# *The State of a Small Amount of Magnesium Contained in Calcareous Shells*

By Yasushi KITANO* and Tsuyako FURUTSU

(Received March 23, 1959)

The distribution of magnesium in calcareous parts of marine organisms was studied by K. E. Chave; he listed the factors which controlled distribution of magnesium in the calcareous skeletal formation of marine organisms[1]. He was also the first to succeed in determining the state of magnesium by using X-ray diffraction technique. The magnesium content of the sample in his study was from 2 to 16% $MgCO_3$ in weight. He concluded that magnesium carbonate was present as a solid solution of calcite and dolomite**[,2]. With his own X-ray diffraction technique, however, Chave was not able to determine the state of magnesium, when the content was more than 16% or less than 2% $MgCO_3$. There are a large number of calcareous shells having a magnesium carbonate content less than 2%. One of the authors, Kitano, was the first to devise a new method for determining the state of a small amount of magnesium contained in calcium carbonate deposits from hot springs, as reported in earlier papers[5-7]. This technique was called the "Dissolution Method". In the present paper the same method is applied for calcareous shells. The process greatly simplifies the determination of the state of magnesium in calcareous shells.

## Principle of Dissolution Method

As to the state of magnesium*** in calcareous shells or organisms, there are only three possible forms, magnesium carbonate, dolomite and a solid solution of calcite and dolomite. When the authors closely examine the three forms from the crystallographic point of view, magnesium carbonate can not be expected, and consequently there are only two forms, dolomite and a solid solution, to be determined. When carbon dioxide gas is passed into a suspension of calcite mixed with dolomite or a suspension of calcite with a solid solution of calcite and dolomite, the dissolved quantity of magnesium can be expected to differ for each of the two magnesium compounds. Therefore, the state of magnesium present in calcareous shells can be determined by knowing the quantity of magnesium dissolved by carbon dioxide aerated water.

## Experimental

**Materials.** — *Calcite.* — Commercial reagent of extra pure grade is used without further purification.

*Aragonite.* — The same volume of 1 N $CaCl_2$ solution is added gradually to the boiling solution of 1 N $Na_2CO_3$; the separated precipitate of aragonite is washed with pure water and allowed to dry.

*Magnesium carbonate.* — Since it is difficult to prepare magnesium carbonate, basic magnesium carbonate (extra pure grade) is used instead of magnesium carbonate. When $MgCO_3 \cdot nH_2O$ is suspended in water, it changes quickly into basic magnesium carbonate, which proves that $MgCO_3 \cdot nH_2O$ is more unstable in water than basic magnesium carbonate[8]. Consequently for the purpose of this experiment, the authors use basic magnesium carbonate (MgO 44.2%) instead of magnesium carbonate.

TABLE I. CONTENT OF CALCIUM AND MAGNESIUM IN FOUR KINDS OF SEA URCHINS

| No. | Ca % | $CaCO_3$ % | Mg % | $MgCO_3$ % |
|---|---|---|---|---|
| 1-a | 32.83 | 82.08 | 3.49 | 12.08 |
| 2-a | 34.82 | 87.05 | 3.07 | 11.62 |
| 3-a | 33.51 | 87.78 | 4.05 | 14.01 |
| 4-a | 35.50 | 88.75 | 3.50 | 12.11 |

*Present address: Water Research Laboratory, Faculty of Science, Nagoya University, Chikusa-ku, Nagoya.

1) K. E. Chave, *J. Geol.*, **62**, 266 (1954).

** In this connection, the authors can write "present as a solid solution composed of calcite and magnesite". As to these two expressions there appears to be no essential difference[3,4].

2) K. E. Chave, ibid., **60**, 190 (1952).

3) R. I. Harkey and O. F. Tuttle, *Am. J. Sci.*, **253**, 209 (1955).

4) R. I. Harkey and O. F. Tuttle, ibid., **253**, 274 (1955).

5) Y. Kitano, *J. Chem. Soc. Japan, Pure Chem. Sec.* (*Nippon Kagaku Zasshi*), **77**, 211 (1956).

6) Y. Kitano, ibid., **77**, 215 (1956).

7) Y. Kitano, ibid., **77**, 218 (1956).

*** It seems better to say "magnesium carbonate" instead of "magnesium".

8) Y. Hagino, *Bull. Soc. Salt Science* (*Nippon Shio Gakkai-shi*), 8, 121 (1954).

*Solid solution of calcite and dolomite.*— For this experiment the shells of four kinds of sea urchins are used. The magnesium carbonate in the shells, as found by using X-ray diffraction technique, is contained as a solid solution. The magnesium content of each kind of shell is given in Table I.

*Dolomite.* — Because it is difficult to prepare this material in a laboratory, the authors use the dolomite found in the Kuzuo Mountain District of Tochigi Prefecture.

(*Anal.*: CaO, 33.80; MgO, 19.37; clay, 0.22%.)

An organic substance, a protein, is always present with minerals in shells, and its presence makes the minerals stable. Therefore, when inorganically prepared minerals are suspended in water, they are less stable than minerals containing an organic material. In this experiment the authors would prefer to use minerals which contain an organic material, but since those can not be obtained, inorganic compounds have to be used. Judging from results given in detail later, however, the use of inorganic minerals, calcite and dolomite, is found to be suitable.

**Procedure.** — The best procedure for the determination of the magnesium state is as follows: Two and a half gram of powdered sample, (<325 mesh), are suspended in 200 ml. of pure water. Carbon dioxide gas, washed by passing through water, is passed into the suspension for 25 min., and is allowed to stand for 10 min. After filtering the suspension with No. 6 Toyo filter paper, the magnesium content in the filtrate is determined. By comparing the dissolved quantities of magnesium in shells with those in mixed samples of calcite and possible magnesium compounds in shells, the state of magnesium in calcareous shells can be determined.

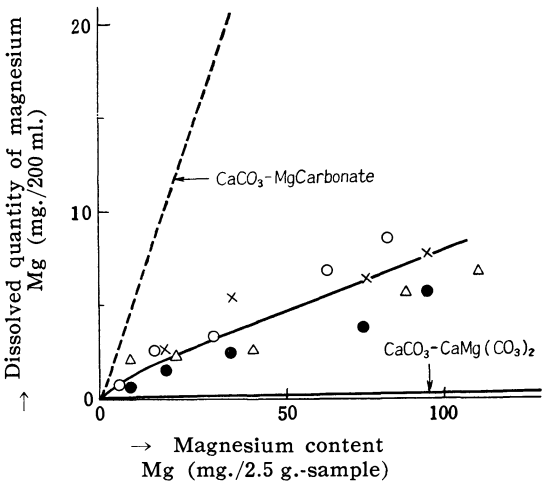



Fig. 1. Relationships between magnesium content and quantity of magnesium dissolved by $CO_2$-aerated water, for possible magnesium compounds in calcareous shells.
× 1-a—e ○ 2-a—e
△ 3-a—e ● 4-a—e

TABLE II. DISSOLVED AMOUNTS OF CALCIUM AND MAGNESIUM IN $CO_2$-AERATED WATER, CALCITE-SHELL OF THE SEA URCHIN, AT ROOM TEMPERATURE

| | Sample | | | | | | | Dissolved quantity | | Ratio in dissolution* | |
|---|---|---|---|---|---|---|---|---|---|---|---|
| | Shell g. | $CaCO_3$ g. | Ca % | Mg % | $MgCO_3$ % | Ca mg. | Mg mg. | Ca mg./200 ml. | Mg mg./200 ml. | Ca, % | Mg, % |
| 1-a | 2.5 | 0.0 | 32.83 | 3.49 | 12.08 | 821 | 87 | 85 | 7.6 | 10 | 8.7 |
| 1-b | 2.0 | 0.5 | 34.26 | 2.78 | 9.62 | 857 | 70 | 82 | 6.4 | 9.6 | 9.1 |
| 1-c | 1.0 | 1.5 | 36.80 | 1.39 | 4.71 | 928 | 35 | 76 | 5.4 | 8.1 | 15 |
| 1-d | 0.5 | 2.0 | 38.58 | 0.70 | 2.42 | 964 | 17 | 74 | 2.6 | 7.7 | 15 |
| 1-e | 0.2 | 2.3 | 39.43 | 0.28 | 0.97 | 986 | 7.0 | 71 | 0.9 | 7.2 | 13 |
| 2-a | 2.5 | 0.0 | 34.82 | 3.07 | 11.62 | 871 | 77 | 82 | 8.5 | 9.4 | 11 |
| 2-b | 2.0 | 0.5 | 35.86 | 2.46 | 8.51 | 896 | 61 | 80 | 6.7 | 8.9 | 11 |
| 2-c | 1.0 | 1.5 | 37.93 | 1.23 | 4.26 | 948 | 31 | 70 | 3.1 | 7.4 | 10 |
| 2-d | 0.5 | 2.0 | 38.96 | 0.61 | 2.11 | 974 | 15 | 70 | 2.0 | 7.2 | 13 |
| 2-e | 0.2 | 2.3 | 39.59 | 0.25 | 0.85 | 990 | 6.1 | 72 | 0.8 | 7.3 | 13 |
| 3-a | 2.5 | 0.0 | 33.51 | 4.05 | 14.01 | 838 | 101 | 76 | 6.8 | 9.0 | 6.6 |
| 3-b | 2.0 | 0.5 | 34.81 | 3.24 | 11.21 | 870 | 81 | 71 | 5.7 | 8.2 | 7.0 |
| 3-c | 1.0 | 1.5 | 37.40 | 1.62 | 5.61 | 935 | 41 | 68 | 2.6 | 7.3 | 6.3 |
| 3-d | 0.5 | 2.0 | 38.70 | 0.81 | 2.80 | 968 | 20 | 67 | 2.3 | 6.9 | 12 |
| 3-e | 0.2 | 2.3 | 39.48 | 0.32 | 1.11 | 987 | 8.1 | 68 | 2.3 | 6.9 | 29 |
| 4-a | 2.5 | 0.0 | 35.50 | 3.50 | 12.11 | 888 | 88 | 82 | 5.6 | 9.2 | 6.4 |
| 4-b | 2.0 | 0.5 | 36.40 | 2.80 | 9.69 | 910 | 70 | 78 | 3.9 | 8.6 | 5.6 |
| 4-c | 1.0 | 1.5 | 38.20 | 1.40 | 4.84 | 955 | 35 | 70 | 2.4 | 7.4 | 6.9 |
| 4-d | 0.5 | 2.0 | 39.10 | 0.70 | 2.42 | 977 | 18 | 65 | 1.5 | 6.6 | 8.7 |
| 4-e | 0.2 | 2.3 | 39.64 | 0.28 | 0.97 | 991 | 7.0 | 68 | 0.6 | 6.9 | 8.1 |

* (dissolved quantity/content in sample) × 100

TABLE III. DISSOLVED AMOUNTS OF CALCIUM AND MAGNESIUM IN $CO_2$-AERATED WATER, VARIOUS KINDS OF CALCAREOUS SHELLS, AT ROOM TEMPERATURE

| Sample Number | Genus | Sample | | | | | Dissolved quantity | | Ratio in dissolution | |
|---|---|---|---|---|---|---|---|---|---|---|
| | | Ca % | Mg % | $MgCO_3$ % | Ca mg./2.5 g. | Mg mg./2.5 g. | Ca mg./200 ml. | Mg mg./200 ml. | Ca % | Mg % |
| 1 | Protothaca jedoesis (Lischke) | 37.89 | 0.81 | 2.80 | 947 | 20 | 77 | 4.0 | 8.1 | 20 |
| 2 | Venerupis Amggdala japonica (Deshdyes) | 36.71 | 0.65 | 2.25 | 918 | 16 | 87 | 0.3 | 9.4 | 1.8 |
| 3 | Meretrix lusorid (Roding) | 36.45 | 0.66 | 2.28 | 911 | 17 | 80 | 0.2 | 8.8 | 1.5 |
| 4 | Paphia euglypta (philippi) | 37.01 | 1.23 | 4.26 | 925 | 31 | 68 | 2.1 | 7.3 | 6.8 |
| 5 | Ostrea (Carssoslraea) gigas Thunberg | 34.60 | 1.79 | 6.19 | 865 | 45 | 75 | 2.6 | 8.6 | 5.7 |
| 6 | Chlamgs mpponensis Kuroda | 36.71 | 0.85 | 2.94 | 918 | 21 | 85 | 1.0 | 9.3 | 4.5 |
| 7 | 〃 (Niotha) levescens | 35.70 | 1.21 | 4.19 | 893 | 30 | 85 | 1.0 | 9.4 | 3.2 |
| 8 | Neverita (glass aulax) didyma | 37.70 | 0.92 | 3.18 | 943 | 23 | 78 | 0.9 | 8.2 | 3.8 |
| 9 | Babyloma japonica (Reeve) | 35.00 | 0.42 | 1.45 | 875 | 11 | 55 | 0.3 | 6.3 | 2.8 |
| 10 | Tonna luteostomo (Kuster) | 36.50 | 0.61 | 3.11 | 913 | 15 | 74 | 1.7 | 8.2 | 11 |
| 11 | Rapana thomasiana Crosse | 38.88 | 0.29 | 1.00 | 972 | 7.3 | 77 | 1.3 | 7.9 | 18 |
| 12 | Mytilus crassitesta Lischke | 36.19 | 0.49 | 1.70 | 905 | 12 | 68 | 1.8 | 7.5 | 15 |
| 13 | Atrina japonica (Reeve) | 36.01 | 0.17 | 0.59 | 900 | 4.3 | 61 | 2.6 | 6.8 | 61 |
| 14 | Ostrea denselamellosa Lischke | 38.79 | 0.00 | 0.00 | 970 | 0.0 | 61 | 0.0 | 6.2 | 0.0 |
| 15 | Saxidomus purpuratus (Sowerby) | 35.73 | 1.90 | 6.57 | 893 | 48 | 79 | 1.6 | 8.9 | 3.4 |
| 16 | Anadara suncrenata (Lischke) | 40.68 | 0.00 | 0.00 | 1017 | 0.0 | 77 | 0.0 | 7.6 | 0.0 |
| 17 | Pinctada Martensi (Dunker) | 35.18 | 0.80 | 2.77 | 880 | 20 | 69 | 3.9 | 7.9 | 15 |
| 18 | Hyriopsis schlegele (Martens) | 37.07 | 0.08 | 0.28 | 926 | 2.0 | 77 | 1.6 | 8.3 | 82 |
| 19 | Mya japonica Jay | 37.84 | 1.08 | 3.74 | 946 | 27 | 73 | 0.6 | 7.8 | 2.1 |
| 20 | Polynices didyma (Röding) | 38.06 | 0.85 | 2.94 | 952 | 21 | 79 | 1.2 | 8.4 | 5.8 |
| 21 | Dosinaia japonica (Reeve) | 37.27 | 1.56 | 5.40 | 932 | 39 | 71 | 1.2 | 7.6 | 3.1 |
| 22 | Babylonia japonica (Reeve) | 38.58 | 1.29 | 4.46 | 965 | 32 | 78 | 2.7 | 8.1 | 8.4 |
| 23 | ? | 38.31 | 0.59 | 2.04 | 958 | 15 | 81 | 0.0 | 8.5 | 0.0 |
| 24 | Rapana thomasiana Crasse | 37.78 | 1.23 | 4.26 | 945 | 31 | 70 | 2.6 | 7.4 | 8.4 |
| 25 | Ostrea sp. | 36.90 | 1.71 | 5.92 | 923 | 43 | 60 | 3.1 | 6.5 | 7.4 |
| 26 | Serpulorlis ? sp. | 34.29 | 2.90 | 10.03 | 857 | 73 | 74 | 1.5 | 8.6 | 2.1 |
| 27 | ? | 37.03 | 1.47 | 5.09 | 926 | 37 | 78 | 2.6 | 8.4 | 7.1 |
| 28 | coral-reef | 37.81 | 0.43 | 1.49 | 945 | 6.5 | 75 | 1.5 | 6.4 | 23 |
| 29 | coral-reef | 36.06 | 1.53 | 5.29 | 902 | 23 | 71 | 3.2 | 7.9 | 14 |
| 30 | Astriclypeus manni Verrill | 33.93 | 3.69 | 12.77 | 848 | 92 | 74 | 7.9 | 8.8 | 8.5 |
| 31 | ? | 38.51 | 0.29 | 1.00 | 963 | 7.3 | 78 | 0.96 | 8.1 | 13 |
| 32 | Callista sinensis (Sowerby) | 38.18 | 0.37 | 1.28 | 955 | 9.3 | 67 | 0.19 | 7.0 | 1.3 |
| 33 | Ciree scripta stutzeri (Donvan) | 38.00 | 0.65 | 2.25 | 950 | 16.2 | 65 | 0.09 | 6.8 | 0.5 |

## Results

Fig. 1 shows the relationship between the amount of magnesium dissolved by carbon dioxide aerated water and the magnesium content in mixed samples of calcite**** and dolomite[5]. In Table II and Fig. 1 the relationship is given for mixed samples[9] of calcite and four kinds of sea urchin shells. When magnesium is contained as dolomite, it is difficult to find any dissolved quantity of magnesium, as is seen from Fig. 1. It may be expected that dolomite becomes more stable and no dissolved quantity of magnesium can be found when it is present with an organic material in calcareous shells. Therefore, it is quite suitable to use in this experiment native dolomite mineral having no organic material.

## Determination of the State of Magnesium Contained in Calcareous Shells

The above procedure is applied to various kinds of calcareous shells and the results are given in Table III and Fig. 2. Fig. 2 includes the result obtained for mixed samples of calcite and dolomite as well as for mixed samples of calcite and a solid solution of calcite and dolomite. From the results given in Fig. 2, it is inferred that a dissolved quantity of magnesium in calcareous shells comes from a solid solution[10]. Therefore, it can be concluded that magnesium carbonate, having a content less than 2% in weight, is contained in calcareous shells as a solid solution. Meanwhile K. E. Chave reported that magnesium carbonate, having a content from 2 to 16% $MgCO_3$, was present in calcareous shells as a solid solution. Kitano reported previously that magnesium in limestone was always present as dolomite[7]. It is known that limestone in nature comes from calcareous shells. Consequently, it may be expected that the natural state of magnesium changes from a solid solution into dolomite during the process of limestone formation from calcareous shells. This finding is important and useful for an understanding of the formation of limestone in nature.

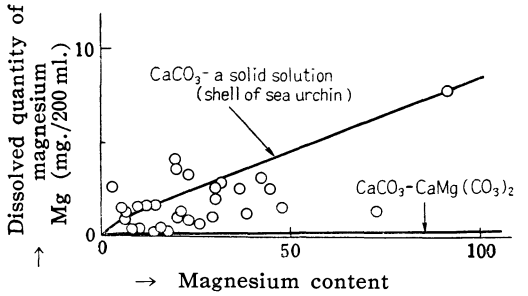



Fig. 2. Relationships between magnesium content and quantity of magnesium dissolved by $CO_2$-aerated water, for various kinds of calcareous shells.

## Summary

An original method (Dissolution Method) for determining small amounts of magnesium contained in calcareous shells has been devised, and the state of magnesium has been determined by this method. As a result, it can be verified that small amounts of magnesium in calcareous shells are always contained as a solid solution of calcite and dolomite.

The authors express their sincere thanks to Mr. Sakae Ichihashi of Osaka City University for his advice given throughout this work.

*Chemical Institute*
*Faculty of Science*
*Kobe University*
*Kobe*

**** Two kinds of calcium carbonate, viz. calcite and aragonite, are used, and no difference between the dissolved quantities of magnesium for these two calcium carbonates can be found. Almost the same amount of calcium carbonate in shells, coexisting with an organic material, as the amount of inorganically prepared calcium carbonate can be dissolved by carbon dioxide aerated water. Hence, the use of inorganically prepared calcite instead of calcium carbonate coexisting with an organic material, is justified.

9) Fig. 1 also shows the relationship in mixed samples of calcium carbonate and magnesium carbonate[5]. It can be expected that the dissolved quantity of magnesium in the solid solution will be higher than that in magnesium carbonate. However, as seen in Fig 1, the latter is in reality higher than the former. That the solid solution used in this experiment is made stable by a coexisting organic material may be responsible for this discrepancy between the presumed and actual results. (The presence of magnesium carbonate can not be expected in calcareous shells, as mentioned earlier).

10) From Fig. 2, it is clear that the dissolved quantity of magnesium in some calcareous shells is less than that in mixed samples of calcium carbonate and shell of four kinds of sea urchins. This can be understood by the following findings: 1) By mixing calcium carbonate with a sea urchin's shell in which 16% $MgCO_3$ is contained as a solid solution, the authors prepare semples containing a small amount of magnesium as a solid solution. It can be expected that the dissolved quantity in the mixed sample will be higher than that in natural shell samples, because a solid solution is less stable with an increase of magnesium content. 2) Since some calcareous shells are not fresh, it appears possible that a part of the solid solution changes to a stable dolomite.

# *Estrogenic Biphenyls. VIII. Preparation and Estrogenic Activity of 4'-(1-Hydroxyalkyl)-4-methoxybiphenyls*

By Takeo SATO

(Received April 20, 1959)

According to the hypothesis presented by Ōki and Urushibara[1] to account for the estrogenic activity of non-steroidal compounds of the stilbene-bibenzyl type, the activity is closely associated with the molecular structure in that the development of strong action requires not only the presence of two active hydrogens or any groups capable of producing such in vivo at the optimum distance from each other, but also optimum thickness and width of the molecule. Therefore, the problems in studying the relation between the physiological action and the molecular structure in a homologous or an analogous series of compounds will be 1) the distance between the active hydrogen atoms in question, 2) the molecular thickness and width, and 3) the nature of the active hydrogens or the groups carrying them.

As for the biphenyl series Dodds and Lawson[2] reported that 4,4'-dihydroxybiphenyl (I) was almost inactive. As the recent X-ray crystallographical investigation[3] of compound I revealed that the molecule of compound I has the unit cell constants of a=10.54 Å, b=5.36 Å and c=7.59 Å, the distance between the two phenolic groups is apparently less than that between the two hydroxyl groups of steroidal hormones or stilbestrol in which the distance between the two oxygens was reported to be 15.5 Å[1b]. Furthermore, the molecule of compound I is planar or nearly planar[4] owing to the full conjugation of the biphenyl system and this is also considered to be unfavorable for the development of strong estrogenic activity. In this respect, 4-hydroxybiphenyl-4'-carboxylic acid (IIa) and its derivatives with two active hydrogens at a longer distance were prepared and found to be estrogenic[5]. While this manuscript was in preparation, however, Y. Osawa[6] observed that compound I, its dimethyl ether and derivatives were considerably active, compound I being active at 500 $\gamma$ in 100% animals (ovariectomized mice), whereas compound IIa was active in 60% animals at the same level[7]. Though the present author can give no comment on this contradiction in the activity of compound I, there might be another optimum distance of two active hydrogens.

The activity of 4-methoxybiphenyl-4'-carboxylic acid (IIb) was enhanced markedly by alkyl substitution, namely, by increasing the molecular thickness and width, and its dialkyl derivatives, in which positions 3' and either 2 or 6' were substituted, produced full estrus in 100% of the mice at a dose of 100 $\gamma$ in spite of the methylation of the phenolic hydroxyl group[5].

In connection with the third problem, 4'-hydroxymethyl-4-methoxybiphenyl (IIIa) has been prepared to obtain a confirmation for the postulation that a compound with a group other than carboxyl but carrying an active hydrogen will be similarly estrogenic, provided that it has two active groups at a similar distance.

A number of analogues of bisdehydrodoisynolic acid methyl ether (IVa), to which the compounds of the present series are structurally related, including the compounds with hydroxymethyl (IVb) and formyl (IVc) groups instead of the carboxyl, have been prepared[8a] and found considerably active though slightly weaker than the carboxylic compound (IVa). The assumption that they are oxidized in vivo to IVa is quite probable and may serve as an explanation for the somewhat

1) (a) M. Ōki and Y. Urushibara, This Bulletin, **25**, 109 (1952). (b) J. Grundy, *Chem. Revs.*, **57**, 281 (1957).

2) E. C. Dodds and W. Lawson, *Proc. Roy. Soc.*, (*London*), **B125**, 222 (1938).

3) S. C. Wallwork and H. M. Powell, *Nature*, **167**, 1072 (1951).

4) Although electron diffraction data indicate the two benzene rings in biphenyl make an angle of about 45° in gas, X-ray diffraction analyses show that biphenyl is a planar molecule when it is solid[1a].

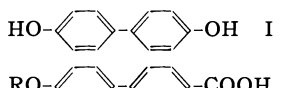
5) See T. Sato and M. Ōki, This Bulletin, **32**, 1289 (1959); also earlier papers of this series.

6) Y. Osawa, Doctorate Thesis, the University of Tokyo (1959).

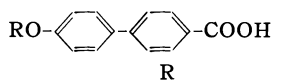
7) M. Ōki and T. Sato, This Bulletin, **30**, 508 (1957).

8) (a) J. Heer and Miesher, *Helv. Chim. Acta*, **30**, 777 (1947). (b) G. Anner and K. Miesher, ibid., **29**, 1071 (1946).

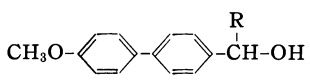
weaker activity. As methyl ketone IVd was found to be very weakly estrogenic[8b], it would be worthwhile to examine a compound with a secondary hydroxyl group which on oxidation would yield a ketone. Such compounds of the present series, namely, IIIb and IIIc have been synthesized. It appears of interest to note a similarity in the bond arrangement of compound IIIc, which is represented as V, with estradiol (VI). Rubin and Wishinsky[9] have already prepared compound VII as a bicyclic analogue of estradiol but not mentioned the activity.



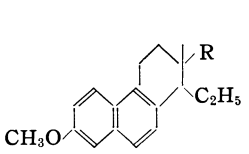
I



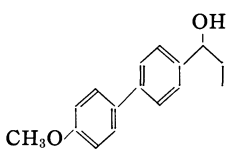
| R | |
|---|---|
| IIa | H |
| b | $CH_3$ |



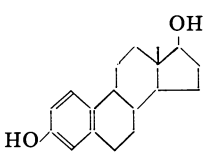
| R | |
|---|---|
| IIIa | H |
| b | $CH_3$ |
| c | $C_2H_5$ |



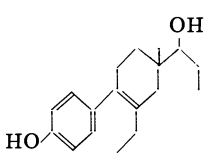
| R | |
|---|---|
| IVa | COOH |
| b | $CH_2OH$ |
| c | CHO |
| d | $COCH_3$ |



V

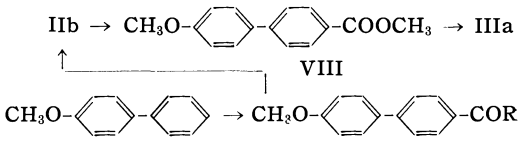


VI



VII

Compound IIIa was obtained through reduction of methyl 4-methoxybiphenyl-4′-carboxylate (VIII)[10,11], prepared from compound IIb, with lithium aluminum hydride in ether. The alkyl homologues IIIb and IIIc were prepared by sodium borohydride reduction of 4′-acetyl-4-methoxybiphenyl (IX) and 4-methoxy-4′-propionylbiphenyl (X), respectively. The methoxyketone IX was prepared from 4-methoxybiphenyl (XI) by Friedel-Crafts reaction according to the literature[10,12]. Similar treatment of compound XI with propionyl chloride and aluminum chloride in carbon disulfide gave the ethyl ketone X, the structure being confirmed by oxidation to the corresponding carboxylic acid IIb likewise the methyl ketone IX[10].



| R | |
|---|---|
| IX | $CH_3$ |
| X | $C_2H_5$ |

→ IIIb or IIIc

Ultraviolet absorption spectra of these alcohols are recorded in Table I with the data of compounds IIb and XI. Compound IIIa showed a strong absorption at 264 m$\mu$ whereas the homologues IIIb and IIIc absorbed at 263 m$\mu$. The curves are very similar and the intensities are nearly the same. As the hydroxymethyl group is only very weakly bathochromic[13], the absorption curves resemble that of 4-methoxybiphenyl (XI) and differ markedly from that of IIb, where additional conjugation with the carboxyl group is possible. These data are also taken as a confirmation of the structures.

TABLE I. ABSORPTION MAXIMA AND ESTROGENIC ACTIVITY

| Compound | m. p. °C | $\lambda_{max}$ m$\mu$ | log $\varepsilon$ | Dose in $\gamma$ (% of response in mice) |
|---|---|---|---|---|
| IIb | 248~249 | 289 | 4.36 | 1000(50) |
| IIIa | 158~159 | 264 | 4.32 | 1000(60) |
| b | 122~123 | 263 | 4.34 | 200(80) |
| c | 91~ 92 | 263 | 4.34 | 200(80) |
| XI | 89 | 260 | 4.31 | ..... |

Compound IIIa was found to be estrogenic to 20% of mice at the dose of 500 $\gamma$ and to 60% at 1 mg., being nearly equally active as compounds IIa[7] and IIb[14]. In compounds IIIb and IIIc, an increase in activity was encountered and they were active to 80% of animals at 200 $\gamma$ level. It is noteworthy that the compounds which are secondary alcohols and racemic

9) M. Rubin and H. Wishinsky, *J. Am. Chem. Soc.*, **68**, 338 (1946).
10) L. F. Fieser and C. K. Bradsher, ibid., **58**, 1738 (1936).
11) L. C. Anderson and W. A. Fisher, ibid., **66**, 594 (1944).
12) W. S. Johnson, C. D. Gutsche and R. O. Offenhauser, ibid., **68**, 1648 (1956).
13) G. H. Beaven, D. M. Hall, M. S. Lesslie and E. E. Turner, *J. Chem. Soc.*, **1952**, 854; G. H. Beaven, D. M. Hall, M. S. Lesslie, E. E. Turner and G. R. Bird, ibid., **1954**, 131.
14) T. Sato and M. Ōki, This Bulletin, **30**, 859 (1957).

are more active than the hydroxymethyl compound.

## Experimental[15]

**Methyl 4-Methoxybiphenyl-4'-carboxylate (VIII).**—The methyl ester was obtained as colorless plates, m. p. 172~173°C, on esterification of 4-methoxybiphenyl-4'-carboxylic acid (IIb) in the usual way. Reported[10,11] melting point is 172~173°C.

**4'-Hydroxymethyl-4-methoxybiphenyl (IIIa).**—To an ethereal slurry made from 100 mg. (0.0026 mol.) of lithium aluminum hydride and 20 ml. of ether, a solution of 240 mg. (0.001 mol.) of compound VIII in 100 ml. of ether was added over a period of 10 min. with efficient stirring. The reaction mixture was gently refluxed on a bath for one hour and then allowed to stand. After the excessive reagent was decomposed with water, 50 ml. of 10% sulfuric acid was added and the aqueous layer was extracted with ether. The ethereal solution was successively washed with water, aqueous sodium hydroxide and water. On evaporation of the solution and recrystallization of the residue from benzene yielded 100 mg. of colorless plates, m. p. 158~159°C.

*Anal.* Found: C, 78.80; H, 7.06. Calcd. for $C_{14}H_{14}O_2$: C, 78.48; H, 6.59%.

*Phenylurethan.*—It was prepared in the usual way as colorless plates melting at 140~141°C on recrystallization from carbon tetrachloride.

*Anal.* Found: N, 4.42. Calcd. for $C_{21}H_{19}O_3N$: N, 4.20%.

**4'-Acetyl-4-methoxybiphenyl (IX).**—4-Methoxybiphenyl (XI), prepared[16] by decomposition of *N*-nitrosoacetanisidide in benzene, was acetylated with acetyl chloride and aluminum chloride in carbon disulfide. Recrystallization from isopropyl alcohol gave compound IX, m. p. 152~153°C. Reported melting point is 153~154°C[10,12].

**4-Methoxy-4'-propionylbiphenyl (X).**—To a mixture of 15g. (0.082 mol.) of compound XI, 13g. (0.098 mol.) of anhydrous aluminum chloride and 100 ml. of carbon disulfide, 8.0 g. (0.086 mol.) of propionyl chloride was added in the course of twenty minutes, while the reaction mixture was gently refluxed. After stirring and refluxing for additional thirty minutes, the mixture was decomposed with ice water containing hydrochloric acid. The product was washed repeatedly with cold ether and recrystallized from ethanol, colorless plates, m. p. 146~147°C. Yield, 11 g. (56% of the theoretical).

*Anal.* Found: C, 79.86; H, 6.84. Calcd for $C_{16}H_{16}O_2$: C, 79.97; H, 6.71%.

On oxidation with potassium permanganate and sodium hydroxide, compound X yielded a carboxylic acid, which did not depress the melting point of an authentic specimen of 4-methoxybiphenyl-4'-carboxylic acid (248~249°C).

*2,4-Dinitrophenylhydrazone.*—It was prepared in the usual way and recrystallized from ethyl acetate, deep red plates, m. p. 201~202°C.

*Anal.* Found: N, 13.42. Calcd. for $C_{22}H_{20}O_5N_4$: N, 13.33%.

**4'-(1-Hydroxyethyl)-4-methoxybiphenyl (IIIb).**—To a suspension of 3 g. (0.016 mol.) of compound IX in 200 ml. of methanol, 0.5 g. (0.013 mol.) of sodium borohydride and 50 ml. of methanol was added in the course of 10 min. After the addition was complete, the mixture was warmed to 60°C and stirred for two hours. Aqueous sodium hydroxide was added and a part of methanol was removed on a steam bath. The residue was diluted with water and the solid was collected. Recrystallization from aqueous ethanol gave 2.5 g. (68% of the theoretical) of colorless plates, melting at 122~123°C.

*Anal.* Found: C, 78.62; H, 6.97. Calcd. for $C_{15}H_{16}O_2$: C, 78.92; H, 7.06%.

*Phenylurethan.*—Colorless plates, melting at 162~163°C, on recrystallization from carbon tetrachloride.

*Anal.* Found: N, 3.82. Calcd. for $C_{22}H_{21}O_3N$: N, 4.03%.

**4'-(1-Hydroxypropyl)-4-methoxybiphenyl (IIIc).**—In the same way as described above, 10 g. (0.042 mol.) of compound X in 400 ml. of methanol was reduced with 1.5 g. (0.040 mol.) of sodium borohydride in 100 ml. of methanol to yield 7.5 g. (74% of the theoretical) of colorless plates, melting at 91~92°C on recrystallization from aqueous ethanol.

*Anal.* Found: C, 79.28; H, 7.37. Calcd. for $C_{16}H_{18}O_2$: C, 79.31; H, 7.49%.

*Phenylurethan.*—It was prepared in the usual way and recrystallized from carbon tetrachloride, colorless plates, m. p. 165~166°C.

*Anal.* Found: N, 3.96. Calcd. for $C_{23}H_{23}O_3N$: N, 3.88%.

**Ultraviolet Absorption Spectra.**—The ultraviolet absorption spectra were measured in 95% ethanol with a Hitachi EPU-2 photo-electric spectrophotometer.

The author wishes to express his hearty thanks to Professor K. Hata, Tokyo Metropolitan University, and Professors Y. Urushibara and M. Ōki, the University of Tokyo, for their kind guidance and encouragement and to the Research Department of Teikoku Hormone Manufacturing Co., Ltd., Kawasaki, for bioassays. The author's thanks are also due to the Ministry of Education for the Grant in Aid for Fundamental Scientific Research.

*Department of Chemistry*
*Faculty of Science*
*Tokyo Metropolitan University*
*Setagaya-ku, Tokyo*

15) All melting points are uncorrected. The author wishes to thank Mr. T. Mizushima of this laboratory for microanalyses.

16) J. W. Haworth and D. H. Hey, *J. Chem. Soc.*, **1940**. 361.

# *Effect of Additives on the Hydrogen Reduction of Nickel Oxide*

By Yoshio IIDA and Kenzo SHIMADA

(Received April 30, 1959)

The effect of additives on hydrogen reduction of metal oxide was previously studied in view of the dissociation pressure of the oxide by Grube[1] and Sano[2]. Parravano[3] recently studied the effect of additives on the reductive properties of nickel oxide from the point of view of a semiconductor and concluded that a direct correlation exists between the activation energy and the type of additives for the hydrogen reduction of nickel oxide.

The present investigation has been undertaken to determine the effect of additives on the temperature at which nickel oxide begins to be reduced by hydrogen, and to ascertain whether or not the properties of a semiconductor are related to the reductive properties of nickel oxide.

## Experimental

Nickel nitrate recrystallized four times was heated at 800°C for 10 hr. to obtain nickel oxide powder. The average particle size of nickel oxide powder was about 0.5 $\mu$ according to an electron micrograph. Aluminum oxide powder obtained by heating c. p. aluminum hydroxide at 800°C for 10 hr. Cupric oxide powder was obtained by heating c. p. nitrate salt at 800°C for 10 hr.

Powders were mixed and pressed at a pressure of 1000 kg./cm$^2$ into tablets $10\times10^{\phi}$ mm. The compacts were heated at various temperatures in a silicon carbide furnace with a sintered corundum tubing.

Weight loss during the reduction process was measured by a thermobalance which had a sensitivity of 0.5 mg. and could be used in hydrogen, vacuum and, if necessary, in oxygen. Hydrogen was used from a commercially available tank after being purified with concentrated sulfuric acid, hot platinum asbestos, potassium hydroxide, and phosphorous pentoxide.

Electrical resistance was measured by a Wheatstone bridge in the range of room temperature to 400°C in air.

## Results

**Effect of Additive Aluminum Oxide.**—In order to study the effect of additive aluminum oxide on reduction of nickel oxide, the reduction-temperature curves were obtained at the rate of heating of 100°C/hr. NiO-$Al_2O_3$ mixtures of 99 : 1, 95 : 5, and 50 : 50 mol. were heated at 1100°C for 4 hr. It is seen from Fig. 1 that the mixtures begin to be reduced at 300°C whereas pure nickel oxide begins to be reduced at 200°C. The reduction-temperature curve of the mixture 50 : 50 mol. ratio consisted of two stages. At the first stage the reduction takes place in the range of 300 to 400°C and the second stage reduction begins at 700°C.

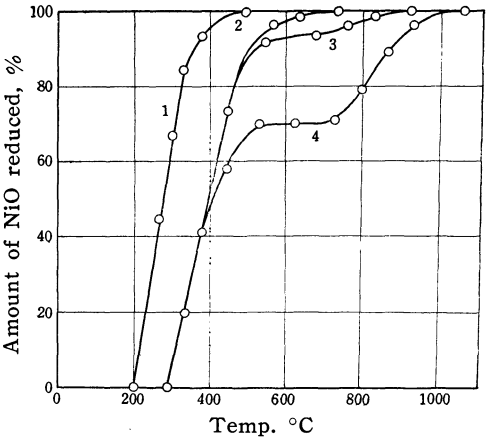



Fig. 1. Reduction-temperature curves of NiO-$Al_2O_3$ mixtures heated at 1100°C for 4 hr. Curve 1 is for pure NiO and curves 2, 3 and 4 are for the mixtures containing 1, 5 and 50 mol. % of $Al_2O_3$, respectively.

**Effect of Additive Lithium Oxide.**—A NiO-$Li_2O$ mixture of 95 : 5 mol. ratio was heated for 4 hr. at 1100°C and the reduction-temperature curve was determined in the same way as described above. It is seen from Fig. 2 that the beginning temperature of reduction of the NiO-$Li_2O$ mixture is about 260°C and is higher that of pure nickel oxide and lower than that of the NiO-$Al_2O_3$ mixture. The temperature at which reduction is completed is 800°C for the NiO-$Li_2O$ mixture and is higher by 400°C than that of pure nickel oxide. It

1) G. Grube, O. Kuvashewuski and K. Zwinaues, *Z. Elektrochem.*, **45**, 881 (1939).
2) K. Sano, *J. Japan Inst. Metals (Nippon Kinzoku Gakukai-shi)*, **6**, 339 (1942).
3) G. Parravano, *J. Am. Chem. Soc.*, **74**, 1194 (1952).

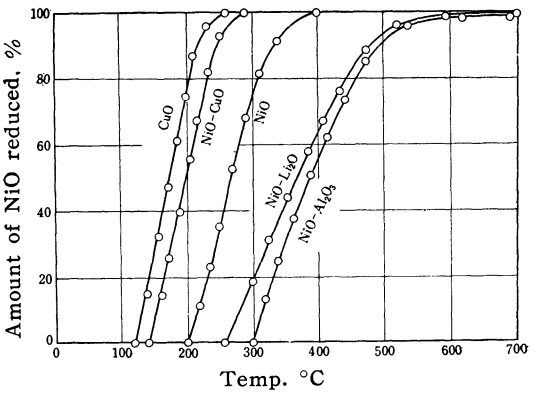



Fig. 2. Reduction-temperature curves of CuO, NiO and mixtures of NiO and 5 mol. % of CuO, $Li_2O$ and $Al_2O_3$, respectively. CuO, NiO and the mixtures were heated at 1100°C for 4 hr.

may be concluded that the heated NiO-$Li_2O$ mixture becomes more difficult to reduce than to do pure nickel oxide.

**Effect of Additive Cupric Oxide.** — The reduction-temperature curve for the NiO-CuO mixture of 95 : 5 mol. ratio heated for four hours at 1100°C was determined at the same rate of heating. It is seen from Fig. 2 that the beginning temperature of reduction for the NiO-CuO mixture is 160°C and is lower than that for nickel oxide. To confirm the fact more evidently, the isotherms of reduction at 160, 140 and 120°C were obtained using the same samples described above. The result is shown in Fig. 3. Pure nickel oxide started to be reduced after an induction period of two hours at 180°C and the amount of nickel oxide reduced was about 80% even after a reducing period of 10 hr. at 180°C. NiO-CuO compact of 95 : 5 mol. ratio heated at 1100°C, however, could be reduced completely after a two hour reducing period at 160°C without an induction period. At 140°C the amount of reduced nickel oxide was 100% after an eight hour reducing period, and even at 120°C the reduction occurred slowly after a two hour induction period. It may be concluded that nickel oxide in the heated NiO-CuO mixture can be reduced at a lower temperature than pure nickel oxide.

In order to see how additive cupric oxide enhances the reduction of nickel oxide by hydrogen, the isotherms of reduction at 140°C for NiO-CuO mixtures of 95 : 5 mol. ratio heated at 700 and 1100°C are compared with the unheated mixtures. The result is shown in Fig. 4. The unheated mixture was reduced by 5% at 140°C for one hour and then ceased to be reduced. Although the mixture heated at 700°C behaves at the initial time of reduction in the same way as the unheated mixture, the one heated at 700°C can be reduced again after a two hour reducing period. The mixture heated at 1100°C can be reduced more rapidly and is reduced by 100% for eight hours at 140°C. It is concluded from the experimental results that cupric oxide in the unheated mixture does not enhance the reduction of nickel oxide but cupric

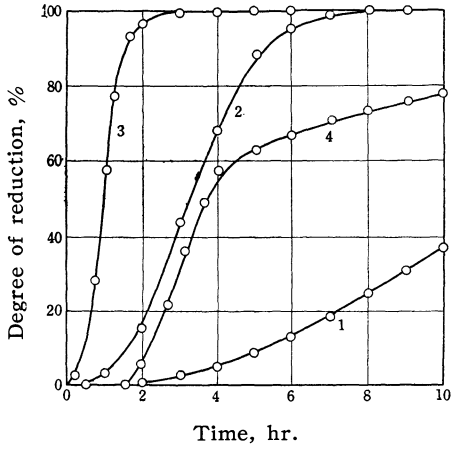



Fig. 3. Comparison between isothermal reduction of NiO-CuO mixture of 95:5 mol. ratio heated at 1100°C and that of pure NiO. Curves 1, 2 and 3 represent reduction of the NiO-CuO mixture at 120, 140 and 160°C, respectively. Curve 4 represents reduction of pure NiO at 180°C.

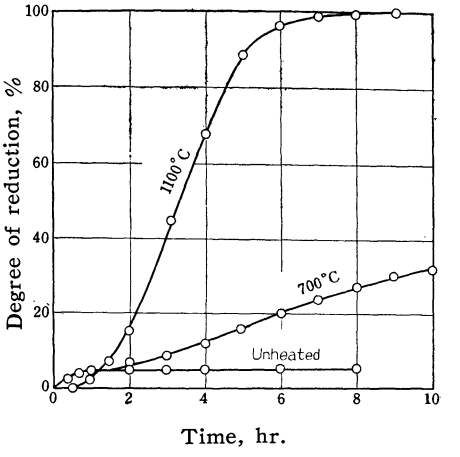



Fig. 4. Isothermal reduction of NiO-CuO mixture of 95:5 mol. ratio heated at 700 and 1100°C, respectively for 4 hr. and of that unheated. The reduction temperature is 140°C.

oxide in the heated mixture enhances the reduction.

## Discussion

In an earlier paper[4] dealing with the solid state reaction of nickel oxide with aluminum oxide, it was shown that when the mixture $NiO$-$Al_2O_3$ was heated, a solid solution of aluminum oxide in nickel oxide and a spinel $NiAl_2O_4$ were formed. From these facts it is concluded that nickel in pure nickel oxide starts to be reduced at 200°C whereas nickel in the solid solution and that in the spinel starts to be reduced at 300 and 700°C, respectively.

Fensham[5] showed that a solid solution is formed when a mixture of nickel oxide and lithium oxide is heated at 1100°C. It was also shown[6] that a solid solution is formed when a mixture of nickel oxide and cupric oxide is heated at 1100°C.

Parravano[3] showed that by incorporation of 5 mol. % of aluminum oxide, the activation energy and the rate of hydrogen reduction of nickel oxide did not differ from those of pure nickel oxide. This result seems to be inconsistent with the result of the present investigation. In Parravano's experiment the mixture of $NiO$-$Al_2O_3$ was heated at 600°C to dissolve aluminum oxide into the nickel oxide crystal, while in this study the mixture was heated at 1100°C. The temperature 600°C seems to be too low to form a solid solution of $NiO$-$Al_2O_3$ completely. This may be the reason for the disagreement.

It was shown by Verwey[7] that nickel oxide is a semiconductor of *p*-type and its electrical conductivity is affected by incorporation of foreign ions. According to the principle of valency control[7], the semiconductivity of nickel oxide decreases by the incorporation of cations with higher valency than two, and increases by the incorporation of monovalent cations. The electrical and reductive properties of nickel oxide incorporated with various additives are shown in Table I. Nickel oxide with various additives was heated at 1100°C for 4 hr. Cationic holes in the nickel oxide lattice increase by the incorporation of $Al^{+3}$ ion and decrease by the incorporation of $Li^+$ ion from the point of view of the electron-neutrality principle.

It can be seen that nickel oxide incorporated with $Li^+$ or $Al^{+3}$ is less readily reducible than pure nickel oxide although $Li^+$ ion has the reverse effect on the semiconductivity compared with $Al^{+3}$ ion. On the other hand, nickel oxide incorporated with $Cu^{+2}$ is more easily reducible than pure nickel oxide, although it has a lower semiconductivity than that of pure nickel oxide. In view of the above facts it is concluded that the effect of impurities on the reductive properties of nickel oxide can not be explained reasonably by the properties of a semiconductor.

Previous reports[1,8] on the effect of additives on hydrogen reduction of oxide showed that the reduction is promoted by the formation of a solid solution of a reduced metal into additives. Niobium could be reduced with hydrogen as an Nb-Ni alloy by the addition of nickel powder[1]. In the present study it is, however, shown that the reductive properties of nickel oxide are not affected merely by the addition of cupric oxide, but affected by the dissolution of a small quantity of cupric oxide into nickel oxide crystal by heating. As the reduced nickel can form no solid solution with unreducible lithium oxide or aluminum oxide, the dissolution of lithium oxide or aluminum oxide should have no influence on the hydrogen reduction according to the above mechanism. The experimental results, however, show that the reduction of nickel

TABLE I. ELECTRICAL AND REDUCTIVE PROPERTIES OF NiO AS A FUNCTION OF IMPURITY DISSOLUTION

| | Electrical resistance at 300°C Ω cm. | Activation energy of electrical conductivity kcal./mol. | Change in the number of vacancies | Reduction beginning temp. °C |
|---|---|---|---|---|
| NiO | $10^5$ | 20 | | 200 |
| $NiO+Al_2O_3$ (5 mol. %) | $10^7$ | 22 | Increase | 300 |
| $NiO+Li_2O$ (5 mol. %) | 10 | 4 | Decrease | 260 |
| NiO+CuO (5 mol. %) | $10^2$ | 10 | Unchange | 160 |

4) Y. Iida, *J. Japan Soc. Powder Metallurgy* (*Huntai oyobi Hunmatsu-Yakin*), **6**, 55 (1959). (in English).
5) P. Fensham, *J. Am. Chem. Soc.*, **76**, 968 (1954).
6) Y. Shimomura, *J. Japan Inst. Metals* (*Nippon Kinzoku Gakukai-shi*), **17**, 421 (1953).
7) E. J. Verwey, P. W. Haaijman, P. C. Romijn and G. W. Osterhout, *Philips Res. Reports*, **5**, 173 (1950).
8) Z. Bankloh, *Z. anorg. u. allgem. Chem.*, **233**, 424 (1937).

oxide is retarded by the dissolution of lithium oxide or aluminum oxide. From these considerations it is concluded that the effect of the dissolution of various oxides on the reduction is not explained completely by the formation of a solid solution.

The reduction of a metal oxide has been considered to be an autocatalytic reaction[9]. Therefore, the accelerated reduction by the addition of cupric oxide is thought to be attributed to the catalytic behavior of metallic copper formed predominantly by hydrogen reduction. It is, however, important to note that cupric oxide does not promote the reduction when cupric oxide is mixed in nickel oxide, but cupric oxide dissolved in the nickel oxide lattice promotes the reduction. From this fact, it is concluded that copper formed predominantly in the reduction process exhibits no catalytic behavior.

In order to know the relation between the reductive properties of nickel oxide incorporated with impurities and the heat of formation of these impurities, the heats of formation of nickel oxide, aluminum oxide, lithium oxide and cupric oxide are given in Table II using the values of Seybolt[10]. It can be seen that the beginning temperature of the reduction of nickel oxide incorporated with other oxides with a greater heat of formation than nickel oxide is higher than that of pure nickel oxide whereas an oxide with a smaller heat of formation than nickel oxide has the reverse effect.

TABLE II. HEAT OF FORMATION OF VARIOUS OXIDES AT 298°K (BY SEYBOLT)

| Oxide | NiO | $Li_2O$ | 1/3 $Al_2O_3$ | CuO |
|---|---|---|---|---|
| Heat of formation kcal./mol. | −51.3 | −134.0 | −126 | −30.4 |

Further, it is seen from Fig. 4 that the induction period of both the unheated mixture NiO-CuO and of that heated at 700°C is shorter than the induction period of that heated at 1100°C. It is evident that the reduction of cupric oxide is retarded by the incorporation of nickel oxide, which has a greater heat of formation than that of cupric oxide.

To see whether this explanation applies to the hydrogen reduction of any other oxide, ferric oxide containing 5 mol. % of aluminum oxide and cupric oxide respectively and pure ferric oxide were heated at 1200°C for 3 hr. and reduced at 350°C isothermally. The results are shown in Fig. 5. It is evident that the dissolution of aluminum oxide which has a greater heat of formation than ferric oxide retards the reduction of ferric oxide and the dissolution of cupric oxide which has a smaller heat of formation than ferric oxide promotes the reduction.

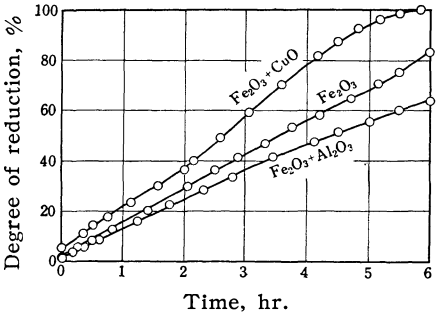



Fig. 5. Isothermal reduction of pure $Fe_2O_3$ and $Fe_2O_3$ containing 5 mol. % of CuO and $Al_2O_3$, respectively. Samples are heated at 1200°C for 3 hr. and reduced at 350°C isothermally.

In view of the above facts the most reasonable conclusion to be drawn from available data is that hydrogen reduction of metal oxide is promoted by the incorporation of another oxide with a greater heat of formation than that of oxide, and is retarded by the incorporation of an oxide with a smaller heat of formation.

## Summary

The effect of additive impurities on the hydrogen reduction of nickel oxide has been studied. The additives have no influence on the reduction unless they dissolve into nickel oxide crystal. The reduction is promoted by the dissolution of cupric oxide and is retarded by the dissolution of lithium oxide and aluminum oxide. The effect of additives on the reduction is not explained reasonably by their catalytic behavior. There is no direct correlation between the reductive properties of nickel oxide and the type of additives from the point of the semiconducting behavior of these materials. The effect of additives on the reduction is related to their heats of formation.

*Government Industrial Research Institute*
*Kita-ku, Nagoya*

9) A. F. Benton and P. H. Emmett. *J. Am. Chem. Soc.*, **46**, 2728 (1924).
10) A. U. Seybolt and J. E. Burke, "Procedures in Experimental Metallurgy", John Wiley & Sons, Inc., New York (1953), p. 175.

# *Polymerization of Methyl Methacrylate Initiated by N-Nitrosophenylurea*

By Ryoichi UEHARA

(Received May 25, 1959)

*N*-Nitrosophenylurea has been prepared by Huisgen[1] by the following reaction of nitrous fumes (a mixture of NO and $NO_2$) and phenylurea:

$$2C_6H_5NHCONH_2 + N_2O_3 = 2C_6H_5N(NO)CONH_2 + H_2O$$

*N*-Nitrosoacylarylamines which are related to *N*-nitrosophenylurea have been noted as sources of free radicals by many investigators[2]. Blomquist[3] has reported polymerizations of methyl methacrylate, styrene and acrylonitrile initiated by several *N*-nitrosoacylarylamines, and suggested that the polymerizations were initiated by aryl radicals which were produced through the decomposition of the *N*-nitrosoacylarylamines. Although *N*-nitrosoacylarylamines were frequently used as initiators during the early period of studies on radical polymerization, they have never since been employed, owing to the facts that they were not efficient as polymerization-initiators and too labile, i.e. they decomposed spontaneously at room temperature. *N*-Nitrosophenylurea is much more stable than *N*-nitrosoacylarylamines, e.g. the half-value periods of *N*-nitrosoacetanilide and *N*-nitrosophenylurea are respectively 99.5 min. at 20°C and 140 min. at 40°C[1].

It has been found by the present author that *N*-nitrosophenylurea is an efficient initiator of the polymerization of methyl methacrylate. In the present paper, results of experiments on the dependence of the initial rate of polymerization upon the concentration of *N*-nitrosophenylurea and methyl methacrylate are given.

The polymerization was carried out in an atmosphere of nitrogen. In Table I, the conversion versus time and average degree of polymerization of polymethyl methacrylate in the bulk polymerization of methyl methacrylate initiated by *N*-nitrosophenylurea $1.21\times10^{-2}$ mol./l. at 60°C are shown. The conversion in the bulk polymerization initiated by benzoyl peroxide $1.30\times10^{-2}$ mol./l. is also shown in Table I. As an initiator of the polymerization of methyl methacrylate, *N*-nitrosophenylurea is more efficient than benzoyl peroxide.

Dependences of the initial rate of polymerization (R) upon the concentration of *N*-nitrosophenylurea ([NPU]) in solution-polymerization in benzene (methyl methacrylate 50%) at temperatures of 40, 50, 60 and 70°C are shown in Fig. 1. It is evident that the square root dependence holds for each case, i.e. the initial rate of polymerization is linearly proportional to the square root of the concentration of *N*-nitrosophenylurea. The relationship between the initial rate of polymerization and the concentration of methyl methacrylate ([MMA]) in benzene (*N*-nitrosophenylurea $1.24\times10^{-2}$ mol./l.) was studied at 60°C. It is clear that the initial rate

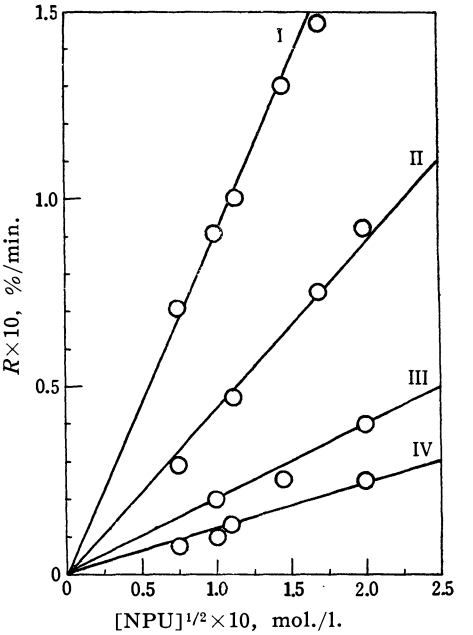



Fig. 1. Correlations of the initial rate of polymerization with the concentration of *N*-nitrosophenylurea (methyl methacrylate 50% in benzene) at 70 (I), 60 (II), 50 (III) and 40°C (IV).

1) R. Huisgen and L. Krause, *Ann.*, **157**, 5474 (1951).
2) See, e.g. W. S. Grieve and D. H. Hey, *J. Chem. Soc.*, **1934**, 1797.
3) A. T. Blomquist et al., *J. Am. Chem. Soc.*, **65**, 2446 (1943).

TABLE I. CONVERSIONS AND AVERAGE DEGREES OF POLYMERIZATION IN THE BULK POLYMERIZATION AT 60°C BY MEANS OF *N*-NITROSOPHENYLUREA $1.21\times10^{-2}$ mol./l.

| Time min. | Conversion, % by NPU | by BPO | Average degree of polymerization* |
|---|---|---|---|
| 30 | 3.8 | 3.1 | 2820 |
| 60 | 5.5 | 4.2 | 4300 |
| 90 | 8.1 | 6.9 | 4210 |
| 120 | 11.1 | 9.3 | 4330 |
| 150 | 15.1 | 13.4 | 4560 |
| 180 | 22.5 | 17.8 | 6020 |
| 210 | 33.4 | 25.9 | 6300 |
| 240 | 53.0 | 45.5 | 7720 |
| 270 | 74.0 | 65.0 | 7900 |
| 300 | 87.1 | 76.2 | 7800 |
| 330 | 93.0 | 82.1 | 6950 |
| 360 | 95.4 | 85.5 | 6300 |

* Polymethyl methacrylate produced by NPU.

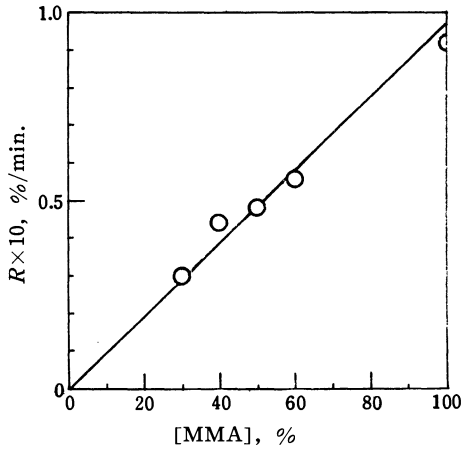



Fig. 2. Correlation of the initial rate of polymerization with the concentration of methyl methacrylate (at 60°C, NPU $1.24\times10^{-2}$ mol./l.)

was linearly proportional to the concentration of methyl methacrylate.

These rate-concentration relationships are quite similar to those which are observed in the polymerizations of vinyl monomers initiated by benzoyl peroxide or $\alpha,\alpha'$-azo-bis-iso-butylonitrile in which unimolecular first order decompositions of the initiators are considered as the initiating reactions by many investigators[4]. Consequently, it is very probable that the polymerization of methyl methacrylate by means of *N*-nitrosophenylurea is initiated by radicals which are produced through the unimolecular first order decomposition of *N*-nitrosophenylurea. The nature of the initiating reaction will be studied in future.

When logarithms of the initial rates of polymerization (methyl methacrylate in benzene 50% and *N*-nitrosophenylurea $1.24\times10^{-2}$ mol./l.) were plotted against reciprocals of temperatures ($1/T$), a good straight line was obtained (Fig. 3). The overall activation energy calculated from the slope in Fig. 3 was found to be 12.8 kcal./mol.

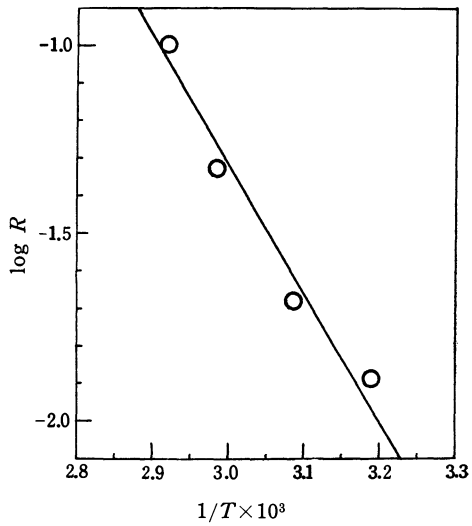



Fig. 3. Correlation of log $R$ with $1/T$ (MMA 50%, NPU $1.24\times10^{-2}$ mol./l.).

## Experimental

**Materials.**—Purification of methyl methacrylate and benzene was carried out as mentioned in a previous paper[5]. *N*-Nitrosophenylurea was prepared through the reaction of nitrous fumes upon phenylurea. Phenylurea (6.8 g.) was suspended in a mixture of glacial acetic acid and acetic anhydride (3 : 1 by volume, 40 cc.) and cooled to 0°C. Nitrous fumes which were produced from arsenious oxide and nitric acid[6] were passed into the suspension until 20 g. of them were absorbed. The crude product was precipitated by pouring the suspension into ice water (200 cc.). The crude product was washed with water (400 cc.) and recrystallized twice from ether, giving pure *N*-nitrosophenylurea (3.1 g.), m. p. 89°C with decomposition. The pure product could be stored in an ice bath for several weeks without any appreciable decomposition.

**Polymerization.**—Details of the procedures of polymerization and the determination of the initial rate of polymerization were given previously[5]. In solution-polymerization, *N*-nitrosophenylurea was dissolved in benzene. Measured amounts of the benzene solution and methyl

4) P. J. Flory, "Principles of Polymer Chemistry", Cornell University Press, Ithaca, N. Y. (1953), p. 116.

5) R. Uehara, This Bulletin., 31, 685 (1958).

6) A. W. Dox, "Organic Syntheses", Col. Vol. 1, John Wiley & Sons, Inc., New York (1941), p. 266.

methacrylate were placed in a test tube and mixed. The test tube was cooled in a dry ice-methanol bath, flashed with nitrogen, evacuated and sealed. Conversions of the polymerization were measured by precipitating and weighing polymethyl methacrylate formed. Degrees of polymerization of polymethyl methacrylate were estimated from their intrinsic viscosities in chloroform according to Sakurada[7].

**Summary**

*N*-Nitrosophenylurea is an efficient initiator of the polymerization of methyl methacrylate. The initial rate of polymerization of methyl methacrylate was linearly dependent upon the concentration of methyl methacrylate and the square root of the concentration of *N*-nitrosophenylurea. These facts suggest that the polymerization is initiated by radicals which are produced through a unimolecular first order decomposition of *N*-nitrosophenylurea.

The author wishes to express his hearty thanks to Professor Osamu Simamura of the University of Tokyo for his interests in this work and Mr. Tsurahide Cho, the President of Tama Kagaku Kogyo Co., for permission to publish, this work.

*Tama Kagaku Kogyo Co.*
*2-28 Minamirokugo*
*Ota-ku, Tokyo*

7) I. Sakurada, *Chem. High Polymers* (*Kobunshi Kagaku*), 2, 253 (1945).

# *Electrode Processes of Nickel(II) Ions at the Mercury Electrode in Concentrated Calcium Chloride Solutions*

By Nobuyuki TANAKA, Reita TAMAMUSHI and Mutsuo KODAMA*

(Received June 8, 1959)

The electrode reaction of nickel(II) ions at the mercury electrode seems to proceed with various mechanisms, depending on the kind of supporting electrolyte present in the solution. It has been known that the reduction of nickel(II) ions at the dropping mercury electrode (DME) in the concentrated solution of chloride occurs with a higher degree of reversibility at the potentials much more positive than those at which the reduction of hydrated nickel(II) ions takes place[1]. Reynolds and his coworkers[2,3] pointed out, from the results of the microcoulometry, that the reduction process of nickel(II) ions at the DME in 5 M calcium chloride solution is represented by

$$Ni^{2+} + 2e \rightarrow Ni$$

Recently, Vlček[4] reported that one continuous redox wave is obtained by the Kalousek's method[5,6] with nickel(II) ions in 6 M calcium chloride solution. From this result, he suggested that nickel(II) ions in 6 M calcium chloride solution is reduced at the mercury electrode to a zero-valent nickel complex, $NiCl_4^{4-}$, the life of which is estimated to be longer than 0.01 sec.

In this paper, an extensive and systematic study on the reduction of nickel(II) ions in concentrated calcium chloride solution at the mercury electrode is presented. The number of electrons which participate in the overall electrode reaction has been accurately determined by the coulometry at constant potential. The reduction product has been investigated by means of the controlled potential electrolysis at the mercury electrode. The reversibility of the electrode reaction is discussed from the analysis of the direct current (d. c.), the alternating current (a. c.) and the Kalousek's polarograms, and a possible mechanism for the reaction is proposed.

* Present address: Department of Chemistry, Faculty of Liberal Arts, Ibaraki University, Mito.

1) I. M. Kolthoff and J. J. Lingane, "Polarography", Vol. II, Interscience Publishers, Inc., New York (1952), p. 486.

2) G. F. Reynolds, H. I. Shalgosky and T. J. Weber, *Anal. Chim. Acta*, 8, 567 (1953).

3) G. F. Reynolds and H. I. Shalgosky, ibid., **10**, 398 (1954).

4) A. A. Vlček, *Z. Elektrochem.*, **61**, 1014 (1957).

5) M. Kalousek, *Collection Czechoslov. Chem. Communs.*, **13**, 105 (1948).

6) R. Tamamushi and N. Tanaka, *Repts. Inst. Sci. Technol. Univ. Tokyo*, **5**, 33 (1951).

## Experimental

**Apparatus.**—Current-voltage curves were measured by a manual polarograph similar to that of Kolthoff and Lingane[7] or recorded automatically by a Yanagimoto Galvarecorder Y-GR 2. The Galvarecorder was also used for recording the a. c. and the Kalousek's polarograms and the current-time curves in coulometry.

The Kalousek's circuit used in this study is schematically shown in Fig. 1. The potential of

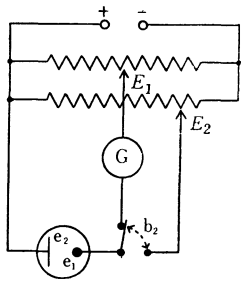



Fig. 1. Circuit of the Kalousek's method: G, Galvarecorder; $e_1$, working electrode (DME); $e_2$, unpolarizable electrode (S. C. E.); $b_2$, exchange switch (contact of relay B in Fig. 2).

the working electrode, $e_1$, is periodically changed from $E_1$ to $E_2$ and vice versa by the exchange switch $b_2$. When the reduction wave is concerned, $E_2$ is usually kept constant at a certain definite value in the potential region of the limiting current plateau. The value of $E_1$ is varied in the same way as in the ordinary polarograph, and only the current which flows when the electrode potential is $E_1$ is recorded. If the reduced substance produced at the electrode is oxidized at the potential of $E_1$, the anodic current is observed.

A simple relay circuit as shown in Fig. 2 was used to exchange the electrode potential instead of a conventional mechanical commutator which consists of a synchronous motor and a rotary switch. Relay B in Fig. 2 has two pairs of contacts, $b_1$ and $b_2$, the latter of which is used for

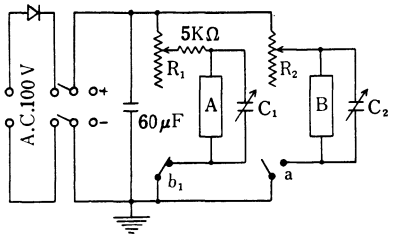



Fig. 2. Circuit of exchange switch: A, B, relay; a, contact of relay A; $b_1$, contact of relay B; $R_1$, $R_2$, 5 kΩ; $C_1$, $C_2$, 5~50 μF.

7) I. M. Kolthoff and J. J. Lingane, "Polarography", Vol. I, Interscience Publishers, Inc., New York (1952), p. 297.

the exchange switch in Fig. 1. The exchange frequency can be easily changed from apporoximately 2 c/s to 30 c/s by adjusting the capacitors $C_1$ and $C_2$. The on-and-off intervals of the switch were made equal by adjusting $R_1$ and $R_2$. This switch proved to be preferable to the conventional mechanical commutator because of the constancy and reliability in its switching action as well as because of its wide range of exchange frequencies. In this study, the exchange frequency of approximately 5.6 c/s was employed unless otherwise stated.

The controlled potential electrolysis was carried out by using a Yanagimoto automatic potentiostat. In the coulometric study the current through the electrolysis cell during the constant potential electrolysis was automatically recorded with a Yanagimoto Galvarecorder[8]. The quantity of electricity was determined by the graphical integration of the current-time curve thus obtained.

A simple beaker type cell was used for all polarographic measurements. A dropping mercury electrode, which had an $m$ value of $1.94_8$ mg./sec. and a drop time $\tau$ of 4.88 sec./drop in an air free 0.1 M potassium chloride solution at −0.60 V. vs. S. C. E., was used for the measurement of current-voltage curves. A saturated calomel electrode of a large surface area was used for the reference electrode, which was connected with the electrolytic solution by a Hume and Harris' type salt bridge[9]. When a. c. polarograms were measured, a platinum plate electrode of a large surface area was inserted in the electrolytic solution as the third electrode, which was terminated at the saturated calomel electrode through a 100 μF capacitor in order to minimize the impedance of the cell[10]. In the controlled potential electrolysis, the cathode was a mercury pool electrode whose surface area was approximately 20 $cm^2$, while the anode was a platinum spiral electrode which was connected with the electrolytic solution through a salt bridge. A saturated calomel electrode was used as a reference electrode, against which the electrode potential of the cathode was controlled.

All measurements were carried out in a thermostat of 25.00±0.01°C, and the dissolved oxygen in the electrolytic solution was removed by bubbling pure nitrogen gas through the solution. The d. c. and the Kalousek's polarograms given in this paper were corrected for the residual current and the ohmic potential drop of the cell circuit.

**Reagents.** — A standard solution of nickel chloride was prepared by the following procedure. An appropriate amount of pure nickel metal (Yokozawa Chemicals Co.: cobalt content, 0.004%) was dissolved in nitric acid, and the excess of nitric acid was removed by evaporation. By dilution with distilled water a nickel nitrate

8) N. Tanaka, T. Nozoe, T. Takamura and S. Kitahara, This Bulletin, 31, 827 (1958).

9) D. N. Hume and W. E. Harris, *Ind. Eng. Chem. Analyt. Ed.*, 15, 465 (1943).

10) B. Breyer, F. Gutmann and S. Hacobian, *Australian J. Sci. Research, Ser. A*, 4, 595 (1951).

solution was obtained, to which a suitable amount of sodium carbonate was added to precipitate nickel(II) as carbonate. The precipitate was filtered off and washed thoroughly with distilled water. The resulting nickel carbonate was dissolved in dilute redistilled hydrochloric acid to prepare the standard solution of an appropriate concentration. The concentration of nickel was accurately determined by the conventional gravimetric method with dimethylglyoxime[11].

Calcium chloride which was free from organic surface-active substances was prepared. Reagent grade calcium chloride dihydrate was heated for 3 hr. at 470°C in an electric oven, and dissolved in redistilled water. After a small amount of insoluble substance was removed by decantation, the pH of the solution was adjusted to about 4.0 by adding hydrochloric acid. The chloride concentration of the solution was determined by the Volhard method[12].

All other chemicals used were of analytical reagent grade. Redistilled water was used to dilute the stock solutions and to prepare the electrolytic solutions.

## Results

In a preliminary investigation, it was found that in 6 M unpurified calcium chloride solution nickel(II) ions are not reduced at the mercury pool electrode at the potentials where they are reduced at the DME. Their reduction at the mercury pool electrode occurred only at much more negative potentials. This phenomenon was not observed when the supporting electrolyte solution was prepared with purified calcium chloride, and therefore it was explained as due to the poisoning effect of surface-active substances which might have been present in the solution prepared with the unpurified reagent. The reduction potential of nickel(II) at the mercury pool electrode was found to shift to negative potentials upon the addition of polyoxyethylene lauryl ether to the electrolytic solution prepared with the purified calcium chloride. This clearly supports the above explanation. In this paper, only the experimental results which were obtained with purified calcium chloride are presented.

The d. c. polarograms of nickel(II) ions which were obtained in the solutions containing various concentrations of calcium chloride are given in Fig. 3. In the presence of 6 M calcium chloride, nickel(II) ions gave a polarogram with a half-wave potential of −0.462 V. vs. S. C. E. A log-

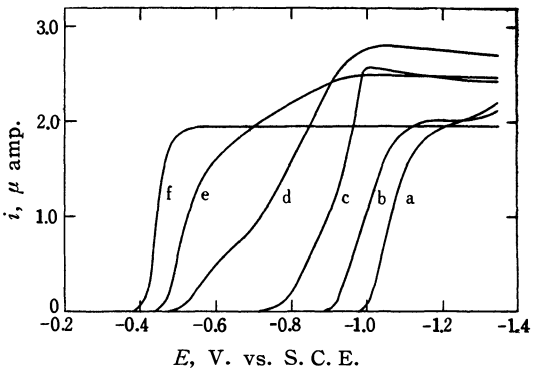



Fig. 3. D. C. polarograms of 0.844 mM Ni(II) ions in the solutions of various concentrations of calcium chloride: a, 1.0 M; b, 2.0 M; c, 3.0 M; d, 4.0 M; e, 5.0 M; f, 6.0 M $CaCl_2$.

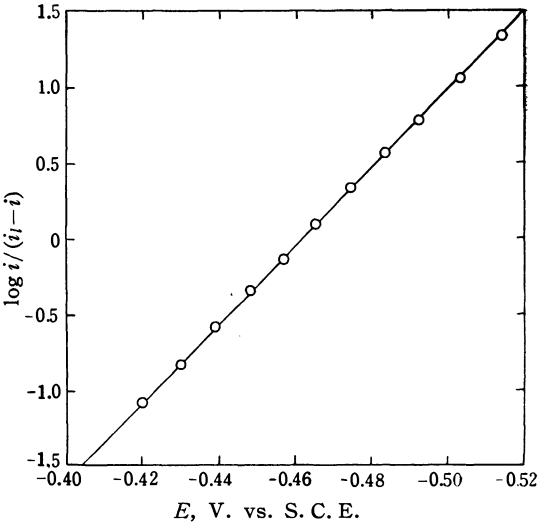



Fig. 4. Log-plot of the d. c. reduction wave of Ni(II) ions in 6 M $CaCl_2$ solution.

plot, i. e. a plot of $\log i/(i_l-i)$ against $E$, of the polarogram gave a straight line with a slope of 38 mV. (Fig. 4). The limiting current was found to be proportional to the bulk concentration of nickel(II) and also to the square-root of the effective pressure on the DME, as shown in Tables I and II.

TABLE I. RELATION BETWEEN THE LIMITING CURRENT $i_l$ AND THE BULK CONCENTRATION $C$ OF NICKEL(II) IONS IN 6 M $CaCl_2$ SOLUTION

| $C$, mM | $i_l$, μ amp. | $i_l/C$, μ amp./mM |
|---|---|---|
| 0.844 | 1.95 | 2.31 |
| $1.68_7$ | 3.89 | 2.31 |
| $2.53_1$ | 5.85 | 2.31 |
| $3.37_5$ | 7.79 | 2.31 |
| $6.75_0$ | 15.58 | 2.31 |

11) F. P. Treadwell and W. T. Hall, "Analytical Chemistry", Vol. 2, John Wiley & Sons, Inc., New York (1951), p. 193.
12) F. P. Treadwell and W. T. Hall, Ibid., p. 650.

TABLE II. RELATION BETWEEN THE LIMITING CURRENT $i_l$ OF 3.37$_5$ mM $NiCl_2$ IN 6 M $CaCl_2$ SOLUTION AND THE EFFECTIVE PRESSURE $h$ ON THE DME

| $h$, cmHg | $i_l$, $\mu$amp. | $i_l/\sqrt{h}$, $\mu$amp. $cm^{-1/2}$ |
|---|---|---|
| 40 | 6.55 | 1.04 |
| 55 | 7.79 | 1.05 |
| 85 | 9.78 | 1.06 |

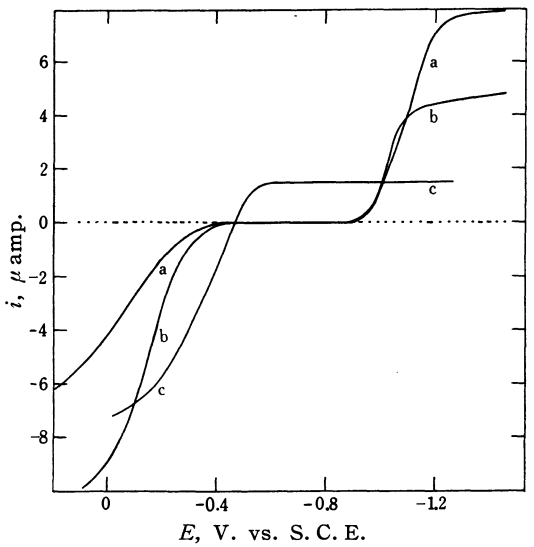



Fig. 5. Kalousek's polarograms of Ni(II) ions obtained at exchange frequency of 5.6 c/s. a; 2.0 mM $Ni(NO_3)_2$ in 0.2 M $KNO_3$, $E_2=-1.45$ V. vs. S. C. E.: b; 1.7 mM $NiCl_2$ in 0.2 M KCl, $E_2=-1.40$ V. vs. S. C. E.: c; 1.7 mM $NiCl_2$ in 6 M $CaCl_2$, $E_2=-0.75$ V. vs. S. C. E.

The Kalousek's polarograms in Fig. 5 were recorded in 6 M calcium chloride, 0.2 M potassium chloride and 0.2 M potassium nitrate solutions. In the 6 M calcium chloride solution one continuous redox wave (Fig. 5, c) was observed as has been reported by Vlček[4], while in the 0.2 M potassium chloride and the 0.2 M potassium nitrate solution no continuous redox wave was obtained, the anodic waves being far separated from the cathodic ones. It may be interesting to note that the potentials at which the anodic waves appear are almost identical in the three different solutions investigated.

In the 6 M calcium chloride solution a typical a. c. polarogram of nickel(II) as shown in Fig. 6 was obtained, the summit potential of which was nearly equal to the half-wave potential of the d. c. polarogram.

An example of the d. c. polarograms of nickel(II) ions obtained at the mercury pool electrode in the 6 M calcium chloride

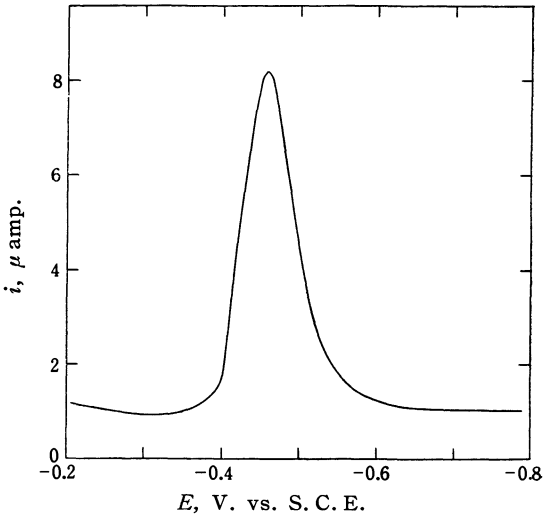



Fig. 6. A. C. polarogram of 3.37$_5$ mM Ni(II) ions in 6 M $CaCl_2$ solution.

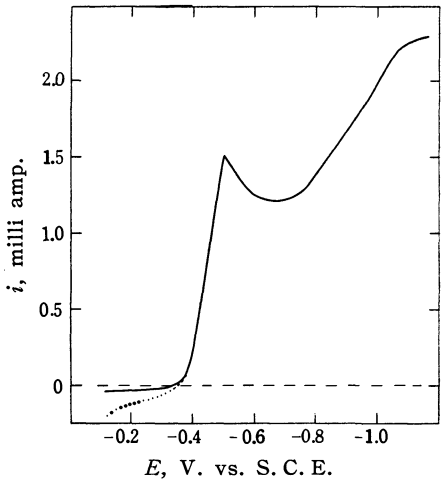



Fig. 7. Current—potential curve of Ni(II) ions in 6 M $CaCl_2$ solution at the mercury pool electrode.

solution is given in Fig. 7. An apparent anodic current was observed when the working electrode was polarized at $-0.1\sim-0.3$ V. vs. S. C. E. immediately after it had been polarized for 20 to 30 min. at the potential where the reduction of nickel(II) takes place (dotted line in Fig. 7). This anodic current remained nearly constant for several minutes if the solution was stirred by nitrogen gas bubbled through it. On the other hand, no anodic current was observed at the dropping mercury electrode with the same solution with which the anodic current was observed at the mercury pool electrode.

The number of electrons $n$ which participate in the overall electrode reaction of

nickel(II) was determined coulometrically by the controlled potential electrolysis. It can be calculated from the relation

$$n = \frac{Q}{FM} \times \frac{(i_d)_1}{(i_d)_1 - (i_d)_2}$$

where $Q$ is the quantity of electricity required for the electrolysis expressed in coulomb, $M$ the initial amount of nickel(II) ions present in the solution expressed in mole, and $(i_d)_1$ and $(i_d)_2$ are the diffusion currents of nickel(II) before and after the electrolysis, respectively. The value of $Q$ was corrected for the quantity of electricity that was measured with the supporting electrolyte solution under the same conditions of actual electrolysis. The results are presented in Table III.

TABLE III. THE NUMBER OF ELECTRONS $n$ CONCERNING THE OVERALL ELECTRODE REDUCTION OF Ni(II) IN 6 M $CaCl_2$ SOLUTION*

| Expt. | $(i_d)_1$, $\mu$ amp. | $(i_d)_2$, $\mu$ amp. | $Q$, coulombs | $n$ |
|---|---|---|---|---|
| 1 | 7.79 | 6.02 | $2.95_9$ | 2.00 |
| 2 | 7.71 | 5.62 | $3.53_2$ | 2.00 |

* The initial amount of Ni(II) was 0.0675 millimol.

In order to know whether the reduced substance of nickel(II) in 6 M calcium chloride solution is contained in the solution or in the mercury of the electrode, the nickel content of the mercury was determined after the electrolysis. Twenty milliliters of $3.37_5$ mM of nickel(II) solution containing 6 M calcium chloride was subjected to the controlled potential electrolysis at −0.80 V. vs. S. C. E. with a mercury pool electrode. After 30 to 40% of the total amount of nickel(II) was reduced, the mercury electrode was separated from the solution, washed carefully with distilled water, and then treated for about 30 hr. with 30 ml. of 3 M hydrochloric acid to extract nickel in the mercury. The precipitate of mercurous chloride produced was filtered off. The volume and pH of the filtrate were adjusted to be about 130 ml. and 6.0~6.5, respectively, by adding distilled water and ammonium hydroxide solution. Then, 15 ml. of 2 M potassium iodide solution was added to the solution, and the solution was kept standing for 30 min. The nickel content of the solution was determined by titration with a 0.01 M ethylenediaminetetraacetate solution using murexide as an indicator[13]. Preliminary experiments indicated that the nickel content can be determined with this procedure in the presence of an excess of mercuric ions. The amounts of nickel(II) ions reduced by the controlled potential electrolysis and those of nickel found in the mercury electrode are given in Table IV.

TABLE IV. DETERMINATION OF THE AMOUNT OF NICKEL IN THE MERCURY POOL ELECTRODE

| Amount of Ni(II) ion reduced, millimol. | Amount of Ni(II) ion found in the mercury pool electrode, millimol. | Recovery of nickel, % |
|---|---|---|
| 0.0287 | 0.0276 | 96 |
| 0.0216 | 0.0203 | 94 |

## Discussion

The color of the solution containing nickel(II) ions and 6 M calcium chloride is yellowish green. This suggests the formation of chloronickel(II) complexes. According to Kiss and his coworkers[14] and Kiseleva and Khodeeva[15], the predominant species of these complexes is considered to be $NiCl_4^{2-}$.

The results given in Table II shows that the limiting current of nickel(II) ions in 6 M calcium chloride solution is diffusion-controlled. The relatively low value of the diffusion current for the unit concentration (Table I) is supposed to be due to the high viscosity of the solution. It is known that the diffusion coefficient of ions in the electrolyte solution is inversely proportional to the viscosity of the solution[16]. If the relation

$$D = D^\circ/\eta$$

where $D^\circ$ is the diffusion coefficient of $Ni^{2+}$ ions at infinite dilution and $\eta$ the viscosity of the 6 M calcium chloride solution referred to that of water as unity, is applied to the present case, the diffusion coefficient $D$ of nickel(II) ions in 6 M calcium chloride solution is calculated to be $8.1 \times 10^{-7}$ cm$^2$/sec., when $6.9 \times 10^{-6}$ cm$^2$/sec. is used for $D^\circ$[17] and 8.5 for $\eta$[18]. With the value of $D$ thus obtained, the number of

13) G. Schwarzenbach, "Die Komplexometrische Titration", Ferdinand Enke, Publisher, Stuttgart (1956), p. 66.
14) Á. v. Kiss and P. Csokán, *Z. anorg. u. allgem. Chem.*, **245**, 355 (1941).
15) E. V. Kiseleva and S. M. Khodeeva, *Trudy Moskov. Khim. Tekhnol. Inst. im. D. E. Mendeleeva*, **1956**, No. 22,89-96; *Chem. Abstr.*, **51**, 16183*e* (1957).
16) I. M. Kolthoff and J. J. Lingane, "Polarography", Vol. I, Interscience Publishers, Inc., New York (1952), p. 97.
17) I. M. Kolthoff and J. J. Lingane, ibid., p. 52.
18) "International Critical Tables", Vol. V, McGraw-Hill Book Co., Inc., New York (1929), p. 14.

electrons which participate in the overall electrode reaction is calculated to be 2.0 with the modified Ilkovič equation[19]

$$i_d = 607\, nD^{1/2}m^{2/3}\tau^{1/6}C\left(1+\frac{34\tau^{1/6}D^{1/2}}{m^{1/3}}\right)$$

This value of $n$ is in agreement with that obtained by coulometry at constant potential (Table III), and leads to a conclusion that the nickel(II) ions in 6 M calcium chloride solution are reduced at the mercury electrode to either nickel metal or some chloro complexes of zero-valent nickel.

It has been reported by Vlček[4] that the anodic wave of the Kalousek's polarogram obtained with nickel(II) ions in 6 M calcium chloride solution is due to the oxidation of zero-valent nickel complex, $NiCl_4^{4-}$, formed on the surface of the electrode. On the other hand, it has been known that nickel amalgam is easily obtained by the reduction of aqueous solutions of nickel chloride or sulfate at the mercury electrode[20,21]. Breckpot[22] reported that the oxidation of nickel amalgam occurred at +0.10 V. vs. N. H. E. at 75°C under the current density of 15 amp./m$^2$. This value of oxidation potential agrees approximately with those which were determined from the Kalousek's polarograms given in Fig. 5. The anodic wave is clearly observed on the Kalousek's polarogram which was obtained at the exchange frequency of about 2 c/s. This seems to be an indication that the life of the substance which is actually oxidized by the Kalousek's method must be longer than 0.5 sec. These facts strongly suggest that the anodic current observed with the Kalousek's method is due to the oxidation of nickel amalgam. It should be noted that the oxidation of nickel amalgam proceeds at almost the same potential in all of the solutions (the 6 M calcium chloride, the 0.2 M potassium chloride and the 0.2 M potassium nitrate solution), while the reduction takes place at entirely different potentials in these three solutions depending on the species and the concentration of supporting electrolyte.

Table IV shows that the amount of nickel reduced at the mercury electrode in 6 M calcium chloride solution is almost completely recovered from the mercury electrode. This excludes any possible contribution of the monovalent nickel compounds to the overall electrode reaction, but supports the conclusion that the reduced substance is nickel metal which is dissolved in mercury as nickel amalgam. However, any possibility that the zero- or monovalent nickel complexes exist as the reaction intermediate of very short lives is not excluded.

The experimental results of the a. c. and the Kalousek's polarograms and the log-plot analysis of the d. c. current-voltage curves indicate that the electrode reaction of nickel(II) ions in 6 M calcium chloride solution proceeds with a relatively high degree of reversibility in comparison with that of hydrated nickel(II) ions. It has been pointed out by Senda[23] et al. that the value of $i_p/(n\sqrt{\tau}\, i_d)$, where $i_p$ is the peak current of the a. c. polarogram, represents the degree of reversibility of the electrode reaction. The value for nickel(II) ions in 6 M calcium chloride solution was calculated to be 0.20, which is smaller than the values for the well-known reversible systems such as cadmium(II) or lead(II) ions in potassium nitrate solutions, but nearly equal to those of quasi-reversible systems such as zinc(II) ions in potassium nitrate solutions.

From the foregoing discussion, it can be concluded that the electrode reaction of nickel(II) ions in 6 M calcium chloride proceeds quasi-reversibly at the mercury electrode according to the reaction

$$NiCl_4^{2-} + 2e + Hg \rightleftarrows Ni(Hg) + 4Cl^-$$

## Summary

A typical reduction wave with a half-wave potential of −0.462 V. vs. S. C. E. was obtained with nickel(II) ions in 6 M calcium chloride solution. The a. c. and the Kalousek's polarograms revealed that the electrode reaction is a quasi-reversible one. From the coulometric measurement carried out at the constant potential, the overall electrode reaction proved to be a two-electron reduction. Nearly the total amount of nickel reduced by the controlled potential electrolysis with the mercury electrode was recovered from the mercury, indicating that the nickel(II) ions are reduced to nickel metal to form probably

19) M. von Stackelberg, *Z. Elektrochem.*, **57**, 338 (1953).
20) J. Jaffray and J. Cariat, *Compt. rend.*, **231**, 1128 (1950).
21) N. Kato, *J. Chem. Soc. Japan, Pure Chem. Sec.* (*Nippon Kagaku Zasshi*), **62**, 29 (1941).
22) R. Breckpot, *Compt. rend. 27e conger. intern. chim. ind.* (*Brussels*), **1954**, 2; *Industrie chim. belge*, **20**, Spec. No., II, 468—472 (1955); *Chem. Abstr.*, **50**, 12700*h* (1956).
23) M. Senda, M. Senda and I. Tachi, *J. Electrochem. Soc. Japan* (*Denki Kagaku*), **27**, 83 (1959).

nickel amalgam. From these experimental results the electrode reaction of nickel(II) ions in 6 M calcium chloride at the mercury electrode was concluded to proceed quasi-reversibly according to the equation

$$NiCl_4^{2-} + 2e + Hg \rightleftarrows Ni(Hg) + 4Cl^-$$

The authors thank the Ministry of Education for the financial support granted for this research.

*Department of Chemistry*
*Faculty of Science*
*Tohoku University*
*Katahira-cho, Sendai*

# *Hot-Atom Chemistry of Halogens in Cobaltammine Complex Salts. I. Hot-Atom Chemistry of Bromine in Bromopentammine Cobalt Complex Salts*

By Nobufusa SAITO, Hirotoshi SANO and Takeshi TOMINAGA

(Received June 22, 1959)

Many attempts have already been made to study the hot-atom effect of central atoms in metal complex salts, while very little attention has so far been paid to the hot-atom effect of ligand atoms[1].

The present authors investigated the behavior of radiobromine in ligands of bromopentammine cobalt complex salts following $(n, \gamma)$ process induced by neutron irradiation. The distribution of radiobromine was studied after the salts were irradiated in different phases and at varied temperatures. The authors were especially interested in the irradiation of the complex ion loaded on a cation exchange resin, because some results were already obtained in their laboratory with respect to the behavior of hot-atoms in ion exchange resins[2].

## Experimental

**Samples.**—Five bromopentammine cobalt complex salts were prepared by methods already known:

1. $[Co(NH_3)_5Br](NO_3)_2$[3]
2. $[Co(NH_3)_5Br](C_2O_4)$[4]
3. $[Co(NH_3)_5Br]Cl_2$[5]
4. $[Co(NH_3)_5Br]Br_2$[6]
5. $[Co(NH_3)_5Br]I_2$[7]

Their composition was checked by the spectrophotometric method and by the determination of halogen contents.

For the irradiation in resin phase, $[Co(NH_3)_5Br]^{2+}$ was adsorbed on Dowex 50 W, cation exchange resin in the hydrogen form, 8% cross-linked, consisting of 100~200 mesh beads. As the bromopentammine cobalt complex salts are aquated in the presence of moisture, the resin loaded with complex ion was dried immediately after washing, by means of suction on a sintered-glass filter for a few hours, or by means of heating at 40~60°C under reduced pressure in an Abderhalden's desiccator with phosphorus pentoxide. However, prolonged procedure of drying, especially, of heating in the Abderhalden's desiccator, caused in the meantime considerable aquation. (The remaining moisture caused aquation even after it was reduced to a very small amount by drying.)

Thus, in the case of the complex ion on the resin, not the pure complex ion but the mixture of $[Co(NH_3)_5Br]^{2+}$ and the aquated products, $[Co(NH_3)_5H_2O]^{3+}$ and $Br^-$, was actually irradiated. The ratio of bromo- and aquo-pentammine complex salts was estimated by determining the amount of $Br^-$ liberated in the aquation reaction 1;

$$[Co(NH_3)_5Br]^{2+} + H_2O \rightarrow [Co(NH_3)_5H_2O]^{3+} + Br^- \quad (1)$$

and was shown in Table III. The procedure of determination was as follows: the dried resin with the mixture was washed with water, and $Br^-$ which had been liberated was extracted and determined volumetrically.

**Irradiation.**—The neutrons produced by Be-D reaction in a cyclotron were thermalized. The flux was approximately $10^7$ neutrons/cm$^2$ sec. The samples were irradiated for two to three hours at room temperature or at a lower temperature (−72°C). For the irradiation at room

1) A. W. Adamson and J. M. Grunland, *J. Am. Chem. Soc.*, **73**, 5508 (1951).
2) N. Saito, M. Furukawa and I. Tomita, *J. Chem. Phys.*, **27**, 1432 (1957); N. Saito, I. Tomita and M. Furukawa, Presented at the 11th Annual Meeting of the Chemical Society of Japan, Tokyo, April, 1958.
3) S. M. Jörgensen, *J. prakt. Chem.*, [2] **19**, 62 (1879).
4) S. M. Jörgensen, ibid., [2] **19**, 67 (1879).
5) S. M. Jörgensen, ibid., [2] **19**, 55 (1879).
6) H. S. Booth, "Inorganic Syntheses", Vol. I, McGraw-Hill Book Co., Inc., New York (1939), p. 186.
7) F. Ephraim, *Ber.*, **56**, 1513 (1923).

temperature, the samples were placed in a paraffin block, while for the irradiation at −72°C, they were put in a test tube immersed in a mixture of dry ice and ethanol in a Dewar's vessel.

The complex salts as aqueous solutions or adsorbed on the resin and dipped in water were irradiated with their container immersed in a mixture of ice and water.

**Procedures of Separation.**—Solid samples were dissolved in water one to four hours after the end of irradiation. (The samples irradiated at a lower temperature were kept at room temperature after the irradiation was over.) The solution was poured into a 1.5 cm.×0.8 $cm^2$ column of Dowex 50 W in the hydrogen form*, 8% cross-linked, 100~200 mesh. The column was then washed with water until the total volume of the effluent amounted to 100 ml. The effluent yielded the first fraction containing anions of the sample solution and radiobromine leached out as anions**. The complex ions were adsorbed on the cation exchange resin so firmly that none of them could be detected spectrophotometrically in the first fraction.

The resin loaded with the complex ions was then immersed in water and digested on a bath at 70 to 85°C for about an hour. As the aquation of the bromopentammines was very rapid at elevated temperatures, ligand bromine including radioisotopes was almost completely aquated with this procedure and was extracted by water as the bromide ion. The extract was separated from the resin and aquo complex ion. The extract and the washing yielded the second fraction.

The complex salts irradiated as solutions were treated in the same way as the solids except that precautions were taken to prevent the aquation before the separation process.

The treatment of the complex ion in the resin phase was as follows. The irradiated resin and complex ion were put into a sintered-glass filter of 1 cm. in diameter containing from about a half to an equal volume of Dowex 50 W, 8% cross-linked, (hydrogen form), at the bottom. The size of the column was about 0.8$cm^2$×4~5cm. The column was immersed in water and then washed by suction with 250~300 ml. of cold water. The washing yielded the first fraction. The resin and the complex ion were digested with water, and the extract yielded the second fraction. In this case, the resin with the aquo complex ion still contained considerable activity which could hardly be removed by further digestion with hot water, or by treatment with inorganic acids or with a reducing agent (0.3 M $NaHSO_2$+0.2 M $H_2SO_4$). This was the third fraction.

Measurements were made on each fraction with respect to the gross activity of $^{80m}Br$ (actually, of its daughter, $^{80}Br$, in equilibrium) and $^{82}Br$, and with respect to the content of bromine.

In order to eliminate the hot-atom effect of $^{80}Br$ ($T_{1/2}$=18 min.) following the isomeric transition from $^{80m}Br$, measurements of activity were made more than three hours after the first fraction had been separated. Thus the gross hot-atom effect of $^{80m}Br$ and $^{82}Br$ was observed in this investigation. The ratio of activities of the two isotopes, $^{80m}Br$ and $^{82}Br$, was about 15 : 1 at the end of irradiation, while 5.5 hr. after the end of irradiation it became 8 : 1. The distribution of activity was calculated for each sample by referring to a definite time (5.5 hr. after the end of irradiation).

Activity was measured with either an immersion-type G-M tube or an end-window G-M tube. Silver bromide precipitates were mounted on counting dishes in the latter case.

Bromide was determined volumetrically by Mohr's method or colorimetrically by the method of Stenger and Kolthoff[8]. The amounts of bromine retained in the resin were estimated by radioactivation analysis.

## Results and Discussion

**Hot-Atom Chemistry in Solids.**—The results of measurements on the solid complex salts are shown in Table I. In any of the complex salts investigated, over eighty per cent of radiobromine atoms was leached out into water with an enrichment factor of at least 50. As the maximum recoil energy of radiobromine resulting from slow neutron capture was calculated to be 174 eV.[9], and this is large enough to break Co–Br bond, such a high extractability may not be unexpected.

The column F-2 in Table I is expected to denote the fraction of radiobromine retained in the ligands of the cobalt complex salts. When a bromine atom in $[Co(NH_3)_5Br]^{2+}$ recoils following the neutron capture, the bond between the metal and the bromine is broken and the resulting hot-atom may have several collisions with the surrounding molecules or atoms before it slows down. In the hot reactions with the recoiling bromine or in the recombination reactions which follow them, complex ions such as $[Co(NH_3)_4BrBr^*]^+$ may probably be produced*** as well as $[Co(NH_3)_5Br^*]^{2+}$ (Br* denotes radiobromine). As

* Potassium form was also used, but the results were not significantly different from those obtained with hydrogen form.

** It was reported by Saito, Tomita and Furukawa that most of radiobromine produced in the neutron irradiation of bromates was found in the form of bromide (presented at the 11th Annual Meeting of the Chemical Society of Japan, Tokyo, April, 1958).

8) V. A Stenger and I. M. Kolthoff, *J. Am. Chem. Soc.*, **57**, 831 (1935).

9) A. C. Wahl and N. A. Bonner, "Radioactivity Applied to Chemistry", John Wiley & Sons, Inc., New York (1951), p. 247.

*** The replacement of an ammine group by hot bromine was proved by the fact that ligand yield as $[Co(NH_3)_5Br]^{2+}$ of about 5% was obtained in the irradiation of $[Co(NH_3)_6]Br_3$ with slow neutrons. Details will be published elsewhere.

TABLE I. DISTRIBUTION OF $^{80m}Br$ AND $^{82}Br$ ACTIVITY AND ENRICHMENT FACTOR IN SOLIDS

| Complex salt | Irradiation at room temp. | | Irradiation at −72°C | | Enrichment factor of F-1 |
|---|---|---|---|---|---|
| | F-1 % | F-2* % | F-1 % | F-2* % | |
| $[Co(NH_3)_5Br](NO_3)_2$ | 83.9 | 16.1 | 87.3 | 12.7 | $1\times10^2$ |
| $[Co(NH_3)_5Br](C_2O_4)$ | 82.6 | 17.4 | — | — | $0.5\times10^2$ |
| $[Co(NH_3)_5Br]Cl_2$ | 82.2 | 17.8 | 84.2 | 15.8 | $0.5\times10^2$ |
| $[Co(NH_3)_5Br]Br_2$ | 82.7 | 17.3 | 82.6 | 17.4 | — |
| $[Co(NH_3)_5Br]I_2$ | 87.6 | 12.4 | — | — | $2\times10^2$ |

* Ligand yield as $[Co(NH_3)_5Br^*]^{2+}$. These values were reproducible in at least three runs within 0.4~0.7% standard deviation.

both complex ions are cationic, the second fraction essentially includes the activity in the form of $[Co(NH_3)_4BrBr^*]^+$ besides $[Co(NH_3)_5Br^*]^{2+}$. The probability of the formation of complex ions containing more than two bromine atoms in ligands may be negligibly small.

For the convenience of discussion, the authors defined a quantity $(L.Y.)_A$, "ligand yield in the form of A", which indicated the fraction of total produced activity retained in the form of the complex ion, A. The value in the second fraction is then the summation of ligand yields of all the complex cations; $(L.Y.)_{[Co(NH_3)_5Br^*]^{2+}}$ and $(L.Y.)_{[Co(NH_3)_4BrBr^*]^+}$ (*cis*- and *trans*-isomers).

In this case, however, all the tetrammine complex salts containing radiobromine are much more unstable and are much more rapidly aquated with liberation of bromine than the pentammine complex salts are. The aquation reactions are

$$[Co(NH_3)_4Br_2]^+ + H_2O \rightarrow [Co(NH_3)_4BrH_2O]^{2+} + Br^- \quad (2)$$

$$[Co(NH_3)_4BrH_2O]^{2+} + H_2O \rightarrow [Co(NH_3)_4(H_2O)_2]^{3+} + Br^- \quad (3)$$

Radiobromine in the tetrammine complex salts is liberated and enters the first fraction, through either of these reactions. Half time of the aquation reactions in nearly neutral aqueous solutions were estimated to be a few minutes at 15~20°C, while that of reaction 1 was estimated to be about a hundred hours[10].

In this investigation, the irradiated complex salts were dissolved in water (pH 5~6) at room temperature and kept in solutions for a sufficiently long time in order to eliminate $(L.Y.)_{[Co(NH_3)_4BrBr^*]^+}$ from the second fraction. When all the unstable complex ions were aquated and only the pentammine remained, the curve for the observed activity of the second fraction vs. the period of separation (period of standing in water) leveled off****. Therefore the distribution of activity in the second fraction in Table I may be taken as almost identical with the ligand yield in the form of $[Co(NH_3)_5Br^*]^{2+}$, or so-called "retention".

As seen in Table I, ligand yield as $[Co(NH_3)_5Br^*]^{2+}$ of the complex salts does not vary appreciably as the anionic component is replaced, except that the iodide shows considerably low yield. The irradiation at a lower temperature decreases the yield in some salts, while in the bromide the yield remains almost unchanged. It is interesting to note that the bromide shows almost the same yield as other salts in the irradiation at room temperature: the hot-atoms resulting from the anions may behave in the same way as those from ligands of the complex salts.

**Hot-Atom Chemistry in Aqueous Solutions.**— The results of measurements of aqueous solutions of the complex salts are shown in Table II. In this case, practically all radiobromine was leached out into the first fraction.

**Hot-Atom Chemistry in Resin Phase.** — As shown in Table III, about 80% of the total activity was extracted into the first fraction with enrichment factors of 3~40 when the irradiated resin and complex ion was washed with water. Nine to thirteen per cent of the activity was retained in the ligands (F-2). More than 9% of the total activity remained in the resin even after the aquation of the complex ion on the resin had been brought to completion (F-3).

10) A. B. Lamb and J. W. Marden, *J. Am. Chem. Soc.*, **33**, 1873 (1911); J. N. Bronsted and R. Livingston, ibid., **49**, 435 (1927).

**** By means of extrapolation of the curves to the separation time zero, approximate values of unstable ligand yields (i. e. as $[Co(NH_3)_4BrBr^*]^+$) were roughly estimated to be about 2~5%.

TABLE II. DISTRIBUTION OF $^{80m}Br$ AND $^{82}Br$ ACTIVITY AND ENRICHMENT FACTOR IN SOLUTIONS

| Complex salt | Concentration | Irradiation at 0~3°C | | Enrichment factor of F-1 |
|---|---|---|---|---|
| | | F-1 % | F-2 % | |
| $[Co(NH_3)_5Br](NO_3)_2$ | $7\times10^{-3}$ M | 99.2 | 0.8±0.6 | $0.4\times10^2$ |
| $[Co(NH_3)_5Br](NO_3)_2$ | $8\times10^{-4}$ M | nearly 100 | nearly 0 | $0.4\times10^2$ |

TABLE III. DISTRIBUTION OF $^{80m}Br$ AND $^{82}Br$ ACTIVITY AND PERCENTAGE OF AQUATION IN RESIN PHASE

| Condition of drying | Temp. of irradiation | Distribution of activity | | | Percentage of aquation (aquo-complex %) |
|---|---|---|---|---|---|
| | | F-1 % | F-2 % | F-3 % | |
| Suction | room temp. | 80.0 | 10.7 | 9.3 | 11~20 |
| | −72°C | 81.1 | 9.3 | 9.6 | 5~ 9 |
| Abderhalden | room temp. | 80.2 | 10.7 | 9.1 | 15~42 |
| | −72°C | 80.5 | 8.9 | 10.6 | 9~21 |
| Without drying | 0~13°C (dipped in water) | 76.5 | 13.0 | 10.5 | 2~ 4 |

As mentioned above, the mixture of bromo- and aquo-pentammine complex ions and the liberated bromine was irradiated on the cation exchange resin. The "percentage of aquation" is shown in Table III. Therefore, the interpretation of the activity in the second fraction is more complicated in the resin phase than in solids. The complex cations possibly produced through the hot-atom effect in the irradiation of the mixture are as follows:

a) from $[Co(NH_3)_5Br]^{2+}$,

$$\begin{cases}[Co(NH_3)_5Br^*]^{2+}\\ [Co(NH_3)_4BrBr^*]^{+}\end{cases}$$

b) from $[Co(NH_3)_5H_2O]^{3+}$,

$$\begin{cases}[Co(NH_3)_5Br^*]^{2+}\\ [Co(NH_3)_4Br^*H_2O]^{2+}\end{cases}$$

Radiobromine in ligands of the unstable complex ions other than the bromopentammine may be considerably aquated during the separation process and eluted into the first fraction. However, these aquation reactions do not proceed as rapidly in the resin in the hydrogen form as in the solutions of the irradiated solids, because the rate of reaction 3 is dependent on the pH of solution and it becomes much slower in acid solutions[11].

In the cation exchange resin in the hydrogen form, the pH of the effluent was measured and found to be less than 3, where half time of reaction 3 was several hundred minutes. Therefore, as far as the products of reactions a) are concerned, only about 50% of $(L.Y.)_{[Co(NH_3)_4BrBr^*]^+}$ may be eliminated from the second fraction through the aquation reaction 2 which is almost completed during the period of separation in this investigation, but reaction 3 may not proceed appreciably in the meantime. Similarly, the products of reactions b) may remain without being aquated during the period of separation.

By making suitable assumptions, the authors estimated ligand yields of the above complex ions separately. According to the investigations now being made in their laboratory[12] a considerable fraction of hot bromine resulting from anionic sphere was enriched in ligands of pentammine cobalt complex salts, $[Co(NH_3)_5Y]Br_{(2\text{ or }3)}$, when they were irradiated with slow neutrons. The value of $(L.Y.)_{[Co(NH_3)_5Br^*]^{2+}}$ for $[Co(NH_3)_5H_2O]Br_3$ sample was 7~8%, which was about a half of that in $[Co(NH_3)_5Br]Br_2$. By assuming that $(L.Y.)_{[Co(NH_3)_5Br^*]^{2+}}$ due to aquo- and bromo- pentammine complex ions in the mixture adsorbed on the resin are in the same ratio (i.e. about 1/2) as those separately obtained in the irradiation of solids of these complex salts, the ligand yields in bromopentammine cobalt complex ion corrected for aquation were calculated and are listed in Table IV. These values, however, may be larger than $(L.Y.)_{[Co(NH_3)_5Br^*]^{2+}}$ by about 50% of $(L.Y.)_{[Co(NH_3)_4BrBr^*]^+}$ (i.e. 1~2%)[13].

11) J. N. Brönsted, *Z. physik. Chem.*, **122**, 383 (1926).

12) Results were partly reported at the 12th Annual Meeting of the Chemical Society of Japan, April, Kyoto, 1959. Details will be published elsewhere.

13) Ligand yields of the tetrammine complex salts were estimated as about 1~4%.

TABLE IV. LIGAND YIELDS IN BROMOPENTAMMINE COBALT COMPLEX ION ON THE RESIN CORRECTED FOR AQUATION

| Condition of drying | Temp. of irradiation | Ligand yields* % |
|---|---|---|
| Suction | room temp. | 12.0 |
| | −72°C | 10.4 |
| Abderhalden | room temp. | 13.4 |
| | −72°C | 10.7 |
| Without drying | 0~13°C (dipped in water) | 13.0 |

* Ligand yields may include (L.Y.)$_{[Co(NH_3)_5Br^*]^{2+}}$ and about 1/2 of (L.Y.)$_{[Co(NH_3)_4BrBr^*]^+}$.

As seen in Table IV, the ligand yields in bromopentammine on the cation exchange resin are 10~13% and lower than those obtained in solids. The yields decreased slightly when the samples were irradiated at a lower temperature. It is interesting to note that the presence of water in the samples did not influence the yields appreciably. Even in the case where the complex and the resin were dipped in water during the irradiation, the yields were not greatly different from those for the samples dried in the Abderhalden's desiccator. This may be understood as indicating that the rate of exchange of ligand bromine of bromopentammine with bromide ion in aqueous solutions is very slow and that the aquation reaction 1 does not disturb the mechanism of recombination from which some portion of the ligand yield may result.

Nearly 10% of the total activity was retained in the irradiated resin after the treatments described above. The enrichment factor of radiobromine in this fraction (F-3) was estimated as at least 100. The exchange reaction between the bromine remaining in the resin and bromide ion in water was regarded as being very slow even at elevated temperatures (70~85°C). The reducing agent decreased the activity in the resin only slightly. The irradiation at a lower temperature increased the activity in the resin slightly.

It was presumed from these observations that most of the radiobromine remaining in the leached resin would be organically combined with the resin matrix: some results in favor of this conclusion were reported by Carlson and Koski[14].

## Summary

The hot-atom effect was investigated on $^{80m}Br$ and $^{82}Br$ resulting from $(n, \gamma)$ processes in ligand bromine of bromopentammine cobalt complex salts. The fraction of radiobromine retained in ligand (ligand yield) was compared for samples irradiated in different phases, and it increased in the following order: solution, resin, solid. It is interesting to note that in the irradiation of solids of bromopentammines $[Co(NH_3)_5Br]Br_2$ showed almost the same ligand yield as other salts. The hot-atoms resulting from the anions may behave in the same way as those from ligands of the complex salts. The exchange of ligand bromine in these complex salts with bromide in water was regarded as being very slow at room temperature.

In the irradiation of the complex ion adsorbed on a cation exchange resin, a considerable fraction of radiobromine was trapped in the resin matrix. Treatments with either inorganic acids or a reducing agent did not remove the activity appreciably. Most of the radiobromine remaining in resin was presumed to be organically combined with the matrix.

*Department of Chemistry*
*Faculty of Science*
*The University of Tokyo*
*Hongo, Tokyo*

14) T. A. Carlson and W. S. Koski, *J. Chem. Phys.*, **23**, 2410 (1955).

# *The Reaction of 3-Oxo-$\Delta^4$-steroids with Isocyanuric Chloride*

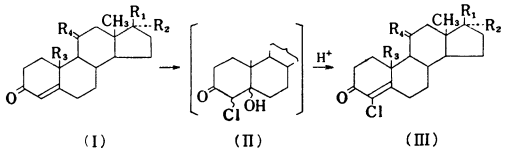
By Fumikazu MUKAWA

(Received May 13, 1959)

It has been reported that 3$\beta$-substituted-$\Delta^5$-steroids gave the corresponding 5$\alpha$-chloro-6$\beta$-hydroxy compounds on treatment with isocyanuric chloride, and that 3-oxo-$\Delta^5$-steroids and their ethyleneketal gave the 6$\beta$-chloro-5$\alpha$-hydroxy compounds[1].

Now, similar studies on the reaction of 3-oxo-$\Delta^4$-steroids (I) with isocyanuric chloride are reported herewith.

Treating the model compound progesterone with isocyanuric chloride in acetone-acetic acid (or perchloric acid) yielded a chloro compound, having an ultraviolet absorption typical for the 4-substituent-4-en-3-one system ($\lambda_{max}^{EtOH}$ 256 m$\mu$, log $\varepsilon$ 4.12)[2-4]. The identity of the product with 4-chloroprogesterone was established by its melting point and the infrared spectrum. Therefore, it appears that 4-chloroprogesterone (Ic) is formed through an intermediate 4$\xi$-chloro-5$\xi$-hydroxy compound (II):



(I) (II) (III)

(a) $R_1$=OAc, $R_2$=H, $R_3$=$CH_3$, $R_4$=$H_2$
(b) $R_1$=$OCOC_2H_5$, $R_2$=H, $R_3$=$CH_3$, $R_4$=$H_2$
(c) $R_1$=$COCH_3$, $R_2$=H, $R_3$=$CH_3$, $R_4$=$H_2$
(d) $R_1$=$COCH_3$, $R_2$=OH, $R_3$=$CH_3$, $R_4$=$H_2$
(e) $R_1$=$COCH_3$, $R_2$=OAc, $R_3$=$CH_3$, $R_4$=$H_2$
(f) $R_1$=OH, $R_2$=$CH_3$, $R_3$=H, $R_4$=$H_2$
(g) $R_1$=$COCH_2OAc$, $R_2$=OH, $R_3$=$CH_3$, $R_4$=O

Extension of this chlorination method to 3-oxo-$\Delta^4$-steroid hormones, led to 4-chloro-derivatives, several of which were characterized by their absorption maximum.

Since this work was completed, Oliveto et al. reported[5] the preparation of 4-chlorocortisone acetate by *N*-chlorosuccinimide and perchloric acid.

4-Chlorotestosterone acetate (IIIa) and 4-chlorotestosterone propionate (IIIb) exhibited greater anabolic and smaller androgenic effect in comparison to administeral testosterone propionate, and showed no inhibitory effects on the gonadotropic secretion upon intraspleenic ovarian transplantation[6].

4-Chloroprogesterone (IIIc) and 4-chloro-17$\alpha$-acetoxyprogesterone (IIIe) showed no progestational activity.

## Experimental*

**5$\alpha$-Chloro-3$\beta$-acetoxy-pregnan-6$\beta$-ol.** — To a mixture consisting of 1.0 g. of pregnenolone acetate, 0.5 g. of isocyanuric chloride and 30 ml. of acetone were added ten drops of 30% acetic acid. The whole was refluxed for 5 min. After cooling to room temperature, the mixture was poured with stirring into 10% aqueous sodium carbonate, and then extracted with ether. The extract was washed with water and dried over magnesium sulfate, after removal of the solvent, the residue was recrystallized from acetone-water to yield 0.6 g. of needles, m. p. 195°C (decomp.), $[\alpha]_D^{17}$ +36 (c. 1.2).

*Anal.* Found: C, 67.26; H, 8.65; Cl, 8.42. Calcd. for $C_{23}H_{35}O_4Cl$: C, 67.37; H, 8.60; Cl, 8.65%.

**Preparation of 4-Chloro-3-oxo-$\Delta^4$-steroids.** — A solution of 0.5 g. of 3-oxo-$\Delta^4$-steroid and 0.3 g. of isocyanuric chloride in 30 ml. of acetone was refluxed for 1 hr. with 3 ml. of acetic acid or 10% perchloric acid. The reaction mixture was then poured into 10% sodium carbonate solution and extracted with ether. Washing of the extract with water, drying over magnesium sulfate, and evaporation of the solvent led to a residue which was purified by recrystallization or chromatography on florisil.

The following 4-chloro-3-oxo-$\Delta^4$-steroids were prepared by this method:

*4-Chlorotestosterone acetate (IIIa)*, needles, m. p. 228°C (from acetone), $\lambda_{max}^{EtOH}$ 255 m$\mu$ (log $\varepsilon$ 4.12);

*4-Chlorotestosterone propionate (IIIb)*, needles, m. p. 164°C (from methanol), $\lambda_{max}^{EtOH}$ 256 m$\mu$ (log $\varepsilon$ 4.12);

1) F. Mukawa, *J. Chem. Soc. Japan, Pure Chem. Sec.* (*Nippon Kagaku Zasshi*) **78**, 452 (1957).
2) B. Camerino, B. Patelli and A. Vercellone, *J. Am. Chem. Soc.*, **78**, 3540 (1956).
3) D. N. Kirk, D. K. Patel and V. Petrow, *J. Chem. Soc.*, **1956**, 1184.
4) J. Ringold, B. Batres, O. Mancera and G. Rosenkranz, *J. Org. Chem.*, **21**, 1432 (1956).
5) E. P. Oliveto, C. Gerold and E. B. Hershberg, *J. Am. Chem. Soc.*, **79**, 3596 (1957).
6) The parabiotic rat technique was reported: V. Clini, G. Baldratti and G. Sala, *Experientia*, **14**, 94 (1958).
* All melting points are uncorrected. Optical rotation was measured in chloroform solution.

*4-Chloroprogesterone (IIIc)*, needles, m. p. 220°C (from acetone), $\lambda_{max}^{EtOH}$ 256 mμ (log ε 4.20);

*4-Chloro-17α-hydroxy-progesterone (IIId)*, needles, m. p. 218°C (from methylene chloride-methanol), $\lambda_{max}^{EtOH}$ 256 mμ (log ε 4.11);

*Anal.* Found: C, 68.90; H, 8.10. Calcd. for $C_{21}H_{29}O_3Cl$: C, 69.29; H, 8.03%.

*4-Chloro-17α-acetoxyprogesterone (IIIe)*, needles, m. p. 194°C (from acetone after being separated by chromatography from benzene on florisil), $\lambda_{max}^{EtOH}$ 256 mμ (log ε 4.20);

*Anal.* Found: C, 67.85; H, 7.53. Calcd. for $C_{23}H_{31}O_4Cl$: C, 68.04; H, 7.70%.

*4-Chloro-17α-methyl-19-nortestosterone (IIIf)*, needles, m. p. 148°C (from ether-hexane after being separated by chromatography from benzene on florisil), $\lambda_{max}^{EtOH}$ 256 mμ (log ε 4.20);

*Anal.* Found: C, 70.93; H, 8.90. Calcd. for $C_{19}H_{27}O_2Cl$: C, 70.87; H, 8.45%.

*4-Chlorocortisone acetate (IIIg)*, needles, m. p. 234°C (from acetone-*n*-hexane), $\lambda_{max}^{EtOH}$ 254 mμ (log ε 4.11).

Ultraviolet spectra and optical rotations were kindly determined by Mr. M. Sawai and Miss S. Imai.

The author wishes to express his sincere thanks to Dr. M. Chuman and Assistant Professor Y. Nomura of the University of Tokyo for their interest in this work. Thanks are also due to Dr. O. Kobayashi of Teikoku Hormone Manufacturing Co., Ltd., and Dr. K. Maekawa of Tokyo Jikeikai School of Medicine for bio-assay.

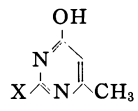
*Tsurumi Research Laboratory of Chemistry*
*Shitanoya-machi, Tsurumi-ku, Yokohama*

# *Wohl-Ziegler Reaction on 6-Methyluracil and its Homologues*

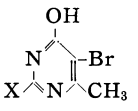
By Tarozaemon NISHIWAKI and Toshinao GOTO

(Received July 6, 1959)

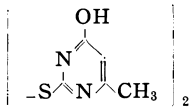
In general, a free radical mechanism has been presented for the Wohl-Ziegler reaction of allylic methyl groups with *N*-bromosuccinimide, but some abnormal reactions such as aromatic nuclear bromination and addition of bromine to olefinic double bonds by this reagent have been believed to proceed via an ionic mechanism. Since hydroxyl groups in the 2-, 4-, or 6-position of pyrimidines tend to increase electron availability at the 5-position in the ring, it seems very interesting to investigate whether such pyrimidines as 6-methyluracil (I), 2-mercapto-6-methyluracil (II), and 2-amino-6-methyluracil (III) are brominated with NBS at allylic side chain or at a nucleus.



(I) X=OH
(II) X=SH
(III) X=$NH_2$



(IV) X=OH
(VI) X=SH
(VII) X=$NH_2$



(V)

The Wohl-Ziegler reactions on methylpyrimidines are scarecely known. 5-Methyl-barbituric acid[1] and 5-methyl-2,4,6-trichloropyrimidine[2] are brominated at the methyl groups while 2-methyl-4H-pyrido-(1,2-a)-4-pyrimidone[3] are brominated at the nucleus. With *N*-chlorosuccinimide (NCS) uracil, thymine and 2-methylmercapto-6-methyluracil gave nuclear-substituted product in glacial acetic acid and allylic side chain substituted-products in chloroform plus benzoyl peroxide[4].

When the reaction of 6-methyluracil (I) and NBS was undertaken under the classical free radical condition, a halogen-containing product, which decomposed at 251°C, was obtained. Analytical values indicated that this was the brominated compound of I. The melting point of 5-bromo-6-methyluracil (IV), however, was reported to be 247°C (decomp.) by Matsukawa et al.[5] and to be 241°C (decomp.)

1) T. Nishiwaki, unpublished work.
2) M. Hasegawa, *Pharm. Bull. (Japan)*, **1**, 387 (1953).
3) R. Adams et al., *J. Am. Chem. Soc.*, **76**, 1845 (1954).
4) R. West et al., ibid, **76**, 3146 (1954).
5) T. Matsukawa et al., *J. Pharm. Soc. Japan (Yakugaku Zasshi)*, **70**, 134 (1950).

by Kurtev et al.[6] The site of the bromine atom in the present compound was concluded to be at $C_5$-position by its unreactive character (e. g. unsuccessful condensation with ethyl malonate)[7] and also by the fact that chlorination of this material yielded 5-bromo-2, 4-dichloro-6-methylpyrimidine[5]. Attempted bromination of 6-methyl-2,4-dichloropyrimidine and 5-bromo-6-methyluracil failed even under illumination with electric light.

2-Mercapto-6-methyluracil (II) was then brominated under the analogous condition. The reaction products were separated by the difference of solubility in ethyl acetate. Ethyl acetate insoluble compound contained no halogen, decomposed gradually over 290°C and could be recrystallized from methanol. From the analytical data, this compound was inferred to be identical with the starting material or with the disulfide (V), solvated with methanol. However, the latter structure was denied because of unsuccessful reduction with sodium borohydride and of the positive reaction for the thiol group with sodium nitroprusside. The reduction of disulfide bond with sodium borohydride was reported by Walton et al.[8] This compound was identified as the starting material by successive benzylation using Bucher's method[9]. From ethyl acetate soluble fraction, a halogen-containing compound with m. p. 256°C (decomp.) was obtained, which was shown to be 5-bromo-2-mercapto-6-methyluracil (VI) by analysis, comparison of its physical data with that reported by Barrett et al.[10,11], positive sodium nitroprusside reaction and failure to brominate this product further, while the expected compound would be susceptible to the further bromination at reactive $C_5$-position, if the bromine had attacked the allylic methyl group. Direct bromination of pyrimidines having alkyl- or aryl-free sulfhydryl group at $C_2$-position had scarecely been reported and Barrett et al. prepared 5-brom-2-mercapto-6-methyluracil (VI) through demethylation of 5-bromo-2-methylmercapto-6-methyluracil by hydrogen iodide. However, it has been revealed that this compound was conveniently prepared by the present method, though in low yield. As 2-methylmercapto-6-methyluracil was substituted at an allylic side chain by NCS, it was also anticipated that this pyrimidine could be brominated at the same position. However, contrary to the authors' expectation, none of the halogen-containing product was obtained, resulting in the quantitative recovery of the starting material.

Under the same condition 2-amino-6-methyluracil (III) was also shown to be brominated at the nucleus by NBS. The reaction product, 5-bromo-2-amino-6-methyluracil (VII), seemed to be unstable in water, because the aqueous solution of this pyrimidine became acidic.

It has also been disclosed that these pyrimidines (I), (II), (III) were brominated at $C_5$-position even in the absence of benzoyl peroxide, in about the same yield as that when benzoyl peroxide was present. From these results it seems possible to conclude that electrophilic attack by NBS took place at $C_5$-position of these three hydroxylpyrimidines.

During the course of this work, the attempt has been made to synthesize 5-bromo-2-benzylmercapto-6-methyluracil. However, this product could not be purified without causing hydrolysis to 5-bromo-6-methyluracil.

## Experimental

**5-Bromo-6-methyluracil (IV).** — Mixtures of 6-methyluracil (12.6 g.), NBS (17.8 g.), benzoyl peroxide (20 mg.) and carbon tetrachloride (100 ml.) were refluxed for 2.5 hr. on a steam bath. After cooling, the solid was collected, and was heated in ethyl acetate (100 ml.) for 50 min. The ethyl acetate insoluble material, after being collected while hot, was successively washed with ethanol (20 ml.), water (10 ml.), and dried at 100°C for one hour, which was recrystallized from glacial acetic acid (charcoal), to give 5-bromo-6-methyluracil, colorless needles, (9.67 g.), m. p. (uncorrected) 251°C (decomp.).

*Anal.* Found: C, 29.61; H, 2.50; N, 13.44. Calcd. for $C_5H_5BrN_2O_2$: C, 29.29; H, 2.45; N, 13.66%.

**5-Bromo-2, 4-dichloro-6-methylpyrimidine.** — The above brominated pyrimidine (IV) (1.50 g.) was heated with mixtures of phosphorous oxychloride (8 ml.) and dimethylaniline (8 ml.) for one hour on an oil bath. The excess of dimethylaniline was removed under reduced pressure, the residue was poured on crushed ice (100 g.). Ether extraction afforded, after removal of the solvent, a compound, b. p. 65~70°C/10 mmHg. It has solidified and then was recrystallized from petroleum ether (b. p. 30~60°C), colorless needles (100 mg.), m. p. (uncorrected) 40~42.5°C. Matsukawa et al. gave m. p. 42~43°C for 5-bromo-2, 4-dichloro-6-methylpyrimidine.

6) B. Kurtev et al., *Chem. Abstr.*, 47, 1607 (1953).
7) None reactivity of halogen atom at $C_5$-position of pyrimidine has been discussed. Cf. J. Chesterfield et al., *J. Chem. Soc.*, **1955**, 3478.
8) E. Walton et al., *J. Am. Chem. Soc.*, **76**, 4748 (1954).
9) K. Bucher, *Pharm. Acta Helv.*, **26**, 145 (1951).
10) H. Barrett, U. S. Pat.. 2,585,615 (1952).
11) H. Barrett et al., *J. Am. Chem. Soc.*, **70**, 1753 (1948).

**Bromination of 2-Mercapto-6-methyluracil.**—Mixtures of 2-mercapto-6-methyluracil [12] (1.4 g.), NBS (1.8 g.), benzoyl peroxide (10 mg.) and carbon tetrachloride (20 ml.) were refluxed for 45 min. on a steam bath. After cooling, the solid was collected, which was again heated with ethyl acetate (20 ml.) for 15 min. The ethyl acetate insoluble material, after being collected while hot, was successively washed with ethanol (10 ml.), water (10 ml.) and dried at 100°C for one hour, which was twice recrystallized from methanol (charcoal) to give light cream-colored rectangulars, (300 mg.). This compound began to decompose over 290°C.

*Anal.* Found: C, 42.22; H, 3.98; N, 18.58. Calcd. for $C_5H_5N_2OS \cdot \frac{1}{4}CH_3OH$ (II): C, 41.98; H, 4.69; N, 18.66%.

Ethyl acetate filtrate was evaporated to dryness and the residue was twice recrystallized from a large volume of ethanol (charcoal) to give 5-bromo-2-mercapto-6-methyluracil, in small needles (100 mg.), m. p. (uncorrected) 256°C (decomp.).

*Anal.* Found: Br, 36.20. Calcd. for $C_5H_5BrN_2OS$: Br, 36.15%.

By concentration of the mother liquor, succinimide (300 mg.) was recovered.

Barrett gave m. p. 260°C (decomp.) for 5-bromo-2-mercapto-6-methyluracil (VI) [10].

**2-Benzylmercapto-6-methyluracil.**—Bucher's preparative method for this compound was slightly modified as follows.

A solution of the above ethyl acetate insoluble, bromine-free pyrimidine (m. p. was over 290°C) (210 mg.) in 0.5 N aqueous sodium hydroxide (3 ml.) was refluxed with benzyl chloride (1 ml.) and ethanol (8 ml.) for 20 min. on a steam bath. After being refrigerated overnight, the precipitate was collected, washed with water and recrystallized from ethanol to give 2-benzylmercapto-6-methyluracil in rods (120 mg.), m. p. (uncorrected) 183~184°C.

Bucher gave m. p. 183~184°C for this compound [9].

**5-Bromo-2-amino-6-methyluracil (VII).**—Mixtures of 2-amino-6-methyluracil [13] (1.25 g.), NBS (1.78 g.), benzoyl peroxide (10 mg.) and carbon tetrachloride (20 ml.) were refluxed for one hour on a steam bath. After cooling, the solid was collected, which was again heated in ethyl acetate (20 ml.) for 20 min. on a steam bath. The ethyl acetate insoluble material, being collected while hot, was washed with water (10 ml.) and dried at 100°C for one hour (1.69 g.). Recrystallization from water (charcoal) gave 5-bromo-2-amino-6-methyluracil as cream-colored plates (220 mg.), m. p. (uncorrected) 249~250°C (decomp.).

Todd et al. gave m. p. 250°C (decomp.) for this *pyrimidine* [14]. The recrystallization mother liquor (pH 4.0) was concentrated at reduced pressure to about 5 ml. (pH 2.6), which was adjusted to pH 7 with 1 N aqueous sodium hydroxide to give colloidal substance.

In the bromination of the above three pyrimidines (I)—(III) in the absence of benzoyl peroxide, yields and melting points were shown in Table I.

TABLE I. BROMINATION OF I, II AND III IN THE ABSENCE OF BENZOYL PEROXIDE with NBS

| Pyrimidines examined | | Yield | m. p. (decomp.), °C |
|---|---|---|---|
| I | (0.6 g.) | (400 mg.) | 249 |
| II | (1.4 g.) | ( 50 mg.) | 256 |
| III | (1.2 g.) | (200 mg.) | 246 |

**Bromination of 2-benzylmercapto-6-methyluracil.**—2-Benzylmercapto-6-methyluracil (4.0 g.) was dissolved in glacial acetic acid (50 ml.) containing acetic anhydride (2.5 ml.). To this solution was added bromine (5 ml.) in glacial acetic acid (20 ml.) with stirring during 10 min. After heating on a steam bath for 15 min. with stirring, a yellow precipitate was collected (3.0 g., m. p. 200°C, decomp.) which was recrystallized from 95% ethanol (charcoal) to give colorless rods, m. p. (uncorrected) 249~250°C (decomp.). Recrystallization from absolute ethanol or glacial acetic acid also gave the same hydrolized compound, 5-bromo-6-methyluracil.

*Anal.* Found: N, 13.58; Br, 38.69. Calcd. for $C_5H_5BrN_2O_2$: N, 13.66; Br, 38.98%.

The authors wish to express their sincere gratitude to Professor Noboru Sugiyama of Tokyo University of Education for his helpful advice. Their thanks are also due to Mr. Ken'ichi Kikuchi, director of this company, who has permitted to publish this work.

*The Research Laboratory*
*Oriental Photo Industrial Co., Ltd.*
*Nishiochiai, Shinjuku-ku, Tokyo*

12) H. Snyder et al., *J. Am. Chem. Soc.*, **76**, 2441 (1954).
13) J. Jaeger, *Ann.*, **262**, 365 (1891).
14) A. Todd et al., *J. Chem. Soc.*, **1947**, 41.

# *Antioxygenic Activity of Lecithin and its Hydrolysis Products. III. Lecithin, Glycerophosphorylcholine, Phosphorylcholine, Phosphatidic Acids, Choline and Glycerol*

By Chieko URAKAMI and Haru KAMEYAMA

(Received May 4, 1959)

It was reported that choline among other hydrolysis products of phosphatides such as glycerol, oleic and linoleic acids, glycerophosphoric acid, and aminoethyl alcohol was the only one active against oils of plant origin[1]. The opinion of other investigators[2,3], however, was that the active entity in the phosphatide molecule is the phosphoric acid residue and that lecithin in which the hydroxyl of the phosphoryl group is involved in zwitterionic combination should show no activity[2,4]. Olcott and Mattill[2], and also Hilditch and Paul[5] reported that purified lecithin was inactive. However, the purities of the substrates as well as those of the samples of lecithin which were employed by these investigators were doubtful.

It has been known that some minor impurities present in substrates or in samples of phosphatides may act synergistically with a compound which has no activity in itself or conversely inhibit activity of a truly active compound. As the authors have demonstrated with the glycerophosphoric acids[6], the method used for purification of the substrate is important in evaluating antioxygenic activity. In this connection, it is of interest to note the recent paper of Olcott[7]. He demonstrated that a minute amount of free fatty acids added to substrates influenced antioxygenic properties of various compounds. Therefore, those results obtained with substrates which had been purified by mere solvent fractionation and distillation would not be trustworthy.

In regard to purification of lecithin, it is fairly recent[8,9] that the separation of phosphatidylcholines from other components of phospholipids and impurities can be achieved by column chromatography, indicating inadequacy of purification by the acetone precipitation method. Therefore, reinvestigation of natural lecithin is desirable in order to ascertain the varied results reported in the literature. The study on its hydrolysis products such as phosphatidic acids, glycerophosphorylcholine, phosphorylcholine, choline and glycerol is also desirable in elucidating structural requirements of phospholipids for antioxygenic activity.

## Experimental

**Materials.**—*Methyl oleate.*—The ester was prepared from olive oil (Nihon Yushi Co.) essentially in the same manner as described previously[6], except that the treatment with urea preceded the fractionation by low temperature crystallization from acetone. The fraction used as substrate had the following constants: b. p., 203~203.5°C/10 mmHg; $n_D^{20}$ 1.4526; Saponification No., 188.9; Iodine No., 89.9. The ultraviolet absorption spectra of this sample in ether showed $E_{1cm}^{1\%}$ 0.930 at 270 m$\mu$, indicating the presence of a small amount of unsaturated fatty acid esters other than the monoethenoid.

*Orthophosphoric acid.* — The analytical reagent grade (approximately 85%) of Mallinckrodt Chemical Works was dried over phosphorus pentoxide in a vacuum desiccator for four days or until a constant weight was attained.

*Glycerol.*—A fraction distilled at 140°C/3 mmHg was dried over phosphorus pentoxide in a vacuum desiccator.

*Choline.* — Free choline was prepared from choline chloride by shaking its aqueous solution with freshly precipitated silver hydroxide[10]. The yield was over 90% of the theoretical.

*$\alpha$- & $\beta$-Glycerophosphoric acids.*—The free acids were prepared from the corresponding sodium salt in the same manner as described in the previous paper[6].

1) R. Strohecker et al., *Z. Untersuch. Lebensm.*, **79**, 23 (1940).
2) H. S. Olcott and H. A. Mattill, *Oil & Soap*, **13**, 98 (1936).
3) H. J. Dutton et al., *J. Am. Oil Chemists' Soc.*, **26**, 441 (1949).
4) V. P. Calkins, *J. Am. Chem. Soc.*, **69**, 384 (1947).
5) T. P. Hilditch and S. Paul, *J. Soc. Chem. Ind.*, **58**, 21 (1939).
6) C. Urakami et al., This Bulletin, **32**, 36 (1959).
7) H. S. Olcott, *J. Am. Oil Chemists' Soc.*, **35**, 597 (1958).
8) D. J. Hanahan et al., *J. Biol. Chem.*, **192**, 623 (1951).
9) D. N. Rhodes and C. H. Lea, *Biochem. J.*, **65**, 526 (1957).
10) H. W. Dudley, *J. Chem. Soc.*, **119**, 1260 (1921).

*Phosphorylcholine chloride.*—The barium salt of phosphorylcholine chloride was synthesized by H. Okura according to the method described by Baer[11]. The barium ion was precipitated as the sulfate and the clear supernatant liquid separated after removing the sulfate by centrifugation was concentrated to a small volume. The residue was treated with 95% ethanol and any precipitate formed was removed completely by centrifugation. The clear filtrate was concentrated to give syrupy material, which was dried over phosphorus pentoxide. The yield was approximately 83%.

*Phosphorylcholine.* — The chloride ion of the barium salt of phosphorylcholine chloride was removed first by precipitating as silver chloride with freshly prepared silver hydroxide (shaking was continued until the aqueous solution showed negative Beilstein test). The barium cation was removed in the manner described above for the preparation of phosphorylcholine chloride from its barium salt.

*Lecithin.* — Crude lecithin isolated from egg yolk by the conventional method of acetone precipitation was purified by slightly modified method of Rhodes and Led[9].

*Phosphatidic acids.*—The sample was prepared by M. Okada by interacting the lecithin prepared as above with lecithinase C (also called phosphatidase C or phospholipase D) of carrot roots in a manner similar to the method described by Kates[12]. Analysis showed that the sample contained about 70% phosphatidic acids and minor amounts of monoacylglycerophosphoric acids and glyceride-like substances.

DL-α-*Glycerophosphorylcholine.* — This compound was also synthesized by H. Okura according to the method of Baer and Kates[13]. A ratio of α-glyceryl ester to choline was found to be 1.03:1.0.

**Autoxidation.**—Each compound was added to the substrate at a concentration of 0.1% with the use of an appropriate solvent. The rest of the procedure employed was exactly the same as that described previously. The bath temperatures of 45 and 60°C were studied, the latter being chosen for comparison of the efficiencies of those found active.

**Peroxide Determination.** — The method previously described was employed.

## Results

Purified ovo-lecithin, known to be L-α-lecithin, and DL-α-glycerophosphorylcholine were found to be inactive at 45°C as shown in Fig. 1. Both compounds were, however, found to be somewhat active at this temperature when methyl oleate purified by the method of low temperature solvent fractionation alone was used (Fig. 2.). Here again it should be emphasized that

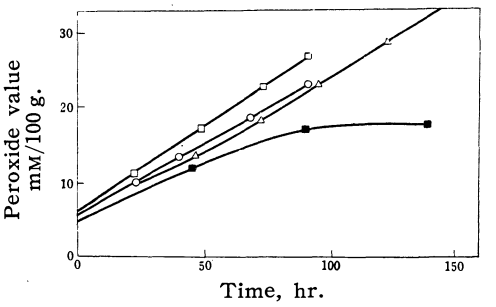



Fig. 1. Peroxide values against time at 45°C.
○: Methyl oleate alone. □: Methyl oleate containing 0.1% ovo-lecithin. △: Methyl oleate containing 0.1% DL-α-glycerophosphorylcholine. ■: Methyl oleate containing 0.1% α-glycerophosphoric acid.

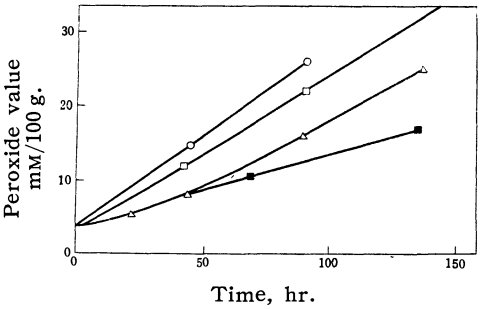



Fig. 2. Peroxide values against time at 45°C, using partially purified methyl oleate.
○: Methyl oleate alone. □: Methyl oleate containing 0.1% ovo-lecithin. △: Methyl oleate containing 0.1% DL-α-glycerophosphorylcholine. ■: Methyl oleate containing 0.1% α-glycerophosphoric acid.

the method of purification of substrates is very important as the authors have advocated.

Choline was found to be inactive both at 45 (Fig. 3) and 60°C (not shown here). It was also found to be inactive in oleic acid at 50°C. Consequently, choline itsef is definitely inactive contrary to the result reported by Strohecker et al.[1]

Glycerol tested at 60°C exhibited no activity and thus is considered to be an inactive compound in purified methyl oleate.

Phosphorylcholine chloride was found to be active both at 45 (Fig. 3) and 60°C (Fig. 4) and the free phosphorylcholine more active than the chloride at 60°C.

The sample of phosphatidic acids employed in this experiment showed an

11) E. Baer, *J. Am. Chem. Soc.*, **69**, 1253 (1947).
12) M. Kates, *Can. J. Biochem. Physiol.*, **33**, 575 (1955).
13) E. Baer and M. Kates, *J. Am. Chem. Soc.*, **70**, 1394 (1948).

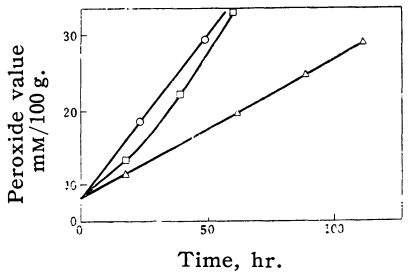



Fig. 3. Peroxide values against time at 45°C.
○: Methyl oleate alone. □: Methyl oleate containing 0.1% choline. △: Methyl oleate containg 0.1% phosphorylcholine chloride.

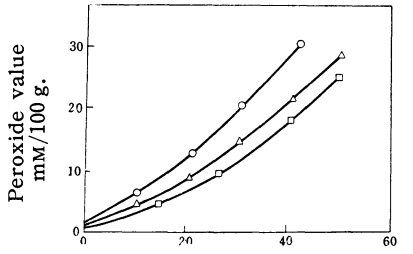



Fig. 4. Peroxide values against time at 60°C.
○: Methyl oleate alone. △: Methyl oleate containing 0.1% phosphorylcholine chloride. □: Methyl oleate containing 0.1% phosphorylcholine.

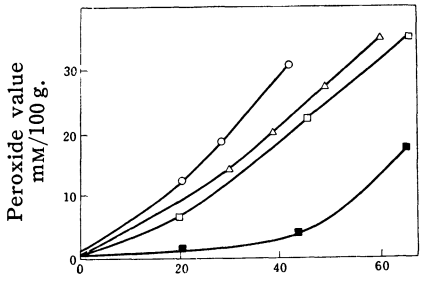



Fig. 5. Peroxide values against time at 60°C.
○: Methyl oleate alone. □: Methyl oleate containing 0.1% phosphatidic acid. △: Methyl oleate containing 0.1% β-glycerophosphoric acid. ■: Methyl oleate containing 0.1% orthophosphoric acid.

activity comparable to that of glycerophosphoric acids (Fig. 5). This result must, however, be considered with some reservation since the control of the purity of the natural free acids was very difficult, just as has been recorded in the literature, i.e. the acids easily lose the fatty acid residues when ethanol or a small amount of moisture is present[14].

The relative efficiencies of the active compounds were compared at 60°C and numerical values obtained by using the following expression: $T_a/T_o$, where $T_a$ is the time required to give 20 mM in peroxide value when 0.1% of an active substance is present and $T_o$ that required to show the same peroxide value by the substrate itself. This method of expression is a modification of that used by Emmanuel et al.[15] As shown in Table I, orthophosphoric acid is the most active one, followed by phosphorylcholine, phosphatidic acid, and phosphorylcholine chloride.

## Discussion

Since glycerol was found to be inactive, the activity observed with the glycerophosphoric acids must be due to the phosphoryl moiety, apparently the glycerol moiety not participating. The absence of activity in DL-α-glycerophosphorylcholine also supports the fact that the glycerol moiety is not involved. This would mean that the alcoholic O-H or C-H linkage of the glycerol moiety is not readily attacked by free radicals, at least not as readily as the α-methylene group of the methyl oleate. This observation is in accord with the order of bond strengths of these three linkages. The bond strength of the O-H linkage is 110 kcal./mol.; that of the C-H of the α-methylene, 80 kcal./mol. or less than 64 when activated by resonance; and that of the C-H in the glycerol moiety, greater than 80 kcal./mol., since an effect produced by the alcoholic hydroxyl group on the C-H linkage is known to be much less than that by the α-double bond.

The activity shown by phosphorylcholine and its chloride is again attributed to the phosphoryl moiety since choline was found to be inactive. It appears that two methylene groups present in the phosphorylcholine molecule are less readily attacked than the α-methylene of the methyl oleate molecule.

It has been reported that ovo-lecithin purified by the method similar to the one the authors employed contained stearic acid in the β-position and an unsaturated acid in the α-position[16]. Since no activity was

14) J. Olley, *Chem. & Ind.*, **73**, 1069 (1954).
15) N. M. Emmanuel et al., *Myasnaya Ind. S. S. S. R.*, **29**, No. 2, 52 (1958); *Chem. Abstr.*, **52**, 177554*h* (1958).
16) D. J. Hanahan, *J. Biol. Chem.*, **211**, 321 (1954).

observed with the sample of lecithin used, it appears that the unsaturated fatty acid moiety in the lecithin does not compete with the $\alpha$-methylene group of the substrate molecule. Thus, participation of the fatty acyl groups of ovo-lecithin can be excluded. However, the behavior of the fatty acids present in the sample of phosphatidic acids may differ from that of the lecithin fatty acyl group although the former was prepared from the same sample of lecithin used for the activity study. Kates[12] states that the isolated phosphatidic acids contain $C_{18}$ fatty acids and about 20% of phosphatidic acid derived from the phospholipids present in the chromoplasts. Since the naturally occurring phosphatidic acids are said to be highly unsaturated, the fatty acid residue present in the sample of phosphatidic acids used is considered to be more highly unsaturated than those present in the lecithin originally subjected to the enzymatic action. Therefore, the activity observed with phosphatidic acids may partly be ascribed to autoxidation of the highly unsaturated fatty acyl group. However, it is highly probable that the phosphoryl residue has played a major role since the glycerophosphoric acids have been shown to be active, almost as active as phosphatidic acids (Fig. 5).

The foregoing discussion leads to the conclusion that the phosphoryl moiety is responsible for antioxygenic activity. A question arises, however, as to the absence of activity in ovo-lecithin and DL-$\alpha$-glycerophosphorylcholine despite the presence of the phosphoryl group in both molecules, The authors tentatively attribute this to the zwitterionic forms of the molecules, as suggested earlier by Olcott and Mattill[2] and Calkins[4]. No definite conclusion concerning this can be drawn at this stage of investigation, for it is necessary to reveal true behavior of cephaline under identical conditions. It is said to be active according to the earlier investigators.

It would be of interest to examine whether the activity ratios, $T_a/T_o$, relate to some characteristics of the molecules of those found to be active such as acidity, the number of the free hydroxyl of the phosphoryl group or the ratio of the molecular weight of phosphoric acid to that of each of the active compounds.

As shown in Table I, an order of acidity is $\beta$-glycerophosphoric acid > $\alpha$-glycerophosphoric acid > orthophosphoric acid phosphatidic acid > phosphorylcholine and its chloride, but this is not in accord with the order of activity ratio, orthophosphoric acid > phosphatidic acid and phosphorylcholine > phosphorylcholine chloride > $\alpha$-glycerophosphoric acid > $\beta$-glycerophosphoric acid. Similarly, no significant relations can be found between the activity ratios and the number of the free hydroxyl of the phosphoryl group in each molecule, e. g. phosphorylcholine which is considered to have only one free hydroxyl, shows a stronger activity than does its chloride or $\beta$-glycerophosphoric acid although orthophosphoric acid with three free hydroxyl groups is exceptionally strongly active. Interaction of the alcoholic hydroxyl with the oxygen and hydroxyl of the phosphoryl group in the $\beta$-glycerophosphoric acid should, of course, be taken into consideration in this connection, but this will be dealt with in a later paper. The ratios of the molecular weight of phosphoric acid to that of each of the active compounds also bear no relation to the activity ratios.

Thus, it appears that other factors must be sought to understand how the phosphoryl group participates in exhibiting antioxygenic activity or in other words to

TABLE I. RELATION OF ACTIVITY RATIOS OF ACTIVE COMPOUNDS WITH SOME OF THEIR CHARACTERISTICS

| | $H_3PO_4$ | PA | PC | PCCl | $\beta$-GP | $\alpha$-GP |
|---|---|---|---|---|---|---|
| $T_a/T_o$ at 60°C | 2.48 | 1.39 | 1.40 | 1.27 | 1.31 | d |
| $pK_{a1}$ | 1.97 | a | b | c | 1.37 | 1.40 |
| No. of free OH available | 3 | 2 | 1 | 2 | 2 | 2 |
| M. wt. of $H_3PO_4$/ that of compound | 1 | 0.14 | 0.54 | 0.44 | 0.57 | 0.57 |

PA represents phosphatidic acids; PC, phosphorylcholine; PCCl, phosphorylcholine chloride; $\alpha$- and $\beta$-GP, $\alpha$- and $\beta$-glycerophosphoric acids. a) This is expected to be somewhat weaker than that of $\alpha$-GP. b) and c) These are weaker than any of the rest of the compounds listed due to the presence of the choline base in their molecules. d) It is expected to be somewhat higher than 1.31 of $\beta$-GP according to the result obtained at 45°C[6].

understand mechanisms involved. For this, the authors have porposed that an oxygenated substrate molecule interact with the phosphoryl group to give highly conjugated compounds which undergo autoxidation much more readily than does the substrate molecule. Further investigation on this problem is underway.

Incidentally, Hanahan et al.[17] reported that phosphorylcholine and glycerophosphoric acids (in conjunction with choline) stimulated oxygen consumption of the isolated rat liver mitochondria, the former being particularly strongly active. Lecithin and glycerophosphorylcholine were found to stimulate some oxygen consumption but only under special conditions. The enzymatic system such as this is far more complex than the system under consideration and in no way should these two systems be compared. However, one can not deny a possibility that reactions taking place in both systems may be found to be related, in view of the recent finding that free radicals are present in biological systems[18,19].

17) M. Rodbell and D. J. Hanahan, ibid., **214**, 595 (1955).
18) B. Commoner et al., *Nature*, **174**, 689 (1954).
19) I. Miyagawa et al., *Proc. Natl. Acad. Sci. U. S.*, **44**, 613 (1958); *Chem. Abstr.*, **53**, 2325e (1959).

**Summary**

Purified ovo-lecithin, DL-α-glycerophosphorylcholine, choline and glycerol were found to exhibit no antioxygenic property against carefully purified methyl oleate. Phosphorylcholine, its chloride and natural phosphatidic acids, on the other hand, showed activity.

The order of activity efficiency at 60°C was found to be orthophosphoric acid > phosphatidic acid and phosphorylcholine > phosphorylcholine chloride > α-glycerophosphoric acid > β-glycerophosphoric acid. The discussion is presented to show that the phosphoryl moiety is predominantly responsible for antioxygenic activity.

The authors are indebted to Misses M. Ishida, J. Kondo, K. Yamaguchi and K. Sakamoto for their technical assistance.

*Faculty of the Science of Living*
*Osaka City University*
*Nishi-ku, Osaka*

# *Synthesis of 1,2,5-Trisubstituted Naphthalene Derivatives**

By Takeshi MATSUMOTO and Akira SUZUKI

(Received February 20, 1959)

Since the elucidation of the structures of Garrya alkaloids by K. Wiesner[1], a number of alkaloids have been shown to be related to the tricyclic diterpenoid[2]. Lycoctonine[3] as well as lucidusculine[4], both of which have been studied in this laboratory under the leadership of Professor H. Suginome for the past several years, are supposed to belong also to this class. Mainly in this connection, the authors became interested in constructing model compounds with the 2-aza-perhydro-1,4a-(propano)-phenanthrene ring system (I). In the present paper the authors describe the preparation of 2-methoxy-5-hydroxy-1-naphthylacetic acid (II) and of other suitably substituted 1,2,5-naphthalene derivatives, which appeared to be potentially useful building blocks for the synthesis of the above skeleton (I). At first, the synthesis of 1-hydroxymethyl-2-methoxy-5-hydroxynaphthalene (III), which would form the B, C ring of the hydrophenanthrene, was attempted.

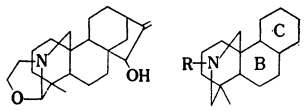
* Approaches to the Synthesis of Diterpenoid Alkaloid Models. I. Part II: T. Matsumoto and A. Suzuki, This Bulletin, **32**, 1283 (1959).

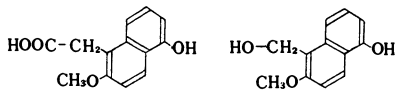
1) K. Wiesner, *Experientia*, **11**, 255 (1955).

2) For reviews, see E. S. Stern in "The Alkaloids", Vol. 4, Academic Press, New York (1954), p. 275; A. R. Pinder, "Annual Reports on the Progress of Chemistry", Vol. 52, The Chemical Society, London (1956), p. 253; G. F. Smith, ibid., Vol. 53, (1957), p. 248; idem., ibid., Vol. 54, (1958), p. 260.

3) H. Suginome, S. Imato, Yamada and N. Katsui, This Bulletin, **32**, 819 (1959).

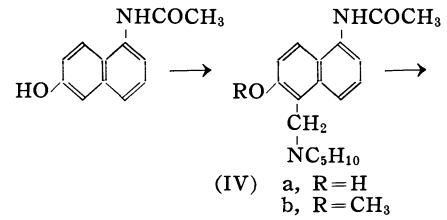
4) T. Amiya, ibid., **30**, 667 (1957); H. Suginome, T. Amiya and T. Shima, ibid., **32**, 824 (1959)



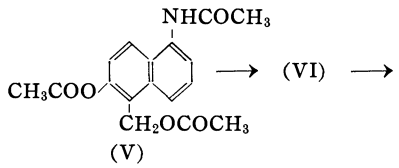




(II) (III)

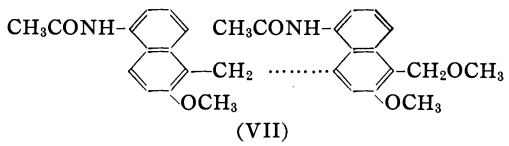
The starting material for this purpose was 1-acetoxymethyl-2-acetoxy-5-acetamidonaphthalene (V), which was prepared from 1-piperidino-methyl-5-acetamido-2-naphthol (IVa) by a slight modification of Cornforth and Robinson's method[5] from 5-acetamido-2-naphthol.



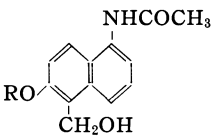

(IV) a, R=H
b, R=CH₃




(V)

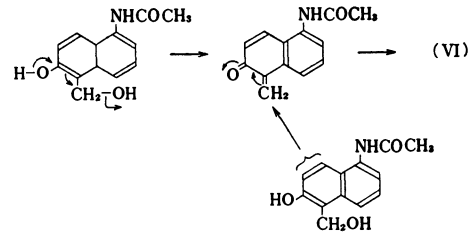



(VII)




(VIII) a, R=H
b, R=CH₃

Attempts to hydrolyze the triacetyl compound V with aqueous alkali however resulted in the formation of an amorphous product VI which could not be caused to crystallize by any means. After methylation with dimethyl sulfate a crystalline methyl derivative was obtained. The derivative was not, however, the expected compound VIIIb. The elemental analysis, determination of the methoxyl group, and measurement of molecular weight of the methyl derivative indicated that its formula corresponds to $C_{26}H_{21}N_2O_2(OMe)_3$. In addition, the compound exhibited infrared absorption in nujol at 3280 (N-H), 1645 (amide I), 1510 (amide II), 1275 (aryl ether), 1100 (alkyl ether), 800 (three adjacent H), 805 $cm^{-1}$ (three adjacent H)[6]. On these grounds formula VII is proposed as a likely structure for this compound, the point of attachment (dotted line) of disubstituted naphthylmethyl moiety however being uncertain. Fromation of this coupled product may be interpreted as follows:




Reaction behaviors of certain phenolic Mannich bases have already been explained in a similar manner[7]. According to the above view, the formation of the coupled product should be controlled through replacement of the phenolic hydroxyl by a methoxyl group. 1-Piperidinomethyl-5-acetamido-2-naphthol methyl ether (IVb), which would form a methoxyl derivative (VIIIb) through acetolysis and hydrolysis, however could not be obtained by treatment of IVa with diazomethane, probably because compound IVa exists almost completely as a zwitter ion. The

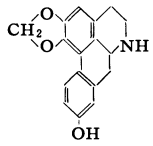
5) J. W. Cornforth, O. Kauder, J. E. Pike and R. Robinson, *J. Chem. Soc.*, **1955**, 3348.

6) The absorption bands at 800 and 805 $cm^{-1}$ suggest the presence of two naphthalene rings which contain three adjacent hydrogen atoms, respectively. See *Note* on p. 37.

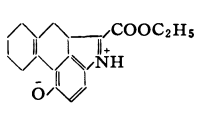
7) (a) K. Auwers, *Ber.*, **36**, 1878 (1903). (b) K. Auwers, *Ann.*, **344**, 131 (1906). (c) K. Auwers and P. Bullmann, *Ber.*, **59**, 2719 (1926); H. R. Snyder and J. H. Brewster, *J. Am. Chem. Soc.*, **70**, 4230 (1948); C. E. Dalgliesh, ibid., **71**, 1697 (1949).

8) L. J. Bellamy, "The Infrared Spectra of Complex Molecules", 2nd Ed., Methuen & Co., Ltd., London (1958), p. 207.

9) Reported infrared spectra of anoboline (i) and the compound (ii) exhibit very weak absorption bands at N-H and O-H stretching vibration region and broad absorption band at 2260~2800 $cm^{-1}$ region. The assignment of 3440 and 3400 $cm^{-1}$ bands of compoud IVa is however not conclusive. One of them might be responsible for the hydroxyl group.

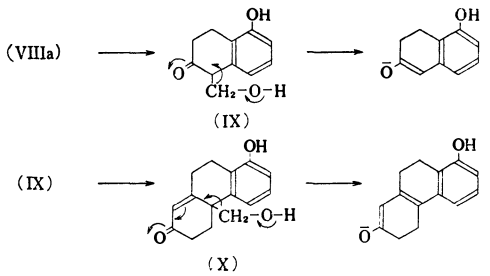



(i)
R. A. Heacock and Léo Marion, *Can. J. Chem.*, **34**, 1782 (1956).




(ii)
H. Pfleininger and H. Kasiwagi, *Ber.*, **88**, 550 (1955).

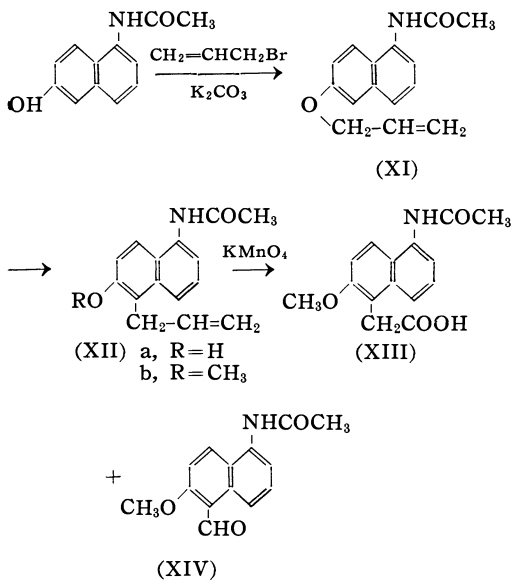
dipolar character seems to be reflected by the infrared absorption of IVa.



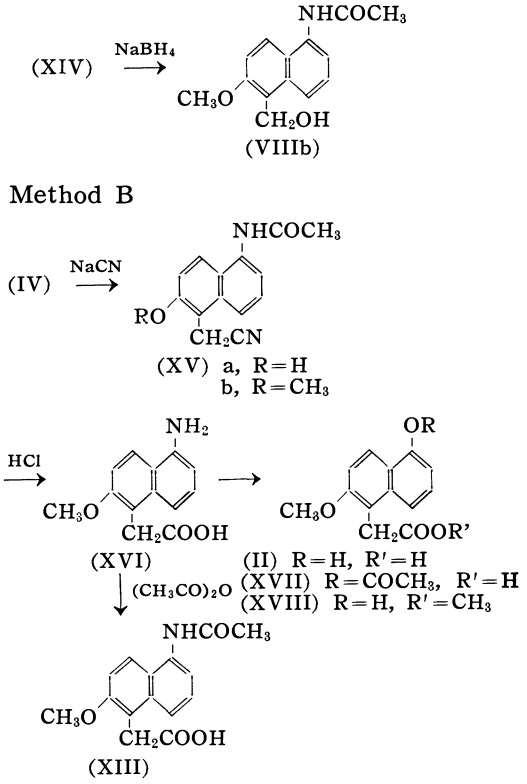
The compound in chloroform exhibited twin secondary amide N-H absorption bands[8] at 3400 and 3440 $cm^{-1}$, a broad weak band extending from 2260 to 2800 $cm^{-1}$, and no absorption band characteristic of the hydroxyl group[9].

Since the first attempt to synthesize 1-hydroxymethyl-2-methoxy-5-naphthol was thus unsuccessful, and moreover, since it was felt that hydronaphthalene (IX) or hydrophenanthrene (X) derived from the naphthol might be likely to undergo carbon-carbon bond cleavage at a certain later stage as illustrated above, the present authors abandoned attempts to find conditions to effect conversion V→VIIIa and turned attention to the preparation of 2-methoxy-5-hydroxy-1-naphthylacetic acid (II) which contains two, rather than one, side chain carbon atoms. Introduction of the carboxymethyl group to naphthalene nucleus has been achieved by two methods. Steps involved are summarized as follows:

Method A



Method B



Of these, method B gave an excellent result.

The reaction of 5-acetamido-2-naphthol with allyl bromide in boiling acetone afforded the allyl ether (XI) in quantitative yield. The latter compound, on being heated in an atmosphere of nitrogen for an hour at 185~195°C, was converted into 1-allyl-5-acetamido-2-naphthol (XIIa) in a yield of 99.5%. The methylation of XIIa with dimethyl sulfate in the presence of alkali proceeded without difficulty (yield, 81.7%). For the formation of naphthylacetic acid, the methyl ether (XIIb) was then treated with potassium permanganate. Oxidation at room temperature resulted in the formation of a difficultly separable mixture, but at below −10°C in ethanol, even though in a yield of 13%, the desired acid (XIII) was obtained along with a non-acidic product (20%). The latter compound was characterized as 2-methoxy-5-acetamido-1-naphthaldehyde (XIV) on the basis of elemental and infrared spectral analyses. The aldehyde was smoothly reduced in a good yield (94%) to the corresponding alcohol (VIIIb) by the use of sodium borohydride. Two promising intermediates, XIII and VIIIb, have thus been obtained. However, for the present purpose, the yield of the oxidation stage

TABLE I

| Substituents | 1650～1500 $cm^{-1}$ | 900～700 $cm^{-1}$ |
|---|---|---|
| 1-NHAc<br>5-Allyl<br>6-OH<br>(XIIa) | a) 1630 (s) 1617 (s) c) 1602 (m) 1580 (m) b) 1533 (s) 1512 (s) | 905 (s) 890 (w) 830 (m) 802 (s) 773 (s) 750 (s) |
| 1-NHAc<br>5-Allyl<br>6-OMe<br>(XIIb) | a) 1645 (s) 1620 (s) c) 1598 (m) 1585 (w) b) 1540 (s) 1505 (s) | 895 (w) 874 (w) 840 (w) 798 (s) 755 (m) 735 (s) |
| 1-NHAc<br>5-$CH_2CO_2H$<br>6-OMe<br>(XIII) | a) 1642 (s) 1620 (m) 1598 (w) 1580 (w) c) b) 1545 (s) 1507 (s) | 890 (w) 875 (w) 840 (w) 795 (s) 760 (m) 725 (m) |
| 1-NHAc<br>5-CHO<br>6-OMe<br>(XIV) | a) 1650 (s) 1620 (m) 1600 (w) 1570 (w) c) b) 1540 (m) 1510 (m) | 890 (w) 845 (w) 820 (m) 800 (s) 755 (s) 720 (s) |
| 1-NHAc<br>5-$CH_2OH$<br>6-OMe<br>(VIIIb) | a) 1645 (s) 1620 (m) 1597 (w) 1590 (w) b) 1545 (m) 1507 (s) | 875 (m) 845 (w) 810 (w) 792 (s) 753 (s) 720 (s) |
| 1-NHAc<br>5-$Pr^n$<br>6-OMe | a) 1640 (s) 1620 (m) 1595 (w) 1580 (w) b) 1532 (m) 1508 (s) | 890 (w) 880 (w) 850 (w) 837 (w) 812 (w) 795 (s) 750 (m) 720 (m) |
| 1-NHAc<br>5-$CH_2CHCH_2$ (Br Br)<br>6-OMe | a) 1640 (s) 1620 (m) 1595 (w) 1580 (w) b) 1540 (m) 1510 (s) | 890 (w) 870 (w) 842 (w) 825 (m) 815 (m) 796 (s) 755 (s) 720 (m) |
| 1-NHAc<br>5-$CH_2OAc$<br>6-OAc<br>(V) | a) 1648 (s) 1624 (m) 1602 (w) 1590 (w) b) 1565 (s) 1510 (m) | 900 (m) 890 (w) 873 (w) 855 (w) 844 (w) 820 (w) 800 (s) 765 (s) 725 (s) |
| 1-NHAc<br>5-$CH_3$<br>6-OH | c) 1635 (m) c) 1620 (s) 1610 (m) 1584 (w) c) 1545 (s) b) 1535 (s) 1510 (s) | 900 (w) 865 (w) 850 (w) 820 (m) 800 (s) 755 (m) 720 (m) |
| 1-NHAc<br>5-$CH_2NC_5H_{10}$<br>6-OH<br>(IVa) | a) 1640 (s) 1617 (s) c) 1600 (w) 1582 (w) b) 1545 (s) 1512 (s) | 895 (w) 879 (w) 870 (w) 858 (w) 843 (w) 818 (s) 796 (s) 783 (s) 745 (s) 720 (w) 707 (w) |
| 1-N($CH_3$)Ac<br>5-$CH_2CN$<br>6-OMe | a) 1647 (s) 1617 (s) 1595 (m) 1580 (m) 1510 (m) | 900 (w) 862 (m) 830 (m) 805 (s) 790 (m) 757 (m) 723 (w) |
| 1-NHAc<br>5-$CH_2CN$<br>6-OH<br>(XVa) | a) 1650 (s) 1620 (s) 1600 (m) 1587 (m) b) 1530 (m) 1508 (s) | 910 (m) 890 (m) 860 (w) 855 (w) 830 (m) 805 (s) 755 (s) 725 (m) |
| 1-NHAc<br>5-$CH_2CN$<br>6-OMe<br>(XVb) | a) 1645 (s) 1623 (m) 1600 (w) 1580 (w) b) 1545 (m) 1510 (s) | 910 (m) 890 (m) 860 (w) 835 (m) 815 (m) 800 (s) 755 (s) 725 (m) |

| | | |
|---|---|---|
| 1-OH<br>5-$CH_2CO_2H$<br>6-OMe<br>(II) | 1625 1600 1582 1520<br>(m) (m) (m) (m) | 875 837 825 805 755 735 723<br>(w) (m) (m) (s) (m) (m) (m) |
| 1-OAc<br>5-$CH_2CO_2H$<br>6-OMe<br>(XVII) | 1625 1600 1580 1515<br>(m) (m) (w) (m) | 900 870 835 818 805 760 735 720<br>(m) (m) (w) (m) (s) (m) (m) (m) |
| 1-OH<br>5-$CH_2CO_2Me$<br>6-OMe<br>(XVIII) | 1625 1595 1580 1520<br>(m) (m) (m) (m) | 876 865 837 820 800 760 725<br>(w) (w) (m) (w) (s) (m) (m) |

TABLE II

| Substituents | 1650~1500 $cm^{-1}$ | 900~700 $cm^{-1}$ |
|---|---|---|
| 1-OH | 1630 1597 1580 1515<br>(m) (s) (s) (m) | 876 862 790 765<br>(m) (m) (s) (s) |
| 2-OH | 1629 1600 1586 1521<br>(s) (s) (m) (s) | 903 875 843 813 765 740<br>(m) (m) (s) (s) (w) (s) |
| 1-OH<br>6-OH | 1630 1605 1585 1515<br>(m) (m) (s) (m) | 872 855 848 832 818 780 747<br>(m) (s) (s) (m) (m) (s) (s) |
| 1-NHAc<br>6-OH | a) c) b)<br>1625 1600 1590 1540 1510<br>(s) (m) (w) (s) (s) | 862 852 822 790 770 750<br>(s) (s) (m) (m) (s) (s) |
| 1-NHAc<br>6-O-Allyl<br>(XI) | a) c) c) b)<br>1645 1630 1602 1590 1550 1507<br>(s) (s) (w) (w) (s) (m) | 890 860 835 826 790 767 750 725<br>(w) (m) (m) (s) (w) (m) (m) (m) |

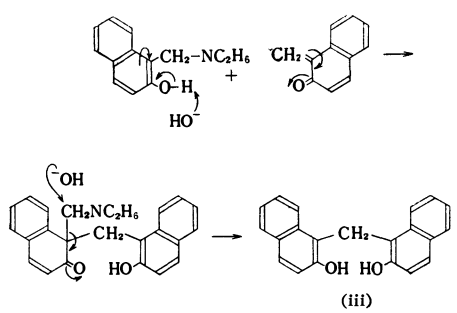
a) amide I b) amide II c) shoulder

was too low. Therefore, plans were again changed and exploration was made of an alternative route, method B.

On treatment of IV with sodium cyanide in aqueous ethanol for 12 hr. under reflux, 1-cyanomethyl-5-acetamido-2-naphthol was obtained in almost quantitative yield[10].

Methylation of XVa to XVb (yield, 93%) by dimethyl sulfate in sodium hydroxide solution, followed by hydrolysis with hydrochloric acid in aqueous ethanol afforded the amino acid hydrochloride (XVI·HCl). In this case, when an excess of dimethyl sulfate and of alkali was used, 1-cyanomethyl-2-methoxy-5-(*N*-methyl)-acetamidonaphthalene was formed as a by-product. The reaction of the amino acid (XVI) with acetic anhydride gave 2-methoxy-5-acetamido-1-naphthylacetic acid, which should be identical with compound XIII obtained by method A. The identity of these products was proved by melting and mixed melting point determinations. Finally, the amino acid hydrochloride (XVI·HCl) was treated under Bucherer conditions. The expected product, 2-methoxy-5-hydroxy-1-naphthylacetic acid (II) was obtained in a 91% yield.

10) In the reaction of 1-dimethylaminomethyl-2-naphthol with sodium cyanide the diarylmethane (iii) is formed at least in 20% yield [J. Brewster, "Organic Reactions", Vol. VII, John Wiley & Sons, Inc., New York (1953), p. 109] clearly through the process outlined below. It is interesting that in the present case, no dinaphthylmethane was produced, although its formation was expected.




(iii)

## A Note on the Infrared Spectra of 1, 2, 5-Trisubstituted Naphthalenes

In the course of the above work, infrared spectra of all the prepared 1,2,5-trisubstituted naphthalenes have been measured. Data on absorption bands at 1650~1500 $cm^{-1}$ (skeletal vibration) and at 900~700 $cm^{-1}$ (C–H out-of-plane vibration) are presented in Table I.

It can be seen that all the 1,2,5-trisubstituted naphthalenes so far examined show a fairly strong band within a narrow frequency range of 800±8 $cm^{-1}$. This band may be attributed to the presence of three

aromatic vicinal hydrogen atoms in these compounds. It is to be expected that these compounds exhibit also a band at 860~800 $cm^{-1}$ (two vicinal hydrogen atoms), but this latter band is obscured owing to the complexity at this region.

In the range of 1650~1500 $cm^{-1}$ the naphthalene derivatives listed above show in common *four* bands. It has been stated[11] that aromatic compounds, in general, exhibit *three* absorption bands in this range[12]. The results given in Table I indicate that the examined naphthalene derivatives present two strong bands at ca. 1620 and ca. 1510 $cm^{-1}$ and two subsidary absorption bands between these wave numbers. Scope and limitation of this generalization are not yet clear. However, it may be mentioned at this point that a number of, of course if not all, naphthalene derivatives except these with electronegative nitro and halogen substituents, exhibit the characteristic four absorption bands between 1650~1500 $cm^{-1}$. Naphthalene itself[13], 1-naphthol[14], 2-naphthol[14], 1,6-dihydroxynaphtalene[14], 1-acetamido-6-hydroxynaphthalene[14] and 1-acetamido-6-allyloxy naphthalene[14] present the above feature. The following naphthalenes, spectra of which appear in the API[15] and DMS[16] cards, fall also in this category (kind and position of substituents, and serial number[17] are given):

1-methyl (762), 2-methyl (763) (1530$cm^{-1}$: weak), 1-ethyl (764), 2-ethyl*,[18] (765), 1,3-dimethyl* (767), 1,5-dimethyl* (769), 1,6-dimethyl* (770), 2,3-dimethyl* (773), 2,7-dimethyl* (775), 2-*n*-propyl* (777), 1-*n*-buthyl (778), 2-*n*-buthyl* (779), 1-*n*-amyl (780), 2-*n*-amyl* (781), 2-methoxy (*1766*), di-1-naphthylmethane (*2777*), 1-cyanoethyl-2-hydroxy (*2640*), di-1-naphthylketone (*2527*) (1621 $cm^{-1}$: sh), 1-benzyl (*2287*) (an extra band at the 1500 $cm^{-1}$ region; attributable to phenyl vibration?), 2-benzyl* (*2288*) (an extra band like 1-isomer), di-2-naphthylketone (*2528*) (1515 $cm^{-1}$: weak).

In the following compounds the subsidary absorption band- or bands- are obscure:

1,4-dimethyl (768), 1,7-dimethyl* (771), 1,8-dimethyl (772), 2,6-dimethyl* (774), 1-*n*-propyl (776), 2,4-dimethyl* (1209).

## Experimental[19]

**1-Piperidinomethyl-5-acetamido-2-naphthol (IVa).**—The procedure of Cornforth and Robinson[5] was slightly modified as follows: Formaldehyde (16.5 ml., 37% solution) was added to a mixture of piperidine (22.5 ml.) 5-acetamido-2-naphthol (37.5 g.) and ethanol (350 ml.). After being kept at room temperature for three days, the crude product, which separated, was collected, washed with a small amount of ethanol and dried. A yield of 88% (49 g.) of piperidino-base was obtained. Recrystallization from isoamyl alcohol gave colorless plates, m. p. 198~199°C. *o-Methylation* of the piperidino-base was attempted by the addition of ethereal solution of excess diazomethane to the base dissolved in chloroform. No generation of nitrogen was observed. On removal of volatile substances after 24 hr., the piperidino-base was recovered in an almost quantitative yield.

**1-Acetoxymethyl-2-acetoxy-5-acetamidonaphthalene (V).**—A mixture of the piperidino-base (IVa) (20 g.) and acetic anhydride (160 cc.) was heated on a steam bath for 3 hr. After addition of water during warming until the solution became clear, the solution was extracted three times with chloroform. The extract was then washed successively with 5% sodium bicarbonate and water, dried and the chloroform removed. The residue was crystallized on being triturated with ether. Recrystallization from ethanol-water gave colorless clustered prisms, m. p. 170~171°C (5.2 g., 24.6%).

**Hydrolysis of V.**—A suspension of 2 g. of V in 20 ml. of 5% aqueous potassium hydroxide was heated at 100°C for several minutes, and then a homogeneous solution was obtained. The solution was then cooled to 0°C and acidified to pH 2 with 6 N hydrochloric acid; an amorphous solid (1.4 g.), which separated, was collected. Methylation was effected as follows: A mixture of the above amorphous solid, sodium hydroxide (0.3 g.) and water (4.2 ml.) was shaken with dimethyl sulfate (0.66 cc.) for half an hour. Additional amount of sodium hydroxide and dimethyl sulfate was then added and shaking continued for a further half hour. The excess of dimethyl sulfate was

11) L. J. Bellamy, "The Infrared Spectra of Complex Molecules", Methuen & Co., Ltd., London (1958), p. 69—79.

12) Since the measurement presented in the table was taken by the nujol mull method, the fourth aromatic skeletal absorption at ca. 1450 $cm^{-1}$ was not taken into account.

13) R. N. Jones and C. Sandorfy, "Chemical Applications of Spectroscopy", Interscience Publishers, Inc., New York (1956), p. 401.

14) See Table II.

15) American Petroleum Institute Research Project 44, Infrared Spectral Data (1943—1958), Carnegie Institue of Technology, Pittsburgh 13, Pa., U. S. A.

16) Documentation of Molecular Spectroscopy, Butterworths Scientific Publications, London (1956—1958).

17) Serial numbers of the DMS cards are given in italics.

18) In the compounds marked with an asterisk, absorption band at the highest frequency (ca. 1620 $cm^{-1}$) splits into two bands of comparable intensity. It may be noted that most of these compounds possess a 2-alkyl group.

19) All melting points are uncorrected. Infrared spectra were taken on a Koken model DS-301 infrared spectrophotometer. The authors wish to thank Mr. O. Yonemitsu of the Pharmaceutical Institute of Hokkaido University for the spectral data and Miss N. Fujino for the microanalyses.

destroyed by gentle heating on a steam bath. Crude methoxyl compound, which separated, amounted to 1.34 g. The product was then dissolved in tetrahydrofuran and chromatographed on alumina (ca. 30 g.). A portion eluted with ethanol was crystallized. For analysis a sample was recrystallized from ethanol; m. p. 285°C (decomp.), colorless small needles.

*Anal.* Found: C, 71.01; H, 6.33; $OCH_3$, 19.07; mol. wt. (Rast), 443.5. Calcd. for $C_{26}H_{21}O_2N_2(OCH_3)_3$: C, 71.58; H, 6.22; $OCH_3$, 19.13%; mol. wt., 486.6.

**5-Acetamido-2-naphthyl Allyl Ether XI.**—5-Acetamido-2-naphthol was converted into allyl ether by heating a mixture of the material (20g.) with allyl bromide (14.4 g.), finely powdered potassium carbonate (28 g.) and purified acetone (600 ml.) for 12 hr. on a steam bath with mechanical stirring. After evaporation of the solvent, the residue was diluted with water and the precipitated allyl ether (24 g., 100%) was collected; m. p. 130~132°C. A portion, recrystallized from aqueous ethanol, gave a pure specimen of XI as colorless needles, m. p. 136°C.

*Anal.* Found: C, 74.96; H, 6.31. Calcd. for $C_{15}H_{16}O_2N$: C, 74.66; H, 6.27%.

**1-Allyl-5-acetamido-2-naphthol (XIIa).**—The crude ether (XI) (18 g.) was heated in an atmosphere of nitrogen for 1 hr. in an oil bath maintained at 185~195°C. The reaction product was then completely dissolved in 10% sodium hydroxide (360 cc.), and the solution was acidified with 6 N hydrochloric acid, the product (17.5 g., 99.5%) being precipitated. Recrystallization from aqueous ethanol gave the naphthol (XIIa) as colorless needles, m. p. 176~177°C.

*Anal.* Found: C, 74.53; H, 6.35. Calcd. for $C_{15}H_{15}O_2N$: C, 74.66; H, 6.27%.

**1-Allyl-2-methoxy-5-acetamidonaphthalene(XIIb).**—A mixture of XIIa (4.4 g.), dimethyl sulfate (4 g.) and aqueous 10% sodium hydroxide (14.5 ml.) was shaken for 0.5 hr., and the precipitated product was filtered, washed with water and dried; yield, 3.8 g. (81.7%). The crude methyl ether was recrystallized from aqueous ethanol as colorless needles, m. p. 147~147.5°C.

*Anal.* Found: C, 75.09; H, 6.85. Calcd. for $C_{16}H_{17}O_2N$: C, 75.27; H, 6.71%.

**1-(2,3-Dibromopropyl)-2-methoxy-5-acetamidonaphthalene.**—To a solution of the methyl ether (XIIb) (0.5 g) in 6 ml. of chloroform, 0.31 g. of bromine dissolved in 4 ml. of chloroform was added drop by drop with shaking. After standing for 1 hr. at room temperature, the solvent was evaporated. The thick sirupy residue solidified upon scratching and was purified by recrystallization from aqueous ethanol; colorless needles, m. p. 168.5~170°C.

*Anal.* Found: C, 45.87; H, 4.41. Calcd. for $C_{16}H_{17}O_2NBr_2$: C, 46.29; H, 4.13%.

**Dihydro Derivative of XIIb.**—Another portion of XIIb (0.8 g.) in ethyl acetate (35 ml.) was hydrogenated over 10% palladized charcoal (0.2 g.). Uptake of hydrogen was completed after about 3 hr. The solution was filtered from the catalyst which was washed with ethyl acetate. The solvent was removed from the combined filtrate and washings under reduced pressure. *1-Propyl-2-methoxy-5-acetamidonaphthalene* was obtained from aqueous ethanol as colorless needles, m. p. 151.5~152.5°C.

*Anal.* Found: C, 74.20; H, 7.71. Calcd. for $C_{16}H_{19}O_2N$: C, 74.68; H, 7.44%.

**Oxidation of XIIb with Potassium Permanganate.**—The methyl ether (XIIb) (5 g.) dissolved in 300 ml. of 95% ethanol and potassium carbonate (1.25 g.) in 12.5 ml. of water were placed in a flask surrounded with an ice-salt bath. A solution of potassium permanganate (10 g.) in 240 ml. of water was then run into the flask at such a rate that the temperature did not rise above −10°C with constant stirring. After the completion of the oxidation, manganese dioxide was filtered off and washed with hot ethanol. The filtrate and washings are combined, the whole was concentrated to about 130 ml., and the residue was extracted three times with chloroform. The combined chloroform extracts were then washed with water, dried and evaporated. A neutral product, *2-methoxy-5-acetamido-1-naphthaldehyde* (*XIV*) was obtained; yield, 1 g. (20%). A pure sample was obtained on recrystallization from ethanol as pale yellow needles and had an m. p. 232~233°C, $\nu_{max}^{nujol}$ 3265 (N-H), 1668 (CHO) and 1655 $cm^{-1}$ (NHCO).

*Anal.* Found: C, 69.18; H, 5.63. Calcd. for $C_{14}H_{14}O_3N$: C, 69.12; H, 5.39%.

To the above aqueous alkaline solution, separated from the chloroform layer, concentrated hydrochloric acid was added in excess to precipitate acidic products; the crude acid was collected (0.5 g.). The filtrate was extracted three times with chloroform, the extracts were combined, dried and evaporated. An additional amount (0.2 g.) of the above acid was obtained. Recrystallization from ethanol gave *2-methoxy-5-acetamido-1-naphthylacetic acid* (*XIII*) as colorless needles, m. p. 245°C.

*Anal.* Found: C, 65.80; H, 5.84. Calcd. for $C_{15}H_{15}O_4N$: C, 65.92; H, 5.53%.

**1-Hydroxymethyl-2-methoxy-5-acetamidonaphthalene (VIIIb).**—The aldehyde (XIV) (190 mg.) was dissolved in 5 ml. of methanol containing a small amount of sodium methoxide and the solution was cooled to produce a fine suspension. On addition of sodium borohydride, the aldehyde dissolved, crystallization of the reduction product began after several minutes, and was completed after 12 hr. The product was collected, washed with water and dried. Removal of the solvent from the filtrate gave further a small quantity of the hydroxymethyl compound. The product weighed 172 mg. (94%) and was purified by recrystallization from ethanol, m. p. 214~215°C.

*Anal.* Found: C, 68.41; H, 6.37. Calcd. for $C_{14}H_{15}O_3N$: C, 68.55; H, 6.16%.

**1-Cyanomethyl-5-acetamido-2-naphthol (XVa).**—A mixture of the piperidino-bass (IV) (9 g.), sodium cyanide (15 g.), ethanol (220 ml.) and water (30 ml.) was refluxed for 12 hr. Water was then added to the reaction mixture, and the solution was concentrated under reduced pressure

to expel ethanol, and acidified with concentrated hydrochloric acid. The solid (7.2 g., 99.5%) which separated was filtered. For analysis a sample was recrystallized from ethanol; m. p. 239°C (decomp.), $\nu_{max}^{nujol}$ 3350 (OH), 3210 (N—H), 2240 (C≡N), and 1660 $cm^{-1}$ (NHCO).

*Anal.* Found: C, 69.54; H, 5.17; N, 11.57. Calcd. for $C_{14}H_{12}O_2N_2$: C, 69.95; H, 5.03; N, 11.66%.

**1-Cyanomethyl-2-methoxy-5-acetamidonaphthalene (XVb).**—The above naphthol (XVa) (6 g.) in aqueous 10% sodium hydroxide (12.5 ml.) was shaken with dimethyl sulfate (3 ml.) for 1 hr., and the reaction mixture was allowed to stand overnight. The methyl ether, which separated, was collected; yield, 5.9 g. (93%); m. p. 211～215°C. Upon recrystallization from ethanol, it formed colorless small needles, m. p. 226～227°C, $\nu_{max}^{nujol}$ 3270 (NH), 2240 (C≡N), and 1660 $cm^{-1}$ (NHCO).

*Anal.* Found: C, 70.70; H, 5.73. Calcd, for $C_{15}H_{14}O_2N_2$: C, 70.85; H, 5.55%.

When a large excess of dimethyl sulfate and of alkali was used, *1-cyanomethyl-2-methoxy-5-(N-methyl)-acetamidonaphthalene* was obtained. Recrystallization from ethanol gave colorless prisms, m. p. 172～173.5°C, $\nu_{max}^{nujol}$ 2240 (C≡N) and 1660 $cm^{-1}$ (NHCO); no appreciable band in the N-H stretching vibration region.

*Anal.* Found: C, 71.58; H, 6.32; N, 10.32. Calcd. for $C_{16}H_{16}O_2N_2$: C, 71.62; H, 6.01; N, 10.44%.

**Hydrolysis of XVb to 2-Methoxy-5-amino-1-naphthylacetic Acid (XVI).**—A mixture consisting of XVb (1.5 g.), ethanol (7.5 ml.), water (5 ml.) and concentrated hydrochloric acid (20 ml.) was refluxed on a steam bath for 5 hr. and was then cooled well with ice. The precipitates were filtered and dried. A yield of 1.52 g. of the amino acid (XVI)·HCl with m. p. 253°C (decomp.) was obtained. The acetate of compound XVI was prepared through the addition of 10% sodium hydroxide solution and acetic anhydride to the aqueous solution of XVI · HCl. The pure sample of the acetate formed colorless needles, m. p. 245°C. No depression in the melting point was observed on admixture of XIII.

**2-Methoxy-5-hydroxy-1-naphthylacetic Acid (II).**—A mixture of the amino acid (XVI) hydrochloride (1.5 g.) and 40% sodium bisulfite solution (85 ml.) in a three-necked flask provided with a reflux condenser and mechanical stirrer, was heated at 95～100°C for 20 hr. At the end of this time 60% aqueous sodium hydroxide (30ml.) was slowly added to the boiling solution with vigorous stirring and the mixture was heated under slightly reduced pressure until the evolution of ammonia had ceased (ca. 3 hr.). After cooling, concentrated hydrochloric acid (85 ml.) was added drop by drop to expel sulfur dioxide and the mixture was heated on a steam bath for 1 hr. The solution was allowed to stand overnight. The crude naphthol (II) (1.23 g., 91%), which separated, was recrystallized from glacial acetic acid as small colorless prisms, m. p. 229～230°C (decomp.), $\nu_{max}^{nujol}$ 3200～3400 (OH), 1710 ($CO_2H$) and 1687 $cm^{-1}$ ($CO_2H$)[20].

*Anal.* Found: C, 67.04; H, 5.32. Calcd. for $C_{13}H_{12}O_4$: C, 67.23; H, 5.21%.

*The methyl ester (XVIII)* was prepared as follows: Fifty milligrams of II was dissolved in 2.5 ml. of 5% methanolic hydrogen chloride. The solution was kept at room temperature. After 48 hr., water and ethyl acetate were added. The ethyl acetate layer was washed with sodium bicarbonate solution, dried and evaporated. The crystalline residue (50 mg., 94.4%), m. p. 150～153°C, was recrystallized from benzene to give a pure sample, m. p. 155.5～156.5°C, $\nu_{max}^{nujol}$ 3400 (OH) and 1720 $cm^{-1}$ (ester).

*Anal.* Found: C, 68.15; H, 5.95. Calcd. for $C_{14}H_{14}O_4$: C, 68.28; H, 5.73%.

**2-Methoxy-5-acetoxy-1-naphthylacetic Acid (XVII).**—The above hydroxy acid (II) (920 mg.) was dissolved in a mixture of anhydrous pyridine (10 ml.) and acetic anhydride (4.5 ml.). After being kept at room temperature overnight, the reaction mixture was concentrated to dryness in vacuo, and the residue was washed with water and dried. Crude acetate (1.02 g., 94%) with m. p. 180～183°C was obtained. The sample for analysis was prepared by recrysallization from benzene; it had m. p. 185.5～186.5°C, $\nu_{max}^{nujol}$ 1755 (phenolic acetate CO), 1200 (phenolic acetate), 1716[20] (carboxyl group) and 1685 $cm^{-1}$ (carboxyl group).

*Anal.* Found: C, 65.31; H, 5.25. Calcd. for $C_{15}H_{14}O_5$: C, 65.69; H, 5.15%.

## Summary

A synthesis of 2-methoxy-5-hydroxy-1-naphthylacetic acid has been described.

The authors are indebted to Dr. Tozo Kubota, Director of the Dyestuffs Division of the Nippon Kayaku Chemicals Co., Ltd. for a generous supply of 1,6-Cleve's acid, from which 2-hydroxy-5-acetamidonaphthalene was prepared.

*Department of Chemistry*
*Faculty of Science*
*Hokkaido University*
*Sapporo*

20) It is interesting to note that both acids, II and XVII, exhibit in nujol two carbonyl bands of comparable strength. Two examples of the similar splitting of carboxyl carbonyl band have been reported in the literature (M. St. C. Flett, *J. Chem. Soc.*, **1951**, 962). This abnormal absorption is probably due to the hydrogen bond of the carboxyl group in the solid state, since i) both the acids exhibit a single absorption in dioxane solution at 1715 $cm^{-1}$ and ii) the abnormal absorption band disappears in the methyl ester (XVIII) of II.

# *Visible and Ultraviolet Absorption Spectra of 1,3,5-Trinitrobenzene in Water in the Presence of Sodium Hydroxide*

By Takehiro ABE

(Received July 1, 1959)

In the previous paper[1,2], the author has reported an absorption spectrum of a red-colored solution produced by adding a few drops of sodium hydroxide solution into an aqueous solution of 1,3,5-trinitrobenzene. In the present paper, an attempt has been made to investigate the interaction of 1,3,5-trinitrobenzene with hydroxyl ion in detail by measuring the absorption spectra of the colored solution at various concentrations of sodium hydroxide, together with an effect of hydrochloric acid on the colored solution.

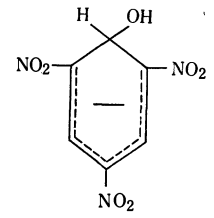
## Experimental

Commercial pure 1,3,5-trinitrobenzene was purified by recrystallizing three times from methanol-water; m. p. 123.1°C. Each colored solution of trinitrobenzene and sodium hydroxide in water was freshly prepared by adding an aqueous solution of sodium hydroxide into an aqueous solution of trinitrobenzene before each measurement. The spectra of the solution were measured with a Hitachi Model EPU-2 spectrophotometer at 25°C or at room temperature. Path length of absorption cells was 1 cm.

## Results and Discussion

**Absorption Spectra of Trinitrobenzene in Water at Various Concentrations of Sodium Hydroxide (Fig. 1).**—As Fig. 1 shows, the aqueous solutions of trinitrobenzene in the presence of sodium hydroxide show absorption bands at 260, 300 and 400~500 mμ. The absorption curve of the colored solution with a sodium hydroxide concentration of 0.393 N resembles that of the red complex between trinitrobenzene and ammonium hydroxide in water[3]. The visible absorption curves of the colored solutions of trinitrobenzene and sodium hydroxide in water are different from that of the solution in acetone, which shows absorption bands at two regions of 450 and 510~590 mμ[4]. The visible absorption curves appreciably resemble that obtained by Caldin et al.[5,6] for the colored solution of trinitrobenzene and ethoxide ion in ethanol, for which a different absorption curve has been obtained by Foster[7].

The color produced by the reaction of trinitrobenzene with sodium hydroxide in water seems to be due to the following structure which is the same as that presented by Meisenheimer[8] for the red product of trinitrobenzene with sodium ethoxide, although the question pointed out in the previous paper[2] still remains.




The structures of Meisenheimer's type have recently been supported for the colored products of many polynitro aromatic hydrocarbons with alkalies[2-4,6,7,9-13].

The absorbances of the visible absorption bands increase with the increasing concentration of sodium hydroxide below the sodium hydroxide concentration, about 0.6 N, but reversely decrease above the sodium hydroxide concentration. The color finally disappears at very high concentration of sodium hydroxide. On the other hand, the bands at 260 and 300 mμ, observed distinctly above the sodium hydroxide concentration, about 0.4 N, become intense, as the sodium hydroxide

1) T. Abe, This Bulletin, **31**, 904 (1958).
2) T. Abe, ibid., **32**, 339 (1959).
3) T. Abe, ibid., **32**, 997 (1959).
4) T. Abe, ibid., **32**, 778 (1959).
5) E. F. Caldin and G. Long, *Proc. Roy. Soc.*, **A228**, 263 (1955).
6) J. B. Ainscough and E. F. Caldin, *J. Chem. Soc.*, **1956**, 2528.
7) R. Foster, *Nature*, **183**, 1042 (1959).
8) J. Meisenheimer, *Ann.*, **323**, 214, 241 (1902).
9) D. L. Hamick and R. Foster, *J. Chem. Soc.*, **1954**, 2153.
10) R. Foster, *Nature*, **175**, 746 (1955).
11) S. Nagakura, S. Oosawa and H. Tsubomura, presented at the Symposium on Electron States of Molecules, Kyoto, October, 1958.
12) S. Nagakura and S. Oosawa, presented at the 12th Annual Meeting of the Chemical Society of Japan, Kyoto, April, 1959.
13) J. F. Bunnett and J. J. Randall, *J. Am. Chem. Soc.*, **80**, 6020 (1958).

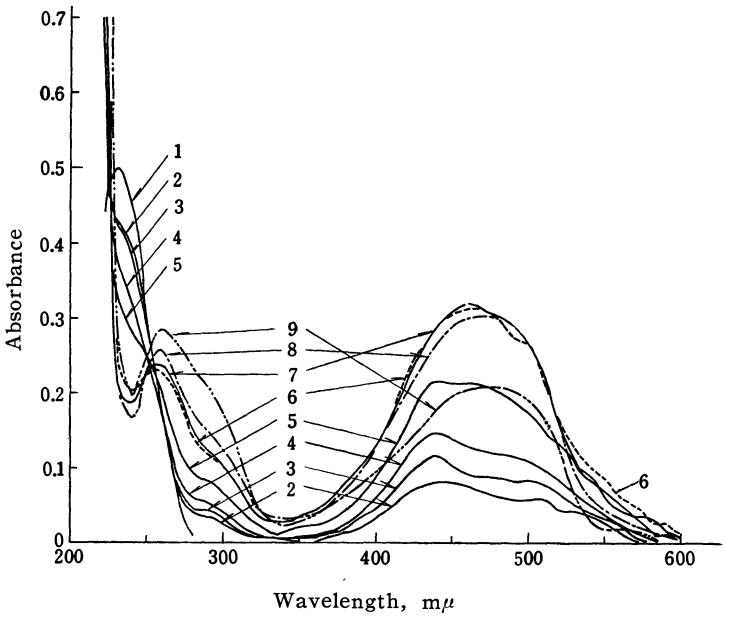
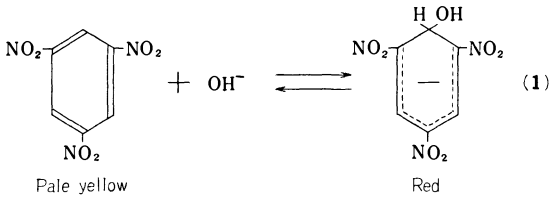
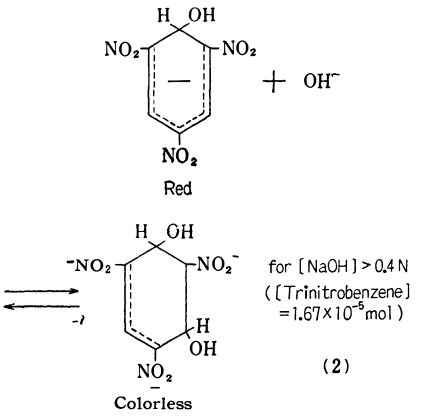


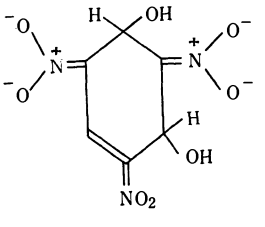

Fig. 1. Absorption spectra of 1,3,5-trinitrobenzene ($1.67\times10^{-5}$ mol.) in water containing various concentrations of sodium hydroxide at 25°C (path length of cells, 1 cm.).
Concentrations of sodium hydroxide:
1) 0; 2) $5.89\times10^{-2}$ N; 3) $7.86\times10^{-2}$ N; 4) $1.18\times10^{-1}$ N; 5) $1.97\times10^{-1}$ N; 6) $3.93\times10^{-1}$ N; 7) $5.89\times10^{-1}$ N; 8) $9.60\times10^{-1}$ N; 9) 1.92 N.

concentration increases. The 260 and 300 mμ bands, as mentioned below, can not be ascribed to a product produced by a further reaction of the colored species, and disappear by addition of an acid. From the above results, the absorption bands may be interpreted as follows. The decrease in the absorbances of the visible absorption bands, considered to be due to [Trinitrobenzene·OH]$^-$, seems to lead to the suggestion that interaction of [Trinitrobenzene·OH]$^-$ with hydroxyl ion results in the formation of [Trinitrobenzene·2OH]$^{2-}$ above the sodium hydroxide concentration, about 0.4 N. The increase in the absorbances of the 260 and 300 mμ bands can be explained by attributing these bands to [Trinitrobenzene·2OH]$^{2-}$. Accordingly, the following reactions may possibly be expected for the interaction of trinitrobenzene with sodium hydroxide in water.




The p$K$ values of 1,3,5-trinitrobenzene solution were determined by Schaal[14] by ultraviolet absorption measurement in an ethylenediamine-water mixture of a known




14) R. Schaal, *Compt. rend.*, **239**, 1036 (1954).

acidity function, with the result of $pK_1=14.40$ and $pK_2=18.00$. The two $pK$ values may support the formations of [Trinitrobenzene·OH]$^-$ and [Trinitrobenzene·2OH]$^{2-}$. Schaal also supposed the formation of the following complex for the $pK_2$.

**An Equilibrium Constant for the Colored Reaction of Trinitrobenzene with Hydroxyl Ion.**—In the previous paper[2] the author has found that the red-colored species of 1,3,5-trinitrobenzene and 2,4,6-trinitrotoluene with sodium hydroxide in water are more stable than those of picryl chloride and 2,4,6-trinitrophenylmethylnitramine (Tetryl). The colored solution of trinitrobenzene and ethoxide ion has been found by Caldin and Long[5] and by Foster[7] to obey Beer's law. An attempt has, therefore, been made to obtain the equilibrium constant $K$ for the colored reaction 1 of trinitrobenzene with sodium hydroxide in water from the result in Fig. 1.

As [NaOH]$\gg$[Trinitrobenzene] in the present measurements, Benesi and Hildebrand's equation[15] can be written as

$$\frac{l[\text{Trinitrobenzene}]}{d}=\frac{1}{\varepsilon K}\cdot\frac{1}{[\text{NaOH}]}+\frac{1}{\varepsilon} \quad (3)$$

Here $l$ represents the path length of absorption cells (1 cm.) and $d$ and $\varepsilon$ are respectively an absorbance and a molar extinction coefficient for the colored species. Fig. 2 is obtained by plotting [Trinitrobenzene]$/d$ against 1/[NaOH]. Although the colored species of trinitrobenzene and hydroxyl ion is comparatively stable, it slowly reacts with hydroxyl ion, as mentioned below. Moreover, the molar extinction coefficient of the colored species may be affected by the concentration of sodium hydroxide, since the absorption curves of the red complexes of trinitrobenzenes with ammonium hydroxide are apt to be greatly influenced with any solvent, as shown in the previous paper[3]. As Fig. 2 shows, [Trinitrobenzene]$/d$, however, is nearly proportional to 1/[NaOH] below the sodium hydroxide concentration, about 0.6 N. The linearities of Benesi and Hildebrand's plots indicate the formation of the 1:1 colored complex between trinitrobenzene and hydroxyl ion, because Benesi and Hildebrand's Eq. 3 is derived for the 1:1 complex. Therefore, the visible absorption bands are undoubtedly owing to the formation

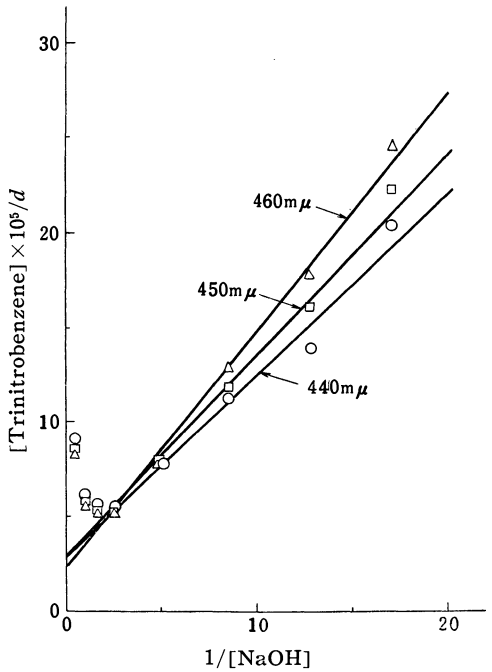



Fig. 2. Benesi and Hildebrand's relation for the result in Fig. 1.

of [Trinitrobenzene·OH]$^-$. Deviations of the plots from the linearities above the sodium hydroxide concentration, about 0.6 N can be interpreted to be owing to the formation of [Trinitrobenzene·2OH]$^{2-}$ according to reaction 2. By Eq. 3 the intercept at 1/[NaOH]=0 and the ratio of the intercept to slope give $1/\varepsilon$ and $1/\varepsilon K$, respectively. From the best straight line for the 450 m$\mu$ absorption band, it is possible to find $\varepsilon_{450}=3.5\times10^4$ and $K=2.7$ at 25°C. The value of $3.5\times10^4$ is larger than the molar extinction coefficient of $9.4\times10^3$ for the maximum absorption band (at 480 m$\mu$) of the red complex of trinitrobenzene with ammonium hydroxide in water[3]. The equilibrium constant of 2.7 is very much smaller as compared with that ($2.4\times10^3$) obtained by Caldin and Long[5] for the color reaction of trinitrobenzene with ethoxide ion in ethanol at 25°C.

**Time Dependence of Absorption Spectra of the Colored Solutions of Trinitrobenzene and Sodium Hydroxide in Water (Fig. 3).**—On standing the colored solutions of trinitrobenzene and sodium hydroxide in water, the absorbances of the visible absorption bands gradually decrease, while an increase in absorbance can be observed at about 350 m$\mu$. The 350 m$\mu$ band is probably due to a product in which [Trinitrobenzene·OH]$^-$ and [Trinitrobenzene·2OH]$^{2-}$ result.

15) H. A. Benesi and J. H. Hildebrand, *J. Am. Chem. Soc.*, **71**, 2703 (1949).

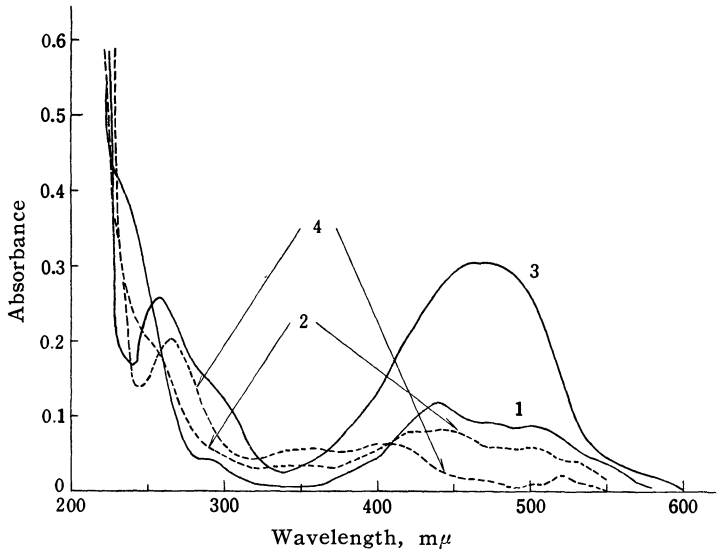



Fig. 3. Absorption spectra of the colored solutions of trinitrobenzene ($1.67\times10^{-5}$ mol.) and sodium hydroxide in water, stood for long hours (at room temperature).
1) A solution with a sodium hydroxide concentration, $7.86\times10^{-2}$ N;
2) The same after two days;
3) A solution with a sodium hydroxide concentration, $9.60\times10^{-1}$ N;
4) The same after a day.

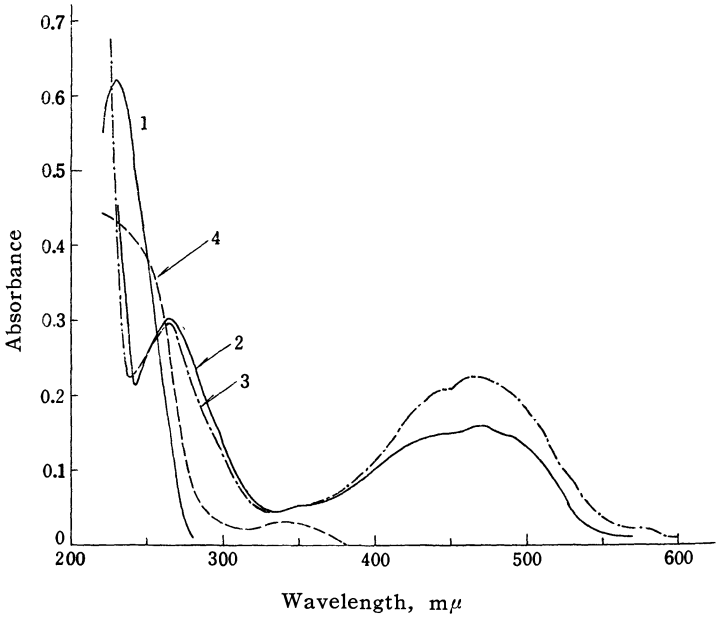



Fig. 4. An effect of hydrochloric acid on the spectrum of the colored solution of trinitrobenzene and sodium hydroxide in water (at room temperature).
1) A solution obtained by adding 2 cc. of water into 2 cc. of an aqueous solution of trinitrobenzene ($4.18\times10^{-5}$ mol.);
2) A solution obtained by adding 2 cc. of water into 2 cc. of a colored solution of trinitrobenzene ($4.18\times10^{-5}$ mol.) and sodium hydroxide (2.88 N);
3) A solution obtained by adding 2 cc. of a 1.77 N aqueous solution of hydrochloric acid into 2 cc. of the same colored solution as in 2);
4) A solution obtained by adding 2 cc. of a 3.55 N aqueous solution of hydrochloric acid into 2 cc. of the same colored solution as in 2).

The 260 and 300 mμ bands and the visible absorption bands may, therefore, be considered to be due to intermediates, that is, [Trinitrobenzene·OH]$^-$ and [Trinitrobenzene·2OH]$^{2-}$ in the reaction of trinitrobenzene with hydroxyl ion to the product giving the 350 mμ band. The absorbances of the visible absorption bands decrease faster in the colored solution with a high sodium hydroxide concentration than in that with a low sodium hydroxide concentration. This suggests that sodium hydroxide plays an important role for the further decoloration reaction of [Trinitrobenzene·OH]$^-$, as mentioned in the previous paper[3].

**An Effect of Hydrochloric Acid on the Spectrum of the Colored Solution of Trinitrobenzene and Sodium Hydroxide (Fig. 4).**—It has been reported by Caldin and Long[5], by Nagakura and Oosawa[12], and by the author[2] that the colored solutions formed on adding alkalies to solutions of aromatic polynitrocompounds are reversibly decolorized by the addition of acids. As Fig. 4 shows, when 2 cc. of 1.77 N aqueous solution of hydrochloric acid is added to the colored solution with a sodium hydroxide concentration, 2.88 N, in which reaction 2 is expected to occur according to the appearance of the distinct 260 mμ band, the absorbances of the visible absorption bands increase, while that of the 260 mμ band slightly decreases. This seems to be due to a reverse reaction of [Trinitrobenzene·2OH]$^{2-}$ to [Trinitrobenzene·OH]$^-$ by addition of hydrochloric acid. If a higher concentrated solution of hydrochloric acid is added to the colored solution, the visible absorption bands disappear and a weak absorption band can be observed 350 mμ. The 350 mμ bands seems to be due to the final product of the reaction between trinitrobenzene and hydroxyl ion, as mentioned above. From the above results, [Trinitrobenzene·2OH]$^{2-}$ may be considered to change into [Trinitrobenzene·OH]$^-$ reversibly by the addition of an acid.

## Summary

(1) Absorption spectra of the colored solutions of 1,3,5-trinitrobenzene and various concentrations of sodium hydroxide in water have been measured at 25°C. The colored solution shows absorption bands at 260, 300 and 440~500mμ. The absorbances of the visible absorption bands increase below the sodium hydroxide concentration, about 0.6 N, but decrease above the sodium hydroxide concentration, as the concentration of sodium hydroxide increases. On the other hand, the 260 and 300 mμ bands, observed above the sodium hydroxide concentration, about 0.4 N, increase their absorbances with an increase in concentration of sodium hydroxide. These lead to the suggestion that the visible absorption bands are due to [Trinitrobenzene·OH]$^-$ and the 260 and 300 mμ bands are due to [Trinitrobenzene·2OH]$^{2-}$.

(2) Below the sodium hydroxide concentration, about 0.6 N, Benesi and Hildebrand's equation holds for the colored solutions, giving an equilibrium constant of 2.7 for the reaction between trinitrobenzene and hydroxyl ion in water at 25°C.

(3) On keeping the colored solution to stand for long hours, the 260 and 300 mμ bands and the visible absorption bands decrease their absorbances, while an absorption band appears at about 350 mμ.

(4) When an aqueous solution of hydrochloric acid is added into the colored solution with a high concentration of sodium hydroxide, the absorbances of the visible absorption bands increase. The 260 mμ band and the visible absorption bands disappear by adding a solution of hydrochloric acid, enough to neutralize the sodium hydroxide contained in the solution. By the addition of acids, [Trinitrobenzene·OH]$^-$ and [Trinitrobenzene·2OH]$^{2-}$ seem to change into trinitrobenzene reversibly.

The author is particularly indebted to Professor Y. Nomura for his suggestions and encouragement throughout this work.

*Department of Chemistry*
*Defense Academy*
*Yokosuka*

# *An Electron Diffraction Investigation on the Molecular Structure of Hydrazine*

By Yonezo MORINO, Takao IIJIMA, and Yoshitada MURATA

(Received July 1, 1959)

The molecular structure of hydrazine was studied in 1943 by Giguére and Schomaker[1] with the visual method of electron diffraction and the N–N distance was found to be 1.47±0.02 Å. Recently Yamaguchi et al.[2] in this Department studied the infrared vibration-rotation spectrum of the molecule and recognized a difficulty in interpreting the spectrum by the use of this distance. Strictly speaking, the moment of inertia can not be fixed uniquely by the vibration-rotation spectrum alone, for there is a wide choice in selecting the $J$ and $K$ numbering without any other information. Thus, precise determination of the N–N distance was desirable for the proper assignment of the spectral lines. The principal object of the research is to determine the N–N distance as accurately as possible by the sector-microphotometer method, and, if possible, to measure the root mean square amplitudes of thermal vibration.

## Experimental

The sample of hydrazine was kindly provided by Dr. Yamaguchi. The apparatus for electron diffraction was the same as that reported in the preceding paper[3]. An $r^3$-sector was used. The camera length was 11.82 cm. and the accelerating voltage used was about 45 kV. The nozzle was heated to about 60°C and the sample holder to about 30°C. The measured range was from 17 to 100 in $q$-unit. The diffraction patterns were traced on a Rigaku-Denki MP-3 microphotometer. During the tracing the photographic plates were rotated rapidly about the center of the diffraction pattern.

## Structure Analysis

Karle's method[4] was applied to a pair of photographs of different exposure (1 : 1.5). The density-intensity calibration curve was found to be linear in the whole range of the measurement. The ratio of density between the two photographs was consistent with the ratio of the time of exposure.

The molecular intensity curves, $qM(q)$, were obtained by the procedure developed by Karle and Karle. The result is shown in Fig. 1. The radial distribution curve (Fig. 2) was calculated by the Fourier transformation of the observed molecular

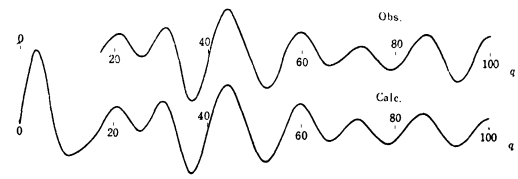



Fig. 1. Observed and calculated molecular intensity curves, $qM(q)$, of hydrazine.

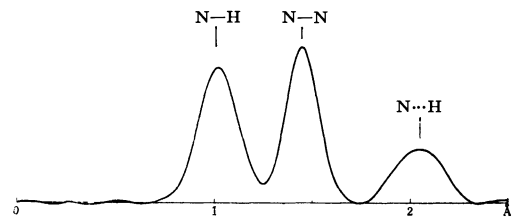



Fig. 2. The modified radial distribution curve of hydrazine.

intensity multiplied by an artificial factor $\exp(-bq^2)$ with $b=0.0002303$, which was assumed so as to reduce the intensity to one tenth of the original at $q=100$. In order to diminish the effect of series termination, the observed intensity curve was spliced with a curve calculated for an assumed model, below 20 and from 90

TABLE I. MOLECULAR PARAMETER OF THE MODEL ASSUMED FIRST FOR THE CALCULATION OF THE SUPPLEMENTARY PART OF THE RADIAL DISTRIBUTION CURVE

| | Atomic distance | Root mean square amplitude |
|---|---|---|
| N–N | 1.47 Å | 0.052 Å |
| N–H | 1.04 Å | 0.074 Å |
| N···H | 2.05 Å | 0.100 Å |

1) P. A. Giguére and V. Schomaker, *J. Am. Chem. Soc.*, **65**, 2025 (1943).
2) A. Yamaguchi, I. Ichishima, T. Shimanouchi and S. Mizushima, *J. Chem. Phys.*, **31**, 843 (1959).
3) Y. Morino and K. Kuchitsu, ibid., **28**, 175 (1958).
4) J. Karle and I. Karle, ibid., **27**, 1052 (1949); **18**, 957 (1950).

to 120 in $q$-scale. The molecular parameters of the starting model are given in Table I. The equilibrium distances were taken from the paper of Giguére and Schomaker. For the mean amplitude of N-N, that of C-O pair in methanol, 0.052 Å, was adopted. The mean amplitude for the pair of N-H, 0.074 Å, was calculated with an N-H diatomic molcule having the frequency of the symmetric stretching vibration of $NH_3$, 3337 $cm^{-1}$. Finally, for the pair of non-bonded N···H the observed value of a C···H pair in $n$-butane, 0.100 Å, was used. The model was refined by successive approximation. The calculations of the molecular intensity curve and of the radial distribution curve were performed with the aid of a parametron computer PC-1.

The index of resolution was found to be about 95%. Each peak of the radial distribution curve was fitted with a Gaussian in shape to obtain $r_m(f)$ from the position of the maximum of the Gaussian peak, and $<\Delta r^2>^{1/2}$ from the width of the peak. The failure of Born approximation was corrected by Bartell-Brockway method[5]. Using the values of $r_m(f)$, $<\Delta r^2>^{1/2}$, and the index of resolution, thus obtained, the theoretical intensity curve was computed. It is compared with the observed in Fig. 1. Agreement is very well up to 90 in $q$-scale. The final values of the molecular constants listed in Table II were established by taking average over the values obtained by four photographs.

TABLE II. FINAL OBSERVED VALUES OF ATOMIC DISTANCES AND THEIR MEAN SQUARE AMPLITUDES

| | $r_m(f)$ | $<\Delta r^2>^{1/2}$ | $r_0$ (spectroscopic)[2] |
|---|---|---|---|
| N-N | 1.449 ±0.004 Å | 0.051 ±0.005 Å | 1.453 ±0.005 Å |
| N-H | 1.022 ±0.006 Å | 0.074 ±0.007 Å | 1.025 ±1.020 Å |
| N···H | 2.063 ±0.015 Å | 0.103 ±0.015 Å | — |
| N-N-H | 112.0 ±1.5° | — | 112 ~112.5° |

## Calculation of Mean Amplitudes

As was shown by one of the present author[6], the mean square amplitude of a distance between a pair of atoms is given by

$$<\Delta R_i^2> = \sum_k L_{ik}^2 <Q_k^2>$$

where $<Q_k^2>$ is the mean spuare amplitude of the $k$-th normal vibration and is given by the normal frequency as follows:

$$<Q_k^2> = \frac{h}{8\pi^2\nu_k} \coth \frac{h\nu_k}{2kT}$$

$L_{ik}$ is the element of the $\boldsymbol{L}$ matrix which transforms the internal coordinates to the normal coordinates. $L_{ik}^2<Q_k^2>$ indicates the contribution of the $k$-th normal vibration to the mean square amplitude of $R_i$.

The $\boldsymbol{L}$ matrix elements of the hydrazine molecule were calculated by Yamaguchi by the use of the frequencies of the normal vibrations obtained by the Raman and infrared spectra. The temperature of the sample was estimated to be 333°K. The calculated values are shown in Table III, with a reference to the observed values.

TABLE III. CALCULATED VALUES OF MEAN SQUARE AMPLITUDES IN THE UNIT OF $10^{-4}$ Å$^2$

| | Frequency ($cm^{-1}$) | Designation | N-N | N-H | N···H |
|---|---|---|---|---|---|
| A | 3280 | N-H sym. stretching | 0.1 | 15.0 | 7.2 |
| | 3325 | N-H antisym. stretching | 0.0 | 12.1 | 5.6 |
| | 1587 | bending | 1.4 | 0.0 | 3.5 |
| | 1275 | twisting | 0.0 | 0.0 | 20.9 |
| | 1098 | N-N stretching | 19.7 | 0.1 | 12.7 |
| | 780 | wagging | 0.6 | 0.0 | 3.1 |
| | 377 | torsion | 0.0 | 0.0 | 0.0 |
| B | 3314 | N-H sym. stretching | — | 10.5 | 7.3 |
| | 3350 | N-H antisym. stretching | — | 16.3 | 9.1 |
| | 1628 | bending | — | 0.2 | 6.2 |
| | 1275 | twisting | — | 0.0 | 11.4 |
| | 966 933 | wagging | — | 0.0 | 10.4 |
| Total | | | 21.8 | 54.2 | 97.4 |
| Observed mean square amplitude | | | 26 | 55 | 106 |

## Discussion

The N-N bond distance was found to be 1.449±0.004 Å. It is apparently smaller than that by Giguére and Schomaker, 1.47 Å, although the difference is of the same order of magnitude as the error of their value. The final assignment of the spectral lines of the infrared spectrum provided 1.453±0.005 Å[2], in good agreement with the value newly obtained. The N-H distance and the angle of N-N-H obtained by both methods are compared in Table II. For the infrared spectrum, it is the moment of inertia that gives the spacings of the spectral lines, and the

5) L. S. Bartell and L. O. Brockway, *Nature*, **171**, 978 (1953).

6) Y. Morino, K. Kuchitsu and T. Shimanouchi, *J. Chem. Phys.*, **20**, 726 (1952); Y. Morino, K. Kuchitsu, A. Takahashi and K. Maeda, *J. Chem. Phys.*, **21**, 1927 (1953).

moment of inertia strongly depends upon the position of the hydrogen atoms which are located at both ends of the molecule. Hence the N–H distance and the N–N–H bond angle may be obtained more accurately by the infrared spectrum. It must be admitted that the non-bonded N···H distance might contain a fairly large error in the electron diffraction measurement, because the halos in the inner region ($<17$ in $q$-scale) have not been measured. In fact, the N···H peak in the radial distribution curve was found to be appreciably deformed from the Gaussian.

For the mean square amplitudes, the agreement between the observed and the calculated is quite satisfactory, as shown in Table III. Large systematic errors would be contained in the observed values, because the effects of non-nuclear scattering and of finite sample size were not corrected for the observed values. It would be of interest to note that the contribution of the N–N stretching mode to the mean amplitude of N–N pair and that of the N–H stretching modes to the bonded N–H mean amplitude are the most predominant, whereas for the non-bonded N···H pair many modes contribute in comparable order of magnitude.

**Summary**

By the sector-microphotometer method of electron diffraction the molecular structure of hydrazine was obtained as shown in Table II. The bond distances are in good agreement with the values obtained by the infrared vibration-rotation spectrum. The mean amplitudes agreed with the calculated values within the limits of errors.

The authors wish to express their gratitude to Professor H. Takahashi and his coworkers, Department of Physics, the University of Tokyo, for the use of the PC-1 Computer, and to Dr. A. Yamaguchi for her kind offer of hydrazine sample and for many helpful discussions. They are also indebted to the Ministry of Education for the research grant.

*Department of Chemistry*
*Faculty of Science*
*The University of Tokyo*
*Hongo, Tokyo*

# *Oxide Formation on Iron Surface Corroded in Non-Oxidizing Acids*

By Jiro KATO and Yoshi ARAI

(Received August 5, 1959)

On corroding an iron specimen in hydrochloric acid solution with an inhibitor, such as propargyl alcohol, it is possible to observe the formation of ferrous oxide on its surface by means of electron diffraction with good reproducibility of results. The propargyl alcohol is known to be an efficient inhibitor for steel against hydrochloric acid solution[1]. Yamamoto[2] assumed that the propargyl alcohol is able to inhibit the dissolution of iron, since it is adsorbed onto the iron surface with its triple bond. A formation of complex compound, such as $HC{=}\underset{\underset{\text{Fe}}{|}}{\overset{\cdot\cdot}{C}}CH_2{-}\underset{\underset{\text{Fe}}{|}}{O}H$, was also suggested by Lüthringhous and Goetz[3]. In their suggestion, they pointed out the effect of hydrochloric acid from the stand point of the organic chemistry. It is of interest, therefore, to examine experimentally whether their assumptions are true or not.

In this investigation the determination of the corrosion products was carried out by means of electron diffraction. The mechanically polished specimens (5×5 mm.) were immersed in 2 N HCl solution with or without propargyl alcohol about 4 hr. at 70°C. The concentration of propargyl alcohol added was about 10 mM. After the corrosion test, the specimens were washed with distilled water, ethanol and petroleum ether successively, and then immediately examined in an electron

1) J. W. Reppe, "Acetylene Chemistry", Charles A. Meyer & Co., Inc., New York (1949), p. 96.
2) K. Yamamoto, This Bulletin, **27**, 379 (1954).
3) A. Lüthringhous and H. Goetze, *Angew. Chem.*, **64**, 661 (1952).

diffraction camera working with 50 kV. electrons. The lattice parameters of the oxide film were determined in reference to those of gold foil. The reflection pattern obtained from the specimen corroded in 2 N HCl solution containing the propargyl alcohol is shown in Fig. 1.

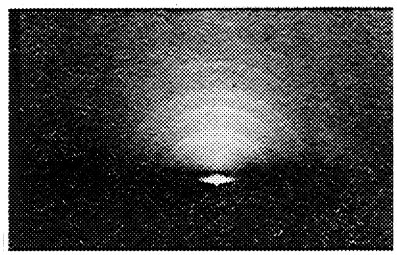


Fig. 1. Diffraction pattern from the iron specimen corroded in 2 N HCl solution containing the propargyl alcohol.
Temperature: 70°C, Immersion time: 4 hr.

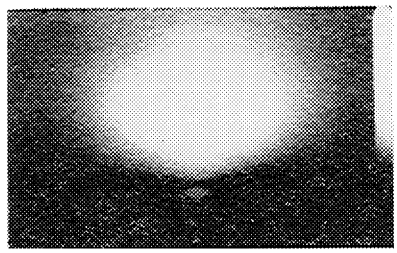


Fig. 2. Diffraction pattern from the iron specimen corroded in 2 N HCl solution containing the propargyl alcohol.
Temperature: 70°C, Immersion time: 8 hr. at 70°C and thereafter 12 hr. at room temperature.

When the specimen was corroded for longer time (about 8 hr.) followed by standing for 12 hr. at room temperature, its surface was coated by $Fe_3O_4$ (or $\gamma$-$Fe_2O_3$). (See Fig. 2.)

Only the iron pattern was observed on the surface of the specimen exposed to 2 N HCl without the propargyl alcohol.

The inhibition mechanism of propargyl alcohol may be explained by considering that oxide films formed on iron surface are protected by the adsorbed propargyl alcohol from a further attack of acid. The oxide films may be always created on the iron surface by dissolved oxygen or OH ions formed at the iron dissolution[4].

In the present investigation the oxide film formation is experimentally observed with the electron diffraction (reflection method). From these results, it is suggested that the oxidation of iron is carried out at the dissolution even in the non-oxidizing acid, such as hydrochloric acid.

The authors wish to express their sincere thanks to Mr. T. Akiba and Dr. A. Nakatuchi for their kind permission to publish this work.

*The Nitto Institute of Chemical Research*
*Kamikizaki, Urawa*

4) K. F. Bonhoeffer and K. E. Heusler, *Z. Elektrochem.* **61**, 122 (1957).

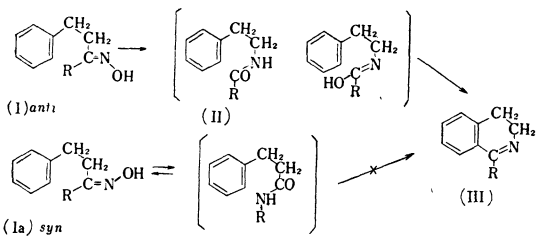
# *The Bischler-Napieralski Reaction in Liquid Sulfur Dioxide. Formation of N, N'-bis-β-Phenethyl Acet- and Benz-amidines and N, N'-Diphenyl Acet- and Benz-amidines*

By Ritsuro TADA, Hisanori SAKURABA and Niichiro TOKURA

(Received May 2, 1959)

It has been shown in a previous paper[1] that dihydroisoquinoline and phenanthridine-derivatives may be produced from the corresponding ketone oximes by simultaneous Beckmann rearrangements and cyclodehydrations in liquid sulfur dioxide under appropriate conditions. As shown in Chart I, the *syn-* and *anti-*configurations of the starting materials should be taken into account in considering the reaction process.

Chart I



In the above-mentioned simultaneous rearrangement and cyclodehydration, the total yield of the condensed ring compound was lower than forty-five per cent and this low yield was apparently due to the presence of a considerable amount of the Ia (*syn*) isomer.

In order to clarify this point, the expected intermediate from the *anti* oxime (I), viz. the acid amide (II), was subjected to the Bischler-Napieralski reaction with phosphorus pentoxide in liquid sulfur dioxide by modifying Bradsher and Sinclair's method of cyclodehydration[2]. In a preliminary examination, it was ascertained that 1-methyl-3,4-dihydroisoquinoline (R=$CH_3$, III) was obtained from *N*-phenethyl acetamide (R=$CH_3$, II) in a maximum yield of 24.5%, and that 10.7% of the acid amide (I) was recovered.

In addition, it was found that the procedure gave a basic substance besides usual Bischler-Napieralski reaction product III.

This result aroused the authors' interest in examining the general behavior of acid amides toward condensing reagents in liquid sulfur dioxide.

Among various reagents examined, phosphorus oxychloride, polyphosphoric acid and thionyl chloride gave no reaction product and only phosphorus pentoxide was effective. The results are shown in Table I.

As is shown in Table I, the relation between the dihydroisoquinoline and the basic substance produced at 20°C in liquid sulfur dioxide explains that the side reaction was induced in preference to the

TABLE I. SYNTHESES OF 1-METHYL-3,4-DIHYDROISOQUINOLINE FROM *N*-β-PHENETHYL ACETAMIDE IN LIQUID $SO_2$[a,b]

| No. | Molar ratio of amide to $P_2O_5$ | Reaction | | Amide, recovered, yield, % | 1-Methyl-3,4-dihydro isoquinoline, yield, % | Basic substance, yield, % |
|---|---|---|---|---|---|---|
| | | Temp. °C | Time hr. | | | |
| 1 | 1 : 5 | 20 | 6 | 35.3 | 3.5 | 23.0 |
| 2 | 1 : 5 | 70 | 6 | 10.7 | 24.5 | 33.8 |
| 3[c] | 1 : 17 | 210 | 0.5 | — | 83 | 0 |

a) Reactions were carried out with 6.5 g. (0.04 mol.) of amide in 100 ml. of liq. $SO_2$ under shaking.

b) $POCl_3$, polyphosphoric acid, or $SOCl_2$ used as the reagent in liq. $SO_2$ (molar ratio of amide to reagent was 1 : 5) at 20°C for 6 hr. or at 70°C for 6 hr., caused no reaction.

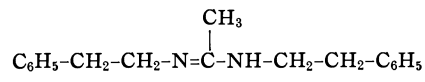
c) Reaction was carried out in tetralin[8].

1) R. Tada, H. Sakuraba and N. Tokura, This Bulletin, **31**, 1003 (1958).

2) C. K. Bradsher and E. F. Sinclair, *J. Org. Chem.*, **22**, 79 (1957).

Bischler-Napieralski reaction.

This basic substance produced was assumed to be the hitherto unknown *N*,*N'*-bis-β-phenethyl acetamidine (IV).

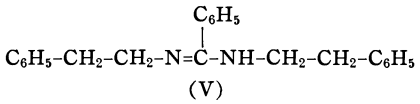


(IV)

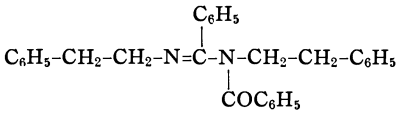
This amidine (IV), distilling at 205~215°C (6~7 mmHg) or 180~190°C (2~3 mmHg) was obtained as a pale yellow oil ($n_D^{15}=1.5748$) and yielded a picrate of m. p. 118~119°C. The elementary analyses of both the base and the picrate satisfied formula IV. The ultraviolet spectrum of the base showed a maximum at $\lambda_{max}^{MeOH}=250\ m\mu$ ($\varepsilon_{max}=385$), indicating the presence of a nonconjugated benzene ring. Its infrared spectrum showed absorption at $\nu_{max}^{KBr}=1635$ (>C=N-), 3440 (>NH), 1352 (methyl), 2915 and 2860 (methylene), and 745 and 695 $cm^{-1}$ (benzene, mono-substituted). The hydrolysis of this base with ten per cent aqueous sodium hydroxide solution, yielded *N*-β-phenethyl acetamide and *N*-β-phenethylamine. Thus the structure of the base was etablished as being IV.

Similarly, it was also shown that a basic substance was afforded by the reaction of *N*-β-phenethyl benzamide (R=$C_6H_5$, II) with phosphorus pentoxide in liquid sulfur dioxide. This basic matter produced was identified as the known *N*,*N'*-bis-β-phenethyl benzamidine (V).

Further, it was also found that another substance was present in the reaction mixture in the latter case. This substance was assumed to be the hitherto unreported *N*-benzoyl-*N*,*N'*-bis-β-phenethyl benzamidine (VI).



(V)

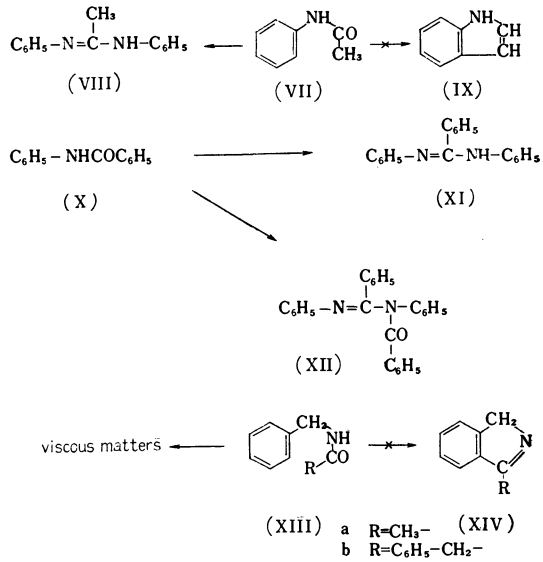


(VI)

This amidine (VI), melting at 110~110.5°C, was obtained as faintly orange crystals. The elementary analysis satisfied formula VI. The ultraviolet spectrum of the amidine showed a maximum at $\lambda_{max}^{MeOH}=241\ m\mu$ ($\varepsilon_{max}=18647$). Its infrared spectrum showed absorptions at $\nu_{max}^{KBr}=1626$ (>C=N-), 1643 (>N-CO-), 2935 and 2860 (methylene), and 747 and 695 $cm^{-1}$ (benzene, mono-substituted). The hydrolysis of this neutral substance with 2 N sulfuric acid gave benzoic acid, *N*-β-phenethyl benzamide and *N*,*N'*-bis-β-phenethyl benzamidine. Thus its structure may be represented by VI.

It was further examined in cases of the other acid amides whether such amidine formations might be encountered generally in liquid sulfur dioxide. When acetanilide (VII) was subjected to this reaction, a similar basic substance was afforded and identified as the known *N*,*N'*-diphenyl acetamidine (VIII). Moreover, when benzanilide (X) was subjected to this reaction, similar substances were obtained and identified as the known *N*,*N'*-diphenyl benzamidine (XI) and *N*-benzoyl-*N*,*N'*-diphenyl benzamidine (XII), respectively. However, when benzyl acet- (XIIIa) and benz-amide (XIIIb) were used, the corresponding amidines were not produced, and viscous substances which were difficult to identify were afforded. The ring closure to IX or XIV was also difficult (Chart II).

Chart II




These results are listed in Table II.

The reason why the formation of dihydroisoquinolines is limited is thus well elucidated as the result of the competitive formation of *N*,*N'*-bis-β-phenethyl amidines. The present authors are not sure that the viscous substances produced from XIII (R=$CH_3$ or $C_6H_5$) might be the polymerization products of the isoindole derivatives which have been known to be very unstable.

TABLE II. REACTION OF PHOSPHORUS PENTOXIDE ON ACID AMIDES IN LIQUID $SO_2$[a]

| Amide | Reaction Temp., °C | Reaction Time, hr. | Amide, recovered, yield, % | Amidine, yield, % | | Other substance produced, yield, % | |
|---|---|---|---|---|---|---|---|
| *N*-β-Phenethyl acetamide | 20 | 6 | 35.3 | 28.3[b] | | 3.5[h] | |
| | 70 | 6 | 10.7 | 41.5[b] | | 24.5[h] | |
| *N*-β-Phenethyl benzamide | 20 | 6 | 48.8 | 12.3[c] | 0[d] | 14.6[i] | 8.3[j] |
| | 70 | 6 | 0 | 9.2[c] | 12.7[d] | 80.6[i] | 8.3[j] |
| Acetanilide | 20 | 6 | 57.4 | 19.0[e] | | 5.5[k] | |
| | 70 | 6 | 35.1 | 30.9[e] | | 11.1[k] | |
| Benzanilide | 20 | 6 | 41.7 | 1.8[f] | 46.6[g] | trace[j] | |
| | 70 | 6 | 5.0 | 46.2[f] | 28.6[g] | 16.6[j] | |
| *N*-Benzyl acetmide | 20 | 6 | — | — | | 57.6[l] | 8.4[m] |
| | 70 | 6 | — | — | | 83.0[l] | 10.8[m] |
| *N*-Benzyl benzamide | 20 | 6 | — | — | | 84.5[l] | 3.5[m] |
| | 70 | 6 | — | — | | 85.7[l] | 3.5[m] |

a) Reaction was carried out with 0.04 mol. of amide in 100 ml. of liq. $SO_2$ under shaking. Molar ratio of amide to $P_2O_5$=1 : 5.
b) The amidine obtained was *N*,*N'*-bis-β-phenethyl acetamidine.
c) The amidine obtained was *N*,*N'*-bis-β-phenethyl benzamidine.
d) The amidine obtained was *N*-benzoyl-*N*,*N'*-bis-β-phenethyl benzamidine.
e) The amidine obtained was *N*,*N'*-diphenyl acetamidine.
f) The amidine obtained was *N*,*N'*-diphenyl benzamidine.
g) The amidine obtained was *N*-benzoyl-*N*,*N'*-diphenyl benzamidine.
h) 1-Methyl-3,4-dihydroisoquinoline.
i) 1-Phenyl-3,4-dihydroisoquinoline.
j) Benzoic acid.
k) Aniline.
l) Viscous neutral substance from benzene extract in the acidic condition.
m) Viscous basic substance from benzene extract in the basic condition.

## Experimental

**Reagents.**—Amides were prepared by acetylation or benzoylation of the corresponding amines according to methods indicated in references; the amides were *N*-β-phenethyl acetamide[3] (b. p. 147~148°C/3~4 mmHg), *N*-β-phenethyl benzamide[3] (m. p. 114.5~115.5°C), *N*-benzyl acetamide[4] (m. p. 61~63°C) and *N*-benzyl benzamide[5] (m. p. 104~105°C). Acetanilide (m. p. 113.5~114.5°C) and benzanilide (m. p. 162.5~163°C) were commercial ones of extra pure grade.

Liquid sulfur dioxide was used as a solvent. A commercial material was dried with sulfuric acid and distilled before use.

The commercial phosphorus -pentoxide, -oxychloride and thionyl chloride of extra pure grade were used. Polyphosphoric acid was prepared by the known method[6].

**Apparatus and General Procedure.**—Glass pressure vessels (300 ml. capacity) equipped with metal joints and needle valves were used as before[1]. A liquid sulfur dioxide solution of an amide was added to a mixture or a solution of the condensing reagent in liquid sulfur dioxide with ice-cooling. Since benzanilide is sparingly soluble in liquid sulfur dioxide, sulfur dioxide was added to the mixture of this amide and phosphorus pentoxide. Then the whole set was thoroughly shaken and kept for a definite time at a definite temperature.

When the reaction was over, the reaction mixture turned into a gelatinous mass. The excessive solvent (sulfur dioxide) was evaporated and the mixture was decomposed with chilled water. Then the products were treated for further examination.

**Reaction of *N*-β-Phenethyl Acetamide (II) (R=$CH_3$) in Liquid Sulfur Dioxide.**—To 50 ml. of sulfur dioxide containing the condensing reagent (five times moles against that of the amide) as indicated in Table I was added a solution of 6.5 g. (0.04 mol.) of *N*-β-phenethyl acetamide (II) (R=$CH_3$) in 50 ml. of sulfur dioxide. After the reaction under a definite condition with shaking, the solvent was evaporated and water was added to the solution with chilling. The acidic mixture was extracted with benzene. The benzene solution, after washing with sodium bicarbonate solution and drying with anhydrous sodium sulfate, was condensed and the residue was distilled in vacuo. The acid amide (II) (R=$CH_3$) was recovered as a pale yellow oil boiling at 160~170°C (6~7 mmHg). Hydrolyzing this acid amide to β-phenethyl amine with hydrochloric acid, a picrate of the amine was prepared, m. p. 167~168°C. Reported melting point is 171°C[7]. The mixed melting point with an authentic sample showed no depression.

3) A. Bischler and B. Napieralski, *Ber.*, **26**, 1903 (1893).
4) J. Strakosch, ibid., **5**, 697 (1872).
5) E. Beckmann, ibid., **23**, 3334 (1890).
6) R. C. Gilmore and W. J. Horton, *J. Am. Chem. Soc.*, **73**, 1412 (1951).
7) H. Decker and W. Kropp, *Ber.*, **42**, 2078 (1909).

The residual aqueous solution was made alkaline with caustic alkali and was extracted with benzene. The benzene solution, after washing with water and drying with anhydrous sodium sulfate, was evaporated and the residue was distilled in vacuo. A colorless oil boiling at 100~105°C (7~8 mmHg) was obtained. This was 1-methyl-3,4-dihydroisoquinoline (III) (R=$CH_3$). Picrate, yellow needles, m. p. 188~189°C. Reported melting point is 188~190°C[8]. No melting point depression was observed when the sample was mixed with an authentic sample.

*Anal.* Base Found: N, 9.72. Calcd. for $C_{10}H_{11}N$: N, 9.65%. Picrate Found: N, 15.10. Calcd. for $C_{16}H_{14}O_7N_4$: N, 14.97%.

Moreover, following the above fraction, a pale yellow oil boiling at 205~215°C (6~7 mmHg) was obtained. This oil was assumed to be *N,N'*-bis-*β*-phenethyl acetamidine (IV), b. p. 180~190°C (2~3 mmHg), $n_D^{15}$=1.5748, I. R. $\nu_{max}^{KBr}$: 3440, 2915, 2860, 1635, 1352, 745 and 695 $cm^{-1}$, U. V. $\lambda_{max}^{MeOH}$: 250 m$\mu$ ($\varepsilon_{max}$ 385). Picrate, yellow needles (from 95% ethanol) m. p. 118~119°C, mol. wt. (by the Counningham method)[9]: 464 (the molar ratio of picric acid : base=1 : 1, calcd. as $C_{24}H_{25}O_7N_6$ 495).

*Anal.* Base Found: N, 10.99. Calcd. for $C_{18}H_{22}N_2$: N, 10.52%. Picrate Found: C, 57.92; H, 4.78; N, 14.29. Calcd. for $C_{24}H_{25}O_7N_5$: C, 58.17; H, 5.09; N, 14.14%.

No production of dihydroisoquinoline or amidine were observed with phosphorus oxychloride, polyphosphoric acid or thionyl chloride in liquid sulfur dioxide from II. Yields obtained with a variety of conditions are listed in Table I.

**Hydrolysis of IV.**—Two grams of this base was heated for 3.5 hr. under refluxing with 20 g. of 10% sodium hydroxide solution, then the mixture was acidified with hydrochloric acid. The mixture was extracted with benzene. The benzene solution, after washing with water and drying with anhydrous sodium sulfate, was concentrated and the residue was distilled in vacuo. A pale yellow oil (0.4 g.), boiling at 154~155°C (4~5 mmHg), was obtained. This was *N*-*β*-phenethyl acetamide. Hydrolyzing this acid amide to *β*-phenethyl amine with hydrochloric acid, a picrate of the amine was prepared. The melting point and the mixed melting point with an authentic sample were 167~168°C[7]. The residual solution was made alkaline with caustic alkali again and the product was extracted with benzene. The benzene extract, after washing with water and drying with anhydrous sodium sulfate, was concentrated and the residue was fractionated in vacuo. Two oils, boiling at 110~115°C (50~51 mmHg) and 205~215°C (6~7 mmHg) were obtained. The first colorless oil (0.4 g.) was *N*-*β*-phenethyl amine. A picrate of the amine was prepared. The melting point and the mixed melting point with an authentic sample were 167~168°C[7]. The second pale yellow oil (0.2 g.) obtained was the recovered *N,N'*-bis-*β*-phenethyl acetamidine. A picrate of the amidine was prepared. The melting point and the mixed melting point with the picrate of the amidine (reaction product in liquid sulfur dioxide) were 118~119°C.

**Preparation of IV from II with Hydrogen Chloride.**—*N*-*β*-Phenethyl acetamide was subjected to a reaction with hydrogen chloride stream at 150°C for two hours according to the preparation method of Wallach[14]. A basic pale yellow oil ($n_D^{15}$=1.5718) boiling at 175~185°C (1~2 mmHg) was obtained and yielded a picrate of m. p. 118~119°C. This melting point was not depressed on mixture with the picrate of the basic substance (b. p. 180~190°C/2~3 mmHg) obtained from *N*-*β*-phenethyl acetamide in liquid sulfur dioxide and assumed to be *N,N'*-bis-*β*-phenethyl acetamidine (IV).

**Reaction of *N*-*β*-Phenethyl Benzamide (II) (R=$C_6H_5$) in Liquid Sulfur Dioxide.**—A solution of 9 g. (0.04 mol.) of *N*-*β*-phenethyl benzamide in 50 ml. of sulfur dioxide was added to 50 ml. of sulfur dioxide containing the reagent (molar ratio of amide to $P_2O_5$ was 1 : 5). After the reaction for six hours and at 20°C with shaking, the solvent was allowed to evaporate and water was added with chilling. The acid mixture was extracted with benzene. The benzene solution, after washing with ammonia water and then with water, was dried with anhydrous sodium sulfate and was evaporated. The residue gave crystals melting at about 115°C. The crystals 4.4 g. (48.8%) were recrystallized from ethanol as colorless leaflets, melting at 116~116.5°C and were identified as the recovered *N*-*β*-phenethyl benzamide. When the reaction was carried out at 70°C, the benzene extract gave crystals of m. p. 110~110.5°C, faintly orange prisms (from ethanol). The crystals (1.1 g., 12.7%) were assumed to be *N*-benzoyl-*N,N'*-bis-*β*-phenethyl benzamidine (VI). I. R. $\nu_{max}^{KBr}$: 2935, 2860, 1643, 1626, 745 and 695 $cm^{-1}$, U. V. $\lambda_{max}^{MeOH}$: 241 m$\mu$($\varepsilon_{max}$ 18647), mol. wt. [Rast's method (camphor)]: 423, calcd. as $C_{30}H_{28}ON_2$, 432.

*Anal.* Found: C, 83.08; H, 6.05; N, 6.41. Calcd. for $C_{30}H_{28}ON_2$: C, 83.30; H, 6.53; N, 6.41%.

The residual acid aqueous solution after benzene extraction was made alkaline with ammonia water and was again extracted with benzene. The benzene solution was dried and concentrated. When 2 N sulfuric acid was added to the residue, an oil was precipitated. The supernatant solution was decanted and ammonia water was added to the oil. The oil changed into crystals. The crystal (0.8 g., 12.3%, reaction at 20°C and 0.6 g., 9.2%, reaction at 70°C) obtained by filtration was recrystallized from ligroin (b. p. 100~120°C) as colorless needles, melting at 79.5~80°C (picrate, yellow plate, m. p. 170~170.5°C) and was identified as *N,N'*-bis-*β*-phenethyl benzamidine[10] (V) (m. p. and mixed m. p. 79.5~80°C) (picrate[11], m. p. and mixed m. p. 170~170.5°C).

8) E. Späth, F. Berger and W. Kuntara, ibid., **63**, 134 (1930).

9) K. G. Cunningham, W. Dawson and F. S. Spring, *J. Chem. Soc.*, **1951**, 2305.

10) G. L. Webster and J. S. Rodia, *J. Am. Chem. Soc.*, **75**, 1762 (1953).

11) C. I. Brodrick and W. F. Short, *J. Chem. Soc.*, **1951**, 1344.

The supernatant solution decanted was made alkaline with ammonia water and was again extracted with benzene. The benzene solution, after washing with water and drying with anhydrous sodium sulfate, was concentrated and the residue was distilled in vacuo. A pale yellow oil ($n_D^{18}=1.6293$) boiling at 150~160°C (2~3 mmHg) was obtained. This base (1.2 g., 14.6%, reaction at 20°C and 6.6 g., 80.4%, reaction at 70°C) was 1-phenyl-3,4-dihydroisoquinoline (III) (R=$C_6H_5$). Picrate, yellow needle, m. p. 173.5~174°C. Reported melting points 173~174°C[12]. No melting point depression was observed when mixed with an authentic sample.

*Anal.* Base Found: N, 6.31. Calcd. for $C_{15}H_{13}N$: N, 6.76%. Picrate Found: N, 12.82. Calcd. for $C_{21}H_{16}O_7N_4$: N, 12.84%.

The results and the related facts observed were shown in Table II.

The residual ammoniacal solution after extraction was acidified with sulfuric acid and was extracted again with benzene. The benzene solution, after washing with water and drying with anhydrous sodium sulfate, yielded a crystal after evaporation. This crystal (0.2 g., 8.3%, reaction at 20°C and 0.2 g., 8.3%, reaction at 70°C) was recrystallized from 50% ethanol to an m. p. of 121~121.5°C and was identified as benzoic acid by a mixed melting point determination.

**Hydrolysis of VI.**—Six tenths gram of VI was heated for two hours on a boiling water bath with 2 N sulfuric acid, then the mixture was made alkaline with ammonia water and was extracted with benzene. The benzene solution, after washing with water and drying with anhydrous sodium sulfate, was concentrated and was triturated with ether. The ether-insoluble residue (0.3 g.) melted at 114~115°C. This was *N*-β-phenethyl benzamide. From the ether solution, a viscous liquid (0.1 g.) was obtained and changed to a crystal melting at 69~70°C (recrystallization from ligroin, b. p. 100~120°C). A picrate of this basic matter was prepared. The melting point and the mixed melting point with the picrate[11] of the *N,N'*-bis-β-phenethyl benzamidine (V) were 170~170.5°C. The residual aqueous solution after extraction was acidified with sulfuric acid and was extracted with benzene. The benzene solution gave a crystal (0.1 g.) melting at 121~121.5°C. This was identified as benzoic acid by a mixed melting point procedure.

**Preparation of VI.**—*N,N'*-bis-β-phenethyl benzamidine[10] was subjected to a reaction for four hours with benzoyl chloride in boiling benzene according to the method[13] of Oxley and Short. A neutral faintly orange prism melting at 110~110.5°C was obtained. This melting point was not depressed on mixture with the neutral substance (m. p. 110~110.5°C) obtained from *N*-β-phenethyl benzamide in liquid sulfur dioxide, thus establishing the structure of the latter to be *N*-benzoyl-*N,N'*-bis-β-phenethyl benzamidine (VI).

**Reaction of Acetanilide (VII) in Liquid Sulfur Dioxide (Table II).**—A solution of 5.4 g. (0.04 mol.) of acetanilide in 50 ml. of sulfur dioxide was added to a mixture of reagent (molar ratio of amide to $P_2O_5$ was 1 : 5) in 50 ml. of sulfur dioxide. When the reaction at 20°C for six hours with shaking was over, the reaction mixture was treated as in the previous case. From the benzene extract of the reaction mixture (acidic condition) there was recovered 3.1 g. (57.4%) of acetanilide, m. p. 113.5~114°C (recrystallization from benzene). No melting point depression was observed when mixed with an authentic sample.

The residual solution was made alkaline by sodium hydroxide solution. From the benzene extract of the solution, there was separated an oil, which changes to a crystalline matter. The crystal (0.8 g., 19.0%) was recrystallized from 50% ethanol as a colorless needle, melting at 131.5~132°C and was identified as *N,N'*-diphenyl acetamidine[14] (VII) (m. p. and mixed m. p. 131.5~132°C). I. R. $\nu_{max}^{KBr}$: 3220, 1637, 1380, 757 and 690 $cm^{-1}$, U. V. $\lambda_{max}^{MeOH}$: 265 mμ ($\varepsilon_{max}$ 18827), mol. wt. [Rast's method (camphor)]: 208, calcd. as $C_{14}H_{14}N_2$, 210. Picrate, yellow needle (from 95% ethanol): m. p. 168.5~169°C[15], mol. wt. (by the Cunningham method)[9]: 475, calcd. as $C_{20}H_{17}O_7N_5$ (the molar ratio, picric acid : base=1 : 1), 439.

*Anal.* Base Found: C, 79.76; H, 6.53; N, 13.55. Calcd. for $C_{14}H_{14}N_2$: C, 79.96; H, 6.71; N, 13.32%. Picrate Found: C, 54.86; H, 4.12; N, 15.76. Calcd. for $C_{20}H_{17}O_7N_5$: C, 54.67; H, 3.90; N, 15.94%.

From the filtrate, 0.3 g. (5.5%) of an oil was obtained by distillation in vacuo. Colorless oil, b. p. 96~102°C (49~50 mmHg) was identified as aniline by its benzoylation[16], m. p. and mixed m. p. 160°C.

When the reaction was conducted at 70°C for six hours, 1.9 g. (35.1%) of the acid amide was recovered and 1.3 g. (30.9%) of the amidine and 0.6 g. (11.1%) of aniline were obtained.

**Reaction of Benzanilide (X) in Liquid Sulfur Dioxide (Table II).**—To a mixture of benzanilide 7.9 g. (0.04 mol.) and the reagent (molar ratio of amide to $P_2O_5$ was 1 : 5), was added 100 ml. of sulfur dioxide. When the reaction at 20°C for six hours with shaking was over, the solvent was allowed to evaporate and water was added with chilling. The acid mixture was filtered. The filtrate was extracted with benzene. From the benzene solution, after washing with water and drying with anhydrous sodium sulfate, a trace of crystal was obtained. The crystal was recrystallized from 50% ethanol as a colorless needle, melting at 121~121.5°C and was identified as benzoic acid by a mixed melting point. The residue, after filtration, was washed with water and dried. Fractional crystallization of the residue from ethanol gave two kinds of crystals melting at about 160 and about 170°C, respectively. The first crystal 3.3g. (41.7%) was recrystallized from ethanol as a colorless leaflet, melting at

12) C. I. Brodrick and W. F. Short, ibid., 1951, 1345.
13) P. Oxley and W. F. Short, *J. Chem. Soc.*, 1948, 1524.
14) O. Wallach, *Ber.*, 15, 208 (1882).
15) P. Oxley and W. F. Short, *J. Chem. Soc.*, 1947, 384.
16) L. Claisen, *Ber.*, 27, 3182 (1894).

162.5~163°C and was identified as the recovered benzanilide.

The second crystal was recrystallized from benzene-ethanol as a faintly yellow prism, melting at 172~172.5°C. This crystal (3.5 g., 46.6%) was identified as *N*-benzoyl-*N*,*N'*-diphenyl benzamidine[13] (XII) (m. p. and mixed m. p. 172~172.5°C). I. R. $\nu_{max}^{KBr}$: 1650, 1626, 763 and 690 $cm^{-1}$, U. V. $\lambda_{max}^{MeOH}$: 255 m$\mu$ ($\varepsilon_{max}$ 20890), mol. wt. [Rast's method (camphor)]: 366, calcd. as $C_{26}H_{20}ON_2$, 376.

*Anal.* Found: C, 83.31; H, 5.25; N, 7.21. Calcd. for $C_{26}H_{20}ON_2$: C, 82.95; H, 5.36; N, 7.44%.

The residual acid aqueous solution was made alkaline with ammonia water and was extracted again with benzene. The benzene solution, after washing with water and drying with anhydrous sodium sulfate, was evaporated and the residue was given as a crystal. The crystal (0.1 g., 1.8%) was recrystallized from benzene as a colorless needle, melting at 146~146.5°C (picrate, yellow plate, m. p. 216.5~217°C with decomp.) and was identified as *N*,*N'*-diphenyl benzamidine[17] (XI) (m. p. and mixed m. p. 146~146.5°C, picrate[18], m. p. and mixed m. p. 216.5~217°C with decomp.).

When the reaction was conducted at 70°C for six hours, 0.4 g. (5.0%) of the acid amide was recovered and 0.4 g. (16.6%) of benzoic acid, 1.4 g. (18.6%) of *N*-benzoyl-*N*,*N'*-diphenyl benzamidine and 2.5 g. (46.2%) of *N*,*N'*-diphenyl benzamidine were obtained.

**Reaction of *N*-Benzyl Acetamide (XIII) (R=$CH_3$) in Liquid Sulfur Dioxide.**—To a mixture of the reagents ($P_2O_5$, 29 g., molar ratio of amide to $P_2O_5$ was 1 : 5) in 50 ml. of liquid sulfur dioxide was added a solution of 5.9 g. (0.04 mol.) of *N*-benzyl acetamide in 50 ml. of liquid sulfur dioxide. The reaction mixture was treated as described above after shaking for six hours at 70°C. A small amount of basic substance and a viscous residue were obtained in the reaction mixture (Table II).

**Reaction of *N*-Benzyl Benzamide (XIII) (R=$C_6H_5$) in Liquid Sulfur Dioxide.** — A solution of 8.4 g. (0.04 mol.) of the *N*-benzyl benzamide in 50 ml. of liquid sulfur dioxide was added to 50 ml. of sulfur dioxide containing the reagent ($P_2O_5$ five times moles against that of the amide). The reaction mixture was treated as in the previous case after shaking for six hours at 20 or 70°C. A small amount of resinous basic substance and a large amount of viscous acidic or neutral substance were separated from the viscous reaction mixture. But they were not further examined.

17) A. C. Hontz and E. C. Wagner, "Organic Syntheses", Vol. 31, John Wiley & Sons, Inc., New York (1951), p. 48.

18) F. C. Cooper, M. W. Partridge and W. F. Short, *J. Chem. Soc.*, **1951**, 401.

## Summary

The Bischler-Napieralski reaction of *N*-$\beta$-phenethyl acetamide in liquid sulfur dioxide resulted in the formation of *N*,*N'*-bis-$\beta$-phenethyl acetamidine in addition to the expected 1-methyl-3,4-dihydroisoquinoline. And the reaction product from *N*-$\beta$-phenethyl benzamide were *N*,*N'*-bis-$\beta$-phenethyl benzamidine and *N*-benzoyl-*N*,*N'*-bis-$\beta$-phenethyl benzamidine in addition to the expected 1-phenyl-3,4-dihydroisoquinoline. In the case of acetanilide, *N*,*N'*-diphenyl acetamidine was produced. Benzanilide afforded *N*,*N'*-diphenyl benzamidine and *N*-benzoyl-*N*,*N'*-diphenyl benzamidine under a similar condition. The similar reaction of benzyl acylamides in liquid sulfur dioxide failed to yield such amidines.

The financial support of this project was granted by the Ministry of Education. Liquid sulfur dioxide was donated by the Befu Chemical Industries Co., Ltd. Ultraviolet absorption spectra were measured by Professor T. Nozoe and his associates of the Department of Chemistry. Infrared absorption spectra were measured by Professor S. Kinumaki and his associates of this Institute. The elementary analyses were performed by Mr. Shinichi Oyama and Miss Yoko Endo. The authors wish to express their thanks to these helps and donations.

*Research Institute of*
*Non-aqueous Solutions*
*Tohoku University*
*Katahira-cho, Sendai*

# *Some Reaction of 2-Mercapto-1, 3-diazaazulene*

By Ichiro MURATA

(Received May 20, 1959)

Nozoe, Mukai and Murata[1] reported that the reaction of tropolone methyl ether and thiourea in ethanol, in the presence of sodium alcoxide, resulted in the condensation to form 2-mercapto-1, 3-diazaazulene (I). Later, the same condensation reaction was carried out on tropolones with methyl[2], isopropyl[3], phenyl[4] and styryl[5], and oxidative desulfurization reaction on 2-mercapto-1,3-diazaazulene thereby formed. No studies, however, have been made on the nature of the mercapto group in 2-position of these compounds and it seemed of interest to examine reactivity of a mercapto group in this kind of new, nitrogenous heterocyclic compound. Therefore, examinations were made with I which has no carbon-containing side chain.

Oxidation of I with nitric acid or 10% hydrogen peroxide with heating affords 1,3-diazaazulene (II)[1] in over 80% yield. Application of 10% hydrogen peroxide at room temperature or of sodium nitrite in acetic acid affords only the 2-disulfide (III)[1] in almost quantitative yield. Application of hydrogen peroxide to III with heating produces II, but the possible intermediate in this reaction, the sulfonic acid or sulfinic acid[6], was not isolated. III is easily reduced to I by aqueous solution of sodium sulfide.

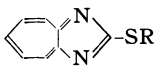
The sodium salt of I undergoes facile reaction in ethanol with various alkyl iodides, polynitrochlorobenzenes, benzyl chloride, chloroacetone, phenacyl chloride, chloroacetic acid, and 2-chloro-1,3-diazaazulene[7] to form the corresponding thioethers (Table I).

TABLE I. 2-SR-1,3-DIAZAAZULENE

| Compd. No. | R | Cryst. form* | m. p., °C | Recrystn. solvent** | Analysis Calcd. C | Calcd. H | Calcd. N | Found C | Found H | Found N |
|---|---|---|---|---|---|---|---|---|---|---|
| IV | $CH_3$ | py. P. | 101~102 | P+B | 61.36 | 4.58 | 15.90 | 61.01 | 4.82 | 16.67 |
| V | $C_2H_5$ | py. P. | 95~ 96 | C+B | 63.15 | 5.30 | 14.73 | 63.32 | 5.01 | 14.38 |
| VI | $n$-$C_3H_7$ | py. N. | 98~ 99 | C+B | 64.69 | 5.92 | 13.72 | 64.61 | 5.46 | 13.65 |
| VII | $n$-$C_4H_9$ | py. N. | 66~ 67 | C | 66.03 | 6.47 | 12.84 | 65.95 | 6.11 | 12.18 |
| VIII | $CH_2$-CH=$CH_2$ | y. P. | 72~ 74 | P+B | 65.33 | 4.98 | 13.86 | 64.84 | 4.94 | 13.82 |
| IX | $CH_2C_6H_5$ | y. N. | 94~ 95 | B+C | 71.41 | 4.80 | 11.11 | 71.25 | 4.84 | 11.09 |
| X | $C_6H_3(NO_2)_2$ | y. N. | 224(d.) | D+A | 51.22 | 2.46 | 17.07 | 51.29 | 2.30 | 17.63 |
| XI | $C_6H_2(NO_2)_3$ | y. N. | 194 | D+A | 45.05 | 1.89 | 18.77 | 44.86 | 2.07 | 15.35 |
| XII | $CH_2COC_6H_5$ | y. N. | 164 | A | 68.56 | 4.32 | 10.00 | 68.50 | 4.47 | 9.70 |
| XIII | $CH_2COCH_3$ | py. S. | 68~ 69 | C | 60.54 | 4.62 | 12.84 | 60.80 | 4.43 | 13.31 |
| XIV | $CH_2COOH$ | py. | 300 | — | 54.55 | 3.66 | | 54.62 | 3.63 | |
| XV | $C_8H_5N_2$ | y. P. | 254(d.) | A | | | 19.30 | | | 19.12 |

* y, yellow; py, pale yellow; N, needles; P, prisms; S, scales.

** A, ethanol; B, benzene; C, cyclohexane; D, dioxane; P, petroleum ether.



(IV)—(XV)

1) T. Nozoe, T. Mukai and I. Murata, *J. Am. Chem. Soc.*, **76**, 3352 (1954).
2) H. Akino, K. Sato and Y. Suzuki, *Science Repts. Tohoku Univ., I*, **40**, 92 (1956).
3) T. Nozoe and T. Sato, unpublished data.
4) K. Kikuchi and T. Muroi, *J. Chem. Soc. Japan, Pure Chem. Sec. (Nippon Kagaku Zasshi)*, **77**, 1081 (1956).
5) H. Matsumura, ibid., **78**, 669 (1957).
6) The intermediate formed by oxidative desulfurization of 2-mercaptoimidazole is said to be a sulfinic acid. Cf. I. E. Balaban and H. King, *J. Chem. Soc.*, **1927**, 1858; I. D. Lamb and F. L. Pyman, ibid., **125**. 706 (1924).
7) T. Nozoe, T. Mukai and I. Murata, *Proc. Japan Acad.*, **30**, 482 (1954).

TABLE II. U. V. ABSORPTION MAXIMA OF 2-SR-1,3-DIAZAAZULENES

| Compd. No. | $\lambda_{max}^{MeOH}$, mμ (log ε) |
|---|---|
| IV | 239(4.47), 270(4.29), 362(4.26) |
| V | 239(4.48), 270(4.30), 362(4.27) |
| VI | 239(4.50), 271(4.32), 362(4.30) |
| VII | 239(4.51), 271(4.32), 364(4.31) |
| VIII | 240(4.41), 268(4.27), 362(4.17), 435(3.74) |
| IX | 240(4.47), 270(4.29), 360(4.28) |
| X | 242(4.59), 270(4.36), 370(4.29) |
| XI | 238(4.58), 270(4.45), 340(4.17), 380(sh.) |
| XII | 241(4.55), 270(4.35), 358(4.26) |
| XIII | 238(4.45), 270(4.35), 358(4.26) |
| XIV | 240(4.40), 270(4.19), 365(4.18) |
| XV | 248(4.72), 275(sh.), 368(4.41) |

The ultraviolet absorption maxima of these thioethers are presented in Table II.

The nucleophilic substitution reaction of I was then examined. Examples of nucleophilic substitution of a mercapto group are extremely rare and only the reaction with ammonia or amine[8] is known. Heating of I with 40% aqueous ammonia or methylamine in a sealed tube for a few hours at 170~180°C only results in quantitative recovery of I. Heating of I with concentrated hydrochloric acid in a sealed tube for 6 hr. at 160°C results in its hydrolysis and 2-hydroxy-1,3-diazaazulene (XVI)[1,7] is obtained in a good yield.

The methylthio group may be considered to undergo more facile nucleophilic substitution than the mercapto group and there is a comparatively large number of examples[9]. Actually, IV reacts with a number of nucleophilic reagents to form the corresponding 2-substituted derivatives (Table III).

## Experimental[10]

**2-Mercapto-1, 3-diazaazulene (I).** — Synthesized from tropolone methyl ether and thiourea according to the method described earlier[1]. Reddish orange microneedles, m. p. >300°C.

**Oxidation of I.**—a) To a suspension of 1 g. of I in 10 cc. of water, 5 cc. of 30% hydrogen peroxide was added and the mixture was warmed on a water bath, by which the reaction proceeded immediately with effervescence to form a clear, orange solution. After cooling, the mixture was rendered weakly alkaline with sodium hydrogen carbonate and extracted with chloroform. The extract was washed with water, dried, and chloroform was evaporated. The residue was dissolved in benzene and passed through a short column of alumina from which 620 mg. of yellow needles, m. p. 110~112°C, was obtained. Mixed fusion with 1,3-diazaazulene (II) showed no depression of the melting point.

b) To a suspension of 100 mg. of I in 1 cc. of water, 1.2 cc. of 10% hydrogen peroxide was added dropwise with stirring at room temperature and the mixture was stirred for further 3 hr. The precipitate formed was collected by filtration and 80 mg. of yellow microneedles (III), m. p. 203°C (decomp.), was obtained.

c) A solution of 45 mg. of sodium nitrite dissolved in 0.5 cc. of water was added dropwise to 100 mg. of I suspended in 2 cc. of glacial acetic acid, cooled in ice. The precipitate formed changed from orange to yellow. After stirring for 2 hr., the precipitate was collected by filtration to 85 mg. of III, m. p. 204°C (decomp.).

**Reaction of Disulfide (III).**—*a) Oxidation with hydrogen peroxide.*—A mixture of 100 mg. of III suspended in 0.5 cc. of water, with 1 cc. of 30% hydrogen peroxide added, was heated on a water bath by which effervescence occurred immediately to form an orange solution. The mixture was neutralized with sodium hydrogen carbonate, extracted with chloroform, and the extract was washed with water. After drying, chloroform was distilled off and 70 mg. of yellow needles, m. p. 110~113°C, was obtained. This showed no

TABLE III. NUCLEOPHILIC SUBSTITUTION OF 2-METHYLTHIO-1,3-DIAZAAZULENE

| Compd. No. | Reagent | Yield, % | m. p., °C | Calcd. | Found | Ref. |
|---|---|---|---|---|---|---|
| XVI | Concd. HCl | 72 | 245 | — | — | 1 |
| XVII | 40% aq. $NH_3$ | 36 | 295(d.) | — | — | 10 |
| XVIII | 40% aq. $NH_2CH_3$ | 55 | 172~173 | 26.40 | 26.32 | — |
| XIX | 40% aq. $NH(CH_3)_2$ | 74 | 133~134 | — | — | 7 |
| XX | 80% aq. $NH_2NH_2$ | 71 | 189 | — | — | 7 |
| XXI | $C_6H_5NH_2$ | 56 | 239 | 18.99 | 19.00 | — |
| XXII | $C_6H_5CH_2NH_2$ | 74 | 175 | 17.86 | 17.92 | — |
| XXIII | $NaOCH_3$ | 27 | 94 | — | — | 7 |

8) G. H. Hitchings and P. B. Russell, *J. Chem. Soc.*, **1949**, 2454; E. C. Taylor, J. A. Carbon and D. R. Hoff, *J. Am. Chem. Soc.*, **75**, 1904 (1953).

9) J. F. Bunnett and R. E. Zahler, *Chem. Revs.*, **49**, 273 (1951).

10) All melting points are uncorrected. Ultraviolet absorption spectra were used for identification of high-melting substances and decomposition products. Measurement was made with a Beckman Model DU spectrophotometer. The microanalyses were carried out by Mr. S. Ohyama and Miss A. Iwanaga, to whom the author's deep gratitude is hereby expressed.

depression in the melting point on admixture with II.

*b) Reduction with sodium sulfide.* — Aqueous solution of 200 mg. of sodium sulfide was added to 65 mg. of III, suspended in 1 cc. of ethanol by which the precipitate disappeared to form an orange solution. The mixture was diluted with 2 cc. of water, acidified with glacial acetic acid, and the precipitate was collected by filtration to give 50 mg. of I, m. p. >300°C.

**Reaction of Sodium Salt of I and Halides.**—*a) General procedure for preparation of methyl- (IV), ethyl- (V), n-propyl- (VI), n-butyl- (VII), allyl- (VIII), benzyl- (IX), phenacyl- (XII) and acetonylthio-1,3-diazaazulene (XIII).* — Ethanolic solution of 1.1 molar equivalents of halide was added to the sodium salt of I dissolved in ethanol and the mixture was refluxed for 0.5~1.0 hr. Ethanol was distilled off, the residue was dissolved in benzene, and the benzene solution was passed through a short column of alumina. The crystalline residue obtained on evaporation of benzene was recrystallized 2~3 times from the solvent listed in Table I.

*b) General procedure for preparation of 2,4-dinitrophenyl- (X), 2,4,6-trinitrophenyl- (XI) and 2-(1,3-diazaazulenylthio)-1,3-diazaazulene (XV).*— Sodium salt of I was mixed with halide in ethanol and the precipitate formed after some time was recrystallized twice from a solvent as listed in Table I.

*c) 2-Carboxymethylthio-1,3-diazaazulene (XIV).* —To a solution of 500 mg. of I dissolved in 2 cc. of 2 N sodium hydroxide, 300 mg. of monochloroacetic acid neutralized with sodium hydrogen carbonate was added and the mixture was heated on a water bath at 90°C for 15 min. After cooling, the mixture was acidified with acetic acid, the yellow precipitate was collected by filtration, and washed with water and then with ethanol, affording 640 mg. of crystalline powder, m. p. >300°C.

**2-Hydroxy-1, 3-diazaazulene (XVI).**—*a) From I.* — A mixture of 100 mg. of I and 2 cc. of concentrated hydrochloric acid was sealed in a tube and heated at 160°C for 6 hr. Evaporation of hydrochloric acid left 120 mg. of colorless crystals, m. p. >300°C, which was dissolved in a small amount of water, and the solution was neutralized with a saturated solution of sodium hydrogen carbonate. The crystalline precipitate thereby formed was collected by filtration and 95 mg. of pale yellow needles, m. p. 234°C, was obtained. Recrystallization from dilute ethanol raised the melting point to 244°C, undepressed on admixture with XVI.

*b) From IV.*—A mixture of 50 mg. of IV and 1 cc. of concentrated hydrochloric acid was refluxed, in an oil bath for 2 hr., hydrochloric acid was evaporated, and the residue was treated as in a) from which 30 mg. of XVI was obtained.

**Nucleophilic Substitution Reaction of IV.**—*a) 2-Amino-1,3-diazaazulene (XVII).*—A mixture of 50 mg. of IV and 1 cc. of ammonia water was sealed in a tube and heated at 100°C for 6 hr. The mixture was allowed to cool overnight and crystals that formed were collected by filtration to 15 mg. of crystals melting at 290°C with decomposition. Recrystallization from hot water afforded yellow needles (XVII), m. p. 294°C (decomp.). Ammonia mother liquor was diluted with 3 cc. of water and extracted with chloroform from which 20 mg. of IV was recovered.

*b) 2-Methylamino- (XVIII) and 2-dimethylamino-1,3-diazaazulene (XIX).*—A mixture of 50 mg. of IV and 40% aqueous solution of monomethylamine or dimethylamine was sealed in a tube and heated at 100°C for 6 hr. The reaction mixture was diluted with water, extracted with chloroform, and the chloroform residue was recrystallized from the benzene-petroleum ether mixture to XVIII, m. p. 173~174°C, or XIX, m.p. 134°C. There was no recovery of IV in this case.

*c) 2-Hydrazino-1,3-diazaazulene (XX).* — To a solution of 70 mg. of IV dissolved in 1 cc. of ethanol, 0.5 cc. of 80% aqueous solution of hydrazine was added and the mixture was refluxed for 2 hr. When cooled, crystals formed, they were collected by filtration and recrystallized from ethanol to 45 mg. of XX, m. p. 187°C (decomp.).

*d) 2-Anilino- (XXI) and 2-benzylamino-1,3-diazaazulene (XXII).*—A mixture of 70 mg. of IV dissolved in 1 cc. of ethanol and 50 mg. of aniline or benzylamine was heated in a sealed tube at 160~170°C for 8 hr. The crystals formed on cooling were recrystallized from benzene to yellow needles (XXI), m. p. 238~239°C, or yellow scales (XXII), m. p. 175°C.

*e) 2-Methoxy-1,3-diazaazulene (XXIII).* — To a solution of 30 mg. of sodium methoxide dissolved in 3 cc. of dehydrated methanol, 90 mg. of IV was added and the mixture was refluxed on a water bath for 25 hr. After evaporation of methanol, the benzene-soluble portion afforded 30 mg. of XXIII and the benzene-insoluble portion afforded 15 mg. of XVI.

The author expresses his deep gratitude to Professor Tetsuo Nozoe of the Faculty of Science of this University for kind and unfailing guidance throughout the course of this work. He is also indebted to Mr. Shinji Iizuka for technical assistance.

*The Chemical Research Institute of Non-aqueous Solutions*
*Tohoku University*
*Katahira-cho, Sendai*

# *On the Structure of Condensation Products of o-Aminophenols with α-Dicarbonyl Compounds. II*

By Ichiro MURASE

(Received June 1, 1959)

It has been reported in the previous paper[1] that 2,2′-bibenzoxazoline and its 2,2′-dimethyl derivative were formed by the condensation of *o*-aminophenol (2 mol.) with glyoxal (1 mol.) and with diacetyl (1 mol.), respectively.

Now, condensation of skeletal derivatives of *o*-aminophenol with several kinds of α-dicarbonyl compounds was studied and the structures of these condensation products were determined.

The condensation reaction proceeded generally in the same way as in the case of 2,2′-bibenzoxazoline previously reported. However it was found that the products were classified into two groups according to the molar ratio of the reactants.

The following investigation led to the conclusion that the compounds of the first group were the condensation products of two moles of *o*-aminophenols with one mole of α-dicarbonyl compounds and the structures proved to be 2,2′-bibenzoxazoline derivatives as in the case previously reported. The second group was equimolar condensation products of each component and the structures proved to be 2-hydroxy 2,3-disubstituted 1,4-benzoxazine derivatives. The structures of these two groups are summarized in Tables I and II, respectively, together with their infrared and ultraviolet absorption spectra. The melting points and analytical data of both groups are listed in Tables III and IV, respectively.

It was found that the more bulky the alkyl groups in the dicarbonyl compounds were, the poorer the yield of the condensation product became. In some cases, such bulky groups affected only benzoxazine type products as the single ones. Acetylisobutylyl reacted only with 4-nitro-2-aminophenol to give a benzoxazine type condensation product. On the other hand, it proved that phenylglyoxal reacted with all *o*-aminophenols examined to give products of the same type in good yields. It was exceptional that acetylbenzoyl despite the bulky groups and though it did not react with any other skeletal derivatives, condensed with two moles of *o*-aminophenol to give a bibenzoxazoline type product. Benzil did not react at all with any of *o*-aminophenols examined.

5-Nitro-2-aminophenol and picrylamine did not react with any α-dicarbonyl compounds examined, while 4-nitro-2-aminophenol was very reactive.

Thus, the ease and the type of the condensation are affected by the basicity of the amino group and the acidity of the hydroxyl group of the *o*-aminophenols and further by the steric factor of the α-dicarbonyl compounds.

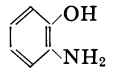
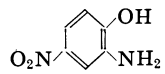
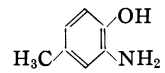
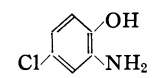
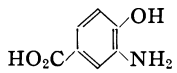
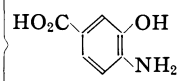
It is interesting to note that in place of methylglyoxal and diacetyl, their monoximes reacted with *o*-aminophenol and 4-nitro-2-aminophenol with elimination of the oximino groups to produce the same condensation products as those obtained from the mother dicarbonyl compounds. But dimethyl glyoxime did not react with them.

The 2,2′-bibenzoxazoline structures were established by means of their infrared and ultraviolet absorption spectra; the sharp NH band and the anilino band were present in each infrared spectrum, which were the same as those of an authentic 2,2′-bibenzoxazoline, and the features of the ultraviolet spectra excellently agreed with each other regarding those of the compounds derived from the same aminophenols (refer to Table I).

Among these bibenzoxazoline derivatives, those which were derived from glyoxal, methylglyoxal and diacetyl were stable toward the cold dilute solution of both mineral acid and aqueous alkali, while higher homologues were more sensitive to these reagents and were hydrolyzed gradually on standing at room temperature. The carboxylic derivatives dissolved in sodium hydrogen carbonate solution to give a colorless solution, and in sodium hydroxide solution with orange coloration.

1) I. Murase, This Bulletin, 32, 827 (1959).

TABLE I. 2,2′-BIBENZOXAZOLINE DERIVATIVES AND THEIR INFRARED AND ULTRAVIOLET ABSORPTION SPECTRA; THOSE OF 2,2′-BIBENZOXAZOLINE AND 2,2′-DIMETHYL-2,2′-BIBENZOXAZOLINE ARE LISTED FOR COMPARISON PURPOSES

| No. | Components: α-Dicarbonyl compounds | Components: o-Aminophenols | R | R′ | X | X′ | UV-spectra (in ethanol) mμ: $\lambda_{max}$ | UV-spectra: ε | IR-spectra (Nujol mull) cm$^{-1}$: NH-band | IR-spectra: Anilino band |
|---|---|---|---|---|---|---|---|---|---|---|
| — | CHOCHO | | H | H | H | H | 236<br>294 | 14340<br>9880 | 3378 | 1613 |
| — | $CH_3COCOCH_3$ | | $CH_3$ | $CH_3$ | H | H | 236<br>293 | 13200<br>9880 | 3358 | 1613 |
| 1 | $CH_3COCHO$ |  | $CH_3$ | H | H | H | 236<br>294 | 12140<br>8798 | | |
| 2 | $CH_3COCOC_2H_5$ | | $CH_3$ | $C_2H_5$ | H | H | 236<br>293 | 12620<br>9273 | | |
| 3 | $C_2H_5COCOC_2H_5$ | | $C_2H_5$ | $C_2H_5$ | H | H | 236<br>294 | 11880<br>8908 | | |
| 4 | $C_6H_5COCOCH_3$ | | $C_6H_5$ | $CH_3$ | H | H | 240<br>292 | 12380<br>9981 | 3390 | 1613 |
| 5 | CHOCHO | | H | H | $NO_2$ | H | 225<br>261<br>305<br>365 | 22930<br>27600<br>11540<br>10070 | 3448<br>3390 | 1623 |
| 6 | $CH_3COCHO$ | | $CH_3$ | H | $NO_2$ | H | 225<br>261<br>306<br>367 | 23600<br>24250<br>10071<br>9184 | | |
| 7 | $CH_3COCOCH_3$ |  | $CH_3$ | $CH_3$ | $NO_2$ | H | 225<br>262<br>306<br>369 | 23210<br>27090<br>11420<br>10860 | | |
| 8 | $CH_3COCOC_2H_5$ | | $CH_3$ | $C_2H_5$ | $NO_2$ | H | 225<br>261<br>306<br>366 | 23610<br>27850<br>11960<br>11100 | | |
| 9 | $C_2H_5COCOC_2H_5$ | | $C_2H_5$ | $C_2H_5$ | $NO_2$ | H | 225<br>262<br>306<br>371 | 23310<br>27370<br>12050<br>10800 | | |
| 10 | CHOCHO |  | H | H | $CH_3$ | H | 238<br>298 | 12250<br>9866 | 3413 | 1621 |
| 11 | $CH_3COCOCH_3$ | | $CH_3$ | $CH_3$ | $CH_3$ | H | 237<br>298 | 11160<br>10280 | | |
| 12 | CHOCHO |  | H | H | Cl | H | 242<br>303 | 11860<br>10880 | 3390 | 1608 |
| 13 | CHOCHO |  | H | H | $CO_2H$ | H | 235<br>261<br>315 | 55910<br>16670<br>10480 | 3425 | 1616 |
| 14 | CHOCHO | | H | H | H | $CO_2H$ | insoluble | | 3401 | 1613 |
| 15 | $CH_3COCOCH_3$ | | $CH_3$ | $CH_3$ | H | $CO_2H$ | 234<br>277<br>309 | 29480<br>21720<br>26050 | 3378 | 1616 |
| 16 | $CH_3COCOC_2H_5$ |  | $CH_3$ | $C_2H_5$ | H | $CO_2H$ | 235<br>278<br>310 | 29010<br>22000<br>26630 | | |
| 17 | $C_2H_5COCOC_2H_5$ | | $C_2H_5$ | $C_2H_5$ | H | $CO_2H$ | 234<br>278<br>310 | 27150<br>21770<br>26510 | | |

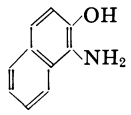
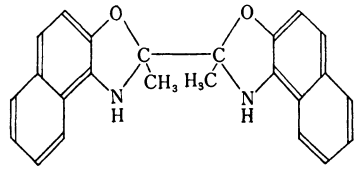
| | | | | | | |
|---|---|---|---|---|---|---|
| 18 | $CH_3COCOCH_3$ |  |  | 234<br>255<br>311<br>346 | 43080<br>79130<br>6534<br>9118 | 3460 | 1626 |

TABLE II. 2-HYDROXY-1,4-BENZOXAZINE DERIVATIVES AND THEIR INFRARED AND ULTRAVIOLET ABSORPTION SPECTRA

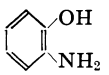
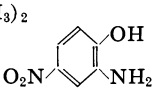
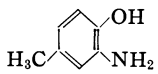
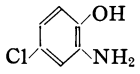
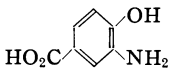
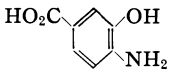
| No. | Components: α-Dicarbonyl compounds | Components: o-Aminophenols | R | R′ | X | X′ | UV-spectra (in ethanol) mμ: $\lambda_{max}$ | UV-spectra (in ethanol) mμ: ε | IR-spectra (Nujol mull): 3000 cm⁻¹ region (broad) | IR-spectra (Nujol mull): 1600 cm⁻¹ region |
|---|---|---|---|---|---|---|---|---|---|---|
| 19 | $C_6H_5COCHO$ |  | H | $C_6H_5$ | H | H | 234<br>281<br>310 | 9924<br>14450<br>12340 | 3300～2600 | 1610<br>1592<br>1563 |
| 20 | $CH_3COCOCH(CH_3)_2$ |  | $CH_3$ | $CH(CH_3)_2$ | $NO_2$ | H | 220<br>260<br>310 | 17890<br>12200<br>7516 | 3400～2700 | 1639<br>1608<br>1600 |
| 21 | $C_6H_5COCHO$ | | H | $C_6H_5$ | $NO_2$ | H | 224<br>286 | 17960<br>30170 | 3200～2500 | 1623<br>1592<br>1567 |
| 22 | $CH_3COCOC_2H_5$ |  | $CH_3$ | $C_2H_5$ | $CH_3$ | H | 217<br>262<br>311 | 20960<br>5000<br>2552 | 3200～2500 | 1634<br>1618<br>1592 |
| 23 | $C_2H_5COCOC_2H_5$ | | $C_2H_5$ | $C_2H_5$ | $CH_3$ | H | 219<br>261<br>305 | 21060<br>5148<br>2756 | 3200～2500 | 1629<br>1618<br>1592 |
| 24 | $C_6H_5COCHO$ | | H | $C_6H_5$ | $CH_3$ | H | 249<br>287<br>320 | 11400<br>15530<br>10800 | 3200～2500 | 1616<br>1613<br>1575 |
| 25 | $CH_3COCOCH_3$ |  | $CH_3$ | $CH_3$ | Cl | H | 251<br>305 | 4678<br>2708 | 3300～2700 | 1639<br>1600<br>1582 |
| 26 | $CH_3COCOC_2H_5$ | | $CH_3$ | $C_2H_5$ | Cl | H | 222<br>256<br>311 | 29630<br>4406<br>2632 | 3300～2700 | 1629<br>1597<br>1582 |
| 27 | $C_6H_5COCHO$ | | H | $C_6H_5$ | Cl | H | 220<br>245<br>285<br>330 | 17720<br>12860<br>17480<br>10430 | 3300～2600 | 1621<br>1595<br>1570 |
| 28 | $C_6H_5COCHO$ |  | H | $C_6H_5$ | $CO_2H$ | H | 219<br>255<br>295 | 19910<br>28780<br>16340 | 3200～2500 | 1618<br>1608<br>1597<br>1585<br>1570 |
| 29 | $C_6H_5COCHO$ |  | H | $C_6H_5$ | H | $CO_2H$ | 297 | 20420 | 3300～2500 | 1623<br>1592<br>1585<br>1570 |

TABLE III. MELTING POINTS AND ANALYTICAL DATA OF 2,2'-BIBENZOXAZOLINE DERIVATIVES LISTED IN TABLE I

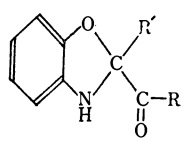
| No. | Formula | m. p. | Anal. Found | | | Calcd. | | |
|---|---|---|---|---|---|---|---|---|
| | | °C | C% | H% | N% | C% | H% | N% |
| 1 | $C_{15}H_{14}N_2O_2$ | 220 | 70.69 | 5.62 | 10.93 | 70.85 | 5.55 | 11.02 |
| 2 | $C_{17}H_{18}N_2O_2$ | 142 | 72.39 | 6.45 | 9.84 | 72.32 | 6.43 | 9.92 |
| 3 | $C_{18}H_{20}N_2O_2$ | 154 | 73.14 | 6.78 | 9.51 | 72.95 | 6.80 | 9.45 |
| 4 | $C_{21}H_{18}N_2O_2$ | 218 | 76.44 | 5.58 | 8.48 | 76.34 | 5.49 | 8.48 |
| 5 | $C_{14}H_{10}N_4O_6$ | 225 | 50.54 | 3.25 | 16.60 | 50.91 | 3.05 | 16.97 |
| 6 | $C_{15}H_{12}N_4O_6$ | 216 | 52.25 | 3.64 | 16.35 | 52.33 | 3.51 | 16.28 |
| 7 | $C_{16}H_{14}N_4O_6$ | 252 | 53.47 | 3.91 | 15.42 | 53.63 | 3.94 | 15.64 |
| 8 | $C_{17}H_{16}N_4O_6$ | 238 | 55.07 | 4.52 | 14.98 | 54.84 | 4.33 | 15.05 |
| 9 | $C_{18}H_{18}N_4O_6$ | 199 | 55.99 | 4.82 | 14.68 | 55.95 | 4.70 | 14.50 |
| 10 | $C_{16}H_{16}N_2O_2$ | 215 | 71.47 | 6.19 | 10.51 | 71.62 | 6.01 | 10.44 |
| 11 | $C_{18}H_{20}N_2O_2$ | 237 | 72.80 | 6.86 | 9.33 | 72.95 | 6.80 | 9.45 |
| 12 | $C_{14}H_{10}N_2O_2Cl_2$ | 208 | 54.50 | 3.49 | 8.64 | 54.39 | 3.26 | 9.06 |
| 13 | $C_{16}H_{12}N_2O_6$ | 237.5 | 58.35 | 3.73 | 8.38 | 58.54 | 3.68 | 8.53 |
| 14 | $C_{16}H_{12}N_2O_6$ | 286 | 58.52 | 3.66 | 8.22 | 58.54 | 3.68 | 8.53 |
| 15 | $C_{18}H_{16}N_2O_6 \cdot 2H_2O$ | 241 | 55.08 | 5.02 | 6.86 | 55.10 | 5.14 | 7.14 |
| 16 | $C_{19}H_{18}N_2O_6 \cdot 2H_2O$ | 221 | 55.95 | 5.53 | 6.58 | 56.15 | 5.46 | 6.89 |
| 17 | $C_{20}H_{20}N_2O_6 \cdot 2H_2O$ | 219 | 56.78 | 6.07 | 6.43 | 57.13 | 5.75 | 6.66 |
| 18 | $C_{24}H_{20}N_2O_2$ | 204 | 78.28 | 5.42 | 7.62 | 78.24 | 5.47 | 7.60 |

TABLE IV. MELTING POINTS AND ANALYTICAL DATA OF 2-HYDROXY-1,4-BENZOXAZINE DERIVATIVES LISTED IN TABLE II

| No. | Formula | m. p. | Anal. Found | | | Calcd. | | |
|---|---|---|---|---|---|---|---|---|
| | | °C | C% | H% | N% | C% | H% | N% |
| 19 | $C_{14}H_{11}NO_2$ | 228 | 74.85 | 4.93 | 6.42 | 74.65 | 4.92 | 6.22 |
| 20 | $C_{12}H_{14}N_2O_4$ | 131 | 57.90 | 5.68 | 11.31 | 57.59 | 5.64 | 11.20 |
| 21 | $C_{14}H_{10}N_2O_4$ | 235 | 62.36 | 3.78 | 10.28 | 62.22 | 3.73 | 10.37 |
| 22 | $C_{12}H_{15}NO_2$ | 151 | 70.58 | 7.46 | 6.77 | 70.22 | 7.37 | 6.82 |
| 23 | $C_{13}H_{17}NO_2$ | 133 | 70.92 | 8.16 | 6.38 | 71.20 | 7.81 | 6.39 |
| 24 | $C_{15}H_{13}NO_2$ | 196 | 75.22 | 5.25 | 5.72 | 75.29 | 5.48 | 5.85 |
| 25 | $C_{10}H_{10}NO_2Cl$ | 172 | 56.72 | 4.89 | 6.40 | 56.75 | 4.76 | 6.62 |
| 26 | $C_{11}H_{12}NO_2Cl$ | 131 | 58.61 | 5.45 | 6.46 | 58.54 | 5.36 | 6.21 |
| 27 | $C_{14}H_{10}NO_2Cl$ | 216 | 64.55 | 4.01 | 5.08 | 64.75 | 3.88 | 5.39 |
| 28 | $C_{15}H_{11}NO_4$ | 241 | 67.02 | 3.90 | 5.41 | 66.91 | 4.12 | 5.20 |
| 29 | $C_{15}H_{11}NO_4$ | 238 | 67.24 | 4.04 | 5.30 | 66.91 | 4.12 | 5.20 |

It is apparent that they were tautomerized to Schiff bases in the latter case as indicated in the previous paper[1].

Concerning the equimolar condensation products (the second group), benzoxazoline structure A was considered at first, since the compounds of this group were insoluble in aqueous alkali except carboxylic derivatives.



(A)

The broad infrared absorption bands found near 3000 $cm^{-1}$ in all spectra indicate the presence of hydrogen bonded OH or NH groups. However carbonyl absorption, the presence of which was expected from formula A, was not found in any spectra, and instead comparatively weak absorptions were present in the 1600 $cm^{-1}$ region. Further, the fact that, in the case of $\alpha$-iminoketones such as $C_6H_5NHCH_2COCH_3$ and $C_6H_5NHC(CH_3)_2COCH_3$, the sharp NH band at 3413 $cm^{-1}$ in the both compounds and the strong C=O band at 1706 $cm^{-1}$ in the former and at 1709 $cm^{-1}$ in the latter existed, excluded the possibility of $\alpha$-iminoketonic formula A.

Therefore, the author proposed the 1,4-benzoxazine structure C and the mode of the reaction indicated.

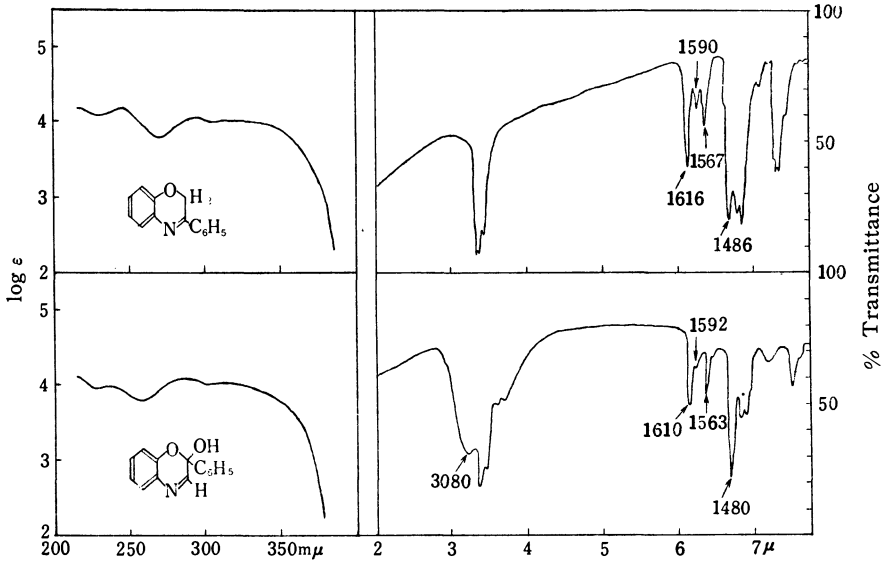
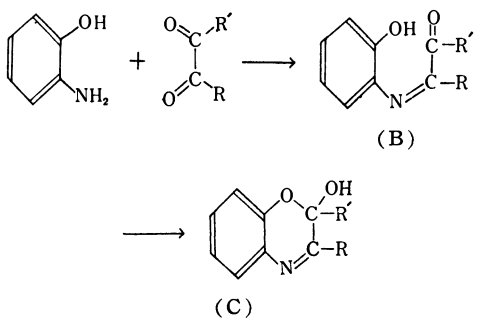



Fig. 1. Ultraviolet (in ethanol) and infrared (Nujol mull) spectra of 19 (bottom) and 3-phenyl-1,4-benzoxazine (top).

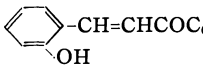


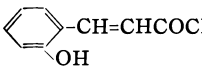
(B)

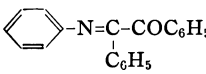


(C)

The intermediate Schiff base structure B was also excluded because the C=O absorption was absent in their infrared spectra and they were insoluble in alkali. This was further supported by the fact that the following compounds of which structures were closely related to B, showed very strong C=O absorptions:

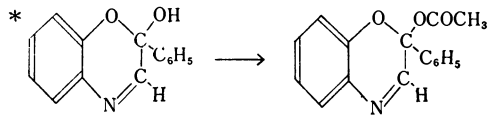
 1645 cm$^{-1}$

 1642 cm$^{-1}$

 1667 cm$^{-1}$
(1645 cm$^{-1}$, C=N)

Thus, the 1,4-benzoxazine structure C carrying no carbonyl group is most favorable and is further supported by the comparison with the known 1,4-benzoxazine structure. While such 2-hydroxyl substituted 1,4-benzoxazines as C have not been reported in literatures so far, 3-phenyl-1,4-benzoxazine is known[2] as one of a few 1,4-benzoxazine compounds and it was found that the condensation product of *o*-aminophenol with phenylglyoxal (19) resembled 3-phenyl-1,4-benzoxazine in the infrared and ultraviolet spectra as shown in Fig. 1.

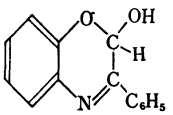
Acetylation of 19 with acetic anhydride gave the acetyl derivative (19a), m. p. 92°C, and the catalytic hydrogenation of 19a afforded the dihydro derivative (19b), m. p. 147°C, one mole of hydrogen being absorbed. The reaction can be explained as follows and the structures of the resulting compounds were consistent with their infrared spectra shown in Fig. 2.



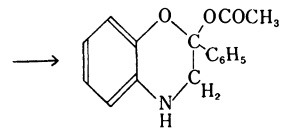
(19) (19a)

2) E. Lellmann and A. Donner, *Ber.*, **23**, 173 (1890).

* In the case of the condensation of *o*-aminophenol with phenylgyoxal, if the amino group reacts with the ketonic carbonyl group to form a Schiff base type product in the first step, and then it undergoes ring-closure to form benzoxazine, the structure should be given as follows:



This isomeric strcuture of 19 was excluded, however, because on potassium permanganate oxidation in boiling acetone, 19 was recovered and the 2-hydroxyl group proved to be attached to a tertiary carbon atom as indicated in the scheme.




(19b)

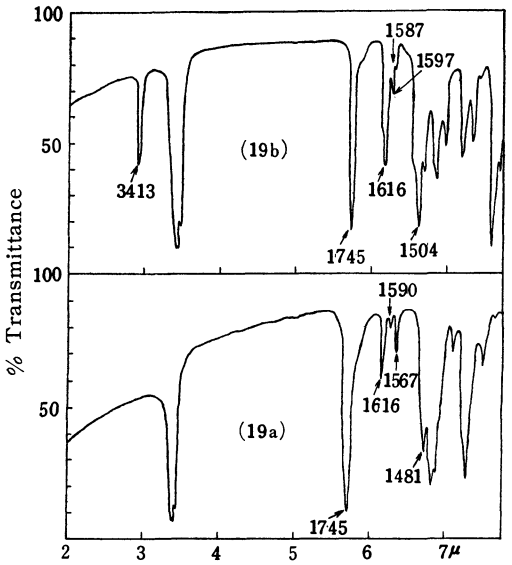
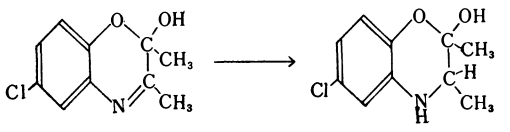



Fig. 2. Infrared spectra of 19a and 19b (Nujol mull).




(25) (25a)

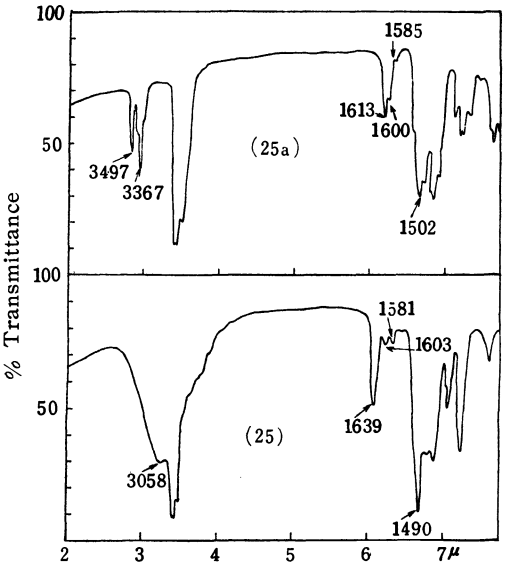



Fig. 3. Infrared spectra of 25 and 25a (Nujol mull).

Definite assignment of C=N absorptions of these 1,4-benzoxazines has remained unsolved, because phenyl ring absorptions were overlapped by other bands in this region, however the bands which were commonly observed in 1,4-benzoxazine derivatives at 1567 $cm^{-1}$ (3-phenyl-1,4-benzoxazine, Fig. 1), 1563 $cm^{-1}$ (19, Fig. 1) and 1567 $cm^{-1}$ (19a, Fig. 2) disappeared by hydrogenation (19b, Fig. 2), and thus the author tentatively assigned these bands to C=N absorptions and other bands in this region which remained even after hydrogenation to phenyl ring absorptions (refer to Table II).

Further, the broad absorption bands in the 3000 $cm^{-1}$ region (19, Fig. 1) should be due to intermolecular hydrogen bond of the hydroxyl group**, because it disappeared by acetylation and the *O*-acetate carbonyl band appeared at 1745 $cm^{-1}$ (19a, Fig. 2).

In the case of the condensation product of 4-chloro-2-aminophenol with diacetyl (25), catalytic hydrogenation was conducted and dihydro derivative (25a), m.p. 135°C, was obtained.

** Because the solubility of 19 in the suitable solvent was very small, it could not be confirmed by taking the infrared spectra with a dilution method.

The structures of 25 and 25a were also consistent with features of their infrared absorption spectra shown in Fig. 3.

Since the others of this second group gave quite similar infrared spectra concerning the 3000 $cm^{-1}$ and the 1600 $cm^{-1}$ regions as shown in Table II, it can be recognized that they should also have the benzoxazine structures.

Thus, it has been concluded that the compounds resulting from the condensation of equimolar *o*-aminophenols and *α*-dicarbonyl compounds have the structure of 2-hydroxy-1,4-benzoxazine derivatives.

The condensation products of asymmetric *α*-diketones such as acetylpropionyl and acetylisobutylyl (20, 22, 26) have not been worked out as regards the position 2- or 3- of the alkyl group in 1,4-benzoxazine. The author tentatively proposed the 3-methyl substituted structure, considering that the carbonyl attached to the methyl group is more reactive than others and reacts with the amino group at first, as shown in the above scheme proposed.

The 2-phenyl derivatives were stable toward 6 N hydrochloric acid at 100°C and dilute alkali at room tempreature, but in the case of 19 it was hydrolyzed to *o*-aminophenol by boiling with 10% sodium

hydroxide solution. On the other hand, 2,3-dialkyl homologues were sensitive to acid and alkali and hydrolyzed gradually even at room temperature.

On applying semicarbazide to 25 and phenylhydrazine to 19, diacetyl disemicarbazone and phenylglyoxal phenylosazone were obtained respectively. Hydrolysis must have occurred in these cases.

## Experimental

**General Procedure of the Condensation Reaction of o-Aminophenols with α-Dicarbonyl Compounds.** —The procedure was equally conducted both in the bibenzoxazoline type and the benzoxazine type condensations.

Freshly prepared *o*-aminophenols were dissolved in a large amount of distilled water which was previously boiled and cooled at 80°C. To this solution, a slight excess of calculated amount of α-dicarbonyl compounds dissolved in a little amount of water was added and mixture was held at this temperature with occasionally shaking for about 1 hr. Precipitates were soon or gradually formed. After cooling, they were filtered and washed with water. Recrystallization from alcohol or dilute alcohol using a Norit gave pure crystalls.

**2-Methyl-2'-ethyl-2, 2'-bibenzoxazoline (2).** — A mixture of *o*-aminophenol (2 g.) and acetylpropionyl (1.5 g.) dissolved in a little amount of alcohol was boiled for 3 hr. The solvent was then distilled off and the remaining tarrish residue was extracted several times with petroleum benzine (80~120°C). The combined extract was decolorized using a Norit and concentrated to form crystals. Recrystallization from dilute alcohol gave prisms, m. p. 142°C.

**2-Methyl-2'-phenyl-2, 2'-bibenzoxazoline (4).** — A solution of *o*-aminophenol (1 g.) and acetylbenzoyl (1.5 g.) in dioxane (15 ml.) was boiled for 2 hr. and then the solvent was distilled off under reduced pressure. The remaining oil soon solidified and was recrystallized from alcohol to give long needles, m. p. 218°C. Mol. wt. (Rast), Found: 329, Calcd.: 330.

**2-Hydroxy-2-isopropyl-3-methyl-7-nitro-1, 4-benzoxazine (20).** — An equivalent portion of 4-nitro-2-aminophenol and acetylisobutylyl was well mixed and heated on a hot plate about at 120°C for 20 min. On cooling, the oily product solidified which was pressed on a clay plate and recrystallized from benzene to give needles, m. p. 131°C.

**Condensation of o-Aminophenol with Isonitrosoacetone; 2-Methyl-2,2'-bibenzoxazoline (1).**—To a solution of *o*-aminophenol (1 g.) in hot water (50 ml.), isonitrosoacetone (1 g.) was added and the mixture was boiled for 1 hr. Precipitates gradually formed and they were recrystallized from alcohol to give fine needles, m. p. 220°C.

The condensations of isonitrosoacetone with 4-nitro-2-aminophenol and diacetyl monoxime with *o*-aminophenol were carried out in the same manner and 5,5'-dinitro-2'-methyl-2,2'-bibenzoxazoline (6) and 2,2'-dimethyl-2,2'-bibenzoxazoline were obtained respectively.

**2-Acetoxy-2-phenyl-1, 4-benzoxazine (19a).** — A solution of 2-hydroxy-2-phenyl-1,4-benzoxazine (19) (1 g.) in acetic anhydride (60 ml.) was boiled for 2 hr. and then the solution was concentrated under reduced pressure. The remaining oily product solidified on standing and was recrystallized from dilute alcohol to give fine prisms, m. p. 92.3°C.

*Anal.* Found: C, 72.12; H, 5.01; N, 5.37. Calcd. for $C_{16}H_{13}NO_3$: C, 72.01; H, 4.88; N, 5.22%.

**Hyrogenation of 19a: 2-Acetoxy-3-phenyl-3,4-dihydro-1,4-benzoxazine (19b).**—A solution of 19a (0.5 g.) in acetic acid (25 ml.) was hydrogenated using Adams calalyst at atmospheric pressure and room temperature. A slightly excessive amount of hydrogen was absorbed after 3 hr. The solvent was removed under reduced pressure and the residue was recrystallized from alcohol to give colorless needles, m. p. 147°C.

*Anal.* Found: C, 71.29; H, 5.71; N, 5.47. Calcd. for $C_{16}H_{15}NO_3$: C, 71.38; H, 5.58; N, 5.20%.

**Action of Phenylhydrazine on 19: Phenylglyoxal Phenylosazone.**—To a suspension of 19 in a little amount of acetic acid, an excess of phenylhydrazine was added and the mixture was heated on water bath, the contents being gradually dissolved. After 30 min., water was added and the resulting precipitates were recrystallized from alcohol. Yellow prisms, m. p. 150~151°C; showed no depression with an authentic phenylglyoxal phenylosazone, m. p. 151°C.

**Hydrogenation of 25: 2-Hydroxy-2,3-dimethyl-6-chloro-3, 4-dihydro-1, 4-benzoxazine (25a).** — A solution of 25 (1 g.) in alcohol (60 ml.) was hydrogenated using Adams catalyst at atmospheric pressure and room temperature. A slightly excessive amount of hydrogen was absorbed after 5 hr. The resulting colorless solution was concentrated under reduced pressure and then water was added. The crystals obtained on cooling of the mixture in an ice box were recrystallized several times from dilute alcohol to give fine plates, m. p. 135°C.

*Anal.* Found: C, 55.92; H, 5.23; N, 6.56. Calcd. for $C_{10}H_{12}NO_2Cl$: C, 56.21; H, 5.62; N, 6.56%.

**Alkali Hydrolysis of 19.**—A suspension of 19 in 5% sodium hydroxide solution was boiled for 20 min., the contents were gradually dissolved and reddish brown solution was obtained. To this solution an excess of acetic anhydride was added and the mixture was evaporated to dryness on a water bath. The resulting residue was washed with water and recrystallized from hot water. Needles, m. p. 201°C, showed no depression with *N*-acetyl-2-aminophenol, m. p. 201°C.

**Action of Semicarbazide on 25: Diacetyl Disemicarbazone.**—To a warm solution of 25 (0.35 g.), semicarbazide hydrochloride (0.3 g.) dissolved in water (1 g.) containing 0.3 g. of sodium acetate was added and the mixture was allowed to stand at room temperature. White precipitates soon formed and they were filtered and well washed

with alcohol. The white crystals, m. p. 279°C, which were almost insoluble in most organic solvents showed no depression with an authentic diacetyl disemicarbazone, m. p. 279°C.

The author wishes to express his thanks to Professor Tokuichi Tsumaki and Professor Takeichi Nishikawa for their exceedingly kind directions to this work. The author also thanks Dr. Yo Ueda and Mr. Hiroshige Yano of the Department of Pharmacy for their measurement of infrared spectra and Mr. Michio Shido and Miss Sachiko Indo for microanalysis. The cost of this research was partly defrayed from the Research Grant of the Ministry of Education, to which the author's thanks are also due.

*General Education Department*
*Kyushu University*
*Otsubo-machi, Fukuoka*

# *Resolution of Amino Acids. II. Resolution of Racemic ε-Acyllysine and δ-Acylornithine Amides by Leucine Aminopeptidase*

By Nobuo IZUMIYA, Hakaru UCHIO and Tetsuo KAMATA

(Received June 8, 1959)

In a previous communication[1], it was shown that racemic phenylalanine and γ-phenyl-α-aminobutyric acid amides can be resolved by leucine aminopeptidase. In this paper, a similar method is described, which is based upon the asymmetric hydrolysis of the amides of ε-benzoyl-DL-lysine, δ-benzoyl-DL-ornithine and δ-carbobenzoxy-DL-ornithine by a partially purified leucine aminopeptidase derived from swine kidney[2].

For the resolution, the initial substrate concentration was set at 0.05 mol., and the course of hydrolysis was followed measuring evolved ammonia. After analysis reveals the theoretical 50% hydrolysis, ω-acyl-L-amino acid was collected by filtration, and ω-acyl-D-amino acid amide in the filtrate was separated by means of ion-exchange resin. In this way, ε-benzoyl-DL-lysine amide was resolved in a good yield. δ-Benzoyl-DL-ornithine amide was hydrolyzed in the same manner. However, the difference of the solubilities in water of δ-carbobenzoxy-L-ornithine and -D-ornithine amide hydrochloride is bigger than that of the corresponding benzoyl derivatives, and therefore the amide of δ-carbobenzoxy-DL-ornithine may be in some cases more suitable for the purpose.

## Experimental

**Preparation of Leucine Aminopeptidase.** — A partially purified enzyme solution of Step 4 by Smith was prepared as described[2]. Its activities against ω-acyl-amino acid amides are shown in Table I, the proteolytic coefficient ($C_1$) of L-leucine amide being included for comparison. The rates of hydrolysis were measured by titration of 0.2 to 0.6 ml. samples with 0.005 N hydrochloric acid by means of the Conway microdiffusion method[3].

As shown in Table I, ω-acyl-L-amino acid amides are hydrolyzed at 1/4~1/7 times the rate

TABLE I. PROTEOLYTIC COEFFICIENT ($C_1$) OF AMINO ACID AMIDES BY PARTIALLY PURIFIED LEUCINE AMINOPEPTIDASE*

| Substrates | $C_1$ at different initial concn. of substrates** | | |
|---|---|---|---|
| | 0.01 M | 0.025 M | 0.05 M |
| L-Leucine amide | 5.6 | 3.2 | 2.0 |
| ε-Benzoyl-DL-lysine amide | 1.3 | 0.84 | 0.49 |
| δ-Benzoyl-DL-ornithine amide | 1.1 | 0.73 | 0.50 |
| δ-Carbobenzoxy-DL-ornithine amide | 0.82 | 0.49 | 0.32 |

* Enzyme was preincubated in 0.1 M Tris buffer of pH 8.0 with 0.008 M manganese chloride for one hour at 38°C. Assays were conducted in 0.1 M Tris buffer of pH 8.0 at 38°C with preincubated enzyme added. $C_1 = \log[100/(100 - \%\ \text{hydrolysis})]/(\text{min.} \times \text{mg. protein } N \text{ per ml. test solution})$.

** Concentrations of L-form of substrates.

1) A. Tanaka and N. Izumiya, This Bulletin, **31**, 529 (1958).

2) E. L. Smith, "Methods in Enzymology", Vol. 2, edited by S. P. Colowick and N. O. Kaplan, Academic Press, Inc., New York (1956), p. 88.

3) R. B. Johnston, M. J. Mycek and J. S. Fruton, *J. Biol. Chem.*, **185**, 629 (1950).

for L-leucine amide, a most sensitive substrate for the enzyme. However, the efficient resolution would be still possible with the susceptibilities of ω-acyl-amino acid amides in the orders described above.

**Synthesis of Compounds.** — *ε-Benzoyl-DL-lysine ethyl ester hydrochloride.* — ε-Benzoyllysine[4,5] (200 g.) was suspended in ethanol (4 l.) and dry hydrogen chloride was introduced to saturation at room temperature. The solution was refluxed for one hour and evaporated in vacuo. The residue was dissolved in ethanol (2 l.), and the same procedure was repeated again. Treatment of the residue with dry ether yielded crystals*. These orystals were recrystallized from ethanol-ether; yield, 236 g. (94%); m. p. 91~94°C.

*Anal.* Found: N, 8.82. Calcd. for $C_{15}H_{23}O_3N_2Cl$: N, 8.90%.

*ε-Benzoyl-DL-lysine amide hydrochloride.* — The above compound (189 g.) was dissolved in methanol (3.4 l.) previously saturated with dry ammonia at 0°C, the solution was kept at room temperature for three days and then concentrated in vacuo to dryness. The residual crystals were collected by the aid of methanol and acetone. This was dissolved in hot water, the solution was concentrated, and additions of methanol and acetone yielded crystals; yield, 108 g. (63%); m. p. 235~237°C (decomp.).

*Anal.* Found: C, 54.73; H, 6.73; N, 14.46. Calcd. for $C_{13}H_{20}O_2N_3Cl$: C, 54.64; H, 7.05; N, 14.71%.

*δ-Benzoyl-DL-ornithine ethyl ester hydrochloride.*— This compound was prepared from δ-benzoyl-ornithine[4-6] (236 g.) in the same way as that for benzoyllysine ethyl ester hydrochloride; yield, 288 g. (96%); m. p. 175~177°C.

*Anal.* Found: N, 9.33. Calcd. for $C_{14}H_{21}O_3N_2Cl$: N, 9.31%.

*α-Carbobenzoxy-δ-benzoyl-DL-ornithine ethyl ester.*— To a suspension of the above compound (9.0 g.) in chloroform (90 ml.) was added triethylamine (9.4 ml.). The compound went into solution immediately, and carbobenzoxy chloride[7] (4.8 ml.) was added to the solution under cooling. The mixture was allowed to react at room temperature overnight, washed with water, dilute bicarbonate solution, dilute hydrochloric acid, and water; the organic layer was dried over sodium sulfate and concentrated in vacuo to yield a syrup which was crystallized by the addition of petroleum ether. This was recrystallized from ethyl acetate-petroleum ether; yield, 10.3 g. (86%); m. p. 110°C.

*Anal.* Found: N, 7.24. Calcd. for $C_{22}H_{26}O_5N_2$: N, 7.03%.

*α-Carbobenzoxy-δ-benzoyl-DL-ornithine amide.* — This compound was prepared from the above compound (6.0 g.) by the same procedure as that for benzoyllysine amide hydrochloride and recrystallized from methanol-ether; yield, 4.7 g. (85%); m. p. 205~206°C.

*Anal.* Found: N, 11.52. Calcd. for $C_{20}H_{23}O_4N_3$: N, 11.38%.

*δ-Benzoyl-DL-ornithine amide hydrochloride.*—This compound was prepared from benzoylornithine ethyl ester hydrochloride (150 g.) in the same way as that for benzoyllysine amide hydrochloride and recrystallized from methanol-ether; yield, 87 g. (64%); m. p. 195~197°C.

*Anal.* Found: C, 53.24; H, 6.68; N, 15.24. Calcd. for $C_{12}H_{18}O_2N_3Cl$: C, 53.04; H, 6.68; N, 15.46%.

This compound was also prepared as follows. α-Carbobenzoxy-δ-benzoylornithine amide (3.7 g.) dissolved in 0.3 N methanolic hydrochloric acid (36 ml.) was treated with dry hydrogen in the presence of palladium black in the usual manner[8]. The filtrate from the catalyst was evaporated in vacuo, and the residual syrup was crystallized easily; yield, 2.5 g. (92%); m. p. 196~197°C.

*Anal.* Found: N, 15.41. Calcd. for $C_{12}H_{18}O_2N_3Cl$: N, 15.46%.

*δ-Carbobenzoxy-DL-ornithine.*—This compound was prepared from ornithine hydrochloride (101 g.) by the same procedure as that for the L-isomer[4,9]; yield, 121 g. (76%); m. p. 250~253°C (decomp.).

*Anal.* Found: N, 10.71. Calcd. for $C_{13}H_{18}O_4N_2$: N, 10.52%.

*δ-Carbobenzoxy-DL-ornithine amide hydrochloride.*— The above compound (106 g.) was treated with 1.5 N methanolic hydrochloric acid (4.4 l.) as described in the case of the L-isomer[10], and the hygroscopic crystalline carbobenzoxyornithine methyl ester hydrochloride obtained was amidated with methanolic ammonia in the usual manner. The product was recrystallized from methanol-acetone; yield, 86 g. (71%); m. p. 153~154°C.

TABLE II. $R_f$ VALUES OF REFERENCE COMPOUNDS

| Compounds | $R_f$* |
|---|---|
| ε-Benzoyllysine (DL, L and D form) | 0.58 |
| ε-Benzoyl-DL-lysine ethyl ester | 0.82 |
| ε-Benzoyllysine amide (DL and D form) | 0.65 |
| Lysine (L and D form) | 0.14 |
| δ-Benzoylornithine (DL, L and D form) | 0.55 |
| δ-Benzoyl-DL-ornithine ethyl ester | 0.80 |
| δ-Benzoylornithine amide (DL and D form) | 0.60 |
| Ornithine (L and D form) | 0.11 |
| δ-Cabobenzoxyornithine (DL and L form) | 0.61 |
| δ-Carbobenzoxyornithine amide (DL and D form) | 0.68 |

* The solvent system of *n*-butanol:acetic acid: pyridine: water (4:1:1:12, by volume) and Toyo filter paper No. 50 were used.

4) A. C. Kurtz, ibid., **180**, 1253 (1950).

5) J. C. Eck and C. S. Marvel, "Organic Syntheses", Col. Vol. 2, edited by A. H. Blatt, John Wiley & Sons, Inc., New York (1948), p. 374; E. E. Howe and E. W. Pietrusza, *J. Am. Chem. Soc.*, **71**, 2581 (1949).

* When the paper chromatography of the crystals shows an additional spot of ε-benzoyllysine except benzoyllysine ester, treatment by dry hydrogen chloride of ethanol solution of the crystals should be repeated again.

6) E. Fischer and G. Zemplen, *Ber.*, **42**, 1022, 2989 (1909).

7) H. E. Carter, R. L. Frank and H. W. Johnston, "Organic Syntheses", Col. Vol. 3, edited by E. C. Horning, John Wiley & Sons, Inc., New York (1955) p. 167.,

8) N. Izumiya and T. Yamashita, *J. Biochem.*, **46**, 19 (1959).

9) R. L. M. Synge, *Biochem. J.*, **42**, 99 (1948).

10) I. Schumann and R. A. Boissonas, *Helv. Chim. Acta*, **35**, 2237 (1952).

*Anal.* Found: C, 51.53; H, 6.68; N, 13.59. Calcd. for $C_{13}H_{20}O_3N_3Cl$: C, 51.74; H, 6.68; N, 13.93%.

***Rf* Values of Compounds.**—The $R_f$ values of the reference compounds are given in Table II.

**Resolution of ε-Benzoyl-DL-lysine Amide.** — *ε-Benzoyl-L-lysine.* — ε-Benzoyl-DL-lysine amide hydrochloride (86.4 g.) was dissolved in water (2 l.) containing manganese chloride tetrahydrate (0.60 g.). The pH was adjusted to about 7.5 with 1 N aqueous ammonia (150 ml.), the enzyme solution containing the equivalent of 16.4 mg. of protein nitrogen was added, and the volume was made up to 6.0 l. After about ten hour incubation at 38°C, the results of ammonia determination indicated complete hydrolysis of the L-amide, when the pH of solution was found to be near 8.5. In the course of the digestion, benzoyl-L-lysine was partly precipitated. The course of hydrolysis is shown in Fig. 1.

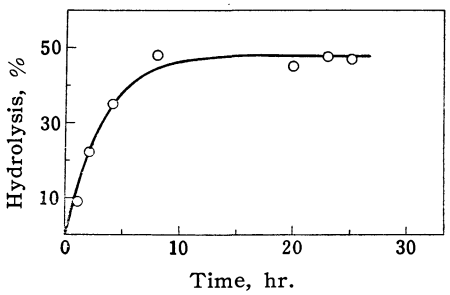



Fig. 1. Time-course of hydrolysis of ε-benzoyl-DL-lysine amide.

It was incubated for another fifteen hours, and its paper chromatography in this stage showed two spots with several solvent systems. The incubation mixture was evaporated in vacuo to a small volume, and the crystals were collected and washed with water (combined filtrate and washings saved for the D-amide). This was recrystallized from hot water; yield, 33.1 g. (88%); m. p. 244~246°C (decomp.); $[\alpha]_D^{15}$ +22.0° ($c$=2, in 5 N hydrochloric acid) (lit.[11] $[\alpha]_D^{25}$ +22.3°).

*Anal.* Found: N, 11.10. Calcd. for $C_{13}H_{18}O_3N_2$: N, 11.29%.

*L-Lysine hydrochloride.* — The above compound (10 g.) was refluxed with 6 N hydrochloric acid (150 ml.) for ten hours, and benzoic acid produced was removed in the usual manner[12]. The solution was evaporated in vacuo, and the residual syrup was dissolved in water. The solution, adjusted to pH 6.4~6.6 by the addition of triethylamine, was evaporated to dryness, and the residue was recrystallized from water-ethanol; yield, 6.7 g. (92%); $[\alpha]_D^{15}$ +20.5° ($c$=2, in 5 N hydrochloric acid) (lit.[13] $[\alpha]_D$ +20.7°).

*Anal.* Found: N, 15.50. Calcd. for $C_6H_{15}O_2N_2Cl$: N, 15.34%.

*ε-Benzoyl-D-lysine amide hydrochloride.* — The filtrate and washing** described already were passed through a column of Amberlite IRA-400 (5 cm.×50 cm.) in the alkaline phase, a strongly basic anion-exchange resin, and water (9 l.) was successively added to the top of the column. The fractions were combined and evaporated to dryness in vacuo. The evaporation was repeated several times with addition of methanol, the residue was dissolved in 1 N methanolic hydrochloric acid (150 ml.), and the solution was concentrated to a small volume, acetone being added. The crystals collected were recrystallized from hot methanol-acetone; yield, 35.5 g. (83%); m. p. 220~221°C (decomp.); $[\alpha]_D^{15}$ −16.8° ($c$=2, in water).

*Anal.* Found: C, 54.61; H, 7.16; N, 14.58. Calcd. for $C_{13}H_{20}O_2N_3Cl$: C, 54.64; H, 7.05; N, 14.71%.

*ε-Benzoyl-D-lysine.*—The above compound (14.3 g.) was refluxed with 2 N hydrochloric acid (210 ml.) for one hour, the solution was evaporated in vacuo, and the residue was dissolved in water, triethylamine being added to neutralization. The crystals collected were recrystallized from hot water; yield, 8.5 g. (68%); m. p. 246~247°C (decomp.); $[\alpha]_D^{15}$ −21.8° ($c$=2, in 5 N hydrochloric acid) (lit.[11] $[\alpha]_D^{30}$ −22.1°).

*Anal.* Found: N, 10.97. Calcd. for $C_{13}H_{18}O_3N_2$: N, 11.19%.

*D-Lysine hydrochloride.*—Benzoyl-D-lysine amide hydrochloride (8.6 g.) was refluxed with 6 N hydrochloric acid for ten hours, benzoic acid was removed, and the solution was evaporated to dryness in vacuo. The evaporation was repeated several times with addition of water and of some triethylamine until free of ammonia, this procedure replacing ammonium chloride with triethylamine hydrochloride which is soluble in ethanol. The product remained was recrystallized from water-ethanol; yield, 4.7 g. (86%); $[\alpha]_D^{15}$ −20.3° ($c$=2, in 5 N hydrochloric acid) (lit.[14] $[\alpha]_D$ −20.7~−21.0°).

*Anal.* Found: N, 15.71. Calcd. for $C_6H_{15}O_2N_2Cl$: N, 15.34%.

**Resolution of δ-Benzoyl-DL-ornithine Amide.**— *δ-Benzoyl-L-ornithine.* — To δ-benzoyl-DL-ornithine amide hydrochloride (54.4 g.) and manganese chloride tetrahydrate (0.40 g.) dissolved in water, pH being brought to 7.5, was added the enzyme

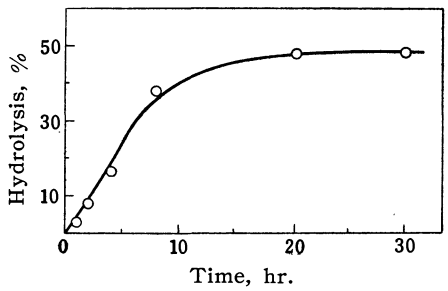



Fig. 2. Time-course of hydrolysis of δ-benzoyl-DL-ornithine amide.

11) N. Izumiya and S. Ota, *J. Chem. Soc. Japan, Pure Chem. Sec.* (*Nippon Kagaku Zasshi*), **72**, 445 (1951).
12) N. Izumiya and K. Kitagawa, ibid., **79**, 65 (1958).
13) J. P. Greenstein, S. M. Birnbaum and M. C. Otey, *J. Biol. Chem.*, **204**, 307 (1953).

** A certain amount of the combined filtrate and washings were evaporated, aqueous sodium hydroxide was added. and the solution was extracted with chloroform as that for D-phenylalanine amide[1], but about 20% of the D-amide could be extracted.

14) S. M. Birnbaum, L. Levintow, R. B. Kingsley and J. P. Greenstein, *J. Biol. Chem.*, **194**, 455 (1952).

containing 12.5 mg. of protein nitrogen. The mixture was made up to 4.0 l. and incubated at 38°C, the course of hydrolysis being shown in Fig. 2. The solution was then evaporated to a small volume, and the resulting crystals were collected and washed with water; yield, 12.8 g. The combined filtrate and washings were passed through a column of Amberlite IRA-400 (4.5 cm.×40 cm.), and the column was washed with water (6 l.) (combined fractions saved for the D-amide). Elution of the additional L-amino acid from the column was accomplished with 2 N hydrochloric acid (7 l.) The eluate was evaporated, the residue was dissolved in water, and the solution was neutralized with triethylamine; yield, 9.7 g. The combined crystals (22.5 g.) were recrystallized from hot water; yield, 20.3 g. (86%); m.p. 243~245°C (decomp.); $[\alpha]_D^{15}$ +26.0° ($c$=2, in 5 N hydrochloric acid) (lit.[15] $[\alpha]_D^{10}$ +19.8°).

*Anal.* Found: N, 11.61. Calcd. for $C_{12}H_{16}O_3N_2$: N, 11.86%.

*L-Ornithine hydrochloride.*—This was prepared from the above compound (11.8 g.) as that for L-lysine hydrochloride; yield, 7.6 g. (90%); $[\alpha]_D^{20}$ +22.0° ($c$=2, in 5 N hydrochloric acid) (lit.[13] $[\alpha]_D$ +22.1°).

*Anal.* Found: N, 16.57. Calcd. for $C_5H_{13}O_2N_2Cl$: N, 16.60%.

*δ-Benzoyl-D-ornithine amide hydrochloride.*—The combined fractions described already were treated in the same way as that for benzoyl-D-lysine amide hydrochloride; yield, 23.4 g. (86%); m. p. 208~210°C; $[\alpha]_D^{15}$ −16.5° ($c$=2, in water).

*Anal.* Found: C, 52.41; H, 6.77; N, 15.38. Calcd. for $C_{12}H_{18}O_2N_3Cl$: C, 53.04; H, 6.68; N, 15.46%.

*δ-Benzoyl-D-ornithine.*—This was prepared from the above compound (13.6 g.) as that for benzoyl-D-lysine; yield, 5.3 g. (45%); m. p. 242~245°C (decomp.); $[\alpha]_D^{15}$ −25.8° ($c$=2, in 5 N hydrochloric acid).

*Anal.* Found: N, 11.73. Calcd. for $C_{12}H_{16}O_3N_2$: N, 11.86%.

*D-Ornithine hydrochloride.*—This was prepared from benzoyl-D-ornithine amide hydrochloride (8.2 g.) as that for D-lysine hydrochloride; yield, 4.5 g. (89%); $[\alpha]_D^{20}$ −21.7° ($c$=2, in 5 N hydrochloric acid) (lit.[14] $[\alpha]_D$ −20.1°).

*Anal.* Found: N, 16.33. Calcd. for $C_5H_{13}O_2N_2Cl$: N, 16.60%.

**Resolution of δ-Carbobenzoxy-DL-ornithine Amide.**— *δ-Carbobenzoxy-L-ornithine.* — δ-Carbobenzoxy-DL-ornithine amide hydrochloride (60.2 g.) was incubated with the enzyme containing 17.4 mg. of protein nitrogen in the similar manner as that for benzoyl-DL-ornithine amide, the course of hydrolysis being shown in Fig. 3. During incubation, the precipitate was deposited gradually. After about sixty hours, the mixture was kept in a refrigerator for two days, and the crystals were collected and washed with cold water (combined filtrate and washings saved for the D-amide). This was recrystallized from dilute hydrochloric acid-aqueous ammonia; yield,

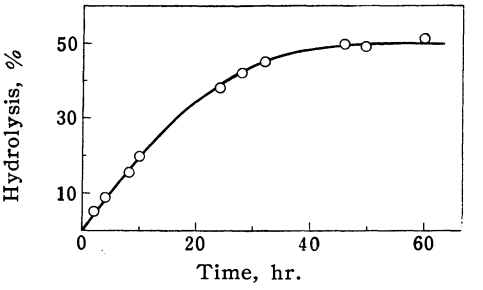



Fig. 3. Time-course of hydrolysis of δ-carbobenzoxy-DL-ornithine amide.

24.5 g. (92%); m. p. 246~248°C (decomp.); $[\alpha]_D^{18}$ +18.1° [$c$=2, in aqueous acetone (1 : 1, by volme) containing two equivalents of of hydrogen chloride] (lit.[9] $[\alpha]_D^{16}$ +17°); $[\alpha]_D^{18}$ +18.9° ($c$=2, in 5 N hydrochloric acid).

*Anal.* Found: N, 10.55. Calcd. for $C_{13}H_{18}O_4N_2$: N, 10.52%.

*L-Ornithine hydrochloride.*—The above compound (5.3 g.) was refluxed with 6 N hydrochloric acid (80 ml.) for four hours, the solution was evaporated to dryness in vacuo, and the residue was treated as that for L-lysine hydrochloride; yield, 2.8 g. (83%); $[\alpha]_D^{20}$ +21.9° ($c$=2, in 5 N hydrochloric acid) (lit.[13] $[\alpha]_D$ +22.1°).

*Anal.* Found: C, 35.89; H, 7.87; N, 16.00. Calcd. for $C_5H_{13}O_2N_2Cl$: C, 35.58; H, 7.77; N, 16.60%.

*δ-Carbobenzoxy-D-ornithine amide hydrochloride.*— The combined filtrate and washings described already were treated in the same way as that for benzoyl-D-lysine amide hydrochloride. The product obtained was recrystallized from hot methanol-ether; yield, 25.7 g. (85%); m. p. 175~176°C; $[\alpha]_D^{18}$ −8.7° ($c$=2, in water).

*Anal.* Found: C, 51.32; H, 6.71; N, 14.04. Calcd. for $C_{13}H_{20}O_3N_3Cl$: C, 51.68; H, 6.68; N, 13.92%.

*D-Ornithine hydrochloride.* — The above compound (6.0 g.) was treated as that for L-ornithine hydrochloride in this section and D-lysine hydrochloride; yield, 2.9 g. (86%); $[\alpha]_D^{20}$ −22.2° ($c$=2, in 5 N hydrochloric acid) (lit.[14] $[\alpha]_D$ −20.1°).

*Anal.* Found: C, 35.91; H, 7.76; N, 15.97. Calcd. for $C_5H_{13}O_2N_2Cl$: C, 35.58; H, 7.77; N, 16.60%.

## Summary

ε-Benzoyl-DL-lysine amide, δ-benzoyl-DL-ornithine amide and δ-carbobenzoxy-DL-orithine amide were resolved to ω-acyl-L-amino acids and ω-acyl-D-amino acid amides by the partially purified leucine aminopeptidase preparation. ω-Acyl-L-amino acids and ω-acyl-D-amino acid amides were hydrolyzed to L- and D-amino acid hydrochlorides, respectively. The parts of ω-benzoyl-D-amino acid amides were changed to ω-benzoyl-D-amino acids by acid hydrolysis.

*Department of Chemistry*
*Faculty of Science*
*Kyushu University*
*Hakozaki, Fukuoka*

15) N. Izumiya, *J. Chem. Soc. Japan, Pure Chem. Sec.* (*Nippon Kagaku Zasshi*), **72**, 150 (1951).

# *Determination of Methyl and Phenyl Groups in Methyl-Phenyl-Siloxane Polymer by NMR Spectroscopy*

By Tsutomu KUBOTA and Tsutomu TAKAMURA

(Received June 22, 1959)

Chemical applications of NMR spectroscopy have been developed rapidly during recent few years. Although many reports have been published on its application to the molecular structure investigation and to the qualitative analysis, quantitative analysis using the NMR method has scarcely been reported[1] at all.

It has already been known that under an appropriate experimental condition the peak area of the resonance spectrum is directly proportional to the number of resonating atoms irrespective of their chemical nature[2,3]. Since the peak area depends both on the volume of specimen inserted in an effective part of a high frequency coil and on whether or not the specimen is placed at the right position in the coil, a calibration must always be performed with the identical sample container if the outer reference method is adopted. If, however, a suitable inner reference is used instead of an outer one, such a disadvantage can be avoided; and in addition to this, the authors have a great advantage that no standard substance is required. The inner reference method is done by mixing a sample material homogeneously with a known amount of any substance which produces a resonance peak and by referring to the peak area produced by the substance as a standard.

Shoolery et al. have pointed out the usefulness of the method, but have not made the actual application[4]. Muller and Goldenson have used the peak area method for their kinetic study of phospher compound[5] and Shaw and Elsken have shown that the peak height of differential form of spectrum can be applied to the quantitative analysis[6], but their purposes seem not to be in the complete examination of the inner reference method.

It is the purpose of the present study to examine the inner reference method and to bring it to a practical use, in which determination of methyl and phenyl groups in methyl-phenyl-siloxane polymer has been carried out. The linear relationship between the peak area and proton concentration has been found to exist in a wide range of experimental conditions, the determination being made without difficulty. The analytical results were compared with those obtained from the infrared analysis and it was found that they were in good agreement within the experimental error.

## Experimental

**Materials.**—Dioxane and benzene of commercial guaranteed reagents were used without further purification. Acetone was purified by drying a commercial guaranteed reagent with unhydrous calcium chloride and by distilling twice. Water was purified by distilling the de-ionized water. All of the organosiloxanes were those synthesized and purified in the Tsurumi Research Laboratory of Tokyo Shibaura Electric Co. The boiling or melting point ranges of siloxanes were within $\pm 0.5°C$.

**Measurements.**—Approximately 0.6 ml. of each sample was poured by means of a syringe into a glass tube of 5 mm. in outer diameter which then was sealed off. If necessary, a glass tube of 2 mm. in outer diameter containing pure water was sealed in the outer tube at the coaxial position. These sealed tubes were offered to measurements. Since according to a preliminary examination, there exists no difference between the proton chemical shift obtained by using a soft lead glass tube as a sample container and that obtained by using a borosilicate glass tube, soft lead glass tubes were used throughout this work becauce of the ease of sealing them.

Proton NMR spectra were recorded with a Japan Electron Optics Laboratory NMR Spectrometer Model JNM-3. The applied resonance frequency was 40 Mc, the field sweep width, 87.5 and 175 milligauss, the sweep rate being controlled to 5 to 10 milligauss per second. All the measurements were carried out in a room whose air temperature was regulated to $25 \pm 1°C$.

1) C. A. Reilly, *Anal. Chem.*, **30**, 839 (1958).
2) N. F. Chamberlain, ibid., **31**, 56 (1959).
3) R. B. Williams, *Ann. N. Y. Acad. Sci.*, **70**, 800 (1958).
4) C. F. Callis, J. R. von Wazer and J. N. Shoolery, *Anal. Chem.*, **28**, 269 (1956).
5) N. Muller and J. Goldenson, *J. Am. Chem. Soc.*, **78**, 5182 (1956).
6) T. M. Shaw and R. H. Elsken, *Anal. Chem.*, **27**, 1983 (1955).

The proton chemical shift described in $\delta$ value was calibrated as follows: The spectrum was recorded for pure acetone using pure water as a reference. The distance between the peaks due to acetone and water was measured from the center of the peaks, the field width corresponding to the distance being decided by using the $\delta$ value of acetone, $\delta = -0.334$, which was given by Allred and Rochow[7]. All the measurements were repeated ten times for one sample, the data being averaged. The proton chemical shift of the methyl group attached to the silicon atom was found to be $\delta = -0.49$ for hexamethylsiloxane and methyl-phenyl-siloxane polymer, and that of the phenyl group to be $\delta = +0.22$ for cyclooctaphenyltetrasiloxane and methyl-phenyl-siloxane polymer.

The infrared spectrum was recorded with an automatic recording spectrometer which was specially designed by Professor H. Yoshinaga of Osaka University. Measurements were carried out with the carbon disulfide solutions of sample at various concentrations and by means of a rock salt cell of 0.1 mm. optical path length for quantitative use. The key bands taken for methyl and phenyl groups were the absorption bands at wave numbers of 2970 and 3030 $cm^{-1}$, respectively.

## Results and Discussion

Prior to the quantitative determination on methyl-phenyl-siloxane polymer, calibration curves were drawn with some standard substances to ascertain that the proportionality really exists between a peak area due to methyl or phenyl group and the number of protons contained in the group. Hexamethylsiloxane and cyclooctaphenyltetrasiloxane were chosen as standards, because the chemical constitution of these substances is similar to that of the siloxane polymer. Although the most favorable case would be one where these substances could be mixed homogeneously at various mixing ratios, the solid of phenyl siloxane is only slightly soluble in methyl siloxane; therefore, benzene and dioxane were used as auxiliary standards. The peak area was measured by varying the mixing ratio for three binary systems, namely, hexamethylsiloxane-benzene, cyclooctaphenyltetrasiloxane-dioxane and benzene-dioxane, where each characteristic peak is well separated. The examples of spectra are shown in Fig. 1.

In the case of the hexamethylsiloxane-benzene system two peaks appeared; the one is due to proton of benzene and the other to that of siloxane. The concentration of siloxane was obtained from the experimental results by taking the ratio of the peak area of benzene to that of siloxane and by multiplying the ratio by

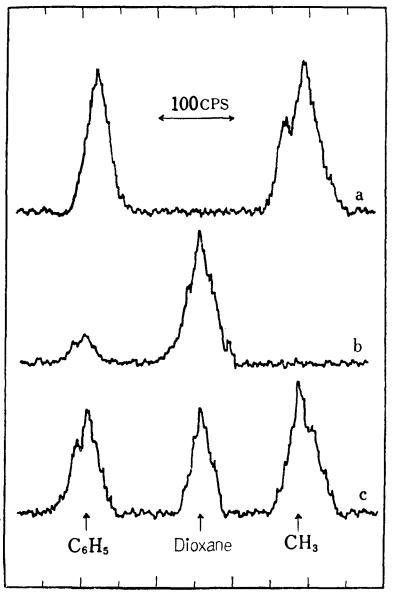



Fig. 1. Proton spin resonance spectra of binary mixtures containing organosiloxanes recorded at 40 Mc. and 25°C.
a) 46.1 weight % of hexamethylsiloxane in benzene;
b) 20.0% of cyclooctaphenyltetrasiloxane in dioxane;
c) 84.1% of methyl-phenyl-siloxane polymer in dioxane.

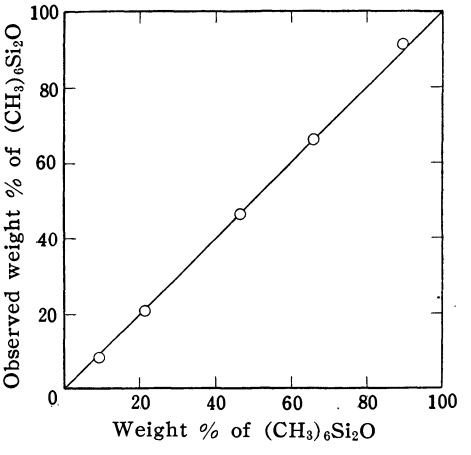



Fig. 2. Plotting of concentration of hexamethylsiloxane in benzene obtained from NMR spectra against that obtained from the mixing ratio.

7) A. L. Allred and E. G. Rochow, *J. Am. Chem. Soc.*, **79**, 5361 (1957).

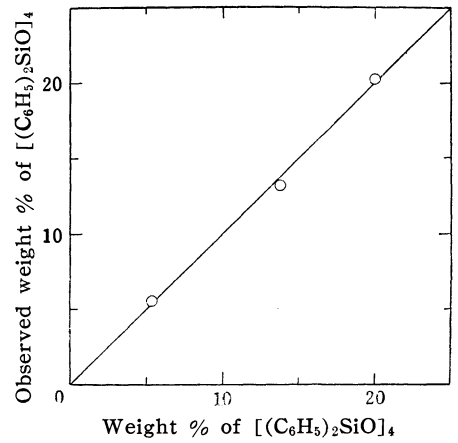



Fig. 3. Plotting of concentration of cyclooctaphenyltetrasiloxane in dioxane obtained from NMR spectra against that obtained from the mixing ratio.

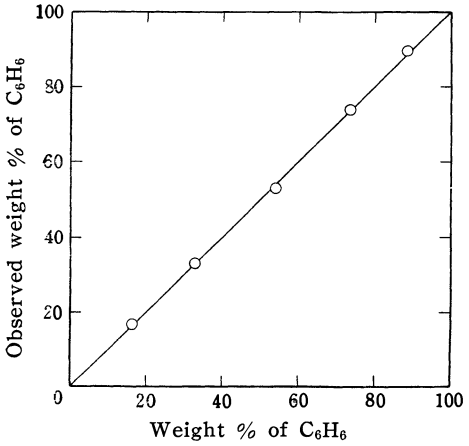



Fig. 4. Plotting of concentration of benzene in dioxane obtained from NMR spectra against that obtained from the mixing ratio.

a factor of 1/2, since benzene and siloxane molecules have six and twelve equivalent hydrogen atoms, respectively. The concentration of siloxane thus obtained was plotted against that determined by the mixing ratio. As seen in Fig. 2, the plots are well on the straight line whose slope is unity, the direct proportionality being confirmed. Similar plottings made on cyclooctaphenyltetrasiloxane-dioxane and benzene-dioxane systems gave also straight lines, the proportionality being ascertained as shown in Figs. 3 and 4. With the results of these experiments parallelly performed the direct proportionality was proved to be maintained in the mixture of hexamethylsiloxane and cyclooctaphenyltetrasiloxane.

The fact that the chemical shift of any respective group shows no difference whether the group is attached to simple siloxane or siloxane polymer shows these compounds to be nearly identical regarding the chemical construction. Therefore, the proportionality is supposed to be maintained also in the case of siloxane polymer.

Since the peak area measured at a definite recording condition depends on the sample volume located in the high frequency coil effectively, as already mentioned, the absolute number of protons can hardly be determined when outer reference is used. Such a difficulty is eliminated by mixing a known amount of a substance having proton with the sample homogeneously. Dioxane was chosen as a suitable reference. The actual measurement was made on the mixture of methylphenylsiloxane polymer and dioxane by varying the mixing ratio. Three well separated peaks appeared in this case as shown in Fig. 1, two from methyl and phenyl groups of siloxane polymer and one from dioxane. The peak area due to one proton can be obtained from the observed area of dioxane whose concentration is known, then, the numbers of methyl and phenyl groups involved in 100 g. of siloxane polymer can be calculated for each mixing ratio from the peak areas. The obtained values are listed in the second and fourth columns in Table I to show the constant value over a wide range of mixing ratio.

On the other hand, the number of each group was also determined with the infrared technique. Cyclooctamethyltetrasiloxane and cyclooctaphenyltetrasiloxane were used as standard substances for methyl and phenyl groups, respectively. Assuming that each extinction coefficient of a respective group in siloxane polymer is identical with that of the corresponding standard substance, the number was

TABLE I. NUMBERS OF METHYL AND PHENYL GROUPS PER 100 g. OF METHYL-PHENYL-SILOXANE POLYMER DETERMINED BY NMR AND INFRARED METHOD

| Weight % of methyl-phenyl-siloxane polymer in dioxane | Number of methyl group | | Number of phenyl group | |
|---|---|---|---|---|
| | NMR | Infrared | NMR | Infrared |
| 84.1 | 1.21 | — | 0.56 | — |
| 54.5 | 1.16 | — | 0.55 | — |
| 44.0 | 1.14 | — | 0.57 | — |
| 30.1 | 1.15 | — | 0.56 | — |
| mean | 1.17 | 1.21 | 0.56 | 0.56 |

determined from the absorptions in carbon disulfide solution of known concentrations. The results averaged are cited in the third and fifth columns of Table I. Agreement of these results obtained from the two different methods is good within the experimental error.

The great advantage of NMR spectroscopy on the quantitative analysis is that no standard to the respective specimen is required because the peak area depends only on the number of protons and, under an appropriate experimental condition, is independent of the nature of molecular configuration. A comparatively large experimental error in the method caused by the crude reproducibility of the spectrum is now being reduced by the rapid development of instrumentation. The group type analysis on the relatively complicated molecule will then be systematized with the accumulation of chemical shift data, each number of atoms having nuclear spin would be determined for each group with the inner reference method, and therefore, the NMR method will display more power in the determination of molecular structure.

## Summary

Proton spin resonance spectra were recorded for the three binary mixtures, benzene-dioxane, benzene-hexamethylsiloxane and dioxane-cyclooctaphenyltetrasiloxane whose mixing ratios were varied. The peak area due to resonating proton of methyl or phenyl group was found to be directly proportional for all systems to the number of protons which give the peak of respective groups over a wide range of recording conditions.

With the results obtained, the determination of methyl and phenyl groups in methyl-phenyl-siloxane polymer was carried out by the use of the inner reference method using dioxane. Siloxane polymer was mixed with dioxane and the spectrum was recorded for the mixture, the number of each group being calculated from the obtained peak area. The results were compared with those obtained from the infrared analysis and they were in good agreement within the experimental error.

The authors express their thanks to Dr. T. Harada, the Manager of Matsuda Research Laboratory, for his permission to publish this paper, to Dr. H. Miyazawa for his advice on the measurement of the NMR spectra and Mr. K. Kawazumi for the preparation and purification of organosilicon compounds.

*Matsuda Research Laboratory*
*Tokyo Shibaura Electric Co.*
*Kawasaki*

# *The Volume Change on Formation of Water from its Ions*[1]

By Akira TSUJIOKA

(Received July 3, 1959)

The reaction between the hydrogen ion and the hydroxyl ion is given by

$$H^+ + OH^- = H_2O \qquad (1)$$

It was noticed by Geffcken et al.[2] that the volume change associated with this reaction in aqueous solution is about 23 cc. per mole at infinite dilution and at 25°C. But there has been no investigation to provide the data at various concentrations and to correlate quantitatively the volume change with concentration. Although the volume changes on formation of water are not susceptible of direct measurement, these values can be determined by using the data on changes of volume on neutralization of a strong acid with a strong base.

In the concentration range of high dilution, there is little or no difference between the volume change on neutralization of aqueous sodium hydroxide with hydrochloric acid and that with hydrobromic or hydroiodic acid[3]. The expansion

1) Presented at the 12th Annual Meeting of the Chemical Society of Japan, Kyoto, April, 1959.

2) W. Geffcken and D. Price, *Z. physik. Chem.*, **B26**, 81 (1934).

3) J. D'Ans and E. Lax, "Taschenbuch für Chemiker und Physiker", 2nd Ed., Springer-Verlag, Berlin (1949), p. 821; Landolt-Börnstein, "Physikalisch-Chemische Tabllen", Erg. B. II, Springer-Verlag, Berlin (1931), p. 274.

in total volume in such cases may be explained as mainly due to the disappearance of electrostriction of charged ions[4], which is caused by the fact that the hydrogen ion combines with the hydroxyl ion to form water. In the higher concentration range, however, the magnitudes of volume change per mole commonly decrease with three different series of reactions mentioned above and the differences among them becomes larger (see the second column in Table II). In order to explain these subjects, it is necessary to derive the relationship between the volume change on formation of water from its ions and the concentrations of acid and base.

With reference to the method employed by Rossini[5], who calculated the heat of ionization of water, i.e. the negative of the heat evolved in reaction 1 at infinite dilution, by combining the data on heats of neutralization and those on heats of dilution, the author has evaluated changes of volume on formation of water from its ions at constant temperature. On the other hand, the author has shown that the volume change on formation of one mole of water from its ions at moderate concentrations is represented by a linear function of the square root of the concentration of ions, by using the Masson-Geffcken relationship[2,6] on the apparent molar volume of electrolytes in solution. The relationship so obtained has been checked with the calculated data. The agreement of the results has been found very satisfactory.

In the present paper the author has utilized the data on changes of volume on neutralization recently obtained by the present author[7], and also the data of Saslawsky et al.[3,8]

## Calculation and Results

In considering the volume changes on neutralization of various acids and bases, the author will deal with both uni-univalent strong electrolytes.

The reaction between a strong acid and a strong base at finite and equal concentrations, $C$ mol./l., is given by

$$HB + MOH = MB + H_2O \qquad (2)$$

This reaction represents the formation of one mole of water from its ions at the initial concentration $C$, and also the dilution of one mole each of $M^+$ and $B^-$ ions from $C$ to $C'$, by which the concentration in moles per liter of the resulting salt solution is denoted.

The volume change for the process is

$$\Delta V_N = \Delta V_F + \Delta V_D \qquad (3)$$

where $\Delta V_N$ is the volume change on neutralization, $\Delta V_F$ is that on formation of water and $\Delta V_D$ is that on dilution. The value of $\Delta V_F$ can be obtained from that of $\Delta V_N$, which is directly measurable, if the corresponding value of $\Delta V_D$ is known. Then, it is assumed that the volume change on dilution of one mole each of $M^+$ and $B^-$ ions from $C$ to $C'$ is equal to that on dilution of one mole of salt MB from $C$ to $C'$. In other words, it is assumed that the sum of the apparent molar volumes of $M^+$ and $B^-$ ions, in the basic and acid solutions respectively, is equal to the apparent molar volume of MB in the neutral salt solution. It will be permissible at the range of concentration here studied, because it would be rightly considered that the difference between $B^-$ ion—$H^+$ ion interaction and $B^-$ ion—$M^+$ ion interaction is small and can be ignored at low or moderate concentrations. Again, a similar assumption is made not only regarding $M^+$ ion, but also regarding $H^+$ and $OH^-$ ions, respectively.

Thus, values of the volume change on formation of water from its ions at various concentrations at 20°C have been computed from those of the volume change, obtained by the present author[7], on neutralization of a hydrochloric acid with a sodium hydroxide solution of equal concentration. In computing these values

TABLE I. CHANGES OF VOLUME ON FORMATION OF WATER FROM ITS IONS AT 20°C[a]

| Initial concn. $C$ mol./l. | Vol. change on neutralization $\Delta V_N$ ml./mol. | Concn. of the resulting soln. $a^*$ % | Vol. change on dilution ($C \rightarrow a^*$) $\Delta V_D$ ml./mol. | Vol. change on formation of water $\Delta V_F$ ml./mol. |
|---|---|---|---|---|
| 1 | 20.04 | 2.841 | −0.58 | 20.62 |
| 2 | 18.16 | 5.530 | −1.00 | 19.16 |
| 3 | 16.91 | 8.093 | −1.25 | 18.16 |
| 4 | 15.87 | 10.544 | −1.45 | 17.32 |
| 5 | 14.97 | 12.895 | −1.63 | 16.60 |

a) Calculated from values of the volume change, obtained by the present author[7], on neutralization of hydrochloric acid with sodium hydroxide solution.

4) I. Uhara, *J. Chem. Soc. Japan, Pure Chem. Sec.* (*Nippon Kagaku Zasshi*), **57**, 53 (1936).
5) F. D. Rossini, *Bur. Standards J. Research*, **6**, 847 (1931).
6) D. O. Masson, *Phil. Mag.*, 8, 218 (1929).
7) A. Tsujioka, This Bulletin, **32**, 685 (1959).
8) J. J. Saslawsky and E. G. Standel, *Z. anorg. u. allgem. Chem.*, **186**, 171 (1930).

given in Table I, the author has taken $\Delta V_D$ as equivalent to the difference between the apparent molar volume of sodium chloride in the aqueous solution, of which the concentration is similar to the one of the acid or the basic solution, and that in the resulting solution, because both the density of the solution to be diluted and that of the resulting salt solution have been known[7,9].

TABLE II. VALUES OF $\Delta V_F$ CALCULATED FROM SASLAWSKY'S DATA[3,8] AT 20°C

(1) Calculated from values of $\Delta V_N$ on reaction: $HCl+NaOH=NaCl+H_2O$.

| Initial concn. $C$ mol./l. | Vol. change on neutralization $\Delta V_N$ ml./mol. | Concn. of the resulting soln. $C^*$ ml./mol. | Vol. change on dilution ($C \rightarrow C^*$) $\Delta V_D$ ml./mol. | Vol. change on formation of water $\Delta V_F$ ml./mol. |
|---|---|---|---|---|
| 1 | 19.6 | 0.495 | −0.7 | 20.3 |
| 2 | 18.0 | 0.982 | −1.0 | 19.0 |
| 3 | 16.7 | 1.463 | −1.2 | 17.9 |
| 4 | 15.9 | 1.938 | −1.4 | 17.3 |
| 5 | 15.0 | 2.409 | −1.6 | 16.6 |

(2) Calculated from values of $\Delta V_N$ on reaction: $HBr+NaOH=NaBr+H_2O$.

| $C$ | $\Delta V_N$ | $C^*$ | $\Delta V_D$ | $\Delta V_F$ |
|---|---|---|---|---|
| 1 | 20.0 | 0.495 | −0.6 | 20.6 |
| 2 | 18.5 | 0.982 | −0.9 | 19.4 |
| 3 | 17.5 | 1.462 | −1.1 | 18.6 |
| 4 | 16.7 | 1.935 | −1.2 | 17.9 |
| 5 | 15.9 | 2.405 | −1.4 | 17.3 |

(3) Calculated from values of $\Delta V_N$ on reaction: $HI+NaOH=NaI+H_2O$.

| $C$ | $\Delta V_N$ | $C^*$ | $\Delta V_D$ | $\Delta V_F$ |
|---|---|---|---|---|
| 1 | 19.4 | 0.495 | −0.5 | 19.9 |
| 2 | 18.4 | 0.982 | −0.7 | 19.1 |
| 3 | 17.9 | 1.461 | −0.9 | 18.8 |
| 4 | 17.1 | 1.934 | −1.0 | 18.1 |
| 5 | 16.0 | 2.404 | −1.1 | 17.1 |

Then, in Table II are shown values of $\Delta V_F$, which have been calculated from the data, obtained by Saslawsky et al.[3,8], on changes of volume on three different series of reactions. In this calculation, the author has evaluated the concentration of the resulting salt solution from the value of $\Delta V_N$, and computed the corresponding value of $\Delta V_D$ by the Masson-Geffcken relationship on the apparent molar volume of electrolyte*. Because the apparent molar volumes of these salts, i. e. sodium chloride, bromide and iodide, confirm satisfactorily this relationship over the range of concentration here treated[10,11].

In Tables I and II-1, the agreement of the results has been found very satisfactory. It is just as predicted from the fact that each of the values of volume change on neutralization obtained by the present author is in good agreement with the corresponding one by Saslawsky et al.[7] Furthermore, each of the values of $\Delta V_F$ shown in Tables II-2 and II-3 is in tolerable agreement with the corresponding one given in Table I or II-1, without an error greater than one or two per cent.

## Discussion

The volume change per mole on reaction 2 is given by[7]

$$\Delta V_N = \Phi_s^* + \Phi_w + \Phi_a - \Phi_b \qquad (4)$$

where $\Phi$ is the apparent molar volume of the solute. The subscripts refer to salt, water, acid and base, respectively, and the asterisk indicates that the salt concentration is $C^*$ mol./l. As has been fully discussed in the previous section, this reaction represents the formation of one mole of water from its ions at the initial concentration, and also the dilution of one mole each of $M^+$ and $B^-$ ions from the initial concentration $C$ to the final one $C'$. Therefore, the changes of volume for these two processes are represented by means of the following equations, respectively.

$$\Delta V_F = \Phi_w - (\Phi_H + \Phi_{OH}) \qquad (5)$$

$$\Delta V_D = \Phi_s^* - (\Phi_M + \Phi_B) = \Phi_s^* - \Phi_s \qquad (6)$$

where $\Phi_H$, $\Phi_{OH}$, $\Phi_M$ and $\Phi_B$ are the apparent molar volumes of $H^+$, $OH^-$, $M^+$ and $B^-$ ions at the initial concentration, respectively.

Substitution of Eqs. 4—6 into Eq. 3 gives the following equation.

$$\Phi_H + \Phi_{OH} = \Phi_a + \Phi_b - \Phi_s \qquad (7)$$

If the apparent molar volumes of these three electrolytes confirm the Masson-Geffcken relationship, $\Phi = \Phi^\circ + S\sqrt{C}$, Eq. 7 can be reduced to

$$\Phi_H + \Phi_{OH} = (\Phi_a^\circ + \Phi_b^\circ - \Phi_s^\circ) + (S_a + S_b - S_s)\sqrt{C} \qquad (8)$$

9) A. Tsujioka, *J. Chem. Soc. Japan, Pure Chem. Sec.* (*Nippon Kagaku Zasshi*), **80**, 467 (1959).

* The limiting slopes are $S_{(NaCl)}=2.32$, $S_{(NaBr)}=2.04$ and $S_{(NaI)}=1.64$ (cf. Ref. 10).

10) A. Tsujioka, *Proc. Faculty Eng., Keio Univ.*, **10**, 63 (1957).

11) H. S. Harned and B. B. Owen, "The Physical Chemistry of Electrolytic Solutions", 2nd Ed., Reinhold Publishing Co., New York (1950), p. 252.

where $\Phi^\circ$ is the apparent molar volume of a solute at infinite dilution, and $S$ is the limiting slope. Again it is the same as in Eq. 4 that the subscripts refer to acid, base and salt, respectively.

It has been found valid for most electrolytes that the Masson-Geffcken relationship holds over a wide range of concentration except on high dilution[2,12]. For aqueous solutions of some acids or lithium salts, however, the apparent molar volumes of the solutes show an unusual dependence on the concentration, especially at high concentrations[13,14]. Hydrogen iodide which has been treated in the present paper is one of these electrolytes, but its deviation from the Masson-Geffcken relationship would be rightly considered to be negligibly small at moderate concentrations[14].

At high dilution, on the other hand, the apparent molar volumes of strong electrolytes in solution confirm the limiting law derived from the Debye-Hückel theory[15,16]. That is, the apparent molar volumes, $\Phi$, of strong electrolytes in solution at high dilution are represented by the following equation.

$$\Phi = \Phi^\circ + S_v\sqrt{C} + kC \qquad (9)$$

where $\Phi^\circ$ is the apparent molar volume of a solute at infinite dilution, $S_v$ is the universal limiting slope which is 1.86 at 25°C for 1—1 electrolyte[17], and $k$ is constant and specific for each electrolyte. If the apparent molar volumes of acid, base and salt confirm Eq. 9**, Eq. 7 can be reduced to

$$\Phi_H + \Phi_{OH} = (\Phi_a^\circ + \Phi_b^\circ - \Phi_s^\circ) + S_v\sqrt{C} + (k_a + k_b - k_s)C \qquad (10)$$

where the subscripts refer to acid, base and salt. Therefore, the sum of the apparent molar volumes of $H^+$ and $OH^-$ ions confirm the limiting Debye-Hückel law at high dilution as same as the 1—1 strong electrolytes.

Now, by using the values of the parameters*** of Masson-Geffcken equations for sodium chloride, hydrogen chloride and sodium hydroxide, Eq. 8 can be reduced to

$$\Phi_H + \Phi_{OH} = -5.47 + 3.10\sqrt{C} \qquad (11)$$

Using Eq. 5, therefore, one obtains the following equation:

$$\Delta V_F = 23.52 - 3.10\sqrt{C} \qquad (12)$$

where $\Delta V_F$ is the volume change in ml./mol. which occurs on reaction 1, and $C$ is the concentration in mol./l. of hydrogen and hydroxyl ions. This equation can be applied to moderate concentrations, i.e. 1~5 mol./l., at 20°C. Again, the numerical term in Eq. 12 does not refer to the value of volume change on formation of water from its ions at infinite dilution.

In Figs. 1 and 2, values of $\Delta V_F$ shown in Tables I and II, as well as those calculated by Eq. 12, have been plotted against the square root of the concentration. The agreement of the results has been found very satisfactory in Fig. 1. In Fig. 2, values of $\Delta V_F$ computed from values of the volume change on neutralization of hydroiodic acid with sodium hydroxide solution are considerably different from the corresponding ones computed from the data in other cases.

The apparent molar volume of hydrogen iodide, at concentrations above 1.5 N, deviate from the values predicted by the Masson-Geffcken relationship[18]. This behavior was attributed to incomplete ionization by Fajans[18], while to ion-ion and

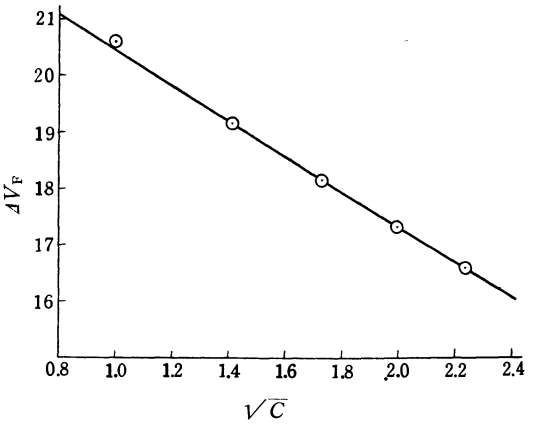



Fig. 1. Volume changes on formation of water, given in Table I, plotted against the square root of the concentration. (——, calculated by Eq. 12).

12) A. F. Scott, *J. Phys. Chem.*, **35**, 2315 (1931).
13) J. Bigeleisen, *J. Phys. & Colloid Chem.*, **51**, 1369 (1947).
14) K. Fajans and O. Johnson, *Trans. Electrochem. Soc.*, **82**, 273 (1942).
15) B. B. Owen and S. R. Brinkley, *Ann. N. Y. Acad. Sci.*, **51**, 753 (1949).
16) O. Redlich and J. Bigeleisen, *Chem. Revs.*, **30**, 171 (1942).
** The limiting law of the molar volume has not been experimentally confirmed for sodium hydroxide. But the limiting slope appears to be the same for NaOH, HCl, NaCl and for other electrolytes of the 1—1 charge type. Because there is no reason to assume any anomaly in NaOH, in view of the theoretical derivation of Eq. 9.
17) O. Redlich and J. Bigeleisen, *J. Am. Chem. Soc.*, **64**, 758 (1942).

*** $\Phi_{(NaCl)} = 15.82 + 2.32\sqrt{C}$; $\Phi_{(HCl)} = 17.80 + 0.87\sqrt{C}$; $\Phi_{(NaOH)} = -7.45 + 4.55\sqrt{C}$ (cf. Ref. 7).
18) K. Fajans, *J. Chem. Phys.*, **9**, 281 (1941).

ion-solvent interactions by Bigeleisen[13]. But it appears to leave much room for discussions[19]. Nevertheless, it would be rightly considered that the less satisfactory linearity of HI, shown in Fig. 2, is due to a reason similar to the one to which its deviation from the Masson-Geffcken rule must be ascribed.

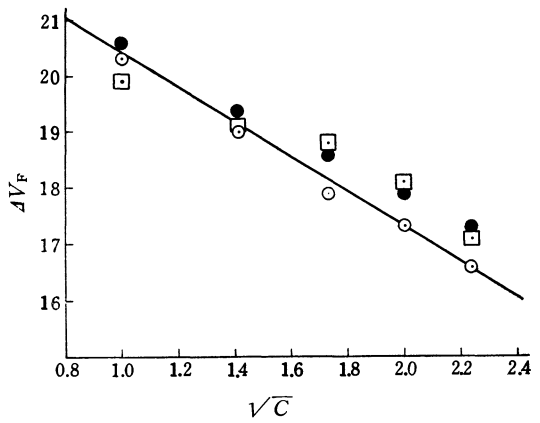



Fig. 2, Concentration dependence of $\Delta V_F$, given in Table II.
(——, calculated by Eq. 12; ○, HCl+NaOH; ●, HBr+NaOH; □, HI+NaOH)

Thus, by using the results obtained in the present work, it is readily possible to predict changes of volume on neutralization of a strong acid with a strong base. The difference among values of the volume change, obtained in different series of reactions between acids and bases at the same conditions, is mainly due to that among the corresponding ones of $\Delta V_D$. Values of $\Delta V_D$ are generally negative, so the expansion in total volume on neutralization gets smaller as the numerical value of $\Delta V_D$ gets larger. The diminution in total volume on dilution ($\Delta V_D$) is proportional to the limiting slope of the salt[10] (cf. Eq. 6). Therefore, the larger the limiting slope for a salt, the smaller the expansion in volume on neutralization is. The correctness of this prediction has been found very satisfactory in Table II*.

19) H. E. Wirth and F. N. Collier, *J. Am. Chem. Soc.*, **72**, 5292 (1950).

## Summary

Values of the changes of volume on formation of water from the hydrogen and hydroxyl ions in aqueous solutions, at various concentrations at 20°C, have been calculated, by combining the data of volume change on neutralization of a strong acid with a strong base and those on dilution of electrolyte solutions. Furthermore, the dependence of the volume change on the concentration has been derived and checked with the calculated data. The volme change on formation of water from its ions at moderate concentrations at 20°C is given by the equation: $\Delta V_F = 23.52 - 3.10\sqrt{C}$ ml. per mole, where $C$ is the concentration of ions in mol./l.

Thus, the author has made it easy to analyze the volume changes on neutralizations of various acids and bases.

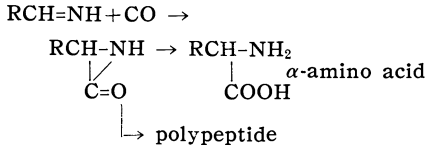
*The Chemical Laboratory*
*Keio University*
*Hiyoshi, Yokohama*

# *Studies on the High Pressure Reaction of Carbon Monoxide. I. On the Reactions of Schiff Bases and Azocompounds with Synthetic Gas*

By Shunsuke MURAHASHI and Shigeki HORIIE*

(Received July 3, 1959)

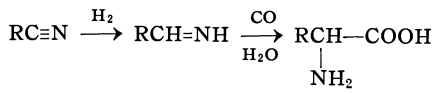
From considerations of the chemical formula, it might be conceivable that if an addition of carbon monoxide to the double bond of Schiff base could occur, there are possibilities of synthesizing α-amino acid on hydrolysis of the addition products with water or peptide with a restricted quantity of water, as indicated below:




The following work was undertaken in the light of such a consideration.

It is well known that the reduction of nitrile proceeds to amine via éte intermediate of Schiff base, and that cobalt carbonyl is able to catalyze oxo-reaction, and furthermore it also catalyzes hydrogenation of aldehyde to alcohol in the presence of carbon monoxide and hydrogen.

On such an account the authors attempted to prove the possibility of obtaining amino acid or polypeptide directly from nitriles.




At the time when the authors started the work, chemical reaction of nitriles under an oxo-condition had not been explored and so benzonitrile and benzylcyanide were subjected to the present examination. The experiments resulted only in giving a small quantity of amines (mixtures of primary and secondary ones) and it revealed that reduction of nitrile would be very difficult to be realized and no reaction product was obtained in which carbon monoxide had been involved. Therefore, the authors have turned the subject to the Schiff base itself and studied to see whether the reaction in this case would take place, giving α-amino acid or peptide as was postulated above.

The general conditions adopted for the experiments are as follows: Catalyst, cobaltcarbonyl; Solvent, benzene or benzene-alcohol (1 : 1); Gas, $CO+H_2$ (1 : 1), 200 atm.; Reaction temperature, 120~130°C.

The results with Schiff bases were shown in Table I which shows conclusively that a reduction of C=N double bond had occured and no reactions were found in which carbon monoxide has participated.

The reduction proceeded very smoothly and did not present any marked difference even when the reactions were carried out at varied conditions, i. e. pressure, temperature and reaction time. As to the effect of reaction medium it was found, that the reaction was faster and began at a somewhat (10~20°C) lower temperature when alcohol-benzene mixture (1 : 1) was used instead of aromatic hydrocarbons.

Benzaldehyde phenylhydrazone did not give any definite result with synthetic gas. The authors, then, studied the reaction of synthetic gas on double bond having nitrogen atom, such as the N=O and N=N-group as well as C=S double bond.

Nitrobenzene and azobenzene was allowed to react with carbon monoxide and was ascertained to give aniline as a principal product. Hydrazobenzene was also subjected to this reaction for reference and it was confirmed that aniline was again the principal product. In all cases the authors found the formation of a considerable quantity of diphenylurea, as shown in Table II.

Thus, it has been confirmed that the four kinds of bond, C=N, N=N, C=S and N=O were all reduced by synthetic gas in the presence of cobalt carbonyl catalyst. The formation of urea derivatives observed in all cases except for the compound involving C=S linkage is

* Present address: Institute of Scientific and Industrial Research, Osaka Univ., Sakai, Osaka.

TABLE I. REACTION OF SYNTHETIC GAS WITH BENZALDEHYDEANILS

| Anil | Solvent | Reaction temp., °C | Reaction time, min. | Product | Yield, % |
|---|---|---|---|---|---|
| $C_6H_5N=CHC_6H_5$ | B | 135 | 110 | $C_6H_5NHCH_2C_6H_5$ | 80 |
| $C_6H_5N=CHC_6H_5$ | A B | 120 | 60 | $C_6H_5NHCH_2C_6H_5$ | 79 |
| $p$-$ClC_6H_4N=CHC_6H_5$ | B | 150 | 70 | $p$-$ClC_6H_4NHCH_2C_6H_5$ | 79 |
| $p$-$ClC_6H_4N=CHC_6H_5$ | A B | 130 | 130 | $p$-$ClC_6H_4NHCH_2C_6H_5$ | 81 |
| $p$-$MeC_6H_4N=CHC_6H_5$ | B | 140 | 90 | $p$-$MeC_6H_4NHCH_2C_6H_5$ | 82 |
| $p$-$MeC_6H_4N=CHC_6H_5$ | A B | 120 | 60 | $p$-$MeC_6H_4NHCH_2C_6H_5$ | 80 |
| $p$-$MeOC_6H_4N=CHC_6H_5$ | B | 130 | 60 | $p$-$MeOC_6H_4NHCH_2C_6H_5$ | 83 |
| $p$-$MeOC_6H_4N=CHC_6H_5$ | A B | 120 | 50 | $p$-$MeOC_6H_4NHCH_2C_6H_5$ | 82 |
| $p$-$NO_2C_6H_4N=CHC_6H_5$ | B | 130 | 80 | $p$-$NO_2C_6H_4NHCH_2C_6H_5$ | 80 |
| $p$-$NO_2C_6H_4N=CHC_6H_5$ | A B | 120 | 70 | $p$-$NO_2C_6H_4NHCH_2C_6H_5$ | 78 |

Catalyst, $[Co(CO)_4]_2$, 0.03 millimol./ml.; Solvent, B=benzene, AB=alcohol-benzene (1:1); Gas, CO(100 atm.)+$H_2$(100 atm.).

TABLE II. FORMATION OF DIPHENYLUREAS BY THE REACTION OF AZOBENZENES AND NITROBENZENE WITH SYNTHETIC GAS

| | $C_6H_5NHCONHC_6H_5$ % | R-$C_6H_4NHCONHC_6H_5$ % | R-$C_6H_4NHCONHC_6H_4$-R % |
|---|---|---|---|
| $C_6H_5NO_2$ | 5～ 6 | | |
| $C_6H_5N=NC_6H_5$ | 15～20 | | |
| $C_6H_5NH-NHC_6H_5$ | 25～30 | | |
| $p$-$ClC_6H_4N=NC_6H_5$ | trace | 5 | 3 |
| $p$-$MeC_6H_4N=NC_6H_5$ | trace | 12 | 5 |

Reaction conditions are the same in Table I.

noteworthy, because it demonstrates, that some new kind of CO-reaction has occurred, and especially the fact that a formation of symmetrically substituted urea derivatives were observed from asymmetrically substituted azo-compounds was of special note.

As the reaction appeared to be a new one, the authors planned further experiments so as to obtain more detailed information about the high pressure reaction of carbon monoxide.

Hydrazobenzene gave 50% yield of azobenzene under the similar condition, at the reaction temperature which was lower than that required for the reduction (80～90°C). From this experiment it could be postulated that urea could have formed from hydrazobenzene via azobenzene. However, the yields of diphenylurea were in all cases higher when hydrazobenzene was used instead of azobenzene. In the case of nitrobenzene, the formation of urea derivative was also observed and its formation could be interpreted by the intermediate formation of either hydrazobenzene or azobenzene.

In order to discuss the possible mechanism for the formation of urea derivative, one has to consider either 1) fission of hydrazo linkage followed by addition of CO, or 2) that the azo group remains without cleavage until CO is added across the double bond and then the -N-N- bond is subjected to fission by hydrogenolysis as will be shown below (Eq. 2). Eq. 1 was suggested earlier by W. Reppe[1] as a possible mechanism of the oxo-reaction and the carboxylation of olefins. Accordingly one might propose Eq. 2 for the urea formation.

$$RCH{=}CH_2 \xrightarrow{CO} RCH(\text{-}CH_2\text{-}C(=O)\text{-}) \longrightarrow RCH(CHO)\text{-}CH_3 \text{ or } RCH_2CH_2CHO \quad (1)$$

$$RN{=}NR' \xrightarrow{CO} RN(\text{-}NR'\text{-}C(=O)\text{-}) \xrightarrow{H_2} RNHCONHR' \quad (2)$$

Since azobenzene is reduced for the most part to aniline, it would be an acceptable argument that the formation of urea could have resulted from the reaction of

1) W. Reppe, *Ann.*, **582**, 40 (1953).

aniline and carbon monoxide. Pino[2] discussed the possibility of formation of urea derivatives from two moles of aniline and one mole of carbon monoxide under a dehydrating condition, and Buckley[3] reported the formation of formylaniline by the reaction of aniline and carbon monoxide.

However, all the authors' tests with aniline and with formylaniline failed to show that the urea-formation is the result of the reaction of aniline and carbon monoxide.

An alternate mechanism would presumably be a fission of the azo-compound by means of carbon monoxide and hydrogen, leading to the primary formation of phenylisocyanate and aniline. However, the authors failed to isolate such an intermediate to prove this mechanism.

As another possibility, hydrazobenzene might well be accounted for the reaction. In this regard the authors will discuss it in later papers.

## Experimental

**1) Reduction of Benzaldehydeanil with Synthetic Gas.** — Benzaldehydeanil (5 g.) was dissolved in 50 ml. of benzene or benzene-alcohol mixture (1:1) and charged in an autoclave of 100 ml. content made of 18-8 stainless steel together with cobalt carbonyl (1.0 g.). After replacement of air, the synthetic gas was compressed up to 200 atm. (CO, 100 atm. and $H_2$, 100 atm.). The autoclave was heated at 120~130°C, when the pressure began to descend, and after completion of gas absorption it was allowed to cool. The content of the autoclave was heated in a flask on a water bath and after decomposition of the cobalt catalyst and filtration the filtrate was distilled in vaccuo, affording 4 g. of benzylaniline, m. p. 38°C, which was identified by the mixed melting point test with an authentic sample.

The essential feature of the experimental procedures are all the same as described above, and thus *p*-chloro, *p*-methyl-, *p*-methoxy- and *p*-nitro-benzaldehydeanil were subjected to examination. The results are given in Table I. The melting points and the boiling points all agree with the values described in the literatures. *p*-Nitrocompound was reduced under the present condition selectively at the anil double bond and the nitro group remained unchanged.

**2) Reaction of 3-Phenyl-2-thioxopropionic Acid and Carbon Monoxide.**—3-Phenyl-2-thioxopropionic acid (3 g.) in benzene (50 ml.) was allowed to react with carbon monoxide and hydrogen of 200 atm. in the presence of cobalt catalyst (1 g.) at 120~130°C for 2 hr. No gas absorption was observed, but after cooling and degassing, it was found that hydrogen sulfide gas had formed. A definite product could not be isolated except 2-phenylpropionic acid amide melting at 102°C.

**3) Formation of Diphenylurea as a By-product in the Reaction of Azobenzene and Synthetic Gas.**—Azobenzene (5 g.) yielded 1.1 g. of diphenylurea (20% yield) in a form of a difficultly soluble product, which was recrystallized from alcohol.

**4) Urea Derivatives from *p*-Chloroazobenzene.** —*p*-Chloroazobenzene (5 g.) was treated as in exp. 1 and from the reaction product 0.6 g. (12%) of a mixture of urea compounds was obtained, and was separated into two parts: *p,p'*-dichlorodiphenylurea as the difficultly soluble part in alcohol in colorless prisms, m. p. 286°C (with decomposition), and as the soluble part *p*-chlorodiphenylurea in scaly crystals, m. p. 244°C.

*Anal.* Found: C, 56.66; H, 3.70; Cl, 25.20; N, 10.36. Calcd. for $C_{13}H_{10}Cl_2N_2O$: C, 56.93; H, 3.64; Cl, 25.26; N, 10.21%.

*Anal.* Found: C, 64.06; H, 4.64; Cl, 14.32; N, 11.55. Calcd. for $C_{13}H_{11}ClN_2O$: C, 64.19; H, 4.52; Cl, 14.40; N, 11.52%.

**5) Urea Derivatives from *p*-Methylazobenzene.** —*p*-Methylazobenzene (5 g.) was treated as in exp. 4 and from the filtrate of the reaction mixture a mixture (1.2 g., 22%) of urea was separated. From a difficultly soluble portion *p,p'*-dimethylphenylurea (0.3 g.) was obtained in colorless needles, m. p. 262°C and from the soluble portion *p*-dimethyldiphenylurea (0.7 g., 12%) was obtained, and further a small quantity of unsubstituted diphenylurea was obtained from the last portion of the soluble residue.

*Anal.* Found: C, 74.81; H, 6.70; N, 11.78. Calcd. for $C_{15}H_{16}N_2O$: C, 75.00; H, 6.66; N, 11.66%.

*Anal.* Found: C, 74.15; H, 6.20; N, 12.51. Calcd. for $C_{14}H_{14}N_2O$: C, 74.33; H, 6.19; N, 12.38%.

*Department of Chemistry*
*Faculty of Science*
*Osaka University*
*Nakanoshima, Osaka*

2) P. Pino and C. Paleari, *Gazz. Chim. Ital.*, 81, 646 (1951); *Chem, Abstr.*, **46**, 7063 (1952).

3) G. D. Buckley and N. H. Ray., *J. Chem. Soc.*, **1949**, 1151.

# *Studies on the High Pressure Reaction of Carbon Monoxide. II. Synthesis of Phthalimidine*

By Shunsuke MURAHASHI, Shigeki HORIIE** and Takashi JŌ**

(Received July 3, 1959)

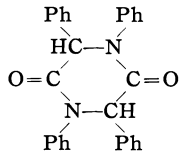
In Part I the reaction of Schiff bases and azobenzene derivatives with synthetic gas was described and it was found that in the case of azobenzene, no insignificant amount of diphenylurea had been formed besides aniline which was the main product.

With the object of obtaining more information on the cause of diphenylurea-formation as well as on the knowledge of reactivity of carbon monoxide with -N=N- bond, the authors studied the reaction with carbon monoxide alone instead of with synthetic gas as reported in Part I. There, it was found that new reactions took place which afforded phthalimidines when Schiff bases were subjected to the reaction with carbon monoxide under the cobalt catalyst, and quinazolones when azocompounds were used. The present paper describes the synthesis of phthalimidine.

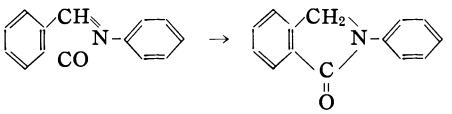
When benzaldehydeanil was dissolved in an aromatic hydrocarbon such as benzene or toluene and heated under carbon monoxide pressure of 100 to 200 atm. at 200~230°C in the presence of cobalt catalyst, it afforded white scaly crystals, m. p. 200°C.

The result of the analysis of these crystals indicated that it had an experimental formula ($C_{14}H_{11}ON$), indicating that 1 mol. of carbon monoxide had entered into every 1 mol. of benzaldehydeanil.

It appeared at the outset to have achieved the synthesis of amino acid in the form of anhydride and to have obtained tetraphenyldiketopiperazine of the following formula:

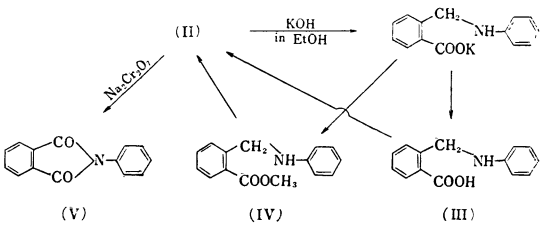


But a detailed study of this substance soon revealed that it was the derivative of phthalimidine (II) and was probably synthesized according to the following scheme:



(I) (II)

Compound II gave on hydrolysis an acid (III) which are so unstable on standing as to return to the original compound. In order to get a stable product, compound II was hydrolyzed with alkali and then the hydrolyzate was esterified directly with dimethylsulfate without acidification. Although the ester of III was separated as an oil, it also returned to its original compound II very easily.



These behaviors did not correspond to the one of diketopiperazine.

The formation of phthalic anhydride by oxidation with potassium permanganate and the formation of *N*-phenylphthalimide by sodium bichromate-oxidation demonstrated eventually that compound II was a phthalimidine derivative as illustrated above.

A conclusive evidence was established by comparison with the authentic sample prepared by other means.

Thus a novel reaction was found, in which CO-attack had taken place on both the benzene rings and on the *N*-atom with simultaneous ring formation. In order to establish the necessary conditions for the achievement of this reaction, several runs were carried out and the results were shown in Table I. The essential features

* Reported briefly in a previous communication: S. Murahashi, S. Horiie, *J. Am. Chem. Soc.*, 77, 6403 (1955).

** Present address: Institute of Scientific and Industrial Research, Osaka Univ., Sakai, Osaka.

TABLE I. REACTION BETWEEN BENZALDEHYDEANIL WITH CO

| Expt. No. | Anil g. | Catalyst | Solvent | CO Pressure atm. | Reaction temp., °C | Reaction time hr. | Yield g. |
|---|---|---|---|---|---|---|---|
| 1 | 5 | — | $C_6H_6$ | 200 | 220～230 | 6 | — |
| 2 | 5 | $[Co(CO)_4]_2$ | 〃 | 〃 | 〃 | 〃 | 4.1 |
| 3 | 3 | Co-acetylacetonate | 〃 | 288 | 〃 | 〃 | 1.2 |
| 4 | 3 | Co-ethylacetoacetate | 〃 | 278 | 〃 | 〃 | 1.7 |
| 5 | 3 | $CoCO_3$ | 〃 | 180 | 〃 | 6 | 2.0 |
| 6 | 5 | $Fe(CO)_5$ | 〃 | 140 | 〃 | 〃 | 0.5 |
| 7 | 3 | $Ni(CO)_4$ | 〃 | 330 | 〃 | 〃 | — |
| 8 | 5[a)] | $[Co(CO)_4]_2$[b)] | 〃 | 200 | 〃 | 6 | 4.1 |
| 9 | 5 | 〃 [c)] | 〃 | 〃 | 〃 | 〃 | 3.9 |
| 10 | 3 | 〃 | 〃 | 155 | 〃 | 3 | 2.0 |
| 11 | 3 | 〃 | 〃 | 84 | 〃 | 1 | 2.0 |
| 12 | 3 | 〃 | 〃 | 45 | 〃 | 3 | 0.5 |
| 13 | 5 | 〃 |  | 200 | 〃 | 6 | — |
| 14 | 5 | 〃 | EtOH | 〃 | 〃 | 〃 | — |
| 15 | 5 | $Ni(CO)_4$ |  | 330 | 〃 | 〃 | — |
| 16 | 5 | $[Co(CO)_4]_2$ | $C_6H_6$, $H_2O$ 1 cc | 185 | 〃 | 6 | — |
| 17 | 5 | 〃 | $C_6H_6$, $H_2O$ 0.5 cc | 160 | 〃 | 〃 | — |
| 18 | 5 | 〃 | $C_6H_6$ | 200 ($0.01\%O_2$) | 〃 | 〃 | 4.1 |
| 19 | 5 | 〃 | 〃 | 200 ($0.15\%O_2$) | 〃 | 〃 | 3.7 |
| 20 | 5 | 〃 | 〃 | 200 | 〃 | 5 | trace |

Concn. of Catalyst: 0.03 millimol./cc.
a) Benzaldehydeanil: 0.028 mol.
b) $[Co(CO)_4]_2$: 0.0015 mol.
c) $[Co(CO)_4]_2$: 0.0045 mol.

of the results are as follows:

a) No reaction without the catalyst (Expt. No. 1). b) Cobalt compound such as dicobalt octacarbonyl, iron pentacarbonyl (less active), metallic cobalt, and cobalt salt or complex and so on, which have the potentiality of forming metal carbonyl, would be effective in promoting the reaction (Expts. No. 2–5). c) Nickel carbonyl is ineffective (Expt. No. 7). d) As a solvent, aromatic hydrocarbons are appropriate and protonic solvents inhibit the reaction (Expts. No. 13–17). e) Temperature of about 200°C is necessary and appropriate temperature of reaction lies in the range of 220～230°C (Expts. No. 10–12). f) Since the change of carbon monoxide pressure in the range of 30～300 atm. did not show any appreciable effect on the reaction, the necessary pressure seems to be that which suffices to maintain the concentration of cobalt carbonyl at the reaction temperature (Expts. No. 10–12). g) Since cobalt carbonyl is decomposed by contact with oxygen, it was inevitably needed to exclude oxygen (Expts. No. 18–19). h) The effect of the inner wall of an autoclave generally was not noticed except at the beginning of its use, when sometimes an irregular behavior was observed.

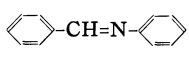
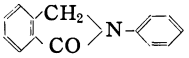
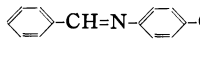
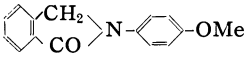
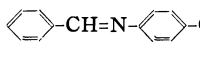
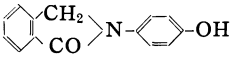
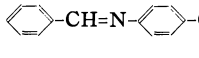
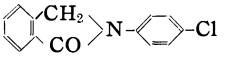
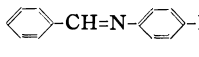
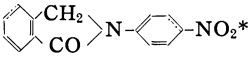
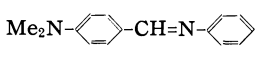
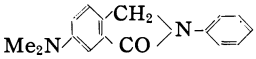
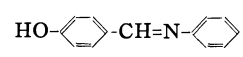
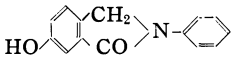
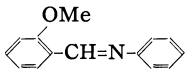
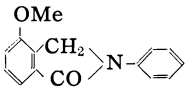
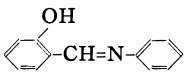
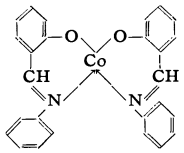
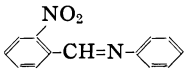
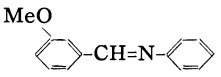
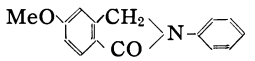
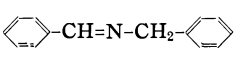
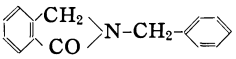
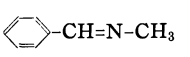
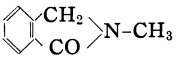
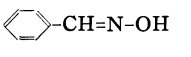
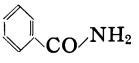
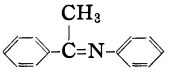
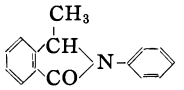
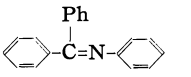
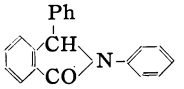
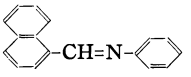
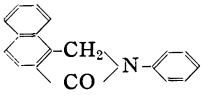
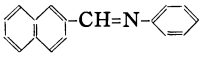
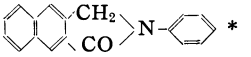
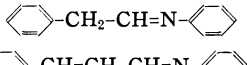
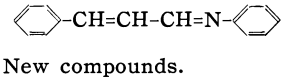
As this reaction is expected to give useful intermediates for dyestuffs and synthetic chemical reagents, the reactions between carbon monoxide and varieties of Schiff bases having various substituents were examined, as shown in Table II.

In both the cases of benzaldehydeanils with substituents (H, OMe, OH, Cl) in the *p*-position of aniline nucleus and those with substituents (OH, $Me_2N$) in the *p*-position of benzaldehyde side, all gave phthalimidines in good yields by the reaction with carbon monoxide, and no appreciable effect of the substituents was observed (Expts. No. 1–4 and 6–7). *o*-Methoxybenzaldehydeanil gave the expected phthalimidine though in a comparatively low yield. (Expt. No. 8).

In the case of salicylaldehydeanil, a stable red-colored complex containing cobalt was formed, and therefore, cobalt compound used as the catalyst did not promote the reaction but appeared only to have been converted to the stable complex compound II with salicylaldehydeanil (Expt. No. 9).

*m*-Methoxybenzaldehydeanil yielded a low yield of phthalimidine. The expected

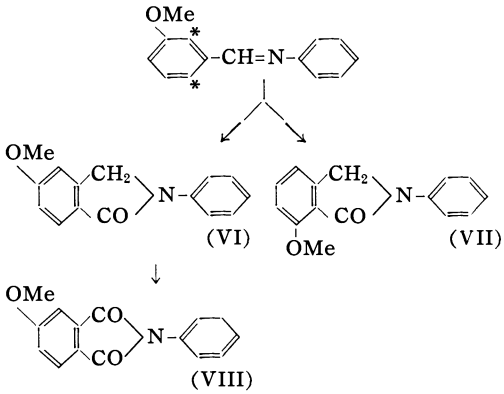
TABLE II. REACTION BETWEEN SCHIFF BASES AND CO

| Expt. No. | Starting material: Schiff base | g. | Product | Yield: g. | Yield: % | m. p.: Author | m. p.: Liter. |
|---|---|---|---|---|---|---|---|
| 1 |  | 5 |  | 4.1 | 71.9 | 164 | 163 |
| 2 |  | 5 |  | 4.8 | 85.7 | 138 | 134 |
| 3 |  | 5 |  | 3.7 | 64.9 | 225 | 228 |
| 4 |  | 5 |  | 4.2 | 75.0 | 182 | 180 |
| 5 |  | 5 |  | — | — | — | — |
| 6 |  | 5 |  | 4.6 | 82.1 | 154 | — |
| 7 |  | 5 |  | 4.4 | 77.2 | 216 | — |
| 8 |  | 5 |  | 1.0 | 17.8 | 146 | — |
| 9 |  | 5 |  | 0.3 | — | 191 | 191 |
| 10 |  | 4 | —— | — | — | — | — |
| 11 |  | 5 |  | 0.3 | 5.3 | 146 | — |
| 12 |  | 5 |  | 4.7 | 82.4 | 91 | 91 |
| 13 |  | 5 |  | 3.0 | 48.6 | 115 | 120 |
| 14 |  | 5 |  | 1.3 | 26.0 | 128 | 128 |
| 15 |  | 5 |  | 3.5 | 61.4 | 82 | 80 |
| 16 |  | 3 |  | 3.2 | 96.9 | 196.5 | — |
| 17 |  | 2 |  | 2.1 | 96.0 | 177 | — |
| 18 |  | 4 |  | 1.5 | 80.0** | 254 | — |
| 19 |  | 5 | —— | — | — | — | — |
| 20 |  | 5 | —— | — | — | — | — |

* New compounds.

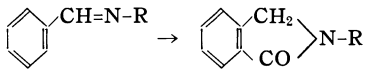
** Yield based on anil consumed.

products could be either VI or VII. Since the product was oxidized with sodium bichromate in acetic acid to yield 4-methoxyphthalic acid anilide (VIII), it was identified as a new compound, *N*-phenyl-5-methoxyphthalimidine (VI) (Expt. No. 11).



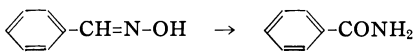

The ring closure is expected to take place at these asterisk positions.

Schiff base derived from aliphatic amine and benzaldehyde also gave the phthalimidine by the reaction with carbon monoxide (Expts. No. 12 and 13).



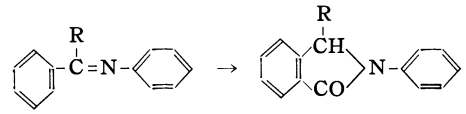

R: $CH_3$ and $PhCH_2$

Benzaldoxime did not give phthalimidine, but gave benzamide. This fact suggests that a part of cobalt carbonyl had been converted to cobalt hydrocarbonyl in the reaction condition and since this is a strong acid*** it might have promoted the Beckmann rearrangement.



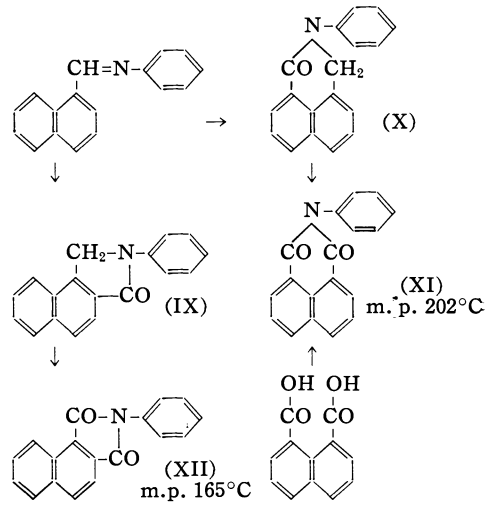

In the case of Schiff base having a nitro group, either on the side of aniline or on the benzaldehyde nucleus, the reaction became very complicated, yielding a deep violet infusible solid**** instead of the expected nitrophthalimidine (Expts. No. 5 and 10). As the model experiment on nitrobenzene (see *Experimental*) shows, the reaction was complicated owing to the presence of the nitro group, but the presence of phthalimidine grouping in the product was demonstrated by the occurrence of phthalic acid among the oxidation products.

Schiff bases, obtained from ketone such as acetophenone and benzophenone and aniline, reacted smoothly with carbon monoxide, yielding the expected phthalimidines (Expts. No. 15 and 16).




R: Me and Ph

Naphthaldehydeanils yielded the corresponding derivatives of phthalimidine in good yields. As 1-naphthaldehydeanil can be expected to ring-close with carbon monoxide at a 2- or 8-position, either one or a mixture of two (IX), (X) will be formed as the product. The product obtained, however, was not a mixture but a pure substance, and was converted to *N*-phenylnaphthalimide (m. p. 165°C) by oxidation with sodium bichromate in acetic acid. *N*-Phenyl-1, 8-naphthalimide (XI) synthesized from 1, 8-naphthalendicarboxylic acid and aniline, which has the melting point of 202°C, does not coincide with the oxidation product. Therefore, the phthalimidine obtained here would be IX and the oxidized product XII. Thus, the ring closure takes place at the 2-position to yield 2-phenylbenz [*e*] isoindolin-1-on (VI),



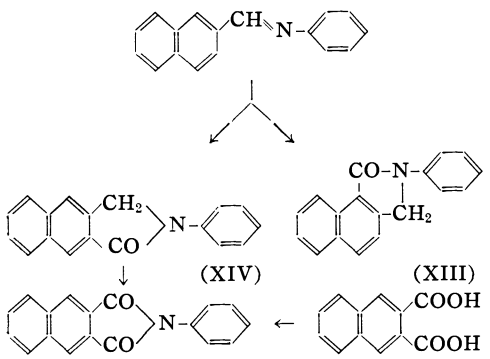

Although the chemical structure of compound IX has not yet been fully

*** Since this rearrangement by cobalt carbonyl or more probably cobalt hydrocarbonyl was considered to be a new fact, the same method was attempted to apply to aliphatic oximes. However, aliphatic oximes were merely reduced and by cyclohexanone oxime, gave dicyclohexylurea besides an amino compouond.

**** It is apparent that the reducing power of carbon monoxide led to the formation of azo-linkage (G. D. Buckley, N. H. Ray; *J. Chem. Soc.*, **1949**, 1154) or of diphenylurea linkage (S. Horiie, unpublished) by the reduction of the nitro group. Reactions as these might be responsible for the reaction between carbon monoxide and the nitrocompound leading to the formation of an insoluble, infusible and deep violet substance.

ascertained by a direct comparison with the synthesized sample, its identity is considered to be well confirmed by the comparison with XV, and this will be described below.

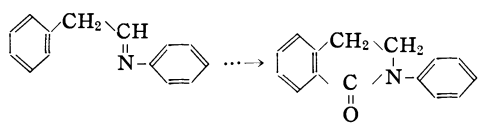
Since, in the case of 2-naphthaldehydeanil, the ring closure takes place at the 1- or 3-position of naphthalene nucleus, the expected product is either XIII of XIV. Only one kind of reaction product was also obtained here and, through the oxidation by sodium bichromate, it gave a *N*-phenylnaphthalimide, which coincided with *N*-phenyl-2, 3-naphthalimide (V), synthesized from 2, 3-naphthalene dicarboxylic acid and aniline. Therefore, the reaction product obtained with 2-naphthaldehydeanil was proved to be 2-phenylbenz[*f*]-isoindolin-1-on (XIV), which occurred as the result of the ring closure at the 3-position.

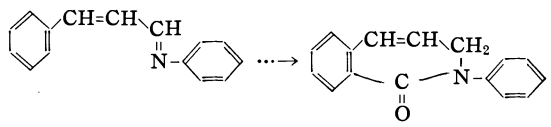



(XV) mp. 278°C

This ring closure by carbon monoxide at the 3-position of the naphthalene derivatives is a very peculiar case and of interest in comparison with the fact that the ring closure usually occurs at the 1-position of 2-substituted naphthalene derivatives.

Starting from phenylacetaldehydeanil and cinnamaldehydeanil, the reaction should analogously be expected to lead to the formation of 6- and 7-membered rings, respectively, but the experiments were carried out in vain. This would suggest that the reaction with carbon monoxide seems to be characteristic of the azomethine group, conjugated with the aromatic ring and is limited to the formation of a 5-membered ring.




## Experimental

**1) Reaction between Benzaldehydeanil and Carbon Monoxide.**—Five grams of benzaldehydeanil was dissolved in 50 ml. of benzene, and placed in an autoclave of 100 ml. content together with a catalytic amount of cobalt carbonyl solution (concn., 0.03 millimol./ml.) and carbon monoxide was pressed after replacement of air up to 100~200 atm., then the autoclave was heated at 220~230°C for 5~6 hr. with constant shaking. After cooling, the excess of carbon monoxide was purged and a greater part of *N*-phenylphthalimidine, which is produced, emitted as crystalline needles or scales and were collected on a filter and washed with a small amount of benzene, the crystal (4.1 g., 72% of theoretical) is almost pure, m. p. 163°C.

*Anal.* Found: C, 80.26; H, 5.47; N, 6.92. Calcd. for $C_{14}H_{11}ON$: C, 80.38; H, 5.26; N, 6.70%.

**2) Hydrolysis of *N*-Phenylphthalimidine and Alkylation of the Hydrolyzed Product.**—One gram of *N*-phenylphthalimidine was boiled with an alcoholic solution of potassium hydroxide (2 g. of potassium hydroxide in 20 ml. of alcohol-water (1 : 1) solu ion) and after 3 hr. the alcohol was distilled off and the remaining water solution was devided into two parts.

When one part of the solution had been made slightly acidic with dilute hydrochloric acid, the oil was separated out, which then crystallized after a while. This crystal (0.45 g.) was proved to be identical with *N*-phenylphthalimidine.

When the other portion of the solution was methylated with 0.6 g. of dimethylsulfate, an oil which gradually changed into crystalls, and which was identified as *N*-phenylphthalimidine, m. p. 162°C oozed out.

**3) Oxidation of Phthalimidine with Bichromate.**—The oxidation carried out referred to the work of Maxwell and Allen[1]. Thus, *N*-phenylphthalimidine (0.5 g.) was dissolved in anhydrous acetic (30 ml.) acid under stirring and warming at 90°C. Sodium bichromate in fine powder was charged slowly until no more color change was observed. After half an hour when the mixture was poured into water, a white crystalline precipitate, which was recrystallized from alcolol, in colorless needles (0.2 g.), m. p. 205°C separated out. The mixed melting point test with an authentic sample proved to be identical with *N*-phenylphthalimide.

**4) *N*-Phenylphthalimidine.** — *N*-Phenylphthalimide, which is obtained by fusion of aniline and phthalic anhydride was reduced with Zn-dust according to the method of Graebe[2] in an acetic acid solution at 80~90°C.

1) C. S. Maxwell and X. F. Allen, "Organic Syntheses", Vol. 24, John Wiley & Sons, Inc., New York (1944), p. 1.
2) C. Graebe, *Ann.*, **247**, 288 (1888).

After reduction, the solution was poured into a large amount of water, and the white crystals separated. The crystals, after recrystallization from alcohol, were found to be identical with the sample obtained from benzaldehydeanil, m. p. 163°C.

**5) Synthesis of *N*-(*p*-Methoxyphenyl)phthalimidine.** — *N*-Benzyl-*p*-methoxyaniline (5 g.) was caused to react with carbon monoxide in the same manner as in the previous paper (Expt. Part 1) in Paper II). After being cooled, the reaction mixture was filtered to yield 4.8 g. of the colorless scaly crystals, m. p. 137~138°C (from methanol). A literature reported the m. p. of 135°C[3].

*Anal.* Found: N, 5.79. Calcd. for $C_{15}H_{13}O_2N$: N, 5.85%.

This crystals (1 g.) suspended in 50 ml. of 1 N sodium hydroxide and oxidized with potassium permanganate, yielded 0.2 g. of phthalic acid which was identified by the mixed melting point test with the authentic sample.

**6) Synthesis of *N*-(*p*-Hydroxyphenyl)phthalimidine.**—The colorless crystals (3.7 g.) were obtained in needles in a similar manner starting from benzal-*p*-hydroxyaniline (5 g.). The product was recrystallized from alcohol, m. p. 224~245°C.

*Anal.* Found: C, 74.65; H, 4.92; N, 6.22. Calcd. for $C_{14}H_{11}O_2N$: C, 74.56; H, 5.12; N, 6.42%.

The crystals (1 g.) were oxidized to phthalic acid (0.2 g.) by alkaline potassium permanganate.

**7) Synthesis of *N*-(*p*-Chlorophenyl)phthalimidine.**—Benzal-*p*-chloroaniline (5 g.) gave in a similar manner 4.2 g. of colorless scaly crystals, which was recrystallized from alcohol, m. p. 181~182°C.

*Anal.* Found: C, 69.14; H, 4.11; N, 5.19. Calcd. for $C_{14}H_{10}ONCl$: C, 69.40; N, 4.44; N, 5.99%.

The crystals (1 g.) were oxidized to phthalic acid (0.25 g.).

**8) Reaction of Carbon Monoxide with Benzal-*p*-nitroaniline.**—In a similar manner, there was obtained an amorphous deep purple substance, which was insoluble in organic and inorganic solvents and was infusible. The fact that oxidation of this substance by potassium permanganate yielded a minor amount of phthalic acid seems to show that the general reaction between benzal-*p*-nitroaniline and carbon monoxide has taken place to some extent.

**9) Synthesis of *N*-Phenyl-6-dimethylaminophthalimidine.**—*p*-Dimethylaminobenzaldehydeanil (5 g.) gave 4.6 g. of colorless needles, which were recrystallized from alcohol, m. p. 154°C.

*Anal.* Found: C, 76.00; H, 6.13; N, 11.30. Calcd. for $C_{16}H_{16}ON_2$: C, 76.16; H, 6.39; N, 11.10%.

**10) Synthesis of *N*-Phenyl-6-hydroxyphthalimidine.** — *p*-Hydroxybenzaldehydeanil (5 g.) also gave 4.4 g. of colorless needles, which were then recrystallized from alcohol, m. p. 215~216°C.

*Anal.* Found: C, 74.65; H, 4.88; N, 6.45. Calcd. for $C_{14}H_{11}O_2N$: C, 74.65; H, 4.92; N, 6.22%.

**11) Synthesis of *N*-Phenyl-4-methoxyphthalimidine.** — The reaction mixture from *o*-methoxybenzaldehydeanil (5 g.) and carbon monoxide, after distillation of benzene and after being kept for several days, gave 1 g. of brownish black crystals, which were then recrystallized from alcohol several times into colorless needles, m. p. 145~146°C.

*Anal.* Found: C, 75.70; H, 5.36; N, 5.96. Calcd. for $C_{15}H_{13}O_2N$: C, 75.30; H, 5.48; N, 5.86%.

**12) Formation of 3-Methoxyphthalic Acid Anil.** —Onto a boiling mixture of *N*-phenyl-4-methoxyphthalimidine (0.4 g.) and glacial acetic acid (10 ml.), sodium bichromate was added portionwise until the color of bichromate ion no longer disappeared, and then the whole mixture was poured onto water. White crystals were filtered off, washed with water and recrystallized from alcohol into colorless scaly crystals (0.2 g.), m. p. 188~189°C, which agreed well with m. p. of a literature[4].

*Anal.* Found: C, 71.00; H, 4.45; N, 5.75. Calcd. for $C_{15}H_{11}O_3N$: C, 71.14; H, 4.37; N, 5.53%.

**13) Formation of Salicylaldehydeanil-cobalt Complex.** — Salicylaldehydeanil (5 g.) gave in a similar manner, after removal of benzene and addition of a small amount of alcohol, 2.1 g. of red crystals, which were recrystallized from alcohol, m. p. 190~191°C. The existence of cobalt was ascertained qualitatively by the borax bead test.

*Anal.* Found: C, 68.55; H, 4.73. Calcd. for $(C_{13}H_{11}ON)_2Co$: C, 68.72; H, 4.84%.

Identification of this compound was carried out by the mixed melting point test with the sample, which was synthesized in the following way: a mixed solution of salicylaldehydeanil (1 g.) in benzene and cobalt carbonyl (1.5 g.), after being kept at room temperature for 3 days, was refluxed in a water bath to decompose the remaining carbonyl and then filtered. After removal of benzene from the filtrate, the remaining brown oil was kept standing with the addition of a small amount of alcohol to yield red crystals, m. p. 190~191°C. This compound showed the same melting point as the one which has been obtained from salicylaldehydeanil and cobalt acetate (m. p. 191°C)[5].

**14) Reaction between *o*-Nitrobenzaldehydeanil and Carbon Monoxide.**—*o*-Nitrobenzaldehydeanil yielded an amorphous deep purple substance just like the one of benzal-*p*-nitroaniline.

**15) Reaction between Nitrobenzene and Carbon Monoxide.**—The reaction mixture of nitrobenzene (40 g.) and cobalt carbonyl (0.5 g.) was subjected to steam distillation, yielding 15 g. of apparently amorphous and deep purple solid as residue, which was insoluble and infusible. An extraction of the solid with alcohol for a prolonged time gave 1.2 g. of diphenylurea.

3) A. T. Peters, G. T. Pringle and F. M. Rowe, *J. Chem. Soc.*, **1948**, 597.

4) W. H. Benteley, R. Robinson and C. Weizmann, ibid., **1907**, 111.

5) Endō, *J. Chem. Soc. Japan, Pure Chem. Sec.* (*Nippon Kagaku Zasshi*), **65**, 428 (1944).

**16) Synthesis of *N*-Phenyl-5-methoxyphthalimidine.**—The reaction mixture of *m*-methoxybenzaldehydeanil (5 g.) and carbon monoxide was refluxed to effect the decomposition of the catalyst, filtered, and evaporated to a brownish oil, which crystallized after standing in a vacuum dessicator (0.3 g.). Repeated recrystallizations from alcohol gave colorless needles, m. p. 145~146°C.

*Anal.* Found: C, 75.10; H, 5.68. Calcd. for $C_{15}H_{13}O_2N$: C, 75.30; H, 5.48; N, 5.86%.

*m*-Methoxybenzaldehydeanil (2.4 g.) was recovered by distillation of the mother liquor at a reduced pressure.

**17) Formation of 4-Methoxyphthalic Acid Anilide.**—*N*-Phenyl-5-methoxyphtalimidine (0.2 g.) in glacial acetic acid (4 ml.) was refluxed with sodium bichromate (2 g.), and the whole mixture was poured into-water, resulting in the formation of white crystals. After washing with water, the crystals were recrystallized from alcohol into colorless needles (0.1 g.), m. p. 177~178°C, which agreed well with the reported melting point of 4-methoxyphthalic acid anilide (179°C)[6]. The crystals showed a depression of melting point with 3-methoxyphthalic acid anilide, and so it was identified as 4-methoxyphthalic acid anilide.

*Anal.* Found: C, 71.32; H, 4.65. Calcd. for $C_{15}H_{11}O_3N$: C, 71.14; H, 4.37%.

**18) Synthesis of *N*-Benzylphthalimidine.** — Starting from benzalbenzylamine (5 g.), crystalline *N*-benzylphthalimidine (4.7 g.) was obtained in a similar manner, m. p. 90~91°C (from alcohol), which agreed well with Gabriel's value (m. p. 90~91°C)[7].

*Anal.* Found: C, 80.40; H, 5.49; N, 6.22. Calcd. for $C_{15}H_{13}ON$: C, 80.69; H, 5.87; N, 6.27%.

Oxidation of the crystals (0.5 g.) by potassium permanganate gave phthalic acid (0.2 g.), which was identified by the mixed melting point test with the known sample.

**19) Synthesis of *N*-Methylphthalimidine.** — Benzalmethylamine (5 g.) was reacted with carbon monoxide in a usual manner, giving *N*-methylphthalimidine (3.0 g.), which was recrystallized from alchohol in colorless cubic crystals, m. p. 114~115°C.

*Anal.* Found: C, 73.15; H, 6.36; N, 9.97. Calcd. for $C_9H_9ON$: C, 73.45; H, 6.16; N, 9.52%.

The crystals (0.5 g.) were oxidized by potassium permanganate to phthalic acid (0.1 g.), which was identified by the mixed melting point test with the known sample.

**20) Reaction between Benzaldoxime and Carbon Monoxide.**— Benzaldoxime (5 g.) gave 1.3 g. of colorless needles by the reaction with carbon monoxide, m. p. 127~128°C (from chloroform). The analytical data showed a good agreement with the composition of the original benzaldoxime, indicating that an additional reaction with carbon monoxide had not taken place. The crystal was considered as benzamide from the fact that its melting point does agree with that of benzamide and that it afforded benzoic acid by hydrolysis. Identification was carried out by the mixed melting point test with a known sample of benzamide.

*Anal.* Found: C, 69.07; H, 6.01; N, 14.01. Calcd. for $C_7H_7ON$: C, 69.40; H, 5.83; N, 11.56%.

**21) Synthesis of *N*-Phenyl-3-methylphthalimidine.**—Acetophenoneanil (5 g.) was reacted with carbon monoxide in a usual manner and, after removal of catalyst and benzene, the residue was extracted with hot petroleum ether. On cooling the extract, there were obtained crystals, which were recrystallized from petroleum ether into colorless needles (315 g.), m. p. 81~82°C.

*Anal.* Found: C, 81.10; H, 5.97; N, 6.21. Calcd. for $C_{15}H_{13}ON$: C, 80.69; H, 5.87; N, 6.27%.

A literature reported the same melting point (80°C)[8].

**22) Synthesis of *N*-Phenyl-3-phenylphthalimidine.**—Benzophenoneanil (5 g.) gave, after the treatment similar to Expt. 17, 2.2 g. of the product in colorless needles (from petroleum ether), m. p. 195~196.5°C.

*Anal.* Found: C, 84.20; H, 5.20; N, 4.98. Calcd. for $C_{20}H_{15}ON$: C, 84.18; H, 5.30; N, 4.91%.

**23) Synthesis of 2-Phenylbenz[*e*]isoindolin-1-on.**—1-Naphthaldehydeanil (2.0 g.) gave, in the usual way, a crystalline product (2.1 g.), m. p. 177°C (from alcohol).

*Anal.* Found: C, 83.68; H, 4.98; N, 5.65. Calcd. for $C_{18}H_{13}ON$: C, 83.38; H, 5.01; N, 5.40%.

**24) Oxidation of 2-Phenylbenz[*e*]isoindolin-1-on.** — The crystals (0.5 g.) were dissolved in 30 ml. of boiling glacial acetic acid and sodium bichromate was added gradually until the color of bichromate ion no longer disappeared. After cooling, the reaction mixture was poured into water, giving white crystals, which was then washed with water and recrystallized from alcohol into colorless needles (0.3 g.), m. p. 165°C.

Since these crystals showed a marked depression of the melting point when mixed with *N*-phenyl-1, 8-naphthalimide (m. p. 202°C), which was synthesized from the known sample of 1, 8-naphthalenedicaboxylic acid and aniline, the product was confirmed to be different from the latter compound.

**25) Synthesis of 2-Phenylbenz[*f*]isoindolin-1-on.** — From the reaction mixture of 2-naphthaldehydeanil (4.0 g.) and carbon monoxide there separated crystals which were recrystallized from alcohol into scaly crystals (1.5 g.), m. p. 254°C.

*Anal.* Found: C, 83.55; H, 5.05; N, 5.28. Calcd. for $C_{18}H_{13}ON$: C, 83.38; H, 5.01; N, 5.40%.

The unreacted 2-naphthaldehydeanil (2.2 g.) was recovered from the filtrate after removal of catalyst and benzene.

**26) Oxidation of 2-Phenylbenz[*f*]isoindolin-1-on.** — The crystal (0.5 g.) was dissolved in 30 ml. of boiling glacial acetic acid, and sodium bichromate added in portions until the color of bichromate ion no longer disappeared. After cooling the reaction mixture was poured into a large quantity of water, yielding white crystals, which

6) W. H. Bentley and C. Weizmann, *J. Chem. Soc.*, **91**, 104 (1907).

7) S. Gabriel, *Ber.*, **45**, 724 (1912).

8) A. Peters, F. M. Rowe and C. I. Brodrick, *J. Chem.* Soc., **1948**, 1259.

was then washed with water and recrystallized from alcohol into colorless needles (0.2 g.), m. p. 278°C. Identification was carried out by the mixed melting point test with a known sample of *N*-phenyl-2, 3-naphthalimide.

*Anal.* Found: C, 78.90; H, 4.29; N, 5.28. Calcd. for $C_{18}H_{11}O_2N$: C, 79.12; H, 4.03; N, 5.12%.

**27) Synthesis of *N*-Phenyl-2, 3-naphthalimide.**—Naphthalene-2, 3-dicarboxylic acid anhydride (0.5 g.), which was obtained by sublimation of naphthalene-2, 3-dicarboxylic acid at 240°C, was mixed with aniline (0.25 g.) and heated in a water bath[9]. The product was recrystallized from alcohol into colorless needles (0.6 g.), m. p. 278°C.

*Department of Chemistry*
*Faculty of Science*
*Osaka University*
*Nakanoshima, Osaka*

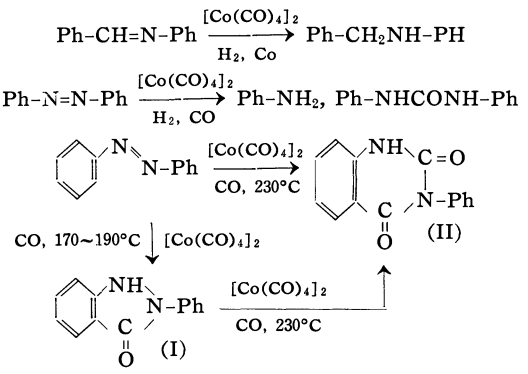
9) M. Freund and K. Fleischer, *Ann.*, **402**, 51 (1914).

# *Studies on the High Pressure Reaction of Carbon Monoxide. III. Reaction between Azocompounds and Carbon Monoxide**

By Shigeki HORIIE** and Shunsuke MURAHASHI

(Received July 3, 1959)

As was reported in Part I of this series, reaction of synthetic gas with Schiff base and with azobenzene principally results in reduction of "C=N" and "N=N" linkage. In the case of azobenzene, however, the principale product aniline was accompanied with a considerable amount of diphenylurea, indicating that azobenzene had reacted in some way with carbon monoxide in the presence of cobalt carbonyl[1]. During the study of the mechanism of diphenylurea-formation, the authors found another new reaction of carbon monoxide, that is, azobenzene gave indazolone and quinazolone by the reaction with carbon monoxide.




The authors wish to report in this paper on the formation of indazolone and quinazolone by the new reaction.

Azobenzene and 100~200 atmospheric pressures of carbon monoxide were heated at 220~230°C in the presence of cobalt carbonyl in aromatic hydrocarbon solvents such as benzene and xylene, resulting in the formation of 3-phenyl-2, 4-dioxo-1, 2, 3, 4-tetrahydroquinazoline (II) (69.2%) (for which, the authors later on will use an abridged expression, quinazolone or quinazolones in general). When the reaction was carried out at the temperature range of 170~190°C, 49.1% of 2-phenylindazolone (I) was obtained.

2-Phenylindazolone thus obtained was reacted again with carbon monoxide according to the condition used for the formation of quinazolone (230°C), yielding a high yield of quinazolone (II) (81.8%). Hence 2-phenylindazolone (I), is considered as an intermediate product in the formation of quinazolone (II) from azobenzene.

Since the formation of 2-phenylindazolone from azobenzene and carbon monoxide was expected from the analogy of formation of phthalimidine from benzaldehydeanil and carbon monoxide, product I was synthesized from another route that is, an azo compound was synthesized by the condensation of anthranilic acid amide and nitrosobenzene, hydrogenated to hydrazo-compound, and then deaminated to 2-phenylindazolone and identified***.

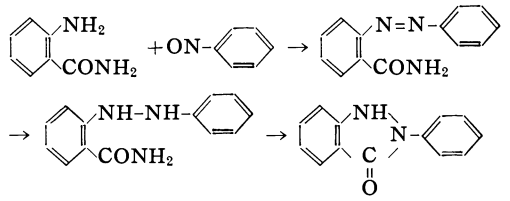
* Reported briefly in a previous communication: S. Murahashi and S. Horiie, *J. Am. Chem. Soc.*, 78, 4416 (1956).

** Present address: Institute of Scientific and Industrial Research, Osaka Univ., Sakai, Osaka.

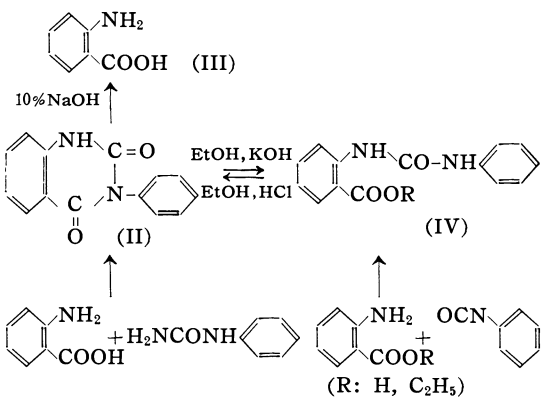
1) S. Murahashi and S. Horiie, *J. Chem. Soc. Japan, Pure Chem. Sec. (Nippon Kagaku Zasshi)*, **79**, 68 (1958).

*** The author synthesized 2-phenylindazolone starting from anthranilic acid amide according to the method of Auwers and Hüttenes[2].

2) K. V. Auwers and K. Hüttenes, *Ber.*, **55**, 2680 (1922).



Identification of 3-phenyl-2, 4-dioxo-1, 2, 3,-4-tetrahydroquinazoline (II) was carried out in the series of reactions which follows: compound II was dissolved in 10% aqueous solution of sodium hydroxie, and was hydrolyzed by boiling the solution for 2~3 hr. to yield anthranilic acid (III) almost quantitatively. Alcoholic potassium hydroxide decomposed compound II to *o*-carboxydiphenylurea (IV), which coincided with the known sample obtained from anthranilic acid and phenylisocyanate. Moreover, compound IV was converted to quinazolone (II) either by fusion of IV or by saturating the alcoholic solution of IV with dry hydrogen chloride.



Compound II was definitely identified as 3-phenyl-2, 4-dioxo-1, 2, 3, 4-tetrahydroquinazoline by comparing with the authentic sample that was synthesized from authranilic acid and phenylurea[3].

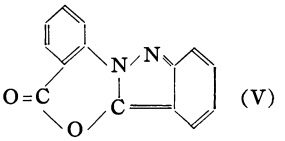
It was found that this new reaction was of value for the synthesis of large varieties of quinazolone derivatives to be elucidated later.

A survey of literatures reveals that the synthetic study of 2-phenylindazolone was meager and the yields were usualy rather low. Although at present our method does not allow high yield of indazolone selectively, being always accompanied with quinazolone and diphenylurea, the method is yet promising for the synthesis of indazolones.

Details of the scope of the reactions with varieties of azobenzene derivatives is described below. Generally, the reaction did not take place in the absence of catalysts. The effective catalysts are iron carbonyl, cobalt carbonyl, or cobalt compound, such as metallic cobalt, cobalt soap, and organic cobalt complex that can be converted into cobalt carbonyl under the reaction condition. Nickel carbonyl did not promote the reaction****. The solvents are preferably aromatic hydrocarbons, such as benzene, toluene, and xylene. The presence of polar substances such as water and alcohol inhibits the reaction[4]. The reaction temperature is preferably in the range of 220~230°C. Below 200°C the proportion of indazolone, which is the intermediate to quinazolone, was pre dominant. Initial charge of carbon monoxide pressure of 100 atmospheric pressures is sufficient for the reaction. As oxygen decomposes the catalyst, it needs to be excluded from the system.

Since quinazolone(III)affords by hydrolysis anthranilic acids in a good yield, the reaction leads to a new and important preparative route of anthranilic acid.

As another by-product in this reaction besides diphenylurea, lactone of 2-(3-hydroxyindazol-2-yl)-benzoic acid (V)[5], and a neutral crystalline substance that has the melting point of 165°C, were obtained. The structure of the latter substance is now under study.



Next, the authors took up the problem of viewing the scope and the extent of this reaction. For this purpose azobenzenes and various kinds of compounds, which seem to be related, were subjected to the reaction. Table II shows the results on the formation of indazolones from substituted azobenzenes RN=NR′, and Table III shows the results of quinazolone-formation. As will be seen from the

3) F. Kunckell, *Ber.*, 43, 1234 (1910).

**** The content of the study was presented at the Meeting of Yūkigōsei-kyokai, November, 1955. In the following year 1956, Prichard and others published a patent (U. S. Pat. 2,769,003), in which they claimed that the reaction of azobenzene with nickel carbonyl yielded mainly lactone of 2-(3-hydroxyindazole-2-yl) benzoic acid being accompanied with small amount of quinazolone and diphenylurea.

4) The effects of various solvents on the reaction will be published in detail in the next paper.

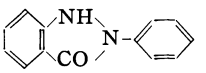
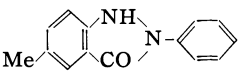
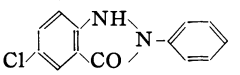
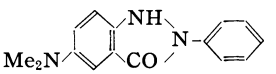
5) The lactone (V) was proved to be identical to the one that was obtained from azobenzene and nickel carbonyl according to the process of Prichard and others.

TABLE I. SYNTHESIS OF QUINAZOLONE*

| Expt. No. | Catalyst | g. | Solvent | Initial atm. | Temp. °C | Time hr. | Quinazolone g. | Quinazolone % | Diphenylurea g. | Diphenylurea % |
|---|---|---|---|---|---|---|---|---|---|---|
| 1 | — | 0 | $C_6H_6$ | 150 | 230 | 3 | 0 | 0 | 0 | 0 |
| 2 | $Ni(CO)_4$ | 3 | $C_6H_6$ | 150 | 230 | 3 | 0 | 0 | 0 | 0 |
| 3 | $Fe(CO)_5$ | 3 | $C_6H_6$ | 180 | 240 | 4 | 0.8 | 12.3 | 0.1 | 1.7 |
| 4 | $[Co(CO)_4]_2$ | 2 | $C_6H_6$ | 150 | 230 | 0.5 | 4.5 | 69.2 | 0.7 | 12.1 |
| 5 | $Co(II)(C_{18}H_{35}O_2)_2$** | 2 | $C_6H_6$ | 160 | 230 | 2.5 | 1.9 | 29.2 | 1.4 | 24.2 |
| 6 | $Co(II)(C_5H_7O_2)_2$*** | 1 | $C_6H_6$ | 150 | 240 | 2 | 1.5 | 23.1 | 0.8 | 13.8 |
| 7 | $[Co(CO)_4]_2$ | 1 | $C_2H_5OH$ | 150 | 230 | 3 | 0 | 0 | 0 | 0 |
| 8 | $[Co(CO)_4]_2$ | 1 | $H_2O$ | 160 | 230 | 3 | 0 | 0 | 0 | 0 |
| 9 | $[Co(CO)_4]_2$ | 1 | $C_6H_6$ | 150 | 190**** | 4 | 0.8 | 17.5 | 0.65 | 16.0 |
| 10 | $[Co(CO)_4]_2$ | 1 | $C_6H_6$ | 100 | 230 | 3 | 3.0 | 46.1 | 0.5 | 8.6 |

* Azobenzene, 5 g., Solvent, 50 ml., 18:8 Stainless autoclave of 100 ml. capacity.
** Co(II)-stearate.
*** Co(II)-acetylacetonate.
**** The main product was 2-phenylindazolone (2.8 g., 49.1%).

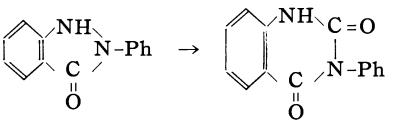
TABLE II. FORMATION OF INDAZOLONES FROM AZO-COMPOUND AND CO.

| R-N=N-R' R | R' | Indazolones | Yield g. | Yield % | m. p. °C |
|---|---|---|---|---|---|
|  |  |  | 2.8 | 49.1 | 204 |
| Me-  | |  | 1.2 | 35.2 | 252 |
| Cl-  | |  | 1.3 | 23.8 | 233 |
| $NMe_2$-  | |  | 4.5 | 80.0 | 217 |

Azo-compound, 5 g.; $[Co(CO)_4]_2$, 0.05 m mol/cc.; CO 150 atm.; solvent, benzene; reaction temperature, 180~190°C; reaction time, 2 hr.; reaction vessel, a 100 ml. rocking autoclave made of 18:8 stainless steel.

tables, the reaction can be applied to various derivatives of azobenzenes. It is interesting to note here that when one of the benzene ring has a substituent of electron-repelling character, the ring closure always occurs on the side of the nucleous having the substituent and where the substituent is electron-attracting the reaction does not take place. This fact suggests strongly that electronegativity of the nitrogen atom, which seems to be the site for the primary act of catalyst, is deeply influenced by these substituents.

The formation of 3-phenyl-2, 4-dioxo-1, 2-3, 4-tetrahydroquinazoline from indazolone is a new reaction, where a five membered ring was enlarged to a six-membered ring under the incorporation of a carbon monoxide molecule. This reaction appears to be formally quite similar to the formation of diphenylurea from hydrazobenzene.

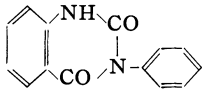
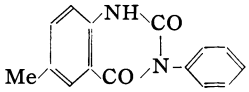
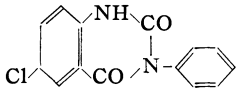
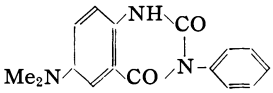
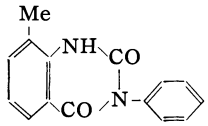
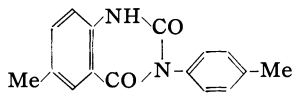
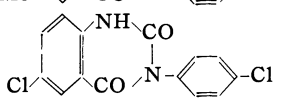
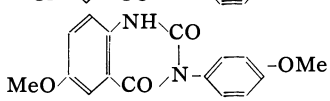
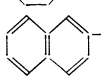
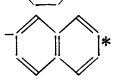


To obtain a further information of the reaction the authors studied several ring compounds with a 5-membered ring under the same condition described as above. Indazol[6], indazolone[6], 2-phenyl-benzoxazol[7] and 2-phenyl-benzimidazole[8] were tested for this purpose. But none of them was found to be feasible for the ring enlargement.

A pyridine and a quinoline derivative, VI and VII[9], which are closely related to

6) E. F. M. Stephenson, "Organic Syntheses", Vol. 29, John Wiley & Sons, Inc., New York (1949), p. 54.
7) L. C. Galatis, *J. Am. Chem. Soc.*, **70**, 1967 (1948).
8) D. Jerchel et al., *Ann.* **575**, 162 (1952).
9) H. K. S. Raw and T. S. Wheeler., *J. Chem. Soc.*, **1938**, 478; P. Ruggli et al., *Helv. Chim. Acta*, 27, 649 (1944).

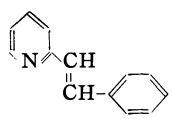
TABLE III. FORMATION OF QUINAZOLONES FROM AZO-COMPOUNDS AND CO.

| R'-N=N-R | | Quinazolone | Yield | | m. p. °C |
|---|---|---|---|---|---|
| R' | R | | g. | % | |
|  | |  | 4.2 | 64.6 | 275 |
| Me-  | |  | 2.3 | 35.9 | 296 |
| Cl-  | |  | 2.7 | 42.8 | 292 |
| |  | | | | |
| $NMe_2$-  | |  | 1.1 | 18.0 | 231 |
| Me  | |  | 1.7 | 26.4 | 256 |
| CN-  | | ? | trace | — | — |
| Me-  |  -Me |  | 2.5 | 40.0 | 285 |
| Cl-  |  -Cl |  | 1.0 | 16.7 | 325 |
| OMe-  |  -OMe |  | 1.6 | 27.7 | 279 |
|  |  * | — | — | — | — |
|  |  * | — | — | — | — |

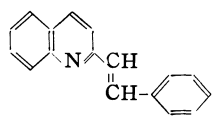
Azo-compound, 5 g.; $[Co(CO)_4]_2$, 0.05 m mol./cc.; CO, 150 atm.; solvent, benzene; reaction temperature, 220~230°C; reaction time, 3 hr.; reaction vessel, a 100 ml. rocking autoclave made of 18:8 stainless steel.

* A small amount of dinaphthylurea was formed.

benzaldehydeanils were studied also under the similar condition.



(VI)



(VII)

In both cases, reactions took place with an uptake of carbon monoxide, but the reaction products thus obtained were colored deep violet-red and unstable solid and could not be crystallized into definite products.

In all cases quinazolone derivatives obtained gave, in good yield, anthranilic acid derivatives. (see *Experimental*)

### On the By-product of the Reaction

As an example shows the following reaction products were obtained by the reaction where benzene was used as the reaction medium.

| | |
|---|---|
| Quinazolone | 64.1% |
| Diphenylurea | 17.2% |
| Lactone | 3.1% |
| Neutral substance | a small quanity |
| Aniline | 〃 |

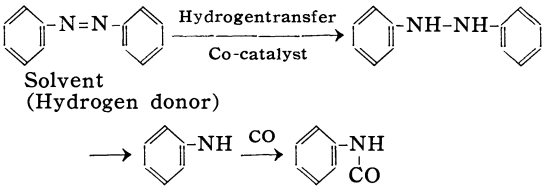
The formation of diphenylurea is significant, and so it would be necessary to learn the cause of its formation and to minimize its formation so as to obtain a complete information on the reaction and to improve the yield of quinazolone. From the result of the experiments it was shown that the formation of diphenylurea could not be observed in the decomposition reaction of quinazolone, and so was the quinazolone formation from diphenylurea and carbon monoxide. Hence it may be concluded that these two reaction products originate from different reaction courses.

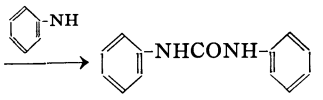
In order to account for the formation of diphenylurea from azobenzene, it is necessary for azobenzene to get one mole of hydrogen from somewhere, since the reactions are carried out with carbon monoxide alone in an anhydrous condition, none of the hydrogen atoms were available except from solvent molecules.

According to the gaschromatographic analysis of carbon monoxide used, the hydrogen in the gas was found to be 0.1% or less, and this quantity was proved to be too low to balance the urea-formation. Therefore, it was considered that solvent molecules are responsible for hydrogen supply. As an approach to this question various solvents were tested, including cyclohexane, *n*-hexane, dioxane, ether, acetonitrile, ethylalcohol, benzene, and naphthalene. Among these, cyclohexane found to produce diphenylurea in much abundance as campared to benzene and the same is also held in a comparison of *n*-hexane and benzene.

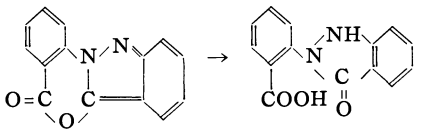
In both of the cases the quantity of urea and also the proportion of urea to quinazolone were increased. These seem to show that the solvent had contributed to the formation of urea by giving up its hydrogen necessary for the formation of urea.

As was described earlier in Part I of this series, the formation of urea was easier by hydrazobenzene than by azobenzene. From this and other facts in early parts of this paper, the authors tentatively propose the possible formation of urea derivatives as to proceed according to the following scheme:




The presence of this lactone [2-(3-hydrooxyindazol-2-yl) benzoic acid lactone] was easily confirmed through its hydrolysis and fomation of 2-(*o*-carboxyphenyl) indazolone. Prichard[10] obtained it by the reaction of azobenzene and carbon monoxide in the presence of nickel carbonyl catalyst and the authors' product was proved to be identical with this.




As was previously stated, the formation of quinazolone is strongly favored in the presence of cobalt catalyst in benzene solution, and the reaction proceeded via indazolone derivative as the intermediate. The same reaction failed when nickel carbonyl was used in a benzene solution.

Prichard has disclosed in his patent that he could observe the formation of this lactone as the main product and of small amount of quinazolone as a by-product, when nickel carbonyl was used as the catalyst in a cyclohexane solution. But, he did not observe anything about the intermediate formation of indazolone.

From the differences of reaction conditions including solvent and of the products which were formed, in quantity as well as in quality, it might be appropriate to conclude that the approach to quinazolone in the authors' experiments was not the same as that of Prichard.

It is well known that cobalt carbonyl is readily convertible to hydrocarbonyl, and so the very nature would be responsible for a hydrogen-transfer reaction. On the other hand, it is not known that nickel carbonyl possesses such a behavior of easy conversion to hydrocarbonyl and such a difference of the property between these two catalysts would be the main cause of differences observed in the authors' and Prichard's results. The authors will consider in detail this point later.

## Experimental

**1) Synthesis of 2-Phenylindazolone by the Reaction of Azobenzene with Carbon Monoxide.** —A solution of azobenzene (5 g.) and cobalt

10) W. W. Prichard, U. S. Pat., 2,769,003 (1956).

carbonyl (1 g.) in benzene (25 ml.) was placed in an autoclave of 100 ml. capacity made of 18:8 stainless steel, and carbon monoxide was charged in up to 150 atmospheric pressures. The autoclave was heated at 180~190°C for 4 hr. under constant shaking. After being cooled, a crystalline substance in the reaction mixture was filtered (3.0 g.). From the filtrate, after removal of catalyst by refluxing on a water bath followed by filtration and removal of benzene, 1.5 g. of azobenzene was recovered. The crystalline substance was treated with 5% aqueous solution of sodium hydroxide, and filtered. The insoluble crystals were to be mainly of diphenylurea (0.65 g., 16%) containing, as contamination, some amount of yellow crystals, which were found to be lactone of 2-(3-hydroxyindazol-2-yl) benzoic acid, m. p. 296°C. Diphenylurea was recrystallized from alcohol (m. p. 240°C) and identified by the mixed melting point test with the sample prepared by an alternative way. The alkaline solution was acidified by either carbon dioxide, hydrochloric acid, or sulfuric acid, and a white crystalline substance separated. The crystalline substance, after filtration, was recrystallized from alcohol, yielding 0.8 g. of quinazolone (17.5%) as the insoluble part and 2.8 g. of 2-phenylindazolone (49.1%) as the soluble part. The latter were colorless needles, m. p. 204°C, and identified by the mixed melting point test with the sample synthesized as described below.

*Anal.* Found: C, 74.03; H, 4.82; N, 13.55. Calcd. for $C_{13}H_{10}N_2O$: C, 74.28; H, 4.76; N, 13.33%.

**2) Synthesis of 2-Phenylindazolone.**—Anthranilic acid was converted to isatoic anhydride[11], which was then treated with 20% aqueous ammonia, and converted to anthranilic acid amide[12] and was used as the starting material of this synthesis. Into a solution of anthranilic acid amide (8.0 g.) in 100 ml. of acetic anhydride, freshly distilled nitrosobenzene[13] (6.2 g.) was added in small portions. The mixture, after being kept at room temperature overnight, was diluted with equal volume of alcohol, and refluxed. Under vigorous stirring zinc powder (20 g.) was added portionwise. The red color of the solution faded out completely after about 1.5 hr. The solution was filtered and poured into a large quantity of water. The separated crystals were filtered off, and recrystallized from alcohol to yield pure 2-phenylindazolone (3.0 g.), m. p. 202~204°C.

**3) Synthesis of 3-Phenyl-2,4-dioxo-1,2,3,4-tetrahydroquinazoline by the Reaction of 2-Phenylindazolone with Carbon Monoxide.**—A mixture of 2-phenylindazolone (2 g.), cobalt carbonyl (1.0 g.) and benzene (50 ml.) was caused to react with 150 atmospheric pressures of carbon monoxide at 230°C for 2 hr. The crude crystals, that were obtained by filtering the reaction mixture after cooling, was recrystallized from alcohol to yield 1.8 g. of pure II (81.8%). Identification was carried out by the melting point test with a known sample.

*Anal.* Found: C, 70.29; H, 4.12; N, 11.66. Calcd. for $C_{14}H_{10}N_2O_2$: C, 70.58; H, 4.20; N, 11.76%.

**4) Synthesis of 3-Phenyl-2,4-dioxo-1,2,3,4-tetrahydroquinazoline by the Reaction of Azobenzene with Carbon Monoxide.**—(i) A mixture of azobenzene (5.0 g.), cobalt carbonyl (2.0 g.) and benzene (45 ml.) was reacted with 150 atomspheric pressures of carbon monoxide at 220~230°C for 0.5 hr. After cooling, a crystalline mass (5.2 g.) in the reaction mixture was filtered off. The filtrate was refluxed on a water bath to effect the decomposition of the catalyst, and removed from inorganic substance by filtration. Yellow crystals, lactone of 2-(3-hydroxyindazol-2-yl) benzoic acid (0.1 g.) was obtained as a comparatively soluble part in benzene. The crystalline mass obtained above was treated with cold 5% aqueous solution of sodium hydroxide[14]. As the insoluble residue, diphenylurea (0.7 g., 12.1%) was obtained, and white crystals precipitated from the alkaline solution by acidifying (pH 4.0) with either carbon dioxide, hydrochloric acid, or sulfuric acid. The crystal was recrystalized from alcohol in colorless needles, m. p. 275°C, which was identified as 3-phenyl-2,4-dioxo-1,2,3,4-tetrahydroquinazoline by the mixed melting point test with the authentic sample.

*Anal.* Found: C, 70.63; H, 4.18; N, 11.90. Calcd. for $C_{14}H_{10}N_2O_2$: C, 70.58; H, 4.20; N, 11.76%.

(ii) A mixture of azobenzene (5.0 g.), iron carbonyl (3.0 g.) and benzene (50 ml.) was heated with 180 atmospheric pressures of carbon monoxide at 240°C for 4 hr. to yield 3-phenyl-2,4-dioxo-1,2,3,4-tetrahydroquinazoline (0.8 g., 12.3%).

(iii) A mixture of azobenzene (5.0 g.), acetylacetone cobalt complex (1.0 g.), and benzene (50 ml.) was heated with 150 atmospheric pressures of carbon monoxide at 240°C for 5 hr. to yield 3-phenyl-2,4-dioxo-1,2,3,4-tetrahydroquinazoline (1.9 g., 29.2%).

(iv) A mixture of azobenzene (5.0 g.), cobalt stearate (2.0 g.) and benzene (50 ml.) was reacted with 160 atmospheric pressures of carbon monoxide at 230°C for 2.5 hr. to yield 1.9 g. of 3-phenyl-2,4-dioxo-1,2,3,4-tetrahydroquinazoline (29.2%).

**5) Hydrolysis of 3-Phenyl-2,4-dioxo-1,2,3,4-tetrahydroquinazoline by Sodium (or Potassium) Hydroxide.**—A solution of quinazolone (2.0 g.) in 10 ml. of 10% sodium (or potassium) hydroxide was refluxed. After 20 min. an oil began to separate, and the mixture was kept boiling for 2.5 hr. After cooling, aniline was removed by extraction with a small amount of ether. The aqueous solution was neutralized to pH 4.0 by diluted hydrochloric acid, and then a white solid precipitate was formed, which was filtered off, washed with water, and dried to yield 0.95 g. of gray crystalline anthranilic acid, m. p. 140°C (86.4%). Identification of the anthranilic was

11) E.C. Wagner and M.F. Fegley, "Organic Syntheses", Vol. 27, John Wiley & Sons, Inc., New York (1947), p. 45.
12) Kolbe, *J. prakt. Chem.*, [2] **30**, 475 (1884).
13) G. H. Coleman, C. M. McCloskey and F. A. Stuart, "Organic Syntheses" Vol. 25, John Wiley & Sons, Inc., New York (1945), p. 80.
14) Upon being warmed. quinazolne might be hydrolyzed to anthrailic acid.

carried out by the mixed melting point test with a known sample.

The filtrate gave by the addition of copper acetate 0.2 g. of copper anthranilate, which corresponds to 0.16 g. of anthranilic acid (10.1%).

**6) Hydrolysis of 3-Phenyl-2, 4-dioxo-1, 2, 3, 4-tetrahydroquinazoline by Alcoholic Potassium Hydroxide.**—A solution of quinazolone (2 g.), potassium hydroxide (8 g.) and 96% alcohol (40 ml.) was refluxed for 20 hr. After removal of alcohol, the residue was dissolved in water and acidified by concentrated hydrochloric acid, when a white solid precipitated. The solid was recrystallized from alcohol yielding as the insoluble part the recovered quinazolone (0.4 g.) and as the soluble part colorless needles, *o*-carboxydiphenylurea (0.8 g., 46.5%). The latter compound was identified by the mixed melting point test with a known sample prepared in the following manner.

*Anal.* Found: C, 65.28; H, 4.70; N, 10.86. Calcd. for $C_{14}H_{12}N_2O_3$: C, 65.62; H, 4.68; N, 10.93%.

**7) Synthesis of *o*-Carboxydiphenylurea.** — A solution of anthranilic acid (2 g.) in dry ether (10 ml.) and a solution of phenylisocyanate (1.8 g.) in dry ether (10 ml.) were combined under ice-cooling and stood at room temperature overnight. Crystals were filtered off and recrystallized from alcohol in colorless needles, *o*-carboxydiphenylurea (3.4 g., 90%), m. p. 187~188°C.

*Anal.* Found: C, 65.60; H, 4.72; N, 10.81. Calcd. for $C_{14}H_{12}N_2O_3$: C, 65.62; H, 4.68; N, 10.93%.

**8) Synthesis of *o*-Carboethoxydiphenylurea.**—Ethyl anthranilate (2 g.) was added gradually into phenylisocyanate (1.5 g.). The reaction was vigorously exothermic. The mixture was heated on a boiling water bath for about 0.5 hr. and the solid thus formed was recrystallized from alcohol in colorless needles, *o*-carboethoxydiphenylurea (3.3 g., 94.3%), m. p. 148°C.

*Anal.* Found: C, 67.30; H, 5.31; N, 10.15. Calcd. for $C_{16}H_{16}O_2N_3$: C, 67.60; H, 5.63; N, 9.86%.

**9) Synthesis of 3-Phenyl-2,4-dioxo-1,2,3,4-tetrahydroquinazoline (II).**—(i) *o*-Carboxydiphenylurea (1.0 g.) was heated for 30 min. at 190°C which is slightly above its melting point. The reaction mass was recrystallized from alcohol in colorless needles, II (0.05 g.), m. p. 273~275°.

(ii) When dry hydrogen chloride was introduced into a solution of *o*-carboxydiphenylurea (1.0 g.) in alcohol (30 ml.) at room temperature (20°C), the temperature of the content rose up to 30~40°C. Introduction of hydrogen chloride was continued for a while and the mixture was kept standing, and then colorless scaly crystals were formed. The crystals, after removal of alcohol and hydrogen chloride, were recrystallized from alcohol into colorless needles (0.9 g., 96.8%), m. p. 274~275°C.

(iii) *o*-Carboethoxydiphenylurea (0.2 g.) was heated at 200°C for 3 hr. in a sealed glass tube. After cooling, the reaction product was solidified at the bottom of the tube and the unreacted starting material was sublimed off on the upper wall of the tube. The product was recrystallized from alcohol into colorless needles (0.03 g., 18.1%), m. p. 273°C.

(iv) A mixture of anthranilic acid (5.0 g.) and phenylurea (5.0 g.) was heated at 200°C for 5 hr. in a sealed glass tube. The reaction product was treated with 100 ml. of 5% sodium hydroxide to remove the insoluble phenylurea. The alkaline solution was acidified by diluted hydrochloric acid, precipitating white crystalline acidic substance which was recrystallized from alcohol into colorless needles (2.5 g., 28.6%), m. p. 274°C.

TABLE IV. FORMATION OF ANTHRANILIC ACIDS FROM QUINAZOLONES

| R | R' | g. | R | Yield g. | Yield % | m. p. °C |
|---|---|---|---|---|---|---|
| H | H | 2.2 | H | 1.1 | 95.6 | 145 |
| Me | H | 2.0 | Me | 1.05 | 88.1 | 172 |
| Cl | H | 2.0 | Cl | 1.0 | 80.0 | 205 |
| MeO | H | 2.0 | MeO | 0.27 | 21.8 | 178 |
| Me | Me | 2.0 | Me | 1.1 | 97.3 | 172 |
| Cl | Cl | 2.0 | Cl | 1.05 | 94.5 | 205 |
| MeO | MeO | 2.0 | MeO | 0.35 | 28.2 | 178 |

**10) Reaction of α-Styrylpyridine and Carbon Monoxide.**—A solution of 3 g. of α-styrylpyridine and 1 g. of dicobalt octacarbonyl in 20 ml. of benzene was heated at 135~145°C under 130 atmospheric pressures of carbon monoxide for one hour to give 1 g. of amorphous product. This product was extracted with dimethylformamide and a reddish purple-colored amorphous substance melted at 200~250°C was obtained.

*Anal.* Found: C, 68.03; H, 5.24; N, 6.59; ash, 11.43%.

A similar experiment with α-styrylquinoline has failed to obtain any definite crystalline product, but resins.

**11) Effect of Solvents.**—For the purification of both naphthalene and *p*-dichlorobenzene, they were recrystallized from ethyl alcohol, and the crystals melting at 80 and 53°C respectively were collected.

Carbon tetrachloride and *n*-butylacetate were carefully fractionated and the fractions boiling at 76 and 126°C respectively were collected. Other solvents such as *n*-hexane, cyclohexane, benzene, toluene, tetraline, dioxane, ether, tetrahydrofuran, chlorobenzene, acetonitrile and ethylalcohol are, after drying over metallic sodium, fractionated. The fractions boiling at 69, 81, 80, 110, 207, 102, 34, 64, 122, 81 and 78°C respectively were collected.

**12) Reaction of Hydrazobenzene and Carbon Monoxide.**—A solution of 2 g. of hydrazobenzene and 1 g. of dicobalt octacarbonyl in 30 ml. of benzene was heated at 220~230°C under 120 atmospheric pressures of carbon monoxide for 4 hr. to give 0.95 g. of diphenylurea (41.3% yield) and 0.2 g. of 3-phenyl-2, 4-dioxo-1, 2, 3, 4-tetrahydroquinazoline (7.7% yield).

*Department of Chemistry*
*Faculty of Science*
*Osaka University*
*Nakanoshima, Osaka*

# *Synthetic and Analytical Studies on Color Reagents. VIII. o-Halogeno-o'-hydroxyazo Compounds*

By Tadashi IWACHIDO*, Haruo MIYATA and Kyoji TOEI

(Received July 3, 1959)

In the previous papers[1-5], a series of *o*-substituted-*o'*-hydroxyazo compounds, having various groups in ortho position were synthetized and their identification limits for various metal ions were determined, and thus the usefulness of these reagents for metal indicators and colorimetric reagents was discussed.

The present paper describes the preparation of *o*-halogeno-*o'*-hydroxyazo compounds and their identification limits for calcium, magnesium and thorium. Especially absorption spectra of *o*-halogenophenylazo-chromotropic acids and their magnesium complexes are determined, and the relation between the absorption spectra and their structures is discussed.

## Experimental

**Syntheses of Reagents.**—*o*-Iodoaniline was prepared by the method of Baeyer[6]. *o*-Iodonitrobenzene was prepared from diazotized *o*-nitroaniline with iodine-potassium iodide solution, and then it was converted into *o*-iodoaniline by the reduction with stannous chloride and purified by the steam distillation. White needles, m. p. 59.5~60°C.

*o*-Bromoaniline[7] was obtained by the reduction of *o*-bromonitrobenzene which was prepared by Sandmeyer's reaction of diazotized *o*-nitroaniline, m. p. 33°C.

*o*-Chloroaniline and aniline were reagent grade products and *o*-fluoroaniline was kindly supplied from Dr. K. Inukai**.

Aniline and *o*-halogenoanilines were dissolved in 6 N hydrochloric solution respectively, cooled in ice, diazotized with an equivalent weight of sodium nitrite, and filtered off when necessary. Coupling reaction had to be carried out immediately. The stability of these diazonium salt solutions seems to decrease in the order of *o*-fluoro-, chloro-, bromo- and iodoaniline.

β-Naphthol, 2-hydroxy-3-naphthoic acid, Scheffer's acid and R-acid were dissolved in about 1 N sodium hydroxide solution, N-W-acid and chromotropic acid in a solution of sodium acetate and G-acid in concentrated aqueous ammonia. These solutions were separated from any insoluble matter by filtration, and then cooled below 5°C. Coupling reaction was carried out by adding the diazonium salt solution into the cooled naphthol or naphtholsulfonic acid solution and the azo compound thus obtained was recrystallized from acetic acid or dilute hydrochloric acid.

**Identification Limits.** — Identification limits for calcium, magnesium and thorium were determined by the method of the previous paper[1]. The reagents coupled with β-naphthol or G-acid indicate no color change with concentrations of 50 γ/ml. magnesium, calcium and thorium, whilst those with Scheffer's acid or N-W-acid change a little or not at all. The identification limits of the reagents coupled with R-acid, 2-hydroxy-3-naphthoic acid and chromotropic acid are relatively low. R-acid reagents do not indicate any color change for 50 γ/ml. thorium, but the identification limits for calcium and magnesium are 5~50 γ/ml. Reagents prepared from 2-hydroxy-3-naphthoic acid for magnesium, calcium and thorium have a limit of 0.1~25 γ/ml. and those from chromotropic acid 0.1~10 γ/ml.

Identification limits of one series of these reagents increase with the atomic weight of the halogen atom at the ortho position. But the values for magnesium and calcium are far greater than those of *o,o'*-dihydroxyazo compounds[1], and are almost the same as those of *o*-trifluoromethyl- or *o*-methyl-*o'*-hydroxyazo[4] and *o*-sulfo-*o'*-hydroxyazo compounds[3]; for thorium they are larger than those of *o*-arsono-*o'*-hydroxyazo compounds[5].

**Absorption Spectra of *o*-Halogenophenylazo-chromotropic Acids and their Magnesium Complexes.** — *Reagent solution.* — The reagents being very hygroscopic, they were dried at 110°C in weighing bottles, cooled in phosphorus pentoxide desiccator, and weighed. A $2.5\times10^{-4}$ mol./l. solution was prepared and stored in the dark.

A 0.25 M magnesium sulfate solution was made from recrystallized $MgSO_4\cdot7H_2O$.

*Procedure and apparatus.*—A series of the reagents and their magnesium complex solutions of varying pH were prepared in the following manner. All solutions were made in a dark room, for the absorption of reagents was retarded by the daylight, especially at a higher pH.

* Present address: The Electrical Communication Laboratory, Musashino-shi, Tokyo.

1) K. Emi, K. Toei and H. Miyata, *J. Chem. Soc. Japan, Pure Chem. Sec.* (*Nippon Kagaku Zasshi*), **78**, 736 (1957).
2) K. Emi, K. Toei and N. Takemoto, ibid., **78**, 741 (1957).
3) K. Emi, K. Toei and H. Miyata, ibid., **78**, 977 (1957).
4) K. Emi, K. Toei and H. Miyata, ibid., **78**, 979 (1957).
5) K. Emi, K. Toei and K. Furukawa, ibid., **79**, 681 (1958).
6) A. Baeyer, *Ber.*, **38**, 2760 (1905).
7) F. Ullman, ibid., **29**, 1880 (1896).

** Government Industrial Research Institute, Nagoya.

Five milliliters of the reagent solution was placed in a 50 ml. volumetric flask, followed by addition of an adequate volume of 1 N hydrochloric acid, 1 M aqueous ammonia, 1 M ammonium chloride or 0.1 N sodium hydroxide to adjust the pH to the desired value and then the volume was made up to 50 ml. with water.

Magnesium complex solutions were similarly prepared with 5 ml. of 0.25 M magnesium sulfate solution. Above pH 11, magnesium hydroxide

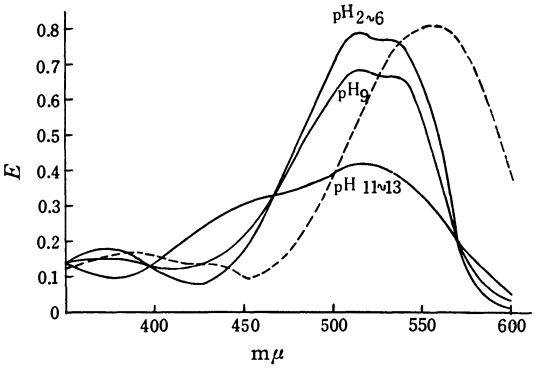



Fig. 1. Absorption curves of phenylazo-chromotropic acid and its magnesium complex (broken line).

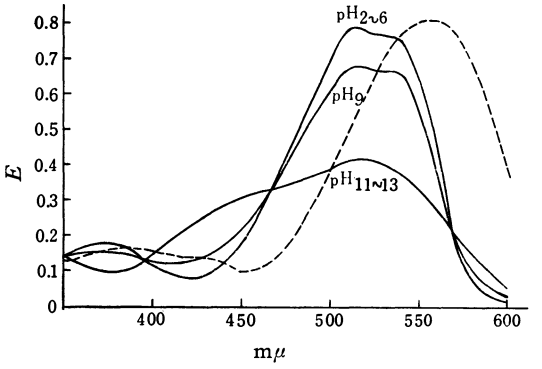



Fig. 2. Absorption curves of *o*-fluorophenylazo-chromotropic acid and its magnesium complex (broken line).

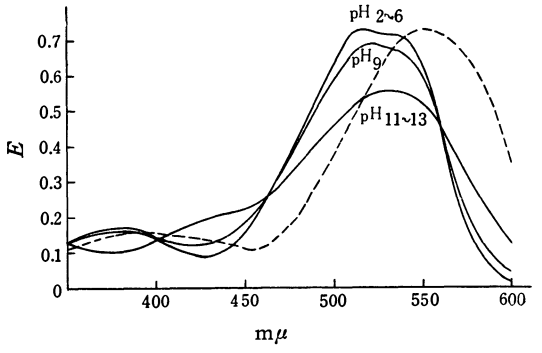



Fig. 3. Absorption curves of *o*-chlorophenylazo-chromotropic acid and its magnesium complex (broken line).

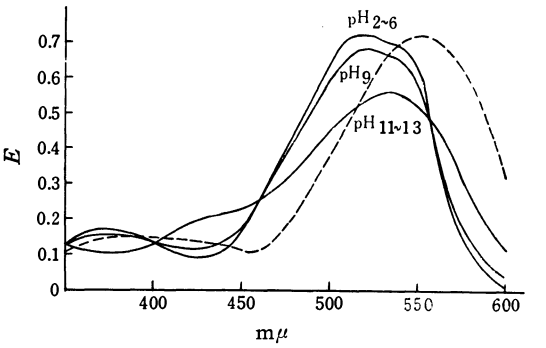



Fig. 4. Absorption curves of *o*-bromophenylazo-chromotropic acid and its magnesium complex (broken line).

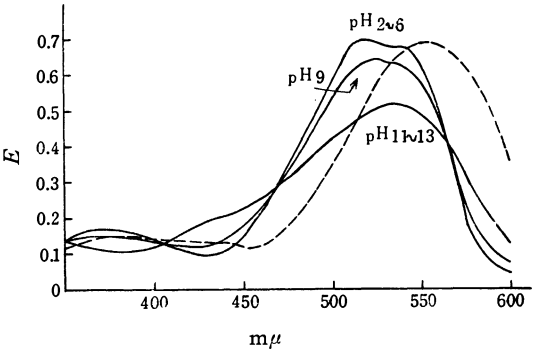



Fig. 5. Absorption curves of *o*-iodophenylazo-chromotropic acid and its magnesium complex (broken line).

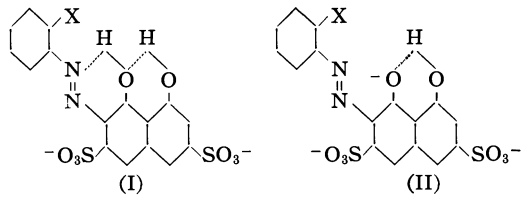
was formed, so the determination could not be made. The pH was measured with Shimadzu Glass Electrode Model GU-1 pH meter and the absorbancy with Shimadzu Spectrophotometer QR-50 type, with 1 cm. cells. Absorption spectra over various pH values are shown in Figs. 1—5.

## Results and Discussion

**Spectral Properties of the Reagents.**—Between pH 2 and 6, the same reagent gives the identical absorption spectra having two absorption maxima at 510~520 and 530~540 mμ (Fig. 1—5). It is considered that electrolytic dissociation of naphtholic OH does not occur. Above pH 7, these maxima shift to form one maximum (at pH≧12) with increasing pH.

From the presence of an isosbestic point in each figure, two structures are expected, and from the electrolytic dissociation of chromotropic acid[8,9] the following structures are presented.

8) H. Zollinger and W. Büchler, *Helv. Chim. Acta*, **34**, 591 (1951).
9) J. Heller and G. Schwarzenbach, ibid., **34**, 1876 (1951).




X=H, F, Cl, Br and I.

Formula I corresponds to the acidic form and II exists at pH more than 12. Azo grouping seems to be *trans*-form. Structure I has two hydrogen bridges; the one between *peri*-oxygen atoms is too strong to dissociate even at pH 12, but the other begins to dissociate at pH 7~8 and completely dissociates at pH 12 to give II. Formula I has a higher co-planarity than formula II.

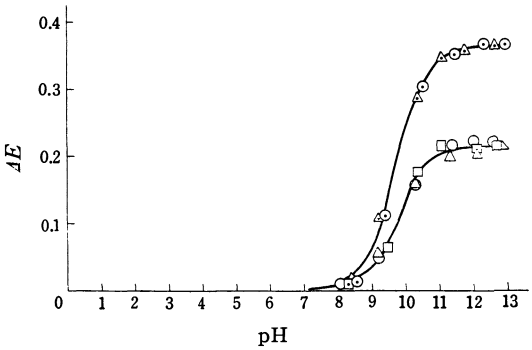



Fig. 6. Relationship between pH and absorption differences at 510 mμ.
⊙, *o*-H-compound; △, *o*-F-compound;
○, *o*-Cl-compound; △, *o*-Br-compound;
□, *o*-I-compound.

Absorption differences at 510 mμ are plotted against pH (Fig. 6). There are two series; the one consists of *o*-hydrogen and *o*-fluoro-compounds, and the other *o*-chloro, *o*-bromo and *o*-iodocompounds. The difference seems to spring from steric hindrance. Namely, in formula II, *o*-halogenophenyl group and chromotropic acid can rotate around each single bond of N-C axis, and hydrogen and fluorine atoms at ortho position are not hindered, but chlorine, bromine and iodine atoms are hindered by the sulfonic group of chromotropic acid according to Stuwart model.

**Spectral Properties of Magnesium Complexes.** —Absorption curves of the mixtures of the reagent and the magnesium solutions are the same as those of the reagent over pH 2~6. This indicates that magnesium complexes can not be formed in an acid medium. Absorption maxima of magnesium complexes at a higher pH are shifted to longer wavelength and to higher absorbancy with increasing amount of magnesium, and thus 1000 times magnesium

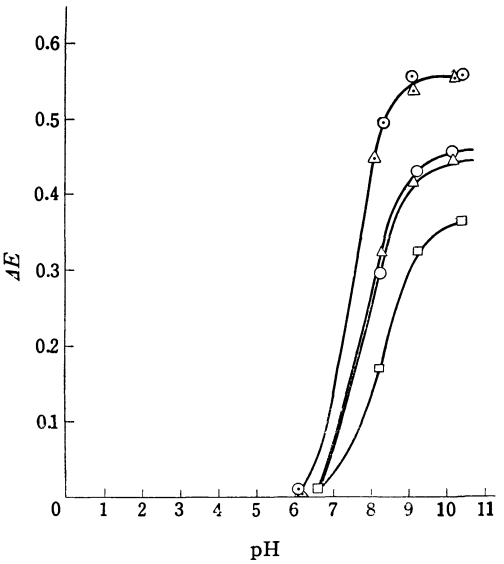



Fig. 7. Relationship between pH and absorption differences at 570 mμ.
⊙, *o*-H-complex; △, *o*-F-complex;
○, *o*-Cl-complex; △, *o*-Br-complex;
□, *o*-I-complex.

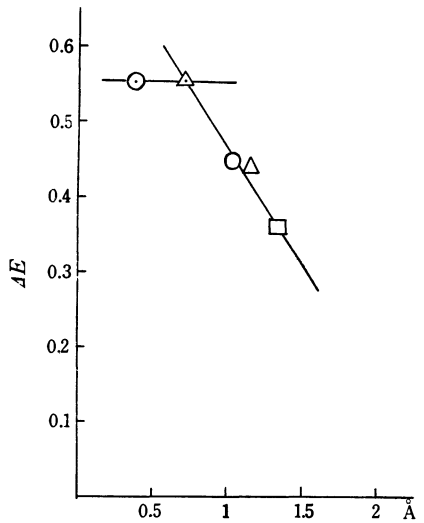



Fig. 8. Relationship between covalent radii of halogen atoms and absorption differences of magnesium complexes at 570 mμ.
⊙, *o*-H-complex; △, *o*-F-complex;
○, *o*-Cl-complex; △, *o*-Br-complex;
□, *o*-I-complex.

was used for the measurement (broken lines in Figs. 1—5).

Absorption differences at 570 mμ are plotted against pH (Fig. 7) and against covalent radii of halogen atoms[10,11](Fig. 8). Absorption differences of *o*-hydrogen and *o*-fluoro-complexes are the same, and the others decrease with the atomic weight of halogen atoms. This also means the presence of steric hindrance.

The authors wish to express their thanks to Professor M. Ishibashi and Professor K. Emi for their encouragement. Also the authors express hearty thanks to Dr. K. Inukai who kindly supplied *o*-fluoroaniline.

*Department of Chemistry*
*Faculty of Science*
*Okayama University*
*Tsushima, Okayama*

10) L. Pauling, "Nature of the Chemical Bond", Cornell Univ. Press, Ithaca, N. Y. (1940), p. 164.
11) V. Schomaker and D. P. Stevenson, *J. Am. Chem. Soc.*, **63**, 37 (1941).

# *Spectrochemical Study of Microscopic Crystals. XX*[1]*. The Dichroism of Tris(ethylenediamine)-cobalt(III) and -chromium(III)*[2]

By Shoichiro YAMADA and Ryutaro TSUCHIDA

(Received July 21, 1959)

Knowledge about the electronic state of metallic complexes is important in understanding theoretically their optical activity, which is quite well-known in the history of the chemistry of coordination compounds. Since the dichroism is closely related to the electronic state of the metallic compounds, the experimental determination of the dichroism with tris-(ethylenediamine)-cobalt(III) and -chromium(III) ions is thought to be useful for elucidating the optical rotatory dispersion as well as the electronic state of the metallic coordination compounds.

In this work, the authors have determined the dichroism with tris(ethylenediamine)-cobalt(III) and -chromium(III) halides in the crystalline state and discussed about the results of the measurements in relation to the above problems.

## Experimental

**Materials.**—Crystals of *d,l*-$[Co\,en_3]Cl_3\cdot 3H_2O$ and *d,l*-$[Co\,en_3]Br_3\cdot 3H_2O$ were prepared according to the method of Grossman and Schück[3]. The hexagonal, prismatic crystals of the compound usually show the well-developed $(10\bar{1}0)$-plane[4]. The crystals show a discernible dichroism on the prism face; they are orange yellow with polarized light having its electric vector along the *c*-axis, and pale yellow with the electric vector perpendicular to the *c*-axis. The dichroism measurements were made on the well-developed prism face.

The optically active *d*-$[Co\,en_3]Br_3\cdot 2H_2O$ was prepared by resolution of the racemic *d,l*-$[Co\,en_3]\cdot Cl_3\cdot 3H_2O$ according to the method of Werner[5]. A slight but definite dichroism was observed under the microscope on the prism face (101), on which the dichroism measurement was carried out.

The racemic *d,l*-$[Cr\,en_3]Cl_3\cdot 3H_2O$ was prepared in yellow, hexagonal prismatic crystals by the method of Rollinson and Bailar[6]. The crystal of the compound appears to be isomorphous with that of *d,l*-$[Co\,en_3]Cl_3\cdot 3H_2O$. It appears yellow with the polarized light having its electric vector along the *c*-axis, and very pale yellow with the electric vector perpendicular to the *c*-axis. The dichroism measurement was carried out on the well-developed prism face.

**Measurements.**—Quantitative dichroism measurements in the visible and ultraviolet regions have been carried out at room temperature by Tsuchida and Kobayashi's microscopic method[7].

The symbols used in the present paper are the same as those in the former papers of this series. Thus the molar absorption coefficient, *K*, was estimated from the following expression: $K=10M\alpha/\rho$.

1) Presented in part before the 4th Annual Meeting of the Chemical Society of Japan, Tokyo, April, 1951.
2) Part XIX of this series: S. Yamada and R. Tsuchida, This Bulletin, **32**, 721 (1959).
3) H. Grossman and B. Schück, *Ber.*, **39**, 1899 (1906).
4) F. M. Jaeger, *Z. Krist.*, **39**, 551 (1904).
5) A. Werner, *Ber.*, **45**, 121 (1912).
6) L. Rollinson and J. C. Bailar, Jr., *J. Am. Chem. Soc.*, **65**, 250 (1943).

## Results

**Dichroism of the Tris(ethylenediamine)-cobalt-(III) Ion.**—The present dichroism measurements with $d,l$-$[Co\,en_3]Cl_3\cdot 3H_2O$ and $d,l$-$[Co\,en_3]Br_3\cdot 3H_2O$ are shown in Figs. 1 and 2, and Tables I and II. Formerly Kobayashi[7a] reported the absorption spectrum of tris(ethylenediamine)-cobalt(III) bromide trihydrate in the crystalline state using natural light. The absorption maxima determined in the present work agree with those formerly reported by Kobayashi, excepting for the region of the short wavelength. According to the crystal structure analysis[8], the $c$-axis in the crystal of $d,l$-$[Co\,en_3]Cl_3\cdot 3H_2O$ is found to be coincident with the threefold axis of the $[Co\,en_3]^{3+}$ ions. Although the crystal structure analysis of $d,l$-$[Co\,en_3]Br_3\cdot 3H_2O$ is not available at present, the bromide trihydrate presumably has the crystal structure of the same type as that of the chloride trihydrate. The $c$-absorption in Figs. 1 and 2, therefore, represents the $z$-absorption of the complex ion, that is, the absorption with the electric vector along the threefold axis of the complex ion.

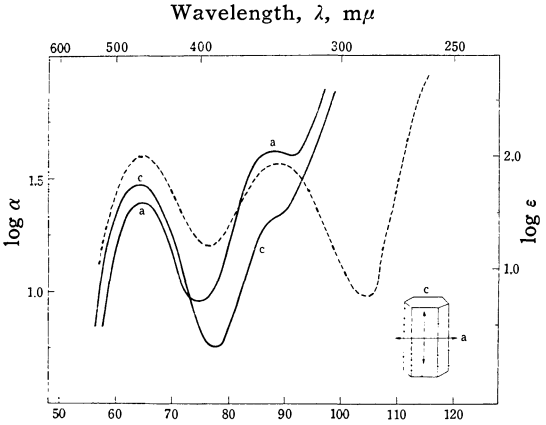



Fig. 1. Absorption spectra of $d,l$-$[Co\,en_3]\cdot Cl_3\cdot 3H_2O$ in the crystalline state (——) and $d,l$-$[Co\,en_3](ClO_4)_3$ in solution (------). The curve of the solution is taken from Ref. 14.

TABLE I. ABSORPTION MAXIMA OF $d,l$-$[Co\,en_3]Cl_3\cdot 3H_2O$

| | $\nu$ | log $\alpha$ | $K$ | $\nu$ | log $\alpha$ | $K$ |
|---|---|---|---|---|---|---|
| $c$-Abs. | 63.8 | 1.49 | $9.55\times10^4$ | (88) | 1.22 | $5.13\times10^4$ |
| $a$-Abs. | 64.0 | 1.33 | $6.62\times10^4$ | 88.8 | 1.61 | $12.5\times10^4$ |
| | $\nu$ | log $\varepsilon$ | $10^3\,\varepsilon$ | $\nu$ | log $\varepsilon$ | $10^3\,\varepsilon$ |
| Solution[a] | 64.4 | 1.99 | $9.96\times10^4$ | 88.5 | 1.94 | $9.73\times10^4$ |

a) M. Linhard, *Z. Elektrochem.*, **50**, 224 (1944).
$\nu$: $10^{13}\,sec^{-1}$.

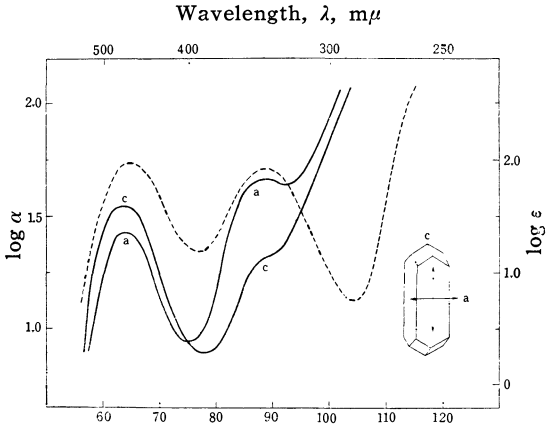



Fig. 2. Absorption spectra of $d,l$-$[Co\,en_3]\cdot Br_3\cdot 3H_2O$ in the crystalline state (——) and $d,l$-$[Co\,en_3](ClO_4)_3$ in solution (------).

TABLE II. ABSORPTION MAXIMA OF $d,l$-$[Co\,en_3]Br_3\cdot 3H_2O$

| | $\nu$ | log $\alpha$ | $K$ | $\nu$ | log $\alpha$ | $K$ |
|---|---|---|---|---|---|---|
| $c$-Abs. | 64.4 | 1.48 | $8.72\times10^4$ | 88 | (1.3) | $5.14\times10^4$ |
| $a$-Abs. | 64.4 | 1.39 | $7.11\times10^4$ | 88 | 1.63 | $12.3\times10^4$ |

$\nu$: $10^{13}\,sec^{-1}$.

From the present measurement, the following relationships are obtained about the dichroism of the $[Co\,en_3]^{3+}$ ion.

(1) For the band at about $64\times10^{13}\,sec^{-1}$ (469 mμ), the $z$-absorption of the complex ion is somewhat stronger than the $x$-absorption.

(2) For the band at about $88\times10^{13}\,sec^{-1}$ (341 mμ), the $x$-absorption is about 2.5

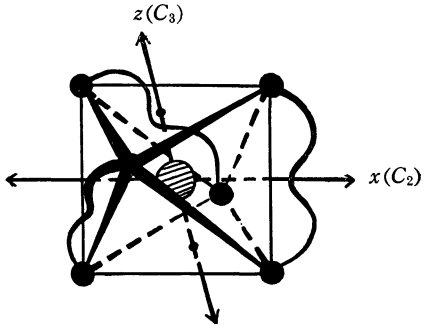



Fig. 3. $[M\,en_3]^{3+}$ ion.

7) (a) R. Tsuchida and M. Kobayashi, "The Color and the Structure of Metallic Compounds" (Kinzoku-kagobutsu no Iro to Kozo), Zoshindo, Osaka (1944), p. 180. (b) R. Tsuchida and M. Kobayashi, This Bulletin, **13**, 619 (1938).

8) K. Nakatsu, Y. Saito and H. Kuroya, This Bulletin, **29**, 428 (1956).

times stronger than the $z$-absorption. The $z$- and the $x$-absorption refer to the directions shown in Fig. 3.

The $[Co\,en_3]^{3+}$ ions in the crystal of $d,l$-$[Co\,en_3]Cl_3\cdot 3H_2O$ are subjected to the field formed by the surrounding ions. However, the dichroism, as here determined, may be assumed in approximation to represent the dichroism of the isolated $[Co\,en_3]^{3+}$ ion itself.

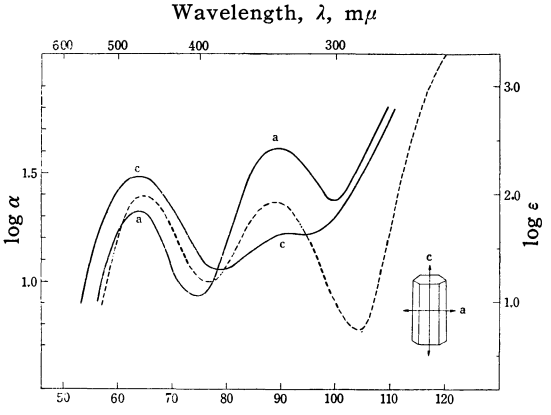



Fig. 4. Absorption spectra of $d$-$[Co\,en_3]\cdot Br_3\cdot 2H_2O$ in the crystalline state (——) and $d,l$-$[Co\,en_3](ClO_4)_3$ in solution (------).

TABLE III. ABSORPTION MAXIMA OF $d$-$[Co\,en_3]Br_3\cdot 2H_2O$

| | $\nu$ | log $\alpha$ | $K$ | $\nu$ | log $\alpha$ | $K$ |
|---|---|---|---|---|---|---|
| $c$-Abs. | 63.9 | 1.54 | $9.07\times10^4$ | 88 | 1.27 | $4.86\times10^4$ |
| $a$-Abs. | 64.1 | 1.43 | $7.03\times10^4$ | 88 | 1.67 | $12.2\times10^4$ |

$\nu$: $10^{13}\,sec^{-1}$.

The dichroism with a crystal of $d$-$[Co\,en_3]Br_3\cdot 2H_2O$ is shown in Fig. 4 and Table III. The arrangement of the complex ions in the crystal of the optically active form is expected to be different from the arrangement in the crystal of its racemic compound, but the dichroism observed with $d$-$[Co\,en_3]Br_3\cdot 2H_2O$ is regarded to represent the main features of the dichroism characteristic of the $d$-$[Co\,en_3]^{3+}$ ion. Comparison of the dichroism of $d$-$[Co\,en_3]Br_3\cdot 2H_2O$ with the dichroism of $d,l$-$[Co\,en_3]Br_3\cdot 3H_2O$ indicates unanimously that the $c$- and the $a$-absorption of the former crystal represent, respectively, the main characteristics of the $z$- and the $x$-absorption of the $d$-$[Co\,en_3]^{3+}$ ion.

From the dichroism with the three compounds above presented, the following relationships may be induced about the dichroism of the $[Co\,en_3]^{3+}$ ion.

(1) For the first absorption band, the $z$-absorption is somewhat stronger than the $x$-absorption.

(2) For the second absorption band, the $x$-absorption is a few times stronger than the $z$-absorption. The polarization is more marked for the second absorption band than for the first band.

(3) The optically active form of the $[Co\,en_3]^{3+}$ ion exhibits the same type of dichroism as the dichroism shown by its racemic complex compounds.

**Dichroism of the Tris(ethylenediamine)-chromium(III) Ion.**—The result of the dichroism measurements with $d,l$-$[Cr\,en_3]Cl_3\cdot 3H_2O$ is shown in Fig. 5 and Table IV. The structure analysis of the crystal has not been reported as yet. The external form and optical property, however, are so closely similar to those of $d,l$-$[Co\,en_3]Cl_3\cdot 3H_2O$ that the crystal of the chromium(III) complex is supposed to be isomorphous with the crystal of the corresponding cobalt(III) compound. Therefore, the $c$-absorption in Fig. 5, the absorption with the electric vector along the $c$-axis, may be regarded as corresponding with the $z$-absorption of the complex ion. Based

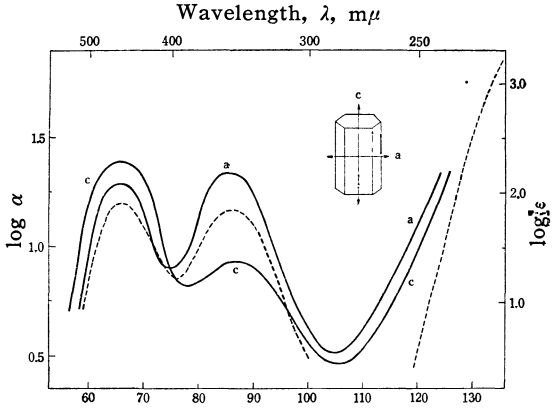



Fig. 5. Absorption spectra of $d,l$-$[Cr\,en_3]\cdot Cl_3\cdot 3H_2O$ in the crystallined state (——) and in solution (-------). The curve of the solution is taken from Ref. 14.

TABLE IV. ABSORPTION MAXIMA OF $d,l$-$[Cr\,en_3]Cl_3\cdot 3H_2O$

| | $\nu$ | log $\alpha$ | $\nu$ | log $\alpha$ |
|---|---|---|---|---|
| $c$-Abs. | 66 | 1.40 | 86 | 0.86 |
| $a$-Abs. | 66.3 | 1.25 | 85.6 | 1.24 |
| | $\nu$ | log $\varepsilon$ | $\nu$ | log $\varepsilon$ |
| Solution[a] | 65.6 | 1.90 | 85.5 | 1.84 |

a) M. Linhard, *Z. Elektrochem.*, **50**, 224 (1944).

$\nu$: $10^{13}\,sec^{-1}$.

on this assumption of the arragement of the complex ions in the crystal, the following relationships are derived about the dichroism of *d,l*-$[Cr\,en_3]Cl_3 \cdot 3H_2O$.

(1) For the band at about $66 \times 10^{13}\,sec^{-1}$ (454 m$\mu$), the *z*-absorption is about 1.5 times stronger than the *x*-absorption.

(2) For the band at about $85.6 \times 10^{13}\,sec^{-1}$ (350 m$\mu$), the *x*-absorption is about 3 times stronger than the *z*-absorption.

These relationships are found to be of a similar type to those for the corresponding cobalt(III) complexes, as is expected from close similarity in absorption spectra between cobalt(III) and chromium(III) complexes in general. The similarity is also expected from consideration on the symmetry of the electronic state as well as the external form of the complex ions.

## Discussion

**Dichroism of the First and the Second Absorption Band.**—The $[Co\,en_3]^{3+}$ ion has symmetry $D_3$, but its spectrum shows that the effective symmetry is much higher and approximates $O_h$. Thus, the absorption curve bears a close resemblance to those of the hexammine-cobalt(III) complexes with $O_h$ symmetry. The ligand field around the $Co^{3+}$ in the $[Co\,en_3]^{3+}$ ion may be represented by the overall symmetry of $O_h$ with a trigonal field of $D_3$ symmetry as a small perturbation term. In the case of the hexammine-cobalt(III) ion, the absorption bands in the long wavelength region are forbidden owing to the $g \leftarrow\!\!|\!\!\rightarrow g$ selection rule, and become allowed in combination, with the vibrational motion of the complex. The $[Co\,en_2]^{3+}$ ion, however, has no center of symmetry, and the unsymmetrical field will allow the slight electric dipole transitions even in the absence of vibrational distortion.

The two absorption bands in the long wavelength region of the $[Co\,en_3]^{3+}$ ion correspond to those of the $[Co(NH_3)_6]^{3+}$ ion, which are due to the electronic transitions $^1A_{1g} \rightarrow {}^1T_{1g}$ and $^1A_{1g} \rightarrow {}^1T_{2g}$. On grounds of energy[9] and from a consideration of the rotatory dispersion[10] of the $[Co\,en_3]^{3+}$ ion, the longer wavelength band around 4700 Å is ascribed to the transition $^1A_{1g} \rightarrow {}^1T_{1g}$ and the shorter wavelength band around 3400 Å to the transition $^1A_{1g} \rightarrow {}^1T_{2g}$, the complex ion being assumed to be approximately of $O_h$ symmetry. It is known that the chromium(III) complexes show absorption spectra quite similar to those of the corresponding cobaltic compounds. The first and the second absorption bands of the hexammine-chromium(III) ion are ascribed to the $^4A_{2g} \rightarrow {}^4T_{2g}$ and $^4A_{2g} \rightarrow {}^4T_{1g}$ transitions, respectively. On the basis of Moffitt's theory, the assignment is found to be in agreement with the rotatory dispersion of the chromium(III) complex ion[11].

In the $D_3$ group, species $A_{1g}$, $A_{2g}$ and E of the $O_h$ group go over into $A_1$, $A_2$ and E, respectively, whereas $T_{1g}$ splits itself into $A_2+E$ and $T_{2g}$ into $A_1+E$. In practice, the degeneracies of the threefold $T_{1g}$ or $T_{2g}$ levels in the hexammines are not perceptibly resolved in their ethylenediamine analogues. The splitting due to the $D_3$ symmetry in these complexes is quite small, as is seen from the present dichroism measurements. Thus the splitting, if any, of the first absorption band under the field of $D_3$ symmetry is found to be very small. Nevertheless the dichroism of the $[M\,en_3]^{3+}$ ion is surely due to the effect of the field with the $D_3$ symmetry.

It might be interesting to point out that the dichroism of the $[Co\,en_3]^{3+}$ and the $[Cr\,en_3]^{3+}$ ion agree, on the basis of the above-mentioned assignment of the absorption bands, with the selection rule which was given by Moffitt[10] from discussion taking only the symmetry of the ground and the excited electronic state into consideration and discarding vibrational modes of the complex ion. This agreement, however, may be rather fortuitous. For complete analysis of the ultraviolet dichroism, account is to be taken of the vibrational modes of the complex ions.

Recently Sugano and Tanabe[12] experimentally determined optical anisotropy with the chromium ruby, in which the field around the $Cr^{3+}$ ion is represented by $C_3$ symmetry and is quite similar to the field encountered in the $[Cr\,en_3]^{3+}$ ion. It was found from their measurements with the chromium ruby that for the first absorption band the *z*-absorption is stronger than the *x*-absorption, and that for the second band the *x*-absorption is stronger than the *z*-absorption, where the *z*- and the *x*-absorptions represent the absorption with polarized light having its electric vector along and perpendicular to the *c*-axis, respectively. This observation was shown to be in good agreement with

9) L. Orgel, *J. Chem. Phys.*, **23**, 1004 (1955) etc.
10) W. Moffitt, ibid., **25**, 1189 (1956).
11) J. P. Mathieu, *J. chim. phys.*, **33**, 78 (1936).
12) S. Sugano and Y. Tanabe, *J. Phys. Soc. Japan*, **13**, 880 (1958).

their theoretical interpretation, which also predicted the same type of dichroism for the $[Cr\,en_3]^{3+}$ and the $[Co\,en_3]^{3+}$ ion. This, however, is not the case with these complex ions. The present measurements indicate that the dichroism with the $[Cr\,en_3]^{3+}$ ion is reverse to the dichroism of thd chromium ruby. The difference in dichroism between the two types of the compounds show that the explanation for one case does not apply, at least in its original form, to the other. The dichroism with the $[Cr\,en_3]^{3+}$ ion may be understood, if this is assumed to belong, for some reason, to the case where the second term of $F_{2u}$ type in the expansion of the hemihedral perturbation field, $V_{trig}$, is much greater than the first term of $F_{1u}$ type in Sugano and Tanabe's treatment[13]. It is expected theoretically that the first term may be much larger than the second term in ordinary cases. The anomaly with the $[Cr\,en_3]^{3+}$ ion is not explained at present.

**Dichroism and Optical Rotatory Dispersion of the Complex Ions.**—The information about the dichroism of the complex ions is expected to be useful for the understanding of the rotatory dispersion[10]. The complex ions of the type here considered show two component absorptions corresponding to the "first absorption band", both of which may possibly be active, at least partly, in the optical rotation. In this case, superposition of the two inversive dispersions due to the component absorptions may be observed in the wavelength region of the first absorption band. In the tris(ethylenediamine)-cobalt(III) and -chromium(III), the splitting of the first absorption band is found from the present dichroism measurements to be quite small, so that the two sorts of Cotton effect due to the two components of the first band are not observed separately, but their superposition appears with only one maximum. On the other hand, the *d*-trioxalatochromate(III) ion shows in the wavelength region of the first absorption band a small, negative component of Cotton effect, in addition to a much larger component of a positive sign[11]. This may be explained qualitatively on the basis of the dichroism. The dichroism measurements, the details of which will be reported later, indicate that the $[Cr\,ox_3]^{3-}$ ion unambiguously shows two maxima at 51.0 and $51.8\times10^{13}\,sec^{-1}$, the splitting of the first band being much greater than in the tris-(ethylenediamine)-cobalt(III) or -chromium(III). The appearance of the small, negative component of Cotton effect may be understood, if it is assumed that the electronic transitions corresponding to the above two component absorptions give rise to Cotton effect of their own, the sign for one being reverse to the sign for the other.

**Comparison of the Crystal Spectra with the Spectra of the Solution.** — It is shown that difference is scarcely recognizable in maximum wavelength between the crystal and the solution. On the other hand, difference is observed in intensity of the first and the second absorption band, the difference being greater for the latter band than for the former. If the authors compare the average of $K_z$ and $K_x$, as the value for the crystal, with $10^3\varepsilon$, which is regared as representing absorption coefficient by the compounds of one formula weight in solution, the present measurements show that intensity is greater for the solution than for the crystal, even when reflection from the surface of the crystal is taken into account. The difference seems to be definite, though it is generally small. This is readily understandable, since the perturbation due to the solvent molecules apparently contributes to absorption coefficient in solution, whereas this kind of contribution to the intensity is lacking in the crystal. The Schwarzschild-Villiger effect might be responsible partly for the difference, but is probably very small in the wavelength region under consideration.

**Absorption Band due to Association of Ions.** —Linhard[14] formerly found a new type of absorption bands in addition to the first and the second absorption band with the tris(ethylenediamine)-cobalt(III) and -chromium(III) complexes in solution. The new absorption band, which appears in the region of wave length slightly shorter than the second absorption band, is found to become stronger as the concentration of the halide ion increases, and is regarded by Linhard and others as due to association of the halide ions with the $[M\,en_3]^{3+}$ ion. The absorption band of this kind is evidently observed in the absorption curves of the complexes in the crystalline state, as reported in the present measurement with a single crystal. The present

13) See Ref. 12. The present authors are indebted to Dr. S. Sugano for the suggestion concerning the difference between the chromium ruby and the complex ions examined in the present work.

14) M. Linhard, *Z. Elektrochem.*, **50**, 224 (1944).

measurements indicate that the tris-(ethylenediamine)-cobalt(III) complexes in the crystalline state show an absorption band in the region of longer wavelength than does $[Co\,en_3](ClO_4)_3$ in solution. Thus *d,l*-$[Co\,en_3]Br_3\cdot 3H_2O$ shows the band at about $100\times 10^{13}\,sec^{-1}$, which is seen to superpose partly on the shorter wavelength side of the second absorption band. The X-ray study shows that in the crystals of the racemic tris(ethylenediamine)-cobalt(III) chloride trihydrate a complex ion is surrounded by nine chloride ions at about 3.2 Å from a nitrogen atom of the complex ions. A similar arrangement of ions is expected for the racemic bromide trihydrate in the crystalline state. The present measurements, therefore, may be regarded as evidence for the view that the new band is due to association of the complex ion with the surrounding halide ions. It is interesting to note here that the interaction takes place at such a distance, which seems to be comparatively great for the interaction. This type of the group composed of the complex ion and the halide ions surrounding it was formerly established to exist from the measurements of rotatory dispersion[15] and absorption spectra with the complex compounds in solution[14].

From the present dichroism measurements, the following relationships are derived about the absorption band due to the association of the ions.

(1) This kind of absorption band lies in the case of the bromide at longer wavelength than in the case of the chloride.

(2) The absorption is stronger with the electric vector along the trigonal axis of the complex than with the electric vector perpendicular to the axis.

(3) The first or the second absorption band undergoes very little effect even when the association band shifts to a longer wavelength region.

(4) The chromium(III) complex shows the association band in much shorter wavelength region than does the corresponding cobalt(III) complex.

15) R. Tsuchida, *J. Chem. Soc. Japan (Nippon Kwagaku Kwaishi)* 58, 621 (1937).

The relationships 1, 3 and 4 are essentially the same as those obtained by Linhard[14] with the complexes in aqueous solution, and in agreement with Linhard's assumption that the association band be ascribed to the electronic transitions due primarily to the halide ions which are deformed under the field of the complex ion.

Since the halide ions without the specific field from the outside absorb in a shorter wavelength, it may be assumed that the absorption of the halide ions is displaced to a longer wavelength in the presence of the field by the complex ions as in the crystals of the compounds here examined. Rrelationship 4 shows that the $[Cr\,en_3]^{3+}$ ion has smaller effect upon the halide ions than has the $[Co\,en_3]^{3+}$ ion, being in agreement with Linhard's observation with the complexes in solution.

## Summary

The dichroism in the visible and ultraviolet region has been quantitatively determined at room temperature by Tsuchida and Kobayashi's microscopic method with a single crystal of *d,l*-$[Co\,en_3]Cl_3\cdot 3H_2O$, *d,l*-$[Co\,en_3]Br_3\cdot 3H_2O$, *d*-$[Co\,en_3]Br_3\cdot 2H_2O$ and *d,l*-$[Cr\,en_3]Cl_3\cdot 3H_2O$.

It has been found that the $[Co\,en_3]^{3+}$ and the $[Cr\,en_3]^{3+}$ ion show a similar type of dichroism. For both the complex ions, the *z*-absorption is slightly stronger than the *x*-absorption in the wavelength region of the first absorption band and much weaker than the *x*-absorption in the region of the second absorption band.

The results of the measurements are discussed in relation to the electronic state and the optical rotatory dispersion of the complex ions.

The present authors wish to thank Dr. S. Sugano of the University of Tokyo for helpful discussion and the Ministry of Education for a grant-in-aid.

*Department of Chemistry*
*Faculty of Science*
*Osaka University*
*Nakanoshima, Osaka*

# *L'effet photovoltaïque des halogénures d'argent*

Par Shinichi KIKUCHI, Hiroshi NOZAKI, Yushi HAMANO et Seiya SAKAINO

(Reçu le 10 juillet 1959)

Quand une électrode métallique est exposée à la lumière dans un liquide ou dans une solution convenable, il se produit un changement du potentiel d'électrode, qui s'appelle l'effet photovoltaïque. Ce phénomène qui s'appelle aussi l'effet Becquerel, d'après le nom de celui qui le mit en évidence, a été étudié par beaucoup de chercheurs[1]. Les raisons de cet effet peuvent être divisées en quatre catégories: a) l'électrode métallique exposée à la lumière donne le potentiel photovoltaïque sans aucun changement macroscopique; b) la réaction photochimique des matières colorantes ou d'autres substances sensibles à la lumière, couvrant l'électrode, donne le potentiel; c) le liquide ou la solution est la cause du potentiel photovoltaïque; d) le semiconducteur solide couvrant la surface du métal donne le potentiel. Le travail de Becquerel doit être classé dans la 2e catégorie, car il traite la production du potentiel par l'électrode d'halogénure d'argent mise dans la solution d'électrolyte. La présente étude doit être classée dans la 3e catégorie, car elle traite l'effet photovoltaïque dans la solution colloïdale d'halogénure d'argent. Sheppard et Vanselow[2] ont étudié en 1938 l'effet photovoltaïque de l'électrode d'halogénure d'argent dans la solution d'électrolytes et développé la théorie de la sensibilisation photographique à partir des résultats de cette étude. Mais le potentiel était de l'ordre de quelques millivolts à quelques dizaines de millivolts. D'ailleurs il était instable et non reproductible surtout quand il y a en suspension des grains d'halogénure d'argent. Nous avons donc adopté l'électrode de platine au lieu de l'électrode d'halogénures d'argent et l'avons mise dans la solution colloïdale d'halogénure d'argent. Dans ce cas le potentiel photovoltaïque était très grand et reproductible et nous a permis d'étudier d'une manière détaillée la vitesse de la réaction photochimique des halogénures d'argent et l'application de cet effet dans les autres domaines.

1) A. W. Copeland, O. D. Black et A. B. Garrett, *Chem. Revs.*, **31**, 177 (1942).

2) W. Vanselow et S. E. Sheppard, *J. Phys. Chem.*, **33**, 331 (1929); S. E. Sheppard, W. Vanselow et V. C. Hall, ibid., **33**, 1403 (1929); S. E. Sheppard, W. Vanselow et G. P. Happ, ibid., **44**, 4411 (1940).

## Expériences

L'appareil que nous avons utilisé dans le présent travail est montré sur la figure 1; les halogénures d'argent sont mis dans une cuve à électrolyse (1), ainsi que la solution colloïdale, et mélangés avec un agitateur magnétique (2). Au-dessus d'une certaine vitesse d'agitation, les halogénures peuvent être considérés comme une suspension homogène. Le bromure et l'iodure d'argent sont préparés en mettant du nitrate d'argent 1 N dans un excès de solution d'halogénures de potassium 1 N. Les précipités sont lavés à l'eau, desséchés et broyés en poudre fine dans le mortier. Une quantité pesée de poudre est mise dans la solution d'électrolyte (la solution d'halogénures alcalins). Quant au chlorure d'argent, une certaine quantité de solution de nitrate d'argent est ajoutée à un petit excès de chlorure de potassium. Le précipité est légèrement chauffé, puis filtré et lavé. Il est entrainé par une solution de KCl 0.1 N dans la cuve à électrolyse à travers un petit trou percé au fond du filtre sur entonnoir. Nous avons essayé de maintenir la même répartition de grains d'halogénures d'argent, en contrôlant les conditions de traitement dans chaque lot d'expériences. Une lampe à mercure (3) est employée comme source. Quelque temps après l'allumage de la lampe, en maintenant la stabilité de luminosité, l'on ouvre l'obturateur (4) et la lumière traverse une distance constante dans l'espace, la paroi du thermostat en résine acrylique (3 mm. d'épaisseur) et ensuite une couche d'eau de 2 cm. avant d'arriver dans la cuve à électrolyse. Dans ce

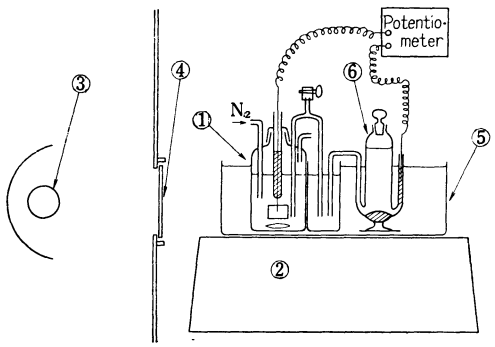



Fig. 1. Le système d'expériences.

rapport, la distance entre le centre de la cuve à électrolyse et celui de la source était maintenue à 20 cm., sauf autre indication, afin qu'une lumière constante entre la cuve. La luminosité de la lampe à mercure a été vérifiée de temps à autre avec un posemètre à sélénium. La cuve à électrolyse est un cylindre de verre de 50 mm. de diamètre. La paroi de verre ne laisse pas passer les rayons plus courts qu'environ 3500 Å. Le potentiel de l'électrode de platine a été mesuré d'une manière potentiométrique en se référent à une électrode au calomel saturé (6). La température du thermostat était de 25°C. Nous avons fait passer de l'azote dans la cuve à électrolyse préalablement à la mesure, afin de chasser l'oxygène dissous dans la solution. Le potentiel de l'électrode de platine peut varier sensiblement, même avant l'exposition à la lumière. Le traitement préalable est donc très important pour obtenir une valeur reproductible. Dans ce travail, l'électrode de platine est trempée dans une solution de soude caustique et de chlorure stanneux pendant 5 min. et mise dans l'acide nitrique concentré. Elle est complètement lavée à l'eau avant l'usage. Quand le potentiel du platine prend sa valeur stable, l'obturateur est ouvert et le potentiel est mesuré de temps à autre jusqu'à ce que le potentiel atteint une valeur constante.

## Résultats des expériences et observations

**1. Allure du potentiel photovoltaïque.**—Au cours de l'exposition, le potentiel de l'électrode de platine mise dans la solution colloïdale d'halogénures d'argent varie le côté positif du potentiel comme l'indique la figure 2 assez rapidement dans les prmières minutes, puis lentement, et il tend vers une valeur de saturation. Même si le potentiel avant l'exposition est différent, il tend vers une valeur déterminée après un certain temps d'exposition.

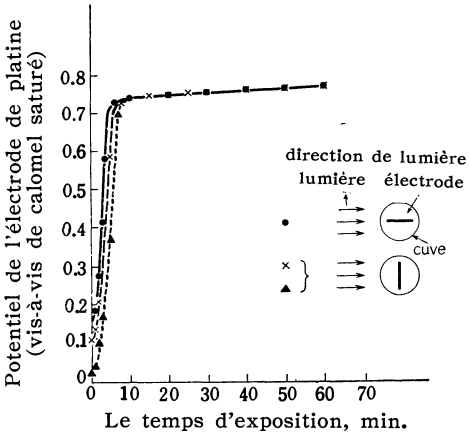



Fig. 2. L'effet photovoltaïque de AgBr 0,1 mol./l. en suspension dans la solution de KBr 0,1 N.

Nous appelons désormais le potentiel du platine mis dans la solution des halogénures d'argent le photopotentiel. Après le moment où le potentiel atteint, la valeur de saturation il ne baisse presque pas, même si l'on cesse d'illuminer la cuve. Il n'y a qu'une diminution de quelques millivolts au bout de 20 heures de repos. Le potentiel reste constant même si l'on arrête l'agitation et si l'halogénure d'argent se dépose au fond de la cuve. La variation de l'aire de l'électrode perpendiculaire à la direction de la lumière n'affecte pas le potentiel de saturation. Le potentiel de l'électrode de platine ne change pas par l'exposition à la lumière s'il n'y a pas d'halogénure d'argent dans la solution d'électrolyte. Ce résultat permet de penser que le photopotentiel ne dépend pas de l'exposition de l'électrode et que la réaction photolytique dans la solution est la raison du changement de potentiel.

**2. Les différents halogénures et le photopotentiel.** — Si l'on suppose que le photopotentiel dépend du potentiel d'oxydation des halogènes, l'ordre des potentiels doit être $AgCl > AgBr > AgI$ et le fluorure d'argent, insensible à la lumière visible, ne doit pas donner le changement du potentiel. Les potentiels normaux des halogènes vis-à-vis de l'électrode à hydrogène normale sont donnés dans le tableau I.

TABLEAU I

| | $\varepsilon_h$ |
|---|---|
| $1/2\,F_2(g)+e \rightleftarrows F^-$ | 2,85 volt |
| $1/2\,Cl_2(g)+e \rightleftarrows Cl^-$ | 1,359 |
| $1/2\,Br_2(a=I)+e \rightleftarrows Br^-$ | 1,085 |
| $1/2\,I_2(s)+e \rightleftarrows I^-$ | 0,536 |

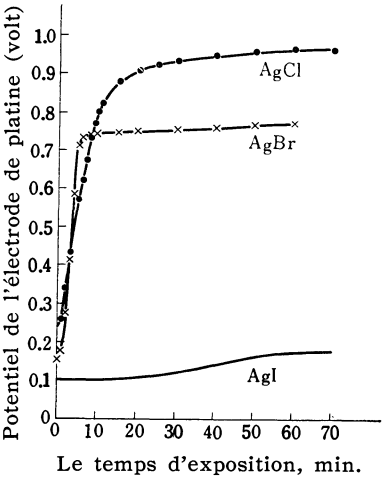



Fig. 3. L'effet photovoltaïque de AgX 0,1 mol./l. en suspension de la solution de KX 0,1 N.

Dans une première série d'expériences, les solutions d'halogénures de potassium 0,1 N contenant 0,05 mol./l. des halogénures d'argent ont donné les photopotentiels comme la figure 3. Le système du fluorure d'argent n'a pas donné d'effet photovoltaïque.

**3. La relation entre la concentration des halogénures dans la solution et l'effet photovoltaïque.**—Si le photopotentiel indique le potentiel d'oxydation d'halogène selon l'équation $1/2\,X_2+e \rightleftarrows X^-$, le potentiel $E$ doit dépendre des concentrations de l'halogène et de l'ion halogène.

$$E=E_0+\boldsymbol{R}T/\boldsymbol{F}\ (\ln [X_2]^{1.2}/[X^-])$$
$$=E_0+\boldsymbol{R}T/2\boldsymbol{F}\ln [X_2]-\boldsymbol{R}T/\boldsymbol{F}\ln [X^-] \quad (1)$$

Si l'on suppose que la concentration des halogénures d'argent en suspension est constante et que la concentration de l'halogène libéré est constante, la formule 1 devient la formule 2.

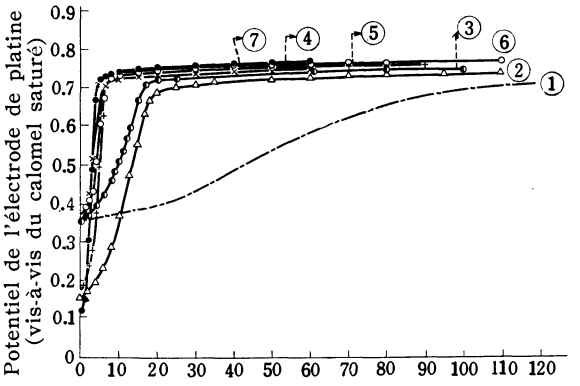
$$E=E_0'-0{,}059\log [X^-] \quad (2)$$

Dans 2e série d'expériences où les auteurs font varier la concentration d'ion, les résultats ont été ceux de la figure 4. La relation entre le photopotentiel mesuré après 60 min. d'exposition et la concentration de l'ion d'halogène est semblable à l'équation 2. Cependant cette relation n'est plus valable au-dessus d'une concentration de 0,3 N. Dans le cas du bromure, la couleur de la solution après l'exposition est sensiblement brune et la couleur du bromure d'argent est aussi grise. Cela montre qu'il y a une certaine quantité de brome dans la solution. Les auteurs supposent que le photopotentiel plus faible dans la solution concentrée de bromure provient de la réduction de la concentration en brome par formation d'ion complexe.

$$Br_2+Br^- \rightleftarrows Br_3^-$$

**4. La relation entre la concentration des halogénures d'argent et le photopotentiel.**—Dans la série suivante, les auteurs ont mesuré le photopotentiel en faisant varie la concentration d'halogénure d'argent, en tenant constante la concentration de l'ion brome. Plus la concentration en bromure d'argent est petite, plus la vitesse de formation du brome est petite et la vitesse d'augmentation du potentiel est également petite (Fig. 5). De la formule 1 on peut tirer la formule 3 en prenant $Br^-$ const.

$$E=E_0''+0{,}0296\log [Br_2] \quad (3)$$




1. $1\times10^{-3}$ mol./l.
2. $3\times10^{-3}$ mol./l.
3. $7\times10^{-3}$ mol./l.
4. $1\times10^{-2}$ mol./l.
5. $5\times10^{-2}$ mol./l.
6. $7\times10^{-2}$ mol./l.
7. $1\times10^{-1}$ mol./l.

Fig. 5. La concentration de AgBr et le photopotentiel (concentration 0,1 N).

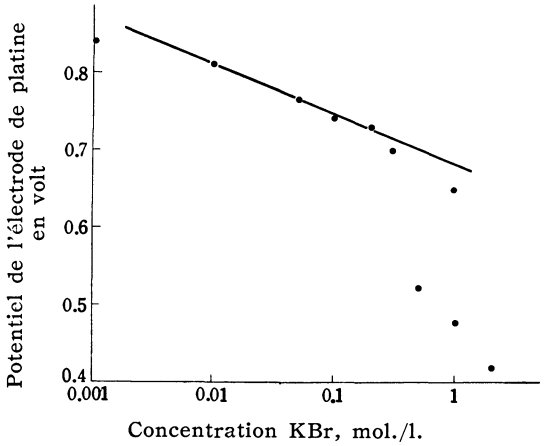



Fig. 4. Photopotentiel de AgBr en suspension 60 min. après l'exposition dans la solution KBr (AgBr 0,05 mol./l.).

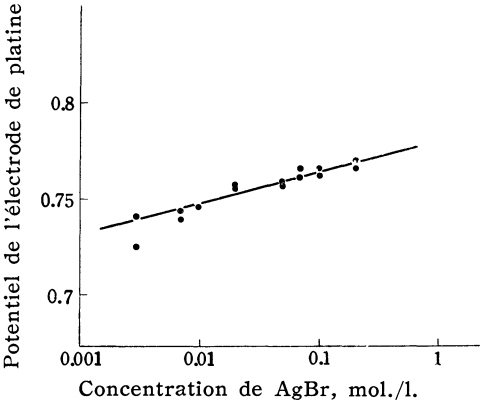



Fig. 6. La concentration de AgBr et le photopotentiel 60 min. après l'exposition (dans KBr 0,1 N).

Comme il y a une réaction de recombinaison d'argent et de brome un effet de filtre de lumière actinique par l'argent déposé, la concentration de brome libéré ne doit pas être proportionnelle à la concentration de bromure d'argent. Mais quand ces effets sont petits, on peut supposer que ces deux concentrations sont proportionelles et la formule 4 devient,

$$E \fallingdotseq E_0''' + 0{,}0296 \log (\mathrm{AgBr}) \qquad (4)$$

En fait la figure 6 montre que le photopotentiel est à peu près une fonction linéaire du logarithme de la concentration de bromure d'argent (Fig. 6).

**5. L'effet de l'intensité de la lumière et de la grandeur des grains d'halogénure d'argent sur le potentiel.** — Quand l'intensité de la lumière qui entre dans le système colloïdal d'halogénure d'argent faiblit, la vitesse d'augmentation du photopotentiel devient moindre et le potentiel final est aussi plus faible (Fig. 7). Il y a un effet identique. Quand la grandeur des grains d'halogénures d'argent augmente, la vitesse d'augmentation du photopotentiel diminue. La figure 8 montre l'allure du photopotentiel pour deux grandeurs de grains de chlorure d'argent, celles de diamètre moyen de moins de 0,1 mm. et de 0,7 mm. On peut en expliquer la raison en disant que la diffusion de chlore libéré dans le gros grain exige plus de temps que dans le petit grain.

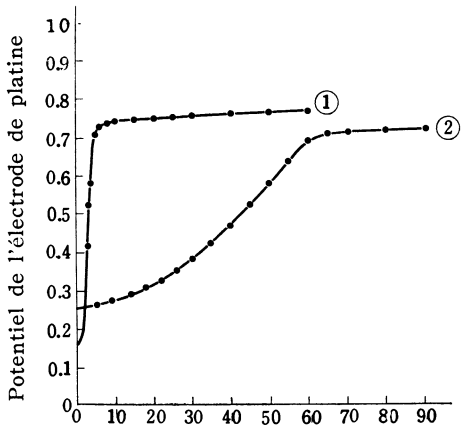



Fig. 7. L'intensité de lumière et l'effet photovoltaïque (0,1 mol./l. AgBr dans 0,1 N KBr).
1) Distance de la source 20 cm.
2) 〃 100 cm.

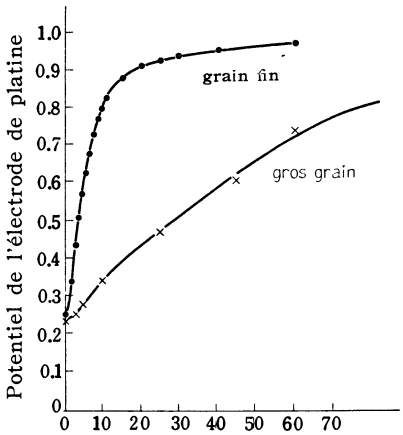



Fig. 8. Grandeur des grains et le photopotentiel (0,1 mol./l. AgCl dans 0,1 N KCl).

**6. Le potentiel après l'arrêt de l'exposition.** —Quand on arrête l'exposition après un certain temps, l'allure du photopotentiel est celle de la figure 9. Quand le potentiel se trouve sur la courbe montante, l'augmentation du potentiel continue même après l'arrêt de l'exposition, puis il commence à redescendre. L'explication est que l'halogène libéré ne se recombine pas tout de suite après l'arrêt de l'exposition et continue à venir dans la solution à cause de la différence de concentration d'halogène entre le cristal et la solution. La redescente peut s'expliquer par la recombinaison du brome avec l'argent. Mais cette explication n'est pas suffisante. Parce qu'une fois que le potentiel se trouve dans la partie de courbe près de la valeur saturée, il ne descend presque pas même après l'arrêt de l'exposition dans le cas du bromure et de l'iodure d'argent. Mais le potentiel de chlorure

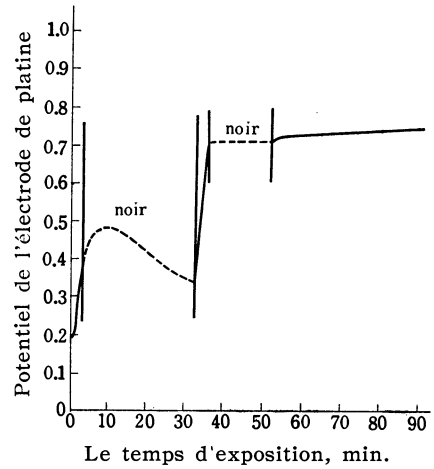



Fig. 9. L'effet photovoltaïque en cas d'interruption de lumière (0,1 mol./l. AgBr dans 0,1 N KBr).
—— exposition, ------ dans le noir

d'argent montre une descente du potentiel. On peut expliquer le phénomène dans le bromure et dans l'iodure d'argent en disant que la quantité d'halogène qui se recombine est minime par rapport à l'halogène libéré dans la solution.

**7. La comparaison du photopotentiel et du potentiel d'électrode d'halogène.**—Les auteurs ont calculé la concentration du brome libéré après 1 heure d'exposition du système colloïdal 0,1 N KBr-AgBr comme dans le tableau II.

TABLEAU II

| Concentration de AgBr mol./l. | Photopotentiel 60 min. après l'exposition vis-à-vis de calomel saturé | Concentration de brome libéré mol./l. |
|---|---|---|
| 0,2 | 0,766 | 2,02 $\times 10^{-5}$ |
| 0,1 | 0,764 | 1,77 〃 |
| 0,07 | 0,761 | 1,37 〃 |
| 0,05 | 0,756 | 0,926 〃 |
| 0,02 | 0,756 | 0,926 〃 |
| 0,01 | 0,746 | 0,424 〃 |
| 0,007 | 0,739 | 0,246 〃 |
| 0,003 | 0,725 | 0,0824 〃 |

On voit que la quantité de brome libéré est minime par rapport à la suspension de AgBr. Pour vérifier si l'électrode de platine indique le potentiel d'oxydoréduction par la réaction,

$$1/2\,Br_2 + e = Br^-$$

dans une solution diluée comme dans le tableau II, nous avons mesuré le potentiel en dissolvant une quantité connue du brome dans des solutions de KBr 0,1 N, 1 N et 3 N. Les résultats se voient sur la figure 10. Dans la solution à 0,1 N de KBr, le potentiel suit la formule 3 au-dessus de 0,72 volt (vis-à-vis du calomel saturé) et au-dessus de la concentration $2\sim3\times10^{-6}$ mol./l. de brome. Au-dessus de 0,72~0,73 volt, le potentiel dévie grandement de la formule 3. Au-dessous de cette concentration de brome, le potentiel est instable à cause du potentiel naturel par suite de l'adsorption d'ions étrangers et pour d'autres raisons. Aux plus fortes concentrations de KBr, comme 1 N ou 3 N, le potentiel devient moindre que le potentiel calculé par la formule 3.

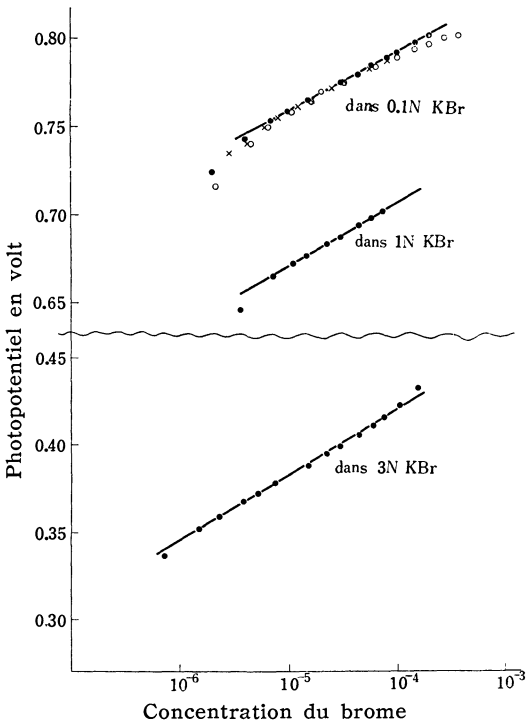



Fig. 10. La concentration du brome et le photopotentiel.

## Conclusion

1. L'exposition à la lumière d'une suspension d'halogénures d'argent dans une solution d'électrolyte donne un grand effet photovoltaïque.

2. Nous avons trouvé par certaines expériences que ce potentiel provient de l'halogène libéré du cristal vers la solution.

3. L'électrode de platine mise dans la solution colloïdale d'halogénure d'argent indique au commencement le potentiel naturel donné par l'état initial de l'électrode. Par l'exposition de AgX à la lumière, l'halogène est libéré vers la solution et il donne le potentiel défini par :

$$1/2\,X_2 + e \rightleftarrows X^-$$

*Institut des Sciences Industrielles*
*L'Université de Tokyo*
*Yayoi-cho, Chiba*

# *Relations between Electronic Absorption Spectra and Spatial Configurations of Conjugated Systems. IV. Polyphenyls*

By Hiroshi SUZUKI

(Received July 7, 1959)

In this part of the series, the electronic absorption spectra and the spatial configurations of polyphenyls are briefly surveyed, and the relation between them is discussed especially for *o*- and *p*-terphenyls, the method applied being analogous to the one for the treatment of biphenyl presented in Part I[1] of this series.

**p-Polyphenyls.**—It is well known that the first intense band in *p*-polyphenyl is shifted progressively toward longer wavelengths and increases in its intensity as the number of benzene rings is increased, no limit having been reached with the first six members which have been studied experimentally[2]. The band is regarded as the conjugation band, and the bathochromic shift and the intensification of this band with the increasing number of benzene rings may be attributed to the increasing extent of conjugation due to the elongation of the conjugated system. It may be stated in this connection that the first four members have been proved to be planar in the crystalline states[3].

The relation between the position of the conjugation band and the number of benzene rings in *p*-polyphenyl has been discussed by several workers on various grounds. Thus, for example, Davydov[4] has treated this problem quantum-mechanically, and derived the following equation:

$$\Delta E_{\min} = A - 2|M||\cos[\pi/(n+1)]|$$

where $\Delta E_{\min}$ is the transition energy corresponding to the conjugation band, $M$ is the matrix element of the interaction between neighboring benzene rings, and $n$ is the number of benzene rings in the molecule. Hence, with increasing $n$, the band should shift toward longer wavelengths, and the magnitude of the shift should decrease. From the experimental data of Gillam and Hey[2] for biphenyl and for sexiphenyl, the values of $A$ and of $M$ have been estimated at 50060 $cm^{-1}$ and at 10300 $cm^{-1}$, respectively, in chloroform, and at 50900 $cm^{-1}$ and at 10200 $cm^{-1}$, respectively, in hexane. Accordingly, when $n$ is $\infty$, the band should be expected to be at about 339 m$\mu$ in chloroform and at about 328 m$\mu$ in hexane. A somewhat similar equation has been derived empirically by Hirayama[5].

Further, Dewar[6] has calculated the wavelengths of the conjugation bands of *p*-polyphenyls by his NBMO method, and obtained values which are in excellent agreement with the experiment.

**m-Polyphenyls.** — The spectra of linear *m*-polyphenyls form a system quite different from that of *p*-polyphenyls. In the meta-series there is virtually no change in the position of the first intense band after biphenyl up to the highest member of the series yet prepared, in which the number of benzene rings is 16, in marked contrast to the para-series. On the other hand, the intensity of the band increases as the series ascends, being roughly proportional to the number of benzene rings in the molecule[2].

The different characteristics of the spectra of the two series have been ascribed to the presence of conjugation which covers the whole molecule in the para- but not in the meta-series. Thus Dewar[6] has considered the *m*-polyphenyls as the cross-conjugated systems according to his definition, and stated that the largest non-cross-conjugated unit present in them is biphenyl. In addition, Dale[7] has described it in line with Dewar's theory as follows; in *m*-terphenyl, one orbital of each of two sets of doubly degenerate $\pi$-orbitals in the central benzene ring will interact mainly with the orbitals in one of the benzene rings

1) H. Suzuki, This Bulletin, **32**, 1340 (1959).
2) A. E. Gillam and D. H. Hey, *J. Chem. Soc.*, **1939**, 1170.
3) L. W. Pickett, *Nature*, **131**, 513 (1933).
4) A. S. Davydov, *Zhur. Eksptl. Teoret. Fiz.* (*J. Exptl. Theoret. Phys.*), 18, 515 (1948); *Chem. Abstr.*, **43**, 3714 (1949).
5) K. Hirayama, *J. Chem. Soc. Japan, Pure Chem. Sec.* (*Nippon Kagaku Zasshi*), **75**, 682 (1954).
6) M. J. S. Dewar, *J. Chem. Soc.*, **1952**, 3544.
7) J. Dale, *Acta Chem. Scand.*, **11**, 971 (1957).

attached to the parent benzene ring, while the other orbital interacts mainly with the orbitals in another benzene ring. These explanations seem considerably satisfactory.

In spite of this, however, Murrell and Longuet-Higgins[8] have proposed a different explanation. They have attempted to account for the main features of the spectra of *m*- and *p*-polyphenyls by electron interaction between the chromophores in these series, and stated that the different characteristics of the spectra of the two series can be interpreted without reference to conjugation between the aromatic rings.

While data of the spatial configurations of linear *m*-polyphenyls appear to have not been available yet, it is of great interest that 1,3,5-triphenylbenzene has been found to be non-planar not only in the vapor state but also in the crystalline state. According to Bastiansen[9], the angle between two adjacent benzene ring planes in this compound in the vapor phase is $46\pm5°$, which is almost completely identical with the value found for biphenyl in the vapor phase[10]. 1,3,5-Triphenylbenzene has been found to have the non-planar configuration even in the crystalline state, in which the interplanar angles are about 25° according to Lonsdale[11] or +34°, −27° and +24° according to Farag[12], in striking contrast to biphenyl which is known to be planar in the crystalline state[13].

**o-Polyphenyls.**—While *p*-polyphenyls have been proved to be planar in the crystalline states, *o*-polyphenyls can not be planar owing to the steric necessities. Actually it has been found that *o*-terphenyl is non-planar in the crystalline state[14]. Consequently, *o*-terphenyl should be less conjugated than the *p*-isomer, and hence the electronic absorption spectrum of the former should be appreciably different from that of the latter. In fact, this has been shown to be the case[15].

**o-Terphenyl, p-Terpheny and Some Related Compounds.**—Now, the relation between the spectra and the most probable spatial configurations of *o*- and *p*-terphenyls and of some related compounds will be discussed below by application of a method analogous to the one used in the treatment of the similar problem of biphenyl in Part I of this series.

The $\pi-\pi$ resonance integral for each of the co-annular bonds in *o*- and *p*-terphenyls is denoted by $\mu\beta$, and by the parameter $\mu$ an allowance is made for a change of the resonance integral associated with changes of the interplanar angle and of the bond length, quite similarly to the case of biphenyl.

*o*-Terphenyl is considered to belong to the symmetry group $C_2$. Seven of nine orbitals belonging to each of the representations $A$ and $B$ vary with $\mu$, and the other two orbitals of each set do not vary with $\mu$ (one of which has energy of $+\beta$, and the other $-\beta$). The highest occupied orbital belongs to $B$, and the lowest vacant one to $A$. The transition between these two orbitals is allowed. On the other hand, *p*-terphenyl is considered to belong to $D_2$. To each of the representations $B_1$ and $B_3$, there belong five orbitals which vary with $\mu$ and one orbital which does not vary with $\mu$ ($B_1$, $+\beta$; $B_3$, $-\beta$). In addition, to each of $A_1$ and $B_2$, three orbitals whose energies do not vary with $\mu$ ($A_1$ $+\beta$, $-\beta$, $-\beta$: $B_2$; $+\beta$, $+\beta$, $-\beta$) belong. The highest occupied orbital belongs to $B_3$, and the lowest vacant one to $B_1$. The transition between these two orbitals is allowed.

The transition between the highest occupied orbital and the lowest vacant one in each compound is considered to correspond to the conjugation band in the spectrum of each compound, and the corresponding transition energy $\Delta E_A$ can be evaluated as a function of $\mu$ by the simple LCAO molecular orbital method. The results of calculations are shown in Table I, in which the data for biphenyl reported previously[1] are included for comparison.

It is evident that the value of $\Delta E_A$ increases in each of the systems as the value of $\mu$ decreases, indicating that the conjugation band should be shifted toward shorter wavelengths with decreasing $\mu$. When $\mu$ is 0, $\Delta E_A$ in each system is $2(-\beta)$, and coincides with the value for benzene.

The difference between the value of $\Delta E_A$ for *o*-terphenyl and that for *p*-terphenyl at the same value of $\mu$ is much smaller than the difference between the

8) J. N. Murrell and H. C. Longuet-Higgins, *J. Chem. Soc.*, **1955**, 2552.
9) O. Bastiansen, *Acta Chem. Scand.*, **6**, 205 (1952).
10) O. Bastiansen, ibid., **3**, 408 (1949).
11) K. Lonsdale, *Z. Kryst.*, **97**, 91 (1937); *Chem. Abstr.*, **31**, 8302 (1937).
12) M. S. Farag, *Acta Cryst.*, **7**, 117 (1954).
13) (a) J. Dhar, *Indian J. Phys.*, **7**, 43 (1932); *Chem. Abstr.*, **26**, 4517 (1932). (b) Idem., *Proc. Natl. Inst. Sci. India*, **15**. 11 (1949); *Chem. Abstr.*, **43**, 4655 (1949).
14) C. J. B. Clews and K. Lonsdale, *Proc. Roy. Soc. (London)*, **A161**, 493 (1937).
15) J. Dale, *Acta Chem. Scand.*, **11**, 650 (1957).

TABLE I

| $\mu$ | $\Delta E_A(-\beta)$ $p$-T | $\Delta E_A(-\beta)$ $o$-T | $\Delta E_A(-\beta)$ B |
|---|---|---|---|
| 1 | 1.1853 | 1.2206 | 1.4092 |
| 0.9 | 1.2527 | 1.2894 | 1.4596 |
| 0.8 | 1.3234 | 1.3611 | 1.5120 |
| 0.7 | 1.3976 | 1.4354 | 1.5666 |
| 0.6 | 1.4750 | 1.5120 | 1.6232 |
| 0.5 | 1.5556 | 1.5908 | 1.6820 |
| 0.4 | 1.6393 | 1.6713 | 1.7424 |
| 0.3 | 1.7258 | 1.7529 | 1.8048 |
| 0.2 | 1.8150 | 1.8353 | 1.8686 |
| 0.1 | 1.9065 | 1.9179 | 1.9338 |
| 0 | 2 | 2 | 2 |

Symbols $p$-T, $o$-T and B represent $p$-terphenyl, $o$-terphenyl, and biphenyl, respectively.

value for biphenyl and that for $o$- or $p$-terphenyl. This fact seems to give some support to the assumption in the treatment of $o$-alkyl- and of $o,o'$-dialkylbiphenyls in the earlier part[16] of this series that the normal electronic bathochromic effect of an $o$-alkyl substituent and that of the corresponding $p$-substituent are approximately of the same magnitude.

According to Dale[15], the ultraviolet absorption spectra of $p$- and of $o$-terphenyls in the crystalline states measured by the pressed KCl-disk technique do not significantly differ from the respectively corresponding solution spectra. Only a normal, or slightly larger than normal, red-shift is observed for each compound. This fact is considered to indicate that the interplanar angles in each compound in solution are not much larger than in the crystalline state. Thus, the spectrum of $p$-terphenyl in hexane shows an intense absorption band without fine structure at 276 m$\mu$ ($\varepsilon$=32100), which is considered to be the conjugation band. (According to the present measurement[17] $\lambda_{max}$ is 276.5 m$\mu$ and $\varepsilon$ is 31800 in $n$-heptane. According to Gillam and Hey[2], $\lambda_{max}$ is 276 m$\mu$ and $\varepsilon$ is 35000 in hexane, and $\lambda_{max}$ is 280 m$\mu$ and $\varepsilon$ is 25000 in chloroform.) On the other hand, the spectrum of the crystalline $p$-terphenyl shows an intense band at 284 m$\mu$. The spectrum of $o$-terphenyl in hexane exhibits a maximum at 232 m$\mu$ ($\varepsilon$=26900), and the spectrum of the crystal at 237 m$\mu$. In addition, the spectra of $o$-terphenyl in both the states show a diffuse maximum or inflection at about 250~260 m$\mu$ (in the hexane solution, $\lambda_{max}$ is about 252 m$\mu$ and $\varepsilon$ is about 11400). Dale has regarded this vestigial band as the $\lambda_1$-band, namely, the "main band" which covers the full chromophore, and the band at 232 m$\mu$ or 237 as the $\lambda_2$-band, namely, the "overtone" or "minor" band.

It is undertaken by applying the author's method to infer the most probable spatial configurations of $o$-terphenyl and of $p$-terphenyl in solution from their spectra. In that case, $p$-terphenyl in the crystalline state is taken as the longer-wavelength-side reference compound, because it has been known to have the planar configuration with the co-annular bond length ($R$) of 1.48 Å [18]. This value of $R$ is equal to that in biphenyl in the crystalline state[13]. Therefore, the value of $\mu$ for the planar $p$-terphenyl molecule is 0.858. This is quite similar to the case of the planar biphenyl[1], and the correspnding value of $\Delta E_A$ is estimated at 1.282($-\beta$), which is referred to as $\Delta E_L$ as usual. The peak wave number of the conjugation band in the spectrum of $p$-terphenyl in the crystalline state measured by the pressed KCl-disk technique, corrected for the normal red-shift[1,15], is taken as the value of the wave number corresponding to $\Delta E_L$ (viz. $\nu_L$). The magnitude of the normal red-shift may be estimated to be about 6 m$\mu$ at 284 m$\mu$ according to the regular relation between the position of the band and the magnitude of the corresponding normal red-shift determined by Dale[15]. Accordingly, the value of $\nu_L$ may be assumed to be 35971 cm$^{-1}$ (278 m$\mu$).

On the other hand, benzene is taken as the shorter-wavelength-side reference compound, similarly to the case of biphenyl. That is, the value of $\Delta E_A$ when $\mu$ is 0 is 2($-\beta$) (viz. $\Delta E_S$), and the corresponding value of $\nu$ (viz. $\nu_S$) is assumed to be 48000 cm$^{-1}$ (the center of gravity of singlets of benzene).

From the positions of the conjugation bands of $o$-terphenyl and of $p$-terphenyl in solution, the respectively corresponding values of $\Delta E_A$ are obtained by the usual procedure (cf. Ref. 1, Eq. 8). (As the conjugation band of $o$-terphenyl the inflection at about 252 m$\mu$ is taken, accepting

16) H. Suzuki, This Bulletin, **32**, 1350 (1959).

17) $p$-Terphenyl was prepared by the reaction of bis-nitrosoacetyl-1,4-phenylenediamine with benzene as described in "Organic Reactions", edited by R. Adams et al., Vol. II, John Wiley & Sons, Inc., New York (1944), p. 252, and purified by sublimation succeeded by repeated recrystallizations from ethanol. The spectrum was measured with a Cary recording spectrophotometer Model 14 M-50.

18) L. W. Pickett, *Proc. Roy. Soc.* (*London*), **A142**, 333 (1933).

TABLE II

| Compound | $\lambda_{max}$, mμ | | $\Delta E_A(-\beta)$ | $\mu$ | $\theta°$ | $R$, Å |
|---|---|---|---|---|---|---|
| *p*-Terphenyl (p) | 278 | (a) | 1.282 | 0.858 | 0 | 1.48 |
| | | (b) | 1.247 | 0.908 | 0 | 1.445 |
| *p*-Terphenyl (s) | 276.5 | (a) | 1.294 | 0.842 | 11 | 1.481 |
| | | (b) | 1.259 | 0.891 | 9.5 | 1.447 |
| | 276 | (a) | 1.298 | 0.836 | 12.5 | 1.482 |
| | | (b) | 1.263 | 0.885 | 11.5 | 1.447 |
| *o*-Terphenyl (s) | (252) | (a) | 1.504 | 0.611 | 43 | 1.496 |
| | | (b) | 1.479 | 0.643 | 42.5 | 1.470 |

Symbols p and s represent the "isolated" planar molecule and the molecule in solution, respectively. Wavelength in parentheses denotes an inflection.

the assignment by Dale, although this would appear to be open to question.) From these values of $\Delta E_A$ the corresponding values of $\mu$ are estimated according to the relations shown in Table I between $\mu$ and $\Delta E_A$ for *o*-terphenyl and for *p*-terphenyl. Then, the corresponding values of $\theta$ (the interplanar angle) and of $R$ are computed according to the relation between $\mu$ and $\theta$ as well as $R$ postulated in Part I of this series (cf. Eqs. 1—7 in Ref. 1). The results of calculations are shown in Table II, being denoted by symbol a.

The fact that the length of the co-annular bonds in the planar molecule of *p*-terphenyl is equal to that in biphenyl would appear to be rather surprising, for it would be expected that the length of the "single" bond might be contracted with the increasing extent of conjugation. This problem will be discussed later. Here, it is tentatively assumed that the co-annular bond length in planar *p*-terphenyl were equal to the "single" bond length, 1.445 Å, in planar *trans*-stilbene, considering that terphenyl as well as stilbene can be regarded as a "tri-conjugated system"[19]. The results of calculation carried out on the basis of this assumption are also shown in Table II, being denoted by symbol b. It is to be noted that the change of the value of the length of the pivot bond of the reference compound from 1.48 to 1.445 Å does not significantly affect the calculated values of the interplanar angles.

According to the result of the X-ray crystal analysis[14], the configuration of *o*-terphenyl in the crystalline state is the one in which the planes of the two outer phenyl groups are turned approximately 50° or less (probably 45~50°) out of the plane of the parent nucleus. Since the interplanar angle in the molecule in solution is considered to be not significantly different from that in the crystalline state in view of the spectral similarity between both the states, it may be said that the calculated value is in considerably good agreement with the experimental value. The interplanar angle in *o*-terphenyl in the vapor phase has been very roughly determined by the electron diffraction method to be about 90°[20].

The most probable configuration of *p*-terphenyl in solution has been inferred to be slightly non-planar, in accordance with the infrared spectroscopic evidence by Dale[21]. It may be noteworthy that the calculated value of the interplanar angle in *p*-terphenyl in solution is considerably smaller than the corresponding one in biphenyl in solution (about 20°)[1]. Furthermore, the value in *p,p'*-quaterphenyl is inferred to be still smaller than that in *p*-terphenyl. According to Dale[15], the position of the conjugation band in the pressed KCl-disk spectrum and that in the hexane solution spectrum (in parentheses) are as follows (wavelengths are in mμ): biphenyl, 253 (246); *p*-terphenyl, 284 (276); *p,p'*-quaterphenyl, 303 (294). On the other hand, the magnitude of the normal red-shift may be estimated to be about 3.5 mμ at 253 mμ, about 6 mμ at 284 mμ, and about 8 mμ at 303 mμ. Accordingly, the position of the conjugation band of the "isolated planar molecule" may be presumed to be 249.5 mμ for biphenyl, 278 mμ for *p*-terphenyl, and 295 mμ for *p,p'*-quaterphenyl, and consequently the differences between the positions of the conjugation bands of the assumed isolated planar molecules and those of the corresponding molecules in solutions are 3.5, 2 and 1 mμ, respectively. This fact may be considered to indicate

19) E. A. Braude and E. S. Waight, "Progress in Stereochemistry", Vol. 1, edited by W. Klyne, Butterworths, Scientific Publications, London (1954), p. 126.

20) I. L. Karle and L. O. Brockway, *J. Am. Chem. Soc.*, **66**, 1974 (1944).

21) J. Dale, *Acta Chem. Scand.*, 11, 640 (1957).

that the degree of the deviation of the most probable configuration of the molecule in solution from the planarity decreases in the order biphenyl > *p*-terphenyl > *p,p'*-quaterphenyl, although it may be somewhat doubtful whether much significance can be attached to the numerical values of these differences themselves mainly because of inevitable uncertainty in the estimation of the magnitude of the normal red-shift.

*o,p'*-Quaterphenyl has two bands at 284 mμ and at 255 mμ in the pressed KCl-disk spectrum, and at 276 mμ and at 248 mμ in the solution spectrum. Dale has interpreted these two bands as $\lambda_1$- and as $\lambda_2$-bands, respectively, on the basis of his concept of the "overtone" band. At any rate, it is of interest that the band at 284 mμ (276 mμ) appears to correspond to the conjugation band of *p*-terphenyl and the band at 255 mμ (248 mμ) to the conjugation band of biphenyl.

**On the Bond Length.**—Lastly, the length of the "single" bond in conjugated systems is briefly discussed. It is noteworthy that the length of the co-annular bond has been proved to be 1.48 Å in each of biphenyl, *p*-terphenyl, and *p,p'*-quaterphenyl[22] in the crystalline state. This fact appears to be in contrast to the expectation that the length of the "single" bond might be contracted with the increasing extent of conjugation, or in other words, with the increasing elongation of the conjugated system, and would be considered to support the striking hypothesis proposed recently by Dewar and coworker[23] that when the distinctions between the bond radius and the energy of bond formation of an $sp^3$ carbon atom and those of an $sp^2$ carbon atom are made it appears that bond lengths and heats of formation can be predicted without considering resonance at all. According to Platt[24], one of the important evidence contributory to Dewar's hypothesis is that the length of the "single" bond 1.48 Å in butadiene represents no shortening of Dewar's $sp^2$–$sp^2$ single bond distance. Butadiene in the vapor phase has been found probably to have almost exclusively the planar *trans*-configuration in which the length of the 2—3 bond is 1.483±0.01 Å [25].

On the other hand, *trans*-stilbene is known to have the planar or nearly planar configuration in which the length of the α-1 "single" bond is 1.44±0.02 Å or 1.45±0.02 Å in the crystalline state[26]. That is, the further shortening of the $sp^2$–$sp^2$ bond occurs in *trans*-stilbene as compared with those in polyphenyls and in butadiene. In addition, Cook[27] has pointed out that the length of the $sp^2$–$sp^2$ "single" bond varies from about 1.44 to about 1.55 Å with the angle between the planar groups joined by such a bond, in accordance with the assumptions made previously by the present author[1,28]. Therefore, in spite of Dewar's new hypothesis, it seems evident that the length of the "single" bond depends on the extent of conjugation, or in other words, on the extent of the π—π interaction across the bond. Hence, the bond length may be to be correlated with the π-bond order as usual after all.

When the actual bond lengths are taken into account, the value of the π-bond order is estimated at 0.319 for the co-annular bond of biphenyl[1] and at 0.384 for the α-1 bond of *trans*-stilbene[29]. On the other hand, when the π—π resonance integral is taken as β for all the bonds, the value of the π-bond order is 0.370 for the co-annular bond of biphenyl[1], is 0.375 for that of *p*-terphenyl[30], and is 0.431 for the α-1 bond of *trans*-stilbene[30]. In view of these values it may not be surprising that the length of the co-annular bond of *p*-terphenyl as well as that of *p,p'*-quaterphenyl is not substantially different from that of biphenyl in spite of the elongation of the conjugated system, and that the length of the "singe" bond of *trans*-stilbene is considerably shorter than those of these polyphenyls. It may be of interest in this connection that Syrkin and Dyatkina[31] have shown by calculations by the molecular orbital method that there is an increase of 0.38(−β) in the resonance energy for each Ph–Ph bond in the formation of biphenyl, terphenyl, or quaterphenyl.

22) L. W. Pickett, *J. Am. Chem. Soc.*, **58**, 2299 (1936).
23) M. J. S. Dewar and H. N. Schmeising, *Tetrahedron*, **5**, 166 (1959).
24) J. R. Platt, *Ann. Rev. Phys. Chem.*, **10**, 349 (1959).
25) A. Almenningen, O. Bastiansen and M. Traetteberg, *Acta Chem. Scand.*, **12**, 1221 (1958).
26) J. M. Robertson and I. Woodward, *Proc. Roy. Soc. (London)*, **A162**, 568 (1937).
27) D. Cook, *J. Chem. Phys.*, **28**, 1001 (1958).
28) H. Suzuki, This Bulletin, **25**, 145 (1952).
29) H. Suzuki, the succeeding part of this series to be published.
30) N. P. Buu-Hoï, C. A. Coulson, P. and R. Daudel, M. Martin, A. and B. Pullman, *Rev. sci.*, **85**, 1041 (1947).
31) Ya. K. Syrkin and M. Dyatkina, *Acta Physicochim. U.S.S.R.*, **21**, 641 (1946); *Chem. Abstr.*, **41**, 1648 (1947).

**Summary**

The ultraviolet absorption spectra and the spatial configurations of polyphenyls have been briefly surveyed, and then the most probable spatial configurations of *p*-terphenyl and of *o*-terphenyl have been inferred from the spectra by application of the method analogous to the one for biphenyl in the first part of this series, resulting in the interplanar angle of about 10° for *p*-terphenyl and in that of about 43° for the *o*-isomer. Some related compounds have also been discussed. Further, it has been shown that the length of the "single" $sp^2$–$sp^2$ bond of the conjugated system depends on the extent of the $\pi$—$\pi$ interaction across the bond, contrary to Dewar's recent hypothesis.

The author thanks Professor Kengo Shiomi for reading the manuscript and for advice.

*Department of Chemistry*
*College of General Education*
*The University of Tokyo*
*Meguro-ku, Tokyo*

# SHORT COMMUNICATIONS

## *Temperature Dependence of Ceric-cerous Gamma-ray Dosimeter*

By Hiroshi HOTTA and Kazuo SHIMADA

(Received August 20, 1959)

The 0.8 N sulfuric acid aqueous solution of ceric sulfate is usually recommended as a gamma-ray dosimeter for high dose. On the other hand, the temperature of irradiated solutions is apt to be raised at high dose rate owing to the absorption of gamma-ray energy. Therefore, in order to examine the temperture effect on the yield of cerous ion, the above solution was irradiated for one or two hours in a water thermostat under various dose rate between about $7\times10^4$ *r*/hr. and $6\times10^6$ *r*/hr. at the Co-60 Irradiation Laboratory of JAERI, and the yield was determined from the decrement of optical density at 314 m$\mu$. Ceric sulfate (Frederick Smith Chem. Co.) without further purification was dissolved in water, distilled triply as usual, in a test tube of hard glass (Hario Glass). A series of the samples was put carefully under the same condition for various temperatures between about 20 and 90°C.

The logarithm of the decrement of optical density of the sample irradiated

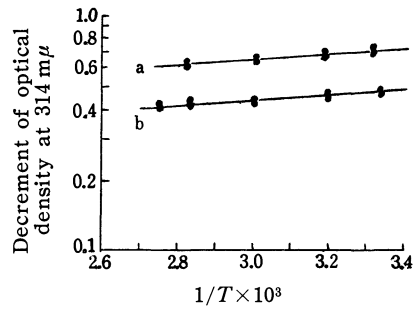



Fig. 1. The observed decrement of optical density of ceric ion by irradiation for 1 hr., against the inverse absolute temperature at (a) $5.6\times10^5$ *r*/hr. and (b) $1.7\times10^6$ *r*/hr. For measuring, the sample was diluted to the suitable concentration, for convenience.

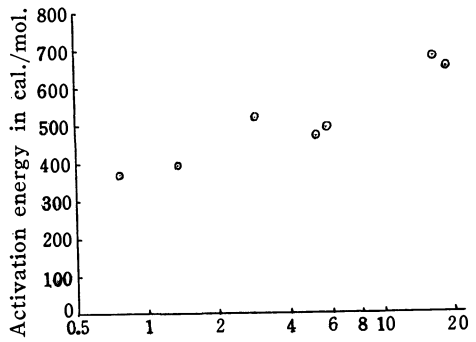



Fig. 2. The apparent activation energy of the reduction of cerous ion at various dose rates.

for one hour at $5.6\times10^5$ and $1.7\times10^6$ $r$/hr., among the observed values at various dose rate is plotted against inverse absolute temperature in Fig. 1. The value at higher dose rate was more reproducible than at the lower one owing to the property of this system. The decrement of the optical density, namely, the yield of cerous ion decreses with the increase of temperature as shown in Fig. 1.

The interpretation of the result is not so easily given, for the various elementary reactions are surposed. According to Hardwick, the apparent activation energy is about −300 cal./mol. at very low dose rate (600 millicurie radium source)[1].

*Japan Atomic Energy Research Institute*
*Tokai, Ibaraki-ken*

1) T. J. Hardwick, *Can. J. Chem.*, **30**, 23 (1952).

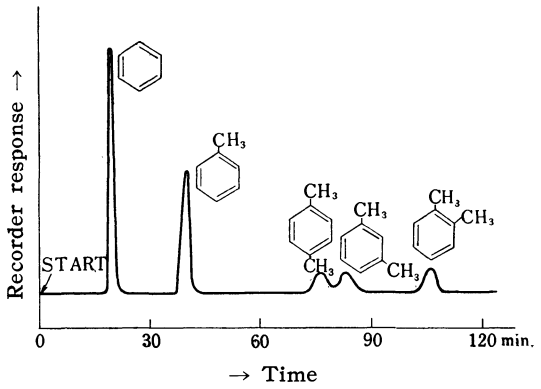



Fig. 1. Chromatogram of aromatic hydrocarbon mixture.
Column; 293 cm.×6 mm. α-naphthylamine (32:100) w/w on C-22 firebrick (50~60 mesh) +7 cm.×6 mm. bare C-22 firebrick (50~60 mesh) at the end of column. Temp., 87°C.
$N_2$ flow rate: 45.7 ml./min., 0.02 ml. of sample was charged.

TABLE I. EXPERIMENTAL DATA OBTAINED

Relative retention volume (toluene=1.00) at 87°C

| Benzene | Toluene | Ethylbenzene |
|---|---|---|
| 0.45 | 1.00 | 1.95 |
| *p*-Xylene | *m*-Xylene | *o*-Xylene |
| 1.97 | 2.13 | 2.76 |

Relative peak separation $S_{12}=0.085$ (*p*-xylene and *m*-xylene).
Resolution $R=0.93$ (*p*-xylene and *m*-xylene).
Theoretical plate number (*o*-xylene); 2800

$$S_{12}=(t_2-t_1)/t_1,\quad R=(t_x\cdot S_{12})/w$$

where $t_1$=elution time of first peak,
$t_2$=elution time of second peak,
$t_x$=elution time of given peak,
$w$=peak width at base line.

## *Gas-Liquid Partition Chromatography of m- and p-Xylenes on α-Naphthylamine*

By Takeo ARAKI and Ryozo GOTO

(Received November 27, 1959)

Recently, Zlatkis, Ling and Kaufman[1] reported the resolution of isomeric xylenes by gas-liquid partition chromatography, and a good separation of *m*- and *p*-xylene was attained by using 1-chloronaphthalene as the liquid substrate. The isomers, *m*- and *p*-xylene have now been resolved. The stationary liquid phase used was α-naphthylamine which is expected to show an ionic character similar to that of 1-chloronaphthalene in the partition of xylenes. A value for the relative peak separtion[2] ($S_{12}=0.085$) for α-naphthylamine was better than the reported value for 1-chloronaphthalene ($S_{12}=0.060$)[1].

Since α-naphthylamine is known to be quite unstable, the end of the column (approximately 7 cm.) was packed with a bare solid support C-22 to maintain a stable base line. When ethylbenzene was present in the aromatic samples, this stationary liquid would not separate *p*-xylene from ethylbenzene. A chromatogram is illustrated in Fig. 1, and experimental conditions and data are listed in Table I.

More detaitled information on this subject will be published elsewhere.

The authors wish to thank the support of Yawata Chemical Industry Co. for assembling the gas-chromatograph instruments used in this study. This work has been carried out by the Scientific Research Grant-in-aid of the Ministry of Education.

*Department of Chemistry*
*Faculty of Science*
*Kyoto University*
*Sakyo-ku Kyoto*

1) A. Zlatkis, S. Ling and H. R. Kaufman, *Anal. Chem.*, **31**, 945 (1959).
2) W. L. Jones and R. Kieselbach, ibid., **30**, 1590 (1958).

## *The Szilard-Chalmers Effect of Calcium and Tungsten Oxinates*

By Hiroshi EBIHARA and Kenji YOSHIHARA

(Received September 30, 1959)

The enrichment of radioactive calcium or tungsten by the Szilard-Chalmers process has not been successful so far. Bruno and Belluco[1] could not find the Szilard-Chalmers effect of calcium ethylenediaminetetraacetate complex. The present authors found enrichment of $^{45}Ca$ and $^{185}W$ during their studies on the Szilard-Chalmers effect of calcium and tungsten complexes of 8-hydroxyquinoline (oxine).

*n*-Butylamine is the best solvent tested for calcium oxinate, but is water-miscible. A preliminary tracer study on the cation exchange behavior of $^{45}Ca$ as bivalent cation in the solvent showed a very high recovery (nearly 100%) of $^{45}Ca$ on the resin. Accordingly the ion-exchange in *n*-butylamine was used in order to catch $^{45}Ca$ in a cationic form leaving the oxinate in the solution. In each experiment about 5.0 g. of dehydrated calcium oxinate irradiated in JRR-1 for about 15 or 60 hr. (neutron flux: $10^{11}$ $n/cm^2 \cdot sec.$, about 95% thermal neutron) was dissolved in *n*-butylamine. The solution was passed through a cation exchange resin column (7.0 mm.$\phi$ $\times$100 mm. of Diaion SK-1, H-form, 100~200 mesh, 1.1 ml./min.). After washing the column with a sufficient volume of *n*-butylamine and water, $^{45}Ca$ on the resin was eluted with 6 N hydrochloric acid. Calcium was precipitated as phosphate for the measurement of radioactivity. The results listed in Table I show that about 6~8% of $^{45}Ca$ is separated in a cationic form from the complex with an enrichment factor of 40~120.

TABLE I. SEPARATION OF $^{45}Ca$ BY THE SZILARD-CHALMERS EFFECT

| Irrad. time | Yield** | Ca taken* | Ca found in the cationic fraction* | Enrichment factor |
|---|---|---|---|---|
| hr. | % | mg. | mg. | |
| 15 | 5.9 | 405 | 0.34 | 70 |
| 15 | 8.3 | 405 | 0.28 | 120 |
| 60 | 8.3 | 390 | 5.13 | 63 |
| 60 | 7.0 | 399 | 6.75 | 41 |
| 60 | 7.4 | 381 | 4.14 | 68 |
| 60 | 8.3 | 376 | 6.61 | 47 |

* The quantity of calcium was determined by the phosphate method.

** Yield=the amount of $^{45}Ca$ in the cationic form/total amount of $^{45}Ca$.

To investigate the Szilard-Chalmers effect of $^{185}W$, about 1.0 g. of dehydrated tungsten oxinate irradiated in JRR-1 for about 15 hr. was dissolved in 150 ml. of chloroform, and the solution was shaken with the buffer solution of various pH values. Thus $^{185}W$ separated from the complex by the Szilard-Chalmers effect was collected in the aqueous solution. The quantities of tungsten were determined colorimetrically. The results are listed in Table II.

TABLE II. EXTRACTION OF $^{185}W$ FROM TUNGSTEN OXINATE

| pH | Yield | W taken*** | W found in the extracted fraction | Enrichment factor |
|---|---|---|---|---|
| | % | mg. | mg. | |
| 1.01 | 37.3 | 38.0 | 0.24 | 59 |
| 2.98 | 34.2 | 38.0 | 0.09 | 144 |
| 4.02 | 33.5 | 38.0 | 0.07 | 196 |
| 5.00 | 33.7 | 38.0 | 0.06 | 233 |
| 5.96 | 33.1 | 38.0 | 0.07 | 194 |
| 7.01 | 33.9 | 38.0 | 0.03 | 429 |
| 9.02 | 38.0 | 38.0 | 0.18 | 80 |
| 10.06 | 44.0 | 38.0 | 0.39 | 43 |

*** The quantity of tungsten was determined by the thiocyanate method.

High enrichment factors were obtained in the pH range between 3~7, and the maximum enrichment factor was 429 at pH 7. The extraction yield was almost constant (34%) in this pH range.

*Division of Isotope Applications*
*Japan Atomic Energy Research Institute*
*Tokai, Ibaraki-ken*

1) M. Bruno and U. Belluco, *Ricerca sci.*, **26**, 2985 (1956).

## *Sorption of Benzene by Isotactic and Atactic Polystyrenes*

By Hisashi Odani, Michio Kurata and Mikio Tamura

(Received November 6, 1959)

In recent years there has been much interest in the physical properties of stereo-specific synthetic polymers. The present authors have recently studied the absorption and desorption of benzene by three isotactic polystyrenes of different degrees of crystallinity and one atactic

polystyrene at 35°C[1]. Sorption isotherm data have been obtained for these systems from both integral and differential kinetic runs*.

An isotactic polystyrene (isotactic-PS) used a sample that had been prepared by stereo-specific polymerization with Ziegler's catalyst. After the purified polymer had been boiled in heptane for thirty hours, the polymer was separated into isotactic and atactic fractions, by extracting the latter with cold methyl ethyl ketone. The isotactic-PS films were obtained by the same procedure reported elsewhere[1]. The polymer films of different degrees of crystallinity were then prepared by annealing these films at three different combinations of temperature and period. These annealing conditions are summarized in Table I, in which the degree of crystallinity of each specimen estimated roughly by the X-ray method are also given. An atactic polystyrene (atactic-PS) sample used was a commercial sample, "Lustrex hi-flow 77-234", and a benzene of A. R. grade was used as penetrant. The sorption apparatus and procedure were practically the same as those reported elsewhere[1].

TABLE I. ANNEALING CONDITIONS AND DEGREES OF CRYSTALLINITY OF ISOTACTIC PS's

| | Annealing condition | | Degree of crystallinity |
|---|---|---|---|
| | Temp. °C | Period hr. | |
| Isotactic PS-I | 120 | 2 | 0.08 |
| Isotactic PS-II | 180 | 0.5 | 0.45 |
| Isotactic PS-III | 160 | 1.5 | 0.50 |

Fig. 1 gives absorption isotherms obtained for the three isotactic-PS's and for the atactic-PS at 35°C. Here the ordinate represents the mass of benzene in grams sorbed per gram of a given polymer at dry state and the abscissa the relative pressure of a given vapor in the external phase. It is seen that the isotherm in the region of medium relative pressure is much steep for atactic-PS and becomes less steep with increase of crystallinity for isotactic-PS's. This feature is analogous to that for isotherms on systems water vapor-celluloses having different

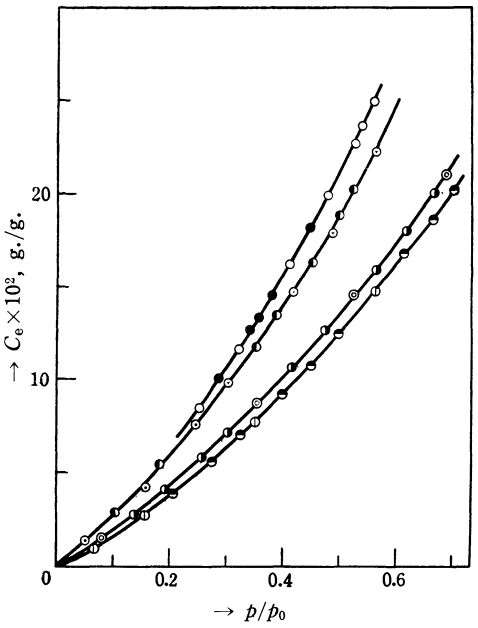



Fig. 1. Absorption isotherms of isotactic PS's and atactic PS-benzene at 35°C.

| | Integral absorption | Differential absorption |
|---|---|---|
| Isotactic PS-I | ⊙ | ◐ |
| Isotactic PS-II | ◎ | ◑ |
| Isotactic PS-III | ⓘ | ◓ |
| Atactic PS | ○ | ● |

degrees of crystallinity[2]. It is also seen that the data from integral absorption experiments and those from differential ones fall well on a single curve for each system.

For any given relative pressure the equilibrium amount of benzene in dry polystyrene decreases with increase in crystallinity. This suggests that benzene is mainly absorbed in amorphous regions of a given sample. If this is the case, there should hold

$$(C_e)_i = (C_e)_a(1-\phi) \qquad (1)$$

where $(C_e)_a$ and $(C_e)_I$ are the equilibrium concentrations of benzene at a given relative pressure in an atactic-PS and in an isotactic-PS in which the volume fraction of crystal region is $\phi$, respectively. The values of $\phi$ may be calculated as a function of relative pressure by applying Eq. 1 to the data of Fig. 1. Within the range where the calculations are possible, $\phi$ is practically independent of $p/p_0$ for each isotactic-PS, giving an average value $0.10_7$, $0.36_4$ and $0.41_0$ for the isotactic-PS-I,

1) A. Kishimoto, H. Fujita, H. Odani, M. Kurata and M. Tamura, *J. Phys. Chem.*, to be published.

* The term "differential" was used to denote experiments in which the difference between initial and final pressures was sufficiently small, while the term "integral" referred to experiments in which this pressure difference was relatively large.

2) P. H. Hermans, "Physics and Chemistry of Cellulose Fibers", Elesevier, New York (1949), Part II, Chap. II.

-II and -III, respectively. It is interesting that these values are reasonably compared to the crystallinities of respective samples shown in Table I, which were estimated from the intensities of the X-ray diffraction peaks.

The authors wish to thank Professor H. Fujita and Dr. A. Kishimoto of this University for their helpful discussions. The isotactic polystyrene sample was supplied to them by Professor J. Furukawa of this University, to whom they express sincere thanks.

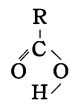
*Department of Industrial Chemistry*
*Faculty of Engineering*
*Kyoto University*
*Sakyo-ku, Kyoto*

## *Intramolecular Hydrogen Bonding in α-Keto- and α-Alkoxy-carboxylic Acids*[1]

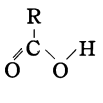
By Michinori Ōki and Minoru Hirota

(Received November 9, 1959)

A number of hydroxylic compounds which carry a proton accepting group at a suitable position have been verified to form an intramolecular hydrogen bonding, but only a few examples of intramolecular hydrogen bonding involving the hydroxyl group of a carboxyl group as a proton donor have been known. The structure of a normal carboxyl group has been suggested to be non-planar, the O–H bond being 30° away from *cis*-planar conformation[2]. However, when an acid has a proton accepting group at α- or β-position to the carboxyl group, the *trans*-structure will be stabilized owing to the formation of an intramolecular hydrogen bonding and will be allowed to exist in spite of the otherwise unfavorable conformation.



(I) *cis*-Structure



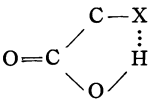
(II) *trans*-Structure

In this regard, the infrared spectra of such compounds including monomethyl oxalate, pyruvic acid, methoxyacetic acid, phenoxyacetic acid, and their homologues were examined with a Perkin Elmer 112G Spectrophotometer in carbon tetrachloride solution[3]. The concentration of the solution was less than 0.002 mol./l. in order to minimize the effect of dimeric association. As summarized in Table I, the results

Table I. $\nu_{O-H}$ Absorption of the carboxyl group of various carboxylic acids

| Acid | $\nu_{O-H}$ Absorption frequencies | | | |
|---|---|---|---|---|
| | Free form | | Hydrogen-bonded form | |
| | $\nu_{max}$ | $\varepsilon_{max}$ | $\nu_{max}$ | $\varepsilon_{max}$ |
| Monomethyl oxalate | 3516.3 | 34 | 3461.1 | 72 |
| Monomethyl malonate | 3529.9 | 58 | | |
| Pyruvic | 3528.9 | 16 | 3430.7 | 69 |
| Acetoacetic | 3530.7 | 60 | | |
| Benzoylformic | 3504.2 | 22 | 3397.2 | 69 |
| Benzoylacetic | 3535.4 | 63 | | |
| Methoxyacetic | 3526.7 | 38 | 3395.8 | 31 |
| β-Methoxypropionic | 3539.0 | 65 | | |
| Phenoxyacetic | 3527.9 | 60 | 3484.7 | 34 |
| β-Phenoxypropionic | 3531.7 | 68 | | |

show that a carboxylic acid which carries a proton accepting group at α-position bear two $\nu_{O-H}$ bands. The results may be interpreted as an evidence for the existence of a hydrogen bonding and consequently for structure II. The peaks at higher frequencies appear between 3550 and 3500 $cm^{-1}$ and are assigned to the $\nu_{O-H}$ bands of free monomeric acids. The peaks at lower frequencies can be assigned to the $\nu_{O-H}$ bands of the intramolecularly hydrogen-bonded forms. It may be also pointed out that the intramolecular hydrogen bonding is observed only when a five membered ring is formed (structure III).



(III)

Since the proton accepting power of an atom is largely influenced by the electron density, the authors expected some electronic effects to be exerted on the hydrogen bonding ability; the spectra of various substituted phenoxyacetic acids were thus measured. The results are in accordance with the expectation, as shown in Table II, where apparent integrated absorption intensities of the two bands

1) Part I: *J. Chem. Soc. Japan, Pure Chem. Sec.* (*Nippon Kagaku Zasshi*), in press.
2) C. P. Smyth, "Dielectric Behavior and Structure", McGraw-Hill Book Co., Inc., New York (1955), p. 306.
3) M. Ōki and H. Iwamura, This Bulletin, **32**, 567 (1959).

TABLE II. $\nu_{O-H}$ ABSORPTION OF *p*-SUBSTITUTED PHENOXYACETIC ACIDS

| Substituents | Free form | | Hydrogen-bonded form | | Intensity ratio* |
|---|---|---|---|---|---|
| | $\nu_{max}$ | $B_f$ | $\nu_{max}$ | $B_h$ | $B_h/B_f$ |
| $CH_3O$ | 3527.7 | 1.28 | 3481.3 | 1.02 | 0.80 |
| $CH_3$ | 3528.8 | 1.21 | 3484.5 | 0.96 | 0.79 |
| H | 3526.9 | 1.54 | 3487.5 | 0.75 | 0.49 |
| Cl | 3524.3 | 2.32 | 3492.9 | 0.74 | 0.32 |
| $C_6H_5CO$ | 3525.6 | 2.5 | 3495.6 | 0.25 | 0.10 |
| $NO_2$ | 3521.8 | | Not found. | | 0 |

* The ratio is a more important factor than the individual integrated intensity in discussing the properties of the bands, since the effect of the dimeric form can not be completely neglected.

were obtained graphically instead of taking the absorption coefficient because of the closeness of the two bands.

Another evidence for the existence of the hydrogen bonding may be obtained from the measurement of the carbonyl region. The measurement revealed that two bands are also found for the monomeric acid when it carries a proton accepting group at the $\alpha$-position and that the higher frequency absorption disappears when no hydrogen bonding is observed in the O-H stretching region. Thus, the peak at about 1790 $cm^{-1}$ is assigned to the $\nu_{C=O}$ band of structure II and that between 1735 and 1730 $cm^{-1}$ to structure I.

The details will be reported in the near future.

*Department of Chemistry*
*Faculty of Science*
*The University of Tokyo*
*Hongo, Tokyo*

## *Behavior of Energetic Radiobromine Atoms Arising from $(n, \gamma)$ Reaction in Cobalt Complex Salts*

By Nobufusa Saito, Takeshi Tominaga and Hirotoshi Sano

(Received November 10, 1959)

In the course of the investigation on the behavior of hot radiobromine atoms ($^{80m}$Br and $^{82}$Br) in bromopentammine cobalt complex salts[1], the present authors found that some of such energetic radiobromine atoms arising from $(n, \gamma)$ reaction either in ligand bromine or in anionic bromine eventually entered ligands of the complexes through formation of chemical bond with the cobalt atom. When solid complex salts, $[Co(NH_3)_5Y]Br_{2,3}$ and $[Co(en)_2Y_2]Br_{1,3}$, were irradiated, the fraction of total produced radiobromine finally retained in ligands (hereafter defined as "ligand yield") was found to vary with changing ligand group, Y. In order to clarify the mechanism of hot-atom behavior of radiobromine in these systems, the present authors investigated the effects of various ligands on the ligand yields in these complex salts.

Experimental procedures were similar to those described in the previous paper[1]. Distribution of radiobromine was determined by a procedure involving separation with a cation exchange resin.

As shown in Tables I and II, enrichment of radiobromine in ligands was observed with these complex salts. On the irradiation of the salts $[Co(NH_3)_5Y] \cdot Br_{2,3}$, several complexes labeled with Br* ($[Co(NH_3)_5Br^*]^{2+}$, $[Co(NH_3)_4YBr^*]^{1,2+}$, etc.) might possibly be produced through reactions of hot radiobromine atoms with the target complex. However, almost all labeled complexes other than $[Co(NH_3)_5 \cdot Br^*]^{2+}$ were extremely unstable to aquotization in aqueous solutions, and it was possible with adequate procedures of separation to obtain the ligand yield without appreciable contribution of yields in the forms of unstable labeled complexes, $[Co(NH_3)_4YBr^*]^{1,2+}$ etc. Therefore, the ligand yield in Table I may be taken as almost identical with the fraction of radiobromine stabilized in the form of $[Co \cdot (NH_3)_5Br^*]^{2+}$, or that obtained through replacement of Y by Br*. On the irradiation of the salts $[Co(en)_2Y_2]Br_{1,3}$, the probability of replacement of ethylenediamine in ligands seemed to be very small. Thus, the ligand yield in Table II may be taken as indicating the fraction of radiobromine in the form of $[Co(en)_2YBr^*]^{1,2+}$. It is interesting that no significant differences were observed between the ligand yields of *cis*- and *trans*-isomers of both $[Co(en)_2(NCS)_2]Br$ and $[Co(en)_2Cl_2]Br$.

To explain the relationship between ligand yield and Y, the present authors proposed a model in which collisions of

1) N. Saito, H. Sano and T. Tominaga, This Bulletin, 33, 20 (1960).

TABLE I. LIGAND YIELD OF SOLID $[Co(NH_3)_5Y]Br_{2,3}$

| No. | Irradiated salt | Ligand yield[a] % | Enrichment factor |
|---|---|---|---|
| 1 | $[Co(NH_3)_6]Br_3$ | 4.8±0.2 | 4 ×10² |
| 2 | $[Co(NH_3)_5NCS]Br_2$ | 5.7±0.3 | 1.2×10² |
| 3 | $[Co(NH_3)_5NO_2]Br_2$ | 8.0±0.3 | 4 ×10² |
| 4 | $[Co(NH_3)_5OH_2]Br_3$ | 7.1±0.7 | 0.2×10² |
| 5 | $[Co(NH_3)_5ONO]Br_2$ | 8.8±0.1 | 9 ×10² |
| 6 | $[Co(NH_3)_5ONO_2]Br_2$ | 9.0±0.3 | 0.3×10² |
| 7 | $[Co(NH_3)_5F]Br_2$ | 7.3±0.6 | 6 ×10² |
| 8 | $[Co(NH_3)_5Cl]Br_2$ | 15.2±0.4 | 3 ×10² |
| 9 | $[Co(NH_3)_5I]Br_2$ | 15.8±0.4 | 5 ×10² |
| 10 | $[Co(NH_3)_5Br]Br_2$ | 17.3±0.6 | — |

a) $\text{Ligand yield} = \frac{\text{Activity of Br* retained in ligands}}{\text{Total activity of Br* produced}} \times 100$

TABLE II. LIGAND YIELD OF SOLID $[Co(en)_2Y_2]Br_{1,3}$

| No. | Irradiated salt | Ligand yield % | Enrichment factor |
|---|---|---|---|
| 11 | $[Co(en)_3]Br_3$ | 0.0±0.1 | — |
| 12 | *trans*-$[Co(en)_2(NH_3)_2]Br_3$ | 0.8±0.1 | 0.8×10² |
| 13 | *trans*-$[Co(en)_2(NCS)_2]Br$ | 4.5±0.2 | 6 ×10² |
| 14 | *cis*-$[Co(en)_2(NCS)_2]Br$ | 5.0±0.1 | 4 ×10² |
| 15 | *trans*-$[Co(en)_2Cl_2]Br$ | 16.6±0.3 | 5 ×10³ |
| 16 | *cis*-$[Co(en)_2Cl_2]Br$ | 17.9±0.3 | 4 ×10³ |
| 17 | *trans*-$[Co(en)_2Br_2]Br$ | 37 ±2 | — |

TABLE III. CALCULATED VALUES OF $\gamma$ FOR THE DONOR ATOM IN Y IN A COLLISION WITH A HOT BROMINE ATOM

| Y | Donor atom | $\gamma = 4MM'/(M+M')^2$ |
|---|---|---|
| $NH_3$, NCS, $NO_2$ | N | 0.50 |
| $OH_2$, ONO, $ONO_2$ | O | 0.56 |
| F | F | 0.64 |
| Cl | Cl | 0.85 |
| I | I | 0.95 |
| Br | Br | 1.00 |

hot bromine atom with the donor atom in Y played an important role. When the masses of the donor atom in ligand Y, and of bromine atom are $M$ and $M'$, respectively, the fraction of the maximum possible loss in the recoiling energy of a hot bromine atom for an elastic collision with the donor atom is given by $\gamma = 4MM'/(M+M')^2$. Calculated values of $\gamma$ for donor atoms in different ligands, Y, are shown in Table III. Fig. 1 shows the relationship between the ligand yield and the $\gamma$ value for the complex salts listed in Tables I and II. As each complex molecule of the salts $[Co(en)_2Y_2]Br_{1,3}$ contains more Y's in ligands than that of $[Co(NH_3)_5Y]Br_{2,3}$, the probability of the collision of a hot bromine atom with Y may be somewhat larger for the former

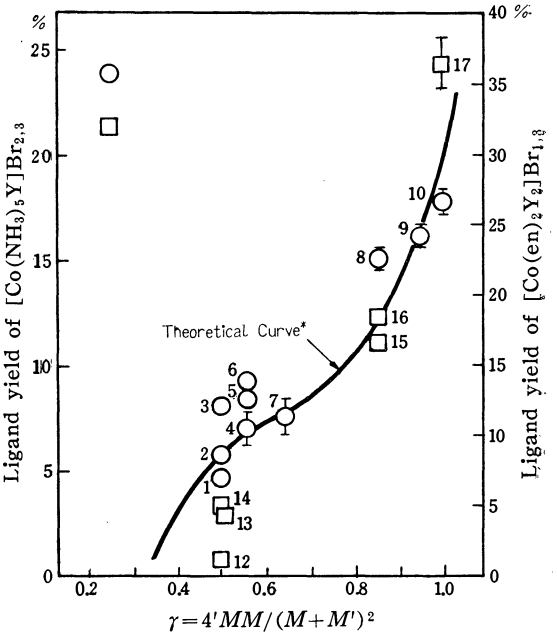



Fig. 1. The relationship between the ligand yield and the value of $\gamma$.
○ $[Co(NH_3)_5Y]Br_{2,3}$
□ $[Co(en)_2Y_2]Br_{1,3}$
* The shape of this curve was theoretically predicated on the basis of the model proposed by the present authors. Details will be published elsewhere.

salts. Based on the crystallochemical data, the ratio of relative collision cross sections of a bromine atom with Y in ligands was estimated as about 1.5 : 1 for $[Co(en)_2Y_2]Br$ and $[Co(NH_3)_5Y]Br_2$. Therefore, different ligand yield scales were used for the two series in Fig. 1 where both are shown together. It is seen in Fig. 1 that the ligand yield seems to increase as the value of $\gamma$ of the donor atom in ligand Y increases: the efficiency of replacement of Y by hot bromine depends mainly on $\gamma$. Therefore, it may be presumed that the kinetic processes play an important role to determine the fate of hot bromine atoms in these systems.

*Department of Chemistry*
*Faculty of Science*
*The University of Tokyo*
*Hongo, Tokyo*

## *Electronic Structure and Antifungal Activity of Quinoline- and Pyridine-N-oxide Derivatives*

By Kenichi FUKUI, Akira IMAMURA and Chikayoshi NAGATA

(Received December 9, 1959)

Many studies have ever been undertaken in order to elucidate the mechamism of action of fungicides or antifungal substances. Albert et al., through the experiments on 8-hydroxyquinoline, concluded that a chelate formation may be involved in the process of fungicidal action[1]. Ikeda found some parallelism between the reduction potential and the fungicidal activity of 1,4-naphthoquinone derivatives and assumed that the binding ability of fungicides with SH group in the body of fungi may be the main factor determining the fungicidal activity[2].

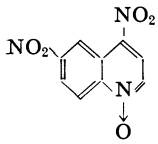
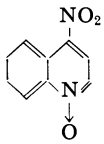
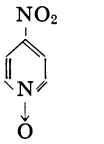
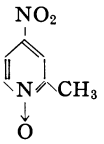
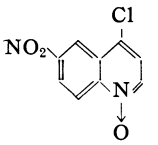
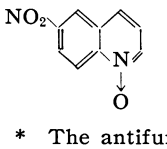
For the purpose of the elucidation of the reaction mechanism involved in the early stage of fungicidal action of quinoline- and pyridine-*N*-oxide derivatives, the present authors have calculated the reactivity indexes, namely, the approximate superdelocalizability ($S'_r$) which is one of the reactivity indexes used in the frontier electron theory and proved to be a good index for discussing the biological actions of carcinogenic compounds and plant growth compounds[3,4].

**Result and Discussion.**—In the present paper the authors dealt with *N*-oxides containing the nitro group such as 4-nitroquinoline-*N*-oxide, 6-nitroquinoline-*N*-oxide, 4,6-dinitroquinoline-*N*-oxide, 4-chloro-6-nitroquinoline-*N*-oxide, 4-nitropyridine-*N*-oxide, and 2-methyl-4-nitropyridine-*N*-oxide whose antifungal activities were tested recently by Okabayashi et al.[5]

From an organic chemical point of view, the most probable reaction is the nucleophilic replacement of the nitro group, since this group is very susceptible to the attack by nucleophilic reagent. If any reaction of this type plays a dominant role in the fungicidal action, the order of antifungal activity must be parallel with the reactivity index of the attacked position. The result of the authors' calculation supports this assumption. That is, the order of approximate superdelocalizability for the nucleophilic attack ($S'^{(N)}$) at the most reactive position in the molecule is nearly parallel with antifungal activity as is seen in Table I. The signs + and − indicate the degree of antifungal activity. The larger the number of + sign is, the greater the activity is. The sign − indicates that the compound has no activity. One exception is inactive 4,6-dinitroquinoline-*N*-oxide whose $S'^{(N)}$ value at position 4 is far larger than the most potent fungicide, 4-nitro-quinoline-*N*-oxide. In order to obviate this difficulty, one can assume that the upper threshold value of reactivity index for occurrence of activity as well as the lower one might exist. Such an interpretation has frequently been made in the theoretical study of biological phenomena, for instance, the carcinogenic action of polycondensed aromatic hydrocarbons and azo compounds. Inactiveness of 4,6-dinitroquinoline-*N*-oxide, therefore, may be understood if the authors suppose that this compound is so reactive that it would react with various groups in the body of fungi before it reaches the reaction center connected with the fungicidal action.

1) A. Albert, S. D. Rubbo, R. J. Goldacre and B. G. Balfour, *Brit. J. Exptl. Path.*, **28**, 69 (1947).
2) N. Ikeda, *J. Pharm. Soc. Japan* (*Yakugaku Zasshi*), **75**, 1073 (1955).
3) C. Nagata, K. Fukui, T. Yonezawa and Y. Tagashira, *Cancer Research*, **15**, 233 (1955).
4) K. Fukui, C. Nagata and T. Yonezawa, *J. Am. Chem. Soc.*, **80**, 2267 (1958).
5) T. Okabayashi, *J. Fermentation Technology* (*Hakkô Kôgaku Zasshi*), **31**, 373 (1953).

TABLE I. RELATION BETWEEN REACTIVITY INDEX AND ANTIFUNGAL ACTIVITY OF QUINOLINE- AND PYRIDINE-*N*-OXIDE DERIVATIVES

| Compound | Approximate superdelocalizability for nucleophilic ($S_r'^{(N)}$) attack | Antifungal activity* |
|---|---|---|
|  | 1.014(4)** | − |
|  | 0.630(4) | +++ |
|  | 0.297(4) | ++ |
|  | 0.279(4) | + |
|  | 0.205(6) | + |
|  | 0.168(6) | − |

* The antifungal activity was tested for Aspergillus oryzae, Tolura utilis, Saccharomyces sake and Zygosaccharomyces soja by Okabayashi, and the signs + and − are given by the present authors considering the experimental activity.

** The figures in the parentheses indicate the position at which the nucleophilic substitution is assumed to take place.

On the other hand, Okabayashi's *in vitro* experiment showed that the nitro group of 4-nitroquinoline-*N*-oxide was easily substituted by the SH group of cystein and the substituted compound lost its antifungal activity. Bearing this fact in mind together with the theoretical result obtained by the present authors, it may be possible to correlate the easiness of nucleophilic substitution at the carbon atom to which the nitro group is attached with the antifungal activity of nitro group-containing quinoline- and pyridine-*N*-oxides.

Parameters for chloro, methyl and nitro groups used in the calculation are the same as those of a previous paper[4]. Since there seem to exist no unambiguous values used for Coulomb integrals of *N*-oxide, the present authors adopt, according to the result of analyses of the ultraviolet spectrum[6], the values $\alpha+\beta$ and $\alpha+1.8\beta$ for nitrogen and oxygen, respectively.

*Faculty of Engineering*
*Kyoto University*
*Sakyo-ku, Kyoto*

6) M. Ito and W. Mizushima, *J. Chem. Phys.*, **24**, 495 (1956).

## *Synthesis of N-Acetyl-O-benzyl-DL-threonine and O-Benzyl-L-threonine*

By Yasuhiro Murase*, Kenji Okawa and Shiro Akabori

(Received December 11, 1959)

Difficulties are encountered in the synthesis of the peptides containing serine or threonine owing to the presence of the hydroxyl group that induces an unexpected side reaction during the synthetic procedure.

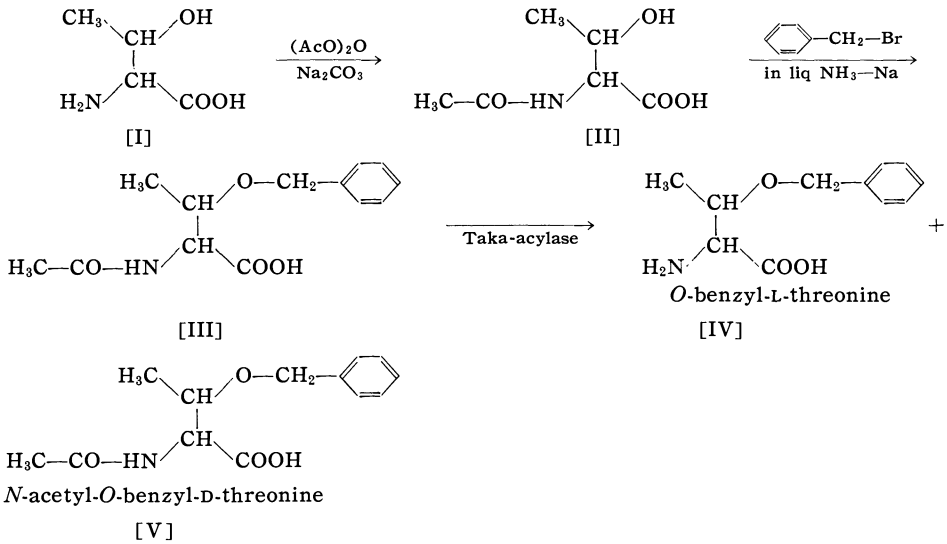
In order to avoid an undesirable side reaction, one of the authors[1] had already synthesized *O*-benzyl-L-serine in which the free hydroxyl group was protected with the benzyl rest.

In this communication, the authors will describe the synthesis of the *O*-benzyl-L-threonine from *N*-acetyl-DL-threonine, which was prepared by the direct acetylation of the DL-threonine with the acetic anhydride method.

**Synthesis of *N*-Acetyl-DL-threonine [II].**—DL-Threonine (12 g.) was dissolved in 200 ml. of an aqueous solution containing sodium carbonate (13.5 g.). Into the above solution was added dropwise acetic anhydride (12 g.) under vigorous stirring at +5°C. After the addition was over, the stirring was continued for about 30 min. at room temperature. When the reaction was over,

* Takamine Laboratory, Sankyo Co., Ltd., Shinagawa-ku, Tokyo.

1) K. Okawa, This Bulletin, **29**, 486 (1956).




[I] [II] [III] [IV]

*N*-acetyl-*O*-benzyl-D-threonine

[V]

about 100 ml. of Dowex 50 (H-form) was added to the reaciton mixture under stirring until the evolution of the carbon dioxide ceased. The resulting mixture was passed through the Dowex 50 (H-form) ion exchange column (7 $cm^2 \times 30$ cm.). By elution with water, the effluent was collected and concentrated in vacuo. The resulting syrupy materials were crystallized with ethylacetate. The crude products weighed 14 g., 87% yield. The recrystallization from ethylacetate containing alcohol gave a pure material (12.9 g.) in 80% yield, m. p. 132~133°C.

*Anal.* Found: C, 44.73; H, 6.96; N, 8.78. Calcd. for $C_6H_{11}O_4N$: C, 44.75; H, 6.88; N, 8.70%.

***N*-Acetyl-*O*-benzyl-DL-threonine [III].** — *N*-Acetyl-DL-threonine (8.5 g.) was dissolved in liquid ammonia (200 ml.), followed by portionwise addition of methallic sodium (2.3 g.) at −60°C. After benzylbromide (18 g.) was added into the above solution, the reaction vessel was taken out from the cooling Dewar's bottle; then the temperature of the reaction mixture raised to −28°C and ammonia was gradually evolved off at this temperature for 2.5 hr. The resulting mixture was dissolved in an aqueous solution of sodium bicarbonate, the aqueous solution extracted with ether being acidified with 6 N hydrochloric acid. The crystals produced were extracted with ethylacetate, and the organic layer was washed with water and dried. By removing the solvent, the crude product (2.0 g.) was obtained in 16% yield. Recrystallization from hot water gave a pure material (1.3 g.), m. p. 141~142°C.

*Anal.* Found: C, 61.69; H, 6.67; N, 541. Calcd. for $C_{13}H_{17}O_4N$: C, 62.13; H. 6.82; N, 5.57%.

**Optical Resolution of *N*-Acetyl-*O*-benzyl-DL-threonine.**—*Preparation of enzyme solution.*—Takadiastase (1 g.) was extracted with 10 ml. of water at 0°C. for 2 hr. and an insoluble part was filtered off using Cellite. The crude enzyme solution was used for the resolution without further purification.

*Enzymic resolution of N-acetyl-O-benzyl-DL-threonine.* — *N*-Acetyl-*O*-benzyl-derivative (1 g.) was dissolved in an aqueous solution of 2 N sodium hydroxide containing a slight excess of sodium hydroxide which brought the solution to pH 7.4. The above enzyme solution, together with the substrate, was incubated at 36.5°C for 24 hr. After incubation was over, the mixture was passed through the Amberlite IR-120 column (H-form). By the first elution with water, the acidic component was removed off, and then the amino acid component was liberated by the second elution with an aqueous 1 N ammonia (about 150 ml.). The latter eluate collected was concentrated in vacuo. The resulting product was dissolved in a small amount of hot water, boiled for 10 min. to remove the contaminant and filtered. The filtrate was concentrated and dried in vacuo. The residual weighed about 330 mg., 79% yield. Crystallization from hot water gave fine crystals of *O*-benzyl-L-threonine which melted at 197°C with decomposition. $[\alpha]_D^{19°} -3.04$ ($c$=1, 1 N HCl).

*Anal.* Found: C, 57.61; H, 7.62; N, 6.31. Calcd. for $C_{11}H_{15}O_3N \cdot H_2O$: C, 58.13; H, 7.54; N, 6.16%.

*Department of Chemistry*
*Faculty of Science*
*Osaka University*
*Nakanoshima, Osaka (K. O.)*

*Institute for Protein Research*
*Osaka University*
*Nishi-ku, Osaka (Y. M. & S. A.)*

## *Molecular Configuration of Poly(m-methylstyrene) and Poly(p-trimethylsilylstyrene)*

By Isamu NITTA, Yōzō CHATANI and Yoshiaki SAKATA*

(Received October 19, 1959)

Syntheses and infrared studies of poly(*m*-methylstyrene) (PMMS) and poly(*p*-trimethylsilylstyrene) (PPTMSS) have already been reported by Murahashi, Nozakura and Tadokoro[1]. In this communication, molecular configuration of these polymers will be reported on the basis of X-ray diffraction evidence.

The fiber period calculated from the layer line spacing is 57.1 Å for PMMS and 60.6 Å for PPTMSS. And by taking photographs of tilted specimens, axial maximum intensity on the 29th layer line was observed (see Fig. 1). The repeat distance of successive monomers along the fiber axis (1.97 Å for PMMS and 2.09 Å for PPTMSS) is much shorter than 2.53 Å found in the case of fully extended chain of singly linked carbon atoms. Therefore, it would be appropriate to conclude that these polymers construct uniform helices in their crystalline regions, indicating one of characteristic features of isotacticity.

To analyze further the helical structure, the authors used the method of Cochran

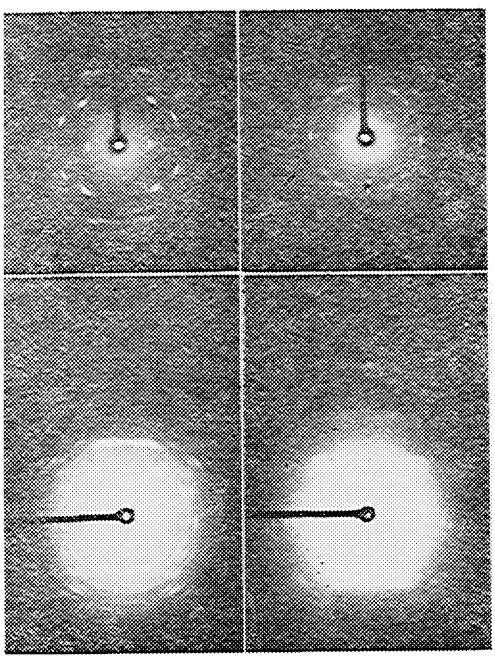


Fig. 1. Fiber diagrams of X-ray diffraction patterns.
Left: Poly(*m*-methylstyrene)
Right: Poly(*p*-trimethylsilylstyrene)
Upper: The axis of specimen is vertical.
Lower: The axis of specimen is inclined at about 23° to the vertical.

TABLE I

| (PMMS) | | | (PPTMSS) | | |
|---|---|---|---|---|---|
| *l** | *I*** | \|*n*\|**** | *l* | *I* | \|*n*\| |
| 0 | *s* | 0 | 0 | *s* | 0 |
| 1 | — | 11 | 1 | — | 13 |
| 2 | — | 7 | 2 | *mw* | 3 |
| 3 | *m* | 4 | 3 | — | 10 |
| 4 | — | 14 | 4 | *w* | 6 |
| 5 | *ms* | 3 | 5 | — | 7 |
| 6 | — | 8 | 6 | — | 9 |
| 7 | — | 10 | 7 | *ms* | 4 |
| 8 | *s* | 1 | 8 | — | 12 |
| 9 | — | 12 | 9 | *s* | 1 |
| 10 | *mw* | 6 | 10 | — | 14 |
| 11 | — | 5 | 11 | *s* | 2 |
| 12 | — | 13 | 12 | — | 11 |
| 13 | *ms* | 2 | 13 | — | 5 |
| 14 | — | 9 | 14 | — | 8 |
| 15 | — | 9 | 15 | — | 8 |
| 16 | — | 2 | 16 | — | 5 |
| 17 | — | 13 | 17 | — | 11 |
| 18 | — | 5 | 18 | *vw* | 2 |
| 19 | — | 6 | 19 | — | 14 |
| 20 | — | 12 | 20 | *w* | 1 |
| 21 | *w* | 1 | 21 | — | 12 |
| 22 | — | 10 | 22 | — | 4 |
| 23 | — | 8 | 23 | — | 9 |
| 24 | — | 3 | 24 | — | 7 |
| 25 | — | 14 | 25 | — | 6 |
| 26 | — | 4 | 26 | — | 10 |
| 27 | — | 7 | 27 | — | 3 |
| 28 | — | 11 | 28 | — | 13 |
| 29 | *m* | 0 | 29 | *m* | 0 |
| 30 | — | 11 | 30 | — | 13 |
| 31 | — | 7 | 31 | — | 3 |
| 32 | — | 4 | 32 | — | 10 |
| 33 | — | 14 | 33 | — | 6 |
| 34 | — | 3 | 34 | — | 7 |
| 35 | — | 8 | 35 | — | 9 |
| 36 | — | 10 | 36 | — | 4 |
| 37 | *vw* | 1 | 37 | — | 12 |
| 38 | — | 12 | 38 | *w* | 1 |
| 39 | — | 6 | 39 | — | 14 |
| 40 | — | 5 | 40 | — | 2 |

* Index of the layer.
** Estimated average intensity of the layer.
*** Order of the Bessel function.

* Present address: Yatsushiro Laboratory, Kokoku Rayon and Pulp Co., Ltd., Yatsushiro-shi, Kumamoto.

1) S. Murahashi, S. Nozakura and H. Tadokoro, This Bulletin, **32**, 534 (1959).

and others[2]. Taking the fiber axis as the $c$ axis and using cylindrical coordinates $R, \phi, l/c$ in the reciprocal space, the structure factor of a helical molecule can be given as follows :

$$F(R, \phi, l/c) = \sum_j \sum_n f_j J_n(2\pi R r_j) \times \exp\left\{i\left[n\left(\phi - \varphi_j + \frac{\pi}{2}\right) + 2\pi l z_j/c\right]\right\} \quad (1)$$

where $r_j, \varphi_j, z_j$ represent the cylindrical coordinates of the $j$-th atom of a monomer, and $J_n$'s are Bessel functions, the order $n$ of which are to be obtained properly for the reflexions on each layer line $l$ by solving the equation ;

$$l = un + vm \quad (n, m ; \text{integers}) \quad (2)$$

where $u$ and $v$ are, respectively, the number of turns and that of monomers in the repeat distance.

Trial consideration** on various possibe types of helices shows that the helix of 8 turns ($u=8$, $v=29$) for PMMS and 9 turns ($u=9$, $v=29$) for PPTMSS will be taken as to account qualitatively for average intensity of each layer line (see Table I). The helical model thus obtained seems to be quite reasonable, because, from the observed value of fiber period and the assumed 1.54 Å of the C-C single bond length, the standard tetrahedral angle (109.5°) comes out in the permissible region of C-C-C bond angle calculated for the C helix. Moreover, the region of intense reflexions conforms to the properties of the selected Bessel function for each layer line. After all such considerations the authors are led to the probable configuration shown in Fig. 2. Although precise orientations of side groups have not been determined from such considerations alone, it would be imagined reasonable that the plane of phenyl radical is so inclined as to be influenced by steric hindrances of neighboring hydrogen atoms.

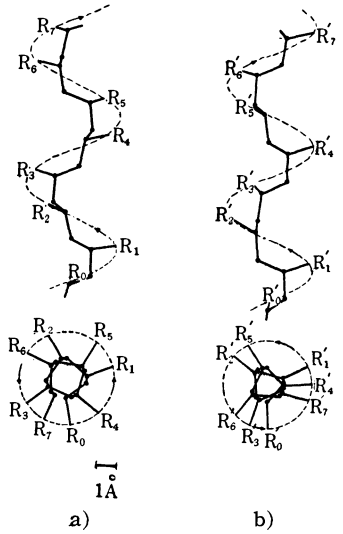



Fig. 2. Chain configuration of the molecule (side and end views of right-handed helix only two turns drawn).
a) Poly($m$-methylstyrene), R=$C_6H_4CH_3$
b) Poly($p$-trimethylsilylstyrene), R'=$C_6H_4Si(CH_3)_3$

The authors wish to express their thanks to Professor S. Murahashi, Dr. S. Nozakura and Dr. H. Tadokoro for the supply of the specimens and the discussion.

*Department of Chemistry*
*Faculty of Science*
*Osaka University*
*Nakanoshima, Osaka*

2) W. Cochran, F. H. C. Crick and V. Vand, *Acta Cryst.*, 5, 581 (1952).

** From Eq. 1, it is shown that on a particular layer line a strong reflexion can occur in a region where $R$ is small only if the corresponding Bessel function is of a low order, so long as a helix dose not take too large a value of any $r_j$.

# *The Abnormality in the Mechanical Behavior of Polyvinyl Acetate-Carbon Tetrachloride Gel*

By Kazuyoshi OGINO

(Received February 23, 1959)

It is well known that many polymeric substances are typically visco-elastic: their stress under constant strain decreases continuously with time; i. e. stress relaxation is observed. In this case, it is usual that the stress deteriorates with time, and this is expected from the following consideration: when a specimen is held under a constant strain, the relative position or the configuration of the molecules changes with time so as to attain a more unstrained position, and thus the stress which corresponds to this strain decreases with time. This is the stress relaxation in "normal" condition.

On the other hand, Tobolsky et al. found[1] that some abnormalities in the stress relaxation under constant elongation appear at about 100°C when natural and several synthetic polymers are heated in the air. Further, they thought that the structural or chemical changes are reflected in the visco-elastic behavior of these substances. This phenomenon is known as the chemorheological process.

Many examples of abnormalities in the mechanical properties of polymeric substances have been interpreted as the result of the scission of the network chain or the cross-linking reaction by oxygen in the air*,[2].

The author found that the mechanical behavior of swollen polyvinyl acetate gels, which were cross-linked slightly with diallyl adipate and swollen in several organic solvents, shows abnormality when carbon-tetrachloride was used as a solvent; i. e. their stress *increases* continuously with time when the temperature was raised above 50°C. When one chooses polyvinyl acetate, polymethyl acrylate, polymethyl methacrylate or polystyrene as the polymeric substance, and chloroform, benzene, toluene, carbon tetrachloride or methanol as the solvent, the combination of polyvinyl acetate and carbon tetrachloride is the only system which causes an increase in stress under constant strain. The purpose of this paper is to report this abnormality, and to make a possible interpretation for this phenomenon.

## Experimental

**Materials.**—Commercial monomeric vinyl acetate was shaken several times with aqueous alkaline solution, and with distilled water. This process was repeated three times. The monomer was then distilled under reduced pressure.

Diallyl adipate was synthesized by esterification of allyl alcohol with adipic acid, and was purified by fractional distillation under reduced pressure**.

Carbon tetrachloride was purified by washing with aqueous alkaline solution and by distillation.

Vinyl acetate monomer mixed with cross-linking agent was polymerized thermally in bulk in a sealed glass tube under the presence of benzoyl peroxide as initiator (about 0.5 wt. %). This had been purified by recrystallization. At the beginning of polymerization, the temperature was kept at about 50°C until the contents were solidified, and was then held at 100°C for 12 hr.

The polymer rod was cut into several pieces, about 1 cm. in length, and was brought to the swelling equilibrium in carbon tetrachloride.

**Apparatus.** — The apparatus used in this

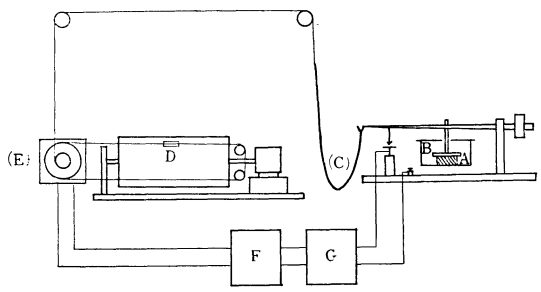



Fig. 1. The apparatus for the measurement of stress relaxation.
A: Specimen. B: Solvent. C: Chain.
D: Rotating drum & pencil.
E: Balancing motor. F: Relay.
G: Amplifying circuit.

1) A. V. Tobolsky and R. D. Andrews, *J. Chem. Phys.*, **13**, 3 (1945).

* The effect of oxygen upon the stress relaxation or creep was studied by the measurement which is known as the intermittent and continuous method.

2) R. D. Andrews, E. E. Hanson and A. V. Tobolsky, *J. Appl. Phys.*, **17**, 352 (1946).

** This cross-linking agent is the same as was used in the previous work; K. Ogino, This Bulletin, **31**, 577 (1958).

experiment is the same as the one used in the previous work[3], and is shown in Fig. 1.

The temperature of the sample was controlled by circulation of water from a water bath, and was read directly by a thermometer immersed in the solvent. The temperature was so high (about 50°C) that in some cases the fluctuation was observed to some extent, but this did not exceed 1°C.

## Results and Discussion

Fig. 2 shows the relation between stress and time at about 50°C under 20% strain. It is clear from this figure that the stress in these gels decreases slightly in the first step and then increases. The degree of this increase in stress becomes larger as the degree of swelling diminishes.

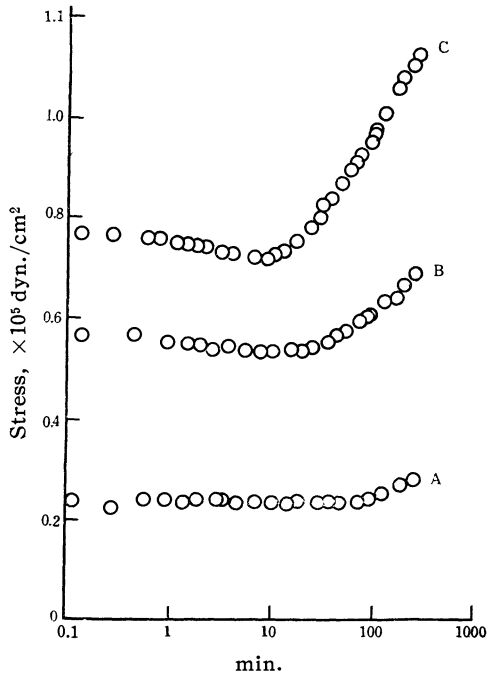



Fig. 2. The relation between stress and time under 20% strain (vertical compression) in $CCl_4$.
A: Volume fraction 0.24 at 48°C.
B: Volume fraction 0.33 at 49°C.
C: Volume fraction 0.42 at 49°C.

Oxygen from the air can not be considered to be the cause of this abnormality, because this occurs only in the system of polyvinyl acetate and carbon tetrachloride, and does not occur in any other polymer-solvent combinations. It is difficulty to find any reason for the effect of atmospheric oxygen being found in this system alone. The structural difference between vinyl acetate and methyl acrylate is only in the position of the carbonyl group. There must consequently be some special meaning for the vinyl acetate system. This can be interpreted as follows.

It is well known that in the solution polymerization, especially when carbon tetrachloride, carbon tetrabromide, chloroform, sulfur dichloride or mercaptane is chosen as solvent, the chain transfer with solvent molecules occurs very easily and each polymer molecule contains fragments of the solvent[4]. Such a compound is known as telomer, and the reaction is called telomerization. Fig. 3 shows the mechanism of the chain transfer with carbon tetrachloride as an example.

On the other hand, the chain transfer with monomeric vinyl acetate takes place in the scheme as shown in Fig. 4.

$$Mn\cdot + CCl_4 \rightarrow MnCl + \cdot CCl_3$$
$$\cdot CCl_3 + M \rightarrow M\cdot CCl_3\cdot \rightarrow MnCCl_3\cdot$$
$$MnCCl_3\cdot + CCl_4 \rightarrow \underset{\text{(Telomer)}}{Cl\cdot Mn\cdot CCl_3} + \cdot CCl_3$$

Fig. 3. The chain transfer with carbon tetrachloride.

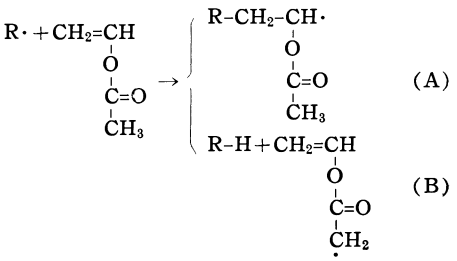



Fig. 4. The chain transfer with vinyl acetate.

In this case, it is noticeable that the radical of type B is produced. This is considered to be the cause of the existence of vinyl groups which are connected to the end of the branching along the long chain molecule of polyvinyl acetate[5]. In the case of the other monomers, such as methyl acrylate, methyl methacrylate or styrene, radicals of this type rarely exist. The existence of this radical, and consequently the possibility of the existence of vinyl groups at the end of each branching in polymer is the characteristic feature of vinyl acetate.

Hence, the polymer which has a structure like that shown schematically in Fig.

3) K. Ogino, This Bulletin, **31**, 580 (1958).

4) P. J. Flory, *J. Am. Chem. Soc.*, **59**, 241 (1937); J. W. Breitenbach and H. Maschin, *Z. physik. Chem.*, **A187**, 175 (1940).

5) O. L. Wheeler, E. Iarin and R. N. Crozier, *J. Polymer Sci.*, **9**, 159 (1952).

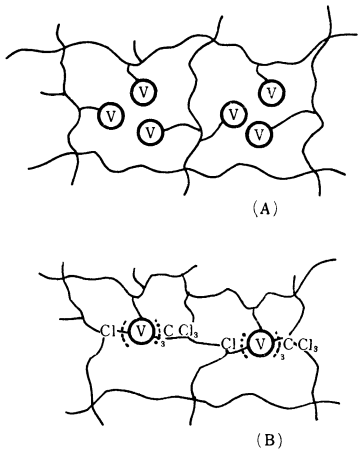



Fig. 5. The schematic diagram to show the internal structure of polyvinyl acetate. ($V$=Vinyl group)

5A will be produced when vinyl acetate is polymerized thermally in bulk in a sealed tube under the presence of benzoyl peroxide as an initiator. Therefore, when this polymer is brought to the swelling equilibrium with carbon tetrachloride, and is maintained at about 50°C, telomer will be formed between carbon tetrachloride and vinyl groups present at the end of each branching. This feature is shown in Fig. 5B. If this reaction occurs, the effective molecular weight between junction points decreases, and so the stress will increase. In order that this reaction, telomerization, may take place, it is necessary that radicals exist in this system. This postulation seems to be satisfied because the initiator which was added initially into the monomer will still remain undecomposed in the polymer, and further, it is demonstrated, for example, by Ingram[6], that radicals which are created in the course of polymerization will remain unchanged.

To confirm this postulation, the mechanical property of polyvinyl acetate, which was swollen at room temperature in carbon tetrachloride with 5% bromine added, was investigated. By this treatment, vinyl groups may be saturated and radicals may be consumed by bromine; i. e. it may be considered that the cause which provokes telomerization will be removed. This result is shown in Fig. 6. It is clear that after the treatment with bromine solution the "normal" relaxation

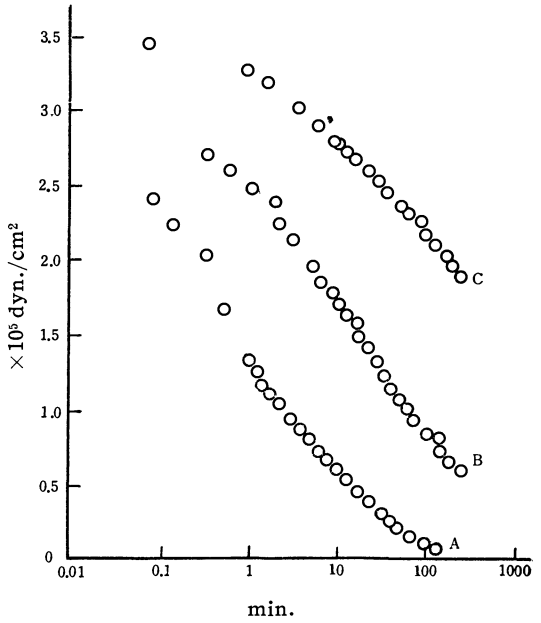



Fig. 6. The relation between stress and time under 20% strain after the treatment by bromine solution in carbon tetrachloride.

of stress is observed. The volume fraction of polymer in bromine solution is larger than that in carbon tetrachloride. This may be due to the polar effect of substituted bromine atoms.

If it may be assumed that the abnormality observed in the system polyvinyl acetate-carbon tetrachloride gel arises from telomerization between vinyl groups and solvent, it is expected that when chloroform is used as a solvent a similar abnormality will be observed. But, as shown in Fig. 7, this was not observed. This may be due to the fact that chloroform is a good solvent for polyvinyl acetate and the degree of swelling becomes very great, so the chain molecules will be fairly far apart from each other in this solvent compared with the case in carbon tetrachloride***.

Tobolsky et al. showed that the splitting or reforming reaction of cross-linkages by oxygen occurs between chain molecules[7], and that if the number of splits per cubic centimeter is a linear function of time, the decay of stress follows the Maxwellian

6) D. J. E. Ingram et al., *Trans. Faraday Soc.*, **54**, 409 (1958).

*** Tobolsky et al. found that the effect of oxygen upon the mechanical property was not observed in swollen polymer, and thought that this might be due to the greater distance of chain molecules in the swollen state than in the dry state[1].

7) A. V. Tobolsky, D. Metz and R. B. Mesrobian, *J. Am. Chem. Soc.*, **72**, 1942 (1950).

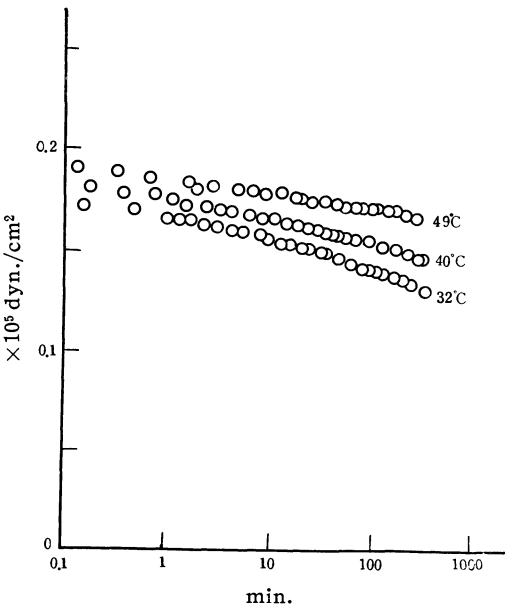



Fig. 7. The relation between stress and time in chloroform. (The volume fraction: 0.020)

decay law[8], or

$$f(t) = f(0) \exp(-kt)$$

where $f(0)$ is the stress at time zero, $f(t)$ the stress at time $t$, and $k$ the rate constant.

Now, for the system polyvinyl acetate-carbon tetrachloride gel, if $a$ is the number of vinyl groups at time zero between junction points, and $x$ of this group are consumed at time $t$ by telomerization, the following equation can be postulated because the rate of telomerization, $dx/dt$, will be primarily dependant upon the distance between chain molecules[1], and as the reaction proceeds, the chance of two vinyl groups meeting with each other will increase by the presence of newly formed cross-linkage. Thus, the rate of reaction will be proportional to the number of vinyl groups which have been cross-linked; i. e.

$$dx/dt = kx$$

therefore,

$$\ln(x/a) = kt$$

The stress at time $t$ can be considered to be proportional to the number of cross-linkages, $x$, which are formed between junction points, and so,

$$\ln\{f(t)/f(0)\} = kt$$

Thus, if one plots the results of Fig. 2 as $\ln(f/f_0)$ against $t$, the curves of Fig. 8 are obtained. The slope in each curve is identical with the rate constant, $k$, if the term of stress relaxation is neglected.

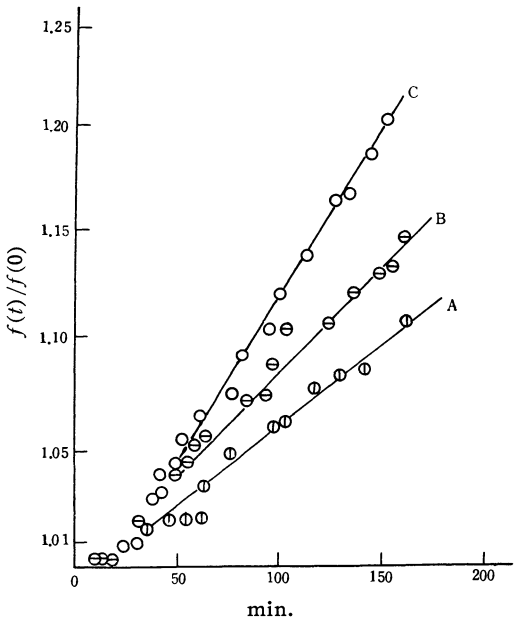



Fig. 8. The plot of $\ln\{f(t)/f(0)\}$ against $t$ at about 50°C.

The abnormality in the mechanical behavior of polyvinyl acetate-carbon tetrachloride gel was interpreted here by telomerization between vinyl groups and solvent.

The author wishes to express his indebtedness to Professor H. Akamatu and Assistant Professor T. Nakagawa for their interest and support, and to Dr. N. Inamoto for his helpful advice and criticism concerning this experiment.

*Department of Chemistry*
*Faculty of Science*
*The University of Tokyo*
*Hongo, Tokyo*

8) M. D. Stern and A. V. Tobolsky, *J. Chem. Phys.*, 14, 93 (1946).

# *Effect of Ionization on the Behavior of Insoluble Monolayers*

By Shoichi IKEDA and Toshizo ISEMURA

(Received March 23, 1959)

It has been observed experimentally that an insoluble monolayer of electrolyte is more condensed on an aqueous subphase of higher concentration of salt while it is more expanded on that of lower concentration. Such an effect of salt on the behavior of ionized monolayer was first elucidated by Davies[1] in the light of the theory of electric double layer, which was based on the Gouy-Chapman's theory of diffuse double layer developed by Derjaguin and Landau[2] and Verwey and Overbeek[3]. Investigations on ionized monolayers have been carried out further along this line[4,5].

In the present paper the authors will show that the same results can be derived from a simpler thermodynamic consideration as well as from the electrostatic theory. The present theory is not only more intuitive and tractable but also is a more general approximation, although it assumes an uncertified model.

An insoluble monolayer may be supposed to be a two-dimensional solution in a surface phase, in which the monolayer substance behaves as a solute, apart from its non-polar side chains. It exerts a surface pressure for maintaining thermodynamic equilibrium with the bulk phase. Thus, for an electrolyte monolayer it may be assumed that its ionized groups are dissolved uniformly in a "surface phase" with a definite thickness, $\delta$, and ions of salt in the aqueous subphase are distributed between the surface and bulk phases, counter ions being concentrated in the surface phase and co-ions being repelled from there into the bulk phase. The distribution of ions between the two phases will be first evaluated by an analogy to the membrane equilibrium and then by an improved approximation. The difference in ionic concentrations between the two phases resulting from the ionization of monolayer contributes to both surface pressure and potential. These contributions will be calculated by means of a thermodynamic procedure.

Consider a uni-univalent type of salt and a monolayer substance whose molecule dissociates into an insoluble cation carrying $i$-univalent ionized groups and $i$ univalent anions common with those of the salt. The ionized groups of the monolayer are assumed to be uniformly distributed in the surface phase. Since the surface phase can not be defined from the present theory alone, its thickness, $\delta$, must be assigned so as to cover the effective thickness of the diffuse double layer, as seen later.

## Membrane Equilibrium for Ionized Monolayer

In the present model it is assumed that the boundary between the surface and bulk phases behaves like a semipermeable membrane in osmotic equilibrium and, to the first approximation, the distribution of diffusible ions between these phases is governed by conditions similar to those in Donnan's membrane equilibrium in colloidal solution[6]. That is, electrochemical potentials of each diffusible ion in both phases are put equal. In the expression of the electrochemical potential functions, activities may be substituted by concentrations, unless they are very high.

Let the concentrations of cation and anion of salt be $\bar{n}_+$ and $\bar{n}_-$ (ions per cm$^3$) in the surface phase, respectively, and those of both ions equally $n$ in the bulk phase. If the electrostatic potential of diffusible ions in the surface phase relative to that in the bulk phase is $\psi_D$, conditions for equilibrium are given by

$$\begin{aligned} kT\ln\bar{n}_+ + e\psi_D &= kT\ln n \\ kT\ln\bar{n}_- - e\psi_D &= kT\ln n \end{aligned} \qquad (1)$$

where $e$ is the elementary charge, $k$ the

1) J. T. Davies, *Proc. Roy. Soc.*, **A208**, 224 (1951).
2) B. Derjaguin and L. Landau, *Acta Physicochim.*, **14**, 633 (1941).
3) E. J. W. Verwey and J. Th. G. Overbeek, "Theory of the Stability of Lyophobic Colloids", Elsevier, Publishing Co., Inc., New York (1948).
4) K. Hamaguchi and T. Isemura, This Bulletin, **28**, 9 (1955).
5) J. N. Phillips and E. Rideal, *Proc. Roy. Soc.*, **A232**, 159 (1955).
6) F. G. Donnan and E. A. Guggenheim, *Z. physik. Chem.*, **A162**, 346 (1932).

Boltzmann constant and $T$ the absolute temperature. Furthermore, it is assumed that the surface phase remains electrically neutral, i.e.

$$\bar{n}_+ + \frac{i\Gamma_M}{\delta} = \bar{n}_- \tag{2}$$

where $\Gamma_M$ (ions per cm$^2$) is the surface concentration of non-diffusible cations, each with $i$ univalent ionized groups, in the surface phase. From Eqs. 1 and 2 the equilibrium concentrations of diffusible ions are obtained as

$$\begin{aligned}\bar{n}_+ &= \frac{1}{2}\left\{-\frac{i\Gamma_M}{\delta} + \sqrt{\left(\frac{i\Gamma_M}{\delta}\right)^2 + 4n^2}\right\} \\ \bar{n}_- &= \frac{1}{2}\left\{\frac{i\Gamma_M}{\delta} + \sqrt{\left(\frac{i\Gamma_M}{\delta}\right)^2 + 4n^2}\right\}\end{aligned} \tag{3}$$

They can also be written as

$$\begin{aligned}\bar{n}_+ &= n\exp(-e\psi_D/kT) \\ \bar{n}_- &= n\exp(e\psi_D/kT)\end{aligned} \tag{4}$$

where

$$i\Gamma_M = 2n\delta\sinh\frac{e\psi_D}{kT} \tag{5}$$

The surface excesses of diffusible ions may be defined as

$$\begin{aligned}\Gamma_+ &= \delta(\bar{n}_+ - n) \\ \Gamma_- &= \delta(\bar{n}_- - n)\end{aligned} \tag{6}$$

and the surface concentration of the ionized group is

$$i\Gamma_M = 1/A \tag{7}$$

where $A$ is the area per ionized group.

In order to determine the thickness of the surface phase, $\delta$, and the potential of ionized groups of monolayer, $\psi_M$, one must take account of the results of the theory of diffuse double layer. According to the theory, concentrations of diffusible ions at the depth, $x$, below the surface, where the electrostatic potential is $\psi$, are given by

$$\begin{aligned}n_+ &= n\exp(-e\psi/kT) \\ n_- &= n\exp(e\psi/kT)\end{aligned} \tag{8}$$

where $n$ is the concentration of each ion or salt far away from the surface. Their surface excesses may be defined by

$$\begin{aligned}\Gamma_+ &= \int_0^\infty (n_+ - n)\mathrm{d}x \\ \Gamma_- &= \int_0^\infty (n_- - n)\mathrm{d}x\end{aligned} \tag{9}$$

which lead to

$$\begin{aligned}\Gamma_+ &= \frac{2n}{\kappa}\left\{\exp\left(-\frac{e\psi_G}{2kT}\right) - 1\right\} \\ \Gamma_- &= \frac{2n}{\kappa}\left\{\exp\left(\frac{e\psi_G}{2kT}\right) - 1\right\}\end{aligned} \tag{10}$$

Here $\psi_G$ is the potential at the surface, $x=0$, and $\kappa$ is the Debye-Hückel parameter

$$\kappa^2 = \frac{8\pi ne^2}{\varepsilon kT} \tag{11}$$

$\varepsilon$ being the dielectric constant. As for the distribution of diffusible ions, the present treatment corresponds to an averaged procedure of the theory of diffuse double layer. Thus, equating Eq. 6 to Eq. 10, it follows that

$$\delta = 2/\kappa \tag{12}$$

and

$$\psi_D = \psi_G/2 \tag{13}$$

The electrostatic potential of ionized groups of monolayer, $\psi_M$, should be equal to the Gouy potential, $\psi_G$. Hence, it is twice as high as the electrostatic potential of diffusible ions, or the membrane potential, $\psi_D$.

$$\psi_M = 2\psi_D \tag{14}$$

It may be assumed generally in the treatment of ionized monolayers based on the present model of surface phase that the thickness of surface phase is given by $2/\kappa$ and the electrostatic potential of ionized groups is twice as high as that of diffusible ions.

### Improved Approximation for the Distribution of Ions

The distribution of diffusible ions obtained in the previous section has been derived from a simple assumption that the surface phase is electrically neutral. In this section one will develop an approximate method when this assumption is removed.

When the surface and bulk phases are distinguished from each other, the electrostatic potential, $\psi$, of diffusible ions follows the Poisson equations

$$\frac{\mathrm{d}^2\psi}{\mathrm{d}x^2} = -\frac{4\pi e}{\varepsilon}\left(\frac{i\Gamma_M}{\delta} + n_+ - n_-\right)$$

for $x \leq \delta$ (surface phase) (15)

$$= -\frac{4\pi e}{\varepsilon}(n_+ - n_-)$$

for $x \geq \delta$ (bulk phase) (16)

where $\delta = 2/\kappa$, and their concentrations are given by equations formally identical with

Eq. 8. Eqs. 8 and 15 imply that the surface phase is not always electrically neutral.

In order to solve the Poisson-Boltzmann equations, Eqs. 15 and 16 with Eqs. 8, it will be assumed that the surface phase deviates slightly from being electroneutral. In such a case the "$\lambda$-method", which was devised for solving the problem of polyelectrolyte solution[7], might be applied to the present equations. Then a quantity $\lambda$ is defined as

$$\frac{i\Gamma_M}{\delta}+n_+-n_-=\frac{i\Gamma_M}{\delta}\lambda \tag{17}$$

$$\lambda \ll 1 \tag{18}$$

Evidently, the problem is reduced to that of the membrane equilibrium, if $\lambda=0$. From Eqs. 8 and 17, it follows that

$$\sinh\frac{e\psi}{kT}=\frac{i\Gamma_M}{2n\delta}(1-\lambda) \tag{19}$$

Expanding $e\psi/kT$ in a series of $\lambda$ using Eq. 19 and ignoring the terms higher than $\lambda$, one obtains

$$\frac{e\psi}{kT}=\ln\frac{i\Gamma_M+\sqrt{(i\Gamma_M)^2+4(n\delta)^2}}{2n\delta}-\frac{i\Gamma_M\lambda}{\sqrt{(i\Gamma_M)^2+4(n\delta)^2}} \tag{20}$$

and

$$\lambda=\frac{\sqrt{(i\Gamma_M)^2+4(n\delta)^2}}{i\Gamma_M}\left[-\frac{e\psi}{kT}+\ln\frac{i\Gamma_M+\sqrt{(i\Gamma_M)^2+4(n\delta)^2}}{2n\delta}\right] \tag{21}$$

Then, instead of Eq. 15, one has a linear equation

$$\frac{d^2\lambda}{dx^2}=\chi^2\lambda \tag{22}$$

or

$$\frac{d^2\psi}{dx^2}=\chi^2(\psi-\psi_D) \tag{23}$$

where

$$\chi^2=\frac{4\pi e^2}{\varepsilon kT}\sqrt{\left(\frac{i\Gamma_M}{\delta}\right)^2+4n^2} \tag{24}$$

and

$$\frac{e\psi_D}{kT}=\ln\frac{i\Gamma_M+\sqrt{(i\Gamma_M)^2+4(n\delta)^2}}{2n\delta} \tag{5a}$$

The most general boundary conditions for Eqs. 15 and 16 are given by

$$(d\psi/dx)_{x=0}=0 \tag{25}$$

$$\psi \text{ and } d\psi/dx \text{ : continuous at } x=\delta \tag{26}$$

and

$$\psi_{x=\infty}=(d\psi/dx)_{x=\infty}=0 \tag{27}$$

Under these conditions one can obtain solutions which correspond to those derivd by Lifson[8] and Nagasawa and Kagawa[9] for the polyelectrolyte solution. For the sake of simplicity, however, a simpler condition

$$\psi_{x=0}=0 \tag{26a}$$

is chosen here instead of the second condition (26). This means that $\psi=0$ and $n_+=n_-=n$ in the bulk phase ($x\geq\delta$). Thus the surface phase ($x\leq\delta$) may be treated separately. The solutions of Eqs. 22 and 23 are found to be

$$\lambda=\frac{\sqrt{(i\Gamma_M)^2+4(n\delta)^2}}{i\Gamma_M}\frac{e\psi_D}{kT}\frac{\cosh\chi x}{\cosh\chi\delta} \tag{28}$$

and

$$\psi=\psi_D\left(1-\frac{\cosh\chi x}{\cosh\chi\delta}\right) \tag{29}$$

respectively.

After this, one will be concerned with the mean concentrations and the mean potential of ions in the surface phase. By a simple averaging procedure or by Gauss's theorem of electrostatics, the mean value of $\lambda$ is calculated to be

$$\langle\lambda\rangle=\frac{\sqrt{(i\Gamma_M)^2+4(n\delta)^2}}{i\Gamma_M}\frac{e\psi_D}{kT}\frac{\tanh\chi\delta}{\chi\delta} \tag{30}$$

The mean concentrations of cation and anion in the surface phase are then represented by

$$\begin{aligned}\langle n_+\rangle&=\frac{1}{2}\left\{-\frac{i\Gamma_M}{\delta}+\sqrt{\left(\frac{i\Gamma_M}{\delta}\right)^2+4n^2}\right\}\times\left\{1+\frac{i\Gamma_M\langle\lambda\rangle}{\sqrt{(i\Gamma_M)^2+4(n\delta)^2}}\right\}\\ \langle n_-\rangle&=\frac{1}{2}\left\{\frac{i\Gamma_M}{\delta}+\sqrt{\left(\frac{i\Gamma_M}{\delta}\right)^2+4n^2}\right\}\times\left\{1-\frac{i\Gamma_M\langle\lambda\rangle}{\sqrt{(i\Gamma_M)^2+4(n\delta)^2}}\right\}\end{aligned} \tag{31}$$

respectively, and their surface excesses are defined by

$$\begin{aligned}\Gamma_+&=\delta(\langle n_+\rangle-n)\\ \Gamma_-&=\delta(\langle n_-\rangle-n)\end{aligned} \tag{32}$$

respectively. The mean electric potential of diffusible ions in the surface phase is given by

$$\langle\psi\rangle=\psi_D\left(1-\frac{\tanh\chi\delta}{\chi\delta}\right) \tag{33}$$

7) F. Oosawa, N. Imai and I. Kagawa, *J. Polymer Sci*., 13, 93 (1953).

8) S. Lifson. *J. Chem. Phys.*, 27, 700 (1957).

9) M. Nagasawa and I. Kagawa, This Bulletin, 31, 961 (1958).

The potential of ionized groups of monolayer is assumed to be defined by

$$\psi_M = 2\langle\psi\rangle \tag{34}$$

as described before. Then one has

$$\langle n_+\rangle/n = n/\langle n_-\rangle = \exp(-e\psi_M/2kT) \tag{35}$$

### Contribution of Ionization to Surface Pressure and Potential

When a monolayer is ionized and charged positively, diffusible ions in aqueous subphase become distributed between the surface and the bulk phase, as given by Eq. 3 or 31, and the electrostatic potential of the monolayer becomes higher than that of the diffusible ions in the bulk phase by the amount $\psi_M$, as given by Eq. 14 or 34. The thermodynamic equilibrium is established by accompanying the decrease in surface free energy, i.e. the increase of surface pressure. The relationship between the increment of surface pressure and the ionic concentrations will be described by an equation such as the Gibbs absorption isotherm. At a constant surface concentration of monolayer, the surface pressure, $\Pi_i$, due to the ionization of monolayer can be expressed by

$$\mathrm{d}\Pi_i = kT(\Gamma_+ + \Gamma_-)\mathrm{d}\ln n + i\Gamma_M \mathrm{d}(e\psi_M) \tag{36}$$

In the following formula one will carry out the integration of Eq. 36 in the case of the $\lambda$-approximation, since the results from the treatment of membrane equilibrium can be derived as a limiting case. Inserting Eqs. 31 and 32 into Eq. 36 and neglecting the terms higher than $\lambda$, it may be written as

$$\mathrm{d}\Pi_i = kT\left\{-2n\delta + \sqrt{(i\Gamma_M)^2 + 4(n\delta)^2} - \frac{(i\Gamma_M)^2\langle\lambda\rangle}{\sqrt{(i\Gamma_M)^2 + 4(n\delta)^2}}\right\}\mathrm{d}\ln n + i\Gamma_M \mathrm{d}(e\psi_M) \tag{37}$$

Integration leads to

$$\Pi_i = 2kT\left\{-2n\delta + \sqrt{(i\Gamma_M)^2 + 4(n\delta)^2} - \frac{(i\Gamma_M)^2\langle\lambda\rangle}{\sqrt{(i\Gamma_M)^2 + 4(n\delta)^2}}\right\} - kT(i\Gamma_M)^2 \int_\infty^n \frac{\langle\lambda\rangle}{\sqrt{(i\Gamma_M)^2 + 4(n\delta)^2}} \frac{\mathrm{d}n}{n} \tag{38}$$

provided that the integration constant is chosen so as to be $\Pi_i = 0$ at the infinite salt concentration. If the last term with a complicated integral is ignored, it follows that

$$\Pi_i = 2kT(\Gamma_+ + \Gamma_-) \tag{39}$$

$$= 2kT\delta(\langle n_+\rangle + \langle n_-\rangle - 2n) \tag{40}$$

In the approximation of membrane equilibrium, $\langle\lambda\rangle = 0$, Eq. 40 reduces to

$$\Pi_i = 2kT\delta(\bar{n}_+ + \bar{n}_- - 2n) \tag{41}$$

Eqs. 40 and 41 represent a colligative nature of surface pressure at a low surface concentration of monolayer. Eqs. 40 and 41 can be rewritten by the use of measurable quantities as

$$\Pi_i = 2kT\left\{-\frac{4n}{\kappa} + \sqrt{\frac{1}{A^2} + \left(\frac{4n}{\kappa}\right)^2} - \frac{1}{A^2}\frac{\langle\lambda\rangle}{\sqrt{\frac{1}{A^2} + \left(\frac{4n}{\kappa}\right)^2}}\right\} \tag{42}$$

and

$$\Pi_i = 2kT\left\{-\frac{4n}{\kappa} + \sqrt{\frac{1}{A^2} + \left(\frac{4n}{\kappa}\right)^2}\right\} \tag{43}$$

respectively, and by the use of the electrostatic potential of monolayer the above two equation become as follows:

$$\Pi_i = 4n\delta kT\left(\cosh\frac{e\psi_M}{2kT} - 1\right) \tag{44}$$

Eq. 44 in the case of $\langle\lambda\rangle = 0$ is in complete agreement with the equation derived from the theory of diffuse double layer

$$\Pi_i = \frac{8nkT}{\kappa}\left(\cosh\frac{e\psi_G}{2kT} - 1\right) \tag{45}$$

which should be expected if Eqs. 12—14 hold.

The situation that the same results follow both from the treatments of membrane equilibrium and of diffuse double layer has also been noticed in the theory of polyelectrolyte solution[9,10]. Further, it would be more plausible to assume that $\delta = 2/\kappa$, although it had always been assumed that $\delta = 1/\kappa$[11].

If the surface pressure of unionized monolayer is $\Pi_0$, the observed surface pressure of ionized monolayer can be expressed by

$$\Pi = \Pi_0 + \Pi_i \tag{46}$$

Thus, the surface pressure of ionized

10) J. J. Hermans and J. Th. G. Overbeek, *Rec. trav. chim.*, **67**, 761 (1948); G. E. Kimball, M. Cutler and H. Samelson, *J. Phys. Chem.*, **56**, 57 (1952); P. J. Flory, "Principles of Polymer Chemistry", Cornell Univ. Press, Ithaca, N. Y. (1953), p. 854 ff.

11) J. F. Danielli, *Biochem. J.*, **35**, 470 (1941); J. T. Davies and E. K. Rideal, *J. Colloid Sci.*, **3**, 313 (1948); J. F. Danielli and J. T. Davies, *Adv. Enzymol.*, **11**, 35 (1951); J. J. Betts and B. A. Pethica, *Trans. Faraday Soc.*, **52**, 1581 (1956).

TABLE I

$T=293°K$, $\varepsilon=80$

1) *Octadecyltrimethylammonium chloride on* NaCl

$A=85$ A$^2$ per long chain ion

| $n$ | $\delta$ | $\Pi_i$(Eq. 43) | $\Pi$ | $\Pi_0$ | $\psi_D$ | $\bar{n}_+$ | $\bar{n}_-$ |
|---|---|---|---|---|---|---|---|
| mol./l. | A | | dyn./cm. | | mV. | mol./l. | |
| 0.033 | 33.6 | 8.46 | 5.8 | −2.66 | 72.4 | 0.00188 | 0.583 |
| 0.10 | 19.3 | 7.80 | 5.3 | −2.50 | 62.0 | 0.00853 | 1.17 |
| 0.50 | 8.62 | 6.18 | 3.8 | −2.38 | 42.4 | 0.0935 | 2.69 |
| 2.0 | 4.32 | 4.28 | 2.7 | −1.58 | 27.2 | 0.676 | 5.88 |

$\Pi_0=-3.5$ (Davies)

2) *Copoly-1 : 3 : 1-(L-lysine, L-phenylalanine, L-glutamic acid) on* KCl *in* 0.005 N HCl

$n=n_{HCl}+n_{KCl}$

$A=20\times5$ A$^2$ per ionized group (L-lysyl residue)

| $n$ | $\delta$ | $\Pi_i$(Eq. 43) | $\Pi$ | $\Pi_0$ | $\psi_D$ | $\bar{n}_+$ | $\bar{n}_-$ |
|---|---|---|---|---|---|---|---|
| mol./l. | A | | dyn./cm. | | mV. | mol./l. | |
| 0.040 | 30.5 | 6.90 | 0.65 | −6.25 | 64.5 | 0.00347 | 0.581 |
| 0.075 | 22.3 | 6.56 | 0.55 | −6.11 | 57.4 | 0.00817 | 0.780 |
| 0.135 | 16.6 | 6·16 | 0.30 | −5.86 | 50.4 | 0.0189 | 1.033 |
| 0.405 | 9.59 | 5.12 | 0.05 | −5.07 | 37.8 | 0·0915 | 1.843 |

$\Pi_0=-5.8$ (Hamaguchi and Isemura)

monolayer is higher at lower salt concentration, and, conversely, it is lower at higher salt concentration. At sufficiently high salt concentrations, $\Pi_i=0$ and, accordingly, $\Pi=\Pi_0$. (A polyelectrolyte monolayer exerts an additional surface pressure due to the elastic deformation of polymer chains on ionization, but the inference mentioned here remains unaltered.)

The surface potential of ionized monolayer measured experimentally has the form[1,12]

$$\Delta V=\frac{4\pi\mu}{A}+\psi_M \tag{47}$$

where $\mu$ is the surface moment per ionized group. At sufficiently high salt concentrations, $\psi_M=0$ and, accordingly, $\Delta V=4\pi\mu/A$. At low salt concentrations,

$$\left(\frac{\partial\Delta V}{\partial\ln n}\right)_{i\Gamma_M \text{ or } A}=\left(\frac{\partial\psi_M}{\partial\ln n}\right)_{i\Gamma_M \text{ or } A}=-\frac{Tk}{e} \tag{48}$$

as already found by Crisp[13].

### Comparison with Experiments

The results obtained above from either treatment for ionized monolayers, the approximation of membrane equilibrium or the $\lambda$-method, can be readily examined with experimental data, by comparing the values of $\Pi_0$ and $\mu$ at various salt concentrations, which can be evaluated by subtracting the calculated values of $\Pi_i$ and $\psi_M$ from the observed values of $\Pi$ and $\Delta V$, respectively. If the treatments were valid, the $\Pi_0$ and $\mu$ values should be independent of salt concentration. One has applied the procedure to the available data on surface pressure of two typically different monolayers, i. e. those of octadecyltrimethylammonium chloride*,[1] and of copoly-1 : 3 : 1-(L-lysine, L-phenylalanine, L-glutamic acid)**,[4].

For the approximation of membrane equilibrium, using Eq. 43 for $\Pi_i$, the results as shown in Table I are obtained. It can be seen that the $\Pi_0$ values are not independent of salt concentration. Further, all these values are found to be negative. The negative $\Pi_0$ values imply that the corresponding unionized monolayers would contract in themselves rather than spread on aqueous surfaces. Davies' suggestion that the ionized monolayers would be condensed into "islands" or micelles is not valid, since the ionized monolayers do not contract but only form condensed films on strong salt solutions. This inconsistency may be ascribed to an overestimate of $\Pi_i$ values. The too high contribution of ionization to monolayer properties

12) J. H. Schulman and A. H. Hughes, *Proc. Roy. Soc.*, **A138**, 430 (1932).

13) D. J. Crisp, Research, "Surface Chemistry", Butterworths Scientific Publications, London (1949), p. 65.

* For this monolayer, a constant value of $\mu$ was noticed by Davies[1]. However, the $\mu$ value appears to be insensitive to salt concentration.

** If the deformation of polymer chains on ionization is taken into account, the $\Pi_0$ values would be lower than those in Table I, in which this contribution is not involved.

comes from the distribution of counter ions being too much concentrated in the surface phase and of co-ions being too much repelled from there. Indeed, the present approximation sometimes leads to concentration of counter ions in the surface phase being more than ten times as high as that in the bulk phase.

It can be expected that this difficulty will be partly avoided by removing the assumption of the electroneutral surface phase. The $\lambda$-approximation has led to the surface pressure due to ionization given by Eq. 42, which is lower than that obtained by the approximation of membrane equilibrium, Eq. 43, by the amount

$$\frac{kT}{A}\ln\left[\frac{1/A+\sqrt{(1/A)^2+(4n/\kappa)^2}}{-1/A+\sqrt{(1/A)^2+(4n/\kappa)^2}}\right]\times\frac{\kappa}{2\chi}\tanh\frac{2\chi}{\kappa}$$

To confirm this, the data for the monolayer of octadecyltrimethylammonium chloride has been treated by Eq. 42 in a manner as previously. The results are shown in Table II. It can be seen that the $\Pi_0$ values are independent of salt concentration and are always positive. Thus, the inconsistency which was encountered previously in the method of membrane equilibrium is not revealed in the $\lambda$-approximation.

TABLE II

*Octadecyltrimethylammonium chloride on* NaCl, $T=293°K$, $\varepsilon=80$, $A=85\ A^2$ per long chain ion

| $n$ mol./l. | $\Pi_i$(Eq. 42) dyn./cm. | $\Pi$ | $\Pi_0$ | $\langle\lambda\rangle$ |
|---|---|---|---|---|
| 0.033 | 3.87 | 5.8 | 1.93 | 0.487 |
| 0.100 | 2.99 | 5.3 | 2.31 | 0.509 |
| 0.50 | 1.40 | 3.8 | 2.40 | 0.539 |
| 2.0 | 0.34 | 2.7 | 2.36 | 0.523 |

The advantage of the $\lambda$-method is, however, only superficial. When the surface concentration of monolayer is not low enough, the last term of an integral in Eq. 38, which can not be easily estimated, becomes significant. Moreover, it is found from Table II that all the $\langle\lambda\rangle$ values are about 0.5 and incompatible with the fundamental assumption, Eq. 18. It may, therefore, be stated that the $\lambda$-method, as well as the approximation of membrane equilibrium, can not explain completely the effect of ionization on the typically expanded monolayer of octadecyltrimethylammonium chloride. The method is also found to be insufficient to elucidate consistently the ionization behavior of the condensed monolayer of copoly-1 : 3 : 1-(L-lysine, L-phenylalanine, L-glutamic acid).

The main purpose of the theory consists in a description of the experimental fact that an ionized monolayer is more condensed on concentrated salt solutions and is more expanded on dilute solutions. The present theory has, however, given explanations of only a part of the observations that higher salt concentrations reduce surface pressure of an ionized monolayer more than lower salt concentrations do. Generally, an ionized monolayer has an area where the reversal of surface pressure occurs, which is independent of salt concentration but dependent on salt species[5]: at the area larger than this, the surface pressure is lower at higher salt concentrations and at the smaller area it is reversed. Hence, the present theory concerns only the region of large area. It seems likely that for a comprehensive interpretation of the behavior of ionized monolayers the assumption of uniformly distributed ionized groups in the surface phase should be modified and penetration of ions into the surface phase, finite dimension of ions, association effect and other individual characteristics of ions should be taken into account.

## Summary

The effect of salt on ionized monolayers is treated with a model of "surface phase", in which ionized groups of monolayers are dissolved uniformly. To obtain the distribution of diffusible ions between the surface and bulk phases, the method of membrane equilibrium and the $\lambda$-approximation are employed. The former method is a special case of the latter. The contribution of ionization to surface pressure is calculated thermodynamically. The results derived from the former method are found to be in complete agreement with those derived from the theory of diffuse double layer, if the thickness of surface phase is chosen as $2/\kappa$ and the electric potential of ionized groups is twice as high as the membrane potential. On examining two typically different monolayers, the former method reveals some contradiction, although it explains experimental data qualitively. The latter method, which is more general, can overcome the difficulty and gives reasonable values for surface pressure of an expanded monolayer. It is

found, however, that even the $\lambda$-approximation is still unsatisfactory to describe the behavior of ionized monolayers in the range of area with which they are ordinarily concerned.

A part of the expense for this work was defrayed by the Ministry of Education, to which the authors' thanks are due.

*Faculty of Science*
*and*
*Institute for Protein Research*
*Osaka University*
*Osaka*

# *The Roles of Prolyl Residue in Polypeptide Monolayers. III. Surface Films of Gelatin*

By Shoichi IKEDA and Toshizo ISEMURA

(Received June 23, 1959)

Collagen and gelatin are unusually rich in prolyl and hydroxyprolyl residues as compared with ordinary globular proteins. Because of the specific structures of these imino acid residues, the configurations of polypeptide chains in these proteins are expected to be quite different from those in other proteins. In fact, such characteristics have been observed in solutions of collagen[1-3] and gelatin[4,5] as well as in collagen fiber[6]. In surface films, if they are spread on aqueous surfaces, collagen and gelatin will likewise show a characteristic behavior.

It was established with synthetic polypetides[7,8] that the presence of prolyl residues in a polypeptide chain makes their surface films more expanded, chiefly due to the decrease in number of hydrogen bonds and, accordingly, the condensed nature of films of ordinary synthetic polypeptides may be ascribed to the hydrogen bonding in films. It has been noticed that most globular proteins form condensed films. If the roles of prolyl residue in polypeptide monolayers are reproduced in protein films, collagen and gelatin should form expanded films on aqueous surfaces.

In the present paper it will be examined by the measurements of surface pressure, potential and viscosity, whether these considerations are valid or not for the surface films of gelatin.

## Experimental

**Materials.**—Gelatin was purified from leaf gelatin of Nihon Hikaku Co., Ltd., by desalting it in acetate buffer at pH 4.8 and then washing it with distilled water. The pH of the solution of gelatin thus obtained was 4.9. Concentrations of gelatin solutions were determined by measuring the dry weight of 0.5% stock solution. Spreading solutions were prepared by diluting the stock solution ten times with distilled water.

**Methods.** — Surface pressure, potential and viscosity were measured by a surface balance of float type, a vibrating electrode and an oscillating rotatory disk, respectively. Surface moment was calculated from surface potential, using the Helmholtz equation.

To adjust pH of aqueous subphases to 2.0, 5.6 and 11.2, 0.01 N hydrochloric acid, distilled water and 0.01 M potassium carbonate were used, respectively. Purified potassium chloride was added to prevent the film from dissolving into aqueous subphases.

## Results

Fig. 1 shows surface pressure-area ($\Pi$-$A$) and surface moment-area ($\mu$-$A$)

1) P. M. Gallop, *Arch. Biochem. Biophys.*, **54**, 486, 501 (1955).
2) H. Boedtker and P. Doty, *J. Am. Chem. Soc.*, **77**, 248 (1955).
3) C. Cohen, *J. Biophys. Biochem. Cytol.*, **1**, 203 (1955); A. G. Szent-Gyorgyi and C. Cohen, *Science*, **126**, 697 (1957).
4) P. Doty and H. Boedtker, *J. Phys. Chem.*, **58**, 968 (1954).
5) E. V. Gouinlock, P. J. Flory and H. A. Scheraga, *J. Polymer Sci.*, **16**, 383 (1955).
6) G. N. Ramachandran and G. Kartha, *Nature*, **176**, 593 (1955); A. Rich and F. H. C. Crick, ibid., **176**, 915 (1955); P. M. Cowan, S. McGavin and A. C. T. North, ibid., **176**, 1062 (1955); R. S. Bear, *J. Biophys. Biochem. Cytol.*, **2**, 363 (1956); G. N. Ramachandran, *Nature*, **177**, 710 (1956); A. Rich and F. H. C. Crick, "Recent Advances in Gelatin and Glue Research", Pergamon Press, London (1958), p. 20.
7) T. Isemura and S. Ikeda, This Bulletin, **32**, 178 (1959).
8) S. Ikeda and T. Isemura, ibid., **32**, 659 (1959).

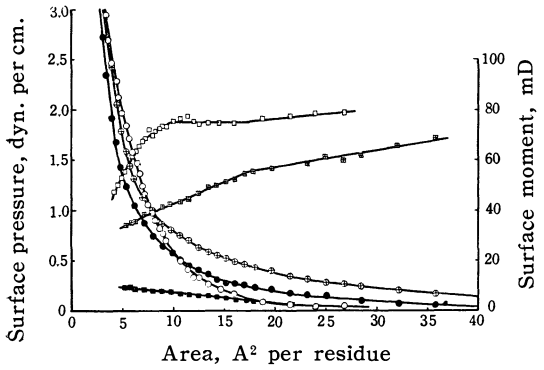



Fig. 1. Surface pressure and moment vs. area curves of gelatin on salt-free solutions at pH 2.0 (⊕, ⊞), 5.6 (○, □) and 11.2 (●, ■): 20°C.

curves of gelatin films on salt-free subphases at three different pH's. Surface pressures of gelatin films on distilled water were scarcely influenced by the temperature of spreading solution and the nature of spreading solvents. Besides a gelatin solution in distilled water at room temperature, a solution in distilled water at 48°C, and solutions in 0.1 M potassium rhodanate, in 40% ethanol and in a mixture of dichloroacetic acid-isopropanol-water (5 : 2 : 3) were examined. Fig. 2 shows the $\Pi$-$A$ and $\mu$-$A$ curves of gelatin films on 1 M potassium chloride solutions at three different pH's. On the alkaline side the film had a slight tendency to dissolve into aqueous subphase, when spreading solution was freshly prepared. The surface viscosity-area ($\eta$-$A$) curve of the film on 1 M potassium chloride is also shown in Fig. 2.

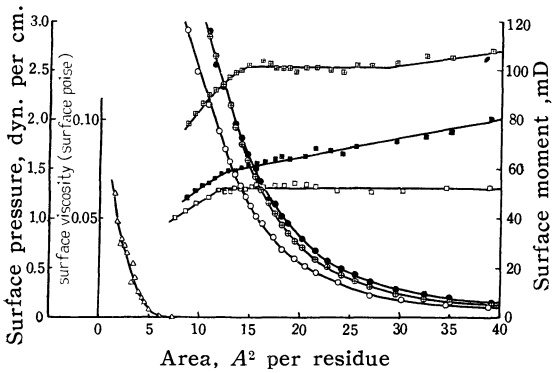



Fig. 2. Surface pressure and moment vs. area curves of gelation on 1 M potassium chloride at pH 2.0 (⊕, ⊞), 5.6 (○, □) and 11.2 (●, ■), and surface viscosity vs. area curve on 1 M potassium chloride at pH 5.6 (△): 20°C.

## Discussion

Both collagen and gelatin are composed of about 30% glycyl residues and about 30% prolyl and hydroxyprolyl residues. In solution a collagen molecule exists as a rigid rod-like particle[1,2] which is also found in collagen fiber from X-ray diffraction studies[6]. On the other hand, a gelatin molecule behaves as a random coil like ordinary polymer molecules but unlike a collagen molecule[4,5].

It was reported, however, that, if collagen and gelatin are spread as surface films, they are indistinguishable from each other: collagen spread from its formic acid solution and gelatin from its aqueous and formic acid solutions give identical $\Pi$-$A$ and $\mu$-$A$ curves on 30% ammonium sulfate solution[9]. This fact is consistent with the present observations that $\Pi$-$A$ curves of gelatin films are independent of the nature of the spreading solutions.

In spite of its hydrophilic nature, gelatin formed a stable film on distilled water, as already noted[10]. The extent of the spreading of film was very incomplete and not very much influenced by the acididity and alkalinity of aqueous subphases. Such behavior of gelatin film is quite different from those of other protein films[11]. Further, molecular expansion of gelatin as was observed in aqueous solutions[12] was not reflected in its surface films. The surface moment of gelatin was higher on distilled water at pH 5.6 than on aqueous subphases at both sides of this pH. This is not consistent with the idea of titration of surface films[13,11], but is in agreement with the result for collagen film on aqueous solutions, the pH's of which were adjusted by hydrochloric acid[9]. Addition of salt into aqueous subphases caused gelatin films to spread more[14]. Even on 1 M potassium chloride, however, gelatin spread still incompletely and appeared to dissolve on compression. The surface pressures at different pH's were nearly identical on such a concentrated salt solution, as was generally expected from the theory of ionized

9) S. C. Ellis and K. G. A. Pankhurst, *Trans. Faraday Soc.*, **50**, 82 (1954).
10) J. Pouradier and M. Abribat, Research, "Surface Chemistry", Butterworths Scientific Publications, London (1949), p. 135.
11) For example, B. S. Harrap, *J. Colloid Sci.*, **9**, 522 (1954).
12) G. Stainsby, *Nature*, **169**, 662 (1952).
13) J. Glazer and M. Z. Dogan, *Trans. Faraday Soc.*, **49**, 448 (1953).
14) H. Kakiyama, *J. Chem. Soc. Japan, Pure Chem. Sec.* (*Nippon Kagaku Zasshi*), **78**, 66 (1957).

monolayers. Apart from these facts, all the surface films of gelatin were found to be of expanded types.

It has been observed that globular proteins, when spread as monolayers, form condensed films, at least, at the isoelectric point and occupy an area of about 15 $A^2$ per residue, which would mean that the protein films are in the $\beta$-configuration[15,11]. The expanded nature of gelatin films may be attributed to the roles of prolyl residues such as are found in the polypeptide monolayers, i. e. to the reduced number of hydrogen bonds[7]. In surface viscosity behavior was exhibited the general property of expanded films showing that the surface viscosity is only manifest at high surface pressure region[8]. The incomplete spreading and pressure-solubility of gelatin films may come from its hydrophility and specific configuration of polypeptide chains.

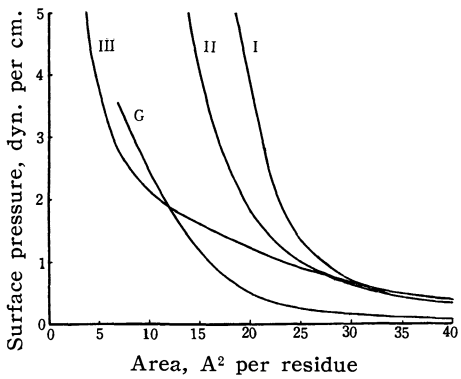



Fig. 3. Comparison of surface pressure-area curve of gelatin with those of some synthetic polypeptides. G: gelatin, I: poly-L-prolyl-L-leucylglycine, II: copoly-1:1:1-(L-proline, L-leucine, DL-alanine), III: poly-L-proline. G and III on 1 M potassium chloride.

Collagen and gelatin molecules were once regarded as consisting of L-prolyl-glycyl-R sequences, on which basis Astbury and Bell[16] suggested a chain configuration in collagen fiber. Recently, Millionova and Andreeva[17] proposed from their X-ray study on poly-glycyl-L-proline that glycyl-L-prolyl sequences are repeated in a collagen molecule. The amino acid analysis on partial hydrolysates of gelatin[18] and collagen[19] has, however, shown that a considerable amount of L-prolyl-L-hydroxyprolyl sequences are found in them, and now it is generally recognized that gelatin and collagen contain these sequences abundantly. At present, a configuration of polypeptide chain in collagen fiber has been established on the basis of the repeated structure of L-prolyl-L-hydroxyprolyl-glycyl sequences[6].

It appears that the surface pressure behavior of gelatin film also supports the presence of these sequences. In Fig. 3 the *II-A* curves of some polypeptide films reported in a previous paper[7] are summarized together with that of gelatin film on 1 M potassium chloride. It will be seen that the extent of expansion or the surface compressibility of gelatin film lies near that of copoly-1 : 1 : 1-(L-proline, L-leucine, DL-alanine) and is lower than that of poly-L-proline. In the former copolypeptide L-prolyl-R-L-prolyl sequences are possible and in the latter polypeptide the successive L-prolyl residues exist. Thus, it is considered that a gelatin molecule consists of L-prolyl-R-L-prolyl or L-prolyl-L-prolyl-R sequences. Since some of the prolyl residues in gelatin are substituted by hydroxyprolyl residues and the presence of hydroxyprolyl residues makes a surface film somewhat condensed, the latter sequence, i. e. L-prolyl-L-hydroxyprolyl-glycyl, may be favorable to explain the extent of expansion of gelatin film, in accordance with the results of chemical analysis.

If L-prolyl-L-hydroxyprolyl bonds are assumed to exsist in a gelatin molecule, the effect of salt on gelatin films can be well interpreted following Harrington's suggestion[20], that most of these bonds are *trans* in distilled water and the addition of salt causes the *trans-cis* transformation of these bonds. If the parts of *cis* bond in a gelatin molecule remain on the surface while the parts of *trans* bond dissolve in aqueous phase and the other parts are either on or in aqueous subphase according as their own hydrophility and their surrounding chain configurations, it can be explained why gelatin can form a stale film even on distilled water in spite of its hydrophilic nature. Further, the presence of salt in subphases would stabilize the *cis* bond more than the *trans* bond, causing the *trans-cis* transformation, and make

15) C. W. N. Cumper and A. E. Alexander, *Trans. Faraday Soc.*, **46**, 235 (1950).
16) W. T. Astbury and F. O. Bell, *Nature*, **169**, 662 (1941).
17) M. I. Millionova and N. S. Andreeva, *Biofizika*, **3**, 259 (1958).
18) W. A. Schroeder, L. M. Kay, J. LeGette, L. Honnen and R. C. Green, *J. Am. Chem. Soc.*, **76**, 2783 (1954).
19) T. D. Kroner, W. Tabroff and J. J. McGarr. ibid., **77**, 3356 (1955).
20) W. F. Harrington, *Nature*, **181**, 997 (1958).

films spread more easily. There considerations are consistent with those made for poly-L-proline film previously[7].

## Summary

Surface films of gelatin, which is very rich in L-prolyl and L-hydroxyprolyl residues, were examined on salt-free and 1 M potassium chloride solutions at three different pH's by the measurements of surface pressure, potential and viscosity. They were found to spread incompletely but to be of expanded types. The incomplete spreading and the other properties of the films were regarded as a manifestation of the specific configuration of gelatin in films. The expanded nature of the films was attributed to the roles of prolyl residue in gelatin such as observed in polypeptides. The extent of expansion of the films appeared to give evidence to support the results from chemical analysis that a gelatin molecule is composed of a large amount of L-prolyl-L-hydroxyprolyl bonds. The behavior of gelatin films was adequately explained by assuming that the parts of *cis* L-prolyl-L-hydroxyprolyl bond form the film and the parts of *trans* bond dissolve in aqueous subphase.

This work was partly supported by a grant given by the Ministry of Education, to which the authors' thanks are due.

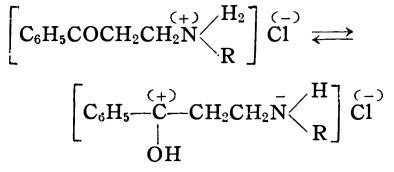
*Faculty of Science*
*and*
*Institute for Protein Research*
*Osaka University*
*Osaka*

# *Studies on the Mannich Reaction. III. On the Formation of Piperidine Derivatives (3)*

By Norito UCHINO

(Received May 4, 1959)

In the previous papers of this series[1], tautomerism of the Mannich compound involving prototropy was proposed as indicated below.



R=H, $CH_3$, $C_6H_5COCH_2CH_2$

The present experiment shows a fact which seems to support the above scheme.

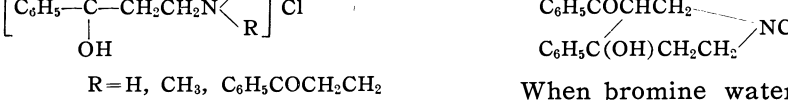
The β-benzoylethylamines[2-4] used are: bis-(β-benzoylethyl)-amine(II), tris-(β-benzoylethyl)-amine(III), 4-oxy-4-phenyl-5-benzoyl-1-(β-benzoylethyl)-piperidine(IV), bis-(β-benzoylethyl)-methylamine(VI) and 4-oxy-4-phenyl-5-benzoyl-1-methyl-piperidine(VII).

$(C_6H_5COCH_2CH_2)_2NH$ (II)

$(C_6H_5COCH_2CH_2)_3N$ (III)

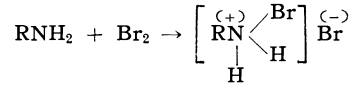
 (IV)

$(C_6H_5COCH_2CH_2)_2NCH_3$ (VI)

 (VII)

When bromine water was added to an aqueous solution of hydrochloride of the above Mannich base, yellow precipitates were produced almost quantitatively. The precipitates thus obtained had an irritative odor, probably that of bromine originated from the compounds. The bromine as molecule was also partly removed by washing with water.

In general, bromine may add to a free amine as the following scheme:



1) N. Uchino, This Bulletin, **32**, 1009 (1959).
2) C. Mannich and S. M. Abdullah, *Ber.*, **68**, 113 (1935).
3) J. T. Plati and W. Wenner, *J. Org. Chem.*, **14**, 543 (1949).
4) C. Mannich and G. Heilner, *Ber.*, **55**, 356 (1922); F. F. Blicke and J. H. Burckhalter, *J. Am. Chem. Soc.*, **64**, 451 (1942).

In the present study, such an addition of bromine seems impossible, because the amine is treated as a hydrochloride. Substitution in a benzene nucleus or addition to a double bond which is formed by enolization of a carbonyl group is not probable, considering the ease of evolution of bromine from the addition products and negative ferric chloride test regarding II·HCl or III·HCl.

The bromine compound from the hydrochloride of the Mannich base could be recrystallized from alcohol if the recrystallization was carried out within a little while, bright yellow crystals being obtained which were of an indistinct melting point. When the crystals were heated to a higher temperature, they decomposed and melted to a dark-brown liquid. The recrystallized addition compound still had a smell of bromine, and reduced potassium iodide.

The acid value, the halogen content and the oxidizing power of the recrystallized bromine addition product of II·HCl are summarized in Table I.

Table I. Analytical results of bromine addition product of II·HCl

| | Found ml./g. | Calcd. ml./g. |
|---|---|---|
| Acid value (N/10-NaOH) | 50.7 | 21.0[c] |
| Oxidizing power[a] (N/10-$Na_2S_2O_3$) | 24.1 | 42.0[d] |
| Halogen content[b] (N/10-$AgNO_3$) | 52.6 | 63.0[d] |

a) The bromine addition product was dissolved in alcohol, and potassium iodide was added to the solution. Iodine produced was titrated with sodium thiosulfate solution.

b) Bacon's method was used.

c) Theoretical value of N/10-NaOH consumed for hydrochloric acid which is present as hydrochloride of the addition compound of one mole of bromine with one mole of II·HCl.

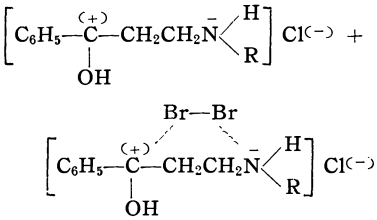
d) Theoretical value for the addition compound of one mole of bromine with one mole of II·HCl.

From the above results, it is considered that at least one mole of bromine is added to one mole of the hydrochloride.

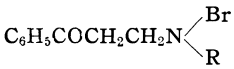
The yellow color of the product from II·HCl or III·HCl disappeared on refluxing the alcoholic solution. On cooling, compound II·HCl was recovered from the solution. When the addition product of II·HCl or III·HCl was treated with alcoholic alkali, base IV was obtained[5]. To obtain the free base of the bromine compound by the alkali treatment, a suspension in water of the additional product of II·HCl or III·HCl was rapidly treated with alkali and the assumed free base produced was immediately extracted with ether. However, the colorless crystals formed proved to be the hydrobromide of II (II·HBr).

The compound II·HCl or III·HCl, however, gave no crystals on the brief treatment with alkali; the ether solution was evaporated to give base IV[5].

On the brief treatment of the bromine addition compound with alkali, a free base containing bromine thus dissolves in ether, and the bromine is partially removed from the original addition product, because the yellow color disappears. Thus the mechanism of the addition of bromine is considered as the following scheme:



The bromine links, in the form of linking astride, on the carbonium ion and on the lone pair of electrons of the nitrogen atom, both of which are formed by the prototropy. When the product is treated with alkali for a little while, the hydrogen chloride and the hydrogen bromide are removed. The free base thus produced may be *N*-bromo-*β*-benzoylethylamine.



The compound of *N*-halogenamine type seems to have an oxidizing power. In the present case, the unstable *N*-bromo-bis-(*β*-benzoylethyl)-amine oxidizes contaminants in the solvent (ether), changing into base II. Base II combines with hydrobromic acid produced, and separates as a hydrobromide.

In order to isolate the unstable *N*-bromoamine, extraction with ether, benzene or carbontetrachloride was attempted without success; the only product obtained was the reduced one II·HBr.

Bromine likewise adds to the free Mannich base. For example, the yellow precipitates readily formed on addition of excessive bromine to an ether solution of base II or III. This product on brief treatment with alkali also yielded the colorless compound II·HBr.

It is known that an amine yields an *N*-bromoamine on treatment with sodium

5) Even if base II or III is produced by the alkali treatment, it changes into base IV; cf. Ref. 2.

hypobromite[6]. Here, compound II·HCl was treated with sodium hypobromite to give II·HBr. This fact also shows the existence of the unstable *N*-bromo-β-benzoylethylamine.

The bromine addition product of III·HCl also gives II·HBr on brief treatment with alkali, probably because of the unstability of the *N*-bromoamine derivative.

## Experimental

**Addition of Bromine to the Salt of the Mannich Base.**—One gram of compound II·HCl or III·HCl was dissolved in 200~300 ml. of water. To the solution was added 500 ml. of bromine water. The yellow precipitates were filtered and dried in vacuo at room temperature in the presence of phosphorous pentoxide; 1.3 g. of bromine addition product of II·HCl or 1.2 g. of that of III·HCl was obtained.

**Recrystallization of the Bromine Addition Product.**—The bromine addition product, which was obtained from 2.0 g. of II·HCl, was recrystallized from alcohol within a little while to give yellow crystals; yield, 1.5 g. The crystals were analyzed after vacuum-drying at room temperature in the presence of phosphorous pentoxide (Table I).

**Decomposition of the Bromine Addition Product by Alcohol.**—In boiling alcohol was dissolved 1.5 g. of bromine addition product of II·HCl, and the solution was refluxed for thirty minutes. After being cooled, 1.2 g. of colorless crystals were obtained, which were recrystallized from alcohol acidified with hydrochloric acid to give II·HCl; m. p. and mixed m. p. 173°C.

*Anal.* Found: C, 67.80; H, 6.52; N, 4.47. Calcd. for $C_{18}H_{20}O_2NCl$: C, 68.02; H, 6.34; N, 4.40%.

The bromine addition product obtained from 1.0 g. of III·HCl was also treated with alcohol giving 0.5 g. of II·HCl; m. p. and mixed m. p. 171~173°C.

**Treatment of the Bromine Addition Product with Alcoholic Alkali.**—The bromine addition product obtained from 1.0 g. of II·HCl was dissolved in hot alcoholic sodium hydroxide, and the solution was poured into a great volume of water. The aqueous solution which became turbid was allowed to stand for one day. The turbid matter coagulated to a resinous matter. The product was dissolved in hot alcohol, and the free base was converted into hydrochloride by adding hydrochloric acid. After being cooled, the hydrochloride was separated by adding a little ether, filtered, and washed with ether. Yield, 0.1 g. The hydrochloride was recrystallized twice from alcohol giving compound IV·HCl; m. p. and mixed m. p. 196~198°C.

*Anal.* Found: C, 71.79; H, 6.05; N, 3.18. Calcd. for $C_{27}H_{28}O_3NCl$: C, 72.06; H, 6.27; N, 3.11%.

The bromine addition product obtained from 1.0 g. of III·HCl was also treated with alcoholic alkali to give 0.2 g. of IV·HCl; m. p. and mixed m. p. 197~199°C. The residual alcohol solution was evaporated giving only a dark-brown resinous matter.

**Short Treatment of the Bromine Addition Product with Alkali.**—The bromine addition product obtained from 2.0 g. of III·HCl was suspended in 100 ml. of water, and an excess of dilute solution of sodium hydroxide was added. The colorless matter produced was quickly extracted with 400 ml. of ether. The organic layer was kept at room temperature; colorless crystals began to separate from the solution. After one day, the crystals were filtered and washed with ether; yield, 0.8 g.; m. p. 166~167°C (from alcohol). The crystals showed a remarkable flame reaction of halogen, and gave precipitates of silver bromide with silver nitrate.

*Anal.* Found: C, 60.30; H, 5.86; N, 3.88. Calcd. for $C_{18}H_{20}O_2NBr$(II·HBr): C, 59.67; H, 5.56; N, 3.86%.

The crystals were converted into hydrochloride by repeated recrystallization from alcoholic hydrogen chloride to give II·HCl; m. p. and mixed m. p. 172~173°C. From these results, the crystals separated from the ether solution were confirmed to be II·HBr.

The residual ether solution was evaporated only to give a dark-brown resinous matter which could not be distilled at the usual reduced pressure. The resinous matter decomposed at a higher temperature.

The bromine addition product obtained from 2.0 g. of II·HCl gave 1.5 g. of II·HBr in the same way as above; m. p. 166~167°C.

*Anal.* Found: C, 60.80; H, 5.72; N, 3.89. Calcd. for $C_{18}H_{20}O_2NBr$: C, 59.67; H, 5.56; N, 3.86%.

In the above reaction, ether, benzene or carbontetrachloride was used as an extracting solvent. All these solvents were sufficiently purified just before use. In this case, compound II·HBr was also separated from the solvent, and the yields were 0.8, 0.2 and 0.3 g., respectively.

**Reaction of the Salt of the Mannich Base with Alkali.**—To 200 ml. of water was added 2.0 g. III·HCl, and an excess of solution of sodium hydroxide. The free base produced was extracted with ether. No crystals separated even when the ether solution was allowed to stand. When the ether solution was evaporated, an oily matter was obtained which solidified after a while. Recrystallization from alcohol gave 1.5 g. of base IV; m. p. and mixed m. p. 149~150°C.

*Anal.* Found: C, 78.63; H, 6.75; N, 3.65. Calcd. for $C_{27}H_{27}O_3N$: C, 78.42; H, 6.58; N, 3.38%.

Two grams of II·HCl gave 1.1 g. of base IV in the same way as above; m. p. and mixed m. p. 149~150°C.

**The Bromine Addition Product of the Free Mannich Base.**—To an ether solution of free base III, which was obtained by treating 3.0 g. of III·HCl with a dilute solution of sodium hydroxide for a little while, was added 1.1 g. of bromine.

6) Cf. R. Willstätter and V. Hottenroth, *Ber.*, **37**, 1783 (1904); F. Rashig, *Ann.*, **230**, 223 (1885).

Yellow precipitates produced were filtered, washed, and dried to give 3.5 g. of yellow powder which emitted an irritating odor of bromine. The bromine content of the precipitates was 26.0% [Theoretical $(C_6H_5COCH_2CH_2)_3NBr_2$, 27.9%]. One gram of this addition product was suspended in ether, and an excess of dilute solution of sodium hydroxide was added with shaking. The bromine addition product turned colorless, and dissolved in ether. The ethereal portion was allowed to stand to give 0.2 g. of II·HBr; m. p. 168~169°C (from alcohol).

*Anal.* Found: C, 59.43; H, 5.63; N, 3.59. Calcd. for $C_{18}H_{20}O_2NBr$: C, 59.67; H, 5.56; N, 3.86%.

The residual ether solution was evaporated to give 0.7 g. of base IV; m. p. and mixed m. p. 149~150°C (from alcohol).

A bromine addition product of base II was produced by the same process as the above one. The bromine content was 44.1% [Theoretical $(C_6H_5COCH_2CH_2)_2NH·Br_2$, 36.2%]. From 0.2 g. of this addition product was obtained 0.1 g. of II·HBr; m. p. 169~170°C (from alcohol).

*Anal.* Found: C, 59.84; H, 5.68; N, 4.08. Calcd. for $C_{18}H_{20}O_2NBr$: C, 59.67; H, 5.56; N, 3.86%.

In the case of bromine addition product of base VI, the results were somewhat different from those of the above reaction. The bromine addition product of base VI, which was obtained from 5.0 g. of VI·HCl, was suspended in ether, and an excess of dilute solution of sodium hydroxide was added to the suspension with shaking. The addition product turned somewhat pale-yellow, but it was hardly soluble in ether. The pale-yellow matter was filtered and dried; yield, 3.5 g. Its bromine content was 27.5%, which is lower than the [theoretical value of $(C_6H_5COCH_2CH_2)_2·NCH_3·Br_2$ (35.1%), and higher than that of VI·HBr (21.2%). Two grams of the above matter was dissolved in 50 ml. of alcohol and refluxed for one hour to give 1.4 g. of VI·HBr; m. p. 188~189°C (from alcohol). The mother liquor was slightly condensed to give an additional amount (0.2 g.) of VI·HBr.

*Anal.* Found: C, 60.65; H, 6.03; N, 3.79. Calcd. for $C_{19}H_{22}O_2NBr$: C, 60.64; H, 5.89; N, 3.72%.

The above crystals were converted into VI·HCl by repeated recrystallization from alcoholic hydrogen chloride; m. p. and mixed m. p. 169~170°C.

The ether layer, which was separated from the bromine addition product, was kept at room temperature to give the same product VI·HBr; m. p. 188~189°C; yield, 0.1 g.

*Anal.* Found: C, 60.36; H, 6.14; N, 3.89. Calcd. for $C_{19}H_{22}O_2NBr$: C, 60.64; H, 5.89; N, 3.72%.

**Reaction of Bis-(β-benzoylethyl)-amine Hydrochloride (II·HCl) with Sodium Hypobromite.**— One gram of II·HCl was added to 100 ml. of water. To this solution was added a solution of sodium hypobromite which was prepared by adding excessive sodium hydroxide to bromine water. The free base produced was extracted with ether. The ether solution was left to stand to produce crystals; yield, 1.0 g. The crystals were recrystallized from alcohol giving II·HBr; m. p. 170°C.

*Anal.* Found: C, 59.96; H, 5.65; N, 3.76. Calcd. for $C_{18}H_{20}O_2NBr$: C, 59.67; H, 5.56; N, 3.86%.

## Summary

i) The addition of bromine to β-benzoylethylamine hydrochloride was studied. It was concluded that bromine molecule was added to β-benzoylethylamine hydrochloride in the form linking astride to the carbionium ion and the lone pair of electrons of the nitrogen atom, both of which were formed by prototropy.

ii) The bromine addition product of β-benzoylethylamine hydrochloride was treated with alkali for a little while to give *N*-bromo-β-benzoylethylamine which was very unstable and decomposed to give β-benzoylethylamine hydrobromide.

The author is particularly indebted to the late Professor Ryuzaburo Nozu and to Professor Ryozo Goto for their discussions and encouragement throught this investigation, and also to Professor Seishi Machida for his encouragement.

*Chemical Laboratory of Textile Fibers*
*Kyoto University of Industrial Arts and Textile Fibers*
*Kita-ku, Kyoto*

# *Selective Reduction of Phosphatides with Lithium Aluminum Hydride. I. Ovolecithin*

By Chieko URAKAMI, Hirochika OKURA and Mitsuko OKADA

(Received May 19, 1959)

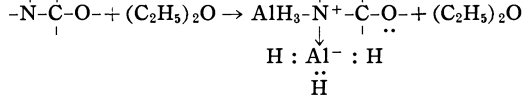
For determination of the structures and the configurations of phosphatides, the following two methods were available. Long and Magure[1] carried out the reactions to derive L-α-glycerylphosphoric acid as described below:

L-α-Lecithin —(Phospholipase C)→ 1,2-Diglyceride
—(Phosphorylation)→ L-α-Phosphatidic acid
—(Hydrolysis)→ L-α-Glycerylphosphoric acid

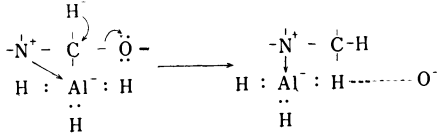
Baer and Maurukas[2] devised the so-called "diazomethol ysis" giving the phosphatidic acid dimethyl ester. In both methods, unsaturated fatty acids, if present, should be hydrogenated before carrying out these reactions. These two methods are, however, not always convenient for general application. The former is far more complicated and would require a sufficient amount of purified phosphatides for analysis of the final product. The latter is, on the other hand, simpler, but it is applicable to those containing the free amino group such as phosphatidyl serine and phosphatidylethanolamine and not to phosphatidylcholine.

The reaction of lecithin with lithium aluminum hydride was carried out by Karrer and Jucker[3] under drastic conditions, at the boiling point of ether. Inorganic phosphorus, phosphine, glycerol and a substance with an amine-like odor were reported to be present in the reaction mixture. Apparently, all ester linkages of the lecithin molecule were cleaved. A number of instances of selective reduction by this reagent were reported, e. g. methyl 4-nitrovalerate was reduced to the corresponding alcohol at −35°C in 20 min., the nitro group being unattacked[4]. A selective reduction similar to this example may possibly be achieved with lecithin under carefully controlled conditions.

The authors' attention was focused on an ionic character of the coordinate covalences of the sulfonyl, nitro and phosphoryl groups. Under mild conditions approach of a hydride ion of lithium aluminum hydride present in ether solution to these groups may encounter some difficulty due to the presence of negatively charged oxygen atoms which are stabilized by resonance. If this plays a part in reduction of the lecithin molecule, the cleavage of the two fatty acid ester linkages would be easier than that of the two ester linkages of the phosphoryl group. However, the nitrogen atom of the choline may also play a role since Trevoy and Brown[5] showed the reaction to be a bimolecular nucleophilic substitution by a hydride ion and Gaylord[6] proposed a mechanism for the reduction of an –N–C–O– group, utilizing the ionic species, $AlH_4^- \rightleftharpoons AlH_3 + H^-$, and the concept of ether participation which have been proposed by Paddock[7], as shown below:

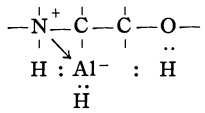


The coordination of $AlH_3$ with the lone pair on nitrogen can occur in the initial step. By analogy with Grignard reaction, the formation of a five-membered quasi-ring is suggested. As the result, nitrogen would become deficient in electron and tend to withdraw electron from the adjacent carbon giving the latter a positive character. The hydride ion could then displace the ethereal oxygen resulting in cleavage of the C–O bond:



1) C. Long and M. F. Magure, *Biochem. J.*, **57**, 223 (1954).
2) E. Baer and J. Maurukas, *J. Biol. Chem.*, **212**, 39 (1955).
3) P. Karrer and E. Jucker, *Helv. Chim. Acta*, **35**, 1586 (1952).
4) H. Feuer and T. J. Kucera, *J. Am. Chem. Soc.*, **77**, 5740 (1955).
5) L. W. Trevoy and W. G. Brown, ibid., **71**, 1675 (1949).
6) N. G. Gaylord, *Experientia*, **10**, 351 (1954).
7) N. L. Paddock, *Nature*, **167**, 1070 (1951).

This mechanism can possibly be applied to the choline moiety of the lecithin molecule, as far as the formation of a six-membered quasi-ring is concerned:



However, an electrostatic effect on the $\beta$-carbon atom would be not as strong as that on the $\alpha$-carbon. The nitrogen atom in this case is already in the cationic form and has no lone pair available for coordination with $AlH_3$ but approach of $AlH_4^-$ would be possible, resulting perhaps in a complex formation*. This may also encounter some difficulty, particularly at low temperatures at which the molecule exists in its ground state, because a hydride ion must overcome zwitterionic and possibly steric effects of the trimethyl group in its approach to the cationic nitrogen. Thus, a higher amount of energy would be required for the cleavage of the phosphoryl-choline linkage than that for the cleavage of the fatty acid ester linkage where no such obstacle exists.

By similar qualitative examination the following speculations may be made on relative ease of cleavage of the two phosphoryl ester linkages. The cleavage of the phosphoryl-glyceryl linkage depends on an attack by a hydride ion on the phosphoryl group only. On the other hand, in the cleavage of the phosphoryl-choline linkage a mechanism involving nitrogen may also participate; this may operate independently of the mechanism involving the phosphoryl group or assist the latter by making oxygen somewhat deficient in electron as a result of the formation of a six-membered quasi-ring. Accordingly the phosphoryl-choline linkage is considered to be cleaved somewhat more readily than the linkage between the phosphoryl and glycerol.

Thus, a step-wise cleavage of the lecithin molecule may be possible, i. e. the cleavage of the fatty acid ester linkages, giving the corresponding alcohols and glycerylphosphorylcholine (with retention of the configuration); or the cleavage of the choline moiety, following the removal of the fatty acids, giving choline and a reduced form of glycerylphosphoric acid**. Accordingly, attempts were made to find suitable reaction conditions to achieve either one of the two possibilities by controlling temperature, time and amounts of lithium aluminum hydride.

* The authors used "$AlH_3$" in a preliminary report on this subject, This Bulletin, **31**, 779 (1958), but presently consider that it must be reserved as such.

## Experimental

**Materials.**—*Lecithin.*—Crude egg yolk lecithin was purified according to Hanahan's method[8], (P : N, 1 : 1.10 and 15.8% choline).

*DL-α-Glycerylphosphorylcholine.*—This compound was synthesized according to the method of Baer and Kates[9], ($\alpha$-glyceryl ester: choline, 1.03 : 1.0).

**Analytical Methods.** — *Choline.* — Choline in glycerylphosphorylcholine was determined by Schmidt's method[10] and in lecithin by Glick's method[11].

*Phosphorus.*—The conventional method of wet incineration, with 10 N sulfuric acid and hydrogen peroxide, was used to convert organic phosphorus to the orthophosphate. The inorganic phosphate was then determined spectrophotometrically according to the method described by Burmaster[12] or by Ernester et al.[13] Concentrations of the reagents were altered, however, as circumstances required.

*Ester.*—The method described by Bauer and Hirsch[14] was employed.

*α-Glycol.*—The periodate oxidation method of Voris et al.[15] was used.

**Reaction of Lecithin with Lithium Aluminum Hydride.**—One hundred milligrams of lithium aluminum hydride was dissolved in 50~60 ml. of dry ether (0.1~0.2% solution). The solution was filtered first through glass wool packed in a glass tubing of about 6 mm. in diameter and then through a sintered glass filter sealed in a glass tubing of about the same diameter and transferred into a specially constructed burette. The filtration and transfer were carried out by applying pressure with dry nitrogen gas. Calcium chloride tubes were provided to keep the entire system in a dry state. A flask of about 100 ml. capacity containing a cooled ether solution of lecithin was attached to the burette and a calculated amount of the reducing agent*** was added in small portions so that the temperature

** A trivalent phosphorus compound may be formed as a result of an attack of $AlH_4^-$ on the positively charged phosphorus atom. This sort of interaction was shown to occur under drastic conditions (the formation of phosphine was recognized)[3] and it may be possible that even under mild conditions this may occur to a certain extent.

8) D. J. Hanahan et al., *J. Biol. Chem.*, **192**, 623 (1951).
9) E. Baer and M. Kates, *J. Am. Chem. Soc.*, **70**, 1394 (1948).
10) G. Schmidt et al., *J. Biol. Chem.*, **197**, 601 (1952).
11) D. Glick, ibid., **156**, 643 (1944).
12) C. F. Burmaster, ibid., **164**, 233 (1946).
13) L. Ernester et al., *Acta Chem. Scand.*, **4**, 942 (1950).
14) F. C. Bauer, Jr. and E. F. Hirsch, *Arch. Biochem.*, **20**, 242 (1949).
15) L. Voris et al., *J. Biol. Chem.*, **133**, 491 (1940).

*** Concentrations of the ether solution were determined from time to time by the conventional method of hydrogen gas liberation. Aliquots were delivered from the burette.

of the reaction mixture could be maintained constant. Stirring with the magnetic stirrer was continued for a desired length of time. The reaction mixture was cooled and decomposed with wet ether. A sufficient amount of water was added to separate the organic layer. The aqueous phase was shaken twice with a small portion of fresh ether and the ether extracts were combined. The aqueous layer was then washed with chloroform to remove lysolecithin (this step was omitted in later experiments since no lysolecithin was found to be present in the chloroform extract). The ether extract was made up to a known volume, usually 25 ml., and aliquots were taken for analyses of organic phosphorus and esters. The aqueous phase was made acid with 10 N sulfuric acid to dissolve the precipitate, the solution filtered and made up to a known volume, usually 50 ml., for analyses of inorganic phosphorus, total phosphorus, free choline and total choline.

**Isolation of L-α-Glycerylphosphorylcholine.** — Lecithin (about 400 mg.) was reduced under the optimum conditions (14°C, Table V). After decomposing the reaction mixture with water, the precipitate formed was removed by centrifugation. The clear solution was passed through a column of IRC-50 and the eluate was analyzed for choline and α-glycol (α-glycol: choline, 1.02: 1.00). The eluate was then concentrated under reduced pressure in the atmosphere of nitrogen and the amorphous cadmium chloride addition complex was prepared according to the procedure described by Baer[9] (Found: P, 5.24%). A solution of the complex was passed through a mixture of 4 ml. of Dowex 3 and 2 ml. of IRC-50 and the solution analyzed for α-glycol, total P and choline (Found: α-glycol : P : choline, 0.97 : 1.00 : 1.02). α-Glycerylphosphorylcholine recovered after passing the resin column was found to be 94%. The crystalline cadmium chloride complex was prepared and analyzed (Found: C, 21.56; H, 4.80) after drying over phosphorus pentoxide at 56°C for 8 hr. under 3 mmHg. The infrared spectrum of this compound was found to be identical with that of the synthetic DL-α-glycerylphosphorylcholine. Its optical rotation was determined on the concentrate of the aqueous solution freshly prepared by repeating the reduction and purification in the same manner as described above [Found: $[\alpha]_D^{24}-2.96\pm0.2°$ (c, 2.2 water); $[\alpha]_D^{23}-2.85\pm0.1°$ (Baer)].

Preliminary experiments with α- and β-glycerylphosphoric acids in the same manner as described for the reduction of lecithin showed that no migration of the phosphoryl group occurred. Similar experiments with glycerylphosphorylcholine was not possible due to technical dfficulties. The migration of the phosphorylcholine groups is, however, unlikely to occur under such mild reaction conditions.

## Results and Discussion

The results shown in Tables I and II indicate that the reaction proceeds through

TABLE I. REDUCTIVE CLEAVAGE OF OVOLECITHIN WITH LITHIUM ALUMINUM HYDRIDE AT 20°C: 15 mol. OF $LiAlH_4$ PER MOLE OF LECITHIN*

| Reaction time (hr.) | 3 | 5 |
|---|---|---|
| Sample wt. (mg.) | 201 | 86 |
| Ch. in sample (mg.) | 31.8±0.3 | 13.9±0.0 |
| Total Ch. (mg.) in aq. phase | 31.8±0.6 | 11.7±0.01 |
| Free Ch. (mg.) in aq. phase | 27.7±0.3 (87) | 11.3±0.2 (81) |
| Inorganic P (mg.) in aq. phase | 0.72±0.00 (9) | 0.56±0.04 (16) |
| Organic P (mg.) in ether phase | 0.00 | 0.00 |
| Organic P (mg.) in chloroform extract | 0.00 | 0.00 |

* For the calculation of the mole ratio 778 was used as an average molecular weight of lecithin. Ch. stands for choline. The figures in parentheses are percentages based on an amount of choline or phosphorus present in each sample weight.

TABLE II. REDUCTIVE CLEAVAGE OF OVOLECITHIN WITH LITHIUM ALUMINUM HYDRIDE AT 20°C: 3 mol. OF $LiAlH_4$ PER MOLE OF LECITHIN

| Reaction time (hr.) | 3 | 5 | 10 |
|---|---|---|---|
| Sample wt. (mg.) | 86 | 113 | 113 |
| Ch. in sample (mg.) | 13.9 ±0.0 | 17.8[a] | 17.8[a] |
| Total Ch. (mg.) in aq. phase | 13.9 ±0.0 | 19.6±0.5 | 15.7±0.3 |
| Free Ch. (mg.) in aq. phase | 5.65±0.2 (41) | 11.3±0.2 (64) | 12.3±0·3 (69) |
| P in sample (mg.)[a] | 3.42 | 4.52 | 4.52 |
| Inorganic P (mg.) in aq. phase | 0.00 | 0.13 (3) | 0.13 (3) |
| Total P (mg.) in aq. phase | 2.12±0.01 (62) | 2.88±0.11 (64) | 3.06±0.1 (68) |
| Total P in ether phase | 0.00 | 0.00 | 0.00 |
| Total P in chloroform extract | 0.00 | 0.00 | 0.00 |

Ch. stands for choline. The figures in parentheses are percentages based on an amount of choline or phosphorus present in each sample weight.

a) Calculated values.

TABLE III. REDUCTIVE CLEAVAGE OF OVOLECITHIN WITH LITHIUM ALUMINUM HYDRIDE AT 18°C: 2 mol. OF $LiAlH_4$ PER MOLE OF LECITHIN

| Reaction time (min.) | 5 | 5 | 10 |
|---|---|---|---|
| Sample wt. (mg.) | 100 | 120 | 120 |
| Ch. in sample (mg.) | 15.3 ±0.3 | 19.3±0.3 | 19.3±0.3 |
| Total Ch. (mg.) in aq. phase | 13.1 ±0.1 | 12.1±0.4 | 20.4±0.0 |
| Free Ch. (mg.) in aq. phase | 3.01±0.1 (19) | 2.1±0.2 (11) | 6.4±0.2 (33) |

Ch. stands for choline. Those figures in parentheses are percentages based on the choline content of the sample.

TABLE IV. REDUCTIVE CLEAVAGE OF OVOLECITHIN WITH LITHIUM ALUMINUM HYDRIDE AT 16°C: 2 mol. OF $LiAlH_4$ PER MOLE OF LECITHIN

| Reaction time (min.) | 30 | 60 |
|---|---|---|
| Sample wt. (mg.) | 113 | 113 |
| Ch. in sample (mg.), calcd. | 17.8 | 17.8 |
| Total Ch. (mg.) in aq. phase | 19.1±0.9 | 19.6±0.5 |
| Free Ch. (mg.) in aq. phase | 4.1±0.2 (23) | 4.4±0.2 (25) |
| P in sample (mg.), calcd. | 4.52 | 4.52 |
| Total P (mg.) in aq. phase | 3.56±0.0 (79) | 3.31±0.2 (73) |
| Total P (mg.) in ether phase | 0.02 | 0.00 |
| Total P (mg.) in chloroform extract | 0.02 | 0.00 |

Ch. stands for choline. Those figures in parentheses are percentages based on an amount of choline or phosphorus present in each sample taken.

TABLE V. REDUCTIVE CLEAVAGE OF OVOLECITHIN WITH LITHIUM ALUMINUM HYDRIDE 2 mol. OF $LiAlH_4$ PER MOLE OF LECITHIN

| Temperature (°C) | 14 | 10 | 10 |
|---|---|---|---|
| Reaction time (min.) | 10 | 20 | 20 |
| Sample wt. (mg.) | 120 | 160.9* | 128.6* |
| Ch. in sample (mg.) | 19.1±0.3 | 22.7[a)] | 18.1[a)] |
| Total Ch. (mg.) in aq. phase | 18.0±0.1 | 23.6±0.1 | 18.3±0.0 |
| Free Ch. (mg.) in aq. phase | 0.8±0.1 (4) | 0.0 | 0.0 |
| P in sample (mg.), calcd. | 4.78 | 6.82 | 5.45 |
| Total P (mg.) in aq. phase | 4.00±0.06 | 7.03±0.07 | 5.40±0.03 |
| Total P (mg.) in ether phase | 0.02±0.00 | 0.04±0.00 | 0.05±0.00 |
| Ester (m. e.), calcd. | | 0.444 | 0.355 |
| Ester (m. e.) in ether phase | | 0.004±0.002 (0.9) | 0.004±0.001 (1.12) |

* The sample of lecithin employed was prepared by the method of Rhodes and Lea, *Biochem. J.*, **65**, 526 (1957), and its analytical results were; choline : P : ester, 1 : 1.17 : 2.50.

a) Calculated values based on the analytical results.

Ch. stands for choline and m. e. for milliequivalent. The figures in parentheses are percentages based on choline or ester content of each sample taken.

the formation of glycerylphosphorylcholine and not phosphorylcholine, since choline containing substances in the aqueous phase release the total amounts of choline present in the samples on acid hydrolysis. Therefore, the experiments under much milder conditions were carried out so that only glycerylphosphorylcholine would be produced. These results are shown in Tables III—V.

It was of interest to see if ether insoluble glycerylphosphorylcholine itself would release the choline moiety by lithium aluminum hydride in ether, the synthetic glycerylphosphorylcholine was, therefore, reacted at 20°C for 3 hr. with 15 mol. of lithium aluminum hydride per mole of the compound. It was found that about 21% free choline was released.

From the results shown in Tables III—V,

the optimum conditions for the reductive cleavage of lecithin giving a 100% yield of glycerylphosphorylcholine appears to be 20 min. at 10°C with a mole ratio of lecithin to lithium aluminum hydride 1 : 2 (Table V). Some phosphorus and ester were found to be present in the ether phase, but this is considered to be due to some impurities present in the sample employed as indicated by its analytical results. According to its optical rotation observed, the glycerylphosphorylcholine formed in the reaction has the L-α-configuration. This method is, therefore, not only simple for the determination of configurations of lecithin, but also a useful method for the preparation of L-α-glycerylphosphorylcholine.

Tables III and V show that the reaction involving the release of the choline moiety is quite sensitive to temperature. With the temperature difference of only four degrees, 18, 14 and 10°C, amounts of choline released decrease from 30 to 4% and finally to 0%, respectively. On the other hand, it is not affected much by reaction time as shown in Tables III, IV and II. It appears then that temperature must be raised higher than 20°C for a complete release of the choline moiety as shown in Table I. The fact that the reaction is sensitive to temperature would mean that an amount of energy required for the cleavage of the phosphoryl-choline linkage is significantly higher than that required for the cleavage of the fatty acid ester linkage. It is quite in accord with what the authors have anticipated.

In those cases where considerable amounts of choline are formed, the total amounts of phosphorus recovered in the aqueous phase are only 62~68% of the calculated amounts (Table II), despite the absence of phosphorus in the organic phase. It is also noticed in the same table that the amounts of the inorganic phosphorus in the aqueous phase are not equivalent to that of the choline moiety released; only 0~3% of the inorganic phosphorus are detected where 41~69% free choline are formed. These results may indicate that some complex mechanisms are involved in the cleavage of the choline moiety.

If a mechanism similar to that proposed by Gaylord[5] operates in the cleavage of the choline moiety, trimethylethylamine should be formed. If, on the other hand, a mechanism involving the phosphoryl moiety participates, choline and a reduced form of α-glycerylphosphoric acid, which may not be detected by the method of analysis employed must be produced. In Table IV, 79 and 73% of phosphorus found in the aqueous phase can be considered to have been derived from 77 and 75% of glycerylphosphorylcholine, respectively. Therefore, 21 and 27% of undetected phosphorus may be ascribed to a reduced form of glycerylphosphoric acid, indicating that the latter mechanism may have played a role. Under such mild conditions, liberation of phosphine would not be possible, for an amount of lithium aluminum hydride used is far less than that required for reduction of the phosphoryl group to its ultimate stage. When three moles of the reducing agent is used (Table II), of 62% total phosphorus detected in the aqueous phase after three hours of reaction time 59% can be accounted for glycerylphosphorylcholine and the remaining 3% may have come from glycerylphosphoric acid (since no inorganic phosphorus is found to be present). Similarly, with 5 and 10 hr. of reaction time 25 and 34%, respectively, may have been derived from glycerylphosphoric acid. Undetected phosphorus would then amount to 38, 36 and 32% for 3, 5 and 10 hr., respectively, of the reaction time in these instances. Therefore, under these conditions, the two mechanisms mentioned above appear to have participated simultaneously, though participation of the latter mechanism seems to predominate in the three hour run. This may indicate that energy requirements for the formation of an intermediary complex with the cationic nitrogen are somewhat higher than that with the phosphoryl group.

Suppose that the formation of the inorganic phosphate is the only indication available for the cleavage of the glycerylphosphoryl linkage, this ester linkage is considered to be the most stable one in the lecithin molecule against lithium aluminum hydride. It may also be pointed out that " free choline " given in the tables constitutes of a mixture of choline itself and the quarternary amine according to the foregoing discussions.

## Summary

The optimum conditions for cleavage of the fatty acid ester linkages in the lecithin molecule were found to be 20 min. at 10°C with the use of two moles of lithium aluminum hydride per mole of lecithin.

The product formed under these conditions was identified to be L-α-glycerylphosphorylcholine when ovolecithin which was shown to be L-α-lecithin[8] was used.

Discussion has been presented as to two mechanisms possibly participating in the cleavage of glycerylphosphorylcholine, one involving a complex formation with the phosphoryl group and the other with the cationic nitrogen atom of the choline base.

*Faculty of the Science of Living*
*Osaka City University*
*Nishi-ku, Osaka*

# *Electrode Kinetics of Indium (III) at the Dropping Mercury Electrode*

By Senkichi INOUYE and Hideo IMAI

(Received May 28, 1959)

The polarographic behavior of indium-(III) has been investigated in various media by many authors. In these investigations two typical electrode processes are noticeable: One is a reversible process which proceeds at about −0.5 V. vs. S. C. E. in the chloride, bromide, iodide or organic acid solution[1,2]. The other is an irreversible process which proceeds at about −1.0 V. vs. S. C. E. in the perchlorate[2] or phosphate[3] solution*. In this report is presented the evaluation of the rate constant of the irreversible electrode process of indium(III) in the perchlorate medium, and the temperature dependence of the rate constant is discussed.

## Experimental

The apparatus used was described in the previous report[4] and was not modified in any detail.

All the reagents were of analytical grade. The stock solution of indium perchlorate was prepared by dissolving indium oxide (weighed as $In_2O_3 \cdot 3H_2O$) in perchloric acid. Indium oxide was prepared from indium chloride by precipitating indium hydroxide with ammonium hydroxide and by desiccating the precipitate to a constant weight at 130°C.

In order to avoid the overlap of the hydrogen wave on the indium wave, the hydrogen-ion concentration was controlled by adding sodium hydroxide. The concentration of the perchlorate ion in the test solution was 0.5 F.

Purified nitrogen was bubbled to remove dissolved oxygen in the test solution prior to submission to polarography.

The temperature was kept constant within the change of ±0.1°C by a thermostat.

## Results and Discussion

**Irreversible Current-Voltage Curve of Indium-(III).**—The irreversible current-voltage curve of indium(III) in the perchlorate medium is illustrated in Fig. 1. Usually, this irreversible wave is accompanied by a pronounced maximum of the first kind. This maximum wave can be suppressed by the addition of a surface active material such as gelatine, methyl red or methyl cellulose. The adsorption of the surface active material on the surface of the dropping mercury electrode (DME), however, seems to change the potential distribution on and near the electrode surface, and this effect results in the variation of the transfer coefficient[3,5]. Moreover, the adsorptive concentration will vary with the change of temperature. Accordingly, the use of a surface active material is not desirable for the purpose of investigating

1) J. Heyrovsky, *Chem. Listy*, **19**, 168 (1925); S. Takagi, *J. Chem. Soc. London*, 301 (1928); J. Tomes, *Collection Czechoslov. Chem. Communs.*, **9**, 12 (1937); J. A. Schufle, M. F. Stubbs and R. Witman, *J. Am. Chem. Soc.*, **73**, 1013 (1951); Z. S. Mukhina, *Zavodskaya Lab.*, **14**, 354 (1948); G. Reinacher and E. Hoschek, *Z. anorg. u. allgem. Chem.*, **268**, 260 (1952); F. Ensslin, *Metall u. Frg.*, **38**, 305 (1941), *Chem. Abstr.*, **36**, 6107 (1942); M. Bulovova, *Collection Czechoslov. Chem. Communs.*, **19**, 1123 (1954).

2) J. J. Lingane, *J. Am. Chem. Soc.*, **61**, 2099 (1939).

3) H. Imai, *J. Sci. Hiroshima Univ.*, **A22**, 291 (1958).

* H. Nakatani has reported that both of the two electrode processes can be observed in one polarogram in the acetic acid—ammonium acetate buffer, and that the second wave is more pronounced with the addition of gelatine [*J. Sci. Hiroshima Univ.*, **A19**, 183 (1955); ibid., **A20**, 49 (1956)].

4) H. Imai, This Bulletin, **30**, 873 (1957).

5) P. Delahay and J. E. Strassner, *J. Am. Chem. Soc.*, **73**, 5219 (1951); H. Imai and S. Chaki, This Bulletin, **29**, 498 (1956).

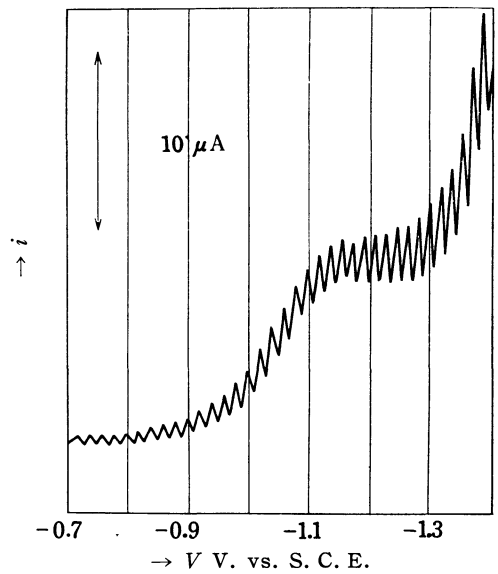



Fig. 1. The current-voltage curve of indium(III) in 0.5 F perchlorate.
Temp.=20°C, $m$=1.8$_1$, $t$=4.9$_0$ (open circuit), [$In^{3+}$]=1 mF.

the temperature dependence of the reaction rate. In this experiment, the lifetime of the DME was elongated by lowering the mercury head, and the supporting electrolyte was appreciably concentrated. Under these conditions, the maximum wave could be satisfactorily minimized. The test solution may be contaminated by the trace of surface active materials which have been accidentally intermixed. After this trace was removed by adding active charcoal, the maximum could not be suppressed in any way. The presence of this trace, however, scarcely affects the value of the transfer coefficient in the temperature range examined, as is illustrated in Table I.

When the hydrogen-ion concentration was too small, the test solution became turbid owing to the formation of indium hydroxide. Even when perchloric acid was added until the turbidity had just disappeared, the current-voltage curve of indium was too greatly extended, from −0.5 to −1.3 V. vs. S. C. E. On the other hand, when the acidity was too great, the hydrogen wave overlapped on the indium wave in question. Therefore, the perchloric acid concentration as great as 0.04 F was preferable.

**Evaluation of Diffusion Constant.** — The value of the diffusion constant of the indium ion is required for the calculation of the rate constant. This value was evaluated from the diffusion-controlled limiting current by Ilkovic's equation, i. e.

$$D^{1/2}=i_d/607\,nCm^{2/3}t^{1/6} \quad (1)$$

where $D$ is the diffusion constant in cm$^2$/sec., $i_d$ is the mean diffusion-controlled current in μA, $n$ is the number of electrons transferred per an ion, $C$ is the bulk concentration of indium(III) in mF, $m$ is the average mass of mercury flowing in mg./sec. and $t$ is the life-time of the DME in sec. The evaluation of the number of electrons transferred per an ion was carried out as follows: When chloride, iodide or acetate was added to the test solution, the irreversible wave was changed to the reversible one, the half-wave potential being simultaneously changed from −1.0 to −0.5 V. vs. S. C. E. It was confirmed that the diffusion-current constants of the two waves were practically equal[3]. In the reversible electrode process the value of $n$ was evaluated to be three from the inclination of the $\log[i/(i_d-i)]$ versus $E$ (the potential of the DME) plot. Accordingly, the value of $n$ in the irreversible electrode process will also be three. The evaluated value of the diffusion constant is given in Table I.

**Evaluation of Transfer Coefficient and Rate Constant.**—The value of $\log[i/(i_d-i)]$ was plotted versus the potential of the DME from the irreversible current-voltage curve. This polt gave a straight line near the half-wave potential. According to Matsuda and Ayabe's theory[6], the inclination of the linear portion of this plot is a function of the transfer coefficient as is given in Eq. 2, i. e.

$$E=\frac{RT}{\alpha nF}\{2.3\log(k_f^\circ f^\circ t^{1/2}D^{-1/2}) -0.12-2.2\log[i/(i_d-i)]\} \quad (2)$$

where $f^\circ$ is the activity coefficient of the depolarizer in the solution and the other symbols are used with their usual significance. The evaluated value of $\alpha n$, which is the product of the transfer coefficient by the number of electrons involved in the rate-determining reaction, is illustrated in Table I.

The rate constant, $k_f^\circ$, referred to 0 V. vs. N. H. E. was evaluated from Eq. 3[6], i. e.

$$E_{1/2}=\frac{RT}{\alpha nF}[2.3\log(k_f^\circ f^\circ D^{-1/2}) +1.15\log t-0.12] \quad (3)$$

6) H. Matsuda and Y. Ayabe, This Bulletin, 28, 422 (1955).

where $E_{1/2}$ is the half-wave potential of the irreversible wave in volts vs. N. H. E. The values of the rate constant at various temperatures ranging from 20 to 30°C are illustrated in Table I.

TABLE I. THE DIFFUSION CONSTANT, THE TRANSFER COEFFICIENT AND THE RATE CONSTANT OF THE ELECTRODE PROCESS OF INDIUM-(III) IN 0.5 F PERCHLORATE

| Temperature $T$°K | Diffusion constant $D$, cm²/sec. | Transfer coefficient $\alpha n$ | Rate constant $k_f^\circ$, cm./sec. |
|---|---|---|---|
| 293.2 | $8.0\times10^{-6}$ | 0.66 | $2.2\times10^{-12}$ |
| 299.7 | $9.6\times10^{-6}$ | 0.66 | $4.7\times10^{-12}$ |
| 303.2 | $10.8\times10^{-6}$ | 0.65 | $7.3\times10^{-12}$ |

**Temperature Dependence of Rate Constant.**— From Table I, the logarithm of the rate constant was plotted versus the reciprocal of the absolute temperature. This plot is satisfactorily linear as is illustrated in Fig. 2. From the inclination of this plot, the heat of activation at constant pressure ($\Delta H^*$) was calculated by Arrhenius's equation, i. e.

$$d\ln k_f^\circ/dt = \Delta H^*/\boldsymbol{R}T^2 \quad \text{or}$$

$$\log k_f^\circ = c - \Delta H^*/2.3\,\boldsymbol{R}T \qquad (4)$$

where $c$ is a constant. The heat of activation at constant volume ($\Delta H^{\ddagger}$) was calculated by Eq. 5 in order to apply the absolute rate expression.

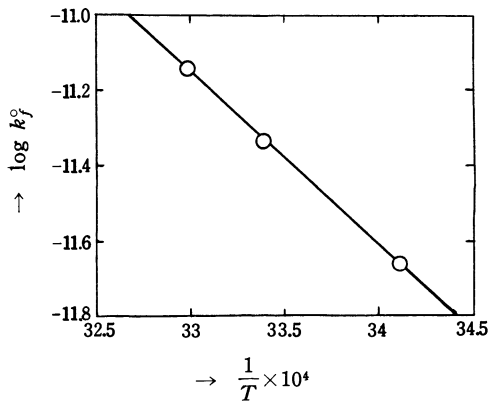



Fig. 2. The temperature dependence of the rate constant of the electrode process of indium(III) in 0.5 F perchlorate.

TABLE II. THE HEAT OF ACTIVATION IN THE ELECTRODE PROCESS OF INDIUM(III) IN 0.5 F PERCHLORATE

| The heat of activation at constant pressure $\Delta H^*$, kcal./mol. | The heat of activation at constant volume $\Delta H^{\ddagger}$, kcal./mol. |
|---|---|
| 21.1 | 20.5 |

$$\Delta H^* = \Delta H^{\ddagger} + \boldsymbol{R}T \qquad (5)$$

These data are illustrated in Table II.

On applying the absolute rate theory to an electrode process, it is noteworthy that the applied potential plays a role as the activation energy of the electron transfer, and that the electrode reaction is a heterogeneous reaction. It is well known that a spontaneous potential difference exists at the mercury-solution interface. Accordingly, the value of the applied potential as the activation energy must be referred to the zero-charge potential, i. e. the Lippmann-potential. Delahay[7] has given a modified expression of the absolute rate theory for an electrode reaction which involves no kinetic complication, as is given in Eq. 6, i. e.

$$k_f^\circ = \frac{e\boldsymbol{k}T}{\boldsymbol{h}}\cdot\rho\cdot\exp(-\Delta H^{\ddagger}/\boldsymbol{R}T) \times\exp(\alpha n\boldsymbol{F}E_m/\boldsymbol{R}T)\cdot\exp(\Delta S^{\ddagger}/\boldsymbol{R}) \qquad (6)$$

where $e$ is the transmission coefficient, $\boldsymbol{k}$ is the Boltzmann constant, $\boldsymbol{h}$ is the Planck constant, $\rho$ is an arbitrary factor in cm., $E_m$ is the Lippmann potential referred to N. H. E.** and $\Delta S^{\ddagger}$ is the entropy of activation in e. u. Eq. 6 involves two arbitrary factors. One of them is the transmission coefficient, the value of which was assumed to be 1 in this calculation. The other arbitrary factor is $\rho$, which was introduced to equalize the dimension of the right side of Eq. 6 to the dimension of the rate constant (cm./sec.).

Delahay has proposed a value as great as that of $2.0\times10^{-8}$ cm. as the mean distance between two depolarizer ions in the bulk solution. It is noteworthy that this value is of the order of the atomic radius. Supposing that the depolarizer at the vicinity of the electrode surface pertains to the rate of the electrode reaction, the above mentioned value of $\rho$ seems to be impossibly small. Accordingly, the value of $\rho$ was evaluated from the depolarizer concentration at the vicinity of the electrode surface. The value amounts to $5.7\times10^{-6}$ cm. as the mean interionic distance between the two depolarizer ions at the vicinity of the electrode surface.

The transmission coefficient does not

7) P. Delahay. *J. Am. Chem. Soc.*, **75**. 1190 (1953); "New Instrumental Methods in Electrochemistry", Interscience Publishers, Inc. New York (1954), p. 41.

** The Lippmann-potential of the DME in 0.5 F perchlorate was evaluated by the "VDME" method[8] as great as $-0.23_7$ V. vs. N. H. E.

8) H. Imai, S. Inouye and S. Chaki, This Bulletin, **31**, 767 (1958); ibid., **32**, 994 (1959).

inherently vary in the order of its magnitude, and accordingly, it does not seriously affect the value of the entropy of activation, while the possible variation of the order of $\rho$-value seriously affects the value of the entropy of activation. In Table III is presented the value of the entropy of activation evaluated in correspondence to the values of $\rho$ as great as $5.7\times10^{-6}$.

TABLE III. THE ENTROPY OF ACTIVATION AND THE FREE ENERGY OF ACTIVATION IN THE ELECTRODE PROCESS OF INDIUM(III) IN 0.5 F PERCHLORATE

| Arbitrary factor $\rho$, cm. | Entropy of activation $S^{\neq}$, e. u. | Free energy of activation $F^{\neq}$, kcal. |
|---|---|---|
| $5.7\times10^{-6}$ | $-5.7$ | 22.2 |

In the above mentioned case the entropy of activation is appreciably negative. Accordingly, it can be assumed that the randomness or disorder in the atomic arrangement of the activated state is less than that of the original state. Lingane[2] has reported that indium(III) is supposed to exist in the form of the aquo complex in the perchlorate solution. Hence, it can be concluded that, when the indium(III) aquo ion enters into the electric field of the electrode surface, the possible coordination of water dipols will be more or less deprived of its randomness prior to the electron transfer.

The reasonable evaluation of $\rho$-value is reserved for the future.

The authors wish to express their hearty gratitude to Professor M. Shinagawa for his valuable advice and to Professor M. Miura for his encouragement throughout this study.

*Department of Chemistry*
*Minami College*
*Hiroshima University*
*Minami-machi, Hiroshima*

# *Density Measurement in Dilute Aqueous Solution of Polyvinyl Alcohol*

By Koichiro NAKANISHI* and Michio KURATA

(Received June 30, 1959)

Precise determination of solution density has an important bearing on the measurements of various physicochemical properties of high polymers in dilute solution. Fragmentary data can be found in literature, but the density measurement itself was scarcely ever chosen as the subject of studies on dilute high polymer solutions, except in the case of a few studies concerning polystyrene[1-5].

Recently a suggestion was made by Kobatake[6] on the possibility of elucidating the polymer-solvent interaction from the density data of dilute solution. According to an equation proposed by Kobatake[6], the polymer-solvent interaction $B_{12}$ can be best estimated from the molecular weight dependence of the solution density. An analysis of Schulz and Hoffmann's data[5] on the apparent specific volume of polystyrene and polymethyl methacrylate was carried out by Kobatake and Inagaki[7] along with this line of approach. Some interesting data concerning molecular interactions in solution were obtained from the values of $B_{12}$. It would seem, therefore, that systematic accumulation of density data should contribute to the problems in dilute high polymer solutions.

In this paper, the density of an aqueous solution of polyvinyl alcohol (PVA) is measured by the use of well defined and fractionated samples, and some analysis

* Present address: Department of Chemistry, Faculty of Science and Technology, Kinki University, Kowakae, Fuse-shi, Osaka.

1) D. J. Streeter and R. F. Boyer, *Ind. Eng. Chem.*, **43**, 1790 (1951).

2) W. Heller and A. C. Thompson, *J. Colloid Sci.*, **6**, 57 (1951).

3) B. Rosen, *J. Polymer Sci.*, **17**, 559 (1955).

4) A. Horth and M. Rinfret, *J. Am. Chem. Soc.*, **77**, 503 (1955).

5) G. V. Schulz and M. Hoffmann, *Makromol. Chem.*, **23**, 220 (1957).

6) Y. Kobatake, *Researches on Chemical Physics (Busseiron Kenkyu)*, **69**, 30 (1953).

7) Y. Kobatake and H. Inagaki, private communication.

of the results are made on the basis of Kobatake's equation[6,7].

In order to determine the solution density, the authors adopted the method of floating equilibria which is the same as that used for the quantitative analysis of heavy water concentration[8,9]. This method was proved to be applicable also to polymer solution. It was rather easy to obtain the solution density and polymer concentration with the same accuracy as that obtained by other methods[2,3,5].

## Experimental

**Preparation of Materials.**—The PVA fractions were obtained by the saponification of polyvinyl acetates which were polymerized in solution under various conditions and fractionated in acetone-water system. Acetyl group content in the resulting PVA samples was less than 0.2%.

The molecular weight of PVA samples was determined from the intrinsic viscosity in water. The viscosity average molecular weight calculated from Nakajima's equation[10] is shown in Table I. In the same table, experimental conditions for polymerization are also tabulated since they have an important bearing on the molecular weight dependence of density.

Unfractionated samples of PVA were also used in the preliminary experiments.

Water as solvent was obtained by the careful distillations of conductivity water.

**Apparatus and Float.**—The apparatus used for the measurement of floating equilibria is based on the one described by Harada[9] for the quantitative analysis of heavy water. The float, made of silicate glass, is spindle-shaped and 2~3 cm. long. The upper spherical part of the float is hollowed, and the apparent specific weight of the whole float is adjusted to a value of the solvent density (water, in this case) near room temperature. The temperature at which the measurements run is always regulated within the accuracy of 0.005°C by a large outer thermostat.

The motion of the float in the sample liquids was followed by a traveling microscope and the equilibrium temperature of the float was read on a Beckmann thermometer.

**Density Measurement.** — (*a*) *Preparation of sample solution.* — The PVA samples, after the saponification, were purified by extraction with methanol in a Soxhlet extractor for three days or longer and dried in vacuo. These samples were dissolved into water in a flask which was placed on a boiling water bath for more than eight hours and about 1% solution was prepared. The solution was then filtered through the glass filters Nos. 2 and 4, and again heated on a boiling water bath. This stock solution was diluted by weight and/or by volume to obtain required concentrations and each solution was stored in a closed tube. Before use, each solution was kept overnight in a thermostat at 80°C. Concentrations of the solution were determined by evaporating the solvent and drying in vacuo at 60°C to constant weight.

(*b*) *Measurement of equilibrium temperature.*— The equilibrium temperature, $T_0$, of the float in water—the temperature which keeps the float both from sinking and floating—is first measured for each float. The "apparent density" of the float is next obtained by comparing this temperature with the density-temperature curve of water (chain-dotted line in Fig. 1). Thus, when the equilibrium temperature in solution, $T$, is again measured for each float of known density, the density-temperature curve of the solution (solid line in Fig. 1) is immediately obtained. The density of solution at any temperature is also determined from this curve.

In practice, the sensitivity of the float to

TABLE I. EXPERIMENTAL CONDITIONS IN POLYMERIZATION, FRACTIONATION AND MOLECULAR WEIGHT OF POLYVINYL ALCOHOL

| | B-5 | T-2 | E-2 | U-1 | U-2 | U-5 |
|---|---|---|---|---|---|---|
| *Polymerization* | | | | | | |
| Solvent | Benzene | Toluene | Ethanol | | | |
| Initiator | 0.1% BPO | 0.1% BPO | 1.0% BPO | | | |
| Monomer, wt.% | 60 | 60 | 30 | Commercial sample | | |
| Temp., °C | 80 | 80 | 70 | | | |
| Time, hr. | 12 | 13.5 | 25 | | | |
| Yield, % | 74 | 44 | 60 | | | |
| *Fractionation* | | | | | | |
| Solvent/precipitant | Acetone/water | | | | | |
| Fractions | 8 | 5 | 5 | Unfractionated | | |
| Temp., °C | 25 | 25 | 25 | | | |
| *Molecular weight* | | | | | | |
| $M_w(\times 10^{-3})$ | 70.4 | 24.2 | 8.4 | 107 | 96.8 | 57.2 |
| $P$ | 1600 | 550 | 190 | 2430 | 2200 | 1300 |

8) T. W. Richards, J. H. Shipley and G. W. Harris, *J. Am. Chem. Soc.*, **34**, 599 (1912).

9) M. Harada, *J. Chem. Soc. Japan. Pure Chem. Sec.* (*Nippon Kagaku Zasshi*), **56**, 811 (1935).

10) A. Nakajima and K. Furutati, *Chemistry of High Polymers* (*Kobunshi Kagaku*), **6**, 460 (1949).

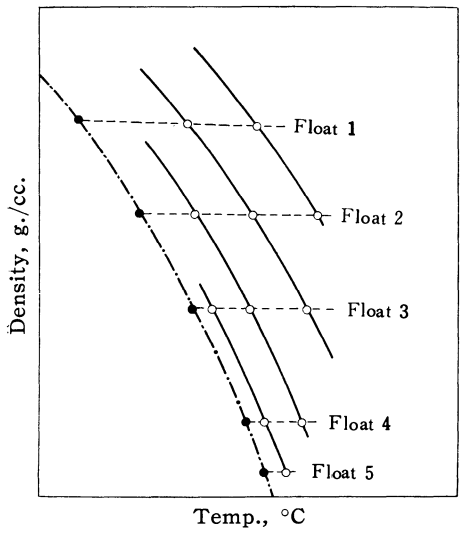



Fig. 1. The method of floating equilibria —— a schematic representation.
● $T_0$ in Eq. 2, ○ $T$ in Eq. 2

temperature variation was higher than the constancy of the thermostat. The equilibrium temperature was then measured in the following two ways; namely, the "quasi-static" and the "dynamic" method[11]. In the former, floating equilibrium is determined directly by a fine adjustment of temperature, while the latter is based on the interpolation of the floating and sinking velocity of the float near the equilibrium temperature.

When the difference between the equilibrium temperature of the solution and that of the solvent is large, a correction for the thermal expansion of the float is required. In this case, the following equation was used,

$$d_t = d_0/(1+\alpha\cdot\Delta T) \quad (1)$$

$$\Delta T \equiv T - T_0 \quad (2)$$

where $d_t$ and $d_0$ are the density of the float at $T$ and $T_0$, respectively, and $\alpha$ is the coefficient of cubic expansion of silicate glass[12].

(c) *Apparent and partial specific volumes.*—Following the procedure given above, the solution density $d_{12}$ can be obtained as a function of polymer concentration $c_2$ (g./cc.) and temperature. For the discussion of experimental data, however, it is convenient to use the apparent specific volume $\phi_2$ (cc./g.) and the partial specific volume $V_2$ (cc./g.) of solute polymer in solution. They can be calculated from the solution density by the following equations,

$$\phi_2 = 1/d_1 - d_{sp}/c_2 \quad (3)$$

$$V_2 = \phi_2 + w_2(1-w_2)\cdot\partial\phi_2/\partial w_2 \quad (4)$$

$$V_2 \cong \phi_2 + c_2\cdot\partial\phi_2/\partial c_2$$

(for dilute aqueous solution) (5)

where $d_1$ is the density of solvent (g./cc.), $w_2$ is the weight fraction of solute polymer and $d_{sp} = (d_{12}-d_1)/d_1$.

**Discussion of the Experimental Error.**—Although the float is sensible to the temperature change of 0.001°C, fluctuation in excess of 0.003°C is inevitable in the determination of equilibrium temperature in both the two methods, quasi-static and dynamic. The error in the density determination, even when the work is very carefully done, is accordingly expected to be about $\pm 2\times 10^{-6}$. In practice, such a degree of precision was easily obtained in the measurement with water in which the "apparent density" of the float was quite stable.

While in PVA solutions, the "apparent density" of the float becomes somewhat unstable, though the cause is uncertain. PVA may be adsorbed to the float and sometimes an insoluble film may be formed on the surface. Under this circumstance, calibration with water is frequently required. Thus, the actual error found in PVA solution was not in excess of $\pm 4\times 10^{-6}$.

Finally, it was often observed that foam grows on the surface of the float and that the quasi-equilibrium of the float is attained especially in the measurement near 20°C. In the temperature region from 25 to 30°C with which the authors' experiment is concerned, however, the appearence of foam was rare and there was practically no experimental difficulty.

## Results and Discussion

**Equilibrium Temperature as Function of Polymer Concentration.** — Fig. 2 shows the temperature difference ($\Delta T$) vs. concentration relationship of PVA aqueous solution up to 1.0 g./100 ml. Each curve in the figure corresponds to the values obtained with using different floats. It is seen at once that the $\Delta T$ vs. concentration relationship can be regarded as almost linear below 0.5 g./100 ml., but convex in the more concentrated region. It can be also observed that the larger the "apparent density" of the float is (namely, the lower the $T_0$ of the float is), the more magnified the temperature difference is for the same sample solution. The molecular weight of PVA affects $\Delta T$, though very minutely and can not be seen in the figure. This point will be discussed later.

The $\Delta T$ vs. concentration curve in Fig. 2 may be used as a calibration curve for the determination of polymer concentration in dilute solution. The temperature difference $\Delta T$ for PVA aqueous solution of 1.0 g./100 ml. reaches to about 9~10°C, while the equilibrium temperature itself can be obtained with a precision of 0.003°C. In this case, accordingly, a concentration difference of at least 0.003 g./100 ml. (i. e.

11) H. Akamatsu, *J. Chem. Soc. Japan (Nippon Kwagaku Kwaishi)*, **61**, 470 (1940).
12) G. W. Morey, "Properties of Glass", Reinhold Publishing Corp., New York (1954), p. 275.

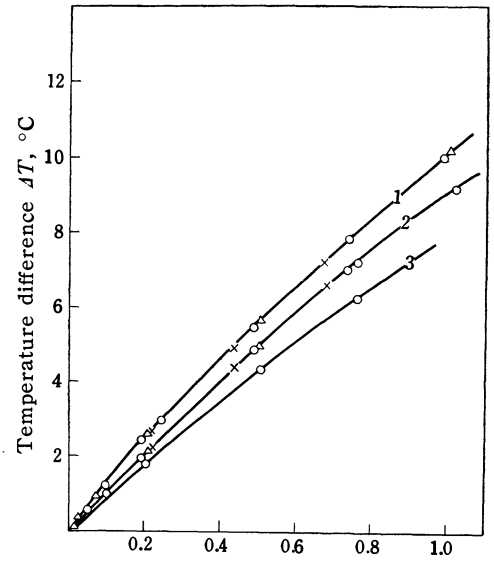



Fig. 2. Equilibrium temperature difference vs. polymer concentration relationship.
○ $P$=1300 × $P$=2200 △ $P$=2430
1 Float 6 ($T_0$=18.47°C)
2 Float 1 ($T_0$=21.29°C)
3 Float 9 ($T_0$=26.21°C)

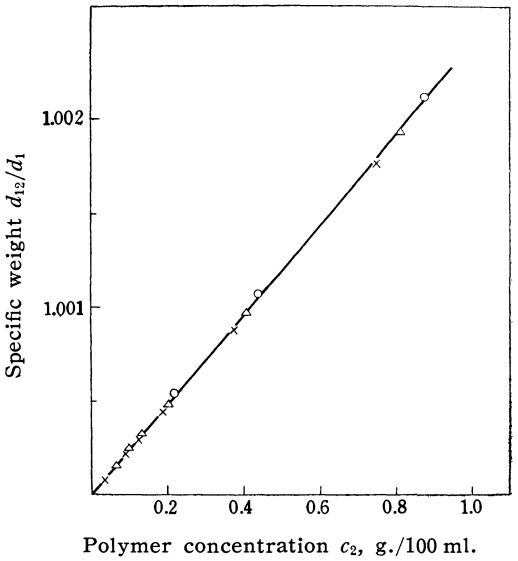



Fig. 3. Solution density vs. polymer concentration relationship for dilute solution of fractionated PVA at 30°C.
○ B-5 $P$=1600 △ T-2 $P$=550
× E-2 $P$=190

0.003 wt. %) will be detectable by the present method.

**Solution Density as Function of Polymer Concentration and Molecular Weight.**—In Fig. 3, the solution density vs. polymer concentration relationship is shown for aqueous solution of fractionated PVA. The data of $d_{12}/d_1$ (specific weight to solvent water) vs. $c_2$ fall on a straight line at least below the polymer concentration of 1.0 g./100 ml., and are slightly dependent on the molecular weight of PVA.

For a clear detection of this dependence, it is convenient to calculate the apparent specific volume $\phi_2$ of PVA in solution. Fig. 4 shows the experimental values of

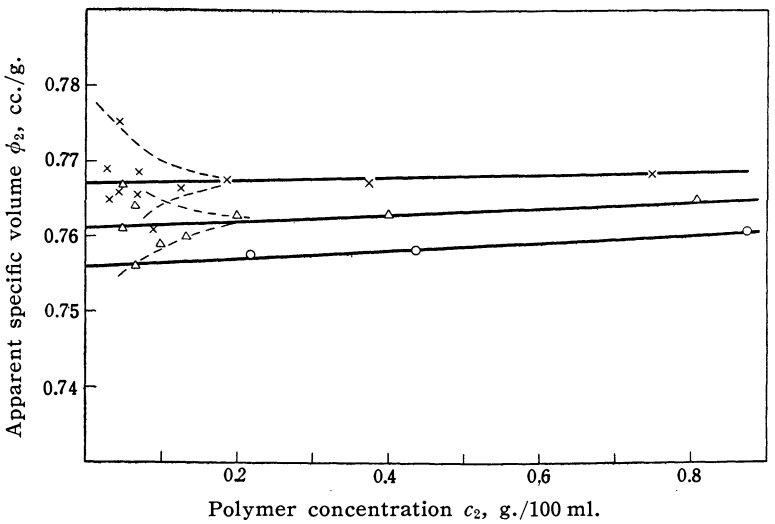



Fig. 4. Apparent specific volume of PVA in aqueous solution, as function of polymer concentration, $c_2$, at 30°C.
○ B-5 $P$=1600 △ T-2 $P$=550 × E-2 $P$=190

$\phi_2$ calculated by Eq. 3 at each concentration. It is seen from the figure that $\phi_2$ increases slightly with $c_2$ for every case concerned, though the data at extreme dilution are somewhat uncertain. It may be thus concluded that a negative second order term, though very small, does exist, if the $d_{12}$ vs. $c_2$ relationship, as usual, is represented by a power series (see Eq. 6).

Another remarkable result seen on Fig. 4 is the clear dependence of $\phi_2$ on the molecular weight of PVA. This dependence is expected from the simple qualitative consideration that the presence of the end-group which is different from the intermediate segment will affect the spatial configuration of the polymer molecule. It is seen that $\phi_2$ decreases with increasing molecular weight, and the fifth decimal place of the solution density $d_{12}$ is influenced by the molecular weight of the solute polymer. As is shown immediately after, $\phi_2$ and the partial specific volume $V_2$ seem to be inversely proportional to the molecular weight of PVA. Taking this molecular weight dependence into account, the experimental formula for the solution density of a dilute solution of PVA at 30°C is proposed as follows:

$$\frac{d_{12}}{d_1} = 1+\left(0.249-\frac{2.47}{P}\right)\cdot c_2 -\left(0.64-\frac{88}{P}\right)\cdot c_2^2 \qquad (6)$$

where $P$ is the polymerization degree of PVA and $c_2$ is the polymer concentration in g./cc. This equation could reproduce the experimental data very well.

Eq. 6 should prove useful for predicting the density of an aqueous solution of PVA, irrespective of the origins of the PVA samples, if the polymerization degree is not too low. However, it is to be remarked here that, if $P$ is lower than 500, the solution density of PVA which is polymerized under different initiators may not be represented by this equation.

From Eq. 4 or 5, the partial specific volume $V_2$ of PVA is easily obtained. Because of scattering in the observed values of $\phi_2$, the accurate determination of $V_2$ and its concentration dependence becomes difficult at concentrations lower than 0.2 g./100 ml., and $V_2$ only at the concentration of 0.5 g./100 ml. was estimated by interpolation. Plotting the experimental values of $V_2$ against $1/P$, a nearly linear relationship is obtained as in Fig. 5.

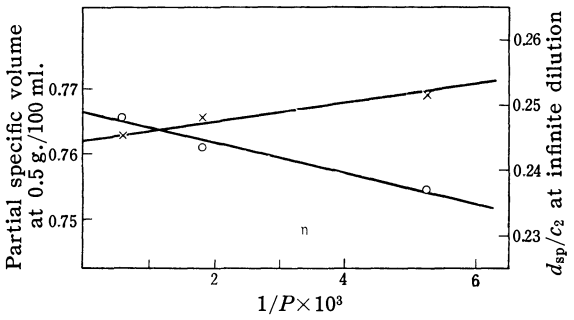



Fig. 5. Molecular weight dependence of $(d_{sp}/c_2)_{c_2\to0}$ and $V_2$ at 0.5 g./100 ml., at 30°C.
○ $\left(\frac{d_{sp}}{c_2}\right)_{c_2\to0}$ × $V_2$ at 0.5 g./100 ml.

In the same figure, the values of $d_{sp}/c_2$ at infinite dilution $(d_{sp}/c_2)_{c_2\to0}$ are also plotted against $1/P$. A linear relationship is observed here. This dependence of $(d_{sp}/c_2)_{c_2\to0}$ on $P$ must be the same as that of $\phi_{2(c_2\to0)}$ as is easily seen from Eq. 3. Thus, one may write

$$\phi_2 = \phi_{2(P\to\infty)}+K/P \qquad (7)$$

at infinite dilution. Here, $\phi_{2(P\to\infty)}$ is the apparent specific volume of the polymer whose polymerization degree $P$ is infinity and $K$ is a constant.

**Estimation of Polymer-Solvent Interaction.**— If the end-segments in the polymer molecule are different in size from the intermediate segments, it is to be expected that $\phi_2$ (or $V_2$) may change inversely proportional to the molecular weight of the polymer.

In fact, Kobatake[6] has derived theoretically an equation which is quite the same in form as Eq. 7. According to his theory, two constants in Eq. 7 can be correlated with the parameters of intermolecular potential as follows:

$$\phi_{2(P\to\infty)} = -\beta_{12}/m_2 \qquad (8)$$

$$K = -2\beta'_{12}+\frac{2\rho_1 B_{11}+1}{\rho_1} \qquad (9)$$

$$B_{12} = 2\beta'_{12}+P\beta_{12} \qquad (10)$$

where $B_{11}$ is the excluded volume (or McMillan-Mayer's "irreducible integral"[13]) between two solvent molecules, $B_{12}$ is the excluded volume between solvent- and polymer molecules, $\beta_{12}$ is the excluded volume between solvent molecule and intermediate segment, $\beta'_{12}$ is the excess excluded volume representing the end-group effect, $m_2$ is the molecular weight

13) W. G. McMillan, Jr. and J. E. Mayer, *J. Chem. Phys.*, **13**, 276 (1945).

TABLE II. EXPERIMENTAL VALUES OF APPARENT AND PARTIAL SPECIFIC VOLUMES AND POLYMER-SOLVENT EXCLUDED VOLUMES

| $P$ | $(d_{sp}/c_2)_{c_2\to 0}$ | $\phi_{2(c_2\to 0)}$ | $V_2$ | $-B_{12}(\times 10^{-3})$ | $-\beta_{12}$ | $-\beta'_{12}$ |
|---|---|---|---|---|---|---|
| 1600 | 0.248 | 0.756 | 0.763 | 1.21 | | |
| 550 | 0.243 | 0.761 | 0.766 | 0.415 | 0.755 | 1.20 |
| 190 | 0.237 | 0.767 | 0.769 | 0.143 | | |

of monomer, and $\rho_1$ is the density (number density) of the solvent.

According to Orstein and Zernike[14], the $B_{11}$ in Eq. 9 is correlated with the isothermal compressibility $\kappa_1$ as follows:

$$\frac{2\rho_1 B_{11}+1}{\rho_1} = kT\kappa_1 \qquad (11)$$

where $k$ is the Boltzmann constant and $T$ is the absolute temperature in °K. One can then calculate $\beta_{12}$ and $\beta'_{12}$ by Eqs. 8 and 9, and finally $B_{12}$ by Eq. 10.

The authors will first estimate the second term $(2\rho_1 B_{11}+1)/\rho_1$ in Eq. 9. Using Eq. 11, the value of $(2\rho_1 B_{11}+1)/\rho_1$ for water is estimated to be 0.068 cc./g. from the experimental data of $\kappa$ at ordinary pressure[15]. Thus, Eq. 9 can be reduced to

$$K = -2\beta'_{12}+0.068 \qquad (12)$$

Using the experimental results of $\phi_{2(c_2\to 0)}$ (extrapolated values of $\phi_2$ to infinite dilution) and its molecular weight dependence, the authors calculate the values of $\beta_{12}$, $\beta'_{12}$ and $B_{12}$, which are listed in Table II.

The value of $\beta_{12}$ represents the "free volume" of PVA molecule per monomer unit, while $\beta'_{12}$ is related to the excess contribution by end-segments. It may be concluded from the comparison between them that the contribution of the end-group in the polymer molecule to total interaction differs markedly from that of the intermediate segment and can not be neglected.

Furthermore, it is to be remarked here that a linear relationship between $\phi_2$ and $1/P$ can also be expected from Eq. 9 even when the end-group effect is negligible. However, for the present case, $\beta'_{12}$ have a large value in comparison with the second term in Eq. 9; the experimental value of $K$ is estimated to be 2.47 cc./g., $-2\beta'_{12}$ is thus estimated to be 2.40 cc./g. which is to be compared with 0.068 cc./g. for the second term. Therefore, a greater part of molecular weight dependence of $\phi_2$ may be attributed to the end-group effect.

Finally, the authors will make a comparison between $V_2$ (see Table II) and the specific volume of solid PVA, $V_2^\circ$. The specific volume of completely amorphous PVA is estimated to be 0.787 from the extrapolation of the experimental values for PVA-film having different crystallinity[16]. A volume contraction in solution is clearly observed in the present case.

14) S. Orstein and F. Zernike, *Physik. Z.*, **27**, 261(1926).
15) The Chemical Society of Japan, "A Handbook of Chemistry (Kagaku Binran)", Maruzen Co., Ltd., Tokyo (1958), p. 461.

## Summary

The solution density of polyvinyl alcohol dilute aqueous solution is measured by the use of the method of floating equilibria. This method is proved to be useful for the purpose of precise density and concentration determination of PVA dilute solution. An experimental formula for the density of PVA aqueous solution both as a function of the concentration and polymerization degree of PVA is proposed. The excluded volumes between solute and solvent are estimated from the molecular weight dependence of apparent and partial specific volumes obtained.

The authors wish to express their hearty thanks to Dr. Y. Kobatake of Tokyo Institute of Technology who calls their attention to the present problem; also to thank Professor M. Tamura of Kyoto University for his interest and guidance. They are also thankful to Dr. A. Nakajima of Kyoto University for his valuable suggestions in preparing the materials.

*Department of Industrial Chemistry*
*Faculty of Engineering*
*Kyoto University*
*Sakyo-ku, Kyoto*

16) I. Sakurada, Y. Nukushina and N. Mori, *Chemistry of High Polymers (Kobunshi Kagaku)*, **12**, 302 (1955).

# *Microwave Spectrum of Malononitrile, $CH_2(CN)_2$. I. The Molecular Structure in the Ground Vibrational State*

By Eizi HIROTA and Yonezo MORINO

(Received July 7, 1959)

The vibration-rotation interaction in polyatomic molecules has been studied extensively by Nielsen and others[1]. The interaction manifests itself in several ways in the observed spectra; for example, the rotational constant differs slightly in each vibrational state and the centrifugal force results in the elongation of molecules. An interesting feature of the interaction is given by the Coriolis force which can be observed most clearly in the degenerate vibrational states. Microwave investigation has been made on the Coriolis interaction in linear and symmetric top molecules, in the name of *l*-type doubling[2]. However, it may be pointed out that, if the two vibrational states are nearly or accidentally degenerate, the Coriolis interaction is expected to become large. Malononitrile has been studied for this purpose, since the Coriolis interactions are expected between four low-lying C—C≡N bending modes[3].

The Raman effect of malononitrile was observed by Kohlrausch and Ypsilanti[4] and the infrared absorption spectrum was measured by Halverson and Francel[5]. The latter authors assigned the spectra and carried out the normal coordinate analysis. However, no data have yet been reported on the structure of the molecule. The present paper will give the molecular structure in the ground vibrational state. The vibration-rotation interaction will be treated in the near future.

## Experimental

The apparatus used was a conventional Stark modulation spectrograph, a 100 kc. sine wave being used for simplicity[6]. In addition to the normal molecule, three kinds of molecules isotopically substituted, $CHD(CN)_2$, $CD_2(CN)_2$, and $CH_2CNC^{15}N$, were synthesized to observe their rotational spectra. The hydrogen atoms of malononitrile exchange readily with the hydrogen of water; thus, the deuterated molecules were obtained by mixing the normal malononitrile with heavy water, made slightly alkaline by adding a small quantity of anhydrous sodium carbonate. The $^{15}N$ substituted molecules were obtained as follows. Ammonium sulfate containing 23.5% $^{15}N$ was mixed with barium hydroxide and heated. The ammonia thus evolved was led into cold water. The reaction of aqueous ammonia with ethylcyanoacetate gave cyanoacetic amide, which was dehydrated by phosphorous oxychloride to $CH_2CNC^{15}N$[7].

## Rotational Spectra and Rotational Constants

The malononitrile molecule has a two-fold symmetry axis and the moment of inertia about this axis is of an intermediate magnitude. Thus, the selection rule allows only the *b*-type rotational transitions. The *a*-axis lies on a plane made by the two cyano groups and the central carbon atom. The *c*-type transitions are allowed for $CHD(CN)_2$ and the *a*-type transitions for $CH_2CNC^{15}N$, but neither of them was observed. Microwave absorption was observed only at room temperature since the vapor pressure is low. Owing to the large dipole moment (~3.6 D), the small rotational constants, and the presence of many vibrational states of low energies, the molecule was found to have many rotational lines: at least, one absorption line was observed in every 10 Mc./sec. Hence, the assignment seemed at first to be difficult. Fortunately, a *Q*-branch series $J_{0,J} \rightarrow J_{1\,J-1}$ was found to be assigned most easily*: the Stark effects are large and the intensities, in particular of high $J$ members, are very strong. It was possible to resolve three or four Stark components of $J=5$, 6 and

1) H. H. Nielsen, *Revs. Modern Phys.*, **23**, 90 (1951).
2) See, for example, R. G. Shulman and C. H. Townes, *Phys. Rev.*, **77**, 421 (1950).
3) E. B. Wilson, Jr., *J. Chem. Phys.*, **4**, 313 (1936).
4) K. W. F. Kohlrausch and Gr. P. Ypsilanti, *Z. physik. Chem.*, **B29**, 274 (1935).
5) F. Halverson and R. J. Francel, *J. Chem. Phys.*, **17**, 694 (1949).
6) E. Hirota, T. Oka and Y. Morino, ibid., **29**, 444 (1958); This Bulletin, to be published.
7) H. Gilman, "Organic Syntheses", Vol. 1, John Wiley & Sons, Inc., New York (1948), p. 179; A. H. Blatt, ibid., Vol. 2 (1948), p. 379; A. R. Surrey, ibid., Vol. 25 (1945), p. 63.

* It can be easily shown by use of the rotational constants that the $J_{0,J} \rightarrow J_{1,J-1}$ transitions are the single series of the *Q*-branch of this molecule in the region accessible by the present technique, 7000 to 30000 Mc./sec.

TABLE I. OBSERVED AND CALCULATED FREQUENCIES (Mc./sec.)

| Transition | $CH_2(CN)_2$ | | $CH_2CNC^{15}N$ | | $CHD(CN)_2$ | | $CD_2(CN)_2$ | | $CH_2CN^{13}CN$ |
|---|---|---|---|---|---|---|---|---|---|
| | obsd. | calcd. | obsd. | calcd. | obsd. | calcd. | obsd. | calcd. | obsd. |
| $1_{01} \rightarrow 1_{10}$ | 18265.36 | 18265.36 | 18088.67 | 18088.66 | 15916.73 | 15916.82 | 14077.66 | 14077.62 | |
| $2_{02} \rightarrow 2_{11}$ | 18595.54 | 18595.46 | 18405.56 | 18405.88 | 16268.84 | 16268.81 | 14444.84 | 14444.81 | |
| $3_{03} \rightarrow 3_{12}$ | 19098.79 | 19098.82 | 18889.37 | 18889.37 | 16807.95 | 16807.47 | 15008.56 | 15008.67 | |
| $4_{04} \rightarrow 4_{13}$ | 19785.23 | 19785.23 | 19548.66 | 19548.23 | 17545.41 | 17545.45 | 15784.72 | 15784.65 | |
| $5_{05} \rightarrow 5_{14}$ | 20667.93 | 20667.53 | 20394.99 | 20394.50 | 18498.82 | 18499.29 | 16791.92 | 16792.84 | |
| $6_{06} \rightarrow 6_{15}$ | 21761.79 | 21761.37 | 21443.07 | 21442.81 | 19688.76 | 19688.98 | 18055.72 | 18057.16 | |
| $7_{07} \rightarrow 7_{16}$ | 23084.25 | 23084.74 | 22709.58 | 22710.03 | 21135.78 | 21137.12 | 19601.55 | 19604.16 | |
| $8_{08} \rightarrow 8_{17}$ | 24656.01 | 24657.52 | 24213.27 | 24214.85 | 22864.92 | 22867.70 | 21456.12 | 21461.10 | |
| $9_{09} \rightarrow 9_{18}$ | 26497.38 | 26500.21 | 25973.43 | 25976.61 | 24899.76 | 24904.63 | 23645.34 | 23653.46 | 26367.03 |
| $10_{0,10} \rightarrow 10_{19}$ | 28626.87 | 28632.98 | 28008.57 | 28014.56 | 27261.51 | 27269.52 | 26189.70 | 26202.06 | 28456.41 |
| $0_{00} \rightarrow 1_{11}$ | 23498.82 | 23498.91 | 23189.52 | 23189.62 | 21086.78 | 21086.64 | 19191.00 | 19191.03 | |
| $1_{01} \rightarrow 2_{12}$ | 28732.50 | 28732.46 | 28290.63 | 28290.58 | 26256.39 | 26256.46 | 24304.47 | 24304.45 | |
| $5_{15} \rightarrow 6_{06}$ | 17414.02 | 17419.57 | | | | | | | |
| $6_{16} \rightarrow 7_{07}$ | 23738.22 | 23746.58 | | | | | | | |
| $5_{14} \rightarrow 4_{23}$ | 24093.24 | 24096.38 | | | | | | | |
| $6_{15} \rightarrow 5_{24}$ | 17595.24 | 17586.45 | | | | | | | |

TABLE II. ROTATIONAL CONSTANTS AND PRINCIPAL MOMENTS OF INERTIA[a)]

| | $CH_2(CN)_2$ | $CH_2CNC^{15}N$ | $CD_2(CN)_2$ | $CHD(CN)_2$ |
|---|---|---|---|---|
| $A$ | 20882.137 | 20639.146 | 16634.324 | 18501.730 |
| $B$ | 2942.477 | 2863.585 | 2916.905 | 2931.189 |
| $C$ | 2616.774 | 2550.477 | 2556.710 | 2584.910 |
| $b$ | $-8.9961\times10^{-3}$ | $-8.7304\times10^{-3}$ | $-1.29590\times10^{-2}$ | $-1.09974\times10^{-2}$ |
| $I_a$ | 24.208777 | 24.493794 | 30.390835 | 27.323445 |
| $I_b$ | 171.8046 | 176.5378 | 173.3108 | 172.4662 |
| $I_c$ | 193.1886 | 198.2104 | 197.7272 | 195.5701 |

$CH_2CN^{13}CN$

$A-(B+C)/2 = 18120.8\pm5.$ Mc./sec.

$(B-C)/2 = 160.3\pm4.$ Mc./sec.

a) Rotational constants are given in Mc./sec. and principal moments of inertia in amu Å$^2$. Conversion factor 505531 Mc. amu Å$^2$ is used.

7 lines and thus to check the $J$ numbers of these lines by the technique of Golden and Wilson[8)]. Six low $J$ transitions of $P$- and $R$-branches were also observed for $CH_2(CN)_2$, and two $R$-branch transitions for isotopically substituted molecules. The $Q$-branch members, $9_{09} \rightarrow 9_{18}$ and $10_{0,10} \rightarrow 10_{19}$ of the $CH_2CN^{13}CN$ molecule in natural abundance were measured and assigned. The measured frequencies are listed in Table I.

The rotational constants given in Table II were determined by four $Q$-branch ($J=$ 1 to 4) and two $R$-branch ($0_{00} \rightarrow 1_{11}$ and $1_{01} \rightarrow 2_{12}$) transitions, the centrifugal distortion being neglected. $A-(B+C)/2$ and $(B-C)/2$ were obtained for $CH_2CN^{13}CN$. The results are also given in Table II. The frequencies calculated by using the constants obtained above are compared with the observed frequencies in Table I.

8) S. Golden and E. B. Wilson, Jr., *J. Chem. Phys.*, 16, 669 (1948).

### Structure Analysis

The structure of malononitrile is specified by five parameters: the C—H, the C—C, and the C≡N bond length, and the HCH and the CCC bond angle. If the linearity of the C—C≡N group is abandoned, an additional parameter, ∠CCN, is necessary.

For convenience a Cartesian coordinate system is fixed in the molecule; its origin coincides with the center of gravity and the $x$-axis is taken along to the $c$-axis, the $y$-axis to the $a$-axis, and the $z$-axis to the $b$-axis, respectively (see Fig. 1). For isotopically substituted molecules the origin is shifted to the new center of gravity,

TABLE III. THE $x$-, $y$- AND $z$-MOMENTS (amu Å$^2$)

| | $CH_2(CN)_2$ | $CH_2CNC^{15}N$ | $CD_2(CN)_2$ | $CHD(CN)_2$ |
|---|---|---|---|---|
| $\sum m_i x_i^2$ | 1.4124 | 1.4106 | 2.9872 | 2.1805 |
| $\sum m_i y_i^2$ | 170.3922 | 175.1228 | 170.3236 | 170.3564 |
| $\sum m_i z_i^2$ | 22.7964 | 23.0876 | 27.4036 | 25.1430 |

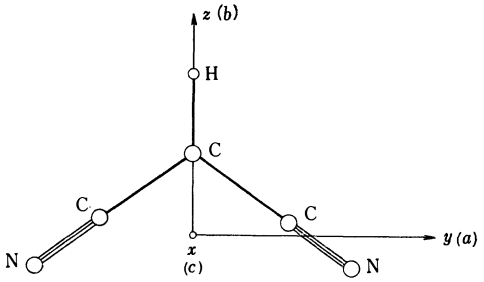



Fig. 1. Schematic diagram of malononitrile molecule.

but the $x$-, $y$-, and $z$-axes are kept parallel to those in the original molecule. For $CD_2(CN)_2$ the ($x$, $y$, $z$) system evidently coincides with the principal axes of moment of inertia, but for $CHD(CN)_2$ and $CH_2CNC^{15}N$ a slight rotation of axes is necessary, in transforming from the ($a$, $b$, $c$) system to the ($x$, $y$, $z$) system. Thus, in evaluating $\sum m_i x_i^2$, $\sum m_i y_i^2$, and $\sum m_i z_i^2$ (which are called the $x$-moment, the $y$-moment, and the $z$-moment, respectively) from $I_a$, $I_b$ and $I_c$ for the latter two molecules, some minor corrections are necessary and they are easily calculated by assuming a structure close to the real one. The $x$-, $y$- and $z$-moments thus obtained are listed in Table III.

**a) $x$-Coordinates.** — The $x$-moment is a function only of the $x$-coordinate of the hydrogen atom, $x_H$: that is,

$$\sum m_i x_i^2 = 2m x_H^2 \qquad (1)$$

where $2m = 2m_H$ for $CH_2(CN)_2$ and $CH_2CN\cdot C^{15}N$, $2m = [(3m_C + 2m_N)(m_D + m_H) + 4m_D m_H]/(3m_C + 2m_N + m_D + m_H)$ for $CHD(CN)_2$, and $2m = 2m_D$ for $CD_2(CN)_2$. The value of $x_H$, given in Table IV, increases with the mass of hydrogen, just as in the case of methylene chloride. Laurie[9] has explained this effect by the inertia defect, in analogy with planar molecules. By taking into consideration the inertia defect $\Delta$, Eq. 1 is modified as follows:

$$\sum m_i x_i^2 + (1/2)\Delta = 2m x_H^2 \qquad (1')$$

where a single value of the inertia defect $\Delta$ is assumed for all molecules, since the inertia defect is considered to originate from the in-plane vibrations of low frequencies. In fact, four observed $x$-moments can be reproduced by Eq. 1′, if two parameters, $x_H$ and $\Delta$, are assumed to be 0.8847 Å and 0.3379 amu Å$^2$, respectively. The calculated $x$-moments are compared with those observed in Table V. The

TABLE IV. VALUES OF $x_H$ DETERMINED WITHOUT THE INERTIA DEFECT CORRECTION (Å)

| Molecule | $x_H$ |
|---|---|
| $CH_2(CN)_2$ | 0·8370 |
| $CH_2CNC^{15}N$ | 0.8364 |
| $CHD(CN)_2$ | 0.8514 |
| $CD_2(CN)_2$ | 0.8610 |

TABLE V. OBSERVED AND CALCULATED $x$-MOMENTS (amu Å$^2$)

| Molecule | $\sum m_i x_i^2$ | |
|---|---|---|
| | obsd. | calcd.[a] |
| $CH_2(CN)_2$ | 1.4124 | 1.4091 |
| $CH_2CNC^{15}N$ | 1.4106 | 1.4091 |
| $CHD(CN)_2$ | 2.1805 | 2.1851 |
| $CD_2(CN)_2$ | 2.9872 | 2.9848 |

a) $x_H = 0.8847$ Å and $\Delta = 0.3379$ amu Å$^2$ are assumed.

inertia defect $\Delta$ of 0.3379 amu Å$^2$ is large compared with that of methylene chloride 0.167 amu Å$^2$, or of other molecules[9]. It is consistent with the fact that there are more normal modes of low frequencies in malononitrile.

Myers and Gwinn[10] have analyzed their data on methylene chloride by plotting $x_H$ against $1/2m$. The meaning of this procedure is evident from Eq. 1′; if $\Delta \ll \sum m_i x_i^2$ is assumed, $x_H$ is given by $(\sum m_i x_i^2/2m)^{1/2} \cdot (1 + \Delta/4\sum m_i x_i^2) = x_H^0 + (\Delta/4x_H^0)(1/2m)$, where $x_H^0 = (\sum m_i x_i^2/2m)^{1/2}$ means the value of $x_H$, when $\Delta$ is ignored. Thus, the $x_H$ obtained here corresponds to $x_H^0$ in the limit of $1/2m \to 0$.

**b) $y$-Coordinates.** — If the effect of zero-point vibration is negligible, the same $y$-moment should be obtained for three molecules; $CH_2(CN)_2$, $CHD(CN)_2$ and $CD_2(CN)_2$, since the $y$-moment is a function depending only upon the coordinates of the cyano groups. The observed $y$-moments,

9) V. W. Laurie, ibid., 28, 704 (1958).

10) R. J. Myers and W. D. Gwinn, ibid., 20, 1420 (1952).

170.3922, 170.3564 and 170.3236 amu Å$^2$, show a small discrepancy, presumably due to zero-point vibration, but the effect is not so large as in the $x$-moment.

By combining the $y$-moment for $CH_2CN\cdot C^{15}N$, $(\sum m_i y_i^2)_{15}$, with that of $CH_2(CN)_2$, $(\sum m_i y_i^2)_{14}$, the $y$-coordinate of nitrogen, $y_N$, in the normal molecule is obtained as follows:

$$y_N^2 = [(M+\Delta m_N)/M\Delta m_N] \times [(\sum m_i y_i^2)_{15} - (\sum m_i y_i^2)_{14}] \quad (2)$$

where $M$ is the total mass of $CH_2(CN)_2$, and $\Delta m_N$ is the mass difference of $^{15}N$ and $^{14}N$. Then $y_N$ is found to be 2.1943 Å.

In order to determine the $y$-coordinate of the carbon atom in a cyano group, $y_C$, it is desirable to substitute the carbon atom with its isotope, $^{13}C$[11]. As mentioned earlier, two $Q$-branch transitions have been observed for $CH_2CN^{13}CN$ molecule, but the rotational constants could not be determined accurately enough for the structure analysis. Hence $y_C$ is evaluated through the $y$-moment combined with the value of $y_N$ obtained above. Three values of the $y$-moments for $CH_2(CN)_2$, $CHD(CN)_2$, and $CD_2(CN)_2$ give accordingly three $y_C$'s: 1.2161, 1.2155 and 1.2149 Å, respectively. As the difference between them is not large, the average of the three values is used for $y_C$: that is, 1.2155 Å.

**c) $z$-Coordinates.** — The $z$-moments of $CH_2(CN)_2$, $(\sum m_i z_i^2)_2$, and of $CHD(CN)_2$, $(\sum m_i z_i^2)_3$, give the $z$-coordinate of hydrogen in the normal molecule, $z_H$, by the relation similar to Eq. 2:

$$z_H^2 = [(M+\Delta m_H)/M\Delta m_H] \times [(\sum m_i z_i^2)_3 - (\sum m_i z_i^2)_2] \quad (3)$$

where $\Delta m_H$ is the mass difference of D and H. If the $z$-moment of $CD_2(CN)_2$, $(\sum m_i z_i^2)_4$, is used in place of $(\sum m_i z_i^2)_3$, the equation

$$z_H^2 = [(M+2\Delta m_H)/2M\Delta m_H] \times [(\sum m_i z_i^2)_4 - (\sum m_i z_i^2)_2] \quad (4)$$

must be applied. Eq. 3 gives $z_H$ of 1.5384 Å, whereas Eq. 4 gives 1.5357 Å. The average value, 1.5371 Å, is used in the following analysis of the structure.

A similar procedure is used to determine the $z$-coordinate of the nitrogen atom, $z_N$. The relevant equation is

$$z_N^2 = [(M+\Delta m_N)/M\Delta m_N] \times [(\sum m_i z_i^2)_{15} - (\sum m_i z_i^2)_{14}] \quad (5)$$

where $(\sum m_i z_i^2)_{14}$ means $(\sum m_i z_i^2)_2$ in Eqs. 3 and 4. It may be noted that, since the effect of zero-point vibration entering in $\sum m_i x_i^2$ is probably similar for the two molecules $CH_2(CN)_2$ and $CH_2CNC^{15}N$, $I_{yy}$ is used in place of $(\sum m_i z_i^2)$. In doing so, the accuracy attained becomes considerably better, for the value of $I_{yy}$ is determined by the rotational constant $A$, whereas $\sum m_i z_i^2$ is evaluated by three rotational constants, $A$, $B$ and $C$. Under this assumption $z_N$ is found to be $-0.5427_3$ Å.

Since adequate substitutions are not yet available, a procedure similar to that used for the determination of $z_H$ and $z_N$ can not be applied to the $z$-coordinates of carbon atoms. Moreover, whatever substitution is possible, the $z$-coordinate of the carbon atom of the cyano group is close to zero, and the procedure becomes less powerful. Hence the first moment equation and the relation giving the $z$-moment of $CH_2(CN)_2$ are used to evaluate the $z$-coordinates of the apex carbon atom, $z_0$, and of the carbon atom in the cyano group, $z_C$[11]. They are 0.8994 and 0.0545 Å, respectively.

All the coodinates necessary for the structure determination are thus obtained and listed in Table VI. The bond length

Table VI. Coordinates of atoms in $CH_2(CN)_2$ and molecular structure

| Atom | $x_i$ | $y_i$ | $z_i$ |
|---|---|---|---|
| H | ±0.8847 Å | 0 Å | +1.5371 Å |
| C (apex) | 0 | 0 | +0.8994 |
| C (cyano) | 0 | ±1.2155 | +0.0545 |
| N | 0 | ±2.1943 | $-0.5427_3$ |

| | | | |
|---|---|---|---|
| C—C | $1.480_3$±0.0056 Å | ∠CCC | 110°24′±24′ |
| C≡N | $1.146_6$±0.0064 Å | ∠HCH | 108°26′±26′ |
| C—H | $1.090_6$±0.0034 Å | ∠CCN | 180°−(3°24′±26′) (outside) |

of C—H is found to be 1.091 Å, that of C—C 1.480 Å, and that of C≡N 1.147 Å. The bond angle of CCC, 110°24′, is about 1° wider than the tetrahedral angle, whereas that of HCH, 108°26′, is smaller than the tetrahedral angle by the same order of magnitude. Myers and Gwinn[10] reported the C—H bond length and the HCH bond angle in methylene chloride to be 1.082 Å and 112°58′, respectively, whereas Lide, Jr.[12], obtained 1.092 Å and 111°52′, for the corresponding quantities in methylene fluoride. The C—H bond length of malononitrile, 1.091 Å, is closer to that of methylene fluoride, rather than to that of methylene chloride, but the

11) C. C. Costain, ibid., **29**, 864 (1958).

12) D. R. Lide, Jr., *J. Am. Chem. Soc.*, **74**, 3548 (1952).

HCH bond angle 108°26′ is definitely smaller than those of methylene halides. It is noteworthy that the linearity of C—C≡N groups does not hold, the cyano groups being bent outside by about 3.5°. Though zero-point vibration may modify considerably the equilibrium configuration, it seems reasonable to assume an electrostatic repulsion between two electronegative groups such as cyano radicals. Somewhat longer C—C, somewhat shorter C≡N bond length, and the bent C—C≡N indicate that the electron configuration in the cyano groups might be more or less different from that in acetonitrile. In fact, Casabella and Bray[13] found, in the solid state, a quadrupole coupling constant and an asymmetry parameter, definitely larger than those of acetonitrile and of ethyl cyanide.

### Dipole Moment

The dipole moment of $CH_2(CN)_2$ was obtained from the Stark effects of the six transitions: four $Q$-branch lines of $J=1$ to 4 and two $R$-branch transitions, $0_{00} \rightarrow 1_{11}$ and $1_{01} \rightarrow 2_{12}$. The field strength was calibrated by the $J=1 \rightarrow 2$ transition of OCS, the dipole moment of OCS being assumed to be 0.7124 D[14]. The values of the dipole moment obtained from the six transitions agree well with each other (Table VII). The average of them is 3.735 D, which is compared with 3.6 D obtained by the dielectric constant measurement in benzene solutions[15].

13) P. A. Casabella and P. J. Bray, *J. Chem. Phys.*, **29**, 1105 (1958).
14) S. A. Marshall and I. Weber, *Phys. Rev.*, **105**, 1502 (1957).

TABLE VII. DIPOLE MOMENT (DEBYE)

| Transition | $\mu$ |
|---|---|
| $1_{01} \rightarrow 1_{10}$ | 3.724 |
| $2_{02} \rightarrow 2_{11}$ | 3.735 |
| $3_{03} \rightarrow 3_{12}$ | 3.759 |
| $4_{04} \rightarrow 4_{13}$ | 3.750 |
| $0_{00} \rightarrow 1_{11}$ | 3.704 |
| $1_{01} \rightarrow 2_{12}$ | 3.736 |
| average | 3.735±0.017 |

The authors wish to express their sincere thanks to Dr. Makoto Shima, Institute for Physical and Chemical Research, for supplying them heavy water and ammonium sulfate containing 23.5% $^{15}N$. The expenses of this research were defrayed from the Scientific Research Encouragement Grant of the Ministry of Education to which the authors' thanks are also due.

*Department of Chemistry*
*Faculty of Science*
*The University of Tokyo*
*Hongo, Tokyo*

*Added in Proof:*

October, 1959 Dr. P. W. Moore of Purdue University called the authors' attention to the paper by N. Muller and D. E. Pritchard, *J. Am. Chem. Soc.*, **80**, 3483 (1958). They measured the microwave spectrum of normal species $CH_2(CN)_2$ of malononitrile and obtained rotational constants in close agreement with the authors'. Recently Dr. Muller wrote us that their measurement had been extended to include the rotational spectrum of deuterium substituted species $CD_2(CN)_2$, and the rotational constants obtained were also in agreement with the authors'.

15) P. Trunel, *Ann. chim.*, **12**, 93 (1939).

# *The Adsorption of Dye Mixtures by Cellophane Sheet. I. Temperature and Concentration Dependence of Adsorption from Some Binary Mixtures*

By Yukio HORIKI, Yoshié TANIZAKI and Noboru ANDO

(Received July 13, 1959)

It is well known that the amount of adsorption of dyes from binary mixtures of a direct dye with others is commonly reduced as compared with the adsorbed dye amount when dyed singly[1-3]. Some factors of such reduction of adsorption in mixture dyeing have been variously discussed, and it seems to be most appropriate to consider a mutual interaction between dyes in solution as a principal factor. Neale and Stringfellow have considered that such interaction is attributed to the complex formation[2]. This concept, however, has failed to be accepted, because there is no direct evidence of complex formation in solution at such a high temperature as is practically applied[4]. Derbyshire and Peters[3] have recently shown by the spectroscopic measurements that Chlorazol Sky Blue FF and Chrysophenine G form a 1 : 1 complex in aqueous solution containing no salt at 60°C, and further concluded by the thermodynamic treatment that the complex formation occurs even at a usual dyeing temperature 90°C. Based on this conclusion, they have discussed in a semi-quantitative way the results of mixture dyeing.

In the hope of finding a method to obtain some quantitative information about the interaction between dyes in mixture dyebath, necessary to explain the reduction in adsorption, the authors have studied the single and the mixture dyeings of Chlorazol Sky Blue FF and Chrysophenine G, and of Chlorazol Sky Blue FF and a monoazo acid dye.

## Experimental

Chlorazol Sky Blue FF and Chrysophenine G were used as direct dyes, and *p*-nitroaniline→γ acid (α-coupling) as a monoazo acid dye. Chlorazol Sky Blue FF (called Blue dye for short) and the monoazo acid dye (Acid dye) were the same as those used in the authors' previous works[5,6], and Chrysophenine G (Yellow dye) was prepared by purifing the commercial dye by Robinson and Mills' method[7].

The Cellophane sheet used was that made by Tokyo Cellophane Co., Ltd. It was washed with distilled water at 90°C for 30 min. Pieces of the sheet weighing 15~25 mg. were dyed in 75 g. portions of the dye solution at 50, 70 and 90°C for 24 hr.* The dyed sheets were rinsed in ice-cold water (about 6°C) and then left in a desiccator with 50% sulfuric acid for two days. An accurate weight of the dyed sheet was obtained by dividing its weight under the constant humidity by a known humidity coefficent (e. g. 1.07 at 15°C and 1.10 at 30°C)[8].

Check measurements on solutions of known density in 25% aqueous pyridine showed that the dyes obeyed Beer's law both singly and in mixture, and that the absorption spectra in the mixture were additive. Based on this fact, the dye adsorbed by the sheet was stripped with 25% aqueous pyridine and the dye content of the strip solution was measured by a Shimadzu QR-50 spectrophotometer.

In case of the mixture dyeing, the initial concentration of Blue dye was about $1\times10^{-5}$ mol./l. for every dyebath, and those of Yellow dye and Acid dye were varied from zero to about $35\times10^{-5}$ and $90\times10^{-5}$ mol./l., respectively. The concentration of sodium chloride was 2.0 g./l. for every dyebath.

## Results

The relation between the amount of adsorption of Blue dye and the dyebath concentration of its partners was examined, 24 hr. after mixture dyeing, by the

1) J. Boulton, A. E. Delth, F. Forthergrill and T. H. Morton, *J. Textile Inst.*, **24**, 113 (1933).
2) S. M. Neale and W. A. Stringfellow, *J. Soc. Dyers Colourists*, **59**, 241 (1943).
3) A. N. Derbyshire and R. H. Peters, ibid., **72**, 268 (1956).
4) T. Vickerstaff, "The Physical Chemistry of Dyeing", 2nd Ed., Oliver & Boyd, London (1954), p. 242.
5) Y. Tanizaki, T. Kobayashi and N. Ando, This Bulletin, **32**, 119 (1954).
6) T. Kobayashi, Y. Tanizaki and N. Ando, ibid., **32**, 675 (1959).
7) C. Robinson and H. A. T. Mills, *Proc. Roy. Soc. (London)*, **A131**, 576 (1931).
8) K. Nishida, *J. Soc. Textile Cellulose Ind. Japan (Sen-i Gakkaishi)*, **7**, 539 (1951).
* This time of of dyeing (24 hr.) may be enough for only a qualitative discussion of the behavior of mixture dyeing.

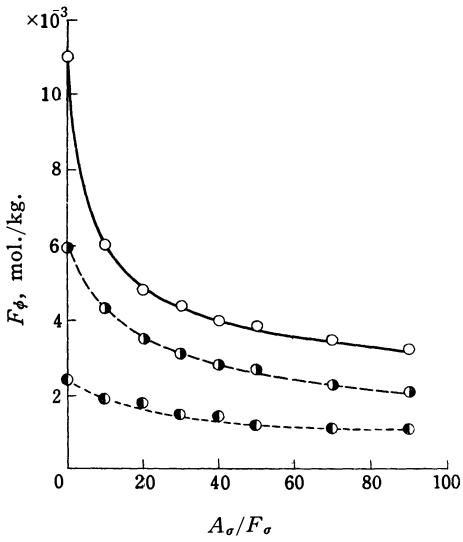



Fig. 1. The relation between the adsorption of Blue dye ($F_\phi$) from a mixture dyebath with Acid dye and the ratio of final dyebath concentration of Acid dye ($A_\sigma$) to that of Blue dye ($F_\sigma$).
—○— 50°C, --◑-- 70°C, ---◐--- 90°C

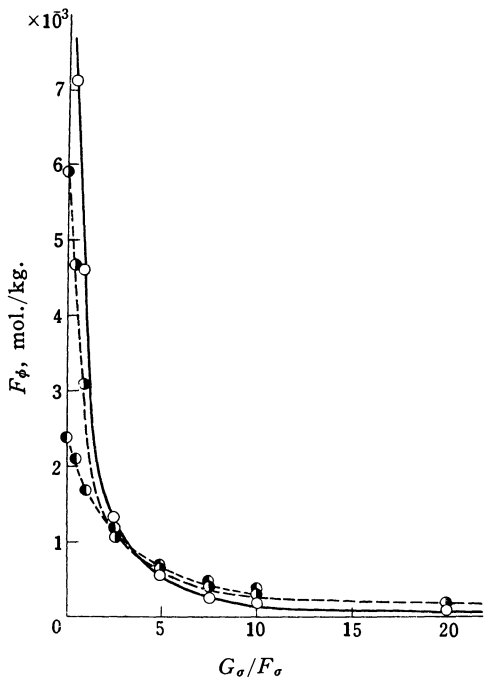



Fig. 2. The relation between the adsorption of Blue dye ($F_\phi$) from mixture dyebath with Yellow dye and the ratio of final dyebath concentration of Yellow dye ($G_\sigma$) to that of Blue dye ($F_\sigma$).
—○— 50°C, --◑-- 70°C, ---◐--- 90°C

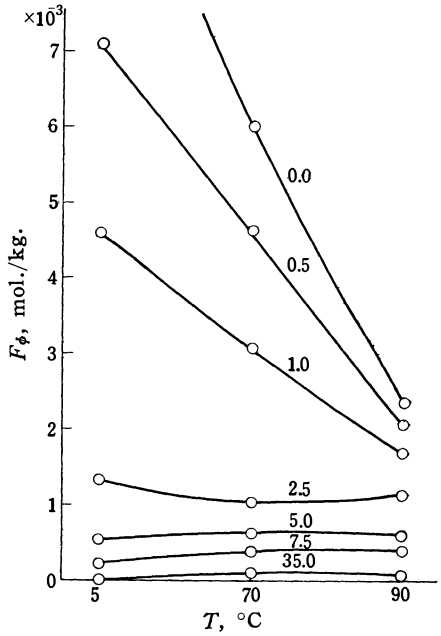



Fig. 3. Effect of temperature on the adsorption of Blue dye from mixture dyebath. The numbers indicate the ratio of the initial dyebath concentration of Yellow dye to that of Blue dye.

adsorption measurements of binary mixtures containing a constant amount of Blue dye. The results are shown in Figs. 1 and 2; the one denotes the pair of Blue dye and Acid dye, and the other Blue dye and Yellow dye. Comparison between these figures shows that the adsorption of Blue dye is not so decreased with an increase in the dyebath concentration of Acid dye (Fig. 1), while it is markedly reduced by the addition of a very small amount of Yellow dye until it rapidly converges to zero (Fig. 2). Furthermore, under the present condition, the adsorption of Blue dye from a dyebath, containing several times as much Yellow dye as Blue dye, slightly increases with a raise in temperature; this is the same tendency as that reported by Neale and Stringfellow[2]. This situation can be recognized by the relation between the adsorption of Blue dye and temperature in Fig. 3.

In case of mixture dyeing with Blue dye the adsorption of the partner, i. e. Yellow dye or Acid dye, is also reduced, as compared with that in the case of its single dyeing. For instance, adsorption curves of Yellow dye from single and mixture dyebaths at 70°C, corresponding to Fig. 2, are shown in Fig. 4a.

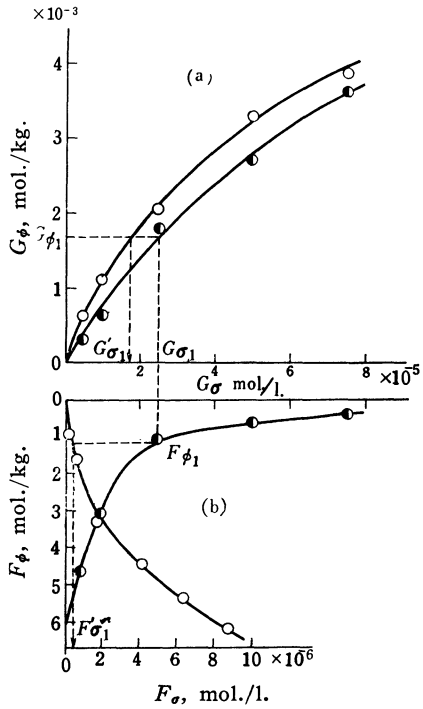



Fig. 4. The adsorptions of Blue dye and Yellow dye from single and mixture dyebaths at 70°C. Here the results of mixture dyeing correspond to those of Fig. 2. Scale ($F_\sigma$) on the abscissa (b) refers to the white circles.

○ Single ◐ Mixture

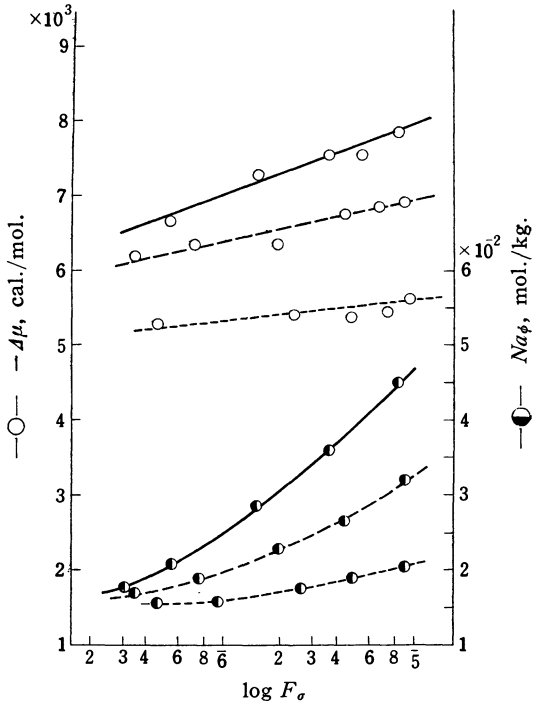



Fig. 5. The relations of the affinity ($-\Delta\mu^0$) of Blue dye for Cellophane (white circles) and of the concentration of sodium ion ($Na_\phi$) in Cellophane (half solid circles) to the logarithm of final dyebath concentration of Blue dye ($F_\sigma$, mol./l.).

—— 50°C, ---- 70°C, ------ 90°C

It has been seen that the affinity of Blue dye**, obtained from its single dyeing (corresponding to the white circles in Fig. 4b), is more or less dependent on its dyebath concentration at constant temperature. The relation between the affinity of Blue dye and its final dye bath concentration at various temperatures in single dyeing is shown in Fig. 5. This figure shows that the affinity, $-\Delta\mu^0$, is approximately proportional to the logarithm of the final dyebath concentration of Blue dye, $F_\sigma$. In this figure is also shown the relation between $\log F_\sigma$ and the concentration of sodium ion in Cellophane, $Na_\phi$**.

## Discussion

Based on the assumption that the reduction of the amount of dyes resulting from the mixture dyeing is due to an interaction between the two dyes, the results described in the preceding section will be discussed. Now, let us assume simply that:

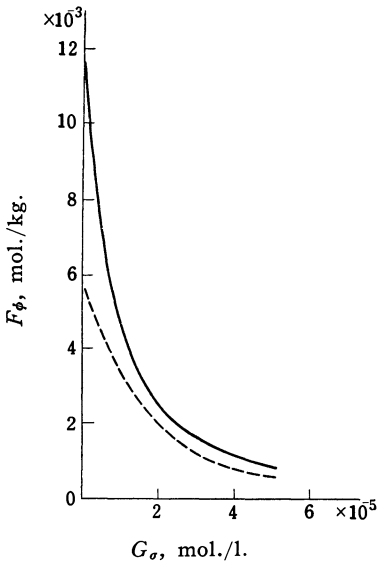



Fig. 6. The relation between the dyebath concentration of Yellow dye and the adsorption of Blue dye calculated from Eqs. 1 and 3. $F_\sigma = 1\times10^{-5}$ mol./l., $K_{50°} = 6\times10^{-7}$ mol./l., $K_{70°} = 1\times10^{-6}$ mol./l.

—— 50°C, ---- 70°C

** $Na_\phi$ and $-\Delta\mu^0$ were calculated from Eqs. 7.19 (p. 200) and 7.26 (p. 206) in Ref. 4. $V$ (surface layer volume) =0.45 l./kg. for each dyeing temperature.

1) The effective dyebath concentration which contributes to adsorption is reduced by an interaction between both dyes in mixture.

2) The amount of the dye adsorbed from the mixture dyebath corresponds to this effective dyebath concentration, and the adsorbing behavior of the dye in mixture dyeing is just the same as that in its single dyeing, so it behaves independently. Consequently, concerning the effective dyebath concentration, the additivity in adsorption comes into being.

These assumptions may be appropriate under the condition that no competition of dyes for the available surface occurs. If the assumptions are accepted, the effective dye bath concentration will be calculated by the following equation, using the amount of dye adsorbed from mixture dyeing and its affinity obtained from single dyeing,

$$D_\phi = Na_\phi^{-z} Na_\sigma^{+z} V^{z+1} D_\sigma' \exp(-\Delta\mu^0/\boldsymbol{R}T) \quad (1)$$

where $D_\phi$ (mol./kg.) is the amount of a dye adsorbed by Cellophane, $D_\sigma'$ (mol./l.) the effective dyebath concentration, $Na_\phi$ (mol./kg.) the sodium ion concentration in Cellophane, $Na_\sigma$ (mol./l.) the sodium ion concentration in dyebath, $V$ (l./kg.) the surface layer volume, $-\Delta\mu^0$ (cal./mol.) the standard affinity, $\boldsymbol{R}$ and $T$ the gas constant and the absolute temperature, respectively, and $z$ the number of sulfonic groups per molecule. The difference $D_c$ (mol./l.) between the total dyebath concentration $D_\sigma$ (mol./l.) and the effective dyebath concentration may be attributed to the interaction of dyes in mixture solution; in other words, $D_c$ may be regarded as the dyebath concentration ineffective to adsorption. If the amount of a dye adsorbed in this mixture dyeing is known, it would be expected that its effective dyebath concentration would be calculated by Eq. 1. However, as the calculated affinity of dyes generally varies more or less with the dyebath concentration, it is undesirable to calculate it directly by Eq. 1. Therefore, it was obtained graphically from the observed values in single and mixture dyeings. Concerning the pair of Blue dye and Yellow dye, for example, its effective dyebath concentration is obtained from Figs. 4a and 4b as follows: when the final total dye bath concentrations of Blue dye and Yellow dye are $F_{\sigma 1}$ and $G_{\sigma 1}$, respectively***, as shown in the figure, the amounts of adsorption of the dyes $F_{\phi 1}$, $G_{\phi 1}$ correspond to $F_{\sigma 1}'$, $G_{\sigma 1}'$ in single dyeing, respectively, which may be regarded as their effective dyebath concentrations. $F_{\sigma 1}-F_{\sigma 1}' \equiv F_{c1}$ and $G_{\sigma 1}-G_{\sigma 1}' \equiv G_{c1}$ may be regarded as the concentrations participated in the interaction, and it follows that $G_{c1}/F_{c1}$ means the mole ratio of both dyes contributed to the interaction. Values obtained in such a way are shown in Tables I and II. Table I shows that $G_c/F_c$ tends to about unity when the relative concentration of Yellow dye to Blue dye increases to a certain value. If it is assumed that the interaction in this range of concentration means the formation of a 1:1 complex, it is possible to calculate the instability constant $K$ of the complex, according to the mass action law,

$$K = \frac{F_\sigma' G_\sigma'}{F_c} = \frac{(F_\sigma - F_c)(G_\sigma - G_c)}{F_c}, \quad (F_c = G_c) \quad (2)$$

Values of $K$ calculated by the equation are shown in Table I.

When the value of $K$ is known, the effective dyebath concentration will be obtained from Eq. 2. For example, $F_\sigma'$ can be given as a function of $F_\sigma$ and $G_\sigma$, by the following equation which was derived from Eq. 2,

$$F_\sigma' = F_\sigma - F_c = \frac{1}{2}\{(G_\sigma - a)^2 + (b^2 - a^2)\}^{1/2} + \frac{1}{2}(a - G_\sigma) \quad (3)$$

where $a = F_\sigma - K$ and $b = F_\sigma + K$. Since $a$ and $b$ are constant when $F_\sigma$ is fixed, $F_\sigma'$ is the function of $G_\sigma$ alone. Further, the value of $F_\phi$ in the mixture of Blue dye and Yellow dye can be obtained by substituting $F_\sigma'$ into Eq. 1.

In order to check the validity of the assumption described above, values of $F_\sigma'$ corresponding to various values of $G_\sigma$ were calculated by Eq. 3; here were used $6\times10^{-7}$ and $1\times10^{-6}$ mol./l. as the values of $K_{50°}$ and $K_{70°}$, respectively, and $1\times10^{-5}$ mol./l. as that of $F_\sigma$ and $0.5\times10^{-5}\sim5\times10^{-5}$ mol./l. as that of $G_\sigma$. The values of $F_\phi$ are also calculated by Eq. 1, using the obtained values of $F_\sigma'$, where $Na_\phi$ and $-\Delta\mu^0$ were obtained graphically from Fig. 5, and $3.42\times10^{-2}$ mol./l. and 0.45 l./kg. were used as the values of $Na_\sigma$ and $V$, respectively. These calculated values of $F_\phi$ against

*** Since the total concentration of Blue dye is nearly constant ($1\times10^{-5}$ mol./l.), $G_{\sigma 1}/F_{\sigma 1}$ is dependent only on $G_{\sigma 1}$. Suffix 1 denotes some fixed values of $F_\sigma$, $G_\sigma$, etc.

TABLE I. RESULTS OF MIXTURE DYEING OF BLUE DYE AND YELLOW DYE

| $T$°C | $F_\sigma$ $\times10^6$ mol./l. | $F_\phi$ $\times10^3$ mol./kg. | $F_\sigma'$ $\times10^6$ mol./l. | $F_c$ $\times10^6$ mol./l. | $G_c/F_c$ | $K$, mol./l. | $G_c$ $\times10^6$ mol./l. | $G_\sigma'$ $\times10^6$ mol./l. | $G_\phi$ $\times10^3$ mol./kg. | $G_\sigma$ $\times10^6$ mol./l. |
|---|---|---|---|---|---|---|---|---|---|---|
| 50 | 8.04 | 7.1 | 3.2 | 4.8 | 0.7 | — | 3.3 | 1.5 | 0.6 | 4.83 |
| | 8.88 | 4.6 | 1.3 | 7.6 | 0.7 | — | 5.1 | 4.6 | 1.3 | 9.70 |
| | 9.75 | 1.3 | 0.4 | 9.4 | 1.2 | $4.7\times10^{-7}$ | 11.0 | 14.0 | 2.8 | 24.5 |
| | 9.87 | 0.6 | 0.2 | 9.7 | 1.2 | $7.4\times10^{-7}$ | 12.0 | 37.0 | 5.2 | 48.8 |
| 70 | 8.59 | 4.6 | 4.6 | 4.0 | 0.7 | — | 2.6 | 2.3 | 0.3 | 4.89 |
| | 9.39 | 3.1 | 2.1 | 7.3 | 0.5 | — | 3.6 | 6.3 | 0.6 | 9.87 |
| | 9.73 | 1.1 | 0.4 | 9.3 | 0.5 | — | 4.6 | 20.0 | 1.8 | 24.6 |
| | 9.86 | 0.6 | 0.3 | 9.6 | 1.3 | $9.6\times10^{-7}$ | 12.0 | 37.0 | 2.7 | 49.4 |
| 90 | 9.90 | 0.4 | 0.9 | 9.0 | 0.9 | $7.4\times10^{-6}$ | 8.0 | 70.0 | 1.7 | 78.0 |
| | 9.96 | 0.2 | 0.7 | 9.3 | 1.0 | $1.4\times10^{-5}$ | 9.0 | 190.0 | 3.5 | 199.0 |

Notations, $F_\sigma$ etc. and $G_\sigma$ etc., refer to Blue dye and Yellow dye, respectively.
$K$ means the instability constant of complex. $(F_c+G_c)/2$ was regarded as the concentration of complex in the range $0.9\leqq G_c/F_c\leqq1.3$.

TABLE II. RESULTS OF MIXTURE DYEING OF BLUE DYE AND ACID DYE

| $T$°C | $F_\sigma$ $\times10^6$ mol./l. | $F_\phi$ $\times10^3$ mol./kg. | $F_\sigma'$ $\times10^6$ mol./l. | $F_c$ $\times10^6$ mol./l. | $A_c/F_c$ | $A_c$ $\times10^6$ mol./l. | $A_\sigma'$ $\times10^5$ mol./l. | $A_\phi$ $\times10^3$ mol./kg. | $A_\sigma$ $\times10^4$ mol./l. |
|---|---|---|---|---|---|---|---|---|---|
| 50 | 8.98 | 4.9 | 1.4 | 7.6 | 1.1 | 8 | 1.2 | 1.6 | 2.0 |
| | 8.96 | 4.4 | 1.2 | 7.8 | 1.2 | 9 | 2.1 | 2.2 | 3.0 |
| | 9.14 | 4.0 | 1.0 | 8.1 | 1.4 | 11 | 2.9 | 2.6 | 4.0 |
| | 9.15 | 3.5 | 0.9 | 8.3 | 1.4 | 28 | 4.2 | 3.2 | 7.0 |
| 70 | 9.25 | 3.1 | 2.0 | 7.3 | 2.3 | 17 | 1.3 | 1.5 | 3.0 |
| | 9.36 | 2.8 | 1.7 | 7.7 | 2.7 | 21 | 1.9 | 1.8 | 4.0 |
| | 9.47 | 2.3 | 1.2 | 8.3 | 3.3 | 27 | 4.3 | 2.6 | 7.0 |
| | 9.55 | 2.1 | 1.1 | 8.5 | 3.4 | 29 | 6.1 | 3.1 | 9.0 |
| 90 | 9.61 | 1.8 | 5.4 | 4.2 | 1.9 | 8 | 1.2 | 0.8 | 2.0 |
| | 9.67 | 1.4 | 3.7 | 6.0 | 2.4 | 14 | 2.6 | 1.3 | 4.0 |
| | 9.73 | 1.3 | 3.1 | 6.6 | 3.0 | 20 | 3.0 | 1.5 | 5.0 |
| | 9.73 | 1.1 | 2.5 | 7.2 | 3.3 | 24 | 4.6 | 1.9 | 7.0 |
| | 9.76 | 1.1 | 2.5 | 7.3 | 3.5 | 25 | 6.5 | 2.3 | 9.0 |

Notations, $F_\sigma$ etc. and $A_\sigma$ etc., refer to Blue dye and Acid dye, respectively.

$G_\sigma$ are given in Fig. 6. Good agreement between the calculated (Fig. 6) and the measured (Fig. 2) values shows that the behavior of dyes in mixture dyeing may be qualitatively explained by the knowledge of single dyeing, if it is possible to know the instability constant.

If the composition of complexes remains constant over the whole concentration range, $K$ should be determined in principle even when the composition is not 1:1. In this way the amount of dyes adsorbed from mixture dyeing may be predicted. In the case of the mixture of Blue dye and Acid dye, however, the composition is gradually varied****, so the instability constant could not be obtained. Therefore, the amount of adsorption of the dyes from mixture dyeing can not be calculated by the above method. But it is expected that the difference between Fig. 1 and Fig. 2 may be understood qualitatively as follows: it is dependent directly on the extent of decrease in the effective dyebath concentration of Blue dye whether the reduction in adsorption of this dye is slow (Fig. 1) or rapid (Fig. 2) with an increase in the dyebath concentration of its partners. This fact may be attributed to the following two factors:

(a) The mole ratio of components in complexes.

(b) The instability constant of the complexes.

It is clear that the smaller the mole ratio ($G_c/F_c$ or $A_c/F_c$), the greater the

**** The spectroscopic measurements for the same mixture free from sodium chloride at room temperature show the same tendency: $A_c/F_c$ gradually increases with an increase in the relative concentration of Acid dye.

TABLE III. EFFECT OF TEMPERATURE ON THE ADSORPTION OF BLUE DYE

| $G_\sigma/F_\sigma$ | $T$°C | $\Delta \ln F_\sigma'/\Delta T$ | $-4\Delta \ln Na_\phi/\Delta T$ | $\Delta(-\Delta\mu^\circ/\boldsymbol{R}T)/\Delta T$ | $\Delta \ln F_\phi/\Delta T$ |
|---|---|---|---|---|---|
| 0.5 | 50 | −0.0005 | +0.0677 | −0.100 | −0.037 |
| | 70 | +0.0154 | +0.0708 | −0.165 | −0.079 |
| | 90 | | | | |
| 5.0 | 50 | +0.0137 | +0.0118 | −0.060 | −0.034 |
| | 70 | +0.1035 | +0.0062 | −0.120 | −0.014 |
| | 90 | | | | |
| 10.0 | 50 | +0.0142 | +0.0121 | −0.045 | −0.019 |
| | 70 | +0.1097 | +0.0129 | −0.115 | +0.008 |
| | 90 | | | | |

decrease in effective dyebath concentration of Blue dye. If one considers only this point, it will apparently be expected from Tables I and II that the reduction of $F_\phi$ is slower in the case of the pair of Acid dye and Blue dye than that of Yellow dye and Blue dye. On the other hand, when the complexes have the same composition, the smaller $K$ is, the greater should be the decrease in the effective dye bath concentration. For instance, it will be expected that in the case of the pair of Acid dye and Blue dye the value of $K$ at a given temperature is greater than in the case of that of Yellow dye and Blue dye in a concentration range, in which only a 1:1 complex seems to be formed in both pairs[9]. Concerning the effect of temperature, the reduction in adsorption of a dye on addition of its partner will become smaller with temperature, since the value of $K$ increases in general with the rise of temperature. This is clearly seen in Figs. 1 and 2.

The relation between the amount of Blue dye adsorbed from the mixture with Yellow dye and dyeing temperature, as shown in Fig. 3, is also remarkable. That is, the amount of Blue dye adsorbed from the mixture, which contains several times as much Yellow dye as Blue dye, tends to increase slightly with the rise of temperature. The interpretation of this result is rendered difficult, but it may be explained at least by the hypothesis of complex formation and the knowledge of single dyeing. In other words, if $Na_\sigma$ and $V$ are independent of temperature, the partial differentiation of Eq. 1 with respect to $T$ leads to

$$\frac{\partial \ln F_\phi}{\partial T} = -4\frac{\partial \ln Na_\phi}{\partial T} + \frac{\partial \ln F_\sigma'}{\partial T} + \frac{\partial}{\partial T}\left(\frac{-\Delta\mu^0}{\boldsymbol{R}T}\right) \tag{4}$$

To see the correspondence of the equation with the results in Fig. 3, the value of each term at the right side of Eq. 4 was calculated for the interval of 20°C (50~70 and 70~90°C). If one takes $1\times10^{-5}$ mol./l. as $F_\sigma$, 1:0.5, 1:5 and 1:10 as $F_\sigma/G_\sigma$, and $5\times10^{-7}$, $1\times10^{-6}$ and $5\times10^{-5}$ mol./l. as $K$ of the 1:1 complex at 50, 70 and 90°C, respectively, then $F_\sigma'$ at each temperature can be calculated from Eq. 3, and $Na_\phi$ and $-\Delta\mu^0$ can be obtained from Fig. 5, also. Therefore, the value of $\Delta \ln F_\phi/\Delta T$ can be obtained from Eq. 4. They are listed in Table III. The result agrees qualitatively with the relation between $F_\phi$ and the temperature shown in Fig. 3. It will be recognized here that the sign of $\partial \ln F_\phi/\partial T$ may be dependent chiefly on the relation between the second and the third terms. In other words, it may mostly be influenced by the dependence of the instability constant and the affinity on temperature.

## Summary

1) The amount of dyes adsorbed by Cellophane from two mixture dyeings of Chlorazol Sky Blue FF and Chrysophenine G, and Chlorazol Sky Blue FF and *p*-nitroaniline→γ acid (α-coupling) was measured. Further, the amount in case of single dyeing was also measured.

2) It was assumed that the reduction in adsorption of dyes from mixture dyeing is due to an interaction between the two dyes in the dyebath, and that this interaction means only the formation of complexes. On this assumption, the instability constant in the case of the pair of Blue dye

9) A value of $K$ of the mixture in aqueous solution of Blue dye and Acid dye calculated at room temperture for a concentration range, in which only a 1:1 complex seems to be formed, is $1.25\times10^{-5}$ (Ref. 6) and that of the mixture of Blue dye and Yellow dye is $4\times10^{-6}$ at 60°C (Ref. 3). If these values are compared with each other at the same temperature, the difference between them will become greater: $K$ of the former may be much greater than that of the latter.

and Yellow dye was calculated, according to the mass action law, but it was impossible to calculate it in the case of the pair of Acid dye and Blue dye, because the composition of complexes of this pair was not constant.

3) How the amount of Blue dye adsorbed from mixture dyeing varies with the sort and the concentration of its partner dye and with the dyeing temperature was discussed from the standpoint of the instability constant and the affinity.

The authors wish to express their sincere thanks to Professor Ikuzo Tanaka and Dr. Tsuneo Yoshino of this Institute for their kind advice, to Assistant Professor Yoshiji Ishii, Gumma University, who gave them Chrysophenine G purified, and to Assistant Professor Kenzo Nishida, Yamagata University, for his helpful suggestion for the treatment of the Cellophane sheet.

*Laboratory of Physical Chemistry*
*Tokyo Institute of Technology*
*Meguro-ku, Tokyo*

# *Chemical Behaviors of the Intermediates Produced during the Reductive Photobleaching of Eosin in the Evacuated Alcoholic Solution*

By Kengo UCHIDA, Shunji KATO and Masao KOIZUMI

(Received July 13, 1959)

One of the present authors (Koizumi) and Imamura[1] investigated kinetically the photobleaching of eosin in the deaerated ethanol solution and concluded that the reaction proceeds via the following primary processes:

$$D \xrightarrow{h\upsilon} D^* \quad \text{(i)}$$

$$D^* \rightarrow D^t \quad \text{(ii)}$$

$$D^t + RH \rightarrow DH\cdot + R\cdot \quad \text{(iii)}$$

$$(DH\cdot \rightarrow \text{final products})$$

Where D: dye ion; $D^*$: singlet excited state of dye ($S^*$); $D^t$: triplet state of dye (T); RH: ethanol; DH·: semiquinone of eosine; R·; radical produced from ethanol.

Now, in order to make clear the details of these elementary reactions, it is essential to study about the chemical behaviors of the intermediates, $D^t$ and DH·. Experiments by the flash technique have already been commenced in the authors' laboratory. However, the ordinary kinetic studies, for example, the investigation about the effect of added substances on the reaction rate are expected to be useful for this purpose to some extent. In the present research, isopentane, *n*-hexane, benzene, cyclohexene, *n*-hexene and cyclooctatetraene (COT) were added to the reaction system and the variation of the rate of photobleaching was examined.

1) M. Koizumi and M. Imamura, This Bulletin, **28**, 117 (1955); **29**, 899 (1956); M. Imamura, ibid., **30**, 249 (1957).

## Experimental

**Materials.**—*Eosine.*—Grübler's product was used. Stock solution $1\times10^{-4}$ M was kept in the dark and this was diluted to $1\times10^{-5}$ M for each experiment. Isopentane, *n*-hexane and benzene were purified by the usual methods. COT prepared kindly by Dr. N. Hagiwara of Osaka University, was further distilled under vacuum three times and was stored in an evacuated ampule.

*n*-Hexene-2 and cyclohexene of Tokyo Kasei were distilled two or three times and were reserved in vacuo.

Ethanol, after being treated with concentrated sulfuric acid, was made free from aldehyde by the addition of silver oxide and dehydrated by calcium oxide.

**Apparatus and Procedures.**—A tungsten projection lamp (75 V. 500 W.) was used as a light source. The voltage was fixed at $45.0\pm0.5$ V. and the intensity was checked by measuring the bleaching rate of the aqueous eosine solution (not deaerated) throughout all the experiments[1]. A yellow glass filter cutting off $< 450$ m$\mu$ and a reaction cell was attached to the metallic case surrounding a glass tube, 6 cm. in diameter, in which the lamp was placed. Degassing of the sample was performed carefully by repeating the vacuum distillation. A Terrex cell for measuring the absorption spectra was used as a reaction vessel, the upper part of which was fused to a tube of hard glass for the cell to be attached to the

above distillation set. After the deaerated sample was poured into the cell it was fused off at a suitable position. The sample was irradiated in a thermostat usually at 25°C and at suitable time intervals the absorption spectra were measured by a Hitachi spectrophotometer (EPU-2A). The measurement of fluorescence spectra was done by the fluorescence attachment of the spectrophotometer.

## Results

**Rate Formula.**—Throughout all the experiments, the absorption spectra of the irradiated solution gradually declined keeping the same shape and particularly with the maximum at the same position as in the original solution. The situations are exactly the same as in the case of the pure alcoholic solution of eosine[1]. One example is shown in Fig. 1.

The rate of bleaching can be expressed by the same formula presented by Koizumi and Imamura[1],

$$-\frac{dc}{dt}=\frac{k}{d}I_0(1-e^{-\alpha cd})\times 10^3 \qquad (1)$$

where $c$ is the concentration of dye in mol./l., $I_0$ the intensity of illuminating light (mol. $cm^{-2}$ $sec^{-1}$), $\alpha$ the average or effective molar absorption coefficient and $d$ the thickness of the solution in cm.

Integrating Eq. 1, one obtains

$$\ln(e^{\alpha c_0 d}-1)-\ln(e^{\alpha cd}-1)=10^3 kI_0\alpha t \qquad (2)$$

By using the properly determined value of $\alpha$, one can obtain $k$ from the inclination of the linear plot of $\ln(e^{\alpha cd}-1)$ against $t$.

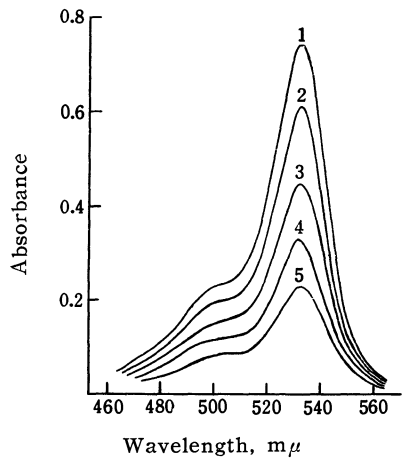



Fig. 1. The absorption spectrum of the irradiated solution of eosin in ethanol with 25% isopentane.
1. initial
2. 10 min.-irradiation
3. 20 min.-irradiation
4. 30 min.-irradiation
5. 40 min.-irradiation

**The Effect of the Added Substance.**—*a) Isopentane, n-hexane, benzene and COT.* — The addition of these substances does not affect appreciably the absorption spectra of eosin in the visible region nor the fluorescence spectra. In the case of high concentration there is a slight decrease

TABLE I

| *Isopentane* | | *n-Hexane* | |
|---|---|---|---|
| Mole fraction | $k\times10^4$ | Mole fraction | $k\times10^4$ |
| 0.334 | 1.18 | 0.309 | 2.55 |
| 0.143 | 2.53 | 0.130 | 2.87 |
| 0.100 | 2.74* | 0.0731 | 3.84 |
| 0.0814 | 4.86 | 0.0472 | 4.36 |
| 0.0529 | 4.94 | 0.0230 | 3.82 |
| 〃 | 3.80* | 0 | 4.30** |
| 0.0254 | 5.66 | | |
| 0 | 5.82** | | |

| *Benzene* | | *Cyclooctatetraene* | |
|---|---|---|---|
| Mole fraction | $k\times10^4$ | Mole fraction $\times10^8$ | $k\times10^4$ |
| 0.220 | 1.23 | 650 | 0 |
| 0.141 | 1.27 | 65 | 0.532 |
| 0.0681 | 1.38 | 32.2 | 0.841 |
| 0.0334 | 1.41 | 8.07 | 1.22 |
| 0.0167 | 1.67 | 5.26 | 1.93 |
| 0.00269 | 2.10 | 0 | 1.97 |
| 0 | 1.85 | | |

* Isopentane purified with utmost caution.
** In these two runs, $k$-value in the pure alcoholic solution is markedly different from that of the other runs (including those in Table II). The cause for this is unknown though it may perhaps be due to the pretreatment of alcohol employed. The effect of the added substance will certainly not be affected seriously by this, since it is essentially related with a relative quantity to the reference alcohol.

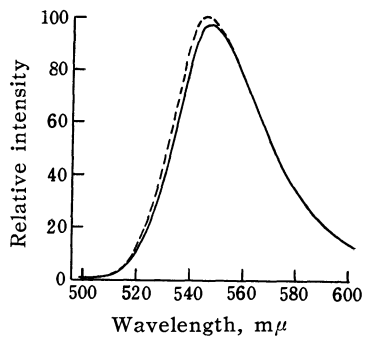



Fig. 2. The effect of addition of isopentane on the fluorescence of eosin.
—— 25% isopentane
------ without isopentane

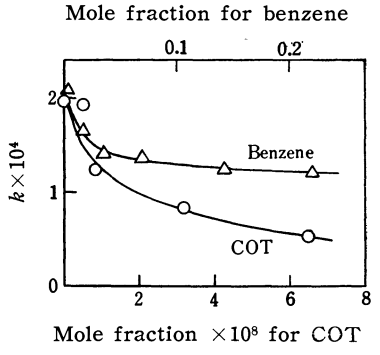



Fig. 3. Plot of $k$ against the concentration of COT and benzene.

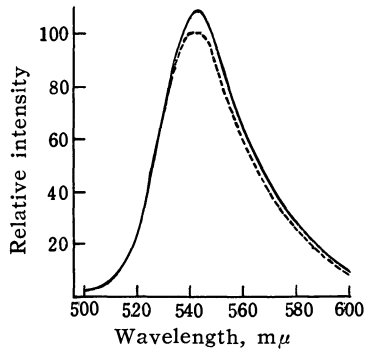



Fig. 4. The effect of addition of cyclohexene on the fluorescence of eosin.
—— 5% cyclohexene
------ pure alcohol

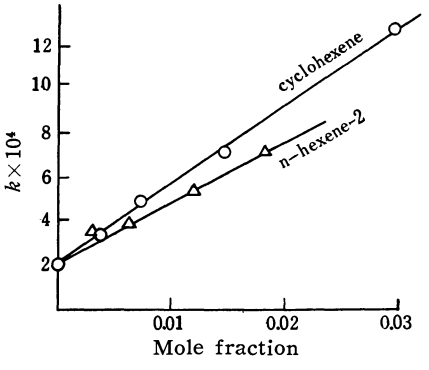



Fig. 5. Plot of $k$ against the concentration of the added substances.

TABLE II

| *Cyclohexene* | | *n-Hexene* | |
|---|---|---|---|
| Mole fraction | $k\times10^4$ | Mole fraction | $k\times10^4$ |
| 0.0295 | 12.8 | 0.0181 | 7.25 |
| 0.0146 | 7.07 | 0.0119 | 5.39 |
| 0.00726 | 4.87 | 0.00593 | 3.98 |
| 0.00362 | 3.42 | 0.00296 | 3.48 |
| 0 | 1.97 | 0 | 2.18 |

in the fluorescence intensity. As an example, the influence of the addition of isopentane upon the fluorescence spectra is shown in Fig. 2. Other substances show more or less similar effects. In Fig. 3 rate constants $k$'s are plotted against the concentration and the data are given in Table I. It is apparent that the above four substances have a retarding effect and among them, COT is by far the most significant inhibitor for the bleaching reaction.

*b) n-Hexene and cyclohexene.* — Neither absorption spectra nor the fluorescence intensity is affected essentially. At higher concentration, the intensity of fluorescence increases slightly as shown in Fig. 4. The values of $k$ are plotted against mole fraction in Fig. 5, which shows that $k$ linearly increases with the concentration of the added substance. The data are given in Table II.

## Discussion

The primary processes were already described in the introduction. The fate of DH· and R· is not yet quite certain but the effect of the added substance on the rate is expected to be due to their interference with one of the above three steps i—iii. Since the mechanism would naturally be different for two groups, the retarding substances (isopentane, *n*-hexane, benzene and COT) and the promoting substances (*n*-hexene and cyclohexene), they will be considered separately.

**The Retarding Effect.**—Since either the absorption spectrum or the intensity of fluorescence is scarcely affected by the addition of the retarding substances, the first two processes in these systems have a rate almost equal to what they have when they are not added. Hence the remaining process iii ought to be eventually retarded by the interference of the added substance. There are two possibilities to be considered for this; the one is the deactivation of $D^t$ and the other is the recovery of D by the removal of hydrogen from DH·. But the latter possibility may safely be ignored from the fact that the above retarders have no tendency to be hydrogenated or scarcely any. Hence the conclusion is that the triplet state of eosin is deprived of its excess energy by the added substance, resulting in the decrease of the bleaching rate. Thus the only process which must be taken into account is the following one

which competes with process iii,

$$D^t + Q \rightarrow D + Q \qquad k_Q[Q] \qquad \text{(iv)}$$

where Q represents an added retarder.

Assuming the steady-state concentration for D* and $D^t$ one can write for $k$ the following:

$$k = \varphi_{S\rightarrow T} \frac{k_a[RH]}{k_a^S[RH] + k_Q[Q]} \qquad (3)$$

where $\varphi_{S\rightarrow T}$ gives the fraction of the singlet state going to the excited triplet, $k_a$ is the rate constant for the effective hydrogenating reaction iii, $k_a^S$, the sum of the rate constants for the genuine reaction and the deactivation of $D^t$ by alcohol. From Fq. 3

$$\frac{1}{k} = \frac{1}{\varphi_{S\rightarrow T}} \frac{k_a^S}{k_a} + \frac{1}{\varphi_{S\rightarrow T}} \frac{k_Q[Q]}{k_a[RH]} \qquad (4)$$

Thus, the plot of $1/k$ against $[Q]/[RH]$ gives a straight line as shown in Fig. 6. From the inclination $k_Q/\varphi_{S\rightarrow T}k_a$ and the intersect with the ordinate $\left(\frac{1}{\varphi_{S\rightarrow T}} \frac{k_a^S}{k_a}\right)$, one can easily evaluate a value of $k_Q/k_a^S$, which gives a measure for the efficiency of the added substances in deactivating $D^t$. The results are shown in Table III.

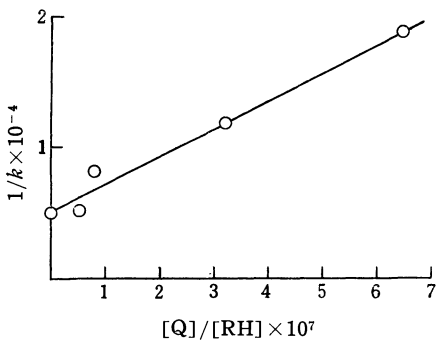



Fig. 6. Plot of $1/k$ against $[Q]/[RH]$ where Q is cyclooctatetraene.

TABLE III. THE KINETIC DATA FOR THE RETARDING SUBSTANCES

| Retarder | $k_Q/\varphi_{S\rightarrow T}\cdot k_a$ | $k_a^S/\varphi_{S\rightarrow T}\cdot k_a$ | $k_Q/k_a^S$ |
|---|---|---|---|
| Isopentane | $5.0\times10^3$ | $1.7\times10^3$ | 2.9 |
| *n*-Hexane | $4.4\times10^3$ | $2.4\times10^3$ | 1.9 |
| Benzene | $3.4\times10^4$ | $5.4\times10^3$ | 6.3 |
| COT | $2.0\times10^{10}$ | $5.5\times10^3$ | $3.7\times10^6$ |
| Water | | | 0.053[1] |

It is interesting that saturated hydrocarbons which are chemically inactive are rather better deactivators than water. The value for COT is enormously large, the result being consistent with that of Schenck[2]. It may be that the electronic excess energy can effectively be transferred to the vibrational energy of COT which has various modes of bending and torsion due to the nonplanarity of its structure.

**The Promoting Effect.** — Cyclohexene and *n*-hexene which promote the bleaching rate have a single double bond. These two substances also give scarcely any influence on the absorption spectrum and fluorescence intensity of eosine, so that they do not have much effect upon the rate of processes i and ii. Furthermore in view of their promoting effect, their action on the T-state of the dye is not thought to be an essentially deactivating one. At first sight, the promoting action might be attributed to the same kind of reaction between D and the added substance (P) as that between D and alcohol represented by iii. But if so, it is very curious that COT, which is exceedingly unsaturated, shows a quite opposite effect. Moreover, since much of the deactivating process would certainly occur along with the genuine reaction (dehydrogenation of P), the overall rate constant $k$ should be represented as follows:

$$k = \varphi_{S\rightarrow T} \frac{k_a[RH] + k_P[P]}{k_a^S[RH] + k_P^S[P]} \qquad (5)$$

where $k_P[P]$ refers to the rate of reaction leading to bleaching and $k_P^S[P]$ is the sum of $k_P[P]$ and that for the deactivating process. Eq. 5 never gives linearity between $k$ and $[P]$ since $k_P^S[P]$ most certainly can not be neglected in view of the rather large value of $k_P[P]$.

Thus, it seems that a plausible interpretation can never be given on the basis of the reaction scheme presented by Koizumi and Imamura[1].

Now, according to the unpublished results for the bleaching reaction of eosine in alcohol by the flash-technique which have been obtained in the authors' laboratory[3], there are two intermediates spectroscopically observed, other than $D^t$, and these have different durations though in the same order of magnitude (few millisec.).

As another intermediate besides semiquinone, the most probable one would be a certain kind of intermolecular complex between $D^t$ and RH, or alternatively, (DH·.....R·) trapped in the same cage. In either case the introduction of another

2) G. O. Schenck and K. Kinkel, *Naturwissenschaften*, 38, 355 (1951).
3) To be published in the near future.

intermediate of this kind modifies the reaction scheme in such a manner that process iii must now be divided into the following ones,

$$D^t + RH \rightarrow X \qquad (iii')$$

$$X \rightarrow D + RH \qquad (iii'')$$

$$X \rightarrow DH\cdot + R\cdot, \quad k_X \qquad (iii''')$$

where X represents either the complex between $D^t$ and RH, or DH· and R· exisitng in the same cage.

In view of a small quantum yield of photobleaching, a large part of X would perhaps decompose into D and RH (process iii'') resulting only in the dissipation of excess energy of $D^t$, while a small fraction of X would complete the bleaching reaction by step iii'''. It is of course undecided whether X is some kind of molecular complex or a transient state in which DH· and R· exist in the same cage, but the two alternatives give exactly the same kinetics.

Now, if one modifies the reaction scheme as above, one can interpret quite rationally the promoting action of the added substance. Thus, if the added substance P attacks X in such a manner that it detaches the R-part from the latter, producing a more stable radical PR· and leaving behind a metastable DH·, then the rate of bleaching would be increased. This type of attack may perhaps be so specific that it would not be accompanied with much of the deactivating process. The process can formally be written as follows:

$$X + P \rightarrow DH\cdot + RP\cdot \qquad (v)$$

Taking into account iii', iii'', iii''' and v instead of iii, one can give the expression for $k$ as follows:

$$k = \varphi_{S\rightarrow T}\varphi_{T\rightarrow X}\frac{k_X + k_P[P]}{k_X^S + k_P[P]} \qquad (6)$$

where $k_X^S$ is the sum of the rate constants for reaction iii'' and iii'''. If one assumes that the action of P on X consists mainly of reaction v and is not of such a nature as to promote reaction iii'' and moreover that $k_X^S \gg k_P$ holds as already discussed above, then Eq. 6 is approximately rewritten as

$$k = \varphi\frac{k_X + k_P[P]}{k_X^S} \quad (\varphi = \varphi_{S\rightarrow T}\varphi_{T\rightarrow X}) \qquad (7)$$

which explains the linear relationship between $k$ and [P] experimentally obtained. From the plot of $k$ against [P], one can evaluate the values of $k_X/k_P$, which are shown in Table IV.

Table IV. The kinetic data for the promoting substances

| Promotor | Inclination | Intersection | $k_P/k_X$ |
|---|---|---|---|
| Cyclohexene | $21.4\times10^{-4}$ | $2.15\times10^{-4}$ | 10.0 |
| *n*-Hexene-2 | $15.3\times10^{-4}$ | $2.50\times10^{-4}$ | 6.1 |

It is to be added that the same relation as Eq. 7 would be obtained, if P attacks $D^t$ in such a specific manner as to produce DH· far more rapidly than to dissipate the excess energy in vain. A relation similar to Eq. 4 would also be obtained for retarding substances if one assumes that X instead of $D^t$ is selectively decomposed by Q into D and RH·. But the assumption is highly improbable that the retarding substances and the promoting substances attack the same one molecular species in a quite different and peculiar fashion. A more natural picture would be that the two groups of the added substances act on different molecular species in a different way as described above. Of course, in order to make the above remark more definitely, it is necessary to study further about the chemical behavior of $D^t$, X and DH· toward many other substances and especially to use the flash technique.

## Summary

The effect of the addition of isopentane, *n*-hexane, benzene, cyclohexene, *n*-hexene and cyclooctatetraene was examined upon the rate of the reductive photobleaching of eosine in the evacuated alcoholic solution. It was found that the saturated hydrocarbons, benzene and COT retard the reaction more or less, COT being most prominent in its effect, while the hydrocarbons with a single double bond (cyclohexene and *n*-hexene) act, contrary to the authors' expectation, as the promotors of the bleaching. The retarding effect of the first group was interpreted to be due to the deactivation of the T-state of dye ion by the added substances, but the promoting action of the second group could not be accounted for rationally on the basis of the above scheme. To fit the present results, therefore, a modified scheme was newly proposed in which a certain kind of molecular complex between $D^t$ and RH is formed prior to DH··

*Department of Chemistry*
*Faculty of Science*
*Tohoku University*
*Katahira-cho, Sendai*

# *Molecular Structure of Acrylonitrile by Electron Diffraction*

By Takahide SAITO and Takeshi UKAJI*

(Received July 20, 1959)

The shortening of a single bond between two multiple bonds has been studied in various cases[1], but not yet in the cases with the structure,

$$C{=}C{-}C{\equiv}N$$

The authors wish to report some results on acrylonitrile (Fig. 1) by the electron diffraction.

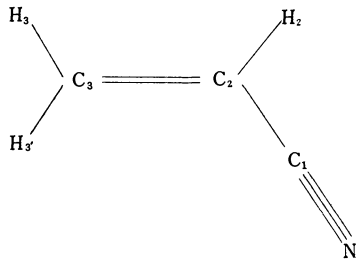



Fig. 1. Molecular scheme of acrylonitrile.

## Experimental

The apparatus of electron diffraction is the same as in the previous reports from the authors' laboratory[2], with the exception of the use of two camera lengths, 9.1 and 10.1 cm. The electron wavelength, about 0.055 Å, was calibrated by gold foil diffraction.

The sample is kindly supplied to the authors' by Professor S. Kambara, b. p.=78°C.

Measurements were carried out by the usual visual method.

## Procedure and Results

The experimental visual curve from eight photographs is shown in Fig. 2. The dotted line for $q>80$ means less accurate observation due to the obscurities of photographs and that for $q<10$ is an assumed line to help the calculation of the radial distribution curve.

The radial distribution curve has been calculated from the visual intensity curve according to the equation[3],

$$r\cdot D(r)=\sum_{q=1,2\cdots}^{q_{max}} I(q)\exp(-aq^2)\sin \pi/10\cdot qr$$

$$q=(4\pi/\lambda)\sin(\theta/2)$$

$$\exp(-aq^2{}_{max})=0.1$$

in which $\theta$ is the scattering angle, and $\lambda$ is the wavelength of the beam. The curve obtained shows the still remaining ghosts. However, it is convenient to assign each peak in this curve for the following trial and error method.

The first peak of 1.16 Å is attributed to the C≡N bond from the consideration of weight**. The second peak of 1.38 Å corresponds to the overlapped contribution of C=C and C—C bonds. The peaks at 2.12 and 3.46 Å correspond to the interatomic distances of nonbonded C···H and C···N, respectively.

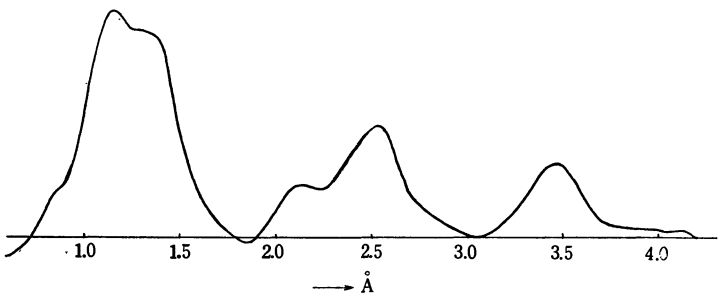



Fig. 2. Radial distribution curve.

* Present address: Department of Chemistry, Faculty of Science, Ibaraki University, Mito.

1) For example, see the following tables: L. E. Sutton and P. W. Allen, *Acta Cryst.*, **3**, 46 (1950); H. Oosaka, "Kagaku Jikkengaku", Vol. 5, Kawade-Shobo, Tokyo (1943), p. 325; Y. Morino, K. Kuchitsu and Y. Hirota, "Jikken Kagaku Koza", Vol. 3, Maruzen Co., Ltd., Tokyo (1958), p. 241. The data for some molecules are given in Table III.

2) T. Yuzawa and M. Yamaha, This Bulletin, **26**, 414 (1953).

3) V. Schomaker et al., *J. Am. Chem. Soc.*, **64**, 2693 (1942).

** The term "weight" means the value of $nZZ/r$ for each interatomic distance, where $n$ is the number of the same interatomic distance $r$ and $Z$ is the atomic number.

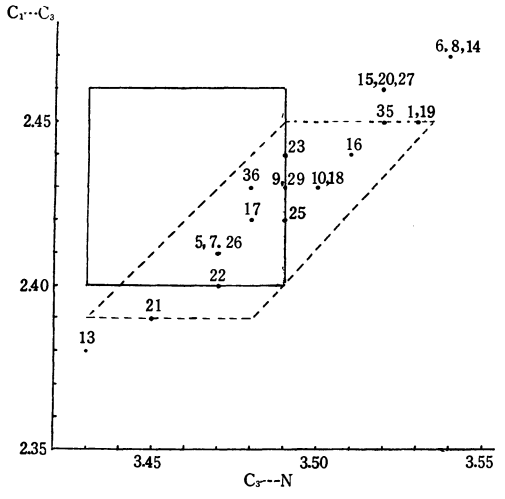



Fig. 3. The parameter chart of $C_1\cdots C_3$ vs. $C_3\cdots N$.

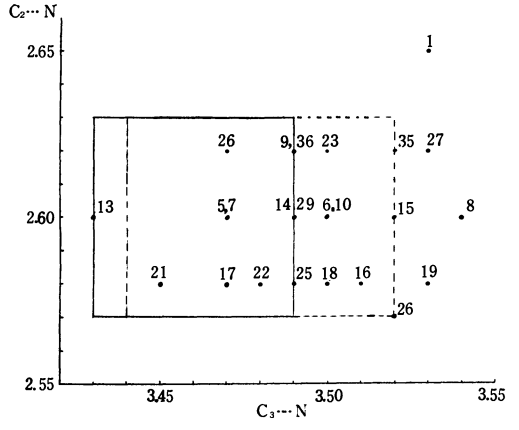



Fig. 4. The parameter chart of $C_2\cdots N$ vs. $C_3\cdots N$.

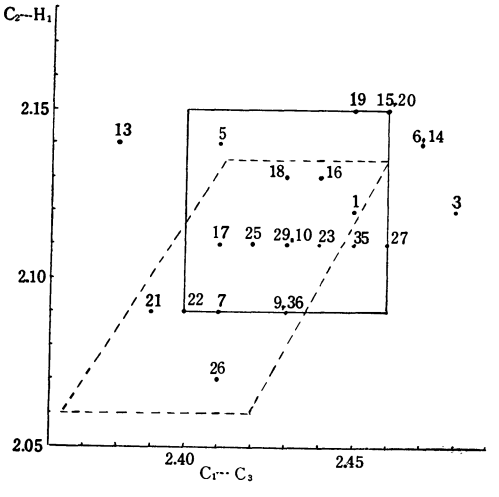



Fig. 5. The parameter chart of $C_2\cdots H_1$ vs. $C_1\cdots C_3$.

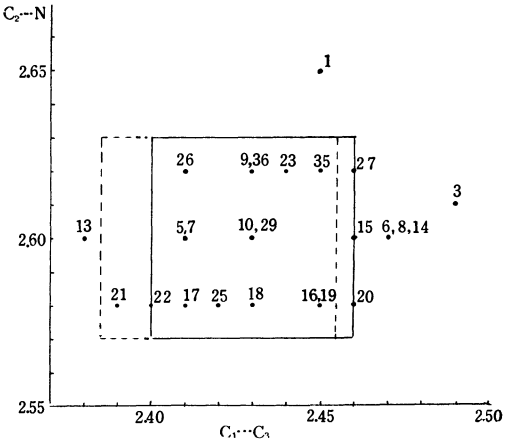



Fig. 6. The parameter chart of $C_2\cdots N$ vs. $C_1\cdots C_3$.

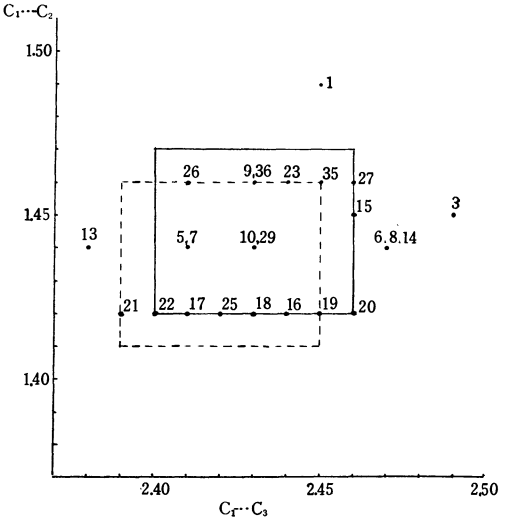



Fig. 7. The parameter chart of $C_1\cdots C_2$ vs. $C_1\cdots C_3$.

The theoretical intensity curve for assumed models has been calculated by the use of the equation[3]

$$I(q)=\sum_{ij}(Z_iZ_j/r_{ij})\exp(-a_{ij}q^2)\sin \pi/10\cdot qr_{ij}$$

$$a_{ij}=(\pi^2/200)l_{ij}$$

where $r_{ij}$ is the distance between the $i$-th and $j$-th atom, $Z_i$ is the atomic number of $i$-th atom and $l_{ij}$ is the mean amplitude of $r_{ij}$.

The coefficient of thermal vibration, $a_{ij}$, is roughly estimated with reference to the calculated data [4-6]. The coefficients used

4) J. Karl, *J. Chem. Phys.*, **20**, 65 (1952).
5) Y. Morino, K. Kuchitsu and T. Shimanouchi, ibid., **20**, 726 (1952).
6) Y. Morino, K. Kuchitsu, A. Takahashi and K. Maeda, ibid., **21**, 1927 (1953).

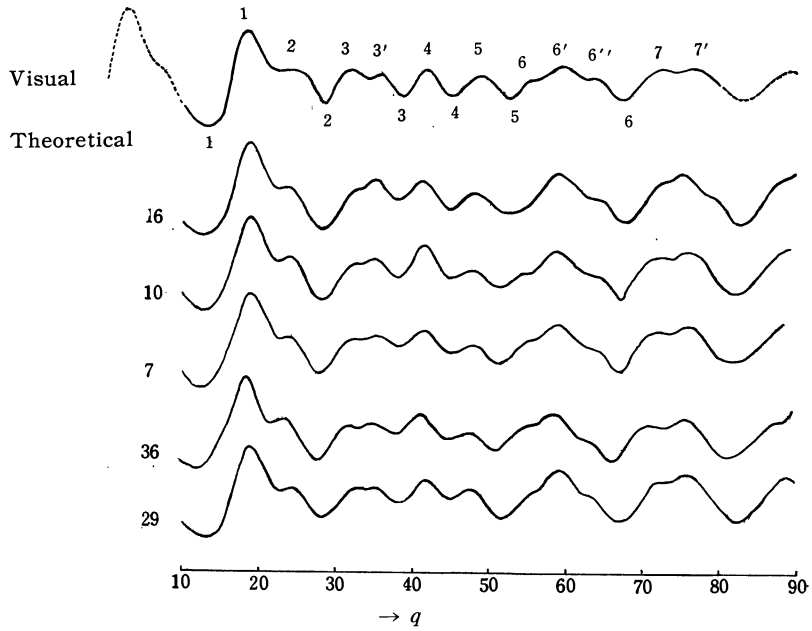



Fig. 8. Theoretical curves and visual curve.

TABLE I. THE COEFFICIENTS OF THERMAL VIBRATION

| Atomic pair | $a$ | Atomic pair | $a$ |
|---|---|---|---|
| C—H | 0.00028 | H···$C_1$ | 0.00013 |
| C=C | 0.00005 | $C_2$···N | 0.00006 |
| C—C | 0.00008 | $C_3$···N | 0.00012 |
| C≡N | 0 | $H_3$···N | 0.00032 |
| $H_3$···$C_2$ | 0.00039 | $H_2$···N | 0.00011 |
| $C_3$···Cl | 0.00016 | | |

TABLE II. THE COMPARISONS WITH EACH MODEL

| Atomic pair | I | II | III | IV | V |
|---|---|---|---|---|---|
| C—C | 1.42 | 1.44 | 1.44 | 1.46 | 1.44 |
| C≡N | 1.16 | 1.16 | 1.16 | 1.16 | 1.16 |
| $C_1$···$C_3$ | 2.44 | 2.43 | 2.41 | 2.43 | 2.43 |
| $C_3$···N | 3.51 | 3.50 | 3.47 | 3.49 | 4.49 |
| $C_2$···N | 2.58 | 2.60 | 2.60 | 2.58 | 2.60 |
| Average of $q_{calcd.}/q_{obsd.}$ | 0.995 | 0.992 | 1.000 | 0.996 | 0.995 |
| Root mean deviation | 0.014 | 0.015 | 0.017 | 0.013 | 0.017 |

The length of atomic pair is given in Å unit.

are shown in Table I. The theoretical curve was calculated to cover the following ranges of parameters, $C_3{\equiv}N$ 1.16, $C_2{=}C_3$ 1.42~1.46, $C_1{\cdots}C_3$ 2.41~2.47 and $C_3{\cdots}N$ 3.46~3.53 Å. In the above calculations, $Z_H$ 1.25 and C—H 1.08 Å were used and each term of H···H was neglected. The theoretical curves, agreeing well with the visual intensity curve and having the values of parameters close to the interatomic distances obtained from the radial distribution curve, are shown in Fig. 2.

In Table II are shown the values of principal parameters in these models. Although these models are more appropriate rather than the others, the agreements with the visual curve are not sufficiently satisfactory. For example, there are considerable disagreements in the following aspects: (1) the relationships of intensity of max. 3 and 3', (2) the relative intensity of max. 7 and 7', (3) the location of min. 5 (the experimental has larger $q$ than all the theoreical), (4) the relationships of intensity of max. 6, 6' and 6''. Therefore, it is difficult to prefer a model to the other form. However, the following ranges for the parameters may be supported in reference to values of the similar molecules (Table III), C≡N 1.15~1.17, C=C 1.32~1.36, C—C 1.42~1.46 and $C_1{\cdots}C_3$ 2.41~2.44 Å. The difficulty in determining the best model may be the result of the uncertain observation of intensity, especially in the range of larger $q$ values.

However, it is probable from the considerations of the parameter charts that the molecule of acrylonitrile has the following interatomic distances:

| | |
|---|---|
| C≡N | 1.16±0.01 Å |
| C=C | 1.34±0.02 Å |
| $C_2{\cdots}C_3$ | 2.43±0.02 Å |
| C—C | 1.44±0.02 Å |

TABLE III. THE INTERATOMIC DISTANCES (Å UNIT) OF SIMILAR COMPOUNDS

| Molecule | Atomic pair C≡N | C—C | C=C | C≡C | Method | Ref. |
|---|---|---|---|---|---|---|
| H—CN | 1.156 | | | | M. W.* | 1 |
| $CH_3 \cdot CN$ | 1.157 | 1.458 | | | M. W. | 2 |
| | 1.16 | 1.49 | | | E. D.** | 3 |
| CN·CN | 1.16 | 1.37 | | | E. D. | 3 |
| $CH_2=CH \cdot CH=CH_2$ | | 1.46 | 1.35 | | E. D. | 3 |
| | | 1.47 | 1.37 | | S. P.*** | 4 |
| $CH_3C \equiv C \cdot CH_3$ | | 1.47 | | 1.20 | E. D. | 3 |
| $CH \equiv C \cdot C \equiv CH$ | | 1.36 | | 1.19 | E. D. | 3 |
| $CH \equiv C \cdot CN$ | 1.157 | 1.382 | | 1.203 | M. W. | 1 |
| $CH_3 \cdot C \equiv C \cdot CH=CH_2$ | | 1.42 | 1.35 | 1.20 | E. D. | 6 |
| | | 1.47 | | | | |

* M. W.; Microwave spectrum.
** E. D.; Electron diffraction.
*** S. P.; Infrared spectrum.

1) W. Gordy et al., *Phys. Rev.*, **86**, 1055 (1952).
2) L. F. Thomas et al., *Trans. Faraday Soc.* **51**, 619 (1955).
3) L. Pauling and L. O. Brockway, *J. Am. Chem. Soc.*, **61**, 927 (1939).
4) O. Bastianssen; these values were quoted from Sutton's Table., L. E. Sutton and P. W. Allen, *Acta. Cryst.*, **3**, 46 (1950).
5) A. A. Westenberg et al., *J. Am. Chem. Soc.*, **72**, 199 (1950).
6) V. Schomaker, *J. Am. Chem. Soc.*, **64**, 2693 (1942).

A further investigation about the structure of this molecule by the use of electron difraction sector microphotometer method will be given in succeeding paper***.

*** During the preparation of this paper the authors read the following paper regarding the molecular structure of acrylonitrile; C. C. Costain and B. P. Stoiceff, *J. Chem. Phys.*, **30**, 777 (1959), which reported the following values about the interatomic distances, C≡N 1.1637, C−C 1.4256 and C=C 1.338$_9$ Å, by the use of microwave spectroscopy. The author's results are very near to their values.

The authors have great pleasure in acknowledging their debts of gratitude to Professor A. Kotera and Professor K. Suzuki for their continued encouragement and advice and to Dr. K. Kuchitsu for his help with the calculation.

*Department of Chemistry*
*Faculty of Science*
*Tokyo University of Education*
*Koishikawa, Tokyo*

# *Determination of Reducing Sugars by Means of Back Titration against Alkaline Copper Solution. I**

By Masahito TAKAHASHI

(Received May 23, 1959)

Since the determination by means of Fehling solution has become used so generally for sugar analysis, different chemists have devised, in consequence of its importance in both practice and research, so many modifications that there is probably no method in analytical chemistry which suffers more from variety of procedure. Numerous modifications have been described which differ in analytical details. Fehling solution is rather unstable, so efforts have been made to improve its stability, and to establish a simpler and more practical procedure.

The amount of copper which is reduced by various sugars has been found to vary according to the alkalinity, the temperature, the rate of ebullition, the time of heating, the type of tartrate, the amount of contact with air, etc. Among them the most important variables are the temperature, the time of heating, and the rate of ebullition. Consequently some methods have devised for heating because it is difficult to standardize the temperature and the rate of ebullition. The indirect heating is frequently employed as in the case of Main's pot method where the temperature is regulated by a boiling water bath and the reduction is carried out in a test tube provided with floats. But this is not a fine procedure, because it requires a complicated operation and demands skilfulness in analyst. Then, the results should be corrected according to the variation of variables rather than a strict standardization of the reacting condition is demanded. Blank titration with a standard sugar solution, which checks the variation of conditions and corrects the results, is most suitable for the present purpose.

Numerous procedures already devised for the determination of the quantity of reduced copper can briefly be divided into a partial reduction method and a total reduction method. In the former a certain volume of Fehling solution is brought into a reaction with a given amount of sugar which does not reduce all the copper, and the cuprous oxide produced is weighed directly or estimated by means of redox titration. The other is a method which, in principle, involves the determination of the volume of sugar solution required to reduce completely a measured volume of alkaline copper solution, the end point being indicated by a spot test or an internal indicator. This is indeed one of the earliest procedures for the determination of the reducing power. Soxhlet heated a known volume of Fehling solution to boiling in an open dish and added the sugar solution until the copper was completely reduced. No great accuracy was possible by this procedure, even in highly skilled hand. The degree of accuracy of this method was considerably increased by various devices, namely, by boiling the solution in a flask instead of an open dish, to diminish back-oxidation, and by using a suitable indicator. Lane and Eynon[1] found that the end point was internally indicated by the reduction of methylene blue to methylene white by minute excess of reducing sugar and determined the weight of each sugar required to reduce the copper completely. These weights, which varied with nature of sugar and with its concentration, constituted their table for analysis. This method, described as "the most convenient, most expeditious, and frequently the most accurate method"[2], has been adopted for industrial and scientific purposes, but seems still to be a complicated and time-consuming procedure with some disadvantages. For instance, it consumes a large volume of sugar solution, and is not available for the determination of a small quantity of sugar, etc.

In general, the total reduction method,

* Partly presented at the Annual Meeting of the Chemical Society of Japan, Tokyo, April, 1957.

1) J. H. Lane and L. Eynon, *J. Soc. Chem. Ind. (London)*, **42**, 32T, 143T (1923); **44**, 150T (1925); **46**, 434T (1927).

2) F. J. Bates et al., "Polarimetry, Saccharimetry and the Sugars", U. S. Government Printing Office, Washington (1942), p. 185.

represented by Lane and Eynon's method, is simpler, more practical, and more accurate than the partial reduction method, represented by the gravimetric method and Bertrand's method. In view of this advantageous quality, the author has endeavored to improve the former procedure and to establish a more convenient method of procedure with a high accuracy on such a way as to confer the maximum possible simplicity of procedure and to eliminate the personal factor as far as possible. To this end a back titration method has been devised.

## Experimental

**Materials.**—The following substances were used for the present investigation. An anhydrous glucose was obtained by recrystallizing a commercial glucose (monohydrate, the Japanese Pharmacopoeia) from water and acetic acid. A pure commercial lactose was recrystallized from water. A pure commercial galactose was recrystallized from water and alcohol. Crystalline copper sulfate ($CuSO_4 \cdot 5H_2O$) of reagent grade was recrystallized from water. A 50% solution of sodium hydroxide (reagent grade) was prepared and allowed to stand until a precipitate of sodium carbonate appeared. By filtering it through asbestos a clear solution was obtained. Benzoic acid, Rochelle salt and methylene blue were all of reagent grade.

**Reagents.** — *I) Standard sugar solution.* — One gram of crystalline benzoic acid and 2.046 g. of crystalline glucose were dissolved in water and made up 1 l. with water.

*II) Copper solution.*—Sixty-six grams of caystalline copper sulfate was dissolved in water and made up to 1 l. with water.

*III) Alkaline solution.*—The calculated amount of sodium hydroxide solution containing 110 g. of sodium hydroxide and 345 g. of Rochelle salt were dissolved in water and made up to 1 l. with water.

*IV) Indicator.*—Half a gram of methylene blue was dissolved in 100 ml. of water.

**Procedure.** — In Soxhlet's method, Lane and Eynon's method and others, a measured volume of the boiling alkaline copper solution is titrated with a sugar solution, the end point being indicated by a spot test or an internal indicator, and the concentration of the sugar solution is estimated from the volume of the sugar solution required to reduce the alkaline copper solution completely. On the other hand, in this back titration method a boiling mixture of a measured volume of the alkaline copper solution and a measured volume of the sugar solution is back-titrated with the standard sugar solution, and the concentration of the sugar solution is estimated from the volume of the standard sugar solution required to reduce the mixture completely.

It is well known, for example, that if the sugar solution is added in portions 5 ml. and the liquid boiled for 10 sec. after each addition, the total volume required will not be exactly the same as if the whole of the sugar solution is added at once. Now in this method nearly the whole of the standard sugar solution is added at once and after boiling the rest quantity is added (normal titration). As in the Lane and Eynon's method, a preliminary titration system is adopted, by which the required volume of the standard sugar solution is found approximately in order that almost the whole of it may be added at one time simultaneously with heating. In the case of the blank titration the required volume is known approximately, so that a preliminary titration is unnecessary.

In a blank titration, a mixture of 20 ml. of water and 10 ml. of an alkaline copper solution is titrated with the standard sugar solution. In the normal titration, the volume of the standard sugar solution can be obtained, which is required to reduce a mixture of the alkaline copper solution (10 ml.) and 20 ml. of the sugar solution. The difference between the two quantities obtained thus represents the concentration of the sugar solution.

*a) Blank titration.*—Equal volumes of solutions II and III are mixed thoroughly. Ten milliliters of the mixed solution and 20 ml. of distilled water are measured into a 100~300 ml. flask and heated over an asbestos wiregauze with a 300~500 W. electric heater charged full voltage. About 23.5 ml. of the standard sugar solution delivered from a 25 ml. burette is added into the flask as soon as possible. For this purpose an automatic burette is very convenient, the outlet of which is connected by melting with a glass tube (about 10 cm.) bent twice at right angles so that the solution in the burette is not heated by the reaction mixture. After the liquid has begun to boil vigorously, it is kept in moderate ebullition by lowering the working voltage. After boiling for two minutes, 3 to 6 drops of the methylene blue indicator are added, and the standard sugar solution is added in small quantities, that is to say, several drops or less at a time, and after the commencement of decolorization, drop by drop. The liquid is boiled for about ten to fifteen seconds between successive addition, and the titration is continued until the color of the indicator is discharged. The titration is completed in about one minute, so that the reaction liquid is boiled altogether for 3 min. without interruption. The decolorization of the methylene blue is easily detected, since the blue color of copper ion has already vanished. The rate of heating is regulated carefully so as to make the precipitate as much as possible. The end point can be determined with accuracy of less than one drop of the standard sugar solution. At the end point the blue color of the methylene blue vanishes suddenly, and the faint purple tint is still observable. The methylene white is rapidly reoxidized by air, particularly at the high alkalinity of this reaction mixture. Hence it is essential that air is excluded during the titration.

This is accomplished by making an uninterrupted current of steam issue from the neck of the flask on which the analysis is performed.

So long as solutions II and III are mixed correctly, the titer of the blank titration is constant; so that the blank titration is unnecessary at each time of mixing. When the sample solution contains materials other than sugars to be determined, a blank titration should be made against the solution containing these materials.

*b*) *Preliminary titration.*—Ten milliliters of the mixed copper solution is boiled in a 100~300 ml. flask after adding 20 ml. of the sample sugar solution. Usually after ten seconds of ebullition the reduction of the copper solution is nearly completed, which can easily be seen from the disappearance of the blue color of cupric ion and the bright red color imparted to the boiling liquid by the suspended cuprous oxide. If it is judged that nearly all the copper has been reduced, boiling is continued for about one minute from the beginning of ebullition, 3 to 5 drops of the methylene blue indicator are added, and then the standard sugar solution is added in small quanties, that is to say, 0.2 ml. or less at a time at regular intervals, the liquid being allowed to boil, until the color of the indicator is discharged. When unreduced copper is still found to be there in large quantity after boiling a mixture of 20 ml. of the sample solution and the copper solution about ten seconds, 3 ml. of the standard sugar solution is added and the whole is allowed to boil for ten seconds and so on, until it is considered unsafe to add a further large increment of the standard sugar solution. Boiling is continued further thirty seconds, after which the indicator is added and the titration is completed by small additions of the standard sugar solution as already mentioned. The indicator should not be added until the end point is nearly reached.

When maximum accuracy is not required, a single preliminary titration gives satisfactory results; the error will, as a rule, not exceed 0.6 mg. per 20 ml. of the sample solution.

*c*) *Normal titration.*—Ten milliliters of the mixed copper solution and 20 ml. of a sample sugar solution are measured into a 100~300 ml. flask, and, as soon as the mixture is heated, almost the whole of the standard sugar solution is added, which required to reduce all the copper, so that if possible not more than 1 ml. is required later to complete the titration. The approximate volume of the standard sugar solution required is estimated by a preliminary titration. After the liquid has begun to boil, it is kept in moderate ebullition for 2 min., and then 3 to 6 drops of the methylene blue indicator are added, and the titration is then completed in 1 min.

## Results

The author has measured the volume of the standard sugar solution required to reduce a mixture of 10 ml. of the alkaline copper solution and 20 ml. of water (*blank titration*), and that of the standard sugar solution required to reduce a mixture of 10 ml. of the alkaline copper solution and 20 ml. of the solution of sugars of various concentrations (*normal titration*). The relationship among the weight ($W$) of sugar in mg. in 20 ml. of sugar solution, the volume ($B$) in ml. of the standard sugar solution required in the blank titration, and the volume ($m$) of the standard sugar solution in the normal titration, has been found to be;

$$W=2(B-m)tf$$

where $t$ is a correction term, and $f$ is a factor of the standard sugar solution.

For the purpose of calculating the weight of sugar from difference ($B-m$), a correction term $t$ has been introduced, which varies with the nature of the sugar and the term ($B-m$). The term $t$ is 1.000 over widely different concentrations, viz. from 1 to 48 mg. per 20 ml. in the case of glucose, but in case of lactose and galactose it varies with the difference ($B-m$), the values of which are shown in Table I.

In the titrations on which Table I is based, the volume of the standard sugar solution added to the reaction mixture after heating was about 0.3~0.5 ml. less than the total volume required, and during the last third minute of ebullition, this complementary quantity was added, two

TABLE I. "$t$" OF LACTOSE AND GALACTOSE

| $B-m$, ml. | Lactose | Galactose |
|---|---|---|
| 1 | 1.32 | 1.03 |
| 2 | 1.32 | 1.03 |
| 3 | 1.32 | 1.03 |
| 4 | 1.32 | 1.03 |
| 5 | 1.32 | 1.03 |
| 6 | 1.32 | 1.03 |
| 7 | 1.318 | 1.030 |
| 8 | 1.315 | 1.031 |
| 9 | 1.314 | 1.031 |
| 10 | 1.312 | 1.032 |
| 11 | 1.310 | 1.032 |
| 12 | 1.309 | 1.032 |
| 13 | 1.308 | 1.032 |
| 14 | 1.307 | 1.033 |
| 15 | 1.307 | 1.033 |
| 16 | 1.307 | 1.033 |
| 17 | 1.306 | 1.034 |
| 18 | 1.306 | 1.034 |
| 19 | 1.036 | 1.034 |
| 20 | 1.306 | 1.034 |
| 21 | 1.306 | 1.034 |
| 22 | 1.305 | 1.035 |
| 23 | 1.305 | 1.035 |
| 24 | 1.305 | 1.035 |

TABLE II. EXAMPLES

| Reducing sugar contained | Weight of reducing sugar in solution mg./20 ml. | Material mixed | $B$ (ml.) required in blank titration | $m$ (ml.) required in normal titration | $f$ factor | $t$ correction term | $2(B-m)ft$ weight of reducing sugar determined mg./20 ml. |
|---|---|---|---|---|---|---|---|
| Glucose | 44.64 | no | 24.30 | 2.45 | 1.021 | 1.000 | 44.62 |
| Lactose | 45.66 | no | 23.98 | 7.30 | 1.047 | 1.307 | 45.64 |
| Glucose | 38.18 | Sucrose 20 g./100 ml. | 20.60 | 1.90 | 1.021 | 1.000 | 38.18 |
| Glucose | 42.24 | Sucrose 5 g./100 ml. | 23.55 | 1.26 | 0.948 | 1.000 | 42.22 |
| Glucose | 21.12 | Sucrose 5 g./100 ml. | 23.55 | 12.40 | 0.948 | 1.000 | 21.10 |

drops at a time at intervals of about 10~15 sec. until the end point was reached.

Operating in this way consistent results have been attained with all the reducing sugars tested, viz. glucose, lactose and galactose. On the basis of these results Table I was prepared. Over the whole of these ranges it is possible to attain a higher degree of precision, and the consistent results may be obtained, the error being within 0.06 ml., namely, 0.12 mg. in the case of glucose.

In the case of the sugar solutions containing other materials whose influence can not be overlooked, blank titration was made against the mixture of 10 ml. of the alkaline copper solution and 20 ml. of a solutions containing all materials of the same concentrations except for reducing sugars to be determined.

Some examples of glucose in solutions containing 5 and 20 g. of sucrose per 100 ml. are shown in Table II. It is important that, in all cases which have been investigated, the correction term $t$ is not affected noticeably by contamination with other materials.

The experimental factor of the standard sugar solution should be 1.000, but a small deviation is inevitable according to the variations of the experimental conditions and personal differences in judging the end point. It is advisable to standardize the standard sugar solution, after its preparation, by titrating against a weighed pure glucose. If the deviation be large, adjustment of the standard sugar solution should be made so as to make the value of the factor approximately equal to one by adding glucose or water to the standard sugar solution.

On the other hand, it is possible to estimate the sugar content in a solution of unknown concentration. The quantity $2(B-m)tf$ gives the weight in mg. of the sugar in 20 ml. of the solution.

Some remarks should be made. Very stable and reproducible heating is possible by use of an electric heater. A reagent grade preparation of sodium hydroxide ordinally containing carbonate may be used, although the decolorization of methylene blue is somewhat slower than it is in the presence of carbonate free sodium hydroxide.

## Summary

A new volumetric method determining reducing sugars has been developed by titrating a boiling mixture of modified Fehling solution and sugar solution with a standard sugar solution. By the method the concentration of sugar solution can be determined rapidly with high degree of precision.

Errors caused by variables of analytical conditions automatically being corrected, the maximum degree of accuracy will be possible by this procedure even in an unskilled hand.

There are several advantages over Lane and Eynon's method and other methods; the method is applicable over a wide range of sugar concentrations, especialy dilute solution, and in addition the difficulty in changing or washing a burette for a new solution, etc., is eliminated.

The author wishes to express his sincere thanks to Professor Y. Tsuzuki of Tokyo College of Science for his kind advice, and to Professors S. Kusunoki and T. Kinugasa of Kobe University for their encouragement throughout this work.

*Department of Biology*
*Faculty of Science*
*Kobe University*
*Mikage, Kobe*

# *Biochemical Studies on Pearl. VIII. Occurence of Calcite, Aragonite and Dolomite in Pearl and Shell*

By Shozo TANAKA, Hiroyuki HATANO* and Osamu ITASAKA**

(Received July 20, 1959)

Among many kinds of bivalved molluscs which are available in the pearl culture industry, *Pinctada martensii* (Dünker), the Japanese pearl oyster, is one of the most important species in Japan. In the previous papers of biochemical studies on pearl, physiological properties of the pearl oyster were reported to have a marked resemblance to the ordinary oyster[1,2] and the chemical mechanism of pearl formation was discussed from a view-point of comparative biochemisrty upon the calcification of invertebrata and vertebrata[3-5].

Several analytical results on the pearl and the shell materials of the pearl oyster have been reported[1-10], but few observations have been made on the nature of chemical constituents in the pearl and the shell.

In the present work, investigations have been made on the chemical compositions of the nacre of pearl, the nacreous portion of the shell or "mother-of-pearl", which forms an innermost layer of the shell, and the prismatic substance of an outer layer of the shell (Fig. 1). Furthermore, crystalline forms of calcium carbonate in the pearl and the shell were determined by the X-ray diffraction method. Also, a minute amount of magnesium was found in the shell and occurrence of dolomite was ascertained by a chemical method.

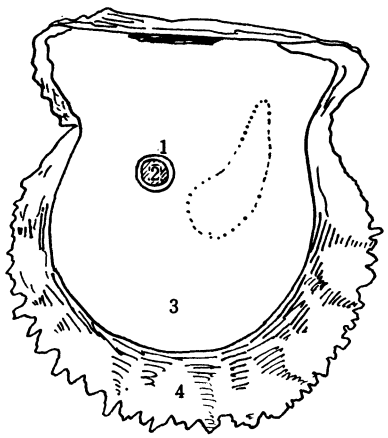



Fig. 1. A schematic diagram of the pearl and the shell of the pearl oyster.
1) The nacre of the pearl; 2) The nuclei of the pearl; 3) The nacreous layer of the shell; 4) The prismatic layer of the shell.

## Experimental

**Materials.**—Cultured pearls used in the following experiments were collected from three-year old Japanese pearl oysters, while shell samples were obtained from pearl oysters of two winters***.

The cultured pearls were separated into nacres and nuclei mechanically, the latter being put aside. By scraping off the outer layers with a grinding-wheel, a nacreous substance of the inner layers of shells was prepared. A prismatic substance of the outer layers was obtained mechanically from thin posterior shell margins. These materials were first crushed into pieces by means of a porcelain mortar and, then, pulverized after drying at room temperature for a few days.

Calcium carbonate crystals for the X-ray diffraction analysis were prepared from the pearls and the shell substances by immersing the pulverized materials in one per cent sodium hypochlorite solutions for a few hours to remove organic substances.

**Methods.**—The chemical compositions of the

* A part of this study was carried out by the author, at Kobe University, Kobe.

** Present address: School of Chemistry, Shiga University, Otsu.

1) S. Tanaka and H. Hatano, *J. Chem. Soc. Japan, Pure Chem. Sec.* (*Nippon Kagaku Zasshi*), **73**, 870 (1952).
2) S. Tanaka and H. Hatano, ibid., **74**, 74 (1953).
3) S. Tanaka and H. Hatano, *Publ. Seto Mar. Biol. Lab. Kyoto Univ.*, **II** (2), 341 (1952).
4) S. Tanaka and H. Hatano, *J. Chem. Soc. Japan, Pure Chem. Sec.* (*Nippon Kagaku Zasshi*), **76**, 602 (1955).
5) S. Tanaka and H. Hatano, *Proc. 1st Symposium on Isotopes. Japan*, **B-1**, 307 (1956).
6) U. Okuda and K. Takeuchi, *J. Chem. Soc. Japan* (*Nippon Kwagaku Kwaishi*), **38**, 819, (1919).
7) J. Tsutsumi, *Mem. Coll. Sci. Kyoto Univ., Ser. A.* **11**, 217, 401 (1928); **12**, 199 (1929).
8) J. Ogushi, "Studies on Pearl (Shinju no Kenkyu)", Ito Bunshindo, Tokyo (1938), p. 143.
9) K. Wada, *Bull. Natl. Pearl Res. Lab. Japan*, **1**, 1, 7 (1956); **2**, 74 (1957).
10) Y. Sawada, ibid., **2**, 68 (1957).

*** The authors wish to express their hearty thanks to Mr. K. Isowa, the president of the Nippon Pearl Co., at Matoya Bay near Kashikojima in Mie-ken for his kind presentation of these materials.

pearl and the shell materials were determined by the methods reported in the previous papers[1,2]; moisture was determined by measuring the decrease in weight on drying at 105°C for about 24 hr. until the weight came to a definite constant; total nitrogen was determined by a semi-micro-Kjeldahl's technique; total ashes were determined by igniting any sample to a constant weight at approximately 700°C and making a correction for the ignition loss of carbonate. Inorganic constituents in the ashes were determined as follows: phosphate as ammonium phosphomolybdate, calcium as calcium oxalate, sulfate as barium sulfate, and magnesium as ammonium magnesium phosphate after being separated from calcium, respectively; the carbonate content was calculated from the amount of carbon dioxide determined by the Conway's microdiffusion method[11].

Conchiolin, a screloprotein contained in the pearl and the shell, was estimated from the amount of residue remaining after the inorganic constituents were dissolved in dilute hydrochloric acid[12].

X-ray diffraction patterns of crystalline calcium carbonate in the pearl and the shell were recorded by the Norelco's X-ray diffractometer and were compared with those of the standard crystals of calcite and aragonite.

The state of chemical combination of a minute amount of magnesium which was found in the pearl as well as the shell was determined by the chemical method established by Kitano[13]. The principle of his method is as follows. When a small amount of magnesium is contained in calcareous shells, it is expected to be present in one of the only two possible forms, i.e. dolomite $CaMg(CO_3)_2$ and a solid solution of calcite and dolomite. Now, when carbon dioxide gas is passed into mixed suspensions of calcium

TABLE I. AMOUNTS OF CALCIUM AND MAGNESIUM DISSOLVED INTO SUSPENSIONS WHICH CONTAIN MAGNESIUM COMPOUNDS, UNDER THE CONDITION OF BEING SATURATED WITH CARBON DIOXIDE[a]

| Suspension | | | | | Dissolved quantity | | Ratio[e] | |
|---|---|---|---|---|---|---|---|---|
| $CaCO_3$[b] g. | Shell[c] g. | $CaMg(CO_3)_2$[d] g. | Ca mg. | Mg mg. | Ca mg./200 ml. | Mg | Ca % | Mg % |
| *1.61 | — | 0.89 | 841 | 117 | 91 | 1.0 | 10.9 | 0.9 |
| *1.97 | — | 0.53 | 904 | 70 | 99 | 0.8 | 10.9 | 1.1 |
| *2.06 | — | 0.44 | 920 | 58 | 91 | 0.5 | 9.9 | 0.8 |
| *2.33 | — | 0.17 | 967 | 23 | 90 | 0.3 | 9.3 | 1.4 |
| *2.39 | — | 0.11 | 980 | 14 | 100 | 0.2 | 10.2 | 1.1 |
| **2.5 | 0.0 | — | 838 | 101 | 76 | 6.8 | 9.0 | 6.6 |
| **2.0 | 0.5 | — | 870 | 81 | 71 | 5.7 | 8.2 | 7.0 |
| **1.0 | 1.5 | — | 935 | 41 | 68 | 2.6 | 7.3 | 6.3 |
| **0.5 | 2.0 | — | 968 | 20 | 67 | 2.3 | 6.9 | 12 |
| **0.2 | 2.3 | — | 987 | 8.1 | 68 | 2.3 | 6.9 | 29 |

a) Into a suspension containing 2.5 g. of magnesium preparation in 200 ml. of distilled water, purified carbon dioxide was passed for 25 min. After being allowed to stand for 10 min., the suspension was filtered through a sheet of Toyo Roshi No. 6 filter paper. Total quantities of calcium and magnesium ions in the filtrate were determined by the volumetric method using EDTA, while the amount of calcium ion was estimated as calcium oxalate, and then the amount of magnesium ion was calculated from these two values, or was determined directly by the volumetric method using oxim reagents.

b) Extra pure reagents of calcite and aragonite prepared by Y. Kitano were used in this experiment.

c) As a standard preparation of a solid solution of calcite and aragonite, were used shells of four kinds of sea urchins, in which the magnesium had been found to be present in the form of a solid solution by X-ray diffraction techniques.

d) A dolomite preparation found at Kuzuo, Tochigi-ken, was used. The analytical results are as follows: CaO, 33.80; MgO, 19.37; clay, 0.22%.

e) [g. of $Ca^{2+}(Mg^{2+})$ dissolved into 200 ml. of a suspension] × 100/[g. of $Ca^{2+}(Mg^{2+})$ in 2.5 g. of a suspension].

* See Ref. 13.

** Y. Kitano, unpublished data (1958).

11) E.J. Conway, "Microdiffusion Analysis and Volumetric Error", Crosby Lockwood & Son, Ltd., London (1950), p. 87; E. J. Conway and A. Byrne, *Biochem. J.*, **27**, 419 (1933).

12) S. Tanaka et al., *J. Chem. Soc. Japan, Pure Chem. Sec.* (*Nippon Kagaku Zasshi*), **74**, 193 (1953).

13) Y. Kitano, ibid., **77**, 211 (1956).

carbonate with dolomite or into those of calcium carbonate with a solid solution of calcite and dolomite, the quantities of magnesium dissolved into the suspensions are not the same for two cases. The data obtained by Kitano[13] are given in Table I. On the basis of these results, therefore, the state of chemical combination of magnesium present in calcareous shells can be determined by measuring the quantity of magnesium dissolved in water saturated with carbon dioxide.

## Results and Discussion

**Chemical Composition.** — The chemical compositions of the pearl and the shell of the pearl oyster are shown in Table II, which indicates that the pearl as well as the shell contain about ninety per cent of calcium carbonate and a few per cent of conchiolin. It seems to be noticeably

TABLE II. THE CHEMICAL COMPOSITIONS OF THE NACRE OF THE PEARL AND OF THE SHELL VALVES OF THE JAPANESE PEARL OYSTER, *Pinctada martensii* (DÜNKER)*

| | Cultured pearl nacre % | Shell | |
|---|---|---|---|
| | | Nacreous layer % | Prismatic layer % |
| Total nitrogen | 0.43 | 0.53 | 1.01 |
| Conchiolin | 2.72 | 2.83 | 9.61 |
| Pigments | ± | ± | +++ |
| Reducing substance | 0.00 | 0.00 | 0.02 |
| Total ashes | 80.60 | 89.60 | 76.00 |
| Calcium | 27.71 | 29.35 | 27.47 |
| Magnesium | 0.12 | 0.12 | 0.59 |
| Carbonate | 56.95 | 58.19 | 56.41 |
| Phosphate | 0.01 | 0.06 | 0.06 |
| Sulfate | 0.66 | 0.59 | 1.09 |

* Free from water content.

characteristic that, contrary to various calcareous tissues of vertebrata, there are little or only minute amounts of phosphate and sulfate in the pearl and the shell of the pearl oyster. Less content of conchiolin and a larger amount of calcium carbonate in the nacre than in the prismatic substance are observed. Scant amounts of pigments are present in the pearl and the nacreous oyster, while plenty of coloring substances can be found in prismatic substances[14]. Compared with the case of the nacre, relatively large amounts of magnesium are contained in the prismatic layer of the shell.

The curves shown in Fig. 2 indicate the X-ray diffraction patterns, recorded by

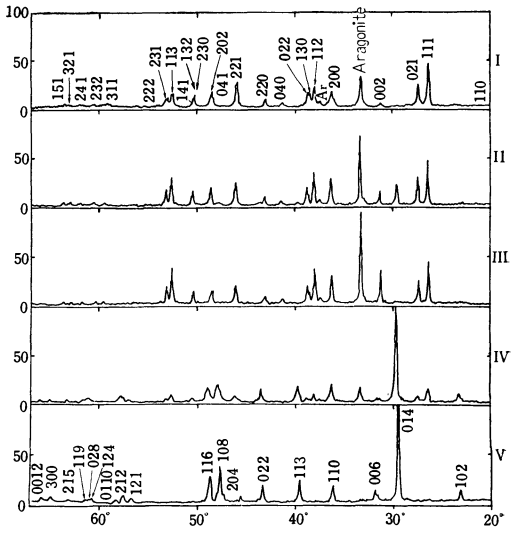



Fig. 2. X-ray diffraction patterns of calcium carbonate crystals in the nacre of pearl and in the shell material of the pearl oyster, *Pinctada martensii*. Pattern I: standard aragonite crystals; II: crystals in the nacre of the pearl; III: crystals in the nacreous layer of the shell; IV: crystals in the prismatic material; V: standard calcite crystal.

Norelco's apparatus****, of crystalline preparations of calcium carbonate from the pearl and shell materials. The crystals of calcium carbonate existing in the nacre of pearl and in the nacreous layer of shell were identified as aragonite crystals of a rhombohedral lattice, and those in the prismatic layer as calcite crystals of a rhombic lattice.

Calcite is known to form the most stable lattice of calcium carbonate while aragonite is less stable under usual crystallographical conditions. For aragonite crystal to be produced, therefore, certain special conditions should be given such as higher temperature, higher pH value of surrounding media, or a larger growing rate of crystals due to sudden supply of materials[15,16]. In connection with these requirements, it may be considered that the presence of relatively large amounts of magnesium ion is favorable to the formation of aragonite crystals.

Magnesium preparations prepared from the pearl and the shell were treated by the same procedure and the results obtained

**** The authors wish to express their thanks to the operating committee of this apparatus in Osaka University, for these measurements.

14) Y. Takagi and S. Tanaka, ibid., **76**, 406 (1955).

15) Y. Kitano and M. Nishimura, ibid., **76**, 581 (1955).

16) Y. Kitano, *J. Chem. Soc. Japan, Ind. Chem. Sec.* (*Kogyo Kagaku Zasshi*), **59**, 1346 (1956).

TABLE III. RESULTS SHOWING THE OCCURRENCE OF DOLOMITE IN THE PEARL AND THE SHELL MATERIALS OF THE PEARL OYSTER*

| Preparation | Suspension | | | Dissolved quantity | | Ratio | |
|---|---|---|---|---|---|---|---|
| | Sample mg. | Ca mg. | Mg mg. | Ca mg./200 ml. | Mg | Ca % | Mg % |
| Pearl, nacre | 952.2 | 240.8 | 1.14 | 20.0 | 0.01 | 8.3 | 0.9 |
| Shell, nacreous substance | 954.6 | 287.0 | 1.14 | 16.3 | 0.0 | 5.7 | 0 |
| Shell, prismatic substance | 973.8 | 267.5 | 5.84 | 14.3 | 1.72 | 5.3 | 29.3 |

* The procedure of this analysis is quite identical with that in Table I.

are presented in Table III. Comparing these results with the data in Table I, it has been determined that magnesium in the nacre of pearls and in the nacreous layer of shells exists as dolomite and that in the prismatic layer as a solid solution of calcite and dolomite.

Several experiments have been carried out on the formation of calcareous skeletons in marine organisms and it is demonstrated that the temperature is one of the most effective factors on differentiation of the composition of calciferous skeleton in some marine invertebrates[17,18]. Any other possible factors may be expected to alter the modification and the chemical composition of a crystal.

According to the experimental data in Table III, the fact that magnesium carbonate is difficult to crystallize in a rhombic lattice owing to a geometrical correlation of constituent atoms, seems to have some relations with the mode of crystallization of calcium carbonate in the pearl oyster.

## Summary

The chemical compositions of the pearl and the shell of the Japanese pearl oyster were investigated from a crystallographical and biochemical point of view.

By the X-ray diffraction analysis, crystals of calcium carbonate in the nacre of pearl and in the nacreous layer of shell were determined to be aragonite, while those in the prismatic layer were shown to be calcite.

The state of chemical combination of minute amounts of magnesium present in the pearl and the shell materials was examined by a chemical method. In the nacreous substances, magnesium is present as dolomite, while in the prismatic material it exists as a solid solution of calcite and dolomite.

The state of crystals of calcium carbonate and magnesium carbonate occurring in the pearl oyster has been discussed with respect to the formation of the pearl and the shell of the pearl oyster.

The authors wish to express their gratitude to Dr. Y. Kitano, Nagoya University, Nagoya, for his kind permission to quote his unpublished data in Table I and also for his advice which was given throughout the course of this research.

*Department of Chemistry*
*Faculty of Science*
*Kyoto University*
*Sakyo-ku, Kyoto*

17) H. A. Lowenstam, *J. Geol.*, **62**, 284 (1954).
18) K. E. Chave, ibid., **62**, 266, 587 (1954).

# *Ionic Character and Hybridization in the Hydrogen Cyanide Molecule*

By Yoshifumi KATO*, Utaro FURUKANE and Haruo TAKEYAMA

(Received July 20, 1959)

It is well known that the nuclear quadrupole coupling constant $eQq$ is intimately related to the electronic structure near the nucleus of a molecule. Townes and Dailey[1] have explained especially the ionic character and the hybridization of an atom from the analysis of the experimental values of the nuclear quadrupole constants. They have considered that the existence of a field gradient $q$ is attributable to unbalanced electrons, i.e. $p$ or $d$ electrons in the valence shell.

Schatz has studied the ionic character and the hybridization of chlorine in discussing the chlorine, hydrogen chloride and methyl chloride molecules[2], using the experimental values of the dipole moment besides the quadrupole coupling constant, and has stressed the importance of including the overlap integral for the estimation of the quadrupole coupling constant. However, his calculations of the field gradient are essentially based on the theory by Townes and Dailey[1]. Namely, he assumed the total quadrupole coupling constant dependent upon only the $3p$ and $3d$ electrons of chlorine and ignored the effects of other electrons and nuclei in the molecule.

In this paper, the ionic character and the $s$ character of the nitrogen atom in a hydrogen cyanide molecule have been investigated by means of the theoretical evaluation of the dipole moment and the quadrupole coupling constant taking into account the effects of all the electrons and nuclei in a hydrogen cyanide molecule.

## Calculation Method

**Basic Wave Function.** — The hydrogen cyanide molecule is a linear molecule having an NC bond distance equal to 1.156 Å and a CH bond distance equal to 1.1064 Å as determined by microwave measurements[3]. The hydrogen cyanide molecule is taken to lie along the $Z$ axis with its nitrogen atom at the origin. The total wave function used is the following valence bond function including an ionic term ($N^-=C^+$), that is,

$$\Psi_T = A\left[\Psi_{cov} + \lambda_1 \Psi_{\sigma ion} + \lambda_2(\Psi_{\pi x ion} + \Psi_{\pi y ion})\right] \quad (1)$$

Where $A$ is the normalization factor and four state functions appearing in Eq. 1 are taken as simple products of the following electron pair bond functions with the Heitler-London type:

$$\left.\begin{aligned}
\Psi_{cov} &= (NC:\sigma)^2(CH:\sigma)^2(N_2:\sigma)^2 \\
&\quad \times (NC:\pi_x)^2(NC:\pi_y)^2 \\
\Psi_{\sigma ion} &= (N_1:\sigma)^2(CH:\sigma)^2(N_2:\sigma)^2 \\
&\quad \times (NC:\pi_x)^2(NC:\pi_y)^2 \\
\Psi_{\pi x ion} &= (NC:\sigma)^2(CH:\sigma)^2(N_2:\sigma)^2 \\
&\quad \times (N:\pi_x)^2(NC:\pi_y)^2 \\
\Psi_{\pi y ion} &= (NC:\sigma)^2(CH:\sigma)^2(N_2:\sigma)^2 \\
&\quad \times (NC:\pi_x)^2(N:\pi_y)^2
\end{aligned}\right\} \quad (2)$$

and

$$\left.\begin{aligned}
(NC:\sigma)^2 &= A_1[n_1(i)c_2(j) + c_2(i)n_1(j)] \\
(CH:\sigma)^2 &= A_2[c_1(i)h(j) + h(i)c_1(j)] \\
(NC:\pi_x)^2 &= A_3[n_{\pi x}(i)c_{\pi x}(j) \\
&\quad + c_{\pi x}(i)n_{\pi x}(j)] \\
(N:\pi_x)^2 &= n_{\pi x}(i)n_{\pi x}(j) \\
(N_1:\sigma)^2 &= n_1(i)n_1(j)
\end{aligned}\right\} \quad (3)$$

$(NC:\pi_y)^2$, $(N:\pi_y)^2$ and $(N_2:\sigma)^2$ are taken with the analogous definitions to $(NC:\pi_x)^2$, $(N:\pi_x)^2$ and $(N_1:\sigma)^2$, respectively. Therefore, in the wave function used, the higher order permutation of the electrons is neglected; that is, the orthogonarity among the electron pair bonds is assumed. The coefficients $A_1$, $A_2$ and $A_3$ of the electron pair bond functions are easily shown to be

* Present address: Osaka Municipal Technical Research Institute, Kita-ku, Osaka.

1) C. H. Townes and B. P. Dailey, *J. Chem. Phys.*, **17**, 782 (1949).

2) P. N. Schatz, ibid., **22**, 695 (1954); **22**, 755 (1954); **22**, 1974 (1954).

3) J. W. Simmon, W. E. Anderson and W. Gordy, *Phys. Rev.*, **77**, 77 (1950).

$$\left.\begin{aligned} A_1&=[2(1+S_{n_1c_2}{}^2)]^{-1/2}\\ A_2&=[2(1+S_{c_1h}{}^2)]^{-1/2}\\ A_3&=[2(1+S_{n_\pi c_\pi}{}^2)]^{-1/2}\\ S_{n_1c_2}&=\int n_1c_2\mathrm{d}v \qquad Sc_1h=\int c_1h\mathrm{d}v\\ S_{n_\pi c_\pi}&=\int n_\pi c_\pi \mathrm{d}v \end{aligned}\right\} \quad (4)$$

Futhermore $h$, $c_{\pi x}$, $c_{\pi y}$, $n_{\pi x}$ and $n_{\pi y}$ are atomic orbitals (AO), and $n_1$, $n_2$, $c_1$ and $c_2$ are the following $s-p$ hybridized orbitals:

$$\left.\begin{aligned} n_1&=\alpha^{1/2}(N:2s)+(1-\alpha)^{1/2}(N:2pz)\\ n_2&=(1-\alpha)^{1/2}(N:2s)-\alpha^{1/2}(N:2pz)\\ c_1&=2^{-1/2}[(C:2s)+(C:2pz)]\\ c_2&=2^{-1/2}[(C:2s)-(C:2pz)] \end{aligned}\right\} \quad (5)$$

All the AO's except the $2p$ orbitals of nitrogen are the Slater orbitals[4] (assumed effective nuclear charge $\delta_h=1.17$, $\delta_c=1.625$ and $\delta_n=1.95$). The $2p$ orbitals of nitrogen have a great effect on the field gradient at the nitrogen nucleus. Then, the following analytic function derived from the Hartree-Fock field calculation of the ground state $^4S$ of the nitrogen atom[5] is used for its radial function instead of the Slater orbital,

$$R_{2p}=r[1.809\exp(-1.387r)+6.620\exp(-2.950r)] \quad (6)$$

**Dipole Moment.**—The experimental value of the dipole moment of hydrogen cyanide has been known to be 3.00 D[3] and also it is given by the expression

$$\mu_T=e(\sum_{i=1}^{2} r_i-\sum_{j=1}^{10}\overline{Z}_j) \quad (7)$$

$$\sum_{i=1}^{2} r_i=6.7440\ \text{Å} \quad \overline{Z}_j=\int|\Psi_T|^2Z_j\mathrm{d}v \quad (8)$$

Where $e$ is the protonic charge ($4.80288\times10^{-10}$ esu), the first and the second term in Eq. 7 are, respectively, the contributions of the nuclei and the electrons. When the latter are calculated by the wave function given in Eq. 1, the expression is easily shown to be

$$\sum_{j=1}^{10} Z_j=M_{cov}+M_{\sigma ion}+M_{\pi ion}+M_{trans} \quad (9)$$

where

$$\left.\begin{aligned} M_{cov}&=2[M(NC:\sigma)+M(CH:\sigma)+2M(NC:\pi)+M_{n_2n_2}]\\ M_{\sigma ion}&=2\lambda_1{}^2[M(CH:\sigma)+2M(NC:\pi)]\\ M_{\pi ion}&=4\lambda_2{}^2[M(NC:\sigma)+M(CH:\sigma)+M(NC:\pi)+M_{n_2n_2}]\\ M_{trans}&=4\lambda_1A_1[M_{n_1c_2}+2S_{n_1c_2}\{M(CH:\sigma)+2M(NC:\pi)+1/2M_{n_2n_2}\}]\\ &+8\lambda_2A_3[M_{n_\pi c_\pi}+2S_{n_\pi c_\pi}\{M(NC:\sigma)+M(CH:\sigma)+M(NC:\pi)+M_{n_2n_2}\}]\\ &+16\lambda_1\lambda_2A_1A_3[S_{n_\pi c_\pi}M_{n_1c_2}+S_{n_1c_2}M_{n_\pi c_\pi}+2S_{n_1c_2}S_{n_\pi c_\pi}\times\{M(CH:\sigma)+M(NC:\pi)+1/2M_{n_2n_2}\}] \end{aligned}\right\} \quad (10)$$

and the following abbreviations are adopted:

$$\left.\begin{aligned} M(NC:\sigma)&=A_1{}^2(M_{n_1n_1}+M_{c_2c_2}+2S_{n_1c_2}M_{n_1c_2})\\ M(CH:\sigma)&=A_2{}^2(M_{c_1c_1}+M_{hh}+2S_{c_1h}M_{c_1h})\\ M(NC:\pi)&=A_3{}^2(M_{c_\pi c_\pi}+2S_{n_\pi c_\pi}M_{n_\pi c_\pi}) \end{aligned}\right\} \quad (11)$$

Also the normalization factor $A$ is shown to be

$$A=(1+\lambda_1{}^2+2\lambda_2{}^2+4A_1S_{n_1c_2}\lambda_1+8A_3S_{n_\pi c_\pi}\lambda_2+16A_1A_3S_{n_1c_2}S_{n_\pi c_\pi}\lambda_1\lambda_2)^{-1/2} \quad (12)$$

The necessary integrals of the dipole moment matrices: $M_{ab}=\int\chi_aZ\chi_b\mathrm{d}v$ and the overlap integrals: $S_{ab}=\int\chi_a\chi_b\mathrm{d}v$ are given to Table I. These values are obtained by the ordinary method[6].

**Quadrupole Coupling Constant.**—The experimental value of the nuclear quadrupole coupling constant has been known from the microwave datum to be $-4.58$ Mc.[3] On the other hand, the quadrupole coupling constant is shown to have the following expression:

$$eQq_T=eQ(q_n+q_{el}) \quad (13)$$

$$q_n=0.79295e\ e\ \text{a.u.}$$

$$q_{el}=-e\int|\Psi_T|^2(3\cos^2\theta_z-1)/r^3\mathrm{d}v \quad (14)$$

Where $q_T$ is the average value of $(\partial^2V/\partial Z^2)_{z=0}$, $V$ being all the electrostatic potentials and $Q$ the nuclear quadrupole moment of nitrogen ($=2\times10^{-26}$ cm$^2$)[1]. In Eq. 13, the

4) J. C. Slater, ibid., **36**, 57 (1932).
5) D. R. Hartree and W. Hartree, *Proc. Roy. Soc. (London)*, **A193**, 299 (1948).
6) For example, M. Kotani et al., "Table of Molecular Integrals", Maruzen Co., Ltd., Tokyo (1955).

TABLE I. VALUES OF MOLECULAR INTEGRALS:

$$S_{ab}=\int \chi_a \chi_b \mathrm{d}v, \quad M_{ab}=\int \chi_a Z \chi_b \mathrm{d}v$$

(in Angstrom as unit)

| | | | |
|---|---|---|---|
| $S_{c_sh}$ | 0.50876 | $M_{c_sh}$ | 0.012501 |
| $S_{c_\sigma h}$ | 0.49357 | $M_{c_\sigma h}$ | 0.16891 |
| $S_{n_sc_s}$ | 0.47011 | $M_{n_sc_s}$ | −0.040613 |
| $S_{n_sc_\sigma}$ | −0.49979 | $M_{n_sc_\sigma}$ | 0.18131 |
| $S_{n_\sigma c_s}$ | 0.39765 | $M_{n_\sigma c_s}$ | 0.13353 |
| $S_{n_\sigma c_\sigma}$ | −0.30254 | $M_{n_\sigma c_\sigma}$ | −0.026792 |
| $S_{n_\pi c_\pi}$ | 0.29880 | $M_{n_\pi c_\pi}$ | −0.020225 |
| | | $M_{c_sc_\sigma}$ | 0.47003 |
| | | $M_{n_\sigma n_s}$ | 0.39169 |

The following abbreviated notations for AO's are used; $h=(H:1s)$, $c_s=(C:2s)$, $c_\sigma=(C:2pz)$, $c_\pi=(C:2px$ or $2py)$, $n_s=(N:2s)$, $n_\sigma=(N:2pz)$ and $n_\pi=(N:2px$ or $2py)$. The one-center and the two-center integrals are respectively evaluated with the nucleus in question and the center of internuclear distance as the origin.

first and the second term on the right are, respectively, the contributions of the nuclei except the nitrogen nucleus and the electrons to the field gradient $q_T$. $q_{el}$ is calculated by Eq. 1 as follows:

$$\begin{aligned}
q_{el}=&2[q(NC:\sigma)+q(CH:\sigma)\\
&+2q(NC:\pi)+q_{n_2n_2}]\\
&+2\lambda_1^2[q(CH:\sigma)+2q(NC:\pi)+2q_{n_1n_1}]\\
&+4\lambda_2^2[q(NC:\sigma)+q(CH:\sigma)+q(NC:\pi)\\
&+q_{n_2n_2}+q_{n_\pi n_\pi}]\\
&+4A_1\lambda_1[q_{n_1c_2}+2S_{n_1c_2}\{q(CH:\sigma)\\
&+2q_{n_\pi c_\pi}+3/2\,q_{n_1n_1}\}]\\
&+8A_3\lambda_2[q_{n_\pi c_\pi}+2S_{n_\pi c_\pi}\{q(NC:\sigma)\\
&+q(CH:\sigma)+q_{n_2n_2}+q_{n_\pi c_\pi}+1/2\,q_{n_\pi n_\pi}\}]\\
&+16A_1A_3\lambda_1\lambda_2[S_{n_\pi c_\pi}q_{n_1c_2}+S_{n_1c_2}q_{n_\pi c_\pi}\\
&+2S_{n_1c_2}S_{n_\pi c_\pi}\{q(CH:\sigma)\\
&+q(NC:\pi)+3/2\,q_{n_1n_1}+1/2\,q_{n_\pi n_\pi}\}] \qquad (15)
\end{aligned}$$

Here the following abbreviations are adopted:

$$\left.\begin{aligned}
q(NC:\sigma)&=A_1^2(q_{n_1n_1}+q_{c_2c_2}\\
&\quad+2S_{n_1c_2}q_{n_1c_1})\\
q(CH:\sigma)&=A_2^2(q_{c_1c_1}+q_{hh}+2S_{c_1h}q_{c_1h})\\
q(NC:\pi)&=A_3^2(q_{n_\pi n_\pi}+q_{c_\pi c_\pi}\\
&\quad+2S_{n_\pi c_\pi}q_{n_\pi c_\pi})
\end{aligned}\right\} \qquad (16)$$

All $q_{ab}=-eq_{ab}'=-e\int \chi_a(3\cos^2\theta_z-1)/r^3\chi_b\mathrm{d}v$ are calculated by using the methods of Barnett and Coulson[7]. These values are given in Table II.

TABLE II. VALUES OF FIELD GRADIENT INTEGRALS:

$$q_{ab}'=\int \chi_a(3\cos^2\theta_z-1)/r^3\chi_b\mathrm{d}v \text{ (in atomic unit)}$$

| | | | |
|---|---|---|---|
| $q_{n_\sigma n_\sigma}'$ | 2.36606 | $q_{c_sc_s}'$ | 0.098460 |
| $q_{n_\pi n_\pi}'$ | −1.18303 | $q_{c_sc_\sigma}'$ | −0.048937 |
| $q_{n_sc_s}'$ | 0.030116 | $q_{c_\sigma c_\sigma}'$ | 0.133908 |
| $q_{n_sc_\sigma}'$ | −0.045963 | $q_{c_\pi c_\pi}'$ | 0.080736 |
| $q_{n_\sigma c_s}'$ | 0.102260 | $q_{hh}'$ | 0.011326 |
| $q_{n_\sigma c_\sigma}'$ | −0.160130 | $q_{c_sh}'$ | 0.027928 |
| $q_{n_\pi c_\pi}'$ | −0.012108 | $q_{c_\sigma h}'$ | 0.035842 |

The three-center integrals $q_{c_sh}'$ and $q_{c_\sigma h}'$ are evaluated by Ruedenberg-Mulliken's approximation[8];

$$\int \chi_a 1/r_c^3 \chi_b \mathrm{d}v \approx 1/2\, S_{ab}\left(\int |\chi_a|^2 1/r_c^3 \mathrm{d}v + \int |\chi_b|^2 1/r_c^3 \mathrm{d}v\right)$$

## Results and Discussion

The parameters to be determined are the ionic characters $\lambda_1$, $\lambda_2$ and the $s$—$p$ hybridization of nitrogen $\alpha$. Now, in use of Eqs. 7 and 13, the relation of $\lambda_1$ and $\lambda_2$

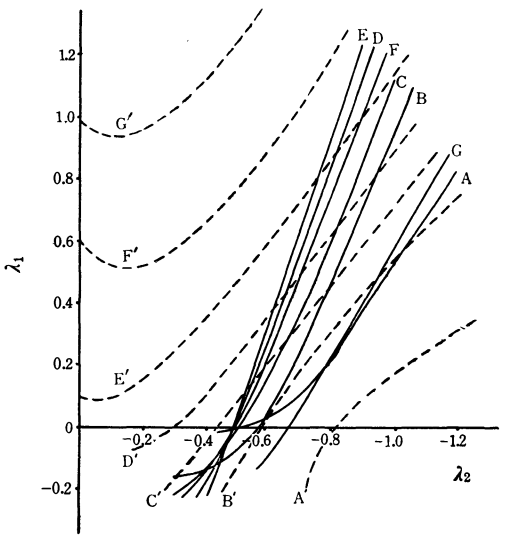



Fig. 1. The relationship between $\lambda_1$ and $\lambda_2$, being chosen in all cases to give the experimental values. $\alpha$ is taken as a parameter. The full and dotted lines are respectively the curves of the dipole moment and the quadrupole coupling constant.

| | | | |
|---|---|---|---|
| A: | $\alpha=0.2$ | A': | $\alpha=0.20$ |
| B: | $\alpha=0.3$ | B': | $\alpha=0.30$ |
| C: | $\alpha=0.4$ | C': | $\alpha=0.35$ |
| D: | $\alpha=0.5$ | D': | $\alpha=0.40$ |
| E: | $\alpha=0.6$ | E': | $\alpha=0.45$ |
| F: | $\alpha=0.7$ | F': | $\alpha=0.50$ |
| G: | $\alpha=0.8$ | G': | $\alpha=0.60$ |

7) M. P. Barnett and C. A. Coulson, *Trans. Roy. Soc. (London)*, **243**, 221 (1951).

8) R. S. Mulliken, *J. chim. phys.*, **46**, 497 (1949); K. Ruedenberg, *J. Chem. Phys.*, **19**, 1433 (1951).

which are taken to coincide with the experimental values is shown in Fig. 1, in which the hybridization $\alpha$ is taken as a parameter. From Fig. 1, it is seen that the dipole moment is not much affected by the *s* character between $\alpha=0.3$ and 0.7, but it depends on the ionicity as a considerable extent. This will explain the well-known fact that there is a possibility to take up the ionic character as a measure of the dipole moment[9]. On the other hand, the *eQq* curves are intensely dependent upon the *s* character, too. The $\alpha$, $\lambda_1$ and $\lambda_2$ values are not determined simultaneously, but it will be clear from Fig. 1 that the region of allowed $\alpha$ value is between about 0.3 and 0.5. Now, it is possible to calculate the NC bond moment under the same scheme as above. The NC bond moments for the reasonable set of $\alpha$, $\lambda_1$ and $\lambda_2$ obtained from Fig. 1 are as follows:

| $\alpha$ | $\lambda_1$ | $\lambda_2$ | NC bond moment |
|---|---|---|---|
| 0.50 | 1.81 | −1.16 | 2.57 D |
| 0.45 | 1.04 | −0.94 | 3.38 D |
| 0.40 | 0.61 | −0.80 | 1.61 D |
| 0.35 | 0.35 | −0.72 | 1.59 D |
| 0.30 | 0.04 | −0.60 | 1.42 D |

The NC bond moment has been estimated to be about 3.5 D by Smyth[10]. If his estimation is correct, a reasonable set of three parameters would be taken to be $\alpha=0.45$, $\lambda_1=1.04$ and $\lambda_2=-0.94$. Then, the experimental value of total molecular dipole moment of the hydrogen cyanide molecule 3.0 D can be explained to be 3.4 D ($N^-C^+$ bond moment) plus −0.4 D ($C^+H^-$ bond moment). The value −0.4 D for the $C^+H^-$ bond moment may be acceptable taking into account the inclusion of the atomic dipole term by Coulson[11].

From the *eQq* data, Townes and Dailey[1] and separately Dailey[12] have estimated the structure of HCN as follows:

| Structure | | Assumed *s* character | Assumed *eQq* per *p* electron** | |
|---|---|---|---|---|
| Covalent | Ionic | | | |
| 90% | 10% | 25% | −24 Mc. | Townes & |
| or 90% | 10% | 50% | −10 Mc. | Dailey |
| 90% | 10% | 45% | — | Dailey |

In both estimates, obviously some arbitrariness exists in the determination of the parameters because of several having been obtained from only one experiment value. On the other hand, Pauling[13] has presumed that the ionicity of the NC bond would probably have about 57% from the experimental values of the dipole moment of alkyl cyanides. The relative weights of structures are expressed in the following two ways; the one is due to the definition that the weights of the covalent and two ionic parts are given in the ratio $1:\lambda_1^2:2\lambda_2^2$ by Coulson[14] (I), and the other includes a transitional structure as well as covalent and ionic by Syrkin and Dyatkina[15] (II). Then, the following results are obtained from the present calculation:

| Structure | | Weight of structure, % By I | By II |
|---|---|---|---|
| Covalent | (A) | 26.0 | 10.2 |
| $\sigma$ ionic | (B) | 28.1 | 11.2 |
| $\pi_x$ & $\pi_y$ ionic | (C) | 45.9 | 18.1 |
| Transitional | (A)—(B) | | 21.3 |
| 〃 | (A)—(C) | | 19.3 |
| 〃 | (B)—(C) | | 20.0 |

Following the definition by Coulson, the present result with 74% as the ionic structure seems rather to support Pauling's conclusion. Here it is interesting to note that in a triple bond NC, each structure with the $\sigma$ or $\pi$ polarized bond has nearly equal weight, notwithstanding the fact that $\sigma$ bond has larger overlap (~0.7) and, on the other hand, $\pi$ bond smaller overlap (~0.3). However, it is probably impossible in the present calculation to state anything about the relationship between the degree of the overlap of each bond in the multiple bond and the polarization of the bond or the mobilities of electron in bond.

Fig. 2 shows the curves of the quadrupole coupling constants calculated, taking into account only *p* electrons of nitrogen and all the charges for the field gradient at the nitrogen nucleus with $\alpha=0.45$. Now, being taken to fix $\lambda_1$ and $\lambda_2$ values, the *eQq* values taking into account the contribution of all the charges are always larger than ones for only *p* electrons. This difference probably depends upon whether or not the charge distribution in the overlap

9) L. Pauling, "The Nature of the Chemical Bond", Cornell Univ. Press, Ithaca, N. Y. (1940), p. 46.
10) C. P. Smyth, *J. Am. Chem. Soc.*, **60**, 183 (1938).
11) C. A. Coulson, *Trans. Faraday Soc.*, **38**, 433 (1942).
12) B. P. Dailey, *J. Phys. Chem.*, **57**, 490 (1953).
** Using Eq. 6, the authors obtain −11.12 Mc. for *eQq* per *2pz* electron; Y. Kato et al., This Bulletin, **32**, 527 (1959).
13) See Ref. 9, p. 75.
14) C. A. Coulson, "Valence", Oxford Univ. Press, London (1952), p. 123.
15) Y. K. Syrkin and M. E. Dyatkina, "Structure of Molecules and the Chemical Bond". Butterworths Scientific Publications, London (1950), p. 205.

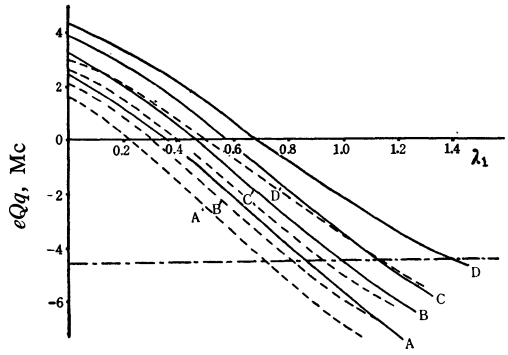



Fig. 2. Quadrupole coupling constant of HCN as a function of $\lambda_1$. $\lambda_2$ is taken as a parameter and $\alpha$ is fixed to 0.45. The horizontal chain line is the experimental value. The full and dotted lines are respectively the curves under the consideration of all the charge and only $p$ electrons for the field gradient at the nitrogen nucleus.

A & A': $\lambda_2 = -0.8$
B & B': $\lambda_2 = -0.9$
C & C': $\lambda_2 = -1.0$
D & D': $\lambda_2 = -1.1$

region is taken into account in evaluating the field gradient. Gordy[16] has argued that the overlap effects should be ignored and has pointed out the merits of his simple relation between the ionicity and quadrupole coupling constant in which the $s$ character is neglected entirely. Certainly the field gradient is proportional to $1/r^3$, but at the same time to the charge density. Therefore, it should be naturally required for the evaluation of the nuclear quadrupole coupling constant to take into account not only the redistribution of the charge near the nucleus due to the formation of the chemical bond, but also the distribution of the charge in bonding region because of its larger density.

In this point, the present results will support Schatz's calculation of $eQq$ including the overlap effects.

One of the authors (Y. K.) wishes to express his gratitude to Professor H. Narumi of Doshisha University and Dr. H. Murata of Osaka Municipal Technical Research Institute for many helpful discussions and their valuable aid during the course of this work.

*Department of Physics*
*Faculty of Science*
*Hiroshima University*
*Hiroshima*

16) W. Gordy, *J. Chem. Phys.*, **19**, 792 (1951); W. Gordy, W. V. Smith and R. F. Trambarulo, "Microwave Spectroscopy", John Wiley & Sons, Inc., New York (1953), p. 272.

# *Spectrophotometric Determination of Nitrous Acid with Disodium 1-(4'-Aminobenzeneazo)-amino-8-hydroxy-naphthalene-2', 6-disulfonate*

By Yukiteru KATSUBE and John H. YOE

(Received July 27, 1959)

Colorimetric methods in general use for a small quantity of nitrous acid are based on the formation of intensely colored azo dyes. Nitrous acid reacts with primary aromatic amines in acid solution to form diazonium salts, which react with a second molecule of the amine to produce colored cations of an aminoazo compound. Although the intense color of the azo dyestuffs formed in this way is available for the determination of nitrous acid, the coupling reagent used has an important influence on the determination.

The best amine that has been used for the determination of nitrous acid is sulfanilic acid (*p*-anilinesulfonic acid), with subsequent coupling of the resulting diazonium compound with $\alpha$-naphthylamine to give the red dyestuff *p*-benzene sulfonic acid-azo-$\alpha$-naphthylamine[1-6].

1) P. Griess, *Ber.*, **12**, 427 (1879).
2) F. L. Hahn and G. Jaeger, ibid., **58**, 2335 (1925).
3) J. Blom, ibid., **59**, 121 (1926).
4) F. P. Treadwell, "Analytical Chemistry", English Ed., Vol. II, John Wiley & Sons, Inc., New York (1951), p. 306.
5) F. Feigl, "Spot Tests", English Ed., Vol. I, Elsevier Publishing Co., New York (1954), p. 302.
6) N. A. Tananaeff and A. M. Schapowalenko, *Z. anal. Chem.*, **100**, 350 (1935).

This paper describes a new method for the determination of trace quantities of nitrous acid based on the formation of a colored compound with disodium 1-(4′-aminobenzeneazo)-2-amino-8-hydroxy-naphthalene-2′, 6-disulfonate.

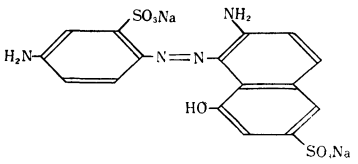



Fig. 1. Disodium 1-(4′-aminobenzeneazo)-2-amino-8-hydroxy-naphthalene-2′, 6-disulfonate.

## Experimental

**Apparatus and Reagents.** — *Spectrophotometer.* — A Shimazdu Spectrophotometer with matched 1 cm. glass cells, was used.

*Standard solution of nitrous acid.* — The standard solution of nitrous acid was prepared according to Treadwell[4]. His instructions are as follows. Add silver nitrate to a concentrated solution of commercial potassium nitrite, filter off the precipitated silver nitrite and wash it several times with cold distilled water. To obtain pure silver nitrite, dissolve the precipitate in as little distilled water as possible and cool quickly. Drain off the mother liquor through a funnel provided with a platinum cone using gentle suction. Wash the silver nitrite on the funnel with a small volume of cold distilled water. Place the washed silver nitrite in a calcium chloride desiccator and allow to dry in the dark. Dissolve 1.5388 g. of the dried silver nitrite in a liter volumetric flask with hot distilled water and add 0.8 g. of pure sodium chloride to convert the silver nitrite into silver chloride and sodium nitrite. After cooling, make the solution up to volume with distilled water and allow the precipitate to settle. Pipet 10 ml. of the clear solution into a second liter-volumetric flask, make up to the mark with distilled water and thoroughly mix. One milliliter of this solution contains 4.7 mg. of nitrous acid.

*Reagent solution.* — Prepare the reagent solution by dissolving disodium 1-(4′-aminobenzeneazo)-2-amino-8-hydroxy-naphthalene-2′, 6-disulfonate in distilled water to give a 0.05% solution. (The reagent may be obtained from the LaMotte Chemical Products Co., Chestertown, Maryland, U. S. A.)

*0.4% Ethylenediaminetetraacetic acid (disodium salt) solution.*

*6 N Hydrochloric acid.*

**Procedure.** — Transfer 20 ml. of EDTA solution to a 25 ml. volumetric flask and add 1 ml. of the sample solution, which has been adjusted so as to contain 5 to 60 p. p. m. of nitrous acid. Add 2.5 ml. of the reagent solution, and 0.3 ml. of 6 N hydrochloric acid and shake well. Make up to the mark with distilled water, thoroughly mix and, after ten minutes, measure the absorbance at 625 mμ, using a reagent blank solution as a reference. Determine the weight or the concentration of nitrous acid in the sample from a calibration curve.

## Results and Discussion

**Absorption Spectra.** — Disodium 1-(4′-aminobenzeneazo) - 2 - amino - 8 - hydroxy - naphthalene-2′, 6-disulfonate is a red-brown solid, soluble in water. It is stable indefinitely in the solid state, and for, at least, three months when dissolved in water. The aqueous solution of the reagent is red; the nitrite ion in hydrochloric acid reacts with it to give a blue solution. Absorption spectra of the reagent solution and of the blue solution produced by the color reaction between the reagent and nitrite in diluted hydrochloric acid solution are given in Fig. 2.

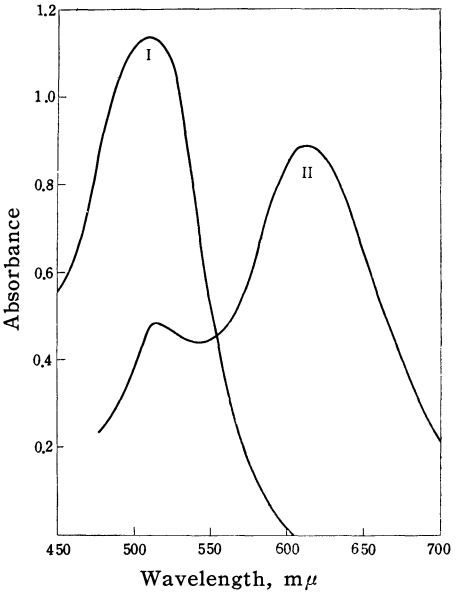



Fig. 2. Absorption spectra.
I. Reagent, 50 p. p. m.
II. Reagent (50 p. p. m.) + $HNO_2$ (2.3 p. p. m.)

As seen in Fig. 2, the compound produced by the color reaction has a maximum absorption at 625 mμ; the reagent solution does not absorb light at this wavelength. Hence, for analytical use absorbance measurements are made at 625 mμ. A large exess of the reagent must be avoided because its solution has a slight absorption at 625 mμ when the reagent concentration is greater than 50 p. p. m. It is not necessary to use exactly the same concentration of the reagent for standards and unknowns so far as the concentration of

unreacted reagent is below 50 p. p. m. and water is used as reference solution. However, color intensities measured with the reagent solution as a blank obey Beer's law better than those with a water blank.

Application of the method of continuous variations[7,8] to this color reaction indicates that the mole ratio of reagent to $NO_2^-$ is 1 to 1. The result is shown in Fig. 3.

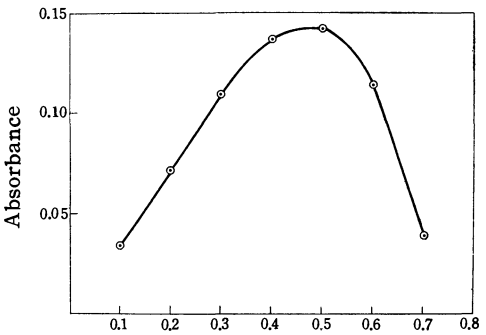



Fig. 3. Application of method of continuous variations: The nitrite and the reagent solutions were mixed in proportion to give the $x$ to $(1-x)$ ratio of component in 1.0 ml. total volume in a 100 ml. volumetric flask, where $x$ is equivalent to ml. of $10^{-3}$ M reagent and $(1-x)$ is equivalent to ml. of $10^{-3}$ M nitrite ion (the concentration of hydrochloric acid in the mixed solution was adjusted to 0.1 N).

**Effect of Concentration of Hydrochloric Acid.** — In order to determine the effect of the concentration of hydrochloric acid on the color reaction, the blue colored solution containing 2.8 p. p. m. of nitrous acid and 50 p.p.m. of the reagent were prepared with hydrochloric acid of various strengths, and absorbances of these solutions were measured. The results are shown in Fig. 4.

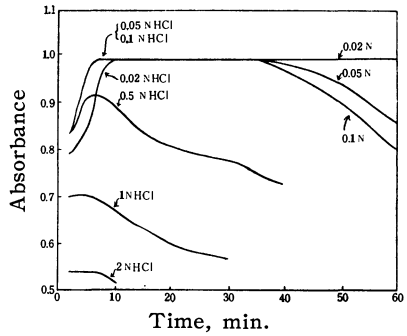



Fig. 4. Effect of hydrochloric acid.

It is seen that the optimum concentration of hydrochloric acid is between 0.05 and 0.1 N and hence, the solution containing nitrite must be adjusted to within this concentration range. Additional acid decreases the color intensity, causing rapid decolorization. With less acid, the color does not attain a maximum intensity within a reasonable time. In the optimum acid concentration, the color increases during the first ten minutes after the preparation of the blue solution, and then remains constant for about thirty minutes. It is necessary, therefore, to allow the solution to stand ten minutes and then to measure the absorbance within thirty minutes.

When sulfuric, phosphoric and acetic acid are used in place of hydrochloric acid, a less intense color is obtained.

**Effect of Temperature.** — There is no variation in the absorbance of the color system over a temperature range of 15 to 30°C. Hence, normal temperature changes in the laboratory introduce no error.

**Interfering Ions.** — The reagent was tested with 67 ions on a spot plate to determine the effect of other ions. The tested ions are given in Table I as the periodic table style.

Sixteen ions shown by italics in Table I were found to cause interference ($As^{+3}$,

TABLE I. EFFECT OF OTHER IONS

| | | | | | | | | | | | | | | | |
|---|---|---|---|---|---|---|---|---|---|---|---|---|---|---|---|
| $Li^+$ | $Be^{+2}$ | | | | | | | | | | $B_4O_7^{-2}$ | $CO_3^{-2}$ | $NO_3^-$ | | $F^-$ |
| $Na^+$ | $Mg^{+2}$ | | | | | | | | | | $Al^{+3}$ | $SiO_3^{-2}$ | $HPO_4^{-2}$ | $S^{-2}$ | $Cl^-$ |
| $K^+$ | $Ca^{+2}$ | $Sc^{+3}$ | *$Ti^{+4}$* | $Cr^{+3}$ | *$Mn^{+2}$* *$MnO_4^-$* | *$Fe^{+3}$* $Fe^{+2}$ | $Co^{+2}$ | $Ni^{+2}$ | $Cu^{+2}$ | $Zn^{+2}$ | $Ga^{+3}$ | $Ge^{+4}$ | *$As^{+3}$* | *$CeO_3^{-2}$* | *$Br^-$* |
| $Rb^+$ | $Sr^{+2}$ | $Y^{+3}$ | *$Zr^{+4}$* | *$MoO_4^{-2}$* | | $Ru^{+3}$ | $Rh^{+3}$ | | | $Cd^{+2}$ | $In^{+3}$ | *$Sn^{+2\ +4}$* | $Sb^{+3}$ | | *$I^-$* |
| $Cs^+$ | $Ba^{+2}$ | | $Hf^{+4}$ | $UO_2^{+2}$ | $ReO_4^-$ | $OsO_5^{-2}$ | $Ir^{+4}$ | | | *$Hg^{+\ +2}$* | $Tl^{+3}$ | $Pb^{+2}$ | $Bi^{+3}$ | | |
| *$La^{+3}$ | *$Ce^{+3}$* | $Pr^{+3}$ | $Nd^{+3}$ | $Sm^{+3}$ | $Eu^{+3}$ | | | $Dy^{+3}$ | | $Er^{+3}$ | $Tm^{+3}$ | $Yb^{+3}$ | | | |

7) P. Job, *Ann. chim.*, (10), **9**, 113 (1928).

8) W. C. Vosburgh and G. R. Cooper, *J. Am. Chem. Soc.*, **63**, 437 (1941).

$Br^-$, $Fe^{+3}$, $Ce^{+3}$, $CeO_3^{-2}$, $F^-$, $Hg^{+,2+}$, $I^-$, $Mn^{+2}$, $MnO_4^-$, $MoO_4^{-2}$, $Sn^{+2,+4}$, $Ti^{+4}$, $Zr^{+4}$). Ferric ions cause a serious error and must be removed before the addition of the reagent. Chemical methods of separation of ferric ions did not yield good results. However, when EDTA solution is added to the sample solution before the addition of the reagent, interference of ferric ions is effectively eliminated. EDTA has no influence on the absorption spectrum of the blue colored solution. The effect of some common ions was tested spectrophotometrically; Table II summerizes the tolerance.

In Table II, the limiting concentration of an ion is taken to be the concentration that causes a deviation of more than 0.01 unit in the absorbance of a solution containing 0.94 p. p. m. of nitrous acid.

Table II. Interferences

| Ion | Added as | Limiting concn., p. p. m. |
|---|---|---|
| $Co^{+2}$ | $CoCl_2$ | 300 |
| $Cr^{+3}$ | $Cr_2(SO_4)_3$ | 200 |
| $Cu^{+2}$ | $CuSO_4$ | 300 |
| $Fe^{+3}$ | $Fe_2(SO_4)_3$ | 100 |
| $Ni^{+2}$ | $NiSO_4$ | 300 |

Table III. Accuracy and precision of the method

| Nitrous acid | | Absorbance** at 625 mμ | Standard deviation*** in absorbance unit | Error % |
|---|---|---|---|---|
| Taken p. p. m. | Found* p. p. m. | | | |
| 0.19 | 0.18 | 0.075 | 0.002 | −5.3 |
| 0.38 | 0.37 | 0.151 | 0.001 | −2.6 |
| 0.56 | 0.57 | 0.231 | 0.001 | +1.8 |
| 0.75 | 0.76 | 0.307 | 0.002 | +1.3 |
| 0.94 | 0.95 | 0.386 | 0.001 | +1.1 |
| 1.13 | 1.14 | 0.463 | 0.002 | +1.0 |
| 1.31 | 1.31 | 0.534 | 0.003 | 0.0 |
| 1.50 | 1.51 | 0.611 | 0.002 | +0.7 |
| 1.69 | 1.65 | 0.669 | 0.003 | −2.4 |
| 1.88 | 1.85 | 0.749 | 0.004 | −1.6 |
| 2.07 | | 0.807 | 0.002 | |
| 2.26 | | 0.864 | 0.002 | |
| 2.63 | | 0.95 | 0.010 | |
| 2.82 | | 0.99 | 0.013 | |
| 3.38 | | 0.15 | 0.018 | |

* These values were calculated by use of 0.405 of average value, from 0.19 to 1.88 p. p. m. $HNO_2$, of absorbances calculated per one p. p. m. $HNO_2$.

** These values are the averages of six replicate determinations.

*** The standard deviations were calculated by the equation, $\sigma = \sqrt{\sum d^2/(n-1)}$, $d$ being the deviation of each absorbance measured from the average and $n$ the number of measurements.

**Calibration Curve and Precision.** — In order to construct a calibration curve and to determine the precision of the method, fifteen series of six replicate determinations were made. The precision, expressed as the standard deviation from the mean for each of the fifteen series, is shown in Table III.

The spectrophotometric sensitivity of the color reaction is 0.004 $\gamma$ of nitrous acid per sq. cm. A more practical sensitivity may be taken as one part of nitrous acid in 10,000,000 parts of solution. A solution containing this concentration has an absorbance of 0.040 unit.

**Beer's Law.** — Beer's law is obeyed up to about 2 p. p. m. of nitrous acid and the absorbances are sufficiently reproducible to allow the range of the determination to be extended to about 3 p. p. m. (see Fig. 5).

**Determination of Nitrous Acid in Synthetic Solutions Containing Various Ions.** — The determination of nitrous acid in the presence of certain other ions has made. The results are given in Table IV.

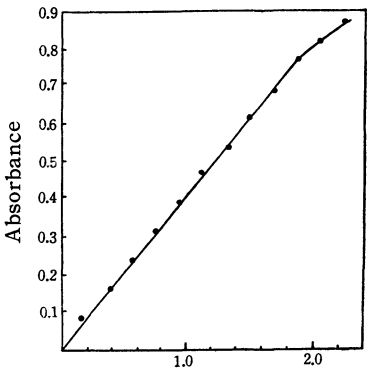



Fig. 5. Beer's law plot.

Table IV. Determination of nitrous acid

| Solutions added | Analyzed p. p. m. | Found $HNO_2$ p. p. m. | Error % |
|---|---|---|---|
| 1) $Fe^{+3}$ | 200 | | |
| $HNO_2$ | 0.20 | 0.21 | +5.0 |
| 2) $Fe^{+2}$ | 400 | | |
| $Fe^{+3}$ | 400 | | |
| $Cu^{+2}$ | 200 | | |
| $HNO_2$ | 0.60 | 0.62 | +3.3 |
| 3) $Cu^{+2}$ | 200 | | |
| $Ni^{+2}$ | 200 | | |
| $Fe^{+3}$ | 500 | | |
| $HNO_2$ | 1.80 | 1.78 | −1.1 |
| 4) $Fe^{+2}$ | 200 | | |
| $Fe^{+3}$ | 200 | | |
| $Ca^{+2}$ | 600 | | |
| $Mg^{+2}$ | 600 | | |
| $HNO_2$ | 0.20 | 0.20 | 0.0 |

**Summary**

A procedure has been developed for the spectrophotometric determination of trace amounts of nitrous acid with disodium 1-(4′-aminobenzeneazo)-2-amino-8-hydroxynaphthalene-2′, 6-disulfonate. The method is accurate and precise and has a sensitivity of 0.004 $\gamma$ of nitrous acid per sq. cm. Beer's law is obeyed up to about 2 p. p. m. of nitrous acid. A study of the effect of many ions on the color reaction has been made. The interference of ferric ions is eliminated by the use of EDTA.

*Himeji Technical Institute, Himeji* (*Y. K.*)

*John Lee Pratt Trace Analysis Laboratory*
*University of Virginia*
*Charlottesville, Va., U. S. A.* (*J. H. Y.*)

# *Estimation of the Energy of Hydrogen Bonds Formed in Crystals. II. Phenols*

By Ariyuki AIHARA

(Received July 20, 1959)

The OH···O bonding is the most familiar of the hydrogen bonds and has already been widely explored; the phenomena in ice (or water), alcohols and acids have been studied in special detail. Nevertheless, data on hydrogen bonds in phenols are not so ample in literatures as those of alcohols and acids, at least so far as the crystalline state is concerned. In this connection the author has chosen, as the first of the series of investigation on the strength of hydrogen bond formed in crystals, a number of phenols of various kinds, and examined them following the procedure proposed in a previous paper[1]. The materials here examined include those the molecules of which have bulky substituents close to hydroxyl groups, preventing the formation of hydrogen bonds, such as *o*-hydroxydiphenyl or 2,4,6-tri-*tert*-butylphenol, and also 1- and 2-naphthols, which may be classified as phenols in a wider sense.

## Experimental

The apparatus used for the measurement of sublimation pressures is the same as was used before[1].

Most of the materials dealt with in this paper are commercial products and purified by fractional sublimation before use. Four of them, i. e. 4-*tert*-butylphenol, 2-*tert*-butyl-4-methylphenol, 2-methyl-4-*tert*-butylphenol and 2,4,6-tri-*tert*-butylphenol were kindly sent by Professor M. Davies, Univ. Wales; these were purified in the same way as the others except 2-methyl-4-*tert*-butylphenol, which was fractionally distilled and measured in liquid state.

## Results and Discussion

**Sublimation Pressures.** — Results of the measurements of sublimation pressures of thirteen phenols are shown in Tables I—XIII, respectively, together with vapor pressure equations obtained by the method of least squares.

TABLE I. SUBLIMATION PRESSURE OF *p*-HYDROXYDIPHENYL

| $T$°K | $P$ (mmHg) $\times 10^4$ | $T$°K | $P$ (mmHg) $\times 10^3$ |
|---|---|---|---|
| 327.6 | 3.88 | 337.7 | 1.10 |
| 329.1 | 4.54 | 339.4 | 1.33 |
| 329.8 | 4.94 | 342.6 | 1.84 |
| 331.2 | 5.67 | 345.6 | 2.46 |
| 335.1 | 8.48 | 347.6 | 3.02 |

$\log P(\text{mmHg}) = 12.056 - 5067.8/T$: m. p. 166°C

TABLE II. SUBLIMATION PRESSURE OF *o*-HYDROXYDIPHENYL

| $T$°K | $P$ (mmHg) $\times 10^3$ | $T$°K | $P$ (mmHg) $\times 10^3$ |
|---|---|---|---|
| 292.0 | 0.819 | 302.4 | 2.71 |
| 294.4 | 1.12 | 304.4 | 3.33 |
| 296.0 | 1.31 | 306.6 | 4.26 |
| 297.3 | 1.55 | 308.3 | 5.13 |
| 299.7 | 2.01 | 310.6 | 6.50 |
| 300.4 | 2.13 | 313.8 | 8.73 |

$\log P(\text{mmHg}) = 11.754 - 4331.0/T$: m. p. 59.0°C

1) A. Aihara, This Bulletin, **32**, 1242 (1959).

TABLE III. SUBLIMATION PRESSURE OF *p*-BENZYLPHENOL

| $T$°K | $P$ (mmHg) $\times 10^4$ | $T$°K | $P$ (mmHg) $\times 10^4$ |
|---|---|---|---|
| 313.8 | 2.75 | 323.8 | 8.48 |
| 315.4 | 3.29 | 326.1 | 10.9 |
| 317.1 | 4.07 | 328.3 | 14.2 |
| 318.5 | 4.71 | 330.7 | 18.1 |
| 320.0 | 5.65 | 332.1 | 21.1 |
| 321.8 | 6.76 | 335.0 | 29.8 |

$\log P\,(\mathrm{mmHg}) = 12.600 - 5072.2/T$: m. p. 85.1°C

TABLE IV. SUBLIMATION PRESSURE OF *p-tert*-BUTYLPHENOL

| $T$°K | $P$ (mmHg) $\times 10^4$ | $T$°K | $P$ (mmHg) $\times 10^4$ |
|---|---|---|---|
| 281.0 | 4.57 | 289.7 | 13.6 |
| 281.5 | 5.04 | 293.5 | 21.3 |
| 282.3 | 5.38 | 295.5 | 27.5 |
| 283.8 | 6.72 | 299.0 | 40.5 |
| 285.1 | 7.78 | 301.2 | 52.4 |
| 287.8 | 10.8 | 303.6 | 67.9 |

$\log P(\mathrm{mmHg}) = 12.332 - 4402.1/T$: m. p. 100.2°C

TABLE V. SUBLIMATION PRESSURE OF 2-*tert*-BUTYL-4-METHYLPHENOL

| $T$°K | $P$ (mmHg) $\times 10^3$ | $T$°K | $P$ (mmHg) $\times 10^3$ |
|---|---|---|---|
| 274.3 | 0.931 | 283.6 | 2.89 |
| 276.5 | 1.22 | 286.1 | 3.85 |
| 279.0 | 1.64 | 288.0 | 4.63 |
| 279.6 | 1.75 | 292.0 | 7.28 |
| 281.0 | 2.13 | 293.4 | 8.46 |

$\log P(\mathrm{mmHg}) = 11.685 - 4035.9/T$: m. p. 53.4°C

TABLE VI. VAPOR PRESSURE OF 2-METHYL-4-*tert*-BUTYLPHENOL

| $T$°K | $P$ (mmHg) $\times 10^3$ | $T$°K | $P$ (mmHg) $\times 10^3$ |
|---|---|---|---|
| 275.3 | 0.692 | 286.9 | 2.59 |
| 277.4 | 0.895 | 288.9 | 3.33 |
| 279.5 | 1.15 | 292.6 | 4.78 |
| 282.9 | 1.69 | 294.5 | 5.74 |
| 285.6 | 2.32 | 297.2 | 8.33 |

$\log P(\mathrm{mmHg}) = 11.199 - 3952.3/T$:
b. p. 125°C (15 mmHg)

TABLE VII. SUBLIMATION PRESSURE OF THYMOL

| $T$°K | $P$ (mmHg) $\times 10^3$ | $T$°K | $P$ (mmHg) $\times 10^3$ |
|---|---|---|---|
| 273.9 | 1.12 | 282.2 | 2.92 |
| 275.1 | 1.26 | 286.6 | 4.86 |
| 276.8 | 1.56 | 290.7 | 7.45 |
| 278.5 | 1.92 | 294.7 | 11.31 |

$\log P(\mathrm{mmHg}) = 11.361 - 3921.0/T$: m. p. 49.5°C

TABLE VIII. SUBLIMATION PRESSURE OF 2,4,6-tri-*tert*-BUTYLPHENOL

| $T$°K | $P$ (mmHg) $\times 10^4$ | $T$°K | $P$ (mmHg) $\times 10^4$ |
|---|---|---|---|
| 291.7 | 3.07 | 301.6 | 9.55 |
| 293.4 | 3.63 | 304.5 | 12.9 |
| 295.2 | 4.52 | 306.2 | 15.6 |
| 297.4 | 5.83 | 309.7 | 22.9 |
| 299.7 | 7.63 | 312.9 | 30.9 |

$\log P(\mathrm{mmHg}) = 11.507 - 4383.1/T$: m. p. 131.2°C

TABLE IX. SUBLIMATION PRESSURE OF *p*-FORMYLPHENOL

| $T$°K | $P$ (mmHg) $\times 10^4$ | $T$°K | $P$ (mmHg) $\times 10^3$ |
|---|---|---|---|
| 312.0 | 3.51 | 322.9 | 1.10 |
| 313.5 | 3.95 | 325.1 | 1.39 |
| 315.1 | 4.89 | 327.4 | 1.74 |
| 316.8 | 5.68 | 331.2 | 2.55 |
| 318.7 | 7.08 | 333.0 | 3.15 |
| 320.8 | 8.95 | 335.9 | 4.32 |

$\log P(\mathrm{mmHg}) = 11.795 - 4762.3/T$: m. p. 118.5°C

TABLE X. SUBLIMATION PRESSURE OF *p*-ACETYLPHENOL

| $T$°K | $P$ (mmHg) $\times 10^4$ | $T$°K | $P$ (mmHg) $\times 10^4$ |
|---|---|---|---|
| 320.5 | 4.07 | 337.5 | 23.8 |
| 323.0 | 5.38 | 339.9 | 32.1 |
| 326.0 | 7.33 | 342.3 | 40.8 |
| 328.3 | 9.47 | 345.0 | 53.0 |
| 332.2 | 14.0 | 347.4 | 65.5 |
| 335.7 | 20.5 | 348.9 | 72.5 |

$\log P(\mathrm{mmHg}) = 12.216 - 5003.5/T$: m. p. 109.8°C

TABLE XI. SUBLIMATION PRESSURE OF *p*-METHOXYPHENOL

| $T$°K | $P$ (mmHg) $\times 10^4$ | $T$°K | $P$ (mmHg) $\times 10^4$ |
|---|---|---|---|
| 278.8 | 3.55 | 288.7 | 12.8 |
| 279.6 | 3.95 | 292.1 | 19.8 |
| 282.1 | 5.33 | 293.9 | 25.4 |
| 283.4 | 6.48 | 295.7 | 30.9 |
| 285.4 | 8.38 | 297.9 | 40.4 |
| 286.9 | 10.2 | 300.1 | 52.9 |

$\log P(\mathrm{mmHg}) = 13.132 - 4624.5/T$: m. p. 56.4°C

TABLE XII. SUBLIMATION PRERSURE OF 1-NAPHTHOL

| $T$°K | $P$ (mmHg) $\times 10^4$ | $T$°K | $P$ (mmHg) $\times 10^4$ |
|---|---|---|---|
| 298.2 | 5.37 | 309.3 | 21.0 |
| 299.6 | 6.49 | 311.3 | 26.6 |
| 300.2 | 7.00 | 312.0 | 28.3 |
| 301.3 | 8.05 | 314.3 | 36.1 |
| 302.4 | 9.25 | 315.1 | 38.9 |
| 303.3 | 10.3 | 317.6 | 51.5 |
| 304.8 | 12.4 | 319.6 | 62.7 |
| 305.3 | 13.1 | 321.8 | 76.7 |
| 306.9 | 15.9 | 323.4 | 89.0 |
| 307.9 | 18.1 | | |

$\log P(\mathrm{mmHg}) = 13.074 - 4873.0/T$,
(below 312.6°K):
$\log P(\mathrm{mmHg}) = 11.526 - 4389.1/T$,
(above 312.6°K):
m. p. 97.0°C: t. p. 39.4°C

TABLE XIII. SUBLIMATION PRESSURE OF 2-NAPHTHOL

| $T$°K | $P$ (mmHg) $\times 10^4$ | $T$°K | $P$ (mmHg) $\times 10^4$ |
|---|---|---|---|
| 298.8 | 1.82 | 307.1 | 5.29 |
| 300.0 | 2.11 | 309.4 | 7.04 |
| 301.9 | 2.73 | 312.0 | 9.57 |
| 302.4 | 2.94 | 314.9 | 13.1 |
| 302.8 | 3.06 | 316.4 | 15.3 |
| 303.6 | 3.36 | 320.0 | 22.5 |
| 304.7 | 3.89 | 324.0 | 33.6 |
| 305.3 | 4.16 | 327.8 | 50.0 |
| 306.5 | 4.90 | 331.8 | 71.4 |

$\log P(\text{mmHg}) = 13.356 - 5108.6/T$, (below 312.3°K):

$\log P(\text{mmHg}) = 11.660 - 4578.9/T$, (above 312.3°K):

m. p. 123°C: t. p. 39.1°C

The linear relation between $\log P$ and $1/T$ has been found quite satisfactory for all the measurements except those of 1- and 2-naphthols, both of which have shown transitional changes of $\log P \sim 1/T$ curves at about 39°C. To confirm this change, careful measurements of sublimation pressures were made repeatedly, and from the intersections of two lines representing $\log P \sim 1/T$ relations for both phases, 39.4 and 39.1°C have been obtained as transition points of 1-naphthol and 2-naphthol, respectively (Fig. 1). As it is not proper to conclude the existence of a transition by the measurement of sublimation pressures alone, especially when the heat of transition is small, a thermal analysis of these substances is now in progress and the results will be published later.

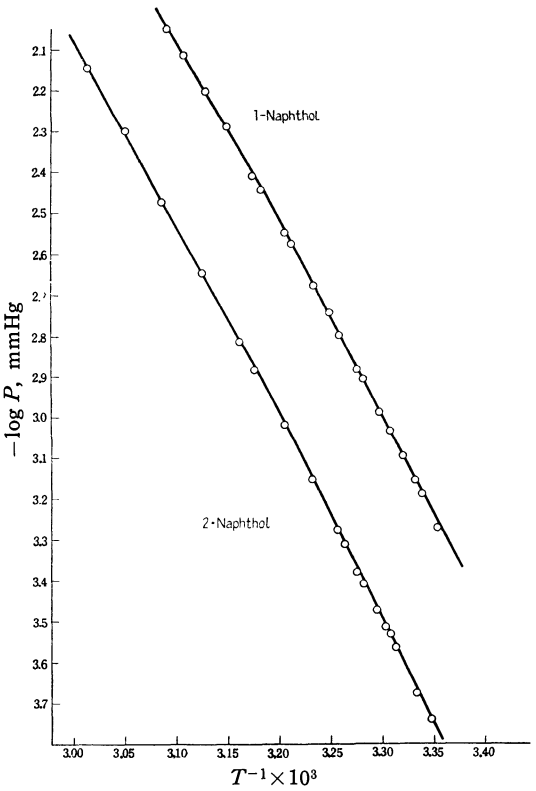



Fig. 1. Sublimation pressures of 1- and 2-naphthols.

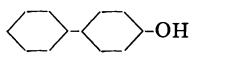
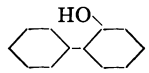
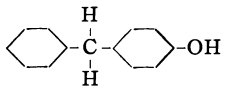
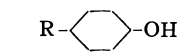
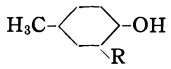
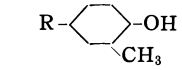
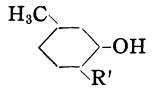
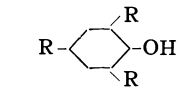
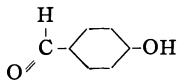
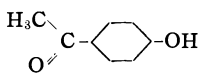
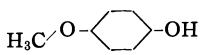
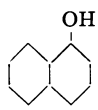
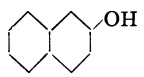
Balson[2] has also measured the sublimation pressure of thymol. However, his result, $\log P = 14.201 - 4766/T$, $\Delta H = 21.8$ kcal./mol., differs appreciably from the author's, the sublimation pressure being lower and the heat of sublimation being greater than the author's in the temperature range of the author's measurement. Considering the structure of this molecule Balson's value for the heat of sublimation of thymol seems to be too large.

**Energy of Hydrogen Bond.**—In Table XIV, the heats of sublimation of thirteen phenols, hypothetical lattice energies obtained assuming the additivity of lattice energies, and the energies of hydrogen bonds estimated by the procedure proposed before are shown by letters, $\Delta H$, $\Delta H'$ and $E$, respectively. The changes of standard free energies at 298.2°K, $\Delta G^{298.2}$, and of entropies, $\Delta S$, on sublimation are also shown in the table.

Let us first consider the case where the formation of OH···O bond seems rather difficult or almost impossible due to the presence of bulky substituted groups, such as phenyl and *tert*-butyl, in the vicinity of OH groups. Four compounds, i. e. *o*-hydroxydiphenyl, 2-*tert*-butyl-4-methylphenol, thymol and 2,4,6-tri-*tert*-butylphenol may fall in this category. As can be seen in Table XIV, the estimated values of hydrogen bonds for *o*-hydroxydiphenyl and 2-*tert*-butyl-4-methylphenol are negligibly small, being in fair agreement with the experimental results of infrared and ultraviolet absorption by Mecke[3], Coggeshall[4] and Josien[5]. According to Coggeshall[4], a phenol with one ortho position occupied by a *tert*-butyl and the other unoccupied, such as 2-*tert*-butyl-4-methylphenol, is partially hindered in forming a hydrogen bond. This means that one might expect, at least, a small

2) E. W. Balson, *Trans. Faraday Soc*. **43**, 54 (1947).
3) R. Mecke and G. Rossmy, *Z. Elektrochem.*, **59**, 866 (1955).
4) N. D. Coggeshall and A. S. Glessner, Jr., *J. Am. Chem. Soc.*, **71**, 3150 (1949); N. D. Coggeshall and E. L. Saier, ibid., **73**, 5414 (1951).
5) M. L. Josien, N. L. Fuson and C. J. Lee, *Phys. Rev.*, **83**, 486 (1951).

TABLE XIV. VALUES OF THERMODYNAMIC FUNCTIONS AND ENERGIES OF HYDROGEN BOND

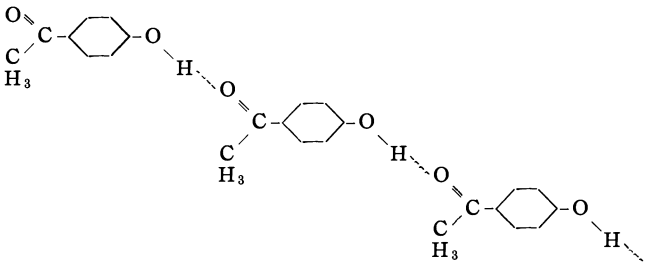
| Compounds | $\Delta H$ kcal./mol. | $\Delta H'$ kcal./mol. | $E$ kcal./mol. | $\Delta G^{298.2°}$ kcal./mol. | $\Delta S$ cal./deg. mol. |
|---|---|---|---|---|---|
|  | 23.19±0.12 | 20.0 | 3.2 | 10.67±0.23 | 42.0±0.4 |
|  | 19.82±0.12 | 20.0 | −0.2 | 7.70±0.24 | 40.6±0.4 |
|  | 23.21±0.15 | 22.0 | 1.2 | 9.94±0.29 | 44.5±0.5 |
|  | 20.14±0.08 | 16.5 | 3.6 | 7.24±0.16 | 43.3±0.3 |
|  | 18.47±0.10 | 18.5 | 0.0 | 6.46±0.21 | 40.3±0.4 |
|  | 18.09*±0.19 | 18.5 | — | 6.74*±0.38 | 38.1*±0.7 |
|  | 17.94±0.09 | 16.5 | 1.4 | 6.37±0.18 | 38.8±0.3 |
|  | 20.06±0.12 | 27.5 | −7.4 | 8.29±0.24 | 39.5±0.4 |
|  | 21.79±0.18 | 14.5 | 7.3 | 9.63±0.35 | 40.8±0.6 |
|  | 22.90±0.16 | 16.5 | 6.4 | 10.16±0.31 | 42.7±0.5 |
|  | 21.16±0.10 | 15.0 | 6.2 | 7.17±0.20 | 46.9±0.3 |
|  | 22.30±0.17<br>(20.08±0.32) | 17.5 | 4.8 | 8.39±0.33<br>(8.28±0.62) | 46.6±0.6<br>(39.6±1.0) |
|  | 23.38±0.12<br>(20.95±0.18) | 17.5 | 5.9 | 9.09±0.24<br>(8.97±0.35) | 47.9±0.4<br>(40.2±0.6) |

R=C(CH$_3$)$_3$, R′=CH(CH$_3$)$_2$

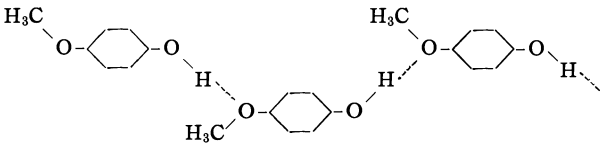
* For liquid state.

value of hydrogen bond energy for this compound instead of zero as shown in Table XIV. This discrepancy must be partly due to the difference in the states of the compound when it was examined, the one being solid and the other in solution, and partly due to the uncertainty of the method of estimation of hydrogen bond energy in this work. Thymol is a phenol with one ortho position occupied by an isopropyl group which is less powerful than *tert*-butyl in hindering the access of OH group of other molecules. Therefore, the energy of hydrogen bond in this compound, 1.4 kcal./mol., would be reasonable. A large negative value was obtained for 2,4,6-tri-*tert*-butylphenol. There will be no objection against believing that the OH group of this molecule is quite free from any intermolecular hydrogen bond, being protected by *tert*-butyl groups on both ortho positions, as was confirmed by Coggeshall[4] and Davies[6], by means of

6) M. Davies and R. J. Meakins, *J. Chem. Phys.*, **26**, 1584 (1957).



or



infrared technique and dielectric method in microwave region, respectively. Therefore, the large difference between $\Delta H$ and $\Delta H'$ for 2,4,6-tri-*tert*-butylphenol must be ascribed to the failure of the assumption, for this compound, of the additivity of lattice energy. This is understandable when the fact is taken into consideration that three *tert*-butyl groups of this molecule are bulky enough to screen a phenyl nucleus, to which they are attached, from the others, thereby causing the decrease of the effect of dispersive force due to the phenyl group to a greater extent. It is likely, therefore, that the *tert*-butyl groups are mainly responsible for dispersive attraction in this case, as was found with a system of $SF_6$ and $CF_4$, where the intermolecular attraction was discussed as due to halogen atoms of the molecules exclusively[7,8].

The heat of vaporization of 2-methyl-4-*tert*-butylphenol, 18.1 kcal./mol., is almost the same as the heat of sublimation of 2-*tert*-butyl-4-methylphenol, 18.5 kcal/mol.; this means that the OH···O bond in the crystal of the former should be stronger than that of the latter, as predicted from their molecular structures.

The hydrogen bond energies for *p*-hydroxydiphenyl and *p*-*tert*-butylphenol, 3.2 and 3.6 kcal./mol., respectively, are almost of the same order of magnitude, but somewhat smaller than the value obtained for phenol by Nitta and Seki, 4.5 kcal./mol.[9] This is probably due to a steric effect of large substituents in para positions rather than to any change of proton donating (or accepting) power of the OH groups. This effect is much more enhanced in the case of *p*-benzylphenol, obtained energy being 1.2 kcal./mol.

Comparatively large values of the energies of hydrogen bonds were obtained for *p*-formylphenol, *p*-acetylphenol and *p*-methoxyphenol, i.e. 7.3, 6.4 and 6.2 kcal./mol., respectively. It is interesting to note that these molecules have a possibility of making head-to-tail associations by hydrogen bonds.

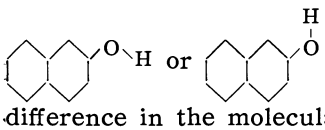
Then, the proton-donating power of OH and, at the same time, the proton-accepting power of O atoms of O=C and O–$CH_3$ groups must be increased appreciably, resulting in the increase of the strength of hydrogen bonds formed. As the crystal structures of these substances have not been analyzed as yet, a definite conclusion can not be drawn with regard to the mode of association of these molecules. Still, it will be quite safe to say that the OH···O bonds formed by these molecules are much stronger than those by other molecules mentioned above. The values for OH···O bonds obtained here can be compared with the energies of association of carboxylic acids in gaseous state, ~7 kcal./mol. (monomer), obtained by Taylor[10] and Nash[11]. Incidentally the $pK_a$ values[12] of *p*-formylphenol, *p*-acetylphenol and *p*-methoxyphenol, which can be taken as the measure of proton-donating power of these molecules, 7.66, 7.95, 10.20, respectively, (in water at 25°C), support the correctness of the order of strength of

7) G. Thomaes, *J. chim. phys.*, **49**, 323 (1952).
8) J. S. Rowlinson, *J. Chem. Phys.*, **20**, 337 (1952).
9) I. Nitta and S. Seki, *J. Chem. Soc. Japan, Pure Chem. Sec.* (*Nippon Kagaku Zasshi*), **69**, 143 (1948); S. Seki, H. Chihara and K. Suzuki, "Hydrogen Bond", Iwanami-Shoten, Publishers, Tokyo (1956), p. 41.
10) M. D. Taylor, *J. Am. Chem. Soc.*, **73**, 315 (1951); M. D. Taylor and J. Bruton, ibid., **74**, 4151 (1952).
11) E. W. Johnson and L. K. Nash, ibid., **72**, 547 (1950); R. E. Lundin, F. E. Harris and L. K. Nash, ibid., **74**, 743, 4654 (1952).
12) E. A. Braud and F. C. Nachod, "Determination of Organic Structures by Physical Methods", Academic Press, Inc., New York (1955), p. 589, 598.

hydrogen bonds for these phenols as revealed here; the $pK_a$ value of phenol is 9.95[12].

The hydrogen bond formed in the crystal of 2-naphthol is stronger than that in 1-naphthol, while the latter seems to be of the same order of strength as the bond in phenol[9]. A similar result was obtained by Nagakura[13] when he studied the proton-donating power of phenols and naphthols by the measurement of near ultraviolet absorption of these substances in appropriate solvents to which some proton-acceptors, such as methylacetate or dioxane were added; his values of the energies of OH···O bonds for phenol, 1-naphthol, and 2-naphthol are 5.3, 5.7 and 6.1 kcal./mol., respectively. These results are rather strange, as Nagakura pointed out, if the fact is considered that the extent of electron migration into the naphthyl ring from oxygen atom is almost of the same order as that into a benzene ring in the case of phenol, and therefore, that the $pK_a$ values[12] and the dipole moments[14-16] of these three compounds are identical; $pK_a$=9.95, 9.85, 9.93 in water at 25°C, $\mu$=1.5, 1.4, 1.5 D, respectively.

The author is inclined to presume that the main factor differentiating 1-naphthol from 2- with regard to the power of forming hydrogen bond is steric hindrance due to a hydrogen atom at 8-position in case of 1-naphthol. Thus, the OH group must be obliged to take only such a direction as to be opposite to the 8-position of the naphthyl nucleus. On the other hand, the OH group in 2-naphthol is quite free from such hindrance as mentioned above, and can take either of the directions,



difference in the molecular structure.

In this connection a comment will be made of the transitions found with 1- and 2-naphthol. The fact of interest is that the transition points of these substances, 39.4 and 39.1°C, respectively, are very close to the melting point of phenol, 40.8°C, and that the heats of transition, 2.2 and 2.4 kcal./mol., respectively, are almost of the same order as the heat of fusion of phenol, 2.7 kcal./mol.[17] This would mean that the transitions and melting of the above substances might occur under the same mechanisms. It is most likely that intramolecular rotation about C–O bond[18] takes place at the melting point of phenol thereby leading to a less ordered state of liquid. As the O–H groups are bound to each other through chains of hydrogen bonds, a rotating part of the molecule will be mostly phenyl nucleus. That the change of entropy on melting at 40.8°C, 8.6 cal./deg. mol.[17], is almost the same as that of benzene at 5.5°C[17], and smaller than that of thiophenol, 10.5 cal./deg. mol. at −14.9 °C[17], may support the above argument. In the case of 1- and 2-naphthol, the onset of intramolecular rotations would lead to a transition in the crystalline states, but not to melting, because the effect of dispersive forces due to naphthyl rings is strong, as was found in the present experiment. Detaits will be published later.

## Summary

The energies of hydrogen bonds formed in the crystalline state of twelve phenols have been estimated by a procedure proposed in a previous paper. The values of energy range from zero to 7 kcal./mol. depending upon the difference of molecular structures: the phenols with bulky substituents in the vicinity of OH groups are non- or weakly-hydrogen-bonded, while those with carbonyl or methoxy groups at para positions are strongly bonded presumably by head-to-tail association. The other phenols fall between the two extremes. Incidentally it is interesting that the highest values of OH···O bond are rather close to the energies of association of carboxylic acids in the gaseous state.

With 1- and 2-naphthols, a parallel relation between the transitions of the above substances and the melting of phenol has been pointed out.

The author is grateful to Professor M. Davies for sending some of the samples

13) S. Nagakura, *J. Chem. Soc. Japan, Pure Chem. Sec.* (*Nippon Kagaku Zasshi*), **74**, 153 (1953); ibid., **75**, 734 (1954); S. Nagakura and M. Gouterman, *J. Chem. Phys.*, **26**. 881 (1957).

14) R. Mecke and K. L. Schupp, *Z. Elektrochem.*, **52**, 54 (1948).

15) S. Nagakura and H. Baba, *J. Am. Chem. Soc.*, **74**, 5693 (1952).

16) R. J. W. Le Fèvre, "Dipole Moment", Methuen & Co., Ltd., London (1953), p. 133.

17) The Chemical Society of Japan, "A Handbook of Chemistry (Kagaku Binran)", Maruzen Co., Ltd., Tokyo (1958), p. 709, 710.

18) A potential barrier hindering the rotation of OH group in phenol is known to amount to 3.2 kcal./mol. [T. Nishikawa, *J. Jap. Chem.* (*Kagaku·no·Ryôiki*), **13**, 385 (1959)]; in 2,4,6-tri-*tert*-butylphenol it is 2.2 kcal./mol. [R. J. Meakins, *Trans. Faraday Soc.*, **52**, 320 (1956)].

dealt with in this work. The cost of the work was partly defrayed by the financial support of the Ministry of Education to which the author's thanks are due.

*Department of Chemistry*
*Faculty of Liberal Arts & Science*
*Shinshu University*
*Agata-machi, Matsumoto*

# *Die absolute Konfiguration des Phyllodulcins*

Von Hisao ARAKAWA

(Eingegangen am 30. April 1959)

Es sind verhältnismässig geringere Dihydroisocoumarinderivate in der Natur gefunden worden; als erstes hatten Asahina und Asano[1] 1931 die Struktur des Phyllodulcins (I), des Süßstoffs der Blätter von *Hydrangea macrophylla* Seringe var. *Thunbergii* MAKINO („Amacha"), festgestellt; seither sind Hydrangenol[1,2], Ochracin[3] (Mellein)[4,5], 3-Me-6-MeO-8-hydroxy-3,4-dihydroisocoumarin[6] und Bergenin[7] als Dihydroisocoumarinderivat charakterisiert und synthetisch sichergestellt worden.

Zur Aufklärung der Beziehung zwischen der optischen Aktivität und der absoluten Konfiguration der Verbindungen dieser Reihe, wählte der Verfasser als Repräsentanten das Phyllodulcin zuerst aus, und beabsichtigte die absolute Konfiguration ihres C-3-Atoms zu bestimmen.

Anderseits hatten vor einigen Jahren Hardegger et al.[8] durch erschöpfende Ozonisierung die absolute Konfiguration des (+)-Catechins, eines Naturstoffs von $C_6$-$C_3$-$C_6$-Gerüst, ähnlich wie I sichergestellt, also wünschte der Verfasser I dieser Methode zu unterwerfen.

Aber es ist schwer, optisch reinstes Präparat von I zu gewinnen. Das von Asahina et al.[1,9] als stärkst drehbares erhaltene Phyllodulcin zeigte den Schmerzp. 120° und $[\alpha]_D$ +67.7~69.70, aber da hatte man nur eine geringere Masse; und es ist dem Verfasser gelungen als stark drehbares Präparat Prismen von Schmerzp. 119~121°C und $[\alpha]_D$ +70.7~80.8°, ausserdem als schwach drehbare Kristalle von $[\alpha]_D$ +22.4° zu erhalten.

Deshalb wurde Phyllodulcin von $[\alpha]_D$ +70.7~80.8° in Essigsäure einer Ozonisierung unterworfen und Oxydation mit Peressigsäure, Entfernung der Oxalsäure und kontinuierliches Extrahieren mit Äther führten zu Äpfelsäure*. Die Veresterung der Säure mit Diazomethan lieferte Methylester von $[\alpha]_D$ +6.5°**, dessen IR-Spektrum mit solchem der authentischen DL-Äpfelsäure identisch ist. Schließlich führte Ammonolyse des Esters zu prismatischem Kristall von Schmerzp. 154~155°C, $[\alpha]_D$ +56.7°. Durch Mischprobe, Vergleichen des IR-Spektrums mit solchem des authentischen Präparates von *R*-Äpfelsäure und spezifische Drehung, ist es sichergestellt, daß das *R*-Äpfelsäure diamid gewonnen worden ist.

Mit der Isolierung der *R*-Äpfelsäure (II) ist es nun bestimmt, daß die absolute Konfiguration des C-3 in Phyllodulcin *R*-Konfiguration ist.

1) Y. Asahina und J. Asano, *Ber.*, **62**, 171 (1929); **63**, 429, 2059 (1930); **64**, 1252 (1931).

2) Hydrangenol: Inhaltstoff von *Hydrangea Hortensia* DC. var. *Otakusa* MAXIM.

3) Stoffwechselprodukt von *Aspergillus ochraceus;* E. Nishikawa, *J. Agric. Soc. Japan* (*Nippon Nôgei-kagaku Kaishi*), **9**, 772, 1059 (1933).

4) Stoffwechselprodukt von *Aspergillus melleus* YUKAWA; T. Yabuta und Y. Sumiki. ebenda. **9**, 1264 (1933); **10**, 703 (1934).

5) J. Blair and G. T. Newbold, *J. Chem. Soc.*, **1955**, 2871.

6) Inhaltstoff der in der Kühle bewahrten Möhren; E. Sondheimer, *J. Am. Chem. Soc.*, **79**, 5036 (1957).

7) J. E. Hay und L. J. Haynes, *J. Chem. Soc.*, **1958**, 2231.

8) E. Hardegger, H. Gempeler und A. Zürst, *Helv. Chim. Acta*, **40**, 1819 (1957).

9) Y. Asahina und S. Ueno, *J. Pharm. Soc. Japan* (*Yakugaku Zasshi*), Nr. **408**, 146 (1916); *Chem. Abstr.*, **10**, 1524 (1916).

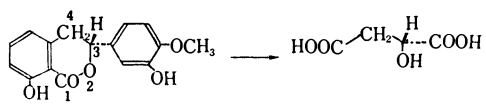
* Papierchromatographisch charakterisierte man als Äpfelsäure. Noch dazu wurde aus dem Kristall von $[\alpha]_D$+22.4° Äpfelsäure als Kristalle erhalten und ihre IR-Spektren stimmten mit solchen der authentischen DL-Äpfelsäure überein und ihre Drehungen in 10-proz. Ammoniummolybdat zeigten links drehend bis $[\alpha]_D$−46.3°. Darum ist die erhaltene Säure ein Gemisch von DL-Körper mit wenigem D-Körper, denn es ist bekannt[10], daß der Drehungssinn einer optisch aktiven Äpfelsäure sich in der Lösung von Ammoniummolybdat umkehrt und ihr Drehungsvermögen mehr als 10-mals vergrößert worden ist.

10) H. D. Dakin, *J. Biol. Chem.*, **59**, 9 (1924).

** Aus dem Phyllodulcin von $[\alpha]_D$+22.4° wurde Methylester von $[\alpha]_D$+2.3° erhalten. (s. Versuche).

TABELLE I

| Fraktion (Ausbeute) | Schmerzp. °C | Optische Aktivität (in Aceton) | Analysenwert | Ber. für $C_{16}H_{14}O_5$ |
|---|---|---|---|---|
| A (11.7 g) | 129～130 | $[\alpha]_D^{16}$ +22.4° (c=1.16) | C 67.27<br>H 5.10 | |
| B ( 1.0 g) | 118～119 | $[\alpha]_D^{19}$ +71.7° (c=1.14) | C 67.06<br>H 5.10 | C 67.12<br>H 4.93 |
| C ( 2.8 g) | 119～121 | $[\alpha]_D^{13}$ +70.7° (c=1.02) | C 67.16<br>H 5.08 | |
| D ( 1.7 g) | 120～121 | $[\alpha]_D^{17}$ +80.8° (c=1.14) | C 66.97<br>H 5.13 | |



(I) (II)

## Beschreibung der Versuche

**Extrahieren des Phyllodulcins.**—Der zu 5.5 kg käufliche „Amacha" wurde mit essigsäurehaltigem wässer. Methanol extrahiert (einmal, einige Tage lang). Nach im Vakuum Abdampfen des Methanols ausgeschiedene grüne rohe Kristalle wurden mit Äther, Chloroform, Äthanol und Methanol gereinigt. Die Kristalle jeder Fraktion wurden mehrmals fraktioniert aus Äthanol umkristallisiert. Es wurden die Prismen erhalten, die rein süß schmecken (Tabelle I).

Die IR-Spektren von B, C, D in Nujol stimmen überein. Die IR-Spektren von A und B in Chloroform sind identisch.

**Ozonspaltung von Fraktion A $[\alpha]_D$ +22.4°.**—Durch eine Lösung von Fraktion A (10 g) in 100 ccm 90-proz. Essigsäure wurde bei 5°C Ozon geleitet. Die Lösung färbte sich bald dunkelbraun und hellte dann auf, schließlich wurde sie nach 67 Stdn. ganz farblos und teils kristallisierte Oxalsäure, die bei 98～100°C schmolz und durch Mischprobe mit authentischem Präparat identifiziert wurde. Nach Zugabe von 15 ccm Perhydrol wurde die Lösung 24 Stdn. lang stehen gelassen und mit 50 ccm Wasser versetzt, dann wurde die Lösung nach Hardegger et al.[8] behandelt und von Oxalsäure befreit und dann im Vakuum eingedampft. Der erhaltene Rückstand wurde nach Zugabe von Wasser wiederholt im Vakuum eingedampft, und der getrocknete Rückstand (6 g) in warmem Wasser gelöst, und dann mit Äther kontinuierlich extrahiert.

Nach Abdampfen von Äther und nack Trocknen dann abfiltriert. Der erhaltene gelbe Rückstand betrug 470 mg. Dreimaliges Umkristallisieren aus Methanol gab 60 mg fast farblose Prismen von Schmerzp. 154～155°C, $[\alpha]_D^{13}$ +56.7° (c=1.18 in Methanol).

war der Extrakt größtenteils kristallisiert. Fraktioniertes Umkristallisieren aus Essigester gab farblose Kristalle (Tabelle II).

TABELLE II

| Schmerzp. C° | Ausbeute g | Spezifisches Drehungsvermögen in 10-proz. Ammoniummolybdat |
|---|---|---|
| 131～132 | 0.3 | —*** |
| 125～127 | 0.2 | $[\alpha]_D^{13}$ −4.9° (c=3.05) |
| 119～121 | 0.4 | $[\alpha]_D^{25}$ −11.7° (c=5.03) |
| 113～116 | 0.1 | $[\alpha]_D^{12}$ −46.3° (c=1.12) |

*** Misch-Schmerzp. mit authentischer DL-Äpfelsäure: 131～132°C.

Nach Trocknen des Kristalls von Schmerzp. 113～116°C bei 80°C im Vakuum.

$C_4H_6O_5$

| | | | | |
|---|---|---|---|---|
| Ber. | C | 35.83 | H | 4.51 |
| Gef. | C | 35.85 | H | 4.63 |

Die Mutterlauge wurde in Vakuum-Exsiccator abgedampft, wonach der Rückstand in Methanol gelöst, mit Diazomethan verestert und mit Natriumsulfat getrocknet. Nach Vorlauf von Kochp. 62°C/2 mmHg wurde 490 mg Hauptfraktion von Kochp. 110～111°C/10 mmHg, $[\alpha]_D^{13}$ +2.7° (c=16.3 in Methanol) erhalten.

$C_6H_{10}O_5$

| | | | | |
|---|---|---|---|---|
| Ber. | C | 44.44 | H | 6.22 |
| Gef. | C | 44.19 | H | 6.42 |

Das IR-Spektrum stimmte mit solchem des authentischen DL-Äpfelsäuredimethylesters von Kochp. 115～117°C/14 mmHg (in $CS_2$, $CCl_4$) überein.

**Abbau der Fraktionen B, C und D von $[\alpha]_D$ +70.7～80.8° mit Ozon und Isolierung von *R*-Äpfelsäure als Diamid aus dem Ätherextrakt.**—Durch eine Lösung von 5.2 g Kristalle (0.9 g B+2.7 g C+1.6 g D) in 50 ccm 95-proz. Essigsäure wurde 3-proz. Ozon 31 Stdn. lang eingeleitet, wonach sie mit 7.5 ccm Perhydrol versetzt, 18 Stdn. lang stehen gelassen und dann wie oben behandelt, mit Äther 20 Stdn. extrahiert. Der erhaltene Rückstand wog 3.3 g und sein Papierchromatogramm (Xylol, Phenol, 85-proz. Ameisensäure, 5:5:2)[11] lieferte die Flecke der Äpfelsäure. Seine Methanollösung wurde dann verestert. Die Destillation des getrockneten Methylesters ergab bei 111～112°C/10 mmHg 700 mg von $[\alpha]_D^{9}$ +6.5° (c=12.89). Das IR-Spektrum stimmt mit solchem von DL-Äpfelsäuredimethylester überein.

666 mg Methylester wurde in verzweigtem Reagenzrohr (unter Abkühlung durch eine Mischung von fester Kohlensäure mit Äthanol) mit 12 ccm von verflüssigtem Ammoniak aus der Bombe versetzt und dann das Reagenzrohr in einem Autoklav geschlossen. Nach Stehenlassen bei Zimmertemperatur 24 Stdn. lang, dampfte man Ammoniak ab und mischte mit Äther und

11) Vgl. H. Kalbe, *Z. physiol. Chem.*, **297**, 19 (1954).

$C_4H_8O_3N_2$

| | | | | | |
|---|---|---|---|---|---|
| Ber. | C | 36.36 | H | 6.10 | N 21.20 |
| Gef. | C | 36.59 | H | 6.34 | N 21.07 |

Misch-Schmerzp. mit authentischem Präparat[12] von Schmerzp. 156°C, $[\alpha]_D$ +60.3° zeigte 154~156°C. Beide IR-Spektren sind praktisch ganz identisch.

12) Herrn Ryonosuke Yoshida, Naturwissenschaftliche Fakultät, Universität Osaka, sei für die freigebige Überlassung des Präparates von *R*-Äpfelsäurediamid gedankt.

Herrn Prof. Dr. Masao Nakazaki danke ich bestens für sein reges Interesse an der vorliegenden Arbeit und seine Unterstützung durch wertvolle Hinweise.

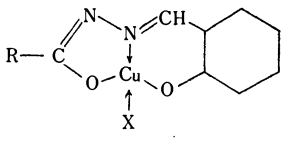
*Organisch-chemisches Laboratorium*
*Institute of Polytechnics*
*Osaka City University*
*Kita-ku, Osaka*

# *Über die Kupferkomplexsalze der Salicylaldehyd-acylhydrazone**

Von Hiroshi OHTA

(Eingegangen am 30. Mai 1959)

In der vorangehenden Mitteilung[1] wurde gezeigt, daß die Salicylaldehyd-aroylhydrazone, welche tuberkulostatische Wirkung besitzen[2], mit 2-wertigem Kupferion im ammoniak-alkalischen Medium die Kupferkomplexsalze der Formel I liefern (I[A]).



I

[A] R=Arylreste, X=$NH_3$ od. $C_5H_5N$.

[B] R= X=$NH_3$ od. 0.

| | | | |
|---|---|---|---|
| (1) | —H | (7) | $-(CH_2)_4\cdot CH_3$ |
| (2) | $-CH_3$ | (8) | $-(CH_2)_6\cdot CH_3$ |
| (3) | $-CH_2\cdot CH_3$ | (9) | $-(CH_2)_8\cdot CH_3$ |
| (4) | $-(CH_2)_2\cdot CH_3$ | (10) | $-(CH_2)_{14}\cdot CH_3$ |
| (5) | $-(CH_2)_3\cdot CH_3$ | (11) | $-CH_2\cdot C_6H_5$ |
| (6) | $-CH_2\cdot CH\cdot (CH_3)_2$ | (12) | $-CH_2\cdot O\cdot C_6H_5$ |

Werden die Aroylreste mit den Acylresten ersetzt, so lassen sich die Salicylaldehyd-acylhydrazone erhalten, die auch, als Chemotherapeutica, in Frage kommen. Durch Anfügen der Acylreste mit längeren Ketten sollen Salicylaldehyd-acylhydrazone lipophile Eigenschaft gewinnen, die den Angriff der Substanzen auf wachsgepanzerte Bakterien erleichtern könnte.

In der vorliegenden Mitteilung sollen die Salicylaldehyd-acylhydrazone, worunter einige noch nicht berichtet worden sind, und deren Kupferkomplexsalze beschrieben werden.

Neue Acylhydrazine und Salicylaldehyd-acylhydrazone wurden in üblicher Weise dargestellt; Acylhydrazine durch Erhitzen der Fettsäureester mit Hydrazinhydrat, Salicylaldehyd-acylhydrazone durch Gemisch des Salicylaldehydes und der Acylhydrazine. Als Ausgangsstoffe für die Komplexsalzdarstellung wurden Salicylaldehyd-formylhydrazon, -acetylhydrazon, -propionylhydrazon, -*n*-butyrylhydrazon, -*n*-valerylhydrazon, -*i*-valerylhydrazon, -*n*-capronylhydrazon, -*n*-caprylylhydrazon, -*n*-caprinylhydrazon, -*n*-palmitylhydrazon, -phenylacetylhydrazon und -phenoxyacetylhydrazon herangezogen. Alle diese Hydrazone sind schneeweiß, und in Äthanol und anderen organischen Lösungsmitteln sehr leicht löslich; sie lassen sich aus Äthanol leicht umkristallisieren.

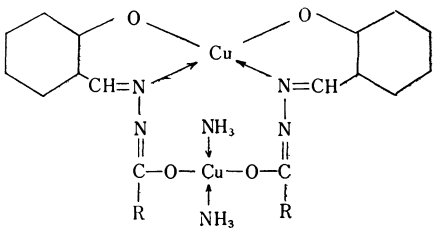
Die Komplexsalze wurden, wie im Versuchsteile näher beschrieben, durch Gemisch der Hydrazone in Äthanol und des Kupferacetats in wässrigem Ammoniak dargestellt. Sie bilden hell- bzw. dunkelgrüne Kristalle, und nach den analytischen Daten kommt ihnen eine allgemeine empirische Formel $[C_8H_5O_2N_2RCu\cdot(NH_3)_{0\text{ oder }1}]$ zu. Die Komplexsalze des Salicylaldehyd-*n*-palmitylhydrazons, -phenylacetylhydrazons und -phenoxyacetylhydrazons enthalten je 1 Mol. Ammoniak und geben es (mit Ausnahme vom Komplexsalze des Salicylaldehyd-phenoxyacetylhydrazons) beim Erhitzen im Vakuum leicht ab; deren

* Organische Metallkomplexsalze III. Vorgetragen in Kyoto auf der XII. Jahresversammlung der Japanischen Chemischen Gesellschaft, am 3. April 1959.

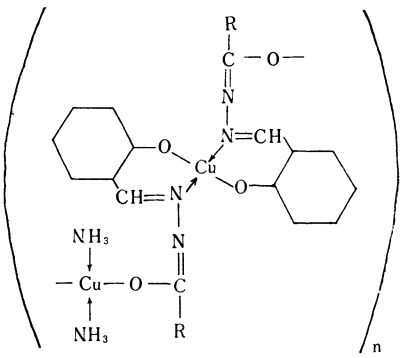
1) II. Mitteilung: H. Ohta, Dieses Bulletin, **31**, 1056 (1958).

2) Ng. Ph. Buu-Hoï und Mitarbb., *J. Chem. Soc.*, **1953**, 1358.

Farbe schlägt vom Hellgrün nach Olivgrün um. Das Ammoniak muß daher koordinativ mit dem Kupferatom gebunden sein. Aus Rücksicht auf die Koordinationszahl des Kupfers und die Struktur des Liganden können diese Komplex salze mit der Formel I formuliert werden. Die Formeln II und III werden als unwahrscheinlich ausgeschlossen, weil 1) die Ausbildung der



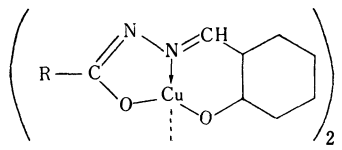
II



III

Salze von der Formel II bzw. III sterisch nicht oder sehr schwer möglich ist, und 2) die Salze der Formel III nur als amorphes Pulver erhalten würden.

Die anderen übrigen Komplexsalze enthalten kein Ammoniak und sind dunkelgrün gefärbt. Diese und diejenigen, die durch Erhitzen im Vakuum das Ammoniak verloren haben, gehören zu den „Kupferkomplexsalzen der Koordinationszahl 3". Von ihnen sind die des Salicylaldehyd-*n*-caprinylhydrazons und -*n*-palmitylhydrazons in Campher löslich. Die Molekulargewichte beider Salze wurden nach Rast durch die kryoskopische Methode bestimmt. Die Resultate zeigten, daß sie dimer sind. Da die Formel II undenkbar ist, könnten diese Komplexsalze mit der Formel IV zum Ausdruck gebracht werden. Wahrscheinlich zwischen den beiden Kupferatomen wäre irgendeine Art Wechselwirkung vorhanden. Auch die magnetischen Messungen



IV

wurden mit diesen zwei Verbindungen in festem Zustand ausgeführt. Wegen der technischen Schwierigkeiten — *N*-Salicyliden-*N'*-*n*-palmityl-hydrazino-kupfer (II) konnte nicht, *N*-Salicyliden-*N'*-*n*-caprinil-hydrazino-kupfer(II) konnte nur äußerst schwer, pulverisiert werden — wurden jedoch keine befriedigenden Ergebnisse erhalten.

## Beschreibung der Versuche

**Acylhydrazine und Salicylaldehyd-acylhydrazone.** —Acylhydrazine können in üblicher Weise durch Kochen von Fettsäureestern mit etwas überschüssigem Hydrazinhydrat leicht synthetisiert werden. Die neuen Acylhydrazine wurden als Salicylidenderivate (Salicylaldehydacylhydrazone) charakterisiert.

Salicylaldehyd-acylhydrazone werden durch Gemische berechneter Mengen Salicylaldehyd und Acylhydrazine in Äthanol dargestellt und daraus umkristallisiert.

*Salicylaldehyd-acetylhydrazon.* — Weiße Nadeln. Schmp. 201~202°C (unkorr.).

$C_9H_{10}O_2N_2$

Ber. C 60.66 H 5.66 N 15.72
Gef. C 60.84 H 5.81 N 15.71

*Salicylaldehyd-n-butyrylhydrazon.*—Weiße, feine Nadeln. Schmp. 138~139°C (unkorr.).

$C_{11}H_{14}O_2N_2$

Ber. C 64.06 H 6.84 N 13.58
Gef. C 64.21 H 7.01 N 13.64

*Salicylaldehyd-n-valerylhydrazon.*—Weiße, feine Nadeln. Schmp. 140~141°C (unkorr.).

$C_{12}H_{16}O_2N_2$

Ber. C 65.43 H 7.32 N 12.72
Gef. C 65.68 H 7.18 N 12.79

*Salicylaldehyd - n - capronylhydrazon.* — Weiße Nadeln. Schmp. 123~124°C (unkorr.).

$C_{13}H_{18}O_2N_2$

Ber. C 66.64 H 7.74 N 11.96
Gef. C 66.86 H 7.71 N 12.09

*Salicylaldehyd-n-caprylhydrazon.*—Weiße, zarte Nadeln. Schmp. 104~105°C (unkorr.).

$C_{15}H_{22}O_2N_2$

Ber. C 68.67 H 8.45 N 10.68
Gef. C 68.94 H 8.22 N 10.67

*Salicylaldehyd - n - caprinylhydrazon.* — Weiße Nadeln. Schmp. 101~102°C (unkorr.).

$C_{17}H_{26}O_2N_2$

Ber. C 70.31 H 9.02 N 9.65
Gef. C 70.10 H 8.92 N 9.64

*Salicylaldehyd - phenoxyacetylhydrazon.* — Weiße, feine Nadeln. Schmp. 171~172°C (unkorr.).

$C_{15}H_{14}O_3N_2$

Ber. C 66.66 H 5.22 N 10.36
Gef. C 66.53 H 5.09 N 10.25

**Kupferkomplexsalze.** — *N-Salicyliden-N'-formyl-hydrazino-kupfer (II)*.—Man gibt 4 ccm Ammoniakwasser (28%) zur Lösung von 164 mg Salicylaldehyd-formylhydrazon in 6 ccm Äthanol. Die Farbe der Lösung wird gelb. Zu dieser gelben Lösung setzt man eine Lösung von 200 mg Kupferacetat (Monohydrat) in 5 ccm Äthanol-Ammoniakwasser-Gemische (Volumverhältnis: 2 : 1) hinzu. Die so entstandene, grünschwarze Lösung engt man auf dem Wasserbade allmählich ein. Dunkelgrüne Nädelchen. Man kann sie durch Lösen in Alkohol-Ammoniakwasser-Gemisch und Eindunsten der Lösung auf dem Wasserbade reinigen.

$C_8H_6O_2N_2$

Ber. C 42.57 H 2.68 N 12.41 Cu 28.15
Gef. C 42.69 H 3.14 N 12.27 Cu 28.00

*N-Salicyliden-N'-acetyl-hydrazino-kupfer (II)*.— Man fügt zur Lösung von 178 mg Salicylaldehyd-acetylhydrazon in 10 ccm Äthanol eine Lösung von 200 mg Kupferacetat in 5 ccm Ammoniakwasser zu. Es entsteht sofort eine grünschwarze, klare Lösung, die man auf dem Wasserbade einengt. Dunkelgrüne, glänzende Nädelchen.

$C_9H_8O_2N_2Cu$

Ber. C 45.09 H 3.36 N 11.69 Cu 26.51
Gef. C 44.87 H 3.41 N 11.78 Cu 26.37

*N-Salicyliden-N'-propionyl-hydrazino-kupfer (II)*.— Zu einer Lösung von 192 mg Salicylaldehyd-propionyl-hydrazon in 10 ccm Äthanol fügt man eine Lösung von 200 mg Kupferacetat in 5 ccm Ammoniakwasser zu und engt die so erhaltene, grünschwarze, klare Lösung auf dem Wasserbade allmählich ein. Dunkelgrüne Nädelchen.

$C_{10}H_{10}O_2N_2Cu$

Ber. C 47.33 H 3.97 N 11.04 Cu 25.04
Gef. C 47.23 H 4.29 N 11.26 Cu 24.98

*N-Salicyliden-N'-n-butyryl-hydrazino-kupfer (II)*.— Man fügt zur Lösung von 206 mg Salicylaldehyd-*n*-butyryl-hydrazon in 10 ccm Äthanol, 200 mg Kupferacetat gelöst in 5 ccm Ammoniakwasser zu. Eine schwarzgrüne Lösung entsteht, die man auf dem Wasserbade einengt. Grünschwarze Kristallle.

$C_{11}H_{12}O_2N_2Cu \cdot 1/2\ H_2O$

Ber. C 47.73 H 4.73 N 10.12 Cu 22.96 $H_2O$ 3.25
Gef. C 47.57 H 4.68 N 9.97 Cu 23.24 $H_2O$ 3.28

*N-Salicyliden-N'-n-valeryl-hydrazino-kupfer (II)*.— Man gibt zur Lösung von 220 mg Salcylaldehyd-*n*-valeryl-hydrazon in 10 ccm Äthanol eine Lösung von 200 mg Kupferacetat in 5 ccm Ammoniakwasser. Es entsteht eine schwarzgrüne, klare Lösung die man auf dem Wasserbade allmählich einengt. Dunkelgrüne, fast schwarz erscheinende Plättchen.

$C_{12}H_{14}O_2N_2Cu$

Ber. C 51.15 H 5.01 N 9.94 Cu 22.55
Gef. C 51.02 H 5.09 N 9.73 Cu 22.71

*N-Salicyliden-N'-i-valerly-hydrazino-kupfer (II)*.— Dies wird gleicherweise wie beim *N*-Salicyliden-*N'*-*n*-valeryl-hydrazino-kupfer(II) dargestellt. Dunkelgrüne, fast schwarze, glänzende Plättchen.

$C_{12}H_{14}O_2N_2Cu \cdot H_2O$

Ber. C 48.07 H 5.38 N 9.34 Cu 21.19 $H_2O$ 6.01
Gef. C 48.86 H 5.54 N 9.48 Cu 21.25 $H_2O$ 5.98

*N-Salicyliden-N'-n-capronyl-hydrazino-kupfer (II)*. —Dies wird ähnlich wie bei den obenerwähnten Komplexsalzen, aus 234 mg Salicylaldehyde-*n*-capronylhydrazon in 10 ccm Äthanol und 200 mg Kupferacetat in 5 ccm Ammoniakwasser dargestellt. Schwärzlich-dunkelgrüne Kristalle.

$C_{13}H_{16}O_2N_2Cu \cdot 1/2\ H_2O$

Ber. C 51.22 H 5.62 N 9.19 Cu 20.84 $H_2O$ 2.96
Gef. C 51.31 H 5.86 N 9.00 Cu 20.63 $H_2O$ 3.00

*N-Salicyliden-N'-n-caprylyl-hydrazino-kupfer (II)*. —Man trägt in eine Lösung von 262 mg Salicylaldehyd-*n*-caprylylhydrazon in 10 ccm Äthanol, 200 mg Kupferacetat gelöst in 5 ccm Ammoniakwasser ein und fügt zur so erhaltenen, grünschwarzen Lösung 15 ccm Ammoniakwasser allmählich zu. Grüne, zarte Nadeln, die aber keine stöchiometrische Menge Ammoniak enthalten. Analysiert wurde eine Substanzprobe, die durch 1-stündiges Erhitzen auf 110～120°C/25 mmHg als braunischgrünes Pulver erhalten worden war.

$C_{15}H_{20}O_2N_2Cu$

Ber. C 55.63 H 6.22 N 8.65 Cu 19.62
Gef. C 55.51 H 6.48 N 8.66 Cu 19.52

*N-Salicyliden-N'-n-caprinyl-hydrazino-kupfer (II)*. —Man fügt zur Lösung von 290 mg Salicylaldehyd-*n*-caprinyl-hydrazon in 5 ccm Äthanol eine Lösung von 200 mg Kupferacetat in 5 ccm ammoniakwasser zu. Dunkelgrüne, zarte Nädelchen.

$C_{17}H_{24}O_2N_2Cu$

Ber. C 58.02 H 6.87 N 7.96 Cu 18.05
Gef. C 57.78 H 7.02 N 7.84 Cu 17.94

*N-Salicyliden-N'-n-palmityl-hydrazino-monoammin-kupfer(II)-monohydrat*.—Fügt man zur Lösung von 375 mg Salicylaldehyd-*n*-palmitylhydrazon in 10 ccm Äthanol eine Lösung von 200 mg Kupferacetat in 5 ccm Ammoniakwasser zu, so scheiden sich sogleich graugrüne Kristalle aus, die man aus Äthanol-Ammoniakwasser-Gemische (Volumverhältnis: 2 : 1) umkristallisiert. Hellgraugrüne, zarte Nadeln.

$C_{23}H_{36}O_2N_2 \cdot NH_3 \cdot Cu \cdot H_2O$

Ber. C 58.63 H 8.77 N 8.92 Cu 13.49 $NH_3+H_2O$ 7.44
Gef. C 58.93 H 8.87 N 8.80 Cu 13.15 $NH_2+H_2O$ (1 Stunde auf 110°C/25 mmHg) 7.54

*N-Salicyliden-N'-n-palmityl-hydrazino-kupfer (II)*. —Man erhitzt *N*-Salicyliden-*N'*-*n*-palmityl-hydrazino-monoammin-kupfer(II)-monohydrat eine Stunde auf 110°C/25 mmHg. Dunkelgrüne Nadeln.

$C_{23}H_{36}O_2N_2Cu$

Ber. C 63.35 H 8.32 N 6.42 Cu 14.57
Gef. C 63.31 H 8.56 N 6.42 Cu 14.23

*N-Salicyliden-N'-phenylacetyl-hydrazino-monoammin-kupfer(II)-monohydrat*.—Man fügt zur Lösung von 255 mg Salicylaldehyd-phenylacetylhydrazon in 10 ccm warmem Äthanol, eine Lösung von 200 mg Kupferacetat in 5 ccm Ammoniakwasser zu.

Tabelle

| Verbindung und Molekulargewicht ber. | Einwaage Komplex mg | Einwaage Campher mg | $\Delta T$ °C | Molekulargewicht gef. |
|---|---|---|---|---|
| *N*-Salicyliden-*N'*-*n*-caprinyl-hydrazino-kupfer(II) 351.9×2=703.8 | 3.6 | 40.4 | 5 | 713 |
| | 3.3 | 55.6 | 3.5 | 678 |
| *N*-Salicyliden-*N'*-*n*-palmityl-hydrazino-kupfer(II) 436.1×2=872.2 | 4.5 | 41.8 | 5 | 861 |
| | 4.1 | 43.1 | 4 | 951 |
| | 2.7 | 20.9 | 6 | 864 |

Man engt die so erhaltene, grünschwarze, klare Lösung auf dem Wasserbade ziemlich stark ein und läßt erkalten. Graulich braungrüne Nädelchen.

$C_{15}H_{12}O_2N_2 \cdot NH_3 \cdot Cu \cdot H_2O$

Ber. C 51.35 H 4.88 N 11.98 Cu 18.11 $NH_3+H_3O$ 9.99

Gef. C 51.78 H 5.00 N 11.90 Cu 18.00 $NH_3+H_2O$ (1 Stunde auf 110°C/25 mmHg) 9.90

Das wasser- und ammoniakfreie Salz ist bräunlich grün.

*N-Salicyliden-N'-phenoxyacetyl-hydrazino-monoammin-kupfer(II).*—Man fügt zur Lösung von 270 mg Salicylaldehyd-phenoxyacetylhydrazon in 15 ccm warmem Äthanol, 200 mg Kupferacetat gelöst in 5 ccm Ammoniakwasser zu und läßt erkalten. Aus der anfangs entstandenen, grüschwarzen, klaren Lösung scheiden sich feine, hellbraune Nadeln aus, die auch beim Erhitzen unter vermindertem Drucke (2 Stunden auf 130~140°C/25 mmHg) keinen Gewichtsverlust erleiden.

$C_{15}H_{12}O_3N_2 \cdot NH_3 \cdot Cu$

Ber. C 51.64 H 4.33 N 12.05 Cu 18.21

Gef. C 51.46 H 4.47 N 11.87 Cu 18.30

**Molekulargewichtsbestimmungen an den Komplexsalzen.**—Die Molekulargewichtsbestimmungen wurden nach der Rastschen Methode ausgeführt, wobei die Gefrierpunkte gemessen wurden. Brauchbare Ergebnisse konnten aus Löslichkeitsgründen nur mit dem *N*-Salicyliden-*N'*-*n*-caprinyl-hydrazino-kupfer(II) und dem *N*-Salicyliden-*N'*-*n*-palmityl-hydrazino-kupfer(II) erzielt werden; bei ersterem machte sich Anwendung eines 20-fachen Campherüberschusses nötig.

Die Tabelle zeigt die erhaltenen Werte:

Meinem Lehrer, Herrn Professor Dr. Tokuichi Tsumaki danke ich herzlich für die Unterstützung und Förderung dieser Arbeit. Herrn Dr. Yasushi Koga (Laboratorium für Physikalische Chemie, Chemisches Institut, Naturwissenschaftliche Fakultät, Kyushu Universität) bin ich für die magnetischen Messungen zu großem Dank verpflichtet. Herrn Michio Shido und Frl. Sachiko Indo (Laboratorium der Elementaranalyse, Kyushu Universität) verdanke ich die Durchführung der C-, H- und N-Bestimmungen.

*Chemisches Institut*
*Naturwissenschaftliche Fakultät*
*Universität Kyushu*
*Hakozaki, Fukuoka*

# *Darstellung von o-Diacetylbenzol durch Diels-Alder-Reaktion*

By Eturô MAEKAWA

(Eingegangen am 1. August, 1959)

*o*-Diacylbenzole sind nicht nur als Ausgangsprodukte der Naphthochinonsynthese[1] von präparativer Bedeutung, sondern bilden auch wegen ihrer intensiven Farbreaktion mit Aminosäuren[2,3] und auch mit primären Aminen[4,5] sehr interessante Verbindungen. Die Farbreaktion von *o*-Diacylbenzolen ist so stark, daß man mit ihnen z. B. 20~50 $\gamma$ Aminosäuren[2] oder 1 $\gamma$ aromatische primäre Amine[44] auf Papierchromatogrammen einwandfrei nachweisen kann. Sie lassen sich darstellen aus *o*-*n*-Alkylacylbenzolen durch Oxydation mit Permanganat[1,2] oder aus 3-Alkylphthaliden durch Umsetzung mit Alkylmagnesiumhalogeniden und durch direkte Oxydation

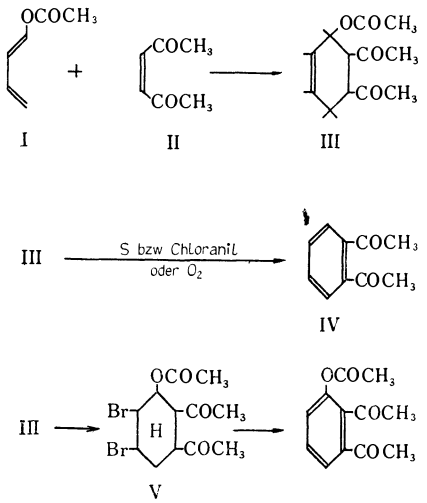
1) F. Weygand, H. Weber und E. Maekawa, *Chem. Ber.*, **90**, 1879 (1957).
2) R. Riemenschneider und C. Weygand, *Monatsh. Chem.*, **86**, 201 (1955).
3) W. Winkler, *Chem. Ber.*, **81**, 256 (1948).
4) F. Weygand, H. Weber und G. Eberhard, *Angew. Chem.*, **66**, 680 (1954).
5) F. Weygand, H. Weber, E. Maekawa und G. Eberhard, *Chem. Ber.*, **89**, 1994 (1956).

des gebildeten Magnesiumsalzes der 1-Oxy-1.3-dialkylphthalane mit Permanganat[1]. Obgleich die Darstellung von *o*-Diacylbenzolen stark verbessert wurde[4,5], geht sie noch immer in ziemlich schlechter Ausbeute vor sich. Außerdem sind die Oxydationsbedingungen bei der ersten Methode so stark, daß diese auf die Ausgangsprodukte mit leicht oxydierbaren Substituenten schwer anwendbar ist. Das zweite Verfahren wird unter milderen Bedingungen durchgeführt, liefert aber nur unreine Produkte.

Wie von F. Weygand u. a. berichtet wurde[1], aromatisiert das Addukt aus 1-Acetoxybutadien-(1.3)[6] und 2.3-Dimethoxy-*p*-benzochinon in siedendem Alkohol automatisch unter Abspaltung von Essigsäure und Wasserstoff zu 2.3-Dimethoxynaphthochinon-(1.4). Diese Tatsache erweckte die Hoffnung, *o*-Diacetylbenzol aus 1-Acetoxybutadien-(1.3) und $\alpha.\beta$-Diacetyläthylen[7,8] durch Diensynthese herstellen zu können. 1-Acetoxybutadien-(1.3) und $\alpha.\beta$-Diacetyläthylen geben beim Kochen der alkoholischen Lösung in guter Ausbeute des Addukt, 3-Acetoxy-1.2.3.6-tetrahydro-1.2-diacetylbenzol, das gegen Erwarten stabil und bei 15 Torr ohne Zersetzung destillierbar ist.

Erhitzt man das Addukt mit Schwefel auf etwa 180°C, so wird zuerst Schwefelwasserstoff- und später Essigsäureentwicklung deutlich bemerkt. *o*-Diacetylbenzol müßte also in zwei Stufen entstanden sein. Aus dem Reaktionsgemisch wird eine schwach gelbe, klebrige Flüssigkeit mit demselben Siedepunkt wie *o*-Diacetylbenzol herausdestilliert. Diese Flüssigkeit, deren Elementaranalyse mit den für *o*-Diacetylbenzol berechneten gut übereinstimmt, zeigt sehr intensive violette Farbreaktion mit Anilin in essigsaurer Lösung in der Kälte und gibt ein Disemicarbazon, das beim Mischschmelzpunkt mit dem reinen *o*-Diacetylbenzol[5] keine Depression zeigt. Obgleich weitere Reinigung dieser Flüssigkeit sehr schwierig war, kristallisierte sie bei längegerem Stehen im Eisschrank—etwa über ein Jahr—zum Teil in schönen Nadeln, die nach einer Umkristallisation aus Petroläther einen Schmelzpunkt von 37°C zeigten[9]. Auch beim Erhitzen des Adduktes in der Luft unter normalem Druck bildete sich *o*-Diacetylbenzol, das als Disemicarbazon identifiziert werden konnte.

Chloranil und dessen Homologe werden oft als Aromatisierungsmittel empfohlen[10,11]. Wenn man das Addukt, 3-Acetoxy-1.2.3.6-tetrahydro-1.2-diacetylbenzol mit zwei molekularer Menge Chloranil in Xylol erhitzt, wird Essigsäureentwicklung beobachtet. Obwohl das Produkt auch starke Farbreaktion mit Anilin in essigsaurer Lösung zeigte und das erwartete *o*-Diacetylbenzol als Disemicarbazon identifiziert werden konnte, ließ es sich noch nicht genügend reinigen. Andere Versuche, z. B. Erwärmen mit Natriumhydrogencarbonat oder mit Selendioxyd, zerstörten die Substanz mehr oder weniger.




Ein Versuch zur Bromierung des Adduktes in der Allylstelle mit *N*-Bromsuccinimid in Tetrachlorkohlenstoff führte nur zur Harzbildung. Während sich beim Versetzen des Adduktes mit Brom in Tetrachlorkohlenstoff ein Harz unter Entwicklung des Bromwasserstoffs bildete—das Reaktionsgemisch zeigte jedoch mit Anilin violette Farbreaktion — wurde durch Versetzen mit Brom unter Zusatz von Pyridin eine kristallinische Dibromverbindung erhalten, die beim Aromatisieren unter Abspalten von Bromwasserstoff 3-Acetoxy-1.2-diacetylbenzol ergeben könne. Das aus der Dibromverbindung durch Erhitzen mit Pyridin hergestellte Produkt zeigte mit Anilin eine violette Farbreaktion und scheint nach Elementaranalyse ein noch unreines Präparat von 3-Acetoxy-1.2-diacetylbenzol zu sein.

6) A. Wacker, Ges. f. Elektrochem. Ind. GmbH., Engl. Pat., 493,196; *Chem. Zentr.*, **1939**, I, 796.
7) G. O. Schenk, *Ber.*, **77**, 661 (1944).
8) K. F. Armstrong und P. Robinson, *J. Chem. Soc.*, **1934**, 1650.
9) Vgl. die zu 3) angegebene Literatur, Fp. 38°C.
10) E. A. Braude, A. G. Brook und R. R. Linstead, *J. Chem. Soc.*, **1954**, 3569.
11) U. Eisner und R. R. Linstead, ebenda, **1955**, 3753.

Bemerkenswert ist, daß das Addukt selbst mit Anilin in essigsaurer Lösung beim Kochen eine intensive rote Farbreaktion zeigt. In der Kälte gibt es in verdünnter Essigsäure nach längerem Stehen mit Anilin eine rote Färbung, die sehr langsam in violette übergeht. Unter Erhitzen der Mischung findet die Veränderung der Farbe viel schneller statt als in der Kälte. Sowohl verschiedene Amine als auch Aminosäuren, die mit *o*-Diacetylbenzol eine violette Farbreaktion zeigen[5], reagierten auch mit dem Addukt zuerst unter einer Rotfärbung: die Farbe wurde beim Stehen langsam tiefer. Mit diesem Addukt konnten $10^{-4}$ bis $10^{-5}$ g primäre Amine auf Papierchromatogramme nachgewiesen werden. Zwar ist die Grenze des Nachweises praktisch gleicher Ordnung wie beim Nachweis mit *o*-Diacetylbenzol, es besteht aber der Nachteil des Adduktes als Nachweisreagens darin, daß für die Färbung längere Zeit benötigt wird. Der Nachteil ist jedoch nicht sehr entscheidend, weil das Addukt als *o*-Diacetylbenzol viel leichter und auch in viel größerem Maßstab hergestellt werden kann.

$\alpha.\beta$-Diacetyläthylen ergab Diels-Alder-Addukte weder mit Furan noch mit 2.3-Dimethoxybutadien-(1.3), soweit versucht wurde.

### Beschreibung der Versuche

**1. $\alpha.\beta$-Diacetyläthylen (I)**[7,8].—Fp. 75.5～76.5°C (Lit.[8] 75.5～76.5°C) (aus Petroläther schwach gelbe Nadeln).

**2. 1-Acetoxybutadien-(1.3)(II)**[6].—$Kp._{30}$ 51～52°C.

**3. 3-Acetoxy-1.2.3.6-tetrahydro-1.2-diacetylbenzol (III).**—40 g I wurden in 300 ccm Äthanol mit 50 g II 24 Std. am Rückfluß in Abwesenheit von Feuchtigkeit gekocht, das Lösungsmittel im Vakuum abgedampft und der Rückstand im Vakuum zweimal fraktioniert, $Kp._{12}$ 156～159°C, Ausbeute 65 g (82%).

$C_{12}H_{16}O_4$ (224.2)

Ber. C 64.27 H 7.19
Gef. C 65.50 H 7.43

Diese Verbindung zeigt mit Anilin in essigsaurer Lösung in der Kälte eine rote Farbreaktion. Die Farbe wird langsam violett.

**4. Versuch zur Aromatisierung von III zu *o*-Diacetylbenzol (IV).**—(a) Mit Schwefel 25 g III wurden 5 Std. mit 3.5 g Schwefel bei 100 Torr auf 160～180°C erhitzt, wobei rege Schwefelwasserstoff- und Essigsäureentwicklung beobachtet wurden. Bei der Destillation des Reaktionsgemisches im Hochvakuum gingen 18 g schwach gelbes Öl bei 105°C und 0.05 Torr über.

$C_{10}H_{10}O_2$ (152.2) (*o*-Diacetylbenzol)

Ber. C 73.92 H 6.21
Gef. C 73.68 H 6.34

Dieses Öl zeigte eine intensive violette Farbreaktion mit Anilin-Essigsäure in der Kälte und kristallisierte zum Teil bei längerem Stehen im Eisschrank (über ein Jahr bei −5°C) in Nadeln, die aus Petroläther umkristallisiert wurden, Fp. 37°C (Lit.[3] 38°C), Ausbeute 2.3 g Disemicarbazon, Fp. 150°C (Lit.[3] 150°C).

(b) Mit Chloranil 4.5 g III wurden 40 Std. mit 9.4 g Chloranil in 500 ccm Xylol am Rückfluß erhitzt, wobei Essigsäureentwicklung beobachtet wurde. Das Reaktionsgemisch wurde abfiltriert, das Filtrat eingeengt und der Rückstand mit Petroläther ausgezogen. Die Petrolätherlösung zeigte eine intensive violette Farbreaktion mit Anilin-Essigsäure in der Kälte. Obgleich keine Kristalle von IV nach dem Abdampfen des Petroläthers erhalten wurden, konnte IV als Disemicarbazon (0.13 g) identifiziert werden.

(c) Mit der Luft 4.5 g III wurden 48 Std. auf ca. 150～160°C erhitzt. Obgleich der Petrolätherauszug des Reaktionsgemisches eine intensive violette Farbreaktion mit Anilin in essigsaurer Lösung zeigte und Disemicarbazon (0.25 g) von IV gibt, blieb der Versuch zur Reinigung des Produktes erfolglos.

(d) Mit Selendioxyd 1 g III wurde 1 Std. mit 200 mg Selendioxyd in 20 ccm Äthanol am Rückfluß erhitzt. Es wurde keine Farbreaktion mit Anilin mehr beobachtet.

(e) Mit Natriumhydrogencarbonat 450 mg III wurden 10 Min. mit 150 mg Natriumhydrogencarbonat in Äthanol-Wasser (1:1) erhitzt. Nach dem Ansäuern mit Essigsäure zeigte das Gemisch nur schwache violette Farbreaktion mit Anilin.

**5. 3-Acetoxy-4.5-dibrom-1.2-diacetylcyclohexan (V).**—1.6 g III wurden in 30 ccm Tetrachlorkohlenstoff mit Brom bei Raumtemperatur versetzt, wobei das Gemisch unter Bromwasserstoffentwicklung ein Harz bildet. Das Produkt zeigte jedoch mit Anilin in essigsaurer Lösung eine intensive Farbreaktion. Unter Zusatz von Pyridin und unter Eiskühlung findet aber beim Versetzen mit Brom Harzbildung kaum statt. Das Gemisch wurde nach Stehenlassen über Nacht abfiltriert, das Lösungsmittel im Vakuum abgedampft und der Rückstand aus Methanol umkristallisiert, farblose Nadeln, Ausbeute 0.9 g (35%), Fp. 90～92°C (Zers.).

$C_{12}H_{16}Br_2O_4$ (384.1)

Ber. C 37.52 H 4.20 Br 41.61
Gef. C 37.63 H 4.39 Br 42.60

**6. Versuch zur Aromatisierung von V: 3-Acetoxy-1.2-diacetylbenzol.**—2 g V wurden in 20 ccm Pyridin 20 Std. am Rückfluß erhitzt, das Lösungsmittel im Vakuum abgedampft, der harzige Rückstand mit Wasser gewaschen und im kleinen Destillationsapparat im Hochvakuum zweimal destilliert. Die schwach gelbe Flüssigkeit, die bei 130°C (Badetemperatur) und 0.05 Torr überging, war halogenfrei und zeigte mit Anilin in essigsaurer Lösung eine violette Farbreaktion, Ausbeute 0.05 g.

$C_{12}H_{12}O_4$ (220.2)

Ber. C 65.45 H 5.49
Gef. C 66.10 H 5.14

Das Produkt scheint ein noch unreines Präparat von 3-Acetoxy-1.2-diacetylbenzol, zu sein konnte

jedoch wegen sehr schlechter Ausbeute nicht mehr gereinigt werden.

## Zusammenfassung

1-Acetoxybutadien-(1.3) gibt mit $\alpha.\beta$-Diacetyläthylen das Addukt: 1-Acetoxy-1.2.3.6-tetrahydro-1.2-diacetylbenzol, das durch Schwefel zu *o*-Diacetylbenzol aromatisiert werden konnte. Die Synthese ist in großem Maßstab leicht durchzuführen. Das Addukt reagiert mit primären Aminen unter einer roten Färbung und die Farbe geht langsam in violette über. Es wurden noch Reaktionen des Adduktes mit Brom untersucht.

Herrn Prof. Dr. F. Weygand, München, sage ich an dieser Stelle meinen aufrichtigsten Dank für Anregung und Anleitung zu vorstehender Arbeit.

*Organisch-Chemisches Laboratorium*
*der Technischen Hochschule Nagoya*
*Syôwa-ku, Nagoya*

# *Studies on Arsenic Trisulfide Glass*

By Jiro MATSUDA

(Received August 11, 1959)

The arsenic trisulfide glass has been studied as one of the new optical materials, because it can transmit infrared rays very well and has marked resistance to water and acid, and is more easily manufactured than single crystals[1-5].

The author once studied some different methods of preparation for technical arsenic trisulfide glass, and found the transmission value to be about 70% between 2 and 12 $\mu$ for 1 mm. thickness[6]. This figure is the maximum of the transmission value of this glass and the rather low transparency in this case results from the surface reflection and high refractive index[7]. If this glass can be properly coated on the surface, it will be more suitable for optical purposes, for this process must assist in reducing the reflection at the surface and raising the poor resistance to alkali.

Apart from the question of optical materials, the arsenic trisulfide glass is the interesting experimental glass composed of one component which melts at low temperature (about 300°C). Since the publication of the theory by Zachariasen[8] and the introduction of the X-ray analysis by Warren[9], glassy substances are explained as homogeneous polymers which characterize the amorphous substances consisting of network formers and modifiers, but some writers have insisted that glass is composed of a microheterogeneous system by microcrystalline structure[10]. These different views are closely related to the process of the transition of solids[11]. What process of transition occurs in glassy substances? The solution of this problem is very interesting and necessary in investigating the structure of glass. The various physical properties have frequently been studied on this point. The color of arsenic trisulfide has been found to be remarkably sensitive to changes in temperature. When it is heated yellow arsenic trisulfide is transformed to red and then to black. At 100°C, red aesenic trisulfide and at 170°C black substances can be obtained[12,13].

The author studied the thermal expansion values of red arsenic trisulfide glass

1) R. Frerichs, *Phys. Rev.*, **78**, 643 (1950).
2) W. A. Fraser, *J. Opt. Soc. Am.*, **43**, 322 (1953).
3) W. A. Fraser, ibid., **43**, 823 (1953).
4) R. Frerichs, ibid., **43**, 1153 (1953).
5) M. H. Bloch, *J. Research Natl. Bur. Standards*, **59**, 2774 (1957).
6) Presented before the Annual Conference on the Artificial Minerals, Nagoya, October, 1958. This result was published in *the Review of Physical Chemistry of Japan*, **29**, 22 (1959).
7) 2.43 at 5$\mu$.
8) W. H. Zachariasen, *J. Am. Chem. Soc.*, **54**, 3841 (1932).
9) B. E. Warren et al., *J. Am. Ceram. Soc.*, **21**, 49 (1935).
10) For example, K. S. Evstropyev, "The Structure of Glass", Consultants Bureau, Inc., New York (1958), p. 9.
11) F. C. Kracer, "Phase Transformations in Solids", John Wiley & Sons, Inc., New York (1951), p. 257.
12) H. Winter, *Z. anorg. u. allgem. Chem.*, **34**, 228 (1904).
13) E. W. Blank, *J. Chem. Educ.*, **20**, 171 (1943).

at transition temperatures by the quenching method and investigated the process of the transition.

## Experimental

The preparation of techincal arsenic trisulfide, the casting and the polishing of the glass were done by the same methods as mentioned in the previous report (Ref. 6).

Terylene film was used to coat the surface of the glass, because it can form the transparent, thin and filmy state easily at fairly low temperature and has a proper refractive index to remove the surface loss peculiar to the arsenic trisulfide glass. Terylene was dissolved in *o*-chlorophenol and this dilute solution was dropped on the glass which was horizontally rotated by an electric motor. Such treated glass was dried at 80°C in an air bath. The chemical durability of the glass to alkali was measured by spectroscopic method; that is, some pieces of glass were experimentally dipped in aqueous solution of sodium hydroxide for a limited time. After such etching they were washed and dried and measured on the falling of the transmittance at 2 $\mu$ wavelength.

The thermal expansion was measured by the ordinary optical lever method. Throughout the measuring, the samples were heated in succession at the constant rate of 2°C a minute. Before heating they were annealed at the constant temperature (187°C) for three days and allowed to cool very slowly to room temperature about 60 hr. in the electric annealing oven. They were then reheated for several hours at various temperatures ranging from 153 to 180°C and were quenched in the air.

The heating was made always in an mobile oil bath to prevent arsenic trisulfide from oxidizing.

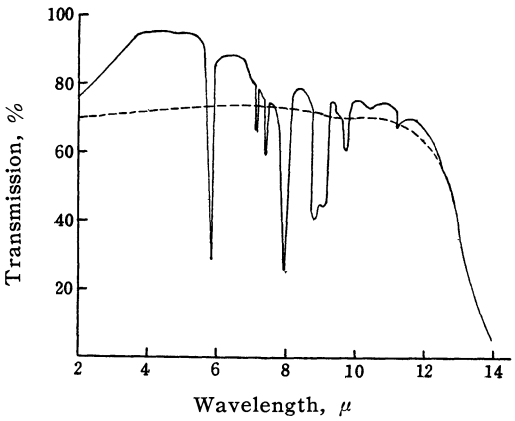



Fig. 1. Effect of coating on the arsenic trisulfide glass of 1 mm. thickness.
——: coated.
----: not coated.

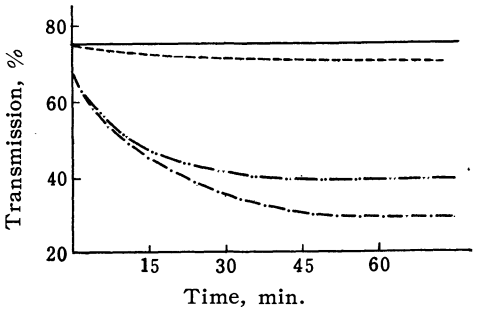



Fig. 2. Transmission after treatment in alkali.
—— and ----: coated glass treated in 0.05 and 0.1 N, respectively.
·—· and ·—·: uncoated glass treated in 0.05 and 0.1 N, respectively.

## Results and Discussion

**Coating of the Surface.** — As shown in Fig. 1, the effect of the coating is very remarkable in the range of short wavelengths, while it gradually decreases in the wavelengths which are over 7 $\mu$ and many absorption bands of surface film appear. If the film coated on the surface is so thin that interference color can be seen, the efficacy of the treatment in the rays of the short wavelengths is very conspicuous. In that case the transmittance is 75 to 95% between 2 and 5.7 $\mu$. Moreover, even such a thin film markedly increases durability to alkali. As shown in Fig. 2, when dipped in 0.05 N alkaline solution, the coated glass is hardly affected at all. After 15 hr. etching the transmittance decreases by about only 4%.

In the case of 0.1 N, the coated glass is affected in some degree, but even after dipping for 30 min. the transmittance decreases by only 1~2%. All these decreases of the transmission were observed to be caused by etching pits which grew up from mechanical scratches on the film. These results mean that terylene film has sufficient protecting action against alkaline etching in such concentrations. As these results show, such coated arsenic trisulfide glass is of good use as optical material of the cell in the infrared between 2 and 5.7 $\mu$ and as seen in Fig. 1, the uncoated glass can be utilized as basic glass to study infrared absorption of various substances. Besides the terylene film, by proper coating of other materials the arsenic trisulfide glass seems to be the more valuable optical material.

**Thermal Expansion.** — The physical properties of glass are affected remarkably by different thermal histories. The abnormal thermal expansion of borosilicate

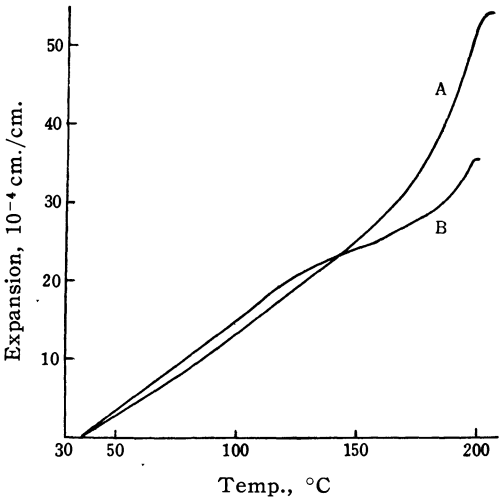



Fig. 3. Thermal expansion.
A: annealed, B: chilled.

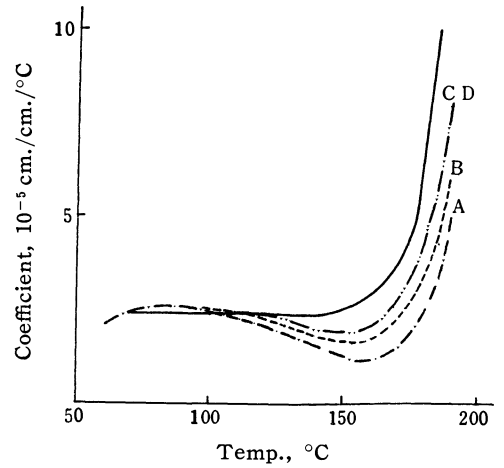



Fig. 4. Different coefficients among annealed and chilled glass.
——: annealed glass.
A, B, C and D are quenched at 180, 174, 164, and 153°C, respectively.

glass is one of the well-known examples of these sorts. As shown in Fig. 3, the annealed arsenic trisulfide glass shows transformation point at 170°C. The meaning of the transformation point in glass is not always the same in crystallography, but it is an undoubted fact that the structure of glass may change to a certain extent near the point. On the other hand, the precipitated arsenic trisulfide is said to have transformation points near 100 and 170°C[12-14]. However, in the case of the glassy state, the transformation appeared only at 170°C. Accordingly in order to study the common transformation point of these different solid states, the various coefficients of expansion were measured by the quenching method. A, B, C and D shown in Fig. 4. represent respectively the quenched specimens at 180, 174, 164 and 153°C. In Fig. 4, both A and B indicate larger values of the coefficients than in annealed glass below 100°C, but C and D almost the same values as annealed glass; that is, the quenching effect does not appear in the case of C and D.

In the high temperature range, the higher the quenching temperature becomes, the smaller the coefficient becomes, arriving at the minimum value near 160°C, but no substantial difference can be found among A, B, C and D curves and these results suggest that there is no intrinsic difference among the internal structures of the four specimens; that is, the difference of the coefficients shows the extent of their polymerization, and the higher the quenching temperature becomes, the more insufficient the polymerization becomes. This fact is guessed also from the difference among their exact temperatures at which the graduation of the dilatometer begins to show shrinking.

TABLE I. QUENCHING EFFECT ON THE EXACT TEMPERATURE AT WHICH THE ELONGATION CURVE ON THE DILATOMETER BEGINS TO SHOW SHRINKING

| Sample | Temp., °C |
|---|---|
| A | 200 |
| B | 200 |
| C | 202 |
| D | 206 |
| annealed | 209 |

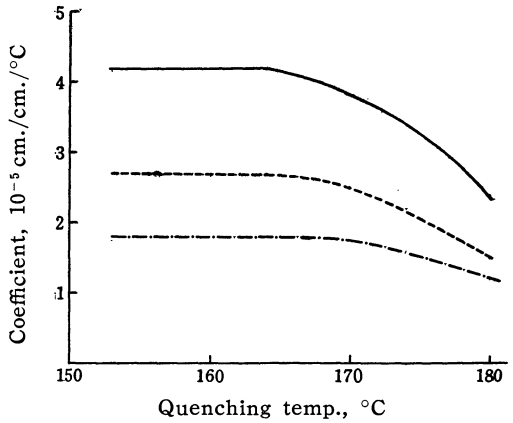



Fig. 5
——, ----, and —·—: measured at 180, 170 and 160°C, respectively.

14) W. A. Jonker, *Z. anorg. u. allgem. Chem.*, **62** 89, (1909).

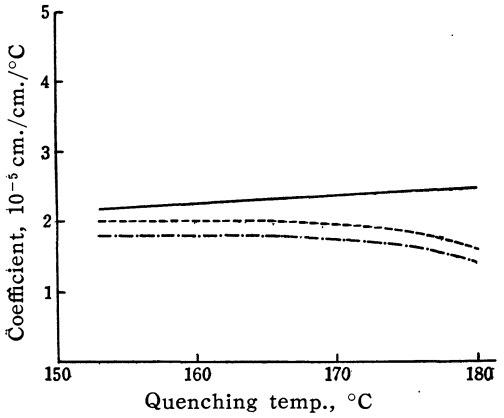



Fig. 6

——, ----, and —·—: measured at 100, 140 and 150°C, respectively.

These results are given in the table. As can been seen, the higher the quenching temperature becomes, the lower the exact temperature becomes; that is, the less sufficient the polymerization becomes.

Figs. 5 and 6 show the interrelation between the quenching temperature and the temperature in measuring of the coefficients. The abscissa means the quenching temperature. The differences among four specimens are notable at 180°C of measuring-temperature and become smaller at low temperature and at 100°C almost disappear. In all specimens the coefficients measured above 160°C, increase as the temperature rises, but this phenomenon appears in reverse below 150°C. Consequently all specimens show the minimum coefficient between 150 and 160°C. However, while the quenching temperature rises, the coefficients decrease in all cases above 100°C.

## Summary

Arsenic trisulfide glass shows 70% of transmittance between 2 and 12 $\mu$. This transmittance is somewhat insufficient for the optical cell in the infrared. Moreover, the chemical durability to alkali is very weak. These defects can be removed by proper coating on the surface. For instance, it can be of good use between 2 and 5.7 $\mu$ by using terylene film.

In thermal expansion, the transformation point of glassy arsenic trisulfide is nearly 170°C. In order to study what process of transformation occurs in the glass, the quenching method was applied. Some pieces of annealed glass were experimentally quenched at 180, 174, 164 and 153°C. Thermal expansion was measured on these quenched glasses.

Because of their various controls of expansion by temperature, glassy transformation at 170°C has no connection with transformation at the same temperature in arsenic trisulfide.

The author wishes to express his thanks to Mr. S. Matsuzaki for valuable cooperation and to Maruzen Oil Co., Ltd. for their kindness in the measuring of transmittance in the infrared.

*Department of Chemistry*
*Faculty of Science and Literature*
*Ehime University*
*Matsuyama*

# *Surface Tension and Spinnability of Molten Poly-ε-capramide*

By Naoya OGATA

(Received August 13, 1959)

Surface tension of a liquid means the tension in the boundary between a liquid and a gas or the free energy of the surface. As surface tension tends to make the area of surface as small as possible, it is expected that the spinnability of a liquid would have relation with its surface tension and hence physical properties concerning its surface can be estimated. Surface tension of molten ε-caprolactam and poly-ε-capramide has been measured and their surface properties have been studied.

## Experimental

**Polymerization of ε-Caprolactam.** — ε-Caprolactam was polymerized at 257°C for 15 hr. in the presence of 5% of ε-aminocaproic acid and 2, 1 or 0.5 mol. % of benzoic acid. The degree of polymerization of polymers was estimated from the solution viscosity in *m*-cresol at 25°C by the following equation[1].

$$\bar{P}=127[\eta]^{1.435} \quad (1)$$

**Measurement of Surface Tension.** — Surface tension of molten ε-caprolactam or poly-ε-capramide was measured by the method of maximum bubble pressure[2]. When a capillary is immersed in a liquid and gas pressure is raised slowly, a bubble is formed at the tip of the capillary. If gas pressure is further raised, the bubble breaks away from the tip and the pressure decreases. Hence, the pressure passes through a maximum. When the main radius of curvature at the largest bubble is $R$ and the depth of the tip of the capillary is $h$, the maximum pressure is given by the following equation.

$$P=2\gamma/R+Dgh \quad (2)$$

where $\gamma$, $g$ and $D$ mean surface tension, gravity constant and density, respectively. If the radius of a capillary is narrow enough, $R$ can be approximated to the capillary radius $r$.

The tip of the capillary of 0.02~0.05 cm. radius was immersed in the melted substance at 1 cm. in depth and nitrogen gas was introduced slowly at the pressure rate of 0.1 cm. $H_2O$/min. and the maximum bubble pressure was measured.

**Measurement of Spinnability.**—The apparatus is shown in Fig. 1. A glass stick of radius of 0.2 cm. was immersed in molten poly-ε-capramide at 0.5 cm. in depth and was pulled up at the constant rate. The clutch was cut off immediately at the break of the thread and the length was measured.

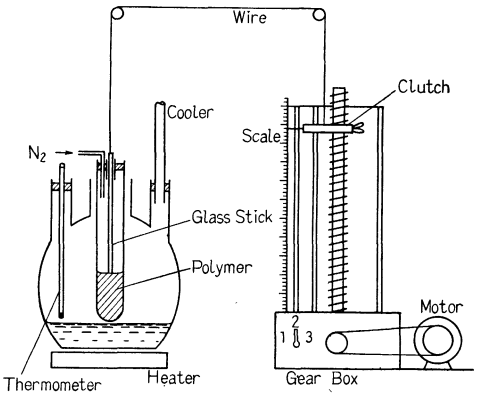



Fig. 1. Apparatus for the measurement of spinnability of poly-ε-capramide.

## Results

**Surface Tension of Molten ε-Caprolactam and Poly-ε-capramide.** — Surface tension values of molten ε-caprolactam and *N*-acetyl-ε-aminocaproic acid to nitrogen gas at various temperatues are shown in Fig. 2.

Surface tension values of poly-ε-capramide of various polymerization degrees and at various temperatures are shown in Figs. 3 and 4. The poly-ε-capramide

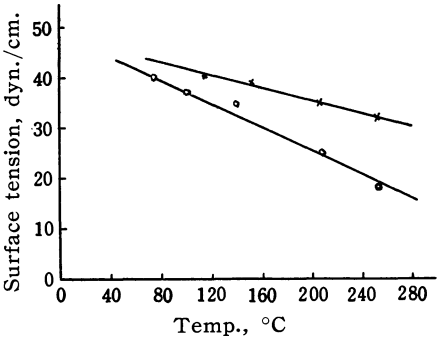



Fig. 2. Surface tension of ε-caprolactam and *N*-acetyl-ε-aminocaproic acid at various temperatures.
× *N*-Acetyl-ε-caprolactam
○ ε-Caprolactam

1) O. Fukumoto, *J. Polymer Sci.*, **22**, 263 (1956).
2) J. J. Bikerman, "Surface Tension", 2nd Ed., Academic Press, Inc., New York (1948), p. 17.

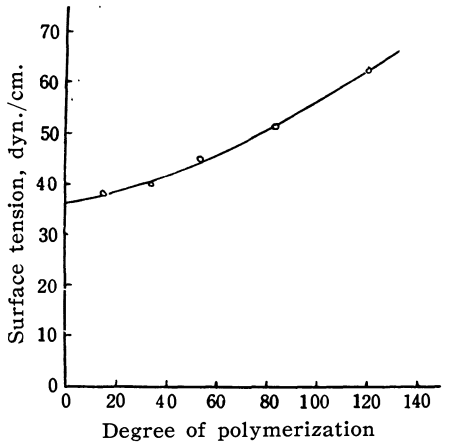



Fig. 3. Surface tension of poly-ε-capramide.

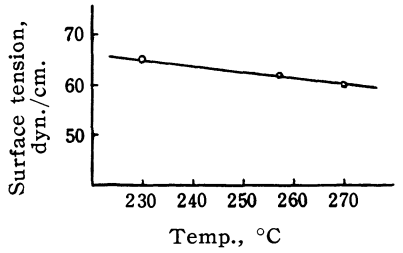



Fig. 4. Surface tension of poly-ε-capramide ($\bar{P}_n$=120) at various temperatures.

used was an equilibrium polymer containing about 10% of ε-caprolactam and its oligomers.

**Thread Length of Poly-ε-capramide.**—The thread lengths of poly-ε-capramide of various polymerization degrees at 230 or 257°C and at various pulling rates are shown in Fig. 5. The thread length of poly-ε-capramide ($\bar{P}$=120) at 257°C and at the pulling rate of 0.74 cm./sec. is proportional to the radius of a glass stick as shown in Fig. 6. Each polymer contained about 10% of ε-caprolactam and its oligomers.

## Discussion

Ramsay and Shields[3] found a linear relation between surface tension of a liquid and temperature as the following equation:

$$\gamma(M/D)^{2/3}=k(T_c-T-6) \qquad (3)$$

where $\gamma$ is surface tension, $M$ is molecular weight, $D$ is density, $T_c$ is critical temperature and $k$ is a constant characteristic for a liquid.

3) W. Ramsay and J. Shields, *Z. physik. Chem.*, **12**, 433 (1893).

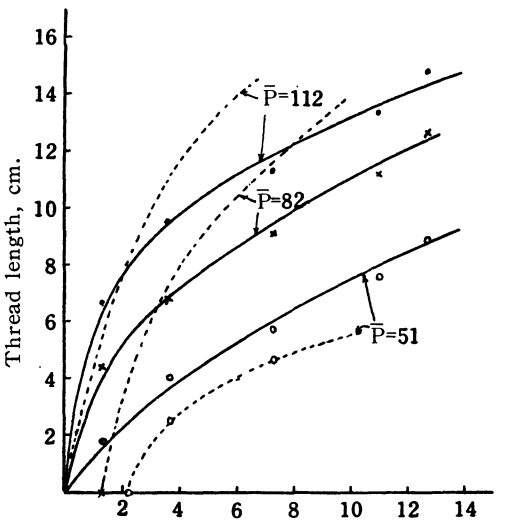



Fig. 5. Thread length at various pulling rates.
—— 230°C, ------ 257°C.

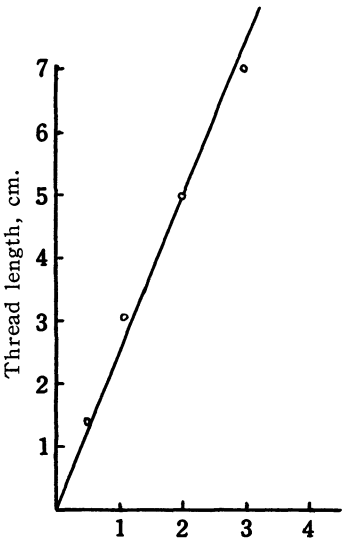



Fig. 6. The relation between thread length and radius of glass stick.
($\bar{P}$=120, $V$=0.74 cm./sec., $t$=257°C)

The value of $k$ for a normal liquid is usually about 2.12. The value of $k$ and the critical temperature of ε-caprolactam is estimated to be 2.77 and 463°C, respectively.

Surface tension of poly-ε-capramide increases as the degree of polymerization increases. When the logarithms of surface-tension $\gamma$ are plotted against the polymerization degree $\bar{P}$, a linear relation is

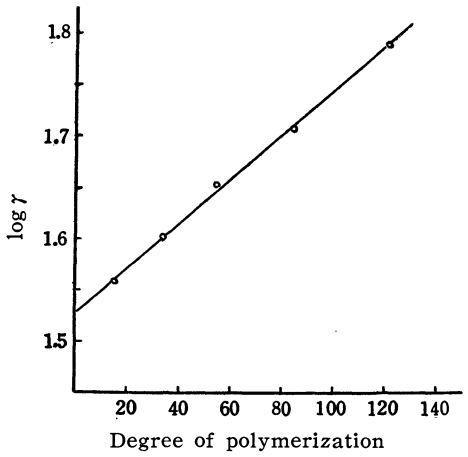



Fig. 7. Relation between $\log \gamma$ and $\bar{P}$.

obtained as shown in Fig. 7 and the following equation is obtained at 257°C.

$$\log \gamma = 0.0022\bar{P} + 1.53 \quad (5)$$

As the surface tension of poly-ε-capramide ($\bar{P}=120$) is nearly proportional to temperature from Fig. 4, the value of $d\gamma/dT$ is about −0.06 dyn./cm. deg. and that of *N*-acetyl-ε-aminocaproic acid is also −0.06 dyn./cm. deg. Therefore, the value of $d\gamma/dT$ of linear poly-ε-capramide is expected to be −0.06 dyn./cm. deg. independent of the polymerization degree, and the following equation is obtained, where $t$ is temperature in degrees centigrade.

$$\gamma = 10^{(0.0022\bar{P}+1.53)} + 0.06(257-t) \quad (6)$$

Surface tension of ε-aminocaproic acid at 252°C is estimated from Eq. 6 to be about 34 dyn./cm. This value is not consistent with the surface tension value of ε-caprolactam (18 dyn./cm.), but is nearly approximated to that of *N*-acetyl-ε-aminocaproic acid (32 dyn./cm.). Therefore, it is expected that the surface tension of ε-aminocaproic acid is about 16 dyn./cm. greater than that of ε-caprolactam.

Since surface tension means intermolecular forces among molecules, this result suggests that the intermolecular force of ε-aminocaproic acid is greater than that of ε-caprolactam.

The total surface energy $U$ is given[2] by

$$U = \gamma - T\partial\gamma/\partial T \quad (7)$$

The total surface energies of ε-caprolactam, *N*-acetyl-ε-aminocaproic acid and poly-ε-capramide are shown in Tables I and II.

The total surface energy of ε-aminocaproic acid is estimated to be about 66 erg/cm² from Table I and is 16 erg/cm² smaller than that of ε-caprolactam. This result is very interesting in relation to the exothermic reaction of the ε-caprolactam polymerization[4,5].

Table I. Total surface energy of ε-caprolactam, *N*-acetyl-ε-aminocaproic acid and poly-ε-capramide

| Sample | Temp. °C | γ(dyn./cm.) | ∂γ/∂T | U(erg/cm²) |
|---|---|---|---|---|
| ε-Caprolactam | 76 | 40 | −0.12 | 82 |
| | 100 | 37 | −0.12 | 82 |
| | 140 | 35 | −0.12 | 85 |
| | 208 | 25 | −0.12 | 83 |
| | 252 | 18 | −0.12 | 81 |
| Mean value | — | — | −0.12 | 82 |
| *N*-Acetyl-ε-aminocaproic acid | 116 | 40 | −0.06 | 63 |
| | 152 | 39 | −0.06 | 65 |
| | 205 | 35 | −0.06 | 64 |
| | 252 | 32 | −0.06 | 64 |
| Mean value | — | — | −0.06 | 64 |
| Poly-ε-capramide ($\bar{P}$=120) | 230 | 65 | −0.06 | 95 |
| | 257 | 62 | −0.06 | 94 |
| | 270 | 60 | −0.06 | 93 |
| Mean value | — | — | −0.06 | 94 |

Table II. Total surface energy of poly-ε-capramide

| $\bar{P}$ | γ(dyn./cm.) | U(erg/cm²) |
|---|---|---|
| 15 | 38 | 70 |
| 34 | 40 | 72 |
| 54 | 45 | 77 |
| 84 | 51 | 83 |
| 121 | 62 | 94 |

It is presumed that the increase in surface tension of poly-ε-capramide with the increase of its polymerization degree may be caused by the difference in thermal movement of macromolecules.

It is assumed that the thread of molten poly-ε-capramide may be broken at the point at which the surface energy reaches equilibrium with the friction energy of viscous liquid. Hirai[6] introduced the following equation in relation to surface tension $\gamma$ and thread length $L$, and ascertained this equation for the thread length of glycerine.

$$L = R_0 V\mu/\gamma \quad (8)$$

4) S. M. Skuratov et al., *Kolloid Zhur.*, **14**, 185 (1952); *Faserforsch. u. Textiltech.*, **4**, 390 (1953).
5) H. Yumoto, This Bulletin, **28**, 94 (1955).
6) N. Hirai, *J. Chem. Soc. Japan, Pure Chem. Sec.* (*Nippon Kagaku Zasshi*), **75**, 1019 (1954); *Chem. Abstr.*, **46**, 9357*h* (1955).

In this equation $R_0$ is the radius of a glass stick, $\mu$ is the viscosity and $V$ is the pulling rate. In case of poly-ε-capramide, $L$ is not proportional to $V$ as shown in Fig. 5. However, a linear relation is obtained by plotting $\log L$ against $\log V$, as shown in Fig. 8.

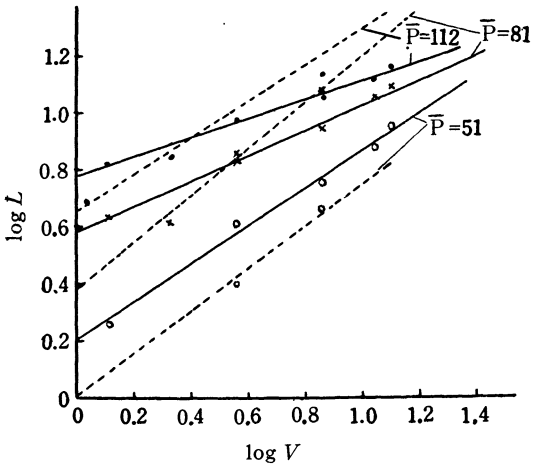



Fig. 8. Relation between $\log L$ and $\log V$.
—— 230°C, ------ 257°C.

Since $L$ was proportional to the radius $R_0$ of a glass stick, the following equation is given:

$$L=kR_0V^a \tag{9}$$

The values of $k$ and $a$ at various polymerization degrees and temperatures are shown in Table III, where $R_0$ and $V$ are given in cm. and cm./sec. units, respectively.

TABLE III. THE VALUES OF $k$ AND $a$ IN $L=kR_0V^a$

| Temp., °C | $\bar{P}$ | $k$ | $a$ |
|---|---|---|---|
| 230 | 51 | 8 | 0.6 |
| | 82 | 16 | 0.4 |
| | 112 | 30 | 0.4 |
| 257 | 51 | 5 | 0.7 |
| | 82 | 12 | 0.7 |
| | 112 | 23 | 0.6 |

The value of $a$ is almost invariable and its mean value is 0.5. Therefore, the thread length is proportional to the square root of the pulling rate.

The values of $\mu/\gamma$, which are shown in Table IV, were estimated from the following equation derived by K. Hoshino[7].

$$\log\mu=-7+2300/T+6.2([\eta]^{25°C}_{cresol})^{1/2} \tag{10}$$

7) K. Hoshino and S. Fujii, *Chem. High Polymers (Kobunshi Kagaku)*, **1**, 14 (1944); *Chem. Abstr.*, **44**, 5147*b* (1950).

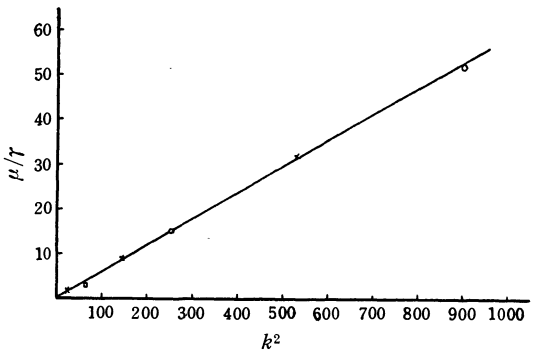



Fig. 9. The relation between $k^2$ and $\mu/\gamma$.

TABLE IV. THE VALUE OF $\mu/\gamma$

| Temp. °C | $\bar{P}$ | $[\eta]^{25°C}_{cresol}$ | $\mu$(poise) | $\mu/\gamma$ | $k^2$ |
|---|---|---|---|---|---|
| 230 | 51 | 0.53 | 123 | 3 | 64 |
| | 82 | 0.74 | 810 | 15 | 256 |
| | 112 | 0.92 | 3240 | 52 | 900 |
| 257 | 51 | 0.53 | 73 | 2 | 25 |
| | 82 | 0.74 | 480 | 9 | 144 |
| | 112 | 0.92 | 1900 | 32 | 529 |

When the value of $k^2$ is plotted against $\mu/\gamma$, a linear relation is obtained as shown in Fig. 9 and the following equation is given.

$$\mu/\gamma=0.059k^2 \tag{11}$$

From Eqs. 9 and 11, the thread length of poly-ε-capramide can be represented as follows:

$$L=4.13R_0(\mu V/\gamma)^{1/2} \tag{12}$$

It can be estimated from the above-mentioned results that the thread length of molten poly-ε-capramide of $\bar{P}=100\sim120$ at 257°C may be approximately 12 cm., when the polymer is spun at the rate of 400 m./min. from a nozzle of 0.02 cm. radius, and the fiber must be cooled within this length to obtain a continuous filament.

## Summary

Surface tension of molten ε-caprolactam and poly-ε-capramide has been measured by the method of maximum bubble pressure. Surface tension of ε-caprolactam at 252°C is 18 dyn./cm. and it is 16 dyn./cm. smaller than that of ε-aminocaproic acid (34 dyn./cm.). It is estimated from the Ramsay-Shields' equation that the critical temperature of ε-caprolactam is 463°C. Surface tension of poly-ε-capramide of the polymerization degree $\bar{P}$ is given by the following equation.

$$\gamma=10^{(0.0022\bar{P}+1.53)}+0.06(257-t)$$

The thread length of molten poly-ε-capramide has been measured by pulling up a glass stick and is represented by the following equation, where $L$ (cm.) is thread length, $R_0$ (cm.) radius of a glass stick, $\mu$ (poise) melt viscosity, $\gamma$ (dyn./cm.) surface tension and $V$ (cm./sec.) pulling rate:

$$L=4.13R_0(\mu V/\gamma)^{1/2}$$

The author wishes to thank Dr. K. Hoshino and Dr. H. Kobayashi who instructed him in this study and permitted the publication of these results. He also thanks Mr. M. Nakata who collaborated with him in experiments.

*Research Department*
*Toyo Rayon Co., Ltd.*
*Minato-ku, Nagoya*

# *Phase Equilibrium on Liquidus Surface of the System $3CaO \cdot P_2O_5$-$CaO \cdot MgO \cdot 2SiO_2$-$MgO \cdot SiO_2$*

By Toshiyuki SATA

(Received August 15, 1959)

As a continuation of the author's preceding reports, which were on the phase relationship in the systems $3CaO \cdot P_2O_5$–$MgO \cdot SiO_2$–$SiO_2$[1] and $3CaO \cdot P_2O_5$–$CaO \cdot MgO \cdot 2SiO_2$–$SiO_2$[2], an equilibrium study on the system $3CaO \cdot P_2O_5$–$CaO \cdot MgO \cdot 2SiO_2$–$MgO \cdot SiO_2$, a side plane of a tetrahedron of a system $3CaO \cdot P_2O_5$–$CaO \cdot MgO \cdot 2SiO_2$–$MgO \cdot SiO_2$–$SiO_2$, was carried out by the usual quenching method. On the phase relationship of this 3-component system, no paper has ever been presented.

Of the three component system concerned, data of the two partial systems, $3CaO \cdot P_2O_5$–$CaO \cdot MgO \cdot 2SiO_2$ and $3CaO \cdot P_2O_5$–$MgO \cdot SiO_2$, were already given by the author's reports. Another partial system $CaO \cdot MgO \cdot 2SiO_2$–$MgO \cdot SiO_2$ was investigated by Bowen[3]. In his phase diagram, it is characterized that forsterite is a primary phase at 22~100% of $MgO \cdot SiO_2$. However, in the phase diagram published in 1952 by Atlas[4], who studied the matter by adding LiF, the primary phase may be a solid solution at overall range, which is decomposed to a clinoenstatite, diopside, protoenstatite or rhombic enstatite solid solution in a crystalline phase. In this report the author followed Bowen's diagram, and constructed the phase diagram on the liquidus surface of this system.

1) T. Sata, This Bulletin, **31**, 408 (1958).
2) T. Sata, ibid, **32**, 105 (1959).
3) N. L. Bowen, *Z. anorg. u. allgem. Chem.*, **90**, 1—66 (1914).
4) L. Atlas, *J. Geology*, **60**, 140 (1952).

## Experimental

The nine compositions taken on the system $CaO \cdot MgO \cdot 2SiO_2$–$MgO \cdot SiO_2$ are listed in Table I. Then on the line joining these nine compositions with $3CaO \cdot P_2O_5$ point, thirty-two sample points were taken in the system $3CaO \cdot P_2O_5$–$CaO \cdot MgO \cdot 2SiO_2$–$MgO \cdot SiO_2$ and plotted in Fig. 1.

Powdered batches of these compositions, prepared by quenching into a glass after being kept at above their melting points, were again held at constant temperatures in a silicon carbide resister furnace and then quenched in water. Thenceforth the equilibrium phases found therein were determined by optical and X-ray examination. For measuring the temperature a thermocouple of platinum-platinum rhodium (10%) was used. Details of the experimental procedures are similar to those already described in the preceding report[1].

TABLE I. COMPOSITIONS OF SAMPLES TAKEN FROM THE SYSTEM $CaO \cdot MgO \cdot 2SiO_2$–$MgO \cdot SiO_2$

| No. | $CaO \cdot MgO \cdot 2SiO_2$ | $MgO \cdot SiO_2$ |
|---|---|---|
| | wt. % | |
| 225 | 85 | 15 |
| 240 | 80 | 20 |
| — | 75 | 25 |
| 209 | 70 | 30 |
| 230 | 60 | 40 |
| 210 | 50 | 50 |
| 238 | 40 | 60 |
| 211 | 20 | 80 |

## Results

Data on the quenching runs for this 3-component system are listed in Table II,

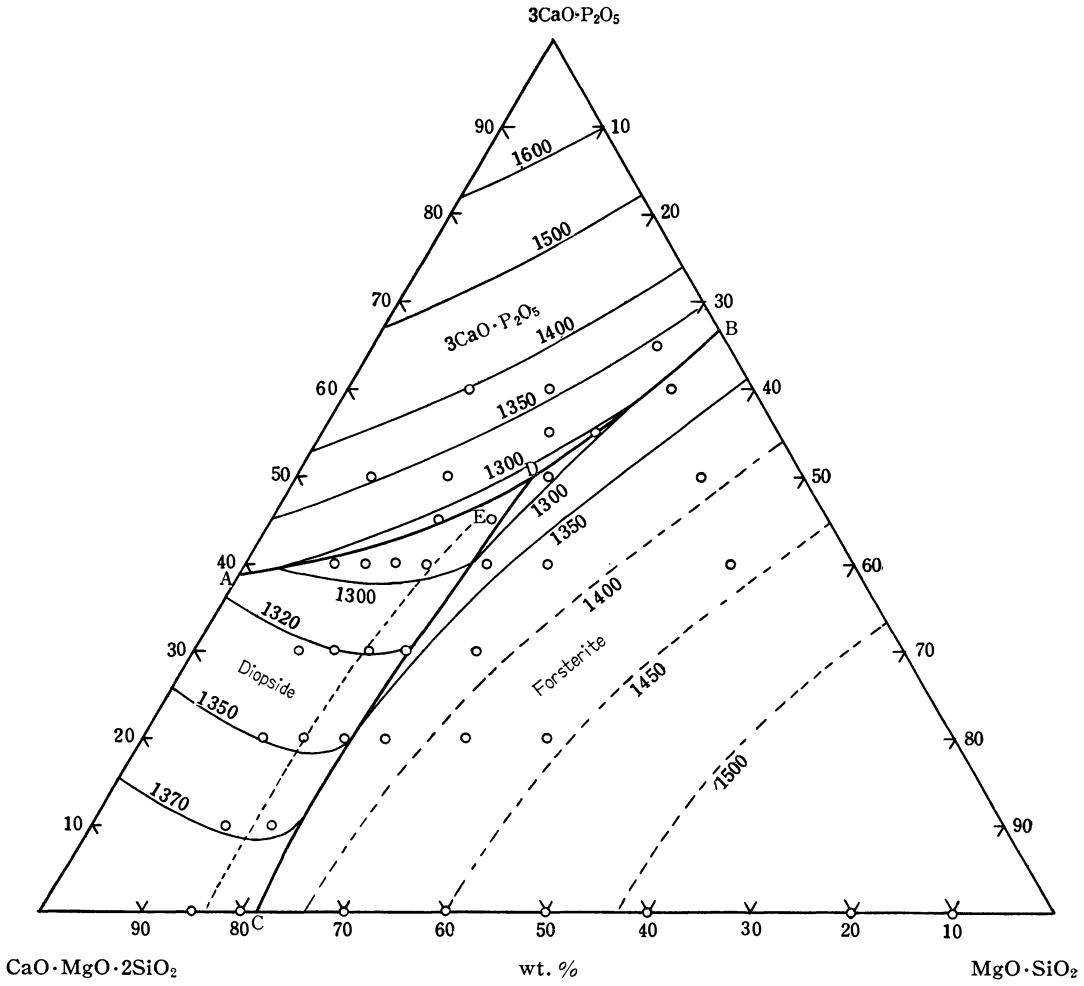



Fig. 1. The system $3CaO \cdot P_2O_5$-$CaO \cdot MgO \cdot 2SiO_2$-$MgO \cdot SiO_2$.
(A: 1314°C, B: 1308°C, C: 1390°C)

from which the equilibrium diagram on the liquidus surface was constructed as shown in Fig. 1. Primary crystals in this system are tricalcium phosphate ($\alpha$ or $\beta$), diopside and forsterite, respectively, and forsterite occupies a wide field. Accordingly it is found that this system is not a ternary one.

A lower liquidus temperature range is located in the center of this triangle, its minimum temperature being 1277±5°C. A temperature minimum at 1389°C in the system $CaO \cdot MgO \cdot 2SiO_2$-$MgO \cdot SiO_2$ falls slowly toward the neighborhood of this lowest point as shown by a dotted line. However, it can not be decided in this report whether this valley of temperature attains to this point or not. Clinoenstatite does not appear as a primary crystal on the liquidus surface. Hence a decomposition of pyroxene solid solution to colinoenstatite may occur under the liquidus.

## Summary

The phase relationship on the liquidus surface of the system $3CaO \cdot P_2O_5$-$CaO \cdot MgO \cdot 2SiO_2$-$MgO \cdot SiO_2$ was investigated by the usual quenching method. The three primary crystals are $\alpha$- or $\beta$-tricalcium phosphate, diopside and forsterite, and the range of the lowest temperature is located at the center of this triangle (1277°C). From these results, it is found that this system should be considered as a partial system in the 4-component system $3CaO \cdot P_2O_5$-$CaO \cdot MgO \cdot 2SiO_2$-$2MgO \cdot SiO_2$-$SiO_2$.

TABLE II. QUENCHING DATA IN THE SYSTEM $3CaO \cdot P_2O_5$-$CaO \cdot MgO \cdot 2SiO_2$-$MgO \cdot SiO_2$

| No. | Composition wt. % | | $C_3P$ | $CMS_2$ wt. % | MS* | Holding temp. °C | Holding time min. | Phases present |
|---|---|---|---|---|---|---|---|---|
| | $C_3P$ No. 225 | | | | | | | |
| 226 | 50 | 50 | 50 | 42.5 | 7.5 | 1347 | 30 | gl.* |
| | | | | | | 1340 | 30 | $\beta$-$C_3P$, gl. |
| 227 | 40 | 60 | 40 | 51.0 | 9.0 | 1307 | 30 | gl. |
| | | | | | | 1298 | 30 | faint diopside, gl. |
| | | | | | | 1290 | 40 | diopside, gl. |
| | | | | | | 1282 | 40 | all crystal |
| 228 | 30 | 70 | 30 | 59.5 | 10.5 | 1332 | 60 | gl. |
| | | | | | | 1325 | 30 | small diopside, gl. |
| | | | | | | 1290 | 30 | diopside, gl. |
| | | | | | | 1282 | 30 | all crystal |
| 235 | 20 | 80 | 20 | 68.0 | 12.0 | 1356 | 30 | gl. |
| | | | | | | 1347 | 30 | faint diopside, gl. |
| 236 | 10 | 90 | 10 | 76.5 | 13.5 | 1372 | 30 | gl. |
| | | | | | | 1364 | 30 | diopside, gl. |
| | | | | | | 1340 | 30 | diopside, small gl. |
| | $C_3P$ No. 240 | | | | | | | |
| 241 | 40 | 60 | 40 | 48 | 12 | 1307 | 30 | faint diopside, gl. |
| | | | | | | 1290 | 30 | diopside, gl. |
| 242 | 30 | 70 | 30 | 56 | 14 | 1332 | 60 | gl. |
| | | | | | | 1325 | 30 | small diopside, gl. |
| | | | | | | 1307 | 30 | diopside, gl. |
| 243 | 20 | 80 | 20 | 64 | 16 | 1356 | 20 | gl. |
| | | | | | | 1347 | 30 | small diopside, gl. |
| 244 | 10 | 90 | 10 | 72 | 18 | 1372 | 30 | gl. |
| | | | | | | 1364 | 30 | diopside, gl. |
| 245** | | | 40 | 45 | 15 | 1302 | 30 | small diopside, gl. |
| | | | | | | 1294 | 30 | diopside, gl. |
| | | | | | | 1286 | 30 | diopside, gl. |
| 246** | | | 30 | 52.5 | 17.5 | 1314 | 40 | gl. |
| | | | | | | 1307 | 40 | diopside, gl. |
| 247** | | | 20 | 60 | 20 | 1357 | 50 | gl. |
| | | | | | | 1347 | 30 | faint diopside, gl. |
| | $C_3P$ No. 209 | | | | | | | |
| 212 | 60 | 40 | 60 | 28 | 12 | 1356 | 40 | gl. |
| | | | | | | 1348 | 40 | $\beta$-$C_3P$, gl. |
| | | | | | | 1282 | 40 | $\beta$-$C_3P$, gl. |
| 213 | 50 | 50 | 50 | 35 | 15 | 1330 | 40 | gl. |
| | | | | | | 1307 | 40 | small $C_3P$, gl. |
| | | | | | | 1282 | 40 | $\beta$-$C_3P$, gl. |
| | | | | | | 1273 | 30 | all crystal |
| 221 | 45 | 55 | 45 | 38.5 | 16.5 | 1307 | 30 | gl. |
| | | | | | | 1282 | 30 | small $C_3P$, gl. |
| | | | | | | 1274 | 50 | all crystal |
| 214 | 40 | 60 | 40 | 42 | 18 | 1302 | 30 | gl. |
| | | | | | | 1294 | 30 | faint diopside, gl. |
| | | | | | | 1286 | 30 | small diopside, gl. |
| | | | | | | 1273 | 30 | all crystal |

* Abbreviations: $C_3P = 3CaO \cdot P_2O_5$; $CMS_2 = CaO \cdot MgO \cdot 2SiO_2$; $MS = MgO \cdot SiO_2$; gl. = glass.

** No. 245, 246, 247 were prepared from 1 : 1 mixture of No. 241—No. 214, No. 242—No. 222, No. 243—No. 229, respectively.

| | | | | | | | | |
|---|---|---|---|---|---|---|---|---|
| 222 | 30 | 70 | 30 | 49 | 21 | 1324 | 40 | gl. |
| | | | | | | 1314 | 40 | faint diopside, gl. |
| | | | | | | 1282 | 40 | diopside, small gl. |
| 229 | 20 | 80 | 20 | 56 | 24 | 1407 | 30 | gl. |
| | | | | | | 1397 | 40 | small forsterite, gl. |
| | | | | | | 1340 | 50 | forsterite, gl. |
| | | | | | | 1332 | 60 | forsterite, diopside, gl. |
| | | | | | | 1322 | 60 | forsterite, diopside, gl. |
| | $C_3P$ No. 230 | | | | | | | |
| 231 | 45 | 55 | 45 | 33 | 22 | 1290 | 30 | gl. |
| | | | | | | 1282 | 30 | small diopside, gl. |
| | | | | | | 1272 | 30 | diopside, $\beta$-$C_3P$, gl. |
| | | | | | | 1265 | 30 | all crystal |
| 232 | 40 | 60 | 40 | 36 | 24 | 1323 | 60 | gl. |
| | | | | | | 1314 | 60 | small forsterite, gl. |
| | | | | | | 1299 | 60 | forsterite, gl. |
| | | | | | | 1290 | 40 | forsterite, diopside, gl. |
| 233 | 30 | 70 | 30 | 42 | 28 | 1397 | 40 | gl. |
| | | | | | | 1390 | 30 | small forsterite, gl. |
| | | | | | | 1323 | 30 | forsterite, gl. |
| | | | | | | 1314 | 60 | forsterite, small diopside, gl. |
| | | | | | | 1250 | 60 | forsterite, diopside, $\beta$-$C_3P$ |
| 234 | 20 | 80 | 20 | 48 | 32 | 1460 | 30 | gl. |
| | | | | | | 1450 | 30 | small forsterite, gl. |
| | $C_3P$ No. 210 | | | | | | | |
| 215 | 60 | 40 | 60 | 20 | 20 | 1348 | 40 | gl. |
| | | | | | | 1340 | 40 | very small $C_3P$, gl. |
| | | | | | | 1332 | 40 | small $C_3P$, gl. |
| 223 | 55 | 45 | 55 | 22.5 | 22.5 | 1314 | 40 | gl. |
| | | | | | | 1307 | 30 | small $C_3P$, gl. |
| 216 | 50 | 50 | 50 | 25 | 25 | 1298 | 30 | gl. |
| | | | | | | 1290 | 30 | faint forsterite, gl. |
| | | | | | | 1282 | 20 | forsterite, gl. |
| | | | | | | 1277 | 30 | forsterite, $C_3P$, gl. |
| 217 | 40 | 60 | 40 | 30 | 30 | 1365 | 50 | gl. |
| | | | | | | 1356 | 40 | small forsterite, gl. |
| 237 | 20 | 80 | 20 | 40 | 40 | 1499 | 15 | gl. |
| | | | | | | 1480 | 20 | small forsterite, gl. |
| | $C_3P$ No. 238 | | | | | | | |
| 239 | 55 | 45 | 55 | 18 | 27 | 1297 | 30 | faint $C_3P$, forsterite, gl. |
| | | | | | | 1290 | 30 | $C_3P$, forsterite, gl. |
| | $C_3P$ No. 211 | | | | | | | |
| 224 | 65 | 35 | 65 | 28 | 7 | 1340 | 30 | gl. |
| | | | | | | 1332 | 40 | small $C_3P$, gl. |
| | | | | | | 1299 | 30 | $\beta$-$C_3P$, gl. |
| | | | | | | 1290 | 30 | $\beta$-$C_3P$, forsterite, gl. |
| 218 | 60 | 40 | 60 | 32 | 8 | 1314 | 40 | gl. |
| | | | | | | 1307 | 50 | small forsterite, $C_3P$, gl. |
| 219 | 50 | 50 | 50 | 40 | 10 | 1422 | 30 | gl. |
| | | | | | | 1407 | 30 | small forsterite, gl. |
| | | | | | | 1365 | 50 | forsterite gl. |
| | | | | | | 1250 | 60 | forsterite, $\beta$-$C_3P$, diopside |
| 220 | 40 | 60 | 40 | 48 | 12 | 1479 | 15 | gl. |
| | | | | | | 1460 | 20 | small forsterite, gl. |
| | | | | | | 1432 | 20 | forsterite, gl. |

The author acknowledges the constant help and encouragement given by Professor R. Kiyoura, Tokyo Institute of Technology. This work was conducted as a program to investigate the corrosion problems of various refractory bricks in the manufacture of fused phosphate fertilizer.

*Research Laboratory of*
*Engineering Materials*
*Tokyo Institute of Technology*
*Meguro-ku, Tokyo*

# *Ultraviolet Absorption Spectra of o-, m- and p-Dinitrobenzene*

By Takehiro ABE

(Received May 15, 1959)

Introduction of a substituent group for hydrogen in a benzene nucleus has been considered to shift in general the spectrum of the original benzene derivative to longer wavelengths. In the previous papers[1,2], however, the author found that absorption maximum bands of *m*-dinitrobenzene, 1,3,5-trinitrobenzene and 2,4,6-trinitrotoluene shifted to the blue as compared with the intense 260 m$\mu$ band of nitrobenzene.

In the present paper, an attempt has been made to investigate the influence of the introduction of one more nitro group in the ortho-, meta-, or para-position upon the spectrum of nitrobenzene.

## Experimental

**Materials.**—*o*-Dinitrobenzene, Tokyo Kasei Co. guaranteed reagent, was used directly; m.p. 118.1°C (lit. 118°C). Commercial pure *m*-dinitrobenzene was recrystallized three times from ethanol; m.p. 90.4°C (lit. 90°C). *p*-Dinitrobenzene, Tokyo Kasei Co. guaranteed reagent, was recrystallized once from methanol; m.p. 174.7°C (lit. 174°C). Commercial guaranteed ethanol was fractionally distilled after the usual treatment.

**Spectra.**—The spectra of the dinitrobenzenes in ethanol were measured with a Hitachi quartz spectrophotometer, Model EPU-2 at room temperature. Path length of absorption cells was 1 cm.

## Results and Discussion

As indicated in Fig. 1 and Table I, the maximum absorption band of *m*-dinitrobenzene is at a shorter wavelength and has a greater molar extinction coefficient than that of nitrobenzene, while the

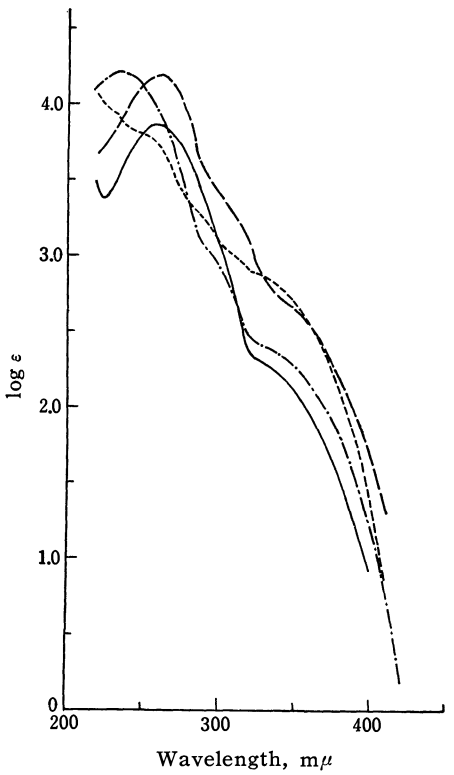



Fig. 1. Absorption spectra of nitrobenzene (——), *o*-dinitrobenzene (------), *m*-dinitrobenzene (—·—), and *p*-dinitrobenzene (— —), all in ethanol.

TABLE I. VALUES OF THE ABSORPTION MAXIMA OF DINITROBENZENES IN ETHANOL

| | $\lambda_{max}$, m$\mu$ | $\varepsilon$ |
|---|---|---|
| Nitrobenzene | 260 | 8140 |
| *o*-Dinitrobenzene | — | — |
| *m*-Dinitrobenzene | 233 | 17200 |
| *p*-Dinitrobenzene | 261 | 15600 |

1) T. Abe, This Bulletin, **31**, 904 (1958).
2) T. Abe, ibid., **32**, 339 (1959).

absorption maximum of *p*-dinitrobenzene gives a more intense absorption band at the same region as the 260 m$\mu$ band of nitrobenzene. The 260 m$\mu$ band of nitrobenzene has been interpreted by Doub and Vandenbelt[3] and later by Wenzel[4] to correspond to the 200 m$\mu$ band of benzene which has the same intensity, but has been interpreted by Nagakura and Tanaka[5] in terms of the intramolecular charge transfer involving an excitation of a bonding electron of the highest occupied energy-level of benzene to the vacant energy-level of the nitro group.

From the concept of the intramolecular charge transfer, the maximum absorption bands of *m*- and *p*-dinitrobenzene will be discussed by considering interactions between the highest occupied energy-levels of nitrobenzene and the vacant level of the nitro group on substituting the second nitro group in the meta- or para-carbon atom of nitrobenzene. According to the energy level diagrams given by Nagakura and Tanaka[6,7], the vacant energy-level ($V_{NO_2}=-6.85$ eV.) of the nitro group is lower than the lowest vacant energy-level ($V_N=-4.65$ eV.) of nitrobenzene, to which the $V_{NO_2}$ mainly contributes. On introducing one more nitro group in nitrobenzene, the energy-levels of nitrobenzene, indicated in Fig. 2, may be approximately affected by only the vacant level ($V_{NO_2}$) of the nitro group with such interaction as was given by Nagakura and Tanaka[5], because interactions with other occupied levels of the nitro group, which are remote or of different symmetry, are negligibly small. According to Nagakura and Tanaka's theory, as a result of the interaction with the $V_{NO_2}$, an energy-level ($E=H_{N1}$ or $H_{N2}$) of nitrobenzene shifts below by the following magnitude:

$$\Delta E=1/2[(E-V_{NO_2})+\{(E-V_{NO_2})^2+4C_N^2C_{NO_2}^2\beta^2\}^{1/2}] \quad (1)$$

Here $C_N$ and $C_{NO_2}$ are a coefficient of an atomic orbital of a carbon atom in the molecular orbital of $E$ and a coefficient of an atomic orbital of the nitrogen atom in the molecular orbital of $V_{NO_2}$, respectively, where the carbon atom and the nitrogen one are joined together. The $\beta$ is the resonance integral between the atomic orbital of the carbon atom and the orbital of the nitrogen atom. It is obvious that the $\Delta E$ increases as $C_N$ increases or as $(E-V_{NO_2})$ decreases. On the other hand, the $V_{NO_2}$ of the nitro group similarly interacts with the levels of nitrobenzene, especially with the $H_{N1}$, $H_{N2}$ and the $V_N$ that is nearest to the $V_{NO_2}$. When the nitro group is substituted in the meta-position of nitrobenzene, two intense absorption bands of intramolecular charge transfer can be expected to appear at longer wavelengths for *m*-dinitrobenzene owing to transitions involving excitations of bonding electrons of the occupied levels ($H_{m1}$ and $H_{m2}$) to the lowest vacant level ($V_m$), because the $V_{NO_2}$ interacts with both the levels of $H_{N1}$ and $H_{N2}$, as in the case of some disubstituted benzenes[6]. On substituting the nitro group in the para-position of nitrobenzene, a transition of a bonding electron in $H_{p2}$ to the lowest vacant level ($V_p$) can be predicted to show only an intense band of intramolecular charge transfer at a longer wavelength, the $B_1$-level ($H_{N1}$) in nitrobenzene being intact. The blue shift of 260 m$\mu$ band of nitrobenzene for

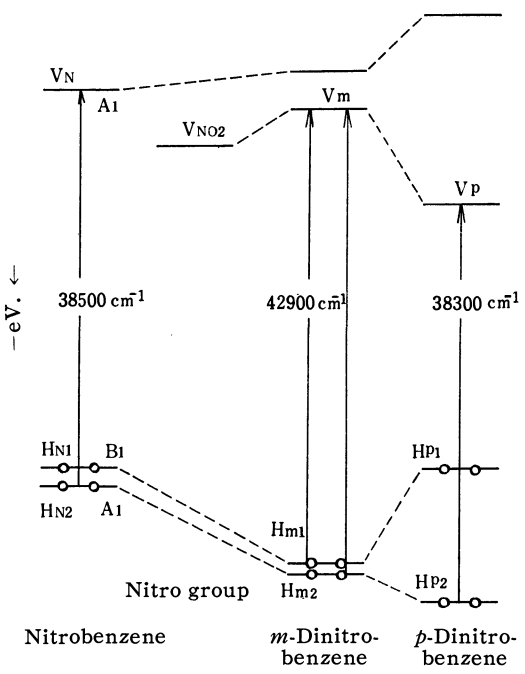



Fig. 2. Spectra of intramolecular charge transfer in dinitrobenzenes.

3) L. Doub and J. M. Vandenbelt, *J. Am. Chem. Soc.*, **69**, 2714 (1947).
4) A. Wenzel, *J. Chem. Phys.*, **22**, 1623 (1954).
5) S. Nagakura and J. Tanaka, ibid., **22**, 236 (1954); *J. Chem. Soc. Japan, Pure Chem. Sec.* (*Nippon Kagaku Zasshi*), **75**, 331 (1954).
6) J. Tanaka and S. Nagakura, *J. Chem. Phys.*, **24**, 1274 (1956); *J. Chem. Soc. Japan, Pure Chem. Sec.* (*Nippon Kagaku Zasshi*), **78**, 1200 (1957).
7) S. Nagakura and J. Tanaka, This Bulletin, **32**, 734 (1959).

*m*-dinitrobenzene means the great interaction of $V_{NO_2}$ with $H_{m_1}$ and $H_{m_2}$. Consequently, these levels will shift in nitrobenzene as indicated Fig. 2. In this case, the occupied $B_1$-level ($H_{N_1}$) as well as the $A_1$-level ($H_{N_2}$) in nitrobenzene may be predicted to become low in *m*-dinitrobenzene, because the coefficient of the atomic orbital belonging to the meta-carbon atom in the molecular orbital of the occupied $B_1$-level ($H_{N_1}$) of nitrobenzene is greater than the corresponding coefficient in the $A_1$-level, although the $H_{N_1}$ is slightly higher than the $H_{N_2}$. In the molecular orbital of the occupied $A_1$-level ($H_{N_2}$) of nitrobenzene, the coefficient of the atomic orbital for the para-carbon atom is apparently greater than that for the meta-carbon atom. Accordingly, the $A_1$-level ($H_{N_2}$) of nitrobenzene can be considered to become lower in *p*-dinitrobenzene than in *m*-dinitrobenzene, as given from Eq. 1. The maximum absorption band of *p*-dinitrobenzene lies at the wavelength close to that of nitrobenzene. From these it may be expected that the $V_{NO_2}$-level shifts below to the same extent, as compared with the $H_{N_2}$, in *p*-dinitrobenzene, owing to the great interaction between the $V_{NO_2}$ and the $V_N$. In comparison with the case of *m*-dinitrobenzene, it is known that the coefficient of the atomic orbital of the para-carbon atom is probably much greater than that of the meta-carbon atom in the molecular orbital of the vacant $A_1$-level ($V_N$) of nitrobenzene. From the above discussion, the maximum absorption bands of dinitrobenzenes may be interpreted to be owing to the electronic transitions illustrated in Fig. 2.

An ortho-substituted benzene usually shows a spectrum resembling that of a meta-substituted benzene[6], while the absorption curve of *o*-dinitrobenzene is different from that of *m*-dinitrobenzene, giving only shoulders at 250, 290, 310 and 360 m$\mu$. This may be understood in terms of steric hindrance by the adjacent large nitro groups of *o*-dinitrobenzene. This steric hindrance may interfere with a coplanar arrangement of the nitro groups with benzene nucleus.

The weak shoulder of nitrobenzene at 290 m$\mu$, which has been interpreted by Nagakura and Tanaka[6,8] to be related to the 260 m$\mu$ band of benzene, becomes more distinct in *m*- and *p*-dinitrobenzene.

The molar extinction coefficients of the 360 m$\mu$ bands for *o*- and *p*-dinitrobenzene are greater than those of *m*-dinitrobenzene, which are slightly larger than the corresponding molar extinction coefficient for nitrobenzene. The 360 m$\mu$ band of nitrobenzene has been interpreted by Wenzel[4] to be due to the nitro group.

## Summary

In ethanol, *m*-dinitrobenzene shows the maximum absorption band at shorter wavelengths than nitrobenzene, while *p*-dinitrobenzene gives the absorption maximum at the wavelength near to that of nitrobenzene. These bands have briefly been discussed from the concept of the intramolecular charge transfer. The absorption curve of *o*-dinitrobenzene, indicating no absorption maximum but shoulders, are different from those of the other dinitrobenzenes, probably owing to steric hindrance by the adjacent large nitro groups.

The author is particulary indebted to Professor Yōkan Nomura for his suggestion and encouragement.

*Department of Chemistry*
*Defense Academy*
*Yokosuka*

8) J. Tanaka, *J. Chem. Soc. Japan, Pure Chem. Sec.* (*Nippon Kagaku Zasshi*), **79**, 1114 (1958).

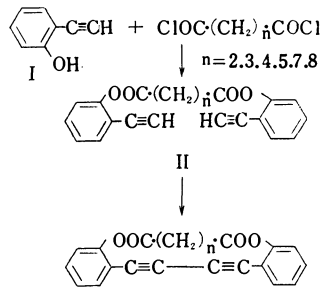
# *Cyclic Acetylenes. I. Cyclic Derivatives of o,o'-Dihydroxydiphenyldiacetylene. An Example of a Strained Cyclic Diacetylene**

By Fumio TODA and Masazumi NAKAGAWA

(Received July 21, 1959)

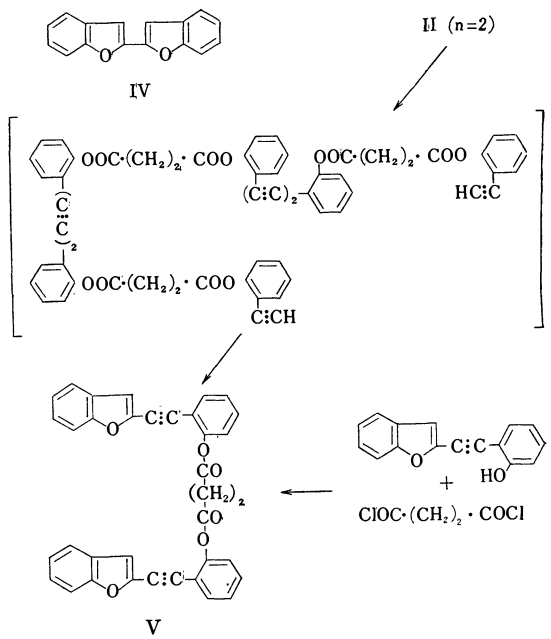
It is of interest to compare the physical and chemical properties of a strained acetylenic compound with that of a strainless analogue in relation to the reactive nature of benzyne intermediate[1]. Along with this line the authors have studied the synthesis of a cyclic diacetylene in which the structure of the molecule forces to bend the diacetylenic linkage. Recently a fairly large variety of cyclic polyacetylenes have been synthesized by several investigators[2], but most of these macrocycles seem to be strainless with regard to the triple bond.

A series of cyclic derivatives of *o,o'*-dihydroxydiphenyldiacetylene have been synthesized according to the following scheme. *o*-Hydroxyphenylacetylene (I)[3] was converted into the polymethylene dicarboxylate (II) by the reaction with the corresponding diacid dichloride in alkaline media. By oxidative coupling of II ($n$=2, 3, 4, 5, 7 and 8) according to the procedure of Eglinton[2] the authors have obtained $III_a$, $III_b$, $III_c$, $III_d$ and $III_{d'}$ in 20, 40, 21 and 7.5% ($III_d$+$III_{d'}$) yield, respectively. Two isomers were found in the case of $n$=7. The low-melting isomer ($III_d$, m. p. 111°C) completely changed to the high-melting isomer ($III_{d'}$, m. p. 125~127°C) on standing at room temperature for two weeks.




The structures of compounds III were inferred from analyses, molecular weight determinations, ultraviolet and infrared spectroscopy. The cyclic nature of III was also confirmed by the absence of free ethynyl absorption in infrared spectra (ca. 3300 $cm^{-1}$) and by titration against silver nitrate.

In the case of $n$=3, 2, 2'-dibenzofuranyl (IV)[4] was isolated in 25% yield together with $III_a$. IV was also obtained from the products of the coupling reaction of II ($n$=2) in 57% yield together with a small amount of compound V. The ultraviolet spectrum of V closely resembles that of 2-(2'-benzoyloxyphenylethynyl)-benzofurane[4] as illustrated in Fig. 1. The structure of V was confirmed by the




* For a preliminary announcement of a part of this work, see *Chem. & Ind.*, **1959**, 458.

1) G. Wittig, *Angew. Chem.*, **68**, 245 (1957); J. D. Roberts, "Chemical Society Symposia Bristol 1958", The Chemical Society, London (1958), p. 115.

2) G. Eglinton and A. R. Galbraith, *Chem. & Ind.*, **1956**, 737; *J. Chem. Soc.*, **1959**, 889; F. Sondheimer, Y. Amiel and R. Wolovsky, *J. Am. Chem. Soc.*, **79**, 4274 (1957) and preceding papers.

3) V. Prey and G. Pieh, *Monatsh. Chem.*, **80**, 790 (1949).

4) F. Toda and M. Nakagawa, This Bulletin, **32**, 514 (1959).

identity with a synthetic specimen which was obtained by the reaction of 2-(2'-hydroxyphenylethynyl)-benzofurane[4] and succinic acid dichloride in alkaline media.

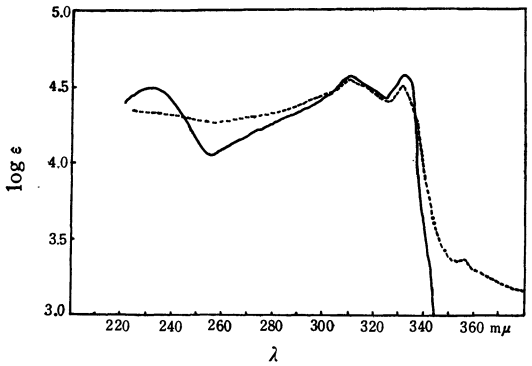
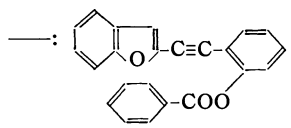


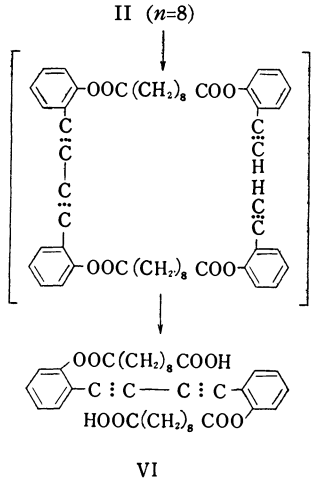

Fig. 1. The ultraviolet spectra of 2-(2'-benzoyloxyphenylethynyl)-benzofurane and V. The curve of V was drawn using the reduced ε values corresponding to the diyne-unit.




----: V

The mechanism of the formation of IV is not yet clear, but it may be formed from highly strained III cleaving the ester linkages simultaneously accompanying the benzofurane ring formation. It has been reported by the present authors that IV is formed in a quantitative yield from *o*, *o'*-dihydroxydiphenyldiacetylene on treatment with alkali[4]. IV and adipic acid are formed on the alkaline hydrolysis of $III_b$, but the formation of IV from *o*, *o'*-dihydroxydiphenyldiacetylene under the condition of Eglinton's oxidative coupling was not observed. Therefore, the simple interpretation such as the intramolecular cyclization to IV of *o*, *o'*-dihydroxydiphenyldiacetylene which is formed by the ring fission of the cyclic diyne is not acceptable as the mechanism of the formation of IV under the condition of the coupling reaction. Also the formation of V may be attributed to the fission of the ester linkages presumably in the course of cyclic trimerization of II ($n=2$).

The attempt to prepare III ($n=8$) have failed. In this case the only identified product was VI, and the formation of VI is also probably associated with the fission of the ester linkages during the course of cyclic dimerization of II ($n=8$).




VI

The most striking property of $III_a$ is its high sensitivity to light in the solid state making a sharp contrast to the photostable nature of $III_b$, $III_c$, $III_d$ and $III_{d'}$. The surface of the colorless crystals of $III_a$ was rapidly coated with red colored, insoluble and high melting point material when the solid was exposed to a diffused light in the laboratory. But the solution of $III_a$ was found to be fairly stable. These properties are closely related to those of some polyacetylene compounds[5].

Examination of the scale models of III indicates that $III_b$ is a rigid and planar molecule with the two phenyl groups held in the same plane. On the other hand, the phenyl groups in $III_c$ are not readily able to become coplanar on account of the bridging chain. The model of $III_a$ clearly shows that the diacetylenic linkage is forced to bend owing to the short methylene chain holding its phenyl groups in a coplanar position. The anomalous photosensitivity of $III_a$ may be attributed therefore to the bending of the diacetylenic bond. It has already been suggested by Bohlmann that the stabilization of a certain polyacetylenic compound bearing two bulky terminal groups is associated with the steric effect of the bulky groups retarding the formation of cross linkings[6]. The diacetylenic linkage in $III_a$ seems to be more exposed to the outer environment of the molecule on account of its bending as compared with that linkage of the corresponding less strained cyclic diynes. Therefore the intermolecular approach to form cross linkings which is facilitated

5) Cf. J. B. Armitage, C. L. Cook, N. Entwistle, E. R. H. Jones and M. C. Whiting, *J. Chem. Soc.*, **1952**, 1998.
6) F. Bohlmann and E. Inhoffen, *Chem. Ber.*, **89**, 1276 (1956).

by the presence of the distorted diacetylenic bond is, though it is not decisive, a possible cause of the unstable nature of $III_a$.

The catalytic reduction of 2,2′-diacetoxydiphenyldiacetylene (VII), $III_a$ and $III_b$ were carried out using a palladium on charcoal catalyst. It was hoped that $III_a$ might exhibit some abnormalities in the course of hydrogenation resulting from the ring strain, but the experimental results indicated no marked difference in the rates of hydrogenation as illustrated in Fig. 2. The fact that the hydrogenation of $III_a$ stopped after absorption of ca. 90% of theoretical amount of hydrogen is probably ascribed to the formation of minor amount of the above mentioned photopolymer during the course of reduction.

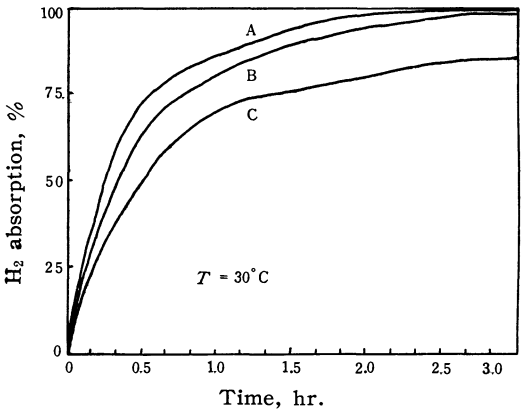



Fig. 2. The rates of hydrogenation of VII, $III_a$ and $III_b$.
A: VII B: $III_b$ C: $III_a$

These situations seem to be reflected in the ultraviolet spectra of $III_a$, $III_b$, $III_c$ and $III_d$. VII was used as a comparison for an open chain analogue of III. As indicated in Table I and Fig. 3, the ultraviolet spectra of these diacetylene are closely related and are different only in the absorption intensities without any significant wavelength displacements. The extinction coefficients $\varepsilon$ of $\lambda_{max}$ of the long wavelength region (290~340 m$\mu$) of $III_b$ are larger than that of VII, but the $\varepsilon$ values of $III_a$, $III_c$, $III_d$ and $III_{d'}$ in the same region are smaller than that of VII.

TABLE I

| Compound | Absorption | | | | | | | | | |
|---|---|---|---|---|---|---|---|---|---|---|
| VII | | | | 250 (479) | 260 (483) | 275 (240) | 291 (337) | 310 (445) | 331 (398) | |
| $III_a$ | 229.5 (304) | **235** (260) | | | | **275** (88) | 292 (198) | 310 (322) | 331 (292) | |
| $III_b$ | | | | | | 275 (113) | 291 (290) | 310 (535) | 332 (541) | |
| $III_c$ | | | | 248.5 (267) | | **275** (122) | 293 (171) | 310 (216) | 331 (174) | |
| $III_d$ | | | | 248 (301) | 260 (304) | 275 (152) | 290 (227) | 309 (337) | 331 (304) | |
| $III_{d'}$ | | | | 249 (325) | 260 (322) | | 292 (197) | 310 (241) | 331 (200) | |
| V | | | | | | | | 310 (343)* | 331 (315)* | |
| VI | | | | 250 (361) | 260 (364) | **275** (155) | 292 (204) | 310 (248) | 331 (216) | |
| $VIII_a$ | | | | 250 (305) | 260 (316) | 275 (153) | 290 (219) | 309 (288) | 331 (255) | |
| $VIII_b$ | | | | 250 (277) | 260 (284) | 275 (124) | 291.5 (205) | 309.5 (284) | 331 (244) | |
| $IX_a$ | | | | | 260 (294) | 275 (112) | **310** (207) | 326 (316) | 349 (267) | |
| $IX_b$ | | | | | 260 (272) | 275 (95) | **310** (190) | 327 (293) | 349 (251) | |
| $X_a$ | | | **240** (204) | | 260 (213) | **275** (85) | 305 (168) | 323 (270) | 345 (236) | |
| $X_b$ | | | **240** (204) | | 260 (216) | **275** (97) | **305** (166) | 323 (252) | 345 (218) | |

The figures indicate the $\lambda_{max}$ in m$\mu$.
The figures in parentheses are $\varepsilon_{max} \times 10^{-2}$.
Asterisk indicates the $\varepsilon$ value of per dyne unit.
The bold figures indicate shoulders.
All spectra were measured in 95% ethanol.

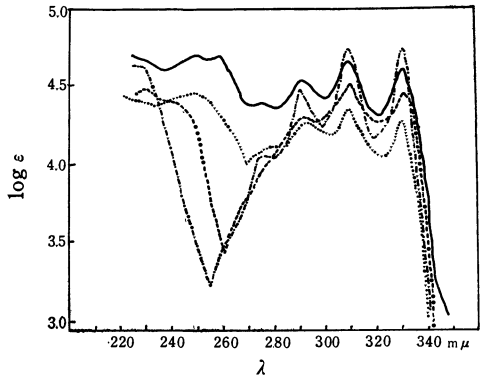
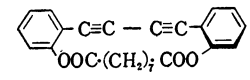


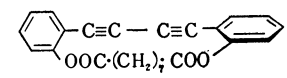

Fig. 3. The ultraviolet spectra of VII and the cyclic diacetylenes ($III_a$, $III_b$ and $III_c$).
——: VII -----: $III_a$
-·-·-: $III_b$ ·····: $III_c$

The decrease of the ε values are in the sequence of $III_b > VII > III_a > III_c$ indicating the important role of the uniplanar phenyl groups in affecting the intensity of absorption. This fact suggests that the spectra associate with transitions between non-planar ground states and near planar excited states[7]. The largest ε values of $III_b$ in this region may be due to the rigid and planar structure of the molecule having maximum conjugation between the two phenyl groups and the acetylenic bonds. On the other hand, the smaller ε values of $III_a$ as compared with VII may be attributed to the diminished probability of excitation of the molecule to an excitation state in which the diacetylenic linkage should take a linear configuration. The low intensity of absorption of $III_c$, $III_d$ and $III_{d'}$ may also be regarded as the twisted position of the phenyl groups in these molecules affecting to reduce the probability to a uniplanar state of excitation.

The ultraviolet spectra of $III_d$ and $III_{d'}$ are different as shown in Table I and Fig. 4. The absorption intensity in the long wavelength region of $III_{d'}$ is much lower than that of $III_d$ indicating the presence of a larger degree of twist of the phenyl groups in $III_{d'}$ as illustrated in the following formulae. Examination of the scale models of $III_d$ and $III_{d'}$ indicates that the methylene chain in $III_d$ is much more crowded than in $III_{d'}$. Therefore, the relief of compression energy of methylene chain seems to be responsible to the




$III_d$




$III_{d'}$

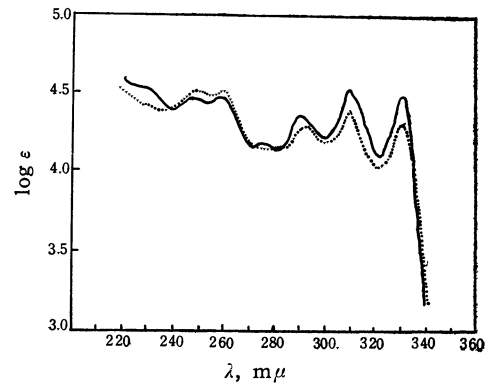
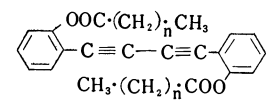


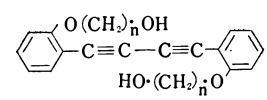

Fig. 4. The ultraviolet spectra of the isomeric cyclic diacetylene ($III_d$ and $III_{d'}$).
——: $III_d$ ·····: $III_{d'}$

stabilization of $III_d$ to $III_{d'}$. The isolation of $III_d$ and $III_{d'}$ may be regarded as the first example of the presence of a new type of conformational isomers in which the diacetylenic linkage behaves as pivot bond.

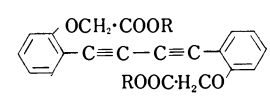
The low absorption intensity in the ultraviolet spectrum of VI is also explained by the hypochromic effect of non-coplanar




VII : n=0
$VIII_a$ : n=1
$VIII_b$ : n=2




$IX_a$ : n=2
$IX_b$ : n=3




$X_a$ : R=$CH_3$
$X_b$ : R=$C_2H_5$

7) E. Braude, F. Sondheimer and W. F. Forbes, *Nature*, 173, 117 (1954); Also cf. E. Heilbronner and R. Gerdil, *Helv. Chim. Acta*, 39, 1996 (1956).

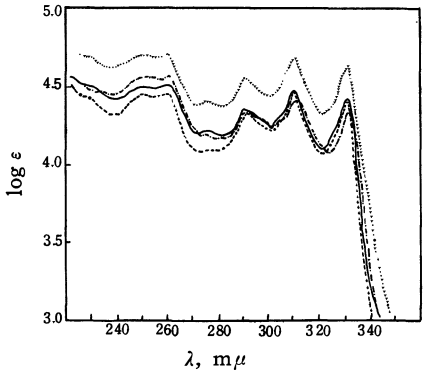



Fig. 5. The ultraviolet spectra of 2,2'-diacyloxydiphenyldiacetylenes.
·····: VII ——: $VIII_a$
----: $VIII_b$ -·-·: VI

phenyl groups. Further examples of the effect are obtained in the series of VIII, IX and X. As illustrated in Fig. 5 and Table I, the increase in the number of methylene group in VIII resulted in the decrease of the intensity of absorption. The steric effect of the acyl group affecting the hypochromic shift of the ultraviolet spectra of VIII seems to show a tendency approaching to a definite value when the steric requirement of the group reaches a certain degree, namely, the differences of $\varepsilon$ values between VII and $VIII_a$, $VIII_b$ and the differences between VII and VI are quite large, while the difference between $VIII_a$ and $VIII_b$ and that of VI and $VIII_a$, $VIII_b$ are relatively small.

The same trend is also observed in the case of $IX_a$, $IX_b$, $X_a$ and $X_b$ as indicated in Figs. 6 and 7 and in Table I.

The characteristic feature in the ultraviolet spectra of $III_a$ and $III_b$ are the presence of a sharp and intense $\lambda_{min}$ at ca. 260 mμ, the $\varepsilon$ values are only one-

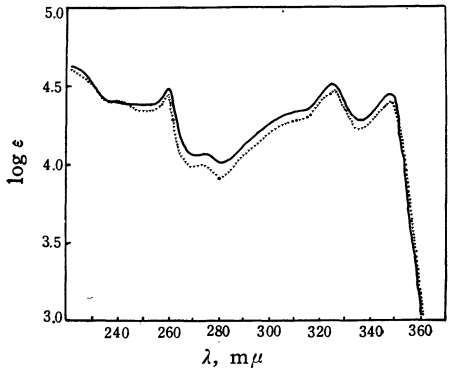



Fig. 6. The ultraviolet spectra of 2,2'-di-ω-hydroxyalkyloxydiphenyldiacetylenes.
——: $IX_a$ ·····: $IX_b$

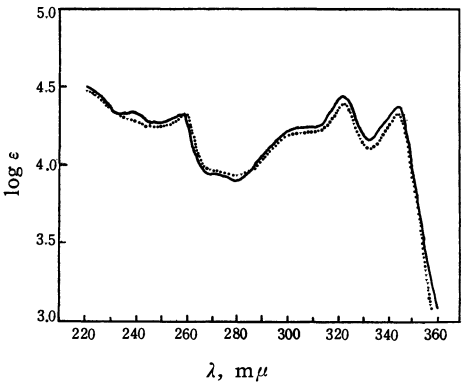



Fig. 7. The ultraviolet spectra of 2,2'-di-(alkyloxycarbonylmethoxy-diphenyl-diacetylenes.
——: $X_a$ ·····: $X_b$

tenth of the corresponding $\varepsilon$ of $III_c$ and $III_d$. The proximity effect of *o,o'*-bridging chain which is held closely parallel with the diacetylenic linkage may be a possible explanation of this fact, but it is premature to deduce a conclusion from these few examples.

Further studies in the same direction are now in progress.

## Experimental**

**General Procedure of the Preparation of Di-*o*-ethynyl-phenyl Polymethylene Dioate (II, $n=2$, 3, 4, 5, 7 and 8).**—Polymethylene dioic acid chloride (2 mol.) was added to the solution of *o*-hydroxy-phenylacetylene[4] (I, 1 mol.) in 10% aqueous solution of potassium hydroxide (7 equiv.). The mixture was shaken under ice cooling. The oily material separated was extracted with ether, washed with aqueous potassium hydroxide and water successively. The colorless viscous oil obtained on evaporating the solvent was used without further purification. For example, in the case of $n=7$, azelaic acid chloride (9.0 g., 0.04 mol.) was added in one portion to the solution of I (2.4 g., 0.02 mol.) in 10% aqueous solution of potassium hydroxide (7.8 g., 0.14 mol.), and the mixture was shaken for 1 hr. The reaction mixture was extracted with ether, washed with aqueous potassium hydroxide and water. The ether extract was dried over anhydrous magnesium sulfate. A colorless oil was obtained by the evaporation of the solvent (3.3 g., 85%). The crude II [$n=7$, I. R. max., 3260 (-C≡CH), 2860, 2920 ($-CH_2-$), 1762 $cm^{-1}$ (ester)] gave yellow cuprous acetylide by Ilosvay's reagent, and gave white silver salt by an alcoholic silver nitrate solution.

**Oxidative Coupling of Di-*o*-ethynylphenyl Adipate ($n=4$).** — The mixture of II ($n=4$, 1.5 g.), cupric

** Not all melting points are corrected. Infrared spectra were measured using liquid film or nujol mull method.

acetate monohydrate (15 g.) and pyridine (150 g.) was stirred for 4 hr. at 55°C. The stirring was continued for additional 1 hr. at room temperature. Most of the pyridine was removed from the reaction mixture under reduced pressure. Water (1000 ml.) was added to the residue and extracted with ether (1000 ml.). The ether extract was washed with aqueous cupric acetate and water, successively. The ethereal solution was dried over anhydrous magnesium sulfate. The solvent was removed and the residual solid was recrystallized from ethanol giving $III_b$ (0.6 g., 40%) as colorless needles, m. p. 123.5°C.

*Anal.* Found: C, 76.83; H, 4.54; mol. wt. (Rast), 325. Calcd. for $C_{22}H_{16}O_4$: C, 76.73; H, 4.68%; mol. wt., 344.

I. R. max., 1758 $cm^{-1}$ (ester).

$III_b$ gave no precipitation with alcohlic silver nitrate solution.

**Hydrolysis of $III_b$.** — $III_b$ (0.1 g.) was dissolved in an aqueous alcoholic solution of potassium hydroxide (ethanol 15 ml., water 2 ml. and potassium hydroxide 0.3 g.). The solution was refluxed for 3 hr. on a boiling water bath. The crystals were recrystallized from ethanol yielding colorless needles, m. p. 194.5~195.5°C which showed no depression of the mixed melting point with an authentic sample of 2,2'-dibenzofuranyl (IV)[4]. The filtrate was washed with ether and the aqueous layer was acidified with 2 N hydrochloric acid, extracted with ether. Treatment of the ether extract gave adipic acid, m. p. 148~150°C. The mixed melting point with pure adipic acid showed no depression.

**Oxidative Coupling of Di-*o*-ethynylphenyl Glutarate (II, $n=3$).** — II ($n=3$, 2.5 g.) was mixed with cupric acetate monohydrate (20 g.) and pyridine (200 g.). The mixture was agitated for 4 hr. at 55°C. The insoluble precipitate was removed from the reaction mixture by filtration and was washed with ether. The filtrate was distilled under reduced pressure to remove pyridine. The residue was extracted with ether (600 ml.). The ether extract and the ethereal washing was combined and washed with a saturated aqueous solution of cupric acetate and water. The ether solution was dried over anhydrous magnesium sulfate and concentrated to 100 ml. The crystals deposited at this stage were filtered (m. p. 194.5~195.5°C, 0.2 g.). The crystals were identified as 2,2'-dibenzofuranyl (IV) by the mixed melting point determination. The solvent was removed from the filtrate and the residue was recrystallized from ethanol employing active charcoal, giving colorless needles mixed with hexagonal plates. Further recrystallization of the mixed crystals from ethanol (50 ml.) gave 0.2 g. of IV. The total yield of IV was found as 0.4 g. (25%). Slightly impure $III_a$ was obtained as hexagonal plates (m. p. 133~134°C, 0.5 g., 20%) on standing the alcoholic filtrate. Recrystallization of this material gave pure $III_a$, m. p. 135~136°C.

*Anal.* Found: C, 76.33; H, 4.08; mol. wt. (Rast), 350. Calcd. for $C_{21}H_{14}O_4$: C, 76.35; H, 4.27%; mol. wt., 330.

I. R. max., 1755 $cm^{-1}$.

The surface of the crystals of $III_a$ changed to red on exposure to a diffused light in the laboratory. An amorphous, high melting material remained when the colored crystals were dissolved in ethanol.

**Oxidative Coupling of Di-*o*-ethynylphenyl Pimelate (II, $n=5$).** — II ($n=5$, 1.4 g.) was oxidized with cupric acetate monohydrate (1.5 g.) in pyridine (150 g.) at 55°C. After 3 hr., the reaction mixture was treated similarly as described above yielding a viscous oil (1.3 g.). The mixture of the oil with methanol (2 ml.) gradually solidified on standing. Repeated recrystallization from methanol using active charcoal gave $III_c$ as colorless needles, m. p. 120.5~121.5°C, 0.3 g (21%).

*Anal.* Found: C, 76.94; H, 5.06; mol. wt. (Rast), 364. Calcd. for $C_{23}H_{18}O_4$: C, 77.08; H, 5.06%; mol. wt., 358.

I. R. max., 1760 $cm^{-1}$.

$III_c$ gave no precipitation with alcoholic silver nitrate.

***o,o'*-Diacetoxydiphenyldiacetylene (VII).** — Acetic anhydride (2.0 g.) was introduced in one portion to the solution of *o,o'*-dihydroxydiphenyldiacetylene (0.4 g.) in aqueous potassium hydroxide (water 40 ml., potassium hydroxide 1.4 g.). The mixture was shaken under ice cooling. The solid deposited was collected by filtration and recrystallized from ethanol yielding VII as colorless needles, m. p. 134°C.

*Anal.* Found: C, 75.33; H, 4.31. Calcd. for $C_{20}H_{14}O_4$: C, 75.46; H, 4.43%.

I. R. max., 1755 $cm^{-1}$ (ester).

**Oxidative Coupling of Di-*o*-ethynylphenyl Succinate (II, $n=2$).** — The mixture of II ($n=2$, 2.5 g.) was stirred for 3 hr. at 55°C and the stirring was continued further 30 min. at room temperature. The most of pyridine was removed under reduced pressure. Water was added to the residue and the mixture was extracted with ether (1000 ml.). The extract was washed with saturated solution of cupric acetate and water, successively. The dried ether extract was reduced to 100 ml. and the needle-like crystals deposited (0.4 g., m. p. 194.5~195.5°C) were collected by filtration. This was identified as IV by mixed melting point determination. The solvent was removed from the filtrate resulting in a mixture of viscous oil and crystals. The crystals separated by filtration were washed with hot ethanol, giving IV (0.7 g.). The recrystallization of the combined IV from benzene using charcoal, yielded 1.0 g. (57%) of IV. The oily filtrate gradually solidified on standing. The solid was treated with ethanol and charcoal to result in V, colorless needles, m. p. 157.5~158.5°C, 20 mg. (ca. 1%).

*Anal.* Found: C, 78.23; H, 4.09; mol. wt. (Rast), 517. Calcd. for $C_{36}H_{22}O_6$: C, 78.54; H, 4.03%; mol. wt., 550.

I. R. max., 1755 $cm^{-1}$ (ester).

V gave a negative test against alcoholic silver nitrate.

**Synthesis of Di-2-(2'-benzofuranylethynyl)-phenyl Succinate (V).** — 2-(2'-Hydroxyphenylethynyl)-benzofurane[4] (50 mg.) was dissolved in the solution of potassium hydroxide (0.35 g.) in water (10 ml.). Succinoyl chloride (0.31 g.) was added in one portion to the alkaline solution and was shaken to result in a crystalline solid. The solid was collected by filtration, washed with water and alcohol. Recrystallization from ethanol gave colorless needles, m. p. 157.5~158.5°C, 30 mg. (51%). The mixed melting point with V, the product of the oxidative coupling of II ($n$=2), showed no depression. The infrared spectra of these two substances were found as identical over the entire region of wavelength.

**Oxidative Coupling of Di-*o*-ethynylphenyl Nonanedioate (II, $n$=7).** — The mixture of II ($n$=7, 2.0 g.), cupric acetate monohydrate (15 g.) and pyridine (150 g.) was stirred for 3.5 hr. at 55°C. Pyridine was removed under reduced pressure. Water (1000 ml.) was added to the residue and the mixture was extracted with ether (1000 ml.). The ethereal layer was washed with saturated solution of cupric acetate and water, successively, and dried over anhydrous magnesium sulfate. A viscous oil (0.5 g.) obtained by removing the solvent was mixed with ethanol (2.0 ml.). The mixture was kept to result crystallization. The crystals were collected by filtration (filtrate A). The crystals were recrystallized from ethanol and separated by filtration (filtrate B). Further recrystallization from ethanol gave $III_{d'}$ as colorless needles, m. p. 125~127°C, 50 mg. (2.5%).

*Anal.* Found: C, 77.20; H, 5.73. Calcd. for $C_{25}H_{22}O_4$: C, 77.70; H, 5 74%.

The crude crystals obtained by the concentration of the combined filtrates A and B were treated with ethanol and charcoal and recrystallized from ethanol, resulting in $III_d$ as colorless needles, m. p. 111°C, 100 mg. (5%).

*Anal.* Found: C, 77.56; H, 5.68; mol. wt. (Rast), 399. Calcd. for $C_{25}H_{22}O_4$: C, 77.70; H, 5.74% mol. wt., 386.

After being kept for two weeks at room temperature the melting point of $III_d$ raised to 125~127°C and the mixed melting point of the material with $III_{d'}$ showed no depression. The ultraviolet spectra of $III_d$ and $III_{d'}$ measured after 4 days from the isolation are listed in Table I.

**Oxidative Coupling of Di-*o*-ethynylphenyl Decanedioate (II, $n$=8).** — II ($n$=8, 2.5 g.) was treated with cupric acetate monohydrate (15 g.) in pyridine (200 g.) at 55°C for 4 hr. The same treatment of the reaction mixture as stated in the case of II ($n$=7) resulted a crystalline solid. Recrystallization of the solid from ethanol employing charcoal yielded VI as amorphous powder, m. p. 149~151.5°C, 0.3 g. (16%).

*Anal.* Found: C, 72.29; H, 6.83. Calcd. for $C_{36}H_{42}O_8$: C, 71.74; H, 7.02%.

I. R. max. (measured in hexachlorobutadiene), 2920, 2850 (-$CH_2$-), 2650 (carboxyl OH), 1755 (ester) and 1703 $cm^{-1}$ (carboxyl CO).

VI is readily soluble in aqueous sodium hydrogen carbonate and sodium hydroxide solution and gave a negative test against an ethanolic silver nitrate.

**2,2'-Dipropionyloxydiphenyldiacetylene ($VIII_a$).** — Propionic anhydride (2.6 g.) was added in one portion to the solution of 2,2'-dihydroxydiphenyldiacetylene[4] (0.47 g.) in water (20 ml.) and potassium hydroxide (1.6 g.). The mixture was shaken with occasional cooling with ice water. The solid separated was recrystallized from ethanol to result in $VIII_a$, m. p. 56°C, 0.5 g. (70%).

*Anal.* Found: C, 76.06; H, 5.29. Calcd. for $C_{22}H_{18}O_4$: C, 76.28; H, 5.24%.

I. R. max., 1770 $cm^{-1}$ (ester).

**2,2'-Dibutyloxydiphenyldiacetylene ($VIII_b$).** — 2,2'-Dihydroxydiphenyldiacetylene (1.2 g.) was reacted with butyric anhydride (8.0 g.) according to the same procedure described above for the preparation of $VIII_a$. The reaction mixture was extracted with ether and the extract was washed with aqueous alkali and water. The solvent was evaporated from the dried extract yielding crude crystals. Recrystallization of the crude material from aqueous ethanol resulted in $VIII_b$, m. p. 51°C, 1.4 g. (75%).

*Anal.* Found: C, 76.61; H, 5.93. Calcd. for $C_{24}H_{22}O_4$: C, 76.98; H, 5.92%.

I. R. max., 1755 $cm^{-1}$ (ester).

**2,2'-Di-(β-hydroxyethoxy)-diphenyldiacetylene ($IX_a$).** — The reaction of *o,o'*-dihydroxydiphenyldiacetylene with ethylenechlorohydrine in the presence of sodium ethoxide gave $IX_a$. $IX_a$ thus obtained was separated into two forms, labile form (m. p. 75~76°C) and stable form (m. p. 90~91°C). The labile crystals readily changed to the stable form on standing at room temperature.

*Anal.* Found: C, 74.64; H, 5.57. Calcd. for $C_{20}H_{18}O_4$: C, 74.52; H, 5.63%.

I. R. max., 3350 (-OH), 2145 (-C≡C-) and 1244 $cm^{-1}$ (=C-O-).

**2,2'-Di-(γ-hydroxypropoxy)-diphenyldiacetylene ($IX_b$).** — *o*-(γ-Hydroxypropoxy)-phenylacetylene (b. p. 142~143°C/7 mmHg) which was obtained in 88% yield by the reaction of *o*-hydroxyphenylacetylene[1] and 3-bromo-1-propanol in the presence of sodium ethoxide was oxidatively coupled according to the method of Sörensen[8]. Treatment of the reaction mixture resulted in $IX_b$ as colorless needles in 57% yield, m. p. 103°C.

*Anal.* Found: C, 75.54; H, 6.01. Calcd. for $C_{22}H_{22}O_4$: C, 75.41; H, 6.33%.

I. R. max., 3320 (-OH), 2145 (-C≡C-), 1252 $cm^{-1}$ (=C-O-).

**2,2'-Di-(alkyloxycarbonylmethoxy)-diphenyldiacetylene ($X_a$ and $X_b$).** — The reaction of *o,o'*-dihydroxydiphenyldiacetylene with methyl bromoacetate in the presence of sodium ethoxide resulted in $X_a$ as colorless needles in 75% yield, m. p. 143°C.

*Anal.* Found: C, 70.04; H, 4.90. Calcd. for $C_{22}H_{18}O_6$: C, 69.83; H, 4.80%.

I. R. max., 1745 $cm^{-1}$ (ester).

$X_b$ was prepared in the same manner employing

8) T. Bruun, T. Morthei and N. A. Sörensen, *Acta Chem. Scand.*, 4, 850 (1950).

ethyl bromoacetate, m. p. 98.5～99°C, colorless needles.

*Anal.* Found: C, 70.57; H, 5.36. Calcd. for $C_{24}H_{26}O_6$: C, 70.92; H, 5.46%.

The authors are grateful to the Shiono Perfume Industry Co., Osaka for generous quantities of coumalin and to Messrs. T. Shiba and M. Okumiya and Miss K. Koike for performing the elementary analyses.

This work is supported by the grant-in-aid of the Ministry of Education and by the research fund of Kaiseikai, to whom they express their sincere thanks.

*Department of Chemistry*
*Faculty of Science*
*Osaka University*
*Nakanoshima, Osaka*

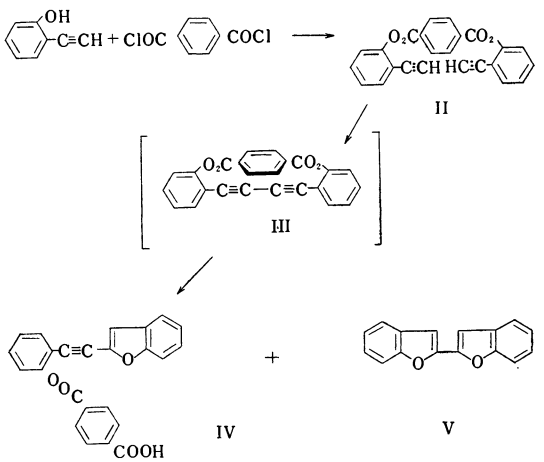
# *Cyclic Acetylenes. II. Attempted Synthesis of Cyclic Terephthalate of o, o'-Dihydroxydiphenyldiacetylene*

By Fumio TODA and Masazumi NAKAGAWA

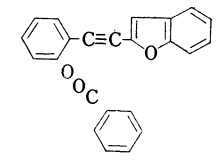
(Received July 21, 1959)

Cyclic terephthalate of *o, o'*-dihydroxydiphenyldiacetylene (III) may offer a suitable model substance for the investigation of transannular phenomena between the $\pi$-electron system of the benzene nucleus of terephthalic acid residue and that of diacetylenic linkage, because the scale model of this molecule indicates that the molecule is rigid, holding the terephthalate group closely in parallel with the diacetylenic linkage.

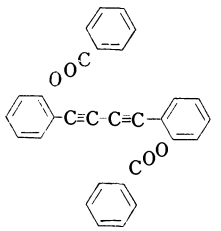
The synthesis of III has been attempted according to the following series of reactions. Di-2-ethynylphenyl terephthalate (II) was obtained in good yield by the reaction of *o*-hydroxyphenylacetylene (I)[1] with terephthaloyl chloride in aqueous acetone in the presence of sodium hydroxide.



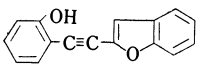
The oxidative coupling according to the Eglinton's procedure[2] at a reaction temperature of 55°C resulted in 2-(2'-benzofuranylethynyl)-phenyl hydrogen terephthlate (IV) in 5% yield. 2, 2'-Dibenzofuranyl (V)[3] and IV were isolated from the reaction products in 15 and 3% yield, respectively, when the reaction was carried out at a temperature of 60°C.



VI



VII



VIII

1) V. Prey and G. Pieh, *Monatsh. Chem.*, **80**, 790 (1949).
2) G. Eglinton and A. R. Galbraith, *Chem. & Ind.*, **1956**, 737.
3) F. Toda and M. Nakagawa, This Bulletin, **32**, 514 (1959).

The ultraviolet spectra of VIII[3] have three maxima in the long wavelength region (290~340 mμ), whereas the spectra of VI and di-2-(2'-benzofuranylethynyl-phenyl succinate[4] have only two peaks in the same region lacking the maximum at ca. 290 mμ indicating that the presence of the free hydroxyl group is responsible for the appearance of the maximum at ca. 290 mμ in the ultraviolet spectra of 2-phenylethynylbenzofurane type compounds. On the other hand, ester derivatives of *o,o'*-dihydroxydiphenyldiacetylene such as VII and *o,o'*-diacetoxydiphenyldiacetylene have

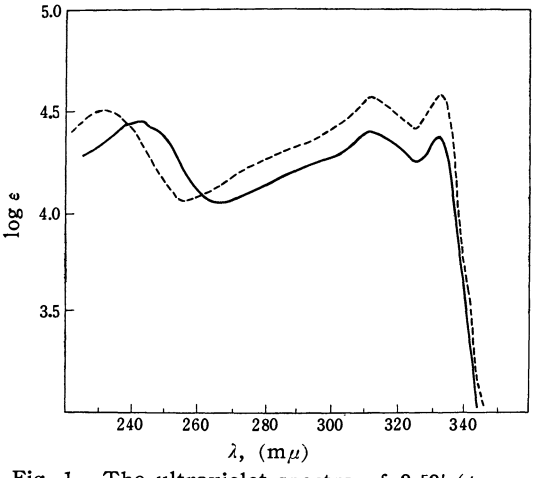



Fig. 1. The ultraviolet spectra of 2-[2'-(*p*-carboxybenzoyloxy)-phenylethynyl]-benzofurane (IV) and 2-(2'-benzoyloxyphenylethynyl)-benzofurane (VI).
——: IV ------: VI

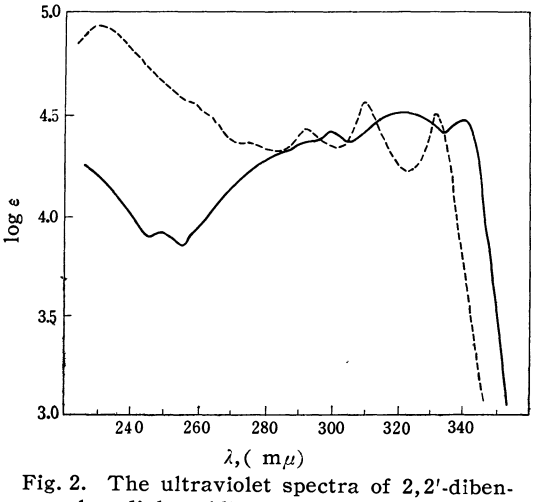



Fig. 2. The ultraviolet spectra of 2,2'-dibenzoyloxydiphenyldiacetylene (VII) and 2-(2'-hydroxyphenylethynyl)-benzofurane (VIII).
------: VII ——: VIII

4) F. Toda and M. Nakagawa, This Bulletin, **33**, 223 (1960).

TABLE I

| Compound | Absorption, mμ | | | | |
|---|---|---|---|---|---|
| IV | 242 (282) | | | 311 (253) | 332 (245) |
| VI | 230 (308) | | | 311 (364) | 332 (371) |
| VII | 230 (815) | **275** (229) | 293 (265) | 311 (346) | 332 (299) |
| II | 240 (1075) | **270** (146) | | | |
| VIII | 250 (79) | | 298 (265) | 318 (297) | 340 (284) |

All spectra were measured in 95% ethanol. The figures in parentheses are $\varepsilon_{max} \times 10^{-2}$. The bold figures indicate shoulder.

always three $\lambda_{max}$ in the long wavelength region. The ultraviolet spectrum of IV is closely related to that of VI lacking the absorption near 290 mμ (cf. Table I; Figs. 1 and 2). The infrared spectrum of IV indicates the presence of a carboxyl group ($\nu_{OH}$, 2655, 2520 $cm^{-1}$; $\nu_{CO}$, 1696 $cm^{-1}$) and ester group ($\nu_{CO}$, 1735 $cm^{-1}$). From these findings the structure of hydrogen terephthalate of VIII was assigned to IV. Presumably internal strains resulting from steric or a dipolar replusion between the terephthalate group and the diacetylenic bond caused the cleavage of one or both of the ester linkage of III yielding IV or V. The same type of fission of ester linkage during the course of intramolecular oxidative coupling of a series of dialkynyl terephthalate was recently reported by Eglinton and Galbraith[5].

It is interesting to note that the infrared spectrum of VIII shows the absorption of disubstituted acetylenic bond at 2207 $cm^{-1}$, but the corresponding absorption disappears in the spectra of IV, VI and VII. The low intensity of absorption in ultraviolet region of IV, as compared with that of VI, is attributable to the hypochromic influence of the more bulky terephthalic acid group as discussed in the previous paper of the series[4].

Further studies on the synthesis of cyclic derivatives of *o,o'*-dihydroxydiphenyldiacetylene containing a para-disubstituted benzene as the *o,o'*-bridging chain are now in progress.

## Experimental*

**2-Ethynylphenyl Terephthalate (II).**—*o*-Hydroxyphenylacetylene (I, 0.6 g) was dissolved in a mixture of sodium hydroxide (0.2 g.), acetone (10 ml.)

5) G. Eglinton and A. R. Galbraith, *J. Chem. Soc.*, **1959**, 889.

* Not all melting points are corrected.

and water (1.0 ml.). Terephthaloyl chloride (0.5 g.) in acetone (10 ml.) was added to the solution at a time. The mixture was shaken with occasional cooling with ice. The solid deposited was filtered to yield somewhat crude II, m.p. 177°C (decomp.), 0.9 g. (97%), which was recrystallized from ethanol to give pure II, colorless leaflets, m.p. 177.5°C (decomp.).

*Anal.* Found: C, 78.25; H, 3.70. Calcd. for $C_{24}H_{14}O_4$: C, 78.68; H, 3.85%.

I.R. max., 3265 $cm^{-1}$ ($-C\equiv CH$), 1741 $cm^{-1}$ (ester), 1248, 1264 $cm^{-1}$ ($=C-O-$).

II gives yellow cuprous acetylide with Ilosvay's reagent and white silver salt with ethanolic silver nitrate solution.

**Oxidative Coupring of II at 55°C.**—II (2.0 g.) in pyridine (50 g.) was added to the solution of cupric acetate monohydrate (15 g.) in pyridine (100 g.). The mixture was kept at 55°C for 5 hr. The precipitate was removed and most of the solvent was removed under reduced pressure. The residue was mixed with water (1000 ml.) and extracted with ether (1000 ml.). The extract was washed with a saturated solution of cupric acetate and water, successively. The dried ethereal solution was concentrated to 100 ml., and the greenish yellow precipitate formed was removed. Concentration of the filtrate yielded crude crystals. After treatment with acetone and charcoal, the crude material was repeatedly recrystallized from xylene to give pure IV, colorless needles, m.p. 222.5~223°C (decomp.), 0.1 g. (5%).

*Anal.* Found: C, 75.38; H, 3.86; mol. wt. (Rast), 343. Calcd. for $C_{24}H_{14}O_5$: C, 75.39; H, 3.69%; mol. wt., 382.

**Oxidative Coupling of II at 60°C.**—II (3.0 g.) in pyridine (150 g.) was added through a Hershberg type dropping funnel to the vigorously stirred solution of cupric acetate monohydrate (15 g.) in pyridine (150 g.) at 60°C over a period of 4 hr., and stirring was continued for additional 1.5 hr. at the same temperature. The precipitate formed was removed by filtration. After removal of pyridine in vacuo, the residue was diluted with water and extracted with benzene (400 ml.). The benzene layer was treated according to the usual manner. Evaporation of the solvent gave a greenish black solid. The solid was digested with ether, and the solvent was removed to give crystals, which were refluxed with ethanol (20 ml.) and the insoluble material was removed by filtration. The filtrate was cooled to yield crystals, which were repeatedly recrystallized from xylene to yield IV, m.p. 222.5~223°C (decomp.), 100 mg. (3%). On concentration of the mother liquor, V, colorless needles, m.p. 190~194°C, 0.3 g. (15%) was obtained, which undepressed the melting point of an authentic sample[3].

The authors wish to thank Messrs. T. Shiba and M. Okumiya and Miss K. Koike for performing the elementary analyses.

*Department of Chemistry*
*Faculty of Science*
*Osaka University*
*Nakanoshima Osaka*

# *High Pressure Reduction of Organic Compounds with Urushibara Catalyst. VI*[1]*. A New Type of Urushibara Nickel Catalyst*

By Izumi MOTOYAMA

(Received August 15, 1959)

In 1952 Urushibara and Chuman discovered a new catalyst, which was prepared from precipitated nickel. Aqueous nickel chloride solution was treated with zinc dust, and the precipitated nickel was digested with caustic alkali to obtain the active catalyst for hydrogenation[2]. The procedure for the preparation of this catalyst has been successively modified to obtain the more active catalyst. It was also found that a highly active catalyst can be obtained by digesting the precipitated nickel with either aqueous caustic alkali or aqueous acetic acid, and the former was named Urushibara nickel B or U-Ni-B in abbreviation[3], and the latter Urushibara nickel A or U-Ni-A in abbreviation[4]. Recently it was proved that the activity of the U-Ni-B is comparable with that of Raney nickel catalyst for hydrogenation under ordinary pressure[5].

An application of Urushibara nickel catalyst to the hydrogenation of various organic compunds under high pressure

1) Part V: K. Hata, S. Taira and I. Motoyama, This Bulletin, **31**, 776 (1958).
2) Y. Urushibara, ibid., **25**, 280 (1952).
3) Y. Urushibara and S. Nishimura, ibid., **27**, 480 (1954).
4) Y. Urushibara, S. Nishimura and H. Uehara, ibid., **28**, 446 (1955).
5) S. Nishimura, *J. Chem. Soc. Japan, Pure Chem. Sec.* (*Nippon Kagaku Zasshi*), **78**, 1741 (1957).

has been investigated since 1954. During the successive investigations it was noticed that this catalyst could not hydrogenate aromatic compounds such as benzene, aniline, etc., even under severe conditions, although it was very effective for the hydrogenation of ethylenic compounds, aldehydes, ketones, nitro compounds, oximes, nitriles and simple phenols[6-9]. To get rid of this defect, an attempt was made to prepare a new type of Urushibara catalyst from nickel chloride and aluminum instead of zinc. Some information on the new Urushibara catalyst thus obtained, named Urushibara nickel BA or U-Ni-BA in abbreviation, was reported briefly in the preceding paper[1].

In the present paper, the hydrogenation of several aromatic compounds with this new catalyst and certain useful modifications of procedure for the preparation of this new catalyst are described.

## Hydrogenation of Aromatic Compounds

The Urushibara nickel BA was found to be effective for the hydrogenation of aromatic nucleus which had not been hydrogenated with U-Ni-B or U-Ni-A. The results of the hydrogenation of some aromatic compounds are summarized in Table I. The hydrogenation of phenol can also be attained with either U-Ni-B or U-Ni-A, but it takes much time to complete the reaction with these catalysts even under considerable high temperature. With U-Ni-BA, however, phenol can be easily hydrogenated at lower temperature. It is evident from these results that the U-Ni-BA has a high activity for the hydrogenation of aromatic nucleus, and that the use of aluminum grains instead of zinc dust brings about a favorable change on the property of Urushibara catalyst. It is obvious that the difference between the properties of these two kinds of Urushibara catalysts is due to the difference of the metal combined with nickel in each catalyst.

## Preservability of Urushibara Catalyst

Preparation of catalyst has been generally thought to be troublesome and difficult, but it is not true for the preparation of Urushibara nickel catalyst, because it is prepared by simple operations in only an hour or less. However, the preparation of U-Ni-BA from nickel chloride and aluminum grains requires somewhat longer time than that of the other Urushibara catalysts from nickel chloride and zinc dust. A certain useful modification has been made in the procedure for the

TABLE I. HYDROGENATION OF ORGANIC COMPOUNDS

Catalyst: U-Ni-BA containing about 2 g. of nickel,
Sample: 10 g., Solvent: 99% ethanol 50 cc.

| Sample | mol. | Initial pressure atm. | Temp. °C | Time hr. | Hydrogen absorbed mol. | Products & Yield* % |
|---|---|---|---|---|---|---|
| Phenol | 0.106 | 66 | 70~110 | 1.0 | 0.355 | Cyclohexanol (79) |
| Methyl salicylate | 0.066 | 65 | 84~115 | 2.0 | 0.190 | Ethyl hexahydrosalicylate** (65) |
| Ethyl benzoate | 0.066 | 54 | 106~150 | 2.5 | 0.231 | Ethyl hexahydrobenzoate (82) |
| Diethyl phthalate | 0.045 | 68 | 114~154 | 3.0 | 0.145 | Diethyl hexahydrophthalate (91) |
| Benzene | 0.128 | 100 | 100~142 | 3.0 | 0.403 | Cyclohexane (70) |
| Ethylbenzene | 0.094 | 70 | 100~143 | 4.0 | 0.308 | Ethylcyclohexane (63) |
| Aniline | 0.108 | 96 | 150~209 | 3.5 | 0.334 | *N*-Ethylcyclohexylamine*** (71) Dicyclohexylamine |
| Acetanilide | 0.074 | 75 | 120~206 | 5.0 | 0.236 | Hexahydroacetanilide (77) |

* Increased yields may be obtained in case of large scale operations.

** Ester exchange was observed during hydrogenation, and yet the product was found to contain an appreciable amount of methyl ester.

*** *N*-Ethylation was observed during hydrogenation (cf. H. I. Cramer et al., Ref. 10)

6) K. Hata et al., ibid., **77**, 1405 (1956).
7) K. Hata, S. Taira and T. Higase, ibid., **78**, 186 (1957).
8) I. Motoyama, ibid., **79**, 1296 (1958).
9) K. Hata, S. Taira and Y. Satomi, ibid., **79**, 1298 (1958).
10) H. I. Cramer and H. Adkins, *J. Am. Chem. Soc.*, **52**, 4354 (1930).

TABLE II. HYDROGENATION OF PHENOL TO CYCLOHEXANOL

Catalyst: U-Ni-BA (2 g. Ni), Sample: phenol 10 g.,
Solvent: ethanol 50 cc. A small amount of NaOH was added.

| Solvent for preservation | Period of preservation day | Initial pressure atm. | Temp. °C | Time hr. | Hydrogen absorbed l. at 20 °C, 1 atm. | Isolated cyclohexanol g. |
|---|---|---|---|---|---|---|
| (Not preserved) | 0 | 66 | 70~110 | 1.0 | 8.6 | 7.9 |
| Water | 6 | 50 | 76~117 | 1.5 | 7.8 | 8.5 |
| 〃 | 90 | 75 | 79~120 | 1.5 | 8.0 | 8.2 |
| Ethanol | 6 | 50 | 68~119 | 1.5 | 7.6 | 8.3 |
| 〃 | 90 | 77 | 74~120 | 1.7 | 7.9 | 7.9 |
| None (dry) | 1 | 65 | 66~112 | 1.5 | 7.5 | 7.7 |
| 〃 | 15 | 82 | 70~120 | 1.3 | 7.9 | 6.3 |
| | | | | | (calcd. 7.7 | 10.6) |

TABLE III. HYDROGENATION OF ORGANIC COMPOUNDS

Catalyst: U-Ni-BA (2 g. Ni) prepared from the precipitated nickel preserved in dry state.

| Sample | mol. | Solvent | Initial pressure atm. | Temp. °C | Time hr. | Products & Yield % |
|---|---|---|---|---|---|---|
| Benzene | 0.27 | None | 80 | 90~150 | 2.5 | Cyclohexane (77) |
| Aniline | 0.11 | Ethanol | 75 | 150~208 | 3.0 | *N*-Ethylcyclohexylamine (69)<br>Dicyclohexylamine |
| Aniline | 0.11 | Cyclohexane | 70 | 150~215 | 3.0 | Cyclohexylamine (35)<br>Dicyclohexylamine (38) |
| Pyridine | 0.10 | Cyclohexane | 65 | 150~218 | 3.0 | Piperidine (86) |

preparation of U-Ni-BA catalyst, so as to shorten the time required for the preparation. The principle of the modification is to prepare the U-Ni-BA catalyst from preserved nickel precipitate, which is previously made in large quantities. After the ion-exchange reaction between nickel chloride and aluminum grains, the precipitated nickel is preseved in a proper manner, and then treated with aqueous alkali to make up the U-Ni-BA catalyst when it is used for hydrogenation. Such preservation of the precipitate, however, was expected to cause deactivation of the catalyst, because it is presumed that active nickel surface are inherently present in the precipitate but are covered with certain water-insoluble substances, and consequently the precipitated nickel itself, as it is precipitated, is ineffective as catalyst, unless it is treated with alkali or acid[4].

The activity of the catalyst prepared from the preserved precipitate was examined by the hydrogenation of phenol. The precipitate was preserved from a day to three months in the following three ways: in distilled water, in 99% ethanol and in dry state. Each preserved precipitate was then treated with 20% aqueous sodium hydroxide solution to prepare the catalyst. The results of the hydrogenation of phenol are summarized in Table II. As shown in Table II, each 3 mol. of hydrogen were absorbed with the catalyst prepared from the preserved precipitate as well as with that immediately treated with alkali after the ion-exchange reaction, although the time required for hydrogenation was somewhat longer with the former catalyst. About 8 g. of cyclohexanol were isolated similarly from every reaction mixture. Thus, contrary to expectation, no remarkable deactivation was found with U-Ni-BA catalyst by any preservation of the precipitated nickel. The precipitate preserved in dry state is more convenient for use than those preserved in water or ethanol.

When the dried precipitate is exposed to air under ordinary pressure, it is rapidly oxidized generating a considerable amount of heat. Therefore, it is desirable to keep it under reduced pressure, especially in case of a large scale operation.

Additional results of the hydrogenation with the catalyst prepared in this way are summarized in Table III. It can be seen from these results that this catalyst still maintains the similar catalytic activity as the catalyst prepared from precipitated

TABLE IV. PHYSICAL CONSTANTS OF THE PRODUCTS

| Compound | b. p. °C/mmHg. | Refractive index (°C) | Derivative (m.p., °C) |
|---|---|---|---|
| Cyclohexanol | 157~162 | | 3,5-Dinitrobenzoate (112) |
| Ethyl hexahydrosalicylate | 115~119/19 | 1.4674(16.0) | |
| Ethyl hexahydrobenzoate | 87~88/20~21 | 1.4437(22.0) | Amide (183~187) |
| Diethyl hexahydrophthalate | 145.5/20 | 1.4523(22.0) | Free acid (197~198) |
| Cyclohexane | 78~ 80 | 1.4315(23.0) | |
| Ethylcyclohexane | 125~132 | 1.4315(27.5) | |
| *N*-Ethylcyclohexylamine | 160~167 | | Hydrochloride (183~185) |
| Cyclohexylamine | 130~136 | 1.4673(13.5) | *N*-Acetyl (104~105) |
| Dicyclohexylamine | | | Hydrochloride (above 210) (Found: N, 6.56%) |
| Hexahydroacetanilide | 103~104 (m. p.) | | |
| Piperidine | | | *N*-Benzenesulfonyl (93.5) |

nickel immediately after the ion-exchange reaction (cf. Table I).

It is quite interesting that the U-Ni-BA catalyst prepared from the precipitated nickel being kept in air for a long time maintains its high catalytic activity for the hydrogenation of aromatic compounds.

The modification in this way can be applied not only to the new Urushibara catalyst but also to the old ones.

## Experimental

**Apparatus.**—Hydrogenation was carried out in an autoclave of stainless steel with a magnetic stirrer (capacity: 200 cc., rate of stirring: about 60 strokes per min.).

**Catalyst.**—Catalyst was prepared according to the procedure previously reported[1] and washed thrice with 99% ethanol, when the hydrogenation was carried out in ethanol. When another solvent was employed, the catalyst was washed first thrice with 99% ethanol and then thrice with the solvent.

**Preservation in Dry State.** — The precipitate, obtained from 100 ml. of aqueous nickel chloride solution containing 40 g. of $NiCl_2 \cdot 6H_2O$ and 50 g. of aluminum grains (40~80 meshes), was washed well with distilled water, then collected on Büchner funnel and dried under reduced pressure. Final weight of the precipitate was about 70 g.* in all. Each 14 g. of the dry precipitate, which contains 2 g. of nickel, was treated with 250 g. of 20% aqueous sodium hydroxide solution before the application for hydrogenation.

**Materials.**—All substances used for hydrogenation were purified by redistillation or recrystallization except those with special indication.

Methyl salicylate, ethyl benzoate and diethyl phthalate were respectively prepared by usual esterification[11] from corresponding acids.

Benzene was purified by treatment first twice with anhydrous aluminum chloride[12], then with a large amount of U-Ni-A[13]. The purified benzene was redistilled before hydrogenation.

**Products.**—Reduction products were fractionally distilled except those with special indication, and were identified through appropriate derivatives. When the products were liquid, their refractive indices were measured. Physical constants of the products are summarized in Table IV.

Cyclohexane and ethylcyclohexane were respectively separated from the solvent by adding a large quantity of water to the reaction mixture, dried over anhydrous calcium chloride and distilled.

Piperidine was converted to its hydrochloride by adding an excess of concentrated hydrochloric acid to the reaction mixture after removal of catalyst. The solvent was distilled off and the residue was completely dried up under reduced pressure. Then, the resulting piperidine hydrochloride was purified by recrystallization from 99% ethanol.

## Summary

A new Urushibara nickel catalyst, U-Ni-BA, was prepared from nickel chloride and aluminum grains. This new catalyst was found to be highly active for the hydrogenation of aromatic nucleus, contrary to the older Urushibara nickel catalyst, U-Ni-A or U-Ni-B.

The preservability of the catalyst was examined: the precipitate, obtained by the reaction of nickel chloride with aluminum grains (or zinc dust), was kept for a long time in solvent or in dry state, and a similarly active catalyst could be obtained by digesting the preserved precipitate with aqueous caustic alkali.

The author wishes to express his hearty thanks to Professor K. Hata for his kind guidance and valuable suggestion throughout the course of this study, and to Mr.

* This weight varies with experimental condition.

11) E. Fischer and A. Speier, *Ber.*, **28**, 3253 (1895).

12) R. J. Graul and J. V. Karabinos, *Science*, **104**, 557 (1946).

13) H. N. Holmes and N. Beeman, *Ind. Eng. Chem.*, **26**, 172 (1934).

S. Taira for his useful advice. The cost of this investigation was defrayed from the Scientific Research Expenditure of the Minstiry of Education.

*Department of Chemistry*
*Faculty of Science*
*Tokyo Metropolitan University*
*Setagaya-ku, Tokyo*

# *An Approximate Method of Calculating Localization Energies in Alternant Hydrocarbons*

By Hiroaki BABA

(Received August 18, 1959)

Since the localization theory was first proposed by Wheland[1], it has been one of the most effective means of dealing with the chemical reactivity in conjugated organic compounds. The only fault found with this theory is that the calculation of localization energies is frequently an arduous task, especially when one is treating a large molecule. By taking into consideration the characteristic property of nonbonding molecular orbitals, Dewar[2] developed a convenient method of obtaining approximate values of localization energies for alternant hydrocarbons, and successfully applied it to some organic reactions[3]. However, the values obtained by this method of approximation are in general numerically far from being the exact values.

In a previous paper[4] it was made clear that in an alternant hydrocarbon the exact value of localization energy has an intimate correlation with Dewar's approximate one, and also with the value of free valence, the latter quantity being an important index of chemical reactivity[5]. In connection with this problem, another approximate method of computing localization energies in alternant hydrocarbons will be described in the present article.

## Definition

The present treatment is based on the simple LCAO molecular orbital method with neglect of overlap integrals; the notation is the same as that used in the preceding papers[4,6].

Consider a carbon atom $r$ in an alternant hydrocarbon, and denote the carbon atoms adjacent to atom $r$ by $t$, $t'$, ……. Suppose that $\beta_{rt}$, $\beta_{rt'}$, …… simultaneously change from their initial value $\beta$ to a certain value $\beta_r$, and that the other coulomb and resonance integrals remain unchanged. Then, bond number $N_r$ can be regarded as a continuous function of $\beta_r$. If this function is represented by $N_r(\beta_r)$, the localization energy of atom $r$ is expressed as[4]

$$L^{(r)}=\int_{\beta}^{0} 2N_r(\beta_r)\mathrm{d}\beta_r. \tag{1}$$

Next, reference will be made to two known approximate values[4] of $L^{(r)}$. One is

$$L^{(r)\prime}=-2N_r{}^0\beta \tag{2}$$

where $N_r{}^0[\equiv N_r(\beta)]$ is the bond number in the initial state, and is connected with free valence $F_r{}^0$ by the relation $N_r{}^0=\sqrt{3}-F_r{}^0$. The other is

$$L^{(r)\prime\prime}=-2N_r(0)\beta \tag{3}$$

where

$$N_r(0)=\lim_{\beta_r\to 0} N_r(\beta_r)$$

As was proved in the previous paper[4], $L^{(r)\prime\prime}$ defined by Eq. 3 agrees with Dewar's approximate value mentioned in the introductory paragraph.

In the simple molecular orbital procedure, the total energy for the ground state of a system of electrons is obtained as the sum of the energies of the ground-state molecular orbitals to which the individual electrons belong. If the orbital energies are determined by the usual variation method, the total energy obtained in this way corresponds to its absolute minimum under the restriction that the orbitals form

1) G. W. Wheland, *J. Am. Chem. Soc.*, **64**, 900 (1942).
2) M. J. S. Dewar, ibid., **74**, 3357 (1952).
3) P. M. G. Bavin and M. J. S. Dewar, *J. Chem. Soc.*, **1956**, 164; M. J. S. Dewar, T. Mole and E. W. T. Warford, ibid., **1956**, 3581, and related papers.
4) H. Baba, This Bulletin, **30**, 154 (1957).
5) See, for instance, B. Pullman and A. Pullman, "Progress in Organic Chemistry", Vol. 4, edited by J. W. Cook, Butterworths Scientific Publications, London (1958), pp. 31—71.
6) H. Baba, This Bulletin, **30**, 147 (1957).

an orthonormal set. If one keeps this fact in mind, it is easily verified that $N_r$ decreases monotonously as $\beta_r$ increases. Hence

$$N_r^0 > N_r(\beta_r) > N_r(0) \quad (\beta < \beta_r < 0) \tag{4}$$

so that from Eqs. 1—3

$$L^{(r)\prime} > L^{(r)} > L^{(r)\prime\prime} \tag{5}$$

Let us now consider a new quantity $\boldsymbol{L}^{(r)}$ defined as follows:

$$\boldsymbol{L}^{(r)} = -(N_r^0 + N_r(0))\beta \tag{6}$$

Then, from Eqs. 2 and 3

$$\boldsymbol{L}^{(r)} = \frac{1}{2}(L^{(r)\prime} + L^{(r)\prime\prime}) \tag{7}$$

Since both $L^{(r)\prime}$ and $L^{(r)\prime\prime}$ are approximate values of $L^{(r)}$, $\boldsymbol{L}^{(r)}$ will also be an approximation of $L^{(r)}$.

The relation of $\boldsymbol{L}^{(r)}$ with other quantities may be understood by Fig. 1, where the full line curve aeb represents the relation between $\beta_r$ and $2N_r(\beta_r)$. $L^{(r)}$ is, of course, equal to the area under the curve, $L^{(r)\prime}$ to the area of rectangle agcd, and $L^{(r)\prime\prime}$ to that of rectangle hbcd, while $\boldsymbol{L}^{(r)}$ is equal to the area of trapezoid afbcd.

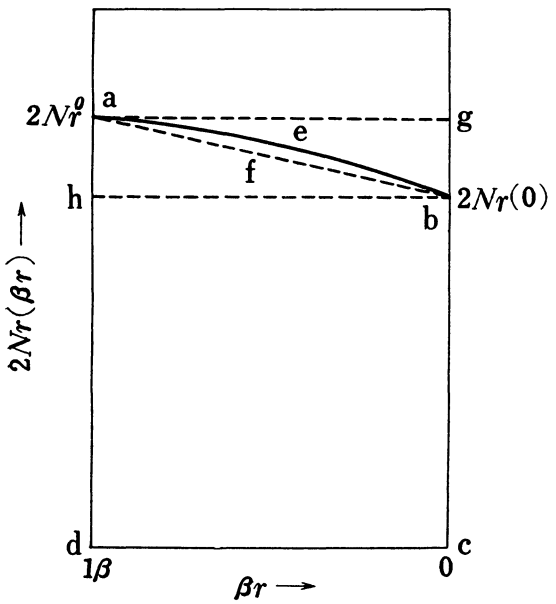



Fig. 1.

## Examples and Discussion

In Table I are listed the values of $\boldsymbol{L}^{(r)}$ and other related quantities for three positions of anthracene. In Fig. 2 $\boldsymbol{L}^{(r)}$, $L^{(r)\prime}$ and $L^{(r)\prime\prime}$ are plotted against $L^{(r)}$ for a number of alternant hydrocarbons. The values of $L^{(r)}$ for primary, secondary and tertiary carbon atoms fall within the ranges 1.0 to 1.8, 1.8 to 2.6 and 2.6 to 3.1, respectively. The examples presented in this table and figure clearly show that $\boldsymbol{L}^{(r)}$ is superior to $L^{(r)\prime}$ and $L^{(r)\prime\prime}$ as an approximation of $L^{(r)}$.

TABLE I. LOCALIZATION ENERGIES IN UNITS OF $-\beta$ FOR ANTHRACENE

| Position | $L^{(r)}$ | $\boldsymbol{L}^{(r)}$ | $L^{(r)\prime}$ | $L^{(r)\prime\prime}$ |
|---|---|---|---|---|
| 1 | 2.25 | 2.06 | 2.55 | 1.57 |
| 2 | 2.40 | 2.27 | 2.65 | 1.89 |
| 9 | 2.01 | 1.84 | 2.42 | 1.26 |

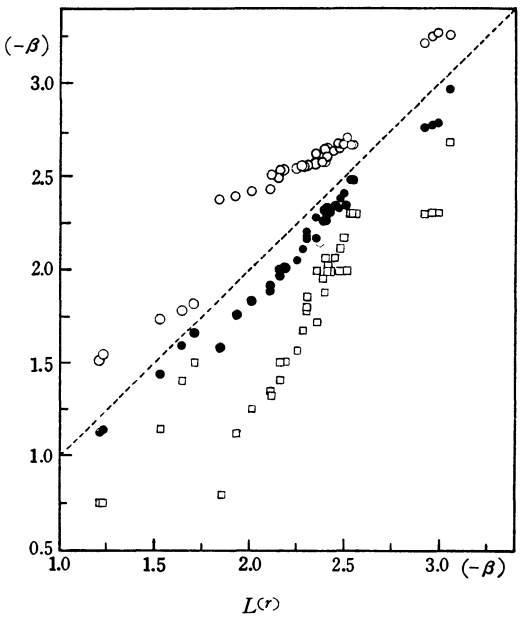



Fig. 2. Relations between $L^{(r)}$ and $\boldsymbol{L}^{(r)}$, $L^{(r)\prime}$ and $L^{(r)\prime\prime}$.
●, $\boldsymbol{L}^{(r)}$; ○, $L^{(r)\prime}$; □, $L^{(r)\prime\prime}$.
$L^{(r)}$ and $L^{(r)\prime}$: Taken from references 5 and 6, and "Dictionary of Values of Molecular Constants", Vol. II, edited by C. A. Coulson and R. Daudel.
$L^{(r)\prime\prime}$: Taken from reference 2, and calculated by the present author.

Previously it was shown by the present author[4,6] and also by Fukui et al.[7] that under certain conditions there is a definite parallelism among the quantum mechanical quantities, including $L^{(r)\prime}$ and $L^{(r)\prime\prime}$, which are related to the reactivity of an alternant hydrocarbon. Considering the definition of $\boldsymbol{L}^{(r)}$, one may at once reach the conclusion that the same parallelism exists between $\boldsymbol{L}^{(r)}$ and any other quantity mentioned above.

*Research Institute of Applied Electricity*
*Hokkaido University, Sapporo*

7) K. Fukui, T. Yonezawa and C. Nagata, *J. Chem. Phys.*, **26**, 831 (1957).

# *Tropones. IV.* Ultraviolet Absorption Spectra of Reaction Products of Tropones and Carbonyl Reagents***

By Toshio MUKAI

(Received June 8, 1959)

The reaction products of tropone and carbonyl reagents, such as oxime, semicarbazone, thiosemicarbazone, phenylhydrazone, and nitrophenylhydrazone form peculiar conjugation systems and they are of interest in the study of ultraviolet spectrum. These compounds generally have deep color, ranging from orange to dusky purple. The present paper describes observations on the ultraviolet spectra of products obtained on the reaction of tropone and tropones possessing the methyl, phenyl, naphthyl, *o*-tolyl, or benzyl group in 2-position, and carbonyl reagents, measured in methanol, acidic and alkaline solutions.

The ultraviolet spectrum of tropone oxime[1], of tropone semicarbazone[1] and of tropone thiosemicarbazone are shown in Figs. 1—3, respectively. These three compounds possess a C=N- group in place of the carbonyl group in tropone and show two typical absorption maxima as tropone itself does[1]. The maximum absorption in methanol solution shifts to longer wavelengths in the order of the oxime, semicarbazone and thiosemicarbazone, and this tendency is the same as that in the case of unsaturated ketone derivaives in general[2]. All three compounds have fairly deep color which must be due to the broad absorption appearing at the wavelength region above 400 m$\mu$.

The ultraviolet spectra of the oxime and semicarbazone in hydrochloric acid solution show a shift to a longer wavelength region and that of the thiosemicarbazone to slightly shorter wavelengths. The absorption maxima lie near 240 and 330 m$\mu$ in all three compounds and the value of their intensity is also similar.

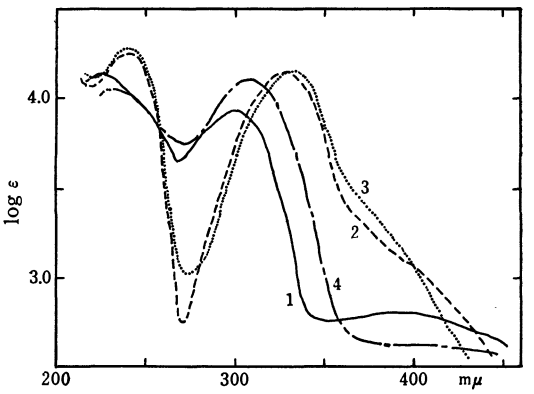



Fig. 1. Ultraviolet absorption spectra of tropone oxime: (1) in methanol, (2) in 0.1 N HCl, (3) in 6 N HCl and (4) in 0.1 N NaOH solution.

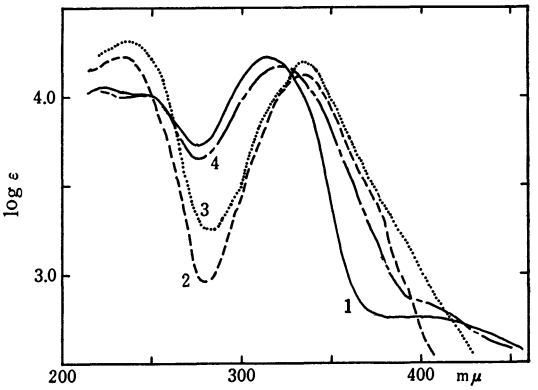



Fig. 2. Ultraviolet absorption spectra of semicarbazone of tropone: (1) in methanol, (2) in 0.1 N HCl, (3) in 6 N HCl and (4) in 0.1N NaOH solution.

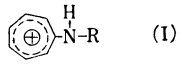
This fact indicates that they all have a structure of conjugate acid like I and that their absorptions are not so greatly affected by group R. The fact that there is no shift of the absorption curve according to the concentration of hydrocholric acid (in 0.1 or 6 N), suggests that the formation of the conjugate acid (I) is almost complete even in dilute acid solution such as 0.1 N solution.

* Part I: Ref. 1; Part II: T. Mukai, This Bulletin, 31, 846 (1958); Part III: Ref. 3.

** Presented before the 39th Tohoku Local Meeting of the Chemical Socity of Japan, Sendai, May, 1956.

1) T. Nozoe, T. Mukai and T. Takase, *Sci. Repts. Tohoku Univ., First Ser.*, **39**, 164 (1956).

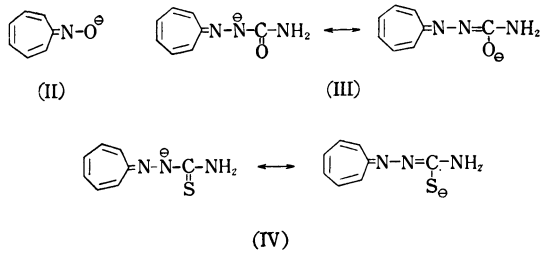
2) A. E. Gillam and E. S. Stern, "An Introduction to Electronic Absorption Spectroscopy in Organic Chemistry", Edward Arnold Publishers, Ltd., London (1955), p. 100.



(I)

R=OH.NHCONH$_2$.NHCSNH$_2$

In alkaline solution, the absorption curves of the oxime, semicarbazone and thiosemicarbazone, all show a shift to a longer wavelength region. It has already been pointed out that the oxime has an amphoteric property, is stable, and dissolves both in acids and in alkalis[1], and this shift is assumed to be due to the formation of an anion (II). Similarly, formation of anions (III) and (IV) can be expected for the semicarbazone and thiosemicarbazone.



(II) (III)

(IV)

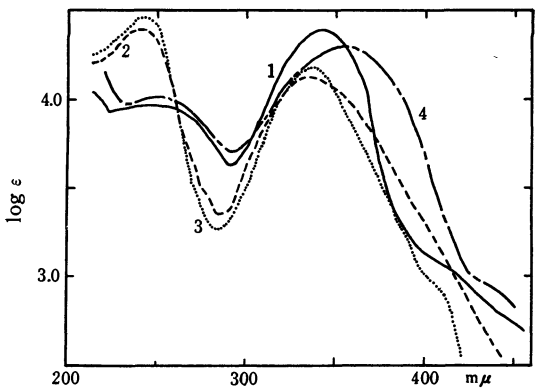



Fig. 3. Ultraviolet absorption spectra of thiosemicarbazone of tropone: (1) in methanol, (2) in 0.1 N HCl, (3) in 6 N HCl and (4) in 0.1N NaOH solution.

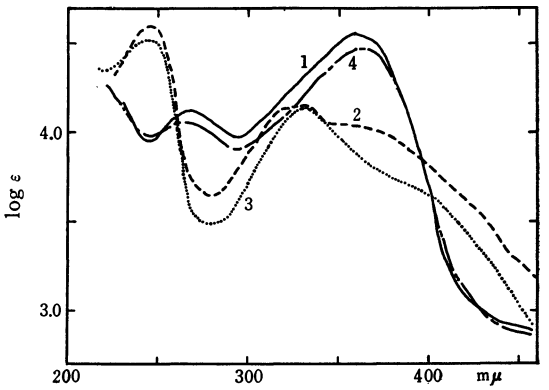



Fig. 4. Ultraviolet absorption spectra of *p*-bromophenylhydrazone of tropone: (1) in methanol, (2) in 0.1 N HCl (3) in 6 N HCl and (4) in 0.1 N NaOH solution.

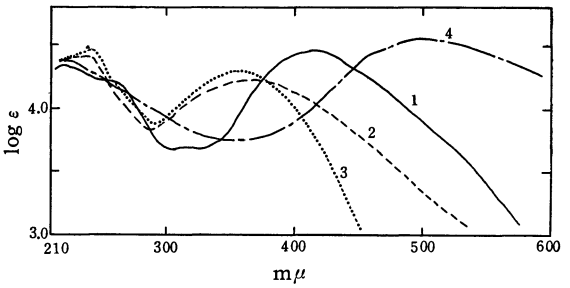



Fig. 5. Ultraviolet absorption spectra of 2,4-dinitrophenylhydrazone of tropone: (1) in methanol, (2) in 0.1 N HCl, (3) in 6 N HCl and (4) in 0.1 N NaOH solution.

Ultraviolet absorption spectra of the phenylhydrazone[1] and *p*-bromophenylhydrazone[1] of tropone are shown in Table I and Fig. 4 and those of *p*-nitrophenylhydrazone[1] and 2,4-dinitrophenylhydrazone[1] of tropone in Table I and Fig. 5. These phenylhydrazones exhibit absorption maximum at a longer wavelength region than the oxime and semicarbazone do. Further it is seen that the introduction of a nitro group in the

TABLE I. ABSORPTION MAXIMA OF TROPONE DERIVATIVES IN mμ (log ε)

| | MeOH | 0.1 N HCl | 6 N HCl | 0.1 N NaOH |
|---|---|---|---|---|
| Phenylhydrazone | 256(4.11) | 240(4.41) | | 252(3.97) |
| | 355(4.43) | 328(4.05) | | 355(4.33) |
| *p*-Nitrophenylhydrazone | 255(inf) | 237(4.42) | 237(4.42) | 255(sh) |
| | 315(3.78) | 356(4.40) | 350(4.27) | 303(3.83) |
| | 383(3.83) | | | 510(4.27) |
| | 429(4.55) | | | |
| 2,4-Dinitrophenylhydrazone | 219(4.34) | 237(4.40) | 238(4.45) | 220(sh) |
| | 260(4.20) | 363(4.23) | 353(4.29) | 500(4.53) |
| | 315(3.70) | | | |
| | 413(4.45) | | | |

TABLE II. ABSORPTION MAXIMA OF OXIMES IN mμ (lon ε)

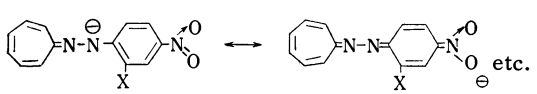
| | MeOH | 0.1 N HCl | 6 N HCl | 0.1 N NaOH |
|---|---|---|---|---|
| 2-Methyltropone | 228(4.24) | 243(4.31) | 243(4.36) | 236(4.16) |
| | 300(3.85) | 338(4.09) | 338(4.11) | 303(3.90) |
| | 360(2.91)* | | | |
| | 390(2.91)* | | | |
| 2-Phenyltropone | 222(4.20) | 237(4.23) | 238(4.33) | 235(4.14) |
| | 260(4.04) | 345(3.95) | 341(4.06) | 265(4.05) |
| | 307(3.75) | | | 308(3.70) |
| 2-Benzyltropone | 228(4.21) | 240(4.27) | 243(4.35) | 243(4.15) |
| | 300(3.78) | 339(3.98) | 340(4.11) | 303(3.85) |
| | 358(2.93)* | | | |
| | 380(2.93)* | | | |
| 2-α-Naphthyltropone | 222(4.89) | 222(4.92) | 224(4.86) | 223(4.84) |
| | 293(4.04) | 240(4.28) | 245(4.30) | 297(3.97) |
| | 380(3.17)* | 280(3.83) | 334(3.99) | |
| | | 336(4.01) | | |
| 2-o-Tolyltropone | 295(3.82) | 240(4.27) | 240(4.37) | 238(4.21) |
| | ca. 355(3.10)* | 340(4.00) | 339(4.11) | 308(3.90) |

* Broad band. These bands can not be compared with each other.

ortho- or para-position of the phenyl ring results in a further shift of the maximum to a longer wavelengths (above 400 mμ).

In hydrochloric acid solution, they all show a shift originating in the formation of a conjugate acid [I: R= $-NH-C_6H_5$, $-NH-C_6H_4Br(p)$, $-NH-C_6H_4NO_2(p)$, $-NH-C_6H_3(NO_2)_2(2,4)$]. In *p*-nitro- and 2,4-dinitrophenylhydrazones, there is a shift of 6~10 mμ when the concentration changes from 0.1 to 6 N hydrocholric acid. This is probably due to the weakened basicity of these compounds by the introduction of a nitro group which has an effect on the formation of the conjugate acid (I).

In alkaline solution, the absorption maxima of *p*-nitro and 2,4-dinitrophenylhydrazone shift to a longer wavelength region (above 500 mμ) and this is due to the formation of an anion (V) with a long chain of conjugation. The formation of an anion (V) is supported by the fact that phenylhydrazone and *p*-bromophenylhydrazone hardly show any shift in alkaline solution (see Fig. 4).



(V) X=H, $NO_2$

The ultraviolet absorption spectra of *p*-nitrophenylhydrazone in methanol and alkaline solution exhibit maxima at somewhat longer wavelength than that of 2,4-dinitrophenylhydrazone and this is due to the steric hindrance of the nitro group in 2-position of the phenyl ring. However, the maximum of 2,4-dinitrophenylhydrazone appears in a longer wavelength than that of *p*-nitrophenylhydrazone in acid solution. This is probably due to the fact that resonance represented by V occurs only to a small extent in acid solution and consequently the interference of the nitro group in 2-position of the phenyl group does not give an effect on the spectrum.

Of these products from reaction with carbonyl reagents, oxime and 2,4-dinitrophenylhydrazone are easily formed in tropones possessing alkyl or aryl radical in its 2-position. Effect of a substituent on the ultraviolet spectrum was examined with oximes. Ultraviolet spectra of oximes are shown in Table II.

The absorption maxima of 2-methyltropone oxime[3] in longer wavelength region shift to a slightly shorter wavelengths than those of tropone oxime when measured in methanol or 0.1 N sodium hydroxide solution but conversely shift to a longer wavelength in hydrochloric acid solution. Of these oximes, the interesting thing is the absorption of 2-phenyltropone oxime[4]. As will be seen from Fig. 6, the curve appears different since new absorption maxima appear at

3) T. Mukai, *J. Chem. Soc. Japan, Pure Chem. Sec.* (*Nippon Kagaku Zasshi*), **79**, 1547 (1958).

4) T. Nozoe, T. Mukai, J. Minegishi and T. Fujisawa, *Sci. Repts. Tohoku Univ., First Ser.*, **37**, 388 (1954).

TABLE III. ABSORPTION MAXIMA OF 2,4-DINITROPHENYLHYDRAZONE IN mμ (log ε)

| | MeOH | 0.1 N HCl | 6 N HCl | 0.1 N NaOH |
|---|---|---|---|---|
| 2-Methyltropone | 222(4.36) | 239(4.44) | 243(4.56) | 491(4.40) |
| | 317(3.65) | 391(4.24) | 354(4.36) | |
| | 410(4.43) | | | |
| 2-Phenyltropone | 232(4.43) | 228(4.20) | 238(4.25) | ca. 250(4.20) |
| | 405(4.44) | 257(4.08) | 363(4.05) | 498(4.30) |
| | | 403(4.12) | | |
| 2-Benzyltropone | 260(4.17) | 410(4.35) | 243(4.43) | 255(4.30) |
| | 411(4.36) | | 358(4.23) | 490(4.45) |
| 2-α-Naphthyltropone | 222(4.97) | 222(4.96) | 222(4.93) | 223(4.94) |
| | 260(4.28) | 406(4.32) | 241(4.50) | 490(4.37) |
| | 410(4.38) | | 355(4.30) | |
| 2-o-Tolyltropone | 260(4.26) | 240(4.41) | 242(4.51) | 480(4.17) |
| | 408(4.42) | 401(4.33) | 358(4.32) | |

260 and 265 mμ in methanol and alkali solution. It is considered that the absorption in this region is due to the coplanarity of the seven-membered ring and phenyl ring, as in the case of 2-phenyltropone itself[3,7].

On the other hand, the absorption of 2-benzyltropone oxime[5] is very similar to that of 2-methyltropone by the introduction of a methylene group, while the absorption of 2-α-naphthyltropone oxime does not exhibit the maximum at around 260 mμ seen in the case of 2-phenyltropone oxime, irrespective of the presence of the naphthyl group. Moreover, the second absorption maximum of 2-naphthyltropone oxime have shifted to a shorter wavelength region than the corresponding absorption maximum of 2-phenyltropone oxime in methanol solution (Table II) and a steric interference between the tropone ring and the naphthyl group at peri-position may be considered at its cause. The absorption maximum at 222~224 mμ of strong intensity seen in 2-α-naphthyltropone oxime is thought to be the absorption of naphthalene itself[8]. The ultraviolet spectrum of 2-o-tolyltropone oxime[3] also suggests the presence of a steric hindrance by the methyl group in the ortho-position of the phenyl ring. Owing to this effect, this compound has a maximum at 295 mμ which is considerably shifted toward shorter wavelength compared with a maximum of phenyltropone oxime at 307 mμ.

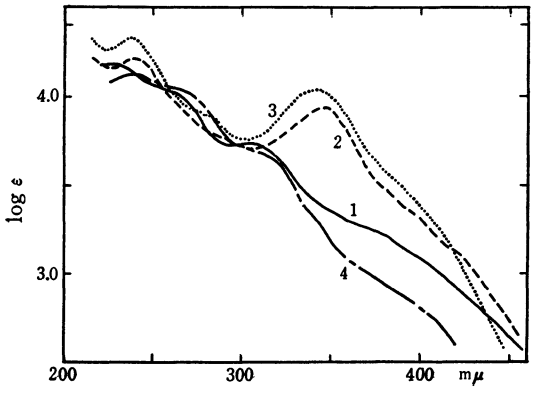



Fig. 6. Ultraviolet absorption spectra of oxime of 2-phenyltropone: (1) in methanol, (2) in 0.1 N HCl, (3) in 6 N HCl and (4) in 0.1 N NaOH solution.

Ultaviolet absorption spectra of 2,4-dinitrophenylhydrazones of various tropones are shown in Table III. In these cases also, the direction of the shift in hydrochloric acid and alkali solutions are the same as in the case of 2,4-dinitrophenylhydrazone of tropone, but the relationship between the shift of absorption and kind of substituents is complicated and conclusive explanation is difficult. The marked tendency of these is the small of shift in the absorption of 2-phenyl-, 2-benzyl- and 2-α-naphthyl-tropone derivatives measured in 0.1 N hydrochloric acid solution. The reason for this is the smallness in basicity and it may be considered that the stronger the basicity, the larger will be the shift. In 6 N hydrochloric acid solution, all the compounds

5) T. Nozoe, T. Mukai and I. Murata, *Proc. Japan Acad.*, **29**, 169 (1953).
6) K. Kikuchi, *J. Chem. Soc. Japan, Pure Chem. Sec.* (*Nippon Kagaku Zasshi*), **77**, 1439 (1956).
7) R. D. Haworth and P. B. Tinker, *J. Chem. Soc.*, **1955**, 911.
8) A. E. Gillam and E. S. Stern, "An Introduction to Electronic Absorption Spectroscopy in Organic Chemistry", Edward Arnold Publishers. Ltd., Londno (1955), p. 122.

have absorption maximum at about 360 mμ and formation of conjugate acids of similar structure may, therefore, be assumed. The absorption maximum of 2-α-naphthyltropone derivative at 222~223 mμ of strong intensity is that of naphthalene itself[8], as was stated earlier.

The author takes this opportunity to express his sincere gratitude Professor Tetsuo Nozoe for his kind guidance throughout the course of this work, and to Professor Shuichi Seto and Assistant Professor Yoshio Kitahara for much helpful advice.

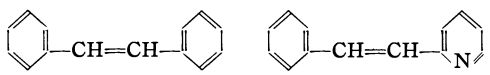
*Department of Chemistry*
*Faculty of Science*
*Tohoku University*
*Katahiracho, Sendai*

# *Geometrical Isomers of α-Stilbazole*

By Takumi KATSUMOTO

(Received August 8, 1959)

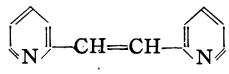
There is a series of stilbene derivatives which are substituted by one or two α-pyridyl groups for the phenyl groups of the stilbene. They are stilbene (I), α-stilbazole (II) and α-pyridostilbene, i.e. 1-2-bis-(α-pyridyl)-ethylene (III).



(I)



(II)



(III)

They are expected to exist in *cis*- and *trans*-structures as they are all 1,2-disubstituted ethylenes. Among the six isomers, *cis*- and *trans*-stilbene (I) are well known and recently the author reported two geometrical isomers of α-pyridostilbene (III)[1]. However, regarding α-stilbazole hitherto only one species which melts at 91°C has been known to us.

The author presumed that in the course of the preparation of the known species of α-stilbazole, the other isomer would be prepared as one of the by-products and then removed in some processes. The course was re-examined and it was found that the last recrystallization process removed completely the other isomer from the main product. Now, he has recovered the other isomer from the the filtrate, and then determined that the known species of α-stilbazole is a *trans*-isomer and the other is a *cis*-isomer on the basis of the data of the elementary analyses, the melting points, the ultraviolet and the infrared spectra.

## Experimental

**Syntheses of *cis*- & *trans*-α-Stilbazole.**—A mixture of freshly purified benzaldehyde (b.p. 179~180°C), α-picoline (b.p. 129.3°C) and anhydrous zinc chloride in the ratio 3 : 2 : 1 was heated in in an autoclave at 200°C for 24 hr.[2] After being cooled, the dark brown and viscid product was dissolved in aqueous hydrochloric acid, steam distilled to remove benzaldehyde and basified with sodium hydroxide, followed by steam distillation to remove the residual α-picoline. The solution separated raw and purplish red stilbazole, which was extracted with chloroform. The chloroform extract was dried over anhydrous sodium sulfate. After the chloroform was evaporated, the residue was distilled under 10 mmHg pressure. Pale yellow liquid passed over the interval 170~180°C and condensed in a receiver. No α-stilbazole could be found in the fore-run which was collected separately in three traps kept at 0, −20 and −80°C, respectively. The main distillate in the receiver was recrystallized from boiling ethanol. The precipitate (**A**) melts at 91°C and corresponds to the known species of α-stilbazole. The yield was 60% theoretical. After ethanol was evaporated from the filtrate, there remained the brown oil. It was purified repeatedly by the elution chromatography (alumina, 2×40 cm., chloroform) until it showed the constant ultraviolet absorption spectrum. The purified oil (**B**) is colorless and melts at −50.0°C. The yield was nearly 3% theoretical.

**Other Materials.**—*cis*- & *trans*-*Stilbene.*—*cis*-Stilbene[3] was prepared from *cis*-α-phenylcinnamic

1) T. Katsumoto, This Bulletin, **32**, 1019 (1959).
2) G. H. Lénárt, *Ann.*, **410**, 95 (1915).
3) C. C. Price, "Organic Syntheses", Vol. 33, John Wiley & Sons, Inc., New York (1953), p. 88.

acid and *trans*-stilbene[4] from benzoin, according to the methods of "Organic Syntheses". They were purified by the same method as the above. Their melting and boiling points are shown in Table II.

*cis- & trans-α-Pyridostilbene.*—The same samples that were synthesized in the preceding experiment[1] were used.

**Analyses and Measurements.**—Analytical data of the elementary analyses were determined by the Elementary Analyses Center of Kyoto University.

Melting points below the room temperature were measured in the following method, because the samples were so transparent even in the solid state as in the liquid state that the appearances did not change at the melting points. A liquid sample was packed as usual in a capillary tube which was then attached to a thermometer centered in a methanol bath. Dry air was sent into the bath to stir the methanol. A very thin and long glass wire was inserted in the capillary tube. As the bath was cooled in a dry ice-acetone mixture to −70°C, the sample solidified and the glass wire was fixed in it. Then, the methanol bath was transferred to an acetone bath that had been cooled near −40°C. The melting point was clearly observed as the glass wire could not be pulled out until the sample began to melt. *cis*-Stilbene and *cis*-stilbazole were viscid near the melting point.

Boiling points under reduced pressure were measured by Garcia's method[5] as described in the preceding paper[1].

The ultraviolet absorption spectra (in cyclohexane) were made with a Shimadzu QB-50 quartz spectrophotometer. The wavelengths of this photometer were calibrated with the absorption band at 301 mμ of an aqueous potassium nitrate solution. The infrared absorption spectra were obtained with a Hilger or a Leitz spectrophotometer equipped with a rock-salt prism. Readings were taken in the region of 1700~670 $cm^{-1}$ and always calibrated with the absorption bands of polystyrene.

## Results and Discussion

As described above, the colorless liquid (**B**) was recovered from the filtrate of the recrystallization of the known species of α-stilbazole (A). The analytical data of the elementary analyses of the liquid (**B**) are shown in Table I and are in good

Table I. Results of the elementary analyses of **B**

| | C | H | N |
|---|---|---|---|
| Found: | 85.95% | 6.32% | 7.93% |
| Calcd. for $C_{13}H_{11}N$: | 86.16 | 6.12 | 7.73 |

Table II. The m.p.'s. and b.p.'s. of the geometrical isomers

| | Stilbene (I) | | α-Stilbazole (II) | | α-Pyridostilbene (III) | |
|---|---|---|---|---|---|---|
| | *cis* | *trans* | **B**(*cis*) | **A**(*trans*) | *cis* | *trans* |
| m.p. | −54.0°C | 125.0°C | −50.0°C | 91.0°C | 48.5°C | 121.0°C |
| b.p. | 142°C/ 10 mmHg | | 141°C/ 10 mmHg | 171°C/ 10 mmHg | 149°C/ 15 mmHg | 197°C/ 15 mmHg |

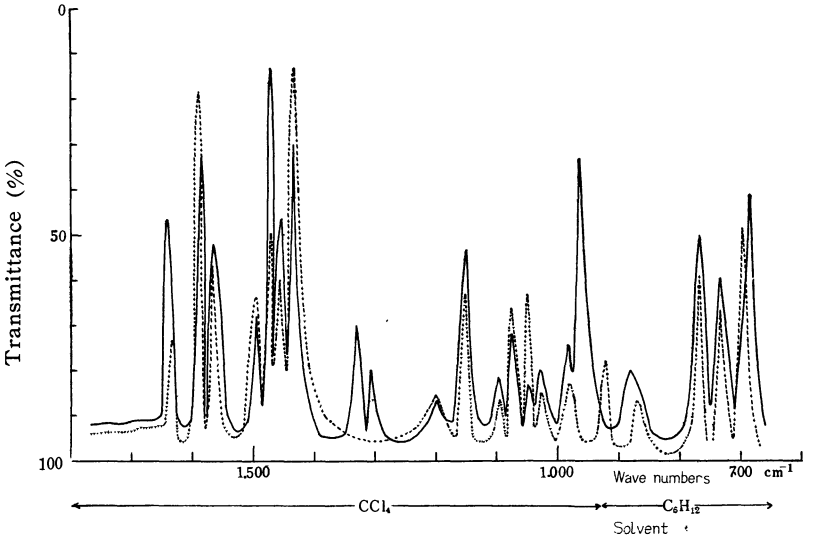



Fig. 1. Infrared absorption spectra of α-stilbazole.
—— **A** (*trans*) ---- **B** (*cis*)

4) L. I. Smith, ibid., Vol. 23 (1943), p. 86.

5) C. Garcia, *Ind. Eng. Chem., Anal. Ed.*, **15**, 648 (1943).

agreement with the calculated values for stilbazole $C_{13}H_{11}N$. It seems that **B** is also a species of $\alpha$-stilbazole. **B** melts at $-50.0°C$, which is much lower as compared with the melting point of **A** (91°C). As a *cis*-isomer always melts at much lower temperature than a *trans*-isomer does (Table II and Ref. 6), **A** is a *trans*-isomer and **B** is a *cis*-isomer.

Fig. 1 shows the infrared absorption spectra of **A** and **B** in carbon tetrachloride or in cyclohexane. Each band of **A** is in good agreement with corresponding band of **B**, except two bands at 1330 and 965 $cm^{-1}$ which will be discussed later. The good agreement indicates that **B** is the other isomer of **A**. Furthermore, this determination is made sure by the assignments of these absorption comparing their absorptions with those of the related compounds, stilbene (I) and $\alpha$-pyridostilbene (III) as shown in Table III.

The fundamental studies[7-9] on benzene vibrations have shown that the characteristic skeletal stretching modes of the semi-unsaturated carbon-carbon bonds lead to the appearance of a group of four bands between 1650~1450 $cm^{-1}$. Four absorptions corresponding to them are also expected theoretically in the case of pyridine and have been found in the similar range of the spectra of many pyridine derivatives[10,11], although the vibrations are mostly found to shift to somewhat lower frequencies on passing from benzene to pyridine. In these ranges each of **A** and **B** shows seven absorptions due to BR-1, 3, 4 and PR-1, 2, 3, 4 vibration modes (Table III). The letters B and P in the table denote the vibrations arising from a benzene and a pyridine ring, respectively. These spectra show that **A** and **B** each consist of a benzene and a pyridine ring. Randall et al.[12] regarded a bond in the range 1587~1575 $cm^{-1}$, namely, BR-2 in Table III, as an indication of the conjugation of an ethylenic double bond with an aromatic ring. In the spectra of $\alpha$-stilbazole the BR-2 vibration is obscure, because the absorption range is very similar to that of the PR-1 vibration and they overlap one another, but the PR-2 vibration corresponding to the BR-2 vibration in the sense of the conjugation, is clearly seen. This shows that a pyridine ring in the $\alpha$-stilbazole is conjugated with an ethylenic double bond.

In the range 1225~950 $cm^{-1}$, aromatic compounds all show a series of relatively weak but sharp bands, the positions of which vary with the type of substitution and are independent of the nature of substituents[11]. Randle and Whiffen[13,14] have shown that they arise from the CH in-plane bending modes. Generally, mono-substituted benzenes show three absorptions in the ranges 1175~1125, 1110~1070 and 1070~1000 $cm^{-1}$ [11,14,15]. In the case of $\alpha$-substituted pyridines the similar absorptions also appear in the ranges 1151~1140, 1050~1040 and 998~986 $cm^{-1}$ [10]. Five absorptions at **A** and **B** are located in the above absorption ranges of the mono-substituted benzenes and the $\alpha$-substituted pyridines, and correspond to the BHI-2, 3 and the PHI-1, 2, 3 vibration modes. The absorptions due to the BHI-1 seem to be masked with those due to the PHI-1 mode (Table III). These absorptions show that the benzene and the pyridine ring of **A** and **B** are a mono-substituted benzene and an $\alpha$-substituted pyridine ring.

Mono-substituted benzenes show two strong absorptions in the ranges of 770~730 $cm^{-1}$ [11,12] and 710~690 $cm^{-1}$ [11,12,15]. They are assigned to the out-of-plane CH bending vibrations of five adjacent ring hydrogen atoms remaining on the benzene ring, and the absence of the latter band is a strong evidence of the latter band is a strong evidence of the absence of a mono-substituted benzene. On the other hand, $\alpha$-substituted pyridines having four adjacent hydrogen atoms on the ring behave like an ortho-substituted benzene and absorb strongly in the range of 780~740 $cm^{-1}$ [10,11]. The three strong bands corresponding to the above bands appear in the spectra of **A** and **B** (BHO-1, 2 and PHO in Table III).

Thus, **A** and **B** are both disubstituted ethylenes with a phenyl and an $\alpha$-pyridyl radical, i.e. $\alpha$-stilbazole.

Generally, *trans*-ethylenic double bonds give rise to two medium to strong bands in the ranges of 990~965 $cm^{-1}$ [11,16] and 1310

6) M. Murakami, "Organic Stereochemistry (Kōzō Yūki-kagaku)", Asakura Publishers, Tokyo (1956), p. 181.
7) R. C. Lord et al., *J. Chem. Phys.*, **21**, 1170 (1953).
8) F. A. Andersen et al., ibid., **23**, 1047 (1955).
9) F. A. Miller et al., ibid., **24**, 996 (1956).
10) H. Shindo, *Pharm. Bull. (Japan)*, **5**, 472 (1957).
11) L. J. Bellamy, "The Infrared Spectra of Complex Molecules", 2nd Ed., John Wiley & Sons, Inc., New York (1958).
12) H. M. Randall et al., "The Infrared Determination of Organic Structures", van Nostrand, New York (1949).
13) D. H. Whiffen, *J. Chem. Soc.*, **1956**, 1350.
14) D. H. Whiffen et al., *Trans. Faraday Soc.*, **52**, 9 (1956).
15) R. B. Barnes et al., "Infrared Spectroscopy", Reinhold Publishing Corp., New York (1944).
16) R. S.. Rasmussen and R. R. Brattain, *J. Chem. Phys.*, **15**, 131, 135 (1947).

TABLE III. INFRARED ABSORPTIONS OF THE THREE PAIRS OF GEOMETRICAL ISOMERS ($cm^{-1}$)

| Stilbene (I) | | α-Stilbazole (II) | | | α-Pyridostilbene (III) | | Assignment* |
|---|---|---|---|---|---|---|---|
| *cis*[a,**] | *trans*[b] | B (*cis*)[c] | A (*trans*)[c] | A (*trans*)[b] | *cis*[b] | *trans*[b] | |
| | | 1632 m | 1643 s | 1636 s | | | |
| 1607 m | 1599 m | | | 1598 sh | | | BR-1 |
| | | 1590 vs | 1586 vvs | 1583 vvs | 1585 vs | 1582 s | PR-1 |
| 1578 w | 1578 m | | | | | | BR-2 |
| | | 1570 s | 1565 s | 1566 sh | 1569 vvs | 1567 vs | PR-2 |
| 1496 s | 1493 vs | 1497 s | 1497 m | 1492 s | | | BR-3 |
| | | 1471 s | 1471 vvs | 1466 vs | 1467 vs | 1468 vs | PR-3 |
| 1455 s | 1453 vs | 1453 m | 1453 s | 1453 vs | | | BR-4 |
| | | 1435 vs | 1433 vs | 1428 vs | 1438 vvs | 1436 vs | PR-4 |
| 1412 m | | | | | 1403 sh | | *cis*-EHI |
| | 1333 m | | 1331 vs | 1330 s | | 1326 s | *trans*-EHI |
| | 1302 m | | 1307 m | 1305 s | 1307 m | 1303 m | |
| | | | | 1237 m | | 1234 w | |
| 1183 w | | 1200 w | 1198 w | 1198 s | | | |
| 1158 w | 1157 m | | | | | | BHI-1 |
| | | 1147 s | 1148 s | 1147 s | 1157 s | 1146 s | PHI-1 |
| | | 1093 w | 1095 w | 1095 m | 1081 m | 1090 m | PHI |
| 1077 s | 1073 s | 1075 m | 1074 m | 1075 m | | | BHI-2 |
| | | 1050 s | 1049 w | 1053 m | 1053 m | 1053 m | PHI-2 |
| 1033 m | 1032 m | 1030 w | 1030 w | 1033 w | | | BHI-3 |
| | | 993 w | 986 w | | 994 s | 996 sh | PHI-3 |
| | 961 vvs | | 965 vvs | 983 vvs | | 976 vvs | *trans*-EHO |
| 924 s | 912 m | 923 m | | | | | |
| | 880 w | | 880 w | 893 m | 893 w | 880 m | |
| 864 m | 860 w | 867 w | | 868 m | | | |
| | | | | | 786 vs | 788 s | |
| 777 vvs | 764 vvs | 779 vs | 772 vvs | 779 vvs | | | BHO-1 |
| | | 740 vs | 735 vs | 735 vvs | 754 vvs | 745 vs | PHO |
| 694 vvs | 685 vs | 697 vs | 688 vs | 685 vs | | | BHO-2 |
| | | | | 676 vs | | | |

* BR and PR mean the stretching vibrations of a benzene and a pyridine ring; EHI, BHI and PHI mean the in-plane bending vibrations and EHO, BHO and PHO mean the out-of-plane bending vibrations, of the hydrogen atoms remaining on an ethylene, a benzene and a pyridine ring, respectively.

** The letters, a, b, c, denote the state of the samples in measurements: a, liquid condition without solvent; b, powder in a potassium bromide disk; c, carbon tetrachloride or cyclohexane solution.

TABLE IV. ULTRAVIOLET ABSORPTIONS OF THE THREE PAIRS OF THE GEOMETRICAL ISOMER (IN CYCLOHEXANE)

| Compound | *cis*-Form | | | | *trans*-Form | | | |
|---|---|---|---|---|---|---|---|---|
| | E-band | | K-band | | E-band | | K-band | |
| | $\lambda_{max}$, mμ | ε | $\lambda_{max}$, mμ | ε | $\lambda_{max}$, mμ | ε | $\lambda_{max}$, mμ | ε |
| Stilbene (I) | 207 | 19450 | 275 | 10730 | 228 | 15900 | 295 | 26600 |
| | 224 | 22600 | | | | | 306 | 24600 |
| α-Stilbazole (II) | 220 | 14860 | 285 | 9630 | 222 | 10570 | 275 | 15620 |
| | | | | | 228 | 11130 | 285 | 16470 |
| | | | | | 235 | 8570 | 314 | 24220 |
| α-Pyridostilbene (III) | 211 | 9920 | 257 | 5790 | 221 | 8770 | 267 | 15750 |
| | | | 262 | 5910 | 226 | 6620 | 316 | 28470 |
| | | | 268 | 4420 | | | 331 | 20510 |

~1290 $cm^{-1}$ [11]. The former band was assigned by Kilpatrick and Pitzer to the out-of-plane bending vibration[11], while the latter was assigned by Sheppard and Sutherland[17] to the in-plane bending vibration, of the hydrogen atoms remaining on the *trans*-disubstituted ethylene. Especially the absence of the former band can be regarded as the conclusive evidence of the *trans*-ethylenic linkage. Not any absorptions corresponding to the above absorptions are found in the spectrum of **B**, while **A** gives rise to the two strong absorptions at 965 and 1330 $cm^{-1}$ due to the *trans*-substituted ethylene (EHO, EHI in Table III). Thus, **B** is *cis*-α-stilbazole and **A** is *trans*-α-stibazole.

The ultraviolet spectra of **A** and **B** are compared with those of *cis*- and *trans*-isomers of stilbene (I) and α-pyridostilbene (III) in Table IV and Figs. 2–4. Each spectrum of stilbene and α-pyridostilbene consists of the E(ethylenic)-band and the K(conjugated)-band (Figs. 2 and 3). All the E-bands of both *cis*- and trans-isomers lie near 220 mμ. However, every K-band of the *trans*-isomer lies at a longer wavelength than that of the *cis*-isomer does. In addition, the intensity of the K-band is always much stronger in the *trans*-isomer than in the *cis*-isomer. The bathochromic displacements and much increase of the absorption intensities arise from the coplanarity of the molecular structure and then from the high degree of resonance on passing from the *cis*-structure to the

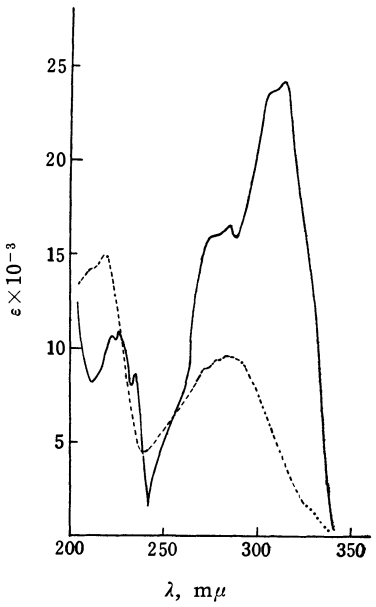



Fig. 3. Ultraviolet absorption spectra of α-stilbazole.
—— **A** (*trans*) ---- **B** (*cis*)

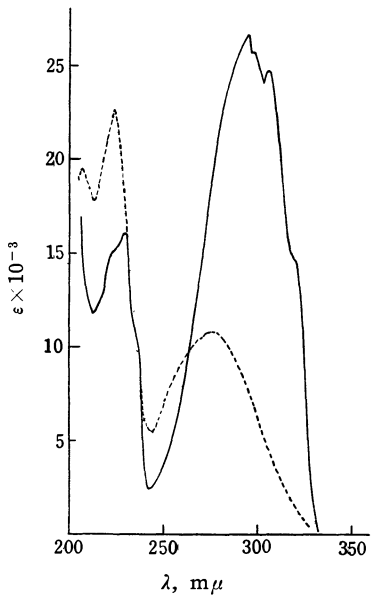



Fig. 2. Ultraviolet absorption spectra of stilbene.
—— *trans*-Fom ---- *cis*-Form

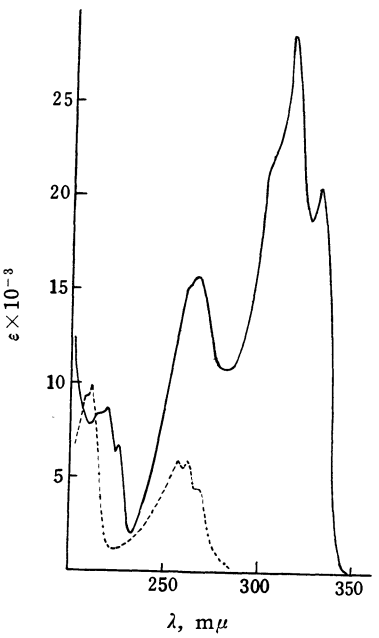



Fig. 4. Ultraviolet absorption spectra of α-pyridostilbene.
—— *trans*-Form ---- *cis*-Form

17) N. Sheppard and G. Sutherland, *Proc. Roy. Soc.*, **A196**, 195 (1949).

*trans*-structure[18]. Robertson and Woodward[19] indicated that, as the results of X-ray diffraction measurements, in *trans*-stilbene the bond joining the phenyl groups to the ethylenic group are 1.45 Å long. As the bond is considerably shorter than the usual saturated carbon-carbon bond (1.54Å), it is therefore a hybrid type, and two phenyl groups in *trans*-stilbene must exist almost in the plane in which ethylenic carbon and hydrogen atoms lie. Such configurations are expected in the cases of α-stilbazole (II) and α-pyridostilbene (III).

The spectra of **A** and **B** are typical of the *trans*- and the *cis*-structure (Fig. 3) and make sure of the above determination.

The conclusion is that a known species of α-stilbazole (**A**) is the *trans*-isomer and the other species (**B**) which was separated by the present author is the *cis*-isomer.

The author wishes to thank Professor S. Kimura of Kyoto University for encouragement, Professor T. Matsu'ura of Hiroshima University and Dr. H. Murata of the Osaka Municipal Technical Research Institute for recording infrared spectra, and Mr. M. Yamaguchi of this laboratory for his helpful assistance.

*Chemical Laboratory*
*Kwansei Gakuin University*
*Nishinomiya-shi, Hyogo*

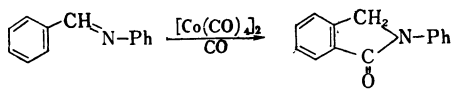
18) R. N. Jones, *J. Am. Chem. Soc.*, **65**, 1818 (1943).
19) J. M. Robertson and I. Woodward, *Proc. Roy. Soc.*, **A162**, 568 (1937).

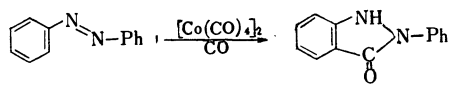
# *Studies on the High Pressure Reaction of Carbon Monoxide. IV. On the Mechanism of Phthalimidine and Indazolone Formation*

By Shigeki HORIIE* and Shunsuke MURAHASHI

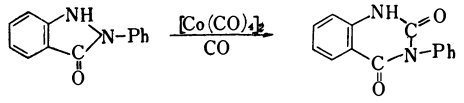
(Received July 3, 1959)

Both the formation of phthalimidines and of indazolones from Schiff bases or azocompounds are considered formally to be the same type of reactions, in which one molecule of carbon monoxide was incorporated into, and then underwent ring closure.





The formation of quinazolons from indazolone is considered to proceed via the reaction of ring enlargement, and has to be considered as another type of reaction and will be mentioned later.

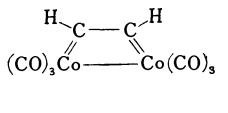


In view of avoiding confusion arising from by-products formation, the reaction of Schiff base was preferably chosen as the subject of this investigation because of the simplicity of the reaction—in the latter case the only reaction product was phthalimidine. From an experiment with Schiff base in continuous run, there could be observed the formation of a complex compound, which was soluble in benzene and was appreciably stable. It was shown in the previous reports that both in the cases of Schiff bases and azobenzenes the more electronegative the "C=N" or "N=N" bond is, the easier the reaction proceeds. These observations seem to indicate that some relation could exist between the ease of complex formation and the feasibility of reaction, and if this argument holds true, the two alternative methods of thinking on the attachment of catalyst on the reactive center of the substrate might be conceivable.

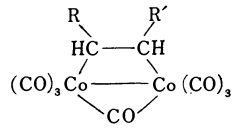
a) The one is that complex formation gives rise to the attachment of cobalt carbonyl across the $\pi$-bond of C=N or N=N. In this case a steric requirement

* Present address: Institute of Scientific and Industrial Research. Osaka Univ., Sakai, Osaka.

should necessarily be considered as was reported by Wender et al. in the case of oxo-synthesis. They observed the formation of a definite complex[1] from acetylene and cobalt carbonyl of the following constitution and, from this fact they postulated the same kind of complex formation by oxo-reaction, when olefins and cobalt carbonyl were reacted II[2],



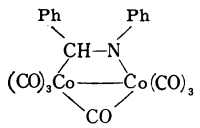
(I)



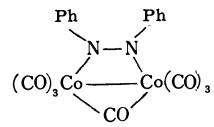
(II)

and they reasonably explained the observed differences of reaction velocity on various olefins on the steric ground, which inevitably affects the ease of intermediate complex formation.

If the same arguments are accepted in the authors' case, the intermediate complex would be such as III or IV, and marked steric effect might well be consiedered when Schiff bases or azocompounds were subjected to the experiment.



(III)



(IV)

On this account, the authors have compared the velocity of phthalimidine formation reaction, taking benzaldehyde-anil, acetophenone and benzophenone-anil as reactants, and the results are illustrated in Fig. 1. There has been no difference on the velocity and no sterically hindered effect of the phenyl group was discernible. Hence, the formation of this type of complex III would hardly be acceptable.

b) An alternative way of thinking would be that, an attachment of cobalt carbonyl takes place on the lone pair of nitrogen, which gives rise to the formation of a complex, acting as an intermediate for the reaction. Such consideration seems to explain much better the experimental facts which are described below. Although in the case of benzalcyclohexylamine gave in good yield phthalimidine as shown in

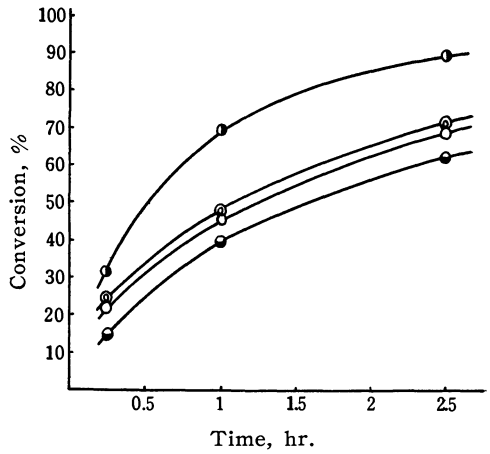
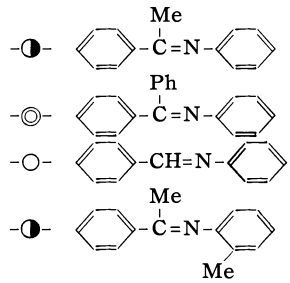
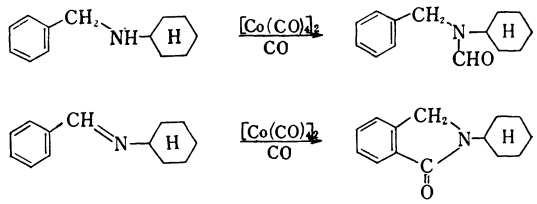



Fig. 1. Reactions of acetophenone-anil and benzophenone-anil with carbon monoxide.



Concn. of Schiff bases: 0.55 millimol/cc.
Concn. of $[Co(CO)_4]_2$: 0.03 millimol/cc.
Pressure of CO : 150 atm.
Solvent : benzene
Reaction temp. : 230°C

formula below, benzyl cyclohexylamine did not give rise to phthalimidine, but only gave *N*-formyl compound by the treatment with carbon monoxide in the presence of cobalt catalyst, under the same condition. Recently, Wender and his collaborators[3] also observed the formation of formyl compounds by the reaction of dimethylamine or piperidine with carbon monoxide, in the presence of cobalt carbonyl catalyst.



In those cases it seems to be appropriate to postulate that an intermediate

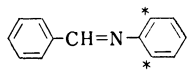
1) H. W. Sternberg, H. Greenfield, R. A. Friedel, J. Wotiz, R. Markby and I. Wender, *J. Am. Chem. Soc.*, **76**, 1457 (1954).

2) I. Wender, S. Metlin, S. Ergun, H. W. Sternberg and H. Greenfield, ibid., **78**, 5401 (1956).

3) H. W. Sternberg, I. Wender. R. A. Friedel and M. Orchin, ibid., **75**, 3148 (1953).

$$\begin{matrix}CH_3\\CH_3\end{matrix}\!\!>\!NH \xrightarrow[CO]{[Co(CO)_4]_2} \begin{matrix}CH_3\\CH_3\end{matrix}\!\!>\!N\text{-}CHO$$

formation of a complex occurred resulting from the coordination of the lone pair of the nitrogen atom with cobalt carbonyl, which in turn stabilized to yield formyl compound. Then, as a possible mechanism for the formation of phthalimidine and indazolone, the same argument would be worth while for consideration and for experimentation.



That is, in this case the initial step of the reaction is the coordination of cobalt carbonyl and nitrogen atom of anil bond CH=N, and the steric effect of ortho-position, which are marked with asterisks,

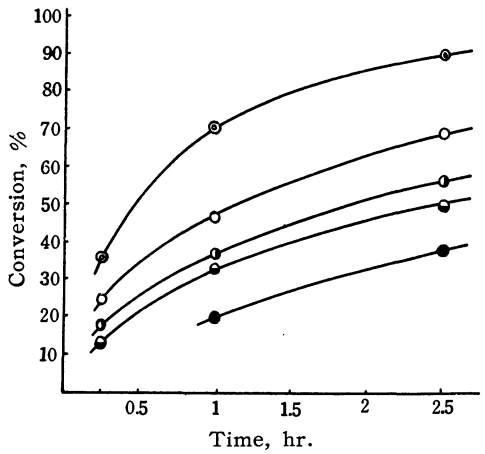
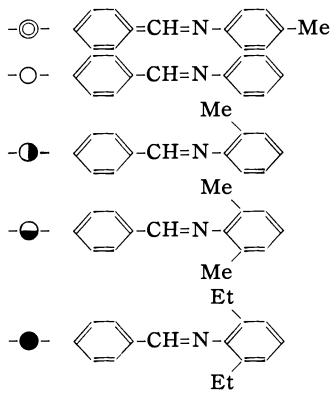



Fig. 2 Reactions of substituted benzaldehyde-anil and carbon monoxide.




Concn. of Schiff bases : 0.55 millimol./cc.
Concn. of $[Co(CO)_4]_2$ : 0.03 millimol./cc.
Solvent : benzene
Pressure of CO : 150 atm.
Reaction temp. 230°C

would become very influential to the reaction. Thus, several *o*-substituted anils were subjected to the reaction so as to see whether the steric effect of the substituents was operative. The results of the experiments were illustrated in Fig. 2, where the effect caused by the methyl or ethyl substituent group were visualized in percentage of conversion of anils to phthalimidines, which were followed by the reaction time. It was expected mono-ortho-substituted anil yields lower conversion than unsubstituted one and ortho-dimethyl substituted anil would exhibit a still lesser conversion

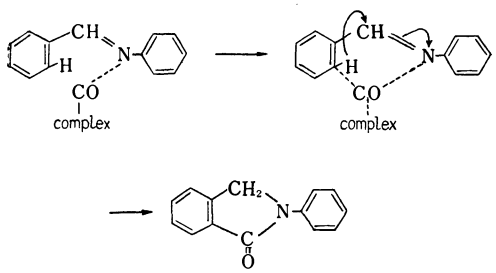
The experiment with *p*-methyl substituted anil has shown that methyl group had rather promoting effect, when it comes on para position, free from steric effect. The fact that in the case of ortho-substituted anil had shown marked low conversion in spite of having a methyl group of promoting action, shows that the steric effect is pronounced in these reactions. Hence it appeared as mentioned above, the primary step would be the addition of cobalt-carbonyl on the lone pair of nitrogen which is hindered by *o*-substituent of large steric requirement.

On the other hand, the reduction of a double bond of anils by means of synthetic gas and cobalt carbonyl go generally smoothly even if in the case where the substituents at the ortho position had shown to exhibit greatest resistance for the formation of phthalimidine, and no distinct steric effect was observed here.

The clear distinction of both reactions should indicate that the fundamental differences might exist in both reactions on the behavior of catalytic action. From the consideration above, the phthalimidine or indazolone formation can eventually be explained as follows.

1) Some kind of complex formation occurred at first between a lone pair of nitrogen atom of the anil or of azo-double bond, and here a steric effect was operative.

2) The formation of N-CO bond was then stabilized with the formation of a 5-membered ring with the carbon atom of benzene with simultaneous transfer of the hydrogen atom of ortho position of benzene to the unsaturated bond of C=N or N=N. Here the presence of such suitable acceptor of hydrogen atom was essential, and these might, side by side, have assisted the ring formation. In the case of benzyl cyclohexylamine as stated above, there is lacking such an accepting group and hence



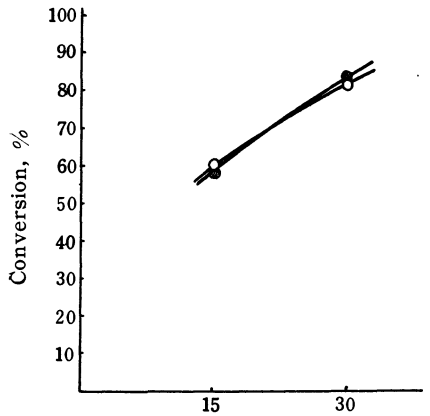
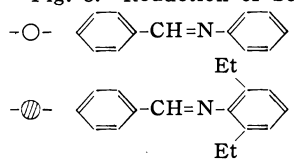




Fig. 3. Reduction of Schiff bases.




Concn. of Schiff bases : 0.5 mmol./cc.
Concn. of $[Co(CO)_4]_2$ : 0.03 mmol./cc.
Pressure of synthetic gas : 180 atm.
$CO/H_2=1/1$
Solvent : benzene
Reaction temp. : 120°C

after the formation of the complex would stabilize by converting to formyl benzyl amine.

Concerning the formation of quinazolone from indazolone as the authors stated earlier, it is believed to have formed by a ring-enlargement reaction, and such a reaction, as far as the authors are aware, has not yet been described. A glance at this reaction seems to be similar to the reaction of the formation of diphenylurea from hydrazobenzene, but the mechanism of this enlargement is not yet fully understood.

## Experimental

**1) Reactions of Schiff Bases and Carbon Monoxide.** — *General procedure.* — A solution of 0.0275 mol. of Schiff base and 1.5 millimol. of dicobalt octacarbonyl in 50 ml. benzene was heated at 230°C under 150 atmospheric pressure of carbon monoxide. After the reaction, benzene solution was heated under atmospheric pressure in a water bath so as to decompose cobalt carbonyl and filtered. After removal of benzene by distillation and then under reduced pressure, the residue was analyzed.

On each run, conversions from Schiff base into phthalimidine was determined for every 15, 60 and 150 min.

*(i) On benzaldehyde-anil.* — Conversions (%) into 2-phenylphthalimidine were 22.9, 46.2 and 68.1, respectively.

*(ii) On acetophenone-anil.* — Conversions (%) into 2-phenyl-3-methylphthalimidine melted at 82°C were 31.5, 68.5 and 89.0, respectively.

*Anal.* Found: C, 80.29; H. 5.99. Calcd. for $C_{15}N_{13}ON$: C, 80.69; H, 5.87%.

*(iii) On benzophenone-anil.*— Conversions (%) into 2,3-diphenyl-phthalimidine melted at 196.5°C were 24.8, 48.6 and 70.2, respectively.

*(iv) On acetophenone o-tolylimide.*—Conversions (%) into 2-*o*-tolyl-3-methylphthalimidine melted at 108°C were 14.3, 10.0 and 63.5, respectively.

*Anal.* Found: C, 80.68; H, 6.15. Calcd. for $C_{16}H_{15}ON$: C, 80.98; H, 6.37%.

*(v) On benzaldehyde p-tolylimide.*—Conversions (%) into 2-*p*-tolylphthalimidine were 36.8, 69.9 and 87.9, respectively.

*(vi) On benzaldehyde o-tolylimide.*—Conversions (%) into 2-*o*-tolylphthalimidine were 18.2, 36.0 and 53.0, respectively.

*(vii) On benzaldehyde o, o-xylidylimide.* — Conversions (%) into 2-*o*, *o*-xylidylphthalimidine melted at 103°C were 14.5, 32.8 and 49.8, respectively.

*Anal.* Found: N, 5.85. Calcd. for $C_{16}H_{15}ON$: N, 5.90%.

*(viii) On benzal-o, o-diethylaniline.*—Conversions (%) into 2-*o*, *o*-diethylphthalimidine melted at 140°C were 18.6 and 35.9, respectively.

*Anal.* Found: N, 5.02. Calcd. for $C_{18}H_{19}ON$: 5.28%.

**2) Reactions of Benzylcyclohexylamine and Carbon Monoxide.**—A solution of 5 g. of benzylcyclohexylamine and 1 g. of dicobalt octacarbonyl in 45 ml. of benzene was heated at 230°C under 140 atmospheric pressure of carbon monoxide to give 1.6 g. (28.1%) of benzylcyclohexylformylamine boiling at 135~140°C/3 mmHg.

*Anal.* Found: N, 5.99. Calcd. for $C_{14}H_{13}ON$: N, 6.63%.

**3) Reaction of Schiff Base and Water Gas.**— *General procedure.*—A solution of 0.025 mol. of Schiff base and 1.5 millimol. of dicobalt octacarbonyl in 50 ml. of benzene was heated at 120°C under 180 atmospheric pressure of synthetic gas (CO : H=1 : 1).

A benzene solution obtained was hydrolyzed with 4 N sulfuric acid. Benzaldehyde liberated was determined by the method of Bennett and Salamon[4] (hydroxylamine) to get the amount of unreacted Schiff base.

4) C. T. Bennett and M. S. Salamon; *Analyst*, **52**, 693 (1927).

The percentage conversions of benzal compound to benzyl compound were estimated from the value of Schiff base remaining after 15 and 30 min. in each run.

*(i) On benzaldehyde-anil.* — Conversions (%) from benzaldehyde-anil into benzylaniline were 59.8 and 80.0, respectively.

*(ii) On benzal-o, o-diethylaniline.*—Conversions (%) from benzal-*o*, *o*-diethylaniline into benzyl-*o*,*o*-diethylaniline were 58.0 and 81.9, respectively.

*Department of Chemistry*
*Faculty of Science*
*Osaka University*
*Nakanoshima, Osaka*

# *Radiation-induced Polymerization of α-Methylstyrene**

By Kozo HIROTA, Kenji MAKINO, Keiji KUWATA and Gisuke MESHITSUKA

(Received July 31, 1959)

It has been considered till recently that α-methylstyrene (αMS) is not easily polymerizable, i. e. it can not be polymerized by radical initiators, but can be polymerized by cationic[1] or anionic initiators[2] at low temperatures. Therefore, it will be interesting to study the effect of ionizing radiation on αMS, i. e. to investigate the possibility of radiation-induced polymerization*, and to make clear the kind of mechanism, if it can be polymerized. After the research was advanced to some extent[3], it was found, however, that the first problem was answered affirmatively, and also that the polymerization seemed to proceed by a radical mechanism[3b]. Therefore, a new problem was encountered. This was why αMS did not polymerize by use of such a radical initiator as benzoyl peroxide. It is the object of the present paper to investigate the three problems mentioned above.

## Experimental

**Materials.** — α-Methylstyrene of guaranteed grade of Tokyo Kasei Kogyo K. K. was used. It was treated with aqueous solutions of 20% NaOH and of 20% $NaHSO_3$ successively. Then, it was dried with dehydrated calcium chloride and also with potassium hydroxide freshly fused, and vacuum-distilled under nitrogen atmosphere. The sample thus purified was stored in a closed vessel. According to gas chromatographic analysis, the water content in it was negligible (<0.002%). Naphthalene of chemical pure grade was used after repeated recrystallization. Other reagents (carbon tetrachloride, benzoquinone, cyclohexane and nitrobenzene) were of guaranteed grade and were used without further purification.

**Procedure of Irradiation.**—Two γ-ray irradiation sources of Co-60 were used; one was 350 curie source, while the other 1000 curie source**. Samples will therefore be classified in series B or J, according as the irradiation was carried out at the former or at the latter. In order to avoid direct contact with air and water, αMS was always vacuum-distilled ($10^{-4}$ mmHg) into irradiation tubes. However, as it is known that the presence of oxygen and water brings about an undesirable effect on polymerization, one of the samples (J 9) was distilled over an evaporated film of sodium in advance of irradiation for the sake of comparison. The irradiation tube was made of hard glass and could contain 5~16 g. of αMS. Being required by the discussion on the mechanism of polymerization, ultraviolet irradiation was also attempted by utilizing the sunlight in summer, enclosing the sample in a quartz ampoule.

**Treatment of the Irradiated Samples.** — The irradiated sample was taken out by opening the tube and was poured into methanol, which was five times as much as the sample in volume. White polymers thus precipitated were filtered, washed with methanol, and dried in vacuo at room temperature until the weight became constant. The molecular weight of the polymer was determined with the osmotic pressure method or the viscosity method. In the latter method,

* When the authors' preliminary research was announced at the 11th Annual Meeting of the Chemical Society of Japan, Tokyo, April, 1958, they could not find any research of this kind in literature.

1) D. J. Worsfold and S. Bywater, *J. Am. Chem. Soc.*, **79**, 4917 (1957); S. Okamura et al., Presented at the 7th Annual Meeting of the Society of Highpolymer Science of Japan, Tokyo, May, 1958.

2) G. C. Jones et al., *Ind. Eng. Chem.*, **48**, 2123 (1956).

3) (a) K. Hirota, K. Kuwata and K. Makino, *Isotopes and Radiation (Tokyo)*, **1**, 104 (1959). (b) Presented at the Symposium of Radiation Chemistry, Tokyo, Nov., 1958.

** The 350 curie source is installed at Institute for Microbial Diseases of Osaka Univ., and the 1000 curie source at Osaka Laboratory of Japanese Association for Radiation Research on Polymers. The authors express sincere thanks to Drs. T. Noguchi, H. Hayashi and M. Hatada for the help in irradiation procedure.

TABLE I. CO-GAMMA IRRADIATION. TOTAL DOSE: $6\times10^6$ $r$

| | Additives: Compounds | Additives: Mole fraction % | Conversion % | $\bar{M}_n$ | m. p. of polymers °C |
|---|---|---|---|---|---|
| B-1 | None | — | 4.4 | $3.8\times10^4$ | 220 |
| B-2 | Carbon tetrachloride | 18.1 | 8.2 | $1.4\times10^4$ | 185 |
| B-3 | Naphthalene | 7.9 | 0.27 | $6.0\times10^4$ | 195 |
| B-4 | Oxygen | air-saturated | 0[a)] | — | — |
| B-5 | *p*-Benzoquinone[b)] | 0.41 | 0 | — | — |

a) However, when the irradiated sample was poured into methanol, a turbid solution was obtained.

b) Total dose of $7.3\times10^6$ $r$; dose rate of $5.3\times10^4$ $r$/hr.

the following viscosity formula was used[4].

$$[\eta]=3.50\times10^{-5}(\bar{M}_n) \quad (1)$$

$\bar{M}_n$: average molecular weight

As the molecular weight of the polymer was low in case of photopolymerization, the cryoscopic method was adopted.

## Results

**Preliminary Experiments.** — As shown in Table I, it has been found that αMS polymerizes with total dose of $6\times10^6$ $r$, dose rate being $1.2\times10^5$ $r$/hr. The polymer obtained is of fairly high molecular weight. Its melting point is also high if compared with the polymer obtained by photo-polymerization[5]. Moreover, it has been found that polymerization was sensitized by the addition of carbon tetrachloride, but was retarded by the presence of naphthalene and perfectly inhibited by oxygen and benzophenone. Such effects of additives seem to suggest that the polymerization proceeds by the radical initiation of γ-rays.

**Effect of Total Dose.** — In Table II, the effect of total dose on conversion and intrinsic viscosity is shown by keeping the dose rate constant. Conversion of polymerization increases linearly with the total dose after an induction period (ca. 5 hr.). On the other hand, judging from the relation between the intrinsic viscosity and total dose, the molecular weight of the polymer seems to be constant.

TABLE II. EFFECTS OF TOTAL DOSE ON CONVERSION AND INTRINSIC VISCOSITY

| Run | Dose rate $r$/hr. | Dose $r$ | Conversion, % | $[\eta]$ |
|---|---|---|---|---|
| J 6-1 | $1.56\times10^5$ | $5.8\times10^6$ | 28.2 | 0.110 |
| J 6-2 | $1.56\times10^5$ | $4.34\times10^6$ | 21.4 | 0.116 |
| J 6-3 | $1.56\times10^5$ | $1.74\times10^6$ | 4.4 | 0.113 |

4) C. P. Brown and A. R. Mathieson, *J. Chem. Soc.*, **1958**, 3445.

5) C. E. Schildknecht, *Ind. Eng. Chem.*, **50**, 107 (1958).

**Effect of Dose Rate.** — In Table III, the effect of dose rate on conversion is shown. In order to investigate the effect of dose rate on velocity of polymerization in detail, the conversion rate $V_p$ is plotted against dose rate $I$ in Fig. 1. It is clear that the velocity of polymerization of αMS is first order of $I$ on the assumption that it is proportional to the rate of conversion. For the sake of comparison, the result of

TABLE III. EFFECT OF DOSE RATE ON CONVERSION

| Run | Dose rate $r$/hr. | Dose $r$ | Conversion, % | $[\eta]$ |
|---|---|---|---|---|
| J 1-2 | $2.6\times10^4$ | $3.5\times10^6$ | 8.6 | 0.105 |
| J 1-3 | $1.4\times10^4$ | $1.8\times10^6$ | 4.6 | 0.106 |
| J 1-4 | $8.8\times10^3$ | $1.2\times10^6$ | 7.5 | 0.115 |
| J 7-3 | $1.6\times10^5$ | $3.3\times10^6$ | 20.5 | 0.118 |
| J 7-4 | $1.6\times10^5$ | $7.6\times10^6$ | 19.1 | 0.116 |

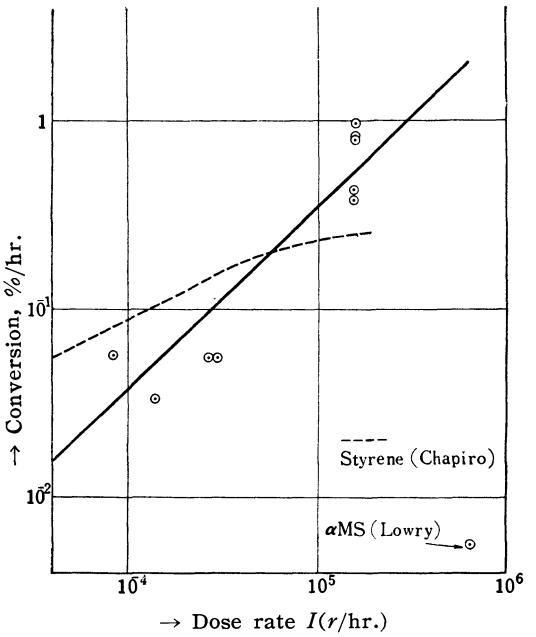



Fig. 1. Conversion per hour vs. dose rate.

Chapiro[6] on styrene is plotted as a broken line, by which it is shown that the order of polymerization of styrene is one half if the dose rate is small. The same order is often reported in the γ-ray-induced polymerization. Therefore, it may be noteworthy that an exceptional order of reaction has been obtained in the present research. This problem will be taken up again in the part of discussion in relation to the mechanism of polymerization. However, the polymerization velocity seems of the same degree in both monomers, while the recent data of Lowry[7] on αMS is very small as compared with that of the present research. The intrinsic viscosity $[\eta]$ is shown to be independent of dose, i. e. 0.110, being similar to that of Lowry. The molecular weight of poly-α-methylstyrene is smaller than that of polystyrene by Chapiro.

**Effect of Solvent.** — As mentioned in the part of the preliminary experiment, effect of several solvents on the reaction rate was already investigated. However, an additional experiment was carried out in other solvents, in order to make the mechanism of polymerization clearer. To meet this requirement, nitrobenzene and cyclohexane were selected as the solvents to be studied, each dielectric constant being 36 and 1.9, respectively. If the reaction proceeds by an anionic or cationic mechanism, αMS will polymerize very rapidly in a solvent of high dielectric constant[8] such as nitrobenzene, while if the reaction proceeds by a radical mechanism, the polymerization must be inhibited by the solvent on the contrary. According to the result shown in Table IV, nitrobenzene behaves as an inhibitor, while cyclohexane behaves as a simple diluent. The result, in addition to the preliminary experiments, confirms the conclusion that the reaction proceeds by a radical mechanism.

**Effect of Temperatures.**—Hitherto, radical polymerization of αMS has been attempted at higher temperatures, but the result was found always negative. Though the data here obtained seem to contradict the above results, the situation may be brought about by the condition that the irradiation was carried out at ordinary temperature. Such being the case, the effect of temperature on radiation-induced polymerization was investigated over the range 9~72°C, the result being summarized in Table V.

As shown by the value of intrinsic

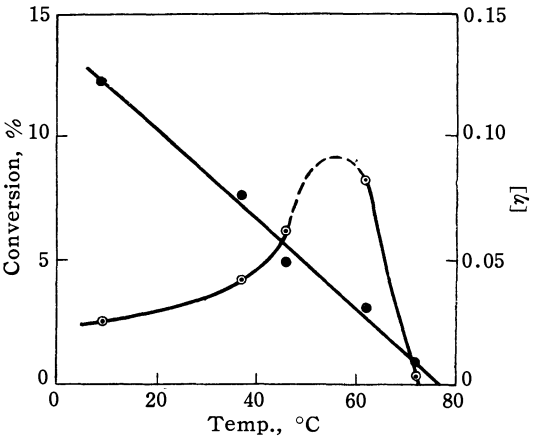



Fig. 2. Conversion and intrinsic viscosity vs. temperature.
⊙: Conversion, %
●: Intrinsic viscosity, $[\eta]$

TABLE IV. EFFECT OF SOLVENT ON THE RATE OF POLYMERIZATION

| Run | Additive compounds | Mol. % | Dose rate $r$/hr. | Dose $r$ | Conversion % | $[\eta]$ |
|---|---|---|---|---|---|---|
| J 7-1 | Cyclohexane | 29.0 | $1.6\times10^5$ | $3.4\times10^6$ | 13.2 | 0.101 |
| J 7-2 | Nitrobenzene | 37.3 | 1.6 〃 | 3.4 〃 | 0 | — |

TABLE V. EFFECT OF TEMPERATURE ON CONVERSION etc.

| Run | Temp. °C | Dose rate $r$/hr. | Dose $r$ | Conversion % | $[\eta]$ | $\overline{DP}$ |
|---|---|---|---|---|---|---|
| J 9-1 | 9 | $3.1\times10^4$ | $1.2\times10^6$ | 2.5 | 0.123 | 29.6 |
| J 9-2 | 37 | 〃 | 〃 | 4.2 | 0.076 | 18.6 |
| J 9-3 | 46 | 〃 | 〃 | 6.1 | 0.049 | 11.9 |
| J 9-4 | 62 | 〃 | 〃 | 8.2 | 0.030 | 7.3 |
| J 9-5 | 72 | 〃 | 〃 | 0.33 | 0.009 | 2.2 |

6) A. Chapiro and P. Wahl, *Compt. rend.*, **238**, 1803 (1954).
7) G. G. Lowry, *J. Polymer Sci.*, **31**, 187 (1958).
8) D. C. Pepper, *Trans. Faraday Soc.*, **45**, 397 (1949).

viscosity, it seems that the degree of polymerization $\overline{DP}$ decreases linearly with temperature, and will became practically zero at 77°C. This tendency may be clearly shown by Fig. 2 where conversion and $[\eta]$ are plotted against temperature. It may be estimated that the degree of polymerization at 77°C will be less than five, because telomers of such low polymerization degree are soluble in methanol. On the other hand, the amount of conversion has a maximum and will be zero at 72°C (cf. Fig. 2). The phenomenon here observed must be ascribed to the peculiar property of αMS, and will serve as a key to the mechanism of polymerization***.

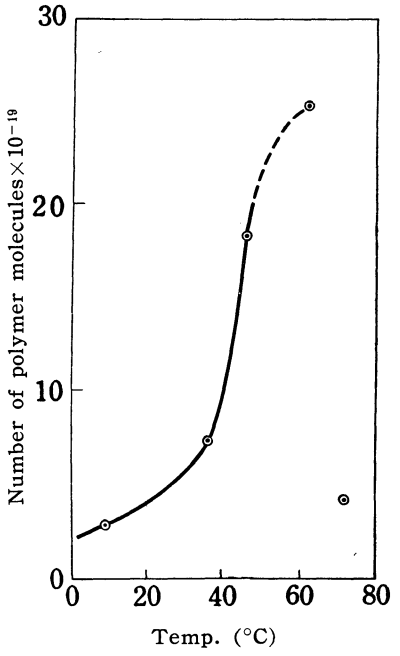



Fig. 3. The effect of temperature on the number of polymer molecules.

Assuming that Eq. 1 can be applied on the poly-αMS, as far as the relative value of average molecular weight is concerned, the number of polymer ($n$) produced at each temperature was calculated, and it was found that $n$ increases very rapidly if temperature decreases as shown in Fig. 3.

**Photopolymerizations.** — Recently, it was reported that Schildknecht[5] succeeded to polymerize αMS by irradiating it with ultraviolet light, the detail being not described. Therefore, similar research was carried out by use of the sunlight for the sake of confirmation. Polymers of 0.38 g. in weight could be obtained from the starting material of (αMS 15.7 g.+di-*tert*-BPO 4.0 g.). The molecular weight of the polymers was ca. 640 (cryoscopic method).

## Discussion

**Mechanism of Polymerization.**—Considering the effects of additives and solvents on the yield of polymers, it may be reasonable to conclude that the radiation-induced polymerization of αMS proceeds by a radical mechanism, as already mentioned. Polymerizing power of ultraviolet light also supports the mechanism, though telomers obtained are of low molecular weight. In the course of the present research this conclusion has been justified independently by Lowry[7] who could obtain polymers having the molecular weight of 50000 at 0°C by the redox polymerization method.

Thus, the present research seems merely to have added an example of radiation-induced polymerization, but it may be noteworthy to have found that the polymerization of this monomer has a peculiar dependency upon temperature, especially it will practically stop at higher temperatures than ca. 70°C. Now, it may be clear why the attempts to polymerize αMS did not succeed hitherto. In these attempts the temperatures to supply radical initiators to the sample were too high to obtain polymers. The phenomenon of this kind called "ceiling temperature" was already pointed out experimentally by Snow and Frey[9] in the copolymerization of olefins and sulfur dioxide. Later Dainton and Ivin[10] explained it by assuming the equilibrium

$$M_j + M \rightleftarrows M_{j+1}$$

and derived the existence of a temperature beyond which the reaction chains will fail to grow. Thermodynamically the ceiling temperature $T_c$ may generally be given by

$$T_c = -\Delta H_p / -\Delta S_p = \frac{\Delta H}{\Delta S^\circ + 2.30 \boldsymbol{R} \log_{10}[M]} \quad (2)$$

where $\Delta H_p$ and $\Delta S_p$ denote, respectively, changes of enthalpy and entropy of polymerization, [M] denotes the concentration

*** Detailed discussion on the relations of conversion and intrinsic viscosity with temperature will be omitted, because it was published already [K. Makino, G. Meshitsuka, K. Kuwata and K. Hirota, *Isotopes and Radiation (Tokyo)*, 2, 322 (1959)].

9) R. P. Snow and F. E. Frey, *Ind. Eng. Chem.*, **30**, 176 (1938); *J. Am. Chem. Soc.*, **65**, 2417 (1943); cf. F. E. Mathews and H. M. Elder, Brit. Pat., 11,635 (1914).
10) F. S. Dainton and K. Ivin, *Nature*, **162**, 705 (1948).

of monomer, and $S^\circ$ denotes the quantity referred to monomer in a standard state of pure liquid. Recently McCormic[11] determined $T_c$ of αMS to be 61°C from the polymerization in tetrahydrofuran solution by use of a sodium naphthalene complex as initiator. Though the temperature is slightly lower than that of the present research, the discrepancy can be explained by Eq. 2, if it is considered that the degree of polymerization of the present sample is lower than that of McCormic (cf. the formula[12] giving the relation between $\Delta H_p$ and average molecular weight $\overline{M}_n$: $-\Delta H_p = 8.424 + 2194/\overline{M}_n$). It is rather interesting that $T_c$ of such a low temperature is obtained in both experiments, notwithstanding the fact that the active species are different in the course of polymerization. Now, a problem remains why $T_c$ of poly-α-methylstyrene is much lower than that of polystyrene. It may be ascribed to the small values of $-\Delta H_p$ for this monomer as compared with other monomers: e. g. αMS 9.0, styrene 16.0 and ethylene 22, respectively in kcal./mol. per monomer, in spite of the order of magnitude of its $\Delta S_p$ comparable to the other monomers[13].

**Kinetic Formula of Polymerization.** — From the above discussion, it seems to be without ambiguity that radiation-induced polymerization of αMS proceeds by a radical mechanism, but an important experimental result still remains to be unexplained. In the pioneer work of Chapiro[6] on the gamma-ray-induced polymerization of styrene and other monomers, he found that velocity $V_p$ of the polymerization can be expressed by the formula

$$V_p \propto I^{1/2} \qquad (3)$$

where $I$ is the dose rate. The formula is generally accepted to be applicable to all the radiation-induced polymerization. Nevertheless, in the present research as shown in Fig. 1, the velocity derived from the conversion (%) is not proportional to $I^{1/2}$ but rather to $I$. The above result, though it seems to be exceptional, can be understood by the mechanism in which a degradative chain transfer proceeds more frequently than the chain termination between radicals. Therefore, each step of the elementary processes of the present reaction will be summarized as follows:

Initiation: $\mathrm{M} \xrightarrow{\phi I} \mathrm{R}\cdot$

$\mathrm{R}\cdot + \mathrm{M} \xrightarrow{k'_i} \mathrm{M}^*$

Propagation: $\mathrm{M}^*_j + \mathrm{M} \xrightarrow{k_p} \mathrm{M}^*_{j+1}$

Depropagation: $\mathrm{M}^*_{j+1} \xrightarrow{k_d} \mathrm{M}^*_j + \mathrm{M}$

Chain transfer to monomer:

$\mathrm{M}^*_j + \mathrm{M} \xrightarrow{k_{tr}} \mathrm{M}_j + \mathrm{M}^*$

Degradative chain transfer:

$\mathrm{M}^*_j + \mathrm{M} \xrightarrow{k_t} \mathrm{M}_j + \mathrm{M}$

where $\mathrm{M}^*_j$ denotes active polymers of $j$ subunits and $\phi$ radicals produced per unit $I$ in unit volume of monomers. Applying the steady state treatment to the mechanism mentioned above, the kinetic formula may be derived easily:

$$V_p = (\phi I/k_t)(k_p[\mathrm{M}] - k_d)$$

i. e. $V_p$ is proportional to $I$.

## Summary

It has been shown that (a) α-methylstyrene polymerizes at room temperatures by gamma-ray irradiation; that (b) the reaction proceeds by a radical mechanism, considering from the effect of solvents, additives and ultraviolet light; that (c) ceiling temperature for this monomer is exceptionally low (ca. 70°C) among vinyl monomers, so that it is hard to obtain high polymers by the usual method; that (d) the experimental fact that the velocity of polymerization is proportional to dose rate and not to square root of dose rate can be explained by the assumption that degradative chain transfer occurs more frequently than the termination between active polymers.

A part of the expense for the present experiment has been defrayed from a grant given by the Ministry of Education, to which the authors' thanks are due.

*Department of Chemistry*
*Faculty of Science*
*Osaka University*
*Nakanoshima, Osaka*

11) H. W. McCormick, *J. Polymer Sci.*, **25**, 488 (1957).
12) D. E. Roberts and R. S. Jessup, *J. Res. Natl. Bur. Standards*, **38**, 627 (1947).
13) C. Walling, "Free Radicals in Solutions", John Wiley & Sons, Inc., New York (1957), p. 213; F. S. Dainton and K. J. Ivin, *Quart. Revs.*, **12**, 61 (1958).

# *Solvent Effect on the Intrinsic Viscosity of Polymers*

By Tetsuya ISHIKAWA

(Received July 7, 1959)

It is well known that the intrinsic viscosity, $[\eta]$, of a polymer takes high values in good solvents and low values in poor solvents. If the experimental precautions to be observed in order to obtain reliable data are taken, such difference may be attributed quantitatively to the solvent character which the existing theories of dilute solution viscosity of polymers do not deal with.

## Analytical Procedure

In the last report[1], the author derived from his ideal mixture law for viscosity the following form for $[\eta]$, $cm^3\,g^{-1}$:

$$[\eta]=\frac{(K_v)_0}{d_2}\left(\frac{\eta_2}{\eta_1}\right),$$

$$(K_v)_0=\left|\frac{(1-z_v)(\eta-\eta_1)}{z_v(\eta_2-\eta)}\right|_{z_v\to 0} \qquad (1)$$

in which $\eta_1$, $\eta_2$ and $\eta$ denote the viscosities of a solvent, solute of high molecular weight whose density is $d_2$, and the solution respectively, and $z_v$ is the volume fraction of the solute before mixing.

For an ideal mixture composed of two liquids of low molecular weights, $(K_v)_0=(K_v)_1=K_v$, a constant for all concentrations, and the probable values of $K_v$ relative to benzene of 32 liquids can be computed from $K$ values relative to benzene obtained before[2], by means of the equality:

$$K_v=K\frac{M_1d_2}{M_2d_1} \qquad (2)$$

where $M_1$, $M_2$, and $d_1$, $d_2$ are the molecular weights and densities of components 1 and 2, respectively, benzene being taken as component 1 in this case.

Combining Eq. 1 with Eq. 2, the following assumption is made:

Since $[\eta]$ is an extrapolated value at infinite dilution of a polymer with a given solvent where solvent molecules suffer presumably no change in association, $(K_v)_0$ of polymer/solvent may be inversely proportional to $K_v$ of solvent/benzene, and therefore $[\eta]$ may be inversely proportional to the product

$$\eta_1\times(K_v \text{ of solvent/benzene})$$

so long as $(K_v)_0\times(K_v$ of solvent/benzene) which signifies the solute character term at infinite dilution retains a constant value in different solvents.

In other words, between the intrinsic viscosities of the same polymer in solvent 1 and in solvent 2, there may exist the equation:

$$\frac{[\eta] \text{ in solvent 1}}{[\eta] \text{ in solvent 2}}=\frac{(\eta\times K_v \text{ rel. to benzene) of solvent 2}}{(\eta\times K_v \text{ rel. to benzene) of solvent 1}} \qquad (3)$$

## Verifications

In order to verify Eq. 3, one quotes from Wales, Marshall and Weissberg's report on the intrinsic viscosities of dextran in water and in formamide at 25°C[3], as one has $K=0.67$ for water and $K=0.34$ for formamide at 25~40°C[2].

Now, one has for benzene ($M=78.11$) $d=0.87875$(20/4), 0.86805(30/4); for water ($M=18.02$) $d=0.99823$ (20/4), 0.99568 (30/4), $\eta=0.01005$ poise (20°C), 0.00802 poise (30°C); and for formamide ($M=45.04$) $d=1.1349$ (20/4), 1.1266(30/4), $\eta=0.0375$ poise (20°C), 0.0294 poise (30°C)[4,5].

From these values one obtains

$$\frac{(\eta\times K_v \text{ rel. to benzene) of water}}{(\eta\times K_v \text{ rel. to benzene) of formamide}}=1.16(20°C),\ 1.19(30°C)$$

On the other hand, the inverse ratios of intrinsic viscosity values, $100\,cm^3\,g^{-1}$, in formamide to those in water taken from

1) T. Ishikawa, This Bulletin, **31**, 791 (1958).
2) T. Ishikawa and T. Baba, ibid., **11**, 64 (1936); see also T. Ishikawa, ibid., **31**, 524 (1958).
3) M. Wales, P. A. Marshall and S. G. Weissberg, *J. Polymer Sci.*, **10**, 229 (1953).
4) "International Critical Tables", III, (1928), pp. 25, 27—30.
5) F. Henning, "Wärmetechnische Richtwerte", Vdi-Verlag G.m.b.H. (1938), pp. 40—45.

Wales, Marshall and Weissberg's data for dextran of four different molecular weights, $M$, are:

$$\frac{[\eta] \text{ in formamide}}{[\eta] \text{ in water}} = \frac{0.121}{0.097} = 1.25 \text{ for } M = 11000$$

$$= \frac{0.341}{0.271} = 1.26 \text{ for } M = 71000$$

$$= \frac{0.446}{0.384} = 1.16 \text{ for } M = 153000$$

$$= \frac{0.492}{0.421} = 1.17 \text{ for } M = 185000$$

Comparing these values with the above obtained values, it is seen that the coincidence is satisfactory, especially for dextran of higher molecular weights.

The following is another test applied to the data of the toluene and methyl ethyl ketone (MEK) solutions of one polystyrene sample distributed to several laboratories from the International Union of Pure and Applied Chemistry (IUPAC)[6]. The average values of $[\eta]$, $cm^3g^{-1}$, assembled by Frank and Mark were 148.3±2.3 for toluene at an average temperature 25.5°C (25°C in eight laboratories, 30°C in one laboratory, and 24.7°C in one laboratory), and 82.9±2.8 for MEK at an average temperature 25.5°C (25°C in seven laboratories, 30°C in one laboratory, and 24.7°C in one laboratory).

For toluene one has $\eta=0.00551$ poise (25°C)[7], and $K=1.24$ (15~35°C)[2], from which one gets $K_v=1.03$ (25°C) by putting toluene ($M=92.13$) and benzene ($M=78.11$) densities to be 0.86122 (25/4) and 0.87340 (25/4), respectively; for MEK one has $\eta=0.00383$ poise (25°C) but $K$ is unknown because of lack of binary mixtures composed of this liquid as one component in the literature, and, under the author's direction, viscosity measurements on the binary system of benzene (1)-MEK(2) have been carried out by M. Ikeda, lecturer of Nagasaki Prefectural Junior College.

Benzene and MEK used for the present measurements were the guaranteed reagents of Kanto Chemical Co., Inc., the former having test No. 4E033294 and the latter having test No. 3E088722, and both were used without further purification.

Densities and viscosities were measured at 25°C with an automatically regulated thermostat, T-3 type of Shimadzu Seisakusho Ltd., with a Gay-Lussac pycnometer of 25 $cm^3$, and with a Ostwald viscometer with 10 $cm^3$ efflux volume which has given efflux time of 54.70 sec. for water.

To convert density (25/25) to density (25/4) and relative viscosity to absolute viscosity, the author used density of water at 25°C=0.99707[4], and viscosity of water at 25°C=0.008941 poise[8].

TABLE I. BENZENE(1)—METHYL ETHYL KETONE(2), 25°C

| $z_v$ | $d_4^{25}$ | $\eta_{obs}$ | $K_v$ obs. | $K_v$ cacld. | $\eta_{calcd}$ |
|---|---|---|---|---|---|
| 0.000 | 0.8733 | 0.006158 | | (1.79) | — |
| 0.125 | 0.8646 | 0.005655 | 2.16 | 1.86 | 0.005710 |
| 0.250 | 0.8557 | 0.005323 | 1.93 | 1.94 | 0.005320 |
| 0.375 | 0.8467 | 0.004977 | 2.07 | 2.03 | 0.004982 |
| 0.500 | 0.8377 | 0.004727 | 2.04 | 2.13 | 0.004713 |
| 0.625 | 0.8286 | 0.004511 | 2.02 | 2.23 | 0.004477 |
| 0.750 | 0.8191 | 0.004296 | 2.28 | 2.35 | 0.004294 |
| 0.875 | 0.8096 | 0.004137 | 2.55 | 2.48 | 0.004145 |
| 1.000 | 0.7999 | 0.004024 | | (2.63) | — |

The experimental results are given in Table I. As seen from the observed $K_v$ values in Table I, this system belongs to the case where the association degree of either of the components decreases with the dilution of the other, and either of the extrapolated values of $K_v$ at $z_v=0$ or $z_v=1$ gives the normal $K_v$ for the mixture. Mixtures of phenol, guaiacol, or benzyl benzoate with benzene or toluene in which the former components suffer molecular dissociation are examples for this case. The formulation of viscosity vs. composition curves of such mixtures can not be generally done, yet a particular case can be solved by a particular means, that is to say, $K_v$ or its reciprocal at each composition to test whether they are in linear relationship with composition or not[9]. For the present case, reciprocal values of $K_v$ against $z_v$ appear to lie nearly on a straight line, $1/K_v=0.56-0.18z_v$, hence one has obtained $(K_v)_0=1.79$ and $(K_v)_1=2.63$. Compare the observed and calculated viscosity values in Table I, the deviations being at most less than 1%. It is doubtful, however, that either of components, benzene or MEK, suffers molecular dissociation, so the author refers to the results by making use of Fischler's viscosity data on benzene

6) IUPAC, *J. Polymer Sci.*, **17**, 1 (1938).
7) T. E. Thorpe and J. W. Rodger, *Phil. Trans. Roy. Soc. London. Ser.* **A185**, 397 (1894); J. Batschinski, *Z. physik. Chem.*, **84**, 643 (1913).
8) "Landolt-Börnstein Tabellen", Eg. I, p. 83.
9) T. Ishikawa, This Bulletin, **4**, 288 (1929); refer also to 2).

(1)-acetone(2) system[10] as found in the literature (see Table II). Since in this system benzene suffers no molecular change throughout the concentration, giving a constant value 2.06±0.05 which is an intermediate value between $(K_v)_0$ and $(K_v)_1$ for MEK/benzene, the same liquid in the benzene(1)-MEK(2) system may also be considered to suffer no molecular change, and therefore $(K_v)_1=2.63$ can be decided as the normal value, $K_v$, for MEK/benzene, the corresponding association degree of MEK being estimated to be 2.78.

TABLE II. BENZENE(1)—ACETONE(2), 25°C (FISCHLER)

| $z_v$ | $\eta$ | $K_v$ |
|---|---|---|
| 0.00 | 0.005758 | |
| 0.25 | 0.004715 | 2.00 |
| 0.50 | 0.003997 | 2.08 |
| 0.75 | 0.003507 | 2.10 |
| 1.00 | 0.003150 | |
| | | 2.06±0.05 |

Taking $K_v=2.63$ and $\eta=0.00383$ poise at 25°C for MEK and the above values for toluene, one obtains

$$\frac{(\eta\times K_v \text{ rel. to benzene) of MEK}}{(\eta\times K_v \text{ rel. to benzene) of toluene}}=1.77$$

whereas

$$\frac{[\eta] \text{ in toluene}}{[\eta] \text{ in MEK}}=\frac{148.3}{82.9}=1.79$$

for $M=560000\sim590000$

Also from the similar data on four polystyrene fractions in the previous report[11] from IUPAC, the same ratios in respective laboratories are:

$$\frac{[\eta] \text{ in toluene}}{[\eta] \text{ in MEK}}=1.88,\ 1.99 \text{ for } M=860000$$
$$=2.11,\ 2.01 \text{ for } M=655000$$
$$=1.54,\ 1.61 \text{ for } M=234000$$
$$=1.64,\ 1.60 \text{ for } M=82500$$

with an average of 1.80 which is nearly equal to the preceding result. Hence the coincidence is fairly good between the ratios taken from intrinsic viscosity data and from the present theory.

## Conclusion

The foregoing verifications lead us to the conclusion that an intrinsic viscosity equation $[\eta]=(K_v)_0(\eta_2/\eta_1)/d_2$ is valid for polymer solutions, and therfore that $[\eta]$ of a polymer in a solvent can be converted to $[\eta]$ of the same polymer in a standard solvent, e. g. benzene, or toluene, or acetone; this procedure will give a reliable value to be further analyzed, if normal $K_v$ values of these solvents relative to the standard solvent are known.

The author is indebted to Nagasaki American Cultural Center for having made it possible for him to obtain, by mail from Tokyo, Journal of Polymer Science, Vol. X, 1953; and also to Mr. M. Ikeda for his viscosity measurements on the binary system of benzene and methyl ethyl ketone.

*Junior College of Commerce*
*Nagasaki University*
*Nagasaki*

10) J. Fischler, *Z. Elektrochem.*, **19**, 126 (1913).
11) IUPAC, *J. Polymer Sci.*, **10**, 129 (1953).

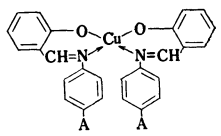
# *Some Addition Compounds of Salicylaldehyde-ethylenediimine-copper*. IV.*

By Tsuguo TANAKA

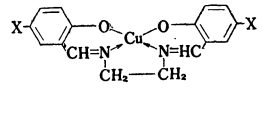
(Received August 17, 1959)

Recently, some observation have been reported[1] about the influence of substituents in the ligand molecules on the physical and chemical properties of their metal chelates. Calvin et al.[2] presented the following order about the stability of the chelates, which he explained on the basis of mesomeric effect, among the substituents A in a metal chelate of salicylaldehyde-anil (I) by the measurement of their half wave potential.

$$OCH_3 > OH > CH_3 > H > C_6H_5 > SO_3Na > NO_2$$



(I)



(II)

An analogous but not identical order of substituents was also observed by the present author[3] about the tendency of the formation of the addition compounds of 5,5′-disubstituted salicylaldehyde-ethylenediimine-copper (II) with propionic acid, phenol and chloroform; the order was

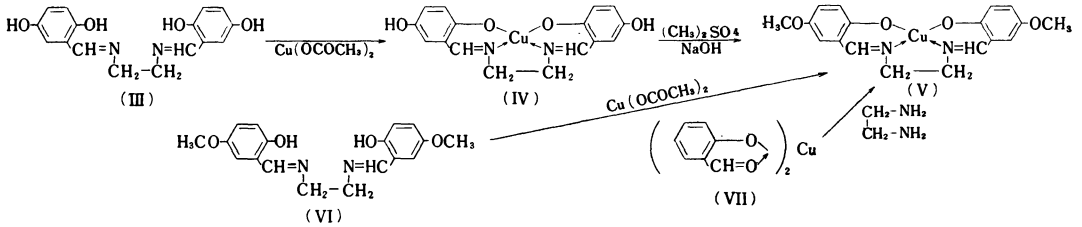
$$5,5'\text{-}CH_3 > 5,5'\text{-}H > 5,5'\text{-}NO_2 > 5,5'\text{-}Cl$$

Now, it was attempted to obtain a further illustration about the influence of the 5,5′-substituent groups in salicylaldehyde-ethylenediimine-copper on the formation of the addition compounds.

5,5′-Dibromo-, 5,5′-diiodo- and 5,5′-dimethoxy-salicylaldehyde-ethylenediimine-copper were synthesized according to the usual procedure[3,4]. 5,5′-Dibromosalicylaldehyde-ethylenediimine-copper was obtained as a purple addition compound with chloroform when it was recrystallized from chloroform, which was eliminated on standing in the air to give a pure green 5,5′-dibromo-salicylaldehyde-ethylenediimine-copper.

The metal chelate which was obtained by the reaction of 5-iodosalicylaldehyde-copper with ethylenediamine-monohydrate in an ethanolic solution was a purple addition compound of 5,5′-diiodosalicylaldehyde-ethylenediimine-copper with ethanol which lost ethanol, when heated at 110°C for thirty minutes, to give dark green 5,5′-diiodosalicylaldehyde-ethylenediimine-copper. Free 5,5′-diiodosalicylaldehyde-ethylenediimine-copper formed addition compounds with ethanol and chloroform.

But the reaction of 5-hydroxysalicylaldehyde with copper acetate in an ethanolic solution resulted in the formation of a black polymeric copper salt, which could not be converted into 5,5′-dihydroxysalicylaldehyde-ethylenediimine-copper by a reaction with ethylenediamine in ethanol. Therefore, 5-hydroxysalicylaldehyde was treated with ethylenediamine-monohydrate in an ethanol to give 5,5′-dihydroxysalicylaldehyde-ethylenediimine (III), which on warming in ethanol with an aqueous solution of copper acetate produced dark blue crystals of the copper salt (IV)[5]. The structure of 5,5′-dihydroxysalicylaldehyde-ethylenediimine-copper (IV) was



(III) (IV) (V) (VI) (VII)

* Bis-salicylaldehyde-ethylenediimine-copper.

1) M. Calvin and K. W. Wilson, *J. Am. Chem. Soc.*, **67**, 2003 (1945). L. G. G. van Uitert, W. C. Fernelius and B. E. Douglas, ibid., **75**, 457 (1953).

2) M. Calvin and R. H. Bailes, ibid., **68**, 953 (1946).

3) T. Tanaka, ibid., **80**, 4108 (1958).

4) P. Pfeiffer, E. Breith, E. Lübbe and T. Tsumaki, *Ann.*, **503**, 85 (1933).

5) C. S. Marvel and N. Tarkoy, *J. Am. Chem. Soc.*, **80**, 832 (1958).

TABLE I. ADDITION COMPOUNDS OF SALICYLALDEHYDE-ETHYLENEDIIMINE-COPPER DERIVATIVES

| Substituents | Color of complex | Addition compounds Color (time required for formation, min.) | | | |
|---|---|---|---|---|---|
| | | Propionic acid | Phenol | Chloroform | Ethanol |
| 5,5'-$OCH_3$[a] | yellow green | purple brown (2) | purple (0.5) | — | — |
| 5,5'-I | dark green | purple (6) | purple (0.5) | purple (0.5) | purple[b] |
| 5,5'-OH[a] | gray green | — | purple brown (0.5) | — | — |
| 5,5'-Br | green | — | purple (0.5) | purple[b] | — |

a) Powdered sample. b) Recrystallization.

confirmed by the following synthesis.

5,5'-Dihydroxysalicylaldehyde-ethylenediimine-copper (IV) was methylated by treating it with dimethylsulfate and aqueous sodium hydroxide[6], when 5,5'-dimethoxysalicylaldehyde-ethylenediimine-copper (V) was obtained. V was also obtained either by the reaction of 5,5'-dimethoxysalicylaldehyde-ethylenediimine (VI) with an aqueous solution of copper acetate in ethanolic solution, or by the reaction of 5-methoxysalicylaldehyde-copper (VII) with ethylenediamine-monohydrate. Identity of these products was proved by the observation of the absorption spectra.

The formation of the addition compounds of these metal chelates with propionic acid, phenol, chloroform and ethanol was examined and the results were summarized in Table I.

Peculiar behavior of 5,5'-diiodosalicylaldehyde-ethylenediimine-copper was noted; it formed addition compounds with propionic acid as well as with chloroform and ethanol in contrast to other derivatives.

Comparing these results with those already reported, the tendency of the formation of addition compounds is in the following order,

$$5,5'\text{-}CH_3 \underset{(+)}{>} 5,5'\text{-}OCH_3 \underset{(-)}{>} 5,5'\text{-}I \underset{(-)}{>} 5,5'\text{-}H >$$
$$5,5'\text{-}OH \underset{(-)}{>} 5,5'\text{-}Br \underset{(-)}{>} 5,5'\text{-}NO_2 \underset{(-)}{>} 5,5'\text{-}Cl$$

where (+) indicates electron releasing and (−) electron attracting inductive effects[7].

## Experimental

5-Iodosalicylaldehyde was obtained as its sodium salt by the reaction of *p*-iodophenol (10 g.) with chloroform (9 g.) in aqueous sodium hydroxide[8] (9.1 g. sodium hydroxide in 40 ml. water) at 55~65°C. Yield, 14%.

**5, 5'-Dihydroxysalicylaldehyde - ethylenediimine.** —To a solution of 5-methoxysalicylaldehyde (1.6 g. in 41 ml. ethanol) was added ethylenediamine-monohydrate (520 mg. in 5 ml. ethanol). In the meantime a yellow precipitate separated, which was filtered and dried (1.5 g.). It was dissolved in ethanol and water was added to it drop by drop until turbidity occurred; the product was left to stand for a while, until yellow needles separated, which were filtered and dried. Yield, 0.9 g.; m. p. 250°C (decomp.). It is easily air-oxidized in an ethanolic solution, when left to stand for one day and the color changes into orange to red.

*Anal.* Found: C, 60.63; H, 5.77; N, 8.00. Calcd. for $C_{16}H_{16}O_4N_2$-$H_2O$: C, 60.37; H, 5.70; N, 8.80%.

**5,5'-Dimethoxysalicylaldehyde - ethylenediimine.** —To a solution of 5-methoxysalicylaldehyde (900 mg. in 20 ml. ethanol) was added ethylenediamine-monohydrate (100 mg. in 3 ml. ethanol). In the meantime the whole mass solidified, which was filtered, washed with a little water and recrystallized from ethanol. Yield, 700 mg.; m. p. 165°C.

*Anal.* Found: C, 65.95; H, 6.38; N, 8.29. Calcd. for $C_{18}H_{20}O_4N_2$: C, 65.84; H, 6.14; N, 8.53%.

5,5'-Dibromo-, 5,5'-diiodo-, 5,5'-dimethoxysalicylaldehyde-ethylenediimine-copper were obtained by the usual procedure[3,4].

**5, 5' - Dibromosalicylaldehyde - ethylenediimine - copper.** — Gold orange 5-bromosalicylaldehyde-copper was converted into green 5,5'-dibromosalicylaldehyde-ethylenediimine-copper. Recrystallization of the product from chloroform produced a purple addition compound with chloroform which, upon standing in air, gradually (in two days) lost chloroform to yield the green, pure 5,5'-dibromo-complex.

*Anal.* Found: C, 39.99; H, 2.86; N, 5.91; Cu, 13.04. Calcd. for $C_{16}H_{12}O_2N_2Br_2Cu$: C, 39.42; H, 2.48; N, 5.75; Cu, 12.97%.

**5, 5' - Diiodosalicylaldehyde - ethylenediimine - copper.**—Gold yellow 5-iodosalicylaldehyde-copper suspended in boiling ethanol was treated with ethylenediamine-monohydrate; immediately transient green coloration was observed, but the color turned purple and the purple addition compound of 5,5' - diiodosalicylaldehyde - ethylenediimine-copper with ethanol precipitated, which was filtered and recrystallized from ethanol. By heating the addition compound at 110°C for thirty minutes, dark green pure 5,5'-diiodosalicylaldehyde-ethylenediimine-copper was obtained.

6) H. Decker and O. Koch, *Ber.*, **40**, 4794 (1907).
7) C. K. Ingold, *Ann. Repts.*, **23**, 129 (1926).
8) Cf. also H. H. Hodgson and T. A. Jenkinson, *J. Chem. Soc.*, **1927**, 1740; ibid., **1929**, 469.

*Anal.* Found: C, 33.25; H, 2.42; N, 4.17; Cu, 10.40. Calcd. for $C_{16}H_{12}O_2N_2I_2Cu$: C, 33.04; H, 2.08; N, 4.82; Cu, 10.93%.

**5, 5'-Dimethoxysalicylaldehyde - ethylenediimine-copper.**—(a) It is obtained from yellow 5-methoxysalicylaldehyde-copper as described above. Recrystallization from chloroform gave green plates. $\lambda_{max}^{C_5H_5N}$ 400, 585 m$\mu$[9].

*Anal.* Found: C, 53.74; H, 4.59; N, 6.77; Cu, 16.91. Calcd. for $C_{18}H_{18}O_4N_2Cu$: C, 54.45; H, 4.65; N, 7.19; Cu, 16.30%.

(b) 5,5'-Dimethoxysalicylaldehyde - ethylene - diimine (600 mg.) in boiling ethanol (80 ml.) was treated with a saturated aqueous solution containing copper acetate (400 mg.) and the mixture was boiled for thirty minutes on a water bath. After cooling, the precipitates were filtered and recrystallized from chloroform.

(c) To an intimate mixture of 5,5'-dihydroxysalicylaldehyde-ethylenediimine-copper (400 mg.) and dimethylsulfate (400 mg.) was added 0.8 ml. of 10% aqueous sodium hydroxide solution; it reacted exothermically at once, stirred thoroughly to complete the reaction. After an hour, the paste was filtered, washed with water, dried and recrystallized from chloroform.

**5, 5'-Dihydroxysalicylaldehyde-ethylenediimine-copper.**—To a boiling solution of 5,5'-dihydroxysalicylaldehyde-ethylenediimine (1.2 g. in 215 ml. ethanol) was added copper acetate (0.96 g. in 20 ml. water) and the mixture heated for twenty minutes on a water bath. After the mixture was cooled, the precipitate was filtered and recrystallized from ethanol. It showed blue purple as needles but a gray green color appeared when powdered. Yield, 1 g.

*Anal.* Found: C, 50.15; H, 4.47; N, 6.64; Cu, 17.27. Calcd. for $C_{16}H_{14}N_2O_4Cu$-$H_2O$: C, 50.61; H, 4.25; N, 7.38; Cu, 16.74%.

**Addition Compound with Propionic Acid**[3].—*5, 5'-Diiodosalicylaldehyde-ethylenediimine-copper.*

*Anal.* Found: C, 33.49; H, 2.70; N, 4.53. Calcd. for $C_{16}H_{12}O_2N_2I_2Cu$-$C_3H_6O_2$: C, 34.79; H, 2.77; N, 4.27%.

*5, 5' - Dimethoxysalicylaldehyde - ethylenediimine - copper.*

*Anal.* Found: C, 54.20; H, 5.39; N, 6.10. Calcd. for $C_{18}H_{18}O_4N_2Cu$-$C_3H_6O_2$: C, 54.35; H, 5.21; N, 6.04%.

**Addition Compounds with Phenol**[3].—*5, 5'-Diiodosalicylaldehyde-ethylenediimine-copper.*

*Anal.* Found: C, 40.16; H, 2.92; N, 4.18. Calcd. for $C_{16}H_{12}O_2N_2I_2Cu$-$C_6H_6O$: C, 39.09; H, 2.68; N, 4.15%.

*5, 5' - Dimethoxysalicylaldehyde - ethylenediimine - copper.*

*Anal.* Found: C, 58.48; H, 4.85; N, 5.63. Calcd. for $C_{18}H_{18}O_4N_2Cu$-$C_6H_6O$: C, 59.54; H, 5.00; N, 5.79%.

*5, 5' - Dibromosalicylaldehyde-ethylenediimine - copper.*—The reaction product was purified by washing with benzene or by recrystallization from chloroform containing phenol.

*Anal.* Found: C, 43.89, H, 2.92; N, 4.74. Calcd. for $C_{16}H_{12}O_2N_2Br_2Cu$-$C_6H_6O$: C, 45.41; H, 3.12; N, 4.82%.

*5, 5' - Dihydroxysalicylaldehyde - ethylenediimine - copper.*—The reaction product was purified by washing repeatedly with benzene, and was not recrystallized.

*Anal.* Found: C, 55.98; H, 4.89; N, 5.00. Calcd. for $C_{16}H_{14}O_4N_2Cu$-$C_6H_6O$: C, 57.95; H, 4.42; N, 6.15%.

**Addition Compounds with Chloroform.**—*5, 5'-Dibromosalicylaldehyde-ethylenediimine-copper.*

*Anal.* Found: C, 36.23, 36.06; H, 2.48, 2.42; N, 5.56, 5.61. Calcd. for $C_{16}H_{12}O_2N_2Br_2Cu$-$\frac{1}{2}CHCl_3$: C, 36.21; H, 2.30; N, 5.12%. Weight decrease at 110°C. Found: 11.13. Calcd. for $C_{16}H_{12}O_2N_2Br_2Cu$-$\frac{1}{2}CHCl_3$: 10.91%.

*5, 5'-Diiodosalicylaldehyde-ethylenediimine - copper.*—Recrystallized from chloroform.

*Anal.* Found: C, 28.54; H, 3.35; N, 4.42. Calcd. for $C_{16}H_{12}O_2N_2I_2Cu$-$CHCl_3$: C, 29.13; H, 3.35; N, 4.00%.

**Addition Compound with Ethanol.**—*5, 5'-Diiodosalicylaldehyde-ethylenediimine-copper.*

*Anal.* Found: C, 32.43; H, 2.88; N, 4.62. Calcd. for $C_{16}H_{12}O_2N_2I_2Cu$-$C_2H_6O$: C, 34.44; H, 2.89; N, 4.46%. Weight decrease at 110°C. Found: 6.34. Calcd. for $C_{16}H_{12}O_2N_2I_2Cu$-$C_2H_6O$: 7.34%.

The author is grateful to Mr. M. Shito and Miss S. Indo for the microanalysis.

*Faculty of Liberal Arts*
*Saga University*
*Honjo, Saga*

9) Beckman E. P. U. spectrophotometer.

# *Primary Processes in the Photobleaching of Eosin as Revealed by the Flash Technique*

By Shunji KATO, Teiko WATANABE, Shigeo NAGAKI and Masao KOIZUMI

(Received August 17, 1959)

A few years ago, Imamura and Koizumi[1] investigated kinetically the reductive photobleaching of xanthen dyes and proposed a reaction scheme which involved the formation of semiquinone radical with a lifetime of millisecond order. Now, techniques of flash photolysis and flash spectroscopy have been introduced in order to get direct evidence for their conclusion and to obtain more detailed information about the primary processes. The present paper is concerned chiefly with the spectra of the transient intermediates and their assignment along with some discussions about the reaction scheme. A rather remarkable result was that two types of intermediates with a lifetime of millisecond order were observed spectroscopically. One of these was assigned to semiquinone and the other to a certain kind of complex between dye and ethanol.

## Experimental

**Flash Lamps.** — A photolysis flash lamp, six turn helical Terex tube, 10 mm. in diameter, the total length of which was about 1 m., was filled with argon at 4.5 cmHg pressure. It was surrounded by a cylindrical magnesia reflector. A spectroflash lamp was a Terex tube, 20 cm. in length and 15 mm. in diameter, having a flat quartz window, the argon pressure being 20 cmHg. Five 10 $\mu$F oil condensers were used for photolysis flash and one condenser of the same capacity for spectroflash, and both of them were charged up to 4 kV. Flashes were triggered by induction coils operated by strobo discharge tubes. The interval of firing was controlled from 0.3 to 700 millisec. by an electronic device. The half height widths of the flashes were measured by an oscilloscope and found to be approximately 60 and $<20$ $\mu$ sec., respectively, a crystal oscillator being used as a time measure.

**Spectroscopic.**—A Shimazdu QF-60 quartz spectrograph and Fuji Neopan plates were used.

**Reaction Vessels.** — The vessels were of 10 cm. length and 1 cm. diameter glass tubes with quartz plates cemented on both ends. The glass part of the vessel cuts off shorter wavelengths than 300 m$\mu$.

**Materials.** — Merck eosin and Wako Pure Chemical Industries G. R. grade ethanol were used. The latter was transparent up to 260 m$\mu$ for a 10 cm. path. Throughout the investigation, $1\times10^{-5}$ mol./l. ethanolic solution of eosin was degassed by repeated distillation in high vacuum, sealed in a reaction vessel and then was placed at the center of the helical flash lamp.

**Calibration of the Flash Intensity.** — Although the flashing condition was made as nearly the same as possible by monitoring the condenser voltage, some variation in intensity could not be avoided. To evaluate correctly the absorption spectra of the transient species from the trace of a microphotometer, the variation of the spectro-flash intensity was taken into account in the following way. From the readings of the trace for the solvent and solution, the logarithm of exposure was determined in the usual way. When the difference in the logarithm of exposure was plotted against the molar extinction coefficient ($\varepsilon_\lambda$) of eosin, a linear relationship was found to hold in the wavelength region above 480 m$\mu$, where the transient species had no absorption. Since the relation

$$\Delta S_\lambda = \log I_\lambda - \log I'_\lambda + \varepsilon_\lambda cd$$

holds, where $\Delta S_\lambda$ is the difference in logarithm of exposure, $I_\lambda$ and $I'_\lambda$ are the intensity of the spectro-flash for solvent and solution, respectively; the intercept of the ordinate gives the value $\log I_\lambda - \log I'_\lambda$, which allows one to calibrate the intensity variation of the spectro-flash.

## Results

The absorption spectra are shown in Fig. 1. The spectra of the initial solution were obtained by a Hitachi spectrophotometer EPU-2A. The time interval written is that between the start of the two flashes. As seen from the figure, after 0.6 millisec., the main absorption of eosin decreases to 60% of the initial solution, and at the same time a definite transient absorption comes into existence. Substracting from this the absorbance due to the remaining eosin, the quantity of which

1) M. Koizumi and M. Imamura, This Bulletin, **28**, 117 (1955); **29**, 899 (1956).

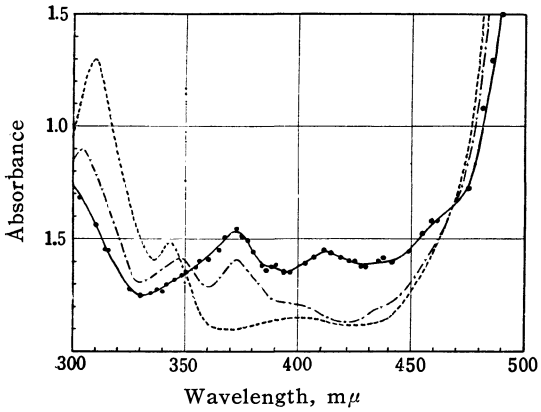



Fig. 1. Transient spectra of eosin.
——: 0.6 millisec.
—·—: 5 millisec.
----: before flash

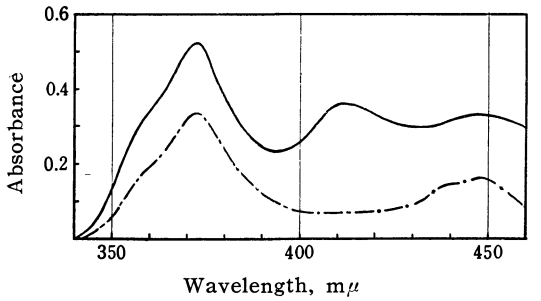



Fig. 2. Absorption spectra of transient species of eosin.
——: 0.6 millisec.
—·—: 5 millisec.

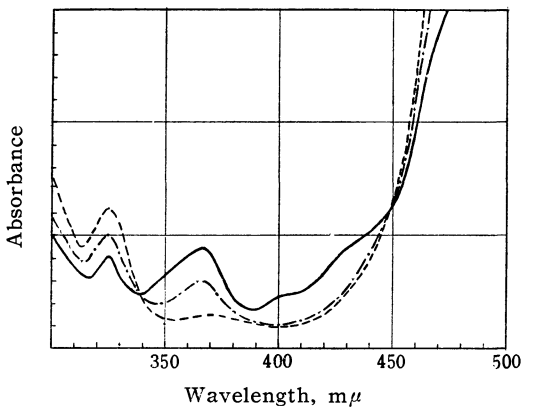



Fig. 3. Transient spectra of uranin.
——: 0.6 millisec.
—·—: 5 millisec.
----: before flash

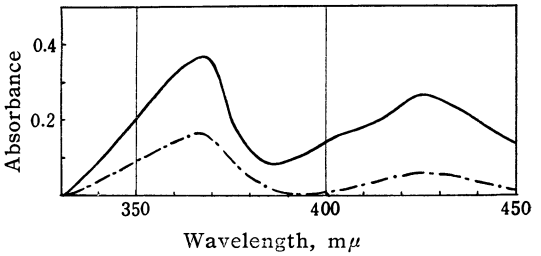



Fig. 4. Absorption spectra of transient species of ulanin.
——: 0.6 millisec.
—·—: 5 millisec.

can be evaluated from the depression of the absorbance in the region longer than 480 mμ, one can obtain the genuine spectra of transient species, which are shown in Fig. 2.

Three peaks are seen at 373, 410 and about 450 mμ. After 5 millisec., the 373 and 450 mμ peaks, which will be called A band from now on, still maintain considerable intensity, whereas the 410 mμ peak (B band) has disappeared. After several minutes, these transient absorption bands thoroughly vanish and the eosin spectra are recovered up to about 88% of the original solution. Twelve per cent loss is attributable, without doubt, to permanent bleaching.

In the presence of air, neither transient spectral change nor permanent bleaching was observed. The deaerated aqueous solution of eosin showed a slight transient depression of eosin absorption spectra, but no new spectra were observed in the region of the above mentioned A and B bands.

For uranin in ethanol also, transient spectra were observed by the flash illumination, but at 0.6 millisec. no clear peak corresponding to the 410 mμ peak of eosin was found (Figs. 3 and 4).

It is worth adding here that when only a photolysis flash is fired, a fluorescence spectrum can be taken on a plate, and it is to be noted that the fluorescence intensity varies markedly according to whether the sample is aerobic or not. On the contrary, the measurement by an ordinary fluorimeter (an accessory of the spectrophotometer), shows no such difference.

TABLE I. RELATIVE FLUORESCENCE INTENSITY AT THE PEAK WAVELENGTH

| | Flash | Fluorimeter |
|---|---|---|
| Aerobic | 100 | 100 |
| In vacuo | 5 | 100 |

## Discussion

The appearance of two spectral bands A and B with different lifetimes indicates that at least two transient species are formed in the initial stage of the reductive photobleaching of eosin.

As regards the assignment of these two bands, there scarcely exists any doubt that the A band is due to the semiquinone radical of eosin on the basis of the kinetic studies of Imamura and Koizumi. The assignment of band B, however, is not so clear-cut. A question may arise whether this absorption is caused by the triplet state of dye, but this possibility can be denied from the following two reasons. The first reason is that the lifetime of the band, being some tenths of a millisecond, would be too long for a triplet. Considered from the results already published in literature, for instance, as reported by Porter et al.[2], triplet states have usually too short a lifetime at room temperature and in ordinary solvents of common fluidity, to be observed by the present apparatus. The second reason is that if it were due to triplet state, the similar band should be observed in aqueous solution because of lower reactivity of water to the triplet state than ethanol, a fact which has been established by kinetic studies of photobleaching[1].

The B band must, therefore, be attributed to some unknown molecular species which perhaps is formed prior to semiquinone. Now, as reported elsewhere[3], the influence of added substances on the bleaching rate of eosin strongly suggests the formation of a certain kind of molecular complex between the excited state of the dye and ethanol. If this scheme is accepted, it is quite natural to attribute the B band to the complex in question.

Furthermore, in order to interpret the other experimental results reported in this paper, it is quite desirable, indeed it seems rather indispensable, to introduce such a complex in the reaction scheme, as will be shown below.

1) From the result that at 0.6 millisec. after the firing of the main flash the quantity of the existent dye drops to about 60% of that of the initial solution, it is very natural to consider that at a certain early period after flashing, nearly all the dye molecules exist as intermediates whose lives are in the order of $10^{-3}$ sec. or so.

Supposing that a semiquinone is the only one species as such an intermediate, then nearly 50% of dye would be bleached permanently, if one assumes, as is plausible, that semiquinone is stabilized by a dismutation process, $2DH \rightarrow D + DH_2$. Contrary to this expectation, only 12% permanent bleaching is produced by a single flash. In other words, about 24% of the dye is converted into semiquinone by one flash, hence this result necessitates that some other transient species like the complex considered above be existent, and that most of this transient species be deactivated without going to the reaction product.

2) The absence of photobleaching as well as of transient spectrum in aerobic condition is intimately connected with the fact formerly reported, that the reductive photobleaching is completely inhibited by the existence of a very small quantity of oxygen[1]. Imamura and Koizumi who at that time did not conceive of the formation of the complex, estimating the lifetime of the species attacked by oxygen to be $10^{-3}$ sec. or so from the quantity of oxygen necessary to suppress completely the bleaching reaction, concluded that semiquinone be mainly destroyed by oxygen, rejecting the possibility of the triplet state (with much shorter lifetime) being deactivated. But if so, B band should still be observed in flashing the aerated alcoholic solution. Thus, their scheme is not consistent with the present results and it is necessary to consider that the molecular complex now introduced be deactivated effectively by oxygen.

3) The results of fluorescence measurements are also consistent with the formation of such a complex. Thus by flash illumination in vacuo, a major part of the dye is converted into the complex at an early stage and survives at the end of the flash. Consequently, the illumination has poor efficiency for the fluorescence, since only a little part of dye remains in the ground state throughout the later period of flash. Whereas the complex is rapidly destroyed into its components by the attack of oxygen, yielding the dye molecule in the ground state. This process enables each molecule of dye to emit fluorescence repeatedly many times in the duration of the flash, resulting in a large increase of the fluorescence intensity. Such a situation is not expected if one assumes that

2) Cf. N. K. Bridge and G. Porter, *Proc. Roy. Soc.*, **A244**, 259 (1958).
3) K. Uchida, S. Kato and M. Koizumi, This Bulletin, **33**, 169 (1960).

oxygen mainly attacks the semiquinone radical. In measurements by an ordinary fluorimeter on the other hand, the low intensity of exciting light causes almost no change in the population of the ground state irrespective of whether a sample is free from air or not, hence the same fluorescence intensity results in the two cases.

The above qualitative discussion, though it seems quite plausible, is in fact not conclusive so long as only the fluorescence experiments for ethanol solutions are concerned, because the results are equally well interpreted if one assumes that the triplet state instead of the complex is efficiently deactivated by oxygen. The problem will be clarified if a quantitative comparison is made for the fluorescence intensity of the evacuated and aerated aqueous solution, where neither semiquinone nor complex is formed. At the present stage of investigation, the complex-decomposition-scheme may be said, in view of the discussion in 2), to be more plausible than the triplet state-deactivation-scheme, although the latter process may perhaps take place to some extent.

Summarizing the above discussion one can conclude the following reaction scheme for the reductive photo-bleaching of eosin.

$$D + h\nu \rightarrow D^* \quad (1)$$

$$D^* \rightarrow D + h\nu' \quad (2)$$

$$D^* \rightarrow D^t \quad (3)$$

$$D^t + RH \rightarrow X \quad (4)$$

$$X \rightarrow D + RH \quad (5)$$

$$X \rightarrow DH\cdot + R\cdot \quad (6)$$

$$2DH\cdot \rightarrow D + DH_2 \quad (7)$$

In the presence of air

$$X + O_2 \rightarrow D + RH + O_2 \quad (8)$$

and in addition to reaction 8, perhaps, $D^t$ may also be deactivated to a lesser extent. The process of reaction 8 is faster than reaction 5 or 6 even when the oxygen content is very small.

For uranin also, a similar scheme may hold, but the lifetime of X seems to be much shorter.

## Summary

Reductive photobleaching of eosin and uranin in ethanol solutions was studied by the flash technique. Transient spectra of semiquinone with a lifetime of millisecond order was established. In addition, another transient spectra with a life of the same order was observed in the case of eosin. This was interpreted to be due to a certain complex intermediate between ethanol and eosin, formed prior to semiquinone. The aerated alcoholic solution and the evacuated aqueous solution, when illuminated by a flash, showed no transient spectra in the wavelength region of the above two intermediates. The fluorescence of the aerated ethanol solution produced by the flash had about twenty times as large intensity as that of the evacuated solution induced under otherwise similar condition. A scheme for the primary processes of the reductive photobleaching involving the above complex can interpret all these results satisfactorily.

The authors express their gratitude to the Mainichi Press for a grant of subsidy.

*Department of Chemistry*
*Faculty of Science*
*Tohoku University*
*Katahira-cho, Sendai*

# *Studies on Antibiotics and Related Substances. IX. Synthesis of Methyl 5-Methylenecyclopentanone-2-acetate, an Antitumor Substance and Related Compounds*

By Sumio UMEZAWA and Mitsuhiro KINOSHITA

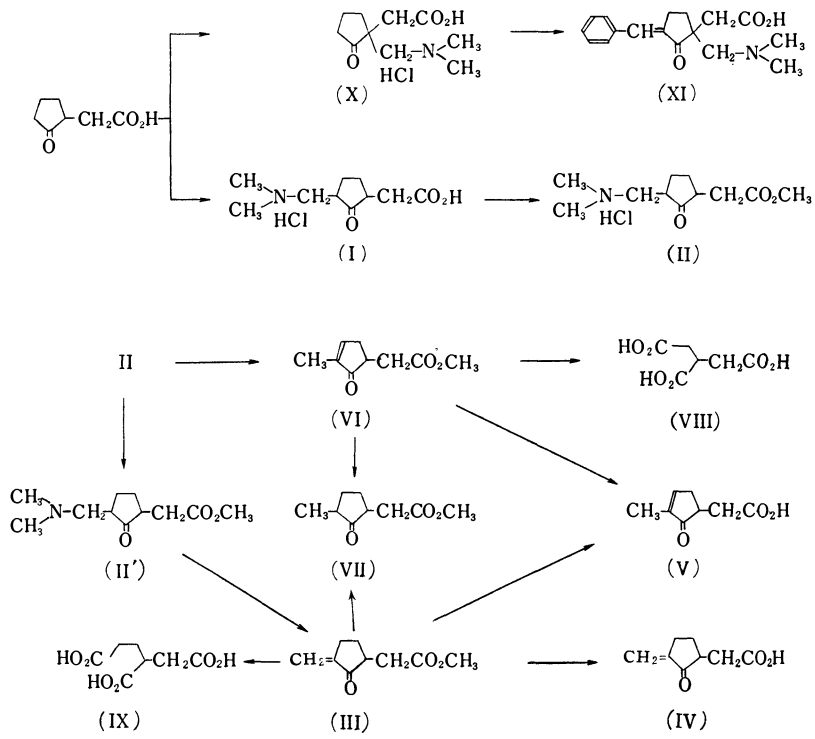
(Received September 3, 1959)

Recent publication[1] from this laboratory described the syntheses and antitumor activities of the methylene derivatives of cyclopentanone-3-carboxylic acid, relating to sarkomycin[2], an antitumor antibiotic. The present paper is concerned with an extention of this work in which the syntheses and antitumor activities of 5-methylenecyclopentanone-2-acetic acid and its ester are described.

Cyclopentanone-2-acetic acid was prepared by the Linstead and Meade's method[3]. A mixture of cyclopentanone-2-acetic acid, paraformaldehyde and dimethylamine hydrochloride was fused to give two kinds of Mannich base hydrochlorides; 2-(dimethylaminomethyl)cyclopentanone-2-acetic acid hydrochloride (X) crystallized at first from the absolute ethanol solution of the reaction mixture and 5-dimethylaminomethyl isomer (I), the desired product, was obtained from the mother liquor in a 24.2% yield.

On treating with benzaldehyde in the presence of sodium hydroxide, the 2-dimethylaminomethyl isomer (X) afforded a benzylidene derivative (XI), indicating[4] the presence of an activated methylene group in VIII.

Thermal decomposition of the methyl




1) S. Umezawa and M. Kinoshita, This Bulletin, **30**, 267 (1957); ibid., **32**, 223 (1959).

2) H. Umezawa, T. Yamamoto, T. Takeuchi, T. Okami, S. Yamaoka, T. Okuda, K. Nitta, K. Yagishita, R. Utahara and S. Umezawa, *Antibiotics & Chemotherapy*, **4**, 514 (1954).

3) R. P. Linstead E. M. Meade, *J. Chem. Soc.*, **1934**, 940.

4) Benzaldehyde condenses readily on the two activated methylene groups of cyclopentanone; C. Mentzel, *Ber.*, **36**, 1499 (1903); R. Cornubert, *Compt. rend.*, **190**, 440 (1930).

ester (II) of 5-dimethylaminomethyl isomer (I) afforded a colorless oil (48%) which gave analyses for $C_9H_{12}O_3$ but had neither antitumor nor antibacterial activity. The product contained a carbonyl group as shown by the formation of a semicarbazone of m. p. 162~163°C. The ultraviolet absorption suggested the presence of an $\alpha,\beta$-unsaturated carbonyl group, showing maxima at 228 and 307 m$\mu$ and the infrared spectrum also indicated a conjugated carbonyl system (Figs. 1 and 2). Ozonolysis yielded tricarballylic acid (VIII) but no formaldehyde. These data led to the conclusion that the destructive distillation of II produced a rearrangement of the exocyclic double bond formed by elimination of dimethylamine to a more stable conjugated system to give methyl 5-methyl-4-cyclopenten-1-one-2-acetate (VI).

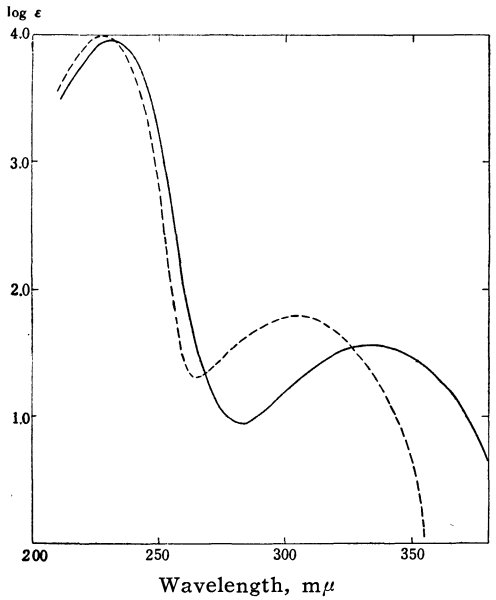



Fig. 1. Ultraviolet absorption spectra of methyl 5-methylenecyclopentanone-2-acetate (——) and methyl 5-methyl-4-cyclopenten-1-one-2-acetate (----) in methanol.

When the free base (II') obtained from II by treatment with ammonia in chloroform was subjected to destructive distillation, the desired methyl ester (III) of 5-methylenecyclopentanone-2-acetic acid was obtained in a 42.7% yield.

Acid hydrolysis of III with 5% hydrochloric acid-acetone solution produced a rearrangement of exocyclic double bond as well as hydrolysis, giving 5-methyl-4-cyclopenten-1-one-2-acetic acid (V) which was found to be identical with the product obtained from VI by alkaline hydrolysis, as judged by mixed melting point determination and by comparison of ultraviolet and infrared absorption spectra. Hydrogenation of III with platinum catalyst in methanol solution afforded methyl 5-methylcyclopentanone-2-acetate (VII); the semicarbazone, m. p. 149~149.5°C, of VII was found to be identical with the semicarbazone of the product obtained from VI by catalytic hydrogenation, as judged by mixed melting point determination. Ozonolysis of III gave formaldehyde (isolated as the methone derivative) and butane-1, 2, 4-tricarboxylic acid (IX); formation of the former established the presence of an exomethylene group in III.

The infrared absorption spectrum of III indicated a conjugated carbonyl system and the ultraviolet absorption data also suggested the presence of the $\alpha,\beta$-unsaturated carbonyl group, showing maxima at 232 and 333 m$\mu$ (Figs. 1 and 3). The accumulated data provided definite proof that the decomposition product III from the free base of II was methyl 5-methylenecyclopentanone-2-acetate.

Mild hydrolysis of III with dilute sulfuric acid followed by extraction with ethyl acetate and evaporation of the solvent in vacuo gave a 16.8% yield of a crude product of 5-methylenecyclopentanone-2-acetic acid

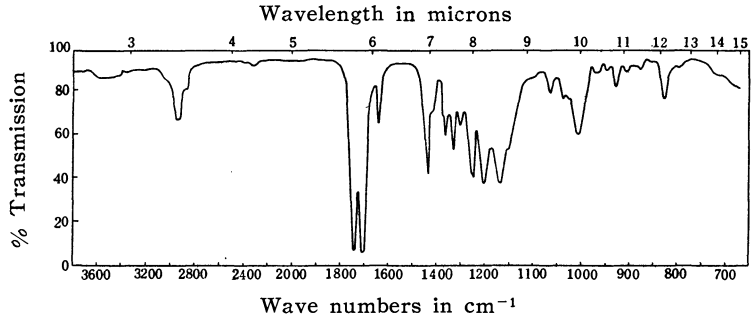



Fig. 2. Infrared absorption spectrum of methyl 5-methyl-4-cyclopenten-1-one-2-acetate (liquid).

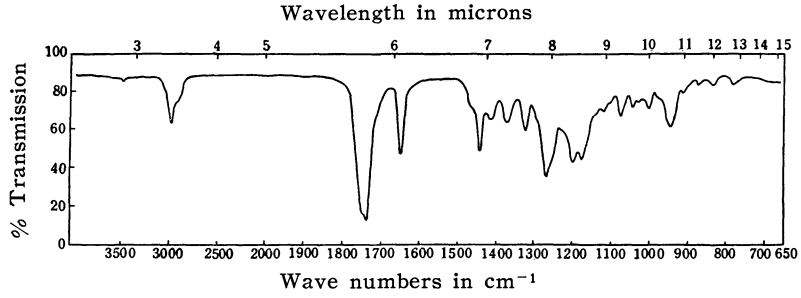



Fig. 3. Infrared absorption spectrum of methyl 5-methylenecyclopentanone-2-acetate (liquid).

(IV), a pale yellow, viscous liquid, which spontaneously polymerized so readily that further purification could not be accomplished. With the crude product, absorptions in the infrared spectrum indicated a conjugated carbonyl system, and the ultraviolet absorption data also suggested the presence of the $\alpha,\beta$-unsaturated cabonyl group, showing a maximum at 230 m$\mu$.

Both 5-methylenecyclopentanone-2-acetic acid and its ester (III) were found to possess antitumor and antimicrobial activities. As in the case of 5-methylenecyclopentanone-3-carboxylic acid[1], the methyl ester (III) was more potent than the corresponding free acid (IV).

## Experimental

**2-(Dimethylaminomethyl)cyclopentanone-2-acetic Acid Hydrochloride (X).** — A mixture of cyclopentanone-2-acetic acid[3] (14.2 g.) and dimethylamine hydrochloride (8.2 g.) was heated to 75°C. To the resulting melt was added paraformaldehyde (3.0 g.) and the mixture stirred at 75°C for 3 hr. and evaporated in vacuo to remove moisture. The resulting syrup was dissolved in hot absolute ethanol and filtered. After cooling, some seeds of pure X were added to the filtrate and the mixture was stored in an ice box. The first crystalline crop was separated, and washed with acetone-ethanol (3 : 1). The product (5.5 g.) was triturated with hot absolute ethanol (10 cc.). After standing at room temperature, filtration followed by washing with cold ethanol (5 cc.) gave 3.4 g. (14.4%) of 2-(dimethylaminomethyl)-cyclopentanone-2-acetic acid hydrochloride (X), m. p. 145~147°C (decomp.). An analytical sample was obtained by recrystallization from methanol, m. p. 150~150.7°C (decomp.).

*Anal.* Found: C, 51.05; H, 7.42; N, 5.72. Calcd. for $C_{10}H_{18}O_3NCl$: C, 50.95; H, 7.64; N, 5.95%.

**5-Benzylidene-2-(dimethylaminomethyl)cyclopentanone-2-acetic Acid (XI).** — To a solution of 2-(dimethylaminomethyl) cyclopentanone-2-acetic acid hydrochloride (X) (200 mg.) in 2.5 N sodium hydroxide (1.6 cc.) was added benzaldehyde (100 mg.) and the mixture stirred at 20°C for one hour. The resulting yellow solution was adjusted to pH 3 with 3 N hydrochloric acid, and shaken with ether. The water-layer was evaporated to dryness in vacuo and then extracted with absolute ethanol. Evaporation of ethanol solution afforded a crude hydrochloride of XI, very hygroscopic yellow amorphous powder; yield, 210 mg. (77%); characteristic strong absorption in ultraviolet spectrum at $\lambda_{max}^{MeOH}$ 308~309 m$\mu$ ($E_{1cm}^{1\%}$ 304). To a solution of the crude hydrochloride (200 mg.) in methanol (1.6 cc.) was added picric acid (200 mg.) in hot methanol (2.4 cc.). Water was added until the solution appeared turbid, and the mixture was allowed to stand overnight in a refrigerator to afford short prisms of picrate of XI; yield, 183 mg. (42% based on the crude hydrochloride of XI), m. p. 149~150°C (decomp.). Two recrystallizations from methanol-water gave a pure sample, m. p. 150~151°C (decomp.).

*Anal.* Found: C, 53.65; H, 4.45; N, 10.82. Calcd. for $C_{23}H_{24}O_{10}N_4$: C, 53.49; H, 4.68; N, 10.85%.

**5-(Dimethylaminomethyl)cyclopentanone-2-acetic Acid Hydrochloride (I).** — The mother liquor of the above-mentioned first crop (X) was stored in an ice box for 3 days to afford the second crop, which was collected, washed with acetone-ethanol (3 : 1) and dried; yield, 6.6 g.; m. p. 130~135°C (decomp.). Recrystallization from ethanol-acetone gave 5.6 g. of 5-(dimethylaminomethyl)cyclopentanone-2-acetic acid hydrochloride (I) (24.2%), m. p. 135~137°C (decomp). An analytical sample was obtained by recrystallization from methanol, m. p. 137~138.5°C (decomp.).

*Anal.* Found: C, 51.31; H, 7.56; N, 6.08. Calcd. for $C_{10}H_{18}O_3NCl$: C, 50.95, H, 7.64; N, 5.95%.

**Methyl 5-(Dimethylaminomethyl)cyclopentanone-2-acetate Hydrochloride (II).** — A mixture of 5-(dimethylaminomethyl)cyclopentanone-2-acetic acid (I) (6.1 g.) and absolute methanol (60 cc.) was saturated with dry hydrogen chloride and allowed to stand overnight. The solvent was removed by distillation at about 40°C in vacuo and the residue was dried in vacuo over phosphorus pentoxide. The resulting crystals were dissolved in a small quantity of absolute methanol by warming and the solution was diluted with absolute ether, whereupon there separated a crystalline precipitate of methyl 5-(dimethylaminomethyl)cyclopentanone-2-acetate hydrochloride (II), m. p. 117~121°C. Yield, 6.0 g. (93%). Two recrystallizations from methanol-ether, m. p. 123.5~124.5°C.

*Anal.* Found: C, 52.54; H, 7.87; N, 5.76. Calcd. for $C_{11}H_{20}O_3NCl$: C, 52.88; H, 8.07; N, 5.61%.

**Methyl 5-Methylenecyclopentanone-2-acetate (III).** — To a solution of methyl 5-(dimethylaminomethyl)cyclopentanone-2-acetate hydrochloride (II) (3.0 g.) in chloroform (10 cc.) was added saturated ammonia-chloroform solution (6.3 cc.), whereupon ammonium chloride immediately precipitated. The chloroform-layer was separated and concentrated under reduced pressure. The residue was heated at 108°C in an oil bath under highly reduced pressure (0.1~0.01 mmHg). Colorless distillate (1.4 g.), which was collected in a receiver cooled in a dry ice-methanol bath, was dissolved in ether (6.5 cc.) and shaken with dilute hydrochloric acid to remove dimethylamine and unreacted free amine-ester (II'). The ether-layer was dried over anhydrous sodium sulfate, and the solvent was removed in vacuo to afford a crude product of methyl 5-methylenecyclopentanone-2-acetate (III) (810 mg., 42.7%). Vacuum distillation of the crude product gave a low yield of pure sample of III, b. p. 60~65°C (bath temp.)/0.01 mmHg. There was much residue in the distillation flask, indicating the ready polymerization of III.

*Absorption spectra*: ultraviolet, $\lambda_{max}^{MeOH}$ 232 ($\varepsilon$ 9100) and 333 m$\mu$ ($\varepsilon$ 36.9); infrared, $\nu_{max}^{liq}$ 1733 (ester and conjugated carbonyl) and 1643 cm$^{-1}$ (C=C).

*Anal.* Found: C, 63.81; H, 7.16. Calcd. for $C_9H_{12}O_3$: C, 64.27; H, 7.19%.

**Catalytic Hydrogenation of III.** — A solution of freshly prepared III (300 mg.) in methanol (3 cc.) was shaken with platinum oxide (24 mg.) and hydrogen; 44 cc. (11°C, 766.1 mmHg, 95% based on theoretical amount) of hydrogen was absorbed in 18 min. The mixture was filtered and concentrated under reduced pressure and distilled in vacuo to give methyl 5-methylcyclopentanone-2-acetate (VII) (235 mg., 77.6%), b. p. 62°C (bath temp.)/0.01 mmHg.

*Anal.* Found: C, 63.84; H, 8.63. Calcd. for $C_9H_{14}O_3$: C, 63.51; H, 8.29%.

*Semicarbazone* of methyl 5-methylcyclopentanone-2-acetate; colorless needle from ethyl acetate, m. p. 149~149.5°C.

*Anal.* Found: C, 52.95; H, 7.37; N, 18.63. Calcd. for $C_{10}H_{17}O_3N_3$: C, 52.85; H, 7.54; N, 18.49%.

**Ozonolysis of III.** — a) A solution of 100 mg. of III in ethyl acetate (5 cc.) was treated with an approximately 2% (by weight) ozone-oxygen mixture at 0°C at a rate of 500cc./min. for 2 hr. The resulting solution was mixed with water (5 cc.) and zinc dust (150 mg.) and the mixture was refluxed for 30 min. The reaction mixture was filtered while hot into a solution of methone (150 mg.) in 5 cc. of ethanol. Dilution with 10 cc. of water afforded the needles of formaldehyde methone, m. p. 185~187°C. Recrystallization from methanol-water; m. p. 188~189°C; yield, 30 mg. Admixing with an authentic specimen of formaldehyde methone showed no change of melting point.

b) A solution of 300 mg. of freshly prepared III in ethyl acetate (14 cc.) was treated with ozone as mentioned above a) at −15°C. The resulting yellow solution was concentrated in vacuo below 10°C to afford a viscous yellow oil, which was heated with 1.6 cc. of 30% hydrogen peroxide at 90°C for one hour. The colorless solution was evaporated under reduced pressure. Addition of water to the residue followed by evaporation was repeated to remove excess of hydrogen peroxide. The final residue was refluxed with 3.5 cc. of 10% methanolic potassium hydroxide for 2 hr. Methanol was removed, acidified to pH 2.4 with dilute hydrochloric acid, saturated with ammonium sulfate and extracted with ether continuously for 3 hr. After the extract was dried over anhydrous sodium sulfate, the ether was distilled off. The residue immediately crystallized; yield, 200 mg. (59%); m. p. 108~112°C. A paper chromatography of this product with xylene-phenol-85% formic acid (7 : 3 : 1) showed only the distinct spot which had the same $R_f$ value as that of an authentic butane-1,2,4-tricarboxylic acid[5] (IX). Recrystallization from ethyl acetate gave 51 mg. of pure butane-1,2,4-tricarboxylic acid, m. p. 119.5~120.8°C, mixed m. p. 120~120.8°C.

**5-Methylenecyclopentanone-2-acetic Acid (IV).** — A mixture of freshly prepared methyl 5-methylenecyclopentanone-2-acetate (III) (994 mg.) and 1.5 N sulfuric acid (20 cc.) was stirred at 28~32°C for 2.5 hr. After removal of a considerable amount of resinous material (527 mg.) by decantation, the resulting solution was adjusted to pH 8.0 with a saturated solution of sodium bicarbonate, and shaken with two 15 cc. portions of ether to remove any unchanged ester. The water-layer was adjusted to pH 2.4 with 1.5 N sulfuric acid and extracted with two 15 cc. portions of ethyl acetate. After the extract was dried over anhydrous sodium sulfate, the ethyl acetate was removed by distillation in vacuo at about 0°C to yield a crude product of IV, a pale yellow viscous oil; yield, 153 mg. (16.8%). The freshly prepared sample was soluble in water and methanol. However, on standing at room temperature, the product rapidly polymerized and became much less soluble in water and methanol. It resisted attempts to recrystallize it. The ultraviolet absorption spectrum of the product showed a strong absorption at 230 m$\mu$ ($E_{1cm}^{1\%}$ 197) in methanol, indicating the presence of an $\alpha,\beta$-unsaturated ketone group. Infrared spectrum in liquid showed maxima at 1735 (carboxyl and conjugated carbonyl), 1642 (C=C) and 2700~2500 cm$^{-1}$ (carboxyl OH).

**5-Methyl-4-cyclopenten-1-one-2-acetic Acid (V).** — a) A mixture of methyl 5-methyl-4-cyclopenten-1-one-2-acetate (VI) (200 mg.) and 10% sodium hydroxide solution (0.45 cc.) was stirred at 17°C for one hour. The resulting solution was acidified to pH 2.0 by addition of dilute hydrochloric acid, saturated with ammonium sulfate, and extracted with three 1 cc. portions of ether. The dried extract was concentrated to afford a pale yellow oil (160 mg.) which, on standing, slowly

5) This was prepared by the method of Tawney and Prill: P. O. Tawney and E. J. Prill, *J. Am. Chem. Soc.*, **70**, 2828 (1948).

turned to a solid mass of crystals intermixed with oil. The crude crystals were drained on porous porcelain to remove an oily material; yield, 50 mg. (27%), m. p. 43~47°C. A pure sample of 5-methyl-4-cyclopenten-1-one-2-acetic acid (V) was obtained by recrystallization from ether-benzine, colorless prism, m. p. 48~49°C.

*Absorption spectra*: Ultraviolet, $\lambda_{max}^{MeOH}$ 228~229 (ε 9850) and 310 mμ (ε 48.4); infrared, $\nu_{max}^{Nujol}$ 1670 (conjugated carbonyl), 1630 (C=C), 2700~2500 (carboxyl OH) and 1738 $cm^{-1}$ (carboxyl C=O).

*Anal.* Found: C, 62.21; H, 6.69. Calcd. for $C_8H_{10}O_3$: C, 62.32; H, 6.54%.

b) A solution of freshly prepared methyl 5-methylenecyclopentanone-2-acetate (III) (1.4 g.) in 14.5 cc. of acetone-hydrochloric acid mixture (6 : 1 by weight) was allowed to stand at 20°C for 10 hr. To a resulting solution, water (30 cc.) and sodium bicarbonate (3 g.) were added under ice-cooling. After removal of acetone under reduced pressure below 5°C, the aqueous layer was extracted with two 10 cc. portions of ether, acidified to pH 2.4 with 3 N hydrochloric acid and again extracted with three 10 cc. portions of ethyl acetate. The dried ethyl acetate solution was concentrated under reduced pressure to afford a pale yellow oil (560 mg.) which crystallized gradually on standing. Treatment on a porous porcelain gave crude crystals (70 mg.), which was recrystallized from ether-benzine, m. p. 48~49°C and mixed m. p. with V obtained in a) 48~49°C. The ethereal extract was concentrated, and then treated in the same manner as described above in a) to afford a viscous oil (500 mg.). Distillation gave a fraction (70 mg.) of b. p. 125~128°C (bath temp.)/0.005 mmHg, which crystallized immediately. Recrystallization from ether-benzine yielded a pure sample of V, m. p. and mixed m. p. 48~49°C.

**Methyl 5-Methyl-4-cyclopenten-1-one-2-acetate (VI).** — Methyl 5-(dimethylaminomethyl)cyclopentanone-2-acetate hydrochloride (II) (1.0 g.) was placed in a round-bottom flask and heated in an oil bath at 150°C for 15 min. The resulting orange colored product was cautiously distilled at 150°C/0.01 mmHg to afford a colorless liquid (VI) in a receiver cooled in a dry ice-methanol bath. By redistillation of the liquid, pure sample of VI was obtained; yield, 325 mg. (48%); b. p. (bath temp.) 80°C/0.01 mmHg.

*Absorption spectra*: Ultraviolet, $\lambda_{max}^{MeOH}$ 228 mμ (ε 9750) and 307 mμ (ε 62.7); infrared, $\nu_{max}^{liq}$ 1712 (conjugated carbonyl), 1640 (C=C) and 1745 $cm^{-1}$ (ester C=O).

*Anal.* Found: C, 63.85; H, 7.41. Calcd. for $C_9H_{12}O_3$: C, 64.27; H, 7.19%.

*Semicarbazone* of VI; colorless needles, m. p. 162~163°C.

*Anal.* Found: C, 53.15; H, 6.49; N, 18.45. Calcd. for $C_{10}H_{15}O_3N_3$: C, 53.25; H, 6.72; N, 18.64%.

**Catalytic Hydrogenation of VI.** — A sample (300 mg.) in methanol (3 cc.) absorbed theoretical amount of hydrogen in the presence of platinum oxide (24 mg.) in 12 min. The reduced product was purified by distillation under reduced pressure to give methyl 5-methylcyclopentanone-2-acetate (VII) (282 mg., 93%), b. p. (bath temp.) 85~89°C/0.03 mmHg. The sample readily afforded a *semicarbazone*, m. p. 149~149.5°C, which did not depress the melting point of the corresponding derivative of the hydrogenation product of III.

Ozonolysis of VI was carried out in the same manner as described in the ozonolysis of III: a) The compound (200 mg.) did not give any formaldehyde methone, indicating the absence of a terminal methylene group. b) The compound (200 mg.) gave a crude crystalline product (117 mg. 56%) which afforded only the distinct spot of tricarballylic acid (VIII) by paper chromatography. Recrystallization from ether gave pure tricarballylic acid; m. p. and mixed m. p. 161~162°C.

**Bioassays.** — Preliminary results have indicated that methyl 5-methylenecyclopentanone-2-acetate (III) completely inhibits the growth of *M. pyogenes var. aureus* 209-p, *E. coli*, *Saccharomyces sake* and *Penicillium* 408,701 in a dilution of 1 : 16000. 5-Methylenecyclopentanone-2-acetic acid (IV) completely inhibited the growth of *Trichophyton mentagrophytes* in a dilution of 1 : 32000, but had comparatively weak activities against other fungi and bacteria tested.

5-Methyl-4-cyclopenten-1-one-2-acetate had no antimicrobial and antitumor activity, as expected from the fact that 2-methyl-2-cyclopenten-1-one-3-carboxylic acid obtained from sarkomycin (2-methylenecyclopentanone-3-carboxylic acid) by thermal isomerization had no biological activity[6].

It is interesting to find that III and IV possess antitumor activity[7]. The minimum necessary concentrations of III and IV for the anti-HeLa-cell effect were 15.6 and 125 μg/cc.

A detailed report on the biological activities of III and IV will be published elsewhere.

## Summary

1) 5-(Dimethylaminomethyl)cyclopentanone-2-acetic acid hydrochloride (I) and 2-dimethylaminomethyl isomer (X) have been synthesized from cyclopentanone-2-acetic acid by means of the Mannich reaction.

2) Methyl 5-(dimethylaminomethyl) cyclopentanone-2-acetate (II′) has been degraded to give methyl 5-methylenecyclopentanone-2-acetate (III), which has been hydrolyzed into 5-methylenecyclopentanone-2-acetic acid (IV), a homologue of isosarkomycin.

3) Destructive distillation of the hydrochloride (I) afforded methyl 5-methyl-4-cyclopenten-1-one-2-acetate (VI), an isomer of III.

6) I. R. Hooper, L. C. Cheney, M. J. Cron, O. B. Fardig, D. A. Johnson, D. I. Johnson, F. M. Palermiti, H. Schmitz and W. B. Wheatley, *Antibiotics & Chemotherapy*, 5, 590 (1955).

7) Private communication from Prof. H. Umezawa of National Institute of Health, Tokyo.

4) It has been found that III and IV possess antitumor and antimicrobial activities.

The authors are indebted to Professor H. Umezawa, National Institute of Health, Tokyo, for antitumor assays.

*Department of Applied Chemistry*
*Faculty of Engineering*
*Keio University*
*Koganei-shi, Tokyo*

# SHORT COMMUNICATIONS

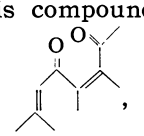
## *Chemical Structure of Miliacin*

By Shokichi ABE

(Received October 7, 1959)

A crystalline substance (I, $C_{31}H_{52}O$, m.p. 282°C, $[\alpha]_D$+8.0°) was isolated from *Panicum miliaceum L.* and from *Syntherisma sanguinalis Dulac var. calialis Honda* by Ito[1] and was named miliacin.

Its ultraviolet absorption spectrum did not indicate the presence of conjugated double bond system, but the color reaction with tetranitromethane suggested the presence of double bond. From its infrared absorption spectrum (9.0 $\mu$) its oxygen linkage was supposed to be an ether type. The oxidation product, miliacin oxide (II, $C_{31}H_{52}O_2$, m.p. 285.5~286°C, $[\alpha]_D$+52.3°) was obtained by the action of perbenzoic acid in chloroform, this oxide did not show the color reaction with tetranitromethane. It follows that miliacin is a pentacyclic compound having a double bond.

Upon oxidation with selenium dioxide, miliacin and miliacin oxide afforded a diendione (III, $C_{31}H_{46}O_3$, m.p. 253°C, $[\alpha]_D$−87.6°, $\lambda_{max}$ 281 m$\mu$ log $\varepsilon$ 4.2), whose infrared absorption spectrum (9.0 $\mu$) revealed the existence of the ether linkage. The ultraviolet absorption spectrum of this compound was similar to that of $\beta$-amyradiendionol. This fact means that this compound contains a partial structure,  , characteristic of compound derived from $\beta$-amyrin-oleanane series. Therefore, it may be concluded that miliacin is a member of $\beta$-amyrin-oleanane series and its ester linkage does not participate with the carbon atoms at positions 9, 11—13, 18 and 19.

Upon treatment with hydrogen chloride in chloroform, miliacin oxide afforded compound (IV, $C_{31}H_{50}O$, m.p. 210~211°C, $[\alpha]_D$ −63.0°, $\lambda_{max}$ 243 m$\mu$ log $\varepsilon$ 4.3, 250 m$\mu$ log $\varepsilon$ 4.4, 260 m$\mu$ log $\varepsilon$ 4.2). Its infrared (9.0 $\mu$) and ultraviolet absorption spectrum and optical rotation difference suggested the presence of an ether linkage and $\Delta^{11:13(18)}$ conjugated double bond. On the other hand, miliacin was changed to its isomer (V, $C_{31}H_{52}O$, m.p. 189°C, $[\alpha]_D$−23.4°) by the same treatment. This isomer gave an oxide (VI, $C_{31}H_{52}O_2$, m.p. 262°C, $[\alpha]_D$+42.7°), which showed no color reaction with tetranitromethane. From the infrared absorption spectrum and the optical rotation difference of this isomer, it was assumed that the double bond of miliacin had rearranged to $\Delta^{13(18)}$ by this treatment.

By the action of boron trifluoride-acetic acid or *p*-toluenesulfonic acid in acetic anhydride-acetic acid, miliacin afforded a diene hydrocarbon (VII, $C_{30}H_{48}$, m.p. 125°C, $[\alpha]_D$+41.2°), which gave a dioxide (VIII, $C_{30}H_{48}O_2$, m.p. 203°C, $[\alpha]_D$+73.5°) by the oxidation with perbenzoic acid. This diene was prepared by David[2] from germanicol and has the structure 8 : 10 : 14-trimethylnovoleana-3(5) : 8-diene. By the action of *p*-toluenesulfonic acid miliacin oxide gave 5 : 8 : 14-trimethylnovoleana-9(10) : 11 : 13(18)-triene[3] (IX, $C_{30}H_{46}$, m.p. 137°C).

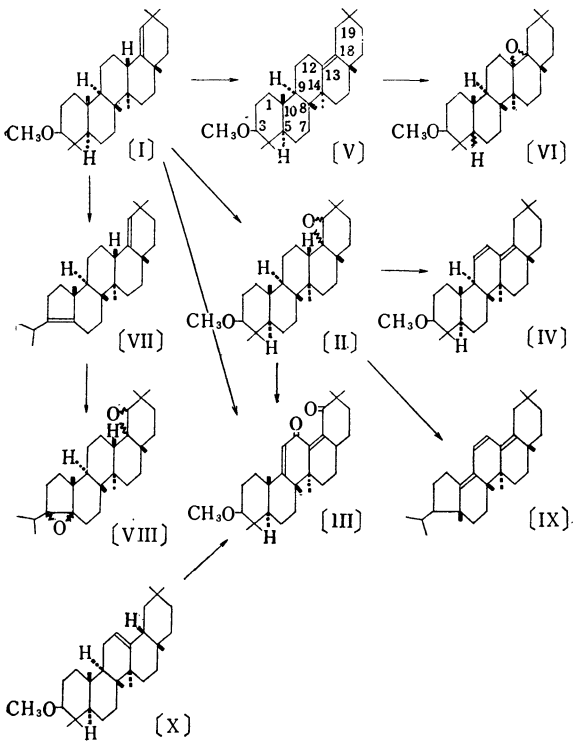
1) H. Ito, *J. Faculty Agr. Hokkaido Imp. Univ.*, **37**, 1 (1934); *J. Chem. Soc. Japan (Nippon Kwagaku Kwaishi)*, **59**, 274 (1938).

2) S. David, *Bull. soc. chim. France*, **1949**, 427.

3) G. G. Allan, M. B. E. Fayez, F. S. Spring and R. Stevenson, *J. Chem. Soc.*, **1956**, 456.

Isosawamilletin[4] (X, 3$\beta$-methoxyolean-12-ene) was oxidized with selenium dioxide to a diendione, which was identical with compound III.

It was deduced from the foregoing experimental results that miliacin was 3$\beta$-methoxygermanicene (I, 3$\beta$-methoxyolean-18-ene), the conjugated diene was 3$\beta$-methoxyoleana-11 : 13(18)-diene [IV], and the isomer derived from miliacin by the action of hydrogen chloride was 3$\beta$-methoxyolean-13(18)-ene [V], as indicated in the next figure.




*Chemical Laboratory*
*Thuru College*
*Thuru-shi, Yamanashi*

4) T. Obara and S. Abe, *Bull. Agr. Chem. Soc. Japan*, **21**, 388 (1957); I. M. Morice and J. C. E. Simpson, *J. Chem. Soc.*, **1942**, 198.

# *On the Model Form of the Catalytic Wave of Proteins**

By Mutsuaki Shinagawa
and Hiroyuki Nezu

(Received December 8, 1959)

In order to extend the knowledge about the nature of the catalytic wave of protein[1,2] a model experiment was undertaken, and the following three points were emphasized in this experiment: 1) hydrogen sulfide and cystine were used as typical sulfhydryl compounds; 2) the influence of methyl cellulose and gelatin on the catalytic wave of cystine was examined polarographically; and 3) the influence of glucose, sucrose, glucosamine and glycogen on the cystine wave was similarly examined. In the latter case, these sugars were used as model compounds for the carbohydrates contained in the mucoprotein molecule, which is said to be an effective substance for the demonstration of the serum filtrate.

From such experiments, the various wave patterns analogous to those of the protein wave were obtained by regulating the amounts of each of the constituents in the test solutions (Table I).

**Single Rounded Cystine-like Wave.**—Hydrogen sulfide, which may be considered as one of the simplest of the sulfhydryl compounds, was examined polarographically over a large range of concentrations in the buffered cobaltous solutions, i.e. 0.1 M $NH_4OH$, 0.1 M $NH_4Cl$ and $10^{-3}$ M $CoCl_2$. When hydrogen sulfide was added to the solution containing gelatin, the single rounded wave analogous to the cystine wave appeared and the diffusion current of cobalt disappeared. When hydrogen sulfide was added to the solution, and then gelatin was added, the single rounded wave did not appear. If the solution contains large amounts of gelatin, the wave analogous to that of cystine did not appear and the diffusion current of cobalt disappeared (Fig. 1A). This cystine-like wave was observed even at the limiting concentrations of hydrogen sulfide as low as $10^{-7}$ M.

* Presented at the Polarographic Discussion Meeting, Kyoto, October, 1957.

1) R. Brdicka, *Research* (*London*), **1**, 25—35 (1948).
2) M. Brezina and P. Zuman, "Die Polarographie in der Medizin, Biochemie und Pharmazie", Akademische Verlagsgeselleschaft, Leipzig (1956), pp. 532—618.

TABLE I. POLAROGRAPHIC EFFECTS OF GELATIN AND CARBOHYDRATES ON THE CATALYTIC WAVE OF HYDROGEN SULFIDE AND CYSTINE IN THE AMMONIACAL BUFFERED COBALTOUS SOLUTION

| Case | Geratin | Carbo-hydrate | Sulfhydryl compound | Single wave (or 2nd wave), V. | Double wave | Unknown wave, V. |
|---|---|---|---|---|---|---|
| 1 | — | — | H | — | — | — |
| 2 | G | — | H | −1.6 | — | −0.95 |
| 3 | G | — | H | — | — | — |
| 4 | — | M | H | −1.6 | — | −0.7 |
| 5 | — | Gl | H | −1.6 | — | −0.7 |
| 6 | — | — | C | poorly defined | — | — |
| 7 | G | — | C | −1.75 | — | −1.0 |
| 8 | — | M | C | −1.75 | well defined | −1.0 |
| 9 | G | M | C | −1.75 | well defined | −1.0 |
| 10 | — | Gl | C | −1.75 | poorly defined | −1.0 |
| 11 | — | S | C | −1.75 | poorly defined | −1.0 |
| 12 | — | Gs | C | −1.75 | poorly defined | −1.0 |
| 13 | — | Gg | C | −1.75 | poorly defined | −1.0 |

C: $10^{-3}$ M Cystine Gl: 0.1% Glucose M: 0.1% Methyl cellulose
G: 0.1% Gelatin Gs: 0.1% Glucosamine S: 0.1% Sucrose
Gg: 0.1% Glycogen H: Hydrogen sulfide

**Protein-like Wave.**—When methyl cellulose was added to the buffered cobaltous solution, the polarographic double wave similar to the protein double wave appeared as shown Fig. 1B. Other carbohydrates such as glucose, sucrose, glucosamine and glycogen were examined in order to determine whether their activities were similar to that of methyl cellulose on the formation of the wave analogous to the protein wave (Table I). Further quantitative experiments were initiated in order to examine the influence of methyl cellulose and gelatin on the cystine wave (Fig. 2).

It seems that Brdicka's mechanism[3], generally accepted since 1933, is unsatisfactory to explain these phenomena for the following reasons: 1) It might be difficult to supply hydrogen ions to the electrode surface from the bulk of an ammoniacal buffered solution at about pH 9. 2) At a potential of about −1.6 V. where the two peaks of the double wave appear, the cobalt-ammine ion is rapidly reduced to metallic cobalt at the electrode surface but the cobaltocysteinate ion may not be reduced to metallic cobalt. So the most delicate point in the interpretation of the whole catalytic electrode process involved in the polarographic "protein wave" consists in the elucidation of the role of cobalt. 3) Even if these waves depend on the catalytic reduction of hydrogen it is difficult to explain how, in the case of protein, two maxima are observed.

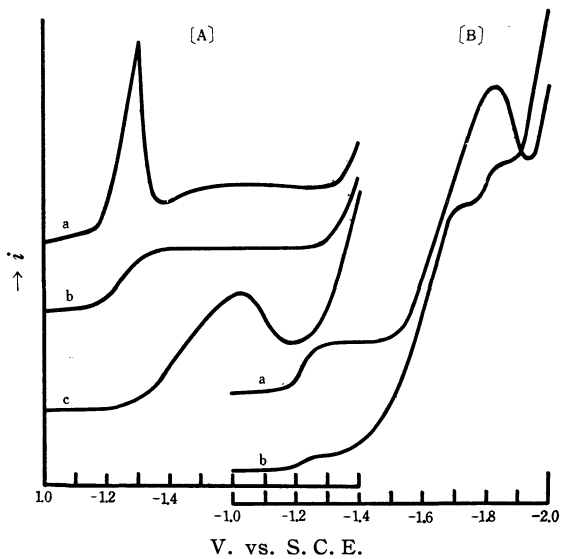



Fig. 1. Polarograms demonstrating the catalytic wave.
(A) a) $1 \cdot 10^{-2}$ M $CoCl_2$ + 1 M $NH_4OH$ 1 ml. + 1 M $NH_4Cl$ 1 ml. + $H_2O$ 7 ml.
b) (a) + 1% gelatin 5 drops
c) (b) + $H_2S$
(B) a) (A, b) + $1 \cdot 10^{-2}$ M cystine 1 ml.
b) (a) + 1% methyl cellulose 10 drops

However, the coexistence of constituents (cobalt ion, cystine, carbohydrate, gelatin and ammonia) in the ammoniacal buffered solution is necessary to obtain the wave analogous to the protein wave. In view of the above experimental facts, it seems reasonable to assume that these five essential constituents in the ammoniacal buffered

3) R. Brdicka, *Collection Czechoslov. Chem. Communs.*, 5, 148—164 (1933).

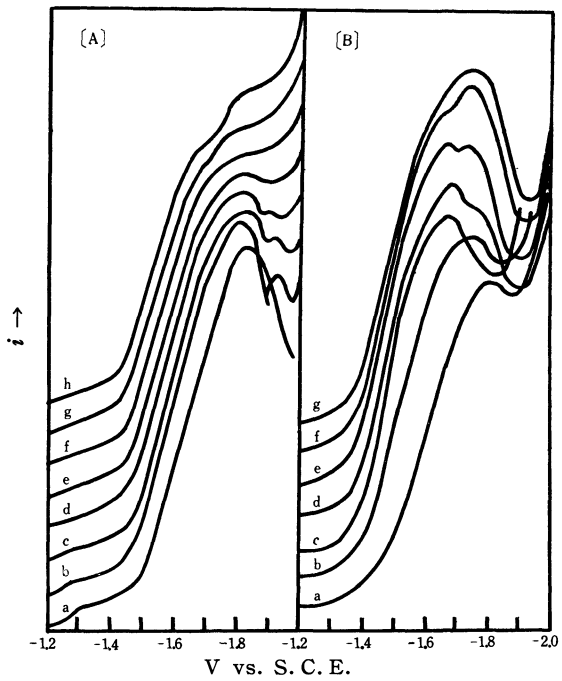



Fig. 2. Polarograms demonstrating the influence of methyl cellulose and gelatin on the cystine wave.

(A) 1% methyl cellulose 30 drops+$10^{-2}$ M $CoCl_2$ 0.5 ml.+1 M $NH_4OH$ 1 ml.+1 M $NH_4Cl$ 1 ml.+$H_2O$: total volume 10 ml. $2\cdot10^{-2}$ M cystine:
a) 0.03 ml., b) 0.06 ml., c) 0.12 ml., d) 0.18 ml., e) 0.24 ml., f) 0.30 ml., g) 0.36 ml., h) 0.42 ml.

(B) a) $2\cdot10^{-2}$ M cystine 0.1 ml.+$10^{-2}$ M $CoCl_2$ 0.5 ml.+1 M $NH_4OH$ 1 ml.+1 M $NH_4Cl$ 1 ml. + $H_2O$: total volume 10 ml.
b) (a)+1% methyl cellulose 1 drop
c) (a)+1% methyl cellulose 2 drops
d) (c)+1% gelatin 2 drops
e) (d)+1% gelatin 2 drops
f) (e)+1% gelatin 2 drops
g) (e)+1% gelatin 2 drops

system make a certain contribution to the electrode reaction either through their chemical interactions in the vicinity of the electrode surface and their adsorptive activities at the surface.

In conclusion, this mechanism may be considered in terms of the two following ideals: a) There may be some competition among the constituents which react with the cobaltous ions to yield complex ions or salts of extremely low solubility. Such competition in the vicinity of the electrode surface has a great effect on the currents of electroreduction and reoxidation of cobalt. b) The surface activities of these competing constituents have characteristic effects on the currents.

*Department of Chemistry*
*Faculty of Science*
*Hiroshima University*
*Hiroshima*

# *Note on the Monomeric Friction Coefficient of Poly-n-butyl Methacrylate in Diethyl Phthalate*

By Hiroshi FUJITA and Akira KISHIMOTO

(Received December 19, 1959)

From dynamic mechanical measurements encompassing the glass to rubber transition region Saunders et al.[1] have recently shown that the monomeric friction coefficient $\zeta_0$ (in dyne sec./cm.) of poly-*n*-butyl methacrylate in diethyl phthalate at 0°C varied with the polymer concentration $c$ (in g./ml. of solution), according to the relation:

$$\zeta_0 = 5.8 \times 10^{-10} \exp(24c) \qquad (1)$$

They state that there appears to be no theoretical expectation for the form of this relation. The purpose of the present communication is to show that their $\zeta_0$ data can be interpreted reasonably in terms of a free volume theory described recently by Fujita and Kishimoto[2], if the original theory is modified so that the diluent concentration $C$ (in grams of diluent per gram of dry polymer) is replaced by the volume fraction of diluent $v$[3]. Thus, the starting assumption of the modified theory is that the fractional free volume, $f$, in the polymer-diluent mixture at a fixed temperature $T$ is a linear function of $v$, i.e.

$$f = f(T, 0) + \beta'(T)v \qquad (2)$$

where $f(T, 0)$ is the free volume fraction in the pure polymer at temperature $T$ and

1) P. R. Saunders, D. M. Stern, S. F. Kurath, C. Sakookim and J. D. Ferry, *J. Colloid Sci.*, **14**, 222 (1959).
2) H. Fujita and A. Kishimoto, *J. Polymer Sci.*, **28**, 547 (1958).
3) The modification of the original theory, involving derivations of the new equations, and applications of the modified theory to viscosity data on concentrated polymer solutions will be described in detail in a forthcoming publication.

$\beta'(T)$ is a parameter (dependent on temperature) similar in nature to the parameter $\beta$ defined previously[2]. The physical meaning of the new parameter $\beta'$ will be given in a forthcoming article[3].

If one starts with Eq. 2 and uses a similar procedure to that described in Ref. 2, one can derive the relation:

$$-\frac{2.303[f(T,0)]^2 \log a_v}{1+2.303f(T,0)\log a_v}=\beta'(T)v \qquad (3)$$

Here $a_v$ is the concentration shift factor with the pure polymer as a standard and may be evaluated, in a manner described previously[2], from appropriate viscoelastic measurements obtained as a function of diluent concentration. Eq. 3 may be rewritten in the form:

$$-(1/\log a_v)=2.303f(T,0)+\{2.303[f(T,0)]^2/\beta'(T)\}(1/v) \qquad (4)$$

This indicates that plots of $-1/\log a_v$ vs. $1/v$ form a straight line and $f(T, 0)$ and $\beta'(T)$ can be determined from its slope and intercept at $1/v=0$.

Under the assumption that all the relaxation mechanisms—at least, those contributing to the mechanical behavior in the particular region concerned—have the same dependence on diluent concentration in the polymer, the shift factor $a_v$ may be evaluated from the ratio of the monomeric friction coefficient of the mixture at diluent concentration $v$ to that of the pure polymer ($v=0$) at the same temperature. The authors calculated $a_v$ for the system poly-*n*-butyl methacrylate+diethyl phthalate at 27°C (this is the glass transition temperature of pure poly-*n*-butyl methacrylate[4]) from the $\zeta_0$ data of Saunders et al.[1] and of Child and Ferry[4]. The latter study gives the $\zeta_0$ values for the pure polymer at 27°C. The former data, which were originally given for the temperature 0°C have been converted to the desired temperature by using the WLF equation[5] with the numerical constants recorded in Table II of Ref. 1. Fig. 1 shows the plot of $-1/\log a_v$ vs. $1/v$ obtained from these data. It is seen that the plotted points follow a straight line reasonably well, in agreement with the prediction of Eq. 4. From the solid line drawn one finds that $f(T_g^0, 0)=0.023$ and $\beta'(T_g^0)=0.05_0$; here $T_g^0$ denotes the glass transition temperature of the pure

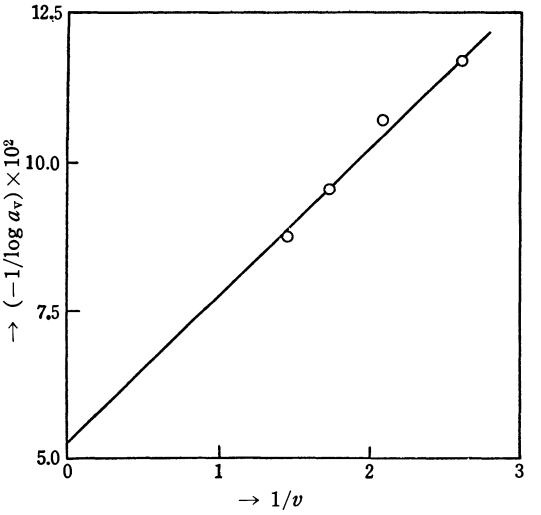



Fig. 1. Plot of $-1/\log a_v$ vs. $1/v$ for the system poly-*n*-butyl methacrylate + diethyl phthalate at 27°C; $v$ is the volume fraction of diethyl phthalate in the mixture.

polymer. It is of interest to see that the value of $f(T_g^0, 0)$ obtained, which was denoted by $f_g^0$ in Ref. 2, is quite close to the approximately) universal value 0.025.

Eq. 4 may be used to evaluate $f(T, 0)$ and $\beta'(T)$ when the steady-flow viscosity, $\eta$, of the polymer-diluent mixture is known as a function of diluent volume fraction $v$. In this case the shift factor $a_v$ may be taken as the ratio $\eta/[(1-v)\eta_0]$, where $\eta_0$ is the value of $\eta$ for the pure polymer at the same temperature $T$. The authors applied Eq. 4 to Bueche's data[6] for the steady-flow viscosity on the system polymethyl methacrylate+diethyl phthalate at 100°C, the glass transition temperatue of this polymer[7]. A very satisfactory straight line was obtained between $-1/\log a_v$ and $1/v$ and yielded $f(T_g^0, 0)=0.017$ and $\beta'(T_g^0)=0.051$, where $T_g^0=100$°C. This low value of $f_g^0$ is consistent with a similar low value obtained previously[7] for this methacrylate polymer. Of interest is the result that the $\beta'$ value derived here is very close to the one obtained above from the analysis of the friction coefficient data for the poly-*n*-butyl methacrylate+diethyl phthalate system. Although the definite conclusion must be reserved, it appears that to a first approximation the parameter $\beta'(T)$ is characteristic of the diluent

4) W. C. Child, Jr. and J. D. Ferry, *J. Colloid Sci.*, **12**, 327 (1957).
5) M. L. Williams, R. F. Landel and J. D. Ferry, *J. Am. Chem. Soc.*, **77**, 3701 (1955).
6) F. Bueche, *J. Applied Phys.*, **26**, 738 (1955).
7) H. Fujita and A. Kishimoto, *J. Colloid Sci.*, **13**, 418 (1958).

species, when camparison is made at $T_g$ of respective polymers.

*Physical Chemistry Laboratory*
*Department of Fisheries*
*Kyoto University*
*Maizuru*

# *Evolution of Atomic Oxygen from Platinum Surface Treated Previously with Discharged Oxygen Gas*

By Kazuo MITANI and Yoshio HARANŌ

(Received January 5, 1960)

Fryburg[1] investigated an enhanced oxidation of platinum by treating a platinum strip with discharged oxygen gas at a temperature of 1000°C. He found that when the temperature of a platinum strip is higher than 800°C, a brown deposit of platinum dioxide appears on the wall of the enclosing glass tube in the immediate vicinity of the heated platinum strip.

After treating platinum surface with discharged oxygen gas, it is found that atomic oxygen evolves from it when heated in vacco.

The main part of the apparatus is shown in Fig. 1. D is a discharge tube. The reaction vessel V contains a platinum ribbon (0.024×0.28×363 mm.) capable of being heated by electric current. Atomic oxygen given off is detected by the change of color of molybdenum trioxide deposited on a glass plate P according to the following equation[2]:

$$3\,MoO_3 + O = Mo_3O_8 + O_2$$

Discharged oxygen gas is made to pass through the reaction vessel at a pressure of 0.1~1 mmHg for 20 min., without heating the platinum ribbon by electric current. Then the discharge being stopped, the

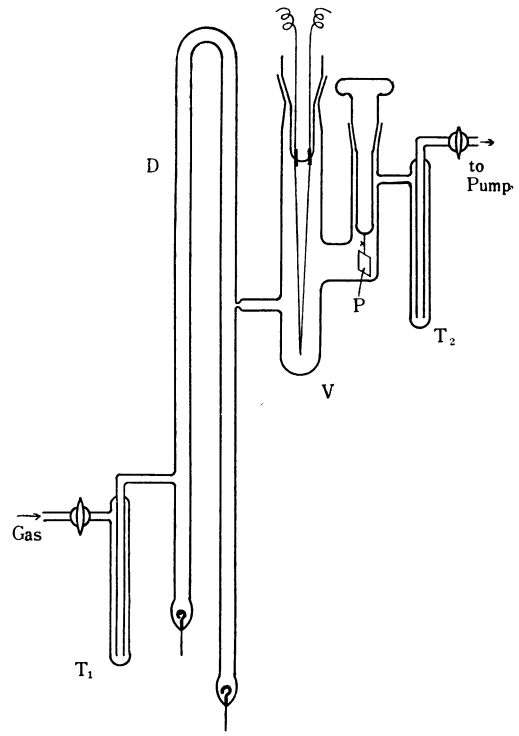



Fig. 1

reaction vessel is evacuated by a diffusion pump through a trap cooled by dry ice. In this condition, molybdenum trioxide remains to be pale yellow. While the evacuation is continued, the platinum ribbon is heated to 1400°C. Then, molybdenum trioxide in the side tube changes its color distinctly from pale yellow to deep blue within 20 min. This is an evidence that atomic oxygen is given off from the platinum surface. The authors will report in a later paper that adsorbed oxygen atoms desorb in molecular form when heated in vacuo. Therefore, taking account of Fryburg's experement[3], it is believed that the platinum surface covered with platinum dioxide, and that atomic oxygen is given off by the decomposition of platinum dioxide when the ribbon is heated to a high temperature in vacuo.

*Institute of Chemistry*
*Kyoto Prefectural University of Medicine*
*Taishōgun, Kita-ku, Kyoto*

1) G. C. Fryburg, *J. Chem. Phys.*, **24**, 175 (1956).
2) W. H. Rodebush and W. A. Nichols, *J. Am. Chem. Soc.*, **52**, 3864 (1930).
3) Loc. cit.

# *Determination of Thallium(I) with Iodate in the Presence of Mercuric Ions and with Iodate and Permanganate via Bromide*

By Bechu SHARMA

(Received August 31, 1959)

Most of the current methods, to determine thallium(I), have certain inherent defects. Willm's method[1] based upon titration of thallium(I) in hydrochloric acid with permanganate has been used extensively, but various authors reported unfavorable results. The procedure used by Marshall[2] is tedious. Kolthoff[3], Zintl and Rienacher[4], however, titrated it accurately with bromate in hydrochloric acid using methyl orange as indicator. Willard and Young[5] determined it against ceric sulfate. Berry[6] titrated various thallous salts with iodate using iodine monochloride end point and reported low results by about 2%. Swift and Garner[7] employed iodine monochloride procedure in the determination of thallium(I) with iodate, permanganate and ceric sulfate, but precise results were obtained only with iodate. Recently a general application of the amperometric Dead Stop End Point to direct and indirect determination with iodate in the presence of mercuric ions has been reported. Arsenious oxide and hydrazine sulfate are used as direct primary standards and thiosulfate, thiocyanate and thiourea are determined by excessive iodate[8]. Investigations were therefore carried out to adopt the above procedure (iodate procedure in the presence of mercuric ions) in the determination of thallium. Oxidation titration of hydrazine sulfate with permanganate and ceric sulfate in hydrochloric acid via bromide has been carried out amperometrically using "Dead Stop End Point" written as D.S.E.P.[9] This also suggested a similar oxidizability of thallium.

1) Willm, *Bull. soc. chim. France*, **1863**, 352; *Ann.c him. phys.*, **5**, (1863).
2) H. Marshall, *J. Soc. Chem. Ind.*, **19**, 994 (1900).
3) I. M. Kolthoff, *Rec. trav. chim.*, **41**, 172 (1922).
4) E. Zintl and G. Rienacher, *Z. anorg. u. allgem. Chem.*, **153**, 276 (1926).
5) H. H. Willard and P. Young, *J. Am. Chem. Soc.*, **52**, 36 (1930).
6) A. J. Berry, *Analyst*, **51**, 137 (1926).
7) E. H. Swift and C. S. Garner, *J. Am. Chem. Soc.*, **58**, 113 (1936).
8) M. G. Bapat and B. Sharma, *Z. anal. Chem.*, **157**, 258 (1957).
9) M. G. Bapat and B. Sharma, *J. Sci. Res. (B.H.U.)*, **VII** (2), 267 (1956—1957).

## Experimental

A 0.1 N (0.025 M) solution of potassium iodate was prepared from E. Merck (G. R.) reagent. Its strength was checked against 0.1 N arsenious oxide prepared from E. Merck (G. R.) reagent using iodine monochloride end point. Approximately 0.1 N potassium permanganate solution, prepared from British Drag House (L. R.) reagent, was standardized against 0.1 N arsenious oxide. A 1% thallous acetate solution was prepared from B.D.H. reagent and its strength was determined against potassium iodate using iodine monochloride procedure.

**Direct Titration Procedure.** — An aliquot of iodate solution was transferred to a 100 ml. titrating vessel, 25～35 ml. of mercuric chloride (8～9%) solution was added followed by such a volume of 12 N hydrochloric acid as to adjust the overall acidity between 0.7～1.5 N. The contents of the vessel were cooled to 25°C completely. The reaction mixture was finally titrated against thallous acetate using the amperometric D.S.E.P. A potential of 0.1 V. was impressed across the indicator electrodes. The indicator current increased toward a maximum as the addition of thallous acetate solution was continued and finally decreased to a minimum at the equivalence point. As iodate is reduced to iodide, the equivalent weight in these titrations is 1/6 the formula weight.

**Reverse Titration Procedure.** — An aliquot of thallous acetate was taken in a titrating vessel, and mixed with 30～35 ml. mercuric chloride solution (8～9%) and 12 M hydrochloric acid (to maintain overall acidity between 1～2 N). The contents of the vessel were cooled to 25°C completely. The reaction mixture was finally titrated against standard iodate solution using the same electrometric end point. Near the equivalence point the indicator current showed a sudden increase in its value.

A series of experiments in which the acidity and mercuric chloride concentration were varied over a wide range, revealed that 1～2 N overall acid concentration and 25～35 ml. mercuric chloride gave accurate results. The results of one typical series of experiments are summarized in Tables I and II. Direct as well as reverse procedure may be extended to iodine monochloride end point (second end point), the acidity (hydrochloric acid) of the reaction mixture being raised at the iodide end point (first end point) to about 5～6 N.

**Determination of Thallium(I) with Iodate and Permanganate via Bromide.**—An aliquot of thallous

TABLE I. DIRECT TITRATION OF THALLIUM(I) WITH IODATE IN THE PRESENCE OF MERCURIC IONS

| ml. of 0.025 M iodate | ml. of 8~9% mercuric chloride | Overall acidity N | ml. of thallous acetate | | % Difference |
|---|---|---|---|---|---|
| | | | Reqd. | Calcd. | |
| 2 | 30~35 | 0.5~1.5 | 2.78 | 2.75 | 1.00 |
| 4 | 30~35 | 0.5~1.5 | 5.55 | 5.50 | 0.91 |
| 5 | 30~35 | 0.5~1.5 | 6.95 | 7.00 | 0.71 |
| 6 | 30~35 | 0.5~1.5 | 8.30 | 8.25 | 0.60 |
| 8 | 30~35 | 0.5~1.5 | 11.06 | 11.00 | 0.55 |
| 10 | 30~35 | 0.5~1.5 | 13.82 | 13.75 | 0.51 |

TABLE II. REVERSE TITRATION OF THALLIUM(I) WITH IODATE IN THE PRESENCE OF MERCURIC IONS

| ml. of thallous acetate | ml. of 8~9% mercuric chloride | Overall acidity N | ml. of 0.025 M iodate | | % Difference |
|---|---|---|---|---|---|
| | | | Reqd. | Calcd. | |
| 2 | 25~35 | 0.5~1.5 | 1.50 | 1.46 | 2.78 |
| 4 | 25~35 | 0.5~1.5 | 2.95 | 2.92 | 1.03 |
| 6 | 25~35 | 0.5~1.5 | 4.40 | 4.38 | 0.45 |
| 8 | 25~35 | 0.5~1.5 | 5.85 | 5.84 | 0.17 |
| 10 | 25~35 | 0.5~1.5 | 7.30 | 7.30 | nil |

TABLE III. DETERMINATION OF THALLIUM(I) WITH IODATE VIA BROMIDE IN HYDROCHLORIC ACID SOLUTION

| ml. of thallium(I) | Wt. of potassium bromide in grams | Overall acidity N | ml. of 0.1 N iodate | | % Difference |
|---|---|---|---|---|---|
| | | | Reqd. | Calcd. | |
| 20 | 2~3 | 1.50 | 15.05 | 15.20 | 0.95 |
| 20 | 2~3 | 2.00 | 15.05 | 15.20 | 0.98 |
| 20 | 2~3 | 3.00 | 15.10 | 15.20 | 0.66 |
| 20 | 2~3 | 4.00 | 15.15 | 15.20 | 0.33 |
| 20 | 2~3 | 5.00 | 15.15 | 15.20 | 0.33 |

TABLE IV. DETERMINATION OF THALLIUM(I) WITH PERMANGANATE VIA BROMIDE IN HYDROCHLORIC ACID SOLUTION

| ml. of thallium(I) | Wt. of potassium bromide in grams | Overall acidity N | ml. of permanganate solution | | % Difference |
|---|---|---|---|---|---|
| | | | Reqd. | Calcd. | |
| 20 | 2~3 | 2.0 | 12.60 | 12.65 | 0.39 |
| 20 | 2~3 | 3.0 | 12.65 | 12.65 | nil |
| 20 | 2~3 | 4.0 | 12.70 | 12.65 | 0.39 |
| 20 | 2~3 | 5.0 | 12.75 | 12.65 | 0.79 |
| 20 | 2~3 | 6.0 | 12.85 | 12.65 | 1.59 |

acetate was taken in a titrating vessel and 25~35 ml. 12 M hydrochloric acid was added to maintain the final acidity as indicated in Tables III and IV followed by 2~3 g. of potassium bromide. The reaction mixture was then titrated againt standard permanganate or iodate using the amperometric D.S.E.P. A potential of 0.1 V. was impressed across the indicator electrodes. The indicator current remained constant throughout the titration and finally at the equivalent point it showed a sudden increase in its value. Series of experiments in which the acidity was varied over a wide range revealed that the method is accurate for the determination of thallium(I) with iodate and permanganate via bromide at an overall acidity between 3~5 N. In the titration of thallous salt with permanganate at a high acid concentration (above 4 N), the amount of permanganate solution consumed was too high owing to (catalytic) oxidation of hydrochloric acid by permanganate.

## Summary

Oxidation of thallium(I) is carried out with iodate in the presence of mercuric ions using the amperometric D.S.E.P. Thallium is oxidized to thallium(III) and iodate is quantitatively reduced to iodide. The procedure is valuable because it gives correct determination for thallium(I) at

a low acid concentration. Oxidation of thallium(I) with permanganate and iodate in hydrochloric acid via bromide is also found to be accurate and quantitative.

The author wishes to thank Professor S. S. Joshi for his kind interest in this work.

*Chemical Laboratories*
*Banaras Hindu University*
*India*

# *Pre-oxidation by Iodine Monochloride—Potassium Hydroxide and Use of Iodine Monochloride End Point in the Determination of Hydrazine, Thiocyanate, Thiosulfate and Glucose*

By Bechu SHARMA

(Received August 31, 1959)

Iodate procedures introduced by Andrews[1] and later developed by Jamieson[2] and Lang[3], involve essentially the formation of iodine (+). Although applicable to a variety of common reductants, in a number of cases, iodate is not capable of bringing about direct oxidation. Thus ferrous iron and ferrocyanide bring about an apparent state of equilibrium which changes only slowly. Lang[3-4] proposed for such reductants a preoxidation by iodine monochloride solution prepared from iodide and iodate in the presence of chloride. Lang further found applicability of this method to an alkaline medium, wherein some cases hypoiodite acts more efficiently, e. g. for the determination of hydrogen peroxide[4] and formaldehyde[5]. An additional advantage of this procedure is that the back titrations can as well be followed with permanganate and ceric sulfate which are standared volumetric oxidizing agents. This point has been emphasized by Swift[6] and his coworkers in the determination of arsenic(III) wherein excessive iodine monochloride was followed in an acid medium. An earlier communication described the "iodine monochloride+sodium hydroxide" oxidation and iodine monochloride end point using iodate, permanganate and ceric sulfate for the determination of thiourea and its derivatives[7]. Subsequent investigations revealed that thiosulfate which is oxidized by alkaline hypoiodite could as well be determined. In an alkaline medium, thiosulfate is oxidized to sulfate which provides an advantage of a high conversion factor. The direct oxidation of thiocyanate by iodate, stops at cyanide stage alone while by alkaline hypoiodite it is converted into cyanate. Herein then, the modified procedure would provide an advantage of higher molecular ratio. Again, the oxidation of hydrazine sulfate, which is an ideal primary standard on account of its stability, ease of purification and various acidimetric and oxidimetric applications, was subjected to restricted conditions of acidity when titrated by iodine monochloride procedure. On the other hand, however, it could be easily oxidized by hypoiodite. Glucose is not oxidized by iodate in an acid medium, but iodine in weakly alkaline medium is capable of oxidizing it to gluconic acid. This principle was therefore applied to the determination of glucose as well. It may be pointed out that there are no direct titrimetric procedures for glucose, whose oxidation, except by iodine, hardly stops at the gluconic acid stage and the complete oxidation by drastic oxidants like permanganate and ceric sulfate in an acid medium and by ferricyanide in an alkaline medium, requires critical operative conditions for quantitative conversion into carbon dioxide and water.

1) L. W. Andrews, *J. Am. Chem. Soc.*, **25**, 756 (1903).
2) G. S. Jamieson, *Am. J. Sci.*, **33**, 352 (1912).
3) R. Lang, *Z. anorg. u. allgem. Chem.*, **142**, 229 (1925).
4) R. Lang, ibid., **142**, 280 (1925).
5) R. Lang, *Z. anal. Chem.*, **106**, 12 (1936).
6) E. H. Swift and C. H. Gregory, *J. Am. Chem. Soc.*, **52**, 901 (1930).
7) G. S. Deshmukh and M. G. Bapat, *Z. anal. Chem.*, **156**, 276 (1957).

## Experimental

A 0.5 M iodine monochloride solution was prepared by dissolving 17.5 g. of potassium iodate, and 22.7 g. of potassium iodide in 250 ml. of water to which 150 ml. 12 M hydrochloric acid was added. The solution was titrated with iodate or iodide solution using carbon tetrachloride till the organic layer was colorless. A 0.1 M potassium thiocyanate solution was prepared and standardized as usual by titration with standard silver nitrate solution. Sodium thiosulfate solution was standardized against potassium dichromate as well as with 0.1 N potassium iodate using iodine monochloride end point. The latter was found to be a better check due to the oxidation of thiosulfate to sulfate, which was subsequently achieved by hypoiodite oxidation. A 0.1 N hydrazine sulfate solution was prepared from British Drng House (L.R.) reagent recrystallized from water twice and dried at 140°C. A 1% glucose solution was prepared from E. Merck (L.R.) sample and was standardized by iodimetric determination. Potassium permanganate and ceric sulfate solutions were prepared and standardized as usual. Except for glucose the following

TABLE I. OXIDATION OF HYDRAZINE BY IODINE MONOCHLORIDE+POTASSIUM HYDROXIDE

| ml. 0.1 N (0.025 M) hydrazine sulfate | ml. 0.5 M iodine monochloride | Overall alkali % | Reaction time in min. | ml. 0.025 M iodate | Diff. % |
|---|---|---|---|---|---|
| (*a*) *Effect of excessive oxidant* | | | | | |
| 10 | 3 | 1 | 5 | 9.60 | 4.00 |
| 10 | 4 | 1 | 5 | 9.80 | 2.00 |
| 10 | 5 | 1 | 5 | 9.95 | 0.50 |
| 15 | 10 | 1 | 5 | 14.95 | 0.33 |
| (*b*) *Effect of hydrazine concentration* | | | | | |
| 10 | 5 | 2 | 5 | 10.00 | — |
| 15 | 8 | 2 | 5 | 14.95 | 0.33 |
| 20 | 10 | 2 | 5 | 20.00 | — |
| (*c*) *Test analysis* | | | | | |
| | | | | ml. 0.1 N permanganate | |
| 5 | 2 | 1 | 5 | 4.95 | 1.00 |
| 10 | 5 | 1 | 5 | 9.95 | 0.50 |
| 15 | 7 | 2 | 5 | 15.00 | 0.00 |
| 25 | 10 | 2 | 10 | 24.90 | 0.04 |

In all the experiments, hydrazine sulfate+iodine monochloride+potassium hydroxide was the order followed, in order to utilize the oxidant both in an acid and an alkaline medium.

TABLE II. OXIDATION OF THIOCYANATE BY IODINE MONOCHLORIDE+POTASSIUM HYDROXIDE

| ml. 0.01 M thiocyanate | ml. 0.5 M iodine monochloride | Overall alkali % | Reaction time in min. | ml. 0.025 M iodate | Diff. % |
|---|---|---|---|---|---|
| (*a*) *Effect of excessive oxidant* | | | | | |
| 10 | 2 | 1 | 5 | 7.20 | −10.00 |
| 10 | 5 | 1 | 5 | 7.80 | − 2.50 |
| 10 | 5 | 1 | 10 | 7.80 | − 2.50 |
| 10 | 10 | 1 | 10 | 7.85 | − 1.88 |
| (*b*) *Effect of alkali concentration* | | | | | |
| 10 | 2 | 3 | 10 | 7.50 | − 6.25 |
| 10 | 4 | 4 | 10 | 7.80 | − 2.50 |
| 10 | 5 | 4 | 10 | 7.90 | − 1.25 |
| 10 | 5 | 6 | 10 | 7.95 | − 0.62 |
| (*c*) *Test analysis* | | | | | |
| 5 | 3 | 4 | 10 | 3.95 | − 1.25 |
| 7.5 | 5 | 5 | 10 | 5.90 | − 1.56 |
| 10 | 10 | 5 | 10 | 7.95 | − 0.62 |
| 10 | 10 | 5 | 10 | 7.95 | − 0.62 |

The order of mixing was thiocyanate, iodine monochloride and alkali, in order to utilize the oxidant in acid and alkali medium.

general procedure was adopted. An aliquot of the reductant solution was taken in an Erlenmeyer flask to which an amount of iodine monochloride (at least 3/2 times that calculated on the reduction to iodide) and finally 25% (potassuim hydroxide solution were added to render the solution 1~2 N in alkali. Advantage of the addition of iodine monochloride was that the oxidant was available in an acid as well as in an alkaline medium. However, with thiosulfate, sulfur precipitates and the oxidation hardly goes to completion. The addition of alkali prior to iodine monochloride avoided this and the oxidation was found to be smooth. After being kept for 5~10 min. the solution was transferred to a 150 ml. beaker, acidified with 12 M hydrochloric acid to give an overall 5~6 N acidity and was titrated with iodate, permanganate or ceric sulfate by

TABLE III. OXIDATION OF THIOSULFATE BY IODINE MONOCHLORIDE+POTASSIUM HYDROXIDE

| ml. 0.01 M thiosulfate | ml. 0.5 M iodine monochloride | Overall alkalinity % | Reaction time in min. | ml. 0.025 M iodate | Diff. % |
|---|---|---|---|---|---|
| (*a*) *Effect of excessive oxidant* | | | | | |
| 5 | 2 | 1 | 5 | 3.80 | − 5.00 |
| 5 | 3 | 1 | 5 | 3.80 | − 5.00 |
| 5 | 4 | 1 | 5 | 3.85 | − 3.75 |
| 10 | 10 | 1 | 10 | 7.85 | − 1.88 |
| (*b*) *Effect of alkali concentration* | | | | | |
| 5 | 2 | 1 | 10 | 3.90 | − 2.50 |
| 5 | 2 | 2 | 10 | 3.95 | − 1.25 |
| 5 | 2 | 4 | 10 | 3.95 | − 1.25 |
| 10 | 5 | 4 | 10 | 7.95 | − 0.62 |
| (*c*) *Test analysis* | | | | | |
| | | | | ml. 0.1 M ceric sulfate | |
| 5 | 2 | 4 | 15 | 3.95 | − 1.25 |
| 7.5 | 4 | 4 | 10 | 5.95 | − 0.83 |
| 10 | 8 | 4 | 10 | 7.95 | − 0.62 |
| 10 | 10 | 4 | 10 | 7.95 | − 0.62 |

*Order of mixing.*—Iodine monochloride+thiosulfate+alkali.—On slow addition of iodine monochloride to thiosulfate, part of sulfur separates, due to high acidity in contact with thiosulfate.

TABLE IV. OXIDATION OF GLUCOSE BY IODINE MONOCHLORIDE+POTASSIUM HYDROXIDE

| ml. of 1% glucose | ml. 0.5 M iodine monochloride | Overall alkalinity % | Reaction time in min. | ml. 0.025 M iodate | Diff. % |
|---|---|---|---|---|---|
| (*a*) *Effect of excessive oxidant* | | | | | |
| 10 | 3 | Just alkaline to dissolve iodine* | 5 | 10.70 | 3.17 |
| 10 | 5 | 〃 | 5 | 10.95 | 0.90 |
| 15 | 7 | 〃 | 10 | 16.40 | 1.05 |
| 15 | 8 | 〃 | 10 | 16.55 | 0.15 |
| (*b*) *Effect of alkali concentration* | | | | | |
| 10 | 3 | 1 | 5 | 10.60 | 4.07 |
| 10 | 5 | 2 | 5 | 10.75 | 2.71 |
| 10 | 5 | 2 | 10 | 10.75 | 2.71 |
| (*c*) *Test analysis* | | | | | |
| 10 | 5 | as in (*a*) | 10 | 10.95 | 0.90 |
| 15 | 10 | 〃 | 10 | 16.55 | 0.15 |
| 20 | 10 | 〃 | 10 | 22.00 | 0.45 |
| 20 | 10 | 〃 | 5 | 21.70 | 1.81 |

10 ml. of 1% glucose require 11.05 ml. 0.025 M iodate.

* As in the presence of excess of alkali, hypoiodite does not act smoothly on glucose, the order of mixing was "glucose+iodine monochloride", to which only just sufficient alkali was added to dissolve the liberated iodine. Finally little more alkali was added to convert iodine into hypoiodite.

the amperometric "Dead Stop End Point". The unit was the simple form of the one described by Foulk and Bawden[8]. One tenth volt was the impressed potential across the indicator electrodes between which a mechanical stirrer served to mix thoroughly the reaction mixture. The current measurements were made by a sensitive galvanometer with a lamp-and-scale arrangement. The current increased to a maximum and then decreased to a minimum where the conversion of iodine and iodide to iodine (+) was complete. In the oxidation of glucose, the control of alkalinity was most critical. This was achieved by careful addition of alkali to the mixture of glucose and iodine monochloride to the point where the iodine that separated just dissolved. The reverse order glucose-alkali-iodine-monochloride was found to give variable results. In glucose determination, the final titration was possible only with iodate because other oxidants, permangante and ceric sulfate, attacked the gluconic acid. The results of one typical series of experiments are summarized in Tables I—IV.

8) C. W. Foulk and A. T. Bawden, *J. Am. Chem. Soc.*, 48, 2045 (1926).

**Summary**

The principle of hypoiodite (iodine monochloride+potassium hydroxide) pre-oxidation and iodine monochloride end point has been adopted to the determination of hydrazine, thiocyanate, thiosulfate and glucose. The availability of alternative standard titrating solutions (iodate, permanganate and ceric sulfate) and applicability over a range of reductant concentrations are essential features of this procedure.

The author wishes to thank Professor S. S. Joshi, for his kind interest in the work.

*Chemical Laboratories*
*Banaras Hindu University*
*India*

# *Heats of Formation of Lower Members of Dimethyl- and Methylisopropoxy-cyclopolysiloxanes*

By Toshio TANAKA

(Received July 30, 1959)

From the investigation on the redistribution equilibrium between dimethylcyclopolysiloxanes and linear polysiloxanes catalyzed by sulfuric acid, it was concluded by Scott that the ring in the trimer of cyclosiloxanes had a slight strain, while the ring structures of tetramer and the polymer of larger size were probably free from strain. He attributed this strain to the deformation of normally large Si-O-Si angle in forming the small-membered ring[1]. Before and after that, it was indicated from X-ray[2,3] and electron[4] diffraction studies that the six-membered ring in the trimer was planer or nearly planar. While, the siloxane rings of the tetramer[5] and the octamer[6] were reported to have *zigzag* form from X-ray diffraction study, and the former ring was supposed to have *cradle* (rather than *crown*) form from electron diffraction study[7]. As the results of these studies, the difference between the molecular structures of the cyclic trimer and the cyclic tetramer exist in the Si-O-Si angle, which is 125° for the former and 140° for the latter, and it has been supposed that a value of about 140° would be probable for a strain free Si-O-Si valency angle[7].

In this paper, the heats of combustion of the members represented by $C_n$ and $D_n$ (see below) have been measured at 20°C and a constant volume, and the corresponding heats of combustion and formation in isobaric process have been calculated. From the results, it will be indicated

1) D. W. Scott, *J. Am. Chem. Soc.*, **69**, 803 (1947).
2) G. Peyronel, *Atti accad. nazl. Lincei. Rend., Classe sci. fis., mat. e nat.*, **15**, 402 (1953); **16**, 78, 231 (1954); *Chem. Abstr.*, **48**, 7971*b*, 10401*h* (1954).
3) W. L. Roth and D. Harker, *Acta Cryst.*, **1**, 34 (1948).
4) E. H. Aggarwal and S. H. Bauer, *J. Chem. Phys.*, **18**, 420 (1950).
5) H. Steinfink, B. Post and I. Fankuchen, *Acta Cryst.*, **5**, 802 (1954).
6) L. K. Frevel and M. J. Hunter, *J. Am. Chem. Soc.*, **67**, 2275 (1945).
7) M. Yokoi, This Bulletin, **30**, 100 (1957).

TABLE I. PHYSICAL CONSTANTS AND ANALYTICAL DATA OF $C_n$

| Compound | b.p. °C/mmHg | $d_4^{20}$ | $n_D^{20}$ | Mol. wt. Found[a] (Calcd.) | $MR_D$ Found (Calcd.)[b] | Si % Found (Calcd.) |
|---|---|---|---|---|---|---|
| $C_3$ | 67/1 | 0.9912 | 1.3973 | 348 (355) | 86.23 (85.98) | 23.80 (23.76) |
| $C_4$ | 97/1 | 1.0009 | 1.4023 | — (473) | 115.09 (114.64) | 23.77 (23.76) |

a) Cryoscopic measurement in benzene.
b) Calculated from bond refractivities by E. W. Warrick, *J. Am. Chem. Soc.*, **68**, 2455 (1946).

that the cyclotetrasiloxane and the cyclopentasiloxane are free from strain, while the cyclotrisiloxane will have a slight strain.

$C_n$: $\left[\begin{array}{l}CH_3\\ |\\ Si\cdot O\\ |\\ OC_3H_7\text{-}i\end{array}\right]_n$, $n=3, 4$; $D_n$: $\left[\begin{array}{l}CH_3\\ |\\ Si\cdot O\\ |\\ CH_3\end{array}\right]_n$, $n=4, 5$

## Experimental

**Materials.**—The members of $C_n$ were prepared by hydrolyzing methylisopropoxydichlorosilane with considerable dropping rate using pyridine as an acid acceptor and were characterized*. The physical constants and the analytical data are shown in Table I.

The members of $D_n$, supplied from Shin-etsu Chem. Ind. Co., have been rigorously fractionated through a semi-micro Stedman column of about 20 theoretical plates and the physical constants have been compared with them reported in the literature of the subject. The results are shown in Table II.

TABLE II. PHYSICAL CONSTANTS OF $D_n$[a]

| Compound | b.p. °C/mmHg | $d_4^{20}$ | $n_D^{20}$ | Mol. wt. Found[b] (Calcd.) |
|---|---|---|---|---|
| $D_4$ | 70/18 [175/760] | 0.9558 [0.9558] | 1.3968 [1.3968] | 291 (297) |
| $D_5$ | 80/8 [210/760] | 0.9596 [0.9593] | 1.3984 [1.3982] | 362 (371) |

a) The values in brackets are those reported in the publication; E. G. Rochow, "An Introduction to the Chemistry of the Silicones", 2nd Ed., John Wiley & Sons, Inc., New York (1951), p. 185.
b) Cryoscopic measurements in benzene.

**Calorimetry.**—The apparatus used in this experiment was described elsewhere[8]. Each liquid sample has been weighed in a gelatine capsule and it has been burned by electrical ignition, as described in the case of methylethoxypolysiloxane in the previous paper[9]. After the burning of the samples, a bulky product, consisting of silica and incomplete combustion products of a part, are yielded in the combustion vessel. The incomplete combustion products in the experiments of $C_3$, $C_4$ and $D_4$ have been found to contain amorphous carbon and, sometimes, a trace of carborundum**. In addition to these products, a polymer-like substance containing a silicon atom has been yielded in the combustion experiment of $D_5$, as in the case of 1,3,5,7,9-pentamethylcyclopentasiloxane[10]. The incomplete combustion products included in the silica have been determined in quantities and the thermal corrections for them have been calculated according to the method in the previous paper[9,10].

## Results and Discussion

Five to six combustion experiments have been carried out with each liquid sample of the same material, and the results are shown in Table III, excepting that of $D_5$.

The result of the combustion experiment of $D_5$ is shown in Table IV.

In Table IV, the energy evolved per gram at 20°C and a constant volume is represented by $-\Delta U_B^{low}$, in which the thermal corrections for carbon and, sometimes, for carborundum have been made, but the correction for the polymer-like substance only is not taken into account;

TABLE III. EXPERIMENTAL RESULTS OF $C_3$, $C_4$ AND $D_4$

| Compound | cal./g. Heat of combustion | | | | | | Mean | Relative mean deviation % |
|---|---|---|---|---|---|---|---|---|
| $C_3$ | 6140 | 6133 | 6121 | 6126 | 6113 | 6138 | 6129 | ±0.14 |
| $C_4$ | 6099 | 6077 | 6096 | 6088 | 6090 | — | 6090 | ±0.06 |
| $D_4$ | 6357 | 6336 | 6355 | 6346 | 6332 | — | 6345 | ±0.09 |

* Details of the preparation of these compounds will soon be published by Dr. Ōkawara.
8) T. Tanaka and T. Watase, This Bulletin, **28**, 258 (1955).
9) T. Tanaka, ibid., **32**, 1258 (1959).
** In the combustion experiment of $D_4$, polymer-like substance, though only a trace in quantity, has sometimes been found in the combustion product, as in the case of $D_5$ described below, but such an experimental result of $D_4$ has been rejected here.
10) T. Tanaka, *Technol. Repts. Osaka Univ.*, **8**, 437 (1958).

TABLE IV. EXPERIMENTAL RESULTS OF $D_5$

| Wt. of sample | $-\Delta U_B^{low}$ | Amount of $SiO_2$ produced from the polymer-like substance | | $-\Delta U_B^{high}$ |
|---|---|---|---|---|
| g. | cal./g. | mg. | $\alpha$(%) | cal./g. |
| 0.45543 | 6326 | 1.90 | 0.52 | 6359 |
| 0.45763 | 6277 | 2.75 | 0.74 | 6323 |
| 0.44446 | 6317 | 2.03 | 0.56 | 6352 |
| 0.45899 | 6292 | 1.79 | 0.48 | 6322 |
| 0.45121 | 6311 | 1.48 | 0.41 | 6337 |
| 0.45404 | 6321 | 1.52 | 0.41 | 6347 |
| Mean | 6307 | | | 6340 |
| Average value | | 6324 | | |

$-\Delta U_B^{low}$, will be therefore considered as underestimated value for the heat of combustion of $D_5$. The third column in this table is the number of grams of silica produced from the polymer-like substance by the further ignition in the course of analysis of incomplete combustion product, and the fourth column indicated by $\alpha$ is its percentage for the amount of silica equivalent to the weight of the sample in each run. As the thermal correction for the formation of the polymer-like substance could not be evaluated exactly in this experiment, it has been calculated under the assumption that the amount of sample equivalent to the amount of silica produced from the polymer-like substance remained, not burned at all, and $-\Delta U_B^{high}$ in th last column of the Table IV has been obtained by the following expression:

$$-\Delta U_B^{high} = -\Delta U_B^{low}(1+\alpha\cdot 10^{-2}).$$

This will be evidently overestimated value for its heat of combustion. Accordingly, the average value of these $-\Delta U_B^{low}$ and $-\Delta U_B^{high}$ values has here been adopted as the reasonable one for the heat of combustion of $D_5$.

Table V is a summary of thermal data of $C_n$ and $D_n$ calculated from the combustion results.

Notations in this table are as follows: $-\Delta U_R$, the heat of combustion at standard constant volume process, where the reactants are one atmospheric pressure; $-\Delta H_f$, the heats of formation of the members of $C_n$ and $D_n$ in the liquid state from standard elements; $-\Sigma E$, the heats of formation of those in the gaseous state from mono-atomic gases. These energy values have been calculated by the method described in the previous paper[8]. In the calculation of $-\Sigma E$, values of 52.1, 59.2, 171.7 and 89.9 kcal./g.-atom have been adopted for the heats of atomization of hydrogen, oxygen, carbon and silicon, respectively, which are the same values used in the previous paper[8]. And then, values of 10.9[11] and 11.2[12] kcal./mol. have been used for the heats of vaporization of $D_4$ and $D_5$, respectively, and the corresponding energy values of $C_3$ and $C_4$ have been estimated to be 10.1 and 11.0 kcal./mol. from the Trouton's rule, respectively. The $-\Sigma E/n$ in the last column of the Table V, derived in this manner, will be considered as the sums of bond energies in structural units*** of $\left[\begin{matrix}CH_3\\ i\text{-}C_3H_7O\end{matrix}\!\!>\!Si\!<\!\begin{matrix}O\\ O\end{matrix}\right]$ for $C_n$ and of $\left[\begin{matrix}CH_3\\ CH_3\end{matrix}\!\!>\!Si\!<\!\begin{matrix}O\\ O\end{matrix}\right]$ for $D_n$.

**No Strain in the Cyclic-tetramer and -pentamer.** —If the $-\Sigma E/n$ of $D_5$ in Table V, though involving a considerable uncertainty, will be accepted as the reasonable value for the sum of bond energies in its structural unit, this is somewhat higher than the corresponding value of $D_4$. Such an energy difference between these compounds will perhaps be attributed to the difference between their polymer sizes, as in the case of methylmethoxypolysiloxanes, $CH_3O\cdot[(CH_3)(CH_3O)SiO]_nCH_3$[9], and methoxy end-blocked dimethylpolysiloxanes, $CH_3O\cdot[(CH_3)_2SiO]_nCH_3$[13], in which the values of

TABLE V. HEATS OF COMBUSTION AND FORMATION OF $C_n$ AND $D_n$

| Compound | Mol. wt. | kcal./mol. | | | | |
|---|---|---|---|---|---|---|
| | | $-\Delta U_R$ | $-\Delta H_c$ | $-\Delta H_f$ | $-\Sigma E$ | $-\Sigma E/n$ |
| $C_3$ | 354.63 | 2173 | 2177 | 601 | 4839 | 1613 |
| $C_4$ | 472.84 | 2879 | 2885 | 819 | 6473 | 1618 |
| $D_4$ | 296.63 | 1882 | 1887 | 518 | 3728 | 932 |
| $D_5$ | 370.79 | 2344 | 2350 | 656 | 4670 | 934 |

11) R. C. Osthoff, W. T. Grubb and C. A. Burkhard, *J. Am. Chem. Soc.*, **75**, 2227 (1953).
12) D. F. Wilcock, ibid., **68**, 691 (1946).
*** For example, in $D_n$, the term of "structural unit" will be used for $[(CH_3)_2SiO_2]$, but not $[(CH_3)_2SiO]$, on the number of each chemical bond in the compounds.
13) T. Tanaka, to be published in *J. Inorg. & Nuclear Chem.*

$-E\left[\begin{smallmatrix}C\\O\end{smallmatrix}\!\!>\!Si<\!\!\begin{smallmatrix}O\\O\end{smallmatrix}\right]$**** and $-E\left[\begin{smallmatrix}C\\C\end{smallmatrix}\!\!>\!Si<\!\!\begin{smallmatrix}O\\O\end{smallmatrix}\right]$**** were found to be increasing with their polymer sizes, respectively.

If the value of 98.8 kcal./mol.[9,10] is here adopted for C–H bond energy in $D_n$, the values of $-E\left[\begin{smallmatrix}C\\C\end{smallmatrix}\!\!>\!Si<\!\!\begin{smallmatrix}O\\O\end{smallmatrix}\right]$ for $D_4$ and $D_5$ result in 339 and 341 kcal./mol., respectively. While, the corresponding values in methoxy end-blocked dimethylpolysiloxanes, which are linear compounds, were obtained to be 329, 335 and 336 kcal./mol. for the monomer, the dimer and the trimer, respectively[13]. The value of $-E\left[\begin{smallmatrix}C\\C\end{smallmatrix}\!\!>\!Si<\!\!\begin{smallmatrix}O\\O\end{smallmatrix}\right]$ in the cyclic tetramer is somewhat larger than that in the linear trimer, and the energy difference between them will be attributed to the difference between their polymer sizes and, if possible, partly to the difference between the cyclic and the linear structures. As the linear polysiloxanes under consideration will probably have no strain in their molecular structures, the ring structures of the cyclic-tetramer and -pentamer may also be free from strain, when one compares the $-E\left[\begin{smallmatrix}C\\C\end{smallmatrix}\!\!>\!Si<\!\!\begin{smallmatrix}O\\O\end{smallmatrix}\right]$ with those in the linear compounds.

**Strain in the Cyclic Trimer.**—The value of $-\Sigma E/n$ in $C_3$ is 5 kcal. lower than that in $C_4$, as shown in Table V. The energy difference will not by itself correspond to the strain per the structural unit of $\left[\begin{smallmatrix}CH_3\\i\text{-}C_3H_7O\end{smallmatrix}\!\!>\!Si<\!\!\begin{smallmatrix}O\\O\end{smallmatrix}\right]$ in $C_3$, because it must be taken into consideration that the value of $-\Sigma E/n$ in $C_n$ will also increase with increasing of the polymer size, as in the case of $D_n$. Now, if it is assumed that the $-\Sigma E/n$ for $C_3$ should be 2 kcal. lower than that for $C_4$, by applying the energy difference in $-\Sigma E/n$ between $D_4$ and $D_5$, the extra lowering energy in $C_3$ comparing from $C_4$, 3 kcal. per the structural unit, will be due to the strain in the cyclic trimer; the ring of cyclic trimer, then, will be anticipated to have a strain corresponding to 9 kcal./mol. as a whole. However, the incremental change in $-\Sigma E/n$ between the cyclic-trimer ($C_3$) and -tetramer ($C_4$), attributed to the difference of their polymer sizes, will perhaps be larger than that between the cyclic-tetramer ($D_4$) and -pentamer ($D_5$), because the incremental change in energy between the neighboring members will be decreasing as their polymer sizes increase, as observed in the previous works on the linear polysiloxanes[9,13]. It has also been found in the previous paper[9] that the value of $-E\left[\begin{smallmatrix}C\\O\end{smallmatrix}\!\!>\!Si<\!\!\begin{smallmatrix}O\\O\end{smallmatrix}\right]$ in the first member of methylmethoxypolysiloxanes were 4 kcal. lower than that in the second member. As the cyclic trimer is the smallest-membered ring in the cyclopolysiloxanes, the larger part of the incremental change (5 kcal.) in $-\Sigma E/n$ between $C_3$ and $C_4$ may be attributed to the difference of their polymer sizes. Thus, the ring of the cyclic trimer will be considered to have a strain corresponding to a few or several kcal./mol. at most, being fairly smaller than 9 kcal./mol.

Though the Si–O–Si angle in the cyclic trimer has been considered to be subjected to a considerable distortion in comparing with its normal angle, the magnitude of energy due to strain obtained here seems to be too small. Such a slight strain in the six-membered ring will however be explained as due to the siloxane linkage having the nature represented by the term of "*ball and joined socket*", as explained previously by Roth and Harker[3].

The energy due to strain derived here comes out from the small difference between large quantities, so that it may not be a conclusive value. Notwithstanding, it may be said that the above results are parallel with the conclusions obtained from the investigation on redistribution equilibrium[1] and on molecular structures of cyclopolysiloxanes[2-7].

**** Sums of bond energies in the structural units of $CSiO_3$ and $C_2SiO_2$, in which C-H and C-O bonds are excepted, in methylmethoxypolysiloxanes and methoxy end-blocked dimethylpolysiloxanes, respectively. These sums were obtained under the assumption that the C-H and the C-O bond energies were not varied from molecule to molecule in the previous papers[9,13].


## Summary

Heats of combustion of lower members of dimethyl- and methylisopropoxy-cyclopolysiloxanes have been measured at 20°C and a constant volume, and the corresponding heats of combustion and formation in isobaric process have been calculated. From the results, the heats of formation of structural units, $\left[\begin{smallmatrix}CH_3\\CH_3\end{smallmatrix}\!\!>\!Si<\!\!\begin{smallmatrix}O\\O\end{smallmatrix}\right]$ and $\left[\begin{smallmatrix}CH_3\\i\text{-}C_3H_7O\end{smallmatrix}\!\!>\!Si<\!\!\begin{smallmatrix}O\\O\end{smallmatrix}\right]$, of these compounds from mono-atomic gases have been derived, and it has been found that the ring structures

of the cyclic-tetramer and pentamer would be free from strain. Further, the effect of distortion of Si–O–Si valency angle in the cyclic trimer on the heat of formation has been discussed.

The author wishes to express his sincere thanks to Professor T. Watase, Dr. R. Ōkawara and Dr. M. Kakudo for their helpful discussions, and to Mr. H. Mimura for his aid in a part of this work.

*Department of Applied Chemistry*
*Faculty of Engineering*
*Osaka University*
*Miyakojima-ku, Osaka*

# *Studies on Organic Reagents for Inorganic Analysis. VI. Absorption Spectrum of Phenylfluorone-Metal Chelate and the Nature of the Chelating Bond*

By Hirotoshi SANO

(Received July 2, 1959)

For many organic dyes used for the colorimetry of metals, the color change is ascribable to the shift of the $\pi \rightarrow \pi'$ absorption spectra of the organic system caused by the chelating. With respect to the nature of such color change, there have been many papers published recently. Molecular orbital (LCAO) method was applied successfully by Belford, Martell and Calvin[1] to compute the effect of metal ion upon the $\beta$-diketone-metal chelate. The absorption spectra of metal oxalates were interpreted by Graddon[2] on the basis of a simple electrostatic effect. Dortashaeppi, Hürzeler and Treadwell[3] tried to apply a free electron gas model method to the alizarin chelates of several metals. Based on the amperometric titration data, the absorption spectra of alizarin S and its metal chelate were also discussed by Larsen and Hirozawa[4].

In the treatment of the problem, however, the effect of the nature of the chelating bond has been almost neglected, although it seems sometimes to have considerable influence on the absorption spectra. The author reported previously that the maximum wavelengths of the absorption spectra of phenylfluorone metal chelates shift toward the longer side with the decrease in the electronegativity of the metal chelated[5]. In this paper, the correlation of the maximum wavelength with the ionic character of the chelating bond was treated theoretically with the aid of the free electron gas model approximation.

## Fundamental Consideration

The author has adopted Kuhn's free electron gas model method[6,7] for the present purpose, because the model can be conveniently applied to the subject although the value of the model must not be overestimated. According to Kuhn, the electron gas suffers a disturbance in the case of polyenes, unsymmetrical cyanines, etc., and the $\pi$-electrons are thought to be placed in a one-dimensional potential having a sine curve periodicity. The wavelength of absorption maximum is expressed by the following equation.

$$\frac{1}{\lambda_{\max}} = \frac{V_0}{\boldsymbol{h}\cdot\boldsymbol{c}}\left(1-\frac{1}{N}\right)+\frac{\boldsymbol{h}}{8m\boldsymbol{c}}\cdot\frac{N+1}{L^2} \qquad (1)$$

where, $L$ is the length of the path of the free $\pi$-electron measured along the conjugated chain, $N$, the number of $\pi$-electrons, $m$, the mass of the electron, $\boldsymbol{c}$, the velocity of light, $\boldsymbol{h}$, Planck's universal constant, and $V_0$, the amplitude of the sine-shaped potential along the chain.

1) R. L. Belford, A. E. Martell and M. Calvin, *J. Inorg. & Nuclear Chem.*, **2**, 11 (1956).
2) D. P. Graddon, ibid., **3**, 308 (1956).
3) Y. Dortashaeppi, H. Hürzeler and W. D. Treadwell, *Helv. Chim. Acta*, **34**, 797 (1951).
4) E. M. Larsen and S. T. Hirozawa, *J. Inorg. & Nuclear Chem.*, **3**, 198 (1956).
5) Part II of this series: H. Sano, This Bulletin, **30**, 790 (1957).
6) H. Kuhn, *Helv. Chim. Acta*, **31**, 1441 (1948); *J. Chem. Phys.*, **16**, 840 (1948).
7) H. Kuhn, *Z. Elektrochem.*, **53**, 165 (1949); *J. Chem. Phys.*, **17**, 1198 (1949).

Suppose that the dye is resonating between two limiting structures Ia and Ib. When each of the two structures makes the same contribution to the normal state of the dye, as seemed to be the case for symmetrical polymethine dyes, each conjugated C–C bond should have an equal bond length*, and the value of $V_0$ should be zero.

$$\cdots\text{-}\underset{1}{C}=\underset{2}{C}\text{-}\underset{3}{C}=\underset{4}{C}\text{-}\underset{5}{C}=\cdots \leftrightarrow \cdots=\underset{1'}{C}\text{-}\underset{2'}{C}=\underset{3'}{C}\text{-}\underset{4'}{C}=\underset{5'}{C}\text{-}\cdots$$

Ia Ib

On the other hand, when Ia and Ib do not make equal contribution to the normal state, as seemed to be the case for polyene etc., a longer C–C bond (so-called "single bond") and a shorter bond (so-called "double bond") appear alternatively along the conjugated chain, and $V_0$ has a definite value.

If the mean bond length of the longer C–C bond and the shorter bond is represented with $\overline{R}'$ and $\overline{R}''$, respectively, the relation mentioned above is summarized as follows:

$$V_0=0, \text{ when } \overline{R}'-\overline{R}''=0 \quad (2)$$

$$V_0>0, \text{ when } \Delta R=\overline{R}'-\overline{R}''>0 \quad (3)$$

**The Relation between $V_0$ and $\Delta R$.**—It was difficult to obtain theoretically the relation between $V_0$ and $\Delta R$. Therefore, the problem was solved with the aid of empirical treatment. The difference between the mean "double-" and mean "single-" bond length in polyenes, $\Delta R$, was obtained by calculation based on Coulson's semi-empirical theory[8], because few observed values for the bond length of polyenes were reported. The results are shown in Table I**.

TABLE I. CALCULATED VALUES OF $\overline{R}'$, $\overline{R}''$ AND $\Delta R$

| $j$ | $\overline{R}'$, Å | $\overline{R}''$, Å | $\Delta R$, Å |
|---|---|---|---|
| 1 | — | 1.330 | — |
| 2 | 1.432 | 1.347 | 0.085 |
| 3 | 1.424 | 1.356 | 0.068 |
| 4 | 1.420 | 1.362 | 0.058 |
| 5 | 1.415 | 1.365 | 0.050 |
| 6 | 1.414 | 1.369 | 0.045 |
| 7 | 1.412 | 1.371 | 0.041 |
| 8 | 1.411 | 1.373 | 0.037 |
| 9 | 1.410 | 1.375 | 0.034 |
| 10 | 1.409 | 1.376 | 0.032 |
| 11 | 1.408 | 1.377 | 0.030 |
| 12 | 1.407 | 1.378 | 0.029 |
| — | — | — | — |
| 22 | 1.402 | 1.384 | 0.017 |

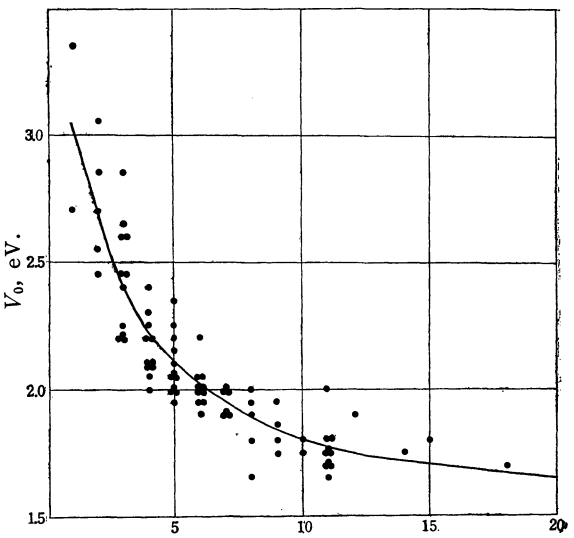
The values of $V_0$ calculated from the experimentally determined absorption maxima of a number of polyenes*** have been collected in Fig. 1, which shows the relationship between $V_0$ and the number of conjugated double bonds. It is found that the values of $V_0$ distribute in a narrow range hyperbolically with the increasing number of the conjugated double bonds.

Based on the values $\Delta R$ obtained in Table I and the values of $V_0$ estimated from Fig. 1, an empirical equation for the $\Delta R$-relation is derived as follows:

$$V_0=3-3\left(1-\frac{\Delta R}{0.21}\right)^5 \quad (4)$$

Fig. 2 illustrates the value of $V_0$ as a function of $\Delta R$.

In practice, the small value of $V_0$ is useful for the following discussion, because the value of $V_0$ is smaller than one electron volt in the dye-metal chelate. Therefore, Eq. 4 can be reduced to




Number of conjugated double bond ($j$)

Fig. 1. Relation between $V_0$ and the number of conjugated double bond.

* This approximation is not strictly correct, but no objection is found in the following consideration, because the corresponding bond length in both structures strictly equal, namely, $C_1$-$C_2$, $C_2$-$C_3$, $C_3$-$C_4$,.....equal to $C_{1'}$-$C_{2'}$, $C_{2'}$-$C_{3'}$, $C_{3'}$-$C_{4'}$,....., respectively.

** The value of bond length for the "single" bond is underestimated, because the calculation used here includes no self-consistent treatment, whereas that of "double" bond is considered to be practically equal to the true value.

*** The absorption maxima were taken from the follwing: A. E. Gillam and E. S. Stern, "An Introduction to Electronic Absorption Spectroscopy in Organic Chemistry", Edward Arnold Publishers, Ltd.. London (1954); Y. Urushibara, "Organic Chemistry II (Yûki Kagaku)", Kyôritsu Shuppan, Tokyo (1955).

8) C. A. Coulson, *Proc. Roy. Soc.*, **A169**, 413 (1939).

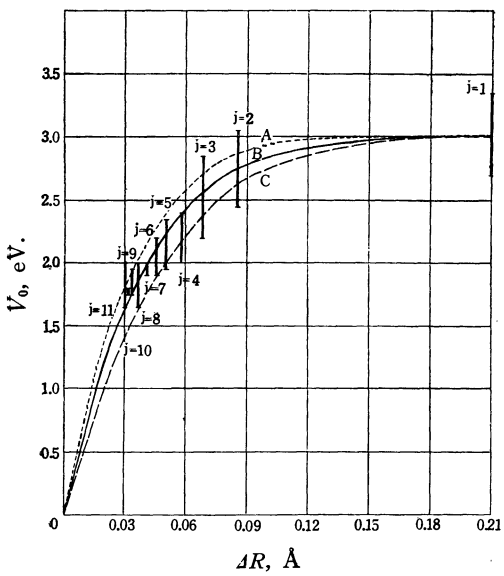



Fig. 2. Relation between $V_0$ and $\Delta R$.
Curve A: $V_0=3-3(1-\Delta R/0.21)^6$
Curve B: $V_0=3-3(1-\Delta R/0.21)^5$
Curve C: $V_0=3-3(1-\Delta R/0.21)^4$

$$V_0 \simeq 71.4\Delta R - 680\Delta R^2 \qquad (5)$$

Deviation from Eq. 4 is 5%, at $\Delta R<0.03$Å, $V_0<1.8$ eV.,

$$\text{or} \qquad \Delta R \simeq \frac{V_0}{71.4}\left(1+\frac{680}{71.4^2}\cdot V_0\right) \qquad (6)$$

**The Relation between $V_0$ and the Ionic Character of the Chelating Bond.**—As is well known, a bond length, $R$, is expressed as follows:

$$R=R_1-(R_1-R_2)\frac{3x}{2x+1} \qquad (7)$$

where $R_1$ is the C-C bond length of pure single bond of ethane, $R_2$ is that of pure double bond of ethylene and $(1+x)$ is the bond order of the C-C bond in question based on the valence bond theory[9]. For instance, $x$ should be expected to be 0.5 when $\Delta R$ is zero.

Suppose that $(1+x)$ represents the bond order of the "double" bond, the bond length, $R''$, is

$$R''=R_1-(R_1-R_2)\frac{3x}{2x+1}, \quad x>0.5 \qquad (8)$$

Similarly, the bond length corresponding to "single bond", $R'$, is

$$R'=R_1-(R_1-R_2)\frac{3(1-x)}{3-2x} \qquad (9)$$

Then,

$$\Delta R=3(R_1-R_2)\frac{2x-1}{4-(2x-1)^2} \qquad (10)$$

substituting numerical data for $R_1$ and $R_2$ in Eq. 10, it is seen that

$$\Delta R=0.63\frac{2x-1}{4-(2x-1)^2}$$
$$(R_1: 1.54\text{Å}, R_2: 1.32\text{ Å}) \qquad (11)$$

By rewriting this expression it is seen that

$$x=\frac{1}{2}+\frac{2}{0.63}\Delta R-\frac{8}{0.63^3}\Delta R^3+\frac{64}{0.63^5}\Delta R^5-\cdots \qquad (12)$$

$$x\simeq\frac{1}{2}+\frac{2}{0.63}\Delta R, \qquad \Delta R<0.16\text{ Å} \qquad (12')$$

On the other hand, the value of $x$ may be connected with the ionic character of the bond between the metal and the donor atom of the dye as follows:

IIa IIIa

O=C-C=···=C-O$^-$ M$^+$ $\leftrightarrow$ O=C-C=···=C-O-M

$\updownarrow$ $\updownarrow$

$^-$O-C=C-···-C=O M$^+$ $^-$O-C=C-···-C=O$^+$-M

IIb IIIb

In the four formulae, IIa and IIb represent two limiting structure of the metal-dye compound combined with a pure ionic bond, whereas IIIa and IIIb represent two limiting structures of compound combined with a pure covalent bond.

When the metal-donor bond has a pure covalency, the conjugated system is considered to be similar to that of polyene ($V_0=V_{0n}$, $\Delta R=\Delta R_n$, and $x=x_n$) which has the same number, $N$, of conjugated $\pi$-electron, whereas it becomes equal to that of symmetrical polymethine ($\Delta V_0=0$, $\Delta R=0$, $x=0.5$) when the bond is pure ionic.

On the whole, therefore, each of two structures, II and III, contributes to the normal state of the dye-metal compound, in proportion to the ionic character and covalent character, respectively. The mean bond order for "double" bonds of the dye-metal chelate, $1+x$, will be expressed as follows:

$$1+x=(1-i)(1+x_n)+1.5i \qquad (13)$$

where $i$ is the ionic character. The value of $x_n$, the mean bond order of the polyene, is obtained from Table 1, Eq. 9 or 10, and the mean bond length $\overline{R'}$ or $\overline{R''}$ of the polyene, which possesses the same number of conjugated $\pi$-electron as the system. Based on Eqs. 6, 12' and 13, the relation between $i$ and $V_0$ can be derived as follows:

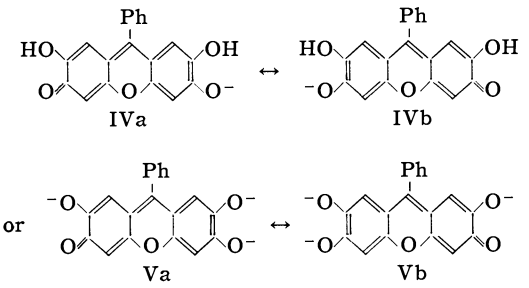
9) L. Pauling, "The Nature of the Chemical Bond", Cornell Univ. Press, Ithaca, N. Y. (1939).

$$1-i=(0.044\ V_0+0.006\ V_0^2)/(x_n-0.5) \quad (14)$$

The absorption maximum of the dye-metal complex is also connected with the ionic character of the dye-metal bond through $V_0$ in Eqs. 1 and 14.

### Application to Experimental Results

It is necessary to know the conjugated system responsible for the absorption maximum of the dye anion to calculate the length of the conjugated chain, $L$, based on the number of $\pi$-electrons in the system. The phenylfluorone anion is considered to be resonating between IVa and IVb or Va and Vb, each of which makes the same contribution to the normal state of the anion, because of its symmetrical structure.

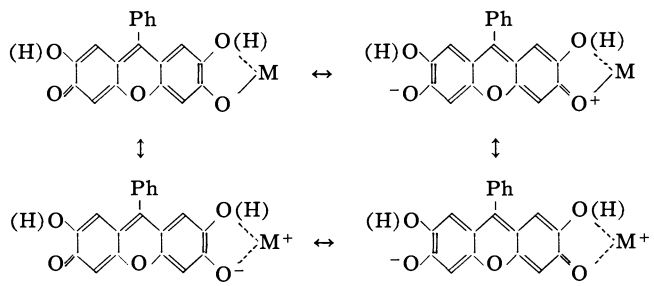



In the present study, $L$ was calculated from the observed wavelength of the absorption maximum of the phenylfluorone anion ($N=12$, and $V_0=0$ based on the following equation,

$$\lambda_{max}=\frac{8mc}{h}\cdot\frac{L^2}{N+1} \quad (1')$$

and this value was used in calculating the value of $V_0$ for the metal chelates.

The possible structures of phenylfluorone metal chelate**** are




The wavelength of absorption maxima of the 2,3,7-trihydroxy-9-phenylfluorone chelates were shown in Table II together with other properties.

As is found in Table II, the shift of the absorption maximum is rather independent of the ionic radii of metals. This suggests that the electrostatic effect on the shift is not predominant in this case.

In the previous work[5] the author showed empirically that $V_0$ of each phenylfluoronate increased with the decrease in the ionic character estimated from the difference of electronegativity between metal and oxygen atoms. The value of the ionic character obtained through the process

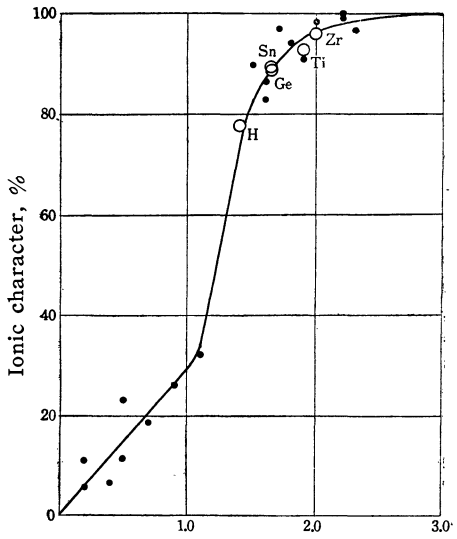



Fig. 3[10]. Relation between electronegativity difference and ionic character in the chelating bond.
○ Data obtained from metal phenylfluoronate.
● Values obtained from nuclear quadrupole coupling data by Dailey and Townes.

**** The infrared spectrum data of germanium phenylfluoronate support this structure: M. Shima, *J. Chem. Soc. Japan, Pure Chem. Soc.* (*Nippon Kagaku Zasshi*), **79**, 1049 (1958).

TABLE II

| Metal | $\lambda_{max}$ Å | Reagent/Metal | $V_0$ (eV.) | $i$ | Ionic radius[a] Å | Electronegativity[b] |
|---|---|---|---|---|---|---|
| H | 4680 | — | 0.473 | $0.77_7$ | — | 2.1 |
| Ge | 5080 | 2 : 1 | 0.246 | $0.88_8$ | 0.53~0.52 | 1.8~1.9 |
| Si | 5100 | — | 0.236 | $0.89_2$ | 0.71 | 1.8~1.9 |
| Ti | 5250 | 2 : 1 | 0.160 | $0.92_3$ | 0.68 | 1.6 |
| Zr | 5400 | 4 : 1 | 0.0891 | $0.95_8$ | 0.80~0.828 | 1.5 |
| Ionic | 5600 | — | 0 | $1.00_0$ | — | — |

a) L. Pauling, *J. Am. Chem. Soc.*, **49**, 765 (1927); E. Kordes, *Z. physik. Chem.*, **B48**, 91 (1941).
b) H. O. Pritchard and H. A. Skinner, *Chem. Revs.*, **55**, 745 (1955).

mentioned above is shown in Fig. 3, together with the results obtained from the nuclear quadrupole coupling data by Dailey and Townes[11], for comparison.

The agreement between two independent results is too close to be accidental. This will be due to the fact that the metal-dye chelate has the structure in which the electrostatic effect by metal is negligibly small, and the effect of the perturbation caused by metal is predominant.

Some phenylfluorone derivatives which possess some substituent in the phenyl group react with metals, and the relationship among the absorption maxima of the metal chelates is similar to that in the phenylfluorone metal chelates[12].

## Experimental

Metal solutions were prepared from metal oxides (germanium, titanium), chloride (tin), or oxychloride (zirconium), and standardized gravimetrically. These stock solutions contain sufficient amounts of hydrochloric acid to prevent the hydrolysis of metals, being free from foreign ions. A working solution was prepared by dilution of an aliquot of each stock solution with water or dilute hydrochloric acid.

Phenylfluorone solution was prepared by dissolving 0.120 g. of phenylfluorone in 150 ml. of ethanol containing 1 ml. of 5.0 N hydrochloric acid, and the resulting solution was diluted to 200 ml. with ethanol.

Absorbance values of the sample and the blank solution were measured with a Beckman Model DU spectrophotometer, using 1 cm. glass cells. Distilled water or blank solution was used as a reference solution. The absorption maxima show practically no variation with the change in the acidity of the solution or the amount of the dyes and metals in solution[14].

## Summary

The absorption spectra of phenylfluorone-fourth group metal chelates were investigated by the acid of Kuhn's free electron gas model method. If the chelating bond formation does not cause an essential change in the $\pi$-electron system of the dye molecule, in the more ionic chelating bond, the absorption maximum of the chelate must be closer to the maximum wavelength of the dye anion. Based on the conception in valence-bond method and ionic-covalent resonance, it was theoretically and experimentaly shown that there was a certain relationship between the absorption maximum wavelength of the chelate and the ionicity of the chelating bond. (The ionicity of the bond was estimated from the difference of electronegativity between the metal and the terminal oxygen atom). The results obtained here for the relationship between the ionicity and the electronegativity difference show too close an agreement with the results obtained from the nuclear quadrupole coupling data by Dailey and Townes.

The author is indebted to Dr. Kenjiro Kimura, Professor Emeritus, and Professor Nobufusa Saito in this laboratory, for their generous encouragement in carrying out this study. The author is also grateful for a grant from the Ministry of Education.

*Department of Chemistry*
*Faculty of Science*
*The University of Tokyo*
*Hongo, Tokyo*

10) As the value of electronegativity, Dailey and Townes adopted the value reported by Huggins[13], but the author adopted here the value reported by Pritchard and Skinner as "best value" (see Table II). The value of electronegativity for the quadrupole spectrum data in Fig. 3 was rearranged in accordance with Pritchard and Skinner's scale.
11) B. P. Dailey and C. H. Townes, *J. Chem. Phys.*, **23**, 118 (1955).
12) H. Sano, This Bulletin, **30**, 672 (1957); **31**, 974 (1958).
13) M. J. Huggins, *J. Am. Chem. Soc.* **75**, 4123 (1953).
14) For other detailed procedures and experimental descriptions, see previous work of the present author[5].

# *Studies on the Chemical Constitution of Agar-agar. XXI*[1]. *Re-investigation of Methylated Agarose of Gelidium Amansii*

By Choji ARAKI and Susumu HIRASE

(Received August 24, 1959)

It has been suggested by Araki[2], one of the present authors, that agar is a mixture of at least two different polysaccharides, one of which is termed agarose having a linear structure composed alternatively of β-D-galactopyranose and 3,6-anhydro-α-L-galactopyranose residues. The structure assignment to the agarose has been partly based on the fact that complete methanolysis of methylated agarose led to the isolation of methyl 2,4,6-tri-*O*-methyl-D-galactoside[3,4] and 2-*O*-methyl-3,6-anhydro-L-galactose dimethylacetal[5]. But the separation of the cleavage fragments was incomplete and the latter fragment was isolated only in a yield insufficient to interpret the whole molecule of agarose. This paper is concerned with the examination of the agarose structure by carefully re-investigating the methanolysis products of methylated agarose prepared from the *Gelidium amansii* agar.

Following the complete methanolysis of the methylated polysaccharide with 3% methanolic hydrogen chloride, the products were separated into neutral and acidic components by means of ion-exchange resins. The acidic component was obtained in too small a yield to be of structural significance. The mixture of neutral sugar derivatives was solved into its components by fractionation with petroleum ether followed by chromatography on charcoal-Celite columns. The mixture was found to contain methyl 2-*O*-methyl-3,6-anhydro-β-L-galactopyranoside in addition to the previously isolated 2-*O*-methyl-3,6-anhydro-L-galactose dimethylacetal and methyl 2,4,6-tri-*O*-methyl-D-galactoside. It was of significance to observe that, well in agreement with the fore-going Araki's formula of agarose, the 2-*O*-methyl-3,6-anhydro-L-galactose derivatives could be obtained in molar quantities equivalent to the 2,4,6-tri-*O*-methyl-D-galactose derivative.

The methyl 2-*O*-methyl-3,6-anhydro-β-L-galactopyranoside, a new compound, was obtained as crystals, melting at 67~69°C and showing a specific rotation $[\alpha]_D^{12}$ +66° in water. Its structure was assigned by the rotation, by the hydrolysis to give 2-*O*-methyl-3,6-anhydro-L-galactose, which was identified as crystalline 2-*O*-methyl-3,6-anhydro-L-galactonic acid and its methyl ester and amide, and by further methylation to give crystalline methyl 2,4-di-*O*-methyl-3,6-anhydro-β-L-galactoside. The finding of the methyl 2-*O*-methyl-3,6-anhydro-β-L-galactopyranoside among the methanolysis products of the methylated agarose accounts for the direct origin of methyl 2,4-di-*O*-methyl-3,6-anhydro-β-L-galactoside, which had been isolated[6] after methanolysis and subsequent re-methylation of the methylated polysaccharide.

If the agarose molecule were branched, it would be expected that either methyl di-*O*-methyl-D-galactoside or 3,6-anhydro-L-galactose dimethylacetal or both would be derived from units of branch points when the methylated polysaccharide was subjected to methanolysis. In spite of careful examination, however, neither of them could be detected among the methanolysis products under investigation. It is therefore convincing that the molecule is a chain as previously suggested by Araki[2]. As for the non-reducing end of the chain, repeated experiments failed to detect any of the fully methylated component sugars among the methanolysis products of the methylated polysaccharide with the exception of only one experiment, in which 2,3,4,6-tetra-*O*-methyl-D-galactose was isolated as its crystalline aniline derivative in a yield of twelve milligrams from fifteen grams of the methylated polysaccharide. This exception, however, suffers from the

1) Part XX: C. Araki and K. Arai, This Bulletin, **30**, 287 (1957).
2) C. Araki, This Bulletin, **29**, 543 (1956); *Memoirs Fac. Ind. Arts, Kyoto Tech. Univ.*, **5**, 21 (1956).
3) C. Araki, *J. Chem. Soc. Japan (Nippon Kwagaku Kwaishi)*, **58**, 1362 (1937).
4) E. G. V. Percival and J. C. Somerville, *J. Chem. Soc.*, **1937**, 1615.
5) C. Araki, *J. Chem. Soc. Japan (Nippon Kwagaku Kwaishi)*, **61**, 775 (1940).
6) (a) C. Araki, ibid., **59**, 304 (1938). (b) C. Araki and K. Arai, ibid., **61**, 503 (1940). (c) S. Hands and S. Peat, *Nature*, **142**, 797 (1938). (d) E. G. V. Percival, J. C. Somerville and I. A. Forbes, ibid., **142**, 797 (1938).

possibility that the polysaccharide molecule might have been degraded before or during the methylation process. Percival and his coworkers reported, that no tetra-*O*-methyl-D-galactose could be detected among the products of hydrolysis of the methylated polysaccharide[7]. Consequently, it may be still difficult at this time to decide whether D-galactose and 3,6-anhydro-L-galactose constitutes the non-reducing end of the molecule. In any case, since the end group, if present, would exist only in a trace quantity, it seems likely that agarose is a chain with a very high degree of polymerization, although the possibility is not completely excluded yet that the polysaccharide may have an endless, closed loop-structure.

In connection with the methylation data mentioned above, the information concerning the paper chromatography of the methylated derivatives of 3,6-anhydro-L-galactose is also reported here in. Cyclohexanol saturated with water was found to serve as an effective solvent for separating the anhydrosugar derivatives, the spots of which could be easily revealed when chromatograms were sprayed with an *o*-aminophenol reagent previously reported from this laboratory[8]. Table I shows the $R_f$ values and the colors of spots observed by this method for some available samples of the anhydrosugar derivatives.

TABLE I. PAPER CHROMATOGRAPHY OF SOME 3,6-ANHYDRO-L-GALACTOSE DERIVATIVES

| Compound | $R_f$ | Color |
|---|---|---|
| Methyl 2-*O*-methyl-3,6-anhydro-$\beta$-L-galactopyranoside | 0.77 | brown |
| 2-*O*-Methyl-3,6-anhydro-L-galactose dimethylacetal | 0.67 | brown |
| Methyl 2,4-di-*O*-methyl-3,6-anhydro-$\beta$-L-galoctoside | 0.84 | brown |
| 2,4-Di-*O*-methyl-3,6-anhydro-L-galactose dimethylacetal | 0.84 | yellow |
| 2,5-Di-*O*-methyl-3,6-anhydro-L-galactose dimethylacetal | 0.84 | brown |

Filter paper used: Tōyō Filter Paper No. 52.
Developing solvent: cyclohexanol saturated with water.
Spraying reagent: *o*-aminophenol in aqueous ethanol acidified with phosphoric acid[8].

## Experimental

**General Procedure.**—Evaporation and concentration of solutions were carried out below 40°C under reduced pressure. Specific rotations were measured in aqueous solutions unless otherwise stated. Melting points are uncorrected.

**Paper Chromatography.**—Paper chromatograms were run in cyclohexanol saturated with water and sprayed with *o*-aminophenol in aqueous ethanol acidified with phosphoric acid[8] for the purpose of identifying 3,6-anhydro-L-galactose derivatives; while, they were run in *n*-butanol-ethanol-water (4 : 1 : 2 V./V.) and sprayed with aniline hydrogen phthalate in moist *n*-butanol[9] for the purpose of identifying reducing D-galactose derivatives.

**Methylated Agarose.**—Methylated agarose was prepared by acetylating the *Gelidium amansii* agar with acetic anhydride and pyridine, extracting the agarose acetate from the resulting acetylation products with chloroform and then treating the agarose acetate repeatedly with dimethylsulfate and sodium hydroxide as previously described by Araki[10], one of the present writers. The methoxyl value found was 33.8% in reasonable agreement with the value 34.3% calculated for $[C_{12}H_{14}O_5(OCH_3)_4]_n$.

**Methanolysis of Methylated Agarose and Separation of Neutral and Acidic Components.**—Methylated agarose (15.0 g.) was suspended in 3% methanolic hydrogen chloride (100 ml.) and heated under reflux for 35 hr. The resulting brown solution was neutralized with silver carbonate, filtered and evaporated to a sirup. It was then dissolved in 0.2 N barium hydroxide solution (100 ml.) and heated for 2 hr. at 60°C to saponify the methyl ester of the acidic component. After removal of the excess of barium hydroxide by neutralization with carbon dioxide and subsequent filtration, the solution was allowed to pass through columns of Amberlite IR-120 (80 ml.) and IR-4B (100 ml.) in succession, and the columns were thoroughly washed with water. The effluent and washings were combined and evaporated to dryness, when the mixture of neutral sugar derivatives was obtained as a colorless sirup; yield, 15.2 g., $[\alpha]_D^{20}+60.0°$ ($c$ 1.20).

The anion-exchange resin used above was transferred to a beaker, stirred with 2 N sulfuric acid (100 ml.) for a few minutes under ice-cooling to displace the acidic component, and re-transferred to a glass tube to form a column. After the excess of the liquid was allowed to drain from the column, the resin was washed with additional 40 ml. of 2 N sulfuric acid followed by water (600 ml.). All the effluents and washings were combined and immediately neutralized with a saturated barium hydroxide solution, the precipitates of barium sulfate were removed by filtration, and the filtrate was evaporated to dryness. The acidic component in a barium salt form was obtained as a thick sirup; yield, 0.42 g., $[\alpha]_D^{20}$ +2.7° ($c$ 0.75). It showed positive color reactions both for ketose and uronic acid. But the yield was so small that no further investigation was carried out.

**Fractionation of the Neutral Components with Petroleum Ether.**—The mixture of the neutral

7) E. G. V. Percival and T. G. H. Thomson, *J. Chem. Soc.*, **1942**, 750.
8) S. Hirase, C. Araki and S. Nakanishi, This Bulletin, **26**, 183 (1953).
9) S. M. Partridge, *Nature*, **164**, 443 (1949).
10) C. Araki, *J. Chem. Soc. Japan* (*Nippon Kwagaku Kwaishi*), **58**, 1338, 1351 (1937).

sugar derivatives (15.2 g.) obtained above was dissolved in water (80 ml.). The solution was continuously extracted with petroleum ether (b. p. 30~37°C) for 30 hr. in a Soxhlet's apparatus. The extract was evaporated to a thin sirup, which on standing crystallized partly; yield, 2.05 g., $[\alpha]_D^{22}$ +76.1° (*c* 0.71). The residual aqueous solution was also evaporated to a sirup; yield, 13.0 g., $[\alpha]_D^{22}$ +56.0° (*c* 1.0).

**Chromatographic Separation of the Components Insoluble in Petroleum Ether.**—One third quantity of the petroleum ether-insoluble components obtained above was chromatographed at 20~22°C on a column (5.2×22 cm.) packed with a mixture of charcoal (50 g.) and Celite (40 g.). The solvents used for elution were water and ethanol of successively increasing concentrations in water. The effluents were collected of every one liter in separate receivers and concentrated to give 100 ml. fractions, which were then examined both polarimetrically and paper chromatographically. The fractions showing the same contents were combined and evaporated to recover components, which were then purified by dissolution in acetone, filtration and re-evaporation to a constant weight. The total recovery amounted to 4.12 g. or 93% of the applied sample. The recovered components were determined for methoxyl content and specific rotation. The results are shown in Table II. None of the fractions showed on a paper chromatogram the presence of non-methylated or fully methylated 3,6-anhydro-L-galactose derivatives, which might be, derived from units of branch points or the non-reducing end of the methylated polysaccharide molecule, respectively.

**Identification of the Components Insoluble in Petroleum Ether.**—*(a) 2-O-Methyl-3,6-anhydro-L-galactose Dimethylacetal.*—Fraction II in Table II was a colorless sirup showing a refractive index $n_D^{25}$ 1.4620. When examined on a paper chromatogram, it showed a single spot having $R_f$ 0.67. The methoxyl value found was in good agreement with the value 41.90% calculated for $C_6H_9O_3 \cdot (OCH_3)_3$. The fraction was therefore considered to be pure 2-*O*-methyl-3,6-anhydro-L-galactose dimethylacetal. One of the present writers has reported $[\alpha]_D^{8}$ −13.79° and $n_D^{25}$ 1.4647 about the previously isolated sample of 2-*O*-methyl-3,6-anhydro-L-galactose dimethylacetal[5].

Fraction III in Table II was a colorless sirup, which on standing crystallized partly. When examined on a paper chromatogram, it showed the presence of two spots having $R_f$ 0.67 and 0.77, respectively, one agreed with the dimethylacetal obtained above, the other with methyl 2-*O*-methyl-3,6-anhydro-β-L-galactopyranoside. Since the optical rotations of these pure compounds are −30.7° and +66.0°, respectively, as reported herein, the fraction was considered to be a mixture of 28% of the dimethylacetal (0.14 g.)

TABLE II. CHROMATOGRAPHIC SEPARATION OF THE COMPONENTS INSOLUBLE IN PETROLEUM ETHER

| | Receiver number | Solvent* | Yield g. | $[\alpha]_D^{22}$ ° ($H_2O$) | $OCH_3$ % | Identified component** |
|---|---|---|---|---|---|---|
| I | 1— 3 | W | nil | — | — | — |
| II | 4— 8 | 2.5% E | 1.10 | −30.7 | 42.37 | A |
| III | 9—10 | 2.5% E | 0.50 | +40.3 | 38.15 | A (28%) + B (72%) |
| IV | 11—12 | 5 % E | 0.19 | +66.7 | 32.83 | B |
| V | 13—15 | 5 % E | 0.22 | +92.8 | 44.65 | B (40%) + C (60%) |
| VI | 16—21 | 7.5% E | 0.77 | +110.2 | 52.25 | C |
| VII | 22—28 | 10 % E | 0.90 | +110.9 | 52.32 | C |
| VIII | 29—33 | 15 % E | 0.06 | +111.0 | 52.35 | C |
| IX | 34—38 | 25 % E | 0.25 | −29.0 | 43.11 | ? |
| X | 39—41 | 50 % E | 0.13 | +35.3 | 39.37 | ? |

* W: Water; E: Ethanol.

** A: 2-*O*-Methyl-3,6-anhydro-L-galactose dimethylacetal;
B: Methyl 2-*O*-methyl-3,6-anhydro-β-L-galactopyranoside;
C: Methyl 2,4,6-tri-*O*-methyl-α, β-D-galactoside.

TABLE III. CHROMATOGRAPHIC SEPARATION OF THE COMPONENTS SOLUBLE IN PETROLEUM ETHER

| | Receiver number | Solvent* | Yield g. | $[\alpha]_D^{22}$ ° ($H_2O$) | $OCH_3$ % | Identified components** |
|---|---|---|---|---|---|---|
| I | 1— 3 | 2.5% E | — | — | — | — |
| II | 4— 7 | 5 % E | 0.60 | +71.7 | 48.40 | B (70%) + C (30%) |
| III | 8— 9 | 5 % E | 1.22 | +88.9 | 52.22 | C |
| | 10—14 | 7.5% E | | | | |
| | 15—19 | 10 % E | | | | |
| IV | 20—24 | 15 % E | 0.04 | +96.0 | — | C + D (?) |
| | 25—28 | 30 % E | | | | |

* E: Ethanol.

** B: Methyl 2-*O*-methyl-3, 6-anhydro-β-L-galactopyranoside;
C: Methyl 2,4,6-tri-*O*-methyl-α, β-D-galactoside;
D: Methyl 2,3,4,6-tetra-*O*-methyl-D-galactoside.

and 72% of the methyl glycoside (0.36 g.). This proportion is in agreement with that calculated on the basis of methoxyl values. For the actual separation, the fraction was re-chromatographed on a column (2.5×20 cm.) of charcoal-Celite at 20~22°C. The dimethylacetal was eluted from the column chiefly with 4% ethanol in water; yield, 0.10 g., $[\alpha]_D^{17}$ −30.3° (*c* 0.54), $n_D^{25}$ 1.4615, $OCH_3$ 41.27%; while, the methyl glycoside was removed from the column with 6% ethanol in water and was obtained as crystals; yield, 0.31 g., m. p. 65~67°C, $[\alpha]_D^{17}$ +66.0° (*c* 0.50). Admixture with the sample obtained from fraction IV described below showed no depression of the melting point.

For the identification of 2-*O*-methyl-3,6-anhydro-L-galactose dimethylacetal, the following experiments were carried out:

*i) 2-O-Methyl-3,6-anhydro-L-galactose.* — 2-*O*-Methyl-3,6-anhydro-L-galactose dimethylacetal (0.40 g.) in 0.02 N sulfuric acid (20 ml.) was heated in a boiling water bath for 2 hr., at which time the rotation of the solution reached a constant value ($[\alpha]_D$ −31°→−10°). The solution was neutralized with barium carbonate, filtered and evaporated to a sirup which was then dissolved in acetone. Filtration and evaporation of the acetone solution afforded 2-*O*-methyl-3,6-anhydro-L-galactose as a colorless sirup; yield, 0.35 g., $[\alpha]_D^{12}$ −14.3° (*c* 0.63), $n_D^{25}$ 1.4870, $OCH_3$; found: 17.45% (calcd. for $C_6H_9O_4(OCH_3)$: 17.59%). It reduced a Fehling solution at room temperature and restored the color to a Schiff's reagent. One of the present writers has reported $[\alpha]_D^{34}$ +33.9° of the sugar[5]. The previously reported value in a positive direction seems to be ascribed to some contaminants.

*ii) 2-O-Methyl-3,6-anhydro-L-galactonic acid.*— The reducing sugar (0.30 g.) obtained above was dissolved in water (5 ml.) and bromine (0.4 ml.) was added dropwise during 4 hr. to the solution kept at 40°C. The treatment of the solution in the usual manner afforded 2-*O*-methyl-3,6-anhydro-L-galactonic acid; yield, 0.35 g., m. p. 137~140°C. Recrystallization twice from ethyl acetate furnished the pure compound; m. p. and mixed m. p. 141~142°C, $[\alpha]_D^{12}$ −70.3° (*c* 0.84). One of the present writers has reported m. p. 142°C and $[\alpha]_D^{12}$ −70.0° for 2-*O*-methyl-3,6-anhydro-L-galactonic acid[5].

Found: C, 43.63; H, 6.32; $OCH_3$, 16.34. Calcd. for $C_6H_9O_5(OCH_3)$: C, 43.75; H, 6.27; $OCH_3$, 16.15%.

*iii) Methyl 2-O-methyl-3,6-anhydro-L-galactonate.* —The acid obtained above was converted to the methyl ester by the reaction with methanolic hydrogen chloride in the usual manner. The resulting methyl ester was recrystallized from benzene, forming stout needles; m. p. 90~91°C, $[\alpha]_D^{12}$ −70.8° (*c* 1.06). One of the present writers has reported about m. p. 91°C[1,5] $[\alpha]_D^{10}$ −55.3°[5] and $[\alpha]_D^{24}$ −61.6°[1].

Found: C, 46.54; H, 7.02; $OCH_3$, 30.23. Calcd. for $C_8H_{14}O_6$: C, 46.60; H, 6.84; $OCH_3$, 30.12%.

*iv) 2-O-Methyl-3,6-anhydro-L-galactonamide.* — The amide was prepared from the methyl ester obtained above by the reaction with methanolic ammonia and purified by recrystallization from ethanol; m. p. 171~172°C, $[\alpha]_D^{12}$ −75.4° (*c* 0.53). Araki and Arai have reported m. p. 170~171°C and $[\alpha]_D^{23}$ −74.3° for the amide[1].

Found: C, 43.88; H, 6.95; $OCH_3$, 16.01. Calcd. for $C_7H_{13}O_5N$: C, 43.97; H, 6.85; $OCH_3$, 16.23%.

*(b) Methyl 2-O-Methyl-3,6-anhydro-β-L-galactopyranoside.*—Fraction IV in Table II crystallized completely on standing and melted at 64°C. It showed on a paper chromatogram as a single spot having $R_f$ 0.77. This was combined with the crystals obtained by re-chromatography of fraction III described above and was recrystallized twice from petroleum ether, affording pure methyl 2-*O*-methyl-3,6-anhydro-β-L-galactopyranoside as elongated prisms; m. p. 67~69°C, $[\alpha]_D^{12}$ +66.0° (*c* 1.00).

Found: C, 50.49; H, 7.46; $OCH_3$, 32.55; mol. wt. (Rast), 190. Calcd. for $C_6H_8O_3(OCH_3)_2$: C, 50.52; H, 7.42; $OCH_3$, 32.65%; mol. wt., 190.2.

The structure assignment to this compound has been based on the following experiments:

*i) 2-O-Methyl-3,6-anhydro-L-galactose.* — The methyl glycoside (0.20 g.) obtained above was hydrolyzed with 0.02 N sulfuric acid (20 ml.) for 2 hr. during which time the specific rotation of the solution changed from +66° to −11°, the final value being in good agreement with that observed when 2-*O*-methyl-3,6-anhydro-L-galactose dimethyl-acetal was hydrolyzed. The resulting 2-*O*-methyl-3,6-anhydro-L-galactose was isolated in the same manner as described already; yield, 0.15 g., $[\alpha]_D^{12}$ −15.0° (*c* 0.50), $n_D^{25}$ 1.4867; $OCH_3$ found 17.50%. The sugar was identified as 2-*O*-methyl-3,6-anhydro-L-galactonic acid and its methyl ester and amide in exactly the same manner as described already.

*ii) Methyl 2,4-di-O-methyl-3,6-anhydro-β-L-galactoside.* — Methyl 2-*O*-methyl-3,6-anhydro-β-L-galactopyranoside (0.08 g.) was dissolved in methyl iodide (4 ml.), silver oxide (3 g.) added, and the mixture was refluxed for 6 hr. The reaction mixture was diluted with dry acetone and filtered. Evaporation of the filtrate afforded methyl 2,4-di-*O*-methyl-3,6-anhydro-β-L-galactoside melting at 81~82°C, which was then recrystallized from petroleum ether; yield, 0.07 g., m. p. and mixed m. p. 83°C, $[\alpha]_D^{10}$ +76.7° (*c* 0.60). Methyl 2,4-di-*O*-methyl-3,6-anhydro-β-L-galactoside has been recorded as: m. p. 83°C and $[\alpha]_D^{14}$ +78.1°[6a]; m. p. 82~83°C and $[\alpha]_D$ +73.0°[6c] and m. p. 81°C and $[\alpha]_D$ +75.0°[6d].

Found: C, 53.02; H, 7.88; $OCH_3$, 45.45. Calcd. for $C_6H_7O_2(OCH_3)_3$: C, 52.93; H, 7.90; $OCH_3$, 45.59%.

*(c) Methyl 2,4,6-Tri-O-methyl-α,β-D-galactoside.* —All fractions VI—VIII in Table II were obtained as crystals with ill-defined melting points. Examination on paper chromatograms using the *o*-aminophenol reagent revealed no spot, indicating thereby the absence of any 3,6-anhydro-L-galactose derivative. The methoxyl values found were in good agreement with the value 52.52% calculated for $C_6H_8O_2(OCH_3)_4$. These fractions

were therefore composed entirely of methyl 2,4,6-tri-*O*-methyl-$\alpha,\beta$-D-galactoside.

Fraction V in Table II showed a spot corresponding to methyl 2-*O*-methyl-3,6-anhydro-$\beta$-L-galactopyranoside on a paper chromatogram. When the fraction was hydrolyzed with 1 N sulfuric acid for 5 hr. at 98°C, the product showed a single spot corresponding to 2,4,6-tri-*O*-methyl-D-galactose on a paper chromatogram, the anhydrosugar derivative being completely destroyed during the hydrolysis. Fraction V was therefore a mixture of 40% of methyl 2-*O*-methyl-3,6-anhydro-$\beta$-L-galactopyranoside (0.09 g.) and 60% of methyl 2,4,6-tri-*O*-methyl-$\alpha,\beta$-D-galactoside, the proportion being calculated on the basis of the methoxyl values.

*i) 2,4,6-Tri-O-methyl-α-D-galactose.*—Fractions VI—VIII were combined and hydrolyzed with 1 N sulfuric acid (20 ml.) for 4.5 hr. at 98°C. The reaction solution was then treated in the usual manner, when 2,4,6-tri-*O*-methyl-D-galactose was obtained; yield, 1.40 g., m. p. 104~105°C. Paper chromatographic examination indicated the presence of 2,4,6-tri-*O*-methyl-D-galactose only. Recrystallization, twice from ether, furnished the pure compound; m. p. and mixed m. p. 110~111°C, $[\alpha]_D^{15}$ +115.9° (initial)→+90.7° (after 24 hr., constant) (*c* 1.07). The physical constants are in good agreement with literature values[3,4].

Found: C, 48.56; H, 8.30; $OCH_3$, 41.78. Calcd. for $C_6H_9O_3(OCH_3)_3$: C, 48.64; H, 8.16; $OCH_3$, 41.90%.

*ii) 2,4,6-Tri-O-methyl-N-phenyl-D-galactosylamine.*—The tri-*O*-methyl-D-galactose recovered from the mother liquor of recrystallization mentioned above was converted into its aniline derivative in the usual manner[3,4]; m. p. and mixed m. p. 174°C, $[\alpha]_D^{14}$ −120.0° (initial)→−82.0° (constant) in acetone (*c* 0.50).

*(d) Unidentified Components.*—Fractions IX and X in Table II seemed to be methylated disaccharide derivatives having molecular weight, respectively, 423 and 398. The structures will be studied in the subsequent paper.

**Separation and Identification of the Components Soluble in Petroleum Ether.**—*(a) Separation.*—The sirup (2.05 g.), which had been obtained by extracting the neutral components of the methanolysis products with petroleum ether, was chromatographed at 22~24°C on a column (5.0×15 cm.) packed with charcoal (40 g.) and Celite (28 g.) in exactly the same manner as in the separation of the components insoluble in petroleum ether. The results are shown in Table III.

*(b) Identification.*—Fraction II was a colorless sirup, showing a spot corresponding to methyl 2-*O*-methyl-3,6-anhydro-$\beta$-L-galactopyranoside on a paper chromatogram. When it was hydrolyzed with 1 N sulfuric acid for 5 hr. at 98°C, the resulting product showed a spot corresponding to 2,4,6-tri-*O*-methyl-D-galactose on a paper chromatogram, the anhydrosugar derivative being completely destroyed during the hydrolysis. From these facts, fraction II was considered to be a mixture of 70% of methyl 2-*O*-methyl-3,6-anhydro-$\beta$-L-galactopyranoside (0.42 g.) and 30% of methyl 2,4,6-tri-*O*-methyl-D-galactoside (0.18 g.), the proportion being calculated on the basis of the methoxyl values.

Fraction III was proved to be entirely methyl 2,4,6-tri-*O*-methyl-$\alpha,\beta$-D-galactoside in exactly the same manner as in the case of fractions VI—VIII in Table II.

Fraction IV in Table III gave no spot on a paper chromatogram sprayed with an *o*-aminophenol reagent, indicating thereby the absence of any 3,6-anhydro-L-galactose derivative. On hydrolysis it produced 2,4,6-tri-*O*-methyl-D-galactose which was identified on a paper chromatogram. Fraction IV contained therefore methyl 2,4,6-tri-*O*-methyl-$\alpha,\beta$-D-galactoside only. However, a similar fraction obtained from the other batch was found to contain methyl 2,3,4,6-tetra-*O*-methyl-D-galactoside in addition to the tri-*O*-methyl-D-galactose derivative as described below.

**Confirmation of Methyl 2, 3, 4, 6-Tetra-*O*-methyl-D-galactoside.**—From the other batch of methylated agarose (15 g.), there was obtained a fraction similar to fraction IV of Table III; yield, 0.07 g. Paper chromatographic examination indicated the absence of any 3,6-anhydro-L-galactose derivative. The sirup was hydrolyzed with 1 N sulfuric acid (1 ml.) for 4.5 hr. at 98°C and the product was isolated in the usual manner as a colorless sirup; yield, 62 mg. Examination on a paper chromatogram indicated the presence of both 2,4,6-tri-*O*-methyl-D-galactose and 2,3,4,6-tetra-*O*-methyl-D-galactose. The mixture was resolved into the components on a column (2.5×32 cm.) packed with filter paper powder, a 2-butanone-water azeotrope being used as a mobile phase. A faster moving fraction containing the tetra-*O*-methyl-D-galactose was obtained as a sirup; yield, 20 mg., $[\alpha]_D^{10}$ +44.0° (*c* 0.50). It was dissolved in ethanol (1 ml.), aniline (20 mg.) added, and the solution was refluxed for 3 hr., when 2,3,4,6-tetra-*O*-methyl-*N*-phenyl-D-galactosyl amine was obtained; yield, 12 mg., m. p. 186~189°C. Recrystallization from ethanol afforded the pure compound; m. p. and mixed m. p. 192°C, $[\alpha]_D^{13}$ −75.8° (initial) in acetone (*c* 0.132).

Found: $OCH_3$, 40.18. Calcd. for $C_{16}H_{25}O_5N$: $OCH_3$, 40.51%.

**Yields of the Components.**—As shown in Tables II and III, the yields of 2-*O*-methyl-3,6-anhydro-L-galactose dimethylacetal, methyl 2-*O*-methyl-3,6-anhydro-$\beta$-L-galactopyranoside and methyl 2,4,6-tri-*O*-methyl-$\alpha,\beta$-D-galactoside are 3.72, 2.34 and 7.02 g., respectively, when calculated on the basis of the whole neutral components (15.2 g.). Consequently, the molar proportion of the sum of the former two to the last one is 1 : 1.03.

The authors wish to express their hearty thanks to Mr. K. Arai for micro-combustion and to Mr. T. Itō for assistance.

*Institute of Chemistry*
*Faculty of Industrial Arts*
*Kyoto Technical University*
*Matsugasaki, Kyoto*

# *Studies on the Vibrated Dropping Mercury Electrode. II. Electrocapillary Characteristics of the Current-Voltage Curve*

By Hideo IMAI, Shōkichi CHAKI and Senkichi INOUYE

(Received June 8, 1959)

The theory of the limiting current of the vibrated dropping mercury electrode (VDME) has been given in the previous report[1], and it was shown that the limiting current increases about ten times when the mean velocity of the vibration is of the order of several centimeters per second. This result suggests the potentiality of the "VDME" method for improving the sensitivity of polarographic determinations. The surface charge density of the dropping mercury electrode (DME), however, exerts an influence on the velocity of the vibration, and accordingly, it controls the limiting current. Thus, the linear relation of the limiting current with the depolarizer concentration was not always obtained. Moreover, the remarkable effect of surface active materials on the limiting current and the effect of the vibration on the summit potential of a polarographic maximum or on potential of the electrocapillary maximum (the Lippmann-potential) were observed. These results are presented and discussed in this report.

## Experimental

The apparatus used was described in the previous report[1] and was not modified in any detail.

All the reagents were of analytical grade, and were used after the recrystallization. The test solution was prepared in the same way as that described in the previous report[1].

When the reduction potential of a depolarizer was adjoining the Lippmann-potential, the plateau of the limiting current was not well-defined. On this occasion, the limiting current was measured at a potential optionally determined.

The increase in the current-sensitivity owing to the vibration was expressed by the ratio, $(i_l/i_d)$, of the limiting current against the diffusion-controlled current measured at the same potential. All measurements were made at 25.0±0.1°C.

1) H. Imai, S. Inouye and S. Chaki, This Bulletin, **32**, 994 (1959).

## Results and Discussion

**1. Variation of Limiting Current with Depolarizer Concentration.**—This relation was investigated in the cases of the mercuric, thallous, cadmium, nickel and zinc ions. The concentration ranged from 0.005 to 10 mF. The test solution contained 0.1 F potassium chloride or potassium nitrate as the supporting electrolyte, and a small

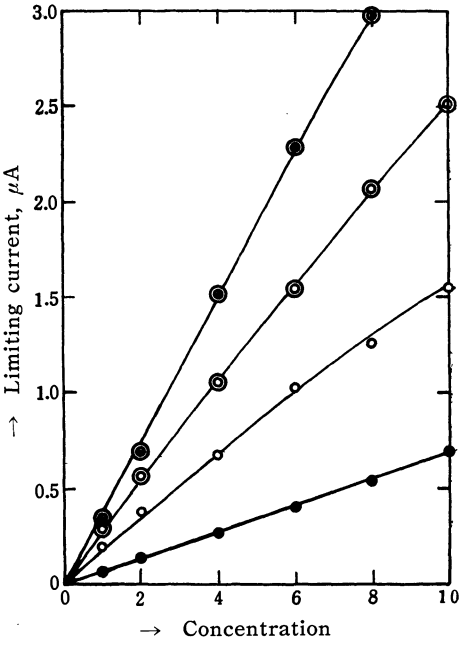



Fig. 1. The variation of the limiting current with the concentration of the zinc ion.
●: $i_d$ of $10^{-3}$, $10^{-4}$ and $10^{-5}$ F order
○: $i_l$ of $10^{-3}$ F order
◎: $i_l$ of $10^{-4}$ F order
◉: $i_l$ of $10^{-5}$ F order
The value of the current in the ordinate must be multiplied by the factor of 100, 10 and 1 μA for the concentration order of $10^{-3}$, $10^{-4}$ and $10^{-5}$ F, respectively. $E$= 0.38 V./cm. (25 c. p. s.). $m$=1.81 mg./sec. $t$=4.1$_9$ sec. (open circuit). The supporting electrolyte=0.1 F KCl. The limiting current was evaluated at −1.2 V. vs. S. C. E.

TABLE I. THE VARIATION OF THE RATIO, $i_l/i_d$, WITH THE DEPOLARIZER CONCENTRATION (25°C)

| Depolarizer concentration, mF | $i_l/i_d$ | | | | |
|---|---|---|---|---|---|
| | $Hg^{2+}$ in KCl | $Tl^{+}$ in $KNO_3$ | $Cd^{2+}$ in KCl | $Ni^{2+}$ in $KNO_3$ | $Zn^{2+}$ in $KNO_3$ |
| 10 | — | — | — | — | 2.0 |
| 5 | — | — | — | — | 2.5 |
| 1 | 5.7 | 3.0 | 3.2 | 3.3 | 3.5 |
| 0.5 | 5.6 | 2.8 | 3.4 | 3.8 | 4.3 |
| 0.1 | 5.7 | 2.8 | 3.3 | 4.0 | 5.0 |
| 0.05 | 5.6 | 2.7 | 3.2 | 4.3 | 6.0 |
| 0.01 | — | 2.8 | 3.2 | 4.6 | 7.0 |
| 0.005 | — | 2.6 | 3.4 | 4.8 | — |
| $E$, V./cm. | 0.4 | 0.38 | 0.38 | 0.38 | 0.38 |
| $t$, sec. | 8.3 | 6.2 | 6.2 | 6.1 | 4.2 |
| $m$, mg./sec. | 0.74 | 1.33 | 1.34 | 1.48 | 1.81 |

$E$ is the intensity of the a. c. electric field (25 c. p. s.), $t$ is the life-time of the DME and $m$ is the rate of mercury flow.

quantity of the sodium sulfite solution was added to remove the trace of dissolved oxygen.

In the cases of the mercuric ion, the thallous ion and the cadmium ion, the plateau of the limiting current was not obtained. This is because the surface charge density of the DME markedly varies near Lippmann-potential which is adjacent to the reduction potential of the depolarizer in question. On the contrary, the nickel ion and the zinc ion developed a fairly well-defined wave except for the increase of the residual current.

The variation of the ratio, $i_l/i_d$, with the depolarizer concentration is given in Table I.

In the former three depolarizers of Table I, the value of $i_l/i_d$ does not appreciably change with the depolarizer concentration. On the contrary, the value of $i_l/i_d$ is inversely proportional to the depolarizer concentration in the latter two depolarizers, and a curvilinear plot of the limiting current versus the concentration is obtained as is shown in Fig. 1.

In this connection, the variation of the life-time of the DME with the depolarizer concentration was investigated, and the result is illustrated in Table II.

TABLE II. THE VARIATION OF THE LIFE-TIME OF THE DME WITH THE CONCENTRATION OF THE ZINC ION (25°C)

| Concentration of the zinc ion, mF | Life-time of the DME, sec. | |
|---|---|---|
| | Open circuit | At −1.2 V. vs. S. C. E. |
| 8 | $4.5_6$ | $4.4_2$ |
| 1 | $4.5_6$ | $4.3_7$ |
| 0.2 | $4.5_7$ | $4.3_4$ |
| 0.01 | $4.5_7$ | $4.2_4$ |
| 0.001 | $4.5_7$ | $3.8_4$ |

In Table II the life-time measured in the open circuit is independent of the depolarizer concentration, while the life-time measured at the more negative potential than the reduction potential of the zinc ion increases as the depolarizer concentration is increased.

The increase of the life-time can be assigned to the increase of the surface tension of the DME.

The surface tension increases as the surface-charge density decreases and the decrease of the surface charge density results in the retardation of the vibration. Thus, the curvilinear relation of Fig. 1 is attributable to the effect of the reductant on the surface charge density of the DME.

**2. Effect of Surface Active Materials.**—*2-i. Variation of limiting current with concentration of surface active materials.*—The variation of the limiting current of 1 mF zinc ion with the concentration of the surface active material such as gelatine, methyl cellulose or polyoxyethylene lauryl ether (LEO, the mean molecular weight= 862) was investigated. The result is illustrated in Fig. 2. In every case the effect of the vibration diminishes by the addition of the surface active material, the limiting current being reduced to the value of the diffusion-controlled current by the addition up to about 0.01%. This effect is attributable to the retardation of the vibration due to the decrease of the surface-charge density. The effect of gelatine is more pronounced than that of methyl cellulose, and the difference of the curvilinear relation in Fig. 2 seems to relate to the adsorption mechanism of the surface

active material on the mercury surface.

*2-ii. Current-voltage curve accompanied with adsorption and desorption of surface acitve material.* — The effect of *n*-octyl alcohol on the current-voltage curve of 1 mF mercuric ion in 0.1 F potassium chloride was investigated. The limiting current markedly changes at two potentials which lie in the region of the anodic polarization and in the region of the cathodic polarization as is illustrated in Fig. 3. The potential of the current change at about −0.2 V. vs. S. C. E. and that of the current change at about −1.5 V. vs. S. C. E. correspond to the potential of the adsorption and that of the desorption of *n*-octyl alcohol, respectively, as is seen in comparison with the tensammetric curve appended in Fig. 3. From the fact that the limiting current changes with the adsorption or the desorption of the surface active material as is previously described in *2-i*, it is concluded that the change of the limiting current at about −0.2 V. vs. S. C. E. and that at about −1.5 V. vs. S. C. E. correspond to the decrease of the anodic current of the chloride ion owing to the adsorption of *n*-octyl alcohol and to the increase of the cathodic current of the mercuric ion owing to the desorption of *n*-octyl alcohol, respectively.

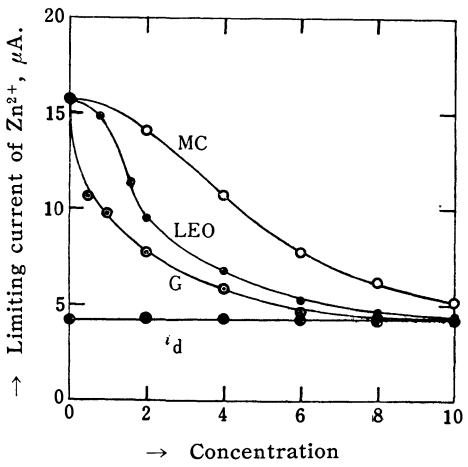



Fig. 2. The variation of the limiting current of the zinc ion with the concentration of the surface active material. The value of the concentration in the abscissa must be multiplied by the factor of $10^{-3}$ % for gelatine (curve G) and methyl cellulose (curve MC) or by the factor of $2.5\times10^{-6}$ F for LEO. $(Zn^{2+})=1\times10^{-3}$ F. Refer the illustration given in Fig. 1 to the other experimental conditions.

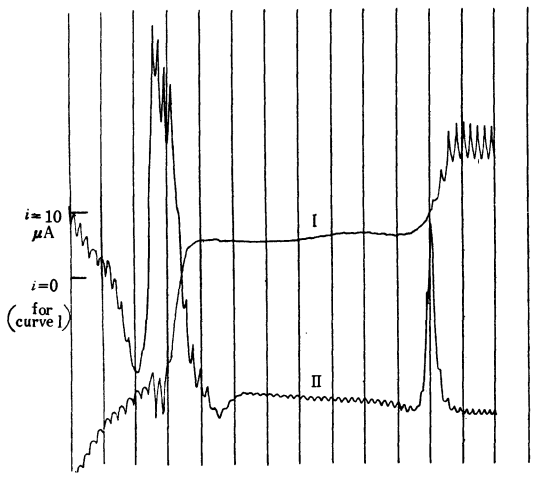



Fig. 3. The "VDME" current-voltage curve of the mercuric ion in the presence of *n*-octyl alcohol (curve I). $(Hg^{2+})=1\times10^{-3}$ F. The supporting electrolyte=0.1 F KCl. Curve II is the tensammetric curve of the same solution. The applied voltage starts from +0.2 V. vs. S. C. E., and each voltage interval corresponds to 0.15 V.

*2-iii. Dependence of limiting current to frequency of vibration and to concentration of*

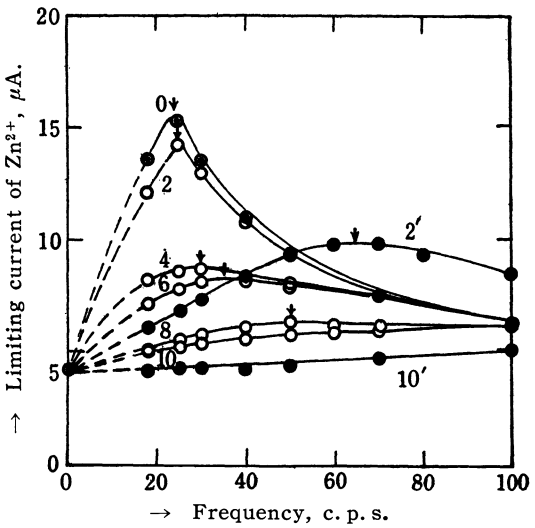



Fig. 4. The effect of the frequency of the a. c. electric field on the limiting current of the zinc ion in the presence of the surface active material. Curve 0 is obtained in the absence of the surface active material. Curves 2, 4, 6, 8 and 10 correspond to the concentration of methyl cellulose as great as 0.002, 0.004, 0.006, 0.008 and 0.01%, respectively. Curves 2′ and 10′ correspond to the concentration of gelatine as great as 0.002 and 0.01%, respectively. The maximum point of curve 10′ appears at about 200 c. p. s. $(Zn^{2+})=1\times10^{-3}$ F. Refer the illustration given in Fig. 1 to the other experimental conditions.

*surface active material.*—The dependence of the limiting current of the zinc ion to the frequency of the vibration was investigated in the presence of gelatine or methyl cellulose of various concentrations. The result is illustrated in Fig. 4. Under the vibration of the frequency less than 20 c. p. s., the mercury droplet is shaken off by the violent vibration in the absence of the surface active material, and the effect of the vibration on the limiting current gradually decreases as the frequency of the vibration increases. Thus, the limiting current gives a maximum at about 25 c. p. s. In the presence of the surface active material, the frequency of the vibration, which gives the maximum limiting current, shifts toward higher frequencies as the concentration of the surface active material increases. In connection with this effect, the difference between gelatine and methyl cellulose is noticeable as is pointed out in *2-ii.*

**3. Effect of Vibration on Maximum Wave.**—It was found that the summit potential of the polarographic maximum of the first kind shifts toward more negative potentials by the vibration.

The test solution contained 1 mF mercuric ion in 0.01 F sodium sulfate solution, and the DME with the comparatively short life-time was preferable in order to obtain reproducible data. The effect of the vibration on the maximum wave of the mercuric ion is illustrated in Fig. 5, and the variation of the summit potential with the intensity of the a. c. electric field is given in Table III.

TABLE III. THE VARIATION OF THE SUMMIT POTENTIAL OF THE POLAROGRAPHIC MAXIMUM WITH THE INTENSITY OF THE a. c. ELECTRIC FIELD ($E_1, E_2, E_3$ and $E_4$ represent the potential given in Fig. 5.)

| The intensity of the electric field, V./cm. | $E_1$ | $E_2$ | $E_3$ | $E_4$ |
|---|---|---|---|---|
| | V. vs. S. C. E. | | | |
| 0 | $-0.37_5$ | $-0.44_8$ | $-0.43_5$ | $-0.36_7$ |
| 0.16 | $-0.39_2$ | $-0.48_0$ | $-0.44_2$ | $-0.37_6$ |
| 0.25 | $-0.43_0$ | $-0.50_3$ | $-0.47_7$ | $-0.41_3$ |
| 0.34 | $-0.49_5$ | $-0.56_1$ | $-0.56_5$ | $-0.50_2$ |

(25 c. p. s. square wave, $t=5.5_6$ sec.)

According to the theory[1] previously reported, the velocity of the vibration is a linear function of the intensity of the a. c. electric field. Accordingly, it seems to be probable that the velocity of the vibration pertains to the shift of the summit potential. In this connection, Heyrovsky and Vascautzanu[2] have pointed out the fact that the summit potential is shifted toward more negative potentials by increasing the mercury head. The authors' observation coincides with this

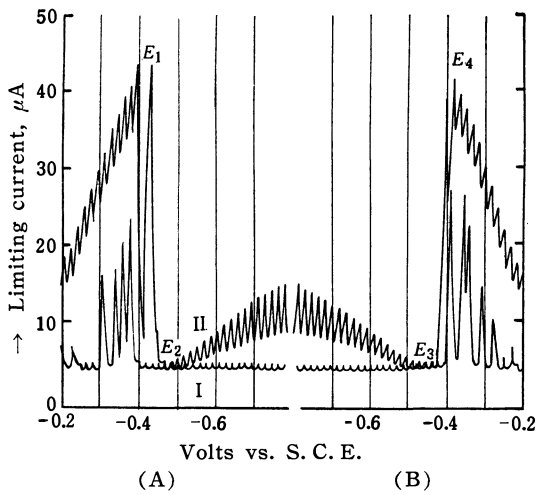



Fig. 5. The effect of the vibration on the summit potential of the maximum wave of $1\times10^{-3}$ F $Hg^{2+}$ in 0.01 F $Na_2SO_4$. The applied voltage is scanned from −0.2 V. to −0.8 V. vs. S. C. E. (A) or from −0.8 V. to −0.2 V. vs. S. C. E. (B). Curves I and II correspond to the cases when the intensity of the applied a. c. electric field is 0 and 0.34 V./cm., respectively. $t=8.0$ sec.

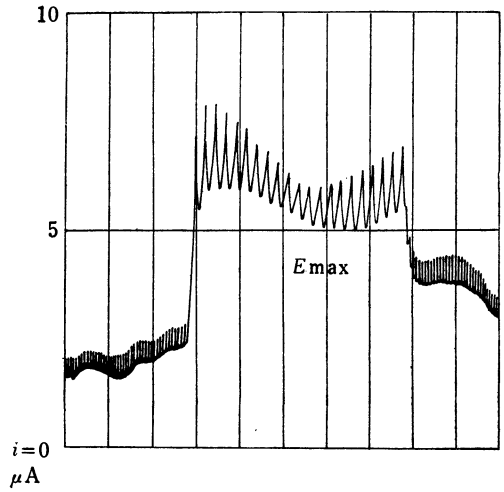



Fig. 6. The current-voltage curve of the mercuric ion under the violent vibration. The voltage starts from 0 V. vs. S. C. E. and each voltage interval corresponds to 0.1 V. $(Hg^{2+})=1\times10^{-4}$ F. The supporting electrolyte=0.1 F KCl. $E=0.38$ V./cm. $t=7$ sec. (open circuit).

2) J. Heyrovsky and E. Vascautzanu, *Collection Czechoslov. Chem. Communs.*, 3, 418 (1931).

effect with respect to the point that the possible change of the $\zeta$-potential due to the movement of the surface of the mercury droplet results in the shift of the summit potential of the maximum.

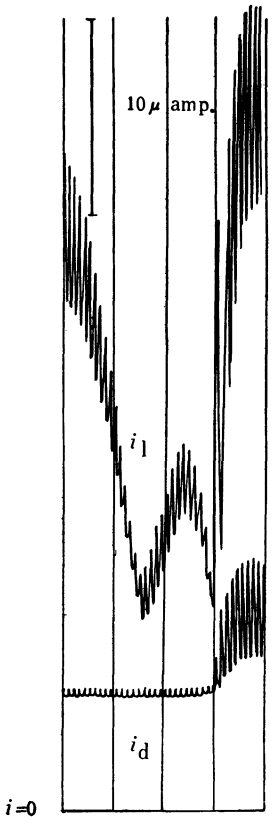



Fig. 7. The "VDME" current-voltage curve of the mercuric ion under the high rate of mercury flow. $i_d$ is the diffusion-controlled current and $i_l$ is the limiting current. $t=5.4_4$ sec. (open circuit). $m=1.34_7$ mg./sec. $(Hg^{2+})=1\times10^{-3}$ F. The supporting electrolyte=0.1 F KCl. The applied voltage starts from $-0.7$ V. vs. S. C. E. and each voltage interval corresponds to 0.1 V.

**4. Anomalous Effect of Vibration on Current-Voltage Curve.** — *4-i. Effect of violent vibration.*—The abrupt change of the limiting current was observed in the current-voltage curve of the mercuric ion under the application of the intense a. c. electric field (cf. Fig. 6). This change is caused by the change of the life-time of the DME. The mercury droplet is attached to the capillary orifice counteracting to the gravity and the vibration, and it is shaken off by the violent vibration caused by the coupled effect of the intense a. c. electric field and the increase of the surface charge density which is a function of the applied potential. Tachi and Okuda[3] have reported a similar phenomenon in the alternating current polarography.

*4-ii. Effect of rapid rate of mercury flow.* —Under the slow rate of the mercury flow, a minimum in the current-voltage curve is observed at the Lippmann-potential by the "VDME" method (cf. **1** and **4**). Under the rapid rate of the mercury flow, however, two minima were observed, the Lippmann-potential lying between them (cf. Fig. 7). It seems to be probable that this effect will be assigned to the variation of the $\zeta$-potential at the mercury-solution interface with the flow of mercury on the surface of the DME.

The authors wish to express their hearty gratitude to Professor Mutsuaki Shinagawa for his valuable advice and encouragement.

*Laboratory of Chemistry*
*Minami College*
*Hiroshima University*
*Minami, Hiroshima*

3) I. Tachi and M. Okuda, This Bulletin, **27**, 310 (1954).
4) H. Imai, S. Inouye and S. Chaki, ibid., **31**, 767 (1958).

# *The Crystal Structure of Phenylarsonic Acid*[1]

By Akira SHIMADA

(Received September 9, 1959)

The chemistry of organoarsenic compounds has an earlier growth than that of others among those of organometallic compounds, and this fact has again attracted much attention of chemists in recent days[2]. However, there are only a few structural studies of the organoarsenic compounds[3-10], and, hence, it may be of interest and importance in this field of chemistry to reveal the spatial configuration and orientation of the molecules in the crystal of phenylarsonic acid, $C_6H_5AsO(OH)_2$, which is one of the fundamental compounds in the organoarsenic compounds. The present work, which provides the first determination of the packing mode of organoarsonic acid, seems of interest also from the standpoint of the hydrogen-bond formation, in comparison with other organic acids.

## Experimental

In a preliminary note, the crystallographic constants were already reported[1]; the crystal of this compound belongs to the orthorhombic system and the space group $D_2^4-P2_12_12_1$ with four chemical units in a unit cell, which has the following dimensions;

$a=10.42\pm0.02$, $b=14.92\pm0.02$, $c=4.70\pm0.02$ Å

The data mentioned above are in fairly good agreement with those recently reported by Bryden[11]. Oscillation and Weissenberg photographs were taken around the principal axes with Cu $K\alpha$ radiation. Intensities were obtained by the multiple-film technique in Weissenberg photographs and were estimated by visual comparison with a calibrated scale. They were corrected by means of the usual Lorentz and polarization factors, while the correction for absorption was evaluated under the assumption that the specimens were cylindrical rods. The absorption effect could not be neglected, especially for $(0\,k\,l)$ and $(h\,0\,l)$ spectra because of the rather high absorption coefficient ($\mu=60.3\,cm^{-1}$) of the crystals and because of their dimensions [cross section with rectangular dimensions: $0.20\times0.25$ mm. for $(h\,k\,0)$, $0.65\times0.40$ mm. for $(0\,k\,l)$, and $0.70\times0.65$ mm. for $(h\,0\,l)$].

## Structure Determination

The structure has been determined by making use of the heavy-atom technique. Thus, the electron density projection $\rho(xy)$, favorable because of the short $c$ axis, were fairly well resolved to reveal the configuration of the molecules, as described in the preliminary note[1]. The electron density projections $\rho(yz)$ and $\rho(xz)$ were easily constructed by the same method, referring to the refined electron density projection $\rho(xy)$. These projections were shown in Figs. 1—3, and the final coordinates are listed in Table I, their refinement being made by the difference syntheses at later stages. In the calculation of structure factors, McWeeny's scattering curves[12] of "valence states" for carbon atom and of $1/3(f^{\parallel}+2f^{\perp})$ for oxygen atom were used, while the scattering curve given by Berghuis et al.[13] was used for arsenic atom. Isotropic temperature factors were estimated to be 3.3 Å$^2$

TABLE I. ATOMIC COORDINATES

| Atom | $x/a$ | $y/b$ | $z/c$ |
|---|---|---|---|
| As | $0.334_4$ | $0.126_5$ | $0.211_2$ |
| $O_1$ | 0.457 | 0.111 | −0.032 |
| $O_2$ | 0.192 | 0.109 | 0.079 |
| $O_3$ | 0.372 | 0.060 | 0.499 |
| $C_1$ | 0.338 | 0.249 | 0.320 |
| $C_2$ | 0.429 | 0.313 | 0.218 |
| $C_3$ | 0.424 | 0.400 | 0.332 |
| $C_4$ | 0.336 | 0.423 | 0.531 |
| $C_5$ | 0.249 | 0.360 | 0.633 |
| $C_6$ | 0.242 | 0.271 | 0.520 |

1) A preliminary account has already appeared in This Bulletin, **32**, 309 (1959).
2) E. G. Rochow, D. T. Hurd and R. N. Lewis, "The Chemistry of Organometallic Compounds", John Wiley & Sons, Inc., New York (1957).
3) R. C. L. Mooney, *J. Am. Chem. Soc.*, **62**, 2955 (1940).
4) R. C. L. Mooney, *Phys. Rev.*, **61**, 739 (1942).
5) H. A. Skinner and L. E. Sutton, *Trans. Faraday Soc.*, **40**, 164 (1944).
6) J. Waser and V. Shomaker, *J. Am. Chem. Soc.*, **67**, 2014 (1945).
7) J. Donohue, G. Humphrey and V. Schomaker, ibid., **69**, 1713 (1947).
8) S. C. Nyburg and J. Hilton, *Acta Cryst.*, 8, 358 (1955).
9) W. Schaffer, ibid., **9**, 401 (1956).
10) R. C. L. Mooney, ibid., **12**, 187 (1959).
11) J. H. Bryden, ibid., **12**, 558 (1959).
12) R. McWeeny, ibid., **4**, 513 (1951).
13) J. Berghuis, I. M. Haanappel, M. Potters, B. O. Loopstra, C. H. MacGillavry and A. L. Veenendaal, ibid., 8, 478 (1955).

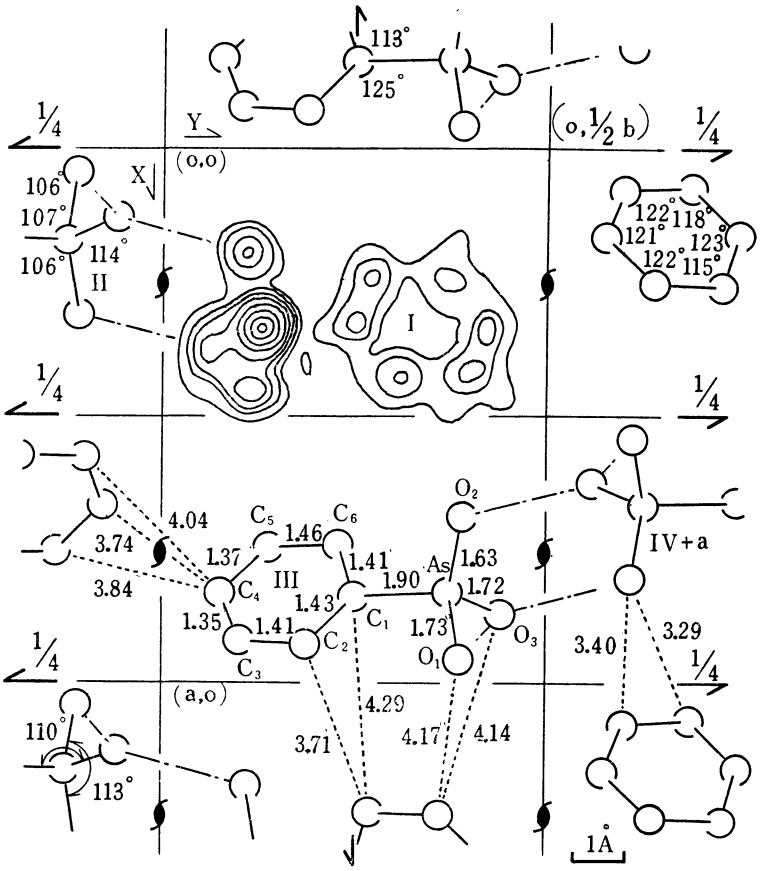



Fig. 1. The structure and the electron-density projection along the *c* axis, with bond angles, intra- and intermolecular distances (Å). Contours at intervals of 2 eÅ$^{-2}$, starting at 2 eÅ$^{-2}$, except at the arsenic atom, where contours above 8 eÅ$^{-2}$ are at intervals of 10 eÅ$^{-2}$. Dot-dash lines indicate hydrogen bonds.

for all atoms in the case of ($h\,k\,0$) and ($0\,k\,l$), and 4.2 Å$^2$ in the case of ($h\,0\,l$). *R* indices for the final coordinates were 18.0, 14.0 and 15.6%, for ($h\,k\,0$), ($0\,k\,l$) and ($h\,0\,l$), respectively, excluding terms too weak to be observed.

### Description of the Structure

The general nature of the structure is shown in Figs. 1—3, which are *c*, *a* and *b* axis projections for this compound. The aresenic atom is surrounded by a group consisting of three oxygen atoms, $O_1$, $O_2$ and $O_3$ of the arsonic acid and one carbon atom $C_1$ of the benzene ring. The average As–O distance is 1.69 Å, and the As–C distance is 1.90 Å. The disposition of bonds from the arsenic atom appears to be nearly tetrahedral, the angles between the bonds being about 110°. The benzene ring is planer and the averge distance between adjacent carbon atoms is 1.41 Å, individual values ranging from 1.35 to 1.46 Å.

Phenylarsonic acid, which has two active hydrogen atoms, forms two hydrogen bonds, one with a length 2.64 Å from the atom $O_3$ of molecule I to the atom $O_2$ of molecule II, the other with a length 2.49 Å from the atom $O_3$ of molecule I to the atom $O_1$ of molecule I+*c* (molecule displaced by the unit vector *c*). This arrangement of these two types of hydrogen bonds links molecules with each other to form endless chains along the twofold axis perpendicular to the (001) plane. The benzene rings are connected through the arsenic atom to these chains which are held together by the van der Waals force only. The shorter distances between neighboring molecules occur between $O_2$ of one molecule and $C_2$, $O_3$ and $C_3$ of adjacent molecules; these distances are 3.29, 3.39 and 3.40 Å, respectively. Other intermolecular distances exceed 3.71 Å.

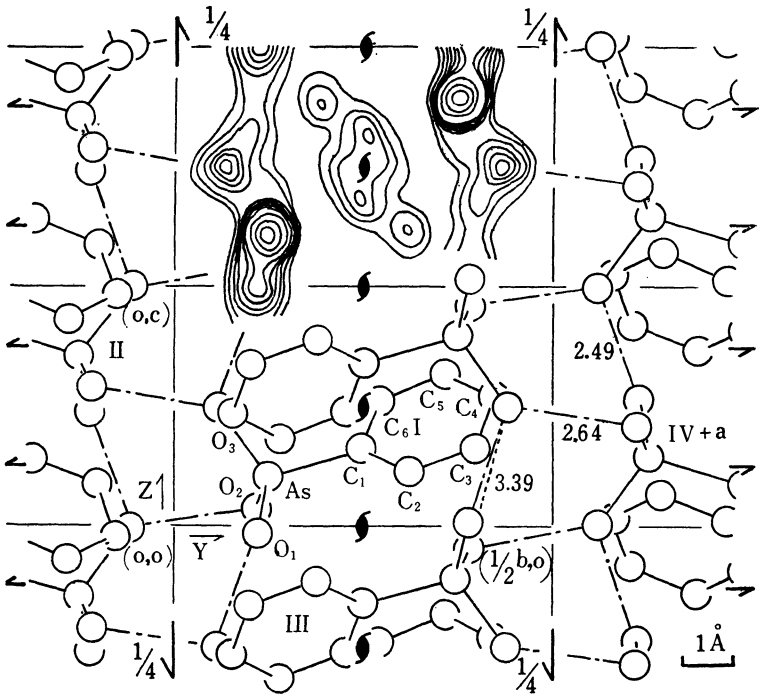



Fig. 2. The structure and the electron-density projection along the *a* axis, with intermolecular distances (Å). Contours at intervals of 2 eÅ$^{-2}$, starting at 4 eÅ$^{-2}$, except at the arsenic atoms, where contours above 16 eÅ$^{-2}$ are at intervals of 10 eÅ$^{-2}$. Dot-dash lines indicate hydrogen bonds.

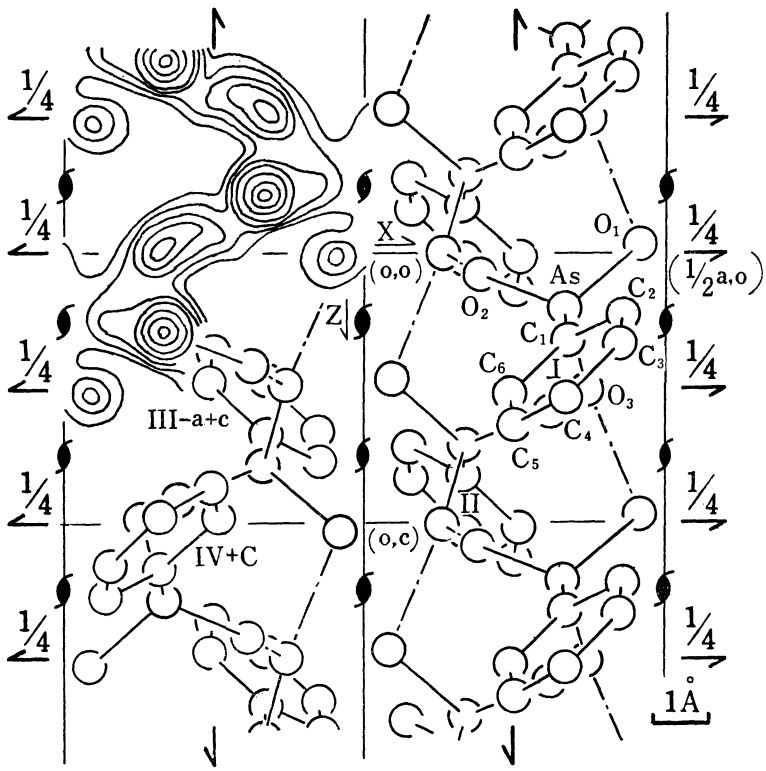



Fig. 3. The structure and the electron-density projection along the *b* axis. Contours at intervals of 3 eÅ$^{-2}$, starting at 5 eÅ$^{-2}$, except at the arsenic atoms, where contours above 11 eÅ$^{-2}$ are at intervals 10 eÅ$^{-2}$. Dot-dash lines indicate hydrogen bonds.

This mode of packing the molecules would explain the cleavages along the planes parallel to the (110) and (100) planes.

The author wishes to express his sincere thanks to Professor I. Nitta and Professor T. Watanabé of Osaka University for their helpful advice, to Professor H. Nakata of Konan University for supplying the specimen, and to other members of this University for their encouragement.

*Department of Chemistry*
*Faculty of Science*
*Konan University*
*Higashinada, Kobe*

# *On the d Orbital of the Sulfur Atom in Thiophene*

By Kôgorô MAEDA

(Received June 17, 1959)

The idea of *pd* hybridization in thiophene has been used successfully in accounting for the general similarity between thiophenes and their benzene analogues[1-3]. In hybridizing the *p*- and *d*-orbitals on the sulfur atom, the fundamental procedure was that the two hybridized orbitals which conjugate with $2p\pi$ orbitals on the carbon atoms are defined so as to be non-orthogonal to each other. A problem which has to be solved, however, results from adopting the *d* orbitals in bonding; it follows what values should be used for nuclear charge parameters of the *d* orbitals. If the use of the free atom parameter required by Slater's rule[4] for an electron in the *d* orbital is to be retained at all, the orbital becomes too diffuse and weakly bound to participate substantially in bonding. For example, when an electron of an unshared pair on the sulfur atom is considered to be in the *d* state, it bears the value 1 as the effective nuclear charge; this fact gives a small value of overlap integral with the $2p\pi$ orbital on the carbon atom, of the order of 0.1[5] and suggests the level of its energy much higher than the ground state. Under this condition, one might not expect the appreciable participation in bonding to occur through the hybridization, from the point of overlap criterion on bonding[6] and from balancing of energy. The eigenfunction of the electron, however, has its radial function whose maximum lies at 9 atomic units. The orbital, therefore, may be regarded as including the full carbon skeleton of thiophene, so that it would be impossible to avoid the influence of the nuclear charges of neighboring carbon atoms. The charges may distort the orbital, contracting it and allowing its participation in the hybridization, as suggested by Craig and Magnusson[7].

In this paper, the influence of perturbing potentials of the charges will be examined, and the possibility of the participation in the hybridization will be inquired into, following the treatment by Craig and Magnusson, who presented a model to represent *d* electrons in an octahedral molecule, and applied it to the consideration of actual examples.

**Orbital Contraction.**—Let us now consider the system in which a bivalent sulfur atom combines with two carbon atoms at an angle. In this model, a single *d* electron will be supposed to move in the field of the sulfur nucleus of charge $Z_s$, and upon this hydrogen-like atom system will be superposed a perturbation consisting of two positive charges of the carbon atoms of magnitude $Z_c$ at the distance of $\sigma$ atomic units. Furthermore, the central hydrogen-like atom will be considered to be surrounded, not by two hydrogen-like atoms of carbon, but just by point charges of magnitude $Z_c$. The actual potential of perturbation consists of the attraction of the surrounding nuclei minus the

1) H. C. Longuet-Higgins, *Trans. Faraday Soc.*, **45**, 173 (1949).
2) K. Kikuchi, *Sci. Repts. Tohoku Univ. Series I*, **40**, 133 (1956).
3) K. Kikuchi, ibid., **41**, 35 (1957).
4) J. C. Slater, *Phys. Rev.*, **36**, 57 (1930).
5) H. H. Jaffé, *J. Chem. Phys.*, **21**, 258 (1953).
6) D. P. Craig, A. Maccoll, R. S. Nyholm, L. E. Orgel and L. E. Sutton, *J. Chem. Soc.*, **1954**, 332.
7) D. P. Craig and E. A. Magnusson, ibid., **1956**, 4895.

coulomb repulsions of their electrons plus exchange terms; hence the dependence on distance of this composite potential will not follow the $r^{-1}$ law at all closely. The system being thus too complicated, the point charge approximation is employed as approximation in this paper; the charge $Z_c$ will be treated rather as a parameter relevant to making up for the imperfection of the approximation, values plausible in wider range being involved. As for the angle between two C-S bonds, $\theta$, the following three cases will be considered apart from the thiophene in question, from a more general point of view, 90°, 120° and further 180°. For $Z_c=0$, the eigenfunction for $d$ electron is, of course, that of the hydrogen-like atom of charge $Z_s$. As the $d$ electron wave function, two of the usual Slater-type atomic functions are taken up for consideration, as follows:

$$\psi_{xz}=(\sqrt{2}/81\sqrt{\pi})\alpha^{7/2}r^2\exp(-\alpha r/3)\times\sin\vartheta\cos\vartheta\cos\varphi$$

$$\psi_{yz}=(\sqrt{2}/81\sqrt{\pi})\alpha^{7/2}r^2\exp(-\alpha r/3)\times\sin\vartheta\cos\vartheta\sin\varphi$$

where, $\alpha$, as will be mentioned later, is a parameter to be determined with respect to energy. Further, the influence upon $3p$ Slater atomic function will be examined in comparison with the case of the $d$ orbitals.

The potential by the outlying charges may be expanded as a sum in the usual $1/r$ series[8], which reduces to the following expressions for the three cases respectively.

$\theta=90°$:

$$V_{r<\sigma}=-(2Z_c/\sigma)-(Z_c/\sigma)(r/\sigma)\times(\cos\varphi+\sin\varphi)\sin\vartheta-(Z_c/2\sigma)(r/\sigma)^2(3\sin^2\vartheta-2)+\cdots\cdots$$

$$V_{r>\sigma}=-(2Z_c/r)-(Z_c/r)(\sigma/r)\times(\cos\varphi+\sin\varphi)\sin\vartheta-(Z_c/2r)(\sigma/r)^2(3\sin^2\vartheta-2)+\cdots\cdots$$

$\theta=120°$:

$$V_{r<\sigma}=-(2Z_c/\sigma)-(Z_c/\sigma)(r/\sigma)\times\cos(\varphi-\pi/3)\sin\vartheta-(Z_c/2\sigma)(r/\sigma)^2\{(15/4)\cos^2\varphi\sin^2\vartheta+(3\sqrt{3}/2)\sin\varphi\cos\varphi\sin^2\vartheta+(9/4)\sin^2\varphi\sin^2\vartheta-2\}+\cdots\cdots$$

$$V_{r>\sigma}=-(2Z_c/r)-(Z_c/r)(\sigma/r)\times\cos(\varphi-\pi/3)\sin\vartheta-(Z_c/2r)(\sigma/r)^2\times\{(15/4)\cos^2\varphi\sin^2\vartheta+(3\sqrt{3}/2)\sin\varphi\cos\varphi\sin^2\vartheta+(9/4)\sin^2\varphi\sin^2\vartheta-2\}+\cdots\cdots$$

$\theta=180°$:

$$V_{r<\sigma}=-(2Z_c/\sigma)-(Z_c/\sigma)(r/\sigma)^2\times(3\cos^2\varphi\sin^2\vartheta-1)+\cdots\cdots$$

$$V_{r>\sigma}=-(2Z_c/r)-(Z_c/r)(\sigma/r)^2(3\cos^2\varphi\sin^2\vartheta-1)+\cdots\cdots$$

Each expression shows that the perturbing potential has its symmetrical plane bisecting the angle between two C-S bonds, $\theta$. The perturbation energy due to the outlying potential is given by $\int\psi V\psi d\tau$, where $\psi$ and $V$ are both shown above. Hence, after integrating over the angular parts excepting the radial one, it is found that the expressions for $3p_z$ orbitals have the same forms, and that the $3d_{xz}$ and $3d_{yz}$ orbitals are exposed respectively to the same fields of the outlying potentials when $\theta=90°$. Both of these can naturally be expected from their symmetric characters. In integrating with respect to the radial part, the terms higher than 2nd may be neglected because of their small contribution to the potential. Hence, the perturbation energy $E'$ is given by the following, for example, for $3d_{xz}$ when $\theta=180°$;

$$E'=(8Z_c/81^2\times15)\int_0^\sigma\alpha^7r^6\{-2/6-(2/7)\times(r^2/\sigma^3)\}\exp(-2\alpha r/3)dr+(8Z_c/81^2\times15)\int_\sigma^\infty\alpha^7r^5\{-2-(2/7)\times(\sigma^2/r^2)\}\exp(-2\alpha r/3)dr$$
$$=-(2Z_c/\sigma)(2\alpha\sigma/3)^7(1/6)[\{6!(3/2\alpha\sigma)^7-A_6(2\alpha\sigma/3)+A_5(2\alpha\sigma/3)\}+(1/7)\{8!(3/2\alpha\sigma)^9-A_8(2\alpha\sigma/3)+A_3(2\alpha\sigma/3)\}]$$

where

$$A_n(\omega)=\int_1^\infty r^n\exp(-\omega r)dr$$

Hereupon, using the auxiliary function presented by Craig and Magnesson[7],

$$R^p{}_{nn}(\alpha\sigma)=(1/\sigma)(2\alpha\sigma/n)^{2n+1}\{1/(2n)!\}\times\{(2n+p)!(n/2\alpha\sigma)^{2n+p+1}-A_{2n+p}(2\alpha\sigma/n)+A_{2n-p-1}(2\alpha\sigma/n)\}$$

8) H. Eyring, J. Walter and G. E. Kimball, "Quantum Chemistry", John Wiley & Sons, Inc., New York (1944), p. 369.

$$E' = -(2Z_c/\sigma)\{\sigma K^0_{33}(\alpha\sigma) - (1/7)\sigma R^2_{33}(\alpha\sigma)\}$$

For $3d_{yz}$ when $\theta=180°$,

$$E' = -(2Z_c/\sigma)\{\sigma K^0_{33}(\alpha\sigma) - (2/7)\sigma R^2_{33}(\alpha\sigma)\}$$

Similarly, when $\theta=120°$, for $3d_{xz}$

$$E' = -(2Z_c/\sigma)\{\sigma K^0_{33}(\alpha\sigma) - (1/56)\sigma R^2_{33}(\alpha\sigma)\}$$

and also for $3d_{yz}$,

$$E' = -(2Z_c/\sigma)\{\sigma K^0_{33}(\alpha\sigma) - (1/8)\sigma R^2_{33}(\alpha\sigma)\}$$

As mentioned above, the $3d_{xz}$ and the $3d_{yz}$ orbitals have the same potentials of perturbation when $\theta=90°$, and so their energies are given in the same form,

$$E' = -(2Z_c/\sigma)\{\sigma K^0_{33}(\alpha\sigma) - (1/14)\sigma R^2_{33}(\alpha\sigma)\}$$

In the case of the $3p$ orbitals, they have the same energies for three cases of the angle $\theta$ because of their symmetric characters, that is;

$$E' = -(2Z_c/\sigma)\{\sigma R^0_{33}(\alpha\sigma) - (1/5)\sigma R^2_{33}(\alpha\sigma)\}$$

The total energy is the sum of the perturbation energy $E'$ and the unperturbed given by

$$W = (\alpha/3^2)(\alpha/2 - Z_s)$$

for the hydrogen-like orbital of free atom parameter $Z_s$.

The procedure to be performed now is to find the new value of effective nuclear charge for which the total energy is a minimum for given magnitude of $\sigma$, $Z_c$ and $Z_s$, i.e. to minimize the energy with respect to the exponent $\alpha$. The increase in $\alpha$ over $Z_s$ corresponds to a contraction of the orbital and the decrease to an expansion, since Slater radial functions have their maxima at $r_m = n^2/\alpha$. As the value of $Z_s$, the following two are chosen, 1 and 2 for $3d$ orbital, and 5 and 6 for $3p$. The distance $\sigma$ is assigned to three values, 4, 3 and 2 atomic units, the first two come from actual examples containing the sulfur atoms, and the last is taken for the purpose of comparison with the first two. With respect to the value of $Z_c$, it is difficult to determine the straightforwardly equivalent parameter of the outlying potential, because, as mentioned above, the real field is not truly coulombic but much more complicated. Furthermore, there is, in general, a considerable difference between so-called potential- and field-determined nuclear charges on the same atom[9]. Therefore, in this paper, three values are assumed, $Z_c=1$, 2 and 3, which are of course treated as tentative parameters, and the last is introduced from the well-known value of Slater's rule for the $2p$ orbital of carbon. In finding the minimum of the total energy, it is necessary to evaluate the values of $\sigma R^p_{nn}(\alpha\sigma)$, which are tabulated in *Appendix*.

In Tables I and II are given the results. It is shown in these tables that the $3d$ orbitals are largely contracted, while the $3p$ orbitals are little affected by the outlying perturbing charges, and that the contraction is more sensitive to the bond distance $\sigma$ than to the effective charge $Z_c$. The magnitude of the contraction is less for a greater bond distance and for a greater value of $Z_s$. This may be expected for the model employed here. Fig. 1 illustrates the rapid decrease in increment $(\alpha - Z_s)$ with increasing $\sigma$ and

TABLE I. EFFECTIVE NUCLEAR CHARGE $\alpha$ of $3d$ ORBITAL WHEN $\theta=180°$ AND $120°$

| $\theta$ | $Z_s$ | $Z_c$ | $\sigma=2$ | $\sigma=3$ | $\sigma=4$ |
|---|---|---|---|---|---|
| I. $3d_{xz}$ | | | | | |
| 180° | 1 | 1 | 2.85 | 2.50 | 2.15 |
| 〃 | 〃 | 2 | 3.76 | 3.00 | 2.45 |
| 〃 | 〃 | 3 | 4.20 | 3.25 | 2.50 |
| 〃 | 2 | 1 | 3.66 | 2.96 | 2.64 |
| 〃 | 〃 | 2 | 4.25 | 3.48 | 2.93 |
| 〃 | 〃 | 3 | 4.50 | 3.65 | 3.10 |
| 120° | 1 | 1 | 2.63 | 2.30 | 2.09 |
| 〃 | 〃 | 2 | 3.56 | 2.93 | 2.48 |
| 〃 | 〃 | 3 | 4.14 | 3.20 | 2.70 |
| 〃 | 2 | 1 | 3.40 | 2.94 | 2.58 |
| 〃 | 〃 | 2 | 4.14 | 3.42 | 2.90 |
| 〃 | 〃 | 3 | 4.60 | 3.60 | 3.05 |
| II. $3d_{yz}$ | | | | | |
| 180° | 1 | 1 | 2.30 | 2.10 | 1.95 |
| 〃 | 〃 | 2 | 3.12 | 2.68 | 2.24 |
| 〃 | 〃 | 3 | 3.78 | 3.05 | 2.62 |
| 〃 | 2 | 1 | 3.08 | 2.84 | 2.59 |
| 〃 | 〃 | 2 | 3.75 | 3.14 | 2.96 |
| 〃 | 〃 | 3 | 4.10 | 3.06 | 3.15 |
| 120° | 1 | 1 | 2.54 | 2.20 | 1.98 |
| 〃 | 〃 | 2 | 3.45 | 2.80 | 2.51 |
| 〃 | 〃 | 3 | 3.90 | 3.16 | 2.65 |
| 〃 | 2 | 1 | 3.28 | 2.87 | 2.68 |
| 〃 | 〃 | 2 | 3.95 | 3.27 | 2.84 |
| 〃 | 〃 | 3 | 4.40 | 3.56 | 2.94 |

TABLE II. EFFECTIVE NUCLEAR CHARGE $\alpha$ of $3p_z$ ORBITAL

| $Z_s$ | $Z_c$ | $\sigma=2$ | $\sigma=3$ | $\sigma=4$ |
|---|---|---|---|---|
| 5 | 1 | 5.47 | 5.22 | 5.15 |
| 〃 | 2 | 5.93 | 5.52 | 5.20 |
| 〃 | 3 | 6.20 | 5.55 | 5.24 |
| 6 | 1 | 6.32 | 6.13 | 6.00 |
| 〃 | 2 | 6.63 | 6.20 | 6.12 |
| 〃 | 3 | 6.90 | 6.25 | 6.18 |

9) For example, see: F. W. Brown, *Phys. Rev.*, 44, 214 (1933).

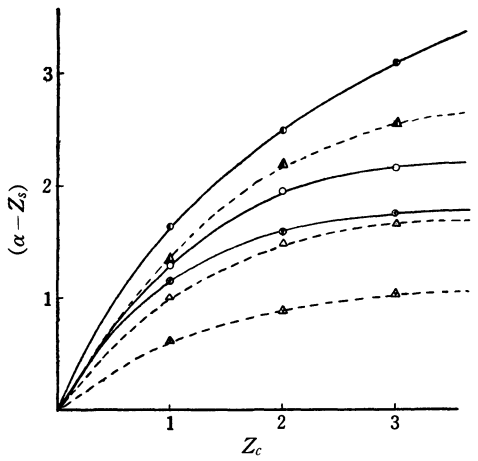



Fig. 1. Values of the increment $(\alpha - Z_s)$ for $3d_{xz}$ and $3d_{yz}$ orbitals when $\theta = 90°$.

—◐— $Z_c=1$ $\sigma=2$
—○— 〃 $\sigma=3$
—⊙— 〃 $\sigma=4$
--◭-- $Z_s=2$ $\sigma=2$
--△-- 〃 $\sigma=3$
--◬-- 〃 $\sigma=4$

$Z_s$, when $\theta=90°$ (the case of thiophene[10]). The figure also shows that the increment of effective nuclear charge by the perturbation is little altered by $Z_c$ in the range $Z_c=2\sim3$ which are most plausible as the equivalent parameter, $\sigma=3$ and 4 corresponding to the actual molecule containing the sulfur atom.

From these results, it might be inferred in any case that in hybridizing the $d$ orbital on the sulfur atom as in thiophene the effective nuclear charge for the $d$ orbital would not bear the free atom parameter, but it should bear at least a greater value, for example, $\alpha \fallingdotseq 3$ for that in thiophene. Of course, it must be emphasized that this discussion on the effective value for $\alpha$ is by all means tentative under the point charge approximation. Furthermore, the value of $\alpha$ appropriate to the real system should be determined precisely with respect to the whole energy of the molecule. The value obtained through the approximation, however, may be used as the first step of the calculation about the molecular energy.

On the other hand, for the $3p$ orbital, the free atom parameter may be used directly in calculating the molecular energy, because it is little affected by the surrounding nuclei. In general, the contraction of orbital is large only when the orbital with highly screened and loosely bound electrons lies under the perturbation. For the $2p\pi$ orbital of carbon, an argument similar to the case for $3p$ orbital can be applied as follows; the perturbation energy $E'$ for the $2p$ orbital with nuclear charge $Z=3$ is given as

$$E' = -(2Z_c/\sigma)\{\sigma R^0_{22}(\alpha\sigma) - (1/5)\sigma R^2_{22}(\alpha\sigma)\}$$

when $\theta=120°$. Using the values $\sigma R^0_{22}$ and $\sigma R^2_{22}$ (see *Appendix*), the perturbed nuclear charge can be obtained, which is given in Table III for $\sigma=2$, 3 and 4 atomic units. It is seen that the orbital is not altered at all. The free atom parameter for the $2p$ orbital of carbon may be used securely as usual in the molecular energy calculation.

TABLE III. EFFECTIVE NUCLEAR CHARGE $\alpha$ OF $2p_z$ ORBITAL WHEN $\theta=120°$

| $Z$ | $Z_c$ | $\sigma=2$ | $\sigma=3$ | $\sigma=4$ |
|---|---|---|---|---|
| 3 | 1 | 3.26 | 3.14 | 3.07 |
| 〃 | 2 | 3.46 | 3.22 | 3.10 |
| 〃 | 3 | 3.64 | 3.33 | 3.14 |

It is of interest to notice that the radial maxima of the $3d$ orbitals contracted lie nearly at the bond distance $\sigma$.

**Overlap Integral.**—The overlap criterion[6] may be used conveniently in discussing the bond formation, because it is generally impracticable to calculate accurately the energy of formation of a bond between two centers, and, as much used and discussed by Mulliken and his collaborators[11], it gives some measure of the concentration of electronic charge between the nuclei. It can be used not only for the discussion of covalent bond, but also can be well applied to that of $\pi$ bonding. An amount of increase in overlap integral means to strengthen the bond to some extent. Further the increase in overlap integral of a $d$ orbital with an orbital on the neighboring atom will be associated by large contribution to the hybridization in which the $d$ orbital participates, because the integral of the hybrid orbital may be written as a sum of those of participating orbitals.

The values of the integral for the contracted and unperturbed $3d\pi$ orbitals with the $2p\pi$ orbitals of carbon are summarized in Table IV, together with those for $3p\pi$ orbitals. In calculating these values, numerical tables given by Jaffé[5] and

10) Y. Schomaker and L. Pauling, *J. Am. Chem. Soc.*, **61**, 1779 (1939).

11) For example, F. S. Mulliken, *J. Phys. Chem.*, **56**, 295 (1952).

TABLE IV. OVERLAP INTEGRALS OF 3*d* ORBITALS WITH 2*p* ORBITALS OF CARBON, WHEN $\theta=90°$*

| $Z_s$ | $Z_c$ | $\sigma=2$ | $\sigma=3$ | $\sigma=4$ |
|---|---|---|---|---|
| I. $3d_{xz}$ and $3d_{yz}$ | | | | |
| 1 | 0 | 0.109 | 0.129 | 0.127 |
| 1 | 1 | 0.438 | 0.425 | 0.290 |
| 1 | 2 | 0.537 | 0.428 | 0.309 |
| 1 | 3 | | | |
| 2 | 0 | 0.319 | 0.326 | 0.279 |
| 2 | 1 | 0.525 | 0.426 | 0.308 |
| 2 | 2 | 0.566 | 0.439 | 0.315 |
| 2 | 3 | | | |
| II. $3p_z$ | | | | |
| 5 | 0 | 0.492 | 0.242 | 0.109 |
| 5 | 1 | 0.484 | 0.241 | 0.099 |
| 5 | 2 | 0.477 | 0.220 | 0.098 |
| 5 | 3 | | | |
| 6 | 0 | 0.477 | 0.202 | 0.081 |
| 6 | 1 | 0.444 | 0.192 | 0.079 |
| 6 | 2 | 0.426 | 0.192 | 0.074 |
| 6 | 3 | | | |

* In calculating the overlap integral involving *d* orbital, one must pay some attention to the special symmetric character of the orbital; in this table are given only the values when $\theta=90°$, because both other cases may cause some confusion in the calculation. Cf. Ref. 2.

Mulliken et al.[12] were used. The results show that the values of integral for the contracted 3*d* orbitals are enlarged without exception. Although it does not necessarily signify a very great possibility of bonding by the *d* orbital, it may be said at least that such $d\pi-p\pi$ bonding is likely to be more commom and important than has ever been considered, and that, therefore, the participation of the *d* orbitals in the hybridization is more probable than expected through the direct employment of free atom parameter by Slater's rule. In an actual system such as the sulfur atom in thiophene, the extent to which the *d* orbital participates in bonding will be of the order same as, or less than, that of the 3*p* orbital, despite the greater value of the integral. Because the mixing coefficient of the *d* orbital in the hybridization is not great, and also the balancing of energy is unfavorable; this will be examined in the next section.

**Balancing of Energy.**—Slater's rule seems to be insufficient for the accurate calculation of energy levels of an atom, although it suffices for the discussion of orbital size and overlap of atoms. For example, according to the rule, one has the values 45 and 1.5 eV. for 3*p* and 3*d* orbitals on the sulfur atom, respectively. They are very different from spectroscopic data[13], though these data are not always precisely corresponding to the so-called valence states of the atom. Spectroscopically the ionization energy of the atom is 10.36 eV. and the difference between 3*p* and 3*d* states is about 8.5 eV.

The discussion dealing with the final determining factor in bonding, i.e. the energy, can not be free from some ambiguity, since the general relationships between the overlap and the bond energy, and between the effective nuclear charge and the energy level, are not yet well established. If one should be allowed to assume that the free atom parameters $Z_s=5.45$ and 1 may correspond to the energy values 10.36 and 1.86 eV., respectively, the levels of the contracted *d* orbitals will be settled at about 5 eV. above the ground state. Of course, this estimation is merely tentative. However, it might be said that the level of energy of the *d* orbital will be drawn to some extent near to that of the 3*p* orbital as the result of the contraction by the perturbation, so that the possibility of participation in the hybridization will become greater, setting aside the question of extra promotion energy suggested by Craig and Magnusson[7], who estimated the energy directly by Slater's rule. It is well known that the closer the two energy levels are drawn to each other, the greater the interaction between them[14].

All the discussions above are those under the point charge approximation. It is more or less inevitable that the results obtained in this paper are not so readily available for an accurate discussion of bond formation in the real system. Further, in thiophene, there are two other perturbing charges which are included by the diffuse *d* orbital on the sulfur atom.

Nevertheless, the results will be sufficiently valid for approximate and semiquantitative discussion on the possibility of participation of the *d* orbital in hybridization.

## Summary

The influence of neighboring atoms upon the diffuse *d* orbital on the sulfur atom

12) R. S. Mulliken, C. A. Rieke, D. Orloff and H. Orloff, *J. Chem. Phys.*, **17**, 1248 (1949).

13) C. E. Moore, *Natl. Bur. Standards (U. S.), Circ.* **467**, 181 (1949).

14) C. A. Coulson, "Valence", Oxford University Press, London (1952), p. 195.

and the possibility of the participation in the hybridization were examined. It might be expected that, with respect to the sulfur atom in thiophene, the participation of *d* orbitals in the hybridization would take place to a greater extent than predicted by the direct application of free atom parameter by Slater's rule, owing to the contraction by the perturbation of neighboring carbon atoms.

The author wishes to express his sincere thanks to Dr. S. Nagakura for his kind advice and helpful discussions. Thanks are also due to Dr. K. Saito for his kind inspection and revision of this manuscript.

*Electrotechnical Laboratory*
*Tanashi P. O., Tokyo*

***Appendix*** THE VALUES OF AUXILIARY FUNCTIONS

| $\alpha\sigma$* | $\sigma R^0_{22}$ | $\sigma R^2_{22}$ | $\sigma R^0_{33}$ | $\sigma R^2_{33}$ |
|---|---|---|---|---|
| 1.5 | | | 0.1665 | 0.0082 |
| 2.0 | 0.4799 | 0.1693 | | |
| 2.25 | | | 0.2498 | 0.0269 |
| 3.0 | 0.6702 | 0.2287 | 0.3323 | 0.0611 |
| 3.75 | | | 0.4133 | 0.1088 |
| 4.0 | 0.8046 | 0.4517 | | |
| 4.5 | | | 0.4915 | 0.1698 |
| 5.0 | 0.8908 | 0.4958 | | |
| 5.25 | | | 0.5656 | 0.2368 |
| 6.0 | 0.9417 | 0.4843 | 0.6341 | 0.3061 |
| 6.75 | | | 0.6961 | 0.3714 |
| 7.0 | 0.9701 | 0.4412 | | |
| 7.5 | | | 0.7511 | 0.4286 |
| 8.0 | 0.9851 | 0.3863 | | |
| 8.25 | | | 0.7988 | 0.4752 |
| 9.0 | 0.9928 | 0.3313 | 0.8394 | 0.5098 |
| 10.0 | 0.9966 | 0.2817 | | |
| 10.5 | | | 0.9011 | 0.5433 |
| 11.0 | 0.9984 | 0.2396 | | |
| 12.0 | 0.9993 | 0.2045 | 0.9416 | 0.5373 |
| 13.0 | 0.9996 | 0.1758 | | |
| 13.5 | | | 0.9667 | 0.5053 |
| 14.0 | 0.9999 | 0.1524 | | |
| 15.0 | 1.0004 | 0.1364 | 0.9817 | 0.4598 |
| 18.0 | | | 0.9949 | 0.3616 |
| 21.0 | | | 0.9987 | 0.2850 |
| 24.0 | | | 0.9997 | 0.2169 |
| 27.0 | | | 0.9999 | 0.1725 |

* The values for $\alpha\sigma$ in the table given by Craig and Magnusson should be multiplied by 1.5.

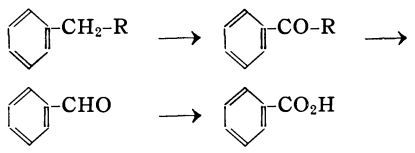
# *Vapor Phase Oxidation of Alkyl Benzenes*[1]

By Shigeru MORITA

(Received September 7, 1959)

Phthalic anhydride is produced commercially by vapor phase oxidation of naphthalene. By the same process, maleic anhydride is obtained from benzene, anthraquinone from anthracene. Production of benzoic acid from toluene and of phthalic anhydride from *o*-xylene by the oxidation has been studied, but the oxidation of benzene which contains an alkyl group with a longer chain than the methyl group has not been examined.

It has been published that, based on liquid phase oxidation of ethyl benzene, the mechanism of vapor phase oxidation of alkyl benzenes is assumed to be as follows[2]:




R: alkyl group

The author studied the mechanism of vapor phase oxidation of alkyl benzenes and others.

## Experimental

**Apparatus.**—As shown in Fig. 1, a reactor was a steel U tube 18 mm. in diameter, immersed in a molten nitrate bath.

1) This is a summary of the report published in *J. Chem. Soc. Japan, Pure Chem. Sec.* (*Nippon Kagaku Zasshi*), **78**, 1746 (1957); **79**, 1081, 1230, 1406 (1958).

2) L. F. Marek and D. A. Hahn, "The Catalytic Oxidation of Organic Compound in the Vapor Phase", Am. Chem. Soc. Monograph No. 61, Chemical Catalog Co., New York (1932), p. 356.

TABLE I. PHYSICAL CONSTANTS OF SUBSTANCES

| | | °C | $d_4^{20}$ |
|---|---|---|---|
| Toluene | b.p. | 110.5 | 0.864 |
| Ethyl benzene | b.p. | 136.2 | 0.867 |
| Styrene | $b.p._{40}$ | 44.5～45.5 | 0.908 |
| *n*-Propyl benzene | b.p. | 159.6 | 0.862 |
| *iso*-Propyl benzene | b.p. | 152.5 | 0.862 |
| *n*-Butyl benzene | b.p. | 183.2 | 0.860 |
| *sec*-Butyl benzene | b.p. | 173.5～173.8 | 0.862 |
| *tert*-Butyl benzene | b.p. | 170.0～170.5 | 0.866 |
| *sec*-Amyl benzene | b.p. | 192.0～192.8 | 0.862 |
| 3-Phenyl pentane | b.p. | 191.0 | 0.864 |
| *tert*-Amyl benzene | b.p. | 189.0～189.5 | 0.873 |
| *n*-Hexyl benzene | b.p. | 225.4 | 0.857 |
| 2-Phenyl-*n*-hexane | b.p. | 214 | 0.861 |
| Dodecyl benzene | $b.p._{20}$ | 165～185 | 0.862 |
| Phenyl cyclohexane | b.p. | 235～236 | 0.943 |
| Diphenyl | m.p. | 70.3 | — |
| Propiophenone | b.p. | 218 | 1.005 |
| Phenyl acetone | b.p. | 216 | 1.004 |
| Hydrocinnamic acid | m.p. | 48 | — |
| Cinnamic acid | m.p. | 133 | — |
| α-Hydrindone | m.p. | 41 | — |
| Butyrophenone | b.p. | 220～221 | 0.988 |
| Benzyl ethyl ketone | $b.p._{16}$ | 109～111 | 1.001 |
| Benzyl acetone | $b.p._{13}$ | 115 | 0.985 |
| γ-Phenyl butyric acid | m.p. | 51 | — |
| Tetralone | $b.p._{13}$ | 127 | 1.092 |

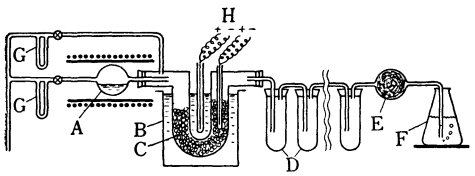



Fig. 1. Apparatus used for vapor phase oxidation.
A. Evaporator
B. Salt bath
C. Reactor
D. Air condensers and ice-cooled condensers
E. Glass wool
F. Water bubbler
G. Flowmeters
H. Thermocouples

**Catalyst.**—The Catalyst was, throughout the present experiments, a mixture of vanadium pentoxide and molybdenum trioxide on pumice stone, which was prepared from ammonium metavanadate (5 g.), ammonium molybdate (5 g.) and puric stone (100 ml.) by the method described before[3].

**Experimental Conditions.**—The air rate was 150 l./hr. and the feed rate of reactants 1.5 g./hr.; the range of reactor temperatures was 300～500°C and the volume of catalyst was 50 ml. Duration of an experimental run was 3 hr. Substances oxidized are listed in Table I.

**Analysis of Reaction Products.**—Oxidation products, mainly a mixture of phthalic and maleic anhydrides and benzoic acid, after having been dissolved in hot water (and filtered, if necessary,) were dried in vacuo and weighed. Then, using a portion of the dried product, the neutralization equivalent of the whole mixture was ascertained. Another portion of the product was taken, benzoic acid was removed completely by microsublimation apparatus at 65～70°C, and the neutralization equivalent of the remaining product was ascertained. From these values the amounts of phthalic, benzoic, and maleic acids were figured out.

The same procedure was repeated using a known mixture of three acids and the experimental values were found to be within 15% of the theoretical values.

## Results and Discussion

**Vapor Phase Oxidation of Monoalkyl Benzenes.**—Toluene, ethyl benzene, propyl benzenes butyl benzenes, amyl benzenes, hexyl benzenes, and dodecyl benzenes were oxidized under the same conditions. The mole percentage yields of products are listed in Table II.

Table II shows that

1) Ethyl benzene is more easily oxidized

3) H. Sasayama, *J. Chem. Soc. Japan, Ind. Chem. Sec.* (*Kogyo Kagaku Zasshi*), **56**, 281 (1953).

TABLE II. EXPERIMENTAL RESULTS OF VAPOR PHASE OXIDATION OF ALKYL BENZENES

| | Reaction temp. °C | Products | | |
|---|---|---|---|---|
| | | Phthalic anhydride mol. % | Benzoic acid mol. % | Maleic anhydride mol. % |
| Toluene | 300 | 0 | 7 | 8 |
| Toluene | 350 | trace | 12 | 45 |
| Ethyl benzene | 300 | 0 | 35 | 12 |
| Ethyl benzene | 400 | 0 | 9 | 41 |
| Styrene | 300 | 0 | 35 | 5 |
| Styrene | 400 | 0 | trace | 49 |
| *n*-Propyl benzene | 350 | 18 | 6 | 34 |
| *n*-Propyl benzene | 400 | 24 | 2 | 35 |
| *iso*-Propyl benzene | 400 | 0 | 21 | 38 |
| *n*-Butyl benzene | 350 | 27 | 7 | 25 |
| *n*-Butyl benzene | 400 | 26 | 2 | 30 |
| *sec*-Butyl benzene | 350 | 35 | 9 | 23 |
| *sec*-Butyl benzene | 400 | 36 | 3 | 26 |
| *tert*-Butyl benzene | 400 | trace | 0 | 24 |
| *sec*-Amyl benzene | 350 | 23 | 5 | 22 |
| *sec*-Amyl benzene | 400 | 24 | 1 | 29 |
| 3-Phenyl pentane | 400 | 20 | 2 | 30 |
| *tert*-Amyl benzene | 350 | 3 | 0 | 38 |
| *tert*-Amyl benzene | 400 | 4 | trace | 44 |
| *n*-Hexyl benzene | 350 | 14 | 1 | 50 |
| *n*-Hexyl benzene | 400 | 19 | trace | 65 |
| 2-Phenyl-*n*-hexane | 350 | 7 | 3 | 25 |
| 2-Phenyl-*n*-hexane | 400 | 35 | 1 | 26 |
| Dodecyl benzene | 400 | 17 | 1 | 45 |
| Phenyl cyclohexane | 400 | 8 | 2 | 20* |
| Phenyl cyclohexane | 500 | 10 | 0 | 16 |
| Diphenyl | 400 | 14 | 2 | 35 |

* and 18 mol. % of diphenyl is produced.

than toluene. And benzoic acid and maleic anhydride are obtained from ethyl benzene in the same yields as that from styrene.

2) When the number of carbons in the longest chain of the alkyl group is three or more, for instance, *n*-propyl, *n*-butyl, *sec*-butyl, amyl, hexyl, etc., phthalic anhydride (25~36%), benzoic acid and maleic anhydride are obtained by vapor phase oxidation. When it is two or less, for instance, methyl, ethyl, *i*-propyl, no phthalic anhydride is obtained.

3) The yield of phthalic anhydride obtained from *n*-alkyl benzenes is lower than that from *sec*-alkyl benzenes, and that from *tert*-alkyl benzenes is very small.

4) No benzoic acid is obtained from *tert*-alkyl benzenes by vapor phase oxidation.

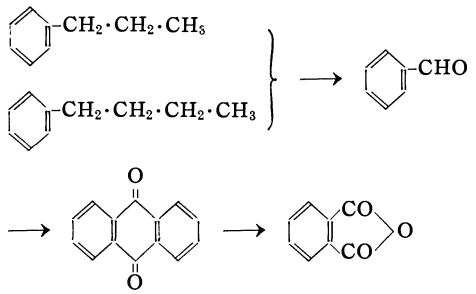
**The Reaction Mechanism of Vapor Phase Oxidation of *n*-Propyl Benzene and *n*-Butyl Benzene.** — *n*-Propyl benzene or *n*-butyl benzene has only one alkyl group. Oxidation of either of these two compounds produces phthalic anhydride in which the benzene ring has two side chains containing carbon atoms. This strange phenomenon, however, can not be explained by the mechanism that has been advocated by Marek, Hahn[2] and others so far.

The range of temperatures of vapor phase oxidation is 350~500°C and a reactant is passed with air through the vanadium pentoxide catalyst zone in vapor phase. Therefore, it is supposed that oxidation, pyrolysis and condensation would occur at the same time.

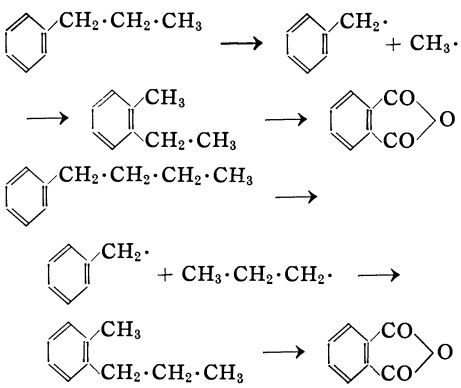
Concerning the above-mentioned strange reaction the author examined accordingly the following three mechanisms *a*, *b* and *c*.

*Mechanism a.* — *n*-Propyl benzene or *n*-butyl benzene would be oxidized to benzaldehyde. The two molecules of the aldehyde may be condensed to form anthraquinone as Parks[4] observed, and then this would be oxidized to from phthalic anhydride.

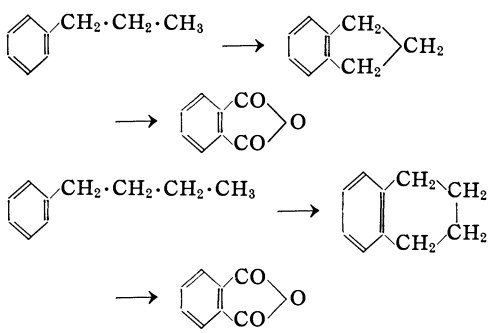
4) W. G. Parks et al., *Ind. Eng. Chem.*, **33**, 891 (1941); C. R. Downs, *J. Soc. Chem. Ind.*, **46**, 388, T (1927).



*Mechanism b.* — *n*-Propyl benzene or *n*-butyl benzene would be dissociated to form benzyl and ethyl or propyl radicals, as given in the papers by Szwarc[5], then the alkyl radical would be attached to the ortho position of benzyl radical to form dialkyl benzene[6]. This would be oxidized to phthalic anhydride.



*Mechanism c.*—As already reported by Tonomura[7], Murphy[8] and Nametkin[9], *n*-propyl benzene or *n*-butyl benzene would produce hydrindene or tetralin by cyclization and then this would be oxidized to phthalic anhydride.



The author examimed these mechanisms.

*On mechanism a.*—Oxidation products of *n*-propyl benzene or *n*-butyl benzene contained no anthraquinone, and when the mechanism is true, ethyl benzene would have to produce phthalic anhydride through the same mechanisms. But the experimental results showed that no phthalic anhydride was produced from ethyl benzene. From these facts, it is supposed that this mechanism is not true.

*On mechanism b.*—If this mechanism is correct, ethyl benzene must produce phthalic anhydride by the oxidation. The experiments showed that ethyl benzene did not produce it, and therefore this mechanism is not correct. To ascertain this conclusion, ethyl benzene was oxidized in the vapor phase with air containing vapor of methanol or ethanol, etc., both of which are liable to form a free radical[10], but no phthalic anhydride was obtained.

*On mechanism c.*—*n*-Propyl benzene was passed through the pumice (carrier) bed which contained no vanadium pentoxide under the same conditions as those of the oxidation (temperature, air rate and feed rate). The ultraviolet spectrum of the product showed that it contained styrene but no hydrindene. Moreover, when this product was oxidized in the liquid phase with aqueous solution of potassium permanganate[11], only benzoic acid was found but no phthalic acid. As to *n*-butyl benzene, the spectrum showed the presence of alkenyl benzene (presumably propenyl benzene). Thus the mechanism *c* is incorrect.

With these three mechanisms, the formation of phthalic anhydride from *n*-propyl benzene or *n*-butyl benzene by the oxidation can not be explained.

The author studied the following reactions.

*Mechanism d·1.*—The first carbon atom attacked by oxygen in the alkyl group of *n*-propyl benzene, and *n*-butyl benzene.

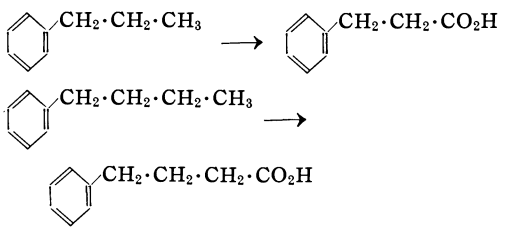
Propiophenone $C_6H_5\cdot CO\cdot CH_2\cdot CH_3$, phenyl acetone $C_6H_5\cdot CH_2\cdot CO\cdot CH_3$, hydrocinnamic acid $C_6H_5\cdot CH_2\cdot CH_2\cdot CO_2H$, butyrophenone $C_6H_5\cdot CO\cdot CH_2\cdot CH_2\cdot CH_3$, benzyl ethyl ketone $C_6H_5\cdot CH_2\cdot CO\cdot CH_2CH_3$, benzyl acetone $C_6H_5\cdot CH_2\cdot CH_2\cdot CO\cdot CH_3$ and $\gamma$-phenyl butyric acid $C_6H_5\cdot CH_2\cdot CH_2\cdot CH_2\cdot CO_2H$ were oxidized in vapor phase under the same conditions. The experimental results are given in Table III.

5) M. Szwarc, *Chem. Revs.*, **47**, 75 (1950); C. H. Leigh et al., *J. Chem. Phys.*, **20**, 407 (1952).
6) V. N. Ipatieff et al., *J. Am. Chem. Soc.*, **75**, 3323 (1953).
7) S. Tonomura, *J. Sci. Research Inst. (Tokyo)*, **21**, 794 (1942); **25**, 256 (1949).
8) M. T. Murphy et al., *J. Am. Chem. Soc.*, **71**, 3347 (1947).
9) S. S. Nametkin, *Chem. Abstr.*, **42**, 3339 (1948).
10) W. A. Waters, "The Chemistry of Free Radicals", Clarendon Press, Oxford (1948), p. 127.
11) S. P. Mulliken, "Identification of Pure Organic Compounds", Vol. I, John Wiley & Sons, Inc., New York, p. 197.

TABLE III. EXPERIMENTAL RESULTS OF VAPOR PHASE OXIDATION OF COMPOUNDS RELATED TO ALKYL BENZENE

| Material | Reaction temp. °C | Products | | |
|---|---|---|---|---|
| | | Phthalic anhydride mol. % | Benzoic acid mol. % | Maleic anhydride mol. % |
| Propiophenone | 300 | 0 | 45 | 39 |
| Propiophenone | 400 | trace | 2 | 49 |
| Phenyl acetone | 400 | trace | 20 | 42 |
| Hydrocinnamic acid | 400 | 20 | 2 | 44 |
| Cinnamic acid | 400 | 15 | 2 | 55 |
| $\alpha$-Hydrindone | 400 | 77 | 0 | 11 |
| Butyrophenone | 300 | trace | 62 | 29 |
| Butyrophenone | 400 | trace | 6 | 42 |
| Benzyl ethyl ketone | 300 | 0 | 18 | 23 |
| Benzyl ethyl ketone | 400 | 0 | 6 | 43 |
| Benzyl acetone | 400 | 18 | 3 | 46 |
| $\gamma$-Phenyl butyric acid | 400 | 30 | trace | 22 |
| Tetralone | 400 | 62 | trace | 12 |

As shown in Table III, propiophenone, butyrophenone, phenyl acetone and benzyl ethyl ketone, of which $C_1$ or $C_2$ contains oxygen atom, produced no phthalic anhydride. While hydrocinnamic acid, benzyl acetone and $\gamma$-phenyl butyric acid whose $C_3$ or $C_4$ has an oxygen atom, produced phthalic anhydride in a yield of 20~30%. From these results, it is concluded that only when the oxidation was initiated at $C_3$ of *n*- propyl benzene or at $C_3$ or $C_4$ of *n*-buthyl benzene, phthalic anhydride was obtained. The waste gas of oxidation of *n*-propyl benzene had a strong odor of hydrocinnamic acid. *n*-Butyl benzene was passed with air through the catalyst bed which contained a very small quantity of vanadium pentoxide, and the presence of $\gamma$-phenyl butyric acid was confirmed by the ultraviolet spectrum of the product.



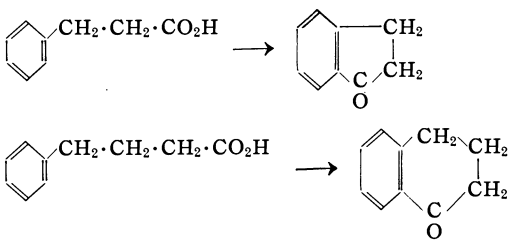

The mechanism given in *d·1* is different from the already published mechanism where only $C_1$ is oxidized in liquid phase or vapor phase oxidation.

*Mechanism d·2.*—On cyclization of hydrocinnamic acid and $\gamma$-phenyl butyric acid.

Hydrocinnamic acid produces hydrindone by cyclization in the presence of hydrogen fluoride[12], poly-phosphoric acid[13] or 80% phosphoric acid[14] catalyst, and tetralone is obtained from $\gamma$-phenyl butyric acid by the action of concentrated sulfuric acid[15]. However, it has not been reported that the cyclization takes place under conditions of vapor phase oxidation.

The author performed the experiment that a mixture of hydrocinnamic acid or $\gamma$-phenyl butyric acid vapor and air was passed through the bed of catalyst at 400°C which contained a very small quantity of vanadium pentoxide. Among the reaction products hydrindone and tetralone were identified as phenyl hydrazone and 2, 4-dinitrophenylhydrazone, respectively.

This indicates that cyclization took place. To ascertain this results, the reaction product was oxidized by aqueous solution of potassium permanganate, and phthalic acid was obtained.




*Mechanism d·3.*—On vapor phase oxidation of hydrindone and tetralone.

By catalytic air oxidation hydrindone and tetralone gave phthalic anhydride in yields of 77, 62% and maleic anhydride 11, 12%, respectively. From these results (*d·1*, *d·2* and *d·3*), the mechanism through

12) F. Fieser et al., *J. Am. Chem. Soc.*, **61**, 2172 (1937).
13) M. R. Snyder et al., ibid., **72**, 2965 (1950); E. C. Horning, ibid., **73**, 5879 (1951).
14) J. C. Hillyer, *J. Org. Chem.*, **17**, 600 (1952).
15) K. Krollpfeiffer et al., *Ber.*, **56**, 620 (1922).

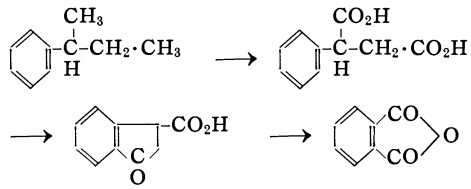
which phthalic anhydride is obtained by the oxidation of *n*-propyl benzene and *n*-butyl benzenes, is as follows:

*n*-propyl benzene → hydrocinnamic acid → α-hydrindone → phthalic anhydride

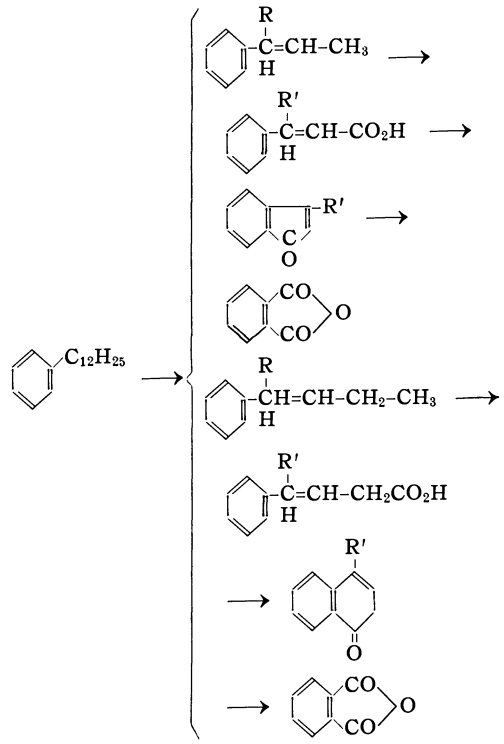
*n*-butyl benzene → γ-phenyl butyric acid → tetralone → phthalic anhydride

*iso*-Propyl benzene and *tert*-butyl benzene gave no phthalic anhydride by the oxidation. They have only two carbon atoms in the longest chain of the alkyl group, and therefore cyclization will be impossible to occur.

The yield of phthalic anhydride from *sec*-butyl benzene was higher than that from *n*-propyl benzene. This will probably be due to the fact that cyclization of hydrocinnamic acid takes place more easily when it has a substituent group than when it has none[16].

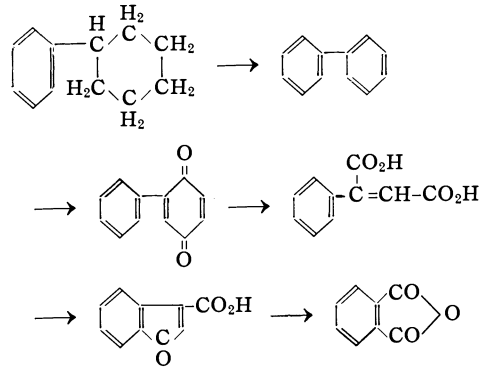


**Vapor Phase Oxidation of Amyl Benzenes, Hexyl Benzenes and Dodecyl Benzenes and Others.**—The number of carbons in the longest chain of these alkyl groups is at least 3 or more. For the same reason, phthalic anhydride is obtained by the oxidation of these alkyl benzenes (Table II). The product that was obtained by passing dodecyl benzene through the pumice stone (carrier) zone at 400°C, was separated by distillation into three fractions, boiling at about 162, 182 and 230°C, respectively. These produced benzoic acid by oxidation with aqueous solution of potassium permanganate and were absorbed by 90% sulfuric acid and their ultraviolet spectra were characteristic. These were possibly alkenyl benzene (the number of carbons of the alkenyl group was 4—6). As the result it is apparent that such long-chain alkyl benzene as dodecyl benzene is decomposed by heat into short-chain alkenyl benzenes and then phthalic anhydride is produced by oxidation through the above mentioned mechanism.




Benzoic acid was not produced from *tert*-alkyl benzenes. This is possibly due to dissociation[17] into benzene nucleus and the alkyl group.

It is supposed that phenyl cyclohexane produced phthalic anhydride by oxidation through the following mechanism.



The author is particularly indebted to Professor S. Kimura of Kyoto University, Dr. T. Yoshida, Superintendent of Tobata Chemical Works and Mr. O. Hibino, Manager of the Laboratory Department of the Yawata Chemical Industry Co., Ltd.

*Tobata Works*
*Yawata Chemical Industry Co., Ltd.*
*Yawata-shi, Fukuoka*

16) Richter-Anschütz, "Organishe Chemie", Band II. Friedrich Cohen Bonn (1913), p. 615.
17) N. Tanaka et al., *J. Chem. Soc. Japan, Ind. Chem. Sec.* (*Kogyo Kagaku Zasshi*), **55**, 443 (1952).

# *Fluorine-19 Nuclear Magnetic Shielding in Some Monofluorinated Compounds*

By Kazuo Ito, Kan Inukai and Taro Isobe

(Received July 20, 1959)

The chemical shifts in the proton magnetic resonance spectra of aromatic compounds have been studied by several authors both experimentally[1,2] and theoretically[2-8]. The magnetically non-equivalent nature of protons in these compounds has been essentially interpreted in terms of the interaction between a proton magnetic moment and diamagnetic currents induced on aromatic rings by an external magnetic field. On the other hand, Isobe, Inukai and Ito[9] have shown that the fluorine atoms in fluorobenzene, 1- and 2-fluoronaphthalenes are also magnetically non-equivalent. They have concluded tentatively that the non-equivalent nature of the fluorine atoms can not be attributed to the induced diamagnetic ring current mentioned above but may be attributed to the variation in polarity of the C–F $\sigma$-bonds. As a criterion for predicting such a variation in polarity of C–F bonds, the $\pi$-electron density of McWeeny's sense[10] has been suggested. Recently, however, Fukui and his coworkers[11] have proposed the qualitative assumption that the larger the $\pi$-electron conjugation of a fluorine atom with a neighboring atom or group of atoms and consequently the smaller the $\pi$-electron density on the fluorine atom, the more the fluorine nucleus is magnetically shielded. The $^{19}$F chemical shifts in some aromatic fluoro compounds, including 1- and 2-fluoronaphthalenes, have been interpreted in terms of this assumption, although the variation in polarity of C–F $\sigma$-bonds has also been introduced in order to interpret the $^{19}$F chemical shifts in *p*-nitrofluorobenzene and 1-fluoro-4-nitronaphthalene for which the assumption predicts results contradictory to those of the experiments.

In the present paper the $^{19}$F NMR spectra of 2- and 3-fluoropyridines, 1-fluoropyrene[12] and cyclohexylfluoride are studied and the $^{19}$F chemical shifts in these compounds, together with those in fluorobenzene, 1- and 2-fluoronaphthalenes, are discussed. The spectra of 9-fluoroanthracene and 12-fluorochrysene[12] have also been studied but no signal has been obtained.

## Experimental

**Materials.**—The samples of 1-fluoropyrene and 12-fluorochrysene were kindly provided by Prof. G. M. Badger[13] of the University of Adelaide, South Australia, that of 9-fluoroanthracene by Dr. C. F. H. Allen[14], Eastman Kodak Co., Rochester, U. S. A. and that of cyclohexylfluoride by Dr. K. Okuhara of Government Industrial Research Institute, Nagoya, Japan, to whom the authors are much indebted. The samples of fluorobenzene[15], *m*-nitrofluorobenzene[16], 1- and 2-fluoronaphthalenes[15,17], 2- and 3-fluoropyridines[18] were prepared by the method of the Schiemann reaction. Since no NMR signal was found in 9-fluoroanthracene, the preparation of another sample of the compound was attempted by the general method of Garvey, Halley and Allen[14]. The reaction repeated under the conditions given was followed by some yellowing of the solution but no substance with the melting point specified for 9-fluoroanthracene was obtained.

**Apparatus and Procedure.**—The $^{19}$F NMR spectra were measured with a Varian V-4300-B High Resolution Spectrometer operating at a fixed frequency of 40 Mc./sec. and equipped with a Varian Field Stabilizer. The sample was dissolved in

1) H. J. Bernstein and W. G. Schneider, *J. Chem. Phys.*, **24**, 468 (1956).
2) H. J. Bernstein, W. G. Schneider and J. A. Pople, *Proc. Roy. Soc. (London)*, **A236**, 515 (1956).
3) J. A. Pople, *J. Chem. Phys.* **24**, 1111 (1956).
4) G. Hazato, ibid., **27**, 605 (1957).
5) J. C. Waugh and R. W. Fessenden, *J. Am. Chem. Soc.*, **79**, 846 (1957).
6) K. Ito, ibid., **80**, 3502 (1958).
7) R. McWeeny, *Molec. Phys.*, **1**, 312 (1958).
8) C. E. Johnson, Jr. and F. A. Bovey, *J. Chem. Phys.*, **29**, 1012 (1958).
9) T. Isobe, K. Inukai and K. Ito, ibid., **27**, 1215 (1957).
10) R. McWeeny, ibid., **19**, 1614 (1951).
11) K. Fukui, S. Hattori, T. Yonezawa, R. Kusaka and H. Kitano, *J. Chem. Soc. Japan, Pure Chem. Sec.*, (*Nippon Kagaku Zasshi*), **80**, 541 (1959).
12) All compounds are numbered in accordance with A. M. Patterson and L. T. Capell, "The Ring Index", Reinhold Publishing Corp., New York (1940).
13) G. M. Badger and J. F. Stephens, *J. Chem. Soc.*, **1956**, 3637.
14) B. S. Garvey, Jr., L. F. Hally and C. F. H. Allen, *J. Am. Chem. Soc.*, **59**, 1827 (1937).
15) G. Balz and G. Schiemann, *Ber.*, **60**, 1186 (1927).
16) K. Inukai and Y. Maki, *J. Chem. Soc. Japan, Pure Chem. Sec. (Nippon Kagaku Zasshi)*, **78**, 1305 (1957).
17) G. Schiemann, W. Gueffroy and W. Winkelmüller, *Ann.*, **487**, 270 (1930).
18) A. Roy and G. F. Hawkins, *J. Am. Chem. Soc.*, **69**, 2443 (1947).

about the same amount of another fluoro compound, *m*-nitrofluorobenzene in most cases, which provides an internal standard for determining the chemical shift $\delta$ of the sample defined as $\delta = 10^5 \times (H_c - H_r)/H_r$ where $H_c$ is the applied magnetic field for the $^{19}F$ resonance in the sample and $H_r$ is that for the reference. The chemical shift was determined by adjusting that of 1-fluoronaphthalene[9] to +1.32, refered to *m*-nitrofluorobenzene. The value of 1.32 was re-determined for the present work on the basis of the chemical shift of fluorobenzene[19] +0.33, agreeing with the previous one[9].

In the previous work[9], the $\delta$-values obtained from the solutions, 1-fluoronaphthalene+*m*-nitrofluorobenzene, 2-fluoronaphthalene+*m*-nitrofluorobenzene and 1-fluoronaphthalene + 2-fluoronaphthalene, were found to be consistent in themselves. In the present work, the results obtained from the solutions, 2-fluoropyridine+*m*-nitrofluorobenzene, 3-fluoropyridine+*m*-nitrofluorobenzene and 2-fluoropyridine+3-fluoropyridine were, also consistent in themselves. Therefore, the bulk effects[20] for the chemical shifts were assumed to be insignificant in the present experiments.

A 33 mol. per cent solution of 9-fluoroanthracene in *m*-nitrofluorobenzene heated for increasing the solubility gave no signal except that of the solvent which was not greatly deformed compared with that of pure *m*-nitrofluorobenzene. Also no signal was obtained on a solution of 12-fluorochrysene in *m*-nitrofluorobenzene because of its low solubility. Both samples will be examined further.

## Results and Discussion

It is known experimentally[21,22] that the magnetic shielding of an $^{19}F$ nucleus is quite sensitive to the nature of the bond between the fluorine atom in question and the atom to which the fluorine is bound. The simple and direct correlation[23] of $^{19}F$ magnetic shielding in para-substituted fluorobenzenes with the $\pi$-electron densities or Hamett's sigma constants for the para-position in the corresponding non-fluorinated compounds may also be attributed to the dependence of the shielding on the bonding nature of C–F bonds. On the other hand, Saika and Slichter[24] have shown theoretically that the $^{19}F$ magnetic shielding must have a close relation with the nature of the $\sigma$-bond by which the fluorine is bound to another atom. The qualitative extension of their theory suggests readily that a $\pi$-bond character in the bond by which the fluorine in question is bound to another atom would also have a significant effect on $^{19}F$ magnetic shielding. In order to discuss the present results, therefore, it would be necessary to take into account both $\sigma$- and $\pi$-bonding characters of C—F bonds. Since, however, correct estimations of $\sigma$- or $\pi$-bonding characters of C—F bonds in the compounds studied are very difficult, the following three molecular indexes which may serve as measures of $\sigma$- and $\pi$-bonding characters of C–F bonds are taken into account: (1) the $\pi$-electron density $q$ on the ring carbon to which the fluorine in question is bound, (2) the $\pi$-electron "atom charge" density of McWeeny's sense[10] $q'$ on the ring carbon mentioned above, and (3) the $\pi$-electron density $q$ on the carbon atom of a $CH_2^-$ group in a hypothetical molecule in which the fluorine atom of the fluoro compound studied is replaced by a $CH_2^-$ group.

The $\pi$-electron densities on ring carbons may serve as a criterion for predicting chemical differences in these carbons and, consequently, differences in the $\sigma$-bonding nature of C–F bonds. The $\pi$-electron "atom charge" densities may also be usable from the same point of view. The latter, however, may be especially useful in alternant hydrocarbons in which the former fails to interpret chemical differences in ring carbons, being equal to unity on all carbons on the basis of the simple LCAO calculation. It would be worth noting that the $\pi$-electron "atom charge" densities on the 1- and 2-positions of naphthalene show a tendency consistent with the experimental observation[25]. The $\pi$-electron density on the carbon atom of the $CH_2^-$ group in the hypothetical molecule mentioned above may serve as a measure of the $\pi$-conjugation of the fluorine atom substituted at the corresponding position. The smaller the $\pi$-electron density on the $CH^-_2$ group, the greater would be the $\pi$-conjugation of the fluorine atom with the remainder of the molecule.

The $^{19}F$ chemical shifts obtained in the present work are given in Table I, together with those of 1- and 2-fluoronaphthalenes. Three molecular indexes mentioned above are given in Tables II—IV, respectively. The parameters used in these tables for

19) H. S. Gutowsky, D. W. McCall, B. R. McGarvey and L. H. Meyer, ibid., **74**, 4809 (1952).
20) B. P. Daily and J. N. Shoolery, ibid., **77**, 3977 (1955); H. J. Bernstein and W. G. Schneider, *Nature*, **178**, 1328 (1956).
21) H. S. Gutowsky and C. J. Hoffman, *J. Chem. Phys.*, **19**, 1259 (1951).
22) L. H. Meyer and H. S. Gutowsky, *J. Phys. Chem.*, **57**, 481 (1953).
23) H. S. Gutowsky, D. W. McCall, B. R. McGarvey and L. H. Meyer, *J. Am. Chem. Soc.*, **74**, 4809 (1952).
24) A. Saika and C. P. Slichter, *J. Chem. Phys.*, **22**, 26 (1954).
25) S. C. Abrahams, J. M. Robertson and J. G. White, *Acta Cryst.*, **2**, 238 (1949).

TABLE I. $^{19}F$ CHEMICAL SHIFTS IN SOME MONOFLUORINATED COMPOUNDS

| Compound | 2-Fluoro-pyridine | Fluoro-benzene | 2-Fluoro-naphthalene | 1-Fluoro-pyrene | 1-Fluoro-naphthalene | 3-Fluoro-pyridine | Cyclohexyl-fluoride |
|---|---|---|---|---|---|---|---|
| $\delta$ | −4.27 | 0 | 0.16 | 0.97 | 0.99 | 1.25 | 5.63 |

TABLE II. THE $\pi$-ELECTRON DENSITIES ON RING CARBONS

| Compound / Position | Pyridine 2 | Benzene | Naphthalene 2 | Pyrene 1 | Naphthalene 1 | Pyridine 3 | Ref. |
|---|---|---|---|---|---|---|---|
| Simple LCAO with[e] | | | | | | | |
| $\delta_N=1$, $\delta_{C'}=0$ | 0.855 | 1.000 | 1.000 | 1.000 | 1.000 | 1.008 | a) |
| $\delta_N=1$, $\delta_{C'}=0.1$ | 0.893 | 1.000 | 1.000 | 1.000 | 1.000 | 0.984 | b) |
| Jaffe's parameters | 0.970 | 1.000 | 0.989 | | 0.999 | 0.977 | c) |
| SCF LCAO | | 1.000 | 1.003 | | 0.967 | | d) |

a) K. Higashi and H. Baba, "Quantum Organic Chemistry (Ryoshi Yuki Kagaku)", Asakura Publishing Co., Tokyo (1956).
b) Calculated by the present authors.
c) H. H. Jaffe, *J. Chem. Phys.*, **20**, 279, 778, 1554 (1952).
d) C. M. Moser, *J. chim. phys.*, **52**, 24 (1955).
e) The Coulomb integral of a nitrogen atom is given by $\alpha_N=\alpha_C+\delta_N\beta_{CC}$ where $\alpha_C$ is the Coulomb integral of a carbon atom and $\beta_{CC}$ is the resonance integral of a C-C bond. The Coulomb integral of the carbon atom bonded to the nitrogen atom is given by $\alpha_{C'}=\alpha_C+\delta_{C'}\beta_{CC}$.

TABLE III. THE $\pi$-ELECTRON "ATOM CHARGE" DENSITIES ON RING CARBONS

| Compound / Position | Pyridine 2 | Benzene | Naphthalene 2 | Pyrene 1 | Naphthalene 1 | Pyridine 3 |
|---|---|---|---|---|---|---|
| Simple LCAO with | | | | | | |
| $\delta_N=1$, $\delta_{C'}=0$ | 0.644 | 0.756 | 0.757 | 0.771 | 0.767 | 0.784 |
| $\delta_N=1$, $\delta_{C'}=0.1$ | 0.672 | 0.756 | 0.757 | 0.771 | 0.767 | 0.767[a] |

a) If the inductive effect of nitrogen on $\beta$-carbon is taken into account as $\delta_C(\beta)=(0.1)^2$, this value takes 0.770

TABLE IV. THE $\pi$-ELECTRON DENSITY ON THE CARBON ATOM OF A $CH_2^-$ GROUP SUBSTITUTED IN AN AROMATIC COMPOUND

| Parent compound | Pyridine | Benzene | Naphthalene | Pyrene | Naphthalene | Pyridine |
|---|---|---|---|---|---|---|
| Position of substitution | 2 | | 2 | 1 | 1 | 3 |
| Charge density on $CH_2^-$ | 1.499[a] | 1.571[d] | 1.529[d] | 1.364[d] | 1.450[d] | 1.561[a] |
| | 1.485[b] | | | | | 1.542[b] |
| | 1.464[c] | | | | | 1.504[c] |

a) Calculated with $\delta_N=1$, $\delta_{C'}=0$.
b) Calculated with $\delta_N=1$, $\delta_{C'}=0.1$.
c) Calculated with $\delta_N=2$, $\delta_{C'}=0.25$. This set of parameters was used by H. C. Longuet-Higgins and C. A. Coulson, *Trans. Faraday Soc.*, **43**, 87 (1947). These parameters would overestimate the electronegative effect of nitrogen (see Refs. 26 and 27), but were used here in order to show an extreme case.
d) Calculated by the method of H. C. Longuet-Higgins, *J. Chem. Phys.*, **18**, 265 (1950).

calculating the indexes of pyridine are their representative values[26,27]. The resonance integral of a C-N bond was assumed to be equal to that of a C-C bond, because small changes in resonance integrals have only negligible effects on the indexes in the tables. The values given in the second and the seventh columns of Table IV were calculated by the use of the mutual atom polarizabilities in a benzyl anion which are shown in Table V.

**Fluorobenzene, 1- and 2-Fluoronaphthalenes, 1-Fluoropyrene and 3-Fluoropyridine.** — The sequence of $\delta$-values for these compounds is, as shown in Table I, fluorobenzene < 2-fluoronaphthalene < 1-fluoropyrene, 1-fluoronaphthalene < 3-fluoropyridine. As seen from Table II, the $\pi$-electron density on the ring carbon to which the fluorine atom is bound fails to explain the

26) R. D. Brown, *Quart. Revs.*, **6**, 63 (1952).
27) L. E. Orgel, T. L. Cottrell, W. Dick and L. E. Sutton, *Trans. Faraday Soc.*, **47**, 113 (1951).

TABLE V. MUTUAL ATOM POLARIZABILITIES IN A BENZYL ANION

| $r-s$[a] | $\pi_{r,s}\times\beta$ |
|---|---|
| 1—1′ | −0.1324 |
| 2—1′ | −0.0716 |
| 3—1′ | −0.0099 |
| 4—1′ | −0.1162 |
| 1′—1′ | 0.4116 |

a) 1′ denotes a $CH_2^-$ group, 1 the carbon atom bonded to the $CH_2^-$ group and 2, 3 and 4 denote the $\alpha$, $\beta$ and $\gamma$ carbon atoms, respectively.

sequence of $\delta$, because the densities in benzene, naphthalene and pyrene are all equal to unity. The $\pi$-conjugation of fluorine atoms, the rough measure of which is seen from Table IV, fails also to interpret the sequence of $\delta$. As far as one restricts the attention only to fluorobenzene, 1- and 2-fluoronaphthalenes, one may find a possible interpretation in terms of the assumption[11] that the greater the $\pi$-electron conjugation of a fluorine atom with a neighboring atom or group of atoms, the greater the value of $\delta$. However, this assumption fails also definitely to interpret the sequence of $\delta$ if one takes into account 1-fluoropyrene and 3-fluoropyridine. On the other hand, the sequence of the $\pi$-electon "atom charge" density (Table III), benzene<2-position of naphthalene < 1-position of naphthalene < 1-position of pyrene < 3-position of pyridine, shows a fairly good parallel tendency with the sequence of $\delta$ mentioned above. Although the parallelism between two sequences is not very good in pyrene, the $\pi$-electron "atom charge" density may be rather satisfactory for interpreting the sequence of $\delta$ compared with other indexes, in the sense that the "atom charge" densities of the 1-position of pyrene and the 1-position of naphthalene are fairly close to each other and that the "atom charge" density of the 3-position of pyridine can be larger than that of the 1-position of naphthalene within the reasonable limits[26,27] of parameters $\delta_N$ and $\delta_{C'}$ (see Table III and footnote e) of Table II). Since the greater the value of $q'$, the more ionic would be the C–F $\sigma$-bond, the increasing tendency of $\delta$ with $q'$ is reasonable[24].

**2-Fluoropyridine.**—This compound has the smallest $\delta$-value. This tendency can be interpreted in terms of any index given in Tables II—IV. However, the $\pi$-electon density would be rather worthless for this case too, because this index is very poor for interpreting the sequence of $\delta$-values as discussed above. The effect of the $\pi$-conjugation of the fluorine atom substituted at the 2-position of pyridine is of interest from the point of view that the $^{35}Cl$ pure quadrupole resonance of 2-chloropyridine[28] has been explained, emphasizing the larger $\pi$-bonding character in the C-halogen bond at the 2-position compared with the $\pi$-bonding characters in those at other positions. The $\pi$-conjugation of the fluorine atom, however, may not be the main cause of the small $\delta$-value of 2-fluoropyridine. Because, if it is so, the $\delta$-value of 1-fluoronaphthalene must also very small contrary to the experiments. Therefore, the $\pi$-electron "atom charge" density and the inductive effect of nitrogen, which has the significant effect on proton NMR spectra of nitrogen heterocycles[29-31], would be responsible for the $^{19}F$ magnetic shielding of 2-fluoropyridine.

**Cyclohexylfluoride.**—This compound has a very great $\delta$-value compared with that of benzene. It is obvious that this difference in $\delta$ is too great to be interpreted in terms of the diamagnetic ring current induced on benzene[2,3]. The assumption of Fukui et al. on the correlation of $\delta$ with the $\pi$-conjugation of the fluorine atom fails also to interpret the $\delta$-value of this compound which is greater than that of fluorobenzene. A possible explanation is that the C–F bond in cyclohexylfluoride is more ionic than that in fluorobenzene. Such an explanation may be rather probable, since it is known that[32] the nature of the $\sigma$-bonding in a C($sp^3$)-Cl bond is more ionic than that in a C($sp^2$)-Cl bond and that[32,33] the ring hydrogens of benzene are more protonic than the hydrogens of C($sp^3$)-H bonds.

In the arguments given above, it has been shown that the $^{19}F$ magnetic shielding of the compounds studied in the present work is correlated most probably with the $\pi$-electron "atom charge" density. Hereupon, it would be worth while to note

28) P. J. Bray, R. G. Barnes and S. L. Segel, *J. Chem. Phys.*, **28**, 99 (1958).
29) H. J. Bernstein and W. G. Schneider, ibid., **24**, 469 (1956).
30) L. H. Meyer, A. Saika and H. S. Gutowsky, *J. Am. Chem. Soc.*, **75**, 4567 (1953).
31) H. S. Gutowsky, R. L. Rutledge and M. Tamres, ibid., **76**, 4242 (1954).
32) Y. Kurita, *J. Japanese Chem.* (*Kagaku no Ryoiki*), **10**, 24 (1956). See also J. Duchesne, *J. Chem. Phys.*, **19**, 246 (1951).
33) H. W. Thompson, *Trans. Faraday Soc.*, **46**, 103 (1950); G. M. Barrow and D. C. McKean, *Proc. Roy. Soc.* (*London*), **A213**, 27 (1952); I. M. Mills and H. W. Thompson, ibid, **A228**, 287 (1955).

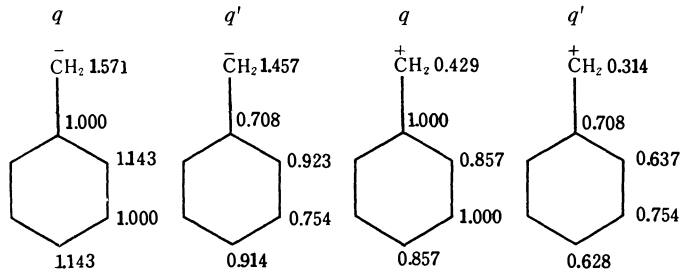



Fig. 1. The $\pi$-electron densities ($q$) and $\pi$-electron "atom charge" densities ($q'$) in a benzyl anion and cation

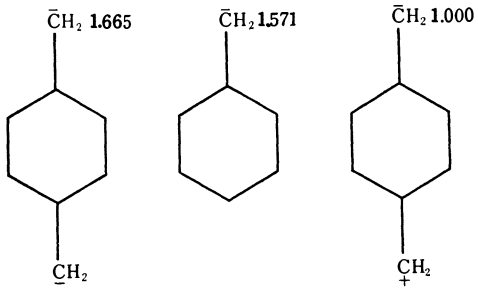



Fig. 2. $\pi$-electron densities in some carbions

that the $^{19}F$ magnetic shielding in substituted fluorobenzenes[23], which has been correlated simply with the $\pi$-electron density $q$, may also be correlated with the $\pi$-electron "atom charge" density $q'$, because $q$ and $q'$ have the parallel tendency as shown in Fig. 1. On the other hand, Fig. 2 predicts that the $\pi$-conjugation of a fluorine atom, which is represented by $CH_2^-$ in the figure, may be reduced by the para-substitution of $-E$ substituents (halogens, OH, $NH_2$, etc.) and is increased by that of $+E$ substituents ($NO_2$, CN, etc.). These predictions suggest that the assumption[11] of Fukui et al. may lead to the contradictory results with the experiments. The pure nuclear quadrupole resonance experiments on para-substituted chlorobenzenes[34] and iodobenzenes[35] have shown that the $\sigma$-bond character of a C–halogen bond is made more ionic by the para-substitution of $-E$ substitution and less ionic by that of $+E$ substituents, whereas the double-bond character of the C–halogen bonds is reduced by the para-substitution of $-E$ substituents and is increased by that of $+E$ substituents. These results support the interpretation of $^{19}F$ magnetic shielding in para-substituted fluorobenzenes in terms of $q'$ or ionicity in C–F bonds, but do not support the interpretation of the same subject in terms of the assumption of Fukui et al. It would also be worth noting that the relative magnetic shielding of $CF_4$ and $CF_3Cl$, which has been one of the important experimental evidences for supporting the assumption of Fukui et al., is not necessarily interpreted merely by their assumption, but is also interpreted by the variation in polarity in C–F bonds as argued in the original paper[36].

34) H. C. Meal, *J. Chem. Phys.*, **24**, 1011 (1956); C. Dean, *Phys. Rev.*, **86**, 607 (1952); Y. Kurita, *Chemistry (Kagaku)*, **12**, 556 (1957).
35) G. W. Ludwig, *J. Chem. Phys.*, **25**, 159 (1956).

**Summary**

The $^{19}F$ NMR spectra of 2- and 3-fluoropyridines, 1-fluoropyrene, cyclohexylfluoride, 9-fluoroanthracene and 12-fluorochrysene were studied. No signal was obtained for the latter two compounds. The magnetic shielding constants obtained were attempted, together with those for fluorobenzene, 1- and 2-fluoronaphthalenes, to be correlated with some molecular indexes. It was found that the $\pi$-electron density in McWeeny's sense ($\pi$-electron "atom charge" density) on the ring carbon atom, to which the fluorine in question is bound, is must probably correlated with the magnetic shielding of the fluorine nucleus. This result suggests that the variation in $^{19}F$ magnetic shielding constants in these compounds may be attributed mainly to the variation in polarity in C–F $\sigma$-bonds. It was noted that such an idea is supported by nuclear quadrupole resonance experiments.

*Department of Chemistry*
*Nagoya University*
*Nagoya (K. Ito)*

*Government Industrial Research Institute,*
*Nagoya (K. Inukai)*

*Chemical Research Institute of*
*Non-Aqueous Solutions*
*Tohoku University*
*Sendai (T. Isobe)*

36) L. H. Meyer and H. S. Gutowsky, *J. Phys. Chem.*, **57**, 481 (1953).

# *Neutron Activation Analysis of Iodine in Silicon*

By Tadashi NOZAKI, Hideo BABA and Hidemaro ARAKI

(Received June 27, 1959)

The determination of trace impurities in silicon is of great importance in the research and industry of the semiconductor material. The neutron activation analysis has played an important role in this field, being used for many kinds of impurity and even in routine work[1]. Among the numerous reports, however, none, as far as listed in the "*Analytical Abstracts* (Society for Analyt. Chem. England)" up to Vol. 6 No. 3 (March, 1959) has dealt with halogens in silicon, though the semiconductor material has been purified through one of its halogen compounds. The present authors determined iodine in silicon purified by the iodide or the chloride method.

Natural iodine consists entirely of $^{127}I$, which is activated by thermal neutrons into $^{128}I$ [$\sigma=6$ barn, $T_{1/2}=25$ min., $\beta$ 2.12 (76%), etc., $\gamma$ 0.45 (17%) etc.]. When more than a few p.p.m. of iodine is present with outany other appreciable amount of impurity that emits $\gamma$-rays or positrons, the $\gamma$-ray spectrometry with a multichannel pulse-height analyzer provides an easy method for quantitative analysis[2]. But when the iodine content is lower, chemical separation becomes necessary, because the photo-peak of $^{128}I$ is masked by the "Bremsung" of $\beta$-rays from $^{31}Si$ ($T_{1/2}=2.62$ hr., $E_{max}=1.48$ MeV.).

The separation method must be checked carefully, because iodine has many oxidation states, which involve complicated behavior of isotopic exchange, and because, molecular iodine as well as hydrogen iodide is volatile. The treatment of silicon with a mixture of hydrofluoric and nitric acid, a suitable process for many cases, cannot be used here. On the other hand, there is an advantageous rule that any kind of iodine oxide, at least in an ordinary concentration, reacts instantaneously and stoichiometrically with an excess of iodide in an acid solution to give molecular iodine. Fusion of the silicon with potassium hydroxide containing potassium iodide as the carrier, followed by treatment with sulfuric acid, and oxidation with sodium nitrite to molecular iodine, provides a method of chemical separation, the last being distilled and converted into silver iodide. Its usefulness was checked by the use of $^{131}I$ produced carrier free in silicon by the neutron irradiation of tellurium diffused in the silicon.

## Experimental

**Sample.**—About 1 g. portion of metallic silicon, prepared by the thermal decomposition of silicon tetraiodide or by the reduction of silicon tetrachloride with zinc was used for each analysis. Details concerning each of the samples are described later.

**Irradiation.**—The sample and reference standard were put side by side in a poly ethylene capsule and irradiated in JRR-1 (Japan Research Reactor 1) under a thermal neutron flux of about $6\times10^{11}$n/cm$^2$·sec. The activity of $^{128}I$ reaches about 80% of its saturation by one hour irradiation.

**Self-shielding Effect.**—Thermal neutrons for which the absorption cross section of natural silicon is only $0.13\pm0.03$ barns, traverse one centimeter in this material, thereby decreasing the flux by only less than 1%. Thus with an ordinary quantity of the sample, the self-shielding effect can legitimately be neglected.

**Chemical Separation of Iodine.**—The irradiated silicon was immediately powdered in a special mortar made of iron. A weighed amount (about 0.8 g.) of the silicon powder was slowly added to potassium hydroxide (about 10 g.) which is maintained just above its melting point, and contained a known quantity (several milligrams) of potassium iodide as the carrier. When the vigorous reaction with the evolution of hydrogen became feeble, the mixture was carefully heated to complete the reaction rapidly. The fused matter was treated with 100 ml. of 5 N sulfuric acid containing a few milligram of sodium chloride and potassium bromide as a hold-back carrier. A solution of sodium nitrite was added to the product, and the liberated iodine distilled into a dilute solution of sodium sulfite. This distillate was treated again with sulfuric acid and sodium nitrite, and the molecular iodine was extracted with xylene, washed with dilute sul-

1) B. A. Thompson et al., *Anal. Chem.*, **30**, 1023 (1958).
2) T. Ichimiya et al., *Radioisotopes* (Jap. R. I. Association), 7, 281 (1958).
3) For example, A. C. Wahl, "Radioactivity Applied to Chemistry", John Wiley & Sons, Inc., New York (1951), p. 32.

furic acid and water, and extracted back into an aqueous solution containing a small excess of sodium sulfite, from which silver iodide was precipitated by the addition of acetic acid, silver nitrate and nitric acid. The precipitate was filtered off through a glass filter (No. 3), washed with a very dilute nitric acid, water, ethanol and ether. The entire process required an hour, or, properly operated, slightly less, with a chemical yield of 50 to 70%.

**Radioactivation Standard.**—A weighed crop of potassium iodide in a polyethylene envelope was irradiated together with the silicon, and dissolved into a solution containing a known amount of inactive potassium iodide. A part of this solution was oxidized as above, and the molecular iodine extracted with xylene, washed with an aqueous potassium hydrogen sulfate and water, and similarly converted into silver iodide.

**Counting.**—A simple G-M counter with an end window tube served very conveniently, when the iodine content was more than 0.01 $\mu$g., while a $2\pi$ counter of gas flow type was used for less iodine. By the use of the latter, whose counting efficiency is several times higher than the former, 3/4 or more of the total disintegration could be detected by virtue of the back-scattering of the $\beta$-rays, when the sample was placed on such a heavy metal plate as tin, with negligible loss due to self-absorption. The activity was measured at short time intervals for about 150 min.

**Check on the Chemical Process.**—The chemical process was checked by the use of silicon containing $^{131}$I, which was prepared by the irradiation of silicon doped with tellurium. The following reactions take place,

$$^{130}\mathrm{Te}\ (n,\gamma)\ ^{131}\mathrm{Te} \xrightarrow[25\ \mathrm{min.}]{\beta^-,\gamma} {}^{131}\mathrm{I} \xrightarrow[8.06\ \mathrm{d.}]{\beta^-,\gamma} {}^{131}\mathrm{Xe}\ (\mathrm{stable})$$

or,

$$^{130}\mathrm{Te}\ (n,\gamma)\ ^{131\mathrm{m}}\mathrm{Te} \xrightarrow[30\ \mathrm{hr.}]{} {}^{131}\mathrm{Te} \longrightarrow {}^{131}\mathrm{I} \longrightarrow {}^{131}\mathrm{Xe}.$$

$^{131}$I emits various $\gamma$-rays, among which that of 0.364 MeV. is predominant, and with the irradiated tellurium the area covered by this photo-peak in the $\gamma$-ray spectrum decayed with the half-life of $^{131}$I, while other peaks of lower energies due to other radioactive nuclides of tellurium (mostly of metastable state) survived longer. It would be reasonable to assume that the two radioisotopes, $^{128}$I and $^{131}$I, formed in the silicon, pass the so-called hot atom state and behave similarly throughout the chemical process.

Very pure silicon and a small quantity of metallic tellurium in an evacuated silica ampoule were heated over 1000°C for many hours, to cause the latter to diffuse into the former. The ampoule was kept in the reactor for a week. After several days, the silicon was washed with aqua regia and slightly etched with a mixture of hydrofluoric and nitric acids to remove surface contamination. The activity in the silicon was counted with a scintillation counter with a well-type crystal and a single channel analyzer (the region between 0.32 and 0.41 MeV.). The silicon without tellurium contained but negligible activity. After the same chemical process described above, the activity of $^{131}$I in the silver iodide was measured under the same condition. The chemical yield being taken into account, the separation method was proved satisfactory within a standard error due to counting, which amounted to 3% in this case.

## Results

The results are shown in the table, where I in the column of sample denotes that the silicons were purified by the iodide process, and Cl by the chloride process. The iodide process has been carried out in the Electrical Communication Laboratory in order to obtain semiconductor grade silicon. This method consists of converting a raw silicon into silicon tetraiodide, of purifying the iodide by various techniques, and of thermal decomposition of the iodide with continuous evacuation. The samples I-1 were silicons just after this stage. I-2 was obtained by keeping molten I-1 containing 4.5 p. p. m. of iodine in a silica vessel for an hour under an argon gas flow. I-3 were taken out of the tail of a single crystal made by the cooling method from I-1 containing 1.3 p. p. m. of iodine. The tail end of the crystal contained much more iodine (2.0 p. p. m.) than a part several millimeters above it (0.32 p. p. m.). These silicons were usually of type N. Floating zone refining has also been applied to obtain a material of higher quality. The samples denoted by Cl were silicons of transistor grade prepared by the chloride process in a certain foreign country, and this silicon is now widely used as the transistor material.

| Sample | Number of different samples assayed | Iodine content (p. p. m.) |
|---|---|---|
| I-1 | 3 | 1.3, 4.5, 4.5 |
| I-2 | 1 | 0.35 |
| I-3 | 2 | 2.0, 0.32 |
| Cl | 2 | 0.005, 0.05 |

## Discussion

After the chemical process, the decay curve of the silver iodide is usually straight on a semilog plot in accordance with the theoretical half-life. However, when the iodine content is lower than 0.01 $\mu$g. and the distillation is carried out carelessly, the separated silver iodide is contaminated with radioactive silica. Without the distillation, the precipitate

of silver iodide is by no means free from silica (about 10 $\mu$g. of silicon); without the extraction, about 1 $\mu$g. of silicon enters the precipitate.

When 0.002 $\mu$g. of iodine is present in silicon, it gives an activity of about 100 cpm to the $2\pi$ counter after the chemical treatments, and is enough for quantitative analysis and the measurement of the decay curve. If a reactor with a higher neutron flux were available, less iodine could be determined; however, the problem of decontamination from radioactive silicon would become more important. In such a case, repetition of the distillation would be necessary.

Determination of segregation constant of iodine and analysis of chlorine and bromine, with a slight modification of the method, in silicon are now under planning.

**Summary**

A trace quantity of iodine in silicon was determined by the neutron activation analysis. A chemical separation process, which involves potassium hydroxide fusion with potassium iodide as a carrier, was proved satisfactory by the use of $^{131}I$ produced by the neutron irradiation of tellurium diffused in silicon. By this method, the iodine was converted into silver iodide ready for counting and weighing within an hour, with a yield exceeding 50%. When it is assumed that a counting rate of 100 cpm is enough for accurate detection of activities, the limit of detection is 0.002 $\mu$g. of iodine with a neutron flux of $6\times10^{11}$ n/cm$^2$ sec. and by the use of a $2\pi$ counter.

The authors acknowledge the help given by the members of the staff of Japan the Atomic Research Institute.

*The Electrical Communication Laboratory*
*Nippon Telegraph and*
*Telephone Public Corporation*
*Musashino-shi, Tokyo*

# *Viscometric Study on Polystyrenesulfonic Acid Solutions*

By Masaaki KATO, Tsurutaro NAKAGAWA and Hideo AKAMATU

(Received August 17, 1959)

Among the physico-chemical properties of polyelectrolytes their flow property makes an important field of study from the viewpoint of polymer science and of electrolyte theory, and many theoretical and experimental investigations on viscosity behavior of various polyelectrolyte solutions have since been reported. Of these, however, comparatively few works have been done on polyelectrolytes of the sulfonic acid type.

It seems, therefore, to be interesting to compare the authors' viscosity data on the polystyrenesulfonic acid, which itself is a strong polymeric acid, with other workers' experimental and theoretical results previously reported, chiefly on sodium salts of polycarboxylic acids or polyquaternary halides.

This paper presents a viscometric study on polystyrenesulfonic acid in various solvents: water, water-dioxane mixed solvent, and aqueous solutions of sodium chloride and some other inorganic salts.

## Part I. Viscosity Behavior of PSA Solution

### Experimental

**Samples.**—For the preparation of polystyrenesulfonic acid, polystyrene pellets manufactured by the American Bakelite Company were used. Its viscosity-average molecular weight is about 180,000 from the viscosity measurement in benzene solution at 25°C.

The main feature of the sulfonation procedure is analogous to that of Neihof[1].

In a 500 cc. conical flask 10 g. of polystyrene pellets and 0.2 g. of silver sulfate as catalyst were taken. To this was added 200 cc. of concentrated sulfuric acid, and the flask was completely corked to exclude moisture and was immersed in a constant temperature bath at 100°C with frequent stirring for 20 hr. By this treatment, polystyrene is completely dissolved in concentrated sulfuric

1) R. Neihof, *J. Phys. Chem.*, 58, 916 (1954).

acid and the content of the flask becomes brown in color and very viscous. The reaction product (i. e. mixture of polystyrenesulfonic acid, sulfuric acid and silver sulfate) is poured into cold distilled water. Then polystyrene sulfonic acid precipitates in the form of a white gummy mass, which is quickly washed with water several times until heat emergence is no longer felt. The precipitate of polystyrenesulfonic acid was then completely dissolved into 500 cc. of distilled water. The large excess of sulfuric acid present could be removed by prolonged dialysis of the aqueous solution using a cellophane membrane. The last trace of remaining sulfuric acid was removed by successive electrodialysis. The presence of sulfuric acid was detected by adding barium chloride solution to the dialyzed polystyrenesulfonic acid solution[2]; a white precipitate which does not dissolve on heating indicates the presence of sulfuric acid. Barium salt of polystyrenesulfonic acid appears also as white precipitate, but it dissolves away on heating. This test was negative after the electrodialysis for three days.

Another sample of polystyrenesulfonic acid was obtained by making the above-mentioned mixture (polystyrene, silver sulfate and conc. sulfuric acid) react in the dark and at the room temperature with frequent stirring for long days, and the following procedure was the same as above-described. The authors will hereafter refer to this as PSA-R and the sample prepared at 100°C as PSA-100.

Determination of the concentration was carried out by completely evaporating the weighed solution to dryness on a steam bath and then drying in an air oven at 110°C until the constant weight was reached.

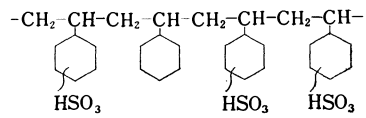
The degree of sulfonation was determined by the back titration of the PSA solution, to which excess alkali was added, with hydrochloric acid using methyl red as an indicator. The results are:

91% for PSA-100
85% for PSA-R

where 100% is assumed for PSA having one sulfonic acid group on each benzene ring.

A solid sample of the polystyrenesulfonic acid was obtained by freeze-drying of the solution as a white cotton-like material. But throughout the present measurement, PSA as the state of aqueous solution was used.

The polystyrenesulfonic acid, thus prepared, is considered to have the structure shown below.




The degree of sulfonation depends, as was mentioned above, upon the condition of sulfonation.

**Viscometers.**—All our viscosity measurements were carried out at 30°C by using four viscometers of Ostwald type. Their flow time for water (ca. 2 cc.) is about 147, 153, 193 and 254 sec., respectively.

**Effect of Rate of Shear.** — Recently many investigators[3-6] have pointed out the pronounced shear dependence of the observed viscosity of linear chain polyelectrolyte solutions at low ionic strength. But, according to the results of our viscosity measurement with a horizontal capillary viscometer in the range of 80~1400/sec. of velocity gradient, our PSA sample exhibited

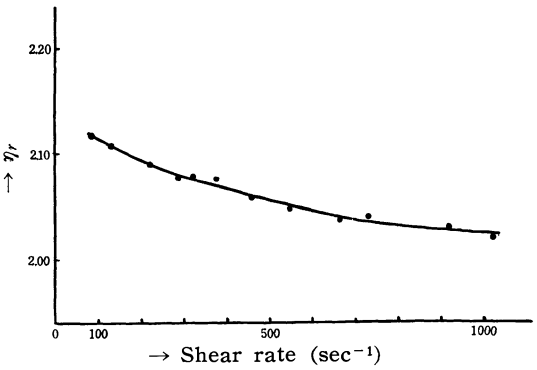



Fig. 1. Effect of rate of shear on relative viscosity. (0.0531%)

TABLE I. EFFECT OF RATE OF SHEAR ON RELATIVE VISCOSITY (0.385%)

| Rate of shear $q$(/sec.) | Relative viscosity $\eta_r \times 10$ |
|---|---|
| 623 | 38.2 |
| 600 | 38.6 |
| 586 | 38.7 |
| 554 | 38.5 |
| 541 | 38.5 |
| 525 | 38.6 |
| 505 | 38.5 |
| 478 | 38.5 |
| 450 | 38.5 |
| 430 | 38.5 |
| 401 | 38.5 |
| 368 | 38.5 |
| 340 | 38.5 |
| 310 | 38.5 |
| 280 | 38.5 |
| 254 | 38.5 |
| 230 | 38.5 |
| 209 | 38.5 |
| 169 | 38.4 |
| 125.0 | 38.5 |
| 98.0 | 38.6 |
| 62.8 | 38.2 |
| 36.1 | 39.0 |

2) H. H. Waxman, B. R. Sundheim and H. P. Gregor, ibid., **57**, 969 (1953).

3) R. M. Fuoss and U. P. Strauss, *J. Polymer Sci.*, **8**, 593 (1952).
4) R. M. Fuoss and W. N. Maclay, ibid., **6**, 305 (1951).
5) A. Katchalsky and N. Sternberg, ibid., **10**, 253 (1953).
6) H. Fujita and T. Homma, ibid., **15**, 277 (1955).

only a very slight shear rate effect even in the absence of added electrolytes.

Fig. 1 shows an example* of the shear rate effect. Table I is another example** of viscosity measurement by varying the rate of shear. Here the influence of shear rate is not observed. ($\eta_r$ is relative viscosity, and $q$ is rate of shear.)

It may therefore be accepted that the following data are free from shear-rate dependence to the first approximation. The kinetic energy correction was negligible in all cases studied.

## Results and Discussion

**In Aqueous Solution.**—The viscosity data obtained for the aqueous solutions are shown in Fig. 2, where reduced viscosity

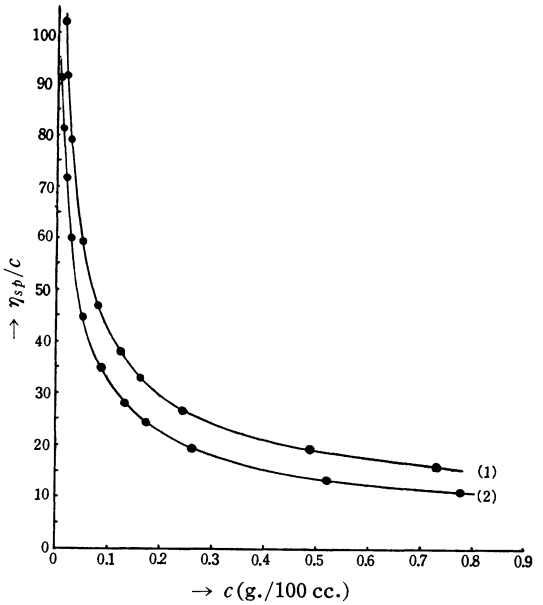



Fig. 2. Reduced viscosity vs. concentration curves.
curve (1) for PSA-100
〃 (2) for PSA-R

$\eta_{sp}/c$ is plotted against concentration $c$ (g./100 cc.). It is noticed that the PSA aqueous solutions have abnormally large $\eta_{sp}/c$ value compared with ordinary non-polar polymer solutions in which $\eta_{sp}/c$ is 2 or 3 at most. $\eta_{sp}/c-c$ plot exhibits a curve strongly concave upward, which is characteristic of polyelectrolyte solutions. In the experimental curves the tendency of decreasing in the low concentration range was not observed.

Considering that the reduced viscosity is a measure of the extention of a polymer coil in solution, the curves show that the size of a polymer becomes larger upon dilution. This phenomenon is generally explained as follows. As the concentration of PSA decreases, the negative net charge on a polyanion increases as a result of increasing dissociation of sulfonic acid groups, and so polymer chains extend more and more, due to the enhanced intramolecular repulsive force between like charges.

The relation between reduced viscosity and concentration of PSA is satisfactorily described by the formula

$$\frac{\eta_{sp}}{c}=\frac{A}{1+B\sqrt{c}} \qquad (1)$$

proposed by Fuoss[7,8]. Here, $A$ and $B$ are empirical constants. $A$ has a meaning of intrinsic viscosity $[\eta]$, and $B$ is a constant dependent on inter-ionic forces. The agreement of the experimental data with Eq. 1 is shown in Fig. 3. The value $A$ is 400 for both PSA samples. The value $B$ is

28 for PSA-100 and
41 for PSA-R

That the two PSA samples of different degrees of sulfonation have the same $A$ value (400) is understandable by recalling that both PSA samples were prepared from the same polystyrene as a starting material and by assuming that no chain scission or cross-link formation through a

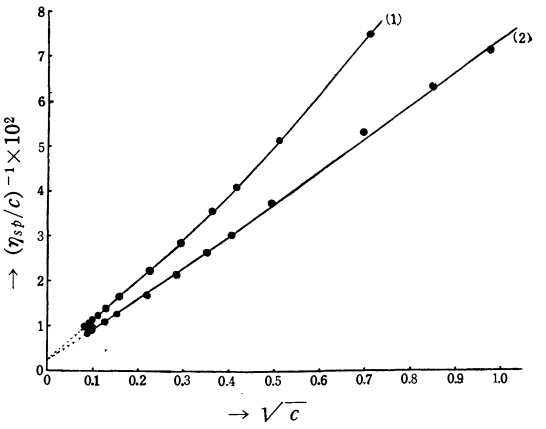



Fig. 3. Reciprocal reduced viscosity vs. $\sqrt{c}$ curves (Fuoss plot).
(1): for PSA-100
(2): for PSA-R

*,**) Samples from Koppers' polystyrene (viscosity-average molecular weight $3\times10^5$). Sulfonation for two weeks at room temperature. Degree of sulfonation 36.8 %. Viscosity measurement at 25°C.

7) R. M. Fuoss and G. I. Cather, *J. Polymer Sci.*, **4**, 97 (1949).
8) R. M. Fuoss, ibid., **3**, 603 (1948).

sulfone bridge during the course of sulfonation reaction occurred.

**Water-Dioxane Mixed Solvent.** — Viscosity data of PSA-R for water-dioxane mixed solvent of various mixing ratio are shown in Fig. 4.

$\eta_{sp}/c$ vs. $c$ relation in all the solvents studied is well described by Fuoss' Eq. 1 (cf. Fig. 5). The values $A$ and $B$ obtained are summarized in Table II together with the dielectric constant $\varepsilon$ of the solvents. Values of $\varepsilon$ of the mixed solvents are those borrowed from the published data on the $\varepsilon$-mixing ratio relationship by G. Åkerlöf and O. A. Short[9].

From Fig. 4 it is seen that the reduced

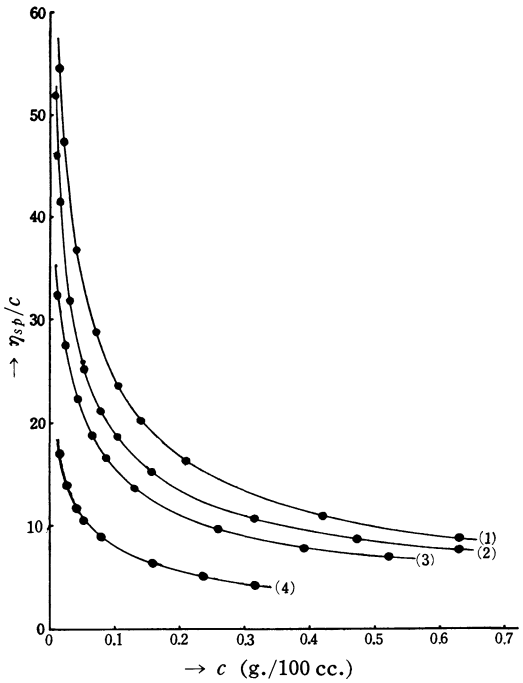



Fig. 4. Effect of dielectric constant of solvent on reduced viscosity.

PSA-R
(for $\varepsilon$=76.7 see Fig. 2)
(1) $\varepsilon$=58.9
(2) $\varepsilon$=40.9
(3) $\varepsilon$=32.4
(4) $\varepsilon$=16.9

TABLE II

| $\varepsilon$ | $B$ | $A$ | $1/\varepsilon^2\times10^3$ |
|---|---|---|---|
| 16.9 | 147 | 400 | 3.50 |
| 32.4 | 74.6 | 400 | 0.952 |
| 40.9 | 68.6 | 400 | 0.598 |
| 58.9 | 59.6 | 400 | 0.288 |
| 76.7 | 41.3 | 400 | 0.170 |

9) G. Åkerlöf and O. A. Short, *J. Am. Chem. Soc.*, 58, 1241 (1936).

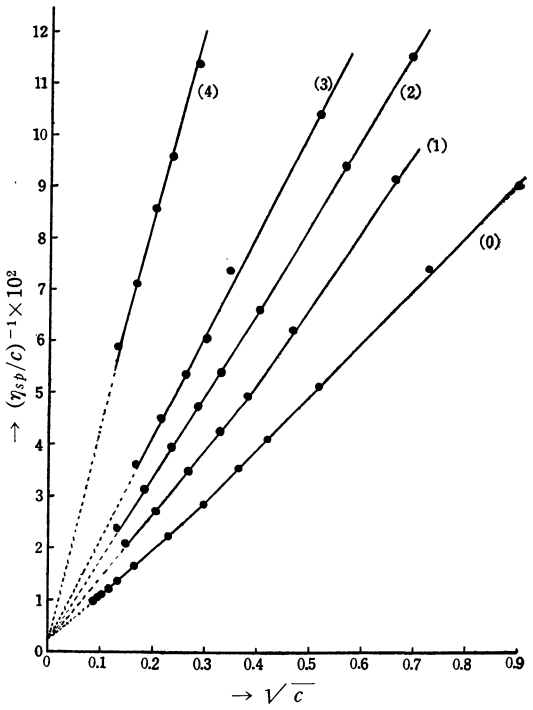



Fig. 5. Fuoss plot for the curves of Fig. 4.

PSA-R
(0) $\varepsilon$=76.7
(1) $\varepsilon$=58.9
(2) $\varepsilon$=40.9
(3) $\varepsilon$=32.4
(4) $\varepsilon$=16.9

viscosity decreases with the decrease of dielectric constant of solvent. This may be explained as follows. The dissociation $-SO_3H \rightarrow -SO_3^- + H^+$ is diminished as $\varepsilon$ decreases, and consequently the negative net charge on a polyanion decreases, so that the polymer coil becomes more contracted in a low $\varepsilon$ solvent than in a solvent of high $\varepsilon$. As the dioxane content in water increases, the Coulombic repulsive force between charged groups becomes stronger due to the decrease of dielectric constant of the medium. This effect to expand a polymer coil, however, may be less dominant than the effect of diminished dissociation of the sulfonic acid group.

Furthermore $B$ vs. $1/\varepsilon^2$ plot is approximated by linear relation (cf. Fig. 6).

The parameter $A$ has the same value 400 in any solvent. This may indicate that PSA molecule has the same size at infinite dilution in any solvent studied here.

**In Sodium Chloride Aqueous Solution.**—Plot of $\eta_{sp}/c$ vs. $c$ is shown in Figs. 7 and 8 for

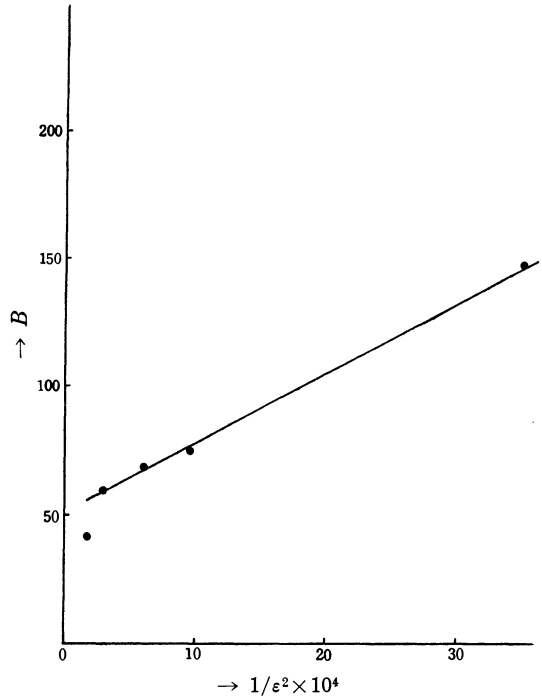



Fig. 6. Constant $B$ of Fuoss' formula plotted against $1/\varepsilon^2$.

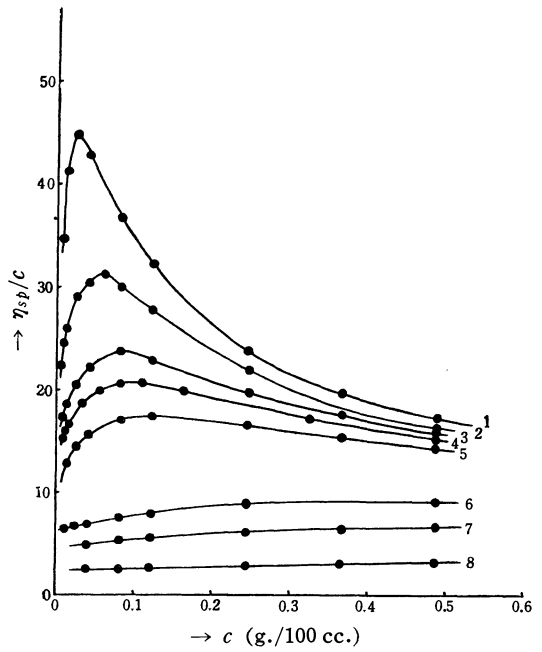



Fig. 7. Effect of salt on reduced viscosity. (PSA-100)

1) 0.000126 N NaCl aq. soln.
2) 0.000314 〃
3) 0.000628 〃
4) 0.000840 〃
5) 0.00126 〃
6) 0.00628 〃
7) 0.0126 〃
8) 0.0628 〃

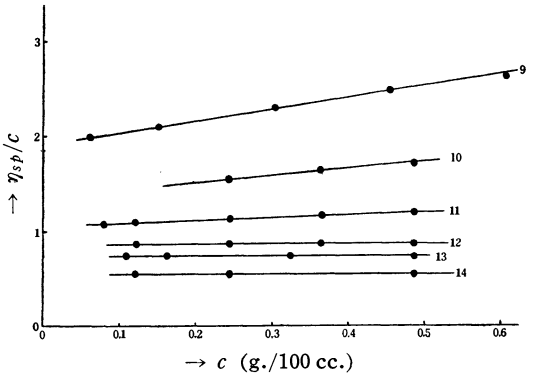



Fig. 8. Effect of salt on reduced viscosity. (PSA-100)

9) 0.0942 N NaCl aq. soln.
10) 0.2573 〃
11) 0.500 〃
12) 1.00 〃
13) 1.33 〃
14) 2.00 〃

solutions of PSA-100 in various concentration of aqueous sodium chloride in the range of 0.000126 to 2.00 N. Reduced viscosity is strongly affected by the presence of sodium chloride and diminished as the sodium chloride content in solution increases. When the sodium chloride concentration is small, the curves exhibit a maximum, which vanishes, however, with the increasing content of sodium chloride and the curves approach those for ordinary non-polar polymers. These behaviors of PSA are characteristic of many other polyelectrolytes. The qualitative explanation was given above. (See, for example, references 10 and 11).

Sodium chloride normality $x$ and PSA normality $c_m$ at the maximum of reduced viscosity are shown in Table III. PSA normality is greater by $10^1$ than sodium chloride normality.

Values of intrinsic viscosity and sodium chloride concentration $x$ (mol./l.) in solution are summarized in Table IV.

TABLE III

| $c$ at $(\eta_{sp}/c)_{max}$ (g./100 cc.) | $(\eta_{sp}/c)_{max}$ | $x\times10^3$ | $c_m\times10^3$ |
|---|---|---|---|
| 0.022 | 45.0 | 0.126 | 1.13 |
| 0.061 | 31.3 | 0.314 | 3.14 |
| 0.081 | 23.8 | 0.628 | 4.16 |
| 0.090 | 20.7 | 0.840 | 4.63 |
| 0.10 | 17.3 | 1.26 | 5.14 |

10) R. M. Fuoss and U. P. Strauss, *J. Polymer Sci.*, **3**, 602 (1948).
11) D. T. F. Pals and J. J. Hermans, *Rec. trav. chim.* **71**, 433 (1952),

TABLE IV

| $x$ | $[\eta]$ | $x$ | $[\eta]$ | $x$ | $[\eta]$ |
|---|---|---|---|---|---|
| 0.000126 | 25.0 | 0.00628 | 6.10 | 0.500 | 1.05 |
| 0.000314 | 18.0 | 0.0126 | 4.80 | 1.00 | 0.86 |
| 0.000628 | 15.7 | 0.0628 | 2.30 | 1.33 | 0.75 |
| 0.000840 | 13.3 | 0.0942 | 1.90 | 2.00 | 0.55 |
| 0.00126 | 8.82 | 0.2573 | 1.36 | | |

$[\eta]$ values for low sodium chloride concentration are unreliable due to difficulty in extrapolating to zero concentration.

The relation between $[\eta]$ and $x$ can be approximately described by the formula

$$[\eta]^{1/3} = a + \frac{b}{\sqrt{x}}$$

presented by Fuoss and Strauss[10] in the range of comparatively high sodium chloride concentration (Fig. 9).

In the Hermans-Overbeek theory[12] the polyion is considered as a sphere in which the separate charges are replaced by a continuous charge distribution, and the small ions are assumed to be governed by the Poisson-Boltzmann equation. Applying the result of the theory to the case in which the polymer coil is free-draining and the added salt concentration is not so low, it is concluded that $[\eta]$ vs. $1/\sqrt{x}$ relation is linear[11]. For the PSA sample a linear relation between $[\eta]$ and $1/\sqrt{x}$ is obtained in the range of concentration above ca. 0.006 N (Fig. 10).

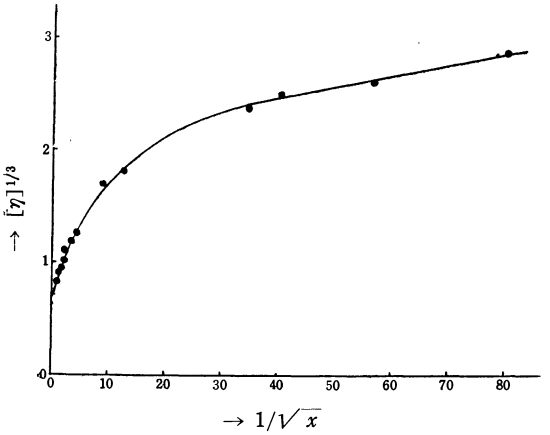



Fig. 9. Effect of salt concentration on the intrinsic viscosity (1).

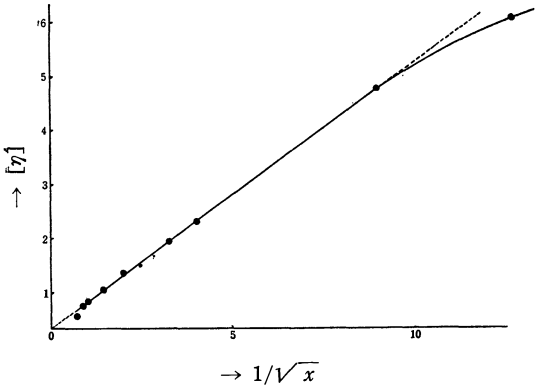



Fig. 10. Effect of salt concentration on the intrinsic viscosity (2).

**In Sodium Bromide and Sodium Sulfate Aqueous Solution.**—In sodium bromide and sodium sulfate aqueous solution the viscosity behavior of PSA-100 is nearly the same as in sodium chloride aqueous solution.

The effect of viscosity depression, i. e. the effect for inducing the contraction of polymer coil is strong in the order NaCl $>$ NaBr $\approx$ $Na_2SO_4$, although the difference is very slight (Table V). No distinct lyotropic effect is observed here.

TABLE V. INTRINSIC VISCOSITY OF PSA-100 IN VARIOUS SOLVENTS

| Solvent | | $[\eta]$ |
|---|---|---|
| $Na_2SO_4$ | 1.491 N aq. soln. | 0.81 |
| 〃 | 0.745 〃 | 1.06 |
| 〃 | 0.373 〃 | 1.31 |
| NaBr | 2.93 N aq. soln. | 0.39 |
| 〃 | 1.46 〃 | 0.82 |
| 〃 | 0.73 〃 | 1.23 |
| NaCl | 2.00 N aq. soln. | 0.55 |
| 〃 | 1.33 〃 | 0.75 |
| 〃 | 1.00 〃 | 0.86 |
| 〃 | 0.50 〃 | 1.05 |

## Part II. Viscosity Equation for PSA

As was stated in the previous part, PSA behaves like ordinary non-polar polymers in its viscosity character when the concentration of the added salt in the solution is high; here $\eta_{sp}/c$ vs. $c$ relation becomes linear. Hence in this circumstance it is possible to obtain Sakurada-Houwink's viscosity equation for PSA.

In this part it is aimed to prepare various PSA samples of the same charge density and different degrees of polymerization and to obtain the viscosity equation which holds between their degree of polymerization and their intrinsic viscosity in 0.52 N hydrochloric acid and 0.5 N sodium chloride aqueous solution.

For the preparation of PSA samples,

12) J. J. Hermans and J. Th. G. Overbeek, ibid., **67**, 761 (1948).

TABLE VI

| PSA | [η] of PS before sulfonation in benzene soln. at 25°C | P | [η] of PSA in 0.5 N NaCl | [η] of PSA in 0.52 N HCl |
|---|---|---|---|---|
| From Fract. 2 | 1.025 | 2534 | 1.41 | 1.64 |
| 〃 〃 4 | 0.672 | 1421 | 0.84 | 0.89 |
| 〃 〃 5 | 0.544 | 1063 | 0.61 | 0.67 |

polystyrene (average molecular weight= 180,000; American Bakelite Company) was fractionated into several fractions and these were sulfonated under the same condition as was described above.

As the authors have some evidence from the previous experiments (Part I) that neither chain scission nor sulfone bridge formation occurs during the course of sulfonation, the degree of polymerization of the fractionated polystyrenes before and after sulfonation was assumed to be unchanged. The degree of polymerization of the fractionated polystyrenes was determined from the viscosity measurement in benzene solution at 25°C.

## Experimental Results

**Fractionation of Polystyrene.**—30 g. of polystyrene pellets was dissolved into 1.2 l. of methyl ethyl ketone in a 2 l. flask and the solution was filtered with a No. 4 glass filter. At room temperature, methanol was slowly added to the solution with stirring until the solution became turbid and then an additional 6 cc. of methanol was added. The flask was set in a thermostat and the bath temperature was raised up until the solution became clear. Then the bath was gradually cooled to the room temperature with stirring. At the room temperature the mixture was allowed to come to equilibrium, and the precipitate was separated by decantation and then an additional 11 cc. of methanol was added to the solution. This process was repeated six times. The amount of methanol used in each precipitation process was 6, 11, 16, 26, 40 and 150 cc., respectively. Each fraction was redissolved into toluene and reprecipitated by a great excess of methanol and finally dried up to a constant weight in vacuo at 50°C.

**Sulfonation.** — Silver sulfate and concentrated sulfuric acid were added to each fraction in the proportion polystyrene : $Ag_2SO_4$ : conc. $H_2SO_4$=10 : 0.2 : 110 by weight. Each mixture was put into a conical flask, which was compactly sealed to prevent the entrance of moisture. The flask was set in a thermostat at 50°C. The following procedure was the same as described in Part I.

It was expected that PSA's, of the same degree of sulfonation would be obtained, but this was unsuccessful. This may be ascribed to the fact that the texture or structure of the precipitated mass is different for each fraction. (There was no regularity between their reactivity and their molecular weight.) Only the PSA's prepared from Fractions No. 2, 4 and 5 had about the same degree of sulfonation, 85%, so that these PSA's were used for viscosity measurement. The viscosity data obtained are shown in Table VI and Fig. 11.

**Viscosity Equation.**—Molecular weight $M$ of the fractionated polystyrene (before sulfonation) was determined by the viscosity formula by C. Bawn et al.[13]

$$[\eta] = 1.13 \times 10^{-4} \cdot M^{0.73}$$

(in benzene at 25°C, $c$ in g./100 ml.)

which seems to be most reliable.

The relation between $\log[\eta]$ and $\log P$ of PSA is well approximated by a straight line and we obtained the following viscosity equations (cf. Fig. 11).

$$[\eta] = 6.35 \times 10^{-4} \cdot P \quad \text{(in 0.52 N HCl aq.)} \qquad (2)$$

$$[\eta] = 5.75 \times 10^{-4} \cdot P \quad \text{(in 0.50 N NaCl aq.)} \qquad (3)$$

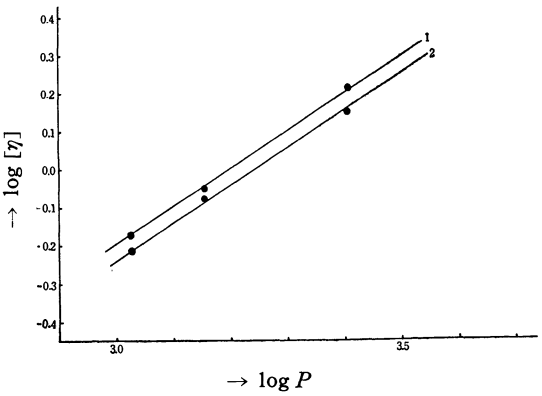



Fig. 11. Intrinsic viscosity vs. polymerization degree relation in salt solution.
1) in 0.52 N HCl
2) in 0.50 N NaCl

13) C. Bawn, R. Freeman and A. Kamaladin, *Trans. Faraday Soc.*, **46**, 1107 (1950).

Here $P$ is the degree of polymerization of PSA. Eq. 2 is for 0.52 N HCl aqueous solution, and Eq. 3 for 0.50 N NaCl aqueous solution.

It is noticeable that $[\eta]$ is directly proportional to the first power of the degree of polymerization.

Calculating the degree of polymerization by Eq. 2 from the viscosity data obtained by Mock and Marshall[14] for vinyltoluene-styrene copolymer sulfonic acid ($P=2036$ by osmotic measurement in methyl ethyl ketone; $[\eta]=1.58$ in 0.54 N HCl at 25°C), $P=2490$ is obtained.

If the authors calculate the degree of polymerization of PSA-R used in the present study ($P=1730$ by viscosity measurement in benzene solution at 25°C before sulfonation; $[\eta]=1.07$ at 25°C in 0.5 N NaCl aq. soln.; degree of sulfonation=85%) by Eq. 3, $P=1860$ is obtained.

Hence Eq. 2 or 3 may be used for calculating roughly the degree of polymerization of highly sulfonated polystyrene-sulfonic acid from its intrinsic viscosity in 0.5 N HCl or 0.5 N NaCl aqueous solution.

The cost of this research has been partly defrayed from the Scientific Research Encouragement Grant from the Ministry of Education, to which the authors' thanks are due.

*Department of Chemistry*
*Faculty of Science*
*The University of Tokyo*
*Hongo, Tokyo*

14) R. A. Mock and C. A. Marshall, *J. Polymer Sci.*, **13**, 263 (1954).

# *Rapid Colorimetric Determination of Mercury by Tin(II)-Strong Phosphoric Acid Reduction Method*

By Toshiyasu KIBA, Ikuko AKAZA and Osamu KINOSHITA

(Received August 28, 1959)

Tin(II)-strong phosphoric acid, a new powerful decomposing and reducing agent first described by the present authors[1], has been widely employed in this country for the determination of sulfur in various materials; e. g. sulfates[2], sulfide ores[3], iron and steel[4], organic compounds[5], rayon staple fiber, acetylcellulose[6] and proteins[7]. The reagent has also been applied for rapid determination of selenium in various forms. The selenium is reduced by the reagent into gaseous hydrogen selenide, which is absorbed in an alkaline solution, and then the amount is determined colorimetrically[8].

1) T. Kiba et al., This Bulletin, **28**, 641 (1955).
2) T. Kiba, and I. Akaza ibid., **30** 53 (1957).
3) T. Kiba, I. Akaza and N. Sugishita, ibid., **30**, 972 (1957).
4) K. Kitagawa and Shibata, *Japan Analyst* (*Bunseki Kagaku*), **7**, 181 (1958).
5) T. Kiba and I. Kishi (present surname, Akaza), This Bulletin, **30**, 482 (1957); S. Ohashi, ibid., **28**, 645 (1955).
6) H. Terada and M. Yoshida, *J. Chem. Soc. Japan, Ind. Chem. Sec.* (*Kogyo Kagaku Zasshi*), **61**, 1301 (1958).
7) S. Akabori and T. Fujiwara, *Bull. Chem. Biolog.*, **40**, 1983 (1958).
8) T. Kiba, I. Akaza and H. Hachino, This Bulletin **32**, 641 (1959).

A further attempt was made by the present authors to reduce mercury in various compounds to the metallic state by treating the samples with tin(II)-strong phosphoric acid. The mercury was driven out from the reaction medium by heating and its vapor was carried in a current of carbon dioxide into an absorbing solution containing sulfuric acid and potassium permanganate. The mercury retained in the solution as mercury(II) ions was determined colorimetrically by the usual dithizone method. This new method is very rapid and simple, and moreover, the error caused by the volatillization of mercury during the digestion of the samples by ordinary methods is totally eliminated for the analysis is carried out in a closed system in carbon dioxide.

## Experimental

**Apparatus.**—The apparatus used in this study is shown in Fig. 1. It is composed of two parts, a reaction vessel (A) and an absorbing part (B). The reaction vessel (A) is a round-bottomed flask of hard glass having a glass cap fitted to its top

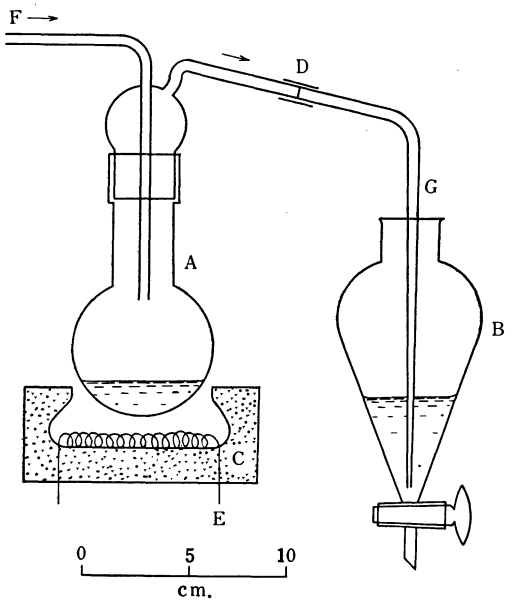



Fig. 1. Apparatus for reduction of mercury compounds and absorption of mercury vapor evolved.
A: Reaction vessel, a round bottomed flask.
B: A separatory funnel.
C: Electric heater.
D: Short piece of rubber tubing.
E: A. C. electric current regulated by a variable transformer.
F: Carbon dioxide gas introduced into A.
G: Gas-delivery tube.

and provided with an inlet and an outlet tube for the gas. The absorbing part (B) is a separatory funnel of about 100 ml. capacity. A gas delivery tube (C) is connected with a piece of rubber tubing (D) to the outlet arm of the reaction vessel (A) and inserted into the absorbing solution in the separatory funnel. A Kipp's apparatus is employed for the production of carbon dioxide, which is purified by three gas-washing bottles (not shown in Fig. 1) and introduced into the reaction vessel through the inlet arm. The solutions used for the purification of carbon dioxide are described later.

*Photoelectric colorimeter.*—A "Hirama photoelectric colorimeter" with 1 cm. cells was used with a filter of 517 mμ.

**Reagents.**—*Strong phosphoric acid.*—Four hundred grams of commercial ortho phosphoric acid of extra pure grade ($d$=1.7) is placed in a 300 ml. conical beaker, and dehydrated by heating on a 500 W. hot plate until a thermometer dipped in the liquid indicates 300°C. If the heating takes too long the liquid will become turbid and viscous and useless for the purposed in view. During the heating, the water vapor and the mist of phosphoric acid coming off should be rapidly removed from the neighborhood of the liquid surface, through a glass tube, one end of which is held near the surface of the liquid, the other end being connected to a suction pump. This saves much time in the dehydration.

*Tin(II)-strong phosphoric acid.*—Fifty grams of tin(II) chloride dihydrate of extra pure grade is placed in a 300 ml. conical beaker and on it is poured 250 g. of the strong phosphoric acid prepared as described above. The content is heated to 300°C within 30 min. in the manner of the preparation of the strong phosphoric acid. After cooling the tin(II)-strong phosphoric acid thus obtained, a very viscous and possibly slightly turbid liquid is produced, which may be stored in a closed vessel.

*Carbon dioxide.*—Carbon dioxide produced in the Kipp's apparatus is purified by passing through three gas-washing bottles containing, respectively, water, 2% vanadium(II) sulfate solution in 6 N sulfuric acid, 1% potassium permanganate solution in 10% sodium carbonate. This is introduced into the reaction vessel through a glass tube.

*Standard mercuric chloride solution.*—A 1.3539 g. portion of mercuric chloride of pure chemical grade dried in a vacuum desiccator is weighed accurately and dissolved in one liter of distilled water. This solution is used as a stock solution. One milliliter of the solution is diluted to 100 ml. with water before use. One milliliter of this diluted solution contains 10 μg. of mercury. According to Sandell[9] the mercuric ion is usually absorbed on the glass wall of the vessel, especially when the solution is extremely diluted. However, the effect is not noticeable when the diluted solution is employed soon after the preparation.

*Dithizone chloroform solution.*—A 0.001% (w/v) and a 0.005% (w/v) solution are prepared according to Sandell[9], and the former is used for 0 to 20 μg. of mercury and the latter for 0 to 50 μg. of the metal.

*Hydroxylamine hydrochloride solution.*—Twenty grams of hydroxylamine hydrochloride is dissolved in 65 ml. of water, and neutralized with aqueous ammonia using thymol blue as indicator. The solution is transferred into a separatory funnel and 10 ml. of 4% sodium diethyldithiocarbamate solution is added to it and mixed well. After a few minutes, 10 ml. of chloroform is poured into the vessel and the content is shaken vigorously to transfer the metal chelates into the organic layer. After the two layers are disengaged, the chloroform layer is rejected. To the aqueous layer, hydrochloric acid is added drop by drop till the red color of the indicator appears. This solution may be employed for the experiment.

*Potassium permanganate solution.*—A suitable amount of solid potassium permanganate of extra pure grade is dissolved in water and filtered through a glass-sintered crucible to make 0.1, 0.5 and 1 N solution.

*Sulfuric acid.*—Concentrated sulfuric acid of pure grade is diluted with water to a concentration of 10%.

*Acetic acid solution.*—6 N.

9) E. B. Sandell, "Colorimetric Determination of Traces of Metals", 2nd Ed., Interscience Publishers, Inc., New York (1950), pp. 441-452.

*Ferric chloride solution.*—Ferric chloride hexahydrate is dissolved in water to make a solution containing 10 mg. of iron(III) ion per ml.

*Cadmium chloride solution.*—Crystalline cadmium chloride is dissolved in water to make a solution containing 3.5 mg. of cadmium ion per ml.

*Mercuric oxide.*—Mercuric oxide of extra pure grade is used as a powder, and the mercury content was estimated by the ordinary potassium thiocyanate titration method as 97.30% pure.

*Alumina.* — As a diluent of solid samples, powdered alumina of utmost purity for chromatography is used.

*Various samples containing mercury.*—Commercial products, especially water-soluble insecticides and fungicides, are used as the samples of analysis, their mercury content having been determined by other methods.

**Procedure.** — Take an accurately measured sample containing mercury of 0 to 50 $\mu$g.—pipet a solution; weigh a solid—and put it into the reaction vessel (A in Fig. 1). The volume of the vessel should be varied according to the amount of the sample to be analyzed. Pour 5 to 10 ml. of the tin(II)-strong phosphoric acid over the sample. Put into the separatory funnel (B in Fig. 1) 5 ml. of 0.1 N potassium permanganate solution and 5 ml. of 10% sulfuric acid and mix well. Connect all the apparatus as shown in Fig. 1. Pass carbon dioxide very rapidly through the apparatus for two or three minutes to expel the air from the apparatus. The end of the gas-delivery tube (G) should reach the bottom of the separatory funnel. Reduce the flow of gas to a rate of one bubble per second, and heat the bottom of the reaction vessel by passing an electric current through the nichrome wire (E) placed in the diatomaceous block (C). Regulate the voltage of the current by a variable transformer. It is unnecessary to keep the temperature constant but it should be high enough to ensure that the content of the reaction vessel exhibits a white turbidity near the end of the reaction. After about fifteen minutes stop the heating, but continue the passing of the gas about five minutes longer.

Remove the separatory funnel, and pour into it about 15 ml. of 1 N sulfuric acid. To the colored solution add 1 ml. of 20% hydroxylamine hydrochloride solution to reduce the permanganate and, moreover, 2 ml. of 6 N acetic acid to stabilize the dithizonate which will be formed hereafter. Add 5 ml. of chloroform to the aqueous solution in the funnel and shake it vigorously for a while to saturate the aqueous phase with chloroform. After the layers are disengaged by standing the vessel for several minutes, reject the lower chloroform layer from the stem of the funnel. Then, add exactly 10 ml. of 0.05% dithizone-chloroform reagent using a pipet. Shake the vessel vigorously with an electric shaking machine for about two minutes. Allow the vessel to stand for several minutes and then drain the organic layer into an Erlenmyer flask containing unhydrous sodium sulfate as a dehydrant. Set it aside for a while till the water contained in the organic phase is absorbed and the layer becomes clear. Transfer the colored organic phase in a 1 cm. cell and read the absorbancy of the layer in a photoelectric colorimeter with a filter of 517 m$\mu$. A blank test should be conducted with the dithizone-chloroform solution undergoing the same procedure without mercury.

## Results and Discussion

**Recovery of Mercury by This Method.**— Employing an aliquot of the standard mercuric chloride solution, the determination of mercury in the amount between 5 and 50 $\mu$g. was made by carrying out all the procedure described above. Another aliquot of the standard solution was directly treated with dithizone-chloroform reagent and the absorbancy of the organic layer was read as described in the latter part of the procedure, which is similar to the ordinary method for the determination of mercury in solutions. The absorbancies measured on the same amount of mercury by the two methods are tabulated together in Table I, which shows good coincidence

TABLE I. COMPARISON OF THE ABSORBANCIES OF MERCURIC DITHIZONATE FOR THE SAME AMOUNT OF MERCURY

| Amount of Hg $\mu$g./100 ml. $CHCl_3$ | Absorbancy measured | |
|---|---|---|
| | Ordinary direct colorimetry | Via this reduction & evolution method |
| 5 | 0.0928 | 0.0930 |
| 10 | 0.1722 | 0.1716 |
| 15 | 0.2580 | 0.2464 |
| 20 | 0.3172 | 0.3301 |
| 25 | 0.4205 | 0.4200 |
| 30 | 0.4878 | 0.4813 |
| 35 | 0.5695 | 0.5690 |
| 40 | 0.6475 | 0.6420 |
| 45 | 0.7190 | 0.7210 |
| 50 | 0.7975 | 0.7960 |

within the error unavoidable in colorimetry. The calibration curves obtained by the two methods can be represented by the following equations. In case ordinary colorimetry of the dithizone-chloroform phase was used:

$$y = 0.0168 + 0.01569\,x$$

and if colorimetry following this reduction and evolution method was used:

$$y = 0.0156 + 0.01569\,x$$

where $y$ is the absorbancy measured and $x$ the amount of mercury taken in micrograms. The numerical values in the equations were calculated by the method of the least squares from the experimental

data of more than two determinations of the same amount of the metal. In conclusion, it may be pointed out that only a negligible amount of mercury is lost in this reduction and evolution method, and a calibration curve prepared by the ordinary method with a standard solution of mercuric salt can be employed in this method as well.

**Determination of Minute Amounts of Mercuric Oxide.**—A definite amount of mercuric oxide was mixed with a large amount of alumina and the mixture was analyzed by the tin(II)-strong phosphoric acid method. Minute amounts of mercury could be determined by this method as shown in Table II.

TABLE II. DETERMINATION OF MERCURY IN MIXTURE OF MERCURIC OXIDE AND ALUMINA

| Sample taken mg. | Hg content μg. | Hg found μg. |
|---|---|---|
| 15.90 | 30.7 | 30.2 |
| 13.32 | 25.7 | 25.5 |
| 14.59 | 28.2 | 28.3 |
| 14.65 | 28.3 | 28.4 |
| 14.73 | 28.4 | 28.7 |

**Determination of Minute Amounts of Mercury in Solution.**—Because of their volatility, mercury compounds can not be dried or their solutions evaporated without affecting the analytical result. So the co-precipitation method was employed to concentrate the mercuric ion using ferric hydroxide or cadmium sulfide as gathering agent. A suitable volume of a solution containing 20 μg. of mercury as chloride, and a suitable volume of ferric chloride solution containing 10 mg. of iron(III) ion per ml. were placed together in the reaction vessel. Sodium hydroxide solution was added dropwise to complete the ferric hydroxide precipitate, and the mixture was set aside from two hours to overnight till the precipitate settled. The supernatant solution was sucked out by means of a suction pump through a filter stick, a short glass tube containing an asbestos plug near one end, the precipitate being allowed to remain in the reaction vessel. The precipitate caught on the asbestos plug was transferred from the filter stick into the reaction vessel by pushing out the plug with a slender glass rod inserted through the other end of the glass tube. The analysis of mercury caught in the ferric hydroxide precipitate was carried out according to the procedure in which the asbestos plug was completely decomposed by heating with tin(II)-strong phosphoric acid as shown by the clear solution obtained.

Cadmium sulfide can also be employed as the co-precipitant. In this case a suitable volume of a solution containing a minute amount of mercury and of cadmium chloride containing 3.5 mg. of cadmium per ml. were put together in the reaction vessel. The pH of the solution was adjusted to about 1 by adding hydrochloric acid, and then hydrogen sulfide was introduced into the solution to precipitate cadmium sulfide. After the solution was left for several hours to let the precipitate settle, it was filtered by means of the filter stick as described above, and the asbestos plug was transferred to the reaction vessel containing the precipitate. The analysis was then carried out according to the procedure.

Both the ferric hydroxide and the cadmium sulfide co-precipitation method give good recovery of mercury in the solution as shown in Table III. In these cases some problems remain about the reaction of tin(II)-strong phosphoric acid with ferric ions and the metallic sulfides. The ferric ion is reduced to the ferrous by the reagent intended for the reduction of the mercuric ion, and excessive consumption of the reagent occurs if a larger amount of iron(III) ion is present. But when only about ten milligrams of iron(III) is used for the co-precipitation, the amount of the tin(II) ion in the reagent used is far in excess of the need of the iron(III) ion, and the reduction of mercury is not hindered.

TABLE III. RECOVERY OF 20 μg. OF MERCURY BY COPECIPITATION METHOD

Ferric oxide was used as a collector:

| Amount of $Fe^{3+}$ mg. | Hg found μg. | Recovery % |
|---|---|---|
| 10 | 19.9 | 99.5 |
| 20 | 19.2 | 96.0 |
| 30 | 19.7 | 98.5 |
| 30 | 19.7 | 98.5 |

Cadmium sulfide was used as a collector:

| Amount of $Cd^{2+}$ mg. | Hg found μg. | Recovery % |
|---|---|---|
| 3.5 | 19.3 | 96.5 |
| 〃 | 19.5 | 97.5 |
| 〃 | 19.3 | 96.5 |
| 5 | 19.2 | 96.0 |
| 〃 | 18.6 | 93.0 |

When cadmium sulfide is treated with the tin(II)-strong phosphoric acid, gaseous

hydrogen sulfide is evolved at the same time, and the gas is carried with the carbon dioxide into the absorbing solution of potassium permanganate and sulfuric acid. The gas consumes the permanganate and the absorbing power of the solution for mercury vapor is markedly lowered. In this case a large amount of permanganate should be persent in the absorbing solution to oxidize the sulfide in the sample and keep adequate absorbing power for mercury vapor. This applies also to the analysis of mercury in sulfates. The question is what concentration of potassium permanganate should be kept in the absorbing solution for various amounts of sulfur in the sample. Fig. 2 shows the results of experiments

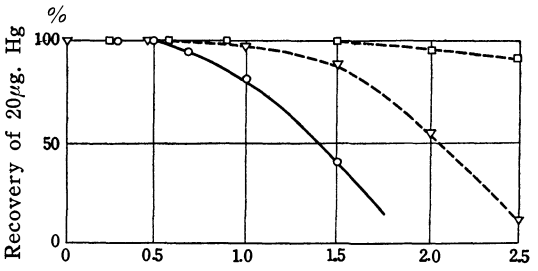



Fig. 2. Dependence of potassium permanganate concentration in the absorbing solution on the recovery of mercury.
Composition of the absorbing solution:
○: 5 ml. 0.1 N $KMnO_4$+5 ml. 10% $H_2SO_4$
▽: 5 ml. 0.5 N $KMnO_4$+5 ml. 10% $H_2SO_4$
□: 5 ml. 1 N $KMnO_4$+5 ml. 10% $H_2SO_4$

to estimate the concentration of permanganate for good recovery of mercury in the presence of various amounts of sulfur as sulfate. When 1 N potassium permanganate solution is used as 1:1 mixture with 10% sulfuric acid, less than 2.0 mg. of sulfur can be allowed to be present in the sample without any hindrance to the determination of 20 μg. of mercury.

**Effect of Chloride for the Analysis.**—The colorimetry of mercury dithizonate is usually dependent on the concentration of the chloride ion in the aqueous solution. In this evolution method, when a sample contains a large amount of chloride, the chloride is given off as hydrogen chloride and absorbed in the absorbing solution. Many papers have been published on the dependence of the accuracy of the dithizone method on the chloride ion concentration, and a suitable pH range for the extraction of mercuric dithizonate by chloroform was reported[10]. However, when the amount of chlorides in the sample is not known, it is very difficult to make the absorbing solution in suitable composition for the colorimetric determination of mercury. In such cases the co-precipitation method is to be preferred.

**Determination of Mercury in Organic Fungicides and Medicines.**—Various methods have already been employed for the determination of mercury in organic compounds, but when the compounds are present mixed with large amounts of other substances or in the form of a solution of extremely low concentration, it is very hard to get an accurate result. Moreover, the decomposition of the compound is usually carried out by strong oxidizing acid with a reflux condenser, through which some of the mercury inevitably escapes during the treatment. If the tin(II)-strong phosphoric acid method is applied for the purpose, the powerful decomposing and reducing power of the reagent acts on the sample instantly, and the mercury vapor is evolved, leaving other interfering metals in the phosphoric acid medium. The procedure of the analysis is the same as in the case of inorganic substances.

**Mercurochrome.** — Crystals of mercurochrome were weighed and dissolved in water to give a solution containing 10 μg. of mercury per ml. Two or three milliliters of the solution was taken in the reaction vessel, and the analysis was carried out according to the procedure. The purity of the sample was estimated by iodometric titration using a large amount of the sample.

**Ethylmercuric Phosphate.**—A substance in tablet form having the trade name "Luberon" (Hokko Chemical Co.) which contains ethylmercuric phosphate among other substances, was employed for the analysis. A 0.4597 g. portion of the sample was dissolved in 1 l. of water, and 2 ml. of the solution was put in a run.

***p*-Toluolsulfonaniline Phenyl Mercury, Ethylmercuric Phosphate and Ethylmercuric Urea.**—A mixture of these compounds, some binding material, some surface active agent and coloring matter, is marketed with the trade name "Fumiron" (Hokko Chemical Co.). A 0.4952 g. portion of the sample was dissolved in 1 l. of water and 2 ml. of the solution was taken for analysis.

**Methoxyethylmercuric Chloride.** — A tablet having the trade name "Usplon" (Japan Special Fungicide Co.) which contains

10) T. Kato, N. Takei and A. Okagami, *Japan Analyst (Bunseki Kagaku)*, **5**, 689 (1956).

TABLE IV. DETERMINATION OF MERCURY IN VARIOUS FUNGICIDES AND MEDICINES

| Sample | | Taken | Diluted to | An aliquot for analysis, | Mercury | |
|---|---|---|---|---|---|---|
| Trade name | Compound contained | g. | l. | ml. | Found μg. | % |
| Luberon (Hg content denoted : 2.5%) | Ethylmercuric phosphate | 0.4597 | 1 | 2 | 23.9<br>23.9<br>24.5<br>23.5 | |
| | | | | | av. 23.95 | ……2.50 |
| Fumiron (Hg content denoted : 2.5%) | *p*-Toluolsulfonaniline phenyl mercury Ethylmercuric phosphate Ethylmercuric urea | 0.4952 | 1 | 2 | 24.0<br>25.5<br>25.4 | |
| | | | | | av. 24.97 | ……2.52 |
| Usplon (Hg content : 2.5%) | Methylethylmercuric chloride | 0.4683 | 1 | 2 | 22.8<br>23.0<br>23.0 | |
| | | | | | av. 23.93 | ……2.55 |
| Mell (Tablet) (Hg content : 4.08%) | Dinaphthylmethane disulfonic acid phenyl mercury | 0.3005 | 1 | 2 | 25.5<br>25.0<br>25.9 | |
| | | | | | av. 25.47 | ……4.24 |
| Mell (Powder) (Hg content : 0.15%) | 〃 | 0.01993<br>0.01923<br>0.01555 | —<br>—<br>— | —<br>—<br>— | 27.5<br>26.4<br>21.4 | ……0.137 |
| Thimerosal (Hg content : 48.3～49.7%) | Ethylmercuric sodium thiosalcylate | 1.15081 | 2.5 | 2 | 22.8<br>22.8<br>22.8 | |
| | | | | | av. 22.8 | ……49.5 |
| Mercurochrome | Dibromohydroxy mercurifluorescein disodium salt | 0.37411 | 10 | 2 | 20.9<br>20.1<br>20.9<br>20.6<br>20.3 | |
| | | | | | av. 20.56 | ……25.88 |

2.5% of mercury was used as a sample. A 0.4683 g. portion of the sample was dissolved in 1 l. of water and 1 ml. of the solution was taken for analysis.

**Dinaphtholmethane Disulfonic Acid Phenylmercuric Salt.**—This compound is contained in "Mell" (Takeda Pharmaceutical Co.) which is solid in two forms. One is a tablet containing the compound in high concentration, and the other is a powder of lower concentration. A 0.3005 g. portion of the tablet was weighed and dissolved in 1 l. of water, 2 ml. of which was used for analysis. The powder was weighed and placed directly in the reaction vessel.

**Ethylmercury Thiosalicylate.** — A sample dried in a vacuum desiccator containing sulfuric acid was weighed (1.1508 g.) and dissolved in water to a concentration of 1 : 25000. Two milliliters of the solution was pipetted into the reaction vessel and the analysis was carried out.

The data obtained by the above analyses are tabulated together in Table IV. This shows good reproducibility, and a run of the analysis for each sample can be carried out within thirty minutes without any difficulty. Various methods have been proposed by other authors[11-14] for each sample, but some of them are not versatile enough for different substances and the others are very tedious. By the tin(II)-strong phosphoric acid method, analysis can be carried out with inorganic and organic compounds in various forms without any pre-treatments or precaution.

## Summary

A simple and rapid method for the determination of a minute amount of

11) J. Kanazawa and R. Sato, ibid., 8, 440 (1959).
12) D. Polley and V. L. Miller, *Anal. Chem.*, **24**, 1622 (1952).
13) V. L. Miller and and D. Polley, ibid., **26**, 1333 (1954); **27**, 1162 (1955).
14) H. Friedeberg, ibid., **27**, 305 (1955).

mercury in organic and inorganic compounds was established. This method uses the powerful decomposing and reducing power of tin(II)-strong phosphoric acid. In this method the sample is heated with the reagent in a round bottomed flask in a current of carbon dioxide. The mercury vapor evolved is carried with the carbon dioxide into an absorbing vessel which is a separatory funnel containing 10 ml. of 0.1 N potassium permanganate solution and 10 ml. of 10% sulfuric acid. The mercury vapor is oxidized again to the mercuric state and the ion is determined colorimetrically by the usual dithizone-chloroform method. After extracting the mercuric dithizonate with chloroform, the absorbancy of the organic layer is measured by a photoelectric colorimeter with a 517 mμ filter. Some organic compounds containing mercury and some inorganic mercuric compounds as mercuric chloride and mercuric oxide were analyzed by this method in extremely low concentrations, and satisfactory results were obtained. This method may be applied to various kinds of samples without special pre-treatments.

A part of the expenses for this study was defrayed by a grant from the Ministry of Education, to which the authors' thanks are due.

*Department of Chemistry*
*Faculty of Science*
*Kanazawa University*
*Kanazawa*

# *Effect of Cupric Ion on Oxidation of Benzene Aqueous Solution by Cobalt-60 Gamma-rays*

By Hiroshi HOTTA and Akira TERAKAWA

(Received July 3, 1959)

The oxidation of benzene aqueous solution by Cobalt-60 gamma-rays has been studied by some investigators[1-4]. The yields of phenol and biphenyl are affected by the presence of some metallic ions[5-7]. The effect of cupric ions will be interpreted in the present paper.

## Experimental

Triply distilled water was saturated with benzene purified by sulfuric acid and then by freezing, by shaking in a separate funnel. Then some solutions were aerated in a gas-wash bottle on covering the solution with benzene. Other inorganic reagents were used without further purification. The concentrations of initial benzene and produced phenol were measured directly by optical density at 253.5 and 270 m$\mu$, respectively.

The solution in a test tube of hard glass (Hario Glass) was irradiated at the Cobalt-60 Irradiation Laboratory of Japan Atomic Energy Research Institute at room temperature (ca. 20°C). The dose, which was measured chemically as mentioned elsewhere[8], was changed not by its irradiation time, but by irradiation for one hour at various positions, namely, at various dose rates. Therefore, the abscissa of Fig. 1 gives the value of the dose in $r$ as well as the value of dose rate in $r$/hr.

## Results

The results of aerated benzene-saturated aqueous solution containing (a) 0.8 N sulfuric acid or (b) nothing are shown in Fig. 1. These curves were linear up to ca. $4\times10^4 r$ for both solutions. The white precipitate, which smelled like biphenyl, was found in the solution irradiated by more than $7\times10^4 r$, and was separated by means of a centrifuge for the measurement of optical density. The corresponding G-value of phenol is listed in Table I with the composition of each solution.

1) P. V. Phung and M. Burton, *Radiation Research*, 7, 199 (1957).
2) K. C. Kurien, P. V. Phung and M. Burton, ibid., in press.
3) G. Stein and J. Weiss, *J. Chem. Soc.*, **1949**, 3241.
4) M. A. Proskyrnin, *Atomnaya Energiya (USSR)*, **5**, 321 (1958).
5) M. A. Proskyrnin and E. V. Barelko, *Nuclear Sci. Abstr.*, **13**. 1020 (1959).
6) J. H. Baxendale and D. Smithies, *J. Chem. Soc.*, **1959**, 779.
7) T. Yumoto, Y. Bono and T. Matsuda, *Mem. Gov. Ind. Research Inst. Nagoya* (in Japanese), 8, 296 (1959).
8) H. Hotta, A. Terakawa and S. Ōno, to be published.

TABLE I. YIELD OF PHENOL

| Name | Solute (in M) | | | | Treatment | G-value | |
|---|---|---|---|---|---|---|---|
| | Cupric sulfate | Cupric chloride | Sulfuric acid | Benzene | | At low dose | At high dose |
| a | 0 | 0 | 0.4 | Saturated | Aerated | 2.63 | 0.33 |
| b | 0 | 0 | 0 | Saturated | Aerated | 2.63 | (0.64)* |
| c | 0.01 | 0 | 0.4 | 0.0115 | Not-aerated | 5.98±1.1 | 0.68±0.03 |
| d | 0 | 0.01 | 0.4 | 0.0132 | Not-aerated | 3.63±0.9 | 0.55±0.14 |
| Burton[1] | 0 | 0 | 0.4 | Saturated | — | (2.64±0.04)** | (0.35±0.02)*** |

* Less reliable; ** Aerated; *** Oxygen-free.

The G-value of solution b) at a high dose was less reliable.

The results of benzene-saturated 0.8 N sulfuric acid solutions containing (c) 0.01 M cupric sulfate or (d) 0.01 M cupric chloride, which were not aerated, are also shown in Fig. 1. These curves were linear up to ca. $6\times10^4$ $r$ for both solutions. These solutions smelled somewhat like biphenyl at a higher does than that corresponding to the break point of the curve. However, nothing was found as precipitate even at the highest dose in spite of the presence of a break point. The corresponding G-value is greater than that in the absence of any cupric ion as listed in Table I.

The earlier result by Burton et al. is listed in the same table for reference[1].

According to the examination of the analytical method by Goodman and Steigman[9], the spectroscopic method without solvent extraction as employed in the present work unavoidably gives a higher G-value of phenol (ca. 29% higher). However, the following discussion might not be proved valueless qualitatively by this uncertainty. Kurien, Phung and Burton indicate that their initial G-value of phenol is very correctly 2.64[2], which is nearly equal to the present value.

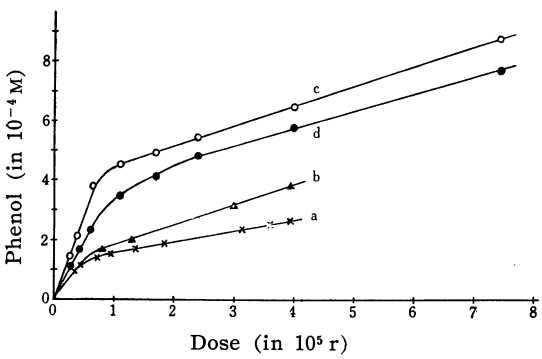



Fig. 1. Oxidation of aqueous benzene solutions. The name of each curve corresponds to the condition in Table. 1.

## Discussion

According to Burton et al.[1,2], phenol and hydrogen peroxide are produced by irradiation of aerated aqueous solution saturated with benzene like the present solutions a) and b). They interpret this fact with the following reactions:

$$H_2O \rightsquigarrow H,\ OH,\ H_2,\ H_2O_2 \qquad (0)$$

$$PhH+OH=Ph+H_2O \qquad (1)$$

$$Ph+O_2=PhO_2 \qquad (2)$$

$$PhO_2+H_2O=PhOH+HO_2 \qquad (3)$$

$$H+O_2=HO_2 \qquad (4)$$

and $$2HO_2=H_2O_2+O_2 \qquad (5)$$

Furthermore, the reactions,

$$Ph+OH=PhOH \qquad (6)$$

$$Ph+Ph=Ph_2 \qquad (7)$$

$$PhH+H=PhH_2 \longrightarrow \text{Polymer} \qquad (8)$$

and $$Ph+H=PhH \qquad (9)$$

must be considered in the oxygen-free or -nearly free solution. Reactions 7 and 8 give some insoluble products. According to Baxendale and Magee[10], the reaction

$$Ph+H_2O_2=PhOH+OH \qquad (10)$$

does not occur. Ph in the above equations denotes phenyl radical ($C_6H_5$).

The above interpretation is based on the assumption that, since the oxygen molecule scavenges all of the phenyl radical as well as H atoms, reactions 7 and 8 are suppressed by oxygen. The yield of phenyl depends not on the concentration of benzene but on that of oxygen. The concentrations at the break point of the curve are supposed to be about $1\times10^{-2}$ M and $1\times10^{-4}$ M for benzene and oxygen, respectively, from the former

9) J. Goodman and J. Steigman, *J. Phys. Chem.*, **62**, 1020 (1958).

10) J. H. Baxendale and J. Magee, *Discussions Faraday Soc.*, **14**, 160 (1953).

and the present experiments[1,11]. In a concentration of oxygen lower than this, phenol radicals are consumed by reactions 6—9[1,6]. The yield of phenol by the above reactions is at the highest $G_w(OH)=2.92$, which is the G-value of the OH radical induced from water. In fact, the experimental G-value supports this restriction, and indicates the partial re-hydrogenation of the phenyl radical to benzene by reaction 9, since the value is smaller than $G_w(OH)$.

In the presence of a cupric ion, the yield of phenol is larger than $G_w(OH)$, and no insoluble product is yielded even at the highest dose. The large yield of phenol can be interpreted by the following reactions,

$$Cu^{2+}+H=Cu^{+}+H^{+} \quad (11)$$

and then

$$Cu^{+}+H_2O_2=Cu^{2+}+OH^{-}+OH \quad (12)$$

The highest yield of phenol from this interpretation is $G_w(OH)+G(H_2O_2)=2.92+2.84=5.76$, where $G(H_2O_2)$ denotes the G-value of hydrogen peroxide by reaction 5 as well as reaction 0 and is estimated from datum by Phung and Burton[1]. Of course, a part of OH radicals may be consumed by the reaction

$$Cu^{+}+OH=Cu^{2+}+OH^{-} \quad (13)$$

This highest G-value is nearly equal to the present observed value of solution c) in Table I. The rate constant of reaction 11 is quantitatively confirmed to be great in the experiment of aqueous ferrous-cupric solution[8].

The concentration of benzene is not necessarily slight at the break point, and benzene should scavenge almost all of the OH radical by reaction 1 even after the break point as well as in the initial stage. Therefore, since the yield of phenyl radical is independent of oxygen, the fate of phenyl radicals, which are not dimerized to biphenyl by reaction 7 in virtue of the presence of the cupric ion, must be considered beside reaction 9. Moreover, reaction 11 suppresses reaction 9. Although reaction 11 suppresses also reaction 8, it is independent of phenyl radical. When the negative phenyl ion, $Ph^{-}$, is assumed to be a more stable form than phenyl radical, the promotion of re-hydrogenation to benzene without dimerization due to the cupric ion can be interpreted by the reactions,

$$Ph+Cu^{+}=Ph^{-}+Cu^{2+} \quad (14)$$

and then

$$Ph^{-}+H^{+}=PhH \quad (15)$$

through reaction 11. An analogous reaction is assumed for ferrous ion by Baxendale and Magee[10]. If almost all of the radical induced from water is scavenged by reactions 1 and 11 in the present condition, reactions 14 and 15 enable them to understand why no precipitate is found even at the highest dose in the presence of a cupric ion. The decomposition of phenol is slight according to Kurien, Phung and Burton[2]. There was no difference for the characteristics of absorption curve between 200~300 mμ for the solution through the whole range of dose.

Next, the effect of a chloride ion on the yield of phenol is noticed for solution d). A chloride ion is usually considered to react with OH radical in an acidic aqueous solution[12] as

$$Cl^{-}+H^{+}+OH=Cl+H_2O \quad (16)$$

and then

$$Cl+H_2O_2=Cl^{-}+H^{+}+HO_2 \quad (17)$$

or

$$Cl+H=Cl^{-}+H^{+} \quad (18)$$

Since reaction 16 competes with reaction 1, the yield of phenol is reduced. The reaction between phenyl and chloride radicals is ignored. The detailed study of the effect of chloride ions on the radiolysis of aqueous solution will be given in a later paper[8].

Since the present experiment is not exhaustive, the detailed study will follow.

## Summary

The effect of a cupric ion on the radiolysis of benzene aqueous solution can be interpreted by the following reactions of a cuprous ion produced in reaction $Cu^{2+}+H=Cu^{+}+H^{+}$. That is, the larger yield of phenol than $G_w(OH)$ in the presence of oxygen is due to the increment of OH radical by reaction $Cu^{+}+H_2O_2=Cu^{2+}+OH^{-}+OH$, and no precipitation in the absence of oxygen is due to re-hydrogenation by reactions $Ph+Cu^{+}=Ph^{-}+Cu^{2+}$ and $Ph^{-}+H^{+}=PhH$, respectively.

*Japan Atomic Energy Research Institute*
*Tokai, Ibaraki-ken*

11) N. A. Lange, "Handbook of Chemistry", Handbook Publishers, Inc., Sandusky, Ohio (1956), p. 1091.

12) T. J. Sworski, *Radiation Research*, **2**, 26 (1955).

# *The Molecular Cross-sectional Areas for the Determination of Specific Surface Areas of Solids. II. Titania and Silica*

By Kumasaburo KODERA and Yoshito ONISHI

(Received August 5, 1959)

As for the determination of the specific surface areas of solids by the B.E.T. method[1], it is generally experienced that the values obtained by different adsorbate gases do not always coincide among themselves. In the preceding paper[2], specific surface areas of carbon blacks were estimated by means of the B.E.T. method using several gases, and by comparing them with those from electron microscopy, the molecular cross-sectional areas of the gases which would give the consistent surface areas with different gases and also with those from electron microscopy were determined. In this paper, similar studies with titania and silica as adsorbents will be mentioned.

## Experimental Method and Results

A series of ten commercial titania samples and five silica samples listed in column 2 of Table I were used. Nitrogen, argon, oxygen, carbon dioxide and *n*-butane were chosen as adsorbate gases, and the adsorption isotherms were measured as in the preceding paper. B.E.T. plots obtained from the isotherms are classified in four types from I to IV as shown in the preceding paper, in which, curves I and III are similar in form excepting that the former has a longer linear portion that the latter, curve II is a normal form with a length of linear portion being intermediate between I and III, and curve IV has a special form with shortest linear part. In Table I, types of isotherms are listed together with the appearance of the hysteresis in the measured pressure range, where "?" shows that the existence of hysteresis is not clear because the desorption isotherm was not measured in these cases. Estimated specific surface areas from the isotherms using the molecular cross-sectional areas[3] listed in column 4 of Table V, i.e. the values calculated from the densities of liquid state, are shown in Table II. Values under $S_{N_2}/S$ in the table are ratios between the surface areas estimated by nitrogen and by other gases. Surface areas* calculated from $d_3 = K\sum nd^3/\sum nd^2$ determined by electron microscopy by Suito and Arakawa[4] are also listed in the table**. It should be noted that in the calculation an equation $S = 6/d_3\rho$ was used. This can be applied only for spherical or cubic particles. In this equation, $S$ represents the specific surface area and $\rho$ the specific gravity of the sample. Values of $\rho$ used were 3.9 for anatase, 4.2 for rutile and 2.0 for silica.

In order to study the effect of the degree of crystallization or other surface states of the sample, surface areas of ten titania samples specially prepared under different conditions were measured by nitrogen, argon, oxygen and carbon dioxide, and the results are given in Table III. These samples were prepared by Kennedy's method[5], namely, titanium dioxide precipitated by hydrolysis of titanium tetrachloride was dried for five hr. at 100°C and then heated at different temperatures under the current of various gases***.

## Discussion

From Table I, it is seen that the isotherms to which the B.E.T. equation can be applied most satisfactorily are those obtained by argon and oxygen, and then those by nitrogen and carbon dioxide; but for *n*-butane, about half of the isotherms are of special types. As in the case of carbon black in the preceding paper, the isotherms of nitrogen and argon generally show no hysteresis, whereas by other gases, hystereses of isotherms are seen in nearly half of the cases.

As are shown in Table II, the average values of $S_{N_2}/S$ for argon at two temperatures are 1.26 and 1.25 and their standard deviations are small. For oxygen, the deviation is also small despite the rather great value for the carbon black but those for *n*-butane and carbon dioxide are great. In these the ratios in parentheses were excluded from the average. This

1) S. Brunauer, P. H. Emmett and E. Teller, *J. Am. Chem. Soc.*, **60**, 309 (1938).
2) K. Kodera and Y. Onishi, This Bulletin, **32**, 356 (1959).
3) P. H. Emmett and S. Brunauer, *J. Am. Chem. Soc.*, **59**, 1553 (1937).
* Ti-8, 9, 10 were measured by the present authors.
** '*d*' represents the particle diameter measured on an electron micrograph.
4) E. Suito and M. Arakawa, unpublished.
5) D. R. Kennedy, M. Ritchie and J. Mackenzie, *Trans. Faraday Soc.*, **54**, 119 (1958).
*** These samples have been prepared by Prof. I. Uei and Prof. F. Mashio of Kyoto Technical University.

TABLE I. TYPES OF B.E.T. CURVES

| No. | Samples | $N_2(-196°C)$ | | $Ar(-196°C)$ | | $Ar(-183°C)$ | | $O_2(-183°C)$ | | $CO_2(-78°C)$ | | $n\text{-}C_4H_{10}(0°C)$ | |
|---|---|---|---|---|---|---|---|---|---|---|---|---|---|
| | | Type | Hyst. | Type | Hyst. | Type | Hyst. | Type | Hyst. | Type | Hyst. | Type | Hyst. |
| Ti- 1 | Ishihara A-100 | I | − | II | − | II | − | II | − | III | − | II | + |
| 〃 2 | Ishihara R-810 | I | − | I | − | II | − | II | − | II | − | II | − |
| 〃 3 | Tochigi TP-53 | III | − | I | − | I | − | II | − | III | − | I | − |
| 〃 4 | Tochigi TP-53C | III | + | II | + | I | + | II | + | III | + | IV | + |
| 〃 5 | Furukawa Anatase-F | II | − | II | − | II | − | II | + | III | − | II | − |
| 〃 6 | Furukawa Rutile-F | II | − | II | − | II | − | II | + | II | − | II | + |
| 〃 7 | Chitan-kogyo Cronos | II | − | II | − | II | − | II | − | III | − | II | − |
| 〃 8 | TFM | II | ? | II | ? | II | ? | II | ? | III | + | — | — |
| 〃 9 | Titanox RA-Nc | II | ? | II | ? | II | ? | II | ? | III | ? | — | — |
| 〃 10 | Unitane O-220 | II | ? | II | ? | II | ? | II | ? | III | − | — | — |
| Si- 1 | Hisil-101 | III | − | II | − | II | − | II | ? | III | − | IV | ? |
| 〃 2 | Aerosil | III | − | II | − | II | − | II | ? | III | + | IV | ? |
| 〃 3 | Carplex 1120 | III | + | II | − | II | − | II | ? | III | + | IV | ? |
| 〃 4 | Microsil B-55 | III | − | II | − | II | − | II | ? | III | + | IV | ? |
| 〃 5 | Nisil F-1 | III | − | II | − | II | − | II | ? | II | + | IV | ? |

TABLE II. SPECIFIC SURFACE AREAS MEASURED BY VARIOUS GASES

| No. | $N_2(-196°C)$ $S_{N_2}$ $m^2/g.$ | $Ar(-196°C)$ | | $Ar(-183°C)$ | | $O_2(-183°C)$ | | $CO_2(-78°C)$ | | $n\text{-}C_4H_{10}(0°C)$ | | Electron microscope $m^2/g.$ |
|---|---|---|---|---|---|---|---|---|---|---|---|---|
| | | $S$, $m^2/g.$ | $S_{N_2}/S$ | $S$, $m^2/g.$ | $S_{N_2}/S$ | $S$, $m^2/g.$ | $S_{N_2}/S$ | $S$, $m^2/g.$ | $S_{N_2}/S$ | $S$, $m^2/g.$ | $S_{N_2}/S$ | |
| Ti- 1 | 9.48 | 7.60 | 1.25 | 7.71 | 1.23 | 8.06 | 1.17 | 6.95 | 1.36 | 7.18 | 1.32 | 8.93 |
| 2 | 6.41 | 5.32 | 1.21 | 5.32 | 1.21 | 5.45 | 1.18 | 4.29 | 1.49 | 4.33 | 1.48 | 3.40 |
| 3 | 8.14 | 6.47 | 1.26 | 6.57 | 1.24 | 7.09 | 1.15 | 6.28 | 1.30 | 5.91 | 1.38 | 8.58 |
| 4 | 7.61 | 5.90 | 1.29 | 5.91 | 1.29 | 6.31 | 1.21 | 4.90 | 1.55 | 5.27 | 1.45 | 8.67 |
| 5 | 10.97 | 8.60 | 1.28 | 8.90 | 1.23 | 9.22 | 1.19 | 6.13 | 1.79 | 7.70 | 1.43 | 8.82 |
| 6 | 8.57 | 6.88 | 1.25 | 7.21 | 1.19 | 7.20 | 1.19 | 3.87 | (2.21) | 5.48 | 1.56 | 6.53 |
| 7 | 9.88 | 7.88 | 1.25 | 7.99 | 1.24 | 7.97 | 1.24 | 5.69 | 1.74 | 7.02 | 1.41 | 8.82 |
| 8 | 16.90 | 13.70 | 1.23 | 13.55 | 1.25 | 13.70 | 1.23 | 9.78 | 1.73 | — | — | 9.50 |
| 9 | 8.89 | 7.03 | 1.26 | 7.06 | 1.26 | 7.00 | 1.27 | 6.21 | 1.43 | — | — | 6.14 |
| 10 | 8.50 | 6.68 | 1.27 | 6.80 | 1.25 | 6.84 | 1.24 | 4.71 | 1.81 | — | — | 6.14 |
| Si- 1 | 93.3 | 73.9 | 1.26 | 73.9 | 1.26 | 79.4 | 1.18 | 68.7 | 1.36 | 61.6 | 1.51 | 100.0 |
| 2 | 118.7 | 92.7 | 1.28 | 94.0 | 1.26 | 97.3 | 1.22 | 82.8 | 1.44 | 88.2 | 1.35 | 77.3 |
| 3 | 86.0 | 67.8 | 1.27 | 69.0 | 1.25 | 73.4 | 1.17 | 65.3 | 1.32 | 55.6 | 1.55 | 126.4 |
| 4 | 117.8 | 91.0 | 1.29 | 91.4 | 1.29 | 97.4 | 1.21 | 87.9 | 1.34 | 74.0 | 1.59 | 64.9 |
| 5 | 24.7 | 19.3 | 1.28 | 19.9 | 1.24 | 20.2 | 1.22 | 8.5 | (2.91) | 15.6 | 1.58 | — |
| Average | | | 1.26 | | 1.25 | | 1.21 | | 1.51 | | 1.47 | |
| Standard deviation | | | 0.02 | | 0.03 | | 0.03 | | 0.17 | | 0.08 | |

TABLE III. SURFACE AREAS OF SPECIALLY PREPARED $TiO_2$

| Heat treatments of samples | | | $N_2(-196°C)$ $m^2/g.$ | $Ar(-183°C)$ | | $O_2(-183°C)$ | | $CO_2(-78°C)$ | |
|---|---|---|---|---|---|---|---|---|---|
| | | | | $m^2/g.$ | $S_{N_2}/S_{Ar}$ | $m^2/g.$ | $S_{N_2}/S_{O_2}$ | $m^2/g.$ | $S_{N_2}/S_{CO_2}$ |
| Vacuum | 200°C | 5 hr. | 59.3 | 47.2 | 1.26 | 49.5 | 1.20 | 49.1 | 1.21 |
| $O_2$ | 385 | 5 | 31.4 | 25.3 | 1.24 | 26.6 | 1.18 | 34.3 | 0.92 |
| $O_2$ | 585 | 5 | 12.80 | 10.34 | 1.24 | 10.55 | 1.21 | 14.5 | 0.88 |
| $O_2$ | 790 | 5 | 4.30 | 3.42 | 1.26 | 3.52 | 1.22 | 3.65 | 1.18 |
| $O_2$ | 1000 | 3 | 2.82 | 2.29 | 1.23 | 2.46 | 1.15 | 2.15 | 1.31 |
| $N_2$ | 900 | 3 | 6.85 | 5.48 | 1.25 | 5.70 | 1.20 | — | — |
| $N_2$ | 1000 | 3 | 4.29 | 3.47 | 1.24 | 3.55 | 1.21 | 3.81 | 1.13 |
| $N_2$-$O_2$(1:1) | 1000 | 3 | 4.70 | 3.88 | 1.21 | 3.97 | 1.18 | — | — |
| $N_2$-$O_2$(4:1) | 1000 | 3 | 4.55 | 3.66 | 1.24 | 3.74 | 1.22 | — | — |
| $N_2$-$O_2$(9:1) | 1000 | 3 | 3.96 | 3.08 | 1.29 | 3.25 | 1.22 | — | — |
| | | | Average | | 1.25 | | 1.20 | — | — |

TABLE IVa. COMPARISON OF SURFACE AREAS FROM THE B.E.T. METHOD AND ELECTRON MICROSCOPY

Ratio of area by B.E.T. to area by electron microscopy

| No. | $N_2$ | $Ar(-196°C)$ | $Ar(-183°C)$ | $O_2$ | $CO_2$ | $n$-$C_4H_{10}$ |
|---|---|---|---|---|---|---|
| Ti-1 | 1.06 | 0.85 | 0.86 | 0.90 | 0.78 | 0.81 |
| 2 | (1.89) | (1.57) | (1.57) | (1.61) | (1.26) | (1.27) |
| 3 | 0.95 | 0.75 | 0.77 | 0.83 | 0.73 | 0.69 |
| 4 | 0.88 | 0.68 | 0.68 | 0.73 | 0.57 | 0.61 |
| 5 | 1.25 | 0.98 | 1.01 | 1.05 | 0.70 | 0.87 |
| 6 | 1.31 | 1.05 | 1.10 | 1.10 | 0.59 | 0.84 |
| 7 | 1.12 | 0.89 | 0.91 | 0.90 | 0.65 | 0.80 |
| 8 | 1.77 | 1.44 | 1.43 | 1.44 | 1.03 | — |
| 9 | 1.45 | 1.15 | 1.15 | 1.14 | 1.01 | — |
| 10 | 1.39 | 1.09 | 1.11 | 1.11 | 0.77 | — |
| Average | 1.24 | 0.99 | 1.00 | 1.02 | 0.76 | 0.77 |
| Molecular cross-section | 13.1 | 13.9 | 14.4 | 13.8 | 22.4 | 41.7 Å² |

TABLE IVb.

| | | | | | | |
|---|---|---|---|---|---|---|
| Si- 1 | 0.93 | 0.74 | 0.74 | 0.79 | 0.69 | 0.62 |
| 2 | 1.54 | 1.20 | 1.22 | 1.26 | 1.07 | 1.14 |
| 3 | 0.68 | 0.54 | 0.55 | 0.58 | 0.52 | 0.44 |
| 4 | 1.82 | 1.40 | 1.41 | 1.50 | 1.35 | 1.14 |
| Average | 1.24 | 0.97 | 0.98 | 1.03 | 0.91 | 0.84 |

anomaly for carbon dioxide has been observed also for the carbon black. From the comparison with the preceding paper, it is seen that the ratio in Table II is 7~11% greater than those for carbon black; therefore, the discrepancy between surface areas by nitrogen and those by other gases increased further.

With the titanias prepared under various conditions shown in Table III, nitrogen, argon, and oxygen give surface areas parallel to each other, i.e. the area ratios $S_{N_2}/S$ are nearly constant, and equal to the values in Table II. This fact suggests that these gases give reliable areas despite the difference in the surface state of the samples. For carbon dioxide, however, ratios vary considerably, and in a few cases give values smaller than 1. Such deviations of ratios by carbon dioxide have been observed also for samples of carbon black, silica and other solids in our laboratory. It seems, therefore, that the adsorptions of carbon dioxide change considerably by some slight change in the surface state of the solid, thus, it is concluded that this gas is not suitable for use in the B.E.T. method.

For the reason mentioned above and for the same reason as in the preceding paper, argon may be taken as the standard gas. To determine the molecular cross-sectional areas of the standard gas and of the other gases, the specific surface areas estimated by the B.E.T. method, were compared with those from electron microscopy, the

TABLE V. MOLECULAR CROSS-SECTIONAL AREAS

| Gas | Temp. | Van der Waals' const. | From liquid density | Livingston's | Present authors' | | |
|---|---|---|---|---|---|---|---|
| | | | | | $TiO_2$, $SiO_2$ | Carbon black[2] | Average |
| $N_2$ | −196°C | 15.4 Å² | 16.2 Å² | 15.4 Å² | 12.9 Å² | 14.2 Å² | — |
| Ar | −196 | 13.6 | 13.8 | 14.6 | 13.8 | 13.8 | 13.8 Å² |
| Ar | −183 | 13.6 | 14.4 | 15.5 | 14.3 | 14.4 | 14.4 |
| $O_2$ | −183 | 13.5 | 14.1 | 14.6 | 13.5 | 13.5 | 13.5 |
| $CO_2$ | − 78 | 16.5 | 17.0 | 19.5 | 20.4 | 20.8 | 20.6 |
| $n$-$C_4H_{10}$ | 0 | 33.0 | 32.1 | 44.6 | 37.4 | 38.6 | 38.0 |

TABLE VI. MOLECULAR CROSS-SECTIONS CALCULATED FROM THE COMPARISON WITH THE ABSOLUTE METHOD

| Gas | Temp. | Molecular cross-sections | | Ratio | Literature |
|---|---|---|---|---|---|
| | | From the liquid dens. | From the absolute method | | |
| $N_2$ | −196°C | 16.2 Å² | 16.2 Å²<br>16.27 | 1.00<br>1.00 | 6, 7, 8<br>9 |
| Ar | −196 | 13.8 | 16.6<br>16.88 | 1.20<br>1.22 | 8<br>9 |
| Ar | −183 | 14.4 | 18.19 | 1.26 | 9 |
| $O_2$ | −196 | 13.2 | 17.5 | 1.33 | 7 |
| Kr | −196 | 15.3 | 19.5<br>21.78 | 1.28<br>1.42 | 6<br>9 |
| $CO_2$ | − 78 | 17.0 | 24.39 | 1.43 | 9 |

method independent of the former. The results are shown in Tables IVa and IVb, where figures represent ratios of surface areas estimated by the B.E.T. method and by electron microscopy. In the table, values of Ti-2 were excluded from the average, because it contained needle-like parallel piped particles. Since only a few samples of silica have been measured and the values in the table scatter rather badly, they were used only to verify those with the titanias. These scattered values for the silicas may be explained by the fact that they consist of far smaller particles than the titanias, so that the measurement of the particle diameters on an electron micrograph would yield more series errors. The values shown in the lowest part of Table IVa are obtained by dividing the molecular cross-sections from the liquid densities (column 4, Table V) by respective average ratios in the table. These values should give the consistent surface areas with those from electron microscopy. Since the molecular cross-sections of argon at −196°C thus obtained agree fairly well with both van der Waals' constant and that from liquid density, the value 13.8 Å² from the liquid density was employed as the standard as in the preceding paper. Molecular cross-sections for the other gases are calculated from this value and the values of $S_{N_2}/S$ in Table II, and are shown in column 6 of Table V. From Table IVb it is seen that these values might be applied for silica as well. Since these values, except for that for nitrogen, agree very well with those for the carbon black, average values for both adsorbents can be used for both solids and are shown in the last column. It is seen that these values agree very well with those in Table IV. Agreement with those from the liquid densities also are fairly good, and the value for oxygen agrees with van der Waals' constant. The value for nitrogen, 12.9 Å², however, is considerably smaller than that for the carbon black, 14.2 Å², and deviation from the widely used value, 16.2 Å², from the liquid density is even greater. This deviation amounts to 26% and will be discussed below.

Beebe[6], Arnold[7], Corrin[8], and Pickering et al.[9] determined the molecular cross-sections of several gases for use in the surface area measurement by the B.E.T. method. In their studies, anatase used by Harkins and Jura[10] and determined to

6) R. A. Beebe, J. B. Beckwith and J. M. Honig, *J. Am. Chem. Soc.*, **67**, 1554 (1945).
7) J. R. Arnold, ibid., **71**, 104 (1949).
8) M. L. Corrin, ibid., **73**, 4061 (1951).
9) H. L. Pickering and H. C. Eckstrom, ibid., **74**, 4775 (1952).
10) W. D. Harkins and G. Jura, ibid., **66**, 1362 (1944).

TABLE VII. SPECIFIC SURFACE AREAS

| No. | $N_2$ $m^2/g.$ | Ar(−196°C) $m^2/g.$ | Ar(−183°C) $m^2/g.$ | $O_2$ $m^2/g.$ | $CO_2$ $m^2/g.$ | $n$-$C_4H_{10}$ $m^2/g.$ | B.E.T. mean $m^2/g.$ | Elec. micro. $m^2/g.$ |
|---|---|---|---|---|---|---|---|---|
| Ti- 1 | 7.55 | 7.60 | 7.71 | 7.72 | 8.42 | 8.50 | 7.92 | 8.93 |
| 2 | 5.10 | 5.32 | 5.32 | 5.22 | 5.20 | 5.12 | 5.21 | 3.40 |
| 3 | 6.48 | 6.47 | 6.57 | 6.79 | 7.61 | 7.00 | 6.82 | 8.58 |
| 4 | 6.06 | 5.90 | 5.91 | 6.04 | 5.94 | 6.24 | 6.02 | 8.67 |
| 5 | 8.74 | 8.60 | 8.90 | 8.83 | 7.43 | 9.11 | 8.60 | 8.82 |
| 6 | 6.83 | 6.88 | 7.21 | 6.89 | (4.69) | 6.49 | 6.86 | 6.53 |
| 7 | 7.87 | 7.88 | 7.99 | 7.63 | 6.89 | 8.31 | 7.76 | 8.82 |
| 8 | 13.45 | 13.70 | 13.55 | 13.12 | 11.85 | — | 13.13 | 9.50 |
| 9 | 7.08 | 7.03 | 7.06 | 6.70 | 7.52 | — | 7.08 | 6.14 |
| 10 | 6.77 | 6.68 | 6.80 | 6.55 | 5.71 | — | 6.50 | 6.14 |
| Si- 1 | 74.3 | 73.9 | 73.9 | 76.0 | 83.2 | 73.0 | 75.7 | 100.0 |
| 2 | 94.5 | 92.7 | 94.0 | 93.1 | 100.3 | 104.3 | 96.5 | 77.3 |
| 3 | 68.5 | 67.8 | 69.0 | 70.2 | 79.1 | 65.8 | 70.1 | 126.1 |
| 4 | 93.8 | 91.0 | 91.4 | 93.2 | 106.5 | 87.6 | 93.9 | 64.9 |
| 5 | 19.7 | 19.3 | 19.9 | 19.3 | (10.3) | 18.5 | 19.3 | — |

have the specific surface area of 13.8 $m^2/g$.**** by their absolute method was chosen as a standard solid of the known surface area. They measured adsorption isotherms on this sample by several adsorbates, and calculated $V_m$ by the B.E.T. equation. Dividing 13.8 $m^2$ by $V_m$ they determined the cross-sectional area of adsorbate gas molecule. Areas thus obtained for various adsorbate gases are shown in Table VI together with the respective ratios to the areas from the liquid densities. These cross-sections have been proved by the above authors to give consistent surface areas for various solids examined, which include carbon black, rouge, rutile, etc. As are shown in column 5, the ratio of nitrogen is naturally 1, but all other values are greater than 1, i.e. from 1.20 to 1.43. From these ratios it is clear that, except for carbon dioxide and one of kryptons, the deviations of 26% for nitrogen mentioned above will nearly compensate deviations indicated by the ratios in the table, if 12.9 $Å^2$ were used for the cross-section of nitrogen. Moreover, ratios of the cross-sections of argon at two temperatures and carbon dioxide to that of nitrogen are 1.04, 1.12, and 1.50, respectively, by Pickering et al.[9], and 1.07, 1.12, and 1.58, respectively, by the present study. This fact also shows the agreement of the relative molecular cross-sections between both cases. Alexander et al.[11] measured surface area of six silica samples by the B.E.T. method, and determined their mean volume surface diameters ($d_3$) from electron microscopy. The ratios of the specific surface areas by nitrogen adsorption given in Table II in their paper and those calculated from $d_3$ in the same table give 1.27 on an average. Therefore, if the areas by electron microscopy are correct, the cross-section of nitrogen must be larger by 27% and agrees with the present study again.

From those discussed above the relative values of the molecular cross-sections estimated by the present authors are in fair agreement with those by the others, but from comparison with electron microscopy 16.2 $Å^2$ for nitrogen at −196°C seems to be too great and better agreement might be attained by choosing argon as a standard and giving 13.8 $Å^2$ for its cross-section at −196°C.

The specific surface areas of all the samples calculated by the cross-sections shown in column 8, Table V, are shown in Table VIII. The average value for each sample together with that from electron microscopy are also listed. In general, the surface areas from the different gases and from electron microscopy are in fair agreement with each other, except for a few cases which are shown in parentheses under carbon dioxide and excluded from the average. Especially for samples of titania, the agreement is satisfactory. Anomalous results obtained by carbon dioxide in certain cases may be explained by some difference in the surface state as in the case of the carbon black. Anomalous ratios in Table III for carbon dioxide are also explained similarly as was discussed above.

**** The same sample gave 13.9 $m^2/g.$ by the B. E. T. method using nitrogen as the adsorbate and by assuming 16.2 $Å^2$ for its molecular cross-section.

11) G. B. Alexander and R. K. Iler, *J. Phys. Chem.*, **57**, 932 (1953).

## Conclusion

For the estimation of the specific surface areas of titania and silica, argon, nitrogen, and oxygen are suitable for adsorbate gases and *n*-butane may also be available, but carbon dioxide must be used carefully as it gives unreliable results in some cases. The molecular cross-sectional areas given in Table V, column 6, are in fair agreement with those obtained for the carbon black except for that of nitrogen. The discrepancy by nitrogen would need further investigation, but for other gases, average values shown in column 8 may be expected to give consistent surface areas for many kinds of solids by different gases.

This research has been carried out by the research fund for science donated by the Ministry of Education.

*Department of Chemistry*
*Faculty of Industrial Arts*
*Kyoto Technical University*
*Sakyo-ku, Kyoto*

# *The Molecular Structure of Hexachlorobenzene by Electron Diffraction*

By Takahide SAITO

(Received July 20, 1959)

An early electron diffraction investigation of the structure of haxachlorobenzene by the usual visual method was reported by Brockway and Palmer[1], observing the scattering in a range of $q$* less than 60 and using the trial and error method, led to the conclusion that the molecule has the planar configuration as a whole. In contrast with their opinion, Bastianssen and Hassel[2] re-investigated the molecule by the sector method and reported that the non-planar structure, illustrated in Fig. 1, is supported on the basis of interpretation of the peaks in the radial distribution curve, but they did not apply the trial and error method to their investigations. The above contradictory results are compared in Table 1, containing the distances of the principal atomic pairs**. Although it is generally recognized that the sector method is superior to the visual method, it is not perfectly meaningless to re-investigate the molecule by the visual method and the trial and error process, if it is possible to obtain the photographs with rings extending to higher scattering angle, that is, if it is possible to observe the rings of larger $q$ values than the previous reports.

## Experimental

The apparatus of electron diffraction is the same as that in the previous reports[3] and the diffraction can be easily observed over the broad range of $q$. The electron wavelength, about 0.055 Å, was calibrated with gold foil diffraction.

The sample was prepared by Holleman's method[4], m. p. 227°C. Measurements of the photographs were carried out by the usual visual method.

TABLE I. A COMPARISON OF TWO REPORTS

| Investigater | $\theta$ | C-Cl | C'-Cl | C''-Cl | Cl-Cl | Cl'-Cl |
|---|---|---|---|---|---|---|
| Brockway, Palmer | 0 | 1.70 | 2.69 | 4.00 | 3.11 | 5.39 |
| Bastianssen, Hassel | 12 | 1.72 | 2.68 | 3.99 | 3.15 | 5.39 |

The unit of interatomic distance is Å.

$\theta$ is the angle between the direction of C-Cl and the benzene plane.

1) L. O. Brockway and K. J. Palmer, *J. Am. Chem. Soc.*, **59**, 2181 (1937).

2) O. Bastianssen and O. Hassel, *Acta Chem. Scand.*, **1**, 489 (1947).

* $q=(10/\pi)s$, $s=(4\pi/\lambda)\sin\theta/2$, which $\lambda$ is the wavelength.

** The term "principal" is used for the atomic pair having the larger values of $nZZ/r$, in which $n$ is the number of the pair, $Z$ is the atomic number and $r$ is the length of atomic pair.

3) T. Yuzawa and M. Yamaha, This Bulletin, **26**, 414 (1953).

4) M. Holleman, *Rec. trav. chim.*, **39**, 763 (1920).

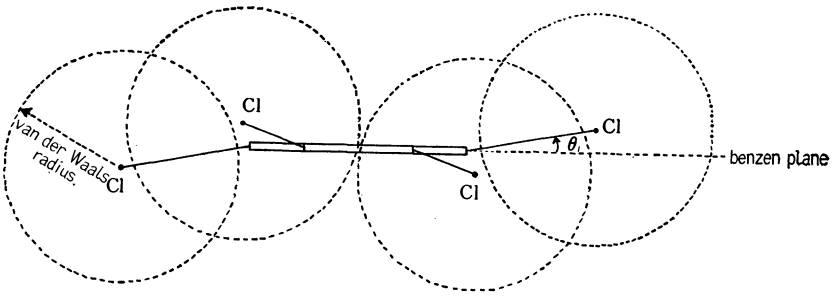



Fig. 1. The schema of deviation of Cl atoms from the benzene plane.

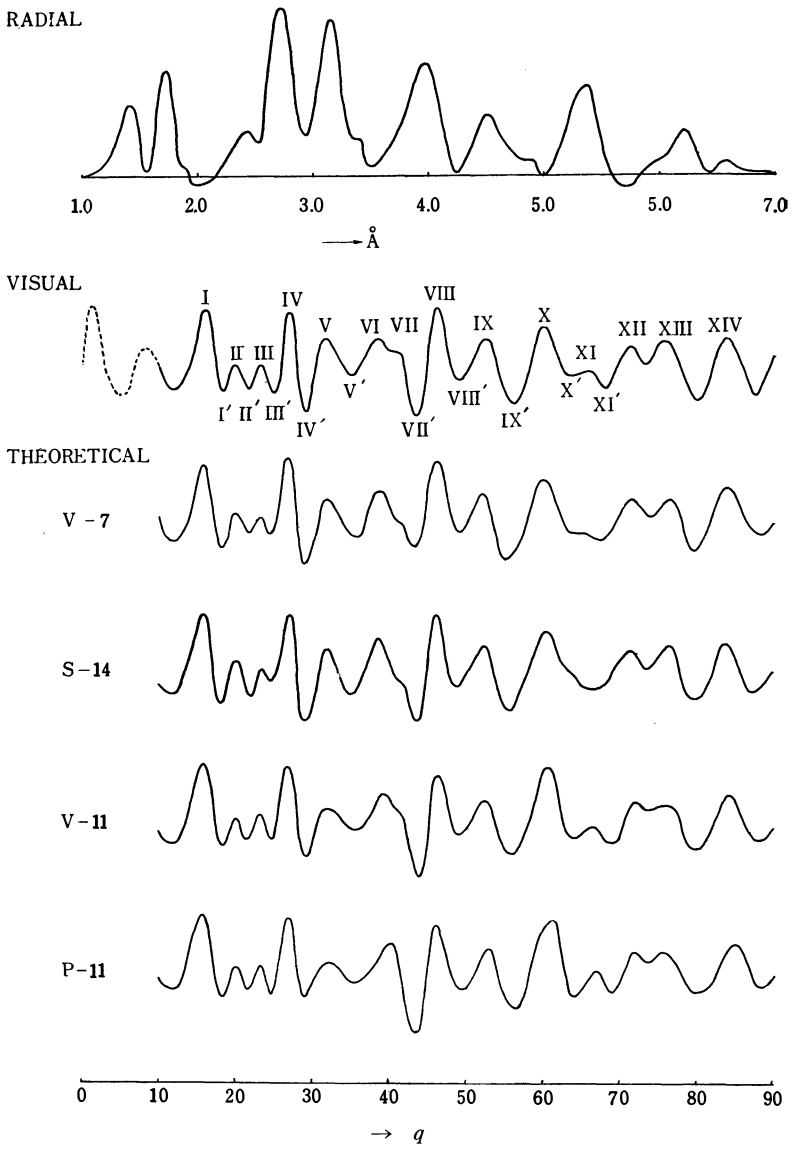



Fig. 2. The radial distribution curve, visual curve and various theoretical curves.

### Procedure and Results

The experimental visual curve is shown in Fig. 2: fourteen maxima and ten minima have been observed in the range of $q$ from 15 to 95. From the visual intensity curve, the radial distribution curve has been calculated according to the equation[5]

$$rD(r)=\sum_{q=1}^{q_{max}} I(q)\exp(-aq^2)\sin(\pi qr/10)$$

$$\exp(-aq^2{}_{max})=0.1$$

$$q=(10/\pi)s \qquad s=(4\pi/\lambda)\sin(\theta/2)$$

in which $\theta$ is the scattering angle and $a$ is a constant. The radial curve shows remaining ghosts, but has clearly six principal peaks at 1.40, 1.72, 2.70, 3.99, 3.15 and 5.36 Å. They correspond to the interatomic distances of C-C, C-Cl, C′-Cl, C″-Cl, Cl-Cl and Cl′-Cl, respectively.

Theoretical intensity curve for the molecular models have been calculated by the use of the equation[5]

$$I(q)=\sum_i\sum_j (Z_iZ_j/r_{ij})\exp(-a_{ij}q^2)\sin(\pi qr_{ij}/10)$$

$$a_{ij}=(\pi^2/200)l^2{}_{ij}$$

where $l_{ij}$ is the mean amplitude of the atomic distance $r_{ij}$. The coefficients of thermal vibration, $a_{ij}$, roughly estimated in reference to the calculated aliphatic data[6-8] is introduced into each model, for $q>30$. The values of coefficients are shown in Table II. The theoretical curves were

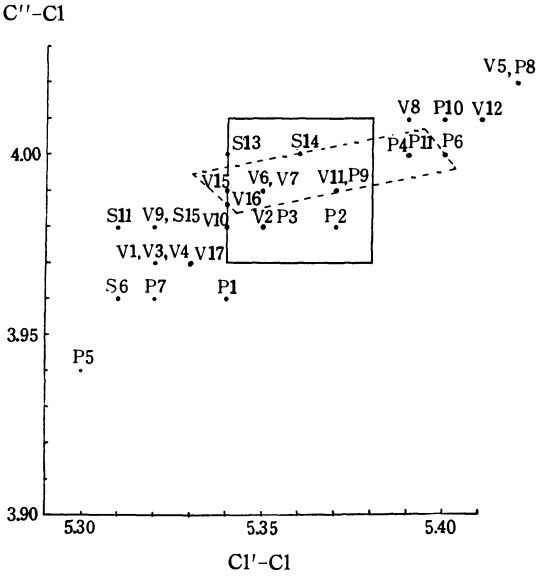



Fig. 3. The parameter chart of C″-Cl vs. Cl′-Cl.

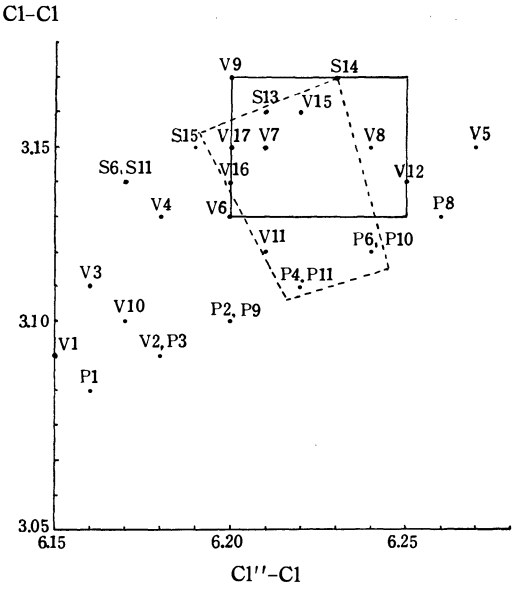



Fig. 4. The perameter chart of Cl-Cl vs. Cl″-Cl

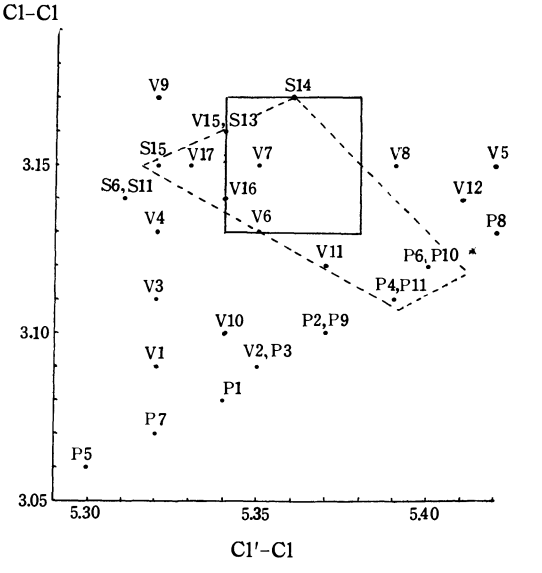



Fig. 5. The parameter chart of Cl-Cl vs. Cl′-Cl.

calculated to cover the following ranges of the principal parameters: C′-Cl=2.66～2.72 Å, C″-Cl=3.94～4.02 Å, Cl-Cl=3.06～3.17 Å and Cl′-Cl=5.30～5.42 Å. In Fig. 2 are shown some of the theoretical curves, which agree comparatively well with the visual intensity curve and have the close

5) R. Spurr and V. Schomaker, *J. Am. Chem. Soc.*, **64**, 2693 (1942).

6) J. Karle, *J. Chem. Phys.*, **20**, 65 (1952).

7) Y. Morino, K. Kuchitsu and T. Shimanouchi, ibid., **20**, 726 (1952).

8) Y. Morino, K. Kuchitsu, A. Takahashi and K. Maeda, ibid., **21**, 1927 (1953).

TABLE II. THE COEFFICIENTS OF THERMAL VIBRATION TERMS

| Atomic pair | $a_{ij}$ | Atomic pair | $a_{ij}$ |
|---|---|---|---|
| C-C | 0 | C''-Cl | 0.00022 |
| C'-C | 0.00007 | C-Cl | 0.00033 |
| C''-C | 0.00015 | Cl-Cl | 0.00011 |
| C-Cl | 0 | Cl'-Cl | 0.00046 |
| C'-Cl | 0.00008 | Cl''-Cl | 0.00062 |

TABLE III. RESULTS OF QUOTED MODELS AND RADIAL DISTRIBUTION CURVE

| Atomic pair | Model number | | | | Radial |
|---|---|---|---|---|---|
| | V-7 | S-14 | P-11 | V-11 | |
| C-Cl | 1.72 | 1.72 | 1.70 | 1.71 | 1.72 |
| C-Cl | 2.70 | 2.70 | 2.69 | 2.70 | 2.70 |
| C-Cl | 3.99 | 3.99 | 4.00 | 3.99 | 3.99 |
| Cl-Cl | 3.15 | 3.16 | 3.11 | 3.12 | 3.15 |
| Cl-Cl | 5.35 | 5.34 | 5.39 | 5.37 | 5.36 |
| Av. of $q_{calc}/q_{obs}$ | 1.001 | 0.996 | 1.005 | 1.005 | |
| Mean deviation | 0.008 | 0.008 | 0.016 | 0.005 | |

V-7, S-14 and V-11 are the non-planar models. P-11 is the plane model.

values of parameters to those of the interatomic distances from the radial distribution curve.

The values of principal parameters of models are shown in Table III. No distinct differences in the theoretical curves to contribute to any decisive choice can be observed, and the observable, relatively small, difference are as follows: (1) the relative shapes and positions of max. V—VII; (2) the relationships of max. VI and min. XI. The theoretical curves of the non-planar models show the good agreements rather than the curves of the plane models in the shapes of the above respects and in the values of $q_{calc}/q_{obs}$ and of interatomic distances.

## Summary

The non-planar structure of hexachlorobenzene is fairly suitable rather than the planar structure and the values of principal interatomic distances are

C-Cl=1.72±0.01 Å

C'-Cl=2.69±0.02 Å

Cl-Cl=3.15±0.02 Å

They are in agreement with Hassel's data.

The author thinks that the re-investigation of the molecular structure of hexachlorobenzene by the precise sector method is necessary.

The author has great pleasure in acknowledging his debts of gratutude to Professor A. Kotera and Professor K. Suzuki for their continued encouragement and advice, and to Dr. M. Igarashi and Dr. H. Sekine for their kind discussions and to Dr. K. Kuchitsu for his kindness in the calculations. A part of the cost of this research has been defrayed from the Scientific Research Encouragement Grant from the Ministry of Education, to which the author's thanks are due.

*Department of Chemistry*
*Faculty of Science*
*Tokyo University of Education*
*Koishikawa, Tokyo*

# *Studies on Thixotropy. I*. On the Thixotropic Gelation Process*

By Takehiko WATANABE

(Received August 10, 1959)

A number of studies concerning thixotropy, have been carried out by various kinds of methods. Taking as an example the bentonite-water system, which may be regarded as a typical thixotropic system, the studies have been made by the analysis of flow curve[1-9], the measurement of time required for gelation[10-14], and by both the rate constant of thixotropic gelation and the maximum gel strength (maximum yield value) developed as a consequence of completion of gel formation[15-18].

The third method may be said to be the one by which the process of gel formation can be actually followed and expressed in proper terms. The author et al.[16] have also made studies on bentonite (Gumma Bentonite) and some other clays, employing a method of the same kind and found that the thixotropic gel formation of clays generally proceeds in two first order processes which take place successively. Later, as phenomena similar to the above, in the case of the surface film of high polymer, Tachibana et al.[19] found that the thixotropic recovery of the surface elasticity or the surface pressure proceeds also in two steps.

In the present experiments, the author has also made studies on other thixotropic systems than bentonite, e.g. vanadium pentoxide sol, graphite suspension, etc., and found that in any system, in which the form of dispersed particles is plate- or rod-like, the thixotropic gelation generally proceeds in two steps. The conditions, under which the thixotropic gel formation proceeds thus in two steps, are examined and discussed.

## Experimental

**Materials.** — *Bentonite.* — Gumma Bentonite; a product from Gumma Prefecture, which was a finely ground powder, was used. A 10% aqueous suspension of the bentonite was let stand for 5 days and after the removal of the larger sized particles by sedimentation, the suspension (concn. about 5%) was collected and concentrated on a water bath at about 60°C.

Yamagata Bentonite: a 3% aqueous suspension of an original soil from Yamagata Prefecture which was eventually let stand for 5 years after preparation was used. The upper part of the suspension was first filtered by cotton wool and the filtrate (concn. about 1%) was concentrated.

Volclay (Wyoming Bentonite): after sedimentation of a 7% aqueous suspension of the powdery product for 5 days, its upper part (concn. about 3%) was taken and concentrated.

Tixoton: a product of the firm "Deutsche Bentonit" was used as an aqueous suspension.

The order of the capacity of swelling of the above four bentonites is as follows.

Yamagata Bentonite>Volclay>Tixoton>Gumma Bentonite.

The X-ray spectrographic analysis showed that Yamagata Bentonite contained no appreciable impurity, while Volclay contained small amounts of impurity which may be $\alpha$-quartz and $\alpha$-crystobalite, and Tixoton a small amounts of $\alpha$-quartz and Gumma Bentonite a relatively large amount of $\alpha$-crystobalite compared with the other three.

*Kaolin.*—Three kinds of products from Tochigi Prefecture (Kampaku mine), Korea and Hongkong, respectively, were used as aqueous suspensions.

*Sericite.* — The original powdery product from Niigata Prefecture was sieved through 250 mesh and used as an aqueous suspension.

* Presented in part at the Symposium on Colloid Chemistry of the Chemical Society of Japan, Kanazawa, October, 1957.

1) O. Kimura, *J. Chem. Soc. Japan, Pure Chem. Sec.* (*Nippon Kagaku Zasshi*), **56**, 1346 (1935).
2) B. Tamamushi ibid., **61**, 280 (1940).
3) H. Akamatu, ibid., **63**, 1275 (1942).
4) T. Alfrey, Jr. and C. W. Rodewald, *J. Colloid Sci.*, **4**, 283 (1949).
5) P. Rehbinder, *Discussions Faraday Soc.*, **18**, 151 (1954).
6) H. van Olphen, "Proceedings of the Fourth National Conference on Clays and Clay Minerals", publication 456, National Academy of Sciences, National Research Council, Washington (1956), p. 204.
7) S. Peter and I. Stolle, *Z. physik. Chem.* (*Frankfurt*), **11**, 251 (1957).
8) Sven-Eric Dahlgren, *J. Colloid Sci.*, **13**, 151, (1958).
9) H. Enneking, *Rheologica Acta.* **1**, 234 (1958).
10) E. A. Hauser, *Kolloid-Z.*, **48**, 57 (1929).
11) H. Freundlich, O. Schmidt and G. Lindau, *Kolloid-Beih.*, **36**, 43 (1932).
12) U. Hofmann, *Kolloid-Z.*, **125**, 86 (1952).
13) S. Ono and T. Watanabe, *J. Chem. Soc. Japan, Pure Chem. Sec.* (*Nippon Kagaku Zasshi*), **74**, 463 (1953).
14) H. v. Platen and H. G. F. Winkler, *Kolloid-Z.*, **158**, 3 (1958).
15) H. Braune and I. Richter, ibid., **113**, 20 (1949).
16) T. Watanabe and S. Matsumoto, *J. Chem. Soc. Japan, Pure Chem. Sec.* (*Nippon Kagaku Zasshi*), **76**, 1215 (1955).
17) A. Packter, *Kolloid-Z.*, **150**, 60 (1957).
18) T. Watanabe and Y. Takasaki, *Naturwissenschaften*, **45**, 334 (1958).
19) T. Tachibana and N. Okuda, presented at the 9th (1956) and the 10th (1957) Annual Meetings of the Chemical Society of Japan.

*Vanadium pentoxide.* An aqueous sol was prepared according to Biltz's method, and the heat treatment of the sol was carried out at 96°C for 10 hr. as suggested by Sato[20]. Afterwards the sol was let stand for one month.

*Graphite.* — Flaky powder was used as an aqueous suspension.

In the case of experiments with the suspension in the electrolyte solution, the electrolyte solution was added to the above aqueous suspension until its requisite concentration was attained.

*Organophilic Bentonite.*—Gumma Bentonite was converted into an organophilic bentonite by cation-exchange reaction using oleyl-picolinium chloride or lauryl-picolinium chloride as cation active agent. A dried powdery product was obtained and used as a benzene suspension.

**Apparatus and Procedure.** — The measurement of yield value of the above mentioned suspensions was carried out using Du Noüy torsion balance. The length and diameter of the torsion wire are 40 and 0.025 cm., respectively. A small glass sphere (diameter about 0.7 cm.) is hung from the hook of the apparatus with a thin palladium wire (diameter 0.1 mm.). The force which causes the glass sphere to move upward, is given by twisting the torsion wire and is read on the dial scale.

In kinetic studies, measurements should be carried out at constant temperature. In the present experiments, however, all the measurements were made at room temperature, since the characteristics of the observed phenomena and also the maximum yield value are only slightly influenced by the change of temperature in the neighborhood of room temperature.

Experiments have been made as follows. The suspension is taken into a test tube (inner diameter 2.1 cm.) and thoroughly shaken or stirred. Then the glass sphere is immersed into the suspension about 3 cm. below the meniscus. Then, force is added until the glass sphere begins to show a minute upward movement (about 1/60 mm.). The preceding procedure should be performed within 30 sec. after stopping the stirring. The moment at which the above procedure was done, is regarded as the starting point of the experiment. Then, at 5 min. intervals, the force is superimposingly added in the same manner as stated above. In this experiment, the yield value (unit, dyn./cm$^2$) is expressed with the value obtained by dividing the force with the equatorial cross-section of the glass sphere. The yield value is taken versus the value obtained in the same manner as the above only with the dispersion medium. To observe the upward movement of the glass sphere, a small mirror was attached to the top of the hook and its movement was observed under twenty times enlargement using a lamp and scale. In the course of the application of the additional force, no upward movement of the glass sphere is observed until the total amount of the force has exceeded a certain amount. The force with which the upward movement of the glass sphere of about 1/60 mm. (i.e. that of 0.3 mm. on the scale) is brought about, is used to evaluate the yield value. It was observed that if the excess of force which caused the upward movement was removed immediately after the movement had been induced, the glass sphere returned to the position before the movement. Therefore, it may be said that the experiment has been carried out under the condition where the deformation applied to the suspension is within elastic limit.

With some of the samples used, experiments were also made using the torsion wire of 15 cm. besides one of 40 cm. In these cases, sensibility to detect a minute deformation was poor so that the amount of the added force became inevitably about two times greater than the case of 40 cm. Therefore, after the cessation of the additional increase of the force at the point where the upward movement of 0.3 mm. on the scale had been observed, a further gradual upward movement of 0.3~0.5 mm. was followed during the ensuing interval of about one minute. This movement may be a visco-elastic flow accompanied with the deformation over elastic limit induced by the force above stated.

## Results

Experiments have been made with the various kinds of suspensions stated above. In Fig. 1 the yield value is plotted versus

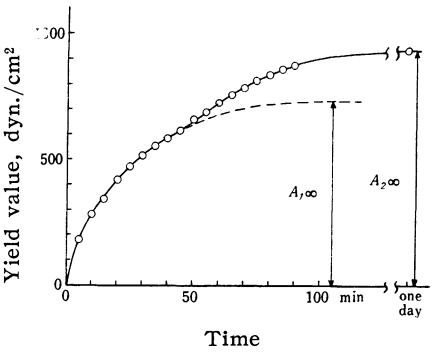



Fig. 1. The process of thixotropic gel formation (result obtained with 3.4% Yamagata Bentonite aqueous suspension).

the setting time. The curve shows that the increase of yield value with time proceeds in two processes which take place successively. The first process starts to develop immediately after the cessation of stirring or shaking. The second one reveals itself successively after some development of the first.

The increase of the yield value varies according to the first order kinetics for each separate process. These may be expressed as follows:

20) K. Sato, "Symposium on Colloid Science (Kōshitsu-gaku Ronsō", Kawade Shobō, Tokyo (1943), p. 93.

$$k_1 = \ln \frac{A_{1\infty}}{A_{1\infty} - A_t} \cdot \frac{1}{t}$$

$$k_2 = \ln \frac{A_{2\infty}}{A_{2\infty} - A_t} \cdot \frac{1}{t}$$

where $A_t$ is the yield value at time $t$ and $A_{1\infty}$ is the maximum yield value of the first process which is obtained from the curve as shown in Fig. 1. $A_{2\infty}$ is the maximum yield value of the second process. $k_1$ and $k_2$ are the rate constants for the first and the second processes, respectively. Similar plots such as that shown in Fig. 1 were generally obtained with the system where the dispersed particles have plate- or rod-like forms. In Table I the systems in which the increase of the yield value proceeds in two steps are collected. In the system to which an electrolyte was added, the two step process was detected, when no marked coagulation of the dispersed particles was observed. On the other hand, in the case where marked coagulation was observed, for example, Gumma Bentonite in 0.01 M $FeCl_3$, the process of the thixotropic gel formation was completed in a single step. The same phenomenon was also observed with the thixotropic sol of ferric oxide in 0.1 M NaCl.

TABLE I. THE SYSTEMS IN WHICH THE THIXOTROPIC GEL FORMATION PROCEEDS IN TWO STEPS

| Dispersed particles | Medium* |
|---|---|
| Gumma Bentonite | Water, 0.1 M NaCl, 0.4 M NaCl, 0.1 M LiCl |
| Yamagata Bentonite | Water |
| Volclay | Water, 0.1 M NaCl, 0.01 M $FeCl_3$, 0.005 M $Th(NO_3)_4$ |
| Tixoton | Water, 0.1 M NaCl, 0.01 M $FeCl_3$, 0.005 M $Th(NO_3)_4$ |
| Organophilic Bentonite | Benzene |
| Kaolin | Water |
| Sericite | Water |
| Vanadium pentoxide | Water |
| Graphite | Water, 0.1 M NaCl, 0.05 M $FeCl_3$ |

* The resulting preparations may contain small amounts of some ions other than those listed, which are due to the nature of the dispersed particles.

For some systems, experiments were carried out at several concentrations of dispersed particles. These results are shown in Table II. And the relation between $A_{1\infty}$ or $A_{2\infty}$ and the concentration ($C$) was derived as shown in Table III.

Another experiment was made by using torsion wires of 15 and 40 cm., respectively. For example, results obtained with 3.1%

TABLE II. EXPERIMENTAL RESULTS WITH YAMAGATA BENTONITE-, VOLCLAY-, AND VANADIUM PENTOXIDE-WATER SYSTEMS

(Temp., room temp. i. e. in the neighborhood of 15°C)

| System | Concn. of disperesed particles g./100 g. | $k_1 \times 10^2$ $min^{-1}$ | $A_{1\infty}$ dyn./cm² | $k_2 \times 10^2$ $min^{-1}$ | $A_{2\infty}$ dyn./cm² |
|---|---|---|---|---|---|
| Yamagata | 3.7 | 2 | 870 | 3 | 1000 |
| Bentonite-water | 3.4 | 4 | 730 | 4 | 930 |
| | 3.1 | 3 | 690 | 4 | 910 |
| | 2.9 | 2 | 600 | 3 | 800 |
| | 2.7 | 3 | 520 | 4 | 750 |
| Volclay-water | 9.3 | 2 | 650 | 6 | 760 |
| | 8.8 | 3 | 540 | 6 | 700 |
| | 8.4 | 2 | 430 | 6 | 620 |
| Vanadium | 2.3 | 6 | 1100 | 5 | 1600 |
| pentoxide-water | 2.1 | 4 | 930 | 7 | 1200 |
| | 1.9 | 4 | 740 | 7 | 920 |
| | 1.8* | 8 | 690 | — | — |

* Complete in a single step.

TABLE III. RELATIONS BETWEEN THE MAXIMUM YIELD VALUE OF THE FIRST STEP ($A_{1\infty}$) OR THE SECOND ($A_{2\infty}$) AND CONCENTRATION ($C$)

| System | Relations |
|---|---|
| Yamagata Bentonite-water | $A_{1\infty} \propto C^2$ & $A_{2\infty} \propto C$ |
| Volclay-water | $A_{1\infty} \propto C^4$ & $A_{2\infty} \propto C^2$ |
| Vanadium pentoxide-water | $A_{1\infty} \propto C^2$ & $A_{2\infty} \propto C^3$ |

TABLE IV. DATA OBTAINED WITH THE SAME SUSPENSION (3.1% YAMAGATA BENTONITE) USING A DIFFERENT LENGTH OF TORSION WIRE

| Wire length, cm. | $k_1\times10^2$, min$^{-1}$ | $A_{1\infty}$, dyn./cm$^2$ | $k_2\times10^2$, min$^{-1}$ | $A_{2\infty}$, dyn./cm$^2$ |
|---|---|---|---|---|
| 40 | 3 | 690 | 4 | 910 |
| 15 | 6 | 1500 | 3 | 2100 |

Yamagata Bentonite aqueous suspension are shown in Table IV. The difference of the value of $k_2$ between the two cases is small but that of $k_1$ is cosiderable. The latter may be due to the following conditions. In the case of 15 cm. wire, the visco-elastic flow has been observed in each measurement as stated above, and consequently the thixotropic gel formation proceeds under small shearing motions which facilitate the formation of the gel structure, i.e. the phenomenon of rheopexy has been observed. In the case of 40 cm. wire such an experimental condition was not established so that the phenomenon of rheopexy was not observed.

## Discussion

In the first place, let us consider the bentonite suspension. As a structure of thixotropic gel, it is adopted in such a network structure that plate-like particles link with each other in a short distance at the junction point. Furthermore as a model of structure, the 'house of cards' structure which was proposed by Hofmann[12] and whose existence in a xerogel was proved by Weiss et al.[21], is recommended.

In the present experiments, it was observed that the dependence on the concentration of $A_{1\infty}$ was different from that of $A_{2\infty}$. This fact can not be explained with the assumption that the yield value of the gel is determined by all the particles in the structure. Therefore, it must be assumed that the particular group of particles contributes to the yield value of the gel. Such a particular particle group which plays the part of a mechanical unit to the yield value, is named 'structural unit' (abbr. S. U.). Further, the particle group which acts as S. U. is classified into two types, i. e. one is the particle group forming linear ribbon and another is that of cross-linkage.

In the structure, the particles are linked at such small distances at any junction point that the steric hindrance caused by the interaction of linking particles must be taken into consideration. In these circumstances, the steric conditions such as freedom of rotation or flexibility around the junction point, may be the same as each other, in any particle group, so far as the co-operation between particles is concerned.

Considering the steric conditions, the association of plate-like particles may be classified into three types as follows.

P-1 association : Two adjacent particles are linked with each other at one point.

P-2 association : Two adjacent particles are linked at two or more points belonging to one straight line.

P-3 association : Two adjacent particles are linked at three or more points so that they are associated with surface-to-surface linkage.

By the third type of association a voluminous structure can not be expected to be formed, so that the discussions are undertaken leaving the third type out of consideration.

Next, it may be assumed that the magnitude of the cohesive force at junction points of S. U., remains constant in a given system unless the range of concentration studied is great. Therefore, as a first approximation, it may be assumed that the contribution to the yield value of each of the same kind of particle group, i. e. the strength of ($b$) the corresponding S. U. is constant, and the yield value ($A$) of any system will be determined by the number ($N_s$) of the S. U. in unit volume as follows :

$$A = bN_s \qquad (1)$$

In this case, the evaluation of the value of $N_s$ is necessary. At first, probability of permanent junction between adjacent particles (abbr. probability of junction) will be considered. The probability of junction where a given particle in a gel is linked to an adjacent one with P-1 association, will be determined by the number of free dispersed particles in unit volume ($N_p$) which may exist when the gel is transformed to sol by stirring etc. In other words, the probability of junction will vary as the concentration of the dispersed particles ($C$). Generally, the probability of junction between a particle and

21) A. Weiss, R. Fahn and U. Hofmann, *Naturwissenschaften*, **39**, 351 (1952); *Ber. deut. keram. Ges.*, **30**, 21 (1953).

its adjacent $l$ particles with P-1 association will vary as $C^l$, where $l \ll N_p$ and $l$ is a positive integer.

The probability of junction will be evaluated in the case of P-2 association. In this case, the above probability will be determined by the following two probabilities. The one is that of orientation of the particle in sol state to the position where the particle can be linked with P-2 association to a given particle. The other is that of formation of junction between particles. The two probabilities will be proportional to $N_p$, i. e. $C$. Therefore, the discussed probability of junction should vary as $C \times C = C^2$. Generally, the probability of junction between a particle and its adjacent $m$ particles in the same manner as stated above will vary as $C^{2m}$, where $m$ is a positive integer.

Let us consider the linear ribbons which act as S. U. The linear ribbons are formed from the aligned particles and in order to act as S. U. they must also be linked to two or more other linear ribbons. In general the linear ribbons are not formed from exactly equal numbers of particles. However, in the present case, the cohesive force between particles is considered to remain constant, so that the yield value may be determined by the number of junction points between particles in unit volume of the gel. The assumptions are made on the way whereby the linear ribbons are formed, i. e. how many particles are separately linked with what type of association to any one particle. And the relations between the yield value and the concentration in the case where the assumed linear ribbons act as S. U., are derived on the basis of the knowledge on the probability of junction above stated. The results are shown in Table V.

The consideration will be given to the cross-linkage. Cross-linkage is a particle group which plays the part of junction between the linear ribbons in structure. When it contributes to the yield value as S. U., it may be expected that one of the particles forming cross-linkage, could not move in accordance with the deformation of the gel under the applied force, but would behave as if it were restricted at a fixed position. Therefore, the characteristics of the cross-linkage are determined by two factors. One of them is the number of effective linear ribbons linked to the above fixed particle and the other is the type of association between particles forming the cross-linkage. In addition, it may be assumed that the degrees of steric hindrance of the junction points between the particles forming a cross-linkage must be the same as each other and further they must be the same as, or higher than, that of forming the linear ribbons participating in the cross-linkage. According to the above considerations, the relations between the yield value and the concentration of the gel are derived from the knowledge of the probability of junction and shown in Table VI. In this table the necessary type of association of the particles forming linear ribbons is also listed.

Considering the process of development of gel structure which is applicable for the two cases of Yamagata Bentonite and Volclay, it must be assumed that S. U. in

TABLE V. THE RELATION BETWEEN THE YIELD VALUE ($A$) AND THE CONCENTRATION ($C$) OF THE GEL IN WHICH THE LINEAR RIBBON ACTS AS STRUCTURAL UNIT

| Nomenclature of structural unit | Mode of formation of linear ribbon | Relations between $A$ and $C$ |
|---|---|---|
| L-1 | P-1 association $l=1$ | $A \propto C$ |
| L-2 | $l=2$ | $A \propto C^2$ |
| L-3 | $l=3$ | $A \propto C^3$ |
| L-4 | P-2 association $m=1$ | $A \propto C^2$ |
| L-5 | $m=2$ | $A \propto C^4$ |

TABLE VI. THE RELATION BETWEEN THE YIELD VALUE ($A$) AND THE CONCENTRATION ($C$) OF THE GEL IN WHICH THE CROSS-LINKAGE ACTS AS STRUCTURAL UNIT

| Nomenclature of structural unit | Mode of formation of cross-linkage | Relations between $A$ and $C$ | Necessary type of association of linear ribbon |
|---|---|---|---|
| M-1 | P-1 association $l=2$ | $A \propto C^2$ | P-1 |
| M-2 | $l=3$ | $A \propto C^3$ | P-1 |
| M-3 | $l=4$ | $A \propto C^4$ | P-1 |
| M-4 | P-2 association $m=1$ | $A \propto C^2$ | P-1 |
| M-5 | $m=2$ | $A \propto C^4$ | P-1, P-2 |

the first step of gel formation is cross-linkage and that of the second is linear ribbon. Therefore, in the case of Yamagata Bentonite having $A_{1\infty} \propto C^2$ and $A_{2\infty} \propto C$, the S. U. for the first step is M-1 or M-4 in Table VI and that of the second is L-1 in Table V, since the linear ribbons of this sample must be formed from the particles linked together by P-1 association. Also in the case of Volclay, the linear ribbons are formed by P-2 association, and the S. U. of the first step is M-5 and that of the second is L-4, since this sample shows the relation, $A_{1\infty} \propto C^4$ and $A_{2\infty} \propto C^2$.

According to the above considerations, it may be explained that the thixotropic gel formation of bentonite will proceed as follows. During the first step, some of the dispersed particles align to form linear ribbons, and the latter further cross-link with neighboring ones to develop into a loose gel structure. In the second step, many particles or linear ribbons having no part in the formation of the first loose gel structure, begin to participate in structure to complete a rigid gel structure. On the other hand, in the first step, the increase of yield value is proportional to the increase in number of cross-linkage and the latter will be accelerated under small shearing motions so that the phenomenon of rheopexy will markedly appear. In the second step, both the increase in number of cross-linkage and that of linear ribbons participating in the formation of the cross-linkage, will simultaneously occur and these will lead to the increase of continuity of the linear ribbons in the gel structure so that the linear ribbons will come to act as S. U. Therefore, though the cross-linkage acting as S. U. in the first step, does not decrease in number nor disappear, its contribution to the yield value as S. U. gradually diminishes in the second step. Moreover, the rheopectic phenomenon can not be observed distinctly in the second step, since the rate of increase of yield value of this step is not determined by the rate of increase of the cross-linkage as in the case of the first step.

In the case of vanadium pentoxide sol, the experimental facts may be explained as follows. It is not necessary to make such a distinction between P-1 and P-2 association as in the case of bentonite, since the vanadium pentoxide particle has a thin rod-like form. It may be assumed that the particle group which acts as S. U. both in the first and in the second step, is the particle group forming cross-linkage. During the first step, a loose gel structure may be developed, in which the dispersed particles are linearly associated and a relatively small number of cross-linkage or entanglement can be seen between the linear chains of particles, and in the second step, it reaches another structure, i. e. a rigid gel structure which may be due to the appreciable increase of cross-linkage between chains. The difference in structure between the loose and rigid one is due to the variance in number of linear chains participating in the formation of the cross-linkage which acts as S. U. The number of linear chains linked to the fixed particle of the cross-linkage is two in the former structure and is three in the latter one, since this sample shows the relation, $A_{1\infty} \propto C^2$ and $A_{2\infty} \propto C^3$. In the course where the rigid gel structure is developed from the loose one, cross-linkage which contributes to the yield value proportional to $C^2$ is transformed to the cross-linkage proportional to $C^3$, according to the increase in number of linear chains linked to form the cross-linkage.

## Summary

(1) In this system, in which the form of dispersed particles is plate- or rod-like, the thixotropic gelation generally proceeds in two steps.

(2) During the first step of thixotropic gel formation, a loose gel structure may be developed and a rigid gel structure in the second step.

(3) In the case of bentonite, the structural unit which contributes to the yield value of the gel in the first step is cross-linkage and that of the second is linear ribbon.

(4) In the case of vanadium pentoxide, the structural unit is cross-linkage both in the first and in the second step.

The author would like to express his gratitude to Professor Sôzaburo Ono for his kind guidance and discussion throughout this work and to Mr. Yoshiyuki Takasaki for his kind assistance in the experiment.

*Laboratory of Biophysical Chemistry*
*College of Agriculture*
*University of Osaka Prefecture*
*Sakai, Osaka*

# *A Simple Method for the Preparation of Crystalline D-Mannose*

By Toshihito FUJITA and Tetsuo SATŌ

(Received August 18, 1959)

In the recent studies on the reaction of carbohydrates with boric acid, the present authors have required a large quantity of crystalline D-mannose. This is usually obtained by the hydrolysis of polysaccharides, such as mannan and glucomannan[1].

A better source of the sugar are the corms of *Amorphophallus* konjac, which contain mannose as glucomannan and are commercially available as "Konjac Flour". According to the previous methods[2] for the preparation of the sugar from this source, D-mannose is isolated in the form of its crystalline phenylhydrazone, purified as easily crystallizable methyl-*a*-D-mannoside, and then the glycoside is hydrolyzed to free sugar. This phenylhydrazone method is quite expensive, and not suitable for preparation on a large scale.

The phenylhydrazone method is based on the unusual low solubility in water of mannose phenylhydrazone. *N*-phenylmannosylamine, like the hydrazone, is insoluble and easily crystallized from an aqueous solution[3]. Moreover, the *N*-glycoside is very easily hydrolyzed under neutral conditions in the presence of formaldehyde or benzaldehyde. The authors have used *N*-phenyl-D-mannosylamine in isolating D-mannose from "Konjac Flour" and made certain improvements for the preparatory purpose of D-mannose.

The "Konjac Flour" has been hydrolyzed with concentrated or with dilute acid solution. The best results bave been obtained by refluxing it in 1 N acid solution. From the acid hydrolysate D-mannose has been isolated as crystalline *N*-phenylmannosylamine, and the *N*-mannoside has been readily hydrolyzed to free sugar in the usual manner[4]. The yield of sugar from this method is nearly equal to that of the phenylhydrazone method.

## Experimental

**Preparation of *N*-Phenyl-D-mannosylamine.**—*Procedure-A.*—One hundred grams of "Konjac Flour" was mixed with 60 ml. of cold 75% sulfuric acid under cooling, allowed to stand overnight at room temperature and then added to 1 liter of water. The diluted solution was refluxed for 6 hr. The solution was neutralized with barium carbonate to pH 4~5 and the precipitate was filtered off. The filtrate was decolorized with active charcoal and concentrated to 100 ml. in vacuo. Aniline (16 ml.) in 100 ml. of ethanol was added to it. The mixture was kept overnight in a refrigerator. The crystals formed were collected and recrystallized from 50% ethanol. Yield 24 g., m.p. 180~181°C. It was identified with an authentic sample[3].

*Procedure-B.*—"Konjac Flour" (100 g.) was suspended in 1 liter of 1 N sulfuric acid and the mixture was boiled for 10 hr. under refluxing. The dark brown solution was neutralized to pH 4~5 with barium carbonate. The *N*-mannoside was obtained as described above. Yield, 33 g.

**Isolation of D-Mannose from *N*-Phenyl-D-mannosylamine.**—Fifty grams of *N*-phenyl-D-mannosylamine was dissolved in water at 60~70°C and 35% formaldehyde (25 ml.) was added to it. A white precipitate was soon deposited. The mixture was allowed to stand for 24 hr. at room temperature. The white resinous substance was removed and the filtrate was evaporated to a thick sirup. The colorless sirup was dissolved in methanol and *n*-propanol (1 : 1) and seeded with *a*-D-mannose. The crystals were separated and recrystallized from ethanol or acetic acid. Yield, 30 g. (85%), m.p. 130~131°C. $[\alpha]_D^{30}$: 28.4° →+13.3° (*c* 3.9, in water).

Found: C, 40.18; H, 6.84. Calcd. for $C_6H_{12}O_6$: C, 40.00; H, 6.71%.

*Laboratory of Organic Chemistry*
*Tokyo Institute of Technology*
*Meguro-ku, Tokyo*

1) J. Sowden, "The Carbohydrates", Academic Press, Inc., New York (1957), p. 94.

2) K. Nishida and H. Hagima, *J. Agr. Chem. Soc. Japan* (*Nippon Nōgei-kagaku Kaishi*), 6, 1065 (1930); C. Araki, "Experiments in Chemistry" (*Kagaku Zikkengaku*)", Vol. II, Kawade Shobō, Tokyo (1942), p. 154.

3) G. P. Ellis and J. Honeyman, "Advances in Carbohydrate Chemistry", Vol. 10, Academic Press, New York (1955), p. 95.

4) L. Berger and J. Lee, *J. Org. Chem.*, 11, 91 (1946).

# *The Crystal Structure of trans-*[*Cr* $en_2Cl_2$]*Cl·HCl·*$2H_2O$

By Shun'ichiro Ooi, Yoshimichi Komiyama and Hisao Kuroya

(Received September 22, 1959)

The crystal structures of the two cobalt(III)-complexes, which are of the type *trans*-[Co $en_2X_2$]$X\cdot HX\cdot 2H_2O$ (X=Cl, Br)[1], were determined by Saito, Kuroya and their collaborators during the past several years[2,3]. In connection with this, it seems really interesting and important to investigate the crystal structures of the chromium(III)-analogues, which have a great resemblance to the cobalt(III)-complexes in various respects; particularly, it may be very instructive to examine what discrepancies can be found between the bond lengths M–N and M–X in these compounds, where M denotes a central metallic ion and N a nitrogen atom of the coordinated ethylenediamine molecule.

The present authors took up the *trans*-dichloro-bis-ethylenediamine-chromium(III) chloride hydrochloride dihydrate, *trans*-[Cr $en_2Cl_2$]$Cl\cdot HCl\cdot 2H_2O$, in the first place, and made an attempt to analyze the crystal structure of this compound by means of X-rays. This paper is to report the results obtained.

## Experimental

The crystal of [Cr $en_2Cl_2$]$Cl\cdot HCl\cdot 2H_2O$ was prepared by the method of Pfeiffer et al.[4] The crystals are bluish-green tablets and show marked dichroism like the crystals of [Co $en_2Cl_2$]-$Cl\cdot HCl\cdot 2H_2O$. From oscillation and Weissenberg photographs the unit cell dimensions were found to be:

$$a=10.97,\quad b=7.88,\quad c=9.12\ \text{Å},\quad \beta=111.5°.$$

The space group was determined to be No. 14 $P2_{1/c}$ from the systematic extinctions of reflections. The unit cell contains two formula units ($\rho_{calcd}=1.59$, $\rho_{obs}=1.54$ g./cm$^3$). The photographs were taken with Cu$K\alpha$ radiation using multiple film technique. All intensities were estimated visually by comparison with standard scales. The usual correction factors were applied by means of a chart given by Cochran and relative $|F_o|$ values were obtained.

## Structure Determination

The structure determination was carried out using $(h\,k\,0)$ and $(h\,0\,l)$ reflections from Weissenberg data. It was observed that the intensity of each reflection is similar to the corresponding one of the cobalt-analogue at low-angle reflections. This had been expected from the dichroism mentioned above and the crystallographic data, and the outline of the crystal structure was determined without difficulty.

At the stage of refinement, the method of successive difference syntheses was employed. The atomic coordinates obtained are shown in Table I. These parameters gave the reliability index $R=\sum||F_o|-|F_c||/\sum|F_o|$ of 0.131 and 0.121 for $(h\,k\,0)$ and $(h\,0\,l)$ respectively, excluding (100) reflection which could not be observed with full certainty. Calculated and observed structure factors are listed in Table II. In the calculation of structure factors, atomic scattering factors listed in the International Table (1935) were used. Overall temperature factors of the form exp $[-B(\sin\theta/\lambda)^2]$, where $B=2.7$ Å$^2$, were applied in the final calculation of structure factors. Final electron density projections on (010) and (001) are shown in Figs. 1 and 2.

Table I. Final atomic coordinates

| | $x/a$ | $y/b$ | $z/c$ |
|---|---|---|---|
| Cr | 0 | 0 | 0 |
| Cl(1) | 0.050 | 0.038 | 0.269 |
| Cl(2) | 0.345 | 0.387 | 0.272 |
| N(1) | 0.100 | −0.235 | 0.042 |
| N(2) | 0.185 | 0.106 | 0.023 |
| C(1) | 0.227 | −0.200 | 0.037 |
| C(2) | 0.288 | −0.022 | 0.100 |
| O | 0.478 | 0.150 | 0.538 |

1) N. Fogel and S. D. Christian reported in *J. Am. Chem. Soc.*, **80**, 2356 (1958) that the dichloro-complex should be given a composition formula [Co $en_2Cl_2$]Cl·$HCl\cdot 6H_2O$ instead of [Co $en_2Cl_2$]$\cdot Cl\cdot HCl\cdot 2H_2O$. However, no other formula than the latter can give any satisfactory agreement between the measured and calculated values of density, and furthermore, between $|F_o|$ and $|F_c|$, i. e., the observed and calculated intensities of X-ray diffraction.

2) A. Nakahara, Y. Saito and H. Kuroya, This Bulletin, **25**, 331 (1952).

3) S. Ooi, Y. Komiyama, Y. Saito and H. Kuroya, ibid., **32**, 263 (1959).

4) P. Pfeiffer et al., *Ber.*, **37**, 4255 (1904).

TABLE II. OBSERVED AND CALCULATED STRUCTURE AMPLITUDES

| *h k l* | $F_o$ | $F_c$ | *h k l* | $F_o$ | $F_c$ | *h k l* | $F_o$ | $F_c$ |
|---|---|---|---|---|---|---|---|---|
| 100 | 39.2 | 68.4 | 480 | <5.2 | −2.4 | 1130 | 9.6 | 9.6 |
| 200 | 38.4 | 51.6 | 490 | 4.8 | −4.4 | 1140 | <3.6 | −0.8 |
| 300 | 70.0 | 72.4 | | | | 1150 | 5.2 | 4.0 |
| 400 | 36.4 | 33.6 | 510 | 23.2 | 16.8 | | | |
| 500 | 9.6 | 5.2 | 520 | 28.0 | 28.8 | 1210 | 3.2 | −2.8 |
| 600 | 42.4 | 42.8 | 530 | <3.6 | 3.6 | 1220 | <3.6 | −1.6 |
| 700 | 21.6 | −27.6 | 540 | 11.2 | 14.0 | 1230 | <3.6 | −4.0 |
| 800 | 4.0 | −0.4 | 550 | 23.2 | −22.0 | | | |
| 900 | 4.4 | 10.0 | 560 | 13.2 | 10.8 | 002 | 19.2 | 16.8 |
| 1000 | <5.4 | −9.2 | 570 | 29.2 | −28.4 | 004 | 114.3 | 114.9 |
| 1100 | 10.4 | 8.0 | 580 | 6.0 | 3.6 | 006 | 14.8 | −13.3 |
| 1200 | 2.4 | 4.4 | 590 | 10.0 | −8.8 | 008 | 28.4 | 26.8 |
| | | | | | | 0010 | <4.0 | −2.0 |
| 020 | 75.2 | 72.4 | 610 | 23.6 | −12.0 | | | |
| 040 | 21.2 | 11.6 | 620 | 30.8 | 26.4 | 102 | <4.0 | 0.4 |
| 060 | 9.6 | 12.4 | 630 | 27.2 | −27.6 | 10$\bar{2}$ | 47.2 | 40.8 |
| 080 | 23.2 | 22.8 | 640 | 14.0 | −22.4 | 104 | <4.0 | −3.6 |
| 0100 | 7.6 | 6.4 | 650 | 19.2 | −23.2 | 10$\bar{4}$ | 96.4 | 96.8 |
| | | | 660 | 7.2 | 7.2 | 106 | 15.6 | 18.8 |
| 110 | 12.4 | −19.2 | 670 | 2.8 | −3.6 | 10$\bar{6}$ | <5.6 | 6.4 |
| 120 | 59.2 | 64.4 | 680 | 18.4 | 18.8 | 108 | <5.6 | −5.6 |
| 130 | 64.4 | −61.2 | | | | 10$\bar{8}$ | 41.2 | 43.2 |
| 140 | 77.2 | 78.0 | 710 | 38.4 | −33.6 | 1010 | <4.0 | 10.4 |
| 150 | 10.8 | 12.8 | 720 | 19.6 | 15.6 | 10$\bar{1}\bar{0}$ | <4.0 | −1.6 |
| 160 | 17.6 | 11.6 | 730 | 22.0 | −21.2 | | | |
| 170 | 15.2 | 16.8 | 740 | 28.8 | 28.0 | 202 | <5.6 | 2.4 |
| 180 | <5.2 | 0.4 | 750 | 11.2 | −7.6 | 20$\bar{2}$ | 19.2 | 23.2 |
| 190 | <3.6 | −2.4 | 760 | 18.0 | 14.8 | 204 | 37.6 | 37.2 |
| | | | 770 | <3.6 | −0.4 | 20$\bar{4}$ | 51.6 | 54.4 |
| 210 | 43.6 | 44.8 | 780 | 6.0 | 2.4 | 206 | <5.6 | −7.2 |
| 220 | 52.0 | 49.6 | | | | 20$\bar{6}$ | 32.0 | 32.8 |
| 230 | 14.0 | −8.8 | 810 | <5.2 | 6.4 | 208 | 8.8 | 10.0 |
| 240 | 42.8 | 40.8 | 820 | <5.2 | −6.0 | 20$\bar{8}$ | 23.2 | 17.6 |
| 250 | 21.2 | −20.8 | 830 | 19.6 | 18.8 | 2010 | <4.0 | −4.8 |
| 260 | 28.0 | 25.2 | 840 | 8.8 | 6.0 | 20$\bar{1}\bar{0}$ | <4.0 | 9.2 |
| 270 | 28.4 | −26.8 | 850 | 18.0 | −19.2 | | | |
| 280 | 9.6 | 4.8 | 860 | 18.0 | 9.6 | 302 | 44.8 | −48.4 |
| 290 | <3.6 | −3.2 | 870 | 10.8 | −12.0 | 30$\bar{2}$ | 98.0 | −96.8 |
| | | | | | | 304 | 20.8 | 24.0 |
| 310 | 18.4 | −15.2 | 910 | 9.6 | −13.2 | 30$\bar{4}$ | 74.4 | 69.6 |
| 320 | 76.0 | 76.4 | 920 | 8.0 | −9.2 | 306 | <5.6 | −4.8 |
| 330 | 38.4 | −33.6 | 930 | 8.4 | −8.4 | 30$\bar{6}$ | 29.6 | −29.6 |
| 340 | 28.0 | 22.8 | 940 | 6.0 | −4.0 | 308 | <5.6 | 6.8 |
| 350 | 9.6 | −9.2 | 950 | <5.2 | −0.4 | 30$\bar{8}$ | 48.8 | 50.8 |
| 360 | 15.2 | 8.8 | 960 | <3.6 | 0.8 | 30$\bar{1}\bar{0}$ | <5.6 | −2.4 |
| 370 | 20.4 | −20.4 | 970 | <3.6 | 0.4 | | | |
| 380 | 17.2 | 16.0 | | | | 402 | 59.6 | 60.4 |
| 390 | 5.6 | −6.4 | 1010 | 6.0 | 4.8 | 40$\bar{2}$ | 44.4 | 46.0 |
| | | | 1020 | <5.2 | −5.2 | 404 | <5.6 | −4.0 |
| 410 | 5.2 | −4.4 | 1030 | <5.2 | −2.0 | 40$\bar{4}$ | 35.2 | 38.0 |
| 420 | 38.8 | 38.4 | 1040 | 20.0 | 15.2 | 406 | 29.2 | 42.4 |
| 430 | 24.8 | −27.6 | 1050 | <3.6 | −3.6 | 40$\bar{6}$ | 16.8 | −16.8 |
| 440 | 37.6 | 37.2 | 1060 | 10.4 | 7.6 | 408 | <4.0 | −2.8 |
| 450 | 12.4 | −13.6 | | | | 40$\bar{8}$ | 33.2 | 25.6 |
| 460 | 31.2 | 32.0 | 1110 | 6.8 | 7.2 | 40$\bar{1}\bar{0}$ | 14.8 | −14.0 |
| 470 | 10.0 | −8.0 | 1120 | 5.6 | 0.8 | | | |

| $hkl$ | $F_o$ | $F_c$ | $hkl$ | $F_o$ | $F_c$ | $hkl$ | $F_o$ | $F_c$ |
|---|---|---|---|---|---|---|---|---|
| 502 | 10.4 | 12.0 | 70$\bar{4}$ | 6.8 | −8.4 | 1002 | 33.6 | 42.0 |
| 50$\bar{2}$ | 32.4 | 35.6 | 706 | 19.6 | 25.2 | 100$\bar{2}$ | 46.0 | 46.8 |
| 504 | 14.0 | 12.0 | 70$\bar{6}$ | 16.8 | 14.4 | 1004 | <4.0 | −7.2 |
| 50$\bar{4}$ | 30.0 | 35.2 | 708 | 26.4 | 23.2 | 100$\bar{4}$ | 12.0 | −16.0 |
| 506 | 11.2 | 12.8 | 70$\bar{1}\bar{0}$ | <4.0 | 6.4 | 100$\bar{6}$ | 32.4 | 26.4 |
| 50$\bar{6}$ | 32.0 | 38.4 | | | | 100$\bar{8}$ | <5.6 | −1.6 |
| 508 | <4.0 | 6.8 | 802 | 22.8 | 26.4 | 100$\bar{1}\bar{0}$ | 9.6 | 6.0 |
| 50$\bar{8}$ | 19.2 | 18.0 | 80$\bar{2}$ | 35.2 | 35.2 | | | |
| 50$\bar{1}\bar{0}$ | 10.0 | 12.4 | 804 | 6.8 | 10.4 | 1102 | 6.8 | 8.4 |
| | | | 80$\bar{4}$ | 7.2 | −15.6 | 110$\bar{2}$ | 32.8 | 34.4 |
| 602 | 25.2 | 22.0 | 806 | 8.0 | 15.6 | 110$\bar{4}$ | <5.6 | 1.2 |
| 60$\bar{2}$ | 10.4 | −11.6 | 80$\bar{6}$ | 17.6 | 13.3 | 110$\bar{6}$ | 36.4 | 34.0 |
| 604 | 11.2 | 17.2 | 80$\bar{8}$ | 11.2 | −18.0 | 110$\bar{8}$ | <4.0 | −5.2 |
| 60$\bar{4}$ | 46.8 | 51.6 | 80$\bar{1}\bar{0}$ | 9.2 | 7.6 | | | |
| 606 | 18.8 | 17.2 | | | | 120$\bar{2}$ | 17.6 | 10.0 |
| 60$\bar{6}$ | 6.8 | −8.4 | 902 | 20.4 | 20.2 | 120$\bar{4}$ | 12.0 | 10.4 |
| 60$\bar{8}$ | 38.8 | 42.8 | 90$\bar{2}$ | 16.8 | 14.0 | 120$\bar{6}$ | 12.0 | 9.2 |
| 60$\bar{1}\bar{0}$ | <5.6 | −4.8 | 904 | <4.0 | 4.4 | 120$\bar{8}$ | 6.0 | 5.6 |
| | | | 90$\bar{4}$ | 24.0 | 24.4 | | | |
| 702 | 40.4 | 40.8 | 90$\bar{6}$ | 9.6 | 8.4 | 130$\bar{2}$ | 16.0 | 22.8 |
| 70$\bar{2}$ | 38.0 | 38.8 | 90$\bar{8}$ | 19.6 | 16.8 | 130$\bar{4}$ | <4.0 | −7.2 |
| 704 | 14.4 | −26.4 | 90$\bar{1}\bar{0}$ | <4.0 | −5.2 | 130$\bar{6}$ | 31.6 | 27.6 |




Fig. 1. Electron density projected along the *b*-axis. Contours are drawn at intervals 10 e. Å$^{-2}$ for peaks Cr and Cl (heavy lines) of 2 e. Å$^{-2}$ for other peaks, zero-electron level being broken.

## Results

The crystal structure determined is isomorphous with $[Co\ en_2Cl_2]Cl\cdot HCl\cdot 2H_2O$ and consists of the following elements: $[Cr\ en_2Cl_2]^+$, $Cl^-$ and $[H_2O\cdots H\cdots H_2O]^+$. The configuration of the complex is as follows. Two enantiomorphous ethylenediamine molecules, taking *gauche* form, are coordinated to a chromium atom with their four nitrogen atoms. The arrangement of nitrogen atoms around the chromium atom is square coplanar. On a line approximately perpendicular to the plane are two chlorine atoms and these are coordinated to the central metal atom. The calculated bond lengths and angles are shown in Table III. The interatomic distance O···O of $[H_2O\cdots H\cdots H_2O]^+$ was found to be 2.56 Å.

A trial was made for the estimation of some coordinate standard deviations by

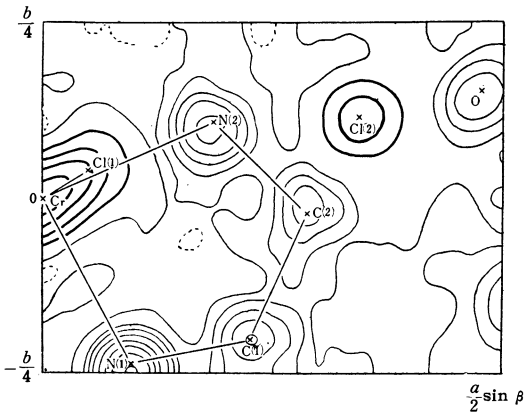



Fig. 2. Electron density projected along the *c*-axis. Contours are drawn in the same manner as Fig. 1.

TABLE III. BOND LENGTHS AND ANGLES

| | |
|---|---|
| Cr-Cl(1) | 2.33 Å |
| Cr-N(1) | 2.11 |
| Cr-N(2) | 2.13 |
| N(1)-C(1) | 1.44 |
| N(2)-C(2) | 1.48 |
| C(1)-C(2) | 1.57 |
| N(1)-Cr-N(2) | 85.2° |
| Cr-N(1)-C(1) | 105.8 |
| Cr-N(2)-C(2) | 108.3 |
| N(1)-C(1)-C(2) | 116.5 |
| N(2)-C(2)-C(1) | 106.8 |

TABLE IV. ESTIMATED COORDINATE STANDARD DEVIATIONS (VALUES IN ANGSTROM UNITS)

| | Cl | N(1) | N(2) |
|---|---|---|---|
| $\sigma(X^*)$ | 0.013** | 0.022 | 0.039 |
| $\sigma(y)$ | 0.010 | 0.054 | 0.032 |
| $\sigma(z)$ | 0.012 | —*** | —*** |

* $X$ is the axis normal to the $yz$-plane.
** 0.013 was estimated from the data for $(h\,0\,l)$, 0.012 from those for $(h\,k\,0)$.
*** $\sigma(z)$ for N(1) and N(2) could not be estimated because of the required tedious calculation**** due to mutual overlaps of atomic peaks (see Fig. 1).
**** D.W.J. Cruickshank, *Acta Cryst.*, 5, 511 (1952).

the method of Cruickshank[5], and the results are listed in Table IV. Regarding the bond lengths of chromium to nitrogen atoms, 2.11 and 2.13 Å are found for Cr-N(1) and Cr-N(2), respectively. These values are greater than the corresponding ones in the cobalt-analogue by ca. 0.1 Å. On this value, then, "significance tests"[3] were tried. At a rough approximation with $\sigma(z)$ of N(1) and N(2) ignored, the standard deviations of bond lengths $\sigma(l)$'s could be calculated from the data given in Table IV.

$$\sigma(\text{Cr-N(1)})=0.049, \quad \sigma(\text{Cr-N(2)})=0.037\ \text{Å}.$$

Similar treatments on the data of cobalt-analogues gave

$$\text{N(1)}: \sigma(X)=0.068, \quad \sigma(y)=0.084\ \text{Å},$$

and $$\text{N(2)}: \sigma(X)=0.100, \quad \sigma(y)=0.108\ \text{Å},$$

from which were obtained the values:

$$\sigma(\text{Co-N(1)})=0.080, \quad \sigma(\text{Co-N(2)})=0.099\ \text{Å}.$$

The values of $|l_1-l_2|/\{\sigma(l_1)^2+\sigma(l_2)^2\}^{1/2}$ were estimated to be 1.4 for Cr-N(1) and Co-N(1), and 1.2 for Cr-N(2) and Co-N(2), where $l_1$ and $l_2$ are bond lengths of Cr-N and Co-N, respectively. According to the levels given by Cruickshank, these values indicate that the difference between $l_1$ and $l_2$ is not significant.

The bond length found for Cr-Cl(1) is 2.33 Å which is the same as that found in the cobalt-analogue, and the estimated $\sigma$(Cr-Cl(1)) is 0.012 Å. The cell dimensions of cobalt-analogue are

$$a=10.68, \quad b=7.89, \quad c=9.09\ \text{Å}, \quad \beta=110.4°,$$

and $a$ is shorter than that of the present crystal by ca. 0.3 Å which is apparently beyond the experimental error while no remarkable discrepancies can be found between the values of $b$'s, $c$'s and $\beta$'s, respectively, of the two paired coordination compounds of Cr(III) and Co(III).

Thus, it has been evidenced that the substitution of metal causes the deformation of the unit cell. It is probably not unduly bold to consider that the effect of a metal substitution takes place first of all in the nearest neighbor of the metal. However, since the accuracy is not high enough as can be seen above, the authors' opinion is that it is going too far to give a definite conclusion to this problem.

The present authors wish to express their sincere thanks to Professor Y. Saito for his kind advice and encouragement throughout this work. Part of the cost of this investigation was defrayed from the Fund for Scientific Resarch Expenditure of the Ministry of Education, to which the authors' thanks are also due.

*Institute of Polytechnics*
*Osaka City University*
*Kita-ku, Osaka*

5) D. W. J. Cruickshank and A. P. Robertson, *Acta Cryst.*, 6, 698 (1953).

# *Catalytic Activity for Methanol Synthesis of Zinc Oxide-Chromium Oxide-Copper Oxide Catalysts and its Structural Dependency*

By Yoshisada OGINO, Masaaki OBA and Hiroshi UCHIDA

(Received September 19, 1959)

Because of their higher catalytic activity for methanol synthesis than that of zinc oxide-chromium oxide catalysts, three component catalysts, consisting of oxides of zinc, chromium, and copper, are in industrial use in this country. A few papers[1-3] have already appeared dealing with the catalysts. However, only the papers by Natta and Ivanov described the catalysts from a structural view point, and dependency of catalytic activity upon catalyst structures has remained unclarified as yet. The present study attempts to assemble a number of experimental data in this respect, and to approach complete understanding of the promoting action of copper oxide in the three component catalysts.

In this paper a preparative procedure somewhat different from the usual ones is proposed. The major part of the determinations on catalyst structures as well as on catalytic activity are made on the catalysts prepared by the procedure.

## Experimental

Preparations of a series of zinc oxide-chromium oxide-copper oxide catalysts of varying chemical compositions were made by a procedure somewhat different from the usual ones: namely, a commercial zinc oxide powder was kneaded with a chromic acid solution, in which an appropriate amount of cupric oxide had been dissolved, into a paste, which was allowed to dry at room temperature. The resulting cake was crushed, and screened to 2 to 2.5 mm. granules. Another catalyst, denoted by catalyst R, manufactured by a usual procedure was also prepared. According to the procedure, a mixture of powders of zinc oxide and copper oxide was kneaded with a chromic acid solution into a paste, which was then treated similarly to finished catalyst granules.

Chemical compositions of the catalysts used in this study are listed in Table I. Because of rather poor solubility of copper oxide in a chromic acid solution, a catalyst of Cu/Zn ratio in excess of 0.25 could not be obtained.

Catalytic activity for the methanol synthesis was determined according to the same procedure as described in the previous paper[4]. Among the by-products of the synthesis, formaldehyde was determined by a chemical analysis, while water and higher alcohols were determined by means of a gas chromatography.

Catalyst bed density was determined on the catalyst after the synthesis as follows: an amount of the catalyst granules was placed in a graduated cylinder, which was vibrated by hand till no more reduction in volume of the catalyst bed was observed. The density is given by the value of catalyst weight (g.) divided by volume (cc.) at the end of the vibration.

Specific surface area of the catalyst was determined from nitrogen adsorption data plotted according to the BET theory. In addition, volumes were measured by the water- and the mercury-displacement method[5], from values of which true and bulk densities, and pore volume could be evaluated.

Some of the catalysts, the raw as well as the reduced ones, were subjected to an X-ray study by means of a Geiger-counter spectrometer using filtered $K_\alpha$ ray.

TABLE I. CATALYST COMPOSITION

| Catalyst | No. 1 | No. 2 | No. 3 | No. 4 | No. 5 | No. 6 | No. 7 |
|---|---|---|---|---|---|---|---|
| Cr/Zn, mol. | 0.39 | 0.39 | 0.44 | 0.49 | 0.49 | 0.49 | 0.49 |
| Cu/Zn, mol. | 0.09 | 0.16 | 0.17 | 0.08 | 0.13 | 0.16 | 0.21 |
| Catalyst | No. 8 | No. 9 | No. 10 | No. 11 | No. 12 | No. 13 | R |
| Cr/Zn, mol. | 0.49 | 0.55 | 0.55 | 0.65 | 0.65 | 0.65 | 0.49 |
| Cu/Zn, mol. | 0.25 | 0.13 | 0.16 | 0.21 | 0.16 | 0.25 | 0.16 |

1) M. R. Fenske and P. K. Frolich, *Ind. Eng. Chem.*, **21**, 1052 (1929).
2) G. Natta and his coworkers, "Catalysis", III, Rheinhold Publishing Corp., New York (1955), p. 375.
3) K. N. Ivanov. ibid., p. 375.
4) H. Uchida and Y. Ogino, This Bulletin, **31**, 49 (1958).
5) A. J. Juhola and E. O. Wiig, *J. Am. Chem. Soc.*, **71**, 2078 (1949).

## Results

**Catalytic Activity for Methanol Synthesis.** — Some of the results are exemplified in Fig. 1 which, for the sake of comparison, includes the authors' previous results[6] on a zinc oxide-chromium oxide catalyst. Besides the well-known fact that an addition of copper oxide is very effective in improving the catalytic activity of a zinc oxide-chromium oxide catalyst, the figure reveals that a zinc oxide-chromium oxide-copper oxide catalyst exists in either one of two states, A or B, of different activities. State-A appears immediately after reduction of the raw catalyst at temperatures lower than 280°C, and it is not until the reduced catalyst is heated above this temperature that catalytic activity is decreased to a lower level. Being heated beyond 280°C, the catalyst suffers a rapid activity decline until a steady state, state-B, is established. There is little tendency to further decrease in activity, even though the catalyst in state-B heated as high as 360°C.

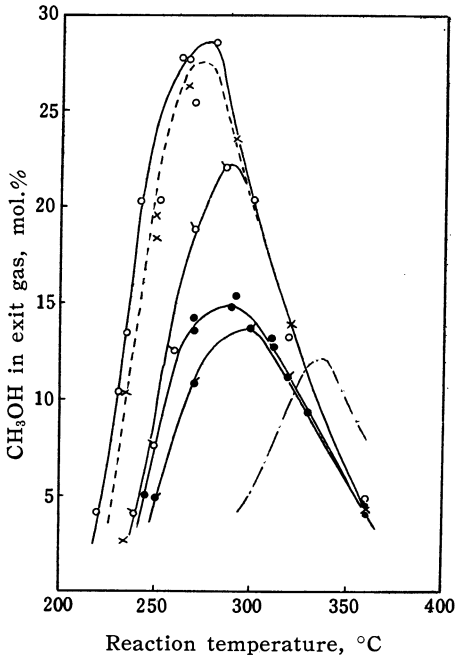



Fig. 1. Methanol concentration as a function of reaction temperature at 150 kg./cm² and S. V. of 1.10⁴.
○, cat. No. 6 (state A), ⫰, cat. No. 6 (B), ×, cat. No. 6 (A′), ●, cat. R (A), ⫰, cat R (B), —·—·, a zinc oxide-chromium oxide catalyst.

6) Y. Ogino, M. Oba and H. Uchida, This Bulletin, 32, 284 (1959).

Fig. 1 also indicates that after slow oxidation at low temperatures the catalyst in state-B recovers the activity to such a level that it is approximate to the initial activity in state-A (catalyst in state-A′). Being compared with catalyst No. 6, catalyst R of the same chemical composition as, but of a different manufacturing procedure from, catalyst No. 6 gives a considerably lower activity.

It is more desirable to express catalytic activity in terms of the rate constant of the synthesis than the methanol concentration in the exist gas. The reason for this is the difficulties of arranging experiments at a constant space velocity (based on catalyst bed volume after the synthesis), since the catalyst bed volume is apt to shrink, during the synthesis, in an extent that can not exactly be predicted before the synthesis. Usually the extents of shrinkage are in the range of 15 to 25% of the original bed volume of the raw catalyst. The rate constant can be calculated from a methanol concentration by the aid of the rate equation proposed by the present authors[4].

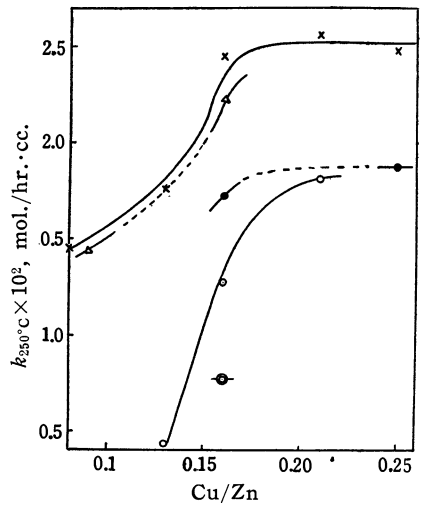



Fig. 2. Catalytic activity as a function of Cu/Zn ratio.
×, Cr/Zn=0.49, △, Cr/Zn=0.89,
●, Cr/Zn=0.65, ○, Cr/Zn=0.55,
◎, cat. R.

The activity thus defined is plotted as a function of chemical composition of the catalysts in Fig. 2. Regarding a series of catalysts of Cr/Zn ratio of 0.49 with varying Cu/Zn ratios, curves in the figure show a rapid initial increase in activity with increasing Cu/Zn ratio, followed by a portion with a smaller slope, and finally

no further increase in the range of Cu/Zn ratios higher than 0.17, while with a series of catalysts with the fixed Cu/Zn ratio of 0.16 and with varying Cr/Zn ratios they show a maximum activity appearing at the Cr/Zn ratio of 0.49.

By-products, such as water and isobutanol, are extremely small in amount (less than 0.7%) in the products at temperatures lower than 270°C, and it makes little difference, whether the catalyst is in state-A or state-B. At higher temperatures the amounts become greater, e. g. attaining to contents of 10% water and 1.4% isobutanol in the product at 360°C. There have been found no alcohols other than isobutanol. Very small quantities of formaldehyde (less than 0.1%) have always been found in the products of the present study.

**Catalyst Bed Density.** — The catalyst bed density after the synthesis is plotted against the chemical composition of the catalyst in Fig. 3, in which it may be seen that the bed density rises with Cr/Zn ratio up to the high value of 1.47 for a catalyst of an appropriate composition. In contrast to this, catalysts of the usual manufacturing procedures, such as catalyst R and a pelleted catalyst in an industrial use, give lower bed densities of 0.808 and 1.15, respectively.

Naturally the catalyst bed density parallels the bulk density of catalyst granules. It is not because the true density

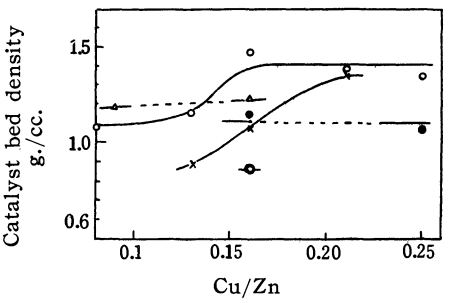



Fig. 3. Catalyst bed density as a function of Cu/Zn.
○, Cr/Zn=0.49, △, Cr/Zn=0.39,
×, Cr/Zn=0.55, ●, Cr/Zn=0.65,
◎, cat. R.

of catalyst granules is high, but because the pore volume in the granules is extremely small, that the present catalyst gives a high value of the bulk density (refer to Table III). As shown in the table, the bulk density of a raw catalyst can not be correlated directly to that of a reduced one, since the raw one contains an appreciable indefinite quantity of crystallization water.

**Specific Surface Area.** — Specific surface areas of the raw and the reduced catalysts are summarized in Table II. The table discloses that the specific surface area is enlarged remarkably by reduction of the raw catalyst to state-A, and further, but in less degree, by subsequent reduction to

TABLE II. CATALYST BED DENSITY AND SPECIFIC SURFACE AREA

| Catalyst | | No. 1 | No. 2 | No. 3 | No. 4 | No. 5 | No. 6 |
|---|---|---|---|---|---|---|---|
| Catalyst bed density, g.*/cc. | | 1.297 | 1.231 | 1.423 | 1.082 | 1.328 | 1.470 |
| Specific surface area (raw), $m^2/g.$ | | — | 10.85 | 0.54 | 8.90 | 5.65 | 1.69 |
| Specific surface area (reduced), $m.^2/g.$ | A | 112 | 132 | 133 | 115 | 113 | 113 |
| | B | — | — | — | 124 | 151 | 147 |

| Catalyst | | No. 7 | No. 8 | No. 10 | No. 11 | No. 12 | R |
|---|---|---|---|---|---|---|---|
| Catalyst bed density, g.*/cc. | | 1.381 | 1.328 | 1.067 | 1.361 | 1.162 | 0.808 |
| Specific surface area (raw), $m^2/g.$ | | 1.08 | 0.24 | 9.20 | — | 5.67 | 26.5 |
| Specific surface area (reduced), $m.^2/g.$ | A | 104 | 113 | 104 | 101 | 116 | 94 |
| | B | 120 | 151 | 120 | — | 140 | 137 |

* With reduced catalysts.

TABLE III. DENSITIES AND PORE VOLUME OF CATALYSTS No. 6 AND R

| Catalyst | | Bed density g./cc. | Density g./cc. | Bulk density g./cc. | Pore volume cc./g. | Average pore dia. Å |
|---|---|---|---|---|---|---|
| No. 6 (raw) | | 1.78 | 3.4122 | 3.0883 | 0.0307 | 728 |
| R (raw) | | 1.03 | 2.9813 | 1.1849 | 0.5085 | 768 |
| No. 6 (reduced) | A | 1.47 | 4.7325 | 3.042 | 0.1190 | 21 |
| | B | 1.43 | 5.4079 | 2.806 | 0.1725 | 23 |
| R (reduced) | A | 0.808 | 4.9221 | 2.9716 | 0.1333 | 28 |
| | B | 0.799 | 5.4477 | 1.8609 | 0.3538 | 52 |

state-B. The present catalysts give much higher surface areas than the zinc oxide-chromium oxide catalysts in the authors' previous paper.

A high extent of specific surface area once obtained on a catalyst in state-B is diminished, by slow oxidation of state-B to state-A, to a smaller area which is approximate to the former area of the catalyst in state-A, with simultaneous recovery of the activity.

**Loss and Gain of Oxygen with Reduction and Oxidation of Catalyst.**—The different states of a catalyst, state-A, −B, and −A′, appeared to be related to different oxygen contents of the catalyst. In this respect, changes in weight of catalyst No. 6 with repeated reduction and oxidation have been pursued in some detail. The results are given in Fig. 4, in which changes in

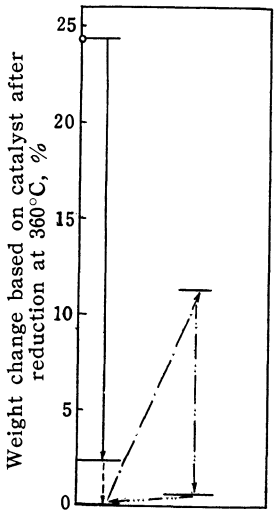



Fig. 4. Changes in weight of catalyst with reduction and oxidation.
○, raw catalyst, ——, reduction at 250°C, ------, reduction at 360°C, —·—·, oxidation at room temperature, —··—··, reduction at 250°C, ——···——, reduction at 360°C.

weight are expressed in per cent increase based on the catalyst weight in state-B. By reduction of the raw catalyst at 250°C, decrease in weight takes place to a remarkable extent, the major part of which is presumably due to release of crystallisation water from the raw catalyst. Subsequent reduction from state-A to state-B accompanies the further decrease in weight, whose major part may probably be due to loss of oxygen[7]. After slow oxidation of the resulting catalyst in dry air at room temperature, gradual take-up of oxygen takes place till it, after a week, attains to as great an amount as 11.3% weight increase. The major part of the oxygen can readily be liberated by reduction at 250°C, and state-A′ is established. On the other hand, it should be emphasized that the gradual oxygen take-up is also observed for zinc oxide-chromium oxide catalysts, though it is of a much smaller amount, e. g. 2.4% increase for a catalyst of Cr/Zn ratio of 0.5.

**Catalyst Structure Revealed by X-ray Diffraction Patterns.** — Among the catalysts, catalysts No. 6 and R were subjected to an X-ray examination. Both of the raw catalysts gave diffraction lines due to zinchydroxychromates I$\beta$ and II$\beta$, with no signs of oxides of copper. With catalyst No. 6 the latter hydroxychromate develops to greater crystallites than the former one, whereas with catalyst R the situation is the opposite. In this respect the authors' previous paper reported that a catalyst of Cr/Zn ratio of 0.49, with no copper, consisted of zinchydroxychromate I$\beta$ alone, and that zinchydroxychromate II$\beta$, together with zinchydroxychromate I$\beta$, appeared only in a catalyst of the smaller ratio. In the present catalysts of high Cr/Zn ratios, zinchydroxychromate II$\beta$ may gradually appear, because the part of chromic acid is consumed by the preferential combination with copper oxide to produce copper chromate. However, no evidence of either copper chromate or cupric chromite has been found in the diffraction diagram, even after the sintering of the catalyst at 600°C[8]. The results also show that in the manufacturing of the present catalysts chromic acid tends to combine with copper oxide more readily than it does in that of catalyst R.

After the synthesis, catalysts No. 6 and R gave no diffraction lines other than the diffused ones due to cuprous oxide[9]. This does not necessarily indicate that the crystallite, such as those of oxides of zinc and chromium or those of zinc chromite, are completely absent in the catalyst

7) The decreases are in the range of 1~3.5% for individual catalyst of the present series. No definite relationship between the extent of decrease and chemical composition has been found.

8) Refer to Stroupe's paper: J. D. Stroupe, *J. Am. Chem. Soc.*, 71, 589 (1949).

9) The crystallites of cuprous oxide may perhaps be produced, during the taking of the diagram, by reoxidation of copper crystallites produced by reduction, though necessary care, such as the leaching of the specimen in methanol, has been taken.

granules, but that the crystallites are too finely dispersed to be detected by an X-ray examination. The diffration lines of cuprous oxide remain essentially unchaned, whether the catalysts are in state-A or state-B. From the diffusivity of the diffraction lines, a rough calculation of the width of cuprous oxide crystallites was made by the aid of Scherrer's formula. The width has proved to be about 50 Å.

## Discussion

**Catalytic Activity and Catalyst Bed Density.**—Fig. 5. presents the relationship between the catalytic activity and the catalyst bed

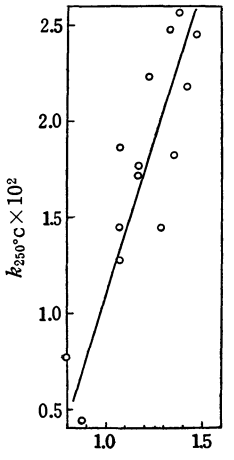



Fig. 5. Relationship between catalytic activity and catalyst bed density.

density, and an approximate proportionality has been found existing between them. The present catalyst owes the fact that it has such a high catalytic activity mainly to the high catalyst bed density. The high catalyst bed density is characteristic of the catalysts made by the present procedure.

**Specific Surface Area and Specific Catalytic Activity.**—With the present catalysts, hardly any relationship between catalytic activity and the extent of the specific surface area has been found. On the other hand, specific activity, namely, activity expressed per unit surface area, tends to increase slowly with copper content throughout the range of the present study (refer to Fig. 6). The tendency, however, is only a minor factor influencing the catalytic activity which is considered on the basis of unit volume of the catalyst bed or unit mass of the catalyst granules. Catalyst R gives a very low specific activity.

**Activation Energy and Frequency Factor of Synthesis.**—Arrhenius' plots are linear with slopes corresponding to an activation energy of 16.6 kcal./mol. for individual catalysts in state-A, and another one of 21.9 kcal./mol. for individual ones in state-B, respectively. Present values of the activation energy are much lower than those of zinc oxide (34.6 kcal./mol.) and zinc oxide-chromium oxide catalysts (e. g. 27.4 kcal./mol. for a catalyst of the Cr/Zn ratio of 0.5).

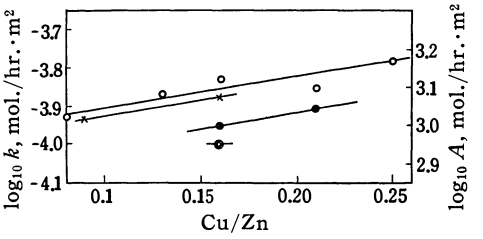



Fig. 6. Specific catalytic activity or frequency factor per unit surface area as a function of Cu/Zn.
○, Cr/Zn=0.49, ×, Cr/Zn=0.39,
●, Cr/Zn=0.55, ◎, cat. R.

By the choice of an adequate scale for the ordinate, the same straight line as cited in Fig. 6 can reveal the relationship between the frequency factor based on unit surface area and the Cu/Zn ratio, since the catalysts give a constant activation energy independently of the varying Cu/Zn ratios[10]. In contrast to the present catalysts, the zinc oxide-chromium oxide catalysts usually showed much higher values of the frequency factor per unit surface area (e. g. $0.5^{-2}$ mol./hr.·m² for the catalyst of Cr/Zn ratio of 0.5). This enables the authors to expect a steep rise of the frequency factor with decreasing Cu/Zn ratios in a range of the extremely low ratios, when the above mentioned straight line relationship is also taken into account. No experimental data, however, are available to demonstrate the expectation as yet.

The catalyst always changes its state from A to B with simultaneous increase of both the activation energy and the frequency factor per unit surface area.

**State-A and State-B of Catalyst.**—It is not because of the sintering of the catalyst granules that a decrease in catalytic

10) From the results, a premise is possible that all active centers are alike, appearing more frequently on the catalyst surface with increasing copper content.

activity appears with the change of the catalyst state from state-A to B, but it is because of a decrease in specific catalytic activity per unit catalyst surface. This is apparent from the rather larger specific surface area for the catalyst in state-B. At first sight, the sintering of copper crystallites, as revealed by the appearance of the diffraction lines due to cuprous oxide in the diagram, seemed to have a great influence upon the specific catalytic activity. This, however, can not be true, because the same diffraction lines appear in the diagram of the catalyst in state-A' of an activity approximate to state-A.

Among structural factors of the catalyst here investigated, only the oxygen content of catalysts seems to have an influence upon the specific catalytic activity. Oxygen of this kind is remarkably increased in amount by an addition of copper oxide. It is increased to such an extent that it is much greater than that estimated to be produced by the reduction of cupric oxide to copper. The oxygen may thus come partly from copper oxide, but also from some other kinds of oxides of high oxidation stage at which the oxygen is rather loosely bound, namely, oxide of chromium. In this respect, the X-ray diffraction diagram has revealed that, by an addition of copper oxide, crystallites of chromium oxide or zinc chromite become more finely dispersed in the catalyst. Chromium oxide in extremely fine dispersion is reasonably expected to be capable of being oxidized more readily to high valency states (refer to the papers of Selwood[11] and others[12,13]).

## Summary

A preparative procedure in which copper oxide is introduced into the catalyst by a different way from the usual ones has presented the catalyst of high catalytic activity for the methanol synthesis. The catalyst owes its high catalytic activity to three structural factors, namely, a high catalyst bed density, a larger extent of specific surface area, and a great amount of oxygen loosely bond in catalyst oxides, among which the first factor plays the most important role. The last is effective in improving the specific catalytic activity based on unit surface area, and is in a close relation to the two states, A and B, of different catalytic activities.

The authors of this paper wish to thank Mr. S. Kato of Tokyo Institute of Technology for taking X-ray diagrams.

*Government Chemical Industrial Research Institute, Tokyo*
*Shibuya-ku, Tokyo*

11) P. W. Selwood, "Advances in Catalysis", Vol. III, Academic Press, Inc., New York (1951), p. 42.
12) Y. Matsunaga, This Bulletin, **31**, 58, 145 (1958).
13) S. Sida et al., Abstracts of the 7th Annual Meeting of the Chemical Society of Japan, (1954), p. 157.

# *On The Mechanism of the Extraction of Uranyl Nitrate by TBP* (Partition Study)*

By Keiji NAITO

(Received July 23, 1959)

The TBP (tri-*n*-butyl phosphate) extraction has been extensively employed for the uranium refining and the reprocessing of reactor spent fuel. A number of researches on this subject have appeared[1], and the mechanism of the uranium extraction by TBP was already proposed by Moore[2] as follows:

$$UO_2^{2+}(aq.) + 2NO_3^-(aq.) + 2TBP(org.) \rightleftarrows UO_2(NO_3)_2(TBP)_2(org.) \quad (1)$$

The more rigorous analysis for the mechanism of TBP extraction was made by McKay et al.[3-5] and the mechanism of uranium extraction was confirmed as Eq. 1 proposed by Moore.

* This study was presented at the 1st Symposium on Atomic Energy, Tokyo, January 13, 1957, and the 1st Symposium on Radiochemistry, Tokyo, December 21, 1957.

1) For example, R. I. Smith, TID-3502.

2) R. L. Moore, AECD-3196 (1951).

3) K. Alcock et al., *Trans. Faraday Soc.*, **52**, 39 (1956).

4) T. V. Healy and H. A. C. McKay, ibid., **52**, 633 (1956).

5) E. Hesford and H. A. C. McKay, ibid., **54**, 573 (1958).

The extraction of the nitric acid by TBP was also observed by Moore[2] and the following mechanism was proposed,

$$HNO_3(aq.) + TBP(org.) \rightleftarrows HNO_3 \cdot TBP(org.) \quad (2)$$

The formation of the complex $HNO_3 \cdot TBP$ was supported by McKay et al.[3] and the behavior of uranium on the TBP extraction from a nitric acid solution was concluded as a result of the competition of uranium and nitric acid[4].

The object of the present work is to propose a method of analysis to confirm the formation of a complex and to apply this analysis to the extractions of uranyl nitrate and nitric acid with TBP. The discussion for the extraction behavior of uranium from nitric acid solution by TBP is the second object of this work and thirdly the thermochemical functions for this kind of complex formation are to be determined.

## Experimental

**Reagents.**—The reagents used in these experiments are as follows:

*A) TBP.*—The TBP (tri-*n*-butyl phosphate) was used after vacuum distillation.

*B) Uranyl nitrate.*—Uranyl nitrate was obtained from British Drug Houses Ltd. and was used after recrystallization.

*C) Diluents.*—As diluents, carbontetrachloride and kerosene were used. Boiling point range of kerosene used in the experiments is 190~260°C, specific gravity (15/4°C) is 0.8094.

**Equipment and Method.**—The Measurements of the distribution equilibrium were always made at constant temperature using a thermostated water bath. The separatory funnels were specially designed in order to be easily dipped into the water bath. The method for the measurement of distribution coefficients was the following. The necessary volumes of both aqueous and organic phases were put into a separatory funnel, which was dipped in the water bath. After the temperature had reached equilibrium, shaking of about one minute was repeated at intervals of fifteen or twenty minutes. Both phases were separated rapidly after an equilibrium time of about three or four hours. A centrifuge was used in the case where the separation was difficult. The distribution coefficients of both uranium and nitric acid were obtained by analyzing both in the aqueous phase.

The methods of analysis are the following. For uranium, the alkaline peroxide method[6] was adopted and a Hitachi EPU-2 spectrophotometer was used for the determination (at $\lambda = 400\ m\mu$). For nitric acid, the uranium peroxide precipitation method[7] was taken.

**Notation.**—$C_M$ and $C'_M$ denote the equilibrium concentrations of a species M in aqueous and organic phases respectively. $Kd(M)$ denotes the distribution coefficient of the species M ($=C'_M/C_M$). $a_M$ is the activity of the species M in aqueous phase or organic phase, and $f_M$ is its activity coefficient.

## Results and Discussion

**Distribution Equilibrium.**—Prior to a discussion about the extraction mechanism, a general survey of distribution equilibrium of uranium between the aqueous and TBP phase was made. The results of the measurement can be summarized briefly as the following.

(a) In case nitric acid is added, the distribution coefficient of uranium is constant when the uranium concentration is low and the nitric acid concentration is kept constant, on the other hand, when nitric acid is absent, a constant distribution coefficient can not be obtained.

(b) The uranium concentration in organic phase increases with the uranium concentration in aqueous phase and reaches a constant which corresponds to the uranium concentration of $UO_2(NO_3)_2 \cdot (TBP)_2$ in organic phase as pointed out by Moore[2].

(c) The distribution coefficients of uranium increases with the nitric acid concentration in aqueous phase and reaches a maximum value, and then decreases gradually. Fig. 1 shows the influence of nitric acid concentration upon the distribution coefficient of uranium at various uranium concentrations.

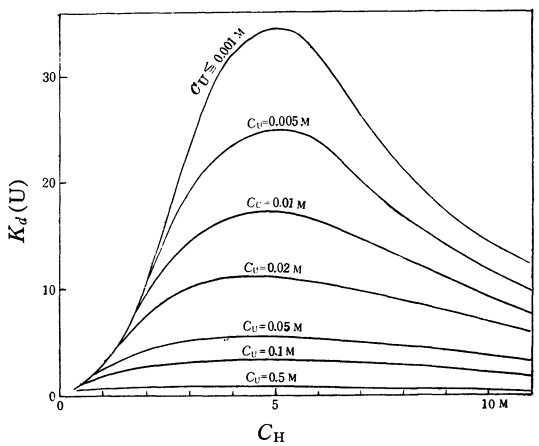



Fig. 1. Influence of nitric acid concentration upon the distribution coefficient of uranium at various concentrations.

6) C. J. Rodden and J. C. Warf, "Analytical Chemistry of the Manhattan Project", (National Nuclear Energy Series VIII-1(1950)).

7) R. E. Connik, MDDC-1245 (1945).

(d) The distribution coefficient of uranium is nearly proportional to the square of the TBP concentration in the organic phase when the concentrations of uranium and nitric acid are low and the nitrate concentration is held constant.

(e) The distribution coefficient of uranium decreases with the increase of temperature.

(f) The distribution coefficient of nitric acid coexisting with uranium decreases gradually with the increase of the uranium concentration in aqueous phase, but in the case where the nitric acid concentration is low the distribution coefficient of uranium reaches a maximum value and then decreases gradually.

(g) The influence of the nitric acid concentration in the aqueous phase on the distribution coefficient of nitric acid is markable when the uranium concentration is low. However, this influence becomes smaller with the increase of the uranium concentration in aqueous phase, and finally the distribution coefficient of nitric acid becomes nearly constant against the concentration of nitric acid in aqueous phase when the uranium concentration is higher than 0.1 M (Fig. 2).

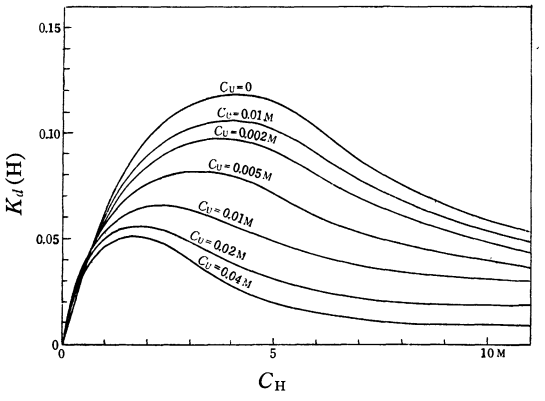



Fig. 2. The distribution coefficient of nitric acid coexisting with uranium.

From the above-mentioned distribution equilibrium of uranium, several pieces of information about the mechanism of the extraction of uranium can be obtained.

Facts b) and d) indicate that formation of the uranium complex with TBP in organic phase is likely. Therefore, it is possible to expect the following complex formation reaction considering the salting-out effect of nitrates on the extraction of uranium,

$$\mu UO_2^{2+}(aq.) + 2\mu NO_3^-(aq.) + \nu TBP(org.) \rightleftarrows [UO_2(NO_3)_2]_\mu(TBP)_\nu(org.) \quad (3)$$

where $\mu$ and $\nu$ are positive integers. The determination of $\mu$ and $\nu$ will be discussed later.

It is estimated from fact e) that this reaction should be an exothermic reaction.

Facts c) and f) also suggest that nitric acid is extracted together with uranium by TBP and both of these extraction reactions take place competitively.

**Method of Analysis for an Extraction Mechanism.**—Although there are several types of mechanisms by which a solute in aqueous phase can be extracted by organic solvent, one is the " mass-action " reaction between the solute ions and the organic solvent molecules as shown by Eq. 3.

This kind of extraction mechanism such as Eq. 3 is written as the following general expression,

$$\mu M^{n+}(aq.) + (n/m)\mu X^{m-}(aq.) + \nu S(org.) \rightleftarrows (MX_{n/m})_\mu S_\nu(org.) \quad (4)$$

where

$M_mX_n$=inorganic solute ($M^{n+}$=cation, $X^{m-}$=anion)

S=organic solvent (extractant)

$\mu$ and $\nu$=positive integers.

The purpose of the analysis is to obtain the value of $\mu$ and $\nu$ respectively without contradiction. The equilibrium constant ($K$) for Eq. 4 is given as

$$K=(a_{complex})/(a_M)^\mu(a_X)^{(n/m)\mu}(a_S)^\nu, \quad (5)$$

where $a$ is the activity in aqueous phase or in organic phase and $a=fC$.

When the concentration of the solute is low, the ratio of the number of bonded solvent molecules to that of free solvent molecules is very small, so that Eq. 5 becomes

$$K=(f_{complex})(C_{complex})/(f_MC_M)^\mu(a_X)^{(n/m)\mu}(a_S^0)^\nu \quad (6)$$

where $a_S^0$ is the activity of the extractant solvent which corresponds to the initial concentration of extractant solvent in organic phase. In Eq. 6, $f_{complex}$ is determined by the concentration of solvent in organic phase so that both $f_{complex}$ and $a_S^0$ are constant at constant concentration of solvent.

If it is assumed that all M ions in organic phase are related to the formation of the complex, the following relation is obtained :

$$C_{complex}=C_M'/\mu \quad (7)$$

Then from Eqs. 6 and 7, considering the relation: $C_{complex}/C_M=Kd(M)$

$$Kd(M)=\text{const.}\ (f_M{}^{\mu}/f_{complex})\cdot (C_M)^{\mu-1}(a_X)^{(n/m)\mu}(a_S{}^0)^{\nu} \quad (8)$$

From Eq. 8, the integers in Eq. 4 are determined experimentally as follows.

*(1) Determination of* $\mu$.—In the case where the salting-out agent is absent, the activity $a_X$ can be replaced with the concentration $C_X$, and $f_M$ becomes unity, and $C_X$ is determined uniquely by $C_M$ as $(n/m)C_M$. When the distribution coefficient of M is measured at constant solvent concentration, $f_{complex}$ and $a_S{}^0$ are constant, as has been stated, so that Eq. 8 becomes

$$Kd(M)\cong\text{const.}\ (C_M)^{(1+n/m)\mu-1} \quad (9)$$

Thus by plotting $\log Kd(M)$ against $\log C_M$ the slope of the line indicates the value of $(1+n/m)\mu-1$, from which $\mu$ can be determined.

In the case where the salting-out agent exists, $C_X$ is determined by both $C_M$ and the concentration of the salting-out agent. If one adds a large amount of salting-out agent compared with $C_M$ (which is low), both $C_X$ and the ionic strength of the aqueous solution are mainly determined by the concentrationof the salting-out agent. Thus, when the distribution coefficient of M is measured at constant solvent concentration keeping the concentration of salting-out agent constant, Eq. 8 becomes

$$Kd(M)\cong\text{const.}\ (C_M)^{\mu-1} \quad (10)$$

because $f_M$ and $a_X$ are constant at costant ionic strength of the aqueous phase and $f_{complex}$ and $a_S{}^0$ are constant at constant solvent concentration. Thus, by plotting $\log Kd(M)$ against $\log C_M$ one can determine $\mu$ from the slope of the line.

*(2) Determination of* $\nu$.—When the distribution coefficient of M is measured, keeping the aqueous phase concentration of M constant, and also keeping the concentration of the salting-out agent constant (if the salting-out agent exists), Eq. 8 becomes

$$Kd(M)\cong\text{const.}\ ((f_S{}^0)^{\nu}/f_{complex})(C_S{}^0)^{\nu} \quad (11)$$

where $f_S{}^0$ is the activity coefficient for $C_S{}^0$. Unfortunately both $f_S{}^0$ and $f_{complex}$ are the function of the solvent concentration $C_S{}^0$, and the determination of these activity coefficints for various solvent concentrations is not easy. However, if the measurement is made at low solvent concentration, the slope which is obtained by plotting $\log Kd(M)$ against $\log C_S{}^0$ roughly indicates the value of $\nu$, because the deviation from the ideal solution becomes smaller according to the dilution of the solution.

The above-mentioned method is applicable to any reaction of the type of Eq. 4; however, it should be noticed that this method stands upon the assumption that all M ions in organic phase are combined with the solvent molecules. If this assumption does not exist, the method of analysis will become more complicated. On the other hand, when one can determine the integers $\mu$ and $\nu$ without contradiction under this assumption, one recognizes the validity of this assumption. An attention should be given to the case in which the successive complex formation by anion takes place according to the increase of the anion concentration, for example,

$$UO_2{}^{2+}+NO_3{}^- \rightleftarrows UO_2(NO_3)^+,$$

$$UO_2(NO_3)^+ + NO_3{}^- \rightleftarrows UO_2(NO_3)_2$$

Since the above-mentioned method of analysis is adopted for a low concentration region of the solute, this method can be applied without correction in case the salting-out agent is absent. In the case salting-out agent is added, the successive formation of the complex by anion will be expected, but the method is still applicable without correction, because the ionic strength of the solution is kept nearly constant. However, if an anionic complex such as $UO_2(NO_3)_3{}^-$, $UO_2(NO_3)_4{}^{2-}$, etc., is formed, the treatment must be changed.

Although this kind of method of analysis was used at first by Moore[2], the treatment was not rigorous. Eq. 11 was also derived by McKey et al.[5] and $\nu$ was called the solvation number. It is important, however, to confirm the existence of "mass-action" reaction for the solvent extraction process by applying the above-mentioned analysis.

**Mechanisms of the Extraction for Uranium and Nitric Acid.**—*(1) Uranyl nitrate extraction by TBP.*—The integers $\mu$ and $\nu$ in Eq. 3 were determined by applying the abovementioned method in the following way.

$\mu$ is determined easily as $\mu=1$ from fact a) and Eq. 10 in case the salting-out agent exists. However, in case the salting-out agent is absent, no linear relation between $\log Kd(U)$ and $\log C_U$ was observed while a linear relation was expected from Eq. 9. This means that the mechanism of extraction in this case is not consistent with

the mechanism postulated in Eq. 3, and uranyl nitrate must be hydrolyzed, especially in the low concentration region and in the case where no acid exists, so that the mechanism of extraction must change.

$\nu$ was determined as $\nu = 2$ by applying Eq. 11. The linear relation between $\log[Kd(\mathrm{U})/(a_{\mathrm{NO_3}})^2]$ and $\log C^0_{\mathrm{TBP}}$ was observed as $\nu=2$ for the low TBP concentration region.

Accordingly one obtained the same mechanism as that proposed by Moore for uranyl nitrate extraction by TBP. Though the same result was obtained, it should be noticed that the existence of this mechanism was confrimed beyond doubt by this analysis and this mechanism does not exist when the hydrolysis of uranium takes place.

On the extraction of uranium from a nitric acid solution by TBP, it was already observed that nitric acid coexisting with uranium is not only effective as a salting-out agent, also extractable together with uranium by TBP, so that the mechanism of the extraction of nitric acid should also be studied in order to clarify the mechanism of the extraction of the U-$HNO_3$-TBP system.

*(2) Nitric acid extraction by TBP.*—One can expect the reaction of nitric acid with TBP molecules as expected in the case of uranyl nitrate extraction, then

$$\mu H^+(\mathrm{aq.}) + \mu NO_3^-(\mathrm{aq.}) + \nu \mathrm{TBP(org.)} \rightleftarrows (HNO_3)_\mu(\mathrm{TBP})_\nu(\mathrm{org.}) \qquad (12)$$

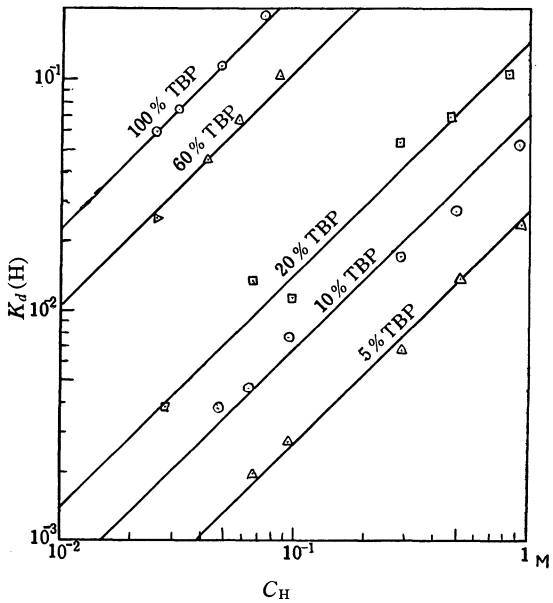



Fig. 3. Determination of $\mu$ in case the salting-out agent is absent.

The integers $\mu$ and $\nu$ in Eq. 12 can be determined as follows.

*(a) Determination of $\mu$.*—In the case where the salting-out agent exists, $\mu$ is determined by Eq. 10. The result of the measurement of $Kd$(H) for dilute nitric acid when sodium nitrate is added as a salting-out agent shows that $Kd$(H) is constant independent of $C_H$ when the concentration of salting-out agent is kept constant. Then, by applying to Eq. 10, $\mu$ is determined as $\mu=1$.

In the case where the salting-out agent is absent, $\mu$ is determined by Eq. 9, Fig. 3 was obtained by plotting $Kd$(H) againts $\log C_H$ at 25°C for TBP-kerosene system. The existence of a linear relation is observed and the slope of this line is 1 independently with TBP concentration. An essentially the same result was obtained when the diluent is carbon tetrachloride. Then, from Eq. 9, $\mu$ is determined again as $\mu=1$.

*(b) Determination of $\nu$.*—The value of $\nu$ is determined by using Eq. 11. Fig. 4 was obtained by plotting $\log Kd$(H) against $\log C^0_{\mathrm{TBP}}$ at 25°C, where the diluent is carbon tetrachloride. In this figure, the lines A and A′ are for the case no

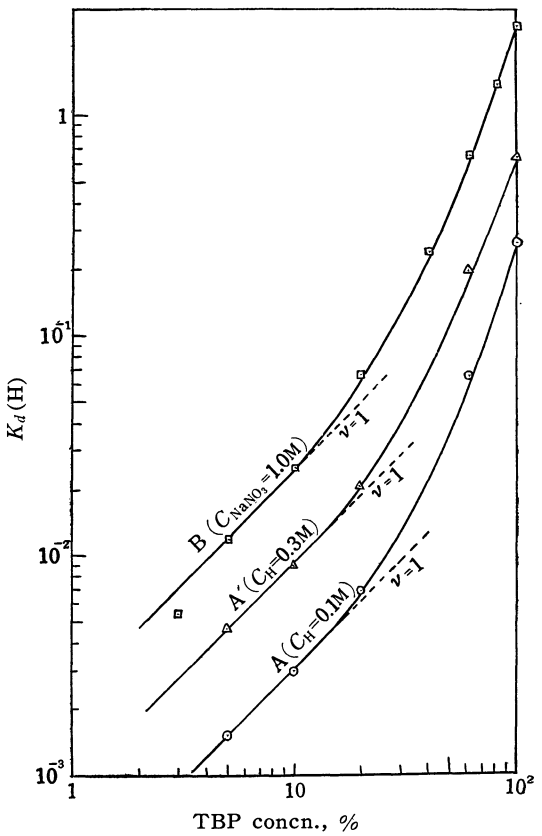



Fig. 4. Determination of $\nu$.

salting-out agent exists and the line B is for the case the salting-out agent exists (1 M $NaNO_3$). It is noteworthy that both A (A′) and B give nearly the same results. For a region where the TBP concentration is low, the linear relations are obtained and slopes are 1 for each case. The essentially the same results are obtained in case the diluent is kerosene. Then, from Eq. 11, $\nu$ is determined as $\nu=1$.

However, in a region where the TBP concentration is higher, the slopes are changing from one to two. It is not clear at the present stage whether this is based upon the change of activity coefficients ($f_S^0/f_{complex}$) in Eq. 11 or the formation of a complex $HNO_3(TBP)_2$.

As a result of above-mentioned analysis for the $HNO_3$–TBP system, the mechanism of the nitric acid extraction by TBP was confirmed as

$$H^+(aq.) + NO_3^-(aq.) + TBP(org.) \rightleftarrows HNO_3 \cdot TBP(org.) \quad (13)$$

On the other hand, Moore proposed Eq. 2 as the mechanism of nitric acid extraction by TBP. This mechanism was derived from the fact that $Kd$(H) is nearly constant, independent of the nitric acid concentration in the case of uranium extraction. However, as shown in fact g) this is true only in case the uranium concentration is higher than about 0.1 M, and his observation was made just in this range ($C_U=0.1\sim0.4$ M). So it is not suitable to discuss the mechanism of nitric acid extraction basing only on this fact. It may be reasonable to interpret this fact as a result of the competition of uranium and nitric acid as will be discussed later.

**Competition of Uranium and Nitric Acid.**—It has been clarified that both uranium and nitric acid are extracted according to the above-mentioned mechanisms. With these mechanisms, the behavior of both uranium and nitric acid during the extraction process should be interpreted as follows.

*(1) Simultaneous partition of uranium and nitric acid.*—In case uranium is extracted from a nitric acid solution by TBP, the distribution equilibria of Eqs. 1 and 13 should be established simultaneously. Then, one obtains the following simultaneous equations,

$$K(U) = [f_{complex}(U)/(f_{\pm}(U))^3] \cdot [Kd(U)/C_{NO_3})^2(a_{TBP})^2] \quad (14)$$

$$K(H) = [f_{complex}(H)/(f_{\pm}(H))^2] \cdot [Kd(H)/(C_{NO_3})(a_{TBP})] \quad (15)$$

where $K$(U) and $K$(H) are the equilibrium constants of uranium for Eq. 1 and of nitric acid for Eq. 13, $f_{\pm}$(U) and $f_{\pm}$(H) are the mean activity coefficients of uranyl nitrate and of nitric acid.

When the concentrations of both uranium and nitric acid are low, if one keeps the ionic strength of solution constant, the activity coefficient in aqueous phase is kept nearly constant, and the activity coeficients of the complex in organic phase are nearly constant because the concentration is very low. In such a case, the following relation is obtained :

$$\log Kd(H) \cong (1/2) \log Kd(U) + \text{const.} \quad (16)$$

This relation was confirmed by Fig. 5

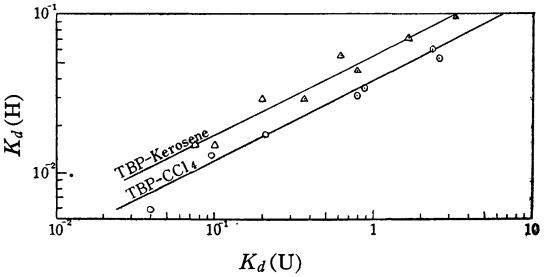



Fig. 5. Existence of simultaneous partition of both uranium and nitric acid.

which was obtained from the measurements under the uranium concentration range : 0.005~0.05 M, and the nitric acid concentration range : 0.1~1 M and at TBP 20%, 25°C. Though this measurement was made at various ionic strengths, the linear relationship is still observed in both the TBP-$CCl_4$ system and the TBP-kerosene system, and the slopes are both 1/2.

By this analysis, it was confirmed that when uranium is extracted from a nitric acid solution by TBP, both the extraction reaction of uranium shown by Eq. 1 and the extraction reaction of nitric acid shown by Eq. 13 take place simultaneously.

*(2) The influence of the nitric acid concentration upon Kd(U).*—In the distribution equilibrium of uranyl nitrate, $Kd$(U) has its maximum value against the change of $C_H$ as shown by fact c). This can be interpreted as a result of the competition of both uranium and nitric acid in the following way.

In the case where the concentration is low, if one replaces the activity by the concentration in order to make the discussion simple, the following simultaneous equations exist approximately,

$$K(U) \cong Kd(U)/C_H^2(C^0_{TBP} - C_H')^2 \quad (17)$$

$$K(\mathrm{H}) \cong C_{\mathrm{H}}'/C_{\mathrm{H}}^2(C^0{}_{\mathrm{TBP}}-C_{\mathrm{H}}') \qquad (18)$$

where $C^0{}_{\mathrm{TBP}}$ represents the initial concentration of TBP in organic phase. From Eqs. 17 and 18 by eliminating $C_{\mathrm{H}}'$,

$$Kd(\mathrm{U}) = K(\mathrm{U})\,[C_{\mathrm{H}}C^0{}_{\mathrm{TBP}}/(1+K(\mathrm{H})C_{\mathrm{H}}^2)]^2 \qquad (19)$$

Eq. 19 gives the relation between $Kd$(U) and $C_{\mathrm{H}}$ in a region where the uranium concentration is low. It can easily be shown from Eq. 19 that $Kd$(U) increases with the increase of $C_{\mathrm{H}}$, reaches a maximum value, then decreases gradually. Furthermore, the maximum value of $Kd$(U) is obtained from Eq. 19 as $K(\mathrm{U})\,(C^0{}_{\mathrm{TBP}})^2/4K(\mathrm{H})$ at $C_{\mathrm{H}}=1/\sqrt{K(\mathrm{H})}$. If one takes $K(\mathrm{U})=27$, $K(\mathrm{H})=0.08$ as the values of equilibrium constants respectively at 25°C, TBP 20% (these values were obtained tentatively as the equilibrium constants), one obtains as the calculated values: $Kd(\mathrm{U})_{\max}=45$ at $C_{\mathrm{H}}=3.5$ M. These correspond to the following experimental values: $Kd(\mathrm{U})_{\max}=34$ at $C_{\mathrm{H}}=5$ M. Considering that this calculation was made using the concentration instead of the activity, the agreement seems to be fairly good.

In case the uranium concentration is higher, although the calculation becomes more complicated, one can obtain a similar result.

Accordingly, it was confirmed that fact c) is interpreted as the result of the competition of both uranium and nitric acid as was pointed out by Moore[2] and McKay[4,8]. From this point of view, facts f) and g) are also interpreted as the result of the competition of both.

*(3) Nitric acid and sodium nitrate as salting-out agent.* — On the extraction of uranium from a nitric acid solution, it was clarified that both uranium and nitric acid are extracted by TBP competitively. Accordingly, it is interesting to observe the behavior of the extraction of uranium when the salting-out agent which is not extractable by TBP is added.

Sodium nitrate was chosen as one of those agents that are suitable for this purpose. The salting-out effects of both nitric acid and sodium nitrate for diluted uranyl nitrate are shown in Fig. 6 which was made at 25°C, TBP 20% (in the case of sodium nitrate, 0.5 M nitric acid is added in order to prevent the hydrolysis of uranium).

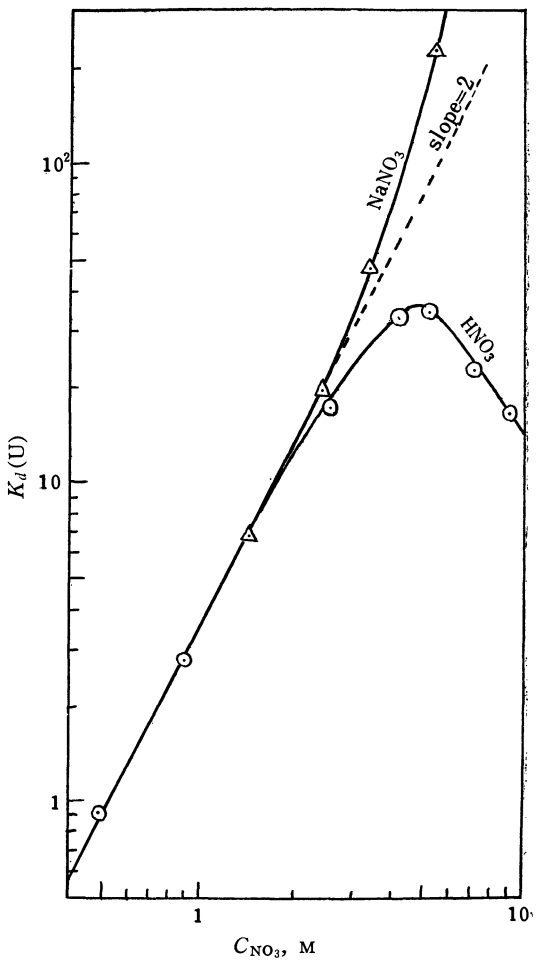



Fig. 6. The salting-out effect of both nitric acid and sodium nitrate for diluted uranyl nitrate.

It is obvious from Fig. 6 that, in the case of nitric acid, $Kd$(U) has the maximum at $C_{NO_3}$ of nearly 5 M; and in the case of sodium nitrate, $Kd$(U) increases monotonously and is nearly proportional to the square of $C_{NO_3}$.

When the salting-out agent is not extracted by TBP and contributes only to the increase of the concentration of $NO_3^-$, one obtains the relation: $Kd(\mathrm{U}) = \text{const.} \times (C_{NO_3})^2$ from Eq. 14 by ignoring the activity coefficient. Then $Kd$(U) is nearly proportional to $(C_{NO_3})^2$. It can also be understood from this analysis that little sodium nitrate is extracted by TBP and is effective only as a salting-out agent for the uranium extraction.

However, it is noteworthy that when the concentration of nitric acid is low, nitric acid is also effective mainly as a salting-out agent. This is observed from

8) H. A. C. McKay, "Int. Conf. Peaceful Uses of Atomic Energy", United Nations, (1955), p./441.

Fig. 6 and is also derived from Eq. 19 as $Kd(U)=\text{const.}(C_H)^2$ by considering $C_H$ is small. This relation just corresponds to the relation $Kd(U)=\text{const.}(C_{NO_3})^2$, therefore, nitric acid is effective mainly as a salting-out agent when its concentration is low.

**Rough Determination of the Thermochemical Functions of the Reaction of Uranyl Nitrate and TBP.**—Although the existence of the complex with TBP such as $UO_2(NO_3)_2(TBP)_2$, $HNO_3 \cdot TBP$ was confirmed, the nature of these complexes remains uncertain. At first the measurement of the thermochemical functions was tried.

$\Delta H^0$, $\Delta F^0$ and $\Delta S^0$ are defined as the enthalpy change, the Gibbs' free energy change and the entropy change respectively for Eq. 1 when the activities of each species of Eq. 1 are unity. These thermodynamical functions are determined roughly by using the distribution coefficient as the following.

*(1) Enthalpy change.* — By applying a thermodynamical relation for the reaction of Eq. 1

$$(\partial \ln K(U)/\partial T)_P = \Delta H^0/\boldsymbol{R}T^2 \qquad (20)$$

The equilibrium constant $K(U)$ is given as Eq. 14. If one keeps both the concentration of salting-out agent and the concentration of TBP constant, the equilibrium constant $K(U)$ becomes

$$K(U)=\text{const.}\,[f_{\text{complex}}/(f_{\pm}(U))^3 \times (f_{TBP})^2]\,Kd(U) \qquad (21)$$

When the concentration is low, the temperature dependence of the activity coefficient is very small, so that one can obtain the following relation from Eqs. 20 and 21

$$(\partial \ln Kd(U)/\partial T)_P \cong \Delta H^0/\boldsymbol{R}T^2 \qquad (22)$$

If one assumes that $\Delta H^0$ is constant for the integration range, from Eq. 22

$$\ln Kd(U) \cong \text{const.} - \Delta H^0/\boldsymbol{R}T \qquad (23)$$

Thus by plotting $\log Kd(U)$ vs. $1/T$ the slope of the line indicates the value $-\Delta H^0/\boldsymbol{R}$, from which $\Delta H^0$ can be obtained.

The measurement of the distribution coefficient of uranium was made at 10, 25 and 50°C, respectively. The concentration of uranium in this measurement is low enough to neglect the temperature dependence of the activity coefficient and to keep the concentration of TBP constant.

The linearity between $\log Kd(U)$ and $1/T$ was observed obviously in both the TBP-$CCl_4$ system and the TBP-kerosene system, and the slopes in both systems were exactly the same. Then, the enthalpy change $\Delta H^0$ was obtained by measuring the slope of the line as

$$\Delta H^0 = -4.3\,\text{kcal.} \quad (10\sim50°C)$$

This value has nearly the same order of the bonding energy of the hydrogen bond, so that it can be estimated that the bond strength or stability of this complex should be of nearly the same order as those of the hydrogen bond.

*(2) Gibbs' free energy change.* — Gibbs' free energy change $\Delta F^0$ for the reaction of Eq. 1 is given as

$$\Delta F^0 = -\boldsymbol{R}T \ln K(U) \qquad (24)$$

The equilibrium constant $K(U)$ is given as Eq. 14 and it is necessary to know the value of the activity coefficient of each species in order to calculate the $Kd(U)$. Unfortunately the activity coefficient of the organic phase is not clear though the activity coefficient of the aqueous phase is available. However, in organic phase, the activity coefficients of each species can be considered as nearly unity so far as the concentration is very low.

It is necessary to make the solution acidic in order to prevent the hydrolysis of uranium, otherwise the mechanism of extraction will change as has been stated already. Therfore, the measurement of the distribution equilibrium of uranium must be made under slightly acidic condition.

The equilibrium constant was calculated by using activity coefficients of uranyl nitrate and nitric acid in aqueous phase and by assuming the activity coefficients of the complex and TBP in organic phase as unity.

The results obtained are the following: $Kd(U)$ are 25.6, 25.2, 21.6 and 20.2 when the initial concentrations of nitric acid are 0.05, 0.1, 0.2 and 0.3 M, respectively. So one can observe that the equilibrium constant of uranium decreases gradually according to the increase of the concentration of nitric acid. This is considered as the result of the extraction of nitric acid into organic phase which causes the deviation of the activity coefficient in organic phase from unity.

Accordingly the following value is obtained as the rough value of $Kd(U)$ at 25°C by extrapolating to the zero nitric acid concentration: $K(U)=27$ (25°C). From this $K(U)$ value, one obtains Gibbs' free energy change of Eq. 1 by using Eq. 24 as

$$\Delta F^0 \cong -2.0 \text{ kcal. } (25°C)$$

This small change of $\Delta F^0$ suggests that uranium can be transferred easily between aqueous and TBP phases by changing the concentration of salting-out agent.

*(3) Entropy change.*—The entropy change $\Delta S^0$ for Eq. 1 is given as

$$\Delta S^0 = (\Delta H^0 - \Delta F^0)/T \qquad (25)$$

If $\Delta H^0 \cong -4.3$ kcal. which was obtained as the average value for 10~50°C is used as the value at 25°C, the entropy change at 25°C is obtained as

$$\Delta S^0 = -7.7 \text{ e. u. } (25°C)$$

## Summary

The method of analysis using the distribution coefficient to confirm the mechanism of extraction was proposed and the formation of the complex $UO_2(NO_3)_2 \cdot (TBP)_2$ and $HNO_3 \cdot TBP$ was confirmed. The extraction behavior of uranium from a nitric acid solution was concluded as a result of the competition of uranium and nitric acid. The thermochemical functions $\Delta H^0$, $\Delta F^0$ and $\Delta S^0$ for the complex formation reaction:

$$UO_2^{+2}(aq.) + 2NO_3^-(aq.) + 2TBP(org.) = UO_2(NO_3)_2(TBP)_2(org.)$$

were determined roughly from the measurement of the distribution coefficient as follows: $\Delta H^0(25°C) \cong -4.3$ kcal., $\Delta F^0(25°C) \cong -2.0$ kcal., $\Delta S^0(\sim 25°C) \cong -7.7$ e.u.

The author would like to express his gratitude to Dr. K. Kimura, Dr. T. Nakai, Dr. K. Oshima and Dr. R. Hara for their invaluable assistance and advice in this work. He also thanks Mr. T. Suzuki for his help during the experiment.

*Japan Atomic Energy Research Institute*
*Tokai, Ibaraki*

# *The Effect of Metallic Ions on Surface Chemical Phenomena. III. Solubility of Various Metal Dodecyl Sulfates in Water*

By Shigeru MIYAMOTO

(Received August 26, 1959)

In the preceding paper[1] a study was made of the effects of various inorganic electrolytes on the stability and type of emulsions stabilized with sodium dodecyl sulfate. Added polyvalent cations were found to cause phase inversion of the emulsions. These effects can hardly be explained without taking into consideration the properties of corresponding metal dodecyl sulfates formed as the consequence of the reaction of sodium dodecyl sulfate with these cations. In order to understand the nature of the effect of metallic ions in these systems it is, therefore, necessary to investigate fully the properties of various metal dodecyl sulfates, more generally metal alkyl sulfates in aqueous solutions.

Some studies have been reported regarding their properties up to the present. Nishizawa and Tomizuka[2] studied the compositions and crystallographic habits of hexadecyl sulfates of potassium, sodium, ammonium, magnesium and calcium. They also made reference qualitatively to the solubility of these compounds in various solvents. Ueno, Yokoyama and Iwakura[3] found that solubilities of ammonium-, sodium- and potassium dodecyl sulfates and hexadecyl sulfates decrease in this order. They studied also the foam formation, surface tension, interfacial tension at oil-water interface and detergent action of these metal dodecyl sulfates. Yoshizaki and Terashima[4] studied the change of foam volume on aqueous solutions of sodium hexadecyl sulfate with the course of time. Measurement of foam of ammonium-, magnesium- and calcium dodecyl sulfate and hexadecyl sulfate

1) S. Miyamoto, *Mem. Fac. Sci. Kyushu Univ., Series C, Chem.*, in press.

2) K. Nishizawa and T. Tomizuka, *J. Chem. Soc. Japan, Ind. Chem. Sec.* (*Kogyo Kagaku Zasshi*), **35**, 1368 (1923).

3) S. Ueno, S. Yokoyama and Y. Iwakura, ibid., **38**, 1333 (1935).

4) T. Yoshizaki and H. Terashima, ibid., **55**, 350 (1952).

solutions was made by Nakashima[5]. Lottermoser et al.[6] synthesized metal alkyl sulfates and undertook measurements of conductance, potential, surface tension and interfacial tension of their aqueous solution. These authors gave consideration to the change of dissolved state with the change of concentration of the solution. Further, Giers and Boido[7] measured cloud point, viscosity, pH, contact angle, wetting speed and foaming property of ammonium-, sodium-, potassium-, magnesium-, calcium- and zinc dodecyl sulfates. As regards solubility, sodium dodecyl sulfate, tetradecyl sulfate and hexadecyl sulfate were studied by Hutchinson et al.[8] at various temperatures. On the solubility of metal alkyl sulfates, however, only a few data have been reported. The solubility of calcium dodecyl sulfate was given as 0.03~0.04% at 25°C by Lenher[9], 0.00457 mol./1000 g. $H_2O$ at 50°C by Tartar and Cadle[10] and 0.5 g./l. at 53°C and 1.0~5.0 g./l. at 54°C[11].

In the preceding paper reported by the author[1] values of solubility of sodium-, calcium-, barium-, aluminum-, iron- and thorium dodecyl sulfates were given at 25°C. It seems, however, that further studies are necessary to obtain full knowledge regarding the values of solubility of many other metal dodecyl sulfates. So one has conducted the measurements of solubility of calcium-, strontium-, lead-, barium-, copper, manganese-, magnesium- and cobalt dodecyl sulfates at various temperatures. It is the purpose of the present paper to report the results of the solubility measurement of these metal dodecyl sulfates and to undertake some discussions concerning them.

## Experimental

**Materials.**—Metal dodecyl sulfates were synthesized from pure sodium dodecyl sulfate (abbreviated as SDS) which was synthesized from pure dodecyl alcohol and a guaranteed reagent of concentric sulfuric acid according to the method described in the papers already reported[1,12]. Pure dodecyl alcohol used was obtained by fractional distillations in vacuo. Synthesized SDS was freed from unsulfated dodecyl alcohol by extraction with ethyl ether for about forty hours in a Soxhlet extractor. The purity of the SDS sample was ascertained from the absence of the minimum in the curve representing surface tension of its aqueous solutions versus its concentration and also from results of elementary analysis of the sample. From these results[1], it was found that the SDS sample was highly pure surface-chemically. Metal dodecyl sulfates were precipitated from SDS aqueous solution by adding concentrated aqueous solutions of magnesium-, calcium-, strontium-, barium-, cupric-, lead-, manganous- and cobaltous chlorides. All these electrolytes had been purified before they were used for the preparation of corresponding metal dodecyl sulfates. The precipitated metal dodecyl sulfates were taken out by filtration by a glass filter and then they were recrystallized further three times except in the case of barium salt which was found to be soluble only in small amount even at high temperatures. Washing with water was carried out fully after every recrystallization. Readily soluble metal dodecyl sulfates were washed with cold water. After purification, they were brought into the air-dried state. Elementary analysis and metal content analysis were conducted on these air-dried samples.

**Method.**—Measurements of solubility were performed as usual by weighing the amounts of solute contained after drying up known weights of the saturated solution at 50°C. It was found that long periods of time were necessary to attain true equilibrium of solubility, so the bottle containing the sample was shaken to accelerate the attainment of equilibrium. The process of attainment of equilibrium is shown in Fig. 1 with magnesium-, calcium-, strontium-, lead- and barium dodecyl sulfates.

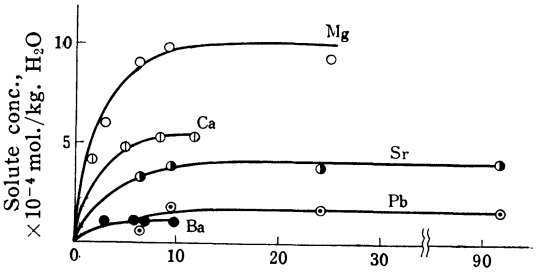



Fig. 1. Attaiment of equilibrium of the solubility in solution of Mg-, Ca-, Sr-, Pb- and Ba dodecyl sulfates in water with the course of stirring time.

## Results

At first, elementary analyses of carbon, hydrogen and metal contents of air-dried metal dodecyl sulfates were carried out.

5) H. Nakashima, ibid., **56**, 611 (1953).
6) A. Lottermoser and F. Püschel, *Kolloid-Z.*, **63**, 175 (1933); A. Lottermoser and F. Stoll, ibid., **63**, 49(1933).
7) S. Giers and D. Boido, *Soap Chem. Specialities*, **30**, 38, 179 (1954).
8) E. Hutchinson, K. E. Manchester and L. Winslow, *J. Phys. Chem.*, **58**, 1124 (1954).
9) S. Lenher, *Am. Dyestuff Reptr.*, **22**, 663 (1933).
10) H. V. Tartar and R. D. Cadle, *J. Phys. Chem.*, **43**, 1173 (1939).
11) K. Kanamaru, "Surface Active Agents (Kaimen Kassei Zai)", Maki Shoten, Tokyo (1955), p. 47.
12) R. Matuura, H. Kimizuka, S. Miyamoto and R. Shimozawa, This Bulletin, **31**, 532 (1958).

TABLE I. RESULTS OF ELEMENTARY ANALYSIS AND METAL CONTENT ANALYSIS OF AIR-DRIED METAL DODECYL SULFATES

| Metal | | Metal content % | Elementary analysis C, % | H, % |
|---|---|---|---|---|
| Ca | Found | 9.33 | 49.10 | 8.65 |
| | Calcd. as $Ca(DS)_2$ | 9.38 | 49.19 | 8.60 |
| Sr | Found | 14.22 | 46.95 | 8.11 |
| | Calcd. as $Sr(DS)_2$ | 14.18 | 46.59 | 8.15 |
| Ba | Found | 20.53 | 43.36 | 7.77 |
| | Calcd. as $Ba(DS)_2$ | 20.57 | 43.12 | 7.55 |
| Pb | Found | 28.04 | 38.90 | 6.89 |
| | Calcd. as $Pb(DS)_2$ | 28.09 | 39.04 | 6.83 |
| Mn | Found | 9.33 | 49.10 | 8.65 |
| | Calcd. as $Mn(DS)_2$ | 9.38 | 49.19 | 8.60 |
| Mg | Found | 3.67 | 43.43 | 9.47 |
| | Calcd. as $Mg(DS)_2 \cdot 6H_2O$ | 3.77 | 43.48 | 9.35 |
| Co | Found | 8.65 | 41.23 | 8.95 |
| | Calcd. as $Co(DS)_2 \cdot 6H_2O$ | 8.45 | 41.29 | 8.96 |
| Cu | Found | — | 43.09 | 8.86 |
| | Calcd. as $Cu(DS)_2 \cdot 4H_2O$ | — | 43.23 | 8.78 |

TABLE II. VALUES OF SOLUBILITY (mol./1000 g. $H_2O$) OF METAL DODECYL SULFATES AT VARIOUS TEMPERATURES (THOSE OF GREATER SOLUBILITY)

| Temp., °C | $Cu(DS)_2 \cdot 4H_2O$ | $Mn(DS)_2$ | $Co(DS)_2 \cdot 6H_2O$ | $Mg(DS)_2 \cdot 6H_2O$ |
|---|---|---|---|---|
| 5.0 | $1.99\times10^{-2}$ | $2.12\times10^{-3}$ | — | — |
| 10.0 | $2.46\times10^{-2}$ | $4.15\times10^{-3}$ | — | $6.39\times10^{-4}$ |
| 13.0 | — | $5.26\times10^{-3}$ | — | — |
| 15.0 | $3.48\times10^{-2}$ | $6.35\times10^{-3}$ | $8.08\times10^{-4}$ | $8.06\times10^{-4}$ |
| 16.0 | — | $1.75\times10^{-2}$ | — | — |
| 17.0 | — | $8.92\times10^{-1}$ | — | — |
| 20.0 | — | $8.99\times10^{-1}$ | $9.01\times10^{-4}$ | $9.27\times10^{-4}$ |
| 23.0 | $4.12\times10^{-2}$ | — | $9.78\times10^{-4}$ | $9.58\times10^{-4}$ |
| 25.0 | $6.53\times10^{-2}$ | — | $2.53\times10^{-3}$ | $9.58\times10^{-4}$ |
| 25.8 | $9.30\times10^{-1}$ | — | — | — |
| 26.5 | $9.68\times10^{-1}$ | — | — | — |
| 28.0 | — | — | $9.81\times10^{-3}$ | $4.98\times10^{-3}$ |
| 31.0 | — | — | $4.17\times10^{-2}$ | $4.46\times10^{-2}$ |

TABLE III. VALUES OF SOLUBILITY (mol./1000 g. $H_2O$) METAL DODECYL SULFATES AT VARIOUS TEMPERATURES (THOSE OF SMALLER SOLUBILITY)

| Temp., °C | $Ca(DS)_2$ | $Sr(DS)_2$ | $Pb(DS)_2$ | $Ba(DS)_2$ |
|---|---|---|---|---|
| 25.0 | $4.61\times10^{-4}$ | $4.05\times10^{-4}$ | $1.76\times10^{-4}$ | $1.15\times10^{-4}$ |
| 35.0 | $7.31\times10^{-4}$ | $5.39\times10^{-4}$ | $1.21\times10^{-4}$ | $1.74\times10^{-4}$ |
| 40.0 | $9.33\times10^{-4}$ | — | — | — |
| 45.0 | — | $8.10\times10^{-4}$ | $2.81\times10^{-4}$ | $2.55\times10^{-4}$ |
| 50.0 | $1.62\times10^{-3}$ | — | — | — |
| 51.0 | $2.09\times10^{-2}$ | — | — | — |
| 52.6 | $2.30\times10^{-2}$ | — | — | — |
| 54.0 | — | — | $1.18\times10^{-3}$ | — |
| 55.0 | $2.45\times10^{-2}$ | $1.09\times10^{-3}$ | $3.43\times10^{-3}$ | — |
| 58.0 | — | — | $6.37\times10^{-2}$ | — |
| 60.0 | — | $1.40\times10^{-3}$ | $6.54\times10^{-2}$ | — |
| 65.0 | — | $3.59\times10^{-3}$ | $7.82\times10^{-2}$ | $5.06\times10^{-4}$ |
| 65.5 | — | $3.59\times10^{-2}$ | — | — |
| 66.0 | — | $6.25\times10^{-2}$ | — | — |
| 67.0 | — | $7.46\times10^{-2}$ | — | — |
| 70.0 | — | — | — | $6.74\times10^{-4}$ |
| 75.4 | — | — | — | $8.02\times10^{-4}$ |
| 100.0 | — | — | — | $1.66\times10^{-3}$ |

and the results are shown in Table I. From these results the compositions of metal dodecyl sulfates were determined. That is, they were found to have the following formulae. $Ca(DS)_2$, $Sr(DS)_2$, $Ba(DS)_2$, $Pb(DS)_2$, $Mn(DS)_2$, $Mg(DS)_2 \cdot 6H_2O$, $Co(DS)_2 \cdot 6H_2O$ and $Cu(DS)_2 \cdot 4H_2O$, where the abbreviation DS represents the dodecyl sulfate radical.

Values of solubility of these metal dodecyl sulfates were obtained at various temperatures and they are shown in Table II (greater solubility) and Table III (smaller solubility).

It has been well known that soaps have the Krafft point above which their solubilities increase enormously. The Krafft point has also been observed generally with the surface active agents such as sodium alkyl sulfates[8], sodium alkyl sulfonates[13], anisidine sodium sulfonates, alkyl pyridinium halides and alkyl trimethylammonium halides[14]. Metal dodecyl sulfates are considered to be surface active agents also, so they are expected to have a Krafft point. To examine whether they have a Krafft point or not, plots of logarithms of solubility versus reciprocals of temperature were drawn as shown in Fig. 2. In this figure, the intersections of two straight lines are seen, which show the Krafft points. The values of Krafft points thus obtained are shown in Table IV.

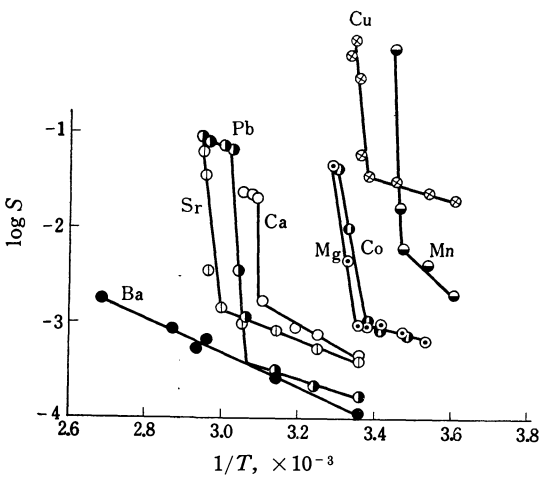



Fig. 2. Relation between the logarithms of solubility of various metal dodecyl sulfates and the reciprocals of absolute temperature.

13) H. V. Tartar and K. A. Wright, *J. Am. Chem. Soc.*, **61**, 539 (1939).
14) N. K. Adam and K. G. A. Pankhurst, *Trans. Faraday Soc.*, **42**, 523 (1946).

TABLE IV. KRAFFT POINTS OF VARIOUS METAL DODECYL SULFATES

| Substance | Krafft point, °C |
|---|---|
| $Mn(DS)_2$ | 16 |
| $Co(DS)_2 \cdot 6H_2O$ | 23 |
| $Cu(DS)_2 \cdot 4H_2O$ | 24 |
| $Mg(DS)_2 \cdot 6H_2O$ | 25 |
| $Ca(DS)_2$ | 50 |
| $Pb(DS)_2$ | 53 |
| $Sr(DS)_2$ | 64 |
| $Ba(DS)_2$ | —* |

* Krafft point of $Ba(DS)_2$ was not observed below 100°C.

## Discussion

From the results of the composition of various metal dodecyl sulfates shown in Table I it is confirmed that calcium-, barium, magnesium- and cupric dodecyl sulfates have the same formulae as those already given by Lottermoser et al.[6] It is noted that some of them have crystalline water. All metal dodecyl sulfates examined were found to have the two dodecyl sulfate radicals in their molecules, presumably showing no hydrolysis of the cations contained in them throughout the process of preparation.

The values of solubility of metal dodecyl sulfates examined were found to increase rapidly with the increase of temperature above the respective Krafft point, except for the case of barium dodecyl sulfate as shown in Fig. 2. The Krafft point could be obtained as the intersect of two straight lines in the diagrams of logarithms of solubility versus the reciprocals of temperature. This method of obtaining the Krafft point has been known to be applicable to many surface active substances in general. From their behaviors in solution, metal dodecyl sulfates are considered to be also a group of the surface active substances.

The values of solubility of magnesium-, calcium-, strontium- and barium dodecyl sulfates in water below the respective Krafft point decrease in this order, which is the same order as that of the values of solubility in water of the inorganic metal sulfates having these cations and also the same as the order of increase of ionic radii of these cations. This series of gegenions is also applied to the values of Krafft point of these metal dodecyl sulfates. These correspondences are, however, not to be extended to manganese-, lead-, cobalt- and copper dodecyl sulfates. As a whole, the Krafft points of various metal dodecyl

sulfates seem to become higher as their solubilities decrease. At a temperature above the Krafft point the micelles of a surface active substance may be formed in the aqueous solution as explained by Murray and Hartley[15]. It has been found from the surface tension vs. concentration diagrams that the critical concentration for micelle formation of the solution of metal dodecyl sulfates of divalent cations is almost the same irrespective of the difference in the kind and type of gegenions. (The details of the surface tension measurement will be reported in a separate paper.) A sparingly soluble metal dodecyl sulfate can let its concentration reach the critical concentration for micelle formation at higher temperatures than more soluble metal dodecyl sulfate.

15) R. C. Murray and G. S. Hartley, ibid., **31**, 183 (1935).

**Summary**

Calcium, strontium-, barium-, lead-, manganese-, magnesium-, cobalt- and copper dodecyl sulfates were synthesized and their compositions were determined from the results of their elementary analysis and metal content analysis. Further, the solubility of these metal dodecyl sulfates was measured at various temperatures. From these data, these metal dodecyl sulfates except barium salt were found to have the Krafft points, values of which were shown also.

The author expresses his sincere gratitude to Professor R. Matuura of Kyushu University for his guidance and encouragement.

*Department of Chemistry*
*Faculty of Science*
*Kyushu University*
*Hakozaki, Fukuoka*

# *The Effect of Metallic Ions on Surface Chemical Phenomena. IV. Surface Tension Measurement on Aqueous Solutions of Metal Dodecyl Sulfates*

By Shigeru MIYAMOTO

(Received August 26, 1959)

In the preceding paper[1a], the effect of metal ions on the properties of the emulsion stabilized with sodium dodecyl sulfate was investigated and in connection with it the solubility of various metal dodecyl sulfates was studied[1b]. Metal dodecyl sulfates should be formed in many systems containing sodium dodecyl sulfate and metal ions as a result of a reaction of the former with the latter. They were supposed to constitute also a group of surface active substances from the existence of their Krafft points measured by the temperature change of their solubilities in water. To explain the Krafft point, the presence of micelles of the solute has been assumed. It is therefore expected that metal dodecyl sulfates begin to form the micelles at a relatively narrow concentration range, referred to as critical micelle concentration (abbreviated as cmc) as is the case with sodium dodecyl sulfate.

In the present paper, measurements of surface tension were performed to examine how far they lower the surface tension of their aqueous solution and whether or not they would actually show cmc as expected from the Krafft phenomena. Although Lottermoser and Stoll[2] made the surface tension measurements of aqueous solutions of dodecyl sulfates of silver, magnesium, copper, zinc and iron(II), their data were obtained with the samples synthesized from impure sodium dodecyl sulfate as illustrated from the presence of the minimum in the diagram of surface tension of its aqueous solution versus concentration. So it seems to be necessary to undertake measurements with pure samples in order to obtain further knowledge of properties of metal dodecyl sulfates, on which only

1) (a) S. Miyamoto, *Mem. Fac. Sci. Kyushu Univ., Series C, Chem.*, in press.
(b) S. Miyamoto, This Bulletin, **33**, 371 (1960).

2) A. Lottermoser and F. Stoll, *Kolloid-Z.*, **63**, 49 (1933).

a few studies have been made up to the present[3].

## Experimental

Metal dodecyl sulfates were synthesized from pure sodium dodecyl sulfate and then purified as described in the preceding paper[1a,b].

Measurements of surface tension of aqueous solutions of metal dodecyl sulfates were conducted with a Du Noüy's tensiometer at various temperatures kept constant with a water thermostat. The sample solution was contained in a bottle having a narrow neck and this was immersed in the thermostat up to the brim. The solution had been heated to a temperature above the temperature of the measurement of surface tension. In the measurement of surface tension, the ring of the tensiometer was suspended by a thin platinum wire from the bar of the tensiometer and was made to have contact with the surface of the solution prior to the measurement of surface tension. After the attainment of equilibrium of temperature of the solution with that of the thermostat, the measurement was started. At high temperatures, the measurement had to be carried out as rapidly as possible to avoid evaporation of the solvent.

From the data of surface tension, the cmc of each metal dodecyl sulfate solution could be determined and it was compared with the one measured by the dye titration method. The dye titration method was conducted by using pinacyanol chloride and rhodamine 6G and observing the change of their color with the change of the detergent concentration.

## Results and Discussion

The values of surface tension of aqueous solutions of various metal dodecyl sulfates at various temperature are shown graphically in Fig. 1—7 as a function of their concentration. It is seen that every curve represents a kink and no minimum near

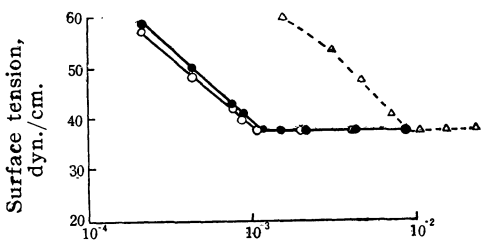



Fig. 1. Relation between surface tension and concentration of magnesium dodecyl sulfate solutions at 40°C (○) and 54°C (●). The dotted line represents the curve obtained with sodium dodecyl sulfate at 54°C.

3) Literatures cited in 1b.

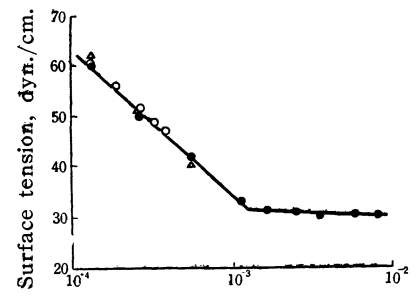



Fig. 2. Relation between surface tension and concentration of calcium dodecyl sulfate. Measurements of surface tension were conducted at 25°C (○), 35°C (△) and 54°C (●).

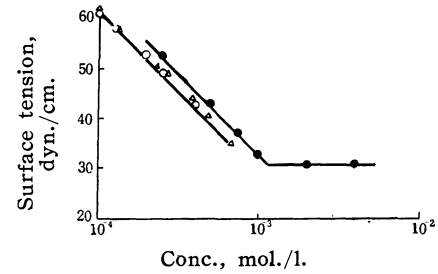



Fig. 3. Relation between surface tension and concentration of strontium dodecyl sulfate. Measurements of surface tension were conducted at 25°C (○), 54°C (△) and 67°C (●).

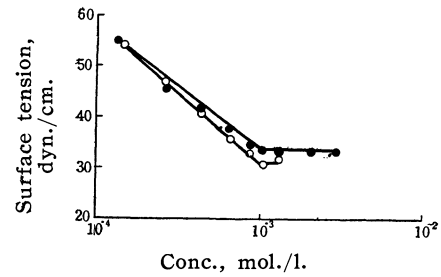



Fig. 4. Relation between surface tension and concentration of lead dodecyl sulfate. Measurements of surface tension were conducted at 54°C (○) and 67°C (●).

the kink point. The absence of the minimum is considered to show the absence of more surface active impurities than these metal dodecyl sulfates. The value of cmc can be obtained as the concentration at the kink point of every curve. These values of cmc of various metal dodecyl sulfates at various temperatures are shown in Table I. It can be seen from Table I that the temperature dependence of the value of cmc of each

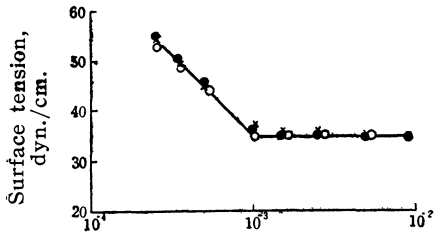



Fig. 5. Relation between surface tension and concentration of manganese dodecyl sulfate. Measurements of surface tension were conducted at 25°C (×), 40°C (○) and 54°C(●).

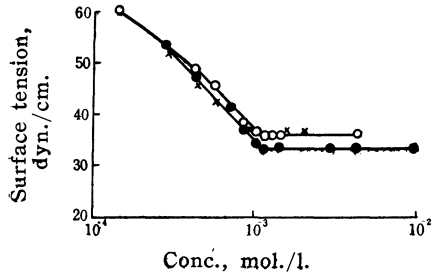



Fig. 6. Relation between surface tension and concentration of cobaltous dodecyl sulfate. Measurements of surface tension were conducted at 25°C (×), 40°C (○) and 54°C (●).

metal dodecyl sulfate of divalent cation is not so remarkable and also the values of dodecyl sulfates of various cations are almost the same, independent of the kind and type of cations contained in the molecules of these metal dodecyl sulfates.

These metal dodecyl sulfates were found to have their Krafft points as already reported[1b]. It is generally accepted with surfactant solutions that only at the temperatures above the Krafft point the micelles are formed. It seems true for some metal dodecyl sulfates studied in the

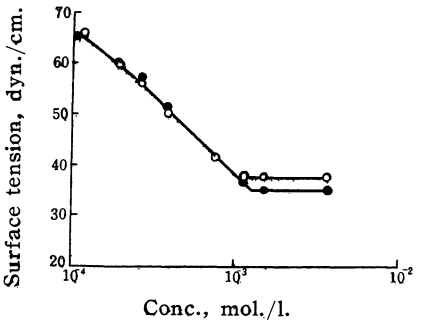



Fig. 7. Relation between surface tension and concentration of cupric dodecyl sulfate. Measurements of surface tension were conducted at 25°C (○) and 40°C (●).

present experiment. For example, calcium dodecyl sulfate was found to show its cmc at 54°C, as illustrated by the kink point of the surface tension-concentration curve (Fig. 2), but at 35°C which is below its Krafft point 50°C, the solution was saturated before its cmc had been reached. Referring to the diagram of Fig. 2 in the preceding paper[1b], it is found that the solubility of magnesium-, calcium-, strontium- and cobalt dodecyl sulfates at each Krafft point is nearly equal to the cmc of each solution which has been determined in the present experiment. In the case of lead salt, however, the solubility at its Krafft point is a little smaller than its cmc, and copper- and manganese salts show considerably larger solubilities than their corresponding value of cmc. It is not clear at the present why these metal dodecyl sulfates show anomalous behaviors. It will be necessary to make measurements of the existence of micelles over a much wider range of temperatures in order to elucidate the relation between the Krafft point and the micelle formation with these metal dodecyl sulfates.

As mentioned above, the dependence of

TABLE I. VALUES OF cmc (mol./l.) OF METAL DODECYL SULFATES AT VARIOUS TEMPERATURES DETERMINED BY SURFACE TENSION MEASUREMENTS

| Subst. | cmc (mol./l.) | | | |
|---|---|---|---|---|
| | 25°C | 40°C | 54°C | 67°C |
| NaDS | $7.4\times10^{-3}$ | — | $9.2\times10^{-3}$ | — |
| $Mg(DS)_2\cdot6H_2O$ | $8.8\times10^{-4}$ | $1.1\times10^{-3}$ | $1.1\times10^{-3}$ | — |
| $Ca(DS)_2$ | — | — | $1.3\times10^{-3}$ | — |
| $Sr(DS)_2$ | — | — | — | $1.1\times10^{-3}$ |
| $Pb(DS)_2$ | — | — | $1.0\times10^{-3}$ | $9.8\times10^{-4}$ |
| $Mn(DS)_2$ | $1.1\times10^{-3}$ | $1.1\times10^{-3}$ | $1.1\times10^{-3}$ | — |
| $Co(DS)_2\cdot6H_2O$ | $8.3\times10^{-4}$ | $9.7\times10^{-4}$ | $1.1\times10^{-3}$ | — |
| $Cu(DS)_2\cdot4H_2O$ | $1.0\times10^{-3}$ | $1.2\times10^{-3}$ | — | — |

the values of cmc of various metal dodecyl sulfates on the kind of divalent cations contained in them is not explicitly found, the cmc being all nearly $1\times10^{-3}$ mol./l. On the contrary, the values of cmc of alkali metal dodecyl sulfates measured by the electrical conductance method have been reported by Meguro et al.[4] to vary with the kind of alkali metal cations; i. e. they reported 7.8, 8.9 and 10.5 millimol./l. as the values of cmc of potassium-, sodium- and lithium dodecyl sulfates, respectively. These authors explained the dependence of cmc on the kind of monovalent cations as being due to the difference in hydration of these monovalent cations. This explanation might be applied also to the case of the metal dodecyl sulfates having the divalent cations examined in this experiment, but actually this effect seems so small that it can hardly be detected in this experiment. Metal dodecyl sulfates having divalent cations show far smaller values of cmc than those of the metal dodecyl sulfates having monovalent cations. This fact shows that the former sulfates have a less hydrophilic nature because of the two hydrocarbon chains for a metal, than the latter ones, and thus they have a tendency to form their micelles in solutions more easily. This may be a reason for the independence of their cmc's on the kind of divalent gegenions.

The value of surface tension of the solution above cmc is nearly constant. It ranges only from 31 to 37 dyn. per cm., depending on the temperature and the kind of metal dodecyl sulfates. In general a salt which is more soluble in water shows a larger value of saturation surface tension.

The cmc of a surface active substance has well been known to be obtained by the dye titration method as well as by the surface tension measurement. To examine the possibility of obtaining the values of cmc of the metal dodecyl sulfates by the dye titration method, measurements were conducted using pinacyanol chloride or rhodamine 6G as the indicator of the dye titration method. It was found that this method can also be applied to metal dodecyl sulfates. The values of cmc of the various metal dodecyl sulfates thus obtained are shown in Table II.

From Table II, the values of cmc obtained by pinacyanol chloride and rhodamine 6G are seen to be in good agreement with each other.

TABLE II. VALUES OF cmc (mol./l.) OF VARIOUS METAL DODECYL SULFATES* AT 40°C OBTAINED BY THE DYE TITRATION METHOD USING PINACYANOL CHLORIDE AND RHODAMINE 6G

| Subst. | cmc (mol./l.) By pinacyanol chloride | cmc (mol./l.) By rhodamine 6G |
|---|---|---|
| NaDS | $6.1\times10^{-3}$ | $6.1\times10^{-3}$ |
| $Mg(DS)_2\cdot6H_2O$ | $1.0\times10^{-3}$ | $1.1\times10^{-3}$ |
| $Ca(DS)_2$ | $1.3\times10^{-3}$ (at 54°C) | — |
| $Mn(DS)_2$ | $1.2\times10^{-3}$ | $1.1\times10^{-3}$ |
| $Co(DS)_2\cdot6H_2O$ | $1.0\times10^{-3}$ | $1.3\times10^{-3}$ |
| $Cu(DS)_2\cdot4H_2O$ | $1.2\times10^{-3}$ | $1.3\times10^{-3}$ |
| $Zn(DS)_2\cdot6H_2O$ | $1.1\times10^{-3}$ | $1.1\times10^{-3}$ |

* Measurements were not performed on strontium- and lead dodecyl sulfates because of their high Krafft points.

Comparing the values obtained by the dye titration method with those shown in Table I, obtained from surface tension measurements, it is found that these two methods of measuring cmc give values approximately coinciding with each other.

As described above, metal dodecyl sulfates with divalent cations are found to lower the surface tension of their solutions exceedingly and have far smaller cmc values than those of the salts of monovalent cations. Relatively soluble salts such as cupric-, manganese-, cobaltous- and magnesium dodecyl sulfates, therefore, may be useful for many purposes based on their strong surface activity.

## Summary

The surface tension of aqueous solutions of various metal dodecyl sulfates with divalent cations was measured at various temperatures with a Du Noüy's tensiometer. The values of surface tension were observed to decrease steeply with the increase of their concentrations up to their cmc's, which are all nearly equal to $1\times10^{-3}$ mol./l. These values of cmc of the metal dodecyl sulfates with divalent cations were found to be practically independent of temperature and the kind of these cations. Further, the dye titration methods were also performed to obtain the values of cmc of these metal dodecyl sulfates using pinacyanol chloride and rhodamine 6G. The values of cmc obtained by these methods were found to coincide with those from the surface tension measurements.

4) K. Meguro, T. Kondo, O. Yoda, T. Ino and N. Ohba, *J. Chem. Soc. Japan, Pure Chem. Sec. (Nippon Kagaku Zasshi)*, 77, 1236 (1956).

The author wishes to express his sincere thanks to Professor R. Matuura of Kyushu University for his encouragement and guidance.

*Department of Chemistry*
*Faculty of Science*
*Kyushu University*
*Hakozaki, Fukuoka*

# *Relations between Electronic Absorption Spectra and Spatial Configurations of Conjugated Systems. V. Stilbene*

By Hiroshi SUZUKI

(Received August 15, 1959)

Previously[1] the present author explained successfully the hypsochromic shifts of the conjugation band observed in the ultraviolet absorption spectra of *cis*-stilbene and of some $\alpha$-alkyl- and $\alpha,\alpha'$-dialkylstilbenes as compared with *trans*-stilbene by correlating those with the most probable spatial configurations of the molecules on the basis of the calculations by the simple LCAO molecular orbital method. Thus, he determined by his calculations the relation between the interplaner angle $\theta$ (that is, the angle through which the plane of each phenyl group rotates out of the plane of the central essentially double bond) and the electronic transition energy correspondinng to the conjugation band, and clarified the fact that the perfect coplanarity of the molecular configuration is not prerequisite to an occurrence of conjugation and hence not prerequisite to the appearance of the conjugation band and that the conjugation band is progressively shifted toward shorter wavelengths with increasing $\theta$. He showed also that the value of the interplanar angle of a given compound of the type concerned can satisfactorily be computed from the position of the conjugation band and vice versa. Further, he showed that the earlier interpretations[2,3] of these hypsochromic shifts in terms of " partial chromophores " are to be rejected.

The calculations were carried out on the basis of the assumption that the absorption maximum at about 294 m$\mu$ in the spectrum of *trans*-stilbene in solution was due to the transition in the planar molecule of *trans*-stilbene. According to the X-ray crystal analysis by Robertson and Woodward[4], *trans*-stilbene in the crystalline state has a nearly planar or probably completely planar configuration. Strictly speaking, however, it seems that there is no evidence to indicate that the most probable configuration of *trans*-stilbene in solution is also planar. The observation by Wiegand and Merkel[5] that the absorption curve of *trans*-stilbene in solution is closely similar to that of 2-phenylindene in which one of the phenyl groups of *trans*-stilbene may be considered to be maintained in the coplanar or nearly coplanar position with the central ethylenic bond by the methylene bridge is somewhat interesting in this connection, but it should not be considered as a proof of the planarity of the whole configuration of *trans*-stilbene in solution. As already discussed in the first part[6] of this series, biphenyl is probably non-planar in solution, while it is known to be planar in the crystalline state. In view of this fact, the spectrum of *trans*-stilbene in solution should not be considered without sufficient consideration to be due to the planar molecule.

In this part of the series, the results of measurements of the spectra of *trans*-stilbene in various solvents and in the crystalline state carried out from these considerations are reported, and these spectra as well as the vapor spectrum of *trans*-stilbene are discussed with special emphasis on the relation of the spectra to the spatial configuration of the molecule.

1) H. Suzuki, This Bulletin, **25**, 145 (1952).
2) R. N. Jones, *J. Am. Chem. Soc.*, **65**, 1818 (1943).
3) E. A. Braude, *J. Chem. Soc.*, **1949**, 1902.
4) J. M. Robertson and I. Woodward, *Proc. Roy. Soc. (London)*, **A162**, 568 (1937).
5) C. Wiegand and E. Merkel, *Ann.*, **550**, 175 (1942).
6) H. Suzuki, This Bulletin, **32**, 1340 (1959).

TABLE I. SOLUTION SPECTRA OF *trans*- AND *cis*-STILBENES

| Solvent | | A-band $\lambda_{max}$, mμ | A-band ε | B-band $\lambda_{max}$, mμ | B-band ε | $\varepsilon_\beta/\varepsilon_T$ |
|---|---|---|---|---|---|---|
| *trans-Stilbene* | | | | | | |
| *n*-Heptane | α | (320.5) | 16000 | (236) | 10400 | 0.949 |
| | β | 306.9 | 26500 | △228.5 | 16200 | |
| | γ | △294.1 | 27950 | (222) | 15500 | |
| | δ | (283) | 24500 | | | |
| Ethanol (95%) | α | 321.0 | 16980 | 236 | 11150 | 0.977 |
| | β | 307.3 | 27200 | △228.8 | 16400 | |
| | γ | △294.5 | 27850 | 222.5 | 15370 | |
| | δ | (284) | 25200 | | | |
| Methanol | α | 319.5 | 17380 | 236.1 | 11200 | 0.975 |
| | β | 306.8 | 27350 | △228.3 | 16500 | |
| | γ | △294.0 | 28050 | (222) | 15500 | |
| | δ | (283) | 24150 | | | |
| Chloroform | α | (323.5) | 16400 | | | 0.989 |
| | β | 309.9 | 27150 | | | |
| | γ | △297.9 | 27450 | | | |
| | δ | (286.5) | 23200 | | | |
| Carbon tetrachloride | α | (324.5) | 15500 | | | 0.988 |
| | β | 311.8 | 24750 | | | |
| | γ | △299.4 | 25050 | | | |
| | δ | (290) | 22100 | | | |
| Benzene | α | (324.5) | 15400 | | | 1.010 |
| | β | △311.2 | 25600 | | | |
| | γ | 298.8 | 25340 | | | |
| | δ | (289) | 21700 | | | |
| Mixed alcohols[7] (−130°C) | α | 326.2 | 25000 | | | 1.711 |
| | β | 311.2 | 38500 | | | |
| | γ | 297.5 | 22500 | | | |
| *cis-Stilbene* | | | | | | |
| Ethanol (100%)[7] | | 280 | 10450 | 224 | 24400 | |

Wavelengths in parentheses denote inflections.
Symbol △ denotes the most intense maximum of the fine structure.

Further, on the basis of the results, the relation between the spectrum and the spatial configuration of *cis*-stilbene is discussed by application of the usual method.

## Spectra of *trans*-Stilbene in Various States

**Solution Spectra of *trans*-Stilbene.**—Data of the spectra of *trans*-stilbene in various solvents measured at room temperature are given in Table I, in which data of the spectrum of *trans*-stilbene at low temperature as well as those of *cis*-stilbene measured by Beale and Roe[7] are also included for comparison. The notation of the absorption bands is according to Beale and Roe. The A-bands are considered to be the conjugation bands. In addition to the bands shown in Table I, the spectrum of *trans*-stilbene in *n*-heptane exhibits a band at about 201.5 mμ ($\varepsilon$=23900), and that in ethanol at about 201.0 mμ ($\varepsilon$=23800). These are termed the C-bands.

The absorption curves of the spectra of the *n*-heptane solution and of the benzene solution of *trans*-stilbene are shown in Fig. 1 as the representatives of the solution spectra of *trans*-stilbene. In Fig. 1 the curve of the spectrum of *cis*-stilbene is also shown for comparison. The spectra of *trans*-stilbene in the other solvents resemble that in *n*-heptane on the whole, although especially the A-α-band in the spectrum in carbon tetrachloride as well as in chloroform is somewhat more diffuse than in the spectra in *n*-heptane and in alcohols.

It is notable that th A-band has a fine structure. The somewhat similar pattern of fine structure is seen also in the B-band. Beale and Roe[7] have concluded that the fine structure originates in the stretching frequency of the ethylenic bond. On the

7) R. N. Beale and E. M. F. Roe, *J. Chem. Soc.*, **1953**, 2755.

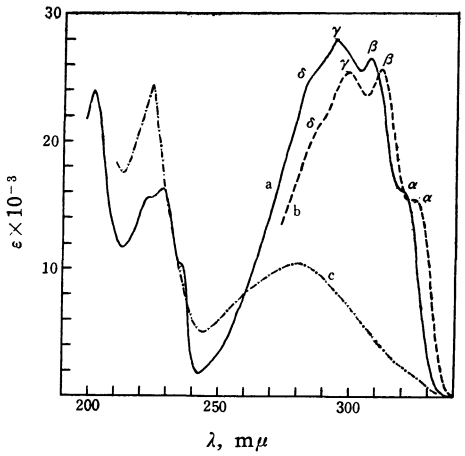



Fig. 1. Solution spectra of *trans*- and *cis*-stilbenes (cf. Table I).
a ——, *trans*-stilbene in *n*-heptane.
b ----, *trans*-stilbene in benzene.
c -·-·-, *cis*-stilbene in ethanol.

other hand, in sharp contrast to *trans*-stilbene, *cis*-stilbene as well as $\alpha$- and $\alpha, \alpha'$-substituted stilbenes which will be treated in a later part of this series shows no fine structure. These compounds are considered to be non-planar as will be shown later. Accordingly it would be expected that an appearance of fine structure might be related to the planarity of the molecular configuration or to its rigidity as the hypotheses proposed by Wiegand and Merkel[8] and by Kortüm and Dreesen[9]. However, such a relation has not yet been established.

In comparison with *n*-heptane, methanol exerts almost no, or a very small, hypsochromic effect, and ethanol exerts a small bathochromic effect. The magnitude of the bathochromic shift is considerably greater in chloroform, and is extraordinarily great in carbon tetrachloride as well as in benzene.

The great bathochromic effect of benzene may be especially noteworthy. According to Bayliss[10], a magnitude of wavelength displacement of a band of a nonpolar molecule by a nonpolar solvent is related to the refractivity of the solvent. The refractivity of benzene is slightly greater than that of *n*-heptane. However, it seems that the great bathochromic effect of benzene relative to *n*-heptane can not be attributed wholly to the difference of refractivity alone.

In this connection, it may be noted that the distribution of intensity among the vibrational bands of the A-band varies considerably with the solvent. The ratio of the intensity of the $\beta$-band to that of the $\gamma$-band for each solvent is listed in the last column of Table I. It is seen that the ratio increases in the order *n*-heptane < ethanol ≈ methanol < chloroform ≈ carbon tetrachloride < benzene. It may be noteworthy that while in solvents other than benzene the $\gamma$-band is the most intense maximum of the A-band, in benzene the $\beta$-band is the most intense maximum.

These facts appear to suggest the presence of a special interaction between the $\pi$-orbitals (or $\pi$-electrons) of the solute molecule and those of benzene. This problem will be discussed in somewhat greater detail in a later part of this series.

**Solution Spectra of Some *p*-Substituted *trans*-Stilbenes.** — The special solvent effect of benzene is seen also in the spectra of some *p*-substituted *trans*-stilbenes. The results of measurements of the spectra of *p*-methoxy-*trans*-stilbene and of *p*-nitro-*trans*-stilbene in *n*-heptane as well as in benzene are shown in Table II and Figs. 2 and 3. These spectra, especially those in *n*-heptane, bear a certain similarity in shape to that of *trans*-stilbene, showing similar patterns of fine structure. The magnitudes of the bathochromic displacements of the bands associated with the change of solvent from *n*-heptane to benzene are considerably

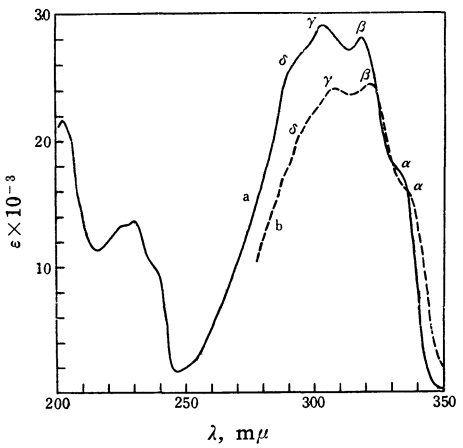



Fig. 2. Solution spectra of *p*-methoxy-*trans*-stilbene (cf. Table II).
a ——, in *n*-heptane.
b ----, in benzene.

8) (a) C. Wiegand and E. Merkel, *Ann.*, **557**, 242 (1947). (b) E. Merkel and C. Wiegand, *Naturwissenschaften*, **34**, 122 (1947). (c) E. Merkel and C. Wiegand, *Z. Naturforsch.*, **3b**, 93 (1948).
9) G. Kortüm and G. Dreesen, *Chem. Ber.*, **84**, 182 (1951).
10) N. S. Bayliss, *J. Chem. Phys.*, **18**, 292 (1950).

TABLE II. SOLUTION SPECTRA OF *p*-SUBSTITUTED *trans*-STILBENES

| Solvent | | A-band $\lambda_{max}$, mμ | A-band ε | B-band $\lambda_{max}$, mμ | B-band ε |
|---|---|---|---|---|---|
| *p-Methoxy-trans-stilbene* | | | | | |
| *n*-Heptane | α | (332.5) | 17700 | (238) | 9830 |
| | β | 317.8 | 28100 | △230.0 | 13600 |
| | γ | △302.7 | 28950 | (225) | 13250 |
| | δ | (291) | 25800 | | |
| Benzene | α | (337) | 15700 | | |
| | β | △322.0 | 24500 | | |
| | γ | 307.7 | 24100 | | |
| | δ | (295.5) | 21000 | | |
| *p-Nitro-trans-stilbene* | | | | | |
| *n*-Heptane | α | (363) | 14200 | 262.0 | 7860 |
| | β | △345.0 | 23820 | △240.0 | 11760 |
| | γ | 332.0 | 23420 | △233.7 | 11760 |
| | δ | (318) | 17850 | (215) | 13770 |
| Benzene | (β) | △350.5 | 17420 | | |

Wavelengths in parentheses denote inflections.
Symbol △ denotes the most intense maximum of the fine structure.

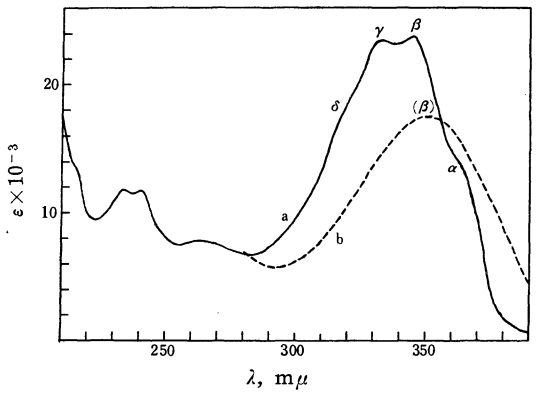



Fig. 3. Solution spectra of *p*-nitro-*trans*-stilbene (cf. Table II).
a ——, in *n*-heptane.
b ----, in benzene.

great (about 5 mμ) also with these compounds. Furthermore, in the spectra of *p*-methoxy-*trans*-stilbene a marked redistribution of intensity between the β-band and the γ-band occurs, quite similarly to the one observed in the spectra of *trans*-stilbene. It is also noteworthy that the fine structure of the A-band of *p*-nitro-*trans*-stilbene disappears almost completely in the spectrum in benzene.

**Crystal Spectra of *trans*-Stilbene.** — The spectrum of *trans*-stilbene in the crystalline state was measured by the pressed KCl-disk technique. The values of the molecular extinction coefficients were not reproducible and were considerably smaller than th corresponding values in the solution spectra. Thus, the former values varied from about 1/3 to about 1/30 of the latter ones from disk to disk. This fact may be considered to indicate the dependence of the extinction values on the condition of dispersion of the micro-crystals or the sizes of the micro-crystals, in view of the somewhat similar phenomenon observed by Weigl[11] in his study on the absorption spectra of some crystalline cationic dyes. In addition, this lowering of the extinction values may be partly due to the possible loss of the organic substance during grinding and evacuation of the press, as stated by Dale[12]. In spite of this, the reproducibility of the positions of the absorption maxima and inflections was almost completely satisfactory except for the α-band of the A-band. As representatives the results of measurements on the two disks of different thicknesses made from the same mixture (cf. *Experimental*) are shown in Table III and Fig. 4.

The crystal spectra differ considerably in the shape of the absorption curve from the solution spectra. In the crystal spectra the most intense maximum in the fine structure of the A-band is the δ-band, neither the γ-band as in the spectra in *n*-heptane etc., nor the β-band as in the spectrum in benzene. In this connection it may be of interest that in the solution spectrum measured by Beale and Roe[7] at low temperature (−130°C) the β-band is the most intense one, the fine structure being much more sharply resolved.

11) J. W. Weigl, ibid., **24**, 364 (1956).
12) J. Dale, *Acta Chem. Scand.*, **11**, 650 (1957).

TABLE III. CRYSTAL SPECTRA OF *trans*-STILBENE MEASURED BY THE KCl-DISK TECHNIQUE

| Disk* | | A-band | | B-band | |
|---|---|---|---|---|---|
| | | $\lambda_{max}$, m$\mu$ | $A$ | $\lambda_{max}$, m$\mu$ | $A$ |
| (*a*) | $\alpha$ | (327.5) | 0.276 | (241.5) | 0.407 |
| | $\beta$ | (312.5) | 0.430 | △233.0 | 0.478 |
| | $\gamma$ | (298.5) | 0.502 | (225.5) | 0.470 |
| | $\delta$ | △287.0 | 0.511 | | |
| | $\varepsilon$ | (276) | 0.460 | | |
| (*b*) | $\alpha$ | (332) | 0.090 | 242 | 0.195 |
| | $\beta$ | (313) | 0.182 | △233.5 | 0.216 |
| | $\gamma$ | (298.5) | 0.245 | (225.5) | 0.190 |
| | $\delta$ | △286 | 0.273 | | |
| | $\varepsilon$ | (276) | 0.254 | | |

* See *Experimental.*

Symbol $A$ represents the absorbance.

Wavelengths in parentheses denote inflections.

Symbol △ denotes most intense maximum of fine structure.

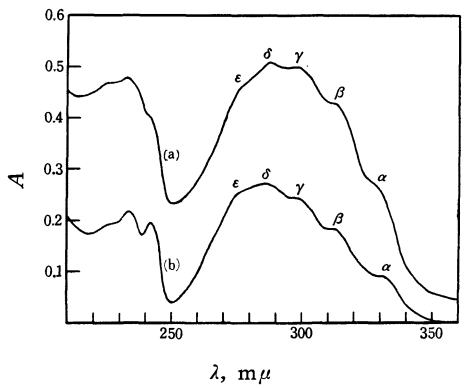



Fig. 4. Crystal spectra of *trans*-stilbene measured by the KCl-disk technique (cf. Table III).

The bands in the crystal spectrum are at longer wavelengths than the corresponding ones in the spectrum in *n*-heptane. The magnitude of the bathochromic shift is about 4.5 m$\mu$ for the $\gamma$-band and about 5.5 or 6 m$\mu$ for the $\beta$-band. These values probably corresponding to the "normal red-shift"[12] of the conjugation band are considerably smaller than those (about 8 m$\mu$ for the $\gamma$-band and about 9 m$\mu$ for the $\beta$-band) anticipated from the regular relation between the magnitude of the shift and the position of the band determined by Dale[12] for rigid molecules. This fact may be considered to indicate that the most probable spatial configuration of *trans*-stilbene in solution does not significantly differ from the one in the crystalline state and hence is planar or nearly planer.

Therefore, in order to infer the most probable spatial configurations of *cis*-stilbene and some related compounds of stilbene in solution by application of our method, the spectrum of *trans*-stilbene in *n*-heptane is taken as the spectrum of the planar reference compound, and the spectra of the *n*-heptane solutions are compared in principle as far as the data are available. In cases of absence of the data of the spectrum of the *n*-heptane solution, the data of the ethanol solution are used. As already mentioned, the spectra of *cis*-stilbene and the stilbene derivatives with substituents at the $\alpha$- and $\alpha'$-positions or at the ortho positions treated in this series all exhibit the structureless conjugation bands in contrast to that of *trans*-stilbene. Therefore, the question arises which maximum of fine structure of the conjugation band in the spectrum of *trans*-stilbene should be taken as the reference for the comparison. In the present treatment the $\gamma$-band at 294.1 m$\mu$ is tentatively chosen as the reference. This band is not only the most intense maximum of fine structure of the conjugation band in the spectrum of the *n*-heptane solution but also probably the central one.

Besides the above mentioned spectra by the pressed KCl-disk technique, the author attempted to measure the crystal spectrum of *trans*-stilbene also on thin films prepared on quartz plates by sublimation of crystals as well as by evaporation of a thin layer of solution, but these attempts were unsuccessful. Thus, the absorption curves obtained were very diffuse and indicated only indistinctly the presence of a band or bands at near 295~335 m$\mu$. This failure of revelation of the conjugation band is probably due to the effect of the orientation of the molecules in the crystals as discussed by Dale[12] in the case of biphenyl.

Pesteil[13] measured the spectrum of *trans*-stilbene on thin crystal plates with polarized light and found a feeble band with two principal maxima at 367 and 387 mμ in addition to the stronger bands below 360 mμ. Jaffé and others[14] have stated that it appears reasonable to assume this feeble band to be the singlet-triplet absorption. Brodin and others[15] measured the spectrum of crystalline *trans*-stilbene at 20°K and found many vibrational frequencies.

**Vapor Spectrum of *trans*-Stilbene.**—According to Kanda[16], the vapor spectrum of *trans*-stilbene prossesses a discontinuous band with nine maxima at the region from 284.4 to 265.6 mμ, of which the most intense maxima are at 284.4 and 283.4 mμ, and a discontinuous band with ten maxima at the region from 244.3 to 233.5 mμ, of which the most intense maximum is at 240.5 mμ. The former band may be considered to be the conjugation band, viz. the A-band, and the latter the B-band. It is noteworthy that the conjugation band in the vapor spectrum is at considerably shorter wavelengths than the corresponding one in the solution spectra as well as the crystal spectrum. This fact probably indicates that the most likely configuration of *trans*-stilbene in the vapor state deviates considerably from the coplanarity, analogously to biphenyl[6].

## Calculation

The relation between the spatial configurations and the electronic absorption spectra of stilbenes can be determined by the following calculations. The procedures of the calculations are the same in principle as the ones described previously[1]. The description is given here in a somewhat more refined form as the basis for the treatments not only in the present part but also in the succeeding parts of this series.

**Determination of the Parameters for the Resonance Integrals as Functions of the Bond Length and the Interplanar Angle.**—The $\pi-\pi$ resonance integral for the central ethylenic bond, namely the $\alpha-\alpha'$ bond, is denoted by $\eta\beta$, and the one for the $\alpha-1$ bond as well as the $\alpha'-1'$ bond by $\rho\beta$. (Symbols $\alpha$ and $\gamma$ in the previous paper were replaced by $\rho$ and $\eta$, respectively). Symbol $\beta$ represents the $\pi-\pi$ resonance integral for the C-C bond in the benzene ring, and $\eta$ and $\rho$ are parameters by which allowances are made for changes of the resonance integrals associated with changes of the bond length and the interplanar angle.

The length of the $\alpha-\alpha'$ bond in *trans*-stilbene was estimated at 1.33±0.04 Å by Robertson and Woodward[4]. The length of the C=C bond in ethylene was recently found to be 1.337 Å[17], and the length of the "double" bonds in butadiene to be 1.337±0.005 Å[18]. Therefore, it may be presumed that the length of the ethylenic "double" bond does not significantly vary with the extent of conjugation. Hence the round value of 1.34 Å is taken as the length of the $\alpha-\alpha'$ bond in *trans*-stilbene as well as the related compounds throughout the present treatment. Consequently, the value of the parameter $\eta$ is estimated at 1.080 from Mulliken's Tables[19] on the basis of the approximate proportionality of the $\pi-\pi$ resonance integral for C-C bond to the $\pi-\pi$ overlap integral.

The parameter $\rho$ can be expressed approximately by the following equation, quite analogously to Eq. 1 in the first part[6] of this series;

$$\rho = S(R,\ 0°)\cos\theta / S(1.39,\ 0°) \qquad (1)$$

where $S(1.39,0°)$ represents the $\pi-\pi$ overlap integral for the C-C bond in the benzene ring and $S(R,\ 0°)$ represents the one in the case where the bond length is $R$ and the interplanar angle is 0°.

According to the result of the X-ray crystal analysis of *trans*-stilbene by Robertson and Woodward[4], two molecules contribute to the asymmetric unit of the crystal, and these molecules have different appearances in the electron density maps. Thus, the length of the "single" bonds joining the phenyl groups to the ethylenic carbon atoms, namely the $\alpha-1$ and $\alpha'-1'$ bonds, and the interplanar angle were estimated at 1.44±0.02 Å and 3°, respectively, for one molecule and at 1.45±0.02 Å and 10°, respectively, for the other. Robertson and Woodward have, however, concluded that the apparent differences are due to the relative orientation of the

13) (a) P. Pesteil, *Compt. rend.*, **233**, 377 (1951). (b) Idem., ibid., **233**, 924 (1951).
14) H. H. Jaffé, Si-Jung Yeh and R. W. Gardner, *J. Molecular Spectroscopy*, **2**, 120 (1958).
15) M. S. Brodin, O. S. Pakhomova and A. F. Prikhot'ko, *Optika i Spektroskopiya*, **5**, 123 (1958); *Chem. Abstr.*, **53**, 48 (1959).
16) Y. Kanda, *Mem. Faculty Sci., Kyushu Univ. Ser. C, Chem.*, **1**, 189 (1950).
17) (a) L. S. Bartell and R. A. Bonham, *J. Chem. Phys.*, **27**, 1414 (1957). (b) H. C. Allen and E. K. Plyler, *J. Am. Chem. Soc.*, **80**, 2673 (1958). (c) J. M. Dowling and B. P. Stoicheff, *Bull. Am. Phys. Soc.*, **II3**, 373 (1958).
18) A. Almenningen, O. Bastiansen and M. Traetteberg, *Acta Chem. Scand.*, **12**, 1221 (1958).
19) R. S. Mulliken, C. A. Rieke, D. Orloff and H. Orlott, *J. Chem. Phys.*, **17**, 1248 (1949).

molecules and not to any appreciable differences in their shape or dimensions, and that the molecules are nearly planar and may be exactly planar within the limits of experimental error.

Therefore, the values of $\theta$ (the interplanar angle) and of $R$ (the length of the $\alpha-1$ bond) may safely be assumed in the present treatment to be 0° and 1.445 Å, respectively, in the configuration of *trans*-stilbene in the crystalline state and hence in the most probable configuration of the molecule in solution. Accordingly, the relation between $\theta$ and $R$ is assumed as follows, quite analogously to Eq. 4 in Part I[6].

$$\{S(R, 0^\circ)-S(1.54, 0^\circ)\}/\{S(1.445, 0^\circ)-S(1.54, 0^\circ)\}=\cos\theta \quad (2)$$

Then, from Eqs. 1 & 2 and Eq. 3 in Part I, one obtains

$$\rho=\cos\theta\times 0.77108+\cos^2\theta\times(1.54-1.445)\times 1.4458 \quad (3)$$

which is quite analogous to Eq. 7 in Part I. Accordingly, the value of $\rho$ is computed to be 0.9084 when $\theta$ is 0° and $R$ is 1.445 Å. It is evident that the value of $\rho$ becomes smaller with increasing $\theta$ and that it is 0 when $\theta$ is 90°.

**Solution of the Secular Equation for the Determination of the Molecular Orbitals.**— By solving the secular equation for the determination of the molecular orbitals as linear combinations of $2p\pi$ atomic orbitals, one can obtain the values of energies of the molecular orbitals corresponding to the value of the parameter $\rho$. Consequently, the values of the extra-resonance energy (subsequently referred to as *R.E.*), of the coefficients of the $2p\pi$ atomic orbitals in the molecular orbital functions, and of the quantities such as the $\pi$-bond orders corresponding to the molecular configuration prescribed by the value of $\rho$ can also be obtained by the usual procedures.

The stilbene-type conjugated system can be considered as belonging to the symmetry group $D_2$ in the present treatment. Then, the highest occupied $\pi$-orbital ($\pi_1$) belongs to the representation $B_1$, and coincides with the $\varphi_1$ orbital in benzene when $\rho$ is 0. On the other hand, the lowest vacant $\pi$-orbital ($\pi_1^*$) belongs to $B_3$, and coincides with the $\varphi_2$ orbital in benzene when $\rho$ is 0. (The notation for orbitals in benzene is according to Sklar[20].) Transitions from orbitals belonging to $B_1$ to those belonging to $B_3$ are allowed by absorption of light polarized along the direction of the long axis of the molecule. Accordingly, the energy difference between the lowest vacant orbital $\pi_1^*$ and the highest occupied orbital $\pi_1$ (referred to as $\Delta E_A$) is considered to be the transition energy corresponding to the conjugation band (viz. the A-band). The value of $\Delta E_A$ (in $-\beta$) is, of course, twice the absolute value of the enegy (in $-\beta$) of one of the two orbitals.

In addition to the ten orbitals belonging to $B_1$ and $B_3$, whose energies vary with $\rho$ (cf. Fig. 2 in Ref. 1), there are two sets of doubly degenerate orbitals belonging to $A_1$ and $B_2$, whose energies do not vary with $\rho$. These orbitals may be considered as ones localized in the benzene rings. Thus, one ($\varphi$) of the two orbitals belonging to either $A_1$ or $B_2$ has the energy of $+\beta$ and corresponds to the $\varphi_{-1}$ orbital in benzene, while the other orbital ($\varphi^*$) has the energy of $-\beta$ and corresponds to the $\varphi_{-2}$ orbital in benzene. Transitions from the $\pi_1$ orbital ($B_1$) to the $\varphi^*$ orbital belonging to $B_2$ or from the $\varphi$ orbital belonging to $A_1$ to the $\pi_1^*$ orbital ($B_3$) are allowed by absorption of light polarized along the direction of the short-axis of the molecule. These transitions may be considered as corresponding to the B-band, as suggested by Dale[21]. The value of the corresponding transition energy $\Delta E_B(-\beta)$ can evidently be expressed as $1+\Delta E_A(-\beta)/2$.

Transitions between the orbitals belonging to $A_1$ and those belonging to $B_2$ are allowed by absorption of light polarized along the direction of the long-axis of the molecule, and correspond probably to the C-band at about 200 m$\mu$.

The results of the calculations are summarized in Table IV. In this table, $\Delta E_A(-\beta)$ and $R.E.(-\beta)$ are values obtained by ignoring the $\pi-\pi$ overlap integral, and $\Delta E_A(-\gamma)$ and $R.E.(-\gamma)$ are values obtained by taking the overlap integral into account, assuming the value of the overlap integral for the C–C bond in benzene as 0.25. The symbols $p_{\alpha-\alpha'}$ and $p_{\alpha-1}$ represent the $\pi$-bond orders of the $\alpha-\alpha'$ bond and of the $\alpha-1$ as well as the $\alpha'-1'$ bond, respectively.

It is evident that the values of $\Delta E_A$ and hence of $\Delta E_B$ increase with decreasing $\rho$ and agree with the values for benzene when $\rho$ is 0. This means that A-band as well as the B-bond is gradually shifted toward shorter wavelengths as the value

20) A. L. Sklar, ibid., 7, 984 (1939).

21) J. Dale, *Acta Chem. Scand.*, **11**, 971 (1957).

TABLE IV

| | | | | | | |
|---|---|---|---|---|---|---|
| $\rho$ | 1.1 | 1.0 | 0.9 | 0.8 | 0.7 | 0.6 |
| $\Delta E_A(-\beta)$ | 0.9920 | 1.0680 | 1.1492 | 1.2352 | 1.3262 | 1.4216 |
| $\Delta E_A(-\gamma)$ | 1.0075 | 1.0874 | 1.1734 | 1.2654 | 1.3637 | 1.4679 |
| $R.E.(-\beta)$ | 1.0252 | 0.8500 | 0.6904 | 0.5464 | 0.4190 | 0.3084 |
| $R.E.(-\gamma)$ | 0.3532 | 0.2922 | 0.2368 | 0.1870 | 0.1432 | 0.1048 |
| $p_{\alpha-\alpha'}$ | | (0.829) | 0.858 | 0.8865 | 0.912 | 0.934 |
| $p_{\alpha-1}$ | | (0.423) | 0.381 | 0.340 | 0.298 | 0.255 |
| $\rho$ | 0.5 | 0.4 | 0.3 | 0.2 | 0.1 | 0 |
| $\Delta E_A(-\beta)$ | 1.5212 | 1.6246 | 1.7306 | 1.8376 | 1.9398 | 2 |
| $\Delta E_A(-\gamma)$ | 1.5783 | 1.6945 | 1.8156 | 1.9400 | 2.0610 | 2.1333 |
| $R.E.(-\beta)$ | 0.2140 | 0.1372 | 0.0772 | 0.0342 | 0.0084 | 0 |
| $R.E.(-\gamma)$ | 0.0726 | 0.0466 | 0.0262 | 0.0118 | 0.0028 | 0 |
| $p_{\alpha-\alpha'}$ | 0.954 | (0.9705) | | | | 1 |
| $p_{\alpha-1}$ | 0.213 | (0.170) | (0.1275) | (0.085) | (0.0425) | 0 |

The values of the $\pi$-bond orders in parentheses were obtained by either interpolation or extrapolation.

TABLE V

| Stilbene | $\lambda_A$ m$\mu$ | $\nu_A$ cm$^{-1}$ | $\Delta E_A$ $-\beta$ | $\rho$ | $\theta$° | $R$ Å | $R.E.$ $-\beta$ | $p_{\alpha-1}$ | $p_{\alpha-\alpha'}$ |
|---|---|---|---|---|---|---|---|---|---|
| *trans-* | 294.1 | 34002 | 1.1423 | 0.9084 | 0 | 1.445 | 0.704 | 0.384 | 0.8555 |
| *cis-* | 280 | 35714 | 1.247 | 0.787 | 28 | 1.456 | 0.530 | 0.333 | 0.890 |

$\rho$ decreases and therefore as the value of $\theta$ increases, and that these bands will coincide with those of benzene when $\rho$ is 0 and therefore when $\theta$ is 90°.

It appears that there is no simple quantitative relation between $\rho$ and $\Delta E_A$, or between $\Delta E_A$ and $R.E.$ On the other hand, $R.E.(-\beta)$ is almost completely proportional to $\rho^2$ and can approximately be expressed as $0.8473\times\rho^2$. In addition, $p_{\alpha-1}$ is roughly proportional to $\rho$ and can roughly be expressed as $0.425\times\rho$.

**Correlation of the Calculated Transition Energy with the Observed Position of the Conjugation Band.**—The value of $\rho$ when $\theta$ is 0° and $R$ is 1.445 Å is 0.9084, and the corresponding value of $\Delta E_A$ is $1.1423(-\beta)$, which is subsequently referred to as $\Delta E_L$. The value of the wave number corresponding to $\Delta E_L$, namely $\nu_L$, is assumed to be 34002 cm$^{-1}$ (294.1 m$\mu$) which is the wave number of the A-$\gamma$-band in the spectrum of *trans*-stilbene in *n*-heptane, on the basis of the considerations mentioned already.

On the other hand, the value of $\Delta E_A$ when $\rho$ is 0, namely $\Delta E_S$, is $2(-\beta)$, and the corresponding value of the wave number, namely $\nu_S$, is assumed to be 48000 cm$^{-1}$ (208.3 m$\mu$), the center of gravity of singlets of benzene, as usual.

Then, the value of $\Delta E_A$ $(-\beta)$ for a given compound of the stilbene-type is obtained from the observed position ($\nu_A$ in wave number) of the conjugation band by Eq. 8 in the first part[6] of this series. Consequently, the corresponding value of the parameter $\rho$ and then the values of $\theta$, $R.E.$, $p$, etc. can be obtained in turn.

### Spectrum of *cis*-Stilbene

The solution spectrum of *cis*-stilbene (cf. Table I and Fig. 1 and also Refs. 1 and 7) differs considerably from that of the *trans*-isomer. The conjugation band (A-band) in the former is structureless in contrast to the one in the latter, and at a considerably shorter wavelength and of lower intensity than the one in the latter. This hypsochromic shift of the band is explained as being due to the non-planarity of the most probable configuration of *cis*-stilbene. The B-band of *cis*-stilbene is also structureless and at a shorter wavelength than the corresponding band of the *trans*-isomer, while the former is more intense than the latter.

### Application of Calculation and Discussion

Data of the spectrum of the *n*-heptane solution of *cis*-stilbene are not available. Hence, the position of the conjugation band (280 m$\mu$) in the spectrum of the ethanol solution is used as the basis of calculation for *cis*-stilbene, since the solvent effect of ethanol on the position of the band is considered not to differ significantly from

that of *n*-heptane on the analogy of the observation in the case of *trans*-stilbene. The results of application of the calculations to *cis*- and *trans*-stilbenes are shown in Table V.

The value of about 28° for the interplanar angles in *cis*-stilbene is in fairly good agreement with the value of about 25° estimated from the scale model[1].

At these values of the interplanar angles the steric repulsion between the two phenyl groups may be almost completely relieved. The difference between the stabilities of the isomers may be considered as the sum of the difference of extra-resonance (stabilization) energy and the difference of steric repulsion (destabilization) energy. If it is assumed that the difference of steric repulsion energy is small in the most probable configurations of the two isomers, the difference of stability is ascribed mainly to the difference of extra-resonance energy. When the value of $-\beta$ is tentatively assumed as 20 kcal./mol., the extra-resonance energy in *trans*-stilbene is evaluated as 14.07 kcal./mol. and that in the *cis*-isomer as 10.60 kcal./mol. The former value agrees fairly well with the value of 15 kcal./mol.[22] estimated from the heat of formation as well as the value of 12.5 kcal./mol.[23] estimated from the heat of hydrogenation[24], although the estimations of resonance energy, in general, do not seem to be entirely free from ambiguity. The difference between the extra-resonance energies of the two isomers is evaluated as about 3.5 kcal./mol. This value is also in satisfactory agreement with the experimental value of the energy difference between the isomers, 3 kcal./mol., estimated from the equilibrium of the thermal isomerization by Kistiakowsky and Smith[25] and by Taylor and Murray[26].

With a view to explaining the fact that the conjugation band of *cis*-stilbene is at a shorter wavelength and is of lower intensity than the corresponding one of the *trans*-isomer, Braude and other[27] have stated as follows: "Assuming that the wavelength shift of 150 Å from *trans*- to *cis*-stilbene is wholly due to steric hindrance, the differential de-stabilization amounts to about 6 kcal./mol., a value remarkably close to the resonance energy of *trans*-stilbene". That is, it seems that they have attempted to correlate the shift with the resonance energy or/and the steric repulsion energy. However, as already mentioned, there is no direct relation between the resonance energy and the electronic transition energy. And further, as mentioned in the earlier parts[6,28] of this series, there is also no direct relation between the steric repulsion energy and the transition energy. It seems evident that Braude and other's attempt was unsuccessful.

The values of $\Delta E_B(-\beta)$ for *trans*- and *cis*-stilbenes are estimated at 1.571 and 1.624, respectively. From these values the B-bands of these compounds are expected to be at 41001 $cm^{-1}$ (243.9 m$\mu$) and 41864 $cm^{-1}$ (238.9 m$\mu$), respectively, by application of the relation between $\Delta E$ and $\nu$ postulated above originally for the A-band. Considering the approximation used, it may be said that the agreement between these expected positions and the observed positions of the B-bands is nearly perfect.

## Experimental

**Measurements of Spectra.** — All the spectra were measured with a Cary recording spectrophotometer Model 14 M-50.

The crystal spectra of *trans*-stilbene were measured by the pressed KCl-disk technique described by Dale[12]. The potassium chloride used had been precipitated from water solution with hydrochloric acid to obtain small particle size and dried at 400 to 450°C for about 6 hr., according to Hales and Kynaston[29]. As an example of the procedures of the preparation of the mixtures, that for the disks on which the spectra shown in Fig. 4 as well as Table III were measured will be described below. About 3.5 mg. of pure *trans*-stilbene was thoroughly ground in an agate mortar with about 200 mg. of potassium chloride. About 10.5 mg. of the mixture was then ground with about 350 mg. of potassium chloride, and pressed under vacuum in the usual manner into transparent disks (a radius, 0.65 cm.). The disk (a) weighed 140.4 mg. (the thickness, about 0.532 mm.), and the disk (b) weighed 111.1 mg. (the thickness, about 0.421 mm.).

**Preparations of *p*-Substituted *trans*-Stilbenes.**— *p*-Methoxy-*trans*-stilbene was prepared by the

22) L. Pauling and J. Sherman, *J. Chem. Phys.*, **1**, 606 (1933).
23) M. M. Kreevoy and R. W. Taft, Jr., *J. Am. Chem. Soc.*, **79**, 4016 (1957).
24) G. W. Wheland, "Resonance in Organic Chemistry", John Wiley & Sons, Inc., New York (1955), p. 80.
25) G. B. Kistiakowsky and W. R. Smith, *J. Am. Chem. Soc.*, **56**, 638 (1934).
26) T. W. J. Taylor and A. R. Murray, *J. Chem. Soc.*, **1938**, 2078.
27) W. Klyne (Ed.), "Progress in Stereochemistry", Vol. 1, Butterworths Scientific Publications, London (1954), p. 131, (E. A. Braude and E. S. Waight).
28) H. Suzuki, This Bulletin, **32**, 1350 (1959).
29) J. L. Hales and W. Kynaston, *Analyst*, **79**, 702 (1954).

Meerwein reaction[30] after the procedure of the preparation of *p*-methoxycarbonyl-*trans*-stilbene described by Fuson and Cooke[31]. The diazonium salt of *p*-anisidine was prepared by adding dropwise a solution of 27 g. of sodium nitrite in 45 ml. of water to a mixture of 150 ml. of 25% hydrochloric acid, 46.2 g. of *p*-anisidine, and 150 g. of ice. Throughout this experiment the reaction mixture was well stirred. An ice bath was placed around the reaction flask and 91.8 g. of crystalline sodium acetate was added. A solution of 55.5 g. of cinnamic acid in 450 ml. of acetone was added and the ice bath was removed. Five minutes later a solution of 20.3 g. of cupric chloride in 45 ml. of water was added dropwise and the mixture was stirred for about two hours at room temperature. After removal of a large amount of acetone, the residue was extracted with benzene. The benzene solution was washed in turn with a dilute solution of sodium carbonate, with dilute hydrochloric acid, and with water, and then dried on calcium chloride. After removal of the solvent, about 33 g. of a dark brown solid product was obtained. Treatment of the crude product with activated charcoal and repeated recrystallization from ethanol gave 23 g. of white crystals of *p*-methoxy-*trans*-stilbene, m.p. 136.8~137.5°C; yield, 29.2%.

*p*-Nitro-*trans*-stilbene was prepared from *p*-nitroaniline by the Meerwein reaction, quite analogously to the synthesis of the methoxy-analogue mentioned above. The purified product, yellow crystals, melted at 156~157°C; yield, about 15%.

## Summary

(1) The quantitative relations between the degree of deviation from the coplanarity of the molecular configuration and the ultraviolet absorption spectrum as well as the quantities such as the extra-resonance energy and the $\pi$-bond orders have been determined for the stilbene-type compounds by calculations based on the simple LCAO molecular orbital method.

(2) The ultraviolet absorption spectra of *trans*-stilbene in the crystalline state, in the solution state, and in the vapor state have been discussed in reference to the spatial configurations of the molecule in the various states. The conjugation band in the vapor spectrum is at considerably shorter wavelengths than that in the solution spectra as well as the crystal spectra, a fact which has been considered as probably indicating that the most likely configuration of the molecule in the vapor state deviates considerably from coplanarity. The magnitude of the red-shift of the conjugation band in the crystal spectra measured by the pressed KCl-disk technique relative to the band in the spectrum of the *n*-heptane solution has been found to be smaller than the value anticipated for the rigid molecule. From this fact it has been inferred that the most probable configuration of *trans*-stilbene in solution does not significantly differ from the one in the crystalline state and is planar or nearly planar.

(3) On the basis of the above inference, the calculations have been applied to *cis*- and *trans*-stilbenes, and the interplanar angles in the most probable configuration of *cis*-stilbene have been estimated at about 28° from the position of the conjugation band, in fairly good agreement with the value estimated from the scale model. The results of the calculations have been discussed.

(4) In addition, the solvent effects of various solvents on the spectra of *trans*-stilbene and its *p*-methoxy- and *p*-nitro-derivatives have been discussed with special reference to the effect of benzene which has been found to cause a large bathochromic displacement of the conjugation band and a remarkable redistribution of intensity among the vibrational bands of the conjugation band of each compound.

The author desires to thank Professor Osamu Simamura for his encouragement, Dr. Yoshiya Kanda of Kyushu University for valuable advice, and also Professor Kengo Shiomi for reading the manuscript and for valuable advice.

*Department of Chemistry*
*College of General Education*
*The University of Tokyo*
*Meguro-ku, Tokyo*

30) H. Meerwein, E. Buchner and K. van Emster, *J. prakt. Chem.*, **152**, 237 (1939); *Chem. Abstr.*, **33**, 6261. See also: F. Bergmann et al., *J. Org. Chem.*, **6**, 134 (1941); **9**, 408, 415 (1944); **12**, 57 (1947).

31) R. C. Fuson and H. G. Cooke, Jr., *J. Am. Chem. Soc.*, **62**, 1180 (1940).

# *Relations between Electronic Absorption Spectra and Spatial Configurations of Conjugated Systems. VI. Triphenylethylene, Tetraphenylethylene and Tolan*

By Hiroshi SUZUKI

(Received August 15, 1959)

The method developed in the preceding part[1] of this series is applied to triphenylethylene, tetraphenylethylene and tolan, and the relation between the ultraviolet absorption spectra and the spatial configurations of these compounds is discussed.

## Triphenylethylene and Tetraphenylethylene

**Spectra.** — The ultraviolet absorption spectra of tri- and tetraphenylethylene in chloroform were formerly measured by Arends[2]. According to the results, the spectra differ only slightly from the spectrum of *trans*-stilbene. Jones[3] explained this spectral similarity as follows. "The three phenyl groups of triphenylethylene and the four phenyl groups of tetraphenyl ethylene can not be accommodated in a strainless planar structure; the strain can be eased either by a small rotation of all of the phenyl groups along their 1, 4-axes, or by a larger displacement of one of the phenyl groups of triphenylethylene or two of the *trans*-related phenyl groups of tetraphenylethylene, leaving two remaining *trans*-phenyl groups in the plane of the ethylenic bond. This second hypothesis leaves the molecule of tetraphenylethylene with a *trans*-stilbene chromophoric system together with two *insulated* phenyl groups, the absorption of which is too feeble to affect the spectrum".

The spectra of these compounds in *n*-heptane and in benzene have been newly measured by the present author. The results are shown in Table I and Fig. 1, in which the spectra of *trans*-stilbene[1] are included for comparison.

The A-band (conjugation band) of triphenylethylene as well as that of tetraphenylethylene has no distinct fine structure in contrast to that of *trans*-stilbene. The B-band, on the other hand, of triphenylethylene has a pattern of fine

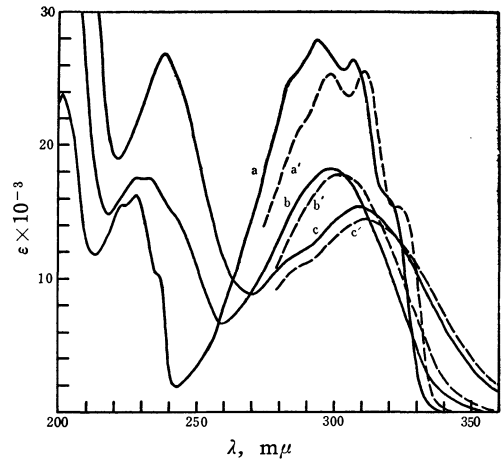



Fig. 1. Ultraviolet absorption spectra of *trans*-stilbene (a, in *n*-heptane; a', in benzene), triphenylethylene (b, in *n*-heptane; *b'*, in benzene), and tetraphenylethylene (c, in *n*-heptane; *c'*, in benzene) (cf. Table I).

structure closely similar to that of *trans*-stilbene.

Assuming that the maxima of the A-bands in the spectra of tri- and tetraphenylethylene in *n*-heptane are to be compared with the most intense maximum, viz. the $\gamma$-band, of fine structure of the A-band of *trans*-stilbene in the same solvent, the position of the maximum of the conjugation band is progressively shifted toward longer wavelengths as the number of phenyl groups in a molecule increases. The B-band is also shifted toward longer wavelengths in the same sequence. On the other hand, while the molecular extinction coefficient of the A-band decreases in the sequence, that of the B-band as well as that of the C-band increases markedly in the sequence.

**Calculation and Discussion.** — When it is assumed that triphenylethylene as well as tetraphenylethylene has a configuration in which the two *trans*-related phenyl groups are coplanar with the plane of the ethylenic bond according to Jones' second

1) H. Suzuki, This Bulletin, **33**, 379 (1960).
2) B. Arends, *Ber.*, **64**, 1936 (1931).
3) R. N. Jones, *J. Am. Chem. Soc.*, **65**, 1818 (1943).

TABLE I. ULTRAVIOLET ABSORPTION SPECTRA OF *trans*-STILBENE, TRIPHENYLETHYLENE AND TETRAPHENYLETHYLENE

| Compound | | A-band | | B-band | | C-band | |
|---|---|---|---|---|---|---|---|
| Solvent | | $\lambda_{max}$, m$\mu$ | $\varepsilon$ | $\lambda_{max}$, m$\mu$ | $\varepsilon$ | $\lambda_{max}$, m$\mu$ | $\varepsilon$ |
| *trans-Stilbene* | | | | | | | |
| *n*-Heptane | $\alpha$ | (320.5) | 16000 | (236) | 10400 | 201.5 | 23900 |
| | $\beta$ | 306.9 | 26500 | 228.5 | 16200 | | |
| | $\gamma$ | 294.1 | 27950 | (222) | 15500 | | |
| Benzene | $\alpha$ | (324.5) | 15400 | | | | |
| | $\beta$ | 311.2 | 25600 | | | | |
| | $\gamma$ | 298.8 | 25340 | | | | |
| *Triphenylethylene* | | | | | | | |
| *n*-Heptane | | 298.5 | 18220 | (242.5) | 14570 | (200) | 40200 |
| | | | | 232.0 | 17580 | | |
| | | | | (228) | 17540 | | |
| Benzene | | 301.8 | 17700 | | | | |
| *Tetraphenylethylene* | | | | | | | |
| *n*-Heptane | | 308.7 | 15300 | 238.5 | 26800 | (203) | 62500 |
| | | (285.8) | 11700 | | | | |
| Benzene | | 311.2 | 14350 | | | | |
| | | (288) | 10900 | | | | |

Wavelengths in parentheses denote inflections.

TABLE II. RESULTS OF CALCULATIONS

| | *trans-Stilbene* | | *Triphenylethylene* | | *Tetraphenylethylene* | |
|---|---|---|---|---|---|---|
| | ($\gamma$) | ($\beta$) | ($\gamma$) | ($\beta$) | ($\gamma$) | ($\beta$) |
| $\lambda_{max}$, m$\mu$ | 294.1 | 306.9 | 298.5 | | 308.7 | |
| $\Delta E_A(-\beta)$ | 1.1423 | | 1.112 | 1.193 | 1.044 | 1.132 |
| $\rho$ | 0.9084 | | 0.946 | 0.849 | 1.032 | 0.922 |
| $\rho'$ | — | | 0.669 | 0.529 | 0.730 | 0.652 |
| $\theta^\circ$ | 0 | | 40 | 52 | 34.5 | 42 |
| $R$, Å | 1.445 | | 1.467 | 1.481 | 1.462 | 1.469 |
| $R.\ E.\ (-\beta)$ | 0.704 | | 0.764 | 0.610 | 0.906 | 0.720 |
| $p_{\alpha-\alpha'}$ | 0.8555 | | 0.845 | 0.873 | 0.820 | 0.852 |
| $p_{\alpha-1}$ | 0.384 | | ($\rho$) 0.400 | 0.359 | 0.310 | 0.277 |
| | | | ($\rho'$) 0.285 | 0.225 | | |
| $\Delta E_B(-\beta)$ | 1.571 | | 1.556 | 1.597 | 1.522 | 1.566 |

hypothesis, it is evident that calculations quite similar to the one for stilbene described in the preceding part of this series can be applied to these compounds.

Alternatively, when it is assumed that in tetraphenylethylene all of the phenyl groups are rotated out of the plane of the ethylenic bond to the same extent as each other according to Jones' first hypothesis, the secular equation for the determination of the molecular orbitals as linear combinations of $2p\pi$ atomic orbitals is factorized into one equation identical in form with the one for stilbene and two equations for benzene, when $\rho'$ is $1/\sqrt{2}\times\rho$, $\rho'\beta$ representing the $\pi-\pi$ resonance integral for each bond connecting a phenyl group to a ethylenic carbon atom.

Similarly, when it is assumed that $\rho'$ is equal to $1/\sqrt{2}\times\rho$ also in triphenylethylene, in which the $\pi-\pi$ exchange integral for each of the bonds connecting two phenyl groups to the same ethylenic carbon atom and that for the bond connecting the other phenyl group to the other ethylenic carbon atom are denoted by $\rho'\beta$ and $\rho\beta$, respectively, the secular equation for this molecule can be factorized into an equation identical in form with the one for stilbene and the equation for benzene.

Therefore, whichever the configurations may be, the calculation based on the same equation as the one for stilbene can be applied to these compounds. Thus, after the procedure described in the preceding part of this series, the values of $\rho$ can be computed from the observed positions of the A-bands.

Since the A-bands of these compounds

are at longer wavelengths than the A-$\gamma$-band of *trans*-stilbene as the reference, the values of $\rho$ for the former compounds should be larger than that for the latter. If the models according to Jones' second hypothesis are chosen, the large values of $\rho$ for tri- and tetraphenylethylene relative to the value for *trans*-stilbene must be explained only by the assumption that the lengths of the bonds linking the coplanar *trans*-related phenyl groups to the ethylenic carbon atoms in tri- and tetraphenylethylene were shorter than the corresponding one in *trans*-stilbene, since the most probable configuration of *trans*-stilbene is considered to be already planar. This is undoubtedly implausible.

The inference that Jones' second hypothesis is implausible seems to be supported also by the following consideration. Thus, as is seen in Table I and Fig. 1, the molecular extinction coefficient of the A-band decreases markedly in the order *trans*-stilbene > triphenylethylene > tetraphenylethylene. If there were any *trans*-stilbene chromophore in these compounds, all these compounds would show the almost identical molecular extinction coefficient at least approximately.

Now, when the alternative models according to Jones' first hypothesis are assumed for the most probable configurations of tri- and tetraphenylethylene, the values of $\rho'$ are obtained from the values of $\rho$, and then, from the values of $\rho'$ the values of $\theta$, $R$ and $p_{\alpha-1}$ can be obtained by the procedure analogous to the one for stilbene in the preceding part of this series. The results of calculations are shown in Table II, in which those for *trans*-stilbene are included for comparison. (The symbols have the same significance as in the preceding part.)

The fact that the calculated value of $\theta$ in triphenylethylene is apparently greater than that in tetraphenylethylene is, needless to say, due to the probably unreal starting assumption that one of the phenyl groups in triphenylethylene is coplanar with the plane of the ethylenic bond. The most probable configuration of triphenylethylene is presumed to be the one in which all of the phenyl groups are rotated out of the plane of the ethylenic bond to certain extents. Therefore, no reliance is to be placed on the values of $\theta$, $R$ and $p_{\alpha-1}$ for this compound, while the values of $R.E.$, $p_{\alpha-\alpha'}$ and $\Delta E_B$ can probably be considered as rough approximations.

The above mentioned calculations are based on the assumption that the maxima of the A-bands of tri- and tetraphenylethylene are to be compared with the $\gamma$-band in the A-band of *trans*-stilbene. However, as is seen in Table I and Fig. 1, while the maxima in the spectra of tri- and tetraphenylethylene in benzene are considered to correspond to the maxima in *n*-heptane, the most intense maximum in the spectrum of *trans*-stilbene in benzene is the $\beta$-band and not the $\gamma$-band as in *n*-heptane. Accordingly the possibility that the $\beta$-band instead of the $\gamma$-band is to be taken as the reference can not perhaps be ruled out. In Table II, the results of the calculations carried out by taking the $\beta$-band as the reference are also shown, being denoted by symbol $\beta$, in addition to those mentioned already, which are denoted by symbol $\gamma$. However, in view of the correlations of these results with some properties of the compounds, results $\gamma$ seems more adequate, and hence subsequently the results of the calculations refer solely to results $\gamma$.

The B-bands are probably due to the allowed transitions from the highest occupied orbitals to the vacant orbitals with the energy of $-\beta$, or from the occupied orbitals with the energy of $+\beta$ to the lowest vacant orbitals, similarly to the case of stilbene. The C-bands are probably due to the allowed transitions from the orbitals with the energy of $+\beta$ to the orbitals with the energy of $-\beta$.

The B-band as well as the C-band increases the intensity in the order *trans*-stilbene < triphenylethylene < tetraphenylethylene, with an increasing number of benzene nuclei. It is interesting that the ratio of the molecular extinction coefficients of the C-bands of these compounds are roughly 1:2:3, in accordance with the ratio of the numbers of the orbitals which are considered to participate in these transitions.

In addition, it is of interest that the magnitude of the red-shift of the conjugation band associated with the change of solvent from *n*-heptane to benzene is appreciably smaller in the cases of tri- and tetraphenylethylene than in the case of *trans*-stilbene as well as some para-substituted *trans*-stilbenes which are presumed to be planar. If the presumption in the preceding part of this series that the shift is due to the special interaction between the $\pi$-orbitals of benzene and

those of the solute molecule is correct, this fact may be related to the nonplanarity of the configurations of tri- and tetraphenylethylene. This subject will be discussed more fully in a later part of this series.

**Correlations between the Spatial Configurations and Some Properties of the Compounds.**—The melting point of tetraphenylethylene is 223~224°C, and is considerably lower than that of its positional isomer, *p,p'*-diphenyl-*trans*-stilbene (about 300°C). In addition, the solubilities of the former compound in usual organic solvents are much greater than those of the latter. These facts are probably due to the nonplanarity of the configuration of tetraphenylethylene. The melting point of triphenylethylene is 68~69°C and markedly lower than that of its positional isomer, *p*-phenyl-*trans*-stilbene (about 220°C), and even than that of *trans*-stilbene (125°C). This fact is probably due to the nonplanarity and the unsymmetrical nature of the configuration of triphenylethylene.

According to Everard and others[4], the exaltation of the molecular refraction ($E[R]_D$) of *trans*-stilbene is +6.6, and that of triphenylethylene is about the same as, or only 0.1 at most less than, that of *trans*-stilbene. This fact may be considered to indicate that the extent of conjugation in triphenylethylene is almost equal to that in *trans*-stilbene, almost in complete accordance with the present conclusion deduced from the ultraviolet absorption spectra.

Next, the relations between the spatial configurations and the reactivities of these compounds will be discussed. In general, steric effects in reactions of olefinic compounds may be divided into the two main types: the steric hindrance to the approach of the reagent to the reaction site and the steric hindrance to resonance. The former may be illustrated by the fact that the rate of bromination of neopentylethylene is smaller than that of *t*-butylethylene[5]. That is, the steric effect of this type retards the reactions in most cases.

Tetraphenylethylene does not add bromine[6,7]. This is probably due to the steric effect of the first type mentioned above. That is, it seems that the phenyl groups rotated out of the plane of the central ethylenic bond inhibit the approach of the reagent to the bond.

According to Leavitt and others[8], the "methyl affinity" is 205 for *trans*-stilbene, 85 for triphenylethylene, and less than 25 for tetraphenylethylene. The "methyl affinity" is considered as a measure of reactivity of compounds to the methyl radical, although it is not clear which atoms of the compounds are attacked. The order of the "methyl affinity" mentioned above appears to be well explained in terms of the steric effect of the first type.

The reaction of olefins with perbenzoic acid in nonpolar solvents gives excellent yields of the corresponding epoxides. It has been presumed that in this reaction perbenzoic acid acts as a "double-bond reagent". According to Lynch and Pausacker[9], the reactivity of the series of phenyl-substituted ethylenes toward perbenzoic acid follows the double-bond orders of the olefinic links calculated by Coulson and Jacobs[10] (i.e. styrene>*trans*-stilbene > triphenylethylene> tetraphenylethylene). However, the calculations by Coulson and Jacobs are unacceptable because they are based on unreal planar molecular models even in the cases of tri- and tetraphenylethylene.

In spite of this, the sequence of the $\pi$-bond orders calculated by Coulson and Jacobs agrees qualitatively with the sequence of the $\pi$-bond orders as well as that of the extra-resonance energies (i.e. the bond localization energies of the ethylenic bonds) calculated here by taking the spatial configurations into account. (The $\pi$-bond orders of the ethylenic bonds calculated by Coulson and Jacobs are: *trans*-stilbene, 0.820; triphenylethylene, 0.752; tetraphenylethylene, 0.685. On the other hand, those calculated by the present author are 0.8555, 0.845 and 0.820, respectively.) Therefore, the sequence of the bond order and hence the sequence of the bond localization energy are presumed to determine at least partly the sequence of the reactivity. However, judging from the fact that the differences of the bond order and of the bond localization energy among these compounds are small, the steric effect of the first type may also be a contributory factor to the reactivity. This subject will be discussed in somewhat

4) K. B. Everard, L. Kumar and L. E. Sutton, *J. Chem. Soc.*, **1951**, 2807.
5) P. W. Robertson, J. K. Heyes and B. E. Swedlund, ibid., **1952**, 1014.
6) H. Bauer, *Ber.*, **37**, 3317 (1904).
7) J. Meisenheimer, *Ann.*, **456**, 139 (1927).
8) F. Leavitt, M. Levy, M. Szwarc and V. Stannett, *J. Am. Chem. Soc.*, **77**, 5493 (1955).
9) B. M. Lynch and K. H. Pausacker, *J. Chem. Soc.*, **1955**, 1525.
10) C. A. Coulson and J. Jacobs, ibid., **1949**, 2805.

TABLE III. ULTRAVIOLET ABSORPTION SPECTRA OF TOLAN

*Solution in n-heptane*

| | A-band | | B-band | | C-band | |
|---|---|---|---|---|---|---|
| | $\lambda_{max}$, m$\mu$ | $\varepsilon$ | $\lambda_{max}$, m$\mu$ | $\varepsilon$ | $\lambda_{max}$, m$\mu$ | $\varepsilon$ |
| $\alpha$ | 297.2 | 27500 | 237.2 | 6930 | 196.5 | 38000 |
| $\beta$ | 288.5 | 20800 | 232.2 | 6520 | | |
| $\gamma$ | 279.9 | 30800 | 222.0 | 16500 | | |
| $\delta$ | 272.7 | 22400 | 217.2 | 18500 | | |
| $\varepsilon$ | 265.3 | 20600 | (212) | 19000 | | |

*Crystals (pressed KCl-disk)*

| | A-band | | | | B-band | | | |
|---|---|---|---|---|---|---|---|---|
| | $\lambda_{max}$, m$\mu$ | $\Delta\lambda$ | $A$ | $\varepsilon$ | $\lambda_{max}$, m$\mu$ | $\Delta\lambda$ | $A$ | $\varepsilon$ |
| $\alpha$ | 301.6 | +4.4 | 0.282 | 1920 | (239.0) | +1.8 | 0.100 | 680 |
| $\beta$ | 292.4 | +3.9 | 0.247 | 1680 | | | | |
| $\gamma$ | 283.3 | +3.4 | 0.350 | 2380 | (223.5) | +1.5 | 0.227 | 1540 |
| $\delta$ | (275.8) | +3.1 | 0.288 | 1960 | (218.5) | +1.3 | 0.264 | 1790 |
| $\varepsilon$ | 268.0 | +2.7 | 0.259 | 1760 | | | | |

Wavelengths in parentheses denote inflections.

$\Delta\lambda$ denotes the magnitude of the wavelength displacement (in m$\mu$) of each band relative to the corresponding band in the spectrum in *n*-heptane.

$A$ denotes the absorbance (optical density).

greater detail in the succeeding part of this series.

In the reactions discussed so far, the reactivity decreases in the order *trans*-stilbene > triphenylethylene > tetraphenylethylene. This order coincides not only with the order in which the steric hindrance to the approach of the reagent to the ethylenic bond increases, but also with the order in which the $\pi$-bond order decreases and hence the bond localization energy increases. Both the factors, steric and electronic, will contribute to the reactivity in the same direction.

On the other hand, in the polarographic reduction the effect of conjugation operates in the opposite direction. Thus, the reduction takes place more easily with an increasing extent of conjugation, and the isolated double bond is not reducible. Maccoll[11] has found that there exists a linear relationship between the reduction potential and the energy required to place one or two electrons in the lowest vacant orbital of the molecule, that is, the energy (in $-\beta$) of the lowest vacant orbital, which is evidently half of $\Delta E_A(-\beta)$ in the present treatment. That is, the reduction potential should be related directly to the transition energy corresponding to the conjugation band. According to Laitinen and Wawzonek[12], in the series of phenylated ethylenes the ease of electro-reduction increases with increasing substitution in the order styrene < 1,1-diphenylethylene < *trans*-stilbene < triphenylethylene < tetraphenylethylene. The mean value of the reduction potential $E$ (in V.) is $-2.1425$ for *trans*-stilbene, $-2.1155$ for triphenylethylene, and $-2.046$ for tetraphenylethylene. On the other hand, the energies of the lowest vacant orbitals (in $-\beta$) of these compounds are calculated to be 0.5712, 0.5558 and 0.5219, respectively. There exists a linear relationship between the reduction potential and the energy of the lowest vacant orbital at least in so far as these compounds are concerned. Tolan has a slightly more negative reduction potential ($-2.195$ V.) than *trans*-stilbene. This fact corresponds only qualitatively to the fact that the conjugation band of tolan is at shorter wavelengths than that of *trans*-stilbene as will be shown in the succeeding section (the energy of the lowest vacant orbital of tolan is calculated to be $-0.635\ \beta$).

*trans*-Stilbene forms a colored complex with 1,3,5-trinitrobenzene. According to the qualitative study by Ley and Rinke[13], when an aromatic compound is mixed with 1,3,5-trinitrobenzene in chloroform (both concentrations, 0.02 mol./l.), the solution colors as follows: *trans*-stilbene, intense yellow; triphenylethylene, yellow; tetraphenylethylene, very feeble yellow; (tetraphenylethane, colorless). The extent of coloration is considered to indicate

11) A. Maccoll, *Nature*, **163**, 178 (1949).

12) H. A. Laitinen and S. Wawzonek, *J. Am. Chem. Soc.*, **64**, 1765 (1942).

13) H. Ley and F. Rinke, *Ber.*, **56**, 771 (1923).

qualitatively the extent of the complex formation. Thus, the extent of the complex formation decreases with an increasing number of phenyl groups in the series of phenylated ethylenes, and accordingly may be related to the spatial configurations of these compounds.

## Tolan

**Spectra.** — The ultraviolet absorption spectra of tolan (diphenylacetylene) are shown in Table III and Fig. 2. The spectra exhibit the conjugation band with well-resolved fine structure at considerably shorter wavelengths than the conjugation band of *trans*-stilbene. The spectrum of tolan in the crystalline state measured

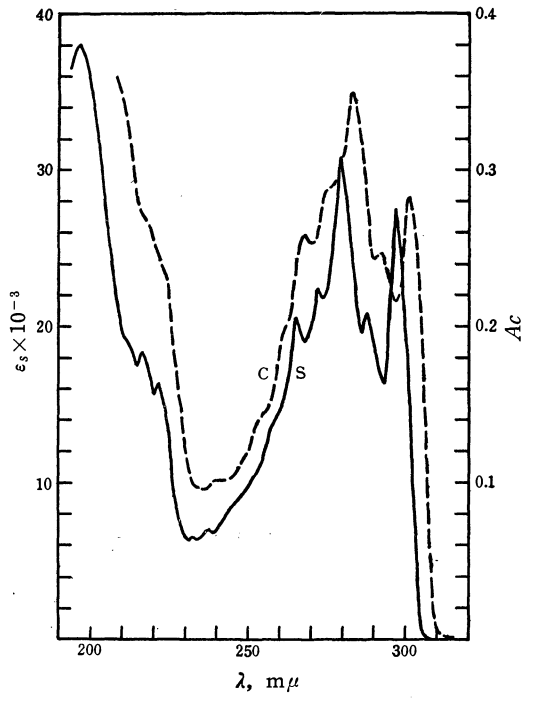



Fig. 2. Ultraviolet absorption spectra of tolan in solution in *n*-heptane (S) and in the crystalline state (the pressed KCl-disk) (C). Note separate ordinates for solution and crystals (cf. Table III).

by the pressed KCl-disk technique resembles the solution spectrum on the whole.

The red-shift of each band associated with the change of the state from the *n*-heptane solution to the crystalline state is seen to increase with almost complete regularity with the wavelength of the band from about 1.3 mμ at 217.2 mμ to about 4.4 mμ at 297.2 mμ, although these shifts are considerably smaller than the values determined by Dale[14] for naphthalene and anthracene (about 2 mμ at 220 mμ to 8 mμ at 300 mμ).

As seen already in the case of *trans*-stilbene in the preceding part of this series, also in the case of tolan, the apparent molecular extinction coefficients in the KCl-disk spectrum are much smaller than the corresponding molecular extinction coefficients in the solution spectrum, the former ones being only about 1/13 of the latter ones.

**Calculation.** — The notation used is as follows: the carbon atoms of the central triple bond, $\alpha$ and $\alpha'$; the carbon atoms attached to $\alpha$ and $\alpha'$, 1 and 1'; the $2p\pi$ atomic orbitals at 1 and 1', $\phi_1$ and $\phi_{1'}$; the two $\pi$-bonds in the triple bond, $(\alpha-\alpha')_x$ and $(\alpha-\alpha')_z$; the corresponding $2p\pi$ atomic orbitals, $\phi_x$, $\phi_{x'}$, $\phi_z$, and $\phi_{z'}$; the $\pi-\pi$ resonance integral for each of $(\alpha-\alpha')_x$ and $(\alpha-\alpha')_z$, $\eta\beta$; the $\pi-\pi$ resonance integral between $\phi_1$ and $\phi_x$ as well as that between $\phi_{1'}$ and $\phi_{x'}$, $\rho_x\beta$; that between $\phi_1$ and $\phi_z$ as well as that between $\phi_{1'}$ and $\phi_{z'}$, $\rho_z\beta$.

The secular equation for the determination of the molecular orbitals of tolan as linear combinations of the $2p\pi$ atomic orbitals can be factorized into the stilbene-type equation and the equation for an isolated $\pi$-bond, either when one of the parameters $\rho_x$ and $\rho_z$ is zero and the other is replaced by $\rho$, or when the parameters are equal to each other and both are replaced by $1/\sqrt{2}\times\rho$. The former requirement means that the two phenyl groups are in conjugation solely with one of the two $\pi$-bonds in the triple bond, leaving the other insulated. The alternative requirement means, needless to say, that the axes of $\phi_1$ and $\phi_{1'}$ form an angle of 45° with the axes of $\phi_x$ and $\phi_{x'}$ as well as the axes of $\phi_z$ and $\phi_{z'}$.

According to the X-ray crystal analysis by Robertson and Woodward[15], tolan in the crystalline state has a planar configuration in which the lengths of the $\alpha-\alpha'$ bond and of the $\alpha-1$ as well as the $\alpha'-1'$ bond are 1.19±0.02 and 1.40±0.02 Å, respectively. The most probable configuration in solution is thought not to differ significantly from the configuration in the crystalline state, in view of the close similarity of the spectra in the two states. From the values of the bond lengths the values of the parameters $\eta$ and $\rho$ are

14) J. Dale, *Acta Chem. Scand.*, **11**, 650 (1957). See also Ref. 1 and Part I of this series: This Bulletin, **32**, 1340 (1959).

15) J. M. Robertson and I. Woodward, *Proc. Roy. Soc.* (*London*), **A164**, 436 (1938).

calculated to be 1.378 and 0.983, respectively, by the usual procedure based on the proportionality between the $\pi-\pi$ resonance integral and the $\pi-\pi$ overlap integral. By solving the secular equation, the following values are obtained: $\Delta E_A(-\beta)$, 1.270; $\Delta E_A(-\gamma)$, 1.303; *R. E.* $(-\beta)$, 0.732; *R. E.* $(-\gamma)$, 0.221; $p_{\alpha-\alpha'}$, 1.868; $p_{\alpha-1}=p_{\alpha'-1'}$, 0.372; $\Delta E_B(-\beta)$, 1.635. (The symbols have the same significance as in the preceding part of this series.)

Whereas the length of the $\alpha-1$ "single" bond in tolan is shorter than the length of the corresponding "single" bond (1.44± 0.02 or 1.45±0.02 Å) in *trans*-stilbene, the $\pi$-bond order of the former is smaller than that of the latter (0.384). This fact is perhaps attributed to the difference of the hybridization of the $\sigma$-orbital at the $\alpha$ carbon atom in these two compounds (tolan, $sp$; stilbene, $sp^2$). Berthier and Pullman[16] reported somewhat different values for the $\pi$-bond orders of these compounds (tolan: $\alpha-\alpha'$, 1.909; $\alpha-1$, 0.307; *trans*-stilbene: $\alpha-\alpha'$, 0.879; $\alpha-1$, 0.352), but the relationship among the values is similar.

By using the linear relation between $\Delta E_A$ and $\nu_A$ postulated for the stilbene-type compounds in the precending part of this series (the longer-wavelength-side reference is the $\gamma$-band in the spectrum of *trans*-stilbene in *n*-heptane and the shorter-wavelength-side reference is the center of gravity of singlets of benzene), the wave number $\nu_A$ corresponding to the value of $\Delta E_A(-\beta)$ for tolan is calculated to be 36086 $cm^{-1}$ (277.1 m$\mu$). This is in good agreement with the observed position (279.9 m$\mu$) of the $\gamma$-band of tolan in *n*-heptane, which is the most intense maximum of fine structure of the conjugation band. In addition, when the $\alpha$-band or the $\beta$-band in the spectrum of *trans*-stilbene in *n*-heptane is taken as the longer-wavelength-side reference, the value of $\nu_A$ is computed to be 33702 $cm^{-1}$ (296.7 m$\mu$) or 34879 $cm^{-1}$ (286.7 m$\mu$), correspondingly, in agreement with the observed positions of the $\alpha$-band (297.2 m$\mu$) and the $\beta$-band (288.5 m$\mu$) in the spectrum of tolan in *n*-heptane. The good agreement between the calculated wavelengths and the observed ones of the bands seems to justify the postulation of the linear relation between $\Delta E_A$ and $\nu_A$.

16) G. Berthier and B. Pullman, *Compt. rend.*, **228**, 397 (1949).

## Experimental

**Measurements of Spectra.**—All the spectra were measured with a Cary recording spectrophotometer Model 14 M-50.

The crystal spectrum of tolan was measured by the pressed KCl-disk technique quite analogously to the case of *trans*-stilbene in the preceding part of this series. About 3 mg. of tolan was thoroughly ground with about 200 mg. of potassium chloride and then about 10 mg. of the mixture was ground with about 350 mg. of potassium chloride and pressed. The disk used weighed 84.7 mg. (the thickness, about 0.321 mm.).

**Materials.**—Triphenylethylene was prepared by dehydration of 1,1,2-triphenylethanol obtained by the reaction of benzophenone with benzyl magnesium chloride[17]. From 27.3 g. (0.15 mol.) of benzophenone, 24.3 g. (0.095 mol.) of triphenylethylene, white crystals melting at 68~69°C, were obtained after recrystallization from 95% ethanol (63.3% of the theoretical amount).

Tetraphenylethylene was prepared by heating diphenyldichloromethane (benzophenone dichloride) with powdered copper in anhydrous benzene[18]. Diphenyldichloromethane was prepared from benzophenone and phosphorus pentachloride[19]. From 9.1 g. (0.05 mol.) of benzophenone, 4.7 g. (0.014 mol., 56.5% of the theoretical amount) of tetraphenylethylene, almost colorless crystals melting at 223~224°C, were obtained after recrystallization from a 1 : 1 by volume mixture of absolute ethanol and benzene.

Tolan was prepared, according to the directions of Schlenk and Bergmann[20], by oxidizing benzil dihydrazone with mercuric oxide. Benzil was prepared by oxidation of benzoin with nitric acid[21]. The yield of pure tolan, colorless crystals melting at 62°C, from 47 g. (0.219 mol.) of benzil was 16.4 g. (0.092 mol., 42% of the theoretical amount) after repeated recrystallization from ethanol.

## Summary

The most probable configuration of triphenylethylene as well as that of tetraphenylethylene has been inferred to be the one in which all of the phenyl groups are rotated out of the plane of the ethylenic bond, on the basis of the analysis of the ultraviolet absorption spectra by application of the method based on the simple LCAO molecular orbital method described in the preceding part of this series. Some physical and chemical properties of these compounds have been

17) L. F. Fieser (Editor-in-Chief), "Organic Syntheses", Vol. XVII, John Wiley & Sons, Inc., New York (1937), p. 89.
18) R. S. Schreiber (Editor-in-Chief), ibid., Vol. 31 (1951), p. 104.
19) C. S. Marvel (Editor-in-Chief), ibid., Vol. XI (1931), p. 95.
20) W. Schlenk and E. Bergmann, *Ann.*, **463**, 76 (1928).
21) R. Adams (Editor-in-Chief), "Organic Syntheses", Vol. I, John Wiley & Sons. Inc., New York (1921), p. 25.

discussed with reference to the spatial configurations.

The method has been applied also to tolan (diphenylacetylene), and it has been shown that the calculated wavelengths of the bands agree fairly well with the observed ones.

In addition, it has been shown that the spectrum of tolan in the crystalline state measured by the pressed KCl-disk technique resembles the spectrum of the solution in *n*-heptane on the whole, and that the red-shift of each band associated with the change of the state from the *n*-heptane solution to the crystalline state increases with almost complete regularity with the wavelength of the band from about 1.3 mμ at 217.2 mμ to about 4.4 mμ at 297.2 mμ, the shifts observed here being appreciably smaller than the analogous shifts observed by Dale in the spectra of naphthalene and anthracene.

The author thanks Professor Kengo Shiomi for reading the manuscript and for advice.

*Department of Chemistry*
*College of General Education*
*The University of Tokyo*
*Meguro-ku, Tokyo*

# *Relations between Electronic Absorption Spectra and Spatial Configurations of Conjugated Systems. VII. α-Substituted and α,α'-Disubstituted Stilbenes*

By Hiroshi SUZUKI

(Received August 15, 1959)

The method developed in Part V[1] of this series is applied to α- and α,α'-substituted stilbenes, some of which were preliminarily treated in an earlier paper[2], and the relations between the ultraviolet absorption spectra and the spatial configurations of these compounds are discussed. Further, the relations between the spatial configurations and some physical and chemical properties of these compounds are discussed in detail with special reference to α,α'-dimethylstilbene.

**Ultraviolet Absorption Spectra.**—The ultraviolet absorption spectra of α-alkyl- and α,α'-dialkylstilbenes in ethanol were reported previously[2]. The spectra of some of these compounds as well as α,α'-dihalostilbenes in *n*-heptane have newly been measured. These are shown in Figs. 1 and 2. In Table I, the data of the spectra are summarized.

The spectra of the alkylated stilbenes in *n*-heptane do not differ significantly from the corresponding spectra in ethanol. Thus, the following generalizations, some of which were not explicitly stated in the earlier paper, can be deduced. (1) The conjugation band is shifted toward shorter wavelengths and is reduced in intensity with increasing number and increasing size of substituents at the ethylenic

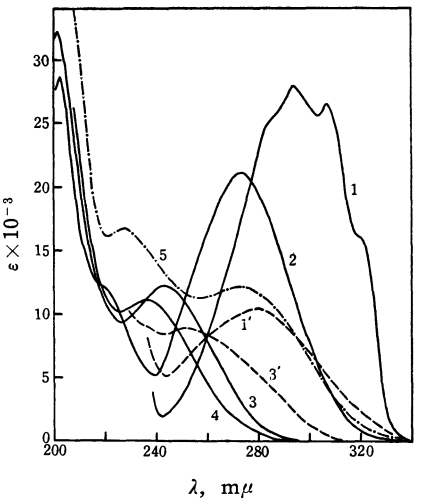



Fig. 1. Ultraviolet absorption spectra of stilbenes in *n*-heptane: 1, *trans*-stilbene; 1', *cis*-stilbene (in ethanol); 2, *trans*-α-methylstilbene; 3, *trans*-α,α'-dimethylstilbene; 3', *cis*-α,α'-dimethylstilbene; 4, *trans*-α,α'-diethylstilbene; 5, methyltriphenylethylene.

1) H. Suzuki, This Bulletin, **33**, 379 (1960).
2) H. Suzuki, ibid., **25**, 145 (1952).

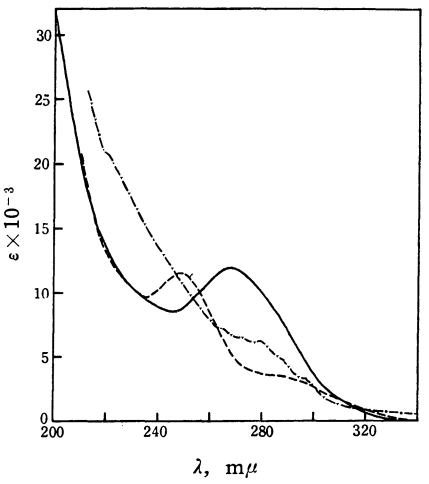



Fig. 2. Ultraviolet absorption spectra of *trans*-α,α'-dihalostilbenes in *n*-heptane: ——, dichlorostilbene; ------, dibromostilbene; —·—·—, diiodostilbene.

carbon atoms in each of the *trans* and the *cis* series. (2) The conjugation band of a *trans* isomer is invariably more intense than that of the corresponding *cis* isomer. (3) With stilbene as well as α-methylstilbene, the conjugation band of the *trans* isomer is at longer wavelengths than that of the *cis* isomer. On the other hand, with α,α'-dimethyl- as well as α,α'-diethylstilbene, the conjugation band of the *trans* isomer is at shorter wavelengths than that of the *cis* isomer. (4) The conjugation bands of these stilbene derivatives have, similarly to that of *cis*-stilbene, no fine structure, in contrast to that of *trans*-stilbene.

Also with *trans*-α,α'-dihalostilbenes, the conjugation band is structureless, and is shifted toward shorter wavelengths as the substituents become larger. *trans*-α,α'-Diiodostilbene in *n*-heptane dissociates

Table I. Ultraviolet absorption maxima

| Stilbene | Solvent | *trans* λ, mμ | *trans* ε | Ref. | *cis* λ, mμ | *cis* ε | Ref. |
|---|---|---|---|---|---|---|---|
| Unsubstituted | H | 294.1* | 27950 | 1) | | | |
| | | (B 228.5* | 16200) | | | | |
| | | (C 201.5 | 23900) | | | | |
| | E | 294.5* | 27850 | 1) | 280 | 10450 | a) |
| | | (B 228.8* | 16400) | | (B 224 | 24400) | |
| | | (C 201.0 | 23800) | | | | |
| α-Methyl- | H | 273.5 | 21100 | b) | | | |
| | | (B (217) | 12530) | | | | |
| | | (C 202.3 | 28700) | | | | |
| | E | 272 | 21000 | 2) | 267 | 9340 | 2) |
| α,α'-Dimethyl- | H | 243.3 | 12270 | b) | 252.0 | 8880 | b) |
| | | (C (201.3) | 32250) | | | | |
| | E | 243.5 | 12260 | 2) | 252 | 8780 | 2) |
| α-Methyl-α'-ethyl- | E | 240 | 11950 | 2) | | | |
| α,α'-Diethyl- | H | 236.6 | 11090 | b) | | | |
| | E | 237.5 | 11020 | 2) | 244 | 7740 | 2) |
| α-Methyl-α'-phenyl- | H | 274.5 | 12200 | b) | | | |
| | | (B 227.5 | 16800) | | | | |
| | E | 275 | 9860 | 2) | | | |
| | | (B 226 | 13720) | | | | |
| α,α'-Dichloro- | H | 268.0 | 12000 | b) | | | |
| α,α'-Dibromo- | H | 248.5 | 11570 | b) | | | |
| α,α'-Diiodo- | H | (220.5) | 20800** | b) | | | |

Solvent: H, *n*-heptane; E, ethanol.

Symbols B and C in parentheses denote the B-band and the C-band, respectively. All the maxima other than the B- and C-bands refer to the conjugation bands (viz. A-bands). Wavelengths in parentheses denote inflections.

* The most intense maximum of fine structure.

** The apparent value. The accurate molecular extinction coefficient could not be determined, because this compound dissociates partly in this solvent into tolan and iodine.

a) R.N. Beale and E.M.F. Roe, *J. Chem. Soc.*, **1953**, 2755.

b) The present work.

TABLE II. RESULTS OF CALCULATION

| Stilbene | Solvent | $\lambda_A$ | $\Delta E_A$ | $\rho$ | $\theta°$ | $R$ | $R.E.$ |
|---|---|---|---|---|---|---|---|
| | | mμ | $-\beta$ | | | Å | $-\beta$ |
| *trans*-α-Methyl- | H | 273.5 | 1.299 | 0.730 | 34.5 | 1.462 | 0.457 |
| *cis*-α-Methyl- | E | 267 | 1.354 | 0.671 | 40 | 1.467 | 0.387 |
| *trans*-α, α'-Dimethyl- | H | 243.3 | 1.577 | 0.446 | 58 | 1.490 | 0.173 |
| *cis*-α, α'-Dimethyl- | H | 252.0 | 1.490 | 0.531 | 51.5 | 1.481 | 0.243 |
| *trans*-α-Methyl-α'-ethyl- | E | 240 | 1.612 | 0.412 | 60.5 | 1.493 | 0.146 |
| *trans*-α, α'-Diethyl- | H | 236.6 | 1.649 | 0.378 | 63 | 1.497 | 0.124 |
| *cis*-α, α'-Diethyl- | E | 244 | 1.570 | 0.453 | 57.5 | 1.489 | 0.178 |
| *trans*-α, α'-Dichloro- | H | 268.0 | 1.345 | 0.680 | 39 | 1.467 | 0.397 |
| *trans*-α, α'-Dibromo- | H | 248.5 | 1.525 | 0.497 | 54.5 | 1.485 | 0.212 |
| *trans*-α, α'-Diiodo- | H | 220.5 | 1.838 | 0.200 | 75.7 | 1.517 | 0.034 |

gradually into tolan and iodine, and consequently the absorption due to tolan is detected in the spectrum (cf. Fig. 2 with Fig. 2 in the preceding part[3] of this series). The inflection at near 220.5 mμ probably indicates the vestigial conjugation band of *trans*-α, α'-diiodostilbene.

**Application of Calculation.**—In the application of the method developed in Part V of this series to these stilbene derivatives, the data of the spectra of *n*-heptane solutions newly measured are used. For the compounds, the spectra of which in *n*-heptane have not yet been measured, the data of the spectra of ethanol solutions are used, since the positions of the bands may be considered not to vary significantly in either of the solvents (cf. Table I and also Parts I[4] and V of this series).

The effects of the substituents upon the spectra must include not only the steric hypsochromic effect due to the steric interferences between the substituents and the phenyl groups but also the electronic (probably bathochromic) effect of the substituents (cf. Part II[5] of this series). However, in view of the fact that the substituents in the compounds treated here are at the positions of cross-conjugation to the conjugated system of the stilbene skeleton, this possible electronic effect is considered to be probably very small compared with the steric hypsochromic effect, especially in the cases of the alkyl substituents, and therefore, is ignored in the present treatment.

In the cases of the halogen substituents, the electronic effect of the lone pair electrons of the halogen atoms may be relatively large campared with the electronic (probably hyperconjugation) effect of the alkyl substituents, and perhaps it should not be ignored. Nevertheless, the possible electronic effect of all the substituents is ignored, for simplification, in the present treatment. That is, it is assumed that the position of the conjugation band is determined solely by the spatial configuration of the stilbene skeleton.

The results of the calculations are shown in Table II. The notation used here is the same as in Part V of this series.

In α-methylstilbene as well as α-methyl-α'-ethylstilbene, the positions of the two phenyl groups are not equivalent, and therefore, their angles of twist must differ from each other. In spite of this, the results for these compounds, obtained on the basis of the assumption that the angles of twist of the two phenyl groups are equal, are also shown for comparison.

It is to be noted that the calculated values of the angle of twist $\theta$ (interplanar angle) in Table II are possibly rather smaller than the actual values because of the neglect of the electronic effect of the substituents mentioned above. In addition, when the β-band instead of the γ-band of *trans*-stilbene is taken as the "longer-wavelength-side reference", the calculated values of $\theta$ will evidently become greater than those in Table II.

## Discussion

As will be expected, Table II shows that the calculated interplanar angle becomes larger with the increasing number and size of substituents. It is of interest that the change of the substituents from methyl groups to ethyl groups affects only rather slightly the position of the conjugation band and consequently the interplanar angle. A somewhat similar phenomenon has been seen in the comparison between *o*-methyl- and *o*-ethylbiphenyl[5]. On the

3) H. Suzuki, ibid., **33**, 389 (1960).
4) H. Suzuki, ibid., **32**, 1340 (1959).
5) H. Suzuki, ibid., **32**, 1350 (1959).

other hand, the replacement of the methyl group in β-methylcinnamic acid by an ethyl group has a greater steric consequence. According to Takahasi[6], the wavelengths (mμ) of the conjugation bands and the molecular extinction coefficients (in parentheses) of the bands of cinnamic acid and its β-alkyl derivatives in 94% ethanol are as follows: cinnamic acid, 273 (22000); β-methylcinnamic acid, 260 (15000); β-ethylcinnamic acid, 244 (10000).

The conjugation band of methyltriphenylethylene (1, 1, 2-triphenylpropene) is at a considerably shorter wavelength than that of triphenylethylene (cf. the preceding part of this series) and coincides in position almost completely with that of *trans*-α-methylstilbene. From this fact, it would be inferred that the most probable configuration of methyltriphenylethylene might be the one in which the phenyl group at the *trans*-position to the methyl group was completely rotated out of the plane of the ethylenic bond, or in other words, was insulated, leaving the two remaining *trans*-related phenyl groups in the configuration analogous to the most probable configuration of *trans*-α-methylstilbene. However, the fact that the intensity of the conjugation band of methyltriphenylethylene is much smaller than that of *trans*-α-methylstilbene suggests that this inference is unlikely. This situation is very similar to that observed in the comparison between the spectra of triphenylethylene and of *trans*-stilbene[3].

As mentioned already, it is especially noteworthy that the conjugation band of *trans*-α, α'-dimethylstilbene as well as its diethyl a analogue is at a shorter wavelength than that of the *cis* isomer, contrary to the generally accepted view that *trans* isomers of conjugated compounds should exhibit the conjugation bands at longer wavelengths than the corresponding *cis* isomers. A similar phenomenon has been observed by Nagai and Simamura[7] with some *p*, *p*'-disubstituted α, α'-dimethylstilbenes. These facts are considered to indicate that with these compounds the *trans* isomers are less conjugated than the corresponding *cis* isomers. In fact, as is seen in Table II, the calculated interplanar angles in the *trans* isomers of α, α'-dimethylstilbene and its diethyl analogue are larger than those of the corresponding *cis* isomers, and the calculated extra-resonance energies of the *trans* isomers are smaller than those of the *cis* isomers. This conclusion deduced here from the absorption spectra seems to be supported by some pieces of information on the properties of these compounds such as the reactivities, the nuclear magnetic resonance spectra, and the exaltations of molecular refraction. Accordingly, the relations between the spatial configurations and some physical and chemical properties of the stilbenes will be discussed in a later section with special emphasis on those for *trans*- and *cis*-α, α'-dimethylstilbenes.

**Correlation of the Calculated Interplanar Angles with the Values Estimated from Scale Models.**—That the calculated interplanar angle (58°) for *trans*-α, α'-dimethylstilbene agrees fairly well with the value estimated from scale models has been described in the earlier paper[2]. Thus, according as one assumes a twisted structure for this compound in which the ortho hydrogen atom of each phenyl group just touches the methyl group attached to the same ethylenic carbon atom as the phenyl group or a structure in which that hydrogen atom just touches the other methyl group, the interplanar angle is estimated at 60° or 56°, in good agreement with the calculated value.

For *trans*-α, α'-dibromostilbene, the interplanar angle is estimated at 48° or 51.5° from analogous models in which the interference radius of a bromine atom is 1.95 Å[8] (van der Waals radius) and the length of a C-Br bond is 1.91 Å[8] (the length of an Alkyl-Br bond). The actual length of the C-Br bond may be shortened more or less from the above normal value by interaction between the bromine atom and the ethylenic bond[9]. When the possible shortening of the bond is taken into account, the interplanar angle estimated from models will become slightly larger. The agreement of the calculated value (54.5°) of the interplanar angle with the value estimated from scale models is not so good as in the case of the dimethyl analogue; still it may be said to be fairly good.

6) M. Takahasi, ibid., 31, 756 (1958).
7) Y. Nagai and O. Simamura, presented at the 11th Annual Meeting of the Chemical Society of Japan, Tokyo, April, 1958.
8) L. Pauling, "The Nature of the Chemical Bond", Cornell University Press, Ithaca, N. Y. (1940).
9) (a) H. de Laszlo, *Proc. Roy. Soc.* (*London*), **A146**, 690 (1934). (b) J. A. C. Hagill, I. E. Coop and L. E. Sutton, *Trans. Faraday Soc.*, **34**, 1518 (1938).

For the dichloro analogue, the interplanar angle is estimated at 43° or 48° from the analogous medels in which the interference radius of a chlorine atom is 1.80 Å[8] (van der Waals radius) and the length of a C–Cl bond is 1.77 Å[8] (the length of a normal Alkyl-Cl bond). The agreement of the calculated interplanar angle (39°) with the value estimated from models is worse than in the cases of the dimethyl and the dibromo analogues. The discrepancy is probably due mainly to the effect of the interaction of the lone pair electrons of the chlorine atoms with the ethylenic bond on the position of the conjugation band, which has been ignored in the present calculations. The interaction may affect not only the estimation of the interplanar angle from scale models by the contraction of the C–Cl bond (the length of the C–Cl bond in chloroethylene, for example, is 1.69 Å[10]), but also may exert a bathochromic effect on the conjugation band. Thus, if it were not for this effect, this compound would exhibit the conjugation band at a shorter wavelength than the observed position, and consequently the calculated interplanar angle would become larger than the value in Table II.

**Correlation of Some Properties with the Spatial Configurations.** — *Exaltation of molecular refraction.*—As Mulliken[11] stated for the case of alkylstyrenes, the exaltation of molecular refraction can be considered as a measure of the extent of conjugation. Some relevant data selected from the data by Auwers[12,13] are shown in Table III.

The exaltation is markedly greater in *trans*-stilbene than in the *cis* isomer. On the other hand, in contrast to the case of stilbene, the exaltation is, though slightly, smaller in *trans*-$\alpha,\alpha'$-dimethylstilbene than in the *cis* isomer. This reversal is similar to what happens to the electronic absorption spectra.

*Nuclear magnetic resonance.* — Curtin and others[14] measured the proton magnetic resonance spectra of stilbene, azobenzene, and diphenylcycloalkanes, and found that the positions of the aromatic proton resonance and those of the $\alpha$-protons provide a new method of assignment of configuration of such compounds.

According to the results of the measurements by them, the $\alpha$-hydrogens of *cis*-stilbene give rise to resonance at a higher magnetic field than those of the *trans* isomer, indicating that the $\alpha$-hydrogens of the *cis* isomer are more shielded than those of the *trans* isomer.

Recently, we measured the proton magnetic resonances of *trans*- and *cis*-$\alpha,\alpha'$-dimethylstilbenes and related compounds[15]. A relevant part of the results are shown in Table IV, together with the data by

TABLE III

| Compound | $EM_\alpha$ | $EM_D$ | $E\Sigma_\alpha$ | $E\Sigma_D$ | Ref. |
|---|---|---|---|---|---|
| *trans*-Stilbene | | | +3.24 | +3.57 | 12, 13) |
| *cis*-Stilbene | +2.26 | +2.74 | +1.26 | +1.52 | 13) |
| *trans*-$\alpha$-Methylstilbene | | | +2.04 | +2.17 | 12) |
| *trans*-$\alpha,\alpha'$-Dimethylstilbene | +2.10 | +2.22 | +1.01 | +1.07 | 13) |
| *cis*-$\alpha,\alpha'$-Dimethylstilbene | +2.12 | +2.27 | +1.02 | +1.09 | 13) |
| Triphenylethylene | +5.17 | +5.68 | +2.02 | +2.22 | 12) |
| Methyltriphenylethylene | +3.64 | +3.98 | +1.35 | +1.47 | 12) |

$EM_\alpha$ and $EM_D$ are exaltations of molecular refraction.
$E\Sigma_\alpha$ and $E\Sigma_D$ are specific exaltations.

TABLE IV. CHEMICAL SHIFTS OF PROTON MAGNETIC RESONANCE (in c.p.s.)

| Compound | Proton | Solvent | *trans* | *cis* | | Standard |
|---|---|---|---|---|---|---|
| Stilbene | $\alpha$-H | CT | −90 | −70 | (at 40 Mc.) | M |
| $\alpha,\alpha'$-Dimethylstilbene | $CH_3$ | B | − 8 | −19 | (at 27 Mc.) | Cy |
| $\alpha,\alpha'$-Diethylstilbene | $CH_2$ | B | −22 | −25 | (at 27 Mc.) | Cy |
| | $CH_3$ | B | +13 | + 5 | (at 27 Mc.) | Cy |

Solvent: CT, carbon tetrachloride; B, benzene.
Standard substance: M, an external methylene chloride; Cy, cyclohexane.

10) L. O. Brockway, J. Y. Beach and L. Pauling, *J. Am. Chem. Soc.*, **57**, 2693 (1935).
11) R. S. Mulliken, *J. Chem. Phys.*, **7**, 356 (1939).
12) K. v. Auwers, *Ber.*, **62**, 693 (1929).
13) K. v. Auwers, *Ann.*, **499**, 123 (1932).
14) D. Y. Curtin, H. Gruen and B. A. Shoulders, *Chem. & Ind.*, 1205 (1958).
15) M. Katayama, S. Fujiwara, H. Suzuki, Y. Nagai, and O. Simamura, presented at the 12th Annual Meeting of the Chemical Society of Japan, Kyoto, April, 1959.

Curtin and others for *trans*- and *cis*-stilbenes.

In contrast to the $\alpha$-hydrogens of *trans*- and *cis*-stilbenes, the hydrogens of the $\alpha$-methyl groups of *cis*-$\alpha,\alpha'$-dimethylstilbene and of the $\alpha$-ethyl groups of *cis*-$\alpha,\alpha'$-diethylstilbene give rise to resonance at lower fields than the corresponding hydrogens of the *trans* isomers. That is, the hydrogens are less shielded in the *cis* isomers than in the corresponding *trans* isomers.

Katayama calculated the magnetic fields due to the circulating $\pi$-electrons' currents for these compounds by making an allowance for the spatial configurations, and found that the calculated differences of the magnetic fields for the *trans* isomers and for the *cis* isomers are smaller than the observed ones. Accordingly, the observed differences may be partly due to the differences of the $\pi$-electron densities at carbon atoms and of the electron densities at the hydrogen atoms concerned, which is, in turn, probably due to the differences of the extent of conjugation as well as hyperconjugation. That is, it appears that the conjugation in the $\pi$-electron systems affects the chemical shift of the nuclear magnetic resonance. At any rate, it is of interest that the observations on the proton resonance mentioned above are considered to correspond to the fact that the sequence of the positions of the conjugation bands of *trans* and *cis* isomers in the case of stilbene is reversed in the cases of $\alpha,\alpha'$-dimethyl- and $\alpha,\alpha'$-diethylstilbene.

*Thermal isomerization.* — As mentioned already in Part V of this series, *trans*-stilbene is thermodynamically much more stable than the *cis* isomer. Thus, according to Taylor and Murray[16], the equilibrium mixture of the *cis-trans* thermal isomerization at 200°C consists of 96% of the *trans* isomer and 4% of the *cis* isomer. In addition, according to Kistiakowsky and Smith[17], the equilibrium mixture at 320~340°C contains 92~94% of the *trans* isomer. The heat of the thermal *cis-trans* isomerization ($-\Delta H$) is about 3 kcal./mol. (In addition, the heat of isomerization at 25°C has been estimated at $7.0 \pm 0.4$ kcal./mol. for *p*-nitrostilbene and at $4.6 \pm 0.3$ kcal./mol. for *p,p'*-dinitrostilbene from the heats of combustion[18]. Also with these compounds, the *trans* isomers are, of course, much more stable than the *cis* isomers.)

The difference of stability between the isomers is by far smaller in the case of $\alpha,\alpha'$-dimethylstilbene than in the case of stilbene. Thus, according to the previous study by Simamura and the present author[2,19], the equilibrium mixture yielded by heating either *trans*- or *cis*-$\alpha,\alpha'$-dimethylstilbene with a little concentrated sulfuric acid for 20 hr. at 210°C contained the *trans* and the *cis* isomers in the ratio of the amounts 55 : 45 or 60 : 40.

The fact that the *trans* isomer is still, though slightly, also more stable in this case than the *cis* isomer would appear, at first sight, to be rather surprising, being contrary to the anticipation from the absorption spectra. As discussed already in the previous paper[2], however, this fact is understandable if one considers that the steric repulsion between the two methyl groups in the *cis* isomer, which can not be reduced by the rotation of the phenyl groups, is also an important contributory factor to the stability besides the resonance stabilization.

According to Taylor and Murray[16], the equilibrium mixture of the *cis-trans* isomerization of $\alpha,\alpha'$-dichlorostilbene at 220~230°C contains 75% of the *cis* isomer. The large stability of the *cis* isomer relative to the *trans* isomer may be partly due to the attractive (London) force between the chlorine atoms in the *cis* isomer as Taylor and Murray stated, and may be partly due to the fact that the difference of the resonance stabilization energy between the two isomers is considered, on the analogy of the case of $\alpha,\alpha'$-dimethylstilbene, to be not so great as in the case of stilbene, the resonance being considerably suppressed in both isomers by the steric factors.

*Reaction with bromine.*—As seen in Tables IV and V in Part V of this series and Table II in the present paper, the extra-resonance energy *R.E.*, i.e. the bond localization energy of the central ethylenic bond, decreases and the $\pi$-bond order of the ethylenic bond $p_{\alpha-\alpha'}$ increases, with decreasing $\rho$, and hence with the increasing interplanar angle. In Table V, the calculated values of *R.E.* and $p_{\alpha-\alpha'}$ for

16) T. W. J. Taylor and A. R. Murray, *J. Chem. Soc.*, **1938**, 2078.
17) G. B. Kistiakowsky and W. R. Smith, *J. Am. Chem. Soc.*, **56**, 638 (1934).
18) C. M. Anderson, L. G. Cole and E. C. Gilbert, ibid., **72**, 1263 (1950).
19) O. Simamura and H. Suzuki, This Bulletin, **27**, 231 (1954).

TABLE V

| Entry No. | Compound | $\rho$ | $R.E.$ $(-\beta)$ | $p_{\alpha-\alpha'}$ |
|---|---|---|---|---|
| 1 | Tetraphenylethylene | 1.032 | 0.906 | 0.820 |
| 2 | Triphenylethylene | 0.946 | 0.764 | 0.845 |
| 3 | *trans*-Stilbene | 0.908 | 0.704 | 0.856 |
| 4 | *cis*-Stilbene | 0.787 | 0.530 | 0.890 |
| 5 | *trans*-$\alpha$-Methylstilbene | 0.730 | 0.457 | 0.904 |
| 6 | *cis*-$\alpha,\alpha'$-Dimethylstilbene | 0.531 | 0.243 | 0.948 |
| 7 | *trans*-$\alpha,\alpha'$-Dimethylstilbene | 0.446 | 0.173 | 0.963 |
| 8 | (Unconjugated olefin) | 0 | 0 | 1 |

*trans*- and *cis*-stilbenes and some related compounds are summarized. The variation of the bond localization energy as well as of the $\pi$-bond order of the ethylenic bond should affect the rates of the reactions of these compounds with the "double-bond reagents"[20]. Thus, the decrease in the bond localization energy as well as the increase in the $\pi$-bond order should facilitate such reactions. This effect is subsequently referred to as the bond localization effect.

On the other hand, the substituents themselves or the phenyl groups rotated out of the plane of the ethylenic bond owing to steric necessities may hinder the approach of the reagent to the reaction site in such reactions. This effect, being purely steric in nature, is referred to as the steric (hindrance) effect in a narrow sense. This effect should, of course, retard such reactions. For example, the fact that $\alpha$-*t*-butylstilbene does not add bromine[21] in contrast to $\alpha$-methyl[19] and $\alpha$-ethyl analogues[22] which add bromine is probably due to this effect.

In addition to the effects mentioned above, the substituents may, of course, exert an electronic effect (e.g. the inductive, mesomeric, or hyperconjugation effect) on the reactions. Therefore, in consideration of the reactions of these stilbene-type compounds, all the effects of the above three types are to be taken into account.

Simamura and the present author found in the earlier study[19] on the action of bromine on stilbenes that *trans*-$\alpha$-methyl stilbene adds bromine much faster than *trans*-stilbene. The extreme slowness of the reaction of *trans*-stilbene with bromine is partly due to the retarding effect of atmospheric oxygen, and when a little catechol is added, the rate increases appreciably. On the other hand, the fastness of the reaction of *trans*-$\alpha$-methylstilbene is ascribed partly to the accelerating effect of a little hydrogen bromide formed as a by-product by substitution, which starts the chain addition reaction of bromine by producing, in co-operation with oxygen, bromine atoms, and this effect is considered to be also suppressed by catechol. However, even when a little catechol is added, the rate of the reaction of *trans*-$\alpha$-methylstilbene with bromine is still much greater than that of *trans*-stilbene[23]. This difference of the rates may be partly due to the electron-donating effect of the methyl group, partly to the unsymmetrical nature of the electronic state of the ethylenic bond in methylstilbene, and partly (perhaps mainly) to the bond localization effect due to the nonplanarity of the configuration of methylstilbene.

The $\pi$-bond order of the ethylenic bond in *trans*-$\alpha,\alpha'$-dimethylstilbene is greater than that in methylstilbene, so that dimethylstilbene would be expected to add bromine more rapidly than methylstilbene. In fact, however, the action of bromine on dimethylstilbene leads to the facile substitution at the methyl groups rather than the addition at the ethylenic bond[19]. This fact seems to be attributable to the steric effect in a narrow sense or the unstability of dimethylstilbene dibromide as the possible intermediate due to the steric strain in the molecule caused by the crowding of bulky groups.

Methyltriphenylethylene does not add bromine, but is substituted at the methyl group only slowly[19]. The absence of the addition is probably due to the steric hindrance effect in a narrow sense.

*Reaction with hydrogen bromide and oxygen.* —It was reported previously that the steric effect plays a predominant role in the

20) G. M. Badger, "The Structures & Reactions of the Aromatic Compounds", The University Press, Cambridge (1954).
21) Ramart-Lucas, *Ann. Chim.*, [8] **30**, 394 (1913).
22) A. Klages and S. Heilmann, *Ber.*, **37**, 1447 (1904).
23) H. Suzuki, unpublished.

TABLE VI. EPOXIDATION OF OLEFINS WITH PERBENZOIC ACID IN BENZENE

| Entry No. | Olefin | $10^4 k$ | $\Delta H^\ddagger$ | $\Delta F^\ddagger$ | $-\Delta S^\ddagger$ | Ref. |
|---|---|---|---|---|---|---|
| 1 | Tetraphenylethylene | 0.28 | 17.2 | 24.1 | 22.6 | 25) |
| 2 | Triphenylethylene | 3.075 | 15.7 | 22.6 | 22.7 | 25) |
| 3 | *trans*-Stilbene | 4.27 | 15.25 | 22.2 | 22.8 | 25) |
| | | | 13.8 | | | 26) |
| 4 | *cis*-Stilbene | 13.35 | 14.1 | 21.75 | 25.2 | 25) |
| 5 | *trans*-$\alpha$-Methylstilbene | 37.42 | 12.6 | 21.1 | 28.1 | 26) |
| 6 | *cis*-$\alpha,\alpha'$-Dimethylstilbene | 219.5 | 10.8 | 20.0 | 30.5 | 26) |
| 7 | *trans*-$\alpha,\alpha'$-Dimethylstilbene | 228 | 11.0 | 20.0 | 29.8 | 26) |
| 8 | Cyclohexene | 263.5 | 12.7 | 19.95 | 24.0 | 25) |

The values of $k$ (in $mol^{-1}$ l. $sec^{-1}$) are those at 30°C. The values of $\Delta F^\ddagger$ (in kcal. $mol^{-1}$) and of $\Delta S^\ddagger$ (in cal. $deg^{-1}$ $mol^{-1}$) are those calculated from the rates at 30°C. The values of $\Delta H^\ddagger$ are in kcal. $mol^{-1}$.

reactions of stilbene and stilbene derivatives with hydrogen bromide and oxygen[24]. The conclusions are summarized as follows.

(1) *trans*-Stilbene and *trans*-$\alpha$-methylstilbene can produce bromine atoms by the combined action of hydrogen bromide and oxygen, and thus can initiate chain reactions, the former yielding mainly its dibromide, and the latter yielding its dibromide along with $\omega$-bromoacetophenone and benzoic acid as the final products.

(2) On the other hand, both *trans*- and *cis*-$\alpha,\alpha'$-dimethylstilbenes as well as *trans*-$\alpha,\alpha'$-diethylstilbene undergo no such reaction in the absence of a catalyst, because they are unable by themselves to produce bromine atoms from hydrogen bromide and oxygen, probably owing to the steric effect which hinders the approach of hydrogen bromide and oxygen to the ethylenic bond. However, once bromine atoms have been produced from hydrogen bromide and a peroxidic initiator, they are active enough to attack the ethylenic bonds of these stilbene derivatives, producing radicals as chain carriers, and resulting in the oxidative cleavage of the double bonds.

(3) Further, methyltriphenylethylene and $\alpha,\alpha'$-bisbromomethylstilbene (1,4-dibromo-2,3-diphenyl-2-butene) appear not to react with hydrogen bromide and oxygen even in the presence of a peroxidic catalyst. That is, the steric hindrance is so great in these compounds that they are not only incapable of such initiation, but also unsusceptible even to the action of bromine atoms, or, if a bromine atom adds to the double bond, unable to propagate the chain reactions efficiently.

24) H. Suzuki, O. Simamura and T. Ichihashi, This Bulletin, **27**, 235 (1954).

*Reaction with perbenzoic acid (epoxidation).*—The reaction of olefins with perbenzoic acid gives excellent yields of the corresponding epoxides. It has been presumed that perbenzoic acid acts as a double-bond reagent, i. e. that the reaction involves attack on the olefinic bond and not on one of the constituting carbon atoms[25]. The correlation of the reactivities of *trans*-stilbene, triphenylethylene and tetraphenylethylene to perbenzoic acid with the $\pi$-bond orders as well as the bond localization energies of the ethylenic bonds of these compounds was briefly discussed already in the preceding part[3] of this series. The discussion will be extended here to other stilbene derivatives.

The relevant data selected from the results of the kinetic studies by Lynch & Pausacker[25] and by Simamura, Fukuyama & Nagai[26] are shown in Table VI.

While *cis*-stilbene is epoxidized much more rapidly than the *trans* isomer, *cis*-$\alpha,\alpha'$-dimethylstilbene is epoxidized slightly more slowly than the *trans* isomer, in accordance with the expectration from the calculated bond localization energies. The difference in the reaction rate among the compounds may, of course, depend not only on the difference of the bond localization energy, but also on the steric effect in a narrow sense (that is, the degree of unfavorableness of the steric situation to the approach of the reagent, or the magnitude of the steric strain in the transition state), and also on the electronic

25) B. M. Lynch and K. H. Pausacker, *J. Chem. Soc.*, **1955**, 1525.

26) The author is indebted to Professor O. Simamura, Dr. M. Fukuyama and Mr. Y. Nagai for communicating with him and allowing him to quote these results in advance of publication. They were presented first by them at the Symposium on the Organic Reaction Mechanism held under the auspices of the Chemical Society of Japan, Fukuoka, October, 1958.

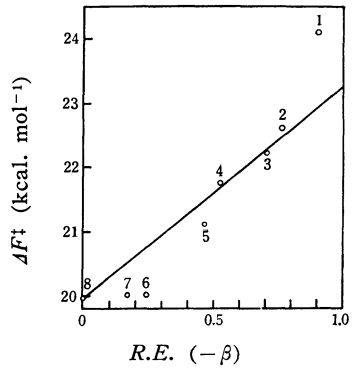



Fig. 3. Relation between the free energy of activation for the reaction of olefins with perbenzoic acid and the bond localization energy. Olefins are represented by the entry numbers in Table V as well as in Table VI.

effect of the substituents (e. g. the electron-donating effect of methyl groups). In spite of this, the sequence of the free energy of activation ($\Delta F^{\ddagger}$) shown in Table VI agrees completely with the sequence of the calculated bond localization energy (*R.E.*) shown in Table V. This fact is seen more clearly in Fig. 3, which shows the values of *R.E.* and $\Delta F^{\ddagger}$ for each compound plotted against one another and numbered according to the entry number in Table VI.

Considering the discrepancy between the experimental value of $\Delta H^{\ddagger}$ for *trans*-stilbene determined by Lynch and Pausacker and that by Simamura and others, it may be somewhat doubtful to compare the data of the different sources. On the other hand, it may also be doubtful to place much reliance on the absolute magnitude of the individual calculated bond localization energy. However, Fig. 3 appears to lead to the following discussions.

The points for *trans*-$\alpha$-methylstilbene and especially for *trans*- and *cis*-$\alpha,\alpha'$-dimethylstilbenes are deviated down from the straight correlation line drawn nearly through the points for cyclohexene, *cis*- and *trans*-stilbenes. That is, the values of $\Delta F^{\ddagger}$ for these methylated stilbenes are smaller than those anticipated from the values of *R.E.* on the basis of the correlation line. These vertical deviations may be considered to indicate the facilitation of the reaction by the hyperconjugation effect or the electron-donating effect of the methyl groups. The steric interference with the approach of the reagent may also exist to some extent in these methylated stilbenes. This interference seems to be revealed by the large absolute values of the entropy of activation for these compounds as compared with *trans*-stilbene.

Tetraphenylethylene and triphenylethylene have greater free energies of activation than anticipated from the calculated bond localization energies on the basis of the correlation line. This fact appears to suggest that the low reactivities of these compounds as compared with *trans*-stilbene are not only due to the larger bond localization energies but also partly to the steric effect in a narrow sense caused by the greater crowding of phenyl groups or by the nonplanarity of the configurations of these compounds. However, in view of the fact that the values of the entropy of activation for these compounds are nearly equal to that for *trans*-stilbene, this possibility may be questionable. Perhaps, the so-called electron-withdrawing effect of the phenyl group relative to the hydrogen atom may be a contributory factor.

Simamura and others measured also the rates of the reaction of many 4,4'-disubstituted $\alpha,\alpha'$-dimethylstilbenes with perbenzoic acid, and found that there exists a linear relation between the logarithms of the rate constants and the sum of the values of Hammett's substituent constant for the 4- and 4'-substituents for each of the *trans* and the *cis* series. According to them, the proportionality constant (Hammett's reaction constant $\rho$) for the *cis* isomers is $-0.88$ at 30°C, $-0.90$ at 20°C, and $-0.93$ at 10°C, and, on the other hand, the value for the *trans* isomers is $-0.80$ at 30°C, $-0.83$ at 20°C, and $-0.86$ at 10°C, meaning that the effect of the 4- and 4'-substituents on the reaction rate constant is stronger in the *cis* series than in the *trans* series. This fact coincides with the present conclusion that the *cis* isomer of $\alpha,\alpha'$-dimethylstilbene is more conjugated than the *trans* isomer. The above mentioned values of Hammett's reaction constant for 4,4'-disubstituted dimethylstilbenes are appreciably smaller than those for 4-substituted *trans*-stilbenes (about $-1.07\sim1.16$, estimated from the data by Lynch and Pausacker). This fact may be correlated with the fact that *trans*-stilbene is more conjugated than *trans*- and *cis*-dimethylstilbenes.

## Experimental

All the spectra were measured with a Cary recording spectrophotometer Model 14 M-50.

The alkylstilbenes were prepared as reported previously[2,19].

*trans*-$\alpha,\alpha'$-Dichlorostilbene was prepared by the addition of chlorine to tolan. To a solution of 10 g. of tolan in 100 cc. of acetic acid, 140 cc. of a 0.4 mol./l. solution of chlorine in acetic acid was added. The reaction mixture was left to stand for about a month, and then poured into water. The crystalline deposits were collected, pressed on a porous plate to remove some adhering oily matter, and repeatedly recrystallized from ethanol. The substance was obtained in colorless crystals melting at 138.5~139.8°C; yield, 2.4 g. (17.2% of the theoretical amount).

*trans*-$\alpha,\alpha'$-Dibromostilbene was prepared by the addition of bromine to tolan. To a solution of 3.4 g. of tolan in 70 cc. of ether, about 2 cc. (in exess) of bromine was added dropwise. The crystalline deposits were collected and washed twice with ether. The substance was obtained in colorless prisms melting at 205~206°C; yield, 5.1 g. (79% of the theoretical amount).

*trans*-$\alpha,\alpha'$-Diiodostilbene was prepared by the addition of iodine to tolan. To a solution of 356 mg. ($2\times10^{-3}$ mol.) of tolan in 10 cc. of acetic acid, a solution of 508 mg. ($2\times10^{-3}$ mol.) of iodine in 22.5 cc. of acetic acid was added and the reaction mixture was left to stand for about a month. The crystalline deposits were collected and carefully recrystallized from acetic acid. The substance was obtained in colorless, bright prisms hardly soluble in most organic solvents and decomposing at about 199°C with the evolution of iodine vapor; yield, 744 mg. (86% of the theoretical amount).

## Summary

The ultraviolet absorption spectra of some $\alpha$- and $\alpha,\alpha'$-substituted stilbenes have been analyzed, and the most probable spatial configurations of these compounds have been inferred from the spectra by application of the calculation method described in the earlier part of this series.

It is especially noteworthy that with $\alpha,\alpha'$-dimethylstilbene as well as its diethyl analogue the *trans* isomer shows the conjugation band at a shorter wavelength than the *cis* isomer, contrary to the generally accepted view that *trans* isomers of conjugated compounds should exhibit the conjugation bands at a longer wavelength than the corresponding *cis* isomers. This fact is considered to indicate that with these compounds the *trans* isomers are less conjugated than the corresponding *cis* isomers, and that the angle of twist of the "single" bond (interplanar angle) is larger in the *trans* isomers than in the corresponding *cis* isomers. This has been confirmed by the results of the calculations. Further, this is supported also by some pieces of information on the properties of these compounds, such as the reactivities, the exaltation of molecular refraction, and the nuclear magnetic resonance. With special emphasis on this respect, the correlation of some physical and chemical properties of these compounds with the spatial configurations of the molecules has been discussed in detail.

The author desires to thank Professor Osamu Simamura and Professor Kengo Shiomi, for reading the manuscript and for valuable advice, and Dr. Makoto Takahasi for encouragement throughout this study.

*Department of Chemistry*
*College of General Education*
*The University of Tokyo*
*Meguro-ku, Tokyo*

# *Relations between Electronic Absorption Spectra and Spatial Configurations of Conjugated Systems. VIII. Stilbene Derivatives with Methyl Groups on the Benzene Nuclei*

By Hiroshi SUZUKI

(Received August 15, 1959)

The method developed in Part V[1] of this series is applied to some stilbene derivatives with methyl groups on the benzene nuclei. With such compounds, the electronic bathochromic effect of the methyl groups on the benzene nuclei should not be ignored. Accordingly, an allowance for this effect is made, analogously to the case of *o*-alkyl- and *o*,*o*'-dialkylbiphenyls in Part II[2] of this series, by choice of the references for correlation between the calculated transition energy $\Delta E_A$ and the observed wave number $\nu_A$ of the conjugation band.

**4-Methyl- and 4, 4'-Dimethyl-*trans*-stilbene.**—In order to determine the longer-wavelength-side reference, the ultraviolet absorption spectra of 4-methyl- and 4, 4'-dimethyl-*trans*-stilbene in *n*-heptane were measured. The results are shown in Table I and Fig. 1. The spectra resemble the spectrum of *trans*-stilbene, on the whole showing fine structures (cf. Table I and Fig. 1 in Part V). The introduction of a methyl group into a para-position of *trans*-stilbene causes the red-shift of about 4.2 m$\mu$ of the maxima of the conjugation band, and the introduction of the second methyl group into the other para-position results in a further red-shift of about 3 m$\mu$.

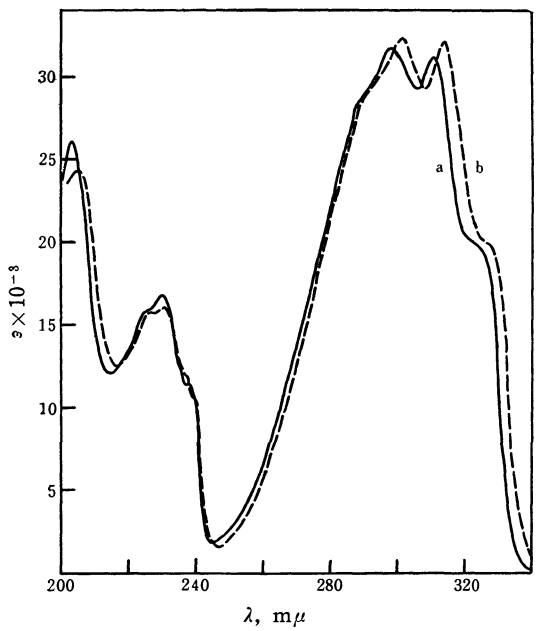



Fig. 1. Ultraviolet absorption spectra (in *n*-heptane): a ——, 4-methyl-*trans*-stilbene; b ------, 4, 4'-dimethyl-*trans*-stilbene.

**4,4',$\alpha$,$\alpha$'-Tetramethylstilbene.**—According to Nagai and Simamura[3], the spectrum of *trans*-4, 4', $\alpha$, $\alpha$'-tetramethylstilbene shows the absorption maximum at 245 m$\mu$ ($\varepsilon$= 15000), and that of the *cis* isomer shows the maximum at 258 m$\mu$ ($\varepsilon$=10000). These maxima are considered as the conjugation bands. Thus, with these compounds, similarly to $\alpha$, $\alpha$'-dimethylstilbene[4], the conjugation band of the *cis* isomer is at a longer wavelength and of lower intensity than that of the *trans* isomer.

In application of our method to these compounds, the possible bathochromic effect of the $\alpha$- and $\alpha$'-methyl groups is provisionally ignored for the same reasons as in the preceding part[4] of this series, and then, in order to make allowance for the bathochromic effect of the *p*- and *p*'-methyl groups, *trans*-4, 4'-dimethylstilbene is taken as the longer-wavelength-side reference compound. That is, the value of $\nu_L$ [wave number corresponding to the calculated transition energy for planar *trans*-stilbene, $\Delta E_L$, 1.1423 ($-\beta$)] is assumed in this case to be 33190 cm$^{-1}$ (301.3 m$\mu$, the $\gamma$-band of *trans*-4, 4'-dimethylstilbene). On the other hand, as the shorter-wavelength-side reference, the value for toluene corresponding to the center of gravity of singlets of benzene is taken. That is, the value of $\nu_S$ [wave number corresponding to the value of $\Delta E_A$ when $\rho$ is 0, $\Delta E_S$,

1) H. Suzuki, This Bulletin, **33**, 379 (1960).
2) H. Suzuki, ibid., **32**, 1350 (1959).
3) Y. Nagai and O. Simamura, presented at the 11th Annual Meeting of the Chemical Society of Japan, Tokyo, April, 1958.
4) H. Suzuki, This Bulletin, 33, 396 (1960).

TABLE I. ABSORPTION MAXIMA OF METHYLATED STILBENES (IN *n*-HEPTANE)

| Compound | A-band | | B-band | | C-band | |
|---|---|---|---|---|---|---|
| | λ, mμ | ε | λ, mμ | ε | λ, mμ | ε |
| 4-Methylstilbene | α (324.5) | 19800 | (238.0) | 11450 | 203.3 | 26100 |
| | β 311.2 | 31200 | △230.2 | 16800 | | |
| | γ △298.3 | 31800 | (225.0) | 15800 | | |
| | δ (292.0) | 29550 | | | | |
| 4,4'-Dimethylstilbene | α (327.5) | 19900 | (239.5) | 10550 | 204.8 | 24350 |
| | β 314.2 | 32100 | (237.0) | 11980 | | |
| | γ △301.3 | 32400 | △230.7 | 16100 | | |
| | δ (293.5) | 29950 | 225.9 | 15730 | | |
| 2,4,6-Trimethylstilbene | 282.7 | 19200 | | | 208.5 | 29600 |
| | | | | | 201.5 | 29700 |
| 2,4,6,2',4',6'-Hexamethylstilbene | 262.7 | 16000 | | | 214.0 | 35700 |

Wavelengths in parentheses denote inflections.
Symbol △ denotes the most intense maximum of fine structure.

TABLE II. RESULTS OF CALCULATION

| Compound | $\lambda_A$ mμ | $\Delta E_A$ $-\beta$ | ρ | θ° | R Å | R. E. $-\beta$ | $p_{\alpha-\alpha'}$ |
|---|---|---|---|---|---|---|---|
| *trans*-Stilbene | 294.1 | 1.1423 | 0.9084 | 0 | 1.445 | 0.704 | 0.856 |
| *trans*-4,4',α,α'-Tetramethylstilbene | 245 | 1.620 | 0.404 | 61 | 1.494 | 0.140 | 0.970 |
| *cis*-4,4',α,α'-Tetramethylstilbene | 258 | 1.491 | 0.530 | 51.7 | 1.481 | 0.242 | 0.948 |
| *trans*-2,4,6,2',4',6'-Hexamethylstilbene | 262.7 | 1.523 | 0.498 | 54.3 | 1.485 | 0.212 | 0.954 |

$2(-\beta)$] is assumed to be 46882 $cm^{-1}$ (213.3 mμ) (cf. Table II in Part II).

On the basis of the above references, calculation by the usual method has been carried out. The results are shown in Table II, in which the notation is the same as in Part V of this series. The calculated values of the interplanar angle θ (the angle of twist of each "single" bond) for *trans*- and *cis*-4,4',α,α'-tetramethylstilbenes agree fairly well with the values for *trans*- and *cis*-α,α'-dimethylstilbenes (58° and 51.5°), respectively (cf. Table II in the preceding part of this series).

**2,4,6-Trimethyl- and 2,4,6,2',4',6'-Hexamethyl-*trans*-stilbene.**—The ultraviolet absorption spectra of 2,4,6-trimethyl-*trans*-stilbene (*trans*-1-mesityl-2-phenylethylene) and 2,4,6,2'4',6'-hexamethyl-*trans*-stilbene (*trans*-1,2-dimesitylethylene) measured in *n*-heptane are shown in Table I and Fig. 2. A comparison of these spectra with the spectrum of *trans*-stilbene[1] reveals that the conjugation band shifts progressively toward shorter wavelengths and reduces the intensity with the increasing number of methyl substituents. This fact is undoubtedly due to the steric interferences

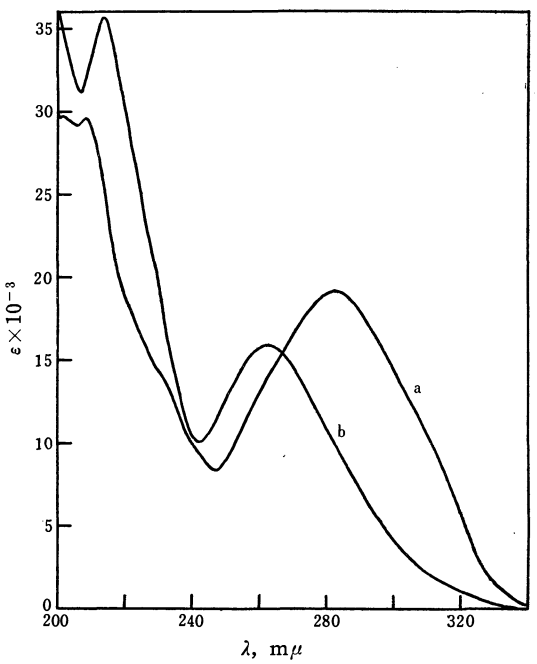



Fig. 2. Ultraviolet absorption spectra (in *n*-heptane): a, 2,4,6-trimethyl-*trans*-stilbene; b, 2,4,6,2',4',6'-hexamethyl-*trans*-stilbene.

of the substituents which prevent the molecule from assuming a planar configuration. It is noteworthy that the conjugation bands of these substituted stilbenes have, similarly to those of *cis*-stilbene[1] and $\alpha$-substituted stilbenes[4], no fine structure, in contrast to that of *trans*-stilbene.

Now, it is assumed that the mean value of the magnitude of the red-shift of the conjugation band caused by substitution of a methyl group at the *o*- or *p*-position of *trans*-stilbene is 3 m$\mu$, and that the effect of methyl substitution is additive analogously to the case of methylbenzenes[5]. Then if the configuration of dimesitylethylene were planar, this compound whould show the conjugation band at a longer wavelength than that of *trans*-stilbene by about 18 m$\mu$ (3×6 m$\mu$). That is, the conjugation band of the hypothetical planar molecule of this compound would be at about 312 m$\mu$ (294+18 m$\mu$). Accordingly, the value of $\nu_L$ is assumed in this case to be 32051 cm$^{-1}$ (312 m$\mu$).

On the other hand, as the shorter-wavelength-side reference compound, mesitylene is taken. While the approximate center of the low-intensity band of benzene in the region between 230 and 270 m$\mu$ is at 255 m$\mu$, the corresponding one of mesitylene is at 266 m$\mu$[6]. In addition, while the 0-0 band of benzene is at 262.54 m$\mu$, that of mesitylene is at 274.06 m$\mu$[5]. That is, the band of mesitylene is at longer wavelengths by about 11 or 11.5 m$\mu$ than that of benzene. On the analogy of the case of toluene as well as ethylbenzene (cf. Table II in Part II), it may be considered that the other bands of mesitylene are probably at longer wavelengths by about 11 or 11.5 m$\mu$ than the corresponding bands of benzene. Accordingly, the value for mesitylene corresponding to the center of gravity of singlets of benzene (48000 cm$^{-1}$, 208.3 m$\mu$) is presumed to be 45600 cm$^{-1}$ (219.3 m$\mu$ = 208.3+11 m$\mu$). Therefore, the value of $\nu_S$ for treatment of dimesitylethylene is assumed to be 45600 cm$^{-1}$.

The results of calculation carried out by the usual procedure on the basis of the above references are shown in Table II. From scale models, it is inferred that the interplanar angle in *trans*-dimesitylethylene should be approximately equal to that in *trans*-$\alpha,\alpha'$-dimethylstilbene. The value calculated here is slightly smaller than that for dimethylstilbene; still it may be said that the agreement is fairly good.

2,4,6-Trimethylstilbene is unsymmetrical, so that the two interplanar angles should be different, and therefore, the resonance integral for the Mes-C bond and that for the Ph-C bond should be different from one another. Therefore, the present method can not be applied to this compound. However, it must be sure that this compound is nonplanar, since the conjugation band is at a considerably shorter wavelength than that of *trans*-stilbene. On the basis of the above assumption that the red-shift caused by a *p*- or *o*-methyl group is about 3 m$\mu$, it is presumed that the conjugation band of this compound would be at about 273.7 m$\mu$ (282.7−9 m$\mu$) if it were not for the red-shift by the electronic effect of the methyl groups. It is of interest that this presumed position coincides almost completely with the observed position of the conjugation band of *trans*-$\alpha$-methylstilbene (273.5 m$\mu$)[4]. It may, therefore, be presumed that the value of the extra-resonance energy *R. E.* of mesitylphenylethylene is approximately equal to that of $\alpha$-methylstilbene [0.457 $(-\beta)$][4] and hence is smaller than that of *trans*-stilbene. This presumption seems to be supported by the following fact. According to Everard and others[7], the exaltation of molecular refraction of *trans*-stilbene is +6.6, and that of 2,4,6-trimethylstilbene is smaller by 1.3 than that of *trans*-stilbene. This fact is considered to indicate that the extent of conjugation is smaller in trimethylstilbene than in stilbene.

Everard and Sutton[8] have found with 4-dimethylaminostilbenes a similar depression of the exaltation caused by *o*-substituents attributable to steric inhibition of resonance. According to them, the exaltation of 4-dimethylaminostilbene is 7.5, and, on the other hand, the values for its 2,2'-dimethyl- and 2',4',6'-trimethyl-derivatives are 3.3 and 1.6, respectively (the values of the exaltation are expressed relative to that of *trans*-stilbene). The value for the 2'-chloro-derivative is much the same as that for the parent compound, indicating that there is negligible inhibition of conjugation in the chloro-compound in contrast to the methyl compounds.

4-Dimethylaminostilbene and related compounds have been studied by several

5) K. F. Herzfeld, *Chem. Revs.*, **41**, 233 (1947).
6) A. E. Gillam and E. S. Stern, "An Introduction to Electronic Absorption Spectroscopy", 2nd Ed., Edward Arnold Publishers, Ltd., London (1957), p. 134.
7) K. B. Everard, L. Kumar and L. E. Sutton. *J. Chem. Soc.*, **1951**, 2807.
8) K. B. Everard and L. E. Sutton, ibid., **1951**, 2816.

workers in England, probably in connection with the carcinogenic activity. Haddow and others[9] have found that the derivatives of 4-dimethylaminostilbene with methyl groups at two *o*-positions in a benzene nucleus are biologically ineffective probably because of the non-planarity of the molecular configurations of these compounds. Beale and Roe[10] have found that the oscillator strength of the longest wavelength band (conjugation band) of *trans*-stilbene as well as 4-dimethylaminostilbene is markedly lowered by substitution of methyl groups at the *o*-positions. Thus, in the 2'-position a methyl group causes a decrement of 0.04 in *f*-value, and successive introductions of further methyl groups into the *o*-positions cause larger decrements in *f* of magnitude varying with the position of substitution. This effect has been attributed to the steric hindrance to planarity of the molecular configuration.

Regarding the reactions of the *o*-methyl substituted stilbenes, only a few data are available. According to the present author's preliminary study[11], the rate of bromination of 2, 4, 6-trimethylstilbene in carbon tetrachloride is markedly greater than that of trans-stilbene, even when a little catechol is added to suppress the retarding effect of atmospheric oxygen[4]. The high reactivity of trimethylstilbene as compared with stilbene is probably partly due to the larger $\pi$-bond order of the ethylenic bond or the lower bond localization energy in trimethylstilbene relative to stilbene.

On the other hand, according to Fuson and others[12], the reactivity to potassium permanganate falls in the order *trans*-stilbene > 2, 4, 6-trimethylstilbene > 2, 4, 6, 2', 4', 6'-hexamethylstilbene. Thus, when 0.1 cc. of a 2% solution of potassium permanganate in water is added to a solution of 0.05 g. of the stilbene in 4 cc. of acetone, the time required for discharging the permanganate color is as follows: *trans*-stilbene, less than one minute; trimethylstilbene, four and one-half hours; hexamethylstilbene, 60 hr. In the methylated stilbenes, there should be a considerably large steric hindrance to the approach of the reagent to the ethylenic bond due to the mesityl or phenyl groups rotated out of the plane of the ethylenic bond. The order of the reactivity can be considered to be in conformity with the magnitude of the steric hindrance.

9) A. Haddow, R. J. C. Harris, G. A. R. Kon and E. M. F. Roe, *Trans. Roy. Soc. (London)*, **A241**, 147 (1948).
10) R. N. Beale and E. M. F. Roe, *J. Am. Chem. Soc.*, **74**, 2302 (1952).
11) H. Suzuki, unpublished.
12) R. C. Fuson, J. J. Denton and C. E. Best, *J. Org. Chem.*, **8**, 64 (1943).

## Experimental

All the spectra were measured with a Cary recording spectrophotometer Model 14 M-50.

*p*-Methylstilbene was prepared by the Meerwein reaction, quite analogously to the synthesis of *p*-methoxystilbene described in Part V of this series. From 53.5 g. of *p*-toluidine, 25.8 g. of the purified product, colorless crystals melting at 121~122°C, was obtained after repeated recrystallization from ethanol (26.5% of the theoretical amount).

*p,p'*-Dimethylstilbene was prepared by reduction of *p,p'*-dimethylbenzoin (*p*-toluoin), quite analogously to the synthesis of *trans*-stilbene from benzoin described in Organic Syntheses[13]. From about 15 g. of *p*-toluoin, the purified product, colorless crystals melting at 177~178°C, was obtained after repeated recrystallization from ethanol; yield, 4.7 g. (32% of the theoretical amount).

Found: C, 92.34; H, 7.86. Calcd. for $C_{16}H_{16}$: C, 92.26; H, 7.74%.

*p*-Toluoin was prepared by the benzoin condensation of *p*-tolualdehyde. To a solution of 82.7 g. of *p*-tolualdehyde in 165 ml. of ethanol, a solution of 18 g. of potassium cyanide in 120 ml. of water was added. The reaction mixture was refluxed for about two hours, and then left to stand for about a month in a refrigerator. The crystalline deposits contaminated with a considerably large amount of orange-colored oily matter were collected and pressed on a porous plate to remove the adhering oily matter. After recrystallization from ethanol, *p*-toluoin was obtained in colorless crystals melting at 87~88°C; yield, 15 g. (18.1% of the theoretical amount).

*p*-Tolualdehyde was prepared according to the method described in Organic Syntheses[14].

2, 4, 6-Trimethylstilbene was prepared, after the procedure described by Fuson and others[12], by dehydration of 1-mesityl-2-phenylethanol prepared by the Grignard reaction of mesitaldehyde with benzyl magnesium chloride. The product was purified by repeated recrystallization from ethanol, and obtained in colorless crystals melting at 56.5~57.5°C.

Mesitaldehyde was prepared, according to the method described in Organic Syntheses[15], by the action of hydrogen chloride on mesitylene in tetrachloroethane in presence of anhydrous aluminum chloride and zinc cyanide.

13) L. I. Smith (Editor-in-Chief), "Organic Syntheses", Vol. 23, John Wiley & Sons, Inc., New York (1943), p. 86.
14) F. C. Whitmore (Editor-in-Chief), ibid., Vol. XII (1932), p. 81.
15) L. I. Smith (Editor-in-Chief), ibid., Vol. 23 (1943), p. 57.

Mesitylene was prepared according to the method described in Organic Syntheses[16].

2,4,6,2',4',6'-Hexamethylstilbene was prepared, according to the method described by Fuson and Best[17], by heating thiomesitaldehyde with copper powder. To a solution of 8.5 g. of mesitaldehyde in 80 ml. of anhydrous ethanol cooled by a freezing mixture, hydrogen chloride was passed for 50 min., and then hydrogen chloride and hydrogen sulfide were passed for one and a third hours at $-5\sim+5$°C. The reaction mixture was left to stand for about two hours. The white deposits were collected and washed repeatedly with anhydrous ethanol. Thus, after being dried in a desiccator, the crude thiomesitaldehyde was obtained as white, apparently amorphous, powder; yield, 4.3 g. About 4.2 g. of the crude thiomesitaldehyde was mixed thoroughly with 3.6 g. of copper powder, and heated for about one hour over an oil bath at 220~230°C. The copper powder turned black. Repeated extraction with hot ligroin afforded, after removal of the solvent, the crude dimesitylethylene. After repeated recrystallization from ethanol and treatment with activated charcoal, the substance was obtained in colorless fine needles melting at 131~132°C; yield, 1.85 g.

The preparation of this compound by dehydration of 1,2-dimesitylethanol was reported by Fuson and others[12]. However, an attempt by the present author to prepare 1,2-dimesitylethanol, according to the directions of Fuson and others, by the Grignard reaction of mesitaldehyde with 2,4,6-trimethylbenzyl magnesium chloride was unsuccessful. 2,4,6-Trimethylbenzyl chloride was prepared from mesitylene according to the directions of Vavon and Bolle[18].

The author desires to thank Professor Kengo Shiomi for reading the manuscript and for advice.

*Department of Chemistry*
*College of General Education*
*The University of Tokyo*
*Meguro-ku, Tokyo*

16) H. Gilman (Editor-in-Chief), ibid., Col. Vol. 1. (1932), p. 334.
17) R. C. Fuson and C. E. Best, *J. Am. Chem. Soc.*, **67**, 155 (1945).
18) G. Vavon and J. Bolle. *Compt. rend.*, **204**, 1826 (1937).

# *Relations between Electronic Absorption Spectra and Spatial Configurations of Conjugated Systems. IX. p-Phenylstilbene, p,p'-Diphenylstilbene, and their Related Compounds*

By Hiroshi SUZUKI

(Received September 21, 1959)

In this part of the series, the results of the measurements of the ultraviolet absorption spectra of *p*-phenylstilbene (1-phenyl-2-*p*-biphenylylethylene), 1-phenyl-2-(2-fluorenyl)-ethylene, *p,p'*-diphenylstilbene (1,2-di-*p*-biphenylylethylene), and its *a,a'*-dimethyl derivative (2,3-di-*p*-biphenylyl-2-butene) are reported, and the calculations based on the simple LCAO molecular orbital method analogous to those for stilbene and related compounds described in the earlier parts[1-4] of this series are applied to these spectra.

In addition, the red-shifts of the conjugation bands observed with these compounds as well as stilbene and related compounds when the solvent is changed from *n*-heptane to benzene are summarized, and the correlation of these shifts with the spatial configurations of the molecules is discussed.

## *p*-Phenylstilbene and 1-Phenyl-2-(2-fluorenyl)-ethylene

The spectra of these compounds (both are probably *trans*) in solutions in benzene and in *n*-heptane are shown in Fig. 1, and the data of the absorption maxima are recorded in Table I. The notation of the bands is analogous to the one in the earlier parts of this series. Thus, the A-band denotes the conjugation band.

These spectra are somewhat similar in shape to that of *trans*-stilbene (cf. Fig. 1 in Part V[1] of this series). The fine

1) H. Suzuki, This Bulletin, **33**, 379 (1960).
2) H. Suzuki, ibid., **33**, 389 (1960).
3) H. Suzuki, ibid., **33**, 396 (1960).
4) H. Suzuki, ibid., **33**, 406 (1960).

TABLE I. ABSORPTION MAXIMA

| Compound | In benzene | | In *n*-heptane | | | |
|---|---|---|---|---|---|---|
| | A-band | | A-band | | B- & C-bands | |
| | λ, mμ | ε | λ, mμ | ε | λ, mμ | ε |
| *p-Phenylstilbene* | | | | | | |
| | [(343.5)] | 22200 | [(338)] | 23200 | 225.5 | 13100 |
| | △327.8 | 35500 | △322.5 | 36000 | | |
| | (317.4) | 32900 | (311.5) | 33200 | 200.3 | 31900 |
| *1-Phenyl-2-(2-fluorenyl)-ethylene* | | | | | | |
| | 356.5 | 28450 | 351.2 | 29100 | 258.9 | 2170 |
| | △341.5 | 42900 | △335.8 | 43100 | 230.0 | 15230 |
| | [(330.5)] | 37000 | [(327.5)] | 37200 | 223.7 | 15420 |
| | [(321)] | 30800 | (318.5) | 32450 | 210.0 | 26950 |
| | [(307)] | 19430 | [(303.5)] | 21000 | 204.5 | 27800 |
| *p, p'-Diphenylstilbene* | | | | | | |
| | [(362)] | 31300 | [(357)] | 0.126* | [(243)] | 0.042* |
| | △343.0 | 49900 | △337.4 | 0.214* | (220.5) | 0.078* |
| | (332.5) | 46200 | (327.5) | 0.199* | (201.8) | 0.254* |
| *p, p'-Diphenyl-α, α'-dimethylstilbene* | | | | | | |
| | 276.2 | 29000 | 273.3 | 0.838* | 203 | 1.826* |

Symbol △ denotes the most intense maximum of fine structure. Wavelengths in parentheses denote inflections, and those in double parentheses denote very indistinct inflections.
Symbol * denotes the intensity in absorbance.

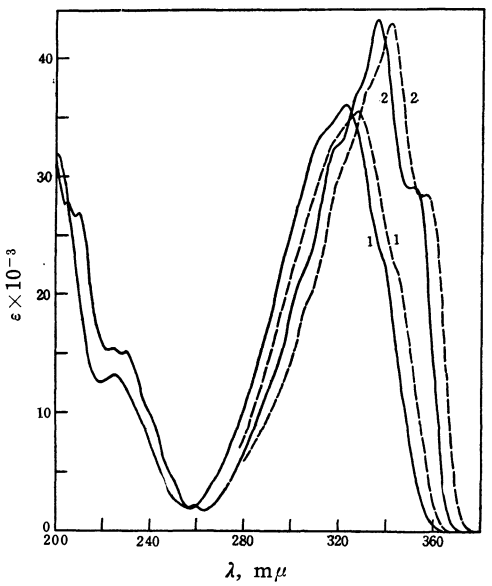



Fig. 1. Ultraviolet absorption spectra: 1, *p*-phenylstilbene; 2, 1-phenyl-2-(2-fluorenyl)-ethylene: ——, in *n*-heptane; ----, in benzene.

structure of the conjugation band of *p*-phenylstilbene is, however, more blurred than that of stilbene. The pattern of the fine structure of the conjugation band of the fluorenyl compound may be said to resemble that of fluorene (cf. Fig. 1 in Part III[5] of this series).

5) H. Suzuki, ibid., 32 1357 (1959).

The maximum of the conjugation band of *p*-phenylstilbene is at a longer wavelength by about 28.4 mμ relative to the most intense maximum (the γ-band) of fine structure of the conjugation band of stilbene, in accordance with the expectation from the length of the conjugated system. The most intense maximum of fine structure of the conjugation band of the fluorenyl compound is at a still longer wavelength by about 13.3 mμ than that of the biphenylyl compound, a fact which may be considered to correspond to the fact that the most intense maximum of fine structure of the conjugation band of fluorene is at a longer wavelength by about 14.5 mμ than the maximum of the conjugation band of biphenyl[5].

Now, the calculation method analogous to the one used so far in this series is applied to these compounds. In the calculation the data of the spectra in *n*-heptane are used as before. The resonance integral for the ethylenic bond is denoted by $\eta\beta$, and as the value of $\eta$ the value of 1.080, corresponding to the bond length 1.34 Å, is taken. The resonance integral for the bonds connecting the benzene rings to the ethylenic carbon atoms is denoted by $\rho\beta$, and as the value of $\rho$, the value of 0.908, corresponding to the bond length 1.445 Å, is tentatively taken as in the case of *trans*-stilbene[1]. The resonance integral for the bond

between the two benzene rings in the biphenyl part is denoted by $\mu\beta$.

When as the value of the variable $\mu$ the corresponding value for fluorene 1.060 is used, the electronic transition energy $\Delta E_A$ (the energy difference between the lowest vacant orbital and the highest occupied orbital) is calculated to be 1.018 $(-\beta)$, by the usual procedure of the simple LCAO molecular orbital method. This calculated value of the transition energy, which is referred to as $\Delta E_L$, is considered to correspond to the wave number of the most intense maximum of the conjugation band of the fluorenyl compound, 29780 $cm^{-1}$ (335.8 m$\mu$), which is referred to as $\nu_L$.

On the other hand, when $\mu$ is zero, the value of $\Delta E_A$ is 1.142 $(-\beta)$, which corresponds conceivably to the wave number of the $\gamma$-band of *trans*-stilbene, 34002 $cm^{-1}$ (294.1 m$\mu$)[1]. These values of the calculated and the corresponding observed transition energies are referred to as $\Delta E_S$ and $\nu_S$, respectively.

On the basis of the above determination of the longer-wavelength-side and the shorter-wavelength-side references, the value of $\Delta E_A$ corresponding to the wave number of the maximum of the conjugation band of the biphenylyl compound, 31008 $cm^{-1}$ (322.5 m$\mu$), is calculated to be 1.054 $(-\beta)$, and the corresponding value of $\mu$ is calculated to be 0.877. This calculated value of $\mu$ is slightly greater than the corresponding value for biphenyl in solution obtained in Part I[6] of this series. This fact would appear to suggest that the length of the bond concerned is shortened and the angle of twist of the bond is decreased in the biphenylyl compound compared with those in biphenyl in solution, owing to the increase in the extent of conjugation. However, it should not be so asserted, since it may be doubtful whether much reliance can be placed on these numerical values, because of the many assumptions made for simplification in the calculation and especially of the peculiar nature of the parameter $\mu$ for fluorene.

### *p,p'*-Diphenylstilbene and its *α,α'*-Dimethyl Derivative

The spectra of these compounds (both are probably the *trans* isomers) in solutions in benzene and in *n*-heptane are shown in Fig. 2, and the data of the absorption maxima are summarized in

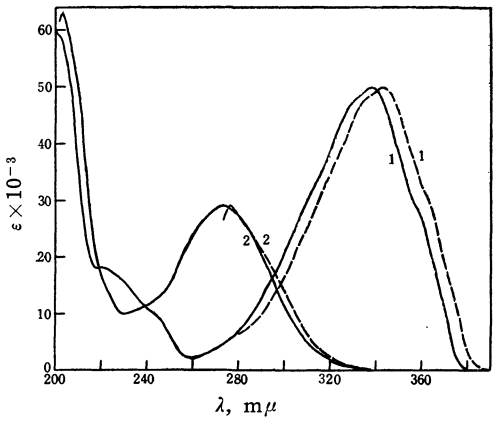



Fig. 2. Ultraviolet absorption spectra: 1, *p,p'*-diphenylstilbene; 2, *p,p'*-diphenyl-*α,α'*-dimethylstilbene: ——, in *n*-heptane; ----, in benzene.

Table I. The solubilities of these compounds in *n*-heptane are so low that the concentrations of the solutions in *n*-heptane and hence the molecular extinction coefficients of the spectra could not be determined. Accordingly, in Table I the intensities of the absorption bands of these compounds in *n*-heptane are represented in absorbance (the solution of the parent compound used is an almost saturated solution, and the solution of the dimethyl derivative is a solution of very roughly quarter the concentration of the saturated solution ; the cell path length is 1 cm.). In Fig. 2, the extinction of the main band of each compound in *n*-heptane has been arbitrarily set to be equal to its extinction in benzene. From these data, it is evident that the solubility of the *α,α'*-dimethyl compound is considerably higher than that of the parent compound. In addition, the melting point of the dimethyl compound (about 240~245°C) is considerably lower than that of the parent compound (about 303~305°C). These facts are very similar to those observed in the comparison between *trans*-stilbene and its *α,α'*-dimethyl derivative[3].

The fine structure of the conjugation band of the diphenylstilbene is further more blurred when compared with that of the phenylstilbene, and the maximum of the former is shifted further toward the longer wavelength than that of the latter. On the other hand, the conjugation band of the dimethyl derivative is almost structureless, and is at a considerably shorter wavelength and of lower intensity than that of the parent compound. This situation is also very similar to that

6) H. Suzuki, ibid., **32**, 1340 (1959).

observed in the comparison between *trans*-stilbene and its $\alpha,\alpha'$-dimethyl derivative[3], and is undoubtedly explained in terms of the steric effect of the methyl substituents.

Similarly to the treatment in the preceding section, the resonance integral for the ethylenic bond is denoted by $\eta\beta$, and the value of $\eta$ is assumed to be 1.080. The resonance integral for the "single" bond between the two benzene rings in each biphenyl part is denoted by $\mu\beta$, and the value of $\mu$ is assumed to be 0.780, being equal to the corresponding value for biphenyl in solution[6]. (This choice of the value is not conclusive, but it is believed that a small change of this value does not alter significantly the final result of the present calculation). The resonance integral for each "single" bond in the stilbene part of the molecule is denoted by $\rho\beta$, in which $\rho$ is the variable in the present calculation.

When as the value of $\rho$ the corresponding value for planar *trans*-stilbene, 0.9084, is taken, the energy of the allowed transition from the highest occupied orbital to the lowest vacant orbital, $\Delta E_A$, is calculated to be 1.0181 $(-\beta)$. This value is $\Delta E_L$ in the present treatment, and is considered to correspond to the wave number of the maximum of the conjugation band of *p,p'*-diphenylstilbene, 29638 $cm^{-1}$ (337.4 m$\mu$). This compound should be more conjugated than *trans*-stilbene as well as biphenyl, and consequently, the lengths of the "single" bonds, the angles of twist of the bonds, and hence the values of $\rho$ and $\mu$ are possibly different from the corresponding ones in *trans*-stilbene and in biphenyl. In spite of this, since it is believed that small changes of the values of $\rho$ and $\mu$ will not significantly alter the final result, on the analogy of the calculation for terphenyls described in Part IV[7] of this series, the calculation is carried out on the basis of the above assumptions.

When $\rho$ is zero, the value of $\Delta E_A$ is 1.523 $(-\beta)$. This value is $\Delta E_S$ in the present calculation, and corresponds to the wave number of the maximum of the conjugation band of biphenyl in *n*-heptane, 40486 $cm^{-1}$ (247.0 m$\mu$)[6].

On the basis of the above references, from the wave numer of the conjugation band of the $\alpha,\alpha'$-dimethyl derivative in *n*-heptane, 36590 $cm^{-1}$ (273.3 m$\mu$), the corresponding value of $\Delta E_A$ is calculated to be 1.342 $(-\beta)$, and then the following corresponding values are obtained by the usual procedure: $\rho$, 0.461; $\theta$, 57°; $R$, 1.488 Å. The calculated value of the interplanar angle $\theta$ between the benzene ring and the ethylenic bond, 57°, for this compound coincides almost completely with the value for *trans*-$\alpha,\alpha'$-dimethylstilbene, 58°[3].

In this connection, it was planned originally to apply a similar method also to 1,2-di-(2-fluorenyl)-ethylene and its 1,2-dimethyl derivative. However, the attempts to prepare these compounds regrettably resulted in failure.

Lastly in this section, the spectra of ketazines may be briefly referred to. Compounds which are probably *p*-biphenylyl methyl ketazine and 2-fluorenyl methyl ketazine were obtained as by-products in the processes of preparation, or in attempts at preparation, of the corresponding dimethylstilbenes, as will be described in the experimental part. The spectra of these ketazines are shown in Fig. 3. These compounds are only very slightly soluble in *n*-heptane, so that the concentrations of the solutions used could not be determined. Consequently, the intensities of absorption are expressed in absorbance (for very roughly saturated solutions; the cell path length, 1 cm.).

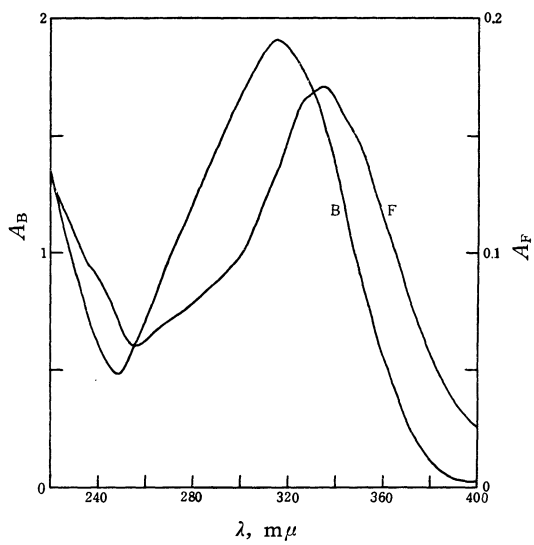



Fig. 3. Ultraviolet absorption spectra: B, *p*-biphenylyl methyl ketazine; F, 2-fluorenyl methyl ketazine. Note separate ordinates for the compounds.

Also in this case, the absorption maximum of the fluorenyl compound (335 m$\mu$) is at a longer wavelength than that of the

7) H. Suzuki, ibid., **33**, 109 (1960).

TABLE II. THE SOLVENT EFFECT OF BENZENE ON THE ULTRAVIOLET ABSORPTION SPECTRA. —The red-shifts of the conjugation bands associated with the change of the solvent from *n*-heptane to benzene.

| Compound | Absorption max. (in *n*-heptane) | | $\Delta\lambda$ mμ | $\Delta\nu$ $cm^{-1}$ | Molecular configuration |
|---|---|---|---|---|---|
| | λ, mμ | ε | | | |
| *p*-Nitrostilbene | 345.0 | 23820 | +5.5 | −455 | planar |
| *p, p'*-Diphenylstilbene | 337.4 | 49900[b)] | +5.6 | −483 | planar |
| 1-Phenyl-2-(2-fluorenyl)-ethylene | 335.8 | 43100 | +5.7 | −497 | planar |
| *p*-Phenylstilbene | 322.5 | 36000 | +5.3 | −502 | planar |
| Tetraphenylethylene | 308.7 | 15300 | +2.5 | −260 | nonplanar |
| *p*-Methoxystilbene | 302.7 | 28950 | +5.0 | −537 | planar |
| Triphenylethylene | 298.5 | 18220 | +3.3 | −366 | nonplanar |
| *trans*-Stilbene | 294.1 | 27950 | +4.7 | −535 | planar |
| *p, p'*-Diphenyl-α, α'-dimethylstilbene | 273.3 | 29000[b)] | +2.9 | −384 | nonplanar |

The values of ε denoted by symbol b represent the values for benzene solutions.

corresponding biphenylyl compound (315 mμ). If these compounds were planar, they would be expected to show the conjugation bands at considerably longer wavelengths than *p,p'*-diphenylstilbene. In fact, however, it is not so. This fact is considered to indicate that these ketazines are conceivably nonplanar.

### Correlation of Solvent Effects of Benzene with Spatial Configurations of Aromatic Solute Molecules

It was previously reported that the conjugation bands of *trans*-stilbene and some related componds are shifted toward considerably longer wavelengths when the solvent is changed from *n*-heptane to benzene[1,2]. A similar phenomenon is observed also with the compounds treated in the present paper. In Table II, the data of the red-shifts observed hitherto are summarized, in which symbols $\Delta\lambda$ and $\Delta\nu$ denote the magnitude of the displacement of the band in wavelength (mμ) and that in wave number, respectively, associated with the change of the solvent from *n*-heptane to benzene. In this table, solely the data on the most intense maximum of the conjugation band of each compound are assembled, the data on the inflections or vestigial bands being excluded.

It is to be noted here that whether or not the apparent absorption maximum of *p,p'*-diphenyl-α, α'-dimethylstilbene in benzene at 276.2 mμ is the true maximum may be somewhat doubtful, because the apparent maximum is so near the shorter-wavelength-side limit (about 270 mμ) of the range in which the measurement of the spectra by using benzene as the solvent is possible. If it is not so, the intrinsic absorption maximum of this compound must be at a shorter wavelength than the apparent maximum. Accordingly, the value of $\Delta\lambda$ for this compound listed in Table II may be considered rather as the upper limit.

Because of inevitable uncertainty in determination of the positions of the absorption maxima, the numerical values of $\Delta\lambda$ as well as $\Delta\nu$ may not be decisive. With such a reservation, however, it seems that the following generalization can be drawn from Table II: whereas the red-shifts for the planar molecules are about 5 mμ, the red-shifts for the probably nonplanar molecules are about 3 mμ and considerably smaller than the values for the planar molecules.

According to Bayliss[8], the magnitude (in $cm^{-1}$) of the red-shift of an absorption band of a nonpolar solute by a nonpolar solvent depends directly on the oscillator strength of the band, inversely on the frequency of the band, therefore, directly on the wavelength of the band, and is related to the refractive index *n* of the solvent at the frequency concerned, depending directly on $(n^2-1)/(2n^2+1)$. Thus, the band is shifted toward lower frequencies and therefore toward longer wavelengths with the increasing refractivity of the solvent.

The refractive index of benzene is greater than that of *n*-heptane. It seems, however, that the great bathochromic effect of benzene relative to *n*-heptane observed here can not be attributed wholly to the difference of refractivity. For

8) N. S. Bayliss, *J. Chem. Phys.*, 18, 292 (1950).

example, by the use of Eq. 12 in Bayliss' paper, the magnitude of the red-shift of the conjugation band of *trans*-stilbene associated with the change of solvent from *n*-heptane to benzene is roughly calculated to be only about 60 $cm^{-1}$. This calculated value is by far smaller than the observed value.

In general, the intensity of the conjugation band of a non-planar compound is considerably smaller than that of the corresponding planar compound. Hence it would be expected that the difference of the magnitude of the red-shift between the planar compounds and the nonplanar compounds might be rather related to the difference of the intensity of the band. This is, however, unlikely, in view of the fact that the conjugation band of *p,p'*-diphenyl-$\alpha,\alpha'$-dimethylstilbene, which is undoubtedly nonplanar, shows a relatively small red-shift in spite of considerably high intensity. Further, as will be evidently seen in Table II, there is no regular relation between the magnitudes of the red-shifts and the wavelengths of the bands.

Therefore, it seems most natural after all to correlate the magnitude of the red-shift with the spatial configuration of the solute molecule, and this correlation seems to suggest, as already mentioned in Part V[1], the presence of a special interaction between the $\pi$-orbitals (or $\pi$-electrons) of the solute molecule and those of benzene.

## Experimental

**Measurements of Spectra.**—The ultraviolet absorption spectra of the olefins were measured with a Cary recording spectrophotometer Model 14 M-50. The spectra of the ketazines were measured with a Beckman type spectrophotometer.

***p*-Phenylstilbene.** — This compound was prepared by the Meerwein reaction. The diazonium salt of *p*-aminobiphenyl was prepared by adding dropwise with stirring a solution of 27 g. of sodium nitrite in 45 ml. of water to a mixture of 300 ml. of 25% hydrochloric acid, 63.4 g. of *p*-aminobiphenyl, and 300 g. of ice. An ice bath was placed around the reaction flask and 235 g. of crystalline sodium acetate was added. A solution of 55.5 g. of cinnamic acid in 900 ml. of acetone was added and the ice bath was removed. Five minutes later a solution of 40.6 g. of cupric chloride in 90 ml. of water was dropwise added and the mixture was stirred for about three hours at room temperature. After being left to stand overnight, the copious green precipitate was collected on a filter and dissolved in a large amount of benzene. The benzene solution was washed in turn with a dilute solution of sodium carbonate, with water, with dilute hydrochloric acid, and then with water, dried on calcium chloride, and treated with activated charcoal. On concentrating the solution by evaporation, pale orange-yellow crystals separated. The crystals were repeatedly recrystallized from benzene. Thus, about 34.5 g. of *p*-phenylstilbene, colorless crystals melting at 220.0~220.5°C, was obtained (about 36% of the theoretical amount). A solution of this compound in benzene shows violet fluorescence.

*p*-Aminobiphenyl was prepared after the procedure described by Schlenk[9] by reducing *p*-nitrobiphenyl in ethanol with stannous chloride and concentrated hydrochloric acid. From 77 g. of *p*-nitrobiphenyl, 64.5 g. of *p*-aminobiphenyl, pale brown-yellow leaflets melting at 53~55°C, was obtained after recrystallization from ethanol (98.6% of the theoretical amount).

*p*-Nitrobiphenyl was prepared, according to the directions of Maki and his coworker[10], by nitration of biphenyl in acetic acid. From 154.2 g. of biphenyl, 91 g. of *p*-nitrobiphenyl, pale yellow needles melting at 114.5~115.3°C, was obtained after recrystallization from ethanol.

**1-Phenyl-2-(2-fluorenyl)-ethylene.** — This compound was prepared by the Meerwein reaction, quite analogously to the preparation of *p*-methoxystilbene described in Part V[1] of this series. From 22.8 g. of 2-aminofluorene, 5.1 g. of the product was obtained after a series of purification processes by treatment with activated charcoal and by repeated recrystallization from benzene; colorless needles melting at 219.5~221.0°C (15.1% of the theoretical amount).

Found: C, 94.04; H, 6.17. Calcd. for $C_{21}H_{16}$: C, 93.99; H, 6.01%.

2-Aminofluorene was prepared by the method described in Organic Syntheses[11], by reducing 2-nitrofluorene in ethanol with zinc dust together with calcium chloride. From 106.3 g. of 2-nitrofluorene, 66.3 g. of 2-aminofluorene, orange-brown needles melting at 125~126.5°C, was obtained (72.7% of the theoretical amount).

2-Nitrofluorene was prepared according to the directions described in Organic Syntheses[11] by nitration of fluorene. From 120 g. of fluorene, 108 g. of the probably somewhat crude product, yellow needles melting at 151~154°C, was obtained (about 71% of the theoretical amount).

***p,p'*-Diphenylstilbene.**—This compound was prepared, after the procedures of preparation of some symmetrical diarylethylenes described by Wood and his coworkers[12] and also the procedures of preparation of 1,2-dimesitylethylene described by Fuson and Best[13], by heating polythio-*p*-phenylbenzaldehyde with copper powder.

9) W. Schlenk, *Ann.*, **368**, 303 (1909).
10) T. Maki and K. Obayashi, *J. Chem. Soc., Japan, Ind. Chem. Sec. (Kogyo Kagaku Zasshi)*, **54**, 375 (1951).
11) W. H. Carothers (Editor-in-Chief), "Organic Syntheses", Vol. XIII, John Wiley & Sons, Inc., New York (1933) p. 74.
12) J. H. Wood, J. A. Bacon, A. W. Meibohm, W. H. Throckmorton and G. P. Turner, *J. Am. Chem. Soc.*, **63**, 1334 (1941).
13) R. C. Fuson and C. E. Best, ibid., **67**, 155 (1945).

A solution of 9.1 g. of *p*-phenylbenzaldehyde in 340 ml. of absolute ethanol was saturated with dry hydrogen chloride. Hydrogen chloride and hydrogen sulfide were then passed into the solution for two and one-half hours at −3∼0°C. The almost white (or pale pink) powder produced in this way was isolated, washed several times with absolute ethanol, and dried in a vacuum desiccator; m. p. 80∼88°C; yield, 9 g. A mixture of 9 g. of the crude thioaldehyde and 26 g. of copper-bronze powder was heated for thirty minutes in a small flask by means of a sand bath at 260∼310°C. The copper powders turned black, and white crystals separated on the surface of the mixture. After cooling, the ethylenic compound was repeatedly extracted with large quantities of boiling xylene. The xylene solution was concentrated to bring about crystallization. Repeated recrystallization from xylene and treatment with activated charcoal gave 0.7 g. of pure *p,p'*-diphenylstilbene, colorless thin plates melting at 301.5∼304.5°C (8.4% of the theoretical amount from the aldehyde). This compound proved to be only slightly soluble in benzene and in xylene, and hardly soluble at all in *n*-heptane and in ethanol. A dilute solution in xylene, benzene, as well as *n*-heptane shows intense violet fluorescence.

Found: C, 94.02; H, 6.28. Calcd. for $C_{26}H_{20}$: C, 93.94; H, 6.06%.

The preparation of *p*-phenylbenzaldehyde, white thin plates melting at 60∼61°C, will be reported in the succeeding part of this series.

The author attempted also to prepare *p,p'*-diphenylstilbene by reducing *p,p'*-diphenylbenzoin with zinc amalgam and hydrochloric acid after the procedures to prepare *trans*-stilbene from benzoin described in Organic Syntheses[14], and also by the method analogous to the one to prepare *trans*-stilbene described by Fieser[15], which involves three steps: replacement of the hydroxyl group of benzoin by chlorine (with thionyl chloride), reduction of the carbonyl group with sodium borohydride to give the chlorohydrin, and elimination of the elements of hypochlorous acid with zinc and acetic acid. These attempts resulted in failure. Thus, by either method, solely an unidentified product, colorless thin plates melting at 227.0∼227.5°C, was obtained in good yield. The ultraviolet absorption spectrum of this compound in *n*-heptane shows a structureless band with the maximum at 275 mμ.

*p,p'*-Diphenylbenzoin was prepared, according to the directions of Gomberg and Natta[16], by the benzoin condensation of *p*-phenylbenzaldehyde. From 42.5 g. of *p*-phenylbenzaldehyde, 25.9 g. of the product purified by repeated recrystallization from xylene and by treatment with activated charcoal, almost colorless or faint yellow crystals melting at 166∼169.5°C, was obtained (61% of the theoretical amount). As a by-product, about 2 g. of *p*-phenylbenzoic acid, colorless needles melting at 219.5∼222°C, was obtained.

***p,p'*-Diphenyl-*α,α'*-dimethylstilbene.**—This compound was prepared from *p*-phenylacetophenone (*p*-biphenylyl methyl ketone) after the Vargha Kovács' method[17]. A mixture of 10 g. of *p*-phenylacetophenone, 100 ml. of isopropyl alcohol, and 25 g. of 80% hydrazine hydrate was refluxed for about 30 hr. A thick white precipitate of the hydrazone was collected and dried in a vacuum desiccator. The hydrazone proved to be soluble with difficulty in petroleum ether. To a solution of the crude hydrazone in about 500 ml. of benzene, 18.1 g. of yellow mercuric oxide was added, and the mixture was stirred for about 9 hr. at room temperature. After filtration, into the pale red-orange solution sulfur dioxide was passed for thirty minutes. After removal of the solvent, the yellow residual solid was extracted with petroleum ether (b.p. 80∼100°C). Repeated recrystallization of the residue from xylene gave 5.8 g. of a compound, yellow, bright, thin plates melting at 274.5°C, which is probably *p*-biphenylyl methyl ketazine. On the other hand, the petroleum ether extract solution was filtered through a chromatographic column of alumina, and then concentrated to bring about crystallization. Fractional recrystallization of the crystals from petroleum ether gave very small quantities of colorless prisms melting at 240∼245°C and small quantities of pale yellow needles melting at about 260∼290°C. Although both the quantities were far too small for complete identification, the former compound (the colorless prisms) is considered probably to be the desired compound. On the other hand, the ultraviolet absorption spectrum of the latter in *n*-heptane shows a band with maxima at 289 and 313.5 mμ, and the spectrum in benzene shows a structureless band at 300 mμ.

The poorness of the yield of the desired compound in the above experiment is considered to originate in imperfection of the oxidation of the hydrazone. The author attempted to oxidize the hydrazone by using lead dioxide instead of mercuric oxide, and also by using petroleum ether as solvent (suspension). However, these attempts resulted in failure, the only isolated product in each experiment being the ketazine.

The author attempted to prepare this dimethyl compound also after the procedures described by Cline and his coworkers[18] to prepare *α,α'*-dimethylstilbene by heating trithioacetophenone with Raney nickel in xylene in an atmosphere of nitrogen. From 6.3 g. of *p*-phenylacetophenone, about 4 g. of the corresponding thio compound, pale grayish yellow powder, was obtained after the procedures of the preparation of trithioacetophenone described by Baumann and Fromm[19].

14) L. I. Smith (Editor-in-Chief), "Organic Syntheses", Vol. 23, John Wiley & Sons, Inc., New York (1943), p. 86.
15) L. F. Fieser, "Experiments in Organic Chemistry", 3rd. Ed., D. C. Heath and Company, New York (1955), p. 179—180.
16) M. Gomberg and F. J. Van Natta, *J. Am. Chem. Soc.*, **51**, 2238 (1929).
17) L. v. Vargha and E. Kovács, *Ber.*, **75B**, 794 (1942).
18) J. K. Cline, E. Campaign and J. W. Spies, *J. Am. Chem. Soc.*, **66**, 1136 (1944).
19) E. Baumann and E. Fromm, *Ber.*, **28**, 895 (1895).

However, the final product obtained by heating the thio compound with Raney nickel was yellow, bright crystals melting at 328.5~330.0°C and soluble with difficulty in usual organic solvents. The ultraviolet absorption spectrum of this product in benzene showed a structureless band with the maximum at 354 mμ.

The preparation of *p*-phenylacetophenone, m.p. 119~121.5°C, will be described in the succeeding part of this series.

**Unsuccessful Attempts to Prepare 1,2-Di-(2-fluorenyl)-ethylene.** — Preparation of this compound by heating polythio-2-formylfluorene with copper powder after the preparation of *p,p'*-diphenylstilbene described above was attempted. However, the only product isolated was pale yellow needles melting at 289~290.5°C, whose spectrum in *n*-heptane resembles the spectum of 2-formylfluorene as well as that of 2-acetylfluorene (cf. the succeeding part of this series), showing a band with well-resolved fine structure, the most intense maximum of which is at about 310.5 mμ. This product is probably not the desired compound, as was revealed by the spectrum.

The preparation of 2-formylfluorene, faint yellow needles melting at 85.5~86.5°C, will be described in the succeeding part of this series.

**Unsuccessful Attempts to Prepare 2,3-Di-(2-fluorenyl)-2-butene.** — Preparation of this compound by the Vargha and Kovács' method analogously to the preparation of 2,3-di-*p*-biphenylyl-2-butene (*p,p'*-diphenyl-α,α'-dimethylstilbene) described above was attempted. However, the attempts to oxidize the hydrazone of 2-fluorenyl methyl ketone (2-acetylfluorene) with mercuric oxide and with lead dioxide were unsuccessful, and the only isolated product was an orange-yellow crystalline compound melting at 301~302°C, which is considered to be 2-fluorenyl methyl ketazine.

The preparation of 2-acetylfluorene, colorless crystals melting at 127.5~128°C, will be described in the succeeding part of this series.

The author desires to thank Professor Kengo Shiomi for reading the manuscript and for advice, and Dr. Makoto Takahasi for his interest and encouragement. The micro-analyses were carried out by Mr. Shozo Masuda.

*Department of Chemistry*
*College of General Education*
*The University of Tokyo*
*Meguro-ku, Tokyo*

# *The Formation Constants of Metal Acetate Complexes. II. Polarographic Determination of the Formation Constants of Acetatocopper(II), Acetatolead(II) and Acetatozinc(II) Complexes*

By Nobuyuki TANAKA and Kiyoko KATO*

(Received September 18, 1959)

In the previous paper[1], a new method for the determination of the formation constants of metal acetate complexes and its application to the study of acetatonickel(II) complexes were presented. The method is based on the polarographic measurement of the sum of the equilibrium concentrations of hydrated metal ions and metal acetate complexes in the presence of an appropriate auxiliary complex-forming substance. Although it has advantages over the conventional methods, its application to other metal acetate complexes seems to be difficult.

In this paper are presented the procedure and the results of the determination of the formation constants of acetatocopper(II), acetatolead(II) and acetatozinc(II) complexes. The procedure is applicable when the formation constants of certain metal acetate complexes are known and can be used as standards.

## Theoretical

Let us consider the acetate buffer solution which contains two different metal ions, $M^{m+}$ and $M'^{m'+}$, and ethylenediaminetetraacetate (EDTA) ions. There exist the following equilibria:

$$M^{m+} + M'Y^{(m'-4)+} \rightleftarrows MY^{(m-4)+} + M'^{m'+} \quad (1)$$

$$MY^{(m-4)+} + H^{+} \rightleftarrows MHY^{(m-3)+} \quad (2)$$

* Present address: The Women's Department, Tokyo College of Pharmacy, 31, Uenosakuragi-cho, Taito-ku, Tokyo.

1) N. Tanaka and K. Kato, This Bulletin, **32**, 516 (1959).

$$M'Y^{(m'-4)+} + H^+ \rightleftarrows M'HY^{(m'-3)+} \quad (3)$$

$$M^{m+} + nOAc^- \rightleftarrows M(OAc)_n^{(m-n)+} \quad (4)$$

$$M'^{m'+} + n'OAc^- \rightleftarrows M'(OAc)_{n'}^{(m'-n')+} \quad (5)$$

where $Y^{4-}$ means a completely dissociated EDTA anion. The overall substitution reaction between $M^{m+}$ and $M'Y^{(m'-4)+}$ in the acetate buffer solution, therefore, may be represented as

$$\left\{\begin{matrix} M^{m+} \\ \uparrow\downarrow \\ M(OAc)_n^{(m-n)+} \end{matrix}\right\} + \left\{\begin{matrix} M'Y^{(m'-4)+} \\ \uparrow\downarrow \\ M'HY^{(m'-3)+} \end{matrix}\right\} \rightleftarrows \left\{\begin{matrix} M'^{m'+} \\ \uparrow\downarrow \\ M'(OAc)_{n'}^{(m'-n')+} \end{matrix}\right\} + \left\{\begin{matrix} MY^{(m-4)+} \\ \uparrow\downarrow \\ MHY^{(m-3)+} \end{matrix}\right\} \quad (6)$$

In the polarographic measurement, the diffusion current of metal ions obtained in acetate media corresponds to the sum of the diffusion current of the hydrated metal ions and that of the acetato complexes[1]. Consequently, the concentrations that can be determined polarographically are $[M^{m+}]_{app}$ and $[M'^{m'+}]_{app}$ given by the equations

$$[M^{m+}]_{app} = [M^{m+}] + \sum_1^n [M(OAc)_n^{(m-n)+}] \quad (7)$$

and

$$[M'^{m'+}]_{app} = [M'^{m'+}] + \sum_1^{n'} [M'(OAc)_{n'}^{(m'-n')+}] \quad (8)$$

respectively.

The total concentrations of metals and EDTA, $[M]_t$, $[M']_t$ and $[EDTA]_t$, in the solution are given in terms of the concentrations of the ionic and molecular species present:

$$[M]_t = [M^{m+}]_{app} + [MY^{(m-4)+}] + [MHY^{(m-3)+}] \quad (9)$$

$$[M']_t = [M'^{m'+}]_{app} + [M'Y^{(m'-4)+}] + [M'HY^{(m'-3)+}] \quad (10)$$

$$[EDTA]_t = [EDTA]_f + [MY^{(m-4)+}] + [MHY^{(m-3)+}] + [M'Y^{(m'-4)+}] + [M'HY^{(m'-3)+}] \quad (11)$$

where $[EDTA]_f$ represents the concentration of the uncomplexed EDTA. Under the condition that $[M]_t + [M']_t > [EDTA]_t$, $[EDTA]_f$ is negligibly small as compared with the concentrations of other species in the solution.

From the polarographic measurement of either $[M^{m+}]_{app}$ or $[M'^{m'+}]_{app}$, the equilibrium constant of Eq. 6

$$K^{M'}_{M,\,app} = \frac{[M'^{m'+}]_{app}\{[MY^{(m-4)+}] + [MHY^{(m-3)+}]\}}{[M^{m+}]_{app}\{[M'Y^{(m'-4)+}] + [M'HY^{(m'-3)+}]\}} \quad (12)$$

is obtained with the relations given by Eqs. 9 to 11, provided that the values of $[M]_t$, $[M']_t$, and $[EDTA]_t$ are known. The constant $K^M_{M',\,app}$ may be called the apparent equilibrium constant of the substitution reaction in question. On the other hand, the equilibrium constant of the substitution reaction given by Eq. 1 is expressed as

$$K^M_{M'} = \frac{[M'^{m'+}]\,[MY^{(m-4)+}]}{[M^{m+}]\,[M'Y^{(m'-4)+}]} \quad (13)$$

Introducing Eqs. 7, 8 and 13 into Eq. 12, $K^M_{M',\,app}$ is rewritten as

$$K^M_{M',\,app} = K^M_{M'} \frac{\beta}{\beta'} \frac{1 + \sum_1^{n'} K_{M'(OAc)_{n'}} [OAc^-]^{n'}}{1 + \sum_1^{n} K_{M(OAc)_n} [OAc^-]^n} \quad (14)$$

$$\beta = 1 + K^H_{MHY}[H^+]$$

$$\beta' = 1 + K^H_{M'HY}[H^+]$$

where $K_{M(OAc)_n}$ and $K_{M'(OAc)_{n'}}$ represent the overall formation constants of $M(OAc)_n^{(m-n)+}$ and $M'(OAc)_{n'}^{(m'-n')+}$, respectively, and $K^H_{MHY}$ and $K^H_{M'HY}$, the equilibrium constants of the reactions of Eqs. 2 and 3, respectively.

If the formation constants of acetato complexes of one of the metals are known, those of the other can be determined with Eq. 14 by the measurement of $K^M_{M',\,app}$ at various acetate concentrations. When the values of $K_{M(OAc)_n}$ are known, Eq. 14 is conveniently arranged as

$$F_0 \equiv K^M_{M',\,app}\left\{1 + \sum_1^n K_{M(OAc)_n}[OAc^-]^n\right\} = K^M_{M'}\frac{\beta}{\beta'}\left\{1 + \sum_1^{n'} K_{M'(OAc)_{n'}}[OAc^-]^{n'}\right\} \quad (15)$$

From the extrapolation of the plot of $F_0$ vs. $[OAc^-]$ to zero acetate concentration, $\frac{\beta}{\beta'}K^M_{M'}$ is obtained. Then, the functions $F_1, F_2, \cdots, F_{n'}$ are defined, which are written as follows:

$$F_1 \equiv \frac{F_0 - \frac{\beta}{\beta'}K^M_{M'}}{\frac{\beta}{\beta'}K^M_{M'}[OAc^-]} = K_{M'OAc} + K_{M'(OAc)_2}[OAc^-] + \cdots\cdots \quad (16)$$

$$F_2 \equiv \frac{F_1 - K_{M'OAc}}{[OAc^-]} = K_{M'(OAc)_2} + K_{M'(OAc)_3}[OAc^-] + \cdots\cdots \quad (17)$$

.....

$$F_{n'} \equiv \frac{F_{n'-1} - K_{M'(OAc)_{n'-1}}}{[OAc^-]} = K_{M'(OAc)_{n'}} \quad (18)$$

$F_1$ is plotted against $[OAc^-]$ and the value of $K_{M'OAc}$ is determined by extrapolating the plot to zero acetate concentration. Further treatment leads to the determination of $K_{M'(OAc)_{n'}}$, if higher acetato complexes are present in the solution.

When the formation constants of $M'(OAc)_{n'}^{(m'-n')+}$ are known, similar relations are derived:

$$F_0' \equiv \frac{1 + \sum_1^{n'} K_{M'(OAc)_{n'}} [OAc^-]^{n'}}{K^M_{M',app}} = \frac{\beta'}{\beta K^M_{M'}} \left\{ 1 + \sum_1^{n} K_{M(OAc)_n} [OAc^-]^n \right\} \quad (15')$$

$$F_1' \equiv \frac{F_0' - \frac{\beta'}{\beta K^M_{M'}}}{\frac{\beta'}{\beta K^M_{M'}} [OAc^-]} = K_{MOAc} + K_{M(OAc)_2} [OAc^-] + \cdots\cdots \quad (16')$$

$$F_2' \equiv \frac{F_1' - K_{MOAc}}{[OAc^-]} = K_{M(OAc)_2} + K_{M(OAc)_3} [OAc^-] + \cdots\cdots \quad (17')$$

The values of $K_{M(OAc)_n}$ can be determined by the same procedure as for those of $K_{M'(OAc)n'}$.

## Experimental

**Reagent.** — Standard solutions of copper(II) nitrate and zinc nitrate were prepared by dissolving known amounts of pure copper and zinc metals, respectively, in a reagent-grade nitric acid. A standard solution of nickel nitrate was the same as used in the previous study[1]. The solution of disodium ethylenediaminetetraacetate was standardized against the standard solution of copper(II) nitrate by amperometric titration[2]. A standard solution of lead nitrate was prepared by dissolving an appropriate quantity of reagent-grade lead nitrate. Its concentration was determined amperometrically with the standardized EDTA solution[2]. For buffers and supporting electrolytes, guaranteed reagents were used without further purification.

**Apparatus and Procedure.** — The polarograph and the dropping mercury electrode used were the same as those described in the previous paper[1]. The dropping mercury electrode had an $m$ value of 1.27 mg./sec. and a drop time $\tau$ of 3.69 sec. in an air-free 0.1 M potassium chloride solution at 25°C with open circuit. The measurements of the diffusion currents of copper(II) in acetate buffer solutions were carried out with the following three reaction mixtures:

(a) copper(II)-nickel(II)-EDTA
(b) copper(II)-lead(II)-EDTA
(c) copper(II)-zinc(II)-EDTA

The measurements were made at 15, 25 and 35°C in acetate buffers of pH 4.7±0.1 in which the acetate concentrations were varied from 0.01 M to 0.2 M. The ionic strength was adjusted to be 0.2 with potassium nitrate. Gelatin was added as a maximum suppressor by 0.01% in concentration.

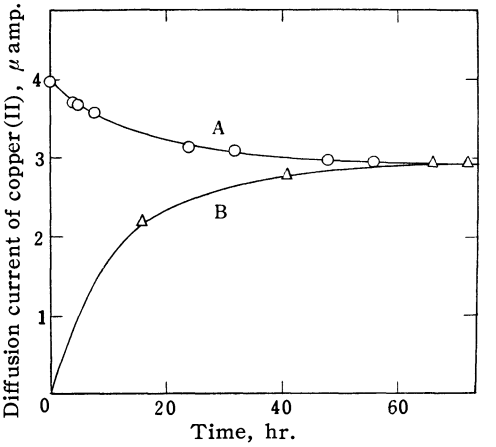



Fig. 1. Relation between the diffusion current of copper(II) and time in the forward (curve A) and the reverse (curve B) reactions of the substitution reaction $Cu^{2+} + NiY^{2-} \rightleftarrows CuY^{2-} + Ni^{2+}$, measured in acetate buffer solutions of pH 4.7 at 15°C. Total concentrations are: $[Cu]_t = 1.00 \times 10^{-3}$ M; $[Ni]_t = 1.50 \times 10^{-3}$ M; $[EDTA]_t = 1.00 \times 10^{-3}$ M.

The substitution reactions involving the EDTA complexes are not always completed instantaneously. The rates of these reactions vary widely according to the system investigated. In systems (b) and (c), the reactions are nearly completed within a few minutes under the experimental conditions. The reaction mixtures, therefore, were subjected to the measurement approximately 3 hours after the preparation. On the other hand, it has often been stated that the exchange or substitution reactions involving the nickel-EDTA complexes proceed at a relatively slow rate[3-7]. This was confirmed also in this study by the fact that the reaction mixtures of system (a) reach the equilibrium extremely slowly. One of the examples is given in Fig. 1, where the change of the polarographic diffusion current of copper(II) in the reaction mixture is plotted against

2) N. Tanaka, M. Kodama, M. Sasaki and M. Sugino, *Japan Analyst (Bunseki Kagaku)*, **6**, 86 (1957).

3) F. A. Long, S. S. Jones and M. Burke, *Brookhaven Conf. Rept. BNE-C-8*, **2**, 106 (1948).

4) C. M. Cook, Jr. and F. A. Long, *J. Am. Chem. Soc.*, **80**, 33 (1958).

5) G. Schwarzenbach, R. Gut and G. Anderegg, *Helv. Chim. Acta*, **37**, 937 (1954).

6) K. Bril and P. Krumholz, *J. Phys. Chem.*, **57**, 874 (1953).

7) N. Tanaka and Y. Sakuma, This Bulletin, **32**, 578 (1959).

the time for the forward and reverse reactions. Fig. 1 shows that the reaction equilibrates approximately 60 hours after the initiation of the reaction. In system (a), therefore, all measurements were made about 3 days after the solutions had been prepared.

## Results

The apparent diffusion current constants of copper(II) were determined by measuring the diffusion current at various acetate concentrations. The values of $[Cu^{2+}]_{app}$ were calculated with the aid of those apparent diffusion current constants from the diffusion currents obtained with the reaction mixtures of systems (a), (b) and (c). Then, the apparent equilibrium constants $K^{M}_{M',app}$ given by Eq. 12 were calculated, with which $F_0$, $F_1$……$F_{n'}$ (or $F_0'$, $F_1'$……$F_{n'}$) were successively obtained. The results obtained for systems (a), (b) and (c) are given below. The values of $\beta/\beta'$ (or $\beta'/\beta$) in Eq. 14 were calculated with the equilibrium constants $K^{H}_{MHY}$ and $K^{H}_{M'HY}$ given by Schwarzenbach et al.[5], with the result that they are approximately unity for all three systems at pH of the present experiments.

**Copper(II) - Nickel(II) - EDTA System.** — In the solution containing acetate up to 0.2 M in concentration, nickel(II) forms only a monoacetato complex, its formation constant $K_{NiOAc}$ at ionic strength 0.2 being 2.6, 2.6 and 2.4 at 15, 25 and 35°C, respectively[1]. With the aid of these values, the formation constants of acetatocopper(II) complexes were obtained by determining the values for $K^{Cu}_{Ni,app}$ at various acetate concentrations. The $K^{Cu}_{Ni,app}$ is given by the equation

$$K^{Cu}_{Ni,app}=\frac{[Ni^{2+}]_{app}[CuY^{2-}]}{[Cu^{2+}]_{app}[NiY^{2-}]}$$

$F_0'$ and $F_1'$ given by Eqs. 15′ and 16′ respectively were calculated and plotted against the acetate ion concentration. These plots for 25°C are shown in Fig. 2, in which the $F_1'$ plot gives a straight line. This fact clearly indicates that no appreciable amount of complexes with three acetates or more co-ordinated is present in the solution under the experimental conditions. From the $F_1'$ plot the formation constants of mono- and diacetatocopper(II) complexes, $K_{CuOAc}$ and $K_{Cu(OAc)_2}$, were determined, the former being determined by the intercept at zero acetate concentration and the latter, by the slope.

Similar relations were also found at 15 and 35°C. The formation constants obtained at various temperatures are given in Table I.

**Copper(II)-Lead(II)-EDTA System.** — The formation constants of acetatolead(II) complexes were determined by the measurement of $K^{Cu}_{Pb,app}$ at various acetate concentrations with the aid of the formation constants of $CuOAc^+$ and $Cu(OAc)_2$ obtained in this study, where $K^{Cu}_{Pb,app}$ is given by the equation

$$K^{Cu}_{Pb,app}=\frac{[Pb^{2+}]_{app}[CuY^{2-}]}{[Cu^{2+}]_{app}[PbY^{2-}]}$$

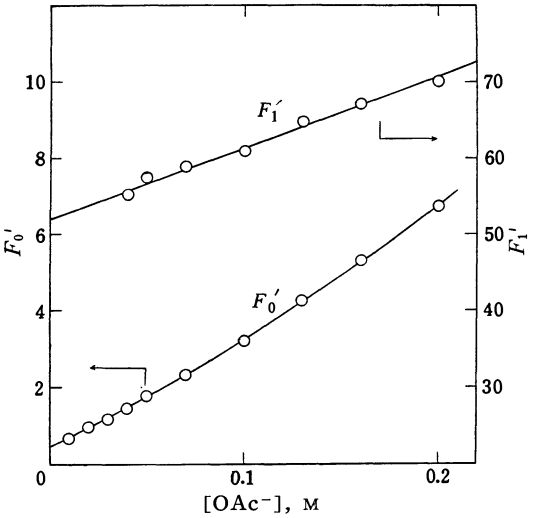



Fig. 2. $F_0'$ (Eq. 15′) and $F_1'$ (Eq. 16′) as a function of the acetate ion concentration in copper(II)-nickel(II)-EDTA system at 25°C.

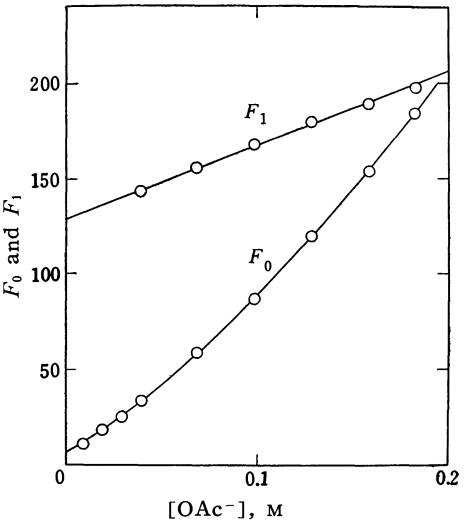



Fig. 3. $F_0$ (Eq. 15) and $F_1$ (Eq. 16) as a function of the acetate ion concentration in copper(II)-lead(II)-EDTA system at 25°C.

In this case $F_0$ and $F_1$ given by Eqs. 15 and 16 were calculated and plotted instead of $F_0'$ and $F_1'$. In Fig. 3 these plots for 25°C are shown, where the $F_1$ plot gives a straight line indicating that $PbOAc^+$ and $Pb(OAc)_2$ are appreciable species of acetatolead(II) complexes present in the solution. Similar plots were obtained at 15 and 35°C. The formation constants of $PbOAc^+$ and $Pb(OAc)_2$ were determined. These are given in Table I.

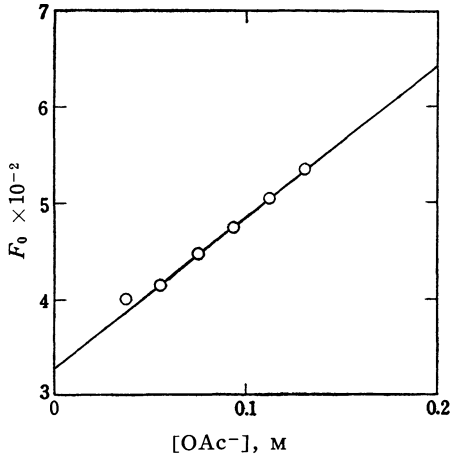



Fig. 4. $F_0$ (Eq. 15) as a function of the acetate ion concentration in copper(II)-zinc(II)-EDTA system at 25°C.

**Copper(II) - Zinc(II) - EDTA System.** — The formation constants of acetatozinc(II) complexes were determined with the same procedure as for the acetatolead(II) complexes. $K^{Cu}_{Zn,\,app}$ which is given by the equation

$$K^{Cu}_{Zn,\,app} = \frac{[Zn^{2+}]_{app}\,[CuY^{2-}]}{[Cu^{2+}]_{app}\,[ZnY^{2-}]}$$

was determined at various acetate concentrations. In this case it was found that

TABLE I. FORMATION CONSTANTS OF ACETATOCOPPER(II), ACETATOLEAD(II) AND ACETATOZINC(II) COMPLEXES AT VARIOUS TEMPERATURES

| Metal ion | Temp.,°C | $K_{MOAc}$ | $K_{M(OAc)_2}$ |
|---|---|---|---|
| Copper(II) | 15 | 41 | 190 |
| | 25 | 52 | 93 |
| | 35 | 69 | 82 |
| Lead(II) | 15 | 130 | 750 |
| | 25 | 130 | 390 |
| | 35 | 120 | 380 |
| Zinc(II) | 15 | 5.7 | — |
| | 25 | 4.6 | — |
| | 35 | 3.7 | — |

TABLE II. SOME EXAMPLES OF THE REPORTED VALUES OF FORMATION CONSTANTS OF ACETATOCOPPER(II), ACETATOLEAD(II) AND ACETATOZINC(II) COMPLEXES

| Metal ion | Investigator | Method | Temp., °C | Ionic strength | $K_{MOAc}$ | $K_{M(OAc)_2}$ | Ref. |
|---|---|---|---|---|---|---|---|
| Copper(II) | Pedersen | Potentiometric | 18 | 0.2 | 46.7 | 316 | 8 |
| | Fronæus | Ion-exchange | 20 | 1 | 45 | 440 | 9 |
| | Sircar et al. | Potentiometric | 29~33 | 0 | 250 | 2000 | 10 |
| | | | | 0.2 | 83* | 350* | (10) |
| Lead(II) | Aditya et al. | Potentiometric | 30 | 0 | 270 | 9000 | 11,12 |
| | | | | 0.2 | 76* | 1300* | (11,12) |
| | Burns et al. | Polarographic | 25 | 1.98 | 150 | 840 | 13 |
| | Siddhanta et al. | Potentiometric | 31~34.5 | 0 | 302 | 9700 | 14 |
| | | | | 0.2 | 85* | 1500* | (14) |
| Zinc(II) | Cannan et al. | Potentiometric | — | 0.2 | 10.7 | — | 15 |
| | Bardhan et al. | Solubility | 35 | 0 | 39 | — | 16 |
| | | | | 0.2 | 13* | | (16) |
| | Bardhan et al. | Potentiometric | 35 | 0 | 29 | — | 16 |
| | | | | 0.2 | 9.6* | | (16) |

* Those values are the formation constants which were calculated by the present authors with the values reported in the literature referred to. In the calculation, the activity coefficients of copper(II), lead(II), zinc(II) and acetate ions were estimated to be 0.33, 0.28, 0.33 and 0.73, respectively, and the activity coefficient of monoacetato complexes was assumed to be equal to that of acetate ions.

8) K. J. Pedersen. *Det Kgl. Danske Viedenskab. Selskab. Math-Fys. Medd.*, **22**, No. 12 (1945).
9) S. Fronæus, *Acta Chem. Scand.*, **5**, 859 (1951).
10) S. C. Sircar. S. Aditya and B. Prasad, *J. Indian Chem. Soc.*, **30**, 633 (1953).
11) N. K. Das, S. Aditya and B. Prasad, ibid., **29**, 169 (1952).
12) S. Aditya and B. Prasad, ibid., **30**, 213 (1953).
13) E. A. Burns and D. N. Hume, *J. Am. Chem. Soc.*, 78, 3958 (1956).
14) S. K. Siddhanta and S. N. Banerjee, *J. Indian Chem. Soc.*, **35**, 323 (1958).
15) R. K. Cannan and A. Kibrick, *J. Am. Chem. Soc.*, **60**, 2314 (1938).
16) S. Bardhan and S. Aditya, *J. Indian Chem. Soc.*, **32**, 105 (1955).

TABLE III. EQUILIBRIUM CONSTANTS FOR THE SUBSTITUTION REACTION (EQ. 1) AT VARIOUS TEMPERATURES COMPARED WITH SCHWARZENBACH'S VALUES

| | | 15°C | 20°C | 25°C | 35°C |
|---|---|---|---|---|---|
| Copper(II)-Nickel(II) | $K^{Cu}_{Ni}$ a) | 2.0 | — | 2.2 | 2.5 |
| | $K^{Cu}_{Ni,app}$ b) | — | 1.5 | — | — |
| | $K^{Cu}_{NI,cor}$ c) | — | 2.1 | — | — |
| Copper(II)-Lead(II) | $K^{Cu}_{Pb}$ a) | 3.2 | — | 5.0 | 8.0 |
| | $K^{Cu}_{Pb,app}$ b) | — | 6.3 | — | — |
| | $K^{Cu}_{Pb,cor}$ c) | — | 4.4 | — | — |
| Copper(II)-Zinc(II) | $K^{Cu}_{Zn}$ a) | $3.2\times10^2$ | — | $3.3\times10^2$ | $3.4\times10^2$ |
| | $K^{Cu}_{Zn,app}$ b) | — | $2.1\times10^2$ | — | — |
| | $K^{Cu}_{Zn,cor}$ c) | — | $2.9\times10^2$ | — | — |

a) Values obtained in the present investigation.
b) Values obtained by Schwarzenbach et al.
c) Values calculated from Schwarzenbach's values with Eq. 14.

the $F_0$ plot gave a straight line, which is shown in Fig. 4. This fact led to the conclusion that at acetate concentration up to 0.2 M, $ZnOAc^+$ is the only species which exists in the solution at an appreciable concentration. Similar relations were obtained also at 15 and 35°C. The formation constants of $ZnOAc^+$ are listed in Table I.

## Discussion

The formation constants of the acetato complexes of copper(II), lead(II) and zinc(II) have been determined by various researchers. Some of them are given in Table II. These are compared with the formation constants given in Table I.

Recently, Yasuda and Yamasaki[18] studied the complex formation of some carboxylic acids by the pH titration method. They compared the stabilities of the complexes of bivalent metal ions and found that the order of Pb > Cu > Zn, Cd > Ni is valid for the complexes which contain co-ordinating groups such as benzoate, phthalate and succinate. The magnitude of the first formation constants of acetato complexes of nickel(II), copper(II), lead(II) and zinc(II) determined by the present authors are in accordance with the above order. This fact supports the validity of the rule proposed by Yasuda and Yamasaki.

The equilibria of the substitution reaction represented by Eq. 1 have been studied. The equilibrium constants so far obtained, however, are considered to be not $K^M_{M'}$, but $K^M_{M',app}$, because they were determined in the acetate media but not corrected for the effect of acetate ions on the equilibria. In the present paper, the values of $K^M_{M'}$ given in Eq. 13 were determined by the extrapolation of the $F_0$ (or $F_0'$) plot to zero acetate concentration. In Table III, the values of $K^M_{M'}$ for the three substitution reactions obtained in this study are summarized together with those obtained by Schwarzenbach et al.[5] for the same reactions. Schwarzenbach and his co-workers studied these equilibria at 20°C in the solution of ionic strength 0.1 with $8\times10^{-3}$ M sodium acetate. The effect of acetato complex formation can be corrected with the relation given by Eq. 14. The original values given by Schwarzenbach et al. were converted to the $K^M_{M'}$ values using the formation constants $K_{M(OAc)_n}$ and $K_{M'(OAc)_{n'}}$ determined in this study. The resulting constants are also given in Table III, which are in satisfactory agreement with the $K^M_{M'}$ values observed experimentally in this study. This fact proves clearly the validity of the procedure and the results presented in this paper.

## Summary

A new procedure for the determination of the formation constants of metal acetate complexes was developed. The procedure is

17) J. Kielland, *J. Am. Chem. Soc.*, **59**, 1675 (1937).
18) M. Yasuda and K. Yamasaki, presented at the Symposium on Metal Complexes, Tokyo, November, 1958.

based on the polarographic measurements of the sum of the equilibrium concentrations of the hydrated metal ions and the metal acetate complexes in the presence of an appropriate auxiliary complex-forming substance and of the reference metal ions of which the formation constants of acetate complexes are known.

The procedure was applied to the study of acetatocopper(II), acetatolead(II) and acetatozinc(II) complexes, EDTA being used as an auxiliary complex-forming substance. The overall formation constants $K_{M(OAc)_n}$ ($n=1$ and 2) for these metal acetate complexes were determined at an ionic strength of 0.2 at 15, 25 and 35°C.

The authors thank the Ministry of Education for the financial support granted for this research.

*Department of Chemistry*
*Faculty of Science*
*Tohoku University*
*Katahira-cho, Sendai*

# SHORT COMMUNICATIONS

## *Confirmation of the Catalytic Deuteration of Methyl Groups of p-Xylene by the Use of the Infrared and NMR Methods*

By Kozo Hirota, Hazime Kusumoto and Tomiko Ueda

(Received November 11, 1959)

It has been considered generally that the catalytic isotopic exchange reaction of hydrogen atoms with deuterium oxide occurs much more difficultly at paraffinoid hydrocarbons than at benzenoid hydrocarbons. However, as reported already[1] the exchange reaction of *p*-xylene catalyzed by nickel powders occurs also at the hydrogen atoms of the methyl groups, judging from the mass-spectrometric and infrared data of the products. In order to confirm such an expected result, the same samples were analyzed by the NMR apparatus of high resolution type (Varian V-4300 B). The conclusion was the same as already obtained. However, it was found that the proton signal of the methyl groups splitted into three or five components. Such a splitting may be not only interesting as a sure evidence of the above conclusions, but also would be noteworthy as a rare case where spin-spin coupling between H and D nuclei attached to the same carbon atom was observed. Although the similar splitting phenomenon has been reported by some researchers[2], the NMR results also will be presented here preliminarily in connection with the essential point of the research.

Nickel powders were prepared by decomposing nickel formate, oxidizing with air at 300°C and reducing at 400°C with hydrogen for 8 hr. Exchange reaction was carried out in a sealed glass tube, which contained a known amount of pure *p*-xylene and deuterium oxide (99.7% $D_2O$) as well as nickel catalyst. During the reaction, the tube was kept in a thermostat without shaking. After the definite time the reaction was stopped, and the *p*-xylene was separated from both heavy water and catalyst.

As an example of the experiment the most deuterated run, (No. 5), in which the reactants *p*-xylene and $D_2O$, were 0.4792 g. and 0.4864 g., respectively, and which were carried out for 150 hr. at 100°C will be referred. The numbers of deuterium ($d_i$) atoms in *p*-xylene molecules, determined by the mass-spectrometer, were as follows (%):

$$d_0=0.2,\ d_1=2.0,\ d_2=9.0,\ d_3=23.5,\ d_4=32.6,$$
$$d_5=24.7,\ d_6=7.9,\ d_7=0.1,\ d_8=d_9=d_{10}=0.0.$$

1) Abstracts of the 12th Annual Meeting of the Chemical Society of Japan (1959), p. 85.

2) (a) M. Karplus, D. H. Anderson, T. C. T. Farrer and H. S. Gutowsky, *J. Chem. Phys.*, **27**, 597 (1957); M. Karplus and D. H. Anderson, ibid., **30**, 6 (1957). (b) J. N. Schoolery, *Svensk. Kem. Tidskr.*, **69**, 185 (1957). (c) G. V. D. Tiers, *J. Chem. Phys.*, **29**, 963 (1958).

By the infrared method, three bands could be observed at the region of the C–D stretching bands, i. e. 2187, 2118 and 2047 $cm^{-1}$ (broad). They can be ascribed to the bands of deuterated methyl groups, because in the case when the exchange reaction had been carried out by use of $D_2SO_4$ in order to deuterate the hydrogen atoms at the benzene ring[3], one C–D band appeared at 2254 $cm^{-1}$. This conclusion is not contradictory to the mass-spectrometric data, because *p*-xylene molecules highly deuterated more than six were negligibly small. Therefore it may be concluded that the exchange reaction proceeded practically at the six hydrogen atoms of the methyl groups (cf. Fig. 1).

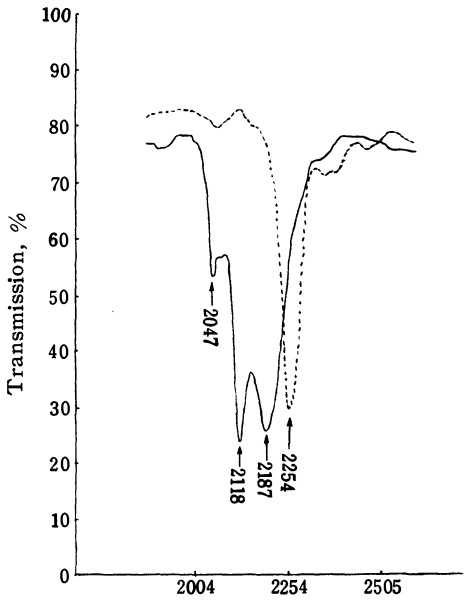



Fig. 1. Infrared absorption spectra of the deuterated samples.
——: Ni catalyst (deuterated degree= 39%)
------: $H_2SO_4$ catalyst (deuterated degree =23%)[3]

By the NMR measurements relative intensity ratio of the proton signals of the methyl and ring groups in the original *p*-xylene should be expected to be 3 : 2 in singlet. This ratio would be expected to change as the deuteration proceeded. Actually the sample in medium process changed it, and moreover the methyl group spectrum had a structure which could be considered as superposed singlet and triplet components. These structures may be assigned to spectra from protons in $CH_3$ groups and those in $CH_2D$ groups, respectively. Though exact measurements were hard, the relative intensity ratio of the ring protons and the methyl ones ($CH_3$ and $CH_2D$) seemed to be almost the same. There was observed no appreciable change in the line shape of the ring protons. It may be difficult to decide whether the ring protons also were exchanged or not. However, the obtained results would suggest that the exchange reaction proceeded easily at the methyl groups. The other features of this spectrum was slight shift of the proton signals of $CH_2D$ to higher field as reported by Tiers[2]. Unfortunately a strong signal from $CH_3$ groups prevented exact measurements of this kind, but the distorted line shape and the slight hump on the central strong component suggested this fact. This tendency was observed more clearly with the more deuterated sample (No. 5). The large sharp central line of the triplet disappeared, and a very weak quintet if compared with the singlet of the ring protons which remained still sharp and strong was observed on the methyl protons. This would suggest at least that the deuteration had proceeded more easily at the two methyl groups than at the ring groups. The observed quintet was very weak and distorted considerably. The observed $J_{H-D}$ was about 2 c. p. s. The distortion might be caused by superimposed structures like singlet, triplet and quintet being slightly shifted each other. These features of NMR measurements confirmed clearly that the deuteration by this method would occur easily at the methyl groups and that the deuteration may take place step by step at the two methyl groups; i. e., roughly speaking, according to the scheme, $CH_3 \rightarrow CH_2D \rightarrow CHD_2 \rightarrow CD_3$.

The authors express their sincere thanks to Professor J. Itoh who gave them valuable suggestions on the NMR spectra.

*Department of Chemistry*
*Faculty of Science*
*Osaka University*
*Nakanoshima, Osaka*
*(K. H.) (T. U.)*

*Research Institute of Industry & Science*
*Osaka University*
*Sakai-shi, Osaka (H. K.)*

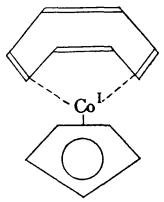
3) T. Ueda, *Catalysts* (*Shokubai*), **1**, 1 (1959).

## *Cyclopentadienyl Cobalt Cyclooctatetraene*

By Akira NAKAMURA and Nobue HAGIHARA

(Received February 4, 1960)

The present authors have previously reported the synthesis of cyclooctatetraene iron tricarbonyl and related compounds[1]. In continuation of the present study, the authors now wish to report a new synthesis of cyclopentadienyl cobalt cyclooctatetraene. Cyclopentadienyl cobalt dicarbonyl was heated at reflux in an excess of cyclooctatetraene under nitrogen for 6 hr. After removal of the unreacted starting materials, brown crystals were obtained by sublimation at 80°C under reduced pressure in 7% yield. These crystals were purified by recrystallization from petroleum ether and by sublimation. The purified sample had a m. p. of 81~82°C. Found: C, 68.32; H, 5.66; mol. wt. (Rast), 256. Calcd. for $C_{13}H_{13}Co$: C, 68.42; H, 5.74%, mol. wt., 228.




(I)

The elemental analysis apparently conformed to the structure, $(C_5H_5)Co(C_8H_8)$, cyclopentadienyl cobalt cyclooctatetraene (I). The same compound (I) could be obtained by irradiation of a mixture of cyclopentadienyl cobalt dicarbonyl and cyclooctatetraene with ultraviolet light under nitrogen for many hours.

I was soluble in common organic solvents and was stable in air. It was also soluble in cold concentrated sulfuric acid and in warm concentrated hydrochloric acid. The solution of I in carbon tetrachloride was decomposed by bromine and by iodine to give green and black precipitates, respectively. I reacted with cyclopentadienyl cobalt dicarbonyl in refluxing dioxane to give dark brown crystals, m.p. >300°C (with decomposition). I readily absorbed 2 mol. of hydrogen in the presence of Raney nickel catalyst at room temperature under ordinary pressure. Orange crystals, m.p. 102°C, were isolated from the hydrogenation mixture by sublimation in a reduced pressure at 80°C. These products of the reaction of I with bromine, iodine, hydrogen, cyclopentadienyl cobalt dicarbonyl and other reagents are now being studied in this laboratory and the results will be reported at a later date.

Three distinct proton resonance peaks were found at 82, 123 and 159 c. p. s, (ratio of the areas; 4.1 : 5 : 4.1), respectively, on the low field side from the proton resonance of cyclohexane. The result of this nuclear magnetic resonance study indicates that three different kinds of protons are present in I in a ratio of 4 : 5 : 4.

The infrared spectrum of I (in Nujol) showed a strong band at 1637 $cm^{-1}$ due to C=C stretching similar to the corresponding 1635 $cm^{-1}$ band of cyclooctatetraene. In the ultraviolet region it had an absorption maximum at 245 m$\mu$ ($\log \varepsilon$ : 4.32, in 95 % alcohol).

These spectral and NMR data together with the chemical reactivity of I are essentially different from those of cyclooctatetraene iron tricarbonyl[1-3]. The double bonds in I which are presumably not used in $\pi$-bonding with the cobalt show usual properties of olefinic double bonds as described above. In contrast to this fact all four double bonds of the cyclooctatetraene moiety in cyclooctatetraene iron tricarbonyl do not show the usual properties of double bonds and they were thought to be affected by $\pi$-complex formation[3]. Accordingly the cyclooctatetraene moiety in I should be different from that of cyclooctatetraene iron tricarbonyl in its spacial and electronic structures. From the above evidences the authors propose the structure shown in the figure for I.

*The Institute of Scientific and Industrial Research*
*Osaka University*
*Sakai-shi, Osaka*

1) A. Nakamura and N. Hagihara, This Bulletin, **32**, 880 (1959); *J. Chem. Soc. Japan, Pure Chem. Sec.* (*Nippon Kagaku Zasshi*), in press; *Mem. Inst. Sci. and Ind. Res. Osaka Univ.*, in press.

2) T. A. Manuel and F. G. A. Stone, *Proc. Chem. Soc.*, **1959**, 90.

3) M. D. Rausch and G. N. Schrauzer, *Chem. & Ind.*, **1959**, 957.

## *The Use of Recoil Fission Rare Gas for the Study of the Change in Crystal Structure*

By Seishi YAJIMA, Sumio ICHIBA, Yuichiro KAMEMOTO and Koreyuki SHIBA

(Received February 5, 1960)

Hahn[1] first investigated the emanation method which used radioactive inert gases $^{222}Rn(T_{1/2}=3.83\ d.)$, $^{220}Rn(T_{1/2}=54.5\ sec.)$ and $^{219}Rn(T_{1/2}=3.92\ sec.)$ as tracers. Since then, crystal structure changes and decomposition reactions were studied by this method[2]. In this method a parent of the radon nuclides is usually incorporated into a solid by coprecipitation with the solid or by deposition on the solid and the correlation between the escaped radioactive inert gas and crystal structure changes was studied.

In the present work, the radioactive fission product rare gases are used in place of radioactive radon nuclides. Uranium dioxide powder (particle size $\sim 0.2\ \mu$) is mixed with the solid powder to be examined, and the mixture is irradiated with thermal neutrons. When the weight ratio of uranium dioxide to the solid is 1 : 30, the fission recoil energy enables about 90% of the fission products to be caught by the surrounding solid powder. The captured fission product rare gases will behave in a similar manner as radon mentioned above, and they will be easily detected because of the relatively high fission-yield of radioactive xenon and krypton.

$\gamma$-Hematite or $\alpha$-hematite and uranium dioxide powder of which the weight ratio is 30 : 1 were mixed and the mixture 500 mg. was irradiated for a total nvt of $\sim 3.5 \times 10^{15}$ thermal neutrons per $cm^2$ in an experimental hole of the JRR-1 reactor. After one-day cooling, the sample was placed in a quartz boat in a quarz tube which was connected with a phosphorus pentoxide drying tube, a dry ice trap (for radioactive iodine), a spiral counting cell inserted into an NaI scintillation crystal well of a $\gamma$-ray spectrometer and a flow rate meter, in the order mentioned. Pure helium gas was passed over the sample at a flow rate of 70 ml./min., and the sample was heated by a furnace surrounding the quartz tube at a rate of 5°C per minute. The radioactive xenon escaping from hematite was carried by helium and the radioactivity was measured by the $\gamma$-ray spectrometer which was previously adjusted to detect 250 keV. $\gamma$-ray of xenon-135 only. The plots of the radioactivity of xenon-135 escaped from $\gamma$-hematite and $\alpha$-hematite versus temperature are shown in Figs. 1 and 2, respectively.

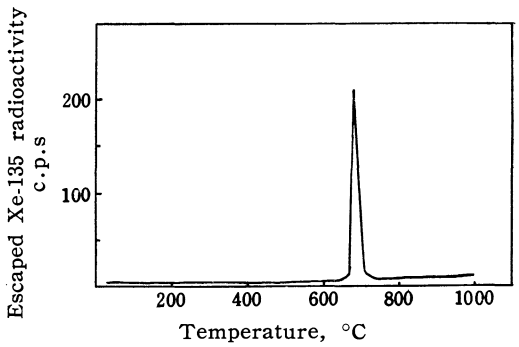



Fig. 1. Heating curve of $\gamma$-hematite. Heating rate, 5°C/min.

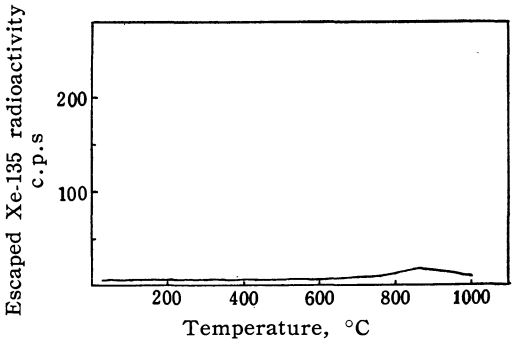



Fig. 2. Heating curve of $\alpha$-hematite. Heating rate, 5°C/min.

The peak at 680°C of $\gamma$-hematite is considered to be related with the crystal change of $\gamma$-hematite to $\alpha$-hematite. An X-ray diffraction method has shown that $\gamma$-hematite changes to $\alpha$-hematite when the former is heated above the temperature at which a peak appears. In the case of $\alpha$-hematite, the peak was not observed, because the crystal structure change is irreversible.

The previous data on the temperature of crystal structure change of $\gamma$-hematite to $\alpha$-hematite are not in good agreement with the present result. The observed peak by the present method may shift with the heating rate, and the temperature

1) O. Hahn and O. Müller, *Z. Elektrochem.*, **29**, 189 (1923).
2) e. g., K. Zimens, *Z. physik. Chem.*, **B37**, 231 (1937).

of crystal structure change may be dependent on the preparation method and on impurities in $\gamma$-hematite.

The emanation method by the use of radioactive fission product rare gases will be applicable to many solids, even metals, because the samples can be prepared without chemical treatment, which are prerequisite to the radon emanation method.

*Division of Chemistry*
*Japan Atomic Energy Research Institute*
*Tokai, Ibaraki-ken*

## *Intramolecular Interaction between Hydroxyl Group and π-Electrons. IX*[1]*. The Energy of the Interaction in Benzyldimethylcarbinol*

By Michinori Ōki and Hiizu Iwamura

(Received February 8, 1960)

The determination of the energy of the intramolecular interaction between hydroxyl group and π-electrons in this laboratory has so far been confined to the phenolic series[1,2]. In a preceding paper[1], it was referred that alcohols having internal interaction show rather complicated O-H stretching absorption bands ($\nu_{O-H}$) consisting of two free $\nu_{O-H}$ corresponding to rotational isomers about the $C_\alpha$-O bond and an interacting $\nu_{O-H}$, and that the present technique[3] of separating the apparent curve into three Lorentz function type curves leaves some ambiguity and makes the evaluation of the energy inaccurate. However, current studies[4] on the effect of molecular conformations on the intramolecular interaction between the alcoholic hydroxyl group and π-electrons have shown that, in order to make more detailed discussions, the strength of the interaction should be expressed quantitatively. To overcome the aforementioned difficulty the authors took advantage of the observation that the rotational isomers of tertiary alcohols can not be distinguished by the present dispersion of the spectrometer[5], and expected that, unlike 2-phenylethanol, the free $\nu_{O-H}$ of benzyldimethylcarbinol would be single[5] and that the apparent $\nu_{O-H}$ curve could be exactly separated into a free and an interacting $\nu_{O-H}$ by the usual method of Ramsay[6]. This expectation proved to be the case and the energy of the interaction was determined by measuring the temperature variation of the absorption as described previously[1]. The least square method was adopted to determine the six parameters; $a_1$, $b_1$, $\nu_1$, $a_2$, $b_2$ and $\nu_2$, in the Lorentz function;

$$D(\nu)=\frac{a_1}{(\nu-\nu_1)^2+b_1^2}+\frac{a_2}{(\nu-\nu_2)^2+b_2^2}$$

The data are summarized in Table I.

Table I. The effect of temperature on the $\nu_{O-H}$ absorption of benzyldimethylcarbinol

| $1/T\times10^3$ | $\nu_{O-H}$ | $\nu$ | $a$ | $b$ | $\ln(A_1/A_2)$ |
|---|---|---|---|---|---|
| 3.37 | 1 | 3593.5 | 16.13 | 8.14 | −0.292 |
| | 2 | 3614.9 | 25.11 | 9.46 | |
| 3.25 | 1 | 3594.3 | 18.46 | 8.97 | −0.268 |
| | 2 | 3615.9 | 26.24 | 9.76 | |
| 3.16 | 1 | 3594.9 | 17.23 | 9.11 | −0.340 |
| | 2 | 3616.0 | 25.93 | 9.76 | |
| 3.04 | 1 | 3595.4 | 17.22 | 9.28 | −0.349 |
| | 2 | 3615.7 | 25.67 | 9.76 | |
| 2.94 | 1 | 3596.3 | 15.86 | 9.14 | −0.397 |
| | 2 | 3617.4 | 24.95 | 9.67 | |

The energy difference ($-\Delta H$) was found to be 0.54±0.13 kcal./mol. This is far less than that of ordinary hydrogen bondings which range from 2.3 to 7 kcal./mol.[7] The energy value is not consistent with those estimated by Goldman and Crisler[8] and by Schleyer and coworkers[9], but is in good agreement with some conformational observations accumulated in this laboratory[10] for β-tetralol, cyclohexen-3-ol and ergosterol. Namely, these compounds only exhibit the free hydroxyl band and

1) Part VIII: M. Ōki and H. Iwamura, This Bulletin, in press.
2) M. Ōki, H. Iwamura and Y. Urushibara, ibid., **31**, 769 (1958).
3) M. Ōki and H. Iwamura, ibid., **32**, 1135 (1959).
4) M. Ōki and H. Iwamura, ibid., **32**, 307 (1959); P. von Schleyer, D. S. Trifan and R. Bacskai, *J. Am. Chem. Soc.*, **80**, 6691 (1958).
5) M. Ōki and H. Iwamura, This Bulletin, **32**, 950 (1959).
6) D. A. Ramsay, *J. Am. Chem. Soc.*, **74**, 72 (1952).
7) C. A. Coulson, *Research*, **10**, 149 (1957).
8) I. M. Goldman and R. O. Crisler, *J. Org. Chem.*, **23**, 751 (1958).
9) While the present work was in progress, P. von Schleyer and his coworkers [*Tetrahedron Letters*, No. 14, (1959), p. 1] alluded that the energy of the intramolecular interaction in 2-phenylethanol was estimated to be about 1.4 kcal./mol. through temperature variation.
10) M. Ōki, H. Iwamura and T. Onoda, unpublished work.

lack the interacting $\nu_{O-H}$. These molecules could have been able to possess an internal interaction if the hydroxyl groups were oriented axially, while the axial conformation is known to be less stable than the equatorial conformation by about one kcal./mol.[11] Thus, if the energy of interaction were more than or at least nearly equal to one kcal./mol., the interaction should have been certainly permitted to exist to some extent. Therefore, the energy of the interaction in these cases must be fairly smaller than one kcal./mol. A full discussion will be given in the near future.

*Department of Chemistry*
*Faculty of Science*
*The University of Tokyo*
*Hongo, Tokyo*

11) D. H. R. Barton, R. C. Cookson, W. Klyne and C. W. Shoppe, *Chem. & Ind.*, **1954**, 21.

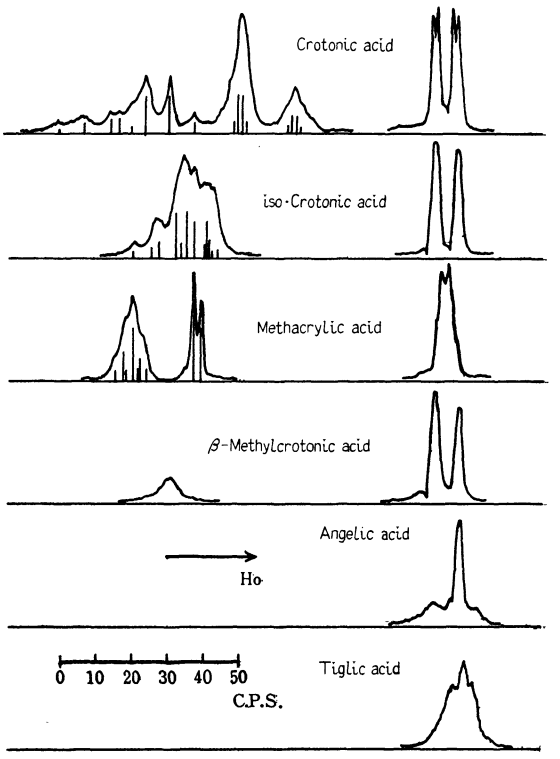



Fig. 1

## *NMR Study of α, β-Unsaturated Fatty Acids*

By Shizuo FUJIWARA, Hiroshi SHIMIZU*, Yoji ARATA* and Sachio AKAHORI**

(Received February 10, 1960)

The NMR spectra of six sorts of α, β-unsaturated acids were measured by the 27 Mc. high-resolution spectrometer constructed in this laboratory. The acids used in this experiment were crotonic acid (I), isocrotonic acid (II), methacrylic acid (III), β-methylcrotonic acid (IV), angelic acid (V) and tiglic acid (VI). Among these, II and III were studied in pure liquids and others as saturated solutions in carbon tetrachloride at 25°C. The observed and calculated spectra are shown in Fig. 1,[1] and the approximate values of chemical shifts and spin coupling constants derived from observed spectra are given in Table I, where the spin coupling constants between H and H, and between H and $CH_3$ are about the same as in ethylenic compounds[1]. From the spectra of I and II, it will be concluded that the α-proton signal appears at the field higher than the β-proton, and that the β-proton *trans* to the carboxyl group is about 1 p.p.m. higher than the *cis* proton. The observed chemical shift between gem protons in methacrylic acid is 0.62 p.p.m., which is considerably larger than that between gem protons in the simple ethylenic compounds with the values of 0.1~0.2 p.p.m.[1] This fact seems to be consistent with the conclusion mentioned above on the chemical shifts for the β-protons of crotonic and isocrotonic acids. The magnitudes of the chemical shifts between the two methyl groups attached to the same carbon atom are not so large as the values between the gem protons.

An interesting solvent effect was observed in the system of β-methylcrotonic acid and benzene; where as the acid was diluted by benzene, the chemical shift between gem methyl groups was observed to increase, and the dilution shift at zero concentration was about 0.45 p.p.m. As reported by Shimizu[2,3] and Fujiwara[2], the active methyl group of saturated fatty

* Faculty of Pharmaceutical Sciences, The University of Tokyo, Hongo, Tokyo.
** Shizuoka College of Pharmacy, Koroku-cho, Shizuoka.

1) J. A. Pople, W. G. Bernstein and H. J. Schneider, "High Resolution Nuclear Magnetic Resonance", McGraw-Hill Book Co., Inc., New York (1959), p. 242.

2) H. Shimizu and S. Fujiwara, *Chem. Pharm. Bull. (Tokyo)*, to be published.

3) H. Shimizu, *J. Chem. Soc. Japan, Pure Chem. Sec. (Nippon Kagaku Zasshi)*, to be published.

TABLE I. SPIN COUPLING CONSTANTS AND CHEMICAL SHIFTS OF $\alpha,\beta$-UNSATURATED FATTY ACIDS

| (3)C=C(2) (4)COOH | Chemical shift p.p.m. | Spin coupling constant, c.p.s. H-H $J_{23}$ | H-H $J_{24}$ | H-H $J_{34}$ | H-$CH_3$ $J_{23}$ | H-$CH_3$ $J_{24}$ | H-$CH_3$ $J_{34}$ |
|---|---|---|---|---|---|---|---|
| $CH_3$, H / H, COOH | $\delta_{H_2}-\delta_{H_4}=1.28$ | | 15.5 | | 1.2 | | 6.1 |
| H, H / $CH_3$, COOH | $\delta_{H_2}-\delta_{H_3}=0.19$ | 9.0 | | | | $\lesssim 1.0$ | 7.0 |
| H, $CH_3$ / H, COOH | $\delta_{H_3}-\delta_{H_4}=0.62$ | | | 1.9 | $\sim 0$ | 1.7 | |
| $CH_3$, H / $CH_3$, COOH | $\delta_{Me_3}-\delta_{Me_4}=0.27$ | | | | $\lesssim 1.0$ | $\lesssim 1.0$ | |
| H, $CH_3$ / $CH_3$, COOH | $\delta_{Me_2}-\delta_{Me_4}=0.2$ | | | | $\sim 0$ | | 6.5 |
| $CH_3$, $CH_3$ / H, COOH | $\delta_{Me_2}-\delta_{Me_3}\simeq 0$ | | | | | $\lesssim 1.0$ | 6.0 |

acid, such as acetic acid shows the high field shift as the result of $\pi$ complex formation with benzene molecule. The *trans* methyl group which is relatively unaffected from a steric point of view will tend to form $\pi$ complex more easily than the *cis* methyl group and, hence, to show the dilution shift. The fact that the $CH_3$-$CH_3$ shift was increased by the dilution will be explained if the methyl group whose signal appeared at the field higher than the other is more shifted toward a high field. Thus, it is suggested from these considerations that the signal at the higher field may be assigned to the *trans* methyl group and the one at the lower field to the *cis* group. This conclusion may seem contrary to the expectation that the active methyl usually resonates at the field lower than the inactive one owing to the less density of the electronic cloud around it. As these unsaturated molecules have planar structures, however, the magnitude of the paramagnetic effect due to the carbonyl group at the *cis* position will exceed that of the paramagnetic effect at the *trans* position whose effect is mainly caused by inductive force of the carbonyl group.

More refined values of chemical shifts and spin coupling constants will be reported in the near future[4] by H. Shimizu, Y. Arata and S. Fujiwara concerning the general discussion of the analyses of the complex NMR spectra.

*University of Electro-Communications*
*Chofu-shi, Tokyo*

4) It will appear in This Bulletin.

## *Remarks on the Mechanism of Ammonia Synthesis*

By Kenzi TAMARU

(Received February 8, 1960)

The importance of adsorption measurements during surface catalysis has recently been emphasized[1] and the adsorption measurements during ammonia synthesis on a doubly promoted iron catalyst has been carried out in a closed circulating system. The apparatus was almost the same with that schematically illustrated in a previous paper[1]. The reaction vessel is 12 cm. in length and 3.5 cm. in internal diameter. The circulation pump has a circulation rate between 4.5 and 8.0 l. (stp) per hour depending upon the pressure,

1) K. Tamaru, This Bulletin, **31**, 666 (1958); *Trans. Faraday Soc.*, **55**, 824, 1191 (1959); *Nature*, **183**, 319 (1959).

reaction temperature and composition of the reaction mixture. The reaction usually proceeded in such a way that the ammonia produced was collected in a trap cooled with liquid oxygen. The composition of the circulating mixture of nitrogen and hydrogen was determined with a thermal conductivity cell connected to the circulating system. The amount of ammonia trapped was determined by releasing it into a space between two stopcocks at room temperature. The amounts of the gases adsorbed on the catalyst surface were estimated from the amount of reactants introduced, the pressure and the composition of the circulating gas, and amount of ammonia trapped. Due allowance was made for the analytical samples removed from the apparatus. The promoted iron catalyst employed was obtained from the Government Industrial Research Institute, Tokyo, and contains 5% $Al_2O_3$ and 1% $K_2O$. The catalyst (198 g.) was powdered to smaller than 20 mesh and was reduced at 500°C for about 1000 hr. in a hydrogen flow of about 36 l. per hour at about atmospheric pressure, water vapor being removed by means of dry ice or liquid oxygen traps in the reaction system. Before each run the catalyst was evacuated for a few hours, treated with circulating hydrogen for 15 hr. in the system, with the traps maintained at liquid oxygen temperature, and then degassed for one hour. All these operations were carried out at 500°C.

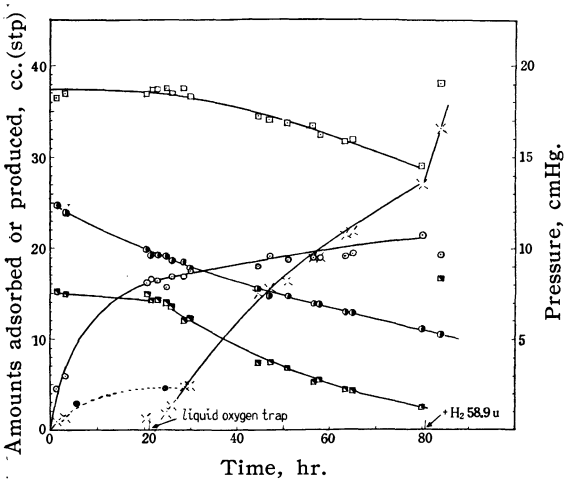



Fig. 1. Adsorption measurements during ammonia synthesis at 180°C. Amounts introduced: Hydrogen, 80.4 cc., Nitrogen, 71.8 cc. (stp).
▣: Hydrogen adsorbed (cc.).
⊙: Nitrogen adsorbed (cc.).
⁘: Ammonia produced (cc.).
◥: Ambient hydrogen pressure (cm.).
◑: Ambient nitrogen pressure (cm.).
●: Nitrogen adsorption in the absence of hydrogen at $P_{N_2}$=15.13 cmHg.

TABLE I

| Flow rate l. (stp)/hr. | Relative reaction rate |
|---|---|
| 11.23 | 1.00 |
| 5.58 | 0.95 |
| 10.18 | 1.00 |
| 4.98 | 1.06 |
| 12.27 | 1.00 |
| 5.56 | 0.89 |
| 7.70 | 1.00 |
| 3.37 | 0.98 |
| 7.39 | 1.00 |
| 2.98 | 0.95 |

Typical results for the experiments at 180°C are shown in Fig. 1 which illustrates experiments in which the ammonia trap was not cooled during the first 21 hr. The reaction rate was measured at a variety of circulation rates including alternately slow and fast rates at 250°C, and the results are shown in Table I, where the total pressure of the circulating reactant was between 22.61 and 11.36 cmHg and the nitrogen content was 28~38%. It is shown in the table that the reaction rate is not very sensitive to the circulation rate in the region in which adsorption was studied. It would appear that in the present studies the circulation rate is so high compared to the reaction rate that the partial pressure of the ammonia produced in the reaction vessel is very small.

According to Scholten and Zwietering[2], the rate of chemisorption of nitrogen on a singly promoted iron catalyst is proportional to the pressure. Hence, if allowance is made for the difference in nitrogen pressure, the results of Fig. 1 show that the rate of adsorption of nitrogen *in the absence of hydrogen* almost corresponds to the rate of ammonia synthesis reported by Emmett and coworkers[3]. This is one reason why they consider nitrogen adsorption to be the rate-determining step in the synthesis. However, as is brought out in Fig. 1, hydrogen causes a marked acceleration in the rate of adsorption of nitrogen. This conclusion is in accordance with the

2) J. J. F. Scholten and P. Zwietering, *Trans. Faraday Soc.*, **53**, 1363 (1957).
3) P. H. Emmett and S. Brunauer, *J. Am. Chem. Soc.*, **56**, 35 (1934); S. Brunauer, K. S. Love and R. G. Keenan, ibid., **64**, 751 (1942).

observations of Joris & Taylor, and Kummer & Emmett[4], that isotopic exchange of nitrogen is accelerated by hydrogen.

As shown in Fig. 1, the removal of ammonia from an equilibrated mixture of nitrogen, hydrogen and ammonia has little effect on the adsorption of either hydrogen or nitrogen. Suppose, for example, that all the nitrogen on the catalyst surface takes part in the reaction, then, if all the ammonia in the equilibrated mixture is removed, the adsorbed nitrogen should be rapidly consumed to form ammonia if nitrogen chemisorption is slow compared to all the other surface reaction, including hydrogen adsorption and that ammonia in the reacting gas is negligible. In actual experiments it may be unrealistic to neglect the ammonia pressure completely, but it is to be expected that if all the gaseous ammonia is trapped out the amount of adsorbed nitrogen should fall by an amount corresponding to the distance from equilibrium. But no sign of this tendency could be detected. Consequently, it seems unlikely, as far as one limits his own discussion to the behavior on the whole surface, that the nitrogen chemisorption only is rate determining, though commonly so accepted at present time[5].

This work was carried out with the financial support from the Mitsubishi Chemical Industries, Ltd., to which the author's thanks are due.

*Department of Chemistry*
*Yokohama National University*
*Minami-ku, Yokohama*

4) G. G. Joris and H. S. Taylor, *J. Chem. Phys.*, **7**, 893 (1939); J. T. Kummer and P. H. Emmett, ibid., **19**, 289 (1951).

5) C. Bokhoven, C. van Heerden, R. Westrik and P. Zwietering, "Catalysis", edited by Emmett, Vol. III, Reinhold Publishing Corp., New York (1955), p. 265.

# *Polymerization of Styrene with the Ziegler-Natta Catalysts in the Presence of Molecular Hydrogen**

By Shunsuke MURAHASHI, Shun'ichi NOZAKURA and Yutaka UTSUHARA**

(Received December 22, 1959)

It appears very important matter to have measures of controlling the molecular weight of isotactic polystyrenes in the polymerization with the Ziegler-Natta catalysts. Isotactic polystyrenes hitherto obtained in this laboratory according to the usual way[1] had the molecular weight of the order of several millions. In the course of this study, polymers having lower molecular weight was needed for the study of solution properties.

Among various factors affecting on molecular weight, such as the concentration of monomer, that of catalysts, and that of transfer agents, molecular hydrogen was chosen in the present work as one of the possible transfer agents, which had been known to be effective for controlling the molecular weight of polyethylene[2].

Recently, Natta has revealed in a paper the effectiveness of molecular hydrogen as controlling agents of molecular weight of polypropylene[3].

It has been found in the present work that isotactic polystyrenes of the low molecular weight could actually be obtained in the presence of hydrogen, although in addition to this there has been found another reaction which is competitive to the polymerization reaction, i.e. hydrogenation of styrene to ethylbenzene.

Polymerizations were carried out in an stainless steel autoclave of 200 ml. capacity. After the autoclave was flashed with nitrogen, $TiCl_3$ (3.0 g., the product of Stauffer Chemical Co.) washed with *n*-heptane was poured in with 30 ml. of *n*-heptane, and $AlEt_3$ (0.6 to 0.7 g.) was injected into the bottom of the autoclave

* Part V in a series on "Stereoregular Polymers": Presented at the 8th Annual Meeting of Society of Polymer Science (Japan), May 30, 1959.

** Present address: Research Laboratories, Kanebo Spinning Co. Ltd., Tomobuchicho, Miyakojima-ku, Osaka.

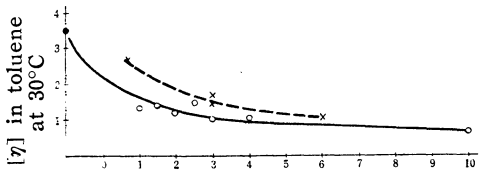
1) S. Murahashi, S. Nozakura, M. Sumi and K. Hatada, This Bulletin, **32**, 1094 (1959).

2) G. Natta, *Chem. & Ind.*, **1957**, 296

3) G. Natta, *J. Polymer Sci.*, **34**, 531 (1959).

from an injection syringe, and then styrene that was placed in a glass bottle was set in the autoclave. Dry hydrogen was charged to the desired pressure, the temperature was raised to 70°C, and then the shaking was commenced to make styrene contact with the catalyst suspension. Isotactic polymer was purified by the usual extraction procedure with methyl ethyl ketone.

It was found that both yields of total polymer and isotactic fraction in total polymer decreased markedly with increasing hydrogen pressure under the condition otherwise unaltered. As expected, however, intrinsic viscosities of isotactic fractions in toluene at 70°C also decreased as illustrated in Fig. 1.




$H_2$ pressure, kg./cm² in gauge

Fig. 1. Variation of intrinsic viscosities of isotactic polystyrenes with hydrogen pressure.
○: Polymerization time, 5 hr.
×: Polymerization time, 21 hr.
●: Polymerization for 5 hr. under a nitrogen atmosphere.

It was also found that the decreasing yields of polymer with increasing hydrogen pressure was mainly attributable to the occurrance of the competitive reaction, i. e. hydrogenation of styrene catalysed by the Ziegler catalyst. In one run, where styrene (9.1 g., 0.087 mol.) was heated with the catalytic system ($AlEt_3$, 0.71 g.; $TiCl_3$, 3 g.) at the constant hydrogen pressure of 8.9 kg./cm², 0.068 mol. of hydrogen was absorbed and gave a product, in which 3.7 g. of ethyl benzene was identified together with 0.474 g. of a pasty polymer and 0.499 g. of a solid polymer.

A modified catalyst system, $AlEt_3$-$Ti(OBu\text{-}n)_4$, produced no appreciable amount of polymer, but smoothly catalyzed the hydrogenation of styrene. Styrene alone, styrene and $AlEt_3$, and styrene and $TiCl_3$ did not show any absorption of hydrogen at the similar conditions.

From the above results, the observed decrease of molecular weight of isotactic polystyrenes with increasing hydrogen pressure may be considered to be due to following two reasons: the first is the effect of hydrogen as a chain transfer agent. Hydrogen probably cleaves a growing carbon-metal bond giving a metal-hydrogen bond and a saturated dead polymer, and the former would be still capable of initiating a new polymer chain. The second is the early lowering of monomer concentration due to the consumption of monomer by the hydrogenation reaction. Dependence of molecular weight on monomer concentration had been definitely demonstrated in the polymerization of propylene with the Natta catalysts[4] and hence the similar feature might be held in this case.

Propylene and butene-1 did not suffer such a hydrogenation reaction and the molecular weights of their polymers were found to be effectively controlled by the hydrogen pressure.

*Department of Polymer Science*
*Faculty of Science*
*Osaka University*
*Nakanoshima, Osaka*

4) G. Natta, I. Pasquon and E. Giachetti, *Makromol. Chem.*, **24**, 258 (1957).

# *Crystalline Adducts of Dicyclohexylamine with Di- and Triols*

By Masazumi NAKAGAWA and Takashi AKAGAMI*

(Received August 6, 1959)

It has been reported briefly in the literatures that dicyclohexylamine forms crystalline addition compounds with hydroxy compounds such as water[1], ethanol[1], cyclohexanols[2] and cyclohexanediols[2]. An accidental observation of the formation of a white precipitate by mixing dicyclohexylamine with ethylene glycol urged the present authors to a more detailed study on the adducts.

When an acetone solution of dicyclohexylamine was mixed with some di- or tri-hydroxy compounds in the same solvent, immediate precipitation of very fine silky needles accompanied by an evolution of heat was observed. The crystals thus obtained could be easily recrystallized from acetone to give a pure adduct. The melting points, the analytical data of nitrogen and the composition of the adducts with various glycols are summarized in Table I.

It is to be noted that in spite of the remarkable change in the structure of glycols, the composition of the adducts with glycols was always in a ratio of 1 : 2. These results are inconsistent with those of Winans[2] who reported the composition of the adducts with diols is 1 : 1 so far as he studied**.

The properties of the adducts with several kind of triols are listed in Table II together with its analytical data.

In these cases the molar ratio of the triol against the amine was found to be 1 : 3 excepting the case of glycerol in which it was found to be 2 : 3.

These adducts are readily soluble in common organic solvents and are especially easily recrystallized from acetone. The adducts are decomposed into the components by the addition of water. The most striking property of the

TABLE I. ADDUCTS OF DICYCLOHEXYLAMINE WITH GLYCOLS

| Glycol | m. p. °C | N(%) Found | N(%) Calcd. | Molar ratio Glycol : Amine |
|---|---|---|---|---|
| Ethylene glycol | 70 | 6.60 | 6.60 | 1 : 2 |
| 1,2-Propanediol | 49～49.5 | 6.28 | 6.39 | 1 : 2 |
| 1,3-Propanediol | 53 | 6.32 | 6.39 | 1 : 2 |
| 1,4-Butanediol | 68～69 | 6.13 | 6.19 | 1 : 2 |
| 2,3-Butanediol | 63.5～64.5 | 6.11 | 6.19 | 1 : 2 |
| 1,3-Butanediol | below room temp | 5.96 | 6.19 | 1 : 2 |
| 2(*cis*)-1,4-Butenediol | 49.5～51 | 6.14 | 6.22 | 1 : 2 |
| 2(*trans*)-1,4-Butenediol | 68～69 | 6.22 | 6.22 | 1 : 2 |
| 2-Butyne-1,4-diol | 59.5 | 6.14 | 6.24 | 1 : 2 |
| 1,5-Pentanediol | 39.5～42 | 6.02 | 6.00 | 1 : 2 |
| 1,6-Hexanediol | 59.5～60.5 | 5.68 | 5.83 | 1 : 2 |
| 2,4-Hexadiyne-1,6-diol | 68.5～69 | 5.96 | 5.95 | 1 : 2 |
| 1,7-Heptanediol | 58～59 | 5.72 | 5.67 | 1 : 2 |
| Diethylene glycol | 25～25.5 | 5.65 | 5.98 | 1 : 2 |
| Hydrocinnamoin | 151.5～152 | 4.63 | 4.45 | 1 : 2 |
| 1,4-Di-(β-phenyl-α-hydroxyethyl)-benzene | 78.5～80 | 3.96 | 4.11 | 1 : 2 |

TABLE II. ADDUCTS OF DICYCLOHEXYLAMINE WITH TRIOLS

| Triol | m. p. °C | N(%) Found | N(%) Calcd. | Molar ratio Triol : Amine |
|---|---|---|---|---|
| Glycerol | 38.5～39.5 | 5.75 | 5.77 | 2 : 3 |
| 1,2,4-Butanetriol | 46～47 | 6.44 | 6.46 | 1 : 3 |
| (−)-1,2,5-Pentanetriol | 27～28 | 6.09 | 6.34 | 1 : 3 |
| 1,2,6-Hexanetriol | 49～50 | 6.04 | 6.20 | 1 : 3 |

* Sansuisoyushi Industrial Co., Ltd., Kyoto.

1) G. Fouque, *Compt. rend.*, **166**, 394 (1918).

2) G. F. Winans, *J. Am. Chem. Soc.*, **61**, 3591 (1939).

** Winans prepared the adducts using petroleum ether or ether as solvent.

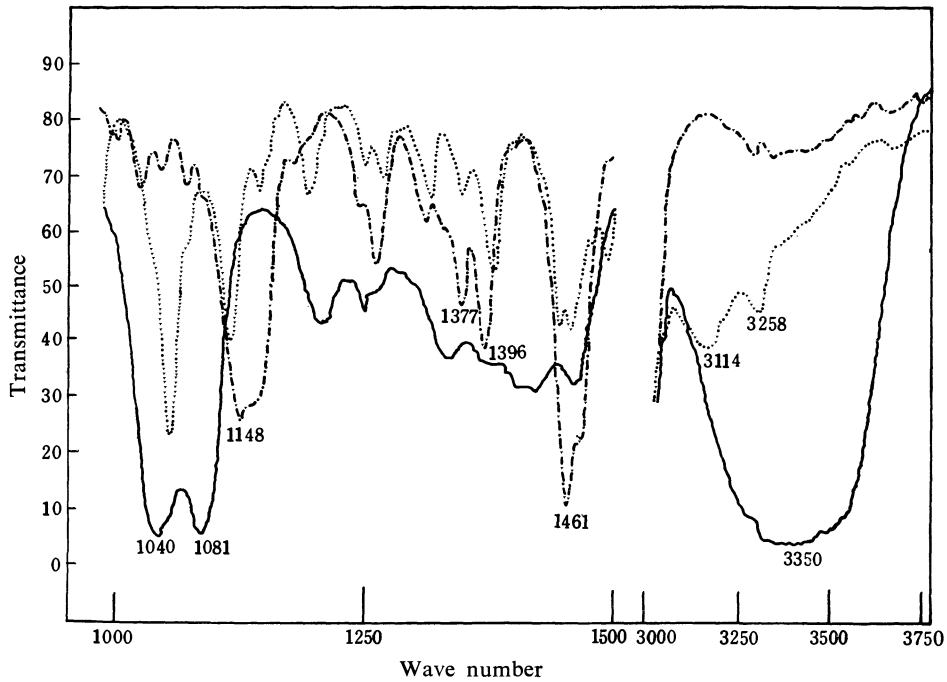



Fig. 1. The I. R. spectra of dicyclohexylamine (·-·-·), ethylene glycol (——) and the adduct with ethylene glycol (····).

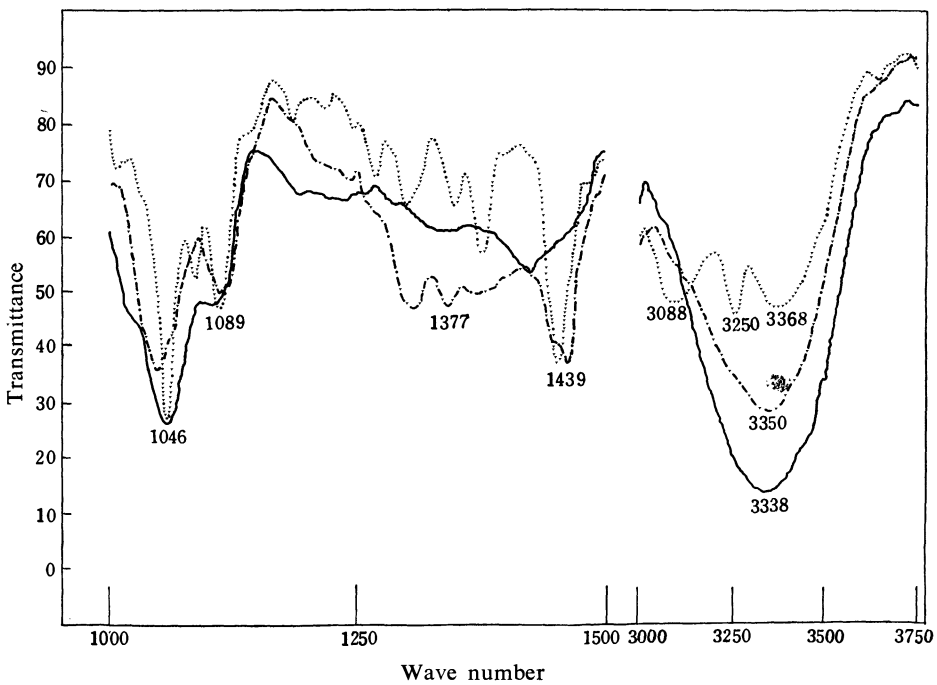



Fig. 2. The I. R. spectra of 1, 2, 4-butanetriol (——), the adduct with 1, 2, 4-butanetriol (····) and the adduct with glycerol (·-·-·).

adducts with diols is its tendency to sublime. When a crystalline adduct with a diol placed in an evacuated sealed tube is heated below its melting point, a rapid growth of beautiful silky needles on the cold wall of the tube can be observed.

The tendency of sublimation is characteristic of the adducts with glycols and can not be seen with the adducts with triols.

The existence of intermolecular polymeric association due to hydrogen bond in hydroxy compounds is well known, and the presence of this type of hydrogen bonds in ethylene glycol and in 1, 2, 4-butanetriol was revealed by the presence of a very broad absorption at 3350 and 3338 $cm^{-1}$ in the infrared spectra of these alcohols as illustrated in Figs. 1 and 2. The diol and the triol also show a broad and strong absorption in the range of 1300~1440 $cm^{-1}$ presumably arising from deformation of the associated hydroxy group or the streching of C–O of the associated hydroxy group. Also the infrared spectrum of dicyclohexylamine shows a broad absorption in the region of 3100~3500 $cm^{-1}$ indicating the presence of associated N–H group. On the other hand, the infrared spectrum of the adduct with ethylene glycol showed two absorption peaks at 3114 and 3258 $cm^{-1}$ instead of the broad absorption band of the glycol at 3350 $cm^{-1}$ (Fig. 1).

Remarkable change in absorption was also observed in the range of 1300~1440 $cm^{-1}$. The broad absorption in the spectrum of ethylene glycol in this region disappeared in the spectrum of the adduct.

These spectroscopic evidences indicate that the formation of amine-glycol adduct is attributed to the formation of new strong intermolecular O—H···N hydrogen bonds destroying the original polymeric intermolecular hydrogen bonds which exist in ethylene glycol and in dicyclohexylamine. These arguments are consistent with the fact that the amine-diol adducts are easy to sublime. The formation of such a type of an "addition compound" in solution has been pointed out by several investigators[3]. The absorption band at ca. 3326 $cm^{-1}$ in the infrared spectrum of the system of alcohol-amine-solvent was attributed to the formation of an amine-alcohol complex by Baker et al.[3c]

The situations are somewhat different in the cases of the adducts with triols. As illustrated in Fig. 2, the infrared spectrum of 1, 2, 4-butanetriol clearly indicates the presence of polymeric intermolecular hydrogen bonds in the triol. However, the infrared spectrum of the adduct with the triol exhibits three absorptions in the range of 3000~3400 $cm^{-1}$ (3368, 3250 and 3088 $cm^{-1}$). Also the adduct with glycerol shows a broad and intense absorption at 3350 $cm^{-1}$ (Fig. 2). These broad absorptions at 3368 or 3350 $cm^{-1}$ seem to indicate the presence of remaining intermolecular polymeric hydrogen bonds in these amine-triol adducts. It is reasonable to conclude that some part of hydrogen bonds is used to associate the amine-triol adduct with each other, giving them the nature of non-sublimation.

Another point of interest in the physical property of the adducts is the oscillation of the melting points. As illustrated in Fig. 3,

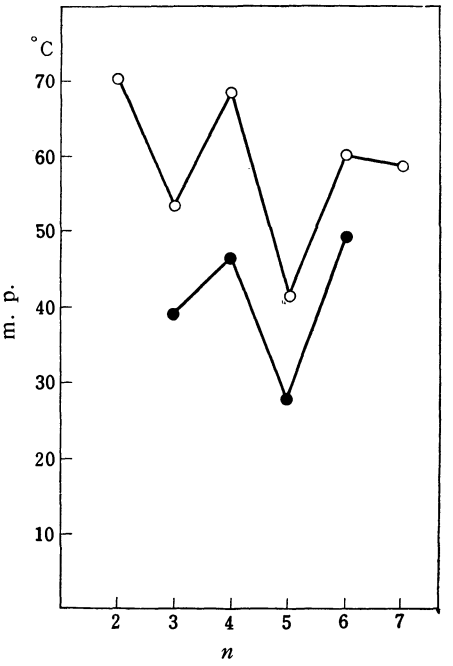



Fig. 3. The melting points of the adducts with $\alpha,\omega$-diols and $\alpha, \beta, \omega$-triols.
○—○ $HO\cdot(CH_2)_n\cdot OH$
●—● $HO\cdot CH_2CH\cdot(CH_2)_{n-2}\cdot OH$
$\quad\quad\quad

TABLE III. DISSOCIATION OF THE ADDUCTS IN SOLUTION

| Alcohol component in adduct | Molecular weight | | | Degree of dissociation, % |
|---|---|---|---|---|
| | Calcd. | A. | B. | |
| Ethylene glycol | 424 | 206<br>207 | 225 | $\alpha_1=100$ or $\alpha_2=50$ |
| 1,4-Di-($\beta$-phenyl-$\alpha$-hydroxyethyl)-benzene | 680 | — | 240 | $\alpha_2=100$ |
| 1,2,6-Hexanetriol | 677 | — | 214 | $\alpha_3=100$ or $\alpha_4=70$ |

A. Cryoscopic method in benzene.
B. Isothermal distillation method in acetone solution.

isothermal distillation methods. The results summarized in Table III indicate the dissociation of the adduct in the solution. These results present no evidence on the nature of dissociation, but the calculated degree of dissociation is tabulated in Table III assuming the following types of dissociation.

$$\text{Diol}\begin{cases}(\text{amine})_2(\text{diol}) \overset{\alpha_1}{\rightleftarrows} (\text{amine})(\text{diol})+(\text{amine}) \\ \text{or} \\ (\text{amine})_2(\text{diol}) \overset{\alpha_2}{\rightleftarrows} 2(\text{amine})+(\text{diol})\end{cases}$$

$$\text{Triol}\begin{cases}(\text{amine})_3(\text{triol}) \overset{\alpha_3}{\rightleftarrows} (\text{amine})(\text{triol})+2(\text{amine}) \\ \text{or} \\ (\text{amine})_3(\text{triol}) \overset{\alpha_4}{\rightleftarrows} 3(\text{amine})+(\text{triol})\end{cases}$$

As stated above, the formation of crystalline adduct with dicyclohexylamine is quite general for primary or secondary diols and triols, but it was found that the tertiary glycols such as 2,4-dimethyl-2,4-butanediol and 1,1',4,4'-tetraphenyl-1,4-butynediol give no crystalline adducts. 2-Amino-ethanol, 1,8-terpin and (−)-menthol also gave no crystalline product even at the temperature in a refrigerator. The last two examples are remarkable as structurally related cyclohexanol itself gave a well defined adduct of m. p. 56~57°C with the composition of 1 : 1 (N, found : 4.87 ; calcd. for 1 : 1-adduct : 4.98%). These findings seem to suggest that the formation of crystalline adduct is influenced by the steric environment around the hydroxyl group.

## Experimental***

**Preparation of the Adducts.**—A mixture of diol (1 mol.) and acetone (equal volume) was added to a solution of dicyclohexylamine (2 mol.) in acetone (equal volume). The mixture was kept for several hours in a refrigerator to complete the crystallization. The crystals formed were filtered and recrystallized from acetone. The molar ratio 1 : 3 (triol : amine) was used in the cases of the preparation of the adducts with triols.

Sublimation under reduced pressure was found as an excellent method of purification of the adducts with diols.

**Measurement of the Infrared Spectra.**—The spectrometer used was a Hilger H 800. The spectra of the hydroxy compounds and the amines were measured by the method of liquid film. The spectra of the adducts were measured employing KBr-disk method.

**Determination of the Molecular Weight.**—*(1) Cryoscopic method.*

a) Adduct with ethylene glycol : 0.01385 g.
Benzene : 2.637 g.
$\Delta T=0.130$°C. Mol. wt., 206

b) Adduct with ethylene glycol : 0.03859 g.
Benzene : 2.637 g.
$\Delta T=0.378$°C. Mol. wt., 207

*(2) Isothermal distillation method.*—A Signer molecular weight apparatus as modified by Clark was used using benzophenone as the standard and acetone as the solvent.

a) Adduct with ethylene glycol : 0.02878 g.
Benzophenon : 0.01220 g.
Final volumes : standard solution, 0.65 ml.
adduct solution, 1.24 ml.
Mol. wt., 225

b) Adduct with 1,2,6-hexanetriol : 0.00905 g.
Benzophenone : 0.00836 g.
Final volumes : standard solution, 1.12 ml.
adduct solution, 1.04 ml.
Mol. wt., 214

c) Adduct with 1,4-di-($\beta$-phenyl-$\alpha$-hydroxyethyl)-benzene : 0.01196 g.
Benzophenone : 0.01449 g.
Final volumes : standard solution, 1.00 ml.
adduct solution, 0.92 ml.
Mol. wt., 240

The authors are grateful to Professor S. Murahashi, Professor T. Kaneko and Mr. H. Katsura of Department of Chemistry of Osaka University and to Mr. H. Yamaguchi of the Nitto Institute of Chemical Research, Urawa for the gift of some of the hydroxy compounds. Acknowledgments are made to Messrs. T. Shiba and M. Okumiya and Miss K. Koike for performing the elementary analyses.

*Department of Chemistry*
*Faculty of Science*
*Osaka University*
*Nakanoshima, Osaka*

*** All melting points are not corrected.

# *Interaction of Surface Active Agent with Amylose*

By Toshio TAKAGI and Toshizo ISEMURA

(Received August 17, 1959)

In the previous papers, one of the authors have reported the interaction of surface active agents with non-ionizable polymers[1] as well as with proteins[2,3]. It was found that the aspect of the interaction of surface active agents with non-ionizable polymers is entirely different from that of the interaction of surface active agents with proteins. Accidently, the authors have found that there is another way of the interaction of the surface active agent with polymer. Actually, they wished to examine the inactivation of Taka-amylase A by surface active agent using amylose as a substrate. As a matter of fact, it was found that amylose is precipitated by sodium dodecyl sulfate (SDS) even in a concentration as low as 0.007% from 0.05% amylose solution in 0.05 M sodium chloride. Accordingly, the cause of this precipitation of amylose was investigated thoroughly.

The precipitate was examined by the X-ray diffraction method and compared with the amorphous amylose precipitated by ethanol. A complex might be formed between amylose and SDS. It was interesting to examine whether such a complex might be formed even in a dissolved state under proper condition. So the possibility was examined from the two standpoints of view as will be described below. The effect of SDS on the coloration of amylose-iodine complex was investigated spectrophotometrically. As the viscosity of polymer solution is a function of the configuration assumed by the dissolved polymer molecules, the solution of amylose containing SDS was studied also by viscosity measurement. From all these experimental findings, the authors have concluded that the precipitation of amylose by the surface active agent should be due to the formation of an adduct between amylose and the surface active agent. The details of the present investigations and inferences based on them will be described hereafter.

## Experimental

**Amylose.**—Amylose was prepared from potato starch by Schoch's butanol precipitating method[4] and was recrystallized three times. The purified amylose was dehydrated by methanol and then dried over calcium chloride in vacuo.

**Amylopectin.** — Amylopectin was precipitated by adding a large amount of methanol to the supernatant separated from amylose prepared by Schoch's method. The precipitate was suspended in methanol for some time to remove butanol and then dried over calcium chloride in vacuo.

**Sodium Dodecyl Sulfate.**—Sodium dodecyl sulfate was prepared by Dreger's method[5] and was recrystallized three times from aqueous butanol.

**X-ray Diffraction Measurement.** — The sample for X-ray diffraction study was prepared as will be described below. One gram of amylose was dissolved in 10 ml. of 1 N sodium hydroxide and kept in a refrigerator overnight to dissolve the amylose completely, and then diluted to about 50 ml. The solution was neutralized with 1 N hydrochloric acid and diluted with distilled water just up to 100 ml. A precipitate was formed by adding 25 ml. of 0.5% SDS solution to the amylose solution and the solution was stood overnight. The precipitate was gathered by centrifugation and dried over calcium chloride in vacuo. On the other hand, amylose was precipitated by adding excess ethanol to the amylose solution prepared just in the same way without the addition of SDS and after washing the precipitate with ether, it was dried over calcium chloride in vacuo. The amylose thus prepared was used as a reference sample without SDS for X-ray diffraction study.

X-ray diffraction patterns were taken by the powder method using "Norelco" recording X-ray diffractometer (Cu-$K_\alpha$ line was used).

**Measurement of Absorption Spectrum of Amylose-iodine Complex.**—Five milliliters of 0.1% solution of amylose which was prepared by Fuwa's method[6] was diluted to about 200 ml. with distilled water, to which the necessary volume of SDS solution was added to assure a desired final concentration and shaken thoroughly. After bringing out the color by the addition of 5 ml. of 0.2% iodine solution (containing 2% potassium iodide), the solution was diluted just up to 250 ml. After standing for about 30 min., the absorption spectra of the solutions were measured by a Hitachi spectrophotometer model EPU-2 or by a Beckman recording spectrophotometer model DK-2.

**Measurement of Viscosity.**—One gram of amylose was suspended in 10 ml. of 1 N sodium hydroxide, was kept in a refrigerator for 2 days and then was diluted with distilled water just up to 100 ml. This solution was diluted with 0.1 N sodium

1) T. Isemura and A. Imanishi, *J. Polymer Sci.*, **33**, 337 (1958).
2) T. Isemura and A. Imanishi, *Mem. Inst. Sci. Ind. Res., Osaka Univ.*, **15**, 173 (1958).
3) T. Isemura and T. Takagi, *J. Biochem.*, **46**, 1637 (1959).
4) T. J. Schoch, *J. Am. Chem. Soc.*, **64**, 2957 (1942).
5) E. E. Dreger et al., *Ind. Eng. Chem.*, **36**, 610 (1944).
6) H. Fuwa, *J. Biochem.*, **41**, 583 (1954).

hydroxide to obtain the solution of various concentrations in respect to amylose. Each solution was mixed with an equal volume of SDS solution of various concentrations. The solutions of various compositions were heated on a water bath at 60~80°C for about 30 min. and kept for 3 hr. in a thermostat at 30±0.05°C. Then, the viscosity of amylose solutions was measured by a viscosimeter of the Ostwald type in the same thermostat.

Viscosity of the amylopectin solutions was measured just in the same manner.

## Results

**Effect of SDS on the X-ray Diffraction Pattern of Amylose.**—The X-ray diffraction pattern of amylose precipitated by SDS is shown in Fig. 1a, while that for amylose precipitated by ethanol in Fig. 1b. In the pattern for the former, two distinct diffraction peaks were found at $2\theta=13$ and 20° ($\theta$=incident angle) which might be attributed to the helical structure of amylose[7-9], whereas in the pattern for the latter, only a broad peak was found which suggests an amorphous structure of amylose.

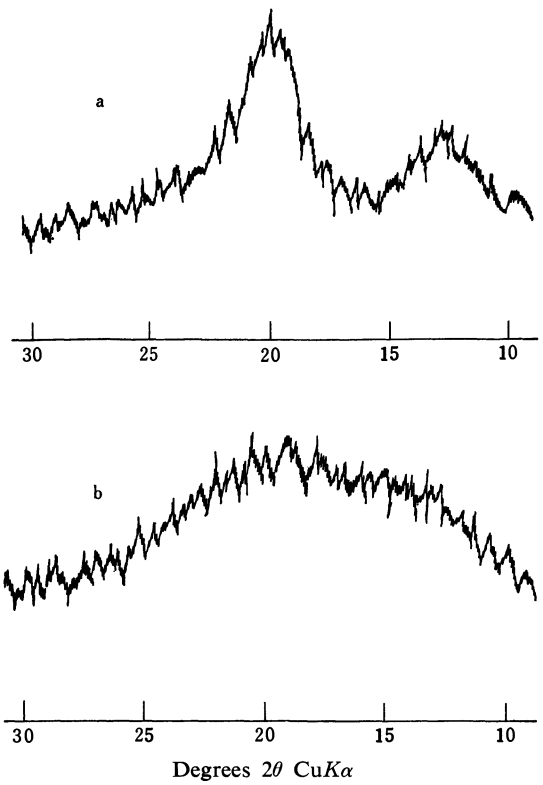



Fig. 1. X-ray diffractometer traces of SDS-treated and non-treated specimens of amylose.
a, precipitated by the addition of SDS.
b, precipitated by the addition of ethanol.

**Effect of SDS on the Coloration of Amylose-iodine Complex.**—If a helical complex is formed between amylose and SDS even in a dissolved state, it is expected that the coloration of amylose-iodine complex may be considerably affected in the presence of SDS. When an aqueous iodine solution was added to the amylose solution to which SDS was added previously, the solution appears at first light yellow assuming the color of $I_3^-$ ion. Then the blue coloration of amylose-iodine complex comes out gradually. It needs about 30 min. to attain the steady coloration. All curves of

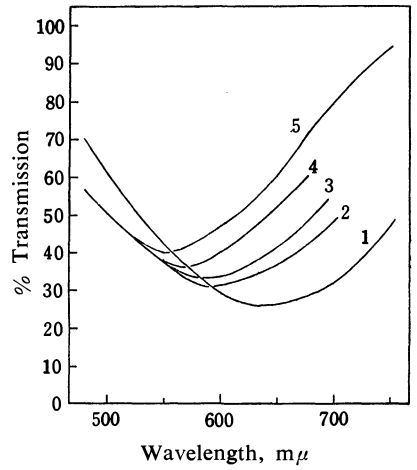



Fig. 2. The effect of the addition of SDS on the absorption spectrum of amylose-iodine complex.
1, 0 M; 2, $2.0\times10^{-5}$; 3, $1.0\times10^{-4}$ M; 4, $6.0\times10^{-4}$ M; 5, $4.2\times10^{-3}$ M. Amylose concentration, $2.0\times10^{-3}$ g./l.

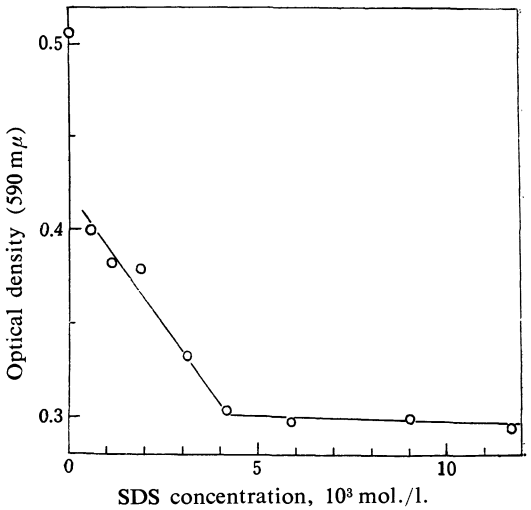



Fig. 3. The inhibitory effect of SDS on the coloration of amylose-iodine complex.

7) R. E. Rundle and D. French, *J. Am. Chem. Soc.*, **65**, 1707 (1943).
8) F. F. Mikus, R. M. Hixon and R. E. Rundle, ibid., **68**, 1115 (1946).
9) R. E. Rundle, ibid., **69**, 1769 (1947).

absorption spectra in Fig. 2 were measured after this steady state was attained. With the increase in the amount of added SDS, the absorption maximum shifts to a shorter wavelength side and the absorption decreases. If one examines the effect of the concentration of SDS by measuring the absorption at 590 mμ over a wide range of the concentration, the effect of SDS increases with the concentration up to $4\times10^{-3}$ M, beyond which the change of the absorption spectra was not found as shown in Fig. 3. The concentration of SDS corresponds nearly to the critical micelle concentration of this surface active agent.

**Effect of SDS on the Viscosity of Amylose Solution.**—As is well known, the viscosity of polymer solution is a function of polymer configuration in solution. So the viscosity of an amylose solution might be profoundly affected by the addition of a small amount of SDS, if amylose changes its configuration from a random coil to a helical structure. The viscosity of amylose solution was measured in the presence of SDS in alkaline solution which is known as a good solvent for amylose and compared with that of amylose solution in the absence of SDS. As shown in Fig. 4., the effect of SDS on the viscosity of amylose solution is very remarkable. On the other hand, amylopectin which can not assume a helical structure because of its branched structure is expected to be scarcely affected by the addition of SDS. The experiment verifies that this is the case, as shown in Fig. 5.

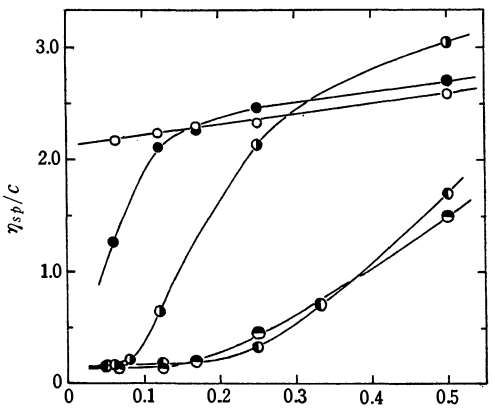



Fig. 4. The effect of the addition of SDS on the viscosity of amylose in 0.1 N KOH. SDS concentration, ○, 0 M; ●, $1.7\times10^{-4}$ M; ◑, $3.5\times10^{-4}$ M; ◐, $5.6\times10^{-4}$; ◓, $7.0\times10^{-4}$ M.

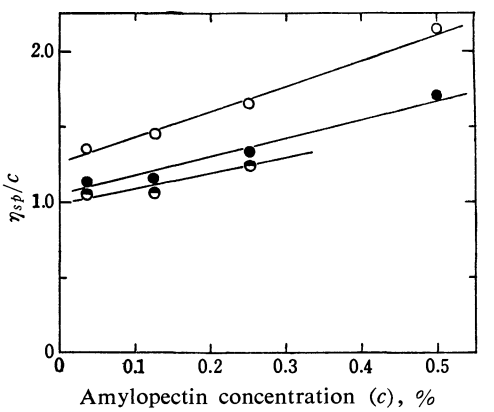



Fig. 5. The effect of the addition of SDS on the viscosity of amylopectin in 0.1 N KOH. SDS concentration, ○, 0 M; ◓, $3.5\times10^{-4}$ M; ●, $7.0\times10^{-4}$ M.

## Discussion

As one of the authors have already reported[1], some surface active agents interact with some polymers causing oriented adsorption on the polymer molecules, often making insoluble polymers soluble. On the other hand, proteins interact with an ionic surface active agent at their ionic sites of the opposite sign[10]. Surface active agents precipitate proteins having opposite electric net charge, changing hydrophilic sites by covering with hydrocarbon chains. However, in the presence of excess surface active agents, surfactant ions are built up on the hydrocarbon tails of surfactant previously combined with protein molecules. Thus, the hydrophobic protein molecules which have been separated from the solution are turned to be hydrophilic again.

In the case of the interaction of amylose with an ionic surface active agent, the ion-ion interaction as in the case of proteins does not occur because of the lack of ionic sites. The oriented adsorption of surfactant ions as in the case of polyvinyl alcohol, as previously reported[1], might be excluded. Also, the dipole-ion interaction between hydroxyl groups of amylose and SDS ions as suggested by Fava and Eyring[11] in the case of adsorption of SDS on cellulose will be refused for the following reasons. In the present case, only an ion of SDS is sufficient to precipitate about 12 glucose residues in amylose. Moreover, it was found in the previous investigation[1] that the interaction of SDS with polyvinyl alcohol which has many hydroxyl groups in a molecule like amylose showed no sign of the insolubilization of the polymer. Further, the insolubilization of amylose can not be ascribed to the adsorption of SDS extending the hydrocarbon tails toward water as in the case of proteins, because of the

10) F. W. Putnam, *Advances in Protein Chem.*, **4**, 83 (1948).
11) A. Fava and H. Eyring, *J. Phys. Chem.*, **60**, 890 (1956).

lack of ionic sites as mentioned above. The precipitation of amylose is also caused by a cationic surface active agent such as cetylbenzyldimethyl amine bromide as well as SDS. On the other hand, the large excess of SDS, even as high as 12% in total concentration does not cause the redissolution of the precipitate. It is also to be noticed that no precipitate was formed by SDS with amylopectin which has a number of branched chains in the molecule.

According to X-ray diffraction study, the amylose precipitate formed by the interaction with SDS gave two distinct peaks at $2\theta=13$ and 20° as shown in Fig. 1a. Rundle and his collaborators[7] concluded from their studies on amylose-iodine complex by X-ray diffraction that amylose forms an adduct with iodine, where amylose assumes a helical structure in which six glucose residues make a turn and iodine molecules lie along the axis of helix, which gives two distinct peaks in X-ray diffraction pattern at $2\theta=13$ and 20°.

Later, they found that amylose forms similar adducts with some higher alcohols and normal fatty acids of moderate chain length[8,9]. As these two diffraction peaks are characteristic of the helical structure of amylose, the amylose precipitate formed by the addition of SDS should be an adduct of amylose including SDS ions in its helical structure. Although the mixture of amylose solution must be heated with higher fatty acid or alcohol at about 70°C and then cooled to obtain the adduct, only the addition of SDS to amylose solution at room temperature is enough in the present case. This difference might originate from the fact that SDS is much more soluble than higher fatty acid or alcohol.

There is another evidence for the formation of the adduct having a helical structure between amylose and surfactant. It is well known that when iodine was added to amylose solution, intensive blue color appears instantaneously. Now it is generally accepted that this characteristic coloration of amylose solution by iodine is caused by the change of an electronic state of iodine molecules lying along the axis of helix of the amylose-iodine complex[12]. The change of the electronic state should be caused by the large polarity of amylose in a helical structure due to the orientation of a large number of hydroxyl groups in glucose residues in a similar direction. As mentioned above, when iodine solution was added to amylose solution containing SDS, the blue color of amylose-iodine complex appears gradually instead of instantaneous coloration as in the case without SDS. It may be expected that it needs some time to exchange SDS ions with iodine in a helix of amylose.

As the authors have mentioned above, the absorption maximum shifts to shorter wavelength-side and absorption decreases with the concentration of SDS. The decrease in absorption is remarkable at the longer wavelength-side. Rundle et al.[13] studied the effect of the molecular weight of amylose on the coloration of amylose with iodine. They found that with the decrease in the molecular weight or the chain length of amylose, the absorption maximum shifts to the shorter wavelength side and the absorption decreases. This change of absorption is remarkable at the longer wavelength side. As iodine competes with SDS in intruding into a helix of amylose, the linear array of iodine molecules which intervened between SDS ions might become shorter with the increase of SDS concentration. The increase of SDS concentration might be assumed to have the same effect as the decrease of the chain length of the amylose molecule forming a helical complex with iodine. Parallel changes in the shift of absorption maximum and the decrease in absorption in both cases mentioned above might be explained in terms of the chain length concerning one continuous unit of the amylose-iodine-complex.

No more change was found in the absorption spectra of amylose-iodine complex, when the concentration of SDS exceeds about $4\times10^{-3}$ M. This concentration almost exactly corresponds to the critical micelle concentration of this surfactant, so that this fact suggests that only the SDS ions are concerned with the formation of the helical complex.

According to the study of the absorption spectra mentioned above, amylose seems to assume a helical configuration in the presence of SDS even in a dissolved state. Viscosity measurments, as well known, give some insights into the configuration of polymer molecules in solution. As shown in Fig. 4., when the reduced viscosity $\eta_{sp}/c$ of amylose solution in the absence of SDS was plotted against amylose concentration, the same linear relation was obtained as in the case of a typical non-electrolytic polymers. However, if SDS is present in the solution, $\eta_{sp}/c$ decreases rapidly with the decrease in amylose concentration and converges to a definite value independent of the concentration of SDS in the low concentration of amylose. The larger the ratio of SDS to amylose is, the larger is the concentration of amylose from which the reduced viscosity begins to decrease. Accordingly, the ratio of SDS to amylose is evidently an important factor to the decrease of the reduced viscosity.

12) R. S. Stein and R. E. Rundle, *J. Chem. Phys.*, **16**, 195 (1948).

13) R. R. Baldwin. R. S. Bear and R. E. Rundle, *J. Am. Chem. Soc.*, **66**, 111 (1949).

In the case of amylopectin, the linear relation between $\eta_{sp}/c$ and $c$ was retained even in the presence of SDS. The line moves parallel, a little downward. Since the intrinsic viscosity of the polymers should be an indication of their volume in the dissolved state, the decrease in the reduced viscosity of amylose suggests the decrease in the effective volume of amylose when SDS was added to the solution. The cause of the decrease in viscosity should be attributed to the formation of a helical complex between amylose and SDS. Owing to the mutual compensation of the polarity of hydroxyl groups in the helical complex, the hydration of amylose might be decreased. This might be one of the reasons why the viscosity of amylose-surfactant-complex decreased.

The minor decrease in viscosity found with amylopectin in the presence of SDS might be caused by the contamination of a small amount of amylose, since the decrease of viscosity is almost the same with the solution containing 0.01% SDS and that containing 0.02% SDS.

In conclusion, it was found experimentally that there are at least three different ways of interaction between surface active agents and polymer, namely, (1) only by van der Waals' force, (2) by electrovalent bonding only or together with van der Waals' force, and (3) by a special combination found in the case of adduct formation. In the case of the interaction of a surface active agent with non-ionizable polymers such as polyvinyl formal or polyvinyl acetate[1], cooperative force between chains of surfactant is very significant. Accordingly, hydrophilic and lypophilic properties of surfactant must be appropriately balanced in this case. The cationic detergent shows poor interaction with polymers, probably because of its stronger hydrophility than that of the anionic detergent.

The electrovalent bonding of the surfactant with polymer is of course encountered with the polymers such as proteins which have ionic sites in the molecules[10]. The surface active agents which can act on the polymers should have the charge of the opposite sign to the polymer. After forming the envelope of the surface active agent of the thickness of a molecule, more layers of surface active agents can be built up on it by van der Waals' force.

The third class of interaction such as these encountered in the case of amylose and surface active agents, some specific steric conditions must be fulfilled. In this case, whether the surface active agent is anion or cation is out of the question. However, non-ionic detergents were found to have scarce interaction with the polymers throughout all these three types of interactions[14].

## Summary

It was found that a specific precipitate is formed when some ionic surface active agents are added to amylose solution and it was confirmed by X-ray diffraction study that this phenomenon is due to the formation of the helical complex between amylose and a surface active agent.

It is also inferred that the same complex is formed even in the dissolved state from the study on the effect of the surface active agent on the viscosity of amylose solution and on the absorption spectrum of amylose-iodine complex.

The authors express their hearty thanks to Dr. S. Hizukuri of the Institute of Scientific and Industrial Research, Osaka Universiy for his valuable advice and cooperation in the X-ray diffraction measurements.

*Division of Physical Chemistry*
*Institute for Protein Research*
*Osaka University*
*Kita-ku, Osaka*

14) Preliminary experiments.

# *Oxidation of Ferrous Ions in the Aqueous Ferrous-Cupric System. I. Effect of Cobalt-60 Gamma-Rays*

By Hiroshi HOTTA, Akira TERAKAWA and Shinichi ŌNO

(Received August 27, 1959)

An irradiation facility with a 10 kilocurie Co-60 gamma-ray source has been in operation at Japan Atomic Energy Research Institute since 1958[1]. Although the characteristics of the source, especially the distribution of radiation intensity around the hollow cylindrical source had to be measured for the public use of this facility, a chemical dosimeter for high dose, which was to be used as the standard, was not studied in Japan. The dose rate inside the present source is about $2\times10^6$ *r*/hr.

For this purpose, the properties of various aqueous solutions were examined to find a suitable chemical dosimeter for high doses. In general, a chemical dosimeter must have certain properties, namely, linearity, reliability, stability, easy standardization and so on[2]. It is concluded from the present experiments that a chemical dosimeter for high doses must have the following properties in addition to the above ones.

The first conclusion is that the oxygen-dependent reaction is not preferable, owing to the restriction of oxygen solubility like ferrous or benzene aqueous solution[3,4]. That is, all components of the system must have great solubility, which determines the upper limit of the appriciable dose. Moreover, the product to be measured should have no secondary reaction such as re-redox reaction and decomposition. Re-redox reactions are considered even for ferric[5] and cerous[6] ions, respectively. Since the temperature of solutions irradiated at a high dose rate is apt to be raised owing to the absorption of radiation energy, it is desirable for the *G*-value to be independent of temperature[7].

It is difficult to find an ideal system having all the above properties. The ceric dosimeter is usually recommended for this purpose, but demands the most careful distillation of water. Moreover, the reagent contains some rare earths occasionally. The ferrous-cupric dosimeter[8] is another one used for high doses. This dosimeter can easily be made from pure and cheap reagents, but this matter is not being so exhaustively studied at present. Therefore, the authors studied the aqueous ferrous-cupric system in detail, and give the results of some discussions concerning it in the present paper.

## Experimental

Triply distilled water was used as usual, but chemical reagents of special grade were used without further purification. The aqueous solutions were irradiated in a test tube of hard glass (Hario Glass) by a 10 kilocurie Co-60 gamma-ray source at the Irradiation Laboratory of Japan Atomic Energy Research Institute at room temperature (ca. 25°C). The solutions were saturated with either oxygen or nitrogen, and sometimes irradiated without any treatment, which is called hereafter the non-treated solution. The concentration of oxygen in distilled water, which was treated similarly with the solution, was measured at 25°C by the Winkler method[9] as listed in Table I. The solubility of oxygen in water is $1.2\times10^{-3}$ M in the handbook[10].

In the present experiment, as mentioned previously[4], the dose was changed not by the irradiation time, but by irradiation for one hour at

TABLE I. INITIAL CONCENTRATIONS OF OXYGEN AND FERRIC ION AT 25°C IN $10^{-3}$ M

| Treatment | Oxygen in water | Ferric ion in ferrous-cupric system | | |
|---|---|---|---|---|
| | | (0)* | ($10^{-3}$)* | ($10^{-2}$)* |
| $N_2$-saturated | 0.019 | 0.2 | 0.2 | 0.2 |
| Non-treated | 0.37 | 0.2 | 1.3 | 1.6 |
| $O_2$-saturated | 1.2 | 0.2 | 2.1 | 2.3 |

Note: The concentration of cupric ion is listed in ( )*.

1) A. Danno, M. Omura, H. Hotta, H. Hirakawa, G. Tsuchihashi and I. Yamaguchi, "The 7th Conf. Hot Lab. and Equipment", Session 6, Cleveland, Ohio, 1959.
2) G. V. Taplin, "Radiation Dosimetry", Ed. by G. J. Hine and G. L. Brownell, Chap. 8 Academic Press, New York (1956).
3) P. V. Phung and M. Burton, *Radiation Research*, 7, 199 (1957).
4) H. Hotta and A. Terakawa, This Bulletin, to be published.
5) T. Rigg, G. Stein and J. Weiss, *Proc. Roy. Soc.*, A211, 127 (1952).
6) J. T. Harian and E. J. Hart, *Radiation Research*, 9, 127 (1958).
7) H. Hotta and K. Shimada, This Bulletin, to be published.
8) E. P. Hart and P. D. Walsh, *Radiation Research*, 1, 342 (1954).
9) Am. Public Health Assoc., "Standard Methods for the Examination of Water, Sewage and Industrial Wastes", Am. Public Health Assoc., New York (1955), p. 252.
10) N. A. Lange, "Handbook of Chemistry", Handbook Publishers, Sandusky, Ohio (1956), p. 1093.

TABLE II. YIELD OF FERRIC ION IN VARIOUS SOLUTIONS

| Run | Solute in M | | | Treatment | G-value | |
|---|---|---|---|---|---|---|
| | Ferrous ammonium sulfate | Cupric sulfate | Sulfuric acid | | at low dose | at high dose |
| a | 0.04 | 0 | 0.4 | $O_2$-saturated | 15.60±0.06 | 8.16±0.03 |
| b | 0.04 | 0 | 0.4 | Non-treated | 15.55±0.02 | 7.94±0.31 |
| c | 0.04 | 0 | 0.4 | $N_2$-saturated | 8.07±0.12 | |
| d | 0.04 | 0.001 | 0.4 | $O_2$-saturated | 14.2 | 6.44±0.2 |
| e | 0.04 | 0.001 | 0.4 | Non-treated | 6.50±0.15 | |
| f | 0.04 | 0.001 | 0.4 | $N_2$-saturated | 6.51±0.07 | |
| g | 0.04 | 0.01 | 0.4 | $O_2$-saturated | 2.60±0.14 | |
| h | 0.04 | 0.01 | 0.4 | Non-treated | 2.4 ±0.05 | |
| i | 0.04 | 0.01 | 0.4 | $N_2$-saturated | 2.34±0.08 | |

various positions, namely, various dose rates. Therefore, the abscissa of all figures gives a value of the dose in $r$ as well as a value of the dose rate in $r$/hr. The deviation of the observed values from the curve is partially due to the uncertainty of the absolute dose rate at a respective position, for samples were not irradiated at a fixed position as is usually done. The absolute dose rate was determined by the ceric dosimeter, which was corrected up to about $1.4\times10^5 r$ by the oxygen-saturated ferrous dosimeter.

The amount of ferric ion was measured by optical density at 304 m$\mu$ ($\varepsilon$=2205 at 25°C). It should be noticed that the ferrous ion was fairly oxidized due to the addition of cupric ions in the presence of oxygen without irradiation as listed in Table I, in which the mean initial concentration of ferric ions in the irradiated solutions is shown[11].

## Results

**Ferrous Solutions.**—The result of aqueous 0.04 M ferrous ammonium sulfate solution containing 0.8 N sulfuric acid and 0.001 M sodium chloride for a) oxygen-saturated, b) non-treated and c) nitrogen-saturated cases are shown in Fig. 1. Their $G$-value is listed with the composition of the solution in Table II. 0.001 M sodium chloride was added as a stabilizer as usual.

**Ferrous-cupric Solutions.** — The results of aqueous 0.04 M ferrous ammonium sulfate solution containing 0.8 N sulfuric acid and 0.001 M cupric sulfate for the above three treatments, d), e) and f), are shown in Fig. 2. Moreover, the results of the similar solution containing 0.01 M cupric sulfate for the same three treatments, g), h) and i), are shown in Fig. 3. Their $G$-value is also listed with the composition of the solution in Table II. The data below about $4\times10^4 r$ were unreliable.

The present results indicate that the non-treated solution is useful as a chemical dosimeter for high doses with good accuracy at

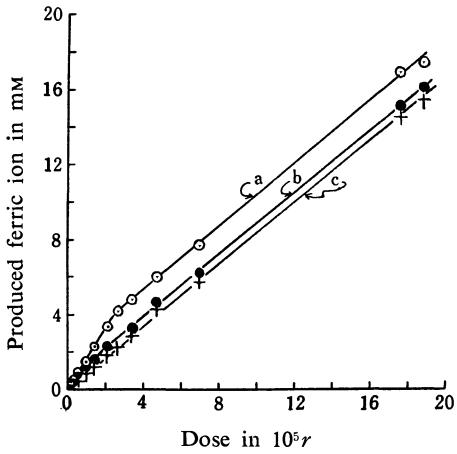



Fig. 1. The oxidation of ferrous ion in 0.04 M ferrous sulfate acidic aqueous solution for (a) oxygen-saturated, (b) non-treated and (c) nitrogen-saturated cases.

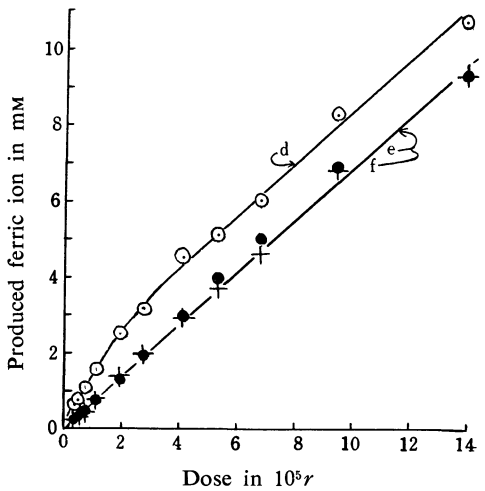



Fig. 2. The oxidation of ferrous ion in 0.04 M ferrous sulfate-0.001 M cupric sulfate acidic aqueous solution for (d) oxygen-saturated (⊙), (e) non-treated (●) and (f) nitrogen-saturated (+) cases.

11) J. W. Mellor, "A Comprehensive Treatise on Inorganic and Theoretical Chemistry", Vol. XIV, Longmans, London (1935), p. 267.

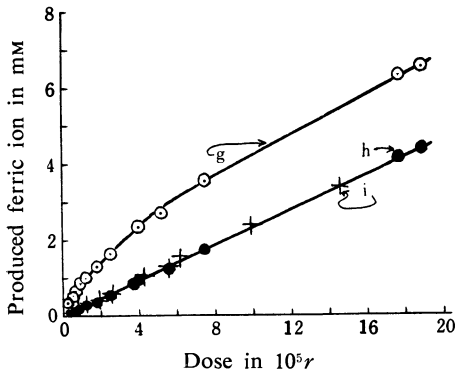



Fig. 3. The oxidation of ferrous ion in 0.04 M ferrous sulfate-0.01 M cupric sulfate acidic aqueous solution for (g) oxygen-saturated (⊙), (h) non-treated (●) and (i) nitrogen-saturated (+) cases.

least up to $2\times10^6 r$ from $4\times10^4 r$. However, the $G$-value is dependent on the composition of the solution[12].

## Discussion

For the primary chemical effects of ionizing radiation on aqueous system,

$$H_2O \rightsquigarrow H_2,\ H_2O_2,\ H \text{ and } OH \qquad (0)$$

the yield of the above products per eV., namely, their $G$-value by Co-60 gamma-rays in the 0.8 N sulfuric acid aqueous system is considered to be $G(H_2)=0.39$, $G(H_2O_2)=0.78$, $G(H)=3.70$ and $G(OH)=2.92$, respectively[13]. The $G$-value of the following reactions, which is shown in parentheses at the right of each equation, is estimated from the above values. The suffix of $G$ denotes the order of reactions included in the $G$-value. For example, $G_{2,1}$ means the total $G$-value of reaction 2 and reaction 1.

The action of OH and $H_2O_2$ in ferrous solution is

$$Fe^{2+}+OH=Fe^{3+}+OH^- \qquad (G_1=2.92) \qquad (1)$$

and

$$Fe^{2+}+H_2O_2=Fe^{3+}+OH^-+OH \qquad (G_{2,1}=2\times0.78) \qquad (2)$$

However, the action of the H atom is very different according to the condition as follows.

**Yield of Ferric Ion in the Absence of Oxygen.**—In the absence of oxygen, the action of the H atom in the acidic solution is

$$H+H^+=H_2^+ \qquad (G_3=3.70) \qquad (3)$$

and then

$$Fe^{2+}+H_2^+=Fe^3+H_2 \qquad (G_4=3.70) \qquad (4)$$

Therefore, the total yield of ferric ion in the absence of oxygen is equal to $G_1+G_{2,1}+G_4=8.18$, as usual. In fact, the observed values at high dose for solutions a), b) and c) in Table I are in good agreement with this value.

In the presence of cupric ion, it reduces the yield of ferric ion by the reaction

$$Cu^2+H=Cu^++H^+ \qquad (5)$$

and then

$$Fe^3+Cu^+=Fe^{2+}+Cu^{2+} \qquad (G_5=G_6) \qquad (6)$$

Reaction 5 competes with reaction 4 within $G_4+G_5=3.70$. Even if the cuprous ion reacts with OH or $H_2O_2$ in addition to reaction 6, the effect of these reactions on the yield of the ferric ion is equivalent to reaction 6. Therefore, these effect are represented by $G_6$.

According to the above interpretation, the $G_5$ for solutions f) and i) are 0.85 and 2.9, respectively. On the assumption that

$$G_4/G_5=k_4K_3(H^+)(Fe^{2+})/k_5(Cu^{2+}) \qquad (i)$$

as pointed out by Hart[12], where $k$, $K$ and parentheses denote rate constant, equilibrium constant and concentration, respectively, the ratios obtained, $k_4K_3(H^+)/k_5$ are 0.084 and 0.069 for solutions f) and i), respectively. If $K_3$ is assumed to be 100 l./mol. according to Hart[12], the ratio, $k_4/k_5$ is estimated to be about $10^{-3}$. It is confirmed from this value that the cupric ion is very reactive for the H atom in comparison with the ferrous ion.

**Yield of Ferric Ions in the Presence of Oxygen.**—In the presence of oxygen, the action of H atom in the acidic solution is

$$H+O_2=HO_2 \qquad (7)$$

$$Fe^{2+}+HO_2=Fe^{3+}+HO_2^- \qquad (8)$$

and then

$$HO_2^-+H^+=H_2O_2 \qquad (G_{7,8,9,2,1}=3\times3.70) \qquad (9)$$

Therefore, the total yield of ferric ions in the presence of oxygen is equal to $G_1+G_{2,1}+G_{7,8,9,2,1}=15.58$, as usual.

In the ferrous and cupric solution, reaction 8 competes with reaction 5 and the reaction

$$Cu^{2+}+HO_2=Cu^++H^++O_2 \qquad (10)$$

and the rate of the consumption of oxygen by reaction 8 is expressed by the equation

$$G(-O_2)_8=G(H)\times\frac{1}{1+\dfrac{k_5(Cu^{2+})}{k_7(O_2)}}\times\frac{1}{1+\dfrac{k_{10}(Cu^{2+})}{k_8(Fe^{2+})}} \qquad (ii)$$

as pointed out by Hart[12]. Therefore, the circumstance of these reactions is complicated.

On the other hand, if $\Delta G$ is considered to be the difference between the observed $G$-value, $G^\circ$, and the ideal one, $G^i$, obtained on the

12) E. J. Hart, *Radiation Research*, 2, 33 (1955).
13) A. O. Allen, 1st Intern. Conf. Peaceful Uses of Atomic Energy", Vol. 7, Geneva, (1956), p. 514.

assumption that cupric ion scavenges all H atoms, it is expressed as

$$\Delta G = G^\circ - G^1 = 4G_8 \qquad \text{(iii)}$$

and

$$G^1 = G_1 + G_{2,1} - G_{5+10} = 0.78$$

Therefore, the consumption of oxygen against the dose in solutions d) and g) is estimated from Eq. iii as shown in Fig. 4. The respective $G$-value of the elementary reactions at the initial stage for both solutions is obtained from the initial slope in Fig. 4 as listed in Table III.

Table III. Yield of elementary reactions at the initial stage for oxygen-saturated ferrous-cupric solutions

| Run | Cupric ion | $G_8$ | $G_{5+10}$ | $G^\circ$ |
|---|---|---|---|---|
| d | $10^{-3}$ M | 3.34 | 0.34 | 14.22 |
| g | $10^{-2}$ M | 2.64 | 1.06 | 11.34 |

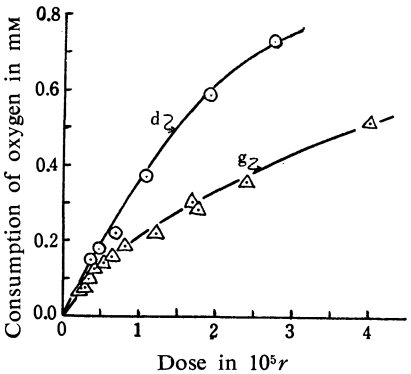



Fig. 4. The consumption of oxygen in oxygen-saturated 0.04 M ferrous sulfate acidic aqueous solution containing (d) 0.001 M and (g) 0.01 M cupric sulfate.

The linearity of the curve at the initial stage in Fig. 4 indicates that the ratios, $k_5(Cu^{2+})/k_7(O_2)$ and $k_{10}(Cu^{2+})/k_8(Fe^{2+})$ should be constant at this stage in Eq. ii, that is,

$$\frac{k_{10}}{k_8} = \frac{G_{10}(Fe^{2+})}{G_8(Cu^{2+})} \qquad \text{(iv)}$$

When the contribution of reaction 5 is assumed to be comparatively slight, $G_{10} \approx G_{5+10}$, in solution d), in which the concentration of cupric ions is low, the ratio, $k_{10}/k_8$ is estimated to be smaller than 4 from Eq. iv on using the values in Table III. According to Hart[12], the ratio, $k_{10}/k_8$ is about 50 for the aqueous solution of $10^{-3}$ M ferrous sulfate and 0.01 N sulfuric acid containing cupric ions between $10^{-6}$ M and $10^{-3}$ M. The disagreement between them may be the pH of the solution.

From the present experiment, $10^{-3}$ M cupric ion is sufficient to suppress the effect of oxygen dissolved naturally. However, it can not be concluded directly from this fact that oxygen is not concerned with the reaction in solution e). It is because the concentration of $HO_2$ radical should be sufficient for a ferrous ion to react with this radical from the result of solution b), and the $G$-value of reaction 10 is not so great as to suppress reaction 8 even in solution d) as listed in Table III. Therefore, it can not be understood why there is no difference between solutions e) and f) in spite of the above condition. However, if the cupric ion scavenges $HO_2^-$ ion by the reaction

$$Cu^{2+} + HO_2^- = Cu^+ + HO_2 \qquad (11)$$

and then $HO_2$ radical or $H_2O_2$ molecule by reaction 9 reacts with ferrous and cupric ions as mentioned already, the effect of oxygen, namely, the difference between reactions 4 and 8 can be actually disregarded. The initial concentration of oxygen in solution e), supposed from Table I, is smaller than the concentration of oxygen at the bend point of solution a), supposed from Fig. 1 and Table I.

## Summary

The oxidation of ferrous ion in ferrous-cupric acidic aqueous solution by Co-60 gamma-rays was studied in order to find a good chemical dosimeter for high doses. Consequently, it is found that the non-treated solution containing the $10^{-3}$ M cupric ion is useful for this purpose, for this amount of cupric ions is sufficient to suppress the effect of oxygen, and that the $G$-value of the ferrous-cupric system is dependent on the composition of the solution. The suppression can be explained by the scavenging of the $HO_2^-$ ion by cupric ions. Furthermore, some discussions regarding the system are given in the present paper.

*Japan Atomic Energy Research Institute*
*Tokai, Ibaraki-ken*

# *Vibrational Spectra of Methyltrimethoxysilane*

By Toshio TANAKA

(Received August 26, 1959)

The group frequency assignments have already been given for the infrared spectra of methyltrimethoxysilane and its higher homologues in the rock salt region[1]. This paper contains the Raman spectrum of methyltrimethoxysilane, the assignment of the observed frequencies and the calculation of the frequencies and the modes of the skeletal vibration. In the calculation a methyl group was regarded as one particle.

The normal coordinate treatment was carried out by the Wilson *FG* matrix method[2] with a Urey-Bradley potential function. The normal vibration has not yet been calculated for any $YM(XZ)_3$ type molecule.

## Experimental

**Material.**—The preparation and the physical constants of methyltrimethoxysilane used in the present work have already been reported elsewhere[3].

**Raman Spectrum.**—The Raman spectrum has been obtained by a Yūki-gōsei Raman spectrograph. The observed frequencies are shown in Table II together with the infrared and the calculated frequencies.

## Normal Coordinate Treatment

For the convenience of the calculation, it has been assumed that the molecule belongs to the point group $C_{3v}$ and has the structure shown in Fig. 1, in which a C–Si–O–C plane and an O–Si–O plane including the same Si–O bond are assumed to have an interplaner angle of 120°. According to the group theory, this molecule has twelve skeletal vibrations, five of $a_1$, one of $a_2$ and six of $e$ species. One of the six skeletal vibrations of the species $e$ is the torsional oscillation of the (Si–)$OCH_3$ group*. All vibrations except the $a_2$ torsional mode are active both in infrared and Raman spectra.

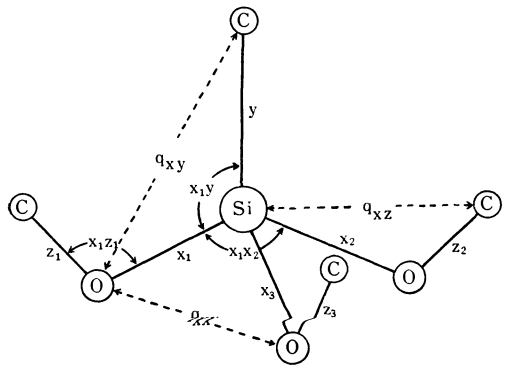



Fig. 1. Internal coordinates of the skeletal of methyltrimethoxysilane.

From the internal coordinates (Fig. 1), the following orthonormal symmetry coordinates have been found:

for the $a_1$ vibrations,

$$R_1=\Delta(z_1+z_2+z_3)/\sqrt{3}$$
$$R_2=\Delta y$$
$$R_3=\Delta(x_1+x_2+x_3)/\sqrt{3}$$
$$R_4=\Delta(x_1x_2+x_1x_3+x_2x_3-x_1y-x_2y-x_3y)/\sqrt{6}$$
$$R_5=\Delta(x_1z_1+x_2z_2+x_3z_3)/\sqrt{3}$$

and for the $e$ vibrations,

$$R_{7a}=\Delta(2z_1-z_2-z_3)/\sqrt{6}$$
$$R_{8a}=\Delta(2x_1-x_2-x_3)/\sqrt{6}$$
$$R_{10a}=\Delta(2x_1z_1-x_2z_2-x_3z_3)/\sqrt{6}$$
$$R_{11a}=\Delta(2x_1x_2-x_1x_3-x_2x_3)/\sqrt{6}$$
$$R_{12a}=\Delta(2x_1y-x_2y-x_3y)/\sqrt{6}$$

The numbering of these symmetry coordinates corresponds to the numbering of the fundamentals in Table II.

From the coefficients of the symmetry coordinates and the potential constants in a Urey-Bradley force field[4], the $F$ matrix elements are obtained as follow:

for the $a_1$ vibrations,

$$F_{11}=K_z+s_{zx}{}^2F_{xz}+t_{zx}{}^2F_{xz}'$$
$$F_{13}=s_{xz}s_{zx}F_{xz}-t_{xz}t_{zx}F_{xz}'$$
$$F_{15}=(s_{zx}t_{xz}F_{xz}+s_{xz}t_{zx}F_{xz}')x$$
$$F_{22}=K_y+3s_{yx}{}^2F_{xy}+3t_{yx}{}^2F_{xy}'$$
$$F_{23}=\sqrt{3}\,(s_{xy}s_{yx}F_{xy}-t_{xy}t_{yx}F_{xy}')$$
$$F_{24}=-\sqrt{3}/2(s_{yx}t_{xy}F_{xy}+s_{xy}t_{yx}F_{xy}')x$$
$$F_{33}=K_x+4s_{xx}{}^2F_{xx}+s_{xy}{}^2F_{xy}+s_{xz}{}^2F_{xz}+t_{xy}{}^2F_{xy}'+t_{xz}{}^2F_{xz}'$$

1) T. Tanaka, This Bulletin, 31, 762 (1958).
2) E. B. Wilson, Jr., *J. Chem. Phys.*, 7, 1047 (1939); 9, 76 (1941).
3) T. Tanaka, A. Tasaka, R. Ōkawara and T. Watase, *Technol. Repts. Osaka Univ.*, 7, 193 (1957).
* It represents the methoxy group attached to the silicon atom.
4) T. Shimanouchi, *J. Chem. Phys.*, 17, 245, 734, 848 (1949).

$$F_{34}=\sqrt{2}s_{xx}t_{xx}(F_{xx}+F_{xx}')x-(s_{xy}t_{yx}F_{xy}+s_{yx}t_{xy}F_{xy}')y/\sqrt{2}$$
$$F_{35}=(s_{xz}t_{zx}F_{xz}+s_{zx}t_{xz}F_{xz}')z$$
$$F_{44}=(H_{xx}+t_{xx}F_{xx}-s_{xx}^2F_{xx}')x^2/2+(H_{xy}+t_{xy}t_{yx}F_{xy}-s_{xy}s_{yx}F_{xy}')xy/2+3\kappa/\sqrt{8}$$
$$F_{55}=(H_{xz}+t_{xz}t_{zx}F_{xz}-s_{xz}s_{zx}F_{xz}')xz$$
$$F_{12}=F_{14}=F_{25}=F_{45}=0$$

and for the $e$ vibrations,

$$F_{77}=K_z+s_{zx}^2F_{xz}+t_{zx}^2F_{xz}'$$
$$F_{78}=s_{xz}s_{zx}F_{xz}-t_{xz}t_{zx}F_{xz}'$$
$$F_{710}=(s_{zx}t_{xz}F_{xz}+s_{xz}t_{zx}F_{xz}')x$$
$$F_{88}=K_x+s_{xx}^2F_{xx}+s_{xy}^2F_{xy}+s_{xz}^2F_{xz}+3t_{xx}^2F_{xx}'+t_{xy}^2F_{xy}'+t_{xz}^2F_{xz}'$$
$$F_{810}=(s_{xz}t_{zx}F_{xz}+s_{zx}t_{xz}F_{xz}')z$$
$$F_{811}=s_{xx}t_{xx}(F_{xx}+F_{xx}')x/2$$
$$F_{812}=(s_{xy}t_{yx}F_{xy}+s_{yx}t_{xy}F_{xy}')y$$
$$F_{1010}=(H_{xz}+t_{xz}t_{zx}F_{xz}-s_{xz}s_{zx}F_{xz}')xz$$
$$F_{1111}=(H_{xx}+t_{xx}^2F_{xx}-s_{xx}^2F_{xx}')x^2+\kappa/\sqrt{8}$$
$$F_{1112}=\sqrt{2}\kappa/4$$
$$F_{1212}=(H_{xy}+t_{xy}t_{yx}F_{xy}-s_{xy}s_{yx}F_{xy}')xy+\kappa/\sqrt{8}$$
$$F_{711}=F_{712}=F_{1011}=F_{1012}=0$$

where the following abbreviations have been adopted:

$$s_{xx}=4x/3q_{xx} \qquad t_{xx}=\sqrt{8}x/3q_{xx}$$
$$s_{xy}=(3x+y)/3q_{xy} \qquad t_{xy}=\sqrt{8}y/3q_{xy}$$
$$s_{yx}=(3y+x)/3q_{xy} \qquad t_{yx}=\sqrt{8}x/3q_{xy}$$
$$s_{xz}=(x-z\cos\theta)/q_{xz} \qquad t_{xz}=z\cos\theta/q_{xz}$$
$$s_{zx}=(z-x\cos\theta)/q_{xz} \qquad t_{zx}=x\cos\theta/q_{xz},$$

and the symbols used for the equilibrium values of the interatomic distances and of the interbond angles are $x$=Si-O, $y$=Si-C, $z$=O-C, $q_{xx}$=O···O, $q_{xy}$=O···C, $q_{xz}$=Si···C and $\theta=\angle$SiOC.

The $G$ matrix elements are obtained by the use of the table of Decius[5] and the method of Crawford[6]. Using the notations $\rho_x$, $\rho_y$ and $\rho_z$ for the reciprocals of Si-O, Si-C and O-C bond lengths, and $\mu_{Si}$, $\mu_O$ and $\mu_C$ for the reciprocals of the masses of silicon and oxygen atoms and methyl group, respectively, the following $G$ matrix elements have been obtained:

for the $a_1$ vibrations,

$$G_{11}=\mu_O+\mu_C$$
$$G_{13}=\mu_O\cos\theta$$
$$G_{14}=-\sqrt{2}\rho_x\mu_O\sin\theta$$
$$G_{15}=-\rho_x\mu_O\sin\theta$$
$$G_{22}=\mu_{Si}+\mu_C$$
$$G_{23}=-\mu_{Si}/\sqrt{3}$$
$$G_{24}=4\rho_x\mu_{Si}/\sqrt{3}$$
$$G_{25}=\sqrt{8/3}\rho_x\mu_{Si}$$
$$G_{33}=\mu_{Si}/3+\mu_O$$
$$G_{34}=-4\rho_x\mu_{Si}/3$$
$$G_{35}=-\sqrt{8}\rho_x\mu_{Si}/3-\rho_z\mu_O\sin\theta$$
$$G_{44}=2\rho_x^2(8\mu_{Si}/3+\mu_O)$$
$$G_{45}=8\sqrt{2}\rho_x^2\mu_{Si}/3+\sqrt{2}\rho_x(\rho_x-\rho_z\cos\theta)\mu_O$$
$$G_{55}=8\rho_x^2\mu_{Si}/3+\rho_z^2\mu_C+(\rho_x^2+\rho_z^2-2\rho_x\rho_z\cos\theta)\mu_O$$
$$G_{12}=0$$

and for the $e$ vibrations,

$$G_{77}=\mu_O+\mu_C$$
$$G_{78}=\mu_O\cos\theta$$
$$G_{710}=-\rho_x\mu_O\sin\theta$$
$$G_{711}=-\rho_x\mu_O\sin\theta/4$$
$$G_{712}=\rho_x\mu_O\sin\theta$$
$$G_{88}=4\mu_{Si}/3+\mu_O$$
$$G_{810}=\sqrt{2}\rho_x\mu_{Si}/3-\rho_z\mu_O\sin\theta$$
$$G_{811}=-\sqrt{8}\rho_x\mu_{Si}/3$$
$$G_{812}=-\sqrt{2}(\rho_x/3+\rho_y)\mu_{Si}$$
$$G_{1010}=\rho_x^2\mu_{Si}/6+\rho_z^2\mu_C+(\rho_x^2+\rho_z^2-2\rho_x\rho_z\cos\theta)\mu_O$$
$$G_{1011}=-\rho_x^2\mu_{Si}/3+\rho_x(\rho_x-\rho_z\cos\theta)\mu_O/4$$
$$G_{1012}=-\rho_x(\rho_x+3\rho_y)\mu_{Si}/6-\rho_x(\rho_x-\rho_z\cos\theta)\mu_O$$

TABLE I. MOLECULAR AND POTENTIAL CONSTANTS OF METHYLTRIMETHOXYSILANE

| Bond distance and angle | Potential constants | |
|---|---|---|
| | Type | md·Å |
| $x$=Si-O | | |
| =1.64 Å[a] | $K_x$(Si-O) | 3.25 |
| $y$=Si-C | $K_y$(Si-$CH_3$) | 3.03 |
| =1.888 Å[b] | $K_z$(O-$CH_3$) | 4.88 |
| $z$=O-C | $H_{xx}$(O-Si-O) | 0.13 |
| =1.42 Å[a] | $H_{xy}$(O-Si-$CH_3$) | 0.12 |
| ∠O-Si-O | $H_{xz}$(Si-O-$CH_3$) | 0.22 |
| =∠O-Si-C | $F_{xx}$(O···O) | 0.13 |
| =109°28′ | $F_{xy}$(O···$CH_3$) | 0.08 |
| ∠Si-O-C | $F_{xz}$(Si···$CH_3$) | 0.21 |
| =113°[a] | $\kappa$ | 0.25 |

a) Values in tetramethoxysilane, Si$(OCH_3)_4$; M. Yokoi, This Bulletin, **30**, 100 (1957).
b) Value in tetramethylsilane, Si$(CH_3)_4$; W. F. Sheehan, Jr. and V. Schomaker, *J. Am. Chem. Soc.*, **74**, 3956 (1952).

5) J. C. Decius, ibid., **16**, 1025 (1948).
6) B. Crawford, ibid., **21**, 1108 (1953).

TABLE II. RAMAN AND INFRARED DATA, CALCULATED WAVE NUMBERS AND THE ASSIGNMENT FOR METHYLTRIMETHOXYSILANE

| $\nu$. Obsvd. | | $\nu$. Calcd. | Assignment | Mode of vibration |
|---|---|---|---|---|
| Raman | Infrared | | | |
| 150(0b) | | 165 | $\nu_5(a_1)$ | SiOC and $CSiO_3$ sym. def. |
| 174(2b) | | 171 | $\nu_{12}(e)$ | $SiO_3$ rocking |
| 268(3bb) | | 286 | $\nu_{11}(e)$ | $SiO_3$ nonsym. def. |
| 336(0) | | 325 | $\nu_4(a_1)$ | $CSiO_3$ and SiOC sym. def. |
| 374(0) | | 371 | $\nu_{10}(e)$ | SiOC nonsym. def. |
| 425(3b) | | — | $\nu_9(e)$ | SiOC nonsym. torsion |
| 628(7) | | 627 | $\nu_3(a_1)$ | Si-O sym. str. |
| 748(2) | | 782 | $\nu_8(e)$ | Si-O nonsym. str. |
| 800(3) | 790(m) | 829 | $\nu_2(a_1)$ | Si-C str. |
| 860(3b) | 845(m) | | | (Si-)$CH_3$ rocking |
| 1072(6) | 1089(s) | 1069 | $\nu_7(e)$ | C-O nonsym. str. |
| | | 1073 | $\nu_1(a_1)$ | C-O sym. str. |
| | 1110(sh) | | | |
| 1148(4) | | | | (O-)$CH_3$ rocking |
| | 1192(m) | | | |
| 1270(4) | 1267(m) | | | (Si-)$CH_3$ and (O-)$CH_3$ def. |
| | 1402(vw) | | | |
| 1430(3) | | | | |
| 1461(4b) | 1459(w) | | | |
| | 2333(b) | | | |
| 2795(1) | 2825(m) | | | (Si-)$CH_3$ and (O-)$CH_3$ str. |
| 2915(5) | 2931(m) | | | |
| 2954(5b) | 2953(sh) | | | |
| 2990(5b) | | | | |

$$G_{1111}=\rho_x^2(8\mu_{Si}/3+5\mu_O/2)$$
$$G_{1112}=\rho_x(\rho_x/3+\rho_y)\mu_{Si}-\rho_x^2\mu_O/4$$
$$G_{1212}=(\rho_x+3\rho_y)^2\mu_{Si}/6+\rho_x^2\mu_O+3\rho_y^2\mu_C/2$$

The geometrical and the potential constants used in the calculation are listed in Table I. As an aid in determining these potential constants, excepting $H_{xz}$ and $F_{xz}$, the results in the previous investigations on tetramethylsilane[7], methoxychlorosilanes[8] and diethylether[9] have been used. However, somewhat lower and higher values for $K_x$ and $K_z$, compared with the corresponding values in methoxychlorosilanes and diethylether, respectively, have been adopted, to obtain better agreement between the observed and the calculated frequencies. The value of $K_z$ adopted here is rather close to that previously obtained in dichloromethylether[10]. The mean value of $H(CH_3\text{–}Si\text{–}CH_3)$ in $Si(CH_3)_4$[7] and $H_{xx}$ in this paper, and that of $F(CH_3\cdots CH_3)$ and $F_{xx}$ have been used as $H_{xy}$ and $F_{xy}$, respectively. The value of $\kappa$ has been derived by means of the proportional allotment from the intramolecular tension of silicon tetrahedron in $Si(CH_3)_4$[7] and that in $Si(OCH_3)_4$[8]. The values of $H_{xz}$ and $F_{xz}$ have been selected so as to give good agreement between the calculated and observed ones. Finally, the value of $F'$ has been assumed to be equal to $-F/10$ by the usual way.

### Assignment of Observed Frequencies

From the $F$ and $G$ matrix elements given above, the fundamental frequencies have been calculated by the use of the molecular and the potential constants listed in Table I, and the results are shown in Table II, together with the observed wave numbers of the Raman and the infrared bands. The skeletal vibrations have been assigned by the calculation of the potential energy distribution in the symmetry coordinates, and also the hydrogen vibrations have been tentatively assigned.

The $L$ matrices and the distribution of potential energy in symmetry coordinates have been calculated for the skeletal normal modes; the results are shown in Table III and IV, respectively.

The calculated frequencies of the skeletal vibrations are in good agreement with their corresponding observed values, except for the Raman line at 425 $cm^{-1}$. This line may be classified as the (Si-)$OCH_3$ torsional oscillation of $e$ species. As shown in Table IV some of

7) T. Shimanouchi, *J. Chem. Soc. Japan, Pure Chem. Sec.* (*Nippon Kagaku Zasshi*), **74**, 266 (1953).
8) H. Murata, ibid., **77**, 893 (1956).
9) M. Hayashi, ibid., **78**, 222 (1957).
10) Y. Morino and M. Katayama, *Reports of Research Institute of Radiation Chemistry, The University of Tokyo* (*Fukusyaken-hôkoku*), **4**, 1 (1947).

TABLE III. THE $L$ MATRICES OF THE SKELETAL NORMAL VIBRATIONS OF METHYLTRIMETHOXYSILANE

*$a_1$ Vibrations*

| | $Q_1$ | $Q_2$ | $Q_3$ | $Q_4$ | $Q_5$ |
|---|---|---|---|---|---|
| $R_1$(C-O sym. str.) | 1.13 | 0.05 | 0.08 | −0.07 | −0.01 |
| $R_2$(Si-C str.) | 0.00 | −0.85 | 0.54 | 0.07 | 0.01 |
| $R_3$(Si-O sym. str.) | −0.29 | 0.58 | 0.55 | −0.15 | 0.03 |
| $R_4$($CSiO_3$ sym. def.) | −0.44 | −0.73 | −0.13 | −0.57 | −0.32 |
| $R_5$(SiOC sym. def.) | −0.27 | −0.81 | −0.56 | −0.53 | 0.33 |

*$e$ Vibrations*

| | $Q_7$ | $Q_8$ | $Q_{10}$ | $Q_{11}$ | $Q_{12}$ |
|---|---|---|---|---|---|
| $R_7$(C-O nonsym. str.) | 1.11 | −0.23 | −0.03 | −0.02 | −0.01 |
| $R_8$(Si-O nonsym. str.) | −0.42 | −0.96 | −0.07 | −0.03 | 0.02 |
| $R_{10}$(SiOC nonsym. def.) | −0.25 | 0.44 | 0.77 | −0.29 | 0.24 |
| $R_{11}$($SiO_3$ nonsym. def.) | −0.03 | 0.26 | −0.42 | −0.85 | −0.13 |
| $R_{12}$($SiO_3$ rocking) | 0.39 | 0.23 | −0.66 | 0.11 | 0.48 |

TABLE IV. POTENTIAL ENERGY DISTRIBUTION $F_{ii}L_{ia}^2/\lambda_a$ FOR THE NORMAL VIBRATION OF SKELETAL IN METHYLTRIMETHOXYSILANE

*$a_1$ Vibrations*

| | $\nu_1$ | $\nu_2$ | $\nu_3$ | $\nu_4$ | $\nu_5$ |
|---|---|---|---|---|---|
| $R_1$(C-O sym. str.) | 0.94 | 0.00 | 0.01 | 0.04 | 0.01 |
| $R_2$(Si-C str.) | 0.00 | 0.57 | 0.40 | 0.03 | 0.00 |
| $R_3$(Si-O sym. str.) | 0.04 | 0.31 | 0.49 | 0.14 | 0.02 |
| $R_4$($CSiO_3$ sym. def.) | 0.02 | 0.09 | 0.01 | 0.39 | 0.49 |
| $R_5$(SiOC sym. def.) | 0.00 | 0.11 | 0.09 | 0.32 | 0.48 |

*$e$ Vibrations*

| | $\nu_7$ | $\nu_8$ | $\nu_{10}$ | $\nu_{11}$ | $\nu_{12}$ |
|---|---|---|---|---|---|
| $R_7$(C-O nonsym. str.) | 0.91 | 0.07 | 0.01 | 0.00 | 0.00 |
| $R_8$(Si-O nonsym. str.) | 0.09 | 0.90 | 0.03 | 0.01 | 0.01 |
| $R_{10}$(SiOC nonsym. def.) | 0.00 | 0.03 | 0.51 | 0.12 | 0.23 |
| $R_{11}$($SiO_3$ nonsym. def.) | 0.00 | 0.01 | 0.13 | 0.87 | 0.05 |
| $R_{12}$($SiO_3$ rocking) | 0.01 | 0.01 | 0.30 | 0.01 | 0.74 |

the symmetry coordinates of totally symmetric species are related to several normal modes to a considerable extent; the $R_2$ and $R_3$ coordinates to both modes of $\nu_2$ and $\nu_3$, and the $R_4$ and $R_5$ coordinates to both modes of $\nu_4$ and $\nu_5$. Especially, in the latter case, the symmetrical deformation of the $CSiO_3$ group and that of the SiOC groups have their equal share in the potential energy of the $\nu_4$ normal mode, and also of the $\nu_5$ mode.

The author wishes to express his sincere thanks to Professor T. Watase of this University, and Dr. H. Murata and Dr. K. Shimizu of Osaka Municipal Technical Research Institute for much valuable discussion.

*Department of Applied Chemistry*
*Faculty of Engineering*
*Osaka University*
*Miyakojima-ku, Osaka*

# 5, 6-Epoxy-cholestane

By Fumikazu MUKAWA

(Received September 22, 1959)

Ruzicka et al.[1] have first obtained 5, 6β-epoxy-5β-cholestane (II), m.p. 53°C, as a by-product of the reaction of cholest-5-ene (I) and peroxyacid. Recently Shoppee et al.[2] have reported that the melting point of 5, 6β-epoxy-5β-cholestane (II) obtained by the above method was 55°C. Henbest and Wrigly[3] have prepared II, m. p. 58°C, $[\alpha]_D$ −9°, by the reduction of 5-bromo-5α-cholestan-6-one with lithium aluminum hydride, while Hallsworth and Henbest[4] have reported that the same epoxycholestane (II) prepared from 5, 6β-diacetoxy-5α-cholestane by the method which was adopted in the preparation of 5, 6β-epoxy-5β-cholestane 3β-ol from 3β, 5, 6β-triacetoxy-5α-cholestane[5] melted at 80°C and showed $[\alpha]_D$ +8°.

Mori and the present author[6] have investigated the addition reaction of hypochlorous acid (isocyanuric chloride-acetic acid) to 3-substituted-$\Delta^5$-steroids and found that the products were 5α-chloro-6β-hydroxy derivatives which have been converted by base to 5β, 6β-epoxides. In the same manner I was expected to be converted to II. However the intermediate 5-chloro-6β-hydroxy-5α-cholestane (III) was not produced but 5, 6β-dichloro-5α-cholestane and oily substance were obtained.

Then, the author has turned to another route to obtain II. Thus, reduction of 5, 6β-epoxy-5β-cholestan-3β-yl halide ($I_a$, halogen=Cl; $I_b$, halogen=Br) with lithium in liquid ammonia or zinc-copper alloy in ethanol has lead to II, m.p. 79°C, $[\alpha]_D$ +80° in 70% yield. The structure of II assigned was confirmed in the following way. Reduction of II with hydroiodic acid (55%) in acetone gave I, and reduction with lithium aluminum hydride in ether gave cholestan-6β-ol. Treatment of II with 1 N sulfuric acid in acetone gave 5, 6β-dihydroxy-5α-cholestane.

It was interesting to notice that the oxide ring at $C_5$~$C_6$ was indifferent to the lithium-ammonia reducing system. By the similar reduction 5, 6α-epoxy-5α-cholestan-3β-yl halide ($IV_a$, halogen=Cl; $IV_b$, halogen=Br) yielded 5,6α-epoxy-5α-cholestan (V), m.p. 76°C, $[\alpha]_D$ −39.9°, which showed no melting point depression upon admixture with an authentic specimen.

It has been reported[7,8] that the reaction of the halohydrins of the steroid series with zinc dust and acetic acid yielded the unsaturated steroids, but 6β-halo (chloro and bromo)-5α-cholestan-3β, 5-diol-3-monoester was exceptional. Thus, the latter was converted into the *trans*-triol 3, 6-diester and $\Delta^5$-derivative was not produced at all. It seems to be noteworthy that in the case of 6β-chloro-5α-cholestan-5-ol (VI), 6β-acetoxy-5α-cholestan-5-ol was obtained being accompanied by a small amount of I[9]. III was converted into I with zinc dust and acetic acid or lithium in liquid ammonia. I was also obtained by the reduction of VI with lithium in liquid ammonia.

## Experimental**

**Attempted Hypochlorous Acid Addition on Cholest-5-ene (I).**—To a mixture consisting of 0.5 g. of I, 0.2 g. of isocyanuric chloride and 15 ml. of acetone were added five drops of 30% aqueous acetic acid. The whole was refluxed for five minutes. After cooling to room temperature, the mixture was poured with stirring into 10% aqueous sodium carbonate, and then extracted with ether. The extract was washed with water and dried over magnesium sulfate. After removal of the solvent, the residue was recrystallized from methanol to yield 0.18 g. of needles, m.p. 120~121°C. The compound did not depress the melting point on admixture with the authentic sample of 5, 6β-dichloro-5α-cholestane. The filtrate was left to stand in a refrigerator for one month. However, only a gum was obtained.

**5, 6β-Epoxy-5β-cholestane (II).**—*i) From 5, 6β-epoxy-5β-cholestan-3β-yl chloride ($I_a$).*—To a well stirred mixture of 50 mg. of lithium and 30 ml. of liquid ammonia, 0.3 g. of $I_a$ in 40 ml. of dry ether was added. After thirty minutes, the excess of

* Present address: Tsurumi Research Laboratory of Chemistry, Tsurumi-ku, Yokohama.

1) L. Ruzicka, M. Furter and G. Thomann, *Helv. Chim. Acta.*, 16, 327 (1933).

2) C. W. Shoppee, R. H. Jenkins and G. H. R. Summer, *J. Chem. Soc.*, 1958, 1657.

3) H. B. Henbest and T. I. Wrigly, ibid., 1957, 4596.

4) A. S. Hallsworth and H. B. Henbest, ibid., 1957, 4606.

5) M. Davis and V. Petrow, ibid., 1949, 2536.

6) S. Mori, *J. Chem. Soc. Japan, Pure Chem. Sec.* (*Nippon Kagaku Zasshi*), 64, 981 (1943); F. Mukawa, ibid., 78. 452 (1957).

7) S. Mori, ibid., 70, 257, 303 (1949); L. Fieser and R. Ettorre, *J. Am. Chem. Soc.*, 75, 1700 (1953) etc.

8) S. Mori and F. Mukawa, *Proc. Japan Acad.*, 31, 532 (1955).

9) Cf. The reaction of epoxy-cholestane derivatives with boronfluoride etherate takes a different course when the substituent is persent at $C_3$. H. B. Henbest et al. *J. Chem. Soc.*, 1957, 4765.

* All melting points are uncorrected.

lithium was destroyed by acetone. After two hours at room temperature, addition of water, extraction of ether and crystallization of the crude product from ethanol afforded II, m.p. 70~73°C, raised by crystallization from ethanol-*n*-hexane to 79°C, $[\alpha]_D$ +8°. It exhibited no absorption of hydroxyl band in the infrared spectrum.

Found: C, 83.85; H, 11.20. Calcd. for $C_{27}H_{46}O$: C, 83.87; H, 11.99%

A mixture of 0.3 g. of $I_a$, 0.2 g. of zinc-copper alloy and 20 ml. of alcohol was heated under reflux for 3 hr. But in this case only starting material was recovered.

*ii) From 5,6β-epoxy-5β-cholestan-3β-yl bromide*[10] *($I_b$).*—To a well stirred mixture of 50 mg. of lithium and 30 ml. of liquid ammonia, 0.3 g. of $I_b$ in 40 ml. of dry ether was added. There were obtained needles which melted at 79°C and did not depress the mixed melting point with the authentic 5,6β-epoxy-5β-cholestane (II). The infrared spectra of the two compounds were identical.

In another rum with 0.5 g. of $I_b$, 0.2 g. of zinc-copper alloy and 30 ml. of ethanol were heated under reflux for 3 hr. There were obtained 0.3 g. of needles with a melting point 78~79°C. There did not depress the mixed melting points with an authentic sample.

**Structure of 5,6β-Epoxy-5β-cholestane (II).**—The product obtained as described above was shown to be 5,6-β-epoxy-5β-cholestane (II) by the following series of reactions.

i) A solution of II (0.2 g.) in acetone (5 ml.) was treated with two drops of hydroiodic acid (55%). After being kept to stand at room temperature (21°C) for 24 hr., the solution was poured into water and was extracted with ether. The extract was washed with sodium thiosulfate solution (5%) and water, dried and evaporated. Crystallization of the residue from alcohol gave 0.1 g. of I, m.p. 90~91°C and mixed m.p. with the authentic specimen showed no depression.

ii) II (0.5 g.) dissolved in anhydrous ether (80 ml.) was added dropwise to lithium aluminum hydride (0.1 g.) in ether for 20 min. at room temperature (20°C) and then refluxed for 5 hr. Chromatography of the product over florisil and elution with ether-methanol gave 5α-cholestan-6β-ol, m.p. 81°C (plates from alcohol), undepressed in m.p. on admixture with the authentic specimen.

iii) A mixture of II (0.3 g.), two drops of sulfuric acid (10%) and 50 ml. of methanol was heated under reflux. After two hours, addition of water, extraction with ether and crystallization of the crude product from alcohol afforded 5α-cholestan-5,6β-diol, m.p. 60~73°C, raised by recrystallization from alcohol to 125°C, undepressed on admixture with the authentic sample.

**5,6α-Epoxy-5α-cholestan-3β-yl Bromide ($IV_b$).**—Cholesteryl bromide (0.5 g.) was added to a cold solution of perbenzoic acid (1.3 equiv.) in 20 ml. of chloroform, the reaction mixture briefly stirred and then allowed to stand at room temperature (18°C) for 48 hr. before pouring into a solution of sodium carbonate. The organic phase was separated, washed with water to neutrality, dried and evaporated. The product crystallized from alcohol to afford $IV_b$, m.p. 87~89°C, $[\alpha]_D = -21.2°$.

Found: C, 68.90; H, 9.70. Calcd. for $C_{27}H_{45}OBr$: C, 69.74; H, 9.75.

**5,6α-Epoxy-5α-cholestane (V).**—The procedure of II was followed. The product was recrystallized from methanol, yielded V, m.p. 76°C, $[\alpha]_D$ −39.9°. It was identified by mixed melting points with the authentic sample.

**5-Chloro-5α-cholestan-6β-ol (III).**—A solution of the epoxy-cholestan II (0.2 g.) in alcohol-free chloroform (2 ml.) was treated with a saturated solution of anhydrous hydrogen chloride in alcohol-free chloroform (10 ml.). After standing at 0°C for 4.5 hr., the solution was evaporated to dryness. The residue was recrystallized from aetone-water to give III, yield, 0.12 g., m.p. 121~123°C, $[\alpha]_D = -12°$.[11]

Found: C, 76.51; H, 11.45. Calcd. for $C_{27}H_{47}OCl$; C, 76.10; H, 11.29%.

*i) With zinc dust.*—A mixture of 0.1 g. of III, 0.2 g. of zinc dust, and 5 ml. of acetic acid was heated under reflux for 3 hr. The solids were filtered off and water was added to produce faint turbidity. The crystals were then crystallized from chloroform-methanol and melted at 91°C. The compound did not depress the melting point with the authentic sample of cholest-5-ene (I).

*ii) With lithium in liquid ammonia.*—The chlorohydrin (III) (0.3 g.) in dry ether was added with vigorous stirring to a solution of lithium (50 mg.) in liquid ammonia (50 ml.). After 30 min., excess lithium was destroyed by acetone. The reaction mixture was then diluted with ether and the ether solution was washed with cold hydrochloric acid solution (1%). Finally the solution was washed with water, dried sodium sulfate and the solvent removed. Crystallization of the product from methanol afforded I, yield, 0.2 g., m.p. 90~91°C, undepressed on admixture with the authentic sample.

**Reduction of 6β-Chloro-5α-cholestan-5-ol (VI).**—*i) With zinc dust.*—A mixture of 1 g. of VI, 0.5 g. of zinc dust and 50 ml. of acetic acid was heated under reflux for 1.5 hr. The solids were filtered off and diluted with water. The product was extracted with ether. The ether solution washed with sodium bicarbonate solution (5%) and then with water, dried, and evaporated. The residue was chromatographed on 20 g. of neutral alumina, the petroleum ether elute yielding, after crystallization from chloroform-methanol, 0.1 g. of I, undepressed on admixture with the authentic sample. Chromatography gave in the ether-methanol (1:1) fractions, 0.4 g. of 6β-acetoxy-5α-cholestan-5-ol, m.p. 80~82°C, $[\alpha]_D = -20°$, the melting point being raised by recrystallization from methanol to 108°C.

Found: C, 77.90; H, 11.00. Calcd. for $C_{29}H_{50}O_3$: C, 77.97; H, 11.28%.

*ii) With lithium in liquid ammonia.*—Reduction of 0.3 g. of VI with lithium in liquid ammonia under conditions described for the 5-chloro-isomer afforded 0.1 g. of I. It was identified by mixed melting point with the authentic sample.

10) S. Mori, *J. Chem. Soc. Japan, Pure Chem. Sec.* (*Nippon Kagaku Zasshi*), **74**, 89 (1953).

11) C. W. Shoppee et al., *J. Chem. Soc.*, **1958**, 1657, reported 108~109°C, $[\alpha]_D$ −22°.

The author wishes to express his sincere thanks to Professor K. Hata for his encouragement and to Assistant Professor Y. Nomura of the Universtiy of Tokyo for reading the manuscript. This work was supported in part by a Grant-in-Aid from the Ministry of Education.

*Department of Chemistry*
*Faculty of Science*
*Tokyo Metropolitan University*
*Setagaya-ku, Tokyo*

# *Detection of Chromatogram by Swelling of Adsorbent*

By Akira HAYAKAWA and Kōji TANAKA

(Received September 17, 1959)

In the field of adsorption chromatography the column chromatography was devised for the first time by Tswett[1] about fifty years ago. Afterwards, in 1950, the chromatostrip as the modifier was introduced by Kirchner et al.[2] and more recently the larger strip called chromatoplate was used by Reitsema[3]. In these methods the adsorbent was sealed with a glass wall or hardened with a binder.

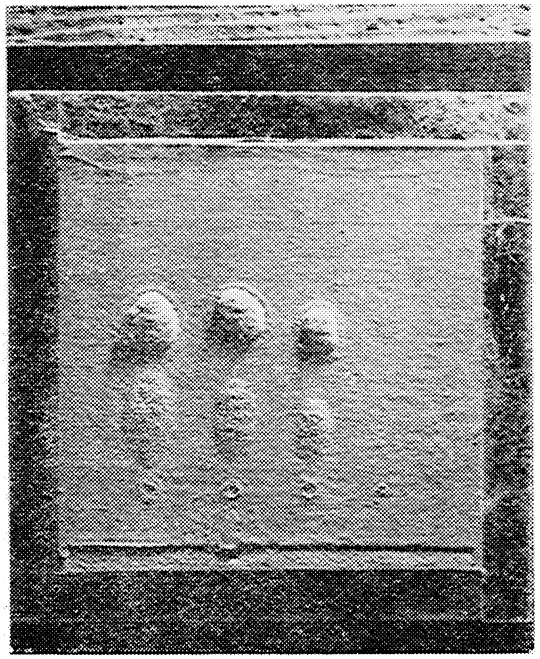


Fig. 1. Swelling of adsorbent by water vapor.
Developer: 10% ethylacetate in *n*-hexane
Adsorbent: Silica gel (about 200 mesh)
Sample : Benzaldehyde
The amount of sample is 15, 10, 5 and 1 drops from left to right, respectively.

Simplifying the operation of the above-mentioned chromatoplate, the authors used the adsorbent alone sprinkled on a glass plate without a binder. As an adsorbent was used silica gel of about 200 mesh. It was sprinkled on the glass plate in constant thickness (2 mm.) and the surface was smoothed with a glass rod. The commercially available pure benzaldehyde was used as a sample. It was developed by 10% ethylacetate in hexane and dried in air to remove the developer.

The present authors happened to discover that the adsorbent of the part of the spot made by benzaldehyde was upheaved by swelling when the plate prepared by the above-described process was left in an enclosed case of high humidity. In order to confirm this phenomenon, the authors left another plate prepared in quite the same way in the sealed case of 100% relative humidity and over a long time observed the change expected to be brought about on it. After 2 to 3 hr. an umbrella-shaped swelling of the adsorbent began to occur at the place of

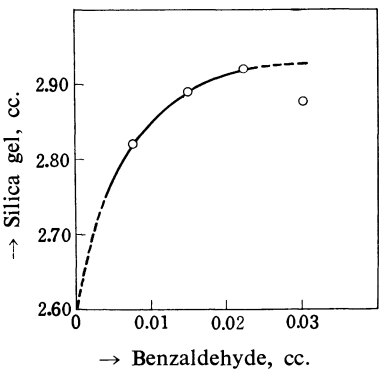



Fig. 2. The apparent volume of silica gel as a function of the amount of benzaldehyde added to 1 g. of silica gel.

1) M. Tswett, *Ber. deut. botan. Ges.*, 24, 384 (1906).
2) J. G. Kirchner and G. J. Keller, *J. Am. Chem. Soc.*, 72, 1867 (1950).
3) R. H. Reitsema, *Anal. Chem.*, 26, 960 (1954).

$R_f$ about 0.5. After one day that of oval shape began to arise at $R_f$ about 0.22 and after three days the rising of ring shape was found around the first one. The second swelling and the third one seem to be caused by derivatives of benzaldehyde or its oxidation products. In either case it is considered that polar groups in these compounds act on polar groups of silica gel and consequently the swelling by water vapor takes place. The condition of the plate after four days is shown in Fig. 1. The amount of the sample dropped on silica gel was 15, 10, 5 and 1 drops from left to right, respectively. In a drip of one drop hardly any upheaval is observed.

Fig. 2 was obtained by plotting the apparent volume of silica gel as a function of the amount of benzaldehyde added to 1 g of silica gel. As is seen in the figure the apparent volume of silica gel increased with the increasing amount of benzal dehyde until it came to 0.025 cc.

The swelling phenomenon was scarcely noted when the relative humidity in the enclosed case was decreased to below 40 or 50%.

So far the expression of the spot of chromatography has been two dimensional or superficial. But the use of the swelling phenomenon above described will make the three dimensional observation possible.

*Department of Chemistry*
*Tokyo College of Science*
*Shinjuku-ku, Tokyo*

# *Structure of Namakochrome. I**

By Toshihiko MUKAI**

(Received September 16, 1959)

In a previous paper[1] of this series the isolation of namakochrome, which would be a new derivative of the polyhydroxynaphthoquinones, from *Polycheira rufescens* was reported.

*Polycheira rufescens* (in Japanese, Murasaki-kuruma-namako) is a sort of tiny sea cucumber, its body being dark purple in color. A crowd of the animals may be frequently found in the stony tidal zone. As preliminary examination assigned the purple coloration of the sea cucumber to a chromoprotein, some methods to isolate the prosthetic group of the protein had been undertaken, and namakochrome was obtained.

Twenty-eight thousand of the sea cucumbers were collected for material at a sea coast near the Amakusa Marine Laboratory, the Faculty of Science, Kyushu University. These animals were dipped into a dilute aqueous solution of acetic acid. The chromoprotein dissolved easily in the aqueous acid to give a red solution. To the red extract, diluted aqueous solution of sodium hydroxide was added till the color of the extract changed to dark purple. After the resulting opaque solution was allowed to stand overnight, a pale yellow supernatant liquid was decanted off and the remaining purple pasty precipitates were collected***. The precipitates were treated with concentrated hydrochloric acid, followed by extraction with ether. Two and thirty-six hundredths grams of crude, orange red pigment of the prosthetic group were obtained. Repeated recrystallization from glacial acetic acid afforded pure namakochrome, a pigment of crimson prisms, m. p. 218°C.

Namakochrome contains only three elements, namely, carbon, hydrogen and oxygen. Its molecular weight determination (by the micro-Rast method with camphorquinone) and elementary analysis yield the result which is in agreement with the molecular formula $C_{11}H_8O_8$. The ultraviolet (ethanol) and infrared (Nujol) absorption spectra are shown in Figs. 1 and 2, respectively. On heating, a greater part of namakochrome sublimes, leaving some carbonized matter. This pigment is easily soluble in solvents of high polarity. It is soluble in mineral acids, to which it is very stable; even in hot concentrated sulfuric acid a red color of the solution lasts for a considerably long time. It is unstable to the solution of weak alkali. With sodium bicarbonate solution it gives a light yellow color, changing gradually to colorless. On the other hand, it dissolves easily in

* "Pigments of Marine Animals", IX. VIII of this series: M. Yamaguchi, This Bulletin, 32, 1171, (1959).

** Present address: Yoshitomi Pharmaceutical Industries, Ltd., Yoshitomi Factory, Yoshitomi-cho, Chikujo-gun, Fukuoka-ken.

1) T. Mukai, *Mem. Fac. Sci., Kyushu Univ., Series C, Chem.*, 3, No. 2, 29 (1958).

*** The same precipitates could be obtained by the addition of methanol instead of aqueous sodium hydroxide, but this caused only imperfect precipitation, and its supernatant liquid still remained deep red.

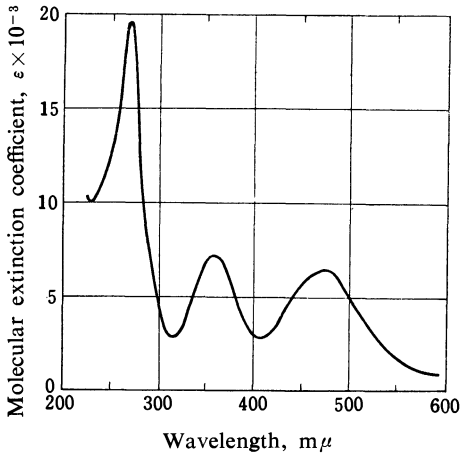



Fig. 1. Absorption curve of namakochrome: solvent, ethanol.

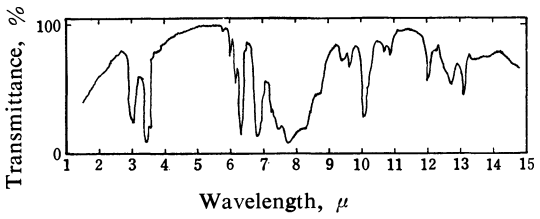



Fig. 2. Infrared spectrum of namakochrome.

dilute solution of strong alkali with orange red color, while with its more concentrated aqueous solution, it forms immediately purplish black salt, which is sparingly soluble in it. With heavy metals also, it gives the difficultly soluble black salts with purple luster. Namakochrome reduces silver nitrate, and gives a dark purple color with ferric chloride. It gives a purple precipitation with neutral lead acetate, a reddish purple precipitation with basic lead acetate, and a dark orange-yellow color with magnesium acetate. On adding zinc dust to a solution of namakochrome in an acetic anhydride pyridine mixture, an original red color soon changes to yellow, then the solution gradually turns colorless, and at last returns to yellow****. This yellow solution becomes red when warmed with concentrated sulfuric acid.

Now, the above-mentioned properties and the molecular formula would suggest that namakochrome is a derivative of polyhydroxynaphthoquinones. To obtain information on the basic structure of the molecular skeleton, zinc dust distillation of namakochrome was carried out, and naphthalene was isolated in a relatively good yield.

Brockmann[2] found that when most of quinone derivatives were hydrogenated in the presence of palladium catalyst on barium sulfate, in aqueous alkaline solution, only the quinone-system prevailed over the other reducible groups in the same molecule. He extended this selective hydrogenation method to a determination of a molecular weight of Actinorhodin, a new hydroxyquinone derivative, isolated from *Streptomyces coeli* color. This method was applied to catalytic hydrogenation of namakochrome, and the result showed that namakochrome shoud have a quinone-system in the molecule, as it absorbed one molecular equivalent of hydrogen. On coming in contact with the air, the resulting pale brown solution changed its color to original red.

In the presence of concentrated sulfuric acid as a catalyst, namakochrome reacts with acetic anhydride to yield a lemon yellow acetyl derivative, m. p. 158~163°C. The acetyl derivative is labile to alkali. When its ethereal solution is brought into contact with aqueous sodium bicarbonate solution even for a short time, decomposition of the acetate occurs and the original material, namakochrome, is isolated. In contrast with namakochrome, the acetate is easily soluble in benzene, sparingly soluble in cold ethanol, and recrystallization from ethanol is very easy. The analytical data[3] obtained for the acetate is in accordance with the formula, $C_{11}H_3O_8(COCH_3)_5$. The infrared absorption spectrum of the acetate is shown in Fig. 3.

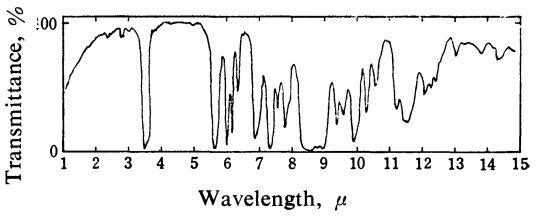



Fig. 3. Infrared spectrum of penta-acetyl namakochrome.

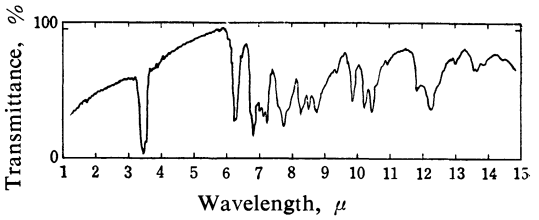



Fig. 4. Infrared spectrum of trimethyl ether of namakochrome.

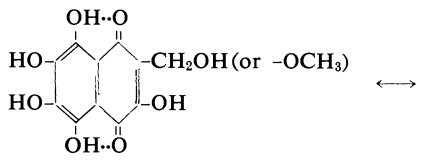
**** There must be a leuco-acetyl derivative of namakochrome in the resulting yellow solution, but no crystalline product is obtained as yet.

2) H. Brockmann et al., *Ber.*, **88**, 781 (1955).

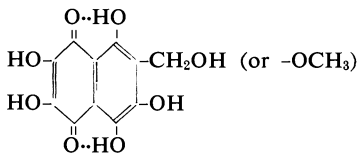
3) In the estimation of acetyl groups of the acetate, 5 N NaOH was emloyed as a saponifying agent. Namakochrome was also treated under the same saponifying condition, because there remained doubt whether this agent degrades namakochrome to acidic volatile substances. It was shown that under these conditions namakochrome which was liberated from the acetate by the saponification, did not suffer an undesirable change.

Since the formation of the acetate evidently shows many hydroxyl groups to be present in the namakochrome molecule, namakochrome was strongly methylated by the Kuroda's method[4]. The resulting ether is of brownish red long needles, melting at 185~187°C. Analysis of the ether yields results which are in accordance with the formula $C_{11}H_5O_5(OCH_3)_3$. The infrared absorption spectrum of the ether is shown in Fig. 4. In the trimethyl ether, two of the hydroxyl groups at the $\alpha$-positions of naphthalene nucleus would, as usual, not be methylated and remain free. Furthermore, the following properties of the ether indicated that the positions of the three methylated hydroxyl groups would be located in 3-, 6- and 7-positions of the naphthalene nucleus. Such properties were of the color reactions, which were introduced by Kuroda[5], and were taken up in the work of Kuhn[6] on the structure of Echinochrome A. That is, namakochrome trimethyl ether, like naphthazarin and $\beta$-alkyl naphthazarin, dissolved in an aqueous solution of sodium hydroxide to give a purplish blue color[7], and did not dissolve in an aqueous solution of sodium bicarbonate. On the contrary, the color reaction and the precipitation reaction of namakochrome itself, already described, could be recognized it as the analogue of naphthopurpurin or $\beta$-alkyl naphthopurpurin.

Although, there is not, as yet, the clue given to the nature of one of the eight oxygen atoms in the namakochrome molecule, this oxygen atom should form a group together with the other remaining one carbon atom and three hydrogen atoms. The unascertained group would, therefore, be either a hydroxymethyl or a methoxyl group, which should locate at the $\beta$-position of the naphthalene nucleus. Namakochrome may be, anyhow, a new derivative of the naphthoquinones, possessing the following structure (I ↔ II).




I




II

4) T. Kuroda, *Nat. Sci. Rep. Ochanomizu Univ., Tokyo*, **2**, 90 (1951).

5) T. Kuroda et al., *Proc. Imp. Acad.*, **12**, 239 (1936); ibid., **13**, 158 (1938).

6) R. Kuhn et al., *Ber.*, **72**, 1407 (1939).

## Experimental

**Distillation of Namakochrome with Zinc Dust.**—Essentially the method of Ochiai and Tsuda[8] was followed for the distillation of namakochrome with zinc dust. Namely, one end of a glass tube (9 mm. in diameter and about 50 mm. in length) was drawn to a capillary about 2 mm. in diameter. A plug of clean asbestos was inserted at the point where the capillary began. Zinc dust was introduced into the tube so that it covered a length of about 10 mm. from the plug, and a mixture of namakochrome and zinc dust was introduced into the tube to fill a length of about 10 mm. of the tube. Zinc dust was last placed in the tube, which was then sealed at the open end. The mixture of 370 mg. of namakochrome and 7 g. of zinc dust was treated with seventeen of the above-mentioned apparatus. The tube containing the materials was heated from the open side to the closed side with continuous rotation, and was finally heated red hot. The distillates were three separate fractions. The first distillate was a waxy substance having a blue fluorescence near the asbestos plug. At a short distance, there was found the second distillate, colorless liquid over which the third colorless leaflets and white solid was lapped. The portions of the crystals and the solid were cut into sections (about 10 mm.) and packed at a sealed end of a glass tube (about 15 mm. in diameter). The other end of the tube had been drawn out to form a capillary, whose length and inside diameter were 70 mm. and 1.5~2 mm., respectively. Then the apparatus was emptied to about 20 mmHg from the open end of the capillary, which was then sealed off. The portion of the larger tube was horizontally inserted in an aluminum block maintained at 95°C, and a wet filter paper condenser was attached at a half of the capillary portion from its closed end. The part of the capillary where the colorless oil separated perfectly, was cut off, and the remainder portions of the capillary were handled again in the same manner as described. Repeated operations afforded the solid which is slightly contaminated with the oil. The solid was then purified by crystallization from ethanol. About 4 mg. of crystals, m. p. 80°C, were obtained. This was naphthalene, whose melting point was unaffected by admixture with an authentic sample.

**Catalytic Hydrogenation.**—In 4 ml. of 1 N sodium hydroxide, 7.65 mg. of namakochrome were hydrogenated in the presence of about 50 mg. of palladium on barium sulfate catalyst.

Found: 1.02 mol. of hydrogen.

**Penta-acetyl Namakochrome.**—One drop of concentrated sulfuric acid was, at room temperature, added to a suspension of namakochrome (50 mg.) in acetic anhydride (1.5 g.), to give a lemon yellow solution. After setting aside for two hours at room temperature, the resulting solution was poured into

7) When the trimethyl ether was catalytically hydrogenated by the Brockmann's method described above, the purplish-blue color caused by the alkali rapidly changed into nearly colorless and again backed to purplish-blue on exposure to air. At this time the trimethyl ether absorbed one molecular equivalent of hydrogen.

8) E. Ochiai and K. Tsuda, "Yuki Biryo Shyoryo Teiryo Bunsekiho", Nanzando, Tokyo (1940), p. 300.

ice water and extracted with benzene. The yellow extracts were concentrated to a small volume under the reduced pressure. The concentrate was filtered through a calcium carbonate column (3×16 cm.). Evaporation of the effluent under reduced pressure, and recrystallization of the resulting yellow residue from ethanol gave penta-acetyl namakochrome as lemon yellow needles (50 mg.), m. p. 158~163°C.

Found: C, 52.68; H, 3.93; AcO, 45.40. Calcd. for $C_{21}H_{18}O_{13}$: C, 52.73; H, 3.79; AcO, 44.99%.

**Trimethyl Ether of Namakochrome.**—A solution of diazomethane (prepared from 5 g. of *N*-methyl-*N*-nitroso-*p*-toluenesulfonamide) in ether (40 ml.) was added dropwise to crystalline namakochrome (300 mg.) spread on a large evaporating dish. When the violence of the reaction abated, and evaporation of the ether slowed, the solvent remaining in the evaporating dish was removed. Addition of the diazomethane solution was then continued. After the addition of the whole ethereal solution of diazomethane, the remaining solvent was evaporated as before. The resulting residue was dissolved in benzene, and filtered through a calcium carbonate column. The red effluent was evaporated to dryness under reduced pressure, and there remained brownish red, fine, long, needles, which, by recrystallization from a mixture of ethanol and benzene, gave trimethyl ether (279 mg.), m. p. 185~187°C.

Found: C, 54.17; H, 4.72. Calcd. for $C_{14}H_{14}O_8$: C, 54.20; H, 4.55%.

The author wishes to express his thanks to Professor Dr. Tokuichi Tsumaki under whose guidance this investigation has been carried out. The expenses of the work were partially covered by the Scientific Research Grant of the Ministry of Education.

*Department of Chemistry*
*Faculty of Science*
*Kyushu University*
*Hakozaki, Fukuoka*

# *Some Characteristics of Zinc Oxide Phosphor*

By Keiji MAEDA

(Received August 31, 1959)

Zinc oxide is well known as a typical oxide semiconductor and many investigations have been made concerning it. Its characteristics are quite complex compared with those of other materials. It may be said that this complexity is due to the divalency of the constituting ions and the difficulty of preparing prefect crystals. Moreover, since zinc oxide is not a purely ionic crystal, one must take into account the homopolar nature of the binding. Although important progress has been made by the recent studies on the single crystal, there remain many ambiguities. A review of the present status has been given by Heiland, Mollwo and Stöckman[1].

On the other hand, zinc oxide has been used for many practical purposes, for instance, as a catalyst and photocatalyst for a series of chemical reactions, and as a phosphor with very fast decay time. In addition, it may play an important role in future in the "Electrofax" process of photographic duplication in which the photoconductivity of zinc oxide is utilized. These applications depend in a direct way on the electronic processes in zinc oxide. As a phosphor, zinc oxide has never been a subject of such extensive investigations as have been made on other similar materials, i.e. zinc and cadmium sulfides. In this report, several characteristics of zinc oxide phosphors will be described.

1) G. Heiland, E. Mollwo and F. Stöckman, "Solid State Physics", Vol. 8, Academic Press, New York (1959), p. 193.

## Experimental and Results

**Sample Preparation.** — The samples were prepared by firing pure zinc oxide at several temperatures from 950 to 1200°C in an atmosphere of air, forming gas, hydrogen or oxygen for various durations. In some samples, many kinds of impurities were intentionally added before firing. Only the phosphors fired in reducing atmosphere give bright green luminescence. The phosphors fired in air emit yellowish green luminescence and those fired in an oxidizing atmosphere dark orange luminescence. Except in the case of a phosphor containing lead as an activator, effects of added impurities on the luminescence spectrum do not appear clearly. Neither chlorine nor bromine functions as a coactivator. A firing in hydrogen atmosphere at 1000°C for 3 min. produced a phosphor emitting intense luminescence. Because of the strong intensity of the green luminescence, one will be concerned with it in the experiments described below.

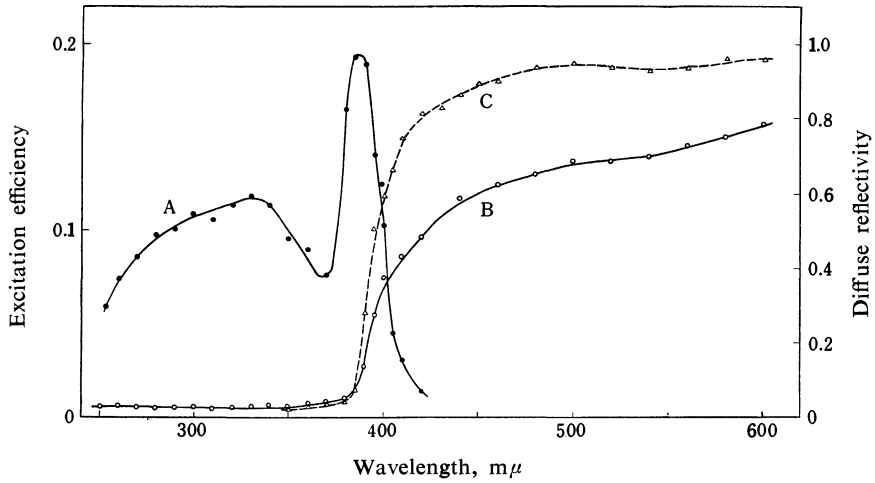



Fig. 1. Excitation and reflectivity spectra of zinc oxide.

A: Excitation efficiency of zinc oxide fired under reducing conditions.
B: Diffuse reflectivity of the same sample as A.
C: Diffuse reflectivity of zinc oxide fired under oxidizing conditions.

**Luminescence Spectrum.**—The luminescence spectrum was measured at both room and liquid air temperatures. The peak of the green luminescence is located at about 5050 Å and does not shift with temperature, but the spectral width decreases with decreasing temperature. This is in agreement with the published data[2].

**Reflection and Excitation Spectra.**—The reflection and excitation spectra were measured with the apparatus made in this laboratory[3]. As examples, some results are shown in Fig. 1. Here, the value of excitation efficiency is defined as the ratio of the number of luminescence photons to that of the incident exciting photons.

The absorption edge of zinc oxide is about 3900 Å at room temperature. The sample fired in an oxidizing atmosphere has a steep rise in reflectivity and a slight absorption at longer wavelengths. On the other hand, for the sample fired in a reducing atmosphere the rise in reflectivity is gradual and a notable absorption extends over the whole wavelength region measured. For the sample fired in stronger reducing condition, a larger absorption results.

There is a remarkable peak in excitation spectrum at the position of the absorption edge. The peak value of the excitation efficiency depends on the sample and amounted to 0.31 in the most efficient phosphor. It has no apparent correlation with the increment in absorption. The excitation decreases with decreasing wavelength of excitation and there are some structures. A similar behavior of excitation spectrum has been reported for zinc sulfide[4] and cadmium sulfide[5].

**Temperature Dependence of Luminescence Intensity.**—The temperature dependence of luminescence intensity was measured under excitation with both 2537 and 3650 Å radiation. As shown in Fig. 2, the characteristics are similar for the

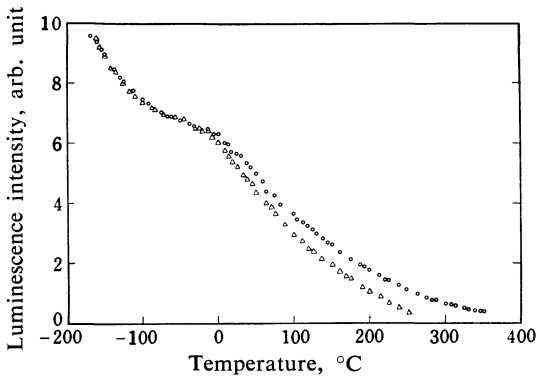



Fig. 2. Temperature dependence of luminescence intensity under 3650 Å excitation (○) and under 2537 Å excitation (△).

two sorts of exciting radiation. The intensity decreases with increasing temperature and the curves have an interesting shape in the neighborhood of 0°C. The author's results are different from those reported by Gobrecht et al.[6]

**Decay of Luminescences.**—The decay of luminescence was measured with an oscilloscope

2) F. J. Studer and L. Gaus, "Soild Luminescent Materials", John Wiley & Sons, Inc., New York (1948), p. 258.
3) Y. Uehara, I. Masuda and Y. Kobuke, to be published.
4) R. H. Bube, *Phys. Rev.*, **90**, 70 (1953).
5) C. C. Klick, ibid., **89**, 274 (1953).
6) H. Gobrecht, D. Hahn and K. Scheffler, *Z. Physik*, **139**, 365 (1954).

Tektronix Model 513D under pulse excitation of cathode ray and care was taken not to distort the fast signal. The luminescence decays very fast and exponentially with time constant of 0.4 $\mu$ sec., which is about an order of magnitude smaller than that reported by Gobrecht et at.[6]

After interruption of photoexcitation it was found a phosphorescence of very weak intensity but with long persistence. This phosphorescence is excited more strongly by 2537 than by 3650 Å radiation. The decay is neither simple monomolecular nor bimolecular type but is represented approximately by $t^{-n}$ for a period of time between 1 and 20 min. following the interruption of excitation. Here $n$ has the value $0.9\pm0.1$ depending on the sample and the condition of excitation. The phosphorescence intensity at one minute after interruption of excitation is smaller by more than three orders of magnitude than the steady state intensity under excitation.

**Atmosphere Dependence of Luminescence Intensity.**—It was found that the luminescence intensity under photoexcitation becomes stronger when the ambient atmosphere of the phosphor is evacuated with a rotary vacuum pump. Fig. 3 illustrates the change of luminescence intensity with time for the processes, excitation on, pumping start, admission of air and excitation off. Average values on several measurements are shown in Table I for the following quantities; the ratio of the luminescence intensity increase $\Delta I$ due to evacuation to the steady state luminescence intensity $I$, in air and the rise time $T_r$ and the decay time $T_d$ of the processes. It was ascertained that $\Delta I/I$ is larger for the weak excitation than for the strong excitation; that is, the proportionality between excitation and luminescence intensities is not satisfied. Here, the intensity ratio of strong to weak excitation is roughly 10. $T_r$ is probably determined by the speed of the evacuating system, and $T_d$ is in dependent on the exciting condition. It could not be detected the slow variation of luminescence intensity compared with $T_r$ and $T_d$ within the experimental accuracy. The light

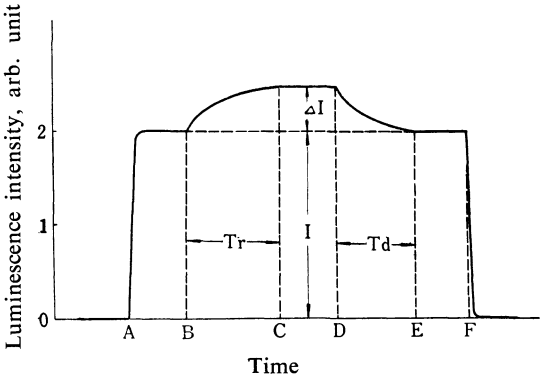



Fig. 3. Variation of luminescence intensity with ambient atmosphere.

A : Excitation on, B : pumping start, C : steady state luminescence intensity in vacuo, D : admission of air, E : steady state luminescence intensity in air and F : excitation off.

TABLE I

| Excitation | $\Delta I/I$ | $T_r$ | $T_d$ |
|---|---|---|---|
| Strong 2537 Å | 0.14 | 1.7 min. | 50 sec. |
| Weak 2537 | 0.18 | 1.8 | 54 |
| Strong 3650 | 0.10 | 1.6 | 62 |
| Weak 3650 | 0.17 | 1.3 | 44 |

intensity reflected from magnesia smoke placed at the same position as the phosphor is independent of the condition of evacuation. Therefore, the variation of luminescence intensity described above can not be attributed to any other causes than the phosphor itself.

Then the author investigated the relationship between the luminescence intensity and the ambient pressure under various kinds of simple atomospheres, such as hydrogen, oxygen, dry air, and mixed vapor of water and ethanol. Of these atmospheres, hydrogen, oxygen or dry air, when passed through a liquid air trap, exhibits no recognizable effect on luminescence intensity. On the other hand, water or ethanol vapor decreases the luminescence intensity

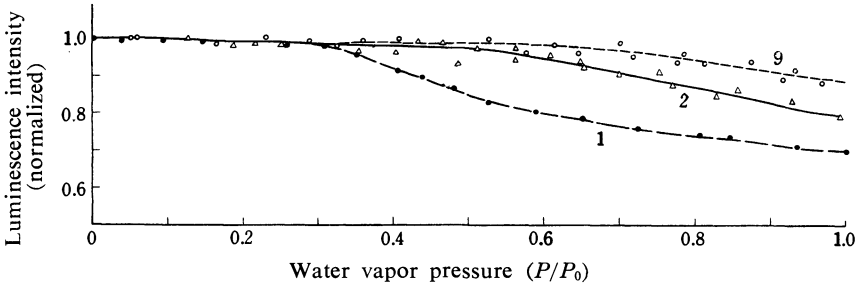



Fig. 4. Dependence of luminescence intensity on water vapor pressure for various exciting intensities (at 30°C). Relative exciting intensity is indicated in the figure and $P_0$ is the saturated vapor pressure.

considerably. Although the results are not always reproduced quantitatively, some of them are shown in Fig. 4 for three excitation intensities. From this figure it is seen that the luminescence intensity suffers quenching for the pressure $P$ which is not so small compared with the saturated vapor pressure $P_0$. In the process of these measurements, photoadsorption or photodesorption of the vapor which gives an effect to luminescence intensity did not occur to a measurable extent.

**Surface Potential.**—It was expected that a change in the surface potential of the phosphor might be accompanied with the variation of the luminescence intensity under the ambient atmosphere. The author measured it by the well known Kelvin method using gold as a reference electrode. When dry or wet air is admitted, the surface potential of zinc oxide becomes more positive compared with that in vacuo.

**X-ray Diffraction.**—From the precise measurements of the lattice constants, it is concluded that the lattice constants are independent of the conditions of preparation within an experimental error. The numerical values are in complete agreement with those reported by Bunn[7].

## Discussion

The green luminescence of zinc oxide is characteristic of phosphors fired under reducing conditions, and it has been reported[8] that a stoichiometric excess of zinc is detected by a chemical analysis from a sample prepared in this way. Although there would be many kinds of lattice defects in the green-emitting zinc oxide, interstitial zinc atoms and oxygen vacancies are considered to be the dominant defects. It is customarily said that the interstitial zinc atom is the luminescence center for the green luminescence. However, according to Mollwo[9], the green luminescence is quenched when the crystal is heated in zinc vapor below 1000°C and zinc atoms diffuse in it. On the contrary, Riehl and Ortman[10] have attributed the green luminescence center to the oxygen vacancy. The energies necessary for formation and migration of the oxygen vacancy would be greater than those of the interstitial zinc atom, since the binding between oxygen and zinc should be broken for the former processes. This consideration agrees with the various conditions for the preparation of the green-emitting phosphor. For example, the efficient phosphor should be fired at higher temperatures than those necessary for the introduction of interstitial zinc atoms.

The oxygen vacancy would be able to accomodate two electrons since it has two effective positive charges in the ionic model of zinc oxide. The same conclusion can be drawn from the covalent model. The first electron would be bound tightly in the vacancy but the second loosely. To be effective as the luminescence center, it would be necessary for the vacancy to have a specific charge. The quenching of green luminescence when the electric conductivity becomes great, for example, by the introduction of excess of zinc as cited above, might be explained by this model.

The ultraviolet emission, which is known to appear in zinc oxide fired under oxidizing conditions, is not observed for these samples. Although Kröger and Meyer[11] attributed this emission to exciton recombination, still more investigations are necessary to arrive at a definite conclusion.

The author has tried an analysis of the one-dimentional configurational coordinate curves[12] based on the experimental result that the peak position of the luminescence spectrum is independent of temperature. From this analysis one may expect an absorption band by the luminescence center in the long wavelength side of the absorption edge. Although an absorption in the expected wavelength region increases as a result of the firing under reducing conditions, one can not observe the excitation of luminescence by this absorption. In additon, the intensity of this absorption does not have any apparent connection with the luminescence efficiency of the phosphor. Therefore, it is considered that this absorption is probably caused by a change of the crystal lattice due to the presence of interstitial zinc atoms.

The decay of luminescence is exponential and the time constant is smaller by one order of magnitude than the reported value. It is considered[1] that the luminescence is emitted by the recombination of electrons at the luminescence center. If it is assumed that the density of the free electron is greater than that of the emptied luminescence center during excitation, the exponential decay and the dependence of time constant upon the sample can be understood.

It might be expected that the temperature dependence of luminescence intensity is different for the two sorts of excitation, i.e. 2537 and 3650 Å radiation, because the author found the structure in the excitation spectrum and the position of the absorption edge shifts toward longer wavelengths with increasing temperature at the

7) C. W. Bunn, *Proc. Phys. Soc.*, **47**, 835 (1935).
8) E. Mollwo and F. Stöckman, *Ann. Physik*, (6), **3**, 223 (1948).
9) E. Mollwo, *Z. Physik*, **138**, 478 (1954).
10) N. Riehl and H. Ortman, *Z. Elektrochem.*, **60**, 149 (1956).
11) F. A. Kröger and H. J. G. Meyer. *Physica*, **20**, 1149 (1954).
12) K. Maeda, *J. Phys. Soc. Japan*, **14**, 478 (1959).

rate of about $10^{-3}$ eV./deg[13]. However, the result is not in accord with the expectation. This suggests that the excitation spectrum changes its shape with temperature. From the temperature dependence shown in Fig. 2, one expects not a single but two kinds of activation energy for the nonradiative de-excitation. In the usual way, one obtains the activation energies of the order of 0.01 and 0.2 eV. by fitting the calculated curve with the observed. However, it is not clear to what process these activation energies correspond.

The slow phosphorescence decay indicates the existence of various metastable states. Considering the *n*-type conductivity of the phosphor, these states are probably deep hole traps.

The effect of atmosphere on the luminescence intensity has been reported only for a case of oxygen on cadmium sulfide[14]. In this case, the photoconductivity of cadmium sulfide is also reduced by the oxygen ambient. It is known that the photoconductivity of zinc oxide is decreased to a large extent by the adsorption of oxygen[16]. However, one found a quenching of luminescence intensity due to molecules having the hydroxyl group but not due to oxygen. Therefore, the above phenomenon seems to have a mechanism of quenching different from that found in cadmium sulfide. As stated in the preceding section, the surface potential of zinc oxide becomes positive when either dry or wet air is admitted relative to that in vacuo. Therefore, the change in the surface potential is not a cause of the luminescence quenching. The adsorbed molecule probably has an effect to accelerate nonradiative recombination of electrons and holes at the surface. Since the absorption constant in the fundamental absorption region is of the order of $10^5$ cm$^{-1}$ [16], electron-hole pairs are created by light absorption to a depth greater than that of a range influenced by surface conditions. Therefore, the amount of quenching is relatively small.

13) E. Mollwo, *Z. angew. Phys.*, **6**, 257 (1954).
14) S. H. Liebson and E. J. West, *J. Chem. Phys.*, **23**, 977 (1955); S. H. Liebson, ibid., **23**, 1732 (1955).
15) D. A. Melnick, *J. Chem. Phys.*, **26**, 1136 (1957).
16) E. Mollwo, *Ann. Physik*, (6) **3**, 230 (1948).

## Summary

Zinc oxide phosphors were prepared under various conditions. From measurements on the characteristics of the green luminescence of the phosphors fired in reducing atmosphere, the following features were observed. (1) In the excitation spectrum, there is a sharp peak at the position of the absorption edge and a gradual decrease toward shorter wavelengths with some structures. The observed maximum value of excitation efficiency is 0.31. (2) The luminescence intensity decreases with increasing temperature. The plot of intensity against temperature has an unusual shape in the neighborhood of 0°C. (3) The decay of luminescence is exponential and the time constant, 0.4 $\mu$ sec., is smaller than that previously reported by an order of magnitude. Long persistent phosphorescence is observed indicating the presence of deep hole traps. (4) The luminescence intensity decreases in a gaseous ambient of molecules having the hydroxyl group.

Standing on the present experimental results, discussions have been undertaken on the luminescence center as well as on the theoretical explanation of the observed characteristics.

The author wishes to express his sincere thanks to Dr. Y. Uehara for his suggestion of this problem, to Mr. Y. Kobuke for the preparation of the samples and to Mr. Y. Hukao for the use of his X-ray apparatus.

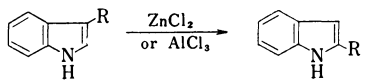
*Matsuda Research Laboratory*
*Tokyo Shibaura Electric Co.*
*Kawasaki*

# *Twofold Wagner-Meerwein Type Rearrangement of 2,3-Disubstituted Indoles*

By Masao NAKAZAKI

(Received August 31, 1959)

Among various interesting reactions of indoles, little attention has been paid to Fischer's rearrangement, which is as old as the discovery of indole itself. In 1888, Fischer and Schmidt[1] reported the conversion of 3-phenylindole (Ia) into 2-phenylindole (IIa) when heated with zinc chloride. Recently, Clemo and Seaton[2] demonstrated the same type of migration of substituents from 3-position to 2-position of indoles on 3-(2-pyridylmethyl) indole (Ib), 3-benzylindole (Ic) and skatole (Id), using aluminum chloride instead of zinc chloride.




Ia R=$C_6H_5$ IIa R=$C_6H_5$
b R=2-pyridylmethyl b R=2-pyridylmethyl
c R=$CH_2C_6H_5$ c R=$CH_2C_6H_5$
d R=$CH_3$ d R=$CH_3$

Fig. 1

These researchers, however, did not dare to inquire into the possible exchange reaction of substituents between 2- and 3-position of 2,3-disubstituted indoles. This paper is concerned with the demonstration of such possibility.

As a simple representative of 2,3-disubstituted indoles, the reaction of 2-methyl-3-phenylindole (III) with aluminum chloride was initially investigated.

2-Methyl-3-phenylindole (III) was prepared from phenylacetone phenylhydrazone by Fischer's method employing zinc chloride[3] or borontrifluoride[4] as catalyst, but the melting point (78~79°C) was inconsistent with the reported melting point (59~60°C) by Trenkler[3] or Ockenden and Schofield[4]. Because of such a great discrepancy of the melting points, an attempt was made to determine the structure of the indole (m. p. 78~79°C) by ozonolysis.

The melting point of *o*-acetoaminobenzophenone (IVa) obtained by ozonolysis of the indole (m. p. 78~79°C) was found 86~88°C in our hands, but Ockenden and Schofield[4] reported it as 71~73°C. There have been disputes about the melting point of IVa: von Auwers and Meyerburg[5] reported that their sample prepared by the acetylation of *o*-aminobenzophenone showed m. p. 72°C, but from the mother liquor there were obtained other crystals melting at 88.5~89°C, although the latter were the only crystals obtained in the repetitions of their experiment by themselves[6] and by others[7].

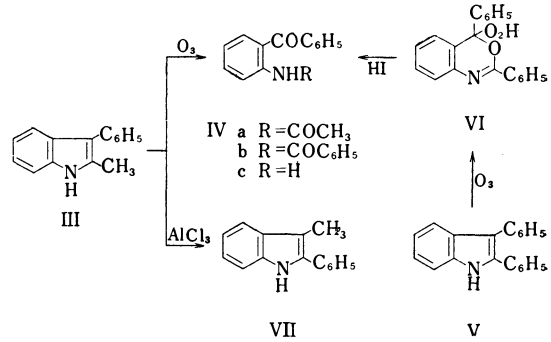



Fig. 2

To secure an authentic sample of *o*-acetoaminobenzophenone for comparison, IVa was synthesized by the process which involved the ozonolysis of 2,3-diphenylindole (V). Although Ockenden and Schofield[4] reported that 2,3-diphenylindole was converted into *o*-benzaminobenzophenone (IVb) (m. p. 85~86°C, 56% yield) when ozone was passed into a solution of V in ethyl acetate at 0°C, our result was found to be another contradiction with their finding.

In our hands, the ozonide VI[8] (m. p. 152

1) E. Fischer and T. Schmidt, *Ber.*, **21**, 1811 (1888).

2) G. R. Clemo and J. C. Seaton, *J. Chem. Soc.* **1954**, 2582. An excellent review about the rearrangement reactions of indoles and indolenines are to be found in P. L. Julian, E. W. Meyer and H. C. Pring, "The Chemistry of Indoles" in R. Elderfield. "Heterocyclic Compounds", Vol. 3, John Wiley & Sons, Inc., New York (1952), p. 1.

3) B. Trenkler, *Ann.*, **248**, 111 (1888).

4) D. W. Ockenden and K. Schofield, *J. Chem. Soc.*, **1953**, 612.

5) K. von Auwers and V. Meyerburg, *Ber.*, **24**, 2384 (1891).

6) K. von Auwers, ibid., **29**, 1263 (1896).

7) A. Bishler and D. Barad, ibid., **25**, 3081 (1892); R. Camps, *Arch. Pharm.*, **237**, 683 (1899).

8) The stable ozonides of indole derivatives were first observed by G. Mentzer, D. Molho and Y. Berguer, *Bull. soc. chim.*, 555 (1950). For details see the exhaustive studies by Witkop on the ozonide of phenylskatole. B. Witkop and J. B. Patrick, *J. Am. Chem. Soc.*, **74**, 3855 (1952); B. Witkop, J. B. Patrick and H. M. Kissman, *Chem. Ber.* **85**, 949 (1952). Remembering that 2-aryl indoles usually afford stable ozonides, it seems rather surprising that Ockenden and Schofield[4] obtained *o*-benzaminobenzophenone (IVb) directly from V. The stable ozonide from 2-(dibenzylmethyl)-3-benzylindole which does not possess the 2-aryl group was reported by M. Nakazaki and K. Tanno, *J. Chem. Soc. Japan, Pure Chem. Sec.* (*Nippon Kagaku Zasshi*), **77**, 952 (1956).

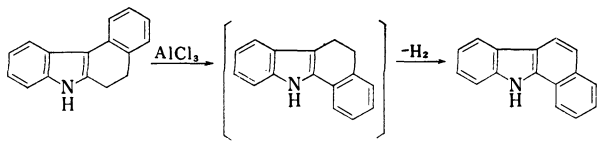



Fig. 3

~154°C, decomp.) of 2, 3-diphenylindole was the only compound isolated following their procedure (in ethyl acetate) or in the ozonolysis in acetic acid. The ozonide VI showed typical reactions of ozonide, and reductive hydrolysis[9] with hydroiodic acid in acetic acid converted it into benzoic acid and *o*-aminobenzophenone (IVc) which was acetylated with acetic anhydride to give *o*-acetoaminobenzophenone (m. p. 86~88°C) which was found identical with IV from 2-methyl-3-phenylindole by mixed melting point determination and comparison of their infrared absorption spectra. Thus being established the structure, 2-methyl-3-phenylindole(III) was subjected to rearrangement by heating with aluminum chloride at 220~240°C for 20 min. The product obtained was found to be identical with 2-phenyl-3-methylindole[10] (VII).

5, 6-Dihydro-7-benzo [*c*] carbazole[11] (VIII) was the next indole derivative tried to demonstrate the analogous rearrangement reaction.

The tetrahydrocarbazole derivative VIII, which was provided from the phenylhydrazone of β-tetralone was heated at 220~240°C for 20 min. with aluminum chloride to give rise to 11-benzo [*a*] carbazole(X), apparently resulted by the dehydrogenation of the intermediate 5, 6-dihydro-11-benzo [*a*] carbazole (IX) with aluminum chloride.

Mechanistically, these rearrangements[12] can be explained by twofold Wager-Meerwein type rearrangement initiated by the electrophilic attack by the Lewis acid (A in Fig. 4.) on the 3-position of indoles (Fig. 4), and the equilibria XI ⇄ XII ⇄ XIII ⇄ XIV are completly parallel to the one to be found in rearrangement of indolenines[13] and Plancher's rearrangement of indolenium compounds[14].

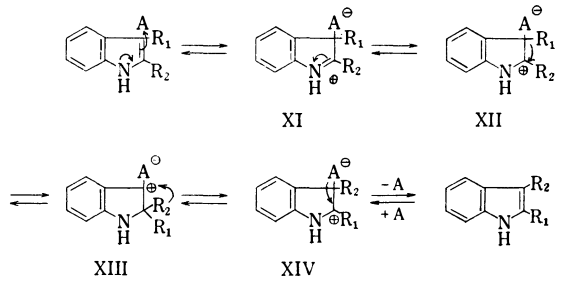



Fig. 4

The *Spiro* type intermediate XV, analogous to the one postulated by Woodward[14] in the dienone-phenol rearrangement, would be the intermediate in the case of 5, 6-dihydro-7-benzo [*c*] carbazole.

Inspection of the ultraviolet spectra (Figs. 6, 7 and 8) and π-electron density in the indole

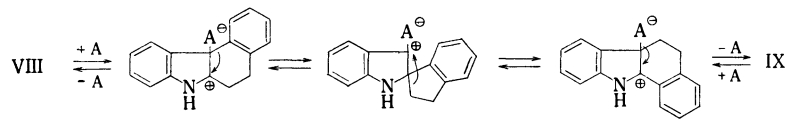



Fig. 5

9) The reductive hydrolysis of the stable ozonide with hydrobromic acid in acetic acid was carried out on the ozonide of 2-(dibenzylmethyl)-3-benzylindole. M. Nakazaki and K. Tanno, Ref. 8.

10) The structure of 2-phenyl-3-methylindole was established by ozonolysis. B. Witkop and J. B. Patrick, *J. Am. Chem. Soc.*, **74**, 3861 (1952); cf. B. Witkop, J. B. Patrick and H. M. Kissman, *Chem. Ber.*, **85**, 949 (1952).

11) Dehydrogenation by heating with 5% palladium-charcoal at 250~260°C converted VIII into the known 7-benzo[*c*] carbazole, m. p. 135~136°C.

12) In Bishler's indole synthesis applied on α-bromo-β-phenylpropiophenone, there was found the formation of two isomeric indoles, i. e. 2-phenyl-3-benzylindole and 2-benzyl-3-phenylindole. [P. L. Julian, E. W. Meyer, A. Magnani and W. Cole, *J. Am. Chem. Soc.*, 67, 1203 (1945); P. L. Julian and J. Pikl, ibid., **55**, 2105 (1953)]. But from a mechanistical standpoint which was worked out recently by Wygand and Richter[*Chem. Ber.*, **88**, 499 (1955)], it is highly improbable to assume the mutual interconversion of these two indoles under the reaction condition *after* they are formed.

13) See the author's papers on Plancher's rearrangement which follow.

14) R. B. Woodward and T. Singh, *J. Am. Chem. Soc.*, 72, 494 (1950). For the dienone-phenol rearrangements of the compounds possessing *spiro* structure, see R. T. Arnold, J. B. Buckley and R. M. Dodson, ibid., 72 3553 (1950); E. N. Marvell and A. O. Geiszler, ibid., **74**, 1259 (1952). Also it is noteworthy to compare the smooth conversion of VIII into X with the dienone-phenol rearrangement of 2-keto-4a-methyl-2, 4a, 5, 6-tetrahydrobenzo[*c*] phenathrene in which the transformation which requires a *spiro* intermediate is inhibited. C. Djerassi and T. T. Grossnickle, *J. Am. Chem., Soc.*, 76, 1741 (1954).

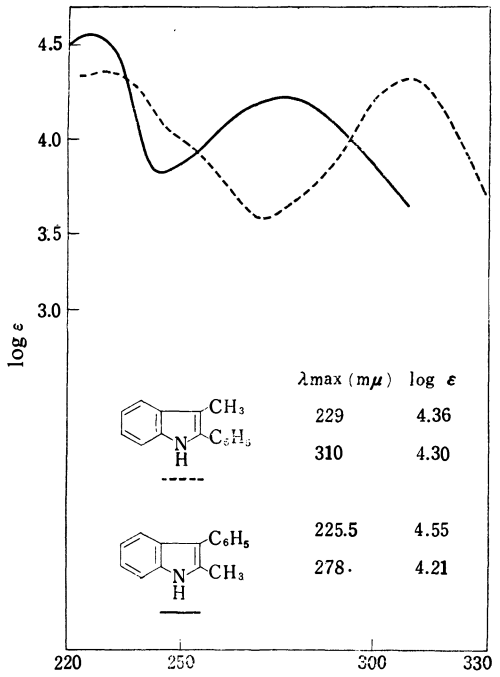



Fig. 6

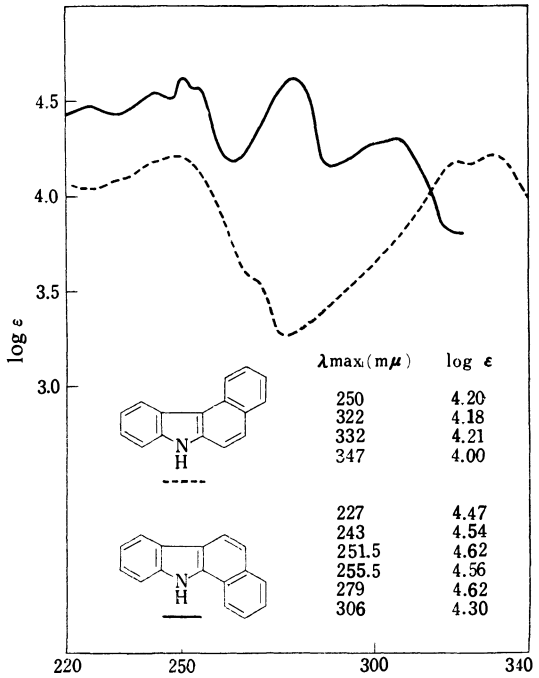



Fig. 8

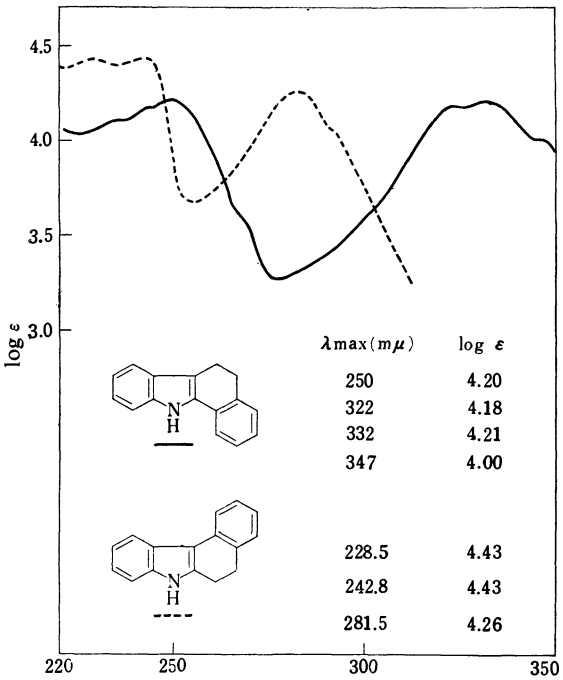



Fig. 7

nucleus[15] (1.059 at 2-position, 1.066 at 3-position) suggest that the driving force of these rearrangement reactions could be sought in the mesomeric stabilization of the products (VII, IX and X) by the phenyl group at 2-position rather than at 3-position.

The same reasoning could be applied to interprete Fischer's rearrangement[1] (migration of hydrogen anion), and the hyperconjugation effect[16] would be the stabilization factor in the case of the rearrangements of the indoles studied by Clemo and Seaton[2].

## Experimental[17]

**2-Methyl-3-phenylindole (III).**—*By borontrifluoride etherate method*[4].—To a solution of 7.0 g. of phenylacetone phenylhydrazone (m. p. 82~83°C) in 70 cc. of acetic acid, 5.1 g. borontrifluoride etherate was added, and the mixture was refluxed on an oil bath for 3 hr. The color of the solution changed from yellow to brown→green→brown. Water was added into the reaction mixture and was extracted with ether. The ethereal extract was washed with water and dried over anhydrous sodium sulfate. Removal of the solvent gave a viscous brown

15) K. Higasi and H. Baba, "Quantum Organic Chemistry (Ryoshi Yuki Kagaku)", Asakura Publishers, Tokyo (1956), p. 406.

16) The formation of *spiro*-(cyclopentane-1, 3'-*pseudo*-2'-methyl-indole) instead of 11-methyltetrahydrocarbazole nine from *spiro*-(cyclopentane-1, 2'-*pseudo*indoxyl) by the action of methyl/magnesium iodide could be interpreted on the same reason. B. Witkop and J. B. Patrick, *J. Am. Chem. Soc.* 75, 2572 (1953).

17) All melting points are not corrected. All ultraviolet spectra were measured by an EPS-2 Hitachi autorecording spectrophotometer and infrared spectra on a Perkin Elmer Model 12C. The analyses were performed in the Microanalytical Laboratory of the Institute of Polytechnics, Osaka City University.

liquid which was distilled in vacuo to afford a pale yellow liquid, b. p. 196~200°C/3 mmHg, 6.2 g. (57.5% yield). The distilate solidified gradually and was recrystallized from petroleum ether (b. p. 60°C) to give crystals, m. p. 78~79°C (literature[3,4]: 59~60°C).

Found: C, 86.77; H, 6.54. Calcd. for $C_{15}H_{13}N$: C, 86.99; H, 6.32%.

U.V. spectrum[18]: $\lambda_{max}$ m$\mu$ (log $\varepsilon$), 225.5 (4.55), 278 (4.21). $\lambda_{min}$ 245.5 m$\mu$ (log 3.82) in methanol (Fig. 6). I.R. spectrum: 2.95 $\mu$.

The picrate was recrystallized from ethanol to give brown needles, m. p. 139~140°C (literature[3,4]: 141~142°C).

Found: C, 57.42; H, 3.84; N, 12.25. Calcd. for $C_{21}H_{16}O_7N_4$: C, 57.80; H, 3.70; N, 12.84%.

*By zinc chloride method.*—Following Trenkler's procedure[3], III was obtained in a yield of 34.6%, m. p. 78~79°C.

**Ozonolysis of 2-Methyl-3-phenylindole (III)**[4]. —To a mixture of 0.7 g. of 2-methyl-3-phenylindole and 35 cc. of acetic acid, a stream of ozone (approximately 5%) was passed for 45 min. at room temperature, during which time the color of the solution was observed to change from yellow to red and then pale yellow again. After water was added, the solution was extracted with ether thrice and the combined ethereal extract was washed with water followed by 5% sodium carbonate solution and saturated sodium chloride solution. Removal of the solvent yielded a viscous residue which could be brought to crystallization by trituration. The crystals were collected and recrystallized from petroleum ether to give crystals melting at 70~72°C (0.291 g.). The melting point was raised to 86~88°C by further recrystallization from water-ethanol.

Found: C, 75.20; H, 5.78. Calcd. for $C_{15}H_{13}O_2N$: C, 75.30; H, 5.48%.

**Stable Ozonide of 2, 3-Diphenylindole VI.** — *In acetic acid solution.*—A stream of ozone (approximately 5%) was passed into a mixture of 1.4 g. of 2,3-diphenylindole (V) and 40 cc. of acetic acid for 1 hr. at room temperature. Completion of the reaction was estimated by the usual color change of the reaction mixture: yellow→red→yellow. Water was added to the reaction mixture to precipitate crystals which were collected and washed with water.

Recrystallization from water-ethanol and ethanol gave colorless crystals (0.47 g.) which darkened in color at 140°C and decomposed at 152~153°C. On the addition of solid potassium iodide to a solution of VI in acetic acid, the formation of iodine was observed.

*In ethyl acetate solution*[4]. — Into a mixture of 2.7 g. of 2,3-diphenylindole and 75 cc. of ethyl acetate, a stream of ozone (approximately 5%) was passed for 1.5 hr. at 0°C. The color of the solution changed from yellow to brown and then to yellow again. After the excess of ozone was blown out by a stream of nitrogen, the solvent was removed in vacuo to give a viscous residue which crystallized by trituration with ethanol.

The crude ozonide (decomp. 148°C) weighed 1.5 g., and was recrystallized from ethanol to afford crystals which decomposed at 152°C.

Found: C, 75.37; H, 5.12; N, 4.54. Calcd. for $C_{20}H_{15}O_3N$: C, 75.69; H, 4.72; N, 4.41%.

**Reductive Hydrolysis of the Ozonide VI.** — A mixture of 1.50 g. of the ozonide VI, 30 cc. of acetic acid and 10 cc. of constant boiling hydroiodic acid solution was refluxed for 5 hr. After water was added, the reaction mixture was extracted with ether, to separate basic and acidic fractions.

*Acidic fraction.*—The ether layer was washed with sodium thiosulfate solution to discharge the color of iodine, and was extracted with 2 N sodium hydroxide solution. The alkaline solution was acidified with 2 N hydrochloric acid solution to precipitate benzoic acid, 0.381 g. Recrystallization from water gave crystals which melted at 120~121°C, alone and admixed with an authentic specimen of benzoic acid.

*Basic fraction.*—The aqueous layer was washed with ether, and was made basic with 2 N sodium hydroxide solution to precipitate *o*-aminobenzophenone (IVc). Extraction with ether afforded 0.81 g. of golden yellow crystals, m. p. 101~104.5°C, which was recrystallized from ethanol-water to give yellow prisms, m. p. 103~105°C (literature[5-7]: 105~106°C).

Found: C, 78.88; H, 5.68. Calcd. for $C_{13}H_{11}ON$: C, 79.16; H, 5.62%.

***o*-Acetoaminobenzophenone (IVa)**.—After a mixture of 0.287 g. of *o*-aminobenzophenone (IVc) and 3 cc. of acetic anhydride was heated on a water bath for 2 hr., water was added to the reaction mixture and was allowed to stand overnight. The precipitate was collected (0.270 g., m. p. 70~75°C) and was recrystallized from ethanol-water to give crystals melting at 86~88°C, alone and admixed with *o*-acetoaminobenzophenone (m. p. 86~88°C) obtained by the ozonolysis of 2-methyl-3-phenylindole (III) mentioned above. The identity was further comfirmed by the comparison of their infrared spectra.

**Rearrangement of 2-Methyl-3-phenylindole (III)**. —A mixture of 0.8 g. of 2-methyl-3-phenylindole, 0.8 g. of aluminum chloride and 0.1 g. of sodium chloride was heated at 220°C for 15 min. and at 220~240°C for 5 min. After water was added to the resulted brown solid mass, the mixture was extracted with ether and the ether extract was washed with water and dried over anhydrous potassium carbonate. After the removal of the solvent, the residue was distilled in vacuo to afford 0.482 g. of a viscous oil, b. p. 194~195°C/2 mmHg., which crystallized on standing. Recrystallization from ethanol-water gave crystals, m. p. 89~90°C, which were found identical with 2-phenyl-3-methylindole[19] by mixed melting point determination and the comparison of infrared

18) Ultraviolet spectrum of phenylskatole: $\lambda_{max}$(log$\varepsilon$), 229 m$\mu$ (4.36), 310 m$\mu$ (4.30), $\lambda_{min}$271.5 m$\mu$ (3.58) in ethanol (Fig. 6). Cf. R. Huisgen and I. Ugi, *Ann.*, **610**, 57 (1957); B. Witkop and J. B. Patrick, *J. Am. Chem. Soc.*, **74**, 3855 (1952).

19) Prepared from propiophenonephenylhydrazone. Fischer's method employing zinc chloride was found to give better yield than the polyphosphoric acid method and borontrifluoride method. [H. M. Kissman, D. W. Farnsworth and B. Witkop, *J. Am. Chem. Soc.*, **74**, 3948 (1952); B. Witkop and J. B. Patrick, ibid, **74**. 3858 (1952)].

spectrum with an authentic specimen. Also, the picrate, m. p. 144~145°C (from ethanol) was prepared to confirm their identity.

**5, 6-Dihydro-11-benzo[*a*]carbazole (IX)**[20]. — 5, 6-Dihydro-11-benzo[*a*]-carbazole was synthesized following the procedure of Organic Syntheses, **30**, 90 (1950), m. p. 163~164°C (from methanol).

U. V. specrum. $\lambda_{max}$ (log $\varepsilon$), 250 m$\mu$ (4.20), 332 m$\mu$ (4.21); $\lambda_{min}$ (log $\varepsilon$), 227 m$\mu$ (4.04), 276 m$\mu$ (3.26) in ethanol (Fig. 7).

The picrate was recrystallized from ethanol to give black needles, m. p. 153~154°C.

Found: N, 12.79. Calcd. for $C_{22}H_{16}O_7N_4$: N, 12.50%.

**11-Benzo[*a*]carbazole (X)**[20].—A mixture of 0.5 g. of 5, 6-dihydro-11-benzo[*a*]carbazole and 0.1 g. of 5% palladium-charcoal was heated at 250~260°C for 20 min. 11-Benzo[*a*]carbazole which resulted was recrystallized from benzene to yield crystals melting at 227~229°C. (literature[21]: 225°C).

U.V. spectrum[21]: $\lambda_{max}$ m$\mu$ (log $\varepsilon$), 227 (4.47), 243 (4.54), 251 (4.62), 279 (4.62), 306 (4.30). $\lambda_{min}$ m$\mu$ (log $\varepsilon$), 234 (4.42), 248.5 (4.51), 263 (4.18), 289 (4.17) in ethanol (Fig. 8).

**5,6-Dihydro-7-benzo[*c*]carbazole (VIII)**[20].—Considerable generation of heat was observed when 15 cc. of acetic acid was added to a mixture of 2.9 g. of $\beta$-tetralone[22] and 2.2 g. of phenylhydrazine, and the reaction mixture was refluxed for 1 hr. After being kept at room temperature overnight, the crystals precipitated were filtered and washed with methanol. Recrystallization from methanol gave 2.4 g. of crystals, m. p. 102~103°C.

Found: C, 87.91; H, 6.15; N, 6.31. Calcd. for $C_{16}H_{13}N$: C, 87.64; H, 5.98; N, 6.39%.

U.V. spectrum: $\lambda_{max}$ m$\mu$ (log $\varepsilon$), 228.5 (4.43), 281.5 (4.26); $\lambda_{min}$ 253.5 m$\mu$ (log $\varepsilon$ 3.68) in ethanol (Fig. 7).

The picrate was recrystallized from ethanol to give black needles, m. p. 129~132°C.

Found: C, 59.11; H, 3.76; N, 12.82. Calcd. for $C_{22}H_{16}O_7N_4$: C, 58.93; H, 3.60; N, 12.50%.

**7-Benzo[*c*]carbazole**[20].—A mixture of 0.5 g. of 5, 6-dihydro-7-benzo[*c*]carbazole and 0.1 g. of 5% palladium-charcoal was heated at 250~260°C for 30 min. The reaction mixture was extracted with boiling benzene. After the solvent was removed, the residue was recrystallized from benzene-ligroin to give 0.27 g. of crystals, m. p. 135~136°C (literature[23]: 135°C). U.V. spectrum: $\lambda_{max}$ m$\mu$ (log $\varepsilon$), 265 (4.69), 285.5 (4.02), 326 (4.09), $\lambda_{min}$ m$\mu$ (log $\varepsilon$), 237 (4.21), 282 (3.86), 295 (3.45) in ethanol (Fig. 8).

**Rearrangement of 5, 6-dihydro-7-benzo[c]carbazole (VIII)**.—A mixture of 1.0 g. of VIII, 1 g. of aluminum chloride and 0.1 g. of sodium chloride was heated at 220°C for 10 min. and at 220~240°C for 5 min. Water was added to the reaction mixture and extracted with ether. The yellow ethereal solution, which exhibited green fluorescence, was washed with water followed with sodium bicarbonate solution and was dried over anhydrous magnesium sulfate. Distillation of the solvent gave a residue which was recrystallized from carbon tetrachloride to give 0.206 g. of crystals, m. p. 210°C. Recrystallization from benzene improved the melting point to 227~228°C which was undepressed when admixed with an authentic specimen of 11-benzo[*c*]carbazole. The identity was further confirmed by the comparison of their infrared spectra which could be overlapped in every detail.

The author is very grateful to Dr. Itaru Mita for his generous supply of phenylacetone. He also feels indebted to Mr. Satosi Kamei for his technical assistance; to Mr. Sachihiko Isoe who kindly measured the ultraviolet absorption spectra.

*Institute of Polytechnics*
*Osaka City University*
*Kita-ku, Osaka*

20) Nomenclature followed A. M. Patterson and L. T. Capell, "The Ring Index", Reinhold Publishing Corp., New York (1940), p. 331.
21) R. Huisgen and I. Ugi, *Ann.*, **616**, 63 (1957).
22) M. D. Soffer et. al., "Organic Syntheses", Vol. 32, John Wiley & Sons, Inc., New York (1952), p. 97.
23) F. R. Japp and W. M. Maitland, *J. Chem. Soc.*, **83**, 270 (1903); H. T. Bucherer and F. Seyde, *J. Prakt. Chem.*, (2) 77. 406 (1908); S. G. P. Plant and S. H. Oakeshott, *J. Chem. Soc.*, **1928**, 1843.

# *Mechanism of Plancher's Rearrangement. I. Twofold Wagner-Meerwein Type Rearrangement of Indolenines*

By Masao NAKAZAKI, Koji YAMAMOTO and Kikuo YAMAGAMI

(Received August 31, 1959)

Although, Plancher's rearrangement, which was described as early as 1898, has been much discussed[1], it is unfortunate that there are found many misunderstandings about the scope of this rearrangement, because of lack of definitive studies. In 1898, Plancher[2] obtained a indolenium iodide, m. p. 237°C, from 2-ethyl-3-methylindole (I) and 2-methyl-3-ethylindole (II) by heating with methyliodide at 120°C.

He assigned the structure of 1, 2, 3-trimethyl-3-ethylindolenium iodide (III) to the indolenium iodide, on a non-confirmative chemical base, but whatever structure it has, migration of the subsituents has to be assumed, in order to explain the formation of the same indolenium iodide, m. p. 237°C, from both I and II.

Another type of rearrangement was established when Plancher[3] obtained two indolenium iodides, m. p. 186° and 232°C, from 2-isopropyl-3-methylindole (IV) by heating with methyliodide at 85~90°C for 2 days.

He posturated the formation of the two intermediate indolenines VII and VIII which would give corresponding indolenium iodides V and VI with methyliodide. Although the structure of the indolenium iodides (V or VI) remained unestablished, the conversion of the indolenium iodide, m. p. 186°C, into the isomeric indolenium iodide, m. p. 232°C, was achieved by heating at 180~190°C for 10 min. From these and other experiments, Plancher could draw the following conclusion[4]: 1) The indolenium iodide with the lower melting point can be converted into the isomeric indolenium iodide with the higher melting point. 2) The heavier substituent migrates to the $\beta$-position. However, his conclusion 2) can be hardly justified without further strenuous studies, since the structures of these indolenium iodides were only presumed on nothing but some analogies, except on one occasion; i.e. 1,2,3-trimethyl-3-phenylindolenium iodide (X). By heating 2-phenylindole (IX) with methyliodide at 120°C, Plancher[5] obtained an indolenium iodide, m. p. 226~227°C, which

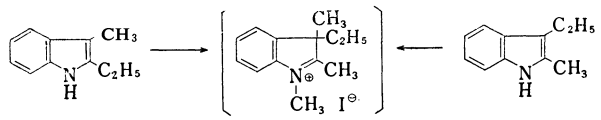



Fig. 1.

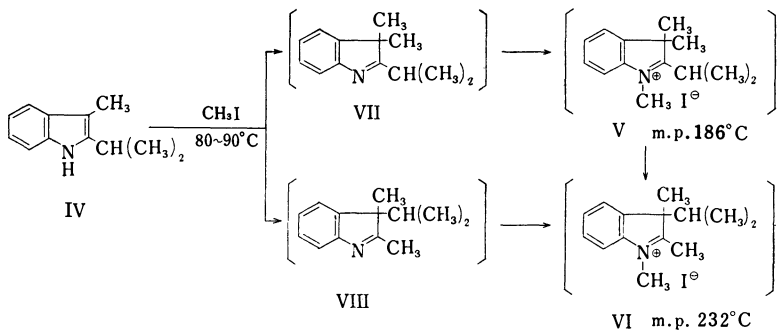



Fig. 2.

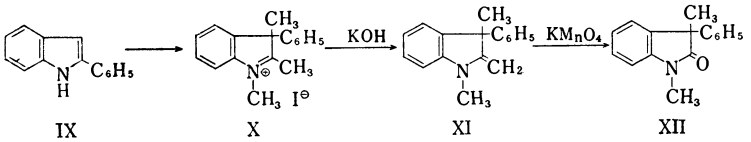
1) For general discussion of Plancher's rearrangement and other related rearrangement reactions, see P. L. Julian, E. W. Meyer and H. C. Pring, "The Chemistry of Indoles" in R. Elderfield, "Heterocyclic Compounds", Vol. 3, John Wiley & Sons., Inc., New York (1952), p. 1.

2) G. Plancher, *Gazz. chim. ital.*, **28**, II, 374 (1898); *Chem.-Zentr.*, **1899**, I, 282.

3) G. Plancher, *Atti. accad. Lincei*, (5), **11**, II, 182 (1902); *Chem.-Zentr.*, **1902**, I, 1322.

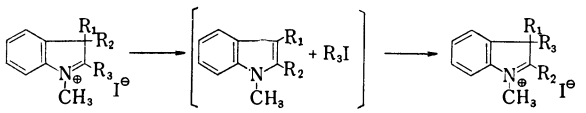
4) G. Plancher, *Atti. acced. Lincei*, (5), **9**, 115 (1900), *Chem.-Zentr.*, **1900**, I, 867. See also a brief discussion of Julian, Ref. 1.

5) G. Plancher, *Gazz. chim. ital.*, **28**, II, 391 (1898); *Chem.-Zentr.*, **1899**, I, 283.



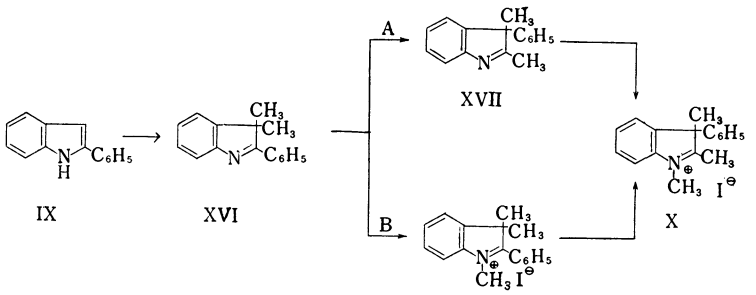
IX X XI XII

Fig. 3.



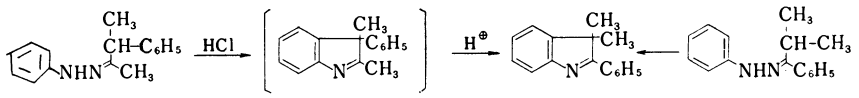
XIII XIV XV

Fig. 4.



IX XVI XVII XVIII X

Fig. 5.



XIX XVII XVI XX

Fig. 6.

he thought to be 1, 2, 3-trimethyl-3-phenylindolenium iodide (X) as the result of rearrangement involving an exchange of methyl with phenyl group. But the structure of this indolenium iodide was left to be determined by chemical means until Boyd-Barrett[6] (1932) repeated Plancher's experiment and oxidized the product with alkaline potassium permanganate (via the intermediate XI) to form 1, 3-dimethyl-3-phenyloxyindole (XII), the nitro derivative of which was found to be identical with the one obtained by the umambiguous synthetic route.

The mechanism of the rearrangement of indolenium compounds proposed by Plancher[7] is illustrated in Fig. 4. According to this mechanism, the formation of iodobenzene and its subsequent reaction with 1,2,3-trimethylindole to secure 1, 2, 3-trimethyl-3-phenylindolenium iodide (X), though it is highly improbable, is an inevitable consequence to explain the formation of X from 2-phenylindole. Julian[8] pointed out another conceivable route from IX to X, assuming that 3, 3-dimethyl-2-phenylindolenine (XVI) is the intermediate and that rearrangement involving an exchange of methyl with the phenyl group takes place at this point (Fig. 5, route A).

This Julian's alternative postulated the migration of the substituents of indolenine which has not been demonstrated in any indolenine with umambiguous constitution[9], and it is unfortunate

6) H. S. Boyd-Barrett, *J. Chem. Soc.*, **1932**, 321.

7) G. Plancher, *Atti, accad. Lincei*, (5), **11**, 183 (1902); *Chem.-Zentr.*, **1902**, I, 1322.

8) See Ref. 1, p. 106.

9) M. Garry, *Ann. chim.*, **17**, 5 (1942); *Chem. Abstr.*, **36**, 6875 (1942), obtained two indolenines; 3,3-diphenyl-2-methylindolenine, m. p. 145°C, picrate, m. p. 210°C, and isomeric indolenine presumingly 2, 3-diphenyl-3-methylindolenine, m. p. 108°C, picrate, m. p. 155°C, from 1-anilino-1-phenylethylketone by heating with aniline and aniline hydrochloride at 160~165°C, but unfortunately she did not mention their possible interconversion. According to Julian's description, "she apparently assumed, and let it to the reader to assume, that the shifts involved in her synthesis took place *before* cyclization to the indolenines". But the recent study of the mechanism of Bishler's indole synthesis seems to suggest that the skeleton change of the anilinoketone would not occur *during* or *before* the cyclization. [F. Weygand and E. Richter, *Chem. Ber.*, **88**, 499 (1955).]. From the present achievement, it is safely assumed that the first formed 3, 3-diphenyl-2-methylindolenine rearranges to give 2, 3-diphenyl-3-methylindolenine under the reaction condition.

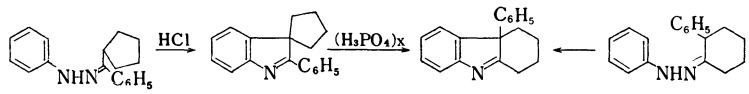



Fig. 7.

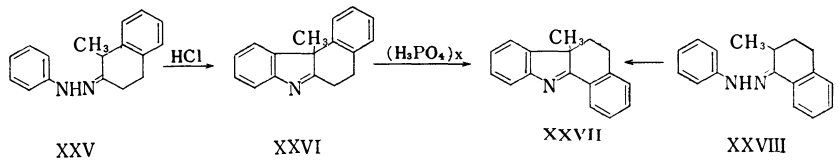



Fig. 8.

that sometimes Plancher's rearrangement was understood as this sort of rearrangement of indolenines only to cause many confusions[10].

This paper is concerned with demonstration of this migration of substituents of indolenines to elucidate the mechanism of Plancher's rearrangement. In order to obtain 2, 3-dimethyl-3-phenylindolenine (XVII), Fisher-Brunner's method was applied on 3-phenylbutane-2-one (XIX) under various conditions using zinc chloride, alcoholic hydrogen chloride and boron-trifluoride etherate as catalyst.

Even under very mild condition (with alcoholic hydrogen chloride at 0°C), all attempts failed only to afford 3, 3-dimethyl-2-phenylindolenine (XVI)[11], apparently resulting from the intermediate indolenine XVII by rearrangement reaction involving an exchange of the phenyl with the methyl group.

The view that 3-phenylbutane-2-one would rearrange to isobutyrophenone and then its phenylhydrazone (XX) would cyclize to XVI seems untenable, since the fact that the entirely reversed process is predominant in acidic condition was firmly established recently[12].

Also it is hard to find any reasonable sequence which would explain a possible migration of substituents in the cyclization steps of Fischer-Brunner's synthesis, which has a common feature with Fischer's indole synthesis extensively studied by Carlin et al.[13] At any rate, route A (Fig. 5) which assumes hypothetical rearrangement XVI → XVII has to be abandoned[14].

Although this is the first case, in which a rearranged indolenine is obtained in Fischer-Brunner's indolenine synthesis, the first example of the rearrangement of an indolenine to the other indolenine, both with established structures, was encountered in the isomerization of XXII to XXIII.

*Spiro*-(cyclopentane-1, 3'-*pseudo*-2'-phenylindole)[15] (XXII) ($\lambda_{max}$ 310 m$\mu$)[16] which was synthesized from cyclopentylphenylketone phenylhydrazone (XXI) by Fischer-Brunner's synthesis by saturating its alcoholic solution with dry hydrogen chloride, was found to convert, when heated with polyphosphoric acid[17], into 11-phenylcarbazolenine (XXIII) which in turn was prepared from 2-phenylcyclohexanone phenylhydrazone (XXIV).

Another interesting rearrangement was demonstrated when 11b-methyl-5, 6-dihydro-11b-benzo-[*c*]carbazole[18] (XXVI) which could be prepared from $\alpha$-methyl-$\beta$-tetralone phenylhydrazone (XXV), was heated with polyphosphoric acid

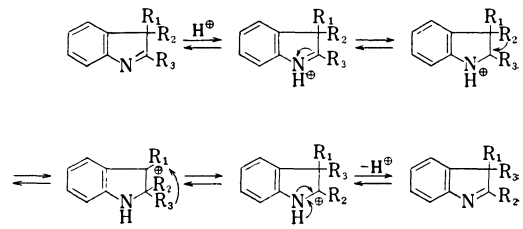



Fig. 9.

10) For example, B. Witkop and J. B. Patrick, *J. Am. Chem. Soc.*, **73**, 1358 (1951), discussed the rearrangement of indolenine as Plancher's rearrangement.

11) An attempt was made to prepare 2, 3-dimethyl-3-phenylindolenine (XVII) by alkylation of 2-methyl-3-phenylindole with sodium amide and methyliodide in liquid ammonia only to afford 1, 2-dimethyl-3-phenylindole. Also another attempt to obtain the indolenine XVII by Grignard synthesis from 2-methyl-3-phenylindole was found fruitless.

12) S. Barton and C. R. Portor, *J. Chem. Soc.*, **1956**, 2483.

13) R. B. Carlin, W. D. Henley and D. P. Carlson, *J. Am. Chem. Soc.*, **79**, 5712, (1957); and also his preceeding papers on the same subject.

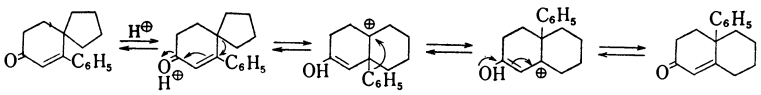
14) The fact that the rearrangement actually takes place by route B (Fig. 5) was established by our experiment which follows. To avoid unnecessary confusion, the term of "Plancher's rearrangement" should be used to indicate solely the *rearrangement of indolenium compounds* such as illustrated XVIII→X (Fig. 5).

15) For the nomenclature of *spiro* compounds, see *Chem. Abstr.*, **39**, 5885, 5888 (1945).

16) U. V. spectrum of 3, 3-dimethyl-2-phenylindolenine: $\lambda_{max}$ 306 m$\mu$ (log $\varepsilon$ 4.177). B. Witkop, J. B. Patrick and H. M. Kissman, *Chem. Ber.*, **85**, 953 (1952).

17) When indolenine synthesis using polyphosphoric acid was applied on cyclopentylphenylketone-phenylhydrazone, 11-phenyltetrahydrocarbazolenine was formed directly.

18) According to the nomenclature of A. M. Patterson and L. T. Capell, "The Ring Index", Reinhold Publishing Corp., New York (1940), p. 331.



XXIX XXX

Fig. 10.

at 180°C for 5 min. The rearranged indolenine was found to be identical with 6a-methyl-5, 6-dihydro-6a-benzo[*a*]carbazole[18] (XXVII) provided from β-methyl-α-tetralone phenylhydrazone (XXVIII) by usual method.

The mechanism of the migration of the substituents of indolenines can be readily explained by twofold Wagner-Meerwein type rearrangement initiated by the attack of a proton on the nitrogen atom of the indolenine nucleus as formulated in Fig. 9[19-21].

Since undoubtedly all steps are in equilibrium, the thermodynamical stability of the products would be the predominant factor to determine the direction of the migration, and it would be safely assumed that mesomeric stabilization of the phenyl group is responsible in the case of XVII → XVI and XXVI → XXVII. The seemingly contradictory attitude of XXII toward acid can be reasoned when the inspection of its Stuart's model reveals that a considerable steric repulsion is observed between the phenyl group and the hydrogens of 3, 4-position of cyclopentyl group of XXII, i. e. this is the case where steric effects suppress mesomeric stabilization of the phenyl group[22].

Harmonious with this result is the smooth transformation[23] of 6-phenyl-*spiro*(4, 5)decen-6-one-8 (XXIX) to 10-phenyl-2-keto-$\Delta^{1,9}$-octahydronaphthalene (XXX) by heating with polyphosphoric acid.

## Experimental[24]

**3-Phenylbutane-2-one.**—A mixture of 16.3 g. of methyliodide and 30 cc. of absolute ether was added dropwise to a mixture of 6.4 g. of magnesium and 30 cc. of absolute ether at room temperature. To the chilled Grignard solution, a mixture of 24.5 g. of α-methyl benzylcyanide[25] and 30 cc. of ether was added, and the reaction mixture was kept at room temperature for 4 hr. The Grignard complex was destroyed by the addition of diluted sulfuric acid and extracted with ether. The ethereal extract was washed with 5% sodium carbonate solution and water and dried over anhydrous sodium sulfate. Removal of the solvent afforded an oil which was distilled in vacuo to give 21.2 g. of 3-phenylbutane-2-one, b. p. 107~115°C/20 mmHg[26].

**3, 3-Dimethyl-2-phenylindolenine (XVI) from 3-Phenylbutane-2-one Phenylhydrazone.**—*By zinc chloride method*[27].—A mixture of 11.8 g. of 3-phenylbutane-2-one and 8.6 g. of phenylhydrazine was heated on a water bath for 40 min. The mixture became turbid and the separation of water drops was observed. Then the mixture was extracted with ether and dried over anhydrous sodium sulfate. After the solvent was evaporated completely, the residue was dissolved in 160 cc. of absolute ethanol and 80 g. of zinc chloride was added. The mixture was refluxed for 20 hr. and the alcohol was removed. The residue was made basic by the addition of concentrated ammonia solution to precipitate basic material. This was extracted with ether, and the ether extract was washed with water and dried over anhydrous potassium carbonate. Removal of the solvent afforded a residue which was distilled in vacuo to give 2.3 g. of a pale yellow liquid, b. p. 110~139°C/2 mmHg.

Found: C, 86.05; H, 7.27; N, 6.77. Calcd. for $C_{16}H_{15}N$: C, 86.84; H, 6.83; N, 6.33%.

The picrate was recrystallized to yield crystals, m. p. 170~172°C, which was found identical with the picrate of 3, 3-dimethyl-2-phenylindolenine, m. p. 167~168°C, prepared from an authentic 3, 3-dimethyl-2-phenylindolenine[28] (XVI), by mixed melting point determination.

19) An intermediate possessing *spiro* structure is to be assumed in the case of XXVI→XXVII, and it seems noteworthy to compare with the dienone-phenol rearrangement of 2-keto-4a-methyl-2, 4a, 5, 6-tetrahydrobenzo[*c*]phenathrene in which the transformation which requires a *spiro* intermediate is inhibited. C. Djerassi and T. T. Grossnickel, *J. Am. Chem. Soc.*, 76, 1741 (1954). See also Ref. 14 in the preceeding paper on the rearrangement of 2, 3-disubstituted indoles.

20) A novel cleavage reaction of benzyl and *t*-butyl group is recently reported when $R_1$ (Fig. 9) is benzyl and *tirt*-butyl, and the same sort of cleavage reaction was demonstrated on 11-benzyltetrahydrocarbazolenine and 11-*tirt*-butyltetrahydrocarbazolenine. M. Nakazaki, S. Isoe and K. Tanno, *J. Chem. Soc. Japan, Pure Chem. Sec.* (*Nippon Kagaku Zasshi*), 76, 1262 (1955).

21) The mechanism of Brunner-Robinson-Suginome's rearrangement (conversion of 3, 3-dimethylindolenine into 2, 3-dimethylindole) is the special case where $R_3$ is a hydrogen atom. K. Brunner, *Monatsh.*, 17, 255 (1896); R. Robinson and H. Suginome, *J. Chem. Soc.*, 1932, 298.

22) B. Witkop and J. B. Patrick, *J. Am. Chem. Soc.*, 73, 1558 (1951), tried the rearrangement of 11-methyltetrahydorocarbazolenine in a hope to get *spiro*-(cyclopentane-1′, 3-*pseudo*-2′-methylindole) but in vain. This can be attributed to the stability of 11-methyltetrahydrocarbazolenine in respect of the steric effect as well as the small migration aptitude of the methyl group.

23) M. Nakazaki and S. Isoe, unpublished experiment.

24) All the melting points are uncorrected values. All ultraviolet spectra were measured with an EPS-2 Hitachi selfrecording spectrophotometer and infrared spectra on a Perkin Elmer Model 12C. The analyses were performed in the Microanalytical Laboratory of the Institute of Polytechnics, Osaka City University.

25) B. p. 106~112°C/11 mmHg or 71~79°C/2 mmHg. Prepared following the procedure of H. M. Crawford, *J. Am. Chem. Soc.*, 56, 140 (1934).

26) W. D. Kumler, L. A. Strait and E. L. Alpen, *J. Am. Chem. Soc.*, 72, 1463 (1950).

27) Following Leuch's procedure to synthesize 3, 3-dimethyl-2-phenylindolenine from isobutyrophenone phenylhydrazone. H. Leuchs, A. Heller and A. Hoffman, *Ber.*, 62, 877, (1929).

28) B. p. 178~182°C/9 mmHg. Picrate, m. p. 167~168°C. Prepared by polyphosphoric acid method. H. M. Kissman, D. W. Farnsworth and B. Witkop, *J. Am. Chem. Soc.*, 74, 3948 (1952).

*By borontrifluoride etherate method*[29].—To a mixture of 2.7 g. of 3-phenylbutane-2-one phenylhydrazone[30] and 30 cc. of acetic acid, 2.1 g. of borontrifluoride etherate was added and refluxed for 3 hr. After the solvent was removed in vacuo, the residue was dissolved in ether and basic material was extracted with 2 N hydrochloric acid solution. To the cooled acidic solution, 2 N sodium hydroxide solution was added to liberate the basic substance, and extracted with ether. After the ethereal solution was washed with water and dried over anhydrous potassium carbonate, the solvent was removed. The residue was distilled in vacuo to give a pale yellow oil, 1.2 g., b. p. 145~155°C/2 mmHg. The picrate, m. p. 168~169°C was prepared to be found identical with the picrate of 3,3-dimethyl-2-phenylindolenine (XVI) by mixed melting point determination.

*Synthesis with hydrochloric acid in ethanol.*—A solution of 2 g. of 3-phenylbutane-2-one phenylhydrazone[30] in 40 cc. of absolute ethanol was chilled in an ice bath and was saturated with dried hydrogen chloride. After being allowed to stand at room temperature for 2 days (15°C), the solvent was removed in vacuo (below 40°C). Water was added to the residue and extracted with ether. The aqueous layer was made basic by the addition of 2 N sodium hydroxide solution and extracted with ether. The ethereal extract was washed with water and dried over anhydrous potassium carbonate. After removal of the solvent, the residue was distilled to afford a liquid, b. p. 135~145°C/1.5 mmHg, infrared spectrum of which could overlap in every detail on that of 3,3-dimethyl-2-phenylindolenine. The identity was further confirmed by the mixed melting point determination of their picrates.

**1,2-Dimethyl-3-phenylindole.**—To a suspension of sodium amide prepared from 200 cc. of liquid ammonia and 0.78 g. of sodium, 5 g. of 2-methyl-3-phenylindole[31] was added with 10 cc. of ether. After a mixture of 3.4 g. of methyliodide and 10 cc. of ether was added dropwise in a period of 20 min., the reaction mixture was allowed to stand at room temperature overnight to evaporate the liquid ammonia. After 200 cc. of water was added, the mixture was extracted with ether. The ethereal extract was washed with 2 N hydrochloric acid to remove basic material (very small amount, discarded). After this has been washed with 5% sodium carbonate solution and water, the ether extract was dried over anhydrous sodium sulfate. Removal of the solvent gave crystals (4 g.), which were recrystallized from ethanol. m. p. 111~112.5°C.

Found: C, 87.38; H, 7.03; N, 6.33. Calcd. for $C_{16}H_{15}N$: C, 86.84; H, 6.38; N, 6.33%.

The picrate was recrystallized from ethanol to give brown black needles, m. p. 199~201°C.

Found: N, 12.40. Calcd. for $C_{22}H_{18}O_7N_4$: N, 12.44%.

***Spiro*-(cyclopentane-1,3'-*pseudo*-2'-phenylindole) (XXII).**—A mixture of 5 g. of cyclopentylphenylketone[32] and 3.4 g. of phenylhydrazine was heated on a water bath for 1 hr. and the water generated was removed by azeotropic distillation with benzene. After the benzene was removed completely in vacuo, the residue was dissolved in 60 cc. of absolute ethanol and the chilled solution was saturated with dry hydrogen chloride. Then 100 cc. of water was added to the semisolid mass, and washed with ether. The aqueous layer was made basic by the addition of 2 N sodium hydroxide solution, and extracted with ether. The ether extract was washed with water and dried over anhydrous sodium sulfate. After the solvent was evaporated, the residue was distilled at reduced pressure to give 4.9 g. of a pale yellow liquid, b. p. 164~167°C/1 mmHg. U. V. spectrum: $\lambda_{max}$ mμ (log ε), 239 (4.28), 247 (4.23), 310 (4.28). $\lambda_{min}$ 258 mμ (log ε 3.89) in ethanol (Fig. 11).

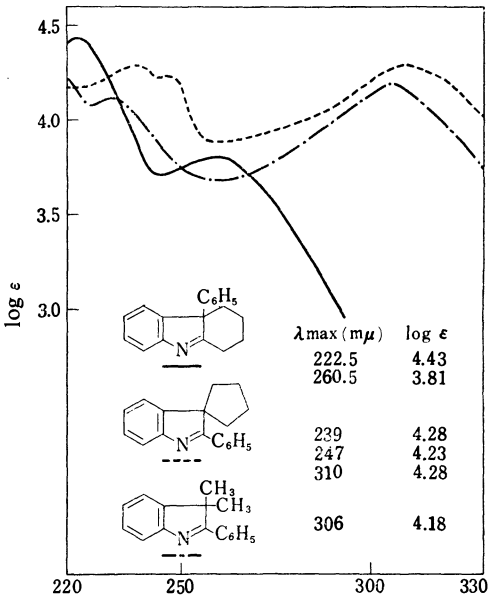



Fig. 11.

Found: C, 87.11; H, 7.21; N, 6.16. Calcd. for $C_{18}H_{17}N$: C, 87.41; H, 6.93; N, 5.55%.

The picrate was recrystallized from ethanol to give yellow crystals, m. p. 175°C.

Found: C, 61.18; H, 4.35; N, 11.74. Calcd. for $C_{24}H_{20}O_7N_4$: C, 60.50; H, 4.23; N, 11.76%.

**11-Phenyltetrahydrocarbazolenine (XXIII).**—*From 2-phenylcyclohexanone phenylhydrazone (XXIV).*—A mixture of 10 g. of 2-phenylcyclohexanone[33] and 7.3 g. of phenylhydrazine was

29) This attempt seems to be the first instance where borontrifluoride etherate was successfully employed for sythesis of indolenine, whereas this reagent has been frequently used for Fisher's indole synthesis. H. R. Snyder and C. W. Smith, ibid., **65**, 2454 (1943).

30) B. p. 160~170°C/2 mmHg; m. p. 76~78.5°C (from ethanol-water). Found: N, 11.83. Calcd. for $C_{16}H_{18}N_2$: N, 11.76%.

31) B. p. 194~196°C/3 mmHg; m. p. 78~79°C. Picrate m. p. 139~141°C. And also see the preceding paper.

32) B. p. 135~136°C/10 mmHg; m. p. of 2,4-dinitrophenylhydrazone, 142°C, [prepared from cyclopentane carboxylic acid chloride by Friedel-Crafts synthesis. (D. H. Hey and O. C. Musgrave, *J. Chem. Soc.*, **1949**, 3156. B. p. 136~140°C/16 mmHg; m. p. of 2,4-dinitrophenylhydrazone, 142~143°C).].

33) B. p. 140~146°C/10 mmHg (60% yield). Prepared following Newman's procedure. M. S. Newman and M. D. Frabman, *J. Am. Chem. Soc.*, **69**, 1550 (1944).

heated on a water bath for 1 hr. The water generated was removed by azeotropic distillation with benzene, and the benzene was removed by distillation in vacuo of a water pump. The residue was dissolved in 100 cc. of absolute ethanol, and saturated with dry hydrogen chloride. A considerable amount of ammonium chloride was observed to precipitate. After the reaction mixture was allowed to stand at room temperature for 10 hr., the solvent was removed in vacuo (below 40~45°C). The residue was dissolved in 250 cc. of water and washed with ether, and the aqueous layer was made basic by the addition of 2 N sodium hydroxide solution and extracted with ether. After the ethereal extract was washed with water and dried over anhydrous potassium carbonate, the solvent was removed to give crystals, which were recrystallized from ethanol-water, m. p. 126~127°C. I. R. spectrum: 6.3 $\mu$. U. V. spectrum: $\lambda_{max}$ m$\mu$ (log $\varepsilon$), 222.5(4.42), 260.5(3.81), $\lambda_{min}$ 245 m$\mu$ (3.72) in ethanol (Fig. 11).

Found: C, 87.47; H, 7.02; N, 5.69. Calcd. for $C_{15}H_{17}N$: C, 87.41; H, 6.93; N, 5.66%.

The picrate was recrystallized from ethanol to give yellow prisms, m. p. 182~183°C.

Found: C, 60.48; H, 4.44; N, 11.78. Calcd. for $C_{24}H_{20}O_7N_4$: C, 60.50; H, 4.23; N, 11.76%.

*From cyclopentylphenylketone phenylhydrazone (XXI).*—To 29 g. of polyphosphoric acid, a mixture of 15 g. of cyclopentylphenylketone[32] and 9.8 g. of phenylhydrazine was added. The temperature of the reaction mixture rose spontaneously up to 150°C, and the reaction mixture was kept at this temperature for 10 min. in an oil bath. The viscous mass was dissolved in water and washed with ether. The acidic aqueous layer was made basic by the addition of 2 N sodium hydroxide solution, and was extracted with ether. After the ether extract was washed with water and dried over anhydrous sodium sulfate, the ether was distilled off. The residue was recrystallized from ethanol-water to give needles, m. p. 122~124°C (7.7 g.) which was proved identical with 11-phenyltetrahydrocarbazolenine (XXIII) prepared from 2-phenylcyclohexanone phenylhydrazone (XXIV).

*From rearrangement of spiro-(cyclopentane-1,3'-pseudo-2'-phenylindole) (XXII).*—A mixture of 1.4 g. of indolenine XXII and 7 g. of polyphosphoric acid was heated at 155°C for 10 min. in an oil bath. The reaction mixture was dissolved in water by warming on a water bath. The acidic aqueous layer was made basic by the addition of 2 N sodium hydroxide solution to precipitate needles (1.0 g.), which were collected and recrystallized from ethanol-water to give m. p. 124°C. The mixed melting point with 11-phenyltetrahydrocarbazolenine was 124°C.

**11b-Methyl-5, 6-dihydro-11b-benzo[*c*]carbazole (XXVI).**—A mixture of 8.1 g. of $\alpha$-methyl-$\beta$-tetralone[34] and 5.5 g. of phenylhydrazine was heated on a water bath for 2 hr., and the generated water was removed by azeotropic distillation with benzene. After the solvent was removed in vacuo, the residue was dissolved in 70 cc. of absolute ethanol, and was saturated with dry hydrogen chloride. After being allowed to stand at 5°C overnight, the reaction mixture was poured into 350 cc. of ice water and washed with ether. The aqueous layer was made basic and was extracted with ether. The ether extract was washed with water and dried over anhydrous potassium carbonate. Removal of the solvent gave a viscous liquid, which was distilled in vacuo to afford 4.1 g. of a viscous pale yellow liquid, b. p. 159~163°C/1 mmHg. I. R. spectrum: 6.3 $\mu$. U. V. spectrum: $\lambda_{max}$ 248 m$\mu$ (log $\varepsilon$ 4.02) in ethanol (Fig. 12).

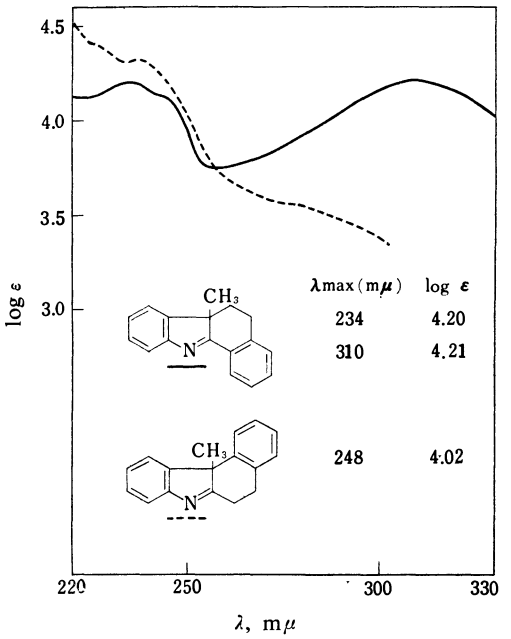



Fig. 12.

Found: C, 86.31; H, 6.83; N, 6.06. Calcd. for $C_{17}H_{15}N$: C, 87.51; H, 6.48; N, 6.00%.

The picrate was recrystallized from ethanol to give yellow prisms, m. p. 167~167.5°C.

Found: C, 59.91; H, 4.03; N, 12.31. Calcd. for $C_{25}H_{18}O_7N_4$: C, 59.74; H, 3.92; N, 12.12%.

**6a-Methyl-5, 6-dihydro-6a-benzo[*a*]carbazole (XXVII).**—When 30 g. of polyphosphoric acid was added to a mixture of 5.2 g. of $\beta$-methyl-$\alpha$-tetralone[35] and 3.6 g. of phenylhydrazine, a considerable generation of heat was observed to cause the reaction temperature to rise to 165°C. After this rather violent reaction subsided, 200 cc. of water was added to dissolve the viscous reaction mass. The acidic aqueous solution was washed with ether, and was made basic to precipitate an oil, which was extracted with ether. The ether extract was washed with water and dried over anhydrous sodium sulfate. Removal of the solvent gave brown viscous residue which was distilled to give 3.4 g. of a pale yellow oil, b. p. 160~164°C/2 mmHg. I. R. spectrum:

34) B. p. 137~142°C/10 mmHg. Prepared following the procedure of J. English and G. Cavaglieri, *J. Am. Chem. Soc.*, 65, 1085 (1943).

35) B. p. 116~120°C/2 mmHg. Prepared following the procedure of W. E. Bachmann and D. G. Thomas, ibid., 63, 598 (1941).

6.5 $\mu$. U. V. spectrum : $\lambda_{max}$ m$\mu$ (log $\varepsilon$), 234(4.20), 310(4.21). $\lambda_{min}$ 256 m$\mu$ (log $\varepsilon$ 3.76) in ethanol (Fig. 12).

Found : C, 86.41 ; H, 6.69 ; N, 6.11. Calcd. for $C_{17}H_{15}N$ : C, 87.51 ; H, 6.48 ; N, 6.00%.

The picrate was recrystallized from ethanol to give yellow prisms, m. p. 169~170°C. The mixed melting point with the picrate of 11b-methyl-5,6-dihydro-11b-benzo[*c*]carbazole (m. p. 167~167.5°C) was 156~159°C.

Found : C, 59.62 ; H, 4.12 ; N, 12.54. Calcd. for $C_{23}H_{18}O_7N_4$ : C, 59.74 ; H, 3.92 ; N, 12.12%.

*From rearrangement of 11b-methyl-5,6-dihydro-11b-benzo[c]carbazole (XXVI)*—A mixture of 0.4 g. of the indolenine XXVI and 2 g. of polyphosphoric acid was heated at 180°C for 15 min. in an oil bath. After water was added, the aqueous solution was freed from a small amount of unsoluble resinous material by filtration.

The solution was made basic with 2 N sodium hydroxide solution, and the turbid mixture was extracted with ether. The ethereal extract was washed with water and dried over anhydrous sodium sulfate. After the ether wae removed, the residue was converted into picrate, without further purification, by the addition of ethanolic picric acid. The picrate was recrystallized from ethanol to give yellow prisms, m. p. 166~167°C, which was proved identical with the picrate of 6a-methyl-5,6-dihydro-6a-benzo[*a*]carbazole (m. p. 169~170°C) by mixed melting point determination.

The authors are very grateful to Mr. Muneo Sato for his technical assistance and to Mr. Sachihiko Isoe who kindly measured the ultraviolet absorption spectra.

*Institute of Polytechnics*
*Osaka City University*
*Kita-ku, Osaka*

# *Mechanism of Plancher's Rearrangement. II*[1]. *Twofold Wagner-Meerwein Type Rearrangement of Indolenium Compounds*

By Masao NAKAZAKI

(Received August 31, 1959)

A novel conversion, by heating at 180~190°C, of an indolenium iodide, m.p. 186°C into an isomeric indolenium iodide, m.p. 232°C, both were obtained by the interaction of 2-isopropyl-3-methylindole and methyliodide was first described by Plancher[2], although the structures of these indolenium iodides were left unsettled.

But on only one occasion was the structure of the rearranged indolenium iodide established: Boyd-Barrett[3] oxidized the indolenium iodide III, obtained from 2-phenylindole (I) by heating with methyliodide at 120°C, to 1, 3-dimethyl-2-phenyloxyindole, and thus confirmed the structure of the rearranged indolenium III proposed by Plancher[4].

Plancher[2] explained the formation of 1, 2, 3-trimethyl-3-phenylindolenium iodide (III) from 2-phenylindole (I) by the sequence of reactions: decomposition of the first formed 1, 3, 3-trimethyl-2-phenylindolenium iodide (II) into iodobenzene and 1, 2, 3-trimethylindole and a recombination of which together with iodobenzene to form III.

It is obvious that such mechanism is hardly tenable, and Julian[5] suggested another mechanism which assumed that 3, 3-dimethyl-2-phenylindolenine is the first intermediate and its rearrangement involving an exchange of the phenyl with the methyl group would give 2, 3-dimethyl-3-phenylindolenine. But the fact that the conversion of 3, 3-dimethyl-2-phenylindolenine into 2,3-dimethyl-2-phenylindolenine, which would give III with methyliodide, however, was proved just opposite to the case[6], leaving only one possible mechanism remaining, i.e. the conversion of the intermediate 1, 3, 3-trimethyl-2-phenylindolenium iodide (II) into III, by a twofold Wagner-Meerwein type rearrangement formulated in Fig. 1. To testify this possibility, Leuch's experiment[7] was repeated in order to obtain 1, 3, 3-trimethyl-2-phenylindolenium iodide (II) from 3, 3-dimethyl-2-phenylindolenine and methyliodide.

1) Part I: M. Nakazaki, K. Yamamoto and K. Yamagami, This Bulletin, **33**, 466 (1960).
2) G. Plancher, *Atti, accad. Lincei*, (5) **11**, III, 182 (1902); *Chem.-Zentr.*, **1902**, I, 1322.
3) H. S. Boyd-Barrett, *J. Chem. Soc.*, **1932**, 321.
4) G. Plancher, *Gazz. chim. ital.*, **28**, II, 391 (1898); *Chem.-Zentr.*, **1899**, I, 283.
5) P. L. Julian, E. W. Meyer and H. C. Pring, "The Chemistry of Indoles", in R. Elderfield, "Heterocyclic Compounds", Vol. 3., John Wiley & Sons, Inc., New York (1952), p. 106. The introductory part of the preceding paper gives a brief historical survey of Plancher's rearrangement.
6) M. Nakazaki, K. Yamamoto and K. Yamagami, This Bulletin, **33** 466 (1960).
7) H. Leuchs, A. Heller and A. Hoffmann, *Ber.*, **62**, 871 (1932).

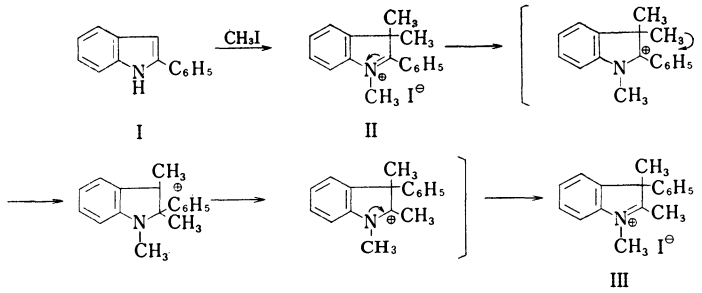


Fig. 1.

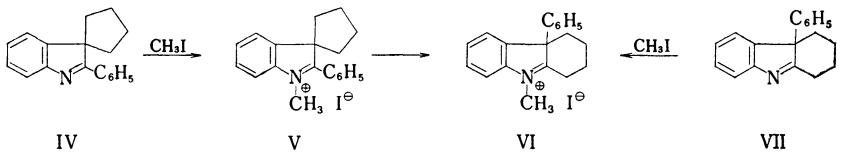


Fig. 2.

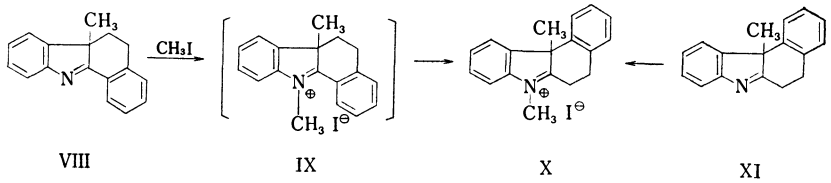


Fig. 3.

When a solution of 3, 3-dimethyl-2-phenylindolenine and methyliodide in methanol was heated at 100°C for 4 hr., there were obtained, in contrary to expectation, colorless prisms, m.p. 226~227°C[8], beside Leuch's indolenium iodide, yellow needles, m.p. 203°C, in about the same amount. Since the indolenium iodide with m.p. 226~227°C was proved to be 1, 2, 3-trimethyl-3-phenylindolenium iodide (III) by Boyd -Barrett's degradative experiment[3], the isomeric yellow indolenium iodide, m. p. 203°C which was a sole product Leuchs could isolate, was to be assigned the structure of 1, 3, 3-trimethyl-2-phenylindolenium iodide (II). These structure assignments were further confirmed by their ultraviolet absorption spectra, which show clearly a bathochromic shift (III, $\lambda_{max}$ 276 m$\mu$ and II, $\lambda_{max}$ 297 m$\mu$) due to conjugation with the phenyl group (Fig. 5).

The conversion of II to III was realised when a methanolic solution of II was heated in a sealed tube at 120~150°C for 1/2 hr., and this is the first case where indolenium compound was rearranged into the isomeric indolenium compound both with known constitutions, exchanging substituents between 2- and 3-position of the indolenium nucleus. Another smooth isomerization was established when *spiro*-(cyclopentane-1, 3'-*pseudo*-2'-phenylindole) methoiodide (V), prepared from the corresponding indolenine IV, with methyliodide, was heated in methanolic solution at 160°C for 3 hr. in a sealed tube to give 11-phenyltetrahydrocarbazolenine methoiodide (VI), which could be prepared from 11-phenyltetrahydrocarbazolenin (VII) and methyliodide.

Although it was unsuccessful to obtain the methoiodide of 6a-methyl-5, 6-dihydro-6a-benzo-[*a*] carbazole (IX) in crystalline form, it could be isomerized by heating its methanolic solution at 150°C for 5 hr. to the isomeric 11b-methyl-5, 6-dihydro-11b-benzo [*c*] carbazole methoiodide (X) provided from the corresponding indolenine XI with methyliodide. The mechanism of these rearrangements of indolenium iodides can be sought in the twofold Wagner-Meerwein type rearrangement[9] illustrated in Fig. 4.

Situated between two substituents at 1- and 3-position of indolenium compounds the substituents at 2-position suffer a considerable steric repulsion from both sides and the most bulky group ($R_3$) would tend to migrate to 2-position,

8) In the repetition of Plancher's experimet, Boyd-Barrett (Ref. 3) obtained a yellow indolenium iodide, m. p. 196°C as a minor product. Apparently this is the intermediate 1, 3, 3-trimethyl-2-phenylindolenium iodide (II), but any structural study as well as its possible rearrangement III was not tried.

9) Twofold Wagner-Meerwein type rearrangement was also demonstrated in indolenines (ref. 6) and 2, 3-disubstituted indoles M. Nakazaki, This Bulletin, 33, 461 (1960) A *spiro* type intermediate has to be assumed in the case of the rearrangement IX→X.

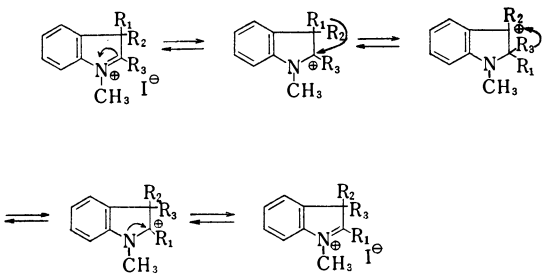


Fig. 4.

compelling the least bulky group ($R_1$) to 2-position (Fig. 4).

This steric effect would be strong enough[10] so as to compensate for the mesomeric stabilization effect of the phenyl group conjugated with the indolenium nucleus.

## Experimental[11]

**1, 3, 3-Trimethyl-2-phenylindolenium Iodide (II) and 1, 2, 3-Trimethyl-3-phenylindolenium Iodide (III).**—A mixture of 12.7 g. of 3, 3-dimethyl-2-phenylindolenine[12], 24.2 g. of methyliodide and 77 cc. of methanol was heated at 100°C. for 4 hr. in a sealed tube. After the solvent was removed on a water bath, the residue was recrystallized from methanol-ethyl acetate. From the more soluble fraction yellow needles were obtained and recrystallization from water (aqueous solution was colorless, whereas the methanolic solution was yellow) gave 3.6 g. of yellow needles, m. p. 202~203°C. (literature[7]: 203°C). Ultraviolet spectrum of 1, 3, 3-trimethyl-2-phenylindolenium iodide: $\lambda_{max}$ 297 m$\mu$ (log $\varepsilon$ 3.97) in methanol (Fig. 5).

Found: C, 56.24; H, 5.07. Calcd. for $C_{17}H_{18}NI$: C, 56.21; H, 4.99%.

From the less soluble fraction, there were obtained colorless prisms which were recrystallized from methanol, m.p. 226~227°C (literature[3]: 227°C). This iodide is rather sensitive to air and gradually changes to pink in color. U. V. spectrum of 1, 2, 3-trimethyl-3-phenylindolenium iodide: $\lambda_{max}$ 276 m$\mu$ (log $\varepsilon$ 3.84) in methanol (Fig. 5).

Found: C, 56.73; H, 5.37. Calcd. for $C_{17}H_{18}NI$: C, 56.21; H, 4.99%.

**Rearrangement of 1,3,3-Trimethyl-2-phenylindolenium Iodide (II).**—The indolenium iodide II (0.5 g.) was dissolved in 6 cc. of methanol and heated at 120~150°C for 3 hr., and then at 180°C for 1/2 hr. in a sealed tube. The original yellow color of the reaction mixture changed to violet-red. After removal of the solvent, the residue was dissolved in a small amount of methanol, and ethyl acetate was added to precipitate prisms (m.p. 222~224°C) with faint pink color, which was recrystallized from methanol to raise the melting point to 224~226°C. This was found identical with 1, 2, 3-trimethyl-3-phenylindolenium iodide (III) by mixed melting point determination and the comparison of infrared spectra.

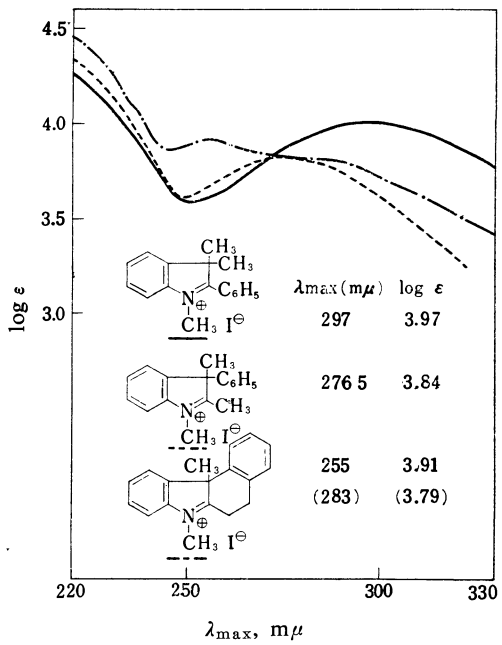



Fig. 5.

***Spiro*-(cyclopentane-1, 3'-*pseudo*-2'-phenylindole)**

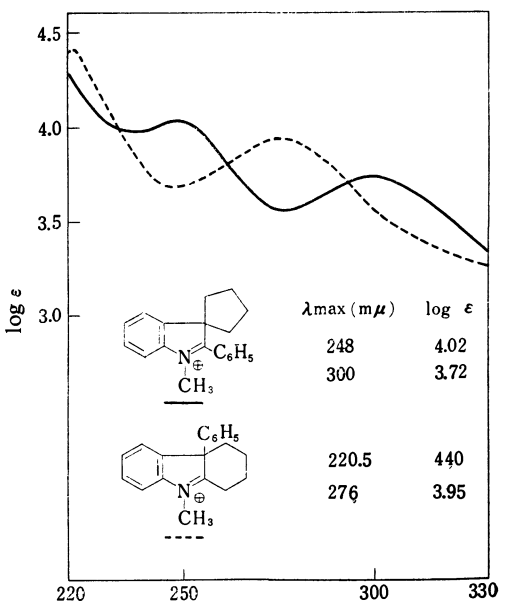



Fig. 6.

10) Even in the indolenine IV, without the repulsion from the substituent at 1-position, the steric strain is sufficient enough to be responsible for the smooth rearrangement of the isomeric indolenine VII (Ref. 6).

11) All the melting points are uncorrected values. All ultraviolet spectra were measured with an EPS-2 Hitachi autorecording spectrophotometer and infrared spectra on a Perkin Elmer Model 12C. The analyses were performed in the Microanalytical Laboratory of the Institute of Ploytechnics, Osaka City University.

12) B. p. 178~179°C/9 mmHg. Picrate, m. p. 167~168°C. Prepared following Witkop's procedure. [H. M. Kissman, D. W. Farnworth and B. Witkop, *J. Am. Chem. Soc.*, 74, 3948 (1952)].

**Methoiodide (V).**—A mixture of 1 g. of *spiro*-(cyclopentane-1, 3'-*pseudo*-2'-phenylindole)[13], 1.0 g. of methyliodide and 10 cc. of methanol was heated at 100°C for 2 hr. in a sealed tube. After the solvent was removed from the dark green reaction mixture, the residue was recrystallized from ethanol to give yellow needles (0.55 g.), m.p. 186.5~188°C. U. V. spectrum: $\lambda_{max}$ m$\mu$(log $\varepsilon$), 248(4.02), 300 (3.72) in ethanol (Fig. 6).

Found: C, 58.51; H, 5.36; N, 3.59. Calcd. for $C_{19}H_{20}N$ I: C, 58.70; H, 5.18; N, 3.60%.

**11-Phenyltetrahydrocarbazolenine Methoiodide (VI).**—A mixture of 1.0 g. of phenyltetrahydrocarbazolenine[14] 1.0 g of methyliodide and 10 cc. of methanol was heated at 100°C. for 3 hr. in a sealed tube. After removal of the solvent, the green residue was dissolved in methanol and decolorized with sulfur dioxide.

Then small amount of water was added to precipitate needles, which were recrystallized from water to give colorless needles, m.p. 116~118°C (decomp.). U. V. spectrum: $\lambda_{max}$ m$\mu$(log $\varepsilon$), 220.5 (4.40), 276(3.95) in ethanol (Fig. 6).

Found: C, 56.26; H, 5.60; N, 3.67. Calcd. for $C_{19}H_{20}NI \cdot H_2O$: C, 56.03; H, 5.45; N, 3.44%.

**Rearrangement of *Spiro*-(cyclopentane-1, 3'-*pseudo*-2'-phenylindole) Methoiodide (V).**—A mixture of 0.4 g. of the indolenium iodide V and 6 cc. of methanol was heated at 160°C for 3 hr. and at 200°C for 15 min. in a sealed tube. After removal of the solvent, the green residue was extracted with boiling water. The aqueous solution was treated with Norit and was concentrated to give colorless needles which were recrystallized from water., m.p. 116~118°C. This was found identical with the 11-phenyltetrahydrocarbazolenine methoiodide (m.p. 116~117°C) by mixed melting point determination (m.p. 116~118°C).

**11b-Methyl-5, 6-dihydro-11b-benzo[*c*]carbazole (X).**—A mixture of 0.2 g. of the indolenine XI[15], 0.4 g. of methyliodide and 4 cc. of methanol was heated at 100°C. for 3 hr. in a sealed tube. After removal of the solvent, a small amount of ether was added to the residue and was allowed to stand with occasional trituration. The crystals precipitated were collected and recrystallized from ethanol to give m.p. 202~204°C. U. V. spectrum: $\lambda_{max}$ 255 m$\mu$(log $\varepsilon$ 3.91) with a plateau at 283 m$\mu$ (3.79) in ethanol (Fig. 5).

Found: C, 57.81; H, 5.18; N, 4.20. Calcd. for $C_{18}H_{15}NI$: C, 57.61; H, 4.83 N, 3.73%.

**Rearrangement of 6a-Methyl-5, 6-dihydro-6a-benzo[$\alpha$]carbazole Methoiodide (IX).**—A mixture of 0.5 g. of the indolenine VIII[16], 1.0 g. of methyliodide and 4 cc. of methanol was heated at 100°C for 3 hr. in a sealed tube. After the solvent was removed at reduced pressure, the residue was washed with ether. After various fruitless attempts to crystallize, the viscous residue was dissolved in 6 cc. of methanol and heated at 150°C for 5 hr. in a sealed tube. The solvent was evaporated and a small amount of ether was added to the residue and triturated. The crystals were collected, and recrystallized from ethanol to give crystals melting at 202~204°C, which was found identical with the indolenium iodide X by mixed melting point determination and the comparison of their infrared spectra.

The author is very grateful to Messrs. Keiji Inui, Koji Yamamoto, Muneo Sato and Kikuo Yamagami for their assistance to prepare various starting materials. He also feels indebted to Mr. Sachihiko Isao for measurement of ultraviolet absorption spectra.

*Institute of Polytechnics*
*Osaka City University*
*Kita-ku, Osaka*

13) B.p. 164~167°C/1 mmHg. Picrate. m.p. 175°C. Ref. 6.
14) M. p. 126°C. Picrate, m. p. 182~183°C. Ref. 6.
15) B. p. 160~165°C/2 mmHg. Picrate. m. p. 167~167.5°C, Ref. 6.
16) B. p. 160~194°C/2 mmHg. Picrate, m. p. 169~170°C. Ref. 6.

# *Theory on the Small Angle Scattering of Light to Determine the Shape, Size and Orientation of High Polymer Molecules in Flow**

By Masayuki NAKAGAKI

(Received October 6, 1959)

As for the small angle scattering of light by high polymer moleculces in a solution at rest, the Zimm plot, that is a double extrapolation method devised by Zimm[1], has been used widely. On the other hand, a theory regarding the deformation of high polymer molecules in flow and on the light scattering by the deformed molecules has been developed by Peterlin, Heller and Nakagaki[2]. On the basis of this theory, it will be shown in the present paper that the Zimm plot can be used for the quantitative determination of the shape, size and orientation of high polymer molecules in flow, and that the photographic pattern of the small angle scattering can be used to determine the orientation of the molecules in flow.

### Initial Slope of the Zimm Plot

The equation of light scattering derived by Debye[3] on the basis of fluctuation theory, and generalized by Zimm[4] is,

$$Kc/R_u(\vec{s}) = 1/MP(\vec{s}) + 2A_2c \tag{1}$$

where $K$ is a constant, $R_u(\vec{s})$ is reduced scattering intensity, $P(\vec{s})$ is interference factor, and $c$, $M$ and $A_2$ are concentration, molecular weight and the second virial coefficient of the polymer. The constant $K$ is given by

$$K = (2\pi^2\mu_1^2/N_0\lambda_0^4)(\mathrm{d}\mu_{12}/\mathrm{d}c)^2 \tag{2}$$

where $\mu_1$ is the refractive index of solvent, $N_0$ is the Avogadro number, $\lambda_0$ is wavelength of light in vacuo and $\mu_{12}$ is refractive index of solution. The reduced scattering intensity $R_u(\vec{s})$ is

$$R_u(\vec{s}) = (I_u(\vec{s})/I_0)/(1+\cos^2\theta) \tag{3}$$

where $I_0$ is the intensity of the unpolarized incident light, $I_u(s)$ is the intensity of light scattered in the direction designated by $\vec{s}$, and $\theta$ is the scattering angle. The scattering vector $\vec{s}$ is given by

$$\vec{s} = \vec{s'} - \vec{s_0} \tag{4}$$

where $\vec{s_0}$ and $\vec{s'}$ are unit vectors in the direction of the incident beam and scattered beam, respectively; and its absolute value, $s$, is

$$s = |\vec{s}| = 2\sin(\theta/2) \tag{5}$$

Here the scattering angle $\theta$ is the angle between $\vec{s_0}$ and $\vec{s'}$.

In the so called Zimm plot, $(Kc/R_u)$ is taken as ordinate and $\sin^2(\theta/2)+kc$ is taken as abscissa, where $k$ is a constant chosen arbitrarily. Therefore, the curve on the Zimm plot for the values extraporated to infinitely dilute concentration gives

$$[Kc/R_u(\vec{s})]_0 = 1/MP(\vec{s}) \tag{6}$$

as a function of $\sigma$ defined by

$$\sigma = \sin^2(\theta/2) \tag{6a}$$

On the other hand, the theoretical expression for the interference factor of streaming polymer molecules derived by Peterlin, Heller and Nakagaki[2] is,

$$P(\vec{s}) = 2\int_0^1 (1-u)\exp[-X(u+\zeta u^2)]\,\mathrm{d}u \tag{7}$$

where

$$X = (8\pi^2/3\lambda^2)R^2\sin^2(\theta/2)\cdot\xi \tag{8}$$

and

$$\zeta = (2/3)\beta^2 \tag{9}$$

Here $\lambda$ is the wavelength of light in the medium, $R$ is the root-mean-square of the end-to-end distance of the polymer molecule at rest, and

$$\xi = \{1+[\beta^2+\beta(1+\beta^2)^{1/2}\cos 2\phi] \times\cos^2(\theta/2)\}/(1+2\beta^2/3) \tag{10}$$

Here $\beta$ is a quantity proportional to the velocity gradient $q$ defined by

$$\beta = (\pi a/6kT)\eta ZR^2q = (M/N_0kT)[\eta]\eta q \tag{11}$$

where $a$ is the hydrodynamic radius of segments, $k$ is the Boltzmann constant, $T$ is the absolute temperature, $\eta$ is the viscosity, $Z$ is the number of segments in a molecule, $M$ is the molecular weight and $[\eta]$ is the intrinsic viscosity. The angle $\phi$ is concerned with the direction of observation as defined in Ref. 2 and will be described later (See Fig. 2).

---

* Presented before the 12th Annual Meeting of the Chemical Society of Japan, Kyoto, April, 1959.

1) B. H. Zimm, *J. Chem. Phys.*, **16**, 1099 (1948).
2) A. Peterlin, W. Heller and M. Nakagaki, ibid., **28**, 470 (1958).
3) P. Debye, *J. Appl. Phys.*, **15**, 338 (1944).
4) B. H. Zimm, *J. Chem. Phys.*, **16**, 1093 (1948).

The value of $[Kc/R_u(0)]_0$, that is the height of the ordinate at which the Zimm plot for infinite dilution intersects and the value of the initial slope of this Zimm plot are obtained by expanding $[Kc/R_u(\vec{s})]_0$ of Eq. 6 as a power series of $\sigma$ of Eq. 6a. These values are:

$$[Kc/R_u(0)]_0 = 1/M \tag{12}$$

and

$$\begin{aligned}(\text{Initial slope}) &= [Kc/R_u(0)]_0 \times (8\pi^2R^2/9\lambda^2) \\ &\times [1+\beta^2+\beta(1+\beta^2)^{1/2}\cos 2\phi] \\ &\times (1+\beta^2/3)/(1+2\beta^2/3)\end{aligned} \tag{13}$$

If a parameter $g$ defined by

$$g = (9\lambda^2/8\pi^2)\ (\text{Initial slope})/[Kc/R_u(0)]_0 \tag{14}$$

is used, the value is

$$\begin{aligned}g &= R^2[1+\beta^2+\beta(1+\beta^2)^{1/2}\cos 2\phi] \\ &\times (1+\beta^2/3)/(1+2\beta^2/3)\end{aligned} \tag{15}$$

Thus, the value of the ordinate at which the Zimm plot intersects is constant irrespective of whether the solution is streaming or not. From this value, the molecular weight may be determined on the basis of Eq. 12. On the other hand, the value of $g$ depends on the velocity gradient or $\beta$. The value of $g$ in the case of the solution at rest, designated by $g_0$, is obtained from Eq. 15 with $\beta=0$. The value is

$$g_0 = R^2 \tag{16}$$

Therefore, it is equal to the mean square end-to-end distance. The value of $g$ for streaming solution depends on the direction of observation or $\phi$ as well as the velocity gradient or $\beta$.

At first, the observation plane is fixed and the variation of $g$ with velocity gradient (or $\beta$) is considered. Since the angle $\phi$ is also a function of $\beta$, angle $\omega$ is used instead (see Fig. 2). The angle $\omega$ is the angle between the direction of flow and the plane of observation, and is related to $\phi$ by the equation:

$$\omega = \phi + 90° - \chi \tag{17}$$

where $\chi$ is the extinction angle varying with $\beta$ according to

$$\beta = -\cot 2\chi \tag{18}$$

Then, Eq. 15 is rewritten to

$$\begin{aligned}g/g_0 &= (1+\beta^2+\beta\sin 2\omega+\beta^2\cos 2\omega) \\ &\times (1+\beta^2/3)/(1+2\beta^2/3)\end{aligned} \tag{19}$$

The variation of $g/g_0$ due to $\beta$ for several values of $\omega$ are shown in Fig. 1 with solid curves. Then, at a constant value of $\beta$, the maximum and minimum value of $g/g_0$ are calculated. The results are:

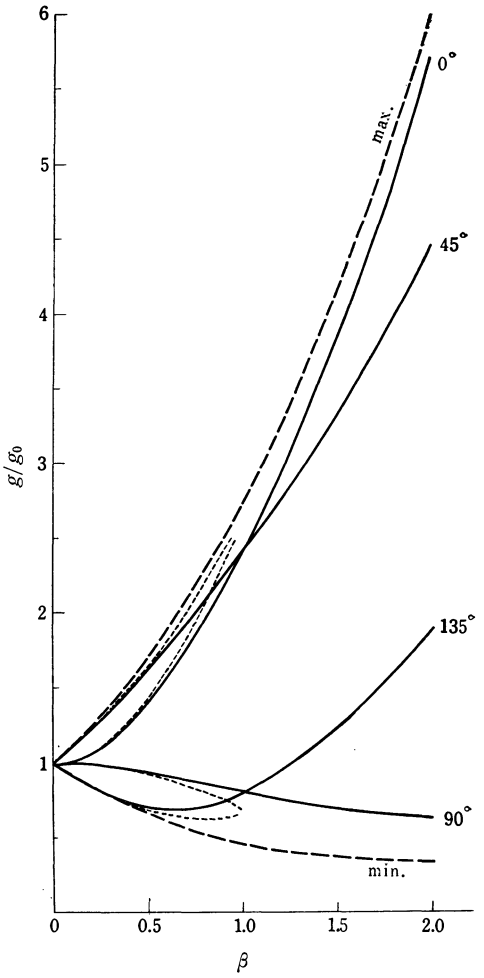



Fig. 1. The relationship between $g/g_0$ and $\beta$.

$$\left.\begin{aligned}g_{max}/g_0 &= [1+\beta^2+\beta(1+\beta^2)^{1/2}] \\ &\times (1+\beta^2/3)/(1+2\beta^2/3) \\ &\text{at}\quad \phi = 0°,\ 180° \\ g_{min}/g_0 &= [1+\beta^2-\beta(1+\beta^2)^{1/2}] \\ &\times (1+\beta^2/3)/(1+2\beta^2/3) \\ &\text{at}\quad \phi = \pm 90°\end{aligned}\right\} \tag{20}$$

These values are shown in Fig. 1 with broken lines.

It may be instructive to estimate here the order of magnitude of $\beta$. If $[\eta]=100$, $\eta=1$ c.p.s., $M=3\times10^5$ and $q=1\times10^4$ sec$^{-1}$, the value of $\beta$ calculated by Eq. 11 is 0.12. Therefore, the usual value of $\beta$ seems to be smaller than unity. If $\beta \ll 1$, Eq. 19 is reduced to

$$g/g_0 \fallingdotseq 1+\beta\sin 2\omega+\beta^2(2/3+\cos 2\omega) \tag{21}$$

The error committed by this approximate equation is less than 5% as far as $\beta \lesssim 0.7$. The values calculated by this equation are shown in Fig. 1 with dotted curves.

As already mentioned, the quantity $\beta$ is proportional to the velocity gradient $q$. When a concentric cylinder apparatus is used, $\beta$ is, therefore, proportional to the rate of rotation $\Omega(\sec^{-1})$, that is

$$\beta = k_1 q = k_2 \Omega \tag{22}$$

with

$$k_2 = k_1(2\pi\rho/d) \tag{23}$$

where $\rho$ is the radius of the rotating cylinder, $d$ is the width of the gap of the concentric cylinder, and the value of $k_1$ is readily obtained from Eq. 11. Thus, there are three methods to determine the value of $k_2$ (or $k_1$). The first is to calculate the value of $k_1$ by Eq. 11. The second is to measure the extinction angle $\chi$ by a streaming double refraction measurement in order to obtain the value of $\beta$ on the basis of Eq. 18. The values of $\beta$ for various values of $q$ or $\Omega$ will give the value of $k_1$ or $k_2$ by Eq. 22. The third and the most direct method for the present experiment is to use the equation derived from Eq. 21, that is:

$$(g/g_0 - 1)/\Omega = A + B\Omega \tag{24}$$

where

$$\left.\begin{aligned} A &= k_2 \sin 2\omega \\ B &= k_2^2(2/3 + \cos 2\omega) \end{aligned}\right\} \tag{25}$$

From the value of $A$ or $B$ determined experimentally, the value of $k_2$ will be obtained.

## A Method for Measurement of the Semi-Major and Minor Axes of Flexible High Polymer Molecules

The extension of high polymer molecules in solution is expressed by the probability distribution of end-to-end distance, that is the probability $\psi$ per unit volume to find one end of the high polymer molecule in a volume element when the other end is fixed at the origin. In the case of freely flexible high polymer molecules, it is well known that the function $\psi$ is Gaussian:

$$\left.\begin{aligned} \psi &= (\mu/\pi)^{3/2} \exp(-\mu r^2) \\ \mu &= 3/2R^2 \end{aligned}\right\} \tag{26}$$

where $r$ is the distance to the volume element from the origin and $R$ is the root mean square end-to-end distance. On the other hand, it is often assumed that the distribution of segments around the center of gravity of the molecule is also Gaussian. The probability $W$ to find a segment in a unit volume of a volume element is then:

$$\left.\begin{aligned} W &= Z(\mu^*/\pi)^{3/2} \exp(-\mu^* r^2) \\ \mu^* &= 6\mu \end{aligned}\right\} \tag{27}$$

where $Z$ is the number of segments in one molecule, and $r$ in this case is the distance between the volume element and the center of gravity. The relation between $\mu^*$ and $\mu$ shown in Eq. 27 is based on the fact established by Debye[5] that the root mean square distance $S$ of a segment from the center of gravity of the molecule is

$$S = R/\sqrt{6} \tag{28}$$

On the other hand, Debye and Bueche[6] concluded from the study of intrinsic viscosity that the radius $R_s$ of a high polymer molecule considered as a sphere should be

$$R_s = \sqrt{5/18}\, R \tag{29}$$

Now, by assuming that the distribution of segments is homogeneous in a sphere of radius $R_s$ the root mean square distance of a segment from the center of gravity of the molecule is readily calculated and the result is

$$S = \sqrt{3/5}\, R_s \tag{30}$$

This result together with Eq. 29 yields a relation exactly the same as that of Eq. 28, the latter being obtained originally on the basis of the Gaussian distribution formulated in Eq. 27.

On the basis of these facts, one may say that the shape of a high polymer molecule in a solution at rest is a sphere with the radius of $R_s$. Then the value of $W$ at the surface of the sphere ($W_s$) relative to the value of $W$ at the center of gravity of the molecule ($W_0$) is,

$$W_s/W_0 = \exp(-5/2) = 0.082 \tag{31}$$

Therefore, to assume a high polymer molecule as a sphere of radius $R_s$ corresponds to the assumption that the surface of the molecule is defined by the points at which $W_s/W_0 = 0.082$ in the Gaussian distribution.

Now, considering high polymer molecules in a streaming solution, Peterlin, Heller and

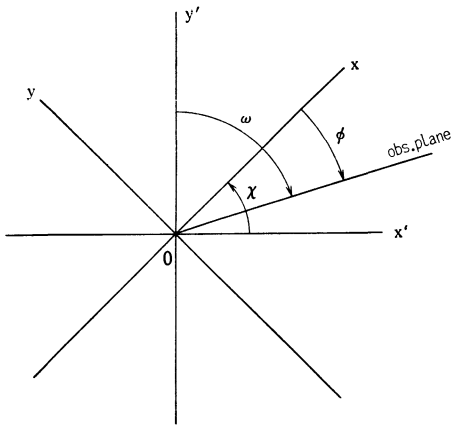



Fig. 2. The coordinate system and angles used.

5) P. Debye, ibid., **14**, 636 (1946).
6) P. Debye and A. M. Bueche, ibid., **16**, 573 (1948).

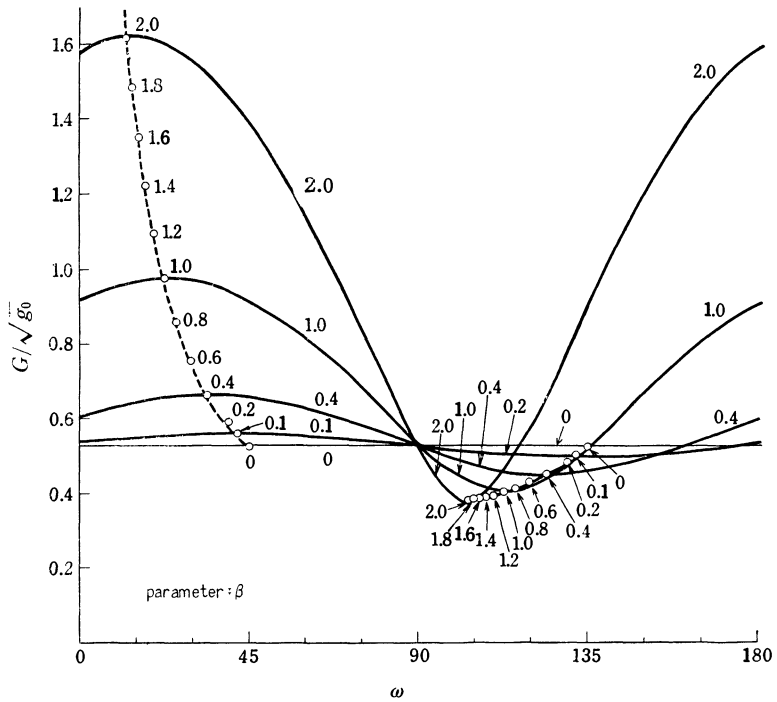



Fig. 3. The relationship between $G/\sqrt{g_0}$ and $\omega$. Parameter: $\beta$.

Nakagaki[2] gave the probability distribution of end-to-end distance by the equation:

$$\psi=\frac{1}{abc}\left(\frac{\mu}{\pi}\right)^{3/2}\times\exp\{-\mu[(x/a)^2+(y/b)^2+(z/c)^2]\} \quad (32)$$

where

$$\left.\begin{aligned} a^2&=\sqrt{1+\beta^2}(\sqrt{1+\beta^2}+\beta)\\ b^2&=\sqrt{1+\beta^2}(\sqrt{1+\beta^2}-\beta)\\ c^2&=1\end{aligned}\right\} \quad (33)$$

Here, the coordinate system $x, y, z$ is that obtained by rotating the coordinate system $x'$, $y'$, $z$ by the angle $\chi$ around the $z$-axis, as shown in Fig. 2, $x'$ and $y'$ being the direction of velocity gradient and velocity, respectively. Eq. 32 is reduced to the usual Gaussian distribution (Eq. 26) when $\beta=0$.

The distribution of segments around the center of gravity of the molecule may then be assumed to be

$$W=\frac{Z}{abc}\left(\frac{\mu^*}{\pi}\right)^{3/2}\times\exp\{-\mu^*[(x/a)^2+(y/b)^2+(z/c)^2]\} \quad (34)$$

with $\mu^*=6\mu$, in analogy to Eq. 27. By the assumption that the surface of the molecule is defined by the points at which $W_s/W_0=\exp(-5/2)$, the molecule should be an ellipsoid expressed by the equation:

$$\mu^*[(x/a)^2+(y/b)^2+(z/c)^2]=5/2 \quad (35)$$

the semi-axes of the ellipsoid $R_a$, $R_b$, and $R_c$ being in the direction of the coordinate axes $x$, $y$ and $z$, respectively, and the values being[7]

$$\left.\begin{aligned} R_a&=\sqrt{5/18}\,aR\\ R_b&=\sqrt{5/18}\,bR\\ R_c&=\sqrt{5/18}\,cR\end{aligned}\right\} \quad (36)$$

When $\beta=0$,

$$R_a=R_b=R_c=R_s \quad (37)$$

since $a=b=c=1$.

In order to determine the values of $R_a$, $R_b$, and $R_c$ experimentally, a quantity $G$ defined by

$$G=\sqrt{(5/18)g(1+2\beta^2/3)/(1+\beta^2/3)} \quad (38)$$

is introduced. Here $g$ is obtainable experimentally from the measurement of the initial slope by using Eq. 14, and $\beta$ is obtainable experimentally by Eq. 22 as a quantity proportional to the rate of rotation $\Omega$. Therefore, the quantity $G$ is a measurable quantity. The theoretical expression for $G$ may be obtained by using Eq. 15 and the result is:

$$G=\sqrt{5/18}\,R\sqrt{1+\beta^2+\beta\sqrt{1+\beta^2}\cos 2\phi} \quad (39)$$

Thus, $G$ as a function of the direction of observation plane, $\omega$, has one maximum and one

7) The quantity $R$ is the root mean square end-to-end distance at rest. The value in flow is $\langle r^2\rangle=R^2(1+2\beta^2/3)$.

minimum in the range $\omega=0\sim180°$. The maximum of $G$ occurs at $\phi=0$, that is, $\omega=90°-\chi$ or the direction of $x$-axis. The maximum value of $G$ is

$$G_{max}=R_a \quad \text{at} \quad \omega_{max}=90°-\chi \tag{40}$$

On the other hand, the minimum value of $G$ occurs at $\phi=90°$, that is the direction of $y$-axis, at which,

$$G_{min}=R_b \quad \text{at} \quad \omega_{min}=180°-\chi \tag{41}$$

The value of $\chi$ can be predetermined theoretically by Eq. 18. Thus, the major and minor semi-axes of the ellipsoidal molecule, $R_a$ and $R_b$, are obtained experimentally from the values of $G_{max}$ and $G_{min}$, and the direction of the major and minor axes of the molecule coinside with $\omega_{max}$ and $\omega_{min}$. The value of $R_c$ is equal to the value of $G$ for $\beta=0$, that is the value for the solution at rest:

$$G_0=R_c \tag{42}$$

The values of $G/\sqrt{g_0}$ are shown in Fig. 3, where $g_0$ is the value of $g$ for the solution at rest. $G_{max}$ and $G_{min}$ are shown by open circles. The numerical values of $G_{max}/\sqrt{g_0}$ and $G_{min}/\sqrt{g_0}$ are shown in Table I for perfectly flexible molecules.

TABLE I. THE MAXIMUM AND MINIMUM OF $G$ FOR PERFECTLY FLEXIBLE HIGH POLYMER MOLECULE

| $\beta$ | $\omega_{max}$ | $G_{max}/\sqrt{g_0}$ | $\omega_{min}$ | $G_{min}/\sqrt{g_0}$ |
|---|---|---|---|---|
| 0 | 45.00° | 0.52705 | 135.00° | 0.52705 |
| 0.1 | 42.14 | 0.55540 | 132.14 | 0.50263 |
| 0.2 | 39.34 | 0.58784 | 129.34 | 0.48190 |
| 0.4 | 34.10 | 0.66475 | 124.10 | 0.45007 |
| 0.6 | 29.52 | 0.75642 | 119.52 | 0.42827 |
| 0.8 | 25.67 | 0.86032 | 115.67 | 0.41349 |
| 1.0 | 22.50 | 0.97388 | 112.50 | 0.40339 |
| 1.2 | 19.91 | 1.0948 | 109.91 | 0.39185 |
| 1.4 | 17.77 | 1.2212 | 107.77 | 0.39134 |
| 1.6 | 16.01 | 1.3518 | 106.01 | 0.38769 |
| 1.8 | 14.53 | 1.4857 | 104.53 | 0.38500 |
| 2.0 | 13.28 | 1.6221 | 103.28 | 0.38290 |

## Expectation from Photographic Study of Small Angle Scattering

The shape of the pattern to be obtained by photographing the small angle scattering from a streaming solution will be discussed here. Let the distance from the specimen (a streaming solution) to the photographic plate be $D$, and the coordinate of one point $P$ on the plate be $(x', y')$. Here the origin of the coordinate system is placed on the point where the primary beam hit the plate, the $x'$-axis being parallel to the direction of the velocity gradient, $\vec{q}$, and the $y'$-axis being parallel to the direction of flow, $\vec{v}$, and the direction of the primary beam being perpendicular to the plate.

Since the small angle scattering only is considered here, $\theta \ll 1$ or $r/D \ll 1$. Therefore,

$$\left.\begin{aligned}\sin(\theta/2) &\fallingdotseq r/2D \\ \cos\theta &\fallingdotseq 1-r^2/2D^2\end{aligned}\right\} \tag{43}$$

The intensity $I_u$ of light per unit solid angle scattered to the direction SP in Fig. 4 is

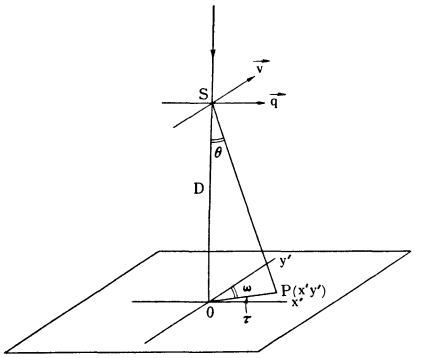



Fig. 4. Illustration of coordinate systems and angles.

$$I_u=I_0(1+\cos^2\theta)\,R_u \tag{44}$$

where $I_0$ is the intensity of the unpolarized incident light, and $R_u$ is the reduced scattering intensity as defined by Eq. 3. Then, the intensity, $I_u'$ of scattered light per unit area on the plate is

$$I_u'=I_u\cos\theta/(D^2+r^2) \tag{45}$$

Now, using Eq. 6 for sufficiently dilute solution, expanding the interference factor $P$ in a power series of $r/D$ and using Eq. 43,

$$I_u'=(2I_0KcM/D^2)\,[1-(r^2/2D^2)\{4+E \times(1+\beta^2+\beta\sqrt{1+\beta^2}\cos 2\phi)\}] \tag{46}$$

where

$$E=(4\pi^2R^2/9\lambda^2)\,(1+\beta^2/3)/(1+2\beta^2/3) \tag{47}$$

The contrast to be obtained on the photographic plate is probably not very great, although it will be the greater, the greater the value of $R/\lambda$ is. Let us, however, expect that the contrast can be emphasized sufficiently by using adequate photographic technique. Here, the shape of the pattern obtained by connecting the points of equal blackness on the plate is discussed. Since $I_u'$ is constant for these points, the value of $h$ defined by

$$h=1-(D^2/2KcM)\,(I_u'/I_0) \tag{48}$$

is constant. Now changing the coordinate system from $(x', y')$ to $(x, y)$ shown in Fig. 2,

$$x^2/\{2D^2h/[4+E(1+\beta^2+\beta\sqrt{1+\beta^2})\} +y^2/\{2D^2h/[4+E(1+\beta^2-\beta\sqrt{1+\beta^2})]\}=1 \tag{49}$$

is obtained from Eqs. 46 and 48. Therefore, the shape of the pattern to be obtained on the plate is an ellipse. The direction of the major axis of the ellipse is parallel to the direction of the minor axis of the molecule ($y$-direction) and the direction of the minor axis of the pattern is parallel to the direction of the major axis of the molecule ($x$-direction). Thus, the orientation of the flexible high polymer molecules in flow can be determined by photographing the small angle scattering of light.

## Summary

Small angle scattering of light by streaming flexible high polymer molecules is studied theoretically. It is concluded that the position at which the Zimm plot for infinite dilution cuts the ordinate does not change with the velocity gradient and is equal to $1/M$. The initial slope of the Zimm plot, however, varies with the velocity gradient as well as the direction of the observation plane. The quantity $g$ proportional to the initial slope varies with the rate of rotation $\Omega$ of a concentric cylinder apparatus according to the approximation equation:

$$(g/g_0-1)/\Omega=A+B\Omega$$

where $g_0$ is the value of $g$ at $\beta=0$, and $A$ and $B$ are parameters depending upon the direction of observation.

Now, when a quantity $G$:

$$G=\sqrt{(5/18)\ g\ (1+2\beta^2/3)/(1+\beta^2/3)}$$

(where $\beta$ is a quantity proportional to the velocity gradient, the proportionality constant being obtained from the value of $A$ or $B$) is measured, the value of $G_{max}$ is equal to the length of the semi-major axis of the molecule, the observation plane for this $G_{max}$ being parallel to the direction of the major axis of the molecule, while the value of $G_{min}$ is equal to the length of the semi-minor axis of the molecule, the observation plane for this value being parallel to the direction of the minor axis of the molecule.

The pattern to be obtained by photographing the small angle scattering from a streaming solution of high polymer is discussed. The pattern is expected to be an ellipse, the orientation of the pattern is expected to be rotated by exactly 90° from the orientation of the molecule.

*Faculty of the Science of Living*
*Osaka City University*
*Nishi-ku, Osaka*

# *Absorption Spectra of Metallic Complexes with Aromatic Molecules*

By Shoichiro YAMADA, Hiroshi YAMAZAKI[1], Hiroaki NISHIKAWA and Ryutaro TSUCHIDA

(Received September 30, 1959)

Ever since the first preparation of bis-(benzene)-chromium[2] and confirmation with X-rays of the sandwish structure of this compound[3], a number of metallic complexes with aromatic molecules have been synthesized. The study of these compounds is thought to be interesting because of the peculiar bonding involved in the compounds which may be quite similar to that in the ferrocene-type compounds. Many articles have been presented concerning various properties of the compounds, but there have been very few reports available which discuss their absorption spectra in relation to the bonding[4].

In the present work, the authors have determined quantitatively absorption spectra of some chromium compounds containing aromatic molecules and discussed the results of the measurements in relation to the bonding involved in the metal-arenes in general.

## Experimental

**Materials.** — Bis-(benzene)-chromium(I) iodide was prepared in yellow crystals from bis-(benzene)-chromium(0), which was obtained according to the method of Fischer[2]. Dichroism of the compound was reported in the earlier paper[4].

Bis-(toluene)-chromium(I) iodide was prepared

1) Present address: Institute of Scientific and Industrial Research, Osaka Univ., Kitahanada-cho, Sakai-shi, Osaka.

2) E. O. Fischer and W. Hafner, *Z. Naturforsch.*, **10b**, 665 (1955).

3) E. Weiss and E. O. Fischer, *Z. anorg. u. allgem. Chem.*, **286**, 142 (1956).

4) S. Yamada, H. Nakamura and R. Tsuchida, This Bulletin, **30**, 647 (1957).

by the method of Fischer and Seus[5] from bis-(toluene)-chromium(0). The yellow, prismatic crystals of the compound show a straight extinction and a slight but definite dichroism on the well-developed prism face.

Monobenzene-chromium tricarbonyl was prepared in yellow, plate-like crystals by the method of Fischer and Öfel[6] from chromium hexacarbonyl and bis-(benzene)-chromium(0) in a sealed tube. The crystals show a slight dichroism on the face, on which the dichroism measurement was carried out.

Chromium hexacarbonyl was prepared in colorless crystals according to the method of Natta et al.[7]

**Measurements.** — Dichroism in the visible and ultraviolet regions of $Cr(C_6H_6)(CO)_3$ was determined on the above-mentioned face with Tsuchida and Kobayashi's microscopic method[8] using polarized light.

Ultraviolet absorption spectra in solution were determined with a Beckman DU spectrophotometer.

Infrared spectra of the compounds in Nujol mulls and in potassium bromide discs were determined in the rock salt region with a Hilger H800 infrared spectrophotometer.

The notations in the present paper are the same as those used in the former papers of this series.

## Results and Discussion

**Ultraviolet Absorption Spectra of Metal Carbonyls.** — Absorption spectra of chromium hexacarbonyl in various solvents have been determined in the present work, and are shown in Fig. 1. The present measurement indicates that there is a very weak absorption band at about $50\times10^{13}$ $sec^{-1}$, which was not reported by the previous investigators[9]. The weak absorption band of this sort, which is observed in the absorption spectra of $Cr(C_6H_6)(CO)_3$, $[Cr(C_6H_6)_2]^+$ and $[Cr(C_6H_5CH_3)_2]^+$, may belong to a "spin-forbidden absorption band" and is discussed in the later part of the present paper.

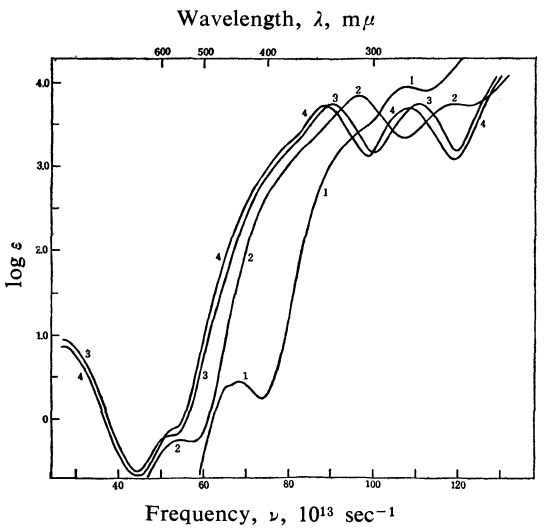



Fig. 1. Ultraviolet absorption spectra: 1, $Cr(CO)_6$ in methanol; 2, $Cr(C_6H_6)(CO)_3$ in methanol; 3, $Cr(C_6H_6)_2I$ in water; 4, $Cr(C_6H_5CH_3)_2I$ in water.

Milazzo and Scheibe[9] believed that most of the intense absorption bands of $Cr(CO)_6$ in the shorter wavelength, excepting the first inflation which they regarded as due to the carbonyl molecule itself, might be due to the decomposition products formed by photo-dissociation from the original molecule. Their conclusion was based upon the absence of a fine structure in the absorption curve. In the opinion of the present authors, however, the absence of a fine structure alone seems to be insufficient for such a conclusion. Such a flat absorption curve may be ascribed rather to the extraordinary nature of the ligand or, in other words, of the metal-to-ligand bond. Flat absorption curves similar to the spectrum of chromium hexacarbonyl are often exhibited; for example, by complexes of transition elements with ligands such as cyanide, isonitriles, ethylene, dimethylglyoxime and so forth.

Generally speaking, absorption spectra of carbonyls of transition elements may be regarded as a superposition of "ligand field absorption bands", due mainly to the metal under the field of the CO molecules, and absorption bands due to the electronic transitions which are closely related with the CO-groups under the field of the metal atom with which they are linked. Thus, the inflation at about $92\times10^{13}$ $sec^{-1}$ of $Cr(CO)_6$, which is found in Fig. 1, may be regarded as corresponding to a "ligand field band", and the absorption bands in shorter wavelength may be due to the electronic transitions closely related with the CO-groups under the field of the central metal. Absorption bands of the latter type, however, can not be ascribed to the CO-groups alone, since the present measurement shows that the absorption bands of $Cr(CO)_6$ undergo a slight "red shift" on changing a solvent from a less polar to a more polar one, whereas the carbonyl-group in ketones, for example, suffers a "blue shift"[10]. The authors are inclined to assume that the bands may most probably be due to electronic transitions from a level related principally with

5) E. O. Fischer and D. Seus, *Chem. Ber.*, **89**, 1809 (1956).
6) E. O. Fischer and K. Öfel, ibid., **90**, 2532 (1957).
7) G. Natta, R. Ercoli, F. Calderazzo and A. Rabizzoni, *J. Am. Chem. Soc.*, **79**, 3611 (1957).
8) R. Tsuchida and M. Kobayashi, This Bulletin, **13**, 619 (1938); "The Colour and the Structure of Metallic Compounds" (Kinzokukagobutsu no Iro to Kozo), Zoshindo, Osaka (1944), p. 180.
9) G. Milazzo and G. Scheibe, *Z. physhik. Chem.*, **B31**, 431 (1936).
10) G. Scheibe, *Ber.*, **58**, 587 (1925).

the metal to excited levels of the CO-groups in the metallic complex.

In connection with the chromium hexacarbonyl, it seems to be interesting to discuss here about the absorption spectrum of $Co_2(CO)_8$. Hieber et al.[11] reported the absorption spectrum of the compound in solution, only pointing out that the binuclear complex showed an absorption spectrum different from that of the corresponding mononuclear complexes. The spectra of the compound in the gaseous and solution states were later determined and discussed in combination with the infrared spectrum, the bibridged structure being regarded as most probable[12]. On re-examination of the ultraviolet spectra reported by the former investigators, it is readily recognized that $Co_2(CO)_8$ exhibits absorption in the wavelength region much longer than the corresponding mononuclear $[Co(CO)_4]^-$ ion. It is known from data so far obtained that the absorption spectrum of bibridged complexes without special interaction between the two metal atoms may be regarded as a superposition of the two mononuclear complexes of which the binuclear complex is assumed to be composed. Thus, the absorption spectrum of the bibridged, binuclear complex is known to show no greatly bathochromic displacement from the spectrum of the corresponding mononuclear complexes. This may be recognized; for example, in comparing absorption spectra of dicobalt-$\mu$, $\mu'$-diol, diplatinum-$\mu$, $\mu'$-dichloro, dipalladium-$\mu$, $\mu'$-dichloro and dichromium-$\mu$,-$\mu'$-diol complexes with the spectra of the corresponding mononuclear complexes[13]. The displacement of the absorption spectrum of $Co_2(CO)_8$ from that of $[Co(CO)_4]^-$ seems to be too great for an ordinary type of binuclear complex without special interaction. Thus, the appearance of the absorption in the enormously long wavelength region may be taken as evidence for the assumption of the direct interaction between the cobalt atoms in the $Co_2(CO)_8$.

**Ultraviolet Absorption Spectra of Bis-(benzene)- and Bis-(toluene)-chromium(I) Iodide.**— Ultraviolet absorption spectra of bis-(benzene)- and bis-(toluene)-chromium(I) iodide, which have been determined in the present work, are shown in Fig. 2 and Table I. The absorption spectrum of $[Cr(C_6H_6)_2]I$ in solution was formerly reported by the present authors, but the measurement has been extended to the longer wavelength region in the present work.

It is seen in Fig. 2 and Table I that the absorption spectrum of $[Cr(C_6H_5CH_3)_2]I$ bears

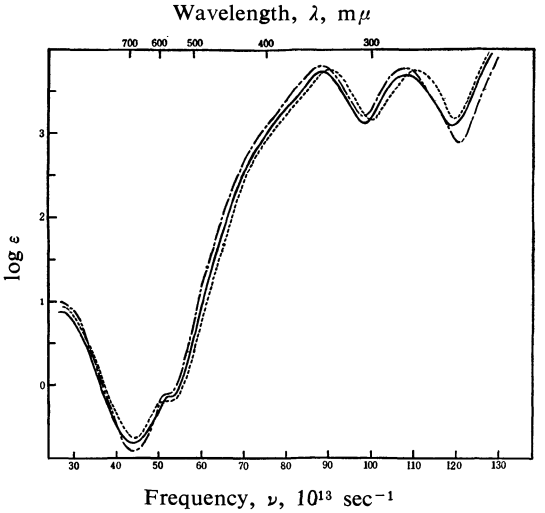



Fig. 2. Ultraviolet absorption spectra: ——, $Cr(C_6H_5CH_3)_2I$ in water; – – –, $Cr(C_6H_5CH_3)_2I$ in ethanol; ------, $Cr(C_6H_6)_2I$ in water.

a close resemblance to the spectrum of $[Cr(C_6H_6)_2]I$. Thus, between the two curves there is only a very slight difference in the wavelength and the intensity of the band maxima. In addition, the solvent effect on absorption bands is also the same for the two compounds, as seen in Table I. It may safely be concluded that the $[Cr(C_6H_5CH_3)_2]^+$ ion has the same structure and bonding as the $[Cr(C_6H_6)_2]^+$ ion. Both the complex ions may most probably have the sandwich structure.

Free benzene and toluene are known to show a characteristic band at about 260 m$\mu$ with a fine structure. On the contrary, both the $[Cr(C_6H_6)_2]^+$ and the $[Cr(C_6H_5CH_3)_2]^+$ ion are found to show no absorption bands of the above sort. The absorption bands of the chromium(I)-complexes in the corresponding wavelength region are much more intense than the band of benzene or toluene, and do not show such a fine structure as is observed in the spectra of the aromatic molecules themselves. Moreover, Bands II and III of the chromium(I)-complexes undergo a slight "blue shift", whereas the absorption band of the benzene ring with a fine structure undergoes a slight "red shift". These facts seem to show that the electronic state of the benzene rings in the chromium(I)-complexes is quite different from that of a benzene ring in the free benzene derivatives. The dichroism of the $[Cr(C_6H_6)_2]^+$ ion also seems to be consistent with this assumption[4]. If the aromaticity of the benzene rings in the chromium(I)-complex were comparatively remarkable, a dichroism similar to the benzene rings would be observed, just as in ordinary benzene derivatives. Since a dichroism of this

11) W. Hieber and K. K. Hofmann, *Z. anorg. u. allgem. Chem.*, 270, 49 (1952).
12) R. A. Friedel, I. Wender, S. L. Shufler and H. W. Sternberg, *J. Am. Chem. Soc.*, 77, 3951 (1955); J. W. Cable, R. S. Nyholm and R. K. Sheline, ibid., 76, 3373 (1954).
13) S. Yamada and R. Tsuchida, unpublished.

TABLE I. ABSORPTION MAXIMA OF CHROMIUM COMPOUNDS WITH AROMATIC MOLECULES

| Compound | Solvent | Band I′ $\nu$(log $\varepsilon$) | Band I $\nu$(log $\varepsilon$) | Band II $\nu$(log $\varepsilon$) | Band III $\nu$(log $\varepsilon$) |
|---|---|---|---|---|---|
| $[Cr(C_6H_5CH_3)_2]I$[a] | water | 27(0.82) | 75(2.9) | 88.0(3.72) | 108.1(3.69) |
| | ethanol | 27(1.00) | 76(3.0) | 87.6(3.80) | 107.8(3.77) |
| | solvent effect | very slight | very slight | slight blue shift | slight blue shift |
| $[Cr(C_6H_6)_2]I$[a,b] | water | 26(0.95) | 76(2.75) | 90 (3.76) | 110.6(3.75) |
| | solvent effect | very slight | very slight | slight blue shift | slight blue shift |
| | stronger component | | Z | Z | Z |
| $[Cr(C_6H_6)(CO)_3]$[a] | methanol | | 80(3.3) | 96.3(3.86) | 118.3(3.74) |
| | ethanol | | 80(3.4) | 96.1(3.54) | 118.1(3.67) |
| | solvent effect | | very slight | slight blue shift | slight blue shift |
| | stronger component | | Z | Z | (Z) |
| $[Cr(C_6H_5\cdot C_6H_5)_2]I$ | ethanol[c] | | | 87.7(4.01) | 120(3.39) |
| | ——[d] | | | 86.2(3.8) | 120(4.5) |
| $[Cr(C_6H_5\cdot C_6H_5)_2](OC_6H_5)$ | ethanol[c] | | | 87.0(——) | 121(——) |
| $[Cr(C_6H_6)(C_6H_5\cdot C_6H_5)]I$ | ethanol[c] | | | 87.5(——) | 111(——) |

$\nu$: $10^{13}\times sec^{-1}$

a) The present measurement.

b) Ref. 4 in the text.

c) Taken from H. H. Zeiss and M. Tsutsui, *J. Am. Chem. Soc.*, **79**, 3062 (1957).

d) Taken from Ref. 5, in which the solvent is not given. In the curve there is observed inflation at about $116\times10^{13}$ $sec^{-1}$ (log $\varepsilon$ 4.3).

sort or a band with a fine structure characteristic of the free benzene derivatives is not observed, the electronic state of the benzene rings in this chromium(I)-complex seems to be comparatively far apart from the state of the free benzene molecule. It is most likely, as is shown in the later part of this paper, that the $\pi$-electrons on the benzene rings are attracted to a considerable extent toward the central chromium ion to form firm linkage with it.

The present measurement also indicates that both $[Cr(C_6H_6)_2]I$ and $[Cr(C_6H_5CH_3)_2]I$ exhibit an absorption band (Band I′) in the near-infrared region. Since it is known that neither free benzene, toluene nor iodide ion in solution has any absorption bands of this sort, Band I′ in the infrared region can be ascribed to the $[Cr(C_6H_6)_2]^+$ and $[Cr(C_6H_5CH_3)_2]^+$ ion. Band I′ may be characteristic of the chromium(I)-complexes, since the present measurement indicates that $Cr(C_6H_6)(CO)_3$ or $Cr(CO)_6$ has no absorption bands in the corresponding wavelength region.

It is known that, when a metal ion having an unfilled *d*-electron shell forms a complex-group with ligands, a few absorption bands of moderate intensity, rather characteristic of the metal ion, must generally appear in the visible or near-ultraviolet region. In terms of the "ligand field theory", these absorption bands, Bands I and I′, may be ascribed to electronic transitions between the energy levels which are produced by splitting the lowest levels of the free metal ion under the field of the ligands. The chromium(I) ion with a $3d^5$ configuration has an $^2F_2$ level as its lowest level in the very strong ligand field[14]. Therefore, a few ligand field bands should appear corresponding to electronic transitions from the lowest level to the upper levels of the metal with the same multiplicity which might be regarded, in approximation, as produced by splitting from the original $^2I$ of the free chromium(I) ion under the very strong ligand field[14]. Band I′ in the near-infrared region and the inflation at about 76 to $78\times10^{13}$ $sec^{-1}$ (Band I( of $[Cr(C_6H_6)_2]^+$ and $[Cr(C_6H_5CH_3)_2]^+$ seem to belong to this sort of absorption bands.

The appearance of the ligand field bands, rather characteristic of the metal in ordinary metallic coordination compounds, seems to show

14) Y. Tanabe and S. Sugano, *J. Phys. Soc. Japan*, **9**, 766 (1954).

that *the linkage between chromium and the aromatic molecules in the chromium-complexes discussed here is rather similar, at least essentially, to the linkage in complexes of transition elements of a Werner-type, so that the π-electrons on the benzene rings in these compounds are withdrawn to a considerable extent toward the central chromium.*

Bands II and III may be different in their origin from the ligand field bands, judging from their intensity, which seems to be rather too great for the ligand field bands. The two bands seem to be due most probably to electronic transitions closely related with the benzene rings, but may not be regarded as belonging to those bands that are quite identical in their origin to the typical absorption band of free benzene, since Bands II and III show a slight but definite "blue shift" when the solvent is changed from a less polar to a more polar one, whereas the band of free benzene rings is known to show a slight "red shift". It may be assumed that Bands II and III are due to electronic transitions from the orbital principally related with the central metal ion to the excited levels of the benzene rings in the complexes. The fact that the difference $\nu_{III}-\nu_{II}$ is nearly constant for the $[Cr(C_6H_6)_2]^+$ and the $[Cr(C_6H_5CH_3)_2]^+$ ion may be consistent with the assumption presented in this paper about the origin of these absorption bands. The assumption also is borne out by the observation in the present work that the value $\nu_{III}-\nu_{II}$ for $[Cr(C_6H_6)_2]^+$ and $[Cr(C_6H_5CH_3)_2]^+$ is nearly equal to the value for $Cr(C_6H_6)(CO)_3$. This will be reported in the next paragraph of the present paper.

**Ultraviolet Absorption Spectra of Monobenzene-chromium(0) Tricarbonyl.** — Ultraviolet absorption spectra of $Cr(C_6H_6)(CO)_3$ have been determined and are shown in Fig. 3 and Table I. Since the chromium(0) atom in $Cr(C_6H_6)(CO)_3$ with a $3d^6$ configuration has $^1A_1$ as its lowest level in the case of very strong ligand field, the chromium(0)-complexes are expected to show a few ligand field bands which are due to electronic transitions from the $^1A_1$ level to the upper levels of the metal atom with the same multiplicity. In fact, the present measurement indicates that no absorption bands of this sort are apparently observed in the absorption curve of $Cr(C_6H_6)(CO)_3$ in solution. In the opinion of the present authors, the ligand field bands of the compound are situated possibly in the comparatively short wavelength region and seem to be covered partly under the more intense absorption bands. The inflation at about $80\times10^{13}$ sec$^{-1}$ in the curve of the solution most probably represents a ligand field band superposed by more intense absorption bands. A distinct maximum corresponding to the ligand field band is recognized at about the same wavelength in the absorption curve of the crystal, as seen in Fig. 3.

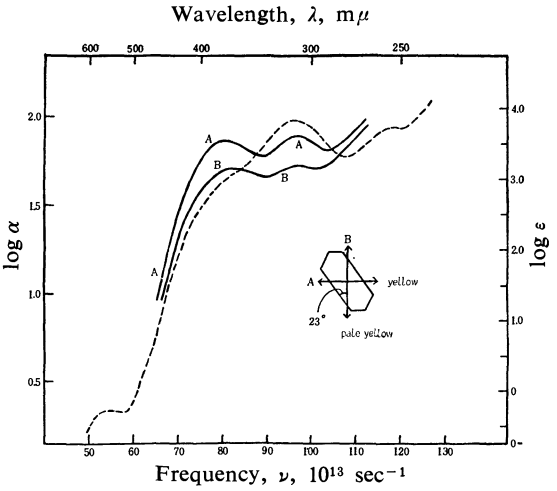



Fig. 3. Ultraviolet absorption spectra of $Cr(C_6H_6)(CO)_3$ in the crystalline state (——) and in methanol (------).

The ultraviolet absorption curve of $Cr(C_6H_6)(CO)_3$ bears a resemblance to that of the $[Cr(C_6H_6)_2]^+$ or the $[Cr(C_6H_5CH_3)_2]^+$ ion excepting that the absorption band in the infrared region, which is observed in the latter complexes, is absent in the former. Thus, the absorption bands at about 86 and $111\times10^{13}$ sec$^{-1}$ of $Cr(C_6H_6)(CO)_3$ in solution apparently correspond to Bands II and III of the $[Cr(C_6H_6)_2]^+$ or the $[Cr(C_6H_5CH_3)_2]^+$ ion, and are regarded as due to the electronic transitions from a level closely related with the central metal to two excited levels of the benzene rings in combination with the metal. It is found that *the difference $\nu_{III}-\nu_{II}$ is almost constant for $[Cr(C_6H_6)_2]I$, $[Cr(C_6H_5CH_3)_2]I$ and $Cr(C_6H_6)(CO)_3$*, it being in agreement with the present assumption about the origin of Bands II and III. The fact that $Cr(C_6H_6)(CO)_3$ shows absorption bands corresponding closely to those of $[Cr(C_6H_6)_2]I$, in spite of the oxidation state of chromium in the former compound which is different from the oxidation state in the latter, seems to indicate that *the linkage of chromium with the aromatic molecule is essentially alike in the above three compounds.* In fact, a recent study with X-rays[15] indicates that a molecule of $Cr(C_6H_6)(CO)_3$ has a structure similar to that of the $[Cr(C_6H_6)_2]^+$ ion having possibly the sandwich structure, the benzene ring in the molecule being parallel to the plane in which the three oxygen atoms are contained.

On the other hand, the absorption spectrum of

15) P. Corradini and G. Allegra, *J. Am. Chem. Soc.*, 81, 2271 (1959).

$Cr(C_6H_6)(CO)_3$ is found to be quite different from the spectrum of $Cr(CO)_6$. Thus, the absorption bands in the ultraviolet region, which are rather characteristic of the metal carbonyls such as $Cr(CO)_6$ and may be due to the electronic transitions closely related with the excited levels of the CO molecules, are missing in $Cr(C_6H_6)(CO)_3$. This fact seems to show that *the linkage of chromium with the CO molecules in* $Cr(C_6H_6)(CO)_3$ *may be different in its nature from the corresponding linkage in* $Cr(CO)_6$. In connection with this, it may be worth noting that mixed carbonyls of wolfram and iron with some isonitriles show

TABLE II. CO STRETCHING FREQUENCIES

| Compound | Freq. $cm^{-1}$ |
|---|---|
| CO | 2143[a] |
| $Cr(CO)_6$ | 2108, 2019, 2000[b] (1965, weak)[c] |
| $Cr(C_6H_6)(CO)_3$ | 1955[d] |

a) Cf. L. J. Bellamy, "The Infra-red Spectra of Complex Molecules", Methuen & Co., London (1954).
b) N. J. Hawkins, H. C. Mattraw, W. W. Sabot and D. R. Carpenter, *J. Chem. Phys.*, **23**, 2422 (1955).
c) S. L. Shufler, H. W. Sternberg and R. A. Friedel, *J. Am. Chem. Soc.*, **78**, 2687 (1956).
d) The present measurement.

TABLE III. C-C SKELETAL VIBRATIONS OF BENZENE NUCLEUS

| Compound | Skeletal vibr. $cm^{-1}$ |
|---|---|
| $Cr(C_6H_6)(CO)_3$ | 1445[a] |
| $[Cr(C_6H_6)_2]I$ | 1428[b] |
| $Fe(C_5H_5)_2$ | 1410[c] |
| $C_6H_6$ | 1500[d] |
| C-C double | 1600～1680[d] |
| C-C single | 800～1200[d] |

a) The present measurement.
b) Ref. 4 in the text.
c) L. Kaplan, W. L. Kester and J. Katz, *J. Am. Chem. Soc.*, **74**, 5531 (1952); E. R. Lippincott and R. D. Nelson, *J. Chem. Phys.*, **21**, 1307 (1953).
d) Cf. L. J. Bellamy, loc. cit.

absorption spectra similar to those of $W(CO)_6$ and $Fe(CO)_5$, respectively. The linkage of the metal with the CO molecules in these mixed carbonyls is found to be rather similar to the linkage in the corresponding metal carbonyls.

As seen in Table II, comparison of a CO stretching frequency of $Cr(C_6H_6)(CO)_3$ with the corresponding values of its related compounds gives the following order: free CO > $Cr(CO)_6$ > $Cr(C_6H_6)(CO)_3$. Since the stronger linkage between the carbon and the chromium atom would loosen the linkage between the carbon and the oxygen atom more greatly, the above frequency shift seems to show, at least qualitatively, that *the metal-to-carbon bond in* $Cr(C_6H_6)(CO)_3$ *may be stronger than the corresponding bond in* $Cr(CO)_6$.

As seen in Table III, comparison of a skeletal C–C vibration of a benzene nucleus gives the following order: free $C_6H_6$ > $Cr(C_6H_6)(CO)_3$ > $[Cr(C_6H_6)_2]^+$. Since the displacement of the skeletal C–C vibration from the vibration of free $C_6H_6$ is less in $Cr(C_6H_6)(CO)_3$ than in $[Cr(C_6H_6)_2]^+$, *the linkage of the chromium atom with the benzene molecule may be stronger in the latter than in the former.*

The conclusion that the linkage between the chromium and the carbon of CO is stronger in $Cr(C_6H_6)(CO)_3$ than in $Cr(CO)_6$ is found to be in accordance with the fact that the Cr-C(in CO) distance is shorter in $Cr(C_6H_6)(CO)_3$[15] than in $Cr(CO)_6$[16]. It may also be worth noting that the Cr-C(in $C_6H_6$) distance is longer in $Cr(C_6H_6)(CO)_3$ than in the neutral molecule of $Cr(C_6H_6)_2$[17].

**Dichroism of Monobenzene-chromium Tricarbonyl.**—The results of the dichroism measurement are shown in Fig. 3. A preliminary report on the crystal structure of $Cr(C_6H_6)(CO)_3$ has recently been published, but the more detailed description of the crystal structure is not available. Comparison of the absorption spectra of $Cr(C_6H_6)(CO)_3$ with the spectra of $[Cr(C_6H_6)_2]I$, however, has enabled one to derive the main characteristics of the component absorptions of the former as referred to the principal axes of the molecule. Actually the molecules are not arranged in the crystal with their corresponding molecular axes completely parallel to each other. However, the dichroism of the crystal, as determined in the present work, may be thought to represent the main features of the component absorptions of the molecule.

The absorption band at about $80\times10^{13}$ $sec^{-1}$ of the crystal probably corresponds to the inflation at about the same frequency in the absorption curve of the compound in solution. This band may be regarded as corresponding to the absorption band at about $70\times10^{13}$ $sec^{-1}$ of $[Cr(C_6H_6)_2]I$ in the crystalline state, and may be assigned to one of ligand field bands. It is to be noted that Band II is found to be much weaker in the crystalline state than in solution, as was also found to be the case with $[Cr(C_6H_6)_2]I$.

16) L. O. Brockway, R. V. G. Ewens and M. W. Lister, *Trans. Faraday Soc.*, **34**, 1350 (1938).
17) E. Weiss and E. O. Fischer, *Z. anorg. u. allgem. Chem.*, **286**, 142 (1956).
18) The Z-direction refers to the threefold axis of the molecule of $Cr(C_6H_6)(CO)_3$.

The dichroism for Bands I and II of $Cr(C_6H_6)(CO)_3$ is found to be quite similar to that of $[Cr(C_6H_6)_2]I$ on suitable assumption of the crystal structure. Thus, if it is assumed that A- and B- absorptions in Fig. 3 represent, respectively, the main features characteristic of Z- and X, Y-absorption of the complex-molecule[18], the dichroism of $Cr(C_6H_6)(CO)_3$ seems to be coincident with the dichroism of $[Cr(C_6H_6)_2]^+$. The following relationship may be derived on the dichroism of $[Cr(C_6H_6)_2]I$ and $Cr(C_6H_6)(CO)_3$.

*Z-absorption is stronger than X, Y-absorption for Bands I and II.*

The absorption spectra and the dichroism of these compounds are evidently different from those of free benzene rings. If much aromaticity were kept in the benzene rings within the chromium-complexes, a dichroism similar to the dichroism of the free benzene rings would be observed, just as in most benzene derivatives. Since the dichroism characteristic of the free benzene rings or a band with a fine structure is not observed, the electronic state of the benzene rings in these compounds seems to be far from the state of the free benzene molecule.

The observation that Z-absorption is stronger than X, or Y-absorption for Bands I and II seems to be in good agreement with the concept that *the $\pi$-electrons on the benzene rings in $Cr(C_6H_6)(CO)_3$ are strongly withdrawn toward the chromium atom to form linkage with it.*

A similar type of dichroism was formerly reported with bis-(cyclopentadienyl)-iron(II) and cobalt(III) complexes, where Z-absorption is stronger than X- and Y-absorptions of the complexes for the two absorption bands in the long wavelength region[19]. This relationship also was taken as evidence that the $\pi$-electrons on the pentagonal rings are withdrawn considerably toward the metal atom to form firm bonds with it.

**Weak Absorption Bands in the Long Wavelength Region.**—The present measurement indicates that $Cr(CO)_6$, $[Cr(C_6H_6)_2]^+$ and $[Cr(C_6H_5CH_3)_2]^+$ all display a very weak band system in the long wavelength side. A part in the shorter wavelength region of the weak band is covered by much stronger absorption bands. It is theoretically known that the electronic transitions between levels with different multiplicities are strictly forbidden, appearing in most cases as very weak absorption bands. Thus, chromium(III)-complexes are known to display a spin-forbidden band with very small intensity to the long wavelength side of the ligand field absorption band[20]. In a similar way, the very weak absorption band systems of $Cr(CO)_6$ or $[Cr(C_6H_6)_2]^+$ may most probably correspond to the spin-forbidden bands which are due principally to chromium(0) or chromium(I). The spin-forbidden bands may tentatively be assigned to electronic transitions from the ground state $^1A_1$ to $^3F_1$ and $^3F_2$ in the case of chromium(0), and to transitions from the ground state $^2F_2$ to $^4F_1$ and $^4F_2$ in the case of chromium(I).

The solvent effect upon this type of the weak absorption bands has been examined, and is shown in Table IV. It is found that the band undergoes a slight "red shift" with the compounds examined here.

TABLE IV. SPIN-FORBIDDEN ABSORPTION BANDS

| Compounds | Solvent | $\nu$ | log $\varepsilon$ |
|---|---|---|---|
| $[Cr(C_6H_6)_2]I$ | water | 52 | $\bar{1}.80$ |
| $[Cr(C_6H_5CH_3)_2]I$ | water | 52.5 | $\bar{1}.90$ |
| | ethanol | 53 | $\bar{1}.90$ |
| $Cr(C_6H_6)(CO)_3$ | methanol | 53-4 | $\bar{1}.8$ |
| | ethanol | 55-6 | — |
| $Cr(CO)_6$ | methanol | 67.5 | 0.47 |
| | ethanol | 68.5 | 0.45 |

$\nu$: $10^{13}$ $sec^{-1}$

The present measurement also indicates that the spin-forbidden bands are displaced to the shorter wavelength region, as the ligand field bands are displaced to the same direction in the following series: $[Cr(C_6H_6)_2]^+$, $Cr(C_6H_6)(CO)_3$, $Cr(CO)_6$.

**Ultraviolet Absorption Spectra of Hein's Polyphenyl-chromium Compounds.**— Hein[21] reported a number of polyphenyl chromium compounds with general composition of $Cr(C_6H_5)_n$ and $Cr(C_6H_5)_n$ X, where $n$ is equal to 3 or 4, and X denotes an anion such as iodide and anthranilate. It was only after the discovery of numerous compounds with a ferrocene-like structure that the suggestion was presented that Hein's compounds might contain chromium(I)-complexes having a sandwich structure with benzene, biphenyl, terphenyl or similar aromatic molecules[22]. Identificaion of one of Hein's compounds, $Cr(C_6H_5)_4I$, with the complex $[Cr(C_6H_5 \cdot C_6H_5)_2]I$, which was prepared from chromium(III) chloride, aluminum and biphenyl as starting materials, was made by comparison of their infrared and ultraviolet absorption spectra, X-ray absorption edges and magnetic properties[5]. Absorption spectra as well as other properties

19) S. Yamada, A. Nakahara and R. Tsuchida, *J. Chem. Phys.*, **22**, 1620 (1954); This Bulletin, **28**, 465 (1955).
20) C. K. Jørgensen, *Acta Chem. Scand.*, **8**, 1502 (1954).
21) F. Hein et al., *Ber.*, **61**, 730 (1928); ibid., **62**, 1151 (1929); *Z. anorg. u. allgem. Chem.*, **273**, 209 (1953); etc.
22) H. H. Zeiss and W. Herwing, *Ann.*, **606**, 209 (1957); H. H. Zeiss and M. Tsutsui, *J. Am. Chem. Soc.*, **79**, 3062 (1957); H. H. Zeiss, M. Tsutsui and L. Onsager, "Abstr. 126th Meeting *Am. Chem. Soc.*", New York (1954), p. 29.

of Hein's compounds were formerly reported, but the detailed discussion about ultraviolet spectra of the compounds has not been presented up to the present. In the following, a brief discussion will be given about the absorption spectra of these compounds on the basis of the relationships which have been obtained in the present work.

It was reported in the earlier part of the present paper that the benzene rings in combination with chromium in the compounds having linkage characteristic of the sandwich molecules show two absorption bands, which are due presumably to electronic transitions from an orbital concerned mainly with the central chromium to the two excited levels of the benzene rings. In support of this idea seems to be the fact that the frequency difference between two such transitions is nearly constant for the chromium compounds with benzene rings.

When benzene is replaced by biphenyl in a similar type of compound, a similar type of relationship may exist about the frequency difference, if the sandwich structure is kept in the biphenyl-compounds. Thus, the magnitude of the corresponding frequency difference may be constant for the compounds of chromium with biphenyl, but different from the magnitude in the case of the chromium(I)-compounds with benzene rings. Based on the concept presented here, absorption spectra of Hein's polyphenyl compounds of chromium(I) seem to be understood well if it is assumed that they contain chromium(I)-complexes with aromatic molecules, having the sandwich structure of a ferrocene-type.

In the case of $[Cr(C_6H_6)(C_6H_5\cdot C_6H_5)]^+$, for example, which has both benzene and biphenyl in combination with chromium(I), electronic transitions to the two excited levels of benzene and to a few levels of biphenyl may be possible, their superposition being observed in the absorption curve of this compound. In fact, $\nu_{III}-\nu_{II}$ obtained from the observed curve[22] of $[Cr(C_6H_6)(C_6H_5\cdot C_6H_5)]^+$ is found to be nearly equal to the value for $[Cr(C_6H_6)_2]^+$, as seen in Table I. This observation may be readily understandable on the basis of the assumption presented in this paper. Thus, if it is assumed that the maximum frequency of Band III, $\nu_{III}$, of the chromium compound is greater with biphenyl than with benzene rings, the difference $\nu_{III}-\nu_{II}$, which is obtained directly from the absorption spectrum of $[Cr(C_6H_6)(C_6H_5\cdot C_6H_5)]^+$, may correspond to the frequency difference between the two excited levels of the benzene ring in combination with the chromium. This is in agreement with the above-mentioned observation. The observation that $[Cr(C_6H_5\cdot C_6H_5)_2]^+$ shows larger $\nu_{III}-\nu_{II}$ than $[Cr(C_6H_6)_2]^+$ does may be understood in a similar way.

The fact that the absorption spectra of Hein's compounds may be explained in this way seems to indicate that *Hein's polyphenyl chromium-(I)-compounds have complex-ions with a sandwich structure similar to that of* $[Cr(C_6H_6)_2]^+$ *or* $[Cr(C_6H_5CH_3)_2]^+$.

It is to be noted that Hein's chromium(I)-complexes all show Band II at about 86 to $88\times10^{13}$ $sec^{-1}$, which is very close to the value for Band II of $[Cr(C_6H_6)_2]^+$, $[Cr(C_6H_5CH_3)_2]^+$ and $Cr(C_6H_6)(CO)_3$. This seems to indicate that *the linkage of the aromatic molecules with the central chromium is remarkably alike in these complexes.*

It was found in the preceding part of the present paper that the chromium(I)-complexes with aromatic molecules exhibit a very weak absorption band, due possibly to spin-forbidden transitions, in the long wavelength region and one of the ligand field bands in the near-infrared. The former investigators did not report a very weak absorption band in the visible or an absorption band in the infrared region for Hein's polyphenyl compounds of chromium(I). In the opinion of the present authors, however, there is good reason to expect that the "polyphenyl compounds of chromium(I)" show a spin-forbidden absorption band at about 50 to $55\times10^{13}$ $sec^{-1}$, and two of the ligand field bands, one in the infrared and the other as inflation at about $80\times10^{13}$ $sec^{-1}$, just like the bis-(benzene)- and bis-(toluene)-chromium(I) complexes.

**General Aspects of Absorption Spectra of Metal-arenes.**—In the next place, the authors will discuss the general aspects of absorption spectra of metallic complexes with aromatic molecules and related compounds on the basis of these measurements with the aid of the data by the former investigators. It may be assumed that these compounds in general display "ligand field absorption bands", due mainly to the central metal under the strong ligand field surrounding it, and absorption bands corresponding to the electronic transitions to the excited levels of the ligand groups in combination with the metal. A part of the former is often covered by more intense absorption of the latter type. The absorption bands of the latter type seem to be rather dependent upon the ligand and sensitive to the nature of its linkage with the metal. Thus, in the case of the cyclopentadienyl-radical, the latter bands are found to undergo a marked shift as the central metal is exchanged, while little change in this type of bands is given rise to when a benzene molecule combined with chromium is replaced by a biphenyl molecule

in the chromium-arenes.

Besides these two types of absorption bands, there is usually observed a very weak absorption band system in the long wavelength region, corresponding to spin-forbidden bands due mainly to the central metal. A part of this band system is also covered by the other absorption bands with much greater intensity.

With an ordinary type of metallic complex, the order of ligands is known as the "spectrochemical series"[23], which represent the decreasing order as to the magnitude of their hypsochromic effect on the ligand field bands of the metallic complexes. In the following, discussion will be undertaken concerning metallic compounds with ligands which are coordinated to a metal atom through their carbon atom. Unambiguous assignments of absorption bands to particular electronic transitions are sometimes quite difficult, but a general trend concerning the above effect may be readily derived. Thus reviewing a series of compounds, $Cr(CO)_6$, $Cr(C_6H_6)(CO)_3$ and $Cr(C_6H_6)_2$, the authors may be able to obtain the following order as to the hypsochromic effect of the ligands: $CO > C_6H_6$. In a similar way, it is easily shown that CO has a greater hypsochromic effect than a cyclopentadienyl-radical: $CO > C_5H_5^-$. It is thus seen that CO stands extremely high in the spectrochemical series, probably even higher than $CN^-$. Comparison also reveals that $C_5H_5^-$ is very close to, but only a little higher than, $C_6H_6$ in the spectrochemical series. In summary, the following order may be derived: $CO > C_5H_5^- > C_6H_6$.

It is interesting to note that the following order also is derived from the previous data[24] about mixed carbonyls of iron and wolfram: $CO > CN\cdot CH_3 > CN\cdot C_6H_5$. Comparison of the isonitriles with $C_6H_6$ and $C_5H_5^-$ as to their hypsochromic effect seems to be difficult for the present.

With the same ligands, the order of transition metal elements as to their hypsochromic effect may also be derived in a similar way. With ligands such as CO, $C_5H_5^-$ and $C_6H_6$, light absorption is found to be displaced to a shorter wavelength, as the authors go down the periodic table for elements belonging to one and the same sub-group. More or less marked hypsochromic shift is observed when a metal atom is replaced by another which stands lower in the same sub-group for a series of elements such as (Cr, Mo, W), (Fe, Ru, Os) and (Co, Rh, Ir). Absorption maxima of all these compounds are not reported, but a difference in color seems to indicate the above trend without exception. The same trend was reported with many other ligands of an ordinary type[25].

## Summary

Ultraviolet absorption spectra of $Cr(CO)_6$, $Cr(C_6H_6)(CO)_3$, $[Cr(C_6H_6)_2]I$ and $[Cr(C_6H_5CH_3)_2]I$ have been determined in various solvents. Dichroism in the visible and ultraviolet region of $Cr(C_6H_6)(CO)_3$ has been determined at room temperature by Tsuchida and Kobayashi's microscopic method with a single crystal of the compound.

The absorption spectrum of $Cr(C_6H_6)(CO)_3$ shows main features similar to those of the spectrum of the $[Cr(C_6H_6)_2]^+$ ion.

These compounds all show a weak absorption band to the long wavelength side of the intense absorption bands.

The results of the measurements have been discussed in relation to the bonding involved in these compounds. Discussion also has been undertaken about Hein's polyphenyl-compounds of chromium(I) on the basis of the present measurements. Absorption spectra of Hein's compounds of chromium(I) seem to be in agreement with the assumption of the sandwich structure.

*Department of Chemistry*
*Faculty of Science*
*Osaka University*
*Nakanoshima, Osaka*

23) R. Tsuchida, This Bulletin, 13, 395 (1938); *J. Chem. Soc. Japan, Pure Chem. Soc.* (*Nippon Kagaku Zasshi*), 59, 586, 731, 819 (1938); R. Tsuchida and Y. Shimura, This Bulletin, 25, 49 (1953).

24) W. Hieber and D. von Pigenot, *Chem. Ber.*, 89, 616 (1956).

25) C. K. Jørgensen, "Technical Report on Absorption Spectra of Complexes of Heavy Metals", U. S. Depratment of the Army, Contract No. DA-91-508-EUC-247, FTR No. 1 (1958), p. 50.

# *Vinyl Polymerization. XLIII. Polymerization of Styrene with Vinylmagnesium Chloride*

By Minoru IMOTO and Masayoshi KINOSHITA

(Received September 21, 1959)

It was reported by Beaman[1] and others that Grignard reagents could polymerize some vinyl monomers. Recently, a synthetic method of Grignard reagent from vinyl chloride was published[2]. In this paper the authors prepared vinylmagnesium chloride after Ramsden[2] and carried out the kinetic study of the polymerization of some vinyl monomers.

## Experimental

**Materials.** — Commercial tetrahydrofuran (THF) was refluxed over potassium hydroxide and then over sodium. After distillation it was stored in the presence of lithium aluminum hydride. Before, use, it was redistilled in a stream of nitrogen. Commercial vinyl chloride was dried with potassium hydroxide, calcium chloride and then with phosphorus pentoxide.

**Vinylmagnesium Chloride.** — Vinyl chloride gas was passed into THF (507 g.) until 144 g. were absorbed. Ethyl bromide (2 ml.) was dropped into a mixture of 44 g. of magnesium turnings and 15 ml. of the vinyl chloride-THF solution was then added as rapidly as possible. After the reaction was completed, excess vinyl chloride was distilled out and the unreacted magnesium was filtered off. The homogeneous solution of vinylmagnesium chloride was stored in a brown bottle. The Grignard solution thus obtained had a concentration of 2.07 mol./l. by Gilman's titration[3] (81% yield). After a month, the concentration decreased to 2.01 mol./l. From these values it was considered that the concentration of the reagent might be kept constant throughout the experiment.

**Change of Vinylmagnesium Chloride into Acrylic Acid.** — A solution of vinylmagnesium chloride in THF was added into a large excess of powdered dry ice. After being acidified, the organic layer was distilled to give an acid, having a stimulus odor, and boiling at 84~88°C/82 mmHg, ($n^{20}=1.4223$). The acid could be polymerized easily. From these facts, it was confirmed that the acid was acrylic acid (in literature 4, $b.p._{88}=81°C$, $n^{20}=1.4224$) and the Grignard reagent was vinylmagnesium chloride.

**Polymerization.**—Styrene and methyl methacrylate were polymerized in a sealed glass tube, and acrylonitrile in a 3-necked flask equipped with a stirrer and a nitrogen inlet tube.

In the case of glass tube method, the tube was first substituted with dry nitrogen and fed with Grignard reagent from a burette, into which the reagent had been fed with the aid of nitrogen pressure. Then, the monomer and solvent were charged. The usual degassing procedure followed. These tubes were set in a water bath at constant temperature and shaken during polymerization. The reacted mixture was poured into methanol, containing excess hydrochloric acid. Polystyrene and polymethyl methacrylate were purified by reprecipitation from benzene solution by methanol. To obtain a sample of polymethyl methacrylate for infrared absorption spectrum, a freezing technique was used.

When acrylonitrile was contacted with the Grignard reagent, so much heat was evolved that the following procedure was used. To a cold mixture of Grignard reagent and a large volume of solvent (THF), the monomer was added through a long glass tube surrounded by dry ice. These operations were carried out under the atmosphere of dry nitrogen.

The intrinsic viscosities shown in Table I are the values at 30°C measured in benzene solution, using a Ubberohde viscometer.

## Results and Discussion

**Polymerization of Vinylmagnesium Chloride.** —As shown in Table I, vinylmagnesium chloride could not be polymerized by the usual methods.

TABLE I. PORYMERIZATION OF VINYLMAGNESIUM CHLORIDE

| Initiator | VMgCl* ml. | THF** ml. | $T$°C | Time hr. | Polymer |
|---|---|---|---|---|---|
| AIBN*** | 50 | 0 | 60 | 10 | None |
| BPO**** | 50 | 0 | 60 | 10 | None |
| None | 50 | 0 | 60 | 10 | None |
| UV 3600 A | 50 | 0 | 30 | 10 | None |

* Vinylmagnesium chloride
** Tetrahydrofuran
*** 2,2'-Azobisisobutylonitrile
**** Benzoylperoxide

**Copolymerization of Vinylmagnesium Chloride with Styren or Methyl Methacrylate.**—The white polymers obtained from the systems consisting of styrene and vinylmagnesium chloride had the same analytical results with styrene or methyl methacrylate homopolymer within the limit of experimental error (Table II). To introduce carboxyl groups to the copolymer, the polymerization mixtures were poured onto a large

1) R. G. Beaman, *J. Am. Chem. Soc.*, **70**, 3115 (1949).
2) H. E. Ramsden, *J. Org. Chem.*, **22**, 1602 (1957).
3) H. Gilman, *J. Am. Chem. Soc.*, **51**, 1676 (1929).

TABLE II. POLYMERIZATION OF SOME VINYL MONOMERS WITH VINYLMAGNESIUM CHLORIDE

| VMgCl | Monomer | | THF | Temp. | Time | Polymer | | |
|---|---|---|---|---|---|---|---|---|
| ml. | ml. | | ml. | °C | hr. | g. | Yield, % | [η]* |
| 60 | Vinylchloride | 10** | 50 | 30 | 20 | | | |
| 90 | Styrene | 50 | 0 | 50 | 6 | 48 | 100 | 0.136 |
| 5 | Styrene | 10 | 0 | 50 | 6 | 8.7 | 96 | |
| 0 | Styrene | 10 | 5 | 50 | 6 | 0.16 | 1.7 | 2.9 |
| 0 | Styrene | 15 | 0 | 50 | 6 | 0.1 | 0.7 | 4.7 |
| 6 | Styrene | 5 | 0 | 50 | 5 | 2.9 | 65 | 0.26 |
| 30 | Methylmethacrylate | 20 | 50 | −60 | 18 | 6.8 | 36 | 2.2 |
| 30 | Methylmethacrylate | 20 | 50 | 10 | 18 | 1.3 | 7.0 | 2.6 |
| | | | | | | | | N %*** |
| 20 | Acrylonitrile | 50 | 50 | 30 | **** | 9.3 | 23 | 19.49 |
| 10 | Acrylonitrile | 10 | 0 | 30 | | 4.4 | 55 | 16.83 |
| 30 | Acrylonitrile | 20 | 50 | −10 | | 8.4 | 52 | 13.07 |

* [η] was measured in benzene at 30°C using a Ubberohde viscometer.
** Under UV irradiation, the mixture gave needle crystals gradually but no polymer.
*** By the Kjeldahl method. Calcd. value is 26.40%.
**** Dropping acrylonitrile into Grignard mixture, yellow polymer precipitated immediately.

*Polystyrene* Found: C, 92.09; H, 8.12.
Calcd. for $C_8H_8$: C, 92.27; H, 7.74%.
*Polymethylmethacrylate* Found: C, 59.78; H, 8.27.
Calcd. for $C_5H_8O_2$: C, 59.98; H, 8.05%.

excess of dry ice, acidified with hydrochloric acid and the polymer was reprecipitated. But the infrared absorption spectra of the polymers had no absorption characteristic of the hydroxyl group in carboxylic acid and were identical to those of each homopolymer.

**Polymerization of Vinyl Chloride Initiated by Vinylmagnesium Chloride.** — The mixture of vinylmagnesium chloride and vinyl chloride was sealed in a glass tube and irradiated by ultraviolet ray of 3600 Å but no polymer was obtained.

**Polymerization of Acrylonitrile Initiated by Vinylmagnesium Chloride.** — Acrylonitrile polymerized vigorously to yellow powder which contained a much smaller quantity of nitrogen than polyacrylonitrile.

**Polymerization of Styrene Initiated by Vinylmagnesium Chloride.**—In the presence of vinylmagnesium chloride styrene hardly polymerized at room temperature, but did so easily above 40°C. Fig. 1 shows the process of polymerization. As the concentration of vinylmagnesium chloride increased, the rate of polymerization also increased. Figs. 2—4 are the time-conversion curves at 50, 60 and 70°C, respectively. Fig. 5 shows the dependence of rate on monomer concentration. At a monomer concentration, the rate becomes maximum but the reason is not clear.

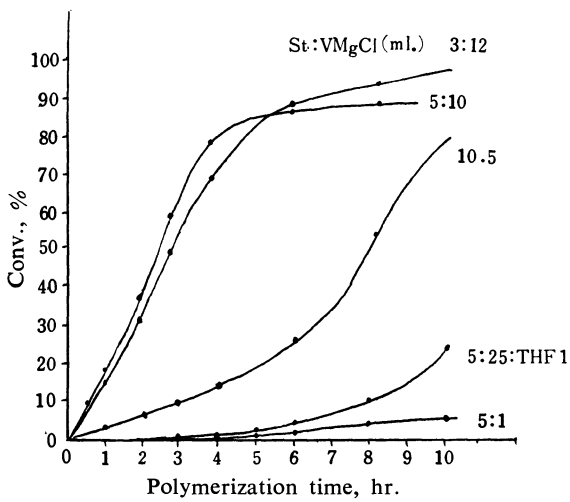



Fig. 1. Polymerization of styrene at 60°C.

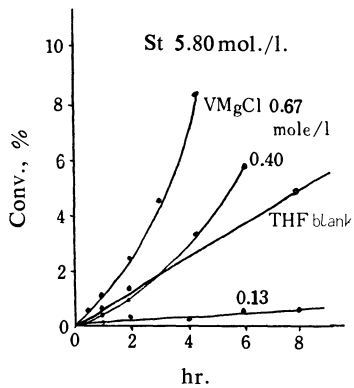



Fig. 2. Polymerization of styrene at 50°C.

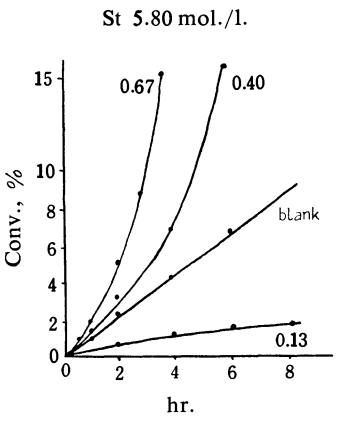



Fig. 3. Polymerization of styrene at 60°C.

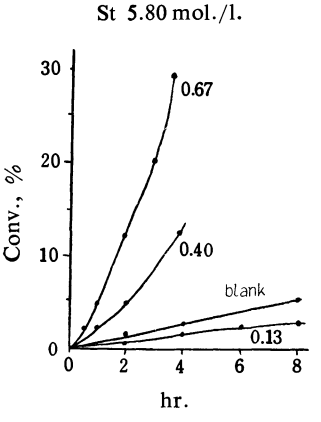



Fig. 4. Polymerization of styrene at 70°C.

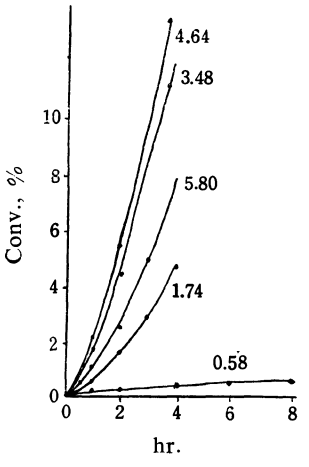



Fig. 5. Polymerization of styrene at constant initiator concentration at 50°C.

The rate of the polymerization of styrene in the absence of vinylmagnesium chloride was abnormally large, as shown in Figs. 2—4, as "blank test". The rapid rate was caused by the addition of THF instead of vinylmagnesium chloride solution. It may be considered that THF included THF-peroxide. In order to testify to this consideration, the THF above used was compared with oxygen absorbed THF. Oxygen was bubbled into THF under the irradiation of ultraviolet ray at room temperature for three days. The effects of the treatment was shown in Fig. 6. When the quantity of vinylmagnesium chloride was small, the rate decreased greatly. This was due to the consumption of the activities of Grignard reagent and peroxide by the mutual reaction.

Observation on the relation between the rate of polymerization and the concentration of vinylmagnesium chloride was carried out. As the curves for time vs. conversion were not straight, the conversions after two hours were plotted against the concentration of vinylmagnesium chloride. Straight lines were obtained as shown in Fig. 7. From the slope of these lines the following equation was derived.

$$Rp = k[C]^{1.4}$$

The overall activation energy of polymerization was about 12 kcal./mol. (Fig. 8).

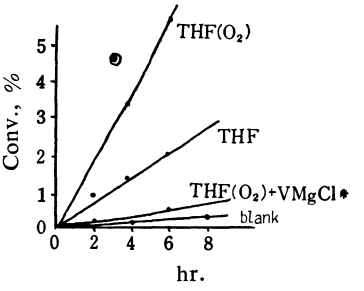



Fig. 6. Polymerization of styrene with $O_2$ treated tetrahydrofuran.
Double circle shows one carried out with the oily residue which was obtained by evaporation of THF treated with $O_2$.
* About 0.5 ml. VMgCl to 5 ml. THF($O_2$).

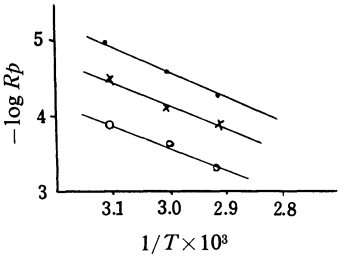



Fig. 7. The relation between the rate of polymerization and the concentration of vinylmagnesium chloride.
● 50°C × 60°C ○ 70°C

4) C. Moreau, M. Murat and N. Tampier, *Ann. chim.*, [9], 15, 221 (1921).
5) R. Criege, *Angew. Chem.*, 62, 120 (1950).

TABLE III. COPOLYMERIZATION OF STYRENE WITH METHYLMETHACRYLATE

| No. | Styrene | | Methylmethacrylate | | Styrene | Time | Polymer | Styrene mol. % in copolymer |
|---|---|---|---|---|---|---|---|---|
| | ml. | mol.×10² | ml. | mol.×10² | mol. % | min. | g. | |
| 1 | 10 | 8.70 | 0 | 0 | 100 | 710 | 0.134 | 100 |
| 2 | 9.5 | 8.26 | 0.53 | 0.49 | 94.4 | 570 | 0.029 | 70.46 |
| 3 | 9 | 7.83 | 1 | 0.94 | 89.3 | 380 | 0.088 | 19.75 |
| 4 | 8 | 6.96 | 2 | 1.87 | 78.8 | 150 | 0.141 | 4.80 |
| 5 | 7 | 6.09 | 3 | 2.80 | 68.5 | 70 | 0.339 | 4.80 |
| 6 | 6 | 5.22 | 4 | 3.74 | 58.3 | 60 | 0.492 | 2.50 |
| 7 | 5 | 4.35 | 5 | 4.67 | 48.2 | 60 | 0.612 | 2.09 |
| 8 | 4 | 3.48 | 6 | 5.61 | 38.3 | 50 | 1.404 | 0.71 |
| 9 | 3 | 2.61 | 7 | 6.54 | 28.5 | 50 | 1.556 | 2.47 |
| 10 | 2 | 1.74 | 8 | 7.48 | 18.9 | 50 | 1.108 | 0.48 |
| 11 | 1 | 0.87 | 9 | 8.41 | 9.38 | 20 | 0.996 | 1.99 |
| 12 | 0 | 0 | 10 | 9.36 | 0 | 20 | 1.095 | 1.58 |

Polymerization temperature ; 10°C.
Grignard concentration ; 0.67 mol./l.
Styrene contents in copolymer were calculated from the carbon contents.

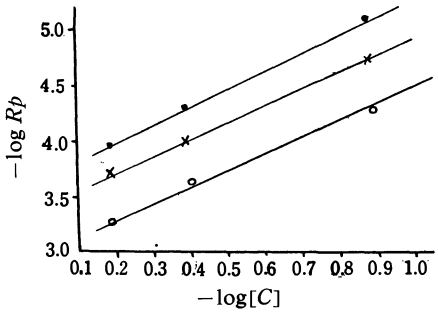



Fig. 8. Overall activation energy of polymerization.
● 50°C × 60°C ○ 70°C

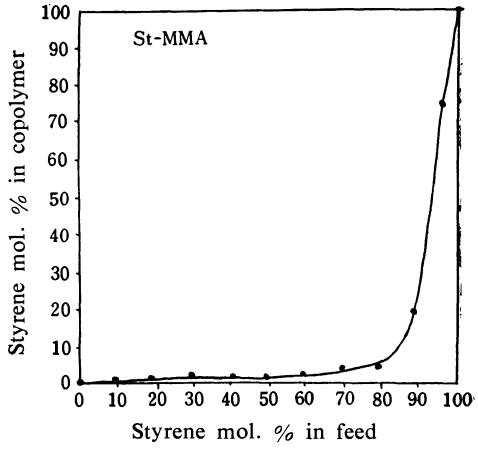



Fig. 9. The composition of styrene-methyl methacrylate copolymer.

**Copolymerization of Styrene with Methyl Methacrylate.**—In 1949, Beaman stated that the polymerization initiated by Grignard reagents proceeded through anionic mechanism. This idea has been generally accepted. To confirm the anionic mechanism in these systems, the authors carried out the copolymerization of styrene with methyl methacrylate at 10°C. From the carbon contents of copolymers their composition were calculated and plotted against the compositions in feed (Table III and Fig. 9). It was confirmed from the results in Fig. 9 that the polymerization initiated by vinyl magnesium chloride proceeded by anionic mechanism.

By the Beilstein test, it was found that no chlorine existed in the molecule of copolymer.

From the results stated above, it was possible to state that the order of the rate of polymerization was as follows:

acrylonitrile > methyl methacrylate ≫ styrene > vinyl chloride = 0

*Department of Applied Chemistry*
*Faculty of Engineering*
*Osaka City University*
*Kita-ku, Osaka*

# *The Behavior of Fission Products Captured in Graphite Powder by Nuclear Recoil. I. The Stability of the Fission Products toward Nitric Acid Solution*

By Toshio NAKAI, Seishi YAJIMA, Koreyuki SHIBA, Jiro OSUGI and Daisaburo SHINODA

(Received September 22, 1959)

In his pioneering study McMillan[1] placed a thin film of uranium oxide powder between filters or cigarette papers and irradiated it with cyclotron neutrons. He found that most of the fission products recoiled out of the film and were captured in the paper. This separation made it possible to identify the strong activity of neptunium-239 with a half life of 2.3 days that had been left behind.

If a fission reaction is caused to proceed in particles of uranium oxide with maximum dimensions smaller than the minimum range* of the fission products, these products will probably recoil out of the uranium oxide. On the other hand, heavier nuclei formed by neutron capture and beta decay will have a much shorter range and remain within the original particles. This means that in a suitable heterogeneous system the fission products will be completely separated from the actinide elements without complicated chemical treatment. Since McMillan's work appeared in a journal, several investigators studied the separation of the fission products and the actinide by nuclear recoil using several kinds of heterogeneous systems.

The authors have been investigating the possibility of the utility of the dispersion-type nuclear fuel element which consists of a mixture of graphite and uranium dioxide. In such a fuel, the behavior of fission products is most characteristic compared with the other solid-type nuclear fuels. If the dimensions of uranium oxide powder are smaller than the minimum range of fission products and the weight ratio of graphite powder to uranium oxide powder is great enough to prevent the penetration of the fission fragments into the neighboring uranium oxide particles and if uranium oxide particles are uniformly dispersed in graphite powder, the fission products produced in uranium oxide powder will be thoroughly recoiled out of them and captured by graphite powder. In the previous paper[2], it was made obvious that when the weight ratio of graphite (particle size is about 50 microns) to uranium dioxide (particle size is about 0.1 microns) was 10, approximately 70% of the overall fission product activity remained in graphite powder and that when the ratio was 30, approximately 95% was captured. Mixtures of graphite and uranium dioxide were irradiated with JRR-1 neutrons (Japan Research Reactor-1, a water boiler type) and after the addition of saturated zinc bromide solution (hydrochloric acid was slightly added), these mixtures were centrifuged. The graphite powder of these mixtures gathered on the upper layer and the uranium oxide powder settled at the bottom. The distribution of the fission products in these fractions was determined using gamma ray spectrometry. From the results, the possibility of a brief reprocessing of the dispersion-type spent fuel was suggested.

The present study was undertaken to investigate the variation of the gross gamma ray spectra of the fission products captured in graphite powder at various cooling times after irradiation, and the stability of the fission products captured in graphite toward nitric acid of several different concentrations at varying durations of immersion at a constant temperature.

## Experimental

**The Gross Gamma Ray Spectra of the Fission Products Captured in Graphite Powder.** — *Procedure 1.*—Twenty milligrams of uranium dioxide (particle size, about 0.1 microns) was mixed with 600 mg. of natural graphite prepared by the Nippon Carbon Co., (particle size, about 50 microns), and the mixture was irradiated in the No. 16 experimental hole of JRR-1 under a thermal neutron flux of about $5\times10^{11}$ neutrons/cm$^2$ sec. for about three minutes. The irradiated mixture was transferred to a centrifuging tube with 70 ml. of a saturated zinc bromide solution which contained a small amount of hydrochloric acid. After centrifugal separation, the graphite powder fraction which was collected on the upper side was transferred into a polyethylene tube (1.5 cm. in diameter and 7 cm. in length) and was gamma-assayed by the RCL

1) E. McMillan, *Phys. Rev.*, **55**, 510 (1939).

* The minimum range of the fission products in uranium dioxide is 8 microns.

2) T. Nakai and S. Yajima, *J. Chem. Soc. Japan, Pure Chem. Sec.* (*Nippon Kagaku Zasshi*), **79**, 1267 (1958).

256-channel gamma ray scintillation spectrometer with a welll-type sodium iodide crystal (2 in. ×1.75 in. diameter) as scintillator. The separation procedure was commenced after 20 min. cooling, and finished within 30 min. after irradiation. Gamma ray spectra were measured at appropriate intervals for two days.

*Procedure 2.*—Instead of the centrifugal separation, the irradiated mixture was treated for 5 min. with 50 ml. of 4 N hot nitric acid solution in order to dissolve uranium dioxide and neptunium formed by neutron capture and beta decay. The residual graphite powder was filtered and washed twice with 20 ml. of 0.1 N nitric acid solution, and then the graphite sample was gamma-assayed by the same method as above mentioned. In this case, the separation procedure was commenced after 20 min. cooling, and finished within 15 min.

*Procedure 3.*—The abundance of the fission nuclides contained in graphite powder varied with the cooling time, and also the state of each nuclide which was captured in a graphite crystal might vary. In this experiment, the irradiated mixtures were cooled for one day after irradiation and then submitted to the centrifugal separation or the nitric acid treatment. The obtained gamma ray spectra were compared with the spectra of the samples which were treated after 20 min. cooling and then cooled for 23 hr. Comparison of gamma ray spectra of the above mentioned treatments gave a good agreement.

Several gamma ray spectra of the gross fission products obtained by procedure 2 are shown in Fig. 1.

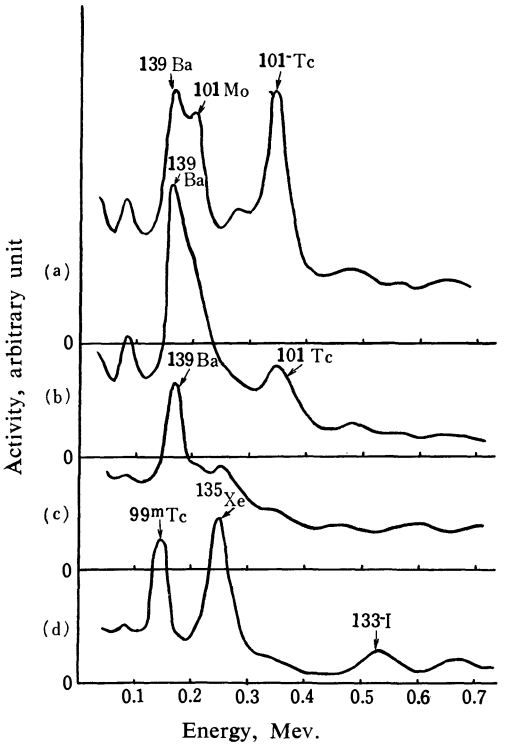



Fig. 1. Gamma ray spectrum of the fission products in graphite (a) at 26 min., (b) at 60 min., (c) at 160 min. and (d) at 20 hr. after irradiation.

The short lived nuclides in the fission products identified by these spectrodiagrams give a good agreement with those deduced from Peirson's experiment[3].

The respective abundance and the cross sections of uranium-238 and of uranium-235 are such that the irradiation of natural uranium by thermal neutrons leads to a temporary obliteration of the low energy portion of the fission products spectra by more intense X-rays and gamma rays emitted from neptunium-239 (half life 2.3 days). If a chemical treatment was used to eliminate the interfering neptunium-239, gaseous fission products such as xenon-135 would escape, and the complete spectrum of the gross fission products could not be obtained. For this reason, in Peirson's experiment[3] the gross gamma ray spectrum was measured by using a uranium, fifty times enriched in uranium-235. However, in this experiment the measurement of the gross gamma ray spectrum can be performed satisfactorily by using nautral uranium**.

The gamma ray spectrum of the fission products obtained by procedure 1 was similar to those obtained by procedures 2 and 3. From these results, it is evident that the centrifugal separation or the nitric acid treatment for such a short period can not affect the state of fission products captured in a graphite crystal. The effect of long time nitric acid treatment will be described in the next section.

**Leaching of Fission Products out of Graphite by Nitric Acid Solution.**—*Procedure.*—The graphite samples used in this experiment are artificial graphite

Table I. Particle size of graphite

| Sample | Particle size, micron |
|---|---|
| Artificial graphite (A. G.) | 30 |
| Natural graphite (N. G.—1) | 1 |
| Natural graphite (N. G.—2) | 50 |

Table II. Analytical data of impurities in graphite

| Impurity | A.G. | N.G.-1 | N.G.-2 |
|---|---|---|---|
| Ash (total) | 0.07% | 0.3% | 0.8% |
| $SiO_2$ | 250 p.p.m | 220 p.p.m | 3700 p.p.m |
| $Al_2O_3$ | 210 〃 | 60 〃 | 3500 〃 |
| $Fe_2O_3$ | 130 〃 | 24 〃 | 300 〃 |
| MgO | 15 〃 | 24 〃 | 100 〃 |
| CaO | 70 〃 | 36 〃 | 300 〃 |
| $V_2O_5$ | — 〃 | 0.12〃 | 0.5〃 |
| MnO | — 〃 | — 〃 | — 〃 |
| $Na_2O$ | 20 〃 | 12 〃 | 25 〃 |
| $K_2O$ | 15 〃 | 12 〃 | 20 〃 |
| NiO | — 〃 | 0.06〃 | — 〃 |
| $ThO_2$ | — 〃 | 2.4〃 | — 〃 |
| CuO | — 〃 | — 〃 | — 〃 |
| $B_2O_5$ | 0.1〃 | 0.02〃 | 0.5〃 |

3) D. H. Peirson, *Brit. J. Appl. Phys.*, 6, 444 (1955).

** It has been confirmed that the gaseous fission products captured in a graphite crystal did not diffuse at room temperature, and the results will be reported in the next article. The activity of fission products can not be recognized in the zinc bromide solution which has been used for the centrifugal separation.

TABLE III. LEACHING OF FISSION PRODUCTS

| Conc. of $HNO_3$ (normality) | Digestion time hr. | 120~160 keV. photo peak main nuclide Tc-99m leaching, % | 490~580 keV. photo peak main nuclide I-133, La-140 leaching, % | 630~720 keV. photo peak main nuclide I-132, Nb-97 leaching, % |
|---|---|---|---|---|
| Sample A.G. (not heated) | | | | |
| | 1 | 0.37 | | |
| 0 | 2 | 0.37 | 0.25 | |
| | 4 | 0.38 | 0.27 | 0.31 |
| | 1 | 0.51 | 0.44 | 0.44 |
| 1 | 2 | 0.49 | 0.51 | 0.71 |
| | 4 | 0.68 | 0.51 | 0.85 |
| | 1 | 0.79 | 0.36 | 0.78 |
| 5 | 2 | 0.85 | 0.36 | 0.75 |
| | 4 | 0.97 | 0.36 | 0.54 |
| | 1 | 0.81 | | 0.76 |
| 10 | 2 | 1.33 | | 0.89 |
| | 4 | 1.57 | 0.36 | 0.73 |
| Sample N.G.-1 (not heated) | | | | |
| | 1 | 0.64 | | |
| 0 | 2 | | | |
| | 4 | 0.69 | | |
| | 1 | 0.90 | | |
| 1 | 2 | 1.01 | | |
| | 4 | 0.88 | 0.76 | |
| | 1 | 1.26 | 0.86 | |
| 5 | 2 | 1.28 | 0.86 | 1.71 |
| | | 1.26 | 1.15 | 1.71 |
| | 1 | 1.37 | 0.96 | 1.54 |
| 10 | 2 | 1.37 | 1.96 | 2.05 |
| | 4 | 1.39 | 2.29 | 2.05 |
| Sample N.G.-2 (not heated) | | | | |
| | 1 | 2.03 | 0.52 | 0.74 |
| 0 | 2 | 1.90 | 1.03 | |
| | 4 | 1.90 | 1.03 | |
| | 1 | 2.33 | 1.03 | |
| 1 | 2 | | | |
| | 4 | | | |
| | 1 | | | |
| 5 | 2 | | | |
| | 4 | 3.71 | 1.55 | 1.97 |
| | 1 | 3.88 | 1.81 | |
| 10 | 2 | 3.79 | 1.55 | 3.94 |
| | 4 | | | |
| Sample N.G.-1 (heated) | | | | |
| | 1 | 2.19 | 10.29 | 1.13 |
| 0 | 2 | 2.18 | 8.82 | 1.35 |
| | 4 | 3.06 | 6.40 | 1.58 |
| | 1 | 3.10 | 11.76 | 1.35 |
| 1 | 2 | 3.26 | 11.76 | 1.35 |
| | 4 | 3.93 | 12.94 | 2.70 |
| | 1 | 3.50 | 10.59 | 6.31 |
| 5 | 2 | 6.70 | 10.59 | 6.31 |
| | 4 | 6.53 | 14.12 | 8.11 |
| | 1 | 7.16 | 11.76 | 9.91 |
| 10 | 2 | 8.20 | 11.76 | 9.91 |
| | 4 | 8.71 | 9.41 | 9.01 |
| Sample N.G.-2 (heated) | | | | |
| | 1 | 5.99 | 3.80 | 2.83 |
| 0 | 2 | 5.65 | 3.80 | 2.54 |
| | 4 | 5.54 | 5.06 | 2.83 |
| | 1 | 5.04 | 5.06 | 2.12 |
| 1 | 2 | 5.60 | 6.33 | 1.41 |
| | 4 | 4.05 | 3.80 | 7.76 |
| | 1 | 5.16 | 7.60 | 1.70 |
| 5 | 2 | 7.15 | 7.60 | 9.89 |
| | 4 | 8.09 | 5.06 | 9.89 |
| | 1 | 8.20 | 5.06 | 11.31 |
| 10 | 2 | 8.65 | 5.06 | 11.31 |
| | 4 | 8.87 | 5.06 | 14.13 |

made from petroleum coke, and two kinds of natural graphite. Grain sizes of the samples are shown in Table I and impurities contained in the samples in Table II.

A mixture of 5 g. of graphite and 0.5 g. of uranium dioxide was irradiated for one hour under the same condition mentioned above. The irradiated mixture was transferred into a centrifuging tube with a saturated zinc bromide solution which contained a small amount of hydrochloric acid. After a centrifugal separation, the graphite was washed rapidly with a diluted hydrochloric acid solution. After being dried at 70°C or heated at 1000°C for four hours in an argon gas stream, it was divided into portions of 100 mg. each. They were immersed in 30 ml. nitric acid solution of 0~10 N concentration at 80°C for a period of 1~4 hr. After the immersion, the solution were filtered the filtrates were evaporated to 3 ml.; this volume was suitable for gamma ray spectrometry. The gamma ray spectrum of fission products in filtrates and precipitates was measured by the RCL 256 channel gamma ray spectrometer with a well-type sodium iodide crystal (2 in.×1.75 in. diameter) as scintillator. By comparing the gamma ray spectra of the filtrates with their total spectra (filtrate+precipitate), the leaching of fission products in nitric acid solution was made clear.

## Results

Experimental data are summarized in Table III. Based on these data the following results. are elucidated.

1) Fission products captured in graphite are leached with difficulty in a nitric acid solution under various conditions of immersion; however, the leaching of all the nuclides is slightly increased with the nitric acid concentration.

2) There is no difference due to varying graphite samples.

3) When the samples were heated at a high temperature, the leaching of fission products increased with acid concentration. For example, 10% of the fission products was leached by 10 N nitric acid solution.

4) However, the fraction of the fission products leached is almost constant regardless of immersion time.

From the results, it is considered that fission products in graphite are very stable toward nitric acid and such stabilities are attributed to a hindrance effect because most fission products are captured in a graphite crystal. It is not yet clearly demonstrated that the leaching is increased with acid concentration when samples are heated at a high temperature.

The authors wish to thank Dr. Kenjiro Kimura for his encouragement.

*Division of Chemistry*
*Japan Atomic Energy*
*Research Institute*
*Tokai, Ibaraki-ken*
*(T. N., S. Y. & K. S.)*

*Department of Chemistry*
*Faculty of Science*
*Kyoto University*
*Sakyo-ku, Kyoto*
*(J. O. & D. S.)*

# *The Behavior of Fission Products Captured in Graphite by Nuclear Recoil. II. The Diffusion of Xenon-135 in Graphite at a High Temperature*

By Toshio NAKAI, Seishi YAJIMA, Koreyuki SHIBA, Jiro OSUGI and Daisaburo Shinoda

(Received September 22, 1959)

In the previous study[1], it was shown that, when a mixture of uranium dioxide and graphite in a weight ratio of 1 : 30 was irradiated with JRR-1 (Japan Research Reactor-1) neutrons, about 95% of the fission products recoiled out of uranium oxide powder into graphite. The orbital electrons of the recoiled fission fragments are partially stripped, and the initial velocities of fission fragments are about $10^9$ cm./sec. It has also been shown that they are highly ionized, bearing ionic charges of 20 or more. Because of this high velocity and the charge, the fission fragments interact readily with matter.

One of the practical problems connected with the operation of a reactor that employs a dispersion type fuel is the determination of the extent of diffusion of radioactive fission products from the fuel pellet when the mixture of graphite and uranium dioxide is pressed to give a density of about 1.8. Since the release of gaseous fission products from the fuel pellet will cause the destruction of the pellet and the radioactive contamination of the coolant and other establishments, it is important to study the behavior of gaseous fission products captured in graphite particles. Likewise the build-up of xenon-135 in a pellet is of some importance because of its abnormally large absorption cross section. In this case continuous elimination of xenon-135 from the pellet through some adequate process should be favorable in relation to the neutron economy of a reactor. Because of these reasons the firm retention and the continuous elimination of gaseous fission products would be of the greatest importance for the dispersion type fuel. Investigators of the North American Aviation Laboratory studied the diffusion of xenon-133 from graphite[2]. When discs of graphite, 0.84 cm. in diameter and 0.064~0.5 cm. in thickness, impregnated with uranium carbide to a concentration of about 520 mg./cc., were heated to 900~1500°C, the leakage rate of xenon varied from approximately 2% per 3 hr. of heating at 900°C to approximately 50% per 3 hr. at 1500°C.

However, an investigation of the state of

1) T. Nakai and S. Yajima, *J. Chem. Soc. Japan, Pure Chem. Sec.* (*Nippon Kagaku Zasshi*), **79**, 1267 (1958).

2) G. A. Cowan and C. J. Orth, *A/CONF.*, 15/p/613 (1958).

TABLE I. ANALYTICAL DATA OF IMPURITIES IN GRAPHITE

| Impurity | Natural graphite-1 (N.G.-1) | Natural graphite-2 (N.G.-2) | Natural graphite-3 (N.G.-3) | Artificial graphite (A.G.) | Amorphous carbon (A.C.) |
|---|---|---|---|---|---|
| Particle size, micron | 1 | 50 | 50 | 30 | 20 |
| Ash (total) | 0.3% | 0.6% | 0.8% | 0.07% | 0.1% |
| $SiO_2$ | 220 p.p.m. | 2600 p.p.m. | 3700 p.p.m. | 250 p.p.m. | 350 p.p.m. |
| $Al_2O_3$ | 60 〃 | 2300 〃 | 3500 〃 | 210 〃 | 100 〃 |
| $Fe_2O_3$ | 24 〃 | 250 〃 | 300 〃 | 130 〃 | 250 〃 |
| MgO | 24 〃 | 80 〃 | 100 〃 | 15 〃 | 10 〃 |
| CaO | 36 〃 | 290 〃 | 300 〃 | 70 〃 | 150 〃 |
| $V_2O_5$ | 0.12〃 | 5.5〃 | 0.5〃 | — 〃 | 50 〃 |
| MnO | — 〃 | — 〃 | — 〃 | — 〃 | — 〃 |
| $Na_2O$ | 12 〃 | 15 〃 | 25 〃 | 20 〃 | 35 〃 |
| $K_2O$ | 12 〃 | 17 〃 | 20 〃 | 15 〃 | 30 〃 |
| NiO | 0.06〃 | — 〃 | — 〃 | — 〃 | — 〃 |
| $ThO_2$ | 2.4 〃 | — 〃 | — 〃 | — 〃 | — 〃 |
| CuO | — 〃 | — 〃 | — 〃 | — 〃 | — 〃 |
| $B_2O_5$ | 0.02〃 | 0.3〃 | 0.5〃 | 0.1〃 | 3 〃 |

gaseous fission products diffusing from the graphite particles is thought to be worth while. Consequently, the present work has been carried out to study the diffusion, at 400, 800 and 1200°C, of xenon-135 captured in several kinds of graphite powder.

## Experimental

**Preparation of Samples.**—The mixture of 1 g. of graphite and 50 mg. of uranium dioxide was irradiated with thermal neutrons for about one hr. in an experimental hole (thermal neutron flux, about $5 \times 10^{11}$ neutrons/cm$^2$ sec.), JRR-1. After irradiation, the mixture was washed with a hot 4 N nitric acid solution in order to dissolve uranium and neptunium, and dried at 70°C. The fission products captured in graphite particles were not leached with a 4 N nitric acid solution within the short time procedure[1]. The fission products in graphite were cooled for twenty hours after irradiation and used for the diffusion experiment. During such a cooling time iodine-135, which is the precursor of xenon-135, decayed sufficiently and the xenon-135 was predominantly built up. The graphite samples used in this experiment are tabulated in Table I.

**Determination of the Diffusion of Xenon-135.**—For the escape rate of xenon-135 from graphite powder to be determined at a high temperature, graphite samples into which fission products recoiled were heated in a stream of argon. The furnace, in which the heating in argon took place, consisted of a silicon carbide heater and a silica tube. The temperature of the furnace was measured with a platinum, platinum-rhodium thermocouple and controlled with a regulator. In the range 400 to 1200°C, the temperature of the furnace was found to remain constant within 10°C throughout the experiment. Argon gas was purified through sponge titanium at about 700°C and through phosphorous pentoxide to prevent the oxidation of the graphite surface. The flow rate of argon gas was checked with a glass capillary flow meter and maintained at a constant rate. The xenon released from graphite was trapped in a charcoal trap cooled with a dry ice-benzene mixture. At appropriate intervals the trap was replaced by a new one. Xenon-135 activity in the charcoal trap was determined with a gamma ray spectrometer. In this experiment an RCL 256 channel gamma ray scintillation spectrometer with a well-type sodium iodide scintillator (2 in. × 1.75 in. diameter) was used.

The gross gamma ray spectrum of fission products in graphite after twenty hours cooling, of the trapped xenon and of the fission products which remained in graphite after the diffusion run are shown in Fig. 1. The amount of the diffused xenon was determined by comparing the heights of

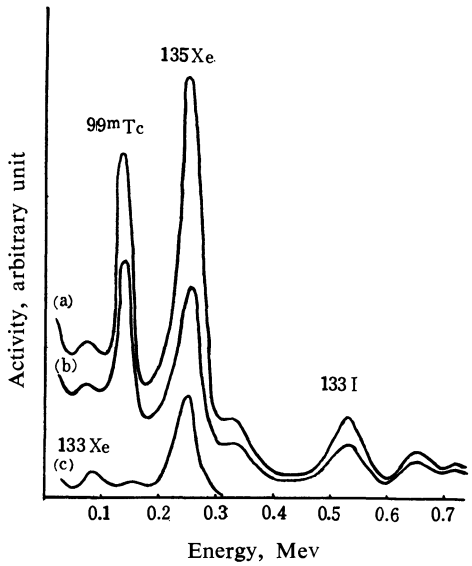



Fig. 1. Gamma-ray spectrum of the fission products in graphite.
(a) Fission products before diffusion.
(b) Fission products remained after diffusion.
(c) Trapped xenon.

the photoelectric peak of xenon-135 of the charcoal trap and of a standard graphite sample of a known weight which was not heat-treated.

## Results

As already mentioned, the results were obtained from gamma ray spectra at appropriate time intervals. The photoelectric peak of gamma ray spectra is proportional to the amount of xenon that escaped from graphite. On the other hand, the initial amount of xenon in graphite was obtained from the gross gamma ray spectrum of the standard graphite sample. Therefore, the fraction of xenon which escaped can be calculated as a function of time. The diffusion rates of xenon-135 from the several kinds of graphite at 400, 800 and 1200°C are shown in Figs. 2—4, respectively.

To analyze these diffusion curves the relation between the logarithmic values of the remaining amounts of xenon-135 and the time intervals at 400, 800 and 1200°C was obtained and shown in Figs. 5—7, respectively.

From these figures it is seen that the curves consist of two fractions which are a steep slope

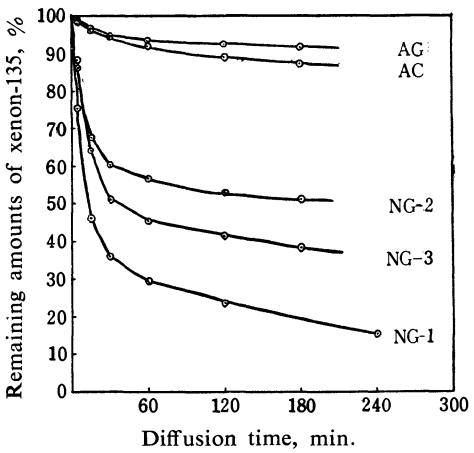



Fig. 4. Diffusion rates of xenon-135 at 1200°C.

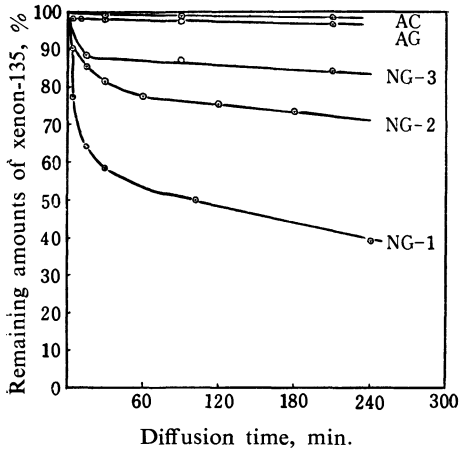



Fig. 2. Diffusion rates of xenon-135 at 400°C.

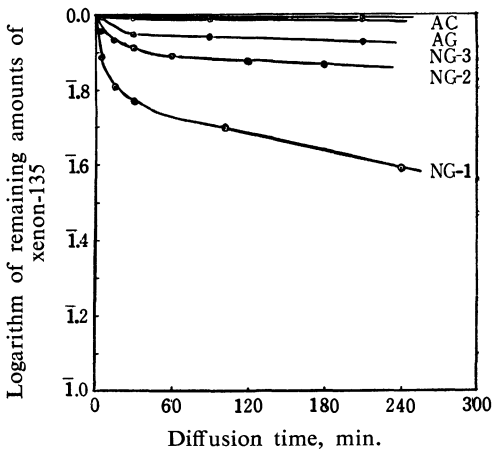



Fig. 5. Results at 400°C.

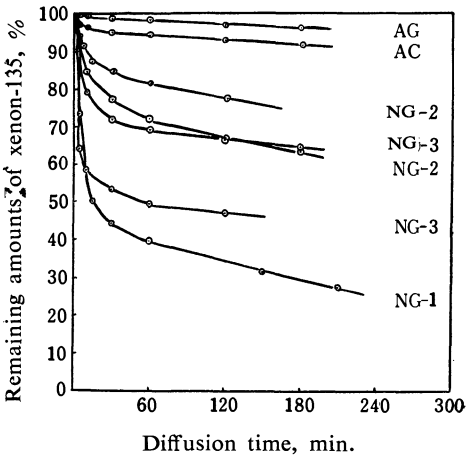



Fig. 3. Diffusion rates of xenon-135 at 800°C.

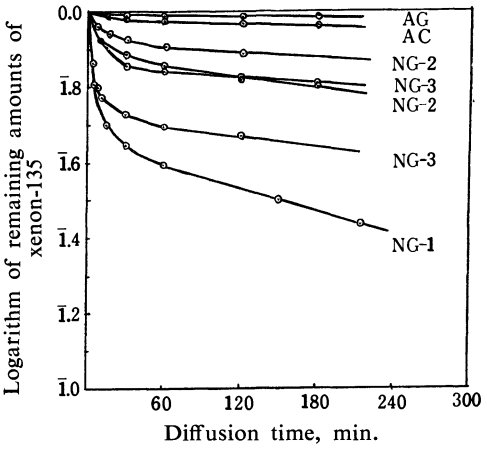



Fig. 6. Results at 800°C.

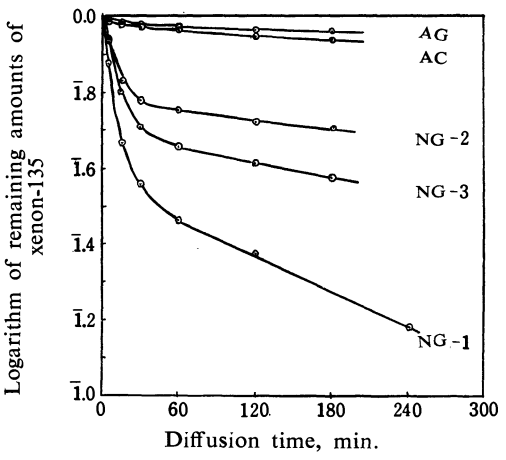



Fig. 7. Results at 1200°C.

curve for one hour and a slow inclination line after one hour. The results show that there are two mechanisms for diffusion in a graphite grain; they are a rapid and a slow diffusion.

The amounts of diffusion of xenon-135 for rapid diffusion are appreciably greater than those for slow diffusion and the amounts vary with the temperature and the kinds of sample. The amounts of diffusion from the natural graphite samples are appreciably greater than those from the artificial graphite or the amorphous carbon samples. The dependency of diffusion amounts on the kinds of sample will be discussed later.

The diffusion rate of a straight line fraction may be used to evaluate a diffusion constant of xenon-135 as shown in the following. In Figs. 5—7 the apparent inclination of a straight line fraction depends on the diffusion constant of xenon-135. Further, from the slope of the linear line for each sample, a diffusion constant is obtained, and they are summarized in Table II. Eq. 1 shows the relation between the diffusion constant and the activation energy, and from this equation the activation energy can be obtained as the inclination of the values of the logarithm of diffusion constants against the reciprocal of the absolute temperatures.

$$D = D_0 \exp\left(-\frac{\Delta H}{RT}\right) \qquad (1)$$

TABLE II. THE ACTIVATION ENERGY OF XENON-135

| Sample | Inclination | Activation energy cal./mol. |
|---|---|---|
| Natural graphite-1 | $0.50\times10^3$ | $2.3\times10^3$ |
| Natural graphite-2 | $0.50\times10^3$ | $2.3\times10^3$ |
| Natural graphite-3 | $0.58\times10^3$ | $2.7\times10^3$ |
| Artificial graphite | $0.51\times10^3$ | $2.3\times10^3$ |
| Amorphous carbon | $1.06\times10^3$ | $4.9\times10^3$ |

where $D$: diffusion constant, $D_0$: diffusion constant at 0 of absolute temperature degree, $R$: gas constant, $T$: absolute temperature degree and $H$: activation energy.

The apparent activation energy of diffusion calculation from the slow inclination of these straight lines is shown in Table II.

## Discussion

If one assumes that xenon diffuses along the interlaminar spaces in a perfect graphite crystal, the activation energy of diffusion can be calculated theoretically. An elementary process of xenon diffusion in graphite is the migration of xenon from position 1 to position 3 through position 2 in Fig. 8. As the activation energy is

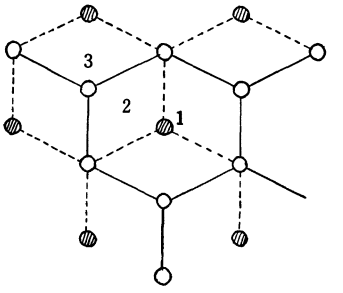



Fig. 8. A pertect graphite crystal.

represented to be the energy difference between position 1 and position 2, the activation energy can be obtained by use of the strain energy of each position. The strain energy is calculated by the interatomic force evaluated from an elastic constant as a specific heat at a low temperature. According to Suzuki[3], the activation energy calculated is about 2000 cal./mol. and is of the same order as the values obtained in this experiment. On the other hand, the calculated activation energy of diffusion across carbon layers is also about 200000 cal./mol. From this high value, the assumption that the diffusion occurs entirely along the interlaminar spaces is justified.

It is well known that graphite, in general, has a small mosaic, particularly in artificial graphite. Dislocation density in graphite is high along the boundary of mosaic structure. Xenon is trapped in trapping centers around a dislocation line rather than a interstitial site in a crystal at room temperature, because it is evident in the present experiment that the activation energy of xenon is fairly small. Therefore, the actual process of diffusion must be discussed with reference to the chemical potential of the trapping centers including the

3) H. Suzuki, private communication.

effect of a stress field as well as the concentration gradient in a sample.

The mosaic size of the graphite samples was determined by the X-ray diffraction method and the electron diffraction method. As a result, the mosaic size of the natural graphite is appreciably larger than those of the artificial graphite and of the amorphous carbon. It is evident that the dislocation density in the region of the mosaic boundary of the natural graphite is appreciably smaller than those of artificial graphite and of amorphous carbon. Therefore, in the case of the natural graphite, xenon-135 which was not captured by the trapping center, diffuses with a high concentration gradient. After that, xenon-135, which was captured by the center is successively released and slowly diffuses along the interlaminar space of a crystal. In this case, because the concentration gradient of xenon-135 in the sample is very small, it is very likely that the gradient is constant, and this warrants the calculation of activation energy.

Since the number of the trapping center of artificial graphite and of amorphous carbon and the amount of xenon-135 which was trapped in the trapping center are greater than those in the case of the natural graphite, the diffusion amounts of a rapid diffusion fraction of the amorphous carbon and the artificial graphite are relatively small.

The diffusion of gaseous fission products of dispersion type fuel will be related to the mosaic size of graphite material. It may be pointed out that, on the basis of the above discussion, the problem of xenon poisoning will be solved.

The authors wish to thank Dr. Kenjiro Kimura for his encouragement.

*Division of Chemistry*
*Japan Atomic Energy*
*Research Institute*
*Tokai, Ibaraki-ken*
*(T. N., S. Y. & K. S.)*

*Department of Chemistry*
*Faculty of Science*
*Kyoto University*
*Sakyo-ku, Kyoto*
*(J. O. & D. S.)*

# *Conformation of Biaryls. Dipole Moment Measurements of o-Methylbiphenyls*

By Takeo SATO

(Received September 22, 1959)

Since the structure of biphenyl in crystals had been determined by X-ray crystal analysis[1], it was a subject of interest for many workers to elucidate the conformation of substituted biphenyls by using various physical methods. As the result of extensive works on biphenyl derivatives especially halogenobiphenyls, their conformations have been determined under various conditions. By X-ray method planar structure was advanced for 3, 3′-dichlorobenzidine[2] in accordance with the conclusion of Dhar on biphenyl itself, of which the result can be compared with a skew conformation found for 2, 2′-dichlorobenzidine[3]. For the knowledge of the free molecules, electron diffraction investigation was undertaken, and it was reported that the biphenyls without any substituent at position 2 were also non-planar[4,5] as well as 2, 2′-dihalogenobiphenyls[6]. Dipole moment measurements of 2-halogeno-[7,8], 2, 2′-dihalogeno-[7,9] and 3, 3′-dihalogenobiphenyls[9] were also reported and rotated molecular conformations were advanced for each case and the mean angles were calculated. It seemed, however, that the information on the structure of 2, 2′-dialkylbiphenyls were very limited, only two examples were reported, at present. Namely, Hargreaves et al.[10] have reported the X-ray

1) N. R. Dhar, *Indian J. Physics*, 7, 43 (1932). Cf. J. Hengstenberg and H. Mark, *Z. Krist.*, 70, 283 (1929); G. L. Clark and L. W. Pickett, *J. Am. Chem. Soc.*, 53, 167 (1931); N. R. Dhar, *Proc. Nat. Inst. Sci. India*, 15, 11 (1949).

2) J. Toussaint, *Acta Cryst.*, 1, 43 (1948).

3) D. L. Smare, ibid., 1, 150 (1948).

4) J. Karle and L. O. Brockway, *J. Am. Chem. Soc.*, 66, 1974 (1944).

5) O. Bastiansen, *Acta Chem. Scand.*, 3, 408 (1949).

6) Idem., ibid., 4, 926 (1950).

7) G. C. Hampson and A. Weissberger, *J. Am. Chem. Soc.*, 58, 2111 (1936).

8) A. C. Littlejohn and J. W. Smith, *J. Chem. Soc.*, 2456 (1953).

9) Idem., ibid., 2552 (1954).

10) F. Fowwether and A. Hargreaves, *Acta Cryst.*, 3. 81 (1950); A. Hargreaves and W. H. Taylor, *J. Sci. Instruments*, 18, 138 (1941).

crystal analysis of 2,2'-dimethylbenzidine dihydrochloride and found that the compound has a rotated angle of 70.6°. Suzuki[11] has also computed the interplanar angle of biphenyls with methyl groups at position 2 (and 2') based on the ultraviolet absorption spectra and found an angle of 70.5° for 2,2'-dimethylbiphenyl.

While, in the course of synthetic studies of estrogenic biphenyl derivatives, it has been reported that 2,2'-dimethylbiphenyls[12,13] failed to show a conjugation band of biphenyl system in the near ultraviolet region[14-16]. This result was explained by the steric interference of the two methyl groups which forced the benzene nuclei into non-planar arrangement, and the mean angle between the rings was assumed to be nearly perpendicular to each other.

In an effort to verify the above postulation, this communication records the results of the dipole moment measurement and the calculation of the interplanar angle of 2-methyl- and 2,2'-dimethylbiphenyls. Dipole moment of 2,2'-dimethylbiphenyl was reported to be 0.66 D[17]. The value, however, would not be large enough for the safer calculation of the angle, when one considered the small dipole moment found for toluene (0.34 D[18]) and the experimental error of this measurement. Thus for favorable compounds, 5,5'-disubstituted 2,2'-dimethylbiphenyls (II) were prepared from the corresponding iodo-compound (I) by the Ullmann reaction. Suitable substituents at the meta positions will increase the moment of the system and alter it markedly according to the rotation around the axis of the biaryl without affecting the steric environment. The method of preparations were described in the *Experimental Part.*

The measurement was carried out for a benzene solution at 25°C. The values found for the dimethylbiphenyls are given in Table I. The moments of benzene component used for the calculations were 1.94 D for *p*-chlorotoluene[19] and 4.52 D for *p*-nitrotoluene[20]. The calculated values for *cis*-planar and perpendicular conformations are given in Table I. As can be seen, the observed values for compound II (X=Cl and $NO_2$) were essentially the same for the calculated ones for the perpendicular arrangement as long as the rings are coaxial. The present results is in good agreement with the assumption derived from the ultraviolet absorption spectra of 2,2'-dimethylbiphenyls[12,13].

It should, however, be pointed out that the calculated values would be modified in a minor degree by considering the induction effects[8,9,21-23], which comprised the effects already present in the component benzene, the effect of each dipole on the second ring and the moment induced at each dipolar substituent by the presence of the other. These inductive effects will be rather large when the polar groups are located at ortho positions as in the case of 2,2'-disubstituted biphenyls. Thus, the values of the angle for 2,2'-dichlorobiphenyl were 88° when all induction effects were ignored but 69~84° when they were considered[9]. However, as can be easily assumed, both values

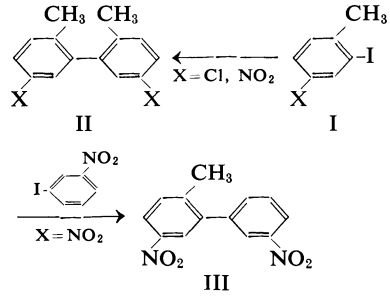



TABLE I. COMPARISON OF OBSERVED[a] WITH CALCULATED DIPOLE MOMENTS FOR 5,5'-DISUBSTITUTED 2,2'-DIMETHYLBIPHENYLS (II) AND 2-METHYL-3',5-DINITROBIPHENYL (III)

| Compound | $\mu$, D observed | $\mu$, D, calculated | | Mean angle between planes of rings |
|---|---|---|---|---|
| | | Rings *cis*-planar | Rings perpendicular | |
| II X=H | 0.66[b] | | | |
| Cl | 2.37 | 3.36 | 2.38 | 90° |
| $NO_2$ | 5.53 | 7.83 | 5.54 | 90° |
| III | 4.55 | 7.35 | 5.21 | 104° |

a) Benzene solution, at 25°C. b) See Ref. 17.

11) H. Suzuki, This Bulletin, 27, 597 (1954).
12) T. Sato, ibid., 32, 1130 (1959).
13) T. Sato and M. Ōki, ibid., 32, 1289 (1959).
14) M. Ōki and T. Sato, ibid., 30, 508 (1957).
15) T. Sato and M. Ōki, ibid., 30, 859 (1957).
16) Idem, ibid., 30, 958 (1957).
17) R. J. W. Le Fèvre and H. Vine, *J. Chem. Soc.*, 1938, 967.
18) C. G. Le Fèvre, R. J. W. Le Fèvre and K. W. Robertson, ibid., 480 (1935).
19) L. Tiganik, *Z. physik. Chem.* B13, 425 (1931).
20) G. R. Paranjpe and D. J. Davar, *Indian J. Physics*, 15, 173 (1941).
21) H. M. Smallwood and K. F. Herzfeld, *J. Am. Chem. Soc.*, 52, 1919 (1930).
22) F. C. Frank, *Proc. Roy. Soc.*, A152, 171 (1935).
23) G. C. Hampson and A. Weissberger, *J. Chem. Soc.*, 1936, 393.

were essentially the same for 3, 3′-disubstituted biphenyls[9], to which the present series are structurally related.

It is quite natural to consider that the conformation of 2-methylbiphenyl is located somewhat between 2,2′-dimethylbiphenyls (II) and biphenyl without ortho substituent owing to the decrease in steric hindrance given by the ortho substituent compared with compound II. The same measurement was applied to 2-methyl-3′, 5-dinitrobiphenyl (III) of which preparation was illustrated in the diagram and described in the *Experimental Part.* For the calculation of the theoretical moment of the system, dipoles moments of nitrobenzene and *p*-nitrotoluene were taken as 3.96[24] and 4.52D[20], respectively.

The observed value, 4.55 D, is smaller than the calculated ones for the conformations in which both rings are in *cis*-planar and perpendicular arrangement. These facts suggest that the molecule takes conformation in which two benzene rings are twisted further from the perpendicular position to *trans*-relationship in respect to two nitro groups. The observed value agreed with the calculated one for the conformation with the rings inclined at an angle of 104°. Therefore, the molecule can be regarded to have a slightly *trans*-arrangement with inclined benzene rings at an angle of 76°. The present result might be compared with the value found for 3, 3′-dinitrobiphenyl, which was reported to have a non-planar structure with an interplanar angle of 106°[9]. The reduction in the rotation angle found in compound III compared with the dimethyl compounds (II) was quite reasonable, but it remained unexplained whether the preferred *trans*-conformation of compound III was given by the steric effect of ortho groups or by the presence of meta substituents.

## Experimental[25]

**2, 2′-Dimethyl-5, 5′-dinitrobiphenyl (II, X=$NO_2$).**—It was obtained by the Ullmann reaction of 2-iodo-4-nitrotoluene, b. p. 138~140°C/3 mmHg, m. p. 58°C (reported melting point is 58°C[26]) according to the modified method given in the literature[27]. One hundred grams (0.38 mol.) of 2-iodo-4-nitrotoluene and 150 g. of dry clean sand were preheated to 215°C and to this mixture was added with good stirring 100 g. (1.6 atoms) of activated copper bronze during one hour while the temperature was maintained at 215~220°C. It was then heated to 250°C and kept at that temperature for one and a half hour. After the reaction was over the mixture was poured onto dry sand and extracted with ethanol. The extract was recrystallized from acetic acid or acetone for several times with the aid of active charcoal. Pale yellow needles, m. p. 177~178°C, were obtained in a low yield.

**5, 5′-Dichloro-2, 2′-dimethylbiphenyl (II, X=Cl).**—Sixteen grams (0.063 mol.) of 4-chloro-2-iodotoluene, b. p. 108~109°C/10 mmHg, $n^{19}$ 1.6231 obtained from 4-chloro-2-toluidine[28] according to Wroblewski[29] or from 2-iodo-4-toluidine[30] by Sandmeyer reaction was heated at 240~250°C with stirring and 20 g. (0.32 atom) of activated copper bronze was added over a period of one hour. The reaction mixture was then heated and kept at 280~290°C for forty minutes. It was extracted with acetone and the extract was distilled to give an oil which boiled first at 140~155°C/4 mmHg, and then at 142~144°C/3 mmHg., $n^{20}$ 1.5961 on redistillation. Yield was 4 g. or 50% of the theory.

Found: C, 66.75; H, 4.74. Calcd. for $C_{14}H_{12}Cl_2$: C, 66.95; H, 4.82%.

**2-Methyl-3′, 5-dinitrobiphenyl (III).**—Under good stirring 15 g. (0.24 atom) of activated copper bronze was added to a mixture of 21 g. (0.080 mol.) of 2-iodo-4-nitrotoluene and 7.5 g. (0.030 mol.) of *m*-nitroiodobenzene in the course of thirty minutes, while the temperature was kept at 220~230°C. It was then heated to 240~250°C and kept for additional thirty minutes at that temperature. After the reaction was over, the mixture was extracted with acetone and the solution was treated with active charcoal. The solvent was evaporated and the remainder was recrystallized from ethanol for several times. Compound III was obtained as pale yellow plates, m. p. 145~146°C.

Found: N, 10.70. Calcd. for $C_{13}H_{10}O_4N_2$: N, 10.85%.

When the above reaction was conducted with an equimolar amount of iodo compounds the main product was found to be 3, 3′-dinitrobiphenyl.

The author wishes to express his hearty thanks to Drs. T. Chiba and T. Shimozawa, the University of Tokyo, for carrying out the measurements. The author's thanks are also due to Professors K. Hata, Tokyo Metropolitan University, and M. Ōki, the University of Tokyo, for their continued interest throughout this study.

*Department of Chemistry*
*Faculty of Science*
*Tokyo Metropolitan University*
*Setagaya, Tokyo*

24) R. Davis, H. S. Bridge and W. J. Svirbely, *J. Am. Chem. Soc.*, 65, 857 (1943).
25) All boiling and melting points are uncorrected. The author wishes to thank Mr. T. Mizushima for microanalyse and Mr. M. Fujii for preparations of the materials.
26) C. Willgerodt and B. R. Kok, *Ber.*, 41, 2077 (1908).
27) R. Pummerer, H. Puttfarcken and P. Schöpflocher, ibid., 58, 1808 (1925).
28) H. Goldschmidt and M. Hönig, ibid., 19, 2438 (1886).
29) E. Wroblewski, *Ann.*, 168, 147 (1873).
30) B. H. Nicolet and R. B. Sandin, *J. Am. Chem. Soc.*, 49, 1806 (1927).

# *Expansion of Nakano's Results on High Frequency Titration Using the Resistance-type Instrument*

By Sadaharu TOYODA

(Received March 25, 1959)

There have been many papers[1-7] on high frequency titration. Many interesting results have been shown by Nakano's paper[8] on this subject. It was based on an experiment using the resistance-type instrument[9]. According to the experimental results of Figs. 2 and 4, which have been obtained by Nakano, the relation between the value of variable resistance, consisting of platinum wire and mercury column, and the concentration of solution shows a minimum point in a case of the condenser-type instrument, and minimum and maximum points in a case of the coil-type instrument. Nakano proved that there exists a relation $\omega C_0 R = 1$, at the minimum point for both cases of condenser-type and coil-type instruments. These results and others have been obtained by using the equivalent circuit without the variable resistance which makes a component of the resistance-type instrument. It is, therefore, significant to see if much more accurate results are obtained by using the equivalent circuit with the variable resistance. The present paper is concerned with the results of the calculation of the equivalent circuit containing the variable resistance.

## Calculation for Condenser-type Instrument

Fig. 1 shows the equivalent circuit for the components of the portion containing the sample solution (refer to Fig. 7a). This equivalent circuit is the same as the one in Nakano's paper[8] except $R_1$ referring to the variable resistance of the platinum wire. Therefore, the physical meaning of $C$, $C_0$, $R$ and $L$ are omitted. If $Z$ denotes the impedance for the condenser

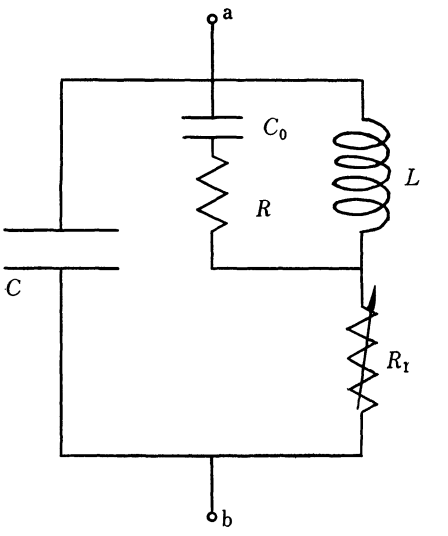



Fig. 1. Equivalent circuit for condenser-type.

element ($C_0$, $R$) and the coil ($L$), the following relation is obtained.

$$\frac{1}{Z}=\frac{(\omega C_0)^2 R}{1+(\omega C_0 R)^2}+\boldsymbol{j}\left\{\frac{\omega C_0}{1+(\omega C_0 R)^2}-\frac{1}{\omega L}\right\} \tag{1}$$

The total admittance between point a and point b in Fig. 1 is written as

$$Y=\boldsymbol{j}\omega C+\frac{1}{Z+R_1} \tag{2}$$

Putting the following expressions for the real and the imaginary parts of $1/Z$

$$A\equiv\frac{(\omega C_0)^2 R}{1+(\omega C_0 R)^2} \qquad B\equiv\frac{\omega C_0}{1+(\omega C_0 R)^2}-\frac{1}{\omega L} \tag{3}$$

and for those of $Z$

$$Z=\frac{A}{A^2+B^2}-\boldsymbol{j}\frac{B}{A^2+B^2}\equiv U-\boldsymbol{j}V \tag{4}$$

the real and imaginary parts of $Y$ can be separated as follows:

$$Y_{\text{real}}=\frac{U+R_1}{(U+R_1)^2+V^2} \tag{5}$$

$$Y_{\text{imag}}=\frac{V}{(U+R_1)^2+V^2}+\omega C \tag{6}$$

1) W. J. Blaedel and H. V. Malmstadt, *Anal. Chem.*, **22**, 734 (1950).
2) K. Anderson, E. S. Bettis and D. Revinson, ibid., **22**, 743 (1950).
3) P. W. West, T. S. Burkhalter and L. Broussard, ibid., **22**, 469 (1950).
4) C. N. Reilley and W. H. McCurdy, Jr., ibid., **25**, 86 (1953).
5) S. Fujiwara and S. Hayashi, ibid., **26**, 239 (1954); S. Fujiwara and S. Hayashi, *J. Chem. Soc. Japan, Pure Chem. Sec.* (*Nippon Kagaku Zasshi*), **74**, 171 (1953).
6) K. Nakano, ibid., **74**, 172 (1953).
7) T. Yano, S. Musya, T. Wada and T. Hino, *Chem. Eng.* (*Kagaku Kôgaku*), **20**, 339 (1956).
8) K. Nakano, *J. Chem. Soc. Japan, Pure Chem. Sec.* (*Nippon Kagaku Zasshi*), **75**, 776 (1954).
9) K. Nakano, ibid., **74**, 227 (1953); K. Nakano, R. Hara and K. Yashiro, *Anal. Chem.*, **26**, 636 (1954).

The frequency of oscillation is determined by the assumption that the imaginary part of $Y$ is equal to zero as in the previous paper[8]. Substituting this condition into Fq. 5, one finds

$$(A^2+B^2)R_1=-\frac{Y_{\text{real}}}{\omega C}B-A \tag{7}$$

On the other hand, the change of plate current takes place by putting the beaker containing the aqueous solution into the condenser-type electrode or the coil. In the previous experiment the change of plate current is compensated by adjusting $R_1$. This manipulation suggests that the value of $Y_{\text{real}}$ is kept constant. In the special case when the beaker is empty ($R=\infty$) the values of $A$ and $B$ are 0 and $-1/\omega_\infty L$, respectively. Applying these values to Eq. 7, $Y_{\text{real}}$ is obtained as follows:

$$Y_{\text{real}}=R_{1\infty}\frac{C}{L} \tag{8}$$

where $R_{1\infty}$ and $\omega_\infty$ denote the variable resistance and the angular frequency in the special case, respectively. Thus Eq. 7 becomes

$$(A^2+B^2)R_1=-\frac{R_{1\infty}}{\omega L}B-A \tag{9}$$

Substituting the above equation into $Y_{\text{imag}}=0$, the following relation between $\omega$ and $R$ will be easily obtained:

$$\omega C=-B\frac{1+(A/B)^2}{1+(R_{1\infty}/\omega L)^2} \tag{10}$$

Of course, both Eqs. 9 and 10 should be used simultaneously in order to find how $R_1$ and $\omega$ change with the concentration of solution.

The distributed capacity between the electrode and the solution, $C_0$, is determined by using the boundary conditions when the beaker is empty or full of the mercury as in the case of Nakano's experiment. From Eq. 10, one obtains

$$\begin{cases} \dfrac{1}{\omega_\infty^2 L}=C\left\{1+\left(\dfrac{R_{1\infty}}{\omega_\infty L}\right)^2\right\} \\ \dfrac{1}{\omega_0^2 L}=C\left\{1+\left(\dfrac{R_{1\infty}}{\omega_0 L}\right)^2\right\}+C_0 \end{cases} \tag{11}$$

where $\omega_\infty$ and $\omega_0$ are the angular frequency when $R=\infty$ and $R=0$, respectively, and $R_{1\infty}\approx 10\,\Omega$. Hence, the distributed capacity, $C_0$, is calculated by the following expression:

$$C_0\fallingdotseq\frac{1}{\omega_0^2 L}-\frac{1}{\omega_\infty^2 L} \tag{12}$$

which means the same as the method shown in the previous paper[8]. Referring to Table I, of course, it is clear that the following term can be neglected, if $R_{1\infty}$ is $100\,\Omega$ and $C$ is 60 $\mu\mu$F:

$$C\left|\left(\frac{R_{1\infty}}{\omega_0 L}\right)^2-\left(\frac{R_{1\infty}}{\omega_\infty L}\right)^2\right|<0.012\ \mu\mu\text{F} \tag{13}$$

Thus the average value of $C_0$ is 2.3 $\mu\mu$F.

Eq. 9 can be rearranged as follows:

$$\left\{1-\frac{2\omega^2LC_0}{1+(\omega C_0R)^2}+\frac{(\omega^2LC_0)^2}{1+(\omega C_0R)^2}\right\}R_1$$
$$=R_{1\infty}\left\{1-\frac{\omega^2LC_0}{1+(\omega C_0R)^2}-\frac{\omega C_0R}{1+(\omega C_0R)^2}\frac{\omega C_0\omega^2L^2}{R_{1\infty}}\right\} \tag{14}$$

Since the variation of frequency is fairly small as shown by the experiment[10], the frequency can be taken as constant. With this assumption, one differentiates Eq. 14 with respect to $R$, then puts it equal to zero, and finally obtains the condition which gives the minimum point of $R_1$

$$R\fallingdotseq\left(1-\alpha+\frac{\alpha}{\beta}\right)\frac{1}{\omega C_0} \tag{15}$$

where $\alpha\equiv\omega^2LC_0$ and $\beta\equiv\omega C_0\omega^2L^2/R_{1\infty}$.

Neglecting $\alpha$ and $\alpha/\beta$ which are much smaller than unity according to Table II, one obtains the condition, $\omega C_0R=1$, which is the conclusion of the previous paper[8]. The depth of $R_1$ at minimum point predominantly depends upon the third term in the right-hand side of Eq. 14. Substituting the condition, $\omega C_0R=1$, into the third term, it becomes $\beta/2$. Then, the following results can be easily found. (a) Using the same coil, the depth of $R_1$ at minimum point increases with the increase of frequency. (b) Using the same frequency, which is approximately determined by the expression, $\omega^2LC=1$, the depth increases with the increase of $L/C$. (c) Even though the same frequency is used, the concentration of aqueous solution at the minimum point varies with the salts in solution.

Investigating the results of Fig. 2 in detail, it is noticed that $R_1$ of curve 9 or 10 is a little larger than $R_{1\infty}$ when the concentration increases.

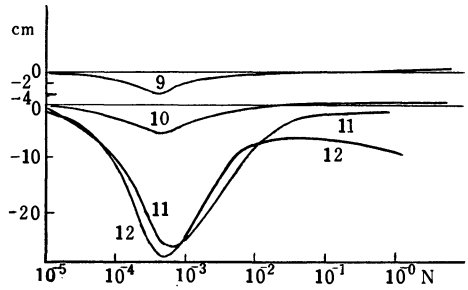



Fig. 2. Relation (Ref. 8) between change of length (resistance) of platinum wire and concentration of salt in aqueous solution for condenser-type.
9, 10, 11 : Ammonium nitrate solution.
12 : Sodium chloride solution.

10) K. Nakano, private communication.

TABLE I

| Nos. of turn of coil | Material in beaker | Freq. Kc | $\omega_\infty^2/\omega_0^2$ | $100^2/\omega_\infty^2L^2$ / $100^2/\omega_0^2L^2$ | $10^{12}/\omega_\infty^2L$ / $10^{12}/\omega_0^2L$ | $C_0$ / $p$ |
|---|---|---|---|---|---|---|
| 100 ($L=4.3\times10^{-4}$H) | air | 1050 | $4.35\times10^{13}$ | $1.24\times10^{-3}$ | $53.4_4$ | $2.1_1$ |
| | mercury | 1030 | 4.19 〃 | 1.29 〃 | $55\cdot5_5$ | |
| 70 ($L=2.9\times10^{-4}$H) | air | 1280 | 6.47 〃 | 1.84 〃 | $53.3_1$ | $2.6_1$ |
| | mercury | 1250 | 6.17 〃 | 1.93 〃 | $55.9_2$ | |
| 40 ($L=1.3\times10^{-4}$H) | air | 1872 | $1.38\times10^{14}$ | 4.28 〃 | $55.6_2$ | $2.2_6$ |
| | mercury | 1835 | 1.33 〃 | 4.45 〃 | $57.8_8$ | |

TABLE II

| No. of curve | Salt | Nos. of turn of coil | $L$ henry | Freq. cycle | $\omega$ | $\alpha$ | $\alpha/\beta$ | $\frac{\omega C_0\omega^2L^2}{2\times10}$ |
|---|---|---|---|---|---|---|---|---|
| 9 | $NH_4NO_3$ | 100 | $4.3\times10^{-4}$ | $1.12\times10^6$ | $7.037\times10^6$ | $4.90\times10^{-2}$ | $3.30\times10^{-3}$ | 7.40 |
| 10 | 〃 | 40 | $1.3\times10^{-4}$ | 1.27 〃 | 7.979 〃 | 1.90 〃 | 9.64 〃 | 0.986 |
| 11 | 〃 | 40 | 〃 | 1.88 〃 | 1.181 〃 | 4.17 〃 | 6.51 〃 | 3.20 |
| 12 | NaCl | 70 | $2.9\times10^{-4}$ | 1.26 〃 | 7.916 〃 | 4.18 〃 | 4.35 〃 | 4.79 |

This fact is attributed to the second term in the left-hand side of Eq. 14, though the right-hand side of Eq. 14 contains half the value of the same term. It is very desirable to calculate the value of $R_1$ at the minimum point, which is nearly equal to $R_{1\infty}(1-\beta/2)$. According to Table II, however, they should have a negative value except in the case of curve 10 and this is hard to be explained. Therefore, it is necessary to examine the equivalent circuit again more in detail and the results will be discussed later.

### Calculation for Coil-type Instrument

Fig. 3 is considered as the equivalent circuit for the coil-type instrument (refer to Fig. 7b). This equivalent circuit except when including $R_1$ is the same as the one in the previous paper[8] which contains the element $KLR$ showing the effect of eddy current. According to the same consideration of the equivalent circuit, the following results may be obtained:

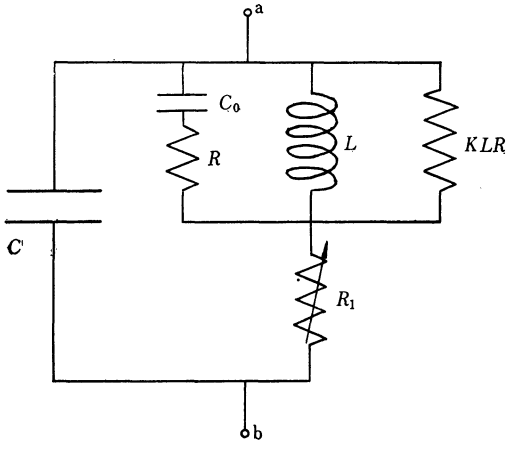



Fig. 3. Equivalent circuit for coil-type.

$$\frac{1}{Z}=\left\{\frac{(\omega C_0)^2R}{1+(\omega C_0R)^2}+\frac{1}{KLR}\right\}+j\left\{\frac{\omega C_0}{1+(\omega C_0R)^2}-\frac{1}{\omega L}\right\}\equiv A+jB \tag{16}$$

$$(A^2+B^2)R_1=-\frac{R_{1\infty}}{\omega L}B-A \tag{17}$$

$$\omega C=-B\frac{1+(A/B)^2}{1+(R_{1\infty}/\omega L)^2} \tag{18}$$

As it is rather difficult to determine the distributed capacity of coil, $C_0$, by these relations, the value shown in the previous paper[8] will be used in the following discussions.

As mentioned above, the change of frequency is expected to be caused by the change of $R$. But it is neglected, as the change of frequency was experimentally[10] found to be not so large. After the rearrangement of Eq. 17, it is written as

$$\left\{1-\frac{2\omega^2LC_0}{1+(\omega C_0R)^2}+\left(\frac{\omega L}{KLR}\right)^2+\frac{(\omega^2LC_0)^2(1+2/KL)}{1+(\omega C_0R)^2}\right\}R_1=R_{1\infty}\left\{1-\frac{\omega^2LC_0}{1+(\omega C_0R)^2}-\frac{\omega C_0R}{1+(\omega C_0R)^2}\frac{\omega C_0\omega^2L^2}{R_{1\infty}}-\frac{1}{KLR}\frac{\omega^2L^2}{R_{1\infty}}\right\} \tag{19}$$

As the first order approximation, the following expression to show the behaviors of all curves for the coil-type instrument is obtained:

$$R_1=R_{1\infty}\left\{1-\frac{\omega C_0R}{1+(\omega C_0R)^2}\frac{\omega C_0\omega^2L^2}{R_{1\infty}}-\frac{1}{KLR}\frac{\omega^2L^2}{R_{1\infty}}\right\} \tag{20}$$

The conditions which give the minimum and the maximum points are the same as the one

TABLE III

| No. of curve | Nos. of turn of coil | Freq. cycle | $\omega$ | $C_0$ / $p$ | $\alpha$ | $\frac{\omega C_0 \omega^2 L^2}{2\times 10}$ |
|---|---|---|---|---|---|---|
| 2 | 40 | $1.45\times10^6$ | $9.111\times10^6$ | 0.0665 | $7.18\times10^{-4}$ | 0.0425 |
| 3 | 70 | 〃 | 〃 | 0.126 | $3.03\times10^{-3}$ | 0.401 |
| 4 | 100 | $1.46\times10^6$ | $9.173\times10^6$ | 0.50 | $1.81\times10^{-2}$ | 3.57 |
| 5 | 100 | $7.575\times10^5$ | 4.759 〃 | 〃 | $4.87\times10^{-3}$ | 0.498 |
| 6 | 70 | 9.05 〃 | 5.686 〃 | 0.126 | $1.18\times10^{-3}$ | 0.0973 |
| 7 | 40 | $1.40\times10^6$ | 8.796 〃 | 0.0665 | $6.69\times10^{-4}$ | 0.0382 |

in the previous paper[8]

$$R=\frac{1}{\omega C_0}\sqrt{\frac{KL-2\pm\sqrt{(KL-2)^2-4(KL+1)}}{2(KL+1)}} \tag{21}$$

where positive and negative signs show minimum and maximum, respectively.

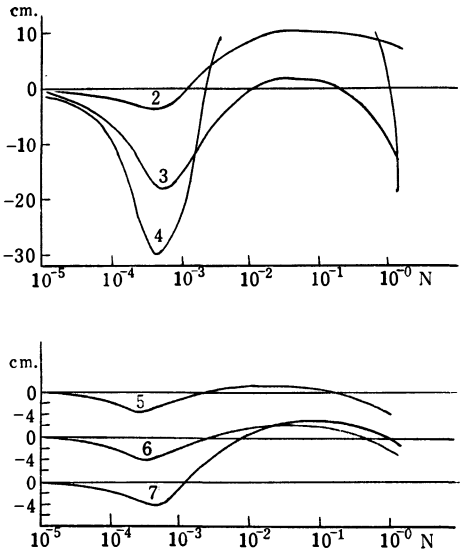



Fig. 4. Relation (Ref. 8) between change of length (resistance) of platinum wire and concentration of sodium chloride in aqueous solution for coil-type.

Investigating the curve in Fig. 4, it is noticed that the maximum value of $R_1$ is larger than the initial value $R_{1\infty}$. This fact should be ascribed to the second terms of the two sides in Eq. 19. But the value of $\alpha(\equiv\omega^2LC_0)$ in Table III is too small for this conclusion. In Table III the values of $\beta/2$ $(\equiv\omega C_0\omega^2L^2/2R_{1\infty})$ which cause the minimum points are smaller than unity except in the case of curve 4.

### Re-examination of Equivalent Circuit

It is difficult to understand, for the condenser-type and the coil-type instruments, why the value of $\beta/2$ is greater than unity. The question arises, thus, whether the resistance value of platinum wire at high frequency would be much greater than the value at direct current or not. Even if only the coil-type is taken up, it is difficult to consider that the value at about one megacycle becomes greater than four times the value at direct current. Now, let us consider the loss of coil itself. Assuming that the low resistance, $R_l$, is connected in series with the inductance of the coil, $L$, the equivalent circuit for the coil-type instrument becomes Fig. 5, in

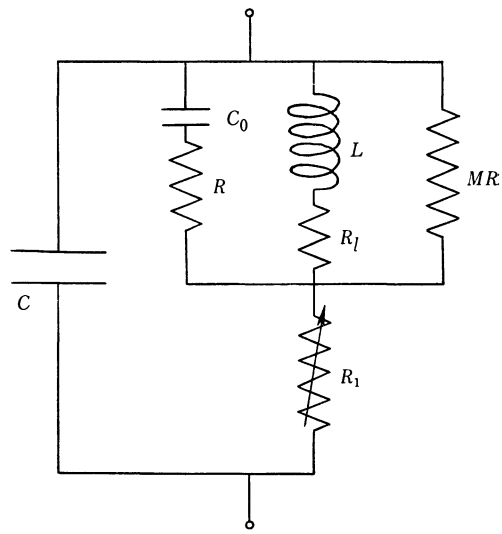



Fig. 5. Equivalent circuit with low resistance showing loss of coil.

which notation, $M$, means $KL$. The equivalent circuit for the condenser-type instrument is easily obtained by setting $M=\infty$. Repeating the calculation as before, one obtains

$$\frac{1}{Z}=\left\{\frac{(\omega C_0)^2R}{1+(\omega C_0R)^2}+\frac{R_l}{(\omega L)^2+R_l^2}+\frac{1}{MR}\right\}+j\left\{\frac{\omega C_0}{1+(\omega C_0R)^2}-\frac{\omega L}{(\omega L)^2+R_l^2}\right\}\equiv A+jB \tag{22}$$

$$(A^2+B^2)R_1=-\frac{Y_{\text{real}}}{\omega C}B-A \tag{23}$$

$$\omega C=-B\frac{1+(A/B)^2}{1+(Y_{\text{real}}/\omega C)^2} \tag{24}$$

where

$$Y_{\text{real}}=\frac{C}{L}(R_{1\infty}+R_l)$$

After the rearrangement, Eq. 23 is written as follows:

$$\left\{1-\frac{2\alpha}{1+x^2}+\frac{2\alpha x Q^{-1}}{1+x^2}+\frac{2\alpha Q^{-1}}{Mx}+\frac{\alpha^2(1+Q^{-2})}{(Mx)^2}+\frac{\alpha^2(1+Q^{-2})(1+2/M)}{1+x^2}\right\}R_1$$
$$=R_{1\infty}\left\{1-\frac{\alpha(1+Q^{-2})(R_{1\infty}+R_l)}{(1+x^2)R_{1\infty}}-\frac{x}{1+x^2}\frac{\omega C_0(\omega L)^2(1+Q^{-2})}{R_{1\infty}}-\frac{\omega C_0(\omega L)^2(1+Q^{-2})}{MxR_{1\infty}}\right\} \quad (25)$$

where $x\equiv\omega C_0R$, $\alpha\equiv\omega^2LC_0$ and $Q^{-1}\equiv R_l/\omega L$.

In Eq. 25, the term which gives the minimum value for the resistance $R_1$ is the same as the one in Eq. 19 except for the factor, $1+Q^{-2}$, being greater than unity. Therefore, it seems impossible in this procedure to find that the term in question has a value smaller than unity.

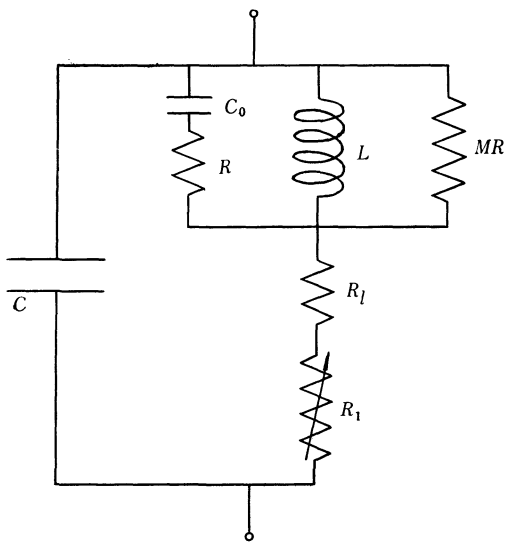



Fig. 6. Another equivalent circuit with low resistance showing loss of coil.

Now, Fig. 6 is considered instead of Fig. 5. In Eq. 19, substituting as follows $R_1\rightarrow R_1+R_l$, $R_{1\infty}\rightarrow R_{1\infty}+R_l$, the following equation is obtained:

$$\left\{1-\frac{2\omega^2LC_0}{1+(\omega C_0R)^2}+\left(\frac{\omega L}{MR}\right)^2+\frac{(\omega^2LC_0)^2(1+2/M)}{1+(\omega C_0R)^2}\right\}(R_1+R_l)$$
$$=(R_{1\infty}+R_l)\left\{1-\frac{\omega^2LC_0}{1+(\omega C_0R)^2}-\frac{\omega C_0R}{1+(\omega C_0R)^2}\frac{\omega C_0\omega^2L^2}{(R_{1\infty}+R_l)}-\frac{\omega^2L^2}{MR(R_{1\infty}+R_l)}\right\} \quad (26)$$

The $Q$ of the coil shows $\omega L/R_l$ and then $R_l$ is calculated from $Q$ at the corresponding frequency. Two cases[10] are considered for the $Q$ of the coil. One of them is to measure only the coil, and the other case is to measure the coil containing distilled water. The former should be considered for the condenser-type instrument, whereas the latter for the coil-type instrument with the assumption that the loss by distilled water is contained in $Q(=\omega L/R_l)$. In Table IV the values of the terms in question for the coil-type instrument are less than unity. The resistance value of platinum wire is 0.2 Ω/cm. and $M\approx10^3$ as shown in the previous paper[8]. The calculated values of the depth at minimum point agree with the experimental values in the case of curves 3 and 6 in Table IV. But the values of curves 4 and 5 are too great in comparison with the experimental ones, though the values of curves 2 and 7 are not discussed.

The calculated values for the condenser-type instrument are shown in Table V. In this case, the values of the terms in question become smaller than the previous value, but some of them are still greater than unity. Therefore, this equivalent circuit seems not to be useful

TABLE IV

| No. of curve | $\omega L$ | $Q$* | $R_l$ | $\frac{\omega C_0\omega^2L^2}{2(R_{1\infty}+R_l)}$ | Depth** of curve Ω | Depth** of curve cm. | Exp. value |
|---|---|---|---|---|---|---|---|
| 2 | 1186 | 68.0 | 17.4 | 0.0155 | −0.415 | −2.07 | −4.0 |
| 3 | 2642 | 77.5 | 34.1 | 0.0908 | −3.95 | −19.7 | −18.5 |
| 4 | 3944 | 91.5 | 43.1 | 0.672 | −35.7 | −179 | −31 |
| 5 | 2046 | 119.5 | 17.1 | 0.184 | −4.94 | −24.7 | −3.5 |
| 6 | 1648 | 88.0 | 18.7 | 0.0339 | −0.956 | −4.78 | −4.0 |
| 7 | 1143 | 68.0 | 16.8 | 0.0143 | −0.374 | −1.87 | −4.5 |

* According to K. Nakano[10]

** $(R_1)_{\min}-R_{1\infty}\fallingdotseq(R_{1\infty}+R_l)\left\{\frac{\alpha}{2}-\frac{\omega C_0\omega^2L^2}{2(R_{1\infty}+R_l)}\right\}/(1-\alpha)$

for the calculation of the depth of the condenser-type instrument, though $Q$ is the value of the coil without the condenser-type electrode.

TABLE V

| No. of curve | $\omega L$ | $Q$* | $R_l$ | $\frac{\omega C_0 \omega^2 L^2}{2(R_{l\infty}+R_l)}$ |
|---|---|---|---|---|
| 9 | 3026 | 112.8 | 26.8 | 2.01 |
| 10 | 1037 | 71.5 | 14.5 | 0.403 |
| 11 | 1535 | 67.8 | 22.6 | 0.982 |
| 12 | 2296 | 88 | 26.1 | 1.33 |

* According to K. Nakano[10]

The calculation on high frequency titration has been extended on the basis of Nakano's paper[8]. As a result of calculation, the relation between the variable resistance, $R_1$, and the high frequency resistance, $R$, having some connection with the concentration of solution becomes clear in some degree, including the condition, $\omega C_0 R = 1$. The term $\omega^2 LC_0/1+(\omega C_0 R)^2$, seems to cause the fact that $R_1$ becomes greater than $R_{1\infty}$ in the case of concentrated solution. Some of the calculated values of depth at minimum point are considerably great in comparison with the experimental one in the case of the coil-type instrument and can not be obtained in the case of the condenser-type instrument. Hence, it seems necessary to take into account another factor in the calculation of the equivalent circuit in order to obtain better agreement with the experimental results.

The sample solution in the condenser-type electrode or the coil has the capacitance together with the resistance as shown in Nakano's paper[8]. The former was omitted in Nakano's paper, under the assumption that the effect of the former is negligible when the value of the latter is not so great. Now, let us consider the equivalent circuit (Fig. 8) on the basis of Figs. 7a and 7b. This equivalent circuit is of the same physical meaning as in the case of Fig. 5 except in the

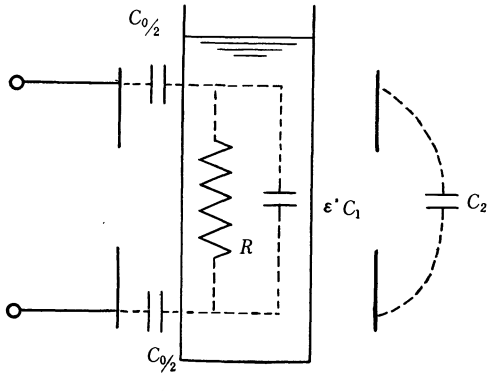



Fig. 7 (a). Relation between sample solution in condenser-type electrode and equivalent circuit.

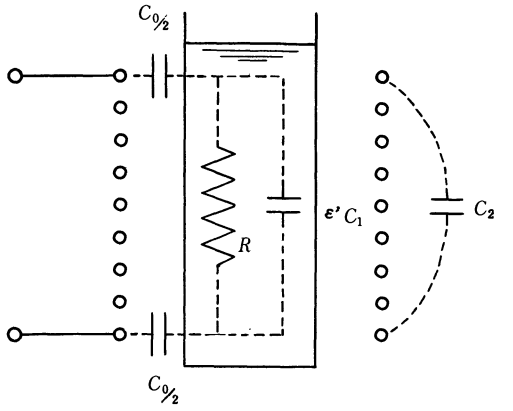



Fig. 7 (b). Relation between sample solution in coil and equivalent circuit.

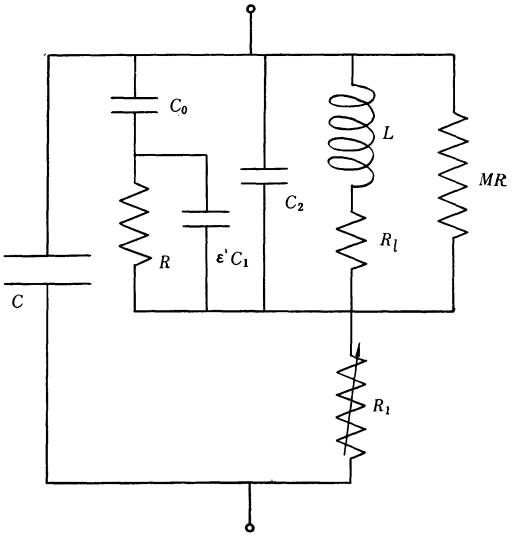



Fig. 8. Equivalent circuit taking into account another factor.

case of the capacitance, $\varepsilon' C_1$, $C_2$, which are visualized by Figs. 7a and 7b, where the notation $\varepsilon'$ means the dielectric constant (real part) of the sample solution. As mentioned above, the sample solution in the condenser-type electrode or the coil has the capacitance, which is shown by the notation $\varepsilon' C_1$ in Figs. 7a or 7b (and Fig. 8) instead of $C_1$ in Nakano's paper. The notation $C_2$ shows the rest of the capacitance of the condenser-type electrode in Fig. 7a and the rest of the self capacitance of the coil in Fig. 7b, which has also been shown by $C_3$ in the recent paper[11].

Again one repeats the similar calculation of this equivalent circuit containing another factor $\varepsilon' C_1$ and $C_2$. As a result of calculation, the following equation is easily obtained:

11) P. F. Knewstubb and T. M. Sugden, *Trans. Faraday Soc.*, **54**, 372 (1958).

$$\frac{1}{Z}=\left\{\frac{(\omega C_0)^2R}{1+\omega^2(\varepsilon'C_1+C_0)^2R^2}+\frac{R_l}{R_l^2+(\omega L)^2}+\frac{1}{MR}\right\}$$
$$+j\left[\frac{\omega C_0\{1+\omega^2\varepsilon'C_1(\varepsilon'C_1+C_0)R^2\}}{1+\omega^2(\varepsilon'C_1+C_0)^2R^2}\right.$$
$$\left.+\omega C_2-\frac{\omega L}{R_l^2+(\omega L)^2}\right]\equiv A+jB \qquad (27)$$

$$(A^2+B^2)R_1=-\frac{Y_{\text{real}}}{\omega C}B-A \qquad (28)$$

$$\omega C=-B\frac{1+(A/B)^2}{1+(Y_{\text{real}}/\omega C)^2} \qquad (29)$$

$$Y_{\text{real}}=\frac{C}{L}\frac{\{1-2\alpha_\infty+\alpha^2{}_\infty(1+Q_{\infty 1}^{-2})\}R_{1\infty}+R_l}{1-\alpha_\infty(1+Q_{\infty 1}^{-2})} \qquad (30)$$

where $Q_{\infty 1}\equiv\omega_{\infty 1}L/R_l$, $\alpha_\infty\equiv\omega^2{}_{\infty 1}L\left(C_2+\frac{C_0C_1}{C_1+C_0}\right)$, $\omega_{\infty 1}$ and $R_{1\infty}$ are the angular frequency $\omega$ and the variable resistance $R_1$, when $R=\infty$ and $\varepsilon'=1$, respectively. After the rearrangement of Eq. 28, it is written as the following expression corresponding to Eq. 25:

$$\left[1-2\alpha_2+\alpha_2^2(1+Q^{-2})-\frac{2\alpha(1+qx^2)}{1+x^2}\right.$$
$$+\frac{2\alpha pxQ^{-1}}{1+x^2}$$
$$+\frac{2\alpha\{\alpha_2(1+qx^2)+p\omega L/M_0\}(1+Q^{-2})}{1+x^2}$$
$$+\frac{\alpha^2(1+Q^{-2})\{(px)^2+(1+qx^2)^2\}}{(1+x^2)^2}$$
$$\left.+\frac{2Q^{-1}\omega L}{M_0x}+\left(\frac{\omega L}{M_0x}\right)^2(1+Q^{-2})\right]R_1$$
$$=\frac{\xi R_{1\infty}+\eta R_l}{1-\eta}\left[1-\frac{\xi R_{1\infty}+R_l}{\xi R_{1\infty}+\eta R_l}\left\{\alpha_2+\frac{\alpha(1+qx^2)}{1+x^2}\right\}\right.$$
$$\left.\times(1+Q^{-2})-\left(\frac{\alpha px\omega L}{1+x^2}+\frac{\omega^2L^2}{M_0x}\right)\frac{(1+Q^{-2})(1-\eta)}{\xi R_{1\infty}+\eta R_l}\right] \qquad (31)$$

where

$$x\equiv\omega(\varepsilon'C_1+C_0)R,\ Q\equiv\omega L/R_l,$$
$$M_0\equiv M/\omega(\varepsilon'C_1+C_0)$$
$$p\equiv\frac{C_0}{\varepsilon'C_1+C_0},\quad q\equiv\frac{\varepsilon'C_1}{\varepsilon'C_1+C_0}$$
$$\alpha\equiv\omega^2LC_0\qquad\alpha_2\equiv\omega^2LC_2$$
$$\xi\equiv 1-2\alpha_\infty+\alpha^2{}_\infty(1+Q_{\infty 1}^{-2}),\ \eta\equiv\alpha_\infty(1+Q_{\infty 1}^{-2})$$

Thus, the term in question becomes

$$\frac{\alpha px\omega L}{1+x^2}\frac{1+Q^{-2}}{R_{1\infty}} \qquad (32)$$

assuming that $\xi$ and $\eta$ are approximately equal to unity and zero, respectively. It seems that the condition giving the minimum point is almost entirely determined by this term taking the rest into account. This term contains the significant factor $p$, which contains $\varepsilon'C_1$ and $C_0$, as compared to the corresponding term in Eq. 25. The capacitance of the sample solution, $\varepsilon'C_1$, will be comparable to or larger than $C_0$, when the sample solution is an aqueous solution which has a large value of dielectric constant, though $C_1$ is considerably smaller than $C_0$. Thus, it is possible to find the possibility that the factor $p$ has a value somewhat smaller than unity, since the capacitance of the sample solution, $\varepsilon'C_1$, can not be neglected in comparison with the capacitance $C_0$. It seems likely that the consideration of the factor, $\varepsilon'C_1$, is helpful for the solution of the problem being discussed in this paper.

The author desires to thank Dr. K. Nakano for his support and advice. His numerous suggestions and interest have contributed much to this investigation. The author also desires to thank Dr. H. Honda for his kind encouragement throughout the investigation.

*Shigengijutsu-Shikenjo*
*Resources Research Institute*
*Kawaguchi-shi, Saitama*

# *Vapor Phase Oxidation of Methyl Naphthalenes*[1]

By Shigeru MORITA

(Received September 23, 1959)

In 1916, Wohl[2] and Gibbs & Conover[3] discovered that, in the presence of vanadium pentoxide, naphthalene is oxidized to phthalic anhydride at 350 to 550°C. The ever-increasing demand for phthalic anhydride has in recent years stimulated the search for alternative raw materials. A patent claim was made that phthalic anhydride appears in the products of the catalytic air oxidation of methyl naphthalenes and phenanthrene. Methyl naphthalene oil[4] (a mixture of methyl naphthalene isomers, naphthalene and others) gave phthalic anhydride in the yield of 50~60%, but both pure 1- and 2-methyl naphthalenes[5] produced it in 30~40%. This yield is very low, in comparison with that from naphthalene (60~80%)[6]. The cause has not been studied. Reaction heat from methyl naphthalenes to phthalic anhydride is 605 kcal./mol. and is larger than that from naphthalene (450 kcal./mol.). Some investigators[7] accordingly proposed that the catalyst zone was superheated and phthalic anhydride once produced was decomposed, and the yield was lowered as a consequence.

The author studied the reaction mechanism of the vapor phase oxidation of methyl naphthalenes and related compounds and clarified the cause of the low yield.

## Experimental

**Apparatus.**—It is the same as that reported before[8].

**Experimental Conditions.**—The air rate was 150 l. per hour, the feed rate 1.5 g. per hour; the range of reaction temperatures was 350~500°C, and the catalyst volume was 50 ml.

The method of preparing the catalyst[8] was also reported before ($V_2O_5$-$MoO_3$-pumice stone).

The physical constants of reactants are listed in Table I.

## Results and Discussion

**Vapor Phase Oxidation of Methyl Benzenes.**—Methyl naphthalenes have two benzene rings condensed, whereas phthalic anhydride has one. Therefore, in order for methyl naphthalenes to produce phthalic anhydride by vapor phase oxidation, one of the two benzene rings of methyl

TABLE I. PHYSICAL CONSTANTS OF MATERIAL USED FOR VAPOR PHASE OXIDATION

| Materials | °C | °C |
|---|---|---|
| Naphthalene | m.p. 80.3 | |
| 1-Methyl naphthalene | f.p. −32.0 | b.p. 245.0 |
| 2-Methyl naphthalene | m.p. 32.0 | b.p. 241.6 |
| *o*-Xylene | f.p. −26 | b.p. 143~144 |
| 1, 2, 3-Trimethyl benzene | f.p. −19.8 | b.p. 173.4~174.5 |
| 1, 2, 4-Trimethyl benzene | b.p. 168.0~168.5 | $d_4^{20}$ 0.8755 |
| 1, 2, 4-Benzene-tricarboxylic acid | b.p. 216~217 | |
| Naphthalene-1-carboxylic acid | m.p. 160.5 | |
| Naphthalene-2-carboxylic acid | m.p. 183.5~184.0 | |
| Tetralone | $b.p._{.13}$ 127 | $d_4^{20}$ 1.092 |
| 2-Methyl-1, 4-naphthoquinone | m.p. 34.2 | |
| 2, 6-Dimethyl naphthalene | m.p. 109.5~110.0 | |
| 2, 7-Dimethyl naphthalene | m.p. 95.5~96.5 | |
| Dimethyl naphthalene oil | b.p. 260~268 | |
| Acenaphthene | m.p. 94.5 | |

1) This is a summary of reports published in *J. Chem. Soc. Japan, Pure Chem. Sec.* (*Nippon Kagaku Zasshi*), **80**, 509, 514 (1959).
2) A. Wohl, Ger. Pat., 379,882 (Sep. 4, 1916).
3) H. D. Gibbs and C. Conover, Brit. Pat., 119,518 (Oct. 1, 1918).
4) J. Shelmerdine et al., *J. Appl. Chem.*, **3**, 513 (1953); T. Yatagai, *J. Japan, Tar Ind. Assoc.* (*Coal Tar*), **9**, 648, (1957).
5) R. Norris et al., *Ind. Eng. Chem.*, **35**, 279 (1943); C. R. Kinney et al., ibid., **43**, 3880 (1951).
6) L. F. Marek and D. A. Hahn, "The Catalytic Oxidation of Organic Compound in the Vapor Phase", American Chemical Society Monograph No. 61., Chemical Catalog Co., New York (1932), p. 404.
7) H. Sasayama, *J. Chem. Soc. Japan, Ind. Chem. Sec.* (*Kogyo Kagaku Zasshi*), **46**, 1225 (1943).
8) S. Morita, This Bulletin, **33**, 309 (1960); O. Hibino and S. Morita, *J. Chem. Soc. Japan, Pure Chem. Sec.* (*Nippon Kagaku Zasshi*), **78**, 1766 (1957).

TABLE II. VAPOR PHASE OXIDATION OF METHYL BENZENES AND THE RELATED COMPOUNDS

| Materials | Reaction temp. °C | Products | | | Material unreacted |
|---|---|---|---|---|---|
| | | Phthalic anhydride mol. % | Maleic anhydride mol. % | Benzene tricarboxylic acid | |
| *o*-Xylene | 400 | 66 | 7 | 0 | 0 |
| 1, 2, 3-Trimethyl benzene | 400 | 0 | 3 | trace | 0 |
| 1, 2, 4-Trimethyl benzene | 400 | 0 | 3 | trace | 0 |
| 1, 2, 4-Benzene-tricarboxylic acid | 400 | 0 | 5 | 0 | 0 |

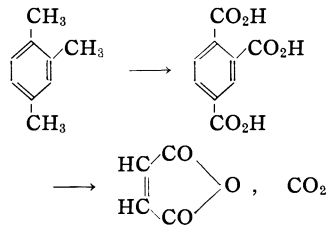
naphthalenes has to be cleaved to form benzene containing two side chains, followed by oxidation to the acid. The author studied the behavior of the side chains of the benzene ring during the vapor phase oxidation.

Toluene, *o*-xylene, 1, 2, 3- and 1, 2, 4-trimethyl benzenes were oxidized in vapor phase under the same conditions mentioned earlier. The results are listed in Table II.

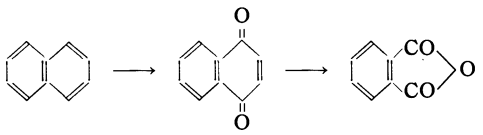
As shown in Table II, phthalic anhydride was produced from *o*-xylene, and benzoic acid from toluene. Therefore, it is apparent that the methyl group is oxidized to carboxylic acid before the benzene ring is cleaved. Sasayama[9] reported that oxidation of trimethyl benzene proceeded stepwise as follows:

trimethyl benzene → benzene-tricarboxylic acid → phthalic anhydride → benzoic acid → benzene → maleic anhydride.

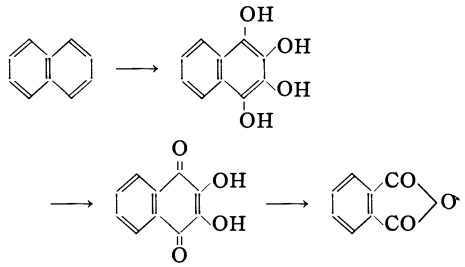
The results obtained by the author showed that both 1, 2, 3- and 1, 2, 4-trimethyl benzenes, on vapor phase oxidation, gave maleic anhydride (in 3% yield) and carbon dioxide, accompanied by very small amounts of 1, 2, 3- and 1, 2, 4-benzene-tricarboxylic acids, respectively, but gave neither phthalic anhydride nor benzoic acid. Furthermore, 1, 2, 4-benzene-tricarboxylic acid gave no phthalic anhydride, but only maleic, anhydride (in 5% yield) and carbon dioxide and no unreacted material was found. The yield of maleic anhydride in this case was comparable with that from 1, 2, 4-trimethyl benzene; therefore, benzene-tricarboxylic acid was presumably formed as an intermediate in the oxidative degradation of trimethyl benzene. However, decarboxylation of the extra carbonyl group did not ensue and the benzene ring was cleaved by the oxidation to form maleic anhydride and carbon dioxide.




**Vapor Phase Oxidation of Methyl Naphthalenes and their Related Compounds.**—The mechanism[10] of the vapor phase oxidation of naphthalene is described as follows:




Meanwhile, Pongratz[11] proposed the following route:




In either case, a carbon-hydrogen bond in one of two benzene rings is broken and a new carbon-oxygen bond is formed in its place, and then the benzene ring containing oxygen is cleaved.

Two benzene rings of naphthalene are equivalent reaction-wise but those of methyl naphthalenes are not, due to the presence of the methyl group in one ring.

Pongratz[11] studied the vapor phase oxidation of chloro-, nitro-, and hydroxy-naphthalenes and found that both 1- and 2-chloronaphthalenes produced phthalic anhydride and monochlorophthalic anhydride. These results show that chlorinated as well as unsubstituted benzene rings were cleaved, but he also obtained phthalic anhydride from 1, 5-dichloronaphthalene and concluded that dechlorination took place during the oxidation.

So far, no report has been made on the mechanism of vapor phase oxidation of methyl naphthalenes. The author examined four conceivable mechanisms (**a**, **b**, **c** and **d**) of vapor phase oxidation of methyl naphthalenes.

*Mechanism* ***a***.—Kato[12] and coworkers obtained naphthalene-carboxylic acids in 86% yield

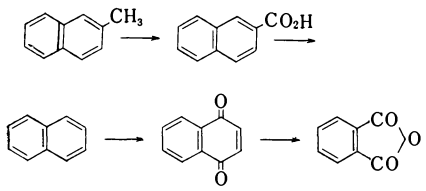
9) H. Sasayama, *J. Chem. Soc. Japan, Ind. Chem. Sec.* (*Kogyo Kagaku Zasshi*), **56**, 281 (1953).

10) C. R. Downs, *J. Soc. Chem. Ind.*, **46**, 383 T(1927).

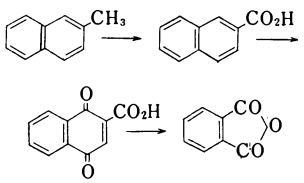
11) A. Pongratz, *Angew. Chem.*, **54**, 22 (1941).

12) S. Kato et al., "Abstracts of the 11th Annual Meeting of Chem. Soc. Japan", Tokyo (1958), p. 18.

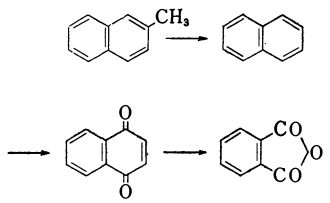
by heating methyl naphthalenes to 250°C with an aqueous solution of sodium dichromate in an autoclave. Pickering[13] et al. obtained the acid by oxidation of alkyl naphthalene with barium permanganate. In the same manner, in the vapor phase methyl naphthalene would first be oxidized to naphthalene-carboxylic acid, and then phthalic anhydride is produced as follows:



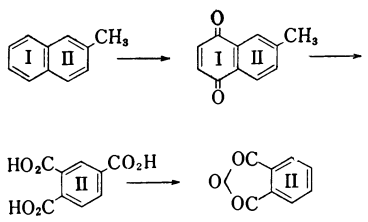
or



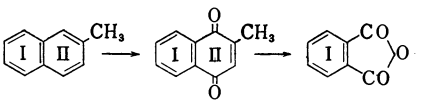
*Mechanism* ***b***.—Madison[14] obtained naphthalene by one-hour pyrolysis of 1- or 2-methyl naphthalene at 475°C, whereas Kynaston[15] obtained the same compound by passing acenaphthene with steam over a catalyst such as zinc oxide, chromium oxide or alumina. In the same way, methyl naphthalene would produce naphthalene by demethylation as an initial step and naphthalene would then be oxidized to phthalic anhydride:



*Mechanism* ***c***.—Unsubstituted benzene ring (I) of methyl naphthalene would be oxidized and produce phthalic anhydride with the concomitant decarboxylation of one of the three carboxyl groups.



*Mechanism* ***d***.—Benzene ring bearing the methyl group would be cleaved by oxidation and produce phthalic anhydride:



The author will discuss these four mechanisms.

*On mechanism* ***a***.—2-Methyl naphthalene was catalytically oxidized in the vapor phase under the same conditions at 350°C and the product contained 2-methyl-1, 4-naphthoquinone (identified as 2, 4-dinitrophenyl-hydrazone; m.p. 274°C uncor., no depression in mixed m.p.) but no naphthalene carboxylic acid. This result agrees with that obtained by Fieser[16].

Since decarboxylation is assumed in this mechanism, the possible occurrence of decarboxylation was examined. Naphthalene-1- or 2-carboxylic acid was passed through a reaction tube filled with pumice stone containing no vanadium pentoxide under the same conditions as in vapor phase oxidation (temperature, feed rate and air rate). The product did not contain naphthalene at all. In the same way, the acids were passed through the oxidation catalyst zone with a stream of carbon dioxide instead of air under the same conditions, but naphthalene was not obtained. Therefore, decarboxylation does not occur in the oxidation of naphthalene-carboxylic acid. This result is similar to the one obtained in the case of benzene-tricarboxylic acid.

From these results, it is supposed that mechanism **a** is incorrect.

*On mechanism* ***b***.—In order to check the assumption of demethylation, the following reaction was performed: methyl naphthalene was passed through a pumice stone zone with air or through an oxidation catalyst zone with carbon dioxide instead of air under the same conditions as in the vapor phase oxidation (temperature, feed rate and gas rate).

The products were carefully distilled, but naphthalene was not found. The density and refractive index of the product were identical with those of the starting material.

Madison's experiment[14] showed the formation of naphthalene from methyl naphthalenes but the heating period in his case was more than one hour. In vapor phase oxidation, the contact time was less than one second, and it is assumed that naphthalene was not formed in such a short time.

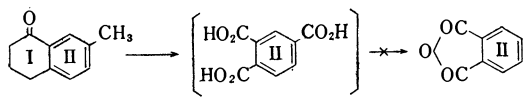
13) G. B. Pickering et al., *Rec. trav. chim.* **69**, 535 (1950); *Chem. Abstr.*, **44**, 838 (1950).
14) J. J. Madison et al., *Ind. Eng. Chem.*, **50**, 237 (1958).
15) W. Kynaston, *J. Soc. Chem. Ind.*, **68**, 225 (1949).
16) L. F. Fieser, *J. Am. Chem. Soc.*, **75**, 4377 (1953).

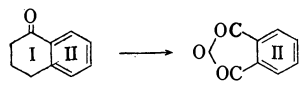
TABLE III. VAPOR PHASE OXIDATION OF METHYL NAPHTHALENES AND THEIR RELATED COMPOUNDS

| Materials | Reaction temp. °C | Products | | | | Material unreacted |
|---|---|---|---|---|---|---|
| | | Phthalic anhydride mol. % | Maleic anhydride mol. % | Benzene tricarboxylic acid | Others | |
| Naphthalene | 450 | 68 | 7 | 0 | — | 0 |
| 1-Methyl naphthalene | 400 | 26 | 4 | trace | a) | 0 |
| 2-Methyl naphthalene | 450 | 42 | 6 | trace | b) | 0 |
| Naphthalene-1-carboxylic acid | 400 | 27 | 21 | — | — | 4 |
| Naphthalene-2-carboxylic acid | 400 | 36 | 16 | — | — | 2 |
| Tetralone | 400 | 62 | 8 | 0 | — | 0 |
| 2-Methyl-1, 4-naphthoquinone | 400 | 65 | 8 | 0 | — | 0 |
| 7-Methyl tetralone | 400 | 0 | 3 | trace | — | 0 |

a) Trace of quinones
b) Trace of 2-methyl-1, 4-naphthoquinone

*On mechanism* **c**.—If the oxidation proceeds according to mechanism **c**, 1, 2, 4-benzene-tricarboxylic acid must produce phthalic anhydride. Consequently mechanism **c** is unlikely. To ascertain this conclusion, 7-methyl tetralone and tetralone were catalytically oxidized in the vapor phase under the same conditions. Tetralone produced phthalic anhydride in the same yield as that from naphthalene, but 7-methyl tetralone did not (Table III). The hydrogenated benzene ring of tetralone has an oxygen atom, and, on oxidation, this ring must have been cleaved in order to form phathalic anhydride. If the reaction proceeds similarly in the case of 7-methyl tetralone, the hydrogenated ring containing oxygen would be cleaved. This is the same course which 2-methyl naphthalene follows when it is oxidized through mechanism **c**.





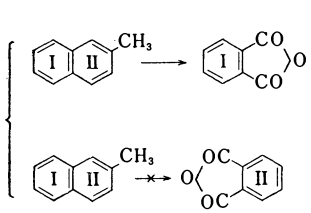
The oxidation products of 2-methyl naphthalene and 7-methyl tetralone caught in the hot part of an air condenser (collector of product) contained a trace of 1, 2, 4-benzene-tricarboxylic acid, which was identified by its melting point and neutralization equivalent. Thus, it is obvious that the benzene ring of methyl naphthalenes having no methyl group was cleaved, but no phthalic anhydride was produced.

*On mechanism* **d**.—If the benzene ring (II) of methyl naphthalenes having the methyl group is cleaved first and the resulting benzene ring (I) containing two side chains is oxidized, phthalic anhydride would be produced in the same way as from *o*-xylene. The benzene ring (II) of 2-methyl-1, 4-naphthoquinone which has a methyl group, contains two oxygen atoms. Therefore, by catalytic vapor phase oxidation, the benzene ring (II) is cleaved and the reaction follows only mechanism **d**.

The experiment showed that 2-methyl-1, 4-naphthoquinone produced phthalic anhydride in the yield of 65% which is the same as that obtained in the case of naphthalene and *o*-xylene. Accordingly, it is obvious that methyl naphthalenes produce phthalic anhydride only when it is oxidized through mechanism **d**.

From these experimental results it is seen that methyl naphthalenes do not produce phthalic anhydride by mechanism **c** but produce it in 60～70% yield by mechanism **d**.

The yield of phthalic anhydride obtained from methyl naphthalenes is about 30～40% by the catalyst used in these experiments ($V_2O_5$–$MoO_3$–pumice), German catalyst ($V_2O_5$–$K_2SO_4$–silica gel) or American catalyst ($V_2O_5$–alumina) and is about one half of that from naphthalene. It is conceivable that both reactions through mechanism **c** and **d** occur simultaneously to the same extent, as the presence of a trace of benzene-tricarboxylic acid was confirmed in the products.



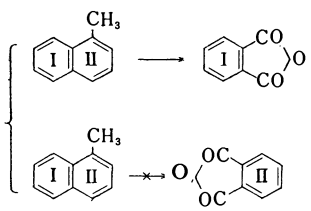
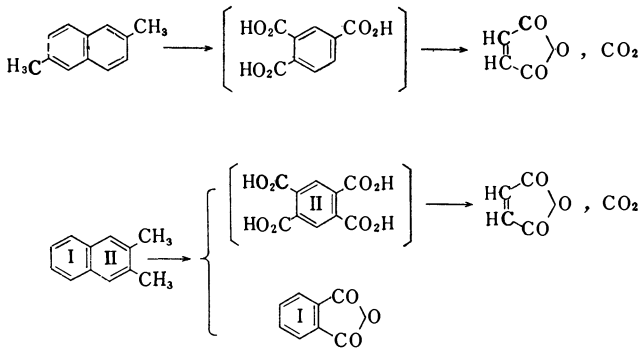


TABLE IV. VAPOR PHASE OXIDATION OF DIMETHYL NAPHTHALENES AND OTHERS

| Materials | Reaction temp. °C | Products | | | |
|---|---|---|---|---|---|
| | | Phthalic anhydride mol. % | Maleic anhydride mol. % | Naphthalic anhydride mol. % | Benzene tricarboxylic acid |
| 2, 6-Dimethyl naphthalene | 450 | 0 | 18 | 0 | trace |
| 2, 7-Dimethyl naphthalene | 450 | 0 | 20 | 0 | trace |
| Acenaphthene | 450 | 0 | 14 | 39 | 0 |
| Dimethyl naphthalene oil | 400 | 15 | 8 | 0 | trace |
| 2, 3-Dimethyl naphthalene[a)] | 375 | 43 | 7 | 0 | — |

a) This result was obtained by Kinney et al. ($V_2O_5$–$K_2SO_4$–silica gel).



If it is desired to produce phthalic anhydride in high yield from methyl naphthalenes, it is necessary to find the catalyst that is capable of cleaving only the benzene ring of methyl naphthalenes which have a methyl group.

**Vapor Phase Oxidation of Dimethyl Naphthalenes and Others.**—Kinney[5)] and coworkers obtained phthalic anhydride from 2, 3-dimethyl naphthalene in yields of 43% and 28% by the American and the German catalysts, respectively. Furthermore they obtained the anhydride in a 30% yield from a fraction (boiling in the 235~270°C range) of coal tar.

The author oxidized 2, 6- and 2, 7-dimethyl naphthalenes and obtained no phthalic anhydride but maleic anhydride in yields of 18 and 20%, respectively, and very small amounts of benzenetricarboxylic acid. He also obtained phthalic anhydride in a 15% yield by vapor phase oxidation of dimethyl naphthalene oil (boiling range, 260~268°C) of coal tar (Table IV).

Each of the two benzene rings of 2, 6-dimethyl naphthalene has one methyl group. Therefore, when either of them is cleaved by the oxidation, the resulting benzene ring has three side chains, and no phthalic anhydride would result according to the above-mentioned mechanism **c**. This conclusion agrees with the experimental results.

In the case of 2, 3-dimethyl naphthalene, one (II) of the two benzene rings has two methyl groups, and the other (I) has none. Therefore, when the benzene ring (II) which has two methyl groups is cleaved by vapor phase oxidation, phthalic anhydride would be produced by mechanism **d**, but when a benzene ring having no methyl group is cleaved, no phthalic anhydride would be produced by mechanism **c**. This conclusion agrees with the experimental results obtained by Kinney et al.

Acenaphthene is the compound that has an ethylidene group connecting positions 1 and 8 of naphthalene. Therefore, it is not conceivable that phthalic anhydride is formed. The author obtained naphthalic and maleic anhydrides but no phthalic anhydride.

From all the experiments mentioned above, it is concluded that the stability of rings and substituents against vapor phase oxidation in the decreasing order is as follows:

benzene ring > methyl group
> naphthalene ring > ethylidene group

The author is particularly indebted to Professor S. Kimura of Kyoto University, Dr. T. Yoshida, Superintendent of Tobata Chemical Works, and Mr. O. Hibino, Manager of Laboratory Department of the Yawata Chemical Industry Co., Ltd.

*Tobata Works*
*Yawata Chemical Industry Co., Ltd.*
*Yawata-shi, Fukuoka*

# *The Nitrogen Isotopic Equilibrium between Ammonia and Ammonium Ion**

By Tatsujiro ISHIMORI

(Received September 21, 1959)

A number of studies have been reported on the enrichment of $^{15}N$ with the isotopic exchange reaction between ammonia gas and aqueous ammonium ion. The fractionation factor for this exchange reaction has been reported[1-3]. A separation of nitrogen isotopes has been made by the use of cation exchange resins[4]. One of the equilibria involved in the separation process is the equilibrium of nitrogen isotopes between ammonia and ammonium ion in aqueous solution. This paper is a report on the investigation of the equilibrium by the use of cation exchanger. The equilibrium constants and enthalpy of the reaction have been measured. It is found that the use of ion exchanger will be useful to study such an equilibrium existing in aqueous solution. Further, the measurement of the equilibrium of nitrogen isotopes between ammonia gas and ammonium ion of its solid chloride has been carried out and is described in this paper.

In an aqueous solution of ammonia and ammonium ion at isotopic equilibrium with the ammonium ion adsorbed on a cation exchange resin, the equilibria involved are described by the equations:

$$^{15}NH_{3(aq)} + {}^{14}NH_{4(aq)}^{+} = {}^{14}NH_{3(aq)} + {}^{15}NH_{4(aq)}^{+} \qquad K_1 \quad (1)$$

$$^{14}NH_4R + {}^{15}NH_{4(aq)}^{+} = {}^{15}NH_4R + {}^{14}NH_{4(aq)}^{+} \qquad K_2 \quad (2)$$

$$^{14}NH_4R + {}^{15}NH_{3(R)} = {}^{15}NH_4R + {}^{14}NH_{3(R)} \quad (3)$$

$$^{15}NH_{3(aq)} + {}^{14}NH_{3(R)} = {}^{14}NH_{3(aq)} + {}^{15}NH_{3(R)} \quad (4)$$

where $NH_4R$ represents ammonium ion taken up into the cation exchanger phase by ion-exchange mechanism and $NH_{3(R)}$ ammonia adsorbed on an ion exchange resin. Equilibria 3 and 4 can be neglected in a solution of low pH, while they exist with the solution of high pH. However, the concentration of $NH_{3(R)}$ is small compared to that of $NH_4R$ when the concentration of $NH_{3(aq)}$ is low. The amount of $NH_{3(R)}$ is also smaller than that of $NH_{3(aq)}$ if the volume of the exchanger is smaller than that of the solution. Thus, the fractionation factor between the exchanger and solution phase may not greatly involve the contribution by $NH_{3(R)}$. Further, the equation

$$^{14}NH_4R + {}^{15}NH_{3(aq)} = {}^{15}NH_4R + {}^{14}NH_{3(aq)} \quad (5)$$

which is the sum of Eqs. 3 and 4, results also from Eqs. 1 and 2. Hence, Eqs. 1 and 2 are enough to represent the equilibria involved in the system of an aqueous solution of ammonia and ammonium ion, and an exchanger of ammonium ion form.

The following quantity can be measured conveniently:

$$\frac{(^{15}N/^{14}N)_{solution} - (^{15}N/^{14}N)_{exchanger}}{(^{15}N/^{14}N)_{exchanger}} = \delta \quad (6)$$

where $(^{15}N/^{14}N)_{exchanger}$ and $(^{15}N/^{14}N)_{solution}$ are the nitrogen isotope ratios in the exchanger and solution phase, respectively. The fractionation factor between the exchanger and solution phase is defined as follows:

$$K = \frac{(^{15}N/^{14}N)_{exchanger}}{(^{15}N/^{14}N)_{solution}} = \frac{1}{1+\delta} \quad (7)$$

This value can be obtained experimentally. Let the following concentrations be represented by the associated symbols:

$$(^{15}NH_{3(aq)}) = a', \quad (^{15}NH_{4(aq)}^{+}) = b', \quad (^{15}NH_4R) = c'$$

$$(^{14}NH_{3(aq)}) = a, \quad (^{14}NH_{4(aq)}^{+}) = b, \quad (^{14}NH_4R) = c$$

Then, the following relationship between $K_1$, $K_2$ and K can be readily derived:

$$\frac{1}{K} = \frac{a}{a+b}\left[\frac{1}{K_1K_2} + \frac{b}{aK_2}\right] \quad (8)$$

The value of $a/(a+b)$ and $b/a$ can be calculated from the dissociation constants of ammonia and water: $K_{dis}$ and $K_w$; if the pH value of the solution is known:

$$\frac{b}{a} \simeq \frac{b+b'}{a+a'} = \frac{K_{dis}}{K_w}(H^+) \quad (9)$$

$$\frac{a}{a+b} \simeq \frac{1}{1+\frac{K_{dis}}{K_w}(H^+)} \quad (10)$$

* This study has been done in the Chemistry Department of the University of Arkansas, Arkansas, U. S. A.

1) H. G. Thode, R. L. Graham and J. A. Ziegler, *Can. J. Research*, **B23**, 40 (1945).

2) E. W. Becker and H. Baumgartel, *Z. Naturforsch.*, **1**, 514 (1946).

3) I. Kirshenbaum, J. S. Smith, T. Crowell, J. Graff and R. McKee, *J. Chem. Phys.*, **15**, 440 (1947).

4) F. H. Spedding, J. E. Powell and H. J. Svec, *J. Am. Chem. Soc.*, 77, 6125 (1955).

It is assumed that $a \simeq a+a'$ and $b \simeq b+b'$ are held since nitrogen with natural isotopic abundance is used and the $^{15}N$ content is about 0.36%[5]. The numerical value of $K_{dis}/K_w$ is $1.04 \times 10^9$ at 30°C[6].

If the pH of the solution phase is less than 5, the concentration of $NH_{3(aq)}$ is negligibly small. Hence,

$$K = K_2 \qquad (11)$$

for the low pH. The value of $K_1$ can be calculated from Eq. 8, using the values of $K_2$, $K$ and pH value.

If the value of $K$ is measured at high pH, the concentration of ammonium ion is very low: $b \ll a$. Hence, Eq. 8 can be written as

$$K_1 = K/K_2 \qquad (12)$$

for the value of $K$ at high pH of the solution. This relation gives approximately the value of $K_1$. Spedding, Powell and Svec[4] have evaluated the fractionation factor, $K$, in the above-mentioned condition.

## Experimental

The ammonia solution was purified by distillation. The other chemicals were of analytical grade. The cation exchange resin used was Dowex 50, X-8.

The conventional water bath for a constant temperature was used. The temperature was controlled within ±0.2°C at the vicinity of the room temperature. The air bath was used to keep the elevated temperatures constant at 200°C to 275°C within ±2°C.

The mass spectrometer used was a Nier type, 60° sector, double collecter instrument designed to measure small differences in isotopic ratio as described by McKinney et al.[7] and Dole[8]. Measurements were made on the ions of mass 28 and 29 ($^{14}N^{14}N^+$ and $^{15}N^{14}N^+$). The result of each isotopic analysis is estimated to have a precision of ±0.0003 in the quantity of $\delta$.

A solution of ammonium chloride and ammonia was added to the cation exchange resin of the ammonium ion form. This mixture was allowed to stand for ten to twelve hours in the constant temperature bath with shaking and brought to isotopic equilibrium. Then, the solution phase was pipetted and acidified with sulfuric acid solution. The resin was separated from the solution by suction filtration. In each experiment, the solution or resin phase contained one to two milligram equivalents of nitrogen. Ammonium ion was converted to nitrogen gas by the oxidation with sodium hypobromite[9]. The resulting nitrogen gas was purified by repeatedly passing the gas over copper oxide at 800°C and through the liquid air[10]. A set of nitrogen gases from the solution and resin phase was analyzed with a mass spectrometer.

The isotopic equilibrium between gaseous ammonia and solid ammonium chloride was measured. The containing vessel was made of Pyrex glass and had two 200 ml. bulbs (Bulbs A and B). A vacuum stopcock (Stopcock 1) connected Bulbs A and B. On the opposite side of Stopcock 1, Bulb A had a well to insert a thermometer and Bulb B had another vacuum stopcock (Stopcock 2). The silicon grease used in the stopcocks was satisfactory at 200 to 275°C. Water vapor and gaseous ammonia were added, at 20 to 25 mmHg and 200 to 275 mmHg, respectively, to 50 to 100 mg. ammonium chloride in Bulb A and allowed to stand for 13 to 62 hr.

It was difficult to know whether or not isotopic equilibrium had been established. The equilibrium was considered to be established if the equilibrium constant did not increase with a longer period of standing at the same temperature. The vapor pressure of ammonium chloride is 117 mmHg at 275°C and 6 mmHg at 200°C[10]. Extra gaseous ammonia was added to get a large enough sample of gas phase for analysis. Water vapor was added to help isotopic equilibrium to be established[11].

After the establishment of isotopic equilibrium, the gas phase was collected in the evacuated Bulb B through Stopcock 1. The stopcock was turned through the window of the air bath. The vessel was taken out of the air bath and cooled with water. A sufficient amount of sulfuric acid was introduced into Bulb B through Stopcock 2 and gaseous ammonia was collected as ammonium ion in aqueous solution. Bulb A was disconnected and the ammonia gas in it was evacuated and replaced with air. Then, the solid ammonium chloride was dissolved with water.

## Experimental Results

The experimental fractionation factors between resin and the solution phase are listed in Table I with the pH values of the solution phases. The value of $K_1$ is calculated by Eq. 8 using the values of the experimental fractionation

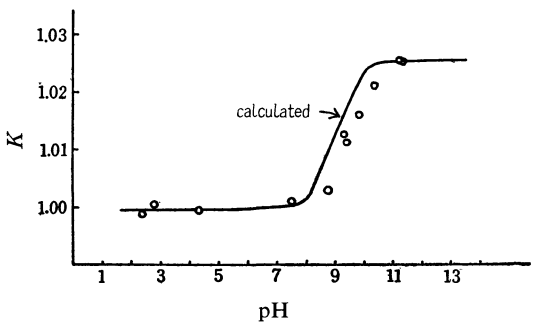



Fig. 1. Fractionation factor and pH.

5) K. T. Bainbridge and A. O. Nier, *Natl. Research Council (U. S.) Prelim. Rept.* 9, (1950).
6) W. M. Latimer, "Oxidation Potential", Prentice-Hall, Inc., New York (1953), Chaps. 3 and 7.
7) C. R. McKinney, J. M. McCrea, S. Epstein, H. A. Allen and H. C. Urey, *Rev. Sci. Instr.*, 21, 724 (1950).
8) M. Dole, *Chem. Revs.*, 51, 263 (1952).
9) D. Rittenberg, "Preparation and Measurement of Isotopic Tracers", Edwards Bros., Ann Arbor, Michigan (1947), p. 31.
10) T. C. Hoering, *Science*, 122, 1233.
11) W. H. Rodebush and J. C. Michalek, *J. Am. Chem. Soc.*, 51, 752 (1929).

TABLE I. EFFECT OF pH OF THE SOLUTION PHASE ON THE FRACTIONATION FACTOR BETWEEN THE RESIN AND SOLUTION PHASE, $K$, AT 30°C

| Run | pH | Concentration of solution ($NH_3+NH_4^+$) mol./l. | Fractionation factor $K$ |
|---|---|---|---|
| 1 | 11.3 | 0.496 | 1.0255 |
| 2 | 11.3 | 0.496 | 1.0250 |
| 3 | 11.2 | 0.196 | 1.0257 |
| 4 | 11.2 | 0.196 | 1.0253 |
| 5 | 10.3 | 0.196 | 1.0210 |
| 6 | 10.3 | 0.196 | 1.0208 |
| 7 | 9.76 | 0.496 | 1.0163 |
| 8 | 9.76 | 0.496 | 1.0156 |
| 9 | 9.72 | 0.496 | 1.0160 |
| 10 | 9.34 | 0.196 | 1.0112 |
| 11 | 9.28 | 0.516 | 1.0125 |
| 12 | 8.66 | 0.516 | 1.0029 |
| 13 | 7.47 | 0.196 | 1.0010 |
| 14 | 7.46 | 0.196 | 1.0010 |
| 15 | 4.30 | 0.483 | 0.9997 |
| 16 | 2.75 | 0.196 | 1.0007 |
| 17 | 2.72 | 0.196 | 0.9997 |
| 18 | 2.35 | 0.196 | 0.9992 |
| 19 | 2.34 | 0.196 | 0.9992 |
| 20 | 1.17 | 0.516 | 0.9999 |

TABLE II. EFFECT OF THE CONCENTRATION OF THE SOLUTION ON THE FRACTIONATION FACTOR BETWEEN RESIN AND SOLUTION PHASE AT 30°C

| Run | pH | Concentration of solution ($NH_3+NH_4^+$) mol./l. | Fractionation factor $K$ |
|---|---|---|---|
| 15 | 4.30 | 0.483 | 0.9997 |
| 21 | 4.40 | 0.0966 | 1.0000 |
| 22 | 5.40 | 0.0097 | 1.0000 |
| 23 | basic | 3.23 | 1.0279 |
| 24 | basic | 1.29 | 1.0269 |
| 25 | basic | 0.515 | 1.0265 |
| 26 | basic | 0.208 | 1.0257 |

" basic " shows that pH value is larger than 11.2.

factor of Run 1 to 4:

$$K_1 = 1.0256 \pm 0.0006 \text{ at } 30°C$$

The error shown is the average deviation. The fractionation factors of Run 1 to 20 are plotted against their pH values of the solution phase in Fig. 1, on which the calculated line is drawn by Eq. 8 using the $K_1$ and $K_2$ obtained.

The effects of the concentration of the solution phase are shown in Table II.

The effects of temperature on the fractionation factor between the resin and solution phase are shown in Table III. The equilibrium constants, $K_1$, are calculated by Eq. 12 with the fractionation factors at the solution of low pH value,

TABLE III. EFFECT OF TEMPERATURE ON THE FRACTIONATION FACTOR BETWEEN RESIN AND SOLUTION PHASE, $K$

| $T$°C | Acidic solution (pH less than 6) ($NH_{4(aq)}^+$) = 0.107 M | | | Basic solution (pH = 11.2) ($NH_{3(aq)}$) = 0.196 M | | |
|---|---|---|---|---|---|---|
| | Run | $\delta \times 1000$ | $K$ | Run | $\delta \times 1000$ | $K$ |
| 50 | 27 | 0 | | 32 | −21.9 | |
| | 28 | −0.5 | 1.0002 | 33 | −21.9 | 1.0224 |
| 40 | 29 | 0 | 1.0000 | 34 | −22.3 | |
| | | | | 35 | −23.1 | 1.0232 |
| 30 | * | | 0.9997 | 36 | −24.7 | |
| | | | | 37 | −25.0 | 1.0255 |
| 0.2 | 30 | −0.8 | | 38 | −25.0 | |
| | 31 | +0.3 | 1.0003 | 39 | −25.8 | |
| | | | | 40 | −25.2 | 1.0260 |

* Average of Run 15 to 20 in Table I.

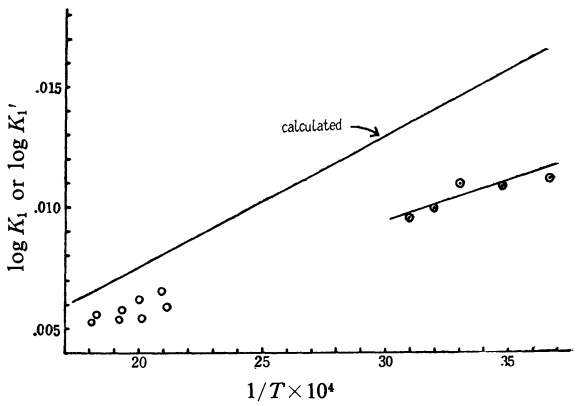



Fig. 2. Equilibrium constant and $1/T$.
○ Represents the equilibrium constant measured for the exchange reaction between gaseous ammonia and solid ammonium chloride.
⊙ Represents the average value of the equilibrium constant measured for the exchange reaction between ammonia and ammonium ion in an aqueous solution.

and the logarithms of the equilibrium constants are plotted against the reciprocal of the absolute temperature, $1/T$, to get the heat of the exchange reaction 1 in Fig. 2:

$$\Delta H \doteq -13.8 \text{ cal./mol.}$$

The effect of temperature on the fractionation factor between gaseous ammonia and solid ammonium chloride is shown in Table IV with the experimental conditions. In this case, these fractionation factors are the equilibrium constant of the equation:

$$^{15}NH_{3(gas)} + {}^{14}NH_4Cl_{(solid)} = {}^{14}NH_{3(gas)} + {}^{15}NH_4Cl_{(solid)} \qquad K_1' \quad (13)$$

The logarithms of the equilibrium constants are

TABLE IV. EFFECT OF TEMPERATURE ON THE FRACTIONATION FACTOR BETWEEN AMMONIA GAS AND SOLID AMMONIUM CHLORIDE

| Run | $NH_4Cl$[1] mg. | $NH_3$[2] mmHg | $T$°C | Period hr. | Fractionation factor, $K_1'$ |
|---|---|---|---|---|---|
| 41 | 100 | 100 | 275 | 27 | 1.0123 |
| 42 | 50 | 200 | 274 | 22 | 1.0130 |
| 43 | 50 | 255 | 245 | 13 | 1.0135 |
| 44 | 50 | 250 | 248 | 21 | 1.0124 |
| 45 | 50 | 200 | 247 | 62 | 1.0132 |
| 46 | 50 | 200 | 227 | 18 | 1.0144 |
| 47 | 50 | 260 | 224 | 38 | 1.0125 |
| 48 | 50 | 250 | 203 | 21 | 1.0137 |
| 49 | 50 | 300 | 206 | 49 | 1.0155 |

1: Amount of ammonium chloride used
2: Pressure of ammonia added at room temperature.

also plotted against the reciprocal of the absolute temperature in Fig. 2. The equilibrium constant between ammonia and ammonium ion, both in the gaseous state, has been calculated by Urey[12]. The calculated values are also plotted in Fig. 2.

## Discussion

The equilibrium constant for the equation

$$^{15}NH_{3(gas)} + {}^{14}NH_{4(aq)}^{+} = {}^{14}NH_{3(gas)} + {}^{15}NH_{4(aq)}^{+} \quad (14)$$

has been measured and found to be 1.034 at 25°C by Kirshenbaum et al.[3] The equilibrium constant for the equation

$$^{14}NH_{3(aq)} + {}^{15}NH_{3(gas)} = {}^{15}NH_{3(aq)} + {}^{14}NH_{3(gas)} \quad (15)$$

has been obtained and found to be 1.005 at 25°C[3]. From the data by Kirshenbaum et al. the equilibrium constant for Eq. 1 is calculated to be 1.029 at 25°C. The value of $K_1$ obtained by the author compares well with the values reported in literature. Further, Fig. 1 shows that Eq. 8 is well satisfied by the experimental fractionation factors and Eqs. 1 and 2 are enough to represent the equilibria involved in the aqueous ammonia-ammonium ion solution and the exchanger of ammonium ion form.

In the equations which involved ammonia in aqueous solution the unionized ammonium hydroxide, $NH_4OH$, is assumed not to exist in the aqueous solution. Instead, $NH_{3(aq)}$ is assumed to represent ammonia in the aqueous solution. There is some uncertainity in regard to the interpretation of "ammonium hydroxide". However, the relatively weakly basic character of "ammonium hydroxide" solution is interpreted recently as resulting simply from the fact that the ammonia molecule is a weaker than the hydroxide ion. There must be a hydrogen bond between the nitrogen of ammonia in aqueous solution and hydrogen of solvent water.

The value of the equilibrium constant $K_1$ is smaller than that of the calculated equilibrium constant with the gaseous partition functions of the isotopic ammonia and ammonium ion as shown in Fig. 2. This difference may be chiefly contributed by the difference of ammonia in the aqueous state from the gaseous state. The equilibrium constant for Eq. 14 by Kirshenbaum et al.[3]: 1.005; is considered to be large enough to explain the difference of the isotopic equilibrium constant $K_1$ from the calculated values. There may not be a large isotope effect on the difference between the gaseous and aqueous ammonium ions, since the nitrogen atom is surrounded by the hydrogen atoms and the nitrogen isotope effect on the solvation in the aqueous ammonium ion may be very small.

The effect of the concentration of the solution phase on the fractionation factor between resin and solution phase (Table II) shows that there is no effect upon acidic solution or ammonium ion and that the concentration of ammonia in the aqueous solution has the tendency to increase the value of the fractionation factor.

The slope of $\log K_1$ versus $1/T$ gives $\Delta H = -13.8$ cal. per mole for the exchange reaction 1. The measurements of the equilibrium constants $K_1'$ for the gas-solid exchange reaction have some difficulty in separating phases at elevated temperatures. The data are not sufficient to determine the accurate value of the heat of the exchange reaction.

In Fig. 2, it is seen that the equilibrium constants measured are located below the line of the calculated equilibrium constants. However, the differences between the measured and the calculated values at the same temperature are smaller with the measured values of the gas-solid exchange reaction than with those of the exchange reaction in aqueous solution. This fact may be partly understood by the presence of the hydrogen bond of ammonia molecules in aqueous solution.

This work was made possible by the support of the U. S. Atomic Energy Commission. The invaluable advice and encouragement from Dr. T. C. Hoering are acknowledged with thanks.

*Department of Chemistry*
*College of Science*
*Rikkyo University*
*Toshima-ku, Tokyo*

12) H. C. Urey, *J. Chem. Soc.*, 1947, 562.

# *Nitrogen Isotopic Equilibria between Ammonia and Metal-ammine Complex Ions in Aqueous Solution**

By Tatsujiro ISHIMORI

(Received September 21, 1959)

The isotopic exchange of ions or molecules dissolved in solution with those coordinated in complex ions have been studied on the carbon isotopes between carbonate or bicarbonate ion and the carbonate coordinated in the cobalt complex ions[1,2], the oxygen isotopes between water as solvent and that in cobalt complex ion[3], and the nitrogen isotopes between ammonia as solvent and metal-ammine complex ions in liquid ammonia[4]. These studies have given data on the nature of the bond in complex ions. This paper reports on the nitrogen isotope effect in the formation of a series of metal-ammine complex ions with ammonia in aqueous solution. Copper-, zinc-, cadmium-, silver- and nickel-ammine complex ions were studied. The experimental method using ion exchangers[5] has been employed. A theoretical relation has been derived between the isotopic equilibrium constant and the first dissociation constant of the complex ion of the stable form.

## Experimental

Using the nitrogen compound with natural isotopic abundance, the equilibrium to be measured is written as

$$\mathrm{M(^{14}NH_3)_{n-1}(^{14}NH_3)^{+p}} + \mathrm{^{15}NH_{3(aq)}} = \mathrm{M(^{14}NH_3)_{n-1}(^{15}NH_3)^{+p}} + \mathrm{^{14}NH_{3(aq)}} \qquad K_1 \quad (1)$$

where $\mathrm{M(NH_3)_n^{+p}}$ represents a metal-ammine complex ion, $K_1$ the equilibrium constant. The cation exchanger of the metal-ammine complex ion form can be brought to isotope equilibrium with the metal-ammine complex ion or ammonia in solution The equilibria are written by the equations:

$$\mathrm{M(^{14}NH_3)_{n-1}(^{15}NH_3)^{+p}} + \mathrm{M(^{14}NH_3)_{n-1}(^{14}NH_3)R} = \mathrm{M(^{14}NH_3)_{n-1}(^{14}NH_3)^{+p}} + \mathrm{M(^{14}NH_3)_{n-1}(^{15}NH_3)R}, \qquad K_2 \quad (2)$$

$$\mathrm{M(^{14}NH_3)_{n-1}(^{14}NH)R} + \mathrm{^{15}NH_{3(aq)}} = \mathrm{M(^{14}NH_3)_{n-1}(^{15}NH_3)R} + \mathrm{^{14}NH_{3(aq)}} \qquad K_3 \quad (3)$$

where $\mathrm{M(NH_3)_nR}$'s represent the metal-ammine complex ions adsorbed on the cation exchanger, $K_2$ and $K_3$ the equilibrium constant for Eqs. 2 and 3, respectively.

The following quantity can be measured conveniently:

$$\delta = \frac{(^{15}N/^{14}N)_{solution} - (^{15}N/^{14}N)_{resin}}{(^{15}N/^{14}N)_{resin}} \qquad (4)$$

where $(^{15}N/^{14}N)_{resin}$ and $(^{15}N/^{14}N)_{solution}$ are the ratio of the nitrogen isotopes in resin and solution, respectively. The value of $\delta$ for Eq. 2 can be measured directly for the system of the complex ion adsorbed on the resin and the solution of the complex ion, if the complex ion is stable without free ammonia or with a negligible amount of the excess ammonia. The equilibrium constant for Eq. 2 can be written

$$K_2 = \frac{\mathrm{M(^{14}NH_3)_{n-1}(^{15}NH_3)R}}{\mathrm{M(^{14}NH_3)_{n-1}(^{14}NH_3)R}} \Big/ \frac{\mathrm{M(^{14}NH_3)_{n-1}(^{15}NH_3)^{+p}}}{\mathrm{M(^{14}NH_3)_{n-1}(^{14}NH_3)^{+p}}} \simeq (^{15}N/^{14}N)_{resin}/(^{15}N/^{14}N)_{solution} = 1/(1+\delta_2) \qquad (5)$$

Eq. 3 describes the equilibrium of the complex ion adsorbed on the resin with excess ammonia in aqueous solution. Using the symbols $\delta_3$ for this case, the equilibrium constant of Eq. 3, $K_3$, is given by the following equation:

$$K_3 = \frac{\mathrm{M(^{14}NH_3)_{n-1}(^{15}NH_3)R}}{\mathrm{M(^{14}NH_3)_{n-1}(^{14}NH_3)R}} \Big/ \frac{\mathrm{^{15}NH_{3(aq)}}}{\mathrm{^{14}NH_{3(aq)}}} \simeq n(^{15}N/^{14}N)_{resin}/(^{15}N/^{14}N)_{solution} = n/(1+\delta_3) \qquad (6)$$

In this equation, $(^{15}N/^{14}N)_{resin}$ is assumed to represent the isotope ratio in only the exchanged complex ions, since the amount of the free ammonia in the resin is negligibly small compared with that of ammonia coordinated in the exchanged compelx ions. It is not necessary to consider ammonium ion in this equilibrium if the pH of the aqueous solution is high.

Now, $K_1$ is given with $\delta_2$ and $\delta_3$;

$$K_1 = \frac{\mathrm{M(^{14}NH_3)_{n-1}(^{15}NH_3)^{+p}}}{\mathrm{M(^{14}NH_3)_{n-1}(^{14}NH_3)^{+p}}} \Big/ \frac{\mathrm{^{15}NH_{3(aq)}}}{\mathrm{^{14}NH_{3(aq)}}} = K_3/K_2 = n(1+\delta_2)/(1+\delta_3)$$

The value of the fractionation factor, $(1+\delta_2)/(1+\delta_3)$, can be experimentally obtained.

The metal-ammine complex ion may undergo successive dissociations. However, many of the complex ions, in general, have one stable form

* This study has been done in the Chemistry Department of the University of Arkansas, Arkansas, U. S. A.

1) D. R. Stranks and G. W. Harris, *J. Chem. Phys.*, **19**, 257 (1951); *J. Phys. Chem.*, **56**, 906 (1952).

2) P. E. Yankwich and J. E. McNamara, *J. Chem. Phys.*, **20**, 1325 (1952).

3) A. Rutenberg and H. Taube, ibid., **20**, 825 (1952).

4) H. U. D. Wiesendanger, W. H. Jones and C. S. Garner, ibid., **27**, 668 (1957).

5) T. Ishimori, This Bulletin, **33**, 516 (1960).

TABLE I. FRACTIONATION FACTORS OF NITROGEN ISOTOPES BETWEEN METAL-AMMINE COMPLEX IONS AND AMMONIA IN AQUEOUS SOLUTION AT 30°C

| Complex ion | Composition of solution, M | | $\delta \times 10^3$ | $\frac{K_1}{n}$ |
|---|---|---|---|---|
| | Complex ion | Ammonia | | |
| *(I) Experiments using cation exchanger* | | | | |
| $Cu(NH_3)_4^{2+}$ | 0.259 | 0.00024 | $\delta_2 = -0.4 \pm 0.1$ | |
| | 0 | 0.236 | $\delta_3 = -11.9 \pm 0.4$ | 1.0117 |
| $Zn(NH_3)_4^{2+}$ | — | — | $\delta_2 \equiv 0$ | |
| | 0 | 0.270 | $\delta_3 = -11.5 \pm 0.4$ | 1.0116 |
| $Cd(NH_3)_4^{2+}$ | — | — | $\delta_2 \equiv 0$ | |
| | 0 | 0.270 | $\delta_3 = -10.2 \pm 0.9$ | 1.0103 |
| $Ag(NH_3)_2^{2+}$ | 0.250 | 0 | $\delta_2 = -0.1 \pm 0.3$ | |
| | 0 | 0.237 | $\delta_3 = -9.3 \pm 0.6$ | 1.0093 |
| *(II) Experiments by salting out complex ions* | | | | |
| $Cu(NH_3)_4^{2+}$ | 0.0455 | 0.276 | $\delta = -11.9 \pm 0.4$ | 1.0120 |
| $Ni(NH_3)_n^{2+}$ | 0.250 | 0.540 | $\delta = -7.4 \pm 0.3$ | 1.0076 |

which exists predominantly in aqueous solution. In such a case, the isotopic equilibrium constant measured will present the equilibrium constant of the stable form of the complex ion.

Copper quadrammine sulfate was prepared[6] and its solution was made by dissolving the prepared crystal in a very dilute ammonia solution. The other complex solutions: zinc, cadmium and silver complex solution were made by dissolving the slight excess of metal sulfate in an ammonia solution and filtering the insoluble residue out. The cation exchanger used was Dowex 50, X-8. The exchanger of a complex ion form was made by passing the metal-ammine complex- ammonia solution through the exchanger column. The exchangers were washed with ammonia solution on the glass filter with a suction of water jet pump.

The general procedures were the same as described in the previous report[5]. The exchanger of the complex ion form was added to the solution of the complex ion or ammonia and allowed to stand in the constant temperature bath at 30°C over one or two nights. The periods may be long enough for the attainment of the equilibria of the exchange reactions in this experiment, which are supposed to be rapid by the rapid exchanges of ammonia between solvent liquid ammonia and copper-, silver- or nickel-ammine complex ion[4]. After the attainment of the equilibria, the exchangers were separated from the solution with suction filtration, and washed with a limited amount of water to avoid the hydrolysis of the exchanged complex ions. The washed exchanger was put into the sulfuric acid solution to convert to the metal ion and ammonium ion. Then, the exchanger and the solution were poured on the exchanger column in the hydrogen form. The ammonium ion was recovered by eluting with 0.5 N potassium sulfate-0.5 M sulfuric acid solution. Through this process, the greater part of the metal ion was removed. The ammonia solution separated from the exchanger at equilibrium was acidified with sulfuric acid solution and used for the isotopic analysis. The complex ion solution was acidified with sulfuric acid solution and treated by the same procedure as described for the complex ion exchanged.

For copper and nickel complex ions, the complex ions were separated from the complex-ammonia mixed solutions by salting out the complex salts with the addition of the large amount of alcohol and centrifuging the complex salts. The isotopic measurements were carried out for the supernatant solution and complex salts centrifuged.

The isotope ratio measurements were made in the same way as described in the previous report[5].

## Results

The experimental results are shown in Table I with the experimental conditions. In the experiments of cadmium and zinc complex ion, the value of $\delta_2$ could not be measured since these complex ions were not stable in aqueous solution without a large excess of ammonia. Their equilibrium constants were calculated by assuming the value of $\delta_2$ to be zero. This assumption seems to be reasonable since the equilibrium constant of isotopic ions between the exchanger and solution phase is nearly unity.

The experiments were carried out by the technique of salting out the complex ion from the complex ion-ammonia mixture solution with the addition of alcohol for copper and nickel complex ions. In this technique, the equilibrium constant can be readily obtained from the measured value of $\delta$:

$$\delta = [(^{15}N/^{14}N)_{solution} - (^{15}N/^{14}N)_{salt}] / (^{15}N/^{14}N)_{salt}$$

The results are also shown in Table I. Both the techniques of using cation exchanger and

6) G. Brauer, "Handbuch der Praeparativen Anorganischen Chemie", Ferdinand Bnke Verlag, Stuttgart (1954), p. 757.

salting out the complex ion gave a good agreement on the value of $K_1$. The agreement shows that the technique with cation exchanger can be efficiently used in measurements of this kind.

## Theoretical and Discussion

A theoretical relationship can be derived between the isotopic equilibrium constant of Eq. 1, $K_1$, and the first dissociation constants of the stable ammine complex ions, $k$ and $k'$ for the dissociations:

$$M(^{14}NH_3)_{n-1}(^{15}NH_3)^{+p} = M(^{14}NH_3)_{n-1}^{+p} + {}^{15}NH_{3(aq)} \quad k \quad (8)$$

$$M(^{14}NH_3)_{n-1}(^{14}NH_3)^{+p} = M(^{14}NH_3)_{n-1}^{+p} + {}^{14}NH_{3(aq)} \quad k' \quad (9)$$

The value which is defined as a ratio of the partition functions of isotopic molecules by Biegeleisen and Mayer[7], is written as,

$$\frac{s}{s'} f = 1 + \Sigma_1 G_1 \Delta u_1 \quad (10)$$

where $s$ and $s'$ are the symmetry number of isotopic molecules. The primed notation refers to the light molecule. The $G$ function relates to the difference in free energy of the formation of isotopic molecules from the isolated gaseous atoms[7]:

$$\frac{\Delta F^0 - \Delta F^{0\prime}}{RT} = -\Sigma_1 G_1 \Delta u_1 + \ln \frac{s}{s'} \quad (11)$$

The following equation can be obtained from Eqs. 10 and 11:

$$f = \frac{s'}{s}\left(1 - \frac{\Delta F^0 - \Delta F^{0\prime}}{RT} + \ln \frac{s}{s'}\right) \quad (12)$$

Then Eq. 12 is applied to the isotopic complex ions in aqueous solution, the ratio of their symmetry numbers, $s'/s$, can be replaced by the number of the ammonia molecules coordinated in the stable complex ions. Further, if Eqs. 8 and 9 are compared the difference of the free energies of formation of the complex ions becomes

$$\Delta F^0{}_c - \Delta F^{0\prime}{}_c = \Delta F^0{}_a - \Delta F^{0\prime}{}_a - RT \ln (k'/k) \quad (13)$$

where the subscripts $c$ and $a$ refer to the complex ion and ammonia, respectively. The $f$ function of the complex ion is written as

$$f_c = n\left(1 + \ln k'/k - \frac{\Delta F^0{}_a - \Delta F^{0\prime}{}_a}{RT} - \ln n\right) \quad (14)$$

For the isotopic ammonia molecules, the ratio of the symmetry numbers is one and its $f$ function is given by

$$f_a = 1 - \frac{\Delta F^0{}_a - \Delta F^{0\prime}{}_a}{RT} \quad (15)$$

With Eq. 15, the $f$ function of the complex ion is rewritten as

$$f_c = n(\ln k'/k + f_a - \ln n) \quad (16)$$

Now the equilibrium constant, $K_1$, which is the ratio of the $f$ function of the complex ion to that of ammonia, can be expressed with the dissociation constants of the stable complex ions, $k$ and $k'$:

$$K_1 = n\left[1 + \ln\left(\frac{k'}{n} \Big/ k\right) \Big/ f_a\right] \quad (17)$$

The quantity of $k'/n$ in this equation is equivalent to $k$ if the probabilities of the dissociations of the isotopic complex ions are taken into account. Both $k'/n$ and $k$ are a measure of the strength of the bond between metal and nitrogen in the complex ions which appeared at the first dissociation.

The measured fractionation factors can be compared with the relationship of Eq. 17, provided a form of the complex ion among the successively dissociated ions is predominantly stable. The successive dissociation constants have been measured[8]. The values of the dissociation constants are listed with the measured fractionation factors in Table II. Copper, zinc, cadmium and silver complex ions have one stable form. However, in the case of nickel complex ion, the successively dissociated ion may exist with comparable concentrations and they effect the value of the measured fractionation factor as an average.

TABLE II. FRACTIONATION FACTORS AND THE FIRST DISSOCIATION CONSTANTS OF COMPLEX IONS

| Complex ion | $\frac{K_1}{n}$ | $\log k'$ | $\log \frac{k'}{n}$ |
|---|---|---|---|
| $Cu(NH_3)_4^{2+}$ | 1.0117 | −2.13 | −2.73 |
| $Zn(NH_3)_4^{2+}$ | 1.0116 | −2.15 | −2.75 |
| $Cd(NH_3)_4^{2+}$ | 1.0103 | −0.93 | −1.53 |
| $Ag(NH_3)_2^{2+}$ | 1.0093 | −3.83 | −4.13 |
| $Ni(NH_3)_n^{2+}$ | 1.0076 | −0.03 for $n=6$ | −0.81 |
| | | −0.75 for $n=5$ | −1.45 |
| | | −1.19 for $n=4$ | −1.79 |

In Table II, the tendency is noted that the smaller value of $k'$ causes the greater fractionation factor or the greater value of the ratio of $k'/n$ to $k$. An exception is in the case of the silver complex ion although the reason is not clear. The greater isotope effect is found in the more tightly bound complex ion which agrees with the general rule of the isotope effects.

7) J. Biegeleisen and M. C. Mayer, *J. Chem. Phys.*, **15**, 261 (1947).

8) J. Bjerrum, *Chem. Revs.*, **46**, 381 (1950).

This work was made possible by the support of the U. S. Atomic Energy Commison. The invaluable advice and encouragement from Dr. T. C. Hoering are acknowledged with thanks.

*Department of Chemistry*
*College of Science*
*Rikkyo University*
*Toshima-ku, Tokyo*

# *Studies on Thixotropy. II.**[1] *On the Thixotropic Gel Structure of Bentonite*

By Takehiko WATANABE

(Received August 10, 1959)

There are two kinds of structure which are currently taken as a model for thixotropic gel of bentonite. One of them is the structure in which dispersed plate-like particles are linked together at a short distance to build up a network. The other[2,3] is the structure in which particles are regularly oriented to each other at a considerable distance. According to the latter structure, however, it was difficult to explain the process of thixotropic gel formation which proceeds in two steps as described in the previous paper[1]. By making light-scattering, birefringence and viscoelastic studies on mono-disperse sol of Wyoming Bentonite, M'Ewen et al.[4] have suggested that particles are oriented edge-to-edge in the form of flat ribbons. Olphen[5] has also concluded from the results obtained by the study of the surface conductance of bentonite suspension that particles are linked with each other at a short distance. These results show that the former structure, e. g. "house of cards" structure[6] in which the particles are linked at

TABLE I. RELATIONS BETWEEN RHEOLOGICAL PROPERTIES AND CONCENTRATION

| Investigator | Apparatus or Method | Relation presented | Relation derived by the present author |
|---|---|---|---|
| Braune et al.[7] | Kämpf viscometer | $A_\infty \propto C^2$ | |
| Peter et al.[8] | Couette viscometer | $\tau_B \propto C^2$ | at low concn. $\tau_B \propto C^2$<br>at high concn. $\tau_B \propto C^4$ |
| Olphen[9] | Stormer viscometer | $\tau_B \propto (C-C_m)^2$ | at low concn. $\tau_B \propto C^2$<br>at high concn. $\tau_B \propto C^4$ |
| | Shear propagation | $\mu \propto (C-C_m)^3$ | $\mu \propto C^6$ |
| Packter[10] | Stormer viscometer | $S_\infty \propto C^6$ | |
| Watanabe[1] | Torsion balance | $\begin{cases} A_{1\infty} \propto C^2, \\ A_{2\infty} \propto C \end{cases}$ | |
| | | or $\begin{cases} A_{1\infty} \propto C^4, \\ A_{2\infty} \propto C^2 \end{cases}$ | |

$A_\infty$: max. yield value; $\tau_B$: Bingham yield stress; $\mu$: modulus of elasticity; $S_\infty$: max. gel strength: $A_{1\infty}$ and $A_{2\infty}$: max. yield value for the first and the second step of gel formation, respectively; $C$: concentration; $C_m$: a constant.

* Presented at the 12th Annual Meeting of the Chemical Society of Japan, Kyoto, April, 1959.

1) Part I: T. Watanabe, This Bulletin, 33, 347 (1960).

2) E. A. Hauser and D. S. LeBeau, *J. Phys. Chem.*, 45, 54 (1941); E. A. Hauser, "Silicic Science", D. van Nostrand Co., Inc., Princeton, New Jersey (1955), p.36.

3) E. Forslind, "Proceedings of the Second International Congress on Rheology", Butterworths Scientific Publications, London (1954), p. 50.

4) M. B. M'Ewen and M. I. Pratt, *Trans. Faraday Soc.*, 53, 535 (1957); M. B. M'Ewen and D. L. Mould, ibid., 53, 548 (1957).

5) H. van Olphen, *J. Phys. Chem.*, 61, 1276 (1957); H. van Olphen and M. H. Waxman, "Fifth National Conference on Clays and Clay Minerals", Publ. 566, National Academy of Sciences, National Research Council, Washington (1958), p. 61.

6) U. Hofmann, *Kolloid-Z.*, 125, 86 (1952).

7) H. Braune and I. Richter, ibid., 113, 20 (1949).

8) S. Peter and I. Stolle, *Z. physik. Chem.* [*N. F.*], 11, 251 (1957).

9) H. van Olphen, "Proceedings of the Fourth National Conference on Clays and Clay Minerals", Publ. 456, National Academy of Sciences, National Research Council, Washington (1956), p. 204.

10) A. Packter, *Kolloid-Z.*, 150, 60 (1957).

a short distance, is favored. Therefore, in this report, discussions will be carried out on this structure on the basis of the rheological data.

### Discussion and Proposal of Gel Structure

In Table I are collected the relations between the rheological properties and the concentration of thixotropic gel of bentonite presented by different investigators, and those derived by the present author using the data obtained by other authors. Furthermore, from the experimental data provided by Peter et al.[8] the relations between shearing stress ($\tau$) and concentration ($C$) at a fixed rate of shear ($q$) are derived and given in Table II. The relation between $\tau$ and $C$ is also dependent on C. Referring to the study of Enneking[11], in which he discussed experimental conditions similar to Peter's, in the range where the values of $\tau$ in Table II are proportional to $C^6$, the flow may be induced not in the whole but in a localized part of the gel. Therefore, it may be said that in the flowing part, the actual value of $q$ is higher than those listed. Consequently, this high $q$ is to be suddenly induced to the set gel. It may further be reasonable to assume that the experimental conditions, under which some of the measurements for Table I were carried out, must be essentially similar to those above stated. Therefore, $\mu$ and $S_\infty$ can be proportional to $C^6$.

TABLE II. RELATIONS BETWEEN $\pi$ (SHEARING STRESS) AND $C$ (CONCENTRATION) AT FIXED $q$ (RATE OF SHEAR) VALUES, DERIVED FROM THE DATA OF PETER ET AL.[8]

Geisenheim Bentonite in Water

| $q$(sec$^{-1}$) \ $C$(%) | 1 | 2 | 3 | 3.47 | 3.92 |
|---|---|---|---|---|---|
| 4.16 | $\tau \propto C^2$ | $\tau \propto C^4$ | | $\tau \propto C^6$ | |
| 25.7 | $\tau \propto C^2$ | | | $\tau \propto C^6$ | |
| 102.9 | $\tau \propto C^2$ | | | $\tau \propto C^4$ | |
| 662 | $\tau \propto C$ | | $\tau \propto C^2$ | | |

Algeria Bentonite in water

| $q$(sec$^{-1}$) \ $C$(%) | 1.79 | 2.71 | 3.61 | 4.49 | 5.10 | 5.92 |
|---|---|---|---|---|---|---|
| 4.16 | $\tau \propto C^2$ | | | $\tau \propto C^6$ | | |
| 6.44 | $\tau \propto C^2$ | | | $\tau \propto C^6$ | | |
| 66.5 | $\tau \propto C^2$ | | | $\tau \propto C^4$ | | |
| 411 | $\tau \propto C$ | $\tau \propto C^2$ | | | | |

11) H. Enneking, *Rheologica Acta*, 1, 234 (1958).

Tables I and II show that the relations between rheological properties (in the following, represented by "strength") and concentration are dependent on the condition of measurement, so that it may be expected that the particles constituting the gel do not orientate so regularly as ions in crystal lattice but link with each other at random to build up the gel structure. This leads to the conclusion that, in the gel, several kinds of agglomerated particle groups can coexist. It may also be expected that under a certain experimental condition, the gel strength is determined by a particular particle group in the gel. Namely, if the observed gel strength is proportional to $C^p$ where $p$ is a positive integer, there exists a particular particle group which performs the role of structural unit. And in this case, provided that the contribution to the gel strength is equal in each particle group of the same kind, it may be concluded that the number of the particle group per unit volume of the gel varies as $C^p$. In other words, the probability of the existence of this particle group is proportional to $C^p$. In the following discussion, a particle group such as stated above will be named structural unit-$C^p$ (abbr. S. U.-$C^p$). If many kinds of particle groups which act as S. U.-$C^p$, exist in the system, the gel strength may be determined by one of them, or by a set of particle groups which make equal contribution to the gel strength in cooperation with each other.

Since the form of bentonite particle is platelike, the association between particles may be classified into three types based on the steric condition of the junction point as described in the previous paper[1]. In the first type, two particles are linked with each other at one point (P-1 association); while, in the second, particles are linked at two or more points belonging to one straight line (P-2 association) and, in the third, particles are linked at three or more points belonging to one plane (P-3 association). Also the number of junction points in unit volume in which two adjacent particles are linked with P-1, P-2 or P-3 association is proportional to $C$, $C^2$ or $C^3$, respectively.

In the first place, it is assumed that, in the gel structure, all particles are linked to each other with P-1 association. In this case, consideration is made based on the experimental results with Yamagata Bentonite reported in the previous paper[1]. This sample shows the maximum yield value proportional to $C^2$, or $C$ according to the first or the second gelation process, respectively. Therefore, it is concluded that S. U.-$C^2$ contributes to the gel strength in the first step and S. U.-$C$ in the second. Furthermore, from the results discussed in the

previous paper[1], it has been ascertained that the particle group which acts as a structural unit in the first step does not disappear, but its contribution to the yield value diminishes in the second step under the experimental method employed. Considering the process of gel formation, the structure developed in the second step is doubtless more rigid than that of the first. S. U.-$C^2$ in the first step, is the cross-linkage in which two linear ribbons are linked to the hypothetical fixed particle which behaves as if it were restricted at a fixed position when the cross-linkage acts as structural unit. Therefore, in the second step, the existence of cross-linkage may be expected, of which more than two linear ribbons are linked to the fixed particle. Namely, there exists the S. U.-$C^p$ where $p>2$ in the second step. Consequently, the structure which satisfies all the relations listed in Tables I and II, may be as follows. The structure is formed by cross-linking of the linear ribbons which are formed of the aligned particles linked by P-1 association. For the cross-linkage, there must coexist at least five kinds of cross-linkage in which two to six linear ribbons, respectively, are linked to the fixed particle.

Based on the above consideration on the structure, in the case of Yamagata Bentonite, the structural unit is S. U.-$C$, namely, the linear ribbons; since the maximum yield value developed in the second step ($A_{2\infty}$) varies as $C$. The result obtained with Volclay[1] where $A_{2\infty} \propto C^2$ and also with Braune's results, $A_\infty \propto C^2$, may be explained as follows. The structural unit is S. U.-$C^2$, that is, the cross-linkage formed by two linear ribbons linking to the fixed particle.

Next, it is assumed that all particles in structure are linked by P-2 association. In this case, the consideration must be made based on the results obtained with Volclay in the previous paper[1]. By treatment similar to that described above in completely set gel, there must exist S. U.-$C^6$ besides S. U.-$C^2$ and S. U.-$C^4$. S. U.-$C^2$ is the linear ribbons which are formed by the aligned particles linked by P-2 association. S. U.-$C^4$ or S. U.-$C^6$ is the cross-linkage in which two or three linear ribbons, respectively, link to the fixed particle. Using this model of structure, it is possible to explain all the experimental results listed in Tables I and II except that of Yamagata Bentonite. However, as to the S. U.-$C^6$ it is not enough to consider such a simple model as that mentioned above, it must satisfy the following requirements.

(1) Among the strengths of bentonite gel measured by various methods, the one proportional to $C^6$ has the largest value of $p$. Therefore, the particle group which acts as S.U.-$C^6$ must be the one which plays the part of constituting a rigid gel structure.

(2) Packter[10] has suggested that the rate of gel formation varies as $C^6$ in the case where the maximum gel strength $S_\infty$ is proportional to $C^6$ as shown in Table I. To satisfy this fact, S. U.-$C^6$ must be the cross-linkage formed in the process where six adjacent particles which participate in the formation of separate linear ribbons, orientate to the fixed particle.

Considering the above requirements, the cross-linkage which acts as S. U.-$C^6$ will be as follows.

The fixed particle is linked to three linear ribbons composed of a certain number of particles, of which each one nearest to the fixed particle must be further linked to another different linear ribbon. The particle group formed in such a way as stated above is an overlapping assembly of the four particle groups, each of which is expected to act as S. U.-$C^6$.

Considering such a particle group, it is safely assumed that such a cross-linkage plays an important role in the rigid gel structure which satisfies requirement 1, and the rate of formation of the cross-linkage varies as $C^6$ and requirement 2 is also fulfiled.

In the above consideration, only the case of P-2 association is treated. However, provided that similar structural conditions exist in the case of P-1 association, it may be expected that a rigid gel structure is built up from the three kinds of particle groups which will be able to act as S. U.-$C$, S. U.-$C^2$ and S. U.-$C^3$, respectively.

Now, it is assumed that four states of particle agglomerate will appear in the course of thixotropic gel-sol-gel transformation. Possible

TABLE III. STRUCTURAL UNITS WHICH EXIST IN FOUR RHEOLOGICAL STATES OF THIXOTROPIC GEL-SOL-GEL TRANSFORMATION

| Type of structure | Type of association | Rheological state | | | |
|---|---|---|---|---|---|
| | | Rigid gel | Loose gel | Sol I | Sol II |
| I | P-1 | S. U.-$C$<br>S. U.-$C^2$<br>S. U.-$C^3$ | S. U.-$C$<br>S. U.-$C^2$ | S. U.-$C$ | Dispersed particles |
| II | P-2 | S. U.-$C^2$<br>S. U.-$C^4$<br>S. U.-$C^6$ | S. U.-$C^2$<br>S. U.-$C^4$ | S. U.-$C^2$ | Dispersed particles |

S. U.-$C^p$ which may contribute to the strength at each state is collected in Table III. In the state where two or more structural units exist, the strength is determined by one of them, depending on the experimental condition. S. U.-$C$ in type I structure and S. U.-$C^2$ in type II are listed on both gel and sol states. These are the linear ribbons which participate in the structure in the gel state and are free in the sol state.

As described in the previous paper[1], during the first step of the thixotropic gel formation, the increase of the yield value of the gel in the loose gel state with setting time was measured and during the second step that of the gel in the rigid gel state was measured. In the case of the second step, experiments have been made to measure the yield value corresponding to the stress necessary to induce a fixed elastic deformation to the gel in which linear ribbons act as the structural unit. This deformation may be classified as a complete, recoverable, non-ideal one[12]. Therefore, the gel at this step shows retarded elasticity. Accordingly, if the deformation within the elastic limit has been induced gradually to the gel in rigid gel state of type II, its strength varies as $C^2$ since the linear ribbons act as the structural unit. On the contrary, when the deformation has been induced to the gel under the condition where the stress is suddenly applied to the system accompanying a fairly high rate of shear, the linear ribbons may not respond to this deformation, and as a result they come to play no role as the structural unit. The cross-linkage then comes to act as the structural unit so that the strength of the gel varies as $C^6$.

When experiments are carried out to obtain a flow curve, the rate of shear induced to the system is gradually increased and the stress corresponding to a given rate of shear is estimated. In this case, the observations are made on the variation of the state, starting from the rigid gel state and ending at the sol state II, listed in Table III. In the course of this experiment, a breakdown of the cross-linkage will occur at the initial stage and will be followed by the disintegration of the linear ribbons into individual particles at a later stage. Therefore, the results derived from the curve reported by Peter et al. or Olphen as shown in Tables I and II are explained as follows.

In these experiments, it may be expected that these systems take a structure of type II shown in Table III. From the results given in Table II, the relations between the stress and the concentration at a fixed rate of shear are dependent on the concentration of the system. Similar dependence on the above is also observed with the relation between the Bingham yield stress and the concentration as shown in Table I. It was observed in the previous experiment[1] that both the ratio of $A_{2\infty}$ to $A_{1\infty}$ and the difference between the values of $A_{2\infty}$ and $A_{1\infty}$ are larger in the case of the lower concentration. Therefore, it may be expected that in the gel which is in the rigid gel state, the ratio of the number of S. U.-$C^2$ to that of S. U.-$C^4$ or S. U.-$C^6$ of low concentration is larger than that of high concentration. Hence, at low concentrations, even the gel standing for a long period has a structure of either a loose gel state or a state not strictly distinguishable from sol state I. According to the above consideration, the relations listed in Table II may be elucidated with the concept given in Table III. The Bingham yield stress ($\tau_B$) is obtained from the intersection of the extraporated straight line with the stress axis so that the relation between $\tau_B$ and concentration is determined by the kind of structural unit in the range in which a linear relationship between the rates of shear and stress is obtained.

There has been no information regarding the condition under which the particles take either the structure of type I or II. However, it may be assumed that if the dispersed bentonite particles are in the form of unit layer, they will constitute a structure of type I, and if the dispersed particles are composed of stacking of several unit layers, a structure of type II will be formed.

P-1 association may be represented typically by the edge-to-edge linkage and P-2 association by the edge-to-surface linkage.

Packter[10] has reported that the maximum gel strength is proportional to $C^3$ in non-hetero-coagulated system where polyanion is added to the bentonite suspension. The results can be clearly explained by the assumption that the particles in the structure are linked by P-3 association. However, the gel structure which is formed by the particles linked by P-3 association is a very compact one compared with those listed in Table III and it is inadequate to accept this structure as that of thixotropic gel.

## Summary

(1) Discussions are carried out on the structure of the thixotropic gel of bentonite on the basis of the relation between the gel strength and the concentration, and the steric conditions of the junction point between two particles participating in structure.

(2) The gel strength is determined by the

12) J. M. Burgers and G. W. Scott Blair, "Report on the Principles of Rheological Nomenclature", North-Holland Publishing Co., Amsterdam (1949), p. 49.

particular group of particles in the structure which acts as the structural unit.

(3) The particle group which plays the part of the structural unit is not limited to one kind but more than one may coexist in a system. The gel strength is determined by one kind of the particle groups according to the experimental method used.

(4) The structure of the thixotropic gel of bentonite is classified into two types according to the mode of association between particles. One of them is the structure in which linear ribbons, which act as structural units, are formed by the aligned particles linking each other at one point. The other is the structure in which linear ribbons are formed by the particles linking at two or more points on one straight line.

The author would like to express his gratitude to Professor Sôzaburo Ono for his kind guidance and discussion throughout this work.

*Laboratory of Biophysical Chemistry*
*College of Agriculture*
*University of Osaka Prefecture*
*Sakai-shi, Osaka*

# *Hydrolysis of 7-Anilinobenzyl-8-quinolinol*

By Motoko Ito

(Received August 21, 1959)

On heating with 4 N hydrochloric, acid 7-anilinobenzyl-8-quinolinol (I) gave 7-hydroxybenzyl-8-quinolinol (II) and aniline as major products. The formation of benzaldehyde was found to be very scanty at this reaction though a distinct odor of benzaldehyde was noticed, suggesting that dissociation into three components of the Mannich base proceeded only to a negligible extent. On further heating with hydrochloric acid, II produced neither 8-quinolinol nor benzaldehyde but gave undefined matter (m.p. 118~119°C, foaming at 125°C). The bromination of II produced 5, 7-dibromo-8-quinolinol and benzaldehyde.

The dissociation of I by 4 N hydrochloric acid was first studied by Phillips et al.[1], however, it was considered at that time that I dissociated into three components in one step.

## Experimental

**7-Hydroxybenzyl-8-quinolinol (II).**—A hot solution of I (0.5 g.) in 4 N hydrochloric acid (10 ml.) was kept at around 85°C for 16 min. (when an odor of benzaldehyde was noticed). After being cooled, the solution was diluted with water (50 ml.) and then sodium acetate (6 g.) was added to it. The resulting precipitate was filtered after standing overnight (when no odor of benzaldehyde was noticeable). The filtrate gave a deep violet color with bleaching powder. The crude product was heated with ligroin (20 ml.) and filtered. From the filtrate on working up a colorless solid (0.15 g.), m.p. 88~100°C, foaming at 120~130°C, was isolated. This may be an impure bakelite-type condensation product.

The undissolved II was crystallized from five hundred times its weight of hot ligroin as colorless prismatic needles, m.p. 128°C.

Found: C, 76.52; H, 5.30; N, 5.20. Calcd. for $C_{16}H_{13}NO_2$: C, 76.49; H, 5.18; N, 5.58%.

When crystallized from benzene (20 ml.), it contained a mole of the solvent, m.p. 126~127°C; yield, 0.25 g. (66%) and when crystallized from carbon tetrachloride and dried in vacuo at room temperature, it also contained the solvent.

Found: C, 80.09; H, 5.65; N, 3.85. Calcd. for $C_{16}H_{13}NO_2 \cdot C_6H_6$: C, 80.24; H, 5.78; N, 4.26%.

Found: C, 53.84; H, 4.01. Calcd. for $C_{16}H_{13}NO_2 \cdot 0.8CCl_4$: C, 53.87; H, 3.47%.

*The hydrochloride* was obtained as colorless needles by the reaction of the base and hydrogen chloride, both in ethereal solution in the cold. It gave no definite m.p., began to sinter at 265°C and became a tar at 302°C.

Found: N, 4.73. Calcd. for $C_{16}H_{13}NO_2 \cdot HCl$: N, 4.87%.

*The picrate* was crystallized from benzene as prisms, m.p. 169°C.

Found: N, 11.50. Calcd. for $C_{16}H_{13}NO_2 \cdot C_6H_3N_3O_7$: N, 11.67%

**Acetyl Derivatives.**—A mixture of II (0.2 g.), freshly fused sodium acetate (0.2 g.), acetic anhydride (0.4 ml.) and ether (20 ml.) was allowed to stand at room temperature for 3 days, ether was evaporated and then water was added to the reaction mixture. The resulting precipitate was filtered; yield, 0.26 g.

The crude product was treated with ether (50 ml.) and the undissolved solid was crystallized from benzene as thick plates, m.p. 135°C. Analysis proved it to be a monoacetyl compound. It gave no color reaction with ferric chloride. This suggests that phenolic hydroxyl was acetylated.

Found: C, 73.89; H, 4.89; N, 4.71. Calcd. for $C_{18}H_{15}NO_3$: C, 73.72; H, 5.12; N, 4.78%.

1) J. P. Phillips and A. L. Duckwall, *J. Am. Chem. Soc.*, 77, 5505 (1955).

The crude product obtained from the ether extract by evaporating the solvent, was carefully recrystallized from ether as colorless prisms, m.p. 109～110°C. The analytical figures corresponded to those of the diacetyl derivatives.

Found: C, 71.49; H, 5.00; N, 4.06. Calcd. for $C_{20}H_{17}NO_4$: C, 71.64; H, 5.07; N, 4.18%.

II (m.p. 126～127°C) on heating with 4 N hydrochloric acid for 10 min. when no odor of benzaldehyde was noticed and further working gave a product m.p. 118～119°C foaming at 125°C.

**5, 7-Dibromo-8-quinolinol.**—*Method A.*—A mixture of the Mannich base (I) (0.33 g., 0.001 mol.) and 4 N hydrochloric acid (7 ml.) was treated in the same manner as that of Phillips[1]. The reaction mixture was neutralized with sodium acetate and the separated solid was filtered; yield, 0.65 g., m.p. 105～170°C. When it was crystallized from ethanol, it gave needles (0.17 g.) melting at 194～15°C alone or on admixture with a sample of 5, 7-dibromo-8-quinolinol which was prepared by bromination of 8-quinolinol.

*Method B.*—To a mixture of II (0.33 g. 0.001 mol.) and 4 N hydrochloric acid (7 ml.) after it was diluted with water (50 ml.), one half normal bromate-bromide solution (8 ml.) was added dropwise.

After standing for 2 hr., the resulting solid (80 mg.) was filtered and crystallized from ethanol to give colorless needles, m.p. with a sample of 5, 7-dibromo-8-quinolinol 194～195°C. A mixture of the filtrate of the crude product and an ethanolic solution of dinitro-phenylhydrazine (0.1 g.), on mild warming and long standing gave a solid, which crystallized from ethanol as orange elongated plates, m.p. 235～236.5°C and identified as benzaldehyde dinitrophenylhydrazone by mixed m.p. method.

The author wishes to thank Mr. Konomu Matsumura for help and advice throughout this work.

*Chemical Laboratory*
*Kitasato Institute*
*Minato-ku, Tokyo*

# *The Photochemical Addition Reaction. VI. The Mechanism of the Addition Reaction of n-Butyl Mercaptan to Vinyl Acetate*

By Kazuo YAMAGISHI, Kunio ARAKI, Tadao SUZUKI and Toshio HOSHINO

(Received September 15, 1959)

Many synthetic investigations have been made on the addition reaction of mercaptans to olefins, yielding the products of $\beta$-alkylthioethyl derivatives with anti-Markownikov configuration under the influence of oxygen, peroxides and light[1]. It has been reported that, by the action of ultraviolet light, the addition of mercaptans to olefins such as vinyl acetate, vinyl chloride and allyl alcohol, proceeds according to the following overall reaction[2];

$$RSH + CH_2:CHR' \xrightarrow{h\nu} RSCH_2CH_2R' \quad (1)$$

Recently Sivertz et al.[3] studied the kinetics of the photosensitized addition reaction of a mercaptan to various olefins in order to explain the reaction mechanism kinetically, although the identification of the reaction products was not involved in their study.

The purpose of the present study is to elucidate the mechanism of the addition reaction of mercaptans to vinyl compounds. Attention has been paid to identifying the termination product as follows: In the presence of a large excess of mercaptan, butyldisulfide has been assumed as the termination product by Sivertz et al.[3] This compound, however, has been found to decompose under ultraviolet light, which was employed for the initiation of the reaction studied. It is impossible to assume that the disulfide is the final product. Hence, the formation of the cross termination product, $\alpha$, $\beta$-dibutylthioethyl derivative could not be ignored. In this connection, the analysis of all the products in the reaction has been carried out. Vinyl acetate and *n*-butyl mercaptan were chosen as the reactants, because they form 1 : 1 adduct quantitatively with no teromer formation during the reaction.

The molar ratio of vinyl acetate to mercaptan in this experiment was 1 : 20. Samples were purified by vacuum distillation for the purpose of excluding water, oxygen and oxides. The reaction mixture was irradiated with ultraviolet light of 3660 Å for forty hours. The mixture

1) S. O. Jones and E. E. Reid, *J. Am. Chem. Soc.*, **60**, 2452 (1938); M. S. Kharasch, W. Nudenberg and G. J. Mantell, *J. Org. Chem.*, **16**, 524 (1951).

2) T. Hoshino, K. Yamagishi and Y. Ichikawa, *J. Chem. Soc. Japan, Pure Chem. Sec.* (*Nippon Kagaku Zasshi*), **74**, 510 (1953); K. Yamagishi and N. Nakajima, ibid., **75**, 1086, (1954).

3) R. H. Pallen and C. Sivertz, *Can. J. Chem.*, **35**, 723 (1957).

irradiated was first divided into gas (fraction I) and liquid at room temperature. By the distillation of the liquid fraction at 20°C (20 mmHg) it was futher divided into two parts (named fractions II and III). One was the distillate (fraction II) consisting of excessively used mercaptan and unreacted vinyl acetate, which were collected in a cold trap (−78°C), and the other was the residue (fraction III) consisting mostly of the main product, β-butylthioethyl acetate, and the termination product, α, β-dibutylthioethyl acetate.

The mass-spectroscopic analysis of fraction I showed the mass number 2 and 88, which correspond to hydrogen and ethyl acetate, respectively. By the rectification of fraction II ethyl acetate was isolated from the mixture of unreacted vinyl acetate and excessively used mercaptan. This ethyl acetate was identified by Dragendorff's xanthate color test.[4] It is, therefore, certain that the mercaptan decomposed directly under the influence of ultraviolet light, yielding hydrogen atom and thyl radical by the primary initiation reaction of Eq. 2.

Prim. init.

$$RSH \xrightarrow{h\nu} RS\cdot + H\cdot \qquad (2)$$

The hydrogen atom may subsequently react with vinyl acetate and mercaptan by the secondary initiation mechanisms a) and b).

a) When a hydrogen atom is added at the double bond of a vinyl acetate molecule, the acetoxyethyl radical is produced (Eq. 3) and the acetoxyethyl radical thus formed reacts with the mercaptan giving the thyl radical and the ethyl acetate (Eq. 4).

Sec. init. a)

$$H\cdot + CH_2:CHOAc \rightarrow CH_3\dot{C}HOAc \qquad (3)$$

$$CH_3\dot{C}HOAc + RSH \rightarrow RS\cdot + CH_3CH_2OAc \qquad (4)$$

b) When a hydrogen atom abstracts the hydrogen atom from a mercaptan molecule, a thyl radical and a hydrogen molecule are produced (Eq. 5).

Sec. init. b)

$$H\cdot + RSH \rightarrow RS\cdot + H_2 \qquad (5)$$

In either secondary initiation a) or b), the thyl radical is produced ultimately, and the radical initiates the propagation reaction of Eqs. 6 and 7.

Prop.

$$RS\cdot + CH_2:CHOAc \rightarrow RSCH_2\dot{C}HOAc \qquad (6)$$

$$RSCH_2\dot{C}HOAc + RSH \rightarrow RS\cdot + RSCH_2CH_2OAc \qquad (7)$$

By the rectification of fraction III, the main product, β-butylthioethyl acetate was obtained in a good yield with a small amount of heavy colorless liquid (b. p. 110°C at 2 mmHg), which was identical with the authentic sample of α, β-dibutylthioethyl acetate. The identification of α, β-dibutylthioethyl acetate was performed as follows: (a) The physical properties of the sample were compared with those of the authentic sample, which was prepared by the reaction of vinyl acetate with butyldisulfide under the irradiation of ultraviolet light of 3660 Å at room temperature for forty hours (Table I). (b) α, β-Dibutylthioethyl acetate was hydrolyzed to butylthioacetaldehyde. This gave the hydrazone (m. p. 63~64°C) with 2, 4-dinitrophenyl hydrazine and no depression of the melting point when mixed with the hydrazone of the authentic sample. The authentic sample of the aldehyde was prepared from bromacetaldehyde dimethyl acetal[8] and sodium mercaptid.

These facts indicate that β-butylthioethyl acetate is produced by the chain propagation reaction of Eqs. 6 and 7. The isolation of α, β-dibutylthioethyl acetate from the reaction mixture supports the view that termination reaction occurred by the mechanism shown in Eq. 8.

Term.

$$RS\cdot + RSCH_2\dot{C}HOAc \rightarrow RSCH_2CH(SR)OAc \qquad (8)$$

Further support of the initiation reaction was obtained by means of the experiment with oxygen as the quencher of atomic hydrogen. By the mass-spectroscopic analysis of fraction I, no ethyl acetate was identified, although traces of water and hydrogen were detected. This result suggests that the hydrogen atom combined with oxygen and the hydrogenperoxyl radical ($HO_2\cdot$) thus formed produced the thyl radical and hydrogen peroxide. More thyl radicals may be produced by $H_2O_2$ (Eq. 11).

$$H\cdot + O_2 \rightarrow HO_2\cdot \qquad (9)$$

$$HO_2\cdot + RSH \rightarrow RS\cdot + H_2O_2 \qquad (10)$$

$$H_2O_2 + RSH \rightarrow RS\cdot + H_2O \qquad (11)$$

## Experimental

**Materials.**—*n-Butyl mercaptan.*—By the hydrolysis of *S*-butylthiuronium hydrobromide *n*-butyl mercaptan was obtained (b. p. 98°C)[5].

*Vinyl acetate.*—After removing the impurities in a commercial product by Matheson's prepolymerization method[6], the remaining monomer was

4) F. Feigl, "Spot Tests in Organic Analysis", Elsevier Publ. Co., Amsterdam (1956), p. 174.

5) H. Backer, *Rec. trav. chim.*, **51**, 289 (1932).

6) M. S. Matheson, E. E. Auer, E. B. Bevilacqua and E. J. Hart, *J. Am. Chem. Soc.*, **71**, 2610 (1949).

TABLE I.

| α,β-Dibutylthioethyl acetate | Boiling point °C at mmHg | Refractive index $n_D$ | Anal. Found C | H |
|---|---|---|---|---|
| The sample from reaction products | 107/0.3 | 1.4958 (20°C) | 54.58 | 9.29 |
| The authentic sample | 109/0.3 | 1.4948 (24°C) | 54.22 | 9.25 |
| Calcd. for $C_{12}H_{24}O_2S_2$: | | | 54.53 | 9.15 |

fractionated and the fraction of b. p. 72.6°C was collected and the sample was stored in vacuo.

The purification of these two samples was effected at first by fractional distillation under nitrogen through a Steadmann type of glass column with 100 plates and the distillate was further purified of a high vacuum system. The out gassing of the liquid sample in the vacuum distillation was achieved by repeated freezing and pumping until no more non-condensible gas was evolved. The liquid sample in the system was then distilled into a vacuum reactor.

The purity of the vinyl acetate was checked by measuring the absorption spectrum. The original crude sample showed two bands at 2680 and 2590 Å, in which the band at 2590 Å was decided to be due to the acetaldehyde present in the sample. These impurity bands were completely removed by the purification described above and no band appeared between 2500 and 3000 Å in the spectrum of the purified sample. The purified sample showed no induction period in the polymerization initiated by 2,2'-azo-bis-*iso*-butyronitrile in the concentration of $10^{-4}$ mol. per liter. This is also an indication of the high purity of the sample.

**Apparatus.** — The parallel light from a Gleiter high pressure mercury lamp (SHL-200 W.) with a condenser was filtered with a Matsuda-UVD2 filter to obtain monochromatic light of 3660 Å. The intensity of the light was measured by a photoelectric tube and was kept constant by controlling the current through the lamp. The mass spectra were observed by a modified Hitachi RMA mass spectrometer. For the study of absorption spectra, a Beckman DU Spectrophotometer was used with 1 cm. cells.

**Procedure.**—The purified vinyl acetate (5.83 g.) and *n*-butyl mercaptan (122 g.) were measured in calibrated tubes and were mixed in a reaction cell in the molecular ratio of olefin to mercaptan 1 : 20.

The reaction cell with a reaction mixture was sealed off from the vacuum line and was irradiated with ultraviolet light of 3660 Å for forty hours. The irradiated mixture which was collected from three reaction cells, was first divided into gas (fraction I) and liquid at room temperature. By the distillation of the liquid fraction at 20°C (20 mmHg), it was further divided into two parts (named fractions II and III). One was the distillate (fraction II) consisting of excessively used mercaptan and unreacted vinyl acetate, which were collected in a cold trap (−78°C), and the other was residue (fraction III), consisting mostly of the main product, β-butylthioethyl acetate, and the termination product, α,β-dibutylthioethyl acetate.

The mass-spectroscopic analysis of fraction I showed the mass numbers 2 and 88, which correspond to hydrogen and ethyl acetate, respectively.

Fraction II was distilled fractionally with a Steadmann type glass column at an atmospheric pressure under nitrogen. One gram of crude ethyl acetate (b. p. 78.1~83.0°C) and 0.5 g. of unreacted vinyl acetate (b. p. 72.1~73.0°C) were obtained together with mercaptan. In order to confirm the existence of ethyl acetate, Dragendorff's xanthate color test[6] was carried out on the crude fraction (b. p. 78.1~83.0°C). The test showed violet color, the indication of ethoxyl residue. The same color test gave us no color with vinyl acetate and blue color with mercaptan.

Fraction III was fractionated under reduced pressure. Thirty-two grams of β-butylthioethyl acetate (b. p. 62°C at 0.7 mmHg $n_D^{25}$ 1.4954) was obtained as the main product. Another product of α,β-dibutylthioethyl acetate (0.3 g.) was identified as follows.

(a) The physical properties of the sample were compared with those of the authentic sample (Table I). The authentic sample was prepared in 30% yield by the reaction of vinyl acetate (0.1 mol.) with butyldisulfide[7] (0.5 mol.) under the irradiation of ultraviolet light of 3660 Å at room temperature for forty hours.

(b) α,β-Dibutylthioethyl acetate was hydrolyzed to butylthioacetaldehyde by steam distillation with a drop of sulfuric acid. The aldehyde gave a hydrazone (m.p. 63~64°C) with 2,4-dinitrophenyl hydrazine and no depression of the melting point when mixed with the hydrazone of the authentic sample. The authentic sample was prepared as follows: The solution of sodium mercaptid (0.5 mol.) in ethanol (200 ml.) was added to the solution of bromoacetaldehyde dimethyl acetal[8] (0.5 mol.) in ethanol (30 ml.) at room temperature. After refluxing for half an hour, sodium bromide and ethanol were removed and *n*-butylthioacetaldehyde diethyl acetal (b. p. 75°C at 0.1 mmHg, $n_D^{25}$ 1.4532) was obtained in the yield of 60.0%.

Found: C, 54.02; H, 10.43. Calcd. for $C_8H_{18}O_2S$: C, 53.91; H, 10.18%.

*n*-Butylthioacetaldehyde dimethylacetal was hydrolyzed by refluxing with dilute sulfuric acid. *n*-Butylthioacetaldehyde (b. p. 88°C at 24 mmHg) was obtained from the reaction mixture by steam distillation in the yield of 77.6%. The 2,4-dinitrophenyl hydrazone of this substance had m. p. 62.0~63.0°C.

Found: N, 17.53. Calcd. for $C_{12}H_{16}O_4N_4S$: N, 17.94%.

When oxygen was used as the quencher of atomic hydrogen the reaction mixture was exposed to dry air in the reaction cell before the irradiation and

7) L. D. Small, J. H. Bailey and C. J. Cavallito, ibid., **69**, 1711 (1947).
8) P. Z. Bedoukian, ibid., **66**, 651 (1944).

the cell was sealed off from the vacuum line at −78°C. By the analysis of fraction I no ethyl acetate was identified, although traces of water and hydrogen were detected.

The authors are indebted to Mr. Asaji Kondo for the elementary analyses and to Mr. Haruyoshi Sakurai for the mass spectroscopic analyses. The authors' thanks are also due to Dr. Shoji Shida and Dr. Saburo Fujii for their helpful discussions in carrying out this study.

*Laboratory of Organic Chemistry*
*Tokyo Institute of Technology*
*Meguro-ku, Tokyo*

# *Synthesis and Physical Properties of Normal Higher Alcohols. II. Synthesis of Normal Higher Primary Alcohols of Odd Carbon Numbers from Heptacosanol to Heptatriacontanol*

By Akira WATANABE*

(Received August 17, 1959)

In continuation of the work described in the preceding paper[1], synthesis of the normal higher primary alcohols of odd carbon numbers containing from twenty-seven to thirty-seven carbon atoms were undertaken and gave the desired products as pure as practicable.

Heptacosanol was prepared by Bowman's method[2], which was outlined in the first paper[1], from arachidic acid and ethyl ε-bromocaproate. The reaction is shown in the following equations.

$$C_2H_5O_2C(CH_2)_nBr \xrightarrow{\text{Ethyl malonate}}$$
(I)

$$C_2H_5O_2C(CH_2)_nCH(CO_2C_2H_5)_2 \xrightarrow{C_6H_5CH_2OH}$$
(II)

$$C_6H_5CH_2O_2C(CH_2)_nCNa(CO_2CH_2C_6H_5)_2 \xrightarrow{RCOCl}$$
(III)

$$C_6H_5CH_2O_2C(CH_2)_nC(CO_2CH_2C_6H_5)COR \xrightarrow{H_2}$$
(IV)

$$HO_2C(CH_2)_nC(CO_2H)COR \xrightarrow{-CO_2}$$
(V)

$$RCO(CH_2)_{n+1}CO_2H \xrightarrow{\text{Huang-Minlon}}$$
(VI)

$$R(CH_2)_{n+2}CO_2H \xrightarrow{C_2H_5OH}$$
(VII)

$$R(CH_2)_{n+2}CO_2C_2H_5 \xrightarrow{LiAlH_4} R(CH_2)_{n+3}OH$$
(VIII) (IX)

By means of the same series of reactions but starting with higher fatty acids and ω-bromoacids, higher alcohols than heptacosanol were synthesized. Since the use of ω-bromoacids is restricted by the difficulty of their preparation in pure state when the carbon chain is considerably long, the author has used a series of long chain fatty acids along with the ω-bromoacids I where $n$ is 5, 7 and 10.

The three bromoacid ethyl esters required for condensation with ethyl malonate were prepared by the following methods. Ethyl ω-bromocaproate was obtained by the method described in the first paper. Ethyl ω-bromooctanoate was prepared, with some modification, according to Hunsdiecker's method[3]. Silver salt of ethyl hydrogen azelaate was added to the carbon tetrachloride solution of bromine in reverse of the customary procedure. The yield was 80% which was better as compared with those of the analogous synthesis of Hunsdiecker (69.7%).

Ethyl ω-bromoundecanoate was obtained from undecylenic acid by addition of dry hydrogen bromide in the presence of benzoyl peroxide followed by exhaustive esterification, according to Jones' method[4].

Besides commercially available fatty acids, the long chain fatty acids such as arachidic ($C_{20}$), tricosanoic ($C_{23}$), tetracosanoic ($C_{24}$) and pentacosanoic ($C_{25}$) acids were synthesized from octadecyl bromide, heneicosyl bromide, and docosyl bromide by repetition of the modified malonic ester synthesis[5].

The condensation products of benzyl alkanetricarboxylates with acid chlorides were semisolid brown materials which were subjected to

* Some parts of this wark were performed at the Department of Chemistry, Faculty of Science, Kyoto University; Sakyo-ku, Kyoto.

1) A. Watanabe, This Bulletin, **32**, 1295 (1959).
2) R. E. Bowman, *J. Chem. Soc.*, **1950**, 174.
3) H. Hunsdiecker et al., *Ber.*, **75B**, 29 (1947).
4) R. G. Jones, *J. Am. Chem. Soc.*, **69**, 2350 (1947).
5) W. Bleyberg et al., *Ber.*, **64**, 2506 (1931).

TABLE I

| Alcohols | Formula | Calcd. C | Calcd. H | Found C | Found H | m. p., °C | f. p. °C | t. p. °C |
|---|---|---|---|---|---|---|---|---|
| Heptacosyl | $C_{27}H_{56}O$ | 81.74 | 14.23 | 81.59 | 14.36 | 80.5(81.0)[a] | 80.0 | 7.25 |
| Nonacosyl | $C_{29}H_{60}O$ | 82.10 | 14.24 | 81.30 | 14.03 | 83.5(83.8)[b] | 82.5 | 75.0 |
| Hentriacontyl | $C_{31}H_{64}O$ | 82.22 | 14.25 | 81.97 | 13.95 | 87.0(87.0)[b] | 85.8 | 78.5 |
| Tritriacontyl | $C_{33}H_{68}O$ | 82.42 | 14.25 | 82.19 | 14.35 | 88.5(88.6)[b] | 87.8 | |
| Pentatriacontyl | $C_{35}H_{72}O$ | 82.60 | 14.26 | 82.83 | 14.01 | 91.2(91.5)[b] | 89.5 | |
| Heptatriacontyl | $C_{37}H_{76}O$ | 82.75 | 14.27 | 82.92 | 14.15 | 92.7 | 91.6 | |

Melting points are uncorrected.

When a sample is cooled below its freezing point, transition appears with change of the transparent waxy material into opaque crystalline state. Transition points of $C_{33}$, $C_{35}$, $C_{37}$ alcohols could not be observed.

a) S. Shiina, *J. Soc. Chem. Ind. Japan* (*Kogyo Kwagaku Zasshi*), **39**, 345 (1936).

b) R. G. Johns, *J. Am. Chem. Soc.*, **69**, 2350 (1947).

TABLE II

| Ethyl alkane-tricarboxylates | Acid chlorides | Cno. | Kotonic acids | m. p. °C | Fatty acids | m. p., °C |
|---|---|---|---|---|---|---|
| *n*-Hexane | Eicosanoyl($C_{20}$) | 27 | $CH_3(CH_2)_{18}CO(CH_2)_6CO_2H$ | 99.5 | Heptacosanoic | 86.6(87)* |
| | Docosanoyl($C_{22}$) | 29 | $CH_3(CH_2)_{20}CO(CH_2)_6CO_2H$ | 101 | Nonacosanoic | 98.7(89.2)* |
| *n*-Octane | | 31 | $CH_3(CH_2)_{20}CO(CH_2)_8CO_2H$ | 105 | Hentriacontanoic | 92.5 |
| | Tetracosanoyl($C_{24}$) | 33 | $CH_3(CH_2)_{24}CO(CH_2)_8CO_2H$ | 107 | Tritriacontanoic | 96.0 |
| *n*-Undecane | Tricosanoyl($C_{23}$) | 35 | $CH_3(CH_2)_{21}CO(CH_2)_{11}CO_2H$ | 109 | Pentatriacontanoic | 98.0 |
| | Pentacosanoic($C_{25}$) | 37 | $CH_3(CH_2)_{23}CO(CH_2)_{11}CO_2H$ | 110 | Heptatriacontanoic | 98.7 |

* S. Shiina, *J. Soc. Chem. Ind. Jap.* (*Kogyo Kwagaku Zassi*), **39**, 345 (1936).

TABLE III

| Starting materials: Fatty acids | m. p. °C | Intermediates: Alcohols | m.p., °C | Bromides[a] m.p., °C | Malonic[b] acids m.p., °C | Products: Fatty acids[c] | m. p., °C | Yields to bromides % |
|---|---|---|---|---|---|---|---|---|
| Stearic | 68.5 | Octadecyl | 58 | 28.5 | 109 | Eicosanoic | 75(75.5[d]) | 75 |
| Behenic | 79 | Docosyl | 71.5 | 44.0 | 125 | Tetracosanoic | 85(86.0[e]) | 50 |
| Tricosanoic | 78.5 | Tricosyl | 72.0 | 51.0 | — | Pentacosanoic | 83.5(85[e]) | 42 |

a) Bromination of the alcohols was modelled after Reid. [E. E. Reid et al., "Organic Syntheses" Vol. 15, John Willey & Sons, Inc., New York (1935), p. 26]. Hydrogen bromide was passed for 15 hr. in each alcohol.

b) Recrystallized from benzene.

c) The malonic acids were decarboxylated in vacuo and the resulting fatty acids were recrystallized from benzene.

d) F. Adam et al., *J. Chem. Soc.*, **1926**, 72.

e) P. A. Levene et al., *J. Biol. Chem.*, **59**, 921 (1924).

hydrogenation without purification, since it is known[2] that the compounds of this type can not be purified. Therefore, for the successful hydrogenation of the compounds, it is essential to purify the acid chlorides by distillation. However, since arachidyl and higher acid chlorides were found to decompose even under vacuum distillation at 2 mmHg, these acid chlorides were subjected to further reaction without distillation. In this case, oxalyl chloride proved to be superior for the preparation of acid chlorides to thionyl chloride because it furnished cleaner products. On hydrogenation considerable poisoning of the catalyst was found even when distilled acid chloride was used. After debenzylation and decarboxylation, the desired ketonic acids were obtained in low yield of about 35%, considerable amount of the starting fatty acids being recovered. Huang-Minlon reduction[6] of the ketonic acids took place readily to give the corresponding fatty acids which, after conversion to their ethyl esters, were led to the final products by reduction with lithium aluminum hydride.

6) Huang-Minlon, *J. Am. Chem. Soc.*, 68, 2487 (1946).

Repeated recrystallizations of the alcohols from benzene or toluene gave products having sharp melting points and excellent analytical values. For hentriacontanol $C_{31}H_{63}OH$ and higher alcohols high vacuum distillation as well as recrystallization was employed. In order to prevent thermal degradation during distillation, the pressure was reduced to $2\times10^{-3}$ mmHg so as to maintain the bath temperature below 210°C.

Melting points, transition points and analytical data of these alcohols are given in Table I. Heptatriacontanol $C_{37}H_{75}OH$ has not been reported previously. All the transition points have been unknown. Combination of the starting materials and the melting points of the intermediate ketonic acids and fatty acids are given in Table II. The physical properties of these alcohols are being investigated and the results will be reported in a separated communication.

## Experimental

**Preparation of ω-Bromo Acids and their Condensation with Ethyl Malonate.** — *Ethyl ε-bromocaproate.*—It was prepared from caprolactone by the method described in Part I[1]. The physical constants are as follows: b. p. 118°C/14 mmHg or 98°C/4.5 mmHg, $n_D^{32}$ 1.4561.

*Ethyl ω-bromooctanoate.*—The procedure of Hunsdiecker[3] was followed with some modification to give increased yield. Pure azelaic acid (m. p. 104~106°C) obtained by repeated recrystallizations of commercial specimen from aqueous ethanol was converted to its ethyl ester by exhaustive esterification. Boiling point of the ester was 135~137°C at 6.5 mmHg (reported: 130~132°C at 5 mmHg)[7]. Above acid (130 g.) and its ethyl ester (98 g.) were treated in the same manner as described in Organic Syntheses[8] for the preparation of ethyl hydrogen sebacate and yielded 62 g. of the monoester; b. p. 161 ~ 163°C/1 mmHg (reported: 169 ~ 170°C/2 mmHg)[9]. Silver salt of the monoester was prepared by an analogous manner described in Part I[1] for the preparation of silver heneicosanoate. The thoroughly dried silver salt (85 g.) was added portionwise to a solution of 60 g. of bromine in 100 ml. of carbon tetrachloride under strict exclusion of moisture. A vigorous reaction ensued with evolution of carbon dioxide. When no more gas evolved, the solution was filtered, washed with water, aqueous solution of sodium hydroxide, again water, and dried over sodium sulfate. Following evaporation of the solvent the residue was distilled through a short Widmer column to give a liquid having a boiling point of 125°C at 3.5 mmHg. $n_D^{27}$, 1.4572: Yield, 53 g. (80%), (reported: 69.7% for methyl compound)[3].

*Ethyl ω-bromoundecanoate.* — The preparation of the corresponding acid was essentially the same as the method described by Jones[4]. The melting point of the acid was 48~49.5°C (reported: 49~50°C).

Ethylester of the acid was obtained in an almost quantitative yield by exhaustive esterification. b. p. 148~150°C/5 mmHg, m. p. 11.5~13.5°C, $n_D^{20}$ 1.4651.

The three ethyl esters of ω-bromo acids mentioned above were condensed with sodiomalonic ester by an usual method to give ethyl alkanetricarboxylates in good yields. The constants are: *Ethyl n-hexane-1, 1, 6-tricarboxylate* (II where $n$ is 5): b. p. 150~151°C/1 mmHg, $n_D^{28}$ 1.4360. *Ethyl n-octane-1, 1, 8-tricarboxylate* (II where $n$ is 7): b. p. 170~172°C/1.5 mmHg, $n_D^{28}$ 1.4380. *Ethyl n-undecane-1, 1, 11-tricarboxylate* (II where $n$ is 10): b. p. 187°C/1 mmHg, $n_D^{28}$ 1.4435.

**Preparation of Long Chain Fatty Acids.**—Except heneicosyl bromide which was prepared from behenic acid by degradative bromination[1], a long chain alkyl bromides were made by the reduction of the corresponding acid esters to the alcohols by high pressure hydrogenation or using lithium aluminum hydride followed by treatment with hydrogen bromide. Further treatment of the alkyl bromides with sodiomalonic ester in butanol[5] in place of ethanol led to the acids of two additional carbon atoms. Since these reactions are relatively well known, detailed descriptions of the experiments were omitted and the results are summarized in Table III.

**Preparation of Higher Alcohols.** — General procedures of the synthesis are very similar throughout the series, so only an example for the preparation of heptatriacontanol $C_{37}H_{75}OH$ is described in detail.

*Benzyl n-undecane-1, 1, 11-tricarboxylate.* — To a suspension of sodium ethoxide (prepared from 0.38 g. of freshly cut sodium and 10 ml. of absolute ethanol) in benzene was added 6.15 g. of ethyl undecane-1, 1, 11-tricarboxylate. After the sodium ethoxide dissolved 5.35 g. of purified benzyl alcohol was added, the mixture was distilled through a Fenske column until the boiling point reached to 80°C. During this time an almost theoretical quantity of ethanol was removed.

*13-Keto-heptatriacontanoic acid* $C_{24}H_{49}CO(CH_2)_{11}\cdot CO_2H$.—To the benzene solution of the above tribenzyl esters was added gradually 6 g. of pentacosanoyl chloride in benzene (prepared from 5.8 g. of pentacosanoic acid and 7.5 g. of oxalyl chloride, and excess of the oxalyl chloride was removed under reduced pressure at 100°C). The reaction mixture was refluxed for 1 hr. After cooling, the solution was washed with ice water to neutral reaction and then dried over sodium sulfate. The solvent was removed under reduced pressure at 50°C of bath temperature to give a brown colored oil which solidified on standing at room temperature. Yield, 20 g. Hydrogenation of the above compounds in 60 ml. of ethyl acetate over Pd-C (5 g.) and Pd-$SrCO_3$ (5 g.) took place at a slightly positive hydrogen pressure, accompanying a considerable poisoning of the catalysts. A nearly theoretical amount of hydrogen was absorbed within 3 hr. The catalyst was filtered off, then the ethyl acetate solution was refluxed for 1 hr. to decarboxylate compound V. Upon cooling to room temperature, small crystals were separated. They were recrystallized twice from ethyl acetate to give the product

7) Jones et al., *J. Chem. Soc.*, **1928**, 68.
8) S. Swann, "Orgamic Syntheses", Vol. 19, John Wiley & Sons, Inc., New York (1938), p. 45.
9) M. Asano, *J. Pharm. Soc. Japan*, **504**, 8 (1924).

having a melting point of 105 to 107°C. Further recrystallizations from benzene gave a pure acid. m. p. 108~109°C. Yield, 3.2 g. (37%). From the mother liquor, 2.5 g. of the pentacosanoic acid was recovered.

*Heptatriacontanoic acid* $C_{36}H_{73}CO_2H$.—The Hung-Minlon reduction of long chain ketonic acid was found to be superior to the Clemmensen reduction[4], because of its effectiveness and simplicity. The experimental conditions were essentially the same as those described in the first paper. A mixture of 3 g. of the ketonic acid, 3 g. of potassium hydroxide, 3 ml. of 85% hydrazine hydrate and 25 ml. of diethylene glycol (b. p. 250°C) was refluxed for 1 hr. After removing the water formed, the temperature of the mixture was gradually raised to 200°C and the refluxing was continued at this temperature for 6 hr. When the mixture was cooled to about 80°C. it was poured into a 100 ml. of water containing 15 ml. of hydrochloric acid with stirring. A white solid separated was collected and washed with water, and then dried. Yield of the crude acid was nearly quantitative. Repeated recrystallizations from benzene and then toluene gave a pure product with little loss of the material, m. p. 97.5~98.5°C.

Found: C, 78.42; H, 13.10. Calcd. for $C_{37}H_{72}O_3$: C, 78.66; H, 12.85%.

*Heptatriacontanol* $C_{37}H_{75}OH$.—Ethyl heptatriacontanoate (2.5 g.) was readily reduced to the alcohol with lithium aluminum hydride in absolute ether[1]. The reaction mixture was hydrolyzed to remove the small amount of unchanged ester, but traces of alkali or soap could not be removed from the product by crystallization. Pure alcohol could be obtained by high vacuum distillation at $2\times10^{-3}$ mmHg followed by repeated crystallizations from toluene, m. p. 92~92.7°C. Yield, 1.8 g.

The author expresses his sincere thanks to Professor Ryozo Goto, Kyoto University, for his kind guidance throughout this study. Thanks are also due to the Ministry of Education for a Grant-in-Aid for Scientific Research.

*Department of Applied Chemistry*
*Himeji Technical College*
*Idei, Himeji*

# *Benzylideneaniline. I. Structure and Ultraviolet Absorption Spectrum of Benzylideneaniline*

By Nozomu EBARA

(Received July 31, 1959)

Benzylideneaniline has been believed to assume a planar structure without any experimental proof, as it has a similar molecular constitution as stilbene or azobenzene, of which the geometries are proved to be planar by the aid of X-ray diffraction method[1]. Benzylideneaniline, however, has many unusual properties which can not be accounted for by the planar structure.

1) Imoto[2] measured the p$K$ values of the several carboxyl derivatives of substituted benzylideneanilines and found that the conduction of the effects of the substituents across the central C=N double bond is extraordinarily small. His data show that *N*-(substituted benzylidene)-*p*-aminobenzoic acid has the p$K$ value almost equal to that of *p*-aminobenzoic acid.

2) Hertel and Schinzel[3] investigated the reaction of methyl iodide with the lone pair electron of N atom in benzylideneaniline and found that the substituents on the aniline ring exert remarkable effects on reaction velocity, while the effects of the substituents on the other ring are negligibly small.

3) The dipole moment of *p,p'*-dinitrobenzylideneaniline was reported to have the intermediate value between those expected for *trans* and *cis* forms[4].

4) Benzylideneaniline seems to show no geometrical isomerism, in contrast to stilbene, azobenzene and azoxybenzene, of which the two isomers can be detected and easily separated. Wyman[5], by means of the rotating-shutter technique, found that the solution of this substance does not show any spectral change when exposed to light. Gaouck and LeFèvre[6] investigated the polymorphic crystals of the derivatives of benzylideneaniline by means of

1) (a) J. M. Robertson and I. Woodward, *Proc. Roy. Soc.*. **162A**, 568 (1937). (b) J. M. Robertson, *J. Chem. Soc.*, 1939, 232.

2) E. Imoto et al., Presented at the 12th Annual Meeting of Chemical Society of Japan, Kyoto, April, 1959.

3) E. Hertel and M. Schinzel, *Z. physik. Chem.*, **B48**, 289 (1941).

4) K. A. Jensen and N. Hofman-Bang, *Ann.*, **548**, 106 (1941).

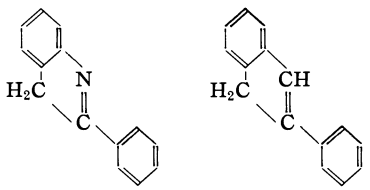
5) G. M. Wyman, *Chem. Revs.*, 55, 625, (1955).

6) V. De Gaouk and R. J. W. LeFèvre, *J. Chem. Soc.*, **1938**, 741.

the measurements of dipole moments and of absorption spectra, and concluded that these molecules exist exclusively in *trans* forms.

5) It has been shown[7] that the phase diagrams of the admixtures of benzylideneaniline with *trans*-stilbene, *trans*-azobenzene, phenanthridine or bibenzyl[8] involve discontinuous curves, while those of the admixtures between *trans*-stilbene, *trans*-azobenzene and bibenzyl speak for the perfect miscibility. This fact is likely to show that the structure of benzylideneaniline corresponds to neither *trans* nor *cis* form.

6) The shape of the ultraviolet absorption spectrum of benzylideneaniline is quite different from those of stilbene, azobenzene and azoxybenzene, which resemble each other very closely. Wiegand and Merkel[7] found that the spectrum of 2-phenylbenzimidazole (I) exhibits a similarity to stilbene and not to benzylideneaniline, while that of 2-phenylindene (II) is very much similar to that of stilbene, where I and II must have planar *trans* structures. They proposed a linear planar structure for benzylideneaniline, but it seems inadequate, as it has no theoretical basis and is energetically less favorable.




I II

7) Benzylideneaniline shows no $n-\pi^*$ transition at the longer wavelength region. Jaffé[9] has assumed that this transition is hidden under the long tapering end of the absorption curve of 315 m$\mu$ band, but it appears that the strong experimental support is lacking for this assumption.

These experimental facts are not consistent with the generally accepted stilbene-type structure, and yet very few works have been carried out with regard to the very nature of the benzylideneanilinemolecule. Therefore, series of experiments are now undertaken to explain some fundamental problems of benzylideneaniline.

## Results and Discussion

Measurements were carried out on the ultraviolet absorption spectra of benzylideneaniline, stilbene, azobenzene and azoxybenzene in *n*-heptane, ethanol and 50% mixture of ethanol and concentrated hydrochloric acid, together with their variations caused by the substituent groups, and for comparison, spectra of some aromatic compounds were also measured. The results are shown in Tables I and II and in Fig. 1.

If benzylideneaniline assumes the stilbene-type planar structure, there must be some substantial similarity in behavior between the spectra of benzylideneaniline and of stilbene, azobenzene or azoxybenzene.

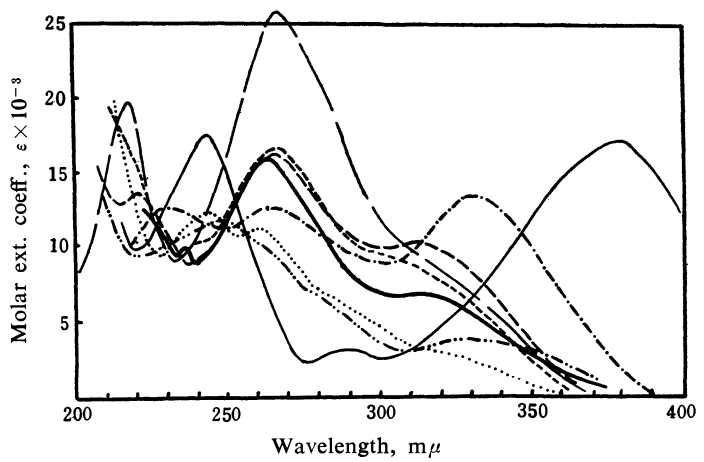
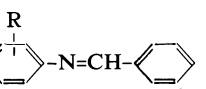
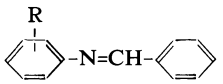



Fig. 1. Spectra of benzylideneanilines:  (in $C_2H_5OH$)

R = ——— H ; —— *p*-$NO_3$ ; —— *m*-$NO_3$ ; -·-· *p*-$OCH_3$ ; -···· *o*-$OCH_3$ ; ---- *p*-Cl ; ------ *m*-Cl ; ····· *o*-Cl.

7) C. Wiegand and E. Merkel, *Ann.*, **550**, 175 (1942).
8) Bibenzyl is found to have the planar *trans* conformation (Ref. 1b).
9) H. H. Jaffé, S. Yeh and R. W. Gardner, *J. Molecular Spectroscopy*, **2**, 120 (1958).

Table I. Wavelengths and intensities of ultraviolet absorption maxima (in $C_2H_5OH$)



| R | Free bases abs. max. λ, mμ | $\varepsilon_{max}$ | Conjugate acids abs. max. λ, mμ | $\varepsilon_{max}$ |
|---|---|---|---|---|
| H | 236 | 10100 | 250 | 13900 |
| | 263 | 16400 | 290 | 2000 |
| | 315 | 6200 | 360 | — |
| *o*-Cl | 244 | 12400 | 220 | 7400 |
| | 260 | 11200 | 250 | 10300 |
| | 290 | — | 290 | 2800 |
| | 330 | 2700 | 360 | — |
| *m*-Cl | 240 | 10300 | 220 | 7200 |
| | 264 | 16900 | 250 | 13900 |
| | 310 | 8800 | 290 | 3200 |
| | | | 360 | — |
| *p*-Cl | 223 | 13800 | 220 | 8800 |
| | 264 | 16600 | 250 | 14600 |
| | 314 | 10400 | 290 | 2250 |
| | | | 360 | — |
| *o*-$OCH_3$ | 246 | 11700 | 220 | 10800 |
| | 263 | — | 250 | 15700 |
| | 330 | 3850 | 290 | — |
| | | | 373 | — |
| *p*-$OCH_3$ | 229 | 12900 | 223 | 11500 |
| | 264 | 13100 | 250 | 15500 |
| | 330 | 13300 | 290 | — |
| | | | 360 | — |
| *m*-$NO_3$ | 218 | 19900 | 252 | 22900 |
| | 267 | 25900 | 290 | — |
| | 325 | 6730 | 355 | — |
| *p*-$NO_3$ | 243 | 17300 | 252 | 22200 |
| | 290 | 3040 | 290 | — |
| | 380 | 16800 | 335 | — |

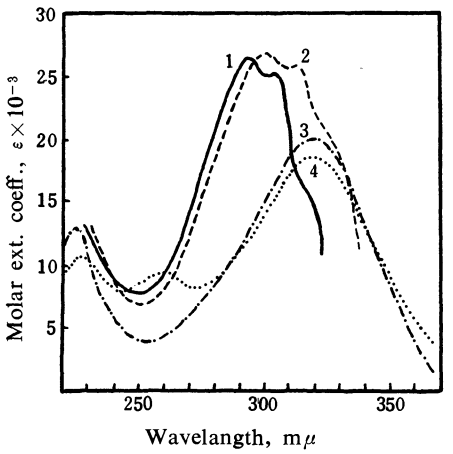
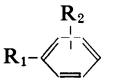



Fig. 2. Spectra of: 1, —— stilbene; 2, ---- *p*-methoxystilbene; 3, -·-· azobenzene; 4, ····· azoxybenzene. (in $C_2H_5OH$)

Table II. Wavelengths and intensities of some aromatic compounds (in $C_2H_5OH$)



| $R_1$ | $R_2$ | λ, mμ | $\varepsilon_{max}$ |
|---|---|---|---|
| Cl | H* | 209.5 | 7400 |
| | | 263.5 | 190 |
| $OCH_3$ | H | 220 | 7020 |
| | | 271 | 1830 |
| $NO_3$ | H* | 268.5 | 7800 |
| $NH_2$ | H | 235 | 8100 |
| | | 285 | 1400 |
| | *o*-Cl | 238 | 8740 |
| | | 292 | 2480 |
| | *m*-Cl | 245 | 9000 |
| | | 295 | 2300 |
| | *p*-Cl | 239 | 11700 |
| | | 290 | 1500 |
| | *o*-$OCH_3$ | 235 | 10000 |
| | | 285 | 3700 |
| | *p*-$OCH_3$ | 235 | 8450 |
| | | 300 | 2580 |
| | *o*-$NO_3$ | 230 | 13100 |
| | | 278 | 4220 |
| | | 406 | 4250 |
| | *m*-$NO_3$ | 234 | 14900 |
| | | 282 | 3560 |
| | | 373 | 1310 |
| | *p*-$NO_3$ | 230 | 6600 |
| | | 368 | 15200 |
| CHO | H* | 249.5 | 11400 |
| | | 285 | — |
| $NH^+_3$ | H* | 203 | 7500 |
| | | 254 | 160 |
| | *p*-Cl* | 215.5 | 9200 |
| | | 263 | 360 |
| | *p*-$NO_3$* | 208 | 7800 |
| | | 258 | 8700 |

* L. Doub and J. M. Vandenbelt, *J. Am. Chem. Soc.*, **69**, 2714 (1947).

Stilbene, as well as azobenzene and azoxybenzene, shows an intense absorption maximum near 300~320 mμ, which has been interpreted to be the $\pi-\pi^*$ transition[9-12]. This band shifts toward longer wavelength when *p*-position is substituted. The spectrum of azobenzene in concentrated sulfuric acid was measured by several authors, and it was suggested that the band at 320 mμ in neutral solvent shifts to 420 mμ in acidic medium, whereby its intensity also increases considerably. This shift has been explained by Jaffé[9] in terms of the LCAO

10) P. P. Birnbaum, J. H. Linfold and D. W. G. Style, *Trans. Faraday Soc.*, **49**, 735 (1953).
11) H. Suzuki, This Bulletin, **25**, 145 (1952).
12) W. Maier, A. Saupe and A. Englert, *Z. physik. Chem., N. F.*, **10**, 273 (1957).

method by taking into account the increase of Coulombic integral of the nitrogen atom when proton attaches to it.

In the present experiment the activity of proton seems to be insufficient to convert the substance completely into its conjugate acid, and it can be inferred from Fig. 3 that there is

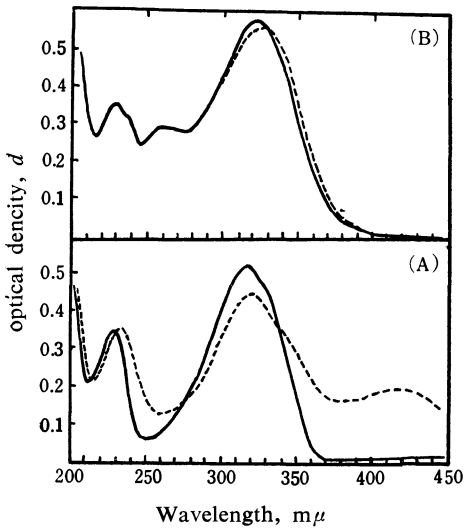



Fig. 3. Spectra of (A) azobenzene and (B) azoxybenzene in —— $C_2H_5OH$ and in ------ $C_2H_5OH$+conc. HCl

an equilibrium between azobenzene and its conjugate acid. In the same condition, azoxybenzene does not undergo any remarkable change in spectrum. This fact may be explained by the consideration that owing to the inductive effect of N→O coordination, basicity of this molecule is greatly reduced compared with that of azobenzene. But the inspection of the shape of the spectrum is likely to tell that also in this case a red shift occurs when conjugate acid is formed.

Benzylideneaniline shows an intense band at 263 mμ and a weak band at about 315 mμ, the latter has been assigned as the $\pi-\pi^*$ transition which corresponds to that of stilbene near 300 mμ[9]. But it can hardly be accepted when one compares it with those of azobenzene or azoxybenzene, as the reduction of symmetry in benzylideneaniline would not reduce the intensity more than that of azoxybenzene. Also it is difficult to assume the 263 mμ band as this transition, as its wavelength is too short and the substituents on the ring exert too little effects upon this band as compared with stilbene or azobenzene. In addition to this, these interpretation can not account for the aforementioned spectrum of 2-phenylbenzimidazole (I), for which the planar *trans* structure is to be assumed. Moreover, acidic medium causes large

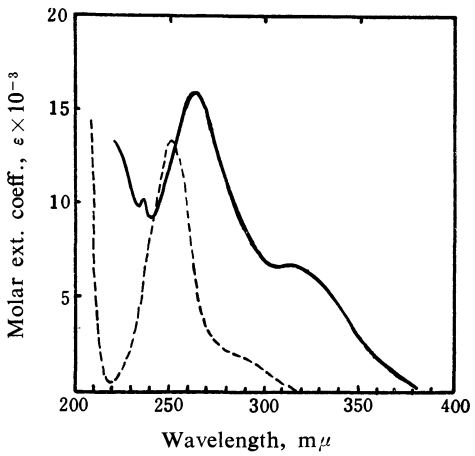



Fig. 4. Spectra of benzylideneaniline —— and its conjugate acid ---- (in $C_2H_5OH$)

unexpected change on these bands (Fig. 4): these bands become weak and shift toward shorter wavelengths, and the spectrum of free base diminishes completely. Measurements were made with various acid concentrations, but no change occurs unless acid concentration was reduced below $\cdot 10^{-3}$ mol./l. (the base concentration remaining about $10^{-4}$ mol./l.). In addition to this, these shifted bands are at the same position even when the aniline ring is substituted. As there is no time-dependence in spectrum during the measurements, and the decomposition rate of this molecule is found to be not so large, this spectrum must be attributed to the conjugate acid.

To explain these experimental results, together with the peculiarities cited above, an alternative geometrical structure must be proposed for this molecule. One possible structure may be such that the benzene ring at the N side is nearly perpendicular to the rest of the molecule (which accounts for problem 5 cited above).

When this structure is assumed, there may be a strong aniline-type resonance interaction, and, as a result, the $n-\pi^*$ transition is necessarily missing (problem 7). In addition, the interaction of benzene rings across the C=N double bond would be reduced to a large extent (problem 1), and the ultraviolet absorption spectrum would become close to the superposition of those of its components, aniline-type and styrene-type (problem 6). Then the substituent on the aniline ring would exert a large influence upon the lone-pair electron, whereas that on the other ring would not (problem 2).

The absence of geometrical isomerism can also be explained with this model. The C–N–C bond angle may be 120° with $sp^2$ hybridization, 180° with $sp$ hybridization or intermediate with higher order hybridization. If it is 180°, there can be no geometrical isomerism at all; if it is

120° or intermediate, there may be bending isomerization through intermediate *sp* structure, where the benzene ring would become absolutely perpendicular so as to reduce the energy of this state by the increase of resonance interaction between nitrogen non-bonding orbital and benzene $\pi$ orbital, and this would permit the undetectably fast reaction (problem 4). Probably the hybridization and the angle of the twist of the benzene ring would be such as to minimize the energy of the molecule, and when the ring is almost perpendicular, the hybridization will be close to *sp*.

Whether this is the case or not may be inferred also from the examination of the absorption spectra.

The spectra of the conjugate acids must be similar to the superposition of those of substituted anilinium ions and the conjugate acid of *N*-benzylidene-alkylamine, with a slight modification caused by the small interaction between these two. In benzylideneaniline, the former should have the absorption maximum at 254 m$\mu$, of which the intensity is so weak that it should be hidden under the intense band of the latter. The latter is isoelectronic with benzaldehyde and the bands of conjugate acids at 250 and 290 m$\mu$ can be compared with 249.5 and 285 m$\mu$ bands of benzaldehyde, respectively (247 m$\mu$ of benzylidene-methylamine). In the case of the conjugate acids of benzylidene-*m*- and -*p*-nitroaniline, 252 m$\mu$ band is very intense, perhaps owing to the overlap of the intense 268.5 m$\mu$ band of nitrobenzene component, as its extinction coefficient is just in the same magnitude as the sum of those of two components. For the conjugate acid of benzylidene-*o*- and -*p*-anisidine, there is an additional band at 220 m$\mu$ which coincides with 217 m$\mu$ band of anisole, intensified by the substituent ($-N^+=$). Also the 220 m$\mu$ band of chlorine-substituted conjugate acids can be compared with the 210 m$\mu$ band of chlorobenzene (216 m$\mu$ of *p*-chloranilinium ion).

The assignment of the bands near 360~370 m$\mu$ are not certain, but one tentative explanation is that they may be the transitions between orbitals of the two components, as their intensities are of the order of $n-\pi^*$ transition**.

The assignment of the spectra of free bases is more obscure, but the bands near 315 m$\mu$ experience considerable perturbation due to the introduction of substituents and can presumably be compared with the 285 m$\mu$ band of aniline (296 m$\mu$ of dimethylaniline). The latter is found to correspond with $A_{1g}$–$B_{2u}$ transition of benzene at 260 m$\mu$, allowed by the perturbation of the amino-substituent group, and becomes more intense and shifts toward red by successive substitution, because perturbation becomes larger. In the case of benzylideneanilines, the orbitals will mix to some extent with those of the other benzaldehyde-type part; therefore, one can probably expect that their positions and intensities may be such as these.

The band at 264 m$\mu$ is more difficult to interprete, but the absence of the effects of the substituents on this band is likely to show that this band comes from the styrene-type part; i.e. corresponds to the 250 m$\mu$ band. It seems at first unlikely that in the conjugate acid the band shifts toward shorter wavelength. However, this can probably be accepted when one assumes that the nitrogen valence orbital is nearly *sp* in free base but becomes $sp^2$ when conjugate acid is formed, and that the C=N bond length is longer in *sp* than in $sp^2$. Calculation was carried out for the transition energy of R–N=CH–$C_6H_5$ (R=alkyl) by the simple LCAO method, assuming that for the conjugate acid the Coulombic integral of N atom is $\alpha+\beta$, the exchange integral of C=N bond, which must have strong double bond character, $1.2\beta$, and that of C–$C_{ring}$, which is predominantly single, $0.6\beta$ and for the free base, these integrals are $\alpha+\beta/2$, $\beta$ and $0.6\beta$, respectively; where $\alpha$ and $\beta$ represent their usual meanings (Fig. 5). The

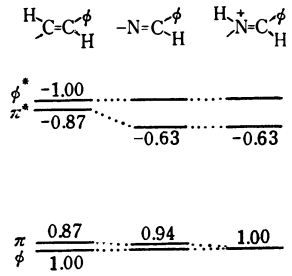



Fig. 5. Energy diagram (in $\beta$ unit).

result shows that the effect of the change in C=N bond length offsets the reverse effect of the change in Coulombic integral of the nitrogen atom, and the hypsochromic shift will occur when conjugate acid is formed.

Other bands near 230~240 m$\mu$ may be attributed to the aniline-type part, as their positions coincide and their intensities are of comparable magnitude.

The spectrum of benzylidene-*p*-nitroaniline exhibits the striking feature that it changes greatly with the solvent, whereas those of chloro-, methoxy- or unsubstituted benzylideneaniline does not. The 380 m$\mu$ band in ethanol shifts to 320 m$\mu$ in *n*-heptane, and its intensity decreases. This is not the case in *p*-nitrostilbene or -azobenzene, and it is highly likely that this band corresponds to 370 m$\mu$ *p*-nitroaniline charge-transfer band, and that the band at 243

** Or it may be that they come from the decomposition products.

mμ is the superposition of 230 mμ of *p*-nitroaniline and 250 mμ of styrene-type part. Their intensities are also consistent with this assumption. In this case, owing to the large charge-transfer resonance interaction between nitro group and nitrogen non-bonding electron, the molecule would assume almost perpendicular conformation with the result that the spectrum of this molecule is much more similar to the superposition of those of components as compared with those of any other benzylideneanilines.

There are some experimental evidences which seem to contradict this assumption. For example, Raman spectra show that the frequencies of C=N stretching vibrations of R–C=N–R′ type compounds decrease in the order R–C=N–R′> R–C=N–Ar> Ar–C=N–Ar, where R and R′ denote alkyl groups—the fact which is parallel to that of the corresponding C=C compounds[13]. This fact is at first likely to show that benzylideneaniline has the planar conformation and the increase of the number of benzene rings causes the increase of resonance interaction, and therefore decreases the force constant of vibration. But in the present model, the resonance interaction will increase though to a smaller extent, and in addition to this, hybridization-change will occur when R′ is replaced by $C_6H_5$, which would also tend to reduce the force constant.

Another strong objection to this assumption is the evidence of photoisomerism of this substance at low temperature[14]. It is not certain whether this is *cis-trans* isomerism, but if it is so, one explanation is that the bending isomerization is frozen at low temperature.

Some question may arise why benzylideneaniline can assume this structure, while azobenzene can not, and why it does not return to the planar structure when proton attaches to it. In this respect, the author has the impression, though merely speculative at this stage, that azobenzene also behaves in somewhat like manner in solution, and its thermal *cis-trans* isomerization is the mixture of ordinary and bending ones, because it belongs to neither of the two types classified by Eyring[15]. This point will be investigated in future.

## Experimental

Benzylideneanilines were prepared by direct condensation of benzaldehyde with corresponding anilines. Stilbene and azobenzene were prepared by recrystallization of commercial substances. *p*-Methoxy-stilbene was kindly supplied by Mr. H. Suzuki. Azoxybenzene was prepared by treating nitrosobenzene with ethanol and sodium hydroxide.

Absorption spectra were measured by Cary self-recording spectrophotometer model 14 M using 1 cm. quartz cell.

## Summary

The ultraviolet absorption spectra of benzylideneanilines, as well as of their conjugate acids, have been measured.

These spectra can not be explained with the ever believed stilbene-type planar structures of these molecules.

An alternative structure is proposed for benzylideneaniline with the benzene ring of aniline part nearly perpendicular to the rest of the molecule.

This structure also adequately explains many experimental evidences, which have been investigated previously but are not accounted for by the planar structure.

The author wishes to express his sincere thanks to Professor S. Nagakura for his kind instruction throughout this study. Thanks are also due to Professor K. Shiomi and to the members of his laboratory for their fruitful discussions.

*Department of Chemistry*
*College of General Education*
*The University of Tokyo*
*Meguro-ku, Tokyo*

13) A. Kirrman and P. Laurent, *Bull. soc. chim. France*, 6, 1657 (1939).
14) E. Fischer and Y. Frei, *J. Chem. Phys.*, 27, 808 (1957).
15) J. L. Magee, W. S. Shand, Jr., and H. Eyring, *J. Am. Chem. Soc.*, 63, 677 (1941).

# *Benzylideneaniline. II. Iodine Complexes of Benzylideneaniline and its Derivatives*

By Nozomu EBARA

(Received July 31, 1959)

In the preceding paper the author proposed for benzylideneaniline a structure with the benzene ring of N side nearly perpendicular to the rest of the molecule. Then the non-bonding electron will migrate into the benzene ring to a large extent, and the ionization potential of the lone-pair electron will increase and its donor ability will decrease compared with the case where there is no interaction. To examine the validity of this assumption, the nature of the lone-pair electron is now investigated by means of the measurement of the equilibrium constant of iodine complex.

**Iodine Complex.**—The interaction between iodine molecule and aromatic compounds was firstly suggested by Benesi and Hildebrand[1] to be the acid-base type interaction, where the iodine molecule behaves as an acid and the aromatic molecule as a base. It has been shown by Mulliken[2] that this type of interaction is based upon charge-transfer resonance stablilization, and the new absorption band in the ultraviolet region, which was absent in both component molecules but now comes into appearence in the complex, can be interpreted as the charge-transfar band, for which this resonance interaction is responsible. This band was also explained by Kuboyama and Nagakura[3] from the LCMO treatment to be due to the electron transition from the perturbed higest filled orbital of the donor component to the lowest vacant $\sigma_u$ MO of iodine component. Also the absorption band of $I_2$ shifts toward shorter wavelengths when a complex is formed, which again can be interpreted from the consideration that the $\sigma_u$ MO of $I_2$ is raised while the $\pi_g$ MO is not so much affected[4]. This phenomenon has been investigated extensively by many authors[2-7] for a large variety of compounds including as bases those with lone pair electrons or $\pi$-electrons, and the equilibrium constants, as well as heats and entropies of formation of these complexes have been measured[8-10].

Hastings, Franklin, Schiller and Matsen[11] and McConnell, Ham and Platt[12] correlated the positions of charge-transfer absorption maxima with the ionization potentials of the donor molecules and found an excellent agreement between theory and experiments.

When benzylideneaniline is used as the base, the donor orbital may be non-bonding orbital, $\pi$-orbital or both, and the position of the charge-transfer band will be the fingerpost for assuming the ionization potential of the donor orbital, and the equilibrium constant will serve as a criterion of the geometry of this molecule.

## Results and Discussion

The spectra of the mixtures of iodine and benzylideneaniline in various concentrations in

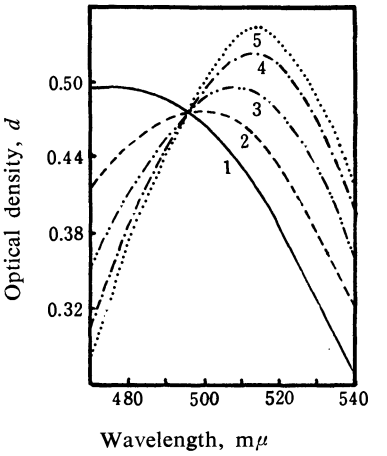



Fig. 1. Spectra of benzylideneaniline+$I_2$ in $CCl_4$; Base concentration: 1, —— 1.10; 2, ---- 0.55; 3, ·····- 0.275; 4, -·-· 0.138; 5, ····· 0.069 mol./l. $I_2$ concentration $1.74 \times 10^{-4}$ mol./l.

1) H. A. Benesi and J. H. Hildebrand, *J. Am. Chem. Soc.*, **70**, 2832 (1948).
2) R. S. Mulliken, ibid., **72**, 600 (1950); **74**, 811 (1952); *J. Phys. Chem.*, **56**, 801 (1952).
3) A. Kuboyama anb S. Nagakura, *J. Chem. Soc. Japan, Pure Chem. Sec. (Nippon Kagaku Zasshi)*, **75**, 1082 (1954).
4) S. Nagakura, *J. Am. Chem. Soc.*, **80**, 520 (1958).
5) H. A. Benesi and J. H. Hildebrand, ibid., **71**, 2703 (1949); **72**, 2273 (1950).
6) R. M. Keefer and L. J. Andrews, ibid., **74**, 458, 1891, 4500 (1952); **75**, 3561 (1953).
7) C. Reid and R. S. Mulliken, ibid., **76**, 3869 (1954).
8) R. M. Keefer and L. J, Andrews, ibid., **77**, 2164 (1955).
9) N. Ogimachi, L. J. Andrews and R. M. Keefer, ibid., **77**, 4205 (1955).
10) T. M. Cromwell, ibid., **72**, 3825 (1950).
11) S. H. Hastings, J. L. Franklin, J. C. Schiller and F. A. Matsen, ibid., **75**, 2900 (1953).
12) H. McConnell, J. S. Ham and J. R. Platt, *J. Chem. Phys.*, **21**, 66 (1953).

carbon tetrachloride in the visible region is shown in Fig. 1, the concentration of the former being constant. It shows an apparent isosbestic point, which proves the formation of 1 : 1 complex. Regrettably enough, as benzylideneaniline absorbs light considerably in the region below 400 mμ, and the equilibrium constant of the complex at the room temperature is found to be very small, no charge-transfer band could be observed on account of experimental difficulty. But the shift of $I_2$ band is considerable, from which the equilibrium constant could be calculated.

The equilibrium constant can be calculated by means of the equation

$$d=C_1\varepsilon_c+(C_1\varepsilon_i-d)/C_2K$$

where $d$ is the optical density of the mixture solution at the measured wavelength, $C_1$ and $C_2$ are the concentrations of iodine and benzylideneaniline, respectively, $\varepsilon_i$ and $\varepsilon_c$ are the molar extinction coefficients of iodine and complex, respectively, at the wavelength, and $K$ is the equilibrium constant. This equation can easily be derived from the law of mass action of 1 : 1 complex, with the consideration that the concentration of benzylideneaniline is actually not altered, as it is so high compared with that of iodine, and that the observed optical density is the sum of those of iodine and a complex. As the absorption due to benzylideneaniline can not be ignored, measurements were carried out with the benzylideneaniline solutions as references.

The values of $d$ are plotted against $(C_1\varepsilon_i-d)/C_2$ (Fig. 2). They fall on straight lines which are parallel to each other, of which the slope indicates $1/K$.

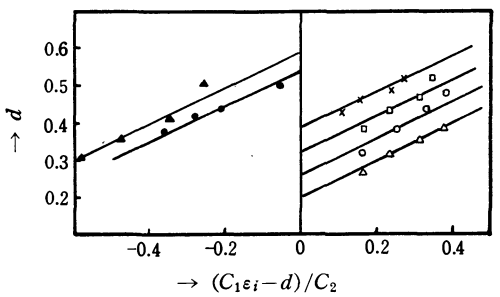



Fig. 2. Plots of $d$ values against $(C_1\varepsilon_i-d)/C_2$.

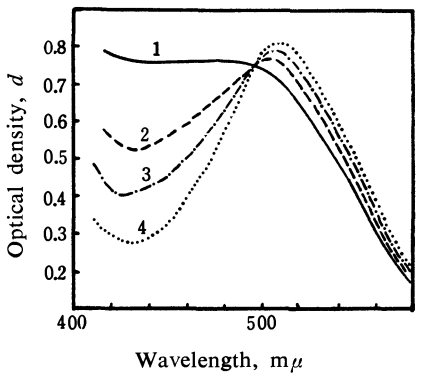



Fig. 3. Spectra of benzylidene-*p*-anisidine+$I_2$ in $CCl_4$; Base concentration: 1, —— 0.83; 2, ---- 0.42; 3, -·-· 0.21; 4, ····· 0.10 mol./l. $I_2$ concentration $2.68\times10^{-4}$ mol./l.

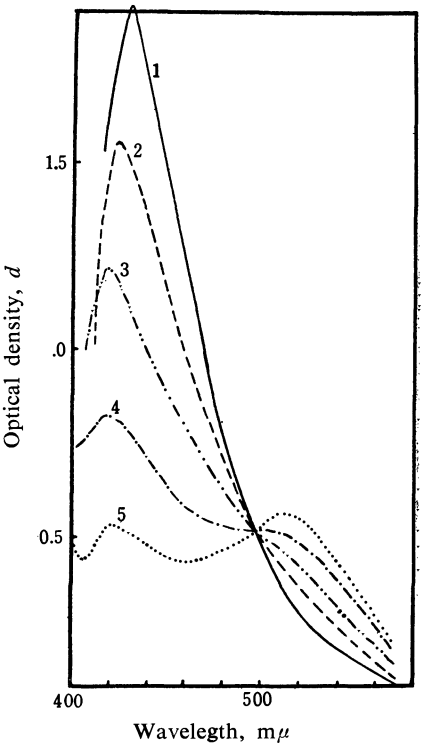



Fig. 4. Spectra of benzylidene-*o*-anisidine+$I_2$ in $CCl_4$; Base concentration: 1, —— 0.83; 2, ---- 0.42; 3, ·····-0.21; 4, ·-·- 0.10; 5, ····· 0.05 mol./l. $I_2$ concentration $1.93\times10^{-4}$ mol./l.

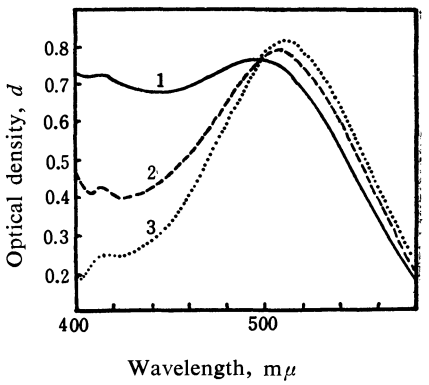
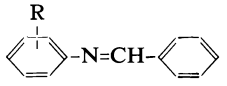



Fig. 5. Spectra of benzylidene-*o*-chloroaniline +$I_2$ in $CCl_4$; Base concentration: 1, —— 0.83; 2, ---- 0.42; 3, ····· 0.21 mol./l. $I_2$ concentration $2.68\times10^{-4}$ mol./l.

The spectra of iodine complexes of benzylidene-*p*- and *o*-anisidine are shown in Figs. 3 and 4. There is a maximum near 420~430 mμ for the latter, which is too intense to be a perturbed iodine transition, and probably it is the charge-transfer band. For the former compound, this band seems to appear at shorter wavelength. The spectra of the chlorine derivatives also show the same peculiarity for the ortho-compound (Fig. 5).

The appropriate values are listed in Table I.

TABLE I. EQUILIBRIUM CONSTANTS OF IODINE COMPLEXES OF BENZYLIDENEANILINES IN $CCl_4$ AT 11.0°C



| R | $K$ |
|---|---|
| H | 2.0 |
| *o*-$OCH_3$ | 10.6 |
| *p*-$OCH_3$ | 9.2 |
| *o*-Cl | 2.4 |
| *m*-Cl | 2.0 |
| *p*-Cl | 2.7 |

The positions of $I_2$ absorption maxima could not strictly be defined, as, at the shorter wavelengths, the absorption due to the free base and presumably due to the charge-transfer band becomes large and the exact calculations are not feasible. But the color of the solutions is bright golden yellow and the calculation shows that their positions should not be above 460 mμ. As the shifts of $I_2$ band in aromatic hydrocarbons are usually not more than 10~20 mμ, it can probably be safe to say that the iodine molecule attaches predominantly to the lone-pair orbital, which is to be more favored, if the steric requirement is fulfilled.

The influence of the methoxyl group in the aniline ring is remarkable. One explanation is that the iodine molecule attaches to the oxygen atom of the substituent, but this is not likely to be the case, because the increment of $K$ is too large to be interpreted under this assumption. Moreover, it can not account for the larger values of $K$ and longer wavelengths of the charge-transfer bands of ortho-derivatives.

If the proposed structure is assumed, it may be said that the methoxyl group will reduce the ionization potential of the lone-pair electron of the nitrogen atom and facilitate complex formation, and for *o*-methoxy-derivative, in addition to this, the two parallel and closely standing non-bonding orbitals with almost the same size will interact strongly with the iodine molecule and stabilize the complex. For the chlorine derivatives, the effects of the substituent would be small and the $K$ values not much different from that of the unsubstituted molecule as expected, and for the *o*-chloro-compound, owing to the large size of chlorine atom, the steric hindrance will predominate over other factors affecting the equilibrium.

The equilibrium constant of benzylideneaniline is unexpectedly small and can be compared with those of the hydrocarbons. But for dimethylaniline, $K$ is also small[13], and this is probably partly due to the increase of the ionization potential of the lone-pair electron caused by its migration into the benzene ring and partly due to the steric inhibition rather than to the complex formation with π-orbital as the donor, as other evidences tend to support the former model.

When the almost perpendicular structure is assumed, the hybridization of nitrogen-valence-orbitals will approach largely to the *sp*-type, then the non-bonding orbital will be almost of the *p*-type. Furthermore, as the interaction of the latter with the benzene ring is of the order of perturbation, it must retain largely its original *p* structure. This orbital is less concentrated along one direction than $sp^2$ orbital, and can not overlap well with $I_2$ orbital unless this comes nearer. This would cause the increase of steric hindrance and decrease the equilibrium constants.

## Experimental

Preparations of benzylideneanilines were described in the previous paper. Iodine was sublimed two times from the G. R. grade commercial substance.

Absorption spectra were measured by a Cary self-recording spectro photometer model 14 M and a Hitachi EPU 2 type spectrophotometer using 1 cm. quartz cell. Measurements were made as soon as the solutions were prepared, so as to avoid the change due to the reaction. Reaction occurs in considerable extent when the mixture is left standing for a long time, but in the course of measurement no remarkable change was observed.

## Summary

Absorption spectra of the mixtures of iodine with benzylideneanilines in various concentrations have been measured, and from the optical densities of the solutions the equilibrium constants have been calculated.

The equilibrium constants are unexpectedly small. But for methoxy-derivatives and especially for ortho-compound, the equilibrium constants are considerably large.

For *o*-methoxy- and *o*-chloro-derivatives, the charge-transfer bands appear at the longer wavelengths.

13) H. Tsubomura, Private communication to Professor S. Nagakura to whom the author is very much indebted for having been allowed to refer to it.

These experimental evidences are also adequately explained by the perpendicular structure of benzylideneaniline.

The author expresses his sincere thanks to Professor S. Nagakura for his kind help throughout this study.

*Department of Chemistry*
*College of General Education*
*The University of Tokyo*
*Meguro-ku, Tokyo*

# *Biochemical Studies on Pearl. IX. Amino Acid Composition of Conchiolin in Pearl and Shell*

By Shozo TANAKA, Hiroyuki HATANO and Osamu ITASAKA*

(Received August 4, 1959)

An organic constituent of shells of molluscs was first named conchiolin by Frémy, and then it was recognized as a kind of protein by Schlossberger and Voit[1]. The amino acid constituents of this protein were studied by Krukenberg & Engel[1], Wetzel[2], Stary & Andratschke[3] and Friza[4]; and the presence of glycine, leucine, tyrosine, tryptophane and arginine was found in hydrolysates of conchiolin. Amino acid components of conchiolin prepared from different species of molluscs were also studied by Roche, Ranson & Eysseric-Lafon[5] and by Grégoire, Duchâteau & Florkin[6]. The composition of various kinds of conchiolin was reported to differ with the kinds of molluscs from which they were prepared. The authors have reported that about fifteen kinds of amino acids were found in hydrolysates of conchiolin prepared from the pearls and the shells of pearl oysters[7]. Halogen-containing amino acids, iodotyrosine and bromotyrosine, which are known as the peculiar components of screloproteins obtained from calciferous skeletons of marine invertebrata such as sponge and gorgonia, were not found in conchiolin of pearls and shells[7].

Electron-microscopic studies on conchiolin by Grégoire, Duchâteau & Florkin[6] and also by Grégoire[8] alone showed that the physical structure of conchiolin in the shells was reticulated unlike that of keratin or collagen which has fibrous structure. Conchiolin has been reported to be successfully fractionated into several preparations by suitable chemical reagents[6,9]. From chemical and crystallographical studies on the pearls and the shells of pearl oysters, the nacre of pearls was found to be identical with the nacreous layer of shells but quite different from the prismatic layer of shells[10]. These results may be of interest in studying the correlation between physical observations and chemical structures. This paper deals with the results of quantitative analyses of amino acids in the hydrolysates of conchiolin prepared from the pearl and the two layers of the shell of an oyster.

## Experimental

**Materials.**—*The pearl and the shell of the pearl oyster.*—The pearls were harvested from the pearl oysters, *Pinctada martensii* (Dünker)**, which had been cultured in the pearl farm at Matoya Bay near Kashikojima during two winters after culture operations. The shells were obtained from the same pearl oysters. Both were rinsed thoroughly with tap water and with distilled water, and then dried at room temperature.

*The nacreous substance of pearls.*—This substance was obtained from crushed pearls, from which nuclei had been mechanically taken away.

*The nacreous substance of shells.*—This substance was obtained from shell valves by grinding off prismatic substances after removing the sea-weed

* Present address: School of Chemistry, Shiga University, Otsu.

1) E. Abderhalden, "Handbuch der Biologischen Arbeitsmethoden", Urban & Schwarzenberg, Berlin Bd. I-8, (1922), p. 554.
2) G. Wetzel. *Z. physiol. Chem.*, **29**, 386 (1900).
3) Z. Stary and I. Andratschke, *Z. physiol. Chem.*, **148**, 83 (1925).
4) F. Friza, *Biochem. Z.*, **246**, 29 (1932).
5) J. Roche, G. Ranson and M. Eysseric-Lafon, *Compt. rend. soc. biol.*, **145**, 1474 (1951).
6) C. Grégoire, G. Duchâteau and M. Florkin, *Ann. inst. oceanog.*, (*Paris*), **31**, 1 (1955).
7) S. Tanaka et al., *J. Chem. Soc. Japan, Pure Chem. Sec.* (*Nippon Kagaku Zasshi*), **74**, 193 (1953).
8) C. Grégoire, *J. Biophys. Biochem. Cytol*,, **3**, 797 (1957).
9) S. Tanaka, H. Hatano and G. Suzue, *J. Biochem.*, **47**, 117 (1960).
10) S. Tanaka, H. Hatano and O. Itasaka, This Bulletin, **33**, 182 (1960).

** The authors wish to express their hearty thanks to Mr. K. Isowa, the president of Nippon Pearl Co., for his kind donation of the pearls and the pearl oysters for this experiment.

and other adhering materials from the surface.

*The prismatic substance of shells.*—This substance was obtained from the thin posterior shell margins. All materials were crushed and pulverized into powder of about ten mesh, washed with tap water, and dried at room temperature.

**Conchiolin.** — Conchiolin was prepared from the above materials by the method described in the previous paper[7]. The materials were immersed in 1 N hydrochloric acid solutions, which were frequently renewed, until no more evolution of carbon dioxide was observed in vacuo. Insoluble matter was washed several times with distilled water and was dialyzed against running water until the chloride ion in the dialyzate became undetectable. The conchiolin prepared from the nacre of pearls and from the nacreous substance of shells had a faint yellowish color, but that from the prismatic layer of shells, had a reddish-brown tint.

**Methods.**—*Preparation of the conchiolin hydrolysates.*—About 50 mg. of pulverized conchiolin was hydrolyzed with 5 ml. of 6 N hydrochloric acid at 100°C in a sealed tube for 30 hr. After small amounts of humin formed were filtered off, the hydrochloric acid was evaporated in vacuo repeatedly. The hydrolysate was dissolved into a mixture of *n*-butanol, *n*-propanol, and 0.1 N hydrochloric acid (1 : 2 : 1, v/v).

**Amino Acid Analysis.**—The analyses were carried out chromatographically by Stein and Moore's method on starch columns[11-13]. The preparatory procedure of the columns of potato starch (150 mesh), the selection of solvents and also the procedure for chromatography followed the description by Stein and Moore[11-13]. Columns of 0.9 cm. × 40 cm. of starch containing 30% of water were prepared and were washed under pressure of 150 mmHg until the washings became negative to a ninhydrin test. The hydrolysate was poured on the columns under pressure of 150 mmHg. Two kinds of solvent were used for elution. Solvent I was a mixture of *n*-butanol, *n*-propanol, and 0.1 N hydrochloric acid (1 : 2 : 1, v/v) and Solvent II was composed of *n*-propanol and 0.5 N hydrochloric acid (2 : 1, v/v). The eluting rate had been controlled as 1.5 ml. of the effluent per hour at the optimum velocity.

Each 0.5 ml. of the effluent fractions was collected by an automatic fraction collector. The amount of amino acids in each effluent fraction was estimated by the colorimetric ninhydrin method[14]. A solution of 250 ml. of ethylcellosolve containing 5 ml. of 0.01 M potassium cyanate, a solution of 2.5 g. ninhydrin in 50 ml. of ethylcellosolve and a 0.2 M citrate buffer solution adjusted to pH 5.4 with 1 N sodium hydroxide, were mixed. After each 0.5 ml. of the effluent aliquot was adjusted to pH 5.4 with 1 N sodium hydroxide in the case of Solvent II, though the pH was not controlled in the case of Solvent I, 0.5 ml. of the citrate buffer solution and 0.5 ml. of the ninhydrin reagent were added to the effluent. The mixed solution was allowed to stand for 20 min. in a boiling water bath. By heating the definite volume of the reaction mixture (5 ml.) with 60% ethanol, violet color was developed. Colorimetric determination was carried out by measuring the optical density of the coloring solution at 570 mμ by using a Beckman model DU spectrophotometer. Only for proline, the measurement was done at 440 mμ. The color yield of each amino acid was determined by comparing it with that of pure amino acid, respectively.

11) W. H. Stein and S. Moore, *J. Biol. Chem.*, **176**, 337 (1948).
12) S. Moore and W. H. Stein, ibid., **176**, 367 (1948).
13) S. Moore and W. H. Stein, ibid., **178**, 53 (1949).
14) E. W. Yemm and E. C. Cocking, *Biochem. J.*, **58**, xii (1954); *Analyst*, **80**, 209 (1955).

## Results and Discussion

The mensuration curves obtained with the hydrolysates of conchiolin from the nacre of pearls, the nacreous substance and the prismatic substance of shells, are shown in Fig. 1.

It was noticed that relatively large amounts of leucines, alanine, glycine, and cystine are contained in both conchiolin from the pearls and the shells. Proline was not recognized in conchiolin from the nacre of the pearl and the nacreous layer of the shell, while its existence was proved in conchiolin from the prismatic substance of the shell.

It is of interest that a relatively large amount of cystine is found in conchiolin. The fact may suggest a fibrous structure of conchiolin, like keratin in the hair and the skin which

TABLE I. AMINO ACID COMPOSITION OF CONCHIOLIN PREPARED FROM THE NACRE OF PEARLS, THE NACREOUS SUBSTANCE OF SHELLS AND THE PRISMATIC SUBSTANCE OF SHELLS*

| Amino acid residue | Conchiolin** | | |
|---|---|---|---|
| | Nacre of pearl | Nacreous substance of shell | Prismatic substance of shell |
| Leucines | 9.2 | 13.6 | 9.0 |
| Phenylalanine | 1.1 | 0.0 | 16.9 |
| Valine | 2.1 | 0.5 | 1.0 |
| Tyrosine | 2.7 | 7.2 | 3.0 |
| Methionine | 0.4 | 0.4 | 0.0 |
| Proline | 0.0 | 0.0 | 7.9 |
| Alanine | 14.0 | 16.3 | 4.6 |
| Glutamic acid | 3.1 | 1.5 | 1.5 |
| Threonine*** | 0.6 | 9.3 | 0.3 |
| Aspartic acid | 6.2 | 2.2 | 3.7 |
| Serine*** | 5.4 | 2.1 | 3.5 |
| Glycine | 24.3 | 12.8 | 16.8 |
| Ammonia | 0.7 | 0.5 | 0.1 |
| Arginine | 7.2 | 15.3 | 10.2 |
| Lysine | 7.4 | 3.3 | 1.5 |
| Histidine | 0.5 | 0.0 | 1.0 |
| Cystine/2 | 12.2 | 11.8 | 14.7 |

* Determined by chromatography of the acid hydrolysates on columns of starch.
** Presented as gram of amino acid residue per 100 g. of protein.
*** Corrected to the hydrolytic damage of threonine (5%) and serine (10%).

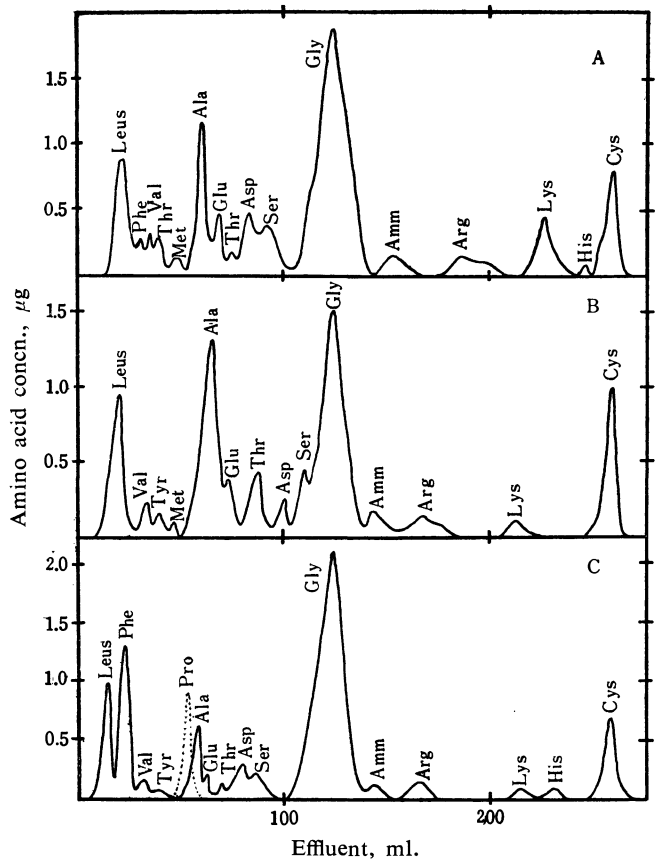



Fig. 1. Starch column chromatography of each 30 hr. hydrolysate of conchiolin prepared from the nacre of pearls (A), the nacreous substance of shells (B) and the prismatic substance of shells (C). Optical density at 570 mμ is plotted on the ordinate for the effluent fractions separated by a 0.9 cm. × 40 cm. column of starch, after treatment with the ninhydrin reagent. The values of optical densities have been corrected by baseline absorption.

causes the elasticity of the tissues. As shown in Table I, conchiolin in the nacreous layer of the shell and that in the pearl contain less phenylalanine and proline, and more alanine than that in the prismatic layer.

## Summary

Conchiolin, a kind of screloprotein, was isolated from the pearl and the shell of the pearl oysters. The amino acid composition of conchiolin was determined by the chromatographic method with the starch column. Relatively large amounts of leucines, alanine, glycine and cystine were found in conchiolin.

Remarkable differences were found in the contents of phenylalanine, alanine and proline between conchiolin from the nacreous substance and that from the prismatic substance.

*Department of Chemistry*
*Faculty of Science*
*Kyoto University*
*Sakyo-ku, Kyoto*

# *Chemisorption of Hydrogen on Zinc Oxide. I. Rate of Desorption and Adsorption Isotherm*

By Yutaka KUBOKAWA

(Received September 9, 1959)

The rate of adsorption and adsorption equilibrium have been measured for various chemisorption systems by many workers. As regards the rate of desorption, however, few quantitative measurements have been carried out with powdered catalysts[1]. For these catalysts the activation energy of desorption is usually taken as the sum of the activation energy of adsorption and the heat of adsorption obtained from the rate of adsorption and adsorption equilibrium, respectively. It is however frequently encountered in chemisorption that the slow attainment of equilibrium and the occurrence of bulk or surface diffusion process introduce considerable uncertainty in the values of the activation energy of adsorption and the heat of adsorption. If the activation energy of desorption is determined by direct measurements of the rate of desorption and compared with the activation energy of adsorption and the heat of adsorption, the information concerning the energy relation for a given chemisorption will be much improved. The present study was undertaken to present such an attempt for the chemisorption of hydrogen on zinc oxide. This paper reports the activation energies for desorption obtained from the rate of desorption at various temperatures, together with adsorption equilibrium data. The rate of adsorption and its relation to the results here reported, will be dealt with in a forthcoming paper.

## Experimental

**Materials.**—For zinc oxide two samples, ZnO I and ZnO II were used. ZnO I was prepared as follows: Zinc oxalate was precipitated from the solutions of ammonium oxalate and zinc nitrate. The precipitate was washed, filtered, dried at 110°C and finally converted to the oxide by heating in air at 400°C. ZnO II was prepared from zinc nitrate and sodium carbonate by the method similar to ZnO I. The reagents were of Extra Pure grade. Hydrogen was obtained by the electrolysis of 30% solution of potassium hydroxide, purified by passing through heated palladium asbestos, phosphorus pentoxide, and finally, through a trap immersed in liquid nitrogen. Nitrogen was prepared by the thermal decomposition of sodium azide, and purified by passing through phosphorus pentoxide. Helium was obtained from commercial sources, and was used without further purification.

**Apparatus and Procedure.**—The adsorbed amount was determined by using a conventional constant volume apparatus, as shown in Fig. 1. The volume of the dead space was measured by the expansion of a known volume of helium over the whole range of temperatures and pressures employed. The mercury manometer $M_1$ and the Mcleod gauge $M_2$ covered a wide range of pressure from $10^{-5}$ to 70 mmHg.

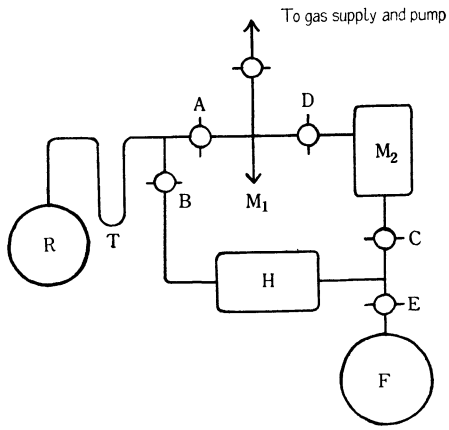



Fig. 1.

The rate of desorption was measured as follows: Before starting a measurement of desorption rate, the pressure in the adsorption vessel R was adjusted to a range of several mmHg by pumping out a known amount of gas through the Mcleod gauge $M_2$ and mercury manometer $M_1$. Then, stop-cocks A and D were closed, B and C opened, and the gas desorbed by mercury diffusion pump H was collected into $M_2$, whose pressure was followed at definite intervals. During a desorption experiment trap T was cooled to −78°C. By using the volume of H at its working state which was determined by an independent measurement, the rate of desorption was calculated from the pressure increase in $M_2$. When gas was accumulated in $M_2$ to such an extent that the rate of desorption might be affected by readsorption, the stopcock D was opened and C closed for a short time to pump out the gas in $M_2$, after which the measurement of desorption was continued. The pressure in the adsorption vessel R during the desorption experiment was measured

1) J. Weber and K. J. Laidler, *J. Chem. Phys.*, **19**, 1089 (1951); J. J. F. Scholten and P. Zwietering, *Trans. Faraday Soc.*, **53**, 1363 (1957); K. Tamaru and M. Boudart, "Advances in Catalysis", Vol. 9, Academic Press, Inc., New York (1957), p. 699.

by closing stopcock C, opening E, A and D, and leading the desorbed gas to flask F, instead of Mcleod gauge $M_2$.

The adsorption vessel was maintained at various required temperatures in the following manner; for the range above room temperature an electric furnace was used, with the constancy of $\pm 1°C$; for the range below room temperature, solid carbon dioxide in ethanol and melting chlorobenzene and bromobenzene were used; a bath for $-60°C$ was obtained by cooling acetone by the addition of a small amount of dry ice from time to time.

Preceding to the chemisorption experiment, the adsorbent was subjected to alternating evacuation and exposure to hydrogen at 400°C several times, and then evacuated for five hours at 420°C. The surface area of the adsorbents was determined by the B. E. T. method using nitrogen as an adsorbate with the following results; ZnO I, 6.6 $m^2/g$.; ZnO II, 5.2 $m^2/g$. The weight of the adsorbent was 14.64 g. (ZnO I) or 11.60 g. (ZnO II).

## Results and Discussion

**Rates and Activation Energies of Desorption at Various Coverages.**—Since the observed rate of desorption is that substracted by the rate of the reverse process, i. e. readsorption, the activation energy of desorption can not be determined from the observed rates unless the rate of readsorption is negligible. As a test to decide whether this condition is satisfied, the following experiment was carried out. After measuring the pressure in adsorption vessel during desorption rate measurements, the pressure increase caused by isolating the adsorption vessel from the mercury diffusion pump was observed. Fig. 2 represents a typical experiment carried out at room temperature. Although adsorption equilibrium was not easily attained, the rapid pressure increase observed suggests that the pressure in the adsorption vessel at the moment when the diffusion pump was cut off would have been negligible compared with the equilibrium pressure corresponding to the adsorbed amount at that moment, and hence that the rate of readsorption was negligible compared with that of desorption. The same was also found to be the case for desorption under other experimental conditions.

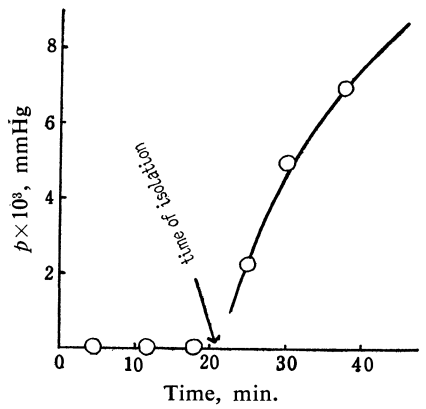



Fig. 2. Pressure increase on isolating the adsorption vessel from the mercury diffusion pump. Pressure in the adsorption vessel before the isolation was $1.3\times10^{-4}$ mmHg.

After hydrogen was allowed to be adsorbed at about 300°C and 20~25 mmHg, the system was cooled down to 209 or 22°C, at which temperature the rate of desorption was measured with the results shown in Fig. 3. Fig. 4 represents the same results as the plots of the logarithm of desorption rate $\log R_{dep}$ against desorbed amount $q$. As to the data given in Fig. 3 a simple unimolecular or bimolecular rate law was found to be inapplicable. This results, together with the fact that the plot of $\log R_{dep}$ against $q$ in Fig. 4 is nearly linear, will be explained by the increase of activation energy for desorption with decreasing amount

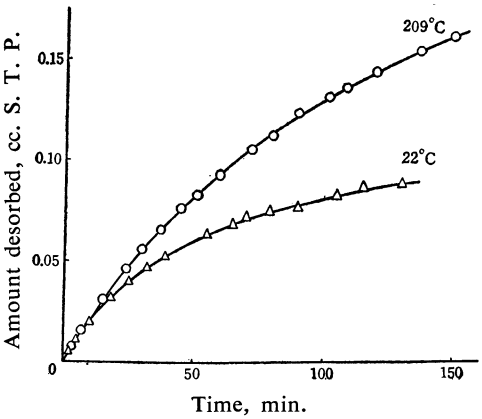



Fig. 3. Rates of desorption of hydrogen chemisorbed on ZnO II. The amount adsorbed at $t=0$ was 0.51 cc. at 209°C and 1.12 cc. at 22°C.

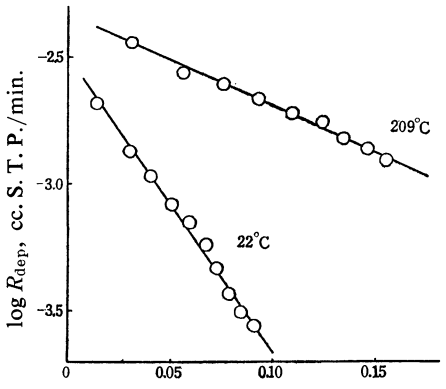



Fig. 4. Plots of $\log R_{dep}$ against the amount desorbed $q$ for the data in Fig. 3.

adsorbed, and its quantitative relationship will also be shown later.

The activation energy of desorption was determined as a function of adsorbed amount by the following procedure: The temperature of desorption was lowered abruptly during the rate measurement, as shown in Fig. 5 (hydrogen chemisorption before the desorption experiment was carried out in a similar manner to that in Fig. 3); the plot of $\log R_{dep}$ against $q$ for the curve before the temperature drop, such as shown in the figure, was extrapolated to a smaller amount adsorbed where the rate measurements after the temperature drop were carried out. Thus, the rates at the two different temperatures corresponding to the same amount adsorbed and, consequently, the activation energy of desorption were obtained.

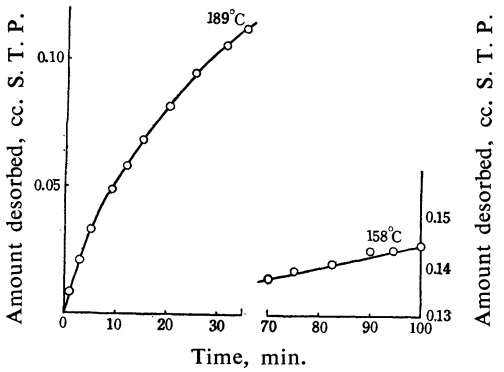



Fig. 5. Determination of the activation energy of desorption. The amount adsorbed at $t=0$ was 0.72 cc. The activation energy was estimated as 23.5 kcal./mol.

The initial admission of hydrogen was usually made at about 300°C and 30~40 mmHg, after which the temperature of the system was lowered to room temperature, and after about 10 hr. it was raised up to 400°C in stages, at each of which the activation energy of desorption was determined in the above mentioned manner. The results obtained with ZnO II are shown in Fig. 6. Fig. 7 shows similar results obtained with ZnO I[2] for a range of higher coverage where desorption was measurable at lower temperatures. It follows from the two figures that the activation energy of desorption increases with decreasing amount adsorbed, up to 31 kcal./mol., and thereafter remains nearly constant[3].

It may be noted that such behavior of the activation energy toward coverage is responsible

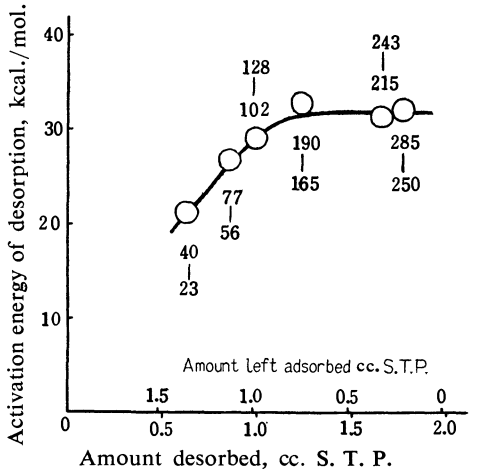



Fig. 6. Activation energies of desorption of hydrogen chemisorbed on ZnO II. The amount adsorbed before desorption at room temperature was 1.98 cc. Figures indicate the temperature interval where the activation energy was determined.

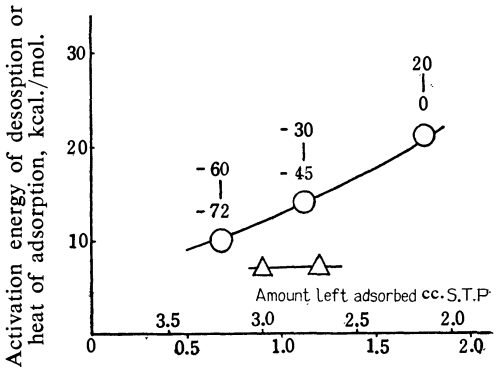



Fig. 7. Activation energies of desorption and heats of adsorption of hydrogen on ZnO I at high coverage. Figures indicate the temperature interval where the activation energy was determined. The amount adsorbed and the equilibrium pressure at room temperature before desorption were 3.90 cc. and 29.5 mmHg respectively. -○-, activation energy of desorption; -△-, heat of adsorption.

for the fact that the slope of the plot $\log R_{dep}-q$ is smaller in the higher temperature range, as seen in Fig. 4.

**Adsorption Isotherms at Various Temperatures.** —An adsorption isotherm obtained in the usual manner, i. e. by admitting a small amount of gas to an evacuated sample successively, was found to be different from that obtained in the reverse way, i. e. by successive withdrawals of the gas. These may be called the adsorption and the desorption branches of the isotherm, respectively. An example at 370°C is given in Fig. 8. This result was obtained with ZnO II

2) Results with ZnO II were similar.

3) The fact that a simple unimolecular or bimolecular rate law was not applicable to the data above 200°C, where the approximately constant activation energy was observed, appears to have resulted from a slight change of the activation energy with the amount desorbed, within the experimental error, ±2 kcal./mol.

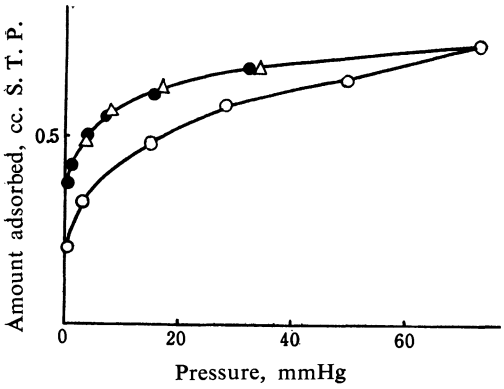



Fig. 8. Adsorption isotherms on the adsorption and desorption branch for the hydrogen chemisorption on ZnO II at 370°C. -○-, initial adsorption; -●-, desorption; -△-, readsorption.

which had been evacuated for five hours at 420°C. On the desorption branch the adsorption equilibrium was rapidly established and reproduced on decreasing or increasing pressure in the pressure range lower than the maximum pressure employed on the adsorption branch. It may therefore be concluded that the isotherm obtained on the desorption branch represents a true equilibrium. The isotherm at varied temperatures was obtained in the following way. After recording the equilibrium pressure at a particular temperature, the temperature was lowered and the new equilibrium pressure at a lower temperature was obtained; a certain amount of hydrogen was then pumped out and the measurements were repeated. The results obtained with ZnO II are shown in Fig. 9. It follows from this figure that the heat of adsorption is nearly constant and equal to 18 kcal./

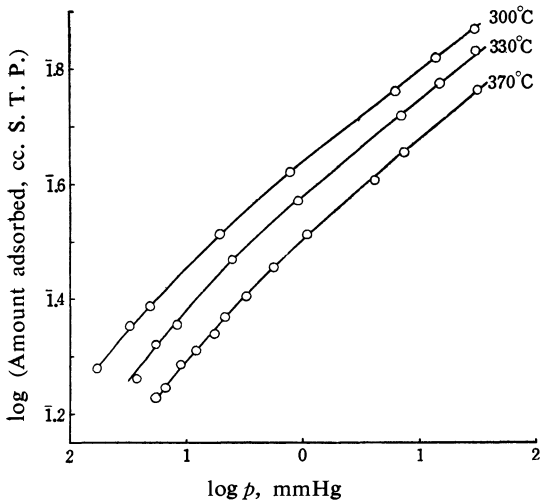



Fig. 9. Adsorption isotherms for hydrogen on ZnO II.

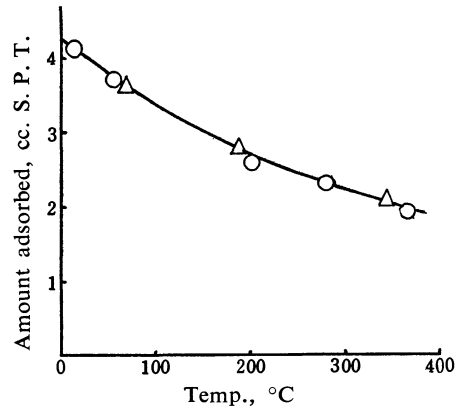



Fig. 10. Adsorption isobar for hydrogen on ZnO I in the pressure range 40~70 mmHg. -△-, on raising temperature; -○-, on lowering temperature.

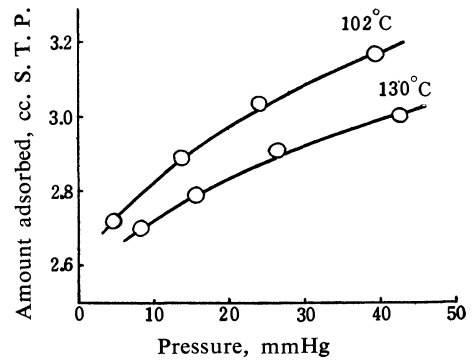



Fig. 11. Adsorption isotherms for hydrogen on ZnO I at 102 and 130°C. The amount adsorbed and the equilibrium pressure at room temperature were 3.76 cc. and 32.8 mmHg respectively.

mol. The same value of the heat of adsorption was obtained with ZnO I.

The adsorption isobar for this system was obtained in the following way: After hydrogen was allowed to be adsorbed at about 350°C, the temperature was lowered in stages down to room temperature and then raised again to 350°C. The results obtained with ZnO I are shown in Fig. 10. It is seen in the figure that the isobars obtained by lowering and raising the temperature nearly coincide, indicating that, once hydrogen is adsorbed at a high temperature, adsorption equilibrium is nearly attained even at considerably lower temperatures, and hence that approximate adsorption isotherms can also be obtained at such low temperatures. Fig. 11 represents such isotherms at 102 and 130°C obtained with ZnO I after hydrogen adsorption at about 300°C, determined in the manner already described for the higher temperature range. Though these low temperature isotherms may be less accurate, the heat of adsorption is

estimated from these as 6~8 kcal./mol.

The activation energy of adsorption may be estimated by combining the activation energy of desorption and the heat of adsorption. As described above, the maximum value of activation energy for desorption and the heat of adsorption are 31 and 18 kcal./mol., respectively. The maximum activation energy of adsorption is, therefore, estimated as 13 kcal./mol.

For the range where the activation energy of adsorption or desorption varies with the amount adsorbed, it seems necessary to take into account the fact that on a heterogeneous surface equal amounts adsorbed do not necessarily mean identical states of adsorption. As described in Figs. 7 and 11, however, adsorbed amount and equilibrium pressure at room temperature differs a little between these two runs, suggesting that in this case the states of hydrogen adsorbed to an equal amount may be compared. Thus, in Fig. 7, the values of the heat of adsorption in the low temperature range described above were shown as a function of the adsorbed amount, together with the activation energy of desorption. It follows from this figure that the activation energy of adsorption in this range is about 5~7 kcal./mol. This figure also suggests that most part of hydrogen chemisorption on zinc oxide is an activated adsorption, although it is doubtful whether the same argument is valid for the fraction which desorbs rapidly below −72°C.

**Summary**

The rate of desorption of hydrogen chemisorbed on zinc oxide was measured over a wide range of temperatures. The rate at a constant temperature was found to obey approximately the kinetics of the Elovich type. The activation energy of desorption was determined at various coverages, with the result that it increased with decreasing amount from at least about 10~31 kcal./mol. and then remained constant. The heat of adsorption obtained from adsorption isotherms in the temperature range 300~370°C was found to be 18 kcal./mol., being roughly constant. Meanwhile, from the isotherms at about 100°C, a heat of adsorption of 6~8 kcal./mol. was obtained. Comparison between the activation energy of desorption and the heat of adsorption suggests that most part of hydrogen chemisorption on zinc oxide involves an activation energy, its highest value being estimated as 13 kcal./mol.

The author wishes to express his sincere thanks to Professor O. Toyama for his guidance and encouragement throughout the course of this study.

*Department of Applied Chemistry*
*College of Engineering*
*University of Osaka Prefecture*
*Sakai-shi, Osaka*

# *Chemisorption of Hydrogen on Zinc Oxide. II. Rate of Chemisorption and Heterogeneity of the Surface of Zinc Oxide*

By Yutaka KUBOKAWA

(Received September 9, 1959)

Taylor and coworkers[1], in a study of hydrogen chemisorption on zinc oxide and other catalysts, found a rapid desorption followed by a slow adsorption and explained these phenomena in terms of a heterogeneity of the surface. As pointed out by various workers[2], however, there are other possibilities leading to such phenomena, which, therefore, may not be regarded as a proof of the existence of any surface heterogeneity. As a proof in relation to this problem, it seems to be promising to investigate the behavior of desorption of the chemisorbed hydrogen in the manner described in a previous report[3], since surface heterogeneity may affect seriously its behavior. The purpose of the present work is to clarify the nature of slow chemisorption by measuring not only the rate of adsorption, but also that of desorption under various experimental conditions, and to obtain, on the basis of these results combined with those described in the previous paper[3], definite conclusions as to the heterogeneity of zinc oxide surface in hydrogen chemisorption.

1) H. S. Taylor and S. C. Liang, *J. Am. Chem. Soc.*, 69, 1306 (1947); H. S. Taylor, "Advances in Catalysis", Vol. 1, Academic Press, Inc., New York (1948), p. 1.

2) J. H. de Boer, ibid., Vol. 8, (1956), p. 18; O. Beeck, ibid., Vol. 2, (1950), p. 151.

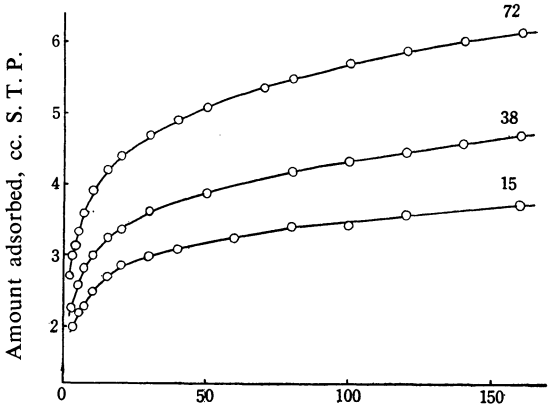
3) Y. Kubokawa, This Bulletin, 33, 546 (1960).

## Experimental

The details of materials, apparatus and procedure were described in the previous paper[3].

## Results and Discussion

**Dependence of Chemisorption Rate on Pressure and Temperature.**—In early experiments, the rate of chemisorption was measured in the usual manner, i.e. by admitting a known amount of hydrogen to an evacuated sample and measuring the pressure change in the system at a constant volume. Some examples of the results obtained at a constant temperature and various pressures are shown in Fig. 1[4]. It might be expected that comparison of the times required for the adsorption of a certain amount, determind from such plots, would give the pressure dependence of the rate at the given temperature. However,




Fig, 1. Rate of adsorption of hydrogen on zinc oxide at 140°C. Figures indicate the initial pressures in mmHg. Different samples were used in these runs.

when the rate thus obtained is represented as proportional to $p^n$, it is found that not only the exponent $n$ increases with the adsorbed amount, but is also greater than unity. The explanation for such unexpected behavior will be given below, according to which experiments such as shown in Fig. 1 do not reflect the true pressure dependence of the adsorption rate. From a similar argument, it will be shown that a series of rate measurements at a constant pressure and various temperatures does not give the true temperature dependence of the rate. Consequently, in the following experiments, the dependence of the rate on pressure or temperature was determined by observing the change in rate caused by an abrupt change of pressure or temperature during adsorption.

4) The pressure decrease due to adsorption was no more than 10~20% of the initial pressure.

The results concerning the pressure dependence are shown in Figs. 2 and 3. As seen in these figures, on increasing pressure an instantaneous adsorption followed by a slow process takes place. Hence, by extrapolation of the rates to the time when a sudden pressure change occurs, the rates at different pressures corresponding

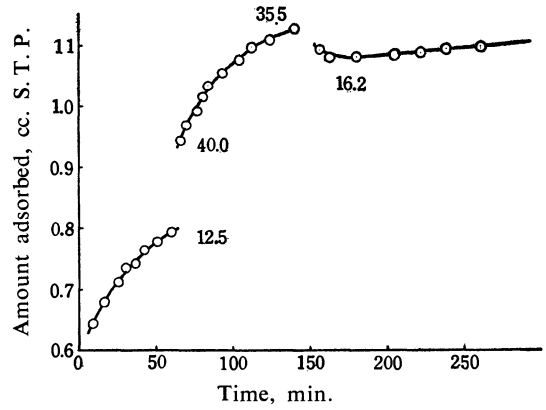



Fig. 2. Effect of the pressure change during adsorption on the rate of adsorption of hydrogen on ZnO II at 18°C. Pressure range, 10~40 mmHg. Figures indicate the pressure before and after the pressure change in mmHg.

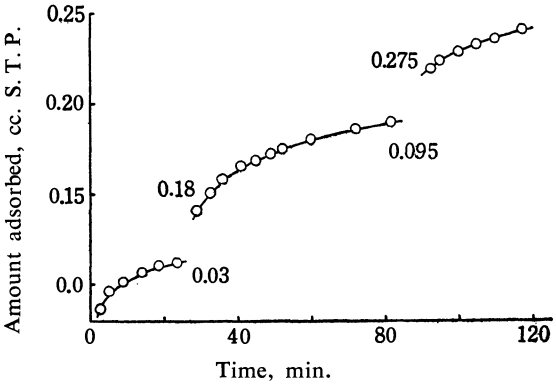



Fig. 3. Effect of the pressure change during adsorption on the rate of adsorption of hydrogen on ZnO I at 18°C. Pressure range, 0.03~0.30 mmHg. Figures indicate the pressure before and after the pressure change in mmHg.

Table I. Values of $n$ in the expression, rate $\propto p^n$ for the data shown in Figs. 2 and 3

| | Pressure before and after the pressure change | $n$ |
|---|---|---|
| Fig. 2 | 12.5 → 40.0 | 1.0±0.1 |
| | 35.5 → 16.2 | 2.0±0.3 |
| Fig. 3 | 0.03 → 0.18 | 1.1±0.1 |
| | 0.095→ 0.275 | 0.9±0.1 |

to equal amounts of slow chemisorption were evaluated. The results are shown in Table I, which shows that the rate is proportional to $p^{0.9\sim1.1}$ on increasing pressure. This relationship was found to be applicable in the whole temperature range studied. As seen in Table I, on decreasing pressure the rate decreases more markedly than is expected from the results obtained on increasing pressure.

The results concerning the temperature dependence obtained with ZnO I in the pressure range 50～70 mm Hg are represented in Fig. 4. It is seen in this figure that on an abrupt temperature change[5], as suggested by Taylor and Liang[1], a rapid desorption followed by a slow adsorption takes place. The activation energy for the slow process was determined in the same manner as for the pressure dependence, with the results shown in Table II. The activation energy

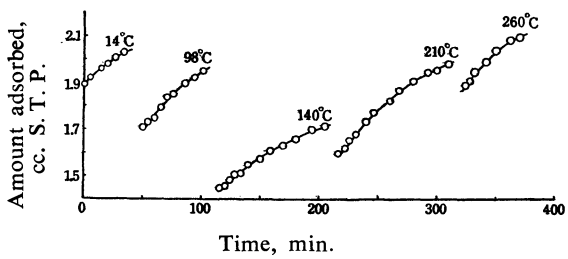



Fig. 4. Effect of the temperature elevation during adsorption on the rate of adsorption of hydrogen on ZnO I. Pressure range, 50～70 mmHg.

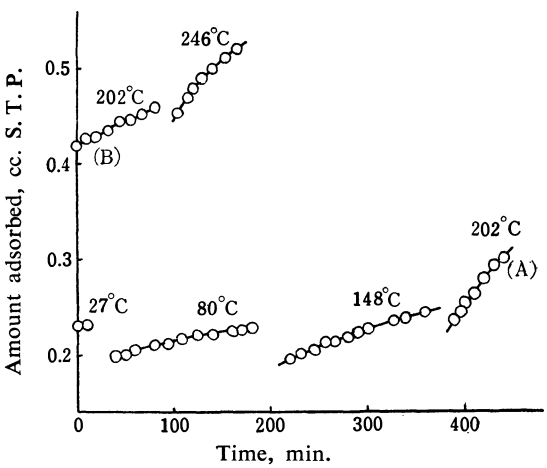



Fig. 5. Effect of the temperature elevation during adsorption on the rate of adsorption of hydrogen on ZnO I. Pressure range, 0.1～0.2 mmHg. Between the runs A and B, the sample was kept at room temperature for 10 hours.

5) A blank experiment carried out with helium in place of hydrogen showed that on such an abrupt temperature change the temperature equilibrium was attained in less than three minutes.

TABLE II. ACTIVATION ENERGIES OF ADSORPTION FOR THE DATA SHOWN IN FIGS. 4 AND 5

| Pressure | Temp. | Activation energy |
|---|---|---|
| 50～70 (Fig. 4) | 14～ 98 | 5.5±1.5 |
| | 98～140 | 7.5±1.0 |
| | 140～210 | 11.0±1.5 |
| | 210～260 | 14.5±1.5 |
| 0.1～0.2 (Fig. 5) | 80～148 | 6.3±1.0 |
| | 148～202 | 13.0±1.0 |
| | 202～246 | 15.0±1.0 |

increases steadily as the temperature becomes higher. As shown in Fig. 5 and Table II, the results obtained in the pressure range 0.1～0.2 mmHg are similar except for the smaller amount of rapid desorption on raising temperature.

In view of the occurrence of hydrogen-deuterium exchange reaction on zinc oxide and, in addition, from a comparison of the energy values for the system of hydrogen on zinc oxide described previously[3] with the information concerning the hydrogen chemisorption on metals given by Gomer and other workers[6], hydrogen chemisorption on zinc oxide at room temperature or above may be assumed to be a dissociative adsorption. Hence, if the rate-determining step of the slow process were a surface migration of the adsorbate, the exponent $n$ in the rate expression Rate $\propto p^n$ would be lower than 0.5. Such expectation is evidently inconsistent with what was observed. It may therefore be concluded that the rate-determining step is not a sort of surface migration, but an adsorption.

As described above, the pressure dependence obtained by increasing pressure differs markedly from that by decreasing pressure. This suggests that desorption can not be neglected during adsorption[7]. Because of this effect, the pressure dependence obtained by increasing pressure, may be somewhat larger than the true value, although the difference may be small compared with that in the case of decreasing pressure.

**Heterogeneity of the Surface of Zinc Oxide in Hydrogen Chemisorption.**—The considerations given above indicate that the slow process is a chemisorption with an appreciable activation energy which increases with adsorbed amount, judged from the considerable change of the activation energy of desorption as described in

6) R. Gomer et al., *J. Chem. Phys.*, 26, 1147 (1957); 27, 1099 (1957); O. Beeck, loc. cit., etc.

7) Taking into account of desorption, the rate of dissociative adsoption on a homogeneous surface will be

$$kp(1-\theta)^2[1-(p_e/p)]$$

where $p_e$ is the equilibrium pressure corresponding to a coverage $\theta$. The term $1-(p_e/p)$ is a correction for desorption. This equation predicts such behavior as observed on an abrupt pressure change during the adsorption rate measurements: In the case where desorption takes place considerably during adsorption, the decrease in the value of $1-(p_e/p)$ on decreasing pressure will be markedly larger than its increase on increasing pressure.

the previous paper[3]. With respect to the behavior observed on raising temperature during adsorption, there are apparently two possible explanations, as the rate-determining step of the slow process is confined to adsorption; one is a heterogeneity of the surface emphasized by Taylor et al. and the other is the coexistence of two types of bonding on a homogeneous surface as frequently proposed by various workers[8]

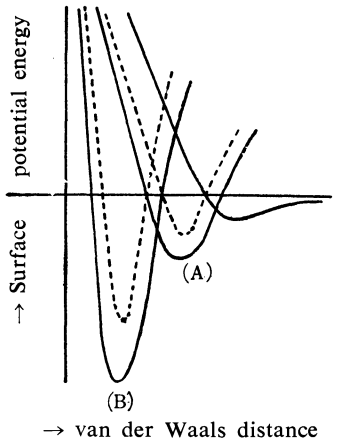



Fig. 6. Energy relation for the two types of chemisorption. Full line, for bared surface; broken line, for covered surface.

(Fig. 6). In the latter case the increase of activation energy of adsorption is attributed to the decrease of heat of adsorption with coverage. According to this model the chemisorption of type A has a low heat of adsorption and negligible activation energy, and hence the adsorption equilibrium is nearly realized throughout the course of slow adsorption, while that of type B involves an appreciable activation energy increasing with coverage and is responsible for the slow process. The behavior observed in this work on raising temperature might be explained by this model in terms of the rapid desorption of the A-type adsorbate followed by the slow adsorption of type B. On the other hand, as regards the rate of desorption, the observed slow process would solely be the desorption of the B-type adsorbate, since that of type A would be probably rapid; the rate of slow desorption would thus be determined only by the adsorbed amount at a given time, irrespective of other experimental conditions.

In order to examine if such a prediction is realized, the following experiments were carried out: At room temperature hydrogen was allowed to be left in contact with the adsorbent for 15 min. in one experiment and 16 hr. in the other one; after which, pumping out a known amount

8) E. Wicke, *Z. Elektrochem.*, 53, 279 (1949); J. H. de Boer, loc. cit.; P. M. Gundry and F. C. Tompkins., *Trans. Faraday Soc.*, 52, 1609 (1956); etc.

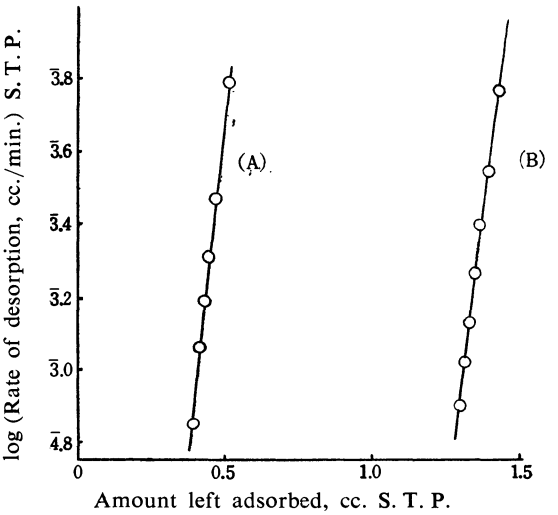



Fig. 7. Rate of desorption as a function of the amount left adorbed. Temp., 16°C.

| | Time of contact | Amount adsorbed before desorption in cc. |
|---|---|---|
| Run A | 15 min. | 1.67 |
| Run B | 16 hr. | 2.65 |

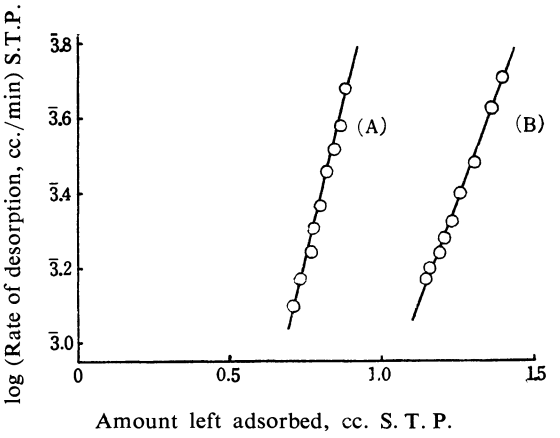



Fig. 8. Rate of desorption as a function of the amount left adsorbed. Temp., 188°C

| | Time of contact | Amount adsorbed before desorption in cc. |
|---|---|---|
| Run A | 15 min. | 1.38 |
| Run B | 16 hr. | 1.85 |

of hydrogen from the system, the rate of desorption was measured in the manner described in the previous paper[3]. The results are shown in Fig. 7, where, contrary to what has been predicted above, the desorption rates corresponding to equal amounts adsorbed differ markedly from each other, indicating that the postulate of two types of chemisorption can not be applied to this system. Similar results were obtained by the experiments at higher temperatures, an example at 188°C being given in Fig. 8.

Of the two alternatives given above, there remains now the postulate of heterogeneity of the surface to be accepted[9,10]. In view of the continuous variation of the activation energy of desorption with adsorbed amount, the pattern of this heterogeneity seems to be characterized by a continuous distribution function of sites with the heats of adsorption and the activation energies of adsorption varying in the same direction as proposed by Halsey[11]. According to this model, on the sites with a low activation energy, the heat of adsorption is also low and adsorption equilibrium will immediately be established after admission of hydrogen. Whilst, those with a high activation energy are covered by a slow process and the activation energy becomes higher as the adsorption proceeds. On raising the temperature during adsorption, a rapid desorption takes place on the sites with a low activation energy, but on the sites with a high activation energy the slow adsorption continues. In this way this model can explain the phenomena found by Taylor and Liang[1]. Furthermore, the observation such as the marked difference in the rates of desorption corresponding to equal amounts adsorbed in the two experiments with different times of contact with hydrogen and the unexpected pressure dependence of the rate of adsorption obtained in the usual manner may be explained as follows: under different experimental conditions, e.g. different times for adsorption or different initial pressures, different sets of sites may be covered to different extents. Hence, the states of equal amounts adsorbed are not necessarily comparable.

**Activation Energy of Adsorption.**—The temperature dependence of slow chemisorption given in Table II will give the true activation energy of adsorption, if desorption is negligible. As described above, this condition is not satisfied in this system. However, in view of the nature of surface heterogeneity given above, the situation before and after a temperature raise may be supposed as follows. Before the temperature raise adsorption proceeds mainly on the sites with a particular value of activation energy, since on those with a lower activation energy the adsorption equilibrium must be almost established, while those with a higher activation energy must be nearly bare. On raising temperature, coverage on these sites may become close to the equilibrium value. Hence, adsorption now proceeds mainly on those with a higher activation energy. Since the heat of adsorption changes in parallel with the activation energy, it seems unlikely that the effect of desorption is markedly altered on raising temperature. Thus, the temperature dependence obtained by extrapolating these rates to the time of a rapid temperature change will give the activation energy not greatly in error. In fact, as described in the previous report[3], the maximum value of the activation energy of adsorption estimated from the activation energy of desorption and the heat of adsorption is 13 kcal./mol., in agreement with 15 kcal./mol. obtained directly from the adsorption rate measurements.

9) An assumption of the coexistence of three or more types of bonding on a homogeneous surface in a limited temperature range might explain the observed behavior. It is, however, difficult to work out plausible physical models for such various types of bonding.

10) The experiments described above, of course, can not decide between the two possibilities, one-type and two-type chemisorption on a heterogeneous surface. As will be shown in a later paper, there is no convincing evidence to support the latter at present.

11) G. D. Halsey, *J. Phys. Chem.*, 55, 21 (1951).

## Summary

With respect to hydrogen chemisorption on zinc oxide, the dependence of adsorption rate on pressure and temperature was determined by an abrupt change of pressure or temperature during adsorption. The pressure dependence obtained on increasing pressure differed markedly from that on decreasing pressure, indicating that desorption can not be neglected. The apparent activation energy of slow chemisorption increased from 6 to 15 kcal./mol. as the temperature range becomes higher. Marked differences were found between the rates corresponding to equal amounts adsorbed in the two experiments where the times of contact with hydrogen were different. On the basis of these results, combined with the variation of activation energy of desorption with the amount adsorbed previously, it was shown that for this system the concept of the two types of chemisorption on a uniform surface can not be applied. Instead a postulate of a heterogeneous surface where the activation energy of adsorption and the heat of adsorption varies in the same direction was found to be able to explain all the results obtained.

The author wishes to express his sincere thanks to Professor O. Toyama for his guidance and encouragement throughout the course of this study.

*Department of Applied Chemistry*
*College of Engineering*
*University of Osaka Prefecture*
*Sakai-shi Osaka*

# *Carbon Monoxide Chemisorption on Zinc Oxide*

By Yutaka KUBOKAWA

(Received September 9, 1959)

Carbon monoxide chemisorption on zinc oxide at room temperature has been investigated by Garner and coworker[1] who reported that the heat of adsorption obtained from the adsorption isotherms is 10~14 kcal./mol., and that the chemisorption is instantaneous and completely reversible at room temperature. Few studies[2] have hitherto been reported on the carbon monoxide chemisorption at high temperatures, which appears to play an important role in the reaction of carbon monoxide, e. g. the oxidation of carbon monoxide. The present work has therefore been undertaken to obtain quantitative information concerning this chemisorption over a wide temperature range by measuring the rate of adsorption and adsorption equilibrium as well as the rate of desorption in the manner described in previous papers[3,4]. Moreover, in this paper, the nature of surface heterogeneity in this system is discussed on the basis of the results obtained, and especially those of the desorption under various experimental conditions which proved to be useful in clarifying the nature of the heterogeneneity of zinc oxide surface in the hydrogen chemisorption[4].

## Experimental

**Materials.**—Zinc oxide was prepared from zinc oxalate in a manner similar to that described in the previous paper[3]. The weight of adsorbent was 16.72 g. and the surface area determined by the B. E. T. method was 6.1 $m^2/g$. Carbon monoxide was prepared by the reaction of air-free formic acid and concentrated sulfuric acid, purified by passing through soda lime and phosphorus pentoxide, and finally through a trap immersed in liquid nitrogen.

**Apparatus and Procedure.** — Details of the apparatus and procedure were described in the previous paper[3]. Before a series of experiments, the pretreatment of the sample with carbon monoxide at 400°C followed by evacuation at this temperature were repeated several times.

## Results and Discussion

**Adsorption Isotherms at About Room Temperature.**—According to the investigations by Garner et al.[1], carbon monoxide chemisorption at room temperature is instantaneous and involves no appreciable activation energy. The results obtained in the present study were similar to their results except for the occurrence of a slow uptake even at room temperature, though its amount was very small. The adsorption isotherm obtained by successive

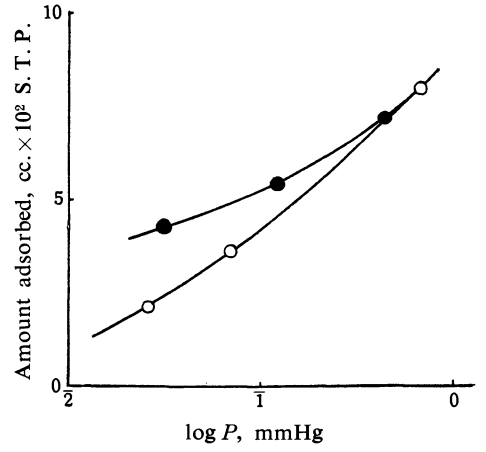



Fig. 1. Adsorption isotherms on the adsorption and desorption branches for the chemisorption of CO on ZnO at 22°C. -○-, on adsorption; -●-, on desorption.

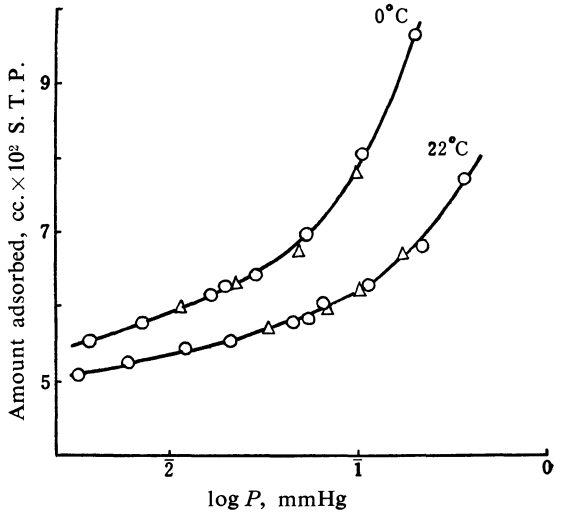



Fig. 2. Adsorption isotherms of CO on ZnO at 0 and 22°C. -○-, on decreasing pressure; -△-, on increasing pressure.

1) W. E. Garner and J. Maggs, *Trans. Faraday Soc.*, **32**, 1744 (1936).
2) R. L. Burwell and H. S. Taylor, *J. Am. Chem. Soc.*, **59**, 697 (1937); E. R. S. Winter, "Chemisorption", edited by W. E. Garner, Butterworths Scientific Publications, London (1957), p. 189.
3) Y. Kubokawa, This Bulletin, **33**, 546 (1960).
4) Y. Kubokawa, ibid., **33**, 550 (1960).

additions of the gas in the usual manner was found to be different from that obtained in the reverse way, i.e., by successive withdrawals of the gas, as shown in Fig. 1. However, the isotherms determined by the latter method were reproducible on increasing or decreasing pressure as found for the hydrogen chemisorption described in the previous paper[3]. Fig. 2 shows the results obtained, which give the heat of adsorption as 10~12 kcal./mol.

**Dependence of the Rate of Adsorption on Pressure and Temperature.**—Carbon monoxide was introduced at room temperature and its adsorption followed, the temperature being raised in stages up to about 300°C. The results obtained are shown in Fig. 3, which shows that the rate of slow uptake increases markedly with temperature, and that above 100°C only a slight rapid desorption takes place on raising the temperature, in contrast with the case of hydrogen chemisorption previously reported[4]. The pressure dependence of the slow process was obtained in a manner similar to that for hydrogen chemisorption, i.e. by comparison of the rates at equal amounts of slow chemisorption between before and after a rapid pressure change during the adsorption rate measurements. A typical result is shown in Fig. 4 and Table I. The rate is proportional to $p^{0.8\sim0.9}$ on both increasing and decreasing pressures, indicating that desorption is negligible during adsorption.

The temperature dependence of the slow process was obtained by a comparison of the rates corresponding to the equal amounts of slow chemisorption at different temperatures. The results evaluated from Fig. 3 are shown

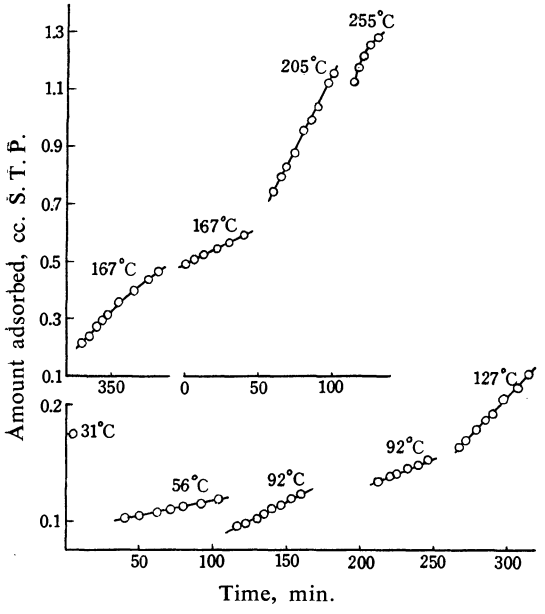



Fig. 3. Effect of the temperature change during adsorption on the rate of chemisorption of CO on ZnO. Pressure, 0.2~0.4 mmHg. Runs at 92 and 167°C were interrupted by reducing pressure or temperature.

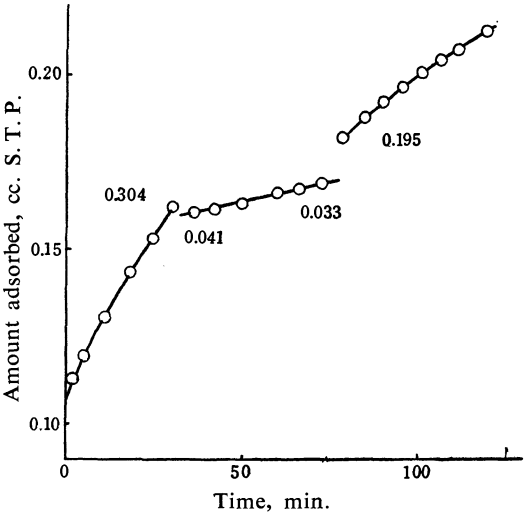



Fig. 4. Effect of the pressure change during adsorption on the rate of chemisorption of CO on ZnO. Temp., 120°C. Figures indicate the pressure before and after the pressure change in mmHg.

TABLE I. VALUES OF $n$ IN THE EXPRESSION, RATE $\propto P^n$ FOR THE DATA IN FIG. 4

| Pressure before and after the pressure change, mmHg | $n$ |
|---|---|
| 0.304 → 0.041 | 0.89±0.06 |
| 0.033 → 0.195 | 0.86±0.06 |

TABLE II. ACTIVATION ENERGIES OF ADSORPTION FOR THE DATA IN FIG. 3

| Temp. range, °C | Activation energy kcal./mol. |
|---|---|
| 56~ 92 | 5.5±1.0 |
| 92~127 | 7.5±1.0 |
| 127~167 | 11.5±0.7 |
| 167~205 | 16.5±0.7 |

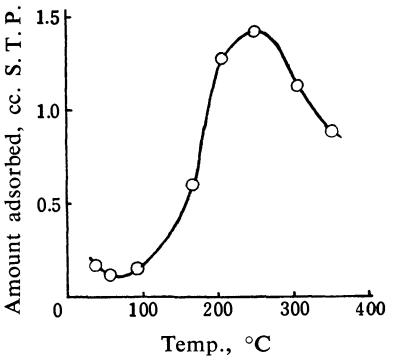



Fig. 5. Adsorption isobar of CO on ZnO at 0.2~0.4 mmHg.

in Table II, which indicates that the activation energy of the slow process increases as the temperature range becomes higher.

The adsorption isobar at approximately constant pressure 0.2~0.4 mmHg was obtained from the amount adsorbed after 1 hour at each temperature. Fig. 5 illustrates this isobar which shows a minimum at about 70°C and a maximum at about 250°C.

**Activation Energies of Desorption at Various Coverages.**—The temperature of the adsorbent which had already adsorbed carbon monoxide at about 300°C was raised from −72 to about 400°C in stages, at each of which the activation energy of desorption was determined in the manner described in the previous paper[3]. The variation of the activation energy for desorption with the amount desorbed is shown in Fig. 6. As seen in this figure, the curve of activation energy of desorption against the desorbed amount is composed of two parts, one corresponding to the desorption below room temperature with the activation energy of 2.5 kcal./mol., and the other to that above 200°C with the activation energy of approximately 40 kcal./mol. The former value is essentially the same as the heat of adsorption derived from the isotherms around room temperature, indicating that the chemisorption at room temperature involves no activation energy, as may be expected. In the latter case, the activation energy of desorption increases somewhat with decreasing coverage.

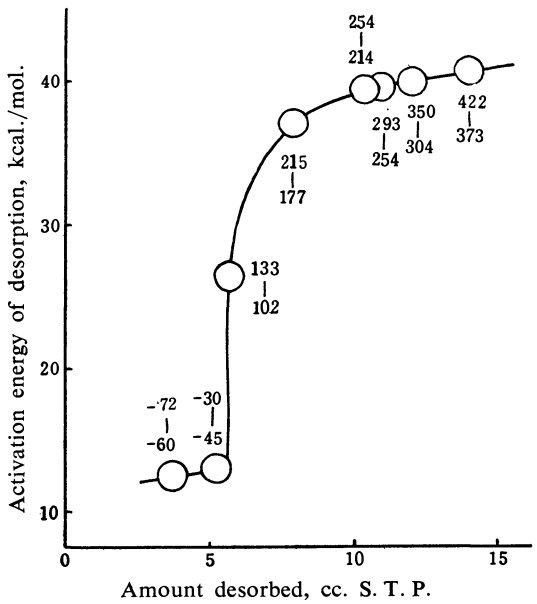



Fig. 6. Activation energies of desorption of CO chemisorbed on ZnO. Figures indicate the temperature interval where the activation energy was determined. The amount adsorbed at room temperature before desorption was 15.81 cc.

This conclusion is based on the assumption that the measured rate of desorption is not affected by the reverse reaction. This was confirmed in the manner previously described[3], i. e., by observing the pressure increase caused by isolating the adsorption vessel from the mercury diffusion pump. In the temperature range above room temperature the observed behavior was almost the some as that of the hydrogen chemisorption previously[3] described, indicating that adsorption is negligible during the desorption rate measurement. Whilst in the temperature range below room temperature, somewhat different behavior was observed as represented in Fig. 7. This shows that an equilibrium pressure $P_e$ is here easily attained, and moreover that the pressure in the adsorption vessel during the desorption experiment $P$, is now comparable to $P_e$. However, the ratio $P_e/P$ was found not to vary seriously by an abrupt change of temperature. From the data given in Fig. 7 this ratio was estimated to be 3.5 at −30°C, while the similar measurements at −45°C following these experiments gave the value of 2.6. The error introduced in the activation energy of desorption by this difference in $P_e/P$ was estimated to be at most 1 kcal./mol. It may therefore be concluded that the activation energy of desorption obtained below room temperature is also nearly equal to the true value.

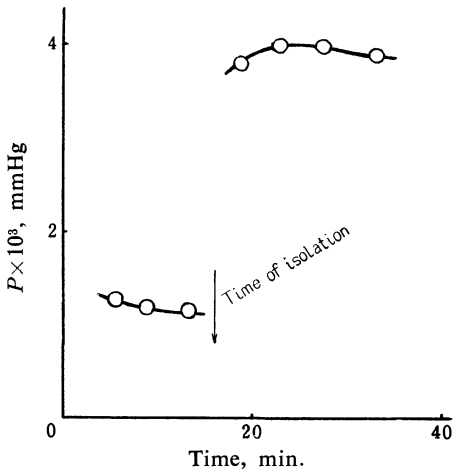



Fig. 7. Results obtained by isolating the adsorption vessel from the mercury diffusion pump. Temp., −30°C.

In order to confirm the reversibility of chemisorption the content of carbon dioxide in the desorbed gas was examined by immersing the trap attached to the MacLeod gauge in liquid nitrogen. The absence of carbon dioxide was confirmed below 350°C, while above this temperature its content amounted to the fraction 1/3~1/2 of the desorbed gas.

**Adsorption Isotherms at Higher Temperature**[5]. —The adsorption isotherms in temperature 300~370°C were determined by successive withdrawals of the gas as described for low temperature isotherms. These isotherms are strictly reproduced on increasing or decreasing pressure, as shown in Fig. 8. Fig. 9 represents the fact that the heat of adsorption derived from these isotherms decreases with the increasing amount adsorbed from 38 to 25 kcal./mol.

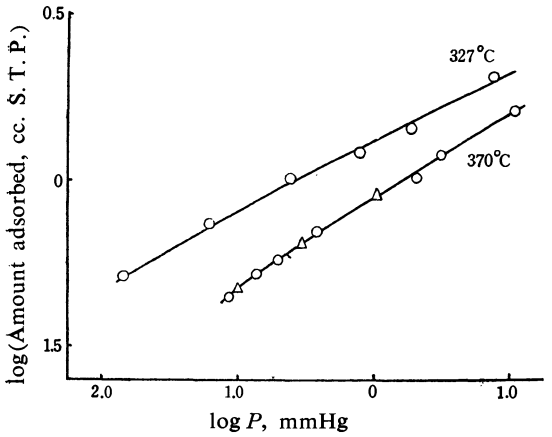



Fig. 8. Adsorption isotherms of CO on ZnO at 327 and 370°C. -○-, on decreasing pressure; -△-, on increasing pressure.

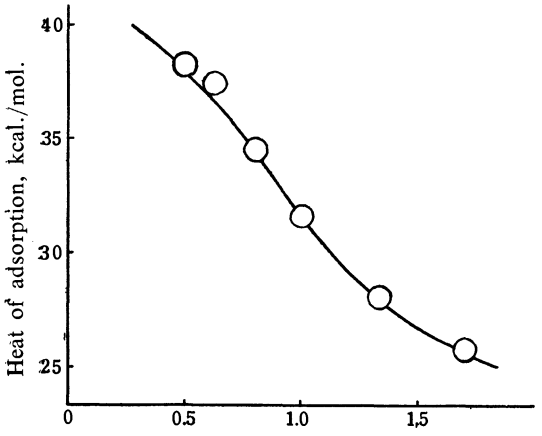



Fig. 9. Heats of adsorption of CO on ZnO.

**Two Types of Carbon Monoxide Chemisorption on Zinc Oxide.**—The plots of the activation energy for desorption against the amount adsorbed shown in Fig. 6, together with the adsorption isobar shown in Fig. 5, suggest that the two types of chemisorption are operating, one being a non-activated type predominating at a lower temperature, and the other an activated type occurring at a higher temperature. Moreover, not only the former, but also a considerable fraction of the latter is reversible, i.e. desorbed as such. Such behavior of the high temperature chemisorption appears to be inconsistent with the investigations by Garner and coworkers[6], who report that on a number of oxide catalysts the high temperature chemisorption takes place on the oxygen ion and the desorbed gas consists of carbon dioxide. However, the exchange reaction of the oxygen atom between carbon monoxide and the oxide surfaces have recently been investigated by Winter[2], who shows that the high temperature chemisorption does not necessarily lead to the desorption of carbon dioxide, in agreement with the results in the present work.

On the other hand, as described above, there is a slow uptake at room temperature which seems to imply that the chemisorption with the lower activation energy occurs even at room temperature. The phenomena of hysteresis observed at room temperature may then be accounted for, since the high temperature type is considered to be irreversible at this temperature.

**Nature of Heterogeneity of the Surface.**—The problem was dealt with in the same manner as previously reported for the hydrogen chemisorption[4]: At 192°C a known amount of carbon monoxide was left in contact with the adsorbent for fifteen minutes in one case and for fifteen hours in the other case; then, by pumping out a known amount of the gas from the system, the desorption rates in the two cases were compared with the results shown in Fig. 10, where curves A and B represent desorption rates after fifteen minute and fifteen hour contacts, respectively. After desorption B a certain amount of carbon monoxide was further pumped out at a higher temperature until the remaining amount adsorbed became comparable to that left after desorption A; thereupon, the temperature was lowered down to 192°C, and desorption rate measurements were carried out. Their results, denoted by C, are also shown in Fig. 10. It follows from this figure that the rate of desorption is greater on the surface where the larger amount is adsorbed, and is determined by the remaining amount adsorbed alone, independent of the conditions employed for the adsorption, in contrast with the behavior of hydrogen described in the previous paper[4].

These results might be explained in terms of the concept that the increase of the activation

5) During the adsorption isotherm measurements, the formation of carbon dioxide was negligibly small and darkening of zinc oxide was not observed, suggesting that the reaction $2CO \rightarrow C+CO_2$ scarcely takes place at all, in disagreement with the results obtained by Taylor and Burwell[2]. Such discrepancy appears to be explained by the severe carbon monoxide treatment in the present work, since the authors cited above reported a marked decrease in the activity toward this reaction after the carbon monoxide treatment.

6) W. E. Garner, *J. Chem. Soc.*, **1947**, 1239.

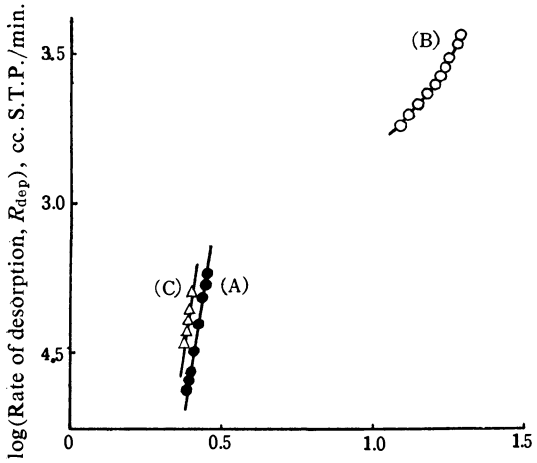



Fig. 10. Rate of desorption as a function of the amount left adsorbed. Temp, 192°C.

energy of adsorption with the adsorbed amount is due to the decrease of the heat of adsorption with coverage, without the concept of an *a priori* heterogeneity. However, the fact that the value of $d \log R_{dep}/dq$ differs markedly between the two runs, A and B, as shown in Fig. 10, can not be explained in terms of the induced heterogeneity[7] above mentioned, because there is no marked difference in the coverage $\theta$ between these two runs, considering that the adsorbed amount at $\theta=1$ estimated from Fig. 8 is about 10 cc. With respect to this problem, the following experimental results may be mentioned. From the plots of $\log R_{dep}-q$ at varied temperatures which were determined for the purpose of determining the activation energy of desorption at various coverages, the values of $d \log R_{dep}/dq$ at different adsorbed amount were estimated as shown in Fig. 11. This considerable change[8] can not be expected from the concept of induced heterogeneity. It may therefore be concluded that in this system again the variation of the heat of adsorption

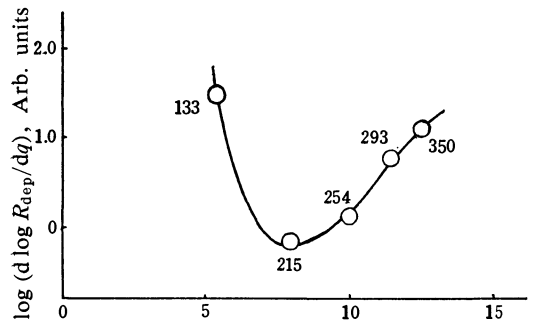



Fig. 11. Values of $d(\log R_{dep})/dq$ at various amounts adsorbed. Figures indicate the temperature in °C where the rate of desorption was measured.

with the adsorbed amount will arise mainly from *a priori* heterogeneity, the nature of which is such that the activation energy of adsorption and the heat of adsorption varies conversely to each other, in contrast with hydrogen chemisorption. Such a correlation between the activation energy of adsorption and the heat of adsorption requires that the maximum activation energy of adsorption 16 kcal./mol. should correspond to the minimum activation energy of desorption 37 kcal./mol. and the minimum of the former 5 kcal./mol. to the maximum of the latter 41 kcal./mol. This gives as the heats of adsorption 36 and 21 kcal./mol. in fair agreement with the values directly obtained from the adsorption isotherms[9].

## Summary

The rates of adsorption and desorption, and the adsorption equilibrium for carbon monoxide chemisorption on zinc oxide were measured over a wide range of temperatures as in the previous study of hydrogen chemisorption on zinc oxide. The behavior of desorption indicated the existence of two types of chemisorption; the non-activated type and the activated type. For the former type the heat of adsorption was estimated as 10~12 kcal./mol. from the adsorption isotherms, in agreement with the activation energy of desorption. The considerable fraction of the latter type was reversible, i.e. desorbed as such. For this type, the activation energy of adsorption increased with the adsorbed amount from 5 to 16 kcal./mol., and the rate was proportional to $P^{0.8\sim0.9}$. Moreover, the heat of adsorption obtained from the adsorption isotherms ranged from 25 to 38 kcal./mol., in fair agreement with those estimated from the activation energy of adsorption and desorption. The behavior of desorption suggested the predominance of surface heterogeneity, the nature of which was such that the activation energy of adsorption and the heat of adsorption varied conversely to each other.

The author wishes to express his sincere thanks to Professor O. Toyama for his guidance and encouragement throughout the course of this study.

*Department of Applied Chemistry*
*College of Engineering*
*University of Osaka Prefecture*
*Sakai-shi, Osaka*

7) M. Boudart, *J. Am. Chem. Soc.*, 74, 3556 (1952).

8) It will be shown in a forthcoming paper that this considerable change inevitably arises on a surface where *a priori* heterogeneity is predominating.

9) In Figs. 3, 6 and 9, the states of the carbon monoxide adsorbed to an equal amount can not be be compared, since the surface has a heterogeneous character, and moreover the observed amount of adsorption includes the irreversible one, the extent of which varies with the experimental conditions.

# SHORT COMMUNICATIONS

## *Formation of Mullite from Kaolin Minerals at Low Temperature*

By Hiroshi OKUDA

(Received February 27, 1960)

Mechanism of the mullite formation has not been explained completely, and there is a widespread disagreement concerning the formation temperature in the literatures[1-4]. It was reported that the formation of mullite from well-crystallized kaolinite occurs above 950°C and the formation of mullite from poorly crystallized kaolinite and halloysite occurs at a higher temperature[5,6]. Colegrave and Rigby[7] showed that traces of mullite were formed, when kaolinite was mixed with 2% of boric oxide and heated at 900°C. for 200 hr. No literature reported that the formation of mullite from kaolin minerals occured below 900°C.

During the course of an investigation of the effects of additive on the mullite formation of kaolin minerals[8], it was found that fluoride of alkali and alkaline earth elements promoted the formation and lithium fluoride was most effective. The present experiment has been carried out to find the effect of additive lithium fluoride on the temperature of mullite formation.

A well-crystallized kaolinite from Kampaku, Tochigi Prefecture, Japan and halloysite from Korea were used. The dried minerals were mixed with 2.5, 5 and 10% of lithium fluoride. The mixtures were heated for 5 hr. at 500, 550, 600, 700, 800 and 900°C. The heated samples were examined by an X-ray diffractometer, and the results are shown in Fig. 1 and Table I.

When 2.5% of lithium fluoride was added to kaolin, mullite and β-spodumene started to be formed at 800°C. The kaolin mixed with 5% of lithium fluoride was converted into β-spodumene above 600°C and into mullite above 700°C. It was found that β-spodumene was formed at 500°C and a small amount of mullite was formed at 550°C, when kaolin was mixed with 10% of lithium fluoride.

It is concluded that by the addition of lithium fluoride the kaolin minerals form mullite at a extremely lower temperature than that reported in the literature. Further experiment, however,

TABLE I. PHASE FOR KAOLIN MINERALS CONTAINING LITHIUM FLUORIDE HEATED AT VARIOUS TEMPERATURES FOR 5 HR.

| Sample | Temp. (°C) | | | | | |
|---|---|---|---|---|---|---|
| | 500 | 550 | 600 | 700 | 800 | 900 |
| Halloysite +2.5% LiF | halloysite | metakaolin | metakaolin | metakaolin | β-sp. mull. | β-sp. mull. |
| Halloysite +5% LiF | halloysite | metakaolin | β-sp. | β-sp. mull. | β-sp. mull. | β-sp. mull. |
| Halloysite +10% LiF | halloysite β-sp. | β-sp. mull. | β-sp. mull. | β-sp. mull. | β-sp. mull. | β-sp. mull. |
| Kaolinite +2.5% LiF | kaolinite | metakaolin | metakaolin | metakaolin | β-sp. mull. | β-sp. mull. |
| Kaolinite +5% LiF | kaolinite | metakaolin | β-sp. | β-sp. mull. | β-sp. mull. | β-sp. mull. |
| Kaolinite +10% LiF | kaolinite β-sp. | β-sp. mull. | β-sp. mull. | β-sp. mull. | β-sp. mull. | β-sp. mull. |

β-sp.: β-spondumene, mull.: mullite

1) A. H.Jay, *Trans. Brit. Ceram. Soc.*, **38**, 455 (1939).
2) H. M. Richardson and F. G. Wilde, ibid., **51**, 387 (1952).
3) G. W. Brindley and K. Hunter, *Mineralog. Mag.*, **30**, 574 (1955).
4) G. W. Brindley and M. Nakahira, *J. Am. Ceram. Soc.*, **42**, 311 (1959).
5) W. D. Johns, *Mineralog. Mag.*, **30**, 186 (1953).
6) H. D. Glass, *Am. Mineralogist*, **39**, 193 (1954).
7) E. B. Colegrave and G. R. Rigby, *Trans. Brit. Ceram. Soc.*, **51**, 355 (1952).
8) H. Okuda, M. Haga and S. Kato, *Reports of the Government Industrial Research Institute, Nagoya* (Nagoya Kogyogijutsu-shikenjo Hokoku), **6**, 60 (1957); ibid., **7**, 74 (1958).

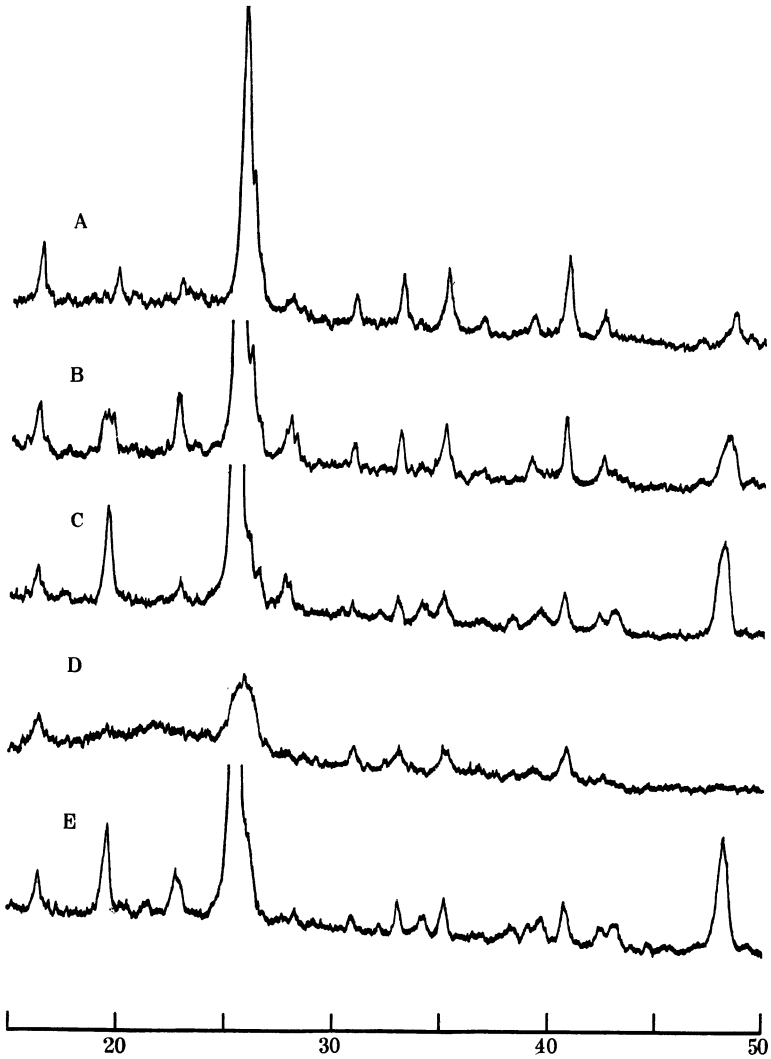



Fig. 1. X-ray diffraction patterns of kaolin minerals containing lithium fluoride.
A, is for the mixture of halloysite and 2.5% LiF heated at 800°C: B, the mixture of halloysite and 5% LiF heated at 700°C: C, the mixture of halloysite and 10% LiF heated at 550°C: D, the mixture of kaolinite and 2.5% LiF heated at 800°C: and E, the mixture of kaolinite and 10% LiF heated at 550°C. Heating period is 5 hr. in all cases.

is necessary to understand the mechanism of the mullite formation and to explain the effect of the addition of lithium fluoride on the formation.

*Government Industrial Research Institute*
*Kita-ku, Nagoya*

# *A New Application of Neutron Activation Analysis to the Polarography of Holmium*

By Hiroshi HAMAGUCHI, Jinzo HASHIMOTO, Kyoichi HOSOHARA and Yoshio NARUSAWA

(Received February 16, 1960)

In general, two stepped reduction waves are observed in the polarograms of lanthanide elements. Conflicting explanations for the mechanism of electrode reaction have been reported as summarized in Table 1.

The present authors introduced a new method for the study of the electrode reduction process of holmium by utilizing a neutron activation technique. Assuming the electrode reaction of holmium to be $Ho^{3+}_{aq}+3e+Hg \rightarrow Ho(Hg)$, the amount of holmium $m(\mu g.)$ amalgamated in one drop of mercury is calculated by

$$m = i_1 \cdot \tau \cdot 164.94/3F$$

where $i_1$ is the limiting current (microamp.), $\tau$ the drop time (sec.), 164.94 the atomic weight of holmium and $F$ the Faraday constant. In the case of the experimental condition shown in Fig. 1, the amount of holmium that would be deposited is calculated as 0.022 $\mu$g. ($\tau$=3.08 sec.) for the first wave and 0.023 $\mu$g. ($\tau$=2.67 sec.) for the second wave. These amounts are well above the sensitivity limit of the activation analysis of the element[9].

One drop of mercury taken up immediately after electrode reaction* was sealed in a vinyl bag, and irradiated for two days with a neutron flux of $\sim 10^{11}$ $n/cm^2/sec.$ in the JRR-1 reactor. After irradiation, the induced radionuclide $^{166}Ho$ was purified by going through decontamination chemistry, and the amount of holmium was then determined by comparing the $\beta$ activity of holmium from the sample with that of the monitor.

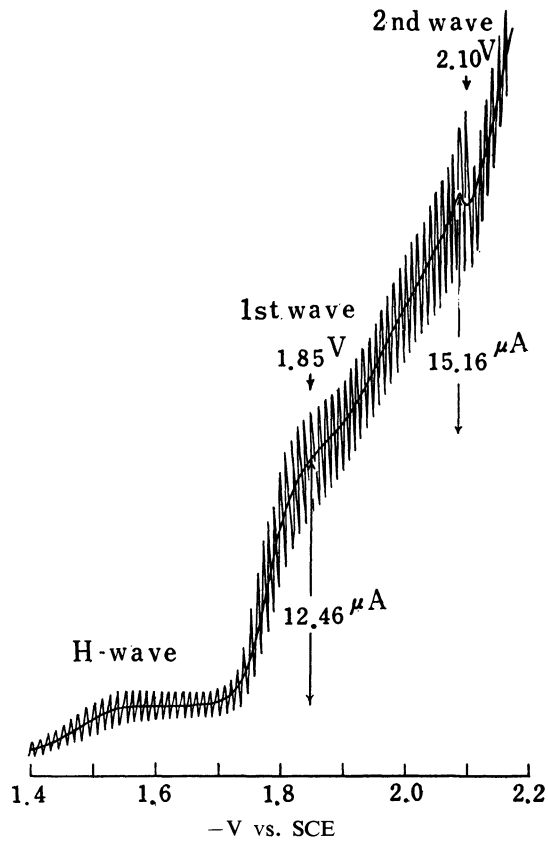



Fig. 1. Polarogram of $2.32\times10^{-3}$ mol./l. $Ho^{3+}$. aq. in 0.1 N LiCl soln. containing 0.01% gelatine. Temp. 25.0±0.01 °C.
The 1st wave: Number of electron 3(pH< 3.1), temp. coeff. 3.0%, linear relationship between wave height and concentration is obtained. Reversible at pH<3.10, quasi-reversible at 3.10<pH<3.90, irreversible at pH>3.90 are explained by Matsuda-Ayabe's theory. $E_{1/2}$ shifts toward more negative with decreasing of pH.
The 2nd wave: Followed by a maximum wave, no linear relation between wave height and concentration is obtained, although the correlation between them is held. The ratio of wave height of the 2nd to that of the 1st is not 2 : 1.

Contrary to the earlier reports that had suggested a reduction of lanthanides to the metallic state, extremely smaller amount of holmium than was expected was found at both reduction steps as shown in Table II.

In the light of the above data and of the polarographic behavior shown in Fig. 1, it should reasonably be considered that the polarographic reduction of holmium is not the reduction of the holmium aquo-complex ion to a metallic state but the discharge of hydrogen ions

1) W. Noddack and A. Brukle, *Angew. Chem.*, **50**, 362 (1937).
2) L. Holleck, *Z. Elektrochem.*, **46**, 69 (1940).
3) I. M. Kolthoff and J. J. Lingane, "Polarography", Vol. II, Interscience Publisher, New York (1952), p. 435.
4) G. Glockler et al., *J. Am. Chem. Soc.*, **70**, 1342, 1345 (1948); **71**, 1641 (1949).
5) S. Misumi and A. Iwase, ibid., **76**, 1231 (1955), **77**, 640 (1956).
6) A. Purushottam and B. H. S. V. Raghava Rao, *Anal. Chim. Acta*, **12**, 589 (1955).
7) A. Iwase, *J. Chem. Soc. Japan, Pure Chem. Sec. (Nippon Kagaku Zasshi)*, **78**, 114 (1957).
8) H. Hamaguchi, J. Hashimoto and Y. Narusawa, *J. Chem. Soc. Japan, Pure Chem. Sec. (Nippon Kagaku Zasshi)*, **80**, 43 (1959).
9) H. Hamaguchi, *J. Japanese Chem. (Kagaku-no-Ryoiki)*, **13**, 316 (1959).

* The method of collecting a drop of mercury is the same as that by J. J. Lingane and I. M. Kolthoff, *J. Am. Chem. Soc.*, **61**, 825 (1939).
In the present communication the re-dissolution of the deposited metal into the regulating solution, though possible, has not been taken into consideration.

TABLE 1. PROPOSED EXPLANATIONS FOR ELECTRODE REACTIONS OF LANTHANIDE ELEMENTS AT A DROPPING MERCURY ELECTRODE

| Element studied | First wave | Second wave | Investigators |
|---|---|---|---|
| Sc, Y, La, etc. | $M^{3+}+e \rightarrow M^{2+}$ | $M^{2+}+2e \rightarrow M^{0}$ | Noddack, Bruckle[1,2] |
| Lanthanides except Eu, Yb | Hydrogen wave | $M^{3+}+3e \rightarrow M^{0}$ | Kolthoff, Lingane[3] |
| La, Pr, Nd, Sm, Gd | $M^{3+}+3e \rightarrow M^{0}$ | ? | Glocker, et al.[4,5] |
| | $M^{3+}+e \rightarrow M^{2+}$<br>$M^{2+}+H_2O \rightarrow M^{3+}+OH^{-}+H^{0}$ | $M^{2+}+2e \rightarrow M^{0}$ | Purushottum, Raghava Rao[6] |
| Sm | $M(OH)^{2+}+3e \rightarrow M^{0}+OH^{-}$ | ? | Iwase[7] |
| Y | $M(OH_2)_6^{3+}+3e$<br>$\rightarrow M(OH)_3(OH_2)_3+3H^{0}$ | ? | Authors[8] |

TABLE II. THE AMOUNT OF HOLMIUM ($\mu$g.) FOUND IN A DROP OF MERCURY*

| First wave | | Second wave | |
|---|---|---|---|
| $m_{Ho}$(found) | $m_{Ho}$(calcd.) | $m_{Ho}$(found) | $m_{Ho}$(calcd.) |
| 0.0050 | 0.0218 | 0.0010 | 0.0230 |

* Values are corrected for the blank (0.0050 $\mu$g. Ho) in a drop of mercury.

produced by the dissociation of the aquo-complex ion. Details will be published later.

We are indebted to the members of the radiochemistry division, Japan Atomic Energy Research Institute for their co-operation with the irradiation. A part of the expense was defrayed from a grant from the Ministry of Education.

*Department of Chemistry*
*Faculty of Science*
*Tokyo University of Education*
*Bunkyo-ku, Tokyo*

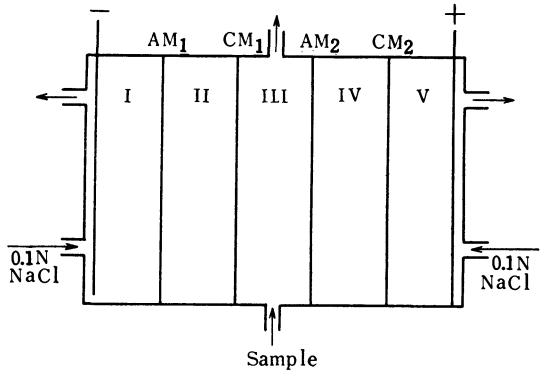
## *Transport Behavior of Ferric, Aluminum and Cupric Ions across the Alginate and the Other Membranes*

By Manabu Senō, Tazuko Saitō and Takeo Yamabe

(Received January 26, 1960)

Recently many attempts have been undertaken to separate various species of ions by the electrodialyses using the ion-selective membranes, but there is no report as to the selective permeability of heavy metal ions. One of the objects of this study is to describe the transport behavior of ferric, aluminum and cupric ions across the ion-selective membranes. Another is to examine the permeability of ferric ion across the alginate membrane which is prepared from alginic acid. It is known that alginic acid adsorbs preferentially the ferric ion[1].

The electrodialyses were carried out at the constant current densities, $(0.33\sim2.50)\times10^{-2}$ amp./cm$^2$, for one hour, using a five-compartment cell which was schematically Shown in Fig. 1.




$AM_1$, SAM ; $CM_2$, SCM

Fig. 1. A five-compartment cell for the electrodialyses.

Into the central compartment, the solution containing 5~10 meq./l. of ferric and aluminum chloride or ferric and cupric chloride and being adjusted to be about pH 1.3 (ca. 0.05N HCl) were fed at the flow-rate of about 1 l./hr. The amounts of ions transferred to the adjacent compartments, which were filled with the same solution beforehand, across the ion-selective membranes were measured. The analyses were done by the simultaneous colorimetric methods[2]. The ion-selective membranes were heterogeneous and were prepared from Amberlite resins in the authors' laboratory*. The alginate membrane

1) M. Senō and T. Yamabe, This Bulletin, to be published.

2) R. E. Kitson, *Anal. Chem.*, **22**, 664 (1950); K. Motojima, *J. Chem. Soc. Japan, Pure Chem. Sec.* (*Nippon Kagaku Zasshi*), **76**, 903 (1955).

* From the four kinds of Amberlite resins, IR-120, IRC-50, IRA-400 and IR-4B, the corresponding ion exchange membranes were prepared. These are a strongly and a weakly dissociated cation-selective membrane and a strongly and a weakly dissociated anion-selective membrane, which are abbreviated as SCM, WCM, SAM and WAM. Similarly the alginate membrane is designated as ACM in Table II.

was prepared from polyvinylchloride and alginic acid crosslinked with formaldehyde[3], using cyclohexanone as a mixing agent. The obserbed membrane potentials of these membranes are 80~90% of the theoretical (S.C.E. | 0.1N KCl | memb. | 0.01N KCl | S.C.E.).

A part of the experimental results was given in Tables I and II. The following facts are to be noticed.

TABLE I. PERMEABILITIES OF HYDROGEN, FERRIC, ALUMINUM AND CUPRIC IONS ACROSS A STRONGLY DISSOCIATED CATION-SELECTIVE MEMBRANE

| Current densities | Concentration ratios* | | | | | |
|---|---|---|---|---|---|---|
| | Fe-Al system | | | Fe-Cu system | | |
| amp./cm$^2$×10$^2$ | H | Fe | Al | H | Fe | Cu |
| 0.33 | 1.99 | 0.84 | 0.79 | 1.88 | 0.78 | 0.72 |
| 0.83 | 2.60 | 1.02 | 1.26 | 2.41 | 1.13 | 1.78 |
| 1.67 | 3.36 | 1.15 | 1.39 | 4.28 | 2.18 | 3.28 |
| 2.50 | 4.90 | 2.26 | 2.49 | 4.70 | 2.41 | 4.30 |

* These are ratios of concentrations of a given ion in the compartment II before and after electrodialysing.

TABLE II. PERMSELLCTIVITY COEFFICIENTS ACROSS THE VARIOUS ION-SELECTIVE MEMBRANES AT 0.0083 amp./cm$^2$

| Ion-selective membrane system (CM1-AM2) | Permselectivity coefficients* | | | |
|---|---|---|---|---|
| | $T^{Al}_{Fe}$ | $T^{Cu}_{Fe}$ | $T^{H}_{Fe}$ | |
| SCM-SAM | 1.23 | 1.57 | 2.55 | 2.13 |
| WCM-SAM | 1.27 | 1.32 | 2.49 | 2.00 |
| WCM-WAM | 1.07 | 1.30 | 2.06 | 2.35 |
| ACM-SAM | 1.03 | 1.70 | 1.72 | 2.50 |
| ACM-WAM | 1.01 | 1.51 | 1.75 | 2.06 |

* $T^{B}_{A}=\dfrac{[B]_f[A]_i}{[B]_i[A]_f}$

where $[A]_i$, $[B]_i$; concentration of A or B ion in the initial solution filling the compartment II, respectively; $[A]_f$, $[B]_f$; concentration of ion A or B in the final (concentrated) solution in the compartment II, respectively.

** In the first column, the values obtained for Fe-Al system were shown and in the second column, those for Fe-Cu system were presented.

(1) The order of permeabilities of these cations across the cation-selective membranes is as follows; $Fe^{3+}<Al^{3+}<Cu^{2+}<H^{+}$, excepting the case at the lowest current density**.

(2) This order remains invariable, independently of the various combinations of the ion-selective membranes. The permeability of the ferric ion across the alginate membrane is nearly the same as that in the other membrane systems. There is no parallel relationship between the selectivity in the ion exchange equilibria[1] and the permselectivity in this experiment, of the various ion-selective membranes.

(3) Some amount of the ferric ion transports across the anion-exchange membranes and this behavior seems to be due to the formation of a complex anion. A further investigation is carried out now, for the experimental error of this research prevents from giving a final conclusion to this problem.

The full data will be presented in the near future.

The authors wish to express their thanks to Professor T. Takahashi for his continuous advice, and to the Ministry of Education for grand-in-aid.

*Institute of Industrial Science*
*The University of Tokyo*
*Yayoi-cho, Chiba*

3) T. Yamabe, Y. Tanka and M. Senō, *Industrial Science (Seisan Kenkyu)*, **9**, 476 (1959).

** This order does not depend on the current density higher than 0.0083 amp./cm$^2$. The diffusion of ions through membrane and the migration of water due to the electro-osmosis make a contribution to the transport behavior to some extent. On this account, the concentration ratio of the metal ions shown in Table I is smaller than unity at the current density, 0.0033 amp./cm$^2$. When the current density is high enough and the same membrane used as AM1, the permselectivity coefficient $T^{B}_{A}$ defined in Table II is considered to be a relative measure of the permeabilities of the cations across the cation-exchange membrane CM1.

## *Two Types of Antifoamers and their Cooperating Action*

By Satiko OKAZAKI and Tsunetaka SASAKI

(Received February 18, 1960)

The present authors pointed out[1] that attention should he drawn to two factors, foam stability and foam producing power, to explain the phenomena of foam formation, and also that two factors should be taken into account, i. e., foam breaking action and foam inhibiting action, to elucidate the phenomena of antifoaming. In this relation we have already shown[2] that when an aqueous solution of saponin which is marked for its foam stabilizing action is mixed with an aqueous solution of alcohol which is marked for its foam producing power, a pronounced foam formation, presumably due to their cooperative or syergistic action, can be observed even in such a dilute solution as they can exhibit only

1) T. Sasaki and S. Okazaki, *Kolloid-Z.*, **159**, 11 (1958).
2) T. Sasaki, This Bulletin., **15**, 449 (1940).

TABLE I. ACTION OF ANTIFOAMERS TOWARDS AQUEOUS SAPONIN AND SODIUM DODECYL SULFATE FOAMS

Saponin Foam (0.5% aqueous solution)

| Antifoamers | Foam height in cm. Before addition | 10 sec. after addition | 3 sec. after shaken again |
|---|---|---|---|
| Silicone | 10 | 9.4 | 0 |
| *i*-Amyl alcohol | 10 | 1.7 | 10 |
| *i*-Amyl alcohol +silicone* | 10 | 2.2 | 0 |
| Ethyl acetate | 10 | 5.5 | 10.6 |
| Ethyl acetate +silicone* | 10 | 5.6 | 0 |
| Ethanol | 10 | 7.3 | 11 |
| Ethanol +silicone* | 10 | 6.8 | 0 |

Sodium dodecyl sulfate foam ($10^{-2}$ mol./l. aqueous solution)

| Antifoamers | Foam height in cm. Before addition | 10 sec. after addition | 3 sec. after shaken again |
|---|---|---|---|
| Silicone | 12 | 7.0 | 0 |
| *i*-Amyl alcohol | 12 | 0.7 | 12 |
| *i*-Amyl alcohol +silicone* | 12 | 2.0 | 0.6 |
| Ethyl acetate | 12 | 4.3 | 12 |
| Ethyl acetate +silicone* | 12 | 3.3 | 0.3 |
| Ethanol | 12 | 8.7 | 12 |
| Ethanol +silicone* | 12 | 6.7 | 0.8 |

* Composition of mixtures being 1 : 1 in weight. Room temperature : 16°C

a poor foam formation when each of them exists separately.

Now we can demonstrate a similar experiment also in the case of antifoaming. As we have shown,[1] silicone oil antifoamer is a well-known excellent foam inhibitor but is not always a good foam breaker, while *i*-amyl alcohol is a strong foam breaker but is not a good foam inhibitor* when added in a small amount. Now, when these two antifoamers of rather mutually opposite in the types of their actions are mixed together and a drop of the mixture is appleid onto the aqueous saponin and sodium dodecyl sulfate foams, a remarkable foam breaking action and foam inhibiting action are observed simultaneously. The results of these experiments are shown in Table 1. Similar instances may be shown for other pairs of antifoamers of the same relation. In this table we can also confirm a slight difference in antifoaming action of a given antifoamer towards different types of foams, i. e., saponin and sodium dodecyl sulfate foams. Anyhow, we can confirm distinctly the existence of two different types of antifoaming actions, i. e., foam breaking and foam inhibiting ones which have been reported merely qualitatively in many literatures,[3] and also confirm their cooperating action, though actually we can only make a rough distinction between two types of antifoamers according to these actions.

The authors thank the Ministry of Education for the Scientific Research Expenditure given to T. Sasaki.

*Department of Chemistry*
*Faculty of Science*
*Tokyo Metropolitan University*
*Setagaya-ku, Tokyo*

* Detailed behavior of antifoamers will be reported elsewhere.

3) For instance, S. Ross and J. W. McBain, *Ind. Eng. Chem.*, **36**, 570 (1944).

## *Preparation of a New Phototropic Substance*

By Taro HAYASHI and Koko MAEDA

(Received March 1, 1960)

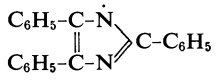
Under the investigation of the mechanism of chemiluminescence which occurred when lophine (2, 4, 5-triphenyl-imidazole) was oxidized in an ethanol solution of potassium hydroxide with an oxidizing agent, there was isolated a new phototropic substance which was considerd to be an imidazole derivative. To the solution of lophine (1 g.) in a solution of potassium hydroxide (12 g.) in ethanol (100 cc.), 450 cc. of 1% potassium ferricyanide aqueous solution was added during a period of 1.5 hr. with stirring by a stream of oxygen at room temperature. The violet color of the solution, which initially appeared, gradually disappeared and white precipitates, having a tinge of pale violet, separated out. When the oxidation was carried out in a dark place, a weak greenish blue chemiluminescence was observed. The precipitates were filtered and then washed with water repeatedly until the washing showed no reaction of ferricyanide ion. The precipitates, dried in vacuo (0.9g.) were dissolved in benzene to yield a deep red violet solution. When the solution was concentrated under reduced pressure, a lemon yellow crystalline substance separated out. It was recrystallized from ethanol as lemon yellow prisms, m. p. 199~201°C.

Found: C, 85.20; H, 5.50; N, 9.41. Calcd. for $C_{21}H_{15}N_2$: C, 85.38; H, 5.11; N, 9.49%.

The molecular weight in benzene solution was determined to be about 290 by a cryoscopic method. Although this compound had the composition nearly equal to that of lophine, properties of these compounds were different from each other, showing that this compound was different from lophine. This compound was soluble in ordinary solvents, giving a pale yellow or almost colorless solution. Its ultraviolet absorption spectrum showed an absorption maximum at ca 267 m$\mu$ in ethanol. This compound was also obtained by the oxidation of lophine with an ethanol solution of bromine. In this case, the bromine solution was mixed in benzene with a solution of lophine in ethanolic potassium hydroxide. A mixture of ethanol solution of this compound with 4% aqueous solution of potassium ferrocyanide, which yielded white precipitates, was warmed in a water bath for 1 hr. and then water was added until white precipitates dissolved in a solution. The solution was evaporated to give white precipitates which were recrystallized from ethanol and identified to be lophine.

This compound showed a marked phototropy; when it was irradiated with sun light or light of mercury lamp in a solution of organic solvent as well as in solid at room temperature, it rapidly turned red violet, both in air and in vacuo. The absorption spectrum of the red violet solution showed absorption maxima at 350 and 550 m$\mu$ in benzene. In solid the red violet color faded slowly at room temperature but rapidly when the colored substance was warmed in a water bath. In solution the color faded rather rapidly even at room temperature. When the benzene solution of this phototropic substance was irradiated, no change of the molecular weight was observed. When nitrogen oxide gas was passed through the red violet benzene solution, the color immediately disappeared. This fact shows that the red violet coloration is due to the formation of a free radical. Electron spin resonance absorption was detected with this red violet substance in benzene solution as well as in solid[1]. The solution of this compound exhibited thermochromism.

From the results mentioned above, it is considered that the red violet form is an oxidation product of lophine which is a free radical $C_{21}H_{15}N_2$ (I), while the lemon yellow form may be a rather labile meso ionic form.



(I)

*Department of Chemistry*
*Faculty of Science*
*Ochanomizu University*
*Bunkyo-ku, Tokyo.*

1) The results of the investigation by electron spin resonance absorption and spectroscopic methods will be published in the near future, T. Hayashi and K. Maeda, *J. Chem. Phys.*, in press.

# *Hydrogenation and Hydrogenolysis. III*[1]. *Rhodium-Platinum Oxide as a Catalyst for the Hydrogenation of the Aromatic Nucleus*

By Shigeo NISHIMURA

(Received March 10, 1960)

It has been shown in these two decades that rhodium is useful as a catalyst for the hydrogenation of various organic compounds[2], and recently that it is specially effective for the hydrogenation of the aromatic nucleus[3-5]. However, most of the works on rhodium catalysts are concerned with the use of colloidal or supported rhodium, and none with the use of rhodium oxide of Adams' type. It seem that this is because of the difficulty of reducing rhodium oxide to the metal form under mild conditions[6].

The present author prepared a useful catalyst consisting of rhodium oxide and platinum oxide in a ratio of 3 : 1 by the weights of the metals, by fusion of the mixture of rhodium chloride and chloroplatinic acid or ammonium chloroplatinate with sodium nitrate exactly in the same way as in the preparation of Adams platinum oxide[7]. This rhodium-platinum oxide[8] can be reduced with hydrogen to rhodium-platinum

1) Part II of this series: S. Nishimura, This Bulletin, 32, 1155 (1959).
2) For earlier literatures, see Refs. 3 and 5.
3) L. D. Freedman, G. O. Doak and E. L. Petit, *J. Am. Chem. Soc.*, 77, 4262 (1955).
4) H. A. Smith and R. G. Thompson, "Advances in Catalysis", Vol. 9, Academic Press Inc., New York (1957), p. 727.
5) G. Gilman and G. Cohn, ibid., p. 733.
6) Cf. Ref. 4, p. 732. This difficulty was also confirmed by the present author.
7) R. Adams, V. Voorhees and R. L. Shriner, "Organic Syntheses", Col. Vol. 1, 2nd Ed., John Wiley & Sons, Inc., New York (1941), p. 463.
8) The mixed oxide thus prepared is not identical with the mere mixture of rhodium oxide and platinum oxide, the former being reduced with hydrogen much more rapidly and uniformly than the latter.

TABLE I. HYDROGENATION OF AROMATIC COMPOUNDS WITH RHODIUM-PLATINUM OXIDE AND PLATINUM OXIDE AS CATALYSTS AT THE ORDINARY TEMPERATURE AND PRESSURE[a]

| Compound | Amount, g. | Catalyst, g. | Hydrogen uptake, mol./mol. | Time for complete hydrogenation, min. |
|---|---|---|---|---|
| Methylphenylcarbinol | 0.611 | Rh-Pt, 0.05 | 3.04 | 36 |
| 〃 | 〃 | Pt, 0.20 | 3.87 | 80 |
| Benzhydrol | 0.553 | Rh-Pt, 0.05 | 6.03 | 105 |
| 〃 | 〃 | Pt, 0.20 | 6.73 | 120 |
| Phenol | 0.471 | Rh-Pt, 0.05 | 3.04 | 14 |
| 〃 | 〃 | Pt, 〃 | 3.35 | 40 |
| Anisole[b] | 0.541 | Rh-Pt, 〃 | 3.04 | 18 |
| 〃 | 〃 | Pt, 〃 | 3.45 | 85 |
| Cinnamyl alcohol[c] | 1.342 | Rh-Pt, 〃 | 1.04 | 11 |
| 〃 | 〃 | Pt, 〃 | 1.31 | 26 |
| Benzene[d] | 0.781 | Rh-Pt, 〃 | 2.99 | 20 |
| 〃 | 〃 | Pt, 〃 | 2.99 | 80 |
| Ethyl benzoate | 0.751 | Rh-Pt, 〃 | 3.02 | 21 |
| 〃 | 〃 | Pt, 〃 | 3.00 | 120 |

a) 20 cc. of glacial acetic acid was used as solvent.
b) Smith and Thompson (Ref. 4) reported that anisole absorbed 3.06 mol. of hydrogen with 5% rhodium on alumina and 3.40 mol. with Adams platinum oxide in acetic acid at 30°C under initial hydrogen pressures of 40–60 p. s. i.
c) Reduction to 3-phenyl-1-propanol and propylbenzene.
d) Gilman and Cohn (Ref. 5) reported that 5 ml. of benzene was hydrogenated four times as rapidly with 1 g. of 5% rhodium on alumina as with 1 g. of 5% platinum on alumina in acetic acid under ordinary conditions.

black in neutral ethanolic or acetic acid suspension at the ordinary temperature and pressure. The reduction begins in about twenty minutes and completes in about forty minutes in acetic acid at 25°C. The rhodium-platinum black thus prepared is an excellent catalyst in the hydrogenation of various aromatic compounds in acetic acid under ordinary conditions as shown in Table I. With this catalyst, methylphenylcarbinol, benzhydrol, phenol, anisole and cinnamyl alcohol are reduced rapidly and quantitatively to the corresponding saturated compounds with far less portions of hydrogenolysis than with Adams platinum oxide as indicated by the moles of hydrogen absorbed. The catalyst is four and six times as active as Adams platinum oxide in the hydrogenation of benzene and ethyl benzoate, respectively, where the hydrogen uptake is equally 3 mol. with both catalysts. Thus the results show that the rhodium-platinum catalyst retains to a large extent the nature of pure rhodium catalysts and is substantially superior to Adams platinum oxide both in activity and in selectivity in the hydrogenation of the aromatic nucleus. Details will follow.

The author wishes to express his hearty thanks to Professor Y. Urushibara for his continued encouragement.

*Department of Chemistry*
*Faculty of Science*
*The University of Tokyo*
*Hongo, Tokyo*

## *The Synthesis of the Pterocarpin Ring System*[1]

By Hiroshi SUGINOME and Tsukasa IWADARE

(Received March 1, 1960)

The structures of pterocarpin and homopterocarpin, the minor principles of *pterocarpus santalinus*, were elucidated in 1940 by Robertson and Whalley and by Späth and Schläger[2] as III, $R_1$=$R_4$=OMe, $R_2$, $R_3$=–O–$CH_2$–O–, and III, $R_1$=$R_3$=OMe, $R_2$=$R_4$=H, respectively. However, the syntheses of pterocarpin and homopterocarpin have not been hitherto completed.

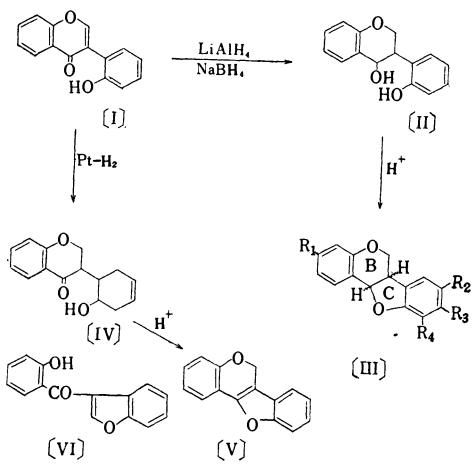
This paper presents the syntheses of the

1) Oxygen heterocycles. (II). Previous paper in this series, Hiroshi Suginome, *J. Org. Chem.*, **24**, 1655 (1959).

2) A. Robertson and W. B. Whalley, *J. Chem. Soc.*, **1940**, 787; **1954**, 1440; E. Späth and J. Schläger, *Chem. Ber.*, **73**, 1 (1940).

simple core of pterocarpin, III, $R_1=R_2=R_3=R_4=H$, and compound V, as shown in the annexed chart, which establish a synthetic route to DL-pterocarpin and DL-homopterocarpin or their isomers.

In view of a possible biogenetic link[1,3,4] of pterocarpin and homopterocarpin to naturally occurring 2'-hydroxyisoflavonoids, the synthetic sequence, I→II→III, is of particular interest.




Mild acid hydrolysis of 2,2'-bis(methoxymethoxy) benzoin, m. p. 104~104.5°[5]. (Found: C, 64.79; H, 5.59. Calcd. for $C_{18}H_{20}O_6$: C, 65.09; H, 6.02%) afforded 2,2'-dihydroxybenzoin, m. p. 161~163°C[6] (Found: C, 68.48; H, 5.02. Calcd. for $C_{14}H_{12}O_4$: C, 68.84; H, 4.95%), accompanied by a small amount of an unidentified substance, m. p. 156~157°C, I. R. bands at 1627 $cm^{-1}$ (conjugated carbonyl) and 3200 $cm^{-1}$ (broad hydroxyl band).

2,2'-Dihydroxydesoxybenzoin, m. p. 102~103°C, readily prepared from above 2,2'-dihydroxybenzoin and from the unidentified substance, m. p. 156~157°C, by zinc-alkali reduction, was converted into 2'-hydroxyisoflavone (I), m. p. 153°C (Found: C, 75.67; H, 4.45. Calcd. for $C_{15}H_{10}O_3$: C, 75.62; H, 4.23%), I. R. bands at 1621 $cm^{-1}$ ($\gamma$-pyrone carbonyl) and 3187 $cm^{-1}$ (phenolic hydroxyl), with ethyl formate and sodium. No isomeric 3-benzoylcoumarone (VI) could be isolated from the reaction mixture. The isoflavone (I) was reduced to an amorphous stereoisomeric mixture of 2'-hydroxyisoflavan-4-ol (U. V. spectrum: $\lambda_{max}$(ethanol) 275 m$\mu$) by $NaBH_4$[7] or $LiAlH_4$.

The successful intramolecular dehydrocyclization of this amorphous diol by mild treatment in acidic medium, led to compound III, $R_1=R_2=R_3=R_4=H$, m. p. 125~126.5° (Found: C, 79.83; H, 5.49. Calcd. for $C_{15}H_{12}O_2$: C, 80.33; H, 5.39%) (U. V. spectrum; $\lambda_{max}$(ethanol) 278 m$\mu$($\varepsilon$; 3260). I. R. No band in the region 3000~3500 $cm^{-1}$), without any proof of stereochemical assignment of B/C ring junction.

On the other hand, catalytic hydrogenation of 2'-hydroxyisoflavone (I) in glacial acetic acid with Adams's platinum oxide as a catalyst, gave the corresponding 2'-hydroxyisoflavanone, m. p. 118~122°C. I. R. bands at 1660 $cm^{-1}$ (conjugated carbonyl) and 3297 $cm^{-1}$ (associated phenolic hydroxyl), which was converted into anhydro-compound V,[1] m. p. 80~83°, U. V. spectrum; $\lambda_{max}$(ethanol) 331, 299, 286, and 239 m$\mu$ ($\varepsilon$; 11190, 7350, 7240, and 11740), in a good yield by treatment in acidic medium.

The synthesis of homopterocarpin along the above synthetic line is now in progress.

Full details of this work will appear shortly.

The authors are grateful to Professors Toshi Irie, Takeshi Matsumoto and Tadashi Masamune for their interest and encouragement in this work.

*Department of Chemistry*
*Faculty of Science*
*Hokkaido University*
*Sapporo*

3) W. B. Whalley, *J. Chem. Soc.*, **1956**, 3224.
4) Also cf. R. Robinson, "The Structural Relations of Natural Products", Oxford Univ. Press, London (1955), p. 41.
5) F. B. Laforge, *J. Am. Chem. Soc.*, **55**, 3040 (1933). F. B. Laforge records b. p. 200~210°C/1 mmHg.
6) F. B. Laforge records m. p. 142~149°C. (Ref. 4).
7) M. Miyano and M. Matsui, *Chem. Ber.*, **91**, 2044 (1958).

# *Separation of Uranium and Protactinium from Thorium by Amine Extraction*

By Fujio ICHIKAWA and Shinobu URUNO

(Received September 18, 1959)

Preuss and Saunders[1] reported the extraction of uranium from sulfuric acid solution with amines. The use of primary amine as an extractant for thorium from sulfuric acid was reported by Crous and Denis[2]. Moore and his coworkers studied the liquid-liquid extraction of protactinium, niobium, tantalum, cobalt and zinc by amine[3-5].

In this paper, the extraction of thorium, protactinium and uranium from hydrochloric, nitric and sulfuric acid of various concentrations with secondary amine is studied. Amberlite LA-1 in kerosene diluent is used as an extractant.

The free-base form of Amberlite LA-1 removes acids from aqueous solutions by neutralization as illustrated by reaction 1,

$$(RR'NH)_{org}+H^{+}+A^{-}\rightleftarrows(RR'NH_2A)_{org} \quad (1)$$

where the ions, $H^+$ and $A^-$, refer to the aqueous phase and "org" refers to the amine salt dissolved in the organic solvent. When the amine salt formed through neutralization is brought into contact with an aqueous solution which contains another anion, the exchange of anions associated with the amine salt takes place as shown by reaction 2,

$$(RR'NH_2A)_{org}+B^{-}\rightleftarrows(RR'NH_2B)_{org}+A^{-} \quad (2)$$

where $A^-$ and $B^-$ represent two different anions.

When an element exists as a complex anion in an aqueous medium, it will be extracted by the amine according to this exchange process. Then it is of interest to compare the acid dependency of the extraction coefficient of an element by the amine with that of the distribution coefficient of the same element by the anion exchange resin. From the result of the extraction study, it is found that under the optimum conditions uranium, protactinium and thorium can be separated from each other. This separation procedure will be suitable for the recovery of uranium-233 from irradiated thorium blanket fuel. Consequently, the radiation damage of Amberlite LA-1 and LA-2 is studied by two methods.

## The Extraction Coefficient of Thorium, Protactinium and Uranium from Hydrochloric, Nitric and Sulfuric Acid of Various Concentrations by Amberlite LA-1

**Experimental.**—Two milliliters each of 5% Amberlite LA-1 in a kerosene diluent is shaken in a small glass-stopped tube for 1 min. with the same volume of an acid solution of the sample. After centrifuging, 1 ml. each of the aqueous and the organic phases are pipetted out and the concentration of the element is measured as follows. Thorium-234 ($UX_1$) and protactinium-233 are used as tracers for thorium and protactinium, and the $\gamma$-ray activity is measured with a well-type scintillation counter. Uranium nitrate is used as the starting material

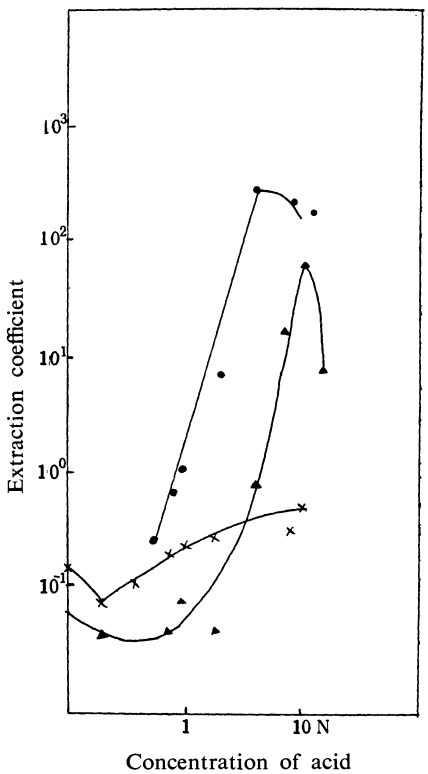



Fig. 1. Extraction coefficient of Th, Pa and U from HCl with Amberlite LA-1.
U —●—, Pa —▲—, Th —×—

1) A. Preuss and J. Saunders, RMO-2533 (1955).
2) D. J. Crous and J. O. Denis, ORNL-1859 (1955).
3) J. Y. Ellenburg, G. W. Leddicotte and F. L. Moore, *Anal. Chem.*, **26**, 1045 (1954).
4) H. A. Mahlman, G. W. Leddicotte and F. L. Moore, ibid., **26**, 1939 (1954).
5) F. L. Moore, ibid., **27**, 70 (1955).

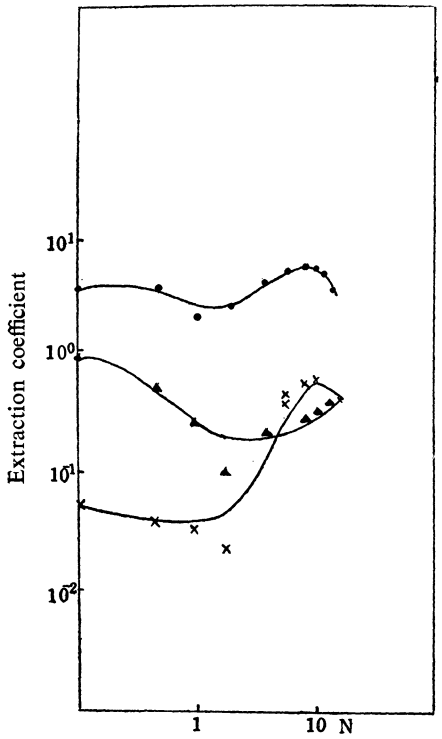



Fig. 2. Extraction coefficient of Th, Pa and U from $HNO_3$ with Amberlite LA-1.
U —●—, Pa —▲—, Th —×—

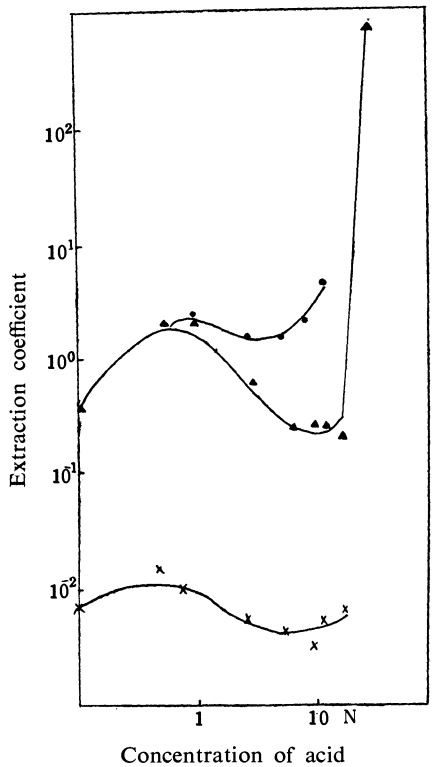



Fig. 3. Extraction coefficient of Th, Pa and U from $H_2SO_4$ with Amberlite LA-1.
U —●—, Pa —▲—, Th —×—

for extraction and its concentration is determined colorimetrically with hydrogen peroxide. The extraction coefficient is calculated by the following equation,

$$E = \frac{\text{Concentration of U, Th or Pa in organic phase/ml.}}{\text{Concentration of U, Th or Pa in aqueous phase/ml.}}$$

where $E$ is the extraction coefficient. The results are shown in Figs. 1—3.

**Results.**—The maximum extraction coefficient of uranium is about 200 at 6～12 N hydrochloric acid and below this concentration the extraction coefficient decreases with a slope of 3. From nitric acid solution, uranium is extractable in all the concentration ranges examined, giving an extraction coefficient of 2～5. The extraction coefficient of 1～3 is also found from 1～12 N sulfuric acid solution. Thorium is not extracted from these acids except 6～15 N nitric acid, but the extraction coefficient is only 0.5 even under this condition. Protactinium is favorably extracted from hydrochloric acid of higher concentration with a maximum extraction coefficient of 60. From nitric or sulfuric acid the extraction coefficient of protactinium is very low.

## Comparison of Extraction Coefficient with Distribution Coefficient

If the amine extraction is based on the anion exchange mechanism, it is valuable to compare the amine extraction curve with the acid dependency of the distribution coefficient of these elements by anion exchange resin. From this view-point, the distribution coefficient ($K$d) of thorium, protactinium and uranium between hydrochloric, nitric and sulfuric acids of various concentrations and anion exchange resin are measured by the following method.

**Experimental.**—Dowex 1 ×8 (100～200 mesh) is used as an anion exchange resin. It is treated with 10% sodium hydroxide solution, washed with water and then converted into the desired form with hydrochloric, nitric or sulfuric acid. Half a gram of dried resin is placed for 24 hr. in 5 ml. of the acid solution of thorium, protactinium or uranium. The solution is filtered and the concentration of 1 ml. of filtrate is compared with that of the reference solution which contains no resin. $K$d is calculated by the following equation,

$$K\text{d} = \frac{\text{C(1 g. of resin)}}{\text{C(1 ml. of solution)}} = \frac{\text{C(reference)} - \text{C(filtrate)}}{\text{C(filtrate)}} \times 10$$

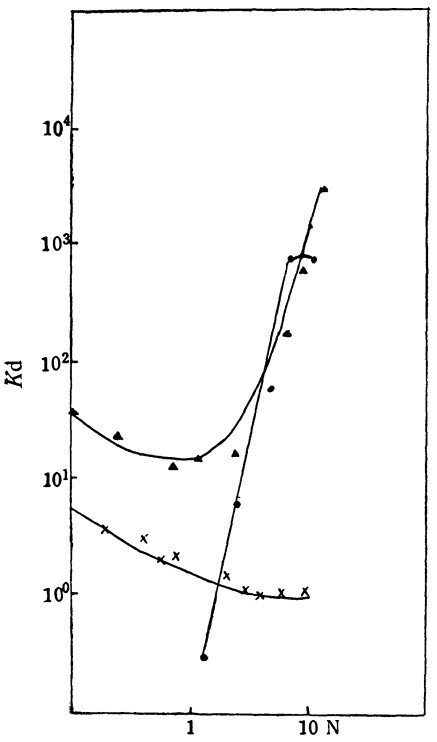



Fig. 4. Distribution coefficient of Th, Pa and U between Dowex 1 and HCl.
U —●—, Pa —▲—, Th —×—

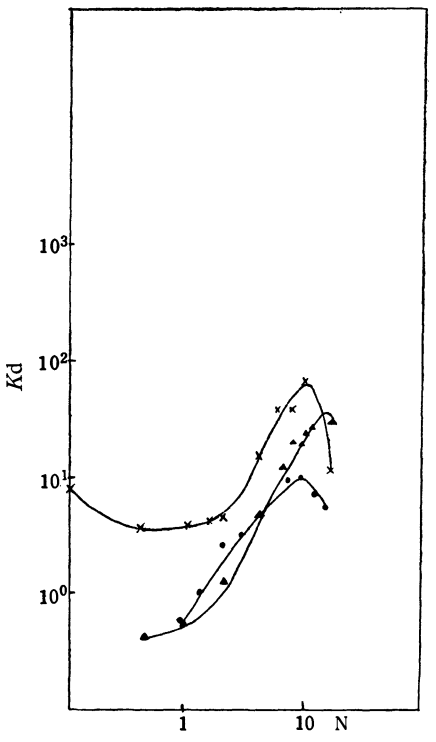



Fig. 5. Distribution coefficient of Th, Pa and U between Dowex 1 and $HNO_3$.
U —●—, Pa —▲—, Th —×—

where C means the concentration.

$UX_1$ and Pa-233 are used as tracers for thorium and protactinium, respectively. Their $\gamma$-ray activities are measured to determine the concentration. The concentration of uranium is determined by the colorimetric method.

**Results.**—The results are shown in Figs. 4—6. Concerning the anion exchange of these elements, some studies have already been reported by Kraus, Nelson and Danon[6,7]. In hydrochloric acid solution, the shapes of *K*d curves resemble those of extraction curves by LA-1, but the extraction coefficient of uranium is relatively very high. In a more concentrated nitric acid, Fig. 5 shows the order of adsorption as Th> Pa>U, but Fig. 2 shows the order of extraction as U>Th>Pa. In sulfuric acid, uranium is most favorably extractable with the amine, but Fig. 6 shows nearly the same *K*d value of uranium and protactinium.

These facts show that Amberlite LA-1 is selective in the extraction of uranium. It is not clear from these data whether or not this selectivity is due to the difference in the mechanism of amine extraction and anion exchange.

6) K. A. Kraus and F. Nelson, A/Conf. 8/P/837 (1955).
7) J. Danon, *J. Am. Chem. Soc.*, 78, 5935 (1956).

## The Separation of Uranium, Protactinium and Thorium by Amberlite LA-1

According to the study of the extraction coefficient, uranium and protactinium are sufficiently extracted from 8 N hydrochloric acid, but thorium is not extracted from hydrochloric acid of any concentration. At 3 N hydrochloric acid, the extraction coefficients are about 35, 0.1 and 0.05 for uranium, protactinium and thorium, respectively. From these facts, the separation of these elements is studied as follows.

**Experimental.**—*a) The separation of thorium and protactinium from 8N hydrochloric acid.*—Fifty milligrams of thorium nitrate is irradiated in the JRR-1 Reactor for 2 hr. at a flux of $10^{11}$ neutrons/$cm^2$/sec. The irradiated sample is dissolved in 2 ml. of 8 N hydrochloric acid and extracted with 5% Amberlite LA-1 (HCl form) in kerosene. The organic phase is scrubbed three times with 3 ml. each of 8 N hydrochloric acid, then stripped three times with 2 ml. each of 0.1 N hydrochloric acid. $\gamma$-Ray activity of about $3.8\times10^6$ c. p. m. of protactinium is collected in the stripping solution and thorium is not detected by thorin in this solution. The recovery of protactinium is about 80%.

*b) The effect of kerosene diluent on the extraction coefficient.*—The effect of kerosene diluent is tested

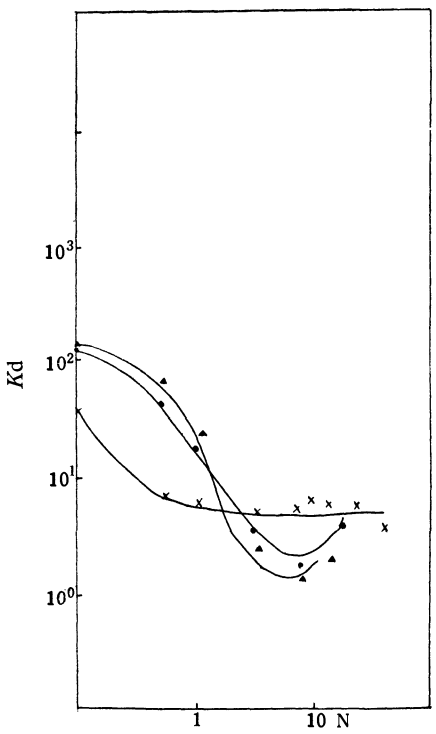



Fig. 6. Distribution coefficient of Th, Pa and U between Dowex 1 and $H_2SO_4$.
U —●—, Pa —▲—, Th —×—

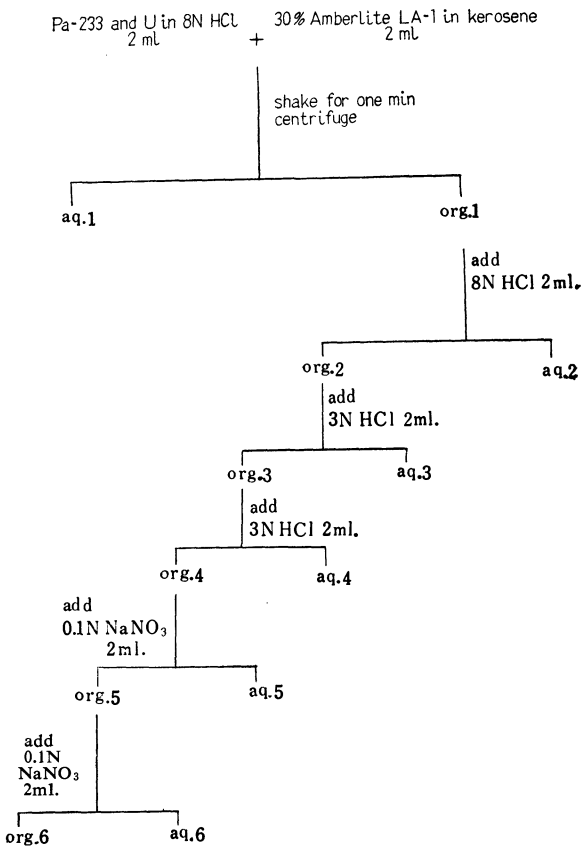



Fig. 7. Procedure of separating uranium and protactinium.

by calculating the extraction coefficient of protactinium from 8 N hydrochloric acid. From zero to 37.5% LA-1 in kerosene is used as an extractant. Two milliliters each of aqueous and organic phases are shaken for 1 min. and centrifuged. The extraction coefficient is determined as explained above. The results are shown in Table I. The effect of the diluent is negligible within the concentration of 2.5 to 37.5% LA-1 in kerosene.

TABLE I. THE EFFECT OF DILUENT TO THE EXTRACTION COEFFICIENT OF PROTACTINIUM FROM 8 N HCl

| The concentration of Amberlite LA-1 in kerosene | Extraction coefficient of Pa from 8 N HCl |
|---|---|
| 0 % | 0.05 |
| 0.5 | 27 |
| 2.5 | 194 |
| 5.0 | 150 |
| 7.5 | 158 |
| 12.5 | 256 |
| 17.0 | 143 |
| 37.5 | 197 |

*c) Stripping of uranium.*—About 10 mg. of uranium is extracted from 2 ml. of 8 N hydrochloric acid with 2 ml. of 30% Amberlite LA-1 in kerosene. Then, uranium is stripped from the organic phase with sodium nitrate, ammonium sulfate and sodium carbonate of various concentrations. The concentration of uranium in aqueous phase is measured colorimetrically with hydrogen peroxide. The results are shown in Table II.

Table II shows that uranium is completely stripped from the organic phase with 0.1 N sodium nitrate.

TABLE II. RECOVERY OF URANIUM FROM 30% AMBERLITE LA-1 IN KEROSENE

| Concentration of stripping agent | Distilled water | $NaNO_3$ | $(NH_4)_2SO_4$ | $Na_2CO_3$ |
|---|---|---|---|---|
| 0 N | 106% | — | — | — |
| 〃 | 119 | — | — | — |
| 〃 | 120 | — | — | — |
| 0.1 | — | 100 % | 88.4% | 82.0% |
| 〃 | — | 102 | — | — |
| 〃 | — | 105 | — | — |
| 0.5 | — | 94.0 | 89.4 | 75.0 |
| 1.0 | — | 89.8 | 54.3 | 94.0 |
| 2.0 | — | 80.5 | 60.5 | — |
| 4.0 | — | 54.6 | — | — |
| 5.0 | — | 30.5 | 54.3 | 87.6 |

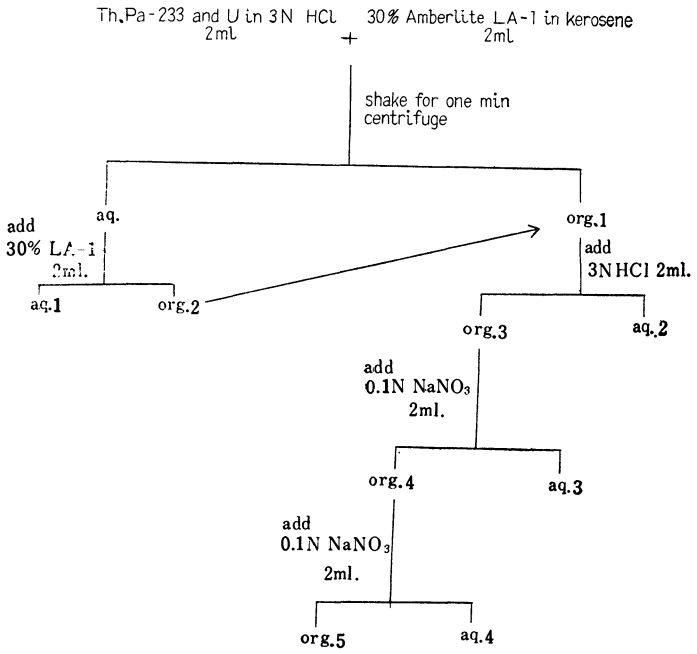



Fig. 8. Procedure of separating uranium from irradiated thorium.

Recovery with 0.1 N ammonium sulfate is 88.4%. The recovery of uranium decreases with the increase of the concentration of sodium nitrate or ammonium sulfate. Recovery with sodium carbonate is 75~94 %. When distilled water is used as a stripping agent, two phases do not separate even after centrifugation and colorimetric data show a higher value. Consequently, the best stripping agent is 0.1 N sodium nitrate.

*d) The separation of protactinium and uranium by 3N hydrochloric acid scrubbing.*—The separation scheme is shown in Fig. 7. Two milliliters of 8 N hydrochloric acid solution of protactinium-233 and uranium is shaken with 2 ml. of 30% Amberlite LA-1 in kerosene for 1 min. Most of the protactinium and uranium are extracted in this procedure. The organic phase is scrubbed with 2 ml. of 8 N hydrochloric acid, then protactinium is stripped twice with 3 N hydrochloric acid. Finally uranium is stripped twice with 0.1 N sodium nitrate. The results are shown in Table III. It is seen from these results that protactinium-233 is sufficiently extracted from 8 N hydrochloric acid and easily stripped with 3 N hydrochloric acid and that uranium is also sufficiently extracted from 8 N hydrochloric acid and about 40% of uranium is stripped with 3 N hydrochloric acid. Sixty per cent of the uranium is recovered with a slight contamination of protactinium-233 in this procedure. Thorium is not extracted under the condition explained above.

*e) The extraction of uranium from thorium and protactinium in 3N hydrochloric acid solution.*— About 50 mg. of thorium nitrate is irradiated in the J. R. R.-1 Reactor. After irradiation, 20 mg. of uranium is added to this sample and the mixture is dissolved in 2 ml. of 3 N hydrochloric acid. Two milliliters of Amberlite LA-1 in kerosene is added to this solution and the solution is shaken for 1 min. After centrifuging, the aqueous phase is re-extracted with 2 ml. of 30% LA-1 solution. Two organic phases are scrubbed with 2 ml. of 3 N hydrochloric acid. Uranium is stripped twice with 2 ml. each of 0.1 N sodium nitrate. The activity of protactinium-233 is measured by $\gamma$-ray counting. The Recovery of uranium is determined by the colorimetric method. Fig. 8 shows the separation scheme. Results are shown in Table IV.

TABLE III. RECOVERY* OF PROTACTINIUM AND URANIUM

| Sample No. | Medium | Recovery of Pa-233 | Recovery of U |
|---|---|---|---|
| aq. 1+aq. 2 | 8 N HCl | 1.3% | 8.4% |
| aq. 3+aq. 4 | 3 N HCl | 98.0 | 35.7 |
| aq. 5+aq. 6 | 0.1 N $NaNO_3$ | 0.3 | 70.0 |
| org. 6 | 30% Amberlite LA-1 in kerosene | 0.4 | — |

* This ratio is calculated by two experiments.

Table IV. RECOVERY* OF PROTACTINIUM AND URANIUM

| Sample No. | Medium | Recovery of Pa-233 | Recovery of U |
|---|---|---|---|
| aq. 1+aq. 2 | 3 N HCl | 98.5% | 0% |
| aq. 3+aq. 4 | 0.1 N $NaNO_3$ | 0.5 | 100 |
| Org. 5 | 30% Amberlite LA-1 in kerosene | 0.7 | — |

* This ratio is calculated by two experiments.

TABLE V. RADIATION DAMAGE OF AMBERLITE LA-1 AND LA-2

| Sample No. | Amine | Distance from Co-60 | Dose rate | Irradiation time | Total dose | Exchange capacity | Extraction coefficient of Pa from 8 N HCl |
|---|---|---|---|---|---|---|---|
| | | cm. | $r$/hr. | hr. min. | $r$ | meq./ml. | |
| 1 | Amberlite LA-1 | 12.5 | $5.6\times10^5$ | 89 20 | $5\times10^7$ | 2.03 | 130 |
| 2 | 〃 | 〃 | 〃 | 17 50 | $1\times10^7$ | 2.03 | 125 |
| 3 | 〃 | 10 | $8.1\times10^5$ | 6 16 | $5\times10^6$ | 2.03 | 134 |
| 4 | 〃 | 〃 | 〃 | 1 15 | $1\times10^6$ | 2.03 | 124 |
| 5 | 〃 | 15 | $4.2\times10^5$ | 1 12 | $5\times10^5$ | 2.01 | 122 |
| 6 | 〃 | 30 | $1.3\times10^5$ | 48 | $1\times10^5$ | 2.01 | 152 |
| 7 | 〃 | 50 | $4.4\times10^4$ | 1 08 | $5\times10^4$ | 2.01 | 173 |
| 8 | 〃 | — | 0 | 0 | 0 | 2.03 | 183 |
| 9 | Amberlite LA-2 | 12.5 | $5.6\times10^5$ | 89 20 | $5\times10^7$ | 2.03 | 83 |
| 10 | 〃 | 〃 | 〃 | 17 50 | $1\times10^7$ | 2.03 | 92 |
| 11 | 〃 | 10 | $8.1\times10^5$ | 6 16 | $5\times10^6$ | 2.03 | 110 |
| 12 | 〃 | 〃 | 〃 | 1 15 | $1\times10^6$ | 2.03 | 87 |
| 13 | 〃 | 15 | $4.2\times10^5$ | 1 12 | $5\times10^5$ | 2.01 | 86 |
| 14 | 〃 | 30 | $1.3\times10^5$ | 48 | $1\times10^5$ | 2.01 | 86 |
| 15 | 〃 | 50 | $4.4\times10^4$ | 1 08 | $5\times10^4$ | 2.03 | 87 |
| 16 | 〃 | — | 0 | 0 | 0 | 2.03 | 85 |

Uranium is completely recovered from the first solution by this procedure.

### Radiation Damage of Amberlite LA-1 and LA-2

If these amines are used in reactor fuel reprocessing, radiation damage may occur on the action of high level $\gamma$-rays. Amberlite LA-1 and LA-2 are irradiated by $\gamma$-rays from Co-60 under various conditions (Table V). The degree of radiation damage is measured by extraction of protactinium-233 from 8 N hydrochloric acid and by potentiometric titration in dioxane. Two milliliters of irradiated sample is dissolved in 50 ml. of dioxane and is titrated with 0.2 N perchloric acid in dioxane. The end point is determined by drawing the potentiometric titration curve. A pH meter is used as a potentiometer. A calomel electrode, of which the aqueous solution of potassium chloride is displaced by saturated methanol solution of potassium chloride[8], is used as a reference electrode. A platinum electrode is used as an indicating electrode. The typical titration curve is shown in Fig. 9. The results are shown in Table V. Another method is to measure the extraction coefficient of protactinium-233 from 8 N hydrochloric acid by 30% irradiated amine in kerosene. The extraction coefficient is determined as mentioned above. Results are also shown in Table V. The radiation damage of Amberlite LA-1 and LA-2 is negligible under these conditions (dose rate is $8.1\times10^5$ $r$/h, maximum total dose is $5\times10^7$ $r$).

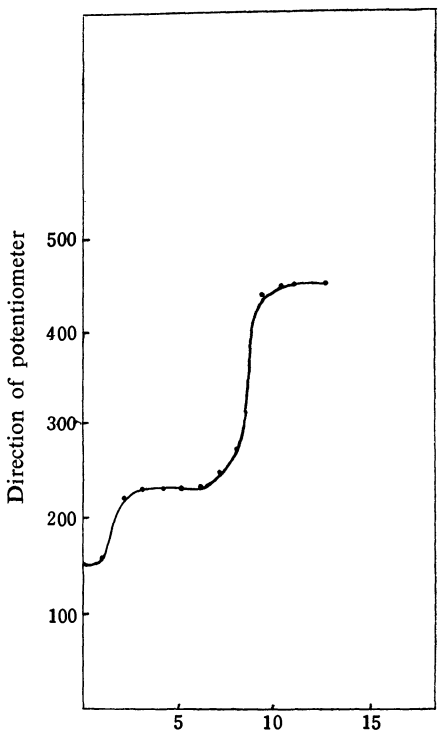



Fig. 9. Typical titration curve of Amberlite LA-1.

### Summary

Uranium, protactinium and thorium are satisfactorily separated from each other by secondary amine extraction. Amberlite LA-1 in kerosene diluent is used as the extractant. Separation from hydrochloric acid solution is superior to that from systems using other acids. The acid

8) J. S. Fritz, A. U. Moye and M. J. Richard, *Anal. Chem.*, **29**, 1685 (1957).

dependency of the extraction coefficient by amine fairly resembles that of the distribution coefficient by anion exchange resin, but the former has a selectivity for uranium. Under the total dose of $5\times10^7$ *r*., the radiation damage of Amberlite LA-1 is negligibly small. From these results, it is evident that there is a possibility of applying the amine extraction to the recovery of uranium-233 from reactor blanket fuel.

The authors wish to express sincere thanks to Dr. Toshio Nakai for his guidance.

*Japan Atomic Energy Research Institute*
*Tokai, Ibaraki-ken*

# *Studies on Seven-Membered Heterocyclic Compounds Containing Nitrogen. III. Reactions of 5-Benzyl-1-oxa-5-azaspiro(5, 2)octane*

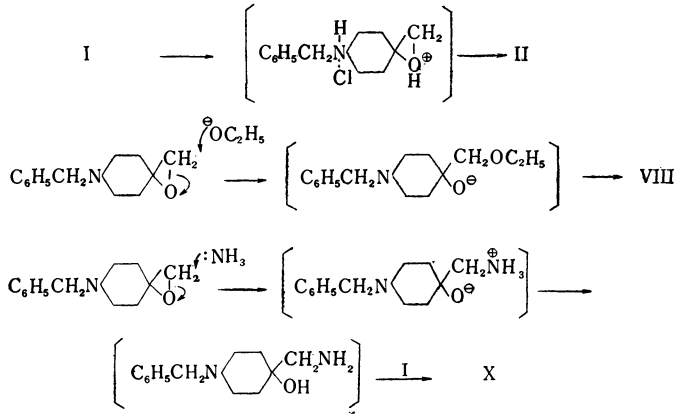
By Shiro MOROSAWA

(Received October 29, 1959)

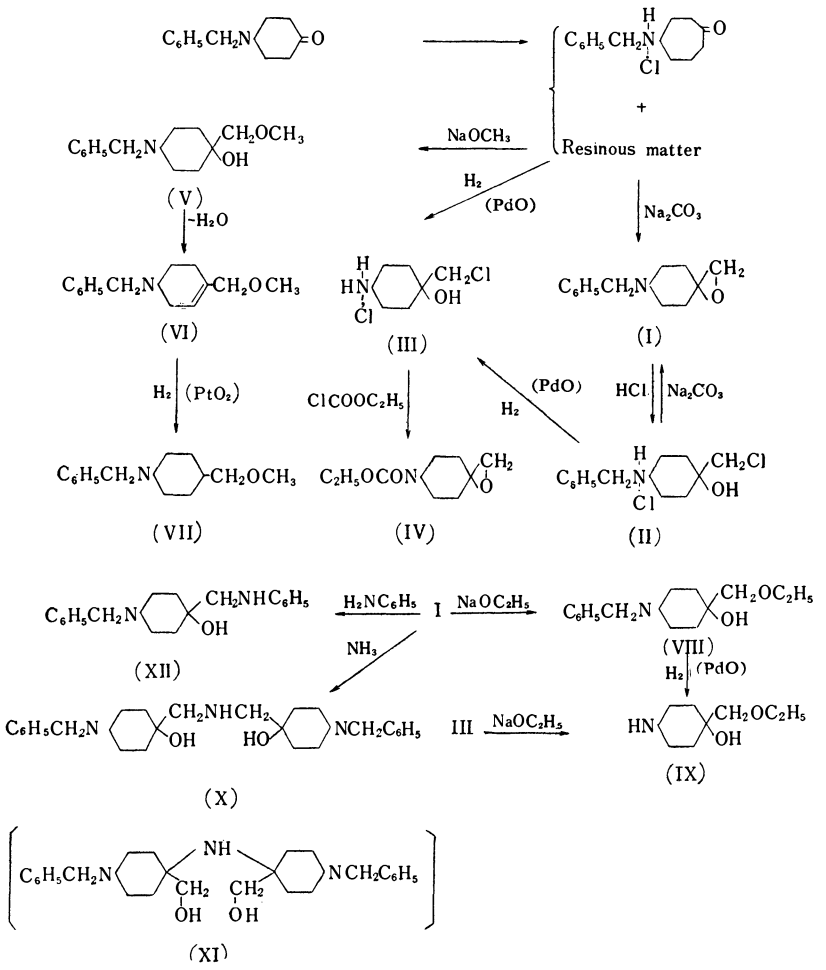
Previously[1] the author reported that 1-benzyl-1-azacycloheptan-4-one was obtained from 1-benzyl-1-azacyclohexan-4-one by ring enlargement and recrystallization as a hydrochloride, followed by the addition of alkali. The present study was undertaken in order to investigate an acidic resinous matter left in a considerable amount on evaporation of mother liquor of the recrystallization, and an epoxy compound was found out. Behaviors of the epoxy group to acid and base were examined.

After treatment of the resinous matter with alkaline water while hot, extraction with benzene yielded an oil, boiling at 119~121°C/0.45 mmHg (I). Infrared absorption spectrum showed that the oil was contaminated with a little ketonic substance even after several recrystallizations as a hydrochloride (II) and liberation by alkali. The oil afforded a sulfonic acid derivative[2] with sodium bisulfite, while 1-benzyl-1-azacycloheptan-4-one a normal addition product. The oil, if necessary, was further treated with 2, 4-dinitrophenylhydrazine and chromatographed on alumina, decolorizing carbon and magnesium sulfate[3]. The infrared absorption spectrum of the purified oil indicated characteristic two bands at 790 $cm^{-1}$ and 895 $cm^{-1}$, which is presumably ascribed to the epoxy group. These two bands disappeared in the infrared absorption spectrum of such compounds derived by opening the epoxy group of I as VIII, X and XII. Judging from the nitrogen analysis and the infrared absorption spectrum, the purified oil, b. p. 114°C/0.43 mmHg, was considered as an epoxy compound, 5-benzyl-1-oxa-5-azaspiro(5, 2)octane, being isomeric with 1-benzyl-1-azacycloheptan-4-one[1].

Reduction of both the resinous matter and



1) S. Morosawa, This Bulletin, **31**, 418 (1958).
2) W. M. Lauer and A. Hill, *J. Am. Chem. Soc.*, **58**, 1873 (1936).
3) R. P. Linstead, J. A. Elvidge and M. Whalley, "A Course in Modern Techniques of Organic Chemistry", Butterworths Scientific Publications, London, (1955), p. 6.




II in the presence of palladous oxide produced an identical substance, m. p. 183~184°C, which was assumed to be III. III afforded a picrolonate, m. p. 228~229°C (decomp.). III and ethyl chlorocarbonate in alkali medium gave an *N*-carbethoxy epoxy compound, b. p. 94~95°C/1 mmHg (IV). The resinous matter and sodium methoxide in absolute methanol gave an oil, b. p. 146~147°C/1 mmHg (V), which was readily dehydrated to an ethylenic compound, b. p. 126°C/0.5 mmHg (VI). VI was then reduced in the presence of platinum oxide to a saturated compound, b. p. 118~120°C/4.5 mmHg (VII). In the formations of II, III and V isomeric abnormal products[4] were not detected.

In view of these facts, it was clear that II was not a primary hydroxy type but a tertiary one, and that the epoxy group of I was opened, when made acidic, and thus I might exist in the resinous matter in the form of II. Ring opening of the epoxide group by the addition of hydrogen chloride was probably due to the normal way.

I and sodium ethoxide in absolute ethanol gave an oil, b. p. 143~144°C/5 mmHg (VIII), which on reduction in the presence of palladous oxide yielded an oil, b. p. 92~93°C/7.5 mmHg (IX). On the one hand, III also gave an oil, b. p. 94°C/7.5 mmHg by the action of sodium ethoxide, which was assumed to accord with IX. This was confirmed by mixed fusion of their picrolonates. It seemed reasonable, therefore, to assume that the addition of ethanol to the epoxy group would proceed as shown below. That the ethoxide anion attacked the methylene carbon and not the spiro carbon is probably due to the steric effect.

I and ammonia in ethanolic solution yielded a crystal, m. p. 142.5°C. Among possible structures corresponding to the crystal, formula X was most probable and the other, for instance XI, could not be constructed in practice into the molecular model owing to the steric interference. The reaction might proceed in the manner like above.

4) R. E. Parker and N. S. Isaacs, *Chem. Revs.*, **59**, 737 (1959).

I and aniline gave a yellow oil, b. p. 202~203°C/0.2 mmHg (m. p. 79.5°C) (XII). This additional reaction also appeared to be the same as in the case of ammonia.

The infrared absorption spectra of VIII, X and XII exhibited characteristic peaks of the tertiary νOH at 1115 $cm^{-1}$ [5].

## Experimental

**5-Benzyl-1-oxa-5-azaspiro(5, 2)octane (I).**—A mixture of 52 g. of the resinous matter, 100 g. of sodium carbonate and 100 cc. of water was stirred for 5 hr. under heating at 70°C. An oily liberated substance was taken up in benzene and dried over potassium carbonate. Evaporation of benzene and rapid vacuum distillation in three batches gave 23 g. of crude epoxide, a colorless oil, b.p. 119~121°C/0.45 mmHg, and when not, much of the substance remained undistilled. (Found: N, 6.99%).

A mixture of 3 g. of the crude epoxide and an excessive saturated solution of sodium bisulfite was shaken vigorously for a short time. Crystals formed were filtered and recrystallized from dilute ethanol to yield 2.3 g. of colorless hexagonal prisms, m. p. 251.5°C (decomp.). It was very soluble in water and did not liberate any oil with acid or alkali.

Found: N, 4.36. Calcd. for $C_{13}H_{17}ON \cdot NaHSO_3$: N, 4.56%.

On the contrary, 1-benzyl-1-azacycloheptan-4-one gave a normal addition product, m.p. 155°C (decomp.). (Found: N, 4.40%).

A mixture of 2.7 g. of the crude epoxide, 0.8 g. of 2, 4-dinitrophenylhydrazine, 0.5 cc. of concentrated hydrochloric acid and 30 cc. of ethanol was boiled on a water bath for two minutes and let stand overnight. Crystals formed were filtered and washed with a little amount of ethanol. The ethanolic solution was passed through Amberlite IRA-400 to remove the hydrochloric acid and evaporated to dryness under reduced pressure. The residual oil was chromatographed on a column packed (from top) with alumina, decolorizing carbon and magnesium sulfate[3] and eluted with dry benzene. The eluate was evaporated and vacuum distillation of the residue yielded 1.7 g. of a colorless oil, b. p. 114°C/0.43 mmHg. Infrared absorption spectrum of the oil showed no carbonyl band.

Found: N, 7.02. Calcd. for $C_{13}H_{17}ON$: N, 6.89%.

**1-Benzyl-4-chloromethyl-4-hydroxy-1-azacyclohexane Hydrochloride (II).**—Through a solution of the crude epoxide in absolute ether was passed dry hydrogen chloride to precipitate a white amorphous hydrochloride. Ether was decanted and the hydrochloride was recrystallized from methanol and ether to give a white crystalline powder. Because of its highly hygroscopic property, it could not be analyzed, but was assumed to be 1-benzyl-4-chloromethyl-4-hydroxy-1-azacyclohexane hydrochloride from the experiment described later. Treatment of the powder with alkaline water as above reformed the epoxide, but not pure.

5) 1-Methylcyclohexane-1-ol gives the peak of the tertiary νOH at 1117 $cm^{-1}$. H. H. Zeiss and M. Tsutsui, *J. Am. Chem. Soc.*, 75, 897 (1953).

**4-Chloromethyl-4-hydroxy-1-azacyclohexane Hydrochloride (III).**—(a) A solution of 5 g. of the acidic resinous matter in 70 cc. of water was reduced under normal temperature and pressure with 0.2 g. of palladous oxide as a catalyst until the theoretical amount of hydrogen had been absorbed. The catalyst was filtered off, and evaporation of water under reduced pressure left light yellow crystals, which were recrystallized from methanol and ether to yield 2 g. of colorless prisms, m. p. 183~184°C.

Found: C, 38.97; H, 7.13; N, 7.52. Calcd. for $C_6H_{13}ONCl_2$: C, 38.73; H, 7.04; N, 7.53%.

III formed a *picrolonate* by heating with a saturated ethanolic solution of picrolonic acid, which was recrystallized from ethanol to give yellow micro prisms, m. p. 228~229°C (decomp.).

Found: N, 15.61. Calcd. for $C_{16}H_{21}O_6N_5Cl_2$: N, 15.55%.

(b) A solution of 10 g. of II in 200 cc. of water was shaken in the hydrogen atmosphere with heating in the presence of 0.2 g. of palladous oxide as a catalyst until the theoretical amount of hydrogen had been absorbed. Light yellow needles were obtained after separation of the catalyst by filtration, followed by evaporation of water. The needles were recrystallized five times from methanol to give 2 g. of colorless prisms, m. p. 183.5~184°C in 30.7% yield, and this did not depress the melting point on admixture with the colorless prisms described above. (Found: N, 7.16%).

A *picrolonate* which derived from the prisms was also not depressed by mixing with the picrolonate mentioned above, m. p. and mixed m. p. 229°C (decomp.). (Found: N, 15.73%).

**5-Carbethoxy-1-oxa-5-azaspiro(5, 2)octane (IV).**—To a solution of 2 g. of III in 10 cc. of water, under stirring and cooling at below 5°C, a solution of 1.3 g. of ethyl chlorocarbonate in 10 cc. of ether and 5 cc. of 30% sodium hydroxide solution were gradually added during 1.5 hr., at such a rate that the two solutions were added simultaneously. After stirring for 15 min. the water layer was separated and extracted three times with a portion of 30 cc. ether each. Combined ethereal solution was dried over potassium carbonate. After evaporation of ether, the vacuum distillation gave 1.4 g. of a colorless oil, b. p. 94~95°C/1 mmHg in 58% yield.

Found: N, 7.29. Calcd. for $C_9H_{15}O_3N$: N, 7.56%.

**1-Benzyl-4-methoxymethyl-4-hydroxy-1-azacyclohexane (V).**—A solution of 14 g. of the resinous matter in 40 cc. of absolute methanol was mixed with a solution of 7 g. of sodium dissolved in 100 cc. of absolute methanol. The resultant mixture was boiled under reflux for 8 hr. After that, 5 cc. of water was added and filtered from the sodium chloride present. The sodium chloride was washed with methanol. Combined methanolic solution was evaporated to leave an oily substance, which was taken up in ether, washed twice with a 10% solution of potassium carbonate and dried over potassium carbonate. Ether was removed and the residual oil was distilled in vacuo to give 7.8 g. of a colorless oil, b. p. 146~147°C/1 mmHg.

Found: N, 5.94. Calcd. for $C_{14}H_{21}O_2N$: N, 5.95%.

**1-Benzyl-4-methoxymethyl-1-azacyclohex-3-ene (VI).**—A mixture of 4.3 g. of V and 6.1 g. of β-naphthalenesulfonic acid was heated for 15 min. on a water bath under reduced pressure (water pump), and then for 1 hr. at 170°C. After cooling, 100 cc. of 10% sodium hydroxide solution was added, extracted in ether and dried over potassium carbonate. Ether was expelled and the vacuum distillation yielded 2.2 g. of a colorless oil, b. p. 126°C/0.5 mmHg. in 56.7% yield, which on standing turned pink immediately.

Found: C, 76.75; H, 8.62; N, 6.55. Calcd. for $C_{14}H_{19}ON$: C, 77.38; H, 8.81; N, 6.45%.

**1-Benzyl-4-methoxymethyl-1-azacyclohexane (VII).**—A solution of 1.1 g. of freshly distilled VI in 50 cc. of methanol containing 0.6 cc. of concentrated hydrochloric acid was reduced in the presence of platinum oxide as a catalyst and the theoretical amount of hydrogen was consumed. After removal of the catalyst by filtration, methanol was distilled off and the residue was made alkaline. Oil thereby liberated was taken up in ether and dried over potassium carbonate. The ether was removed to leave an oil, which on vacuum distillation gave 0.25 g. of a colorless, fluid oil, b. p. 118~120°C/4.5 mmHg.

Found: C, 76.23; H, 9.94; N, 6.31. Calcd. for $C_{14}H_{21}ON$: C, 76.67; H, 9.65; N, 6.39%.

**1-Benzyl-4-ethoxymethyl-4-hydroxy-1-azacyclohexane (VIII).**—A solution of 4 g. of I in 10 cc. of absolute ethanol was mixed with a separately prepared solution of 1.5 g. of sodium in 30 cc. of absolute ethanol and the whole was boiled under reflux for 8 hr. After cooling, 2 cc. of water was added and evaporated under reduced pressure to leave an oil, which was taken up in ether, washed twice with a dilute potassium carbonate solution and dried over potassium carbonate. Oil left on evaporation of ether was distilled in vacuo to yield a colorless oil boiling at 128~136°C/0.5 mmHg, which was redistilled to give 2.5 g. of the oil, b. p. 143~144°C/5 mmHg, in 50.3% yield.

Found: N, 5.77. Calcd. for $C_{15}H_{23}O_2N$: N, 5.62%.

**4-Ethoxymethyl-4-hydroxy-1-azacyclohexane (IX).**—(a) A solution of 2.5 g. of VIII in 50 cc. of water containing 1 cc. of concentrated hydrochloric acid was reduced with heating and in the presence of 0.1 g. of palladous oxide as a catalyst until the theoretical amount of hydrogen had been absorbed. After separation of the catalyst by filtration, a residue left on evaporation of water was dissolved in 10 cc. of water and neutralized with potassium carbonate. A further addition of 2 g. of sodium hydroxide liberated an oil, which was extracted in ether and dried over potassium carbonate. Evaporation of ether and distillation in vacuo gave 0.5 g. of an oil, b. p. 92~93°C/7.5 mmHg in 31% yield.

Found: N, 8.77. Calcd. for $C_8H_{17}O_2N$: N, 8.82%.

IX formed a *picrolonate*, m. p. 209°C (decomp.), which was recrystallized twice from ethanol to yield yellow micro prisms, m. p. 216~217°C (decomp.).

Found: N, 16.31. Calcd. for $C_{18}H_{25}O_7N_5$: N, 16.54%.

(b) A solution of 1 g. of III in 5 cc. of absolute ethanol was mixed with a separately prepared solution of 1 g. of sodium dissolved in 15 cc. of absolute ethanol and the whole was boiled under reflux for 8 hr. After cooling, 2 cc. of water was added and filtered from any solid, which was washed with ethanol. A tan oily substance left on evaporation of ethanol was treated as before to give 0.5 g. of an oil, b. p. 94°C/7.5 mmHg (Found: N, 8.73%).

A *picrolonate* of the oil, m. p. 216~217°C (decomp.) was not depressed on admixture with that described before. (Found: N, 16.37%).

**4-Anilinomethyl-1-benzyl-4-hydroxy-1-azacyclohexane (XII).**—A mixture of 4.2 g. of I and 3.3 g. of freshly distilled aniline was boiled under reflux for 1.5 hr. Excessive aniline was removed under reduced pressure to leave a colored residue. Vacuum distillation of the residue gave 3.7 g. of a light yellow viscous oil boiling at 202~203°C/0.2 mmHg in a 60.5% yield. The oil gradually crystallized on standing and was recrystallized from cyclohexane and benzene in light creamy plates, m. p. 79.5°C.

Found: C, 76.70; H, 8.29; N, 9.44. Calcd. for $C_{19}H_{24}ON_2$: C, 76.99; H, 8.16; N, 9.45%.

XII afforded a *picrate*, m. p. 177.5°C (from ethanol).

Found: N, 14.55. Calcd. for $C_{19}H_{24}ON_2 \cdot (C_6H_3O_7N_3)_2$: N, 14.85%.

**Bis-(4-benzyl-1-hydroxy-4-azacyclohexylmethyl)-amine (X).**—A solution of 2 g. of I in 10 cc. of 99% ethanol was saturated with ammonia at 0°C and let stand for a week at room temperature. An ether insoluble substance left on evaporation of ethanol was recrystallized from dilute ethanol after treating with decolorizing carbon to give 0.6 g. of colorless scales, m. p. 142.5°C in a 30% yield.

Found: C, 73.50; H, 8.96; N, 9.99. Calcd. for $C_{26}H_{37}O_2N_3$: C, 73.72; H, 8.80; N, 9.92%.

Both *picrate*, m. p. 225°C (decomp.) and *picrolonate*, m. p. 247°C (decomp.) were insoluble and difficult to recrystallize from any common solvent.

The author wishes to thank Professor A. Yokoo (this laboratory) for his helpful advice. Thanks are also due to Mr. A. Kondo (The Department of Organic Chemistry of Tokyo Institute of Technology) for carrying out the carbon and hydrogen micro analyses.

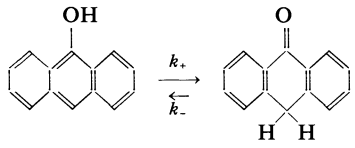
*Chemical Institute*
*Faculty of Science*
*Okayama University*
*Tsushima, Okayama*

# *Kinetic Study on Isomerization of Anthranol to Anthrone*

By Yoshié BANSHO and Kenkichi NUKADA

(Received October 13, 1959)

Only a few studies concerning the physical and chemical properties of anthranol have been reported in literature. K. H. Meyer[1] found in 1911 that in organic solvents anthranol turns to anthrone and after a long time a chemical equilibrium between these substances is established. Bäckström et al.[2] pointed out an iodine titration method for the analysis of anthranol. Le Fèvre et al.[3] investigated the dielectrical properties of the same substance, but its purity was not satisfactory enough to determine the dielectric constant of the solutions.




Anthranol Anthrone

The authors have established the best condition for the preparation of anthranol and measured the dipole moments in several organic solvents[4].

In this paper, the authors present the methods of measuring the velocity constants of the isomerization of anthranol to anthrone by the analytical and dielectrical techniques and the calculated values of the activation energies of the reaction.

## Experimental

**Preparation of Anthranol.** — Improving the original procedures of Meyer[1] and Bäckström et al.[2], the authors have established the best method of preparation of pure anthranol and reported the findings in this Bulletin[4].

**Measurements of Velocity Constants of the Isomerization by Iodometry.**—Bäckström et al. determined the purity of anthranol by iodometric analysis. This suggests that the method may also be used for the measurement of isomerization velocity, because one mole of anthranol reacts exactly with one mole of iodine in some solvents, while anthrone does not react with iodine at all. It has been found that methanol and ethanol were suitable solvents for the measurement of isomerization velocity.

In a stream of nitrogen, 1.0 g. of freshly prepared anthranol was dissolved into 200 cc. of solvent keeping the temperature constant. After appropriate time, 10 cc. of the solution was poured into 5 cc. of 0.1 N iodine-potassium iodide aqueous solution. After a few minutes the remaining iodine was titrated with 0.1 N sodium thiosulfate solution, and thus the content of anthranol in the solution was obtained directly. These operations were repeated until an equilibrium of the reaction was attained.

**Dielectrical Measurement.**—The authors have already measured the apparent dipole moments of anthranol in several organic solvents at 6 and 15°C[4]. At these temperatures, isomerization velocities are so small that anthranol in solvents safely remains unchanged during the measurements.

When the temperature is raised, the reaction velocity of isomerization becomes greater and it becomes impossible to get the real value of dipole moment of anthranol. A kinetic study of isomerization, on the other hand, becomes possible even at elevated temperatures.

Dielectric constants of solutions (in benzene and toluene) at several temperatures were measured several times until they reached maximum values. Although it is necessary also to measure the densities of solutions at every time of measurements of dielectric constants, this procedure is very troublesome. Hence, in this paper, it was assumed that the density of solutions remained constant during the reaction.

## Results and Discussion

**Iodometry.**—First of all, it was assumed that the reaction is reversible and of the first order, so that

$$\frac{dx}{dt}=k_+(a_0-x)-k_-(a_0'+x) \qquad (1)$$

where $x$ is the amount of changed anthranol at the time $t$, $a_0$ and $a_0'$ are the initial amounts of anthranol and anthrone expressed in molar fraction, and $k_+$ and $k_-$ are the velocity constants of normal and reverse reactions, respectively. As the purity of the anthranol was about 98%,

$$a_0 \fallingdotseq 1 \quad \text{and} \quad a_0' \fallingdotseq 0$$

and then

$$K=\frac{k_+}{k_-} \fallingdotseq \frac{a_\infty}{1-a_\infty} \qquad (2)$$

where $K$ is the equilibrium constant and $a_\infty$ is the value of $x$ at the equilibrium ($dx/dt=0$).

1) K. H. Meyer, *Ann.*, **379**, 37 (1911).
2) H. Bäckström and H. Beatty, *J. Phys. Chem.*, **35**, 2549 (1930).
3) C. L. Angyl and R. J. W. Le Fèvre, *J. Chem. Soc.*, **1950**, 562.
4) K. Nukada and Y. Bansho, This Bulletin, **26**, 454 (1953).

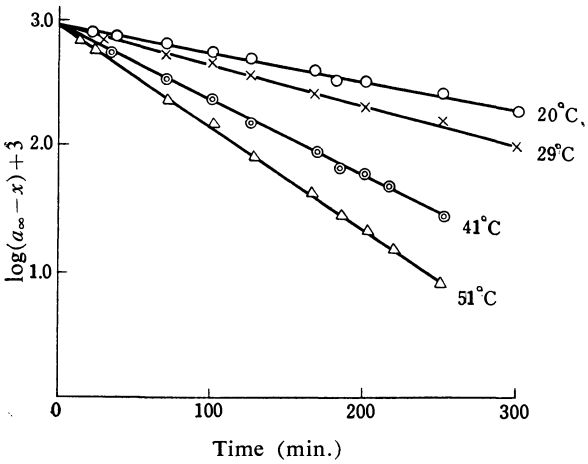



Fig. 1. Kinetics in methanol by iodometry.

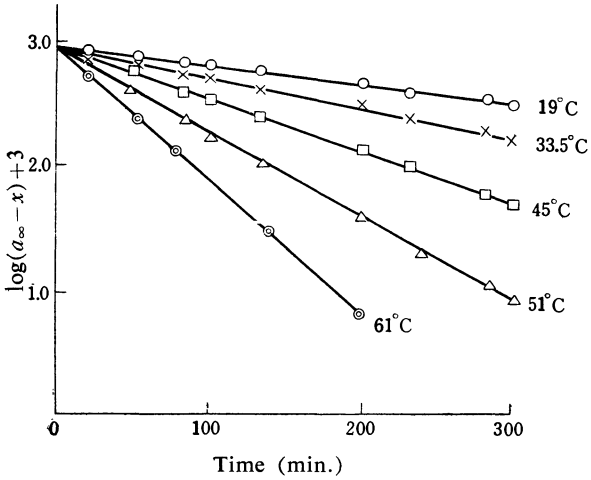



Fig. 2. Kinetics in ethanol by iodometry.

Table I. The velocity constants of isomerization

| Temp., °C | In methanol $k_+$ | In ethanol $k_+$ |
|---|---|---|
| 20 | 0.0050 | 0.0032 |
| 29 | 0.0063 | |
| 36 | | 0.0050 |
| 41 | 0.0125 | 0.0059 |
| 45 | 0.0137 | 0.0079 |
| 51 | 0.0165 | 0.0149 |
| 61 | 0.0256 | 0.0211 |

From Eqs. 1 and 2, the next equation is obtained.

$$k_+ + k_- = 1/t \ln [a_\infty/(a_\infty - x)] \quad (3)$$

From Eqs. 2 and 3, the value of $k_+$ can be obtained. In Figs. 1 and 2, $\log(a_\infty - x)$ are plotted against $t$ at between 20~60°C in methanol and ethanol solutions, respectively. Since rectilinear relationships between $\log(a_\infty - x)$ and $t$ were observed, it is reasonable to assume that the reaction of isomerization is of the first order. The calculated values of $k_+$ are shown in Table I.

According to Arrhenius' equation, the authors plotted the values of $\log k_+$ against the reciprocal of absolute temperature $(1/T)$ as shown in Fig. 3 and calculated the activation energies of the isomerizations of anthranol in methanol and ethanol. Anthranol isomerizes faster in methanol than in ethanol and the obtained values of activation energies are 5.8 and 12.4 kcal./mol. in methanol and ethanol, respectively. This might be due to the fact that ethanol is stronger in basisity than methanol.

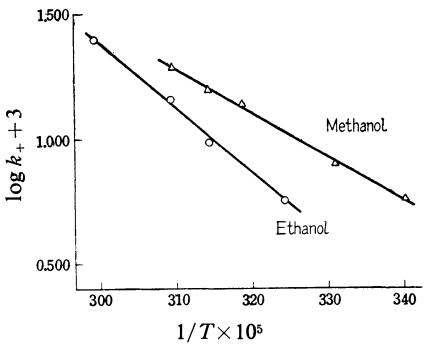



Fig. 3. Measurements of activation energies by iodometry.

The times required for the complete disappearance of fluorescence in diluted anthranol solutions were ca. 50 and 6.5 hr. in ethanol and methanol, respectively[4]. These times are supposed to depend upon the velocities of isomerization.

**Dielectrical Measurement.**—The only measurable quantity with dielectrical measurement is the time dependency of the dielectric constant of solutions at various temperatures. In order to obtain the velocity constants from these measurable quantities, some assumptions are made.

First of all, it was assumed that

$$p_{12}(t) = (1-y)p_1 + yp_2(t) \quad (4)$$

where $p_{12}(t)$, $p_1$ and $p_2(t)$ are the specific molecular polarizations of solution, solvent and solute, respectively, and $y$ is the weight fraction, of solute. The molecular polarization of solute $P_2(t)$ is obtained by substituting the following Eqs. 5—7 into Eq. 4.

$$p_{12}(t) = 1/d_{12} \times (\varepsilon_{12}(t) - 1)/(\varepsilon_{12}(t) + 2) \quad (5)$$

$$p_1 = 1/d_1 \times (\varepsilon_1 - 1)/(\varepsilon_1 + 2) \quad (6)$$

$$p_2 = P_2(t)/M \quad (7)$$

where $\varepsilon_{12}(t)$, $\varepsilon_1$ and $d_{12}$, $d_1$ are dielectric constants and densities of solution and solvent, respectively, and $M$ is a molecular weight of

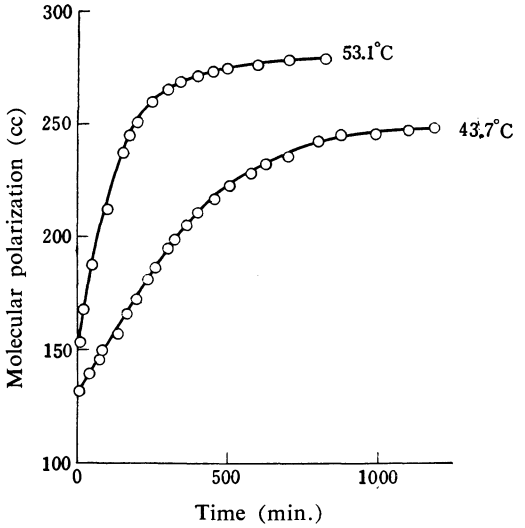



Fig. 4. The change of molecular polarization in benzene.

solute. $p_{12}(t)$, $p_2(t)$, $P_2(t)$ and $\varepsilon_{12}(t)$ mean that these quantities are functions of time. In Fig. 4, $P_2(t) \sim t$ curves are shown.

If the reaction is of the first order, Eq. 3 leads

$$\exp(-kt_i) = 1 - x(t_i)/a_\infty \qquad (8)$$

where $k = k_+ + k_-$ and $i = 1, 2, 3, \ldots\ldots, N$ ($N$ is the number of measurement). If it is possible to measure $x(t)$, the two unknown parameters $k$ and $a_\infty$ in Eq. 8 can be determind by the statistical method of least square, and then with Eq. 2 the normal velocity constant $k_+$ can be calculated. In the dielectrical measurement, however, $x(t_i)$ can not be obtained directly but only $P_2(t)$ can be measured. So it is necessary to combine the above quantities using a further assumption as follows:

$$P_2(t) = P_L[1 - x(t)] + P_N x(t) \qquad (9)$$

where $P_L$ and $P_N$ are the molecular polarizations of pure anthranol and pure anthrone, respectively, and both are unknown parameters. From Eq. 9, it is obtained the following equations.

$$x(t) = (P_2(t) - P_L)/(P_N - P_L) \qquad (10)$$

With $t = \infty$ the authors have $x = a_\infty$, so that

$$a_\infty = (P_2(\infty) - P_L)/(P_N - P_L) \qquad (11)$$

where $P_2(\infty)$ means the saturated $P_2(t)$ value. Substituting Eqs. 10 and 11 to Eq. 8, it is obtained

$$\exp(-kt_i) = (P_2(\infty) - P_2(t_i))/(P_2(\infty) - P_L) \qquad (12)$$

Eq. 12 includes two unknown parameters ($k$ and $P_L$) but they can be obtained by the statistical method of least square. In the present case the velocity constant of the reverse reaction is found to be very small compared with that of the normal reaction*. Therefor, $k_+$ is almost equal to $k$ and the final equation is obtained.

$$k_+ \fallingdotseq k = \frac{\sum_i \ln(P_2(\infty) - P_2(t_i)) \sum_i t_i/N - \sum_i t_i \ln(P_2(\infty) - P_2(t_i))}{\sum_i t_i^2 - (\sum_i t_i)^2/N} \qquad (13)$$

If Arrhenius' equation is also valid in this cace, the curve $\ln k_+ \sim 1/T$ should be linear and the results agree quite well with this requirement (Fig. 5). Activation energies, obtained from Fig. 5 are listed in Table II. These values are of the same order as those obtained in methanol and ethanol solutions by the iodine titration method. It is important to notice that the potential barrier between two isomers is rather small so that the isomerization can occur very easily.

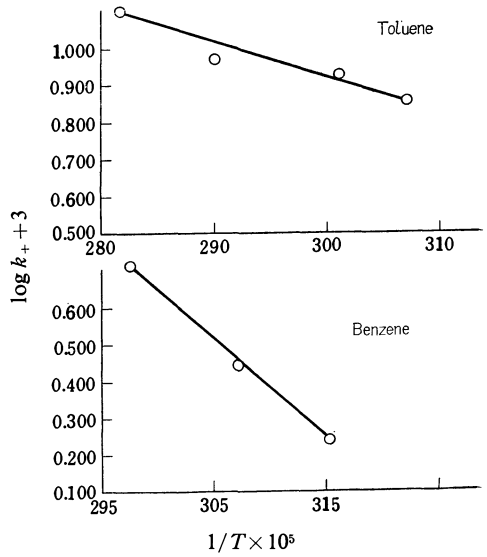



Fig. 5. Measurements of activation energies by dielectrical method.

TABLE II. THE ACTIVATION ENERGIES OF ISOMERIZATION MEASURED IN SEVERAL ORGANIC SOLVENTS

| Solvent | Method of measurement | Activation energies kcal./mol. |
|---|---|---|
| Methanol | Iodometry | 5.8 |
| Ethanol | Iodometry | 12.4 |
| Benzene | Dielectrical method | 12.2 |
| Toluene | Dielectrical method | 4.8 |

The authors could not find common solvents suitable to measure the velocity constant for

* The authors measured the molecular polarization of anthrone in benzene and toluene and ascertained that $P_2(t)$, in this case, maintained its initial value even after a long time, i. e. $k_-$ was almost equal to zero.

both the analytical and dielectrical methods for the following reasons: methanol and ethanol are polar substances and not suitable for the dielectrical measurement, while benzene and toluene are immiscible with water making iodometry titration impossible.

## Conclusion

Pure anthranol was prepared and its isomerization to anthrone was studied by analytical and dielectrical methods. The reaction was found to be of the first order and the observed heat of activations were 5.8, 12.4, 12.2 and 4.8 kcal./mol. in methanol, ethanol, benzene and toluene, respectively. These small values mean that anthranol isomerizes easily in these solvents.

Sincere thanks are tendered to Dr. Y. Mashiko of this Institute for his valuable discussion. The authors also appreciate the help rendered by Mr. Kuang Lieh Huang in performing a part of these experiments.

*Government Chemical Industrial Research Institute of Tokyo*
*Hatagaya, Shibuya-ku, Tokyo*

# β-Hydroxyleucine. I. Synthesis by Means of Copper Complex and Separation of the Diastereomeric Racemates

By Yoshikazu IKUTANI, Tôru OKUDA and Shiro AKABORI

(Received October 19, 1959)

β-Hydroxyleucine has recently been found by Kenner and Sheppard[1] to be a constituent of an antibiotic (I. C. I. No. 13959), which is unusually active against infection of *Trypanosoma congolense*, and they assigned the structure D- or L-threo isomer to the natural product. This is, as they stated, the first time that β-hydroxyleucine has been obtained from natural sources.

A survey of the literature indicates that the procedures reported hitherto for the synthetic preparation of this amino acid are rather complicated and that yields are poor.

It was synthesized by Abderhalden for the first time from isocaproic acid through isopropyl-acrylic acid in an overall yield of 7%[2], by Wieland and coworkers by adding isobutyraldehyde into a melting mixture of glycine and potassium hydroxide in a 20% yield[3], and by Buston and Bishop by hydroxybromination of isopropylacrylic acid in a 12% yield[4]. The authors have succeeded in preparing β-hydroxyleucine as a diastereomeric mixture in a high yield by the copper complex method[5] by which already threonine[5], serine[6] and β-hydroxy-β-methylaspartic acid[7] were successfully synthesized.

Glycine copper complex was allowed to react in the presence of potassium or sodium hydroxide with isobutyraldehyde. The reaction mixture was treated with aqueous ammonia and the copper was removed by means of an ion exchange resin (Dowex 50). The product thus freed from copper was found to contain no by-product but a trace of unreacted glycine by paperchromatographic analysis. Having two asymmetric carbons in α- and β-positions, β-hydroxyleucine has two diastereomeric racemates. The separation of these diastereomers was effected by utilizing the different solubility of their sodium salts in absolute ethanol. The amino acid (A) derived from the insoluble salt showed a decomposition point of 240~241°C and that of (B) from the soluble salt 255~256°C. Although Buston and Bishop[4] reported that β-hydroxyleucine is separable into two isomers with m. p. 240 and 209°C, the authors could never obtain the latter. Paperchromatography in a solvent system of methyl ethyl ketone—*n*-butanol — concentrated ammonia — water (3 : 5 : 1 : 1) permits the definite separation of these

1) G. W. Kenner and R. C. Sheppard, *Nature*, **181**, 48 (1958).
2) E. Abderhalden, *Z. physiol. Chem.*, **251**, 164 (1938).
3) T. Wieland, H. Cords and E. Keck, *Chem. Ber.*, **87**, 1312 (1954).
4) H. W. Buston and J. Bishop, *J. Biol. Chem.*, **215**, 217 (1955).
5) M. Sato, K. Okawa and S. Akabori, This Bulletin, **30**, 937 (1957).
6) S. Akabori, T. T. Otani, R. Marshall, M. Winiz and J. P. Greenstein, *Arch. Biochem, Biophys.*, **83**, 1 (1959).
7) L. Benoiton, M. Winiz, R. F. Colman, S. M. Birnbaum and J. P. Greenstein, *J. Am. Chem. Soc.*, **81**, 1726 (1959).

isomers. (A-form, $R_f=0.49$; B-form, $R_f=0.32$). The ratio of A- to B-form obtained was 1.8～2.8 as measured by the ninhydrin method[8]. These results are shown in Table I. In comparison with threonine it may be assumed that A- and B-forms correspond to the threo and erythro-forms, respectively. The definite assignment of structure is under way and will be reported later.

Table I. Yields and ratios of the diastereomers obtained with various catalysts

| Catalyst | Yield | Form A | Form B | Form A/Form B |
|---|---|---|---|---|
| KOH | 76% | 63.7% | 36.3% | 1.8 |
| NaOH | 69% | 73.5% | 26.5% | 2.8 |
| $Na_2CO_3$ | Trace | — | — | — |
| $H_2N-CH_2-CH_2-NH_2$ | Trace | — | — | — |

## Experimental

**Isobutyraldehyde.**—The aldehyde was prepared according to Whitmore's method[9] with slight modification.

**β-Hydroxyleucine.**—In a 500 cc. flask, 30 g. of freshly distilled isobutyraldehyde was added to a suspension of 23 g. of copper complex of glycine in a solution of 8 g. of potassium hydroxide (or 6 g. of sodium hydroxide) in 40 cc. of water. The suspension was swirled for a few minutes, and then placed in a refrigerator overnight. The reaction mixture was transferred to a mechanical shaker and shaken at room temperature for 5 hr. Two hundred cubic centimeters of water and 170 cc. of concentrated aqueous solution of ammonia were added and the resulted solution was filtered. The filtrate was passed through a column of Dowex 50 which had previously been converted into the ammonium form. Then the column was eluted with 5 N aqueous solution of ammonia, and the eluate was collected until no further positive ninhydrin reaction.

The effluent was concentrated under reduced pressure until the crystallization of β-hydroxyleucine began, and then about three volumes of ethanol were added. After being kept in a refrigerator overnight, the crystals of β-hydroxyleucine were collected, washed with ethanol, and dried in vacuo. When potassium hydroxide was used as catalyst, the yield was 22 g. (76%); and in the case of sodium hydroxide the yield was 20 g. (69%).

The reaction product was contaminated with a small amount of unreacted glycine and it was a mixture of two racemic diastereoisomers.

Synthetic β-hydroxyleucine, when recrystallized from water by the addition of ethanol after decolorization with charcoal, showed an m. p. of 240～241°C (decomp.).

Found: C, 48.55; H, 9.07; N, 9.50. Calcd. for $C_6H_{13}NO_3$: C, 48.96; H, 8.90; N, 9.52%.

Determination of the ratio of A- to B-form was carried out by separating them on paperchromatogram in the solvent system mentioned above and by measuring the optical density of 50% ethanol of each spot treated with ninhydrin.

**Separation of the Diastereomeric Racemates.**—Fourteen and seventenths grams of β-hydroxyleucine was added to a hot solution of sodium ethylate prepared from 2.3 g. of sodium and 50 cc. of absolute ethanol. The suspended mixture was refluxed with agitation for an hour, and placed at room temperature overnight. The mixture was filtered to remove the sodium salt of Form A, and the separeted sodium salt of Form A was added to 50 cc. of ethanol. The mixture was refluxed for an hour and the precipitate was collected and washed with ethanol.

The collected sodium salt of Form A was dissolved in 200 cc. of water and the solution was passed through a column of Amberlite-IRC 50 which had been converted into the H-form. Water was passed through the column until the effluent became ninhydrin negative. The aqueous effluent containing free β-hydroxyleucine (Form A) was concentrated under reduced pressure to a low bulk. Excess ethanol was added, and the resulting precipitate was collected by filtration after storage in a refrigerator overnight and washed with ethanol. The yield was 10 g.

Recrystallization of the product was effected from water by the addition of ethanol after decolorization with a small amount of charcoal. The product, when chromatographed on paper, revealed only a single ninhydrin-positive spot which was identical with Form A, and it showed an m.p. of 240～241°C (decomp.).

Found: C, 48.91; H, 8.72; N, 9.60. Calcd. for $C_6H_{13}NO_3$: C, 48.96; H, 8.90; N, 9.52%.

On the other hand the filtrate, namely, the ethanol solution of sodium salt of Form B was treated in the same manner as described above and its free amino acid was obtained. The yield was 2.3 g. and m. p. 255～256°C (decomp.).

Found: C, 48.95; H, 8.75; N, 9.60. Calcd. for $C_6H_{13}NO_3$: C, 48.96; H, 8.90; N, 9.52%.

**Reduction of β-Hydroxyleucine with Hydriodic Acid.** — In a sealed tube a mixture containing 0.05 g. of β-hydroxyleucine, 0.02 g. of red phosphorous and 3 cc. of hydriodic acid ($d=1.60$) was heated for 10 hr. at 150°C. By paperchromatographic analysis of the reaction product it was confirmed that most of the starting material had been reduced to leucine, but a part of β-hydroxyleucine remained unchanged in the reaction mixture. The paperchromatograms also showed three ninhydrin-positive spots of glycine, and unidentified substances with $R_f$-values 0.22 and 0.00.

8) M. Wolfe, *Biochim. et Biophys. Acta*, **23**, 186 (1957).
9) W. L. Evers, H. S. Rothrock, H. M. Woodburn, E. E. Stanly and F. C. Whitmore, *J. Am. Chem. Soc.*, **55**, 1136 (1933).

*Division of Organic Chemistry*
*Institute for Protein Research*
*Osaka University*
*Nishi-ku, Osaka*

# *The Kinetic Study of Surface-chemical Reactions at Extremely Low Pressures. V. The Thermal Reaction between Water Vapor and a Tungsten Filament. Part V*

By Takuya HAMAMURA

(Received October 20, 1959)

In previous papers[1-4] of this series the reaction of water vapor with tungsten in the 1270 to 1950° K temperature range was presented. Here the data for this reaction from 1950 to 2460° K are given and discussed. The division into two temperature ranges is done for convenience in discussing the result. Below 1950° K a blue deposit having a mean apparent composition of $WO_{2.8}$ is produced on the wall of the vessel. Above 1950° K the ratio O/W of the deposit increases with the rise of the temperature and a colorless deposit is formed at higher temperatures.

## Experimental

The apparatus was the same as that used in previous experiments. Tungsten filaments, 0.114mm. in diameter and 56mm. long, were used for determining the reaction rate and the composition of the reaction product. Procedures of measuring the reaction rate and determining the composition of the reaction products have been described previously. The two-filament method was not used to obtain the reaction probability owing to the too severe influence of hydrogen pressure on the reaction rate. The temperature of the reaction vessel remained at room temperature throughout the experiments.

Uptake of oxygen by the deposit was studied as follows. After the deposit had been produced, water vapor was removed from the vessel by cooling water reservior 1 in Fig. 1* with dry ice and a definite amount of oxygen was introduced into the vessel through cock 12 after the boiler of diffusion pump 7 was cooled. Then the vessel was heated in an electric furnace and the pressure decrease was measured by a McLeod manometer.

Desorption of a permanent gas from the deposit was studied as follows. After the deposit had been produced, water vapor was removed from the vessel in the manner mentioned above. The vessel was then heated in an electric furnace and the permanent gas given off was transferred into the glass balloon by diffusion pump 7. The pressure was measured by a McLeod manometer.

## Results and Discussion

**Reaction Rate.**—Reaction rates were determined from $30\times10^{-5}$ to $103\times10^{-5}$ mmHg initial pressures of water vapor under various pressures of hydrogen in the vessel. It was found that the reaction rate decreased with the increase of hydrogen pressure more steeply as the temperature rose or the pressure of the water vapor decreased in a manner similar to that observed below 1950° K. The cause of decrease of the rate was studied by the following experiment. Two filaments of the same length** and diameter were heated in water vapor of the same initial pressure separately for the same interval of time with the same current under different pressures of hydrogen. The amount of hydrogen produced and the increment of resistance of the respective filaments were determined. Results for 1.5 amp. heating current (about 2350°K) are given in Table VI***. Increments of the resistance are almost the same for two filaments even though the amounts of hydrogen are considerably different. Therefore, it is apparent that the decrease is not caused by the retardation of the reaction of water vapor with tungsten by hydrogen.

The reaction probability at a definite temperature was evaluated from the reaction rate at zero pressure of hydrogen obtained by extrapolating back the rate vs. hydrogen pressure curve to zero pressure of hydrogen. Values of reaction probabilities at $60\times10^{-5}$ mmHg of water vapor are given in Table VII. A probability at 1890°K is also given for comparison. These values are not free from the end effect of the filament.

**Composition of Deposit.**—Results obtained are given in Table VIII. It is obvious that the ratio O/W of the deposit increases with the rise of the temperature, whereas it decreases with the increase of the hydrogen pressure. Properties of deposits are as follows.

1) Deposits having ratio values O/W smaller than 3 appeared blue in transmitted light,

1) N. Sasaki and T. Hamamura, This Bulletin, **29**, 365 (1956).
2) T. Hamamura, ibid., **32**, 845 (1959).
3) T. Hamamura, ibid., **32**, 848 (1959).
4) T. Hamamura, ibid., **32**, 1180 (1959).
* Fig. 1 is presented in the first paper of this series.

** Filaments, 12.8 cm. long, were used for this experiment.
*** Tables in the present paper are numbered after those of previous papers.

Table VI

| Expt. No. | Heating time min. | Initial press. of $H_2O$ mmHg$\times 10^5$ | Press. of $H_2$ in vessel mmHg$\times 10^4$ | Amount of $H_2$ produced mol.$\times 10^5$ | Initial resist. at 25°C ohm | Increment of resist. ohm |
|---|---|---|---|---|---|---|
| 1 | 50 | 91.0 | 5.5 | 1.97 | 1.171 | 0.033 |
| 1′ | 50 | 91.0 | 62.5 | 1.40 | 1.164 | 0.032 |
| 2 | 120 | 56.5 | 2.4 | 2.02 | 1.194 | 0.052 |
| 2′ | 120 | 56.5 | 18.0 | 0.96 | 1.203 | 0.050 |

Table VII. Reaction Probabilities

| Temp. of filament (°K) | 1890 | 2000 | 2100 | 2200 | 2300 |
|---|---|---|---|---|---|
| $k$ | $7.7\times10^{-3}$ | $1.3\times10^{-2}$ | $1.7\times10^{-2}$ | $2.5\times10^{-2}$ | $3.0\times10^{-2}$ |

Table VIII

| Filament temp. °K | Initial press. of $H_2O$ mmHg$\times 10^5$ | Press. of $H_2$ in vessel mmHg$\times 10^5$ | Net weight loss of filament mol.$\times 10^6$ | Amount of $H_2$ produced mol.$\times 10^5$ | Composition in $WO_x$ | Gas mass No., product % |
|---|---|---|---|---|---|---|
| 2000 | 103 | 26 | 7.85 | 2.26 | $WO_{2.88}$ | |
| 2000 | 103 | 108 | 8.26 | 2.35 | $WO_{2.85}$ | |
| 2110 | 58 | 21 | 4.17 | 1.32 | $WO_{3.16}$ | |
| 2110 | 58 | 82 | 4.44 | 1.34 | $WO_{3.01}$ | |
| 2110 | 103 | 19 | 6.95 | 2.10 | $WO_{3.02}$ | |
| 2210 | 60 | 22 | 3.93 | 1.37 | $WO_{3.48}$ | |
| 2310 | 66 | 22 | 3.38 | 1.36 | $WO_{4.03}$ | 28 1.2%<br>32 0.4% |
| 2310 | 66 | 66 | 3.39 | 0.99 | $WO_{2.93}$ | 28 0.6%<br>32 0.6% |
| 2310 | 103 | 37 | 5.27 | 2.02 | $WO_{3.82}$ | |
| 2310 | 103 | 91 | 6.47 | 2.04 | $WO_{3.15}$ | |
| 2430 | 60 | 18 | 3.36 | 1.31 | $WO_{3.90}$ | 28 2.3%<br>32 1.2% |
| 2430 | 60 | 46 | 2.88 | 8.84 | $WO_{3.07}$ | |
| 2460 | 104 | 32 | 5.16 | 2.05 | $WO_{3.98}$ | |

whereas those having ratio values greater than 3 appeared colorless.

2) The deposition of a colorless product revealed a bleaching action upon the blue deposit, that is, when the colorless product was deposited on the blue deposit the blue color faded gradually with the accumulation of the colorless deposit.

3) When $100\times10^{-5}$ mmHg of oxygen was admitted to the blue deposit, oxygen was hardly taken up at all at room temperature, but it was taken up swiftly at 200°C with fading of the blue color.

4) When the blue and the colorless deposits were heated separately in high vacuum at 300°C for two hours, the desorption of a permanent gas and the change of the color were not observed in either case.

The bleaching action of the colorless product upon the blue deposit may be explained by making an assumption that besides the reaction between water vapor and tungsten, the thermal decomposition of water vapor takes place with an increasing rate with the rise of the temperature and oxygen thus produced reacts with the blue deposit to make it colorless. Although the reduction of the deposit by hydrogen must take place at the same time, so long as the oxidation rate predominates over the reduction rate the colorless product is produced. It is shown experimentally that the blue deposit takes up oxygen to become colorless.

It has been stated[4] that the deposit produced below 1950°K has the ratio value O/W of 2.8. On the other hand, at temperatures above 1950 °K the ratio value was found to increase with the rise of the temperature to become greater than 4. The ratio value may increase owing to the formation of a higher oxide or may appear to increase by the production of hydrogen, not being accompanied by the weight loss of the filament, because the ratio value is determined by the amount of hydrogen produced and the weight loss of the filament. The presence of a higher oxide than tungsten trioxide has not been reported in literature. If the deposit was composed of a peroxide, oxygen or hydrogen peroxide would be generated when the deposit was dissolved in sulfuric acid or in aqueous solution of sodium hydroxide. However, the oxygen

evolution was not observed at all and the hydrogen peroxide formation was not detected by luminol[5]. Peroxytungstic acids[6] have been reported by some investigators, but these acids are described as being unstable and as decomposing with the evolution of oxygen by heating. Therefore, it is obvious that the colorless deposit is not composed of these acids. The colorless deposit is composed of tungsten trioxide.

Thermal decomposition of water vapor has been assumed to explain the bleaching action of the colorless product, but if all the oxygen produced reacts with the filament to form tungsten trioxide, the ratio value can not become greater than 3. It is necessary for the ratio value to become greater than 3 that oxygen be consumed by another process than the reaction with the filament. The following processes may be considered for such consumption.

1) Oxygen leaves the reaction vessel to be introduced into the glass balloon. 2) Oxygen produces hydrogen peroxide to be caught by the trap cooled with liquid nitrogen. 3) Oxygen is taken up by the wall of the apparatus or by the deposit on the wall of the vessel.

Results of the analysis by the mass spectrometer are given in Table VIII. It is evident that the amount of oxygen introduced into the balloon is too little to explain the observed ratio value. Hydrogen peroxide[7,8] has been reported to be produced when the water vapor contacts with a Nernst tube at a high temperature or when atomic hydrogen combines with oxygen on a wall cooled with liquid oxygen. Therefore, hydrogen peroxide may be produced in the reaction of water vapor with the tungsten now being studied. The formation of hydrogen peroxide was studied by the following experiment; after a filament was heated at 2310°K in $60\times10^{-5}$ mmHg of water vapor for two hours, the filament and the boiler of diffusion pump 7 were cooled and air was introduced into the apparatus to an atmospheric pressure. Trap 6 was then detached from the apparatus, warmed to room temperature and a luminol reagent was dropped in it within a dark room to detect hydrogen peroxide by its luminescence. As a result, hydrogen peroxide was not detected by this experiment although about $2\times10^{-6}$ mol. of hydrogen peroxide must be produced if the observed ratio value is ascribed to the formation of hydrogen peroxide. A blank test revealed that about $2\times10^{-7}$ mol. of hydrogen peroxide could be detected.

The fact that a permanent gas was not given off from the deposit at 300°C suggested that oxygen had not been physically adsorbed at all or that it had been chemisorbed by the wall of vessel and/or by the deposit. The uptake of oxygen by the wall of the apparatus was studied by carrying out an electrodeless discharge in oxygen within the vessel. The discharge vessel was 30 mm. in diameter and 130 mm. long. The vessel was connected with a trap cooled with liquid nitrogen and the pressure was measured with a McLeod manometer. The electrodeless discharge was carried out by placing the vessel in a coil through which a high frequency current flowed. After evacuating and degassing the apparatus, about 0.2 mmHg of oxygen was introduced into the apparatus. Then the discharge was carried out for two minutes, and the pressure was measured again. Thus, the oxygen pressure was measured every time after the two-minute discharge. The uptake of oxygen by the tungsten trioxide deposit was studied similarly by using a vessel whose wall had been covered with tungsten trioxide deposit formed by heating a tungsten filament mounted along the axis of a vessel in oxygen. As a result, it was found that the tungsten trioxide deposit hardly took up oxygen at all, whereas the wall of the apparatus took up some amount of oxygen. It is evident that excited molecules and atoms of oxygen were produced by the discharge and a part of them were taken up by the wall. In the reaction of water vapor with tungsten, too, excited molecules and atoms of oxygen would be produced and a part of them be taken up by the wall by chemisorption. Langmuir[9] has found that oxygen adsorbed on tungsten evaporates from the surface as atoms when the surface is nearly bare. Therefore, it is most reasonable to consider that the ratio value greater than 3 is caused by the fact that some amount of hydrogen is liberated, not being accompanied by the weight loss of filament, since oxygen is produced by the decomposition of water vapor and is taken up by the wall of the apparatus, and to consider that the reaction rate and the ratio value O/W of deposit decrease with the increase of hydrogen pressure, since oxygen thus taken up reacts with hydrogen to form water vapor.

## Summary

1) Reaction probabilities above 1950°K are determined.

2) The ratio value O/W of the deposit increases with the rise of temperature.

3) The deposit having ratio value O/W greater than 3 appears colorless in transmitted light.

5) W. Langenbeck and U. Ruge, *Ber.* **70**, 367 (1937).

6) J. W. Mellor, "Comprehensive Treatise on Inorganic and Theoretical Chemistry", Vol. XI, Longmans, Green Ltd., London (1954), p. 833.

7) W. Nernst, *Z. Elektrochem.*, **11**, 710 (1905).

8) K. H. Geib and P. Harteck, *Ber.*, **65**, 1551 (1932).

9) I. Langmuir and D. S. Villars, *J. Am. Chem. Soc.*, **53**, 486 (1931).

4) The colorless deposit is composed of tungsten trioxide and the ratio value O/W greater than 3 is ascribed to the production of hydrogen, not being accompanied by the weight loss of filament, since the ratio value is determined from the amount of hydrogen produced and the amount of weight loss of filament.

5) Water vapor decomposes and a part of the oxygen thus produced is taken up by the wall of the apparatus, and hence hydrogen is produced, not being accompanied by the weight loss of filament.

6) The reaction rate and the ratio value O/W of the deposit decrease with the increase of hydrogen pressure, since the oxygen taken up by the wall recombines with hydrogen to form water vapor.

The author wishes to express sincere thanks to Professor N. Sasaki of kyoto University and Professor K. Kodera of Kyoto Technical University for their kind discussion and encouragement, and to Mr. T. Makita of Kyoto University for the mass spectrometer analysis.

*Department of Chemistry*
*Faculty of Industrial Art*
*Kyoto Technical University*
*Sakyo-ku, Kyoto*

# *Investigation on Mixed Complexes. III*[1]*. Spectrophotometric Studies on Platinum(II) Complexes*

By Shigeo KIDA

(Received August 17, 1959)

In general, mixed complexes are easily formed, but it appears that mixed cyano complexes are not easily formed. For instance, many species of mixed ammine complexes of cobalt(III) and platinum(II) are known, but mixed cyano complexes of cobalt(III) and platinum(II) known hitherto are few[2], and they have a strong tendency to become cyano complexes[3].

In the preceeding paper[1] of this series, it was demonstrated that no mixed cyano complexes are formed in the case of nickel(II) and copper(I). However, these are the cases where the parent complexes (for instance, $[Ni\,en_3]^{2+}$ and $[Ni(CN)_4]^{2-}$) have different configuration from each other. In this article an experiment has been carried out on platinum(II) complexes, which have the same configuration, in order to verify whether the mixed cyano complex is formed or not.

## Results and Discussion

It has been known that chloride ions in tetrachloro platinate(II) ion are replaced by cyanide ions in solution at room temperature. Though no mixed cyano complex of platinum(II) has ever been known, a possibility of its formation in solution is still in question. The experiment was undertaken to solve this problem.

A potassium cyanide solution was added to a solution of potassium tetrachloro platinate(II) in the ratios as indicated in Table I, and extinction measurements were carried out on each of the mixed solutions. The results are shown in Fig. 1.

The extinction curves in Fig. 1 show that only the tetracyano platinate(II) and tetrachloro platinate(II) ions are present, no mixed complex ions such as $[Pt\,Cl_3CN]^{2-}$, $[Pt\,Cl_2(CN)_2]^{2-}$ and $[Pt(CN)_3Cl]^{2-}$ being present; if any of the mixed complexes were formed, the absorption curve would be subject to deformation to some degree, or a new absorption maximum would appear correspondingly, in the region where tetracyano platinate(II) ion has no absorption.

TABLE I. THE COMPOSITION OF THE SOLUTIONS (cf. Fig. 1)

| Solution number | (1) | (2) | (3) | (4) | (5) |
|---|---|---|---|---|---|
| 0.03 F $K_2[Pt\,Cl_4]$ and 3 F KCl* | 8 ml. | 8 | 8 | 8 | 8 |
| 0.1220 F KCN | 0 ml. | 2 | 4 | 6 | 8 |
| Water | 8 ml. | 6 | 4 | 2 | 0 |

* KCl is added to supress hydrolysis of $[Pt.Cl_4]^{2-}$.

1) Part II of this series: S. Kida, This Bulletin, 32, 981 (1959).

2) J. C. Bailar, "The Chemistry of the Coordination Compounds", Reinhold Publ. Co., New York (1956), p. 87, "General Survey".

3) This tendency can be seen when one compares the methods of preparation of the two complxes, $[Co(NH_3)_5Cl]^{2+}$ and $[Co(CN)_5Cl]^{3+}$; the pentammine complex is readily prepared from cobaltous salt, ammonia and ammonium chloride in an aqueous solution, while the pentacyano complex is obtained only by substitution of the cyanide ion for ammonia of petammine complex under a very delicate condition.

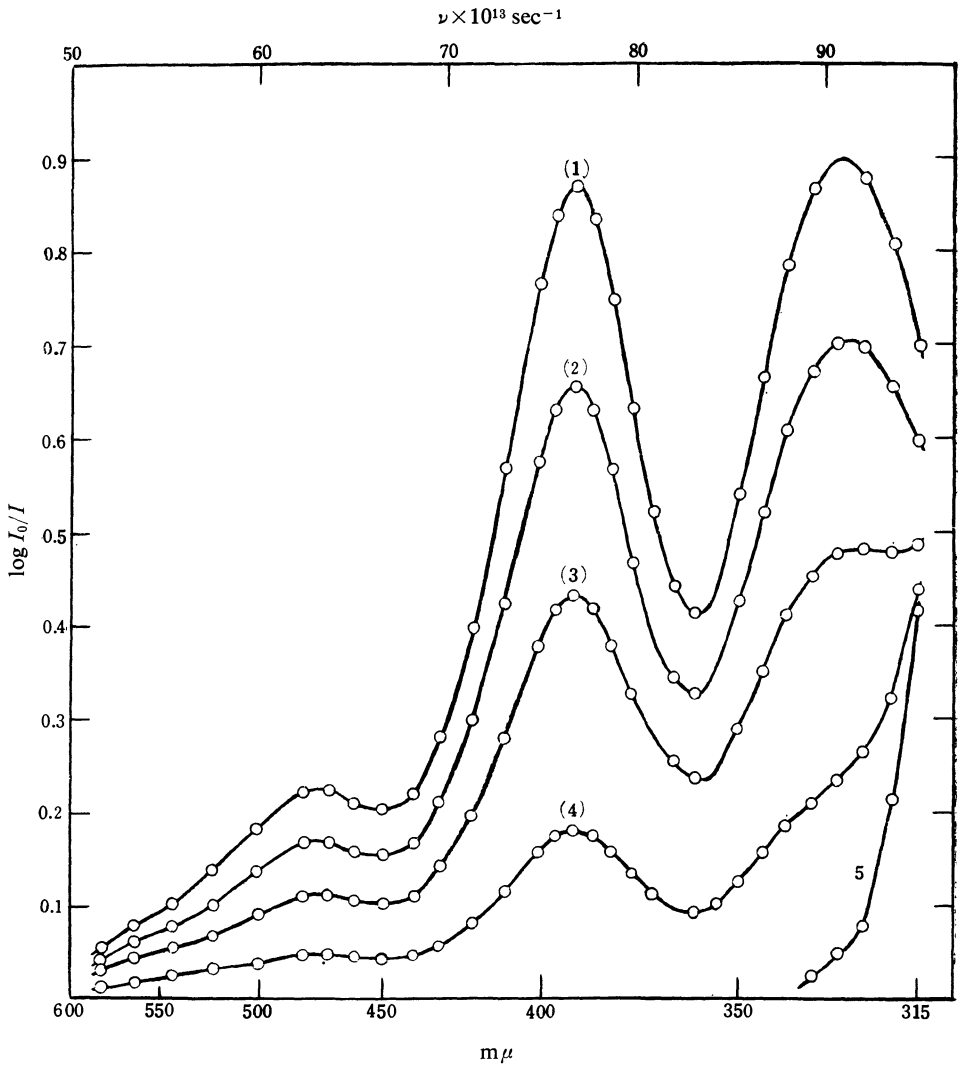



Fig. 1. (cf. Table I).

If it is assumed that all of the added cyanide ions are consumed to form the tetracyano platinate(II) ion, the calculated value of ([Pt] $-1/4$[CN])/[Pt] must accord with the experimentally obtainable value, $D/D_1$[4], where [Pt] and [CN] denote the total concentration of all platinum species and of the added cyanide ion in each solution shown in Table I and Fig. 1. Actually, a satisfactory agreement between the calculated and the experimental value can be found in Table II.

A potassium cyanide solution was added to a solution of potassium tetrabromo platinate(II), in order to examine the substitution of the cyanide ion for the coordinated bromide. The result was the same in the case of the potassium tetrachloro platinate(II); i.e. the absorption curves are not deformed in the region where the tetracyano platinate(II) ion has no absorption, and the calculated value, ([Pt] $-1/4$[CN])/[Pt] accords with the experimental value, $D/D_6$, as is shown in Fig. 2 and Table IV.

TABLE II

| | (1) | (2) | (3) | (4) | (5) |
|---|---|---|---|---|---|
| ([Pt]$-1/4$[CN])/[Pt] | 1.00 | 0.746 | 0.492 | 0.237 | 0 |
| $D/D_1$ for 470 mμ | 1.00 | 0.748 | 0.496 | 0.207 | 0 |
| for 400 mμ | 1.00 | 0.751 | 0.492 | 0.208 | 0 |
| for 390 mμ | 1.00 | 0.753 | 0.499 | 0.209 | 0 |
| for 380 mμ | 1.00 | 0.759 | 0.505 | 0.212 | 0 |

Numbers in the first row denote solution numbers in Table I.

4) If the reaction, $[PtCl_4]^{2-}+4CN^- \rightarrow [Pt(CN)_4]^{2-}+4Cl^-$, takes place quantitatively, optical densities of the solutions are expressed as in the following:
$D=\varepsilon_1([Pt]-1/4[CN])+\varepsilon_2(1/4[CN])$, and for solution 1, $D_1=\varepsilon_1[Pt]$, where $\varepsilon_1$ and $\varepsilon_2$ are extinction coefficients of $[PtCl_4]^{2-}$ and $[Pt(CN)_4]^{2-}$, respectively. However, in the region of 330~600 mμ the ratio $D/D_1$ can be reduced to ([Pt]$-1/4$[CN])/[Pt], since in this region $\varepsilon_2=0$.

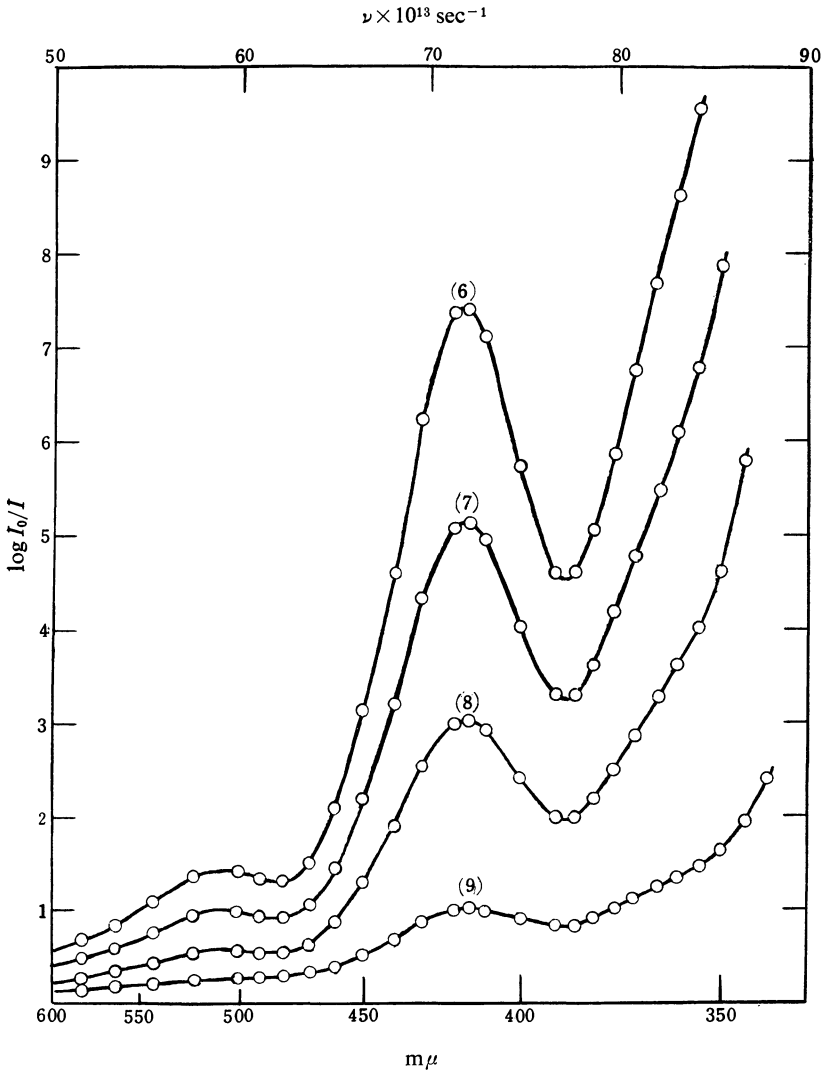



Fig. 2. (cf. Table III).

TABLE III. THE COMPOSITION OF THE SOLUTIONS (cf. Fig. 2)

| Solution number | (6) | (7) | (8) | (9) | (10) |
|---|---|---|---|---|---|
| 0.015 F $K_2[PtBr_4]$ and 1 F KBr** | 8 ml. | 8 | 8 | 8 | 8 |
| 0.0703 F KCN | 0 ml. | 2 | 4 | 6 | 8 |
| Water | 8 ml. | 6 | 4 | 2 | 0 |

** KBr is added to supress hydrolysis of $[PtBr_4]^{2-}$.

TABLE IV

| | (6) | (7) | (8) | (9) | (10) |
|---|---|---|---|---|---|
| ([Pt]−1/4[CN])/[Pt] | 1.00 | 0.707 | 0.414 | 0.121 | 0 |
| $D/D_6$ for 520 mμ | 1.00 | 0.691 | 0.403 | 0.187 | 0 |
| for 420 mμ | 1.00 | 0.690 | 0.407 | 0.137 | 0 |
| for 410 mμ | 1.00 | 0.697 | 0.411 | 0.140 | 0 |

Numbers in the first row denote solution numbers in Table III.

These results are the first example which evidently shows that no mixed complex is formed between the complexes of the same configuration. The cause of this phenomenon will be discussed in the last paper of this series[5].

Further experiments on the other compounds, especially on cobaltic complexes, to find further similar examples, are desirable. Unfortunately, however, it has been found difficult to find appropriate compounds to be examined for the present purpose.

When a potassium cyanide solution is added to a solution of hexammine cobalt(III) chloride, the coordinated ammonia is replaced by the cyanide ion, and the only product obtained is not easily soluble crystals, $[Co(NH_3)_6]\cdot[Co(CN)_6]$. From the above fact alone, one

5) S. Kida, to be published.

can not deduce a conclusion, because there are two probable cases; i.e. 1) the mixed complex is not formed because of its comparatively less stability, 2) although the mixed complexes are easily formed in solution, the least soluble compound, $[Co(NH_3)_6] \cdot [Co(CN)_6]$, separates out, and the equilibrium shifts to produce the crystals, $[Co(NH_3)_6] \cdot [Co(CN)_6]$.

## Experimental

Extinction measurements were made by the Beckman DU Spectrophotometer using 1 cm. qualtz cells at room temperature.

Potassium tetrachloro platinate(II), $K_2[PtCl_4]$, and potassium tetrabromo platinate(II), $K_2[PtBr_4] \cdot 2H_2O$, were prepared according to the literatures[6,7], and their purity was checked by analyzing their quantity of halogen. The concentration of potassium cyanide was determined by a titration with a standard solution of silver nitrate.

6) W. C. Fernelius, "Inorganic Syntheses", Vol. II, McGraw- Hill Book Co., Inc., New York (1954), p. 87.
7) E. Billmann and A. C. Anderson, *Ber.*, **36**, 1566 (1903).

## Summary

The spectrophotometric investigation has shown that in the substitution reactions of cyanide ion for halogens($X^-$) of the complexes, $[PtX_4]^{2-}$, (X=Cl and Br) in solution, no mixed complex is formed.

The author wishes to thank Professor R. Tsuchida of Osaka University for his kind guidance throughout this work. He is also indebted to Dr. H. Yoneda and Dr. J. Fujita for their helpful discussions.

*Department of Chemistry*
*Wakayama University*
*Masago-cho, Wakayama*

# *Adsorption of the Ferric Ion by Weakly Acidic Resins. Preferential Uptake of the Ferric Ion by Alginic Acid*

By Manabu SENŌ and Takeo YAMABE

(Received October 6, 1959)

Weakly acidic ion-exchange resins have strong affinity to the hydrogen ion and it is scarcely exchanged at all for other cations including heavy metal ions. Recently, it has been revealed[1,2] in the course of separation experiments of heavy metal ions that alginic acid adsorbs the ferric ion to a great extent, although it is a weakly dissociated acid.

In this paper, adsorptive properties for ferric ions of weakly acidic ion-exchange resins, Amberlite IRC-50 and alginate resin, are examined and discussed.

## Experimental

The exchange resins used are Amberlite IRC-50 (Rohm and Haas Co., Ltd., U. S. A.) and alginic acid*. They were washed thoroughly with pure water and air-dried, after conditioning with acid and alkali.

All the equilibrium experiments were carried out by the batch-method. Resins of acidic form were used unless otherwise stated. About 0.2 g. of the resin and 50 ml. of the external salt solution were taken in a beaker and allowed to stand for a week or more with stirring occasionally, since the rate of exchange is rather low for weakly dissociated resins as shown by the preliminary test (Fig. 1). To prevent the vaporization of the solution, the beaker was covered with polyvinylchloride sheet. The concentrations of metal ions in the added solutions were about 0.03 meq./ml. except these described otherwise. After equilibrating, the metal and hydrogen ions remaining in solution were assayed and the amount of the metal ions adsorbed on the resin was estimated as usual. The iron, aluminum and copper were analyzed colorimetrically.

All reagents are of commercial special-grade and were used without further purification.

Absorption spectra were measured using a Hitachi EPU-2A spectrophotometer.

## Results and Discussion

**Exchange of the Hydrogen Ion for the Ferric Ion.**—Quantitative data on the adsorption of the ferric ion by weakly acidic resins from chloride solutions of varying initial concentrations of

1) H. Specker and H. Hartkamp, *Z. anal. Chem.*, **140**, 167; **141** 33 (1953).

2) T. Takahashi and S. Emura, *Japan Analyst* (*Bunseki Kagaku*), **7**, 568 (1958).

* It was prepared by treating commerical sodium alginate (Kimitsu Chemical Industry, Co., Ltd.) with 10% hydrochloric acid, after it was once dissolved in water and filtered.

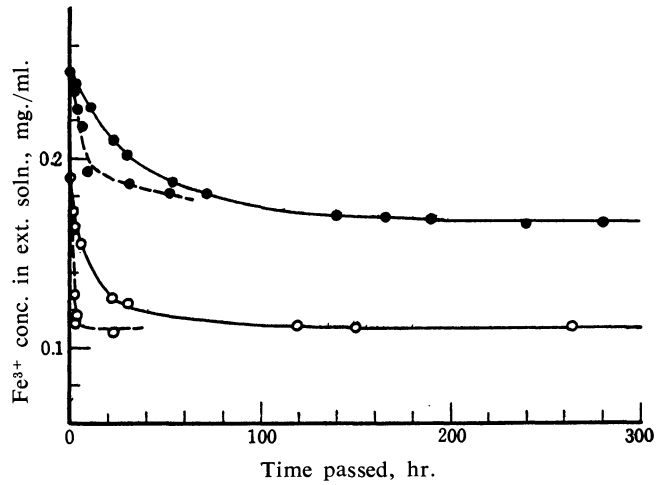



Fig. 1. Rate of exchange
○ Alginate resin, —— in settling
● Amberlite IRC-50, ---- with stirring
Resin, acidic form. Alg. 0.32 g., IRC-50 0.49 g.; Soln., 0.001 N HCl, 150 ml.

TABLE I. EXCHANGE OF THE HYDROGEN ION FOR THE FERRIC ION

| | $Fe^{3+}$ exchanged, meq./g. resin (eq./eq. resin) | | | |
|---|---|---|---|---|
| HCl concn., N | 0 | 0.001 | 0.01 | 0.1 |
| Amberlite IRC-50 | 4.57(0.44) | 2.53(0.24) | 1.06(0.10) | 0.93(0.09) |
| Alginate resin | 6.67(1.17) | 3.88(0.68) | 3.54(0.62) | 2.12(0.37) |
| Amberlite IR-120 | 5.90(1.26) | 5.54(1.18) | 5.13(1.09) | 3.42(0.73) |

Resins, acid form 0.1~0.2 g.
Ferric chloride soln., 0.5 mg. $Fe^{3+}$/ml., 50 ml.

TABLE II. AMOUNTS OF IONS REMAINING IN SOLUTION PHASE BEFORE AND AFTER EQUILIBRIUM

| | Amounts, meq./ml. | | | | | |
|---|---|---|---|---|---|---|
| | Orig. ext. soln. | | | Equil. ext. soln. | | |
| | $H^+$ | $Fe^{3+}$ | $Cl^-$ | $H^+$ | $Fe^{3+}$ | $Cl^-$ |
| Alginate resin (0.21 g.) | 0.0010 | 0 | 0.0012 | 0.0011 | 0 | 0.0012 |
| | 0.0010 | 0.0141 | 0.0152 | 0.0059 | 0.0082 | 0.0153 |
| | 0.0010 | 0.0282 | 0.0302 | 0.0056 | 0.0223 | 0.0303 |
| Amberlite IRC-50 (0.16 g.) | 0.0010 | 0 | 0.0012 | 0.0011 | 0 | 0.0012 |
| | 0.0010 | 0.0141 | 0.0152 | 0.0019 | 0.0135 | 0.0152 |
| | 0.0010 | 0.0282 | 0.0302 | 0.0042 | 0.0250 | 0.0298 |

hydrochloric acid were given in Table I. Alginate resin adsorbs the ferric ion more strongly than Amberlite IRC-50. Amounts of ferric ions adsorbed were markedly dependent on pH of the external solution. For comparison, the data on exchange by a strongly acidic ion-exchange resin, Amberlite IR-120, were also shown in the table.

It is interesting to note that the adsorption capacity for the ferric ion is larger than the total exchange capacity**, which is obtained

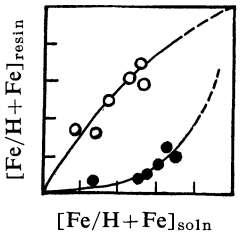



Fig. 2. Exchange diagram between hydrogen and ferric ions.
○ Alginate resin
● Amberlite IRC-50

** The total exchange cepacities are 10 for Amberlite IRC-50, 5.6 for alginate and 4.5 (meq./g. resin) for Amberlite IR-120, respectively.

from a titration curve by alkali, in the case of alginic acid and Amberlite IR-120.

In Fig. 2, the equilibrium diagram of the ferric ion against the hydrogen ion was shown. It is noteworthy that the ferric ion is adsorbed by alginate resin to almost the same extent as the hydrogen ion.

In Table II, the amounts of all ions remaining in external solution before and after equilibrium of the exchange reaction were described. As seen in the table, the adsorption of the ferric ion is intrinsically an exchange reaction of counter-ions of the resins.

**Preferential Adsorption of the Ferric Ion.**—In Table III and Fig. 3, the results of exchange equilibria of other heavy metal ions, $Fe^{2+}$, $Al^{3+}$ and $Cu^{2+}$, for the hydrogen ion were given. As shown already by other investigators[1], who tried successfully to separate the ferric ion from other metal ions by columns of alginic acid powder, alginate resin combines very strongly with the ferric ion compared with other heavy metal ions. This behavior is a remarkable character of alginate resin, in contrast with Amberlite IR-120 and IR C-50; the former adsorbs well all metal ions and the latter has a very strong affinity to the hydrogen ion and, therefore, metal cations replace the hydrogen ion with difficulty.

This result is valid, independently of the acidity of the external solution as seen in Table IV. Of course, as the acidity of a solution becomes very high, these resins can not combine with other cations except in the case of the hydrogen ion.

To confirm this selective uptake of the ferric ion by alginic acid, the exchange equilibria between $Fe^{3+}$ and $Al^{3+}$ or $Cu^{2+}$ were examined under the condition that the concentration of hydrochloric acid in salt solution was kept constant. Also the total concentration of the metal ions in the system was almost kept constant, 0.15 meq./ml. The results were given in Fig. 4. Preferential adsorption of the ferric

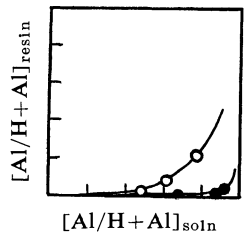



Fig. 3. Exchange diagram between hydrogen and aluminum ions.
○ Alginate resin
● Amberlite IRC-50

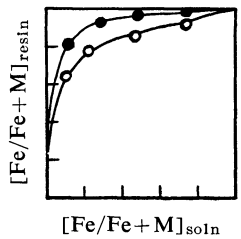



Fig. 4. Exchange equilibria of alginate resin between $Fe^{3+}$ and $Al^{3+}$ or $Cu^{2+}$ at a constant acid concentration, 0.01 N $H_2SO_4$.
○ $Fe^{3+}$~$Cu^{2+}$, ● $Fe^{3+}$~$Al^{3+}$

TABLE III. EXCHANGE OF THE HYDROGEN ION FOR HEAVY METAL IONS IN SOLUTION OF CONSTANT ACID CONCENTRATION, 0.01 N

| | Ions exchanged, meq./g. resin | | | |
|---|---|---|---|---|
| Ions | $Fe^{3+}$ | $Fe^{2+}$ | $Al^{3+}$ | $Cu^{2+}$ |
| Salt form | $FeCl_3$ | $FeCl_2$ | $Al_2(SO_4)_3$ | $CuSO_4$ |
| Amberlite IRC-50 | 1.06 | 0 | 0.20 | 0 |
| Alginate resin | 3.54 | 0.13 | 0.50 | 1.17 |
| Amberlite IR-120 | 5.13 | 4.02 | 4.84 | 4.36 |

Resins, acid form 0.1~0.2 g.
Metal ion soln., ca. 0.03 meq./ml., 50 ml.

TABLE IV. EXCHANGE OF THE HYDROGEN ION FOR THE FERROUS OR THE ALUMINUM ION

| | Ions exchanged, meq./g. resin | | | |
|---|---|---|---|---|
| $Fe^{2+}$, $FeCl_2$-HCl (0.60 mg. $Fe^{2+}$/ml., 50 ml.) | | | | |
| HCl concn., N | 0 | 0.001 | 0.01 | 0.1 |
| Amberlite IRC-50 | 0.12 | 0.05 | 0 | 0 |
| Alginate resin | 0.41 | 0.23 | 0.13 | 0.05 |
| $Al^{3+}$, $Al_2(SO_4)_3$-$H_2SO_4$ (0.25 mg. $Al^{3+}$/ml., 50 ml.) | | | | |
| $H_2SO_4$ concn. N | 0 | 0.0001 | 0.001 | 0.01 |
| Amberlite IRC-50 | 0.28 | 0.22 | 0.19 | 0.17 |
| Alginate resin | 2.18 | 2.06 | 1.49 | 0.47 |

Resin, acid form 0.1~0.2 g.

TABLE V. DESORPTION OF METAL IONS WITH ACID FROM RESINS

| Added soln. | | Ions retained, meq./g. resin $H_2O$ | 0.01 N HCl | 0.1 N HCl | 1.0 N HCl |
|---|---|---|---|---|---|
| Alginate resin | $Fe^{3+}$ | 6.98 | 6.06 | 1.44 | 0 |
| | $Al^{3+}$ | 4.33 | 2.75 | 0.53 | 0 |
| | $Cu^{2+}$ | 4.61 | 3.18 | 0.11 | 0 |
| Amberlite IRC-50 | $Fe^{3+}$ | 6.00 | 4.97 | 0.02 | 0 |
| | $Al^{3+}$ | 5.93 | 3.78 | 0.43 | 0 |
| | $Cu^{2+}$ | 6.33 | 4.00 | 0 | 0 |

Resin, metal salt form 0.3~0.4 g., soln., 100 ml.

TABLE VI. EFFECT OF ANION ON ADSORPTION OF THE FERRIC ION

| Salt form | $FeCl_3$ | $Fe^{3+}$ adsorbed, meq./g. resin $Fe(NO_3)_3$ | $Fe_2(SO_4)_3$ | $FeK(SO_4)_2$ |
|---|---|---|---|---|
| HCl concn., N | $0.0135_6$ | $0.0100_5$ | 0.0110 | 0.0111 |
| Amberlite IRC-50 | 1.07 | 1.07 | 0.98 | 1.05 |
| Alginate resin | 3.24 | 2.96 | 3.14 | 3.09 |

Resin, acid form 0.1~0.2 g.
Ferric ion soln., 0.5 mg./ml., 50 ml.

ion against the aluminum or copper ion is very remarkable and, therefore, it is clear that the ferric ion can easily be separated from these ions by using alginic acid as an ion-exchange resin.

**Desorption of Metal Ions from Resins with Acid.**—Although in all the experiments mentioned above the acidic form resins were equilibrated with salt solution, here salt form resins were treated with acid to examine the reversibility of these exchange reactions. Resin of $Fe^{3+}$-, $Al^{3+}$- or $Cu^{2+}$- salt form was prepared by treating sodium salt form resin with ferric, aluminum or cupric chloride solution respectively, and washing it several times with pure water.

A definite quantity of each salt resin was immersed in an acid solution of known concentration, and the amount of metal ion desorbed from resin was measured. The results were given in Table V.

The reversibility of the exchange equilibrium does not always hold. It must be pointed out that, in the case of Amberlite IRC-50, the amounts of metal ions retained in this elution experiment are larger than those adsorbed in the adsorption experiment, independently of the variety of ion species. Alginate resin adsorbs ferric ion remarkably and the retained quantity is nearly equal to the adsorbed one shown in Table I.

Metal ions are eluted from resins almost with 0.1 N and completely with 1 N hydrochloric acid.

**Effect of Anion.**—The effect of anion on adsorption of the ferric ion by resin was examined and the result was given in Table VI.

In both resins the effect of anion is not remarkable.

**Mechanism of Ferric Ion Adsorption on Resins.**—As mentioned above, alginic acid resin adsorbs the ferric ion more extensively than Amberlite IRC-50 and the ferric ion is more preferentially adsorbed than other heavy metal ions, aluminum and copper ions, by these weakly dissociated resins. Taking into account these facts and the structural character of resins, the mechanism of adsorption of the ferric ion on these resins is examined as follows:

**Adsorption of Chloride Complex Ions, $FeCl_n^{+(3-n)}$.**—It is well-known[3,4] that the ferric ion combines with the chloride ion to form complex ions, $FeCl_n^{+(3-n)}$, where $n$ becomes four at higher chloride concentration. If these complex ions take a part in the exchange reaction, adsorption of the chloride ion must be observed. However, this is not the case as shown in Table II, probably because the chloride concentration is rather low, less than 0.1 N, and the formation of chloride complexes is not predominant.

**Adsorption of Hydroxy Complex Ions, $Fe(OH)_n^{+(3-n)}$.**—Since in this experimental condition the hydrogen ion concentration is low in external medium, the ferric ion is hydrolyzed partially and the hydroxy complex ions, $Fe(OH)^{+2}$, $Fe(OH)_2^{+}$ and $Fe(OH)_3$, may be formed to a large extent[3,5]. Moreover, the fact that the exchanged quantity of the ferric ion is greater than the total exchange capacity leads to the conclusion that the ferric ion is exchanged not as a trivalent cation but as an ion with less valency on the average.

3) E. Rabinowitch and W. H. Stockmayer, *J. Am. Chem. Soc.*, **64**, 335 (1942).
4) G. A. Gamlen and D. O. Jordan, *J. Chem. Soc.*, **1953**, 1435.
5) A. B. Lamb and A. G. Jacques, *J. Am. Chem., Soc.*, **60**, 967, 1215 (1938).

For these reasons, it seems to be a fact that these hydroxy complexes have a part in the exchange reaction. None of the present experiments oppose the above deduction. It supports the probability of this adsorption mechanism that, when alginic acid combines with the ferric ion, it colors to reddish-brown and has a very similar absorption spectrum to that of the ferric hydroxide sol and of $Fe(OH)^{2+}$ given by Rabinowitch et al. (Fig. 5)[3].

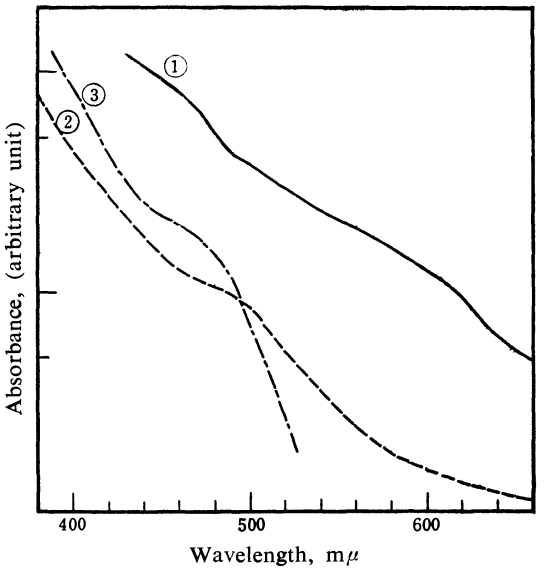



Fig. 5. Absorption spectra of
1. alginate resin membrane adsorbing ferric ion against original alginate membrane,
2. ferric hydroxide sol and
3. $Fe(OH)^{2+}$ given by Rabinowitch et al.[3]

In a case when partially hydrolyzed ions, e. g. $Fe(OH)^{2+}$, play a part in the adsorption reaction, reactions of various types may proceed at the same time. For instance, besides the normal exchange reaction 1

$$2HAlg + Fe(OH)^{2+} \rightleftarrows Fe(OH)Alg_2 + 2H^+ \quad (1)$$

the following reactions including neutralization may occur

$$HAlg + Fe(OH)^{2+} \rightleftarrows Fe(Alg)^{2+} + H_2O$$

$$Fe(Alg)^{2+} + 2HAlg \rightleftarrows Fe(Alg)_3 + 2H^+$$

that is,

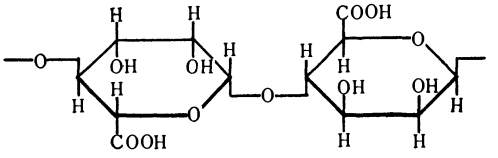
$$3HAlg + Fe(OH)^{2+} \rightleftarrows Fe(Alg)_3 + 2H^+ + H_2O \quad (2)$$

where Alg denotes a structural unit of alginate resin. Taking the hydrolysis of ferric alginate into account, reactions 1 and 2 cause the same result.

Although the present study can not give any confirmative evidence for the occurrence of these reactions, it is probably true that this mechanism may play an important part in the adsorption of the ferric ion by weakly acidic resin, for neutralization reaction can proceed to a large extent in these weakly dissociated resins.

The detailed discussion of such an exchange reaction including reactions of various types must be made clear in future.

**Complex Adsorption.**—As alginic acid has the following structure containing two hydroxyl groups and an oxygen linkage, it may be expected to combine with the ferric ion, forming an inner salt complex. To examine the effect



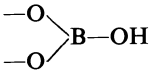

of the hydroxyl groups on the adsorption of the ferric ion by alginic acid, the ferric ion adsorbed on alginate resin was estimated when boric acid was added to the equilibrating system. The result was given in Table VII. The addition

TABLE VII. ADSORPTION OF THE FERRIC ION BY ALGINATE RESIN IN THE PRESENCE OF BORIC ACID

| HCl concn., N | 0 | 0.001 | 0.01 | 0.1 |
|---|---|---|---|---|
| $Fe^{3+}$ adsorbed, meq./g. | 3.28 | 2.84 | 2.04 | 1.99 |

Boric acid, 1.0 meq. (equiv. to alginate)
Alginate resin, 0.2 g.
Ferric chloride soln., 0.5 mg. $Fe^{3+}$/ml., 50 ml.

of boric acid diminishes the adsorbed quantity of ferric ions. Since it is known[6] that alginic acid having a *cis*-diol group combines with boric acid to form a chelate compound,




it is confirmed that the presence of the hydroxyl groups influences the adsorption of the ferric ion.

Moreover, to obtain further knowledge concerning the formation of a chelate compound between alginic acid and the ferric ion, absorption spectra of the ferric ion were measured in the presence of glucuronic acid, which is similar structurally to the unit of alginic acid***. As

6) H. Deuel and M. Neukom, *Makromol. Chem.*, 3, 13 (1949).

*** The structural unit of alginic acid is mannuronic acid and glucuronic acid may be structurally named galacturonic acid. However, it is safely considered that qualitative behaviors toward the ferric ion are similar for both acids.

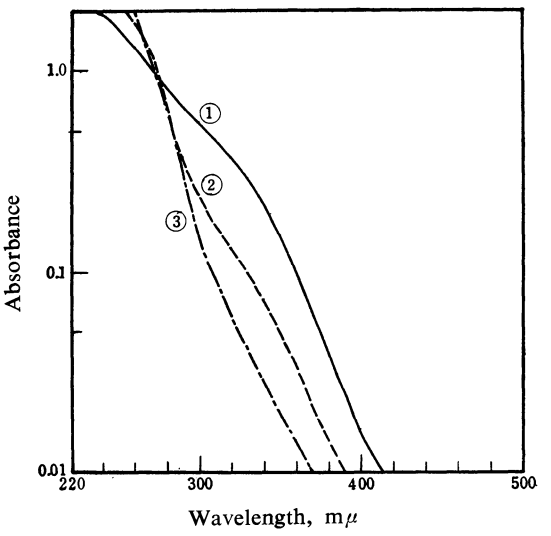



Fig. 6. Absorption spectra of ferric perchlorate $Fe(ClO_4)_3$, 0.0022 meq./ml.; $HClO_4$, 1, 0.007 N; 2, 0.031 N; 3, 0.091 N. Reference, $H_2O$.

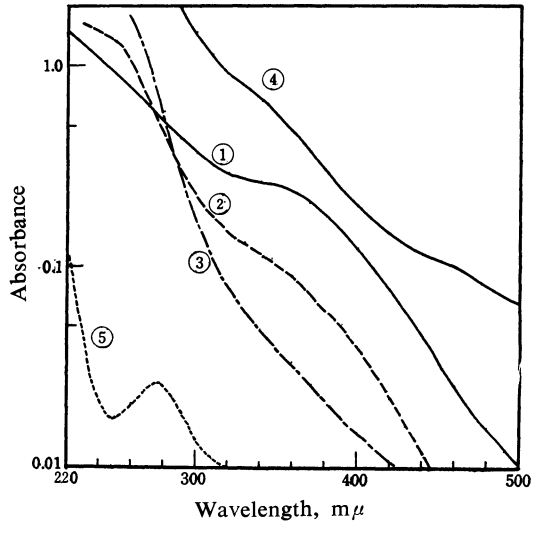



Fig. 7. Absorption spectra of $Fe^{3+}$~glucuronate.

| | $Fe(ClO_4)_3$ | $HClO_4$ | Na glu. |
|---|---|---|---|
| 1 | 0.0022 | 0.007 | 0.0022 meq./ml. |
| 2 | 〃 | 0.031 | 〃 |
| 3 | 〃 | 0.091 | 〃 |
| 4 | 〃 | 0.007 | 0.022 |
| 5 | 0 | 0 | 0.0022 |

reference, $H_2O$.

shown in Figs. 6 and 7, it is apparent that there is a shoulder at 320~340 mμ region of the absorption spectrum of the ferric ion in the presence of the glucuronate ion. That is to say, an absorption band appears at about 330 mμ and becomes weaker as the acidity of the solution increases and disappears at 0.1 N of perchloric acid.

When the concentration of the glucuronate ion is high, a weak absorption is observed over the visible wavelength region and the solution becomes weakly reddish-yellow. The absorption at 330 mμ does not become remarkable and a new weak band appears at 470 mμ.

The visible absorption spectrum**** of alginate membrane adsorbing the ferric ion also has a shoulder at 460~470 mμ, as shown in Fig. 5.

The component ions, ferric (aquo), glucuronate and alginate ions, exhibit no absorption peak in these regions[7]. Therefore, although these spectroscopic characters can not be explained completely in the present stage, it may be concluded that there are some interactions between the ferric ion and the glucuronate or alginate ion besides the simple coulombic one. Thus, it is, partly at least, due to the complex formation that alginate resin adsorbes the ferric ion intensively and preferentially.

It must be noticed that a hydroxy complex of the ferric ion has an absorption spectrum over the visible wavelength region and this spectrum has a shoulder at 460~480 mμ, as revealed from the spectrum of the ferric hydroxide sol and the spectrum of $Fe(OH)^{2+}$ obtained by Rabinowitch et al.[3] Since the concentration of the hydrogen ion is higher in the resin phase than in the external solution, it can not be expected that these hydroxy complexes exist in a free state, but it may be probable that hydroxy complexes are formed between the ferric ion and the glucuronate or alginate ion.

The absorption spectra of the ferric ion in the presence of acetate and *p*-toluene sulfonate ions were shown in Figs. 8 and 9. These ions are structurally similar to a unit of Amberlite IRC-50 and Amberlite IR-120, respectively. The spectrum of the ferric ion is not affected by the addition of the former[8] and the addition of the latter does not change in shape, but shifts the spectrum of the ferric ion to a longer wavelength. From these observations it may be concluded that these ions do not combine with the ferric ion to form chelate compounds.

**** It was measured against the original alginate membrane using opal-glass. Measurements in the region of ultraviolet wavelengths are impossible by this method.

7) Ther is a peak at 270~280 mμ in the absorption spectrum of the glucuronate ion. The chloride complexes of the ferric ion have an absorpion peak at 330~340 mμ.

8) W. Reiss et al.[9] reported that ferric acetate complex exhibits absorption peaks at 337.5 and 465 mμ when the concentration of the acetate ion is high. These peaks were not detected under the present experimental condition.

9) W. Reiss, J. F. Hazel and W. M. McNabb, *Anal. Chem.*, **24**, 1647 (1952).

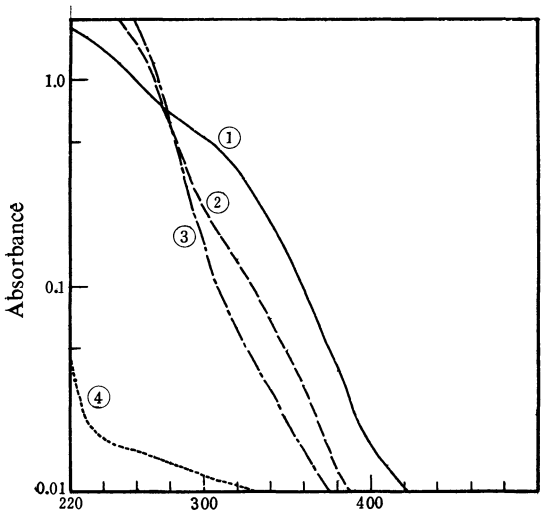



Fig. 8. Absorption spectra of $Fe^{3+}$~acetate.

| | $Fe(ClO_4)_3$ | $HClO_4$ | Na acet. |
|---|---|---|---|
| 1 | 0.0022 | 0.007 | 0.0022 meq./ml. |
| 2 | 〃 | 0.031 | 〃 |
| 3 | 〃 | 0.091 | 〃 |
| 4 | 0 | 0 | 〃 |

reference, $H_2O$.

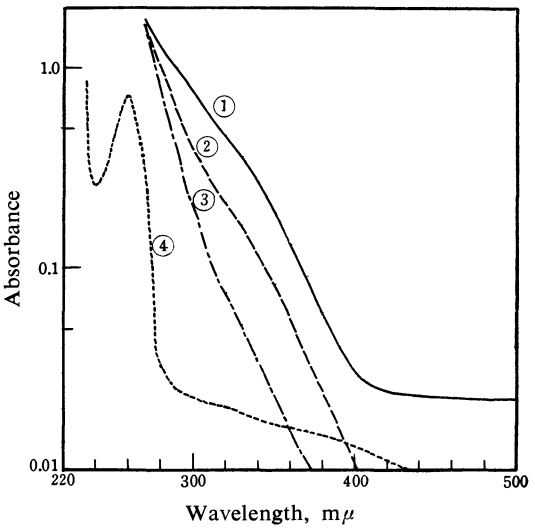



Fig. 9. Absorption spectra of $Fe^{3+}$~*p*-toluene sulfonate.

| | $Fe(ClO_4)_3$ | $HClO_4$ | Na-*p*-TS. |
|---|---|---|---|
| 1 | 0.0022 | 0.007 | 0.0022 meq./ml. |
| 2 | 〃 | 0.031 | 〃 |
| 3 | 〃 | 0.091 | 〃 |
| 4 | 0 | 0 | 〃 |

reference, $H_2O$.


## Summary

The exchange adsorptions of the ferric ion by the cation-exchange resins of carboxylic acid type, Amberlite IRC-50 and alginate resin, were examined. Equilibration experiments revealed that alginate resin adsorbs metal ions more extensively than Amberlite IRC-50 and the ferric ion is preferentially adsorbed by these resins, especially by alginate resin. The mechanism of adsorption of the ferric ion was discussed and it was concluded that the preferential uptake of the ferric ion by alginate resin was due to the partial hydrolysis of the ferric ion and the complex formation between the ferric ion and alginate resin.


In concluding this paper, the authors wish to express their thanks to Professor T. Takahashi for his continuous advice. The cost of the present research has been partly defrayed from the grant of the Ministry of Education, for which the authors' thanks are due.

*Institute of Industrial Science*
*The University of Tokyo*
*Yayoi-cho, Chiba*

# *Studies on the Chemical Constitution of Agar-agar. XXII.*[1] *Partial Methanolysis of Methylated Agarose of Gelidium Amansii*

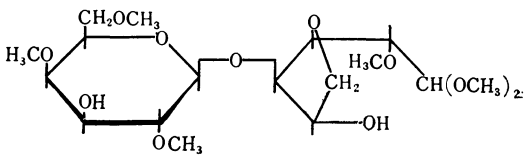
By Choji ARAKI and Susumu HIRASE

(Received October 8, 1959)

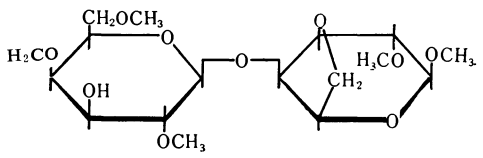
Agarose, a chief polysaccharide of agar, has been suggested by Araki[2], one of the present authors, to be a chain composed of alternating β-D-galactopyranose and 3,6-anhydro-α-L-galactopyranose residues. The preceding paper[1] concerned with the complete methanolysis of methylated agarose of *Gelidium amansii* provided a strong evidence to verify the above mentioned structure of agarose. A further support has now been obtained herein by partial methanolysis of the methylated polysaccharide.

The partial methanolysis was conducted with 0.5% methanolic hydrogen chloride for four hours, during which time 74% of the methylated polysaccharide was concerned in reaction. After treatment with barium hydroxide, the products were separated into neutral and acid components by fractionation with ether. The acidic component in the barium salt was obtained in too small a yield to be of structual significance. Further separation of the neutral components on a charcoal-Celite column led to the isolation of *O*-2, 4, 6-tri-*O*-methyl-β-D-galactopyranosyl-(1→4)-2-*O*-methyl-3, 6-anhydro-L-galactose dimethylacetal (I) and methyl *O*-2, 4, 6-tri-*O*-methyl-β-D-galactopyranosyl-(1→4)-2-*O*-methyl-3, 6-anhydro-β-L-galactopyranoside (II), both being derivatives of agarobiose (4-*O*-β-D-galactopyranosyl-3, 6-anhydro-L-galactose), which constitutes the repeating units of the agarose molecule. The total yield of compounds I and II amounted to 82% of the neutral products by weight.

The dimethylacetal (I) was eluted from the chromatographic column with 10~20% ethanol in water at 26~27°C and isolated in a crystalline form with the empirical formula $C_{12}H_{16}O_5 \cdot (OCH_3)_6$. Further, methylation with methyl iodide and silver oxide afforded hexa-*O*-methylagarobiose dimethylacetal, which on methanolysis yielded methyl 2, 3, 4, 6-tetra-*O*-methyl-α, β-D-galactoside and 2, 5-di-*O*-methyl-3, 6-anhydro-L-galactose dimethylacetal, identifying thereby compound I as a derivative of agarobiose. Hydrolysis with 0.02 N oxalic acid solution removed two methoxyl groups from the molecule to yield tetra-*O*-methylagarobiose, indicating that the compound I was a dimethylacetal. On methanolysis the compound I produced a mixture of methyl 2, 4, 6-tri-*O*-methyl-α, β-D-galactosides, methyl 2-*O*-methyl-3, 6-anhydro-β-L-galactopyranoside and 2-*O*-methyl-3, 6-anhydro-L-galactose dimethylacetal, the separation of the mixture being effected by selective hydrolysis of the anhydrosugar derivatives followed by fractionation with *n*-hexane. This established the positions of the four methoxyl groups connected in ether linkages with the rest of the molecule of compound I.




(I)




(II)

The methyl glycoside (II) was eluted from the charcoal column with 50% ethanol in water at 26~27°C and isolated in a crystalline form with the empirical formula $C_{12}H_{15}O_5(OCH_3)_5$. When treated with boiling methanol containing 3% of hydrogen chloride, it was converted with ease into the fore-going dimethylacetal (I). Hydrolysis of compound II with 0.02 N oxalic acid solution resulted in the formation of the reducing sugar identical with that obtainable from the dimethylacetal (I). These facts have enabled to be assigned structure II to the compound under problem, the β-configuration of the glycosidic methoxyl group being suggested on the basis of the positive value of optical rotation. Moreover, further methylation of compound II with methyl iodide and silver oxide afforded crystalline methyl penta-*O*-methyl-β-agarobioside, which agreed in all respects

1) Part XXI: C. Araki and S. Hirase, This Bulletin, 33, 291 (1960).
2) C. Araki, This Bulletin, 29, 543 (1956); *Memoirs Fac. Ind. Arts, Kyoto Tech. Univ.*, 5, 21 (1956).

with the methylated disaccharide derivative previously isolated by Araki[3], one of the present authors, by re-methylation of the methanolysis products of methylated agarose of *G. amansii*.

The isolation of compounds I and II in a good total yield emphasizes that agarobiose units are repeated through their 1 and 3′ positions in the molecule of agarose of *G. amansii* as previously suggested by Araki.

## Experimental

Evaporation and concentration of solutions were carried out under reduced pressure below 40°C. Melting points are uncorrected.

**Methanolysis of Methylated Agarose.**—Methylated agarose (10 g.) was suspended in methanol (150 ml.) containing 0.5% of hydrogen chloride and the suspension was heated under reflux for four hours, at which time undissolved material was removed by filtration. The filtrate was neutralized with silver carbonate, refiltered and evaporated to afford a sirup, which was then treated with 0.2 N barium hydroxide solution (100 ml.) at 60°C for two hours to saponify the methyl ester of the acidic component. The excess of the barium hydroxide was removed by neutralization with carbon dioxide and subsequent filtration, and the filtrate was evaporated to a sirup (7.4 g.).

**Separation of Neutral and Acidic Components.**—When the sirup obtained above was dissolved in ether (150 ml.), the acidic component was precipitated as a barium salt form. It was filtered off, washed with ether and dried in vacuo; yield, 0.18 g., $[\alpha]_D^{27}$ −26.4° in water (*c* 0.72). Evaporation of the filtrate afforded a mixture of neutral components as a colorless sirup; yield, 7.2 g., $[\alpha]_D^{27}$ −1.21° in water (*c* 0.83).

**Chromatographic Separation of Mixture of Neutral Components.**—The mixture of the neutral components (7.2 g.) obtained above was chromatographed at 25~27°C on a column (5.2×20 cm.) packed with charcoal (60 g.)and Celite (40 g.), successively higher concentrations of ethanol in water being used as developing solvents. The effluents were collected in separate receivers and evaporated to dryness to recover the contents, which were then weighed and the specific optical rotation, the methoxyl content and the molecular weight were measured. The results are shown in Table I.

TABLE I. CHROMATOGRAPHIC SEPARATION OF THE MIXTURE OF NEUTRAL COMPONENTS

| Fraction | Developer %* | Developer l. | Yield g. | $[\alpha]_D^{27}$ (°) $H_2O$ | $OCH_3$ % | M.W.** |
|---|---|---|---|---|---|---|
| I | 5 | 5 | 0.3 | − 0.6 | 42.1 | 211 |
| II | 7.5 | 5 | 0.5 | +97.8 | 48.3 | 225 |
| III | 10 | 5 | 1.6 | −29.3 | 43.3 | 423 |
| IV | 15 | 5 | 1.8 | −30.8 | 43.1 | 423 |
| V | 20 | 5 | 0.8 | −30.9 | 43.2 | 425 |
| VI | 30 | 6 | 0.4 | −11.0 | 40.8 | 410 |
| VII | 50 | 3 | 1.1 | +38.4 | 39.6 | 398 |
| VIII | 70 | 2 | 0.1 | +39.0 | 39.5 | 395 |

* Concentration of ethanol in water.
** Molecular weight was determined by Rast's method.

Fractions I and II were obtained as colorless sirups, but on standing the latter fraction crystallized partly. Papar chromatographic examination, using cyclohexanol saturated with water as a mobile phase[1] and *O*-aminophenol in aqueous ethanol acidified with phosphoric acid as a spraying reagent[4], indicated the presence of 2-*O*-methyl-3,6-anhydro-L-galactose dimethylacetal ($R_f$ 0.67) and methyl 2-*O*-methyl-3,6-anhydro-β-L-galactopyranoside ($R_f$ 0.77) in fraction I and of the latter compound in fraction II. When these were hydrolyzed with 1 N sulfuric acid for five hours in a boiling water bath and subsequently examined on paper chromatograms with *n*-butanol-ethanol-water (4 : 1 : 2) as a mobile phase and aniline hydrogen phthalate in moist *n*-butanol as a spraying reagent, 2,4,6-tri-*O*-methyl-D-galactose was detected in the hydrolyzates of both fractions I and II, the anhydrosugar derivatives being decomposed during the hydrolysis. It was therefore considered that fraction I was a mixture of 2-*O*-methyl-3,6-anhydro-L-galactose dimethylacetal, methyl 2-*O*-methyl-3,6-anhydro-L-galactopyranoside and methyl 2,4,6-tri-*O*-methyl-D-galactoside and that fraction II was a mixture of the latter two.

On the other hand, fractions III—V were proved to be entirely the dimethylacetal (I), and fractions VII and VIII were also proved to be entirely the methyl glycoside (II) as described below. Fraction VI seemed to be a mixture of compounds I and II.

**Tetra-*O*-methylagarobiose Dimethylacetal (I).**—All fractions III—V in Table I crystallized completely on standing and melted at 84~86°C. These were combined and recrystallized twice from ether containing a small amount of petroleum ether, affording the dimethylacetal (I) in prisms; m. p. 88~89°C, $[\alpha]_D^{19}$ −25.2° in water (*c* 1.19), $[\alpha]_D^{10}$ −41.9° in methanol (*c* 1.05) and $[\alpha]_D^{10}$ −46.7° in chloroform (*c* 1.07). The crude yields of the dimethylacetal thus amounted to 58% of the sample applied.

Found: C, 50.65; H, 8.06; $OCH_3$, 43.45; mol. wt., 425. Calcd. for $C_{12}H_{16}O_5(OCH_3)_6$: C, 50.69; H, 8.04; $OCH_3$, 43.67%; mol. wt., 426.5.

**Methanolysis of Dimethylacetal (I).**—The dimethylacetal (I) (1.5 g.) obtained above was dissolved in 3% methanolic hydrogen chloride (30 ml.) and heated under reflux for two hours, at which time the optical rotation of the solution reached a constant value ($[\alpha]_D$ −29° → +42°). The solution was neutralized with silver carbonate, filtered and evaporated to dryness, when a mixture of methyl 2-*O*-methyl-3,6-anhydro-β-L-galactopyranoside, 2-*O*-methyl-3,6-anhydro-L-galactose dimethylacetal and methyl 2,4,6-tri-*O*-methyl-D-galactoside was obtained as a sirup (1.3 g.); $[\alpha]_D^{25}$ +51.0° in water (*c* 1.0).

*a) Identification of methyl 2,4,6-tri-O-methyl-α,β-D-galactosides.*—The sirup obtained above was

3) C. Araki, *J. Chem. Soc. Japan*, (*Nippon Kwagaku Kwaishi*), **26**, 733 (1941).

4) S. Hirase, C. Araki and S. Nakanishi, This Bulletin **26**, 183 (1953).

5) S. M. Partridge, *Nature*, **164**, 443 (1949).

heated with 0.02 N oxalic acid solution for two hours in a boiling water bath to hydrolyze selectively the derivatives of 2-*O*-methyl-3,6-anhydro-L-galactose. The resulting product was isolated as a sirup in the usual manner and then extracted seven times each with 15 ml. of *n*-hexane at 50°C. The extracts were combined and evaporated to dryness, an anomeric mixture of methyl 2,4,6-tri-*O*-methyl-D-galactosides being obtained as crystals; yield, 0.50 g., m. p. 44~60°C, $[\alpha]_D^{27}$ +81.6° in water (*c*. 0.38), $OCH_3$ found: 51.67% (calcd. for $C_6H_8O_2(OCH_3)_4$: 52.52%). The methyl glycoside was identified by conversion in the usual manner into the corresponding reducing sugar[6], m. p. and mixed m. p. 109~110°C, $[\alpha]_D^{26}$ +116° → +90.1° in water (*c* 0.81), and its aniline derivative, m. p. and mixed m. p. 174°C, $[\alpha]_D^{26}$ −103° (initial) in acetone (*c* 0.40).

*b) Identification of 2-O-methyl-3,6-anhydro-L-galactose.* — The residual sirup, which had been separated from the methyl tri-*O*-methyl-D-galactoside by extraction with *n*-hexane as mentioned above was dissolved in acetone (5 ml.) and filtered. Evaporation of the filtrate afforded 2-*O*-methyl-3,6-anhydro-L-galactose[1] (0.65 g.), which seemed to be still contaminated with appreciable quantities of the methyl tri-*O*- methyl-D-galactoside as indicated by its positive value of the optical rotation $[\alpha]_D^{27}$ +24.1° in water (*c* 0.83) and its high methoxyl value 28.43% (calcd. for $C_6H_9O_4(OCH_3)$: 17.59%). But, without further purification, the sugar was oxidized with bromine water in the usual manner, and the resulting 2-*O*-methyl-3,6-anhydro-L-galactonic acid was crystallized from ethyl acetate; yield, 0.41 g., m. p. and mixed m. p. 141~142°, $[\alpha]_D^{25}$ −70.8° in water (*c* 0.72). One of the present authors has reported m. p. 142°C and $[\alpha]_D^{12}$ −70.0° in water for 2-*O*-methyl-3,6-anhydro-L-galactonic acid[7].

**Hexa-*O*-methylagarobiose Dimethylacetal from I.**—The dimethylacetal (I) (1.0 g.) was methylated twice with methyl iodide (15 g.) and silver oxide (10 g.) in the usual manner, giving hexa-*O*-methylagarobiose dimethylacetal as a colorless sirup; yield, 1.0 g., $[\alpha]_D^{10}$ −21.6° in water (*c* 1.11), $[\alpha]_D^{10}$ −37.3° in methanol (*c* 1.10), $[\alpha]_D^{10}$ −40.5° in chloroform (*c* 1.11), $n_D^{25}$ 1.4611, $OCH_3$ found: 54.18% (calcd. for $C_{12}H_{16}O_5(OCH_3)_6$: 54.61%). One of the present authors has reported $[\alpha]_D^{23}$ −11.09° in water, $[\alpha]_D^{23}$ −29.46° in chloroform and $n_D^{25}$ 1.4632 for hexa-*O*-methylagarobiose dimethylacetal[8].

**Methanolysis of Hexa-*O*-methylagarobiose Dimethylacetal.**—Hexa-*O*-methylagarobiose dimethylacetal (0.80 g.) obtained above was subjected to methanolysis with 3% methanolic hydrogen chloride (20 ml.) for twenty five hours. The hydrogen chloride was removed by neutralization with silver carbonate and filtration, and the filtrate on evaporation afforded a mixture of methyl 2,3,4,6-tetra-*O*-methyl-α,β-D-galactosides and 2,5-di-*O*-methyl-3,6-anhydro-L-galactose dimethylacetal; yield, 0.85 g., $[\alpha]_D^{10}$ +48.0° in water (*c* 1.00).

The mixture was separated at 10~13°C on a column (3.7×11 cm.) packed with charcoal and Celite into four fractions shown in Table II. Fraction I was identified as 2,5-di-*O*-methyl-3,6-anhydro-L-galactose dimethylacetal and fractions III and IV were done as methyl 2,3,4,6-tetra-*O*-methyl-α,β-D-galactosides as described below; while, fraction II seemed to be a mixture of the two components.

TABLE II. SEPARATION OF THE PRODUCTS OF METHANOLYSIS OF HEXA-*O*-METHYLAGAROBIOSE DIMETHYLACETAL

| Fraction | Developer %* | l. | Yield g. | $[\alpha]_D^{13}$ (°)$H_2O$ | $n_D^{25}$ | $OCH_3$ % |
|---|---|---|---|---|---|---|
| I | 7.5 | 2.0 | 0.20 | − 30.9 | 1.4547 | 52.31 |
| II | 10 | 2.0 | 0.18 | + 36.0 | 1.4531 | 55.41 |
| III | 10 | 2.5 | 0.12 | +180.0 | 1.4489 | 61.88 |
| IV | 12.5 | 2.0 | 0.06 | +180.0 | 1.4488 | 61.85 |

* Concentration of ethanol in water.

*a) Identification of 2,5-O-methyl-3,6-anhydro-L-galactose Dimethylacetal.*—The properties of fraction I in Table II agree with those of 2,5-di-*O*-methyl-3,6-anhydro-L-galactose dimethylacetal, which have been recorded by the present authors as: $[\alpha]_D^{17}$ −6.90°[8] or $[\alpha]_D^{19}$ −6.67°[9] in water and $n_D^{25}$ 1.4533[8] or $n_D^{20}$ 1.4563[9].

For confirmative identification, the dimethylacetal (0.15 g.) was converted into 2,5-di-*O*-methyl-3,6-anhydro-L-galactonic acid by hydrolyzing with 3% hydrobromic acid for five minutes in a boiling water bath and then oxidizing with bromine in the usual manner. The resulting carboxylic acid (0.16 g.) was purified by recrystallization from ethyl acetate; m. p. and mixed m. p. 160~161°C, $[\alpha]_D^{12}$ −62.2° in water (*c* 0.90). The present authors[3,9] have reported m. p. 161°C, $[\alpha]_D^{23}$ −54.32° in water and $[\alpha]_D^{21}$ −61.9° in water for the compound.

Found: C, 46.45; H, 6.88; $OCH_3$, 30.38. Calcd. for $C_6H_8O_4(OCH_3)_2$: C, 46.60; H, 6.84; $OCH_3$, 30.12%.

*b) Identification of Methyl 2,3,4,6-tetra-O-methyl-D-galactoside.*—Fractions III and IV in Table II agree in properties with methyl 2,3,4,6-tetra-*O*-methyl-D-galactoside. The fractions were combined and hydrolyzed with 1 N sulfuric acid in the usual manner to give the corresponding reducing sugar, which was crystallized from *n*-hexane; m. p. and mixed m. p. 70~72°C, $[\alpha]_D^{12}$ +144.4° (initial) → +120° (final) in water (*c* 0.45).

Found: C, 50.41; H, 8.51; $OCH_3$, 52.45. Calcd. for $C_6H_8O_2(OCH_3)_4$: C, 50.83; H, 8.53; $OCH_3$, 52.52%.

**Methyl Tetra-*O*-methyl-β-agarobioside (II).**—Fractions VII and VIII in Table I crystallized completely and melted at 143~144°C. These were combined and recrystallized twice from ethyl acetate, affording the pure sample of compound II in prisms; m. p. 143~144°C, $[\alpha]_D^{10}$ +41.7° in water (*c* 1.15), $[\alpha]_D^{15}$ +23.6° in methanol (*c* 1.10) and $[\alpha]_D^{10}$ +35.4° in chloroform (*c* 1.13).

Found: C, 51.67; H, 7.53; $OCH_3$, 39.51; mol.

6) C. Araki, *J. Chem. Soc. Japan (Nippon Kwagaku Kwaishi)*, **58**, 1362 (1937); E. G. V. Percival and J. C. Somerville, *J. Chem. Soc.* **1937**, 1615.

7) C. Araki, *J. Chem. Soc., Japan (Nippon Kwagaku Kwaishi)*, **61**, 775 (1940).

8) C. Araki, ibid., **65**, 533, 627 (1944).

9) S. Hirase, This Bulletin, **30**, 75 (1957).

wt., 394. Calcd. for $C_{12}H_{15}O_5(OCH_3)_5$: C, 51.77; H, 7.67; $OCH_3$, 39.35%; mol. wt., 394.4.

**Conversion of the Methyl Glycoside (II) into the Dimethylacetal (I).** — When methyl tetra-*O*-methyl-β-agarobioside (0.20 g.) obtained above was heated in 3% methanolic hydrogen chloride (20 ml.), the specific rotation of the solution changed from +14° to −29° within five minutes, at the end of which time the hydrochloric acid was removed by neutralization with silver carbonate and filtration. Evaporation of the filtrate gave a sirupy mixture of the dimethylacetal (I) and the starting material; yield, 0.20 g., $[\alpha]_D^{10}$ −11.3° in water (*c* 0.53). The mixture was then resolved into the components on a column (2.7×11 cm.) of charcoal and Celite. The dimethylacetal was eluted from the column with 30% ethanol in water and crystallized from ether containing a few drops of petroleum ether; yield, 0.14 g., m. p. 88~89°C, $[\alpha]_D^{10}$ −25.0° in water (*c* 0.80). Admixture with a sample of the dimethylacetal (I) described earlier showed no depression of the melting point. Subsequent elution of the column with 50% ethanol in water led to recovery of a small amount of the starting material.

**Methyl Penta-*O*-methyl-β-agarobioside from II.** —Methyl tetra-*O*-methyl-β-agarobioside (II) (0.30 g.) was methylated twice with methyl iodide (20 g.) and silver oxide (5 g.) in the usual manner. Extraction of the product with acetone followed by evaporation afforded methyl penta-*O*-methyl-β-agarobioside (0.30 g.), which was then recrystallized by dissolving in a small volume of ether and adding petroleum ether; m. p. 98~100°C, $[\alpha]_D^{10}$ +48.1° in water (*c* 1.04). One of the present authors has reported m. p. 99~100°C and $[\alpha]_D^{27}$ +48.32° in water for the methylated disaccharide derivative[3] previously isolated from methylated agarose. Admixture of the two showed no depression of the melting point.

Found: C, 52.85; H, 7.72; $OCH_3$, 45.68. Calcd. for $C_{12}H_{14}O_4(OCH_3)_6$: C, 52.93; H, 7.90; $OCH_3$, 45.59%.

**Tetra-*O*-methylagarobiose.** — *a) From the Dimethylacetal (I).* — The dimethylacetal (I) (0.20 g.) in 0.02 N aqueous oxalic acid solution (20 ml.) was heated in a boiling water bath for one and a half hours, during which time the specific rotation of the solution changed from an initial value −25° to a constant value +12°. The solution was neutralized with calcium carbonate, filtered and evaporated to a sirup, which was then extracted with acetone. Filtration and evaporation of the extract afforded tetra-*O*-methyl-agarobiose as glass; yield, 0.17 g., $[\alpha]_D^{13}$ −15.1° (constant) in water (*c* 0.86), $OCH_3$ found: 41.65% (calcd. for $C_{12}H_{16}O_6(OCH_3)_4$: 42.07%). It was soluble in water and organic solvents except ether and petroleum ether. It slowly reduced the Fehling solution at room temperature and restored the color of Schiffs reagent. Attempt to prepare a crystalline aniline derivative was unsuccessful.

*b) From methyl glycoside (II).* — The methyl glycoside (II) (0.20 g.) was hydrolyzed with 0.02 N oxalic acid solution in a boiling water bath for one and a half hours, during which time the specific rotation of the solution changed from an initial value +41° to a constant value −12°, the final value being in exact agreement with that observed for the hydrolysis of dimethylacetal (I). The eesulting tetra-*O*-methylagarobiose was isolated as glass in exactly the same manner as described above; yield, 0.19 g., $[\alpha]_D^{13}$ −15.6° (constant) in water (*c* 0.64), $OCH_3$ found 41.69%.

The authors wish to express their hearty thanks to Mr. K. Arai for micro-combustion and to Mr. T. Itô for assistance.

*Institute of Chemistry*
*Faculty of Industrial Arts*
*Kyoto Technical University*
*Matsugasaki, Kyoto*

# *The Kinetics of Substitution Reactions Involving Metal Complexes. III. Reaction between Copper(II) and Zinc-Ethylenediaminetetraacetate Complexes in Aqueous Solutions**

By Kiyoko KATO**

(Received October 12, 1959)

In the previous papers[1,2], the substitution reaction of copper(II) ions and lead-ethylenediaminetetraacetate (EDTA) complexes was reported. The rate of the reaction was followed by measuring the change of the polarographic diffusion current of copper(II) ions with the time. The reaction was found to proceed simultaneously through three different reaction paths.

* Requests for the reprint should be addressed to Nobuyuki Tanaka, Department of Chemistry, Faculty of Science, Tohoku University, Katahira-cho, Sendai.

** Present address: The Women's Department, Tokyo College of Pharmacy, 31, Uenosakuragi-cho, Taito-ku, Tokyo.

1) N. Tanaka, K. Kato and R. Tamamushi, This Bulletin, 31, 283 (1958).

2) N. Tanaka and K. Kato, ibid., 32, 1376 (1959).

under the experimental conditions, and the rate constants of the elementary reactions of those reaction paths were determined. The effect of acetate ions on the rate of the substitution reaction was explained quantitatively on the basis of the formation of acetato complexes of copper(II) and lead(II) and on the assumption that the substitution reaction proceeds only through the hydrated metal ions.

Since it seemed worth while to extend the study to the substitution reactions involving EDTA-complexes of other metal ions, the substitution reaction of copper(II) ions and zinc-EDTA complexes

$$Cu^{2+} + ZnY^{2-} \rightleftarrows CuY^{2-} + Zn^{2+}$$

was dealt with. The results are presented in this paper.

## Experimental

The preparation of solutions of copper(II) nitrate and disodium ethylenediaminetetraacetate was described in the previous paper[1]. A solution of zinc nitrate was prepared by dissolving a known amount of pure zinc metal in reagent-grade nitric acid.

The rate of the reaction between copper(II) ions and zinc-EDTA complexes was followed by measuring the change with the time in the polarographic diffusion current of copper(II) ions in acetate buffer solutions. Current-time curves were obtained with a Shimadzu RP-2 pen-recording polarograph. The dropping mercury electrode described in the previous paper[1] was used. This had an $m$ value of 1.27 mg./sec. and a drop time of 3.69 sec. in an air-free solution of 0.1 M potassium chloride at 25°C with open-circuit.

Measurements were made at 15 and 0°C in acetate buffers of pH 4.4 to 5.0 which contained 0.1 M of sodium acetate unless otherwise stated. The ionic strength was adjusted to be 0.2 with potassium nitrate. Gelatin was added as a maximum suppressor by 0.01% in concentration.

## Results and Discussion

In the solution containing acetate ions less than 0.2 M in concentration, copper(II) forms mono- and diacetato complexes, whereas zinc(II) forms only a monoacetato complex[3]. Therefore, the overall substitution reaction of copper(II) ions and zinc-EDTA complexes in acetate buffer solution is represented by the equations

$$Cu^{2+} + 2\,OAc^- \rightleftarrows CuOAc^+ + OAc^- \rightleftarrows Cu(OAc)_2 \quad (1)$$

$$Cu^{2+} + ZnY^{2-} \rightleftarrows CuY^{2-} + Zn^{2+} \quad (2)$$

$$Zn^{2+} + OAc^- \rightleftarrows ZnOAc^+ \quad (3)$$

where $Y^{4-}$ means a completely dissociated EDTA anion. Under the condition that both zinc ions and zinc-EDTA complexes are present in a large excess over copper(II) ions, the substitution reaction 2 can be simplified to

$$Cu^{2+} \underset{k^-}{\overset{k^+}{\rightleftarrows}} CuY^{2-} \quad (4)$$

The rate equation for reaction 4 is expressed as[2]

$$-\frac{d[Cu^{2+}]_{app}}{dt} = k^+ [Cu^{2+}]_{app} - k^- [CuY^{2-}] \quad (5)$$

where $[Cu^{2+}]_{app}$ is the concentration of copper(II) that can be determined polarographically, and given by the equation

$$[Cu^{2+}]_{app} = [Cu^{2+}] + [CuOAc^+] + [Cu(OAc)_2] \quad (6)$$

Integrating Eq. 5,

$$\ln\{[Cu^{2+}]_{app} - [Cu^{2+}]_{e,app}\} = -(k^+ + k^-)t + \ln\{[Cu^{2+}]_{0,app} - [Cu^{2+}]_{e,app}\}$$

is obtained, where subscripts 0 and e denote the initial and the equilibrium conditions, respectively. At the equilibrium of the reaction, the relation

$$\frac{k^+}{k^-} = \frac{[CuY^{2-}]_e}{[Cu^{2+}]_{e,app}} \fallingdotseq K^{Cu}_{Zn,app} \frac{[ZnY^{2-}]_0}{[Zn^{2+}]_{0,app}}$$

may be satisfied, where $K^{Cu}_{Zn,app}$ represents the apparent equilibrium constant expressed as

$$K^{Cu}_{Zn,app} = \frac{[Zn^{2+}]_{e,app}[CuY^{2-}]_e}{[Cu^{2+}]_{e,app}[ZnY^{2-}]_e}$$

The values of $K^{Cu}_{Zn,app}$ were determined polarographically to be 76 at 15°C and 92 at 0°C in acetate buffer solutions which contained 0.1 M of sodium acetate.

The apparent rate constant, $k^+/[ZnY^{2-}]_0$, was obtained at varied pH's at two different concentrations of zinc ions but at constant concentration of other species present. In Fig. 1 the values obtained at 15°C are plotted against the hydrogen ion concentration. This clearly indicates that a linear relation exists between $k^+/[ZnY^{2-}]_0$ and $[H^+]$. A similar relation was also found at 0°C.

On the basis of the dependencies of the observed apparent rate constants on the concentration of uncomplexed zinc ions, which are identical to those of the substitution reaction of copper(II) ions and lead-EDTA complexes[1,2], the following mechanisms were set down for reaction 2:

$$(i)\quad Cu^{2+} + ZnY^{2-} \underset{}{\overset{k_1^+}{\rightleftarrows}} CuY^{2-} + Zn^{2+} \quad (7)$$

$$(ii)\quad ZnY^{2-} + H^+ \rightleftarrows ZnHY^- \quad (8a)$$

3) N. Tanaka and K. Kato, ibid., 33, 417 (1960).

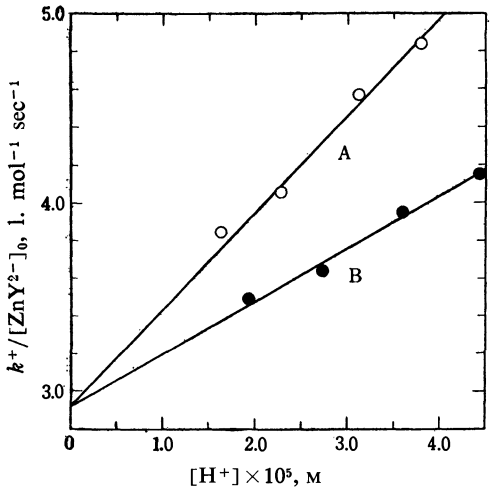



Fig. 1. $k^+/[ZnY^{2-}]_0$ as a function of the hydrogen ion concentration in acetate buffer-potassium nitrate solutions of ionic strength 0.2 at 15°C. Initial concentrations are: $[Cu^{2+}]_{0,app}=1.20\times10^{-4}$ M; $[ZnY^{2-}]_0=4.03\times10^{-3}$ M; $[Zn^{2+}]_{0,app}=1.12\times10^{-2}$ M (curve A) and $2.64\times10^{-2}$ M (curve B). Concentrations of free acetate are: 0.096 M (A) and 0.091 M (B).

$$Cu^{2+} + ZnHY^- \overset{k_{II}^+}{\rightleftarrows} CuHY^- + Zn^{2+} \quad (8b)$$

$$CuHY^- \rightleftarrows CuY^{2-} + H^+ \quad (8c)$$

(iii) $$ZnY^{2-} + H^+ \rightleftarrows Zn^{2+} + HY^{3-} \quad (9a)$$

$$Cu^{2+} + HY^{3-} \overset{k_{III}^+}{\rightleftarrows} CuY^{2-} + H^+ \quad (9b)$$

As has been mentioned previously[2], the concentration which was actually measured polarographically was not the concentration of hydrated copper(II) ions but the sum of the concentrations of hydrated ions and acetato complexes. If it is assumed that the substitution reaction proceeds through only the hydrated metal ions which are in equilibrium with the acetato complexes, the apparent rate of the forward reaction ($v^+=k^+[Cu^{2+}]_{app}$) determined polarographically is expressed as

$$v^+=\left\{\frac{k_1^+ + k_2^+[H^+] + k_3^+[H^+]\dfrac{1+K_{ZnAOc}[OAc^-]}{[Zn^{2+}]_{app}}}{1+\sum_{n=1}^{2}K_{Cu(OAc)_n}[OAc^-]^n}\right\}\times[Cu^{2+}]_{app}[ZnY^{2-}] \quad (10)$$

where

$$k_2^+=k_{II}^+K_{ZnHY}^H, \quad k_3^+=k_{III}^+/(K_{ZnY}K_{HY}) \quad (11)$$

$K_{ZnHY}^H$ represents the equilibrium constant of reaction 8a, $K_{ZnY}$, the formation constant of $ZnY^{2-}$ and $K_{HY}$, the fourth dissociation constant of ethylenediaminetetraacetic acid. $K_{Cu(OAc)_n}$ and $K_{ZnOAc}$ represent the overall formation constants of acetatocopper(II) and acetatozinc-(II) complexes, respectively.

From Eqs. 5 and 10, the relation

$$\frac{k^+}{[ZnY^{2-}]_0}=\frac{k_1^+ + k_2^+[H^+] + k_3^+[H^+]\dfrac{1+K_{ZnOAc}[OAc^-]}{[Zn^{2+}]_{0,app}}}{1+\sum_{n=1}^{2}K_{Cu(OAc)_n}[OAc^-]^n} \quad (12)$$

is obtained, where the initial concentrations, $[Zn^{2+}]_0$ and $[ZnY^{2-}]_0$, are substituted for $[Zn^{2+}]$ and $[ZnY^{2-}]$, respectively. Since both $Zn^{2+}$ and $ZnY^{2-}$ are present in the reaction mixture in a large excess over the concentration of copper-(II), the changes of their concentrations can be neglected.

The rate constants in Eq. 10 were calculated from the plots of $k^+/[ZnY^{2-}]_0$ against hydrogen ion concentration, which are tabulated in Table I. The values of $K_{CuOAc}$, $K_{Cu(OAc)_2}$ and $K_{ZnOAc}$ used in this calculation were 41, 190 and 5.7, respectively. These were all determined polarographically at ionic strength 0.2 at 15°C[3]. The concentration of uncomplexed acetate in the solution was calculated by successive approximation.

Table I. Rate constants in Eq. 10 obtained experimentally at ionic strength 0.2 at various temperatures

| Temp., °C | Rate constant, l. mol$^{-1}$ sec$^{-1}$ | | |
|---|---|---|---|
| | $k_1^+$ | $k_2^+$ | $k_3^+$ |
| 0 | 5.2 | $3\times10^4$ | $7.1\times10^2$ |
| 15 | 19 | $5\times10^4$ | $2.1\times10^3$ |

The rate constants of both elementary reactions 8b and 9b were calculated from the relations given in Eq. 11, using the values of $K_{ZnHY}^H$, $K_{ZnY}$ and $K_{HY}$ in Table II. The value of $K_{ZnHY}^H$ which was determined by Schwarzenbach et al.[4] at 20°C at ionic strength 0.1 was used after correction for ionic strength with the Debye-Hückel equation. The values of $K_{ZnY}$ at 15 and 0°C were obtained by dividing the value of $K_{CuY}$ by those of $K_{Zn}^{Cu}$. As for $K_{CuY}$, the values obtained by Schwarzenbach et al.[4]

4) G. Schwarzenbach, R. Gut and G. Anderegg, *Helv. Chim. Acta*, 37, 937 (1954).

were used after correction for temperature and ionic strength[2]. The equilibrium constants of reaction 2 at zero acetate concentration, $K_{Zn}^{Cu}$, used in this calculation were 320 at 15°C[3] and 310 at 0°C, the latter of which was estimated by extrapolation. The rate constants of three elementary reactions 7, 8b and 9b thus calculated are summarized in Table III.

Table II. Equilibrium constants at ionic strength 0.2 at various temperatures

| Temp., °C | $\log K_{ZnY}$ | $pK_{HY}$ | $\log K_{ZnHY}^{H}$ |
|---|---|---|---|
| 0 | 16.51 | 10.41 | — |
| 15 | 16.17 | 10.20 | — |
| 20 | — | — | 2.9 |

Table III. Rate constants for reactions 7, 8b and 9b at ionic strength 0.2 at various temperatures

| Temp., °C | Rate constant, l. mol$^{-1}$ sec$^{-1}$ | | |
|---|---|---|---|
| | $k_1^+$ | $k_{II}^+$ | $k_{III}^+$ |
| 0 | 5.2 | 40 | $8.9\times10^8$ |
| 15 | 19 | 60 | $2.0\times10^9$ |

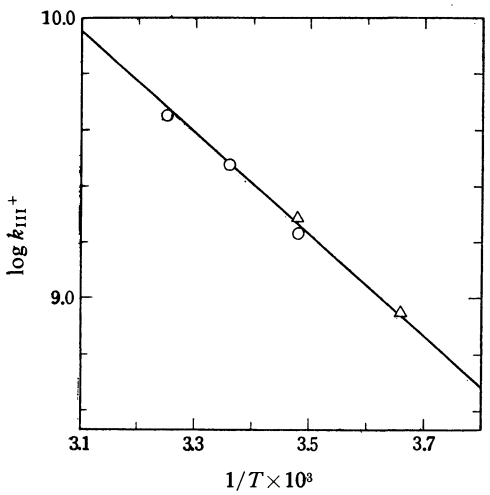



Fig. 2. The relation between the logarithm of rate constant and the reciprocal of absolute temperature for the reaction $Cu^{2+} + HY^{3-} \xrightarrow{k_{III}^+} CuY^{2-} + H^+$. ○ indicates the value obtained in the reaction of copper(II) ions and lead-EDTA complexes and △, in the reaction of copper-(II) ions and zinc-EDTA complexes.

From these results, the rate constants expressed in the form of the Arrhenius equation were derived and the heats of activation and the entropies of activation were calculated for three elementary reactions 7, 8b and 9b. The results are given in Table IV.

The rate constants of reaction 9b were obtained at 15 and 0°C in this study as given in Table III. The logarithmic values of $k_{III}^+$ are plotted against the reciprocal of absolute temperature as shown in Fig. 2. The rate constants of the same reaction were previously obtained at 15, 25 and 35° in the study of the substitution reaction of copper(II) ions and lead-EDTA complexes[2]. They are also shown in Fig. 2, which are in good agreement with the present ones. This fact supports the validity of the method for the determination of the rate constants proposed in this series of papers.

From Eq. 10, it is predicted that the reaction rate decreases with the increase of acetate concentration. Using Eq. 12, the values of $k^+/[ZnY^{2-}]_0$ were calculated at various acetate concentrations with the rate constants given in Table I and

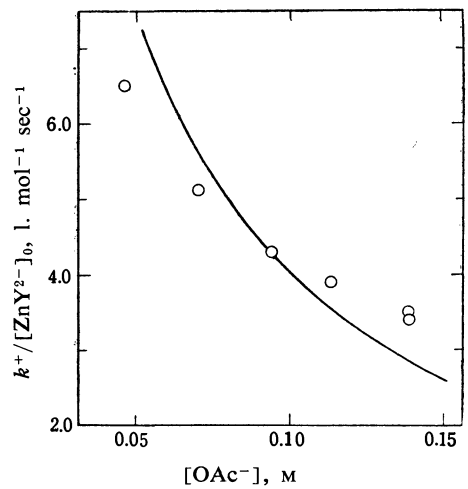



Fig. 3. $k^+/[ZnY^{2-}]_0$ as a function of the acetate concentration in acetate buffer-potassium nitrate solutions of pH 4.70 and ionic strength 0.2 at 15°C. Initial concentrations are:
$[Cu^{2+}]_{0,app} = 1.20\times10^{-4}$ M;
$[ZnY^{2-}]_0 = 4.03\times10^{-3}$ M;
$[Zn^{2+}]_{0,app} = 1.12\times10^{-2}$ M
—— indicates the theoretical curve and ○, the experimental value.

Table IV. Rate constants, heats of activation and entropies of activation for reactions 7, 8b and 9b

| Reaction | Rate constant, expressed in l. mol$^{-1}$ sec$^{-1}$ | $\Delta H^{\ddagger}$, kcal. mol$^{-1}$ | $\Delta S^{\ddagger}$, e. u. |
|---|---|---|---|
| $Cu^{2+} + ZnY^{2-} \rightarrow CuY^{2-} + Zn^{2+}$ | $k_1^+ = 1.5\times10^{11}\exp(-13{,}000/\boldsymbol{R}T)$ | 12 | − 9.3 |
| $Cu^{2+} + ZnHY^- \rightarrow CuHY^- + Zn^{2+}$ | $k_{II}^+ = 6.3\times10^5\exp(-5{,}300/\boldsymbol{R}T)$ | 4.7 | −34 |
| $Cu^{2+} + HY^{3-} \rightarrow CuY^{2-} + H^+$ | $k_{III}^+ = 3.4\times10^{15}\exp(-8{,}200/\boldsymbol{R}T)$ | 7.6 | 11 |

the formation constants of the acetato complexes. In Fig. 3, they are plotted against acetate concentration and compared with the values which were experimentally measured at various acetate concentrations, the other conditions being kept constant. The deviation of the experimental values from the calculated ones is considered as probably due to a contribution of the reactions in which acetatocopper(II) complexes participate.

## Summary

The kinetic study of the substitution reaction of copper(II) and zinc-EDTA complexes in acetate buffer solutions was carried out with the same procedure as reported previously[1,2]. The reaction was found to proceed simultaneously through three different reaction paths under the experimental conditions. The rate constants for three elementary reactions of those reaction paths were determined at 15 and 0°C, and the heats of activation and the entropies of activation for the reactions were calculated.

The author wishes to express her hearty thanks to Professor Nobuyuki Tanaka for his guidance and encouragement in the course of this work.

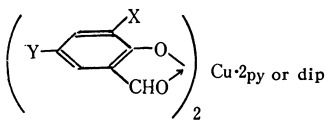
*Department of Chemistry*
*Faculty of Science*
*Tohoku University*
*Katahira-cho, Sendai*

# *The Addition Compounds of Bis-salicylaldehyde Copper(II) and its Derivatives with Pyridine and α, α'-Dipyridyl. II. Some Studies on the Structures*

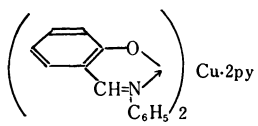
By Yoneichiro MUTO

(Received September 28, 1959)

There are studies by several investigators reporting that copper(II) can form a complex with coordination numbers higher than four[1]. In the first paper[2] of this series, the author has reported the isolation of the addition compounds of bis-salicylaldehyde copper(II) and a number of its derivatives with pyridine or α, α'-dipyridyl having Formula I.




I




II

(X: H, $NO_2$; Y: H, Br, $NO_2$; py: Pyridine; dip: α, α'-Dipyridyl).

Although a hexa-coordinated octahedral configuration has been considered for bis-pyridine-bis-salicylaldehyde nickel by magnetochemical study[3], it is not definitely confirmed whether or not the copper atoms of these addition compounds are coordinated with six donors as yet. This paper presents some studies undertaken in order to investigate the structures of these addition compounds.

**Spectrophotometric Studies.**—Recently, Waters and Hall[4] have suggested that bis-salicylaldehyde copper(II) is solvated in coordinating solvents such as pyridine to give a penta- or hexa-coordinated copper(II) complex from the spectral change in various solvents. On the other hand, Charles[5] has shown that the spectra of some bis-*N*-*n*-alkylsalicylaldimine copper(II) in pyridine are similar to those in dioxane or toluene, although this is not the case with the corresponding nickel complexes. Therefore, he has concluded that no specific interaction (to form hexa-coordinated complexes) is present between the complexes and pyridine. However, the present author has observed that brown

1) H. B. Jonassen, R. E. Reeves and L. Sgal, *J. Am. Chem. Soc.*, 77, 2748 (1955); S. Kirschner, ibid., 78, 2372 (1956); D. E. C. Corbridge and E. G. Cox, *J. Chem. Soc.*, 1956, 594; etc.

2) Y. Muto, This Bulletin, 31, 56 (1958).

3) F. Basolo and W. R. Matoush, *J. Am. Chem. Soc.*, 75, 5663 (1953).

4) T. N. Waters and D. Hall, *J. Chem. Soc.*, 1959, 1200.

5) R. G. Charles, *J. Am. Chem. Soc.*, 81, 1793 (1959).

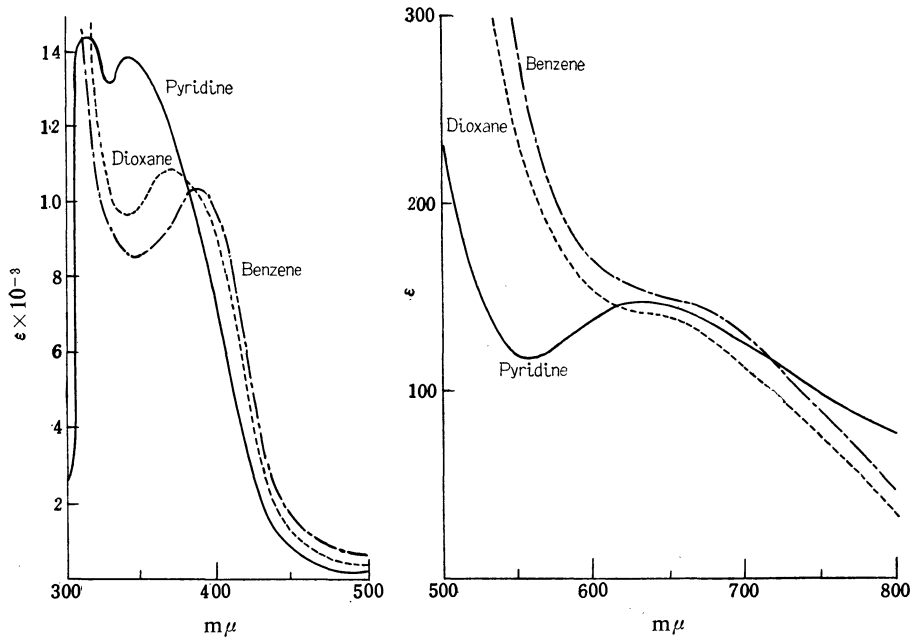


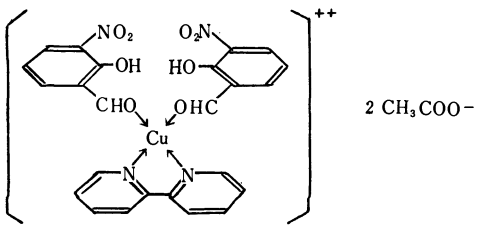

Fig. 1. Absorption spectra of bis-*N*-phenylsalicylaldimine copper(II).

bis-*N*-phenylsalicylaldimine copper(II) forms green crystals of a pyridinate having Formula II[2] and that its spectrum in pyridine is dissimilar to that in dioxane or benzene (Fig. 1). These facts confirm the formation of a hexa-coordination of the copper atom.

In addition, the author has observed that the absorption bands of bis-salicylaldehyde copper (II), a number of its derivatives, and bis-acetylacetone copper(II) in pyridine appear at longer wavelengths than those in dioxane (Figs. 2 and 3 and Table I). Probably, this indicates that the bands shift toward the longer wavelength side, owing to the formation of the hexa-coordinated copper(II) complexes in pyridine*.

**Some Behaviors of the Addition Compounds.** —Assuming that the addition compounds prepared in this study are hexa-coordinated copper-(II) complexes, the bond between the fifth or sixth donor and the copper atom should be weak relatively, as has been guessed from the fact that the usual coordination number of copper(II) is four. Actually, some of the pyridinates readily liberate pyridine. For example, bis-pyridine-bis-salicylaldehyde copper (II) lost pyridine gradually at room temperature. Also, the addition compounds with $\alpha, \alpha'$-dipyridyl were oxidized on heating in organic solvents such as ethanol to yield the derivatives of copper(II) monosalicylate[2], although $\alpha, \alpha'$-dipyridyl could be liberated from them with difficulty. This fact shows that probably the CHO → Cu bond is weak as compared with the N → Cu bond (in which N is a nitrogen atom of $\alpha, \alpha'$-dipyridyl). Namely, the CHO → Cu bond would be broken on heating in organic solvents, and then the aldehyde group would be oxidized, as benzaldehyde readily undergoes oxidation to benzoic acid in the presence of air.

**Addition Compounds of $\alpha, \alpha'$-Dipyridyl-bis-3-nitrosalicylaldehyde Copper(II).** — Among the addition compounds prepared in this study, only $\alpha, \alpha'$-dipyridyl-bis-3-nitrosalicylaldehyde copper(II) formed further addition compounds with chloroform, picric acid and acetic acid. Although no direct evidence has yet been afforded to elucidate the structures of these




III

* It has been noticed by several investigators[6-8] that the absorption bands (from the near infrared to the near ultraviolet) of copper(II) complexes generally appear at longer wavelengths for hexa-coordinated complexes than for tetra-coordinated ones.

6) J. Bjerrum, C. J. Ballhausen and C. K. Jørgensen, *Acta Chem. Scand.*, **8**, 1275 (1954).

7) H. Ito, *J. Chem. Soc. Japan, Pure Chem. Sec. (Nippon Kagaku Zasshi)*, **77**, 1395 (1956).

8) G. Gordon and R. K. Birdwhistell, *J. Am. Chem. Soc.*, **81**, 3567 (1959).

addition compounds by physical methods such as X-ray analysis, Formula III has been presumed for the acetate for the following reasons. First, it was observed that $\alpha,\alpha'$-dipyridyl-bis-3-nitrosalicylaldehyde copper(II) could not be oxidized by heating in organic solvents and that $\alpha,\alpha'$-dipyridyl and 3-nitrosalicylaldehyde could be liberated from this complex with difficulty by the action of acetic acid, although other addition compounds with $\alpha,\alpha'$-dipyridyl were decomposed to give $\alpha,\alpha'$-dipyridyl-copper(II)-acetate. From these results, it seems that CHO → Cu and N → Cu bonds are relatively strong. Secondly, it seems that the bond between copper and phenolic oxygen in $\alpha,\alpha'$-dipyridyl-bis-3-nitrosalicylaldehyde copper(II) has an ionic character to a considerable extent owing to the presence of a nitro and an aldehyde group at the ortho positions. Also, it has been observed that relatively strong acids such as picric acid or acetic acid add to the complex, while very weak acids such as phenol or cresol do not do so**. Therefore, it is possible that the complex forms a salt as shown in III.

TABLE I. ABSORPTION MAXIMA OF BIS-SALICYLALDEHYDE COPPER(II) DERIVATIVES IN THE VISIBLE REGION

| Substituent | Solvents: Dioxane | Pyridine | (Addition compounds with $\alpha,\alpha'$-dipyridyl) Pyridine |
|---|---|---|---|
| 5-Methyl | 675 (1.71) | 750 (2.04) | |
| None | 670 (1.70) | 740 (2.02) | 700 (1.97) |
| 5-Chloro | 621 (1.62) | 759 (1.95) | |
| 5-Bromo | 655 (1.93) | 756 (2.27) | |
| 3-Nitro-5-methyl | 638 (1.65) | 760 (1.92) | 720 (1.97) |
| 3-Nitro | 670 (1.60) | 710 (1.81) | 704 (1.84) |
| 5-Nitro | 619 ( ? ) | 660 (2.45) | 636 (2.40) |
| 3,5-Dinitro | 645 ( ? ) | 675 (2.37) | |
| Salicylaldehyde-ethylenedimine | 576 (2.55) | 602 (2.53) | |
| Bis-acetylacetone | 612 (1.57) | 654 (1.88) | |

The values in parentheses are the logarithms of molar extinction coefficients ($\log \varepsilon$) at the maxima. The value marked with a question mark could not be determined accurately owing to the slight solubility of the complex in dioxane.

## Experimental

**Spectrophotometric Measurements.**—Bis-salicylaldehyde copper(II), its derivatives and bis-acetylacetone copper(II) were prepared by conventional methods. The addition compounds with $\alpha,\alpha'$-dipyridyl were prepared by the method described in the first paper[2] of this study. Although bis-*N*-phenylsalicylaldimine copper(II) was very soluble in various organic solvents, other complexes were soluble in pyridine, slightly soluble in dioxane, and soluble with difficulty in other common organic solvents.

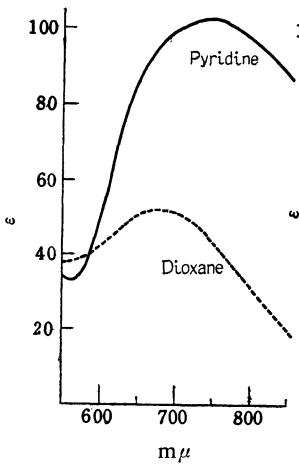



Fig. 2. Absorption spectra of bis-salicylaldehyde copper(II).

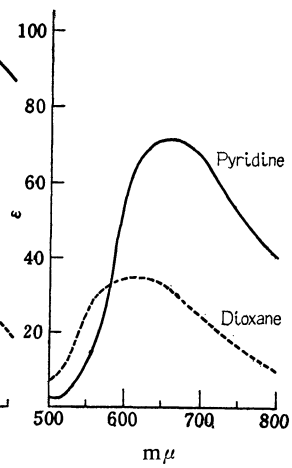



Fig. 3. Absorption spectra of bis-acetylacetone copper(II).

The absorption spectra were determined at 25 ±1°C with a Hitachi spectrophotometer (model EPU-2A) using 1 cm. quartz cells. The concentration of the complexes in solutions ranged from $5\times10^{-5}$ to $3\times10^{-3}$ mol. per liter depending upon the degree of absorption.

*Preparation of additon compounds of $\alpha,\alpha'$-dipyridyl-bis-3-nitrosalicylaldehyde copper(II) with chloroform, picric acid, and acetic acid.*—1) Cu·[O·$C_6H_3(NO_2)$·CHO]$_2$·dip·$CHCl_3$.—$\alpha,\alpha'$-Dipyridyl-bis-3-nitrosalicylaldehyde copper(II) (yellow-brown crystals) (0.6 g.) was dissolved in chloroform (30 ml.) and the resulting brown solution was filtered. The filtrate was allowed to stand overnight in air at room temperature; meanwhile the addition compound crystallized in green prismatic crystals. It was purified by repeated recrystallization from chloroform.

Found: C, 44.67; H, 2.85; N, 8.17; Cu, 8.59; $CHCl_3$, 17.82. Calcd. for $C_{14}H_8O_8N_2$·Cu·$C_{10}H_8N_2$·$CHCl_3$: C, 44.73; H, 2.55; N, 8.35; Cu, 8.56; $CHCl_3$, 17.78%.

Both $\alpha,\alpha'$-dipyridyl-bis-3-nitrosalicylaldehyde cobalt(II) and the corresponding nickel complex prepared by a method of synthesis similar to that employed for the copper(II) complex formed no addition compound with chloroform.

The cobalt complex was isolated in the form of red crystals.

Found: N, 10.16; Co, 10.82. Calcd. for $C_{14}H_8O_8N_2$·Co·$C_{10}H_8N_2$; N, 10.24; Co, 10.77%.

The nickel complex was isolated in the form of orange crystals.

Found: N, 10.29; Ni, 10.56. Calcd. for $C_{14}H_8O_8N_2$·Ni·$C_{10}H_8N_2$; N, 10.24; Ni, 10.73%.

** Although it has been observed that *p*-nitrophenol add to the complex, the addition compound can not be isolated in the pure state.

2) Cu · [O · $C_6H_3(NO_2)$ · CHO]$_2$ · dip · HO · $C_6H_2(NO_2)_3$. —$\alpha,\alpha'$-Dipyridyl-bis-3-nitrosalicylaldehyde copper(II) (0.3 g.) was added to 50 ml. of ether containing 0.2 g. of picric acid. The mixture was refluxed on a water bath for half an hour, meanwhile the addition compound crystallized in green prismatic crystals. The separated crystals were washed with ether repeatedly and then dried in a desiccator over sulfuric acid.

Found: C, 46.40; H, 2.71; N, 12.47; Cu, 8.16. Calcd. for $C_{14}H_8O_8N_2 \cdot Cu \cdot C_{10}H_8N_2 \cdot C_6H_3O_7N_3$; C, 46.13; N, 12.55; Cu, 8.15%.

3) Cu · [O · $C_6H_3(NO_2)$ · CHO]$_2$ · dip · $(CH_3COOH)_2$. —$\alpha,\alpha'$-Dipyridyl-bis-3-nitrosalicylaldehyde copper-(II) (0.6 g.) was dissolved in a mixture of ether (20 ml.) and acetic acid (3 ml.) and the resulting solution was filtered. When 30 ml. of ether was added to the filtrate, the addition compound precipitated in green prismatic crystals. The crystals were separated, washed with ether repeatedly, and then dried in a vacuum desiccator over sulfuric acid.

Found: C, 49.76; H, 3.89; N, 8.23; Cu, 9.26; $CH_3COOH$, 17.73. Calcd. for $C_{14}H_8O_8N_2 \cdot Cu \cdot C_{10}H_8N_2 \cdot C_4H_8O_4$: C, 50.04; H, 3.60; N, 8.34; Cu, 9.45; $CH_3COOH$, 17.87%.

The author is grateful to Mr. Michio Shido of Kyushu University for carrying out the elementary analysis of the compounds prepared.

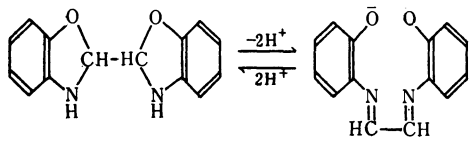
*Chemical Laboratory*
*Faculty of Liberal Arts*
*Saga University*
*Honjo-machi, Saga*

# *On the Structure of Condensation Products of o-Aminophenols with α-Dicarbonyl Compounds. III. Copper Chelates of 2, 2'-Bibenzoxazoline Derivatives*

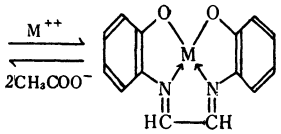
By Ichiro MURASE

(Received October 12, 1959)

In previous papers[1,2], the condensation products of *o*-aminophenols (2 mol.) with *α*-dicarbonyl compounds (1 mol.) were determined to have the structure of 2, 2'-bibenzoxazolines (I). In addition, 2, 2'-bibenzoxazoline tautomerized to the corresponding Schiff base (II) in ethanol solution on addition of alkali, the formation of its metal chelates being explained by the scheme indicated below. The structure of metal chelates was thus in agreement with the one stated by Bayer[3] as the derivatives of glyoxal bis-(2-hydroxy anil) (III).

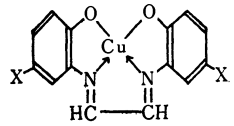


I II



III

Here, the reaction of copper acetate with 2, 2'-bibenzoxazoline derivatives was conducted, obtaining copper chelates of 5, 5'-dinitro (IV), 5, 5'-dimethyl (V) and 5, 5'-dichloro (VI) derivative as deep violet or blue amorphous powder.



IV, X=$NO_2$ V, X=$CH_3$ VI, X=Cl

The absorption spectra in ethanol of these compounds were taken by the method indicated in the experimental part and they are shown in Fig. 1, where $\varepsilon$ of each copper chelate was expediently calculated by means of concentrations of bibenzoxazolines dissolved.

Each spectrum did not represent the true feature of the copper chelate itself since the solution consisted of equilibrium mixture of bibenzoxazoline and copper chelate as suggested from the above scheme. However, the band at

1) I. Murase, This Bulletin, **32**, 827 (1959).
2) I. Murase, ibid., **33**, 59 (1960).
3) E. Bayer, *Ber.*, **90**, 2325 (1957).

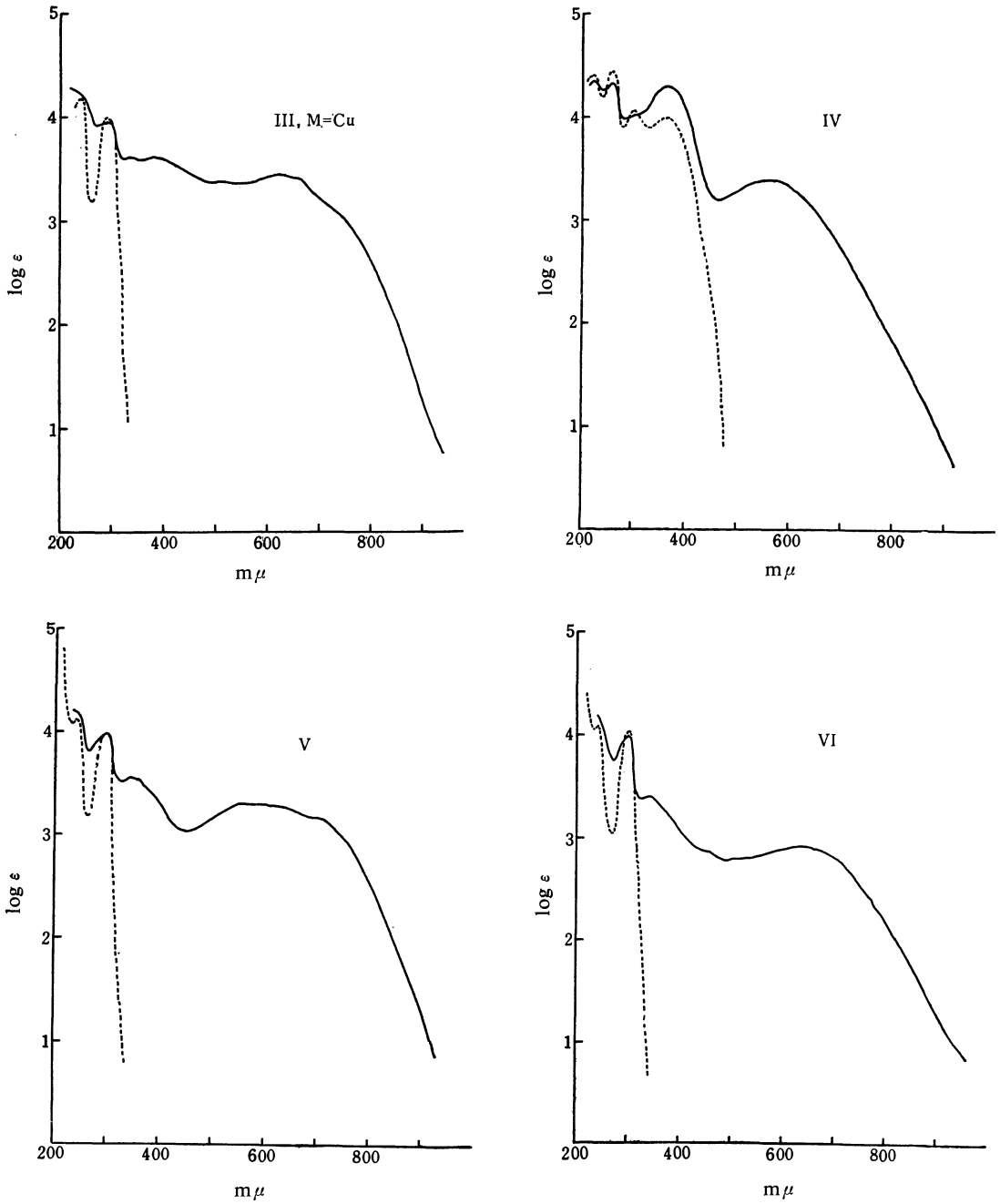


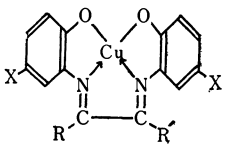

Fig. 1. Ultraviolet and visible absorption spectra of copper chelates of 2,2′-bibenzoxazoline and its derivatives in ethanol, ——; copper chelate, ------; parent bibenzoxazoline or its derivative.

500~600 mμ in each spectrum should be due to metal-ligand linkage and it resembles the authentic one of glyoxal bis-(2-hydroxy anil)-copper (Fig. 1, III, M=Cu), the solution of which was prepared also in the same manner as other chelates. Therefore, it has been assumed from those spectra that these copper chelates have structures IV—VI.

In the case of 2-substituted and 2,2′-disubstituted derivatives of 2,2′-bibenzoxazoline such as 2-methyl-, 5,5′-dinitro-2-methyl-, 2-methyl-2′-ethyl-2,2′-diethyl- and 2-methyl-2′-phenyl-bibenzoxazoline, with the exception of 2,2′-dimethyl derivative, deep violet or blue colored solutions

were obtained by addition of copper acetate to their ethanol solutions. On concentration of these colored solutions, no copper chelates were isolated, instead the oxazolines were recovered unchanged. However, the presence of the chelates in solution was suggested by their coloration and was revealed by their absorption spectra which are shown in Fig. 2, where $\varepsilon$ of each copper chelate was calculated in the same manner as in Fig. 1.

These spectra resemble those in Fig. 1 in having absorption bands at 500~600 m$\mu$, though their absorption intensities varied with substituents in 2, 2′-positions. Thus, the presence of copper chelates in solution of similar structures VII—XII has been recognized.



VII, R=$CH_3$, R′=X=H
IIX, R=$CH_3$ R′=H, X=$NO_2$
IX, R=R′=$CH_3$, X=H
X, R=$CH_3$, R′=$C_2H_5$, X=H
XI, R=R′=$C_2H_5$, X=H
XII, R=$CH_3$, R′=$C_6H_5$, X=H

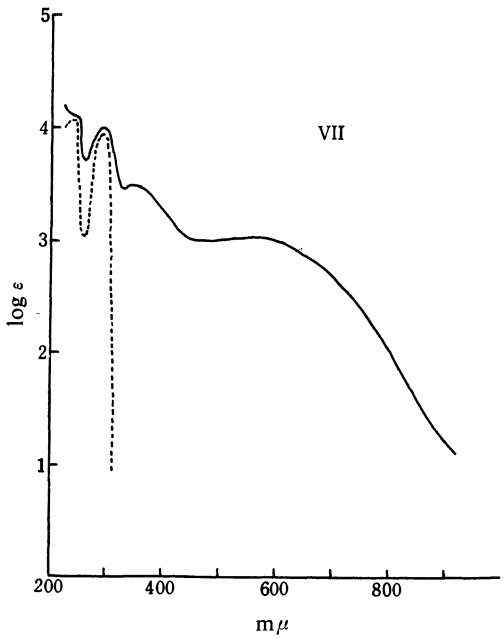
The reason why these copper chelates could not be isolated may be that their formation constant is considerably small. Since the formation constant in each case should be introduced from overall equilibrium consisting of oxazoline, Schiff base and chelate, the proportion of the tautomeric form of oxazoline in the mixture should be considered to be very small.

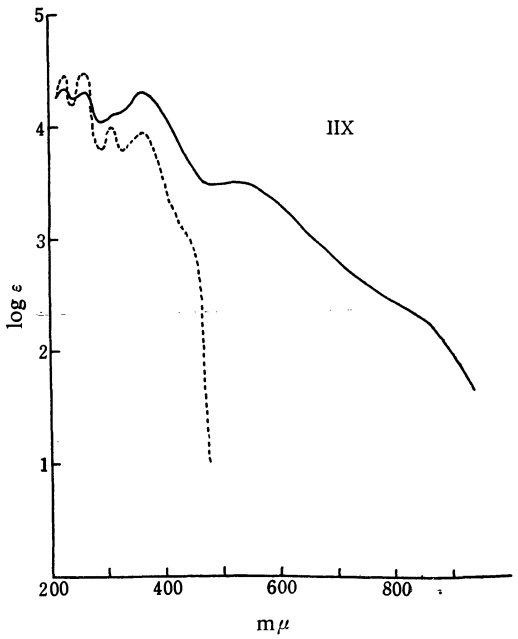
With respect to the condensation product of *o*-aminophenol with diacetyl, Bayer explained its inability to form metal chelate as the result of the hindrance of methyl groups in diacetyl bis-(2-hydroxy anil), but the author previously suggested, from the spectroscopic behavior toward alkali, that 2, 2′-dimethyl-2, 2′-bibenzoxazoline does not tautomerize to diacetyl bis-(2-hydroxy anil) and forms no metal chelates[1].

Apparently no deep coloration was observed when copper acetate was added to this compound in ethanol. Nevertheless, in this case also, the presence of the chelate in solution was suggested from the careful observation of its spectrum (Fig. 2, IX); an absorption maximum was observed at 560 m$\mu$ though in very weak intensity. Thus, it was found that 2, 2′-dimethyl-2, 2′-bibenzoxazoline still possesses a tendency of tautomerism and of formation of copper chelate in solution.

Thus, it is concluded that 2, 2′-bibenzoxazolines acquire an ability of metal chelate formation through tautomerism, which is most remarkable in the case of 2, 2′-unsubstituted derivatives and is hindered by substituents at 2, 2′-position, among which the methyl group is most effective and the phenyl group is not so much.

In the case of carboxy derivatives of bibenzoxazoline, it is interesting to note that 5, 5′-dicarboxy derivative gave reddish violet precipitates on reacting with an equimolar amount



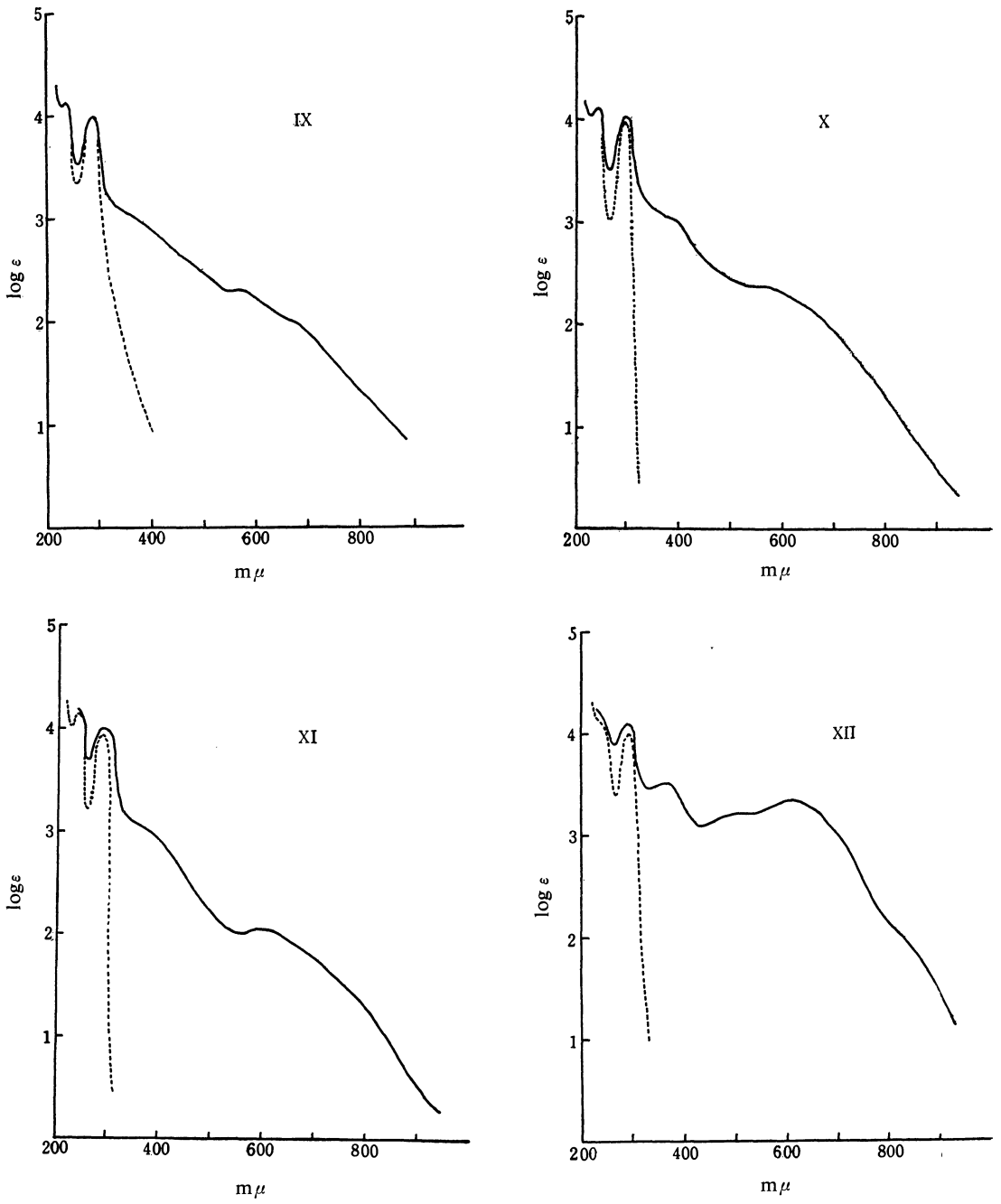



Fig. 2. Ultraviolet and visible absorption spectra of copper chelates of 2, 2'-bibenzoxazoline derivatives in ethanol, ——; copper chelate, ------; parent bibenzoxazoline derivative.

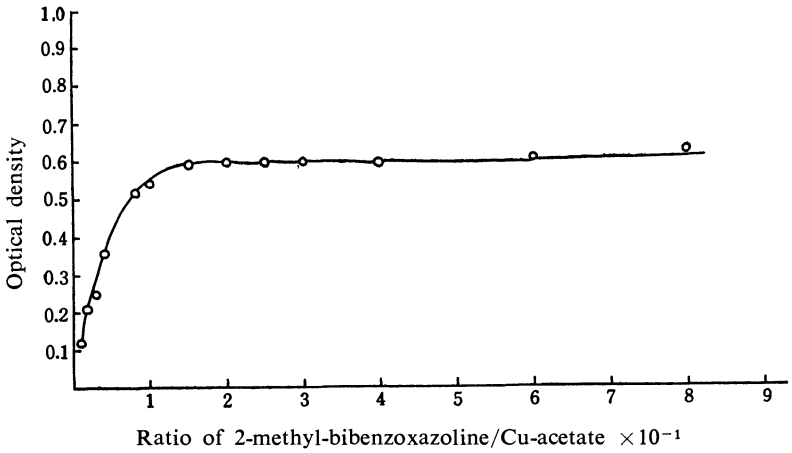



Fig. 3. Optical densities at 540 mμ of various solutions with excess 2-methyl-bibenzoxazoline present: Cu-acetate = $9.99 \times 10^{-5}$ M.

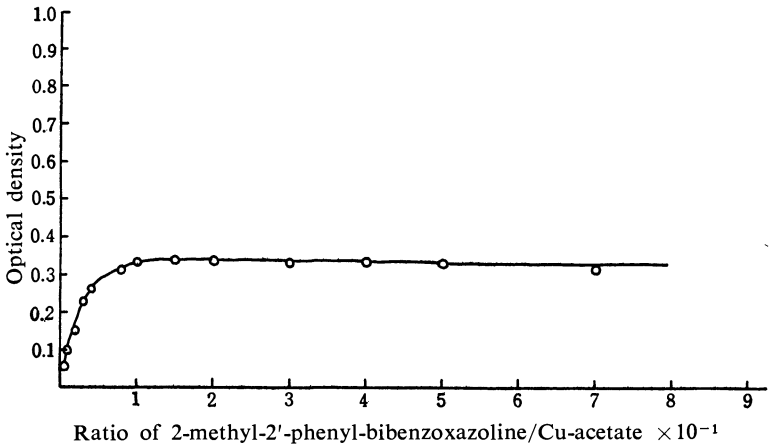
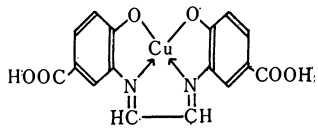
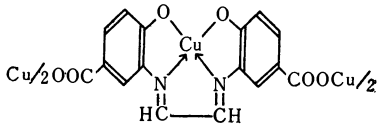



Fig. 4. Optical densities at 600 mμ of various solutions with excess 2-methyl-2'-phenyl-bibenzoxazoline present: Cu-acetate = $4.99 \times 10^{-5}$ M.

of copper acetate. Since a part of the precipitates was soluble in sodium hydrogen carbonate solution with a blue-violet coloration, the precipitates should contain copper chelate of structure XIII* in which the carboxyl groups are free and the copper atom is coordinated with the Schiff base ligand in the same manner as the other chelates. When this dicarboxy derivative reacted with bimolar amounts of copper acetate, blue-violet precipitates were obtained. This substance was insoluble in sodium hydrogen carbonate solution and consisted of two copper atoms to one molecule of ligand. The structure should be given as XIV in which one copper atom chelates and the other combines as carboxylate.




XIII

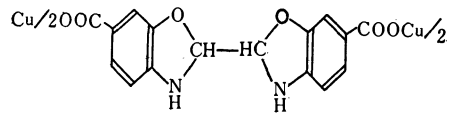



XIV

* The precipitates were treated with sodium hydrogen carbonate solution and the soluble part was reprecipitated by neutralization with acetic acid. The substance obtained did not show reasonable analytical results, possibly due to partial decomposition by this treatment.

Found: C, 44.26; H, 3.48; N, 7.04; Cu, 16.07. Calcd. for $C_{16}H_{10}N_2O_6 \cdot 2H_2O$: C, 45.13; H, 3.31; N, 6.58; Cu, 15.39%.

On the other hand, 6, 6′-dicarboxy derivative gave green precipitates with copper acetate. The substance may have the structure of simple salt of bibenzoxazoline carboxylic acid (XV), because they were insoluble in sodium hydrogen carbonate solution and consisted of one copper atom to one oxazoline molecule. The structure may further be supported by its green color which is seen in ordinary copper carboxylates. It seems that the carboxyl groups at 6, 6′-positions prevent the ring opening of oxazoline to form the Schiff base.



XV

For the determination of metal-ligand proportion in metal chelate in solution, the molar ratio method is known[4]; it consists of the measurement of optical density at a typical wavelength at which an absorption is caused by metal chelate formation, the molar ratio of the ligand being varied to a constant metal ion concentration. If a formation constant of metal chelate is appreciably large, the optical density should reach a constant value at which the metal-ligand proportion is equivalent.

In the case of the above copper chelates, in which the metal-ligand ratio is naturally 1 : 1, the optical densities should be expected to give constant values over the range of more than this ratio.

The experiment was carried out on 2-methyl-bibenzoxazoline and 2-methyl-2′-phenyl-bibenzoxazoline**. The results are shown in Figs. 3 and 4, but they fell short of expectations.

The optical density of each solution gave almost constant value for ratios greater than 20. Since such poly-coordinate chelate is considered to be impossible, these curves should mean that stability constants of these copper chelates are small. Here again, it proved that the equilibrium between bibenzoxazoline and the Schiff base exists in favor of the former.

## Experimental

**Copper Chelate of 5, 5′-Dimethyl-2, 2′-bibenzoxazoline.**—To a solution of 5, 5′-dimethyl-2, 2′-bibenzoxazoline (0.2 g.) in hot methanol (50 ml.), a solution of copper acetate (0.15 g.) in methanol (20 ml.) was added and the mixture was heated on a water bath for 30 min. The resulting deep violet-blue precipitates were centrifuged and washed with methanol and dried over phosphorus pentoxide in vacuo at 110°C.

Found: C, 55.43; H, 4.48; N, 7.98; Cu, 18.61. Calcd. for $C_{16}H_{14}N_2O_2Cu \cdot H_2O$: C, 55.24; H, 4.60; N, 8.04; Cu, 18.26%.

**Copper Chelate of 5, 5′-Dichloro-2, 2′-bibenzoxazoline.**—Prepared from 5, 5′-dichloro-bibenzoxazoline (0.2 g.) and copper acetate (0.13 g.) in the same manner as described in the case of the dimethyl derivative. Deep blue amorphous powder.

Found: C, 43.07; H, 2.71; N, 7.43; Cu, 15.96. Calcd. for $C_{14}H_8N_2O_2Cl_2Cu \cdot H_2O$: C, 43.26; H, 2.57; N, 7.20; Cu, 16.34%.

**Copper Chelate of 5, 5′-Dinitro-2, 2′-bibenzoxazoline.**—Prepared from 5, 5′-dinitro-bibenzoxazoline (0.5 g.) and copper acetate (0.4 g.) in the same manner as described in the case of the dimethyl derivative. Deep reddish violet crystalline powder.

Found: C, 41.12; H, 2.53; N, 13.55; Cu, 15.55. Calcd. for $C_{14}H_8N_4O_6Cu \cdot H_2O$: C, 40.97; H, 2.43; N, 13.65; Cu, 15.51%.

**Copper Chelate of Copper-2, 2′-bibenzoxazoline-5, 5′-dicarboxylate.**—To a solution of 5, 5′-dicarboxy-2, 2′-bibenzoxazoline (0.5 g.) in hot methanol (300 ml.), copper acetate (0.8 g.) in methanol (50 ml.) was added and the mixture was heated on a water bath for 1 hr. After cooling, resulting precipitates were filtered and washed with methanol and dried over phosphorus pentoxide in vacuo at 110°C. Deep blue-violet crystalline powder.

Found: C, 36.84; H, 3.00; N, 5.06; Cu, 24.91. Calcd. for $C_{16}H_8N_2O_6Cu_2 \cdot 4H_2O$: C, 36.71; H, 3.08; N, 5.35; Cu, 24.28%.

**Copper-2, 2′-bibenzoxazoline-6, 6′-dicarboxylate.**—To a suspension of 6, 6′-dicarboxy-2, 2′-bibenzoxazoline (0.2 g.) in ethanol (100 ml.), a solution of copper acetate (0.12 g.) in ethanol and 2 drops of acetic acid were added and the mixture was heated on a water bath for 4 hr. The crystals were gradually diminished and green precipitates were formed. After standing over-night, they were filtered and washed with ethanol and dried over phosphorus pentoxide in vacuo at 60°C.

Found: C, 45.62; H, 3.49; N, 6.21; Cu, 14.96. Calcd. for $C_{16}H_{10}N_2O_6Cu \cdot 2H_2O$: C, 45.13; H, 3.31; N, 6.58; Cu, 15.39%.

**Absorption Spectra.**—The copper chelates III~VI, when once precipitated, were very difficult to dissolve in ethanol. To obtain the ultraviolet and visible absorption spectra in ethanol of these compounds, a method was devised in the preparation of the solution. To ethanol solutions of bibenzoxazolines (ca. 1/5000~1/10000 M), equimolar amounts of copper acetate in ethanol were added and the solutions were heated at 70°C for ten minutes and cooled to room temperature. The coloration of each solution reached almost a maximum by this treatment and further heating resulted in decolorization by decomposition, thus clear colored solutions containing copper chelates being obtained.

4) S. Miyakawa and T. Uemura, This Bulletin, 24, 25 (1951); R. P. Yaffe and A. F. Voigt, *J. Am. Chem. Soc.*, 74, 2503 (1952).

** Since their own spectra have no absorption at a visible region (refer to Fig. 2, VII and XII), the optical densities could be observed without any correction. For the measurements, the solution were prepared in the same manner as the case of the measurement of their spectra and the concentration of coppr acetate was used in place of the copper ion concentration to avoid the ambiguity of the latter in ethanol.

In the case of VII—XII, the solutions were prepared also in the same manner as indicated above. The measurement of absorption spectra and optical densities in the molar ratio method were carried out using a Hitachi EPU-2A spectrophotometer with a 10 mm. quartz cell.

The author wishes to express his thanks to Professor Tokuichi Tsumaki and Professor Takeichi Nishikawa for their exceedingly kind directions of this work. The author also thanks Mr. Michio Shido and Miss Sachiko Indo for the microanalysis.

The cost of this research was defrayed by the Scientific Research Encouragement Grant from the Ministry of Education, to which the author's thanks are due.

*General Education Department*
*Kyushu University*
*Otsubo-machi, Fukuoka*

# *Relations between Electronic Absorption Spectra and Spatial Configurations of Conjugated Systems. X. Benzaldehyde, Acetophenone and Related Compounds*

By Hiroshi SUZUKI

(Received October 30, 1959)

## Benzaldehyde and Acetophenone

In the near ultraviolet absorption spectrum of benzaldehyde as well as that of acetophenone four band systems appear. The weakest band, which appears at about 320 m$\mu$ with the molecular extinction coefficient of the order of ten, is regarded as an $n \rightarrow \pi^*$ transition in the carbonyl group (R-band). The weak band with fine structure, which appears in the range between 270 and 290 m$\mu$ with the molecular extinction coefficient of about 1000~2000, is considered to correspond to the $A_{1g} \rightarrow B_{2u}$ transition in benzene, and therefore, to the "hidden transition" at about 275 m$\mu$ in biphenyl[1] (B-band, or Benzenoid band). The band at about 200 m$\mu$ is considered to correspond to the $A_{1g} \rightarrow B_{1u}$ transition in benzene. The strongest band at near 240 m$\mu$, whose molecular extinction coefficient is about 15000, has been interpreted by Tanaka, Nagakura, and Kobayashi[2] as the "intramolecular charge-transfer absorption", which may be considered as the conjugation band (K-band). (The notation of the bands shown in parentheses is according to Gillam and Stern[3]). The present study is mainly concerned with the last "conjugation band".

O'Shaughnessy and Rodebush[4] found formerly that the introduction of two methyl groups into the ortho positions of acetophenone exerts a marked influence on the absorption spectrum, a fact which was explained in terms of the steric effect. Braude and his coworkers[5-8] have stated, on the basis of their classification of steric effects in ultraviolet absorption spectra, that *o*-methylated acetophenones and benzaldehydes show the steric effects of type 1, i. e. the steric effects which give rise to decreases in absorption intensity alone without causing any wavelength displacement of the bands. According to them, the steric effect of this type occurs when steric interaction is relatively weak, i. e. when the steric repulsion energy for the planar conformation is less than 3 kcal./mol., and is produced by "transitions between nonplanar ground states and uniplanar (or near-planar) excited states".

On the basis of the above mentioned view, they have applied their postulated relation between the intensity of the conjugation band and the angle of twist of the "single" bond to

1) H. Suzuki, This Bulletin, **32**, 1340 (1959).
2) J. Tanaka, S. Nagakura and M. Kobayashi, *J. Chm. Phys.*, **24**, 311 (1956).
3) A. E. Gillam and E. S. Stern, "An Introduction to Electronic Absorption Spectroscopy in Organic Chemistry", 2nd. Ed., Edward Arnold Publishers, Ltd., London (1957), p. 141 and p. 262.
4) M. T.O'Shaughnessy and W. H. Rodebush, *J. Am. Chem. Soc.*, **62**, 2906 (1940).
5) E. A. Braude, F. Sondheimer and W. F. Forbes, *Nature*, **173**, 117 (1954).
6) E. A. Braude and F. Sondheimer, *J. Chem. Soc.*, **1955**, 3754.
7) E. A. Braude and E. S. Waight, "Progress in Stereochemistry", 1, (edited by W. Klyne), Butterworths Scientific Publications, London (1954), p. 144 ff.
8) E. A. Braude, "Determination of Organic Structures by Physical Methods", (edited by E. A. Braude and F. C. Nachod), Academic Press, Inc., Publishers, New York (1955), p. 172 ff.

*o*-substituted benzaldehydes and acetophenones, and found that in the aldehydes the calculated angle of twist $\theta$ (i.e. the interplanar angle between the benzene ring and the carbonyl group) is about 20° in the presence of either the one or the two *o*-methyl groups, and that in the ketones the calculated interplanar angle is about 35° in the presence of the one, and about 60° in the presence of the two, *o*-methyl groups. In the calculations, they have taken the parent compounds, benzaldehyde and acetophenone, as the planar reference compounds for the corresponding derivatives. That is, they have assumed that there is no significant steric hindrance to the coplanarity of the molecular configuration with acetophenone as well as benzaldehyde. This assumption would be considered to be supported by the fact that, according to Braude and others, both the compounds exhibit their conjugation bands at almost the same wavelength (242 m$\mu$, in hexane).

On the other hand, as will be shown in the succeeding part of this series, $\alpha$-methylstyrene exhibits the conjugation band at an appreciably shorter wavelength than its parent compound, styrene. That is, it may be said that the $\alpha$-methyl group in this system exerts the "steric effect of type 2" defined by Braude and others, i.e. the steric effect which causes not only a decrease in the intensity of the conjugation band but also a hypsochromic wavelength displacement of the band. Thus, the most probable configuration of $\alpha$-methylstyrene is inferred to be nonplanar. While the geometry of the relevant part of benzaldehyde is considered to be similar to that of styrene, that of acetophenone is considered to be similar to that of $\alpha$-methylstyrene. Accordingly, it is expected that the steric effects in acetophenone and in $\alpha$-methylstyrene are likely to be very similar. That is, it is presumed, contrary to the opinion of Braude and others, that there should be appreciable steric interaction between the methyl group and the phenyl group in the planar conformation of acetophenone, and that, consequently, the most probable configuration of the molecule is not planar. According to Auwers and Eisenlohr[9], the value of the exaltation of molecular refraction, $EM_D$, for acetophenone (+0.52) is considerably smaller than the value for benzaldehyde (+0.80). This fact may be considered to indicate that acetophenone is less conjugated than benzaldehyde, and therefore, to support the above mentioned view.

It may be somewhat doubtful whether a deviation from the coplanar configuration results in a hypsochromic displacement of the "conjugation band" also in the present conjugated system, because the system containing a hetero-atom O is not quite analogous to the hydrocarbon conjugated systems (termed "normal") treated in the preceding parts of this series. Therefore, it seems to be necessary to make some comment on this point.

According to Nagakura and Tanaka[10], in the conjugated system $C_6H_5$–C=O the interaction between the lowest vacant orbtial of the carbonyl group ($V_S$) and the highest occupied orbital of benzene ($H_B$) is predominant, and to a first approximation the intense absorption bands in the wavelength region 230~260 m$\mu$ are regarded as due to the transition between the two new orbitals $W_n$ and $W_e$ which occur by the interaction between $V_S$ and $H_B$. The new highest occupied orbital $W_n$ is lower than $H_B$, and the new lowest vacant orbital $W_e$ is higher than $V_S$. The energy separation between $W_e$ and $W_n$ will become greater when the interaction between $V_S$ and $H_B$ becomes greater. Accordingly, from this theory, it might be expected that a twist of the "single" bond between the phenyl group and the carbonyl group from the coplanar position would cause a bathochromic shift of the absorption band rather than a hypsochromic shift.

This surmise seems, however, to be denied by the fact that the absorption band maxima of 2-methylbenzaldehyde and of 2-methylacetophenone are at considerably shorter wavelengths than the corresponding 4-isomers. Especially, it is notable that the absorption maximum of 2-methylbenzaldehyde is at a shorter wavelength even than that of the 3-isomer. Thus, according to Braude and Sondheimer[6], the wavelengths (in m$\mu$) of the absorption maxima of these compounds are as follows (figures in parentheses represent the molecular extinction coefficients): 4-methylbenzaldehyde, 251(15000) and 257 (12500); 3-methylbenzaldehyde, 245(13500) and 251(12000); 2-methylbenzaldehyde, 243(12500) and 251(13000); 4-methylacetophenone, 252 (15100); 2-methylacetophenone, 242(8700) and 245(8300). Since the electronic effect of an ortho-methyl group may be said to be approximately equivalent to that of a para-methyl group, it may be quite reasonable to consider the hypsochromic displacements observed above as mainly due to the steric effect of the ortho-methyl groups. Accordingly, it may be said that a deviation of the most probable conffiguration from the coplanarity causes a hypsochromic displacement of the "conjugation band" in the case of the conjugated system $C_6H_5$–C=O, just as in the cases of the normal conjugated systems. Therefore, from the foregoing consideration it may be expected that the conjugation band of acetophenone will be at a

9) K. v. Auwers and F. Eisenlohr, *Ber.*, **43**, 806 (1910).

10) S. Nagakura and J. Tanaka, *J. Chem. Phys.*, **22**, 236 (1954).

TABLE I. ABSORPTION MAXIMA OF BENZALDEHYDE, ACETOPHENONE AND BENZOPHENONE

| Compound | Solvent | "Benzenoid band" | | "Conjugation band" | | Ref. |
|---|---|---|---|---|---|---|
| | | λ, mμ | ε | λ, mμ | ε | |
| Benzaldehyde | Hp | 288.9 | 890 | 248.1 | 8600 | *a* |
| | | 280.6 | 1410 | (240.5) | 13400 | |
| | | 273.8 | 1520 | 236.9 | 14100 | |
| | | | [C-band : | (204.8) | 18900] | |
| | Hx | 289 | 1200 | 248 | 12500 | 5-8 |
| | | 280 | 1400 | 242 | 14000 | |
| | E | 280 | 1500 | 244 | 15000 | 3 |
| Acetophenone | Hp | 286.2 | 1180 | (245.5) | 9690 | *a* |
| | | 278.3 | 1480 | 238.5 | 13130 | |
| | | 275.2 | 1460 | | | |
| | | 271.4 | 1440 | | | |
| | Hp | 279 | 890 | 238 | 12600 | 2 |
| | Hx | | | 242 | 13000 | 5,7,8 |
| | E | 278 | 1000 | 242 | 11750 | 2 |
| | E | 279 | 1200 | 243 | 13200 | 6 |
| | E | 278 | 1100 | 240 | 13000 | 3 |
| Benzophenone | Hp | [(286)] | 1550 | 248.5 | 19550 | *a* |
| | | [(277)] | 2540 | | | |

Solvent: Hp, *n*-heptane; Hx, hexane; E, ethanol. Wavelengths in parentheses denote inflections, and those in double parentheses denote very indistinct inflections. Ref. *a*, the present work.

shorter wavelength than that of benzaldehyde. In this connection, it may be of some interest that in the case of the conjugated system $C_6H_5$–C=N the "conjugation band" maximum of the acetophenone analogue is at a considerably shorter wavelength than the corresponding one of the benzaldehyde analogue. Thus, according to Braude and Sondheimer[6], the wavelengths of the absorption maxima of the semicarbazones of benzaldehyde and of acetophenone are 281 mμ (22000) and 270 mμ (20400), respectively.

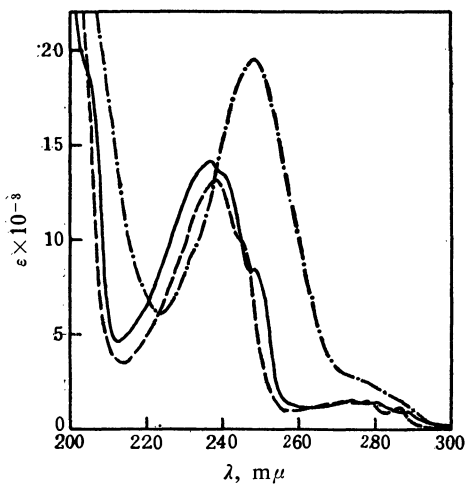



Fig. 1. Ultraviolet absorption spectra (in *n*-heptane): ——, benzaldehyde; ----, acetophenone; -·-·-, benzophenone.

From this point of view, to re-examine the steric effect in acetophenone itself, the ultraviolet absorption spectra of acetophenone and of benzaldehyde in solutions in *n*-heptane have newly been measured. The results are shown in Fig. 1. In Table I, the data of the absorption maxima are summarized together with those found in the literature.

The conjugation bands of these compounds are not structureless, but have, though considerably diffuse, fine structures. The inflection at 245.5 mμ in the spectrum of acetophenone is at a shorter wavelength than the probably corresponding maximum at 248.1 mμ in the spectrum of benzaldehyde, in accordance with the expectation. On the other hand, the maximum at 238.5 mμ in the spectrum of acetophenone appears to correspond to the two bands at 240.5 and 236.9 mμ in the spectrum of benzaldehyde. Therefore, it seems somewhat doubtful which of the two bands of benzaldehyde is to be compared with the band of acetophenone.

### *p*-Biphenylyl and 2-Fluorenyl Carbonyl Compounds

The author prepared *p*-phenylbenzaldehyde and *p*-phenylacetophenone as intermediates in the syntheses of *p*,*p*'-diphenylstilbene and its α,α'-dimethyl derivative, as described in the preceding part[11] of this series. In addition,

11) H. Suzuki, This Bulletin, 33, 410 (1960).

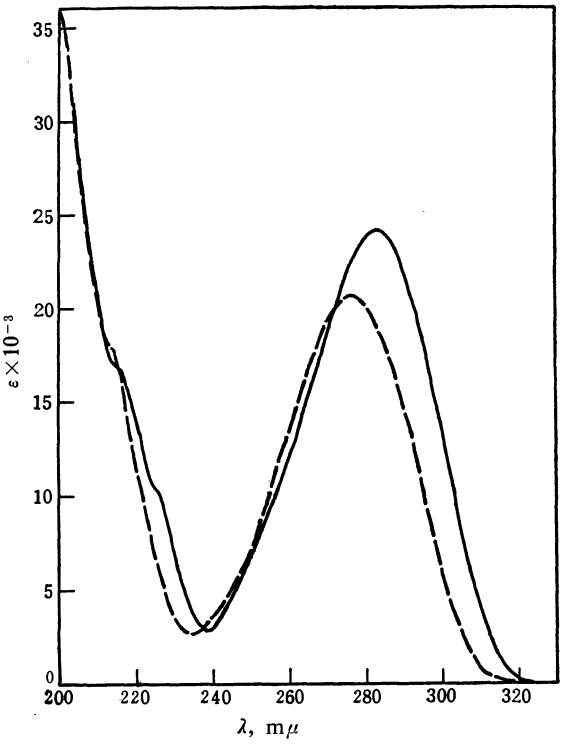



Fig. 2. Ultraviolet absorption spectra (in *n*-heptane): ——, *p*-phenylbenzaldehyde; ----, *p*-phenylacetophenone.

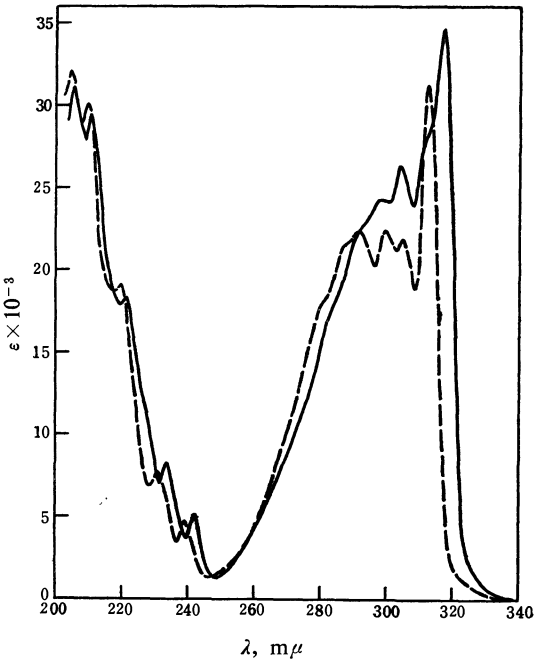



Fig. 3. Ultraviolet absorption spectra (in *n*-heptane): ——, 2-formylfluorene; ----, 2-acetylfluorene.

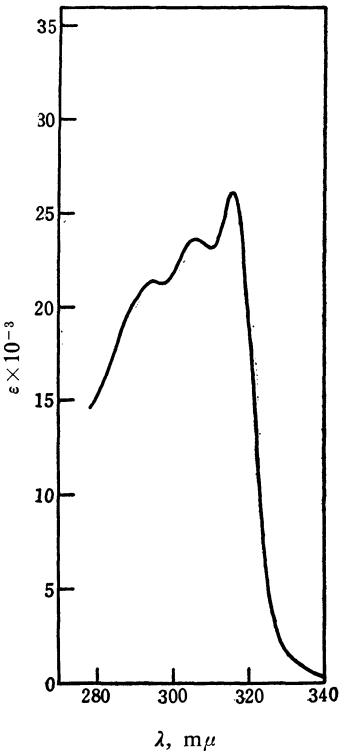



Fig. 4. Ultraviolet absorption spectrum of 2-acetylfluorene in benzene.

2-acetylfluorene and a compound which is considered to be probably 2-formylfluorene were prepared in attempts to prepare 1, 2-di-(2-fluorenyl)-ethylene and its 1, 2-dimethyl derivative. The absorption spectra of these analogues of benzaldehyde and of acetophenone seem to be of interest in connection with the above considerations. The spectra are shown in Figs. 2—4. In Table II, the data of the absorption maxima are summarized.

In the spectra of these compounds, the possible bands corresponding to the bands of benzaldehyde and of acetophenone in the range between 270 and 290 m$\mu$ are completely hidden by the intense conjugation bands. The bands appearing in the range between near 215 m$\mu$ and near 240 m$\mu$ are considered to be probably the ones due to transitions from the highest occupied orbital to the vacant orbitals localized in benzene rings whose energy is $-\beta$, or from the occupied orbitals localized in benzene rings whose energy is $+\beta$ to the lowest vacant orbital, analogously to the bands of stilbene and related compounds appearing in almost the same range[12,13]. It may be noteworthy that the bands at 200~210 m$\mu$ have about double the intensity of the corresponding band of benzaldehyde, in conformity

12) H. Suzuki, ibid., 33, 379 (1960).
13) H. Suzuki, ibid., 33, 389 (1960).

TABLE II. ABSORPTION MAXIMA OF *p*-BIPHENYLYL AND 2-FLUORENYL CARBONYL COMPOUNDS

| Compound | Solvent | A-band | | B-band | | C-band | |
|---|---|---|---|---|---|---|---|
| | | λ, mμ | ε | λ, mμ | ε | λ, mμ | ε |
| *p*-phenylbenzaldehyde | Hp | 283.5 | 24150 | [(226)] | 10100 | | |
| | | | | (215.5) | 16900 | | |
| *p*-Phenylacetophenone | Hp | 276.2 | 20650 | (214.5) | 17750 | 200.0 | 35700 |
| 2-Formylfluorene | Hp | 317.2 | 34600 | 242.3 | 5050 | 210.5 | 29400 |
| | | (312.2) | 28200 | 234.0 | 8220 | 205.2 | 31100 |
| | | 304.4 | 26300 | 221.2 | 18320 | | |
| | | 297.7 | 24200 | | | | |
| | | (293.5) | 22900 | | | | |
| | | [(285)] | 18400 | | | | |
| 2-Acetylfluorene | Hp | 312.8 | 31200 | 239.3 | 4730 | 209.7 | 30500 |
| | | 305.1 | 21850 | 231.1 | 7730 | 204.5 | 32000 |
| | | 299.7 | 22400 | 219.8 | 19100 | | |
| | | 291.8 | 22450 | | | | |
| | | (287.2) | 21450 | | | | |
| | | (280.9) | 18050 | | | | |
| | B | 315.8 | 26100 | | | | |
| | | 305.3 | 23650 | | | | |
| | | 294.8 | 21350 | | | | |
| | | [(289.5)] | 20200 | | | | |

The notation of the bands is quite analogous to the one in the case of stilbenes in Part V of this series: A-band refers to the conjugation band. Solvent: Hp, *n*-heptane; B, benzene. Wavelengths in parentheses denote inflections, and those in double parentheses denote very indistinct inflections.

with the number of benzene rings in a molecule.

The conjugation band of *p*-phenylacetophenone is at an appreciably shorter wavelength than that of *p*-phenylbenzaldehyde, both the bands being structureless, (cf. Fig. 2). The conjugation bands of the two fluorenyl compounds have fine structures. Also with these compounds, the bands of the acetophenone analogue are at shorter wavelengths than the probably corresponding bands of the benzaldehyde analogue (cf. Fig. 3). These hypsochromic shifts of the conjugation bands observed in the comparison of the acetophenone analogues with the corresponding benzaldehyde analogues are considered to be mainly due to the steric effect of the methyl groups. This means that in these acetophenone analogues there exist steric interactions between the methyl groups and the benzene rings which cause the hypsochromic wavelength displacements of the conjugation bands relative to the conjugation bands of the corresponding benzaldehyde analogues, and that, consequently, the most probable configurations of these acetophenones are nonplanar.

By analogy with these facts, it may be inferred that the most probable configuration of acetophenone itself is nonplanar. Probably, the fact that the introduction of a methyl group at the carbonyl carbon atom of benzaldehyde to give acetophenone does not result in any appreciable hypsochromic wavelength displacement of the conjugation band is merely apparent. Further, this fact should not be considered to indicate the absence of the steric interference in acetophenone or the absence of the hypsochromic shift arising from the steric effect. It seems more reasonable to consider that the hypsochromic shift caused by the steric effect is so small that it is compensated by the electronic bathochromic effect of the methyl group. Accordingly, also the apparent absence of hypsochromic shift in *o*-methylated acetophenones, e. g. 2-methylacetophenone and 2, 4, 6-trimethylacetophenone, as compared with acetophenone should probably be interpreted similarly. From this point of view, not only the application of the hypothesis of Braude and others to the acetophenone derivatives but also their classification of steric effects in ultraviolet absorption spectra or their basic theory itself seems to be criticizable. This subject will be discussed more fully in the succeeding part of this series.

It remains to refer to the spectrum of 2-acetylfluorene in benzene shown in Fig. 4. It is of interest that this spectrum differs considerably from the spectrum in *n*-heptane. Thus, when

the solvent is changed from *n*-heptane to benzene, the first (from longer wavelengths side) maximum of fine structure of the conjugation band is reduced markedly in the intensity, and further, the second and the third maxima appear to merge into a maximum. Also with this compound, analogously to the cases of stilbene and related compounds discussed in earlier parts[11-13] of this series, considerably large red-shifts (about 3 m$\mu$) associated with the change of solvent are observed.

### Benzophenone

Lastly, the spectrum of benzophenone, which is shown in Fig. 1 and in Table I, is briefly discussed. It is evident that the two benzene rings in benzophenone can not be simultaneously coplanar with the plane of the carbonyl bond owing to the steric necessities. This situation is very similar to that in the case of 1, 1-diphenylethylene which will be treated in the succeeding part of this series. However, in contrast to the fact that 1, 1-diphenylethylene shows the conjugation band at almost the same position as the conjugation band of styrene, the conjugation band of benzophenone, which is structureless, has the maximum at an appreciably longer wavelength than that of benzaldehyde. This situation is rather similar to that observed in the comparison of the spectrum of tetraphenylethylene with that of *trans*-stilbene, the maximum of the former being at a longer wavelength than that of the latter[13]. Thus, it may be considered that the angle through which each benzene ring in benzophenone is rotated out of the plane of the carbonyl bond is not so large as the corresponding angle in 1, 1-diphenylethylene. However, it can not be asserted so, because the maximum of the conjugation band of benzophenone may be compared, alternatively, with the minor maximum of fine structure of the conjugation band of benzaldehyde at almost the same wavelength (i. e. at 248.1 m$\mu$).

### Experimental

All the spectra were measured with a Cary recording spectrophotometer Model 14 M-50.

The specimens of benzaldehyde and of acetophenone were obtained by distillation of commercial products under reduced pressure.

Benzophenone was prepared by the method described in Organic Syntheses[14]; colorless prisms melting at 48~48.5°C.

*p*-Phenylbenzaldehyde was prepared by the method described in Organic Reactions[15]. From 150 g. of biphenyl, 124 g. of the purified product was obtained after treatment with activated charcoal and repeated recrystallization from petroleum ether (b. p. 80~100°C); colorless thin plates melting at 60~61°C. About 5 g. of biphenyl was recovered.

*p*-Phenylacetophenone was prepared by the method described by Long and Henze[16]. From 77.1 g. of biphenyl, 87.4 g. of the purified product was obtained (89% of the theoretical amount); colorless crystals melting at 119~121.5°C.

2-Formylfluorene was prepared almost analogously to the preparation of *p*-phenylbenzaldehyde. Thus, a stream of dry carbon monoxide and hydrogen chloride was passed for about 4.5 hr. into a well-stirred solution of 42 g. of fluorene in 200 ml. of dry benzene containing 59 g. of anhydrous aluminum chloride and 11 g. of cuprous chloride at 35~40°C. The dark-colored reaction mixture was poured into a mixture of ice and small quantities of concentrated hydrochloric acid. The violet-colored mixture was extracted with benzene. The benzene solution was concentrated to about 300 ml. by evaporation, and the solution was shaken with an excess of a saturated solution of sodium bisulfite and small quantities of ethanol. The brown bisulfite compound was collected, washed repeatedly with ethanol and then with ether, and warmed with aqueous sodium carbonate. The aldehyde was then collected, dried on a porous plate, and crystallized twice from petroleum ether. The yield of faint yellow needles melting at 85.5~86.5°C was 6.3 g. It might be somewhat doubtful whether this product is the desired compound, 2-formylfluorene, because, according to Rodd[17], treatment of fluorene with ethyl formate and potassium ethoxide gives 9-formylfluorene which sinters at about 70°C and melts at about 90°C. However, the ultraviolet absorption spectrum of this product is considered to have revealed that this product is not 9-formylfluorene, but probably 2-formylfluorene.

2-Acetylfluorene was prepared by the method described in Organic Syntheses[18]. From 40 g. of fluorene, 24.4 g. of the product was obtained after purification by treatment with activated charcoal and by twofold recrystallization from ethanol (48.9% of the theoretical amount); colorless crystals melting at 127.5~128°C.

The author desires to thank Professor Kengo Shiomi for reading the manuscript and for valuable advice.

*Department of Chemistry*
*College of General Education*
*The University of Tokyo*
*Meguro-ku, Tokyo*

14) H. Gilman (Editor-in-Chief), "Organic Syntheses", Col. Vol. 1, John Wiley & Sons, Inc., New York (1932), p. 89.
15) R. Adams (Editor-in-Chief) "Organic Reactions", Vol. V, John Wiley & Sons, Inc., New York (1949), p. 298.
16) L. M. Long and H. R. Henze, *J. Am. Chem. Soc.*, 63, 1939 (1941).
17) E. H. Rodd, "Chemistry of Carbon Compounds", Vol. III B, Elsevier Publishing Co., Amsterdam (1956), p. 1454.
18) H. R. Snyder (Editor-in-Chief), "Organic Syntheses", Vol. 28, John Wiley & Sons, Inc., New York (1948), p. 3.

# *Relations between Electronic Absorption Spectra and Spatial Configurations of Conjugated Systems. XI. Styrene, 1, 1-Diphenylethylene and their Methylated Derivatives*

By Hiroshi SUZUKI

(Received October 30, 1959)

An introduction of a substituent into an *o*-, the $\alpha$-, or the *cis*-$\beta$-position of styrene must cause a deviation of the phenyl group from the coplanar position with the plane of the ethylenic bond, owing to the steric interaction between the *o*-substituent and the $\alpha$- or the *cis*-$\beta$-hydrogen or between the $\alpha$- or *cis*-$\beta$-substituent and an *o*-hydrogen. On the other hand, in 1, 1-diphenylethylene, the two phenyl groups can not simultaneously be coplanar with the plane of the ethylenic bond. These steric situations must reveal themselves in the ultraviolet absorption spectra. In this part of the series, the method analogous to the one used so far in the previous parts of this series is applied to methylated styrenes, 1, 1-diphenylethylene, and its methylated derivatives, and the relations between the most probable spatial configurations of these compounds and the ultraviolet absorption spectra are discussed.

## Calculation

The method of calculation is quite analogous to the ones for biphenyls[1], terphenyls[2], and stilbenes[3,4] in the earlier parts of this series. The $\pi-\pi$ resonance integral for the ethylenic bond is denoted by $\eta\beta$, and that for the $\alpha-1$ "single" bond of styrene is denoted by $\rho\beta$, in which $\beta$ represents the $\pi-\pi$ resonance integral for a C–C bond in benzene as usual. By substituting suitable values for $\eta$ and $\rho$ according to the lengths and the angles of twist of the corresponding bonds, and by solving the secular equation for the determination of the molecular orbitals of styrene as linear combination of $2p\pi$ atomic orbitals by the usual procedure, the energy $\Delta E_A$ of the transition from the highest occupied orbital to the lowest vacant orbital, which is allowed by absorption of light polarized along the direction of the long axis of the molecule, is calculated. This value of $\Delta E_A$ is considered to correspond to the transition energy of the intense conjugation band of the molecule of the styrene-type of the configuration prescribed by the values of $\eta$ and $\rho$.

The length of the ethylenic bond is assumed to be 1.34 Å, and hence the value of $\eta$ is assumed to be 1.080 for the styrenes and 1, 1-diphenylethylenes throughout the present treatment, for the same reason as in the case of stilbenes in Part V[3] of this series. By using this value for $\eta$, the value of $\Delta E_A$ is calculated as a function of the variable $\rho$. The results are shown in Table I. It is seen in Table I that the value of $\Delta E_A$ increases with the decreasing value of $\rho$, and that the value of $\Delta E_A$ coincides with the value for benzene, $2(-\beta)$, when the value of $\rho$ is zero.

TABLE I

| $\rho$ | 1 | 0.9 | 0.8 | 0.7 | 0.6 | |
|---|---|---|---|---|---|---|
| $\Delta E_A(-\beta)$ | 1.3958 | 1.4506 | 1.5082 | 1.5684 | 1.6314 | |
| $\rho$ | 0.5 | 0.4 | 0.3 | 0.2 | 0.1 | 0 |
| $\Delta E_A(-\beta)$ | 1.6968 | 1.7646 | 1.8342 | 1.9036 | 1.9672 | 2 |

Although reliable data concerning the spatial configuration of styrene molecule are not yet available, the configuration can be presumed by analogy with the following facts. Butadiene in the vapor phase has recently been found by Almenningen and his collaborators[5] to have probably almost exclusively the planar *trans*-configuration in which the length of the 2-3 "single" bond is 1.483±0.01 Å. On the other hand, biphenyl in the crystalline state has been found to have the planar configuration in which the length of the co-annular "single" bond is 1.48Å[6]. Accordingly, it may be presumed that styrene has probably the planar or nearly planar configuration in which the length of the $\alpha-1$ "single" bond is about 1.48 Å. Even if the presumption of the bond length is not correct, a small change in the bond length for the reference compound is considered not to affect significantly the resultant calculated values for

1) H. Suzuki, This Bulletin, **32**, 1340 (1959).
2) H. Suzuki, ibid., **33**, 109 (1960).
3) H. Suzuki, ibid., **33**, 379 (1960).
4) H. Suzuki, ibid., **33**, 410 (1960).
5) A. Almenningen, O. Bastiansen and M. Traetteberg, *Acta Chem. Scand.*, **12**, 1221 (1958).
6) (a) J. Dhar, *Indian J. Phys.*, **7**, 43 (1932); *Chem. Abstr.*, **26**, 4517 (1932). (b) Idem., *Proc. Natl. Inst. Sci. India*, **15**, 11 (1949); *Chem. Abstr.*, **43**, 4655 (1949).

the angles of twist, as suggested by the results of the similar calculations for terphenyls in Part IV[2] of this series. Therefore, the presumption is adopted in the present treatment. Then, the relation between $\rho$ and the angle of twist $\theta$ (i. e. the interplanar angle between the benzene ring and the ethylenic bond) as well as the length of the "single" bond $R$ is assumed to be quite analogous to the relation between $\mu$ (the variable analogous to $\rho$) and $\theta$ as well as $R$ postulated in the case of biphenyl in Part I[1] of this series. Thus, $\rho$ is expressed as follows:

$$\rho = \cos\theta \times S(R, 0°)/S(1.39, 0°)$$
$$= \cos\theta \times 0.77108 + \cos^2\theta \times (1.54 - 1.48) \times 1.4458$$

where $S(R, 0°)$ represents the $\pi-\pi$ overlap integral for the bond, the length and the angle of twist of which are $R$ (Å) and 0°, respectively, and $S(1.39, 0°)$ represents the overlap integral for a C–C bond in benzene, whose length is 1.39 Å and whose angle of twist is, of course, zero.

Accordingly, the value of $\rho$ when $R$ and $\theta$ are 1.48 Å and 0°, respectively, i. e. the value of $\rho$ for the planar styrene molecule, is calculated to be 0.858, and the corresponding value of $\Delta E_A$ is calculated to be 1.475 $(-\beta)$, which is referred to as $\Delta E_L$. When the wave number $\nu_A$ of the maximum of the conjugation band of a styrene derivative has been correlated with the calculated transition energy $\Delta E_A$, the value of $\rho$ for the compound can be evaluated, and then the corresponding values of $\theta$ and $R$ can be estimated.

## Styrenes

The data of the ultraviolet absorption spectra to be found in the literature for styrene and substituted styrenes are considerably variable. Especially the data of the molecular extinction coefficients are extremely variable, probably owing to the presence of polymeric materials in some of the specimens used, as pointed out already by Braude and Sondheimer[7]. Also with wavelengths of the absorption maxima, different workers using different instruments have reported values which vary by a few mμ. Further, the positions of the maxima vary more or less, depending on the solvent. With consideration for these situations, mainly the data obtained newly by the present author and those obtained recently by Schwartzman and Corson[8], both using Cary recording spectrophotometers and

TABLE II. ABSORPTION MAXIMA OF STYRENES

| Styrene | Solvent | | | Conj. band | | | | Ref. |
|---|---|---|---|---|---|---|---|---|
| | | λ, mμ | ε | λ, mμ | ε | λ, mμ | ε | |
| Unsubstituted | C | | | 248 | | | | 8 |
| *p*-Methyl- | C | | | 253 | | | | 8 |
| *trans*-β-Methyl- | E | 293 | 780 | 250 | 17300 | | | 9 |
| | | 284 | 1100 | | | | | |
| *o*-Methyl- | C | | | 246 | | | | 8 |
| *o,p*-Dimethyl- | C | | | 251 | | | | 8 |
| α-Methyl- | H | 285.7 | 167 | 241.5 | 9780 | 215.4 | 8670 | *a* |
| | | 278.1 | 311 | | | 200.0 | 20950 | |
| α,β-Dimethyl- | E | | | 244 | 8700 | | | 10 |
| *cis*-β-Methyl- | E | 290 | 120 | 240.6 | 13800 | | | 9 |
| β,β-Dimethyl- | H | 288.2 | 550 | 239.4 | 9060 | (216) | 8260 | *a* |
| | | 280.3 | 800 | (247.2) | 6690 | | | |
| | | 264.8 | 890 | | | | | |
| *o,o'*-Dimethyl- | C | | | 238 | | | | 8 |
| *o,p,o'*-Trimethyl- | O | | | 245 | 7000 | | | 11 |
| α,β,β-Trimethyl- | H | 286.0 | 430 | 237.8 | 8440 | | | *a* |
| | | 278.5 | 550 | (245.3) | 6210 | | | |
| | | 275.5 | 550 | | | | | |
| α,*o*-Dimethyl- | E | No max. between 210 and 300 mμ | | | | | | 12 |

Solvent: C, cyclohexane; E, ethanol; H, *n*-heptane; O, octane.
Wavelengths in parentheses denote inflections.
Ref. *a*, the present work.

7) E. A. Braude and F. Sondheimer, *J. Chem. Soc.*, **1955**, 3773.
8) L. H. Schwartzman and B. B. Corson, *J. Am. Chem. Soc.*, **78**, 322 (1956).
9) R. Y. Mixer, R. F. Hech, S. Winstein and W. G. Young, ibid., **75**, 4094 (1953).
10) Y. Hirschberg, ibid., **71**, 3241 (1949).
11) K. C. Bryant, G. T. Kennedy and E. M. Tanner, *J. Chem. Soc.*, **1949**, 2389.
12) (a) M. J. Murray and W. S. Gallaway, *J. Am. Chem. Soc.*, **70**, 3867 (1948). (b) Ramart-Lucas and J. Hoch, *Bull. soc. chim. France*, [5] **5**, 848 (1938).

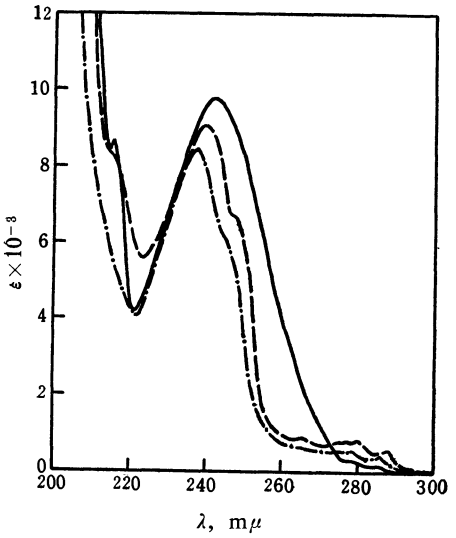



Fig. 1. Ultraviolet absorption spectra (in *n*-heptane): ——, $\alpha$-methylstyrene; ----, $\beta,\beta$-dimethylstyrene; -·-·-, $\alpha,\beta,\beta$-trimethylstyrene.

using saturated hydrocarbons as the solvents, are used in the present treatment. For a few compounds, the data of the spectra of which in solutions in saturated hydrocarbon are not available, the data for ethanol solutions are used. Such data used here are summarized in Table II, and the spectra measured by the present author are shown in Fig. 1.

It is evident that the styrene derivatives with methyl substituents in the sterically hindered positions exhibit the conjugation bands at shorter wavelengths than the conjugation band of the parent compound, styrene. The bands appearing in the range between 270 and 290 m$\mu$ are considered to be the ones corresponding to the $A_{1g} \rightarrow B_{2u}$ transition in benzene, quite similarly to the corresponding bands of benzaldehyde and of acetophenone[13].

In order to infer the spatial configurations of the styrenes from the data of the spectra by applying the above-mentioned calculation method, the electronic bathochromic effect of the methyl groups (probably due to the hyperconjugation effect) should be taken into account, because the wavelength separation between the conjugation band of styrene and the center of gravity of singlets of benzene as the shorter-wavelength-side reference is so small that the magnitude of the bathochromic effect of the methyl groups may not be negligible relatively to the magnitude of the steric hypsochromic effect.

The allowance for the electronic bathochromic effect of the methyl groups is made by the method analogous to the ones used in the treatments of *o*-alkylbiphenyls in Part II[14] of this series and of the stilbene derivatives with methyl groups on the benzene nuclei in Part VIII[15] of this series, i. e. by choosing pertinently the longer-wavelength-side and the shorter-wavelength-side references in the correlation of $\nu_A$ with $\Delta E_A$.

**Longer-wavelength-side Reference.** — As the value of $\nu_A$ corresponding to $\Delta E_L$, viz. $\nu_L$, the wave number, at which the molecule concerned would exhibit the absorption maximum of the conjugation band if the molecule were planar, is taken. Thus, for example, as the value of $\nu_L$ for *o*-methylstyrene, the wave number of the absorption maximum of the conjugation band of *p*-methylstyrene, 39526 cm$^{-1}$ (253 m$\mu$), is taken, since the electronic bathochromic effect of a methyl group can be considered to be approximately equivalent in the *o*- and *p*-positions.

From the comparison of the spectrum of *p*-methylstyrene with that of styrene and the comparison of the spectrum of *o,p*-dimethylstyrene with that of *o*-methylstyrene, it may be presumed that the magnitude of the bathochromic displacement of the conjugation band per a methyl substituent at the *p*- or *o*-position of styrene is about 5 m$\mu$. Further, it may be assumed that the displacement is approximately additive, on the analogy of the case of methylated benzenes[16]. According to Schwartzman and Corson[8], *m*-methylstyrene and *m,m'*-dimethylstyrene in cyclohexane solutions exhibit the conjugation bands at 251 and 254 m$\mu$, respectively. Comparing these wavelengths with that of styrene itself (248 m$\mu$), it is seen that the magnitude of the bathochromic displacement per a methyl group at a *m*-position is 3 m$\mu$, and that the additivity holds good in this case. The magnitude of the bathochromic displacement caused by an *o*-methyl group may, strictly speaking, be not completely equal to that by a *p*-methyl group. Probably, the former is very slightly smaller than the latter, in view of the results of the calculations for *p*- and *o*-terphenyls described in Part IV[2] of this series, but must be considerably larger than the magnitude of the bathochromic displacement caused by a *m*-methyl group. Therefore, the assumption that the magnitude of the displacement per an *o*-methyl group is equal to that per a *p*-methyl group can be considered to be quite satisfactory in the present approximate treatment. When it is assumed so, *o,p*-dimethylstyrene would have the absorption maximum of the conjugation band at about 258 m$\mu$ (248+5×2 m$\mu$) if it were not for

13) H. Suzuki, This Bulletin, 33, 613 (1960).

14) H. Suzuki, ibid., 32, 1350 (1959).
15) H. Suzuki, ibid., 33, 406 (1960).
16) K. F. Herzfeld, *Chem. Revs.*, 41, 233 (1947).

TABLE III. RESULTS OF CALCULATION FOR STYRENES

| Group | Entry No. | Styrene | $\lambda_A$ mμ | $\lambda_L$ mμ | $\lambda_S$ mμ | $\Delta E_A$ $-\beta$ | $\rho$ | $\theta°$ | $R$ Å |
|---|---|---|---|---|---|---|---|---|---|
| I | 1 | Unsubstituted | 248 | | | 1.475 | 0.858 | 0 | 1.48 |
| | 2 | *p*-Methyl- | 253 | | | | | 0 | |
| | 3 | *trans*-β-Methyl- | 250 | | | | | 0 | |
| II | 4 | *o*-Methyl- | 246 | 253 | 213.3 | 1.555 | 0.722 | 31 | 1.489 |
| | 5 | *o,p*-Dimethyl- | 251 | 258 | 217.3 | 1.553 | 0.725 | 30.7 | 1.489 |
| | 6 | α-Methyl- | 241.5 | 250 | 208.3 | 1.567 | 0.702 | 33 | 1.490 |
| | 7 | α,β-Dimethyl- | 244 | 252 | 208.3 | 1.557 | 0.719 | 31.5 | 1.489 |
| III | 8 | *cis*-β-Methyl- | 240.6 | 250 | 208.3 | 1.578 | 0.685 | 35.2 | 1.491 |
| | 9 | β,β-Dimethyl- | 239.4 | 252 | 208.3 | 1.607 | 0.639 | 40 | 1.494 |
| IV | 10 | *o,o'*-Dimethyl- | 238 | 258 | 217.3 | 1.711 | 0.480 | 54 | 1.505 |
| | 11 | *o,p,o'*-Trimethyl- | 245 | 263 | 219.3 | 1.669 | 0.543 | 49 | 1.500 |
| | 12 | α,β,β-Trimethyl- | 237.8 | 254 | 208.3 | 1.638 | 0.590 | 45 | 1.498 |
| V | 13 | α,*o*-Dimethyl- | | | | | | (90) | |

the steric hypsochromic effect. Accordingly, for the treatment of *o,p*-dimethylstyrene, the value of 38760 $cm^{-1}$ (258 mμ) is taken as the value of $\nu_L$.

Further, for example, for *cis*-β-methylstyrene, the wave number of the maximum of *trans*-β-methylstyrene is taken as $\nu_L$. The magnitude of the bathochromic wavelength displacement caused by the introduction of a methyl group into the α-position and that by the introduction into a β-position may be not equal to each other, since the two positions must be not equivalent, the α-methyl group being at the position of cross-conjugation to the conjugated system of the styrene skeleton and, on the other hand, the β-methyl group being at the position of conjugation to the conjugated system. In spite of this, the magnitude of the displacement by an α-methyl as well as a β-methyl group is provisionally assumed to be equal to the difference in wavelength between the maximum of *trans*-β-methylstyrene and that of styrene, 2 mμ, although the data of the maxima of these compounds may be not pertinent to comparison, since they are obtained in different solvents. Further, it is assumed that the additivity holds good also in this case. Then, for example, the value of $\nu_L$ for the treatment of α, β, β-trimethylstyrene becomes 39370 $cm^{-1}$ (254 mμ = 248 + 2 × 3 mμ).

**Shorter-wavelength-side Reference.**—The value of $\Delta E_A$ when $\rho$ is zero, $2(-\beta)$, is denoted by $\Delta E_S$, and the corresponding wave number is denoted by $\nu_S$, as usual. As the value of $\nu_S$ for the treatments of the styrenes which have no methyl substituent on the benzene nuclei, the center of gravity of singlets of benzene, 48000 $cm^{-1}$ (208.3 mμ), is taken, as usual.

As shown in Table II in Part II[14] of this series, the absorption bands of toluene, *m*-xylene, and mesitylene are at longer wavelengths by about 5, 9 and 11 mμ, respectively, than the corresponding bands of benzene. Accordingly, the values for these compounds corresponding to the center of gravity of singlets of benzene are considered to be approximately 46882 $cm^{-1}$ (213.3 mμ = 208.3 + 5 mμ), 46019 $cm^{-1}$ (217.3 mμ = 208.3 + 9 mμ), and 45600 $cm^{-1}$ (219.3 mμ = 208.3 + 11 mμ), respectively. Therefore, for example, as the value of $\nu_S$ for the treatment of *o, p, o'*-trimethylstyrene, the value of 45600 $cm^{-1}$ is taken.

**Application of the Calculation.** — When the references have been determined for each styrene derivative as mentioned above, the value of the calculated transition energy $\Delta E_A$ corresponding to the observed position ($\nu_A$ in wave number) of the maximum of the conjugation band of the compound can be easily obtained by the use of the usual postulated linear relation of $\Delta E_A$ to $\nu_A$ between the two reference points. Consequently, from the value of $\Delta E_A$, the corresponding value of $\rho$ can be obtained according to the relation between $\rho$ and $\Delta E_A$ shown in Table I, and then the corresponding values of $\theta$ and $R$ can be obtained. The results of the calculations are shown in Table III, in which $\lambda_A$ refers to the wavelength of the absorption maximum of the compound concerned, and $\lambda_L$ and $\lambda_S$ refer to the corresponding longer-wavelength-side and the corresponding shorter-wavelength-side references, respectively, in wavelength.

## Discussion

Although much reliance may not be placed on the individual numerical values of the calculated interplanar angles because of the approximation used, the results of the calculations shown in Table III appear to lead to the

conclusion that these styrenes can be classified into the following well-defined groups with respect to the type or the degree of the steric interaction involved in the molecule.

*Group I.* The compounds which have no methyl substituent at hindering positions, i. e. at *o*-, $\alpha$-, and *cis*-$\beta$-positions. To this group, the compounds of the entry numbers 1—3 listed in Table III belong. These compounds are probably planar.

*Group II.* The compounds which have one hindering methyl group either at an *o*-position or at the $\alpha$-position of the molecule. These compounds are considered to involve solely the steric interference either between the *o*-methyl group and the $\alpha$-hydrogen or between the $\alpha$-methyl group and an *o*-hydrogen. To this group, the compounds of the entry numbers 4–7 in Table III belong. The $\beta$-methyl group in "$\alpha$, $\beta$-dimethylstyrene" (entry 7) is probably *trans* to the phenyl group. The calculated interplanar angles for these compounds range from 31° to 33°.

*Group III.* The compounds with one hindering methyl group at the *cis*-$\beta$-position. These compounds involve solely the steric interference between the *cis*-$\beta$-methyl group and an *o*-hydrogen. To this group, the compounds of the entry numbers 8 and 9 belong. For these compounds, the calculated interplanar angles are 35° and 40°, being slightly larger than those for the compounds belonging to Group II.

*Group IV.* The compounds with two hindering methyl groups either at both *o*-positions or at the $\alpha$- and the *cis*-$\beta$-positions. These compounds involve the steric interferences between methyl groups and hydrogen atoms on both the sides of the benzene nucleus. To this group, the compounds of the entry numbers 10–12 in Table III belong. The calculated interplanar angles for these compounds range from 45° to 54°, and are considerably larger than those for the compounds belonging to Group II and those for the compounds belonging to Group III.

*Group V.* To this group, $\alpha$, *o*-dimethylstyrene (entry 13) belongs. If the most probable configuration of this compound were the configuration involving the steric interference between the $\alpha$-methyl group and the *o*-hydrogen and the interference between the *o*-methyl group and the *cis*-$\beta$-hydrogen, this compound would belong to Group IV and not to Group V. In fact, however, this compound has been reported to show no absorption maximum in the range between 210 and 300 m$\mu$, in contrast with the compounds belonging to Group IV. Accordingly, the most probable configuration of this compound is probably the one in which the two methyl groups just contact with each other, and consequently, the interplanar angle is larger than in the compounds belonging to Group IV and probably nearly 90°. This inference seems to be not unlikely, in view of the fact that *o*, *o'*-dimethylbiphenyl has probably the *cis*-like configuration in which the two methyl groups contact with each other as discussed in Part II[14] of this series.

The fact that the calculated interplanar angles for the compounds belonging to Group III are appreciably larger than those for the compounds belonging to Group II is of interest. This fact seems to lead to the conclusion that the steric interference due to the *cis*-$\beta$-methyl group is more effective than that due to the $\alpha$-methyl group.

The geometries of the relevant parts of the compounds belonging to Group IV are considered to be approximately similar to those of *trans*-$\alpha$, $\alpha'$-dimethylstilbene and of *trans*-2, 4, 6, 2', 4', 6'-hexamethylstilbene, except for the possible differences of the bond lengths and of the bond angles. The calculated interplanar angle for $\alpha$, $\beta$, $\beta$-trimethylstyrene (entry 12) is considerably smaller than that for *trans*-$\alpha$, $\alpha'$-dimethylstilbene (58°)[17]. On the other hand, the calculated interplanar angle for *o*, *o'*-dimethylstyrene (entry 10) coincides almost completely with that for *trans*-hexamethylstilbene (54.3°)[15].

At any rate, it is noteworthy that the interplanar angles for the compounds which involve the steric interferences between methyl groups and hydrogen atoms on both sides of the benzene ring (belonging to Group IV) are considerably larger than those for the compounds which involve the steric interference solely on one side of the benzene ring (belonging either to Group II or to Group III). This may mean that in the compounds with the steric interference solely on one side of the benzene ring the steric interference is relieved to some extent probably by changes in the bond angles.

Lastly in this section, it may be concluded that, by making allowance for the electronic bathochromic effect of the methyl substituents, the interplanar angles in the methylated styrenes have been almost satisfactorily inferred from the wavelength positions of the conjugation bands.

## Criticism on Braude and Forbes' Classification of Steric Effects in Ultraviolet Absorption Spectra

Braude and his coworker[18] classified the steric effects of twisting of "single" bonds in conjugated systems on the conjugation bands into

17) H, Suzuki. This Bulletin, 33, 396 (1960).
18) E. A. Braude and F. Sondheimer, *J. Chem. Soc.*, 1955, 3754.

two types: (1) Steric effect which gives rise to intensity changes only, without causing any "unusual" change in wavelength (the steric effect of type 1, or *type 1* steric effect). This effect is caused by relatively small twists. (2) Steric effect which causes changes in both wavelength and intensity (the steric effect of type 2, or *type 2* steric effect). This effect is caused by larger twists than the first effect.

To the above two types, Forbes[19] has recently added a third type; the steric effect occurring when the twist is so large that conjugation across the bond is almost completely inhibited and the molecule absorbs as two distinct entities. This effect has been termed a *type 3* steric effect.

A similar classification of steric effects into three main classes has been proposed also by Turner and Voitle[20], and such a classification appears to have been generally accepted[21].

Braude and Sondheimer have regarded *o*-methylated styrenes and related compounds[7] as well as *o*-methylated benzaldehydes and acetophenones[18] as examples of the compounds exhibiting the steric effect of type 1, and have applied their postulated equation $\cos^2\theta = \varepsilon/\varepsilon_0$ to these compounds, where $\varepsilon$ and $\varepsilon_0$ are the molecular extinction coefficient of the conjugation band of a given compound and that of the corresponding planar reference compound, respectively. According to the results, the estimated interplanar angles between the phenyl group and the CH=CX group in styrenes and related compounds are about 20~30° for one, and about 40~60° for two *o*-methyl substituted compounds.

On the other hand, Braude and Forbes[22] have stated that *o*-methylbiphenyl provides an excellent example of the steric effect of type 2, in contrast with *o*-methylated styrenes and acetophenones, notwithstanding the fact that the geometries of the relevant parts of these systems are quite similar. They have explained this rather strange difference between the biphenyl system on the one hand, and the acetophenone and styrene systems on the other, as follows: "the two possible uniplanar conformations of this compound (*o*-methylbiphenyl) are identical and involve the same extent of steric hindrance, whereas the two uniplanar conformations of 2-methylacetophenone or 2-methylstyrene are not identical and one involves much less steric hindrance than the other. Hence the steric hindrance produced by an *o*-methyl substituent will be effectively much larger in the biphenyl than in the other two systems, and the probability of any *o*-substituted biphenyl molecule's occupying a near-planar vibrational state will be extremely low. Thus, the conditions prerequisite for the display of steric effects of type 1 no longer exist".

This appears to be their main reason, although they have given two additional reasons. If this explanation were acceptable, why do *o,o'*-dimethyl substituted styrenes and acetophenones, e. g. 2, 4, 6-trimethylstyrene, 2, 6-dimethylbenzylideneacetone, and 2, 6-dimethylacetophenone, belong to the group of compounds which exhibit the steric effect of type 1 as Braude and his coworker have stated?

It will be evident, as seen in the present treatment of the styrenes and as discussed for the case of acetophenones in the preceding part[13] of this series, that the electronic bathochromic effect of the substituents is responsible for the apparent absence of an appreciable hypsochromic displacement of the conjugation band in these compounds. That is, it seems that the apparent absence of an appreciable wavelength displacement is not a proof of the absence of the hypsochromic displacement produced by the steric interaction but should be considered as a result of compensation of the hypsochromic effect by the electronic bathochromic effect of the substituents. The apparent bathochromic displacement observed sometimes with hindered compounds should, of course, be considered to be due to the electronic bathochromic effect of the substituents outweighing the steric hypsochromic effect. These considerations imply that the difference between the steric effect of type 1 and the steric effect of type 2 is not the difference in kind or in underlying mechanism as Braude and Forbes have asserted, but merely in degree.

In general, as has been discussed so far in this series, the electronic transition energy and hence the wavelength at which absorption occurs are determined by the spatial configuration or conformation of the molecule. Thus, so far as the conformation about the "single" bond is concerned, the non-planarity of the conformation must in principle produce a more or less large hypsochromic shift of the conjugation band, depending on the degree of the deviation from the coplanarity. On the other hand, the presence of steric interference in the molecule affects invariably the population ratio among conformations, and changes the most probable conformation from the planar conformation to a nonplanar one in most cases. Therefore, the wavelength displacement of the

19) W. F. Forbes, "Steric Effects in Conjugated Systems", edited by G. W. Gray, (Proceedings of a Symposium held at the University, Hull, 15-17 July, 1958 by the Chemical Society), Butterworths Scientific Publications, London (1958), p. 62.
20) R. B. Turner and D. M. Voitle, *J. Am. Chem. Soc.*, 73, 1403 (1951).
21) M. S. Newman (ed.), "Steric Effects in Organic Chemistry", John Wiley & Sons, Inc., New York (1956), p. 484.
22) E. A. Braude and W. F. Forbes, *J. Chem. Soc.*, 1955, 3776.

conjugation band caused by steric interference is not an unusual phenomenon as Braude and others have stated, but rather a usual one.

Either when the steric interference is so weak that the planar or nearly planar conformation is still the most probable one, or when the transition probability in the more probable nonplanar conformation is much smaller than the transition probability in the less probable planar conformation, it might be possible that the absorption maximum in the resultant spectrum of the sterically hindered compound is at the same wavelength as the maximum of the unhindered planar reference compound, the intensity of the former being smaller than that of the latter. However, it is doubtful whether such cases can exist in fact. The so-called steric effect of type 1 is, as mentioned above, merely superficial or spurious with respect to the steric effect, and should be considered as a special case where the steric hypsochromic shift is so small that it is almost completely compensated by the bathochromic shift due to the electronic effect of the substituents. Further, only considering that, as pointed out already in an earlier part[23] of this series, the hypsochromic shifts of the conjugation bands as compared with the bands of the corresponding planar reference compounds are observed even in the spectra cited by Braude and others as examples of the steric effect of type 1, it will be evident that the effect of this type is not clear-cut even phenomenologically.

Attention to the fact that, even when any significant wavelength displacement is apparently not observed, the presence of steric interference in the molecule or the deviation of the most probable molecular configuration from the coplanarity can manifest itself in a decrease in the intensity of the band may be of some practical significance, whatever the underlying mechanism may be. It seems, however, not to be necessary in principle to consider the so-called steric effect of type 1 separately from the so-called steric effect of type 2. Further, the steric effect of type 3 (i. e. the *type 3* steric effect) is merely the extreme case of the steric effect of type 2. Accordingly, it may be concluded that Braude and Forbes' classification of steric effects and their elucidations of the "mechanisms underlying the different types" are quite redundant, as pointed out also by Dewar[24].

### 1, 1-Diphenylethylenes

In 1, 1-diphenylethylene, the two phenyl groups can not be simultaneously coplanar with the ethylenic bond, owing to the steric necessities. Therefore, the most probable configuration of this molecule is presumed to be the configuration in which both of the phenyl groups are rotated out to the same extent as each other from the plane of the ethylenic bond, or alternatively, the configuration in which one of the phenyl groups is almost perpendicularly rotated out of the plane of the ethylenic bond, leaving the other phenyl group coplanar with the ethylenic bond.

The data of the ultraviolet absorption spectra of 1, 1-diphenylethylene and its methylated derivatives are summarized in Table IV, in which the data of the spectrum of styrene are also included for comparison. In addition, the spectra of 1, 1-diphenylethylene and its 2, 2-dimethyl derivative measured by the present author are shown in Fig. 2. These spectra are similar to each other, except for the appearance of the additional band at 235.4 m$\mu$ besides the principal band at 248.0 m$\mu$ in the spectrum of 1, 1-diphenylethylene. It is especially of interest that the absorption maxima of the principal (conjugation) bands of these four compounds appear at the almost identical wavelength.

The close similarity between the spectrum of 1, 1-diphenylethylene and that of styrene would be considered as supporting the second of the two hypotheses mentioned above concerning the

Table IV. Absorption maxima of 1, 1-diphenylethylenes

| 1, 1-Diphenylethylene | Solvent | | | Conjugation band | | Ref. |
|---|---|---|---|---|---|---|
| | | $\lambda$, m$\mu$ | $\varepsilon$ | $\lambda$, m$\mu$ | $\varepsilon$ | |
| Unsubstituted | H | | | 248.0 | 14270 | *a* |
| | | | | 235.4 | 13730 | |
| 2-Methyl- | | | | ca. 248 | ca. 13000 | 25 |
| 2, 2-Dimethyl- | H | (286.5) | 1320 | 248.0 | 11700 | *a* |
| | | (279.0) | 1900 | | | |
| (Styrene) | C | | | 248 | | 8 |

Solvent: H, *n*-heptane; C, cyclohexane. Wavelengths in parentheses denote inflections.
Ref. *a*, the present work.

23) H. Suzuki, This Bulletin, 32, 1357 (1959).
24) M. J. S. Dewar, Ref. 19, p. 71.
25) Ramart-Lucas and P. Amagat, *Bull. soc. chim. France*, [4] 51, 108 (1932).

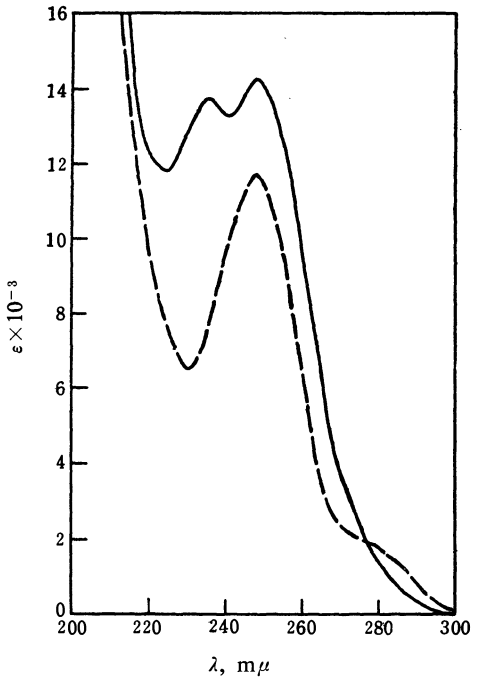



Fig. 2. Ultraviolet absorption spectra (in *n*-heptane): ——, 1,1-diphenylethylene; ----, 1,1-diphenyl-2,2-dimethylethylene.

most probable configuration of 1,1-diphenylethylene. However, the close similarity between the spectrum of 1,1-diphenylethylene and the spectra of its methylated derivatives seems to suggest that the first hypothesis is more plausible, because especially the dimethyl derivative (1,1-diphenyl-2-methylpropene) can not assume the configuration of the second hypothesis owing to the steric interferences between the phenyl groups and the methyl groups at the *cis*-$\beta$-positions relative to the phenyl groups.

Now, when it is assumed that 1,1-diphenylethylene as well as its derivatives has the configuration in which a styrene chromophore is left as the second hypothesis, these compounds can be treated by the calculation quite similar to the one in the case of styrenes.

Alternatively, when it is assumed that each compound has a configuration in which the two phenyl groups are rotated out by the identical degree from the plane of the ethylenic bond as the first hypothesis, the secular equation for the determination of the molecular orbitals as linear combinations of the $2p\pi$ atomic orbitals can be factorized into one equation identical in the form with the one for styrene and one equation for benzene, when $\rho'$ is $1/\sqrt{2} \times \rho$, $\rho'\beta$ representing the $\pi - \pi$ resonance integral for each bond connecting a phenyl group to an ethylenic carbon atom. This situation is very similar to that in the treatment of tetraphenylethylene in Part VI[26] of this series. Accordingly, also in this case, the calculation similar to the one for styrenes can be applied to these 1,1-diphenylethylenes, and from the values of $\rho$ obtained as results of the calculation, the values of $\rho'$ can be obtained. Then, from the values of $\rho'$, the values of $\theta$ and $R$ can be obtained by the use of the relation quite analogous to the one between $\rho$ and $\theta$ as well as $R$ postulated already. The results of the calculation are shown in Table V, in which the symbols have the same significance as in Table III. Allowance for the electronic bathochromic effect of methyl groups has been made by the method quite analogous to the one used in the case of the styrenes. In 1,1-diphenyl-2-methylethylene, the positions of the two phenyl groups are not completely equivalent, and therefore, their angles of twist $\theta$ must differ, though probably very slightly, from each other. In spite of this, the results for this compound obtained on the basis of the assumption that the angles of twist of the two phenyl groups are equal are shown.

It is noteworthy that the introduction ot methyl groups into the 2- or $\beta$-positions of 1,1-diphenylethylene affects only slightly the calculated interplanar angle $\theta$. The presence of the additional steric interference by the methyl groups in spite of the apparent absence of a wavelength displacement of the conjugation band is evident from the fact that the intensity of the band is decreased in the order 1,1-diphenylethylene > 1,1-diphenyl-2-methylethylene > 1,1-diphenyl-2,2-dimethylethylene, with the increasing number of methyl substituents. Thus, also in this case, the apparent absence of a wavelength displacement of the conjugation band is considered as the result of the compensation of the hypsochromic shift due to the steric interference by the bathochromic shift due to the electronic (probably hyperconjugation) effect of the methyl groups. Lastly, it may be mentioned that the calculated interplanar angles for these compounds, especially for the dimethyl compound, are very similar to those for the styrene derivatives belonging to Group IV (cf. Table III).

### Exaltation of Molecular Refraction

Mulliken[27] has indicated that the molecular refractions of positional isomeric alkylstyrenes should roughly parallel the ultraviolet absorption maxima. Following this view, Schwartzman and Corson[8] have correlated the ultraviolet absorption spectra of styrene derivatives with methyl substituents on the benzene nucleus with the molecular refractions. The present author also has frequently referred so far in this series to

26) H. Suzuki, This Bulletin, 33, 389 (1960).
27) R. S. Mulliken, *J. Chem. Phys.*, 7, 356 (1939).

TABLE V. RESULTS OF CALCULATION FOR 1,1-DIPHENYLETHYLENES

| 1,1-Diphenylethylene | $\lambda_A$ mμ | $\lambda_L$ mμ | $\lambda_S$ mμ | $\Delta E_A$ $-\beta$ | $\rho$ | $\rho'$ | $\theta°$ | $R$ Å |
|---|---|---|---|---|---|---|---|---|
| Unsubstituted | 248 | 248 | 208.3 | 1.475 | 0.858 | 0.607 | 43.5 | 1.496 |
| 2-Methyl- | 248 | 250 | 208.3 | 1.496 | 0.821 | 0.581 | 46 | 1.498 |
| 2,2-Dimethyl- | 248 | 252 | 208.3 | 1.515 | 0.788 | 0.557 | 48 | 1.500 |

TABLE VI

| Compound | $EM_\alpha$ | $EM_D$ | $E\Sigma_\alpha$ | $E\Sigma_D$ | Ref. |
|---|---|---|---|---|---|
| *Styrene* | | | | | |
| Unsubstituted | | 1.37 | | | 9 |
| | | 1.10 | | 0.97 | 28 |
| | | | 1.10 | 1.13 | 29 |
| | | | 1.05 | 1.10 | 30 |
| *p*-Methyl- | | | 1.40 | 1.48 | 29 |
| *trans*-β-Methyl- | | 1.87 | | | 9 |
| | | | 1.09 | 1.19 | 30 |
| α-Methyl- | | 0.94 | | | 9 |
| | | 0.64 | | 0.55 | 28 |
| | | | 0.62 | 0.68 | 29, 30 |
| α,β-Dimethyl- | | 0.70 | | | 9 |
| | | | 0.63 | 0.67 | 29, 30 |
| *cis*-β-Methyl- | | 1.00 | | | 9 |
| β,β-Dimethyl- | | | 0.64 | 0.70 | 29, 30 |
| α,β,β-Trimethyl- | | 0.59 | | | 9 |
| | | 0.50 | | 0.34 | 28 |
| | | | 0.44 | 0.48 | 30 |
| *1,1-Diphenylethylene* | | | | | |
| Unsubstituted | | | 0.88 | 0.95 | 30 |
| 2-Methyl- | 1.86 | 2.10 | 0.96 | 1.08 | 30 |
| 2,2-Dimethyl- | 1.39 | 1.53 | 0.67 | 0.74 | 30 |

$EM_\alpha$ and $EM_D$ are exaltations of molecular refraction.
$E\Sigma_\alpha$ and $E\Sigma_D$ are specific exaltations.

the exaltation of the molecular refraction as a measure of the degree of conjugation.

In Table VI, the data of the exaltations found in the literature for the styrenes and the 1,1-diphenylethylenes treated in this part of the series are summarized. The data for some compounds are considerably variable, depending on the worker. In addition, the values of the exaltations are considered to contain not only the conjugation effect but also the hyperconjugation effect of the methyl groups. Therefore, it may not be pertinent to correlate these values of the exaltations directly with the calculated interplanar angles or with the degrees of conjugation which will be inferred from the calculated interplanar angles. Notwithstanding, it will be seen that there exist roughly regular relations among these quantities.

## Experimental

All the spectra were measured with a Cary recording spectrophotometer Model 14 M-50.

α-Methylstyrene (2-phenylpropene) was prepared after the procedure described by Klages[31], and purified by repeated distillation; colorless liquid, b. p. 160~162°C. The value of boiling point is in good agreement with those found in the literature (162°C[31], 160~162°C[32]).

β,β-Dimethylstyrene (1-phenyl-2-methylpropene) was prepared, after the procedure described by Tiffeneau[33], by dehydration of 1-phenyl-2-methylpropanol by heating with oxalic acid, and was purified by repeated distillation; colorless liquid, b. p. 189~193°C. The boiling point of this compound found in the literature is 179~189°C[33]. 1-Phenyl-2-methylpropanol was prepared by the Grignard reaction of benzaldehyde and the Grignard reagent prepared from isopropyl bromide and magnesium.

α,β,β-Trimethylstyrene (2-phenyl-3-methyl-2-butene) was prepared by dehydration of 2-phenyl-3-methyl-2-butanol by distillation, and purified by repeated distillation; colorless liquid, b. p. 189~

28) K. v. Auwers and F. Eisenlohr, *Ber.*, **43**, 806 (1910).
29) K. v. Auwers, ibid., **45**, 2781 (1912).
30) K. v. Auwers, ibid., **62**, 693 (1929).
31) L. Klages, ibid., **35**, 2640 (1902).
32) M. Tiffeneau, *Compt. rend.*, **134**, 845 (1902).
33) M. Tiffeneau, *Ann. Chim.*, [8] **10**, 365 (1907).

191°C. The value of boiling point is in good agreement with the value found in the literature. 2-Phenyl-3-methyl-2-butanol was prepared by the Grignard reaction from acetophenone and isopropyl bromide.

The specimen of 1,1-diphenylethylene used was obtained by re-distillation under reduced pressure of the material prepared by Dr. Takahasi in this laboratory by the method described in Organic Syntheses[34]; colorless thin plates; b. p. 140~143°C/16 mmHg.

1,1-Diphenyl-2,2-dimethylethylene (1,1-diphenyl-2-methylpropene) was prepared by dehydration of 1,1-diphenyl-2-methylpropanol by refluxing with a few pieces of biscuit chips impregnated with concentrated sulfuric acid, and purified by distillation; colorless liquid, b. p. 167~169°C/22 mmHg. The value of boiling point of this compound found in the literature is 150~152°C/15 mmHg[35] and 280~282°C/775 mmHg[36]. 1,1-Diphenyl-2-methylpropanol was prepared by the Grignard reaction from benzophenone and isopropyl bromide.

The author thanks Professor Kengo Shiomi and Professor Saburo Nagakura for reading the manuscript and for valuable advice, and also thanks Dr. Makoto Takahasi for his interest and for a generous supply of 1,1-diphenylethylene.

*Department of Chemistry*
*College of General Education*
*The University of Tokyo*
*Meguro-ku, Tokyo*

34) H. Gilman (Editor-in-Chief), "Organic Syntheses", Col. Vol. 1, John Wiley & Sons, Inc., New York (1932), p. 221.

35) Ramart-Lucas and M. E. Salmon-Legagneur, *Bull. soc. chim. France*, [4] 45, 728 (1929).

36) J. Levy, ibid., [4] 29, 882 (1921).

# *Reaction of Troponoids and Organometallic Compounds. V. Reaction of Bromotropolones and Alkylmagnesium Iodides*

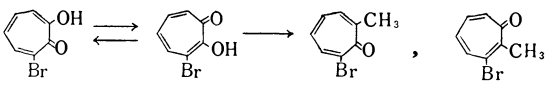
By Katsuo KIKUCHI

(Received October 19, 1959)

It has been reported in a previous paper[1] of this series that bromo derivatives of tropolone methyl ether react with $\alpha$- and $\beta$-naphthylmagnesium bromides to yield corresponding bromo substitution products of 2-$\alpha$- and 2-$\beta$-naphthyltropones and 2-hydroxyphenyl $\alpha$- and $\beta$-naphthyl ketones.

The present paper deals with an investigation on the reaction of bromotropolones and alkyl Grignard reagents.

Reaction of methylmagnesium iodide and 3-bromotropolone (Ia) yielded colorless plates (IIa) whose ultraviolet spectrum was similar to that of tropone[2] (Fig. 1), suggesting that it is monobromo-2-methyltropone. As 3-bromotropolone is in a " high mobile tautomeric " system as represented with A and A′, two isomeric monobromo-2-methyltropone, i.e. 7-bromo-2-methyltropone (B) and 3-bromo-2-methyltropone (B′) should be obtained by this reaction. Actually, treatment of IIa with dilute alkali gave *o*-toluic acid (IIIa) indicating that IIa is 7-bromo-2-methyltropone (B).



A A′ B B′

However, the reaction of 3,7-dibromotropolone and methylmagnesium iodide under similar condition gave only minute amount of unidentified phenolic substance. Similarly, the reaction of 3, 5, 7-tribromotropolone and methylmagnesium iodide afforded only a small amount of dimethyl 3, 5-dibromo-2-hydroxyphenyl carbinol which was proved to be identical with that synthesized by the reaction of methyl 3, 5-dibromosalicylate and methylmagnesium iodide.

On the other hand, by the reaction of 3, 7-dibromotropolone methyl ether (Ib) and methylmagnesium iodide 3, 7-dibromo-2-methyltropone (IIb) was obtained. By treatment with alkali IIb was submitted to rearrangement to give 3-bromo-*o*-toluic acid (IIIb)[3], debromination of which gave IIIa. The ultraviolet absorption spectrum of IIb (Fig. 1) showed bands characteristic of tropone.

1) Part IV: K. Kikuchi, *J. Chem. Soc. Japan, Pure Chem. Sec.* (*Nippon Kagaku Zasshi*), **81**, 505 (1960).
2) T. Nozoe, T. Mukai and K. Takase, *Sci. Repts. Tohoku Univ., Ser.* I, **39**, 164 (1956).
3) D. Peltier, *Compt. rend.*, **237**. 357 (1954).

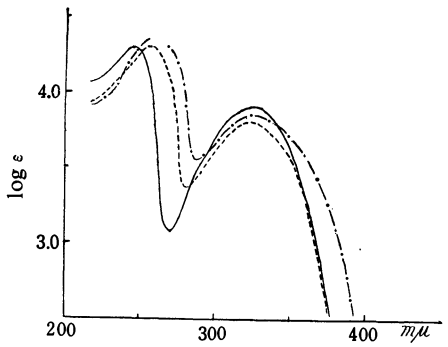
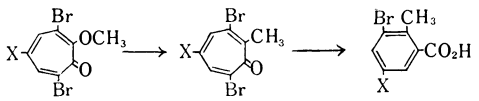


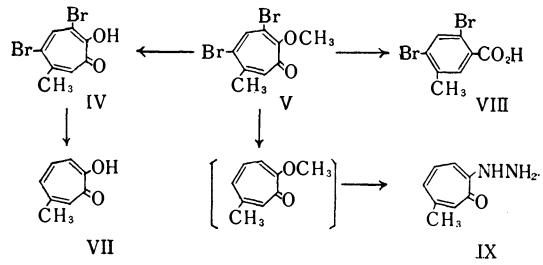

Fig. 1. Ultraviolet absorption spectra of IIa (——), IIb (------) and IIc (—·—·—) in methanol.

Reaction of 3, 5, 7-tribromotropolone methyl ether (Ic) and methylmagnesium iodide afforded four kinds of crystals as follows: pale yellow prisms (IIc), m. p. 63~64°C; colorless needles (IV), m. p. 151.5~153°C; colorless needles (V), m. p. 151~152°C and colorless needles (VI), m. p. 116~117°C. The main product was IIc.

Treatment of IIc with alkali afforded an acid (IIIc) whose debromination gave *o*-toluic acid (IIIa). This fact and the analytical values of IIc and IIIc indicate that IIc and IIIc are 2-methyl-3, 5, 7-tribromotropone and 3, 5-dibromo-*o*-toluic acid, respectively. The ultraviolet spectrum of IIc is shown in Fig 1.




IV showed red coloration with ferric chloride characteristic of tropolone and gave yellow sodium salt with aqueous sodium carbonate. On catalytic debromination, IV afforded 4-methyltropolone (VII)[4,5]. Treatment of V with hydrobromic acid in aqueous acetic acid and with aqueous sodium hydroxide afforded IV and 4, 6-dibromo-*m*-toluic acid (VIII)[6], respectively. Catalytic debromination of V on palladium-charcoal gave colorless crystals which, on treatment with hydrazine hydrate, was converted to 2-hydrazino-6-methyltropone (IX)[7]. These experimental results indicate that IV is 3, 5-dibromo-6-methyltropolone and V is 3, 5-dibromo-2-methoxy-6-methyltropone as shown in the following scheme.




It was reported previously that the reaction of 7-bromo-2-methoxytropone and phenylmagnesium bromide afforded phenyltropolone[8], m. p. 96~97°C, as a by-product. Pauson[9] suggested it to be 4-phenyltropolone and later Kitahara[10] presented the mechanism of its formation. The formation of IV and V also could be explained by his mechanism.

Analysis of VI is in agreement with the formula $C_9H_8OBr_2$ and its ultraviolet absorption spectrum (Fig. 2) is quite similar to those of IIa—IIc, and it is suggested that VI has a tropone nucleus. Presumably VI will be 3, 5-dibromo-2, 7-dimethyltropone or 3, 5-dibromo-2, 6-dimethyltropone formed either by the reaction of excess of methylmagnesium iodide with IIc or V, but the determination of the structure was impossible because of limited amount of the material.

Application of ethylmagnesium iodide to Ib afforded 3, 7-dibromo-2-ethyltropone (IId), as in the case of IIb. IId was converted to 3-bromo-2-ethylbenzoic acid (IIId), and the latter was debrominated to 2-ethylbenzoic acid (IIIe). The same reaction of ethylmagnesium iodide with Ic gave no crystalline product even after chromatographic separation on an alumina column. Ethanolic solution of the oil thereby obtained, however, when treated with dilute alkali, resulted in the formation of dibromo-2-ethylbenzoic acid (IIIf) and its ethyl ester (IIIg). From this fact it seems reasonable to assume that 2-ethyl-3, 5, 7-tribromotropone (IIe) was formed in this reaction as in the case of IIc.

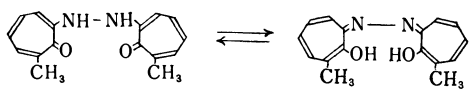
Some nucleophilic reactions on IIa, IIb and IIc were next examined.

Heating of IIa and IIb with *p*-toluidine respectively afforded 2-methyl-7-(*p*-toluidino)-tropone (Xa) as yellow prisms and 3-bromo-2-methyl-7-(*p*-toluidino)-tropone (Xb) as yellow plates. The ultraviolet spectrum of Xa was shown in Fig. 2. Similarly, heating of IIa and IIb with aniline respectively gave 7-anilino-2-methyltropone (Xc) as an oil and 7-anilino-3-bromo-2-methyltropone (Xd) as yellow crystals.

Application of hydrazine hydrate to IIa at

4) R. D. Haworth, B. P. Moore and P. L. Pauson, *J. Chem. Soc.*, **1948**, 1045.
5) T. Nozoe, T. Mukai, M. Kunori, T. Muroi and K. Matsui, *Sci. Repts. Tohoku Univ., Ser.* I, **35**, 242 (1951).
6) R. Fittig, W. Ahrens and L. Mattheides, *Ann.*, **147**, 36 (1868).
7) P. Akroyd, R. D. Haworth and J. D. Hobson, *J. Chem. Soc.*, **1951**, 3427.
8) T. Nozoe, T. Mukai and I. Murata, *Proc. Japan Acad.*, **28**, 142 (1952).
9) P. L. Pauson, *Chem. Revs.*, **55**, 9 (1955).
10) Y. Kitahara, *Sci. Repts, Tohoku Univ., Ser.* I, **39**, 250 (1956).

room temperature afforded yellow needles (XIa) which gave red coloration with ferric chloride. From its analytical value and the ultraviolet absorption spectrum (Fig. 2) it was assumed to be bis-(2-methyltropon-7-yl)-hydrazine (C) or its tautomer (C') but no further study was made.



C C'

Similar treatment of IIb with hydrazine hydrate yielded colorless needles (XIIa) and yellow needles (XIb). The former was assumed to be 3-bromo-*o*-toluic acid hydrazide from its analytical value and its ultraviolet absorption spectrum (Fig. 2) and the latter to have the analogous structure to XIa. On the other hand, treatment of IIc with hydrazine hydrate gave 3,5-dibromo-*o*-toluic acid hydrazide (XIIb) and the compound corresponding to XIa and XIb was not obtained.

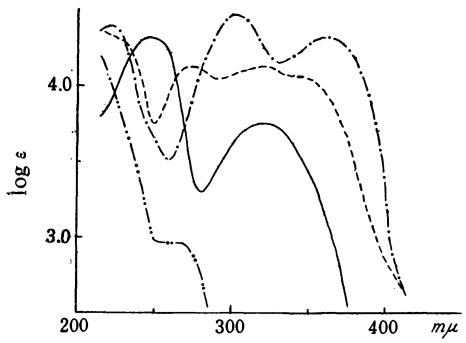



Fig. 2. Ultraviolet absorption spectra of VI (——), Xa (------), XIa (—·—·—·) and XIIa (—··—··—) in methanol.

Several methods[11-15] have already been reported by which 2-halotropones could be converted to tropolones. Application of these methods to IIb and IIc gave no satisfactory results, but by heating of IIb and IIc each with sodium acetate in acetic acid[11] 4-bromo-3-methyltropolone (XIIIa) and 4,6-dibromo-3-methyltropolone (XIIIb) were obtained respectively only with poor yields.

## Experimental

**Reaction of 3-Bromotropolone (Ia) and Methylmagnesium Iodide.**—To a solution of methylmagnesium iodide prepared from 5.0 g. of methyl iodide, 0.84 g. of magnesium and 20 cc. of absolute ether, a solution of 2.0 g. of Ia dissolved in 20 cc. of dehydrated tetrahydrofuran was added in drops under stirring, while chilling with ice. The mixture was stirred for further five hours under ice-chilling, decomposed with dilute sulfuric acid and extracted with chloroform. The chloroform solution was washed with dilute sodium hydroxide solution by which 320 mg. of Ia was recovered. The chloroform solution was then washed with water, dried and the solvent was removed to give 750 mg. of reddish brown oil. This oil was dissolved in benzene, passed through an alumina column, and 470 mg. of 7-bromo-2-methyltropone (IIa), m. p. 43~45°C, was obtained. Recrystallization from cyclohexane gave colorless plates, m. p. 46~47°C.

Found: C, 48.39; H, 3.90. Calcd. for $C_8H_7OBr$: C, 48.22; H, 3.54%.

**Reaction of 7-Bromo-2-methyltropone (IIa) and Alkali.**—A mixture of 50 mg. of IIa and 0.5 cc. of 1 N sodium hydroxide was heated on a water bath for one hour. After removal of the insoluble material, the aqueous layer was acidified with dilute hydrochloric acid and the crystals that separated out were recrystallized from dilute ethanol to give colorless crystals (IIIa), m.p. 99~101°C, undepressed at melting point on admixture with *o*-toluic acid.

**Reaction of 3,7-Dibromotropolone Methyl Ether (Ib) and Methylmagnesium Iodide.**—To a solution of methylmagnesium iodide prepared from 3.0 g. of methyl iodide, 0.5 g. of magnesium and 30 cc. of absolute ether, a solution of 3.0 g. of Ib dissolved in 30 cc. of dehydrated benzene was added in drops and stirring was continued for further two and a half hours. The reaction mixture was poured into dilute sulfuric acid, and the yellow precipitates thereby obtained were filtered off. After washing the organic solvent layer with water, the solvent was removed to give 710 mg. of 3,7-dibromo-2-methyltropone (IIb). By passing the oily portion through an alumina column 150 mg. of a second crop of IIb was obtained. Recrystallization from ethanol gave colorless needles, m. p. 121~122°C.

Found: C, 34.29; H, 2.29. Calcd. for $C_8H_6OBr_2$: C, 34.57; H, 2.18%.

**Reaction of 3,7-Dibromo-2-methyltropone (IIb) and Alkali.**—Similar treatment of IIb with 1 N sodium hydroxide as in the case of IIa gave colorless plates (IIIb), m. p. 150°C. The reported melting point of 3-bromo-*o*-toluic acid is 153°C.

Found: C, 44.88; H, 3.45. Calcd. for $C_8H_7O_2Br$: C, 44.68; H, 3.28%.

IIIb was debrominated catalytically to *o*-toluic acid (IIIa), m. p. 100~102°C, and identified by a mixture melting point determination.

**Reaction of 3,5,7-Tribromotropolone Methyl Ether (Ic) and Methylmagnesium Iodide.**—a) To an ice-chilled solution of methylmagnesium iodide prepared from 1.52 g. of methyl iodide, 0.26 g. of magnesium and 15 cc. of absolute ether, 2.0 g. of Ic dissolved in 15 cc. of benzene was added under stirring. The mixture was stirred further for one

11) T. Nozoe, Y. Kitahara, T. Ando, S. Masamune and H. Abe, ibid., *Ser.* I, 36, 166 (1952).
12) W. E. Doering and J. R. Mayer, *J. Am. Chem. Soc.*, 75, 2387 (1953).
13) S. Seto, *Sci. Repts. Tohoku Univ., Ser.* I, 37, 275 (1953).
14) S. Seto, ibid., 37, 297 (1953).
15) W. E. Doering and C. F. Hiskey, *J. Am. Chem. Soc.*, 74, 5688 (1952).

hour and decomposed with dilute sulfuric acid. After washing the organic solvent layer successively with water, 5% sodium hydrogen carbonate solution and water, the solvent was removed and 2.1 g. of red oil was obtained. The oil was redissolved in a mixture of benzene and petroleum ether and passed through a silica column. Three kinds of crystals were thereby obtained; 670 mg. of 2-methyl-3, 5, 7-tribromotropone (IIc), m. p. 62~64°C; 80 mg. of 3, 5-dibromo-6-methyltropolone (IV), m. p. 148~150°C; 20 mg. of 3, 5-dibromo-2-methoxy-6-methyltropone (V), m. p. 147~149°C.

b) To a solution of methylmagnesium iodide prepared from 3.8 g. of methyl iodide, 4.0 g. of Ic dissolved in benzene was added. Treatment of the reaction mixture as in a) gave 920 mg. of IIc, 120 mg. of IV, 75 mg. of V and 20 mg. of dibromodimethyltropone (VI).

IIc was recrystallized from a mixture of benzene and petroleum ether to give colorless needles, m. p. 64~65°C.

Found: C, 27.26; H, 1.88. Calcd. for $C_8H_5OBr_3$: C, 26.92; H, 1.41%.

Pyridine solution of IIc gives a reddish purple coloration with dilute sodium hydroxide solution.

IV was recrystallized from a mixture of benzene and petroleum ether to give colorless needles, m. p. 151.5~153°C. Benzene solution of IV gives red coloration with ferric chloride.

Found: C, 32.95; H, 2.54. Calcd. for $C_8H_6O_2Br_2$: C, 32.68; H, 2.06%.

V was recrystallized from a mixture of benzene and petroleum ether to give colorless needles, m. p. 151~152°C. Pyridine solution of V colors reddish purple with dilute sodium hydroxide solution.

Found: C, 35.48; H, 3.00. Calcd. for $C_9H_8O_2Br_2$: C, 35.06; H, 2.60%.

VI was recrystallized from ethanol to yield colorless needles, m. p. 116~117°C. Pyridine solution gives deep reddish purple coloration with dilute sodium hydroxide solution.

Found: C, 36.96; H, 3.03. Calcd. for $C_9H_8OBr_2$: C, 36.98; H, 2.73%.

**Reaction of 2-Methyl-3, 5, 7-tribromotropone (IIc) and Alkali.**—Similar treatment of IIc with 2 N sodium hydroxide solution as in the case of IIa gave colorless crystals (IIIc), m. p. 195~197°C.

Found: C, 33.09; H, 2.36. Calcd. for $C_8H_6O_2Br_2$: C, 32.68; H, 2.06%.

IIIc was debrominated to *o*-toluic acid, m. p. 100~102°C.

**Debromination of 3,5-Dibromo-6-methyltropolone (IV).**—Catalytic reduction of 40 mg. of IV dissolved in 6 cc. of methanol, in the presence of 50 mg. of sodium acetate and 20 mg. of 5% palladium-charcoal resulted in absorption of 6 cc. of hydrogen. After removal of the catalyst by filtration, the solvent was removed and the crystalline residue was recrystallized from petroleum ether to give colorless crystals, m. p. 70~72°C. These crystals showed no depression at the melting point on admixture with 4-methyltropolone (VII).

**Acid Hydrolysis of 3, 5-Dibromo-2-methoxy-6-methyltropone (V).**—A suspension of 18 mg. of V in a mixture of 0.5 cc. of acetic acid and 0.1 cc. of hydrobromic acid (sp. g.=1.48) was heated on a water bath for one hour. Addition of water separated 14 mg. of colorless crystals, m. p. 150~151°C. These crystals showed no depression at the melting point on admixture with 3, 5-dibromo-6-methyltropolone (IV).

**Reaction of 3, 5-Dibromo-2-methoxy-6-methyltropone (V) and Alkali.**—Similar treatment of V with dilute aqueous sodium hydroxide as in the case of IIa afforded colorless plates (VIII), m. p. 181~183°C, the melting point remaining unchanged on admixture of 4, 6-dibromo-*m*-toluic acid.

**Reaction of Hydrazine and the Debromination Product of 3, 5-Dibromo-2-methoxy-6-methyltropone (V).**—A solution of 60 mg. of V dissolved in 6 cc. of methanol was catalytically debrominated with the addition of 50 mg. of sodium acetate and 5% palladium-charcoal. After removal of the catalyst by filtration, the solution was diluted with water and extracted with benzene. The benzene layer was washed with water and the solvent was removed. The crystalline residue obtained was dissolved in 0.1 cc. of methanol and two drops of 80% hydrazine hydrate was added. The mixture was warmed on a water bath, cooled and the crystals thereby formed were recrystallized from benzene to give yellow needles, m. p. 121~123°C, which showed no depression at the melting point on admixture with 2-hydrazino-6-methyltropone (IX).

**Reaction of 3, 5, 7-Tribromotropolone and Methylmagnesium Iodide.**—To a solution of Grignard reagent prepared from 1.0 g. of methyl iodide, 0.72 g. of 3, 5, 7-tribromotropolone dissolved in dehydrated tetrahydrofuran was added under chilling with ice. After being stirred for five hours, the reaction mixture was decomposed with dilute sulfuric acid and extracted with chloroform. The chloroform extract was treated with dilute sodium carbonate solution by which 250 mg. of 3, 5, 7-tribromotropolone was recovered. The chloroform solution was further treated with dilute sodium hydroxide and the aqueous layer was acidified with dilute hydrochloric acid and extracted with benzene. Benzene extract afforded, after removal of the solvent, 130 mg. of dark red oil, chromatographic separation of which through an alumina column gave 40 mg. of crystals. Recrystallization from ethanol gave colorless plates, m. p. 133~134°C.

Found: C, 35.05; H, 3.25. Calcd. for $C_9H_{10}O_2Br_2$: C, 34.87; H, 3.25%.

These crystals showed no depression at the melting point on admixture of dimethyl 3, 5-dibromo-2-hydroxyphenyl carbinol prepared from the reaction of methyl 3, 5-dibromosalicylate and methylmagnesium iodide.

**Reaction of 3, 7-Dibromotropolone Methyl Ether (Ib) and Ethylmagnesium Iodide.**—To a solution of ethylmagnesium iodide, prepared from 3.2 g. of ethyl iodide, a solution of 3.0 g. of Ib in benzene was added with stirring at 0°C, and the reaction mixture was treated as in the reaction of Ib and methylmagnesium iodide. 3, 7-Dibromo-2-ethyltropone (IId) was obtained as colorless needles, m. p. 81~82°C. Yield, 730 mg.

Found: C, 37.28; H, 3.02. Calcd. for $C_9H_8OBr_2$: C, 36.98; H, 2.73%.

IId, when heated on a water bath for three hours,

with the addition of dilute aqueous solution of sodium hydroxide, was rearranged to give colorless plates (IIId), m. p. 100~101°C.

Found: C, 47.10; H, 4.00. Calcd. for $C_9H_9O_2Br$: C, 47.18; H, 3.96%.

IIId was catalytically debrominated to 2-ethylbenzoic acid (IIIe), m. p. 64~65°C.

**Reaction of 3, 5, 7-Tribromotropolone Methyl Ether (Ic) and Ethylmagnesium Iodide.**—To a solution of ethylmagnesium iodide, prepared from 1.68 g. of ethyl iodide, 2.0 g. of Ic in benzene was added. After being stirred for one hour under ice-chilling, the reaction mixture was treated as in the case of Ic and methylmagnesium iodide. With the recovery of 350 mg. of 3, 5, 7-tribromotropolone, 1.7 g. of dark red oil was obtained. This oil was dissolved in a mixture of benzene and petroleum ether and passed through a silica column, but none of each fraction of the eluents gave crystalline products.

The red oil (800 mg.), obtained from easily eluated fraction, was then warmed with a mixture of 1 cc. of ethanol and 1.5 cc. of 2 N sodium hydroxide for several minutes and chilled with ice. From the alkali-soluble part 220 mg. of dibromo-2-ethylbenzoic acid (IIIf) was obtained. Recrystallization from ethanol raised the melting point to 145~146°C.

Found: C, 35.01; H, 2.62. Calcd. for $C_9H_8O_2Br_2$: C, 35.10; H, 2.62%.

Alkali-insoluble part gave 300 mg. of ethyl dibromo-2-ethylbenzoate (IIIg). Recrystallization from ethanol raised the melting point to 45~46°C.

Found: C, 38.85; H, 3.57. Calcd. for $C_{11}H_{12}O_2Br_2$: C, 39.32; H, 3.60%.

IIIf was debrominated to 2-ethylbenzoic acid (IIIe), m. p. 63~64°C, and was esterified to IIIg with ethanol in the presence of concentrated sulfuric acid.

**2-Methyl-7-(*p*-toluidino)-tropone (Xa).**—A mixture of 50 mg. of 7-bromo-2-methyltropone (IIa) and 50 mg. of *p*-toluidine was heated at 120~130°C for ten minutes, diluted with benzene and the benzene solution was washed successively with dilute sulfuric acid and water. The crystalline residue, obtained upon removal of benzene, was recrystallized from ethanol to give yellow prisms, m. p. 75~76°C.

Found: N, 6.40. Calcd. for $C_{15}H_{15}ON$: N, 6.22%.

**3-Bromo-2-methyl-7-(*p*-toluidino)-tropone (Xb).**—Obtained from 3, 7-dibromo-2-methyltropone (IIb) and *p*-toluidine as in the case of Xa, and recrystallized from ethanol to give orange yellow prisms, m. p. 105~106°C.

Found: N, 4.89. Calcd. for $C_{15}H_{14}ONBr$: N, 4.59%.

**7-Anilino-2-methyltropone (Xc).**—Obtained from IIa and aniline as in the case of Xa as a red oil. Picrate of Xc was obtained by the usual method and recrystallized from methanol to give yellow microneedles, m. p. 159~160°C.

Found: N, 12.98. Calcd. for $C_{20}H_{16}O_8N_4$: N, 12.72%.

**7-Anilino-3-bromo-2-methyltropone (Xd).**—Obtained from IIb and aniline by the same method as above, and recrystallized from ethanol to give yellow crystals, m. p. 109~110°C.

Found: N, 4.95. Calcd. for $C_{14}H_{12}ONBr$: N, 4.83%.

**Reaction of 7-Bromo-2-methyltropone (IIa) and Hydrazine.**—To a solution of 50 mg. of IIa dissolved in 0.1 cc. of ethanol was added 50 mg. of 80% hydrazine hydrate. After being warmed slightly on a water bath, the reaction mixture was acidified with dilute sulfuric acid. Yellow crystals that separated were collected by filtration and recrystallized from ethanol and then from *n*-butanol to give yellow needles (XIa), m. p. 200~201°C. Ethanolic solution of XIa colors red with ferric chloride.

Found: C, 71.52; H, 5.91; N, 10.57. Calcd. for $C_{16}H_{16}O_2N_2$: C, 71.62; H, 6.01; N, 10.44%.

**Reaction of 3, 7-Dibromo-2-methyltropone (IIb) and Hydrazine.**—To a solution of 100 mg. of IIb dissolved in 0.6 cc. of benzene was added 100 mg. of 80% hydrazine hydrate and the whole was allowed to stand overnight. The crystals that separated out were recrystallized from ethanol to give colorless needles (XIIa), m. p. 157~158°C.

Found: N, 12.15. Calcd. for $C_8H_9ON_2Br$: N, 12.23%.

The filtrate was acidified with dilute sulfuric acid and the crystals that separated out were recrystallized from a mixture of dioxane and *n*-butanol to give yellow needles (XIb), m. p. 283~284°C.

Found: C, 45.10; H, 3.35. Calcd. for $C_{16}H_{14}O_2N_2Br_2$: C, 45.08; H, 3.31%.

**Reaction of 2-Methyl-3, 5, 7-tribromotropone (IIc) and Hydrazine.**—A solution of IIc in benzene was treated with hydrazine hydrate as in the case of IIb. The crystals obtained were recrystallized from ethanol to give colorless needles (XIIb), m. p. 175~176°C.

Found: N, 9.50. Calcd. for $C_8H_8ON_2Br_2$: N, 9.09%.

**4-Bromo-3-methyltropolone (XIIIa).**—A mixture of 100 mg. of IIb, 80 mg. of anhydrous sodium acetate and 1 cc. of glacial acetic acid was heated at 180~200°C for one hour. The solution was then diluted with water, warmed further for a half hour, extracted with benzene and the benzene solution was treated with dilute aqueous sodium hydroxide. Yellow sodium salt that separated out was collected by filtration and acidified with hydrochloric acid. XIIIa thereby liberated was recrystallized from ethanol to give pale brownish crystals, m. p. 100~102°C; yield was very poor (about 5 mg.). XIIIa gives red coloration with ferric chloride.

Found: C, 45.30; H, 3.27. Calcd. for $C_8H_7O_2Br$: C, 44.68; H, 3.28%.

**4, 6-Dibromo-3-methyltropolone (XIIIb).**—Obtained from 40 mg. of IIc as in the case of XIIIa and recrystallized from ethanol to give pale yellow needles, m. p. 121~123°C; yield was about 5 mg.

Found: C, 33.04; H, 2.59. Calcd. for $C_8H_6O_2Br_2$: C, 32.68; H, 2.06%.

The author wishes to express his sincere thanks to Professor T. Nozoe of Tohoku University for his guidance and encouragement throughout this work, as well as to Professor S. Seto, Assistant Professor Y. Kitahara and Assistant Professor T. Mukai of Tohoku University for their kind advices and suggestions. He is also

grateful to Miss K. Kato for the measurements of ultraviolet absorption spectra and to Mr. S. Ohyama and Miss A. Iwanaga for the elemental analyses.

*Department of Chemistry*
*Faculty of Liberal Arts and Science*
*Yamagata University*
*Koshirakawa-cho, Yamagata*

# *Syntheses and Reactions of 2-Bromomethyltropones*

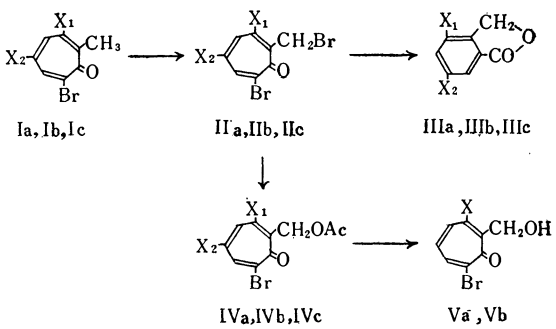
By Katsuo KIKUCHI

(Received October 19, 1959)

Recently it was reported that tropone, 2-phenyltropone and several kinds of their bromine substituted compounds were comparatively easily brominated on their tropone nucleus through addition of bromine to their double bonds and subsequent dehydrobromination (and debromination in some instances), showing the unsaturated properties of the tropone nucleus[1,2].

In the present paper the bromination of 7-bromo-2-methyltropone (Ia), 3, 7-dibromo-2-methyltropone (Ib) and 2-methyl-3, 5, 7-tribromotropone (Ic)[3] was undertaken. The aim of the experiment of this paper is twofold; (1) 2-methyltropone is considered to be a vinylog of methylketone and accordingly it would be important to examine whether bromination occurs on a tropone nucleus or on a methyl group; and (2) 2-bromomethyltropones, if they were obtained, would be easily converted to 2-hydroxymethyltropones, the key intermediates for the preparation of 2-formyltropones.

Application of one molecular equivalent of bromine or *N*-bromosuccinimide on Ia afforded pale yellow needles (IIa) in a good yield. Although attempted conversion of IIa to phthalide (IIIa) directly by treating with alkali failed, the structure of IIa was proved to be 7-bromo-2-bromomethyltropone as described later. Similarly, both Ib and Ic, when treated with bromine, afforded 2-bromomethyl-3, 7-dibromotropone (IIb) and 2-bromomethyl-3, 5, 7-tribromotropone (IIc), respectively. Treatment of IIb with dilute alkali gave 4-bromophthalide (IIIb)[4], which on reduction over palladium charcoal aforded IIIa. Similar treatment of IIc with alkali afforded 4, 6-dibromophthalide (IIIc), whose debromination gave IIIa.




Bromination of IIa gave pale yellow needles (IId), the structure of which is not clear yet. On the other hand, further bromination of IIb was found to be difficult even under prolonged heating on a water bath. This fact is rather interesting from the fact that 3, 7-dibromo-2-phenyltropone was easily brominated to give 2-phenyl-3, 5, 7-tribromotropone[1]. Ultraviolet absorption spectra of IIa, IIb and IIc were shown in Fig. 1.

Although the preparations and reactions of

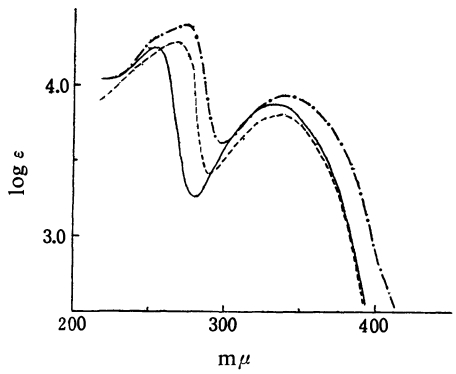



Fig. 1. Ultraviolet absorption spectra of IIa(——), IIb (----) and IIc(-·-·-) in methanol.

1) T. Mukai, *Sci. Repts. Tohoku Univ., Ser.* I, **38**, 280 (1954).
2) T. Nozoe, T. Mukai and K. Takase, ibid., **39**, 164 (1956).
3) K. Kikuchi, This Bulletin, **33**, 628 (1960).
4) J. Tirouflet, *Bull. soc. sci. Bretagne, Spec. No.*, **26**, 7 (1951); *Chem. Abstr.*, **47**, 8693 (1953).

hydroxymethyltropolone[5-7] and formyltropolone[7,8] derivatives have been examined in some detail, 2-hydroxymethyltropone and 2-formyltropone derivatives have remained unknown. Therefore, the synthesis of these materials were next attempted.

Application of silver acetate on IIa in acetic acid gave 2-acetoxymethyl-7-bromotropone (IVa) which, when heated with a mixture of dilute hydrochloric acid and ethanol, easily underwent hydrolysis to give 7-bromo-2-hydroxymethyltropone (Va). Va showed no coloration with ferric chloride characteristic of tropolone. The ultraviolet absorption spectrum of Va reveals that it retains tropone nucleus as shown in Fig. 2. Treatment of Va with dilute alkali gave IIIa though in a poor yield. These facts indicate that Va has the expected structure and that bromination of Ia has undoubtedly occurred on a side chain methyl group as described before.

Similar treatment of IIb with silver acetate or sodium acetate afforded 2-acetoxymthyl-3, 7-dibromotropone (IVb), which was hydrolyzed to 3, 7 - dibromo - 2 - hydroxymethyltropone (Vb). Similarly, treatment of IIc with silver acetate gave 2-acetoxymethyl-3, 5, 7-tribromotropone (IVc). Acid hydrolysis of IVc, however, resulted in the formation of IIIc. This result is curious compared with the fact that 2-halotropones usually do not rearrange to aromatic acids in acidic media.

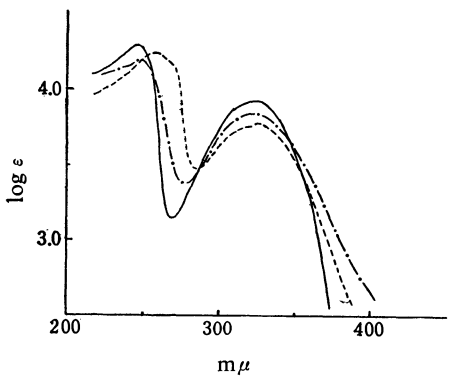
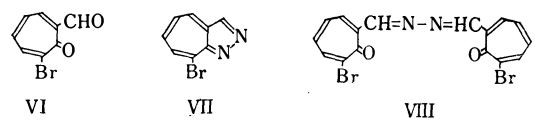



Fig. 2. Ultraviolet absorption spectra of Va(——), Vb(----) and VI(-·-·-) in methanol.

Mild oxidation of Va with activated manganese dioxide in benzene[8] or with chromium trioxide in a mixture of acetic acid and acetic anhydride afforded 7-bromo-2-formyltropone (VI). VI reduces ammoniacal silver nitrate solution and Fehling's solution and gives phenylhydrazone.

An attempted synthesis of 8-bromo-1, 2-diazaazulene (VII) by treating VI with hydrazine has not succeeded, and the only product was yellow crystals which was assumed to be symmetrical azine (VIII) of VI from its analytical value.




VI VII VIII

## Experimental

**7-Bromo-2-bromomethyltropone (IIa).**—a) To a solution of 200 mg. of 7-bromo-2-methyltropone (Ia) in 1.5 cc. of acetic acid was added 170 mg. of bromine and the mixture was heated on a water bath for 30 min. and cooled. The crystals that separated were collected by filtration. Yield, 80 mg. Mother liquor was diluted with water, extracted with benzene and the benzene layer was washed successively with water, 2 N sodium carbonate and water. Removal of the solvent afforded second crop of 60 mg. of crystals. These crystals were combined and recrystallized from ethanol to give colorless needles (IIa), m. p. 103~104°C.

Found: C, 34.50; H, 2.07. Calcd. for $C_8H_6OBr_2$: C, 34.57; H, 2.18%.

b) A mixture of 520 mg. of Ia, 520 mg. of *N*-bromosuccinimide and 6 cc. of carbon tetrachloride was heated to reflux for four and one-half hours under irradiation. The crystals were filtered, washed well with benzene and the combined solution was washed with water. Removal of the solvent provided 500 mg. of crystals, m. p. 97~101°C. These crystals showed no depression of the melting point on admixture with IIa obtained by the method of a).

**2-Bromomethyl-3, 7-dibromotropone (IIb).**—A mixture of 100 mg. of 3, 7-dibromo-2-methyltropone (Ib), 0.8 cc. of acetic acid and 60 mg. of bromine was heated on a water bath for about 30 min. From the reaction mixture 110 mg. of IIb was obtained as pale yellow needles of m. p. 141~143°C. Recrystallization from ethanol raised the melting point to 142~143°C.

Found: C, 27.26; H, 1.88. Calcd. for $C_8H_5OBr_3$: C, 26.92; H, 1.41%.

**2-Bromomethyl-3, 5, 7-tribromotropone (IIc).**—To a solution of 200 mg. of 2-methyl-3, 5, 7-tribromotropone (Ic) dissolved in 1 cc. of acetic acid was added 100 mg. of bromine, and the mixture was heated on a water bath for about 30 min. On cooling, 220 mg. of IIc was obtained as pale yellow plates of m. p. 104~106°C. Recrystallization from ethanol raised the melting point to 107~108°C.

Found: C, 22.13; H, 1.14. Calcd. for $C_8H_4OBr_4$: C, 22.05; H, 0.93%.

**Bromination of 7-Bromo-2-bromomethyltropone (IIa).**—A mixture of 50 mg. of IIa and 35 mg. of bromine in 0.3 cc. of acetic acid was heated on a water bath for about 30 min. and cooled. The crystals that separated were collected by filtration and recrystallized from ethanol to give pale yellow needles

5) T. Nozoe, T. Mukai and K. Matsui, *Proc. Japan Acad.*, 27, 561 (1951).
6) T. Nozoe, T. Mukai and K. Takase, *Sci. Repts. Tohoku Univ., Ser.* I, 36, 40 (1952).
7) S. Seto and K. Ogura, This Bulletin, 32, 493 (1959).
8) E. Sebe and S. Matsumoto, *Sci. Repts. Tohoku Univ., Ser.* I, 38, 308 (1954).

(IId), m. p. 131~133°C. Yield, 45 mg. Further recrystallization from ethanol raised the melting point to 133~134°C.

Found: C, 27.56; H, 1.76. Calcd. for $C_8H_5OBr_3$: C, 26.92; H, 1.41%.

Action of dilute aqueous sodium hydroxide on IId gave only unidentified black resinous matter. Attempted debromination of side chain bromine with zinc and acetic acid also failed.

**Attempted Bromination of 2-Bromomethyl-3, 7-dibromotropone (IIb).**—A mixture of 50 mg. of IIb and 30 mg. of bromine in 0.4 cc. of acetic acid was heated for two hours on a water bath in a closed vessel. On cooling, 20 mg. of pale yellow crystals, m. p. 136~140°C was obtained and identified as starting material by the mixture melting point method. Mother liquor, on being diluted with water, gave pale yellow crystals of m. p. 113~125°C, purification of which was difficult.

**Reaction of 2-Bromomethyl-3, 7-dibromotropone (IIb) and Alkali.**—A mixture of 100 mg. of IIb and 1 cc. of 1 N sodium hydroxide solution was heated on a water bath for one hour, treated with active carbon and filtered. Acidification of the filtrate with dilute hydrochloric acid gave 35 mg. of 4-bromophthalide (IIIb) as colorless plates of m. p. 94~97°C. Recrystallization from cyclohexane raised the melting point to 98~99°C. Reported melting point of IIIb is 103~104°C.

Found: C, 45.39; H, 2.43. Calcd. for $C_8H_5O_2Br$: C, 45.10; H, 2.37%.

Catalytic debromination of IIIb afforded phthalide (IIIa), m. p. 70~71°C, undepressed of melting point on admixture with authentic sample.

**Reaction of 2-Bromomethyl-3, 5, 7-tribromotropone (IIc) and Alkali.**—A mixture of 100 mg. of IIc, 0.6 cc. of 1 N aqueous sodium hydroxide and 0.1 cc. of ethanol was treated as in the case of IIb, and 4, 6-dibromophthalide (IIIc) thereby obtained, was recrystallized from dilute ethanol to give colorless needles, m. p. 112~113°C.

Found: C, 33.15; H, 1.51. Calcd. for $C_8H_4O_2Br_2$: C, 32.91; H, 1.38%.

Debromination of IIIc afforded IIIa, m.p. 71~72°C.

**2-Acetoxymethyl-7-bromotropone (IVa).**—To a solution of 150 mg. of 7-bromo-2-bromomethyltropone (IIa) dissolved in 1.2 cc. of acetic acid 150 mg. of silver acetate was added, and the mixture was heated on a water bath for 15 min. with occasional stirring and filtered. Acetic acid was removed from the filtrate by evaporation, and the residue was extracted with benzene. The benzene solution was washed with water and the solvent evaporated. The crystals thereby obtained were recrystallized from a mixture of benzene and petroleum ether to give colorless needles (IVa), m. p. 108~110°C. Yield, 130 mg. Further recrystallization raised the melting point to 110~111°C.

Found: C, 46.30; H, 3.16. Calcd. for $C_{10}H_9O_3Br$: C, 46.72; H, 3.53%.

**2-Acetoxymethyl-3,7-dibromotropone (IVb).** — a) To a solution of 200 mg. of 2-bromomethyl-3, 7-dibromotropone (IIb) dissolved in 2 cc. of acetic acid was added 160 mg. of sodium acetate, the mixture was heated on a water bath for one and one-half hours and filtered. The filtrate was diluted with water, extracted with benzene, and the benzene extract was washed with water and concentrated. The crystals thereby obtained were recrystallized from ethanol to give colorless crystals (IVb), m. p. 84~87°C. Yield, 160 mg. Further recrystallization from ethanol raised the melting point to 88~89°C.

Found: C, 35.90; H, 2.30. Calcd. for $C_{10}H_8O_3Br_2$: C, 35.74; H, 2.40%.

b) Similar treatment of 200 mg. of IIb with 150 mg. of silver acetate as in the case of IIa afforded 150 mg. of colorless crystals of m. p. 85~88°C, undepressed of the melting point on admixture with IVb obtained in a).

**2-Acetoxymethyl-3, 5, 7-tribromotropone (IVc).**—Similar treatment of 300 mg. of 2-bromomethyl-3, 5, 7-tribromotropone (IIc) with 180 mg. of silver acetate as in the case of IIa afforded 240 mg. of IVc, m. p. 87~90°C. Recrystallization from ethanol gave colorless needles, m. p. 88~90°C.

Found: C, 28.59; H, 1.95 Calcd. for $C_{10}H_7O_3Br_3$; C, 28.95; H, 1.70%.

**7-Bromo-2-hydroxymethyltropone (Va).**—A solution of 330 mg. of 2-acetoxymethyl-7-bromotropone (IVa) dissolved in a mixture of 3 cc. of ethanol and 1.5 cc. of 2 N hydrochloric acid was heated to reflux for 50 min. Evaporation of most of ethanol afforded 260 mg. of pale brown crystals (Va), m. p. 116~118°C (decomp.). Recrystallization from dilute ethanol gave colorless needles, m. p. 120~121°C (decomp.).

Found: C, 44.92; H, 3.74. Calcd. for $C_8H_7O_2Br$: C, 44.68; H, 3.28%.

**Reaction of 7-Bromo-2-hydroxymethyltropone (Va) and Alkali.**—A mixture of 40 mg. of Va and 0.5 cc. of 1 N sodium hydroxide solution was heated on a water bath for 30 min. The resulting clear solution was acidified with hydrochloric acid, treated with charcoal, filtered while hot and cooled. Colorless plates, m. p. 69~71°C, thereby obtained, showed no depression of melting point on admixture with phthalide.

**3, 7-Dibromo-2-hydroxymethyltropone (Vb).** — A solution of 100 mg. of 2-acetoxymethyl-3, 7-dibromotropone (IVb) dissolved in a mixture of 1 cc. of ethanol and 0.5 cc. of 2 N hydrochloric acid was heated on a water bath for one hour. Similar treatment of the reaction mixture as in the case of Va afforded 70 mg. of Vb, m. p. 100~103°C (decomp.). Recrystallization from ethanol gave colorless crystals, m. p. 109~110°C (decomp.).

Found: C, 33.08; H, 2.20. Calcd. for $C_8H_6O_2Br_2$: C, 32.68; H, 2.06%.

**Acid Hydrolysis of 2-Acetoxymethyl-3,5,7-tribromotropone (IVc).**—A solution of 300 mg. of IVc dissolved in a mixture of 2 cc. of ethanol and 1 cc. of 2 N hydrochloric acid was heated on a water bath for two hours and cooled. The crystals thereby obtained were recrystallized from ethanol to give colorless needles, m. p. 112~113°C, which showed no depression of melting point on admixture with IIIc obtained by the action of alkali on IIc.

**7-Bromo-2-formyltropone (VI).**—a) To a solution of 200 mg. of 7-bromo-2-hydroxymethyltropone (Va) dissolved in 10 cc. of benzene was added 800 mg. of active manganese dioxide, and the mixture was stirred for two hours at room temperature and filtered.

Evaporation of the solvent afforded 100 mg. of VI, m. p. 147~149°C (decomp.). Recrystallization from ethanol gave yellow needles, m. p. 148~150°C (decomp.).

Found: C, 45.05; H, 2.74. Calcd. for $C_8H_5O_2Br$: C, 45.10; H, 2.37%.

b) To a suspension of 100 mg. of Va in a mixture of 0.3 cc. each of acetic acid and acetic anhydride was added 0.3 cc. of chromium trioxide solution (prepared by dissolving 1 g. chromium trioxide in a mixture of 5 cc. each of acetic acid and acetic anhydride) at room temperature. The solution was warmed at 35~45°C for 50 min., cooled and the crystals that separated out were collected by filtraton. Yield, 40 mg. Recrystallization from ethanol gave yellow needles, m. p. 146°C (decomp.).

**Phenylhydrazone of 7-Bromo-2-formyltropone (VI).**—To a solution of 50 mg. of VI dissolved in 2 cc. of ethanol was added a solution of 40 mg. of phenylhydrazine hydrochloride in 0.3 cc. of water at room temperature. Phenylhydrazone of VI was obtained as purple needles, m. p. 142°C (decomp.). It was difficult to recrystallize from usual organic solvents.

Found: C, 55.51; H, 3.53; N, 9.15. Calcd. for $C_{14}H_{11}ON_2Br$: C, 55.46; H, 3.66; N, 9.24%.

**Azine (VIII) of 7-Bromo-2-formyltropone (VI).**—To a solution of 50 mg. of VI dissolved in 2.5 cc. of ethanol was added a solution of 20 mg. of hydrazine hydrochloride in 0.3 cc. of water at room temperature. Azine (VIII) was obtained as yellow crystals, m. p. 147~148°C (decomp.), which were difficult to recrystallize from usual organic solvents.

Found: C,45.72; H, 2.47; N, 6.49. Calcd. for $C_{16}H_{10}O_2N_2Br_2$: C, 45.55; H, 2.39; N, 6.64%.

The author wishes to express his sincere thanks to Professor T. Nozoe of Tohoku University for his guidance and encouragement throughout this work, as well as to Professor S. Seto, Assistant Professor Y. Kitahara and Assistant Professor T. Mukai of Tohoku University for their kind advice and suggestions. He is also grateful to Miss K. Kato for the measurements of ultraviolet absorption spectra and to Mr. S. Ohyama and Miss A. Iwanaga for the elemental analyses.

*Department of Chemistry*
*Faculty of Liberal Arts and Science*
*Yamagata University*
*Koshirakawa-cho, Yamagata*

# *Inorganic Extraction Studies on the System between Tri-n-butyl Phosphate* and Hydrochloric Acid*

By Tomitaro ISHIMORI, Kenju WATANABE and Eiko NAKAMURA

(Received October 28, 1959)

During the course of the solvent extraction studies on fission products and actinide elements with TBP, it was felt that the behavior of other common elements ought to be clarified. In the present paper, is studied the behavior of about fifty chemical elements, ranging from sodium to curium, in the TBP-hydrochloric acid system.

## Experimental

**Sources of Materials.**—Tributyl phosphate was purified in the usual way[1-3], and used without any dilution. Hydrochloric acid solutions were prepared by diluting commercial concentrated hydrochloric acid. The acidity was determined volumetrically if necessary.

Table I[4-8] shows the sources of radioactive tracers. Most of the imported tracers were used as received, whereas Y-90, Nb-95[7] and Ra-224 were prepared from imported Sr-90, Zr-95 and Th-228, respectively. Many other tracers were prepared by irradiating suitable targets in JRR-1. In order to avoid complication as far as possible, very pure materials were used as the targets. The subsequent chemical treatments were carried out if necessary; however, in many cases targets were simply dissolved in acids and converted into chloride solutions.

The radiochemical purities were checked by $\gamma$-ray spectrometry, tracing the decay and/or $\beta$ absorption. Nickel and cadmium tracers contained some radiochemical impurities. Accordingly these tracers were measured at photopeaks using a $\gamma$-spectrometer.

* TBP

1) K. Alcock, S. S. Grimley, T. V. Healy, J. Kennedy and H. A. C. McKay, *Trans. Faraday Soc.*, 52, 39 (1956).

2) D. F. Peppard, G. W. Mason and J. L. Maier, *J. Inorg. & Nuclear Chem.*, 3, 215 (1956).

3) D. F. Peppard, W. J. Driscoll, R. J. Sironen and S. McCarty, ibid., 4, 326 (1957).

4) T. Ishimori, K. Yoshihara and H. Nakamura, 3rd Japan Conference on Radioisotope, S-17 (1959).

5) T. Ishimori, H. Nakamura, and E. Nakamura, ibid., S-16 (1959).

6) N. Shibata and K. Yoshihara, This Bulletin, 32, 422 (1959).

7) S. Yajima, ibid., 31, 699 (1958).

8) H. Ebihara and K. Yoshihara, ibid., 33, 116 (1960).

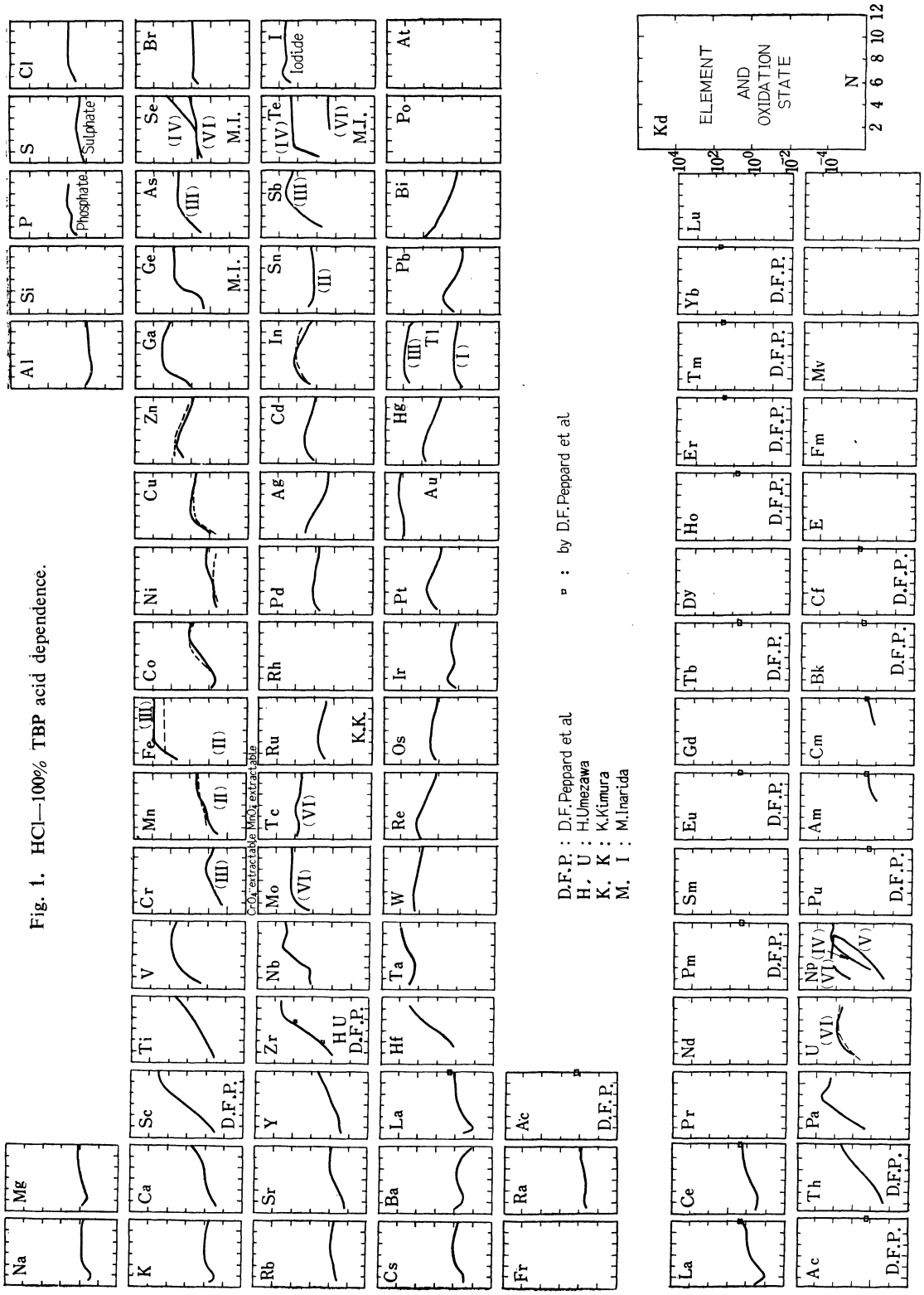
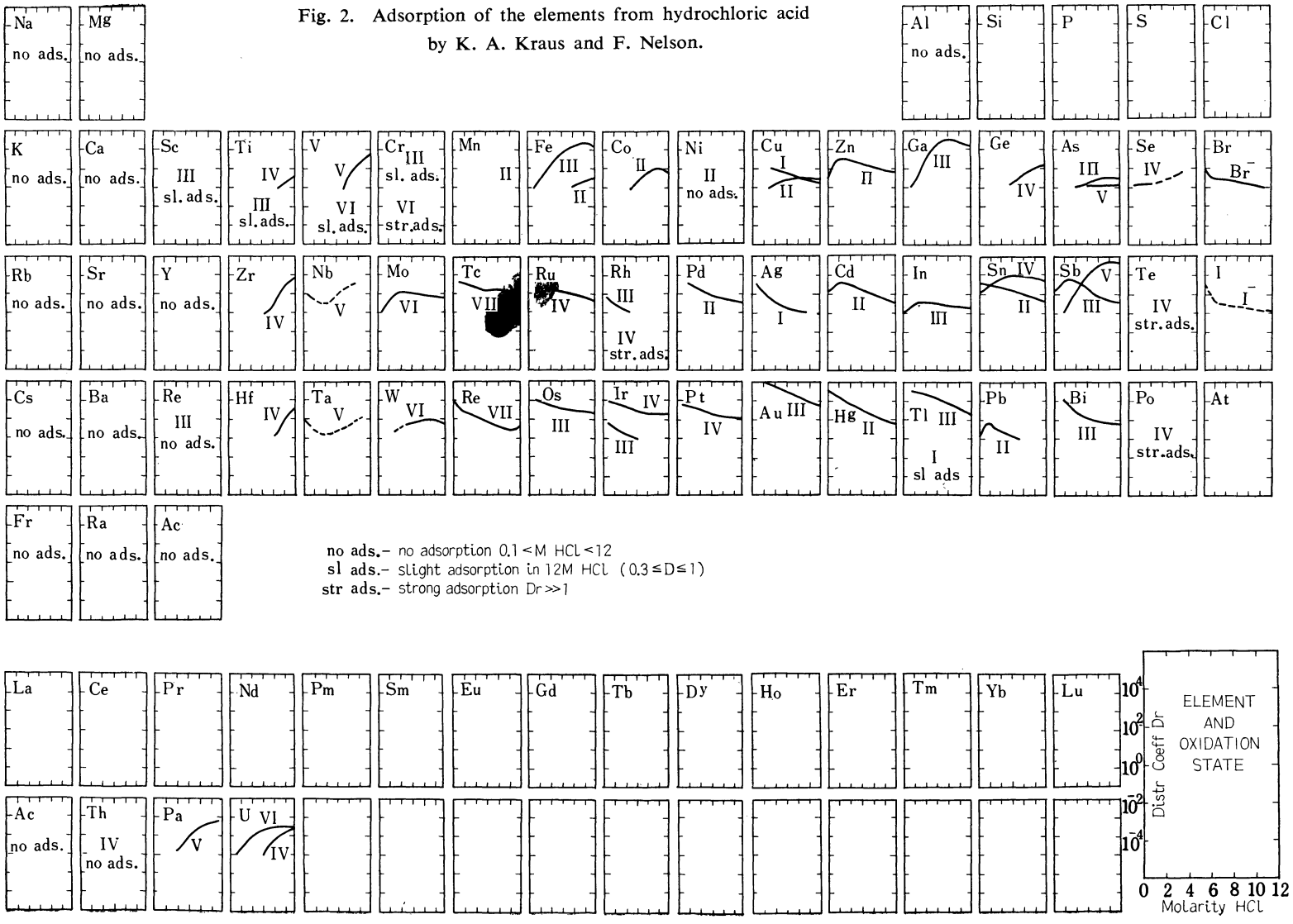



Fig. 1. HCl—100% TBP acid dependence.

Fig. 2. Adsorption of the elements from hydrochloric acid by K. A. Kraus and F. Nelson.



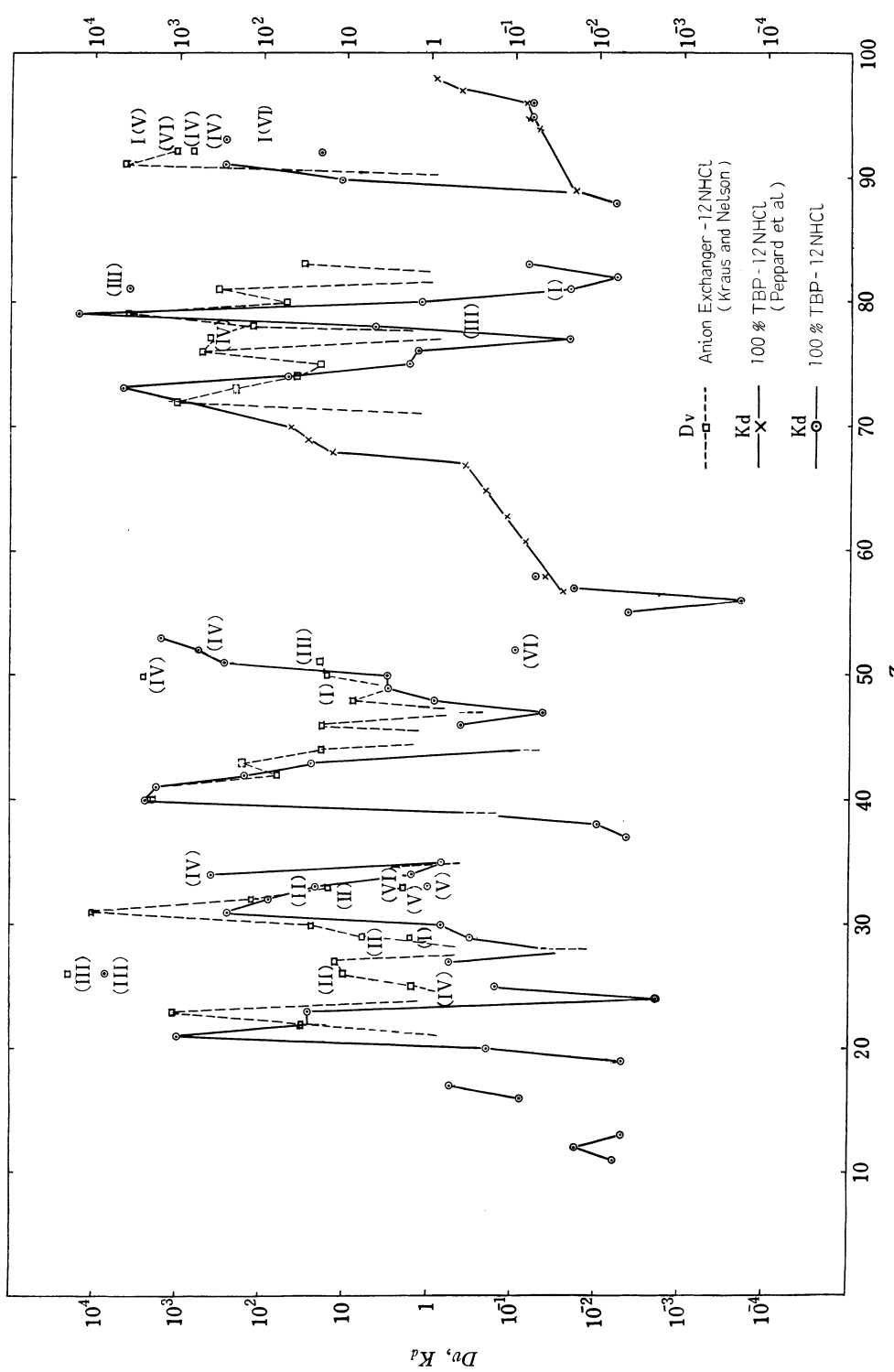



Fig. 3. Solvent extraction and anion exchange at 12 N HCl.

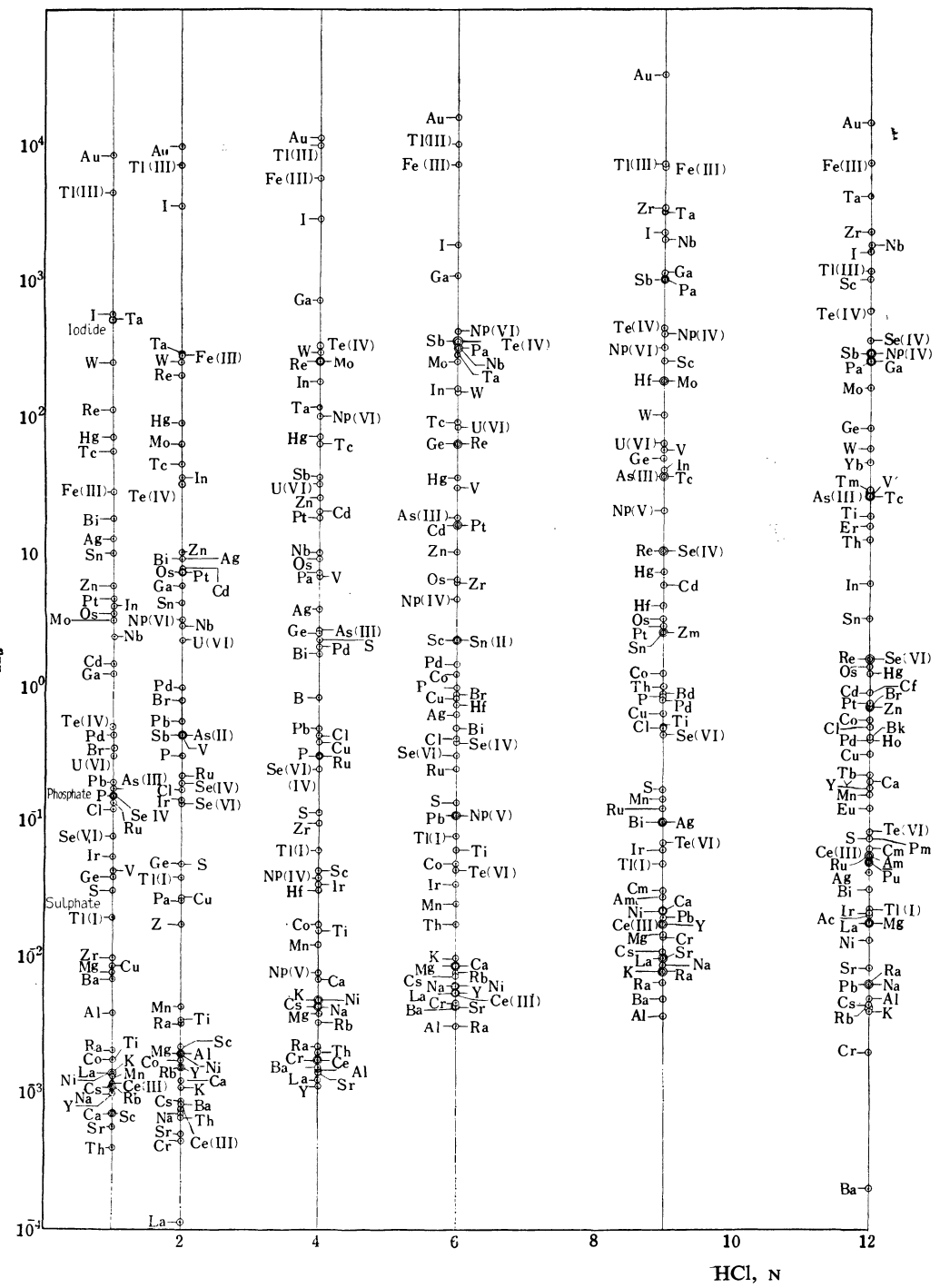



Fig. 4. $K_d$ values in 100% TBP- 1~12 N HCl.

TABLE I. SOURCES OF RADIOACTIVE TRACERS USED

| Element | Tracer | Target | Radiochemical purity was checked by | Remarks |
|---|---|---|---|---|
| Na | Na-24 | $Na_2CO_3$ | $\gamma$-spectrum, $\beta$-decay | |
| Mg | Mg-27 | Mg metal | $\gamma$-decay | |
| Al | Al-28 | Al metal | $\gamma$-decay, $\gamma$-spectrum | |
| P | P-32 | S | $\beta$-decay, absorption | Processed, used as $PO_4$[4] |
| S | S-35 | BHC | $\beta$-decay, absorption | Processed, used as $SO_4$[5] |
| Cl | Cl-38 | $NH_4Cl$ | $\gamma$-decay | |
| K | K-42 | $K_2CO_3$ | $\gamma$-spectrum, $\beta$-decay | Prepared by Isotope Production Group, JAERI |
| Ca | Ca-45 | | | Imported |
| Ti | Ti-51 | $Ti(OH)_4$ | $\gamma$-decay | |
| V | V-52 | $NH_4VO_3$ | $\gamma$-decay | |
| Cr | Cr-51 | | | Prepared by Yoshihara[6], Isotope Production Group, JAERI |
| Mn | Mn-56 | $MnO_2$ | $\gamma$-decay | |
| Fe | Fe-59 | | | Imported |
| Co | Co-60 | | | Imported |
| Ni | Ni-65 | $Ni(NO_3)_2$ | | Counted at 1.49 MeV. |
| Cu | Cu-64 | Cu metal | $\gamma$-decay, $\gamma$-spectrum | |
| Zn | Zn-65 | | | Imported |
| Ga | Ga-72 | $Ga_2O_3$ | $\beta$-decay, $\gamma$-spectrum | |
| As | As-76 | $As_2O_3$ | $\beta$-decay, $\gamma$-spectrum | |
| Br | Br-80 m, 82 | $NH_4Br$ | $\gamma$-decay | |
| Rb | Rb-86, 88 | RbCl | $\gamma$-decay | Cl-38 was removed by ion exchange |
| Sr | Sr-90 | | | Imported |
| Y | Y-90 | | $\beta$-decay, absorption | Milked from imported Sr-90* |
| Nb | Nb-95 | | $\beta$-decay, absorption | Milked from imported Zr-95[7] |
| Mo | Mo-99 | $(NH_4)_2MoO_4$ | $\beta$-decay | |
| Tc | Tc-99 | | | Imported |
| Pd | Pd-109 | Pd metal | $\gamma$-decay | Ag-111 was removed by pptn. of AgCl after addition of Ag carrier |
| Ag | Ag-108 | $AgNO_3$ | $\gamma$-decay | |
| Cd | Cd-115 | Cd metal | $\gamma$-spectum | Counted at 0.5~0.525 MeV. |
| In | In-116 m | In metal | $\gamma$-spectrum, $\beta$-decay | Prepared by Yoshihara, Isotope Production Group, JAERI |
| Sn | Sn-121 | Sn metal | | |
| Sb | Sb-122 | Sb metal | $\gamma$-decay | |
| I | I-131 | | | Imported |
| Cs | Cs-137 | | | Imported |
| Ba | Ba-139 | $BaCO_3$ | $\gamma$-decay | |
| La | La-140 | $La_2O_3$ | $\gamma$-decay | |
| Ce | Ce-144 | | | Imported |
| Hf | Hf-181 | | | Imported |
| Ta | Ta-182 | | | Imported |
| W | W-187, 185 | W-oxinate | $\beta$,$\gamma$-decay | Prepared by Ebihara[8], Isotope Production Group, JAERI, hotchemically |
| Re | Re-186, 188 | Re metal | $\gamma$-decay | |
| Os | Os-191, 193 | Os metal | $\gamma$-decay | |
| Ir | Ir-192, 194 | Ir metal | $\beta$,$\gamma$-decay | Fused with $Na_2O_2$ |
| Pt | Pt-193, 197 | Pt metal | $\beta$,$\gamma$-decay | Au-199 was removed* |
| Au | Au-198 | Au metal | $\gamma$-spectrum, $\beta$-decay | Prepared by Yoshihara, Isotope Production Group, JAERI |
| Hg | Hg-203 | | | Imported |
| Tl | Tl-204 | | | Imported |
| Ra | Ra-224 | | $\alpha$-decay | Milked from Th-228* |

* Procedures are given in the present paper.

Inorganic extraction,
in 100% TBP—HCl system
TBP extraction of,
Na, Mg, Al, $PO_4$, $SO_4$, Cl, K, Ca, Sc, Ti, V, Cr, Mn, Fe, Co, Ni, Cu, Zn, Ga, Ge, As, Se, Br, Rb, Sr, Y, Zr, Nb, Mo, Tc, Ru, Pd, Ag, Cd, In, Sn, Sb, Te, I, Cs, Ba, La, Ce and other rare earth elements, Hf, Ta, W, Re, Os, Ir, Pt, Au, Hg, Tl, Pb, Bi, Ra, Th, Pb, Bi, Ra, Th, Pa, U, Np, Am and Cm

The specific activity of these radiochemical tracers were higher than $10^4$ cpm/100 microgram. Although in some cases the oxidation states and the chemical forms of the tracer could not be clearly defined, for the most part familiar chemical forms were chosen as far as possible.

Distribution ratios were determined radiometrically in the ordinary way[2,3,9].

## Results and Discussion

The results obtained are summarized in Fig. 1 as a series of graphs of $\log K_d$ vs. N HCl, where $K_d$ is the distribution ratio and N the molarity. Fig. 1 was compiled from some published and unpublished results. Curves for scandium[2], zirconium[2], some of the rare earth elements[10,11], thorium[2] and some other actinide elements[10,11] are taken from the work of Peppard and his coworkers. Data for zirconium[12], ruthenium[13], germanium[14], selenium[14] and tellurium[14] are taken from the observations of Umezawa et al., Kimura and Inarida. The curves for lead, bismuth, uranium, americium and curium were obtained by one of the present authors (T. Ishimori) during his stay in the Argonne National Laboratory, Lemont, Ill. U.S.A. Finally the three curves for neptunium (IV), (V) and (VI) are quoted from the previous paper[9]. The curves for iron, cobalt, nickel, copper, zinc, indium and uranyl obtained by Irving et al.[15] are added to Fig. 1 with broken lines. Morris and Bell[16] gave the acid dependence curve for cobalt which coincides with that of the present authors. It is likely that permanganate and chromate have fairly high $K_d$ values. However, their values were not plotted because of the rapid reduction of these ions in the system.

As Fig. 1 shows, the four alkali metal elements behave in a similar way, showing always very low $K_d$ values. Halogen elements keep their $K_d$ values practically constant in the higher acidity range over 4 N. There are some similarities in the shapes of the acid dependence curves for zinc, cadmium and bivalent mercury; ruthenium, palladium, osmium and platinum; and tervalent arsenic and antimony, respectively.

The $K_d$ values of scandium, yttrium and lanthanum increase with their decreasing atomic number, $Z$, at higher acidity range. A similar relationship is seen more clearly among quadrivalent zirconium, hafnium and thorium. In these cases, the element of smaller $Z$ has higher $K_d$ value. On the other hand, the extractability of alkali metal elements or the group of zinc, cadmium and bivalent mercury, does not depend on the value of $Z$. Further, $K_d$ values of chloride, bromide and iodide increase with their increasing atomic number.

Fig. 2 gives the adsorption behavior of the elements on an anion exchange resin from hydrochloric acid solutions. The curves in Fig. 2 are rewritten in a similar scale with that of Fig. 1 based on the original figure proposed by Kraus and Nelson[17]. As they did not give distribution coefficients, $D_v$, less than 1, the curves below $D_v=1$ are not drawn in Fig. 2.

The shapes of the acid dependence curve given in Figs. 1 and 2 are very similar for most elements. The high $K_d$ value of scandium is a rare exception. It is not understandable that the solvent-extraction behavior of tervalent antimony resembles the ion exchange behavior of quinquevalent antimony.

It is likely that the resemblance discussed above shows similar mechanisms of distribution between the anion exchange and the extraction with TBP.

The $K_d$ values at 12 N hydrochloric acid were plotted against the atomic number, $Z$, in Fig. 3. The figure shows that the $K_d$ values vary regularly to some extent, giving two peaks for one long period of the periodic table. The values for lanthanide and tervalent actinide elements are quoted from the work of Peppard et al.[3,10,11] who found the effect of the half-filled shell in the relationship between $K_d$ and $Z$.

The broken lines in Fig. 3 show the relationship between $D_v$ values of anion exchange and $Z$. A close similarity is seen here again between the behaviors of the solvent extraction and the ion exchange.

Fig. 4 gives $K_d$ values in the 100% TBP-hydrochloric acid system. This will be convenient for checking the possibility and efficiency

9) T. Ishimori and E. Nakamura, ibid., 32, 713 (1959).
10) D. F. Peppard, P. R. Gray and M. M. Markus, *J. Am. Chem. Soc.*, 75, 6063 (1953).
11) P. R. Gray, unpublished results quoted in E. K. Hyde, "Proceedings International Conference on Peaceful Uses of Atomic Energy, Geneva", Vol. VII, P/728, United Nations Publication, New York (1956).
12) T. Ishimori, H. Umezawa and K. Watanabe, *J. Atomic Energy Soc. Japan*, 1, 299 (1959).
13) K. Kimura, unpublished.
14) M. Inarida, unpublished.
15) H. Irving and D. N. Edgington, *J. Inorg. & Nuclear Chem.*, 10, 306 (1959).
16) D. F. C. Morris and C. F. Bell, ibid., 10. 337 (1959).
17) K. A. Kraus and F. Nelson, "Proceedings International Conference on Peaceful Uses of Atomic Energy, Geneva, 1955", Vol. VII, P/837, United Nations Publication, New York (1956).

of a mutual separation of a couple of elements chosen arbitrarily. These $K_d$ values are found with tracers of fairly high specific activities. Therefore, optimum conditions of a separation found in Fig. 4 will fit farily well in a tracer scale chemical separation; however, some caution must be exercised in macro-scale separations. For example, $K_d$ for silver of more than 10 at 1 N acidity, is not applicable in a macro-scale separation because of the formation of insoluble silver chloride. Some examples are given in the following, showing how to utilize the $K_d$ values obtained.

## Applications

**a) Preparation of Y-90 (or La-140).**—The solvent extraction behavior of strontium, yttrium, barium, lanthanum and iron in the 100% TBP-hydrochloric acid system are given in Fig. 5. The curves of Fig. 5. show that the direct separation of Y-90 (or La-140) from Sr-90 (or Ba-140) is not easy. However, the difference between $K_d$ values for iron and yttrium (or lanthanum) is so great that yttrium (or lanthanum) is separated from iron very easily. Yttrium-90 (or La-140) is separated from Sr-90 (or Ba-140) by the carrying down with ferric hydroxide. The precipitate is dissolved in 3 N hydrochloric acid. The TBP extraction

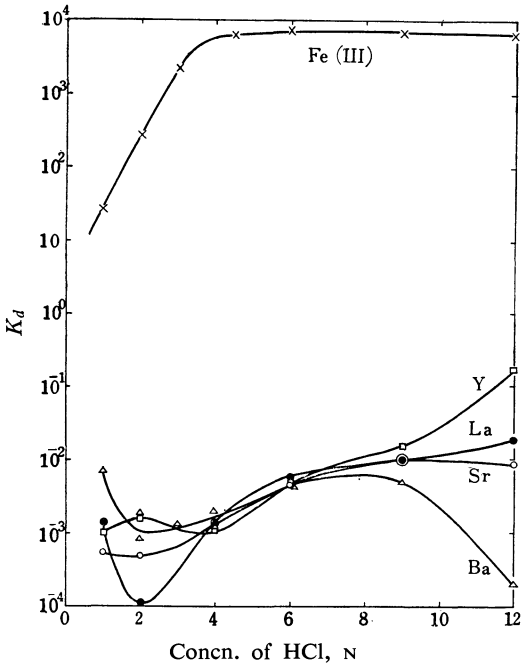



Fig. 5. The $K_d$ valuer of iron, strontium, yttrium, barium and lanthanum.
—×— Fe, —○— Sr, —□— Y, —△— Ba, —●— La

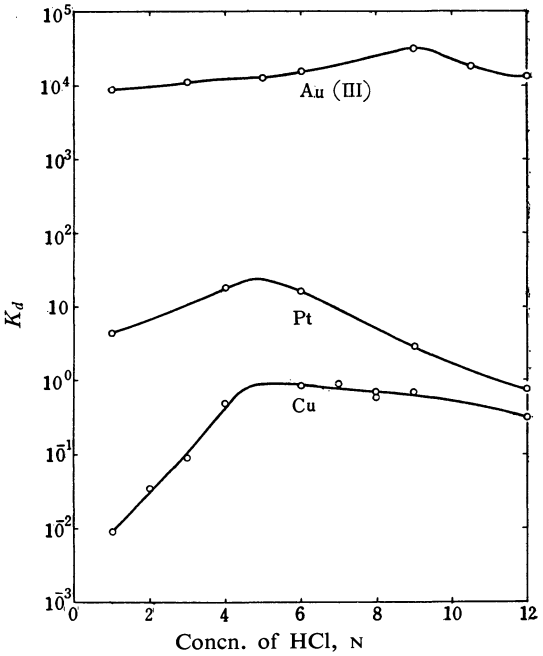



Fig. 6. The $K_d$ values of gold, plutinum and copper.

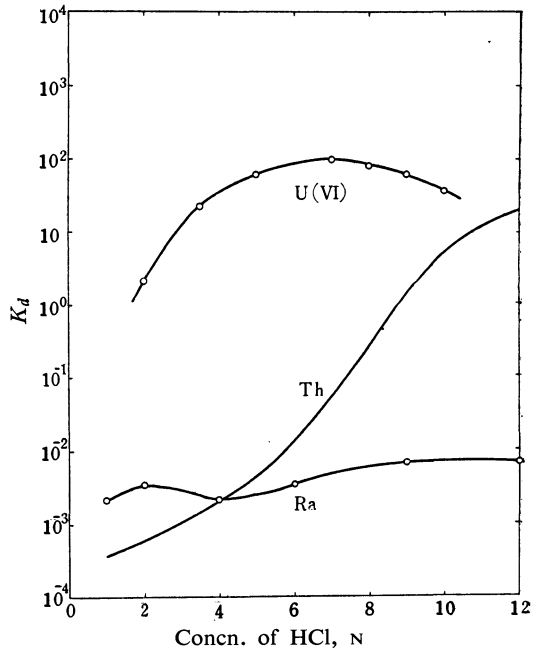



Fig. 7. The $K_d$ values of uranium, thorium and radium in HCl-100% TBP.
The data for thorium was taken from the work of Peppard et al.

removes iron, leaving Y-90 (or La-140) carrier free in the acid solution.

**b) Radiochemical Purification of Pt-197.**— The difference of $K_d$ values between gold and platinum is shown in Fig. 6. As is seen in the figure, $K_d$ values of platinum are too high to keep platinum in the acid quantitatively. Therefore, TBP is diluted with toluene in order to make $K_d$ values for both elements lower. The TBP (1 : 2) works well for the separation of gold from platinum at 1 or 12 N hydrochloric acid.

Irradiated platinum containing Pt-197 and Au-199 is dissolved in aqua regia, and converted into 1 or 12 N hydrochloric acid solution. Extraction of Au-199 with TBP (1 : 2) brings about an aqueous solution of purified Pt-197 tracer. Gold in copper is removed similarly with diluted TBP from 1 N hydrochloric acid solution. (Fig. 6).

**c) Milking of Th-234 from U-238.** — The difference between $K_d$ values for thorium and uranyl ion is shown in Fig. 7.

In the 6 N hydrochloric acid—TBP system uranyl ion is extracted into TBP, whereas thorium remains in the aqueous solution. The TBP solution of uranyl chloride is used conveniently as a cow. In this case the addition of a small amount of bromine prevents the photoreduction of uranyl ion.

**d) Milking of Ra-244 from Th-228.**—As is shown in Fig. 7, radium is not extracted from 12 N hydrochloric acid, while thorium is extractable with a $K_d$ of about 10. Accordingly radium is left in the acid solution after several extractions of thorium with TBP. Both Pb-212 and Bi-212 remain in the acid solution with Ra-224.

*Chemistry Division, Tokai Laboratory*
*Japan Atomic Energy Research Institute*
*Tokai, Ibaraki-ken*

# *The Aconite Alkaloids. XXXIII*. On Lucidusculine. III***

By Takashi AMIYA

(Received October 27, 1959)

In the previous reports some derivatives of lucidusculine (I), $C_{24}H_{35}O_4N$, have been reported and the extended formula of compound I has been proposed[2,3].

Lately the author has investigated the behavior of compound I toward various oxidizing agents, and the previously proposed partial formula[2] is further extended.

Oxidation of compound I with 3% hydrogen peroxide gave lucidusculine *N*-oxide-a (II), $C_{24}H_{35}O_5N \cdot H_2O$, m. p. 191°C (decomp.) in a poor yield. From the procedure for its preparation, compound II seems to contain water of crystallization[4-7].

Further, in order to obtain an epoxide derivative of compound I, perbenzoic acid oxidation has been performed. This oxidation has not given the results expected in the cases of Senecio alkaloids[8] and atisine derivatives[9]. Compound I reacted with only one mole of perbenzoic acid under different conditions and an *N*-oxide, lucidusculine *N*-oxide-b (III), $C_{24}H_{35}O_5N \cdot 1/2H_2O_2$***, m. p. 200°C (decomp.), was yielded. This reaction proceeds similar to that of strychnine[10]. Compound III lost hydrogen peroxide of crystallization on standing for several months, being converted into lucidusculine *N*-oxide-c (IV), $C_{24}H_{35}O_5N$, m. p. 209°C**** (decomp.)[5]. Infrared spectrum of compound

* This paper constitutes a part of a series entitled "The Aconite Alkaloids" by H. Suginome. Part XXX, cf. Foot Note 2). Part XXXII, cf. Foot Note 3).

** Part XXXII corresponds to part II of "On Lucidusculine". A preliminary note on part of the matter of this paper appeared in this Bulletin[1].

1) T. Amiya, This Bulletin, **30**, 677 (1957).

2) H. Suginome, T. Amiya and T. Shima, ibid., **32**, 824 (1959).

3) T. Amiya, ibid., **32**, 1133 (1959).

4) K. Bodendorf and B. Binder, *Arch. Pharm.*, **287**, 326 (1954).

5) D. W. Henry and E. Leete, *J. Am. Chem. Soc.*, **79**, 5254 (1957).

6) A. S. Bailey and R. Robinson, *J. Chem. Soc.*, **1948**, 703; R. H. F. Manske and H. L. Holmes, "The Alkaloids", Vol. II, Academic Press, Inc., Publishers, New York (1952), p. 522.

7) M. Oesterlin, *Ber.*, **76**, 224 (1943).

8) L. J. Dry, M. J. Koekemoer and F. L. Warren, *J. Chem. Soc.*, **1955**, 59.

9) C. F. Huebner and W. A. Jacobs, *J. Biol. Chem.*, **170**, 515 (1947).

*** Compound III does not contain water of crystallization[1] but does contain hydrogen peroxide.

10) M. Kotake and T. Mitsuwa, *J. Chem. Soc. Japan*, **57**, 236 (1936); R. N. Chakravarti and R. Robinson, *J. Chem. Soc.*, **1947**, 78.

**** The previously reported d. p. is revised to this.

IV showed a band at 10.47$\mu$ characteristic of an *N*-oxide group[11,12]. Its ultraviolet absorption spectrum showed only end absorption.

Compound III was readily reduced with zinc dust and dilute sulfuric acid to compound I normally.

Oxidation of compound I with *N*-bromosuccinimide afforded dehydroluciduscuiline (V), $C_{24}H_{33}O_4N$, m. p. 175~180°C, with loss of two hydrogens. Its infrared spectrum showed sharp bands at 10.15 and 11.34$\mu$ which were probably indicative of a cyclic ether[13,14]. Compound I lacks the bands corresponding to these (10.15 and 11.34$\mu$) of compound V. It is, therefore, probable that the reaction proceeds as in the case of each delcosine[13] and delsoline[14] with formation of a cyclic carbinolamine internal ether between carbinolamine hydroxyl and one of the hydroxyls in compound I. This may be supported by the fact mentioned below that luciduscuiline *N*-oxide was found to change to compound V. Its ultraviolet absorptions spectrum showed end absorption.

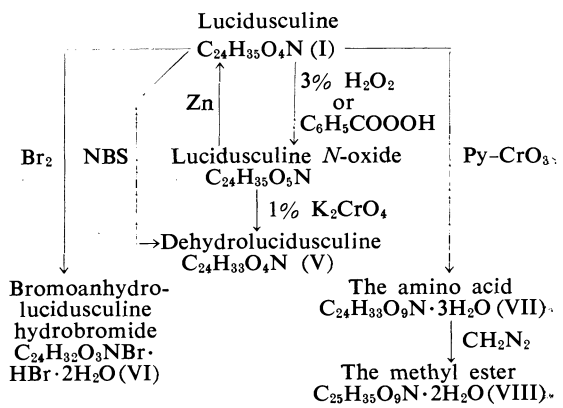
Strychnine *N*-oxide has been rearranged to a carbinolamine, pseudostrychnine[6]. Crow[15] mentioned the transformation of sparteine *N*-oxide to three possible carbinolamines. Therefore compound III was treated under the same conditions as in the case of the isomerization of strychnine *N*-oxide. Although an expected carbinolamine was not obtained, compound V was yielded. From these facts, it is supposed that an initially formed carbinolamine is changed to compound V with loss of one mole of water and with simultaneous formation of a carbinolamine internal ether.

In contrast to isoatisine[9], on bromination of compoud I no expected dibromo derivative was obtained. In this case a hydrobromide of a monobromo derivative, bromoanhydrolucidusculine hydrobromide (VI), $C_{24}H_{32}O_3NBr \cdot HBr \cdot 2H_2O$, m. p. 210°C (decomp.) was produced. Thus, the behavior of compound I on bromination is noted. Its infrared absorption spectrum showed the disappearance of a band which was characteristic of a terminal methylene group and corresponded to that (11.07$\mu$)[16] of compound I[3]. From the observation of the molecular formula and its infrared spectrum, compound VI is perhaps yielded from an intermediate dibromo derivative, which is produced from compound I by the normal addition of one mole of bromine to a terminal methylene group, with simultaneous elimination of one mole each of water and hydrogen bromide. The ultraviolet absorption spectrum of compound VI does not correspond to that of a conjugated diene (Fig. 1). Although some interpretation of this observation might be presented, it will be left to a later occasion.

The oxidation of some of the aconite alkaloids, viz., atisine, isoatisine, kobusine and hypognavine with chromium trioxide-pyridine complex has been reported to give $\alpha,\beta$-unsaturated ketone bases[19-21]. Furthermore, delpheline and lucaconine have been shown to be oxidized to lactams[22,23] by the same reagent.

On the other hand, the action of chromium trioxide-pyridine complex on compound I yielded an amino acid, $C_{24}H_{33}O_9N \cdot 3H_2O$, (VII), which showed no definite m. p. nor d. p., and gradually

TABLE I




11) L. J. Bellamy, "The Infra-red Spectra of Complex Molecules", 2nd. Ed.. Methuen & Co., Ltd., London (1958), p. 308.
12) R. H. Wiley and S. C. Slaymaker, *J. Am. Chem. Soc.*, 79, 2233 (1957).
13) R. Anet, D. W. Clayton and Léo Marion, *Can. J. Chem.*, 35, 397 (1957).
14) F. Sparatore, R. Greenhalgh and Léo Marion, *Tetrahedron*, 4, 157 (1958).
15) See A. Albert, G. M. Badger and C. W. Shoppee, "Current Trends in Heterocyclic Chemistry", Butterworths Scientific Publications, London (1958), p. 116.
16) From the observation of infrared spectra of luciculine[2,8] and isoluciculine[17], of two bands near wavelength 11$\mu$ the one at 11.02$\mu$ corresponds to that of the terminal methylene group of luciculine, whilst the other at 11.27 $\mu$[2,3] does not correspond. Normally, each of the compounds of the type $R_1R_2C=CH_2$[18] shows a band due to a terminal methylene group near this wavelength (11.27 $\mu$). This shift from the normal wavelength is explicable by the fact that luciculine includes an allyl alcohol moiety, HO—C(H)—C=$CH_2$[17] which contains a polar group in the $\alpha$-carbon atom to the double bond[18]. Similarly, a band characteristic of a terminal methylene group of compound I is not that at 11.26 $\mu$[3] but that at 11.07 $\mu$. Furthermore, luciduscuiline diacetate, luciculine methiodide, isomesoluciculine and bromolucidusculine cyanamide[3] show the bands attributable to the terminal methylene groups at 11.07, 10.98, 11.03 and 10.95 $\mu$ in the infrared spectra, respectively.
17) T. Amiya, This Bulletin, 32, 421 (1959).
18) L. J. Bellamy, "The Infra-red Spectra of Complex Molecules", 2nd. Ed., Methuen & Co., Ltd., London (1958), p. 51.
19) W. A. Jacobs and S. W. Pelletier, *J. Am. Chem. Soc.*, 76, 4496 (1954).
20) T. Okamoto, *Chem. Pharm. Bull.*, 7, 44 (1959).
21) S. Sakai, ibid., 7, 51 (1959).
22) R. C. Cookson and M. E. Trevett, *Chem. & Ind.*, 1954 1324 ; *J. Chem. Soc.*, 1956, 2689.
23) T. Amiya and T. Shima, This Bulletin, 31, 1083 (1958).

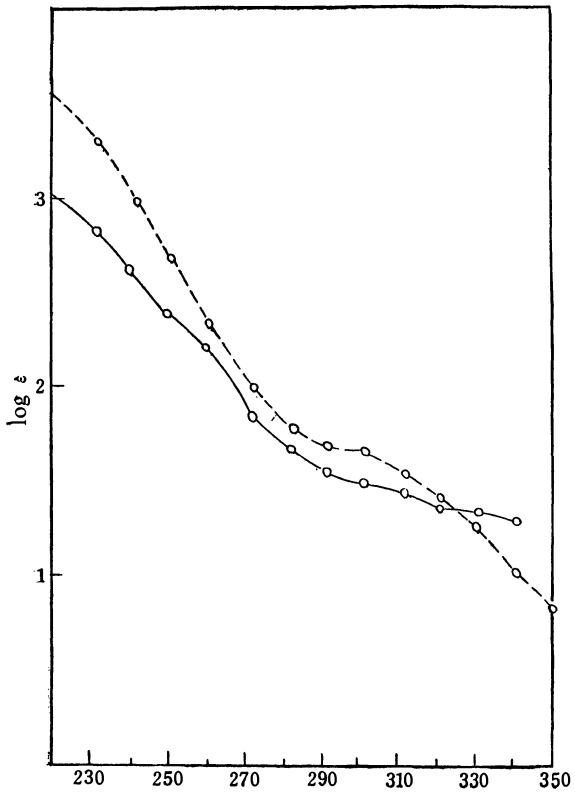



Fig. 1.

The amino acid (VII) --○--○--
Bromoanhydroluciduscuiline hydrobromide (VI) —○—○—

became black above 350°C. It is soluble in methanol and water but insoluble in ethanol and almost all other organic solvents. Although it showed no characteristic absorption maximum of a ketone carbonyl group in the ultraviolet spectrum (Fig. 1), its infrared spectrum showed a strong absorption near 5.85$\mu$, indicating the presence of a ketone carbonyl group in a six-membered ring.

Methylation of compound VII with diazomethane gave a methyl ester (VIII), $C_{25}H_{35}O_9N \cdot 2H_2O$, which gradually swelled with decomposition near 288°C. The ultraviolet spectrum of compound VIII is similar to that of compound VII.

The oxidation of compound I with this milder reagent appears to convert the primary hydroxyl group to a carboxyl group as in the case of oxidation of a dodecahydrophenanthrene derivative[24], and probably the secondary one to the above mentioned ketone carbonyl group. Furthermore, the examination of the molecular formula, $C_{24}H_{33}O_9N \cdot 3H_2O$, and the infrared absorption spectrum of compound VII suggest that this oxidation reaction may cause formation of four new hydroxyl groups. Two of them seem to be introduced into the terminal methylene group as a vicinal glycol system. This is supported by the infrared absorption specteum of compound VII. The spectrum does not indicate a band due to a terminal methylene group near 11$\mu$.

These results indicate that, of two hydroxyl groups in compound I, one is primary, and the other is secondary and is attached to a carbon atom in a six-membered ring.

Subsequently, the previously proposed partial formula[2] of I may be further summarized as[25],

$C_{16}H_{20}$ < $CH_2OH$, $OCOCH_3$, $>CH(OH)$, $>N\text{-}C_2H_5$, $>C{=}CH_2$

Lucidusculine (I)

## Experimental

**Lucidusculine *N*-Oxide-a (II).**—Powdered lucidusculine (0.5 g.) was suspended in 50 cc. of about 3% hydrogen peroxide and stirred under warming. After one hour the base was dissolved, and the resulting solution was further stirred for 1.5 hr. without warming. The excessive hydrogen peroxide was then decomposed in contact with a small quantity of freshly prepared manganese dioxide. After removal of the manganese dioxide, the solution was further decolorized with active carbon. After removal of the active carbon by filtration, the solution was evaporated to dryness in vacuo, and the residue was crystallized from aqueous methanol. It was recrystallized from methanol. It showed m. p. 191°C (decomp.).

Found: C, 65.94; H, 8.37; $H_2O$, 3.31. Calcd. for $C_{24}H_{35}O_5N \cdot H_2O$: C, 66.18; H, 8.56; $H_2O$, 4.13%.

From the above described procedure, it is probable that the substance does not contain hydrogen peroxide but water of crystallization as strychnine *N*-oxide does[6,7].

**Lucidusculine *N*-Oxide-b (III).**—Lucidusculine (0.5 g.) dissolved in chloroform (10 cc.) was added to 12 cc. of chloroform solution of perbenzoic acid (about 4 mol. equiv.). The reaction mixture was allowed to stand in a refrigerator for 6 days, and then was evaporated to dryness. To the residue, ether, about 1 cc. of 2 N hydrochloric acid and a small quantity of water were simultaneously added and the mixture was shaken. The aqueous layer separated from ether layer was passed through a column 17 cm. by 2 sq. cm. of anion-exchange resin (Amberite IRA-400) and then the column was eluted with 100, 50 and 25 cc. of water one after the other. From the first fraction (100 cc.) of elute, the residue was obtained, which gave crystals, m. p. 193°C

24) G. I. Poos, W. F. Johns and L. H. Sarett, *J. Am. Chem. Soc.*, 77, 1026 (1955).

25) The partial formula of I in a previous report[1] is revised to this.

(decomp.), on treatment with methanol. On recrystallization from methanol a material, m. p. 200°C (decomp.), $[\alpha]_D^{15}$ −101°, was obtained.

Found: C, 65.30, 65.52; H, 8.53, 8.68. Calcd. for $C_{24}H_{35}O_5N.{}^1/_2H_2O_2$: C, 66.32; H, 8.34%.

From the results described below it seems to contain hydrogen peroxide of crystallization. However, this material should be re-examined more precisely by iodometric titration.

**Lucidusculine *N*-Oxide-c (IV).**—To lucidusculine (1 g.) dissolved in 10 cc. of chloroform, were added 12 cc. of chloroform solution, containing excessive perbenzoic acid, and a few drops of water. After standing overnight, the chloroform was removed. The residue was digested with ether. To the ether-insoluble portion, 2 cc. of 2 N hydrochloric acid, water and chloroform were simultaneously added, and the mixture was shaken. The aqueous layer separated from chloroform layer was passed through the above mentioned column of anion-exchange resin and the column was eluted with water and then methanol. From the first fraction (80 cc. of aqueous elute), 0.7 g. of crystalline material, m. p. 198°C with decomposition was obtained. Subsequently, following fractions were discarded. It liberated iodine from acid solution of potassium iodide. From this fact, it seems to contain hydrogen peroxide of crystallization[4,7]. Recrystallization from methanol gave 0.2 g. of *N*-oxide-b which showed m. p. 205°C (decomp.)*. It was slightly soluble in chloroform and insoluble in ethyl acetate. The specimen several months old had lost hydrogen peroxide, and it showed no diminution of its weight by drying in vacuo at 100~110°C. It melted at 209°C with decomposition. The ultraviolet absorption spectrum of this compound in methanol showed end absorption and no maximum. The infrared absorption spectrum in Nujol showed the presence of hydroxyl groups (3.15 $\mu$), an acetoxyl group (5.82 and 8.09 $\mu$), an *N*-oxide group (10.47 $\mu$) and a terminal methylene group (11.07 $\mu$).

Found: C, 69.32; H, 8.27. Calcd. for $C_{24}H_{35}O_5N$: C, 69.03; H, 8.45%.

**Reduction of Lucidusculine *N*-Oxide.** — The *N*-oxide-b (0.15 g.) freshly prepared from lucidusculine by perbenzoic acid oxidation for 2 days was dissolved in 1.5 cc. of 10% sulfuric acid**. To this solution, a drop of cupper sulfate solution was added and then 0.15 g. of zinc powder was gradually added. After standing for 2.5 hr. the reaction mixture was filtered, made alkaline with aqueous ammonia and extracted with chloroform. After removal of the chloroform, the residue was crystallized from methanol. It melted at 169~173°C and showed no depression of the melting point on admixture with lucidusculine.

**Oxidation of Lucidusculine with *N*-Bromosuccinimide [Dehydrolucidusculine (V)].**—Lucidusculine (0.5 g.) and *N*-bromosuccinimide (0.23 g.) were dissolved in 250 cc. of benzene. After boiling for 3 hr., the formed precipitate was removed by filtration. The filtrate was evaporated to dryness in vacuo. The residue dissolved in chloroform was washed three times with sodium carbonate solution and then three times with water. After removal of the chloroform, the residue was redissolved in chloroform and chromatographed on alumina. The chromatogram was eluted with chloroform and acetone and then methanol. From the chloroform portion (15 cc.), 50 mg. of residue was obtained, which on recrystallization from methanol, melted at 175~180°C. From the acetone portion (30 cc.), impure lucidusculine was obtained. Accordingly, the methanol portion (15 cc.) was discarded. The ultraviolet absorption spectrum of this compound (m. p. 175~180°C) showed end absorption and no maximum. The infrared absorption spectrum in Nujol showed the presence of a hydroxyl group (3.08 $\mu$), an acetoxyl group (5.76 and 8.09 $\mu$), a terminal methylene group (10.75 $\mu$) and a carbinolamine ether (10.15 and 11.34 $\mu$).

Found: C, 71.51; H, 8.41. Calcd. for $C_{24}H_{33}O_4N$: C, 72.15; H, 8.33%.

**Dehydrolucidusculine (V) from Lucidusculine *N*-Oxide.**—To 76 cc. of 1% $K_2CrO_4$ solution, was added lucidusculine *N*-oxide (200 mg.), which was the same sample as that used for the above described reduction. The material was heated on a water bath. The solution, which was transparent at first, became turbid in about thirty minutes. After heating for 1.5 hr., the separated material (50 mg.) was collected by filtration. It was dissolved in chloroform and the filtered solution was concentrated. On addition of methanol, a crystalline substance was obtained. On recrystallization from acetone, it melted at 173~177°C and showed no depression on admixture with sample obtained by the above described NBS oxidation.

Found: C, 72.38; H, 8.74***. Calcd. for $C_{24}H_{33}O_4N$: C, 72.15; H, 8.33%.

**Bromoanhydrolucidusculine Hydrobromide (VI).**—To a solution of lucidusculine (0.5 g.) dissolved in 10 cc. of methanol, a freshly prepared 0.25 M solution of bromine in methanol was added dropwise. Excessive bromine was detected by potassium iodide starch paper. In total 8.5 cc. of reagent were added; after one hour, excessive bromine persisted (1 mol. 5.07 cc.). When the methanol solution was concentrated, it showed acid reaction to Congo red. It was evaporated to dryness in vacuo. The residue, on recrystallization from methanol, gave crystals, m. p. 210°C (decomp.). $[\alpha]_D^{18}$ −64.63°C (methanol). The ultraviolet absorption spectrum of this compound in methanol is graphed in Fig. 1. The infrared absorption spectrum in Nujol had no band attributable to a terminal methylene group; it showed the presence of a hydroxyl group (2.99 $\mu$), an acetoxyl group (5.78 and 8.16 $\mu$) and water (6.05 $\mu$).

Found: C, 50.02; H, 6.74; Br, 29.70; $H_2O$, 5.5. Calcd. for $C_{24}H_{32}O_3NBr \cdot HBr \cdot 2H_2O$: C, 49.73; H, 6.43; Br, 27.57; $H_2O$, 6.2%.

The hydrobromide was soluble in water. The base, liberated from the hydrobromide with aqueous ammonia, could not have been obtained in a crystalline form on treatment with methanol.

**The Amino Acid (VII).**—A mixture of lucidusculine (1.8 g.) and chromium trioxide (2.4 g.) in

* This material seems to be purer than the *N*-oxide-b which showed m. p. 200°C (decomp.).

** For hydrochloric acid[1], 10% sulfuric acid is substituted.

*** The figure, 8.75[1], was misprinted.

pyridine (48 cc.) that had been allowed to stand at room temperature overnight was filtered. The filtrate was evaporated to dryness in vacuo. The residue was treated with water saturated with sulfur dioxide. After standing overnight, the acid solution was made alkaline with saturated baryta water to precipitate chromic hydroxide. The alkaline solution from which the precipitate had been removed by filtration was made slightly acid by the addition of 10% sulfuric acid, and the precipitated barium sulfate was removed. The concentrated filtrate was neutralized with baryta water and was evaporated to dryness. The residue was treated with methanol and the undissolved barium sulfate was removed by filtration. The methanol solution was evaporated to dryness. To a solution of the residue (1.8 g.) dissolved in 9.5 cc. of methanol, 34 cc. of acetone was added. Then a yellow precipitate was formed. The transparent solution separated from the precipitate was concentrated to obtain a crystalline material; it weighed 1.4 g. It was dissolved in methanol (5.5 cc.). Upon the addition of 28 cc. of ethanol, 0.3 g. of a crystalline material was obtained. The mother liquor gave a second crop (0.3 g.) on recrystallization from methanol-ethanol.

The combined crystalline material (0.6 g.) was dissolved in 30 cc. of 70% methanol. The solution was passed through a column of 10 cc. of cation-exchange resin (Dowex 50) and eluted with the same solvent. The elute (280 cc.) was evaporated to dryness and yielded 540 mg. of crystalline residue. It was recrystallized from 70% methanol and gave 200 mg. of pure material. It was soluble in water and methanol but not in ethanol and other organic solvents. It showed no definite m. p. nor d. p. and gradually became black above 350°C. $[\alpha]_D^{16}$ −26.22° (methanol). The ultraviolet absorption spectrum of this compond in methanol is graphed in Fig. 1. The infrared absorption spectrum in Nujol showed the presence of hydroxyl groups (2.92 $\mu$), an acetoxyl group (5.78 and 8.11 $\mu$), a ketone carbonyl group (5.85 $\mu$), water (6.06 $\mu$) and an ionized carboxyl group (6.19 $\mu$).

Found: C, 54.22, 54.60; H, 7.88, 7.69; N, 3.05; $H_2O$, 10.11. Calcd. for $C_{24}H_{33}O_9N \cdot 3H_2O$[26]: C, 54.02; H, 7.36; N, 2.62; $H_2O$, 10.12%.

**The Methyl Ester (VIII).** — To the amino acid (0.25 g.) dissolved in methanol (12.5 cc.), a slight excess of ethereal solution of diazomethane was added. The reaction mixture was allowed to stand overnight and then was evaporated to dryness. The residue was dissolved in 1 N HCl and was precipitated by the addition of aqueous ammonia. The precipitate (0.1 g.) was crystallized from methanol-ethyl acetate and was further recrystallized from methanol. It showed no definite melting point nor definite d. p. and it swelled gradually with decomposition near 288°C. The ultraviolet absorption spectrum of this compound in methanol showed end absorption and no maximum.

Found: C, 57.01; H, 7.70; $H_2O$, 6.01. Calcd. for $C_{25}H_{35}O_9N \cdot 2H_2O$[26]: C, 56.69; H, 7.42; $H_2O$, 6.80%.

26) From the result of determination of water of crystallization the previously reported molecular formula[1] is revised to this.

## Summary

The alkaloid lucidusculine was oxidized by hydrogen peroxide and also by perbenzoic acid to lucidusculine *N*-oxide. The *N*-oxide could be converted back into the original base by reduction. Oxidation of the alkaloid with *N*-bromosuccinimide afforded dehydrolucidusculine which was also produced by transformation of lucidusculine *N*-oxide. Dehydrolucidusculine seems to be a cyclic carbinolamine internal ether. The action of bromine on the alkaloid was noticeable and gave bromoanhydrolucidusculine hydrobromide which was probably obtained from the intermediate dibromide with loss of one mole each of water and hydrogen bromide. Chromium trioxide-pyridine complex oxidized lucidusculine to an amino acid which, on methylation with diazomethane, gave a methyl ester. From these experimental results, the previously proposed partial formula of lucidusculine was further extended.

The author is grateful to Professor Harusada Suginome, President of Hokkaido University, for his unfailing kindness in encouraging this work, to Professor Shin-ichiro Fujise, Tôhoku University, for his kindness in making part of the material available and to Drs. Masao Yamaguchi and Akira Fujino, Institute of Polytechnics, Osaka City University, for their kindness in the determination of the infrared spectra.

*Department of Chemistry*
*Faculty of Science*
*Hokkaido University*
*Sapporo*

# *Untersuchungen über Meso-ionischen Verbindungen. X*[1] *Synthesen von 4-Substituierten 3-(β-Pyridyl)sydnonen*

Von Masaki OHTA und Mitsuo MASAKI

(Engegangen am 16 Oktober, 1959)

*N*-Pyridylglycin, das in der Synthese von 3-(β-Pyridyl)sydnon eine Zwischenverbindung ist, kann nicht durch die gewöhnlichen Reaktionen, z. B. durch die Reaktion von β-Aminopyridin mit Chloressigsäure, gewonnen werden, sondern nur durch Reduktivkondensation von β-Aminopyridin und Glyoxylsäureäthylester im Autoklaven, wie es schon berichtet worden ist[2]. Bisher ist kein 4-substituiertes 3-(β-Pyridyl)sydnon erhalten worden.

Nach der Umsetzungsmethode von Amin über Aminoacetonitril in Aminoessigsäure, die von Knoevenagel[3], Tiemann[4], Bristow[5], u. a. beschrieben worden sind, haben wir *N*-(β-Pyridyl)-*N*-nitrosoglycin (IV-a), *N*-(β-Pyridyl)-*N*-nitroso-α-methylglycin (IV-b), und *N*-(β-Pyridyl)-*N*-nitroso-α-phenylglycin (IV-c) gewonnen, und diese drei *N*-Nitrosoglycine setzen sich durch Erwärmen mit Acetanhydrid in die entsprechenden Meso-ionischen Verbindungen um.

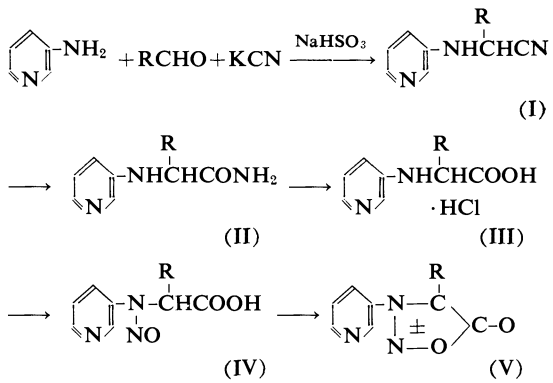
Wir stellten so 3-(β-Pyridyl)sydnon (V-a), 3-(β-Pyridyl)-4-methylsydnon (V-b) und 3-(β-Pyridyl)-4-phenylsydnon (V-c) dar.

In Wasser als Lösungsmittel reagiert β-Aminopyridin mit Bisulfitverbindung des Formaldehyds und Alkalicyanids, und β-Pyridylaminoacetonitril (I-a) wird erhalten, das durch Erhitzen im Reaktiongemisch β-Pyridylaminoacetamid (II-a) liefert, aus dem durch Hydrolyse mit Alkali oder Säure *N*-(β-Pyridyl)glycin zugänglich ist.

Das Glycin wurde durch sein Salzsäuresalz (III-a) festgestellt. Man kann aber das *N*-Nitrosoglycin unmittelbar durch das Zusetzen des Natriumnitrits zu der salzsäuresaueren wässerigen Lösung von Glycin gewinnen, nachdem man das Amid in Alkalilösung erwärmt hat. Das *N*-Nitrosoglycin liefert phototropisches Sydnon, wenn man es mit Acetanhydrid erwärmt, wie J. M. Tien u. a.[2] beschrieben haben.

Ganz analog reagiert β-Aminopyridin mit Bisulfitverbindung des Acetaldehyds oder des Benzaldehyds und Alkalicyanid, wobei α-(β-Pyridylamino)propionitril (I-b) oder α-(β-Pyridylamino)-phenylacetnitril (I-c) entsteht, das sich in das entsprechende Amid durch Auflösen in konz. Schwefelsäure überführen läßt.

Durch das Erhitzen mit Salzsäure läßt sich α-(β-Pyridylamino)phenylacetamid (II-c) in das salzsauere α-(β-Pyridylamino)phenylglycin(III-c) verseifen. Nur α-(β-Pyridylamino)-propionamid (II-b) zersetzt sich bei Erwärmen mit konzentrierter oder verdünnter Salzsäure in braunrotes Öl* und Ammoniumchlorid.



(I) (II) (III) (IV) (V)

-R=-H : a)
-R=-$CH_3$ : b)
-R=-$C_6H_5$ : c)

Die beiden Amide sind aber am besten durch das mehrstündige Erwärmen mit Alkali in die entsprechende Säure unzuwandeln. Wenn man die erhaltenen Lösungen mit Salzsäure und Natriumnitrit unter Kühlen versetzt, so entstehen die entsprechenden *N*-Nitrosoglycine, aus denen durch Dehydratisierung die zwei 4-substituierten 3-(β-Pyridyl)sydnone zugänglich sind. Sie zeigen sich aber nicht phototropisch.

## Beschreibung der Versuche

**3-(β-Pyridyl)sydnon (V-a).**—*β-Pyridylaminoacetonitril (I-a).*—Man versetzt 41 g von etwa 37% Formaldehydlösung mit 13.2 g von ca. 40% Natriumbisulfitlösung und darauf mit 4.7 g β-Aminopyridin. Das Gemisch wurde auf dem Wasserbad eine Std. erwärmt, dann setzt man 4 g Natriumcyanid in konzentrierter, wässeriger Lösung zu. Nach einigem Stehen scheidet sich ein Öl ab, das 2~3 mal mit Chloroform ausgeschüttelt wird. Das nach dem

1) IX. Mitteil. : H. Kato und M. Ohta, Dieses Bulletin, 32, 282 (1959).
2) J. M. Tien und I. M. Hunsberger, *J. Am. Chem. Soc.*, 77, 6604 (1955).
3) E. Knoevenagel *Ber.*, 37, 4073 (1904). E. Knovenagel und Merkin, ebenda, 37, 4090 (1904).
4) F. Tieman und R. Stephan, ebenda, 15, 2028 (1882). F. Tieman u. a., ebenda, 15, 2034 (1882).
5) N. W. Bristow, *J. Chem. Soc.*, 1954, 616.

* Diese Reaktion untersuchen wir noch jetzt.

Abdampfen des Chloroforms zurückgebliebene Nitril wird aus Chloroform umkristallisiert. Farblose Nadeln vom Schmp. 77°C. Ausb. 4.9 g (74% d. Th.)

$C_7H_7N_3$

Ber. N 31.56
Gef. N 31.69

*β-Pyridylaminoacetamid (II-a).* — Ohne Extrahierung mit Chloroform erhitzt man das Nitril in dem oben erhaltenen Reaktionsgemisch auf dem siedenden Wasserbad noch 2~3 Stdn. Das abgeschiedene Öl läßt sich wieder lösen und die Lösung färbt sich braunschwarz, woraus sich beim Erkalten derbe Prismen abscheiden, und dann werden sie abfiltriert und aus dem Wasser umkristallisiert. Farblose derbe Nadeln vom Schmp. 166°C. Ausb. 4.7 g. (63% d. Th.)

$C_7H_9N_3O$

Ber. C 55.61 H 6.00 N 27.80
Gef. C 55.23 H 6.23 N 28.04

*Salzsaures N-(β-Pyridyl)glycin (III-a).*—Man löst 1.5 g β-Pyridylaminoacetamid in einer Mischung von 5 ccm konz. Salzsäure und 3 ccm Äthanol, und erhitzt dieses auf einem Wasserbad 3~4 Stdn. Der beim Erkalten abgeschiedene, farblose Niederschlag, Ammoniumchloride, wurde abfiltriert. Das Filtrat trocknet man durch Eindampfen unter vermindertem Druck, und die zurückgebliebene Kristallmaße kristallisiert sich aus konz. Salzsäure in farblose Prismen vom Schmp. 222~224°C. Ausb. 1.3 g (72% d. Th.).

$C_7H_9N_2O_2Cl$

Ber. N 14.85
Gef. N 14.80

In 14 ccm Wasser löst man 1.3 g. β-Pyridylaminoacetnitril, setzt 0.69 g. $K_2CO_3$ und 0.28 g. CaO zu, und dann wird es 4 Stdn. lang gelinde, unter Anwendung eines Asbestdrahtnetzes erhitzt. Wenn die Entwicklung von Ammoniak aufgehört hat, so kühlt man diese Lösung. Man filtriert den gebildeten farblosen Niederschlag, $CaCO_3$, ab, sättigt dann das Filtrat mit Chlorwasserstoff unter Kühlung, fügt etwa 15 ccm Äthanol hinzu und sätfigt wieder die Flüssigkeit mit Chlorwasserstoff. Der abgeschiedene Niederschlag, KCl, läßt sich abfiltrieren und das Filtrat wird durch Eindampfen im Vakuum getrocknet, wobei salzsaueres *N*-(β-Pyridyl)glycin hinterbleibt.

*N-Nitroso-N-(β-pyridyl)glycin (IV-a).* — Man löst 1.5 g NaOH in 40 ccm Wasser auf, versetzt mit 5.0 g β-Pyridylaminoacetamid, und erwärmt es 5~6 Stdn. unter mechanischem Rühren auf 40~50°C. Hierauf kühlt man die Lösung auf 0°C ab, fügt langsam 7.1 g konz. Salzsäure hinzu, und versetzt dann diese Lösung mit 2.5 g Natriumnitrit, wobei die Temperatur nicht über +1°C steigen soll. Nach einigem Stehen scheidet sich ein farbloser Niederschlag ab, der bei 158°C schmilzt. Die Mischprobe mit dem durch das Verfahren von J. M. Tien[2] erhaltenen *N*-Nitroso-*N*-(β-pyridyl)glycin, zeigt keine Schmelzpunkterniederung.

*3-(β-Pyridyl)sydnon (V-a).*—Eine Mischung von 1.5 g (IV-a) und 20 ccm Essigsäureanhydrid wird auf siedendem Wasserbad erhitzt. Nach einer halben Stunde wird die Lösung unter vermindertem Druck in $N_2$ eingeengt, wobei 3-(β-Pyridyl)sydnon sich abscheidet. Die aus dem Wasser umkristallisierten, farblosen Prismen vom Schmp. 119~121°C sind eine photropische Verbindung.

**3-(β-Pyridyl)-4-methylsydnon (V-b).**—*α-(β-Pyridyl)aminopropionitril (I-b).*—Man versetzt 26.4 g von etwa 40 proz. Natriumbisulfitlösung mit 10 g von 44 proz. Acetaldehyd und dann mit 9.4 g β-Aminopyridin. Zuerst eine halbe Stunde lang bei Raumtemperatur, darauf rührt man eine Stunde lang in einem Wagserbad von 80°C die Mischung um, und nach dam Abkühlen bis zur Raumtemperatur setzt man dazu 6.5 g Kaliumcyanid in wenigem wasser zu. Nach einigem Stehen scheidet sich ein Öl ab. 4~5 Stdn. lang rührt man das Gemisch bei Raumtemperatur um, darauf schüttelt man es 6~7 mal mit Chloroform aus, trocknet die vereinigten Chloroformextrakte mit Natriumsulfat und dampft im Vakuum ein. Es hinterbleiben 8 g α-(β-Pyridyl)-aminopropionitril (Ausb. 54% d. Th.) die zur Analyse 2 mal mit Äther gewaschen werden. Farblose Nadeln vom Schmp. 98~100°C.

$C_8H_9N_3$

Ber. N 28.55
Gef. N 28.50

*α-(β-Pyridyl)aminopropionamid (II-b).*—Man fügt 8 g (I-b) zu 60 g konz. Schwefelsäure unter Umrühren nach und nach hinzu, wobei die Temperatnr nicht über 5°C steigen soll. Nach 4~5 Stdn. Umrühren läßt man die schwefelsäure Lösung einen Tag bei Raumtemperatur stehen, gießt die klare Lösung in 200 g zerstoßenes Eis und versetzt diese mit Ammoniak bis zur neutralen Reaktion. Der nach einigem Stehen abgeschiedene Niederschlag wird abfiltriert und aus Äthanol umkristallisiert. Farblose Prismen vom Schmp. 179°C. Ausb. 6.8 g (76% d. Th.).

$C_8H_{11}N_3O$

Ber. N 25.44
Gef. N 25.84

*N-Nitroso-N-(β-pyidyl)methylglycin (IV-b).*—Eine Mischung von 2 g des fein pulverisierten Amids und 16 ccm ca. 4 proz. Natronlauge ist solange umzurühren und auf einem Wasserbad von 40~50°C zu erwärmen, bis das Amid ganz in Auflösung übergegangen ist. Nach 9~10 Stdn. fügt man unter Kühlung 3 ccm konz. Salzsäure vorsichtig hinzu, und versetzt mit 1 g Natriumnitrit, wobei die Temperatur unter 0°C zu behalten ist. Bald scheidet sich ein Niederschlag ab, der nach einer Stunde abfiltriert wird und den man, wenn notwendig, aus dem Wasser umkristallisieren kann. Farblose Prismen vom Schmp. 135°C. Ausb. 2.2 g (92% d. Th.).

$C_8H_9N_3O_3$

Ber. N 21.53
Gef. N 21.50

*3-(β-Pyridyl)-4-methylsydnon (V-b).*—Man löst 1.7 g (IV-b) in 20 ccm Essigsäureanhydrid durch Erhitzen auf siedendem Wasserbad anf. Nach einer Viertelstunde wird die Lösung unter vermindertem Druck in $N_2$ abgedampft. Es hinterbleibt 1 g 3-(β-Pyridyl)-4-methylsydnon, das mit verdünntem Alkohol gewaschen wird. Aus Wasser umkristallisiert zeigen farblose schuppige Kristalle den Schmp. 143°C. Ausb. 70% d. Th.

$C_8H_7N_3O_2$
Ber. C 54.23 H 3.98 N 23.72
Gef. C 53.98 H 4.26 N 23.83

**3-(β-Pyridyl)-4-phenylsydnon (V-c).** — *α-Phenyl-(β-pyridylamino)acetonitril (I-c).*—Man schüttelt 15 g Benzaldehyd mit 41 g ca. 40% Natriumbisulfitlösung, und der erhaltene Kristallbrei wird mit 15 g β-Aminopyridin versetzt. Dann erwärmt man das Gemisch auf dem Wasserbad solange, bis die wässerige Reaktionsmischung vollständig verflüssigt und klar wird. Dann setzt man 11 g Kaliumcyanid, in wenigem Wasser gelöst, zu. Nach ungefähr 2~3 Stdn. Umrühren wird der gebildete Niederschlag abfiltriert, mit Äther gut gewaschen und aus siedendem Äthanol umkristallisiert. Rotgelbliche Prismen vom Schmp. 117°C. Ausb. 24 g (76% d. Th.).

$C_{13}H_{11}N_3$
Ber. N 20.08
Gef. N 20.19

*α-Phenyl-(β-pyridylamino)acetamid (II-c).*—Zu 160 g konz. Schwefelsäure fügt man 24 g (I-c) unter Kühlung allmählich hinzu, hierbei ist das Gemisch solange umzurühren, bis Nitril völlig in Auflösung gegangen ist. Bei Raumtemperatur läßt man die klare Lösung einen Tag stehen, gießt sie dann in 300 g zerstoßenes Eis, und neutralisiert darauf vorsichtig mit Ammoniak, wobei α-Phenyl-(β-pyridylamino)acetamid sich als ein gelblicher Niederschlag ausscheidet. Aus Äthanol umkristallisiert, erzeugen sich farblose Nädelchen vom Schmp. 191°C. Ausb. 5.2 g (26% d. Th.).

$C_{13}H_{13}N_3O$
Ber. N 18.49
Gef. N 18.44

*Salzsaures α-Phenyl-(β-pyridylamino)essigsäure (III-c).*—Man löst 2 g (II-c) in 18 ccm konz. Salzsäure und erhitzt dies 4~5 Stdn. auf siedendem Wasserbad. Das gebildete Ammoniumchlorid filtriert man ab, und dampft das Filtrat bis zum Trocknen im Vakuum ein. Der Rückstand wird 2~3 mal aus konz. Salzsäure umkristallisiert. Farblose Prismen vom Schmp. 218~220°C. Ausb. 1.7 g (73% d. Th.).

$C_{13}H_{13}O_2N_2Cl$
Ber. N 10.59
Gef. N 10.67

*N-Nitroso-N-(β-pyridyl)phenylglycin (IV-c).* — (1) In 7 ccm Wasser wird 1 g salzsaures *N*-(β-Pyridyl)-phenylglycin gelöst und dann dazu 0.3 g $NaNO_2$ hinzugefügt, wobei die Temperatur unter 0°C bleiben soll. Nach einigem Stehen wird der gebildete, farblose Niederschlag abfiltriert, der bei 147°C schmilzt und zur Analyse vollständig rein ist. Ausb. 0.8 g (84% d. Th.).

$C_{13}H_{11}N_3O_3$
Ber. N 16.34
Gef. N 16.35

(2) Eine Mischung von 5.2 g (II-c) und 40 ccm ca. 2.5 proz. Natronlauge wird unter mechanischem Rühren auf einem Wasserbad von 70~80°C solange erwärmt, bis das Amid vollständig aufgelöst ist. Zur, nach 5~6 Stdn. erhaltenen, klaren, wässerigen Lösung fügt man 5 ccm konz. Salzsäure hinzu und versetzt darauf das Gemisch mit 1.9 g Natriumnitrit, wobei die Temperatur nicht über 0°C steigen soll. Der bald ausgefallene Niederschlag schmilzt bei 147°C, und zeigt bei der Mischprobe mit der aus Glycin hergestellten Verbindung keine Schmelzpunkterniederung. 4.5 g (76% d. Th.).

*3-(β-Pyridyl)-4-phenylsydnon (V-c).*—Man fügt 4.7 g (IV-c) zu 40 ccm Essigsäureanhydrid hinzu, und erhitzt es 20 minutenlang auf siedendem Wasserbad. Die erhaltene, klare, braune Lösung wird unter vermindertem Druck in $N_2$ eingedampft, wobei 3.7 g Rückstand hinterbleibt, der mit ein wenig verd. Alkohol gewaschen wird. Die aus verd. Äthanol umkristallisierte, gelbliche Nadeln zeigen den Schmp. 118~120°C. Ausb. 3.1 g (70% d. Th.).

$C_{13}H_9N_3O_2$
Ber. C 65.26 H 3.79 N 17.57
Gef. C 64.85 H 3.94 N 17.59

Herrn Asaji Kondo danken wir bestens für seine Ausführung der Mikro-analyse.

*Organich-Chemisches Laboratorium*
*Technische Hochschule zu Tokyo*
*Meguro-ku, Tokyo*

# *Hydrogen Abstraction from Hydrogen Sulfide Molecules by Methyl Radicals*

By Naomi IMAI and Osamu TOYAMA

(Received November 1, 1959)

A study of the hydrogen sulfide catalyzed thermal decomposition of acetaldehyde carried out in this laboratory suggested that the catalysis is at least in part ascribed to hydrosulfide radicals produced by the reaction of methyl radicals with hydrogen sulfide molecules. It seemed then desirable to investigate this hydrogen abstraction reaction quantitatively, for only limited information was available on this reaction.

The technique used in this work is one of the competitive methods which have frequently been applied to study reactions of free radicals: acetone vapor has been photolyzed in the presence of varied amounts of hydrogen sulfide; the analysis of the products has yielded the ratio of the rate of the abstraction reaction in question to that of the recombination reaction of methyl radicals; the rate of the former reaction can then be estimated since that of the latter has already been the subject of a number of extensive investigations.

## Experimental

**Materials.**—Acetone used in this experiment was supplied commercially and purified by bulb-to-bulb distillation. Hydrogen sulfide was prepared by dropping water on aluminium sulfide in a vacuum system, dried by passing through a trap at $-78°C$ and purified by bulb-to-bulb distillation. Cupric oxide and cupric sulfate used in analyses were commercial samples.

**Apparatus.** — Photolysis was carried out in a cylindrical quarz vessel of about 110 cc. capacity placed in an electric furnace with a glass window which cuts off the light of a wave length shorter than 2800 Å. Therefore, no light was absorbed by hydrogen sulfide. The reaction vessel was connected to a mercury manometer, to an analytical system, and to a capillary tube of small volume, which had a mercury manometer and was used to measure a small quantity of hydrogen sulfide to be admitted to the vessel. The full light from a medium-pressure mercury arc was used in the present experiment. In order to increase light intensity it was placed at a focus of a half spheroidal mirror and at the other focus the center of the vessel was placed. Light intensity was kept constant by using a voltage stabilizer. The vessel, manometer, storage bulbs and the analytical system were attached to a conventional vacuum line.

**Procedure.**—A small measured quantity of hydrogen sulfide was admitted to the reaction vessel. Acetone vapor with a desired pressure was then added. After a few minutes to allow the gases to mix thoroughly and to come to a desired temperature, light was admitted into the vessel and irradiation was continued for a desired time.

**Analysis.**—After the photolysis, using a Toepler gauge, the reactants and products were passed through a trap at $-78°C$ where the unreacted acetone and low boiling point products were condensed. The uncondensable fraction at $-78°C$ was passed through a trap at $-196°C$ and the quantity of uncondensable fraction at $-196°C$ was measured by Toepler gauge. This fraction contained methane and carbon monoxide and was passed over cupric oxide at 250°C where carbon monoxide was oxidized to carbon dioxide and hydrogen, if any, to water. By the Toepler gauge these gases were passed through a trap at $-78°C$ where water, if any, was condensed, and through another one at $-196°C$ where carbon dioxide was condensed. The uncondensable fraction contained only methane, and its quantity was measured by the Toepler gauge. The condensed carbon dioxide was vaporized at room temperature and its quantity was measured by a McLeod gauge connected with the trap. The quantity of product uncondensable at $-196°C$ was always equal to the sum of quantities of methane and carbon monoxide analyzed within an error of 1%. That no water was found in all the runs showed that no hydrogen was formed in the photolysis. The fraction uncondensable at $-78°C$ and condensable at $-196°C$ contained the remaining hydrogen sulfide, ethane and other products. This fraction was vaporized and led to a trap at $-196°C$ through another one at about $-160°C$. The uncondensable fraction at $-160°C$ was vaporized and measured by the McLeod gauge. This fraction should have contained only hydrogen sulfide and ethane. Hydrogen sulfide was removed by contact with dry cupric sulfate. Thus the quantities of ethane and hydrogen sulfide were determined separately.

## Results and Discussion

A series of preliminary experiments with varied times of irradiation under otherwise constant conditions revealed that all the rates of formation of carbon monoxide, methane and ethane remain nearly constant at least during the initial stage of the photolysis up to about 0.2% conversion, which justifies the computation of initial rates of formation of these products from the analytical results at such low

TABLE I. THE EFFECT OF HYDROGEN SULFIDE ON THE PHOTOLYSIS OF ACETONE

| Temp. °C | Initial concentration mol. cc$^{-1}$ | | Time sec. | Rate of formation mol. cc$^{-1}$ sec$^{-1}$ | | | $R_{CH_4}/R_{C_2H_6}^{1/2}$ $\times 10^6$ |
|---|---|---|---|---|---|---|---|
| | $[Acetone]_0$ $\times 10^6$ | $[H_2S]_0$ $\times 10^9$ | | $R_{CO}$ $\times 10^{12}$ | $R_{CH_4}$ $\times 10^{12}$ | $R_{C_2H_6}$ $\times 10^{12}$ | |
| 50 | 3.87 | 0 | 3000 | 6.01 | 0.968 | 6.52 | 0.38 |
| | 3.92 | 0 | 2000 | 6.00 | 1.05 | 6.45 | 0.41 |
| | 3.85 | 3.02 | 200 | 9.2 | 6.5 | 5.25 | 2.84 |
| | 3.90 | 4.22 | 300 | 6.73 | 8.17 | 3.81 | 4.27 |
| | 3.89 | 4.9 | 300 | 9.1 | 9.0 | 3.77 | 4.64 |
| | 3.89 | 5.3 | 300 | 7.23 | 9.1 | 3.30 | 5.00 |
| | 3.86 | 8.2 | 400 | 5.74 | 11.1 | 2.00 | 7.88 |
| | 3.89 | 9.9 | 500 | 5.40 | 12.5 | 1.80 | 9.33 |
| 90 | 3.92 | 0 | 3000 | 20.6 | 3.28 | 18.6 | 0.752 |
| | 3.87 | 0 | 1000 | 25.4 | 3.77 | 21.0 | 0.823 |
| | 3.90 | 1.57 | 100 | 24.3 | 12.2 | 15.2 | 3.13 |
| | 3.87 | 2.48 | 100 | 24.8 | 15.9 | 13.7 | 4.30 |
| | 3.90 | 3.65 | 100 | 25.0 | 18.3 | 10.7 | 5.6 |
| | 3.90 | 5.0 | 200 | 22.0 | 21.7 | 7.75 | 7.8 |
| | 3.87 | 6.3 | 200 | 22.0 | 24.2 | 7.62 | 8.8 |
| | 3.89 | 9.5 | 200 | 22.5 | 27.3 | 5.12 | 12.1 |
| | 6.94 | 0 | 2000 | 29.3 | 6.80 | 22.5 | 1.43 |
| | 6.92 | 2.83 | 100 | 39.3 | 22.6 | 21.5 | 1.89 |
| | 6.93 | 4.2 | 200 | 37.5 | 28.2 | 18.4 | 6.57 |
| | 6.91 | 6.0 | 100 | 37.0 | 34.9 | 13.5 | 9.51 |
| | 6.90 | 9.1 | 200 | 30.6 | 37.3 | 6.64 | 14.4 |
| | 6.88 | 11.3 | 200 | 28.0 | 38.8 | 5.57 | 16.5 |
| 140 | 3.88 | 0 | 3000 | 39.3 | 15.0 | 29.0 | 2.79 |
| | 3.88 | 0 | 3600 | 41.8 | 15.1 | 28.0 | 2.85 |
| | 3.88 | 1.70 | 100 | 35.2 | 25.4 | 14.5 | 6.06 |
| | 3.89 | 3.80 | 100 | 38.9 | 31.6 | 8.60 | 10.8 |
| | 3.87 | 4.75 | 100 | 31.0 | 32.0 | 6.60 | 12.4 |
| | 3.88 | 6.5 | 200 | 30.0 | 35.4 | 4.62 | 16.5 |
| | 3.88 | 8.5 | 200 | 29.0 | 36.8 | 3.33 | 20.2 |
| 200 | 3.85 | 0 | 1000 | 41.2 | 34.2 | 11.0 | 10.3 |
| | 3.39 | 0 | 2000 | 22.3 | 22.0 | 5.20 | 9.4 |

conversions[1]. In Table I are listed the initial rates of formation of these products thus determined in several series of experiments. Within a series only the initial concentration of hydrogen sulfide was varied to determine the dependence of the rate on its concentration. The intensity of light was kept nearly constant throughout all the runs. As the concentration of hydrogen sulfide was increased, the rate of formation of ethane was decreased as seen in the table. On the other hand, use of too much hydrogen sulfide made its removal by dry cupric sulfate in analysis incomplete so that the rate of ethane formation was then liable to be overestimated. This situation limited the concentration range for hydrogen sulfide to those given in Table I.

It has been established[2-5] that during the photolysis of acetone, metane, ethane and carbon monoxide are produced almost entirely by the following reactions:

$$CH_3COCH_3 + h\nu = CH_3CO + CH_3 \quad (1)$$

$$CH_3CO = CH_3 + CO \quad (2)$$

$$CH_3 + CH_3 = C_2H_6 \quad (3)$$

$$CH_3 + CH_3COCH_3 = CH_4 + CH_3COCH_2 \quad (4)$$

1) It was found in the present work that the hydrogen sulfide initially added is consumed as the photolysis is continued. The ultimate fate of the hydrogen sulfide will be dealt with in a later paper.

2) K. W. Saunders and H. A. Taylor, *J. Chem. Phys.*, **9**, 616 (1941).

3) A. F. Trotman-Dickenson and E. W. R. Steasie, ibid., **18**, 1097 (1950).

4) R. Gomer and G. B. Kistiakowsky, ibid., **19**, 851 (1951).

5) M. T. Jaquiss, J. S. Roberts and M. Szwarc, *J. Am. Chem. Soc.*, **74**, 6005 (1952).

Reactions 3 and 4 lead to the following equation

$$R_{CH_4}/R_{C_2H_6}{}^{1/2} = (k_4/k_3{}^{1/2})\,[CH_3COCH_3] \quad (I)$$

which is in agreement with experimental results. In the presence of hydrogen sulfide, the reaction

$$CH_3 + H_2S = CH_4 + HS \quad (5)$$

may occur[6] and reactions 3, 4 and 5 taken together now yield

$$R_{CH_4}/R_{C_2H_6}{}^{1/2} = (k_4/k_3{}^{1/2})\,[CH_3COCH_3] + (k_5/k_3{}^{1/2})\,[H_2S] \quad (II)$$

When the concentration of acetone is kept constant, the plot of $R_{CH_4}/R_{C_2H_6}{}^{1/2}$ vs. $[H_2S]$ should give a straight line, and its intercept should be equal to the value of $R_{CH_4}/R_{C_2H_6}{}^{1/2}$ in the absence of hydrogen sulfide. Fig. 1 shows such plots of the results given in Table I and it is seen that the above requirements are in fact satisfied. That the slope of the straight line is not affected by a two-fold increase in the acetone concentration at 90°C may be taken as additional evidence for the validity of Eq. II. From the slopes of these straight lines, values of $k_5/k_3{}^{1/2}$ at various temperatures were determined and are shown in Table II together with those of $k_4/k_3{}^{1/2}$ obtained in the absence of hydrogen sulfide.

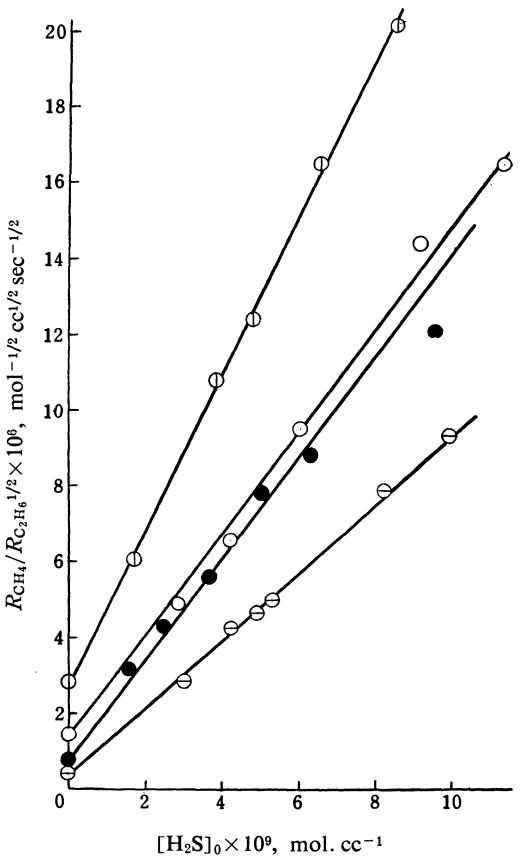



Fig. 1. Dependence of the ratio $R_{CH_4}/R_{C_2H_6}{}^{1/2}$ on the concentration of hydrogen sulfide.
⊖, $[Acetone]_0 = 3.9 \times 10^{-6}$ mol. cc$^{-1}$, 50°C;
●, $[Acetone]_0 = 3.9 \times 10^{-6}$ mol. cc$^{-1}$, 90°C;
○, $[Acetone]_0 = 6.9 \times 10^{-6}$ mol. cc$^{-1}$, 90°C;
Ⓘ, $[Acetone]_0 = 3.9 \times 10^{-6}$ mol. cc$^{-1}$, 140°C.

TABLE II. VALUES OF $k_5/k_3{}^{1/2}$ AND $k_4/k_3{}^{1/2}$

| Temp. °C | $k_5/k_3{}^{1/2}$ mol$^{-1/2}$ cc$^{1/2}$ sec$^{-1/2}$ | $k_4/k_3{}^{1/2}$ mol$^{-1/2}$ cc$^{1/2}$ sec$^{-1/2}$ |
|---|---|---|
| 50 | 880 | 0.102 |
| 90 | 1350 | 0.210 |
| 140 | 2080 | 0.727 |
| 200 | — | 2.71 |

The Arrhenius plot of $k_4/k_3{}^{1/2}$ shows a curvature at temperatures below 100°C as is well known. According to Ausloos and Steacie[7] this falling off in the apparent activation energy at low temperatures presumably arises from a reaction between methyl radicals and adsorbed acetone molecules on the wall and a disproportionation reaction between methyl radicals and acetyl radicals. The excessive value of $k_4/k_3{}^{1/2}$ in question, however, caused no more than 3% error in the value of $k_5/k_3{}^{1/2}$ even at 50°C. The values of $k_4/k_3{}^{1/2}$ at 140° and 200°C are in satisfactory agreement with those previously reported[2-5].

In contrast, the Arrhenius plot of $k_5/k_3{}^{1/2}$ yielded a good straight line from which $E_5 - 1/2E_3 = 2.6$ kcal. mol$^{-1}$ and $A_5/A_3{}^{1/2} = 10^{4.675}$ mol$^{-1/2}$ cc$^{1/2}$ sec$^{-1/2}$ are obtained, where $E$ denotes the activation energy and $A$ the pre-exponential factor. Accepting the values $E_3 = 0$ and $A_3 = 10^{13.38}$ mol$^{-1}$ cc. sec$^{-1}$ as recommended by Shepp[8] we find

$$k_5 = 10^{11.4} \exp(-2{,}600/RT) \text{ mol}^{-1} \text{ cc. sec}^{-1}$$

The value of $A_5 = 10^{11.4}$ mol$^{-1}$ cc. sec$^{-1}$ seems to be reasonable, since most $A$ factors for hydrogen abstraction reactions by methyl radicals are of the order of $10^{11}$ mol$^{-1}$ cc. sec$^{-1}$.

On the other hand, the value of $E_5 = 2.6$ kcal. mol$^{-1}$ might be regarded unexpectedly low. Birrell, Smith, Trotman-Dickenson and Wilkie[9] have reported that the apparent order of reactivities of thiols towards methyl radical are given by

$$Bu^tSH > Pr^iSH > EtSH > MeSH > H_2S$$

6) Subsequent reactions of hydrosulfide radicals formed by reaction 5 are under investigation. There is, however, little indication that these reactions affect the importance of reaction 3 in forming ethane and that any other important source of methane besides reactions 4 and 5 must be considerd.

7) P. Ausloos and E. W. R. Steacie, *Can. J. Chem.*, 33, 47 (1955).

8) A. Shepp, *J. Chem. Phys.*, 24, 939 (1956).

9) R. N. Birrell, R. F. Smith, A. F. Trotman-Dickenson and H. Wilkie, *J. Chem. Soc.*, 1957, 2807.

According to Kerr and Trotman-Dickenson[10], the rate constants of hydrogen abstraction from thiols by methyl radical at 30°C are

MeSH 1.8, EtSH 3.5, Pr$^i$SH 4.1, Bu$^t$SH 5.9

in $10^{-7}$ mol$^{-1}$ cc. sec$^{-1}$. From these values they estimated the activation energies between 4.9 and 5.6 kcal. mol$^{-1}$, assuming $A=10^{11.3}$ mol$^{-1}$ cc. sec$^{-1}$. If the estimations given by these two studies are accepted altogether and the same value of $A$ is assumed for reaction 5, $E_5$ can not be lower than 5.6 kcal. mol$^{-1}$, while a much lower value of 2.6 kcal. mol$^{-1}$ has actually been found in this work. Presumably, there is some error in the order of reactivity estimated by Birrell et al. on the basis of qualitative considerations; although this order of reactivity for a series of thiols from methane thiol to isobutane thiol is in agreement with that of rate constrants found by Kerr and Trotman-Dickenson, and hence may be taken as established, there seems to be no convincing evidence for the least reactivity of hydrogen sulfide[11]. The expression for $k_5$ obtained in the present work gives $k_5=3.3\times10^9$ mol$^{-1}$ cc. sec$^{-1}$ at 30°C, a value far greater than Kerr and Trotman-Dickenson's rate constants for thiols cited above.

The results given in Table I show that the rate of formation of carbon monoxide, on the whole, increases with temperature in agreement with the previous observation[12-14] on the quantum yield of carbon monoxide. There is some indication in the table at low temperatures that the addition of a small quantity of hydrogen sulfide increases the rate of formation of carbon monoxide, while greater concentration of hydrogen sulfide lowers the rate though the effect is not great at high temperatures. The probable explanation for these findings seems to be given by the promotion of the primary decomposition by hydrogen sulfide and the reaction of acetyl radical with hydrogen sulfide, though anything conclusive cannot yet be drawn at present on these problems.

10) J. A. Kerr and A. F. Trotman-Dickenson, ibid., 1957, 3322.
11) Birrell et al. themselves described that their interpretation of the results with hydrogen sulfide was somewhat uncertain.
12) R. Spence and W. Wild, *J. Chem. Soc.*, 1937, 352.
13) D. S. Herr and W. A. Noyes, Jr., *J. Am. Chem. Soc.*, 62, 2052 (1940).
14) H. W. Anderson and G. K.Rollefson, ibid., 63, 816 (1941).

## Summary

Acetone has been photolyzed in the presence of the varied amounts of hydrogen sulfide in the temperature range from 50° to 140°C. From the analysis of the products at low conversions the initial rates of formation of carbon monoxide, methane and ethane have been determined, which, combined with the mechanism of acetone photolysis already established, give the values of $k_5/k_3^{1/2}$, where $k_5$ and $k_3$ are respectively the rate constants for the reactions $CH_3+H_2S=CH_4+HS$ and $CH_3+CH_3=C_2H_6$. Accepting $k_3=10^{13.38}$ mol$^{-1}$ cc. sec$^{-1}$ with zero activation energy as recommended by Shepp, the rate constant of the abstraction reaction is represented by $k_5=10^{11.4}\exp(-2.6\text{ kcal. mol}^{-1}/\boldsymbol{R}T)$ mol$^{-1}$ cc. sec$^{-1}$.

The present study was partly supported by the financial aid of the Ministry of Education, to which the authors' thanks are due.

*Department of Applied Chemistry*
*College of Engineering*
*University of Osaka Prefecture*
*Sakai, Osaka*

# *Temperature Dependence of the Formation of NiO-$Li_2O$ Solid Solution*

By Yoshio IIDA, Shunro OZAKI and Kenzo SHIMADA

(Received November 5, 1959)

Since Verwey[1] extensively studied the semiconductivity of a solid solution of lithium oxide in nickel oxide, many investigators[2,3,4] have studied the physical or catalytic properties of the solid solution. In the previous papers[1,2,3,4] the solid solution of NiO-$Li_2O$ was formed by heating the mixture of nickel oxide and lithium carbonate. Unfortunately, the dissolved lithium oxide was not determined chemically and was thought to be the same as the added lithium oxide. It is expected that the amount of free lithium oxide is high when the sample is heated at a low temperature and the amount of evaporated lithium oxide is high when the sample is heated at a high temperature in the process of the NiO-$Li_2O$ solid solution formation. Accordingly, it is desiarble to determine the amount of the dissolved lithium oxide.

The mixture of nickel oxide and 5 or 10 at. % of lithium was heated and studied in the previous papers[1,4]. In the present experiment about 18 at. % of lithium equivalent to 4.15 wt. % of lithium oxide was mixed. Since the dissolved lithium oxide became constant after a heating period of 3 hr. at 800°C, the mixture of nickel oxide and lithium carbonate which was equivalent to 4.15 wt. % of lithium oxide was heated for 3 hr. at various temperatures. Chemical analysis of lithium oxide was carried out by a flame photometry[5]. Nickel oxide is not soluble in cold dilute acetic acid but lithium carbonate or free lithium oxide is soluble in it. The amount of lithium oxide dissolved in nickel oxide or free oxide was determined by the extraction method and the result is shown in Table I.

Table I shows that the amount of lithium oxide dissolved in nickel oxide is very small when the sample is heated below 600°C and increases with an increase in the heating temperature up to 800°C, but decreases above 1000°C. On the other hand, the amount of free lithium decreases with an increase in the temperature. It is seen that there is a relatively large amount of free lithium oxide present when the sample is heated at high temperatures of 1400 and 1500°C. The amount of lithium oxide evaporated increases remarkably with an increase in the temperature. Table I shows that the mixture heated at 800°C loses one half of the lithium oxide added and the mixtures heated at 1400 and 1500°C have only one tenth of the lithium oxide added. High temperatures are not suitable for the formation

TABLE I. CHEMICAL ANALYSIS AND ELECTRICAL RESISTANCE OF THE MIXTURE HEATED AT VARIOUS TEMPERATURES

| Heating temp. (°C) | Free $Li_2O$ (wt. %) | Dissolved $Li_2O$ (wt. %) | Evaporated $Li_2O$ (wt. %) | Electrical resistance ($\Omega$ cm.) |
|---|---|---|---|---|
| unheated | 4.15 | 0 | 0 | $3.3\times10^{6}$ |
| 200 | 4.15 | 0 | 0 | $3.3\times10^{6}$ |
| 300 | 4.15 | 0 | 0 | $1.2\times10^{6}$ |
| 400 | 4.15 | 0 | 0 | $4.8\times10^{5}$ |
| 500 | 4.15 | 0 | 0 | $1.8\times10^{4}$ |
| 600 | 4.00 | 0.07 | 0.08 | $3.5\times10^{2}$ |
| 800 | 0.60 | 1.39 | 2.16 | $8.0\times10$ |
| 1000 | 0.32 | 1.34 | 2.49 | $8.2\times10$ |
| 1100 | 0.31 | 1.21 | 2.63 | $8.8\times10$ |
| 1200 | 0.26 | 0.84 | 3.05 | $1.3\times10^{2}$ |
| 1300 | 0.18 | 0.78 | 3.19 | $1.8\times10^{2}$ |
| 1400 | 0.11 | 0.34 | 3.70 | $9.2\times10^{2}$ |
| 1500 | 0.10 | 0.22 | 3.83 | $1.1\times10^{2}$ |

1) E. J. Verwey et al., *Philips Res. Rep.*. 5, 173 (1950).
2) A. Cimino et al., *Z. phys. Chem. N. F.*, 16, 101 (1958).
3) G. Parravano, *J. Am. Chem. Soc.*, 75, 1452 (1953).
4) P. Fensham, ibid., 76, 969 (1954).
5) T. Takeuchi et al., *Rep. Government Ind. Res. Inst. Nagoya (Nagoya Kogyo Gijitsu Shikenjo Hokoku)*, 6, 719 (1957).

of the solid solution of lithium oxide in nickel oxide, and a temperature range of 800 to 1000°C is suitable.

Since an amount of lithium oxide less than 0.01 wt. % is not found by the flame photometry, the amount of lithium oxide dissolved in nickel oxide below 600°C could not be determined exactly. The electrical resistance of nickel oxide has been known to be sensitive to the foreign atoms incorporated with the lattice[1]. In order to find the temperature at which lithium oxide starts to dissolve in nickel oxide, the electrical resistance of the mixtures heated at various temperatures was measured at room temperature by a method similar to that described by Griffith[6]. The electrical resistance of the mixtures decreases remarkably with an increase in the temperature up to 800°C, and increases with a temperature above 1000°C. It is clearly seen from Table I that the electrical resistance of the mixture heated at 300°C is smaller than that of the pure nickel oxide. As the pure nickel oxide was prepared from ignition of nickel sulfate at 900°C in air for 10 hrs., its electrical resistance is not thought to vary when the oxide is heated below 900°C in air. It is found that NiO-$Li_2O$ solid solution starts to be formed about 300°C.

In order to confirm the fact, electrical resistance of pure nickel oxide and of the mixture were measured at a heating rate of 100°C/hr. from room temperature to 600°C. Fig. 1 clearly shows that the electrical resistance of the mixture becomes lower about 300°C than that of the pure nickel oxide. It is concluded that lithiuum oxide starts to dissolve in nickel oxide at about 300°C.

Bevan and coworkers[7] have suggested that diffusion in ionic compound only becomes appreciable above 0.5 $T_m$, where $T_m$ is the melting point absolute. Since the melting point of nickel oxide is about 2000°C, the temperature of 300°C is equivalent to 0.25 $T_m$. It is found that the diffusion of lithium oxide in nickel oxide can clearly be observed by this suitable method even at 0.25 $T_m$.

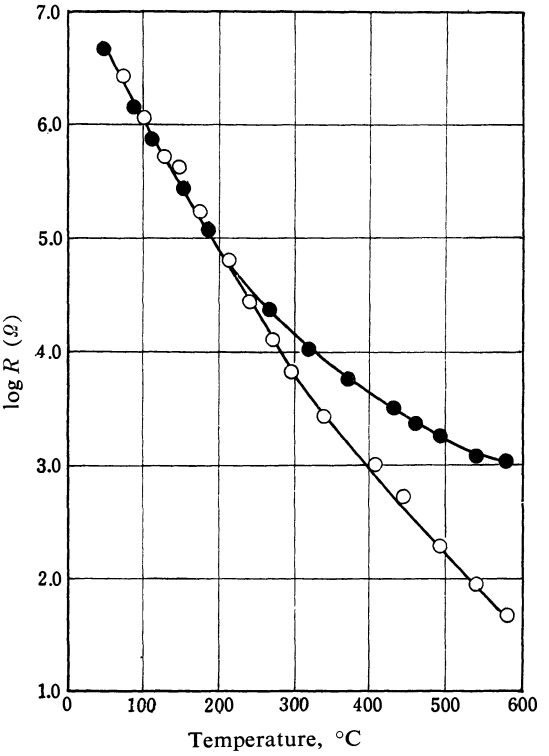



Fig. 1. Electrical resistance of pure nickel oxide (●) and the mixture of nickel oxide and lithium carbonate (○) under heating. A heating rate is 100°C/hr.

*Government Industrial Research Institute*
*Kita-ku, Nagoya*

6) R. H. Griffith, *Disc. Faraday Soc.*, **8**, 258 (1950).
7) D. J. M. Bevan et al., *J. Chem. Soc.*, **1948** 1729.

# *An Attempted Preparation of Optically Active Organometallic Compounds as Polymerization Catalysts**

By Shunsuke MURAHASHI, Shun'ichi NOZAKURA and Shigeru TAKEUCHI

(Received November 13, 1959)

A number of investigations on isotactic polymerization have been carried out in recent years. As regards the mechanism of isotactic polymerization by heterogeneous catalysts, it seems to be of great interest to see if the use of optically active organoaluminum compound in combination with a titanium halide might influence the steric structure of the resulting polymer.

**Polymerization of Styrene with an Optically Active Triamylaluminum.**—From the viewpoint mentioned above, we attempted to prepare trialkylaluminum containing three optically active 2-methylbutyl groups, starting from (−)-2-methylbutanol of 96% optical purity, $[\alpha]_D^{13'}=-5.70°$.

(−)-2-Methylbutanol was purified by repeated fractional distillation of fusel oil through a Stedman column of about 70 theoretical plates. Calculation of the optical purity is based on the value −5.90° for the pure substance[1]. Treatment of the alcohol with thionyl chloride and pyridine gave (+)-2-methylbutyl chloride of 95% purity, $[\alpha]_D^{14'}=+1.62°$ (+1.70° for the pure substance[2]).

A widely used preparative method of organoaluminum compounds is that using the reaction between metallic aluminum and an alkyl halide. The method, however, was by no means feasible in the case of higher alkyl halides, such as amyl chloride, because of the occurrence of vigorous decomposition reaction[3], and hence an alternative method was adopted in the present work as shown in the following equations:

$$HgCl_2+2AmMgCl \rightarrow Hg(Am)_2+2MgCl_2 \quad (1)$$

$$2Al+3Hg(Am)_2 \rightarrow 2Al(Am)_3+3Hg \quad (2)$$

$$(Am=-CH_2-CH(CH_3)-CH_2-CH_3)$$

(+)-Bis-(2-methylbutyl)mercury was obtained in 80% yield by the reaction of Eq. 1. An ethereal solution of 2-methylbutylmagnesium chloride (from 11.0 g. of the active chloride) and mercuric chloride (12 g.) was refluxed for one hour, and then after the removal of ether by distillation the residual mass was heated in an oil bath at 120°C for one hour. The reaction mass was combined with the ether distillate, decomposed by saturated aqueous ammonium chloride, and distilled to yield the product, b. p. 135～7°C (30 mmHg), $d_4^{27.5}=1.657$, $[\alpha]_D^{27.5'}=+7.65°$.

Found: Hg, 56.6%. Calcd. for $C_{10}H_{22}Hg$: Hg, 58.5%.

As the reaction between metallic aluminum and (+)-bis-(2-methylbutyl)mercury was found to be very vigorous, leading occasionally to decomposition of the product, the exothermic reaction was suppressed by the portion-wise addition of granular aluminum into (+)-bis-2-methylbutyl)mercury, which was kept at 100～110°C in an oil bath. The yield of tris-(2-methylbutyl) aluminum was 56% based on (+)-bis-(2-methylbutyl)mercury used, b. p. 85～105°C (0.5 mmHg).

Found: Al, 11.50%. Calcd. for $C_{15}H_{33}Al$: Al, 11.24%.

The optical purity of tris-(2-methylbutyl)-aluminum thus obtained was estimated by the following procedures, i.e., oxidation with oxygen, subsequent hydrolysis to 2-methylbutanol, and checking its optical rotatory power:

$$2Al(Am)_3+3O_2 \rightarrow 2Al(OAm)_3 \quad (3)$$

$$Al(OAm)_3+aq.\,HCl \rightarrow AlCl_3aq.+AmOH \quad (4)$$

The recovered 2-methylbutanol was found to have an optical purity of 27%, $[\alpha]_D^{30'}=-1.58°$, which indicates that an extensive racemization had taken place in some stages of the synthetic process (Eqs. 1 and 2) or of recovering process (Eqs. 3 and 4). In our experiment, therefore, the optical purity of tris-(2-methylbutyl)aluminum should be estimated at 27% at the lowest.

Polymerization of styrene was carried out at 70°C in *n*-heptane using this aluminum compound (0.3 g.) in combination with titanium trichloride (3 g.) for 2 to 7.5 hr. The isotactic fractions of the polymers showed no difference

*) Paper IV in a series on "Stereoregular Polymers". Presented at the Symposium of High Polymers, Osaka October 14, 1958.

1) W. Markwald and A. Mackenzie, *Ber.*, **34**, 485 (1907).

2) A. Mackenzie and G. W. Clough, *J. Chem. Soc.*, **103**, 698 (1913).

3) A. V. Grosse and J. M. Mavity, *J. Org. Chem.*, **5**, 108 (1940).

4) The content of mercury was determined by decomposition of the sample with sulfuric acid in a Kjeldahl flask and by titration of mercuric ions with ammonium rhodanate, M. Hiral and R. Hayatsu, *J. Pharm. Soc. Japan* (*Yakugakuzashi*), **70**, 76 (1950).

in the physical properties, such as melting points, X-ray diffraction pattern and optical rotation in toluene solution, in comparison with isotactic polystyrenes that were prepared with racemic tris-(2-methylbutyl) aluminum and titanium trichloride.

**Polymerization of Styrene with Optically Active Amylsodium.** — In the course of our study on the polymerization of styrene with Alfin catalysts, it was found that amylsodium alone could produce isotactic polystyrene in a suitable solvent, though in a small yield, together with a large amount of atactic polymer. Based on this observation, the amylsodium prepared from optically active amyl chloride was tested in the same way. Amylsodium was prepared from (+)-2-methylbutyl chloride and sodium dispersion in the usual manner[5] and was used as a catalyst in *n*-heptane solvent. However, the isotactic polystyrene here obtained showed again no unusual character and was quite identical with that obtained by an inactive catalyst, isoamylsodium.

*Department of Polymer Science*
*Faculty of Science*
*Osaka University*
*Nakanoshima, Osaka*

5) J. J. R. Williams, J. Van Den Berghe, K. R. Dunham and W. J. Dulmage, *J. Am. Chem. Soc.*, **79**, 1716 (1957).

# *Alkylalkoxypolysiloxanes. VIII.*[1] *Lower Members of Cyclic Methyl- and Ethyl-isopropoxypolysiloxanes*

By Rokuro OKAWARA and Masuo KATAYAMA

(Received November 11, 1959)

Cyclic trisiloxane, the first member of the cyclic polysiloxanes, has been known. While there were found stable compounds such as dialkyl cyclotrisiloxanes and $(C_2H_5Si(OC_2H_5)O)_3$[2], a group of unstable compounds was also known. Spontaneous changes of physical constants were reported with those unstable cyclotrisiloxanes; $((CH_3)HSiO)_3$[3], $((C_2H_5)HSiO)_3$[4], $(CH_3Si(OC_2H_5)O)_3$[2] and $((C_2H_5O)_2SiO)_3$[5].

In this paper, the preparation and properties of cyclic polysiloxanes as indicated by the following formula will be described.

$(RSi(OC_3H_7\text{-}i)O)_n$ $R=CH_3$ and $C_2H_5$; $n=3$ and 4

One of the objects of this paper is to assure that the rapid hydrolysis method[2,5] developed by the author is applicable for the preparation of cyclotrimers, and the other is to obtain some knowledge of their stability.

The results showed that the cyclic trimer together with the tetramer were formed by using a considerable dropping rate. Comparing the yield of cyclotrimers, the ethyl compound is formed more easily than the methyl compound in those conditions. The infrared absorption spectra of those cyclotrimers showed, as in the case of $(CH_3Si(OC_2H_5)O)_3$[2,6] and $(C_2H_5Si(OC_2H_5)O)_3$[2], a strong absorption at 1023 $cm^{-1}$ which would likely be attributed to the vibration of Si-O bond in cyclotrisiloxane ring. Though a measurable strain[7] would be expected in the cyclotrisiloxane ring of those compounds, no increase of the refractive index,

TABLE I. RESULTS OF THE HYDROLYSIS

Dichlorosilane (1 mol.) was added to the ice-cooled hydrolyzing mixture which consisted of pyridine (2 mols.), water (1 mol.) and 250 g. of benzene.

| Expt. | Dichlorosilane | Droppping rate g./min. | Hydrolyzate: Total yield (%) | Composition (%): $C_3$** | $C_4$** | Residue |
|---|---|---|---|---|---|---|
| 1 | I* | 15 | 57 | 13 | 16*** | 71 |
| 2 | I | 30 | 65 | 13 | 20 | 67 |
| 3 | II* | 20 | 75 | 32 | 10 | 58 |

* I: $CH_3(i\text{-}C_3H_7O)SiCl_2$,
II: $C_2H_5(i\text{-}C_3H_7O)SiCl_2$

** $C_3$: Cyclic trimer
$C_4$: Cyclic tetramer

*** Gelation occurred in still-pot after 16% of $C_4$ has distilled out.

1) Part VII of this series, R. Okawara and S. Imaeda, This Bulletin, **13**, 194 (1958).
2) R. Okawara, G. Minami and Z. Oku, ibid, **31**, 22 (1958).
3) S. D. Brewer, *J. Am. Chem. Soc.*, **70**, 3962 (1948).
4) R. Okawara, U. Takahashi and M. Sakiyma, This Bulletin, **30**, 608 (1957).
5) R. Okawara, S. Hotta and T. Shimura, ibid., **28**, 541 (1955).
6) R. Okawara, ibid., **31**, 154 (1958).
7) T. Tanaka, ibid., **34**, 282 (1960).

TABLE II. CYCLIC POLYSILOXANES

| Polymer size $n$ | Boiling point °C/mmHg | Refractive index $n_D^{20}$ | Density $d_D^{20}$ | Molar refraction found (calcd.)* | Molecular weight found (calcd.)** | Anal. Si, % found*** (calcd.) |
|---|---|---|---|---|---|---|
| | $(C_2H_3Si(OC_3H_7\text{-}i)O)_n$ | | | | | |
| 3 | 67/1 | 1.3973 | 0.9912 | 86.23 | 348 | 23.80 |
| | | | | (85.98) | (354.6) | (23.76) |
| 4 | 97/1 | 1.4023 | 1.0009 | 115.09 | — | 23.77 |
| | | | | (114.64) | (472.8) | (23.76) |
| | $(C_2H_5Si(OC_3H_7\text{-}i)O)_n$ | | | | | |
| 3 | 92/1 | 1.4129 | 0.9817 | 100.74 | 407 | 21.22 |
| | | | | (99.87) | (396.7) | (21.24) |
| 4 | 125/1 | 1.4177 | — | — | — | 21.22 |
| | | | | | | (21.24) |

* Calculated from bond refractivities by E. L. Warrick, *J. Am. Chem. Soc.*, **68**, 2455 (1946).
** Cryoscopic measurement in benzene.
*** Silicon was determined by decomposing the sample with concentrated suluric acid.

due to a spontaneous decomposition, was observed with the samples sealed in a soft glass ampule within one year.

## Experimental

**Starting Materials.** — Methyltrichlorosilane used in these experiments was supplied from the Shin-etsu Chem. Ind. Co. Ethyltrichlorosilane was obtained from the product of silicon-ethylchloride reaction. Methylisopropoxydichlorosilane (I) and ethylisopropoxydichlorosilane (II) were prepared by adding 1 mol. of isopropanol to 1 mol. of those trichlorosilanes, respectively. After the addition, the mixture was aerated with stirring to drive off the hydrogen chloride at room temperature. Then the mixture was fractionated through a Stedman column of about 20 theoretical plates. Redistilled dichlorosilanes were taken for the starting materials.

*Methylisopropoxydichlorosilane* (I) b. p. 112.5°~113°C (Reported[8]: b. p. 110°~111°C)

Found: Cl, 41.1. Calcd. for (I): Cl, 41.0%.

*Ethylisopropoxydichlorosilane* (II) b. p. 137°~8°C (Reported[9]: b. p. 67°C/60 mmHg)

Found: Cl, 37.5. Calcd. for (II): Cl, 37.9%.

**Hydrolysis and Fractionation of the Hydrolyzate.**—Hydrolysis was carried out as described in the preceding papers.[2,5] The results are summarized in Table I.

The composition of the hydrolyzate was determined by fractionation through a Stedman column of about 50 theoretical plates. In Expt. 1, gelation occurred in a still-pot after 16% of $C_4$ distilled out; accordingly the fractionation of the other runs were carried out with the distillable fraction which was obtained from the hydrolyzate through a simple distillation. Comparing the yield of $C_3$, the ethyl compound is more easy to be formed than the methyl compound.

The fractions which exhibited constant boiling points and refractive indicies were taken for the samples and their physical constants are given in Table II.

**Infrared Spectra and Stability.** — Infrared absorption spectra were obtained with a Hilger H-800 infrared spectrophotometer with a rock salt prism. In the range 700~1300 $cm^{-1}$, samples were observed as solution in carbon disulfide. The positions of the strong bands which appeared in the range 1000~1100 $cm^{-1}$ are shown in Table III.

TABLE III

| Compound | Absorption Spectra (in $cm^{-1}$) | | |
|---|---|---|---|
| $(CH_3Si(OC_3H_7\text{-}i)O)_3$ | 1023 | 1044 | — |
| ( 〃 )$_4$ | — | 1044 | 1086 |
| $(C_2H_5Si(OC_3H_7\text{-}i)O)_3$ | 1024 | 1045 | — |
| ( 〃 )$_4$ | — | 1043 | 1087 |

All the samples shown in Table II, which were sealed in a glass ampule, gave no changes of refractive index within one year.

## Summary

1) Methyl- and ethyl-isopropoxydichlorosilane were hydrolyzed with considerable dropping rate using pyridine as an acid acceptor.

2) Methyl- and ethyl-isopropoxycyclotrisiloxane have been prepared and characterized. Those compounds were found to be stable.

3) Methyl- and ethyl-isopropoxycyclotetrasiloxane have been prepared and characterized.

*Department of Applied Chemistry*
*Faculty of Engineering, Osaka University*
*Higashinoda Osaka*

8) R. Okawara, *Technol. Repts. Osaka Univ.*, 7, 453 (1957).
9) R. Okawara and I. Ishimaru, This Bulletin, 27, 582 (1954).

# *Absorption Spectra of Dyes. V*[1]. *The Composition and Intermolecular Charge Transfer Spectra of Complexes Formed in Aqueous Solution of the Mixture of Chlorazol Sky Blue FF and Chrysophenine G*

By Teruaki KOBAYASHI, Yoshié TANIZAKI and Noboru ANDO

(Received December 2, 1959)

Most of the binary mixtures of dyes in aqueous solution studied before showed more or less non-additive spectra[1-6]. Of these dyes the pair of Chlorazol Sky Blue FF and Chrysophenine G revealed the most remarkable change in spectrum. This pair was first studied by Neale and Stringfellow[2], and then in more detail by Derbyshire and Peters[4]. According to the latter workers, only a 1:1 complex is formed between Chrysophenine G and Chlorazol Sky Blue FF in equimolar solution or in the presence of an excess of Chlorazol Sky Blue FF at room temperature, while higher complexes are formed to a certain extent in the presence of an excess of Chrysophenine G. However, they made no mention of the composition of these higher complexes. In the hope of obtaining some information about the composition of the higher complexes and then interpreting the spectral change observed on the basis of quantum chemical concept, this combination has been studied in greater detail.

A series of studies of binary mixtures of Chlorazol Sky Blue FF with some other dyes have shown that the relatively small spectral change observed in mixtures of some monoazo and disazo dyes may be explained by the perturbation between molecular orbitals of two component dyes caused by the formation of loose complexes[1,5]. However, it has been impossible to apply this concept to more compact complexes: a large spectral change which appeared in a binary mixture of Chlorazol Sky Blue FF has been unable to be explained without the concept of intermolecular charge transfer[1]. As the authors pointed out before, the mixture of Chlorazol Sky Blue FF and Chrysophenine G also shows a spectral change which implies the occurrence of charge transfer[1]. Therefore, this pair, which is considered to be a typical example of these sorts of dyes having the intermolecular charge transfer phenomenon, seems to be most suitable for our purpose.

## Experimental

**Preparation of Samples.**—The purification of the dyes and the preparation of dye solutions followed the same methods as explained in the previous paper[1].

**Absorption Spectra.**—All the absorption spectra of dye solutions were measured by a Shimadzu QR-50 spectrophtometer at room temperature (27°~30°C). Cells used were 0.2, 0.5 and 1 cm. thick.

Hereafter Chlorazol Sky Blue FF and Chrysophenine G will shortly be called Blue (or B) and Yellow (or G), respectively.

## Results and Discussion

**1. The Composition of Complexes Formed in Solutions.**—As is shown in Fig. 1, absorption spectra of mixtures of Blue and Yellow at

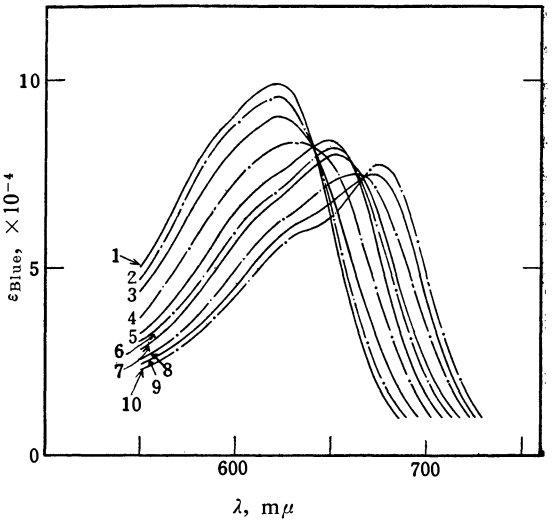



Fig. 1. Absorption spectra of mixtures of Blue and Yellow in aqueous solution at room temperature (ca. 27°C). The concentration of Blue is $1.00\times10^{-5}$ mol./l. The ratio of the concentration of Yellow to that of Blue is 1-0, 2-0.105, 3-0.313, 4-0.610, 5-1.03, 6-1.55, 7-2.07, 8-4.18, 9-8.27 and 10-51.5.

1) Part IV of this series, T. Kobayashi, Y. Tanizaki and N. Ando, This Bulletin, 32, 680 (1959).
2) S. M. Neale and W. A. Stringfellow, *J. Soc. Dyers Col.*, 59, 241 (1943).
3) D. R. Lemin and T. Vickerstaff, *Trans. Faraday Soc.*, 43, 491 (1947).
4) A. N. Derbyshire and R. H. Peters, *J. Soc. Dyers Col.*, 72, 268 (1956).
5) Y. Tanizaki, T. Kobayashi and N. Ando, This Bulletin, 32, 119 (1959).
6) T. Kobayashi, Y. Tanizaki and N. Ando, ibid., 32, 675 (1959).

wavelengths corresponding to the first absorption band of Blue (620 m$\mu$) show a characteristic change, with an increase in the concentration of Yellow added into the solution containing a constant amount of Blue ($1.00\times10^{-5}$ mol./l.). It is already known[4] that, while the concentration of Yellow does not exceed that of Blue, spectra of mixtures of this pair have an isosbestic point at about 640 m$\mu$ accompanied with a new clear absorption band at 650 m$\mu$. Fig. 1 clearly shows that, when the concentration of Yellow has increased more than four times as high as that of Blue, the second isosbestic point appears at about 670 m$\mu$ and 650 m$\mu$ band disappears, followed by the appearance of a new band at 675 m$\mu$. Since Yellow does not absorb light in the wavelength region shown in the figure, these two isosbestic points mean that each molecule responsible for the 650 m$\mu$ band contains in itself one Blue molecule (the first isosbestic point), and that each molecule responsible for the 675 m$\mu$ band contains in itself one molecule of the complex (the second isosbestic point).

As has already been known, the 650 m$\mu$ band is due to a 1 : 1 complex[4]. Then, the molecular species of the 675 m$\mu$ band may be considered to be a complex made up of a 1 : 1 complex and Yellow in the ratio 1 : 1. Now, let us suppose that the molecular species which shows the 675 m$\mu$ band is a 1 : 2 complex richer in Yellow and that the following equilibriums exist in solutions.

$$B+G \rightleftarrows BG \qquad (K_1)$$

$$BG+G \rightleftarrows BG_2 \qquad (K_2)$$

It is possible to calculate the equilibrium constants ($K_1$ and $K_2$) corresponding to the above equilibriums, from observed obtical densities in accordance with the mass action law. They were calculated here by use of the difference $\Delta D$ between the sum of observed optical densities of the component dyes and the optical density of the corresponding mixture at 620 m$\mu$, according to the usual method[3,6]. Since the observed optical density of the mixture is, in practice, the sum of those of the single dyes and the complexes, the calculation is complicated. Therefore, an approximate one was performed. As the figure shows clearly, the amount of 1 : 2 complex is negligibly small in the concentration region [B] > [G] (where [B] and [G] mean the initial concentrations of Blue and Yellow. respectively). Consequently, the value of $K_1$ was calculated from observed optical densities in the region [B] > [G]. The optical density at 620 m$\mu$ decreases with an increrase of [G], approaching to a certain value as [G] becomes large relative to [B]. This value may be considered to be due only to the 1 : 2 complex, $BG_2$. Thus the molecular extinction coefficient of $BG_2$ may be known, and by use of it, $K(=K_1K_2)$, the overall equilibrium constant of the formation of the complexes, may be calculated. $K_2$ can easily be obtained from $K$ and $K_1$. Calculated values of $K_1$ and $K_2$ were about $6\times10^5$ and $5\times10^4$, respectively, at 27°C.

Now as the values of $K_1$ and $K_2$ were thus decided, the concentrations of BG and $BG_2$ corresponding to any amounts of Blue and Yellow will be obtained, according to mass action equations, hence the difference of optical densities $\Delta D$ will be calculated by use of them. Calculated $\Delta D\sim$ [G] curves when the initial concentration of Yellow is varied with that of Blue kept constant are shown by full lines in Fig. 2,

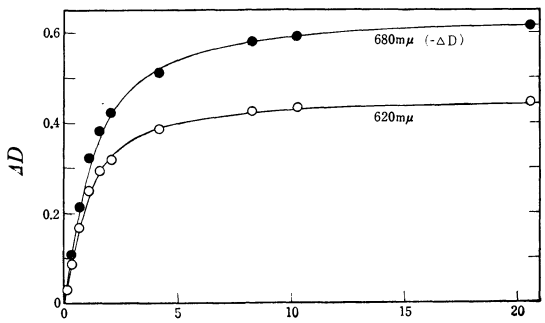



Fig. 2. The difference in optical densities when the concentration of Blue is constant ($1.00\times10^{-5}$ mol./l.) at 27°±1°C. 1 cm. thick.
Full lines: calculated differences
Black and white circles: observed differences corresponding to the respective curves

in which the lower and upper curves show the differencce at 620 m$\mu$ and at 680 m$\mu$, respectively. The latter is described as $-\Delta D$ because it has negative values. Observed values corresponding to each curve are shown by white and black circles. They are coincident well with the respective calculated curves.

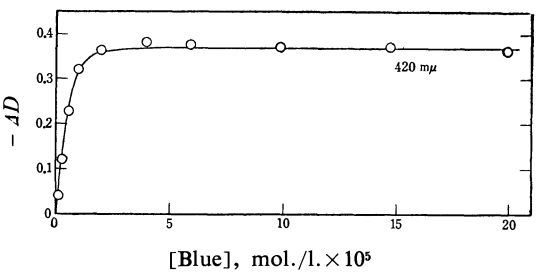



Fig. 3. The difference in optical densities when the concentration of Yellow is constant ($1.00\times10^{-5}$ mol./l.) at 28°±1°C. 1 cm. thick.
Full line: calculated difference
White circles: observed differences corresponding to the calculated curve

A corresponding calculation was then made at 420 mμ, the concentration of Yellow being kept constant. The result ($-\Delta D\sim$ [B] curve) is shown by a full line in Fig. 3, in which the white circles are corresponding observed values. The coincidence between the observed and the calculated values is also satisfactory in this case.

As seen above, each of the $\Delta D\sim$ [G] and the $\sim$ [B] curves calculated by use of $K_1$ and $K_2$, of which values were obtained from the observed optical densities at 620 mμ, explains the observed values well. This satisfactory coincidence between the observed and the calculated values of $\Delta D$ means the propriety of the assumption that a 1 : 1 complex and a 1 : 2 complex are formed in equilibrium in the mixture solution. Further it affirms that the obtained values of $K_1$ and $K_2$ are proper.

Now, it has become clear that two sorts of complexes exist in the mixture solution, in addition to the component dyes. Therefore, the behavior of the spectral change shown in Fig. 1, i. e., the shift of the first absorption band from 620 mμ to 650 mμ and to 675 mμ through the two isosbestic points with an increase in concentration of yellow, may be expressed in the quantitative relation among these components and complexes. The consentrations of Blue and the two complexes change with an increase in amount of Yellow as shown in Fig. 4, in which Curves I, II and III show the concentrations of free Blue, BG and $BG_2$, respectively. As the figure shows, the existence of $BG_2$ is negligible when it is compared with the others, in the region where the amount of Yellow is less than $0.5\times10^{-5}$ mol./l. Consequently the spectral change of the mixture will be governed only by the amounts of free Blue and BG (the first isosbestic point). When the concentration of Yellow is further increased, free Blue decreases to a nigligible amount, hence the spectral change is governed only by the amounts of BG and $BG_2$ (the second isosbestic point). Thus the change in spectra of the mixtures shown in Fig. 1 will well be understood through the relation between the concentrations of the components and the complexes shown in Fig. 4.

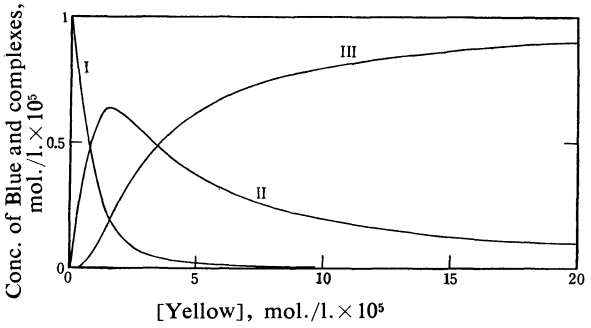



Fig. 4. The changes in concentrations of Blue and the complexes with that of Yellow when the initial concentration of Blue is $1.00\times10^{-5}$ mol./l.
I: free Blue, II: BG, III: $BG_2$

**2. The Change in Absorption Spectra.**—The discussion in the previous section has clarified that a 1 : 1 complex BG and a 1 : 2 complex $BG_2$ are formed in aqueous solution of the mixture of Blue and Yellow. The equilibrium constants ($K_1$ and $K_2$) for these complexes have also been obtained. Therefore, absorption curves of the complexes can be drawn from observed absorption spectra of mixtures. The curves shown in Fig. 5 are the absorption spectra of BG and $BG_2$ thus obtained*. Inspection of the absorption spectra of the components and the complexes

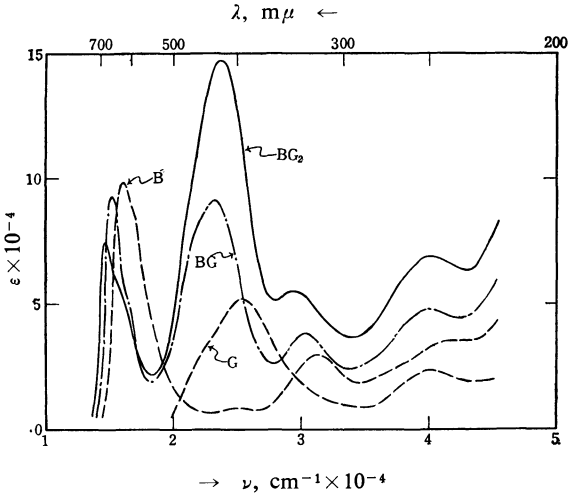



Fig. 5. Absorption spectra of the complexes and the component dyes

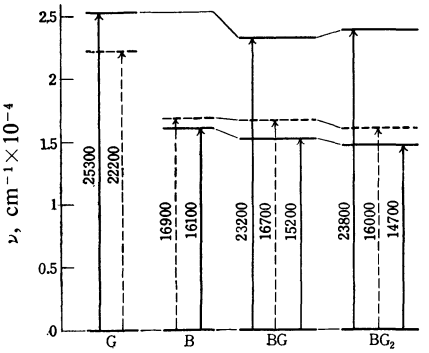



Fig. 6. Observed transition energies ($cm^{-1}$) of Yellow (G), Blue (B) and the complexes (BG and $BG_2$)

* Since these curves were made from absorption specra which were converted from those measured in various cells different in thickness so as to correspond to the unit cell, their molecular extinction coefficients and maximum wavelengths shown in the figure may have some errors.

shows that the first absorption bands shift to longer wavelengths with a change from Blue to $BG_2$; on the other hand, the absorption of BG corresponding to the first absorption band of Yellow (395 m$\mu$) is markedly shifted to longer wavelengths (430 m$\mu$) with a remarkable increase in intensity, while that of $BG_2$ to shorter wavelengths (420 m$\mu$) than that of BG is. To show these changes more clearly, the transition energies ($cm^{-1}$) of Blue, Yellow, BG and $BG_2$ are given in Fig. 6, where the dotted lines mean absorptions corresponding to shoulders. The absorptions illustrated in Fig. 6 seem to show a regular change, except those in the shorter wavelength region, in view of the fact that they shift to longer wavelengths with a change from Blue to $BG_2$. The absorptions of the complexes in the shorter wavelength rigion seem to have an unusual behavior. Perhaps they are charge transfer spectra, as the following discussion will suggest.

The first absorption bands of dyes are generally considered to be due to conjugated double bond chains connected with auxochromes. According to the VB theory, the first absorption bands of Blue and Yellow may be considered to be owing to resonances between the following extreme structures.

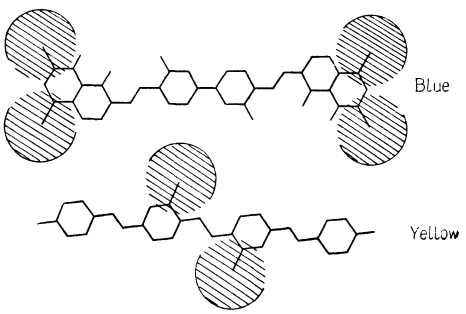
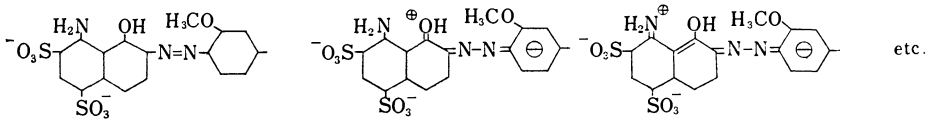
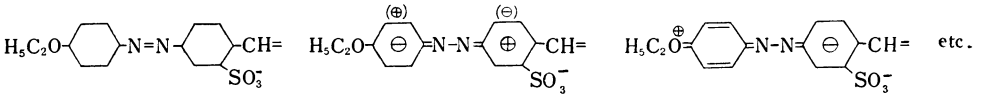



Fig. 7. Models of Blue and Yellow. The shadowed circles mean sulfonic groups.

pointed out before[4] and the structures in Fig. 7 show clearly, Blue and Yellow might approach close each other without accepting the repulsion of their charged groups, if they form complexes with their molecular axes in parallel with each other. In such structures, the auxochromes of Blue may have higher possibility of being covered by the conjugated system of their partners than those of Yellow, so unshared $\pi$-electrons of the auxochromes of Blue may be more affected than those of Yellow. These conditions may make the ground state of Blue unstable, the contribution of structure I to it




I II III




I′ II′ III′

where the half of the structure of each dye is shown. Though there are a number of extreme structures, they are lumped together under the structures of which inner $\pi$-electron systems have negative charge. The first absorption band of each dye may approximately be expressed by a transition from the ground state (mainly I or I′) to an excited state (mainly II or II′)**. As

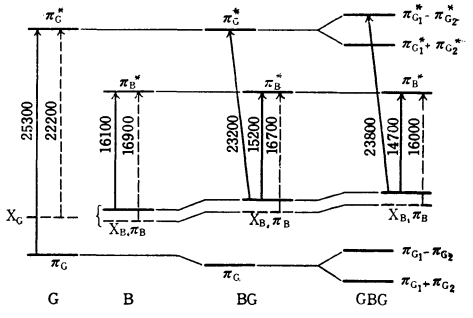
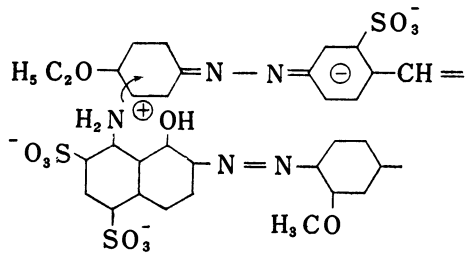



Fig. 8. Schematic representation of electronic transitions among molecular orbitals of Yellow (G), Blue (B) and the complexes (BG and GBG)

** According to empirical facts, auxochromes, which are attached to a naphthalene ring as a coupling component, show, in general, greater effects on absorption spectra, when attached to the inner ring having an azo group. Hence, the excited state of Blue seems to consist mainly of structure II. In case of Yellow, as the effect of $OC_2H_5$ as auxochrome seems to be weak because of its weak electron donating power relative to $NH_2$, ect.,[7] it may approximately be considered that the shoulder of the first absorption hand is due to the resonance I′↔III′ and the peak to I′↔II′.

7) A. E. Gillam and E. S. Stern, "An Introduction to Electronic Absorption Spectroscopy in Orgnic Chemistry", Edward Arnold, London, (1957), p. 129.

smaller, and, at the same time, charge transfer from Blue to Yellow easy. The important structure of an excited state in this case may be



in which a mobile electron of Blue in structure II or III transfers to the inner $\pi$-electron system of Yellow***.

The same discussion will be given on $BG_2$. The structure of $BG_2$ may be considered to be a sandwich type with B in its inside. The two G molecules in this complex are supposed to be close to each other in spite of holding B between them, so it is necessary to take into account an interaction between them: the mixing may occur to some extent between the excited states of G molecules, causing them to split in two different levels. The experimental results suggest that the charge transfer from B may occur to the higher level, though it can not possibly be ascertained.

According to the MO method, the spectral change will be explained as follows. A rough approximation shows that the first absorption bands of the dyes are due to electron transitions of unshared $\pi$-electrons of the auxochromes to the lowest vacant orbitals of the inner $\pi$-electron systems, i. e., the $X \rightarrow \pi^*$ transitions in Fig. 8****. In case of Yellow (G), this is $X_G \rightarrow \pi_G^*$. As the electron donating power of $OC_2H_5$ is weak relative to that of $NH_2$[7], however, this absorption may also be weak. Probably the principal absorption band of G is due to $\pi_G \rightarrow \pi_G^*$. In case of Blue, it is difficult to know which auxochrome $X_B$ corresponds to, because Blue has many auxochromes. Consequently, they are lumped together under $X_B$.

If Bule and Yellow from the complex BG with the structure mentioned above, the first probable change will arise between $\pi_G$ and $X_B$ (and $\pi_B$), because the auxochromes of B may be affected strongly by the inner $\pi$-electron system of G; a repulsion between these MO's will occur to make such a pattern as BG in Fig. 8. It was supposed here that no interaction happens between $\pi_B^*$ and $\pi_G^*$. If a geometrical arrangement of the orbitals $X_B$ and $\pi_G^*$ in the complex is taken into consideration, the $X_B \rightarrow \pi_G^*$ transition, i. e., an intermoleculer charge transfer, may be expected to occur easily.

Concerning the complex $BG_2$, as already mentioned, its structure may be as GBG, with the linear molecules standing side by side. Since the G molecules stand close to each other in spite of B existing between them and parallel with each other, the complex has at least one symmetry. Consequently, the two $\pi_G^*$ orbitals mix to separate into $\pi^*_{G_1} + \pi^*_{G_2}$ and $\pi^*_{G_1} - \pi^*_{G_2}$. As seen in the discussion based on the VB theory, it is also difficult to ascertain to which molecular orbital the charge transfer from B occurs. The experimental results, however, mean that it may be $X_B \rightarrow (\pi^*_{G_1} - \pi^*_{G_2})$. On the other hand, it is clear from the above discussion that the $X_B$ level in GBG is pushed up higher than the one in BG.

Though there is no ground for justifying the relative positions of the molecular orbitals in Fig. 8, the spectral changes shown in Fig. 6 could be explained at least qualitatively by the above discussion based on the MO method. Some parts of the above two discussions were not always perfect, but it should be noted that the spectra of the complexes could not be explained without the concept of charge transfer. Explanation of these specteal changes by a solvent effect caused by the close approach of dye molecules was attempted, without considering the charge transfer, only to fail; the first absorption band of Yellow was insensitive to the change in pH or in solvent. So, it follows that the strong absorptions at about 420 m$\mu$ of the complexes can not be explained by a mere solvent effect.

Thus the absorption spectra of the complexes formed of Blue and Yellow could be explained qualitatively on the basis of those of the components. A binary mixture of Blue, in which the formation of a 1 : 1 complex is proved, also showed a change in spectrum which might not be explained without the concept of charge transfer.[1],***** It cannot always be said, however, that its charge transfer occurs in the same mechanism as is considered in the present work. The main reason will be found in the fact that the partner of Blue has no such symmetry in its structure as Yellow has and that the obvious factors suggesting the arrangement of the component dyes in the complex are not found.

*** Since the amino groups have less effect on the spectrum of Blue than the hydroxyl groups and the electron donating power of the former is stronger than that of the latter, as mentioned in footnote 2, an electron of one of the amino groups may be considered to have high possibility of acting in the intermolecular charge transfer. However, it is impossible and unnecessary to confirm the fact.

**** X and $\pi$ mean the orbital of unshared electrons and the inner $\pi$-orbital, respectively.

***** Blue and Durazol Red 2B forms a 1 : 1 complex in aqueous solution (see Ref. 3), of which spectrum seems not to be understood without considering charge transfer.

**Summary**

1. The change in absorption spectra of mixtures of Chlorazol Sky Blue FF and Chrysophenine G in aqueous solution was stoichiometrically studied in detail and a 1 : 1 complex and a 1 : 2 complex were proved to be formed.

2. The absorption spectra of the complexes were drawn from experimental results by use of the calculated equilibrium constants, and the phenomena of these absorptions were qualitatively explained according to VB and MO methods, with the conclusion that charge transfer spectra from Chlorazol Sky Blue FF to Chrysophenine G appear in the complexes.

The authors wish to express their thanks to Professor Ikuzo Tanaka for his helpful discussion.

*Laboratory of Physical Chemistry*
*Tokyo Institute of Technology*
*Meguro-ku, Tokyo*

# *Sodium Iodide-Acetone and Zinc Bromide-Acetone Molecular Complexes*

By Haruka YAMADA

(Received November 17, 1959)

The molecular compound between sodium iodide and acetone, known as NaI·3 acetone, can be used for the purification of acetone. The nature of the bonding, however, has not been made clear. From conductivity measurements, Rosenthal[1] suggested that the molecular compound was dissociated into $Na^+$ and $(I \cdot 3 \text{ acetone})^-$ in acetone. This may indicate that the compound has an ionic structure as represented by $Na^+$ $(I \cdot 3 \text{ acetone})^-$. By infrared studies, Slovokhotova[2] reported that acetone molecules had the enol form when sodium iodide was added, but her explanation does not seem to be plausible.

On the other hand, the complex formed by the addition of iodine or lithium perchlorate to acetone is known as the charge transfer complex stabilized by the electron donor-acceptor interaction[3,4]. The sodium compounds of salicylaldehyde and methylsalicylate[5] are also known to be formed by the same interaction between the $Na^+$ ion and the C–O and C=O groups, respectively. As for the NaI-acetone complex, the charge transfer force may interpret the intermolecular bonding.

The present study has been undertaken to clarify what sort of force gives rise mainly to the intermolecular bonding of the NaI-acetone and $ZnBr_2$-acetone systems.

1) W. Rosenthal, *Compt. rend.*, **237**, 1537 (1953),
2) N. A. Slovokhotova, *Zhur. Fiz. Kim.*, **25**, 768 (1951), *Chem. Abstr.*, **46**, 2396h (1952).
3) H. Yamada and K. Kozima, *J. Am. Chem. Soc.*, **82**, 1543 (1960).
4) A. D. E. Pullin and J. McC. Pollock, *Trans. Faraday Soc.*, **54**, 11 (1958).
5) H. Yamada, This Bulletin, **32**, 1051 (1959).

## Experimental

Guaranteed commercial anhydrous sodium iodide and zinc bromide were used without further purification. Sodium perchlorate was obtained by heating $NaClO_4 \cdot H_2O$ in an air bath. The anhydrous salts were stored in the dark in a desiccator. Acetone was used after drying over anhydrous sodium sulfate and fractionating. The salts were dissolved into acetone and the thin layers of the solutions were obtained by sandwiching them between polyethylene films. The solid sample was made by cooling with the dry ice-ethanol mixture. The infrared spectra were taken with a Perkin-Elmer Model 112 infrared spectrophotometer in the region $400\,cm^{-1} \sim 4000 cm^{-1}$, using KBr, NaCl, $CaF_2$ and LiF prisms.

The composition of the complex was determined as follows. The salt was dissolved into acetone at room temperature and its concentration was determined by weighing. When the solution was cooled and the complex was crystallized, an excess of acetone was eliminated by suction and the complex was weighed.

## Results and Discussion

The wave numbers of the spectra of the NaI- and $ZnBr_2$-acetone systems are shown in Table I and the curves in Figs. 1—5.

The skeletal vibrations of acetone were influenced noticeably by the addition of the salts, while the other bands were not so affected. Concerning the bands splitting into the two components, one of the components can be attributed to the complex and the other to original acetone. Although the separation of the C=O stretching band in NaI-acetone system

TABLE I. WAVE NUMBERS OF SPECTRA FOR ACETONE, NaI-ACETONE AND $ZnBr_2$-ACETONE

| Acetone (liquid) | NaI-acetone (liquid) | NaI-acetone (solid) | $ZnBr_2$-acetone (liquid) | Assignment* |
|---|---|---|---|---|
| 1717 | 1709 | 1708 | 1697(s) | $A_1$ C=O stretching |
| 785 | 789 | 790 | 789 | $A_1$ C-C sym. stretching |
| 1215 | 1233(s) | 1236(s) | 1236(s) | $B_1$ C-C antisym. stretching |
| 530 | 539(s) | 540(s) | 540(s) | $B_1$ C-C=O bending |
| 3411 | 3405 | 3401 | 3401 | $A_1$ C=O stretching overtone |
| 1092 | 1093 | 1094 | 1091 | |
| 903 | 906 | 910 | 909 | |

(s) indicates the band having two components and the wave number is the value for the complex component.

* T. Miyazawa, *J. Chem. Soc. Japan, Pure Chem. Sec. (Nippon Kagaku Zasshi)*, **74**, 915 (1953).

could not be observed, the observed band with the shifted maximum is interpreted as the complexed band closely overlapped with the non-complexed one. The fact that the band shifts observed on complex formation are small suggests that the acetone molecules in the complex are slightly perturbed. The directions and amounts of the shifts are similar to those observed for the iodine-acetone[3] and lithium perchlorate-acetone complexes[4]. These shifts may be interpreted as being due to the changes of the force constants of C=O stretching and C-C=O bending vibrations caused by the formation of the complex, similarly as the case of the iodine-acetone or lithium perchlorate-acetone complex[6].

Since the spectrum of the NaI-acetone complex exhibited a similarity to that of the $NaClO_4$-acetone complex except the absorption caused by the $ClO_4^-$ ion, the formation of the salt-acetone complex may be due to the bonding between acetone and the $Na^+$ or $Zn^{2+}$ ion.

When the NaI-acetone solution was cooled, the needle crystal was obtained. Its composition was 1 : 5 mole ratio. The spectrum of this crystal contained the original acetone bands and was similar to that of the solution. The C-C antisymmetric stretching band is shown in Fig. 2(b). This curve can be divided into the two Lorentz curves with the maxima at 1236 $cm^{-1}$ and at 1215 $cm^{-1}$. Intensities were calculated from Ramsay's method[7]. It has been shown[3] that, for the iodine-acetone system, this band does not change in intensity on complex formation. The same may be true for this complex. From this property of the band and the fact that the area intensity ratio between the two bands is about 3 : 2, it follows that three acetone molecules are regarded as those of complexed acetone and the other two as those of non-complexed acetone. Probably the $Na^+$ ion forms the tetra-coordinate compound having $I^-$ and three acetone molecules as ligands and the other two acetone molecules will be contained in the crystal without coordinating.

The overtone band of the C=O stretching vibration showed a remarkable change. As shown in Fig. 5, this band became broad and was enhanced very much. By subtracting the two bands at 3520 $cm^{-1}$ and at 3620 $cm^{-1}$ from the observed curve for the NaI-acetone system, the dotted curve was obtained. This may be attributed to the overtone band of C=O stretching vibration and not the OH band, because the similar phenomenon was observed for the overtone band of the C=O stretching vibration of the iodine-acetone complex.

Relatively large shifts were observed for the skeletal vibrations belonging to the $B_1$ type. This differs from the phenomenon observed for the iodine-acetone complex and is probably due to the fact that the mole ratio of the NaI-acetone complex is 1 : 3 even in solution, while that of the iodine-acetone is 1 :1.

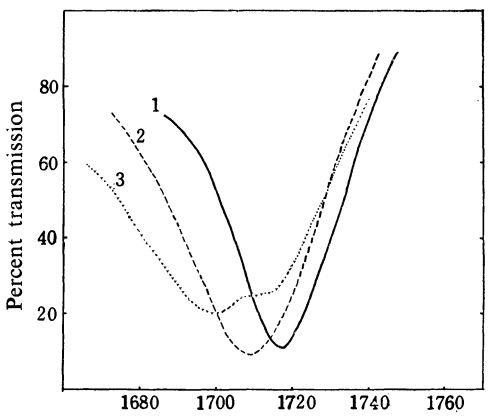
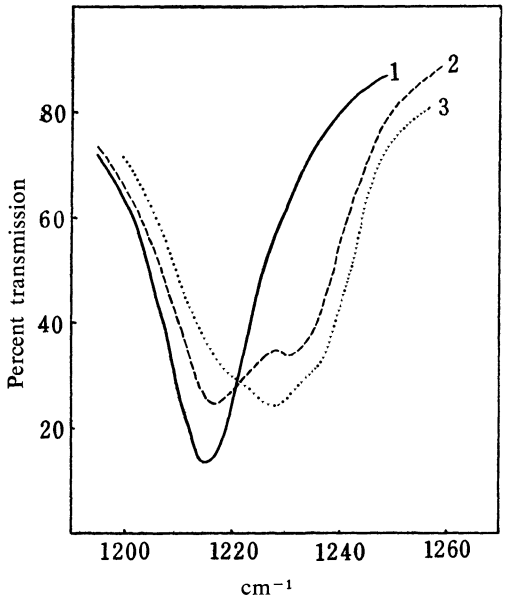
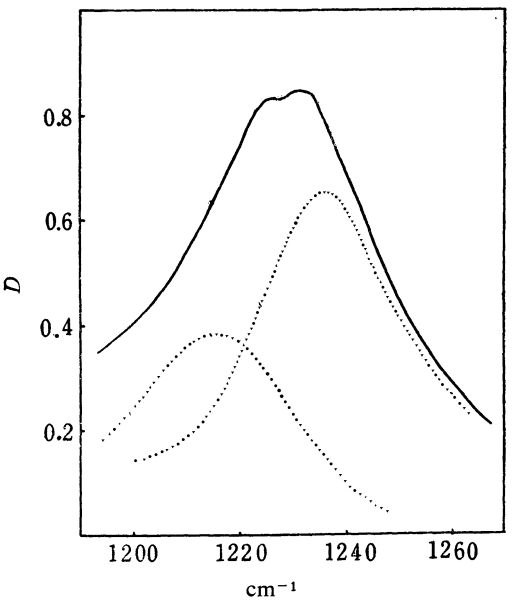



Fig. 1. C=O stretching bands for NaI- and $ZnBr_2$-acetone systems.
1. Pure acetone
2. NaI-acetone solution (saturated)
3. $ZnBr_2$-acetone solution (saturated)

6) K. Kozima and H. Yamada, unpublished.
7) D A. Ramsay, *J. Am. Chem. Soc.*, **74**, 72 (1956).




(a) Liquid state
1. Pure acetone
2. NaI-acetone in 1 : 10 mole ratio
3. NaI-acetone in 1 : 6 mole ratio




(b) Solid state
Unbroken curve is observed for NaI-acetone solid in 1 : 5 mole ratio. Dotted curves are Lorentz curves.

Fig. 2. C-C antisym. stretching bands of NaI-acetone system.

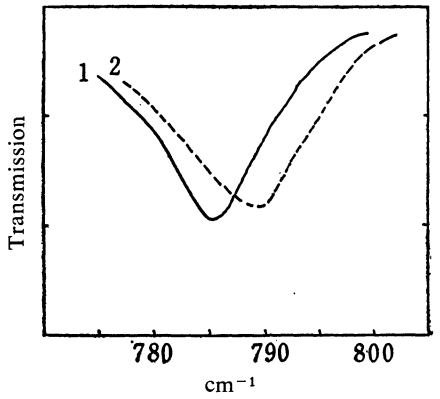



Fig. 3. C-C sym. stretching bands.
1. Pure acetone
2. NaI-acetone solution (saturated)

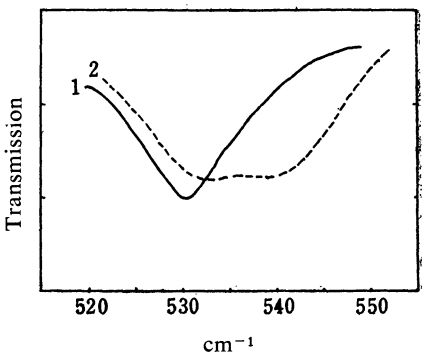



Fig. 4. C-C=O bending bands.
1. Pure acetone
2. NaI-acetone solution (saturated)

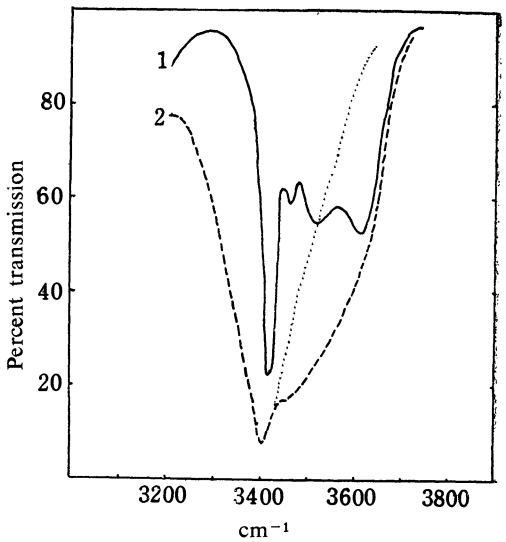
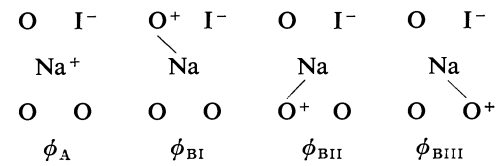



Fig. 5. Overtone bands of C=O stretching vibration.
1. Pure acetone (0.1 mm. cell)
2. NaI-acetone solution (0.1 mm. cell)

From the fact that the frequencies of the acetone band maxima do not vary continuously with salt concentration but the bands show the contour of two components and from the fact that observed shifts are similar to those for the iodine-acetone charge transfer complex, it may be concluded that the formation of the complex is due to the coordination of the lone pair electrons of oxygen atom to the $Na^+$ or $Zn^{2+}$ ion. No evidence for the enolization of acetone was found. As for the intermolecular bonding of these complexes, the charge transfer force, besides ion-dipole interaction etc., should be taken into account. The wave function of the normal state for the complex may be written by

$$\Psi_N = a\phi_A + b(\phi_{BI} + \phi_{BII} + \phi_{BIII}).$$

Here $\phi_A$ expresses the no-bond structure and $\phi_{BI}$, $\phi_{BII}$ and $\phi_{BIII}$ following dative structures.




The author wishes to express her sincere thanks to Professor K. Kozima for his kind guidance during this work.

*Research Laboratory of Spectroscopy*
*Tokyo Institute of Technology*
*Meguro-ku, Tokyo*

# *Synthesis of 1,4,7-Cyclononatrione**

By Sin'iti KAWAI, Sanae TANAKA, Kenji TERAI, Masami TEZUKA and Tarozaemon NISHIWAKI

(Received May 26, 1959)

The hydrocarbon $C_{20}H_{20}$ (III) with the complete skeleton of a regular pentagonal dodecahedron has not yet been known. Since the hydrocarbon, which shall be tentatively called "dodecahedrane", will be a very stable, strainless compound, an attemp of its synthesis has been started with the present work.

For the synthesis of dodecahedrane it is necessary to obtain the hypothetical *d*, *l*-tricyclic compound, I+I′, which shall be temporarily called "tricyclone". Although there are four asymmetric carbon atoms in the molecule of tricyclone, only one pair of optical isomers, I and I′, are possible and synthesis will lead to a racemate. The tricyclone, having three pairs each of carbonyl and active methylene groups, must be a very reactive compound. Condensation will begin with the collision of two molecules of triyclone in the following combination:

(1) I+I′; (2) I+I and (3) I′+I′.

Case 1 may be divided into three divisions, a, b and c.

(a) Addition starts with cyclobutane ring formation, for instance, with addition of 2′ to 1 and of 2 to 1′.

(b) Addition starts with cyclohexane ring formation, for instance, with addition of 2 to 1′ and of 6′ to 3.

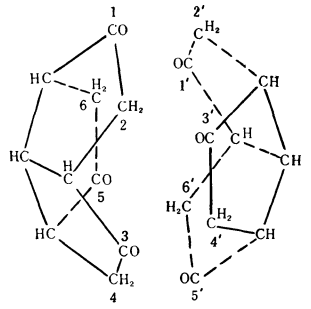
(c) Addition starsts with cyclopentane ring formation, for instance, with addtion of 2 to 3′ and of 4′ to 3.

Both divisions a and b will lead to undefinable polymerization products, while division c may proceed to a dodecahedrane derivative under consecutive additions of 2′ to 1, of 6 to 1′, of 6′ to 5 and of 4 to 5′.

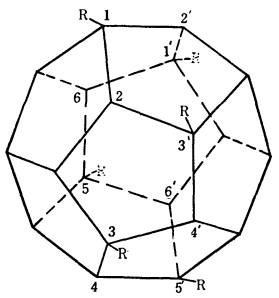
In the presence of an appropriate agent (for instance sodium ethoxide, etc.), I and I′ will be able to add to each other to give a hexahydroxydodecahedrane (II, R=OH) through the narrow reaction route, cace 1, division c, the yield being consequently expected to be small. As soon as the hexahydroxydodecahedrane is formed, it may probably suffer spontaneous dehydration, thus affording dodecahedrahexaene (IV). It is to be noted, that formula IV denotes only a limiting structure, because the conjugated hexaene ring V contained in formula IV will resonate with another limiting structure VA and that the double linkings in the molecule will not be restricted within the one hexaene ring, V↔VA, but will be distributed equally all over the whole system of the twenty carbon atoms. Consequently the dodecahedrahexaene is expected to be a rather stable compound, but its catalytic hydrogenation may afford the desired dodecahedrane (III).

On the other hand, one possibility from case

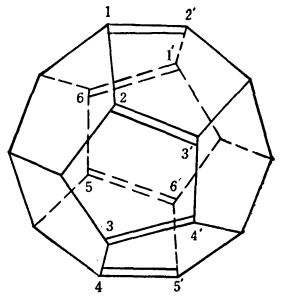
* Read before the Ninth Annual Meeting of the Chemical Society of Japan, Kyoto, April 5, 1956.



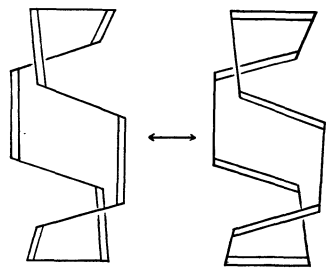
I I′



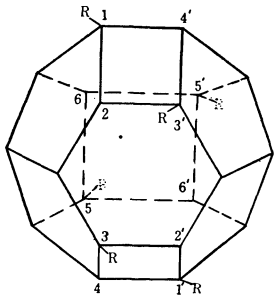
II R=OH ; $C_{20}H_{14}(OH)_6$
III R=H ; $C_{20}H_{20}$



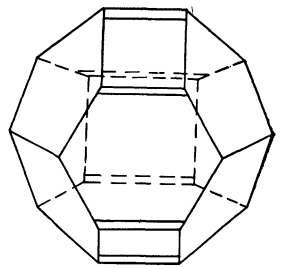
IV $C_{20}H_8$



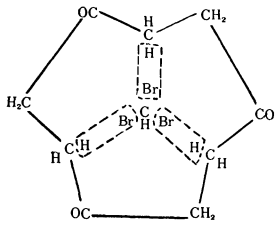
V VA



VI R=OH ; $C_{20}H_{14}(OH)_6$



VII $C_{20}H_8$



VIII

2 will similarly lead to an optically active dimerization product VI (it shall be tentatively named "hexahydroxyisododecahedrane"). The corresponding product from case 3 will be the optical isomer of VI. In both compound VI and its optical isomer not only the cyclobutane rings but also the cyclohexane rings are strongly strained, because the latter may be forced to take an almost coplanar form. Dehydration at the instant of their formation may afford the same optically inactive isododecahedrahexaene $C_{20}H_8$, as shown by formula VII with arbitrary positions of the six double bonds.

Thus *d, l*-tricyclone, I+I′, may produce dodecahedrahexaene and isododecahedrahexaene along with a large amount of undefinable polymerization products from improper collisions among the tricyclone molecules.

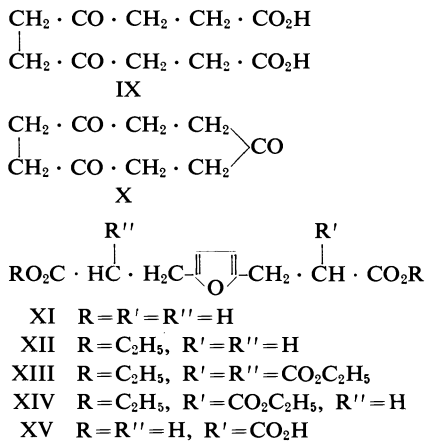
Success depends on our ingenuity in the synthesis of *d, l*-tricyclone because we even expect that the tricyclone, if once formed, may condense spontaneously to give hexaene IV, although it may have to be separated from isohexaene VII. When condensed with bromoform, the compound given in the title of this paper, or 1, 4, 7-cyclononatrione (X), may give *d, l*-tricyclone accompanied by other condensation products (see VIII). This paper communicates the synthetical efforts paid by us for obtaining cyclononatrione (X). The syntheses of the so-called "medium ring"[1] compounds which are composed of 9, 10 or 11 methylenes are known to be difficult[2]. Some simple compounds among them, however, were synthesized recently by Prelog and Stoll's method[2], and it is especially noteworthy, that these medium ring compounds possess particular

1) H. C. Brown and M. Borkowsky, *J. Am. Chem. Soc.*, **74**, 1894 (1952).
2) V. Prelog, *J. Chem. Soc.*, **1950**, 420.

internal strain (transannular effect)[3] when compared with other smaller or larger ring compounds. Apart from the question of transannular effect, there are fears lest cyclononatrione should suffer intramolecular condensation, and yet the first attempt adopted by us lay in the dry distillation of the barium salts of 4, 7-dioxodecanedioic acid (IX) according to Ruzicka's ring ketone syntheses[4]. The acid IX was obtained early by Kehrer et al.,[5] later by Asahina and Fujita[6], and then by Hachihama et al.[7], through hydrolytic furan-ring fission of δ-furfurylidenelevulinic acid.

The acid IX was mixed with barium carbonate and pyrolysis was carried out by heating under reduced pressure. Indeed, a ketone was separated as its semicarbazone (m. p. 184° (decomp.)) from the neutral part of the distillate thus obtained, but the analytical value of its nitrogen content was too small to conclude that the trissemicarbazone of the triketone X was really obtained.

The yield of this undefinable semicarbazone in the above attempt was poor, but the synthesis turned out to be successful by boiling tetraethyl 2, 5 - diethylfuran - β, β, β', β' - tetracarboxylate (XIII) or triethyl 2, 5-diethylfuran-β, β, β'-tricarboxylate (XIV) with hydrobromic acid[8]. The compounds XIII and XIV were synthesized by the following scheme.



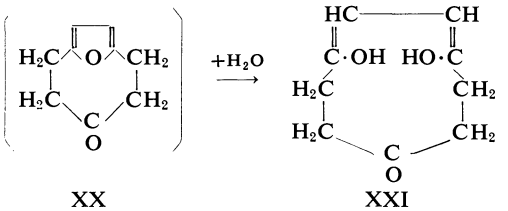
IX



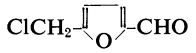
X



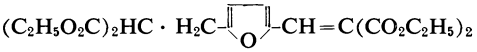
XI R=R'=R''=H
XII R=$C_2H_5$, R'=R''=H
XIII R=$C_2H_5$, R'=R''=$CO_2C_2H_5$
XIV R=$C_2H_5$, R'=$CO_2C_2H_5$, R''=H
XV R=R''=H, R'=$CO_2H$



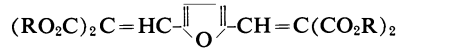
XX XXI



XVI



XVII



XVIII R=$C_2H_5$
XIX R=H

4, 7-Dioxodecanediocic acid (IX), when heated over its melting point, afforded 2, 5-diethylfuran-β, β'-dicarboxylic acid (XI)[6a),7b)], which was converted into its ethyl ester XII. Introduction of an ethoxycarbonyl group into the β-position of the latter was carried out according to Jone's procedure[9]. From the reaction product, XIV was distilled at 132~155°C/0.15~0.27 mmHg in a poor yield. Without further purification the tarry residue was hydrolyzed with alcoholic potash to give 2, 5-diethylfuran-β, β, β'-tricarboxylic acid (XV) which, was identical with the hydrolysis product of XIV. 5-(Chloromethyl)-furfural (XVI)[10], on the other hand, gave tetraethyl 2-ethyl-5-vinylfuran-β, β, β', β'-tetracarboxylate, (XVII) when treated with diethyl malonate. Catalytic reduction of XVII with platinum black afforded XIII. Neither did the latter distill out even in vacuo nor showed any sign of crystallization. It was immediately hydrolyzed with alcoholic potash, and then acidified with dilute sulfuric acid whereupon XV was obtained. These facts revealed that XIII was produced accompanied by XIV. Since it seemed noteworthy that, in the above-mentioned hydrolysis of XIII, only one ethoxycarbonyl group underwent decarboxylation simultaneously with hydrolysis, two more examples of the hydrolysis of related malonic ester derivatives were carried out. When XVII was shaken with aqueous potassium hydroxide at room temperature for a long time, and the reaction mixture was acidified, one ester group remained unchanged and one of the three hydrolyzed carboxyl groups underwent decarboxylation, thus a mono ester of a tricarboxylic

3) (a) V. Prelog and K. Schenker, *Helv. Chim. Acta*, **36**, 896, 1181 (1953); (b) A. C. Cope et al., *J. Am. Chem. Soc.*, **74**, 5885 (1952); (c) R. Robinson et al., *Chem. & Ind.*, **1953**, 944; (d) N. J. Leonard et al., *J. Am. Chem. Soc.*, **76**, 630, 3463, 5708 (1954).

4) L. Ruzicka et al., *Helv. Chim. Acta*, **9**, 249, 499 (1926); ibid., **11**, 496, 670 (1928).

5) (a) A. Ludwig and E. A. Kehrer, *Ber.*, **24**, 2776 (1891); (b) E. Hofacker and E. A. Kehrer, ibid., **28**, 917 (1895); c) E. Hofacker and E. A. Kehrer, *Ann.*, **294**, 165 (1896).

6) (a) Y. Asahina and M. Fujita, *J. Pharm. Soc. Japan*, **448**, 471 (1919); (b) Y. Asahina and M. Fujita, ibid., **470**, 331 (1931); (c) M. Fujita, ibid., **492**, 67 (1923).

7) (a) I. Hayashi, I. Kumashiro and Y. Hachihama, *J. Chem. Soc. Japan, Ind. Chem. Sec.*, (*Kogyo Kagaku Zasshi*), **57**, 299 (1954); (b) I. Hayashi and Y. Hachihama, ibid., **57**, 504 (1954).

8) L. Crombie, J. E. H. Hancok and R. P. Linstead, *J. Chem. Soc.*, **1953**, 3496.

9) V. H. Wallingford, A. H. Homeyer and D. M. Jones, *J. Am. Chem. Soc.*, **63**, 2056 (1941).

10) (a) Org. Syn., **14**, 62 (1934); (b) W. N. Haworth and W. H. H. Jones, *J. Chem. Soc.*, **1944**, 667.

acid (relative positions of its carboxyl and ester groups are ambiguous) was obtained. On the other hand, when tetraethyl 2,5-divinylfuran-$\beta, \beta, \beta', \beta'$-tetracarboxylate (XVIII)[11,12] was hydrolyzed by heating with sodium hydroxide and acidifying with sulfuric acid, 2,5-divinylfuran-$\beta, \beta, \beta', \beta'$-tetracarboxylic acid (XIX) was procured without suffering decarboxylation. Thus the malonic ester derivative (XVIII), in which the $\alpha$-carbon atoms of the malonic ester groups are connected with $\alpha$ double linkings, undergoes only hydrolysis but not decarboxylation.

Now the tricarboxylic acid ester XIV was heated with 48% hydrobromic acid for 30 min. according to Linstead's method[8]. If ring closure occurred XX should be yielded. Although the compound XX is bicyclic with two double bonds at the bridged heads it may be capable of existence, because one of the two rings is eight-membered, hence belonging to an exceptional case of Bredt's rule[2]. As a matter of fact we could isolate the triketone X (or the keto form of XXI) as its trissemicarbazone (m. p. 176~177°C (decomp.)) from the neutral part of the reaction product, thus indicating the intermediate formation of the hypothetical bicyclic compound XX. In this case, only a little amount of XI was recovered from the acidic part, but the major amount became a black polymer which was rather soluble in water. The yield of the trissemicarbazone of X based on XIV ranged from 2 to 4%. Compounds, corresponding to mono- and bis-semicarbazones, were not detected. When the crude material of XIII was used as the starting material, X was obtained with poorer yields (0.5~1%). When XIV or XII were subjected to Dieckmann's ring closure with sodium and sodium methoxide, no ring formation was observed but XI besides the starting material were yielded.

The attempt to obtain the compound X from its semicarbazone was fruitless. When the trissemicarbazone was treated with alcoholic sulfuric acid, only a tarry matter was obtained as a neutral substance, which neither distilled in high vacuum nor gave any simicarbazone when treated with semicarbazide.

## Experimental[13]

**Dry distillation of 4,7-dioxodecanedioic acid.**—A small saber flask, which was wrapped with a copper wire gauze, was attached to a well chilled trap. 4,7-Dioxodecanedioic acid (5 g., 1 mol.) and barium carbonate (4.3 g., 1 mol.) were powdered and intimately mixed and the whole was put into the flask. The flask was heated in vacuo gently at the beginning but later stronger with a free flame under constant moving. The oily distillate has an allyl-alcohol-like disagreeable smell. This pyrolysis was repeated five times and 25 g. in total of 4,7-dioxodecanedioic acid gave 4.3 g. of the distillate. The distillate was dissolved in ether, washed successively with aqeous sodium bicarbonate, 10% sodium carbonate, and 5% sodium hydroxide, and finally with water, dried and evaporated. The yield of the neutral oily substance was 220 mg. Vacuum distillation gave a colorless oil, b. p. 205~248°C/0.1~0.14 mmHg; yield, 110 mg. Its semicarbazone was obtained in an usually way. Recrystallization from chloroform gave grayish white platelets, m. p. 184°C (partly decomp.).

Found: C, 42.68; H, 7.67; N, 34.70. Calcd. for $C_{12}H_{21}N_9O_3$: C, 42.47; H, 6.24; N, 37.15%.

Acidification of the aqueous sodium bicarbonate solution with sulfuric acid gave 50 mg. of an acidic material, m. p. 141~146°. The latter (28 mg.), without further purification, was titrated with 0.098 N sodium hydroxide, 2.8 cc. being consumed. When calculated for a dibasic acid its molecular weight is 230. This value roughly corresponds to that for 2,5-diethylfuran-$\beta, \beta'$-dicarboxylic acid (XI) (m. p. 155°C with partial decomp., molecular weight 212). The sodium carbonate washing was acidified with dil. sulfuric acid and then shaken with ether. The ethereal solution, when evaporated, left an oily substance with strong phenolic smell. The sodium hydroxide washing behaved quite similarly. The phenolic oils of the two origins were therefore combined (250 mg. in total) and treated with *p*-nitrobenzoyl chloride. A small amount of crystals with m. p. 86~91°C was obtained but both its purity and quantity were insufficient for micro analysis.

**Diethyl 2,5-diethylfuran-$\beta, \beta'$-dicarboxylate (XII) and Diethyl 4,7-dioxodecanedioate**—A mixture of 2,5-diethylfuran-$\beta, \beta'$-dicarboxylic acid (XI, 45 g.), absolute alcohol (300 cc.), benzene (150 cc.) and 2 drops of conc. sulfuric acid was subjected to azeotropic distillation. When the main bulk of alcohol distilled out further azeotropic distillation was repeated twice, with the addition of alcohol (100 cc.) and benzene (30 cc.) each time. Then the solvent was removed as much as possible. The residue was dissolved in ether, and the solution was washed successively with aqueous sodium bicarbonate and water, dried and evaporated. Vacuum distillation gave 36 g. (63%) of a colorless liquid, b. p. 155~161°C/4 mmHg. Redistillation gave XII in analytical purity as a liquid of b. p. 147~148°C/3 mmHg.

Found: C, 62.62; H, 7.58. Calcd. for $C_{14}H_{20}O_5$: C, 62.67; H, 7.51%.

During the above written manipulation of vacuum distillation the distillate over 180°C/4 mmHg. solidified in the condenser, and the residue in the distilling flask also solidified. Combined yield, 8 g. (13%). Recrystallization from petroleum ether (b. p. 40~55°C) gave diethyl 4,7-dioxodecanedioate[5b] as colorless scales, m. p. 46~46.5°C. No melting point depression was observed, when mixed with an authentic specimen.

11) W. F. Cooper and W. H. Nuttall, *J. Chem. Soc.*, **101**, 1074 (1912).
12) W. F. Cooper and W. H. Nuttall, ibid., **105**, 2218 (1914).
13) All melting points are uncorrected.

Found: C, 58.77; H, 7.75. Calcd. for $C_{14}H_{22}O_6$: C, 58.73; H, 7.75%.

**Triethyl 2,5-diethylfuran-$\beta,\beta,\beta'$-tricarboxylate (XIV).**—The above compound XII (13 g., 1 mol.) and diethyl carbonate (75 g., 6 mol.) were mixed well in a 500 cc. distilling flask, and to the mixture was slowly added a sodium ethoxide solution [2.3 g. metallic sodium in absolute alcohol (70 cc.)] with stirring. The solution gradually changed to pinkish yellow in color and yielded gray precipitates. Alcohol was removed slowly and carefully in a water bath. Dry benzene (30 cc.) was then added, and the solvent was removed by distillation as much as possible first on a steam bath, finally in an oil-bath (160~170°C) in vacuo. After cooling water was added, the residue was acidified with sulfuric acid, and extracted with ether. The ethereal solution was washed with water, dried and evaporated. High vacuum distillation gave 3.3 g. (20%) of an oil which solidified on standing. B. p. 132~135°C/0.15~0.27 mmHg. Recrystallization from petroleum ether (b. p. 35~45°C) with exterior cooling in dry ice gave XIV as colorless platelets, m. p. 28~29°C.

Found: C, 60.29, H, 6.85. Calcd. for $C_{17}H_{24}O_7$: C, 56.99; H, 7.10%.

**Tetraethyl 2,5-diethylfuran-$\beta,\beta,\beta',\beta'$-tetracarboxylate (XIII).**—5-(Chloromethyl)-furfural (XVI, b. p. 137~138°C/5 mmHg, 16 g., 1 mol.) was added with cooling, to an alcoholic solution of magenesium salt of diethyl malonate [magnesium (2.5 g., 1 atom) dissolved in diethyl malonate (17 g., 1 mol.)]. The whole was kept standing at room temperature, and then refluxed for 1 hr. To this solution were added diethyl malonate (17 g., 1 mol.) and piperidine (0.5 cc.), and the whole was refluxed for 7.5 hr. The solvents were evaporated as thoroughly as possible, and then water was added to the risidue. After acidification with sulfuric acid, the reaction mixture was extracted with ether, washed with water and dried. Removal of the ether gave XVII as a dark red viscous oily substance which did not crystallize nor distil out on high vacuum distillation. The identification was carried out by way of its hydrolysis product (described later). An alcoholic solution (100 cc.) of the crude material of XVII (4.2 g., 0.1 mol.) was subjected to catalytic hydrogenation with platinum black (0.2 g.) as the catalyst, thereby 186 cc. (0°C, 760 mmHg; 0.085 mol.) of hydrogen gas being consumed during 60 min. Filtering off the catalyst and subsequent evaporation of alcohol gave a very viscous oily substance (XIII), its purification being fruitless.

**2,5-Diethylfurane-$\beta,\beta,\beta'$-tricarboxylic acid (XV).**—a) From XIV: A solution of XIV (3 g.) in 20% aqueous sodium hydroxide (50 cc.) was heated on a steam bath for 1 hr. The whole was acidified with sulfuric acid under cooling, salted out with table-salt, and extracted with ether. The ethereal layer was washed with water, dried and evaporated. The residue, after digestion with hot water (1 cc.), was allowed to stand for 2 or 3 days, thus yielding a little amount (0.3 g.) of crystals. Recrystallization from aqueous methanol afforded XV as colorless platelets, m. p. 102~105°C (decomp.).

Found: C, 48.66; H, 5.32. Calcd. for $C_{11}H_{12}O_7 \cdot H_2O$: C, 48.18; H, 5.15%.

An aqueous solution of the above-obtained substance (0.265 g.) was titrated with 0.102 N aqueous sodium hydroxide, phenolphthalein being used as an indicator.

Found: 30.2 cc. Calcd.: 28.4 cc.

b) From XIII: Hydrolysis of the crude material XIII, already described above, gave the same XV.

**Hydrolysis of Tetraethyl 2-ethyl-5-vinylfuran-$\beta,\beta,\beta',\beta'$-tetracarboxylate (XVII).**—The benzene (5 cc.) solution of the crude material of XVII (15 g.) was shaken with 20% aqueous potassium hydroxide (100 cc.) for 17 hr. at room temperature, then the whole was acidified with sulfuric acid under ice-cooling, and was extracted with ether. The ethereal layer was washed with water, dried and evaporated, thus a colorless solid matter (1 g.) was obtained. Recrystallization from wet benzene gave colorless plates, which melt at 148.5~149°C with decomposition. Elementary analysis as well as titration revealed, that this compound ($C_{13}H_{14}O_7 \cdot \frac{1}{2}H_2O$) may be derived from XVII through hydrolysis. Simultaneous decarboxylation occurred in any one of the four ethoxycarbonyl groups contained in the molecule of XVII.

Found: C, 53.40; H, 5.67. Calcd. for $C_{13}H_{14}O_7 \cdot \frac{1}{2}H_2O$: C, 53.61; H, 5.91%.

The above-mentioned substance (0.301 g.) was titrated with 0.102 N aqueons sodium hydroxide, giving the following results.

Found: 22.1 cc. Calcd.: 19.6 cc.

**2,5-Divinylfuran-$\beta,\beta,\beta',\beta'$-tetracarboxylic Acid (XIX).**—Tetraethyl 2,5-divinylfuran-$\beta,\beta,\beta',\beta'$-tetracarboxylate (XVIII) (2 g.), which had been obtained by Cooper's method[12], was dissolved in 27% aqueous sodium hydroxide (50 cc.) and the whole was heated on a steam bath for 1 hr. The solution was then acidified with sulfuric acid, salted out with table-salt, and then extracted with ether. The ethereal layer was washed with water, dried and evaporated. The residue was dissolved in hot water (1 cc.) and then kept in a vacuum desiccator. Crystals which appeared during 10 days were collected, and recrystallized from ethyl acetate and then from hot water. Orange red plates, m. p. 218°C (decomp.); yield, 0.5 g. (39%).

Found: C, 46.01; H, 3.39. Calcd. for $C_{12}H_8O_9 \cdot H_2O$: C, 45.87; H, 3.21%.

The above-mentioned substance (0.317 g.) was titrated with 0.102 N aqueous sodium hydroxide, giving the following result.

Found: 40.5 cc. Calcd.: 39.0 cc.

**Trissemicarbazone of 1,4,7-cyclononatrione (X).**—The tricarboxylic acid triester XIV (5 g.) was mixed with 48% hydrobromic acid (30 cc.) and the whole was refluxed gently for 30 min. After cooling, the dark solution which occasionally contained a black solid matter was treated with water (100 cc.) and ethyl acetate. The ethyl acetate layer was washed successively with water, aqueous sodium bicarbonate, and finally with water, and dried. Removal of the solvent gave a dark orange liquid. Semicarbazone was obtained by the usual method as a gray solid (0.1~0.2 g.), which, when recrystallized from methanol or alcohol, underwent decomposition. Recrystallization from benzene—although the solubility in it was small—gave grayish

white plates, m. p. 176~176.5°C (partly decomp.); yield, 30 mg.

Found: C, 42.08; H, 7.00; N, 36.79. Calcd. for $C_{12}H_{21}O_3N_9$: C, 42.47; H, 6.24; N 37.15%.

The aforesaid washings with aqueous sodium bicarbonate were acidified with sulfuric acid, yielding a grayish white solid. Recrystallization from water gave IX, m. p. 155~156° (partly decomp.). The black polymer, obtained in this reaction, was rather soluble in water, very soluble in alcohol or acetone, but insoluble in ether and ethyl acetate. Further investigation was given up, since the attempts of purification failed.

Since one of us (Kawai) must now give up his laboratory life, in consequence of his personal circumstance, we hope that anyone who feels interested in this field will persue the synthetical attack on the "dodecahedrane", the existence of which is theoretically possible.

We are indebted to the Ajinomoto Co. for the gifts of valuable compounds for the present research. Thanks are also due to the Science Research Institute and the Takamine Kenkyusho in the Sankyo Co. for microanlyses.

*Department of Chemistry*
*Faculty of Science*
*Tokyo University of Education*
*Koishikawa, Tokyo*

# *Bromination of Ethyl Diacetosuccinate*

By Sin'iti KAWAI and Sanae TANAKA

(Received May 26, 1959)

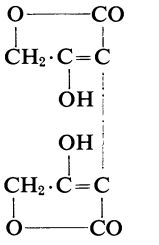
Although the synthesis of 1, 4, 7-cyclononatrione has been realized by us[1], it was isolated only as its trissemicarbazone in a poor yield. We have now chosen another course to attain this cyclic triketone, thus intending at first to obtain ethyl 1, 4, 7-cyclononatrione-2, 3, 6, 8-tetracarboxylate through the condensation of $\gamma,\gamma'$-dibromodiacetosuccinate (II) and ethyl disodioacetonedicarboxylate. This attempt, however, failed presumably owing to the false constitution (II) of the so-called $\gamma,\gamma'$-dibromodiacetosuccinate. Consequently, the bromination of ethyl diaceto succinate (I) had to be reinvestigated and the present paper presents some new aspects as an exceptional example of the bromination of $\beta$-ketoesters.

Informations concerning II can be summarized as follows: Wolff et al.[2] treated ethyl diacetosuccinate (I) with two moles of bromine and ascribed formula II to the pale yellow reaction product because of the fact that the substance in question, when heated at 150~160°C, gave bistetronic acid (V) by giving up two moles of ethyl bromide. On the other hand, Hirst et al. treated the same bromination product with hydrazine and concluded from the estimation of the nitrogen gas evolved that the bromide was a mixture of 21% of $\alpha,\alpha'$-dibromo compound III and 79% of $\gamma,\gamma'$-dibromo compound II[3], in other words, an equilibrium mixture due to an $\alpha,\gamma$-shift of bromine atoms[3-5].

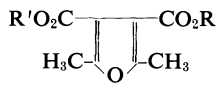
$RCH_2 \cdot CO \cdot CR' \cdot CO_2C_2H_5$

$RCH_2 \cdot CO \cdot CR' \cdot COC_2H_5$

(I) R=R'=H
(II) R=Br, R'=H
(III) R=H, R'=Br
(IV) R=R'=Br



(V)



(VI) R=H, R'=$C_2H_5$
(VII) R=R'=H
(VIII) R=R'=$CH_3$
(IX) R=R'=$C_2H_5$

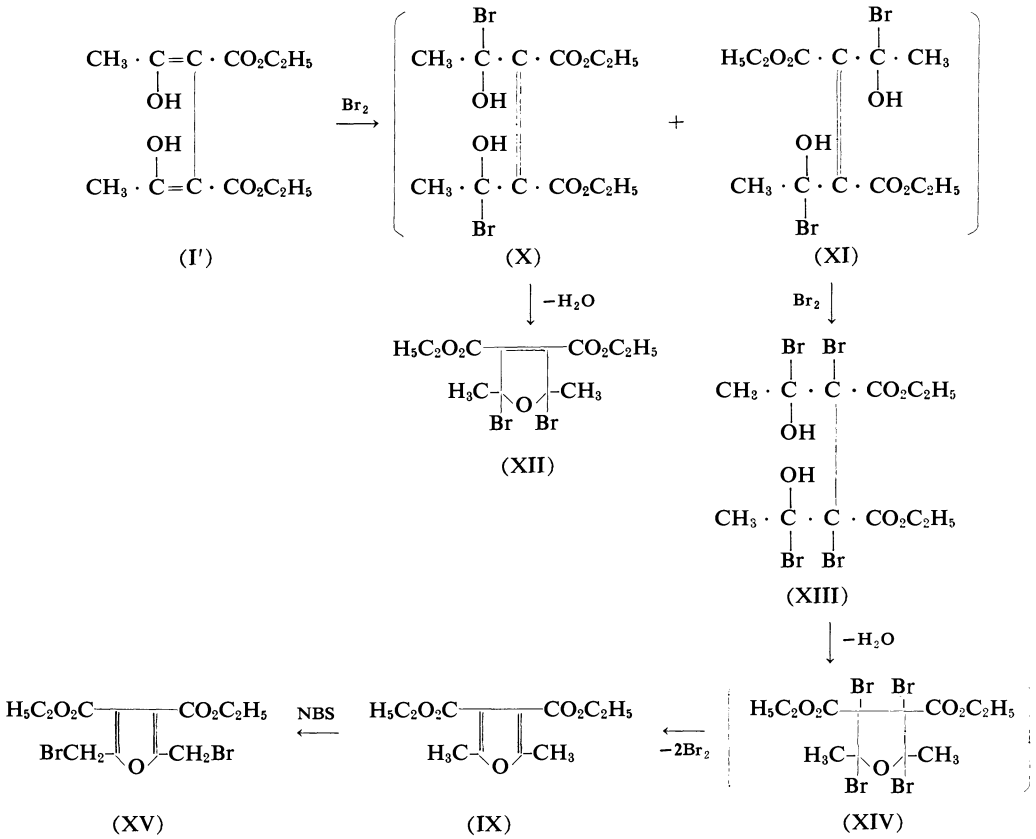
In fact, we could obtain a pale orange yellow viscous oil without hydrogen bromide evolution when we brominated compound I after Wolff's method[2], but the vacuum distillation of this

1) S. Kawai, S. Tanaka, K. Terai, M. Tezuka and T. Nishiwaki, This Bulletin, 33, 669 (1960).
2) L. Wolff and H. Junker, *Ann.*, 399, 311 (1913).
3) E. L. Hirst and A. K. Macbeth, *J. Chem. Soc.*, 121, 2169 (1922). Their conclusion was deduced from the fact that the bromine atom of the $\alpha$-bromide is so reactive that it decomposes hydrazine with the evolution of nitrogen gas quantitatively but the $\gamma$-bromide remains intact.
4) (a) C. Duisberg, *Ann.*, 213, 137 (1882). (b) A. Hantsch, *Ber.*, 27, 356, 3168 (1894). (c) M. Conrad, ibid., 29, 1024 (1896). (d) A. K. Macbeth and D. Trail, *J. Chem. Soc.*, 127, 1118 (1925). (e) M. S. Kharasch, E. Sternfeld and F. R. Mayo, *J. Am. Chem. Soc.*, 59, 1655 (1937). (f) F. Kröhnke and H. Timmler, *Ber.*, 69, 614 (1939).
5) A. Becker, *Helv. Chim. Acta*, 32, 1114, 1584 (1949).

oil gave only a little amount of a distillate at 150~170°C (bath temperature) and then met with a sudden rise of the pressure obviously due to decomposition. The distillate contained monoethyl 2, 5-dimethylfuran-3, 4-dicarboxylate (VI), and the residue included 2, 5-dimethylfuran-3, 4-dicarboxylic acid (VII) as one of its constituents.

Then, we gave up vacuum distillation, and kept the viscous oily bromination product of compound I (it shall be called "I-bromide" hereafter) in a cool place during one month. Crystals which gradually appeared in the meanwhile were collected at appropriate intervals and at least four new compounds, i.e. I-tetrabromide (XIII), monoester VI, dicarboxylic acid VII and the dibromide of diester IX, were isolated.

The I-bromide gave neither any indole derivative when heated with a mixture of aniline and aniline hydrobromide[6], nor a *p*-nitrophenylpyridazine derivative when treated with *p*-nitrophenylhydrazine[5]. These results show the absence of a $\gamma,\gamma'$-dibromide such as II or IV. Since the I-bromide, when heated with resorcinol or with $\alpha$-naphthol, did not give any bromophenol or bromonaphthol, the bromine atom is not so "positive"[7]. Thus the presence of $\alpha,\alpha'$-dibromide derivatives such as III or IV is excluded. The I-bromide, when heated with absolute methanol, gave dimethyl 2, 5-dimethylfuran-3, 4-dicarboxylate (VIII), and a desmotropic form[8] of diacetosuccinic acid (I, H instead of $C_2H_5$) when heated with sodium methoxide. When treated with concentrated sulfuric acid[5,9] the I-bromide did not show any sign of a ketonic hydrolysis but gave the free acid VII. The I-bromide gave no definite product when heated with aqueous potassium carbonate[10]. On the other hand, compound I gave diethyl 2, 5-dimethylfurandicarboxylate (IX) on treatment with concentrated sulfuric acid and acetonylacetone on heating with aqueous potassium carbonate, both in good yields. When hydrogen bromide gas was passed through a benzene solution of compound I, only a very little




6) J. R. Catch and E. R. H. Jones, *J. Chem. Soc.*, **1948**. 272, 276.
7) R. Altschul and P. B. Bartlett, *J. Org. Chem.*, **5**, 623 (1942).
8) Thirteen isomeric forms are theoretically possible for diacetosuccinic acid, but only three are known [L. Knorr, *Ber.*, **22**, 170 (1889); *Ann.*, **293**, 103 (1896)]. The compound obtained above does not agree in the melting point with any of the three.
9) P. Ruggli, A. von Wartburg and H. Erlenmeyer, *Helv. Chim. Acta*, **30**, 348 (1947).
10) L. Knorr, *Ber.*, 33, 1219 (1900).

amount of VII was obtained and the major part of compound I remained unchanged. Therefore, the two compounds, VI and VII, which were isolated from the I-bromide, should never have been derived from the starting material (I) through the catalytic action of the little amount of hydrogen bromide generated during the bromination of compound I.

As has already been mentioned, there is no positive proof for the existence cf $\alpha,\alpha'$-dibromide III and $\gamma,\gamma'$-dibromide II. Hence, the elucidation of the constitution of the I-tetrabromide, found as one constituent of I-bromide, appeared difficult. We are now forced to assume that the dienediol form I′ of compound I gave a mixture of *cis*-dibromide X and *trans*-dibromide XI as the result of 1,4-addition of bromine, and the former (X) passed over to a dihydrofuran XII while the latter (XI) took up another mole of bromine to produce tetrabromide XIII. Then, tetrabromide XIII underwent dehydration catalyzed by hydrogen bromide, thus yielding a tetrabromide XIV, which, as the result of spontaneous debromination, gave furan derivative IX. Compound IX suffered partial and total hydrolysis catalyzed by hydrogen bromide, yielding compounds VI and VII. The precise structure of dibromide XII is further shown by the fact that it is quite different from dibromide XV obtained from the dimethylfuran derivative IX through *N*-bromosuccinimide. Thus, the I-tetrabromide in question may perhaps be represented by formula XIII, because this compound is so unstable that it decomposes (dehydration?) when merely heated or treated with water-miscible solvents.

The proof that the main course involved in this reaction belongs to bromine addition but not bromine substitution can be found in the following facts: (i) during the bromination of compound I evolution of hydrogen bromide was scarcely recognized: (ii) on the other hand, hydrogen bromide evolution was observed during the manipulation of recrystallization of crystals gathered from the I-bromide.

Both Wolff[1] and Hirst[2] observed that bromine substitution took place when ethyl diacetosuccinate was treated with bromine, which does not agree with our experiments. Our observation seems more reasonable, because the more stable conjugated dienediol-form I′ may predominate over the unconjugated diketo-form I in ethyl diacetosuccinate, and the reaction may start with the 1,4- and further 2,3-addition of bromine to the conjugated system but not with bromine substitution.

## Experimental[11]

**Bromination of Ethyl Diacetosuccinate.**—To a solution of ethyl diacetosuccinate[12] (I) (140 g., 1 mol.) in chloroform (300 cc.) bromine (170 g., 1.95 mol.) was added dropwise in 2 hr. with ice-cooling and stirring, and the mixture was stirred for 2 hr. at room temperature. Hydrogen bromide was scarcely evolved, or estimated as only 0.53% of the value calculated for bromine substitution. The chloroform layer was washed successively with water, with 5% sodium thiosulfate and finally with water, dried and evaporated in vacuo on a water bath (below 38°C), giving "I-bromide" as a pale reddish orange substance containing a small amount of colorless crystals. Yield, 290 g.

**I-Tetrabromide (XIII) of Ethyl Diacetosuccinate.**—The small amount of colorless crystals, obtained above, were separated from the oily substance, washed with a small amount of petroleum ether (b. p. 40~50°C), dried and recrystallized from anhydrous benzene to yield the I-tetrabromide as colorless plates, m. p. 189°C (decomp.). Yield, 1.2g.

Found: C, 25.15; H, 2.59; Br, 55.83. Calcd. for $C_{12}H_{18}O_6Br_4$: C, 24.94; H, 3.14; Br, 55.31%.

When the above oily substance was left to stand, further crops of XIII were obtained during 2 or 3 days. The total yield was 2.7 g. On long heating in an attempt to recrystallize from aqueous benzene or anhydrous benzene, XIII changed to an indefinite substance with evolution of hydrogen bromide. On the other hand, when a water-miscible solvent such as methanol, alcohol and acetone, were used, XIII changed to VII.

**Separation of VI, VII and XII from "I-Bromide".**—When XIII was separated from the "I-bromide", and the oily substance was left to stand, crystals gradually separated out during 5~30 days. Addition of a small amount of ether promoted crystallization. Since the colection of the crystals by filtration was quite difficult because of the viscousness of the liquid, the whole was placed on a porcelain plate in spite of the loss of the yield or diluted with ether and then filtered. The solid thus obtained showed various melting points such as m. p. 60~90°C, m. p. 110~115°C (decomp.) and m. p. 130~140°C (partly decomp.), and was a mixture of VI, VII, XII, XIII and I as described below. When the oily substance was kept on standing for more than 3 months, hydrogen bromide and bromine were evolved gradually, yielding a solid which was mainly VII.

The solid obtained above was dissolved in anhydrous benzene, and then an insoluble substance was filtered off. The most soluble part was left to stand, a small amount of crystals being formed in the meanwhile. Filtration and recrystallization from petroleum ether (b. p. 40~50°C) gave VI[13] as colorless long plates, m. p. 83~84°C.

Found: C, 56.60; H, 5.83. Calcd. for $C_{10}H_{12}O_5$: C, 56.60; H, 5.70%.

The filtrate from VI was evaporated, yielding another crystalline substance. Recrystallization from petroleum ether (with active carbon) gave

11) All melting points are uncorrected.

12) (a) E. Fischer, "Anleitung zur Darstellung organischer Prärparate", Berlin, Friedrich Vieweg u. Sonn. (1922), p. 48. (b) L. Knorr and F. Haber, *Ber.*, 27, 1155 (1894). (c) L. Knorr, *Ann.*, 306, 332 (1899).

13) (a) G. H. U. Harrow, *Ann.*, 201, 152 (1880). (b) L. Knorr, *Ber.*, 17, 2864 (1884); ibid., 22, 153 (1889).

unchanged I as colorless scales, m. p. 92~93°C, which was identified by mixed melting point determination.

Found: C, 55.86; H, 6.98. Calcd. for $C_{12}H_{18}O_6$: C, 55.80; H, 7.03%.

When the crystals, separated from the part soluble in benzene, were recrystallized from anhydrous benzene, XII was obtained as colorless long pillars, m. p. 92~96°C (decomp.). It melted at 92~96°C with decomposition to a substance which melted at 128~130°C and gave the positive Beilstein halogen test.

Found: C, 36.20; H, 3.59. Calcd. for $C_{12}H_{16}O_5Br_2$: C, 36.03; H, 4.03%.

From the part more soluble in benzene than XII, a small amount of XIII, previously mentioned, was obtained.

From the part less soluble than XII and from the first insoluble part, a crude material of VII was obtained. During recrystallization XII partly changed to VII, and use of recovered benzene promoted the change. The latter was collected and recrystallized from aqueous methanol or water, yielding VII as colorless pillars of m. p. 234~236°C (partly decomp.).

Found: C, 49.70; H, 4.77. Calcd. for $C_8H_8O_5 \cdot \frac{1}{2}H_2O$: C, 49.74; H, 4.70%.

The yields of VI, I, XII and VII were 2.2 g., 0.8 g., 1.7 g. and 28.5 g., respectively.

**Vacuum Distillation of "I-Bromide".** — After removal of XIII, "I-bromide" (50 cc.) was heated under the reduced pressure of 5~6 mmHg. The pressure dropped to 30~40 mmHg at 150~170°C (bath-temperature) and again rose to 6~7 mmHg after 10 min. A pale orangish oily substance distilled out at ca. 200°C (bath-temperature). When the distillate was triturated with a small amount of ether, it solidified. Recrystallization from aqueous methanol gave VI as colorless long pillars of m. p. 83~84°C, b. p. 100~105°C/0.25~0.3 mmHg. Yield, 2.1 g. It was identified by a mixed melting pont with an authentic sample.

The residue was a very viscous reddish black syrup containing a small amount of a solid and had a distinct smell of hydrogen bromide and bromine. To the residue a small amount of ether was added, and the whole was kept standing in a stoppered flask for 2 or 3 days, yielding crystals gradually. These were collected on a filter and recrystallized from aqueous methanol (1 : 1) to give VII as colorless pillars, m. p. 234~236°C (partly decomp.). Yield, 3.8 g.

**Hydrolysis of VI.**—VI (1.2 g.) was dissolved in alcohol (60 cc.), and 50% sulfuric acid (5 cc.) was added, and the whole was refluxed for 4 hr. After removal of the alcohol, water was added. The precipitate, which formed in the meanwhile, was recrystallized from water, giving VII, m. p. 234~235°C (partly decomp.).

**Reaction of "I-Bromide" with Methanol.**—1) The oily "I-bromide" (2 g.), freed from all the crystals VI, VII, XII and XIII, was mixed with absolute methanol, and the whole was refluxed on a steam bath for 5 hr. After cooling a small amount of crystals were yielded. Recrystallization from water gave VII. The methanolic filtrate from VII was concentrated, giving first a small amount of a colorless substance of m. p. 100~110°C. Recrystallization from petroleum benzine (b. p. 60~75°C) gave colorless long pillars of m. p. 118~119°C, the amount being too little to be analyzed. From the last portion of the methanolic filtrate, colorless long plates of m. p. 45~46°C were obtained. Recrystallization from petroleum ether (b. p. 40~50°C) gave VIII[14] as colorless tetragonal plates, m. p. 58~61°C.

Found: C, 56.53; H, 5.70. Calcd. for $C_{10}H_{12}O_5$: C, 56.60; H, 5.70%.

2) The mixture of the oily "I-bromide" (2 g.), freed from all the crystals, with sodium methoxide (sodium 0.2 g., absolute methanol 50 cc.), was refluxed on a steam bath for 2 hr., and after the methanol was removed as much as possible and water was added, it was acidified with sulfuric acid to yield a white residue. Recrystallization from benzene (with active charcoal) gave a compound of m. p. 120~121°C (partly decomp.) as pale yellow plates, which were analyzed as diacetosuccinic acid.

Found: C, 47.59; H, 4.94. Calcd. for $C_8H_{10}O_6$: C, 47.53; H, 4.99%.

**Hydrolysis of "I-Bromide".**—1) The oily "I-bromide" (1 g.) freed from all the crystals was treated with concentrated sulfuric acid (5 cc.) and the whole was heated on a steam bath for 1 hr. Addition of water yielded grayish white precipitates, which, on recrystallization from benzene and then water, gave VII.

2) The oily "I-bromide" (6 g.) freed from all the crystals was dissolved in aqueous potassium carbonate (protassium carbonate 7 g., water 25 cc.) and the whole was boiled for 2 hr. After addition of water, the whole was acidified with sulfuric acid, and extracted with ether. The ethereal solution was washed with water, dried and evaporated, leaving a grayish white solid (0.2 g.). Recrystallization from ethylene chloride gave a material of m. p. 176~180°C (decomp.), which was not analyzed because of the impurity.

**Cyclization of I by Hydrogen Bromide.**—Through a cooled solution of I (12 g.) in anhydrous benzene (150 cc.) dried hydrogen bromide was passed for 30 min. The whole was placed in a stoppered flask, and kept standing overnight, yielding crystals. These were recrystallized from aqueous methanol to give 0.7g. of VII. When the benzene filtrate was concentrated, 8.5 g. of I was recovered and a small amount of colorless needles of m. p. 105~112°C were obtained, which could not be further investigated because of the scarcity of the sample.

**Ethyl 1-*p*-Nitrophenyl-3, 6-dimethyl-1, 4-dihydropyridazine-4, 5-dicarboxylate (Anhydro-*p*-nitrophenylhydrazone of I).**—A solution of I (2 g.) and *p*-nitrophenylhydrazine (1 g.) in 70% acetic acid, was kept standing for 1 hr. at room temperature. The crystals which were yielded were recrystallized from ethyl acetate, giving pale yellow long pillars, m. p. 122~123°C.

Found: N, 11.57. Calcd. for $C_{18}H_{21}O_6N_3$: N, 11.20%.

14) I. M. Heilbron, E. R. H. Jones, P. Smith and B. C. L. Weedon, *J. Chem. Soc.*, **1946**, 57.

**Ethyl 2, 5-Di(bromomethyl)furan-3, 4-dicarboxylate (XV).**—To a mixture of IX (9.6 g., 1 mol.), *N*-bromosuccinimide (14.3 g., 2 mol.) and carbon tetrachloride (100 cc.), benzoyl peroxide (ca. 0.1 g.) was added. The whole was refluxed gently on a steam bath for 5 hr and allowed to cool. Succinimide which separated was filtered off. The filtrate was concentrated, and the residue was distilled in vacuo, giving XV as a pale yellow, very viscous syrup of b. p. 170~180°C/3 mmHg. Yield, 14.5 g. (91%). When kept standing in an icebox, it solidified, but melted partly at room temperature. The solidified substance was recrystallized from petroleum ether (b. p. 40~50°C) (the solution was kept standing in an icebox to crystallize), giving XV as colorless long plates, m. p. 52~52.5°C.

Found : C, 36.13; H, 3.62. Calcd. for $C_{12}H_{14}O_5Br_2$: C, 36.19 ; H, 3.52%.

*Department of Chemistry*
*Faculty of Science*
*Tokyo University of Education*
*Koishikawa, Tokyo*

# *Near Ultraviolet Absorption Spectra of Acrolein and Crotonaldehyde*

By Kōzō Inuzuka

(Received August 24, 1959)

Near ultraviolet absorption spectra of a number of aldehydes and ketones have been studied by many workers[1]. It is well known that these compounds have a weak absorption in 33300~25000 $cm^{-1}$ region, and that this absorption arises from the transition of an electron from a non-bonding orbital to an excited orbital. We have also studied recently the effects of solvents on the near ultraviolet absorption spectra of some conjugated aldehydes and ketones[2]. In order to study the electronic properties of the carbonyl group in these molecules, we treated in this paper acrolein and crotonaldehyde which have conjugated systems. E. Eastwood and C. P. Snow[3] carried out a vibrational analysis for the n-$\pi^*$ absorption spectrum of acrolein. The purpose of the present paper is to analyze the n-$\pi^*$ absorption bands of acrorlein and crotonaldehyde, and also to estimate the amount of elongation of the C=O bond of these molecules during the n-$\pi^*$ transition from the relative intensities of the C=O progression bands using the method of J. A. Howe and J. H. Goldstein[4].

## Experimental

Acrolein and crotonaldehyde (Tokyo Kasei G. R. grade) were distilled before the experiment.

Carbon tetrachloride used as a solvent was boiled with dilute alkali several times. The carbon disulfide free solvent thus obtained was then washed several times with water, dried over phosphorus pentoxide, and distilled. Absorption spectra were measured by a Hitachi E. P. S. double beam automatic recording spectrometer. The absorption cell of 10 or of 40 cm. was used, depending upon the vapor pressure of the sample. All the absorption measurements were made at room temperature. Solution spectra were obtained with 1 cm. cell. For the purpose of checking that the transition in this region is of the n-$\pi^*$ type, the effects of solvent on the absorption spectra were also studied by changing the solvent from carbon tetrachloride to ethanol.

## Result and Discussion

Both of the compounds have weak absorption in 33300~25000 $cm^{-1}$ region in solution and vapor states. In carbon tetrachloride solution each of the absorption spectra exhibits four distinct shoulders. On addition of ethanol

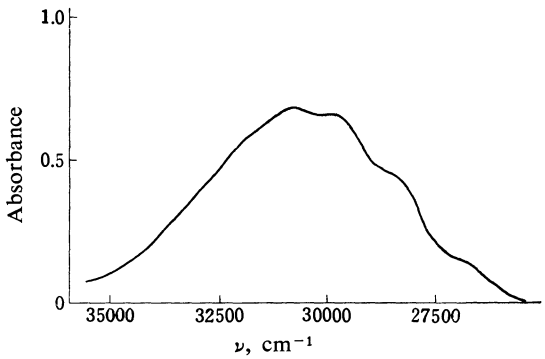



Fig. 1. Spectrum of acrolein in carbon tetrachloride solution.

1) For example, H. L. McMurry, *J. Chem. Phys.*, **9**, 241 (1941); J. W. Sidman, *Chem. Revs.*, **58**, 689 (1958).
2) M. Ito, S. Inuzuka and S. Imanishi, *J. Am. Chem. Soc.* 82, 1317 (1960).
3) E. Eastwood and C. P. Snow, *Proc. Roy. Soc.*, **149A**, 446 (1935).
4) J. A. Howe and J. H. Goldstein, *J. Am. Chem. Soc.*, **80**, 4846 (1958).

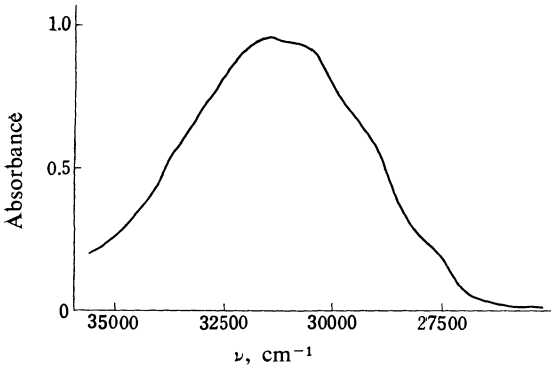



Fig. 2. Spectrum of crotonaldehyde in carbon tetrachloride solution.

to carbon tetrachloride solution the absorption shifts towards shorter wavelengths, and in pure ethanol solution the acrolein maximum shifts to the shorter wavelengths, by 400 $cm^{-1}$ compared with the pure carbon tetrachloride solution. In the case of crotonaldehyde also the blue-shift of 900 $cm^{-1}$ was observed. These blue-shifts indicate the n-$\pi^*$ nature of the electronic transition.

In the vibrational analysis of the vapor spectrum of acrolein we have taken the strong band at 25873 $cm^{-1}$ as the 0—0 band, which is accompanied on its lower frequency side by three very weak bands at 24647, 24912 and 25555 $cm^{-1}$. From the higher frequency region of the 0—0 band, we may pick out three vibrational frequencies of 1427, 1271 and 498 $cm^{-1}$ all of which forming long progressions. The progression formed by 1271 $cm^{-1}$ frequency is the most prominent feature in the spectrum. For crotonaldehyde, the 0—0 band taken at 26518 $cm^{-1}$ which is accompained by no prominent band on its lower frequency side. On the high freguency side there are three progressions with the separations of 1360, 1237 and 450 $cm^{-1}$, respectively, the one with the 1237 $cm^{-1}$ separation being the strongest. For acrolein, E. Eastwood and C. P. Snow[3] found two fundamental vibrational frequencies 1260 and 500 $cm^{-1}$ of the excited state. They assigned the former to the C=O stretching vibration and the latter to an oscillation of the methylene group about the C=C double bond. As it is well known that in ketone and aldehyde n-$\pi^*$ spectra the C=O stretching vibration generally gives rise to the main progression, the frequencies 1271 $cm^{-1}$ in acrolein and 1237 $cm^{-1}$ in crotonaldehyde may be assigned to the C=O stretching vibration in their excited states. Futhermore, since vibrational modes involving the motion of hydrogen generally do not appear prominently in the electronic spectra it seems to be more reasonable that the 498 $cm^{-1}$ in acrolein and the 450 $cm^{-1}$ in crotonaldehyde should be assigned to the skeletal bending modes instead of the assignment otherwise made by E. Eastwood and C. P. Snow. The frequencies 1427 $cm^{-1}$ of acrolein and 1360 $cm^{-1}$ of crotonaldehyde may be assigned to the C=C stretching vibration in the excited state, corresponding to the ground state vibration frequencies 1618[5] $cm^{-1}$ and 1642[6] $cm^{-1}$, respectively, observed in Raman spectra. The blue-shift by 645 $cm^{-1}$ of the 0–0 band of crotonaldehyde relative to that of acrolein is in accordance with the fact that the methyl substitution generally leads to the blue-shift of the n-$\pi^*$ absorption[7,8].

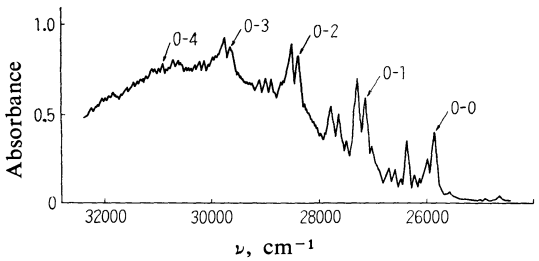



Fig. 3. Absorption spectrum of acrolein vapor.

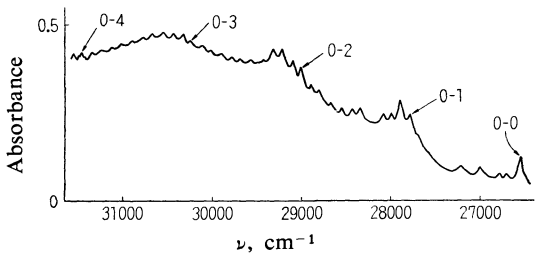



Fig. 4. Absorption spectrum of crotonaldehyde vapor.

In order to check the above assignments, the relative intensities of the member bands in the main C=O progression were calculated with the method used by Hose and Goldstein[4] and were compared with the observed intensities*. Figs. 3 and 4 show the vapor spectra of acrolein and crotonanldehyde. The procedure of this calculation was detailed by D. P. Craig[9]. The C=O group in the molecle was assumed to be a simple diatomic moleclue harmonically bound. The intensity of the 0-$n$ band is given by

5) P. Lambert and J. Lecomtte, *Compt. rend.* **208**, 740 (1939).

6) K. W. F. Kohlrausch und A. Pongratz, *Z. physik. Chem.*. **B27**, 176 (1934).

* The intensity of a band was assumed here to be proportional to the observed optical density value. The intensity contribution from satellite bands was assumed to be the same for all the bonds forming the C=O progression.

7) H. Baba, *J. Chem. Soc. Japan, Pure Chem. Sec.* (*Nippon Kagaku Zasshi*), **72**, 341 (1951).

8) L. E. Orgel, *J. Chem. Soc.*, 121 (1955).

9) D. P. Craig, ibid., 2146 (1950).

$$I_n = (\omega_n/\omega_0)\left[\int \psi_0(\xi_1)\psi_n(\xi_2)\,d\tau\right]^2$$

where $\psi_i(\xi_j)$ is the $i$-th simple harmonic oscillator wave function of the $j$-th electronic state, and $\omega_n$ is a frequency of the $n$-th band in the progression. Craig has given a formula for evaluating the overlap integral as a function of the separation of the origins of coordinate $q$ of the two reduced oscillators in the electronic states 1 and 2, and also as a function of the ratio of frequencies $\rho = \nu_1/\nu_2$ where $\nu_1$ and $\nu_2$ are the C=O stretching frequencies in the ground and excited states.

The results of calculation for acrolein and crotonaldehyde are shown in Tables I and II. As seen in these tables, calculated intensities for acrolein with $q = 0.11$ Å are in fairly good

Table I. Relative intensities of the C=O progression band in acrolein

| Band | $q=$ 0.10 Å | $q=$ 0.11 Å | $q=$ 0.12 Å | Obsd. intensity |
|---|---|---|---|---|
| 0—0 | 1.00 | 1.00 | 1.00 | 1.00 |
| 0—1 | 1.81 | 1.99 | 2.60 | 1.48 |
| 0—2 | 1.90 | 2.27 | 3.76 | 2.07 |
| 0—3 | 1.50 | 1.93 | 3.94 | 2.20 |
| 0—4 | 0.99 | 1.36 | 3.40 | 1.95 |

Table II. Relative intensities of the C=O progression bands in crotonaldehyde

| Band | $q=$ 0.11 Å | $q=$ 0.115 Å | $q=$ 0.12 Å | Obsd. intensity |
|---|---|---|---|---|
| 0—0 | 1.00 | 1.00 | 1.00 | 1.00 |
| 0—1 | 2.17 | 2.37 | 2.62 | 2.00 |
| 0—2 | 2.74 | 3.23 | 3.83 | 3.04 |
| 0—3 | 2.59 | 3.28 | 4.10 | 3.63 |
| 0—4 | 2.04 | 2.74 | 3.65 | 3.35 |

agreement with the observed values listed in the last column of the tables. Similarly, for crotonaldehyde the calculated values with $q = 0.115$ Å are in reasonably good agreement with the observation.

On the other hand, an empirical relation between the C=O bond length and its vibrational frequency has been given by Layton et al.[10]. From using this empirical relation the $q$ values were estimated, and were compared with our calculated $q$ values given in Table III. The agreement is quite satisfactory. From the above results we may conclude that the C=O bond distances of acrolein and crotonaldehyde increase by about 0.1 Å during n-$\pi^*$ transition. In this calculation $q$ values may be correct within 0.01 Å.

Table III.

| | Acrolein | Crotonaldehyde |
|---|---|---|
| $q$(Layton) | 0.11 Å | 0.11 Å |
| $q$(calc.) | 0.11 Å | 0.115 Å |

## Summary

The positions vibrational structures and blue-shifts of absorption spectra of acrolein and crotonaldehyde in 33300~25000 $cm^{-1}$ region suggest that the transition is of the n-$\pi^*$ type. They are similar in vibrational structure except that the crotonaldehyde absorption is shifted towards higher frequencies with respect to that of acrolein. The vapor frequency of the 0-0 band is 25873 $cm^{-1}$ for acrolein, smaller by 654 $cm^{-1}$ than that of crotonaldehyde. The acrolein absorption has 1427, 1271 and 498 $cm^{-1}$ progressions, which are assigned to the C=C stretching frequency, the C=O stretching frequency and skeletal bending frequency in the excited state, respectively. For the crotonaldehyde there are 1360, 1237 and 450 $cm^{-1}$ progressions, which are assigned to the C=C stretching frequency, the C=O stretching and the skeletal bending vibration in the excited state, respectively According to our calculation, the elongation $q$ in the carbonyl bond length during the n-$\pi^*$ transition, is estimated to be approximately 0.1 Å.

The auther wishes to express his sincere thanks to Professor S. Imanishi and Dr. Y. Kanda for their encouragement throughout this work. He is also indebted to Dr. M. Ito and Mr. A. Sadō for their helpful advice and discussions.

*Department of Chemistry,*
*Faculty of Science*
*Kyushu University*
*Hakozaki, Fukuoka*

10) E. M. Layton, J. R. D. Kross and V. A. Fassel, *J. Chem. Phys.*, **25**, 135 (1956).

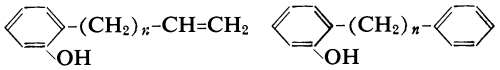
# *Intramolecular Interaction between Hydroxyl Group and π-Electrons. VII*[1]. *Limitation of the Interaction by Chain Length in 2-(ω-Alkenyl)-phenols and 2-(ω-Phenylalkyl)-phenols*

By Michinori Ōki and Hiizu Iwamura

(Received November 16, 1959)

In the previous papers of this series[1,2,3], the authors treated the limitation of the intramolecular interaction between the alcoholic hydroxyl group and π-electrons by the chain length in ω-hydroxy-1-alkenes and ω-phenylalkanols and it has been found that, in the former series, the interaction is observed up to 3-buten-1-ol and in the latter up to 2-phenylethanol[4]. The shift of wave numbers of the O–H stretching vibration ($\nu_{O-H}$) from the free $\nu_{O-H}$ to the interacting one, and the absolute intensities of these bands in the infrared absorption were discussed with respect to the configuration, the energy and the entropy of the interaction.

As the phenolic hydroxyl group has a stronger proton donating power in the hydrogen bonding than the alcoholic one, it is naturally expected that the replacement of the alcoholic hydroxyl group in the compounds already studied by the phenolic one will release the limitation of the interaction to compounds with chains longer by one or more carbon atoms and thus some elucidation of the nature of the interaction may be obtained. In this regard, the present authors have extended the study to the two series of 2-(ω-alkenyl)-phenols (I) and 2-(ω-phenylalkyl)-phenols (II), thus completing all the types of the interaction between the alcoholic and phenolic hydroxyl groups and olefinic and benzenoid π-electrons.



I II

It has been reported that 2-allylphenol, a compound of series I, shows two $\nu_{O-H}$ maxima in the 3 μ region of the infrared absorption spectra[5]. The data for 2-hydroxybiphenyl, the lowest member of the second series II, are also available[6]. These two compounds were re-examined together with others, a high precision grating infrared spectrometer[2] being used.

## Experimental

**Measurement and Calculation.**—They were performed similarly as described previously[2]. For the decision of the disappearance of the weaker bands, the measurements were carried out with a quartz cell of 5 cm. optical length without alteration in concentration, which enables to detect a very weak absorption, even if the extinction coefficients were as small as one.

**Materials.**—The phenols used for the measurement are all known, except 2-(3-butenyl)-phenol, and were prepared in the following ways. The physical constants, after fractional distillation under diminished pressure, well agreed with those in the literature.

*2-Vinylphenol (I, n=0).*—*o*-Coumaric acid was decarboxylated by heating under diminished pressure (ca. 20 mmHg)[7]. B. p. 112°C/17 mmHg, $n_D^{27}$ 1.5775 (lit.[7], b. p. 93~94°C/12 mmHg, $n_D^{25.7}$ 1.577).

*2-Allylphenol (I, n=1).*—Allyl phenyl ether was submitted to Claisen rearrangement[8]. B. p. 109°C/23 mmHg, $n_D^{21}$ 1.5451 (lit[8]., 99°C/12 mmHg, $n_D^{20}$ 1.5453).

*2-(3-Butenyl)-phenol (I. n=2).*—A Grignard reagent was prepared from 31.3 g. (0.2 mol.) of *o*-methoxybenzyl chloride[9], 6 g. (0.25 atom) of magnesium and 150 ml. of ether and the supernatant solution was decanted into a dry flask. To the Grignard solution 24.2 g. (0.2 mol.) of allyl bromide in 50 ml. of ether was added and the mixture was refluxed for two hours to complete the reaction. The mixture was decomposed with aqueous ammonium chloride and the ether layer was dried over potassium carbonate. Fractional distillation gave 19 g. (59% of the theoretical) of 4-(2-methoxyphenyl)-1-butene, b. p. 120~123°C/18 mmHg. To a solution of methylmagnesium iodide prepared from 71 g. (0.5 mol.) of methyl iodide, 12.2 g. (0.5 atom) of magnesium and 200 ml. of ether was added 19 g. of 4-(2-methoxyphenyl)-1-butene. Ether was evaporated and the temperature was gradually raised up to 160° on an oil bath. During this time the mixture became pasty and evolution of ethane was observed. Heating was continued for two hours,

1) Part VI: M. Ōki and H. Iwamura, This Bulletin, **32**, 1135 (1959).
2) Part II: idem, ibid., **32**, 567 (1959).
3) Part V: idem, ibid., **32**, 955 (1959).
4) In γ-arylpropanols with such electron donating ring substituents as amino, methoxyl and methyl groups, the interaction was found to be operative, but in γ-phenylpropanol itself it was indecisive.
5) A. W. Baker and A. T. Shulgin, *J. Am. Chem. Soc.*, **80**, 5358 (1958): R. West, ibid., **81**, 1614 (1959).
6) O. R. Wulf, ibid., **58**, 2290 (1936); V. von Keussler and G, Rossmy, *Z. Elektrochem.*, **60**, 136 (1956).
7) K. Fries and G. Fickewirth, *Ber.*, **41**, 367 (1908).
8) D. S. Tarbell, Org. Reactions, Vol. II, p. 27 (1944), John Wiley & Sons, New York.
9) M. Simonetta and G. Favini, *J. Chem. Soc.*, **1954**, 1840.

until the evolution of the gas practically ended. The mixture was dissolved in dilute acetic acid and extracted with ether. The ether extracts were extracted with aqueous sodium hydroxide. The aqueous layer was shaken with ether, treated with Norite, and then acidified with dilute hydrochloric acid. Ether extraction followed by fractional distillation gave 12.5 g. of the desired phenol (72% of the theoretical), b.p., 78°C/2.5 mmHg, $n_D^{24}$ 1.5347. *Anal.* Found: C, 80.67; H, 8.31%. Calcd. for $C_{10}H_{12}O$: C, 81.04; H, 8.16%.

*2-Hydroxybiphenyl (II, n=0).* — A commercial product was recrystallized from petroleum ether (b. p. 50~70°C). M. p., 59.0°C (lit[10]., 59°C).

*2-Benzylphenol (II, n=1).* — Sodium phenolate was C-benzylated with benzyl chloride in toluene according to the method described by L. Claisen and his co-workers[11]. They obtained dimorph, melting at 21°C and 52°C respectively, while the species used in the present work melted at 21C°.

*2-Phenethylphenol (II, n=2).* — 2-Hydroxystilbene[12] was quantitatively hydrogenated over Raney Ni catalyst. The substance, after recrystallization from benzene, melts at 81°C (lit.,[13] 81°C).

*2-(3-Phenylpropyl)-phenol (II, n=3).* — To a Grignard reagent prepared from 37 g. (0.2 mol.) of phenethyl bromide, 4.8 g. (0.2 atom) of magnesium and 100 ml. of ether, was added 9.2 g. (0.075 mol.) of salicylaldehyde in 50 ml. of ether, and the mixture was refluxed for two hours under stirring and then was decomposed with dilute acetic acid. The ether layer was separated, washed with aqueous sodium carbonate and dried over potassium carbonate. After evaporating the solvent, the residue was recrystallized from ligroin, giving 13.5 g. of 2-(1-hydroxy-3-phenylpropyl)-phenol (80% of the theoretical), m. p., 60~61°C. *Anal.* Found; C, 78.85, H, 7.05%. Calcd. for $C_{15}H_{16}O_2$: C, 78.92, H, 7.06%. 2-(1-Hydroxy-3-phenylpropyl)-phenol (12.15 g., 0.053 mol.) and 4 g. of a palladium-on-carbon catalyst (5% Pd) in 50 ml. of ethanol were shaken with hydrogen under atmospheric pressure. In one and half hours 1.34 l. of hydrogen was absorbed and the absorption practically stopped. After removing the catalyst and evaporating the solvent, the residue was distilled under diminished pressure, b. p., 148 ~150°C/2.5 mmHg. The distillate set to needles and melted at 21°C. The reported melting point is 21°C[14].

## Results and Discussion

The apparent O–H stretching absorption curves of the phenols examined are shown in Figs. 1 and 2, and the data of the two bands in each compounds are recorded in Tables I and II.

It should first be noted that in these phenols the free O–H stretching absorption bands at ca.

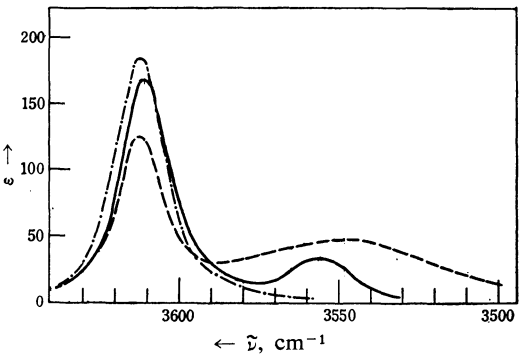



Fig. 1. $\nu_{O-H}$ absorptions of 2-($\omega$-alkenyl)-phenols $o$-$HOC_6H_4(CH_2)_nCH{=}CH_2$.
$n=0$ ——, $n=1$ – – –, $n=2$ —·—·—.

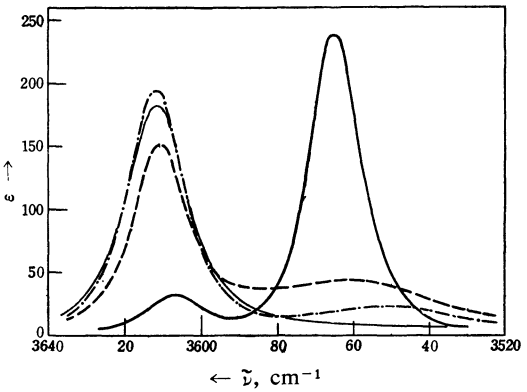



Fig. 2. $\nu_{O-H}$ absorptions of 2-($\omega$-phenylalkyl)-phenols $o$-$HOC_6H_4(CH_2)_nC_6H_5$.
$n=0$ ——, $n=1$ – – –, $n=2$ —·—·—, $n=3$ ——.

3610 $cm^{-1}$ are always absolutely symmetric in contrast to the unsymetric ones in the free O–H stretching absorption bands in alcohols. This fact gives a support to the idea of the existence of the rotational isomers in alcohols, tentatively developed in a previous paper[15] on the unsymmetry of the free $\nu_{O-H}$ bands of almost all alcohols.

In series I, the interaction is effective up to 2-allylphenol (I, $n=1$); the number of the carbon atoms between the hydroxyl group and the nearest carbon atom which carries the $\pi$-electron participating in the interaction is three. It is one more than that in 3-buten-1-ol. In series II, the interaction is discernible up to 2-phenethylphenol (II, $n=2$), the number of the intervening carbon atom being two more than that in 2-phenylethanol. It can, therefore, be said that the limitation by the chain length is released by one or two carbon atoms, when an alcoholic hydroxyl group is replaced by a phenolic one, and the results can be

10) W. Hückel, O. Neunhoeffer, A. Gercke and E. Frank, *Ann.*, **477**, 123 (1930).
11) L. Claisen, F. Kremers F. Roth and E. Tietze, ibid., **442**, 210 (1925).
12) H, P. Kaufmann, ibid., **433**, 237 (1923).
13) St. von Kostanecki, A. Rost and W. Szabranski, *Ber.*, **38**, 743 (1905).
14) A. Greewood and M. Nierenstein, *J. Chem. Soc.*, **1920**, 1595.
15) M. Ōki and H. Iwamura, This Bulletin, **32**, 950 (1959).

TABLE I. $\nu_{O-H}$ ABSORPTIONS OF 2-(ω-ALKENYL)-PHENOLS $o$-$HOC_6H_4(CH_2)_nCH=CH_2$

| $n$ | $\nu_{O-H}$ | $\nu_{max}$ $cm^{-1}$ | $\Delta\nu^a_{1/2}$ $cm^{-1}$ | $A\times10^{-4}$ $mol^{-1}$ l. $cm^{-2}$ | $\Delta\nu_{max}$ $cm^{-1}$ | $A_i/A_f$ |
|---|---|---|---|---|---|---|
| 0 | f. | 3611.0 | 17.8 | 1.08 | 53.9 | 0.26 |
| | i. | 3556.8 | 24.4 | 0.28 | | |
| 1 | f. | 3612.5 | 16.0 | 0.67 | 63.7 | 1.69 |
| | i. | 3548.8 | 67.4 | 1.13 | | |
| 2 | f. | 3612.4 | 17.9 | 1.19 | — | — |

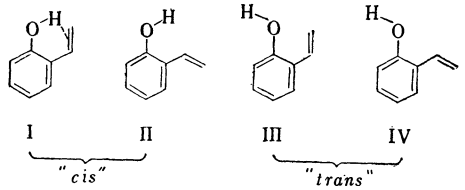
TABLE II. $\nu_{O-H}$ ABSORPTIONS OF 2-(ω-PHENYLALKYL)-PHENOLS $o$-$HOC_6H_4(CH_2)_nC_6H_5$

| $n$ | $\nu_{O-H}$ | $\nu_{max}$ $cm^{-1}$ | $\Delta\nu^a_{1/2}$ $cm^{-1}$ | $A\times10^{-4}$ $mol^{-1}$ l. $cm^{-2}$ | $\Delta\nu_{max}$ $cm^{-1}$ | $A_i/A_f$ |
|---|---|---|---|---|---|---|
| 0 | f. | 3607.0 | 18.2 | 0.20 | 42.0 | 6.4 |
| | i. | 3565.0 | 15.0 | 1.28 | | |
| 1 | f. | 3611.0 | 17.0 | 0.87 | 50.9 | 0.92 |
| | i. | 3560.1 | 56.2 | 0.80 | | |
| 2 | f. | 3612.0 | 17.0 | 1.20 | 61.5 | 0.29 |
| | i. | 3550.5 | 47.4 | 0.35 | | |
| 3 | f. | 3611.7 | 19.5 | 1.28 | — | — |

attributed to the higher acidity and the favorable structure of the phenols. In alcohols, intervening carbon atoms are all those of methylenes and there are many internal rotational degrees of freedom, of which carbon skeletons must take an *eclipsed* or at least a *gauche* form for the interaction. This is disadvantageous not only to the energy but also to the entropy of the interaction. In phenols, however, at least O-C=C-C bonds are fixed in a *cis* conformation which is favorable for the interaction. These two factors can not be evaluated quantitatively so far as the present data are concerned.

Although it has been established[16] that the shifts in wave numbers in similar classes of compounds correspond to the lengthening of the X-H bond and to the energy of the interaction, it is not yet known whether this pinciple is applicable to the phenomenon the present authors are dealing with. The energy difference in the free and the interacting forms will be dealt with in the following paper. Although the relationship between the energy and the wave number shift is ambiguous, the following will be still valid in this interaction as is empirically known; 1) The intensities represent the number of the molecules with the hydroxyl group related to the appropriate bands and are dependent not only on the energy but also on the entropy factor. 2) The half band-widths correspond to the rotational degree of freedom.

The most appreciable difference between 2-(ω-alkenyl)-phenols and 2-(ω-phenylalkyl)-phenols is found in the lowest members of the series. 2-Hydroxybiphenyl has 6.4 times as many molecules of the interacting form as those of the free, while 2-vinylphenol has the ratio of only 0.2, the free form being predominant provided that the light absorption per molecule is equal in both free and interacting forms. This phenomenon could be explained in the following way. It is generally accepted that the hydroxyl hydrogen in phenol is situated in the plane of the benzene ring so that 2pπ electrons on the oxygen atom can conjugate with π-electrons in the benzene ring, and this gives rise to the so-called "*cis*" and "*trans*" isomerism in ortho-substituted phenols[6,17]. In the biphenyl molecule, the "*trans*" form gives normal free O-H stretching vibration, while "*cis*" can not help taking the interacting form. Differing from this situation, 2-vinylphenol can be regarded as the composite of the following four conformations (I~IV) and the hydroxyl group in the




conformation I only can interact with the π-electrons of the vinyl group. Moreover, a full development of conjugation between the benzene ring and the vinyl group will be favored in the conformations II, III and IV which involve less steric interference. Thus the resonance stabilization favors the predominant contribution of II, III and IV in the equilibrium mixture and this is clearly disadvantageous to the interaction. On the other hand, the biphenyl molecule, except in the solid state, has been known not

16) L. P. Kuhn, *J. Am. Chem. Soc.*, **74**, 2492 (1952); R. Badger and S. Bauer, *J. Chem. Phys.*, **5**, 839 (1937).

17) L. Pauling, "The Nature of the Chemical Bond", Cornell University Press, Ithaca, N. Y., 1945, p. 322.

Table III. $\nu_{O-H}$ Absorption of 2-hydroxystilbene

| $\nu_{O-H}$ | $\nu_{max}$ $cm^{-1}$ | $\Delta\nu^{a}_{1/2}$ $cm^{-1}$ | $A\times10^{-4}$ $mol^{-1}$ l. $cm^{-2}$ | $\Delta\nu_{max}$ $cm^{-1}$ | $A_i/A_f$ |
|---|---|---|---|---|---|
| f. | 3609.0 | 17.2 | 1.10 | 54.8 | 0.13 |
| i. | 3554.2 | 21.5 | 0.14 | | |

to exist in the co-planar structure, but in the crossed structure, the angle between the two benzene rings being regarded as large as ca. 50°[18]. This enables the hydrogen atom of the "*cis*" O–H group to come to the very head of the $\pi$-electron clouds. In the interacting conformation of the 2-vinylphenol, the plane of the vinyl group is closely co-planar with that of the benzene ring and the hydrogen atom of the hydroxyl group must approach the $\pi$-electron clouds from the side. This difference in the angle of hydrogen approach in the interaction must have a significance to the amount of the interaction, and this kind of mechanism will be dealt with in future issues.

The half band-widths of the interacting $\nu_{O-H}$ become greater when a methylene chain is introduced between the hydroxyl group and the group carrying the $\pi$-electrons. This is without doubt caused by the participation of many rotational sub-levels to the fundamental transition of the O-H stretching vibration. The interacting forms of these molecules are therefore fairly complicated and have an appreciable degree of freedom.

Inspection of the data obtained with 2-benzylphenol and with 2-allylphenol indicates that these compounds give similar absorption for the interacting form. If this is taken as a significant indication, then it would possibly be the $\pi$-electron nearest[19] to the hydroxyl group that accepts the proton. However, it is not proved which $\pi$-electron interacts with the hydroxyl group. Hence the above mention is only of a reserved significance.

The measurement was extended to 2-hydroxystilbene, which had been proved to be a *trans*-form from the ultraviolet spectrum[12]. The proton acceptor must be the $\pi$-electrons on the central ethylene linkage from the structural requirement. The band properties for O–H stretching vibrations are shown in Table III.

The weaker interaction than that in 2-vinylphenol can be explained on the basis of the electronic effect of the phenyl group attached to the vinyl group, that is, the phenyl group diminishes the electron density on the proton acceptor. This presents a striking contrast to the increased interaction in *o*-propenylphenol, in which the methyl group attached to the vinyl group enriches the $\pi$-electron densities at the latter[20].

The authors are indebted to Professor Y. Urushibara and Professor T. Shimanouchi for their encouragement and discussion throughout this work. The authors' thanks are also due to the Ministry of Education for the Grant in Aid for Fundamental Scientific Research.

*Department of Chemistry*
*Faculty of Science*
*The University of Tokyo*
*Hongo, Tokyo*

18) O. Bastiansen, *Acta Chem. Scand.*, 3, 408 (1949).

19) The authors are meaning the $\pi$-electron to be another than that born on the phenolic ring.

20) M. Ōki and H. Iwamura, unpublished. See also Reference 5).

# *Constitution and Solubility of Vitreous Phosphates and Slags*

By Jumpei ANDO

(Received September 4, 1959)

Recently various sorts of fused phosphates and slags are being used as fertilizers to supply lime, magnesia, phosphorus pentoxide, silica and other components necessary for plants. Most of these fused phosphates and slags are produced by quenching the melts with water and thus are almost vitreous containing little crystalline minerals. The constitution of such vitreous substances have not yet been clarified, though many studies have been made on crystalline minerals.

In the present work, the constitution of such vitreous substances was investigated by X-ray diffraction, and thus citrate solubility or acid solubility of those were clarified.

## Experimental

**Samples.**—More than seventy samples including fused phosphates, slags and glasses produced in large scale or pilot plants or in the laboratory were tested by means of X-ray diffraction and microscope. Samples which were almost completely vitreous containing less than 2~3% crystalline minerals were classified according to their chemical composition (Table I).

Samples marked as CMSP or CMASP are calcium magensium phosphate fused by electric furnaces using phosphate rock and serpentine, or by blast furnaces using phosphate rock, garnierite (nickel magnesium silicate ore) and gypsum to produce nickel matte at the same time[1,2]. Samples marked as CSP are slags of phosphorus production by electric furnaces. Samples marked as CMAFS are slags of nickel production from garnierite, limestone and gypsum. A sample CMAS-6 is a blast furnace slag of iron production.

Samples marked as CP, MP, CMP and NP were prepared by fusion of mixtures of pure chemicals in platinum crucibles. Other samples were fused in graphite crucibles in the laboratory. Each sample was fused at the temperature 100~200°C higher than the softening point (Table I). Most of these were quenched by water and others were quenched by air.

Among these samples CMAFS-1,2 contain 2~3% crystalline minerals such as forstelite etc. CMAS-6 contains 2~3% melilite (Fig. 1). Blast furnace slags containing more lime include more amount of melilite. Other samples are nearly completely vitreous, containing less than 1% crystalline materials.

1) J. Ando, *J. Chem. Soc., Japan, Ind. Chem. Sec.* (*Kogyo Kagaku Zasshi*), **61**, 1134 (1958).
2) J. Ando, *Ind. Eng. Chem.*, **51**, 1267 (1959).

**Measurement of Halos by X-ray Diffractometer.**—X-ray diffraction patterns of all samples were recorded by X-ray diffractometer under conditions described in Fig. 1. Every sample gave single diffraction maximum (halo) between the diffraction angle of 20~40°. At first when recorded by the voltage of 30kV., each sample gave another maximum around 8~15°, which diminished when the voltage was reduced to 15kV. explaining that this maximum

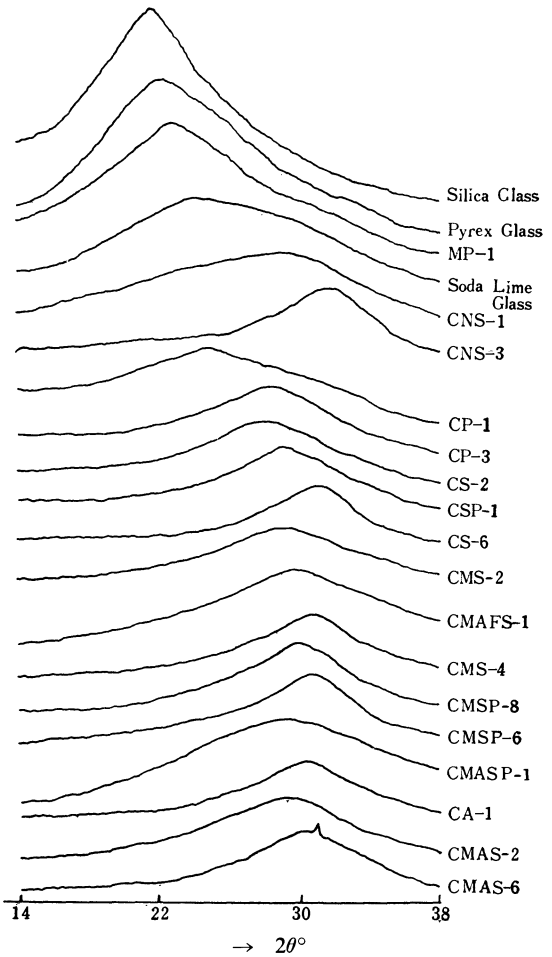



Fig. 1. X-ray diffraction patterns of samples.
Cu ray (15kV., 15 milliamp.), Ni filter
Slit 2.5°, 2.5° and 0.8 mm.
Sample area 16×33 mm.
Time constant 8 sec.
Full scale 400 counts/sec.
Scanning speed 2°/min.
Chart speed 1 cm./min.

TABLE I. CHEMICAL COMPOSITION (%) AND SOFTENING POINT (°C) OF SAMPLES

| Mark | $SiO_2$ | $Al_2O_3$ | FeO | MgO | CaO | $P_2O_5$ | S. P. |
|---|---|---|---|---|---|---|---|
| CP-1 | — | — | — | — | 28.3 | 72.3 | 965 |
| CP-2 | — | — | — | — | 32.7 | 68.0 | — |
| CP-3 | — | — | — | — | 35.8 | 65.4 | 1040 |
| MP-1 | — | — | — | 21.2 | — | 80.2 | 1140 |
| MP-2 | — | — | — | 34.4 | — | 76.4 | 1145 |
| CMP-1 | — | — | — | 14.4 | 17.0 | 68.6 | 990 |
| CMP-2 | — | — | — | 14.4 | 23.2 | 62.2 | — |
| CMP-3 | — | — | — | 24.7 | 19.0 | 56.3 | 1070 |
| CMSP-1 | 42.1 | 0.7 | 1.4 | 13.7 | 25.8 | 12.6 | 1275 |
| CMSP-2 | 40.3 | 1.8 | 0.9 | 15.7 | 26.0 | 12.7 | 1265 |
| CMSP-3 | 34.0 | 0.8 | 0.8 | 15.7 | 27.8 | 19.0 | 1235 |
| CMSP-4 | 39.3 | 0.6 | 1.4 | 16.6 | 26.1 | 12.0 | 1260 |
| CMSP-5 | 39.0 | 0.6 | 1.6 | 15.7 | 27.4 | 11.8 | 1270 |
| CMSP-6 | 26.0 | 2.0 | 1.6 | 18.7 | 30.0 | 19.5 | 1260 |
| CMSP-7 | 23.8 | 1.3 | 4.1 | 17.1 | 31.0 | 20.6 | 1270 |
| CMSP-8 | 21.0 | 2.1 | 0.9 | 10.6 | 38.9 | 25.8 | 1275 |
| CMASP-1 | 43.0 | 6.0 | 6.5 | 21.7 | 17.0 | 5.7 | 1235 |
| CMASP-2 | 29.5 | 7.1 | 3.1 | 11.7 | 30.1 | 18.5 | 1215 |
| CMASP-3 | 38.0 | 5.3 | 6.1 | 16.8 | 22.9 | 9.3 | 1230 |
| CMASP-4 | 32.7 | 5.0 | 6.1 | 15.3 | 28.4 | 13.0 | 1250 |
| CASP-1 | 29.1 | 15.8 | 0.2 | 0.3 | 39.3 | 15.4 | 1350 |
| CASP-2 | 26.5 | 15.1 | 0.2 | 0.4 | 43.5 | 13.6 | 1320 |
| CSP-1 | 49.3 | 1.8 | 0.2 | 0.3 | 45.6 | 2.1 | 1425 |
| CSP-2 | 46.8 | 1.4 | 0.2 | 0.8 | 49.6 | 1.8 | 1410 |
| CS-1 | 65.2 | 0.4 | — | — | 34.8 | — | — |
| CS-2 | 61.3 | 0.4 | — | — | 38.3 | — | 1430 |
| CS-3 | 56.0 | 0.4 | — | — | 43.4 | — | 1460 |
| CS-4 | 53.7 | 0.6 | — | — | 45.9 | — | 1490 |
| CS-5 | 48.5 | 0.5 | — | — | 50.6 | — | 1475 |
| CS-6 | 46.0 | 0.3 | — | — | 53.9 | — | 1440 |
| CS-7 | 44.3 | 0.7 | — | — | 55.0 | — | 1425 |
| CMS-1 | 57.8 | 1.0 | 1.2 | 14.0 | 26.0 | — | — |
| CMS-2 | 55.5 | 0.9 | 0.5 | 12.8 | 29.8 | — | 1330 |
| CMS-3 | 51.3 | 0.9 | 0.6 | 15.7 | 31.2 | — | 1330 |
| CMS-4 | 44.6 | 0.6 | 1.0 | 18.8 | 31.9 | — | 1315 |
| CMS-5 | 44.3 | 1.6 | 1.0 | 17.4 | 35.0 | — | 1380 |
| CMAFS-1 | 44.7 | 6.6 | 6.6 | 18.0 | 23.6 | — | 1270 |
| CMAFS-2 | 45.5 | 5.8 | 6.3 | 17.8 | 25.3 | — | 1285 |
| CA-1 | 5.6 | 53.1 | 2.4 | 0.1 | 37.2 | — | 1420 |
| CA-2 | 5.3 | 50.1 | 2.0 | 0.1 | 40.7 | — | 1340 |
| CA-3 | 5.0 | 48.0 | 1.8 | 3.8 | 39.9 | — | — |
| CA-4 | 5.8 | 45.2 | 1.5 | 0.2 | 46.2 | — | 1385 |
| CAS-1 | 44.9 | 19.9 | 0.5 | 0.2 | 32.9 | — | — |
| CAS-2 | 42.0 | 20.1 | 0.7 | 0.3 | 35.8 | — | — |
| CAS-3 | 38.7 | 19.9 | 0.4 | 0.3 | 39.3 | — | 1270 |
| CAS-4 | 36.3 | 20.0 | 0.3 | 0.3 | 41.7 | — | 1290 |
| CMAS-1 | 45.7 | 13.4 | 0.5 | 6.1 | 32.3 | — | 1180 |
| CMAS-2 | 42.0 | 14.1 | 0.7 | 6.4 | 34.3 | — | 1200 |
| CMAS-3 | 38.9 | 15.0 | 0.5 | 6.8 | 36.3 | — | 1220 |
| CMAS-4 | 35.3 | 15.8 | 0.7 | 7.2 | 38.3 | — | 1320 |
| CMAS-5 | 32.5 | 15.9 | 1.3 | 9.4 | 38.6 | — | 1340 |
| CMAS-6 | 32.1 | 16.5 | 0.7 | 7.5 | 40.2 | — | 1350 |
| NP-1 | — | ($Na_2O$ | 30.4) | — | — | 69.6 | — |
| NP-2 | — | ($Na_2O$ | 36.2) | — | — | 63.8 | — |
| CNS-1 | 67.0 | ($Na_2O$ | 17.3) | — | 15.7 | — | — |
| CNS-2 | 51.0 | ($Na_2O$ | 25.8) | — | 23.2 | — | — |
| CNS-3 | 46.0 | ($Na_2O$ | 33.3) | — | 20.7 | — | — |

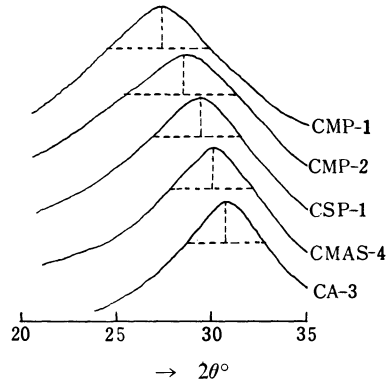



Fig. 2. Precise recording of X-ray halos and measurement of the angle of center of halos.
Cu ray (15kV. 15 milliamp.), Ni filter
Slit 2.5°, 2.5° and 0.8 mm.
Sample area 16×33 mm.
Time constant 16 sec.
Full scale 250 counts/sec.
Scanning speed 0.5°/min.
Chart speed 0.25 cm./min.

was caused by white X-ray which was not cut satisfactorily by nickel filter.

As an interesting relationship of halos to the composition of glasses was found, the halos were recorded more precisely as is illustrated in Fig. 2 in order to measure the angle of the center of halos. The diffraction angles of the center and of maximum of each halo coincide approximately but not exactly.

**Measurement of Solubility.**—All samples were crushed so as to have the following grain sizes: 60～100 mesh 10%, 100～200 mesh 40%, and under 200 mesh 50%. To 1 g. sample 150 ml. of 2% citric acid or N/2 (about 1.8%) hydrochloric acid was added, shaken for 5, 15, 30 or 60 min. at 20 or 30 °C, then filtered quickly using suction. The insoluble residue was dried and weighed. In this case, "Solubility" means the weight loss % measured by such method. "Solubility" when dissolved in a definite time concerns mainly the velocity of dissolution in the case of most vitreous phosphates and slags of basic composition which are dissolved completely by acids ultimately. In such case the solubility of all components of samples, lime, magnesia, alumina, silica, ferrous oxide and phosphorus pentoxide ect., are nearly the same as each other, coinciding with the solubility measured by weight loss of samples.

Some of vitreous samples containing much silica or phosphorus pentoxide are not dissolved by acids completely even when shaken for a long time but leave insoluble residue consisting mainly of a silicic or phosphoric acid component. In such cases solubility of each component was measured by chemical and X-ray analysis of the residue. Citrate solubility (at 65°C) of samples was measured similarly.

**Measurement of Softening Point.**—Samples were shaped into segel cones of 3 cm. height, fixed on chromite holders, and were heated at a rate of 5°C/min. Temperatures at which the cones fell were measured by platinum-platinum · rhodium thermocouple (Table I).

## Results

**Relationship of X-ray Diffraction Halos to Chemical Composition, Construction and Properties of Glasses.**—*Outline.*—It was found that acidic samples such as silica glass, Pyrex glasses, MP-1 or MP-2 revealed a steep maximum of X-ray diffraction pattern at smaller diffraction angle of 22～24° (Fig. 1). The diffraction maximum (halo) shifts to larger angle according to the increase of the basicity of samples. Each of the samples of moderate basicity, CP-1, 2, CMP-1, soda lime glass, etc., reveals a gentle maximum around 25～29°. These samples of moderate basity have a lower softening point and are renderd to glass state most easily.

Every basic sample such as CMSP-5～8, CS-5～7, CA-4, CMAS-4～6, or CNS-3 reveals at larger angle of 30～32° a halo smaller than that of acidic samples but steeper than that of samples of intermediate basicity. The melts of these samples crystallize very quickly, and therefore can not be rendered to complete glass state without quenching. Samples which were more

TABLE II. RATIOS AND THEIR MEANINGS

| | |
|---|---|
| $CR=\frac{Ca+Na+(1-a)Al+(1-b)Mg+(1-c)Fe-0.1P}{1.1P+Si+aAl+bMg+cFe}$ | A ratio of the number of cations which are coordinated by six or eight oxygen ions to that coordinated by four oxygen ions. |
| $OR_0=\frac{O}{1.1P+Si+aAl+bMg+cFe}$ | A ratio of the number of total oxygen ions to that of cations coordinated by four oxygen ions. |
| $OR_1=\frac{O}{P+Si+aAl}$ | A ratio of the number of oxygen ions to that of cations the bond strength of which with oxygen is larger than 80 kcal. (Table IV). |
| $OR_2=\frac{O}{1.05P+Si+(a+0.05)Al+0.5bMg}$ | A part of intermediate cations was added to denominator of $OR_1$ (Table IV). |
| $OR_3=\frac{O}{1.08P+Si+(a+0.15)Al+0.8bMg}$ | Most of intermediate cations was added to denominator of $OR_1$. |

TABLE III. EXAMPLES OF CALCULATION OF RATIOS

| Samples | A.B.N. | *a* | *b* | *c* | CR | $OR_1$ | $OR_2$ | $OR_3$ |
|---|---|---|---|---|---|---|---|---|
| CMP-1 | — | — | 0.30 | — | 0.40 | 3.17 | 2.90 | 2.76 |
| CASP-1 | 44 | 0.50 | 0.08 | 0.05 | 0.96 | 3.14 | 3.05 | 2.92 |
| CMAFS-2 | 49 | 0.60 | 0.10 | 0.07 | 1.09 | 3.18 | 3.09 | 3.00 |
| CMAS-1 | 42 | 0.43 | 0.06 | 0.05 | 0.98 | 3.02 | 2.96 | 2.87 |
| CMAS-6 | 52 | 0.71 | 0.12 | 0.07 | 1.23 | 3.23 | 3.12 | 2.97 |
| CA-2 | 55 | 0.73 | — | 0.08 | 1.28 | 3.00 | 2.80 | 2.55 |

TABLE IV. CALCULATED BOND STRENGTH OF OXIDE COMPONENTS

| M | Valence | Dissociation energy per $MO_x$, kcal. | Coordination number | Single bond strength $B_{M-O}$, kcal. | |
|---|---|---|---|---|---|
| Si | 4 | 424 | 4 | 119 | Glass formers |
| Al | 4 | 402-317 | 4 | 107-79 | |
| P | 5 | 442 | 4 | 111-88 | |
| Al | 3 | 317-402 | 6 | 53-67 | Intermediates |
| Mg | 2 | 222 | 4 | 56 | |
| Ca | 2 | 257 | 4 | 66 | |
| Mg | 2 | 222 | 6 | 37 | Glass modifiers |
| Ca | 2 | 257 | 6 | 43 | |
| Na | 1 | 120 | 6 | 20 | |
| Ca | 2 | 257 | 8 | 32 | |

basic could not be rendered to complete glass even by rapid quenching with water.

The author thinks that halos of these glasses and vitreous substances are chiefly determined by the ratio of the number of cations coordinated by six (or eight) oxygen ions to that coordinated by four oxygen ions. This ratio is shown as "coordination ratio" (CR) in Table II and Fig. 3. X-ray is chiefly diffracted to smaller angle by oxide glasses containing much $SiO_4$, $PO_4$, $MgO_4$ etc. because these tetrahedra are apt to form hexagonal rings or chains having larger spacing. On the contrary, $CaO_6$, $MgO_6$, $NaO_6$ etc. are apt to form tetragonal rings having smaller spacing, and thus diffract X ray to larger angle. When nearly equal amount of $RO_4$ and $RO_6$ is mixed the gentle halo appears in intermediate angle.

The strongest diffraction peaks of the more basic crystalline minerals of each $CaO$-$P_2O_5$, $CaO$-$SiO_2$, $CaO$-$Al_2O_3$, $CaO$-$Al_2O_3$-$SiO_2$ or other systems appear usually at larger angle: e. g. $CP \rightarrow C_2P \rightarrow C_3P$, $S \rightarrow CS \rightarrow C_2S$, $C_3A_5 \rightarrow CA \rightarrow C_3A$, $CAS_2 \rightarrow C_2AS$, etc. Moreover, the diffraction angle of the strongest peak of CP (calcium metaphosphate) coincides with that of the center of the halo of the glass of the same chemical composition similarly as in the case of cristobalite and silica glass. These facts show that there is some relation between the structure of glass and that of crystalline mineral. However, the diffraction peaks of crystalline minerals and halos of glasses of the same composition do not always agree with each other.

*Empirical formula indicating the relation of X-ray halo to chemical composition and constitution of glasses.*—It was found that for every glasses consisting of silica, alumina, lime, phosphorus pentoxide, magnesia, sodium oxide and ferrous oxide there was simple relation between the diffraction angle (or $\lambda/\sin\theta$) of the center of each halo and the value of the above-mentioned coordination ratio (Table II, Fig. 3).

In the ratio Ca, Mg, Al, Si, etc. are the number of each ion (or atom) in a unit volume of glasses. Coefficients a, b and c are given by

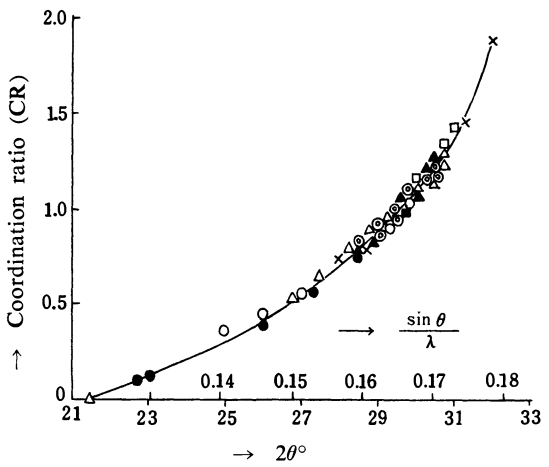



Fig. 3. Relationship of the diffraction angle or $\sin\theta/\lambda$ of center of halo to coordination ratio.
○ CP, CASP ▲ CMS, CMAFS
◎ CMSP, CMASP □ CA, CAS
● MP, CMP ■ CMAS
△ CS, CSP × NP, CNS

Fig. 4 which illustrates the relationship of the coefficients to apparent basicity number A. B. N. (= CaO + MgO + 0.7FeO + 0.25$Al_2O_3$). Here, CaO, MgO, FeO and $Al_2O_3$ of A. B. N. are weight % of each component of glasses. Fig. 4 was plotted empirically by trial-and-error method in consideration of both X-ray halo and solubility of glasses which will be described below. The coefficients a, b or c indicates principally a ratio of numbers of aluminum, magnesium and iron ions which are coordinated by four oxygen ions [these are described as Al(4), Mg(4) and Fe(4) below] to that of total aluminum, magnesium or iron ions respectively.

The apparent basicity number (A. B. N.) of calcium magnesium phosphate, slags of iron, nickel or phosphorus production which are being used as fertilizers is usually 47~52, and therefore, a=0.6~0.7, b=0.10~0.12, and c=0.06~0.07. In the case of aluminous glass containing much alumina the change of the coefficient a is smaller than in the case of glasses containing less alumina (Fig. 4).

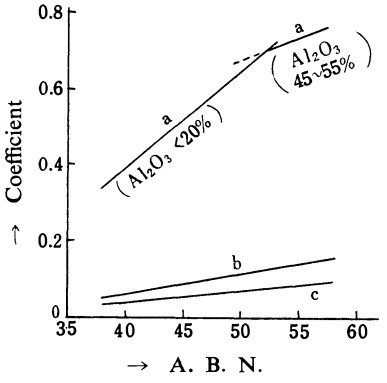



Fig. 4. Relationship of A. B. N. to the coefficients.

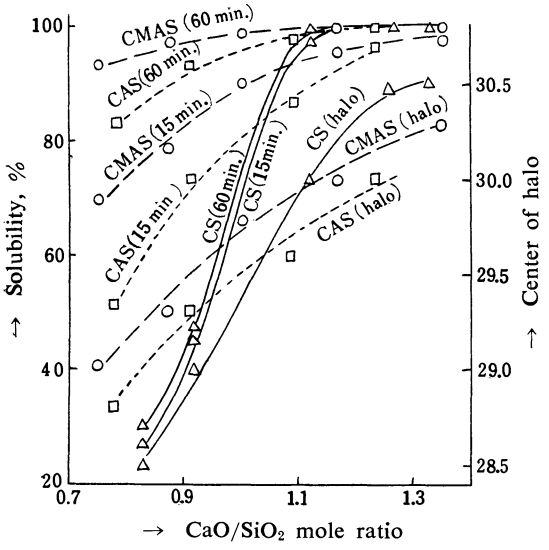



Fig. 5. Relationship of $CaO/SiO_2$ mole ratio to the solubility in N/2 hydrochloric acid (60 min. at 30°C) and to the angle of the center of halo.

As is illustrated by Fig. 5 both the diffraction angle of the center of each halo and hydrochloric acid solubility of samples of CS(CaO-$SiO_2$) system are reduced remarkably according to the decrease of $CaO/SiO_2$ mole ratio. However, the reduction of both the angle and the solubility is far smaller for the samples containing a considerable amount of alumina or magnesia and alumina (samples of CAS or CMAS systems). This is attributable to the change of oxygen coordination number of aluminum and magnesium ions—much Al(4), Mg(4) and less Al(6), Mg(6) occur in basic glasses, less Al(4), Mg(4) and much Al(6), Mg(6) occur in acidic glasses as is illustrated by Fig. 4.

It was found by both X-ray and solubility tests that in glasses which contain phosphorus pentoxide more Mg(4), Al(4) and Fe(4) occurred than in silicate glasses. The amount of such four coordinated ions increases according to the amount of phosphorus pentoxide. It seems that even a part of calcium or sodium is coordinated by four oxygen ions in phosphate glasses. From this standpoint of view, coefficients of phosphorus 1.1 for denominator and −0.1 for numerator were introduced into coordination ratio (Table II) for convenience of calculation of the value of the ratio. In this way X-ray, patterns and solubilities of phosphate glasses are indicated well (Figs. 3 and 9—11).

Especilly in the case of glasses containing magnesia and much phosphorus pentoxide, an extensive amount of magnesium ions seems to be coordinated by four oxygen ions. The X-ray diffraction halos of silica glass and that of MP-1 which consists of nearly equal mole of magnesia and phosphorus pentoxide resemble each other explaining that $MgP_2$ plays a role of $Si_3$. Coefficient b to be used for calculation of coordination ratio of glasses containing more than 40% phosphorus pentoxide is given by Fig.

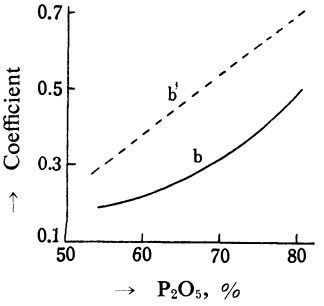



Fig. 6. Relationship of $P_2O_5$ content to coefficients.

6. In the case of phosphate glass the coefficient a, b or c does not indicate the ratio of the number of Al(4), Mg(4) or Fe(4) to that of total Al, Mg or Fe respectively because coefficients of phosphorus 1.1 and −0.1 are used for conveniene. The approximate ratio of the number of Mg(4) to total Mg of samples of CMP and MP systems is shown by dotted curve (b′) in Fig. 6.

*Relationship of glass formation to oxygen ratio.*—Oxygen ratio, a ratio of the number of total oxygen ions to that of network-forming ions, is known to relate deeply to glass formation. It was clarified by the present study that approximate oxygen ratio was calculated by ORo (Table II). Samples with the ratio less than 3.0 could easily be rendered to glass without quenching, because these are composed of long chains or networks of oxygen and network-forming ions and the melts of these are viscous. Samples with the ratio 3.0～3.3 could be rendered to glass state completely by water quenching (CMSP-6～8, CS-6, 7, CMS-4, 5, CA-2, 3, CMAS-5, 6, etc.). As an exception high temperature modification of calcium metasilicate (pseude wollastonite) was crystallized very quickly from the melt of the composition $CaO \cdot SiO_2$, oxygen ratio of which is 3.0. This mineral is composed of small $Si_3O_9$ rings[3] and therefore, is completely soluble in N/2 (about 1.8%) hydrochloric acid, though silicic acid component of the glass of the same composition is not dissolved by the acid.[4] Samples with the ratio larger than 3.3 could not be rendered to complete glass state even by rapid water quenching from high temperature forming crystalline minerals partly. The glass formation is affected by bond strength, too (Table IV).

**Solubility of Glasses.**—*Relationship of bond strength to citric and hydrochloric solubility.*—In Table IV single bond strength between oxygen and various cations[5] is illustrated. Mg(4), Ca(4) and Ca(6) were inserted by the present author into the table. Iron is thought to be intermediate between calcium and magnesium.

It was clarified in the present study that linkage Si-O, P-O or Al(4)-O, the bond strength of which is more than 80 kcal., could scarcely be broken by 2% citric acid or N/2 hydrochloric acid. The linkage Ca(6)-O, Ca(8)-O, Mg(6)-O, or Na-O, the bond strength of which is less than 50 kcal., is broken by the acids quickly. The linkage of intermediate bond strength such as Al(6)-O, Mg(4)-O, or Ca(4)-O is slowly broken by the acids.

Basic glasses containing less intermediate components are dissolved in acids very quickly

3) J. W. Gruner, *Am. Mineral.*, 33, 681 (1948).
4) J. Ando and S. Matsuno. *J. Chem. Soc. Japan, Ind. Chem. Sec.* (*Kogyo Kagaku Zasshi*), 62, 1481 (1959).
5) Kuan-Han Sun, *J. Am. Ceram. Soc.*, 30, 277 (1947).

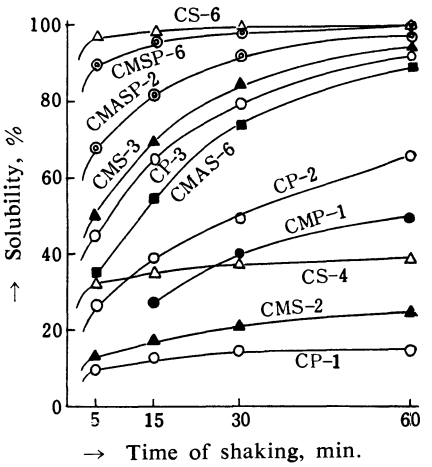



Fig. 7. Citric solubility of samples in various times at 20°C

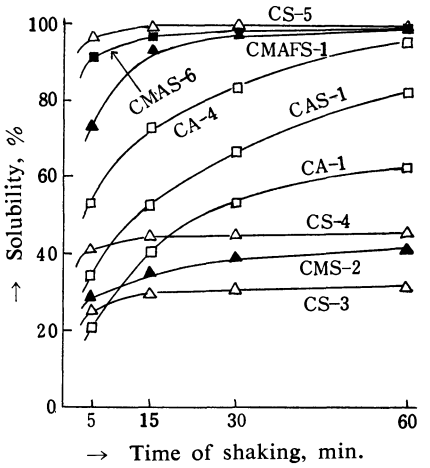



Fig. 8. Solubility of samples in N/2 HCl at 30°C.

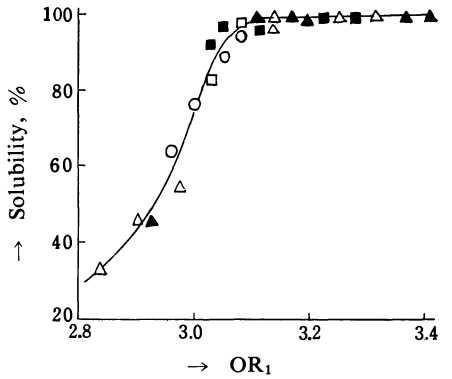



Fig. 9. Relationship of $OR_1$ to hydrochloric solubility in 60 min. at 30°C.
△ CS, CSP ■ CMAS
▲ CMS, CMAFS ○ CA
□ CAS

(CS-6, CMSP-6 in Fig. 7, CS-5 in Fig. 8., etc.). Basic glasses containing much intermediate components dissolve slowly but completely (CMASP-2, CMS-3, CP-3, CMAS-6, CMAFS-1, CA-4, CAS-3, 4, etc.).

Acidic glasses (CP-1, CS-2, 3, 4, CMS-2, etc.) are not dissolved completely by acids but leave mainly hydrated silica or phosphoric acid component undissolved, because such glasses contain large linkage of P-O-P-O or Si-O-Si-O which forms long chains, large rings or networks. Such large linkages, the bond strength in which is larger than 80 kcal., must not be dissolved into liquid but remain as insoluble residue or as colloidal state. On the contrary, small chains or rings must enter into solution by hydration. The magnitude of the linkage is related to oxygen ratio as will be described below.

Fig. 9 illustrates the relationship of $OR_1$ (Table II) to the solubility of glasses when shaken in N/2 HCl for an hour at 30°C. Samples with $OR_1$ larger than 3.2 are dissolved completely. Samples with $OR_1$ smaller than 3.15 leave insoluble residue. $OR_1$ 3.2~3.15 corresponds to $M_5O_{16}$~$M_6O_{19}$ which is the linkage of five ~six $MO_4$ groups and is 10~15 Å in length. It was clarified that the linkages (the bond strength in which is larger than 80 kcal.) smaller than 10 Å entered into solution and that linkages larger than 20 Å did not enter into solution usually but remained undissolved or as colloidal residue.

In citric acid the samples dissolve more slowly than in N/2 HCl. Especially the samples containing much Ca(4), Mg(4) or Al(6) are dissolved slowly and therefore not completely in an hour in 2% citric acid. It was clarified that

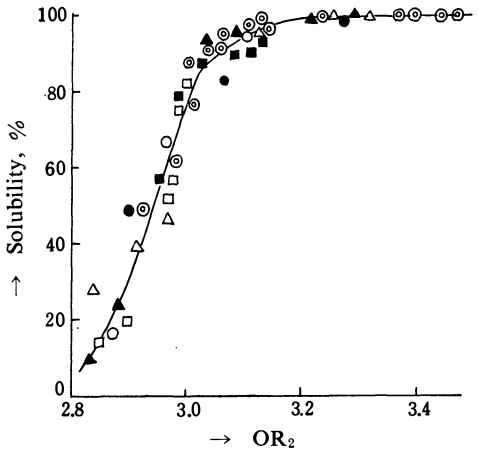



Fig. 10. Relationship of $OR_2$ to citric solubility in 60 min. at 20°C.

○ CP, CASP ▲ CMS, CMAFS
◎ CMSP, CMASP □ CAS, CA
● CMP ■ CMAS
△ CS, CSP

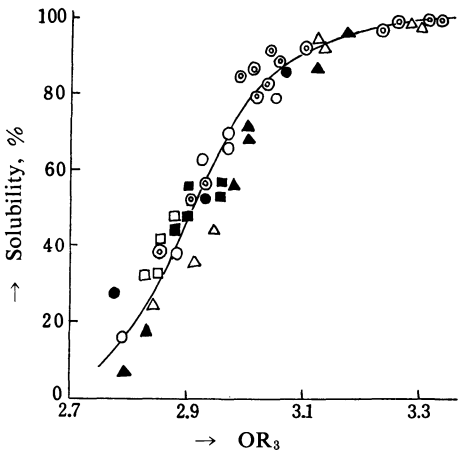



Fig. 11. Relationship $OR_3$ to citric solubility in 15 min. at 20°C.

○ CP, CASP △ CS, CSP
◎ CMSP, CMASP □ CAS
● CMP ■ CMAS
▲ CMS, CMAFS

citric solubility of samples in 60 or 15 min. at 20°C can be indicated by $OR_2$ or $OR_3$ (Table II) as is illustrated by Fig. 10 or 11.

Citric solubility of −200 mesh/inch samples is nearly equal to hydrochloric solubility of −60 mesh/inch samples treated in the same time. Hydrochloric solubility in 15 min. is nearly equal to citric solubility in 60 min. By raising the temperature from 20 to 30°C velocity of dissolution increases somewhat. Thus acid solubility of various vitreous phosphates and slags can be known from chemical composition using above relations.

*Citrate solubility.* — Citrate solubility by American official method and citric or hydrochloric solubility is quite different. For examble, CP-1 is dissolved very quickly in neutral citrate

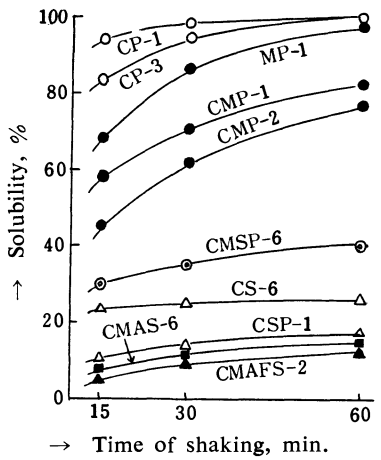



Fig. 12. Citrate solubility of samples in various times at 65°C.

though largely insoluble in acids. Phosphate glasses (CP-1—3, CMP-1—3) are dissolved more quickly in citrate but more slowly in acids when the samples are more acidic containing more phosphorus pentoxide component (Fig. 12). $NH_4^+$ and $OH^-$ of the citrate must break linkages of P-O-P-O.

Silicate or aluminate glasses is dissolved slightly. Calcium magnesium phosphate, a silicophosphate glass, is dissolved intermediately in citrate (Fig. 12).

## Discussion

The relation illustrated in Fig. 3 applies nearly exactly to glasses composed mainly of oxides of sodium, magnesium, aluminum, silicon, phosphorus, potassium and calcium atomic number of which is between 11 and 20. For glasses containing much boron, lithium, lead, barium etc., the atomic number of which is far smaller or far larger than that of the above elements, the relation between X-ray halo and composition of glasses is not so simple. In such cases the X-ray halo must be affected not only by coordination number of cations but also fairly intensely by ionic radius, the number of electron etc.

The above explanations of X-ray halos which was based only on coordination number and especially relations illustrated by Figs. 4 and 6 are not quite exact. However, many facts shown in the present study must be useful to clarify the construction and properties of various glasses and vitreous substances. Moreover, it is possible to determine the chemical composition of glasses by the measurement of X-ray halo.

Quenched phosphates and slags often contain small amount of crystalline minerals which affect the solubility considerably. Usually crystalline minerals dissolve far more slowly than glasses of the same composition. Crystallized forstelite, enstatite, diopside, apatite, anorthite and calcium pyrophosphate scarcely dissolve in citric acid or citrate. Gehlenite dissolves slowly, åkermanite and $\beta$-tricalcium phosphate dissolve fairly quickly in acids.[6,7] $\alpha$-Calcium metasilicate[4] and $\alpha$-tricalcium phosphate dissolve quickly in acids. In citrate $\alpha$ modification of tricalcium phosphate is highly soluble but $\beta$ modification is less soluble because of the difference of velocity of dissolution which is due to the difference of structure.

## Summary

The diffraction angle of center of X-ray halo of glasses composed of silica, phosphorus pentoxide, alumina, lime, magnesia, sodium oxide and ferrous oxide is principally determined by a ratio of the number of cations coordinated by six (or eight) oxygen ions to that coordinated by for oxygen ions.

Approximate ratio of the number of aluminum or magnesium ions which is coordinated by four oxygen ions to that of total aluminum or magnesium ions can be determined by measurement of X-ray halo using above relations.

Glass formation is closely related to oxygen ratio $OR_0$. Solubility of vitreous phosphates and slags in N/2 hydrochloric acid or 2% citric acid is indicated by the ratios $OR_1$, $OR_2$ and $OR_3$ all of which are calculated from chemical composition and above relations.

*Department of Industrial Chemistry*
*Faculty of Engineering*
*Chuo University*
*Bunkyo-ku, Tokyo*

6) J. Ando, *J. Chem. Soc. Japan, Ind. Chem. Sec.* (*Kogyo Kagaku Zasshi*), **63**, 83 (1960).
7) J. Ando, ibid., **60**, 535 (1957).

# *Ternary Liquid Equilibria in System n-Heptane-Thiophene-Liquid Ammonia. New Tie Line Correlation*

By Kiyoharu ISHIDA

(Received October 19, 1959)

The removal of organic sulfur compounds from petroleum products has been one of the most important problems in the petroleum refinery field for many years, although the success of the hydro-refining process has reduced the difficulties of the desulfurization. It has been reported that there is a possibility of the use of liquid ammonia and its mixed solvents as desulfurizing agents on the extraction process[1], but no fundamental data in connection with this matter have been given. This paper presents the equilibrium data at temperatures of 20 and 0°C for the system *n*-heptane-thiophene-liquid ammonia, and a new method correlating tie line data for ternary liquid equilibria has been described.

The method used to obtain data for the construction of phase equilibria was the same analytical method as described in the previous paper[2]. The heterogeneous liquid layers were separated and analyzed after the saturation equilibrium was attained in a constant temperature bath regulated within the range of ±0.05°C throughout the experiment. An aliquot of each layer, which was determined from the difference of weight of the bottle containing the system, was released to the receiver and the ammonia was absorbed by the definite quantity of the 2 N sulfuric acid solution after it was removed from the receiver by volatilization, and then backtitrated with 0.5 N standard hydroxide solution. The compositions of ammonia-free organic liquid were determined by measuring their densities and refractive indices to the nearest 0.0001 unit. The results were adjusted for the slight loss of organic liquid by volatilization by means of the lever rule[3] from the composition of the total mixture and the concentrations of ammonia in both layers. It was observed that when the vaporization loss of binary mixtures of heptane and thiophene was less than about 15%, the compositions of organic binary mixtures were practically unaffected with the vaporization of organic liquid accompanied by the determination of ammonia, though the vapor pressure of thiophene has about twice that of *n*-heptane in the neighborhood of 0°C.

*n*-Heptane used in this investigation was the reference fuel for octane number determination, having the following physical constants, b.p., 98.3°C; $d_4^{20}$, 0.6838; $n_D^{20}$, 1.3878. Commercially available thiophene was dissolved in liquid ammonia, allowed to stand overnight, and then redistilled after the yellowish precipitates were removed; the middle fractions having the constants b. p. 84.1°C, $d_4^{20}$ 1.0638, $n_D^{20}$ 1.5288 were used.

## Results and Discussion

The data of densities and refractive indices for the binary system of *n*-heptane and thiophene from which the compositions of the raffinate and the extract were determined are given in Table I, and the equilibrium data for the ternary system are given in Table II and shown in Figs. 1 and 2. As will be clear from the figures, tie lines are almost parallel to the base of the triangle and in the case of equilibrium at 0°C the distribution ratio changes from more than unity to less than unity as shown in Fig. 2. The maximum selectivity[5] for this system regarding liquid ammonia as a solvent for the separation of thiophene from paraffin are given to be 72.9 and 62.0 wt. % at 0 and 20°C., respectively. The respective maximum concentrations of thiophene in the extract are 89.3 and 78.8 wt.% at 0 and 20°C., then the maximum

TABLE I. DENSITIES AND REFRACTIVE INDICES FOR *n*-HEPTANE-THIOPHENE BINARY SYSTEM

| Thiophene wt. % | $d_4^{20}$ | $n_D^{20}$ |
|---|---|---|
| 0.0 | 0.6838 | 1.3878 |
| 12.73 | 0.7154 | 1.3977 |
| 25.89 | 0.7514 | 1.4103 |
| 31.73 | 0.7688 | 1.4164 |
| 53.36 | 0.8414 | 1.4432 |
| 58.37 | 0.8607 | 1.4508 |
| 62.36 | 0.8766 | 1.4565 |
| 74.19 | 0.9285 | 1.4764 |
| 79.82 | 0.9554 | 1.4865 |
| 85.98 | 0.9866 | 1.4988 |
| 92.71 | 1.0229 | 1.5128 |
| 100.0 | 1.0638 | 1.5288 |

1) V. A. Kalichevsky, *Petroleum Refiner*, **30**, No. 4, 111 (1951).
2) K. Ishida, *J. Chem. Soc. Japan, Ind. Chem. Sec.* (*Kogyo Kagaku Zasshi*), **56**, 469 (1953).
3) D. F. Othmer and P. E. Tobias, *Ind. Eng. Chem.*, **34**, 690 (1942).

TABLE II. EQUILIBRIUM DATA FOR THE SYSTEM *n*-HEPTANE-THIOPHENE-LIQUID AMMONIA AT 20.0 AND 0.0°C., wt. %

| Total mixture | | Hydrocarbon layer | | Solvent layer | |
|---|---|---|---|---|---|
| Thiophene wt. % (Solvent-free basis) | $NH_3$ wt. % | $NH_3$ wt. % | Thiophene wt. % (Solvent-free basis) | $NH_3$ wt. % | Thiophene wt. % (Solvent-free basis |
| | | At 20.0°C | | | |
| 0.0 | — | 4.8 | 0.0 | 96.9 | 0.0 |
| 12.7 | 53.2 | 5.7 | 5.6 | 89.4 | 61.2 |
| 25.9 | 54.1 | 6.7 | 11.5 | 82.9 | 73.4 |
| 44.7 | 51.7 | 8.8 | 22.0 | 71.3 | 78.8 |
| 42.3 | 40.1 | 10.1 | 26.8 | 65.6 | 77.9 |
| 53.4 | 38.9 | 13.6 | 36.0 | 55.0 | 75.0 |
| 50.8 | 30.6 | 15.6 | 40.6 | 49.4 | 72.7 |
| 58.4 | 32.6 | 22.0 | 49.2 | 41.2 | 67.3 |
| 60.7 | 34.8 | 23.8 | 51.1 | 38.8 | 65.5 |
| Plait point[a] | | 30.7 | 58.1 | 30.7 | 58.1 |
| | | At 0.0°C | | | |
| 0.0 | — | 2.7 | 0.0 | 98.2 | 0.0 |
| 8.9 | 45.5 | 2.9 | 4.8 | 93.2 | 74.2[b] |
| 19.3 | 52.0 | 3.4 | 9.4 | 88.6 | 82.4[b] |
| 33.5 | 50.7 | 4.1 | 17.1 | 81.2 | 88.0 |
| 36.0 | 33.7 | 5.3 | 25.2 | 73.3 | 89.3 |
| 50.1 | 34.5 | 7.4 | 35.7 | 63.4 | 88.8 |
| 56.5 | 32.8 | 8.8 | 41.9 | 56.9 | 87.5 |
| 62.4 | 30.0 | 11.4 | 49.8 | 49.0 | 85.0 |
| 63.9 | 30.6 | 11.9 | 50.9 | 48.1 | 84.6 |
| 78.2 | 42.3 | 12.9 | 52.8 | 46.5 | 84.1 |
| 73.6 | 32.8 | 18.2 | 61.9 | 38.4 | 79.8 |
| Plait point[a] | | 28.3 | 72.5 | 28.3 | 72.5 |

a) The plait point was estimated according to Treybal et al.[4]

b) This value was calculated from the concentration of ammonia in both layers and the composition of the total mixture and the raffinate.

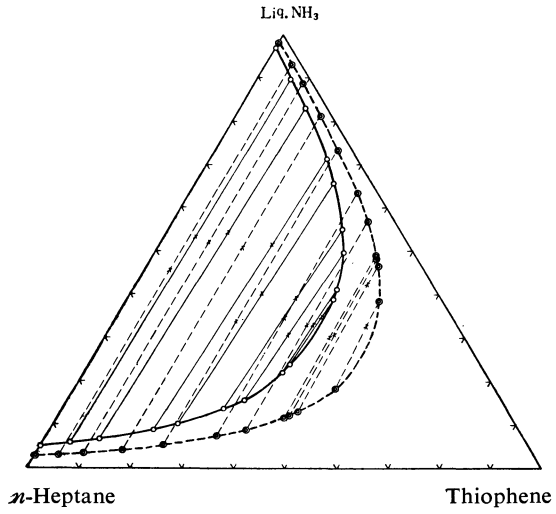



Fig. 1. System *n*-heptane-thiophene-liq. $NH_3$ at 20 and 0°C, wt. %.

—○— 20.0°C --◎-- 0.0°C

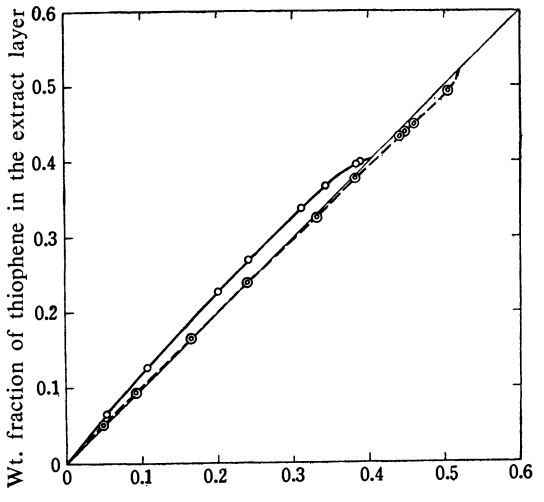



Fig. 2. Equilibrium distribution diagrams for the system *n*-heptane-thiophene-liq. $NH_3$.

—○— 20.0°C --◎-- 0.0°C

4) R. E. Treybal, L. D. Weber and J. F. Daley, ibid., 38, 817 (1946).

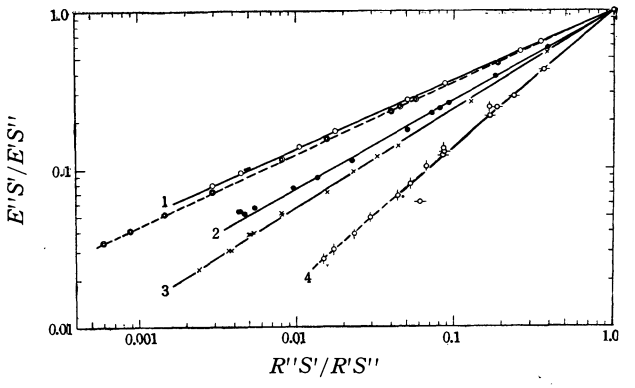



Fig. 3. Plot on logarithmic coordinates $E''S'/E'S''$ against $R''S'/R'S''$ for liquid ammonia systems.

| Number | Symbol | System R — E — S | Temperature, °C | Reference |
|---|---|---|---|---|
| 1 | —○— | *n*-Heptane—Thiophene—Liq. $NH_3$ | 20.0 | |
| | --◎-- | *n*-Heptane—Thiophene—Liq. $NH_3$ | 0.0 | |
| 2 | —●— | *n*-Hexane—Benzene—Liq. $NH_3$ | 20.0 | 5) |
| 3 | —×— | *n*-Heptane—Toluene—Liq. $NH_3$ | 20.0 | 6) |
| 4 | —○- | Ethylbenzene—Styrene—Liq. $NH_3$ | 0.0 | 5) |
| | --⊙-- | Ethylbenzene—Styrene—Liq. $NH_3$ | −15.5 | 5) |

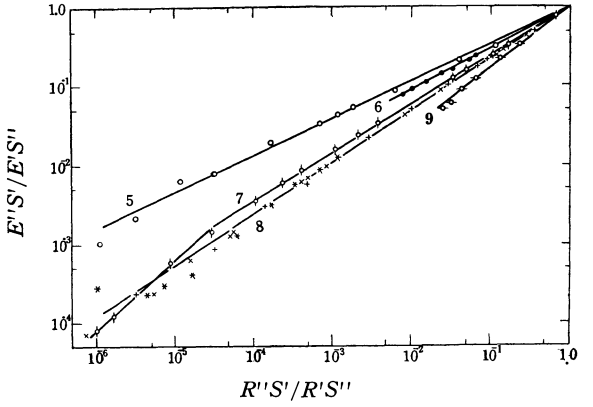



Fig. 4. Plot on logarithmic coordinates of $E''S'/E'S''$ against $R''S'/R'S''$ for systems of various investigators.

| Number | Symbol | System R — E — S | Temperature, °C | Reference |
|---|---|---|---|---|
| 5 | ○ | Benzene—Dioxane—Water | 25 | 7) |
| 6 | ● | Water—Acetic Acid—Furfural | 26.7 | 8) |
| 7 | ⊙ | Water—Acetic Acid—Toluene | 25 | 9) |
| 8 | + | Water—Ethanol—Benzene | 25 | 10) |
| | × | 〃 〃 〃 | 25 | 11) |
| | ✳ | 〃 〃 〃 | 25 | 12) |
| 9 | -○- | Water—Methanol—Butano | 15 | 13) |

5) K. Ishida, This Bulletin, **30**, 612 (1957).
6) K. Ishida, This Bulletin, **29**, 956 (1956).
7) R. J. Berndt and C. C. Lynch, *J. Am. Chem. Soc.*, **66**, 282 (1944).
8) A. E. Skrzec and N. F. Murphy, *Ind. Eng. Chem.*, **46**, 2245 (1954).
9) R. M. Woodman, *J. Phys. Chem.*, **30**, 1283 (1926).
10) Y. -C. Chang and R. W. Moulton, *Ind. Eng. Chem.*, **45**, 2350 (1953).
11) K. A. Varteressian and M. R. Fenske, ibid., **28**, 928 (1936).
12) E. R. Washburn, V. Hnizda and R. Vold, *J. Am. Chem. Soc.*, **53**, 3237 (1931).
13) A. J. Mueller, L. I. Pugsley and J. B. Ferguson, *J. Phys. Chem.*, **35**, 1314 (1931).

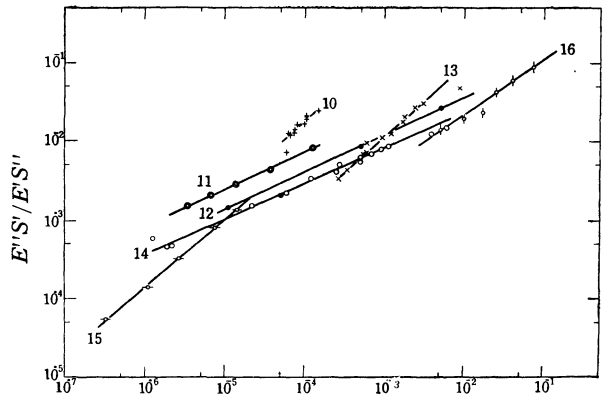



Fig. 5. Plot on logarithmic coordinates of $E''S'/E'S''$ against $R''S'/R'S''$ for systems containing two partially miscible pairs.

| Number | Symbol | System R — E — S | Temperature, °C | Reference |
|---|---|---|---|---|
| 10 | + | *n*-Heptane—Methylcyclohexane—Aniline | 25 | 14) |
| 11 | ◎ | Water—Aetone—Chlorobenzene | 25~26 | 15) |
| 12 | ● | *n*-Hexane—Methyl ethyl ketone—Water | 37.8 | 16) |
| 13 | × | *n*-Heptane—Toluene—Liq. $NH_3$ | −15 | 6) |
| 14 | ○ | Benzene—Butanol—Water | 25 | 17) |
| 15 | -○- | Toluene—Aniline—Water | 25 | 18) |
| 16 | ⊙ | Ethyl acetate—*sec*-Butanol—Water | 20 | 19) |

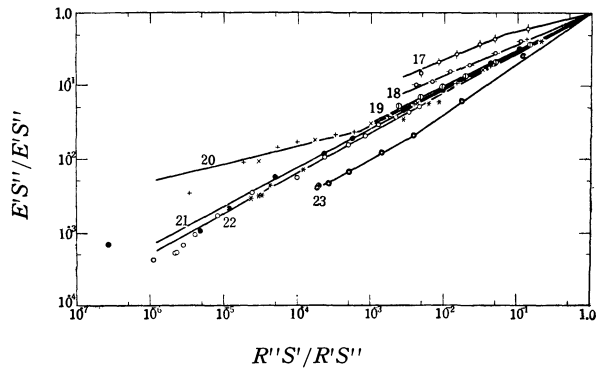



Fig. 6. Plot on logarithmic coordinates of $E''S'/E'S''$ against $R''S'/R'S''$ for solutropic systems.

| Number | Symbol | System R — E — S | Temperature, °C | Reference |
|---|---|---|---|---|
| 17 | ⊙ | Water—*t*-Butanol—Ethyl acetate | 20 | 19) |
| 18 | -○- | Water—Isopropanol—Ethyl acetate | 20 | 19) |
| 19 | ◫ | Water—Acetic acid—Ether | 25 | 20) |
| 20 | + | Water—Pyridine—Benzene | 25 | 21) |
| | × | 〃 〃 〃 | 25 | 22) |
| | ✳ | 〃 〃 〃 | 25 | 23) |
| 21 | ● | Water—*t*-Butanol—Benzene | 25 | 24) |
| 22 | ○ | Water—Isopropanol—Benzene | 25 | 25) |
| 23 | ◎ | Water—Ethanol—3-Heptanol | 25 | 26) |

separation factors[5] become the respective values of 0.650 and 0.488, these values being considerably greater when compared with those in cases of the separation of hydrocarbon mixtures.

### Tie Line Correlation

This system as in the other solutropic systems fails to give a straight line having a definite slope from the appropriate plot of conjugate values at equilibrium according to any method which has been proposed by any one of the many investigators as tie line correlations. The author has found that a straight line results from a plot of logarithm of $E''S'/E'S''$ against logarithm of $R''S'/R'S''$ where $S$, $E$ and $R$ are the respective fractions of the solvent, the solute and the diluent at equilibrium and one prime and two primes denote the diluent-rich layer and the solvent-rich layer, respectively. Plots by this method for the present data are shown in Fig. 3. In Fig. 3, plots for the several systems using liquid ammonia as a solvent are also included. It is observed that these data are correlated by this method satisfactorily.

Several ordinary systems investigated by various workers are plotted in Fig. 4, and plots for systems containing two pairs of partially miscible liquids are given in Fig. 5. Plots by this method for several solutropic systems are shown in Fig. 6. Except for some systems where it seems to be plausible that the data are correlated by two straight lines changing their slopes, the plotted data for most systems fall on straight lines having definite slopes almost within their probable experimental accuracy. When the solvent and the diluent are practically insoluble as in the case of benzene-water binary, values of $S'R''/S''R'$ and $S'E''/S''E'$ become more inaccurate at the lower concentrations of the solute, because the concentrations of the solute are very small and their accurate determinations by ordinary methods are difficult. For this reason, it may be said roughly that plots by this method would give a straight line for most ternary systems.

Since the values of $S'R''/S''R'$ for the binary systems of the diluent and the solvent are located as the abscissa on the left ends of straight lines in these figures, the initial distribution ratio at zero concentration of the solute can be estimated from the ordinate on these points. The ordinate on the right ends of straight lines in Fig. 5 represent the values of $S'E''/S''E'$ for the binary systems of the solute and the solvent, and the abscissa the product of the distribution coefficient at zero concentration of the diluent and the ratio of the concentration of the solvent in the solute rich phase to that in the solvent rich phase.

The straight lines can be represented by equations of the form

$$\log \frac{E''S'}{E'S''} = n \log \frac{R''S'}{R'S''} + k \qquad (1)$$

For the ordinary systems which comprise two miscible pairs of liquids and one partially miscible pair, the value of $k$ should be extremely near zero, since the values of $S'E''/S''E'$ and $S'R''/S''R'$ at the plait point are equal to unity. If the relative distribution ratio is designated by $\beta$,

$$\beta = \frac{E''}{E'} \cdot \frac{R'}{R''} \qquad (2)$$

Then,

$$\log \beta = (n-1) \log \frac{R''S'}{R'S''} + k \qquad (3)$$

Therefore, if a plot is made of the relative distribution ratio against the quotient of the ratio of the concentration of the solvent in the diluent rich phase to that in the solvent rich phase and that of the solute or the diluent on the double logarithmic coordinates, a straight line will be given as well not only for ordinary systems, but also for solutropic systems and those containing two partially miscible pairs.

### Summary

Phase equilibria for the system *n*-heptane-thiophene-liquid ammonia has been determined at temperatures of 0 and 20°C. A new method has been proposed which correlates tie line data in such a manner that a straight line is obtained for most systems including solutropic systems.

*The Chemical Research Institute of Non-Aqueous Solutions*
*Tohoku University*
*Katahira-cho, Sendai*

14) K. A. Varteressian and M. R. Fenske, *Ind. Eng. Chem.*, **29**, 270 (1937).
15) D. F. Othmer, R. E. White and E. Trueger, ibid., **33**, 1240 (1941).
16) J. H. Jones and J. F. McCants, ibid., **46**, 1956 (1954).
17) E. R. Washburn and C. V. Strandskov, *J. Phys. Chem.*, **48**, 241 (1944).
18) J. C. Smith and R. E. Drexel, *Ind. Eng. Chem.*, **37**, 601 (1945).
19) D. G. Beech and S. Glasstone, *J. Chem. Soc.*, 67 (1938).
20) C. J. Major and O. J. Swenson, *Ind. End. Chem.*, **38**, 834 (1946).
21) J. C. Smith, *J. Phys. Chem.*, **46**, 376 (1942).
22) G. N. Vriens and E. C. Medcalf, *Ind. Eng. Chem.*, **45**, 1098 (1953).
23) R. M. Woodman and A. S. Corbet, *J. Chem. Soc.*, **127**, 2461 (1925).
24) D. R. Simonsen and E. R. Washburn, *J. Am. Chem. Soc.*, **68**, 235 (1946).
25) A. L. Olsen and E. R. Washburn, ibid., **57**, 303 (1935).
26) C. M. Qualline, Jr., and M. van Winkle, *Ind. Eng. Chem.*, **44**, 1668 (1952).

# *Polymerization of Methyl Methacrylate Initiated by a Combined Action of p-Tolylsulfonylacetic Acid and Dimethylaniline*

By Ryoichi UEHARA

(Received July 20, 1959)

It has been first reported by Lal et al.[1], that the polymerization of methyl methacrylate is initiated by mixtures of dimethylaniline and various carboxylic acids. In a previous paper by the present author[2], results of studies on the kinetics of the polymerization of methyl methacrylate initiated by a combined action of trichloroacetic acid and dimethylaniline have been reported, and a bimolecular reaction between these two compounds has been suggested as the initial reaction of the polymerization. In the report of Lal, per-cent-conversions after 1 hr. in the bulk polymerization of methyl methacrylate at 58.6°C by using nine carboxylic acids have been given briefly, and six acids, i. e., mono-, di- and trichloroacetic, mercaptoacetic, phenoxyacetic and 1, 4-dichlorobenzoic acids, were found to be effective.

The present author has found that *p*-tolylsulfonylacetic acid, which has been prepared by Gabriel[3] from sodium *p*-toluenesulfinate and monochloroacetic acid, is also effective as a component of the polymerization-initiating system.

$$CH_3C_6H_4SO_2Na + ClCH_2COOH = CH_3C_6H_4SO_2CH_2COOH + NaCl$$

In the present paper, per-cent-conversion of the bulk polymerization of methyl methacrylate initiated by the system of *p*-tolylsulfonylacetic acid and dimethylaniline is given, and the effects of *p*-substituted groups in dimethylaniline upon the polymerization-initiating efficiencies of the two systems, trichloroacetic acid-dimethylaniline and *p*-tolylsulfonylacetic acid-dimethylaniline, are compared.

The polymerization was carried out in the atmosphere of nitrogen. In Table I, per-cent-conversion of the bulk polymerization at 60°C is given. Each of *p*-tolylsulfonylacetic acid, and dimethylaniline alone was not responsible for the initiation of the polymerization. In Fig. 1, per-cent-conversion after 1 hr., in the bulk polymerization, by means of equimolar amounts of *p*-tolylsulfonylacetic acid and dimethylaniline at temperatures of 51, 60 and 70°C are plotted against the concentration of the acid. It is observed that the per-cent-conversion after 1 hr. is linearly dependent upon the concentration of the acid. This fact indicates that, in this polymerization, the linear dependence of the rate of polymerization upon the initial concentration of *p*-tolylsulfonylacetic acid or dimethylaniline holds, as in the case of the

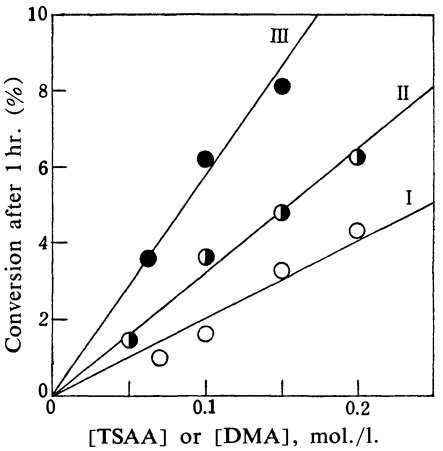



Fig. 1. Correlations of per-cent-conversion after 1 hr. with the concentration of *p*-tolyl-sulfonylacetic acid or dimethyl aniline.
I at 51°C, II at 60°C, III at 70°C

TABLE I. PER-CENT-CONVERSION (*C*) AND AVERAGE DEGREE OF POLYMERIZATION (*DP*) IN THE BULK POLYMERIZATION OF METHYL METHACRYLATE AT 60°C BY MEANS OF *p*-TOLYLSULFONYLACETIC ACID (TSAA) AND DIMETHYLANILINE (DMA)

| mol./l. | | Time, hr. | *C*, % | *DP* |
|---|---|---|---|---|
| TSAA | DMA | | | |
| 0.15 | 0.15 | 1 | 4.8 | |
| 〃 | 〃 | 2 | 10.9 | 2120 |
| 〃 | 〃 | 3 | 15.3 | 2470 |
| 〃 | 〃 | 4 | 21.0 | 2500 |
| 〃 | 〃 | 5 | 27.8 | |
| 〃 | 〃 | 6 | 33.6 | 3900 |
| 〃 | 〃 | 10 | 97.3 | |
| 0.36 | 0 | 1 | 0 | |
| 〃 | 0 | 8 | trace | |
| 0 | 0.18 | 1 | 0 | |
| 0 | 0.30 | 10 | 0 | |

1) J. Lal et al., *J. Polymer Sci.*, **24**, 81 (1957).
2) R. Uehara, This Bulletin., **31**, 685 (1958).
3) S. Gabriel, *Ber.*, **14**. 834 (1881).

polymerization initiated by equimolar amounts of trichloroacetic acid and dimethylaniline[2], because per-cent-conversion after 1 hr., can be considered to be proportional to the initial rate of polymerization.

*p*-Substituted groups in dimethylaniline significantly affect the polymerization-initiating efficiencies of the two systems, *p*-tolylsulfonylacetic acid-dimethylaniline and trichloroacetic acid-dimethylaniline. Table II shows per-cent-conversions after 1 hr. by using various dimethylanilines in bulk polymerizations of methyl methacrylate, in which *p*-tolylsulfonylacetic and trichloroacetic acids were used respectively. Electron-donating groups such as methyl and methoxyl promote, and electron-withdrawing groups such as chloro, bromo and nitroso reduce the efficiencies of the polymerization-initiating systems. In Table II, $C/C_0$ are also shown, where $C_0$ and $C$ are per-cent-conversions in the polymerizations by using dimethylaniline and *p*-substituted dimethylaniline, respectively.

Table II. Relative efficiency of *p*-substituted dimethylaniline in the polymerizations initiated respectively by systems, *p*-tolylsulfonylacetic acid-dimethylaniline and trichloroacetic acid-dimethylaniline

| Substituent | % Conversion* (TSAA and DMA) | $C/C_0$ | % Conversion** (TCA and DMA) | $C/C_0$ |
|---|---|---|---|---|
| $OCH_3$ | 11.3 | 2.35 | 11.4 | 1.752 |
| $CH_3$ | 8.7 | 1.81 | 8.9 | 1.37 |
| H | 4.8 | 1.0 | 6.5 | 1.0 |
| Cl | 2.9 | 0.604 | 4.2 | 0.646 |
| Br | 2.4 | 0.500 | 4.1 | 0.630 |
| NO | 0 | 0 | 0 | 0 |

* 0.15 mol./l. of each of TSAA and DMA were used at 60°C.

** 0.20 mol./l. of each of TCA and DMA were used at 25°C.

For each of the substituted groups, the value of $C/C_0$ in the polymerization by using *p*-tolylsulfonylacetic acid is substantially similar to that in the polymerization, in which trichloroacetic acid was employed, i.e., the relative efficiency of *p*-substituted dimethylaniline is substantially the same in the initiating systems. When the logarithms of $C/C_0$ are plotted against $\sigma$ (substitutent constant of Hammett) of each substituted groups, good straight lines are obtained as are shown in Fig. 2. It is evident that Hammett's rule holds in the two cases.

As has been mentioned above, the dependence of the initial rate of polymerization upon the concentration of *p*-tolylsulfonylacetic acid (or dimethylaniline) and the relative efficiency of the substituted dimethylaniline in the polymerization of methyl methacrylate initiated by the system of *p*-tolylsulfonylacetic acid and dimethylaniline are quite similar to those in the polymerization initiated by a combined action of trichloroacetic acid and dimethylaniline. Therefore, it is conceivable, that the polymerization initiated by *p*-tolylsulfonylacetic acid and dimethylaniline proceeds through the same mechanism as that which has been postulated previously for the polymerization initiated by trichloroacetic acid and dimethylaniline[2].

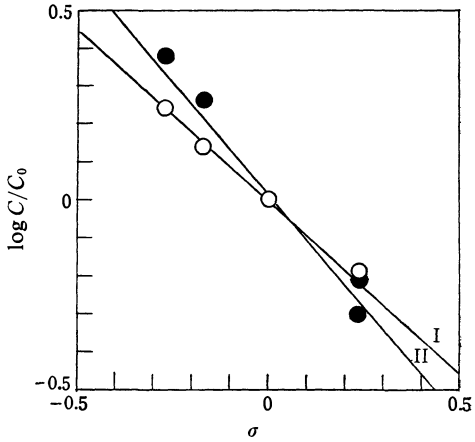



Fig. 2. Correlations of $\log C/C_0$ with $\sigma$.
I for TCA and DMA (○)
II for TSAA and DMA (●)

## Experimental

The polymerization and the purification of methyl methacrylate were carried out as mentioned previously[2]. *p*-Tolylsulfonylacetic acid was prepared by the following procedures; sodium *p*-toluenesulfinate (43 g.) and monochloroacetic acid (19 g.) were mixed with methanol (100 cc.), and sodium hydroxide (8 g.) which was dissolved in water (100 cc.) was added. The mixture was refluxed for 4 hr., and then methanol was distilled off. By treating the residue of the distillation with 30% aqueous hydrochloric acid (50 cc.), an oily material separated. The oil was cooled in an ice salt-bath until it changed into crystalline solids. They were washed with aqueous methanol (1 : 1 by volume) and recrystallized from pure methanol, giving pure *p*-tolylsulfonylacetic acid (17.5 g.), m. p. 86°C. Dimethylaniline and *p*-substituted dimethylaniline were distilled under reduced pressure in the atmosphere of nitrogen or recrystallized from methanol: dimethylaniline b. p. 56°C/5 mmHg, $-CH_3$ b. p. 73.5°C/5 mmHg, $-Cl$ b. p. 86°C/5 mmHg, $-Br$ b. p. 101°C/5 mmHg, $-OCH_3$ m. p. 48.5°C, and $-NO$ m. p. 85°C.

## Summary

It has been found that the polymerization of methyl methacrylate is initiated by the system of *p*-tolylsulfonylacetic acid and dimethylaniline.

In the polymerization initiated by equimolar amounts of *p*-tolylsulfonylacetic acid and dimethylaniline, the initial rate of polymerization is linearly dependent upon the initial concentration of the acid (or dimethylaniline). Hammett's rule holds for the relative efficiency of *p*-substituted dimethylaniline as the component of the polymerization-initiating system. These relationships are quite similar to those which are observed in the polymerization of methyl methacrylate, initiated by trichloroacetic acid and dimethylaniline. It is conceivable that the two polymerization reactions proceed through the same mechanism.

The author wishes to express his thanks to Professor Osamu Simamura of the University of Tokyo, for his interests in this work and Mr. Tsurahide Cho, the President of Tama Kagaku Kogyo Co., for permission to undertake this work.

*Tama Kagaku Kogyo Co.*
2-28 *Minamirokugo,*
*Ota-ku, Tokyo*

# *Kolbe's Reaction of Higher Fatty Acids. I. Electrolysis of Lauric Acid**

By Tikami MIZUTA**, Takeo HISANO and Ryoichi MATSUDA

(Received August 21, 1959)

Kolbe's reaction of fatty acids in general has been studied by many investigators but that of lauric acid[1] in particular not in detail. In the previous paper[2], one of the present authors, R. Matsuda, studied electrolysis of acetic and propionic acids for the purpose of clarifying the mechanism of the reaction. The present study was undertaken to find a clue to approach its true aspect, dealing with higher members of fatty acid.

Four electrolytes were employed which consisted of an ethanolic solution of lauric acid and potassium hydroxide. These were different from each other with respect to the alkali content. In Experiment 1 the effect of changing anodic current density 0.08~1.20 amp./cm$^2$ upon the current efficiency of docosane production which is due to Kolbe's reaction was examined with one of the electrolytes. The increase of current efficiency with that of the anodic current density was observed with nickel anode as well as platinum anode. The former anode resulted in current efficiency which was close, but a little inferior, to that by means of the latter.

In Experiment 2 the effect of the alkalinity of the electrolyte upon the current efficiency was examined with the four solutions, and it was found that the less alkaline the electrolyte, the greater was the current efficiency. Nickel and platinum anodes behaved as in Experiment 1. In the case of lower members of fatty acid, nickel anode is known not to give rise to Kolbe's reaction.

## Experimental

An anode of platinum plate was coupled with a cathode of the same material, and so was an anode of nickel plate with a cathode of the same. The cathode in each case was in the shape of a square box without top or bottom, the horizontal section being 10×20 mm., and the height 20 mm. The anode which was rectangular 5×10 mm. was placed at the center of the cathode in each case. The upper part of the electrlytic cell was cylindrical 100 mm. long and 30 mm. in diameter, and its lower part was 50 mm. long, being flattened so as to have the two faces 25 mm. apart. The vessel was inclined by some 30° when in operation. Such a cell together with the electrodes helped not only to lessen the volume of the electrolyte and the voltage required, but also to ease the agitation of the solution without mechanical device. This sort of agitation might have the disadvantage of not always being uniform, because of the varied amount of evolving gas. It was, however, sufficiently useful for the present purpose. The lauric was 99.9% pure, the neutralization value being 279.5 against the theoretical value of 280.23 and the m. p. 44.1°C. Four solutions were prepared for electrolysis, each of which contained 1 mol. lauric acid and a different portion of potassium hydroxide in a mixture of 800 cc. ethanol and 533 cc. water: Solutions A, B, C and D contained 0.14, 0.34, 0.68 and 1.02 mol. potassium hydroxide respectively.

Each electrolysis was conducted with 40 cc. of the solution at 40°C. An oily mass floated, consisting mainly of docosane, as it was produced by

* Read before the Local Meeting of the Chemical Society of Japan at Tokushima, August 29, 19588.

** Present address, Daitoh Paper Mill Co., Iyo-Mishima, Ehime.

1) J. Petersen, *Z. Electochem.*, 12, 143 (1906); Y. Minami, F. Ono and Y. Toyama, *J. Chem. Soc. Japan, Ind. Chem. Sec.*, (*Kogyo Kagaku Zasshi*), 53, 393 (1950).

2) R. Matsuda, This Bulletin, 7, 18, 297 (1932).

electrolysis. The content of the vessel was cooled after electrolysis, and the coagulated crude docosane was taken out, melted in 70~80°C water, and cooled again. This product was purified by extracting with benzene four to five times, and then by recrystallizing with ethanol three to four times. It was subsequently identified as docosane by the melting point, the elementary analysis and the molecular weight determination. M. p. 44.0~44.5°C (the reported m. p. 44.4°C)[3].

Found: C, 85.30; H, 14.81. Calcd. for $C_{22}H_{46}$: C, 85.39; H, 14.61%. Mol. wt. (Rast's method). Found: 292. Calcd.: 310.31.

**Experiment 1.** Solution C was electrolyzed with the nickel as well as the platinum electrodes. The anodic current density was varied 0.08~1.20 amp./cm² in order to see the influence of anodic current density on Kolbe's reaction, 2200 coulombs were supplied for each electrolysis. This quantity was nearly 90% of that necessary to electrolyze lauric acid in the solution. The docosane production is shown in Table I and Fig. 1.

Table I. Influence of anodic current density upon docosane production

| Anodic current density amp./cm² | Pt-electrodes docosane current efficiency | | Ni-electrodes docosane current efficiency | |
|---|---|---|---|---|
| | g. | % | g. | % |
| 0.08 | 1.20 | 34.0 | 1.12 | 31.8 |
| 0.20 | 1.23 | 34.8 | 1.21 | 34.3 |
| 0.40 | 1.31 | 37.1 | 1.27 | 36.0 |
| 0.80 | 1.39 | 39.4 | 1.30 | 36.8 |
| 1.20 | 1.42 | 40.2 | 1.35 | 38.2 |

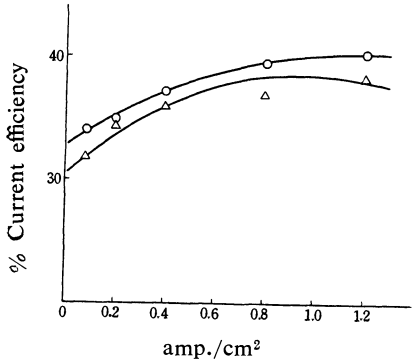



Fig. 1. Influence of anodic current density upon docosane production.
-○- Platinum electrodes.
-△- Nickel electrodes.

**Experiment 2.** In order to see the influence of alkalinity, solutions A, B, C and D were electrolyzed with 2200 coulombs at a constant anodic current density of 0.4 amp./cm², employing the platinum as well as the nickel electrodes. The current efficiency of docosane production in these cases is shown in Table II and Fig. 2.

3) The reported value: 44.0~44.5°C, F. Kraft, *Ber.*, **40**, 4783 (1907).

Table II. Influence of alkalinity of solution upon docosane production

| Solution | Mol. KOH per 1 mol. lauric acid | Pt-electrodes Docosane | C. E. | Ni-electrodes Docosane | C. E. |
|---|---|---|---|---|---|
| A | 0.14 | 2.29g. | 64.9% | 2.23g. | 63.2% |
| B | 0.34 | 1.88 | 53.3 | 1.88 | 53.3 |
| C | 0.68 | 1.31 | 37.1 | 1.27 | 36.0 |
| D | 1.02 | 0.67 | 19.0 | 0.54 | 15.3 |

C. E. denotes current efficiency.

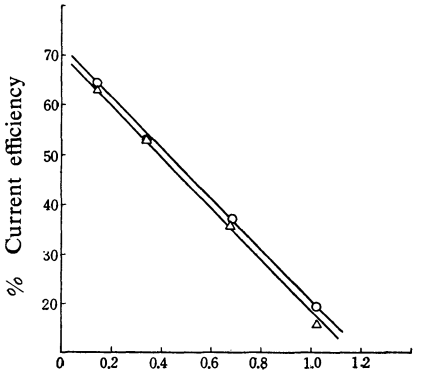



Fig. 2. Influence of alkalinity of solution upon docosane production.
-○- Platinum electrodes.
-△- Nickel electrodes.

## Discussion

According to Experiment I the increase of anodic current density favored Kolbe's reaction, the influence being more noticeable when the current density was smaller. This tendency was also observed with acetic acid, in which case it was mentioned that proper regions of concentration and pH should be maintained[4]. Larger current density means a larger number of anions discharged per unit surface area of the anode. The result of Ex-periment I will be understood if it is assumed that the discharge of lauric acid anions which is responsible for Kolbe's reaction occurs dominantly under the favored condition. When the current density was larger than 1.2 amp./cm², the gas evolution made it impossible to keep the current uniform and to obtain a reliable result. It is presumed that docosane production decreases for the following two reasons: first that with current density above 1.2 amp./cm² the discharge of more easily movable hydroxyl ions might dominate, and second that the migration velocity of lauric acid ions reaches the maximum. Docosane production consequently decreased.

4) R. Matsuda, *J. Chem. Soc. Japan (Nippon Kwagaku Kwaishi)*, **51**, 662 (1930).

Platinum and nickel were compared as anode material. The latter was found as good for Kolbe's reaction of lauric acid as the former, which had been regarded practically as the superlative material for Kolbe's reaction of fatty acid in general.

It was shown by Experiment 2 that docosane production quickly dropped off with the increase of potassium hydroxide, and there was no maximum point in the curves of Fig. 2 as was expected. It seems that the discharge of lauric acid ions steadily gave place to that of hydroxyl ions as potassium hydroxide increased, and docosane production decreased. Platinum and nickel were compared again as anode material and found close to each other with respect to the current efficiency of docosane production, although the former was superior to the latter as in Experiment 1. Fichter[5] considered that oxidation of fatty acid by means of anodic atomic oxygen resulted in Kolbe's reaction. There is, however, a great difference between the oxygen overvoltages of platinum and nickel. If the overvoltage should have anything to do with anodic atomic oxygen, hence with Kolbe's reaction, these two metals would behave differently as anode material, platinum with its high over-voltage being favorable to the reaction. Besides, Kameyama[6] describes that when acetate is electrolyzed with nickel, iron or gold as an anode no Kolbe's reaction takes place, oxygen being the dominant product of the anodic reaction.

In addition to the fact that nickel was available as an good anode for Kolbe's reaction in the present case, dimethlyglyoxime failed to detect nickel ions in the electrolyzed solution, and the nickel anode showed no apparent change after electrolysis. It is likely that the nickel anode assumed the passive state during electrolysis.

The authors wish to express their thanks to Nippon Oils and Fats Co., Ltd. which kindly provided them with lauric acid.

*Department of Applied Chemistry*
*Faculty of Engineering*
*Tokushima University*
*Tokushima*

5) Fr. Fichter, *Trans. Am. Electrochem. Soc.*, **45**, 131 (1924).

6) N. Kameyama, "Theory and Application of Electrochemistry (Denki-Kagaku no Riron oyobi Oyo)" Vol. II. Maruzen, Tokyo (1953), p. 225.

# *Coprecipitation of Neptunium with Lanthanum Trifluoride*

By Eiko NAKAMURA

(Received November 21, 1959)

It is well known that oxidized neptunium does not coprecipitate with lanthanum trifluoride whereas reduced neptunium is carried down almost quantitatively. Although this process is studied and often utilized for the practical separation of neptunium[1-3], its oxidation state is not clearly defined. Some believe that both neptunium(IV) and -(V) are carried down by lanthanum trifluoride[4], whereas others believe that neptunium(V) is not[5]. Sometimes the expression the "lanthanum fluoride carriable state" is used in place of the "oxidation state"[6]. Thus, the coprecipitation behavior of neptunium (V) is open to question.

In the present study, the different modes of coprecipitation behavior of neptunium(IV), -(V) and -(Vl), are studied with the aids of the tracers for neptunium(IV), -(V) and -(Vl). The oxidation state of the neptunium tracer used is determined according to the solvent extraction behavior as well as to the coprecipitation behavior with zirconium phosphate.

## Experimental

**Materials.**—Neptunium-239 separated from neutron irradiated uranyl nitrate[7] is used as the tracer for neptunium. Prior to use, the tracer is treated chemically in order to confirm the fact that neptunium(IV), -(V) and -(VI) tracer is radiochemically pure.

1) G. T. Seaborg and A. C. Wahl, *J. Am. Chem. Soc.*, 70, 1128 (1948).
2) L. B. Magnusson and T. J. LaChapelle, ibid., 70, 3534 (1948).
3) L. B. Magnusson, S. G. Thompson and G. T. Seaborg, *Phys. Rev.*, 78, 363 (1950).
4) L. B. Magnusson, J. C. Hindman and T. J. LaChapelle, AEC Report ANL-4066 (1947).
5) G. T. Seaborg and J. J. Katz, "The Chemistry of the Actinide Elements"; Methuen and Co., Ltd., London (1957), Chap. VI.
6) E. K. Hyde, First United Nations International Conference on the Peaceful Uses of Atomic Energy, Vol. VII, P/728, United Nations Publication, New York (1956).
7) T. Ishimori and E. Nakamura, This Bulletin, 32, 713 (1959).

These chemical treatments are as follows.

*Tetravalent neptunium.*—(A) *In nitirc acid system.* The tracer reduced by granulated zinc in 1 N nitric acid is extracted by TTA*-benzene, stripped by 3 N nitric acid washed with benzene and diluted with distilled water to 2 N. (B) *In hydrochloric acid system.* The tracer is reduced by granulated zinc in 1 N HCl, extracted by TTA-benzene solution, stripped by 1 N HCl in a large volume and washed with benzene.

*Pentavalent neptunium.*—In the nitric acid system, neptunium(V) tracer is prepared in the following four ways. (C) The tracer is prepared as perchloric acid solution and pipetted into 2 N nitric acid. Neptunium is almost all pentavalent in perchloric acid[7], and the neptunium(VI) which might be present is removed by 100% TBP**. (D) The tracer is oxidized with ceric ammoium nitrate[5] in 7 N nitric acid, extracted with 100% TBP, stripped by distilled water after the organic layer is diluted with a large volume of benzene, and reduced by hydrazine[5]. The acid concentration is about 2 N. Neptunium distribution ratios in the TBP nitric acid system are measured when neptunium is treated with oxidizing or reducing agent. (E) The tracer is reduced with sulfur dioxide in perchloric acid solution in order to change all of neptunium into neptunium(V), and pipetted in volume of a few lambda (0.001ml.). The distribution ratio is measured between 100% TBP and 1.7 N perchloric acid tracer solution saturated with sulfur dioxide. (F) The tracer is treated as (D), but reduced with sulfur dioxide instead of with hydrazine[5]. The distribution ratio of this tracer solution is checked between 1.7 N perchloric acid and TBP.

(G, H) In the hydrochloric acid system, the tracer is obtained in perchloric acid solution and a few lambda of it are pipetted into the acid. The acid concentration is 1 N(G) or 4 N(H) of hydrochloric acid.

(I, J) In the perchloric acid system, a perchloric acid tracer solution is used. The perchloric acid concentration is 4.6 N(I) or 1.2 N(J).

*Hexavalent neptunium.*—(K) In nitric acid system. The tracer solution is warmed and oxidized with ceric ammonium netrate in 7 N $HNO_3$[5]. Oxidized neptunium is extracted with 100% TBP. The organic phase obtained is shaken with 7 N nitric acid in order to remove Np(IV) and -(V). Neptunium is backextracted with distilled water and washed with benzene. The acid concentration is about 2 N. The distribution ratio of neptunium between 7 N nitric acid and TBP is measured. (L) In hydrochloric acid system. The tracer is oxidized by potassium chlorate[5] in 8 N hydrochloric acid during the heating of the solution, extracted with 100% TBP, backextracted with a large volume of distilled water, and washed with benzene. The distribution ratio of tracer between 8 N hdyrochloric acid and 100% TBP is checked. (M) In perchloric acid system. Tracer is oxidized with silver peroxide in 1.2 N perchloric acid[5]. Experiments are carried out in the presence of silver peroxide powder. Without silver peroxide, the tracer is carried down with lanthanum fluoride.

The lanthanum carrier solution contains 2 mg. of the lanthanum ion per ml. in acid solution. In order to avoid complexities, lanthanum carrier is dissolved in the same acid as that used for nuptunium tracer solution in every case.

The zirconium carrier solution contains 10 mg. zirconium per ml.

Hydrofluoric acid (47.1%) is used without dilution as precipitant for lanthanum fluoride. It will be seen in Table I that high hydrofluoric acid concentration in the precipitant causes marked coprecipitation of neptunium(V) in nitric acid medium. Thus, the coprecipitation behavior is supposed to be dependent on the concentration of hydrofluoric acid. However, not considering this effect, hydrofluoric acid is used without any dilution or purification in the present study.

1 M diammonium hydrogen phosphate solution is used as precipitant for zirconium phosphate.

**Procedure.**—The coprecipitation experiments are carried out as follows. Two milliliters of acid solution containing neptunium-239 in a desired oxidation state, 1 ml. of carrier solution and 1 ml. of precipitant solution are mixed thoroughly in a centrifuge tube. The hydrofluoric acid corrosion of glass is avoided by using an polyacrylic acid tube. After the white precipitate is removed by centrifugation, 2 ml. of the supernatant solution is taken in a glass tube for the measurement of the gamma activity. This is measured by Philips' scintillation counter.

## Results

The reproducibility is checked by repeating experiments under the same conditions. As is seen in Table I, most values coincide well with

Table I. The effect of hydrofluoric acid concentration

| Acid concn. | Activity remaining / Activity taken | Mean |
|---|---|---|
| conc. HF(47.1%) | 0.0067 | 0.0073 |
| | 0.0068 | |
| | 0.0082 | |
| | 0.0074 | |
| 1 : 1 HF | 0.010 | 0.010 |
| | 0.011 | |
| | 0.0096 | |
| | 0.0096 | |
| 1 : 3 HF | 0.057 | 0.057 |
| | 0.044 | |
| | 0.060 | |
| | 0.060 | |

Given activity for 2 ml. of solution is 61486 cpm. Nitric acid concentration is 2 N. Tracer is Np(V).

Table II. The effect of nitric and concentration

| $HNO_3$, N | Activity remaining / Activity taken |
|---|---|
| 0.5 | 0.0138 |
| 1.0 | 0.0116 |
| 2.0 | 0.0124 |
| 5.0 | 0.0110 |

* Thenoyltrifluoroacetone.
** Tri-*n*-butyl phosphate.

TABLE III. COPRECIPITATION OF NEPTUNIUM

| Acid | Tracer | | $LaF_3$ pptn. | | $ZrH_2(PO_4)_2$ pptn. | |
|---|---|---|---|---|---|---|
| | Solution | Treatment | Ratio* | % Np pptd. | Ratio* | % Np pptd. |
| $HNO_3$ | Np(IV) | A | 0.0096 | 99 | 0.084 | 92 |
| | Np(V) | B | 0.012 | 99 | 0.70 | 30 |
| | Np(V) | C | 0.0064 | 99 | 0.77 | 23 |
| | Np(V) | D | 0.017 | 98 | 0.78 | 22 |
| | Np(V) | E | 0.021 | 98 | 0.85 | 15 |
| | Np(VI) | F | 0.99 | 1 | 0.45 | 55 |
| HCl | Np(IV) | G | 0.016 | 98 | 0.018 | 98 |
| | Np(V) | H | 0.011 | 99 | 0.96 | 4 |
| | Np(V) | I | 0.0099 | 99 | 0.87 | 13 |
| | Np(VI) | J | 0.72 | 28 | 0.75 | 25 |
| $HClO_4$ | Np(V) | K | 0.028 | 97 | 0.97 | 3 |
| | Np(V) | L | 0.026 | 97 | 0.82 | 18 |
| | Np(VI) | M | 0.89 | 11 | 0.66 | 34 |

* $\frac{\text{Activity remaining in solution}}{\text{Activity taken}}$

one another. However, experiments are repeated four times under the same conditions and the mean value of the ratio between the neptunium remaining and the neptunium taken, is calculated.

On the other hand, it is likely that the acidity of the tracer solution would not cause a strong effect on the coprecipitation. Table II shows that the tracer solution of 0.5~5.0 N nitric acid gives reproducible results. All results obtained are summarized in Table III.

The tracers were prepared by solvent extraction with TBP and/or TTA, as described in the experimental part and the oxidation state of the neptunium was determined according to the solvent extraction behavior and also the coprecipitation behavior with zirconium phosphate.

The oxidation state of neptunium(IV) was ascertained by TTA-extraction and zirconium phosphate coprecipitation. It is well known that only neptunium(IV) is extracted by TTA[4-6], and is carried down by zirconium phosphate[3,5,6]. Results show that neptunium(IV) coprecipitates with lanthanum fluoride in nitric and hydrochloric acid solutions. No experiment was carried out in perchloric acid solution, because neptunium(IV) is unstable in perchloric acid solution.

In the series of experiments for neptunium(V) and -(VI), the distribution ratios of the neptuium tracer were measured between mineral acid and 100% TBP. The distribution of neptunium(IV), -(V) and -(VI) between tributyl phosphate and some kinds of mineral acid had been betermined in the previous study[7]. The distribution ratio being measured, the oxidation state is assigned by comparing the distribution ratio measured and that reported. On the other hand, zirconium phosphate can not carry down neptunium(V) and -(VI) quantitatively. These results show that neptunium(V) is carried down with lanthanum fluoride whereas neptunium(VI) is not. An uncertainty may be found in the preparation of $ZrH_2(PO_4)_2$ precipitate, because it is not aged in order to prevent any change in the oxidation state of neptunium.

It will be noted in Table III that both neptuium(IV) and -(V) are carried down by lanthanum fluoride almost completely, while a remarkable amount of neptunium(VI) remains in the supernatant solution. As far as lanthanum fluoride precipitation is concerned, the difference between the behavior of neptunium(IV) and that of neptunium(V) can not be identified separately, but these two oxidation states behave quite differently in TBP-acid solution systems. It is also seen in Table III that they behave differently in coprecipitation with zirconium phosphate.

Results show that neptunium(IV) and -(V) can not be separately identified according to their behavior in being carried down with lanthanum trifluoride, whereas they are identified by the behavior in the solvent extractions or in the coprecipitation with zirconium phosphate. Thus it is presumed that both neptunium(IV) and -(V) are carried down almost completely with lanthanum trifluoride while neptunium(VI) remains in the supernatant solution.

The author wishes to thank Dr. Tomitaro Ishimori for criticism and suggestions which made a major contribution to this work.

*Chemistry Division, Tokai Laboratory*
*Japan Atomic Energy*
*Research Institute,*
*Tokai, Ibaraki-ken*

# *On the Molecular Structure of Malononitrile*

By Eizi HIROTA and Yonezo MORINO

(Received March 28, 1960)

The structure of malononitrile molecule has been investigated by microwave spectroscopy[1], three kinds of isotopic species, $CHD(CN)_2$, $CD_2(CN)_2$, and $CH_2CNC^{15}N$, being used in addition to the normal one, $CH_2(CN)_2$. The CCN group was found to be bent slightly. However, as Dr. N. Muller pointed out in his private communication, the procedure of the analysis applied gave a mixed $r_s$ and $r_o$ structure, that is, the positions of hydrogen and nitrogen atoms were determined by isotopic substitution, on the other hand those of carbon atoms were obtained from the first moment equation and the observed moments of inertia, because the isotopic atom $^{13}C$ was not available[2]. It would be therefore worthwhile to see whether the bent structure of the CCN group is established or not, in the $r_o$ structure including inertia defect. The reanalysis is made by fitting the calculated $x$-, $y$-, and $z$-moments with the observed by the least-squares method. The result is shown in Table I and the molecular structure obtained is listed in Table II. It is found within the mean deviation that the CCN group is bent by $3°40' \pm 2°54'$[3]. The bond lengths C–C and C≡N are nearer to those found in a number of other related molecules than those obtained in the previous paper, though the mean deviations attached are large enough to include the structural parameters determined by the previous analysis.

It is very difficult to estimate the errors in the molecular structure obtained. The effect of zero-point vibration is a serious factor in the determination of molecular structure by the spectroscopic method. The mean deviations given here are considered mostly due to the effect of zero-point vibration. The error in the observed moment of inertia is of minor importance, and was taken into consideration in the previous paper where the effect of zero-point vibration was ignored. The more detailed analysis will be made possible by using the $^{13}C$ species.

TABLE I. THE $x$-, $y$-, AND $z$-MOMENTS (amu Å$^2$)

| | $CH_2(CN)_2$ | | $CH_2CNC^{15}N$ | | $CD_2(CN)_2$ | | $CHD(CN)_2$ | |
|---|---|---|---|---|---|---|---|---|
| | Obsd. | Calcd. | Obsd. | Calcd. | Obsd. | Calcd. | Obsd. | Calcd. |
| $\sum m_i x_i^2$ | 1.4124 | 1.4102 | 1.4106 | 1.4102 | 2.9872 | 2.9847 | 2.1805 | 2.1856 |
| $\sum m_i y_i^2$ | 170.3922 | 170.3574 | 175.1228 | 175.1228 | 170.3236 | 170.3574 | 170.3564 | 170.3574 |
| $\sum m_i z_i^2$ | 22.7964 | 22.7991 | 23.0876 | 23.0877 | 27.4036 | 27.4065 | 25.1430 | 25.1374 |

TABLE II. MOLECULAR STRUCTURE OF MALONONITRILE

| | $r_o$ structure | $r_o$ and $r_s$ structure[a] |
|---|---|---|
| C–C | 1.468±0.034 Å | $1.480_3$±0.0056 Å |
| C≡N | 1.167±0.026 Å | $1.146_6$±0.0064 Å |
| C–H | 1.088±0.010 Å | $1.090_6$±0.0034 Å |
| ∠CCC | 109°22′±2°54′ | 110°24±24′ |
| ∠HCH | 108°42′±1°22′ | 108°26′±26′ |
| ∠CCN | 180° − (3°40′±2°54′) (outside) | 180° − (3°24′±26′) (outside) |
| $\Delta$ | 0.333±0.015 amu Å$^2$ | 0.3379 amu Å$^2$ |

a) See Ref. 1.

1) E. Hirota and Y. Morino, This Bulletin, 33, 158 (1960).
2) C. C. Costain, *J. Chem. Phys.*, 29, 864 (1958).
3) C. C. Costain and J. R. Morton, (ibid., 31, 389 (1959)) have shown that the C-C≡C group in propynal is bent by 1°36′.

*Department of Chemistry*
*Faculty of Science*
*The University of Tokyo*
*Hongo, Tokyo*

# *The Equilibrium between the Sn-Pb Liquid Solution and the $H_2$-$H_2O$ Gaseous Mixture*

By Koji ATARASHIYA*, Masahiro UTA**, Mitsuo SHIMOJI and Kichizo NIWA

(Received September 28, 1959)

The thermodynamic investigation of metallic solutions is very important in order to have a deep understanding of their structure[1]. In the tin-lead system the primary solid solutions have very limited solid solubilities in the respective solvents. The immiscibility of these primary solid solutions is found over a wide range of the concentration[2]. This fact may reflect the fact that the excess heat of the tin-lead liquid solution shows a positive value according to the simple model of solutions, for example, that of the regular solution[3]. Thermodynamic data on this binary system, all of which have been based on calorimetric measurements, enable one to confirm the above expectation. The excess heat of this system has been measured by Magnus and Mannheimer[4], by Kawakami[5], by von Samson-Himmelstjerva[6], and by Kleppa[7].

However, no direct measurement of the excess free energy of this system has so far been carried out. This may presumably be due to some experimental difficulties which accompany the direct methods of measuring the activity of this system such as those of electromotive force and of vapor pressure. The activities of the tin-lead system have been calculated by Elliott and Chipman[8] from the experimental results on the tin-lead-cadmium system.

In this paper the activity of tin in the tin-lead liquid solution is obtained by measuring the equilibrium of the tin-lead system with the hydrogen-water vapor mixture.

The principle of this method is as follows:—

If the hydrogen-water vapor mixture is in equilibrium with liquid tin and its dioxide in accordance with Eq. I,

$$Sn(l) + 2H_2O(g) = SnO_2(s) + 2H_2(g) \qquad (I)$$

one can write, as the equilibrium constant $K$ for reaction I,

$$K = (P_{H_2}/P_{H_2O})^2 \qquad (1)$$

where $P_{H_2}$ and $P_{H_2O}$ are the partial pressures of $H_2$ and $H_2O$ respectively. On the other hand, a similar equation (II) can be given for the tin-lead liquid solution, if the oxide of tin is stable as compared with that of lead.

$$Sn(\text{liq. soln.}) + 2H_2O(g) = SnO_2(s) + 2H_2(g) \qquad (II)$$

Corresponding to Eq. 1, one has

$$K = (P_{H_2}'/P_{H_2O}')^2/a_{Sn} \qquad (2)$$

where $a_{Sn}$ is the activity of tin relative to pure liquid tin, and the prime labeled for the pressures means the equilibrium partial pressure in the tin-lead system. From Eqs. 1 and 2 one obtains

$$a_{Sn} = (P_{H_2}'/P_{H_2O}')^2/(P_{H_2}/P_{H_2O})^2 \qquad (3)$$

Thus, in principle, the activity of tin in this system can be determined by measuring the partial pressures of hydrogen and water vapor in equilibrium with both pure tin and tin-lead.

## Stability of Oxides

It is the fundamental condition for Eq. 3 that the oxide, $SnO_2$, is most stable among all oxides conceivable in the present system. In thermodynamic terms, an oxide should be stable in case the partial pressure of oxygen in equilibrium with the oxide is low. In other words the formation of a stable oxide is associated with a small amount of oxygen. In Table I the partial pressures of oxygen in equilibrium with several oxides are shown, which are calculated from the free energies of formation of respective oxides[9] at 1000°K.

It is readily found that tin oxides are stable

* Present Address, Toho Denka K. K., Shiota, Chiba.
** Present Address, Institute of Mineral Dressing and Metallurgy, Tohoku University, Sendai.

1) K. Niwa and M. Shimoji, *Proceedings of International Symposium on Physical Chemistry of Metallic Solutions and Intermetallic Compounds*, Teddington, England (1958).
2) M. Hansen and K. Anderko, "Constitution of Binary Alloys", McGraw-Hill, New York (1958).
3) E. A. Guggenheim, "Mixtures", Oxford Univ. Press, London (1952).
4) A. Magnus and M. Mannheimer, *Z. physik. Chem.*, **121**, 267 (1926).
5) M. Kawakami, *Z. anorg. allgem. Chem.*, **167**, 345 (1927); *Sci. Rep. Tohoku Imp. Univ.*, **16**, 915 (1927).
6) H. O. von Samson-Himmelstjerva, *Z. Metallkunde*, **28**, 197 (1936).
7) O. J. Kleppa, *J. Phys. Chem.*, **59**, 175 (1955).
8) J. E. Elliott and J. Chipman, *J. Am. Chem. Soc.*, **73**, 2682 (1951).
9) J. P. Coughlin, *Bureau of Mines, Bull.*, No. 542 (1954).

TABLE I. PRESSURES OF OXYGEN IN EQUILIBRIUM WITH TIN- AND LEAD-OXIDES AT 1000°K

| Oxides | | Pressures of oxygen $\log P_{O_2}$ (atm.) |
|---|---|---|
| $SnO_2$ | (s) | −19.6 |
| SnO | (s) | −19.0 |
| SnO | (g) | − 7.1 |
| PbO | (s) | −12.6 |
| $Pb_3O_4$ | (s) | − 8.9 |
| $PbO_2$ | (s) | − 4.5 |

compared with lead oxides. Although the value of SnO(s) is close to that for $SnO_2$(s), the solid SnO is found unstable as compared with $SnO_2$ in other studies[10]. Further, according to the electron diffraction study by Shimaoka and Yamai[11], the oxide film formed on the surface of the tin-lead solution under the condition of temperatures higher than 470°C and of pressures below 1 atmosphere of air, shows complete patterns of the stannic oxide. After the present experiment has been finished, the samples should be examined by means of the X-ray or by the electron diffraction, but the amount of oxides formed by reaction II is too small to be determined in such a way. However, the fact of the stannic oxide being most stable may be assured by the other reasons already described above.

## Experimental

The same apparatus, used in the measurement of equilibrium in $GeO_2$-$H_2$-Ge-$H_2O$ system[12], is employed with a modification of the sizes of both the furnace and the reaction tube.

Metallic solutions are prepared by fusing each mixture of pure metals (Kanto Kagaku, 1st grade) in a closed vessel under vacuum; their concentrations are confirmed by chemical analysis.

The boat of high alumina filled with 3∼4 g. of the powdered sample, which has been dispersed in alumina powder, is set in the reaction tube. After the tube has been evacuated to the pressure of $10^{-5}$ mmHg, water vapor saturated at 18±0.01°C (15.45 mmHg), is introduced for oxidation, while hydrogen, generated by electrolysis of a potassium hydroxide solution, is introduced for reduction. The oxidation method is used for liquid metallic solutions, since there is no assurance of obtaining the required metallic solution from the reduced tin metal. The rate of gas flow is about 200 cc./min. The measurements have been carried out over the range of 700∼800°C.

The whole error in $a_{Sn}$ may be about 3% which is due to the inaccuracies of the furnace temperature (±2°C) and of the temperature of water (±0.01°C), as well as of the reading of the cathetometer (pressure: ±0.01 mmHg), etc. As one of the other sources of error, the change of concentration in liquid solutions should be taken into account, since tin in the solution is oxidized during the reaction. However, the amount of this change estimated from the volume of the reaction system (about 850 ml.) is at most $10^{-5}$ mol., and small compared with the initial amount of tin in solutions (at least $10^{-3}$ mol.). Though the vapor pressure of lead is about $10^{-2}$ mmHg at 700∼800°C, the rate of vaporization is then at most $10^{-5}$ mol./hr. Thus, this effect may be negligible because of the short time taken for the present reaction (1∼5 hr.).

## Results

**Equilibrium in the Sn-$H_2O$-$SnO_2$-$H_2$ System:** —The results for this system are shown in Table

TABLE II. EQUILIBRIUM IN Sn-$H_2O$-$SnO_2$-$H_2$

| Temperature °C | Total pressure* mmHg | Equilibrium constant ($K$) | $\log K$ | Method |
|---|---|---|---|---|
| 875 | 18.75 | 0.0456 | −1.341 | reduction |
| 850 | 19.10 | 0.0558 | −1.258 | 〃 |
| 825 | 19.45 | 0.0670 | −1.174 | 〃 |
| 802 | 19.70 | 0.0757 | −1.121 | oxidation |
| 800 | 19.80 | 0.0793 | −1.101 | reduction |
| 777 | 20.20 | 0.0945 | −1.024 | 〃 |
| 750 | 20.75 | 0.1177 | −0.929 | 〃 |
| 750 | 20.80 | 0.1199 | −0.921 | oxidation |
| 700 | 22.30 | 0.1994 | −0.700 | 〃 |

* The pressure of water vapor is kept constant at 15.45 mmHg.

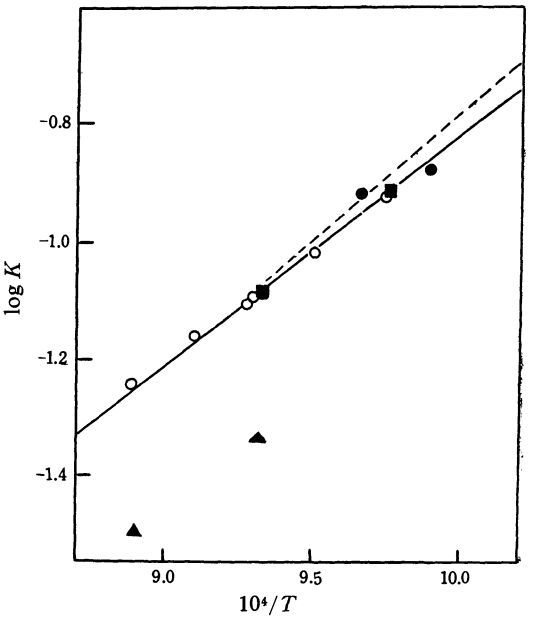



Fig. 1. Temperature dependence of equilibrium constant in the system Sn(pure)-$H_2O$-$SnO_2$-$H_2$
○ Present work. ● Meyer and Scheffer. ■ Emmett and Shultz. ▲ Eastman and Robinson. --- Ishikawa and Ando.

10) K. Niwa, I. Yamai and T. Wada, This Bulletin, **31**, 725 (1958).
11) G. Shimaoka and I. Yamai, *J. Chem. Soc. Japan, Pure Chem. Sec.* (*Nippon Kagaku Zasshi*), **76**, 1139 (1955).
12) T. Yokokawa, M. Koizumi, M. Shimoji and K. Niwa, *J. Am. Chem. Soc.*, **79**, 3365 (1957).

TABLE III. EQUILIBRIUM IN Sn(in soln.)-$H_2O$-$SnO_2$-$H_2$

| Temperature °C | $x_{Sn}$ | Total pressure mmHg | $(P_{H_2}/P_{H_2O})^2$ | Activity of tin | $\bar{G}^e_{Sn}$ |
|---|---|---|---|---|---|
| 750 | 0.0521 | 17.30 | 0.0143 | 0.116 | 1630 |
| 〃 | 0.100 | 17.90 | 0.0251 | 0.204 | 1450 |
| 〃 | 0.151 | 18.35 | 0.0352 | 0.285 | 1290 |
| 〃 | 0.199 | 18.70 | 0.0442 | 0.358 | 1190 |
| 〃 | 0.301 | 19.20 | 0.0589 | 0.477 | 930 |
| 〃 | 0.403 | 19.55 | 0.0704 | 0.570 | 700 |
| 〃 | 0.501 | 19.80 | 0.0793 | 0.642 | 500 |
| 〃 | 0.711 | 20.25 | 0.0965 | 0.781 | 190 |
| 775 | 0.0521 | 17.10 | 0.0114 | 0.115 | 1650 |
| 〃 | 0.100 | 17.65 | 0.0203 | 0.205 | 1490 |
| 〃 | 0.151 | 18.00 | 0.0272 | 0.276 | 1260 |
| 〃 | 0.199 | 18.35 | 0.0352 | 0.356 | 1210 |
| 〃 | 0.301 | 18.75 | 0.0456 | 0.462 | 890 |
| 〃 | 0.403 | 19.10 | 0.0558 | 0.565 | 700 |
| 〃 | 0.501 | 19.30 | 0.0621 | 0.628 | 460 |
| 〃 | 0.711 | 19.74 | 0.0775 | 0.784 | 200 |
| 800 | 0.0521 | 16.90 | 0.0088 | 0.110 | 1600 |
| 〃 | 0.100 | 17.40 | 0.0159 | 0.199 | 1470 |
| 〃 | 0.151 | 17.75 | 0.0222 | 0.277 | 1290 |
| 〃 | 0.199 | 18.00 | 0.0272 | 0.341 | 1140 |
| 〃 | 0.301 | 18.45 | 0.0377 | 0.472 | 960 |
| 〃 | 0.403 | 18.70 | 0.0443 | 0.554 | 690 |
| 〃 | 0.501 | 18.90 | 0.0499 | 0.624 | 480 |
| 〃 | 0.711 | 19.30 | 0.0621 | 0.777 | 180 |

II. If the common logarithms of the equilibrium constant, $K$, thus obtained, are plotted against the reciprocal temperature, as shown in Fig. 1, they lie close about a straight line, which is expressed by Eq. 4. (This equation is established by means of the least square).

$$\log K = 4150/T - 4.965\ (\pm 0.05) \qquad (4)$$

This result is in good agreement with the data of other investigators[13-16]. For example, the following values are obtained by means of Eq. 4.

| $t$, °C | $K$ |
|---|---|
| 750 | 0.1235 |
| 775 | 0.0988 |
| 800 | 0.0799 |

**Equilibrium in Sn (in Soln.)—$H_2O$-$SnO_2$-$H_2$ System**:—The equilibrium constant and the activity of tin, measured in this system, are indicated in Table III. The activity of tin, shows a positive deviation from Raoult's law, as is seen in Fig. 2. The partial excess free energy of tin, $\bar{G}^e_{Sn}$, is related to its activity by

$$\bar{G}^e_{Sn} = \boldsymbol{R}T \ln a_{Sn}/x_{Sn} = \boldsymbol{R}T \ln f_{Sn} \qquad (5)$$

where $\boldsymbol{R}$ is the gas constant, $x_{Sn}$ is the atomic fraction of tin, and $f_{Sn}$ is the actitvity coefficient. If the values of $\bar{G}^e_{Sn}/(1-x_{Sn})^2$ are plotted against $x_{Sn}$, they lie close about a straight line, shown in Fig. 3, which is expressed by Eq. 6 at 775°C.

$$\bar{G}^e_{Sn}/(1-x_{Sn})^2 = 2330 - 600(1-x_{Sn}) \quad (\pm 50\ \text{cal./mol.}) \qquad (6)$$

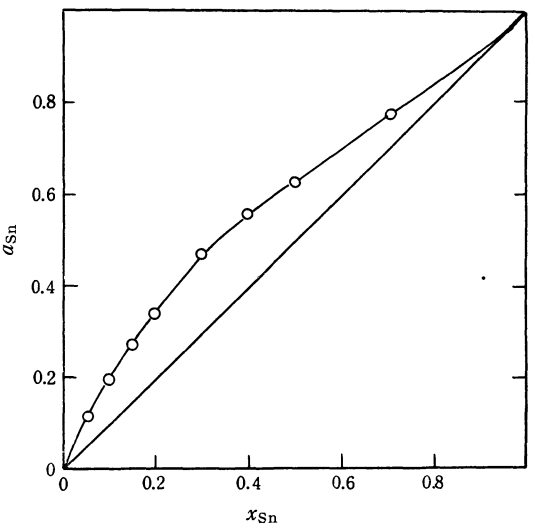



Fig. 2. Observed activity of tin in the tin-lead liquid solution at 800°C.

13) G. Meyer and F. E. C. Scheffer, *Rec. trav. chim.*, **54**, 294 (1935).
14) P. H. Emmett and J. F. Schultz, *J. Am. Chem. Soc.*, **55**, 1390 (1933).
15) E. D. Eastman and P. Robinson, ibid., **50**, 1106 (1928).
16) F. Ishikawa and S. Ando, *Sci. Paper Inst. Phys. Chem.* **34**, 873 (1938).

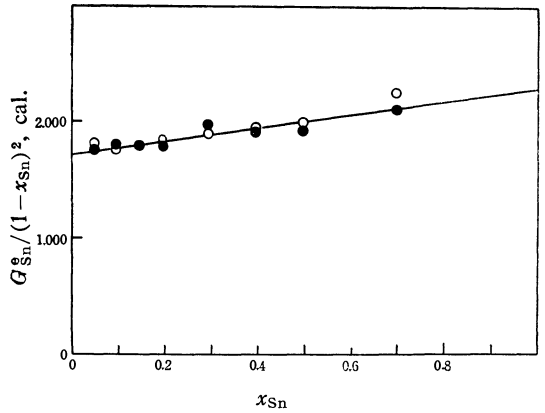



Fig. 3. Concentration dependence of partial molar excess free energy of tin in the tin-lead liquid solution. ○ Observed values at 750°C. ● Observed values at 800°C.

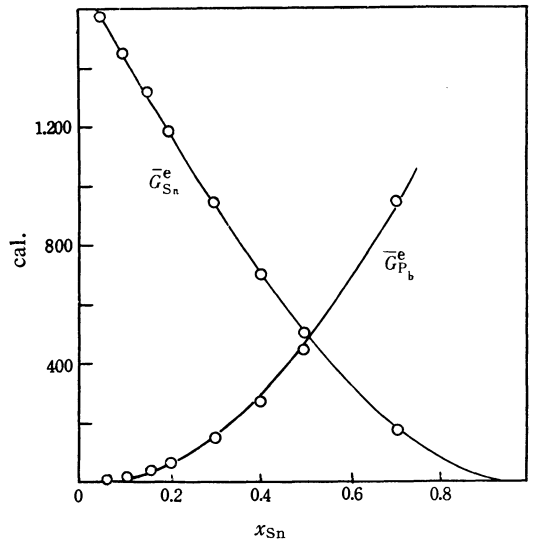



Fig. 4. Partial excess free energies in the tin-lead solution at 775°C.

Applying Gibbs-Duhem's relation to the above results, one obtains not only the partial molar excess free energy of lead, but also the (integral) excess free energy of the solutions, $G^e_m$, as are shown in Figs. 4 and 5 which are expressed respectively by Eqs. 7 and 8 at 775°C

$$\bar{G}^e_{Pb} = 1430\, x_{Sn}{}^2 + 600\, x_{Sn}{}^3 \quad (7)$$

$$G^e_m = x_{Sn} x_{Pb} (1730 + 300 x_{Sn}) \quad (8)$$

Unfortunately, the temperature dependence of $a_{Sn}$ could not be accurately obtained in this experiment owing to the limited range of temperatures (750~800°C). This limitation is due to the fact that the vapor pressure of lead is very high at temperatures above 800°C, while the reaction rate for oxidation is very slow if the temperature is lower than 700°C.

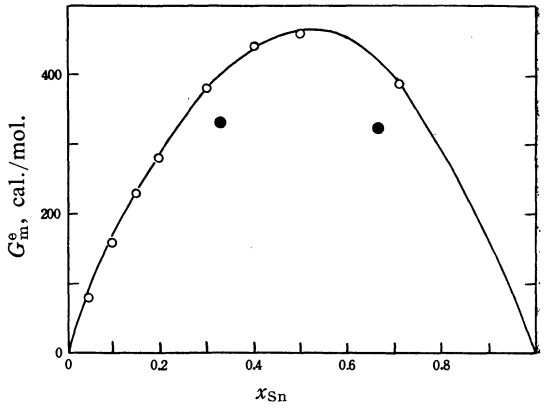



Fig. 5. Excess free energy in the tin-lead liquid solution at 775°C. ○ Observed values. ● Calculated from the data of Elliott and Chipman for the ternary system.

## Discussion

So far as the excess free energy of the tin-lead system is concerned, there are no experimental data available except an indirect result calculated from those of the cadmium-tin-lead system obtained by Elliott and Chipman[8]. They have given only two values of the excess entropy at about 500°C, which can be extrapolated to 775°C. The excess free energy, $G^e_m$, thus obtained is as follows.

| $x_{Sn}$ | 0.333 | 0.667 |
|---|---|---|
| $G^e_m$(cal.) | 333 | 320 |

By a combination of these values with the present results, a comparison is made in Fig. 5. It is found that the results, obtained by Elliott and Chipman for only two concentrations, have a tendency to represent slightly small values compared with the present ones. However, the values of the heat of mixing calculated from those for the cadmium-tin-led system are 15~20% smaller than those directly measured by Kleppa[7]. Hence, if the excess free energy is calculated by combining Kleppa's values for the excess heat with those of Elliott and Chipman for the excess entropy, the agreement between the values thus obtained and those of the present study is quite reasonable. It should be noted that the excess entropy shows a slightly negative deviation from ideal mixing.

It is of interest to examine the excess function on liquid tin-lead solutions from simplified models of metallic solutions. According to Haissinsky[17], the electronegativity of tin is almost in agreement with that of lead. ($Sn^{II}$, 1.65; $Pb^{II}$, 1.6; $Sn^{IV}$, 1.8; $Pb^{IV}$, 1.8.) So the electrochemical effect due to transfer of electrons may be very small in the tin-lead system. For

17) M. Haissinsky, *J. phys.* 7, 7 (1946).

these cases, the theoretical calculation of excess functions can be simplified, as pointed out by Hildebrand and Scott[18].

$$H_m^e = [(L_A/V_A)^{\frac{1}{2}} - (L_B/V_B)^{\frac{1}{2}}]^2 \varphi_A \varphi_B V_S \quad (9)$$

and $$S_m^e = 0 \quad (10)$$

$L_A$ and $L_B$ are the energies of vaporization of pure A and B respectively. $V_A$ and $V_B$ denote their volumes in pure states. $V_S$ represents the volume of the solution. $\varphi_A$ and $\varphi_B$ are the volume fractions respectively.

As the interatomic potential in liquid metals cannot always be expressed by the well known 6-12 potentials or 6-$\infty$ potentials, Shimoji[19] has proposed the following theoretical expression for the excess energy after taking into account the generalized potential.

$$H_m^e = [(L_A/V_A)^{\frac{1}{2}} - (L_B/V_B)^{\frac{1}{2}}]^2 \varphi_A \varphi_B V_S + \frac{nl}{8}\rho^2\left(1+\frac{\delta_v}{2}\right)\frac{L_{AA}}{V_A}\varphi_A\varphi_B V_S \quad (11)$$

Here,

$$\rho = 2(r_B - r_A)/(r_B + r_A)$$

and $$\delta_v = (L_B/V_B - L_A/V_A)/L_A/V_A) \quad (12)$$

$r_i$ means the interatomic distance in the pure state of i. It is found that the parameter $nl$ in Eq. 11 is about 10 or 20 in most liquid metals. If $nl=72$, Eq. 12 corresponds to the one derived by Prigogine[20]. Of course Hildebrand's Eq. 9 can be obtained if the term due to the difference of atomic radii (size factor) is neglected in Eq. 11. Furthermore, the assumption of the geometric mean of energies between unlike atoms used in deriving Eq. 9 might be open to doubt because of metallic forces. If the arithmetic mean is used for the energies, $H_m^e$ should be zero for Eq. 9, (or the first term of Eq. 11 should be zero.) It is noteworthy that Eq. 11 gives a positive excess energy even if the assumption of the arithmetic mean is used.

Table IV. Comparison of calculated values of the excess functions in tin-lead liquid solutions (cal./mol.)

| | Hildebrand | Shimoji ($nl=10$) | 6-12 potential | Expl. |
|---|---|---|---|---|
| $H_m^e$ | 860(0*) | 1050(200*) | 2150(1300*) | 330[7] |
| $G_m^e$ | 860 | 1000 | | 460 |

$H_m^e$: The excess heat at $x_{Sn}=0.5$
$G_m^e$: The excess free energy at $x_{Sn}=0.5$ (at 800°C)
*: Values based upon the arithmetic mean rule.

In Table IV the calculated values of the excess energy and the exsess entropy at $x_{Sn}=0.5$ are compared with the observed ones. The most reasonable approach to the excess energy of an alloy is based on the collective electron theory of metals, such as the cellular approximation etc.[21,22] Unfortunately, no reliable values of the parameters adaptable for these theories have yet been determined either experimentally or theoretically in either the liquid tin or lead systems. However, according to Varley's calculation[21] based on the free electron approximation, the electrochemical factor is nearly zero in the lead-tin system. Then, the size factor indicating the positive excess energy plays an important role in liquid metals as well as in solid alloys. Rigorous estimation in the liquid state can not be achieved because of lack of knowledge concerning the parameters of pure metals, but the same conclusion may thus be obtained either from the theories of the pair bond interaction[18,19] or from those of the free electron approximation based upon the band model of metals.

## Summary

Equilibrium in Sn (in liquid alloy)-$H_2O$-$SnO_2$-$H_2$ system has been determined from 750 to 800°C by measuring the ratio of pressures between $H_2O$ and $H_2$ gas mixtures. From this the activity of tin liquid tin-lead solutions has been calculated, and the following equation has been derived at 775°C.

$$\overline{G}_{Sn}^e = 2330(1-x_{Sn})^2 - 600(1-x_{Sn})^3 \text{ cal./mol.}$$

The temperature dependence of $\overline{G}_{Sn}^e$ could not be determined. However, if this value is calculated by combining Kleppa's value for the excess heat, calorimetrically determined, with that of Elliott and Chipman for the excess entropy, the agreement between the value thus obtained and that of the present investigation is quite reasoable, taking into consideration the accuracies of these experiments. Theoretical considerations have been given for the excess functions of this system. It shonld be emphasized that the electrochemical effect of charge transfer is very small or may be regarded as zero in the lead-tin system and that the size factor is important.

*Department of Chemistry*
*Faculty of Science*
*Hokkaido University*
*Sapporo*

18) J. H. Hildebrand and R. L. Scott, "Solubility of Non-Electrolyte", Reinhold, New York (1950).
19) M. Shimoji, *Proceedings of International Symposium on Physical Chemistry of Metallic Solutions and Intermetallic Compounds*, N. P. L. Teddington, England (1958).
20) I. Prigogine, "Molecular Theory of Solutions", Noth Holland Publishing, (1957).
21) J. H. O. Varley. *Phil. Mag.*, **48**, 446 (1954).
22) M. Shimoji, *J. Phys. Soc. Japan*, **14**, 1525 (1959).

# SHORT COMMUNICATIONS

## *Three Geometrical Isomers of p-Distyrylbenzene*

By Soichi MISUMI and Motoyuki KUWANA

(Received February 24, 1960)

Three geometrical isomers are possible in *p*-distyrylbenzene (I) with regard to the ethylenic double bonds of the molecule. We have studied the synthesis and the photoisomerization of these three isomers with the purpose to compare the physical and chemical properties with those of the recently extensively studied pure polyolefinic systems such as diphenylpolyenes[1] and carotenoids[2].

The *cis, cis*- and *cis, trans*-isomers ($I_c$ and $I_b$) were prepared by the partial hydrogenation of the corresponding acetylenic compounds using Lindlar's catalyst. The *trans, trans*-isomer ($I_a$) was obtained by the dehydration of *p*-bis(β-phenyl-α-hydroxyethyl)benzene. The isomers were purified by repeated recrystallization or chromatography on alumina.

Unexpectedly the sequence of qualitative photostability of these isomers under diffused light was found to be *trans, cis* ($I_b$) ≪ *cis, cis* ($I_c$) ≤ *trans, trans* ($I_a$). Both of the sterically hindered *cis, cis*- and *cis, trans*-isomers ($I_c$ and $I_b$) showed no fine structure in their ultraviolet spectra as illustrated in Fig. 1. The *cis, trans*-isomer ($I_b$) showed the most intense

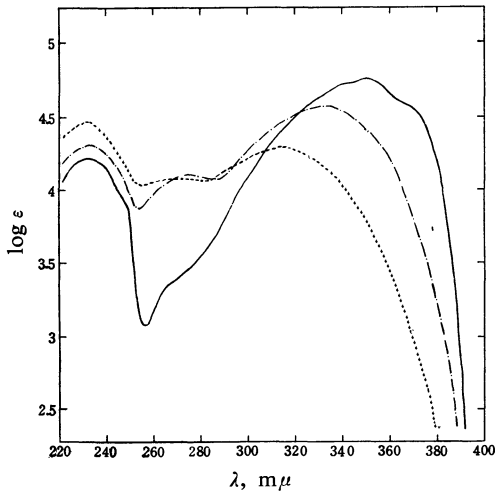



Fig. 1. Ultraviolet absorption spectra of *p*-distyrylbenzene (I) in *n*-hexane: ——, *trans, trans*; —·—, *cis, trans*; ----, *cis, cis*.

*cis*-peak[2b] (ca. 270mμ) in accord with the theory proposed by Zechmeister.

The solutions of the isomers were exposed to light of a fluorescent tube under controlled conditions and the course of the photoisomerization was followed by the change of the intensities of absorption at 270 and 350 mμ. The results are illustrated in Figs. 2 and 3. It is to be noted that the rate of spatial rearrangement of the most hindered *cis, cis*-isomer ($I_c$) is much slower than that of *cis, trans*-isomer ($I_b$). Theoretically, the same equilibrium mixture

TABLE I. PHYSICAL PROPERTIES OF *p*-DISTYRYLBENZENE

| Isomer | *trans, trans*[3] | *trans, cis*[4] | *cis, cis* |
|---|---|---|---|
| m. p. (°C) | 266~267 | 114~114.5 | 86.5~87.5 |
| U. V. $\lambda_{max}$ (mμ) | 232, 350 | 232, 273, 331 | 232, 270, 314 |
| (log ε) | (4.21), (4.76) | (4.09), (4.30), (4.56) | (4.44), (4.04), (4.22) |
| I. R. ($cm^{-1}$) *cis* $\delta_{CH}$ | — | 774 | 774 |
| *trans* $\delta_{CH}$ | 966 | 961 | — |
| Found* C, | 93.59 | 93.58 | 93.79 |
| H, | 6.76 | 6.44 | 6.60 |

* Calcd. for $C_{22}H_{18}$: C, 93.57; H, 6.43%.

1) L. Zechmeister et al., *J. Am. Chem. Soc.*, **64**, 2755 (1942); **69**, 553 (1947); **70**, 1937 (1948); **76**, 2308, 4144 (1954); B. C. L. Weedon et al., *J. Chem. Soc.*, **1959**, 933.

2) a) L. Zechmeister, *Chem. Revs.*, **34**, 267 (1944); *Experientia*, **10**, 1 (1954).
b) L. Zechmeister, A. L. LeRosen, W. A. Schroeder, A. Polgar and L. Pauling, *J. Am. Chem. Soc.*, **65**, 1940 (1943).

3) H. Kaufmann, *Ber.*, **50**, 515 (1917); G. Drefahl and G. Plötner, *Chem. Ber.*, **91**, 1274 (1958); T. W. Campbell and R. N. McDonald, *J. Org. Chem.*, **24**, 1246 (1959).

4) J. Dale, *Acta Chem. Scand.*, **11**, 971 (1957). He suggested that a compound melting at ca. 95°C, isolated from the products of photoisomerization of the *trans, trans*-isomer, may have the *cis, trans*-configuration.

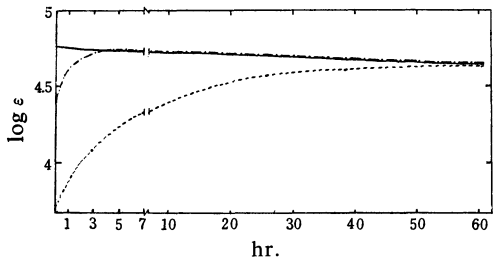



Fig. 2. Change of the extinction value at 350 mμ. of the U. V. spectra of three isomeric *p*-distyrylbenzenes in *n*-hexane by exposure to light: ——, *trans*, *trans*; —·—, *cis*, *trans*; ----, *cis*, *cis*.

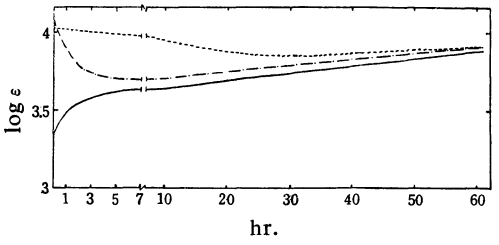



Fig. 3. Change of the extinction value at 270 mμ. of the U. V. spectra of three isomeric *p*-distyrylbenzenes in *n*-hexane by exposure to light: ——, *trans*, *trans*; —·—, *cis*, *trans*; ----, *cis*, *cis*.

might be attained regardless of the geometry of the starting isomers, but the experimental results showed a slight difference in their absorption spectra in final stage. This fact is attributable to the minor degree of decomposition or polymerization of I during the course of photostereomutation.

The experimental detail and the full discussion of this investigation will be published in near future.

The authors wish to express their thanks to Professor Masazumi Nakagawa for his kind advice and encouragement throughout this work.

*Department of Chemistry*
*Faculty of Science*
*Osaka University*
*Kita-ku, Osaka*

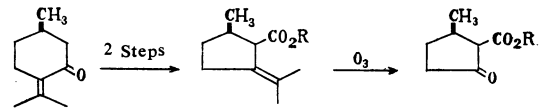
## *The Absolute Structure of Actinidine*

By Takeo SAKAN, Akira FUJINO, Fujio MURAI, Akio SUZUI, Yasuo BUTSUGAN and Yutaka TERASHIMA*

(Received March 26, 1960)

(+)-Actinidine, the enantiomeric from of the levorotatory natural product, has been synthesized from (+)-pulegone through methyl pulegenate (Ib).

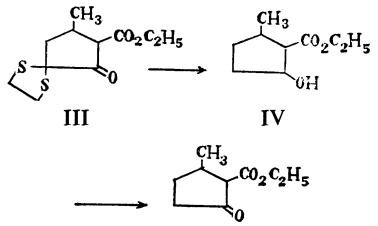
The synthesis was preceded by the scrupulous confirmation of the plane structure of pulegenic acid (Ia), presented by H. Rupe and K. Schäfer[1] to be 2-isopropyliden-5-methyl-cyclopentanecarboxylic acid. The ethyl ester (Ic) of Ia was ozonolyzed to ethyl 2-methyl-5-oxo-cyclopentanecarboxylate (IIc), b. p. 95~96°C/10 mmHg (Found: C, 63.31; H, 8.35. Calcd. for $C_9H_{14}O_3$: C, 63.51; H, 8.29 %), and the racemic form of the latter was synthesized.




I II

a: R=H; b: R=$CH_3$; c: R=$C_2H_5$

The half ethylene dithio-ketal (III), m. p. 63°C (Found: C, 50.53: H, 6.23; S, 24.59. Calcd. for $C_{11}H_{16}O_3S_2$; C, 50.77; H, 6.20; S, 24.62 %) of ethyl 2-methyl-4, 5-dioxocyclopentanecarboxylate[2] was reduced on treatment with Raney nickel to the hydroxy ester (IV) ($\nu_{OH}$ 2.89 $\mu$ in infrared absorption spectrum), which was converted into the corresponding keto ester (IIc′) by the successive oxidation with the complex of chromic oxide-pyridine. IIc and IIc′ were proved to be identical through the mixed fusion test and the comparison of the infrared absorption spectra of their semicarbazones.




III IV

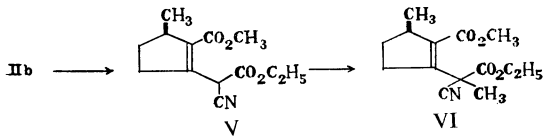
IIc′

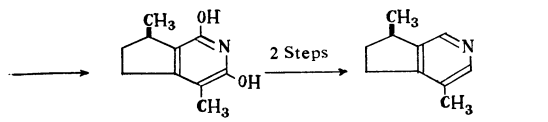
* Institute for Food Chemistry, Kita-ku, Osaka.

1) H. Rupe and K. Schafer, *Helv. Chim. Acta*, 11, 466 (1928).

2) H. Staudinger and L. Ruzicka, ibid., 7, 381 (1924).

The attempts to hydroxylate the isopropyliden group in Ib with selenium dioxide under the various conditions were so all in failure that the authors were impelled to take a rather circuitous route for the purpose. The satisfactory result was achieved when the methyl ester (IIb), b. p. 90~92°C/12 mmHg (Found: C, 61.29; H, 7.91. Calcd. for $C_8H_{12}O_3$: 61.52; H, 7.75 %), was chosen as a key compound and the necessary $C_3$-moiety was re-introduced into IIb as shown below.




The condensation product (V) of IIb with ethyl cyanoacetate was treated with methyl iodide in the ethoxide solution and the methylated diester (VI) was hydrolyzed with acid or alkali to the dihydroxypyridine derivative (VII), m. p. 172~173°C (Found: C, 67.15; H, 7.51; N, 7.98. Calcd. for $C_{10}H_{13}O_2N$: C, 67.02; H, 7.31; N, 7.82%). The chlorination of VII and the successive catalytic hydrogenation of the dichloro-compound, similar to those reported in the synthesis of DL-actinidine[3], yielded the base (VIII), the purified picrate (Found: C, 50.95; H, 4.36; N, 14.91. Calcd. for $C_{16}H_{16}O_7N_4$; C, 51.06; H, 4.29; N, 14.89 %) of which melted at 146~147°C. The regenerated base, b. p. 88~90°C/5 mmHg, from the latter gave the value of $[\alpha]_D^{15}+16.1°$ (c 5.52 chloroform) and the identical infrared absortion chart with the natural alkaloid. Although the absolute values of rotatory power were not equal between these two actinidines obtained, the synthesized one was likely to be in a more purified state.

As the asymmetric center of (+)-pulegone had already been correlated in the stereochemical analysis to D-series[4], the absolute configuration of $C_{(7)}$-carbon atom in natural actinidine (6, 7-dihydro-4, 7-dimethyl-5(*H*)-2-pyrindine) has now been established.

*Institute of Polytechnics*
*Osaka City University*
*Kita-ku, Osaka*

3) T. Sakan, A. Fujino, F. Murai, A. Suzui and Y. Butsugan, This Bulletin, **32**, 1155 (1959).
4) K. Freudenberg and W. Hohmann, *Ann.*, **584**, 54 (1953).

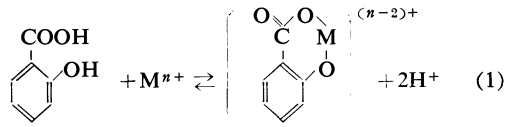
# *Effect of Metal Ions on the Radiation-Induced Decarboxylation of Aqueous Benzoic and Salicylic Acid Solutions*

By Akira SUGIMORI and Gen-ichi TSUCHIHASHI

(Received March 9, 1960)

Remarkable effect of heavy metal ions was observed in the radiolysis of benzene in aqueous solution[1] and other organic compounds[2]. In the systems hitherto studied, the interaction between metal ions and organic molecules is expected to be different from that in the compounds containing metal ions. The effect of metal ions bound to organic molecules on the radiolysis has not yet been studied.

The present authors studied the effects of added ions on the decarboxylation of benzoic and salicylic acids, in order to clarify the difference in the effect between bound and non-bound metal ions. Benzoic acid does not form any chelate compounds with metal ions, whereas salicylic acid gives stable complexes with $Fe^{3+}$, $Cu^{2+}$ and $Al^{3+}$.




(1)

The difference in the effect of heavy metal ions on $G(CO_2)$ was found between benzoic and salicylic acid, and this can be attributed to the difference in the states of ions.

The oxygen free solution containing 0.2 % of either acid and metal salts were irradiated by $^{60}Co$ $\gamma$-rays in the test tube with side cell in which 0.1 N barium hydroxide solution was

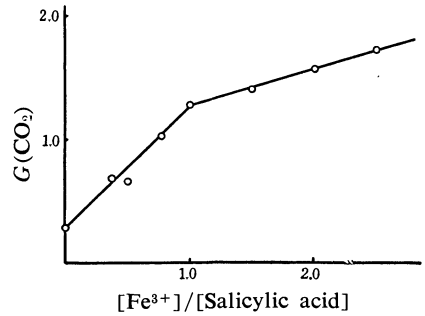



Fig. 1. The effect of $Fe^{3+}$ concentration on $G(CO_2)$ of salicylic acid.

1) J. H. Baxendale and D. Smithies., *J. Chem. Phys.*, **23**, 604 (1955); *J. Chem. Soc.*, **1959**, 779.
2) E. A. Cherniak, E. Collinson, F. S. Dainton and G. M. Meaburn, *Proc. Chem. Soc.*, **1958**, 54.

TABLE I. EFFECTS OF SALTS ADDED ON $G(CO_2)$

| Acid | Salt added | $G(CO_2)$ |
|---|---|---|
| Salicylic acid | — | 0.29 |
| | $FeCl_3$ 1.4 mol. | 1.38 |
| | $FeSO_4$ 1.4 mol. | 0.27 |
| | $CuCl_2$ 1.4 mol. | 0.47 |
| | $AlCl_3$ 1.4 mol. | 0.26 |
| | $CoCl_2$ 1.4 mol. | 0.23 |
| | $NiCl_2$ 1.4 mol. | 0.26 |
| | $ZnCl_2$ 1.4 mol. | 0.28 |
| | $MgCl_2$ 1.4 mol. | 0.28 |
| | $H_2SO_4$ (0.8 N) | 0.55 |
| | $H_2SO_4$ (0.8 N) $FeCl_3$ 1.4 mol. | 0.65 |
| | KF 8.3 mol. $FeCl_3$ 1.4 mol. | 0.11 |
| Benzoic acid | — | 0.66 |
| | $FeCl_3$ 2.8 mol. pH~1 | 0.30 |

placed in order to absorb carbon dioxide formed. Dose rate and total dose were $9.5\times10^4$ r./hr. and $1.57\times10^6$ r., respectively. Carbon dioxide formed was absorbed by barium hydroxide solution and $G(CO_2)$ was measured volumetrically.

The effects of various metal ions are summarized in Table I. In the case of benzoic acid, $Fe^{3+}$ added does not bring about the increase in $G(CO_2)$, while in the case of salicylic acid, it makes $G(CO_2)$ remarkably high. This suggests that $Fe^{3+}$, chelating organic molecules and attacking redicals cooperate in the decarboxylation of the complex. This is also supported by the following experiments.

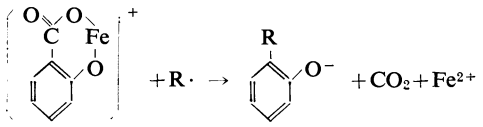
a) Fig. 1 shows the plot of $G(CO_2)$ in the radiolysis of salicylic acid against the amount of $Fe^{3+}$ added. As is shown in the figure, a remarkable break is observed at $[Fe^{3+}]/[\text{Salicylic acid}]=1$, where all of $Fe^{3+}$ ions and salicylic acid mulecules exist as complexes and neither of $Fe^{3+}$ nor salicylic acid remains in excess.

b) The addition of some masking reagents such as $F^-$ and $H^+$ to the complex makes $G(CO_2)$ low.

Based on the above results, the mechanism of the decarboxylation of the complexes is conceivably different from that of free acids.

Therefore the following sequence of reactions can be given for the decarboxylation of the complex.

$$H_2O \xrightarrow{\gamma\text{-rays}} H\cdot + HO\cdot + H_2O_2 \quad \text{etc.} \tag{2}$$



(3)

(where R· represents free radical)

The attacking radical (R·) is not yet identified but this mechanism is supported by the following observations.

a) In this case $Fe^{3+}$ is easily reduced to $Fe^{2+}$, although it is reduced only to small extent in the absence of organic compounds.

b) $Fe^{3+}$ and $Cu^{2+}$ added bring about the increase in $G(CO_2)$ of salicylic acid, whereas added $Al^{3+}$ has only a slight effect. All of them are known as metal ions which give complexes with salicylic acid.

These indicate that both the complex formation and easy reduction of metal ions are essential for this kind of metal catalyzed radiation-induced decarboxylation.

The present authors are very grateful to Dr. K. Kimura and Dr. A. Danno for their helpful discussion.

*Radiation Application Division*
*Japan Atomic Energy Research Institute*
*Tokai, Ibaraki-ken*

# *Separation of Lanthanons by Paper Precipitation Chromatography with 8-Quinolinol. I. Separation and Detection of Lanthanum, Cerium and Praseodymium (Part 1)*

By Hideo NAGAI

(Received September 30, 1959)

The separation of lanthanons by paper chromatography and its analogous column method was studied by Lederer[1-4] and Pollard et al.[5,6], and the separation was effective to some extent. However, the separation of adjacent elements was very difficult, although a few elements have been separated. The difficulties were principally caused by considerable tailing and the close $R_f$ values of the elements. On the other hand, precipitation chromatography with 8-quinolinol (oxine), which the author has studied[7-12], involved fundamentalf actors to reduce these difficulties. The procedure of precipitation chromatography is as follows. One drop of the test solution is applied at the center of a circular filter paper, previously impregnated with oxine, and developed with an adequate developing solvent. As the developing solvent penetrates into the filter paper, the oxine contained in the filter paper dissolves and reacts with the cations in the test solutions; the phenomenon can be compared with the dropwise addition of the precipitating agent to the test solution in the precipitation titration. Accordingly, from the analogous deduction of the precipitation titration, the cation which forms the most stable metal complex with oxine precipitates at the central part of the filter paper. By the precipitation the reaction product is removed from the reaction system. Therefore the reaction proceeds in such a way as to cause the predominant precipitation of the same kind of complex salt to continue, until the greater part of this cation was consumed. Then the deposition of the next stable complex salt in the test solution follows. Such a course of precipitation prevents the overlapping of the bands corresponding to each cation in the test solution.

In addition to the advantage described above, this chromatographic procedure scarcely ever causes any tailing. This phenomenon is probably due to the following reason: when the test solution is applied on the filter paper, nuclei of the precipitate of the cations are formed and grow smoothly during the entire development. On the other hand, the difficulties caused by the coprecipitation are encountered in this procedure, especially, when the lanthanons are treated. Accordingly, an improved procedure was devised so as to utilize the advantages of precipitation chromatography and to avoid as much as possible the coprecipitation of the elements.

## Experimental

**Apparatus.**—The apparatus used for developing the chromatogram is illustrated in Fig. 1.

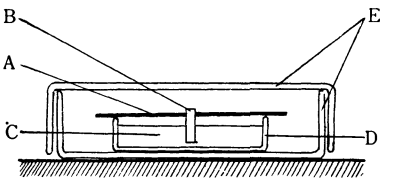



Fig. 1

A is a sheet of filter paper impregnated with oxine, which was prepared as follows. One hundred sheets of circular filter paper 9 cm. in diameter (Toyo filter paper No. 5B) were dipped in an ethanolic solution of oxine containing ca. lg. oxine in 80 ml. of ethanol (95%). After about 10 min. the paper was taken out, and dried in the open air. When the paper was almost dry, it was placed in an electric drier and completely dried. After storage for a few days in a closed vessel, the paper was used for the experiment. B is a narrow strip of untreated filter paper, 1~1.5 mm. in width, inserted in a slit cut at the center of the oxine-treated filter paper where one drop of the test solution, saturated with isobutanol, had been spotted. C is the developing solvent. D is a small Petri dish (the container for the developing solvent). E is a large Petri dish (12~13 cm. in diameter).

**Preparation of Test Solutions.**—The available

1) M. Lederer, *Compt. rend.*, **236**, 1557 (1953).
2) M. Lederer, *Nature*, **176**, 462 (1955).
3) M. Lederer, *Anal. Chim. Acta*, **15**, 46 (1956).
4) M. Lederer, ibid., **15**, 122 (1956).
5) F. H. Pollard, J. F. W. McOmie and H. M. Stevens, *J. Chem. Soc.*, **1952**, 4730.
6) F. H. Pollard, J. F. W. McOmie and H. M. Stevens, ibid., **1954**, 3435.
7) H. Nagai, *J. Chem. Soc. Japan, Pure Chem. Sec.* (*Nippon Kagaku Zasshi*), **76**, 1246 (1955).
8) H. Nagai, ibid., **77**, 1267 (1956).
9) H. Nagai, ibid., **77**, 1794 (1956).
10) H. Nagai, ibid., **78**, 285 (1957).
11) H. Nagai, ibid., **78**, 840 (1957).
12) H. Nagai, ibid., **78**, 1334 (1957).

lanthanon material consisted of lanthanum oxide, praseodymium oxide, and cerous nitrate. Aqueous nitrate solutions were prepared by evaporating to dryness ca. 10 mg. of the required oxide or nitrate with a few drops of 2 N nitric acid, and dissolving the residue in water to produce the test solution containing ca. 10 mg. cation in 1 ml. solution. The following binary mixtures were prepared similarly: La-Ce, La-Pr and Ce-Pr.

**Development.** — Acetic acid-butanol system has been successfully used in a number of cases as the developing solvent for precipitation chromatography in the separation of many metallic cations, but it seemed to show insufficient separability in the case of lanthanons, though identification of each element in binary systems was possible with some difficulty. The lanthanum-cerium system developed with 0.5% acetic acid (by volume) saturated with isobutanol, and the cerium-praseodymium system developed with ca. 0.01% acetic acid and isobutanol (saturation) gave bare identification of the cations. In the separation of lanthanum and praseodymium, 0.01% acetic acid (saturated with isobutanol) was the most suitable solvent for the identification of praseodymium, while ca. 0.5% acetic acid (saturated with isobutanol) was the most suitable for the identification of lanthanum. The use of a solution more concentrated than 2% acetic acid (saturated with isobutanol) as the developing solvent caused irregular deformation of the chromatogram early in the development and then the bands of the chromatogram completely dissolved; thus the identification of the components of the test solution was scarcely ever possible.

Solution of *n*-butyric acid saturated with isobutanol showed far better results in the separation of lanthanons. Solutions of 0.005, 0.01, 0.05, 0.1, 0.5, 1, 2, 3, 5 and 10% *n*-butyric acid (by volume) saturated with isobutanol were used as developing solvent. The results were as follows. When the test solution was developed with 0.005 or 0.01% solution the innermost band was formed without leaving any blank space at the center of the chromatogram, and the bands showed practically no migration during the development. By the use of the solutions of 0.05 and 0.1% *n*-butyric acid, a blank area appeared at the central portion of the chromatogram, and, although the bands migrated a little on development, the results resembled the foregoing two cases. In the development with more than 1% *n*-butyric acid, the appearance of the bands resembled rather the chromatograms of the perfectly dissolved type than the precipitation chromatogram. When solutions of 1, 2 and 3% were used, the patterns of the chromatograms resembed one another, and the most desirable results were obtained generally in these cases (Fig. 2).

When 5% *n*-butyric acid (saturated with isobutanol) was used, the bands mixed together appreciably. And when 10% *n*-butyric acid (saturated with isobutanol) was used, the confusion of the bands became more marked, but the deformation of the chromatogram, which was observed at a higher concentration of acetic acid, was not observed in the *n*-butyric acid system.

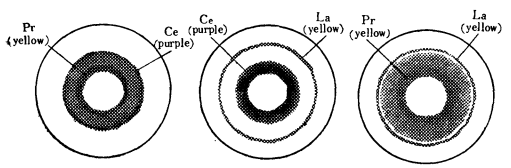



Fig. 2.

The temperature of the developing solvents was 20±1°C. After the development was finished, the chromatogram was subjected to reaction with ammonia vapor so as to stabilize the metal oxinates, and investigated under both visible and ultraviolet light.

## Discussion

When the acetic acid system (saturated with isobutanol) was used as the developing solvent, cerium and praseodymium were identified most readily by the use of 0.01% acid. Since the $R_f$ values of cerium and praseodymium hitherto reported have been the same, this can be regarded as an improvement, though their complete separation has met with little success. On the other hand, lanthanum-praseodymium and lanthanum-cerium whose $R_f$ values were reported to be somewhat different from each other (but the real separation was very difficult owing to their considerable tailing), showed rather better separation at a higher concentration of acetic acid (ca. 0.5% acetic acid).

When the *n*-butyric acid system (saturated with isobutanol) was used as the developing solvent, the separation of cations was achieved at a higher concentration than in the case of the acetic acid system. Accordingly, the chromatogram appeared to be somewhat soluble rather than of complete precipitation but a distinct difference was observed from the perfectly dissolved chromatogram. It was far superior to that of the acetic acid system described above.

These phenomena might be explained as follows. Precipitation chromatography inherently possesses the characteristic of exaggerating the separation factor among the cations, but the coprecipitation is apt to compensate for the advantage of the precipitation chromatography, as the author pointed out at the beginning of this paper. One way to minimize the influence of coprecipitation was to increase the acidity of the developing solvent. When the acidity reached a concentration adequate to prevent coprecipitation and to maintain the ability to form complex salts, the best separability could be expected. Even if the complex salts thus formed do not precipitate completely, their diffusion (migration) velocities in the filter paper decrease so markedly by complex formation that they can not migrate together with the developing front where the reaction between the complexing agent and the cation is predominantly taking place. Accordingly, it would

be reasonable to say that the reaction product (the complex salt formed) was taken out of the reaction system as in the case of precipitation. Thus, the advantages of precipitation chromatography are still retained while its minor disadvantage, coprecipitation, is avoided.

The author wishes to thank Professor T. Sasaki, Tokyo Metropolitan University, Professor N. Saito, the University of Tokyo, Professor J. Yoshimura, Kyushu University, Professor R. Matuura, Kyushu University, Professor K. Ochiai, Kumamoto University, and Assistant Professor H. Kimizuka, Fukuoka Gakugei University, for their encouragement and numerous suggestions throughout the investigation. Also the author expresses hearty thanks to Professor S. Misumi for the gift of lanthanons. The cost of this research was defrayed from the Scientific Research Fund of the Ministry of Education.

*Department of Chemistry*
*Faculty of Science*
*Kumamoto University*
*Kurokami-machi, Kumamoto*

# *Intramolecular Interaction between Hydroxyl Group and π-Electrons. VIII*[1]. *Energetics of the Interaction*

By Michinori Ōki and Hiizu Iwamura

(Received December 11, 1959)

Little is known of the energy of the intramolecular interation between the hydroxyl group and π-electrons in spite of many studies on this phenomenon in a number of compounds. In the first paper[2] of the present series, the authors reported briefly that the energies of the intramolecular interaction in 2-hydroxy-4- and -4′-nitrobiphenyls are 2.5 and 0.93 kcal./mol., respectively. Goldman and Crisler[3] suggested that the strengths of this kind of interaction in 2-phenylethanol and 2-(*p*-methoxyphenyl)-ethanol are 0.88 and 0.98 kcal./mol., respectively, assuming that Badger's postulation, that 70 $cm^{-1}$ shift of the wave number of the hydroxyl stretching bands caused by the hydrogen bond formation corresponds to one kcal./mol. in the energy[4], is operative in this interaction. Necessity of elucidating the true nature of the interaction prompted the authors to examine the energy difference between the free and the interacting forms, since the results would be very useful for the discussion of the relation between band properties and the energy difference and consequently for the discussion of the nature. The present paper deals with some detailed procedures used in the measurement of the energies, which were omitted in the former short communication[2], and reports some data added recently in this laboratory. The materials include 2-allylphenol[1], 2-benzylphenol[1], 2-isopropenylphenol[5] and 2-hydroxybiphenyl[1]. The variation with the temperature of the infrared absorption spectra due to free and interacting hydroxyl groups was measured. These phenols were chosen out of many which possess the internal interaction by considering not only the fundamental structure representing each series, but also some technical advantages. The relative intensities of the free and the interacting O–H stretching absorption bands ($\nu_{O-H}$) at various temperatures can be measured most accurately when the intensities of the two bands are nearly equal. Otherwise, when the most favorable absorbance of one band is secured, the other will be either so weak that it may be affected by the noise of the recording system or so strong that it may exceed saturation. 2-Hydroxybiphenyl does not necessarily fulfill this requirement but the duplicate measurement under the best condition of the spectrometer gave reasonable data, although the probable error was fairly large in this case. To cover all the types of the intramolecular interaction, further combinations of the alcoholic hydroxyl group and the π-electrons of olefins and aromatic rings must be considered. The alcohol, however, as pointed out previously[6], shows rather complicated $\nu_{O-H}$ consisting

1) Part VII: This Bulletin, 33, 681 (1960).
2) M. Ōki, H. Iwamura and Y. Urushibara, ibid., 31, 770 (1958).
3) I. M. Goldman and R. O. Crisler, *J. Org. Chem.*, 23, 751 (1958).
4) R. M. Badger, *J. Chem. Phys.*, 8, 288 (1940).
5) M. Ōki and H. Iwamura, Presented at the Symposium on the Electronic State of Molecules, Tokyo, Sept. 8, 1959.
6) M. Ōki and H. Iwamura, 32, 567 (1959).

of two free $\nu_{O-H}$'s of rotational isomers and one interacting $\nu_{O-H}$ and thus obliges some discretion in dividing the apparent curve into absorptions due to free and interacting forms. This phenomenon caused the authors to give up the study of energy in the alcoholic series in the present work.

## Experimental

**Measurement.**—A Perkin Elmer Model 112 G Double Pass High Precision Grating Infrared Spectrometer was used as previous[6], the spectral slit width being 1.0 $cm^{-1}$ in this region. In a quartz absorption cell of 2 cm. length, having a window of 2.5 cm. diameter and protected with a heating coil covered with asbestos, about 20 ml. of the solution of the sample ($c\sim0.001$ mol./l.) in carbon tetrachloride was placed, and the temperature was controlled by varying the current through the heating coil, kept at each equilibrated temperature within $\pm0.2$°C and read by a thermometer dipped in the solution. The spectrometer being of a single beam type, a background trace was recorded every time immediately before the spectral measurement of the solution and the latter was always referred to the former, which also changed a little with the varying temperature.

**Calculation.**—Separation of the apparent curve and calculation of the integrated intensities of the two bands were made according to Ramsay's first method[6,7] for each of the absorption curves at different temperatures.

$$\text{Free form} \rightleftarrows \text{Interacting form}$$

Then the integrated form of the well-known van't Hoff equation (1) can be applied to obtain the energy difference between the two forms.

$$\ln K = -\frac{\Delta H}{RT} + \frac{\Delta S}{R} \qquad (1)$$

$K$ can be given by

$$K = \frac{C_i}{C_f} = \frac{A_i/a_i}{A_f/a_f} = a\frac{A_i}{A_f} \qquad (2)$$

where $a_i$ and $a_f$ represent intensities per molecule with a free hydroxyl group and an interacting one, respectively, and $A$'s integrated intensities. Combination of Eq. 1 with Eq. 2 gives

$$\ln\frac{A_i}{A_f} = \frac{-\Delta H}{RT} + \left(\frac{\Delta S}{R} - \ln a\right) \qquad (3)$$

The slope of the line obtained by taking $\ln(A_i/A_f)$ on the ordinate and $1/T$ on the abscissa gives the energy of the interaction ($-\Delta H$). Here it is assumed, that $a_i$ and $a_f$, or at least their ratio $a$, should be independent of the temperature, since the temperature range is rather narrow (25~70°C).

**Materials.**—Phenols used in the measurements are all known compounds and their physical constants were already reported previously[1,5].

## Results and Discussion

Apparent absorption curves of 2-isopropenylphenol at various temperatures are shown in Fig. 1 and $\ln(A_i/A_f)$ and temperature relation in Fig. 2.

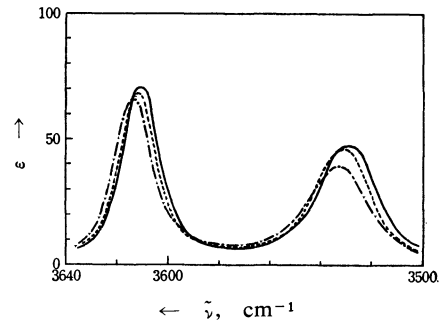



Fig. 1. $\nu_{O-H}$ absorptions of 2-isopropenylphenol at various temperatures.
28.1°C —— 45.3°C ------ 70.5°C -·-·

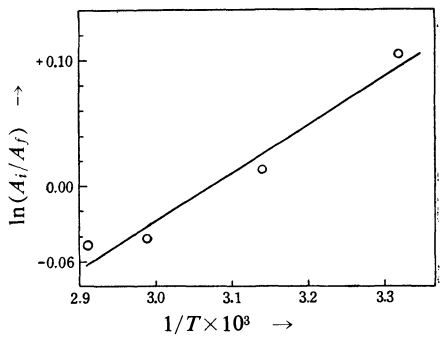



Fig. 2. Relation between $\ln(A_i/A_f)$ and temperature for 2-isopropenylphenol.

The effects of the temperature on the hydroxyl stretching frequencies and on the intensities are summarized in Tables I to IV.

There is always a slight but definite increase in absorption frequencies of both free and interacting $\nu_{O-H}$, accompanied by a decrease in the total integrated intensities ($A_i+A_f$). These effects might be attributed to the rupture of the remaining hydrogen bonding, but, in concentration employed here ($c\sim0.001$ mol./l.), the possibility of the bonding of two phenol molecules can be neglected with certainty. Liddel and Becker[8] already observed an appreciable decrease in the peak intensity and a slight increase in frequency (ca. 6 $cm^{-1}$) of the free $\nu_{O-H}$ of methanol in carbon tetrachloride in the temperature range between $-10$ and 50°C, and suggested that these variations might be considered to be owing to a weak hydrogen bonding to the solvent. This possibility is apparently reasonable because this type of interaction may be very weak and the observed shift of the frequencies is only small, besides it can be ruptured easily with the rising temperature. Tables I to IV show, however, that

7) D. A. Ramsay, *J. Am. Chem. Soc.*, **74**, 72 (1952).

8) U. Liddel and E. D. Becker, *J. Chem. Phys.*, **25**, 173 (1956).

TABLE I. THE EFFECT OF THE TEMPERATURE ON $\nu_{O-H}$'S OF 2-ALLYLPHENOL

| Temperature $1/T\times10^3$(°K$^{-1}$) | $\nu_{max}$ (cm$^{-1}$) | $\Delta\nu^a{}_{1/2}$ (cm$^{-1}$) | $A\times10^{-3}$ (mol$^{-1}$·l.·cm$^{-2}$) | $A_i/A_f$ | $\Delta\nu_{max}$ (cm$^{-1}$) |
|---|---|---|---|---|---|
| 3.31 | 3612.2<br>3547.0 | 17.0<br>62.3 | 6.66<br>8.72 | 1.30 | 65.2 |
| 3.14 | 3613.2<br>3548.6 | 17.4<br>62.8 | 6.58<br>8.55 | 1.30 | 64.6 |
| 3.03 | 3614.1<br>3551.7 | 17.6<br>64.2 | 6.52<br>8.04 | 1.23 | 62.4 |
| 2.92 | 3614.9<br>3556.1 | 18.0<br>65.8 | 6.23<br>7.46 | 1.20 | 58.8 |

TABLE II. THE EFFECT OF THE TEMPERATURE ON $\nu_{O-H}$'S OF 2-BENZYLPHENOL

| Temperature $1/T\times10^3$(°K$^{-1}$) | $\nu_{max}$ (cm$^{-1}$) | $\Delta\nu^a{}_{1/2}$ (cm$^{-1}$) | $A\times10^{-3}$ (mol$^{-1}$·l.·cm$^{-2}$) | $A_i/A_f$ | $\Delta\nu_{max}$ (cm$^{-1}$) |
|---|---|---|---|---|---|
| 3.31 | 3611.1<br>3560.6 | 17.2<br>60.8 | 8.48<br>8.67 | 1.02 | 50.5 |
| 3.14 | 3612.0<br>3561.8 | 17.8<br>59.2 | 8.53<br>8.44 | 0.99 | 50.2 |
| 3.04 | 3612.6<br>3565.8 | 17.8<br>60.8 | 8.07<br>7.90 | 0.98 | 46.8 |
| 2.91 | 3613.4<br>3566.9 | 18.4<br>61.8 | 7.90<br>7.55 | 0.96 | 46.5 |

TABLE III. THE EFFECT OF THE TEMPERATURE ON $\nu_{O-H}$'S OF 2-ISOPROPENYLPHENOL

| Temperature $1/T\times10^3$(°K$^{-1}$) | $\nu_{max}$ (cm$^{-1}$) | $\Delta\nu^a{}_{1/2}$ (cm$^{-1}$) | $A\times10^{-3}$ (mol$^{-1}$·l.·cm$^{-2}$) | $A_i/A_f$ | $\Delta\nu_{max}$ (cm$^{-1}$) |
|---|---|---|---|---|---|
| 3.32 | 3611.0<br>3529.4 | 16.7<br>26.5 | 4.19<br>4.59 | 1.11 | 81.6 |
| 3.14 | 3612.0<br>3531.9 | 16.8<br>26.0 | 4.08<br>4.28 | 1.01 | 80.1 |
| 2.99 | 3612.8<br>3532.4 | 16.8<br>25.8 | 3.99<br>3.83 | 0.96 | 80.4 |
| 2.91 | 3613.8<br>3533.5 | 17.0<br>25.6 | 3.92<br>3.75 | 0.96 | 80.3 |

TABLE IV. THE EFFECT OF THE TEMPERATURE ON $\nu_{O-H}$'S OF 2-HYDROXYBIPHENYL

| Temperature $1/T\times10^3$(°K$^{-1}$) | $\nu_{max}$ (cm$^{-1}$) | $\Delta\nu^a{}_{1/2}$ (cm$^{-1}$) | $A\times10^{-3}$ (mol$^{-1}$·l.·cm$^{-2}$) | $A_i/A_f$ | $\Delta\nu_{max}$ (cm$^{-1}$) |
|---|---|---|---|---|---|
| 3.30 | 3606.9<br>3564.9 | 15.5<br>15.0 | 1.39<br>13.11 | 9.44 | 42.0 |
| 3.19 | 3607.3<br>3565.3 | 15.8<br>15.2 | 1.48<br>12.99 | 8.77 | 42.0 |
| 3.08 | 3607.7<br>3565.9 | 16.0<br>15.2 | 1.63<br>12.57 | 7.72 | 41.8 |
| 3.01 | 3607.9<br>3566.3 | 16.2<br>15.6 | 1.59<br>12.84 | 8.10 | 41.6 |
| 2.90 | 3608.3<br>3566.8 | 17.0<br>15.8 | 1.80<br>12.48 | 6.92 | 41.5 |

TABLE V

| Phenols | $-\Delta H$ (kcal./mol.) | $\Delta S/R-\ln a$ | $\Delta\nu_{max}$(cm$^{-1}$) |
|---|---|---|---|
| 2-Allylphenol | 0.46±0.14 | −0.49±0.22 | 65.5 |
| 2-Benzylphenol | 0.33±0.05 | −0.53±0.10 | 50.8 |
| 2-Isopropenylphenol | 0.76±0.11 | −1.17±0.20 | 82.0 |
| 2-Hydroxybiphenyl | 1.45±0.27 | −0.17±0.42 | 42.0 |

the frequencies of the internally interacting $\nu_{O-H}$ which has no available proton any longer also rise in the same way with the temperature and this fact may be explained from lessening of the dipole-dipole interaction between phenols and solvent molecules by their thermal motion, to which Cole and Macritchie[9] have recently alluded. About a half of the decrease in the total intensity can be attributed to the thermal expansion of the solvent, the volume expansion coefficient of carbon tetrachloride being $1.236 \times 10^{-3}$.

In Table V are listed the energies of the interaction ($-\Delta H$), together with constant $\Delta S/R - \ln a$, obtained by applying Eq. 3 to the above data in Tables I to IV. The shifts (for the room temperature) of the $\nu_{O-H}$ absorption maxima of the interacting form from that of the free one are listed in the last column for comparison of the shifts with the energy.

$-\Delta H$'s are all smaller than the weakest one of the ordinary hydrogen bonding which ranges from 2.3 (NH···N) to 7 (FH···F) kcal./mol.[10] Even the strongest interaction of this kind ever measured, 2.5 kcal./mol. for 2-hydroxy-4-nitrobiphenyl[2], lies at the lowest limit of the energy for the hydrogen bonding. This difference in energy may be the best criterion which differentiates this interaction from the ordinary hydrogen bonding. It seems that at least no simple relation exists between $\Delta\nu_{max}$ and $-\Delta H$. The rotational degree of freedom must be taken into account. In 2-allylphenol, 2-benzylphenol and 2-isopropenylphenol, a loss of energy may be caused by the formation of the internal interaction, because the molecule must take a structure, which is otherwise the sterically unfavored one. The apparent $-\Delta H$, therefore, does not necessarily mean the true energy difference of the interaction. These considerations lead to the reasonable explanation of the arbitrary relation between $\Delta\nu_{max}$ and the energy difference. Some relation may be expected between $\Delta\nu_{max}$ and $-\Delta H$ if the compounds are limited to a certain series, but, it is still clear that the relation is not so simple as a linear one, as is understood from the three compounds in the biphenyl series. Hence, it is dangerous to evaluate the energy of the interaction from the mere comparison of the two frequencies.

Although, for strict understanding of the entropy changes of the interaction ($\Delta S$), another standard band common in frequency and in molecular absorption coefficient to both molecular types must be further used together with these two $\nu_{O-H}$'s, as shown by Mizushima and his collaborators[11], constant $\Delta S/R - \ln a$ obtained by extrapolating $T$ to infinity in the Eq. 3 can be assumed to be a measure of the entropy change, since roughly speaking it can be assumed that constant $a$ in Eq. 2 is equal to unity, when $\ln a$ becomes zero. This assumption is partly supported by the speculation that the changes of the dipole moment accompanying the vibrational motion are much smaller, than in the case of the ordinary hydrogen bonding, and partly by the observation, that the total integrated intensities ($A_i + A_f$) in these phenols possessing different degrees of interaction are about equal to $1.5 \times 10^4$ except that of 2-isopropenylphenol which is rather sterically hindered. Entropy changes accompanying the intramolecular interaction consist of those of the vibrational motion and of the internal rotation, each being estimated to be a few entropy units, when they are perfectly restricted[11,12]. With weak intramolecular interaction between the hydroxyl group and $\pi$-electrons this effect is expected to be less and it is the case in three of the phenols presented above. On the contrary, 2-isopropenylphenol shows an extraordinary great entropy term which can not be explained from the above factors only. It can be well explained by assuming that this phenol exists in four rather stable conformations near coplanarity, and only one of them can be the molecular form favorable for the interaction. Then the ratio of the number of the conformation, 1/3, must be introduced into the entropy term in the form of ln 3 and subtraction of the latter from the former gives a reasonable value ($-0.07$) comparable to the other phenols. Almost equal $\Delta S/R - \ln a$ values in 2-allylphenol and 2-benzylphenol can be understood by considering that the interaction in both cases will occur with the $\pi$-electron at the "$\beta$" carbon atom in respect of the phenol nucleus as already suggested in the previous paper[1]. The small $\Delta S/R - \ln a$ value in 2-hydroxybiphenyl is rather unexpected. One of the most interesting internal motions in this molecule is that of rotation and/or vibration around the pivot bond. This will give rise to an appreciable entropy decrease if perfectly restricted. The observed small amount of the entropy term shows that the contribution of this effect is very small, and the moderate changes in the O-H force constants between free and interacting forms can be accomodated with almost no entropy changes.

The authors wish to express their hearty thanks to Professor Y. Urushibara and Professor

9) A. R. H. Cole and F. Macritchie, *Spectrochim. Acta*, **1959**, 6.
10) C. A. Coulson, *Research*, **10**, 149 (1957).
11) S. Mizushima, T. Shimanouchi, K. Kuratani and T. Miyazawa, *J. Am. Chem. Soc.*, **74**, 1378 (1952).
12) H. H. Jaffé, ibid., **79**, 2373 (1957).

T. Shimanouchi for their valuable suggestions and discussions. The authors are also indebted to the Ministry of Education for the Grant in Aid for Fundamental Scientific Research.

*Department of Chemistry*
*Faculty of Science*
*The University of Tokyo*
*Hongo, Tokyo*

# *Electrophotoluminescence of Zinc Sulfide Phosphors*

By Yoshihide KOTERA and Kiyotaka NARAOKA

(Received October 13, 1959)

Various effects of electric fields on the light emission of zinc sulfide phosphors during or after excitation by ultraviolet or X-rays have been investigated by a number of authors[1-4]. The effects include a quenching or an enhancement of the luminescence under the electric field, a momentary stimulation of luminescence at application or removal of the electric field, and other miscellaneous effects.

If the observations on various phosphors, each having different kinds of activators or different chemical compositions of matrix, for example, hex.-ZnS : Cu, cub.-ZnS : Mn, (Zn, Cd)S : Ag and ZnS : Cu, Pb are carried out under the same conditions, then each phosphor has different influences. The purpose of this paper is to find how the influence of an alternating electric field on luminescence varies with the kinds of activator or chemical composition of the matrix.

Destriau[2] made extensive investigations of these effects, and he reported that it seems that the sulfides with a persistent phosphorescence are very sensitive to momentary stimulation and insensitive to the quenching effect, while the sulfides with brief phosphorescence show an appreciable quenching effect and a slight or even insignificant momentary stimulation. However, he[5] noted that although thermoluminescence and infrared stimulation can occur after the action of the field, application of the field after thermoluminescence or infrared stimulation, on the other hand, does not produce any emission. From this observation, it might be concluded that the electric field acts only on shallow traps but not on deep traps, but he thought that this conclusion is uncertain, because the field obviously has a directional character, whereas temperature or infrared radiation has not.

Matossi[4] has studied the electrophotoluminescence of various zinc sulfide phosphors, but he could not find any systematic dependence of the characteristics of stimulation or quenching on the method of preparation (kind of activator or flux) or on other luminescence properties, such as the time of afterglow.

It is explained by several authors that the momentary field stimulation might be caused by electron traps, from which the electron is released by electric field and returns to luminescent centers to cause emission. Further, phosphorescence, infrared stimulation and thermoluminescence are explained by the action of electron traps. Therefore it is expected that there might be a close relation between momentary stimulation and those characteristics. From this standpoint, we are going to discuss the relations between momentary field stimulation and phosphorescence, infrared stimulation, or thermoluminescence, respectively.

## Experimental

The phosphors were synthesized from the pure zinc sulfide by adding appropriate aqueous solution of activator and two weight percent sodium chloride. The mixtures were stirred well, dried, transferred to a silica crucible and fired for crystallization from 750 to 1200°C in a temperature-controlled furnace in air for half an hour. After crystallization, the preparations were washed free of water-soluble chloride and were dried. The composition of phosphors and the condition of firing are shown in columns 2 and 3 of Table I.

All phosphors were embedded in Acrylite (Polymethylmethacrylate, produced by Mitsubishi Rayon Co.) and investigated in cells of the common construction of the electroluminescent cell with about 10 $cm^2$ area and about 0.5 mm. thickness of the layer. The phosphor-dielectrics layer was held between two electrodes, one of which was conductive glass coated with tin oxide layer, and the other was aluminum

1) G. Destriau, *Phil. Mag.*, **38**, 784 (1947).
2) G. Destriau, ibid., **38**, 880 (1947).
3) I. T. Steinberger. W. Low and E. Alexander, *Phys. Rev.*, **99**, 1219 (1955).
4) F. Matossi, *J. Electrochem. Soc.*, **103**, 122 (1956).
5) G. Destriau and H. F. Ivey, *Proceeding of the IRE*, **43**, 1911 (1955).

TABLE I. THE COMPOSITION OF PHOSPHORS AND THEIR LUMINESCENT CHARACTERISTICS

| No. | Composition | Firing temp. °C | concn. of act. mol./1 mol. ZnS | P. L. | Phospho. | I. R. S. | M. F. S. | F. Q. | Notes |
|---|---|---|---|---|---|---|---|---|---|
| 1 | ZnS : Ag | 1000 | $10^{-5}$ | b | S | | | + | |
| 2 | 〃 | 1150 | $10^{-5}$ | 〃 | 〃 | | | + | |
| 3 | 〃 | 〃 | $10^{-4}$ | 〃 | 〃 | | | + | |
| 4 | 〃 | 〃 | $10^{-3}$ | 〃 | 〃 | | | + | |
| 5 | $(Zn_{0.80}, Cd_{0.20})S$ : Ag | 950 | $10^{-4}$ | g | 〃 | | | + | |
| 6 | $(Zn_{0.50}, Cd_{0.50})S$ : Ag | 〃 | 〃 | y | 〃 | | | + | |
| 7 | $(Zn_{0.20}, Cd_{0.80})S$ : Ag | 〃 | 〃 | r | 〃 | | | − | |
| 8 | $(Zn_{0.63}, Cd_{0.37})S$ : Ag | 1150 | $10^{-5}$ | g | L | | + | + | |
| 9 | 〃 | 〃 | $10^{-4}$ | 〃 | 〃 | | + | + | |
| 10 | 〃 | 〃 | $10^{-3}$ | 〃 | S | | | + | |
| 11 | (Zn, Cd)S : Ag | — | — | y | 〃 | | | + | (a) |
| 12 | ZnS : Zn | 900 | — | b | 〃 | | | + | |
| 13 | ZnS : Cu | 〃 | $10^{-6}$ | g. b. | 〃 | | + | + | |
| 14 | 〃 | 〃 | $3\times10^{-6}$ | g | 〃 | | ++ | + | |
| 15 | 〃 | 〃 | $10^{-5}$ | 〃 | M | | ++ | + | |
| 16 | 〃 | 〃 | $3\times10^{-5}$ | 〃 | 〃 | | ++ | + | |
| 17 | 〃 | 〃 | $10^{-4}$ | 〃 | 〃 | | + | + | |
| 18 | 〃 | 〃 | $3\times10^{-4}$ | 〃 | S | | | + | |
| 19 | 〃 | 〃 | $10^{-3}$ | 〃 | 〃 | | | + | |
| 20 | 〃 | 1000 | $10^{-5}$ | 〃 | M | | ++ | + | (b) |
| 21 | 〃 | 〃 | $10^{-4}$ | 〃 | S | | + | + | (〃) |
| 22 | 〃 | 〃 | $10^{-3}$ | 〃 | 〃 | | | + | (〃) |
| 23 | 〃 | 1200 | $3\times10^{-6}$ | 〃 | L | | | + | |
| 24 | 〃 | 〃 | $10^{-5}$ | 〃 | V. L | + | + | − | |
| 25 | 〃 | 〃 | $3\times10^{-5}$ | 〃 | 〃 | + | + | − | |
| 26 | 〃 | 〃 | $10^{-4}$ | 〃 | L | | | + | |
| 27 | 〃 | 〃 | $3\times10^{-4}$ | 〃 | 〃 | | | + | |
| 28 | 〃 | 〃 | $10^{-3}$ | 〃 | S | | | + | |
| 29 | 〃 | — | — | 〃 | V. L | | | − | (c) |
| 30 | $(Zn_{0.80}, Cd_{0.20})S$ : Cu | 1050 | $10^{-4}$ | y | L | | | + | |
| 31 | $(Zn_{0.50}, Cd_{0.50})S$ : Cu | 〃 | 〃 | r | S | | | − | |
| 32 | Zn(S, Se) : Cu | 780 | $10^{-4}$ | y | 〃 | | | + | |
| 33 | ZnS : Cu, Fe | 1200 | | g | 〃 | | | + | |
| 34 | ZnS : Cu, Pb | 1150 | | 〃 | L | ++ | | − | (d) |
| 35 | 〃 | — | — | 〃 | M | | + | − | (e) |
| 36 | ZnS : Pb | 900 | — | 〃 | 〃 | + | + | + | |
| 37 | 〃 | 1200 | — | 〃 | L | + | | − | |
| 38 | ZnS : Pb, Mn | 1150 | | y | 〃 | + | | − | |
| 39 | ZnS : Mn | 1000 | $10^{-2}$ | o | S | + | | − | |
| 40 | 〃 | | 〃 | 〃 | 〃 | | + | − | (f) |
| 41 | 〃 | 1200 | 〃 | 〃 | 〃 | + | | − | |
| 42 | ZnS, ZnO : Mn | 1000 | 〃 | 〃 | 〃 | | + | − | |
| 43 | $(Zn_{0.80}, Cd_{0.20})S$ : Mn | 〃 | 〃 | 〃 | 〃 | + | | + | |
| 44 | 〃 | 〃 | 〃 | 〃 | 〃 | | | + | (f) |

(a) A commercial product for X-ray.
(b) Fired in nitrogen stream.
(c) A commercial product for phosphorescent paint.
(d) Fonda's phosphor.
(e) Electroluminescent phosphor.
(f) No flux.

TABLE I (continued)

| | |
|---|---|
| P. L.: | Color of photoluminescence<br>b=blue, g=green, y=yellow, r=red, g. b=greenish blue, o=orange. |
| Phospho.: | Phosphorescence<br>S=short persistence, M=medium, L=long, V. L=very long. |
| I. R. S.: | Infrared stimulation<br>+=weak i.r.s., ++=strong i.r.s. |
| M. F. S.: | Momentary field stimulation (the Gudden-Pohl effect)<br>+=considerable m.f.s., ++=strong m.f.s. |
| F. Q.: | Quenching of luminescence by electric field application during excitation<br>−=none or slight, +=considerable field quenching. |

plate. A d-c operated black light lamp with a Corning glass filter 5840 transmitting from 3100 to 4200 Å served as the exciting ultraviolet source. The light emitted by phosphor was allowed to fall upon the cathode of the 1P21 photomultiplier, the anode current from the photomultiplier being measured by means of d-c amplifier and cathode ray oscillograph, and the oscillogram of transient phenomenon for emission at electric field application or removal was observed.

The applied electric field was obtained from 50 c. p. s a-c line, and field intensity was estimated to be about 10000 volts per centimeter. With this field intensity electroluminescence was not detected with the exception of zinc sulfide phosphors which contain $10^{-3}$ mol. or more of copper per 1 mol. ZnS.

## Experimental Results and Discussion

On application of the alternating electric field during continuous ultraviolet excitation, the average brightness of luminescence increases for a moment. After these transitory phenomena the average brightness reaches a new equilibrium level, lower than the luminescent level before application of the filed. Some phosphors show no steady state quenching. The transient variation of emission is shown schematically as a function of time in Fig. 1. The field quenching lasts as long as the field is applied, and recovers gradually, then reaches a steady level.

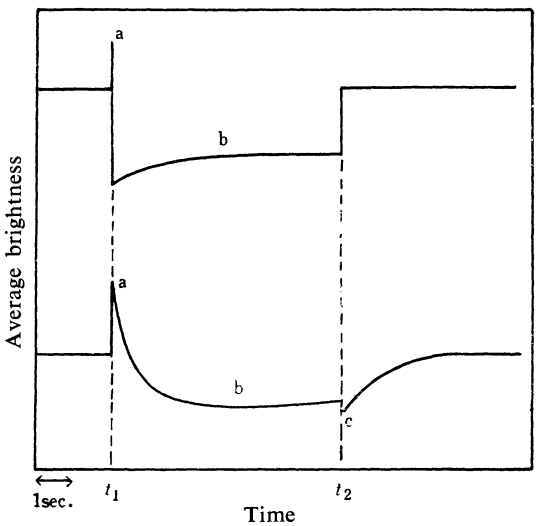



Fig. 1. Average brightness of luminescence when electric field is applied or removed.
$t_1$···field application, $t_2$···field removal,
a···momentary stimulation,
b···field quenching, c···cut-off dip.

The stimulated and quenched brightness were modulated by applied alternating electric field. A frequency of brightness wave was that of applied alternating field or twice this frequency. The modulated frequency for pure zinc sulfide phosphors was 100 c.p.s., while that of zinc-cadmium sulfide phosphors which contained 20 mol. percent cadmium sulfide or more was 50 c.p.s.. Fig. 2 shows the oscillogram of modulated wave for ZnS and (Zn, Cd)S phosphors. The (Zn, Cd)S phosphors which contain below 20 mol. percent cadmium sulfide was not studied.

When the electric field was removed, then the phosphors such as ZnS : Cu, Fe, (Zn, Cd)S : Ag (No. 11), and Zn(S, Se) : Cu (No. 32) had a short flash, while the phosphors such as ZnS : Cu and (Zn, Cd)S : Cu had a dip of brightness. On the other hand, the phosphors such as the many ZnS : Ag and (Zn, Cd)S : Ag phosphors recovered directly without flash or dip. The cut-off stimulation was found by Matossi for almost all phosphors to consist of two components, a very sharp peak and a tail of long duration. We found this cut-off

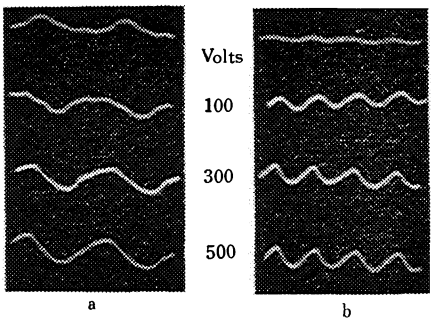
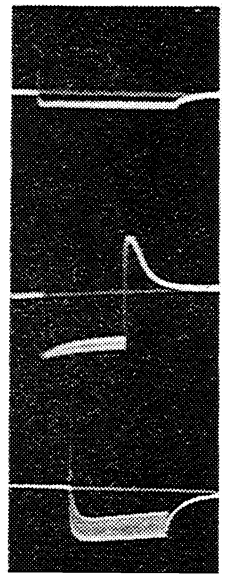



Fig. 2. Oscillogram of quenching brightness wave during 1/25 second at various voltage. The patterns of 'a' show quenching brightness waves of (Zn, Cd)S : Ag, and they are modulated to 50 c.p.s. The patterns of 'b' show the waves of ZnS : Cu, modulated to 100 c.p.s.

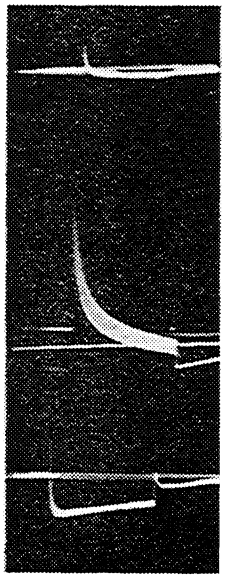


a
Sample
No. 5
(Zn, Cd)S : Ag

b
No. 11
(Zn, Cd)S : Ag

c
No. 30
(Zn, Cd)S : Cu

1 sec.



d
No. 38
ZnS : Cu, Mn

e
No. 20
ZnS : Cu

f
No. 33
ZnS : Cu, Fe

1 sec.

Fig. 3. Oscillogram of brightness at field application and removal. The luminescence of ultraviolet excited phosphors are affected by alternating electric field in following order, 1; steady luminescence, 2; field stimulation during excitation (the Gudden-Pohl effect), 3; field quenching during excitation, 4; cut-off stimulation or dip, 5; recovery.

stimulation only for ZnS : Cu, Fe, while (Zn, Cd)S : Ag (No. 11) and Zn(S, Se) : Cu (No. 32) showed a different kind of cut-off stimulation from Matossi's, and had no sharp peak, but the emission increased gradually with time, reaching a maximum at about one second after removal of the electric field, then decreased slowly to initial brightness. The increased emission at field removal was observed by the naked eye for the (Zn, Cd)S : Ag (No. 11). Their characteristics are shown in Fig. 3b. In Fig. 3 various typical brightness curves of luminescence which are influenced by the electric field are shown. In these figures the coordinate is brightness and the abscissa is time. Steady emission before the application of the electric field, momentary stimulation, field quenching, cut-off stimulation, and recovery are shown from left to right. During this period the phosphor was illuminated continuously by ultraviolet light.

The intensity of first stimulation depends on exciting ultraviolet intensity, the time interval between repeated field applications after first application and so on. The stimulated emission increased with the intensity of excitation and the time interval, and showed saturation. Fig. 4 shows stimulated emission as a function of the time interval at various exciting intensities.

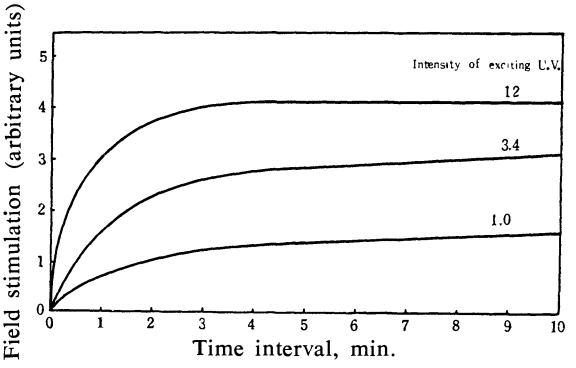



Fig. 4. Momentary field stimulation during excitation as a function of excited time interval at various intensity of ultraviolet. Phosphor ZnS : Cu (No. 17).

The time of application was about 10 sec. and in that time the momentary stimulation was over.

For the Gudden-Pohl effect after removal of the ultraviolet radiation the form of brightness pulse and dependence on kinds of activator and chemical composition of phosphors are similar to the first momentary stimulation during excitation.

The behavior under electric field, phosphorescence and infrared stimulation are shown in Table I. From this table, it is possible to compare the influence of electric field on the different phosphors. This is summarized as follows:

1. Many of the ZnS : Ag and (Zn, Cd)S : Ag phosphors with short persistent afterglow show appreciable field quenching during excitation, estimated to be 40% at a field intensity

of 10000 volts per cm., and have slight momentary stimulation. (Zn, Cd)S : Ag phosphors with longer afterglow show large momentary stimulation, but the quenching ratio does not decrease.

2. ZnS : Mn and (Zn, Cd)S : Mn which show considerable infrared stimulation have no field quenching, while ZnS : Mn which incorporates ZnO and also shows short afterglow and no infrared stimulation has a momentary stimulation whose duration is very short.

3. Cub.-ZnS : Pb with a short persistent phosphorescence and some infrared stimulation shows a strong field stimulation and a small field quenching, while hex.-ZnS : Pb with a long persistence and a strong infrared stimulation shows feeble field stimulation and no field quenching. ZnS : Cu, Pb (Fonda's phosphor) has a most remarkable infrared stimulation but shows feeble field stimulation and no field quenching.

4. The field sensitivity of ZnS : Cu and ZnS : Ag phosphors decreases by substitution of a large amount of cadmium for zinc, for example, $(Zn_{0.20}, Cd_{0.80})S : Ag$ (red) and $(Zn_{0.50}, Cd_{0.50})S : Cu$ (red) have no field stimulation and also no field quenching. But zinc-cadmium sulfide phosphors with medium substitution of cadmium for zinc still have considerable field sensitivity.

5. The influence on ZnS : Cu phosphors is very complicated. The zinc sulfide fired at 1020°C or higher is expected to have hexagonal structure, while sulfide fired below 1020°C is expected to have cubic structure. In this observation, the sulfide was fired at 1200°C for the hexagonal phosphor, and at 900°C for the cubic.

Their phosphorescence, infrared stimulation, and momentary stimulation during decay at field application are shown in Fig. 5 as a function of copper concentration. In this figure, the phosphorescence is plotted as an afterglow intensity after a lapse of one minute from removal of ultraviolet excitation, and the infrared stimulation as an initial flash-up intensity under infrared illumination also after one minute's decay, and the integral of light flash at field application (the area under the curve obtained in Fig. 6, in which the abscissa is time and the ordinate is the photocurrent from the photomultiplier) was taken as the measure of the Gudden-Pohl effect.

In hex.-ZnS : Cu, the phosphorescence is found to be increased by increasing the copper content and to reach a maximum at copper content of $3\times10^{-5}$ mol. per one mol. of ZnS, and Gudden-Pohl stimulation is also increased by increasing the copper content and reaches a maximum at a copper content of $10^{-5}$ mol.

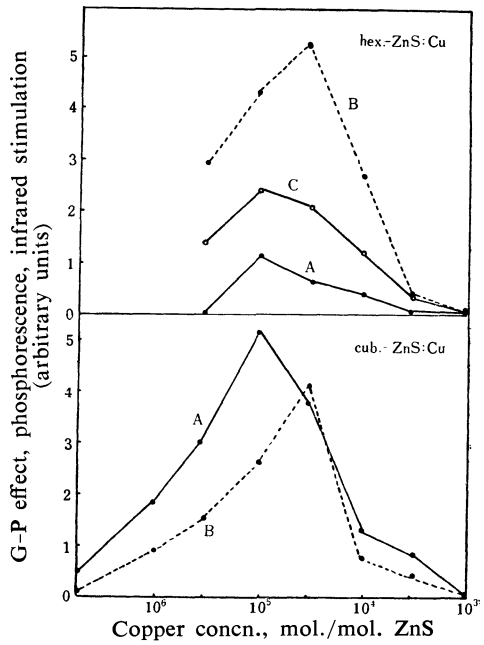



Fig. 5. The Gudden-Pohl effect during decay, phosphorescence and infrared stimulation as a function of copper concentration in hex. and cub. zinc sulfide phosphors.
A. The Gudden-Pohl effect,
B. phosphorescence, C. infrared stimulation.

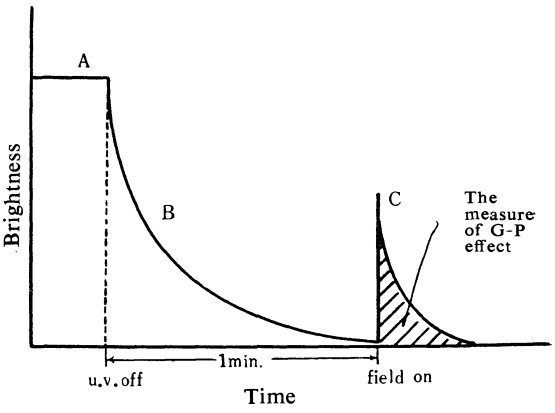



Fig. 6. The Gudden-Pohl effect (C) after removal of ultraviolet excitation.
A : steady state luminescence, B : decay.

The zinc sulfide with $3\times10^{-5}$ mol. copper has a very long persistent phosphorescence and the strongest infrared stimulation among the zinc sulfide phosphors activated with copper, but it shows weak field stimulation. Independent of the copper content the momentary field stimulation of hex.-ZnS : Cu is weaker than that of cub.-ZnS : Cu. The field stimulation of cub.-ZnS : Cu phosphors as a function of copper concentration is similar to that of hexagonal phosphors, but infrared stimulation is so feeble

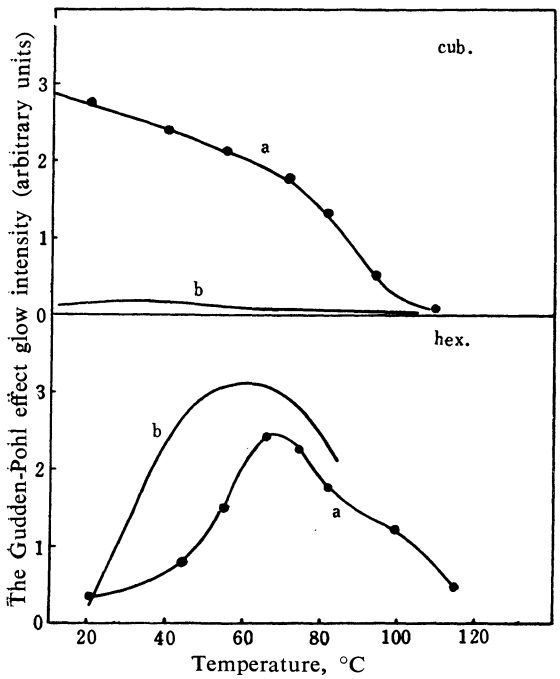



Fig. 7. The Gudden-Pohl stimulation as a function of temperature and glow curve. a: the Gudden-Pohl effect, b: glow intensity. Sample, cub.···ZnS: Cu(No. 16), hex.···ZnS: Cu (No. 24).

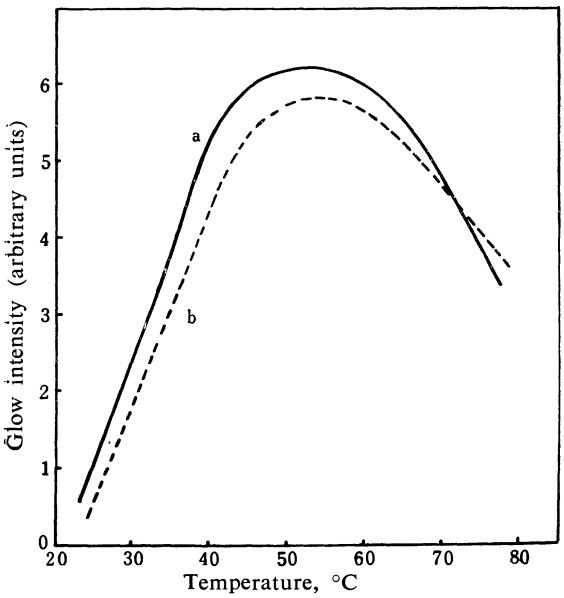



Fig. 8. Glow curves depending upon whether an electric field has been previously applied or not. Sample ZnS: Cu (No. 24). a: previously applied, b: not applied.

that it can not be detected. The Gudden-Pohl effect of cub.-ZnS: Cu with a suitable amount of copper is strong and shows relatively long duration, and it takes about one second to fall from flash-up to quenching level, and also several seconds to recover to initial brightness.

The intensity and decay of the flash by the electric field depend on temperature, that is, at higher temperature momentary stimulation at field application is sharper and its decay is more rapid. In Fig. 7 field stimulation is plotted as a function of temperature, and glow curves of phosphors which were excited and caused to decay at room temperature are shown in the same figure. The heating rate of glow curves was 0.2°C per second. In cub.-ZnS: Cu, the higher the temperature is, the smaller is the field stimulation between 20° and 120°C, and there is no peak in this temperature range. The momentary stimulation of hex.-ZnS: Cu increases with temperature reaching a maximum at 70°C, while the glow curve has a peak at 55°C.

Some knowledge of traps has been obtained from glow curve measurements by Bube[6]. He proposed that a large number of traps are present in self-activated ZnS phosphors with no added copper impurity. The incorporation of copper up to $1.7\times10^{-4}$ mol. (0.01%) causes the appearance of traps which are deeper than those present before the addition of copper. Incorporation of copper in amounts of more than $1.7\times10^{-4}$ mol. causes disappearance of the deep traps due to copper.

Comparing our experimental results with the knowledge about traps, it could be considered that there is a maximum of momentary stimulation as a function of copper concentration at $10^{-5}$ mol. copper content and the number of deeper traps has a maximum value at $1.7\times10^{-4}$ mol. copper content, that is, two maxima are uncoincident. So the deeper traps might not be contributing to the momentary stimulation.

Two glow curves of hex.-ZnS: Cu (24) depending upon whether or not the electric field has been previously are shown in Fig. 8. The application of the field was done after removal of excitation, and the time of application was ten seconds. A similar experiment was carried out by Destriau[5]. In our observation, it can be seen that the maxima of two glow curves have about the same height. From this observation, we might assume that the deeper trap which corresponds to the glow peak at 55°C does not contribute to momentary stimulation at room temperature. Rather the increase of momentary stimulation at higher temperature may be ascribed to the effect of emptying the deeper

6) R. H. Bube, *Phys. Rev.*, **80**, 655 (1950).

traps which can release their electron thermally at higher temperature.

**Summary**

The effects of the electric field on the luminescence of ultra-violet excited zinc sulfide phosphors are shown as a function of kinds of activator and chemical composition of matrix. All phosphors were measured in an electroluminescent cell of common construction. The electric field was obtained from 50 c.p.s. alternating line. The Gudden-Pohl effect of both hexagonal and cubic ZnS : Cu increased with increasing copper content and reached a maximum at a content of $10^{-5}$ mol. The effect of cubic ZnS : Cu ($10^{-5}$) is the strongest in the zinc sulfide phosphors at room temperature. Cubic sulfide phosphors activated by copper are sensitive to both momentary stimulation and field quenching.

Further, a relation between electron traps and the Gudden-Pohl effect was studied. From the temperature dependence of the Gudden-Pohl effect and glow curves, it might be assumed that the deeper trap which corresponds to a glow peak at 55°C does not produce the Gudden-Pohl effect at room temperature, rather the increase of the effect at higher temperature may be ascribed to the emptying of the deeper traps which can release their electrons thermally at higher temperature.

*Government Chemical Industrial Research Institute*
*Hatagaya, Tokyo*

# *Polyethers. I. Stereospecific Polymerization of Epihalohydrins*†

By Shin'ichi ISHIDA*

(Received October 3, 1959)

Recenctly a number of publications have appeared which describe the polymerization of propylene oxide with different catalysts to give a product which contains crystalline polypropyleneoxide[1-5]. On the contrary, there has been no publication on stereospecific polymerization of epihalohydrins. In the earlier work[6] or epihalohydrin, using Friedel-Crafts catalysts such as stannic chloride, it was reported to produce only viscous liquid or pasty resins of low molecular weight.

In the present paper, the author wishes to report on the synthesis of crystalline polymers of epichlorohydrin and epifluorohydrin.

The attempted stereospecific polymerization of epiiodohydrin was unsuccessful.

## Experimentals

**Epichlorohydrin and Propylene Oxide.** — Commercial materials were dried over a molecular sieve and fractionally distilled before use.

**Epifluorohydrin.**—It was prepared from epichlorohydrin and anhydrous potassium fluoride by Gryszkiewicz-Trochimowsky's method[7]. The yield was lower than that reported; only 7 g. of the product boiling at 85~86°C was obtained from 100 g. of epichlorohydrin and 100 g. of anhydrous potassium fluoride.

**Epiiodohydrin.**—It was prepared according to the direction given by E. Wedekind.[8] Epichlorohydrin (48.5 g.) was mixed with a solution of dry sodium iodide (78.5 g.) in acetone (530 ml.) and this mixture was refluxed for 30 hr. The yield of the product boiling at 62°C (24 mmHg) was 40% (37 g.). $n_D^{20}$ 1.5418.

**Ferric Chloride Complex Catalyst.**—A complex of ferric chloride with propyleneoxide was prepared immediately before use according to the procedure of Price[1]. Analogous complexes of ferric chloride with epichlorohydrin and with epifluorohydrin were prepared in a similar manner. A pasty complex catalyst was weighed and dissolved into anhydrous acetone. (about 10% by weight.)

**Polymerization by Ferric Chloride Complex**

† Presented at the 8th Annual Meeting of the Society of Polymer Science, Tokyo, May, 1959.

* Present address: Textile Research Laboratory, Asahi Chem. Ind. Co. Ltd., 118, Ama, Takatsuki, Osaka.

1) C. C. Price and M. Osgan, *J. Am. Chem. Soc.* **78**, 4787 (1956).

2) S. Kambara and M. Hatano, *J. Polymer Sci.*, **27**, 586 (1958).

3) M. Osgan and C. C. Price, *J. Polymer Sci.*, **34**, 153 (1959).

4) R. O. Colclough, G. Gee, W. C. E. Higginson, J. B. Jackson and M. Litt, *J. Polymer Sci.*, **34**, 171 (1959).

5) J. Furukawa, T. Tsuruta, T. Saegusa and G. Kakogawa, *J. Polymer Sci.*, **36**, 541 (1959).

6) "Epichlorohydrin", Shell Chem. Corp. Technical Booklet (1949).

7) MM. E. Gryszkiewicz-Trochimowski, A. Spoizynski and J. Wnuk, *Rec. trav. chim.*, **66**, 413 (1947).

8) E. Wedekind and E. Bruch, *Ann.*, **471**, 97 (1929).

TABLE I. POLYMERIZATION OF EPICHLOROHYDRIN AND PROPYLENEOXIDE BY THE $FeCl_3$ COMPLEXES AT 80°C WITHOUT SOLVENT

| No. | Catalyst | wt. % | Time hr. | Total conversion % | Fraction, % I | II | III | m. p. of of I, °C |
|---|---|---|---|---|---|---|---|---|
| Epichlorohydrin | | | | | | | | |
| Ep-9 | $FeCl_3$-PO | 5 | 41 | 78.5 | 60.7 | 12.2 | 27.1 | 115 |
| Ep-27 | $FeCl_3$PO | 5 | 48 | 61.0 | 55.0 | 10.7 | 34.3 | 108 |
| Ep-101 | $FeCl_3$-EpCl | 10 | 68 | 46.0 | 38.0 | nil* | 62.0 | 104 |
| Ep-104 | $FeCl_3$-EpCl | 5 | 68 | 31.7 | 41.3 | nil* | 58.7 | 111 |
| Propyleneoxide | | | | | | | | |
| Fp-22 | $FeCl_3$-PO | 5 | 68 | 34.6 | 28.2 | nil† | 71.8 | — |
| PO-10 | $FeCl_3$-PO | 2.5 | 96 | 81.8 | 44.7 | nil† | 55.3 | 59 |
| Ep-105 | $FeCl_3$-EpCl | 5 | 68 | 29.0 | 18.0 | nil† | 82.0 | 61 |

* No case of the complex with epichlorohydrin has been obtained fraction II.

† In the case of propylene oxide, there was found no fraction II.

**Catalyst.**—The general procedures were as follows: A catalyst solution of known concentration was injected into a glass tube and then the solvent was evaporated in vacuo at room temperature. In cooling, monomer was poured into tubes. The tubes were flushed with nitrogen and sealed and then placed in a constant temperature bath at 80±0.5°C.

**Polymer Purification.**—At the end of the reaction time the tube was cooled and opened. The polymer produced was fractionated into three parts by the following procedure.

*Fraction I.*—To the reaction mixture was added acidified (HCl) acetone. The insoluble material was collected, washed with dilute HCl-acetone and methanol successively, and then reprecipitated from tetrahydrofuran solution by adding methanol as precipitant.

*Fraction II.*—Acetone solution separated from fraction I was added dropwise with stirring to a large volume of methanol. A white powder, in some cases a pasty mass, separated out of the solution. The precipitate was further fractionated by washing with methanol in which it was partly soluble. The insoluble residue (Fraction II) was reprecipitated from acetone solution with metanol.

*Fraction III.*—The acetone-methanol solution separated from fraction II and methanol washing of fraction II, were combined, concentrated to a small volume and poured into a large excess of water, then centrifuged to give the third fraction III which was a viscous liquid or in some cases a paste.

**Polymerization by Organometallic Compounds.**—In all cases, the catalyst was added to the monomer or the solution of monomer in *n*-hexane or benzene, which was placed in the glass tube cooling in Dry-Ice acetone under nitrogen atmosphere, and then the tube was sealed and placed in a constant temperature bath. The polymers were isolated by an appropriate reprecipitation procedure.

## Results and Discussion

Epichlorohydrin was polymerized using a complex catalyst of ferric chloride and propylene oxide ($FeCl_3$–PO) or an analogous complex catalyst of ferric chloride and epichlorohydrin ($FeCl_3$–EpCl) without solvent at 80±0.5°C. Some results were shown in Table I, in which the results of polymerization of propylene oxide by the same catalysts were compared.

The product was fractionated to three fractions, an acetone-insoluble (at room temperature) fraction (I), an acetone-soluble and methanol-insoluble fraction (II) and a methanol-soluble fraction (III).

Fraction I, a white and non-tacky solid, was insoluble in boiling methanol, ethanol, and diethyl ether and cold acetone, but soluble in boiling acetone, tetrahydrofuran and benzene. This fraction was shown by X-ray diagram to be crystalline. The melting point of the fraction I obtained from the different conditions varied from 109 to 115°C, but a purified sample showed the melting point of 119°C by capillary method. The molten polymer could be formed into a strong fiber and a tough film which showed a high degree of orientation after drawing. The drawn fiber had an identity period of 7.05±0.1 Å.

This value is nearly equal to the period of 7.16 Å on polypropyleneoxide[9].

Fraction II was a white solid, melting at

TABLE II. ELEMENTAL ANALYSIS OF THREE FRACTIONS AND LIQUID POLYMERS OBTAINED BY $BF_3$-ETHERATE

| Fraction | C | H | Cl |
|---|---|---|---|
| I | 38.85 | 5.44 | 38.06 |
| II | 38.39 | 5.13 | 37.35 |
| III | 40.17 | 5.86 | 36.54 |
| liquid polymer | 38.85 | 5.62 | 38.76 |
| calcd. for $(-CH_2-\underset{\displaystyle CH_2Cl}{\underset{\vert}{CH}}-O-)$ | 38.94 | 5.45 | 38.32 |

9) G. Natta, *Angew. Chem.*, 68, 393 (1956).

about 75°C, or in some case, a tacky semi-solid from which a strong film or fiber could not be obtained. Usually, it was possible to obtain an additional crystalline polymer from this fraction by redissolving it in acetone and chilling the solution to −30°C. The amorphous polymer was recovered by evaporation of the filtrate to dryness.

Fraction III was a viscous liquid or a paste and was not found to be crystalline.

All these fractions mentioned above were confirmed to be polyepichlorohydrin by the elemental analysis (Table II).

The infrared spectra of fraction I differ from those of fractions II and III and also from an amorphous liquid polymer which was obtained by a polymerization using $BF_3$-etherate as a catalyst, and the differences might well be attributed to the presence of crystalline-sensitive bands. As may be seen in Fig. 1, the spectral difference between the amorphous and crystalline polymers is striking, several bands at 1472(w), 1336(sh.w), 1277(s), 1232(s), 1173(s), 1036(m), 972(s) and 900(s) $cm^{-1}$ were observed only in spectra of the crystalline fraction. A similar feature was found in the case of polypropylene-oxide: bands at 1480(s),1330(m),1240(s),1140(s), 1039(m) and 931(m) $cm^{-1}$ were observed only

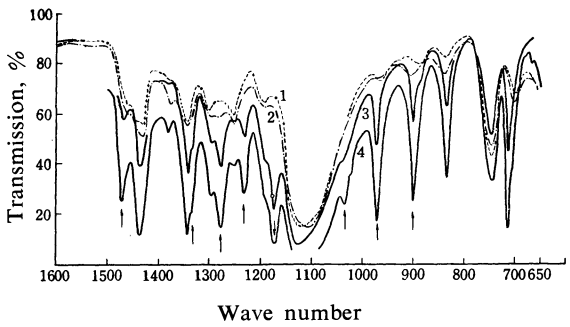



Fig. 1. Infrared spectra of the polymers of epichlorohydrin. Curve 1 ------: liquid polymer by $BF_3$-etherate, curve 2 -·-·-: fraction III, curve 3 ——: fraction I (KBr disk), curve 4 ——: fraction I (film). The curve of fraction II (pasty) was almost identical to that of fraction III.

TABLE III. POLYMERIZATION OF EPICHLOROHYDRIN BY SOME ORGANOMETALLIC COMPOUNDS

| No. | Catalyst | % | Time, hr. | Temp., °C | Solvent | Total conv., % wt. | Fraction % I | II | III |
|---|---|---|---|---|---|---|---|---|---|
| 50 | AIP-$ZnCl_2$ | 2 | 96 | 80 | — | 37.2 | 8.6 | 9.2 | 82.2 |
| 401 | $AlEt_3$ | 2 | 20 | r.t. | — | 41.3 | nil | 100 | nil |
| 410 | $AlEt_3$ | 2 | 6 days* | −78∼r.t. | *n*-hexane | 72.7 | 56.2 | 17.5 | 26.3 |
| 403 | $AlEt_3$-$ZnCl_2$ | 2 | 4 days* | 80 | benzene | ca.100 | 2.2 | 11.1 | 86.7 |
| 405 | $AlEt_3$-$FeCl_3$ | 2 | 4 days* | 80 | benzene | 50.9 | 10.5 | 17.0 | 72.5 |
| 13 | $ZnEt_2$ | 2 | 8 | r.t. | — | 81.8 | nil | 0.5 | 99.5 |
| 14 | $ZnEt_2$-Alumina | | 18 days | r.t. | — | none | — | — | — |
| 40 | $ZnEt_2$-$ZnCl_2$ | 2 | 8 days* | r.t. | benzene | 29.2 | nil | 4.6 | 95.6 |

* After solidification of reaction mixture (two days), these had been kept standing with catalytic systems.

TABLE IV. X-RAY PATTERNS OF CRYSTALLINE POLYMERS

| Propylene oxide | | Epifluorohydrin | | Epichlorohydrin | |
|---|---|---|---|---|---|
| Spacing (in Å) | Relative intensity | Spacing (in Å) | Relative intensity | Spacing (in Å) | Relative intensity |
| 5.17 | s | 5.44 | m | | |
| | | 4.35 | w | 4.56 | s |
| 4.23 | s | 4.33 | s | | |
| 4.05 | w | | | 3.83 | m |
| 3.63 | w | 3.67 | m | | |
| 3.46 | w | 3.21 | w | | |
| 3.10 | w | | | | |
| | | 2.85 | m | 3.09 | w |
| 2.78 | w | 2.69 | m | | |
| | | 2.49 | w | | |
| | | 2.35 | w | | |
| | | 2.20 | w | | |
| | | 1.87 | w | | |
| | | 1.81 | w | | |
| | | 1.75 | w | | |

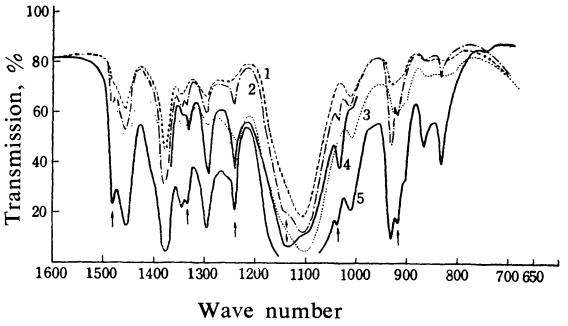



Fig. 2. Infrared spectra of the polymers of propylene oxide. Curve 1 ------: fraction III (viscous liquid), curve 2 -·-·: fraction II (pasty), curve 3 ·····: fraction III (pasty), curve 4 ——: fraction I (KBr disk), curves ——: fraction I (film).

in the crystalline fraction (Fig. 2).

Among organometallic compounds, some, such as aluminum triethyl, zinc diethyl and aluminum isopropoxide in conjunction with zinc chloride were found to be effective catalysts in converting epichlorohydrin to its polymer. The details were given in Table III. The polymerization proceeded rapidly at room temperature with the first two catalysts and went on fairly below room temperature, while with the last catalyst it was necessary to operate at higher temperatures. But in all cases, it was found that the amount of the crystalline fraction (fraction I) of the polymer obtained by these three catalysts was less than that of the $FeCl_3$-PO catalyst.

In the case of epifluorohydrin, ferric chloride complex catalyst was used. The polymer obtained was a solid powder which was soluble in acetone, and was insoluble in methanol, carbon tetrachloride and carbon disulfide. The polymer melted at about 68°C and was highly crystalline, a feature confirmed by X-ray examination. The molten polymer could be formed into a fiber and a film.

Table IV records the data from the X-ray

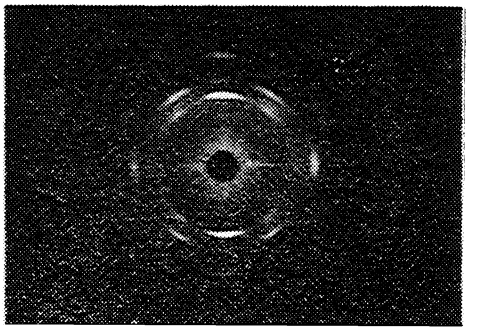


Fig. 3. X-ray pattern of a drawn fiber of polyepichlorohydrin. (fraction I).

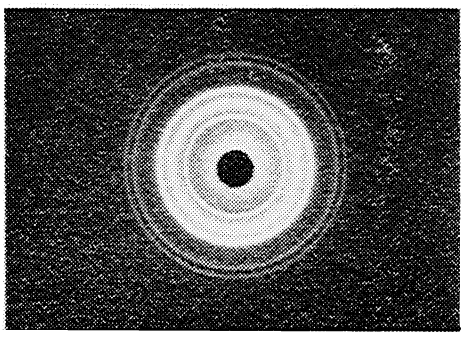


Fig. 4. X-ray pattern of polyepifluorohydrin.

patterns of the crystalline polymers of epichlorohydrin and epifluorohydrin together with that of crystalline polymer of propylene oxide for reference. X-ray diffraction patterns of the former two are shown in Figs. 3 and 4.

The author wishes to express his sincere thanks to Professor S. Murahashi for his guidance and encouragement throughout this work. Thanks are also due to Dr. S. Nozakura for his helpful discussions and to Mr. K. Katayama (Textile Research Laboratory, Asahi Chem. Ind, Co., Ltd.) for X-ray examinations.

*Department of Polymer Science*
*Faculty of Science*
*Osaka University*
*Nakanoshima, Osaka*

# *Polyethers. II. Copolymerizations of Propylene Oxide with Epihalohydrins**

By Shin'ichi ISHIDA†

(Received October 22, 1959)

Although copolymerization of vinyl monomers has been extensively studied, none of the detailed information on the copolymerization of olefine oxide or polymerizable epoxy compounds has been published. The work to be reported here was undertaken for the purpose of investigating the copolymerization of epoxides using a catalyst which commonly stereospecifically catalyzes to individual monomers.

It has been reported that propylene oxide[1-3] epichlorohydrin[4] and epifluorohydrin[4] can be polymerized by ferric chloride complex catalyst to give products which are of crystalline nature.

The present paper deals with the copolymerization of propylene oxide with epichlorohydrin using the ferric chloride complex catalyst ($FeCl_3$–PO)[1] which has been shown to be the common stereospecific catalyst. An attempted copolymerization of epifluorohydrin with propylene oxide is also contained.

## Experimental

**Monomers and Catalyst.**—Commercial epichlorohydrin and propylene oxide were dried over a molecular sieve, fractionally distilled before use. Epifluorohydrin was prepared from epichlorohydrin and anhydrous potassium fluoride by Cryszkiewicz-Trochmowski's method[5], b. p. 85~86°C. The catalyst was prepared as previously reported by Price's procedure[1,4].

**Copolymerization.** — All copolymerizations were carried out, as in our previous report on the stereospecific polymerization of epihalohydrins, in sealed glass tubes containing 10 g. of the varied monomer compositions and 5% by weight of catalyst. The tubes were thoroughly flushed with nitrogen before sealing and they were maintained at 85°C in an oil bath.

**Purification of Polymer.** — At the end of the reaction time, tubes were cooled and opened. The products were fractionated into three parts by the following procedure.

*Fraction I.*—To the reaction mixture was added acidified (HCl) acetone, and the insoluble material was filtered and washed with dilute HCl-acetone and methanol successively, and then reprecipitated from a hot acetone solution with methanol.

*Fraction II.*—The acetone solution separated from fraction I was added dropwise under stirring to a large volume of methanol. A tacky mass, or in some cases a paste, separated out from the solution.

*Fraction III.*—The acetone-methanol solution separated from fraction II and the methanol washing of fraction II were combined, concentrated to a small volume and poured into a large excess of water, then centrifuged to give fraction III which was a viscous liquid.

## Results and Discussion

The copolymerization of epichlorohydrin with propylene oxide was studied over a wide range of monomer compositions in the presence of $FeCl_3$–PO catalyst. Results were given in Table I. The products usually were able to be fractionally separated into three fractions; an acetone-insoluble (at room temperature) fraction (I), an acetone-soluble but methanol-insoluble fraction (II), and a methanol-soluble fraction (III).

TABLE I. COPOLYMERIZATION OF EPICHLOROHYDRIN (EpCl) WITH PROPYLENE OXIDE BY $FeCl_3$-PO CATALYST

| No. | EpCl in comonomer mole % | Total conversion wt. % | Fraction % | | |
|---|---|---|---|---|---|
| | | | I | II | III |
| 37 | 100 | 62.5 | 55.0 | 10.7 | 34.3 |
| 39 | 85.4 | 35.0 | 27.8 | 15.4 | 56.8 |
| 30 | 72.2 | 26.3 | 11.2 | 15.9 | 72.9 |
| 31 | 48.6 | 26.7 | 0.8 | 14.2 | 85.0 |
| 32 | 38.6 | 38.9 | 0.1 | 12.4 | 87.5 |
| 33 | 29.5 | — | trace | 5.5 | 94.5 |
| 34 | 21.2 | 47.0 | 0.4 | 1.0 | 98.6 |
| 35 | 13.6 | 50.7 | nil | nil | 100 |
| 36 | 6.5 | 59.0 | nil | nil | 100 |
| 38 | 0 | 70.2 | 45.0 | nil | 55.0 |

Polymerization was carried out at 85°C in bulk for 96 hr.

The acetone-insoluble fraction (I) was a solid, the yield of which was markedly affected by the composition of epichlorohydrin in comonomer mixture. Fractions II and III were a pasty mass or a viscous liquid and their purification and

* Presented at the 8th Annual Meeting of the Society of Polymer Science, Tokyo, May, 1959.

† Present address; Textile Research Laboratory, Asahi Chem. Ind. Co., Ltd., Takatsuki, Osaka.

1) C. Price et al., *J. Am. Chem. Soc.*, 78, 4787 (1956); *J. Polymer Sci.*, 34, 153 (1959).
2) R. Colclough et al., ibid., 34, 171 (1959).
3) J. Furukawa et al., ibid., 34, 541 (1959).
4) S. Ishida, This Bulletin, 33, 727 (1960)
5) MM. E. Cryszkiewicz-Trochimowski et al., *Rec. trav. chim.*, 66, 413 (1947).

exact fractionation and its evaluation appeared to be difficult. Accordingly in this paper only fraction I was investigated in some details, and the other fractions left untouched because of the difficulties of handling.

The relationships between mole per cent of epichlorohydrin in comonomer and the yield of total product as well as the percentage relationships of each fraction were shown in Fig. 1.

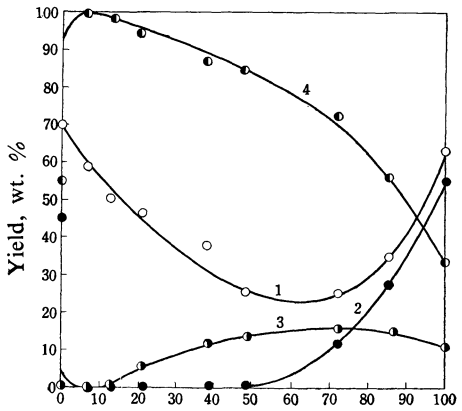



Fig. 1. The plots of yield of each fraction versus the mole % of epichlorohydrin in the comonomer.
Curve 1: total conversion, curve 2: fraction I, curve 3: fraction II, curve 4: fraction III.

Since an amorphous polypropyleneoxide is soluble in acetone and methanol, it can hardly be suspected to be contained in fraction I. Fraction I was therefore further purified by extraction with boiling ether so as to remove the crystalline homopolymer of propylene oxide. The products thus treated were white, crystalline solids. As they were believed to be true copolymers from the following evidences, they were referred as "copolymer" and were discriminated from Fraction I. Artificial mixtures of each homopolymer (crystalline polypropylene oxide : Crystalline polyepichlorohydrin =1:1 and 1:3 by weight) could be separated completely to the original components by an extraction with boiling ether.

The further evidence that the "copolymer" was not a mixture of homopolymer of epichlorohydrin and a copolymer but a genuine copolymer, was proved by the analysis of the fractions from the "copolymer"; a successive, careful fractionation of the "copolymer" from a tetrahydrofuran solution using methanol and water as precipitants gave fractions having almost the same chlorine contents. (Table II)

All "copolymers" exhibited the X-ray patterns contributed solely by the polyepichlorohydrin part, while an artificial co-precipitated mixture

TABLE II. FRACTIONATION AND ANALYSIS OF A "COPOLYMER"

| Fraction | wt. % | Cl % | EpCl mole % |
|---|---|---|---|
| "copolymer" | origin | 29.89 | 69.3 |
| F11 | 2.8 | 32.10 | 76.0 |
| F12 | 27.6 | 29.76 | 67.2 |
| F2 | 53.7 | 29.86 | 69.2 |
| F3 | 15.9 | 27.47 | 61.9 |

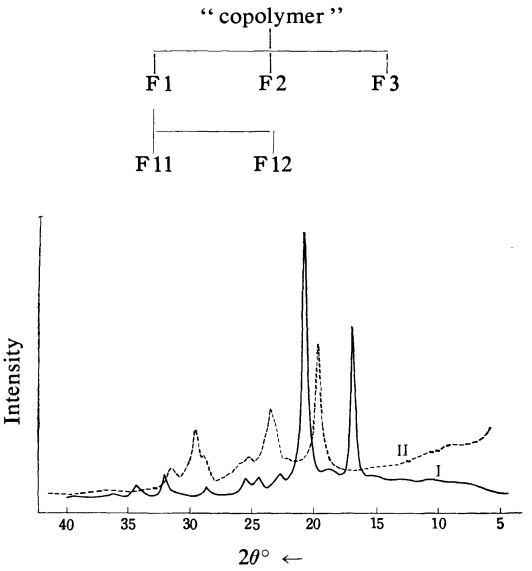



Fig. 2. X-ray diffraction spectra of the crystalline polymers.
I) Crystalline polypropylene oxide (full line).
II) Crystalline polyepichlorohydrin (dotted line).

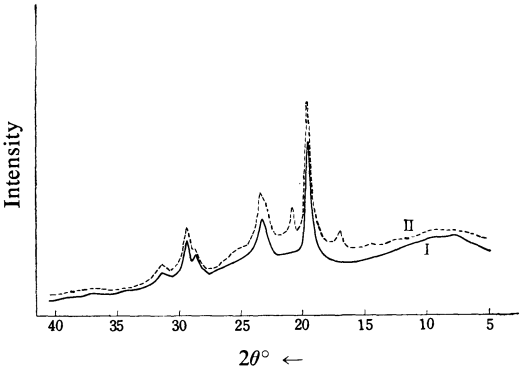



Fig. 3. X-ray diffraction spectra of the "copolymer" and "artificial mixture" of the homopolymers.
I) "Copolymer" (Found. EpCl mole % 67.2; full line).
II) "Artificial mixture" (poly-EpCl; 65 mole %, poly-PO; 35 mole %; dotted line).

of both the crystalline homopolymers which had the composition corresponding to that of the "copolymer", showed a superposed pattern of two crystalline homopolymers.

A comparison of a "copolymer" of 67.2 mole % of epichlorohydrin content with an artificial mixture of 65 mole % of crystalline polyepichlorohydrin and 35 mole % of crystalline polypropyleneoxide was shown Figs. 2 and 3, together with both crystalline homopolymers.

The experimental data were presented in Table III and the copolymer composition curve for this system together with the melting points of the "copolymers" by the capillary method were illustrated in Fig. 4.

TABLE III. COMPOSITIONS OF "COPOLYMERS" AND THEIR MELTING POINTS

| No. | Comonomer EpCl mole % | "Copolymer" Cl % | "Copolymer" EpCl mole % | "Copolymer" m. p. °C |
|---|---|---|---|---|
| 16 | 17.3 | 29.21 | 67.3 | 87 |
| 25 | 33.3 | 30.46 | 71.0 | 88 |
| 13 | 36.0 | 31.66 | 75.3 | 88 |
| 14 | 56.2 | 32.74 | 79.0 | 91 |
| 30 | 72.2 | 34.06 | 83.7 | — |
| 15 | 78.2 | 34.31 | 85.0 | 95 |
| 39 | 85.4 | 35.49 | 92.6 | 102 |
| 37 | 100 | 38.32 | 100 | 117 |

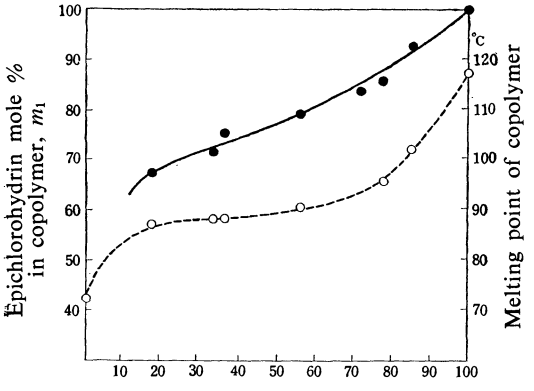



Fig. 4. Copolymer composition curve (● full line) for a system of epichlorohydrin and propylene oxide together with melting points of "copolymers" (○ dotted line).

From these data, the monomer reactivity ratios of epichlorohydrin and propylene oxide in copolymerization to crystalline "copolymer" were estimated by Mayo's method[6].

$$r_1(\text{epichlorohydrin}) = 1.8 \pm 0.3$$

$$r_2(\text{propylene oxide}) = 0.6 \pm 0.5$$

A soild non-tacky product which had been obtained by polymerization of equimolar mixture of propylene oxide and epifluorohydrin using $FeCl_3$–PO catalyst was purified by reprecipitation from an acetone solution with methanol-water. Then a fraction which was insoluble in methanol was separated from the acetone solution of the above product by adding a large excess of methanol. This fraction was a white non-tacky powder, and could not be further fractionated by reprecipitation using the same solvents and precipitants. It seemed to be possible that a crystalline polypropyleneoxide and a crystalline polyepifluorohydrin were contained in this fraction, as may be seen from the solubility data of both homopolymers in the preceding paper[4].

In fact, it was found by X-ray examination, that this fraction showed a superposed pattern of each specimen and so it might be a mixture of both the crystalline homopolymers. The attempted separation was unsuccessful because the author could not find a suitable solvent for the separation.

Attempts to copolymerize epichlorohydrin with 1, 1-dimethylethylene oxide by aluminum triethyl as catalyst did not give a copolymer but a mixture of each homopolymer.

The author wishes to express his sincere thanks to Professor S. Murahashi for his guidance and encouragement throughout this work. He is also indebted to Dr. S. Nozakura for his helpful discussions and suggestions and to Mr. K. Katayama (Textile Research Laboratory, Asahi Chem. Ind. Co., Ltd.) for X-ray examinations.

*Department of Polymer Science*
*Faculty of Science*
*Osaka University*
*Nakanoshima, Osaka*

6) F. R. Mayo and F. M. Lewis, *J. Am. Chem. Soc.*, **66**, 1594 (1944).

# *An Interpretation of the Elovich Equation for the Rate of Chemisorption on the Basis of Surface Heterogeneity*

By Yutaka KUBOKAWA

(Received September 9, 1959)

Taylor and Thon[1] showed that a number of chemisorption rate data are represented by the Elovich equation

$$dq/dt = ae^{-bq}$$

where $q$ is the amount of gas adsorbed and $a$ and $b$ are constants. In order to explain this equation, they postulated the annihilation of adsorption sites in the course of adsorption. Being stimulated by this work, various workers[2] discussed the applicability of this equation for chemisorption processes and presented various models leading to this equation. Although there is, of course, no reason to believe that only one and the same mechanism is operative in all systems to which the Elovich equation is applicable, the most probable interpretation of the equation seems to be the one based on surface heterogeneity at least for the adsorbents for which the existence and the effect of surface heterogeneity have been established.

Such an interpretation has been proposed by Porter and Tompkins[2] for a simple case where the distribution function of adsorption site is constant and the rate of desorption is negligibly small. The purpose of the present paper is to elaborate a similar interpretation for more complex cases where the distribution is variable and/or the rate of desorption can not be neglected and to discuss some available data with respect to the variation of constant $b$ in the Elovich equation with pressure and temperature.

**Adsorption Rate on a Heterogeneous Surface.** —For a heterogeneous surface the adsorption sites over the whole surface may be divided into a number of sets, each of which consists of sites of the same kind; the number of sites in each set is given by a distribution function which may, in the present case, be assumed to be a function of the activation energy $E$ for a given chemisorption. Taking account of desorption, the net rate of adsorption on any set of sites may be given by

$$v = d\theta/dt = kp(1-\theta) - k'\theta$$

where $\theta$ is the fraction of the sites covered and $p$ the pressure in the gas phase. Since $\theta = 0$ when $t = 0$, this rate gives on integration at a constant pressure

$$\theta = \theta_e[1 - e^{-(kp+k')t}]$$

where $\theta_e$ is the equilibrium coverage. Differentiating with respect to time

$$v = (kp + k')\theta_e e^{-(kp+k')t} = kpe^{-(kp/\theta_e)t} \quad (1)$$

The rate for the whole surface may be obtained by integration, by assuming a continuous distribution function of sites. First, let us consider the simplest case where desorption is negligible and the distribution function $N$ is constant. Since $\theta_e = 1$ in this case, Eq. 1 becomes

$$v = Ke^{-Kt} \quad (2)$$

where $K = kp$. The rate for the whole surface under such conditions will be

$$N\int_0^\infty v(E)\,dE = N\int_\infty^0 [v(E)\,dE/dK]\,dK \quad (3)$$

From the expression $k = \text{const.}\, e^{-E/RT}$, it follows that

$$dE/dK = -RT/K \quad (4)$$

Introduction of Eqs. 2 and 4 into Eq. 3 gives

$$N\int_0^\infty v(E)\,dE = -NRT\int_\infty^0 e^{-Kt}dK = NRT/t \quad (5)$$

On the sites with a high value of $E$ the rate will naturally be small, while on those with a low value of $E$ it will again be small because the coverage is here close to the equilibrium value. For a particular set of sites with an intermediate magnitude of $E$, therefore, the rate will pass through a maximum. This condition may be written as

$$\frac{dv}{dE} = \frac{dv}{dK}\frac{dK}{dE} = e^{-Kt}(1-Kt)\left(-\frac{K}{RT}\right) = 0$$

Consequently, $v$ shows a maximum at $Kt = 1$. The maximum rate, being equal to $NKe^{-1}$ or $N/te$, is proportional to the rate over the whole surface represented by Eq. 5.

When the distribution function is not constant and the rate of desorption can not be ignored, the over-all rate can not easily be integrated. However, it may be assumed as a first approximation that in this case the over-all rate is also

1) H. A. Taylor and N. Thon, *J. Am. Chem. Soc.*, 74, 4169 (1952).

2) A. S. Porter and F. C. Tompkins, *Proc. Roy. Soc.* A217, 529 (1953); H. J. Engell and K. Hauffe, *Z. Elektrochem.*, 57, 762 (1953); R. T. Landsberg, *J. Chem. Phys.*, 23, 1079 (1955); D. D. Eley, *Trans. Faraday Soc.*, 49, 643 (1953) etc.

proportional to the maximum rate.

As described above, the rate for any set of sites can be represented by

$$v = NK\mathrm{e}^{-Kt/\theta}$$

where $\theta$ is written for $\theta_e$ for brevity. The condition for the maximum rate is

$$\frac{dv}{dE} = \frac{dv}{dK}\frac{dK}{dE} = \left(-\frac{K}{\boldsymbol{RT}}\right)N\mathrm{e}^{-Kt/\theta}\left[1 + \frac{dN}{N}\frac{K}{dK} - Kt\frac{d(K/\theta)}{dK}\right] = 0$$

The dependence of $K$ on $\theta$ is determined by the relation between the activation energy of adsorption $E$ and the heat of adsorption $Q$, which is assumed to be given by

$$E - E_0 = (1/\alpha)(Q - Q_0)$$

where $\alpha$ is a constant and $Q_0$ is the heat of adsorption on the sites with the lowest activation energy $E_0$. Assuming the Langmuir isotherm to be applicable,

$$1/\theta = 1 + (A/P)\mathrm{e}^{-Q/RT}$$

so that

$$\frac{d(1/\theta)}{d(-Q/\boldsymbol{RT})} = \frac{A}{p}\mathrm{e}^{-Q/RT} = \frac{1}{\theta} - 1$$

It follows then

$$\frac{d\theta}{dK} = \frac{d\theta}{d(1/\theta)}\frac{d(1/\theta)}{d(-Q/\boldsymbol{RT})}\frac{d(-Q/\boldsymbol{RT})}{d(-E/\boldsymbol{RT})}\frac{d(-E/\boldsymbol{RT})}{dK} = \alpha\left(\frac{1}{\theta} - 1\right)\left(-\frac{\theta^2}{K}\right) \quad (6)$$

Hence

$$\frac{d(K/\theta)}{dK} = \frac{1}{\theta} - \frac{K}{\theta^2}\frac{d\theta}{dK} = \frac{1 + \alpha - \alpha\theta}{\theta}$$

By defining $\beta = (dN/N)(K/dK)$, we find that the rate $v$ shows a maximum at

$$Kt = [(1+\beta)\theta]/(1 + \alpha - \alpha\theta) = F\theta \quad (7)$$

where $F = (1+\beta)/(1+\alpha-\alpha\theta)$. So that the maximum rate $v_m$ is

$$v_m = NK\mathrm{e}^{-F} \quad (8)$$

Taking the logarithm of Eq. 8 and differentiating it with respect to $\ln K$

$$\frac{d\ln v_m}{d\ln K} = 1 + \beta - \frac{dF}{d\ln K}$$

Hence, we may write,

$$\frac{d\ln v_m}{dq} = \frac{d\ln v_m}{d\ln K}\frac{d\ln K}{dE}\frac{dE}{dq} = \left(1 + \beta - \frac{dF}{d\ln K}\right)\left(-\frac{1}{\boldsymbol{RT}}\right)\frac{dE}{dq} \quad (9)$$

where $q$ is the amount adsorbed at a given time. Taking the logarithm of Eq. 7, differentiating it with respect to time,

$$\frac{d\ln K}{dE}\frac{dE}{dt} + \frac{1}{t} = \frac{1}{F}\frac{dF}{d\ln K}\frac{d\ln K}{dE}\frac{dE}{dt} + \frac{1}{\theta}\frac{d\theta}{dK}\frac{dK}{dE}\frac{dE}{dt} \quad (10)$$

Inserting Eqs. 6 and 4 in Eq. 10, and rearranging

$$\frac{dE}{dt} = \left(\frac{\boldsymbol{RT}}{t}\right)\left(1 + \alpha - \alpha\theta - \frac{1}{F}\frac{dF}{d\ln K}\right)^{-1} \quad (11)$$

Using the definition of $F$, we can write Eq. 11 as

$$\frac{dE}{dt} = \left(\frac{\boldsymbol{RT}}{t}\right)F\left(1 + \beta - \frac{dF}{d\ln K}\right)^{-1} \quad (12)$$

Eqs. 7 and 8 give

$$v_m = (N/t)F\theta\mathrm{e}^{-F}$$

As was described above, a relationship $v_t = cv_m$ holds where $v_t$ is the over-all rate and $C$ a constant. Hence,

$$v_t = \frac{dq}{dt} = C(N/t)F\theta\mathrm{e}^{-F} \quad (13)$$

comparing Eq. 12 with Eq. 13, we obtain

$$\frac{dE}{dq} = \frac{\boldsymbol{RT}}{CN\theta}\left[\frac{\mathrm{e}^F}{1 + \beta - (dF/d\ln K)}\right]$$

Inserting this expression into Eq. (9)

$$\frac{d\ln v_m}{dq} = \frac{d\ln v_t}{dq} = -\frac{1}{CN\theta}\mathrm{e}^F \quad (14)$$

When desorption is negligible and $N$ is constant, Eq. 13 becomes

$$dq/dt = CN/t\mathrm{e}$$

Comparing this expression with Eq. 5, we obtain $C = \boldsymbol{RT}\mathrm{e}$. Hence, Eq. 14 becomes

$$\frac{d\ln v}{dq} = -\left(\frac{1}{N\theta\boldsymbol{RT}\mathrm{e}}\right)\mathrm{e}^F = -\left(\frac{1}{N\theta\boldsymbol{RT}\mathrm{e}}\right)\mathrm{e}^{\frac{1+\beta}{1+\alpha-\alpha\theta}} \quad (15)$$

where $v$ is written for $v_t$ for the sake of simplicity of representation. Eq. 15 gives the physical meaning of constant $b$ of the Elovich equation on the basis of surface heterogeneity.

**Variation of the Constant $b$ of the Elovich Equation with Temperature and Pressure.**—For the sake of simplicity, let us assume the values of $\alpha$ and $\beta$ to remain constant on changing pressure or temperature in the rate measurements, and discuss the dependence of $b$ on temperature and pressure for the following four different cases.

Case 1: Desorption is negligible and $N$ is constant. In this case Eq. 15 becomes

$$\frac{d\ln v}{dq} = -\frac{1}{N\boldsymbol{RT}} = \text{const}$$

Accordingly, strict applicability of the Elovich equation is expected. As described by various

workers[2], the value of $b$ should be independent of pressure and vary in proportion to $1/T$.

Case 2: Desorption is negligible but $N$ is not constant. In this case Eq. 15 becomes

$$\frac{\mathrm{d}\ln v}{\mathrm{d}q}=-\left(\frac{1}{NRT}\right)\mathrm{e}^{\beta}$$

The right hand side of this equation varies as adsorption proceeds. However, if the range of coverage is limited, and the change of $N$ during adsorption is not marked, we may expect that the Elovich equation will still, though approximately, be obeyed. Variation in the value of $b$ expected in this case may be as follows: If $N$ increases with $E$, the value of $N$ for the sites mainly responsible for adsorption may increase with pressure or temperature, since the set of sites with a higher value of $E$ may be covered at a higher pressure or temperature. This increase of $N$ will result in the decrease of $b$ with increasing pressure or temperature.

Case 3: Desorption can not be neglected but $N$ is constant. In this case, Eq. 15 becomes

$$\frac{\mathrm{d}\ln v}{\mathrm{d}q}=-\left(\frac{1}{N\theta RT\mathrm{e}}\right)\mathrm{e}^{\frac{1}{1+\alpha-\alpha\theta}}$$

As described in Case 2, the Elovich equation will approximately be obeyed in a limited range of coverage. Let us consider the pressure dependence of $b$ for the case $1<\alpha<2$, which seems to be the most probable case for $\alpha$ positive. Plotting $\theta\mathrm{e}^{\frac{-1}{1+\alpha-\alpha\theta}}$ against $\theta$ for the two different values of $\alpha$, $\alpha=1$ and $\alpha=2$, we obtain Fig. 1, which shows that, except in the range $\theta\simeq1$, $\theta\mathrm{e}^{\frac{-1}{1+\alpha-\alpha\theta}}$ increases with $\theta$. This result together with the fact that the sites with a higher value of $E$, i. e., with a larger value of $\theta$ come to operate at a higher pressure leads to the conclusion that the value of $b$ decreases with increasing pressure.

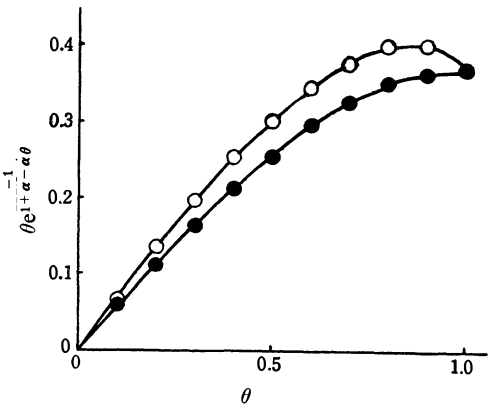



Fig. 1. Plot of $\theta\mathrm{e}^{\frac{-1}{1+\alpha-\alpha\theta}}$ against $\theta$.
—●—, $\alpha=1$; —○—, $\alpha=2$

Case 4: Desorption can not be neglected and, in addition, $N$ is not constant. Let us consider only the special case when both conditions, $\mathrm{d}N/\mathrm{d}E>0$ and $1<\alpha<2$, are satisfied. Remembering that $\beta<0$ in this case, the following conclusion in the pressure dependence of $b$ may be drawn. The extent of decrease of $b$ with increasing pressure may be greater than that in the case where either $N$ or $\theta$ alone varies, i. e., in Case 2 or 3 described above.

So far we have tacitly assumed an undissociative adsorption. For a dissociative adsorption, the adsorption rate corrected for desorption may be given by $k\sqrt{p}\,(1-\theta)-k'\theta$, or $kp(1-\theta)^2-k'\theta^2$. It is clear that the former equation leads to the same expression for the maximum rate as in the undissociative adsorption, except for the term $\sqrt{p}$. As regards the latter equation, it may also easily be shown that, in case desorption is negligible, this gives a similar expression for the maximum rate to that for the undissociative adsorption. It may therefore be expected that qualitative conclusions concerning the pressure dependence of $b$ described in Cases 3 and 4 will not be altered for the dissociative adsorption.

**A Criterion for the Negligible Desorption.**—It follows from Eq. 15 that

$$\frac{-\mathrm{d}(\ln v-\ln v_0)}{\mathrm{d}q}=\frac{\mathrm{e}^{\frac{1+\beta}{1+\alpha-\alpha\theta}}}{N\theta RT\mathrm{e}}=\frac{\mathrm{e}^{\gamma}}{N\theta RT}$$

where $\gamma=(1+\beta)/(1+\alpha-\alpha\theta)-1$ and $v_0$ represents the initial rate when $t=0$ or $q=0$, that is, the adsorption rate on the set of sites with the lowest value of $E$. Integration of this equation gives

$$q=RT\int N\theta\mathrm{e}^{-\gamma}\mathrm{d}(\ln v_0-\ln v)$$

Substituting the expression, $\ln v_0=\ln p+\ln v_0'$, where $v_0'$ represents the pressure independent terms in $v_0$, we obtain

$$q=RT\int N\theta\mathrm{e}^{-\gamma}\mathrm{d}\left[\ln v_0'-(\ln v-\ln p)\right]$$

This equation leads to the conclusion that if desorption can be neglected, i. e., the conditions $\theta=1$ and $\gamma=\beta$ are satisfied, the plots of $q$ against $\ln v-\ln p$ at different pressures should lie on the same curve, provided that the temperature is constant. On the contrary, if desorption is not negligible, such plots will give separate curves.

**Discussion of Some Available Data with Respect to Variation of $b$ with Pressure.**—*1) Hydrogen on Zinc Oxide.*—Values of constant $b$ for this system were obtained from the following integrated form of the Elovich equation

$$q=(2.3/b)\log(t+t_0)-(2.3/b)\log t_0,\quad t_0=1/ab$$

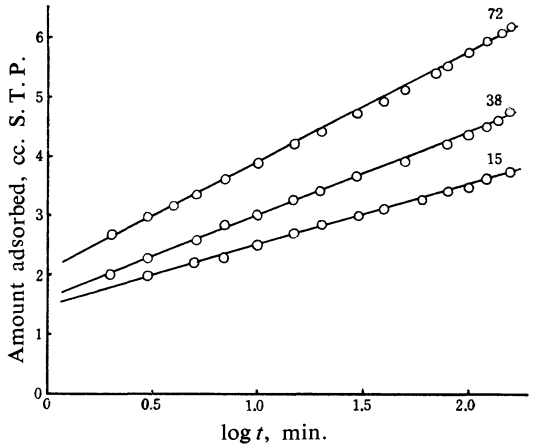



Fig. 2. Elovich plots for the hydrogen chemisorption on zinc oxide at 140°C. Figures indicate the initial pressure in mmHg.

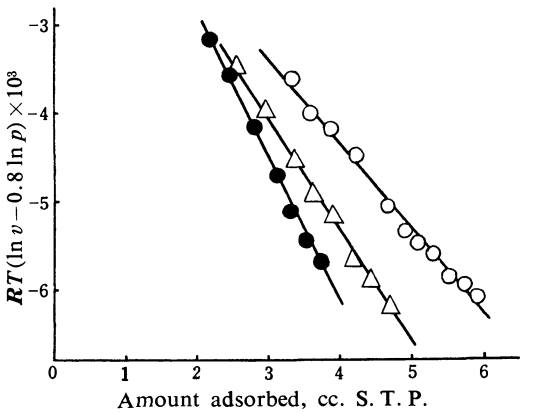



Fig. 3. Plots for the hydrogen chemisorption on zinc oxide at 140°C. —○—, 72 mmHg; —△—, 38 mmHg; —●—, 15 mmHg.

Plotting $\log(t+t_0)$ against $q$ with $t_0$ adjusted to give a linear plot, the value of $b$ was determined from the slope. The results shown in Fig. 2 indicate that the slope $2.3/b$ increases with initial pressure[3].

The same data are shown in Fig. 3 as the plots of $q$ against $\ln v - 0.8 \ln p$. The term $\ln p$ is here multiplied by a factor of 0.8, for the rate was found to be proportional to $p^{0.8}$ as reported previously[4]. As seen in this figure, the plots at different pressures give distinctly separate curves, indicating that appreciable desorption takes place during adsorption rate measurements, which is also expected from the results described in the previous paper[4].

3) The adsorption rate was measured by pressure change, using an adsorption apparatus of constant volume. The pressure decrease due to adsorption was no more than 10~20% of the initial pressure. The latter quantity was measured one minute later than the time of admission of hydrogen into the vessel.

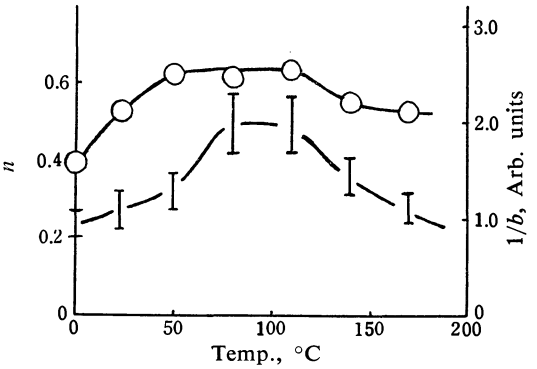



Fig. 4. Variation with temperature of the exponent $n$ and $1/b$ at the pressure 65 mmHg. —I—, $n$; —○—, $1/b$

The pressure dependence of $1/b$ for this chemisorption was found to be approximately represented by $1/b \propto p^n$. As shown in Fig. 4, the exponent $n$ varies with temperature and passes through a maximum, indicating that the pressure dependence of $1/b$ is considerably influenced by temperature. As given together in the figure, $1/b$ itself obtained at a particular pressure shows a similar dependence on temperature. It seems impossible to explain such behavior in terms of the concept that only the value of $\theta$ varies with pressure but the distribution function $N$ is constant[5]. It may therefore be concluded that hydrogen chemisorption on zinc oxide belongs to the case where both $N$ and $\theta$ change, i.e., to Case 4.

*2) Hydrogen on Chromic Oxide Gel.*—As an example for the case where the rate of desorption is negligibly small, we may mention the chemisorption of hydrogen on chromic oxide gel investigated by Burwell and Taylor[6]. Taking into account that the rate of adsorption for this system was found to be proportional to $p^{0.8}$ by these investigators, their data have been reexamined by plotting $q$ against $\ln v - 0.8 \ln p$ with the results shown in Fig. 5. As seen in the figure, all of the plots at different pressures lie on a single curve. In addition, $-\mathrm{d} \ln v/\mathrm{d}q$ increases with decreasing value of $E$[7]. We

4) Y. Kubokawa, This Bulletin, 33, 550 (1960).

5) If the value of $\theta$ alone were variable, such a marked increase in $n$ with increasing temperature from 20 to 80°C as seen in Fig. 4 would be accompanied by decrease in $1/b$ at a particular pressure, in contradiction to what was observed.

6) R. L. Burwell and H. S. Taylor, *J. Am. Chem. Soc.*, 58, 697 (1936).

7) Strictly speaking, this conclusion is valid provided that $\beta$ is unaltered with decreasing value of $N$. Even if $\beta$ is altered, however, it seems unlikely that the decrease in $e^{\beta}$ offsets the effect of the decrease in $N$, since in most cases $|\beta|$, i.e., $|\mathrm{d}\ln N/\mathrm{d}\ln K|$ may be less than 1, and the change of $\beta$ may be small compared with that of $N$. It will be shown in a later paper that the inference given here is reasonable for this adsorption.

may therefore regard this chemisorption as an example for Case 2 with $N$ increasing with $E$. In fact, the value of $b$ obtained by applying the integrated form of the Elovich equation decreases with increasing pressure as shown in Table I, in accordance with the above statement.

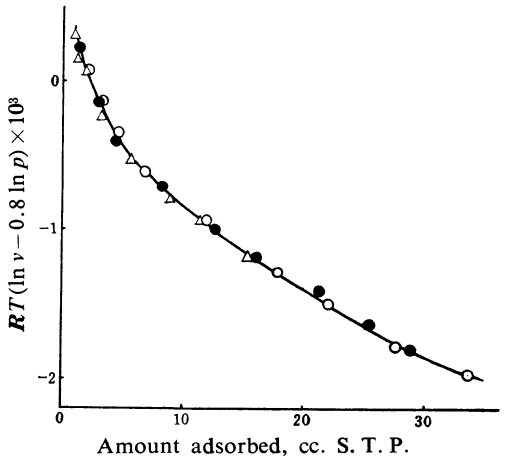



Fig. 5. Plots for the hydrogen chemisorption on chromic oxide gel at 457°K.
—○—, 1 atm.; —●—, 0.5 atm.; —△—, 0.25 atm.

TABLE I. VALUES OF $b$ OBTAINED FROM THE INTEGRATED FORM OF THE ELOVICH EQUATION FOR THE HYDROGEN CHEMISORPTION ON CHROMIC OXIDE GEL AT 457°K

| Pressure, atm. | $b$, 1/cc. |
|---|---|
| 1 | 0.061 |
| 0.5 | 0.065 |
| 0.25 | 0.091 |

**On the Constant $t_0$ in the Integrated Form of the Elovich Equation.**—As described in a previous section, if desorption is negligible and $N$ is constant, we may write

$$dq/dt = RTN/t$$

Hence,

$$d \ln t/dq = (d \ln t/dt)(dt/dq) = 1/RTN$$

It is clear from this equation that, in this case, the plot $q - \log t$ is linear. Consequently, the constant $t_0$ in the integrated form of the Elovich equation should be very small in this case. Furthermore, as described above, Case 1 is the only case to which the Elovich equation is expected to apply strictly. We may therefore conclude as follows: So far as the present interpretation of the Elovich equation is applicable, the constant $t_0$ of an appreciable magnitude such as is frequently employed to make the plot $q - \log(t+t_0)$ linear implies that in such cases, the equation holds only approximately, and the constant $b$ thus determined can not be given any physical meaning such as stated above, although the equation may be useful for evaluating initial rates.

## Summary

For the heterogeneous surface where the distribution function was variable and/or desorption could not be neglected, the rate of adsorption was derived and the physical meaning of constant $b$ in the Elovich equation was given. It was shown that in complicated case the Elovich equation is expected to apply only approximately in a limited range of coverage. The variation in constant $b$ with pressure or temperature was qualitatively explained in terms of the concept that on changing pressure or temperature, different sets of sites are covered and/or the contribution of desorption in adsorption rate measurements, is altered. The chemisorption of hydrogen on zinc oxide and on chromic oxide gel was discussed on the basis of the present interpretation of the Elovich equation. Finally, it was shown that, on the basis of surface heterogeneity, the constant $b$ obtained from the integrated form of the Elovich equation can not be given any physical meaning when the constant $t_0$ of an appreciable magnitude is required.

The author wishes to express his sincere thanks to Professor O. Toyama for his guidance and encouragement throughout the course of this study.

*Department of Applied Chemistry*
*College of Engineering*
*University of Osaka Prefecture*
*Sakai-shi, Osaka*

# *Effect of Hydrogen and Carbon Monoxide on the Electrical Conductivity of Zinc Oxide*

By Yutaka KUBOKAWA

(Received September 9, 1959)

The increase in electrical conductivity of zinc oxide caused by hydrogen was investigated in previous works[1,2] in order to get a clue to the nature of the chemisorption of hydrogen, with the results summarized as follows: On admission of hydrogen no significant change in the conductivity is observed below 100°C, while at higher temperatures a marked increase takes place; moreover, the rate and the amount of chemisorption decrease with increasing temperature up to 110°C but increase at higher temperatures. On the basis of these results, it was suggested that two types of hydrogen chemisorption exist on zinc oxide; one is predominating at higher temperatures and responsible for the increase in conductivity, and the other is observed at lower temperatures, with little effect on conductivity. Making use of the rate of increase in conductivity, the activation energy for the chemisorption of the high temperature type was estimated as 25 kcal./mol.

However, the existence of two such types of chemisorption can not yet be regarded as established, since later studies[3,4] on the rate of desorption and the adsorption isotherm in addition to those on the rate of adsorption, covering wide ranges of pressure and temperature, showed that the heterogeneity of zinc oxide surface should be taken into account. The aim in the present work has been to reinvestigate the relation between the hydrogen chemisorption and the conductivity change by more extensive experiments.

## Experimental

**Materials.**—Zinc oxide was prepared as described previously[3]. The experiments with hydrogen were carried out with zinc oxide sintered at 800°C for 5 hr., while non-sintered zinc oxide was used for the study with carbon monoxide. Hydrogen and carbon monoxide were obtained as given in previous papers[3,5].

**Apparatus and Procedure.**—Conductivity measurements were made with a powdered specimen held between two electrodes, by means of a Wheatstone bridge. Details of the apparatus and procedure were described in the previous paper[2]. In the measurements of the rate of conductivity decrease, an auxiliary heater of nickel wire was mounted in the reaction vessel for the purpose of changing the temperature rapidly, taking into account the slow attainment of thermal equilibrium at low pressures.

## Results and Discussion

**Relationship between the Rate of Conductivity Increase and that of the Formation of Donors.**—There seems to be little doubt that the observed increase in conductivity of zinc oxide brought in contact with hydrogen is related to the formation of donors of a certain type. In view of the well-known difficulties, especially in the case of a powdered sample such as used in the present work, it seems questionable to discuss the kinetics of the formation of donors, from the conductivity-time curves at a constant temperature, on the assumption of a relationship between conductivity and the number of donors. However, as shown in the previous paper[2], the activation energy of the formation of donors may be obtained in the following way. The rate of formation of donors at the time when the number of donors present is $c$ may be written as

$$(dn/dt)_c = (dn/d\kappa)_c (d\kappa/dt)_c$$

where $\kappa$ is the conductivity and $n$ the number of donors. The activation energy for the formation of donors, $E$ is therefore given by $E=E_2-E_1$, where $E_1$ and $E_2$ are the activation energies of conductivity itself and of conductivity increase, respectively, both referring to the number of donors $c$. Using this equation, we can obtain the value of $E$ provided that $E_1$ and $E_2$ are known.

**Temperature Coefficient of Conductivity.**—$E_1$ decreases with increasing number of donors as described by various workers. The value for the state with a negligible number of donors was estimated from the temperature coefficient of conductivity with the specimen evacuated at about 400°C. Fig. 1 shows a typical result, which gives a value of 1.2 kcal./mol. Values

1) Y. Kubokawa and O. Toyama, *Bull. Naniwa Univ.* (at present *Bull. Univ. Osaka Prefecture*) **A2**, 103 (1954).
2) Y. Kubokawa and O. Toyama, *J. Phys. Chem.*, **60**, 833 (1956).
3) Y. Kubokawa, This Bulletin, **33**, 546 (1960).
4) Y. Kubokawa, ibid., **33**, 550 (1960).
5) Y. Kubokawa, ibid., **33**, 555 (1960).

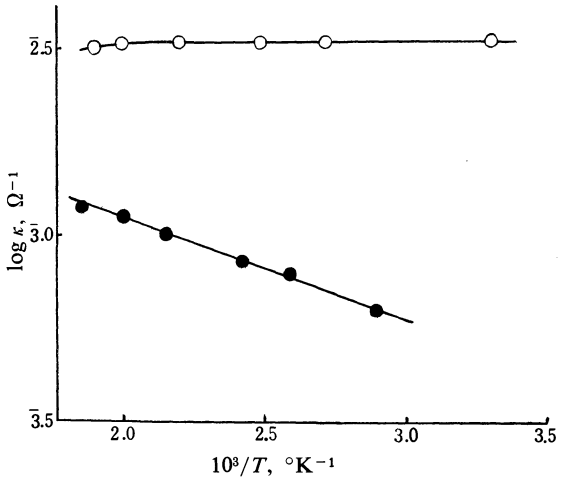



Fig. 1. Conductivity as a function of temperature.
—●—, in vacuo; —○—, in $H_2$.

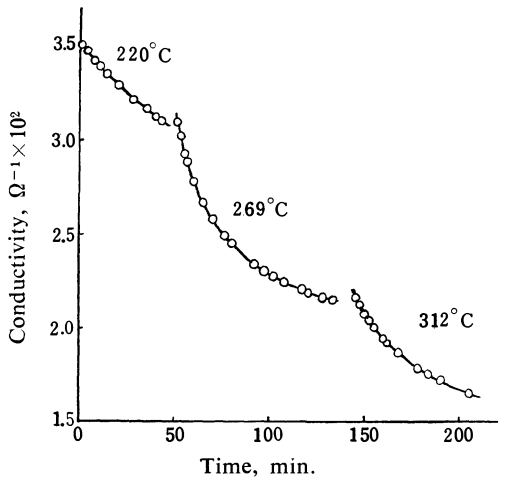



Fig. 2. Conductivity decrease by reducing pressure and the effect of a sudden temperature change.

TABLE I. VALUES OF $E_1$ AND THE ACTIVATION ENERGY OF CONDUCTIVITY DECREASE FOR THE DATA IN FIG. 2

| Temp. range (°C) | 220～269 | 269～312 |
|---|---|---|
| $E_1$ (kcal./mol.) | 0.4±0.1 | 0.7±0.2 |
| Activation energy of cond. decrease (kcal./mol.) | 31±2 | 31±2 |

of $E_1$ at an appreciable number of donors can not easily be obtained because the temperature coefficient in hydrogen such as shown in Fig. 1 does not give the true value of $E_1$, since in this case the change of conductivity with temperature may arise from two factors, i. e., from the temperature coefficient of conductivity itself and from the variation of the number of donors with temperature. However, approximate values of $E_1$ may be obtained as follows.

After hydrogen was introduced at about 400°C, the whole vessel was cooled down to a lower temperature, where the conductivity decrease by evacuation was followed for some time. Then the vessel was abruptly heated to a higher temperature, where the conductivity measurement was continued. The results are shown in Fig. 2. As described in a previous paper[4], by extrapolation of the $\kappa \sim t$ curves to the time of the abrupt change in temperature, the conductivities at different temperatures corresponding to equal numbers of donors were obtained. Values of $E_1$ thus determined are given in Table I. They are appreciably less than the value determined at the evacuated state.

**Dependence of the Rate of Conductivity Increase on Temperature.**—This was determined in two ways, i. e., by measuring the initial rates of conductivity increase at varied temperatures as described previously[2] and by observing the rate increase caused by an abrupt temperature elevation during the conductivity increase measurements. The latter method is similar in principle to that used in the adsorption rate measurements[4]. By extrapolation of the rates

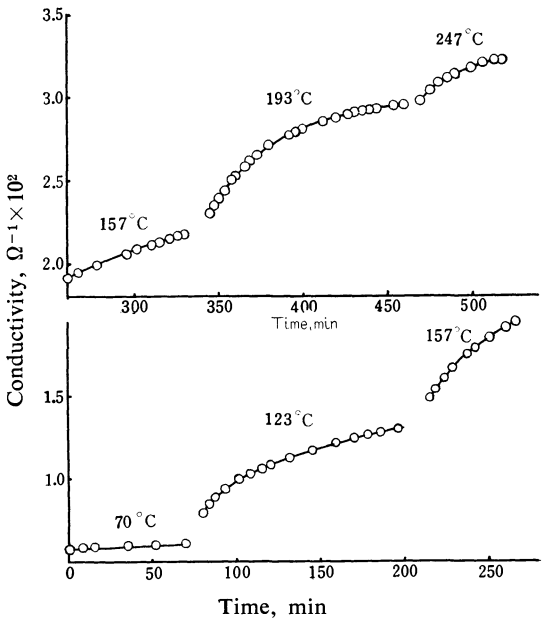



Fig. 3. Conductivity increase by hydrogen and the effect of a sudden temperature change. Pressure, 56 mmHg.

TABLE II. VALUES OF $E_2$ FOR THE DATA IN FIG. 3

| Temp. range (°C) | 70～123 | 123～157 | 157～193 |
|---|---|---|---|
| $E_2$ (kcal./mol.) | 18±1.5 | 21.7±1.5 | 20.5±1.5 |

to the time of the abrupt change, the rate at the two different temperatures corresponding to equal numbers of donors and consequently $E_2$ for that number of donors were obtained. In a typical example shown in Fig. 3, the temperature was raised in stages up to about 300°C after hydrogen was admitted at room temperature. The value of $E_2$ found here was about 21 kcal./mol., being roughly constant in the temperature range 120~200°C (Table II). $E_2$ is therefore of much greater magnitude compared with $E_1$ described above, indicating that the activation energy of the formation of donors is almost equal to that of conductivity increase.

The initial rate measurements, i. e., the other one of the two methods mentioned above, gave a value of 20 kcal./mol. for $E_2$, in agreement with that obtained by a rapid temperature elevation. The conductivity-time curves obtained were similar to those described in the previous paper[2].

**Dependence of the Rate of Conductivity Increase on Pressure.**—This was determined in two ways similar to those used for the temperature dependence. Fig. 4 shows the results obtained by a rapid pressure change during the measurements of conductivity increase. The pressure dependence was supposed to take the form $p^n$ and the values of the exponent $n$ were determined from this figure, as given in Table III. It is seen that the rate of conductivity increase is proportional to $p^{0.85}$ at increasing as well as decreasing pressure. The measurements of the initial rates of conductivity increase gave a similar pressure dependence.

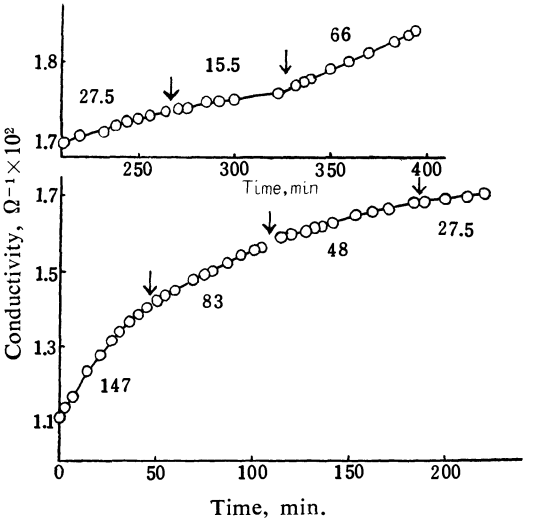



Fig. 4. Conductivity increase by hydrogen at 130°C and the effect of a sudden pressure change. Figures indicate the pressure in mmHg.

TABLE III. VALUES OF $n$ IN THE EXPRESSION, RATE $\propto p^n$ FOR THE DATA IN FIG. 4

| Pressure before and after the pressure change (mmHg) | $n$ |
|---|---|
| 147 ⟶ 83 | 0.82 |
| 83 ⟶ 48 | 0.85 |
| 48 ⟶ 27.5 | 0.85 |
| 27.5 ⟶ 15.5 | 0.88 |
| 15.5 ⟶ 66 | 0.93 |

An upper limit of the experimental error was ±10%.

**Dependence of the Rate of Conductivity Decrease by Reducing Pressure on Temperature.**—This may be estimated by the comparison of the rates at different temperatures corresponding to equal numbers of donors. For this purpose we may utilize the results described in Fig. 2, which were used for the determination of $E_1$. In the same manner as described above, the activation energy of conductivity decrease was estimated as 31 kcal./mol. (Table I).

**Variation of the Conductivity with Hydrogen Pressure.**—Above 300°C, the rate of conductivity increase on admitting hydrogen was found to be very great, suggesting that in this temperature range the conductivity increased to an equilibrium value may be obtained as a function of pressure in a manner similar to the adsorption equilibrium measurements. Thus hydrogen was introduced at 350°C, and the conductivity was measured at various pressures and a constant temperature by decreasing pressure successively. The results were reproducible when pressure was inversely increased as shown in Fig. 5.

**Conductivity Increase by Carbon Monoxide.**—Using carbon monoxide, in place of hydrogen, similar measurements were performed. Fig. 6 shows the $\kappa \sim t$ curves at varied temperatures and an approximately constant initial pressure, which gives a value of 25 kcal./mol. for the activation energy of conductivity increase. This

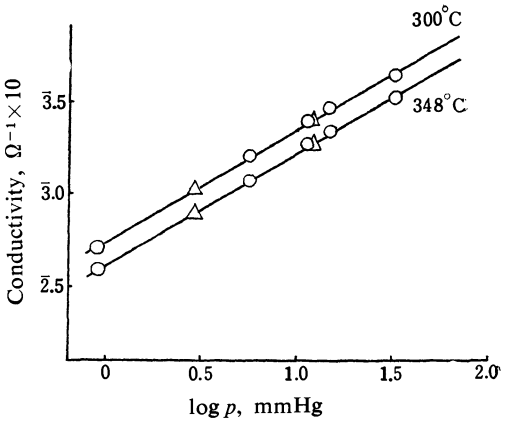



Fig. 5. Conductivity as a function of hydrogen pressure. —○—, on decreasing pressure; —△—, on increasing pressure.

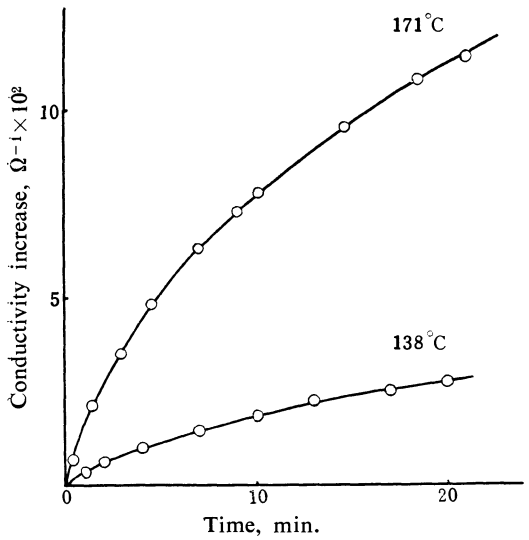



Fig. 6. Conductivity increase by carbon monoxide. Pressure, 1.4 mmHg. The activation energy was estimated as 25 kcal./mol.

may be regarded approximately as that of the formation of donors because of the negligible value of $E_1$. Almost the same value of activation energy was obtained in the method of a rapid temperature elevation. The conductivity increase was reversible as with hydrogen: by evacuation at 400°C the original conductivity was restored.

**Relation between the Hydrogen Chemisorption and the Conductivity Increase.**—As described in the previous paper[2], the conductivity enhanced by hydrogen was restored nearly to the original value by pumping out at 400°C. In addition, the conductivity increased to an equilibrium value varies reproducibly on increasing as well as decreasing pressure. These results, together with the fact that the amount of hydrogen adsorbed is almost completely desorbed as such, appear to indicate that this conductivity increase may not arise from the reduction of zinc oxide, but from the hydrogen adsorption of a certain type.

However, from the results obtained in this work, the assumption that the conductivity increase is due to a sort of chemisorption leads to the heat of chemisorption of 10 kcal./mol. and the activation energy of 21 kcal./mol. Relative magnitudes of these values are quite unusual for a chemisorption. Moreover, the activation energy of hydrogen chemisorption obtained from adsorption measurements[4] is 7～10 kcal./mol. in the comparable temperature range 100～140°C, and hence markedly less than the above value of 21 kcal./mol. These considerations suggest that the conductivity increase is not directly related to the hydrogen chemisorption of any type, and that the hydrogen uptake associated with the conductivity increase, if any, is only a negligible portion of the total uptake. It seems therefore necessary to modify the conclusion drawn from the earlier conductivity measurements[2] that two types of chemisorption exist, one of them being responsible for the conductivity increase while the other is not.

As described in the previous paper[2], the rate of adsorption and the adsorbed amount decrease with any increase in temperature up to 110°C, but increase at higher temperatures. Although such behavior, apparently, is adequately explainable in terms of the two types of chemisorption, this can not be the only explanation. Now that the heterogeneity of zinc oxide surface is undeniable through desorption measurements, the concept of single type chemisorption on a heterogeneous surface seems to present a more probable explanation. In addition, as previously described[3], the change in the activation energy of desorption is continuous, in contrast with that of carbon monoxide for which the presence of the two types of chemisorption was confirmed[5]. This again appears to favor the concept of single type chemisorption on a heterogeneous surface.

**Nature of the Conductivity Increase by Hydrogen.**—As regards the nature of the conductivity increase, an interpretation is that hydrogen atoms diffuse as protons into the lattice close to the surface, as suggested by various workers[6]. However, such an interpretation may not easily be reconciled with the following results obtained: The rate of conductivity increase is proportional to $p^{0.85}$; essentially the same behavior is observed with carbon monoxide on zinc oxide where there is no possibility of dissolution into crystals; in addition, this conductivity increase is an exothermic phenomenon, in contrast with hydrogen dissolution into a crystal of zinc oxide which is an endothermic phenomenon, as reported by Mollwo and others[7].

At present, the most plausible interpretation of the conductivity increase seems to be that proposed by Thomas et al.[8], who attributed it to the surface reduction of zinc oxide. This possibility was excluded previously on the basis of the fact that no water vapor was detected on desorption and that the conductivity increase was reversible. However, the amount of hydrogen uptake is a negligible portion of the total uptake as shown above. Hence such a

6) e. g., F. S. Stone, "Chemisorption", edited by W. E. Garner, Butterworths Scientific Publications, London (1957), p. 181.
7) E. Mollwo, *Z. Physik.*, **138**, 478 (1954); D. G. Thomas and J. J. Lander, *J. Chem. Phys.*, **25**, 1136 (1956).
8) D. G. Thomas and J. J. Lander, *J. Phys. Chem. Solids*, **2**, 318 (1957).

small amount of water vapor will not be detectable. Moreover, the recovery of the original conductivity by pumping out at high temperature and the reproduction of the conductivity on increasing and decreasing pressure may be explained on the assumption that zinc atoms produced by reduction evaporate rapidly at high temperature. This seems to be a plausible assumption, since the reduction is probably confined to the surface layer[9,10].

This interpretation may be applied in the temperature range above 100°C, but a slight conductivity change observed below this temperature described in the previous paper[2] probably arises from the chemisorption of hydrogen, although this behavior has not been studied in detail.

## Summary

The rate of increase in conductivity of zinc oxide caused by hydrogen was found to be proportional to $p^{0.85}$ and to have an activation energy of 21 kcal./mol. For this system the activation energy of the increase of donors was shown to be almost the same as that of the conductivity increase. The activation energy of the decrease of donors by evacuation was 31 kcal./mol. A similar conductivity increase was observed with carbon monoxide. On the basis of these results together with those of adsorption measurements reported previously, it was concluded that the conductivity increase was scarcely related at all to the hydrogen chemisorption, indicating that it is untenable to postulate two such types of hydrogen chemisorption as was believed in the previous work, i. e., one responsible for the conductivity increase and the other without such effect. As for the cause of the conductivity increase, the surface reduction of zinc oxide was suggested.

The author wishes to express his sincere thanks to Prefessor O. Toyama for his guidance and encouragement throughout the course of this study.

*Department of Applied Chemistry*
*College of Engineering*
*University of Osaka Prefecture*
*Sakai-shi, Osaka*

9) The conductivity increase observed on the oxidized state described in a previous paper[1] may also be attributed to the surface reduction of zinc oxide.

10) According to the previous work[2], the activation energy of the conductivity increase is 25 kcal./mol., being somewhat different from the value of 21 kcal./mol. found in the present work. Considering that this activation energy is a composite quantity including the activation energy of adsorption and that of the surface reduction, this difference may be explained by different proportions of the contributions of the two processes.

# *Effect of Oxygen Pretreatment on Hydrogen and Carbon Monoxide Chemisorption on Zinc Oxide*

By Yutaka KUBOKAWA

(Received September 9, 1959)

Since the treatment of an electron barrier layer was suggested for the chemisorption on semiconductors by Hauffe, Weisz, and others[1], the chemisorption and catalysis on oxide catalysts have been discussed on the basis of this model, and the relation between the catalytic activities of oxides and their properties as semiconductors have been emphasized by a number of workers[2,3]. As for the catalysis by zinc oxide, Parravano and others[4] found that the activity towards hydrogen-deuterium exchange reaction increases with its electrical conductivity. On the basis of these results, Hauffe[2] emphasized the fact that the properties of oxides as semiconductors play a large part in determining the activity towards this reaction.

However, for hydrogen or carbon monoxide chemisorption on zinc oxide which belongs to a "cumulative chemisorption", the barrier is so thin that it is doubtful whether this model

1) K. Hauffe and H. J. Engell, *Z. Elektrochem.*, **56**, 366 (1952); **57**, 763, 773 (1953); P. Aigrain and C. Dugas, ibid., **56**, 363 (1952); P. B. Weisz, *J. Chem. Phys.*, **21**, 1531 (1953).

2) K. Hauffe, *Angew. Chem.*, **67**, 189 (1955).

3) F. S. Stone, "Chemistry of the Solid State", edited by W. E. Garner, Butterworths Scientific Publications, London (1955), p. 367; T. Takaishi, *Z. Naturforsch.*, **11a**, 286, 297 (1956).

4) E. Molinari and G. Parravano, *J. Am. Chem. Soc.*, **75**, 5233 (1953); L. F. Heckelsberg, A. Clark and G. C. Bailey, *J. Phys. Chem.*, **60**, 559 (1956).

will be applicable to such systems. It appears more likely that covalent-bonding, similar to that in the chemisorption on metals determines the behavior of these systems, as pointed out by several workers[5].

It was aimed in the present work to obtain unambiguous information on the relation between the electronic state of zinc oxide and the chemisorption of hydrogen as well as carbon monoxide. For this purpose, the effect of high temperature oxygen treatment of zinc oxide was investigated, inasmuch as it is well established that such treatment markedly reduces the electrical conductivity of zinc oxide.

The present work was designed with another object in addition to that stated above. As regards hydrogen chemisorption on zinc oxide, Morrison[6] proposed a model, according to which the chemisorption means nothing but an interaction of hydrogen with adsorbed oxygen remaining after high temperature evacuation in the form of $O^-_{ads}$ or $O^{2-}_{ads}$. This mechanism may be written as

$$O^-_{ads} + 1/2\,H_2 \rightarrow OH^-_{ads}$$

$$O^{2-}_{ads} + 1/2\,H_2 \rightarrow OH^-_{ads} + \text{electron}$$

He is of the opinion that the two types of chemisorption for this system as described by Taylor et al.[7], may be explained in terms of these two processes. According to Garner[8], however, $OH_{ads}$ produced by the interaction of hydrogen with adsorbed oxygen is irreversible, in contradiction to Morrison's view. It may then be expected that the present study of the effect of oxygen treatment on hydrogen chemisorption would also serve to solve this problem.

## Experimental

**Materials.**—For zinc oxide, ZnO I described in a previous paper[9] was used. Hydrogen and carbon monoxide were prepared and purified as in the previous work[9,10]. Oxygen was obtained by the electrolysis of 30% potassium hydroxide solution, and purified in the same manner as hydrogen.

**Apparatus and Procedure.**—The apparatus used in the present work was the same as that used in the previous work[9] except that a Pirani gauge was attached to the flask in which the gas desorbed was collected. By measuring the voltage required to balance the bridge, the composition of the desorbed gas could be calculated from the calibration curves for hydrogen and oxygen.

## Results

**Effect of Oxygen Pretreatment on the Amount of Hydrogen Adsorbed.**—After oxygen adsorption was allowed to proceed for 3 hr. at 450°C and at a pressure of 30 mmHg, the temperature was lowered to 260°C. The system was evacuated for 30 min. at this temperature, and then the chemisorption rate measurements were carried out at room temperature (Run A). After this run, the system was evacuated for 1 hr. at 500°C and similar measurements were taken (Run B). Run B was further followed by evacuation for 15 hr. at 500°C and thereafter the chemisorption rate measurements were repeated (Run C). The results are shown in

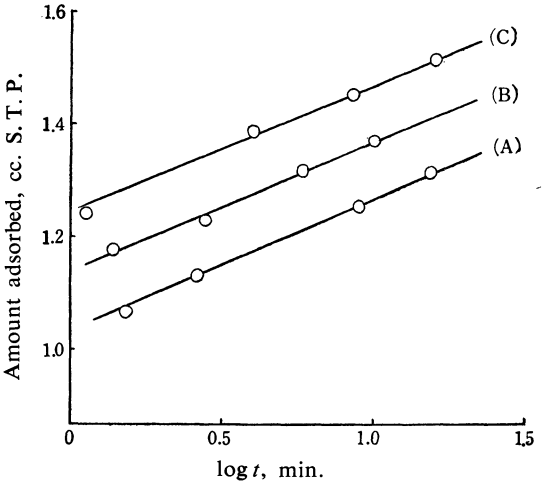



Fig. 1. Effect of oxygen pretreatment on the amount of hydrogen adsorbed at 14°C. Pressure, 20~25 mmHg.

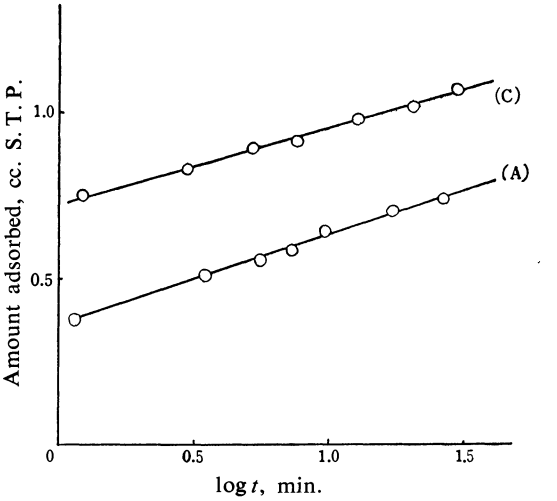



Fig. 2. Effect of oxygen pretreatment on the amount of hydrogen adsorbed at 189°C. Pressure, 20~25 mmHg.

5) D. A. Dowden, N. Mackenzie and B. M. W. Trapnell, *Proc. Roy. Soc.* A237, 245 (1956); F. S. Stone, loc. cit.
6) S. R. Morrion, "Advances in Catalysis", Vol, 7, Academic Press Inc., New York (1955), p. 259.
7) H. S. Taylor and C. O. Strother, *J. Am. Chem. Soc.*, 56, 586 (1934); H. S. Taylor and S. C. Liang, ibid., 69, 1306 (1947).
8) W. E. Garner, *J. Chem. Soc.*, 1947, 1239.
9) Y. Kubokawa, This Bulletin, 33, 546, 550 (1960).
10) Y. Kubokawa, This Bulletin, 33, 555 (1960).

Fig. 1. In these runs the order of the amounts of oxygen adsorbed is expected to be A>B>C. As seen in this figure, the amount adsorbed at a particular time also increases in this order. The amount adsorbed after 16 hr. was 1.95 cc. in run A and 2.21 cc. in run C, showing a slight difference. Fig. 2 represents the results obtained at a higher temperature. It follows from the figure that, in this case too, the decrease in the amount adsorbed after oxygen treatment will become unmarked in a later stage of adsorption.

**Effect of Oxygen Pretreatment on the Rate of Desorption of Hydrogen.**—After hydrogen was allowed to be chemisorbed at room temperature on the specimen pretreated with oxygen at 450°C followed by evacuation at 260°C, the activation energies of desorption at various coverages were determined in the manner described previously[9]. For comparison, similar measurements were carried out with the specimen before such pretreatment. Allowing for the different amounts initially adsorbed on these specimens, the activation energy of desorption was plotted in each case against the ratio of the amount desorbed to that initially adsorbed. As seen in Fig. 3, the results obtained with the two specimens were essentially indentical. Moreover, the comparison at various temperatures between the amount desorbed from the two specimens before the rates of desorption fell to a particular value shows, as seen in Table I, that there is no marked difference between the rates of desorption from these

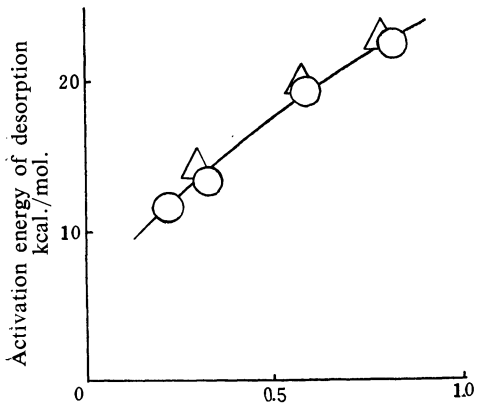



Fig. 3. Effect of oxygen pretreatment on the activation energy of desorption of hydrogen.
-○-, before oxygen pretreatment; -△-, after oxygen pretreatment. The amount of hydrogen adsorbed before desorption was 2.15 cc. before pretreatment and 1.82 cc. after pretreatment.

Table I. Ratio of the amount desorbed before the rate of desorption fell to $3.73\times10^{-3}$ cc. S. T. P./min. to the amount adsorbed before desorption

| Temp. of desorption (°C) | −30 | 20 | 71 |
|---|---|---|---|
| Before oxygen pretreatment | 0.323 | 0.572 | 0.759 |
| After oxygen pretreatment | 0.295 | 0.582 | 0.741 |

specimens. It may therefore be concluded that the rate of desorption as well as its activation energy is scarcely affected at all by oxygen treatment of the adsorbent at a temperature as high as 450°C.

**Interaction of Hydrogen with Adsorbed Oxygen.**—After hydrogen was allowed to be chemisorbed at room temperature, the temperature of the system was raised up to 400°C, and after several hours it was again lowered to room temperature. Then the amount of gas desorbed during the temperature elevation up to 400°C was measured and its composition was analyzed by means of the Pirani gauge. These measurements were carried out with a specimen which had been subjected to the same oxygen treatment as that used in the experiment shown in Fig. 1. The results are shown in Table II. In the Runs A and B the gas desorbed below 400°C consisted solely of hydrogen, while above 400°C a considerable amount of water was detected in the gas desorbed and its uncondensable fraction was found to be almost entirely oxygen. This indicates the occurrence of an irreversible chemisorption of hydrogen, the extent of which may be estimated from the amounts not removed by pumping out at 400°C. As seen in Table II, the amount of irreversible

Table II

| | Amount absorbed at room temp. before desorption (1) | Amount desorbed below 400°C (2) | Residual amount adsorbed (1)—(2) |
|---|---|---|---|
| Run A | 3.94 | 3.48 | 0.46 |
| Run B | 3.85 | 3.54 | 0.31 |
| Run C | 4.10 | 3.96 | 0.14 |

Amount adsorbed is in cc. S. T. P. The order of the amounts of oxygen adsorbed is A>B>C.

chemisorption increases with that of the oxygen adsorbed. On the other hand, in Run C where little or no oxygen remained adsorbed, no water vapor was detected even above 400°C, suggesting that hydrogen chemisorption was completely reversible in this case.

**Effect of Oxygen Pretreatment on Carbon Monoxide Chemisorption.**—As described in the

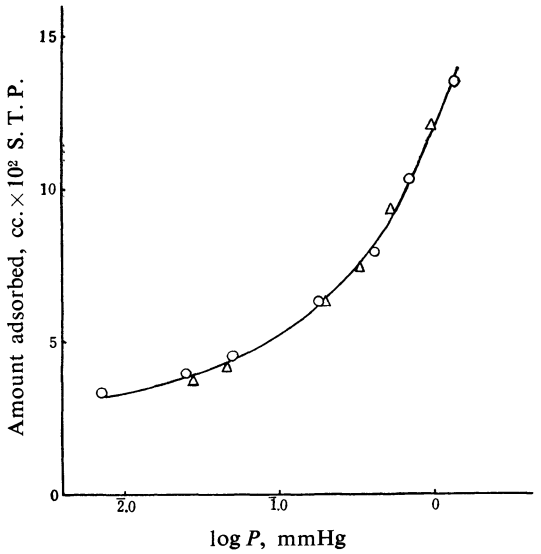



Fig. 4. Effect of oxygen pretreatment on carbon monoxide chemisorption at 15°C. -○-, before oxygen pretreatment; -△-, after oxygen pretreatment.

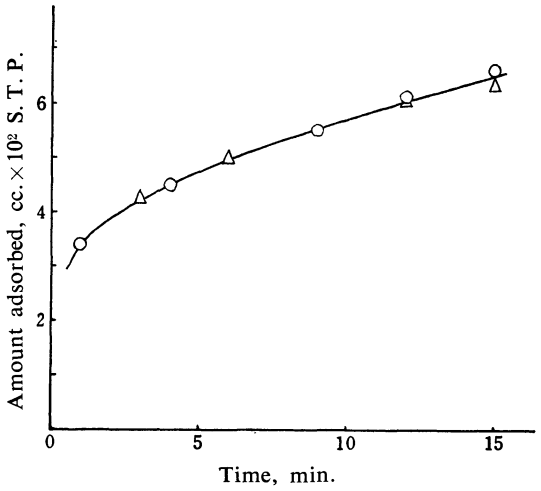



Fig. 5. Effect of oxygen pretreatment on carbon monoxide chemisorption at 90°C. -○-, before oxygen pretreatment; -△-, after oxygen pretreatment. Pressure, 0.1 ~0.2 mmHg.

previous paper[10], there are two types of chemisorption for carbon monoxide, one of them being a non-activated adsorption at low temperature, and the other an activated absorption at high temperature. The effect of oxygen treatment was therefore investigated in the following two ways. Fig. 4 shows the effect on the adsorption isotherm at room temperature obtained on a desorption branch, such as was described previously. It follows from this figure that the oxygen treatment has no effect on the chemisorption of low temperature type, in agreement with the results obtained by Garner et al.[11] For the chemisorption of high temperature type, similar results were obtained, as shown in Fig. 5. Oxygen treatment in this case was conducted at 450°C, followed by evacuation at 260°C.

## Discussion

If the electronic state of zinc oxide had played a large part in determining the behavior of hydrogen chemisorption, the amount adsorbed as well as the rate of desorption of hydrogen would have been seriously affected by oxygen treatment at high temperature, in contradiction to what was found actually in this work. It may therefore be concluded that the change of the electronic state of zinc oxide has little or no effect on hydrogen chemisorption.

This conclusion in turn suggests that a slight decrease in the amount adsorbed caused by the oxygen treatment is not due to the change of the concentrations of electrons. In view of the existence of surface heterogeneity in this system as revealed in a previous work[9], this decrease may probably be ascribed to the variation of the distribution function of sites, although details of the variation are unknown at present.

According to Parravano et al.[4], the activity of zinc oxide towards hydrogen-deuterium exchange reaction decreases markedly after oxygen treatment. On the basis of the considerations given above, it seems unlikely that this decrease in the catalytic activity is attributed to the change of the concentrations of free electrons. In addition, the extent of decrease in the activity after oxygen treatment as reported by these authors appears to be markedly greater than that in the amount of hydrogen adsorbed in the present work, although there may be more or less uncertainty in such comparisons, as no measurements with the same specimen of zinc oxide were carried out. Such a marked difference, if it is real, suggests that only a negligible portion of the total amount of hydrogen adsorbed is responsible for the exchange reaction, in agreement with what may be expected from the surface heterogeneity established for this system.

Various workers[12] have emphasized the fact that hydrogen chemisorption on zinc oxide is confined to interstitial zinc atoms or F-centers which probably exist after evacuation at high temperature. The observation in this work

11) W. E. Garner and J. Maggs, *Trans. Faraday Soc.*, **32**, 1744 (1936).
12) J. H. de Boer, "Advances in Catalysis", Vol. 8 (1956), p. 18; W. E. Garner, "Advances in Catalyss", Vol. 9 (1957), p. 169.

that the amount adsorbed is not seriously affected by the oxygen treatment indicates that such interpretation is unjustifiable.

The decrease in the amount of hydrogen adsorbed after oxygen treatment and the increase of the extent of irreversible adsorption with the increasing amount of oxygen adsorbed suggest that Morrison's mechanism is unjustifiable and that $OH_{ads}$, produced by the interaction of hydrogen with adsorbed oxygen, is irreversible and desorbed as water above 400°C, in accordance with Garner's view.

As for carbon monoxide chemisorption, the results obtained in the present work indicate again and still more clearly that this chemisorption is not affected by the electronic state of zinc oxide. Moreover, these results together with the fact that the amount adsorbed at $\theta=1$, estimated from the isotherms, amount to about a half of the amount of nitrogen adsorbed in a monolayer determined by the B. E. T. method as previously described[10] suggest that carbon monoxide chemisorption is not confined to special active sites, e. g., interstitial zinc atoms or F-centers, but the entire surface of zinc oxide participates in the chemisorption.

Finally, with respect to the change of the catalytic activity of zinc oxide caused by the addition of small amounts of $Li_2O$ or $Al_2O_3$ as shown by a number of workers, the results presented here, seem to indicate that it is doubtful in some cases that this effect can be attributed to the change of the electronic state of zinc oxide caused by the addition.

## Summary

The effect of oxygen treatment at about 500°C of zinc oxide upon the chemisorption of hydrogen as well as of carbon monoxide was investigated in order to clarify the relation between the electronic state of the adsorbent and the chemisorption. In the case of hydrogen chemisorption, the amount adsorbed was reduced only slightly and the rate of desorption remained practically unaltered after oxygen treatment. On carbon monoxide chemisorption the oxygen treatment gave no effect. It was concluded from these results that both the chemisorption of hydrogen and that of carbon monoxide are essentially independent of the electronic state of zinc oxide. On the basis of such a conclusion combined with other results, the inapplicability of the model of hydrogen chemisorption proposed by Morrison was pointed out.

The author wishes to express his sincere thanks to Professor O. Toyama for his guidance and encouragement throughout the course of this study.

*Department of Applied Chemistry*
*College of Engineering*
*University of Osaka Prefecture*
*Sakai-shi, Osaka*

# *Hydrogen Chemisorption on $ZnO \cdot Cr_2O_3$, $ZnO \cdot MoO_3$ and $Cr_2O_3$*

By Yutaka KUBOKAWA

(Received September 9, 1959)

In previous papers[1] hydrogen chemisorption on zinc oxide was studied by measuring the rate of adsorption, adsorption equilibrium and the rate of desorption, which made it possible to obtain quantitative information on the energy relation for this system. The behavior of desorption under various experimental conditions suggested the existence of a heterogeneity of the surface, the nature of which was such that the activation energy of adsorption and the heat of adrorption varied in the same direction, in contrast with carbon monoxide chemisorption on zinc oxide where these quantities varied in the reverse direction to each other.

It seemed then desirable to ascertain whether the conclusion obtained with zinc oxide is generally applicable to hydrogen chemisorption on oxides or not. As a first step in such an investigation, the hydrogen chemisorption was measured with $ZnO \cdot Cr_2O_3$, $ZnO \cdot MoO_3$ and $Cr_2O_3$, in the same manner as with zinc oxide and the results obtained are reported in this paper.

## Experimental

**Materials.** — $ZnO \cdot Cr_2O_3$ and $ZnO \cdot MoO_3$ were prepared in the same way as described in the previous work[2]. $Cr_2O_3$ was prepared by controlled

1) Y. Kubokawa, This Bulletin, 33, 546, 550 (1960).

2) Y. Kubokawa and O. Toyama, *J. Phys. Chem.*, **60**, 833 (1956).

ignition of $CrO_3$ of extra pure grade in a stream of dry air at 450°C as described by Bevan et al.[3] The gases were obtained as described in the previous papers[1]. The weight of the adsorbent and surface area determined by the B. E. T. method using nitrogen adsorption were as follows: $ZnO \cdot Cr_2O_3$, 6.71 g., 28 $m^2$/g.; $ZnO \cdot MoO_3$, 8.83 g., 13 $m^2$/g.; $Cr_2O_3$, 14.13 g., 17 $m^2$/g.

**Apparatus and Procedure.**—Details of the apparatus and procedure were described in the previous papers[1]. Before a series of experiments, all the adsorbents were subjected to repeated pretreatments with hydrogen at 450°C followed by evacuation at this temperature.

## Results and Discussion

**Dependence of Chemisorption Rate on Temperature.**—The problem was investigated in two ways, one comparing, as usual, the rate at varied temperatures after admission of a known amount of hydrogen to a degassed sample and the other observing the rate increase caused by an abrupt temperature elevation during an adsorption rate measurement as previously applied to hydrogen chemisorption on zinc oxide. Measurements making use of the former method were already carried out in the previous work[2] with the following results: With $ZnO \cdot Cr_2O_3$ an instantaneous chemisorption followed by a slow process occurred and apparent activation energies of adsorption in the low and high temperature ranges were 7 and 13~16 kcal./mol., respectively, while with $ZnO \cdot MoO_3$, only a slow chemisorption with an activation energy of 28 kcal./mol. was observed.

Figs. 1 and 2 represent the results obtained by the latter method: After hydrogen was allowed to be adsorbed at room temperature, the temperature was raised up in stages. As seen in Fig. 1, in the case of $ZnO \cdot MoO_3$ the amount of rapid desorption due to the abrupt temperature raise is negligibly small, and the rate of slow uptake increases steadily with temperature as in the carbon monoxide chemisorption on zinc oxide described previously[4]. Similar behavior was observed on $Cr_2O_3$. On the other hand, the result obtained with $ZnO \cdot Cr_2O_3$ is similar to that for hydrogen chemisorption on zinc oxide, as seen in Fig. 2. Here on increasing the temperature a rapid desorption was followed by the occurrence of a slow

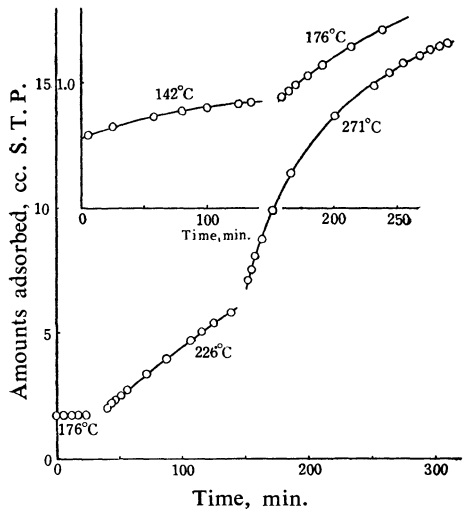



Fig. 1. Effect of temperature change during adsorption on the rate of hydrogen chemisorption on $ZnO \cdot MoO_3$. Pressure, 60~80 mmHg. Run at 176°C was interrupted by cooling the adsorbent to room temperature.

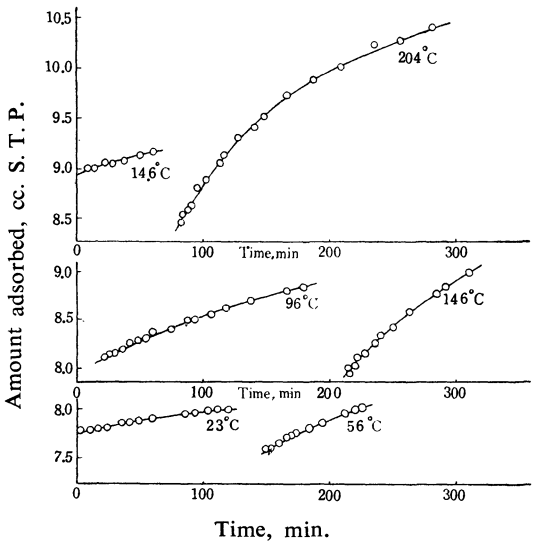



Fig. 2. Effect of temperature change during adsorption on the rate of hydrogen chemisorption on $ZnO \cdot Cr_2O_3$. Pressure, 60~80 mmHg. Both after the run at 56°C and during that at 146°C, the rate measurement was interrupted by cooling the adsorbent to room temperature.

TABLE I. ACTIVATION ENERGIES OF ADSORPTION

| Adsorbent | Temp. range °C | Activation energy of adsorption kcal./mol. |
|---|---|---|
| $ZnO \cdot MoO_3$ (Fig. 1) | 142~176 | 14.5±1.0 |
| | 176~226 | 23 ±1.5 |
| | 226~271 | 25 ±1.5 |
| $Cr_2O_3$ | 160~205 | 13 ±1.5 |
| $ZnO \cdot Cr_2O_3$ (Fig. 2) | 23~ 56 | 8.0±1.0 |
| | 96~146 | 9.5±1.0 |
| | 146~204 | 12 ±1.0 |

3) J. M. Bevan, J. P. Shelton and J. S. Anderson, *J. Chem. Soc.*, **1948**, 1729.

4) Y. Kubokawa, This Bulletin, 33, 555 (1960).

uptake. Apparent activation energies were determined by a method similar to that described in the previous papers[1], i. e., by comparison of the rates at different temperatures, corresponding to equal amounts of the slow chemisorption. The results obtained are shown in Table I.

Although a rapid desorption on an abrupt temperature raise is observed with $ZnO \cdot Cr_2O_3$, which shows, on the whole, a normal pattern of an activated adsorption according to the previous work[2], i. e., except in the temperature range 80~110°C, the rate of adsorption increases steadily with temperature. In addition, both methods of obtaining the dependence of rate on temperature give similar values of activation energy, contrary to the results for zinc oxide. This may be attributed to a much smaller proportion of the amount desorbed rapidly on raising the temperature to the amount adsorbed before the temperature rise.

**Dependence of Chemisorption Rate on Pressure.**—As described in previous papers[1,4], the pressure dependence was determined by observing the rate change caused by an abrupt pressure change during adsorption. As an example, the results obtained with $ZnO \cdot MoO_3$ are shown in Fig. 3. The comparison of the rates at different pressures corresponding to equal amounts of slow uptake gives the pressure dependence, with the results listed in Table II.

With $ZnO \cdot MoO_3$, the rate was found to be proportional to $P^{0.8}$ on both increasing and decreasing pressure, indicating that desorption is negligible during adsorption. The results obtained with $Cr_2O_3$ were similar. In the case of $ZnO \cdot Cr_2O_3$, it is clear that desorption can not be neglected, since on decreasing pressure the exponent $n$ in the expression Rate $\propto P^n$ is, markedly larger than the value when desorption is negligible, namely 0.8, and on increasing pressure too, a value somewhat greater than 0.8 was obtained, as seen in Table II.

**Activation Energies of Desorption at Various Coverages.**—The temperature of the adsorbent which had already adsorbed hydrogen at about

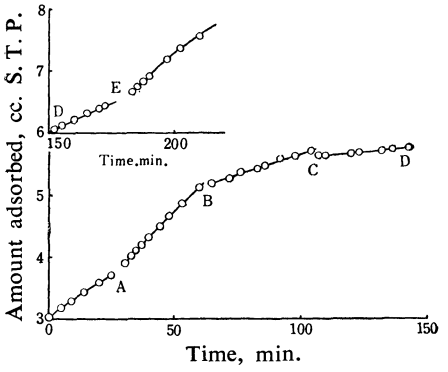



Fig. 3. Effect of pressure change during adsorption on the rate of hydrogen chemisorption on $ZnO \cdot MoO_3$. Temp., 228°C. Pressures before and after the pressure change are shown in Table II.

TABLE II. VALUES OF $n$ IN THE EXPRESSION, RATE $\propto P^n$

| Adsorbent | Pressure before and after the pressure change, mmHg | $n$ |
|---|---|---|
| $ZnO \cdot MoO_3$* | (A) 27.0→73.2 | 0.77 |
| (Fig. 3) | (B) 64.8→19.0 | 0.80 |
| | (C) 15.4→ 4.6 | 0.81 |
| | (D) 3.7→27.7 | 0.83 |
| | (E) 24.2→67.5 | 0.79 |
| $ZnO \cdot Cr_2O_3$ | 20.5→86.5 | 0.95±0.1 |
| | 77.1→49.2 | 2.5 ±0.5 |

* An upper limit of the error was ±7%.

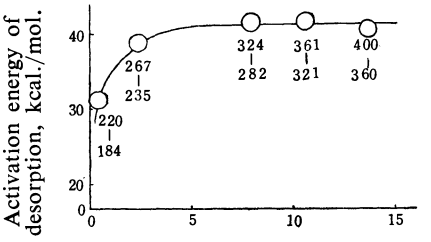



Fig. 4. Activation energies of desorption of hydrogen chemisorbed on $ZnO \cdot MoO_3$. The amount adsorbed and equilibrium pressure at room temperature before desorption were 15.42 cc. and 22.0 mmHg, respectively. Figures indicate the temperature interval where the activation energy was determined.

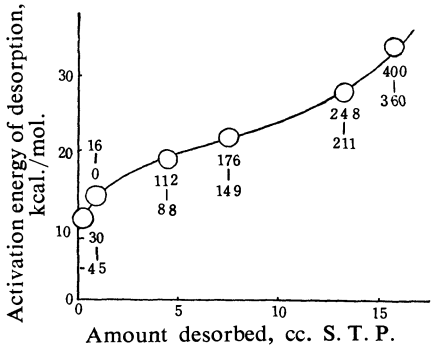



Fig. 5. Activation energies of desorption of hydrogen chemisorbed on $ZnO \cdot Cr_2O_3$. The amount adsorbed and equilibrium pressure at room temperature before desorption were 16.82 cc. and 42.3 mmHg respectively. Figures indicate the temperature interval where the activation energy was determined.

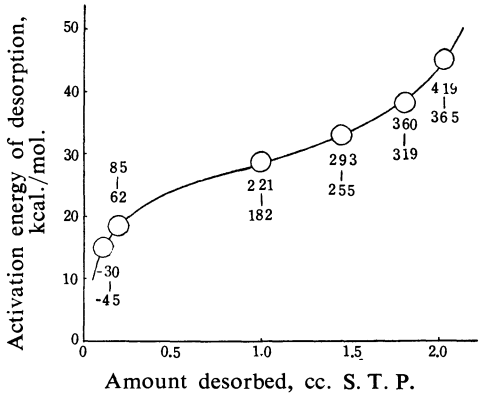



Fig. 6. Activation energies of desorption of hydrogen chemisorbed on $Cr_2O_3$. The amount adsorbed and equilibrium pressure at room temperature before desorption were 2.18 cc. and 36.4 mmHg respectively. Figures indicate the temperature interval where the activation energy was determined.

400°C was raised up from −72 to about 400°C in stages at each of which the activation energy of desorption was determined in the same manner as described previously[1]. The results obtained are shown in Figs. 4, 5 and 6. For all the systems studied in the present work, it was confirmed that adsorption could be neglected during desorption rate measurement as in the case of hydrogen chemisorption on zinc oxide. In the case of $ZnO \cdot MoO_3$, the amount desorbed with an activation energy less than 30 kcal./mol. is a negligible fraction of the total amount desorbed. In addition, the greater part of the chemisorbed hydrogen desorbs with an approximately constant activation energy of 41 kcal./mol. On the other hand, for the other systems, the activation energy of desorption varies considerably with the amount desorbed, i. e., for $ZnO \cdot Cr_2O_3$ from 10 to 35 kcal./mol. and for $Cr_2O_3$ from 15 to 45 kcal./mol. Moreover, in the former case a considerable fraction of chemisorbed hydrogen desorbs with a low activation energy of desorption (<20 kcal./mol.), while in the latter, this fraction is negligibly small.

**Adsorption Isotherms.** — After hydrogen was allowed to be adsorbed at a high temperature, the adsorption isotherm was determined by successive withdrawals of the gas. The isotherm thus determined on the desorption branch was, as in the case of hydrogen chemisorption on zinc oxide, reproducible at increasing as well as decreasing pressure. The results obtained with $ZnO \cdot Cr_2O_3$ and $ZnO \cdot MoO_3$ are shown in Figs. 7 and 8[5]. The

5) The isotherm for $Cr_2O_3$ was not determined.

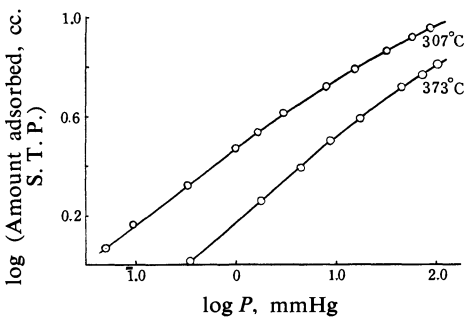



Fig. 7. Adsorption isotherms of hydrogen on $ZnO \cdot Cr_2O_3$ at 307 and 373°C.

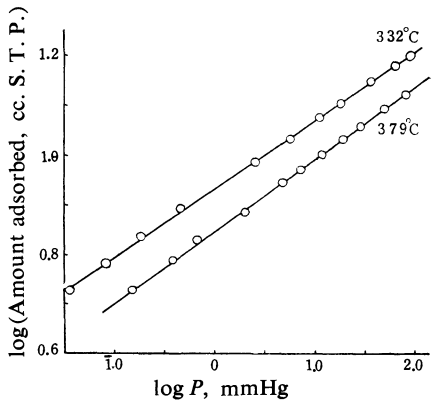



Fig. 8. Adsorption isotherms of hydrogen on $ZnO \cdot MoO_3$.

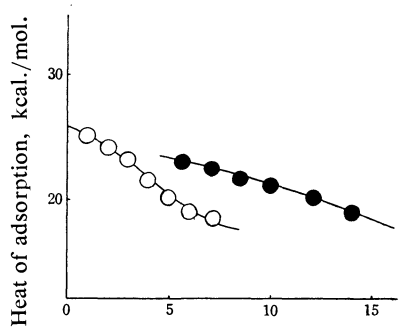



Fig. 9. Heats of adsorption of hydrogen on $ZnO \cdot Cr_2O_3$ and $ZnO \cdot MoO_3$. -○-, $ZnO \cdot Cr_2O_3$; -●-, $ZnO \cdot MoO_3$.

variations of the heat of adsorption determined from these isotherms with the amount adsorbed are represented in Fig. 9.

As seen in Fig. 5, with $ZnO \cdot Cr_2O_3$, the chemisorption with a low activation energy of desorption occurs to a considerable extent. The heat of adsorption for such chemisorption was estimated from the adsorption isotherms at 115 and 85°C, determined in desorption branch with the specimen which had chemisorbed hydrogen at about 300°C. The result

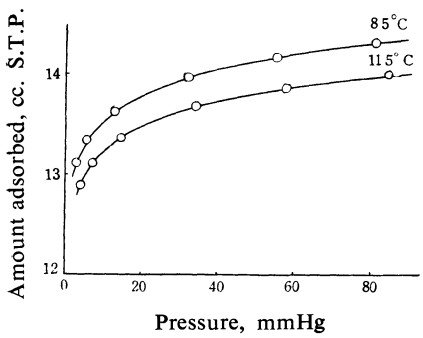



Fig. 10. Adsorption isotherms of hydrogen on $ZnO \cdot Cr_2O_3$ at 85 and 115°C.

obtained is shown in Fig. 10, from which the heat of adsorption is estimated as 7~8 kcal./mol.

**Nature of Heterogeneity of the Surface.**— The problem was dealt with as described in the previous papers[1,4]: At a particular temperature, hydrogen was left in contact with the adsorbent for some time; then, by pumping a known amount of gas from the system, the desorption rate was measured. The measurement was conducted with various times for each adsorbent. The results obtained with $ZnO \cdot MoO_3$, as shown in Fig. 11, are similar to those for carbon monoxide chemisorption on zinc oxide: The rate of desorption is greater on the surface with a larger amount adsorbed and there is a marked difference between the value of $d \log R_{dep}/dq$ for the runs of different times of contact with hydrogen. This suggests the existence of a heterogeneity of the surface where the heat of adsorption and the activation energy of adsorption vary inversely to each other as described in the previous paper[4].

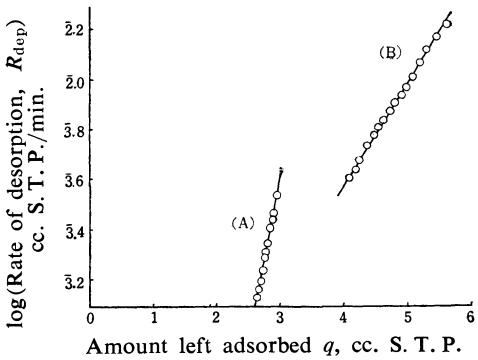



Fig. 11. Rate of desorption of hydrogen chemisorbed on $ZnO \cdot MoO_3$ as a function of the amount left adsorbed. Temp., 266°C. The weight of adsorbent used in these runs was 3.81 g. The amount adsorbed at room temperature before desorption was 3.54 cc. in Run A and 6.41 cc. in Run B. (A) After 30 min.; (B) After 3 hr.

In contrast to the case with $ZnO \cdot MoO_3$, the behavior observed on $ZnO \cdot Cr_2O_3$ was almost identical with that of hydrogen chemisorption on zinc oxide, i. e., a marked difference between the rates of desorption at equal amounts adsorbed after different contact times. Such behavior together with a rapid desorption observed on raising temperature suggests that the existence of an a priori heterogeneity of the surface where the activation energy of adsorption and the heat of adsorption vary in the same direction as was concluded in the previous work[1].

In the case of $Cr_2O_3$, although the result obtained at 162°C was similar to that with $ZnO \cdot MoO_3$ mentioned above (Fig. 11), at 206°C, somewhat different behavior was observed, as seen in Fig. 12 and Table III. Here in an early stage of adsorption, the proportion of the amount desorbed rapidly to the total amount adsorbed increases as adsorption proceeds, while after one hour since the admission of hydrogen, the situation is reversed, i. e., this proportion is now smaller on the surface with a larger amount adsorbed, indicating that the sites with a higher heat of adsorption are covered in a later stage. This behavior may be explained by assuming that the sites

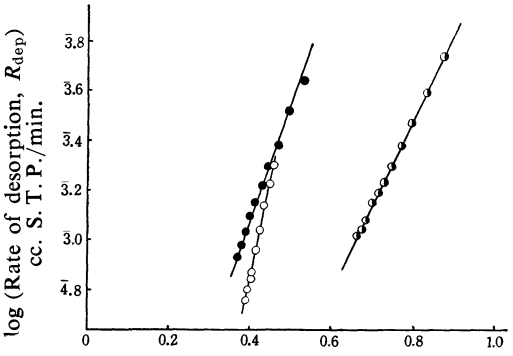



Fig. 12. Rate of desorption of hydrogen chemisorbed on $Cr_2O_3$ as a function of the amount left adsorbed. Temp., 206°C. Time of contact: -○-, 15 min.; -●-, 50 min.; -◑-, 15 hr.

TABLE III.

| Time of contact | Amount desorbed rapidly* cc. | Amount adsorbed at room temp. before desorption cc. |
|---|---|---|
| 15 min. | 0.04 | 0.55 |
| 50 min. | 0.27 | 0.77 |
| 15 hr. | 0.21 | 1.05 |

* This amount was estimated by the amount desorbed before $\log R_{dep}$ fell to $\bar{3}.64$. (cc. S. T. P./min.)

with the highest heat of adsorption are not accessible to the gas phase, but can be reached by a surface or bulk diffusion process from the sites with a lower heat of adsorption. Such an explanation may be more plausible than one assuming that the relationship between the heat of adsorption and the activation energy of adsorption changes abruptly in the final stage of adsorption. Irrespective of the explanation for this phenomenon, it may be concluded that the nature of surface heterogeneity in this system is, in principle, such that the heat of adsorption varies inversely to the activation energy of adsorption, since the desorbed amount in question is only a small fraction of the total amount desorbed.

On the basis of the relationship between the heat of adsorption and the activation energy of adsorption described above, we can estimate the activation energy of adsorption indirectly from the heat of adsorption and the activation energy of desorption. In the case of $ZnO \cdot MoO_3$, from the maximum value of heat of adsorption, 26 kcal./mol., and that of the activation energy of desorption, 41 kcal./mol., the minimum value of the activation energy of adsorption can be estimated as 15 kcal./mol., in agreement with that obtained directly from adsorption measurements. Similar estimation with $ZnO \cdot Cr_2O_3$ yields 10 kcal./mol. as the maximum activation energy of adsorption, in approximate agreement with that directly determined. Considering that for the latter system the minimum activation energy of desorption is 10 kcal./mol. and the minimum heat of adsorption will be below 7 kcal./mol., it may be concluded, as in the case of hydrogen chemisorption on zinc oxide, that almost the whole process of chemisorption involves activation energy.

It may be noted that the following correlation is obtained from the results described above and in previous papers[1,4]: When desorption can not be neglected during adsorption, a rapid desorption on an abrupt temperature raise always takes place. Moreover, the presence of the fraction with a low activation energy of desorption is always associated with a rapid desorption on raising the temperature. Such correlation can be expected for the surface heterogeneity, the pattern of which is characterized by a continuous distribution function of sites with the heats of adsorption varying in the same direction with the activation energy of adsorption.

**Hydrogen Chemisorption on Oxides.** — From the results presented here, combined with those described in previous papers[1], the following common features for hydrogen chemisorption on oxides may be mentioned:

1) On oxides of reduced state, hydrogen chemisorption is reversible, in the sense that hydrogen is desorbed as such. For zinc oxide, this was already described in the previous work[6]. For $ZnO \cdot Cr_2O_3$, $ZnO \cdot MoO_3$ and $CrO_3$, essentially the same conclusion was obtained although the complete desorption requires a very long time.

2) When desorption is negligible, the rate of chemisorption is proportional to $P^{0.8}$ over a wide range of temperatures, indicating that the rate-determining step is not a sort of surface migration but an adsorption.

3) Almost the whole process of hydrogen chemisorption on oxides involves activation energy which becomes higher as the adsorption proceeds, although its magnitude varies from one oxide to another.

4) There is no evidence to support the existence of two types of hydrogen chemisorption which was believed to exist previously[2]. Although extensive conductivity measurements were not made with $ZnO \cdot Cr_2O_3$ and $ZnO \cdot MoO_3$ as in the case of zinc oxide, the concept of two types chemisorption is not required for these systems either, since all the results can be explained by the concept of single type chemisorption on a heterogeneous surface. The fact that the variation of activation energy of desorption is continuous over the whole range of the amount adsorbed appears to favour this concept.

5) The change of activation energy of adsorption with the amount adsorbed mainly arises from an a priori heterogeneity of the surface and not from the induced heterogeneity or the formation of electrical double layer owing to charge transfer between the gas adsorbed and the surface. At present the reason for the fact that the relation between the heat of adsorption and the activation energy of adsorption varies from one oxide to another is unknown. As regards the chemisorption of hydrogen on oxides other than those studied by the present author, the results obtained in this work may serve to make some prediction. In the cases of MnO and $MnO \cdot Cr_2O_3$ investigated by Taylor et al.[7], the activation energy of adsorption and the heat of adsorption will vary inversely to each other, since a rapid desorption on raising temperature is not observed. The situation with $V_2O_3$ studied by Tarama and Teranishi[8], may be similar, since the general features of the chemisorption are similar to those with $ZnO \cdot MoO_3$, i. e., the chemisorption measurement is possible

6) Y. Kubokawa, This Bulletin, 33, 743 (1960).
7) H. S. Taylor and A. T. Williamson, *J. Am. Chem. Soc.*, 53, 2168 (1931).
8) K. Tarama and S. Teranishi, *J. Chem. Soc. Japan, Ind. Chem. Sec.*, (*Kogyo Kagagu Zasshi*), 55, 376 (1952).

only above 200°C, and the rate increases steadily with increasing temperature. It may be concluded that the variation of the activation energy and the heat of adsorption in the reverse direction is more frequently encountered in hydrogen chemisorption on oxides.

## Summary

For hydrogen chemisorption on $ZnO \cdot Cr_2O_3$, $ZnO \cdot MoO_3$ and $Cr_2O_3$, the rates of adsorption and desorption, and adsorption equilibrium were investigated. The activation energy of adsorption ranged from 8 to 12 kcal./mol. for $ZnO \cdot Cr_2O_3$, and from 15 to 25 kcal./mol. for $ZnO \cdot MoO_3$. The value for $Cr_2O_3$ was about 13 kcal./mol. In the cases of $ZnO \cdot MoO_3$ and $Cr_2O_3$, where desorption is negligible during adsorption, the rate of adsorption was proportional to $P^{0.8}$, while with $ZnO \cdot Cr_2O_3$ desorption was found to occur appreciably. The activation energy of desorption increased with a decreasing amount adsorbed from 10 to 35 kcal./mol. for $ZnO \cdot Cr_2O_3$, and from 15 to 45 kcal./mol. for $Cr_2O_3$, while an approximately constant value of 41 kcal./mol. was obtained with $ZnO \cdot MoO_3$ except in the initial stage of desorption. The maximum heat of adsorption estimated from adsorption isotherms was about 25 kcal./mol. for both $ZnO \cdot Cr_2O_3$ and $ZnO \cdot MoO_3$. For all the systems studied, desorption experiments suggested the existence of surface heterogeneity with the activation energy of adsorption and heat of adsorption varying inversely in the cases of $ZnO \cdot MoO_3$ and $Cr_2O_3$, while with $ZnO \cdot Cr_2O_3$ the variation in the same direction was observed. On the basis of the results hitherto obtained, the general characteristics of hydrogen chemisorption on oxides were discussed.

The author wishes to express his sincere thanks to Professor O. Toyama for his guidance and encouragement throughout the course of this study.

*Department of Applied Chemistry*
*College of Engineering*
*University of Osaka Prefecture*
*Sakai-shi Osaka*

# *Monolayers of Some Cyclic Peptides. Fungisporin and Gramicidin $J_1$*

By Shoichi IKEDA and Toshizo ISEMURA

(Received September 19, 1959)

Chemical structures of many naturally occurring cyclic peptides and their modes of biological action have been investigated and elucidated in recent years. While many informations concerning the chain configuration and other properties of linear polypeptides in spread monolayer are obtained, the studies on cyclic peptides on surface are relatively deficient and stimulate our interest in several respects. Spread linear polypeptides are generally accepted to take the $\beta$-configuration[1,2] but spread cyclic peptides, unless the size of their rings is large enough, can not accomodate with this configuration. Thus it is desired to examine the configuration of cyclic peptides in the monolayer. Further, it is noticed that while ordinary linear polypeptides form monolayers of a condensed type owing to the intramolecular hydrogen bonding, the presence of prolyl residue[3] or ionized amino acid residue[4] in amino acid sequence, causes their monolayers to expand more. It is of importance to investigate whether or not this effect is exhibited in the monolayers of cyclic peptides.

Some investigations on the monolayers of cyclic peptides have been performed mainly by Few[5], but their configurations on the surface have so far been discussed only in the cases of tyrocidine A and B and gramicidin SA and SB[6].

From these points of view, the monolayers of two cyclic peptides, i. e., fungisporin and gramicidin $J_1$, have been studied by measuring surface pressure, potential and viscosity. Fungisporin[7],

1) C. W. N. Cumper and A. E. Alexander, *Trans. Faraday Soc.*, **46**, 235 (1950).
2) J. T. Davies, *Biochim. Biophys. Acta*, **11**, 165 (1953).
3) T. Isemura and S. Ikeda, This Bulletin, **32**, 178 (1959).
4) T. Isemura and K. Hamaguchi, ibid., **27**, 339 (1954); K. Hamaguchi and T. Isemura, ibid., **28**, 9 (1955); T. Isemura, K. Hamaguchi and S. Ikeda, *J. Polymer Sci.*, **23**, 651 (1957).
5) A. V. Few and J. H. Schulman, *Biochem. J.*, **54**, 171 (1953); A. V. Few, *Biochim. Biophys. Acta*, **16**, 137 (1955); idem., *Proc. Second Int. Cong. Surface Activity*, **2**, CZ 168 (1957), Butterworths Scientific Publications, London.
6) A. V. Few, *Trans. Faraday Soc.*, **53**, 848 (1957).
7) Y. Sumiki and K. Miyao, *J. Agr. Chem. Soc. Japan (Nippon Nogei-kagaku Kaishi)* **26**, 27 (1952); K. Miyao, *Bull. Agr. Chem. Soc. Japan*, **19**, 86 (1955).

isolated from spores of some species of *Penicillium* and *Aspergillus*, is an octapeptide, cyclo-(D-Phe-L-Phe-D-Val-L-Val)$_2$[8]. Gramicidin $J_1$[9] is a heptapeptide, cyclo-(D-Orn-L-Val-L-Orn-D-Phe-D-Leu-L-Phe-L-Pro)[10]. Fungisporin has given a monolayer of condensed type, whereas gramicidin $J_1$ that of an expanded type. The behavior of these monolayers has been discussed in the light of the configurations of these cyclic peptides.

## Experimental

Fungisporin was prepared by Dr. Miyao and was offered to our disposal. It is soluble only in dichloroacetic acid. As its spreading solvent was used a dichloroacetic acid-benzene (1 : 1 v/v) mixture which was found to be the most suitable for the surface potential measurement. Gramicidin $J_1$ dihydrochloride was a gift of Professor Otani. It was spread from a methanol solution.

Surface pressure, $\Pi$, was measured by a balance of a hanging plate type in higher pressure region, but it was measured by a balance of a float type of a better sensitivity in lower pressure or dilute region. The surface potential, $\Delta V$, was measured by the vibrating electrode method and surface viscosity, $\eta$, by the damped rotatory oscillation of a disk. From surface potential, the apparent surface moment, $\mu$, was calculated by the Helmholtz equation

$$\Delta V = \frac{4\pi\mu}{A}$$

where $A$ was the area per amino acid residue.

## Results

**Fungisporin.**—The $\Pi-A$, $\Delta V-A$, $\mu-A$ and $\eta-A$ curves of fungisporin on 0.01 M potassium chloride are shown in Fig. 1. The monolayer was found to be of a condensed type. The condensation of the film may be ascribed mainly to the hydrogen bonding and partly to the cohesion between hydrocarbon side chains. At the region of rise of the $\Pi-A$ curve the surface pressure declined gradually with time after each compression. In Fig. 1 the values at 1 min. per interval are plotted. The delay for attaining a steady surface pressure after each compression has been noticed in some condensed films of long chain substances and of high polymers with long side chain and is, therefore, closely related to the structure of fungisporin. The surface potential was reproducible only at the areas smaller than about 40 Å$^2$. This is also commonly observed for condensed films of low molecular weight substances, and consequently, consistent with the fact that fungisporin is a small molecule, an octapeptide. The surface viscosity was manifest at the areas below

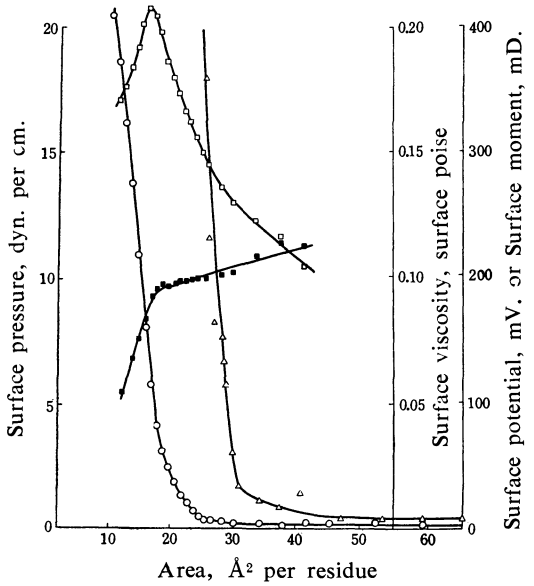



Fig. 1. Monolayer of fungisporin on 0.01 M potassium chloride (14°C). ○ surface pressure; □ surface potential; ■ surface moment; △ surface viscosity.

40 Å$^2$, where a surface potential was found to be reproducible.

The area, $A_\mu$, where the slope of $\mu-A$ curve suddenly changed was found to be 17.5 Å$^2$ and the area, $A_\Pi$, of the minimum surface compressibility was 16.0 Å$^2$. These areas are nearly identical with each other and will represent the area occupied by an amino acid residue. The surface moment, $\mu_c$, at the area, $A_\mu$, was 200 mD. Both the area and surface moment are larger than those found for linear polypeptide monolayers.

**Gramicidin $J_1$.**—Since gramicidin $J_1$ contains two ornithyl residues in a molecule, it forms an ionized monolayer on distilled water and an unionized monolayer on aqueous solution at pH higher than 10.5.

The unionized monolayer of gramicidin $J_1$ on 0.01 M potassium carbonate at pH 11.2 showed a characteristic feature, when a neutral salt such as potassium chloride was added into the aqueous subphase. The effect of the concentration of potassium chloride on the $\Pi-A$ curve is illustrated in Fig. 2. The $\Pi-A$ curve in the absence of neutral salt was smooth, but a break point appeared when potassium chloride was present. The break point was found to be independent of salt concentration and was 27 Å$^2$ and 5.6 dyn. per cm. In the absence of salt or on 0.001 M potassium chloride, slight time effects were observed in the region of surface pressure higher than the break point. The $\Pi-A$ curves were not altered by salt concentration between 0.01 M and 1 M. In Fig. 3 are

8) K. Miyao, ibid., 24, 23 (1960).
9) S. Otani and Y. Saito, *Proc. Japan Acad.*, 30, 991 (1954).
10) S. Otani, "Chemistry of Proteins" ed. by S. Akabori and S. Mizushima, Vol. 5, Kyoritsu Shuppan Co., Ltd., Tokyo (1957), p. 297.

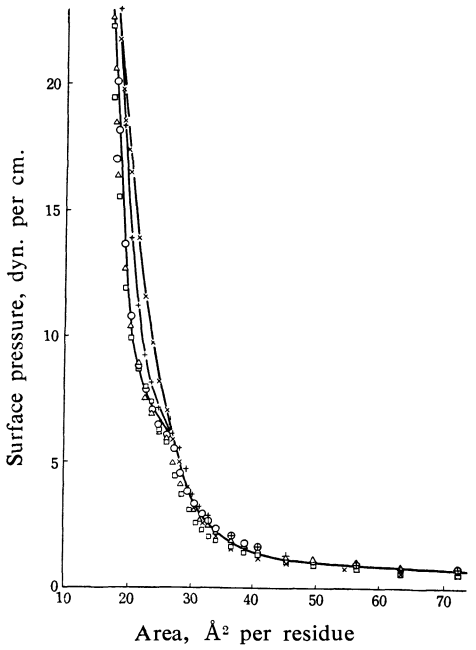



Fig. 2. Effect of potassium chloride on the surface pressure-area curve of gramicidin $J_1$ on 0.01 M potassium carbonate (15°C). × no salt; + 0.001 M; ○ 0.01 M; △ 0.1 M; □ 1 M.

shown the $\Pi-A$, $\Delta V-A$, $\mu-A$ and $\eta-A$ curves on 0.01 M potassium carbonate when 0.01 M potassium chloride are added. Surface potential was scarcely affected by salt concentration and the corresponding break point such as observed in the $\Pi-A$ curve was not found in both $\Delta V-A$ and $\mu-A$ curves.

It was noticed that the $\Pi-A$ curves of gramicidin SA and SB likewise exhibited the same kind of break points on 1 M potassium chloride at pH 12.5, and the break was attributed to the reorientation of side chains of ornithyl residues[6]. However, no break on the $\Delta V-A$ and $\mu-A$ curves for gramicidin $J_1$ suggests that the break on the $\Pi-A$ curve would not come from the reorientation of ornithyl residues but presumably from the micelle formation as proposed for fatty acid monolayers[11].

At pH 11.2 where they were unionized, the monolayers of gramicidin $J_1$ were of an expanded type, as shown in Fig. 2. Correspondingly, the surface viscosity was manifest first in the region of high surface pressures[4,12] as shown in Fig. 3. A constant value of the surface moment was observed over a wide area. The smallest area, $A_\mu$, of constant surface moment was found to be 19.0 Å², the area, $A_\Pi$, of minimum surface compressibility to be 20.5 Å² and the gelling area, $A_\eta$, to be 20.0 Å². All these areas were scarcely dependent on salt concentrations not less than 0.01 M and nearly identical

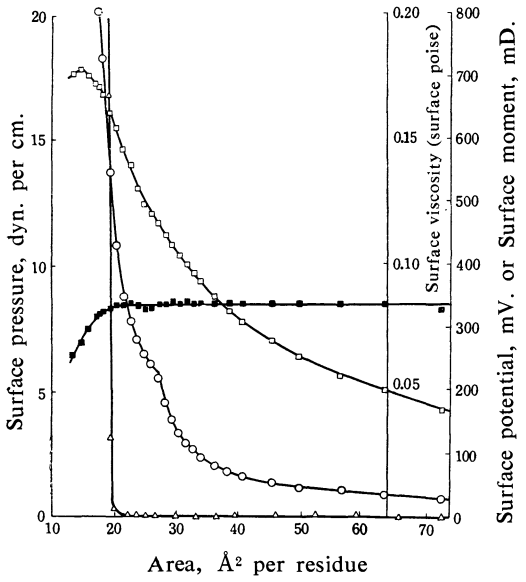



Fig. 3. Monolayer of gramicidin $J_1$ on 0.01 M potassium carbonate in the presence of 0.01 M potassium chloride (15°C). ○ surface pressure; □ surface potential; ■ surface moment; △ surface viscosity.

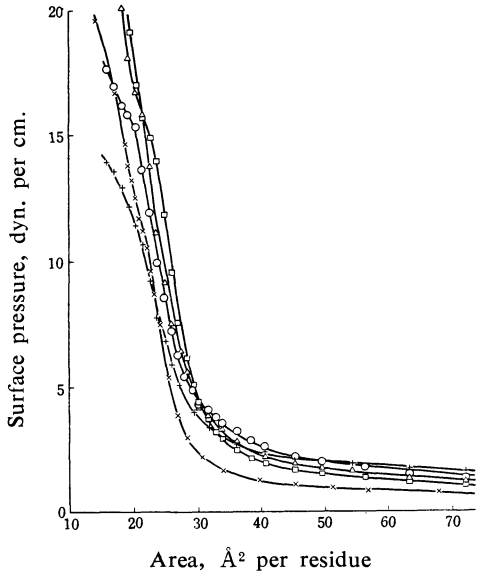



Fig. 4. Effect of potassium chloride on the surface pressure-area curve of gramicidin $J_1$ on distilled water (15°C). × no salt; + 0.001 M; ○ 0.01 M; △ 0.1 M; □ 1 M.

11) I. Langmuir, *J. Chem. Phys.*, **1**, 756 (1933).
12) S. Ikeda and T. Isemura, This Bulletin, **32**, 659 (1959).

with one another. Consequently, they represent the area occupied by an amino acid residue. The constant surface moment, $\mu_c$, was about 340 mD.

On distilled water at pH 5.6 gramicidin $J_1$ forms an ionized monolayer. In this case, the monolayer behaves unlike the unionized monolayer but in a quite specific manner, as the salt concentration is varied. The variation of the $\Pi-A$ curves with the concentration of patassium chloride is shown in Fig. 4. In the absence of salt or on 0.001 M potassium chloride, the monolayers were somewhat unstable and had a tendency to dissolve into aqueous subphases on compression. On potassium chloride of the concentrations of 0.01 M to 1 M, however, the monolayers exhibited a typical behavior of ionized monolayer. Monolayers were more condensed at higher salt concentrations and more expanded at lower concentations. The $\Pi-A$ curves pass a reversal point[13], 30.5 Å$^2$ and 4.3 dyn. per cm.

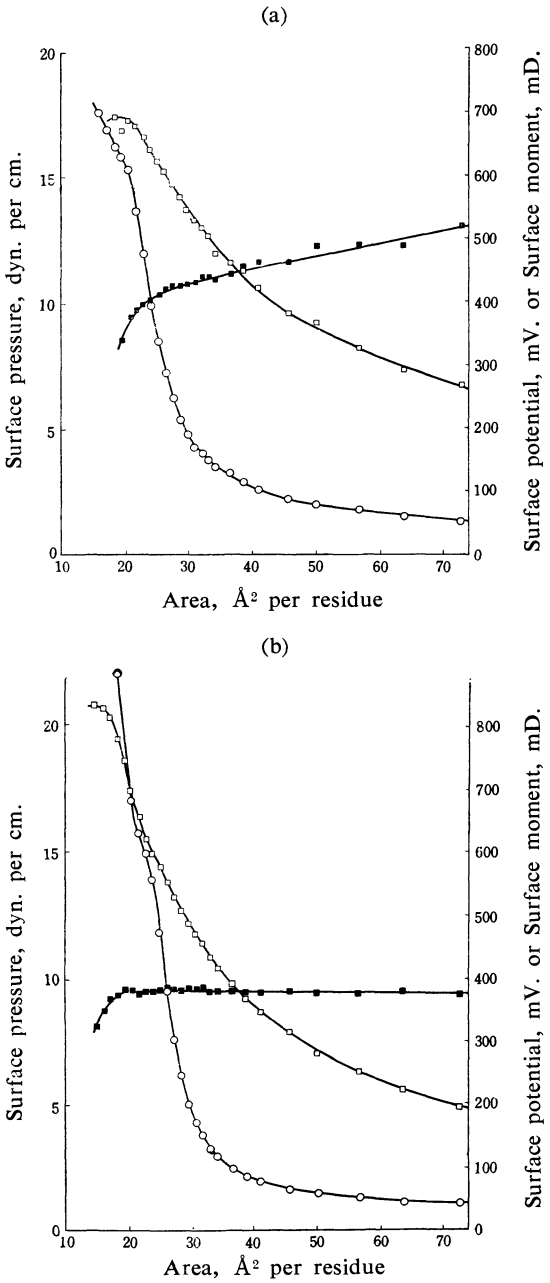



Fig. 5. Monolayers of gramicidin $J_1$ on distilled water in the presence of potassium chloride (15°C). a, 0.01 M; b, 1 M. ○ surface pressure; □ surface potential; ■ surface moment.

In Fig. 5 are illustrated some of the $\Delta V-A$ and $\mu-A$ curves together with the $\Pi-A$ curves. The surface moment gave no constant value on 0.01 M potassium chloride but a constant value, 380 mD, on 1 M potassium chloride. On the $\Delta V-A$ and $\mu-A$ curves no significant change was observed at the area corresponding to the reversal point on the $\Pi-A$ curve. The surface viscosity was very low and not detected even at an area as small as 10 Å$^2$ on 0.01 M potassium chloride.

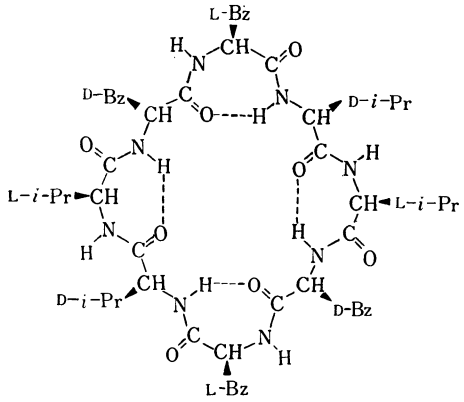
In the presence of 0.01 M potassium chloride, the ionized monolayer of gramicidin $J_1$ on neutral subphase was more expanded than the unionized monolayer on 0.01 M potassium carbonate and the surface potential of the former was higher than that of the latter.

## Discussion

**Configurations of Cyclic Peptides in Monolayer.**—The molecular configuration of cyclic peptide has so far been investigated by a polarized infrared spectra[14] and an X-ray diffraction[15] on gramicidin S crystal. The infrared study suggested, that a gramicidin S molecule consists of ten seven-membered rings, each with a hydrogen bond between the imino and carbonyl groups. Few[6] has proposed the configurations of tyrocidines and gramicidin SA in a monolayer in such a way, as the maximum number seven-membered of rings can be formed in a plane and the other peptide bonds can take the $\beta$-configuration. We can deduce the configurations of fungisporin and gramicidin $J_1$ in monolayer in the same way.

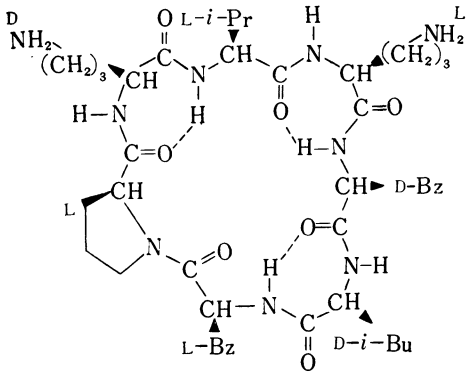
In accordance with the above conditions, the configurations of fungisporin in a monolayer are confined to be square-like ones. One of them is illustrated as follows:

13) J. N. Philips and E. Rideal, *Proc. Roy. Soc.*, **A232**, 159 (1955).
14) N. B. Abbott and E. J. Ambrose, ibid., **A219**, 17 (1953).
15) D. Crowfoot-Hodgkin, *Cold Spring Harbor Symp. Quant. Biol.*, **14**, 65 (1950).



An alternative configuration is obtained by shifting each side chain one by one, in either sence, along the perimeter of this configuration, the orientation of side chains being altered. The other possibilities can be obtained by turning each of these two configurations over. It can not be distinguished which side of the molecular plane is exposed to the air or to the aqueous phase, when the molecule is put on surfaces, and consequently all of these four configurations are equally probable.

The unionized gramicidin $J_1$ molecule can take only one confiugration in the monolayer, subject to the foregoing requirements:



An alternative is obtained by turning of this configuration. In considering the difference of D-leucyl and L-valyl residues in hydrophilic nature, it is a little more favorable to choose the latter configuration (if the air is above the plane).

In all these cases of fungisporin and gramicidin, the areas occupied by a residue are consistent with those obtained experimentally. It is remarkable to note that the side chains of all the D-amino acid residues orientate oppositely to these of all the L-residues with respect to the plane of a molecule. Thus, if the side chain of the L-ornithyl residue in gramicidin $J_1$ tends towards the aqueous phase, that of the D-ornithyl residue is directed to the air.

Since the formation of a seven-membered ring will force the carbonyl groups to direct towards the aqueous phase, the surface moment is expected to be higher than that of the $\beta$-configuration. The surface moment of fungisporin is mainly composed of two different orientations of the carbonyl groups, one hydrogen bonded intramolecularly and the other not participating in hydrogen bonding. It was found to be about 200 mD, which is actually higher than that of the $\beta$-configuration, 160 mD[3]. On the other hand, the surface moment of gramicidin $J_1$ is a mean value of three orientations of carbonyl groups, hydrogen bonded, not hydrogen bonded and belonging to L-phenylalanyl residue, and two amino groups of D- and L-ornithyl residues. The experimental value was very high and 340 mD. It is much higher than 273 mD and 274 mD for gramicidin SA and SB[6]. If the contribution of each carbonyl group is assumed to be equally 200 mD, as in fungisporin, the two amino groups must contribute about 980 mD or, in the average, an amino group about 490 mD. This value would be compared with the surface moments of long chain amines, 300 to 400 mD[16]. However, this value is too high if the opposite directions of two ornithyl residues are taken into account. The reason for this and, accordingly, for the large values of the surface moment, as compared with those of gramicidin SA is not clear.

**Condensation and Expansion of the Monolayers.** — Fungisporin gave a monolayer of

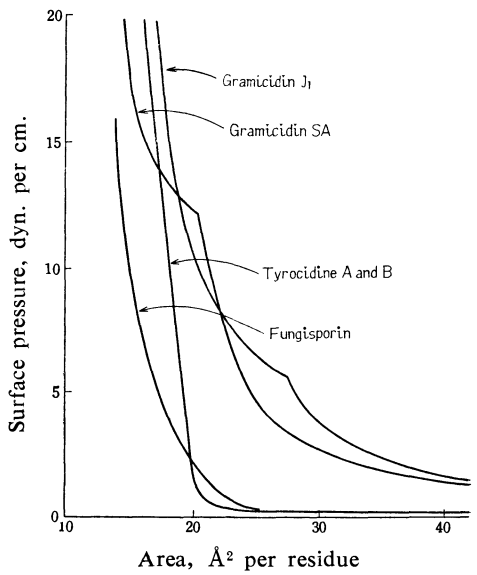



Fig. 6. Surface pressure-area curves of some cyclic peptides. Gramicidin SB gives a nearly identical curve with gramicidin SA.

16) E. F. Porter, *J. Am. Chem. Soc.*, **59**, 1883 (1937); J. Glazer and M. Z. Dogan, *Trans. Faraday Soc.*, **49**, 448 (1953).

condensed type but gramicidin $J_1$ gave an unionized monolayer of expanded type. It was noticed[6] that tyrocidine A and B formed condensed films on aqueous subphases at the ionic strength 1.0, irrespective of pH, but gramicidin SA and SB formed expanded films under the same condition. These results are summarized in Fig. 6. It was concluded by Few[6] that the expansion of films of cyclic peptides is closely related to the content of ornithyl residues. It is, however, known in the case of unionized linear polypeptides[4] that the L-lysyl residue, which has a longer side chain than the ornithyl residue only by one methylene group, does not influence the type of monolayers but remains to be of a condensed type. We, therefore, no longer regard his proposed explanation as adequate. We have previously observed that the monolayers of synthetic linear polypeptides are transformed gradually from a condensed type to an expanded type as the content of prolyl residue is increased[3,12] and further, this effect is virtually demonstrated in the case of protein films such as gelatin[17]. It can be seen that even for the monolayers of cyclic peptide the prolyl residue plays the same role as for linear polypeptides. In comparing the amino acid composition, fungisporin contains no prolyl residue in a heptapeptide[8], gramicidin $J_1$ one in an octapeptide[10], both tyrocidine A and B one in a decapeptide[18,19] and gramicidin SA two in a decapeptide[20]. The proportion of prolyl residues in gramicidins are higher than in fungisporin and tyrocidines. Thus the former peptides give more expanded monolayers than the latter. On the contrary, gramicidin SB, whose complete structure is still unknown, but whose monolayer expands to the same extent as gramicidin SA, will have two prolyl residues if it is a decapeptide.

**Ionization of Dilute Gramicidin $J_1$ Monolayer.**—Because of the expanded nature of gramicidin $J_1$ monolayers, it was possible to measure accurately the surface pressure and potential at the region of very large areas. Then the behavior of dilute ionized monolayers of gramicidin $J_1$ when spread on neutral salt solution can be treated in terms of the theory of the ionized monolayer so far presented.

In general, the surface pressure of an ionized monolayer can be divided into two parts:

$$\Pi = \Pi_0 + \Pi_i$$

where $\Pi_0$ is the surface pressure of an unionized monolayer, which is independent of salt concentration, when the other effect is ignored. In this equation the contribution of deformation due to the electric repulsion is not included. The surface pressure due to ionization, $\Pi_i$, is, according to the theory of the electric double layer[21,22], given by

$$\Pi_i = 2kT\left\{-\frac{2n}{\kappa}+\sqrt{\left(\frac{2n}{\kappa}\right)^2+\frac{1}{A_i^2}}\right\}$$

where $k$ is the Boltzmann constant, $T$ the absolute temperature, $n$ the salt concentration (molecules per $cm^3$) and $\kappa$ the Debye-Hückel parameter. Here $A_i$ is the area per ionized group. Evidently, the surface pressure is lower, as neutral salt is more concentrated in an aqueous phase. However, values of the surface

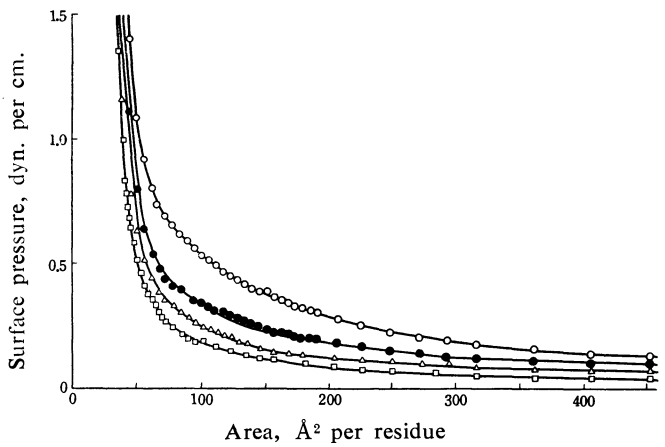



Fig. 7. Effect of potassium chloride on the surface pressure-area curve of dilute gramicidin $J_1$ monolayer on distilled water (15°C). ○ 0.01 M; ● 0.025 M; △ 0.1 M; □ 1 M.

17) S. Ikeda and T. Isemura, This Bulletin, 33, 137 (1960).
18) A. Paladini and L. C. Craig, *J. Am. Chem. Soc.*, 76, 688 (1954).
19) T. P. King and L. C. Craig, ibid., 77, 6627 (1955).
20) R. Consden, A. H. Gordon, A. J. P. Martin and R. L. M. Synge, *Biochem. J.*, 41, 596 (1947); A. R. Battersby and L. C. Craig, *J. Am. Chem. Soc.*, 73, 1887 (1951).
21) J. T. Davies, *Proc. Roy. Soc.*, A208, 224 (1951).
22) S. Ikeda and T. Isemura, This Bulletin, 33, 131 (1960).

Table I. Surface pressure due to ionization at 200 Å² per residue

| $n$ | $\Pi$ | (A) an ionized residue $\Pi_i$ | $\Pi_0$ | (B) two ionized residues $\Pi_i$ | $\Pi_0$ |
|---|---|---|---|---|---|
| mol./l. | dyn./cm. | dyn./cm. | | dyn./cm. | |
| 0.01 | 0.29 | 0.230 | 0.06 | 0.699 | −0.41 |
| 0.025 | 0.19 | 0.159 | 0.03 | 0.550 | −0.35 |
| 0.1 | 0.12 | 0.087 | 0.03 | 0.326 | −0.21 |
| 1 | 0.07 | 0.032 | 0.04 | 0.111 | −0.04 |

pressure, $\Pi_0$, at a constant area, which are obtained by subtracting the calculated values of $\Pi_i$ from the experimental values of $\Pi$, should be independent of salt concentration, even if the salt concentration is varied.

The $\Pi-A$ curves of dilute ionized gramicidin $J_1$ monolayers on potassium chloride solutions of various concentrations are shown in Fig. 7. The surface pressure is virtually lower at higher salt concentrations. In the monolayer of gramicidin $J_1$ in an unionized state the two amino groups of ornithyl residues, which are responsible for the ionization of the molecule, are assumed to be oppositely directed to each other. If this configration is still retained in the state of ionization, the electric double layer will be concerned with only one amino group, probably of the L-ornithyl residue. Taking account of this, we have estimated the values of $\Pi_0$ at an area, $A=200$ Å², by the foregoing procedure for both cases, that only one ionized amino group ($A_i=7A$) and two ionized groups ($A_i=(7/2)A$) are assumed to concern the electric double layer. The results are given in Table I. In the former case the obtained values of $\Pi_0$ are nearly constant and positive, unlike in the latter case. Thus it is likely, that the electric double layer is formed by the ionization of only one amino group and not related to that of the other. This might support the proposed configuration of gramicidin $J_1$ in monolayer.

According to Schulman and Hughes[23], the surface potential of an ionized monolayer can be expressed by

$$\Delta V=\frac{4\pi\mu_M}{A_i}+\psi_M$$

where $\mu_M$ is the surface moment of an ionized group (one or two seventh of the moment per amino acid residue according as one or two ionized ornithyl residues) and $\psi_M$ is the potential of the monolayer. In this equation the first term assumes the ordinary Helmholtz equation and the second term is, according to the theory of electric double layer[21,22], expressed by

$$\psi_M=\frac{2kT}{e}\sinh^{-1}\frac{\kappa}{4nA_i}$$

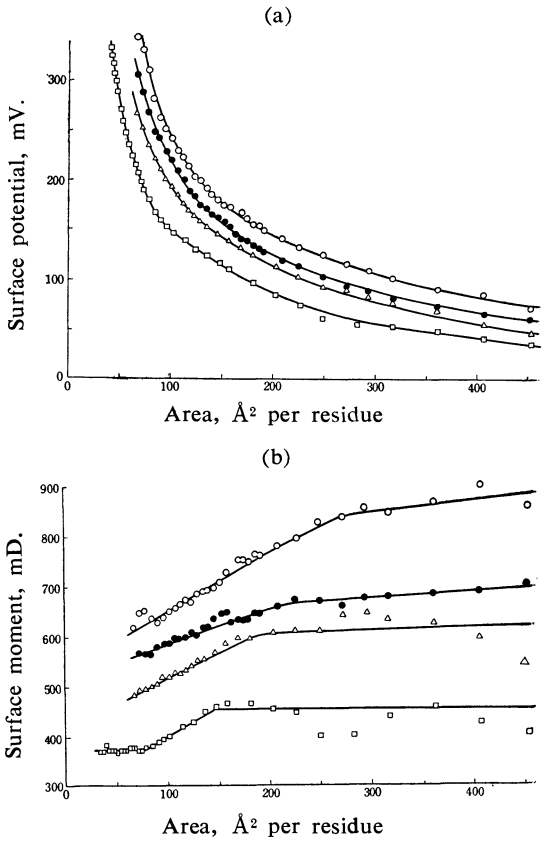



Fig. 8. Effect of potassium chloride on dilute monolayer of gramicidin $J_1$ (15°C). a, surface potential; b, apparent surface moment. ○ 0.01 M; ● 0.025 M; △ 0.1 M; □ 1 M.

where $e$ is the elementary charge. These equations indicate that the surface potential is lower, as neutral salt is more concentrated in the aqueous phase. In Fig. 8a is shown the variation of the $\Delta V-A$ curves with concentration of potassium chloride in the aqueous phase, which is in accord with the above indication. We have found, however, that the same procedure as done for the surface pressure is not suitable to distinguish whether one or two ornithyl residues concern the electric double layer, since the surface potential can not be measured with sufficient accuracy so as to allow it. Instead of doing so, we have tested the above equations by another method. These

23) J. H. Schulman and A. H. Hughes, *Proc. Roy. Soc.*, A138, 430 (1932).

equations show that the apparent surface moment, $\mu$, calculated from $A \cdot \Delta V/4\pi$, generally falls on compression and its value is lower at higher salt concentrations. On highly concentrated salt solutions the apparent surface moment should be constant over a wide region of areas, In Fig. 8b is shown the $\mu-A$ curves for gramicidin $J_1$ on potassium chloride solutions. Although a minor error in surface potential measurement causes a marked scatter of the surface moment at large areas, it can be seen that the general trend of the $\mu-A$ curves is consistent with the prediction. On such a concentrated salt solution as 1 M, however, the Helmholtz equation appears to be obeyed by the ionized monolayer at areas smaller than 90 Å$^2$ but fails to hold at larger areas.

In addition, it was found that only at moderate areas the ionized monolayer obeys the electrochemical equation[24]

$$\left(\frac{\partial \Delta V}{\partial \ln n}\right)_A = -\frac{kT}{e}$$

as illustrated in Fig. 9.

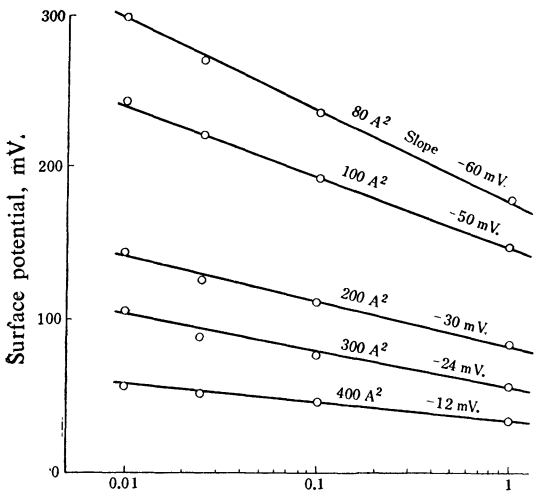



Fig. 9. Surface potential plotted against logarithm of concentration of potassium chloride. Theoretical slope at moderate areas, −57 mV. at 15°C.

## Summary

Monolayers of two naturally occurring cyclic peptides, fungisporin and gramicidin $J_1$, were investigated by the measurements of surface pressure, potential, and viscosity. Fungisporin, an octapeptide composed of phenylalanyl and valyl residues, gave a monolayer of a condensed type. Gramicidin $J_1$, an electrolytic heptapeptide containing a prolyl and two ornithyl residues, gave an unionized monolayer of an expanded type on an alkaline subphase. It behaved in a somewhat specific manner when neutral salt such as potassium chloride was present.

The configurations of these cyclic peptides in monolayer were suggested in such a way as intramolecular hydrogen bonding could cause a maximum number of seven-membered rings. Then fungisporin can take four possible square-like configurations, which are equally probable, and gramicidin $J_1$ can take two possible configurations. When these configurations of both peptides are put on surfaces, side chains of all the D-residues always orientate oppositely to those of all the L-residues with respect to the surfaces.

In taking account of the condensation and expansion of these monolayers, together with those of tyrocidine A and B and gramicidin SA, it was concluded that cyclic peptides give more condensed monolayers as the contents of prolyl residue are higher. Thus a prolyl residue plays the same role in cyclic peptides as in linear polypeptides.

Gramicidin $J_1$ gave a monolayer of more expanded type on a neutral subphase, and exhibited a characteristic behavior common with ionized monolayers when neutral salt such as potassium chloride was added. At very large areas the the behavior was adequately explained by the theory of the electric double layer, when only one ionized residue was assumed to concern the double layer.

The authors are indebted to Professor S. Otani of the Medical School, Osaka City University, and to Dr. K. Miyao of the Faculty of Agriculture, the University of Tokyo, for the gifts of valuable peptides. This work was partly supported by a grant from the Ministry of Education, to which the authors' thanks are also due.

*Faculty of Science and*
*Institute for Protein Research*
*Osaka University, Osaka*

24) D. J. Crisp, Research, "Surface Chemistry", Butterworths Scientific Publications, London (1949), p. 65.

# *Spectrophotometric Determination of Tellurium(IV) by Extraction with Tributylphosphate*

By Seiichiro HIKIME

(Received October 21, 1959)

Several spectrophotometric methods for tellurium determination have been reported[1-7]. However these methods have still some disadvantages, e. g. troubles in separation by precipitation.

In the study of separation of tellurium from iron[8], the authors have found that tellurium-(IV) complex with thiourea is extracted by tributylphosphate (TBP) from a dilute hydrochloric acid solution in the presence of potassium thiocyanate and the yellow color develops more deeply in the TBP phase than in the aqueous phase. When thiourea or potassium thiocyanate exists alone in the solution, tellurium complex is not extracted by TBP, whereas in case where a large excess of thiocyanate ions exists in the solution whose hydrochloric acid concentration is more than 0.1 N, even a small amount of tellurium is extracted by TBP. The coloration thus developed in TBP was applied to the spectrophotometric determination of tellurium.

## Experimental

**Reagents, Materials and Apparatus.**—*Hydrochloric acid and nitric acid.*—A guaranteed reagent is diluted with pure water to the required concentrations.

*Potassium thiocyanate solution.*—The guaranteed reagent 500 g. is dissolved in pure water and diluted to 1000 ml.

*Thiourea solution.*—The guaranteed reagent 80 g. is dissolved in water at 70°C and diluted to 1000 ml.

*Standard solutions of tellurium(IV).*—Metallic tellurium (2 g.) supplied by Nippon Kogyo Co. Ltd., is dissolved in 30 ml. of aqua regia and the solution is evaporated on a water bath. Concentrated hydrochlorlc acid (10 ml.) is added to the residue and the liquid is evaporated to dryness; this procedure is repeated twice in order to expel any traces of nitric acid from the solution. The residue is again dissolved in hydrochloric acid and diluted with pure water. By this procedure two solutions of tellurium are prepared as a stock solution, i. e., 6 N hydrochloric acid solution containing tellurium in a concentration of 10 g./l. and 3 N hydrochloric acid solution containing 2 g. Te/l. Several standard series of tellurium are prepared by diluting one of these stock solutions with dilute hydrochloric acid.

*n-Tributyl phosphate (TBP).*—TBP is purified by the method reported by Alock et al.[9], and used without dilution after saturation with the reagent solutions under experimental conditions.

A Beckman DU spectrophotometer with 10 mm. cell was used for the measurements of absorbances. pH values were determined by Horiba H-type pH-meter with a glass electrode.

*Procedure.*—The same volume of TBP with that of the sample solution was used for a single extraction without any organic diluent. Although under the experimental conditions tellurium complex is extracted completely with TBP by shaking in a separatory funnel for 30 sec. The shaking was continued for 2 min. to ensure the extraction. The extraction was carried out only at room temperature.

After extraction, both TBP- and aqueous-phase became turbid to some extent, the extent depending on the initial acidity of the aqueous solution. A clean solution, however, was obtained by centrifuge; this treatment gave no remarkable volume change of the two phases.

Potassium thiocyanate solution is added to a sample solution whose pH was controlled to about 1, to which thiourea solution is added. The solution is finally fitted to a constant volume (10 or 20 ml.) and the pH value adjusted to 1 with hydrochloric acid. After 20 min., the same volume of TBP as that of the aqueous solution is added and the mixture shaken for 2 min. with a shaker. When the TBP phase is separated from the aqueous phase, the former is taken out with a centrifugal separator and the absorbance of tellurium(IV) complex in TBP is measured at 400 m$\mu$.

## Results and Discussion

**Absorption Spectrum of Tellurium(IV) Complex in TBP.**—Hydrochloric acid solutions containing 20, 50 and 100 $\gamma$ of tellurium per ml. were prepared, and to its 10 ml. portion were added 5 ml. of potassium thiocyanate solution and 4 ml. of thiourea solution. The

1) E. A. Golubtsova, *Zavodskaya Lab.*, **16**, 623 (1950).
2) M. Inarida, *J. Chem. Soc. Japan, Pure Chem. Sec. (Nippon Kagaku Zasshi)*, **79**, 968 (1958).
3) M. W. Hanson, W. C. Dradbury and J. K. Corlton, *Anal. Chem.*, **29**, 490 (1957).
4) W. Nielsch and G. Böltz, *Z. Metallkunde*, **45**, 380 (1954).
5) H. Goto and Y. Kakita, *Japan Analyst (Bunseki Kagaku)*, **3**, 299 (1958).
6) K. Geiersberget and A. Durst, *Z. anal. Chem.*, **135**, 11 (1952).
7) E. G. Brown, *Analyst*, **79**, 50 (1954).
8) S. Hikime, H. Yoshida and Y. Uzumasa, *Japan Analyst (Bunseki Kagaku)*, **8**, 531 (1959).
9) K. Alcock, S. S. Grimley, T. V. Healy, J. Kennedy and H. A. C. McKay, *Trans. Faraday Soc.*, **52**, 39 (1956).

solution was made pH 1.0 with hydrochloric acid and made up to 20 ml. with 0.1 N hydrochloric acid. After 20 min., 20 ml. of TBP was added to the solution, and this mixture was shaken for 2 min. so that the tellurium complex could be extracted to the TBP phase thoroughly. The TBP phase was colored more deeply yellow than that obtained by the use of thiourea solution alone. This coloration was stable at least for 2.5 hr. The absorbance of the solution was measured spectrophotometrically over the range of wavelength, 330 m$\mu$ to 560 m$\mu$. The results are shown in Fig. 1.

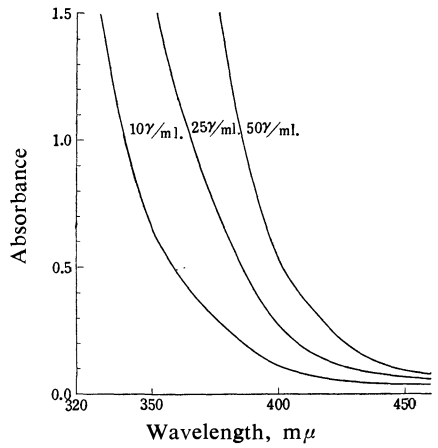



Fig. 1. Absorption curves of tellurium(IV) complex in TBP. KSCN 5 ml., $(NH_2)_2CS$ 4 ml., pH 1, total volume 20 ml., TBP 20 ml.

As shown in Fig. 1, tellurium complex in TBP has strong absorption in ultraviolet region. Although these absorption spectra are similar to those of tellurium-thiourea complex in dilute hydrochloric acid solution, absorbances of the former are several times greater than those of the latter.

**Effect of Potassium Thiocyanate.**—Varying amounts of potassium thiocyanate solution were added to solutions each containing 500 $\gamma$ of tellurium and 4 ml. of thiourea solution. The pH of the solutions was kept about 1. The final volume of each solution was then made up to 20 ml.

Table I shows the absorbance of these solutions as a function of the amount of the reagent added. Constant absorbances were obtained adding more than 2 ml. of the reagent solution; one gram of the reagent, therefore, is sufficient for extracting thoroughly 500 $\gamma$ of tellurium. To refer the effect of potassium thiocyanate on the extraction of tellurium, the amounts of tellurium remaining in the aqueous phase were determined also by thiourea method and the percentages of tellurium extracted were calculated from those values. The results agree with those obtained by the absorbance measurements.

In the absence of potassium thiocyanate, tellurium complex is not extracted with TBP under the experimental condition. However when potassium thiocyanate exists together with thiourea in the tellurium solution, percentage of the extracted tellurium increases with increasing amount of the reagent added, and the tellurium complex is extracted almost completely with TBP, when more than 1 ml. of the reagent is added.

TABLE I. EFFECT OF POTASSIUM THIOCYANATE

| KSCN solution ml. | Absorbance of TBP-phase at 400 m$\mu$ | Te | | |
|---|---|---|---|---|
| | | Taken $\gamma$ | Found, aq. phase $\gamma$ | Extracted % |
| — | 0.000 | 500 | 497 | 0.6 |
| 0.01* | 0.004 | 500 | 479 | 4.8 |
| 0.02* | 0.013 | 500 | 450 | 10.0 |
| 0.05* | 0.037 | 500 | 398 | 20.4 |
| 0.5 | 0.221 | 500 | 47 | 90.6 |
| 1.0 | 0.262 | 500 | 7.5 | 98.5 |
| 2.0 | 0.278 | 500 | 0.5 | 99.9 |
| 4.0 | 0.279 | 500 | 0.5 | 99.9 |
| 8.0 | 0.284 | 500 | 0.0 | 100 |

Thiourea solution 4 ml., pH 1, total volume 20 ml., TBP 20 ml.
* Added after dilution of the stock solution.

**Effect of Thiourea.**—Since the amount of thiourea also affects the color development of tellurium complex in dilute hydrochloric acid solution, several experiments were carried out to determine its effect. Measurements of the absorbance of the TBP phase showed that 80 mg. of thiourea is sufficient for complexing thoroughly 500 $\gamma$ of tellurium and absorbances are constant beyond this concentration of thiourea.

In order to ensure the results, the amounts of tellurium remaining in the aqueous phase were determined and the percentage of tellurium extracted into TBP phase was calculated. (Table II) The results agree with those obtained by the absorbance measurements.

TABLE II. EFFECT OF THIOUREA

| Thiourea solution ml. | Absorbance of TBP-phase at 400 m$\mu$ | Te | | |
|---|---|---|---|---|
| | | Taken $\gamma$ | Found, aq. phase $\gamma$ | Extracted % |
| — | 0.002 | 500 | 420 | 16 |
| 0.5 | 0.071 | 500 | 289 | 42 |
| 1 | 0.277 | 500 | 2 | 99.6 |
| 2 | 0.278 | 500 | 0 | 100 |
| 3 | 0.276 | 500 | 4 | 99.2 |
| 5 | 0.277 | 500 | 0 | 100 |
| 8 | 0.276 | 500 | 2 | 99.6 |

Potassium thiocyanate solution 2 ml., pH 1, total volume 20 ml., TBP 20 ml.

**Effect of pH.**—In view of possible decomposion of either potassium thiocyanate or thiourea in an acid solution, experiments were carried out in low acidity solutions. A series of solutions were prepared, containing 500 $\gamma$ of tellurium, 2 ml. of potassium thiocyanate solution and 2 ml. of thiourea sulution. The pH values of these solutions were controlled around 1 with hydrochloric acid and similarly extracted with TBP. Results are shown in Table III. The absorbance at 400 m$\mu$ remains constant in the range from pH 0.6 to 1.7, indicating that tellurium complex is extracted with TBP so that it is possibe to extract and determine tellurium over this pH range.

TABLE III. EFFECT OF pH

| pH values before extraction | Absorbance of TBP-phase at 400 m$\mu$ | Te | |
|---|---|---|---|
| | | Found, aq. phase $\gamma$ | Extracted % |
| 0.34 | 0.262 | 2 | 99.6 |
| 0.6 | 0.275 | 0 | 100 |
| 1.0 | 0.278 | 0 | 100 |
| 1.3 | 0.277 | 1 | 99.8 |
| 1.7 | 0.275 | 2 | 99.6 |

Te 500 $\gamma$, KSCN soln. 2 ml., thiourea soln. 2 ml., total volume. 2 ml., TBP 20 ml.

**Stability of Color.**—The yellow color of tellurium complex extracted into TBP phase is very stable and is several times as deep as that of the complex formed with thiourea in dilute hydrochloric acid solution. Four solutions containing 5, 12.5, 25 and 50 $\gamma$ of tellurium per milliliter respectively were prepared and, after extraction, the stability of the color of each solution was tested. No changes were found in the absorbance after exposure in diffused light for 150 min.

**Recommended Procedure.**—To 15 ml. of a sample solution (ca. 0.1 N hydrochloric acid solution containing up to 500 $\gamma$ of tellurium), add 2 ml. of potassium thiocyanate solutions (500 g./l.) and 2 ml. of thiourea solution (80 g./l.). Adjust pH to 1, and make the final volume of the solution to 20 ml. with 0.1 N hydrochloric acid. After 20 min. add 20 ml. of TBP to the solution, and shake for 2 min.

When the TBP phase separates from the aqueous phase, centrifuge the former for 2 min. The absorbance of TBP phase is measured at 400 m$\mu$ with a spectrophotometer with 10 mm. cells.

**Calibration Curves.**—Prior to the determination of tellurium in the sample solution, calibration curves were prepared with a series of solutions containing 1 to 75 $\gamma$ of tellurium per milliliter. The curves are shown in Fig. 2.

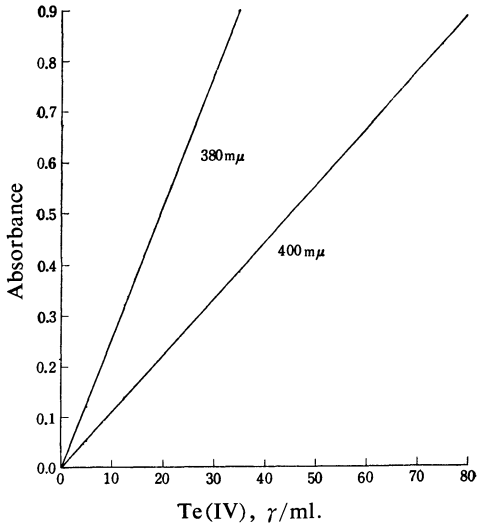



Fig. 2. Calibration curve for tellurium.

TABLE IV. ANALYSIS OF SAMPLES OF TELLURIUM

| Absorbance vs. blanc | Te | | Difference $\gamma$ |
|---|---|---|---|
| | added $\gamma$ | found $\gamma$ | |
| 0.277 | 250 | 249 | − 1 |
| 0.275 | 〃 | 247 | − 3 |
| 0.277 | 〃 | 249 | − 1 |
| 0.279 | 〃 | 251 | 1 |
| 0.278 | 〃 | 250 | 0 |
| 0.270 | 〃 | 243 | − 7 |
| 0.282 | 〃 | 254 | 4 |
| 0.285 | 〃 | 257 | 7 |
| 0.273 | 〃 | 247 | − 3 |
| 0.279 | 〃 | 251 | 1 |
| | mean | 249.7 | − 0.2 |
| 0.552 | 500 | 497 | − 3 |
| 0.553 | 〃 | 498 | − 2 |
| 0.570 | 〃 | 514 | 14 |
| 0.556 | 〃 | 501 | 1 |
| 0.539 | 〃 | 485 | −15 |
| 0.544 | 〃 | 490 | −10 |
| 0.546 | 〃 | 492 | − 8 |
| 0.552 | 〃 | 497 | − 3 |
| 0.564 | 〃 | 508 | 8 |
| 0.558 | 〃 | 503 | 3 |
| 0.545 | 〃 | 491 | − 9 |
| 0.548 | 〃 | 494 | − 6 |
| 0.554 | 〃 | 499 | − 1 |
| 0.546 | 〃 | 492 | − 8 |
| 0.565 | 〃 | 509 | 9 |
| 0.554 | 〃 | 499 | − 1 |
| 0.548 | 〃 | 494 | − 6 |
| 0.558 | 〃 | 503 | 3 |
| 0.564 | 〃 | 508 | 8 |
| 0.546 | 〃 | 492 | − 8 |
| | mean | 498.3 | − 1.7 |

TABLE V. INTERFERENCE STUDY OF DIVERSE IONS ON ABSORBANCE OBTAINED WITH 25 p.p.m. OF TELLURIUM

| Ions present | Added as | Concentration p.p.m. | Difference of absorbance ×1000 | Tolerance p.p.m. |
|---|---|---|---|---|
| $Bi^{3+}$ | $Bi(NO_3)_3$ | 2.5 | 21 | 0 |
| | | 5.0 | 36 | |
| $Cu^{2+}$ | $CuSO_4$ | 10 | 0 | 10 |
| | | 25 | 7 | |
| | | 100 | 34 | |
| $Ni^{2+}$ | $Ni(NO_3)_2$ | 50 | 0 | 50 |
| | | 125 | 4 | |
| | | 250 | 16 | |
| $Te^{6+}$ | $Na_2TeO_4$ | 75 | 6 | 75 |
| $Co^{2+}$ | $CoCl_2$ | 50 | − 2 | 500 |
| | | 500 | − 3 | |
| $Fe^{3+}$ | $FeCl_3$ | 0.3 | 0 | 0.3 |
| | | 0.9 | 20 | |
| $Cr^{3+}$ | $CrCl_3$ | 50 | 2 | 50 |
| | | 250 | 7 | |
| $Hg^{2+}$ | $HgCl_2$ | 400 | 1 | large excess |
| $Zn^{2+}$ | $ZnCl_2$ | 50 | 0 | 500 |
| | | 500 | − 3 | |
| $Cd^{2+}$ | $CdCl_2$ | 500 | 0 | large excess |
| $Mn^{2+}$ | $MnSO_4$ | 250 | 0 | 〃 |
| $Al^{3+}$ | $AlCl_3$ | 500 | 0 | 〃 |
| $Mg^{2+}$ | $MgCl_2$ | 50 | 0 | 〃 |
| | | 500 | − 2 | |
| $PO_4^{3-}$ | $H_3PO_4$ | 1400 | 0 | 〃 |
| $SO_4^{2-}$ | $H_2SO_4$ | 1250 | − 2 | 〃 |
| $NO_3^-$ | $HNO_3$ | 500 | 0 | 〃 |
| $WO_4^{2-}$ | $Na_2WO_4$ | 50 | − 1 | 50 |
| | | 500 | −45 | |
| $VO_3^-$ | $NH_4VO_3$ | 10 | 3 | 10 |
| | | 50 | 17 | |
| $CrO_4^{2-}$ | $K_2CrO_4$ | 50 | −54 | 0 |

A linear relationship exists between the absorbance and the tellurium concentration over the range investigated. In many respect, however, measurement at 400 mμ is preferable to that at 380 mμ.

**Reproducibility.**—Several samples were prepared separately in the same way as unknown samples and analysed by the recommended procedure. As shown in Table IV, the reproducibility of this procedure is satisfactory.

**Effect of Diverse Ions.**—Separate tests were made to elucidate the interference of various cations as well as anions on the tellurium determination. The results are shown in Table V. In this table, by "tolerance" is meant the value that gives no significant interference. Under these values the difference between the absorbance of tellurium of the test solution and that of the standard containing no other ions is less than 3%.

A pre-extraction test was also made in which a previous attempt to remove $Bi^{3+}$, $Cu^{2+}$, $Ni^{2+}$ and $Fe^{3+}$ was made, since these ions were considered to have relatively larger interfering behavior. In this experiment, only potassium thiocyanate and no thiourea was added first to the solution of tellurium containing these ions. After a single extraction with the same volume of TBP at pH 1, the organic layer was separated off and the remaining aqueous solution was used to determine the amount of tellurium. Some more potassium thiocyanate and also a necessary amount of thiourea were added to this aqueous solution; tellurium was shaken out to the TBP layer according to the recommended procedure, and then determined spectrophotometrically. As shown in Table VI, a single pre-extraction treatment is not sufficient to give a satisfactory value for tellurium, since about 6% positive error results in the absorbance of tellurium. This means that even after the pre-extraction, there remain some fractions of these ions which are transferred to the TBP layer when the recommended procedure is applied. In the single pre-extraction, $Cu^{2+}$ and $Ni^{2+}$ seems to be extracted only partly although $Fe^{3+}$ and $Bi^{3+}$ may be extracted fairly well. It would be possible, however, to eliminate them to such an extent that they give little effect on the determination

of tellurium, if a better experimental condition were further sought.

TABLE VI. PRE-EXTRACTION TEST

| Te taken p.p.m. | Ions added p.p.m. | Absorbance at 400 mμ in TBP |
|---|---|---|
| 25 | — | 0.139 |
| 25 | $Bi^{3+}$ 5, $Cu^{2+}$ 25, $Ni^{2+}$ 50, $Fe^{3+}$ 1.3 | 0.147 |
| — | $Bi^{3+}$ 5, $Cu^{2+}$ 25, $Ni^{2+}$ 50, $Fe^{3+}$ 1.3 | 0.006 |

## Summary

Spectrophotometric determination of tellurium-(IV) by means of extraction with 100% TBP was studied. Tellurium forms yellow complex, as seen in the literature, with thiourea in a dilute hydrochloric acid solution, and the complex is extracted into TBP whenever potassium thiocyanate is present in excess in the solution.

Conditions on the extraction and the determination of tellurium were examined. It was found that addition of 2 ml. of thiourea solution (80 g./l.) and 2 ml. of potassium thiocyanate solution (500 g./l.) to the sample solution is enough to extract 1 to 500 γ of tellurium per 20 ml. from the dilute hydrochloric acid solution with 20 ml. TBP. Tellurium complex was extracted thoroughly with TBP at pH 1. For the determination of tellurium, the absorbance of the TBP phase was measured spectrophotometrically at 400 mμ.

The effect of the diverse ions on the absorbance of tellurium complex was examined and also pre-extraction test on the removal of interference ions was carried out.

The author wishes to express his grateful thanks to Professor Y. Uzumasa for his kind encouragement and discussion and to Mr. H. Yoshida for technical assistance in this study.

*Department of Chemistry*
*Faculty of Science*
*Hokkaido University*
*Sapporo*

# *A Rapid Method for Determining Fission Products Contained in Waters Using an Ion Exchanger**

By Hiroyuki TSUBOTA and Yasushi KITANO

(Received November 9, 1959)

It is essential to select a proper elutriant in order to separate many constituents in solutions by ion exchange resins. Many elutriants have been used by various researchers[1-7]; among them citrate buffer is used most extensively. However, most of these methods are time-consuming, and the preparation and preservation of elutriants are sometimes rather difficult. Moreover, it is often troublesome to treat the effluent for further chemical or radiochemical examinations. This paper deals with a procedure for rapid and easy separation of alkali, alkaline earth and rare earth elements contained in mixed fission products, by using the formate buffer solution.

A good elutriant should have the following characteristics: 1) There must be complete separation of elements; degree of separation can be expected from the complexity constants between cations in a sample and the anion of the complexing agent used as an elutriant[2,8,9]. When the complexity constants of various cations in the sample differ considerably from each other, these cations can be eluted separately

* A part of this work was done at Kobe University, Kobe.

1) R. H. Diamond, K. Street, Jr. and G. T. Seaborg, *J. Am. Chem. Soc.*, 76, 1461 (1954).

2) E. R. Tompkins, J. X. Khym and W. E. Cohn, ibid., 69, 2769 (1947).

3) W. E. Cohn, G. W. Parker and E. R. Tompkins, *Nucleonics*, 3, No. 5. 22 (1948).

4) K. Kimura, E. Minami, M. Honda et al., *Japan Analyst (Bunseki Kagaku)*, 3, 335 (1954).

5) B. H. Ketelle and G. E. Boyd, *J. Am. Chem. Soc.* 73, 1862 (1951).

6) E. C. Freiling and L. R. Bunney, ibid., 76, 1021 (1954).

7) R. C. Vickery, *J. Chem. Soc.*, 1952, 4357.

8) F. H. Spedding et al., *J. Am. Chem. Soc.*, 69, 2777 (1947).

9) E. R. Tompkins and S. W. Mayer, ibid., 69, 2859 (1947).

as the elutriant passes through a column of ion exchanger. 2) Buffer solutions having various pH values should be prepared easily and should be stable. 3) The reagent must be vaporized easily and completely because it is essential that all coexisting materials, other than a compound of the element in question, be removed before radioactive assay. 4) Besides these conditions, the reagents of high quality can be obtained at low cost. From the result of this experiment a formate buffer solution was proved to satisfy these conditions* and to be the best elutriant.

## Experimental

**Elutriants.**—The following elutriants were used for the present experiment:

(A) Hydrochloric acid: 0.2 N.

(B) Oxalic acid: 0.5%.

(C) A buffer solution of 1 M formic acid and 1 M ammonium formate (a formate buffer solution): As shown in Fig. 1, the buffer solutions having various pH values can be prepared by mixing 1 M formic acid solution with varying quantities of 1 M ammonium formate solution.

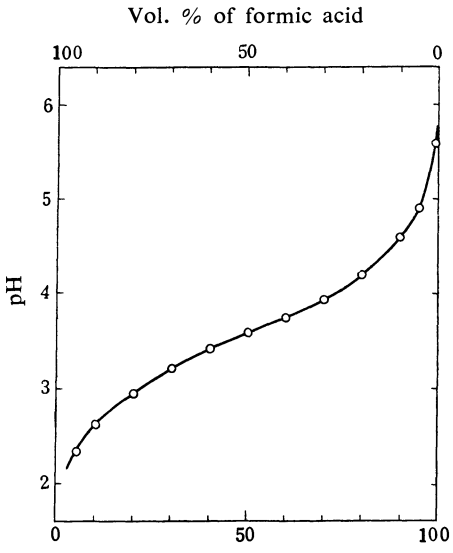



Fig. 1. pH of the buffer solution prepared by mixing 1 M formic acid and 1 M ammonium formate solution.

**Columns.**—Two columns were used:

No. 1, Dowex 50, X8, 100~150 mesh, 1.0×8.0 cm., $H^+$-saturated resin, (exchange capasity, ca. 14 meq.).

No. 2, Dowex 50, X8, 200~250mesh, 1.0×20 cm., $H^+$-saturated resin, (exchange capacity, ca. 35 meq.).

**Flow Rate.**—0.3~0.4 ml./min.

**Sample Solution of Mixed Fission Products.**—The fission products mixture used in this experiment had been supplied from ORNL, U. S. A., and was three years old. Nitric acid was added to the fission product solution, and was evaporated on a water bath. More nitric acid was added to the residue. And 0.1~1 ml. of the nitric acid solution (concentration, approx. 10 μc/ml.) were diluted with 5~10 ml. of 0.2 N hydrochloric acid. This hydrochloric acid solution was used as a sample solution.

**Procedure.**—(A) The sample solution is passed through the column No. 1.

(B) Ruthenium is eluted with about 20 ml. of 0.2 N hydrochloric acid*,[4]. The column is washed by passing 10~20 ml. of distilled water.

(C) Next, zirconium, niobium and uranium are eluted together by passing 50~70 ml. of 0.5% oxalic acid[3,4]. The column is washed with 10~20 ml. of distilled water.

(D) When the formate buffer solution of pH 3.2 (1 M formic acid: 1 M ammonium formate=7:3, in volume) has passed through the column, cesium is eluted in the effluent of a quantity between 50 and 110 ml. Thymol blue is used as indicator because cesium begins to be eluted after the thymol blue indicator in the effluent changes to yellow.

(E) When the formate buffer solution of pH

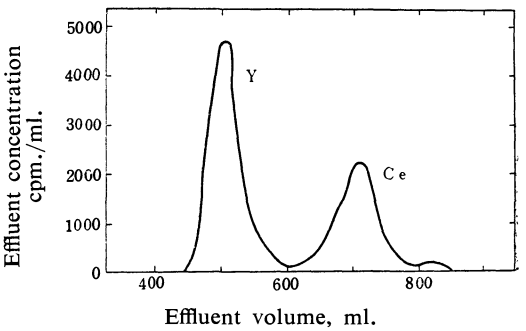



Fig. 2. Separation of rare earth elements.
Column: No. 2.
Elutriant: the buffer solution, pH 3.8.
Flow rate: 0.2~0.3 ml./min.

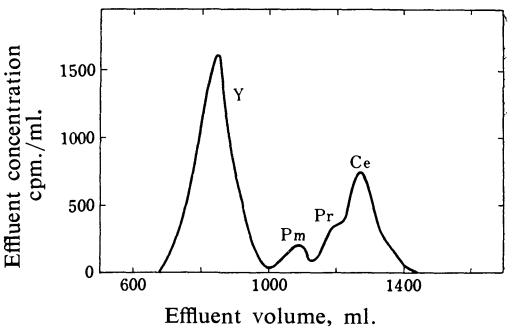



Fig. 3. Separation of rare earth elements.
Column: No. 2.
Elutriant: the buffer solution, pH 3.6.
Flow rate: 0.2~0.3 ml./min.

* They will be discussed in detail elsewhere.

* If I and Te are present, they are eluted together with Ru.

3.8 (1 M formic acid : 1 M ammonium formate=4 : 6, in volume) has passed through the column, all rare earth elements are simultaneously eluted in a fraction between 50 and 170 ml. of the effluent. After this fraction of the effluent has been vaporized, the residue containing rare earth elements is dissolved in a small amount of dilute hydrochloric acid. The resultant solution is passed through the column No. 2, and rare earth elements are adsorbed on it. When the formate buffer solution having pH 3.8 has passed, rare earth elements are separated into yttrium and cerium groups, as shown in Fig. 2. When the formate buffer solution having pH 3.6 (1 M formic acid : 1 M ammonium formate=1 : 1) is used, cerium group elements are further separated into promethium, praseodymium and cerium fractions, as shown in Fig. 3.

(F) After ruthenium, zirconium, niobium and cesium and rare earth elements have been removed, strontium is eluted by passing about 120 ml. of the formate buffer solution of pH 4.2 (1 M formic acid : 1 M ammonium formate=2 : 8) through the column No. 1.

The method is summarized in Table I, and the results are shown in Fig. 4.

**Radioactibity Measurement.** — The effluent is divided into 5 ml.-fractions by means of a fraction collector, and 1~2 ml. of each fraction is transferred into a counting dish. Evaporation and sublimation of the effluent is done by heating the counting dish with an infrared lamp and an electric heater. After the formate is removed completely, the radioactivity is measured by using a G. M. counter. The nuclides can be identified from the decay curves and the absorption curves.

TABLE I. METHOD FOR SEPARATION OF FISSION PRODUCTS WITH CATION EXCHANGE RESIN

Sample (in dil. HCl)

↓

Column No. 1

| | Elutriant | Elements eluted |
|---|---|---|
| 0.2 N HCl | 20 ml. | Ru |
| (washed with water) | | |
| 0.5% oxalic acid | 50~70 ml. | U, Pu, Zr, Nb |
| the buffer solution, pH 3.2 | 110 ml. | Cs (found in a effluent intermediate between 50 and 110 ml.) |
| the buffer solution, pH 3.8 | 170 ml. | Rare earth elements (found in a effluent between 50 and 170 ml.) |
| the buffer solution, pH 4.2 | 100 ml. | Sr |
| 2 M ammonium formate solution | 100 ml. | Ba |

Rare earths fraction
(dissolved in dilute HCl after evaporation)

↓

Column No. 2

1) Y- and Ce-groups can be separated with the buffer solution, pH 3.8.
2) When the buffer solution having pH 3.6 is used, the elements of Ce-group can be separated partially.
3) To separate exactly, use the buffer solution having pH 3.3~3.4 or use a longer column.

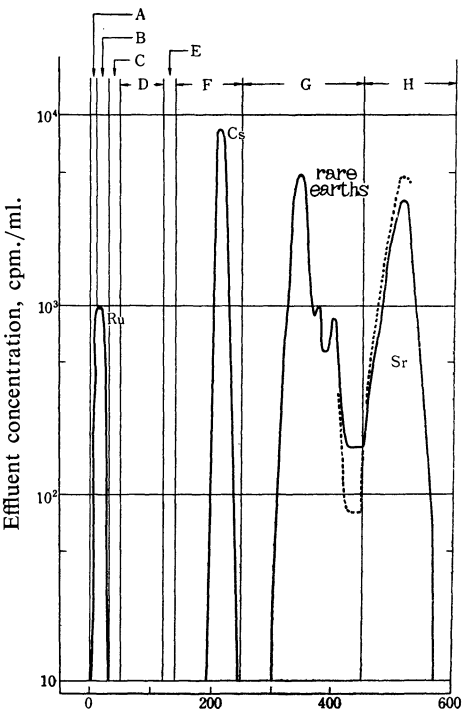



Fig. 4. Separation of fission products.
Column: No. 1.
Influents: A sample solution, B 0.2 N HCl, C $H_2O$, D 0.5% oxalic acid, E $H_2O$, F the buffer solution, pH 3.2, G the buffer solution, pH 3.8, H the buffer solution, pH 4.2.
Flow rate: 0.33 ml./min.
The curve in dotted line shows the radioactivity of each fraction 60 hours after the original measurements.

## Discussion

**Elution of Cesium.**—Up to the present time, the elution of cesium has been conducted with hydrochloric acid or citrate buffer solution[10], but neither of these elutriants is satisfactory for the following reasons. When cesium is completely eluted with hydrochloric acid from the column, the adsorption band of strontium moves downward, and consequently, when a further separation of rare earth and alkaline earth elements is to be carried out, a part of

10) M. Honda, Y. Sasaki and H. Natsume, *Japan Analyst (Bunseki Kagaku)*, **4**, 240 (1955).

strontium is eluted together with the rare earth elements and the separation is incomplete. When a citrate buffer solution is used as the elutriant, the process is complicated because, to avoid the uncertainty of separating rare earth and alkaline earth elements, cesium and rare earth elements must be eluted together, and afterwards cesium and rare earth elements must be separated by resorption and chromatographic elution. Finally, it is very difficut to remove citrate from the effluent. When the formate buffer solution having a pH less than 3.4 is used, the adsorption bands of both rare earth and alkaline earth elements never move downward. Therefore cesium alone can be eluted completely by using the formate buffer solution having pH 3.2, as shown in Fig. 5. Ammonium formate and formic acid sublime easily and completely. Therefore, when the effluent containing cesium is evaporated, and an adequate acid is added to the residue and re-evaporated, pure and carrier-free cesium salts can be obtained.

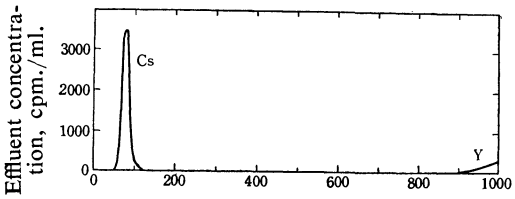



Fig. 5. Elution curve of Cs.
Column: No. 1.
Elutriant: the buffer solution, pH 3.3.
Flow rate: 0.40 ml./min.

**Separation of Rare Earth and Alkaline Earth Elements.**—As shown in Fig. 4, a fairly high radioactivity is found in the effluent intermediate between yttrium and strontium fraction. It is, however, possible to conclude that the radioactivity of this fraction is not due to the incomplete separation of rare earth from alkaline earth elements, but to the elution of $^{90}Y$ coming from $^{90}Sr$ adsorped on the column from the decay of this fraction.

When the formate buffer solution is used, lanthanum is to be eluted last among all rare earth elements to be eluted in the effluent. In other words, amoung rare earth elements lanthanum is the most difficult element to be separated from alkaline earth elements. The solution of fission products used in this experiment is not fresh; hence, it does not contain $^{140}La$ having a half-life of 40 hr. Complete separation of lanthanum from strontium is essential if the sample contains fresh fission products. For this purpose, separation of the two elements was examined by using nonradioactive strontium and lanthanum. One meq. of strontium and 1 meq. of lanthanum are passed through the column No. 1 and are adsorbed, and they are eluted by the formate buffer solution as described above. The effluent is divided into 5 ml.-fractions, and lanthanum and strontium in each fraction are determined by a semi-quantitative method, and the result is obtained as shown in Fig. 6. Fig. 6 also shows the result of 1 meq. of strontium and 1 meq. of mixed rare earth elements, viz., lanthanum, neodymium, praseodymium and cerium. From the figure, it can be seen that strontium is easily and completely separated from lanthanum and also from other rare earth elements by using column No. 1 with the buffer solution having pH 3.8. It can be concluded from this experiment that by using the formate buffer solution, rare earth elements and alkaline earth elements can be separately eluted even when fairly large amounts of carriers are present in the sample to be analysed.

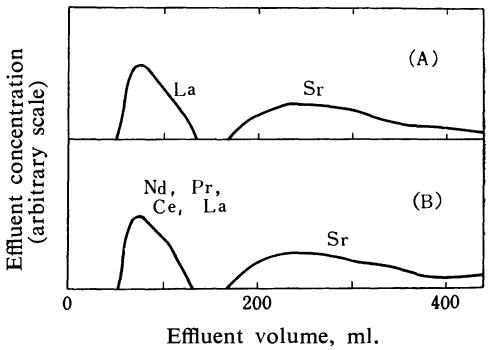



Fig. 6. (A) Separation of La-Sr, (B) Separation of rare earth elements-Sr.
Column: No. 1.
Elutriant: the buffer solution, pH 3.8.
Flow rate: (A) 0.24 ml./min., (B) 0.30 ml./min.

**Separation of Rare Earth Elements.** — Since fresh fission products contain various kinds of the rare earth element, the authors conducted separation of rare earth elements as follows:

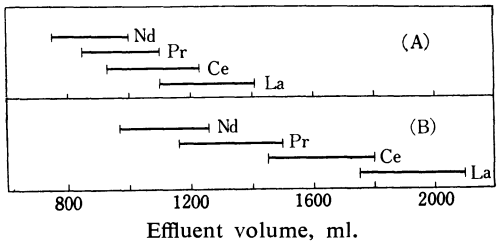



Fig. 7. Separation of rare earth elements.
Column: No. 2.
Elutriant: the buffer solution, (A) pH 3.6, (B) pH 3.4.
Flow rate: 0.25 ml./min.

a mixture of 1 meq. each of neodymium, praseodymium, cerium and lanthanum is adsorbed on column No. 2; the rare earth elements are eluted with the formate buffer solution. The effluent is divided into 10 ml.-fractions, and the elements in each fraction are determined. As shown in Fig. 7, the separation is incomplete when the formate buffer solution having pH 3.6 is used, but when the buffer solution of pH 3.4 is used the separation becomes rather complete. This procedure will be applied for the purification of rare earth elements.

**Separation of Strontium and Barium.**—With the same purpose as described in the preceding section, the authors carried out separation of strontium and barium by adsorbing 1 meq. of strontium and of barium on the column No. 1. As shown in Fig. 8, barium can be separated from strontium very easily and completely.

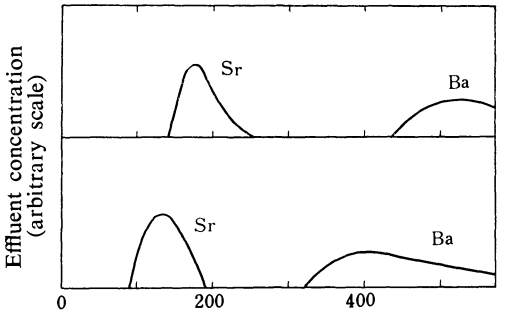



Fig. 8. Separation of Sr-Ba.
Column: No. 1.
Elutriant: the buffer solution, (A) pH 4.0, (B) pH 4.2.
Flow rate: (A) 0.40 ml./min., (B) 0.42 ml./min.

**Separation of Fission Products from Iron.**—To determine exactly fission products in natural waters by ion exchange resin, it is essential that the coexisting elements or carriers must be separated from fission products. Sodium, potassium, magnesium, calcium, ferric and aluminum ions are often found in natural waters, and barium and ferric ions are used as carriers. By using the formate buffer solution fission products can be separated easily from the other metals such as alkali, alkaline earth elements and iron. The separation of alkali and alkaline earth elements will be reported eleswhere[11], and the separation of

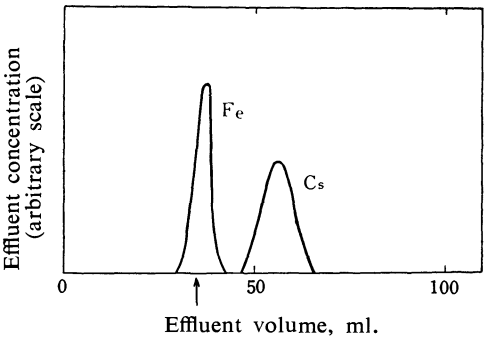



Fig. 9. Separation of Fe(3 meq.) from Cs.
Column: Dowex 50, X8, 1.1×10 cm., (100~150 mesh) $H^+$-saturated resin.
Elutriant: the buffer solution, pH 3.2.
Flow rate: 2.0 ml./min.
Arrow indicates the point at which thymol blue indicator changes to yellow from red.

iron and fission products is reported here; this is particularly important for the determination of fission products in natural waters. As shown in Fig. 9, the ferric ion is completely eluted before thymol blue indicator in the effluent changes from red to yellow. By using the buffer solution of pH 3.2, the ferric ion can be eluted long before cesium is eluted.

## Summary

The essential point of this method is the use of the formate buffer solution. This method would be used for the analysis of fission products in natural waters and for the preparation of pure and carrier-free radioactive elements from mixed fission products.

The authors express their sincere appreciation to Professor Yasuo Miyake of Tokyo University of Education and Mr. Masami Izawa of National Institute of Radiological Sciences for their helpful advice and encouragement throughout this work.

*National Institute of Radiological Sciences*
*Kurosuna-machi, Chiba (H. T.)*
*Water Research Laboratory*
*Faculty of Science*
*Nagoya University*
*Chigusa-ku, Nagoya (Y. K.)*

11) H. Tsubota and Y. Kitano, This Bulletin, 33, 770 (1960).

# *A Rapid Method for Determining Alkali and Alkaline Earth Elements Using an Ion Exchanger**

By Hiroyuki TSUBOTA and Yasushi KITANO

(Received November 9, 1959)

The present authors previously reported[1] that fission products can be separately eluted more easily and rapidly by using a buffer solution of formic acid and ammonium formate as the elutriant than by using any other elutriants. As reported in that paper, even when fission products in a sample coexist with large amounts of other elements or carriers, they can be completely separated.

Many researchers have separated alkali metals[2-7] and alkaline earth elements[8-10] by using an ion exchanger. They have tried to analyse a mixture of alkali and alkaline earth elements containing other metal ions by using an ion exchange resin; moreover, separation of sodium, potassium, magnesium and calcium ions, which are abundant in nature, has been successful[6,11,12]. They did not, however, include in their experiments such rare elements as cesium or barium. Without including the cesium ion in their experiments, some researchers have stated that univalent ions and divalent ions can easily be separated with an ion exchanger[13,14]. However, the separation between cesium and magnesium ions would be difficult because the cesium ion is eluted last among alkali metals and the magnesium ion is eluted first among alkaline earth elements. The authors conducted systematic experiments on these elements with an ion exchanger and finally succeeded by using the buffer solution of 1 M formic acid and 1 M ammonium formate (the formate buffer solution).

## Experimental and Discussion

**Selection of an Elutriant.**—Separation of alkali metals from alkaline earth metals has been conducted by using hydrochloric acid as an elutriant, when cesium was not included. To find out whether efficient separation can be realized when cesium is present, the following experiment was carried out. 0.1~1 meq. of potassium, cesium and magnesium ions, respectively, were mixed and passed into the column, Dowex 50, X12, 200~250 mesh, 1.1×15 cm., $H^+$-saturated resin, (exchange capacity, ca. 37 meq.), and eluted chromatographically with 1 N hydrochloric acid or 0.5 N hydrochloric acid at the flow rate of 1 ml./min. The effluent was divided into 10 ml. fractions. After evaporation of the fractions potassium and cesium in each fraction were determined from chloride content using silver nitrate standard solution and fluorescent indicator, and magnesium was determined by EDTA standard solution and Eriochrom Black T(EBT) indicator after the pH of the fractions had been adjusted to 10 with ammonium hydroxide.

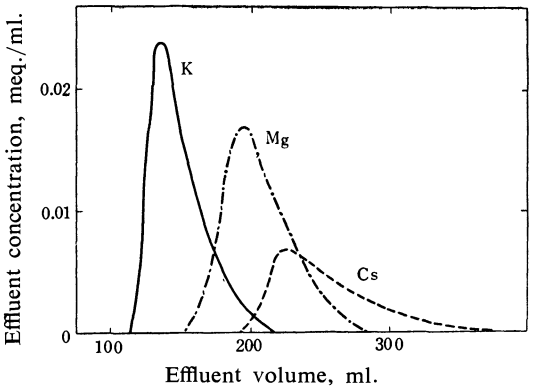



Fig. 1. Elution curves of $K^+$, $Cs^+$ and $Mg^{2+}$ with HCl.
Column: Dowex 50, X12, 200~250 mesh, 1.1×15 cm.
$H^+$-saturated resin.
Elutriant: 1.0 N HCl.
Flow rate: 1.0 ml./min.

* A part of this work was done at Kobe University, Kobe.

1) H. Tsubota and Y. Kitano, This Bulletin, 33, 765 (1960).
2) W. E. Cohn and H. W. Kohn, *J. Am. Chem. Soc.*, 70, 1986 (1948).
3) G. Kayas, *Compt. rend.*, 228, 1002 (1949).
4) G. Kayas, *J. Chim. Phys.*, 47, 408 (1950).
5) H. Okuno, M. Honda and T. Ishimori, *Japan Analyst (Bunseki Kagaku)*, 2, 228 (1953).
6) J. Beukenkamp and W. Rieman III, *Anal. Chem.*, 22, 582 (1950).
7) W. Buser, *Helv. Chim. Acta*, 34, 1635 (1951).
8) D. N. Campbell and C. T. Kenner, *Anal. Chem.*, 26, 560 (1954).
9) M. Lerner and W, Rieman III, ibid., 26, 610 (1954).
10) M. Honda, *Japan Analyst (Bunseki Kagaku)*, 3, 132 (1954).
11) H. Kakihana, *J. Chem. Soc. Japan, Pure Chem. Soc. (Nippon Kagaku Zasshi)*, 72, 203 (1951).
12) R. C. Sweet, W. Rieman III and J. Beukenkamp, *Anal Chem.*, 24, 952 (1952).
13) O. Samuelson, "Ion Exchangers in Analytical Chemistry", John Wiley & Sons, Inc., N. Y. (1954), p. 35.
14) M. Honda, *J. Chem. Soc. Japan, Pure Chem. Sec. (Nippon Kagaku Zasshi)*, 71, 118 (1950).

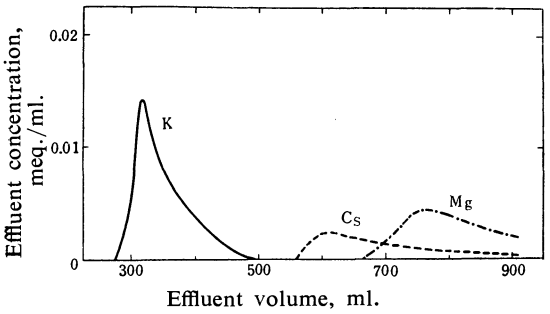



Fig. 2. Elution curves of $K^+$, $Cs^+$ and $Mg^{2+}$ with HCl.
Column: Dowex 50, X12, 200~250 mesh, 1.1×15 cm.
$H^+$-saturated resin.
Elutriant: 0.5 N HCl.
Flow rate: 1.0 ml./min.

When 1 N hydrochloric acid is used, potassium and cesium can be partially separated from each other, but magnesium and cesium can not be separated at all although magnesium begins to be eluted shortly before the elution of cesium (Fig. 1). When 0.5 N hydrochloric acid is used, potassium and cesium can be separated completely, but cesium and magnesium can not be separated although cesium begins to be eluted shortly before the elution of magnesium (Fig. 2). Based on these results, it can be concluded that, when cesium and magnesium are to be separated completely, a much longer column and a larger amount of a very dilute hydrochloric acid must be used. In other words, hydrochloric acid is not a practical elutriant for separating cesium from magnesium. The effect of the concentration of hydrochloric acid on the elution of magnesium, as seen in Figs. 1 and 2, can be understood by the fact that the magnesium ion forms $MgCl^+$ complex ion with the chloride ion. Therefore, in order to separate magnesium from cesium, it is essential to use an acid or salts other than chloride. As previously reported[1], when a formate buffer solution was used as the elutriant, cesium and magnesium were completely separated. This elutriant could be prepared and preserved easily and after-treatment of the effluent was done easily because ammonium formate could be sublimed easily and completely. Thus, it was decided to use the formate buffer solution as the elutriant, and separation of elements by using the buffer solution was examined.

**Examination of Methods for Analyzing Alkali and Alkaline Earth Elements.** — (A) *Alkali metals.*—The following two methods were used for determination of alkali metal ions in an effluent.

i) When an effluent containing alkali metals is evaporated and the residue is heated with infrared lamp or electric heater to remove ammonium formate completely, only alkali formate remains. A small amount of hydrochloric acid is added to the alkali formate and evaporation is repeated. The chloride content of the residue is determined by silver nitrate standard solution and fluorescent indicator;

Table I. The effect of ammonium formate on the determination of alkali ions by silver nitrate titration method

| Metal | Added, mg. | Method of evaporation | Found, mg. | | |
|---|---|---|---|---|---|
| $Na^+$ | 3.63 | Water bath | 3.93 | 5.60 | |
| | 3.63 | Infrared lamp | 3.63 | 3.65 | |
| | 3.63 | Heat after using water bath | 3.63 | 3.62 | 3.63 |
| $K^+$ | 7.53 | 〃 | 7.55 | 7.53 | 7.57 |

Table II. The effect of ammonium formate on the determination of alkali ions by flame photometric method

| Metal | Wavelength | Added, p. p. m. | Brightness of flame in various solutions | | |
|---|---|---|---|---|---|
| | | | $H_2O$ | 0.5 M $NH_4HCOO$ | 1 M $NH_4HCOO$ |
| $Li^+$ | 671 mμ | 10~100 | 100 | 100±1 | 99±1 |
| $Na^+$ | 589 | 10~100 | 100 | 100±1 | 99±1 |
| $K^+$ | 766 | 10~100 | 100 | 100±1 | 99±1 |
| $Rb^+$ | 420 | 10~100 | 100 | 100±5 | 100±5 |
| $Cs^+$ | 455 | 10~100 | 100 | 100±5 | 100±5 |

Apparatus: Shimadzu-flame photometer, Type QB-50.
Fuel: $H_2$ gas
The brightness of ions in distilled water are set on 100.

TABLE III. THE EFFECT OF AMMONIUM FORMATE ON THE DETERMINATION OF ALKALINE EARTH IONS WITH EDTA

| Metal | Indicator | Added, meq. | Found, meq. (average) in various solutions | | | |
|---|---|---|---|---|---|---|
| | | | $H_2O$ | 0.1 M $NH_4HCOO$ | 1 M $NH_4HCOO$ | 2 M $NH_4HCOO$ |
| $Mg^{2+}$ | E. B. T. | 0.225 | 0.225 | 0.225 | 0.224 | |
| $Ca^{2+}$ | E. B. T. | 0.108 | 0.108 | 0.108 | 0.108 | |
| $Sr^{2+}$ | E. B. T. | 0.165 | 0.165 | 0.165 | 0.164 | * |
| | P. C. | | 0.164 | 0.165 | 0.165 | * |
| $Ba^{2+}$ | E. B. T. | 0.148 | 0.15** | 0.15* | 0.15** | * |
| | P. C. | | 0.148 | 0.148 | 0.149 | * |

E. B. T.: Eriochrom Black T
P. C.: Phthalein Complexone
*: End point of titration can not be detected.
**: End point is not clear.

then, alkali content can be determined from the chloride content. The results are shown in Table. I.

ii) Alkali content in an effluent is determined directly by flame photometric method. The effect of a large amount of ammonium and formate ions upon the determination of alkali metals must be carefully examined. As given in Table II, however, interference of ammonium formate is not found in 0.5 M ammonium formate solution, and is found slightly in 1.0 M.

(B) *Alkaline earth elements.*—Alkaline earth elements are titrated by EDTA solution containing the magnesium ion using EBT indicator. The formate ion does not interfere, as shown in Table III. It is necessary to adjust pH over 9.5 for the titration with EDTA. As the effluent has a buffer action, the use of an indicator will be preferable, since it does not obscure the end point of the titration by EDTA and changes its color at pH 9.5. Thymol blue indicator satisfies the conditions. One drop of 0.1% water solution of thymol blue is added to an effluent to be titrated, and ammonium hydroxide is added until the color of the solution changes from yellow to blue and then the solution is titrated by EDTA with EBT indicator. As shown in Table IV, the values obtained by EDTA titration are about 1% lower than the added values, and therefore the observed value must be corrected. In some cases strontium and barium are determined by EDTA standard solution and phthalein-complexone indicator.

TABLE IV. THE EFFECT OF pH-INDICATOR ON THE DETERMINATION OF ALKALINE EARTH IONS WITH EDTA

Sample solution: $Mg^{2+}$ is contained in 50 ml. of 0.5 M ammonium formate solution.
pH-indicator: 0.1% Thymol Blue-water solution; 1 drop
Metal chelate indicator: Eriochrom Black T

| Added; meq., $Mg^{2+}$ | Found; meq., $Mg^{2+}$ | Error, % |
|---|---|---|
| $0.022_5$ | $0.022_3$ | −0.9 |
| $0.045_0$ | $0.044_5$ | −1.1 |
| $0.067_5$ | $0.067_0$ | −0.7 |
| $0.090_0$ | $0.089_0$ | −1.1 |
| $0.112_5$ | $0.111_5$ | −0.9 |
| $0.135_0$ | $0.133_5$ | −1.1 |
| $0.157_5$ | $0.156_0$ | −1.0 |
| $0.180_0$ | $0.178_0$ | −1.1 |
| $0.202_5$ | $0.200_0$ | −1.2 |
| $0.225_0$ | $0.223_5$ | −0.7 |

**Examination of Conditions for the Separation of Alkali and Alkaline Earth Elements.**—It is desirable to use a short column and a small

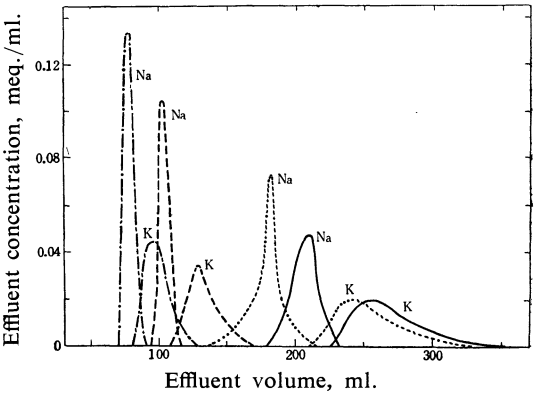



Fig. 3. Elution curves of $Na^+$ and $K^+$.
Column: Dowex 50, X8, 100~150 mesh, 1.1×8 cm.
Flow rate: 1.0~1.1 ml./min.
Resin form and elutriant:
—— $H^+$-saturated resin, with 0.1 M ammonium formate solution
····· $NH_4^+$-saturated resin, with 0.1 M ammonium formate solution
---- $H^+$-saturated resin, with 0.2 M ammonium formate solution
-·-· $H^+$-saturated resin, with the buffer solution, pH 3.2

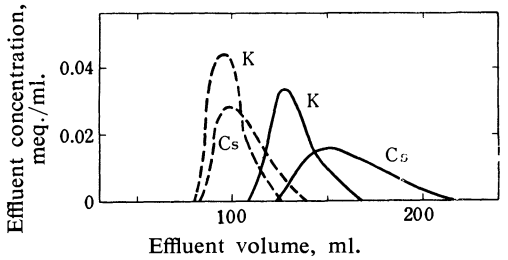



Fig. 4. Elution curves of $K^+$ and $Cs^+$.
Column: Dowex 50, X8, 100~150 mesh, 1.1×8 cm., $H^+$-saturated resin.
Flow rate: 1.0 ml./min.
Elutriants:
—— 0.2 M ammonium formate solution.
---- the buffer solution, pH 3.2.

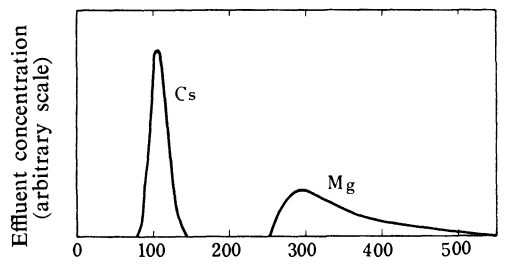



Fig. 5. Elution curves of $Cs^+$ and $Mg^{2+}$.
Column: Dowex 50, X8, 100~150 mesh, 1.1×8 cm., $H^+$-saturated resin.
Elutriant: the buffer solution, pH 3.2.
Flow rate: 0.50 ml./min.

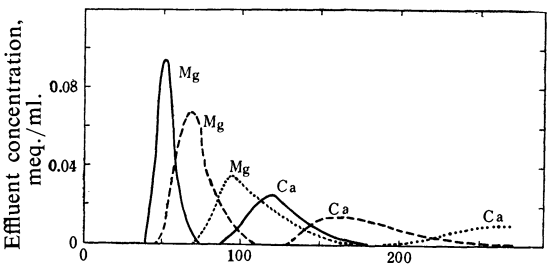



Fig. 6. Elution curves of $Mg^{2+}$ and $Ca^{2+}$.
Column: Dowex 50, X8, 100~150 mesh, 1.1×8.5 cm., $H^+$-saturated resin.
Folw rate: 0.40~0.50 ml./min.
Elutriant: —— the buffer solution, pH 4.0
---- the buffer solution, pH 3.8
····· the buffer solution, pH 3.6

amount of elutriant for separation. To decide a suitable elutriant to be used with a column of Dowex 50, X8, 100~150 mesh, 1.1×8 cm., $H^+$-saturated resin, (exchange capacity, ca. 17 meq.), and at rate of 2~3 ml./min., elution curves were made as follows: An effluent was divided into fractions of 5~10 ml. and elements

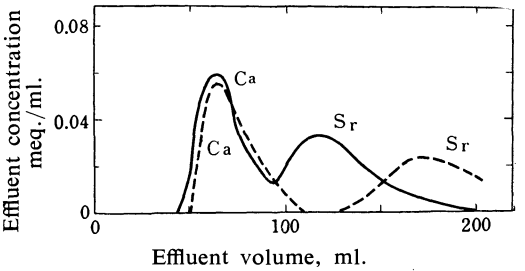



Fig. 7. Elution curves of $Ca^{2+}$ and $Sr^{2+}$.
Column: Dowex 50, X8, 100~150 mesh, 1.1×8.5 cm., $H^+$-saturated resin.
Flow rate: 1.0 ml./min.
Elutriant: —— the buffer solution, pH 4.2
---- the buffer solution, pH 4.1

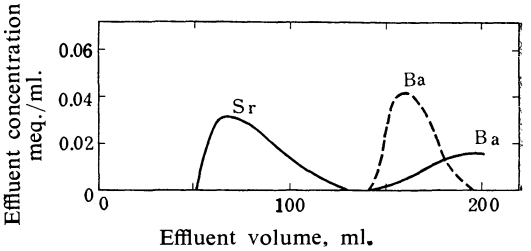



Fig. 8. Elution curves of $Sr^{2+}$ and $Ba^{2+}$.
Column: Dowex 50, X8, 100~150 mesh, 1.1×8.5 cm., $H^+$-saturated resin.
Flow rate: 1.0 ml./min.
Elutriant:
—— the buffer solution, pH 4.5.
---- 2 M ammonium formate solution.

in each fraction were determined by the same method as shown above. The results are as follows:

*(A) Separation of alkali metals.*—It is known that separation factors of sodium, potassium and ammonium in cationic resin of sulphonic type are increased according to the series: sodium < ammonium < potassium. It is, therefore, expected that sodium and potassium can be easily separated when ammonium salt is used as an elutriant. Fig. 3 shows the elution curves of sodium and potassium when ammonium formate solution and the formate buffer solution are used. The separation of potassium and cesium, however, can not be conducted with this buffer solution, as shown in Fig. 4.

*(B) Separation of cesium and magnesium.*—As shown in Fig. 5, cesium and magnesium can be separated completely from each other by using the formate buffer solution having pH 3.2.

*(C) Separation of alkaline earth elements.*—The elution curves of magnesium and calcium, as shown in Fig. 6, are obtained when the formate buffer solutions of various pH are used as an elutriant. From Fig. 6, it can be seen

that magnesium and calcium can be easily separated by the buffer solutions. As shown in Fig. 7, calcium and strontium can be separately eluted by the buffer solution having pH 4.1. Finally, to separate strontium and barium, strontium is first eluted by the buffer solution of pH 4.5, and then barium is eluted by 2 M ammonium formate solution, as shown in Fig. 8.

*(D) Separation of alkali and alkaline earth elements.*—To separate completely alkali and alkaline earth elements, a column of 10 cm. in length may be used. This column length was determined by the plate theory[6] for two ions, sodium and potassium ions which are most difficult to separate in the above experiments.

Sodium and potassium can be separately eluted by using 0.1 M ammonium formate solution. For an early start of elution of sodium, 0.2 M ammonium formate solution may be passed through a column before 0.1 M ammonium formate solution is passed.

To separate potassium and cesium with the formate buffer solution, it is necessary to use a very long column and a large amount of the elutriant. Therefore first it was better to elute

TABLE V. DETERMINATION OF IONS IN MIXTURES

| No. | | $Na^+$ | $K^+$ | $Cs^+$ | $Mg^{2+}$ | $Ca^{2+}$ | $Sr^{2+}$ | $Ba^{2+}$ |
|---|---|---|---|---|---|---|---|---|
| 1 | Added, meq. | 0.481 | 0.493 | | 0.450 | 0.434 | 0.412 | 0.403 |
| | Found, meq. | 0.491 | 0.488 | | 0.453 | 0.432 | 0.424 | 0.40 |
| | Error, % | +2.3 | −1.0 | | +0.7 | −0.5 | +2.9 | |
| 2 | Added, meq. | 0.961 | 0.987 | 0.498 | 0.450 | 0.469 | 0.412 | 0.403 |
| | Found, meq. | 0.953 | 1.491 | | 0.451 | 0.466 | — | 0.40 |
| | Error, % | −0.8 | +0.4 | | +0.2 | −0.6 | | |
| 3 | Added, meq. | 0.481 | 0.493 | 0.498 | 0.450 | 0.469 | 0.412 | 0.403 |
| | Found, meq. | 0.470 | | | 0.448 | 0.472 | 0.397 | 0.40 |
| | | (0.009) | (0.495) | (0.488) | | | | |
| | Error, % | −2.3 | | | −0.4 | +0.6 | −3.6 | |
| | | (−0.4) | (+0.4) | (−2.0) | | | | |
| 4 | Added, meq. | 0.961 | 0.987 | 0.498 | 0.450 | 0.469 | 0.412 | 0.403 |
| | Found, meq. | 0.965 | | | 0.451 | 0.469 | — | 0.40 |
| | | (0.000) | (0.982) | (0.495) | | | | |
| | Error, % | +0.5 | | | +0.2 | −0.0 | | |
| | | | (−0.5) | (−0.6) | | | | |

The values in parenthesis are obtained by resorping the $K^+$ and $Cs^+$ fraction in longer column (1.1×15 cm.) and eluting with 0.5 N HCl separately (as shown in Fig. 2).

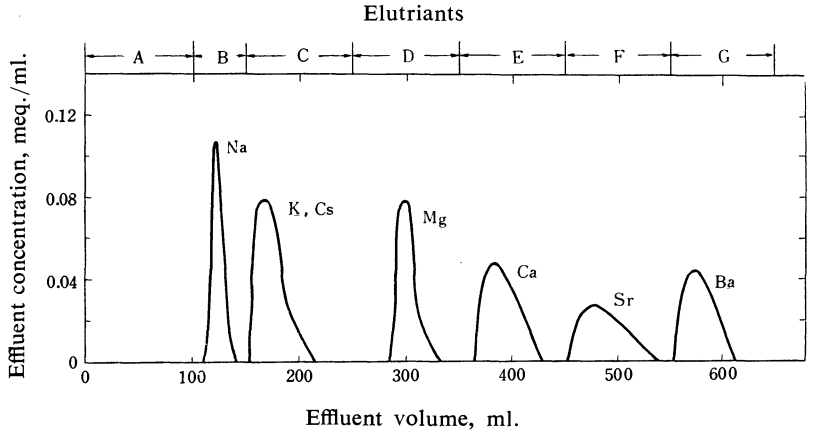



Fig. 9. Elution of alkali and alkaline earth elements.
Column: Dowex 50, X8, 1.1×10 cm., 100~150 mesh, $H^+$-saturated resin.
Flow rate: 2 ml./min.
Elutriants: A 0.2 M ammonium formate solution, B 0.1 M ammonium formate solution, C the buffer solution, pH 3.2, D the buffer solution, pH 4.0, E the buffer solution, pH 4.1, F the buffer solution, pH 4.4, G 2 M ammonium formate solution.

both simultaneously with the formate buffer solution of pH 3.2, and then to separate potassium and cesium by resorption and chromatographic elution with 0.5 N hydrochloric acid.

Cesium and magnesium can be separated by the formate buffer solution having pH 3.2. And the separation of magnesium, calcium, strontium and barium can be conducted by using the same buffer solution with different pH.

Using the column of Dowex 50, X8, or Amberlite IR-120, 100~150 mesh, 1.1×10 cm., and $H^+$-saturated resin, (exchange capacity, ca. 21 meq.), 0.5~1 meq. of sodium, potassium, cesium, magnesium, calcium, strontium and barium ions, respectively, are separated at a flow rate of 2~3 ml./min. The results are shown in Fig. 9 and Table V. Alkali and alkaline earth elements can be successfully separated from each other by the procedure shown in Fig. 9.

**Summary**

Alkali and alkaline earth elements, including their rare elements, can be separately eluted easily, rapidly and completely by the elutriants here described. This procedure and its modified procedures* can be applied to routine analysis of natural waters.

The authors express their sincere appreciation to Professor Yasuo Miyake of Tokyo University of Education and Mr. Masami Izawa of National Institute of Radiological Sciences for their helpful advice and encouragement throughout their work.

*National Institute of Radiological Sciences*
*Kurosuna-machi, Chiba (H. T.)*

*Water Reserch Laboratory, Faculty of Science*
*Nagoya University, Chigusa-ku, Nagoya (Y. K.)*

* The modified procedures will be reported elsewhere.

# *Studies on Organic Peroxides. V. Decomposition of Benzoyl Peroxide by Iron(II)**

By Shigeo HASEGAWA and Norio NISHIMURA

(Received October 28, 1959)

It has been found that the rate of the decomposition of peroxides was greatly accelerated by ferrous ion[1]. In the presence of the latter, the decomposition is supposed to take place according to the Haber-Weiss one-electron transfer mechanism as follows[2]:

$$P + Fe^{2+} \xrightarrow{k_1} RCOO\cdot + RCOO^- + Fe^{3+} \quad (1)$$

where P and R denote benzoyl peroxide and phenyl group respectively. It is noted that this decomposition is not homolytic but semi-ionic. Therefore, it would be expected that the physical properties of solvents play an important role apart from the discussions about the induced decomposition of benzoyl peroxide. In the previous paper[3], this mechanism was postulated in order to explain the dependence of the initial rate of polymerization of vinyl acetate in the benzoyl peroxide-Fe(II)-benzoin redox system on the initial concentration of ferrous ion. In this paper, the analytical method was applied to the ferrous ion catalysed decomposition of peroxide in order to verify this mechanism.

## Experimental

Reagents used were of reagent grade or prepared by the method reported previously[3]. A definite amount of ferrous chloride crystals ($FeCl_2 \cdot 4H_2O$) was dissolved in ethanol (50 ml.) in a three-necked flask provided by a condenser. The reaction was initiated by the addition of ethanolic solution (50 ml.) of benzoyl peroxide. Oxygen-free carbon dioxide gas was bubbled through the reaction mixture for the purpose of stirring the solution and preventing the ferrous ions from being oxidized by air. Reactions were carried out at temperatures between 15 and 32°C. The analytical procedures of benzoyl peroxide was a modification of the method recommended by Nozaki[4]. At specified times after

* Presented at the Annual Meeting of the Chemical Society of Japan, Tokyo, April 5, 1958.

1) M. S. Kharasch, A. Funo and W. Nudenberg, *J. Org. Chem.*, **15**, 763 (1950).

2) F. Haber and P. Weiss, *Proc. Roy. Soc. London*, **A147**, 332 (1934).

3) S. Hasegawa et al., This Bulletin, **31**, 696 (1958).

4) K. Nozaki, *Ind. Eng. Chem., Anal. Ed.*, **19**, 872 (1947).

the beginning of the reaction, aliquots of the reaction mixture were pipetted out from the flask into an Erlenmeyer flask containing 1 ml. of saturated sodium hydrogen phosphate to eliminate ferric ions, which would, otherwise, disturb the correct analysis of benzoyl peroxide. Five milliliters of acetic anhydride in which 0.3 g. of sodium iodide had been dissolved was added and then allowed to stand about half an hour at room temperature. Iodine liberated was titrated with 0.01 N sodium thiosulfate solution adding 1% starch solution towards the last. This method of analysis is favored by the fact that the atmosphere above the solution to be analysed need not be replaced by inert gas.

Ferrous ion is known to react with $\alpha\alpha'$-bipyridyl forming a very stable red complex which has the maximum absorbance at 510 m$\mu$. Colorimetric measurement was, therefore, applied to determine the concentration of the ferrous ion in the reaction mixture. One milliliter of an aqueous solution of 1% $\alpha\alpha'$-bipyridyl was buffered at pH of 4.75 by acetic acid~sodium acetate solution. Ten milliliters of the reaction mixture was added to the solution followed by dilution with water. When it was allowed to stand at room temperature, colloidal particles of benzoyl peroxide appeared which grew up to precipitate after standing for 2~3 hr. This precipitate was filtered off and the absorbance of the solution at 470 m$\mu$ was measured by a photoelectric colorimeter. A plot of the absorbance against the ferrous ion concentration in a series of blank experiments showed a straight line relationship up to about $1.5\times10^{-4}$ mol./l. of ferrous ion, in accordance with Beer's law.

The initial concentration of benzoyl peroxide was $5\times10^{-3}$ mol./l. in each run.

## Results and Discussion

The extent of the decomposition of benzoyl peroxide induced by ferrous ions was plotted against time as shown in Fig. 1. As is seen from the figure, this reaction takes place with considerable rate even at room temperature.

According to the reaction 1, the rate of the ferrous ion induced decomposition of benzoyl peroxide should be expressed as follows:

$$-\mathrm{d}[P]/\mathrm{d}t = k_1[P][\mathrm{Fe}^{2+}] \qquad (2)$$

or rearranging Eq. 2,

$$-\mathrm{d}\ln[P]/\mathrm{d}t = k_1[\mathrm{Fe}^{2+}] \qquad (3)$$

Instead of the extent of the decomposition, the logarithm of the corresponding volume $v$ of sodium thiosulfate consumed in titration, was plotted against time $t$; this is shown in Fig. 2 for various initial ferrous ion concentrations at 25°C. Extrapolated values of each curve evidently correspond to the initial concentration of benzoyl peroxide. It is to be noted from Fig. 2 that the slope of the curves, i. e., d log $[P]/\mathrm{d}t$ has not suffered a marked change during the reaction. This means that the apparent decomposition rate of benzoyl peroxide is

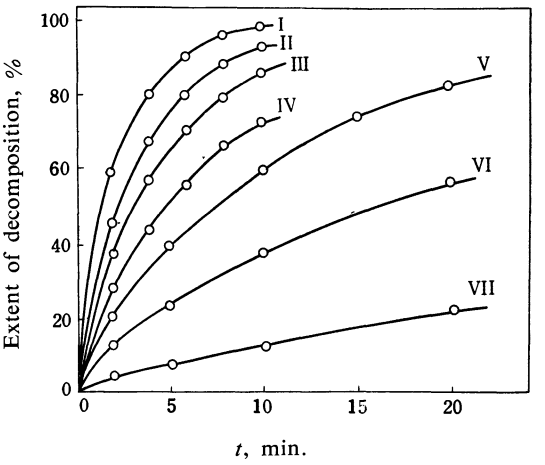



Fig. 1. Extent of decomposition of benzoyl peroxide in ethanol at 25°C. $[FeCl_2]_0\times10^4$: I, 25.1; II, 16.5; III, 13.6; IV, 10.6; 6.8; VI, 5.4; VII, 2.5 mol./l., respectively; $[BPO]_0$: $5\times10^{-3}$ mol./l.

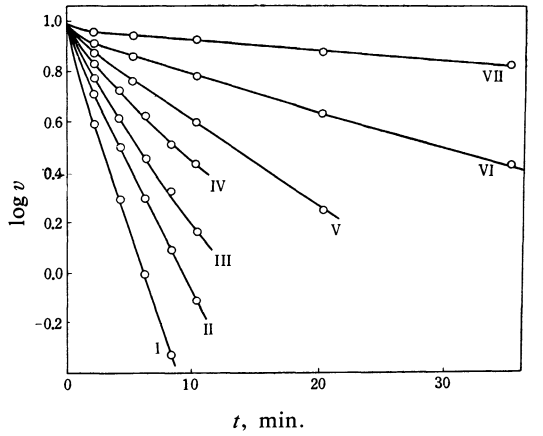



Fig. 2. Relation between log $v$ and $t$. Numbers are identical with those in Fig. 1.

nearly of the first order with respect to benzoyl peroxide. Another evidence for the first order reaction lies in the fact that the slope of the curves in Fig. 3 in which log $v$ was plotted against $t$, seems to be independent of the initial concentration of benzoxyl peroxide.

The slopes of the curves in Fig. 2 seem to be linearly proportional to the initial concentration of ferrous ion. Although care was taken to remove oxygen, the trace of oxygen in the solution might oxidize the ferrous ions. In addition, ferrous ions are oxidized by reaction 1. Therefore, it is necessary to determine the true concentration of ferrous ions in solution.

The ferrous ion concentration in the reaction mixture at any time was determined by the colorimetric method. The slope −d log

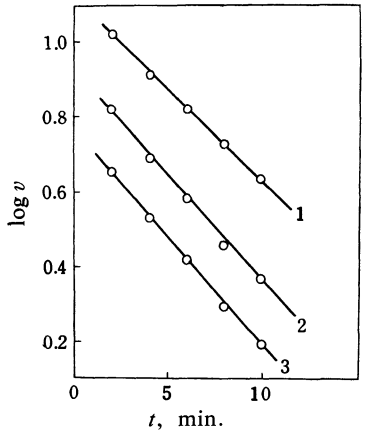



Fig. 3. Relation between $\log v$ and $t$ at 25°C; $[BPO]_0\times10^3$: 1, 7.5; 2, 5.0; 3, 3.3 mol./l., respectively; $[FeCl_2]_0$: $10.1\times10^{-4}$ mol./l.

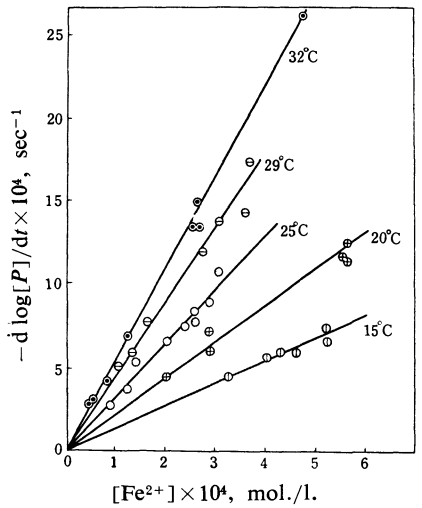



Fig. 4. Plots of $-\mathrm{d}\log[P]/\mathrm{d}t$ against actual ferrous ion concentration in ethanol at various temperatures.

$[P]/\mathrm{d}t$ was plotted against the ferrous ion concentration as shown in Fig. 4. The plots gave straight lines, all of which converged to the origin of the coordinate at each temperature.

Thus it could be said that equation 2 is the complete expression for the reaction rate in accordance with the mechanism postulated above.

Table I shows the numerical values for $[Fe^{2+}]$, $-\mathrm{d}\log[P]/\mathrm{d}t$ and $k_1$ at various temperatures. Fig. 5 shows the Arrhenius plot which gives a straight line. The Arrhenius equation for the decomposition reaction was calculated to be $k_1=2.2\times10^{11}\exp(-14.21\times10^3/\boldsymbol{RT})$ mol.$^{-1}$ l. sec.$^{-1}$ with a standard deviation of 0.40 for $\log A$ and 0.55 kcal. mol.$^{-1}$ for $E$, where $A$ and $E$ represent the frequency factor and the activation energy, respectively.

Table I. Rate constants for benzoyl peroxide-iron(II) reaction

| $t$ °C | $[Fe^{2+}]\times10^4$ mol. l$^{-1}$ | $-\mathrm{d}\log[P]/\mathrm{d}t\times10^4$ sec$^{-1}$ | $k_1$ mol.$^{-1}$ l. sec$^{-1}$ | $k_1$ av. |
|---|---|---|---|---|
| | 4.65 | 29.0 | 14.4 | |
| | 2.65 | 15.0 | 13.0 | |
| | 2.60 | 16.7 | 14.8 | |
| 32 | 2.50 | 15.0 | 13.8 | 14.4±0.2 |
| | 1.20 | 7.67 | 14.7 | |
| | 0.80 | 4.67 | 13.4 | |
| | 0.50 | 3.33 | 15.3 | |
| | 0.43 | 3.00 | 16.1 | |
| | 3.65 | 19.3 | 12.2 | |
| | 3.55 | 16.0 | 10.4 | |
| | 3.05 | 15.3 | 11.6 | |
| 29 | 2.70 | 13.3 | 11.3 | 11.8±0.2 |
| | 1.60 | 8.67 | 12.5 | |
| | 1.30 | 6.67 | 11.8 | |
| | 1.00 | 5.67 | 13.1 | |
| | 3.00 | 12.0 | 9.21 | |
| | 2.85 | 10.0 | 8.08 | |
| | 2.55 | 9.33 | 8.43 | |
| | 2.55 | 8.67 | 7.83 | |
| 25 | 2.35 | 8.33 | 8.16 | 8.44±0.14 |
| | 2.00 | 7.33 | 8.44 | |
| | 1.35 | 5.67 | 9.67 | |
| | 1.20 | 4.17 | 8.00 | |
| | 0.85 | 3.00 | 8.13 | |
| | 5.55 | 14.0 | 5.84 | |
| | 5.55 | 12.7 | 5.27 | |
| 20 | 5.45 | 13.0 | 5.49 | 5.71±0.12 |
| | 2.85 | 8.00 | 6.46 | |
| | 2.85 | 6.67 | 5.39 | |
| | 1.98 | 5.00 | 5.82 | |
| | 5.15 | 8.33 | 3.73 | |
| | 5.15 | 7.33 | 3.28 | |
| 15 | 4.55 | 6.67 | 3.38 | 3.56±0.05 |
| | 4.20 | 6.67 | 3.66 | |
| | 3.95 | 6.33 | 3.69 | |
| | 3.20 | 5.00 | 3.60 | |

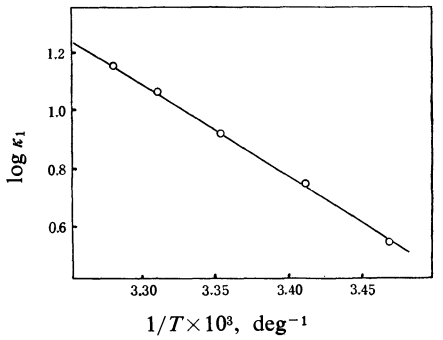



Fig. 5. Arrhenius plot of $\log k_1$ against $1/T$.

As is seen above, the reaction proceeds bimolecularly in accordance with the Haber-Weiss mechanism, and hence the reaction should be of the second order. However, as shown in Fig. 2, the apparent decomposition was approximately of the first order. In order for the reaction to be of the first order, the ferrous ion concentration in Eq. 2 must be kept constant during the reaction. Ferrous ion concentration was decreased rapidly at first, but became nearly contant within 2~3 min. It could be said therefore, that ferrous ion concentration was roughly kept constant during the stationary state.

It is well known that the thermal decomposition rate of peroxides in various solvents can be expressed as[5]

$$-\mathrm{d}[P]/\mathrm{d}t = k_d[P] + k_i[P]^x \qquad (4)$$

where $k_d$ represents the specific rate of spontaneous cleavage, $k_i$ the specific rate constant of induced decomposition and $x$ the order of the induced reaction which may vary between 0.5 and 2.0. In ethanol solution, $x$ was reported to be unity[6], and the apparent decomposition rate was of the first order. In this case, the essential reactions were considered to take place as follows:

$$\mathrm{P} \xrightarrow{k_d} 2\mathrm{RCOO}\cdot \qquad (5)$$

$$\mathrm{RCOO}\cdot + \mathrm{CH_3CH_2OH} \xrightarrow{k_2} \mathrm{RCOOH} + \mathrm{CH_3\dot{C}HOH} \qquad (6)$$

$$\mathrm{CH_3\dot{C}HOH} + \mathrm{P} \xrightarrow{k_3} \mathrm{CH_3CHO} + \mathrm{RCOO}\cdot + \mathrm{RCOOH} \qquad (7)$$

$$\mathrm{CH_3\dot{C}HOH} + \mathrm{RCOO}\cdot \xrightarrow{k_4} \mathrm{RCOOH} + \mathrm{CH_3CHO} \qquad (8)$$

and the apparent decomposition rate was given by

$$-\mathrm{d}[P]/\mathrm{d}t = k'[P] \qquad (9)$$

where $k'$ is a constant including some specific rate constants in the equations given above. The specific rate constant for the spontaneous decomposition $k_d$ may be negligible at room temperature. Hence, in the presence of ferrous ion, reaction 7 will take part in the decomposition of benzoyl peroxide together with reaction 1. The overall rate of the decomposition reaction may be expressed as

$$-\mathrm{d}[P]\,\mathrm{d}t = k_1[P][\mathrm{Fe}^{2+}] + k'[P] \qquad (10)$$

If the reaction 7 occurs predominantly, the mole ratio of benzoyl peroxide decomposed to ferrous ion consumed will be greater than unity. In fact as is seen from Fig. 2, the amount of the peroxide decomposed in each case was much greater than those expected from reaction 1. However, comparing Eq. 10 with Eq. 2 which was confirmed experimentally, the second term of the right hand side in Eq. 10 could be neglected. This indicates that radical-induced decomposition of benzoyl peroxide may be suppressed by the presence of ferrous ions, as in the case of the decomposition of benzoyl peroxide by dimethyl aniline[7].

In order to explain both the first order decomposition and the suppression of reaction 7, reduction of ferric to ferrous ion may be postulated. Since ethanol radical is considered as an electron donor, this reduction would take place through reaction 11:

$$\mathrm{CH_3\dot{C}HOH} + \mathrm{Fe}^{3+} \xrightarrow{k_5} \mathrm{CH_3CHO} + \mathrm{Fe}^{2+} + \mathrm{H}^+ \qquad (11)$$

Thus it may be assumed that the reactions 1, 6, 8 and 11 are predominant. If the stationary state conditions for radicals are applied, then for RCOO·,

$$k_1[P][\mathrm{Fe}^{2+}] = k_2[\mathrm{RCOO}\cdot][\mathrm{CH_3CH_2OH}] + k_4[\mathrm{RCOO}\cdot][\mathrm{CH_3\dot{C}HOH}] \qquad (12)$$

and for $\mathrm{CH_3\dot{C}HOH}$,

$$k_2[\mathrm{RCOO}\cdot][\mathrm{CH_3CH_2OH}] = k_4[\mathrm{RCOO}\cdot][\mathrm{CH_3\dot{C}HOH}] + k_5[\mathrm{CH_3\dot{C}HOH}][\mathrm{Fe}^{3+}] \qquad (13)$$

Therefore, from these equations, it follows

$$k_1[P][\mathrm{Fe}^{2+}] = k_5[\mathrm{CH_3\dot{C}HOH}][\mathrm{Fe}^{3+}] + 2k_4[\mathrm{RCOO}\cdot][\mathrm{CH_3\dot{C}HOH}] \qquad (14)$$

The left hand side in Eq. 14 represents the rate of the oxidation of ferrous ion and the first term of the right hand side is that of reduction of ferric ion. As mentioned earlier, the ferrous ion concentration did not suffer a marked change during the reaction after a stationary state was attained. Hence, the second term of the right hand side in Eq. 14 may be neglected. The main reactions in this study may, therefore, be reduced to reactions 1, 6 and 11. Among these reactions, iron may be considered to serve as electron transferer.

Swain et al.[8] believe that two benzoxy groups

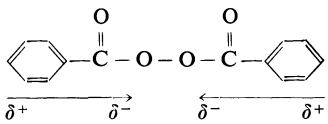
5) P. D. Bartlett and K. Nozaki, *J. Am. Chem. Soc.*, **68**, 1686 (1946); ibid., **69**, 2299 (1947); W. E. Cass, ibid., **68**, 1976 (1946).

6) S. Kato and F. Mashio, *J. Chem. Soc. Japan, Ind. Chem. Sec.* (*Kogyo Kagaku Zasshi*), **59**, 380 (1956).

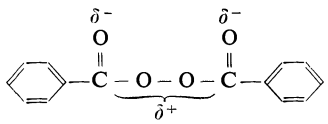
7) M. Imoto and C. Suckon, *Chem. High Polymers* (*Kobunshi Kagaku*) **11**, 396 (1954).

8) C. G. Swain, W. T. Stockmayer and J. T. Clarke, *J. Am. Chem. Soc.*, 72, 5426 (1950); ibid., **68**, 1686 (1946).

in benzoyl peroxide are dipoles attached to one another in such a way as to repel each other:



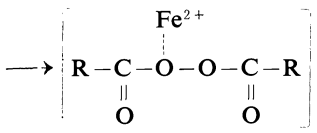
and they ascribed the driving force of the decomposition of the peroxide to the electrostatic repulsion between two benzoxy groups. Whereas, Imoto et al.[7] proposed that the driving force was due to the repulsion between oxygen atoms on carbonyl groups,



and successfully explained the effect of substituents on phenyl rings of benzoyl peroxide upon the rate of decomposition in the presence of dimethyl aniline.

In the reaction of benzoyl peroxide with ferrous ion, as is the case for the reaction between benzoyl peroxide and dimethyl aniline, the two species, when they approach, will interact with each other forming an activated complex:

$$RCOO-OOCR+Fe^{2+}$$



$$\longrightarrow RCOO^- + RCOO\cdot + Fe^{3+} \qquad (15)$$

An electron jump from ferrous ion to either of the oxygen atoms bonded to each other will easily take place. Orr and Williams[9] suggested the formation of the activated complex by coördination of the ferrous ion and hydroperoxide.

The spontaneous decomposition of benzoyl peroxide in various solvents has been widely studied by many authors[10] and they found that the activation energy was 28~30 kcal./mol., which is slightly lower than the O—O bond energy, 34 kcal./mol., calculated by Pitzer[11].

A short discussion of activation entropy may be relevant to the present problem. It is noted that the frequency factor of the thermal decomposition of benzoyl peroxide in various solvents is of the order of $10^{13}$~$10^{15}$ $mol^{-1}$ l. $sec^{-1}$, the value for which is abnormally large owing, probably, to the chain process. But, as already stated, in the present case, the factor $A$ was found to be $2.2\times10^{11}$. This will also suggest the fundamental difference in the reaction mechanisms in two cases. Rollefson[12] considers that the activation entropy is a measure of the bond strength of activated complex. The frequency factor of $2.2\times10^{11}$ corresponds to the entropy loss of about 11.2 e. u. provided the transmission coefficient is unity. The value may be compared with $\Delta S^{\neq}$ of $-10$ e. u. which is accompanied by the loss of only one degree of translational freedom[9]. Accordingly, it seems that ferrous ion forms a weakly combined complex with benzoyl peroxide molecule. From the standpoint of the entropy factor, the decomposition mechanism proposed above could again be considered to be reasonable.

## Summary

An investigation of the rate of decomposition of benzoyl peroxide by ferrous ion in ethanol has been made. The rate of the reaction was linearly proportional to the concentrations of benzoyl peroxide and ferrous ion, in accordance with Haber-Weiss one electron transfer mechanism. But the apparent decomposition rate was of the first order. The Arrhenius equation was $k_1=2.2\times10^{11}\exp(-14{,}210/\boldsymbol{RT})\,mol^{-1}$ l. $sec^{-1}$.

*Department of Chemistry*
*Faculty of Science*
*Okayama University*
*Tsushima, Okayama*

9) R. J. Orr and H. L. Williams, *J. Phys. Chem.*, **57**, 925 (1953).
10) K. Nozaki and P. D. Bartlett, *J. Am. Chem. Soc.*, **68**, 1686 (1946); P. F. Hartman, H. G. Sellers and D. Turnbull, ibid., **69**, 2416 (1947); A. T. Blomquist and A. J. Buselli, ibid., **73**, 3883 (1951).
11) K. S. Pitzer, ibid., **70**, 2140 (1948).
12) G. K. Rollefson, *J. Phys. Chem.* **56**, 976 (1952).

# *Molecular Complexes between Ketones and Alkali Salts*

By Haruka YAMADA

(Received December 14, 1959)

Sodium or lithium perchlorate and sodium iodide have high solubilities in ketones. These salts form a sort of molecular complex with ketones. From infrared studies[1,2] it has been shown that the change of the ketone band with salt concentration differs from that in general solvation case, and the non-complexed ketone band is replaced by the shifted band of the complexed ketone; namely, one absorption maximum falls gradually in intensity to be replaced by another. Further, it has been shown that the separation between the complexed and non-complexed ketone bands is independent of anion species. Based on these facts, it has been understood that the formation of the complex is due to the bonding between the C=O group and metallic cation.

These complexes are of interest, because they will give information upon the covalent bond formation, besides the other intermolecular interactions such as ion-dipole, dipole-dipole interaction, London force etc., of alkali metallic ions with some electron donor molecules. The present studies are undertaken to elucidate the electronic states of the complexes.

In ultraviolet absorption spectra, the shifts caused by the formation of the complexes are measured for the $n\rightarrow\pi^*$ and $\pi\rightarrow\pi^*$ bands. In order to know whether or not the experimental results obtained here are interpreted based on the theory of charge transfer complex[3], the covalent characters and the stabilization energies of the complexes have been estimated by use of Pauling's " bond-length " relation[4]. By these estimated values, the $n\rightarrow\pi^*$ transition energies of the complexes have been calculated and compared with the observed data.

## Experimental

Ultraviolet absorption spectra were taken with a modified* Perkin-Elmer Model 112 Infrared Spectrophotometer equipped with LiF prism. A $H_2$-lamp and a 1P28 photomultiplier were used as light source and detector, respectively. Wavelength calibration was made by means of the spectra of Hg-lamp and benzene vapor. Cells had quartz windows and lead Spacers. The thickness of the cell was measured by interference method. Spectral slit width ranged from 10 $cm^{-1}$ to 20 $cm^{-1}$.

Infrared spectra were taken with the spectrophotometer mentioned above, by use of $CaF_2$ prism.

Organic compounds were purified by fractionating after drying. Guaranteed commercial anhydrous sodium iodide was used without further purification. Anhydrous sodium perchlorate was obtained heating $NaClO_4 \cdot H_2O$ in an air bath. Lithium perchlorate was prepared by neutralizing lithium carbonate with a slight excess of 60% perchlorate acid, and digesting the mixture on a hot plate until evolution of carbon dioxide ceased, and a clear solution remained. The solution was heated to remove excess acid and the white solid remained. The salt was dehydrated by heating in vacuo to approximately 100°C over phosphorus pentoxide. The anhydrous salts were stored in the dark in a desiccator. Measurements were made for pure ketones and the ketone solutions of the salts. No diluent was added, as no suitable solvent for the complexes was found.

## Experimental Results

**Infrared Absorption Spectra.**—The wave numbers for C=O stretching bands are tabulated in Table I. From this table, it can be seen that the wave numbers for the NaI- and the $NaClO_4$-ketone system are about the same and that the observed shifts are larger for lithium salt than for sodium salt and exhibit a similarity between the acetone- and the cyclohexanonesalt system.

TABLE I. WAVE NUMBERS FOR C=O STRETCHING BANDS

| | Pure liquid | NaI-ketone complex | $NaClO_4$-ketone complex | $LiClO_4$-ketone complex |
|---|---|---|---|---|
| Acetone | 1717 | 1709 | 1710 | 1702 |
| Cyclohexanone | 1714 | 1706 | 1706 | 1702 |
| Acetophenone | 1685 | (1684) | (1680) | (1677) |

**Ultraviolet Absorption Spectra.**—The curves obtained for the $NaClO_4$- and the $LiClO_4$-acetone systems both in 1:4 mole ratio are shown in Fig. 1. The non-complexed acetone band attributed to the $n\rightarrow\pi^*$ transition has a maximum at 36400 $cm^{-1}$. By the addition of the salt the band shifts to higher frequencies with

1) A. D. E. Pullin and J. McC. Pollock, *Trans. Faraday Soc.*, **54**, 11 (1958).
2) H. Yamada, This Bulletin, **33**, 666 (1960).
3) R. S. Mulliken, *J. Am. Chem. Soc.*, **72**, 600 (1950); ibid., **74**, 811 (1952); *J. Phys. Chem.*, **56**, 801 (1952).
4) L. Pauling, *J. Am. Chem. Soc.*, **69**, 542 (1947).
* Thanks are due to Mr. W. Suětaka and Mr. S. Saito for their help in this modification.

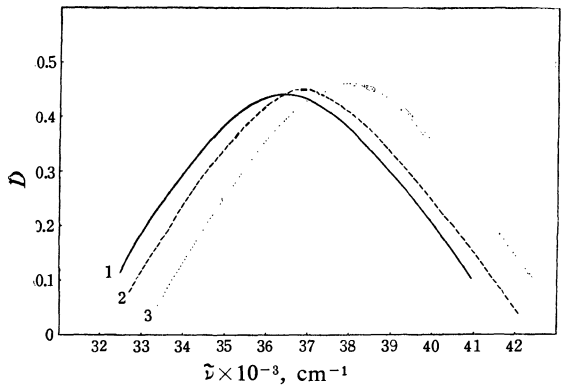



Fig. 1. $n\rightarrow\pi^*$ bands of acetone and acetone-salt solutions.
1. Pure acetone.
2. Acetone-$NaClO_4$ solution (in 4 : 1 mole ratio).
3. Acetone-$LiClO_4$ solution (in 4 : 1 mole ratio).

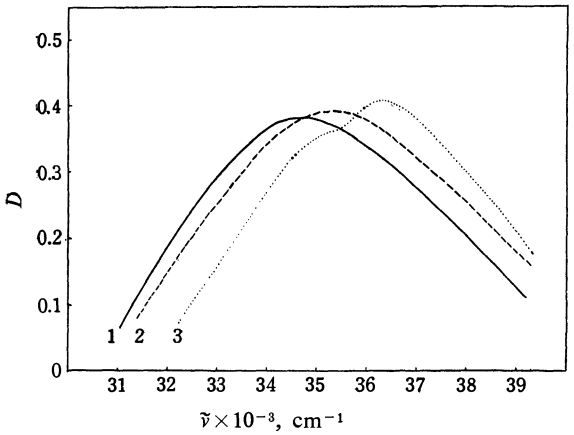



Fig. 2. $n\rightarrow\pi^*$ bands of cyclohexanone and cyclohexanone-salt solutions.
1. Pure cyclohexanone.
2. Cyclohexanone-$NaClO_4$ solution (in 4 : 1 mole ratio).
3. Cyclohexanone-$LiClO_4$ solution (in ca. 6.5 : 1 mole ratio).

the maximum at 36900 $cm^{-1}$ for the $NaClO_4$-acetone system and at 38000 $cm^{-1}$ for the $LiClO_4$-acetone system. The band for the $LiClO_4$-acetone system shows a contour with two peaks at a lower perchlorate concentration. In 1 : 4 mole ratio, almost all the acetone molecules are, therefore, regarded as forming the complex with the salt. For the $NaClO_4$-acetone system the separation between acetone and the complex bands is relatively small and the variation of band contour is not found for changing mole ratio.

The observed curves for the $NaClO_4$- and the $LiClO_4$-cyclohexanone system are shown in Fig. 2. The $n\rightarrow\pi^*$ band maximum of cyclohexanone at 34700 $cm^{-1}$ shifts to 35300 $cm^{-1}$ by the addition of $NaClO_4$ and to 36400 $cm^{-1}$ by that of $LiClO_4$. The curves for the $LiClO_4$-cyclohexanone system measured for various concentrations are shown in Fig. 3. Each band shows the contour of two components. Since all these curves intersect at about 35600 $cm^{-1}$ and the number of cyclohexanone molecules in unit volume, calculated from the specific gravity of the solution, is almost constant over this range of concentration, this point at about 35600 $cm^{-1}$ is the so-called isosbestic point for the $LiClO_4$-cyclohexanone system.

The curves for the $NaClO_4$- and the $LiClO_4$-acetophenone system are shown in Fig. 4. Acetophenone shows a $\pi\rightarrow\pi^*$ band together with the $n\rightarrow\pi^*$ band in ultraviolet region. Although the solubilities of the salts in acetophenone are relatively low, the shifts are observed distinctly. By adding the salt the $n\rightarrow\pi^*$ band, having a maximum at 31250 $cm^{-1}$, shows the blue shift similar to the $n\rightarrow\pi^*$ bands of the other ketones. The red shift of the $\pi\rightarrow\pi^*$ band was observed, although the band maximum was difficult to determine owing to the high intensity. As shown in Fig. 4, the peak of $n\rightarrow\pi^*$ band for the $LiClO_4$-acetophenone system is hardly ever found in 1 : 10 mole ratio and can not be found in 1 : 6 mole ratio, because it is covered with the $\pi\rightarrow\pi^*$ band shifted to lower frequencies.

Although it might be expected from the results of infrared studies that the ultraviolet spectrum of the sodium iodide-ketone system is similar to that of the sodium perchlorate-ketone system, it is not actually the case.

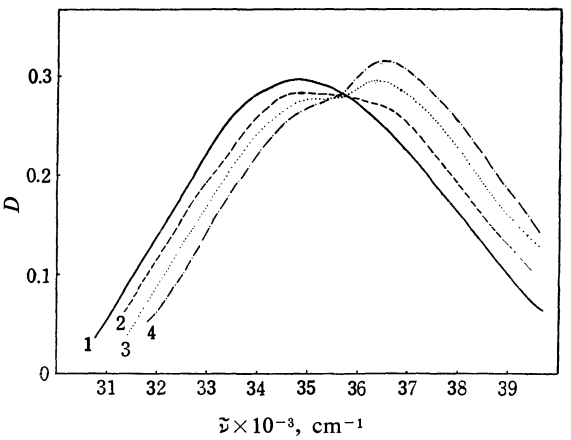



Fig. 3. Curves for cyclohexanone-$LiClO_4$ solutions in various concentrations (27.2 $\mu$ cell).
1. Pure cyclohexanone.
2. ca. 15 : 1 mole ratio.
3. 8.1 : 1 mole ratio.
4. 6.5 : 1 mole ratio (saturated).

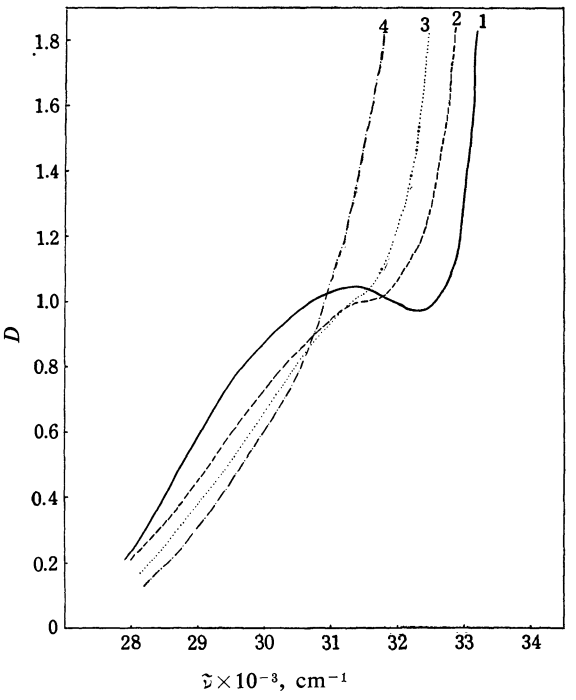



Fig. 4. Spectra of acetophenone and acetophenone-salt solutions.
1. Pure acetophenone.
2. Acetophenone-$NaClO_4$ solution (in ca. 12 : 1 mole ratio).
3. Acetophenone-$LiClO_4$ solution (in ca. 10 : 1 mole ratio).
4. Acetophenone-$LiClO_4$ solution (in ca. 6 : 1 mole ratio).

The curve measured for the sodium iodide-ketone system, however, has a strong absorption ranging from about 31000 $cm^{-1}$ to higher frequencies, which is probably caused by the iodide ion in the solution.

The $n\rightarrow\pi^*$ blue shift and $\pi\rightarrow\pi^*$ red shift phenomena observed here are similar to but generally much larger than those usually observed as general solvent effects. The band contours can be separated into two components. These phenomena are just like those observed for the hydrogen bond formation.

## Interpretations

**Infrared Spectra.**—Although only the C=O bands are shown in Table I, the slight changes for the other ketone bands were also found similar to the sodium iodide-acetone complex[2]. From the fact that the $NaClO_4$-ketone and NaI-ketone complexes show the same frequencies, it follows that the formation of the complexes is independent of anion species. The solubilities of the salts in acetophenone are low and the spectra of the saturated solutions are not those of the complexes but those of the complexed acetophenone overlapped with the non-complexed one. The observed shifts for the acetophenone-salt systems, therefore, are small.

**Covalent Contribution to the Intermolecular Bond.**—By considering a charge transfer force between C=O group and metallic ion, besides the other intermolecular interactions such as ion-dipole, dipole-dipole interaction, London force etc., the intermolecular bonding is expressed as a resonance between following two structures.

$$\text{(A)}\quad C{=}O\quad M^+$$

$$\text{(B)}\quad C{=}\overset{+}{O}{-}M$$

The structure A expresses a no-bond structure and the structure B dative one which is formed by the transfer of the lone pair electrons of oxygen atom to the cation.

To estimate the contribution of the B structure to the complex, Pauling's "bond-length" relation[4] seems to be useful for the complex[5], since this relation holds for intermetallic compounds and also for organic compounds. The relation is represented by

$$R(n)-R(1)=-C\log_{10}n$$

Here, $R$ expresses the atomic radius, $n$ is the number of shared electron pairs involved in the bond and is proportional to the bond order[5], and $C$ a constant. As for the bond length $L$ the following formula is obtained from the formula described above.

$$L(n)-L(1)=-2C\log_{10}n$$

The values of $L(n)$ are estimated to be 2.15 and 2.46 Å for O—$Li^+$ and O—$Na^+$ bonds, respectively. These values are the same as those obtained for $LiClO_4\cdot3H_2O$[6a] and $Na_3SbS_4\cdot9H_2O$[6b] or $Na\cdot Al(SO_4)_2\cdot12H_2O$[6c] crystals in which the $Li^+$ or $Na^+$ ion combines with the ligands of six water molecules by the coordination of the lone pair electrons of oxygen atoms. As $C$ is usually 0.30 for intermetallic compounds and 0.35 for organic compounds, the mean value of them, 0.325, is used for these complexes. By use of the usual covalent radii for $R(1)$[7], the relation $L(1)=R_O(1)+R_M(1)$ and the values of $L(n)$, the values of $n$ are obtained. The suffixes O and M refer to

5) Coulson and Danielson applied in to the hydrogen bonds to estimate the contribution of the B structure, and reported that the results obtained agreed satisfactorily with the results calculated by a semi-empirical method. C. A. Coulson and U. Danielson, *Arkiv För Fysik*, **24**, 239 (1954).

6) a) C. D. West, *Z. Krist.*, **88**, 198 (1934).
b) A. Grund and A. Preisnger, *Acta Cryst.*, **3**, 363 (1950).
c) H. Lipson, *Proc. Roy. Soc.* (*London*), **A151**, 347 (1935).

7) The covalent radii used are $R_O(1)=0.66$, $R_{Li}(1)=1.34$ and $R_{Na}(1)=1.54$ Å.

oxygen and metal, respectively. From the meaning of $n$, the following formula should hold for the complexes,

$$b^2 = n \times (\text{covalent character of the } L(1) \text{ bond})$$

Since the covalent character of the $L(1)$ bond can be estimated from the difference between the electronegativities of two atoms, the covalent character of $L(n)$ bond, $b^2$, is calculated. The results are contained in Table II.

Table II

| | $n$ | Difference of electronegativities | Covalent character of the $L(1)$ bond | $b^2$ |
|---|---|---|---|---|
| O—$Li^+$ | 0.59 | 2.5 | 22% | 0.13 |
| O—$Na^+$ | 0.40 | 2.6 | 20% | 0.08 |

The covalent character of O—$Li^+$ is 13% and that of O—$Na^+$ 8%. It can be seen that these complexes mainly consist of the no-bond structure and the covalent character of O—$Li^+$ is about 1.5 times that of O—$Na^+$.

**Stabilization Energy of the Complex.**—By use of the amount of contribution of the B structure obtained above, the stabilization energy of the complex per one ketone molecule was estimated. According to Mulliken[3], the ground state wave function of the complex is written by

$$\Psi_N = a\phi_A + b\phi_B$$

and the stabilization energy of the complex in ground state is given by

$$W_{AA} - W_N = (W_{BB} - W_{AA})b^2/a^2$$

where $\phi_A$ is the no-bond wave function and $\phi_B$ the dative one,

$$W_{AA} = \int \phi_A H \phi_A d\tau$$

$$W_{BB} = \int \phi_B H \phi_B d\tau = I_P - E_A + V$$

In this case, $I_P$ is the ionization potential of the oxygen atom for lone pair electrons, $E_A$ the electron affinity of the metallic ion and $V$ the energy of the covalent bond between the oxygen atom and the ion. Although the exact values of $I_P$ and $E_A$ are not available, the following ones seem to be reliable, i.e. $I_P = 10.1$ eV., $E_A = 5.39$ eV. for $Li^+$ and 5.14 eV. for $Na^+$. The energy $V$ may be expressed by Morse's function, i. e.

$$V = D_e(e^{-2a(L-L_e)} - 2e^{-a(L-L_e)}), \quad L_e = L(1)$$

where the dissociation energy, $D_e$, is given by the geometric mean of the bond energies $D$(O—O) and $D$(M—M), and $a$ is determined by Badger's rule.

$$a = (k/2D_e)^{1/2}$$

where $k$ expresses the force constant.

Table III

| | $D_e$ (kcal./mol.) | $k$ (dyne/cm.) | $a$ (Å$^{-1}$) | $V$ (eV.) |
|---|---|---|---|---|
| O—$Li^+$ | 30.8 | $0.808 \times 10^5$ | 1.37 | −1.29 |
| O—$Na^+$ | 25.3 | $0.847 \times 10^5$ | 1.55 | −0.977 |

The formation energy of the complex bond, namely the stabilization energy of the lone pair electrons is determined as follows.

$$W_{AA} - W_N = (I_P - E_A + V)b^2/a^2$$
$$= 0.51 \text{ eV. } (O—Li^+)$$
$$0.34 \text{ eV. } (O—Na^+)$$

where $W_{AA}$ is taken to be zero.

**Computation of the $n \rightarrow \pi^*$ Transition Energies of the Acetone-salt Complexes.**—By taking into account the stabilization energies, the $n \rightarrow \pi^*$ transition energies of the complexes can be calculated. As the energy level of lone pair electrons is approximately expressed by the coulomb integral of oxygen atom, the stabilization energy of the complex is due to the decrease of the coulomb integral of oxygen atom. The stabilized energy level may be expressed by

$$\alpha_O' = \alpha_O + (W_{AA} - W_N)/2$$

Here, $\alpha_O$ expresses the coulomb integral of oxygen atom. As for the other numerical values required for the computations, Nagakura's values[8] for acetone molecule are used. They are, $X_C = 2.5$, $X_O = 3.5$, $k = 4.1$, $\alpha_C = 4.35\beta$, $\alpha_O = 5.44\beta$ and $\beta_{CO} = 0.838\beta$ in his notation. The calculated results are shown in Table IV(A), in which the $n \rightarrow \pi^*$ transition energy is expressed by $E_2 - \alpha_O'$. In Table IV(B) the calculated $n \rightarrow \pi$ transition energies are shown in wave number unit, together with the observed data. Here, $\beta = 2.84$ eV. $= 23000$ cm$^{-1}$. It seems more reasonable to compare the calculated

Table IV

(A)

| | Acetone | $NaClO_4$-acetone complex | $LiClO_4$-acetone complex |
|---|---|---|---|
| $E_1$ | $5.895\beta$ | $5.94\beta$ | $5.96\beta$ |
| $E_2$ | 3.895 | 3.91 | 3.92 |
| $\alpha_O'$ | 5.44 | 5.50 | 5.53 |
| $E_2 - \alpha_O'$ | −1.55 | −1.59 | −1.61 |

(B)

| | | | |
|---|---|---|---|
| Cal. | 35600 | 36600 | 37000 |
| Obs. | 35800 (in non-polar solvent) | 36900 | 38000 |
| | 36400 (in liquid) | | |

8) S. Nagakura, This Bulletin, 25, 164 (1952).

value for acetone with the observed value in non-polar solvent than that in liquid.

Although the formation of the complexes is mainly due to the no-bond structures, the $n \rightarrow \pi^*$ blue shift phenomenon is interpreted by use of the results calculated by considering the charge transfer interaction.

The author wishes to express her sincere thanks to Professor K. Kozima for his kind guidance.

*Research Laboratory of Spectroscopy*
*Tokyo Institute of Technology*
*Meguro-ku, Tokyo*

# *Intramolecular Interaction between N–H Group and π-Electrons in N-Benzylanilines*

By Michinori Ōki and Kiyoshi Mutai

(Received December 14, 1959)

The discovery[1] of the rotational isomers and the intramolecular interaction between the hydroxyl group and π-electrons in benzyl alcohol derivatives has prompted the authors to examine the N–H stretching absorption of the benzylamine derivatives, since the situation will be much similar in these two series of compounds. The observation of two $\nu_{N-H}$ bands for *N*-benzylaniline was reported by Ōki and Iwamura[1], while Russel and Thompson[2] had reported the presence of two $\nu_{N-H}$ bands for *N*-benzylaniline and attributed them to the rotational isomerism. Moritz[3] also noticed the existence of two $\nu_{N-H}$ bands for some derivatives of *N*-benzylaniline while the present paper was in preparation and the observation of two $\nu_{N-H}$ bands for *N*-allylaniline by Schleyer et al.[4] may also fall into this category.

The present paper deals with the rotational isomers of *N*-alkylanilines in respect of the $C_{aliph}$–N axis and the intramolecular interaction between the N–H group and π-electrons in N-benzylanilines. Aniline derivatives are not the indispensable choice but are convenient for handling, since they do not absorb carbon dioxide from the air owing to the low basicity.

## Experimental

**Measurement and Calculation.**—They were performed as reported previously[5]. The concentration of the carbon tetrachloride solution ranged from 0.003 to 0.005 mol./l.

**Materials.**—The compounds used in the present study are known compounds unless otherwise stated, and were purified through the known method. Their physical constants agreed well with those reported.

*N-(m-Methoxybenzyl)-aniline.*— *m*-Methoxybenzanilide obtained by heating methyl *m*-methoxybenzoate with aniline was reduced with lithium aluminum hydride in ether and the product was purified through fractional distillation. It is a colorless oil, b. p. 200~202°C/21 mmHg, $n_D^{25.5}$ 1.6039.

Found: C, 78.97; H, 7.34. Calcd. for $C_{14}H_{15}NO$: C, 78.84; H, 7.09%.

*N-(m-Dimethylaminobenzyl)-aniline.*—It was prepared similarly as above, starting from *m*-dimethylaminobenzanilide, and recrystallized from ethanol. It forms colorless needles melting at 60–61°C.

Found: C, 79.65; H, 8.12. Calcd. for $C_{15}H_{18}N_2$: C, 79.60; H, 8.02%.

## Results and Discussion

***N*-Alkylanilines.**—The apparent absorption curves for N–H stretching of *N*-alkylanilines are shown in Fig. 1. The curves for *N*-methylaniline is symmetric, while those for N-ethylaniline and for *N*-isopropylaniline are unsymmetric. The unsymmetric curves are divided, assuming that the curve is an overlap of two symmetric curves which can be expressed by the Lorentz function. The results are summarized in Table I.

Inspection of Table I reveals that the positions of absorption curves can be classified as three categories. Namely, band I is located at about 3444 $cm^{-1}$, band II at about 3421 $cm^{-1}$ and band III, at about 3395 $cm^{-1}$. The origin of the splitting of the $\nu_{N-H}$ absorption cannot be attributed to hydrogen bonding among the solute molecules, because firstly, the low concentration such as 0.005 mol./l.

1) M. Ōki and H. Iwamura, This Bulletin, **32**, 955 (1959).
2) R. A. Russel and H. W. Thompson, *J. Chem. Soc.*, 1955, 483.
3) A. G. Moritz, *Spectrochim. Acta*, **12**, 242 (1959).
4) P. von Schleyer, D. S. Trifan and R. Bacskai, *J. Am. Chem. Soc.*, **80**, 6691 (1958).
5) M. Ōki and H. Iwamura, This Bulletin, **32**, 567 (1959).

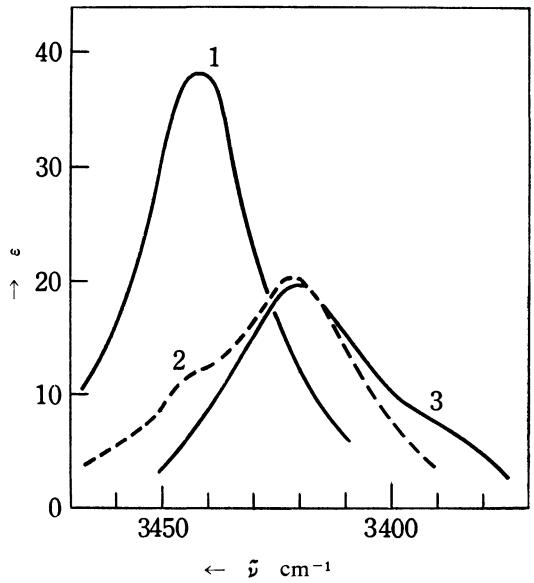



Fig. 1. $\nu_{N-H}$ absorptions of methylaniline (1), ethylaniline (2) and isopropylaniline (3).

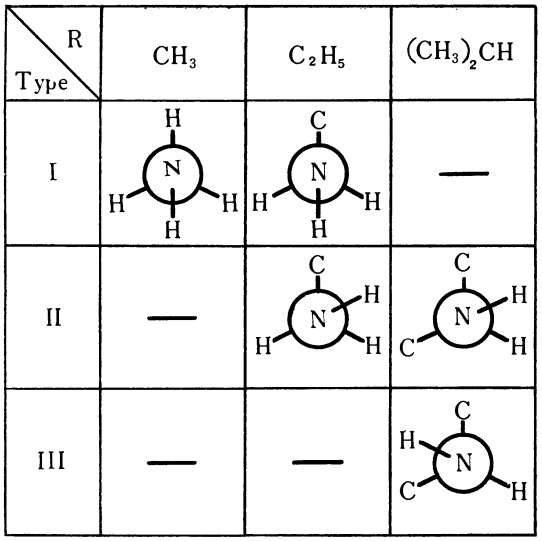



Fig. 2. Classification of rotational isomers in alkylanilines.
The phenyl group is omitted from the diagram for convenience.

TABLE I. $\nu_{N-H}$ ABSORPTION OF *N*-ALKYLANILINES ($RNHC_6H_5$)

| *R* | Band | $\nu_{max}$ cm$^{-1}$ | $\Delta\nu^a_{1/2}$ cm$^{-1}$ | $A\times10^{-3}$ mol$^{-1}$·l.·cm$^{-2}$ |
|---|---|---|---|---|
| $CH_3$ | I | 3442.6 | 29.8 | 4.13 |
| $C_2H_5$ | I | 3445.2 | 18.2 | 0.28 |
| | II | 3421.4 | 34.2 | 2.44 |
| $(CH_3)_2CH$ | II | 3420.5 | 31.2 | 2.19 |
| | III | 3394.5 | 22.0 | 0.30 |

would not permit the dimeric form to exist and secondly any kind of association of the molecules does not explain the symmetry of the absorption curve of *N*-methylaniline examined under the similar conditions as the others.

Thus the variation of the curves must be attributed to the variation of the alkyl group attached to the nitrogen atom and the concept of the rotational isomerism about the $C_{aliph}$–N axis will be valid for the explanation as for a similar phenomenon in the aliphatic alcohols[6].

In Fig. 2, the projection of the molecule through the $C_{aliph}$–N axis, the nitrogen atom being located at the upper side, is shown. A circle indicates a carbon atom as is customary in Newman projection. It is assumed that the molecule does not take an eclipsed form, thence the hydrogen atom of the N-H group in *N*-methylaniline must be in the same situation, because it always comes between the two hydrogen atoms attached to the alpha-carbon atom, no matter what rotational position is taken. On the other hand, when the alkyl group is an ethyl, there are two posibilities, that the hydrogen atom of the N-H group comes either between the two hydrogen atoms of the alpha-carbon atom or between the carbon and the hydrogen atoms combined with the alpha-carbon atom. Thus two rotational isomers are possible for *N*-ethylaniline. Similarly, *N*-isopropylaniline can take two conformations. Band I may be considered to correspond to rotational isomer I, band II to isomer II and band III to isomer III.

The probability of isomer II is 2/3 for both *N*-ethylaniline and *N*-isopropylaniline. However, the observed values widely differ from those expected and isomer II seems to be an overwhelming majority, since it is probable to assume that the light absorption of a molecule is the same irrespective of its conformation. The reason is not completely understood at the present time but it is clear that the steric effect plays an important role, because the nitrogen atom carries a large phenyl group.

**N-Arylmethylanilines.**—*N*-Benzylaniline derivatives have two distinct maxima for N-H stretching absorption and the separation of the two bands are much clearer than in *N*-alkylanilines (compare Fig. 3 with Fig. 1). The apparent absorption curves for *N*-(*p*-nitrobenzyl)-aniline, *N*-benzylaniline and *N*-(*p*-dimethylaminobenzyl)-aniline are shown in Fig. 3.

The electron-withdrawing group such as the nitro group enhances the band at the higher wave number and diminishes the band at the lower wave number. On the other hand, the electron-donating group such as the dimethylamino group shows just the contrary tendency

6) M. Ōki and H. Iwamura, ibid. 32, 950 (1959).

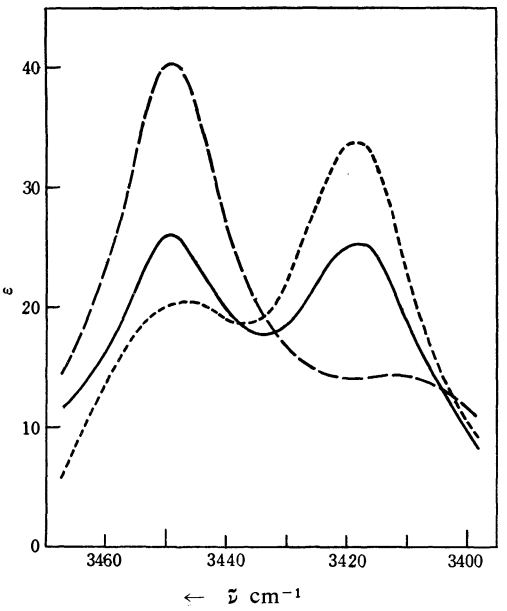



Fig. 3. $\nu_{N-H}$ absorptions of benzylaniline (——), *p*-nitrobenzylaniline (----) and *p*-dimethylaminobenzylaniline (------).

and the absorption at the lower wave number forms the main peak. It is again assumed that the curves are the overlaps of the two symmetric curves which obey the Lorentz function and the apparent curves are divided by Ramsay's first method. The results are shown in Table II.

The ratio $A_i/A_f$, where $A_i$ is the integrated intensity of the absorption due to the interacting form and $A_f$ that of the free form, varies with the electron-donating or electron-withdrawing nature of the substituent and the tendency is indicative of the interaction between the $\pi$-electron and the N-H group. The summation of the integrated intensities due to the two forms also changes when the substituent varies, but this fact may be left out, for comparison of the ratio $A_i/A_f$.

Hammett's $\sigma$ values[7] of the substituents are taken and the relation with $\log(A_i/A_f)$ is compared. $\mathrm{Log}(A_i/A_f)$ instead of $A_i/A_f$ is taken, because the equilibrium between the interacting and the free forms is the subject of the present discussion. As is seen from Fig. 4, the relation is linear when the $\sigma$ constants representing the electron density on the carbon atom[8] ($C_1$), to which the anilinomethyl group is attached, are taken. However, $\sigma$ values for the other carbon atoms or for the position between two carbon atoms are not proportional to $\log(A_i/A_f)$.

Since the benzylaniline derivatives are secondary amines, which belong to the *N*-ethylaniline type (Fig. 2), they should have two

TABLE II. $\nu_{N-H}$ ABSORPTION OF *N*-(ARYLMETHYL)-ANILINES ($x$-$RC_6H_4CH_2NHC_6H_5$)

| *R* | *x* | Band | $\nu_{max}$ cm$^{-1}$ | $\Delta\nu_{max}$ cm$^{-1}$ | $\Delta\nu^a_{1/2}$ cm$^{-1}$ | $A\times10^{-3}$ mol$^{-1}$·l.·cm$^{-2}$ | $\log(A_i/A_f)$ | $\sigma$ |
|---|---|---|---|---|---|---|---|---|
| $(CH_3)_2N$ | *p* | i[a] | 3418.2 | 30.5 | 27.6 | 3.15 | 0.382 | −0.83 |
| | | f[b] | 3448.7 | | 24.2 | 1.31 | | |
| | *m* | i | 3419.0 | 31.8 | 29.6 | 2.86 | 0.276 | −0.20 |
| | | f | 3450.8 | | 25.6 | 1.51 | | (−0.55)[d] |
| $CH_3O$ | *p*[c] | i | 3418.0 | 32.1 | 27.8 | 2.63 | 0.182 | −0.27 |
| | | f | 3450.1 | | 23.7 | 1.73 | | |
| | *m* | i | 3417.0 | 32.4 | 28.4 | 2.22 | 0.017 | 0.12 |
| | | f | 3449.4 | | 26.8 | 2.14 | | |
| H[c] | | i | 3417.4 | 32.8 | 28.6 | 2.24 | 0.025 | 0.00 |
| | | f | 3450.2 | | 25.6 | 2.11 | | |
| Cl | *p* | i | 3415.3 | 34.6 | 37.6 | 2.76 | −0.034 | 0.23 |
| | | f | 3449.9 | | 29.2 | 2.60 | | |
| | *m* | i | 3411.9 | 38.0 | 27.2 | 2.23 | −0.066 | 0.37 |
| | | f | 3449.9 | | 38.4 | 2.60 | | |
| $NO_2$ | *m* | i | 3406.6 | 42.1 | 45.2 | 2.03 | −0.248 | 0.71 |
| | | f | 3448.7 | | 29.4 | 3.58 | | |
| | *p* | i | 3407.9 | 42.2 | 51.6 | 1.94 | −0.244 | 0.78 |
| | | f | 3450.1 | | 25.2 | 3.41 | | |

a) i denotes interacting form of the N-H group.
b) f denotes free form of the N-H group.
c) The values are taken from Ref. 1.
d) See the discussion below.

7) L. P. Hammett, "Physical Organic Chemistry", McGraw-Hill Book Co., Inc., New York, (1940); H. H. Jaffé, *Chem. Revs.*, **53**, 191 (1953); D. M. McDaniel and H. C. Brown, *J. Org. Chem.*, **23**, 420 (1958).

8) H. H. Jaffé, *J. Chem. Phys.*, **20**, 279, 778 (1952); *J. Am. Chem. Soc.*, **76**, 5843 (1954).

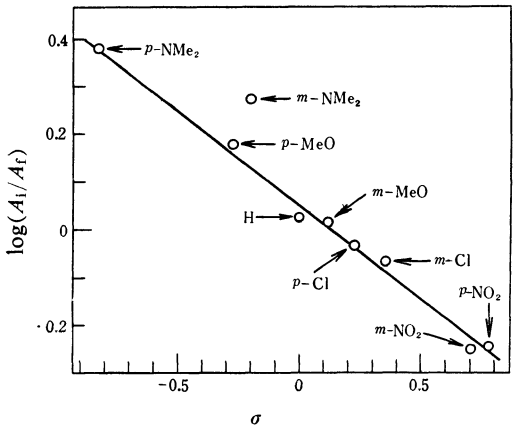
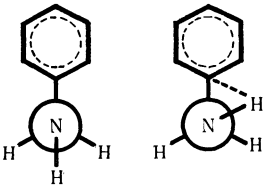



Fig. 4. Comparison of $\log(A_i/A_f)$ of *N*-(arylmethyl)-anilines with $\sigma$-values.




IV V

Fig. 5. Possible rotational isomers of benzylaniline (ring B is abbreviated).

rotational isomers. The absorption due to the free form is closely related to type I of *N*-ethylaniline, because it lies at about 3450 $cm^{-1}$, while type I of *N*-ethylaniline absorbs at 3445 $cm^{-1}$. Thus, the free form of *N*-benzylaniline corresponds to the rotational isomer IV and the interacting form to structure V in Fig. 5. The interaction takes place between the $\pi$-electron on $C_1$ atom and the N-H group, as judged from the relation between $\sigma$ constants and $\log(A_i/A_f)$. Therefore, the structural formula for the interacting form can be represented by structure V.

One problem remains in the above assignment. That is, the number of molecules of the free form of the *N*-benzylaniline derivatives seem to increase in spite of the expectation that the formation of the internal interaction will lessen the free molecules when compared with the number of molecules belonging to type I in *N*-ethylaniline. In the earlier paper[1], it was pointed out that the internal interaction between the hydroxyl group and $\pi$-electrons decreases the number of free molecules. This contradiction may be attributed to the steric effect, since the nitrogen atom carries a large phenyl group. And/or it may be attributed to the difference of the nature of the interactions with the N-H group and with the O-H group series.

The far deviation of the point for *N*(*m*-dimethylaminobenzyl)-aniline might be interpreted in the following way. Jaffé[7] gave $\sigma$ value of −0.20 for the *m*-dimethylamino group and this value is taken in Fig. 4. On the other hand, $\sigma$ value of the *p*-dimethylamino group has been given by Jaffé as −0.60, while the recent paper by McDaniel and Brown[7] gives −0.83. From an analogous consideration, $\sigma_m$ given by Jaffé may be smaller than the true and ambiguous, because of lack of examples. The authors obtain $-0.55\pm0.05$ for the $\sigma_m$ of the dimethylamino group from Fig. 4.

Fluctuation of the position for the interacting $\nu_{H-N}$ will be discussed in "the nature of the interaction".

**N-Benzylarylamines.** — The substituent is introduced into the benzene ring which carries the N-H group to understand the electronic effect. It is expected, that the substituent will vary the nature of the N-H bond. The results are given in Table III.

The effect of the substituent on $A_i/A_f$ is not found in Table III. Thus the electron density at the site of hydrogen approach seems

Table III. $\nu_{N-H}$ absorption of *N*-arylbenzylamine ($C_6H_5CH_2NHC_6H_4R$-*p*)

| *R* | Band | $\nu_{max}$ $cm^{-1}$ | $\Delta\nu_{max}$ $cm^{-1}$ | $\Delta\nu^a_{1/2}$ $cm^{-1}$ | $A\times10^{-3}$ $mol^{-1}\cdot l.\cdot cm^{-2}$ | $A_i/A_f$ | $\sigma$ |
|---|---|---|---|---|---|---|---|
| $CH_3O$ | i | 3405.6 | 37.1 | 35.8 | 1.93 | 1.11 | −0.27 |
| | f | 3442.7 | | 30.5 | 1.74 | | |
| $CH_3$ | i | 3413.5 | 34.8 | 34.6 | 2.34 | 1.30 | −0.17 |
| | f | 3448.3 | | 28.0 | 1.79 | | |
| H[a] | i | 3417.4 | 32.8 | 28.6 | 2.24 | 1.06 | 0.00 |
| | f | 3450.2 | | 25.6 | 2.11 | | |
| Cl | i | 3420.7 | 31.1 | 26.6 | 2.55 | 1.10 | 0.23 |
| | f | 3451.8 | | 23.0 | 2.32 | | |
| Br | i | 3421.5 | 30.0 | 27.4 | 2.75 | 1.08 | 0.23 |
| | f | 3451.5 | | 23.6 | 2.54 | | |
| $NO_2$ | i | 3431.8 | 23.2 | 17.6 | 5.45 | 1.34 | 0.78 |
| | f | 3455.0 | | 17.4 | 4.05 | | |

a) The values are taken from reference 1.

to determine the number of internally interacting molecules.

The things which vary with the varying substituent are the individual absorption peak of the free and the interacting molecules, and the difference of positions of peaks ($\Delta\nu_{max}$) corresponding to each species of the molecule. The absorption maxima of both free and interacting forms move to higher frequencies as the substituent becomes more electronegative, although the relation between the $\sigma$ constants and the frequencies of absorption is not perfectly linear. This result roughly agrees with the data obtained by others[9] who have revealed the relationship in aniline derivatives.

One thing noticeable is that $\Delta\nu_{max}$ between the free and the interacting forms relates linearly with the $\sigma$ value of the substituent (Fig. 6), although the rate of increase or decrease of the frequencies of the free and the interacting forms is not the same and the straight lines, which show the relation between $\sigma$ value and $\nu_{max}$, are not parallel to each other. The phenomenon will be discussed in "the nature of the interaction".

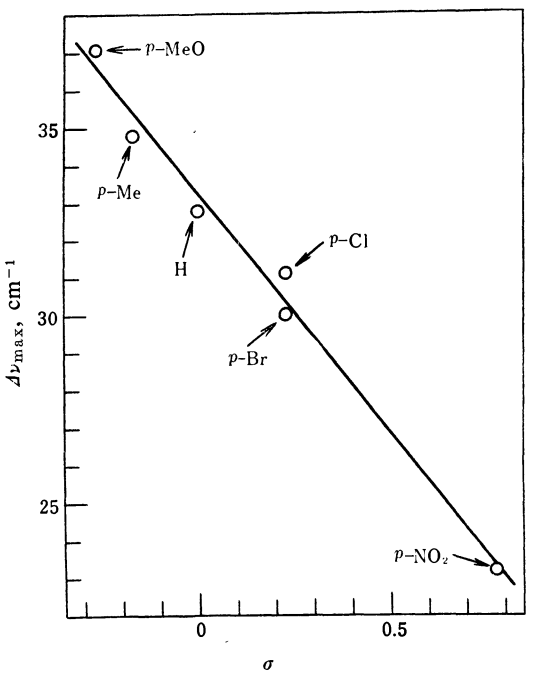
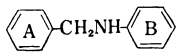



Fig. 6. Comparison of $\Delta\nu_{max}$ of *N*-arylbenzylamines with $\sigma$-values.

**Nature of the Interaction.**—It is now known from Table II that the $\nu_{N-H}$ absorption due to the interacting form does not always appear at the constant wave number, when the substituent is introduced into the benzene ring (ring A) which is included in the benzyl group. This is the striking difference when the situation of the benzyl alcohol derivatives is considered, of which interacting hydroxyl groups




absorb at a reasonably constant frequency. As was already pointed out, the free form absorbs at the constant wave number, ca. 3450 $cm^{-1}$, irrespective of the substituent, indicating the effect of the substituent through the methylene group is negligible.

The relation between $\Delta\nu_{max}$ and $\sigma$ values for the compounds carrying a substituent in ring A, is shown in Fig. 7, which reveals, that the slope of the straight line is not constant but shows a crease at some point. When the electron density on ring A is decreased, $\sigma$ constants and $\Delta\nu_{max}$ are in linear relation, the slope being positive. On the other hand, when $\sigma$ value is below 0.00~0.10, the slope of the straight line is almost zero, i. e., $\Delta\nu_{max}$ seems to have no connection with the substituent.

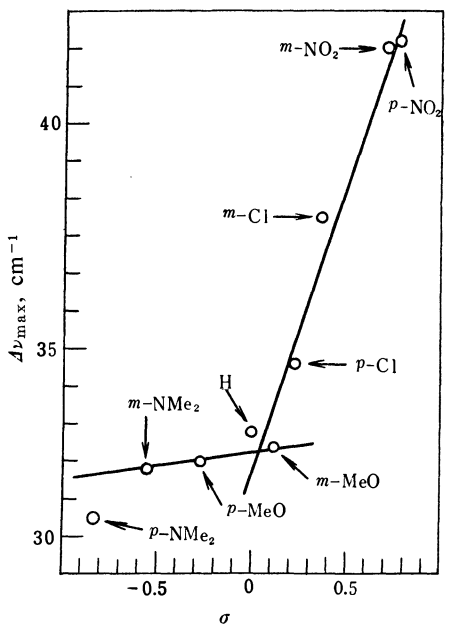



Fig. 7. Comparison of $\Delta\nu_{max}$ of *N*-(arylmethyl)-anilines with $\sigma$-values.

Yet, splitting of the $\nu_{N-H}$ band into two distinct maxima must be attributed to the intramolecular interaction between the N-H group and the $\pi$-electron, no matter which ring carries the substituent. The mechanism of the interaction must also be common in both series of compounds and will satisfy the following conditions. 1) The larger the $\sigma$ constant, the

9) M. St. C. Flett, *Trans. Faraday Soc.*, **40**, 767 (1944); S. Califano and R. Mocca, *Gazz. chim. ital.*, **86**, 1014 (1956); P. J. Krueger and H. W. Thompson, *Proc. Roy. Soc.*, **A243**, 143 (1957).

smaller is the $\Delta\nu_{max}$, when the benzene ring (ring B), which carries the N-H group, bears the substituent. In the case of the substituent involved in ring A, $\Delta\nu_{mnx}$, increases as the $\sigma$ value increases, as far as the $\sigma$ value is larger than 0.1. 2) When a substituent of which the $\sigma$-constant is less than 0.1 is introduced into ring A, $\Delta\nu_{max}$ changes to a negligible extent, regardless of the substituent.

It must be noticed that condition 1 is just the contrary to the case mentioned in $\omega$-arylalkanols[10], In the case of $\omega$-arylalkanols, the hydrogen atom of the hydroxyl group possesses at least a proton-like character and the increasing electron density in the benzene nucleus favors the interaction. The above considerations lead to an idea that is quite different from that developed for the interaction between the hydroxyl group and $\pi$-electrons.

That is, one of the possibilities which will explain the results is the idea of "flow-in" of the electron from the N-H group to ring A. If this idea were taken into consideration, above conditions 1 and 2 would be explained in the following way. The greater the electron-density gap between ring A and the N-H group, the easier the flow of the electron of the latter into the former, as far as the electron density of the N-H group is higher, Thus the force constant of the N-H group is lessened to result in appearance of the N-H band at a lower wave number and also in more $\Delta\nu_{max}$. If the difference of electron densities between ring A and the N-H group approaches zero or the electron density of ring A is higher than that of the latter, the electron of the N-H group does not "flow-out". Then, it will be the field effect that plays the most important role, and $\Delta\nu_{max}$ may appear at the constant wave number, irrespective of the substituent.

Furthermore, if the above assumption is made, it is easier to understand the phenomenon found in *N*-benzylarylamines. When an electron-withdrawing substituent is introduced into ring B, the electron of ring B is attracted to the substituent, hence the electron of the N-H group flows into ring B. The lack of the electron in the N-H group results in a smaller electron-density difference between ring A and the N-H group. This permits the flow of the electron from the N-H group to ring A to a very limited extent, the interaction between $\pi$-electron and N-H group becoming weaker. Thus the strength of the interaction or $\Delta\nu_{max}$ may be proportional to $\sigma$ constant of the substituent, when the substituent is introduced into ring B.

In the above hypothesis, it is assumed, that the interaction takes place as a mere probability. The interaction must be caused by an overlap of the orbitals belonging to the electrons of the N-H group and the $\pi$-electrons of ring A. And the overlap of orbitals will occur more easily, when the electron density of ring A is heightened by the presence of an electron-repelling group. Accordingly, the molecular species which has the internal interaction increases when the electron density of ring A is higher, although the electron flows out of the N-H group into ring A.

A support to the above hypothesis is being sought.

The authors are thankful to Professor Y. Urushibara and Professor T. Shimanouchi for their valuable advice and encouragement and to Mr. H. Iwamura for his technical assistance. The authors are also indebted to the Ministry of Education for the Grant in Aid for the Fundamental Scientific Research.

*Department of Chemistry*
*Faculty of Science*
*The University of Tokyo*
*Hongo, Tokyo*

10) M. Ōki and H. Iwamura, This Bulletin, **32**, 1135 (1959).

# *Hydrogen Reduction of a Single Crystal of Nickel Oxide*

By Yoshio IIDA and Kenzo SHIMADA

(Received November 24, 1959)

In an earlier paper[1] it was shown that the reduction of nickel oxide was strongly affected by a small amount of additive incorporated in the nickel oxide lattice. Little attention has been paid to the mechanism of hydrogen reduction of metal oxide, while the mechanism of oxidation of metal has been studied successfully since Wagner's theory[2]. Recently Baba[3] explained the mechanism of hydrogen reduction of germanium dioxide by assuming that the reduction is governed by an autocatalytic behavior. Murata[4] reported that a diffusion process of cation or anion is a rate-determining process in the hydrogen reduction of iron oxide. In their experiments oxide powder was used as a specimen. As powder exhibits complicate properties resulting from particle size and shape, powder is thought to be unfavorable to the study of the mechanism of the hydrogen reduction. From these points it is desirable to study the hydrogen reduction of a single crystal. In the present study the hydrogen reduction of a single crystal of nickel oxide has been carried out to explain the mechanism of the reduction.

## Experimental Procedure

A single crystal of nickel oxide was prepared by Tochigi-Kagaku Co. in a way similar to Verneuil's method[5]. Rectangle specimens of 6×4×3 mm. were cut out from the raw material. The specimens were not subjected to further treatment.

Nickel nitrate recrystallized four times was heated at 800°C for 10 hr. to obtain nickel oxide powder. The average particle size of the nickel oxide was about 0.5 $\mu$ according to an electron micrograph.

The weight loss during the reduction process was measured by the thermobalance with a sensitivity of 0.5 mg. The apparatus could be used in hydrogen or in vacuo. After the specimen was heated in vacuo at a desired temperature, it was reduced with hydrogen. Hydrogen was used from a commercially available tank after purifying it with concentrated sulfuric acid, hot platinum asbestos, potassium hydroxide and phosphorus pentoxide.

## Results and Discussion

**Time-dependent Study.**—A comparison of a reduction-temperature curve of a single crystal of nickel oxide with that of nickel oxide powder when heated at a velocity of 100°C/hr. is shown in Fig. 1. It is seen that a rate of reduction of the single crystal is much lower than that of the powder. It should be noted that there is the stage at about 500°C in the case of the single crystal where the reduction slows down. In order to elucidate the mechanism of the hydrogen reduction of nickel oxide, the isothermal reduction of the single crystal was studied in the range of 300°C to 800°C. The results are shown in Fig. 2. To see whether

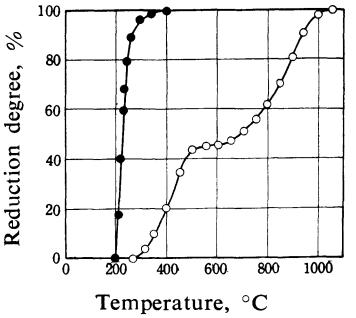



Fig. 1. Reduction-temperature curves of a single crystal of nickel oxide (○) and nickel oxide powder (●).

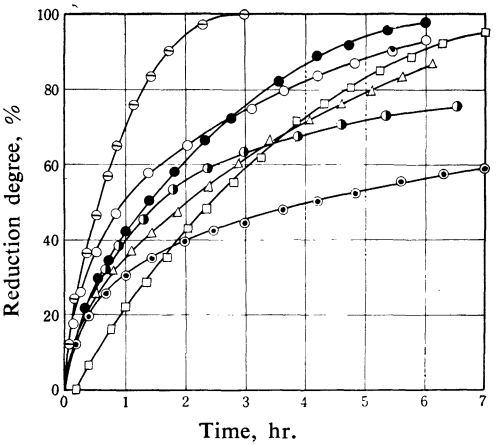



Fig. 2. Isothermal reduction of a single crystal of nickel oxide. □, 300°C: ●, 350°C: △, 400°C: ⊙, 500°C: ◑, 600°C: ○, 700°C: ⊖, 800°C

1) Y. Iida and K. Shimada, This Bulletin, to be published.
2) C. Wagner, *Z. physik. Chem.*, **49**, 735 (1936).
3) H. Baba, This Bulletin, **29**, 789 (1956).
4) Y. Murata and N. Kasaoka, *J. Chem. Soc. Japan, Ind. Chem. Sec.* (*Kogyo Kagaku Zasshi*), **61**, 1440 (1958).
5) J. Nakazumi, ibid., **59**, 1304 (1956).

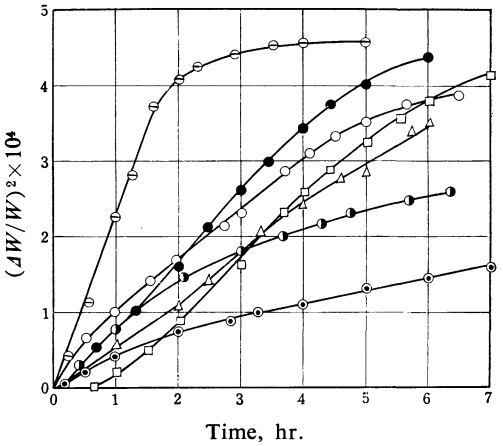



Fig. 3. Parabolic plot of isothermal reduction of a single crystal of nickel oxide. □, 300°C: ●, 350°C: △, 400°C: ⊙, 500°C: ◑, 600°C: ○, 700°C: ⓘ, 800°C.

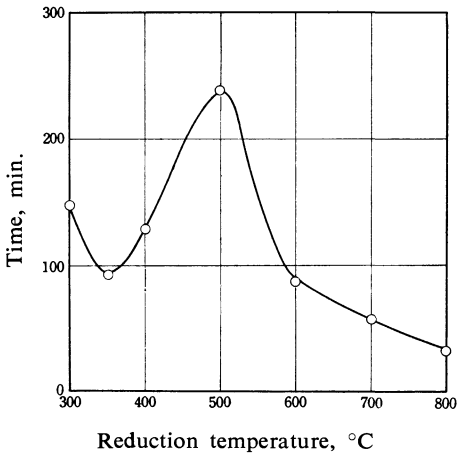



Fig. 4. Time required to obtain 50% reduction at various temperatures.

the isotherms can be expressed by the parabolic law, a square of the reduction loss per gram is plotted against the reduction time. Fig. 3 shows that the reduction of the single crystal does not obey the parabolic law. A rate of reduction of the single crystal does not always increase with an increase in the reduction temperature. In Fig. 4, the time required to obtain 50% reduction is plotted against the reduction temperature. It is seen that the time at 350°C is shorter than that at 300°C whereas the time increases with an increase in the reduction temperature in the range of 350°C to 500°C. Since the time is reversely proportional to the rate of the reduction, the rate is lowest at 500°C and then increases with an increasing temperature as do ordinary chemical reactions. The stage at which the reduction does not proceed in the reduction-temperature curve of the single crystal at 500°C is attributed to the lowest rate of the reduction at 500°C. In the reduction of nickel oxide powder or other metal oxide such as ferric oxide and tungsten oxide powder, these phenomena were not observed.

**Microscopical Examination.** — Reduction of the single crystal oxide proceeds layer by layer as shown in Fig. 5. The specific gravity of

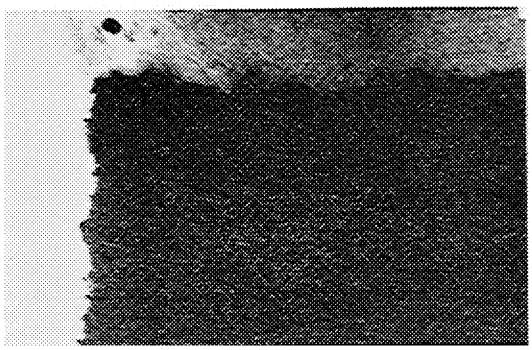


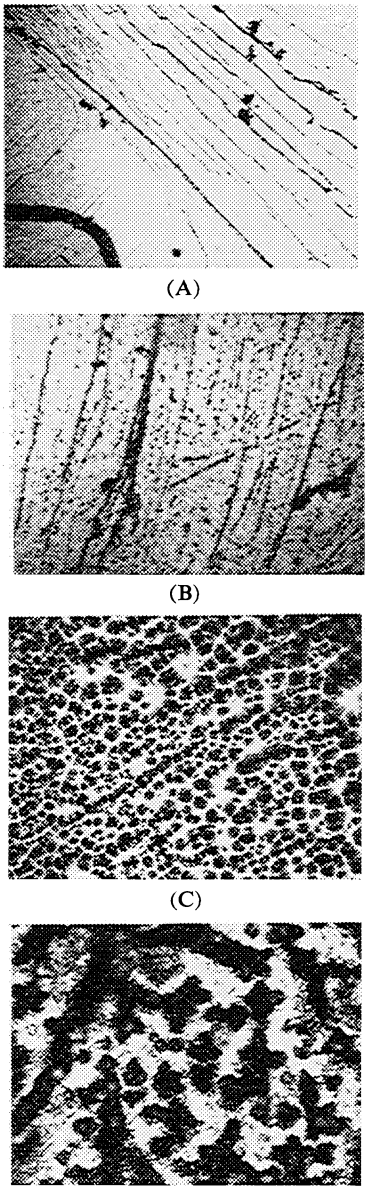
Fig. 5. A section of a single crystal of nickel oxide reduced partially. A white part is a reduced nickel phase and a brack part is an unreduced nickel oxide phase. (×20)

the single crystal of nickel oxide is 6.8 and that of nickel is 8.90. As a volume ratio of nickel oxide is 6.8/8.9=0.76, the specific volume of nickel is lower than that of nickel oxide. Accordingly, the nickel layer formed on the nickel oxide by the hydrogen reduction should be very porous. The reduction mechanism is considered schematically as follows. Hydrogen passes through the porous nickel layer, and reacts with nickel oxide at the boundary of nickel and nikel oxide. The water formed as a result of the reduction is released from the boundary. The penetration of hydrogen through the porous nickel layer is very easy because of its small molecular size. However, the desorption of water through the nickel layer is thought to be very difficult because of its large molecular size. By this reduction schema, the desorption of water formed is considered to be a rate-determining step in the hydrogen reduction process. Nickel formed on the surface of nickel oxide by the reduction is composed of very fine particles, and the particles start to sinter with an increase in the reduction temperature[6,7]. It is expected that the number and size of the pores decrease at higher temperatures by sintering, and the desorption of water through the pores is retarded. It may be attributed to

6) R. Ueda, *J. Japan Inst. Metals (Nippon Kinzoku Gakkai-Shi)*, **23**, 292 (1959).
7) P. H. Emmett, "Catalysis" Vol. I The Waverly Press, Inc., New York (1954), p. 371.

the change of the pores by sintering that the rate of reduction decreases in the range of 350 to 500°C.

While the sintering is enhanced above 500°C, a pressure of water vapor increases and thus the water vapor passes through the nickel layer forming large pores at higher temperatures. Water vapor can easily be released through the large pore and then the reduction process is promoted above 500°C as shown in Fig. 4.

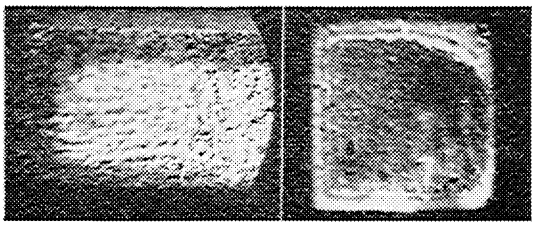


(A) (B) (C) (D)

Fig. 6. Microphotographs of the surface of a single crystal of nickel oxide reduced at various temperatures. (A) is for the unreduced crystal; (B), for the crystal reduced at 400°C: (C), for the crystal reduced at 800°C: and (D), for the crystal reduced at 1000°C. (×400)

A microscopical examination shows that these explanations are correct. Fig. 6a is a microphotograph of the free surface of the unreduced single crystal. Fig. 6b shows that there are many small pores on the surface of the single crystal reduced at 400°C. It is seen in Figs. 6c and 6d that the pores become larger when the single crystal was reduced at 800 and 1000°C. From these facts it is concluded that the release of water from the boundary of the metal and the oxide is a rate-determining step in the hydrogen reduction of the single crystal of nickel oxide.

**Study on the Reduction of Nickel Oxide Powder.**—It is of interest to see whether the reduction of nickel oxide powder can be explained by the above mechanism. Nickel oxide powders of which praticle size was about 1 $\mu$ were compressed to a tablet of 10 $\phi \times 5$ mm. at a pressure of 1000 kg./cm$^2$. The bulk density of the tablet was 3.2 g./cc. and its porosity was 52%, which was thought to be sufficient for the penetration of hydrogen or the release of water. It is expected that each nickel oxide powder can be reduced homogeneously all over the tablet, and the reduction of each powder is governed by the above mechanism. The tablet was reduced at 180 and 250°C. Fig. 7 shows the section of the tablet reduced incompletely. It is seen that the reduction proceeds layer by lager in spite of the porous tablet. At 250°C at which there is no induction period, the reduction starts at the exterior of the tablet. At a reduction temperature of 180°C at which there is an induction period of reduction, the reduction starts at the interior of the tablet. It is generally accepted that a rate of oxidation of nickel is negligibly small below 300°C[8]. The outer oxide layer observed in the reduction of 180°C can not be attributed to the re-oxidation with oxygen contained in hydrogen or with water formed. These facts can not be explained completely by the mechanism reported in the previous literatures[2,3]. At present there is no



(A) (B)

Fig. 7. A section of a compact of nickel oxide powder reduced at 250°C (A) and 180°C (B). (×10)

8) A. E. Gulbransen and K. F. Andrew, *J. Electrochem. Soc.*, **101**, 128 (1954).

alternative but to say that the reduction of nickel oxide powder proceeds topochemically.

**Crystal Growth of Nickel Reduced.**—It is reported[9] that oxide film formed on the metal surface by oxidation has a preferential orientation related to the crystal orientation of the metal. No attention has been paid to the crystal growth of the reduced metal on the metal oxide by the hydrogen reduction from the viewpoint of the crystal orientation of the reduced metal and the metal oxide.

The plane of cleavage of the single crystal of nickel oxide is known to be (100) plane[5]. The nickel layer reduced on the (100) plane of the single crystal of nickel oxide at 1000°C was etched and examined microscopically. The result is shown in Fig. 8, where a square etch pit is seen. It is concluded that nickel formed on (100) plane of nickel oxide by the reduction has (100) plane as perferential orientation.

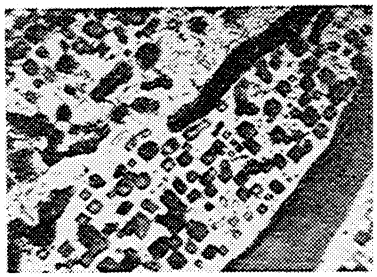


Fig. 8. Etch pit of reduced nickel. The etching reagent is concentrated nitric acid. (×400)

## Summary

In the hydrogen reduction of a single crystal of nickel oxide, the rate of reduction does not always increase with an increase in the reduction temperature. In the range of 350 to 500°C the rate decreases with the temperature, and the rate is the lowest at 500°C. These facts are explained reasonably by the microscopical examination of the surface of the reduced nickel. It is concluded that the desorption of the water formed through the pores is a rate-determining step in the reduction of the single crystal of nickel oxide. The nickel formed on (100) plane of nickel oxide by the reduction has (100) plane as a preferential orientation.

The single crystal of nickel oxide was kindly presented to us by Tochigi Kagaku Kogyo Co.

*Government Industrial Research Institute*
*Kita-ku, Nagoya*

9) I. S. Kerr, *J. Inst. Metals*, **85**, 379 (1956).

# *Partial Molal Volumes of Butyl Alcohols and of Related Compounds in Aqueous Solution*

By Koichiro NAKANISHI

(Received December 4, 1959)

The excess function of any thermodynamic quantities for liquid mixtures is symmetric in form with regards to the mole fraction of component, if the components are the "normal liquids" which consist of the spherical molecule with no specific interaction. However, this symmetry fails when the size and form of one component are different from those of another, or when a specific interaction plays an important role in intermolecular force. In the "associated solution", this specific interaction which is attributed to the formation of hydrogen bonding is predominant, and the anomaly in the behavior of the excess function is often observed for a number of such systems[1].

The same is true for the excess volume (the volume change on mixing). For binary mixtures of the normal liquids the excess volume is generally small and nearly symmetric in form, and the interrelationships with other thermodynamic properties and parameters of the intermolecular force have been also investigated, both experimentally and theoretically, by many authors[2]. On the other hand, large negative excess volume is observed generally for the liquid mixtures containing water, alcohols or other associated liquids as one or both

1) J. A. Barker, *J. Chem. Phys.*, **20**, 794, 1526 (1952); J. A. Barker and F. Smith, ibid., **22**, 375 (1954).

2) G. Scatchard, *Trans. Faraday Soc.*, 33, 160 (1937); J. H. Hildebrand and R. L. Scott, "Solubility of Non-Electrolytes", 3rd. ed., Reinhold Publ. Corp., New York (1950), p. 138; I. Prigognie, "The Molecular Theory of Solution", North-Holland Publ. Co., Amsterdam (1957), p. 176.

TABLE I. DENSITIES OF AQUEOUS SOLUTION OF BUTYL ALCOHOLS AT 20°C

| Normal | | Iso | | Secondary | | Tertiary | |
|---|---|---|---|---|---|---|---|
| Wt. % | Density | Wt. % | Density | Wt. % | Density | Wt. % | Density |
| 1.2684 | 0.99623 | 1.3042 | 0.99610 | 1.2149 | 0.99621 | 1.3139 | 0.99593 |
| 1.9816 | 0.99514 | 2.0761 | 0.99495 | 1.8892 | 0.99522 | 2.3476 | 0.99425 |
| 2.7038 | 0.99405 | 2.7871 | 0.99395 | 2.7195 | 0.99400 | 3.7557 | 0.99199 |
| 3.2835 | 0.99321 | 3.2493 | 0.99319 | 3.4639 | 0.99299 | 4.7743 | 0.99052 |
| 4.0939 | 0.99211 | 3.4096 | 0.99308 | 4.3960 | 0.99173 | 6.2671 | 0.98843 |
| 4.8138 | 0.99114 | 4.1259 | 0.99206 | 4.9808 | 0.99102 | 7.4321 | 0.98689 |
| 5.5200 | 0.99016 | 4.4318 | 0.99154 | 5.7904 | 0.99005 | 8.3009 | 0.98578 |
| 5.6470 | 0.98993 | 4.9319 | 0.99091 | 7.0477 | 0.98848 | 9.4236 | 0.98432 |
| 6.0442 | 0.98950 | 5.2515 | 0.99050 | 8.3458 | 0.98678 | 10.132 | 0.98346 |
| 6.1640 | 0.98924 | 5.6818 | 0.98982 | 8.8445 | 0.98620 | 12.143 | 0.98098 |
| 6.5653 | 0.98878 | 5.9351 | 0.98946 | 9.6519 | 0.98517 | 13.662 | 0.97907 |
| 6.6262 | 0.98862 | 6.5070 | 0.98875 | 10.637 | 0.98396 | 14.612 | 0.97780 |
| 6.7731 | 0.98842 | 6.7836 | 0.98831 | 11.842 | 0.98239 | 15.529 | 0.97671 |
| 7.2231 | 0.98780 | 7.1135 | 0.98798 | 12.753 | 0.98119 | 16.159 | 0.97593 |
| 7.6415 | 0.98722 | 8.0334 | 0.98669 | 13.471 | 0.98019 | 17.943 | 0.97331 |
| 7.7671 | 0.98699 | 8.2184 | 0.98639 | 14.066 | 0.97932 | 19.425 | 0.97100 |
| 78.914 | 0.84872 | 83.448 | 0.83552 | 14.824 | 0.97802 | 21.328 | 0.96754 |
| 90.586 | 0.82837 | 85.353 | 0.83193 | 15.742 | 0.97668 | 24.536 | 0.96115 |
| 100.000 | 0.80973 | 88.757 | 0.82521 | 16.886 | 0.97467 | 30.483 | 0.94841 |
| | | 90.703 | 0.82140 | 18.612 | 0.97211 | 39.115 | 0.92824 |
| | | 94.613 | 0.81375 | 67.968 | 0.87176 | 49.449 | 0.90386 |
| | | 95.391 | 0.81194 | 74.591 | 0.85869 | 58.386 | 0.88322 |
| | | 100.000 | 0.80185 | 82.684 | 0.84231 | 69.937 | 0.85709 |
| | | | | 88.435 | 0.83043 | 79.027 | 0.83481 |
| | | | | 93.948 | 0.81901 | | |
| | | | | 100.000 | 0.80634 | | |

components. The partial volumes of both components show complicated behavior with the variation in the composition of the component. The case of water-ethanol system, which has often been cited in many text-books of chemical thermodynamics, is a well-known example. At present, we have no clear understanding of this phenomenon, although a qualitative explanation[3] accounts for it as the disintegration of structure in water by the solute molecule which is capable of forming the hydrogen bonding with water.

It seems to be natural to expect an anomaly similar to the above for the case of aqueous solutions of alcohols other than ethanol and of other compounds having the hydroxyl group. In the present study, we obtained the dependence of partial molal volumes in water upon the composition for four isomers of butyl alcohol from the density measurement and compared them with that of other alcohols. For comparison's sake, the partial molal volume of ethylene glycol was also evaluated. In each case concerned, the general feature of partial volume vs. composition curve was the same as that for the case of ethanol in water.

3) For example, A. G. Mitchell and W. F. K. Wynne-Jones, *Discussion Faraday Soc.*, No. 15, 161 (1953).

## Experimental

**Purification of Materials.**—*Normal*, *iso*-, *sec*.- and *tert*.-butyl alcohols and ethylene glycol were prepared as follows. The best grade available was dried over dehydrating agents and then fractionally distilled.

*n*-Butyl alcohol was at first treated with dilute sulphuric acid and sodium bisulphate solution for the removal of ketones and aldehydes, and then heated under reflux with a small amount of sodium hydroxide solution for the removal of esters. After the removal of alkali, the material was dried over calcium hydroxide, refluxed with calcium oxide, and then fractionally distilled a few times.

Isobutyl alcohol and *sec*.-butyl alcohol were boiled under reflux over calcium oxide for a few hours, and then fractionally distilled.

*tert*.-Butyl alcohol was dried over anhydrous potassium carbonate at 46°C for a long time, and then fractionally distilled.

Ethylene glycol was distilled under reduced pressure, and the middle fraction was dried over anhydrous sodium sulphate for a long time. The material was then redistilled.

Water was obtained by the repeated distillations of conductivity water.

All the sample liquid were stored in sealed glass containers and redistilled immediately before use. The densities of the sample liquids at 20°C were within 0.00005 g./cc. of the values given in literature.

**Pycnometers.**—The pycnometers used were of ordinary bicapillary type. Type A held slightly more than 25 cc. of liquid, while type B slightly less than 10 cc. The main body of the pycnometer was the usual flat-bottom type. The capillaries were calibrated with a travelling microscope by the conventional method of moving a small mercury column. In the middle of each capillary, a horizontal razor mark was applied and the volume of pycnometer with meniscus on this mark was obtained by the measurement with water.

**Density Measurement.**—The component liquids were mixed in a glass-stoppered weigh-bottle having a narrow mouthpiece. The mole fraction of the sample solution was determined from the weight of each component.

After being kept over night, the sample solution was transfused into the pycnometer by injection with a medical syringe until each of the two meniscus was near the horizontal mark on the capillary. The pycnometer was then placed into the thermostat at $20\pm0.005$°C, and when complete thermal equilibrium was attained, the height difference between the meniscus and the mark was determined by means of a travelling microscope reading to $\pm0.01$ mm.

Immediately after the volume determination, the apparent weights of the pycnometer and the sample solution were determined with an analytical balance. The values were converted into true weights by the cnventional procedure in which the buoyancy corrections were applied.

Thus, the densities of sample solutions were obtained with a precision of $\pm2\times10^{-5}$.

## Results and Discussion

**Densities.**—The density data of butyl alcohol-water and ethylene glycol-water systems are summarized in two tables. Table I shows the densities of aqueous solution of four isomers of butyl alcohol, and Table II shows the densities of ethylene glycol-water system at 20°C. In all cases concerned, the densities of the solution can not be expressed by the conventional power series relation.

Table II. Densities of aqueous solution of ethylene glycol at 20°C

| Wt. % | Density | Wt. % | Density |
|---|---|---|---|
| 1.5193 | 1.00013 | 30.440 | 1.03894 |
| 3.2341 | 1.00231 | 31.957 | 1.04095 |
| 5.7310 | 1.00554 | 36.540 | 1.04717 |
| 8.7395 | 1.00949 | 40.674 | 1.05276 |
| 9.3383 | 1.01019 | 41.410 | 1.05347 |
| 10.807 | 1.01215 | 51.737 | 1.06704 |
| 11.243 | 1.01277 | 58.341 | 1.07474 |
| 14.348 | 1.01693 | 71.378 | 1.08876 |
| 15.768 | 1.01879 | 80.617 | 1.09830 |
| 17.972 | 1.02182 | 87.942 | 1.10459 |
| 21.213 | 1.02621 | 94.169 | 1.10924 |
| 23.957 | 1.03001 | 100.000 | 1.11313 |
| 28.545 | 1.03628 | | |

**Volume of Mixing (Excess Volume).**—Since the specific volumes of both components are known (except for *tert.*-butyl alcohol which has the melting point above 20°C), the volume of the mixing $\Delta V$ is easily calculated from the present data. It is a common characteristic that $\Delta V$ has large negative value in the whole range of composition and that there is an inflection point below the alcohol mole fraction of 0.1. Fig. 1. shows the general feature schematically.

**Partial Volumes.**—Partial specific (molal) volumes of alcohols $V_2$ are calculated from the density data directly by Eq. 1, or from the concentration dependence of apparent specific volume $\phi_2$ by Eq. 2,

$$V_2=(1/d_{12})+(1-w_2)\frac{\partial(1/d_{12})}{\partial w_2} \quad (1)$$

$$V_2=\phi_2+w_2(1-w_2)\frac{\partial\phi_2}{\partial w_2} \quad (2)$$

where the apparent specific volume is defined as follows,

$$\phi_2=(1/d_1)-(d_{12}-d_1)/(d_{12}d_1w_2) \quad (3)$$

and $d_{12}$ is the density of solution, $d_1$ is the density of water and $w_2$ is the weight fraction of alcohols.

As in the well-known example of ethanol-water system, characteristic behaviors of partial molal volume vs. composition curves are obtained with all systems investigated. Partial molal volume of alcohol decreases with increasing its mole fraction, reaches a minimum value and then increases gradualy to the molal volume. In the whole range of composition, it is always smaller than the molal volume $V_2^0$. Partial molal volume of water, on the other hand, increases slightly with increasing the alcohol mole fraction, reaches an indistinct maximum and then decreases gradually.

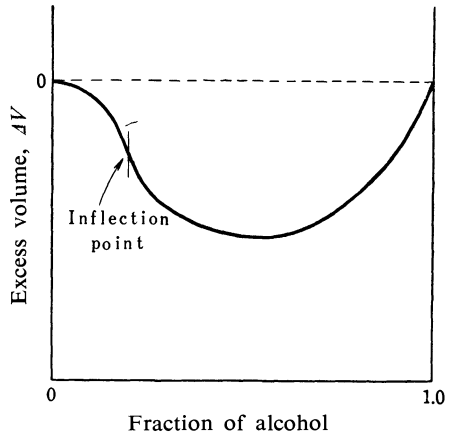



Fig. 1. Schematic diagram of excess function in alcohol-water systems.

The general feature just described above can well be understood by the case of ethylene glycol-water system given in Fig. 2.

For the partial volumes of four isomers of butyl alcohol in water, the diagram is incomplete owing to the phase separation or high melting point. Fig. 3 shows the isomeric variation in the partial volumes of butyl alcohols in their low concentration region where the characteristic behavior is clearly observed.

For comparison's sake, the partial molal volumes of methanol, ethanol, propyl alcohols and glycerol in water are calculated and plotted in Fig. 4 together with the present data. The calculation is made with the ICT data[4]. In

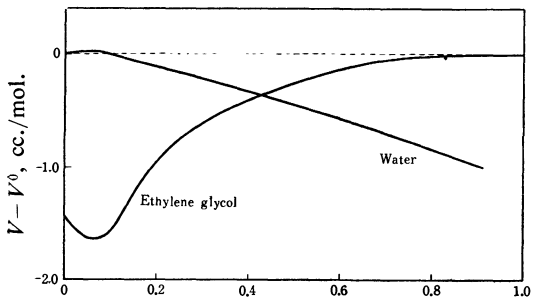



Fig. 2. Partial molal volumes of ethylene glycol-water system at 20°C.

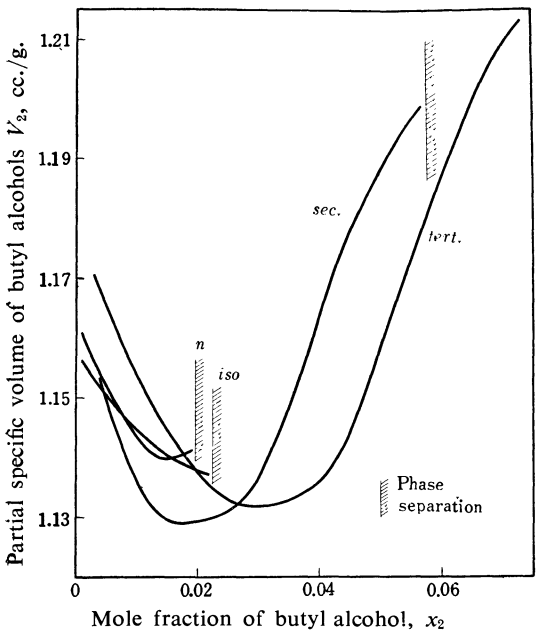



Fig. 3. Partial specific volume of butyl alcohols in water at their low concentration at 20°C.

4) International Critical Table, Vol. III, p. 115~122.

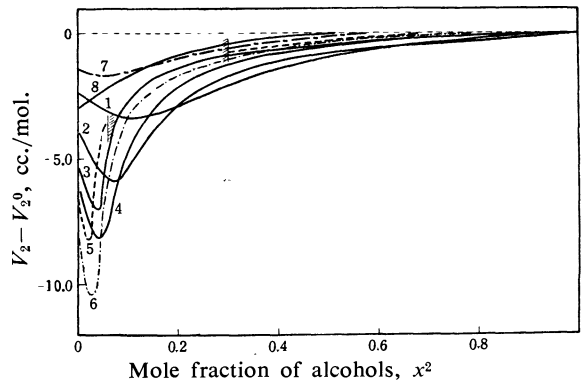



Fig. 4. Partial molal volume of alcohols in water.

1 Methanol (15°C)
2 Ethanol (20°C)
3 *n*-Propyl alcohol (15°C)
4 Isopropyl alcohol (15°C)
5 *sec.*-Butyl alcohol (20°C)
6 *tert.*-Butyl alcohol (20°C)
7 Ethylene glycol (20°C)
8 Glycerol (15°C)

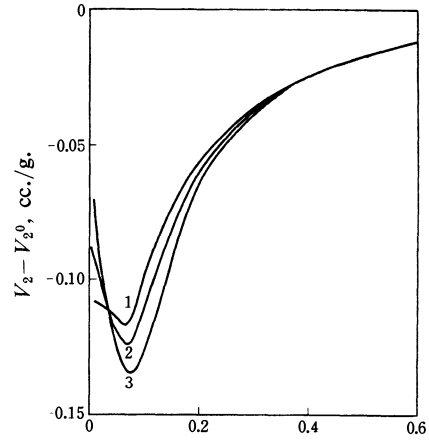



Fig. 5. Partial specific volume of ethanol in water at different temperatures.

1, 40°C; 2, 25°C; 3, 10°C;

addition, an interesting temperature dependence, which is found in ethanol, is shown in Fig. 5.

**Summary of Experimental Observations.**— Partial volume behavior presented above may be summarized as in the following.

1) Partial volumes of alcohols take a minimum value at a definite point. The position of this minimum shifts systematically to the lower concentration of alcohol in the order of BuOH, PrOH, EtOH and MeOH, as is shown in Table III.

2) Depth of the minimum in $V_2-V_2^0$ depends on the kind of alcohol in a more

Table III. Minimum point in the value of $V_2-V_2^0$

| Compound | | Minimum point at mole % | wt. % |
|---|---|---|---|
| Monohydric alcohol | $CH_3OH$ | 10.5 | 17. |
| | $C_2H_5OH$ | 7.0 | 16. |
| | *n*-$C_3H_7OH$ | 4.5 | 14. |
| | *iso*-$C_3H_7OH$ | 5.0 | 15. |
| | *n*-$C_4H_9OH$ | 1.5 | 6. |
| | *iso*-$C_4H_9OH$ | >2.1 | >8. |
| | *sec.*-$C_4H_9OH$ | 1.8 | 7. |
| | *tert.*-$C_4H_9OH$ | 3.0 | 11. |
| Dihydric alcohol | $CH_2OH$ \| $CH_2OH$ | 6.0 | 16. |
| Trihydric alcohol | $CH_2OH$ \| $CHOH$ \| $CH_2OH$ | — | — |

complicated manner than the above. The largest volume contraction is observed with *tert.*-butyl alcohol.

3) Volume contraction of polyhydric alcohols in water is generally smaller than that of monohydric alcohols. Moreover, it is of interest that the partial volume of ethylene glycol has a minimum value near the glycol mole fraction of 0.06, while that of glycerol has no minimum (Fig. 4).

4) Partial volume $V_2$ of ethanol at high dilution (below the alcohol mole fraction of 0.04) has a small temperature coefficient nearly half the value of ethanol itself. Thus, with the raise in temperature, a) the increase in the depth of $V_2-V_2^0$ at high dilution is observed, although b) the value at the minimum point decreases gradually.

**Discussion.**—Examination of all the experimental data available leads us to the conclusion that the partial volume behavior of mono- and dihydric alcohol-water system has a common characteristic. Qualitatively, the abrupt fold in the partial volume vs. composition curve would be interpreted[3] as the disintegration of the hydrogen-bonded structure in water by the increased strain due to the invading alcohol molecule with increasing fraction of the alcohol. It may be that there are two kinds of configuration of alcohol molecule in aqueous solution, one has a specific volume of alcohol itself, while the other has a small effective volume, and the fraction of the two may change with composition in a complicated manner in an alcohol-water system.

In this connection, it is of interest to examine the other properties of aqueous solution of alcohols. For example, ultrasonic absorption in aqueous solution of alcohol has a marked maximum in some definite composition[5]. But, this maximum in absorption does not always correspond to the minimum in partial volume, and moreover the former is found in aqueous solution of acetone which has smoothed partial volume vs. composition curve[6].

Another interesting result to be noted here is the partial volume behavior in dioxane-water system[7] in which a similar anomaly is observed. In this case, however, partial volume of water has a minimum point instead of a maximum as in alcoholic solutions, and the partial volume of dioxan has a maximum. It is an interesting fact that the role of the OH- group in alcohol molecules contrasts remarkably with that of ether bond -O- in the formation of intermolecular hydrogen bonding in aqueous solution.

In conclusion, all the available data seem to comprise only indirect evidences and it is obvious that more direct information about the inner structure of solutions is desirable for the elucidation of this phenomenon.

## Summary

Partial molal volumes of four isomers of butyl alcohol and ethylene glycol in water are evaluated from the density measurement. They are compared with those of other monohydric alcohols and all the available data which have a common characteristic in the dependence upon the alcohol fraction are summarized.

The author wishes to express his sincere gratitude to Professor Mikio Tamura and to Assistant Professor Michio Kurata for their guidance and criticism

*Department of Industrial Chemistry*
*Faculty of Engineering*
*Shinshu University*
*Wakazato* 500, *Nagano*

5) O. Nomoto, *J. Phys. Soc. Japan*, **11**, 827 (1956); ibid., **12**, 300 (1957).
6) V. S. Griffith, *J. Chem. Soc.*, **1953**, 860.
7) G. N. Malcolm and J. S. Rowlinson, *Trans. Faraday Soc.*, **53**, 921 (1957).

# *On the Hydrolysis Products of Abietic Acid-Maleic Anhydride Adduct*

By Masahiro ABO

(Received November 26, 1959)

In 1932 Ruzicka and his coworkers[1] found that the saponification product of methyl abietate-maleic anhydride adduct could not be isolated as tricarboxylic acid but identified with the anhydride adduct directly obtained from the reaction between colophony and maleic anhydride, and they stated that the tricarboxylic acid, which was produced at the beginning of the saponification, had a tendency to convert easily into the anhydride acid in the course of acidification or recrystallization.

It was also reported that *cis*-9, 10-dihydroanthracene-9, 10-endo-$\alpha$, $\beta$-succinic acid[2] and alkyl-1, 4-dihydronaphthalene-1, 4-endo-$\alpha$, $\beta$-succinic acid[3] had similar tendencies. These dibasic acids could not be successfully purified by recrystallization, even from the low-boiling solvents, because of their partial or complete conversion to the corresponding anhydrides. It may be seen that these tendencies are common characteristics of these structural homologues.

In the present work an attempt has been made to isolate the hypothetical tricarboxylic acid which might be directly produced by means of the hydrolysis of the abietic acid-maleic anhydride adduct. Some properties of those hydrolysis products which were obtained in a few ways were compared with those of maleic anhydride- or fumaric acid- adducts with abietic acid and discussion was offered as to their chemical structures.

## Experimental

**Maleic Anhydride Adduct with Abietic Acid.**—60 g. of abietic acid (so-called Steele's acid which was produced by refluxing Chinese gum rosin with acetic acid) and 20 g. of maleic anhydride were heated at 170~180°C with stirring under a slow stream of carbon dioxide for two hours. The reaction mixture was dissolved in 100 ml. of glacial acetic acid, and this was poured into a large amount of water with stirring. The separated yellowish resinous product was refluxed with a small amount of carbon tetrachloride to remove the unreacted abietic acid, and recrystallized from glacial acetic acid. Further recrystallization was carried out from benzene-carbon tetrachloride according to the procedure of Ruzicka and his coworkers[1]. Thirty-two grams of fibrous white needles melting at 226~228°C were obtained.

Found: C, 71.63; H, 7.82. Calcd. for $C_{24}H_{32}O_5$: C, 71.96; H, 8.06%. $[\alpha]_D^{15}$ −31.0° (10% in chloroform).

Besides the above, the most refined sample could be obtained by purification with the aid of sublimation of the above crystal under reduced pressure of 1 mmHg at 190~210°C. Its analytical data are shown in Table I with other properties.

**Fumaric Acid Adduct with Abietic Acid.**—50 g. of abietic acid and 20 g. of fumaric acid were heated at 195~200°C with the same procedure as the above for two hours. The reaction mixture was dissolved in 150 ml. of glacial acetic acid, and this was poured into a large amount of hot water with stirring and filtered through a hot funnel. This procedure was repeated twice. The unreacted abietic acid was removed from the yellowish powder by refluxing in benzene, filtered and the filtrate was recrystallized from glacial acetic acid. An analytical sample was obtained by repeated recrystallization from dioxane. Its properties and analytical results are shown in Table I with others. Purification by the vacuum sublimation method was unsuccessful owing to its thermal decomposition.

**Hydrolysis of Maleic Anhydride Adduct.**—It was carried out in two ways. (1) 30 g. of purified maleic anhydride adduct was dissolved in 100 ml. of acetone and added 30 ml. of water. The flask was immersed in a water bath kept at 60~70°C, and boiled gently under a reflux condenser for two hours. On cooling at room temperature, white crystals began to precipitate. After the crystallizations from acetone-water were repeated, they were filtered and ground into fine powder and then dried at room temperature under reduced pressure (2~5 mmHg). They reached the constant weight after about two hours. The analytical data are shown in Table I with others. (2) Ten grams of purified maleic anhydride adduct was dissolved in excess of 10%, aqueous sodium hydroxide solution and precipitated by acidification with 2 N hydrochloric acid. The precipitate was collected, washed with water repeatedly and recrystallized from acetone. All the procedures after hydrolysis were carried out at room temperature, in order to prevent the reversion to the original anhydride. Drying was carried out under the same condition as above. The analytical data are shown in Table I with others.

**Measurement of Acid Number**[4].—*Total Number.* —0.2~0.3 g. of the sample in about 50 ml. of the

1) L. Ruzicka, P. J. Ankersmit and B. Frank, *Helv. Chim. Acta*, **15**, 1289 (1932).

2) W. E. Bechmann and L. B. Scott, *J. Am. Chem. Soc.*, **60**, 481 (1938); **70**, 1458 (1948).

3) M. C. Kloetzel and H. L. Herzog, ibid., **72**, 1991 (1950).

4) E. F. Siegel and M. K. Moran, ibid., **69**, 1457 (1947); W. Klausch, *Farbe u. Lack*, **63**, 119 (1957).

TABLE I. PROPERTIES AND ANALYSES OF TWO KINDS OF ABIETIC ACID ADDUCT AND HYDROLYSIS PRODUCTS OF MALEIC ANHYDRIDE ADDUCT

| | Adduct of fumaric acid | Adduct of maleic anhydride | Hydrolysis products of maleic anhydride adduct (1)[a] | (2)[b] |
|---|---|---|---|---|
| Melt. pt., °C | 249~252 | 226~228 | 226~228 (187~210[c]) | |
| Analyses, %: | | | | |
| Calcd., C | 68.87 | 71.97 | 68.87[d] | |
| H | 8.19 | 8.05 | 8.19[d] | |
| Found, C | 68.96 | 71.69 | 68.70 | 68.73 |
| H | 8.10 | 7.89 | 8.01 | 8.05 |
| Acid number: | | | | |
| Calcd., Apparent | 393 | 280 | 393[d] | |
| Total | 393 | 420 | 393[d] | |
| Found, Apparent | 387 | 280 | 270 | 273 |
| Total | 395 | 417 | 395 | 397 |
| $[\alpha]_D^{15}$ | +34.0° | −25.2° | −24.0° | −23.6° |
| (g./100 ml. ethanol) | (2.0) | (5.0) | (2.0) | (2.0) |
| Solubility at room temp.: | | | | |
| Chloroform | insol. | sol. | insol. | |
| Benzene | insol. | sol. | insol. | |

a) Refluxed the acetone containing water solution of maleic anhydride adduct for two hours and recrystallized from its solution. b) Precipitated by acidification of the alkali solution of maleic anhydride adduct. c) Measured in a sealed capillary tube. d) Calculated for hypothetical tricarboxylic acid $C_{24}H_{34}O_6$ which may be produced on the hydrolysis process.

mixture of 1 : 3 *tert.*-butyl alcohol and acetone was dissolved, and about 10 ml. of water were added to prevent the turbidity which happened often in titration, and titrated with 0.1 N aqueous sodium hydroxide solution by means of potentiometric titration method. — *Apparent Number.* — 0.2~0.3 g. of the sample was dissolved in about 50 ml. of ethanol and titrated with 0.1 N alcoholic sodium hydroxide.

**Thermal Degradation Curves.**—An apparatus of Honda's thermal balance[5] was used. About 0.5 g. of fine powdered sample was heated at constant rate of 10°C/5 min. and loss of weight of sample was measured.

## Discussion

As was shown in Table I, the elementary analytical data of both hydrolysis products, which were obtained in two ways as mentioned above, were in good agreement with that expected for the aimed tricarboxylic acid $C_{24}H_{34}O_6$ respectively. They were insoluble in benzene or chloroform, similarly to fumaric acid adduct, at room temperature, but soluble at elevated temperature. Their specific rotation was negative like that of the maleic anhydride adduct, and the decrease of the rotation nearly corresponded with the decrease of the concentration of the asymmetric carbons attendant upon the increase of their molecular weights. The melting points which were measured by the ordinary method agreed with that of the maleic anhydride adduct. However, when they were measured in a sealed capillary tube they showed a remarkable depression and were distinct from anhydride.

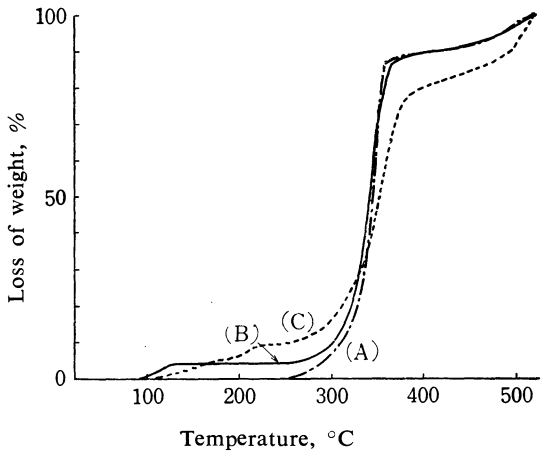



Fig. 1. Thermal degradation curves of (A) abietic acid-maleic anhydride adduct, (B) hydrolysis product of A, and (C) abietic acid-fumaric acid adduct.

Another distinguished difference was observed in the thermal degradation curves of the three kinds of adducts (Fig. 1). The hydrolysis product showed suddenly 4.1 to 4.4% weight loss at about 100 to 120°C (Curve B, Fig. 1), which corresponded approximately to the loss of

5) K. Honda, *Sci. Rep. Tohoku Univ.*, 4, 97 (1915).

one molecule of water from one molecule of the hypothetical tricarboxylic acid. After it was heated at that temperature the weight was kept constant till it began once more to lose the weight nearly along the curve A of anhydride adduct at about 250°C. In the other run, when the heating was stopped at 150°C, it was confirmed that the remaining product was the same one as anhydride adduct by its mixed melting point and infrared spectrum.

Now, if the above mentioned hydrolysis products had the same structure as the hypothetical tricarboxylic acid (I) which corresponded with the abietic acid-maleic acid adduct, it should be expected that there would be no difference in titer between titrations in a primary alcoholic and a tertiary alcoholic medium. Contrary to our expectation, it was found that they titrated only about two thirds of the expected titration in ethanol (Table I).

Incited by this fact, we were led to find more interesting facts: (a) When the titration of above hydrolysis product was carried out in the mixed solution of acetone — *tert.*-butyl alcohol—water, with alcoholic (ethyl) alkali solution as titer, we also obtained only about the apparent acid number, two thirds of the expected one for the tricarboxylic acid I. (b) Even if it was titrated after the solution was kept at its refluxing temperature for two hours, we also found the same result. Under the same condition, ordinary anhydrides, e. g. maleic anhydride and phthalic anhydride etc., were titrated to their own total acid number respectively. (c) Furthermore, it was also confirmed that the maleic anhydride adduct itself showed only an apparent acid number under the same condition as (a) or (b).

From these facts it seems that they have not the expected tricarboxylic acid structure but an anhydride one in spite of their elementary analyses and other evidences mentioned above. And then, it seems that the anhydride adduct cannot be hydrolyzed in a hydrous medium, even at its refluxing temperature, but proceeds readily to monoesterification with primary alcohol included in titer.

On the other hand, the infrared spectra of them, compared with those of maleic anhydride- and fumaric acid- adducts (Fig. 2), supported an existence of five membered ring anhydride structure. And also, it was first revealed by these spectra that there were two forms of products according to their hydrolysis method, (1) or (2). In either case, two characteristic bands due to the carbonyls in five membered anhydride ring appeared near 1770 and 1830 $cm^{-1}$ similar to that found in the anhydride adduct. These results make it possible to explain their anomality in acid number consistently.

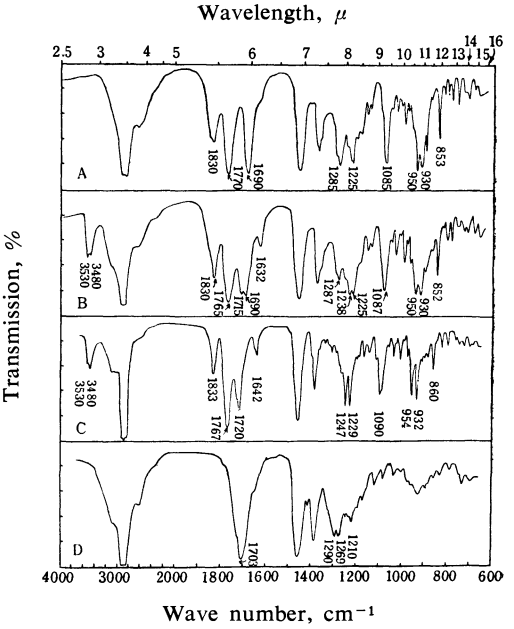
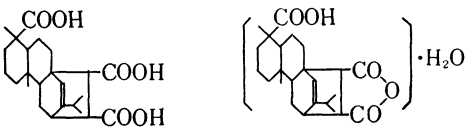



Fig. 2. Infrared spectra in Nujol of (A) abietic acid-maleic anhydride adduct, (B) hydrolysis product (α-form), recrystallized from acetone-water solution of A, (C) hydrolysis product (β-form), precipitated by acidification of the alkali solution of A, (D) abietic acid-fumaric acid adduct.

But if it is so, it becomes difficult to make compatible their elementary analytical data or their thermal degradation curves etc. with an existence of anhydride structure. The only reasonable explanation for this would be that the anhydride adduct had a tendency to form a monohydrate II without opening the anhydride ring in hydrate solution for some reason, e. g. it may be due to the stereochemically unusual approach in positions between the two carbonyl groups belonging to the succinic acid structure added to 6-, 14-carbons of abietic acid.




It was considered that the bands at 3530, 3480 and 1642 $cm^{-1}$ suggested the existence of a hydrated water. Two forms of the hydrolysis products perhaps appeared from the difference in the mode of hydrogen bonding. It is considered that the carbonyl band at 1720 $cm^{-1}$ in β-form is assigned to that of the tertiary carboxyl group under the influence of hydrogen bond caused by the hydrated water. In α-form, it divided in two bands, at 1715 and 1690 $cm^{-1}$.

It seems that one is under the influence of hydrogen bond and the other is not.

It seems to be almost sure that the hydrated water is stoichiometric component in the hydrolysis products, because those products which were dried to the constant weight at room temperature under reduced pressure always showed the reproducible stepwise loss of weight at the range of about 120 to 250°C in the thermal degradation curves, while abietic acid or its fumaric acid adduct which was recrystallized from acetone-water and dried under the same condition showed neither such a stepwise loss of weight in that curve nor the water bands in its infrared spectrum. It seems probable that the hydrated water is the same sort as the zeolitic water by reason of the fact that the collapse of crystals which should happen near their dehydrating temperature can not be observed in an open capillary. It could be also analyzed by Karl Fischer's method. The water content measured by this method was compared with the loss of weight at 150°C in the thermal degradation curve about the samples which were dried under various conditions in Table II.

Table II. Drying time and water content of hydrolysis products of maleic anhydride adduct

| Drying time, hr. (at 2 mmHg/28°C) | Loss of weight at 150°C, % | Water content by means of Karl Fischer's method % |
|---|---|---|
| 1 | 4.43 | 4.20 |
| 2 | 4.32 | — |
| 4 | 4.31 | 4.10 |
| 6 | 4.15 | 4.42 |
| 11 | 4.30 | 3.98 |

Samples: Hydrolysis products precipitated from acetone containing water solution.

## Summary

Hydrolysis of abietic acid-maleic anhydride adduct was carried out in two ways. The elementary analytical data of both resulting products were in good agreement with that calculated for the hypothetical tricarboxylic acid $C_{24}H_{34}O_6$, and at about 100 to 120°C these products lost the weight, which corresponded to the loss of one molecule of water from one molecule of the acid, to revert to the original anhydride adduct. But, they showed only an apparent acid number when the titrations were carried out in ethyl alcohol, similarly to the case of the anhydride adduct. Their infrared spectra suggested an existence of five-membered ring anhydride structure and a hydrated water. On the basis of these facts, we offered an anhydride adduct monohydrate structure II for the above hydrolysis products.

The author wishes to thank Dr. Shiro Tsuruta, Dr. Wataru Koga and Dr. Kiyoshi Sakashita for many stimulating discussions and helpful suggestions.

*Hitachi Insulating Material Works*
*Hitachi Ltd., Hitachi*
*Ibaragi Prefecture*

# *Pyrolysis of Organic Compounds. I. Kinetic Study of the Pyrolysis of Toluene*

By Makoto TAKAHASI

(Received October 16, 1959)

In 1948 Szwarc[1] measured the reaction velocities of the pyrolysis of toluene by the flow technique in the temperature range 738~864°C. He assumed that the reaction is homogeneous, and proposed the following reaction scheme:

$$C_6H_5CH_3 \longrightarrow C_6H_5CH_2\cdot + H\cdot \quad (1)$$
initiation

$$H\cdot + C_6H_5CH_3 \longrightarrow H_2 + C_6H_5CH_2\cdot \quad (2)$$
abstraction by H atom

$$H\cdot + C_6H_5CH_3 \longrightarrow C_6H_6 + CH_3\cdot \quad (3)$$
metathesis

$$CH_3\cdot + C_6H_5CH_3 \longrightarrow CH_4 + C_6H_5CH_2\cdot \quad (4)$$
abstraction by $CH_3$ radical

$$2C_6H_5CH_2\cdot \longrightarrow C_6H_5CH_2CH_2C_6H_5 \quad (5)$$
termination by recombination

He considered that the rate determining step

1) H. Szwarc, *J. Chem. Phys.*, **16**, 128 (1948).

is the unimolecular reaction 1, and assumed that the velocity constant $k$ observed by the flow method corresponds to that of the reaction 1. The activation energy and the temperature independent factor of the reaction 1 obtained by plotting $\log k$ versus $1/T$ are 77.5 kcal./mol. and $2\times10^{13}$ respectively, and he assumed that the activation energy corresponds to the bond dissociation energy, $D(C_6H_5CH_2\text{-}H)$. H. R. Anderson Jr., H. A. Scheraga, and E. R. Van Artsdalen[2] studied the thermal bromination of toluene, and they derived 89.5 kcal./mol. for the upper limit of the bond dissociation energy of toluene. H. Blades, A. T. Blades and E. W. R. Steacie[3] repeated the study of the pyrolysis of toluene in a flow system, and they carried out a more elaborate analysis of the reaction products. Styrene, dimethylbiphenyls and anthracene were obtained in addition to bibenzyl which was reported by Szwarc to be the sole nonvolatile product in the reaction. Steacie and Blades ascribed the origin of the dimethylbiphenyls to the secondary decomposition of bibenzyl. They observed that the first order rate constant increases, as the contact time is increased, and that the rate of the reaction depends upon the condition of the surface of the reaction vessel. They calculated the apparent activation energy to be 90 kcal./mol., keeping the contact time constant at 0.068 sec., although they did not assert that the value corresponds to the true bond dissociation energy of toluene $D(C_6H_5CH_2\text{-}H)$.

Most recently, S. W. Benson and J. H. Buss[4] reviewed various attempts to determine the bond dissociation energy of toluene, and they attempted a measurement of the equilibrium constant for the reaction:

$$C_6H_5CH_3(g)+Br_2(g) \rightleftarrows C_6H_5CH_2Br(g)+HBr(g)$$

at 150°C, and they estimated the bond dissociation energy of toluene to be 84 kcal./mol., together with the known thermal data.

The bond dissociation energy was also obtained by electron impact measurement by D. O. Schissler and D. P. Stevenson[5] as 77.3 kcal./mol., and J. B. Farmer, I. H. S. Henderson, C. A. McDowell and F. P. Lossing[6] criticized the value, and they presumed that the bond dissociation energy is possibly higher by about 20 kcal./mol.

From the theoretical point of view, the present author considers that Szwarc's value of the bond dissociation energy of toluene is somewhat too low, for the difference:

$$D(CH_3-H)-D(C_6H_5CH_2-H) = 103-77.5=22.5 \text{ kcal./mol.}$$

is too large compared with the extra resonance energy of the benzyl radical which was calculated as about 14 kcal./mol.[7] If such an abnormal weakening of toluene bond were assured by experiments, the fact might be an interesting theoretical problem, but at present it seems to be premature to discuss this point, for there remain many points which should be made clear in the experiments.

It is to be noted that the value obtained by Steacie and his collaborators for the activation energy of the pyrolysis of toluene is different from that by Szwarc, although the method was the same. A. F. Trotman-Dickenson[8] pointed out that Steacie and his collaborators measured the rate constant, keeping the contact time far less than in the experiments by Szwarc.

However, the present author considers that it is very unfortunate that the two groups made experiments in the different ranges of the reaction temperatures; that is, Szwarc in the range between 738~864°C, and Steacie and his collaborators between 860~940°C. Therefore, the present experiment was carried out to cover the whole temperature range 737~953°C, and efforts were made to elucidate the cause of the discrepancy of the bond dissociation energies of toluene obtained by the two groups.

## Experimental Procedure

**Materials.**—Both Szwarc's and Steacies groups used toluene prepyrolyzed to remove interfering impurities which would give extra hydrogen and light hydrocarbons by pyrolysis. The present author attempted to obtain toluene of higher purity which is usable without prepyrolysis. Toluene from two sources were examined, the one of which was obtained by the usual purification process combined with azeotropic distillation with acetonitrile to remove interfering impurities which were presumed to be cycloalkanes. This toluene was conceived to be of very high purity, but nevertheless it gave some amount of ethylene and propylene in addition to hydrogen and methane by pyrolysis, if it was subjected to prepyrolysis.

In order to obtain toluene of higher purity which contains no alkanes nor cycloalkanes, the author prepared toluene from toluidine by applying the method described in Organic Syntheses[9]. A cold diazonium solution was prepared from 105 g. of toluidine, 190 ml. of concentrated hydrochloric acid,

2) H. R. Anderson Jr., H. A. Scheraga and E. R. Van Artsdalen, ibid., **21**, 1258 (1953).
3) H. Blades, A. T. Blades and E. W. R. Steacie, *Can. J. Chem.*, **32**, 1142 (1954).
4) S. W. Benson and J. H. Buss, *J. Phys. & Colloid Chem.*, **61**, 104 (1957).
5) D. O. Schissler and D. P. Stevenson, *J. Chem. Phys.*, **22**, 151 (1954).
6) J. B. Farmer, I. H. S. Henderson, C. A. McDowell and F. P. Lossing, ibid., **22**, 1948 (1954).
7) M. Takahasi, This Bulletin, **29**, 625 (1956).
8) A. F. Trotman-Dickenson, "Gas Kinetics", Butterworths Scientific Publications, London (1955), p. 108.

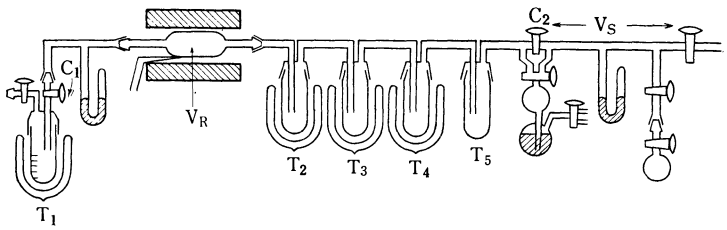



Fig. 1. Apparatus for Pyrolysis.

TABLE I. VELOCITY CONSTANTS IN THE CASE OF THE REACTION VESSEL I

| Exp. No. | Vap. pressure mmHg | Reaction temp., °C | $-\log k$ | Mole ratio of $H_2$ to $CH_4$ | Contact time, sec. |
|---|---|---|---|---|---|
| 95 | 7.24 | 763.5 | 3.24 | | |
| 94 | 8.38 | 787.2 | 2.95 | | |
| 93 | 9.60 | 819.0 | 2.52 | | |
| 40 | 4.98 | 856.5 | 1.81 | | 0.26 |
| 41 | 4.94 | 863.9 | 1.71 | | |
| 42 | 5.24 | 866.3 | 1.65 | | |
| 90 | 8.00 | 879.8 | 1.54 | | |
| 89 | 7.54 | 880.6 | 1.58 | | |
| 91 | 7.00 | 894.0 | 1.34 | | |
| 47 | 5.04 | 912.0 | 1.11 | 2.0 | |
| 48 | 5.15 | 933.1 | 0.78 | | |
| 49 | 5.98 | 936.9 | 0.72 | | |
| 50 | 5.34 | 939.3 | 0.69 | | |

and 69 g. of sodium nitrite in 200 ml. of water, and it was poured into a flask containing 520 g. of sodium hypophosphorite, $NaH_2PO_2 \cdot H_2O$, 256 g. of concentrated hydrochloric acid and 40 g. of water. Evolution of nitrogen was controlled, keeping the solution at 5°C. The flask was placed in a refrigerator overnight, and the reaction product was transfered to a separating funnel, and the upper oil was separated from the aqueous phase. Ether extraction should be avoided, for it causes the contamination of toluene with ether. A fraction boiling at 110°C. was gathered by simple distillation which weighed about 55 g., and then it was distilled through a spinning band fractionating column of 150 cm. in length. This toluene did not give any appreciable amount of ethylene and higher hydrocarbons in the pyrolysis, even if prepyrolysis was not carried out, and therefore the latter toluene was used in the present kinetic study.

**Apparatus and Procedure**—The general arrangement of apparatus for pyrolysis shown in Fig. 1 is similar to that used by Szwarc but with a small modification to improve experimental accuracy. Toluene which had been refluxed with sodium for about one hour was distilled under reduced pressure into the storage vessel $T_1$. This vessel was weighed before and after each run of experiment, to measure the amount of toluene passed in each run, if it was necessary to calculate accurate contact time. In the usual runs, the amount of toluene was determined by volume in the storage flask. During runs, the vessel was kept in a Dewar vessel contaning water maintained at a temperature constant to 0.1°C. Toluene was evaporated from $T_1$ through cock $C_1$ to maintain its vapor pressure 4~10 mmHg, and led into a silica reaction vessel heated by an electric furnace. Contact time was controlled by replacing silica reaction vessels which were designated as I, II, and III. (Table V). The electrical furnace was about 70 cm. long, and the variation of temperature along the reaction vessel was ±2°C. The temperature of the reaction vessel was measured by a calibrated Pt-Rh thermocouple with a potentiometer. It was checked to discover whether temperature difference inside and outside the reaction vessel might be caused by passing toluene, but the difference did not exceed 2°C.

The reaction system was evacuated to $10^{-6}$mmHg before the experiment, and pressure increase in the reaction system in the course of about 20 min. was checked without passing toluene. The increase of pressure was caused mainly by evaporation of toluene previously dissolved in grease of cocks but not by leakage of air, being suppressed to about $10^{-3}$ mmHg in the course of about 20 minutes, a time comparable to that of one usual run of pyrolysis.

The vapor leaving the reaction vessel passed through traps $T_2$ and $T_3$ which were cooled with a mixture of ether and solid carbon dioxide. Toluene and the less volatile products such as bibenzyl and dimethylbiphenyls were almost completely condensed in trap $T_2$. The noncondensable gas passed through trap $T_4$ which was cooled by liquid nitrogen or oxygen. Trap $T_5$ was reserved for distillation, and

9) "Organic Syntheses", Collective Vol. II. John & Willey Sons, Inc., New York, p. 1039.

TABLE II. VELOCITY CONSTANTS IN THE CASE OF THE REACTION VESSEL II

| Exp. No. | Vap. pressure mmHg | Reaction temp., °C | $-\log k$ | Mole ratio of $H_2$ to $CH_4$ | Contact time, sec. |
|---|---|---|---|---|---|
| 13 | 5.02 | 737.8 | 3.43 | | |
| 80 | 8.39 | 741.1 | 3.11 | | |
| 81 | 9.62 | 749.0 | 3.34 | | |
| 88 | 8.14 | 755.2 | 3.24 | | |
| 87 | 8.47 | 763.6 | 3.13 | | |
| 82 | 9.22 | 770.8 | 3.05 | | |
| 12 | 5.76 | 779.0 | 2.91 | | |
| 86 | 8.64 | 791.3 | 2.71 | | |
| 18 | 6.64 | 801.9 | 2.57 | | |
| 19 | 5.88 | 801.9 | 2.54 | 2.1 | |
| 20 | 5.66 | 803.5 | 2.50 | 2.3 | |
| 85 | 9.20 | 814.1 | 2.38 | | |
| 83 | 8.64 | 814.9 | 2.31 | | |
| 11 | 7.14 | 821.4 | 2.32 | | |
| 84 | 9.06 | 828.7 | 2.15 | | |
| 77 | 9.26 | 837.5 | 1.98 | | |
| 78 | 9.10 | 837.5 | 1.90 | | |
| 10 | 7.04 | 839.1 | 2.06 | | |
| 76 | 9.66 | 848.7 | 1.78 | | |
| 79 | 9.10 | 850.3 | 1.92 | | |
| 75 | 9.58 | 851.1 | 1.78 | | |
| 21 | 6.12 | 855.1 | 1.79 | 2.1 | |
| 8 | 6.34 | 859.1 | 1.67 | | 0.11 |
| 35 | 6.40 | 860.7 | 1.67 | | |
| 74 | 9.76 | 860.7 | 1.65 | | |
| 9 | 6.28 | 863.9 | 1.62 | | 0.10 |
| 5 | 5.68 | 863.9 | 1.70 | | 0.09 |
| 72 | 9.00 | 875.0 | 1.48 | | |
| 73 | 10.02 | 875.8 | 1.42 | | |
| 10 | 9.64 | 880.6 | 1.34 | | 0.24 |
| 71 | 9.49 | 890.1 | 1.22 | | |
| 17 | 6.50 | 897.9 | 1.14 | 2.3 | 0.11* |
| 69 | 9.35 | 902.6 | 1.07 | | |
| 6 | 5.40 | 908.1 | 0.94 | | 0.14 |
| 68 | 10.14 | 908.9 | 0.93 | | |
| 64 | 9.28 | 916.7 | 0.85 | | |
| 27 | 6.58 | 918.3 | 0.89 | 2.2 | |
| 38 | 5.80 | 928.4 | 0.72 | 1.8 | |
| 65 | 9.94 | 932.3 | 0.60 | | 0.14 |
| 16 | 6.50 | 937.0 | 0.52 | | |
| 14 | 6.24 | 938.6 | 0.52 | 2.3 | 0.13 |
| 15 | 7.19 | 940.1 | 0.60 | | 0.15 |
| 66 | 9.70 | 944.0 | 0.40 | | |
| 67 | 10.60 | 953.3 | 0.26 | | |
| 24 | 4.34 | 953.7 | 0.25 | 1.9 | |
| 7 | 6.49 | 955.6 | 0.23 | | 0.16 |

* Condensable gas at liquid nitrogen temperature amounted to 2% of total gas product.

kept at room temperature. Noncondensable gas in trap $T_4$ was composed of hydrogen and methane, and it was pumped out by a Toepler pump and collected in a storage vessel of about 100 ml. The quantity of hydrogen and methane produced was given by reading the pressure in the storage vessel with a McLeod gauge or a U tube manometer according to the pressure. The reaction time extended from 3 to 30 minutes, according to the quantity of gas produced. After the flow of toluene vapor was stopped, the trap $T_2$ was warmed to room temperature to distil toluene from trap $T_2$ to $T_3$. All the produced gas, remaining in the reaction system and dissolved in toluene of trap $T_2$, was pumped out by a Toepler pump to the storage vessel. Hydrogen and methane expelled from trap $T_2$ amounted to about 10% of the total gas produced. Operation of Toepler pump was continued for 15 min. after flow of toluene was stopped. After the pressure of a mixture of hydrogen and methane was read, trap $T_4$ was warmed to $-70°C$ by changing the cooling material to a mixture of ether and carbon dioxide. The amount of gas condensable in trap $T_4$ at liquid nitrogen temperature was at most a few per cent of that of condensable gas, if toluene which was synthesized from toluidine as described above was pyrolyzed.

As the experimental conditions were so chosen that the decomposition ranged from 0.001 percent to 0.6 percent of total toluene, the reaction rate constant for the unimolecular reaction was calculated by the equation,

$$k=\frac{P_s\times V_s\times T_R}{P_t\times t\times T_r\times V_R} \tag{6}$$

where $P_t$ is vapor pressure of toluene (mmHg), $T_R$ is reaction temperature (°K), $V_R$ is volume of reaction vessel (l.), $t$ is time of flow (sec.), and $P_s$ is pressure of product gas ($H_2+CH_4$) (mmHg) at $T_r$ °K in a storage vessel of $V_s$. The contact time was calculated according to Eq. 7,

$$\tau=V_R/v=\frac{V_R\times P_t\times t}{m\times 0.082\times T_R\times 760} \tag{7}$$

$$k=\text{fractional decomposition}/\tau \tag{8}$$

where $m$ is moles of toluene passed, and $v$ (l.) is volume of toluene which passed through the reaction vessel per second at $T$ °K. Contact time was calculated in several runs, but not in all runs, because it depends mainly on the value of reaction vessel and vapor pressure of toluene, the latter being varied over a small range.

TABLE III. VELOCITY CONSTANTS IN THE CASE OF THE REACTION VESSEL III

| Exp. No. | Vap. pressure mmHg | Reaction temp., °C | $-\log k$ | Contact time, sec. |
|---|---|---|---|---|
| 101 | 9.88 | 811.7 | 2.34 | |
| 100 | 10.78 | 836.7 | 2.01 | |
| 99 | 10.80 | 868.8 | 1.58 | |
| 98 | 10.95 | 888.8 | 1.30 | |
| 97 | 10.60 | 908.1 | 0.99 | |
| 54 | 7.28 | 925.3 | 0.66 | 0.03 |
| 55 | 6.48 | 925.3 | 0.67 | |
| 56 | 6.36 | 939.3 | 0.61 | |
| 96 | 11.10 | 948.7 | 0.44 | |
| 57 | 6.51 | 958.7 | 0.38 | |
| 61 | 7.22 | 960.3 | 0.33 | |

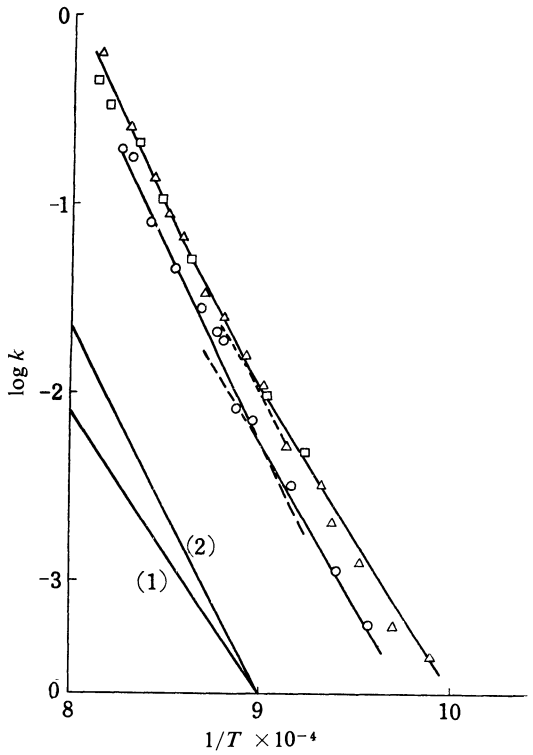



Fig. 2. Relation of $\log k$ versus $1/T$
△ Reaction Vessel I
○ 〃 II
□ 〃 III
(1) gradient corresponding to the activation energy of 70 kcal./mol.
(2) 〃 of 90 kcal./mol.

## Experimental Results

The results are shown in Tables I, II and III, and the relation of $\log k$ versus $1/T$ is shown in Fig. 2. From the figure it may be apparently concluded that the relation was linear, but the more precise analysis makes clear the curve is slightly concave. Therefore, the temperature range was rather arbitrarily divided into three parts, that is, higher, medium, and lower temperature ranges, and a linear relation of $\log k$ versus $1/T$ was assumed in each range, and experimental activation energies and temperature independent factors were calculated by the least square method. The results are summarized in Table IV. Different gradients were obtained in each temperature range, corresponding to different activation energies and different frequency factors. The probable cause of deviation of the relation of

TABLE IV. EXPERIMENTAL ACTIVATION ENERGIES AND $\log A$ OF PYROLYSIS OF TOLUENE UNDER VARIOUS CONDITIONS

| Temp. range °C | Number of experiments | Volume of reaction vessel, ml. | Contact time, sec. | $E$ kcal./mol. | $\log A$ |
|---|---|---|---|---|---|
| 764～843 | 4 | 53.7 | 0.3 | 81.3 | 13.7 |
| 857～894 | 6 | 〃 | 〃 | 69.2 | 11.5 |
| 912～933 | 4 | 〃 | 〃 | 104.9 | 18.1 |
| 738～849 | 19 | 31.0 | 0.1～0.2 | 73.7 | 12.4 |
| 850～898 | 13 | 〃 | 〃 | 93.3 | 16.2 |
| 903～956 | 14 | 〃 | 〃 | 103.5 | 18.0 |
| 812～889 | 4 | 6.4 | 0.02～0.04 | 78.0 | 13.3 |
| 908～960 | 7 | 〃 | 〃 | 76.2 | 13.1 |
| Szwarc[1] | | | | | |
| 738～850 | 27 | not described | 0.2～0.9 | 77.5 | 13.1 |
| Steacie and his collaborators[3] | | | | | |
| 850～940 | 9 | not described | 0.068 | 90 | not described |

$\log K$ versus $1/T$ from linearity is discussed below.

**Identification and Analysis of Products.**—The mole ratio of hydrogen to methane was determined by a mass spectrometer of CEC 21-103A type by using peaks of $m/e$ 2 and 16, although quantitative analysis of hydrogen by the mass spectrometer did not give sufficient accuracy. Complete analysis of solid and oily matters which were obtained in trap $T_2$ was not carried out, but the ultraviolet absorption spectrum (Fig. 3) showed that the main products were composed of bibenzyl and dimethylbiphenyls, and this result agrees with that of Steacie and his collaborators.

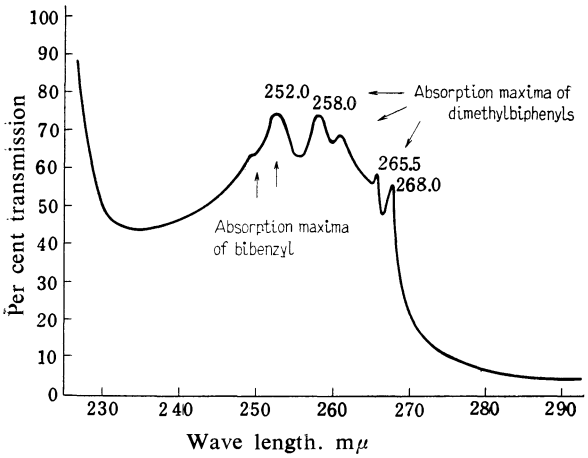



Fig. 3. Absorption spectrum of the nonvolatile reaction products of pyrolysis of toluene in ethanol.

## Discussions

As described above, the present experimental results show that the relation of $\log k$ versus $1/T$ in the temperature range 737～953°C is not strictly linear and that high activation energies and high frequency factors are obtained in the higher temperature range in the series of the experiments which were carried out at contact time of 0.1～0.3 sec. In the case of shorter contact time, 0.02～0.04 sec., (Table IV), the activation energy is obtained only in the higher temperature range 812～960°C, because the experiment in the lower temperature range should give a smaller amount of gas product and involve larger experimental error, compared with the experiments of longer contact time. It is to be noted that the lower activation energy is obtained even in the higher temperature range, compared with the experiment of longer contact time in the same temperature range.

Now the author will discuss the probable cause of systematic deviation of the relation of $\log k$ versus $1/T$ from linearity.

1) Experimental errors: It may be possible that $k$ at lower temperatures involves relatively large error, because the amount of the product gas at lower reaction temperature is very small, even if the reaction time is lengthened. As was described in the experimental part, the pressure increase in the storage vessel in the blank test amounted to about $10^{-3}$ mmHg in the course of about 15 min. Total pressure of product gas which was given by pyrolysis of toluene for ten minutes at the lowest reaction temperature, 738°C, amounted to about 0.06 mmHg (cf. Exp. No. 13). This may mean that the observed velocity constants at lower reaction temperatures should be reduced by some percentage, but such correction seems not to increase so much the activation energy obtained at the lower temperature range.

Alkanes and cycloalkanes which may supposedly exist in commercial toluene may be decomposed more rapidly than toluene, and

such toluene may increase the apparent $k$ at lower reaction temperatures, but the toluene which was synthesized from toluidine may be free from such impurities.

2) Correction by using the more elaborate Arrhenius equation: As was pointed out by many authors[10], under some conditions the frequency factor is a function of the temperature and a more accurate equation 10 than the usual Arrhenius equation 9 should be used.

$$k = A\exp(-E_a/RT) \quad (9)$$

$$k = AT^n\exp(-E/RT) \quad (10)$$

or $$\ln k = -E/RT + n\ln T + \ln A$$

and the difference of the two activation energies is

$$E = E_a - nRT. \quad (11)$$

In the present case, $n$ is not known, but if $n$ is assumed to be 1/2 as in the usual collision theory, $n(\ln T_1 - \ln T_2)$ amounts to 0.042, when $T_1$ and $T_2$ are assumed 953°C and 737°C respectively. This may reduce activation energies in the higher temperature range to some extent, but the correction seems not to contribute so much to reducing the concave nature of the relation of $\log k$ versus $1/T$.

3) Complications due to competitive reactions: H. Blades, A, T. Blades and E. W. R. Steacie[3] pointed out that the first order rate constants for the pyrolysis of toluene depends on the condition of the surface of the reactor, and the contact time, and on the pressure. A. Frost and R. G. Pearson[10] pointed out that a plot of $\log k$ versus $1/T$ shows a curvature if there are two competing reactions with different activation energies.

One case is that where the same reaction occurs both homogeneously and heterogeneously. The homogeneous reaction usually has a higher activation energy, and it is favored at high temperatures whereas the heterogeneous reaction predominates at lower temperatures. In the present experiment, it is shown that $k$ at the same temperature varies slightly as shown in Fig. 2, when the reaction vessel is replaced (I, II, and III). Contact time, volume and surface area of reaction vessel are varied as shown in Table V by replacing the reaction vessel, but it is not yet elucidated how these conditions affect the velocity constant and activation energy of pyrolysis of toluene. The present author presumed that any unfavorable secondary reaction may be suppressed, if the experiment is carried out under a smaller contact time, but such a presumption could not be confirmed in the present experiment.

10) A. A. Frost and R. G. Pearson, "Kinetics and Mechanism", John Wiley Sons, Inc., New York (1953), p. 24.

Table V

| Reaction vessel | Volume ml. | Contact time, sec. | Surface area, $cm^2$ |
|---|---|---|---|
| I | 53.7 | 0.3 | 113 |
| II | 31.0 | 0.2—0.1 | 94 |
| III | 6.4 | 0.03 | 44 |

Thus, the author's efforts to obtain a value as much smaller than $k$ as possible especially in the lower temperature range appeared not to modify the concave nature of $\log k$ versus $1/T$, and another source of complications of the present reaction is now considered in the following. At the higher temperature range between 900~950°C, it may be possible that the observed $k$ becomes rather increased, as the reaction temperature is increased, because some competitive side reaction takes place, giving hydrogen and methane. Already both Szwarc[1] and Steacie[3] considered the following reaction,

$$C_6H_5CH_3 \longrightarrow C_6H_5\cdot + CH_3\cdot$$

as one of possible side reactions, but they considered that such a reaction is less probable, because the ratio of hydrogen to methane does not vary over the whole temperature range. The present experimental results of the ratio of hydrogen to methane appear to support their conclusion. Another possible reaction is one involving the participation of ring-hydrogen in initiation and/or propagation reaction as follows:

$$C_6H_5CH_3 \longrightarrow \cdot C_6H_4CH_3 + H\cdot \quad \text{initiation}$$

$$C_6H_5CH_3 + H\cdot \longrightarrow \cdot C_6H_4CH_3 + H_2$$
abstraction by hydrogen atom

$$C_6H_5CH_3 + CH_3\cdot \longrightarrow \cdot C_6H_4CH_3 + CH_4$$
abstraction by methyl radical

Blades and Steacie[11] pointed out such a possibility in the experiment of pyrolysis of $n$-propylbenzene in the presence of toluene-$\alpha$-$d_3$ at 722°C. They found that the amount of methane in the reaction product is unexpectedly large compared with the amount of methane-$d$. Recently S. H. Wilen and E. L. Eliel[12] assumed abstraction of ring-hydrogen by methyl radicals in the reaction of acetyl peroxide with ring-deuterated toluene at 131~147°C. which gave rise to some methane-$d$. The present author's experiment of toluene-3-$d$ and toluene-4-$d$ which confirms the involvement of ring-hydrogen in the pyrolytic reaction of toluene itself will be reported in the succeeding paper, although it remains unsolved whether the involvement of ring-hydrogen modifies the overall activation energy or not.

11) A. T. Blades and E. W. R. Steacie, *Can. J. Chem.*, 32, 1142 (1954).

12) S. H. Wilen and E. L. Eliel, *J. Am. Chem. Soc.*, 80, 3309 (1958).

**Summary**

Pyrolysis of toluene by the flow technique was carried out under various conditions, and the velocity was measured over the wide temperature range 737~953°C at contact time 0.02~0.3 sec. The relation of log $k$ versus $1/T$ appears to be linear, but the more precise analysis shows a slight concave nature, and therefore activation energy tends to increase, as the reaction temperature is raised. Detailed investigation on its cause was made, and it is presumed that such an increase of activation energy with rise of temperature is mainly brought about by some competitive reaction, but not by experimental conditions. The present author considers that the involvement of ring-hydrogen reaction may compete with the reaction of fission of C–H bond of the methyl group, and such competitive reaction may modify the activation energy of the fission of the methyl bond of toluene, if the experiment is carried out over the wide reaction temperature range.

The author wishes to express his hearty thanks to Professor Y. Urushibara and Professor O. Simamura for their kind guidance and encouragement of the present work. The author is grateful to Dr. M. Kobayashi for experimental help and for stimulating discussions, and to Dr. T. Tamura and Mr. H. Saito for fractional distillation of toluene.

*Department of Chemistry*
*College of General Education*
*The University of Tokyo*
*Meguro-ku, Tokyo*

# *Pyrolysis of Organic Compounds. II. Pyrolysis of Toluene-3-d and Toluene-4-d*

By Makoto TAKAHASI

(Received October 16, 1959)

In recent years the bond dissociation energy of toluene, $D(C_6H_5CH_2\text{–}H)$, has become a topic of considerable dispute, and various attempts to determine the bond dissociation energy were reviewed by Benson & Buss[1] and by the present author[2]. Szwarc[3] estimated the activation energy of the pyrolytic reaction of toluene by the flow method to be 77.5 kcal./mol., and the frequency factor to be $2\times10^{13}$ in the reaction temperature range 738~864°C. H. Blades, A. Blades and Steacie[4] repeated the study of the pyrolysis of toluene by the same method, and they observed that the first order rate constant increases, as the contact time is increased. They calculated the apparent activation energy of the pyrolytic reaction to be 90 kcal./mol., keeping the contact time constant at 0.068 sec. in the reaction temperature range 860~940°C, but they concluded that it is premature to assign any definite value to the bond dissociation energy of toluene. At first, in order to explain the higher activation energy and the occurrence of methane, they suggested reaction 2, which proceeds concurrently with the main reaction 1.

$$C_6H_5CH_3 \rightarrow C_6H_5CH_2\cdot + H\cdot \quad (1)$$

$$C_6H_5CH_3 \rightarrow C_6H_5\cdot + CH_3\cdot \quad (2)$$

Later, however, they[5] approved of Szwarc's view that the contribution of reaction 2 to the apparent activation energy of pyrolysis of toluene is of a minor degree, for they considered the facts that the ratio of hydrogen to methane in the reaction product of pyrolysis of toluene is constant over the reaction temperature range, and that the ratio does not vary even in the decomposition of *n*-propylbenzene in the presence of excessive toluene[6].

The present author[2] carried out the pyrolysis of toluene in both of the temperature ranges, 738~864 and 860~940°C, to elucidate the cause of the discrepancy of the bond dissociation energies of toluene obtained by the two groups, and it was found that the apparent activation energy for the first order rate expression of pyrolysis of toluene increases, as the reaction

1) S. W. Benson and J. H. Buss, *J. Phys. & Colloid Chem.*, **61**, 104 (1957).
2) M. Takahasi, This Bulletin, **33**, 801 (1960).
3) M. Szwarc, *J. Chem. Phys.*, **16**, 128 (1948).
4) H. Blades, A. T. Blades and E. W. R. Steacie. *Can. J. Chem.*, **32**, 298 (1954).
5) A. Blades and E. W. R. Steacie, ibid., **32**, 1142 (1954).
6) C. H. Leigh and M. Szwarc, *J. Chem. Phys.*, **20**, 403 (1952).

temperature was extended to a higher range. The author discussed the possible causes of the nonlinearity of the relation of $\log k$ versus $1/T$, and suggested complication by the involvement of some competitive reaction. Blades and Steacie[5] suggested the same possibility in the reaction, and carried out the pyrolysis of *n*-propylbenzene in an excess of deuterated toluenes (mixture of toluene-$\alpha$-$d_3$: 66%, toluene-$\alpha$-$d_2$: 29%, and toluene-$\alpha$-$d$: 5%) at 722°C at contact time 0.45 sec. They found the products were composed of hydrogen, methane, ethane, ethylene, benzene and bibenzyl, and the ratios of the gaseous products were:

$$H_2 : HD : D_2 = 1 : 1 : 0$$

and

$$CD_4 : CD_3H : CD_2H_2 = 1 : 1.5 : 1$$

respectively.

The large ratio of $H_2$ to HD suggested that hydrogen atoms may be abstracted from the ring as well as from the side chain. In addition, they concluded that concerning two mechanisms 3 and 4 suggested by Szwarc,

$$H\cdot + C_6H_5CD_3 \text{ (or } C_6H_5CD_2H) \rightarrow C_6H_5\cdot + CD_3H \text{ (or } CD_2H_2) \quad (3)$$

$$C_6H_5\cdot + C_6H_5CD_3 \rightarrow C_6H_5D + C_6H_5CD_2\cdot$$

$$H\cdot + C_6H_5CD_3 \text{ (or } C_6H_5CD_2H) \rightarrow CD_3\cdot \text{ (or } CD_2H\cdot) + C_6H_6$$

$$CD_3\cdot \text{(or } CD_2H\cdot) + C_6H_5CD_3 \text{(or } C_6H_5CD_2H) \rightarrow CD_4 + C_6H_5CD_2\cdot \text{(or } CD_3H,\ CD_2H_2) \quad (4)$$

mechanism 3 would give $CD_3H$ and $CD_2H_2$, while mechanism 4 would give $CD_4$, $CD_3H$ and $CD_2H_2$. They considered that the production of $CD_4$ in their experiment is a good evidence for mechanism 4, and that mechanism 3 contributes to a minor degree. As the pyrolysis of toluene itself was not carried out in their experiment, it was not clear whether the initiations reaction of pyrolysis of toluene involves the ring-hydrogen or not. The present author attempted to study the pyrolysis of toluene-3-*d* and toluene-4-*d* in the temperature range 830~955°C, and investigated the reactivities of the meta and para positions of toluene.

## Experimental

**Materials.**—Toluene-3-*d* and -4-*d* were prepared by the reaction of *m*- and *p*-tolylmagnesium bromide with deuterium hydroxide according to Gold[7] with some modifications. The Grignard reagent was prepared from 50 g. of *m*- or *p*-bromotoluene, 7 g. of magnesium and 120 ml. of ethyl ether; and 6 ml. of deuterium hydroxide (99.78 g. $D_2O$/100 g.) was added to the reaction mixture. In adding deuterium hydroxide, care should be taken to continue vigorous stirring to secure the contact of deuterium hydroxide with the Grignard reagent. The reaction mixture was refluxed for about ten minutes, and left to stand overnight. In order to decompose the remaining Grignard reagent, dry carbon dioxide was passed through for some time, and then 7 g. of ammonium chloride solution in 25 ml. of water was added, a solid material being formed. Then 20 ml. of concentrated hydrochloric acid was added to dissolve the solid. Ether layer was separated, and the aqueous layer was extracted with 100 ml. of ether. The combined ether solution was washed with a dilute sodium hydroxide solution and with distilled water successively, and dried with calcium chloride. Ether was removed by distillation with Vigreux's columm, and toluene fraction boiling at 111~112°C was collected, weighing about 15 g. The toluene fraction was then shaken with about 15% hydrochloric acid to remove a trace of ether which interferes with pyrolysis of toluene, and distilled through a spinning band column of 150 cm. in length. Although the deuterated toluenes thus obtained contained about 22% of undeuterated toluene (see the next section), some improvements of isotopic purity may be obtained by the more elaborated method proposed by Weldon[8].

**Determination of Isotopic Purity of Deuterated Toluenes.** — For the determination of the isotopic purity of the deuterated organic compounds, mass spectrometry under reduced ionization voltage[9] is recommended, but the available mass spectrometer of CEC 103 A type operated at ionizing voltage 70 V. was unsuitable for the present purpose. So the present author was obliged to apply the infrared spectra for the determination of the isotopic purity of synthesized deuterated toluenes, in spite of less accuracy of the method. Infrared spectra of toluene, toluene-3-*d* and toluene-4-*d* were already given by Tiers[10] in the region of 693~835 $cm^{-1}$. Comparison of their spectral data of toluene with those of the present author gave good agreement in the wave numbers of the absorption maxima, but not in the intensity, their absorption coefficients at characteristic absorption maxima being larger by about twice than the present author's. While standard toluene-3-*d* and -4-*d* of isotopic purity of more than 99% were not available to us, Tier's data were not proper to be applied to the present analysis, so that the present author adopted the method to determine the content of undeuterated toluene in the synthesized mixture. The infrared spectral data obtained by a Perkin Elmer 112 infrared spectrometer are shown in Table I. The absorption band of toluene at 730 $cm^{-1}$ is too strong to determine the absorption coefficient in liquid state. Therefore, the absorption band at 695 $cm^{-1}$ was used in the analysis of the mixture of toluene and toluene-4-*d*, the latter of which has no characteristic absorption at the wave number. The extinction coefficient of standard

7) V. Gold and D. P. N. Satchell, *J. Chem. Soc.*, **1951**, 2743.

8) L. H. P. Weldon and C. L. Wilson, *J. Chem. Soc.*, **1946**, 235.

9) The Institute of Petroleum, "Applied Mass Spectrometry", London, (1954), p. 91.

10) G. V. D. Tiers and J. H. Tiers, *J. Chem. Phys.*, **20**, 761 (1953).

TABLE I. EXTINCTION COEFFICIENTS OF STANDARD TOLUENE, AND OF MIXTURES OF TOLUENE-3-*d* OR -4-*d* AND TOLUENE

| Wave numbers, $cm^{-1}$ | 3030 | 835 | 798 | 730 | 710 | 695 |
|---|---|---|---|---|---|---|
| Standard toluene | 430 | 0 | 0 | 1470 | 0 | 840 |
| Sample I (toluene+toluene-3-*d*) | 260 | 0 | 540 | 480 | 0 | 800 |
| Sample II (toluene+toluene-4-*d*) | 260 | 640 | 0 | 490 | 200 | 190 |

Extinction coefficient $K_\nu = \log (I_0/I)/d$.
Cell thickness $d = 0.00087$ cm.

TABLE II. COMPARISON OF MASS SPECTRA OF STANDARD TOLUENE, SAMPLES I AND II, WITH API DATA

| *m/e* | Standard toluene | Sample I | Sample II | Toluene* | Toluene-3-*d** | Toluene-4-*d** |
|---|---|---|---|---|---|---|
| 95 | — | 0.21 | 0.26 | — | — | — |
| 94 | 0.16 | 5.38 | 5.49 | 0.16 | — | — |
| 93 | 6.00 | 69.09 | 70.39 | 5.60 | 72.5 | 71.6 |
| 92 | 78.37 | 100 | 100 | 78.5 | 100 | 100 |
| 91 | 100 | 35.15 | 37.07 | 100 | 8.51 | 8.53 |
| 90 | 7.70 | 4.50 | 4.57 | 9.08 | 2.53 | 3.66 |
| 89 | 3.72 | 2.14 | 2.09 | 4.13 | 1.00 | 0.93 |
| 88 | 0.27 | 0.45 | 0.42 | 0.36 | 0.32 | 0.33 |
| 87 | 0.58 | 0.80 | 0.75 | 0.60 | 0.61 | 0.61 |
| 86 | 0.99 | 0.98 | 0.99 | 0.94 | 0.69 | 0.67 |
| 85 | 0.78 | 0.71 | 0.73 | 0.66 | 0.48 | 0.48 |
| 84 | 0.33 | 0.35 | 0.35 | 0.22 | 0.23 | 0.21 |

Ionization voltage: 70 V.
Ionizing current : 10.5 $\mu$A.
* From API Spectral Data, Serial No. 418, 687 and 688.
Components containing $^{13}C$ have been removed in the API Data.

toluene at 695 $cm^{-1}$ being 840, the content of toluene in Sample II (mixture of toluene and toluene-4-*d*) was ascertained as 22%. In the analysis of Sample I (mixture of toluene and toluene-3-*d*) the band at 695 $cm^{-1}$ is unsuitable, for toluene-3-*d* has the absorption band of nearly the same strength as toluene at the position. However, as the extinction coefficient of Sample I at 730 $cm^{-1}$ is accidentally almost the same as that of Sample II, the content of toluene in Sample I was presumed to be nearly the same as that of Sample II, that is, 22%. Mass spectrometric data which are shown in Table II may support the above conclusion, although they are not sufficient for determining the precise isotopic purity.

**Apparatus and Procedure of Pyrolysis.** — They were previously described in Part I. Experiments in the temperature range lower than 830°C and at a contact time less than 0.1 sec. were not carried out, for a sufficient amount of gas for the mass spectrometric analysis was not produced under these conditions.

## Analysis of Gaseous Products and Experimental Results

The gas products of pyrolysis of the mixture of toluene and toluene-3-*d* or -4-*d* consisted of $H_2$, HD, a trace of $D_2$, $CH_4$ and $CH_3D$. No complete method of determination of the ratio of HD to $H_2$ appeared to be established until most recently[11], in the case where the relative abundance of HD to $H_2$ is more than 10% and the total amount of hydrogen is small. Recent development of gas chromatography has made it possible to separate HD from $H_2$, using a very small amount of a sample[12], and this method may be applied to the analysis. In the present experiment, the author was satisfied with determining the ratio approximately. As pure HD for a standard was not available, its mass spectrometric sensitivity at *m/e* 3, was assumed to be equal to that of $H_2$ at *m/e* 2. It has been pointed out that the peak at *m/e* 3 contains the component of $H_3^+$, in addition to that of $HD^+$, but its contribution was not appreciable in the present case, using ionizing current of 10.5 $\mu$A. The contribution of $D^+$ to *m/e* 2 is not known, but it may be neglected.

TABLE III

| *m/e* | 18 | 17 | 16 | 15 | 14 | 13 |
|---|---|---|---|---|---|---|
| | | | $CH_4^+$ | $CH_3^+$ | $CH_2^+$ | $CH^+$ |
| | | $^{13}CH_4^+$ | $^{13}CH_3^+$ | $^{13}CH_2^+$ | $^{13}CH^+$ | $^{13}C^+$ |
| | | $CH_3D^+$ | $CH_2D^+$ | $CHD^+$ | $CD^+$ | $CH^+$ |
| | $^{13}CH_3D^+$ | $^{13}CH_2D^+$ | $^{13}CHD^+$ | $^{13}CD^+$ | $^{13}CH^+$ | $^{13}C^+$ |
| | $P_{18}$ | $P_{17}$ | $P_{16}$ | $P_{15}$ | $P_{14}$ | $P_{13}$ |

11) The Institute of Petroleum, "Applied Mass Spectrometry", London (1954) p. 81.
12) S. Ohkoshi, Y. Fujita and T. Kwan, This Bulletin, 31, 771 (1958).

considering that the relative abundance of $H^+$ produced from $H_2$ is 2.1% to that of $H_2^+$ [13].

The ratio $CH_3D/CH_4$ was determined according to the following procedure. As each peak of the mixture of $CH_4$ and $CH_3D$ at $m/e$ 18~13 is composed of the following several components as shown in Table III, Eqs. 5 and 6

$$P_{17}=\frac{1}{100}\{S_{CH_4}(a_{^{13}CH_4^+}\times 0.0101)X + S_{CH_3D}(b_{CH_3D^+}\times 0.9896+b_{^{13}CH_2D^+}\times 0.0101)Y\} \quad (5)$$

$$P_{16}=\frac{1}{100}[S_{CH_4}(a_{CH_4^+}\times 0.9896+a_{^{13}CH_3^+}\times 0.0101)X + S_{CH_3D}\{b_{CH_2D^+}\times 0.9896+(b_{^{13}CHD^+}+b_{^{13}CH_3^+})\times 0.0101\}Y] \quad (6)$$

are derived, where $P_{17}$ and $P_{16}$ are observed peak heights at $m/e$ 17 and 16, $S_{CH_4}$ and $S_{CH_3D}$ are sensitivities of $CH_4$ and $CH_3D$ at their parent peaks, $a_{R^+}$ and $b_{R^+}$ are relative abundances of ions produced from $CH_4$ and $CH_3D$, and $X$ and $Y$ are pressures of $(CH_4+{}^{13}CH_4)$ and $(CH_3D+{}^{13}CH_3D)$, respectively.

TABLE VI. MASS SPECTRA OF $CH_4$ AND $CH_3D$

| $m/e$ | $CH_4$ ($a$) | $CH_3D$ ($b$) | $CH_4$ ($a'$) |
|---|---|---|---|
| 17 | | 100 | |
| 16 | 100 | 79.8 | 100 |
| 15 | 89.3 | 23.7 | 88.1 |
| 14 | 19.4 | 10.5 | 19.8 |
| | Mohler's data, | this work | |
| | $^{13}CH_4$ component has been removed. | | |

For the measurement of standard $CH_4$ by the present author gave nearly the same cracking pattern $a'$ as $a$ of Mohler[14] (Table IV), the author applied his data $a$ and $b$ to the present analysis. From Eqs. 5 and 6, Eq. 7 is derived assuming $S_{CH_4}=S_{CH_3D}$, and using Mohler's data,

$$Y/X=99.052\frac{(1.00808\,P_{17}-0.0101\,P_{16})}{(98.96\,P_{16}-79.207\,P_{17})} \quad (7)$$

The data of mole ratios $HD/H_2$ and $CH_3D/CH_4$ obtained in the pyrolysis of Samples I and II under various conditions are shown in Table V, where Eq. 7 was applied to the determination of $CH_3D/CH_4$. The determination of the mole ratio $(H_2+HD)/(CH_4+CH_3D)$ was not performed, for sufficient accuracy was not expected for the determination by the mass spectrometric analysis, and from the previous data it may be presumed that the ratio is about 2[2].

Analyses of liquid products were carried out by both infrared and mass spectrometric methods. Toluene recovered from the reaction products of Samples I and II gave nearly the same infrared spectra as the original ones. Therefore, it may be concluded that any transfer of deuterium from the initial position did not occur in the pyrolysis. Mass spectra of the recovered toluene were also nearly the same in the mass range of $C_7$ groups, but some differences were observed in the range of $C_6$ groups as shown in Table VI.

Table VI shows that the peak at $m/e$ 78 includes $C_6H_6^+$, $C_6H_4D^+$ and $C_5{}^{13}CH_5^+$, and the peak at $m/e$ 79 does $C_6H_5D^+$, $C_6H_3D_2^+$ and $C_5{}^{13}CH_6^+$, but it was not carried out to determine the ratio $C_6H_6 : C_6H_5D : C_6H_4D_2$ from these data. It is to be noted that the increase of benzene content due to the rise of the reaction temperature is rather small compared

TABLE V. MOLE RATIOS $HD/H_2$, $D_2/H_2$ AND $CH_3D/CH_4$ IN THE PYROLYSIS OF SAMPLES I AND II

| Expt. No. | Reaction temp., °C | Vapor pressure, mmHg | $k$, $sec^{-1}$ | $HD/H_2$ | $D_2/H_2$ | $CH_3D/CH_4$ |
|---|---|---|---|---|---|---|
| Sample I (mixture of 22% toluene and 78% toluene-3-*d*) | | | | | | |
| I-4 | 830.3 | 8.92 | $(1.0\times10^{-2})$ | — | — | 0.060* |
| I-3 | 832.0 | 7.36 | $1.0\times10^{-2}$ | 0.11 | 0.000 | 0.052 |
| I-1 | 876.6 | 8.80 | $4.2\times10^{-2}$ | 0.14 | 0.004 | 0.077 |
| I-5 | 902.6 | 8.46 | $1.2\times10^{-1}$ | — | — | 0.091* |
| I-2 | 908.1 | 8.82 | $1.3\times10^{-1}$ | 0.13 | 0.004 | 0.075 |
| Sample I′ (toluene recovered from the reaction mixture of Sample I after pyrolysis) | | | | | | |
| I′-1 | 850.3 | 3.66 | — | 0.17 | 0.006 | 0.058 |
| I′-2 | 852.0 | 10.62 | $2.8\times10^{-2}$ | 0.19 | 0.007 | 0.082 |
| I′-3 | 919.0 | 8.96 | $2.9\times10^{-1}$ | 0.18 | 0.007 | 0.085 |
| Sample II (mixture of 22% of toluene and 78% of toluene-4-*d*) | | | | | | |
| II-3 | 834.3 | 7.86 | $1.2\times10^{-2}$ | — | — | 0.053* |
| II-1 | 876.5 | 5.42 | $7.8\times10^{-2}$ | 0.15 | 0.005 | 0.074 |
| II-4 | 907.3 | 5.60 | $1.9\times10^{-1}$ | — | — | 0.098* |
| II-2 | 955.6 | 3.90 | 1.1 | 0.19 | 0.004 | 0.079 |

* In these cases, sensitivity of mass spectrometer was low and unstable particularly for hydrogen.

13) API Mass Spectral Data. No. 452.

14) F. L. Mohler, V. H. Dibeler and E. Quinn, *J. Research Natl. Bur. Standards*, 61, 171 (1958).

TABLE VI. MASS SPECTRA OF UNPYROLYZED AND PYROLYZED TOLUENES

| Sample No. | Reaction temp. °C | m/e 72 | 78 | Δ 78* | 79 | Δ 79* | 80 | 84 | 93 | 94 |
|---|---|---|---|---|---|---|---|---|---|---|
| Sample I | (before pyrolysis) | 0.09 | 1.30 | — | 0.16 | — | 0.00 | 0.35 | 69.1 | 100 |
| I-4 | 830.0 | 0.08 | 1.42 | 0.12 | 0.21 | 0.05 | 0.00 | 0.35 | 68.2 | 〃 |
| I-3 | 832.0 | 0.10 | 1.39 | 0.09 | 0.25 | 0.09 | 0.00 | 0.35 | 70.2 | 〃 |
| I-1 | 876.6 | 0.09 | 1.43 | 0.17 | 0.33 | 0.17 | 0.05 | 0.31 | 71.6 | 〃 |
| I-5 | 902.6 | 0.08 | 1.66 | 0.36 | 0.72 | 0.56 | 0.11 | 0.31 | 69.3 | 〃 |
| I-2 | 908.1 | 0.09 | 1.48 | 0.18 | 0.56 | 0.40 | 0.08 | 0.34 | 71.1 | 〃 |
| Sample II | (before pyrolysis) | 0.09 | 11.30 | — | 0.17 | — | 0.00 | 0.35 | 70.4 | 〃 |
| II-3 | 834.3 | 0.09 | 1.47 | 0.17 | 0.25 | 0.08 | 0.00 | 0.35 | 69.4 | 〃 |
| II-4 | 907.3 | 0.09 | 1.52 | 0.22 | 0.93 | 0.76 | 0.16 | 0.36 | 68.8 | 〃 |

* Δ means increment of relative abundance by pyrolysis.

with the increase of velocity constant in the same reaction temperature range (cf. Table V).

These experimental results are summarized as follows:

1) Toluene-3-*d* and -4-*d* (isotopic purity: 78%) gave $H_2$, HD, a trace of $D_2$, $CH_4$ and $CH_3D$ by pyrolysis, and their mole ratios were determined by mass spectrometric analysis.

2) There was not any distinct difference in the mole ratios of $HD/H_2$ and $CH_3D/CH_4$ in the reaction of either toluene-3-*d* or -4-*d*, and it may be concluded that the reactivities of *m*- and *p*-hydrogen of toluene are of the same order.

3) As the pyrolyzed toluene gave a nearly similar infrared spectra as those of unpyrolyzed one, exchange reaction of hydrogen between toluenes did not occur to an appreciable extent in the temperature range 830~900°C.

The following reaction mechanism may be presented to explain the formation of HD and $CH_3D$.

In the above schemes, statistical weight shows numbers of reacting hydrogens in each set of elementary processes. The production of HD may be explained by one or more of reactions 5'—7, and that of $CH_3D$ by 10 and/or 13. If it is assumed that eight hydrogens of toluene

(toluene-3-*d* or -4-*d* containing 22% toluene)

| | | | | Statistical weight on the assumption of equal reactivity | |
|---|---|---|---|---|---|
| $C_6H_4D\text{-}CH_3$ | ⟶ | $C_6H_4D\text{-}CH_2\cdot + H\cdot$ | (1) | 3 | Initiation |
| 〃 〃 | ⟶ | $\cdot C_6H_3D\text{-}CH_3 + H\cdot$ | (2) | 4 | |
| 〃 〃 | ⟶ | $\cdot C_6H_4\text{-}CH_3 + H\cdot$ | (2') | 1 | |
| 〃 〃 | ⟶ | $\cdot C_6H_4D + CH_3\cdot$ | (3) | | |
| $H\cdot + C_6H_4D\text{-}CH_3$ | ⟶ | $C_6H_4D\text{-}CH_2\cdot + H_2$ | (4) | 3 | Abstraction by H atom |
| 〃 〃 | ⟶ | $\cdot C_6H_3D\text{-}CH_3 + H_2$ | (5) | 4 | |
| 〃 〃 | ⟶ | $\cdot C_6H_4\text{-}CH_3 + HD$ | (5') | 1 | |
| $D\cdot + C_6H_4D\text{-}CH_3$ | ⟶ | $C_6H_4D\text{-}CH_2\cdot + HD$ | (6) | 3 | Abstraction by D atom |
| 〃 〃 | ⟶ | $\cdot C_6H_3D\text{-}CH_3 + HD$ | (7) | 4 | |
| 〃 〃 | ⟶ | $\cdot C_6H_4\text{-}CH_3 + D_2$ | (7') | 1 | |
| $H\cdot + C_6H_4D\text{-}CH_3$ | ⟶ | $\cdot C_6H_4D + CH_4$ | (8) | | Metathesis by H atom |
| 〃 〃 | ⟶ | $C_6H_5D + CH_3\cdot$ | (9) | | |
| $D\cdot + C_6H_4D\text{-}CH_3$ | ⟶ | $\cdot C_6H_4D + CH_3D$ | (10) | | Metathesis by D atom |
| 〃 〃 | ⟶ | $C_6H_4D_2 + CH_3\cdot$ | (11) | | |
| $CH_3\cdot + C_6H_4D\text{-}CH_3$ | ⟶ | $C_6H_4D\text{-}CH_2\cdot + CH_4$ | (12) | 3 | Abstraction by $CH_3$ radical |
| 〃 〃 | ⟶ | $\cdot C_6H_3D\text{-}CH_3 + CH_4$ | (13) | 4 | |
| 〃 〃 | ⟶ | $\cdot C_6H_4\text{-}CH_3 + CH_3D$ | (13') | 1 | |
| $2\cdot C_6H_3D\text{-}CH_3$ (or $\cdot C_6H_4\text{-}CH_3$) | ⟶ | Deuterated and undeuterated dimethylbiphenyls | (14) | | Termination |
| $C_6H_4D\text{-}CH_2\cdot$ (or $C_6H_5\text{-}CH_2\cdot$) | ⟶ | Deuterated and undeuterated bibenzyls | (15) | | |

(The reactions of undeuterated toluene omitted.)

had the reactivities of the same order both in the initiations and propagations, (that is, here both isotope effect and structure effect are neglected), the expected ratio $H_2 : HD : D_2$ in the pyrolysis of toluene-*d* of 100% of isotopic purity might be $7/8\times7/8+7/8\times1/8 : 1/8\times7/8 : 1/8\times1/8 = 1 : 0.29 : 0.02$. On the other hand, if it is assumed that HD was produced only by the abstraction of D atom from benzene ring by hydrogen atom (reaction 5′), not by reactions 6 and 7, the ratio $H_2 : HD : D_2$ might be $7/8 : 1/8 : 0 = 1 : 0.14 : 0$ (natural abundance 0.02% of D is neglected). As the experimental results (Table V) show the ratio, $1 : 0.10\sim0.19 : 0.000\sim0.007$, it is indicated that the ratio is in the middle of the two assumed ratios, and it may be expected that $HD/H_2$ is augmented, if 22% of undeuterated toluene is removed from Samples I and II. Although these results do not suffice to establish the initiation reactions 2 and 2′, they may not be a negative evidence for such processes. A more direct evidence supporting the existence of process 2′ may be obtained by pyrolyzing $C_6D_5CH_3$, for $C_6D_5CH_3$ would give $D_2$ by the successive reactions 2′, 6 and 7 in a high yield.

The ratio $CH_3D : CH_4$ is relatively low compared with that of $HD : H_2$ in the whole reaction temperature range. The possible processes to produce $CH_3D$ may be 10 and/or 13′, and if it is assumed that processes 2 and 2′ gave H and D atoms in the ratio 7 : 1, and that processes 12—13′ proceeded with statistical weights (3 : 4 : 1), the ratio of $CH_3D$ to $CH_4$ obtained by reactions 8 and 10 might be 1/7, and the ratio of $CH_3D$ to $CH_4$ obtained by reactions 12—13′ might be also 1/7. On the other hand, if it is assumed that D atom was not produced by the initiation reaction 2′, $CH_3D$ might be produced only by reaction 13. In this case, the ratio $CH_3D : CH_4$ depends on the relative velocity rate of reactions 8 and 9. If it is assumed that the relative rate ratio is $\alpha : 1$, the ratio $CH_3D/CH_4$ should be $1/(7+8\alpha)$, and less than 1/7.

These experimental results are rather unexpected, considering the generally accepted fact that $D(C_6H_5\text{–}H)$ is larger than $D(C_6H_5CH_2\text{–}H)$. Dr. Kobayashi[15] suggested that the benzyl radical would rearrange to cycloheptatrienyl radical, considering the mass spectrometric evidence of the rearrangement of benzyl cation to cycloheptatrienium cation[16]. If such a rearrangement took place, transfer of deuterium atom in the aromatic ring would be observed. Unfortunately the amount of aromatic products produced by pyrolysis was not sufficient to be analyzed. On the other hand, it has been known that $CH_3$ radical abstracts hydrogen from the benzene ring[17,18], and this fact may explain the production of $CH_3D$. As may be described in the succeeding paper, pyrolysis of benzene proceeds in the relatively low temperature range, and its apparent activation energy is unexpectedly low. Although the reaction mechanism of pyrolysis of benzene is not yet completely established, it may be compatible with the present results.

15) M. Kobayashi, private communication.

## Summary

In order to elucidate the mechanism of the pyrolysis of toluene, pyrolysis of toluene-3-*d* and -4-*d* was carried out by the flow method in the temperature range 830∼955°C, and the mole ratios $D_2 : HD : H_2$ and $CH_3D : CH_4$ were determined by mass spectrometry. The involvement of the reaction of ring-hydrogen in the pyrolysis has been confirmed from the formation of HD and $CH_3D$. As there was not any distinct difference in the mole ratios between the reactions of toluene-3-*d* nor -4-*d*, it is concluded that the reactivities of *m*- and *p*-hydrogens of toluene are of the same order. Considering these results, the possible elementary processes involving ring-hydrogen are discussed.

The author wishes to express his hearty thanks to Professor Y. Urushibara and Professor O. Simamura for their kind guidance and encouragement for the present work. The author is grateful to Professor S. Araki for kind advice in mass spectrometry, to Dr. M. Kawano for measurements of infrared spectra, to Dr. M. Kobayashi for stimulating discussions and also to Mr. A. Suzuki for experimental help.

*Department pf Chemistry*
*College of General Education*
*The University of Tokyo*
*Meguro-ku, Tokyo*

16) P. N. Rylander, S. Meyerson and H. M. Grubb, *J. Am. Chem. Soc.*, **79**, 842 (1957).
17) A. F. Trotman-Dickenson and E. W. R. Steacie, *J. Chem. Phys.*, **19**, 329 (1951).
18) S. H. Wilen and E. L. Eliel, *J. Am. Chem. Soc.*, **80**, 3309 (1958).

# *Studies on Dehydroalanine Derivatives. II. Synthesis of Polydehydroalanine*

By Shumpei SAKAKIBARA

(Received November 30, 1959)

In the preceding paper of this series[1] the synthesis and properties of *N*-carboxy dehydroalanine anhydride (I) were described. The present investigation was designed to synthesize polydehydroalanine using the anhydride I as starting material, and to obtain some information concerning the structure of the polypeptide.

**Synthesis of Polydehydroalanine.** — It was previously observed, that the carbamic acid II, which formed from the *N*-carboxy anhydride I, after hydrolysis or aminolysis was unusually stable as compared with those derived from ordinary amino acids[1]. Therefore, it was expected that the rate of polymerization of the *N*-carboxy anhydride I would be much slower than that of usual *N*-carboxy anhydrides at ordinary temperature. In order to ascertain this expectation, the rate of polymerization of *N*-carboxy dehydroalanine anhydride (I) was compared with that of *N*-carboxy DL-alanine anhydride at 30°C using cyclohexylamine as initiator. As can be seen from Fig. 1, the time-conversion curve of the polymerization of the *N*-carboxy anhydride I reached the 25% line only after 5 hours, and then very slowly approached the 35% line, while the *N*-carboxy DL-alanine anhydride polymerized very quickly, and the curve arrived at the 90% line within half an hour. It was concluded from these findings that the polymerization reaction of the *N*-carboxy anhydride I should be carried out at sufficiently high temperatures to permit a more rapid rate of the decarboxylation reaction, and that tertiary amines should be used as initiators. The tertiary amine used, would overcome the inclination for low conversion of the polymerization reaction which may be induced by the formation of ureide III as the termination reaction. A rapid rate of the polymerization reaction also seemed to be desirable in order to suppress a vinyl-type polymerization.

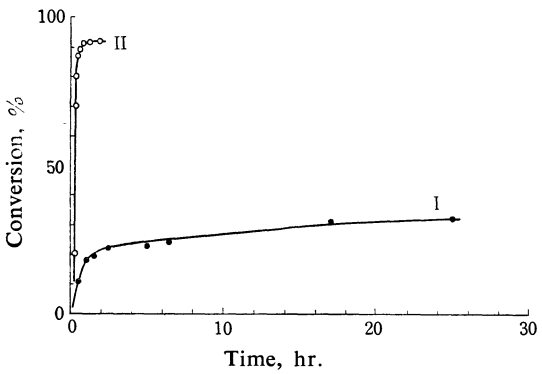
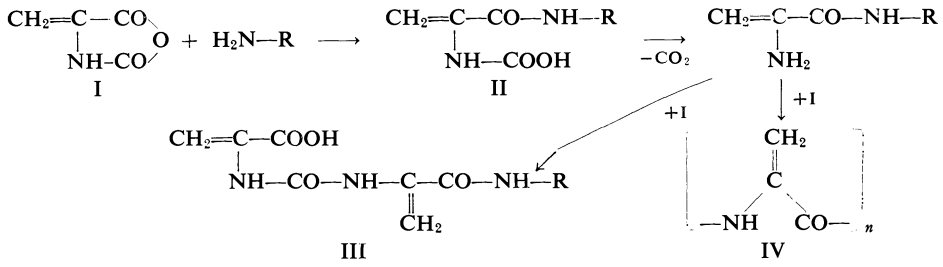



Fig. 1. Polymerization rates of *N*-carboxy anhydrides at 30±0.1°C in dioxane containing cyclohexylamine (10 mol. % against the *N*-carboxy anhydrides): I. *N*-Carboxy dehydroalanine anhydride; II. *N*-Carboxy DL-alanine anhydride.

In the present experiment, polydehydroalanine was prepared by heating a dry pyridine solution of the substance I, at 100°C, or by adding a small amount of triethylamine into a boiling dry toluene solution of the substance I. In the case of the former, the reacting solution gradually became dark-brown as the polymerization reaction proceeded and brown precipitates (IVa) formed. Evolution of carbon dioxide almost ceased after about 2 hr. In the case of the latter, the starting, slight-yellow, clear solutidn suddenly turned into brown, when a small amount of triethylamine was added into




1) S. Sakakibara, This Bulletin, 32, 13 (1959).

the solution. At the same time a vigorous evolution of carbon dioxide was observed and brown precipitates gradually formed. This precipitates were partially insoluble in water, and the water soluble part was collected as polydehydroalanine (IVb).

**Properties of the Polydehydroalanine.** — The freshly formed brown product IV (IVa or IVb) was completely soluble in water, formic acid and dichloroacetic acid, slowly dissolved in dimethylformamide and *m*-cresol, but after complete drying it became partially insoluble in these solvents. Furthermore, about 80% of the substance IV was converted into a water-insoluble form, when preserved under ordinary conditions for about six months. Such a solubility behavior of the substance IV was similar to that of poly-DL-alanine[2,3]. It was, however, found that 34% of the aged substance IV, was completely insoluble even in formic acid, in which the aged poly-DL-alanine is readily soluble[3]. This fact seems to indicate that the substance undergoes not only $\alpha$-$\beta$-configuration change of the polypeptide-bonds, but also the intermolecular cross-linkage formation due to its double bonds. After reprecipitation from water-ethanol, the polypeptide IV was still brown in color, and its ultraviolet absorption spectrum (Fig. 2) suggested the presence of some kinds of conjugated double bonds. When the polypeptide was hydrogenated as described in a later part of this paper, this absorption bands at 230~350 m$\mu$ corresponding to the conjugated double bonds vanished and the brown color extremely reduced at the same time.

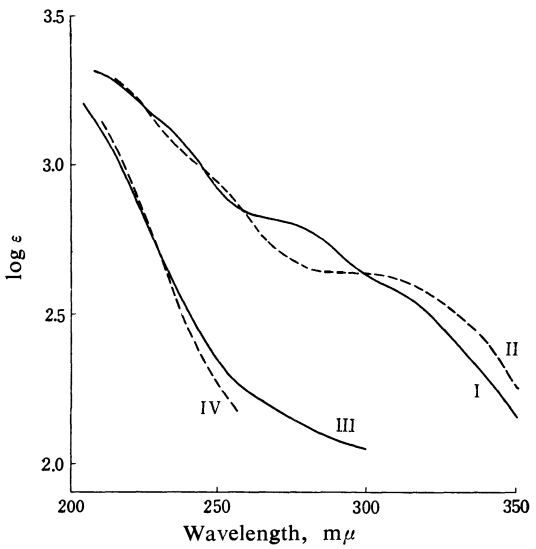



Fig. 2. Ultraviolet absorption spectra recorded on a Beckman DK-2 spectrophotometer: I. Polydehydroalanine (PDA) dissolved in distilled water; II. PDA dissolved in aq. 1 N NaOH solution; III. Hydrogenated PDA dissolved in water; IV. Poly-DL-alanine dissolved in water.

The determination of the molecular weight of the polymer was very difficult. The end-amino group of the polypeptide should not be expected to be present in this material, because of the instability of the *N*-terminal dehydroalanyl group[1]. Therefore, amino-nitrogen determination for calculating the mean molecular weight of the polymer is not significant. When this polymer was titrated with sodium methoxide for determining the end-carboxylic acid, equivalent weights of 330 and 435 were obtained, which corresponded to about 4.7 and 6.2 monomer residues, and these values were much smaller than those calculated hereafter from the expected molecular weight of the polymer. This fact suggested the following two possibilities: (1) Enolization of peptide bonds, which has been mentioned previously by Bergmann, et al. in the cases of dehydroalanyl peptides or diketopiperazines[4]. (2) Partial hydrolysis of pyrolidone rings (VI) which may be formed spontaneously from the dehydroalanyl residues as described in a later part of this paper. The delicate difference between the ultraviolet absorption spectrum of the polymer in 1 N sodium hydroxide solution and that in distilled water would also suggest the fact of enolization. Viscosities of 0.5% dichloroacetic acid solutions of these polymers, IVa and IVb, were determined at 25±0.01°C, and $\eta_{sp}/C = 1.8$ and 0.9 ($C$ expressed in base mol./l.) were obtained, respectively. If an assumption is permitted, that this polymer behaves quite similarly to poly-DL-alanine in dichloroacetic acid, the molecular weight of the polymer may be determined by comparison of the viscosity number with that of known poly-DL-alanine under the same conditions[5]. From the above consideration, about 7000~5000 and 4000~2000 were calculated for their molecular weights, respectively.

**Hydrogenation and Hydrolysis of Polydehydroalanine for Elucidation of the Actual Structure.** —Elucidation of the structure of the polymer was very difficult because double bonds involved in the molecule are expected to be reactive and they may interact with one another within the molecule. If the structure of the polymer is exactly identical with the structural formula

2) C. H. Bamford, A. Elliott and W. E. Hanby, "Synthetic Polypeptide", Academic Press, New York (1956), p. 312.
3) A. Elliott, *Nature*, **170**, 1066 (1952).
4) M. Bergmann and A. Miekeley, *Ann.*, **458**, 40 (1927).
5) C. H. Bamford, A. Elliott and W. E. Hanby, "Synthetic Polypeptide", Academic Press, New York (1956), pp. 299, 314.

IV, poly-DL-alanine should be derived as a result of hydrogenation of the polymer. An attempt of catalytic hydrogenation of the polymer IV under the presence of palladium-charcoal was unsuccessful, since the polymer was adsorbed on the catalyst and separation of the catalyst from the product was very difficult. Recently, Izumi[6] has published an excellent catalyst, which was prepared by reduction of palladium chloride co-ordinated with silk-fibroin. When this catalyst was used, the hydrogenation reaction of the polymer IV, proceeded successfully, and the starting brown solution of the polymer IV turned into a slight-yellow one, after the reaction was finished. Since the palladium atoms have previously adsorbed between peptide layers of silk-protein, no more polypeptide was adsorbed on the catalyst during the reaction. From the hydrochloric acid hydrolyzate of the product V, alanine was detected in a yield of about 5% of the theoretical by the Dowex 50 column chromatography under the condtions of Moore and Stein[7] (Fig. 3).

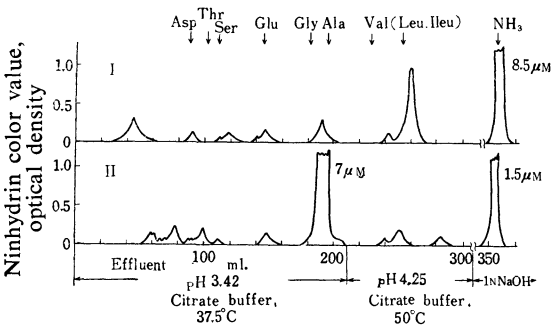
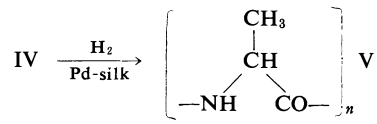
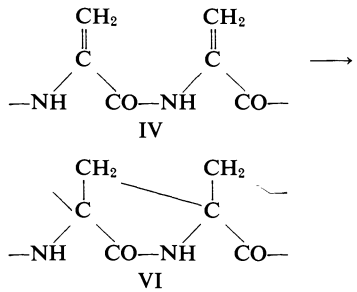



Fig. 3. Chromatographic analysis of ninhydrin-positive materials of the HCl-hydrolyzates: I. Polydehydroalanine (10 mg.); II. Catalytic hydrogenated polydehydroalanine (10 mg.). Arrows indicate the position of the peaks of standard amino acids.




The ultraviolet absorption spectrum of the hydrogenated product V (Fig. 2) was similar to that of the poly-DL-alanine and the absorption bands corresponding to the conjugated double bonds at 250~350 mμ disappeared after hydrogenation as described previously. The infrared spectrum of the hydrogenated product V (Fig. 4), however, was neither quite different from that of the starting polymer, nor similar to that of poly-DL-alanine. This infrared spectrum resembled rather that of poly-α-amino acrylic acid[8]. Since the actual structure of the poly-α-amino acrylic acid is considered to be polypyrolidone[9], a greater part of the polymer would be composed of such a polypyrolidone-type structure VI, which might form spontaneously from the polydehydroalanine by interaction of the neighboring double bonds. The infrared absorption bands at 1700~1760 $cm^{-1}$ (Fig. 4) supported also the presence of five membered cyclic amide. If the structure of the polydehydroalanine corresponds to the formula IV exactly, its hydrochloric acid hydrolyzate must all be pyruvic acid and ammonia. However,




many kinds of ninhydrin-positive materials, the total yield of which was about 10% of the ideal formula IV, were detected by ion-exchanger column chromatography from the hydrochloric acid hydrolyzate (Fig. 3). Ammonia, which formed in this case was also directly ascertained[10] and amounted to 9.5% of the theoretical. These facts all supported the formation of the non-hydrolyzable material which was considered to be such a polypyrolidone. Actually, the hydrochloric acid hydrolyzate of the polymer IV became dark brown, and this fact indicated a formation of huminic material during the course of the reaction. From the result of the experiments and the above considerations, it may be appropriate to consider that the obtained polymer IV, consists of about 90% of polypyrolidone-type polypeptide and about 10% of dehydroalanyl residues. In other words, the synthesis of polydehydroalanine, which was exactly expressed as the structural formula IV, was unsuccessful in the present experiment. If the preparation of co-polymer of dehydroalanine and another stable amino acid is possible, the interaction of the neighboring double bonds would decrease more

6) Y. Izumi, This Bulletin, 32, 932 926, 942 (1959).

7) S. Moore and W. H. Stein, *J. Biol. Chem.*, 192, 663 (1951).

8) This material was prepared from a vinyl-type polymer of the substance I or from that of α-phthalimido acrylc acid as will be described in a later communication of the series.

9) cf. M. Vrancken and G. Smets, *J. Polymer Sci.*, 14, 521 (1954).

10) J. E. Varner, et al., *Anal. Chem.*, 25, 1528 (1953).

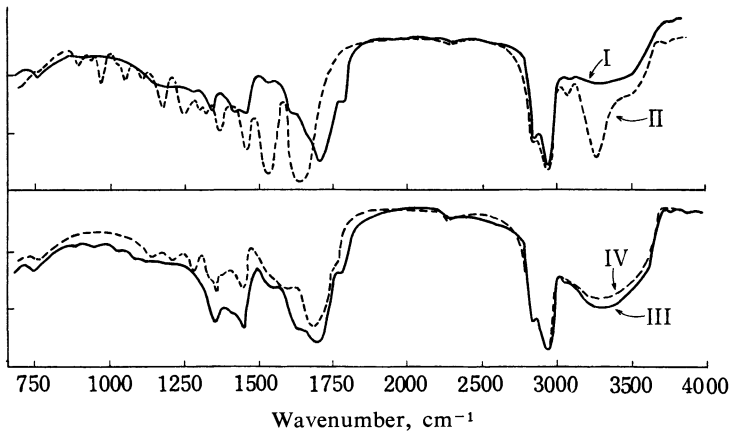



Fig. 4. Infrared absorption spectra recorded on an Adam-Hilger H-80 infrared spectrophotometer: I. Polydehydroalanine; II. Poly-DL-alanine; III. Hydrogenated polydehydroalanine; IV. Poly-$\alpha$-amino acrylic acid. Nujol suspension.

distinctly. A communication on the reactivity of the dehydroalanyl groups involved in the present polymer will be published in the near future.

## Experimental

**Materials.**—*N*-Carboxy dehydroalanine anhydride (I) and *N*-carboxy DL-alanine anhydride were prepared according to the description in the previous paper[1].

**Determination of the Polymerization Rate of I.**—The substance I (350 mg.) was dissolved in freshly distilled dry dioxane (15.00 ml.) containing cyclohexylamine (30.4 mg.). The solution was divided into 14 test tubes so that each tube contains 1.00 ml. of the solution, and the tubes were sealed. Then, they were allowed to react in a bath at 30± 0.1°C, simultaneously. Each of the portions was opened successively at times and dry nitrogen was introduced for about one min. into the solution, which was then titrated with a methanol-benzene solution of sodium methoxide, using thymol blue as an indicator according to the description of Berger, et al.[11] (Fig. 1). The sodium methoxide solution (ca. 0.3 N) was standardized every 5 hr. with purified benzoic acid. *N*-Carboxy DL-alanine anhydride was subjected to the reaction under the same condition described above (Fig. 1).

**Polymerization of I in Pyridine (Preparation of Polydehydroalanine IVa).**—A solution of I (5 g.) in purified dry pyridine (15 ml.) was heated in a boiling water bath for about 2 hr. After cooling to room temperature, the reddish brown reaction mixture was poured into ethyl acetate (100 ml.). The precipitated brown material was centrifuged, washed thoroughly with ethyl acetate and ether, and dried. The brown powder obtained (3.05 g.) was reprecipitated from water-ethanol and dried under reduced pressure at room temperature. The yield was 2.4 g. (64%).

Found: C, 43.8; H, 5.76; N, 15.5; volatile part at 135°C, 17.9. Calcd. for $(C_3H_3ON+14/18\cdot H_2O+1/20\cdot C_2H_6O$ (ethanol)$)_n$: C, 43.7; H, 5.71; N, 16.5; volatile part, 18.8%.

Found*: C, 49.50; H, 4.24; N, 18.86; ash, 1.2%; Na-equiv. wt.[12], 330. Calcd. for $(C_3H_3ON)_n$: C, 52.17; H, 4.35; N, 20.3%.

This material was hard to burn up for analysis.

**Polymerization of I in Toluene (IVb).**—Few drops of triethylamine were added into a boiling toluene solution of I (1 g./20 ml.). The starting clear solution, which was light-yellow, suddenly turned into brown as the reaction occurred and reddish brown precipitates formed immediately under the vigorous evolution of carbon dioxide. After about 30 min., the reaction mixture was cooled and the formed precipitates were filtered off, washed three times with ethyl acetate and dried. The yield was 0.62 g. This material was extracted with sufficient amount of water. The water extract was concentrated to about 5 ml. and brown powder (0.19 g.) (IVb) was reprecipitated with ethanol. The water insoluble part of the material was about 0.18 g. Na-equiv. wt. of the material IVb was 435.

**Hydrogenation of IVa.**—The substance IVa (300 mg.) was dissolved in water (50 ml.) and hydrogenated in an autoclave under 100 atm. of hydrogen at 50~60°C for about 8 hr. using palladium-silk catalyst (200 mg.). After the reaction was complete, the catalyst was filtered off and the filtrate was concentrated to about 10 ml. Ethanol (100 ml.) was added into the concentrate and about 160 mg. of light-yellow powder was precipitated. This material was reprecipitated from water-ethanol and dried under reduced pressure at 118°C.

Found: C, 47.67; H, 5.13; N, 16.68. Calcd. for $(9/10\cdot C_3H_3ON+1/10\cdot C_3H_5ON+2/5\cdot H_2O)_n$: C, 47.1; H, 5.36; N, 18.3%.

11) A. Berger, M. Sela and E. Katchalski, *Anal. Chem.*, 25, 1554 (1953).

12) M. Sela and A. Berger, *J. Am. Chem. Soc.*, 77, 1893 (1955).

*) This material was dried over phosphorus pentoxide under reduced pressure at 135°C, in which procedure a certain extent of decomposition might occur, such as liberation of formaldehyde or ammonia.

The hydrogenated material (10 mg.) was hydrolyzed with 6 N hydrochloric acid for about 20 hr. and the hydrolyzate was concentrated to dryness. The residue was then subjected to column chromatography under the Stein-Moore's condition (Fig. 3). The fraction corresponding to alanine was collected, treated with 2,4-dinitrofluorobenzene and purified by celite column chromatography using ether-phosphate buffer (0.25 M, pH 6.5) as a developer. Infrared spectrum of the purified main fraction was agreed with that of authentic DNP-alanine.

## Summary

The polymerization rate of *N*-carboxy dehydroalanine anhydride (I) was compared with that of *N*-carboxy DL-alanine anhydride, and it was found, that the former was much slower than the latter at 30°C. Polydehydroalanine (IV) was obtained by heating the substance I in dry pyridine at 100°C, or by adding a small amount of triethylamine into the boiling toluene solution of I. The substance IV was water-soluble brown powder, the actual structure of which was supposed to be a pyrolidone-type polypeptide VI containing about 10% of dehydroalanyl residues.

The author wishes to express his thanks to Professor Shiro Akabori and Professor Shunsuke Murahashi for their guidance and encouragement throughout the course of this study.

*Institute for Protein Research*
*Osaka University*
*Nishi-ku, Osaka*

# *Systematic Separation of Fission Products by Solvent Extraction Method*

By Toshiyasu KIBA, Shigeru OHASHI and Toyoo MAEDA

(Received October 27, 1959)

Solvent extraction methods have often been employed for the separation of individual fission products. The purpose of the present investigation was to establish a new scheme of systematic separation of fission products having relatively long half-lives by combining and modifying the solvent extraction methods developed previously. The fission products considered in this investigation were limited to the nuclides, the radioactivities of which are higher than one per cent after all the fission products have been aged for one year. The nuclides which fall in this category are zirconium-niobium-95, cerium - praseodymium - 144, promethium - 147, strontium-yttrium-90, ruthenium-rhodium-106, cesium-137-barium-137$^{m}$, strontium-89, and yttrium-91. Since the chemical behaviors of strontium-89 and yttrium-91 are just the same as those of strontium-90 and yttrium-90, respectively, these were excluded from the scope of the present investigation. All of the other nuclides except promethium-147 are composed of the pairs of parent and daughter. Among these pairs, praseodymium-144, rhodium-106, and barium-137$^{m}$ are relatively short-lived daughters. Therefore, the nuclides considered finally for this study were zirconium-niobium-95, cerium-144, promethium-147, strontium-yttrium-90, ruthenium-106, and cesium-137.

Marinsky, Hume and Ballow[1] reported that zirconium-95 and niobium-95 can be extracted from a hydrochloric acid solution into chloroform with cupferron. Kiba and Kanetani[2] found that rare earth nuclides, cerium-144, promethium-147, and yttrium-90 can be separated from an acetate solution of pH 4 to 5 into chloroform with cupferron. Kiba and Mizukami[3] investigated the separation of strontium-90 and yttrium-90 and found that strontium-90 can be extracted from an acetate solution of pH 8 with TTA dissolved in hexone. Kiba and Hirono[4] reported that ruthenium-106 can be extracted from hydrochloric acid solution into a mixture of TBP and kerosene with diphenyl thiourea. Combining and modifying the methods mentioned above the present authors have presented a new systematic method for the separation of fission products by the liquid-liquid extraction processes.

## Experimental

All of the radioactive nuclides were purchased from the Oak Ridge National Laboratory of the

1) J. A. Marinsky, D. N. Hume and N. E. Ballow, "Radiochemical Studies; The Fission Products", National Nuclear Energy Series IV-9, (1951), p. 1514.
2) T. Kiba and M. Kanetani, This Bulletin, 31, 1013 (1958).
3) T. Kiba and S. Mizukami, ibid., 31, 1007 (1958).
4) T. Kiba and H. Hirono, presented at the 11th Annual Meeting of the Chemical Society of Japan, Tokyo, April 5, 1958.

United States of America. Stock solutions of these unclides were made as follows. The original solution of zirconium-niobium-95 in 0.03 M oxalic acid was diluted with 0.33 M oxalic acid. The original solution of cerium-144 as cerous nitrate in nitric acid, that of promethium-147 in hydrochloric acid, that of strontium-yttrium-90 in nitric acid, that of ruthenium-106 as nitrosyl ruthenium trinitrate in 8 M nitric acid, and that of cesium-137 in 1 M nitric acid were diluted with 3.75 M hydrochloric acid, respectively. About 0.05 to 0.1 $\mu$c of the carrier-free nuclides was used for each experiment.

TBP was purified by distillation. All other chemicals of the guaranteed or the first grade of Japan Industrial Standards were used without further purification. An electric shaker was used for shaking of separatory funnels. Whole or aliquots of both aqueous and organic phases were taken into small porcelain dishes after five to ten minute shaking for each extraction. The content of each dish was evaporated or ignited, and the beta activity was measured with an end-window type GM counter.

## Results and Discussion

The whole scheme of the systematic separation is demonstrated in Table I. The method is composed of four-step extractions. The first

TABLE I. SCHEME OF SYSTEMATIC SEPARATION

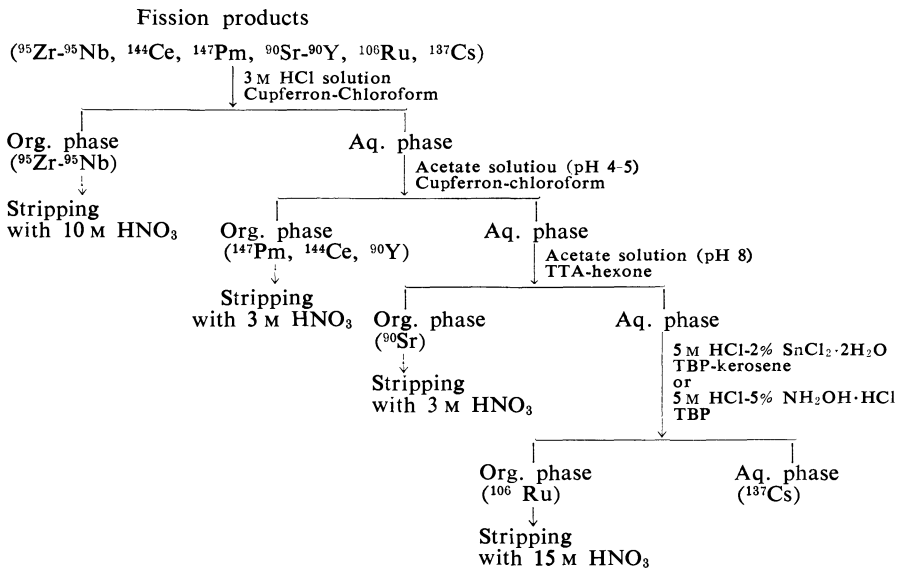



TABLE II. DETAILS OF EXTRACTION CONDITIONS

| Extraction step | Composition of aqueous phase | | Organic phase | |
|---|---|---|---|---|
| 1 | Sample solution | 0.5 ml. | | |
| | 3.75 M HCl—0.043 M $H_2C_2O_4$ | 3.5 ml. | Chloroform | 5 ml. |
| | 20% $NH_2OH \cdot HCl$ | 0.5 ml. | | |
| | 5% Cupferron | 0.5 ml. | | |
| 2 | Aqueous solution after the first step extraction | 5 ml. | | |
| | 9 M $NH_3$ | 1.6 ml. | Chloroform | 5 ml. |
| | 0.9 M $NH_4AcO$ | 10.4 ml. | | |
| | 5% Cupferron | 3 ml. | | |
| | 5% Cupferron | 3 ml. | Chloroform | 5 ml. |
| | 5% Cupferron | 3 ml. | Chloroform | 5 ml. |
| 3 | Aqueous solution after the second step extraction | 27 ml. | 0.05 M TTA in hexone | 10 ml. |
| | 5.4 M $NH_3$ | 1 ml. | | |
| 4A | Aqueous solution after the third step extraction | 27 ml. | TBP-kerosene (1 : 2) | 10 ml. |
| | 11 M HCl—4.4% $SnCl_2 \cdot 2H_2O$ | 23 ml. | | |
| 4B | Aqueous solution after the third step extraction | 27 ml. | TBP | 50 ml. |
| | 11 M HCl—11% $NH_2OH \cdot HCl$ | 23 ml. | | |

TABLE III. EXTRACTION OF FISSION PRODUCTS

| Step | Phase | $^{95}$Zr—$^{95}$Nb | $^{144}$Ce | $^{147}$Pm | $^{90}$Sr—$^{90}$Y | $^{106}$Ru | $^{137}$Cs |
|---|---|---|---|---|---|---|---|
| 1 | Org. phase | 98.9 | 0.3 | 0.0 | 0.0 | 0.0 | 0.4 |
| | Aq. phase | 0.3 | 99.3 | 98.2 | 99.5 | 99.8 | 98.1 |
| 2 | Org. phase | 84.2[a] | 99.4 | 99.6 | 53.2($^{90}$Y) | 0.5 | 0.6 |
| | Aq. phase | 2.0[a] | 0.5 | 0.5 | 46.2($^{90}$Sr) | 99.6 | 101.6 |
| 3 | Org. phase | 60.7 | 100.0 | 99.6 | 99.4 | 1.2 | 0.4 |
| | Aq. phase | 37.8 | 0.0 | 0.6 | 0.5 | 99.6 | 99.6 |
| 4A | Org. phase | 9.3[b] | 1.0[b] | 14.8[b] | 0.8[b] | 98.5[b] | 0.0[b] |
| | Aq. phase | 90.7 | 99.0 | 85.2 | 99.2 | 1.5 | 100.0 |
| 4B | Org. phase | 27.6[b] | 8.8[b] | 13.3[b] | 0.0[b] | 93.9[b] | 0.6[c] |
| | Aq. phase | 72.4 | 91.2 | 86.7 | 100.0 | 6.1 | 82.2 |

a. Some of $^{95}$Zr and/or $^{95}$Nb was lost probably by the adsorption.
b. These values were calculated from the total activities and the activities in the aqueous phase.
c. This value was obtained by the stripping of $^{137}$Cs from the organic phase with 15 M nitric acid. The loss of $^{137}$Cs in the 4B step was unaccountable.

step is the extraction of zirconium-95 and niobium-95 from a 3 M hydrochloric acid solution into chloroform with cupferron. The second step is the extraction of rare earth nuclides, i. e. cerium-144, promethium-147, and yttrium-90 from an acetate buffer solution of pH 4 to 5 into chloroform with cupferron. The third step is the extraction of strontium-90 from an acetate buffer solution of pH 8 into hexone with TTA. The fourth step is the extraction of ruthenium-106 from a 5 M hydrochloric acid solution into a mixture of TBP and kerosene (1 : 2) in the presence of stannous chloride. Another method for the fourth step is the extraction of ruthenium-106 from a 5 M hydrochloric acid solution into TBP in the presence of hydroxylamine. Thus cesium-137 remains is the last aqueous solution. The detailes of the extraction procedures are tabulated in Table II. The distribution of each radioactive nuclide in the aqueous and organic phases in each extraction step was determined. The results are summarized in Table III, in which the data shown under the step-like line in each column were obtained only for reference. Recovery on the stripping of the radioactive nuclides from the organic phase is shown in Table IV. The data given in Tables III and IV are mean values obtained from three or four experiments.

TABLE IV. RECOVERY OF NUCLIDES FROM ORGANIC PHASE BY STRIPPING

| Nuclide | Stripping agent | Number of stripping | Recovery % |
|---|---|---|---|
| $^{95}$Zr—$^{95}$Nb | 10 M $HNO_3$ | 2 | 83.9 |
| $^{144}$Ce | 3 M $HNO_3$ | 1 | 98.4 |
| $^{147}$Pm | 3 M $HNO_3$ | 1 | 88.8 |
| $^{90}$Y | 3 M $HNO_3$ | 1 | 98.8 |
| $^{90}$Sr | 3 M $HNO_3$ | 1 | 98.4 |
| $^{106}$Ru | 15 M $HNO_3$ | 3 | 99.8 |

In the first step oxalic acid is added to the solution to prevent the adsorption of zirconium-95 and niobium-95 onto a glass vessel by forming complexes with these nuclides. Hydroxylamine protects cupferron from oxidation with air and a trace amount of nitric acid. The data disclose that by the first step extraction only zirconium-95 and niobium-95 are extracted as cupferrates into the organic phase and all other nuclides are left in the aqueous phase. The zirconium-95 and niobium-95 extracted in the organic phase can be stripped with 10 M nitric acid as shown in Table IV.

In the second step aqueous ammonia is added to the aqueous phase remaining after the first step extraction to neutralize hydrochloric acid, and then ammonium acetate solution is added to adjust the pH of the aqueous phase to 4~5. In order to complete the separation of rare earth nuclides the concentration of cupferron should be considerably high and the extraction should be repeated three times. Before each extraction with chloroform 3 ml. of a 5% cupferron solution is added to the aqueous phase. By this step cerium-144 and promethium-147 are extracted into the chloroform phase.

Strontium-90 and yttrium-90 in their radioactive equilibrium are separated from each other, the former being in the aqueous phase and the latter in the organic phase, as shown in the sixth column of Table III. The decay or the growth curve and the Harley plot of the activity in each phase indicates that the separation of the nuclides can be carried out completely. The rare earth and yttrium nuclides extracted in the organic phase can easily be stripped with 3 M nitric acid.

After the second step extraction, a small amount of aqueous ammonia is added to the resulting aqueous phase to raise the pH of the

solution up to 8[3]. Then the third step extraction is carried out with a 0.05 M TTA-hexone solution. Two extractions complete the separation of strontium-90. The data in the sixth column of Table III shows that yttrium-90, if it could be present, by the later decay of strontium-90 is also extracted into the organic phase. The strontium-90 extracted in the organic phase can be stripped with 3 M nitric acid.

The fourth step extraction is that of ruthenium-106. It was found in the previous investigation[4] that ruthenium-106 can be extracted from 6 M hydrochloric acid solution with diphenyl thiourea dissolved in a mixed solvent of TBP and kerosene (1 : 2) in the presence of stannous chloride. However, it is difficult to strip the ruthenium-106 extracted in the mixed solvent into an aqueous phase. The present authors reexamined the extraction condition for ruthenium-106 and found that ruthenium-106 can be almost completely extracted, in the presence of stannous chloride from 6M hydrochloric acid solution with the mixed solvent of TBP and kerosene containing no chelating agent such as diphenylthiourea. Almost all of the ruthenium-106 extracted in the organic phase can be stripped with concentrated nitric acid, but a part of stannous chloride which is extracted from into the organic phase is also stripped with concentrated nitric acid. It is difficult to remove the stannous chloride from the nitric acid solution as well as to obtain the salt-free aqueous solution of ruthenium-106. So this method would not be suitable for preparing carrier-free ruthenium-106, but the procedure might be used as an analytical method for ruthenium-106 in the fission products.

Another method for the extraction of ruthenium-106 is as follows: ruthenium-106 can be extracted from 5 M hydrochloric acid solution in the presence of hydroxylamine with TBP which is not diluted with kerosene but is saturated with a 5 M hydrochloric acid solution. By this method about 94 per cent of ruthenium-106 is extracted and almost all of it is stripped with concentrated nitric acid from the organic phase. Some amount of hydroxylamine is also extracted with TBP and then also with concentrated nitric acid. But it is possible to decompose the hydroxylamine stripped together with ruthenium-106 by heating after neutralizing the nitric acid with aqueous ammonia. Then we can get the salt-free aqueous solution of ruthenium-106. Although the yield of ruthenium-106 is less than that obtained by the former method, this method is superior to the former one from the point of view of the preparation of carrier-free ruthenium-106.

## Summary

A new scheme for separating fission products, zirconium-niobium-95, cerium-144, promethium-147, yttrium-90, strontium-90, ruthenium-106 and cesium-137, by the four-step liquid-liquid extractions was presented. First, zirconium-95 and niobium-95 were extracted from a 5 M hydrochloric acid solution into chloroform with cupferron. Second, rare-earth nuclides, cerium-144, promethium-147 and yttrium-90 were extracted from an acetate buffered solution of pH 4 to 5 into chloroform with cupferron. Third, strontium-90 was extracted from an acetate buffered solution of pH 8 into hexone (methyl isobutyl ketone) with TTA (2-thenoyltrifluoroacetone). Fourth, ruthenium-106 was extracted from 5 M hydrochloric acid solution with TBP (tri-*n*-butyl phosphate)-kerosene in the presence of stannous chloride or extracted with TBP in the presence of hydroxylamine. then cesium-137 was left in the last aqueous solution. Strippings of nuclides extracted in the organic phases could be attained by shaking each organic phase with nitric acid.

This study was done as a part of the cooperative research on fission products and fissile materials which was superintended by Prof. N. Saito, the University of Tokyo. The authors wish to express many thanks to him and the Ministry of Education for financial help of this study.

*Department of Chemistry*
*Faculty of Science*
*Kanazawa University*
*Kanazawa*

# *Dielectric Properties of Polypeptide Solutions. Measurement of the Dielectric Properties of the α-Helix by the Low Frequency Bridge Method*

By Akiyoshi WADA

(Received November 6, 1959)

The exhaustive research on the polypeptide solution by Doty, Blout and their co-workers[1] revealed the important fact that the α-helix can exist not only in the solid state but even in solution. One significant implication of their work is that the α-helix, one of the stable configurations of polypeptide molecules described by Pauling, Corey and Branson[2], can be studied in solution where each α-helix exists as a free molecule, that is, almost free from solute-interaction. These results then suggest the possibility and necessity of another type of research, the measurement of the electric dipole moment and the critical frequency of such a molecule with a highly ordered arrangement of residues.

The measurement of the electric dipole moment of the molecule has been considered a useful method of finding the charge distribution and the orientation of the polar groups in a molecule. The method has often been used to determine the molecular structure of a simple molecule in the field of physical chemistry. However, in the usual chain polymer molecule, because of the flexibility of the chain the observed electric dipole moment becomes a complicated function of the internal coordinates and the internal energy of the molecule, and this method does not appear to be as useful as in the case of the simple molecule. For the α-helix, however, if the Pauling-Corey model is given as the proper configuration and if the molecule is rigid as Doty et al. concluded[1], the resultant molecular dipole moment would be proportional to the degree of polymerization, unlike the usual chain polymer, and would have a tremendous value in a highly polymerized molecule.

As the measurement of the dipole moment, which is a vectoral value, is essentially different from investigations on non-directional values such as molecular dimension, the observation will approach the α-helix and related problems from an entirely different angle.

## Description of the Low-Frequency Bridge Circuit

Though the heterodyne beat method or the resonance method has often been used for the measurement of the dielectric constant of solution, they could yield reliable data only in the high-frequency range and would not be adequate for the purpose of the present investigation. Because the solute, the α-helix, is a rigid and highly assymmetric rod-shaped molecule and the relaxation time of over-all molecular rotation in the solvent must be fairly great, the apparatus must be designed to cover the low-frequency range where sufficient time can be allowed for very slow orientation polarization. The bridge method seems to be appropriate for the present purpose and the apparatus by which the dielectric constant and loss factor can be measured from 30 cycle to 20 kilocycle was constructed as described below.

1) **Low-Frequency Bridge.**—The bridge method has been known as the best device for the measurement of the dielectric constant in the low-frequency range.[3] For instance, Cole and Gross[4] developed a transformer bridge, and Hippel et al. employed the Schering bridge method in their comprehensive research on dielectric materials.[5]

The Cole and Gross bridge was designed to fit the guard without the use of the Wagner ground. The measurement of capacitance was obtained by balancing the bridge by changing the capacity of the precision condenser which was set in the conjugated arm of the unknown capacitance. The conductance measurement is performed by a device called the conductance shifter.

The latter, designed by Hippel and his co-workers, has a sample holder in the arm of the precision condenser, and is generally known as a substitution method. In such an apparatus the cell constant used is calibrated by the standard substance. The conductance is given, in this apparatus, by the reading of the dissipation balancing condenser.

For the present purpose the apparatus was designed to combine the substitution method and the conductance shifter. The block diagram of the bridge circuit is shown in Fig. 1.

The low frequency oscillator which continuously

1) P. Doty, A. M. Holtzer, J. H. Bradbury and E. R. Blout, *J. Am. Chem. Soc.*, 76, 4493 (1954); P. Doty, J. H. Bradbury and A. M. Holtzer, ibid., 78, 947 (1956).
2) L. Pauling, R. B. Corey and H. R. Branson, *Proc. Natl. Acad. Sci.* 37, 205 (1951).
3) C. P. Smyth "Dielectric Behavior and Structure", McGraw-Hill Book Co., Inc., New York, N. Y. (1955).
4) R. H. Cole and P. M. Gross, Jr., *Rev. Sci. Instr.* 20, 252 (1949).
5) *Progress Rept. No. 1, Lab. Insulation Res.*, M. I. T., p. 7 (1947).

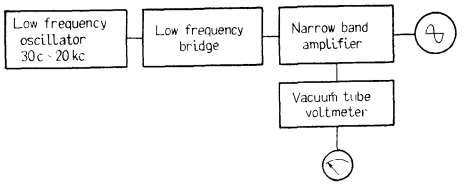



Fig. 1. Block diagram of low frequency bridge.

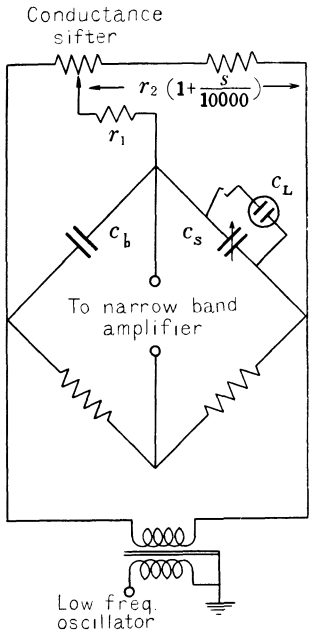



Fig. 2. Low frequency bridge circuit.

generates sine waves in the range of 30 to 20,000 cycles and output voltage from 0 to 20 volts has the same circuit as the Heathkit Model AO-1.

The circuit of the bridge section is shown in Fig. 2. $C_s$ is the liquid cell whose capacitance is compared with that of a portion of the calibrated precision condenser. The precision condenser (Yokogawa Elect. Co. CDS-500 Variable Air Condenser), in which the use of the worm drive makes possible a scale which can be read to one part in 50,000 of full scale, has a maximum capacitance of 500 $\mu\mu$F. By using low resistance for the balancing arm the undesirable effects of stray capacitance and induction from the external field can be suppressed at the sacrifice of sensitivity. In the reading of the conductance shifter, the conductance, $G$, can be given as a three-digit number, $s$, by the following equation

$$G=\frac{(s/10000)/r_1}{1+(r_2/2r_1)\{1-(s/10000)^2\}} \qquad (1)$$

when $s \ll 10000$

$$G\fallingdotseq\frac{(s/10000)/r_1}{1+r_2/2r_1} \qquad (2)$$

where $r_1$ and $r_2$ are the resistances which are shown in Fig. 2. The present apparatus was designed so that $r_1$ can be set at four different values by the use of a rotary switch, which made the measurement of the conductance from $10^{-5}$ to $10^{-9}$ mho possible. The null detector consists of a narrow-band amplifier and vacuum tube voltmeter. The narrow-band amplifier, in which the Wien bridge and the negative feedback system are combined, has a sharp frequency response, an example of which is shown in Fig. 3, and amplifies only the given frequency, cutting out the hamper noise and harmonic frequency. The wave pattern was checked by the cathode-ray oscillograph. The null point can be obtained from the minimum reading of the vacuum tube voltmeter. The relation between the reading of the precision condenser and the vacuum tube voltmeter is plotted for different

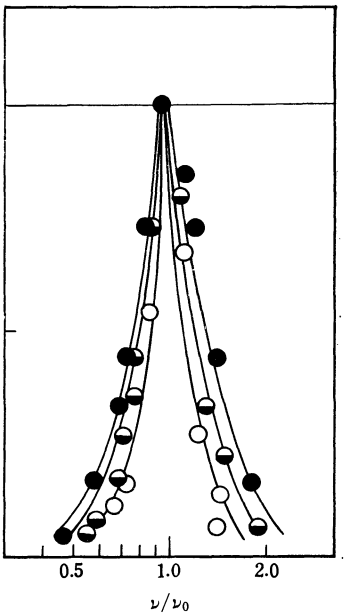



Fig. 3. Frequency response of the narrow band amplifier. Filled circle 90 cycle, half filled circle 1000 cycle, open circle 10000 cycle.

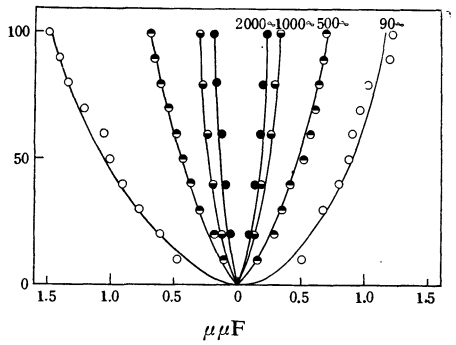



Fig. 4. Reading of vacuum tube voltmeter near null point.

TABLE I. ACCURACY IN CAPACITANCE MEASUREMENT BY BRIDGE METHOD

| Frequency | 100 | 500 | 1000 | 2000 |
|---|---|---|---|---|
| Accuracy | ±0.5 | ±0.2 | ±0.1 | ±0.1 $\mu\mu$F |

frequencies in Fig. 4, and the accuracy of the measurement is given below.*

2) **Liquid Cell.**—The liquid cell consists of a concentric double cylinder of glass as shown in Fig. 5; the inside of the outer cylinder and the outside of the inner cylinder are silver gilt or spattered with gold. The latter was found to be more satisfactory in chemical and mechanical durability.

3) **Calibration.**—Because the substitution method was used here, the cell constant had to be determined by a pure liquid of known dielectric constant. Benzene, the dielectric constant of which has been given as 2.274 at 25°C with a probable accuracy of 0.1%, was used as a standard substance for the calibration.[6]

The dielectric constant of ethylene dichloride and dioxane measured by the calibrated liquid cell are plotted against frequency in Fig. 6. The apparent increase in the dielectric constant at low-frequency range may be due to the polarization capacitance

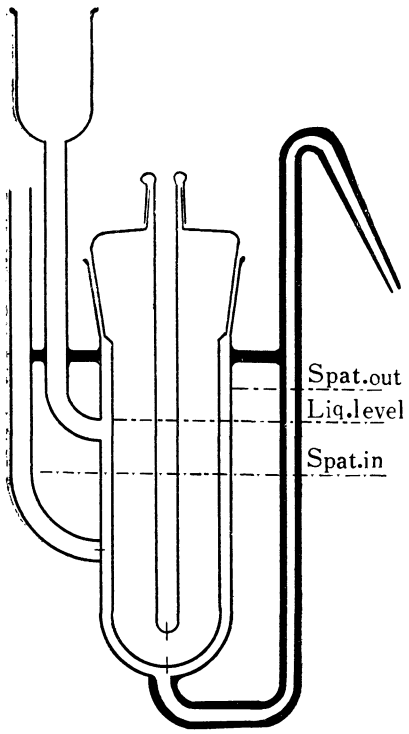



Fig. 5. Liquid cell for the measurement of dielectric constant of solution.

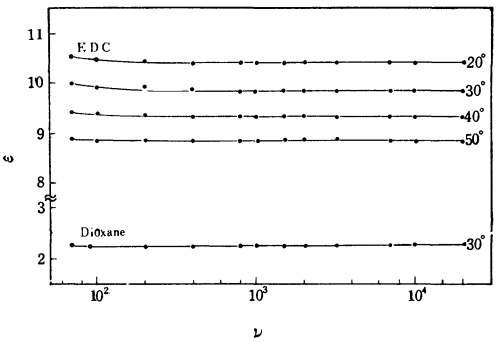



Fig. 6. Dielectric constant of ethylene dichloride and dioxane at various temperatures and frequencies.

on the electrode surface. The polarization effect increases and must be corrected for a liquid of high conductivity but it was negligible for one of small conductivity. The dielectric constants of liquids mentioned above at 1000 cycles where the polarization effect satisfactorily diminished are listed in Table II and were consistent with the values observed by other workers.

TABLE II. DIELECTRIC CONSTANT OF ETHYLENE DICHLORIDE AND DIOXANE

| Ethylene dichloride | | |
|---|---|---|
| Temp., °C | ε (Wada) | ε (Smyth*) |
| 20 | 10.42 | 10.42** |
| 30 | 9.85 | 9.87 |
| 40 | 9.35 | 9.36** |
| 50 | 8.87 | 8.87 |
| **Dioxane** | | |
| Temp., °C | ε (Wada) | ε (Smyth***) |
| 30 | 2.295 | 2.306** |
| 50 | 2.245 | 2.251 |

* C. P. Smyth et al., *J. Am. Chem. Soc.*, **53**, 4242 (1931).
** Interpolated in Smyth's data.
*** C. P. Smyth et al., *J. Am. Chem. Soc.*, **53**, 2115 (1931).

## Characterization of Poly-γ-benzyl-L-glutamate (PBLG)

1) **Polymerization.**—The sample used here was prepared by the Blout-Karlson method[7]. The procedure adopted consisted of polymerizing γ-benzyl-N-carboxy-L-glutamate anhydride, usually 3—5% in dioxane solution, by a sodium methoxide initiater at room temperature. After polymerization was completed the reaction mixture was poured into cold ethanol with vigorous stirring. The precipitate was redissolved in dioxane and precipitated by cold ethanol again. No difference in intrinsic viscosity was found between the reprecipitated

* The bridge was found to be stable enough that the reading of the vacuum-tube voltmeter did not fluctuate more than 3/100 full scale after a 20-min. warm-up of the apparatus.

6) A. A. Maryott and E. A. Smith, "Table of Dielectric Constant of Pure Liquids", *Natl. Bur. Standard* (*Circ.* 514 (1951); A. S. Brown et al., *J. Chem. Phys.* **19**, 1226 (1951).

7) E. R. Blout and R. H. Karlson, *J. Am. Chem. Soc.*, 78, 941 (1956).

PBLG and that liopholyzed from the first dioxane solution.

**2) Solvent.** — Dimethyl formamide (DMF) was used as the solvent for the light scattering measurement because the PBLG was found to exist as a non-associated molecule in this solvent. DMF was dried by dry sodium bicarbonate and fractionally distilled at 47°C (14 mmHg). For the dielectric constant and light scattering measurement dioxane was purified according to the method of Fieser[8] and fractionally distilled after 24 hr. refluxing with sodium. For the polymerization reaction, dioxane was purified by refluxing with sodium for 24 hr. and fractionally distilled just before use. The ethylene dichloride (EDC) for the measurement of the dielectric constant was dried by $P_2O_5$ and fractionally distilled at 84°C.

**3) Light Scattering.** — The Brice Phoenix type light scattering photometer made by the Shimadzu Co. was used to obtain the molecular weight of PBLG. The apparatus was calibrated according to the Rayleigh ratio of pure benzene ($R_{90}=48.4\times10^{-6}$ at 436 m$\mu$.[9]). The spectrophotometric calibration was independently done by Ludox solution and the result was quite consistent with the calibration by benzene. Scattering from DMF solution of PBLG was measured by the Erlenmeyer cell and the circular uniformity of which was checked with clean fluorescein by measuring the angular envelope. The cell used had good circular uniformity as the light intensity from the unit volume of the solution was constant to ±1% from $\theta=30°$ to 135°. The angle made by the side of the Erlenmeyer cell was sufficient to exclude the effects of back reflection, so that no correction for the data was necessary. Centrifuge by a Hitachi Preparative Ultracentrifuge using a polyethylene tube with a specially constructed tefron cap, at about 60,000 $g$ for 1 hr. and filtration by ultra-fine sintered glass filter were performed to make a dust-free solution and solvent respectively. Measurements were made on the solutions obtained by adding a weighed amount of 1% PBLG dust-free solution to a known volume of clean solvent in an Erlenmeyer cell, on which the scattering was already measured. The concentration after each addition was determined gravimetrically relative to the stock solution.*

The refractive index increment $dn/dc$ for the evaluation $K=2\pi^2n_0^2(dn/dc)^2/N\lambda^4$ where $n_0$ is the refractive index of the solvent, $\lambda$ is the wave length of the incident light in vacuo, $N$ is the Avogadro number, was determined by the Debye-type defferential refractometer made by Shimadzu Co. The instrument was usually calibrated before each measurement with a standard KCl solution, $c=\frac{10.8691\,\text{g.}}{H_2O\,(\text{kg.})}$, for which the increment was taken as 0.0015204 on the basis of an extrapolation of data by Kruis.[10]

According to the well known equation established by Zimm,[11]

$$Kc/R_\theta=\{M_wP(\theta)\}^{-1}+2A_2c \qquad (3)$$

the weight average molecular weight $M_w$ can

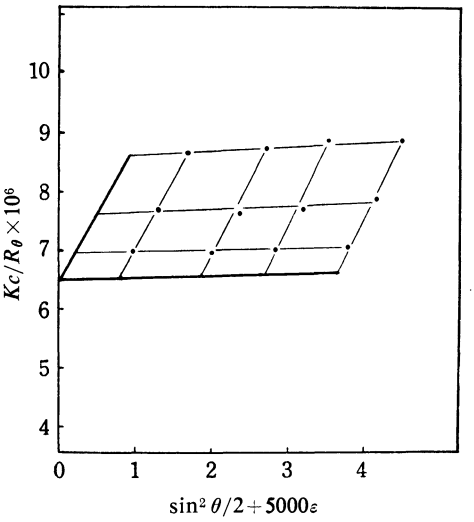



Fig. 7a. Light scattering data for PBLG sample No. 105 in DMF at 23°C.

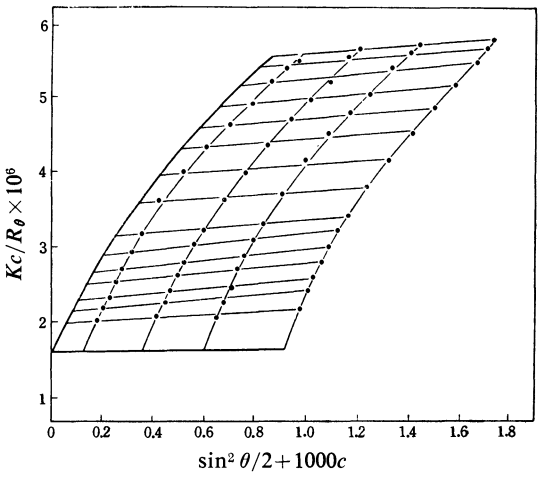



Fig. 7b. Reciprocal angular envelope of solutions PBLG No. 105 in dioxane at 23°C.

8) L. F. Fieser, "Experiments in Organic Chemistry" 2nd ed., D. H. Heath & Co., Boston, Mass., (1941).
9) B. A. Brice and M. Halwer, *J. Opt. Soc. Am.*, **40**, 765 (1950).
* The light scattering measurement was performed following a process established by Professor P. Doty and his coworkers at Harvard University.
10) A. Kruis, *Z. physik. Chem.*, **34B**, 13 (1936).
11) B. H. Zimm, *J. Chem. Phys.*, **16**, 1093, 1099 (1948).

TABLE III. MOLECULAR WEIGHT, MOLECULAR LENGTH, SPECIFIC POLARIZATION, DIPOLE MOMENT AND CRITICAL FREQUENCY OF PBLG IN EDC

| PBLG | $M_w$ | $L_{z,z+1}$ | $P_2^{00}$(cc) | $\mu$(D) | $\mu_0$(D) | $\nu_0$ |
|---|---|---|---|---|---|---|
| 202 | 180,000 | 1350 | 963 | 2910 | 3.54 | 3000 |
| 105 | 154,000 | 1100 | 805 | 2450 | 3.48 | 7000 |
| 102 | 102,000 | 750 | 494 | 1570 | 3.36 | 16000 |
| 201 | 86,000 | 690 | 470 | 1404 | 3.58 | 20000 |
| 103 | 70,000 | 600 | 314 | 1040 | 3.25 | 40000 |

be obtained after extrapolating to $c=0$ and $\theta=0$, where the particle scattering factor $P(\theta)$ is known to be unity. A typical double plot, that is, the so-called Zimm plot, for one of the PBLG samples in DMF is shown in Fig. 7a. Measurements were also conducted for the dioxane solution as one of the Zimm plot and are shown in Fig. 7b. The molecular length, assuming a rigid rod-shaped molecule at present, can be calculated from the initial slope of the angular envelope in the Zimm plot;

$$L^2_{z,z+1}=\frac{9\lambda'^2}{8\pi^2}\frac{(\text{slope})_{c=0,\ \theta=0}}{(\text{intercept})_{c=0,\ \theta=0}} \tag{4}$$

where $\lambda'$ refers to the wave length in solution.

The final results of the measurement of molecular weight and molecular length are listed with the polymerization condition in Table III. The remarkable increase in molecular weight and molecular length in dioxane solution might result from molecular association which will be discussed in detail later.

## Dielectric Properties of PBLG in Ethylene Dichloride and Dioxane

For a long, rigid rod-shaped molecule, the cavity field in the direction of the rod axis can be assumed to be the same as the external field, and in the $\alpha$-helix having point dipoles parallel with the rod axis, only the field of this direction has to be taken into consideration. So the relation between the static dielectric constant of the solution $\varepsilon_{12}^0$ and the specific polarization of the solute $P_2$ is given in terms of the weight fraction of the solute $w_2$, the specific polarization of the solvent $P_1$, and the density of the solution $d_{12}$ as follows[12]

$$P_2^0=[(\varepsilon_{12}-1)/3d_{12}-P_1]/w_2+P_1 \tag{5}$$

The specific polarization extrapolated to zero concentration $P_2^{00}$ and the dipole moment of the $\alpha$-helix in the solvent are related

$$\mu^*=(9k/4\pi N)^{1/2}(P_2^{00}\bar{M}_wT)^{1/2}$$
$$=0.0128(P_2^{00}\bar{M}_wT)^{1/2} \tag{6}$$

In the dipole moment $\mu^*$, the moment induced in the polarizability $\alpha$ by the reaction field $\mu^*R(\varepsilon)$ is taken into consideration and it is given by the moment in vacuo $\mu$.[13]

$$\mu^*=\frac{\mu}{1-\alpha R(\varepsilon)} \tag{7}$$

To obtain the static dielectric constant $\varepsilon^0_{12}$ or specific polarization, those values measured by the bridge method at various frequencies must be extrapolated to zero frequency. In this procedure the following problems must be considered:

1) The relation between $\varepsilon_{12}$ and $\nu$ is not linear.

2) The dispersion curve does not agree, in general, with Debye's theoretical one in which a single relaxation time is assumed.

3) In the low-frequency range, the polarization effect on the electrode surface of the liquid cell can not be negligible. To cope with these problems, three methods for extrapolation are proposed as follows.

I) Assuming an empirical functional relation which gives a linear relation especially at the low-frequency range, we extrapolate it to zero frequency.

II) Extrapolation is made to zero frequency on the Cole-Cole's arc plot.[12] This method, however, does not seem appropriate because of the increase in experimental error of the loss factor at low-frequency.

III) Extrapolation of the flat part at the low-frequency range in $\varepsilon_{12}\sim\nu^{-1}$ plotting to $\nu^{-1}\to 0$.[14] This extrapolation will be useful to exclude electrode polarization because it becomes zero at infinite frequency. An underestimate of the dielectric constant will result when the polydispersity in the $\alpha$-helix is present.[13]

**1) Ethylene Dichloride Solution.** — The dispersion curve of each PBLG sample in EDC is shown in Fig. 8. It can be seen that the critical frequency becomes lower as the specific polarization and the molecular weight become larger.

In Figs. 9a, 9b and 9c three plottings of these samples are shown and the extrapolated values of $P_2$ are compared in Table IV. For

12) A. Wada, *J. Chem. Phys.*, **29**, 674 (1958).

13) A. Wada, ibid., **31**, 495 (1959).

14) J. L. Oncley, *Chem. Revs.*, **30**, 433 (1942).

TABLE IV. SPECIFIC POLARIZATION OF PBLG IN EDC EXTRAPOLATED TO ZERO FREQUENCY

| PBLG | Method of extrapolation I | | II | | III |
|---|---|---|---|---|---|
| | $P_2^{00}$(cc) | $\nu_0$ | $P_2^{00}$(cc) | $\nu_0$ | $P_2^{00}$(cc) |
| 202 | 950 | 3000 | 920 | 3000 | 900 |
| 105 | 800 | 6300 | 770 | 7000 | 780 |
| 103 | 330 | 33000 | 314 | 40000 | 320 |

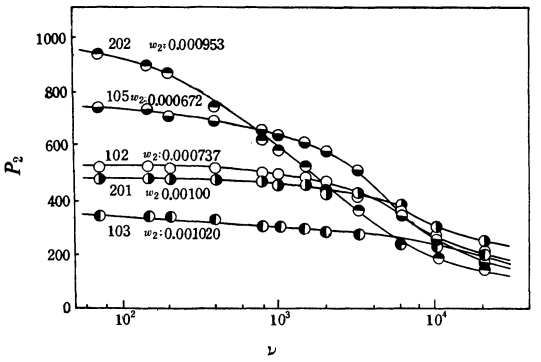



Fig. 8. Dependence of dielectric constant of the EDC solutions of PBLG samples upon frequency at 25°C.

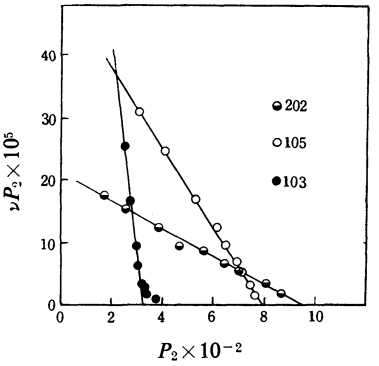



Fig. 9a. Plotting of $\nu P_2$ as a function of $P_2$.

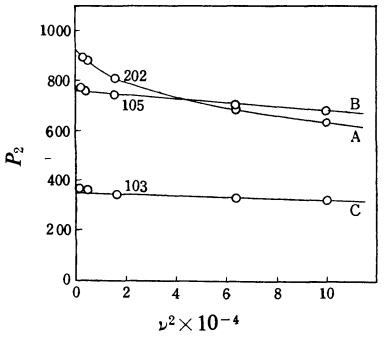



Fig. 9b. Specific polarization of PBLG as a function of $\nu^2$.
A $M_w$: 180,000, B $M_w$: 154,000,
C $M_w$: 70,000.

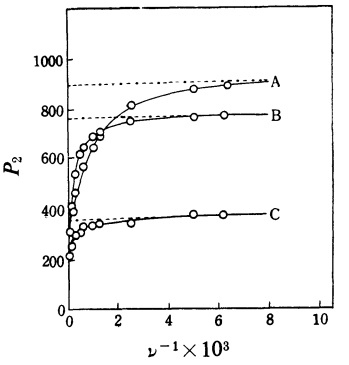



Fig. 9c. Specific polarization of PBLG as a function of $\nu^{-1}$.
A $M_w$: 180,000, B $M_w$: 154,000,
C $M_w$: 70,000.

the first extrapolation method it was incidentally given a linear relation in $P_2\nu \sim P_2$ plot. This means that the relation $P_2 = P_2^0\left(1+\frac{\nu}{\nu_0}\right)^{-1}$ can be maintained in this system and $P_2^0$ and the critical frequency $\nu_0$ are given from the intercept and the slope of this plot respectively. The deviation from the linearity at the low-frequency range may be due to electrode polarization. Though the extrapolated values by these three methods differ slightly, they do not seriously affect the result, as can be seen in Table IV.

For the calculation of the molecular dipole moment, the $P_2^0$ measured in several concentrations were extrapolated to zero concentration. A typical plot is shown in Fig. 10 and

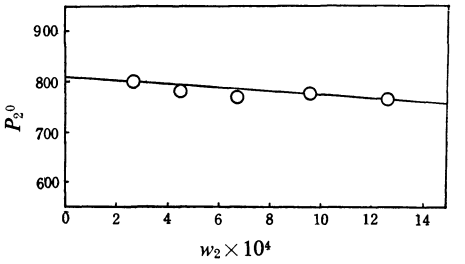



Fig. 10. Concentration dependence of specific polarization of PBLG sample No. 105 in EDC at 25°C.

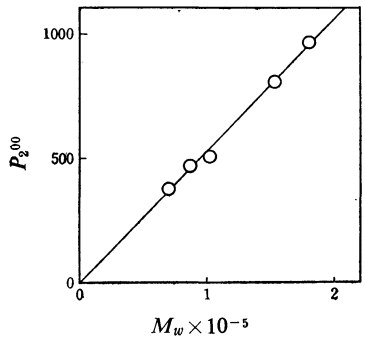



Fig. 11. Dependence of specific polarization of PBLG samples in EDC upon molecular weight.

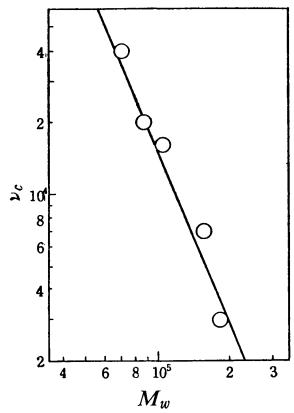
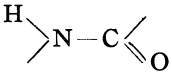



Fig. 12. Double logarithmic plot of critical frequency of PBLG samples in EDC against molecular weight.

the final results are listed with the dipole moment calculated in Table III.

The measured $P_2$ and dipole moments increase proportionately to the molecular weight as shown in Fig. 11. The dipole moment of the amino acid residue in the $\alpha$-helix then can be calculated as 3.5 D. This value is quite consistent with the parallel orientation of the dipole moment of polar groups  in the $\alpha$-helix. Further, the critical frequency, on the other hand, is known to have a linear relation in double logarithmic plot as shown Fig. 12. This behavior is well explained using Perrin's equation with the hydrodynamically equivalent ellipsoid of revolution which has the same volume and length as the $\alpha$-helix. That is

$$\tau_0 = (2\pi\tau)^{-1}$$

$$\tau = \frac{2\tau_0}{3}\,\frac{1}{2\rho^2 \ln(2/\rho) - \rho^2} \qquad (8)$$

$$\rho = b/a, \quad \tau_0 = 4\pi\eta ab^2/kT$$

The solid line in Fig. 13 is the theoretical plot corresponding to 18.3 Å of the minor axis, that is 15 Å for the diameter of the $\alpha$-helix. All of the above results are consistent with and tend to support the belief that in this solvent the PBLG exists as a rigid rod-shaped molecule, the $\alpha$-helix given by Pauling and Corey.

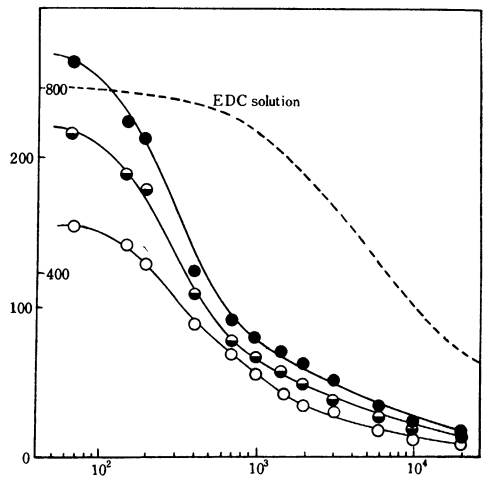



Fig. 13. Dependence of specific polarization of PBLG samples in dioxane solution upon frequency at 30°C.
Filled circle No. 105 $w_2=0.000824$. Half filled circle No. 103 $w_2=0.001282$. Open circle No. 102 $w_2=0.001112$.

**2) Dioxane Solution.** — In dioxane the $\alpha$-helix of PBLG may be in an associated state as Doty et al. concluded.[1] They emphasized that the association is of the end-to-end type but that the rod-like form is not preserved. The increase in the molecular weight and molecular length of PBLG in this solvent, which has been given by the light scattering measurement as shown in Table III, seems to endorse this idea. Moreover, the non-linear relation between the molecular weight and the molecular length suggests that the associated molecule is no longer linear and/or rigid.

For further study on the mechanism of molecular association the information from the electric dipole moment, as a vectoral quantity along the direction of the helical axis, will be useful. Leaving quantitative considerations of this interesting problem to another report[15], we may conclude, however, that the $\alpha$-helix still has a large electric dipole moment in dioxane which is the only non-polar solvent in which PBLG can dissolve.

Examining the dispersion curve of this system in Fig. 13 the critical frequency reveals

15) A. Wada, *J. Polymer Sci.*, (1960), in press.

a remarkable shift to lower frequencies compared with that of the same sample in EDC for which the dispersion curve is plotted in the same figure in a dotted line. Therefore, the third extrapolation method could not be used because the left part of the dispersion curve goes out of the range of measurement. Only the second method, the extrapolation in Cole-Cole's arc plot, is effective, as shown in Fig. 14. A linear relation in the plot which was given in the case of EDC solution no longer holds in dioxane. This discrepancy between dioxane and EDC suggests that the molecular association will change the molecular weight distribution. The molecular weight distribution seems to be more polydisperse than that of the most probable distribution as in the case of EDC solution. The broader distribution may also be suggested from the flat shape of Cole-Cole's arc in this solvent (Fig. 14). This fact means that the molecules preferably aggregate in certain ranges of molecular weight more than in others as Doty et al. mentioned.[1)]

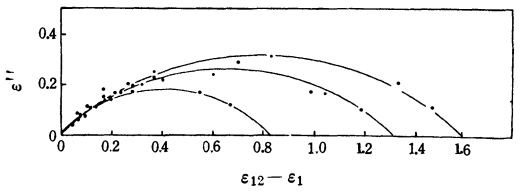



Fig. 14. Cole-Cole's arc plot for the dioxane solution of PBLG No. 105. $w_2=0.003058$, 0.001794, 0.000824.

The $P_2^0$ depends strongly upon the concentration in dioxane as shown in Fig. 15. This strong dependence may originate from the molecular association and/or dipole-dipole interaction which becomes stronger in a nonpolar solvent such as dioxane than in a polar one such as EDC. The absence of concentration dependence in light scattering measurement will support the latter possibility. It is empirically found that the $P_2^{0-1}\sim c$ plot gives a straight line as shown in Fig. 16. From these extrapolated values the electric dipole moment is computed. In Table V the electric dipole moment, calculated from the original molecular weight and from that of the associated molecule, are listed. Though the result is no longer proportional to the molecular weight, the dipole moment 1~3 D per amino acid residue still suggests that the molecule has an ordered form which has a partial $\alpha$-helical configuration.

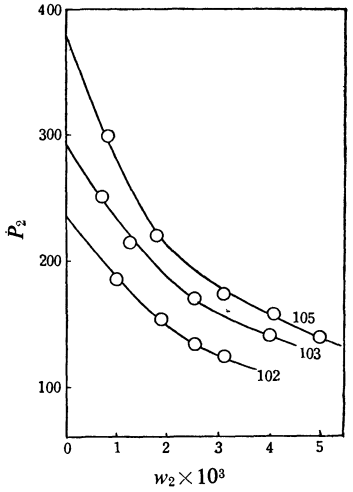



Fig. 15. Concentration dependence of specific polarization of PBLG samples in dioxane at 30°C.

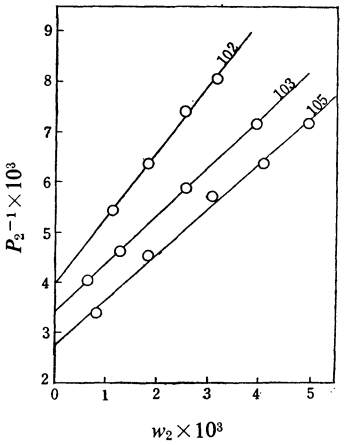



Fig. 16. Reciprocal plot of specific polarization of PBLG samples in dioxane against concentration.

TABLE V. MOLECULAR WEIGHT, SPECIFIC POLARIZATION, CRITICAL FREQUENCY AND DIPOLE MOMENT OF PBLG IN DIOXANE

| PBLG | $\overline{M}_w$ | $P_2^{00}$ (cc.) | $\nu_0$ | Dipole moment calcd. from Original $M_w$ | | Associated $M_w$ | |
|---|---|---|---|---|---|---|---|
| | | | | $\mu$(D) | $\mu_0$(D) | $\mu$(D) | $\mu_0$(D) |
| 105 | 660,000 | 360 | 400 | 1650 | 2.35 | 3407 | 1.13 |
| 102 | 1610,000 | 250 | 600 | 1115 | 2.39 | 4435 | 0.60 |
| 103 | — | 300 | 1100 | 1010 | 3.16 | — | — |

**Summary**

The work described above has produced the following conclusions.

(1) A large electric dipole moment corrospoinding to the $\alpha$-helix described by Pauling, Corey and Branson is found in EDC and dioxane.

(2) A linear relation between the electric dipole moment and the molecular weight in EDC suggests that the molecule is linear and not flexible.

(3) The critical frequency of the orientation polarization was elucidated by using an equivalent ellipsoid model and the equation for the rotatory diffusion constant derived from Perrin's equation. This fact will support the conclusion of Doty, Bradbury and Holtzer that the $\alpha$-helix is fairly rigid in the solution.

(4) In dioxane the $\alpha$-helix can be found to be associated and to have a different distribution in molecular weight.

*Department of Chemistry*
*Ochanomizu University*
*Bunkyo-ku, Tokyo*

# *Spectrophotometric Determination of Traces of Boron in Uranium*

By Hiroshi ONISHI, Nasumi ISHIWATARI and Hitoshi NAGAI

(Received January 7, 1960)

Various methods for determining traces of boron in uranium and its compounds were investigated because of the effect of neutron absorption. Table I summarizes most of the previous literature on the photometric determination of boron in uranium. Spectrographic

TABLE I. SUMMARY OF LITERATURE ON THE PHOTOMETRIC DETERMINATION OF BORON IN URANIUM

| Samples | Reagent | Separation | Range | Reference |
|---|---|---|---|---|
| $U_3O_8$ | Carmine | —* | 0.05—50 $\mu$g. B | 1 |
| $U_3O_8$ | Carmine | — | 1 p.p.m. B detd. (1 g. sample) | 2 |
| $UO_2(NO_3)_2$ | Carmine | Distillation | 0.1—0.5 p.p.m. (4 g. sample) | 3 |
| Al-U | Carminic acid | — | 10—70$\mu$ g. (0.5—2 g. sample) | 4 |
| $U_3O_8$ | 1,1'-Dianthrimide | Ion exchange | 0.2—2 p.p.m. | 5 |
| $UF_6$ | Curcumin | Distillation | | 6 |
| $U_3O_8$ | Turmeric | Distn. from $H_3PO_4$ soln. | 0.1—1.5 $\mu$g. | 7 |
| U, U compds. | Curcumin | Distillation | 0.5—5 $\mu$g. | 8 |
| U | Curcumin | Solvent extn. | >0.1 p.p.m. | 9 |
| U-Zr, U-Zircaloy | Curcumin | EtOH extn. | 0.015% detd. | 10 |
| U, $UO_2Cl_2$ | Crucumin | — | 3—50 p.p.m. (0.1 g. sample) | 11 |
| U | Curcumin | Distn. from HCl soln. | 0.01—0.3 p.p.m (10 g. sample) | 12 |
| Al-U | Curcumin | Distn. from HCl soln. | >30 p.p.m. | 13 |
| U | Curcumin | Ion exchange | | 14 |

* — denotes that separation is not required.

1) R. Cypres and P. Leherte, *Bull. soc. chim. Belges*, **63**, 101 (1954).
2) R. F. Cellini and L. G. Sánchez, *Proc. Intern. Conf. Peaceful Uses Atomic Energy*, **8**, 364 (1956).
3) T. Nowicka-Jankowska and H. Szyszko, *Chemia Analityczna*, **1**, 285 (1956).
4) K. W. Puphal, J. A. Merril, G. L. Booman and J. E. Rein, *Anal. Chem.*, **30**, 1612 (1958).
5) A. R. Eberle, M. W. Lerner and H. Kramer, **NBL-143**, 5 (1958).
6) E. Staple, E. D. Marshall, F. Nelson and W. Simon, **AECD-4212** (1946. Decl. 1955).
7) C. J. Rodden, *Proc. Intern. Conf. Peaceful Uses Atomic Energy*, **8**, 197 (1956).
8) J. F. Possidoni de Albinati and R. H. Rodrguez Pasqués, ibid., **8**, 339 (1956).
9) J. Coursier, J. Huré and R. Platzer, ibid., **8**, 487 (1956).
10) J. Rynasiewicz and V. Consalvo, **KAPL-M-JR-8** (1956).
11) L. Silverman and K. Trego, *Anal. Chim. Acta*, **15**, 439 (1956).
12) Chemical Services Dept., **IGO-AM/S-124** (1958).
13) I. H. Crocker, **CRDC-811** (1958).
14) T. Takeuchi, T. Yoshimori and S. Shibayama, the 12th Annual Meeting of the Chem. Soc. of Japan, April, 1959.

methods are not included in the table. Curcumin methods are generally more sensitive than carmine methods. However, the curcumin methods which have been reported up to the present consist of varied procedures according to different authors. Moreover, the reasons for using each procedure are not always evident. Consequently, in order to obtain optimum conditions, the available methods have been critically studied.

As shown in Table I, a phosphoric acid or a hydrochloric acid medium appears to be widely used for the separation of boron as methyl borate from uranium. In the case of the phosphoric acid medium, that methanol vapor must be passed through a hot sample solution[7] is considered to be disadvantageous, since connection of two distilling flasks is necessary; Otherwise phosphoric acid solutions of uranium form gels. When the hydrochloric acid medium is employed, the removal of excess of water is not easily effected[15].

In the determination of boron in uranyl sulfate, the authors found that a sulfuric acid medium was very suitable for the separation of boron as methyl borate, and that the above-mentioned disadvantage and difficulty could be avoided. Further investigation has shown that satisfactory results of analyses of $U_3O_8$ and uranium metal (after conversion into $U_3O_8$) can be obtained by using the same medium for the dissolution of the sample and distillation of methyl borate. These results are reported in the present paper.

## Experimental

**Apparatus.**—The distilling apparatus (quartz) is shown in Fig. 1. The volume of the flask is about 300 ml. Absorbance measurements were made with a Hitachi Model EPU-2A spectrophotometer, using 1-cm. cells.

**Reagents.** — In purification and preparation of reagents, as well as in analysis, redistilled water was used. For purification by distillation described below, a quartz distilling apparatus was used. All the solutions (except hydrogen peroxide) were kept in polyethylene bottles.

*Water, redistilled.*—Small amounts of mannitol (dissolved in distilled water) are added to the flask for redistillation.

*Sulfuric acid*, 1 : 3.—In a quartz beaker 5 ml. of 48% hydrofluoric acid is added to 100 ml. of concentrated sulfuric acid and heated to strong fumes. After cooling water is added.

*Hydrogen peroxide*, 30%.—Purification was effected by modification of Luke's procedure[16]. A 2.5 g. portion of Amberlite IR-120 ($H^+$ form) and 7.5 g. of Amberlite IRA-400 ($OH^-$ form) are transferred to a 100 ml. polyethylene beaker. While cooling,

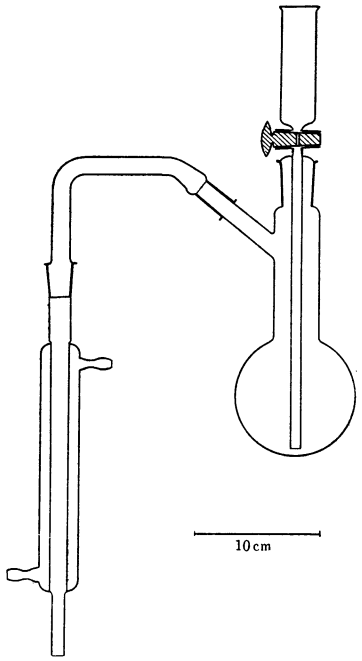



Fig. 1. Distilling apparatus.

60 ml. of cold 30% hydrogen peroxide is added and stirred for 10 min. The product is filtered through a paper (washed with water and dried) to a brown glass bottle and kept in a refrigerator.

*Methanol*, redistilled from sodium hydroxide.

*Calcium hydroxide suspension*, 0.1 N. — Distilled calcium is washed with water and the oxide scraped. One gram of calcium is dropped into a 500 ml. quartz flask and enough water is added cautiously. After cooling the contents are transferred to a bottle and diluted to 500 ml. with water.

*Curcumin-oxalic acid solution*[17,18].—A 0.40 g. portion of finely ground curcumin and 50 g. of oxalic acid are dissolved separately in ethanol. Both solutions are mixed and diluted with ethanol to 1 l.

*Ethanol*, redistilled from sodium hydroxide.

*Standard boron solution.*—A 0.5716 g. portion of boric acid is dissolved in 100 ml. of water (1.00 mg. B/ml.). From this stock solution 1 and 0.2 p.p.m. B solutions are prepared.

**Procedure.** — *Uranium metal.* — Ignite cautiously 1.00 g. of the sample in a platinum crucible at a low temperature. Then heat the crucible in an electric oven at about 800°C for one hour. Cool, and transfer the oxide formed to the distilling flask. Then continue as described below.

$U_3O_8$.—Transfer 1.00 g. of sample to the distilling flask and assemble the distilling apparatus. Place a 100 ml. platinum dish containing 10 ml. of water under the condenser. To the flask add 5 ml. of 1 : 3 sulfuric acid and 1 ml. of 30% hydrogen peroxide. Heat gently with a small flame until the sample is in solution. Replace the burner by an infrared lamp (300~500 W.) and distil excess of

15) H. Onishi, N. Ishiwatari and H. Nagai, the 12th Annual Meeting of the Chem. Soc. of Japan, Kyoto, April, 1959.
16) C. L. Luke, *Anal. Chem.*, 27, 1150 (1955).
17) W. T. Dible, E. Truog and K. C. Berger, *Anal. Chem.*, 26, 418 (1954).
18) I. Muraki and K. Hiiro, *J. Chem. Soc. Japan, Pure Chem. Sec.* (*Nippon Kagaku Zasshi*), 78, 845, 850 (1957).

water. Heat several times the side arm of the flask to remove water droplets. Stop heating when fumes begin to appear. Cool.

Immerse the fiask in a 1 l. beaker containing water (this serves as a water bath). Add 5.0 ml. of 0.1 N calcium hydroxide suspension to the platinum dish and raise the dish so that the tip of the condenser is in the solution. (The dish is protected from the heat of the burner by an appropriate shield.) From the tap funnel add 30 ml. of methanol. Raise the temperature of the bath slowly to approximately 95°C, giving a slow but steady distillation of methyl borate and methanol*. Continue heating until no more liquid comes over. Remove the burner and replace the hot water by cold water. Add 2.0 ml. of 0.1 N calcium hydroxide suspension to the solution in the dish. Add 20 ml. of methanol through the tap funnel and distil again. Lower the dish and wash down the stem of the condenser. Mix the distillate and washings with a quartz stirring rod (confirm that the solution is alkaline), and evaporate gently to dryness on a water bath.

To the residue add 2 ml. of water and 4.0 ml. of curcumin-oxalic acid solution and mix with a quartz stirring rod. Wash the rod with a small amount of water. Evaporate the solution on a water bath at 55±3°C, and allow to remain for 30 min. after the contents are dry. Cool the dish to room temperature (in a desiccator). Extract the colored products with 9 : 1 ethanol by stirring with a quartz rod. Transfer the colored solution to a 25 ml. volumetric flask and make up to volume with 9 : 1 ethanol. Mix, transfer the contents to a centrifuge tube, cover the tube with parchment paper, fasten the paper with a rubber band, and centrifuge at about 3000 r.p.m. for 10 min. Transfer the clear solution to a 1 cm. cell, and measure the absorbance at 550 mμ, using 9 : 1 ethanol as the reference.

Establish the standard curve by taking, for example, 0, 0.2, 0.5, and 1 μg. of boron, adding 7 ml. of 0.1 N calcium hydroxide suspension, and proceeding as described above. Run a blank, preferably in duplicate, throughout the entire procedure. As the recoveries of boron are low, a correction of +15% is advisable. When the standard curve is established by including the separation, this correction is naturally unnecessary.

## Results and Discussion

**Spectrophotometric Determination of Boron.** —In general, it may be summarized that the variable factors in the curcumin methods are use of alkalis (sodium hydroxide[8,12,13,19] and calcium hydroxide[7,18]), addition of hydrochloric acid, amounts of curcumin and oxalic acid, and extractants (ethanol[7,18], methanol[8], acetone[8,11]) of the colored products. Spicer and Strickland[19] used a glycerol-sodium hydroxide reagent, of composition of 1% sodium hydroxride, 0.1% sodium chloride, and 3% glycerol, to collect methyl borate. In this case hydrochloric acid must be added before adding curcumin. Muraki and Hiiro[18] used calcium hydroxide, and did not add hydrochloric acid, while other workers (e. g., Ref. 7) added the acid.

The preparation of curcumin-oxalic acid solution, described by Muraki and Hiiro[18], appears most satisfactory, because the preparation is simple, and the solution is stable. When the solution has been allowed to stand for 2 days after preparation, the absorbance becomes practically constant (Fig. 2). The workers mentioned[18] allowed the solution to stand for 7~10 days before use. The solution can be kept for one month at room temperature in the dark.

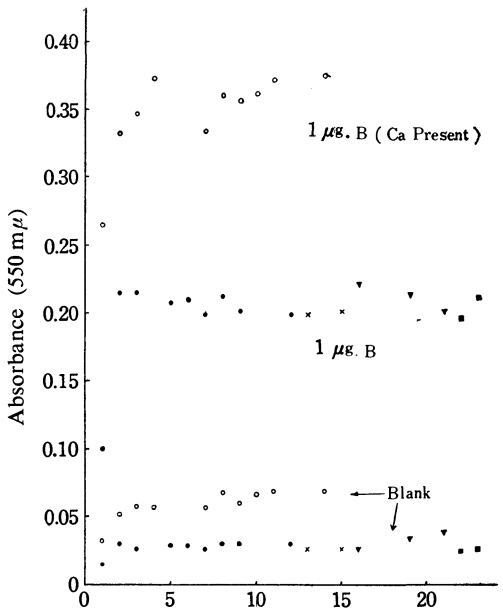



Fig. 2. Aging of curcumin-oxalic acid reagent
○ With Wako-Eastman curcumin and other points with Koso curcumin (cf. Table VII).
●: 97%(v./v.) EtOH, ○ and × : 87% (v./v.) EtOH, ▼ : MeOH, ■ : acetone.

Table II shows the effects of alkalis and extractants on the determination of boron. In each case 4 ml.[18] of curcumin-oxalic acid solution was used. It is seen that the presence of calcium hydroxide increases the absorbance of colored solution*, while that of sodium chloride decreases the absorbance. Addition of hydrochloric acid to calcium hydroxide is not

* This distillation requires about 15 min., and the second distillation about 10 min.

19) G. S. Spicer and J. D. H. Strickland, *Anal. Chim. Acta*, **18**, 523 (1958).

* Data obtained by Muraki and Hiiro[18] also indicate this phenomenon.

TABLE II. EFFECTS OF ALKALIS AND EXTRACTANTS ON THE DETERMINATION OF BORON

| | 97% (v./v.) EtOH | 87% (v./v.) EtOH | MeOH | Acetone |
|---|---|---|---|---|
| Blank | | | | |
| Mean absorbance | 0.029 | 0.028 | 0.034 | 0.026 |
| No. of expts. | 16 | 4 | 6 | 4 |
| Std. deviation, % | 9.0 | 8.6 | 9.4 | 8.7 |
| 1 μg. B | | | | |
| Mean absorbance | 0.208 | 0.200 | 0.214 | 0.204 |
| No. of expts. | 16 | 4 | 6 | 4 |
| Std. deviation, % | 3.7 | 1.8 | 5.6 | 4.7 |
| 5 ml. of 0.1 N $Ca(OH)_2$ was added | | | | |
| Blank | | | | |
| Mean absorbance | 0.038 | 0.039 | 0.053 | 0.039 |
| No. of expts. | 6 | 4 | 4 | 4 |
| Std. deviation, % | 10 | 4.4 | 4.0 | 3.6 |
| 1 μg. B | | | | |
| Mean absorbance | 0.249 | 0.245 | 0.265 | 0.269 |
| No. of expts. | 6 | 4 | 4 | 4 |
| Std. deviation, % | 1.3 | 1.0 | 2.3 | 4.4 |
| 2 ml. of glycerol-NaOH reagent was added. 2 ml. of 1 N HCl was added after removal of glycerol | | | | |
| Blank | | | | |
| Mean absorbance | 0.028 | 0.026 | 0.029 | 0.024 |
| No. of expts. | 4 | 4 | 4 | 4 |
| Std. deviation, % | 18 | 6.9 | 11 | 10 |
| 1 μg. B | | | | |
| Mean absorbance | 0.148 | 0.152 | 0.151 | 0.139 |
| No. of expts. | 4 | 4 | 4 | 4 |
| Std. deviation, % | 4.3 | 3.1 | 3.3 | 4.1 |

TABLE III. COMPARISON OF SEVERAL CURCUMIN PRODUCTS

| | Vol. of 0.1 N $Ca(OH)_2$ soln., ml. | Absorbance* | | |
|---|---|---|---|---|
| | | Blank | 1 μg. B | Difference |
| Koso Chemical Co., Ltd. | 5 | 0.038 | 0.249 | 0.211 |
| Tokyo Kasei Kogyo Co., Ltd. | 5 | 0.072 | 0.380 | 0.308 |
| Tokyo Kasei Kogyo Co., Ltd. | 7 | 0.075 | 0.371 | 0.296 |
| Kanto Chemical Co., Inc. | 7 | 0.069 | 0.367 | 0.298 |
| Wako Pure Chemical Industries, Ltd.-Eastman Kodak Co. | 7 | 0.062 | 0.357 | 0.295 |

* Average of 6—12 determinations.

TABLE IV. EFFECT OF FOREIGN SUBSTANCES ON THE DETERMINATION OF BORON

| Addition | Absorbance | | |
|---|---|---|---|
| | Blank | 1 μg. B | Difference |
| — | 0.072 | 0.380 | 0.308 |
| 1 ml. 0.1 N HCl | 0.053 | 0.373 | 0.320 |
| 2 ml. 1 N HCl | 0.031 | 0.285 | 0.254 |
| 1 ml. 0.2 N $H_2SO_4$ | 0.073 | 0.397 | 0.324 |
| 2.0 ml. 0.2 N $H_2SO_4$ | 0.046 | 0.292 | 0.246 |
| 2.5 ml. 0.2 N $H_2SO_4$ | 0.083 | 0.303 | 0.220 |
| 1 ml. 0.2 N HCOOH | 0.224 | 0.502 | 0.278 |
| 20 ml. $H_2O$, 50 ml. MeOH | 0.082 | 0.374 | 0.292 |
| 1 mg. U (as $UO_2SO_4$) | 0.080 | 0.394 | 0.314 |

TABLE V. DISTILLATION OF BORON AS METHYL BORATE

| Acid solution | B taken, μg. | B found,* μg. | Av. recovery, % |
|---|---|---|---|
| 5 ml. 1 : 3 $H_2SO_4$ | 1.00 | 0.82, 0.79, 0.84, 0.86, 0.89, 0.82 | 84 |
| 5 ml. 1 : 3 $H_2SO_4$, 1 ml. 30% $H_2O_2$ | 0.50 | 0.41, 0.45 | 86 |
| 5 ml. 1 : 3 $H_2SO_4$, 1 ml. 30% $H_2O_2$ | 1.00 | 0.91, 0.83 | 87 |
| 5 ml. 1 : 3 $H_2SO_4$, 1 ml. 30% $H_2O_2$, 1 ml. 0.1 N HCl | 0.20 | 0.20, 0.16 | 90 |
| 5 ml. 1 : 3 $H_2SO_4$, 1 ml. 30% $H_2O_2$, 1 ml. 0.1 N HCl | 0.50 | 0.38, 0.44 | 82 |
| 5 ml. 1 : 3 $H_2SO_4$, 1 ml. 30% $H_2O_2$ 1 ml. 0.1 N HCl | 1.00 | 0.89, 0.81, 0.86, 0.89, 0.89, 0.80 | 86 |

* Based on the standard absorbance obtained by omitting methanol distillation (direct color development).

recommended (cf. Table IV). When the glycerol-sodium hydroxide reagent is used, addition of 2 ml. of 1 N hydrochloric acid gives the maximum absorbance. From the data in Table II, it may be concluded that, on the basis of sensitivity and simplicity in manipulation, calcium hydroxide is superior to glycerol-sodium hydroxide (and sodium hydroxide) and that 87% ethanol (=9 : 1) gives most reproducible results. The method of Silverman and Trego[11] is not sensitive enough to be used for the present purpose.

The absorbances of the colored solutions (ethanol and acetone) remain practically constant for 2 hours after the beginning of extraction of colored products. After that there is a gradual decrease in absorbance. The absorbance of a methanolic solution tends to decrease more rapidly than that of other solutions.

For the purpose of studying the influence of curcumin of different origins, several products were examined (Table III).

The effects of some foreign substances on the determination of boron were investigated (Table IV). Five ml. of 0.1 N calcium hydroxide suspension and the foreign substance, with or without 1 μg. of boron, was evaporated to dryness and then subjected to color development. The addition of 2 milliequivalent of hydrochloric acid to 0.5 milliequivalent of calcium hydroxide resulted in about a 20% decrease in absorbance (1 μg. B). If the same quantity of the acid is added to 0.7 milliequivalent of calcium hydroxide, the absorbance is low by as much as 40%. The effect of formic acid was investigated because of the possible formation formic acid during methanol distillation[20]. During evaporation of the methanolic solution about 5% of boron is lost. A loss of 4% was reported by Spicer and Strickland[19] during evaporation of methanolic solution in the presence of glycerol-sodium hydroxide reagent.

**Separation of Boron from Uranium.** — Table V summarizes the results of methanol distillation from sulfuric acid solution. Excess of water was removed by heating and methanol distillation was carried out as described in the procedure. Larsen[21] states that the addition of chloride in catalytic amounts to a mixture of sulfuric acid and hydrogen peroxide increases the rate of solution of uranium very markedly. This is the reason that 0.1 milliequivalent of hydrochloric acid was added in some cases. The effect of this solution method will be discussed later.

On the basis of the standard absorbance obtained by omitting the methanol distillation (i. e., direct color development), the average recovery of 1 μg. of boron from sulfuric acid solution is 84% (standard deviation 4.2%). Addition of hydrogen peroxide to sulfuric acid does not affect the recovery of boron (average 87%). The weighted average of recovery from the sulfuric acid-hydrogen peroxide-hydrochloric acid mixture is 85% (standard deviation 4.9% for 1 μg. B). The loss may be due to incomplete distillation of methyl borate, volatilization of boron during the evaporation of distillate, and slight difference in the composion between the sample solution and the standard solution. Most of the previous papers (cited in Table I) lack the information

TABLE VI. DETERMINATION OF BORON IN URANYL SULFATE

1.0 g. of U (as $UO_2SO_4$) in 5 ml. of 1 : 3 $H_2SO_4$ was taken in each determination

| B added, μg. | B found, μg. | B recovered, μg. |
|---|---|---|
| 0 | 0.10, 0.10 | |
| 0.20 | 0.26, 0.35 | 0.16, 0.25 |
| 0.50 | 0.48, 0.54 | 0.38, 0.44 |
| 1.00 | 0.99, 0.94 | 0.89, 0.84 |

20) M. Codell and G. Norwitz, *Anal. Chem.*, **25**, 1446 (1953).

21) R. P. Larsen, *Anal. Chem.*, **31**, 545 (1959).

TABLE VII. DETERMINATION OF BORON IN $U_3O_8$ AND URANIUM METAL

| Sample | B present, p. p. m. | B found, p. p. m.*** | | |
|---|---|---|---|---|
| | | 1 | 2 | 3 |
| $U_3O_8$* | 0.5 | 0.59, 0.57 | 0.62, 0.60 | 0.59, 0.57 |
| U metal** | 0.23 | | 0.22, 0.22, 0.23 | |

* New Brunswik Laboratory, NBL-65-3. Certified values of other constituents (in p. p. m.): 0.2 Cd, 12 Cr, 12 Cu, 28 Fe, 6 Mn, 1.0 Mo, 22 Ni, 50 P, 25 Si, 0.6 Ag, 20 V.

** New Brunswick Laboratory analyzed sample No. 16. Other certified values (in p. p. m.): 10 Al, 410 C, 2 Cu, 45 Fe, 1 Pb, 2 Mg, 6 Mn, 45 Ni, 40 N, <1 K, 50 Si, <0.1 Ag, 2 Na, 0.3 Th.

*** Three methods of standardization were studied:

1. Based on the standard curve involving MeOH distillation.
2. Seven ml. of 0.1 N $Ca(OH)_2$ solution evaporated to dryness. Color development followed. +15% correction.
3. Twenty ml. of water and 50 ml. of MeOH evaporated to dryness in the presence of $Ca(OH)_2$. Color development followed. +10% correction.

on the recoveries of boron, and the calibration curves were constructed by including the distillation step. A calculation from the data reported by Muraki and Hiiro[18] gives an apparent recovery of 80% for 0.2~2.0 μg. of boron. Also, a recovery of 75% is calculated from Luke's results[22] that were obtained by the distillation of 0.2~0.6 μg. of boron from chloride solutions.

Known amounts of boron were added to uranyl sulfate (1 g. U) solution and the boron was separated by distillation after removing excess of water (Table VI). A recovery (weighted average) of 87% is obtained with 0.2~1 μg. boron. When a correction factor of +15% (100/87=1.15) is applied, the error is not likely to exceed ±0.1 p. p. m. for this concentration range.

The results of analyses of standard samples of $U_3O_8$ and uranium metal, obtained in applying the proposed method, are shown in Table VII. The reagent blank (against the blank of direct color development) was about 0.1 μg. of boron. The $U_3O_8$ sample dissolved in the mixture of sulfuric acid and hydrogen peroxide readily. Three methods of standardization give essentially the same results.

The mixture of sulfuric acid-hydrogen peroxide-hydrochloric acid, described by Larsen[21], does not dissolve uranium readily unless the sample is very fine or thin. Anodic dissolution of uranium appears promising*. Since the solution of $U_3O_8$ in sulfuric acid and hydrogen peroxide is easily effected, uranium metal was converted in to the oxide by ignition. From the table it is seen that boron is not lost by the heat-treatment. Because the state of this element in uranium is not well known, and other standard metal samples were not available, further experiments were not made.

## Summary

Procedure is described for the spectrophotometric determination of 0.1~1 p. p. m. of boron in uranium (metal, $U_3O_8$, and uranyl sulfate). Uranium metal was first converted to $U_3O_8$, and the oxide was dissolved in sulfuric acid and hydrogen peroxide. Boron was separated by distillation as methyl borate from sulfuric acid solution, and finally determined by the curcumin method.

*Japan Atomic Energy Research Institute*
*Tokai, Ibaraki-ken*

* Larsen[21], and preliminary work of the present authors.

22) C. L. Luke and S. S. Flaschen, *Anal. Chem.*, 30, 1406 (1958).

# *Polarographic Studies on the Rare Earths. III. Yttrium.*

By Seizo MISUMI and Yasushi IDE

(Received October 8, 1959)

Polarographic studies on the reduction of the tripositive yttrium ion had been reported and discussed by Noddack and Brukl[1], Kolthoff and Lingane[2], and Purushottam and Raghava Rao[3], but the electrode reaction in the reduction process was not completely solved, because of the special properties of the aquo yttrium complex ion and of the anomalies of the reduction wave. Noddack and Brukl obtained a double wave for 0.01 M solution of yttrium sulfate, without any supporting electrolyte, having the half-wave potentials of $-1.76$ V. and $-1.84$ V. vs. S. C. E., respectively and concluded the reduction process to be $Y^{3+} \rightarrow Y^{2+} \rightarrow Y^{0}$. However, it is very doubtful. Kolthoff and Lingane suggested that it was more probable that the first wave resulted from the reduction of hydrogen ion produced by the hydrolysis of the aquo yttrium complex ion and the second wave corresponded to the three electron reduction to metal. Purushottam and Raghava Rao also obtained the double wave with yttrium chloride using lithium chloride as supporting electrolyte. From the reciprocal slope of the logarithmic plots of both waves, they concluded that the electrode reaction of the first wave was of one-electron change, and that of the second wave, of two-electron change, that is, $Y^{3+} \rightarrow Y^{2+} \rightarrow Y^{0}$ the same as before. However, all these results were incomplete because the effects of pH and concentration of yttrium ions on the diffusion current, the half-wave potential and further on the electrode reaction in reduction process were not discussed in detail. The present authors, for the purpose of solving the electrode reaction in the reduction process, studied the reduction wave of the aquo tripositive yttrium complex ion in an unbuffered solution under various conditions and obtained a different result from other reports. By the addition of a small amount of dilute acid to prevent the hydrolysis of the aquo yttrium complex ion, the hydrogen wave was completely separated from the reduction wave of the aquo yttrium complex ion, which was generally a single wave in a perchlorate solution and often a double wave in a halide solution. The electrode reaction of the single wave was irreversible and of a three-electron reduction. This wave was due to the reduction of the hydrogen ion which was produced from the dissociation of the aquo yttrium complex ion as the yttrium acid. In the case of the double wave, the first wave was irreversible or quasi-reversible and its electrode reaction was also of a three-electron reduction. The second wave was irreversible and anomalous. The two-stepped wave in the solution of the halide ions, added as supporting electrolyte, was considered to be attributed probably to the reduction of the aquo halo complex ion.

1) W. Noddack and A. Brukl, *Z. Angew. Chem.*, **50**, 362 (1937).
2) I. M. Kolthoff and J. J. Lingane, "Polarography". Vol. II. Interscience Publishers Inc., New York (1952), p. 436.
3) A. Purushottam and Bh. S. V. Raghava Rao, *Anal. Chim. Acta*, **12**, 589 (1955).

## Experimental

All current-voltage curves were recorded by a Yanagimoto photographic polarograph PEL-Model 3. All cathode potentials were referred to a saturated calomel electrode. The capillary used had an *m* value of 0.706 mg./sec. and drop times of 3.25 sec. at $-1.8$ V. and 2.98 sec. at $-1.9$ V. vs. S. C. E., when measured in an air-free 0.1 M lithium perchlorate solution at 57.6 cm. of effective height of mercury. The measurement of pH was done with the Hitachi glass electrode pH meter Model EHM-1 for a micro amount scale. All experiments were carried out in a thermostat of $25.0 \pm 0.1$°C.

An yttrium stock solution was prepared by dissolving pure yttrium perchlorate or sulfate. (As yttrium oxide, the purity was higher than 99.99%.). The concentration of the stock solution was 0.01 M. The lithium perchlorate and tetramethyl ammonium iodide which were used as the supporting electrolytes were guaranteed grade reagents and recrystallized before use. The concentration of these stock solutions were 1 and 0.2 M., respectively. The gelatine solution used as the maximum suppressor was prepared afresh in every experiment. Perchloric acid and sulfuric acid solutions of 0.01 N in concentration were prepared from the analytical pure reagents and used for the adjustment of pH.

To the sample solution of yttrium, appropriate quantities of the supporting electrolyte and gelatine were added to give the final concentrations, 0.1 M and 0.01% respectively. Then a micro amount of 0.01 N acid was added to prevent the hydrolysis of the aquo yttrium complex ion and to adjust the pH at the same time. The total volume of the solution was made up to 5 ml. with distilled water. The concentration of the yttrium ion was in the range from 0.5 to 2.0 millimol./l. and the pH of the solution

was varied from 4.00 to 2.60. Dissolved oxygen was removed by passing purified nitrogen gas through the solution at least for 20 min. The polarograms were recorded at 25.0±0.1°C.

The diffusion coefficient of the yttrium ion was calculated from Nernst's equation, using the value of equivalent conductance at infinite dilution[4].

$D$: $5.721\times10^{-6}$ cm. sec$^{-1}$ (for $Y(ClO_4)_3$)

$D$: $5.764\times10^{-6}$ cm. sec$^{-1}$ (for $Y_2(SO_4)_3$)

## Results and Discussion

*The reduction wave of aquo tripositive yttrium complex ion.*—The reduction wave of the aquo yttrium complex ion (Fig. 1) at pH about 4.5 differed from the true reduction wave owing to the precedence of the hydrogen wave produced by the hydrolysis of the aquo yttrium complex ion. The typical reduction wave was obtained by adding a micro amount of acid to prevent the hydrolysis when the hydrogen wave was completely separated from the reduction wave of the aquo yttrium complex ion under a certain condition. The reduction wave was generally a single wave in a perchlorate medium and often a double wave in a halide (chloride or iodide) medium.

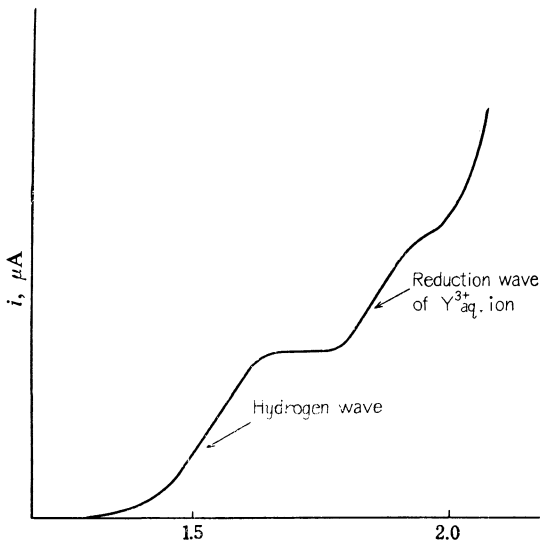



Fig. 1. Reduction wave of the aquo yttrium complex ion. (1) In perchlorate medium
$Y^{3+}$ ion: 1.25 mM in 0.1 M $LiClO_4$ and 0.01% gelatine medium
pH: 2.95 S: 1/200 25.0°±0.1°C

From the results obtained by the variation in pH and the concentration of the yttrium ion, the following common characters of the reduction wave were derived: 1) At a pH higher than 3.4, only a single wave was obtained in both perchlorate and halide medium. 2) At a pH less than 2.7, only a single wave was observed, but as the height of the hydrogen wave became large, the wave was ambiguous. 3) At a pH between 2.7 and 3.4, in a perchlorate solution, only a single wave was obtained clearly and as the pH decreased, there was a tendency for a small maximum wave to appeare ofteh after the reduction wave. In a halide solution, when the two-stepped wave was obtained, the second wave decreased gradually as the pH decreased or the concentration of yttrium ions increased until it finally disappeared.

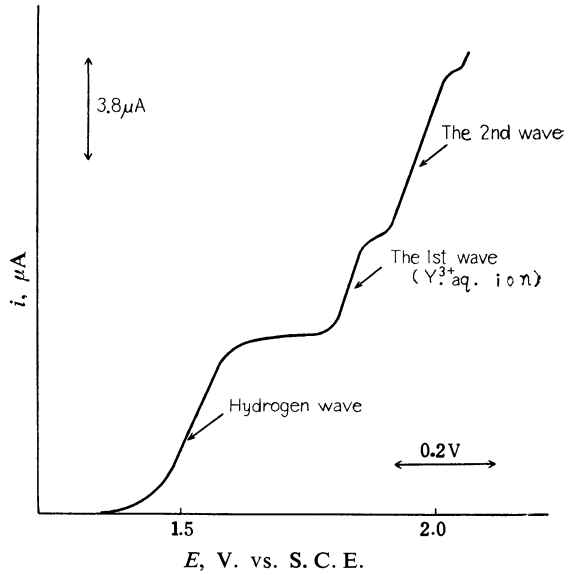



Fig. 1. Reduction wave of the aquo yttrium complex ion. (2) In iodide medium
$Y^{3+}$ ion: 1.03 mM in 0.1 M $(CH_3)_4NI$ and 0.01% gelatine medium
pH: 3.09 S: 1/181 25.0°±0.1°C

*Dependence of the limiting current on the pressure upon the dropping mercury electrode and the influence of temperature on the limiting current and the half-wave potential.*—A relationship between the limiting current and the height of mercury column is shown in Table I. As the limiting current is proportional to the square root of the height of mercury column, the limiting current was diffusion-controlled.

The temperature coefficient of the half-wave potential and that of the diffusion current in the range from 25° to 35°C were 0.7 mV./deg. and 1.86%/deg., respectively, which were nearly in agreement with the values that would be expected in the case of the diffusion-controlled process.

*The plots of E vs. log{$i/(i_d-i)$}.*—The reduction waves of the aquo tripositive yttrium complex ion were analyzed by the logarithmic

4) F. H. Spedding and S. Jaffe, *J. Am. Chem. Soc.*, 76, 882 (1954); ibid., 76, 884 (1954).

Table I. Dependence of limiting currents of the reduction wave on the heights of mercury column

| $h$ cm. | $h$(corr.) cm. | $i_l$ μA | $i_l/\sqrt{h}$ | $h$ cm. | $h$(corr.) cm. | $i_l$ μA | $i_l/\sqrt{h}$ |
|---|---|---|---|---|---|---|---|
| 50 | 47.6 | 3.07 | 0.446 | 50 | 47.5 | 2.96 | 0.431 |
| 60 | 57.7 | 3.39 | 0.448 | 60 | 57.5 | 3.32 | 0.448 |
| 70 | 67.6 | 3.66 | 0.446 | 70 | 67.6 | 3.61 | 0.439 |

$Y^{3+}$ ion: 0.992 mM in 0.1 M $(CH_3)_4NI$ and 0.01% gelatine medium. pH: 3.0.

$Y^{3+}$ ion: 1.257 mM in 0.1 M $LiClO_4$ and 0.01% gelatine medium. pH: 2.9.

Table II. The reciprocal slope of $E$ vs. $\log\{i/(i_d-i)\}$

| pH | Reciprocal slope, V. | | pH | Reciprocal slope, V. 1st wave. | 2nd wave. |
|---|---|---|---|---|---|
| 3.50 | 0.059 | | 3.70 | 0.043 | |
| 3.35 | 0.037 | | 3.35 | 0.020 | |
| 3.00 | 0.027 | | 3.05 | 0.019 | anomalous |
| 2.80 | 0.027 | max. | 2.85 | 0.020 | |
| 2.65 | 0.022 | 〃 | 2.60 | 0.020 | |

$Y^{3+}$ ion: 0.611 mM in 0.1 M $LiClO_4$ and 0.01% gelatine medium.

$Y^{3+}$ ion: 1.00 mM in 0.1 M $(CH_3)_4NI$ and 0.01% gelatine medium.

Table III. The effects of pH on half-wave potential, diffusion current and diffusion current constant

| pH | Half-wave potential, $E_{1/2}$ V. vs. S. C. E. | Diffusion current, $i_d$ μA | Diffusion current constant, $I_d$ |
|---|---|---|---|
| 3.75 | −1.725 | 2.47 | 4.48 |
| 3.50 | −1.727 | 2.43 | 4.36 |
| 3.35 | −1.824 | 2.45 | 4.45 |
| 3.10 | −1.870 | 2.45 | 4.45 |
| 3.00 | −1.865 | 2.45 | 4.45 |
| 2.95 | −1.865 | 2.47 | 4.50 |
| 2.80 | −1.943 | 2.43 | 4.39 |
| 2.65 | −1.945 | 2.47 | 4.53 |

($Y^{3+}$ ion: 0.611 mM in 0.1 M $LiClO_4$ and 0.01% gelatine medium.)

| pH | Half-wave potential V. vs. S. C. E. | | Diffusion current μA | | Diffusion current constant, $I_d$ |
|---|---|---|---|---|---|
| | $(E_1)_{1/2}$ | $(E_2)_{1/2}$ | $i_{\alpha_1}$ | $i_{\alpha_2}$ | |
| 3.70 | −1.737 | | 3.42 | | 3.40 |
| 3.55 | −1.773 | | 3.46 | | 3.51 |
| 3.35 | −1.801 | −1.941 | 3.48 | 3.61 | 3.51 |
| 3.10 | −1.826 | −1.970 | 3.49 | 4.70 | 3.55 |
| 3.05 | −1.834 | −1.976 | 3.44 | 4.92 | 3.52 |
| 2.85 | −1.852 | −2.000 | 3.52 | 4.85 | 3.58 |
| 2.75 | −1.864 | −2.006 | 3.30 | 4.50 | 3.46 |
| 2.70 | −1.878 | −2.012 | 3.34 | 3.84 | 3.40 |

($Y^{3+}$ ion: 1.043 mM in 0.1 M $(CH_3)_4NI$ and 0.01% gelatine medium.)

plot. The results are shown in Table II. With decreasing pH, the value of the reciprocal slope of the reduction wave decreased. In a perchlorate solution, the electrode reaction was irreversible and at a pH less than 3.00, it indicated a tendency to approach to a three-electron reduction, provided that the reduction of the aquo yttrium complex ion is followed by amalgamation at electrode. This tendency was evidently observed in a halide midium. In a halide solution, at a pH less than 3.4, the electrode reaction of the first wave was irreversible, but it approached from irreversible to quasi-reversible and corresponded to three-electron change. The electrode reaction of the second wave was also irreversible and very anomalous.

*The effects of pH on the reduction waves.*—

The reduction waves were recorded at various pH from 4.00 to 2.60 under a certain condition. The results are shown in Table III.

Half-wave potentials of all reduction waves shifted to more negative potentials as pH decreased. It is considered that this was probably due to the increasing stability of hydroxo yttrium complex ion, which was formed by the hydrolysis of the aquo yttrium complex ion owing to the weak basicity of yttrium. This shift was always dependent only on the concentration of the free hydrogen ion. It was observed that at the same pH the half-wave potential was more negative in a perchlorate medium than in a halide medium under a given condition. The diffusion current of the reduction wave, $i_d$, was independent of pH from 3.4 to 2.6 and almost constant in a perchlorate medium. However it was observed that at a pH higher than 3.4, the diffusion current tended to decrease slightly. In the halide medium, at a pH higher than 3.6, there was the same tendency. The diffusion current of the second wave, in a halide medium, increased slightly with the decrease of the pH down to 3.1 and had a small maximum, but with the further decrease of the pH, $i_d$ decreased gradually and anomalously. The diffusion current constant of the reduction wave, $I_d$, was constant at a pH from 3.4 to 2.6 in the perchlorate medium and that of the first wave in the halide medium, $I_{d_1}$, was also constant at a pH less than 3.6. The value of the diffusion current constant of the second wave, $I_{d_2}$, was irregular, and anomalous.

*The effects of concentration of the yttrium ion on the reduction wave and the value of n, calculated from diffusion current constant.*—The reduction waves were recorded in the range of concentration of yttrium ion 0.5 to 2.0 millimol./l. at a constant pH. The results are shown in Table IV.

The half-wave potential of the reduction wave shifted to more negative potentials slightly, with the increasing concentration at a constant pH. The diffusion current, $i_d$, was apparently proportional to the concentration of $Y^{3+}$ ion in the perchlorate medium. The first diffusion current in the halide medium gave a similar result, but the second diffusion current was anomalous. The diffusion current constant of the reduction wave was constant, independent of the concentration of the yttrium ion and its average value was about 4.46 in 0.1 M $LiClO_4$ and about 3.51 in 0.1 M $(CH_3)_4NI$, while the theoretical value of the diffusion current constant is 4.34, which was calculated by assuming that the number of the electrons associated with the electrode reaction of the reduction wave, $n$, was three and the value of the diffusion coefficient of the yttrium ion $D$, $5.721\times10^{-6}$ cm. $sec^{-1}$ ($Y(ClO_4)_3$). It is considered that the average value observed in 0.1 M lithium perchlorate was almost equal to the theoretical one. The diffusion coefficient of the yttrium ion ($Y_2(SO_4)_3$) is $5.764\times10^{-6}$ cm. $sec^{-1}$ and the diffusion current constant was calculated to be 4.35. Although the average value of the diffusion current constant in the halide medium was smaller than the calculated one, it is also considered that the former was closer to the latter than the value which would be expected in the case of $n=2$. From these experimental values of the diffusion current constants, the number of the electrons involved in the electrode reaction, $n$, was calculated. The calculated value of $n$ was 3.06 in the case of 0.1 M lithium perchlorate, where the perchlorate ion has no tendency to complex with cation. Therefore, the electrode reaction was of three-electron change. The calculated value of $n$ for the first wave in the case of 0.1 M tetramethylammonium iodide, where iodide ion forms generally an aquo iodo-

Table IV. The effects of concentration of yttrium ion on the half-wave potential, the diffusion current, and the diffusion current constant

| $Y^{3+}$ ion mM | Half-wave potential, $E_{1/2}$ V. vs. S. C. E. | Diffusion current, $i_d$ μA | Diffusion current constant, $I_d$ |
|---|---|---|---|
| 0.332 | −1.815 | 1.39 | 4.54 |
| 0.428 | −1.819 | 1.69 | 4.41 |
| 0.917 | −1.881 | 3.70 | 4.49 |
| 1.529 | −1.900 | 5.89 | 4.40 |

(pH=3.00, $Y(ClO_4)_3$, in 0.1 M $LiClO_4$ and 0.01% gelatine medium.)

| $Y^{3+}$ ion mM | Half-wave potential V. vs. S. C. E. | | Diffusion current μA | | Diffusion current constant |
|---|---|---|---|---|---|
| | $(E_1)_{1/2}$ | $(E_2)_{1/2}$ | $i_{d_1}$ | $i_{d_2}$ | |
| 0.723 | −1.850 | −1.990 | 2.40 | 3.97 | 3.47 |
| 1.043 | −1.852 | −2.000 | 3.52 | 4.85 | 3.58 |
| 1.984 | −1.857 | −2.005 | 6.65 | 5.34 | 3.50 |

(pH=2.90, $Y_2(SO_5)_3$, in 0.1 M $(CH_3)_4NI$ and 0.01% gelatine medium.)

complex ion, was about 2.60, which seemed apparently smaller than three, owing to the probable formation of the aquo iodo complex ion. The value of the diffusion current constant of the second wave was irregular because of the anomaly of the reduction wave.

*Polarographic depolarizing action of the hydrolyzable aquo yttrium complex ion.*—The aquo tripositive yttrium complex ion, $Y(H_2O)_x^{3+}$ ion, behaves as a weak acid, "yttrium acid," in aqueous solution, owing to its weak basicity. Generally, the half-wave potential of the reduction wave which is due to the deposition of hydrogen from a weak acid, HA, has the following well known equation in excess of an indifferent electrolyte,

$$E_{1/2} = -3\boldsymbol{R}T/2\boldsymbol{F}\cdot\ln i_d/2 + k = -0.089 \log i_d/2 + k$$

where $k$ is a constant. Accordingly, it follows that the half-wave potential of a weak acid should shift to more negative potentials with the increasing acid concentration and $dE_{1/2}/d\log(HA) = -0.089$ V. In fact, as shown in Table IV, the half-wave potential of the reduction wave shifted slightly to more negative potentials with the increasing concentration at a certain pH. The value of $dE_{1/2}/d\log(Y(H_2O)_x^{3+})$ for the reduction wave calculated by extrapolation and given as follows: $dE_{1/2}/d\log(Y(H_2O)_x^{3+})$ equals $-0.090$ V. in perchlorate medium and $-0.088$ V. in an iodide medium. These values are considered to be equal to the theoretical value of $-0.089$ V. This fact indicates that the reduction wave of the aquo yttrium complex ion was the same as the reduction wave of the hydrogen ion from the yttrium acid, that is, the reduction wave was not due to the reduction of the yttrium ion, ($Y^{3+}$ ion), itself, but was attributed to the deposition of hydrogen from the yttrium acid. It is also in accordance with the results of irreversibility and of a three-electron change in electrode reaction. Of course, the hydrogen ion from "the yttrium acid" was at first combined and not free. Since the hydrogen ion was produced by hydrolysis of the aquo yttrium complex ion as the yttrium acid, the following equation would be given:

$$Y(H_2O)_x^{3+} + yH_2O = Y(H_2O)_{x-y}(OH)_y^{(3-y)+} + yH_3O^+$$

where $x$ is the coordination number of the tripositive yttrium ion (usually 6 in the case of a mononuclear yttrium ion), and $y$ is the number of the hydrogen ion produced from the yttrium acid by hydrolysis at a certain pH. The yttrium acid $Y(H_2O)_x^{3+}$ has three hydrogen ions per one molecule to be released and reduced at electrode. Therefore the quantities of electricity to be exchanged by the hydrogen ions at dropping mercury electrode are just the same as those which tervalent yttrium ions require when reduced to metal. Actually, the reduction of the hydrogen ion from the aquo yttrium complex ion at dropping mercury electrode requires a large overpotential, but still the hydrogen ion seems to take an electron more easily than the aquo yttrium complex ion or the hydroxo yttrium complex ion does. Thus the electrode reaction was irreversible (or quasi-reversible in the halide medium) and three-electron change as described above. It is considered that the reduction proceeds for example as follows:

$$Y(H_2O)_x^{3+} + 3e^- \rightarrow 3/2H_2 + Y(H_2O)_3(OH)_3$$

The second wave in the halide medium, if it existed, was supposed also to be the hydrogen wave which is due to the reduction of the hydrogen ion from dissociation of water in the aquo halo complex. This wave was also irreversible. Consequently, it was concluded that the polarographic depolarising action of the aquo yttrium complex ion was indicated by the reduction of the hydrogen ion from the yttrium acid and not by the reduction of the yttrium ion itself to metal.

## Conclusion

The logarithmic plot for the reduction wave of yttrium(III) indicated a straight line, independent of concentration of yttrium(III) at a pH less than 3.4. The value of its reciprocal slope approached the theoretical value for three-electron reduction with decreasing pH. The average value of the diffusion current constant was about 4.46 in 0.1 M lithium perchlorate and 3.60 in 0.1 M tetramethylammonium iodide from which the value of $n$ was calculated to be 3, it being assumed that in the reduction of the aquo yttrium complex ion at dropping mercury electrode, amalgamation would follow. In short, the reduction wave was irreversible and three-electron reduction. However, it was found that the aquo yttrium complex ion behaved as a weak acid, "the yttrium acid", and that the reduction wave was due to the deposition of hydrogen from the hydrolyzable aquo yttrium complex ion as the weak acid. It is also supposed that the second reduction wave, if it appeared in the halide medium, was due to the deposition of hydrogen from dissociation of water in aquo halo yttrium complex formed during the first reduction step. This second reduction wave was irreversible and anomalous.

At pH 3.00, the half-wave potential of the reduction wave was $-1.881$ V. vs. S. C. E. for the concentration of $Y^{3+}$ ion of 0.917 mM in 0.1 M lithium perchlorate and 0.01% gelatine medium.

The authors wish to thank Mr. Y. Masuda for his assistance in this experiment. Their thanks are also due to the Ministry of Education for its financial support of this research.

*Department of Chemistry*
*Faculty of Science*
*Kyushu University*
*Hakozaki, Fukuoka*

# *Thermodynamic Studies on Cobalt Complexes. V. On the Solubility and the Thermal Dissociation of Aquopentamminecobalt(III) Nitrate and Bromide, and on the Thermodynamic Stability of Monoacidopentamminecobalt(III) Complexes**

By Motoshichi Mori and Ryokichi Tsuchiya

(Received December 2, 1959)

In the preceding paper[1] the authors determined the standard free energies of formation of aquopentamminecobalt(III) chloride in the solid state and in aqueous solution. In the present study the standard free energies of formation of aquopentamminecobalt(III) nitrate and bromide in the solid state were determind by measuring their solubilities, and those of nitratopentamminecobalt(III) nitrate and bromopentamminecobalt(III) bromide in the solid state were determined by measuring their dissociation pressures.

On the basis of these data the thermodynamic stability of aquopentamminecobalt(III) chloride, nitrate and bromide, that of monoacidopentamminecobalt(III) complexes and that of their ions in aqueous solution were compared and discussed.

## Experimental

Aquopentamminecobalt(III) nitrate was precipitated with nitric acid from an aqueous solution of its chloride. The bromide was prepared by the double decomposition of its chloride with ammoium bromide in aqueous solution.

Solubilities of these aquopentamminecobalt(III) complexes were obtained by analyzing the cobalt content in their saturated solutions by iodometry in the same manner as described in the second paper[2] of this series. The dissociation pressures of the complexes were measured with the same apparatus as described in the third paper[3].

* Read at the Symposium on Coordination Compounds of the Chemical Society of Japan, Fukuoka, Oct., 1959.

1) M. Mori, R. Tsuchiya and Y. Okano, This Bulletin, 32, 1029 (1959).

2) M. Mori, R. Tsuchiya and Y. Okano, ibid., 32, 462 (1959).

3) M. Mori and R. Tsuchiya, ibid., 32, 467 (1959).

4) M. Mori and R. Tsuchiya, *J. Chem. Soc. Japan, Pure Chem. Sec.* (*Nippon Kagaku Zasshi*), 79, 1164 (1958).

## Results and Calculation

**Solubility of Aquopentamminecobalt(III) Nitrate.**—The results obtained for aquopentamminecobalt(III) nitrate are listed in Table I.

As the activity coefficient of the compound was not known, it was assumed that it was approximately equal to that of hexamminecobalt(III) chloride[4] in relatively lower concentrations. When aquopentamminecobalt(III) nitrate is dissolved in water, the change is expressed by

$$[Co(NH_3)_5OH_2](NO_3)_3\ (s) = [Co(NH_3)_5OH_2]^{3+}(aq.\ a) + 3NO_3^-(aq.\ a)$$

If the solubility of the salt in molality and its mean activity coefficient are expressed by $m$ and $\gamma_\pm$ respectively, the equilibrium constant

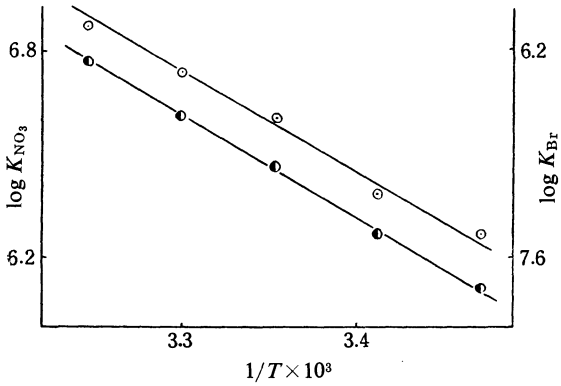



Fig. 1. The relationship between the equilibrium constant of the solution and the temperature.
-⊙-; aquopentamminecobalt(III) nitrate
-◑-; aquopentamminecobalt(III) bromide

Table I. Equilibrium of solution for aquopentamminecobalt(III) nitrate

| Temp. °C | Solubility in Molality $m$ | $1/T\times10^3$ | Mean activity coefficient $\gamma_\pm$ | $K_{NO_3}\times10^6$ | $\log K_{NO_3}$ |
|---|---|---|---|---|---|
| 15 | 0.07443 | 3.471 | 0.217 | 1.837 | $\bar{6}$.2642 |
| 20 | 0.08516 | 3.417 | 0.203 | 2.412 | $\bar{6}$.3823 |
| 25 | 0.1084 | 3.355 | 0.181 | 4.001 | $\bar{6}$.6022 |
| 30 | 0.1284 | 3.299 | 0.166 | 5.539 | $\bar{6}$.7434 |
| 35 | 0.1472 | 3.246 | 0.155 | 7.317 | $\bar{6}$.8643 |

of the solution, $K_{NO_3}$, is given by

$$K_{NO_3}=27m^4\gamma_\pm^4$$

The plots of its logarithm against the reciprocal of the absolute temperature are shown in Fig. 1, giving an almost straight line. Its equation computed by the method of least squares is

$$\log K_{NO_3}=3.884-2774/T$$

From this equation the heat of solution is obtained as $\Delta H=12.7$ kcal.

The standard free energy change of the solution, $\Delta G^0$, is calculated by the following formula,

$$\Delta G^0=-RT\ln K_{NO_3}=12690-17.76T \quad (1)$$

from which the values of the standard free energy change of the solution at 25°C, $\Delta G^0_{298}=7396$ cal. and its entropy change at 25°C, $\Delta S^0_{298}=17.76$ entropy unit are obtained.

On the other hand, the standard free energy of formation of the aquopentamminecobalt(III) ion in unit activity was calculated in the preceding paper[1] as

$$\Delta G_f{}^0=-192900+296.6T \quad (2)$$

and that of the nitrate ion, $NO_3^-$, was obtained in the second paper[2] of this series as

$$\Delta G_f{}^0=-49370+77.03T \quad (3)$$

From formulae 1, 2 and 3, the standard free energy of formation of aquopentamminecobalt(III) nitrate in the solid state is calculated as

$$\Delta G_f{}^0=-353700+545.4T \quad (4)$$

The value at 25°C is $\Delta G^0_{298}=-191100$ cal. and the heat of formation is $\Delta H=353.7$ kcal.

**Dissociation Pressure of Aquopentamminecobalt(III) Nitrate.**—The weight loss of aquopentamminecobalt(III) nitrate upon heating was followed by a thermobalance. The relationship between the weight loss and the temperature is plotted in Fig. 2, together with those of aquopentamminecobalt(III) bromide, chloride and perchlorate. It is found in this figure

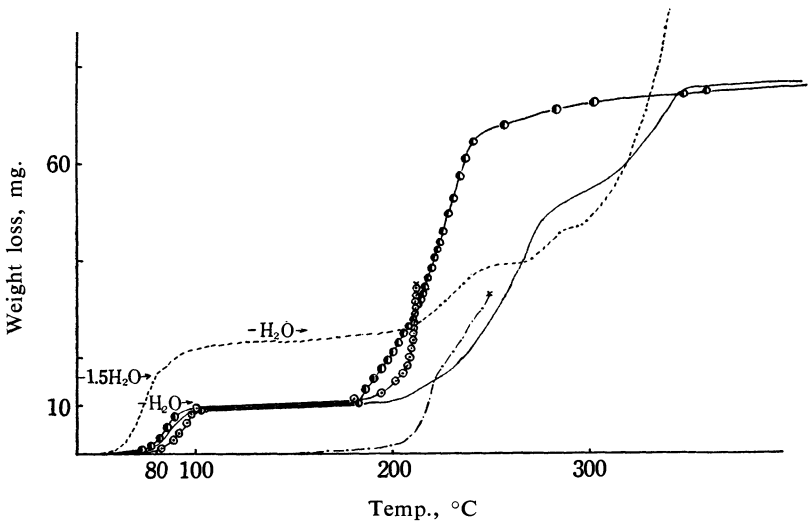



Fig. 2. The relationship between the weight loss and the temperature upon heating for several aquopentamminecobalt(III) complexes by a thermobalance.
-⊙-; aquopentamminecobalt(III) nitrate
-◐-; aquopentamminecobalt(III) bromide
——; aquopentamminecobalt(III) chloride
------; aquopentamminecobalt(III) sulfate hydrate
-·-·-; aquopentamminecobalt(III) perchlorate

that the nitrate decomposes upon heating at 80~100°C to nitratopentamminecobalt(III) nitrate according to the following equation;

$$[Co(NH_3)_5OH_2](NO_3)_3(s) = [Co(NH_3)_5NO_3](NO_3)_2(s) + H_2O(g)$$

The vapor pressure of water produced by this docomposition at 30~68°C, that is, the dissociation pressure of aquopentamminecobalt(III) nitrate measured is shown in Table II.

Table II. Dissociation pressure of aquopentamminecobalt(III) nitrate

| Temp. °C | $1/T\times10^3$ | Dissociation pressure mmHg | $\log p_{mm}$ |
|---|---|---|---|
| 30 | 3.299 | 1.35 | 0.1303 |
| 33 | 3.267 | 1.70 | 0.2305 |
| 39 | 3.204 | 2.19 | 0.3404 |
| 45 | 3.144 | 3.19 | 0.5038 |
| 52 | 3.076 | 4.09 | 0.6117 |
| 56 | 3.039 | 4.59 | 0.6618 |
| 62 | 2.984 | 6.34 | 0.8021 |
| 68 | 2.932 | 8.48 | 0.9284 |

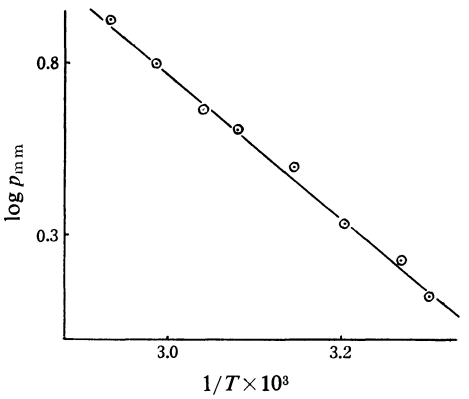



Fig. 3. The relationship between the dissociation pressure and the temperature for aquopentamminecobalt(III) nitrate.

The logarithm of the dissociation pressure, $p_{mm}$, is plotted against the reciprocal of the absolute temperature in Fig. 3, which shows an almost straight line. By the method of least squares the equation of this line is computed as follows:

$$\log p_{mm} = 7.045 - 2091/T$$

From this equation the heat of dissociation is obtained as $\Delta H = 9562$ cal. The standard free energy change of dissociation, $\Delta G^0$, is given by the following formula,

$$\Delta G^0 = -RT \ln p_{atm} = 9562 - 19.05\,T \qquad (5)$$

from which the values of the free energy change of dissociation at 25°C, $\Delta G^0_{298} = 3885$ cal. and the entropy change of the solution at 25°C, $\Delta S^0_{298} = 19.05$ entropy unit are obtained.

The standard free energy of formation of aquopentamminecobalt(III) nitrate in the solid state was already calculated above as formula 4, and that of $H_2O(g)$ was obtained in the preceding paper[1] as

$$\Delta G_f^0 = -57800 + 10.61T \qquad (6)$$

By subtracting formula 6 from the sum of formulae 4 and 5, the standard free energy of formation of nitratopentamminecobalt(III) nitrate in the solid state is calculated as

$$\Delta G_f^0 = -286400 + 515.8T$$

The value at 25°C is

$$\Delta G^0_{f298} = -132600 \text{ cal.} \qquad (7)$$

and the heat of formation is

$$\Delta H_{298} = -286.4 \text{ kcal.}$$

By using the solubility[5] and the heat of solution[6] of nitratopentamminecobalt(III) nitrate and by assuming that its activity coefficient is equal to that of bromopentamminecobalt(III) bromide[7], the free energy change of the solution of the former at 25°C is obtained as

$$G^0_{298} = 7347 \text{ cal.} \qquad (8)$$

Subtracting twice the standard free energy of formation of $NO_3^-$, $-26.41$ kcal.[8], from the sum of the formulae 7 and 8, the free energy of formation of nitratopentamminecobalt(III) ion in unit activity in aqueous solution is obtained as follows:

$$\Delta G^0_{f298} = 72440 \text{ cal.}$$

If $\Delta H = -168.8$ kcal.[9] is used as the heat of formation of its ion, the relationship between the free energy of formation and temperature is expressed by

$$\Delta G_f^0 = -168800 + 323.3T$$

**Solubility of Aquopentamminecobalt(III) Bromide.**—The results obtained for aquopentamminecobalt(III) bromide are listed in Table III.

When the aquopentamminecobalt(III) bromide is dissolved in water, the change is expressed by

$$[Co(NH_3)_5OH_2]Br_3(s) = [Co(NH_3)_5OH_2]^{3+}(aq.\ a) + 3Br^-(aq.\ a)$$

5) J. N. Brönsted and A. Petersen, *J. Am. Chem. Soc.*, **43**, 2265 (1921).
6) A. Lamb and J. Simmons, ibid., **43**, 2188 (1921).
7) B. Adell, *Z. anorg. allgem. Chem.*, **246**, 303 (1941).
8) F. D. Rossini et al., "Selected Values of Chemical Thermodynamic Properties", United States Government Printing Office, Washington (1952), p. 53.
9) K. B. Yatsimirskii and L. L. Pankowa, *Zhur. Obshchei Khim.*, **18**, 2051 (1948); K. B. Yatsimirskii, "Thermochemie von Komplexverbindungen", Akademie-Verlag, Berlin (1956), p. 179.

TABLE III. EQUILIBRIUM OF SOLUTION FOR AQUOPENTAMMINECOBALT(III) BROMIDE

| Temp. °C | Solubility in molality $m$ | $1/T\times10^3$ | Mean activity coefficient $\gamma\pm$ | $K_{Br}\times10^7$ | $\log K_{Br}$ |
|---|---|---|---|---|---|
| 15 | 0.03304 | 3.471 | 0.317 | 3.250 | $\bar{7}.5119$ |
| 20 | 0.03899 | 3.412 | 0.294 | 4.663 | $\bar{7}.6686$ |
| 25 | 0.04771 | 3.355 | 0.268 | 7.218 | $\bar{7}.8584$ |
| 30 | 0.05556 | 3.299 | 0.251 | 10.21 | $\bar{6}.0091$ |
| 35 | 0.06722 | 3.246 | 0.228 | 14.89 | $\bar{6}.1730$ |

The plots of the logarithm of the equilibrium constant, $K_{Br}$, against the reciprocal of the absolute temperature are shown in Fig. 1, giving a straight line. Its equation is calculated as follows

$$\log K_{Br}=3.756-2953/T$$

The heat of solution is obtained as $\Delta H=13.5$ kcal.

The free energy change of solution is given by the following formula,

$$\Delta G^0=-RT\ln K_{Br}=13510-17.18T \qquad (9)$$

and the value at 25°C is $\Delta G^0_{298}=8385$ cal. and the entropy change at 25°C is $\Delta S^0_{298}=17.18$ entropy unit.

As the standard free energy of formation of bromide ion, $Br^-$, was obtained in the second paper[2] of this series as

$$\Delta G_f{}^0=-28900+14.51T \qquad (10)$$

that of aquopentamminecobalt(III) bromide in the solid state is obtained from formulae 2, 9 and 10 as:

$$\Delta G_f{}^0=-293100+357.3T \qquad (11)$$

Its value at 25°C is $\Delta G^0_{f298}=-186600$ cal. and the heat of formation is $\Delta H=-293.1$ kcal.

**Dissociation Pressure of Aquopentamminecobalt(III) Bromide.** — Aquopentamminecobalt(III) bromide changes to bromopentamminecobalt(III) bromide upon heating at 75~95°C as

$$[Co(NH_3)_5OH_2]Br_3(s)=[Co(NH_3)_5Br]Br_2(s)+H_2O(g)$$

The vapor pressure of water produced by the above reaction at 18~32°C, that is, the dissociation pressure of aquopentamminecobalt(III) bromide is listed in Table IV.

TABLE IV. DISSOCIATION PRESSURE OF AQUOPENTAMMINECOBALT(III) BROMIDE

| Temp. °C | $1/T\times10^3$ | Dissociation pressure mmHg | $\log p_{mm}$ |
|---|---|---|---|
| 18 | 3.435 | 3.84 | 0.5843 |
| 20.5 | 3.406 | 5.23 | 0.7185 |
| 24 | 3.366 | 8.40 | 0.9243 |
| 26 | 3.343 | 9.35 | 0.9708 |
| 27 | 3.332 | 12.04 | 1.0806 |
| 29 | 3.310 | 14.75 | 1.1688 |
| 32 | 3.278 | 17.89 | 1.2526 |

The logarithm of the dissociation pressure, $p_{mm}$, is plotted against the reciprocal of the absolute temperature in Fig. 4, which shows an almost straight line. By the method of least squares the equation of this line is computed as:

$$\log p_{mm}=15.65-4382/T$$

From this equation the heat of dissociation is obtained as $\Delta H=9562$ cal.

The standard free energy change of dissociation is given by the formula,

$$\Delta G^0=-RT\ln p_{atm}=20040-58.41T \qquad (12)$$

from which the value at 25°C, $\Delta G^0_{298}=2633$ cal. and the entropy change of solution at 25°C, $\Delta S^0_{298}=58.41$ eutropy unit are obtained.

As the standard free energy of formation of aquopentamminecobalt(III) bromide in the solid state was already calculated above according to formula 11, that of bromopentamminecobalt(III) bromide in the solid state is calculated from formulae 6, 11 and 12 as

$$\Delta G_f{}^0=-215300+288.2T$$

The value at 25°C is

$$\Delta G^0_{f298}=-129300 \text{ cal.} \qquad (13)$$

and the heat of formation is $\Delta H=-215.3$ kcal.

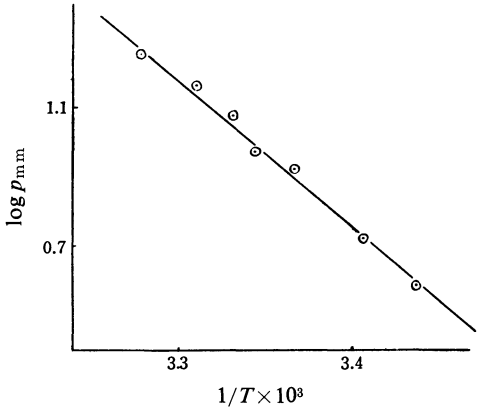



Fig. 4. The relationship between the dissociation pressure and the temperature for aquopentamminecobalt(III) bromide.

By using the solubility[5], the heat of solution[6] and the activity coefficient[7] of bromopentamminecobalt(III) bromide, the free energy change of solution of it at 25°C is obtained as

$$\Delta G^0_{293} = 8855 \text{ cal.} \quad (14)$$

Subtracting twice the free energy of formation of $Br^-$, $\Delta G^0_{293} = -24.57$ kcal.[10], from the sum of formulae 13 and 14, the free energy of formation of bromopentamminecobalt(III) ion in unit activity in aqueous solution is calculated as:

$$\Delta G_{f^0_{298}} = -71340 \text{ cal.}$$

If $\Delta H = -146.8$ kcal.[11] is used as the heat of formation of its ion, the relationship between the free energy of formation and temperature is expressed by

$$\Delta G_f{}^0 = -146800 + 253.2T$$

## Discussion

**Thermodynamic Stability of Aquopentamminecobalt(III) Complexes.** — The standard free energy of formation of aquopentamminecobalt(III) nitrate and bromide in the solid state, the free energy of the solution and the heat of solution of them calculated above together with those of its chloride obtained in the preceding paper[1] and the radii of each anions are again shown in Table V.

According to these values, it will be seen that the thermodynamic stability of these three aquopentamminecobalt(III) complexes in the solid state and aqueous solution decreases in the following order,

$$[Co(NH_3)_5OH_2]Cl_3 > [Co(NH_3)_5OH_2](NO_3)_3 > [Co(NH_3)_5OH_2]Br_3$$

This order is in good agreement with the decreasing order of the thermodynamic stability of hexamminecobalt(III) complexes,

$$[Co(NH_3)_6]Cl_3 > [Co(NH_3)_6](NO_3)_3 > [Co(NH_3)_6]Br_3$$

reported as in the second paper[2] of this series.

The heat of solution of these aquopentamminecobalt(III) complexes increases in the order, chloride < nitrate < bromide, and increases with the radius of anion as shown in Table V. It is generally known[12] that for simple salts of which the radius of the cation is 2.4 Å, the heat of solution increases with the radius of the anion. It is concluded that this relationship is also valid for these aquopentamminecobalt(III) complexes, the radius of the cation, $[Co(NH_3)_5OH_2]^{3+}$, being 2.4 Å.

The solubility of these complexes decreases in the order, chloride > nitrate > bromide. This may be due to the fact that the radius of anions becomes larger and consequently the ionic character of the bond between the complex cation and anion of the salts diminishes in the order, chloride > nitrate > bromide.

**Thermodynamic Stability of Monoacidopentamminecobalt(III) Complexes.** — The standard free energy of formation of nitratopentamminecobalt(III) nitrate and bromopentamminecobalt(III) bromide in the solid state obtained above, that of chloropentamminecobalt(III) chloride obtained in the third paper[3] of this series and that of chloropentamminecobalt(III) nitrate and bromide, nitratopentamminecobalt(III) chloride and bromopentamminecobalt(III) chloride and nitrate calculated from the solubility[5] and the heat of solution[9] in the literature are summarized in Table VI.

TABLE V. STANDARD FREE ENERGY OF FORMATION, FREE ENERGY OF SOLUTION AND HEAT OF SOLUTION OF AQUOPENTAMMINECOBALT(III) CHLORIDE, NITRATE AND BROMIDE, AND THE RADII OF EACH ANIONS

| Complexes | Free energy of formation kcal. | Free energy of solution cal. | Heat of solution kcal. | Radius of anion, Å |
|---|---|---|---|---|
| $[Co(NH_3)_5OH_2]Cl_3$ | −203.0 | 4488 | 8.75 | 1.81 |
| $[Co(NH_3)_5OH_2](NO_3)_3$ | −191.1 | 7396 | 12.7 | 1.89 |
| $[Co(NH_3)_5OH_2]Br_3$ | −186.6 | 8385 | 13.5 | 1.96 |

TABLE VI. STANDARD FREE ENERGY OF FORMATION OF MONOACIDOPENTAMMINECOBALT(III) COMPLEXES

| Complexes | $\Delta G_{f^0_{298}}$, kcal. | Complexes | $\Delta G_{f^0_{298}}$, kcal. |
|---|---|---|---|
| $[Co(NH_3)_5Cl]Cl_2$ | −144.9 | $[Co(NH_3)_5NO_3]Cl_2$ | −141.4 |
| $[Co(NH_3)_5Cl](NO_3)_2$ | −133.7 | $[Co(NH_3)_5NO_3](NO_3)_2$ | −132.6 |
| $[Co(NH_3)_5Cl]Br_2$ | −131.7 | | |
| | | $[Co(NH_3)_5Br]Cl_2$ | −142.1 |
| | | $[Co(NH_3)_5Br](NO_3)_2$ | −131.8 |
| | | $[Co(NH_3)_5Br]Br_2$ | −129.3 |

10) G. Jones and S. Bäckström, *J. Am. Chem. Soc.*, **56**, 1524 (1934).
11) K. B. Yatsimirskii, "Thermochemie von Komplexverbindungen", Akademie-Verlag, Berlin (1956), p. 178.
12) K. B. Yatsimirskii, "Thermochemie von Komplexverbindungen", Akademie-Verlag, Berlin (1956), p. 45.

On the basis of these values, it is found that the thermodynamic stability of these complexes in the solid state decreases in the following order:

$$\begin{array}{ccccc} [Co(NH_3)_5Cl]Cl_2 & > & [Co(NH_3)_5Cl](NO_3)_2 & > & [Co(NH_3)_5Cl]Br_2 \\ \vee & & \vee & & \\ [Co(NH_3)_5NO_3]Cl_2 & > & [Co(NH_3)_5NO_3](NO_3)_2 & & \vee \\ \wedge & & \vee & & \\ [Co(NH_3)_5Br]Cl_2 & > & [Co(NH_3)_5Br](NO_3)_2 & > & [Co(NH_3)_5Br]Br_2 \end{array}$$

The levels of the standard free energy of formation for these complexes are diagrammatized in Fig. 5. From these figures it is found that the decrease of the thermodynamic stability of these monoacidopentamminecobalt(III) complexes is far less for the case when $Cl^-$ in the inner sphere is replaced by $NO_3^-$ or $Br^-$ than for the case when $Cl^-$ in the outer sphere is replaced by $NO_3^-$ or $Br^-$. This fact might be partly interpreted by the increase of the radius of the anion in the outer sphere in the order, $Cl^- < NO_3^- < Br^-$.

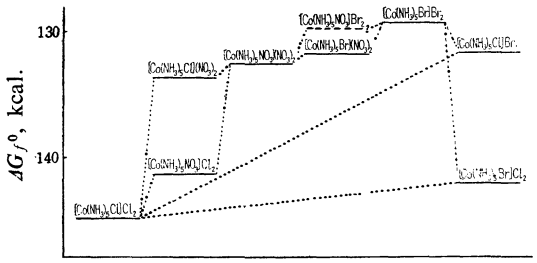



Fig. 5. The levels of the standard free energy of formation for several monoacidopentamminecobalt(III) complexes in the solid state.

**Thermodynamic Stability of Monoacidopentamminecobalt(III) Ions.** — From the standard free energies of formation of nitratopentamminecobalt(III) and bromopentamminecobalt(III) ions obtained above, and those of chloropentamminecobalt(III) ion[1], nitropentamminecobalt(III) ion[13], sulfatopentamminecobalt(III) ion[6], aquopentamminecobalt(III) ion[1] and hexamminecobalt(III) ion[13], the free energy change for the following substitution reactions are calculated:

$$[Co(NH_3)_5OH_2]^{2+} + NO_2^- = [Co(NH_3)_5NO_2]^{2+} + H_2O(l) \qquad \Delta G^0_{298} = -52590 \text{ cal.}$$

$$[Co(NH_3)_5OH_2]^{3+} + SO_4^{--} = [Co(NH_3)_5SO_4]^+ + H_2O(l) \qquad -6750$$

$$[Co(NH_3)_5OH_2]^{3+} + NH_3\ (aq.) = [Co(NH_3)_5NH_3]^{3+} + H_2O(l) \qquad -320$$

$$[Co(NH_3)_5OH_2]^{3+} + Br^- = [Co(NH_3)_5Br]^{2+} + H_2O(l) \qquad 1040$$

$$[Co(NH_3)_5OH_2]^{3+} + NO_3^- = [Co(NH_3)_5NO_3]^{2+} + H_2O(l) \qquad 1780$$

$$[Co(NH_3)_5OH_2]^{3+} + Cl^- = [Co(NH_3)_5Cl]^{2+} + H_2O(l) \qquad 3825$$

From these values it is concluded that the thermodynamic stability decreases in the order:

$$[Co(NH_3)_5NO_2]^{2+} > [Co(NH_3)_5SO_4]^+ > [Co(NH_3)_6]^{3+} > [Co(NH_3)_5OH_2]^{3+} > [Co(NH_3)_5Br]^{2+} > [Co(NO_3)_5NO_3]^{2+} > [Co(NH_3)_5Cl]^{2+}$$

This order is in good agreement with the spectrochemical series[14] with the exception of $[Co(NH_3)_5SO_4]^+$ and $[Co(NH_3)_5Br]^{2+}$.

## Summary

1. By measuring the solubility and the dissociation pressure of aquopentamminecobalt(III) nitrate, the standard free energy of formation of the salt and that of nitratopentamminecobalt(III) nitrate produced by the decomposition of the former in the solid state were determined.

2. In the same way the standard free energy of formation of aquopentamminecobalt(III) bromide and that of bromopentamminecobalt(III) bromide were determined.

3. On the basis of these results, the thermodynamic stabilities of three aquopentamminecobalt(III) complexes, several monoacidopentamminecobalt(III) complexes and their ions were determined.

*Department of Chemistry*
*Faculty of Science*
*Kanazawa University*
*Kanazawa*

13) A. B. Lamb and A. T. Larson, *J. Am. Chem. Soc.*, **42**, 2038 (1920).

14) Y. Shimura and R. Tsuchida, This Bulletin, **29**, 311 (1956).

# *Rotatory Dispersion of Metallic Co-ordination Compounds. II. Absorption Spectra and Rotatory Dispersion of Cobalt(III) Complexes of EDTA*

By Jinsai HIDAKA, Yoichi SHIMURA and Ryutaro TSUCHIDA

(Received November 25, 1959)

It is well known that rotatory dispersion is closely related to the absorption band, and there are many reports[1] concerning the rotatory dispersion of some metallic complex ions but very few on the relation between the partial "inversive dispersion" and the absorption band. In the former paper of this series[2], anomalous rotatory dispersion in the visible and ultraviolet region has been measured for the cobalt(III) ethylenediamine complexes, analyzed in partial "inversive dispersion" and discussed in relation to their absorption band. Furthermore, a possibility of determining the absolute configuration of the complex ion has been suggested from the viewpoint of the inversive dispersion curve in the wavelength region of the first absorption band.

In the present paper, the anomalous rotatory dispersion of D-$Na_2[Co(edta)NO_2]\cdot 3H_2O$, D-K$[Co(edta)]\cdot 3H_2O$ and D-$K_2[Co(edta)Cl]\cdot 3H_2O$, which were recently resolved by Dwyer et al.[3,4], and D-*cis*-$[Co\,en_2(NO_2)_2]$ I will be studied in the visible and ultraviolet region in the same way as was done in the former report[2].

## Experimental

**Measurements.**—The rotatory dispersion measurements were carried out with a Rudolph photoelectric spectropolarimeter, Model 200S-80. The measurements were made in the region from 700 m$\mu$ ($42.8\times10^{13}$/sec.) to 365 m$\mu$ ($82\times10^{13}$/sec.) using mainly the lines of the mercury spectrum. A xenon or a tungsten lamp was also used when necessary. The measurements of D-$[Co(edta)NO_2]^{2-}$ and D-$[Co(edta)]^-$ were made in aqueous solutions of $1/5\times10^2$ F, $1/10^3$ F, $1/2\times10^3$ F, and $1/4\times10^3$ F. The solvent employed for D-$[Co(edta)Cl]^{2-}$ was hydrochloric acid (1 : 1) because this complex ion is not so stable in an aqueous solution that it undergoes aquotization rapidly. The concentration of the solution was $1/5\times10^2$ F or $1/10^3$ F, and the measurements were made as rapidly as possible after preparation of the solution to reduce the reaction of the complex ion with weter to the minimum. The concentration of D-*cis*-$[Co\,en_2(NO_2)_2]^+$ was $1/10^3$ F, $1/3\times10^3$ F and $1/6\times10^3$ F in aqueous solutions. The absorption measurements were made by a Beckman DU spectrophotometer. All measurements were made at room temperature.

**Material.**—Potassium-(ethylenediaminetetraacetato) cobalt(III) trihydrate, $K[Co(edta)]\cdot 3H_2O$, was prepared in violet crystals and resolved by the method of Dwyer et al[3]. Optically active complex ions, D-$[Co(edta)]^-$, were precipitated as a more sparingly soluble salt with D-$[Co\,en_3]^{3+}$.[5] The preparation and resolution of disodium nitro-(ethylenediaminetetraacetato) cobalt(III) trihydrate, $Na_2[Co(edta)NO_2]\cdot 3H_2O$, and dipotassium chloro-(ethylenediaminetetraacetato) cobalt(III) trihydrate, $K_2[Co(edta)Cl]\cdot 3H_2O$, were also made by the direction of Dwyer et al.[4] The D-isomer of both the complex ions was precipitated as a more sparingly soluble salt with L-*cis*-$[Co\,en_2(NO_2)_2]^+$. *cis*-Dinitro-bis-(ethylenediamine) cobalt(III) iodide was prepared and resolved by the method of Werner[6]. The D-isomer was precipitated as a more sparingly soluble salt with *d*-camphorsulphonic acid. These optically active complex ions gave positive value of optical rotation at green lines of a mercury spectrum, and were denoted as a D-isomer.

## Results and Discussion

The rotatory dispersion and the absorption curve of D-$Na_2[Co(edta)NO_2]\cdot 3H_2O$, D-K$[Co(edta)]\cdot 3H_2O$, D-$K_2[Co(edta)Cl]\cdot 3H_2O$ are shown in Figs. 1~3. The structures of these complex ions were well established by Dwyer[4] and other workers[7]. The observed curves were analyzed on the basis of the following consideration. It is assumed that the observed curve is the superposition of the partial inversive dispersion[8] and the tail of a total dispersion which has its inversion center in the far ultraviolet

1) W. Kuhn and K. Bein, *Z. physik. Chem.*, **B24**, 355 (1943); W. Kuhn and K. Bein, *Z. anorg. allg. Chem.*, **216**, 321 (1934); J.-P. Mathieu, *J. chim. phys.*, **33**, 78 (1936); J.-P. Mathieu, *Bull. soc. chim. France*, [5] **3**, 476 (1936); R. Tsuchida, *J. Chem. Soc. Japan (Nippon Kagaku Zasshi)*, **58**, 621 (1937); M. Kobayashi, ibid., **64**, 684 (1943).

2) J. Hidaka, S. Yamada and R. Tsuchida, This Bulletin, **31**, 921 (1958).

3) F. P. Dwyer, E. C. Gyarfas and D. P. Mellor, *J. Phys. Chem.*, **59**, 296 (1955).

4) F. P. Dwyer and F. L. Garvan, *J. Am. Chem. Soc.*, **80**, 4480 (1958).

5) A. Werner, *Ber.*, **45**, 121 (1912).

6) A. Werner, *Ber.*, **44**, 2450 (1911).

7) D. H. Bush and J. C. Bailar, Jr., *J. Am. Chem. Soc.*, 75, 4576 (1953); G. Schwarzenbach, *Helv. Chim. Acta*, **32**, 839 (1949); M. L. Morris and D. H. Bush, *J. Am. Chem. Soc.*, **78**, 5178 (1956).

8) J.-P. Mathieu, *Compt. rend.*, **199**, 278 (1934); J.-P. Mathieu, ibid., **201**, 1183 (1935); J.-P. Mathieu, *Bull. soc. chim. France*, [5] **3**, 476 (1936),

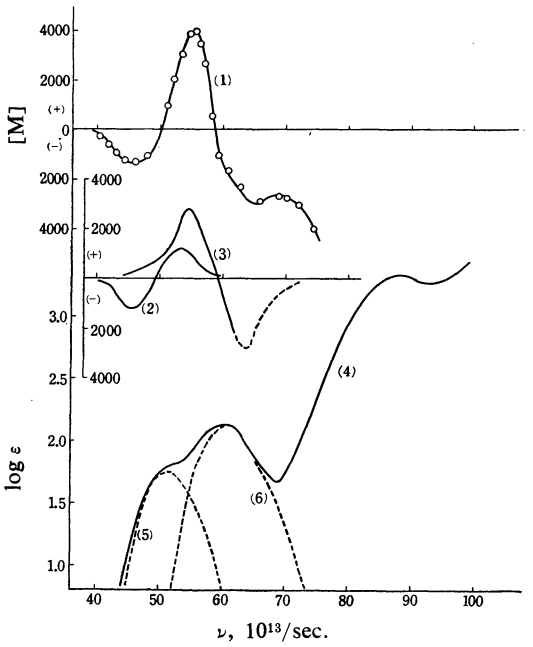



Fig. 1. Rotatory dispersion and absorption of D-$Na_2[Co(edta)NO_2]\cdot 3H_2O$: 1, rotatory dispersion curve; 2—3, curve analyses of the rotatory dispersion curve; 4, absorption curve; 5—6, curve analyses of the first absorption band.

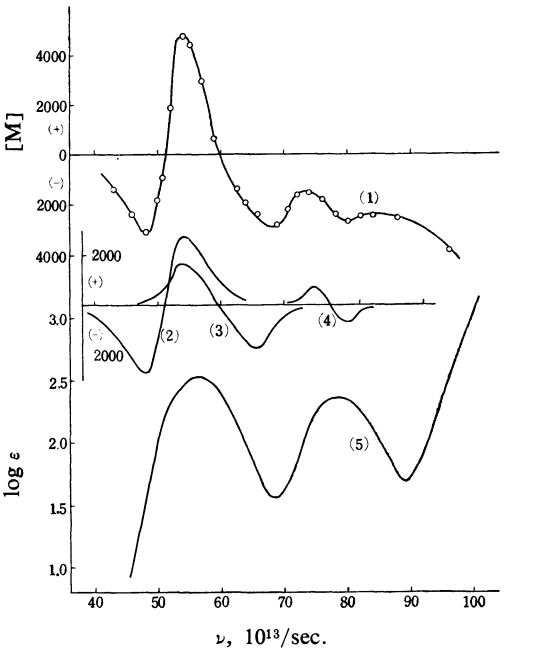



Fig. 2. Rotatory dispersion and absorption of D-$K[Co(edta)]\cdot 3H_2O$: 1, rotatory dispersion curve; 2—4, curve analyses of the rotatory dispersion curve; 5, absorption curve.

region. For the analysis, the method of successive approximation was employed.

D-$Na_2[Co(edta)NO_2]\cdot 3H_2O$. As is seen in Fig. 1, the observed curve indicates that total the dispersion curve is apparently displaced to the negative side on the whole. In the analysis of the curve, therefore it is assumed that the observed curve is the superposition of the partial dispersion in the visible region and the negative tail of a total dispersion concerned in the far ultraviolet region. The shape of the rotatory dispersion curve suggests that an overlapping of two inversive dispersions occurred in its first absorption band. As a result of tentative curve analysis, it was found that two inversive dispersions overlapped with each other in the visible region. The sign of the Cotton effect concerned in the first inversive dispersion is negative. Thus the molar rotation changes from negative (long wavelength side) to positive values (short wavelength side) at about 49 ($\times 10^{13}$/sec.). On the other hand, the second inversive dispersion appears at about 59 ($\times 10^{13}$/sec.) and shows a positive Cotton effect. The magnituds of these two partial dispersions is found to be of the same order. The two inversive dispersions may be regarded as corresponding to the absorption band in these wavelength regions. As is shown in Fig. 1, the first absorption band of $[Co(edta)NO_2]^{2-}$ distinctly splits into two components. The Ia-component is at 60.4 ($\times 10^{13}$/sec.) in the shorter wavelength as compared with the first band of $[Co(edta)]^-$, and the sub-component, Ib, is at 51.4 ($\times 10^{13}$/sec.) in the long wavelength side of the first band of $[Co(edta)]^-$ [9]. It has been reported that the center of the inversive rotatory dispersion was almost always in the longer wavelength region in comparison with the position of the absorption maximum[10]. In this respect, the result of the present measurements is in good agreement.

D-$K[Co(edta)]\cdot 3H_2O$. The rotatory dispersion curve of D-$[Co(edta)]^-$ is shown in Fig. 2. The total dispersion curve is apparently displaced to the negative side. This complex ion also shows two inversive dispersions in the region of the first absorption band. The one, with its center at about 51.5 ($\times 10^{13}$/sec.), has a negative Cotton effect and the other, with its center at 61.0 ($\times 10^{13}$/sec.), a positive Cotton effect. As is seen in Fig. 2, the first absorption band of this complex does not split. Judging from the symmetry of the complex ion, however, it is expected that its first absorption band splits into two component

9) Y. Shimura and R. Tsuchida, This Bulletin, **29**, 643 (1956).
10) Y. Shimura, ibid., **31**, 315 (1957).

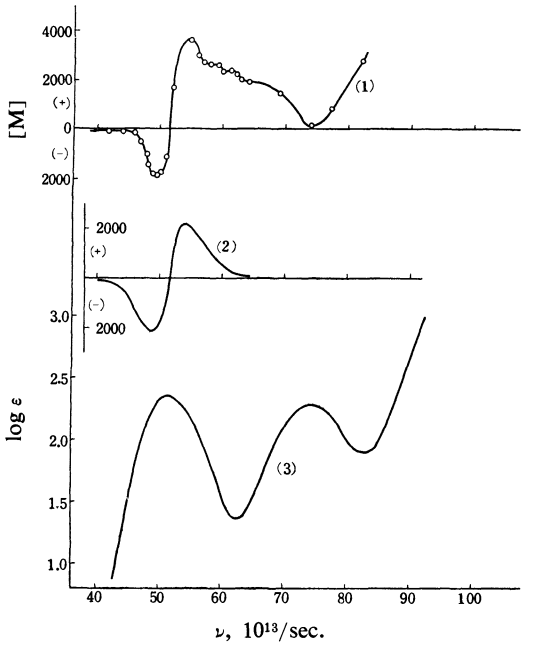



Fig. 3. Rotatory dispersion and absorption of D-$K_2$[Co(edta)Cl]·$3H_2O$: 1, rotatory dispersion curve; 2, curve analyses of the rotatory dispersion curve; 3, absorption curve; first band, $\nu_{max}$=ca. 52.0 ($\log \varepsilon_{max}$=2.35); second band, ca. 74.0 (2.28).

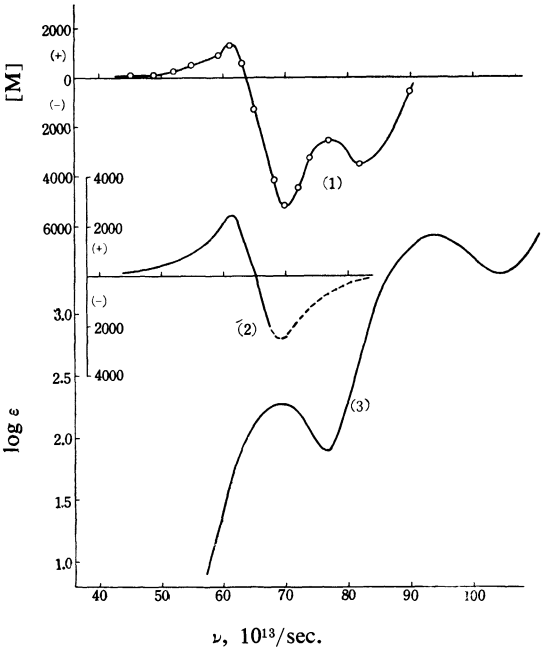



Fig. 4. Rotatory dispersion and absorption of D-*cis*-[Co $en_2(NO_2)_2$]I: 1, rotatory dispersion curve; 2, curve analyses of the rotatory dispersion curve; 3, absorption curve.

absorptions, Ia and Ib. It is considered, therefore, that the two inversive dispersions obtained above probably correspond to the two components of the first absorption band. The optical activity is due to the arrangement of the groups about the central cobalt atom, so the rotatory dispersion curve of complexes of similar configuration should have the same chracteristic. Therefore, the similarity of the rotatory dispersion curve of D-[Co(edta)-$NO_2$]$^{2-}$ and D-[Co(edta)]$^-$ complexes, in the region of the first absorption band, shows that the two complex ions have a similar configuration. There is another small inversive dispersion with its center at about 77 ($\times 10^{13}$/sec.), which probably belongs to the second absorption band.

D-$K_2$[Co(edta)Cl]·$3H_2O$. Contrary to the preceding two complexes, the observed curve is apparently displaced to the positive side by the tail of total dispersion from the far ultraviolet side. The result of the measurement and the analysis is shown in Fig. 3. According to the analysis, the inversive dispersion of the first absorption band occurred at 51.8 ($\times 10^{13}$/sec.), which has a negative Cotton effect. In the shorter wavelength side of the first absorption band at about 57~63 ($\times 10^{13}$/sec.), there is a small hump in the rotatory dispersion curve. This fact shows that the first absorption band has a sub-component in this region, although no evidence is observed in the absorption curve. Because this complex is not so stable toward aquotization in solutions, it was not possible to measure the rotation in the region of a wavelength shorter than 82.5 ($\times 10^{13}$/sec.). However, as regards the behavior of the short wavelength end of the observed curve, it may be considered that an inversive dispersion which belongs to the second absorption band also contributes to the observed rotatory dispersion curve. From the results mentioned above for the cobalt(III) complexes of EDTA, it will easily be understood that the analysis of the rotatory dispersion curve is very useful for the study of the absorption bands, especially for the study of their splitting and overlapping.

D-*cis*-[Co $en_2(NO_2)_2$]I. In the region of the first absorption band, as is shown in Fig. 4, there is an inversive dispersion with its center at about 65.5 ($\times 10^{13}$/sec.), which has a positive Cotton effect, and this result coincides with Methieu's[11]. The behavior of the dispersion curve, that is that the observed curve has apparently one inversive dispersion in the region of the first band, resembles that of D-*cis*-[Co$en_2$Cl $NO_2$]$^+$ [2].

11) J.-P. Mathieu, *Bull. soc. chim. France*, [5] 3, 487 (1936).

This fact is considered as follows. The two components of the first absorption band, which have the positive sign of the Cotton effect, are so close together that a complete overlapping of two inversive dispersions occurred. In the shorter wavelength region, the observed value of the molar rotation is smaller. Judging from the position of the absorption maximum, it may be suggested that there begins in this region an inversive dispersion which belongs to the nitro-specific absorption band too. Similarly, on the observed curve of D-$[Co(edta)NO_2]^{2-}$, the increase of molar rotation for the negative side in the shorter wavelength end may be regarded as originating from the nitro-specific absorption band.

## Summary

The rotatory dispersion measurements have been made for D-$Na_2[Co(edta)NO_2]\cdot 3H_2O$, D-$K[Co(edta)]\cdot 3H_2O$, D-$K_2[Co(edta)Cl]\cdot 3H_2O$ and D-*cis*-$[Co\,en_2(NO_2)_2]I$. On the basis of these measurements, the relation of the splitting of the first absorption band with the so-called anomalous rotatory dispersion has been discussed. In the anomalous rotatory dispersion of D-$[Co(edta)NO_2]^{2-}$, there appear two inversive dispersions due to the component absorption, Ia and Ib, of the split first absorption band. Similarly considered, it has been shown that the first absorption band of $[Co(edta)]^-$ or $[Co(edta)Cl]^{2-}$ may have two component absorptions in accordance with the behavior of its rotatory dispersion curve.

The present authors wish to thank the Ministry of Education for a grant.

*Department of Chemistry*
*Faculty of Science*
*Osaka University*
*Kita-ku, Osaka*

# *Ultraviolet Absorption Spectra of Aqueous Solutions and Single Crystals of Thioacetamide and Thiourea*

By Haruo HOSOYA, Jiro TANAKA and Saburo NAGAKURA

(Received December 15, 1959)

In a series of previous papers by Nagakura and Tanaka[1-4], electronic absorption spectra of various molecules, in which electron donating and accepting groups are connected with each other directly or through a bridge of conjugated double bonds, were discussed from both experimental and theoretical points of view. In these studies, special attention was paid to absorption bands which can be ascribed to neither of the component groups but to the interaction between the electron donating and accepting groups within a molecule. Since the transition corresponding to this kind of absorption band is apparently accompanied by a great amount of electron transfer from the electron donor to the acceptor, it may be called an intramolecular charge-transfer absorption by analogy with intermolecular cases developed by Mulliken[5]. From both experimental results of polarized ultraviolet absorption spectra and theoretical studies based on the LCMO treatment, it was actually shown that the intramolecular charge-transfer absorption can be found with formamide ($O=CH-NH_2$), acrolein ($H_2C=CH-CH=O$), nitramide ($H_2N-NO_2$), nitrobenzene ($C_6H_5-NO_2$), benzoic acid ($C_6H_5-COOH$), *p*-nitroaniline ($O_2N-C_6H_4-NH_2$) and other similar molecules. For example, the strong 370 m$\mu$ band of *p*-nitroaniline could reasonably be interpreted as an intramolecular charge-transfer absorption, in view of the fact that the direction of the transition moment associated with the band is parallel to the molecular axis connecting the two nitrogen atoms. A similar interpretation was applied to the 237 m$\mu$ band of aniline by Longuet-Higgins and Murrell[6].

1) S. Nagakura and J. Tanaka, *J. Chem. Phys.*, **22**, 236 (1954).
2) S. Nagakura, ibid., **23**, 1441 (1955); *Molecular Physics*, to be published.
3) J. Tanaka, S. Nagakura and M. Kobayashi, *J. Chem. Phys.*, **24**, 311 (1956); J. Tanaka and S. Nagakura, ibid., **24**, 1274 (1956).
4) J. Tanaka, *J. Chem. Soc. Japan, Pure Chem. Sec.* (*Nippon Kagaku Zasshi*), **78**, 1636 (1957); **79**, 1373 (1958).
5) R. S. Mulliken, *J. Phys. Chem.*, **56**, 801 (1952) and other papers.
6) H. C. Longuet-Higgins and J. N. Murrell, *Proc. Phys. Soc.*, **A68**, 601 (1955); J. N. Murrell, ibid., **A68**, 969 (1955).

In the present paper, electronic absorption spectra of thioacetamide ($S=C\langle^{CH_3}_{NH_2}$) and thiourea ($S=C\langle^{NH_2}_{NH_2}$) are studied as a subject of much interest from the aspect of intramolecular charge-transfer absorption. In these molecules, the thiocarbonyl (C=S) and amino ($NH_2$) groups are electron acceptor and donor, respectively, and the appearance of the intramolecular charge-transfer absorption may be expected. Especially thiourea seems to be most suitable for studying the effect of so-called cross-conjugation upon the charge-transfer absorption. This is because this molecule shows absorption bands at relatively longer wavelengths than the similar compounds, say urea ($O=C\langle^{NH_2}_{NH_2}$), do. By the way, the absorption bands of urea appear at wavelengths below 190 m$\mu$ and therefore are difficult to be measured with spectrophotometric instruments usually available at present.

Katagiri et al. measured absorption spectra of thioacetamide and thiourea in ethereal solution and pointed out that the weak band of thioacetamide at 318 m$\mu$ is conceivably ascribed to the $n\rightarrow\pi^*$ transition[7]. However, the assignment of the $\pi\rightarrow\pi^*$ transition bands of these two molecules has never been made. In the present paper, it is undertaken to obtain a definite conclusion on the assignment of the absorption bands by measuring the polarized ultraviolet absorption with their crystals and, moreover, by combining the experimental results with theoretical consideration based on the semi-empirical molecular orbital method including configuration interaction.

As is well known, thioacetone ($(H_3C)_2C=S$) can not exist as a stable monomer but usually as a trimer[8]. Therefore, it is difficult to obtain peak wavelengths of the absorption spectrum pertinent to the C=S bond, which is one of the important and basic data indispensable for the present study. In order to remove this difficulty, we have undertaken to measure the absorption spectrum of the conjugate acid of thioacetamide ($S=C\langle^{\overset{+}{N}H_3}_{CH_3}$) which is isoelectronic with thioacetone. In this connection, the equilibrium between thioacetamide and a proton is studied in detail and its equilibrium constant is obtained by means of the spectrophotometric method.

7) S. Katagiri, Y. Amako and H. Azumi, Presented at the Symposium on Structural Chemistry, Kyoto, October, 1958.
8) E. Baumann and E. Fromm, *Ber.*, **22**, 2593 (1889).
9) A. Bernthsen, *Ann.*, **192**, 47 (1878).
10) A. Hantzsch, ibid., **296**, 93 (1897).

## Experimental

**Materials.**—Commercial thioacetamide of G. R. grade was purified by repeating recrystallization from ethyl ether, m. p. 109.5~110.5°C (uncorrected). The reported value is 107.5~108.5°C[9]. After the purification it was subjected to spectrophotometric measurements as soon as possible, because it has a tendency to decompose easily. Commercial thiourea of G. R. grade was recrystallized from ethanol, m. p. 177~178.5°C (uncorrected). The reported value is 180°C[10]. Hydrochloric acid and sulfuric acid, which are both of G. R. grade, were used as solvents without further purification.

**Measurement.** — *Ultraviolet Absorption Spectra of Solutions.* — A Cary recording spectrophotometer model 14 M was used for the ultraviolet absorption measurements of solutions. Measurements were usually carried out at room temperature (20~25°C), the quartz cell with a stopper of 1 cm. light path being used. If necessary, however, the temperature of the absorption cell was kept constant by circulating water of a desired constant temperature through the cell jacket.

*Ultraviolet Absorption Spectra of Crystals.* — An ultraviolet microscope equipped with a Hitachi model EPU monochromator and a polarizer of Rochon prism type was used for the measurement of polarized ultraviolet absorption in the wavelength region of 220~650 m$\mu$[11]. Crystalline axes and planes were identified by the aid of X-ray rotation photographs and of optical examination with a polarizing microscope.

The single crystal of thioacetamide suitable for the measurement of polarized ultraviolet absorption was prepared by sublimation. The crystal showed a well developed (001) cleavage plane and was about 1×2 mm. in size and about 1~2 $\mu$ in thickness. The single crystal of thiourea was prepared directly on a quartz plate by dipping it into the ethanol solution and by evaporating the solvent slowly. Two kinds of crystals were obtained, one of which was hexagonal and the other rectangular. The latter was used for the spectroscopic measurement. Its developed plane was shown to be (110) by X-ray rotation photographs.

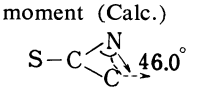
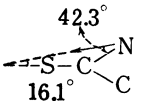
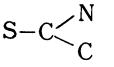
## Experimental Results

**Absorption Spectra of Thioacetamide in Aqueous and Hydrochloric Acid Solutions.** — The results obtained with the aqueous and hydrochloric acid solutions of thioacetamide are summarized in Table I and Figs. 1 and 2. The ultraviolet absorption spectrum of thioacetamide in aqueous solution apparently consists of three bands. Two of them, which appear at 261 and 210 m$\mu$, are fairly strong and may reasonably be attributed to allowed $\pi\rightarrow\pi^*$ transitions. On the other hand, the longest wavelength band at 318 m$\mu$, whose molar extinction coefficient is only 60, may be regarded as an $n\rightarrow\pi^*$ transition band.

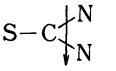
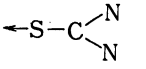
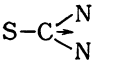
11) For the detail of the instrument, see Ref. 4.

Table I. Absorption spectra of thioacetamide and thiourea in aqueous solutions

a) Thioacetamide

| $\lambda_{max}$ Obs. | $\lambda_{max}$ Calc. | $\log \varepsilon_{max}$* Obs. | $f$ Obs. | $f$ Calc. | Direction of transition moment (Calc.) | Assignment |
|---|---|---|---|---|---|---|
| 210 mμ (5.90 eV) | 167 mμ (7.44 eV) | 3.66 | ~0.13 | 0.198 |   | $E_1 \rightarrow E_3$ |
| 261 (4.75) | 260 (4.77) | 4.08 | 0.216 | 0.515 |   | $E_1 \rightarrow E_2$ |
| 318 shoulder (3.90) | — | 1.8 | — | — |   | $n \rightarrow \pi^*$ |

b) Thiourea

| | | | | | | |
|---|---|---|---|---|---|---|
| 195 mμ (6.36 eV) | 212 mμ (5.84 eV) | 4.11 | >0.3 | 0.600 |   | $W_1 \rightarrow W_4$ |
| 236 (5.25) | 225 (5.51) | 4.08 | 0.227 | 0.529 |   | $W_1 \rightarrow W_2$ |
| ? | 136 (9.11) | ? | ? | 0.025 |   | $W_1 \rightarrow W_3$ |

* $\varepsilon_{max}$ is the molar extinction coefficient at the absorption peak.

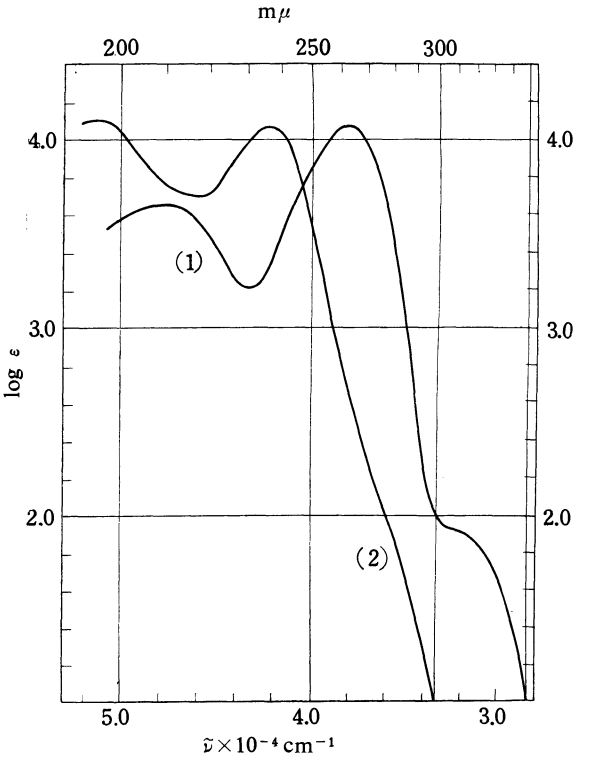



Fig. 1. Ultraviolet absorption spectra of thioacetamide (1) and thiourea (2) in aqueous solutions.

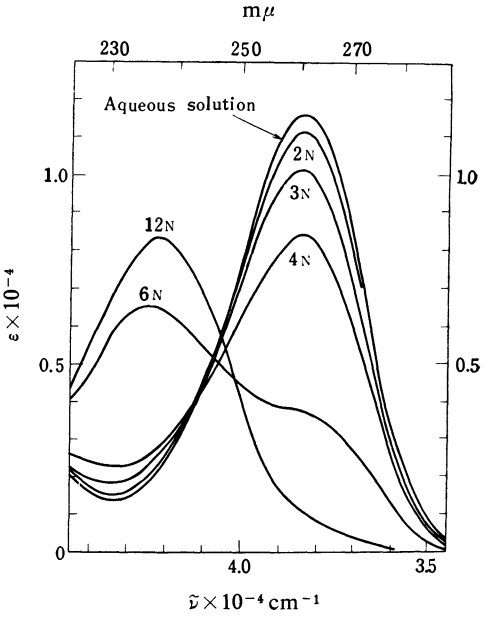



Fig. 2. Ultraviolet absorption spectra of thioacetamide in hydrochloric acid solutions with various acid concentrations.

The absorption spectrum of thioacetamide in hydrochloric acid solution changes considerably from that in aqueous solution. As is seen from Fig. 2, with the increasing concentration of hydrochloric acid, the 261 mμ band gradually decreases its intensity and a new band appears at 237 mμ[12]. Further, an isobestic point can be observed at 245 mμ, though the crossing of absorption curves is not always complete for the solutions of the higher concentrations of hydrochloric acid*. This fact conclusively indicates the existence of an equilibrium between thioacetamide and its conjugate acid. Concerning the mechanism of this equilibrium, there are two possible alternatives which are different from each other in the position where a proton is attached to the parent thioacetamide molecule. They are represented by the following equations:

$$H_2N\text{-}\overset{\overset{S}{\|}}{C}\text{-}CH_3 + H_3O^+ = H_3\overset{+}{N}\text{-}\overset{\overset{S}{\|}}{C}\text{-}CH_3 + H_2O$$

$$H_2N\text{-}\overset{\overset{S}{\|}}{C}\text{-}CH_3 + H_3O^+ = H_2N\text{-}\overset{\overset{{}^+SH}{\|}}{C}\text{-}CH_3 + H_2O$$

Here the former equilibrium is adopted as the more probable one. Some details on this point will be discussed in some later parts of the present paper.

From the experimental results regarding the absorption spectrum of thioacetamide in hydrochloric acid solutions of various concentrations, the basicity constant ($pK_B$) of thioacetamide can be obtained by the aid of the following equations:

$$K_B = (H_3\overset{+}{N}CSCH_3)/(H_2NCSCH_3)(H^+)$$
$$= (\varepsilon - \varepsilon_B)/(\varepsilon_{HB^+} - \varepsilon)(H^+)$$
$$pK_B = \log\{(\varepsilon_{HB^+} - \varepsilon)/(\varepsilon - \varepsilon_B)\} + pH$$

Quantities $(H_2NCSCH_3)$, $(H_3\overset{+}{N}CSCH_3)$ and $(H^+)$ are activities of thioacetamide, its conjugate acid and a proton, respectively. Activity coefficients of thioacetamide and its cation are assumed to be equal to unity because of their low concentrations. The activity of the proton can be evaluated by combining the concentration of the solution determined by titration with the value of activity coefficient taken from the literature[13]. Quantities $\varepsilon$, $\varepsilon_B$ and $\varepsilon_{HB^+}$ represent the apparent molar extinction coefficient of thioacetamide in dilute hydrochloric acid solution, in aqueous solution and in concentrated hydrochloric acid solution, respectively. The values of the above-mentioned quantities actually used for the evaluation of $pK_B$ are listed in Table II, together with the calculated $pK_B$ value.

The average value of $pK_B$ is obtained to be 1.2 at 24.5°C. Concerning the evaluation of this value, there are some ambiguities on the adoption of activity coefficients and on the medium effect upon the absorption spectrum of thioacetamide in concentrated hydrochloric acid. However, the $pK_B$ value of thioacetamide evaluated here seems to be reasonable compared with the value of thiourea quoted in the literature[14].

**Polarized Ultraviolet Absorption Spectra of Thioacetamide Crystal.**—According to the structural analysis data of thioacetamide crystal by Truter[15], the molecules lie on the (001) plane as is schematically shown in Fig. 3. The polarized ultraviolet absorption spectra of thioacetamide parallel to *a* and *b* axes are shown in Fig. 3. From this figure it is easily seen that the 261 mμ band has stronger intensity in the direction of *b*-axis than in the direction of *a*-axis, and that the reverse is the case for the 210 mμ band, though the dichroism is not so conspicuous for this band as for the 261 mμ band. For these two bands, unfortunately, it is

Table II. Evaluation of the $pK_B$ value of thioacetamide

| Concentration of HCl (N) | $(\varepsilon-\varepsilon_B)/(\varepsilon_{HB^+}-\varepsilon)$ 260 mμ | 270 mμ | 280 mμ | Average | $(H^+)$ | $pK_B$ |
|---|---|---|---|---|---|---|
| 3 | 0.156 | 0.157 | 0.146 | 0.153 | 3.665 | 1.38 |
| 4 | 0.406 | 0.393 | 0.372 | 0.390 | 7.104 | 1.26 |
| 6 | 2.90 | 2.45 | 2.68 | 2.68 | 22.41 | 0.92 |

Average $pK_B$ value: 1.19.

* This may be due to the medium effect of the acid.

12) The band corresponding to the 210 mμ band of thioacetamide can not be observed in hydrochloric acid solution, because hydrochloric acid is not transparent in the wavelength region below 220 mμ. However, the spectrum in concentrated sulfuric acid solution which is transparent until 200 mμ shows only one absorption band at 240 mμ, namely the one corresponding to the 237 mμ band in hydrochloric acid solution. This seems to support the opinion that the 210 mμ band of thioacetamide disappears in strongly acidic solution.

13) H. S. Harned and R. W. Ehlers, *J. Am. Chem. Soc.*, 55, 2179 (1933); G. Åkerlöf and J. W. Teare, ibid., 59, 1855 (1937).

14) $pK_B = 1.0$ for thiourea: "Handbook of Chemistry (Kagakubinran)", edited by the the Chemical Society of Japan, Maruzen, Tokyo (1958), p. 871.

15) Private communication from Dr. M. R. Truter.

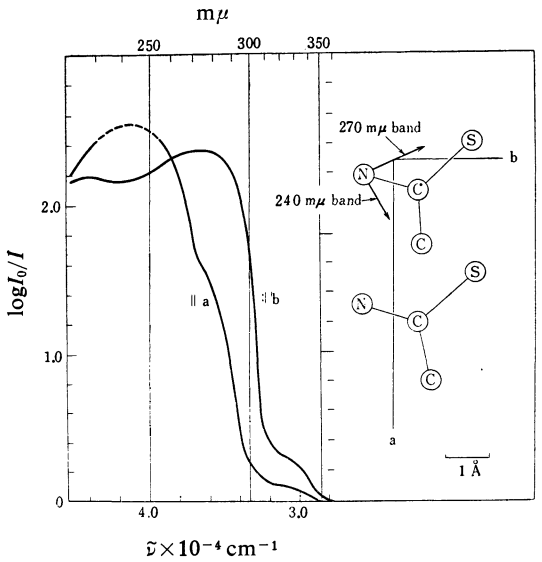



Fig. 3. The polarized ultraviolet absorption spectrum of thioacetamide and the projection of the molecules to the (001) plane. Arrows show the observed directions of transition moments.

difficult to determine exactly the direction of the transition momont from the combination of these spectral data with the crystal analysis result. This is because they overlap with each other and it is difficult to obtain the accurate value of oscillator strength for each band separately. However, it is well accepted that the transition moment of the 261 mμ band is directed very closely to the line connecting the nitrogen and the sulfur atom, thus the absorption intensity being greater in the b-axis spectrum than in the *a*-axis spectrum, while the transition momen of the 210 mμ band is approximately parallel to the line joining the nitrogen atom to the methyl carbon atom, thus the absorption intensity being a little stronger in the *a*-axis apectrum than in the *b*-axis spectrum.

A weak absorption band probably due to $n\rightarrow\pi^*$ transition appears in the 320~340 mμ region and its intensity is much stronger in the direction of *b*-axis than in the direction of *a*-axis. Concerning this weak band, however, one must be careful in determining the direction of the transition moment from the observed absorption intensity ratio, because weak forbidden bands often appear strongly in crystals by borrowing intenisty from allowed transition bands situated nearby[16]. Therefore it seems most likely that the weak band appearing at 320~340 mμ may not exhibit the dichroic property intrinsic to itself but rather the dichroic property characteristic of the 261 mμ band. In fact, the intensity ratio (about 5/1= $I_b/I_a$) measured with the weak band is completely consistent with the above-mentioned direction of transition moment of the 261 mμ band.

**Absorption Spectra of Thiourea in Aqueous Solution.**—As is seen from Table I and Fig. 1, absorption bands of thiourea have a conspicuous tendency to appear at shorter wavelengths compared with the corresponding band of thioacetamide. The same tendency seems to be found also in the case of comparing the absorption spectrum of urea with that of acetamide, though a definite conclusion can not be obtained for the case of these two molecules because of some difficulties from the experimental point of view. Another characteristic of the absorption spectrum of thiourea is the fact that the longest wavelength band of thioacetamide, which is probably associated with $n\rightarrow\pi^*$ transition, disappears.

**Polarized Absorption Spectra of Thiourea Crystal.**—According to the X-ray crystal analysis study by Wyckoff and Corey and by Kunchur and Truter[17], the molecules of thiourea lie on the (110) plane as is shown in Fig. 4. The polarized ultraviolet absorption spectra of thiourea measured by the use of the incident radiation polarized parallel and perpendicular to the *c*-axis of the crystal are shown in Fig. 4. From this figure it is easily

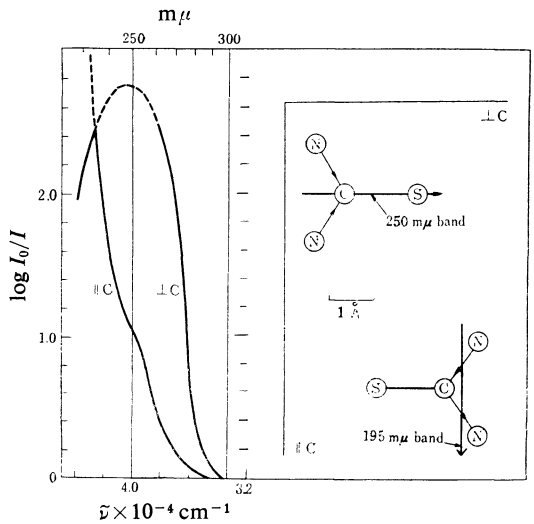



Fig. 4. The polarized ultraviolet absorption spectrum of thiourea and the projection of the molecules to the (110) plane. Arrows show the observed direction of transition moments.

16) D. S. McClure and O. Schnepp, *J. Chem. Phys.*, **23**, 1375 (1955).

17) R. W. G. Wyckoff and R. B. Corey, *Z. Krist.*, **81**, 386 (1932). N. R. Kunchur and M. R. Truter, *J. Chem. Soc.*, **1958**, 2551.

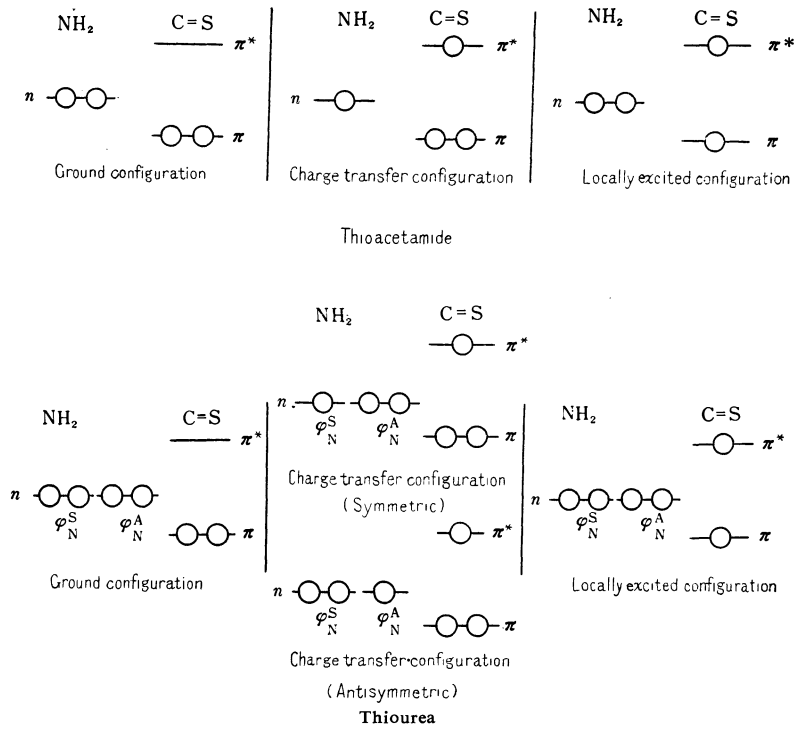



Fig. 5. Electron configurations for thioacetamide and thiourea.

seen that the observed intensity of the longer wavelength band is overwhelmingly great in the direction perpendicular to the *c*-axis compared with that in the direction parallel to the same axis, while the reverse is the case for the shorter wavelength band. This means that the transition moment of the longer wavelength band is evidently perpendicular to the *c*-axis, namely parallel to the C=S bond axis. On the other hand, the transition moment of the shorter wavelength band is determined to be perpendicular to the C=S bond axis.

## Theoretical

In the present calculation, only $\pi$-electrons are taken into account and moreover the approximation of zero-differential overlap is adopted. In actual calculations, four and six $\pi$-electrons are taken for thioacetamide and thiourea, respectively. Now let us explain the actual calculation procedure in some detail, initially taking thioacetamide as an example.

Following Longuet-Higgins and Murrell's procedure[6], three electron configurations are constructed for this molecule in terms of $\pi$-electron molecular orbitals ($\varphi_1$, $\varphi_2$) of the electron accepting groups (C=S) and the nonbonding $2p$ atomiic orbital ($\chi_N$) on the nitrogen atom of the electron donating group ($NH_2$)[18]. These configurations (a), (b) and (c) corresponding to ground, charge-transfer and locally excited configurations, respectively, are schematically shown in Fig. 5. As is well known, the wave functions for these configurations are written as follows:

$$\psi_G = 1/\sqrt{4!}\ \sum(-1)^p P\varphi_1(1)\alpha(1)\varphi_1(2)\beta(2) \times \chi_N(3)\alpha(3)\chi_N(4)\beta(4) \quad (1)$$

$$\psi_{CT} = 1/\sqrt{4!}\ \sum(-1)^p P\varphi_1(1)\alpha(1)\varphi_1(2)\beta(2) \times \chi_N(3)\alpha(3)\varphi_2(4)\beta(4) \quad (2)$$

$$\psi_{LE} = 1/\sqrt{4!}\ \sum(-1)^p P\varphi_1(1)\alpha(1)\varphi_2(2)\beta(2) \times \chi_N(3)\alpha(3)\chi_N(4)\beta(4) \quad (3)$$

Here, $\sum(-1)^p P$ is the usual antisymmetrizing summation over all permutations of the electrons. The wave functions $\varphi_1$ and $\varphi_2$ in Eqs. 1—3. can be determined following the procedure described in the Appendix.

Next one must take into account configuration interaction in terms of the three electron configurations mentioned above. According to this procedure, the energy levels of the molecule turn out to be obtained as solutions of the following secular equation:

18) According to the X-ray crystal analysis data of thioacetamide, hydrogen atoms of amino group are almost coplanar with heavy atoms.[15] This means that the nonbonding electrons of nitrogen may reasonably be assumed to belong to the pure $2p\pi$ atomic orbital.

$$\begin{vmatrix} H_G-E & H_{G\cdot LE} & H_{G\cdot CT} \\ H_{G\cdot LE} & H_{LE}-E & H_{LE\cdot CT} \\ H_{G\cdot CT} & H_{LE\cdot CT} & H_{CT}-E \end{vmatrix}=0 \qquad (4)$$

where, $H_G=\int \psi_G H \psi_G d\tau$, $H_{G\cdot LE}=\int \psi_G H \psi_{LE} d\tau$, etc.

Suppose the energy of the ground configuration is taken as a standard. The value of $H_{CT}$, the energy of the charge-transfer configuration, can be evaluated by the following equation:[2]

$$H_{CT}=I_N-A_{C=S}-\{d^2_{11}(CC \mid NN)+d^2_{12}(SS \mid NN)\} \qquad (5)$$

where $I_N$ and $A_{C=S}$ are the ionization potential of the nonbonding electron of the amino nitrogen atom and the electron affinity of the C=S group, respectively. The former is set equal to the ionization potential of ammonia which is determined as 10.15 eV by Watanabe from the photoionization experiment.[19] The quantities $d_{11}$ and $d_{12}$ are coefficients of atomic orbitals in $\varphi_1$ or $\varphi_2$ molecular orbital and are evaluated to be 0.6902 and 0.7236 (see Appendix), respectively. Two center Coulomb integrals (CC | NN) and (SS | NN) are calculated with the aid of uniformly charged sphere approximation, by taking the C–N and C=S bond distances as 1.324 and 1.713 Å, respectively, and further by taking ∠SCN as 121.6°[15]. The value of $A_{C=S}$ is assumed to be −0.32 eV which seems to be reasonable compared with that of the C=O bond, −1.20 eV.[2]

The energy value of the locally excited configuration, $H_{LE}$, is set equal to the observed excitation energy corresponding to the $\pi\rightarrow\pi^*$ transition pertinent to the C=S group. It is natural to take this value from the experimental result on the absorption spectrum of thioacetone. Unfortunately, however, this expectation can not be satisfied, because thioacetone usually exists as trimer like $Me_2C<^{S-C-Me_2}_{S-C-Me_2}>S$[8]. Then in the present calculation this value is taken to be 5.24 eV from the experimental result of the absorption spectrum of thioacetamide in hydrochloric acid solution. As mentioned above, thioacetamide in this condition exhibits the peak absorption at 237 mμ. This absorption band is conceivably ascribed to the protonated thioacetamide represented by $R>C-\overset{+}{N}H_3$. Since in this protonated cation the resonance effect of the amino group can be neglected to the first approximation, the 237 mμ band may be regarded as due to the $\pi\rightarrow\pi^*$ transition pertinent to the C=S bond. The present consideration on this point is consistent with the observation by Katagiri et al.[7] that thiocamphor shows a peak absorption at 242 mμ (5.12 eV).

Following the procedure developed by Longuet-Higgins and Murrell,[6] and also by Pople,[20] values of $H_{G\cdot CT}$, $H_{G\cdot LE}$ and $H_{CT\cdot LE}$ can easily be evaluated as follows:

$$H_{G\cdot CT}=\sqrt{2}\, d_{12}\beta_{CN}$$
$$=1.414\times 0.7236\times(-2.1)=-2.15 \text{ eV}$$
$$H_{G\cdot LE}=0$$
$$H_{CT\cdot LE}=-d_{11}\beta_{CN}=-0.6902\times(-2.1)=1.45 \text{ eV}$$

Here $\beta_{CN}$ is the core resonance integral between the π-electron orbital of carbon and the nonbonding orbital of nitrogen. In the present calculation $\beta_{CN}$ is assumed to be an appropriate value of −2.1 eV.

By inserting the energy integral values into Eq. 4 and by solving it, the three energy levels of thioacetamide can be determined. Further, wave functions corresponding to these energy levels can easily be evaluated following the usual procedure in the variation method. The results are shown in Table III. Here values in parentheses are squares of coefficients of corresponding component wave functions. In view of the fact that these values represent magnitudes of contributions of electron configurations to a certain state of the molecule, it may be said that the lowest state ($E_1$) is principally composed of the ground configuration and the contribution of the charge-transfer configuration to that state is only 17%.[21] On the other hand, in the $E_2$ state contributions of the charge-transfer and locally excited configurations are almost equal and amount to 43%.

From the energy values for the states of thioacetamide given in Table III, excitation energies corresponding to $E_1\rightarrow E_2$ and $E_1\rightarrow E_3$ transitions can be calculated to be 4.77 eV and 7.44 eV, respectively. Values of the transition moments $Q_{1i}$'s and oscillator strength $f_{1i}$'s associated with these transitions are calculated by the following equations[22]:

$$Q_{1i}=\int \Psi_1 \, er \, \Psi_i \, d\tau \qquad i=2, 3 \qquad (6)$$

$$f_{1i}=4.704\times 10^{-7}\,\tilde{\nu}_{1i}Q^2_{1i} \qquad (7)$$

where $\tilde{\nu}_{1i}$ is the wave number ($cm^{-1}$) of the absorption peak under consideration and $Q_{1i}$ is represented in Debye units. The calculated

19) K. Watanabe, *J. Chem. Phys.*, **26**, 542 (1957).

20) J. A. Pople, *Proc. Phys. Soc.*, **A68**, 81 (1955).

21) This apparently corresponds to the fact that the electronic structure of thioacetamide can be represented by a resonance hybrid between the following two structures:

$H_3C>^{S}C-NH_2 \longleftrightarrow H_3C>^{S^-}C=\overset{+}{N}H_2$

22) R. S. Mulliken, *J. Chem. Phys.*, 7, 14 (1939); J. R. Platt and H. B. Klevens, *Rev. Modern Phys.*, **16**, 182 (1944).

TABLE III. ENERGY LEVELS AND WAVE FUNCTIONS FOR THIOACETAMIDE

| Energy level | Symmetry | Wave function |
|---|---|---|
| $E_1=-0.9929$ eV | $A'$ | $\Psi_1=0.9036\,\phi_G-0.0971\,\phi_{LE}+0.4173\,\phi_{CT}$ (0.8165 0.0094 0.1741) |
| $E_2=3.7811$ eV | $A'$ | $\Psi_2=-0.3740\,\phi_G-0.6538\,\phi_{LE}+0.6578\,\phi_{CT}$ (0.1399 0.4275 0.4327) |
| $E_3=6.4519$ eV | $A'$ | $\Psi_3=-0.2090\,\phi_G+0.7503\,\phi_{LE}+0.6271\,\phi_{CT}$ (0.0437 0.5630 0.3933) |

TABLE IV. ENERGY LEVELS AND WAVE FUNCTIONS FOR THIOUREA

| Energy level | Symmetry | Wave function |
|---|---|---|
| $W_1=-1.7653$ eV | $A_1$ | $\Phi_1=0.8555\,\phi_G-0.1454\,\phi_{LE}+0.4968\,\phi^S{}_{CT}$ (0.7319 0.0211 0.2468) |
| $W_2=3.7397$ eV | $A_1$ | $\Phi_2=-0.4328\,\phi_G-0.7275\,\phi_{LE}+0.5324\,\phi^S{}_{CT}$ (0.1873 0.5293 0.2835) |
| $W_3=7.3357$ eV | $A_1$ | $\Phi_3=-0.2840\,\phi_G+0.6705\,\phi_{LE}+0.6854\,\phi^S{}_{CT}$ (0.0807 0.4496 0.4698) |
| $W_4=4.0700$ eV | $B_1$ | $\Phi_4=\phi^A{}_{CT}$ |

values of $f_{1i}$'s are listed in Table I in comparison with the observed valuse which are obtained from absorption curves with the aid of the following equation:

$$f_{1i}^{obs}=4.32\times10^{-9}\int\varepsilon d\tilde{\nu} \qquad (8)$$

where $\varepsilon$ denotes the molar extinction coefficient. Directions of transition moments can also be evaluated readily from magnitudes of their components parallel and perpendicular to the C=S bond axis in the molecular plane. Consequently it is found that directions of transition moments associated with transitions $E_1\rightarrow E_2$ and $E_1\rightarrow E_3$ are inclined by 16° to the C=S bond and by 46° to the N–C bond, respectively. These theoretical results are schematically shown in Table I.

The calculation of $\pi$-electron structure is carried out also with thiourea by the same method as described in the case of thioacetamide. Therefore, it seems tedious to describe repeatedly the details of the calculation procedure. However, it may be necessary to add some note on the fact that in the case of thiourea two group orbitals, whose wave functions are represented by $\varphi^S{}_N=(\chi_{1N}+\chi_{2N})/\sqrt{2}$ and $\varphi^A{}_N=(\chi_{1N}-\chi_{2N})/\sqrt{2}$, can be obtained from the two nonbonding orbitals belonging to the amino groups. Consequently, in this case two charge-transfer configurations must be taken into account. Suppose that the wave functions of these two charge-transfer configurations and of the ground and locally excited configurations can be designated by $\psi^S{}_{CT}$ and $\psi^A{}_{CT}$[23], $\phi_G$ and and $\phi_{LE}$, respectively (see Fig. 5). Among these wave functions, only $\psi^A{}_{CT}$ is antisymmetric with respect to the symmetry plane perpendicular to the molecular plane and including the C=S bond axis, while $\psi^S{}_{CT}$, $\phi_G$ and $\phi_{LE}$ are all symmetric with the same symmetry plane. Therefore it is readily concluded that the electron configuration represented by $\psi^A{}_{CT}$ can not mix with the other configurations. On the other hand, three configurations represented by $\phi_G$, $\psi^S{}_{CT}$ and $\phi_{LE}$ interact with one another. The configuration interaction in terms of these three configurations finally results in three new states. The energy values and wave functions of these new states are given in Table IV[24].

From the energy values given in Table IV, excitation energies corresponding to $W_1\rightarrow W_2$, $W_1\rightarrow W_4$ and $W_1\rightarrow W_3$ are evaluated to be 5.51, 5.84 and 9.11 eV., respectively. It is inferred from this that the observed two absorption bands (236 and 195 m$\mu$) in near ultraviolet region may reasonably be ascribed to the $W_1\rightarrow W_2$ and $W_1\rightarrow W_4$ transitions. The directions of transition moments for these two transitions

23) $\psi^S{}_{CT}=1/\sqrt{6!}\,\Sigma(-1)^P p\phi_1(1)\alpha(1)\phi_1(2)\beta(2)\phi^S{}_N(3)\alpha(3)\phi_2(4)\beta(4)\phi^A{}_N(5)\alpha(5)\phi^A{}_N(6)\beta(6)$
$\psi^A{}_{CT}=1/\sqrt{6!}\,\Sigma(-1)^P p\phi_1(1)\alpha(1)\phi_1(2)\beta(2)\phi^S{}_N(3)\alpha(3)\phi^S{}_N(4)\beta(4)\phi^A{}_N(5)\alpha(5)\phi_2(6)\beta(6)$

24) The values of matrix elements used for the evaluation of energy levels of thiourea are as follows:
$H_G=0$
$H^S{}_{CT}=H^A{}_{CT}=4.07$ eV.
$H_{LE}=5.24$ eV.
$H_{G\cdot CT}=2d_{12}\beta_{CN}=2\times0.7236\times(-2.1)=-3.04$ eV.
$H_{G\cdot LE}=0$
$H_{LE\cdot CT}=-\sqrt{2}\,d_{11}\beta_{CN}=-1.414\times0.6902\times(-2.1)=2.05$ eV.
The values of $I_N$ and $A_{C=S}$ necessary for the evaluation of $H^S{}_{CT}$ and $H^A{}_{CT}$ are the same as those employed in the case of thioacetamide (see Eq. 5). The values of (NN | CC) and (NN | SS), however, are newly calculated for thiourea by the method as described in the case of thioacetamide, by the use of the C-N and S-N distances determined by X-ray crystal analysis ($d_{C-N}=1.35$ Å, $d_{C=S}=1.64$ Å, $\angle NCS=126°$; see Ref. 16 for these data).

can easily be found from the symmetry properties of the upper and lower states for each transition. That is to say, the direction of transition moment for the $W_1 \rightarrow W_2$ transition is expected to be exactly parallel to the C=S bond axis, while that for the $W_1 \rightarrow W_4$ transition is perpendicular to the same axis. Combining this theoretical expectation with the experimental results regarding polarized ultraviolet absorption, it is possible to determine clearly the assignment of these two absorption bands. This point will be explained in the next chapter.

## Discussion

**Assignment of Absorption Bands of Thioacetamide.** — Experimental and theoretical results concerning the absorption spectra of thioacetamide are summarized in Table I and Figs. 1 and 3. From these results it is seen that the directions of transition moments determined theoretically for $E_1 \rightarrow E_2$ and $E_1 \rightarrow E_3$ transitions, whose excitation energies are calculated to be 4.77 eV. (260 m$\mu$) and 7.44 eV. (167 m$\mu$), respectively, are approximately equal to the directions of transition moments observed with the 261 m$\mu$ and 210 m$\mu$ bands, respectively. This fact gives a powerful support for the assignment that the 261 m$\mu$ and 210 m$\mu$ bands ought to be ascribed to the transitions $E_1 \rightarrow E_2$ and $E_1 \rightarrow E_3$, respectively. According to the above assignment, the agreement between the theoretical and experimental excitation energies is satisfactory for the 261 m$\mu$ band, but some discrepancy is seen for the 210 m$\mu$ band. A principal reason for this discrepancy is thought to be the neglect of electron configurations with higher energies, say configurations including two electron jumps. Although there is the above-mentioned difficulty from the quantitative point of view, the assignment of the two absorption bands of thioacetamide may be thought to be finally determined by the present experimental and theoretical studies.

Concerning the assignment of the weak band at 318 m$\mu$, much can not be said. As pointed out by Katagiri et al.[7], however, this band is tentatively due to an $n \rightarrow \pi^*$ transition, namely due to the excitation of a nonbonding electron of the sulfur atom to the excited $\pi$-electron orbital of the C=S bond.

**Assignment of Absorption Spectrum of Thiourea.** — The results regarding the absorption spectrum of thiourea are given in Table I and Figs. 1 and 4. This molecule shows fairly strong absorption bands at 236 and 195 m$\mu$. Calculated excitation energies for the $W_1 \rightarrow W_2$ and $W_1 \rightarrow W_4$ transitions are 5.51 (225 m$\mu$) and 5.84 eV. (212 m$\mu$), respectively. In this case, it is dangerous to determine the assignment of these two bands from the theoretical excitation energies alone, because the energy difference between $W_2$ and $W_4$ states is only 0.33 eV. and there may be some possibility that energy levels of these two states are reversed with each other by changing to only a small extent some parameters adopted in the present calculation. Fortunately, however, this difficulty is completely removed by considering the result of the polarized ultraviolet absorption measurement on the single crystal.

As is seen from Fig. 4, experimental results on the polarized ultraviolet absorption spectrum shows that the directions of transition moments of the longer and shorter wavelength bands are parallel and perpendicular to the C=S bond axis, respectively. Theoretical consideration in

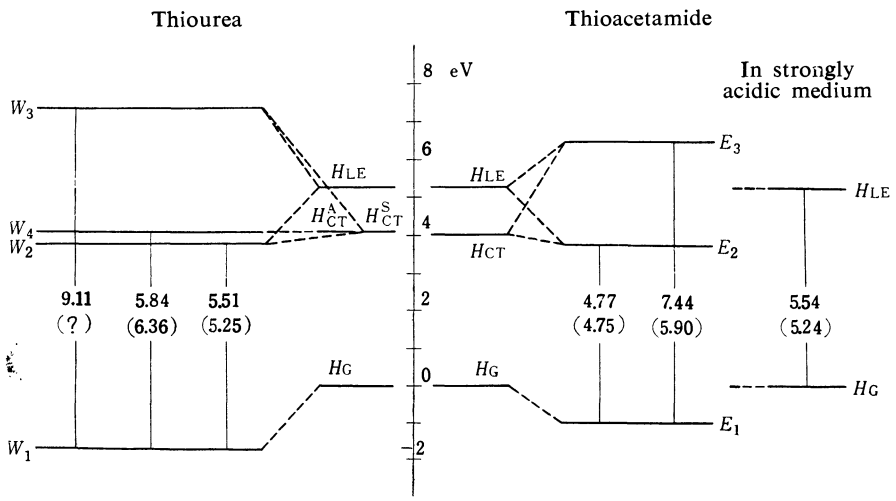
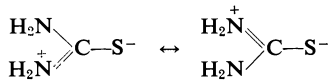



Fig. 6. Energy level diagrams for thioacetamide and thiourea, showing the relation between observed (in parentheses) and calculated transition energies.

the preceding chapter concludes that the transition moments associated with $W_1 \rightarrow W_2$ and $W_1 \rightarrow W_4$ ought to have directions exactly parallel and perpendicular to the C=S bond axis, respectively. These facts lead to the conclusion that the 236 m$\mu$ and 195 m$\mu$ bands correspond to the $W_1 \rightarrow W_2$ and $W_1 \rightarrow W_4$ transitions, respectively.

Of these two absorption bands, the shorter wavelength (195 m$\mu$) band may be called a typical intramolecular charge-transfer band, because the upper state ($W_4$) of the corresponding transition is completely constructed from the charge-transfer configuration. This charge-transfer configuration includes electron transfer from the orbital represented by an antisymmetric combination of the nonbonding electron orbitals of the two nitrogen atoms to the $\varphi_2$ orbital pertinent to the C=S bond. From the resonance viewpoint, this means that the upper state of the 195 m$\mu$ band can be represented approximately by the resonance hybrid between the following two structures:



On the other hand, the 236 m$\mu$ band exhibits strongly the character of the locally (C=S) excited band, because in the excited state corresponding to this band the contribution of the locally excited configuration is great and amounts to 53%. In this sense, the 236 m$\mu$ band of thiourea may be regarded as the shifted one of the 237 m$\mu$ band pertinent to the C=O bond.

The relation between the energy state and the ultraviolet absorption spectrum described hitherto on thioacetamide and thiourea are schematically shown in Fig. 6.

**Absorption Spectrum of Thioacetamide in Hydrochloric Acid Solution.**—The fact that the 261 m$\mu$ and 210 m$\mu$ bands ($E_1 \rightarrow E_2$ and $E_1 \rightarrow E_3$ transitions, respectively) of thioacetamide disappear and a new band appears at 237 m$\mu$ in concentrated hydrochloric acid solution (240 m$\mu$ in concentrated sulfuric acid solution) seems to give an important information regarding the position of the proton attached to the parent molecule. Concerning the position of the proton, there are conceivably two alternatives, namely the nitrogen atom of the amino group and the sulfur atom of the thiocarbonyl group. In the latter case, it may be expected that the electron affinity of the C=S group increases considerably and the energy of the charge-transfer configuration given by Eq. 5 apparently decreases. From this it may be predicted that the 261 m$\mu$ band of thioacetamide will shift toward longer wavelengths if the proton be attached to the sulfur atom. The experimental result is completely reverse to this prediction. This seems to support the other possibility, namely the fact that proton is attached to the nitrogen atom. This conclusion is in agreement with the result obtained from the absorption measurement in the infrared region[25].

## Appendix

**The Molecular Orbital Functions Pertinent to the C=S Bond.** — $\pi$-Electron orbitals of the C=S bond are represented by the linear combination of the $2p$ atomic orbital of carbon ($\chi_C$) and the $3p$ atomic orbital of sulfur ($\chi_S$):

$$\varphi_1 = d_{11}\chi_C + d_{12}\chi_S \tag{9}$$

$$\varphi_2 = d_{12}\chi_C - d_{11}\chi_S \tag{10}$$

The problem is to calculate the values of coefficients $d_{11}$ and $d_{12}$. The calculation is carried out by the aid of the combination of Roothaan's LCAO SCF method[26] with Pariser and Parr's approximation[27]. The values of energy integrals actually adopted to the calculation are as follows:

$$\alpha_C = -I_C + \int \chi_C U_S \chi_C d\tau = -11.54 - 7.76 = -19.30 \text{ eV}. \tag{12}$$

$$\alpha_S = -I_S + \int \chi_S U_C \chi_S d\tau = -12.50 - 7.65 = -20.15 \text{ eV}. \tag{11}$$

$\beta_{CS} = -2.0$ eV. (assumed value)

$$(CC|CC) = \int \chi_C(1)\chi_C(2)\frac{e^2}{r_{12}}\chi_C(1)\chi_C(2)d\tau = 11.54 - 0.46 = 11.08 \text{ eV}.$$

$$(CC \mid SS) = \int \chi_C(1)\chi_S(2)\frac{e^2}{r_{12}}\chi_C(1)\chi_S(2)d\tau = 7.37 \text{ eV}.$$

$$(SS \mid SS) = \int \chi_S(1)\chi_S(2)\frac{e^2}{r_{12}}\chi_S(1)\chi_S(2)d\tau = 12.50 - 2.70 = 9.80 \text{ eV}.$$

Here U and $\alpha$ represent core potential and core Coulomb integral concerning atoms each of which is referred to by a suffix, respectively. $\beta_{CS}$ is the core resonance integral between the $\chi_C$ and $\chi_S$ orbitals. $I_C$ and $I_S$ are the ionization potential of the $2p$ electron of carbon and of the $3p$ electron of sulfur, respectively. These values are taken from Pritchard and Skinner's table[28]. Integrals $\int \chi_C U_S \chi_C d\tau$ and $\int \chi_S U_C \chi_S d\tau$ are assumed to be equal to electrostatic attraction between two spherically charged ($-e/2$ each) tangent balls on one atom and the opposite charge ($+e$) on the other

25) E. Spinner, *Spectrochim. Acta*, **12**, 95 (1959).
26) C. C. J. Roothaan, *Rev. Modern Phys.*, **23**, 69 (1951).
27) R. Pariser and R. G. Parr, *J. Chem. Phys.*, **21**, 466, 767 (1953).
28) H. O. Pritchard and H. A. Skinner, *Chem. Revs.*, **55**, 745 (1955).

atom. Following Pariser and Parr's procedure[27], one center Coulomb repulsion integral, (CC | CC) or (SS | SS) is set equal to the difference between the ionization potential and the electron affinity. These two quantities are taken from Pritchard and Skinner's table. The two center Coulomb repulsion integral (CC | SS) is evaluated under the uniformly charged sphere approximation[29], taking the C=S bond distance as 1.71 Å, the value obtained by Truter from the X-ray analysis data on thioacetamide[15].

In order to obtain more accurate values for the core Coulomb integrals, the polarization effect of the $\sigma$-electrons of the C=S orbital upon them is taken into account. According to Moffit's method[30], the corrected ionization potentials can be obtained by the following equation[31]:

$$I'_C = -11.54 - 0.1436(11.08 - 7.37) = -12.08 \text{ eV}.$$

$$I'_S = -12.50 + 0.1436(9.80 - 7.37) = -12.15 \text{ eV}.$$

Substituting these values for $I_C$ and $I_S$ in Eqs. 11 and 12, the corrected core Coulomb integrals become as follows:

$$\alpha'_C = -19.84 \text{ eV}. \qquad \alpha'_S = -19.80 \text{ eV}.$$

By using these integral values, the iterative procedure following Roothaan's method is continued until self-consistent results are obtained with $d_{11}$, $d_{12}$ and orbital energies ($\varepsilon_1$, $\varepsilon_2$). The final results thus obtained are as follows[32]:

$$d_{11} = 0.6902 \qquad d^2_{11} = 0.4764$$

$$d_{12} = 0.7236 \qquad d^2_{12} = 0.5236$$

$$\varepsilon_1 = -12.946 \text{ eV}. \qquad \varepsilon_2 = -1.566 \text{ eV}.$$

$$\varphi_1 = 0.6902\chi_C + 0.7236\chi_S$$

$$\varphi_2 = 0.7236\chi_C - 0.6902\chi_S$$

Further the excitation energy $\Delta E$ corresponding to the $\varepsilon_1 \rightarrow \varepsilon_2$ transition can be calculated by the following equations:

$$\Delta E = \varepsilon_2 - \varepsilon_1 - (11 \mid 12) + 2(12 \mid 12) = 5.54 \text{ eV}.$$

$$(11 \mid 22) = d^2_{11}d^2_{12}\{(CC \mid CC) + (SS \mid SS)\} + (d^4_{11} + d^4_{12})(CC \mid SS)$$

$$(12 \mid 12) = d^2_{11}d^2_{12}\{(CC \mid CC) + (SS \mid SS) + 2(CC \mid SS)\}$$

The calculated value, 5.54 eV., may be said to be in fairly good agreement with the observed one, 5.24 eV.

29) R. G. Parr, *J. Chem. Phys.*, **20**, 1499 (1952).
30) W. Moffitt, *Proc. Roy. Soc.* (*London*), **A202**, 534 (1950).
31) In this calculation the following energy values are used:

$I^\sigma_S = 20.0$ eV. $\quad A^\sigma_S = 4.0$ eV.
$I^\sigma_C = 15.42$ eV. $\quad A^\sigma_C = 3.32$ eV.
$\beta^\sigma_{CS} = -2.0$ eV.

where $I$ and $A$ represent ionization potential and electron affinity, respectively, and the superscript $\sigma$ means that the corresponding quantity is concerned with $\sigma$-electrons. The quantities on carbon are taken from Pritchard and Skinner's table[28] and those on sulfur are roughly estimated from corresponding values for oxygen which are also obtained from the table.
32) Katagiri et al. calculated independently the wave functions and orbital energies of the C=S bond and obtained the following results:

$\phi_1 = 0.6330\chi_C + 0.7741\chi_S$
$\phi_2 = 0.7741\chi_C - 0.6330\chi_S$
$\varepsilon_1 = -11.98$ eV $\quad \varepsilon_2 = -1.90$ eV

S. Katagiri, Y. Amako and H. Azumi, Presented at the Symposium on Electronic States, Tokyo, September, 1959.


## Summary

Ultraviolet absorption spectra of thioacetamide and thiourea are measured under various conditions. In aqueous solution, three bands (210, 261 and 318 m$\mu$) for thioacetamide and two bands (195 and 236 m$\mu$) for thiourea are observed. Further, polarized ultraviolet absorption spectra are measured with their crystals. On the basis of the results regarding the polarized ultraviolet absorption spectra, the directions of transition moments can be determined as follows: 1) the directions of transition moments of the 261 and 210 m$\mu$ bands of thioacetamide are approximately parallel to the axis connecting the nitrogen and sulfur atoms and connecting the nitrogen and methyl carbon atoms, respectively, 2) the directions of transition moments of the 236 and 195 m$\mu$ bands of thiourea are parallel and perpendicular to the C=S axis, respectively. From the combination of the experimental results concerning the directions of transition moments with theoretical consideration based on semi-empirical LCAO treatment including configuration interaction, the assignment of the four absorption bands under consideration are finally determined. One of the noticeable conclusions is that the 195 m$\mu$ band of thiourea can be regarded as a typical intramolecular charge-transfer absorption.

It is shown that in the hydrochloric acid solution of thioacetamide the 261 m$\mu$ band decreases its intensity and a new band appears at 237 m$\mu$. By measuring the dependence of intensities of these two bands upon the acid strength of the solution, it is concluded that the 237 m$\mu$ band is due to the conjugate acid of thioacetamide. The p$K_B$ value of thioacetamide is determined spectrophotometrically to be 1.2 at 24.5°C. From the comparison of the wavelength of the peak absorption of thioacetamide with that of its conjugate acid, it is seen that the proton is conceivably attached to the amino group.


The authors wish to express their sincere thanks to Dr. M. R. Truter for her kindness in giving valuable information on the X-ray crystal analysis data of thioacetamide prior to publication. Their thanks are also due to Dr. T. Sakurai in our Institute for his kind cooperation in identifying the crystal axis of thiourea.

*The Institute for Solid State Physics*
*The University of Tokyo*
*Shinryudo-cho, Minatoku*
*Tokyo*

# SHORT COMMUNICATIONS

## *The Crystal Structure of Tetra-thiourea-palladium(II) Chloride*, $[Pd(SCN_2H_4)_4]Cl_2$

By Shun'ichiro Ooi, Tsuyoshi Kawase, Kazumi Nakatsu and Hisao Kuroya

(Received April 11, 1960)

It is well known that thiourea is capable of forming a number of coordination compounds with metallic ions. Recently, we reexamined the preparation methods of some of them, the chemical analyses being carried out carefully, and obtained quite well-formed crystals of the palladium(II) complex salt, $Pd(SCN_2H_4)_4Cl_2$. We have therefore, attempted to investigate the crystal structure of this compound. There are only a few structural studies[1-4] of the thiourea coordination compounds.

The crystal was prepared by the method of Kurnakow[5]. The products are monoclinic, showing the predominant (100) face. The crystallographic data are: $a=16.89$, $b=11.18$ $c=8.89$ Å, $\beta=91.5$, $Z=4$, $\rho_{obs}=1.92$ and $\rho_{calc}=1.91$ g./cm$^3$. Space group $C2/c$ or $Cc$ was given by the observation of the systematically absent reflections. However, the method of Howells

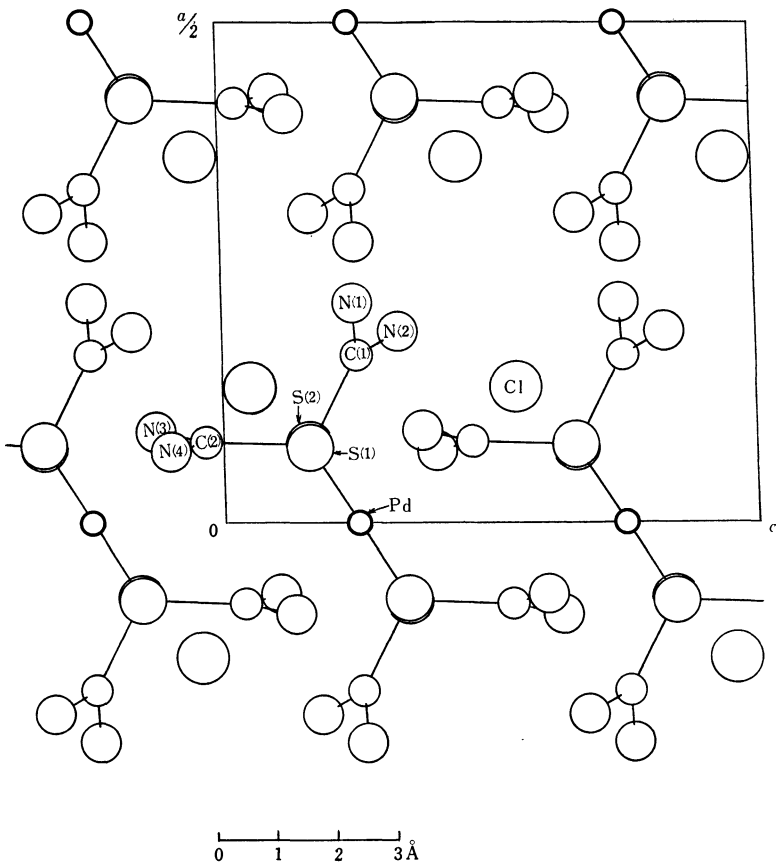



Fig. 1. Projection of the structure upon a plane normal to the *b*-axis.

1) M. Nardelli, L. Cavalca and A. Braibanti, *Gazz. chim. ital.*, **86**, 1037 (1956).
2) M. Nardelli, L. Cavalca and A. Braibanti, ibid., **87**, 137 (1957).
3) C. B. Knobler, Y. Okaya and R. Pepinsky, *Z. Krist.*, **111**, 385 (1959).
4) M. Nardelli and G. Fava, *Acta Cryst.*, **12**, 727 (1959).
5) Kurnakow, *J. prakt. Chem.*, [2] **50**, 496 (1894).

TABLE I. ATOMIC COORDINATES

| | *x/a* | *y/b* | *z/c* |
|---|---|---|---|
| Pd | 0 | 0.324 | 0.250 |
| S (1) | 0.073 | 0.482 | 0.158 |
| S (2) | 0.079 | 0.167 | 0.155 |
| Cl | 0.135 | 0.182 | 0.050 |
| N (1) | 0.220 | 0.561 | 0.242 |
| N (2) | 0.189 | 0.380 | 0.328 |
| N (3) | 0.092 | 0.078 | −0.136 |
| N (4) | 0.071 | 0.288 | −0.105 |
| C (1) | 0.167 | 0.476 | 0.247 |
| C (2) | 0.081 | 0.183 | −0.037 |

et al.[6], applied to (*hk*0) reflections, was indicative of the presence of a center of symmetry, which was, in turn, favorite to $C2/c$. The structure analysis was carried out by using (*h0l*) and (*hk*0) data obtained from Weissenberg photographs which were taken with Cu$K\alpha$ radiation. From Patterson projections on (010) and (001), the positions of palladium, chlorine and sulfur atoms could be deduced. A usual Fourier method was, then, applied to further analysis. Atomic coordinates listed in Table I gave the reliability index $R=0.18$ and 0.16 for (*h0l*) and (*hk*0), respectively.

In Fig. 1, the structure projected on (010) is shown. The crystal is essentially ionic and consisted of $[Pd(SCN_2H_4)_4]^{2+}$ and $Cl^-$. A palladium atom is surrounded by four sulfur atoms in an approximately rectangular configuration with 3.00 and 3.15 Å for the lengths of shorter sides, and 3.50 Å for the longer ones. A complex ion has a two-fold rotation axis bisecting the two shorter sides and passing through the palladium atom. All S—C bonds projected on the plane formed with 4S's and Pd, are parallel to the shorter sides. Bond distances and angles found in a complex ion are: Pd—S=2.33 and 2.35 Å, ∠S—Pd—S=82°, 85° and 97°, ∠Pd—S—C=106 and 107°, S—C=1.72 and 1.75 Å, C—N=1.32, 1.37 and 1.47 Å, ∠S—C—N=120, 121, 123 and 126° and ∠N—C—N 117°. No significant discrepancies could be found in the dimensions between the thiourea molecule reported by Kunchur and Truter[7] on the thiourea crystal and the one in the present work. The bond angles formed at S's can be compared with those in $Cu(SCN_2H_4)_3Cl$[3] and in $Pb(SCN_2H_4)_2Cl_2$[4].

*Institute of Polytechnics*
*Osaka City University*
*Osaka, Japan*

6) E. R. Howells, D. C. Phillips and D. Rogers, *Acta Cryst.*, 3, 210 (1950).
7) N. R. Kunchur and M. Truter, *J. Chem. Soc.*, **1958**, 2551.

# *The Structure and a Novel Type Rearrangement of a Ketol Produced by the Robinson Annelation Reaction*

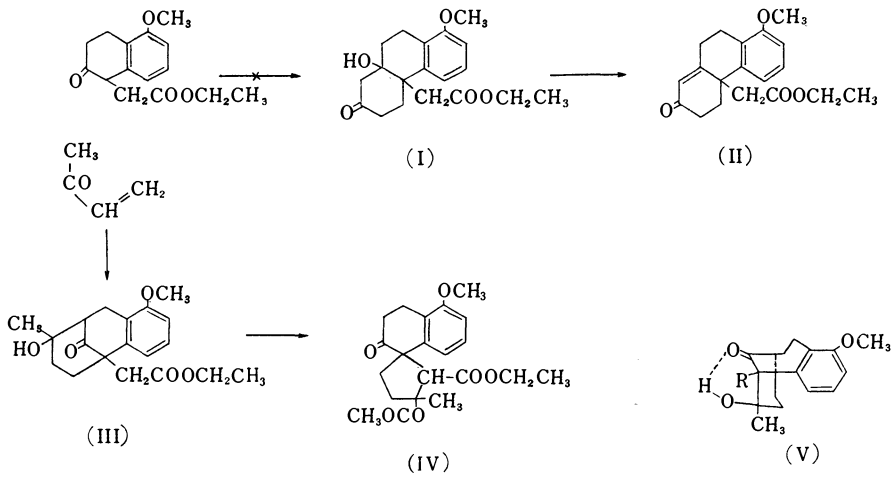
By Takeshi MATSUMOTO and Akira SUZUKI

(Received May 17, 1960)

In the course of a study directed to the synthesis of a certain diterpenoid skeleton[1], the authors condensed ethyl 1, 2, 3, 4-tetrahydro-2-oxo-5-methoxy-1-naphthyl acetate[2] with methyl vinyl ketone, expecting the formation of either ketol I or its dehydration product II. However, the obtained ketol [m. p. 134~135°C; $\nu_{max}^{Nujol}$ 3380 (OH), 1733 and 1185 (ester), and 1700 $cm^{-1}$ (ketone); $\lambda_{max}^{MeOH}$ 271 ($\varepsilon$ 1410) and 278 m$\mu$ ($\varepsilon$ 1310); Found: C, 68.44; H, 7.10. Calcd. for $C_{19}H_{24}O_5$: C, 68.65; H, 7.28%] was actually a bridged ring compound III. Moreover, attempted acetylation of III with isopropenyl acetate in the presence of *p*-toluenesulfonic acid resulted in a remarkable change in the carbon skeleton of compound III, a spirocyclic acetate IV [m. p. 97.5~98.5°C; $\nu_{max}^{Nujol}$ 1730 (ester) and 1715 $cm^{-1}$ (ketone); Found: C, 67.10; H, 6.94. Calcd. for $C_{21}H_{26}O_6$: C, 67.36; H, 7.00%] being produced. The formation of a similar bridged ring ketol system through the Robinson annelation reaction was first disclosed only quite recently by W. S. Johnson and his co-workers[3]. Conversion of the skeletons III to IV seems, so far as the authors are aware, to have never been described in the literature.

The structures of both compounds III and IV were determined by the NMR spectra[4]. The spectrum of ketol III showed one sharp maximum at high applied magnetic field characteristic of proton resonance for the $-\overset{|}{\underset{|}{C}}-CH_3$ group (203 c. p. s., standard, benzene; observed relative peak area, 3.4) and is completely accounted for in terms of structure III. Further, presence of an intramolecular hydrogen bond, as indicated by the infrared spectrum ($\nu_{max}$ 3430 $cm^{-1}$, in 0.0046 M solution in tetrachloroethylene) clearly defines the conformation of the ketol as V. In the NMR spectrum of acetate IV, presence of a $-\overset{|}{\underset{|}{C}}-CH_3$ group and

1) T. Matsumoto and A. Suzuki, This Bulletin, **32**, 1283 (1959); **33**, 33 (1960).
2) T. Matsumoto and A. Suzuki, to be published.
3) W. S. Johnson, J. J. Korst, R. A. Clement and J. Dutta, *J. Am. Chem. Soc.*, **82**, 614 (1960).
4) Taken on a Varian 40 MC instrument in $CDCl_3$ solution.




absence of the $-\overset{|}{\underset{|}{C}}-CH_2-CO_2-$ group are indicated respectively by the appearance of a sharp peak at 190 c. p. s. (relative peak area, 3.1) and by the disappearance of the singlet peak at 151 c. p. s. (relative peak area, 1.7) of III. The only one structure consistent with the observed findings is expressed by formula IV. The resonance line due to $-\overset{|}{\underset{|}{C}}-CH_3$ group of the acetate is shifted to the lower magnetic field by 13 c. p. s. as compared with that of the ketol. This shift might be an indication of the *cis* location of the methyl and ethoxycarbonyl groups.

*Chemistry Department*
*Faculty of Science*
*Hokkaido University*
*Sapporo*

## *The Existence of Acid Centers of a Lewis Type on Silica-Alumina Surface*

By Michio Okuda and Taro Tachibana

(Received May 10, 1960)

Recently, attention has been paid to the nature of acid centers on silica-alumina surface[1]. In order to study this problem spectroscopically, we have measured electronic spectra of some reagents adsorbed from their cyclohexane solutions on silica-alumina according to a procedure described by Robin[2].

A sample of silica-alumina was kindly supplied by Professor Shiba of Tokyo Institute of Technology and stated to contain approximately 13% alumina and no ferric ion. This sample was used as an adsorbent without further heat treatment (SA-1), or after heat treatment for 3 hr. at 110°C (SA-2), for 3 hr. at 430°C (SA-3) in dry air.

By using benzeneazodiphenylamine ($pK_a$: 1.52) as Walling's acid-base indicator, it was found that the adsorbent shows surface acidity. As is clearly seen from Fig. 1, benzeneazodiphenylamine adsorbed exhibits the two absorption bands at 440 m$\mu$ and 538 m$\mu$, which are evidently associated with the free base of the dye and its conjugated acid respectively. The latter specimen is produced by the reaction of the free base with a proton of protonic acid or aluminum atom as Lewis acid. The heat treatment of adsorbents increases the intensity of the acid band, indicating the increase of the amount of acid centers on the silica-alumina surface.

To obtain some information on whether or not these acid centers involve those of a Lewis type, *p*-phenylenediamine, which is a typical electron donor and is suitable for detecting electron accepting ability of the opponent entity, was adsorbed on silica-alumina adsorbents and its absorption spectrum was examined. The absorption spectrum of *p*-phenylenediamine adsorbed showed two characteristic bands at 324 m$\mu$ and 468 m$\mu$, as shown in Fig. 2. The former band was identified with that of *p*-phenylenediamine in alcohol ($\lambda_{max}$: 312 m$\mu$)[3] and the latter band with that of its semiquinone

1) J. E. Mapes and R. P. Eischens, *J. Phys. Chem.*, **58**, 1059 (1954); E. I. Kotov, *Optika i Spektroskopiya*, **3**, 115 (1957).

2) M. Robin, *J. Chem. Educ.*, **33**, 526 (1956).

3) L. C. Anderson and J. W. Steedly, Jr., *J. Am. Chem. Soc.*, **76**, 5144 (1954).

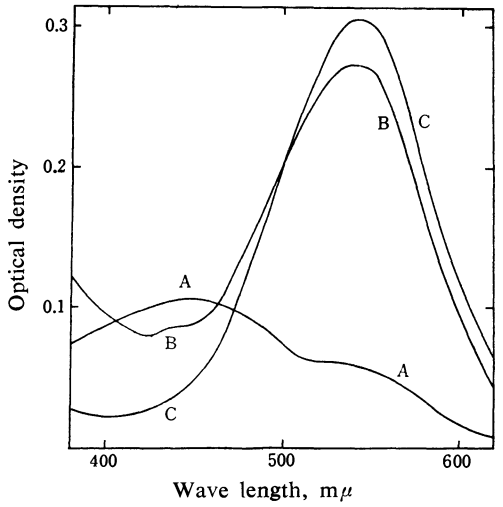



Fig. 1. Absorption spectra of benzeneazodiphenylamine adsorbed on silica-alumina (A, SA-1; B, SA-2; C, SA-3).

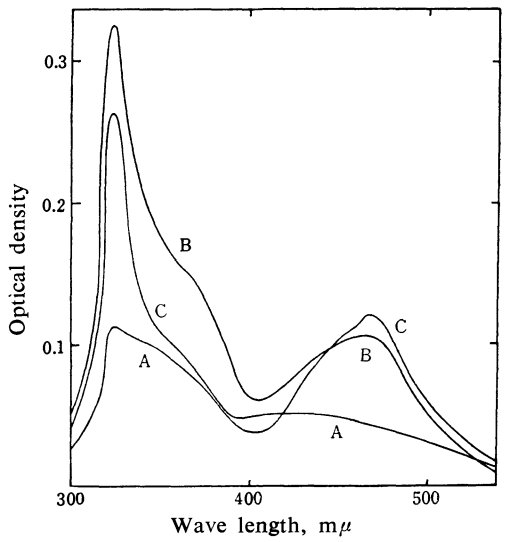



Fig. 2. Absorption spectra of *p*-phenylenediamine adsorbed on silica alumina (A, SA-1; B, SA-2; C, SA-3.)

cation radical $(NH_2C_6H_4NH_2)^+$ in water ($\lambda_{max}$: 462 mμ)[4]. Fig. 2 shows also that the intensity of absorption band of semiquinone increases with the increasing temperatures of heat treatment of adsorbent. The existence of semiquinone radicals on the adsorbent was also confirmed by the appearence of electron spin resonance spectrum. On the other hand, semiquinone radical could not be observed with the absorption spectrum of *p*-phenylenediamine adsorbed on a silica gel sample containing protonic acid.

The present results lead us to consider that the vacant $3p$ orbital of the aluminum atom on silica-alumina surface accepts one electron from the highest occupied $\pi$ orbital of the *p*-phenylenediamine molecule adsorbed and, therefore, aluminum atoms react with a base as Lewis acid centers, the structure of which has been proposed by Mills et al.[5]. It was also shown that the amount of Lewis acid centers increases with the temperature of heat treatment of the silica-alumina sample. The method of electronic spectra studied by us has given a more direct evidence for the existence of Lewis acid centers on silica-alumina sample than that obtained by other methods hitherto reported[1].

*Chemical Laboratory*
*Ochanomizu University*
*Bunkyo-ku, Tokyo*

4) L. Michaelis, M. P. Schubert and S. Granick, ibid., **61**, 1981 (1939).

5) T. H. Milliken, Jr., G. H. Mills and A. G. Oblad, *Disc. Faraday Soc.*, No. 8, 279 (1950).

# *Ein Beitrag zur Entwicklung der Harztüpfelmethode mittels Zentrifugierens der fein zerriebenen Ionenaustauscherteilchen**,[1]

Von Masatoshi FUJIMOTO

(Eingegangen am 6. Mai, 1960)

Beim Zentrifugieren einer mit einem Farbreaktionssystem berührenden, wäßrigen Suspension der fein zerriebenen Ionenaustauscherteilchen lassen sich die an den Austauscher stark adsorbierten, stark sich färbenden Bestandteile der genannten Reaktion an die Spitze des Zentrifugenröhrchens schnell und dicht ausammeln. Durch raffinierte Anwendung dieser Erscheinung auf die Harztüpfelmethode[2] wurde es bei der vorliegenden Arbeit eine Reihe von schnellen und wesentlich empfindlichen Nachweismethoden neu festgestellt.

Die wesentlich größere Ausdehnung der Oberfläche an den fein geteilten Harzteilchen

---

* Mikroanalyse mit Hilfe von Ionenaustauscherharzen. XVI.

1) XV. Mitteilung: M. Fujimoto, *Naturwissenschaften*, **47**, Heft 11, im Druck (1960).

2) In bezug auf die Einzelheiten der Harztüpfelmethode, vgl. M. Fujimoto, *Chemist-Analyst*, **49**, 4 (1960). Vgl. auch hierzu die in 1954—1957 in diesem Bulletin vom Verfasser nacheinander mitgeteilten Veröffentlichungen.

im Vergleich mit der an der gleichen Menge der Harzkugeln mit größerem Durchmesser ist an der hier vorgeschlagenen Methode besonders günstig, denn ein einziger Nachteil der empfindlichsten Harztüpfelmethode, d. h., die langsame Diffusion der gewöhnlich größeren, sich färbenden Ionen in die größeren Harzkugeln mit nur beschränktem Flächeninhalt**, kann erfolgreich beseitigt werden.

**Ausführung:** (*1*) *Darstellung der Harzsuspension mit beinahe gleicher Korngröße.* — 0.5 bzw. 1 g völlig gereinigten, farblosen Ionenaustauscherharzes wird in einem Achatmörser mit geringer Menge entionisierten Wassers etwa 15 Min völlig zerrieben. Das Harz geht in eine weiße und zähe Paste über. Danach wird dieser Harzschleim mit entionisiertem Wasser zur Suspension umgeschüttelt. Diese wird durch wiederholtes Zentrifugieren unter bestimmtem Bereich der Drehungsanzahl, 0∼1000, 1000∼2000 Drgg. pro Min, u. s. w., und jedesmaliges Auswaschen mit entionisiertem Wasser raffiniert, um die Korngröße der Harzteilchen möglichst gleichmäßig regulieren zu lassen. Die hier erhaltenen Harzteilchen werden mit entionisiertem Wasser zur bestgeeigneten Konzentration verdünnt.

(*2*) *Anreicherung der mit den sich färbenden Reaktionsprodukten beladenen Harzteilchen durch Zentrifugieren.*—In einem Spitzröhrchen (Abb. 1) wird ein Tropfen der Probelösung (od. der

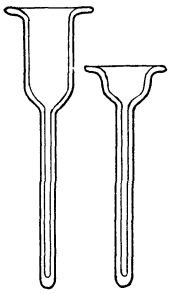


Abb. 1. Mikrospitzröhrchen (1/2 nat. Gr.)

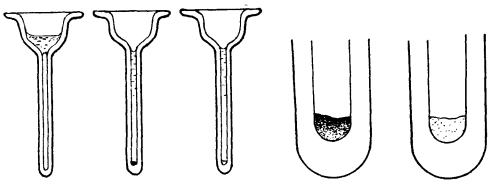



Abb. 2. Die Zustände der Harzteilchen im Mikrospitzröhrchen.
a: Die in dem Gemische der Probe- und Reagens-lösungen schwebenden Harzteilchen.
b: Die an die Spitze abgeschleuderten Harzteilchen beim Nachweise.
c: Diegleichen Harzteilchen beim Blindversuche.
b' und c': Die zehnfach vergrößerten Bilder der Spitzen an b und c.

TABELLE I. VERGLEICHUNG DER BEI DEN VERSCHIEDENEN NACHWEISMETHODEN ERHALTENEN EMPFINDLICHKEITEN

| Ionen | | Kobalt(II) | | Kupfer(II) | |
|---|---|---|---|---|---|
| Reagens | | 1 M $NH_4NCS$ | | 0.001proz. PAN**** | |
| Harzart | | stark basisches Harz in Chloridform | | stark saures Harz in H- od. $NH_4$-Form | |
| Erfassungsgrenze* bei | gewöhnlicher Tüpfelmethode | 0.5 $\mu$g[a)] | (0.30) | 0.004 $\mu$g[c)] | (2.40) |
| | Harztüpfelmethode** | 0.16 $\mu$g[b)] | (0.80) | 0.0016 $\mu$g[c)] | (2.80) |
| | vorliegendem Verfahren*** | 0.023 $\mu$g | (1.64) | 0.00008 $\mu$g | (4.10) |

* Die einklammerten Werte sind die pE. G. entsprechenden Nachweises, worunter man die negativen gemeinen Logarithmen der auf Mikrogramme ausgedrückten Erfassungsgrenze, d. h., $-\log_{10}$ (E. G. in $\mu$g) versteht.

** Die hier gegebenen Erfassungsgrenzen wurden erst 10 bis 20 Min nach der Mischung erlangt.

*** Die hier beobachteten Erfassungsgrenzen wurden schon 1 bis 3 Min nach der Mischung erlangt.

**** 1-(2-Pyridylazo)-2-naphthol.

a) F. Feigl, „Spot Tests in Inorganic Analysis", 5. Aufl., Elsevier Publishing Co., Amsterdam (1958), S. 146ff.
b) M. Fujimoto, Dieses Bulletin, **27**, 48 (1954).
c) M. Fujimoto und T. Iwamoto, unveröffentlichte Resultate.

** Dieser Nachteil wurde dadurch teilweise verbessert, daß man die fein zerriebenen Harzteilchen als Träger der stark sich färbenden Bestandteile an die Grenzfläche zweier flüssigen Phasen ansammeln läßt[1)].

Reagenslösung) mit einem Tropfen der Harzsuspension versetzt. Sodann wird ein Tropfen der Reagenslösung (od. der Probelösung) hinzugefügt, wobei die Harzteilchen eine Weile in der ganzen Lösung schweben und sogleich die in der Lösung vorhandenen, stark sich färbenden Ionen adsorbieren (Abb. 2a). Nach 1 bzw. 3 Min langem Stehen wird das Gemisch etwa 1 Min zentrifugiert. Es ist dabei empfehlenswert, daß man dies unter einer Anzahl der Drehung wesentlich größer als die bei der Reinigung der Harzsuspension abschleudern läßt, um die gefärbten Harzteilchen an die Spitze der Kapillare möglichst scharf, dicht und schnell ansammeln zu lassen. Das 1 Min lange Abschleudern unter höchstens 3000 Drgg. pro Min ist zur Abtrennung des Harzteilchens genügend. Die Farbe der auf solche Weise an die Spitze angesammelten Harzteilchen ist mit einer Lupe (20 mal) leicht zu erkennen.

Weil die kleineren Harzteilchen, die die sich färbenden Bestandteile schneller als die größeren Teilchen anreichern können, sich in der Kapillare langsamer als die größeren fallen, färbt sich die dabei an der Spitze gebildete Harzschicht von unten nach oben allmählich stärker (Abb. 2b'), und infolgedessen wird die Nachweisempfindlichkeit bedeutend erhöht.

Zwei sinnfällige Beispiele für die Erhöhung der Empfindlichkeit des Nachweises mittels oben vorgeschlagenen Verfahrens, sogenannter „Harz-zentrifugierenmethode", stehen in Tabelle I, in der das Erfassungsgrenze beim vorliegenden Verfahren mit dem bei der gewöhnlichen Tüpfelmethode sowie der Harztüpfelmethode verglichen wird.

Die obenerwähnte Methode ist nicht nur der gewöhnlichen Tüpfelmethode sondern auch der Harztüpfelmethode daran weit überlegen, daß man durch einfaches Zentrifugieren der gereinigten Harzsuspension eine wesentlich verbesserte Empfindlichkeit schnell und sicher gewinnen kann. Die große Austauschgeschwindigkeit beim kleinsten Harzteilchen ermöglicht den schnellen und empfindlichsten Nachweis gegen größere Menge der hoch verdünnten Probelösung. Überdies sei es möglich, durch Vergleichung der an der gleichen Menge der Harzteilchen entstehenden Farben mit den einer Reihe von Standards entschieden kleine Stoffmenge ziemlich genau zu bestimmen, worüber der Verfasser zur Zeit einige Versuche durchführt.

*Laboratorium der analytischen Chemie*
*Chemisches Institut der*
*wissenschaftlichen Fakultät*
*Universität zu Tokyo*
*Hongo, Tokyo*

# *Magnetic and Spectrophotometric Studies on Decoloration of Thiocyanato Iron(III) Complexes in Solutions. I*

By Chie MIYAKE*

(Received August 20, 1959)

The reaction between iron(III) and thiocyanate ions has been studied in detail by many authors for more than 30 years. Despite the vast experimental data thus accumulated, no decisive conclusion seems to have been drawn as to the nature of the species which exist in the solutions. In 1953, reviewing all the reports ever published, S. Z. Lewin et al.[1] have shown the following series of equilibria as the basis upon which all of the experimental evidences can be correlated.

$$Fe^{3+} + SCN^- \rightleftharpoons FeSCN^{2+} \quad (1)$$

$$FeSCN^{2+} + SCN^- \rightleftharpoons Fe(SCN)_2^+ \quad (2)$$

$$Fe(SCN)_2^+ + SCN^- \rightleftharpoons Fe(SCN)_3 \text{ or } [1/2Fe_2(SCN)_6] \quad (3)$$

$$Fe(SCN)_3 + SCN^- \rightleftharpoons Fe(SCN)_4^- \quad (4)$$

and probably also:

$$Fe(SCN)_4^- + SCN^- \rightleftharpoons Fe(SCN)_5^{2-} \quad (5)$$

$$Fe(SCN)_5^{2-} + SCN^- \rightleftharpoons Fe(SCN)_6^{3-} \quad (6)$$

On the other hand, in the field of chemical analysis the color reaction between iron(III) and thiocyanate ions has long been used as a proof of the existence of iron(III) ions, as well as being used as the procedure of its quantitative determination. However, in the above-mentioned solutions there exists a gradual color change with time, which makes the quantitative measurements somewhat difficult. And indeed the explanation of this change itself is still in question. In 1952, Hiraki et al.[2] from the spectrophotometric measurements with a Dubosk spectrophotometer, reported that the fading of color is caused by the reduction of iron(III) to iron(II) by thiocyanate ions. If this reaction did exist, there should be a change of magnetic susceptibility of the solutions as the fading of color proceeds. Thus, the decoloration mechanism of the solutions is one of the most interesting subjects to be clarified in the field of magnetochemistry. In this paper were summarized the measurements of the magnetic susceptibility and the visible absorption spectra during the decoloration.

## Experimental

**Materials.**—Iron solution: A given amount of Mohr's salt was dissolved in distilled water containing several drops of conc. sulfuric acid. Adding a small amount of hydrogen peroxide (30%) in order to oxidize iron(II) to iron(III), the solution was heated on a water bath to expel the excess of hydrogen peroxide. After cooling, the solution was diluted to exactly 0.05 M with distilled water.

Potassium thiocyanate: The reagent of analytical grade was dissolved and diluted to 0.5 M with distilled water. The solution obtained was completely colorless and its test by $\alpha\cdot\alpha'$-dipyridyl was also negative. Therefore, neither iron(III) nor iron(II) ions can exist in our prepared solution.

Hydrochloric acid: The hydrochloric acid was purified by distillation until it gave a negative test for iron.

Sample solution: The solution to be measured was prepared by adding a given amount of hydrochloric acid and potassium thiocyanate to the iron stock solution and then was diluted to the desired concentrations.

**Measurements.**—The magnetic susceptibility of the solutions was measured from time to time during the decoloration by the torsion magnetometer with fused silica[3].

Absorption spectra were determined by a Beckman Model DU Spectrophotometer. Matched 10 mm. silica cells with quartz 9.5 mm. thick were used; this gave an effective optical path of 0.5 mm.

## Experimental Results

**Magnetic Data.**—The magnetic moments in Bohr magnetons for total iron in the solutions of thiocyanato iron(III) and thiocyanato iron(II) complexes are shown in Table I. The magnetic moment is calculated from the formula $\mu = 2.84\sqrt{\chi \times T}$ where $\chi$ is the susceptibility per gram atom of total iron in the solutions and $T$ the absolute temperature[4]. Here, any magnetic interaction is neglected, since all of the solutions are magnetically dilute. Fig. 1 shows

* Present address, Nuclear Engineering Department, College of Engineering, Osaka University, Higashinoda, Miyakojima, Osaka.

1) S. Z. Lewin and R. S. Wagner, *J. Chem. Educ.*, **No. 9**, 445 (1953).

2) Y. Hiraki, K. Tamura and M. Katumi, *Sci. Repts. Saikyo Univ.*, **1**, 19 (1952).

3) H. Takaki, N. Kawai, C. Miyake and T. Morita, *J. Phys. Soc. Japan*, **13**, 629 (1958).

4) J. H. Van Vleck. "The Theory of Electric and Magnetic Susceptibilities", Oxford University Press, Oxford (1932), p. 282.

TABLE I. MAGNETIC MOMENTS OF IRON IN BOTH THIOCYANATO IRON(III) AND THIOCYANATO IRON(II) COMPLEXES N HYDROCHLORIC ACID SOLUTIONS*,**

| Magnetic moment(Bohr magneton) | |
|---|---|
| Iron(III) | Iron(II) |
| 5.92 | 5.45 |
| 5.91 | 5.46 |
| 5.91 | 5.44 |

* 0.05 M thiocyanato iron(III) complex, 0.12 N hydrochloric acid solution.

** All of the measurements were made fifteen minutes after the solutions were prepared.

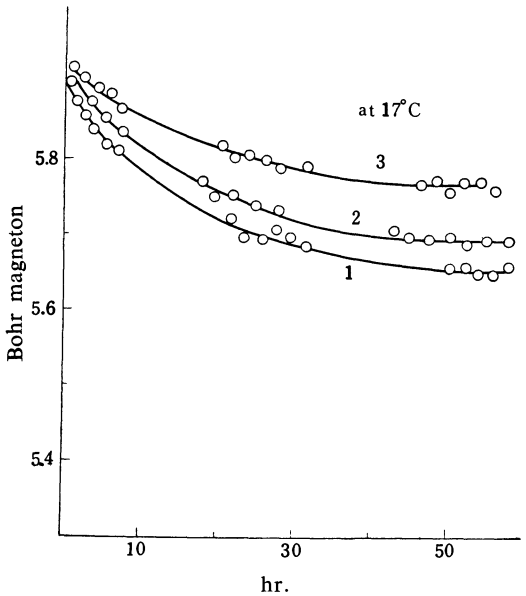



Fig. 1. Dependency of decrease in magnetic moment of iron upon concentration of hydrochloric acid. (0.005 M iron(III), 0.05 M thiocyanate ion solutions).
1: 0.012 N HCl 2: 0.12 N HCl
3: 1.2 N HCl

the decrease in magnetic moment of the solutions with varying concentrations of hydrochloric acid, when the amount of thiocyanate ions in the solutions are held constant. Fig. 2 represents the similar decrease with varying concentrations of thiocyanate ions.

**Spectrophotometric Data.**—Fig. 3 shows the spectral curve of thiocyanato iron(III) complexes and that of thiocyanato iron(II) complexes in hydrochloric acid solutions. Of all the present absorption measurements, some representative curves of thiocyanato iron(III) complexes with varying concentrations of thiocyanate ions are shown in Fig. 4. The maxima of the absorbance at about 470 mμ due to thiocyanato iron(III) complexes shift to the region of longer wave length. This bathochromic effect may be attributed to the increase

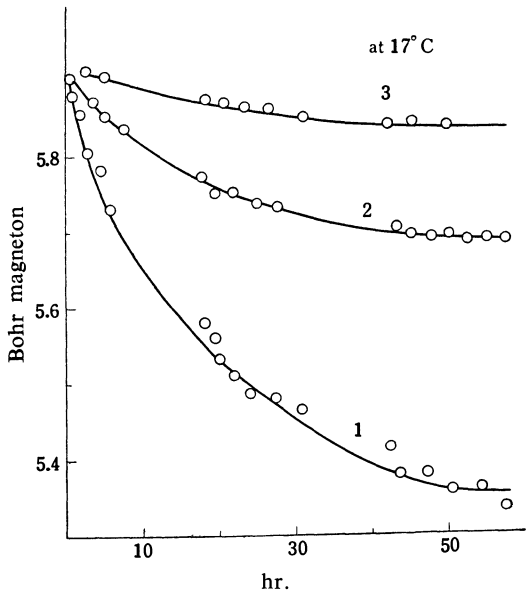



Fig. 2. Dependency of decrease in magnetic moment of iron upon concentration of thiocyanate ions. (0.005 M iron(III), 0.12 N hydrochloric acid solutions).
1: [Fe(III)]/[NCS⁻] = 1 : 100
2: 〃 = 1 : 10
3: 〃 = 1 : 0.14

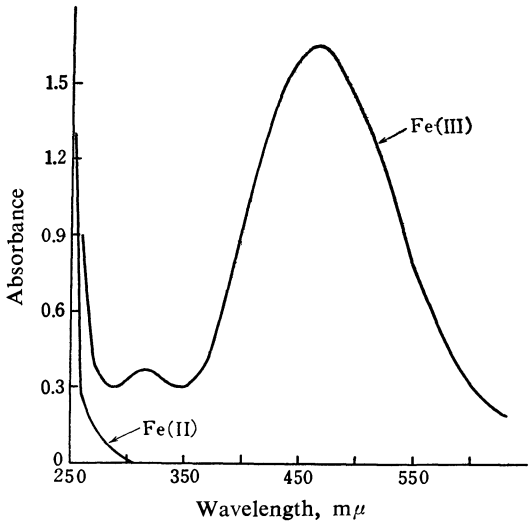



Fig. 3. Absorption spectra of thiocyanate iron(III) and thiocyanato iron(II) complexes in hydrochloric acid solutions.

in ratio of the number of coordinated thiocyanate ions to that of coordinated chloride ions. At the same time, the absorbances at the maxima increase with increasing concentrations of thiocyanate ions. The other absorption maxima at about 320 mμ are probably due to chloro iron(III) complexes as shown

TABLE II. EFFECTS OF CONCENTRATIONS OF BOTH HYDROCHLORIC ACID AND THIOCYANATE IONS TO ABSORBANCES AT ABOUT 470 mμ AND 320 mμ

| | Increase of [$NCS^-$] | Increase of [HCl] |
|---|---|---|
| | Absorbance at about 470 mμ | |
| Wavelength of max. absorbance | bathochromic | constant* |
| absorbance | increase | decrease* |
| Rate of decrease in absorbance | increase | decrease |
| | Absorbance at about 320 mμ | |
| Wavelength of max. absorbance | bathochromic* | bathochromic |
| absorbance | decrease* | increase |
| Rate of decrease in absorbance | constant* | decrease |

* The absence of notable effect.

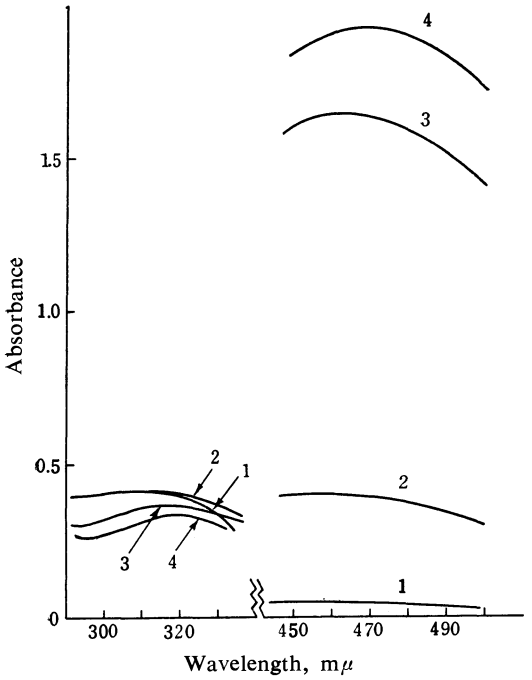



Fig. 4. Absorption spectra of thiocyanato iron(III) complex solutions with varying concentration of thiocyanate ions. (0.005 M iron(III), 0.12 N hydrochloric acid solutions).
1 : 0.0005 M, 2 : 0.005 M, 3 : 0.05 M, 4 : 0.7 M

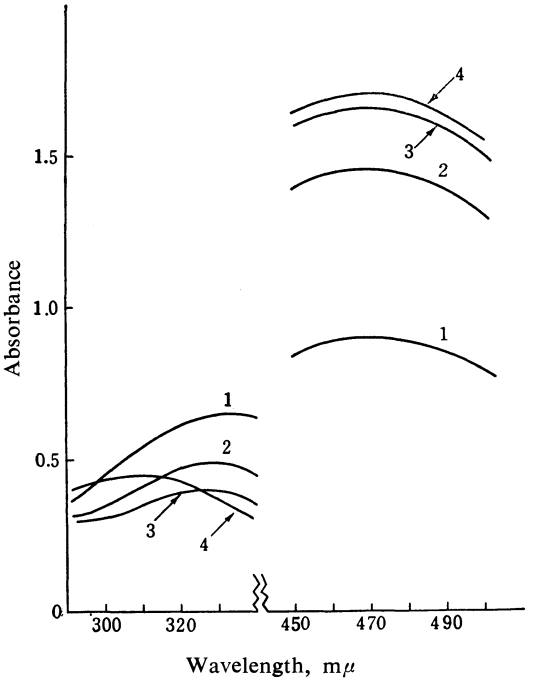



Fig. 5. Absorption spectra of thiocyanato iron(III) complex solutions with varying concentration of hydrochloric acid. (0.005 M iron(III), 0.05 M thiocyanate ion solutions).
1 : 3.6 N, 2 : 1.2 N, 3 : 0.6 N, 4 : 0.12 N

in Fig. 5.[5] In Table II, the results of spectrophotometric measurements are summarized. Here, it seems to be of importance for the following discussion to compare the time-change in magnetic moment (already shown in Figs. 1 and 2) and the similar change in absorbance at about 470 mμ (shown in Fig. 6).

## Discussion

Before going directly into the discussion, the following remarks seem to be necessary.

The magnetic measurement is quite useful and important for determining the electronic spatial configuration in the complex containing transition element. For example, if the complex be assumed to have the inner orbital type of binding, then the 3d-electrons of iron(III) ion are necessarily paired, leaving only one residual electron to be unpaired, giving 1.7 Bohr magnetons (theoretical) to the complex. But on the other hand, when the complex has a binding of the so-called outer orbital type, all of the 3d-electrons of iron(III)

5) M. Ishibashi, T. Shigematsu, Y. Yamamoto, M. Tabushi and T. Kitagawa, This Bulletin, 30, 433 (1957).

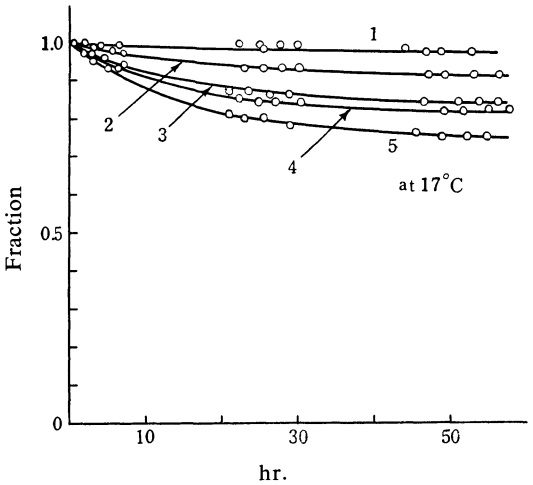


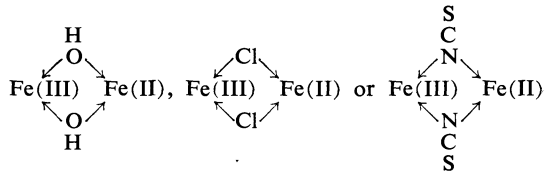

Fig. 6. Decrease of absorbances with time at about 470 mμ of ferric thiocyanate solutions.
1 : corresponds to 3 in Fig. 2
2 : 3 in Fig. 1
3 : 2 in Figs. 1 and 2
4 : 1 in Fig. 1
5 : 1 in Fig. 2

ion are left unpaired, thus giving 5.9 Bohr magnetons (theoretical). In case of iron(II), the complex with the inner orbital type has no magnetic moment and that with the outer orbital type has 4.8 Bohr magnetons (theoretical), respectively. The number of unpaired electrons $n$ of complex can generally be calculated from the magnetic measurements by the formula $\mu=\sqrt{n\times(n+2)}$.

The present magnetic observations which are shown in the preceding section and tabulated in Table I, show that thiocyanato iron(III) complex has five unpaired electrons and thiocyanato iron(II) complex four unpaired electrons, both belonging to the outer orbital type of binding. If the decoloration depends upon the simple reduction of iron(III) to iron(II) by thiocyanate ions, it is required that the magnetic moment decreases by 0.47 Bohr magneton and completely reduced solutions become colorless. This is evident from Fig. 3 in which it is shown that the iron(II) has no absorption in the region of visible light.

Although the magnetic data in Figs. 1 and 2 seem to support the idea that the above-mentioned simple reduction had actually been taking place, the spectrophotometric data are not favourable, because the absorbances at 470 mμ are still greater even after the decrease of the magnetic moment. In order to harmonize the above-mentioned discrepancy there must be another scheme by which all of the obtained data can be consistent. If we assume that the iron(II) ion already reduced in the solutions and the iron(III) ion still remaining were combined through the bridges of hydroxo ions, chloride ions or thiocyanate ions, and also that they were formed in the so-called "binuclear complex" or "dimer", whose unpaired electron is single, the reduction of the magnetic moment in solution and the amount of the remaining color may be plausible, despite the fact that a question still remains whether or not the free iron(III) ion and that combined into the dimer have the same absorbance character in the region of visible light.

The probable formula of the dimer is considered to be one of the following three types:




The study of the problem concerning the determination of the actual type existing in the present solutions must be continued. However, a series of reactions up to the above-mentioned formation of dimer, seems to be initiated in any way by the partial reduction of iron(III) to iron(II) as has already been stated. This argument is directly proved in Figs. 1, 2 and 6, which indicate that the solution with greater decrease in magnetic moment shows a greater decreases in absorbance. At the same time, we can say from the figures that both the decoloration and demagnetization with time proceed almost proportionally to the concentration of thiocyanate ions and inversely proportionally to the acidity of the solutions (hydrochloric acid). The acidity is generally considered to suppress the power of reduction of thiocyanate ions[6]. These tendencies are shown in Table II.

On the basis of the formation of the dimer which the present author has proposed, both the magnetic and spectrophotometric data are summarized in the following way. In the formation of the dimer which we supposed to have the inner orbital type of binding, five unpaired electrons of the original iron(III) ion and six electrons of iron(II) ion are paired with each other, leaving in the dimer only one unpaired electron. The number of the unpaired electrons thus reduced, hence the reduction of magnetic moment, is quite large. Therefore, we can say that the number of the originally unpaired electrons of 2×Fe(III),

6) G. Charlot, "L'analyse qualitative et les réactions en solution", Masson et Cie (1957), p. 334.

ten, are reduced and finally only one unpaired electron is left in the dimer.

Supposing that $\alpha$-fractions of iron(III) in the original solutions are reduced to iron(II) and converted into the 1 : 1 dimer with iron(III), the final number of the unpaired electrons in the dimer is given by

$$5\times(1-2\alpha)+\alpha=5-9\alpha \qquad (1)$$

and the corresponding theoretical magnetic moment by

$$\{5.92^2\times(1-2\alpha)+1.73^2\times\alpha\}^{1/2} \qquad (2)$$

In the above relation only the spin contribution to the magnetic moment is taken into consideration and at the same time for simplicity's sake, the true equilibrium conditions in the formation of the dimer is ignored.

On the other hand, the spectrophotometric fractional absorbances of the solutions can be expressed by

$$\varepsilon\times(1-\alpha) \qquad (3)$$

where $\varepsilon$ is the molar extinction coefficient. Here, the difference of the extinction coefficient between free iron(III) and iron(III) in the dimer are again neglected. The present results of measurements so far obtained seem to show a good agreement with the above relations (2) and (3).

Werbel et al.[7], in their results for the same substance using 0.06 M thiocyanato iron(III) complex in 1.9 M perchloric acid solution, have reported that the magnetic moment of 5.88 Bohr magnetons was obtained about one hour after its preparation and that about one percent of the total amount of iron(III) originally present was converted into iron(II). They have also pointed out that the magnetic moment of thiocyanato complex is too small to account for the reaction due to simple reduction from iron(III) to iron(II), because of the too small difference in magnetic moment between them. The result obtained by Werbel et al. seems, however, to be quite reasonably explained on the present consideration of the existence of dimer.

7) B. Werbel, V. H. Debeler and W. C. Vosborgh, *J. Am. Chem. Soc.*, **65**, 2329 (1943).

## Summary

The decoloration mechanism of thiocyanato iron(III) complex solutions was investigated by means of both the magnetic and spectrophotometric methods. The data for the magnetic measurements supported that the decoloration was caused by the simple reduction of iron(III) to iron(II) by thiocyanate ions. But such a simple model of the reduction was not favourable for the observed decoloration, because the decrease in the absorbance was too small, being only about twenty percent. In order to eliminate this discrepancy, another scheme was proposed, which ascribes the magnetic and spectral observations to the formation of a binuclear complex of iron(III) and iron(II), a so-called dimer, during the decoloring reaction. This dimer possesses only one unpaired electron and accordingly very small magnetic moment, but possesses the significant absorbance due to iron(III). On this model, the greater decrease in magnetic moment and the rather smaller decrease in absorbance which we obtained, were quite satisfactorily clarified.

The author wishes to express her sincere thanks first to Professor H. Takaki for his continuous encouragement and interest throughout the present work. She wishes to convey her sincere thanks to Dr. Y. Yamamoto whose advice and discussions were very fruitful in this experiment. The author's thanks are also tendered to professor M. Ishibashi, whose kind permission to use the Beckman spectrophotometer gave added value to her study.

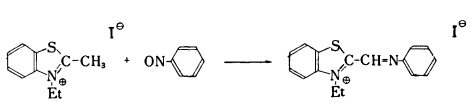
*Department of Chemistry*
*Faculty of Science*
*Kyoto University*
*Sakyo-ku, Kyoto*

# *Synthesis of Dyes with the Neocyanine Structure Presented by Brooker, and Related Dyes. III. Condensation of 3-Ethyl-2-methylbenzothiazolium Iodide and Nitrosobenzene, and the Dyes Obtained from its Condensates*

By Shiro KIMURA

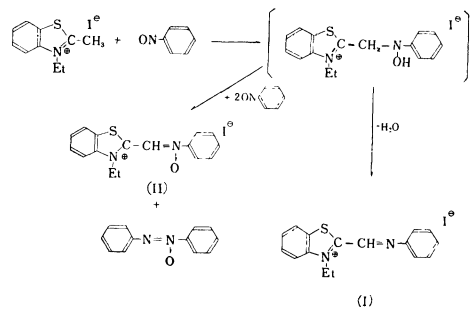
(Received November 17, 1959)

The synthetic process for the "Brooker-type dyes" described in the preceding paper[1] could possibly be improved with regard to the yield and by-product formation. The present series of experiments was carried out in order to obtain some fundamental concept of this reaction. An attempt was first made to prepare the 2-aldehyde anil derivative I of 3-ethyl-2-methyl-benzothiazolium iodide by the condensation of 3-ethyl-2-methylbenzothiazolium iodide and nitrosobenzene. In accordance with the report Katayanagi[2], the condensation of 3-ethyl--2-methylbenzothiazolium iodide and nitrosobenzene was carried out in ethanol with piperidine as a condensation agent. The product of this reaction was obtained as dark purple-needle crystals, m. p. 213–214°C (decomp.) $\lambda_{max}$ 390 m$\mu$ which became bluish purple prisms, m. p. 215°C (decomp.), when recrystallized from acetic anhydride. But this was not the expected anil I and was found to be a nitrone II.



(I)

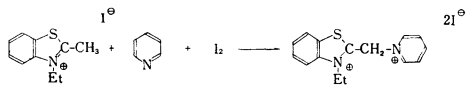
The basic condensation reactions of active methyl and nitroso compounds in general has been known from olden times as the Ehrlish-Sachs reaction[3]. It has been clarified in recent years that this reaction is accompanied by an oxidative reaction to form a nitrone as a by-product, besides the anil. It is also known that these two products are difficult to separate. The nitrone obtained in the present series of experiments was not completely pure and rather difficult to separate. When the impure nitrone was boiled with nitrosobenzene in ethanol, a dark purple substance was obtained which crystallized in reddish brown needles, m. p. 219°C (decomp.). Its analytical values were closer to those of the phenylnitrone. Then a mixture of 1 mol. of 3-ethyl-2-methyl-benzothiazolium iodide and 3 mol. of nitroso-benzene in ethanol was reacted with the addition of piperidine and reddish brown needles, m. p. 219°C (decomp.) were obtained. This was found to be pure nitrone II from its analytical values. The mechanisms of this reaction were shown by the following scheme:



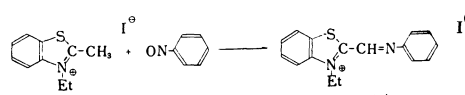
(II)

(I)

Synthesis of the phenylnitrone was also attempted with reference to the general method of synthesis by Kröhnke and others[4] for the phenylnitrone of 1-methyl-2-formylpyridinium iodide, and preparation of *N*-(3-ethyl-1-thia-3-azoniainden-2-ylmethyl) pyridinium diiodide was undertaken, but the product seemed to be labile and the objective was not attained.



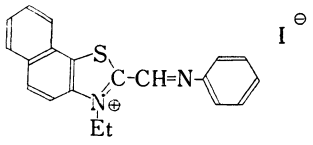
A purely synthetic preparation of the anil from heterocyclic ammonium salts has recently been reported by Mcgookin[5]. This process was applied to 3-ethyl-2-methylbenzothiazolium iodide and pure anil I of 3-ethyl-2-formyl-benzothiazolium iodide was obtained. In this case, equimolecular amounts of 3-ethyl-2-methylbenzothiazolium iodide and nitroso-benzene were reacted in absolute ethanol, with anhydrous potassium carbonate as the condensation agent, and red needles, m. p. 199°C (decomp.) were obtained.



(I)

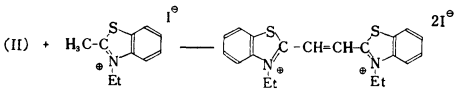
1) S. Kimura, *Bull. Soc. Sci. Phot. Japan*, **9**, 45 (1959).
2) M. Katayanagi, *J. Pharm. Soc. Japan*, **69**, 38 (1949).
3) P. Ehrlich and F. Sachs, *Ber.*, **32**, 2341 (1899).
4) F. Kröhnke and H. Leister, ibid., 71, 2583 (1938).
5) A. Mcgookin, *J. Appl. Chem.*, **5**, 65 (1955).

Similarly, condensation, of 3-ethyl-2-methylnaphtho[2, 1-*d*]-thiazolium iodide and nitrosobenzene afforded the anil III of 3-ethyl-2-formylnaphtho[2, 1-*d*]thiazolium iodide.

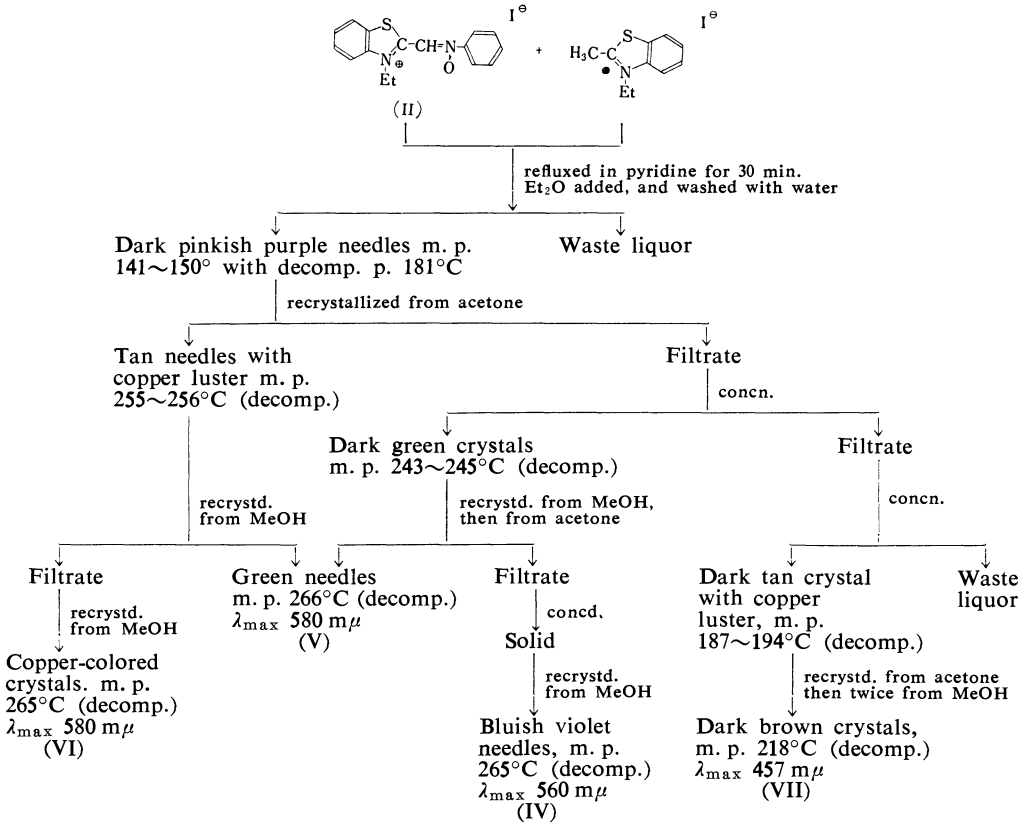


(III)

We then attempted the synthesis of 3, 3′-diethyl-2, 2′-vinylidendibenzothiazolium diiodide as a clue to the synthesis of "Brooker-type dyes", by the condensation of 3-ethyl-2-methylbenzothiazolium iodide with these nitrone derivative obtained above. Unexpectedly, however, this reaction was found to be much more complicated than was anticipated.

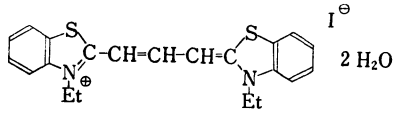


By refluxing an equimolar mixture of this phenylnitrone of 3-ethyl-2-formylbenzothiazolium iodide and 3-ethyl-2-methylbenzothiazolium iodide in pyridine for 30 min., a mixture of four kinds of dyes was obtained: the dyes were purified by fractional crystallization from acetone according to the scheme shown:




These dyes were also examined by paper chromatography and exactly the same four kinds of dyes were found to have been formed.

The structures of these four kinds of dyes

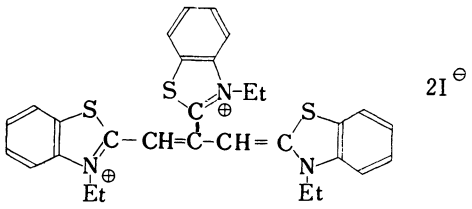


(IV)

were examined from their analytical values and absorption spectra and IV was identified with the known 3,3′-diethylthiacarbocyanine iodide dihydrate by comparison with the dyes prepared by a known route.

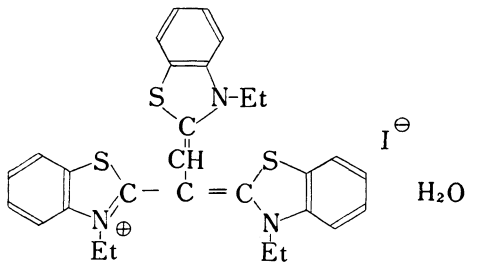
The analytical values of V were very close to those of the known trinuclear carbocyanine, 3, 3′-diethyl-9-(3-ethyl-2-benzothiazolinylidenemethyl)thiacarbocyanine iodide, but the absorption spectra and physical characteristics were entirely different and no presumption could be made of its structure. The analytical

values of VI suggested it to be a diiodide, and accordingly a trinuclear carbocyanine, 3, 3'-dietyl-9-(3-ethyl-1-thia-3-azoniainden-2-yl)-thiacarbocyanine diiodide, was presumed. The dye with this structure had earlier been synthesized by Tanabe[6] who recorded the melting point of 85°C and $\lambda_{max}$ 545 m$\mu$, but these data are entirely different from those of VI and definite conclusion can be drawn. Its 8-substituted isomer was synthesized by Anish[7] and shwos entirely different physical properties.




(VI)

VII was assumed to be a monomethine from its absorption spectrum and analytical values suggested the structure of a trinuclear monomethinecyanine, 3, 3'-diethyl-8-(3-ethyl-2-benzothiazolinylidenemethyl)thiacyanine iodide monohydrate.




(VII)

Chemical evidences for the structure of these four dyes will be discussed in the following paper.

## Experimental

**Preparation of the Phenylnitrone II of 3-Ethyl-2-formylbenzothiazolium Iodide.**—A solution of 50 g. of 3-ethyl-2-methylbenzothiazolium iodide and 18 g. of nitrosobenzene dissolved in 500 ml. of ethanol with warming on a water bath, added with 7 drops of piperidine, was stirred thoroughly and allowed to stand for about 2 hr. The dark purple crystals that separated out were collected by filtration, washed with water and methanol, and 21 g. (yield, 33%) of a dye, m. p. 156~164°C (decomp. at 174°C), was obtained. Recrystallization of this dye from 200 ml. of methanol afforded 7 g. (yield, 11%) of dark purple needles, m. p. 213~214°C (decomp.). Approximately the same result was obtained on repeating this experiment several times.

These dyes were boiled with about 40 volumes of acetic anhydride for 30 min. and the dark bluish purple prismatic crystals thereby formed were collected by filtration. After washing with ether the dye melted at 215°C with decomposition and its analytical value supported the nitrone structure.

Found: C, 46.56; H, 4.07; N, 6.62; I, 29.93. Calcd. for $C_{16}H_{15}ON_2IS$: C, 46.82; H, 3.66; N, 6.83; I, 30.98%.

**Condensation of the Phenylnitrone II of 3-Ethyl-2-formylbenzothiazolium Iodide and 3-Ethyl-2-methylbenzothiazolium Iodide.**—A solution of 6 g. of the phenylnitrone II of 3-ethyl-2-formylbenzothiazolium iodide and 4.8 g. of 3-ethyl-2-methylbenzothiazolium iodide in about 100 ml. of pyridine was refluxed for 30 min. and the major part of pyridine was distilled off under reduced pressure. About 100 ml. of ether was added to the residue, the dark purple crystals that precipitated out were washed with several 300 ml. portions of ether. The residue was mixed with 50 ml. of water, filtered, and the precipitate on the filter was washed with water. The dark pinkish violet crystals, m. p. 141~150°C (decomp. at 181°C) so obtained were dissolved in ca. 1 l. of acetone, concentrated to 400 ml., and 0.5 g. of dark tan crystals with copper luster, m. p. 255~256°C (decomp.) was obtained. Concentration of its mother liquor afforded 0.3 g. of dark green crystals, m. p. 243~245°C (decomp.). Further concentration of its mother liquor to about 50 ml. separated an oily substance which crystallized upon addition of ca. 50 ml. of ether. The crystals were collected by filtration and washed with ca. 30 ml. of ether, affording 0.4 g. of dark tan crystals with copper luster, m. p. 187~197°C (decomp.). These three kinds of crude dyes were purified through fractional crystallization and four kinds of pure dyes were isolated.

**Purification of the Dark Tan Crystals, M. P. 255~256°C (Decomp.).**—A solution of 0.5 g. of the crude dye dissolved in 50 ml. of methanol was concentrated to about 30 ml. and 0.35 g. of green needles, m. p. 260~262°C, separated. This substance was recrystallized twice from methanol to 0.18 g. of green needles V m. p. 266°C (decomp.) $\lambda_{max}$ 580 m$\mu$.

Found: C, 53.31; H, 4.06; N, 6.95; I, 20.53. Calcd. for $C_{28}H_{24}N_3IS_3$: C, 53.75; H, 3.84; N, 6.72; I, 20.25%.

The initial filtrate left after separation of the green crystals was concentrated and the copper-colored crystals m. p. 258°C (decomp.), so formed were recrystallized from methanol to clustered crystals VI m. p. 265°C (decomp.) $\lambda_{max}$ 580 m$\mu$.

Found: C, 45.80; H, 4.29; N, 5.22. Calcd. for $C_{30}H_{29}N_3I_2S_3$: C, 46.10; H, 3.70; N, 5.38%.

**Purification of Dark Green Crystals, M. P. 243~245°C (Decomp.).**—A solution of 0.3 g. of the crude dye dissolved in 60 ml. of methanol was concentrated to about 30 ml. and a mixture of green and bulish purple needle crystal was obtained. The green crystals were comparatively sparingly soluble in acetone and, therefore, the bluish purple crystals

6) Y. Tanabe, *J. Pharm. Soc. Japan*, 74, 814 (1954).
7) A. W. Anish, U. S. Pat. 2,427,177 (1944).

dissolved out with 100 ml. of acetone, leaving 0.1 g. of green needles, m. p. 262°C (decomp.). The acetone solution was concentrated to 80 ml. and 0.05 g. of the same green crystals, m. p. 265°C (decomp.) separated. These green crystals were found to be identical with the dye V described above. The acetone mother liquor was concentrated to 20 ml. and 0.04 g. of bluish purple needles, m. p. 260°C (decomp.), was obtained. This was recrystallized from a small amount of methanol to 0.01 g. of bluish purple needles IV m. p. 265°C (decomp.) $\lambda_{max}$ 560 m$\mu$.

Found: C, 48.03; H, 4.55; N, 5.52; I, 25.61. Calcd. for $C_{21}H_{21}N_2IS_2 \cdot 2H_2O$: C, 47.70; H, 4.73; N, 5.31; I, 24.03%.

**Purification of the Dark Tan Crystals with Copper Luster, M. P. 187~194°C (Decomp.).** —A solution of 0.4 g. of the crude dye dissolved in 300 ml. of acetone was concentrated to 50 ml. and 0.3 g. of dark brown needles, m. p. 210~211°C (decomp.) was obtained. This was mixed with a small amount of bluish purple crystals which were removed and the rest was recrystallized twice from methanol to 0.12 g. of dark brown needles, VII, m. p. 218°C (decomp.) $\lambda_{max}$ 457 m$\mu$.

Found: C, 52.25; H, 4.55; N, 6.c9; I, 19.65. Calcd. for $C_{29}H_{28}N_3IS_3 \cdot H_2O$: C, 52.80; H. 4.55; N, 6.37; I, 19.28%.

**Separation of Dye Mixture by Chromatography.** —Instead of the fractional crystallization as described above, the precipitate obtained from the pyridine reaction mixture was purified through chromatography. A solution of 2 g. of this mixture was dissolved in ca. 200 ml. of acetone concentrated to about 100 ml. and allowed to stand overnight. About 400 ml. of acetone was added to this mixture to dissolve the crystals but sparingly soluble crystals V remained undissolved. The green crystals were removed by filtration, the filtrate was concentrated about 200 ml., and the solution was passed through a column of alumina (Merck), requiring about 1.5 hr., the adsorbed layers separated into pale orange, violet, and pink bands. Each of these bands was eluted with acetone, the acetone elute was concentrated, and separated crystals were recrystallized from methanol. Dark brown needles VII m. p. 216°C(decomp.) $\lambda_{max}$ 457 m$\mu$. were obtained from the pale orange band, green needles V m. p. 260°C (decomp.), $\lambda_{max}$ 580 m$\mu$, from the violet band, and bluish purple needles IV m. p. 267~268°C (decomp.), $\lambda_{max}$ 560 m$\mu$, from the pale pink band. The dye VI obtained by fractional crystallization, was not isolated from this chromatographic separation.

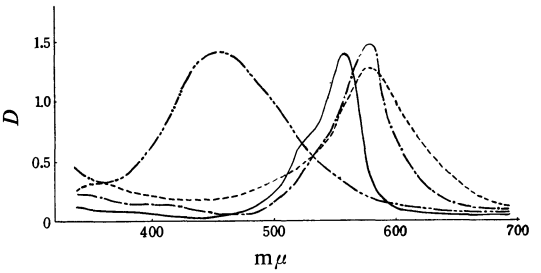



Fig. 1. Absorption spectral curves of IV, V, VI and VII (in ethanol).
—— (IV) —— (V) ---- (VI)
—— (VII)

Chemical evidences for the structure of these four dyes will be discussed in the following paper.

*Research Laboratory*
*Fuji Photo Film Co. Ltd.*
*Minami-Ashigara-machi*
*Kanagawa-ken*

# *Synthesis of Dyes with the Neocyanine Structure Presented by Brooker, and Related Dyes. IV. Structure of the Dyes Obtained by the Condensation of 3-Ethyl-2-methylbenzothiazolium Iodide with Nitrone or Anil Derivatives*

By Shiro KIMURA

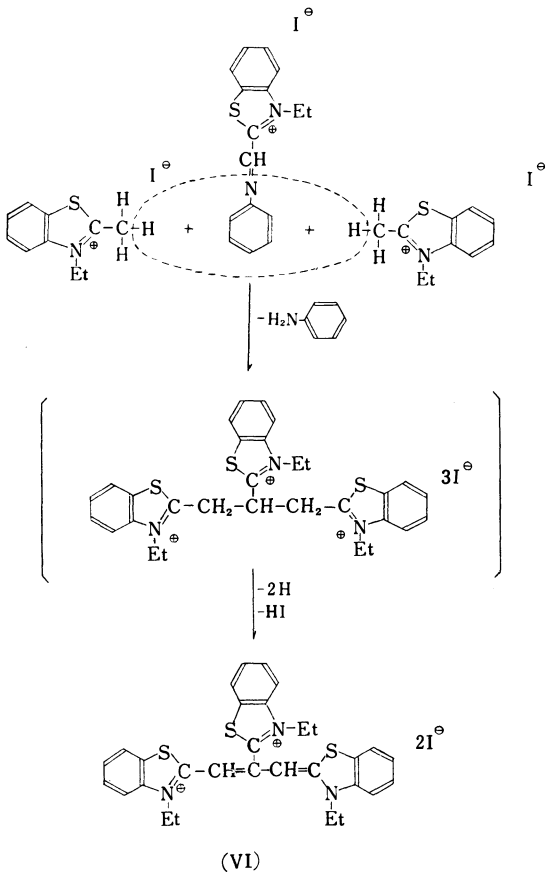
(Received November 17, 1959)

It has been shown in the preceding paper[1] that the condensation of phenylnitrone of 3-ethyl-2-formylbenzothiazolium iodide and 3-ethyl-2-methylbenzothiazolium iodide in pyridine gave four kinds of dyes and their structures were deduced from analytical values and absorption spectra.

In order to examine the formation process of these dyes, the anil I and 3-ethyl-2-methylbenzothiazolium iodide were reacted by refluxing for a short time (8~15 min.) in pyridine and, in this case, 3, 3-diethyl-9-(3-ethyl-1-thia-3-azoniainden-2-yl)thiacarbocyanine diiodide (VI) alone was obtained. This result shows that

1) S. Kimura, This Bulletin, 33, 872 (1960).

this dye VI is initially formed in the early stage of this reaction and its formation mechanism is considered to be as follows:

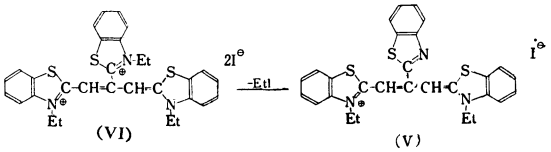


(VI)

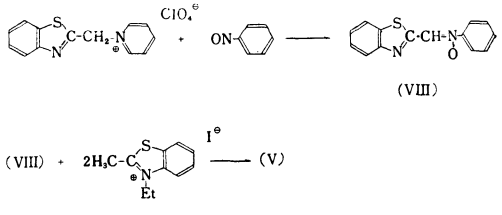
Dehydrogenation of cyanines in pyridine had been observed already by Mills[2] and the present reaction was considered to be of similar mechanism. The dye VI obtained earlier was isolated as an anhydrous salt, but the same dye obtained in the present series of experiments possessed 2 mol. of water of crystallization. The same dye VI was also obtained on replacing the anil I with the nitrone II but the yield of the dye was better when the anil was used.

Tanabe synthesized dyes of this structure and reported the formation of 3-ethyl-2-trichloromethylbenzothiazolium chloride as an intermediate during the reaction of 3-ethyl-2-methylbenzothiazolium iodide and thionyl chloride. On following this reaction, a substance of m. p. 124°C (decomp.), identical with that reported in the literature, was obtained in a good yield. The elemental analytical values, however, did not correspond to those of the objective intermediate and further, iodine was detected besides the chlorine atom. Therefore, this product was not considered to be 3-ethyl-2-trichloromethylbenzothiazolium chloride as reported in the literature. Further, an attempt was made to prepare a dye with this intermediate but a single dye of m. p. 85°C as given in the literature was not obtained and in its stead, a crude dye of m. p. 185°C (decomp.) was obtained. This dye was submitted to paper chromatography and dye spots of yellow, magenta, and purple were separated on the chromatogram, showing the dye to be a mixture. Although further examination of this crude dye mixture was not made, it is certain that the dye VI obtained in the present series of experiments is not the same as the dye obtained by Tanabe.

This dye VI was heated at 130°C for about 12 hr. in the Abderhalden apparatus for the purpose of determining the water of crystallization and the loss in weight was more than that calculated. Therefore, the dried sample was examined by paper chromatography and it was found that the dye VI had changed into the structurally unknown dye V described in the preceding paper. Consideration of this phenomenon showed the necessity of assuming the liberation of ethyl iodide and analytical results supported this assumption. Therefore, the structure of this dye V must be 3,3'-diethyl-9-(2-benzothiazolyl)thiacarbocyanine iodide.



In order to clarify the structure of this dye V an attempt was made to synthesize it by a different route. With reference to the report of Ried and others[3], iodine was applied to 2-methylbenzothiazole in pyridine, and the *N*-(benzothiazol-2-ylmethyl)pyridinium perchlorate obtained therefrom was reacted with nitrosobenzene to form the phenylnitrone VIII of 2-formylbenzothiazole. Condensation of VIII with 2 mol. of 3-ethyl-2-methylbenzothiazolium iodide in pyridine afforded the same dye as V. This fact proves the correctness of the structure of 3,3'-diethyl-9-(2-benzothiazolyl)thiacarbocyanine iodide for V.

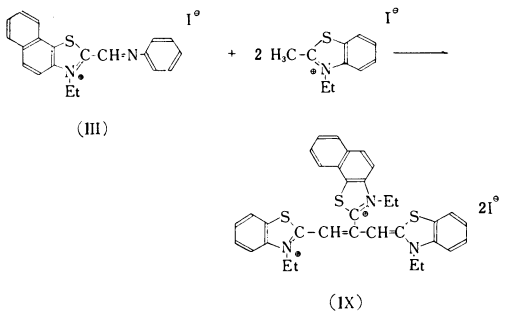


2) W. H. Mills, *J. Chem. Soc.*, **121**, 455 (1922).

3) W. Ried and H. Bender, *Ber.*, **89**, 1893 (1956).

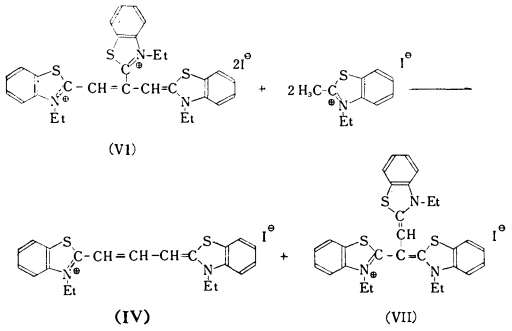
With the identification of the structure of the dye V, the structure of the dye VI also became certain and conversion of this dye VI into V was experimentally proved by refluxing in pyridine for about 2 hr.

Condensation of the anil III of 3-ethyl-2-formylnaphtho-[2, 1-*d*] thiazolium iodide with 2 mols. of 3-ethyl-2-methylbenzothiazolium iodide in pyridine afforded, as anticipated, 3,3'-diethyl-9-(3-ethyl-1-thia-3-azoniacyclopenta-[*a*] naphth-2-yl) thiacarbocyanine diiodide (IX). It was thereby found that this process can be recommended as a general method for the synthesis of dyes of this type.



(III) (IX)

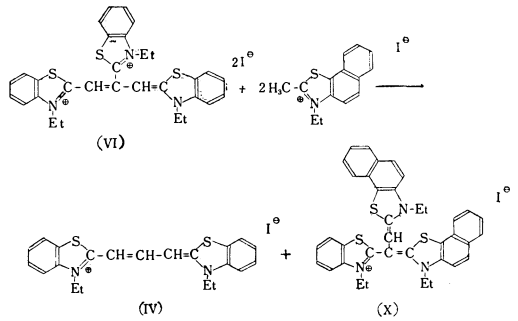
The foregoing experiments have revealed the course of formation of the dyes V and VI in the reaction described in the preceding paper and, consequently, formation of the dyes thought to be 3, 3'-diethylthiacarbocyanine iodide (IV), and 3, 3'-diethyl-8-(3-ethyl-2-benzothiazolinylidenemethyl) thiacyanine iodide (VII) was found to occur through the reaction of 3-ethyl-2-methylbenzothiazolium iodide with 3, 3'-diethyl-9-(3-ethyl-1-thia-3-azoniainden-2-yl)-thiacarbocyanine diiodide (VI) in pyridine.



(VI) (IV) (VII)

The structure of the dye VII was merely presumed from its analytical values and absorption spectrum, and unequivocal establishement of this structure has not succeeded as yet, but it is certain that the dye VI is cleaved at the 9-position to liberate the substituent group to form the dye IV. In order to ascertain this cleavage reaction, the dye VI was refluxed with 3-ethyl-2-methylnaphtho [2, 1-*d*] thiazolium iodide in pyridine and the same dye (IV) was found to be formed. Whether the dye X formed at the same time is the anticipated 3, 3'-diethyl-8-(3-ethyl-2-naphtho [2, 1-*d*] thiazolinyl-idenemethyl)-6', 7'-benzothiacyanine iodide or not is still uncertain since, although the analytical values of the dye X are comparatively close to the theoretical values, its absorption maximum is in a longer wavelength region (650 m$\mu$), and this is unthinkable in the case of monomethine dyes.

Therefore, structural determination of these dyes VII and X must await further studies.



(VI) (IV) (X)

## Experimental

**Reexamination of Synthetic Method Tanabe's for the So-called 3, 3'-Diethyl-9-(3-ethyl-1-thia-3-azoniainden-2-yl) thiacarbocyanine Diiodide.**—The experiments followed Tanabe's report[4]. To 6.1 g. (0.02 mol.) of 3-ethyl-2-methylbenzothiazolium iodide, 24 ml. of thionyl chloride was added dropwise with cooling, by which the iodide turned black and dissolved gradually. Ether was added to this reaction mixture and the yellow precipitate thereby formed was collected to 7 g. of a solid, m. p. 100°C. This was dissolved in thionyl chloride, reprecipitated with ether, and 5 g. (yield, 79%) of yellow powder, m. p. 124°C (decomp.), was obtained. This substance agrees with the so-called 3-ethyl-2-trichloromethylbenzothiazolium chloride, m. p. 125°C (decomp.), reported by Tanabe, but he had assumed this structure from the analytical value of the chlorine alone, and elemental analyses in the present series of experiments gave results which were inconsistent with this structure.

Found: C, 30.81; H, 3.43; N, 3.70. Calcd. for $C_{10}H_9N\,Cl_4S$: C, 37.85; H, 2.84; N, 4.42%.

A solution of 1 g. (0.0032 mol.) of this intermediate product and 2 g. (0.0057 mol.) of 3-ethyl-2-methylbenzothiazolium iodide dissolved in 2.5 ml. of acetic anhydride, added with 1 g. of anhydrous potassium acetate, was heated in an oil bath at 120~130°C for 10 min., cooled, and ether was added to this reaction mixture. The crude dye that precipitated out was collected by filtration washed with water, and the powdery dye so obtained was recrystallized from acetone to 0.5 g. of pale purplish brown powder, m. p. 185°C (decomp.). This dye

4) Y. Tanabe, *J. Pharm. Soc. Japan*, 74, 814 (1954).

is different from that of m. p. 85°C reported in the literature and was found to be a mixture of three kinds of dyes, giving spots colored violet, pink, and yellow by paper chromatography. $R_f$ values were 0.54 (violet), 0.72 (pink), and 0.81 (yellow) (butanol : water=6 : 1). This dye was also different from the dye VI obtained in the present series of experiments.

Results of this reexamination indicated that there is some doubt about the structure of this intermediate and the dye produced in the present series of experiments was never identical with that reported in the literature. Therefore, this examination was not followed further.

**Formation of 3, 3'-Diethyl-9-(2-benzothiazolyl)-thiacarbocyanine Iodide (V) by Liberation of Ethyl Iodide from 3, 3'-Diethyl-9-(3-ethyl-1-thia-3-azonia-inden-2-yl) thiacarbocyanine Diiodide (VI).** — The dye VI was heated in the abdelhalden apparatus at 120~130°C in 20 mmHg for 12 hr. and the loss in weight amounted to 12.22%. The values calculated for 2 mol. of water of crystallization is 4.41%. This dried dye was developed by paper chromatography by which it separated into two kinds of dyes : one a violet zone of $R_f$ 0.44 and the other of reddish violet zone of $R_f$ 0.89 (butanol : water= 6 : 1). The violet zone was that of the starting dye VI and the reddish violet zone agrees with $R_f$ 0.89 of the dye V.

On boiling this dye VI in pyridine for 2 hr., the dye VI completely changed into V and the unity of this dye was proved by the reddish violet single zone of $R_f$ 0.90 in the paper chromatogram.

The fact that the chromatographic purification of the mixture of four kinds of dyes through alumina column only afforded three kinds of dyes, IV, V and VII, as described in the preceding paper, indicates that VI had transited into V.

**Preparation of the Phenylnitrone VIII of 2-Formylbenzothiazole.** — To a solution of 6.52 g. (0.02 mol.) of *N*-(benzothiazolyl-2-methyl)-pyridinium perchlorate and 2.14 g. (0.02 mol.) of nitrosobenzene dissolved in 40 ml. of pyridine, 20 ml. of 2 N sodium hydroxide solution was added and the mixture was stirred, by which process exothermic reaction took place. The mixture was allowed to cool and crystals separated out after 2 hr. The crystals were collected by filtration, washed with ethanol, and 3 g. of yellowish brown needles, m. p. 160~167°C, was obtained. Recrystallization from ethanol afforded 1.1g. (yield, 21.6%) of pale yellowish brown needles, m. p. 163~164°C.

Found : C, 66.28 ; H, 4.17 ; 10.82. Calcd. for $C_{14}H_{10}ON_2S$ : C, 66.15 ; H, 3.98 ; N, 11.02%.

**Preparation of 3, 3'-Diethyl-9-(2-benzothiazolyl)-thiacarbocyanine Iodide (V).**—A solution of 0.254 g. (0.001 mol.) of the phenylnitrone VIII of 2-formylbenzothiazole and 0.61 g. (0.002 mol.) of 3-ethyl-2-methylbenzothiazolium iodide in 3 ml. of pyridine was refluxed in an oil bath of 120°C for 10 min. The color of the reaction mixture changed from the initial yellow through green to purple. Ether was added to the reaction mixture to precipitate the dye formed which was collected by decantation and washed with wather to 0.4 g. of crystalline powder, m. p. 192~195°C (decomp.). Recrystallization from ethanol afforded 0.1 g. (yield, 16%) of green needles, m. p. 266°C (decomp.): $\lambda_{max}$ 580m$\mu$. Paper chromatogram : $R_f$ 0.89 (butanol : water=6 : 1) : single spot of violet, indicating the substance to be identical with dye V among the four kinds of dyes isolated from a mixture.

**Synthesis of 3, 3'-Diethyl-9-(3-ethyl-1-thia-3-azoniacyclopenta[*a*]naphth-2-yl)thiacarbocyanine Diiodide (IX).**—A mixture of 2.2 g. of the anil III of 3-ethyl-2-formylnaphtho[2, 1-*d*]thiazolium iodide and 3.0 g. of 3-ethyl-2-methyl-benzothiazolium iodide in 30 ml. of pyridine was heated in an oil bath of 130°C for 25 min., cooled, and ether was added to this mixture. The precipitate thereby formed was separated by decantation, washed with ether and water, and warmed with a small amount of ethanol. On allowing this solution to cool, navy-blue crystalline powder was obtained which melted once at 185°C, resolidified, and again melted with decomposition at 245°C. Two recrystallizations from ethanol failed to change this mode of melting. Paper chromatogram exhibited a single zone of bluish purple color at $R_f$ 0.51, $\lambda_{max}$ 585 m$\mu$. The analytical values agreed with those calculated as a monohydrate.

Found : C, 48.06 ; H, 4.07 ; N, 5.08 ; I, 29.54. Calcd. for $C_{34}H_{31}N_3I_2S_3 \cdot H_2O$ : C, 48.06 ; H, 3.89 ; N, 4.95 ; I, 29.95%.

**Formation of 3,3'-Diethylthiacarbocyanine Iodide (IV) and 3, 3'-Diethyl-8-(3-ethyl-2-benzothiazolinyl-idenemethyl)thiacyanine Iodide (VII) from the Dye VI and 3-Ethyl-2-methylbenzothiazolium Iodide.**— A mixture of 0.1 g. of VI and 0.075 g. of 3-ethyl-2-methylbenzothiazolium iodide in 30 ml. of pyridine was boiled and an aliquot of this reaction mixture was periodically examined by paper chromatography (butanol : water=6 : 1) to find the formation of dyes. After 30 min., the starting dye still appeared as a spot at $R_f$ 0.35, but this disappeared after 60 min., and the reaction solution contained three kinds of dyes, one of reddish pink zone at $R_f$ 0.75 (dye IV), one of violet zone at $R_f$ 0.86 (dye V), and one of brown zone at $R_f$ 0.93 (dye VII).

**Formation of 3,3'-Diethylthiacarbocyanine Iodide (IV) and 3, 3'-Diethyl-8-(3-ethyl-2-naphtho[2, 1-*d*]-thiazolinylidenemethyl)-6', 7'-benzothiacyanine Iodide (X) from the Dye VI and 3-Ethyl-2-methyl-naphtho[2, 1-*d*]thiazolium Iodide.** — A mixture of 1 g. of IV and 0.9 g. of 3-ethyl-2-methylnaphtho[2, 1-*d*]-thiazolium iodide in 300 ml. of pyridine was boiled at 130°C for 4 hr., pyridine was removed under a reduced pressure, and the residue was washed with 2 portions of ether. The residue was dissolved in acetone and the solution was developed through an alumina column by which the product separated into three bands of greenish black, reddish pink, and violet, from bottom to top. The reddish pink band was eluted with acetone, acetone solution was evaporated, and the residue was treated with ether, affording 0.1 g. of a crude dye, m. p. 200°C (decomp.) : $\lambda_{max}$ 580 m$\mu$ : paper chromatogram : $R_f$ 0.74 (butanol : water=6 : 1). This was identified with the dye IV.

The greenish black zone was eluted with acetone and the residue obtained on evaporation of acetone was treated with ether, affording greenish black

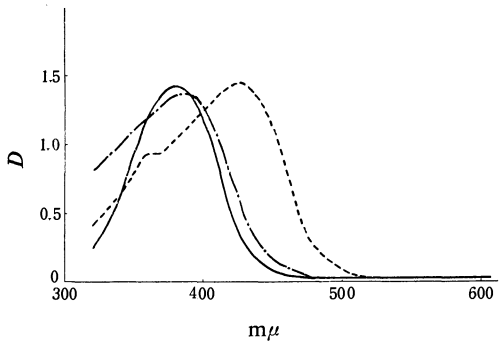



Fig. 1. Absorption spectral curves of I, II and III (in ethanol).
—·— (I), —— (II), ---- (III)

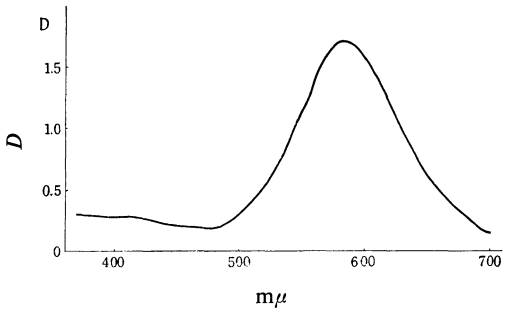



Fig. 2. Absorption spectral curve of IX (in ethanol).

crystalline powder, m. p. 192°C (decomp.). Recrystallization from methanol gave 0.5 g. of a dark green crystalline powder, m. p. 195°C (decomp.): $\lambda_{max}$ 470 and 650 mμ. Paper chromatogram: a single spot of dark green color at $R_f$ 0.94 (butanol: water=6:1).

Found: C, 59.75; H, 4.56; N, 6.00. Calcd. for $C_{37}H_{32}N_3IS_3$: C, 59.90; H, 4.32; N, 5.67%.

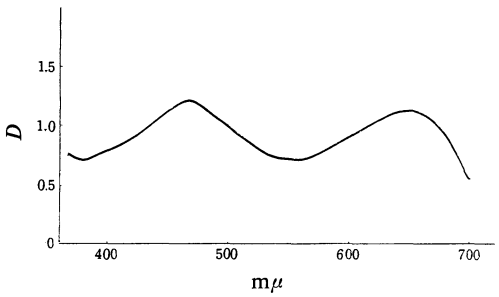



Fig. 3. Absorption spectral curve of X (in ethanol).

*Research Laboratory*
*Fuji Photo Film Co. Ltd.*
*Minami-Ashigara-machi*
*Kanagawa-ken*

# *Synthesis of Dyes with the Neocyanine Structure Presented by Brooker, and Related Dyes. V. Synthesis of the Brooker-type Dyes from the Anil of 3-Ethyl-2-formylbenzothiazolium Iodide*

By Shiro KIMURA

(Received November 17, 1959)

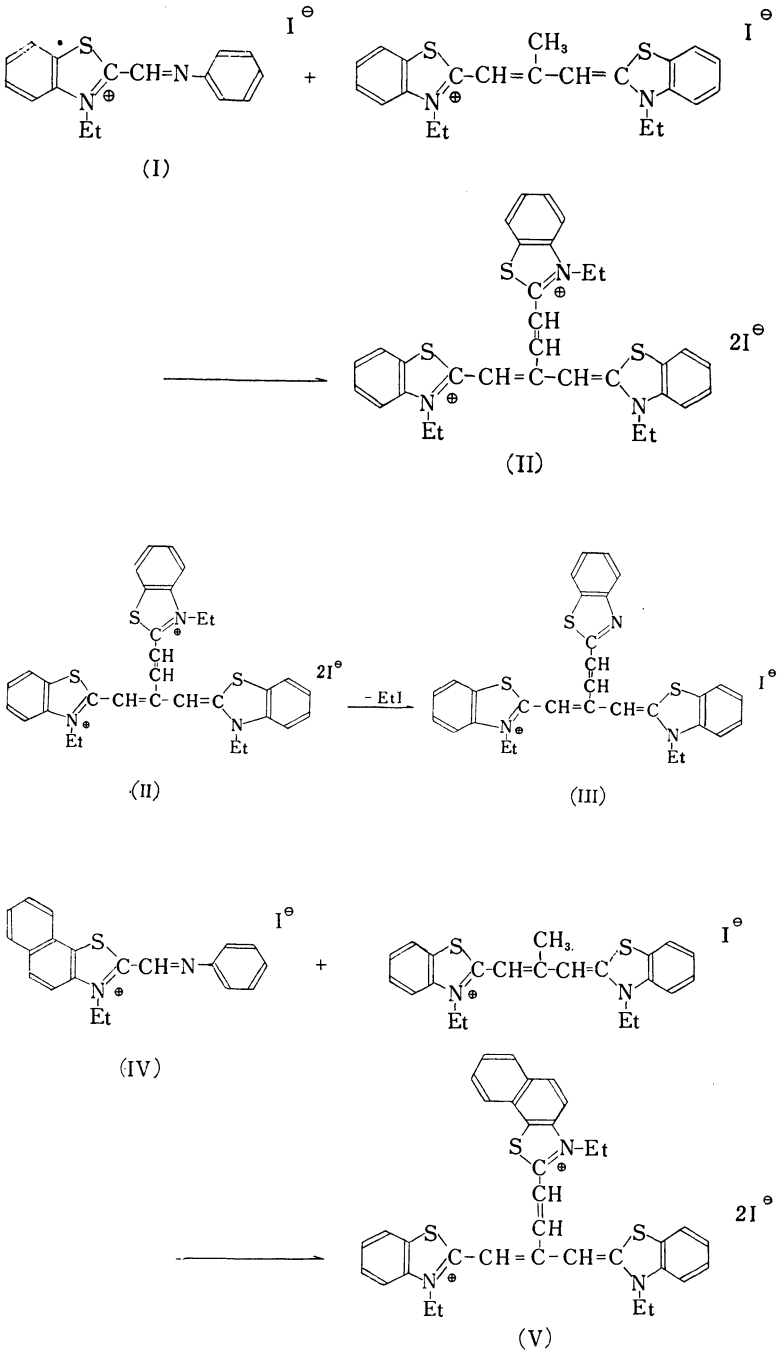
Synthesis of the Brooker-type dye, 3, 3′-diethyl-9-[2-(3-ethyl-1-thia-3-azoniainden-2-yl) vinyl] thiacarbocyanine diiodide (II) in a good yield from the anil I of 3-ethyl-2-formylbenzothiazolium iodide and 3, 3′-diethyl-9-methylthiacarbocyanine iodide is discribed in this paper and this is the reverse of the reaction given in Part II of this series[1] for synthesis of the Brooker-type dyes from the nitrone of 3, 3′-diethyl-9-formylthiacarbocyanine bromide. At the same time, properties of the dye and synthetic process for similar dyes are described.

Pure synthetic process for the anil I was described in the preceding paper[2]. An equimolar mixture of this anil and 3, 3′-diethyl-9-methylthiacarbocyanine iodide was warmed in piperidine at 80～100°C for 5 min. and the dye II was obtained as brownish black leaflet crystal with copper luster, m. p. 257°C (decomp.).

It was shown in II that, during the course of the synthesis of this dye, heating of the mixture in a basic solvent for a long period of time or development of the product through alumina column afforded a dye of m. p. 219°C (decomp.). It was assumed that, similar to the case of 3, 3′-diethyl-9-(3-ethyl-1-thia-3-azonia-

1) S. Kimura, *Bull. Soc. Sci. Phot. Japan*, 9, 45 (1959).

2) S. Kimura, This Bulletin, 33, 872 (1960).



inden-2-yl) thiacarbocyanine diiodide described in the preceding paper, this dye II might also have undergone liberation of ethyl iodide to form 3, 3'-diethyl-9-[2-(2-benzothiazolyl) vinyl] thiacarbocyanine iodide (III). This dye III had already been synthesized by Hamer[3] and examination of her synthetic process showed that they are identical dyes.

Condensation of 3-ethyl-2-formylnaphtho-[2, 1-*d*] thiazolium iodide (IV) and 3, 3'-diethyl-9-methylthiacarbocyanine iodide in pyridine similarly afforded 3, 3'-diethyl-9-[2-(3-ethyl-1-thia-3-azoniacyclopenta [*a*] naphth-2-yl) vinyl] thiacarbocyanine diiodide (V) as purplish black crystalline powder of m. p. 257°C (decomp.): $\lambda_{max}$ 650 m$\mu$.

3) F. M. Hamer, *J. Chem. Soc.*, **1952**, 3197.

This synthetic process for the Brooker-type dyes from anils gives the product in comparatively good yield and can be recommended as a general method of synthesis of this type of dyes.

## Experimental

**Preparation of 3, 3'-Diethyl-9-[2-(3-ethyl-1-thia-3-azoniainden-2-yl) vinyl] thiacarbocyanine Diiodide (II).**—A solution of 0.95 g. of the anil I of 3-ethyl-2-formylbenzothiazolium iodide and 1 g. of 3, 3'-diethyl-9-methylthiacarbocyanine iodide in 80 ml. of pyridine was heated at 80~100°C for 5 min. and cooled; ether was added to the reaction mixture to precipitate the dye formed. The precipitate was collected by filtration, washed with water, and 1.2 g. of the crude dye was obtained as purplish black powder, m.p. 180~190°C (decomp.). Recrystallization from methanol afforded 0.045 g. (yield, 2.8%) of brownish black leaflets, m. p. 257°C (decomp.). Paper chromatogram showed a single zone of violet color at *Rf* 0.37 (butanol : water=6 : 1), $\lambda_{max}$ 560 m$\mu$. This was identified with the dye II whose preparation was described in Part II of this series[1].

Found: C, 47.48; H, 3.91; N, 5.48; I, 30.94. Calcd. for $C_{32}H_{31}N_3I_2S_3$: C, 47.60; H, 3.81; N, 5.21; I, 31.50%.

**Formation of 3, 3'-Diethyl-9-[2-(2-benzothiazolyl) vinyl] thiacarbocyanine Iodide (III) by Liberation of Ethyl Iodide from the Dye II.**—Examinations were made on elementary analytical values of the green needles, m. p. 219°C (decomp.), isolated during alumina chromatography of the product obtained from preparation of the dye II, described in Part II[1], and the values were found to be close to those calculated for III.

Found: C, 55.60; H, 4.82; N, 6.44. Calcd. for $C_{30}H_{26}N_3IS_3$: C, 55.29; H, 4.02; N, 6.45%.

The dye of m. p. 218°C (decomp.), obtained on following the synthetic process of Hamer, exhibited the same absorption curve as this dye III with $\lambda_{max}$ at 563 m$\mu$, proving these dyes to be identical.

**Preparation of 3' 3'-Diethyl-9-[2-(3-ethyl-1-thia-3-azoniacyclopenta [*a*] naphth-2-yl) vinyl] thiacarbocyanine Diiodide (V).**—A mixture of 1 g. of the anil IV of 3-ethyl-2-formylnaphtho[2, 1-*d*]thiazolium iodide and 1 g. of 3, 3'-diethyl-9-methylthiacarbocyanine iodide in 80 ml. of pyridine was heated in an oil bath of 115~120°C for 10 min. Insoluble matter was filtered off, ether was added to the filtrate to precipitate the dye formed, and the mixture was allowed to stand over night. The precipitate was collected by filtration, washed with ether, and 0.8 g. of crude dye, m. p. 185~195°C (decomp.), was obtained. Recrystallization from 50 ml. of methanol afforded, as the first crop, the starting dye as indigo prisms, m. p. 275°C (decomp.), and concentration of this mother liquor to one-half the original volume afforded 0.17 g. of crystals of m. p. 195°C (decomp.). Recrystallization of this second crop of crystals from 30 ml. of methanol gave 0.05 g. of purplish black crystalline powder, m. p. 257°C (decomp.): $\lambda_{max}$ 650 m$\mu$.

Found: C, 50.00; H, 3.94; N, 5.00. Calcd. for $C_{36}H_{33}N_3I_2S_3$: C, 50.40; H, 3.86; N, 4.90%.

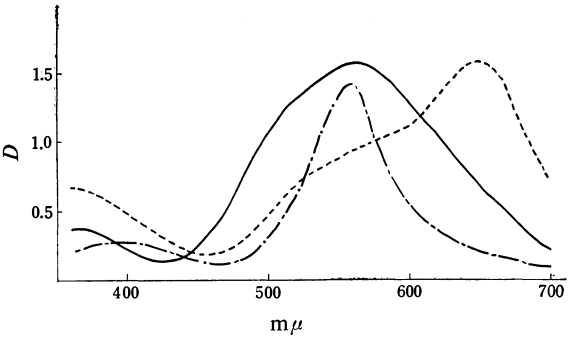



Fig. 1. Absorption spectral curves of II, III and V (in ethanol).

—— (II) —— (III) ---- (V)

*Research Laboratory*
*Fuji Photo Film Co. Ltd.*
*Minami-Ashigara-machi*
*Kanagawa-ken*

# *Rapid Determination of Thorium by Fluoride Titration Using Some Chromotropic Azo Dyes*

By Sachindra Kumar DATTA

(Received January 8, 1960)

Thorium nitrate has been employed by many workers as a reagent for the volumetric analysis of fluoride. Willard and Winter[1] used alizarin sulfonate as indicator in the titration of fluorine with thorium nitrate. This method for the determination of fluorine in minerals and rocks has undergone many modifications in the hands of many workers[2]. Menis and co-workers[3] used alizarin red-S for the titration of fluoride by an automatic spectrophotometric device. Gurev and Ioffe[4] employed the thorium-alizarin red-S lake for the photometric determination of fluorine in zinc concentrates and electrolytes. This dye found application in the determination of this halogen by column chromatography with cellulose supported with alizarin red-S[5]. This thorium-alizarin sulfonate method has also been used by Guntz and Arene[6] for the colorimetric determination of fluorine in waters. Organic fluorine has also been determination by this method by Musgrave and Smith[7] and later the method was modified by Stross and coworkers[8] and also by Ellis and Musgrave[9]. Milton and Liddel[10] employed solochrome Brilliant Blue B. S. as indicator for the estimation of fluorine. Willard and Horton[11] made a comparative study on the use of many indicators for the titration of fluoride with thorium nitrate and showed that purpurin sulfonate and alizarin red-S gave reproducible results. Banerjee[12] used his dye SPADNS as indicator for such titration. The present author employed three dyes: SNADNS-4, di-SNADNS-4 and nitroso-SNADNS-4 for the determination of fluorine present in fluorides and rocks[13].

The reversed procedure, i. e., titration of thorium with a soluble fluoride in presence of a metal indicator is also feasible. Banerjee[14] carried out such a titration using SPADNS dye. The present paper describes a method for the titrimetric determination of thorium with sodium fluoride using three chromotropic azo dyes: nitroso-SNADNS-4, SNADNS-6[15] and CHPADNS[16], prepared from 1-naphthylamine-4-sulfonic acid, 1-naphthylamine-6-sulfonic acid and *p*-aminosalicylic acid respectively. The dyes form pink to violet complexes with thorium, which are decomposed by the addition of a standard fluoride solution resulting in the liberation of the free dyes showing a marked color change at the end point.

## Experimental

**Reagents and Chemicals.**—*Sodium Fluoride.*—A stock solution was prepared from Merck's analytical grade sodium fluoride, previously dried at 120°C to constant weight.

*Thorium Nitrate.*—A thorium nitrate solution of strength 0.0128 M was prepared from thorium nitrate tetrahydrate (E. M.) by standardising gravimetrically with oxalic acid and phenyl acetic acid.

*Dye Solution.*—The dyes were prepared by following methods previously described[15,16]. A 0.1% solution of the dyes was used.

TABLE I. EFFECT OF pH ON THE TITRATION
NaF=0.0526 M

| Th taken mg. | pH | Th found (mg.) with the dyes | | |
|---|---|---|---|---|
| | | Nitroso-SNADNS-4 | SNADNS-6 | CHPADNS |
| 14.85 | 1.81 | 13.20 | 12.81 | 12.63 |
| | 2.01 | 13.51 | 13.45 | 13.52 |
| | 2.25 | 13.92 | 13.86 | 13.94 |
| | 2.43 | 14.84 | 14.82 | 14.83 |
| | 2.62 | 14.86 | 14.83 | 14.84 |
| | 2.83 | 14.84 | 14.86 | 14.86 |
| | 3.22 | 14.75 | 14.72 | 14.74 |

1) H. H. Willard and O. B. Winter, *Ind. Eng., Chem., Anal. Ed.*, 5, 7 (1933).
2) G. Bruinisholz and J. Michod, *Helv. Chim. Acta*, 37, 874 (1954); F. Grimaldi and F. Cutta, *Anal. Chem.*, 27, 918 (1955); G. Pletzka and P. Ehrlich, *Angew. Chem.*, 65, 131 (1953); D. S. Reynolds and W. L. Hill, *Ind. Eng. Chem., Anal. Ed.*, 11, 21 (1939); H. R. Shell and R. L. Craig, *Anal. Chem.*, 26, 996 (1954).
3) O. Menis, D. L. Manning and R. G. Ball, *Anal. Chem.*, 30, 1772 (1958).
4) S. D. Gurev and V. P. Ioffe, *Anal. Abstr.* 6, 159 (1959).
5) S. K. Yasuda and J. L. Rambert, *Anal. Chem.*, 30, 1489 (1958).
6) A. A. Guntz and M. Arene, *Chim. Anal.*, 40, 453 (1958).
7) W. K. R. Musgrave and J. Smith, *J. Chem. Soc.*, 1949, 3026.
8) Stross et al., *Metallurgia*, 36, 346 (1947).
9) J. F. Ellis and W. K. R. Musgrave, *J. Chem. Soc.*, 1950, 1969.
10) R. F. Milton, H. F. Liddel and J. E. Chivers, *Analyst*, 72, 43 (1947).
11) H. H. Willard and C. A. Horton, *Anal. Chem.*, 22, 1190 (1950).
12) G. Banerjee, *Anal. Chem. Acta*, 13, 409 (1955).
13) S. K. Datta, *Z. anal. Chem.* 149, 333 (1956).
14) G. Banerjee, ibid., 146, 417 (1956).
15) S. K. Datta, ibid., 149, 270 (1956).
16) S. K. Datta, ibid., 167, 105 (1959).

TABLE II. DETERMINATION OF THORIUM WITH FLUORIDE

| Th taken mg. | Volume of 0.0263 M NaF: Theoretical ml. | Actually required using the dyes: Nitroso-SNADNS-4 ml. | SNADNS-6 ml. | CHPADNS ml. | Alizarin-S ml. |
|---|---|---|---|---|---|
| 43.07 | 28.24 | 28.19 | 28.17 | 28.18 | 28.17 |
| 31.19 | 20.45 | 20.42 | 20.40 | 20.43 | 20.41 |
| 29.70 | 19.47 | 19.48 | 19.45 | 19.47 | 19.43 |
| 23.76 | 15.58 | 15.60 | 15.59 | 15.61 | 15.57 |
| 11.88 | 7.79 | 7.78 | 7.76 | 7.80 | 7.80 |
| 2.97 | 1.95 | 1.98 | 1.94 | 1.96 | 1.93 |
| 1.49 | 0.98 | 0.96 | 1.00 | 0.94 | 0.95 |

*Buffer Solution.*—Standard acetate buffer mixtures of different pH were prepared as usual.

*Starch Solution.*—A 5% starch solution was prepared when required.

**Optimum Conditions for the Determination of Thorium.**—*Hydrogen Ion Concentration.*—Titration of thorium was carried out in solutions having different pH, adjusted by 0.01 N hydrochloric acid, sodium hydroxide or acetate buffer. It was observed that a pH range from 2.4 to 2.8 was more or less suitable for estimation with these dyes. (Table-I).

*Concentration of the Dyes.*—A. half ml. of 0.1% dye solution was sufficient to give good end points with smaller amounts thorium in 50 ml. volume.

*Concentration of Thorium Solution.*—Reproducible results were obtained when very dilute solutions of thorium were titrated. The end point becomes obscure and a considerable amount of the indicator is absorbed by the increased amount of thorium fluoride precipitate. The quantity of thorium present should not be more than 50 mg. per 50 ml.

*Starch Solution.*—A 5 ml. portion of 5% freshly prepared starch solution should be added per 50 ml. solution to reduce the precipitation of thorium fluoride, acting as a protective colloid[8].

*Volume of Titrating Solution.*—In order to find out the effect of dilution of the volume of the titrating solution on the end point, titrations were carried out by varying the final volume of the solution keeping all other things constant. It was found that titration was best done in 40~50 ml. volume.

*Temperature.*—The titration is to be carried out at room temperature. At higher temperature the end point became indistinct.

**Analytical Procedure.**—An aliquot quantity of thorium nitrate solution was taken in a 250 ml. Erlnmeyer flask to which was added 0.5 ml. of the indicator, the mixture was diluted to 40 ml. the pH was adjusted to 2.5 with 0.01 N sodium hydroxide or hydrochloric acid, 5 ml. of starch solution were added and the volume was finally made up to 50 ml. The titration was carried out rapidly with the standard sodium fluoride solution till the end point was attained. Blank titrations were also carried out side by side. Titration should be completed quickly as the efficacy of the starch solution is soon lost. At the end point the color of the solution with nitroso-SNADNS-4, changed from reddish-pink to yellow, with SNADNS-6 the change was from pinkish-blue to pink and with CHPADNS the color changed from pinkish-violet to red. The end point with nitroso-SNADNS-4 was very sharp and distinct. Some of the representative data given in Table II, show that the method is stoichiometric up to about 50 mg. of thorium, within the limits of experimental error. The results have been compared with those obtained by the use of alizarin red-S indicator at pH 2.9~3 and the results were found to agree favorably.

**Determination of Thorium in Micro Quantities.** The procedure for titrating microgram amounts of thorium was the same as before, excepting that a micro-burette, more dilute solutions of the fluoride and thorium nitrate and 0.5 ml. of 0.05% dye solution per 50 ml. final volume, were used. The end points were sharper in this titration as the bulk of thorium fluoride formed was small. The data recorded in Table III, indicate that as low as 3.8 $\mu$g. of thorium per 50 ml. may be determined using these dyes with fair accuracy.

TABLE III. MICRO-TITRATION OF THORIUM WITH FLUORIDE

| Th taken $\mu$g. | Th found in $\mu$g. (NaF=0.0013 M): Nitroso-SNADNS-4 | SNADNS-6 | CHPADNS |
|---|---|---|---|
| 22.88 | 22.90 | 22.86 | 22.89 |
| 15.26 | 15.22 | 15.19 | 15.21 |
| 11.44 | 11.41 | 11.40 | 11.38 |
| 7.63 | 7.60 | 7.60 | 7.62 |
| 3.81 | 3.78 | 3.74 | 3.76 |

**Effect of Various Ions on the Determination.**—Possible interference in this determination was investigated. The ions that complex thorium or the dyes and also those which react with fluoride, interfere strongly. The elements which caused interference are as follows: lead, mercury(I), alkaline earth metals, iron, tin, manganese, magnesium, cerium, rare earth elements, zirconium, phosphate, borate, oxalate, tartrate and citrate. Determination could be carried out in the presence of other elements like copper, cadmium, aluminum, beryllium, zinc, mercury(II), cobalt, nickel, sodium and potassium. The results have been placed in Table IV.

TABLE IV. DETERMINATION OF THORIUM IN PRESENCE OF DIVERSE IONS

Th taken = 8.91 mg. = 5.84 ml. of 0.0263 M NaF

| Elements | Amount mg. | Titre value (ml.) with | | |
|---|---|---|---|---|
| | | Nitroso-SNADNS-4 | SNADNS-6 | CHPADNS |
| Na | 12.84 | 5.88 | 5.81 | 5.89 |
| K | 13.16 | 5.87 | 5.88 | 5.86 |
| Cu | 5.21 | 5.80 | 5.79 | 5.80 |
| Cd | 9.32 | 5.89 | 5.80 | 5.88 |
| Al | 6.03 | 5.81 | 5.78 | 5.80 |
| Be | 5.71 | 5.80 | 5.79 | 5.79 |
| Zn | 8.72 | 5.82 | 5.88 | 5.81 |
| Hg(II) | 4.32 | 5.83 | 5.80 | 5.86 |
| Co | 8.13 | 5.80 | 5.81 | 5.78 |
| Ni | 6.04 | 5.81 | 5.79 | 5.80 |

**Summary**

The thorium-chromotropic azo dye complexes are found to be fast-reacting with fluorides, in which exchange of dye molecule for fluoride ion takes place. The colored thorium-dye complexes are thereby decomposed with the liberation of the free dye and formation of thorium fluoride. The color changes at the end point enable visual comparison. Three dyes: nitroso-SNADNS-4, SNADNS-6 and CHPADNS have been used here as thorium complexing agents or indicators. The color change with the nitroso-SNADNS-4 at the end point is very sharp. Titrations are best carried out at pH range 2.4~2.8 and thorium present should not be more than 50 mg. per 50 ml. solution. With the increased precipitation of thorium fluoride the dyes are adsorbed in the precipitate and the end point becomes more obscured. Microgram amounts of thorium may also be determined by this method. A large number of cations and anions interfere in the process, of which the most important are: iron, cerium, rare earth elements, alkaline earth elements, phosphates, borates, oxalates, tartrates and citrates. This method is best applicable to thorium solutions from which the interfering elements have been removed.

*Chemical Laboratory*
*Victoria (Government) College*
*Coochbehar, India*

# *Separation of Radioactive Arsenic from Germanium Irradiated with Protons*

By Kazuo SAITO, Shigerô IKEDA and Makoto SAITO

(Received January 26, 1960)

Concerning the preparation of radioactive arsenic including $^{70}As$, $^{71}As$, $^{72}As$ and $^{74}As$, from a germanium target irradiated with protons, a little information is available. Green et al.[1] extracted germanium tetrachloride with benzene and left arsenic in the aqueous phase consisting of 11 N hydrochloric acid. Irvine[2] distilled off germanium tetrachloride in an oxidative atmosphere in the presence of carrier arsenic and hydrochloric acid. These reports, however, give only insufficient information on the preparation of radioactive arsenic of a very high specific activity (e. g. 1 mc in 0.05 ml. of aqueous solution containing less than 10 $\mu$g. of arsenic).

With the aims of measuring the accurate energy of the gamma rays of arsenic $-74$ by the internal conversion method and using the product for a tracer of a high specific activity, the present authors examined the separation of almost carrier-free arsenic by distillation with reference to the rate of distillation; they also applied the solvent extraction method[3] with diethyldithiocarbamate to the present purpose. Since commercial germanium of a high purity contains a very small amount of arsenic (e. g. less than 0.0001%), the product can not be called carrier-free. However this is regarded as practically carrier-free from either a nuclear spectroscopic or a radiochemical viewpoint; never-the-less the term "carrier-free" is not used in this paper.

It was elucidated that the distillation of arsenic trichloride in the absence of germanium, is completed within 5 min. (Table I.) and the

1) M. Green and J. A. Kafalas, *J. Chem. Phys.*, 22, 760 (1954).
2) W. Irvine Jr., *J. Applied Phys.*, 13, 910 (1942).
3) N. Stanford, P. F. Wyatt and F. G. Kershaw, *Analyst*, 70, 232 (1945).

distillate contains no appreciable amount of solute other than hydrogen chloride, hydrogen bromide and radioactive arsenic in an almost carrier-free state. It is often seen that the distillation of a substance is retarded on a micro scale, but this is not the case. It remains uncertain, however, whether the rapid distillation is due to the possible presence of a very small amount of carrier or to the fact that a large amount of hydrogen chloride simultaneously distils out. The distillate can be used as a tracer for arsenic. It was found, however, more convenient to extract arsenic into an organic phase and extract it back into an aqueous layer, for the product to be submitted to conversion electron measurement in a beta-ray spectrometer.

The extraction of diethyldithiocarbamate with carbon tetrachloride provides satisfactory results on such a micro scale, provided that a sufficient amount of the reagent is present. (Fig. 1) The use of an acetate buffer, which is generally involved in the analytical use of this reagent, was not found essential for a quantitative extraction, whenever the pH is duely adjusted. It appears as if the use of a buffer causes the presence of a salt-like substance in the final product, which vitiates the specific activity and hence the conversion electron spectrum. Although the presence of germanium does not interfere with the extraction, most satisfactory results were obtained by the application of the extraction method to the distillate of almost carrier-free arsenic trichloride. Retardation of the extraction, which is often involved in the case of carrier-free separation, was not recognized. The reason is uncertain, but it must be noticed that a large excess of diethyldithio carbamate is essential for a rapid extraction and that a very small amount of the reagent is extracted into the organic phase at the given pH.

When relatively short-lived arsenic-69, 70, 71, 72 and 76 decay after one week, the redioactivity consists of arsenic-74 (half-life, 17.5 days) and arsenic-73 (76 days); the latter gives only two gamma rays of 14 and 54 keV. and does not interfere with the measurement of gamma-rays of arsenic-74 having higher energies, by the scintillation method. Hence the product is satisfactorily used for the study of the decay scheme of $^{74}$As and as a tracer of arsenic having an apparent half-life of 17.5 days. The result of the study of the decay scheme was published elsewhere[5]. A part of the spectrum is shown in Fig. 2, which clearly shows that the source is thin enough to give a resolution of $\pm 0.8\%$. The amount of miscellaneous substances in the final product, including carrier arsenic is less than 10 $\mu$g. for 0.4 mc, the specific activity for $^{74}$As being about 1 mc per 25 $\mu$g. immediately after preparation. The overall yield for $^{74}$As is about 70%.

## Experimental

**Target and Irradiation.**—Elementary germanium of a purity more than 99.99999999% (measured by the Hole effect) (possible chemical purity more than 99.999%) and germanium dioxide (purity more than 99.999%) were used as target. The germanium was placed on a water-cooled detachable stem and covered with a thin (20 $\mu$) foil of aluminum. The oxide was mixed with a dilute solution of glycerin phthalate resin (glyptal) in ethylacetate, mounted on an aluminum plate and dried at 250°C; the plate was fixed on the head of the stem.

Irradiation was made in INS cyclotron (diameter of the magnet pole piece, 163 cm.) with protons of various energies ranging from 10 to 14 MeV. for 2 to 5 hr., the intensity of the beam current being 10 to 20 $\mu$A. The irradiated target was set aside in the vacuum chamber for 1 hr., the head of the stem taken out and the target submitted to chemical separation.

The irradiated unit contained arsenic-70, 71, 72, 73, 74 and 76, germanium-69 and 71 (produced by (p, pn) reaction) and probably a small amount of gallium-67, 68, 70 and 72 (produced by (p, 2p) and (p, $\alpha$) reaction) as radioactive nuclides. The total amount of radioactive substance was of the order of several ten mc immediately after irradiation, when the beam current was 15 $\mu$A and the duration of irradiation was 5 hr.; the amount of arsenic-74 appeared to be 1 mc or a little less. Irradiation was made five times altogether. Chemical behavior of the produced nuclides was carefully checked. Essential parts are described as follows.

**Distillation.**—The elementaryger manium (10 g., in four pieces) was placed in a Clysen-type flask, dissolved in aqua regia (30 ml.) and germanium tetrachloride distilled in a current of chlorine with the addition of 6 N hydrochloric acid (50 ml.) until the volume of the residue is less than 1 ml. The addition of hydrochloric acid and the distillation were repeated three times. Germanium oxide taken off the plate was placed in the flask and similarly distilled. The remaining charred resin did not interfere with the subsequent distillation of arsenic. The removal of germanium was almost complete. The chlorine being removed in a current of nitrogen, the arsenic trichloride was distilled in the presence of 10 N hydrochloric acid (10 ml.) and 9 N hydrobromic acid (5 ml.), into an ice-cooled adapter containing water (10 ml.). The arsenic was found in the first a few milliliters' portion. This fact was clearly demonstrated by a small-scaled distillation

4) C. L. Luke, and M. E. Campbell, *Anal. Chem.*, **25**, 1588 (1953); H. Goto and Y. Kakita, *J. Chem. Soc. Japan, Pure Chem. Sec. (Nippon Kagaku Zasshi)*, 77, 739 (1956).

5) T. Yamazaki et al., *J. Phys. Soc. Japan*, in press. After the completion of the present study, the following two papers have appeared. They concern the decay scheme of $^{74}$As, but not the chemical procedures. E. P. Gligoriev et al., *Izvestia Akad. Nauk, SSSR, Ser. Phys.*, **22**, 831, (1958); D. J. Horen et al., *Phys. Rev.*, **113**, 875 (1959).

TABLE I. DISTILLATION OF ARSENIC TRICHLORIDE*

| Fraction | Distilled ml. | Time of distil. min. | Relative counting rate, c.p.m. | Remarks |
|---|---|---|---|---|
| 1 | 5 | 5 | 10863 | ** |
| 2 | 4 | 8 | 241 | |
| 3 | 5 | 13 | 88 | |
| 4 | 5 | 20 | 56 | |
| 5 | 5 | 24 | 45 | |
| 6 | 5 | 30 | 7 | +HCl 10 ml. +HBr 5 ml. |
| 7 | 5 | 35 | 23 | |
| 8 | 7 | 42 | 16 | |

* The amount of the radioactive As is much smaller than that in the practical separation, but the volume of the aq. soln. is almost the same.

** Initial vol. of the aq. soln. 0.5 ml.; the counting rate, 12100 c.p.m.

shown in Table I. The total recovery was about 94%; most of the remaining radioactive arsenic was found on the surface of the rubber stoppers.

**Solvent Extraction.**—The experimental procedure shown in the original paper[3] was followed.

Since this method has been examined for use in micro analysis of arsenic[4], the following experiments were centered around the rate of extraction on such an ultra-micro scale. The distillate was heated to dryness with sulfuric acid (1 N, 2 ml.) and nitric acid (15 N, 5 ml.), mixed with hydrochloric acid (12 N, 1 ml.) and water (15 ml.) and again heated to 50°C. The product is treated with potassium iodide solution (10%, 3 ml.) and sodium sulfite (1 g.), made pH 5 with sodium acetate (10%, 5 ml.) and aqueous ammonia solution and shaken with carbon tetrachloride for 1 min. (equal volume to the aqueous layer) in the presence of variable amounts of sodium diethyldithiocarbamate solution (0.1%, in water). The results are shown in Fig. 1.

It is clearly seen that the extraction largely depends on the amount of the reagent. No appreciable adsorption of radioactive arsenic was observed on the surface of the glass wares, not excepting the ground parts. A similar extraction curve was obtained in the presence of germanium. A satisfactory extraction of arsenic was also effected in the absence of any buffer, provided that the pH was duely adjusted. Back-extraction of radioactive arsenic was substantiated from the carbon tetrachloride solution, by the use of 8 N nitric acid, 6 N hydrochloric acid or aqueous ammonia solution. Single extraction suffices for the recovery of more than 90% of the radioactive arsenic.

**Measurement of Radioactivity.**—For checking the procedures for separation, a G. M. counter was used, the sample being placed at a reproducible geometry. Since one series of experiments is completed within a few hours, the radiochemical composition of the sample can be regarded as identical, although the sample solution contains, especially at the early stage of separation, several radioactive nuclides. Hence the counting rate was shown in c. p. m. on an arbitrary scale in the figures and tables.

For the measurement of the conversion electron spectrum, the back-extracted arsenic in nitric acid solution was mounted on a trace of insulin on a thin polyvinylchloride foil lined with a thin layer (several $\mu$g. per cm$^2$) of vacuum-evaporated aluminum, dried up under an infrared lamp or in vacuo and attached to a beta-ray spectrometer. (INS-III, $\rho = 18$ cm.)

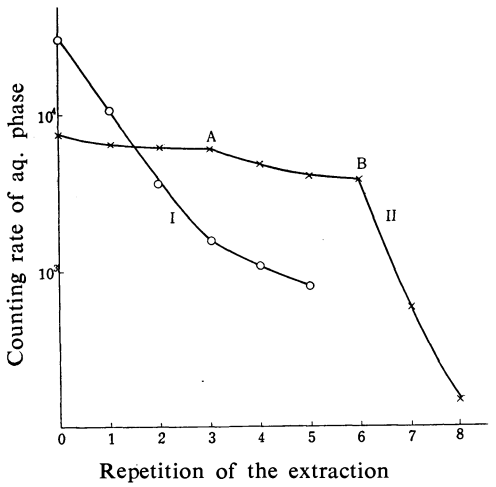



Fig. 1. Extraction of arsenic with carbontetrachloride in the presence of diethyldithiocarbamate.

Curve I. Extraction in the presence of 3 ml. of 0.1% reagent soln.; vol. of the aq. phase, 6 ml.; time of shaking 1 min. each.

Curve II. Extraction in the presence of a less amount of reagent; initial, 0.5 ml.; vol. of the aq. phase, 6 ml.; time of shaking, 1 min. At point A and B, 0.5 ml. and 1.0 ml. of 0.5% reagent soln. were respectively added.

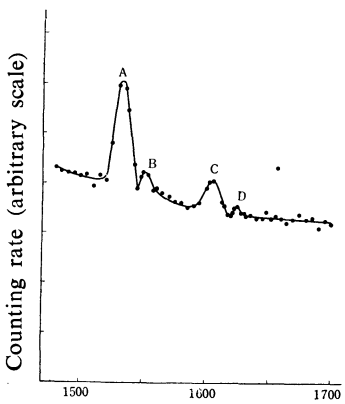



Fig. 2. Conversion electron spectrum of aresenic-74.

A, 596 keV.-K; B, 596 keV.-LM; C, 635 keV.-K; D, 635 keV.-LM.

The experiments were carried out co-operatively by the members of the beta- and gamma-ray group of the Institute for Nuclear Study (Dr. Mitsuo Sakai, Messers. Hidetsugu Ikegami and Toshimitsu Yamazaki), to whom the authors thanks are due. They are also indebted to Professor Hidehiro Goto of Tohoku University for his encouragement. A part of the expenses was defrayed from the Ministry of Education.

*Institute for Nuclear Study*
*The University of Tokyo*
*Tanashi, Tokyo (K. S.)*

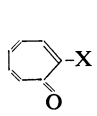
*Institute for Iron,*
*Steel and other Metals*
*Tohoku University*
*Katahira-cho, Sendai*
*(S. I. and M. S.)*

# *The Synthesis of 4-Aminotropone*

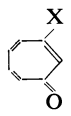
By Kozo Doi

(Received November 17, 1959)

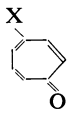
Tropolone[1] (I) and its isomers, 3-hydroxytropone[2] (II) and 4-hydroxytropone[3] (III) have been synthesized and their reactions have also been investigated. The amino homologues, of tropolones, 2-aminotropone[1] (IV) and derivatives, have already been synthesized and their reactions have been studied in detail. The isomeric 3-aminotropone (V) and 4-aminotropone (VI), on the other hand, have sofar not been prepared. The present communication deals briefly with the synthesis of the 4-isomer VI starting from 4-aminotropolone[4] (VII).



I: X=OH IV: X=$NH_2$

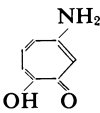


II: X=OH V: X=$NH_2$

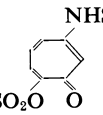


III: X=OH VI: X=$NH_2$

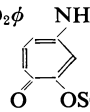
Reaction of 4-aminotropolone sulfate and *p*-toluenesulfonyl chloride in pyridine afforded, with company of a di-*p*-toluenesulfonate (VIII), 4-amino-2-*p*-toluenesulfoxytropone (IX), of which hydrogenolysis[5] over 5% palladized charcoal gave easily 4-aminotropone (VI).



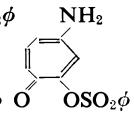
VII



VIIIa



VIIIb



IX

The ultraviolet absorption of the aminotropone VI shows an tropone type of spectrum[6], having maxima at 228 m$\mu$ (log $\varepsilon$ 4.35), 260 (3.89) and 365 (4.38) (Fig. 1).

The structure of the aminotropone VI is more reasonably assumed from the fact, that its infrared spectrum has two absorption bands,

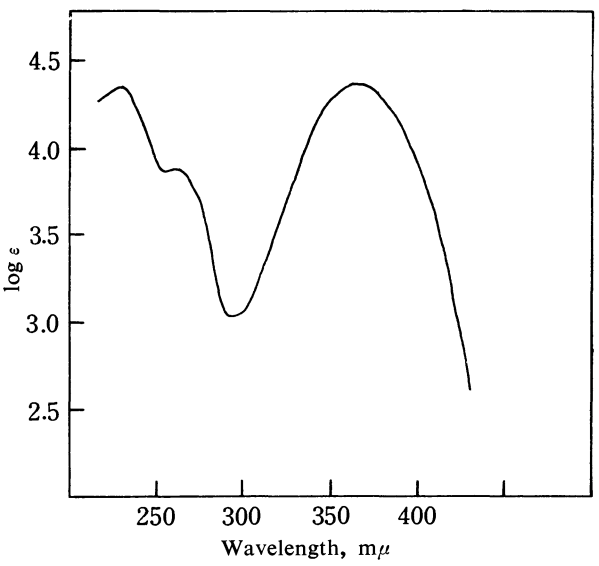



Fig. 1. Ultraviolet absorption spectrum of 4-aminotropone (VI) in methanol.

1) cf. P. L. Pauson, *Chem. Revs.*, **55**, 9 (1955).
2) R. B. Johns, A. W. Johnson and M. Tisler, *J. Chem. Soc.*, **1954**, 4605; A. W. Johnson and M. Tisler, ibid., **1955**, 1841.
3) T. Nozoe, T. Mukai, Y. Ikegami and T. Toda, *Chem. & Ind.*, **1955**, 66; R. B. Johns, A. W. Johnson, A. Langemann and J. Murray, *J. Chem. Soc.*, **1955**, 309.
4) K. Doi, Abstracts of the 12th Annual Meeting of the Chemical Society of Japan, p. 230 (1959).
5) T. Nozoe, S. Seto, T. Sato and S. Ninagawa (to be published) have found the formation of tropones from 2-*p*-toluenesulfoxytropones with a similar hydrogenolysis procedure.
6) M. Tsuboi, This Bulletin, **25**, 369 (1952).

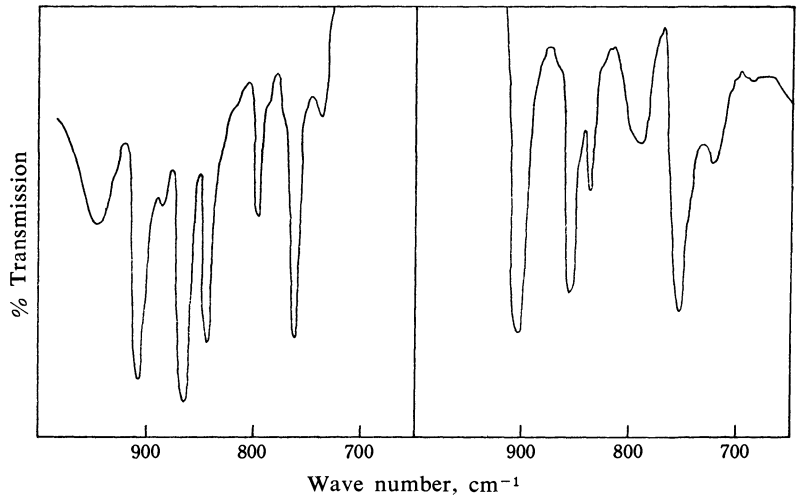



Fig. 2. Infrared absorption spectra of 4-aminotropone (VI, right) and 4-hydroxytropone (III, left).

790 and 903 $cm^{-1}$, which have been assigned[7] to the bands based on the CH out-of-plane vibrations of 4-substituted tropones. It may support the structural assignment above described, that the infrared spectrum of 4-hydroxytropone[7] (III) has two absorption bands, 797 and 865 $cm^{-1}$, and the features of the absorption in this region are closely ressembling to that of the aminotropone VI (Fig. 2).

## Experimental

**4-Amino-2-*p*-toluenesulfoxytropone (IX).**—To a stirred solution of 4-aminotropolone sulfate[4] (2 g.) and pyridine (3 cc.), was added *p*-toluenesulfonylchloride (1.9 g.) for 3 min. at room temperature. After 30 min., dilution with water (20 cc.) and subsequent filtration afforded a pale yellow solid (2.6 g.), m. p. 199~200°C (decomp.), of which fractional recrystallization from methanol gave a less soluble product, a di-*p*-toluenesulfonate (VIII, 1.8 g.), m.p. 213°C (decomp.),

Found : C, 56.37 ; H, 4.54 ; N, 3.56. Calcd. for $C_{21}H_{19}O_6NS_2$ : C, 56.61 ; H, 4.30 ; N, 3.14%.

and more soluble product IX (0.12 g.), yellow needles, m. p. 194°C (decomp.).

Found : C, 57.67 ; H, 4.41 ; N, 5.00. Calcd. for $C_{14}H_{13}O_4NS$ : C, 57.73 ; H, 4.50 ; N, 4.82%.

**4-Aminotropone (VI).**—A mixture of IX (0.3 g.), sodium acetate trihydrate (0.15 g.), 5% palladized charcoal (50 mg.) and methanol (100 cc.) was shaken in the hydrogen atmosphere until absorption of hydrogen ceased. After 8 hr., the catalyst was removed and the filtrate was concentrated in vacuo. The residual solid, after chromatographic purification (ethyl acetate-alumina) followed by crystallization from ethyl acetate, afforded 4-aminotropone (VI, 20 mg.), yellow prisms, m. p. 218°C (decomp.).

Found : C, 69.08 ; H, 5.83 ; N, 11.63. Calcd. for $C_7H_7ON$ : C, 69.40 ; H, 5.83 ; N, 11.56%.

The author thanks Professor Yoshio Kitahara very much for his unfailing guidance, also Mr. Yusaku Ikegami for the infrared spectral analysis and Messrs. Shinichi Ohyama and Yoko Endo for the microanalyses.

*The Chemical Research Institute of Non-Aqueous Solutions*
*Tohoku University*
*Katahira-cho, Sendai*

7) Y. Ikegami *Kagaku-no-Ryoiki* (*J. Japanese Chem.*), Extra No. 38, p. 33, Nankodo Co., Tokyo (1959).

# *Magnetic Susceptibilities of Sulfur, Selenium and Tellurium from Room Temperature to 1100°C*

By Shōtarō Tobisawa

(Received August 18, 1959)

The temperature-dependences of magnetic susceptibilities of sulfur, selenium and tellurium have, hitherto, been investigated by many workers. Some different results can, however, be found among their data. The magnetic susceptibilities of the three elements have, therefore, been measured with the recording magnetic balance to compare the present results with those reported by other investigators and to compare the present results with experimental results observed on the physical properties such as viscosity, specific heat, electrical conductivity and so on.

## Experimental

**Materials.**—*Sulfur.*—Guaranteed sulfur, Kanto Chemical Co. Ltd., was purified by Bacon and Fanelli's procedure[1], and then was treated by Gardner and Fraenkel's method[2] to eliminate magnetic impurities.

*Selenium.*—Guaranteed selenium, Junsei Chemical Co. Ltd., was distilled several times under high vacuum to obtain selenium of spectro grade. A glassy solidified black-selenium (glassy selenium) was prepared by quenching a sample of molten selenium under vacuum of $10^{-5}$ mmHg. This sample was confirmed to have diffused rings without diffraction patterns by X-ray analysis. Hexagonal selenium was obtained by heating a sample of glassy selenium at about 130°C for 48 hr. under vacuum of $10^{-5}$ mmHg. This sample was found to have hexagonal patterns.

*Tellurium.*—Tellurium of Merck (sample A) and a specimen produced by Mitsubishi Ōsaka Refinery (sample B) were distilled three and five times, respectively, to obtain tellurium of spectro grade. Both the samples were crystallized by cooling very slowly from the molten state under vacuum of $10^{-5}$ mmHg. It was ascertained by X-ray examinations that both the samples had hexagonal patterns.

**Measurements.**—Measurements were carried out by using the recording magnetic balance described in detail in the previous report[3]. The dimension of the sample bulb was the same as the previously reported one. The apparatus, which was operated by the Faraday method, was modulated on a recording chart to be able to indicate the changes of

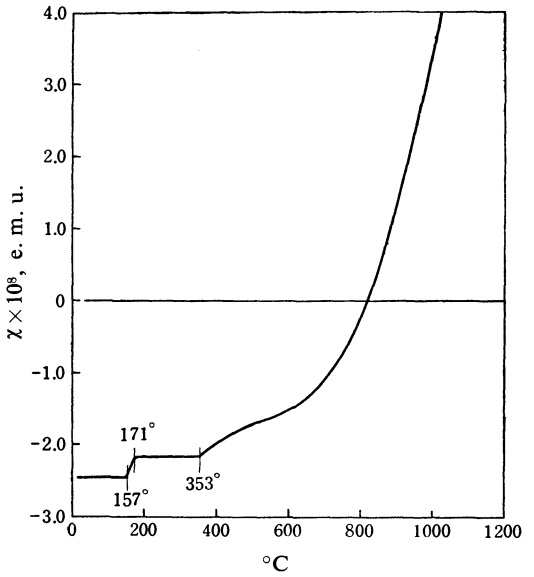



Fig. 1. Magnetic susceptibility-temperature curve for sulfur (50.2 mg. in weight).

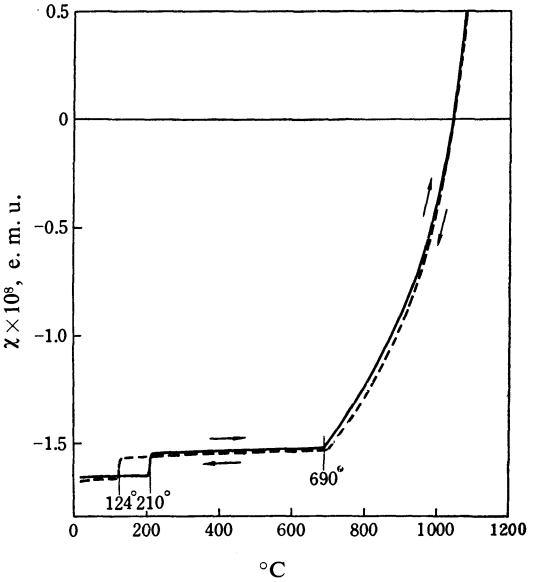



Fig. 2. Magnetic susceptibility-temperature curve for glassy selenium (50.0 mg. in weight).
—— heating ---- cooling

1) R. F. Bacon and R. Fanelli, *J. Am. Chem. Soc.*, **65**, 639 (1943).
2) D. M. Gardner and G. K. Fraenkel, ibid., **76**, 5891 (1954); ibid., **78**, 3279 (1956).
3) S. Tobisawa, This Bulletin, **32**, 1173 (1959).

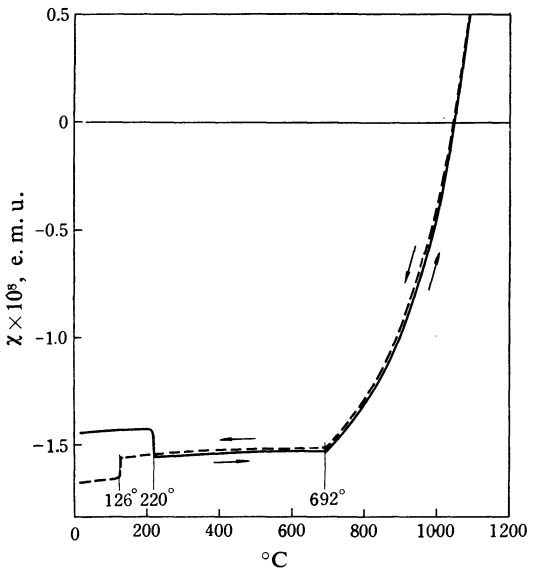



Fig. 3. Magnetic susceptibility-temperature curve for hexagonal selenium (50.2 mg. in weight).
—— heating ---- cooling

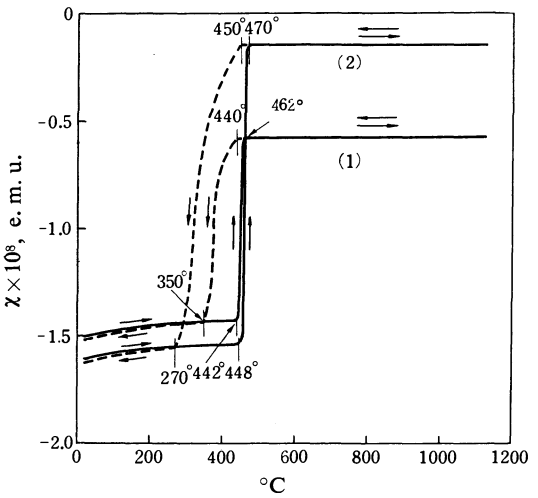



Fig. 4. Magnetic susceptibility-temperature curves for hexagonal tellurium.
(1) sample A (50.0 mg. in weight).
(2) sample B (50.1 mg. in weight).
—— heating ---- cooling

0.1 mA, which corresponded to $-1.3\times10^{-9}$ e.m.u. in magnetic susceptibility. In each experiment, a sample of about 50 mg. was charged into a fused quartz bulb. This bulb was sealed carefully, after having been evacuated to about $10^{-5}$ mmHg. The measurements were made with heating or cooling rates of 300°C per hour, at constant field, 8250 Oersteds. The results obtained are shown in Figs. 1—4.

## Results

**Comparison with the Results Obtained by other Investigators.**—*On the Solid State.*—The magnetic susceptibilities of the three elements obtained at room temperature are given in Table I. The susceptibility of sulfur scarcely changes with temperature, while those of selenium and tellurium change slightly with temperature.

Table I. The magnetic susceptibilities of the three elements

| Sample | $\chi\times10^6$ (per g.) |
|---|---|
| Sulfur | −0.49 |
| Glassy selenium | −0.33 |
| Hexagonal selenium | −0.29 |
| Hexagonal tellurium | −0.30 (Sample A)<br>−0.32 (Sample B) |

*On the Behavior of Susceptibilities at the Melting Points and their Neighborhood.*—(1) The susceptibility of sulfur showed no particular changes at the melting point and its neighborhood. It began to decrease from 157°C, and reached $-0.43\times10^{-6}$ per g. at 171°C. Ishiwara[4] reported that the susceptibility of sulfur decreased at about 160°C, while Honda[5] showed that the susceptibility of sulfur had a minimum value at the melting point.

(2) Busch et al.[6] reported that the volume susceptibility of hexagonal selenium increased on fusion. In Figs. 2 and 3, the susceptibility of glassy selenium decreased slightly at 210°C, while that of hexagonal selenium increased slightly at 220°C. On cooling, both kinds of liquid selenium turned to glassy selenium, showing slight increases in susceptibilities at about 125°C under the present experimental condition. Busch et al. reported that the volume susceptibility of glassy selenium had no abrupt changes despite the fast cooling of molten selenium.

(3) The susceptibility of hexagonal tellurium of sample A began to decrease at 442°C and reached the value of $-0.12\times10^{-6}$ per g. at 462°C. The susceptibility of sample B began to decrease at 448°C and reached the value of $-0.03\times10^{-6}$ per g. at 470°C. The susceptibility-temperature curve for hexagonal tellurium deflected toward sides opposite to that for hexagonal selenium, as shown in Figs. 3 and 4. Under the present experimental condition, sample A was supercooled to 350°C, while sample B was supercooled to 270°C.

*In the Liquid State.*—(1) The susceptibility

4) T. Ishiwara, *Science Repts. Tōhoku Imp. Univ.*, **9**, 233 (1920).
5) K. Honda, ibid., **1**, 1 (1911).
6) G. Busch and O. Vogt, *Helv. Phys. Acta*, **30**, 224 (1957).

of liquid sulfur scarcely changed until 353°C ($-0.43\times10^{-6}$ per g.).

(2) The susceptibility of fused selenium, $-0.31\times10^{-6}$ per g. at 220°C, decreased slightly with temperature. The values reported as the susceptibility of fused selenium are as follows: $-0.31\times10^{-6}$ [7], $-0.304\times10^{-6}$ [8] and $-0.32\times10^{-6}$ per g.[9] Busch et al.[6] showed that the volume susceptibility of fused selenium was $-1.347\times10^{-6}$ per cc. at the melting point. Taking 3.987 g. per $cm^3$ [10] as the density of fused selenium at 220°C, Busch's value corresponded to $-0.338\times10^{-6}$ per g. in mass susceptibility. This value is greater than the present experimental value at 220°C.

(3) The value of liquid tellurium from sample B at 470°C, $-0.03\times10^{-6}$ per g., consistent with the values of liquid tellurium obtained by Honda[11] and Endo[12], was smaller than that of sample A. On the other hand, values reported as the volume susceptibility of liquid tellurium by the other authors were $-0.3\times10^{-6}$ [13] and $-0.767\times10^{-6}$ [6] per cc.

*In the Higher Temperature Range.*—(1) The curve in Fig. 1 deflected toward paramagnetic sides above 353°C. Néel[14] and Scott[15] reported that the diatomic sulfur molecule produced by the dissociation of sulfur at high temperature,

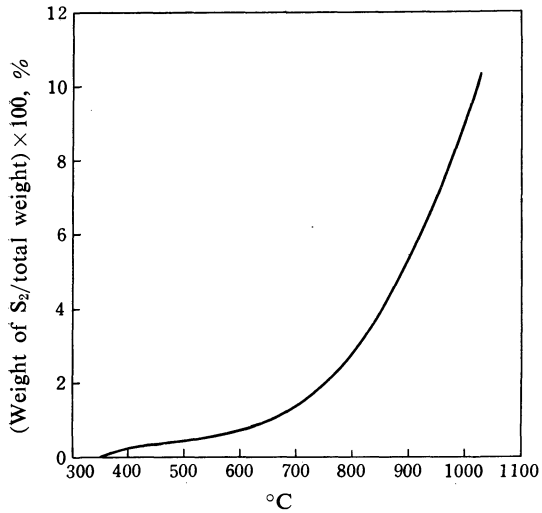



Fig. 5. (Weight of $S_2$/total weight)-temperature curve for sulfur.

was paramagnetic. On the assumption that the deflection toward paramagnetic sides above 353°C is due to the paramagnetism of the diatomic sulfur molecule, an attempt was made to estimate the weight of the diatomic sulfur molecule at every temperature by comparing the experimental value of paramagnetic susceptibility with the value calculated from Van Vleck's equation[16]. The ratios of the weight of the diatomic sulfur molecule to the total weight of sulfur at every temperature, are shown in Fig. 5.

(2) From Figs. 2 and 3, it is clear that selenium shows paramagnetism above 690°C and that the paramagnetic change occurs reversibly with temperature. Bhatnagar et al.[17] found that selenium vapor as well as sulfur vapor was paramagnetic. The ratio of the weight of the diatomic selenium molecule to the total weight of selenium was estimated in the same way as that used for sulfur. The results are given in Fig. 6.

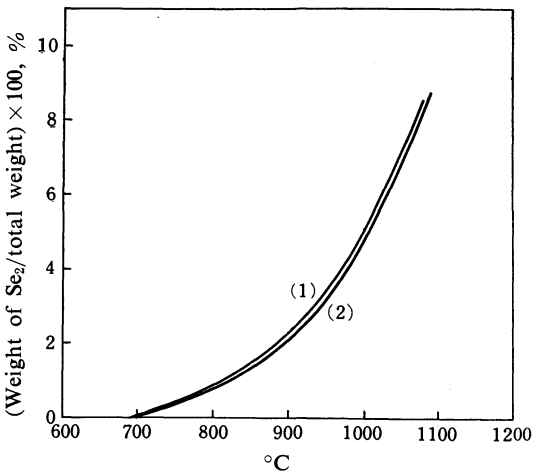



Fig. 6. (Weight of $Se_2$/total weight)-temperature curve for selenium.
(1) for glassy selenium.
(2) for hexagonal selenium.

(3) In contrast with sulfur and selenium, tellurium showed no paramagnetic changes until 1100°C under the present experimental condition. On the other hand, Busch et al. reported that tellurium was paramagnetic above 980°K.

**Reference to Experimental Results Observed on the Physical Properties such as Viscosity, Specific Heat, Electrical Conductivity and so on.** —*Sulfur.*—It is well known that liquid sulfur

7) P. Curie, *Ann. de Chem. et Phys.*, **5**, 289 (1895).
8) K. Honda and T. Sone, *Science Repts. Tōhoku Imp. Univ.*, **2**, 25 (1913).
9) M. Owen, *Ann. Physik*, **37**, 657 (1912).
10) S. Dobinski and J. Wesolowski, *Bull. intern. acad. polon. sci., Classe sci. math. nat.* **No. 8-9A**, 446 (1936).
11) K. Honda, *Ann. Physik*, **32**, 1027 (1910).
12) H. Endo, *Science Repts. Tōhoku Imp. Univ.*, **16**, 206 (1927).
13) S. R. Rao and S. R. Govindarajan, *Proc. Indian Acad. Sci.*, **10A**, 235 (1939).
14) L. Néel. *Compt. rend.*, **194**, 2035 (1932).
15) A. B. Scott, *J. Am. Chem. Soc.*, **71**, 3145 (1949).
16) J. H. Van Vleck, "Electric and Magnetic Susceptibilities", Oxford University Press, Oxford, London (1937), p. 266.
17) S. S. Bhatnagar, H. Lessheim and M. L. Khanna, *Proc. Indian Acad. Sci.*, **6A**, 155 (1937); *Nature*, **140**, 152 (1938).

has anomalies in regard to the physical properties such as viscosity[1,18,19], specific heat[20] and others[19,21] in the vicinity of 160°C. Gee[22] has interpreted these anomalies from the standpoint of the equilibrium between eight-membered sulfur rings and long chain polymers. Gee and his colaborators[23] measured the susceptibility of sulfur to investigate the existence and concentration of free radicals. They could not find any paramagnetic contribution from free radicals. On the other hand, Gardner et al.[2] confirmed the paramagnetism due to free radicals by the paramagnetic resonance absorption measurements over the range from 189° to 414°C, and stated that the paramagnetism increased reversibly with temperature. From the comparison of the present results with various results mentioned above, it can be concluded that the change in susceptibility of liquid sulfur at 157 ~171°C suggests the formation of free radicals due to the scission of the eight-membered sulfur rings. Therefore, it is reasonable to suppose from the curve in Fig. 1 that there occurred no scission of the eight-membered sulfur rings from the melting point to 157°C. Also no scission was acceptable in the temperature range from 171° to 353°C, because the curve in Fig. 1 showed no change in this range. The results mentioned above are supported by the fact that the maximum viscosity of liquid sulfur decreased rapidly with temperature in the corresponding range.

*Selenium.*—The change in susceptibility of hexagonal selenium at 220°C is due to phase transition on fusion, because the melting point of hexagonal selenium reported in the literature is 217.4°[24] or 220.2°C[25]. On the contrary, it is known that glassy selenium has no definite melting point. By X-ray investigations Lark-Horovitz[26] has concluded that glassy selenium consists of supercooled liquid, and that the chain structure was preserved in the liquid states. On the other hand, from X-ray analysis Krebs[27] insists that about one-third of glassy selenium is in the form of eight-membered selenium ring and the rest in poly-membered ring with about one thousand selenium atoms. From the electrical measurements on selenium, glassy selenium is an insulator and liquid selenium is a semiconductor with predominant hole conduction[28]. According to Krebs' interpretation, this difference between the electrical properties for glassy and liquid selenium can be ascribed to the difference between ring structure of glassy selenium and the chain structure of liquid selenium. It is reasonable to conclude that the decrease in susceptibility of glassy selenium at about 210°C can be attributed to the scission of selenium rings similar to the scission of sulfur at 157~171°C, and that the increases in susceptibilities of liquid selenium at about 125°C on cooling are related to the reclosing of chains into rings. No scission was acceptable in the temperature range from 220° to 690°C, because the susceptibility-temperature curves for selenium in Figs. 2 and 3 showed no abrupt changes in this temperature range. This interpretation is supported by the fact that the viscosity of liquid selenium decreases smoothly with temperature, showing no scission of rings[29].

*Tellurium.*—Umino[30] reported an anomaly in specific heat of solid tellurium. By X-ray investigations of tellurium layers in vacuo, Scanlon et al.[31] showed that no structure change of solid tellurium occurred up to fusion. In Fig. 4, the susceptibility-temperature curves for solid tellurium showed no abrupt changes.

Epstein et al.[32] showed that the electrical resistivity, the Hall coefficient and the thermoelectric power of tellurium decreased at the melting point of 445°C. Busch et al.[6] stated that the volume susceptibility of tellurium decreased abruptly together with the decreases in the electrical resistivity, the Hall coefficient and the thermoelectric power. In Fig. 4, the susceptibilities of samples A and B decreased in the ranges from 442° to 462°C and from 448° to 470°C, respectively. On the other hand, as the melting point of tellurium, diversely discordant values from 420° to 455°C have been listed by Machol et al.[33] The results of X-ray investigations[34] on tellurium

18) C. Farr and D. B. Macleod, *Proc. Roy. Soc.*, **A118**, 534 (1928).
19) J. Schenk, *Physica*, **23**, 546 (1957).
20) H. Braune and O. Möller, *Z. Naturforsch.*, **9a**, 210 (1954).
21) A. M. Kellas, *J. Chem. Soc.*, **113**, 903 (1918).
22) G. Gee, *Trans. Faraday Soc.*, **48**, 515 (1952).
23) F. Fairbrother, G. Gee and G. T. Merrall, *J. Polymer Sci.*, **16**, 459 (1955).
24) L. E. Dodd, *J. Am. Chem. Soc.*, **42**, 1579 (1920).
25) E. Berger, *Z. anorg. Chem.*, **85**, 75 (1914).
26) K. Lark-Horovitz and E. P. Miller, *Phys. Rev.*, **51**, 380 (1937).
27) H. Krebs, "Semiconducting Materials", Butterworths, London (1951), p. 246; H. Krebs and F. Schultze-Gebhardt, *Naturwissenschaften*, **41**, 474 (1954); *Acta Cryst.*, **8**, 412 (1955).
28) H. W. Henkel, *Phys. Rev.*, **76**, 1737 (1949); ibid., **77**, 734 (1950); *J. Appl. Phys.*, **21**, 725 (1950); H. W. Henkel and J. Maczuk, ibid., **25**, 1 (1954); P. K. Weimer, *Phys. Rev.*, **79**, 171 (1950); A. I. Blum, N. P. Mokrovskiĭ and A. R. Regel, *Izvest. Akad. Nauk S. S. S. R., Ser. Fiz.*, **16**, 139 (1952); F. Eckart, *Ann. Physik*, **14**, 233 (1954).
29) S. Dobinski and J. Wesolouski, *Bull. intern. acad. polon. sci., Classe sci. math. nat.*, **No. 10A**, 7 (1937).
30) S. Umino, *Kinzoku-no-kenkyu*, **3**, 498 (1926).
31) W. Scanlon and K. Lark-Horovitz, *Phys. Rev.*, **72**, 530 (1947).
32) A. S. Epstein, H. Fritzsche and K. Lark-Horovitz, ibid., **107**, 412 (1957).
33) R. E. Machol and E. F. Westrum, *J. Phys. Chem.*, **62**, 361 (1958).
34) R. Buschert, I. G. Geib and K. Lark-Horovitz, *Phys. Rev.*, **98**, 1157 (1955).

immediately after fusion have shown that the number of nearest neighbors and the distance between the nearest neighbors determined for the crystal persist in the liquid state. This indicates the existence of chain molecules bound by covalent bonds in the liquid. The results of electrical investigations[28,32,35] on tellurium have shown that liquid tellurium shows a semiconducting property in which hole conduction is predominant, and that the semiconductor-metal transition occurs gradually at higher temperatures. From the results of electrical measurements Epstein et al. stated that tellurium atoms bound by covalent bonds into chains of various lengths, tellurium ions, and free electrons will be present in liquid tellurium, and that, as the temperature increases, the chains will be ionized, giving off free electrons which leave behind holes, i. e., missing covalent bonds, which in turn are able to migrate within the chains, until very high temperatures are reached, at which the liquid will be composed of tellurium ions and free electrons. It can, therefore, be considered that the decrease of susceptibility during fusion in Fig. 4 is due to a paramagnetic contribution from unpaired spins produced by incomplete ionization of the valence shell[36]. That the susceptibilities of tellurium after fusion in Fig. 4 are independent of temperature, may be owing to the mixed effects of diamagnetic and paramagnetic contributions associated with the semiconductor-metal transition mentioned above.

## Summary

(1) The susceptibility of sulfur showed the first change at about 157°C, showing no changes at the melting point and its neighborhood. The change is attributed to the radical chains owing to the scission of eight-membered sulfur rings.

(2) On fusion the susceptibility-temperature curve for glassy selenium deflected toward sides opposite to that for hexagonal selenium. It is considered that the decrease in susceptibility of glassy selenium can be ascribed to free radicals produced by the scission of selenium rings. On cooling, liquid selenium turned to glassy selenium, showing the increase in susceptibility at about 125°C. It can be considered that this change is related to the reclosing of chains into rings.

(3) The susceptibility of hexagonal tellurium decreased abruptly on fusion. It may be considered that this change is due to a paramagnetic contribution from unpaired spins produced by incomplete ionization of the valence shell.

(4) The susceptibility-temperature curves for sulfur and selenium were deflected toward paramagnetic sides above 353° and 690°C, respectively. The paramagnetism increased reversibly with temperature, while the susceptibility of tellurium was independent of temperature to 1100°C. On sulfur and selenium, the ratios of the weight of the diatomic molecule to the total weight at every temperature were obtained from the weight of the diatomic molecule estimated by comparing the experimental value of paramagnetic susceptibility with the value calculated from Van Vleck's equation.

The author wishes to express his sincere gratitude to Professor Y. Nomura for his helpful suggestions and encouragement in the course of this work. The author is also indebted to Mr. T. Ashida for his valuable assistance in X-ray analysis and to Mr. S. Uchida for his kind assistance.

*Department of Chemistry*
*Defense Academy*
*Yokosuka*

35) N. P. Mokrovskiĭ and A. R. Regel, *Zhur. Tekh. Fiz.*, **25**, 2093 (1955).
36) G. Busch, H. J. Stocker and O. Vogt, *Helv. Phys. Acta*, **31**, 297 (1958).

# *On the Mechanism of the Extraction of Uranyl Nitrate by Tributyl Phosphate II. Infrared Study*

By Kenkichi NUKADA, Keiji NAITO and Utako MAEDA

(Received January 26, 1960)

The uranium extraction by TBP (tri-*n*-butyl phosphate) has been studied by many workers especially from the standpoint of distribution equilibrium. For the extraction of uranyl nitrate by TBP, the following mechanism was presented by Moore[1].

$$UO_2^{2+}(aq.) + 2NO_3^-(aq.) + 2TBP(org.) \rightleftharpoons [UO_2(NO_3)_2](TBP)_2(org.) \quad (1)$$

Naito, one of the present authors, has given an analytical method for studying the extraction mechanism and applied it to a uranyl nitrate extraction system[2]. As a result of this analysis, it was shown that the extraction of nitric acid (Eq. 2) competes with that of uranyl nitrate (Eq. 1), when uranyl nitrate is extracted by TBP from a nitric acid solution,

$$H^+(aq.) + NO_3^-(aq.) + TBP(org.) \rightleftharpoons HNO_3 \cdot TBP(org.) \quad (2)$$

However, the results obtained by the partition study were not enough to demonstrate how the TBP complex was formed from the species involved in the extracted system. In this paper the authors present the results of the infrared study concerning the mechanism of extraction. At first, discussions for the systems TBP-water, TBP-nitric acid and TBP-uranyl nitrate are given individually, and secondly the extraction mechanism of the system TBP-uranyl nitrate-nitric acid is presented.

## Experimental

Perkin-Elmer Model 12C and 321 Spectrometers equipped with rock salt prisms were used in the infrared measurement. The liquid cell was constructed from spacers and frames made by polyethylene with silver chloride windows, since the usual cell made from metal spacers and frame with alkaline halide windows is attacked by nitric acid and a considerable loss of nitric acid takes place. The above-mentioned non-metallic cell, designed and constructed by the present authors, was quite useful for this experiment and the detail of the design will be reported elsewhere.

The concentration of nitric acid was determined by titration against standard alkali, and the water content in the TBP phase was determined by the Karl-Fisher titration method. The uranium concentration was determined by the alkaline peroxide method. TBP was purified by refluxing with 0.5% aqueous sodium hydroxide according to the method shown by Alcock et al.[3] In some cases, the purified TBP was further distilled in vacuo in order to remove a trace of water. Analytical-grade uranyl nitrate (after recrystallization), nitric acid and carbon tetrachloride were used.

## Results and Discussion

**Spectra of Pure TBP.**—First of all, tentative assignment of TBP itself will be explained in order to analyze the spectra of the systems described below. The spectrum of pure TBP is shown in Fig. 1. Two bands at 2911 and 2840 $cm^{-1}$ are assigned to CH stretching frequencies of *n*-butyl group. Two bands at 1459 and 1382 $cm^{-1}$ are assingned to $CH_3$ and $CH_2$ deformation frequencies of *n*-butyl group, respectively. A strong band at 1270 $cm^{-1}$ is assigned to P=O stretching frequency according to Bellamy[4]. A triplet band at 1059, 1027 and 991 $cm^{-1}$ is assigned to the P–O–C group. The assignment of the weak bands at 1237, 1168, 1149, 1119, 959 and 910 $cm^{-1}$ is not clear at present.

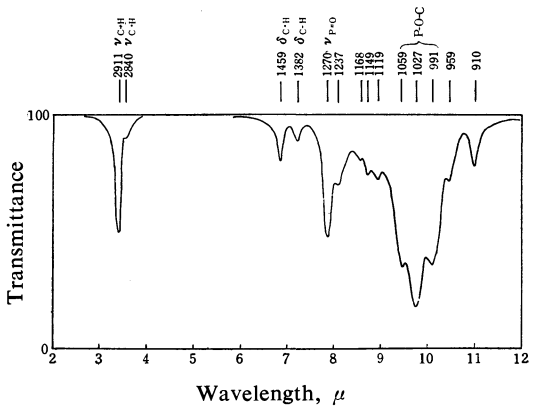



Fig. 1. Infrared spectra of pure TBP capillary.

**TBP-Water System.**—The infrared spectra of the system TBP-water, obtained by Cobb, have

1) R. L. Moore, *AECD-3196* (1951).
2) K. Naito, This Bulletin, 33, 363 (1960).
3) K. Alcock et al., *Trans. Faraday Soc.*, 52, 39 (1956).
4) L. J. Bellamy, "The Infrared Spectra of Complex Molecules", 2nd Ed., John Wiley and Sons, Inc., New York (1958), p. 258.

been mentioned in the paper by Alcock et al.[3] He has shown that as water is added to pure TBP the band due to the P=O group at 1283 $cm^{-1}$ is shifted to 1267 $cm^{-1}$ and a shift of 16 $cm^{-1}$ suggests the formation of weak hydrogen bonding (with water) at P=O oxygen.

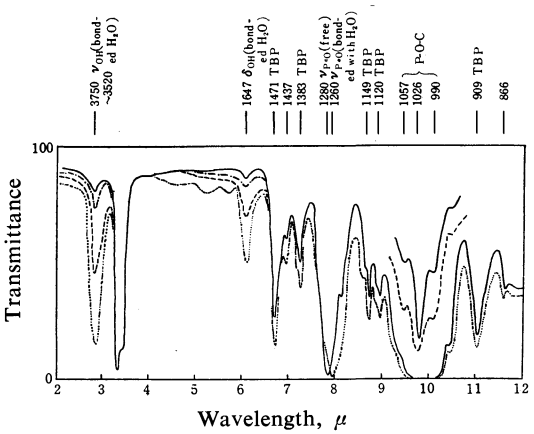



Fig. 2. Infrared spectra of TBP-$H_2O$ system. Thickness : 0.015 mm.
—— No. 1, (0.968 mg. water per ml. of solution)
·-·- No. 2, (5.98 mg. water per ml. of solution)
---- No. 3, (31.9 mg. water per ml. of solution)
····· No. 4, (64.0 mg. water per ml. of solution)

The spectra for this system obtained by the authors are shown in Fig. 2. Samples No. 1, 2, 3 and 4 contain 0.968, 5.93, 31.9 and 64.0 mg. water per ml. of solution, respectively. It is observed from Fig. 2 that as water is added to pure TBP the band due to P=O at 1280 $cm^{-1}$ is shifted to 1260 $cm^{-1}$ in agreement with Cobb's result. At the same time an increase in intensities of bands at 3750~3550 and 1647 $cm^{-1}$, is observed which are assigned to the stretching and deformation vibrations of the OH group respectively. The positions of these two bands are near to those of stretching and deformation vibrations of free water and this fact also suggests the formation of weak hydrogen bonding between P=O oxygen and water molecules.

Since the positions of the absorption bands due to P–O–C at 1057, 1026 and 990 $cm^{-1}$ have no appreciable change by the addition of water, it is concluded that in this system water does not bond with the P–O–C group.

**TBP-Nitric Acid System.**—The samples for TBP-nitric acid system were prepared as follows: 5% carbon tetrachloride solution of TBP was shaken with aqueous solution of nitric acid having various concentrations (where the volume ratio of the organic phase to the aqueous is equal to unity). After separating the organic phase from the aqueous phase, the former was used as a sample. A 5% TBP solution was used for the reason that the adequate intensities of bands can be obtained with 0.1 mm. spacer. The results of analysis for nitric acid and water contents in these samples are summarized in Table I.

Table 1. Result of analysis for the samples of TBP-nitric acid system

| Sample No. | Initial conc. (aqueous phase) of $HNO_3$, M | Equilibrium conc. $HNO_3$, M | (TBP phase) of $H_2O$, M |
|---|---|---|---|
| 1 | 0 | 0 | 0.0250 |
| 2 | 0.995 | 0.0095 | 0.0328 |
| 3 | 3.41 | 0.099 | 0.0368 |
| 4 | 5.14 | 0.151 | 0.0267 |
| 5 | 7.10 | 0.173 | 0.0211 |
| 6 | 9.23 | 0.188 | 0.0239 |
| 7 | 10.83 | 0.192 | 0.0250 |

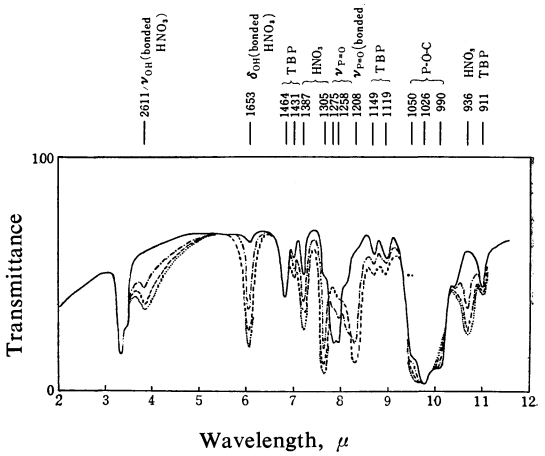



Fig. 3. Infrared spectra of TBP-$HNO_3$ system. Thickness 0.1 mm.
—— No. 2, (0.995 N $HNO_3$)
·-·- No. 3, (3.41 N $HNO_3$)
---- No. 4, (5.14 N $HNO_3$)
····· No. 5, (7.10 N $HNO_3$), No. 6, (9.23 N $HNO_3$) and No. 7, (10.83 N $HNO_3$)

The infrared spectra obtained for these samples are shown in Fig. 3. As the concentration of nitric acid in the TBP phase increases, the intensities of bands due to P=O at 1275 $cm^{-1}$ and 1258 $cm^{-1}$ decrease and one at 1208 $cm^{-1}$ rises in its place. It is not clear at present whether the branches of the doublet due to P=O are assigned to the free and bonded (with water) P=O respectively or are to be considered as a solvent effect caused by dilution with carbon tetrachloride. A new band at 1208 $cm^{-1}$ is assigned to bonded P=O with

nitric acid. The shift amounts to 50~66 $cm^{-1}$ and this fact suggests a strong bonding between P=O and nitric acid. In the case of samples No. 5—7. the bands at 1275 and 1258 $cm^{-1}$ almost disappear and the same spectra are obtained for all of these samples. Accordingly in the case of samples No. 5—7 all molecules of the TBP are entirety bonded with nitric acid at their P=O bonds. This is in agreement with the analytical data shown in Table I.

The triplet band assigned to the P–O–C group (1050, 1026 and 990 $cm^{-1}$) shows a change to some extent in samples No. 2—5 in which the increase in nitric acid content brings the increase in the intensity of the band at 1050 $cm^{-1}$ together with the decrease in that at 990 $cm^{-1}$, whereas the intensity of the band at 1026 $cm^{-1}$ remained unchanged. However, in the case of samples No. 5—7, little change is observed at the P–O–C band. Though it is not easy to interpret the above-mentioned change of spectra due to the P–O–C group, it may be attributed directly to the complex formation at P=O in view of the parallel nature between the spectra of the P–O–C group and that of the P=O group.

The bands at 2611 and 1653 $cm^{-1}$, the intensities of which are roughly proportional to the content of nitric acid in the TBP phase, are assigned to the stretching and deformation vibrations of the OH group, respectively. The band at 2611 $cm^{-1}$ is shifted obviously from the band due to free OH stretching vibration, so that the formation of strong hydrogen bonding is also confirmed.

The intensities of bands at 1387 and 1305 $cm^{-1}$ are also roughly proportional to the nitric acid content although the former band is overlapped with the band due to the deformation vibration of $CH_3$ groups of TBP at 1381 $cm^{-1}$. These two bands are then assigned to the bonds of the bonded nitric acid. It was found by Kamiyama[5] that when an alkaline halide window is used instead of a silver chloride window, a *single band* at 1387 $cm^{-1}$, which is assigned to the absorption due to the nitrate ion, appeared instead of these two bands*. It was interpreted as the result of the exchange reaction between alkaline halide and nitric acid in the TBP phase, which in turn formed nitrate ion at the surface of the window, so that the use of an alkaline halide window in this case should be strictly avoided. Tuck[6] described briefly the infrared spectra of the TBP-nitric acid system and found bands at 1400 and 810 $cm^{-1}$, which are assigned to the ionic organic nitrate. The discrepancy between his result and the authors' may have originated from the fact that he used an alkaline halide window.

The intensity of the band at 936 $cm^{-1}$ is also roughly proportional to the content of nitric acid in the TBP phase. Thus the bands at 2611, 1653, 1387, 1305 and 936 $cm^{-1}$ have the same tendency with respect to the content of nitric acid in the TBP phase, and therefore these bands are useful as the indication for bonded nitric acid in TBP phase.

**TBP-Uranyl Nitrate System.** — The samples used here consist of the following three samples: No. 1; 5% TBP solution (carbon tetrachloride is used as a diluent) saturated with uranyl nitrate monohydrate, No. 2; sample No. 1 was diluted with 5% TBP solution (the volume ratio equals 1 : 1), No. 3; sample No. 1 was diluted with 5% TBP solution (the volume ratio equals 5 : 1).

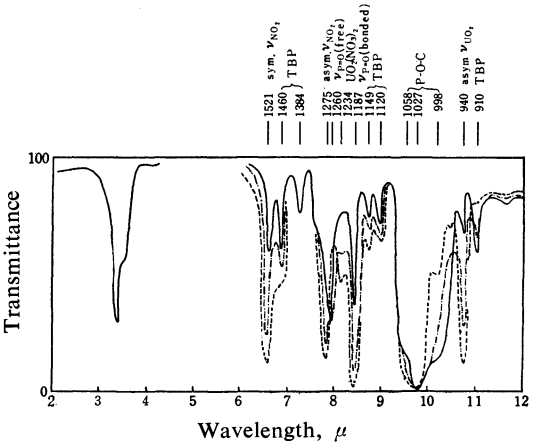



Fig. 4. Infrared spectra of TBP-$UO_2(NO_3)_2$ system. Thickness : 0.1 mm.
---- No. 1 (TBP saturated with $UO_2(NO_3)_2$)
·-·- No. 2 (1/2 diluted solution of No. 1)
—— No. 3 (1/6 diluted solution of No. 1)

The infrared spectra obtained for these samples are shown in Fig. 4. As the solution is diluted, the intensity of the band at 1187 $cm^{-1}$, which the authors assign to P=O bonded with uranyl nitrate, decreases and that at 1260 $cm^{-1}$, due to free or bonded (with water) P=O rises in its place. The shift of frequency between the two bands amounts to 70 $cm^{-1}$ and this fact suggests the strong complex formation between P=O and uranyl nitrate.

The triplet band assigned to P–O–C group at 1058, 1027 and 998 $cm^{-1}$ also shows a similar appreciable change with dilution. As uranyl nitrate content in the TBP phase increases, the intensity of the band at 1058 $cm^{-1}$ increases

5) H. Kamiyama, unpublished.
6) D. G. Tuck, *J. Chem. Soc.*, **1958**, 2783.
* Miller et al. mentioned that the ionic nitrates of alkali metals illustrates the point group $D_{3h}$, where the strong nitrate asymmetrical stretching frequency is centered in the region of 1380 $cm^{-1}$ and no splitting occurs. F. A. Miller and C. H. Wilkins, *Analyt. Chem.*, **24**, 1253 (1952).

and one at 998 $cm^{-1}$ decreases, whereas one at 1027 $cm^{-1}$ shows little change. As in the case of TBP-nitric acid system, the change of P–O–C band may be directly related to the complex formation at P=O.

The intensities of bands at 1521, 1275, 1234 and 940 $cm^{-1}$ are roughly proportional to the uranyl nitrate content. The band at 940 $cm^{-1}$ is assigned to the uranyl group[7]. According to Ferraro, the former two bands are assigned to $NO_2$ asymmetric and symmetric stretching of covalent nitrate, respectively[8]. The assignment of the band at 1234 $cm^{-1}$ is not clear at present.

**TBP-Uranyl Nitrate-Nitric Acid System.**—It is known that when uranyl nitrate is extracted from an aqueous solution of nitric acid by TBP, the extraction peak of uranyl nitrate appears at nitric acid concentration of 5~6 mol./l. in the aqueous phase. As an illustration, the result obtained by McKay is shown in Fig. 5[9]. The existence of such a peak was concluded by Naito as the result of competition to form TBP complex between uranyl nitrate

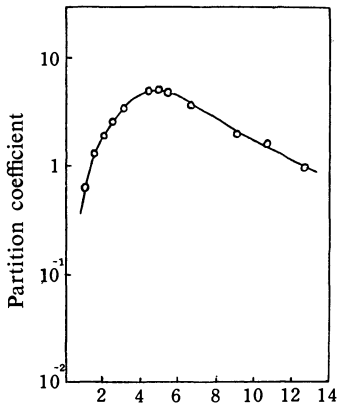



Fig. 5. Extraction of $UO_2(NO_3)_2$ by TBP. Kerosine is used as a diluent. (The original curve by H. A. C. McKay)

and nitric acid[2]. The mechanism of extraction was described as follows; in low nitric acid concentration the extraction of uranyl nitrate predominates over the extraction of nitric acid which serves merely as a salting-out agent, whereas the increase in nitric acid concentration promotes the extraction of nitric acid into the TBP phase with the progressive replacement of uranyl nitrate by nitric acid. This illustrates the existence of the peak in the extraction curve.

The mechanism obtained by the partition study was checked by the infrared spectroscopy as follows:

*Replacement of Nitric Acid by Uranyl Nitrate.*—Fig. 6 shows the infrared spectra in which the replacement of nitric acid by urany nitrate in TBP phase is demonstrated. The samples were prepared as follows: 5% carbon tetrachloride solution of TBP was shaken with aqueous solution of 5 N nitric acid containing uranyl nitrate of various concentrations (where the volume ratio of organic phase to the aqueous equals unity). After separating the organic phase from the aqueous phase, the former was used as a sample. The initial concentrations of uranyl nitrate in aqueous phase for samples No, 1, 2, 3 and 4 were 0.05, 0.1, 0.3 and 0.5 M, respectively.

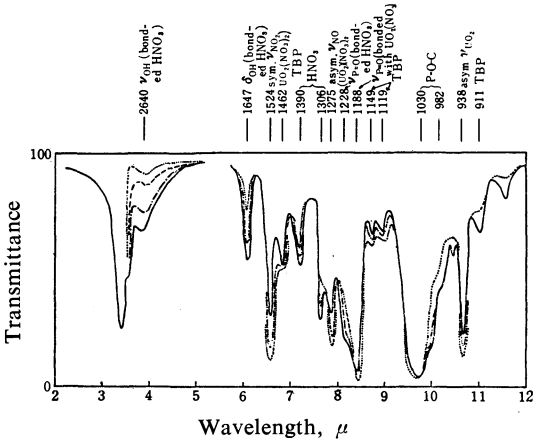



Fig. 6. Infrared spectra of TBP-$UO_2(NO_3)_2$-$HNO_3$ system. (a) Replacement of nitric acid by uranyl nitrate. Thickness: 0.1 mm.
—— No. 1 (Initial concentration of $UO_2(NO_3)_2$: 0.05 mol./l.)
·-·- No. 2 (Initial concentration of $UO_2(NO_3)_2$: 0.1 mol./l.)
---- No. 3 (Initial concentration of $UO_2(NO_3)_2$: 0.3 mol./l.)
····· No. 4 (Initial concentration of $UO_2(NO_3)_2$: 0.5 mol./l.)

In the spectra of Fig. 6, the bands at 1228 and 1188 $cm^{-1}$ are assigned to the P=O bonded with nitric acid and uranyl nitrate respectively as mentioned above. As going from sample No. 1 to No. 4, the intensity of the band at 1228 $cm^{-1}$ decreases and the one at 1188 $cm^{-1}$ rises in its place. At the same, the intensities of the bands at 1524, 1275 and 940 $cm^{-1}$, which are assigned to the vibrations of uranyl nitrate, increase and those of the bands at 2640, 1647, 1390 and 1306 $cm^{-1}$, which are assigned to the vibrations of nitric acid, decrease.

One can obviously observe from these facts that when going from sample No. 1 to No. 4, the concentration of uranyl nitrate in the TBP phase increases, while that of nitric acid decreases, and that all sites at the P=O group initially occupied by nitric acid are progressively replaced by uranyl nitrate.

*Replacement of Uranyl Nitrate by Nitric Acid.*— Fig. 7 shows the infrared spectra of samples in which nitric acid expels uranyl nitrate. The samples were prepared as follows: 5% carbon tetrachloride solution of TBP was shaken with an aqueous solution of uranyl nitrate (0.05 M) containing nitric acid of various concentrations (where the volume ratio of the organic phase to the aqueous one equals unity). The initial concentrations of nitric acid in aqueous phase of sample No. 1, 2 and 3 are 2, 6 and 12 mol./l., respectively.

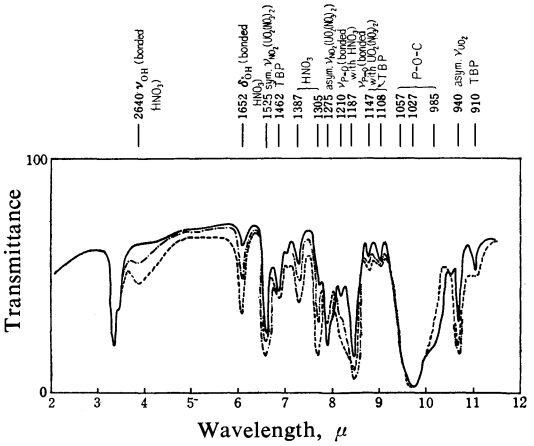



Fig. 7. Infrared spectra of TBP-$UO_2(NO_3)_2$-$HNO_3$ system. (b) Replacement of uranyl nitrate by nitric acid. Thickness: 0.1 mm.
—— No. 1 (Initial concentration of $HNO_3$: 2 mol./l.)
·–·– No. 2 (Initial concentration of $HNO_3$: 6 mol./l.)
---- No. 3 (Initial concentration of $HNO_3$: 12 mol./l.)

When going from sample No. 1 to No. 3, the intensity of the band at 1210 $cm^{-1}$ due to P=O bonded with nitric acid increases, on the other hand that at 1187 $cm^{-1}$ due to P=O bonded with uranyl nitrate shows a maximum in sample No. 2. At the same time, the intensities of the bands at 2640, 1652, 1387 and 1305 $cm^{-1}$, which are assigned to the vibrations of nitric acid, increase and those at 1525, 1275 and 940 $cm^{-1}$, which are assigned to the vibrations of uranyl nitrate, show a maximum at sample No. 2, except for one at 1275 $cm^{-1}$. The band at 1275 $cm^{-1}$ of sample No. 1 is overlapped with the band due to free or bonded (with water) P=O at 1275~1258 $cm^{-1}$, therefore this band only looks to be irregular.

Thus it is evidently seen from these facts that when going from sample No. 1 to No. 3 the concentration of nitric acid in the TBP phase increases monotonously, while that of uranyl nitrate shows a maximum in sample No. 2. Therefore the peak of extraction of uranyl nitrate from nitric acid solution appears at 5~6 M of nitric acid concentration in aqueous phase beyond which the sites of P=O occupied by uranyl nitrate are progressively replaced by nitric acid.

In conclusion, the above-mentioned infrared study confirms the competition between uranyl nitrate and nitric acid in TBP phase and is in good agreement with the result obtained by the partition study.

## Summary

The complex formation of TBP in the systems TBP-water, TBP-nitric acid, and TBP-uranyl nitrate was confirmed by means of infrared spectroscopy. The infrared spectra of uranyl nitrate in the system TBP-nitric acid-uranyl nitrate lead to the conclusion that the competition extraction of both uranyl nitrate and nitric acid takes place during the extraction process.

The authors would like to express their gratitude to Dr. K. Kimura, Dr. Y. Mashiko, Dr. K. Oshima and Dr. R. Hara for their invaluable assistance and advise in this work. They also wish to thank Mr. T. Suzuki for his help in the laboratory work.

*Government Chemical Industrial Research Institute of Tokyo*
*Shibuya, Tokyo*
(Nukada and Maeda)

*Japan Atomic Energy Research Institute*
*Tokai, Ibaragi-ken*
(Naito)

7) e. g. see B. M. Gatehouse and A. E. Comyns, *J. Chem. Soc.*, **1958**, 3965.
8) J. R. Ferraro, *J. Inorg. Nucl. Chem.* **10**, 319 (1959).
9) H. A. C. Mckay, Int. Conf. on the Peaceful Uses of Atomic Energy, Geneva, 1955, vol. 7, p. 314.

# *Effect of Temperature on the Viscosity and the Optical Rotation of Poly-ε-aminocaproyl-α-alanine**

By Mituo EBATA

(Received November 25, 1959)

An interesting property of the synthetic poly-ε-aminocaproyl-α-alanine, an reversible coagulation by heat in acidic or neutral aqueous solution, has been shown by Noguchi and his coworkers[1,2]. In the previous paper[3] the author reported, that the coagulated form of the polymer is much more susceptible than the dissolved form, to the action of trypsin. This fact has been explained by assuming some probable difference which might be present in the structure of both forms of the polymer, although the mechanism of the reversible heat coagulation was not yet clear. Thus, it is interesting to examine the effect of temperature on some physical property of this material, especially the rotatory dispersion for the estimation of the degree of folding of the polymer chain. The present paper deals with the results obtained from experiments on the viscosity and the optical rotation of the D, L- or L-alanine polymer under several temperatures.

## Experimental

The preparation method and some properties of poly-ε-aminocaproyl-D, L-alanine (M. W., 21,800) and poly-ε-aminocaproyl-L-alanine (M. W., 7,000) were described previously[3]. The polymer solution was prepared as follows: To 10 ml. of water 100 mg. of the polymer was added and the mixture was stood for over night. After filtration by a glass filter, polymer concentrations in the solution were determined by the method of Kjeldahl N-analysis. pH value of the solution was adjusted by adding 0.2 volume of M/15 phosphate buffer, if it was necessary, small amounts of N HCl or N NaOH were added.

The viscosity was measured by Ostwald's viscosimeter.

The optical rotation of the polymer was determined with the automatic recording polarimeter[4]. Measurements on the optical dispersion were made at a wavelength of 400, 437, 452, 471, 498, 527, 549 and 589.3 mμ; these were obtained from a tungsten lamp and filters except the last one which was the D line of sodium lamp. As sample tube of the polarimeter the capillary cells of 10 cm. in length were used. Temperature control of the polymer solution was carried out by varying the temperature on the water jacket of the sample tube.

## Results

The specific viscosity of the polymer was found in an acidic or alkaline media as shown in Fig. 1. A minimum value of the viscosity of the D, L-alanine polymer was found at 55°C in all cases, and was independent on pH and on the concentration of the polymer. The coagulation of the polymer occured at 40 and 50°C in curves I and II respectively, while no coagulation was found in the curve III owing to its high pH value of the medium. This indicates, therefore, that the result given by curves I and II at high temperatures might be meaningless. However, an analogous curve, curve III, was obtained by an

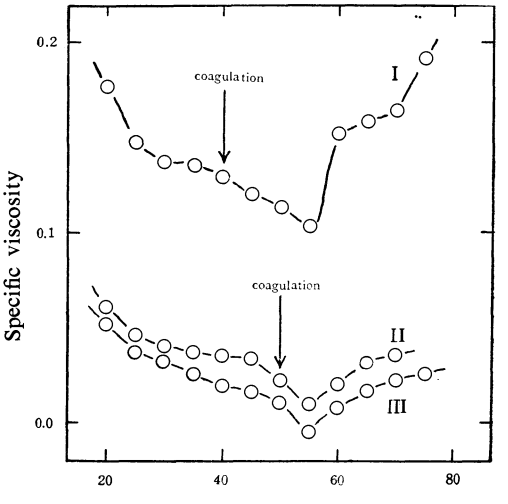



Fig. 1. Effect of temperature on the specific viscosity of the poly-ε-aminocaproyl-DL-alanine.
I: 0.65% polymer, pH 7.1
II: 0.37% polymer, pH 3.7
III: 0.37% polymer, pH 8.7 (no coagulation)
Temperature, ±0.02°C

* This work was presented at the Symposium on Protein Structure, Osaka, October, 1959.

1) J. Noguchi, T. Hayakawa, J. Suzuki and M. Ebata, *J. Chem. Soc. Japan, Pure Chem. Sect.* (*Nippon Kagaku Zasshi*), 76, 648 (1955).
2) J. Noguchi, T. Hayakawa and M. Ebata, *J. Polymer Sci.*, 23, 843 (1957).
3) M. Ebata, *J. Biochem.*, 46, 383 (1959).
4) A. Tsugita, Unpublished (A part appeared in M. Ebata, A. Tsugita and S. Akabori, *Sym. on Enz. Chem. Japan*, 14, (1959), in Japanese).

experiment in the heating process, even under no coagulable conditions. Another experiment in the cooling process agreed with that of the rising one. Curve III shows, that the polymer was transformed to a different type by heating as evidenced by the appearance of a minimum viscosity. The specific viscosity at 55°C in curve III was of a negative value. Thus negative values were often found in the specific viscosity measurement, when the concentrations of the polymer were low although the reason was obscure. Similar curves were also obtained with the viscosity of the L-polymer.

The effect of temperature on the optical rotation of poly-ε-aminocaproyl-L-alanine was studied. The specific rotation of the polymer in aqueous solution was a constant value between 15° to 50°C as shown in Fig. 2. A remarkable increase in *levo*-rotation was found by heating above 53°C. This increase in the rotation was completely reversible with heating and cooling. Addition of a large amount of salts, acids, alkalis and denaturating reagents such as urea did not induce an optical rotation change of the polymer at room temperature, and no coagulation by heat was observed.

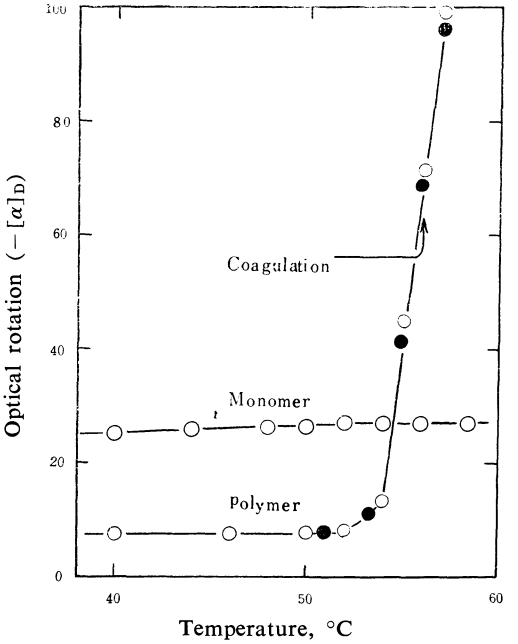



Fig. 2. Optical rotation of poly-ε-aminocaproyl-L-alanine.
Polymer, 0.47% in water (pH 4.0)
Monomer (ε-aminocaproyl-L-alanine), 0.94% in water
○, Points obtained with temperature rising
●, Points obtained with temperature falling
Temperature, ±0.05°C

The rotatory dispersion of the polymer was measured in the aqueous solutions at several different temperatures. When the measurement was made on the solution, its rotatory dispersion was belived to be obeyed Drude's one-term equation, $[\alpha]_\lambda = k_c/(\lambda^2 - \lambda^2_c)$. Where $\lambda$ stands for the wavelength, $[\alpha]_\lambda$ for the specific rotation at $\lambda$, and $k_c$, $\lambda_c$ are the rotation constant and the dispersion constant, respectively. In the present experiment the constants were estimated from the data by the usual manner. The $\lambda_c$ values were 385 mμ (at 30°C), 345 mμ (at 53°C), 315 mμ (at 54°C) and 155 mμ (at 55°C) as can be seen in Fig. 3. No serious coagulation was found at 55°C under the conditions as shown in Fig. 2. Due to the appearance of coagulation, the reasonable value of $\lambda_c$ could not be estimated from the rotatory dispersion measured at 56°C.

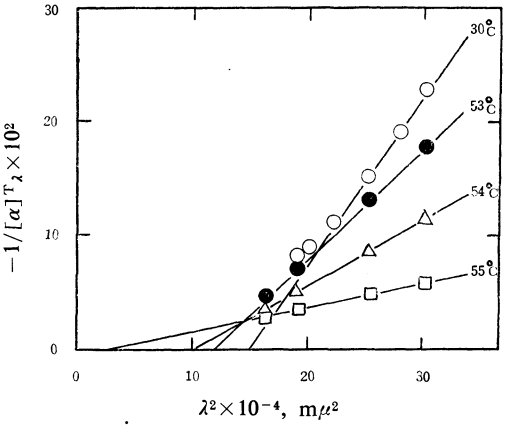



Fig. 3. Rotatory dispersion of poly-ε-aminocaproyl-L-alanine at various temperatures.
Polymer, 0.47% in water (pH 4.0)
Temperature, ±0.05°C

## Discussion

The denaturation of protein is known to be accompanied by an increase in specific viscosity and *levo*-rotation and a shift of its $\lambda_c$ value to shorter wavelength[5,6]. The result on the polymer reported here clearly resembles this information. When the similarity between the protein and the polymer examined here is considered, it is suggested, that a mechanism analogous with protein denaturation might be presented in the nature of the coagulation of the present sample.

According to Doty's results[6,7], a high $\lambda_c$ value is a measure of the high helix content

5) K. Linderstrøm-Lang and J. A. Schellmann, *Biochim. Biophys. Acta*, **15**, 156 (1954).
6) J. T. Yang and P. Doty, *J. Am. Chem. Soc.*, **79**, 761 (1957).
7) P. Doty and R. D. Lundberg, *Proc. Natl. Acad. Sci.*, **43**, 213 (1957).

of a protein molecule. It is therefore reasonable to assume that the polymer has probably a compact structure in aqueous solution at room temperature and the structure is unfolded by heating. Then, an interesting conclusion described previously[3] that, the coagulated form of the polymer is more susceptible than the dissolved form to the action of trypsin, can be explained by this assumption.

## Summary

Viscosity and optical rotation of a synthetic polymer, poly-ε-aminocaproyl-α-alanine, were studied connecting with the reversible heat coagulation. A minimum viscosity of the poly-ε-aminocaproyl-D, L-alanine solution was found at 55°C. Heating of the poly-ε-aminocaproyl-L-alanine solution produces an increase in its *levo*-rotation and a shift of its dispersion constant ($\lambda_c$ value) to shorter wavelength. The mechanism of the reversible heat coagulation of the polymer was discussed to be based on the obtained result.

The author wishes to express his hearty thanks to Professor S. Akabori of our University and Professor J. Noguchi, Kanazawa University, for their interest and encouragement throughout the course of this work.

*Laboratory of Biochemistry*
*Faculty of Science*
*Osaka University*
*Kita-ku, Osaka*

# *Quantitative Spectrochemical Analysis of Minor Elements in Silicates with Double Internal Standards*

By Hiroshi HAMAGUCHI, Rokuro KURODA and Ryokichi NEGISHI

(Received December 3, 1959)

The spectrochemical procedures for determining a number of traces of elements in silicate rocks involve some difficult problems. The fact that many of the geochemical studies on the minor elements in the lithosphere have been carried out with a semiquantitative scheme, may be, in part, attributed to the troublesome problems associated with the accurate simultaneous determination of minor elements in silicate rocks. The main difficulty arises from the different rates of volatilization of the elements from the electrode cavity into the arc column.

Ahrens[1] divided the minor elements into two groups, i. e. volatile and involatile group. For the elements of the volatile group which complete their distillation before or at the same time that the alkali metals complete theirs, Ahrens suggested a general arcing procedure with or without an internal standard. In the former case indium has been chosen as the internal standard for its volatility, satisfactory excitation properties and its extremely low concentration in most silicates. For the involatile group that includes all elements which emit their maximum line intensity after the main phase of alkali metal distillation has subsided, one part of the sample was buffered with two parts of carbon powder containing palladium as the internal standard and the mixture was completely distilled with 7 amp. d. c. carbon arc. Shaw[2] employed the total energy method for determining about 19 minor elements in silicate rocks. He also divided the subject elements into two groups according to the volatility difference of the elements, as was done in the case of Ahrens.

These schemes of quantitative spectrochemical analysis are rather tedious and even without the internal standard two arcing procedures are needed. The selection of suitable internal standards, buffer and excitation conditions may eliminate the necessity of separate arcing for volatile and involatile group. An attempt was made to determine the minor elements differing much in the volatilization rates, i. e. lead, gallium, tin, chromium, vanadium, cobalt, nickel and scandium in silicates in a single arcing procedure by using double internal standards. As a result a method was established without serious loss of precision and with reasonably high sensitivities.

1) L. H. Ahrens, "Quantitative Spectrochemical Analysis of Silicates," Pergamon Press, London (1954), p. 74.

2) D. M. Shaw, *Bull. Geol. Soc. Amer.*, **65**, 1151 (1954).

## Experimental and Results

**Equipment and Procedure.**—To establish the procedure the densitometric and the logarithmic sector method were used. Although the logarithmic sector method is rather obsolete, some special advantages are obtained by this method. The intensity ratio of subject to internal standard lines is generally independent of conditions of exposure, slit width, development and plate calibration. The time required for the analysis is shortened by a factor of 2 or 3, compared with the densitometric method. No expensive densitometer is necessary.

Equipment and excitation conditions are listed in Table I for both calibrating methods.

**Standard, Internal Standard and Buffer.**—As the object for analysis is naturally occurring silicates, the general chemical composition and physical

TABLE I. EQUIPMENT AND EXCITATION CONDITIONS

| Subject | Densitometric method | Logarithmic sector method |
|---|---|---|
| Spectrograph | Shimadzu-QL170 Littrow type quartz spectrograph | Hilger $E_2$, medium type quartz spectrograph |
| Power source | Continuous a. c. arc supplied from the Pfeilsticker type intermittent a. c. arc source unit with radiofrequency spark. | D. c. arc supplied from commercial unit with full wave rectification with radio frequency initiating spark. |
| Power | 8 A | 5 A |
| Working voltage | 210 V. | 100 V. |
| Preburn | None | None |
| Exposure | 60 sec. | 40 sec. |
| Arc gap | 3 mm. | 3 mm. |
| Electrodes | Upper : 1/4 in. diameter graphite rod (National Carbon Co., "Special Grade") The end is a 30° cone. | Upper (cathode) : 5 mm. diameter graphite rod. (Shimadzu Manufacturing Co.) The end is a ca. 60° cone. |
| | Lower : 1/4 in diameter rod containing an axial crater 1/16 in. diameter, 1/6 in deep. (National Carbon Co. "Special Grade") | Lower (anode): 5 mm. diameter. graphite rod containing an axial crater 3 mm. diameter, 2 mm. deep (Shimadzu Manufacturing Co.) |
| Spectral region | 2650 to 4000 Å | ca 2300 to 4500 Å |
| Sector | Five step sector : Step ratio 1 : 2 | Logarithmic sector |
| Slit width | 30 microns | 20 microns |
| Densitometer | Rigaku Denki Co. Ltd. MD-2 type. | None |

TABLE II. INTERNAL STANDARDS AND ANALYSIS LINES

| | Element | Wavelength | Excitation potential, eV. | Analysis range, p.p.m. |
|---|---|---|---|---|
| Volatile group | Sb (internal standard) | 2877.915 | 5.3 | |
| | Ga | 2943.637 | 4.3 | 10～300 (L)<br>10～300 (D) |
| | Pb | 2833.069 | 4.4 | 30～500 (L)<br>10～1000 (D) |
| | Sn | 3175.019 | 4.3 | 10～3900 (D) |
| Involatile group | Pd (internal standard) | 3242.703<br>3481.152 | 4.6<br>4.8 | |
| | Sc | 3613.836 | 10.1 | |
| | Cr | 3593.488 | 3.4 | 5～500 (D) |
| | V | 3183.982 | 3.9 | 10～400 (L)<br>10～1000 (D) |
| | Ni | 3414.765 | 3.6 | 5～300 (L)<br>5～500 (D) |
| | Co | 3453.505 | 4.0 | 5～300 (D)<br>5～1000 (L) |

L : Logarithmic sector method
D : Densitometric method

properties of the standards should approximate as closely as possible those of the unknown ones. Thus, a potash feldspar was used as a base material of the standards for nickel, chromium, cobalt and scandium. It was also possible to use a serpentinite and two specimens of granite as the base materials for lead, gallium, tin and vanadium. Since traces of gallium were apparent on the granite-base material, the granite was analyzed for gallium fluorometrically (Sandell)[3] and a correction was made for the residual impurity of gallium.

For the simultaneous determination of elements with the arc excitation, it is essential to volatilize all elements in approximately the same rate from the electrode cavity. The addition of carbon causes the elements of widely different volatilities to evaporate simultaneously. Though it would be possible to suppress considerably the selective volatilization with the addition of a large amount of carbon, some loss of sensitivities will result in general. In the present work 1 : 1 ratio of carbon to each of standard and sample was selected to maintain the highest sensitivities for most elements. In the presence of such a small amount of carbon buffer the choice of internal standard is highly critical. Consequently, two internal standards were used to assure the similarity in volatilization rates for the selected pairs of subject and internal standard elements; antimony(III) oxide for the elements of volatile group i. e., lead, tin and gallium, and palladium black for the elements of involatile group i. e., nickel, cobalt, chromium, vanadium (and scandium). The carbon powder as the buffer was previously well mixed with antimony-(III) oxide and palladium black to give the concentrations 0.80 per cent for antimony(III) oxide and 0.04 per cent for palladium Selected internal standard and analysis lines are listed in Table II with their excitation potentials and analysis ranges.

**Procedure for Constructing Working Curves.**— To one part of the final standard one part of the carbon powder prepared as described in the previous section is added and the mixtures are excited according to the analytical conditions listed in Table I. The spectrograms are recorded on Fuji Process Hard plate. The plate is developed for 3 min. in Fuji FD 31 developer, placed in a 3% acetic acid stop bath for 30 sec., and fixed in Fuji Fixer for 5 min. After washing for 20 min. with running water, the plate is air-dried.

In the case of the densitometric method, the intensity ratios of analysis pairs were obtained by a self-calibrating method. The working curves are

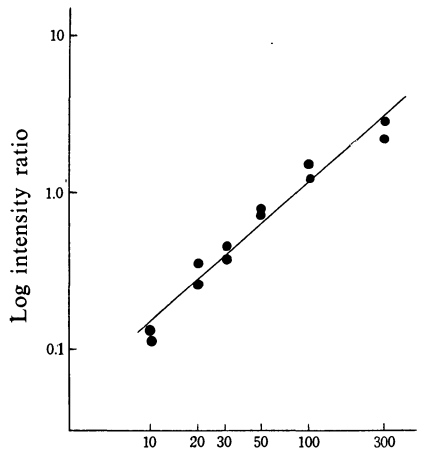



Fig. 1. Working curve for gallium (Densitometric method).
Ga 2943.637 / Sb 2877.915

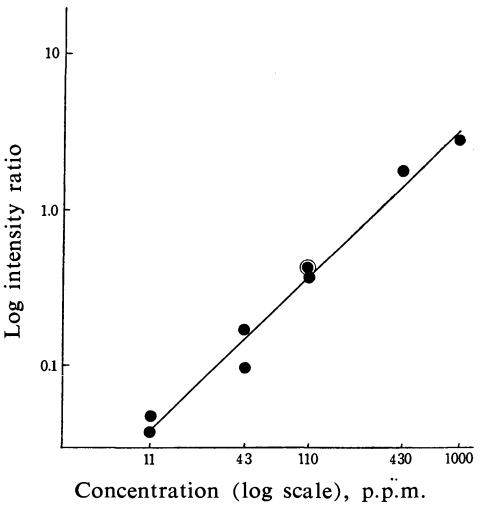



Fig. 2. Working curve for vanadium (Densitometric method).
V 3183.982 / Pd 3242.703

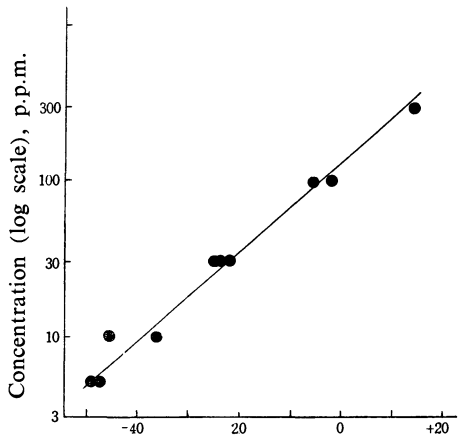



Fig. 3. Working curve for cobalt (Logarithmic method).
Co 3453.505 / Pd 3481.152

3) E. B. Sandell, "Colorimetric Determination of Traces of Metals,", 2nd. Ed., Interscience Publishers, Inc., New York (1950), p. 326.

TABLE III. PRECISION DATA

D: Densitometric method, L: Logarithmic sector method

| Sample | Subject element | Sx* | | Mean p.p.m. | | Confidence limit, 68% | | Concentration range previously reported p.p.m. | Recommended value by Ahrens (1954) p.p.m. | Analysis line pair | |
|---|---|---|---|---|---|---|---|---|---|---|---|
| | | D | L | D | L | D | L | | | D | L |
| W-1 | Ga | 0.038 | 0.124 | 13.6 | 18.4 | 14.8 ~12.5 | 24 ~13 | 11~20 | 14.5 | Ga 2943.637 / Sb 2877.915 | Ga 2943.637 / Sb 2877.915 |
| W-1 | Co | 0.075 | 0.080 | 55 | 53 | 65 ~46 | 63 ~44 | 20~55 | 36 | Co 3453.505 / Pd 3481.152 | Co 3453.505 / Pb 3481.152 |
| Potash-feldspar | Pd | 0.040 | 0.039 | 177 | 164 | 194 ~161 | 180 ~150 | 6~7 | — | Pb 2833.069 / Sb 2877.915 | Pb 2833.069 / Sb 2877.915 |
| W-1 | V | 0.047 | 0.042 | 236 | 160 | 263 ~212 | 176 ~145 | 170~340 | 240 | V 3183.982 / Pd 3242.703 | V 3183.982 / Pd 3481.152 |
| Biotite-gneiss | Sn | 0.088 | 0.084 | 48 | — | 59 ~39 | — | — | — | Sn 3175.019 / Sb 2877.915 | — |
| W-1 | Cr | 0.059 | — | 139 | — | 159 ~121 | — | 100~150 | 130 | Cr 3593.488 / Pd 3481.152 | Cr 3593.488 / Pd 3481.152 |
| W-1 | Ni | 0.042 | 0.110 | 59 | 84 | 65 ~54 | 106 ~65 | 47~150 | 90 | Ni 3414.765 / Pd 3481.152 | Ni 3414.765 / Pd 3481.152 |
| W-1 | Sc | 0.119 | — | 280 | — | 368 ~213 | — | 15~51 | 37 | Sc 3613.836 / Pd 3242.703 | Sc 3613.836 / Pd 3481.152 |

* Sx is the standard deviation of log concentration of a sample for its single analysis.

prepared by plotting the logarithm of the intensity ratios against the logarithm of the concentrations of the elements. Typical results are shown in Figs. 1 and 2.

In the case of the logarithmic sector method, the ratio of intensities between two lines is measured by their difference in lengths. The working curves are obtained in the same manner as by the densitometric method. A typical working curve is shown in Fig. 3.

The procedure for sample analysis is almost the same as that for the standards.

**Precision.**—The precision of the methods was evaluated from the working curve data and from the standard diabase W-1 (U. S. Geological Survey) analysis, following the treatment of the statistical method described by Shaw and Bankier[4]. The results are listed in Table III. As tin and lead were not detected in the standard diabase W-1, a gneiss and a potash feldspar were analyzed instead of the standard W-1.

## Discussion

The procedure presented could be extended to cover further species of minor elements except for extremely involatile elements, e. g., rare earth elements.

To check the accuracy of the methods, the ranges previously reported and the recommended values concerning the contents of minor elements in the standard diabase W-1 are also listed in Table III. Satisfactory agreement is observed with the recommended values by Ahrens except for cobalt, nickel and scandium.

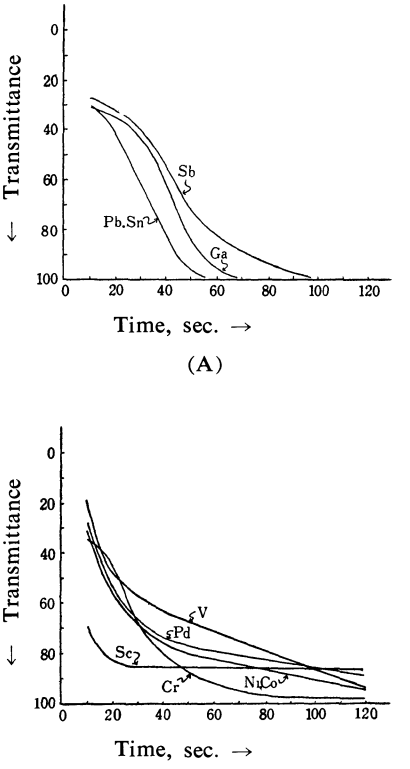



Fig. 4. Volatilization curves for the elements of valatile and involatile groups.
A: Volatile group
B: Involatile group

4) D. M. Shaw and J. D. Bankier, *Geochim. et Cosmochim. Acta*, 5, 111 (1954).

Smales[5] has found the values 54, 52, 50, 46, 46, 45 p. p. m. Co for the W-1 with the radioactivation method of analysis which may be regarded at present as the most reliable tool for the trace analysis. The present figure for cobalt agrees rather well with the values obtained by Smales. The nickel content of the W-1 was also obtained by Smales, who gave the values of 78, 78, 76, 73, 71, 63, p. p. m. Ni. The recommended value for nickel might be somewhat higher. The present figure for scandium is remarkably high and probably in error. The cause may be attributed to the matrix effect depending on the difference in chemical composition between the potash feldspar used as a base material for the standards and the analyzed diabase W-1. The analysis line Sc II 3613.836 is an ionic line having high excitation potential (10.1 eV.) and its intensity may be largely suppressed in the low temperature arc prevailing in the excitation of the alkali-rich feldspar. The low temperature arc also accelerates the selective volatilization of scandium remarkably, as illustrated in Fig. 4. For other elements the matrix effect may not be remarkable, as judged from the comparison of given data with the recommended value by Ahrens in Table III. The matrix effect on scandium can be completely eliminated by the addition of a large amount of carbon buffer, at least three times the weight of each standard and sample, as pointed out previously by Hamaguchi and coworkers[6]. The requirement for the establishment of highly sensitive methods obliges us to compromise with a 1 : 1 weight ratio of each standard or sample to the carbon buffer. Under this circumstance the volatilization trends of the subject and the selected internal standard elements are illustrated in Fig. 4. Reasonably parallel volatilization trends are found for the pairs of the subject element and its internal standard. However, the volatilization curve for scandium differs significantly from that for palladium, as described previously.

Using the medium type spectrograph, available analysis lines are limited because of the rather complex spectrum of silicate rocks. Especially, highly sensitive analysis of tin is practically impossible owing to the coincidence of its sensitive lines with interfering lines. The entire coverage of concentration range of chromium encountered in silicate rocks is also impossible even with the utilization of several spectral lines. Thus the establishment of procedure for chromium and tin with the medium type spectrograph was not attempted.

5) A. A. Smales, ibid., **8**, 300 (1955).
6) H. Hamaguchi, K. Tomura and R. Kuroda, *J. Chem. Soc. Japan, Pure Chem. Sec.* (*Nippon Kagaku Zasshi*), **79**, 504 (1958).

## Summary

Two internal standards have been used in the spectrographic analysis of silicates, antimony(III) oxide for volatile elements and palladium black for the involatile group. The former was used as the standard for the determination of gallium, lead and tin, and the latter for the determination of nickel, cobalt, chromium, vanadium and scandium. A medium spectrograph is not suitable for the determination of chromium or tin, and scandium did not volatilize in a manner parallel to the palladium but it was possible to obtain reasonable results for the other elements.

*Department of Chemistry*
*Faculty of Science*
*Tokyo University of Education*
*Koishikawa, Tokyo*

# *The Transition Polymerization of Acrylamide. I. On the Polymerization Condition and the Property of Polymer**

By Naoya OGATA

(Received November 27, 1959)

Generally, amino acid tends to cause an intermolecular condensation reaction between two molecules to form a ring compound and almost never makes linear polyamide by heating. It was reported by Breslow[1] that acrylamide was polymerized into poly-β-alanine (Nylon 3) of high degree of polymerization in the presence of an alkali catalyst and an inhibitor of the vinyl polymerization. The polymerization proceeds through the transition of an amide hydrogen to a double bond of acrylamide and can be designated as the transition polymerization.

$$n\mathrm{CH_2{=}CHCONH_2} \rightarrow [-\mathrm{CH_2CH_2CONH}-]_n$$

The condition of polymerization and the property of the polymer have been investigated in this study.

## Experimental

**The Effect of Solvent.**—Acrylamide was dissolved in various solvents at the concentration of 10% and the solution was heated at 115°C for 2 hr. in the presence of 1/32 mol./mol. of sodium-*tert*-butyrate and 0.02% of phenyl-β-naphthylamine. Polymer precipitated gradually from the solution after the addition of catalyst and adhered massively to the wall of a reaction vessel or a stirrer. Polymer was extracted with water for an hour and the weight of water-soluble and water-insoluble polymer was determined. The relative viscosity of the polymer was determined for 1% solution in 98% sulfuric acid. Polymer was hydrolyzed by sulfuric acid and the qualitative and quantitative analyses of β-alanine were carried out by paperchromatography, using a mixed solvent of *n*-butanol/ammonia =80/20 as a developer. These results are shown in Table I.

The yields of polymer are larger in the solvents of lower dielectric constant and in aromatic solvents than in aliphatic solvents. The polymerization hardly ever occurs in the solvents with active hydrogen, such as alcohol, amine or amide.

In the case of a *N*-substituted amide such as dimethylformamide or dimethylacetamide, the polymer was obtained in the form of suspension in spherical particles of about 100 μ diameters.

**The Concentration of Monomer and Inhibitor.**—Acrylamide was dissolved in pyridine at various concentrations and the solution was heated in the presence of sodium-*tert*-butyrate. The yield and the relative viscosity of polymer was largest at 10% monomer concentrations, as shown in Table II.

The quantity of an inhibitor of the vinyl polymerization, such as hydroquinone or phenyl-β-naphthylamine, does not necessarily affect the yield of the polymer, and poly-β-alanine is obtained without such inhibitors. These results are shown in Table III.

Contamination of water in the solvents decreases the yield of polymer and the vinyl polymerization occurs in the presence of more than 1% of water in the solvents, as shown in Table IV.

**The Effect of Catalyst.**—The catalytic effect of several alkali compounds was investigated in chlorobenzene at 10% monomer concentrations, which is shown in Table V. The yield of polymer is largest for tertiary alkoxide and the catalytic effect of alkali metals is in the order of K>Na>Li.

The yield of the polymer is approximately in proportion to the square root of the concentration of the catalyst, while the relative viscosity of the polymer does not change markedly, as shown in Table VI and Fig. 1.

**The Rate of Polymerization.**—The rates of polymerization of acrylamide were determined in various solvents at 10% monomer concentrations in the presence of 1/32 mol./mol. of sodium-*tert*-butyrate and 0.02% of phenyl-β-naphthylamine. These

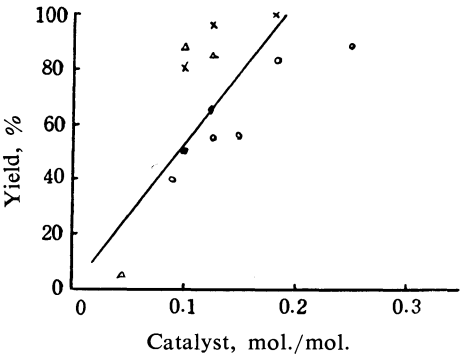



Fig. 1. The relation between the yield of the polymer and the concentration of catalyst.
○ Pyridine
× Monochlorobenzene
△ *N*,*N*-Dimethylaniline
● *N*,*N*-Dimethylformamide

* Presented at the Symposium of High Polymer, held at Tokyo on November 20, 1959, under the auspices of the Chemical Society of Japan.

1) D. S. Breslow, G. E. Hulse and A. S. Matlack, *J. Am. Chem. Soc.*, 79, 3760 (1957).

TABLE I. THE TRANSITION POLYMERIZATION OF ACRYLAMIDE IN VARIOUS SOLVENTS
(○ : colored deeply by ninhydrin)

| Solvent | Dielectric constant of solvent | Water-insoluble polymer % | Water-soluble polymer % | Total polymer % | $\eta_{rel}$ of water-insoluble polymer | Confirmation of β-alanine |
|---|---|---|---|---|---|---|
| Toluene | 2.38(25°C) | 22 | 62 | 84 | — | ○ |
| Dowtherm-A | — | 74 | 22 | 96 | — | ○ |
| Tetraline | 2.66(20°C) | 12 | 81 | 93 | 1.406 | ○ |
| Diphenyl | 2.53(73°C) | 84 | 16 | 100 | 1.813 | ○ |
| Tricresol | 5.0 (24°C) | 0 | 0 | 0 | — | — |
| Aniline | 7.2 (20°C) | 18 | 25 | 43 | 1.483 | ○ |
| Monomethylaniline | 5.97(22°C) | 37 | 30 | 67 | 1.719 | ○ |
| Dimethylaniline | 4.91(20°C) | 60 | 23 | 83 | 1.835 | ○ |
| Chlorobenzene | 5.62(25°C) | 80 | 20 | 100 | 1.903 | ○ |
| *o*-Dichlorobenzene | 7.47(25°C) | 86 | 12 | 98 | 1.736 | ○ |
| *p*-Dichlorobenzene | 2.86(53°C) | 74 | 26 | 100 | 1.837 | ○ |
| Nitrobenzene | 35.8 (20°C) | 2 | 98 | 100 | — | ○ |
| Acetophenone | 18.3 (20°C) | 0 | 5 | 5 | — | ○ |
| Pyridine | 12.3 (25°C) | 43 | 40 | 83 | 1.923 | ○ |
| Quinoline | 9.0 (25°C) | 36 | 40 | 76 | 1.555 | ○ |
| Dioxiane | 2.21(25°C) | 0 | 69 | 69 | — | ○ |
| Methylcellosolve | 16 (30°C) | 0 | 0 | 0 | — | — |
| Methanol | — | 0 | 0 | 0 | — | — |
| *tert*-Butanol | — | 0 | 40 | 40 | — | ○ |
| Formamide | 84 (20°C) | 0 | 0 | 0 | — | — |
| Dimethylformamide | 26.6 (25°C) | 46 | 42 | 88 | 1.714 | ○ |
| Dimethylacetamide | — | 84 | 16 | 100 | 1.670 | ○ |
| Adiponitrile | — | 0 | 16 | 16 | — | — |
| Mareic Anhydride | — | 0 | 0 | 0 | — | — |

TABLE II. THE EFFECT OF MONOMER CONCENTRATION
(Polymerized in the presence of 1/32 mol./mol. of sodium-*tert*-butyrate and 0.02% of phenyl-β-naphthylamine at 115°C for 2 hr.)

| Monomer concentration % | Water-insoluble polymer % | Water-soluble polymer % | Total polymer % | $\eta_{rel}$ of water-insoluble polymer |
|---|---|---|---|---|
| 3.5 | 32 | 24 | 56 | 1.938 |
| 5.0 | 42 | 30 | 72 | 2.043 |
| 6.6 | 39 | 28 | 67 | 2.037 |
| 10.0 | 43 | 40 | 83 | 2.010 |
| 13.4 | 41 | 37 | 78 | 1.962 |
| 20.0 | 43 | 32 | 75 | 1.975 |
| 40.0 | 44 | 32 | 76 | 1.882 |

TABLE III. THE EFFECT OF AN INHIBITOR OF THE VINYL POLYMERIZATION
(Polymerized in pyridine at 10% monomer concentrations at 115°C for 2 hr. in the presence 1/32 mol./mol. of sodium-*tert*-butyrate.)

| Kind of inhibitor | Inhibitor %/monomer | Water-insoluble polymer % | Water-soluble polymer % | Total polymer % | $\eta_{rel}$ of water-insoluble polymer |
|---|---|---|---|---|---|
| Phenyl-β-naphthylamine | 0 | 32 | 34 | 66 | 2.048 |
| | 0.05 | 34 | 27 | 61 | 2.062 |
| | 0.1 | 37 | 24 | 61 | 1.941 |
| | 0.2 | 43 | 40 | 83 | 2.010 |
| | 0.5 | 34 | 26 | 60 | 1.980 |
| | 1.0 | 37 | 31 | 68 | 1.955 |
| Hydroquinone | 0.1 | 40 | — | — | — |
| Diphenylamine | 0.2 | 40 | — | — | — |

TABLE IV. THE EFFECT OF WATER

(Monomer concentration=10%)
(Phenyl-β-naphthylamine=0.02%/monomer)
(Sodium-*tert*-butyrate=1/32 mol.)
(Temperature=115°C)

| Solvent | Water content % | Time hr. | Water-insoluble polymer % | Water-soluble polymer % | Total polymer % | $\eta_{rel}$ of water-insoluble polymer | $\eta_{rel}$ of water-soluble polymer | Confirmation of β-alanine |
|---|---|---|---|---|---|---|---|---|
| Dimethyl-formamide | 0.13 | 1 | 82 | 16 | 98 | 1.624 | 1.067 | ○ |
| | 0.61 | 1 | 70 | 18 | 88 | 1.544 | 1.087 | ○ |
| | 0.85 | 1 | 65 | 20 | 85 | 1.569 | 1.087 | ○ |
| Monochloro-benzene | 0.02 | 2 | 84 | 16 | 100 | 2.063 | 1.488 | ○ |
| | 1.0 | 3 | 9 | 89 | 98 | — | — | × |
| | 10.0 | 1 | — | 90 | 90 | — | — | × |

TABLE V. THE CATALYTIC EFFCT OF ALKALI COMPOUNDS

(Polymerized at the catalyst concentration of 1/32 mol./mol., with 0.02% phenyl-β-naphthylamine, at 115°C for 3 hr.)

| Catalyst | Water-insoluble polymer % | Water-soluble polymer % | Total polymer % | $\eta_{rel}$ of water-insoluble polymer | $\eta_{rel}$ of water-soluble polymer |
|---|---|---|---|---|---|
| $CH_3ONa$ | 25 | 63 | 88 | 1.447 | 1.286 |
| *n*-BuONa | 66 | 20 | 86 | 1.780 | 1.147 |
| *tert*-BuOLi | 67 | 32 | 99 | 1.841 | 1.308 |
| *tert*-BuONa | 84 | 16 | 100 | 2.085 | 1.244 |
| *tert*-BuOK | 86 | 14 | 100 | 2.118 | 1.170 |
| Na | 9 | 89 | 98 | — | 1.357 |
| NaOH | 3 | 89 | 92 | — | 1.283 |
| $Na_2CO_3$ | 0 | 0 | 0 | — | — |

TABLE VI. THE CONCENTRATION OF CATALYST

(Polymerized at 10% monomer concentration in the presence of 0.02% phenyl-β-naphthylamine for 2 hr.)

| Solvent | Temp. °C | Concentration of catalyst (mol./mol.) | Water-insoluble polymer % | Water-soluble polymer % | Total polymer % | $\eta_{rel}$ of water-insoluble polymer | $\eta_{rel}$ of water-soluble polymer |
|---|---|---|---|---|---|---|---|
| Pyridine | 115 | 0 | 0 | 0 | 0 | — | — |
| | | 1/30 | 20 | 20 | 40 | 2.118 | — |
| | | 1/65 | 32 | 23 | 55 | 2.033 | — |
| | | 1/43 | 33 | 23 | 56 | 2.075 | — |
| | | 1/32 | 43 | 40 | 83 | 2.010 | — |
| | | 1/15 | 59 | 27 | 86 | 1.967 | — |
| Monochloro-benzene | 115 | 1/200 | 0 | 0 | 0 | — | — |
| | | 1/100 | 13 | 67 | 80 | 1.820 | 1.601 |
| | | 1/64 | 71 | 25 | 96 | 1.920 | 1.339 |
| | | 1/32 | 84 | 16 | 100 | 2.082 | 1.287 |
| *N*,*N*-dimethyl-aniline | 130 | 1/200 | 0 | 5 | 5 | — | — |
| | | 1/100 | 45 | 43 | 88 | 1.734 | 1.351 |
| | | 1/64 | 62 | 23 | 85 | 1.833 | 1.305 |
| *N*,*N*-dimethyl-formamide | 130 | 1/200 | 0 | 0 | 0 | — | — |
| | | 1/100 | 15 | 35 | 50 | 1.296 | 1.171 |
| | | 1/64 | 35 | 31 | 66 | 1.462 | 1.173 |
| | | 1/32 | 89 | 11 | 100 | 1.614 | 1.063 |

TABLE VII. THE RATE OF POLYMERIZATION IN PYRIDINE AT 115°C

| Time hr. | Water-insoluble polymer % | Water-soluble polymer % | Total polymer % | $\eta_{rel}$ of water-insoluble polymer |
|---|---|---|---|---|
| 0.5 | 17 | 42 | 59 | 1.820 |
| 1 | 36 | 34 | 70 | 1.912 |
| 2 | 43 | 40 | 83 | 2.010 |
| 3 | 43 | 40 | 83 | 1.923 |
| 5 | 46 | 22 | 68 | 1.946 |
| 7.5 | 54 | 27 | 81 | 1.826 |

TABLE VIII. THE RATE OF POLYMERIZATION IN CHLOROBENZENE

| Temp. °C | Time hr. | Water-insoluble polymer % | Water-soluble polymer % | Total polymer % | $\eta_{rel}$ of water-insoluble polymer | $\eta_{rel}$ of water-soluble polymer |
|---|---|---|---|---|---|---|
| 80 | 1 | 0 | 86 | 86 | — | 1.256 |
| | 1.5 | 0 | 95 | 95 | — | 1.251 |
| | 2 | 0 | 97 | 97 | — | 1.306 |
| | 4 | 0 | 95 | 95 | — | 1.314 |
| | 7 | 0 | 100 | 100 | — | 1.314 |
| 100 | 0.5 | 0 | 96 | 96 | — | 1.337 |
| | 1 | 0 | 97 | 97 | — | 1.451 |
| | 1.5 | 0 | 97 | 97 | — | 1.472 |
| | 2 | 4 | 85 | 89 | — | 1.500 |
| | 4 | 48 | 44 | 92 | 1.929 | 1.373 |
| | 7 | 74 | 24 | 98 | 2.035 | 1.318 |
| 115 | 0.5 | 15 | 76 | 91 | 1.905 | 1.488 |
| | 1 | 75 | 21 | 96 | 2.063 | 1.336 |
| | 1.5 | 82 | 18 | 100 | 2.095 | 1.283 |
| | 2 | 84 | 16 | 100 | 2.085 | 1.244 |
| | 4 | 91 | 9 | 100 | 2.123 | 1.244 |
| | 7 | 92 | 8 | 100 | 2.133 | 1.243 |

TABLE IX. THE RATE OF POLYMERIZATION IN *o*-DICHLOROBENZENE

| Temp. °C | Time hr. | Water-insoluble polymer % | Water-soluble polymer % | Total polymer % | $\eta_{rel}$ of water-insoluble polymer | $\eta_{rel}$ of water-soluble polymer |
|---|---|---|---|---|---|---|
| 100 | 0.25 | 0 | 86 | 86 | — | 1.343 |
| | 0.5 | 0 | 82 | 82 | — | 1.390 |
| | 0.75 | 0 | 86 | 86 | — | 1.435 |
| | 1 | 0 | 86 | 86 | — | 1.435 |
| | 1.5 | 0 | 92 | 92 | — | 1.493 |
| | 2 | 3 | 87 | 90 | — | 1.543 |
| | 4 | 43 | 42 | 85 | 2.014 | 1.493 |
| | 7 | 71 | 29 | 100 | 2.061 | 1.340 |
| 115 | 0.25 | 0 | 91 | 91 | — | 1.543 |
| | 0.5 | 9 | 89 | 98 | — | 1.555 |
| | 0.75 | 59 | 30 | 89 | 1.998 | 1.377 |
| | 1 | 69 | 23 | 92 | 2.082 | 1.417 |
| | 1.5 | 76 | 24 | 100 | 2.072 | 1.324 |
| | 2 | 86 | 12 | 98 | 2.205 | 1.298 |
| | 4 | 93 | 17 | 100 | 2.035 | 1.309 |

TABLE X. THE RATE OF POLYMERIZATION IN *p*-DICHLOROBENZENE

| Temp. °C | Time hr. | Water-insoluble polymer % | Water-soluble polymer % | Total polymer % | $\eta_{rel}$ of water-insoluble polymer | $\eta_{rel}$ of water-soluble polymer |
|---|---|---|---|---|---|---|
| 100 | 0.25 | 0.4 | 85 | 85 | — | 1.326 |
| | 0.50 | — | 94 | 94 | — | 1.390 |
| | 0.75 | 0.5 | 93 | 93 | — | 1.397 |
| | 1 | 0.7 | 93 | 94 | — | 1.433 |
| | 1.5 | 0.8 | 81 | 82 | — | 1.454 |
| | 2 | 17 | 78 | 95 | 1.946 | 1.452 |
| | 4 | 41 | 57 | 98 | 2.021 | 1.403 |
| | 7 | 59 | 41 | 100 | 2.071 | 1.343 |
| 115 | 0.25 | 2 | 96 | 98 | — | 1.428 |
| | 0.50 | 14 | 80 | 94 | 2.003 | 1.444 |
| | 0.75 | 43 | 49 | 92 | 1.976 | 1.404 |
| | 1 | 70 | 27 | 97 | 2.072 | 1.336 |
| | 1.5 | 82 | 18 | 100 | 2.120 | 1.316 |
| | 2 | 80 | 20 | 100 | 2.086 | 1.310 |
| | 4 | 91 | 9 | 100 | 2.163 | 1.315 |

TABLE XI. THE RATE OF POLYMERIZATION IN *N,N*-DIMETHYLFORMAMIDE

| Temp. °C | Time min. | Water-insoluble polymer % | Water-soluble polymer % | Total polymer % | $\eta_{rel}$ of water-insoluble polymer | $\eta_{rel}$ of water-soluble polymer |
|---|---|---|---|---|---|---|
| 115 | 30 | 0 | 37 | 37 | — | 1.223 |
| | 60 | 0 | 52 | 52 | — | 1.250 |
| | 90 | 41 | 37 | 78 | 1.525 | 1.200 |
| | 120 | 37 | 40 | 77 | 1.475 | 1.221 |
| | 240 | 59 | 21 | 80 | 1.500 | 1.100 |
| | 420 | 45 | 34 | 79 | 1.505 | 1.176 |
| 130 | 5 | 7 | 61 | 68 | — | 1.226 |
| | 10 | 75 | 17 | 92 | 1.485 | 1.087 |
| | 20 | 79 | 16 | 95 | 1.521 | 1.067 |
| | 30 | 83 | 14 | 97 | 1.605 | 1.061 |
| | 60 | 82 | 16 | 98 | 1.624 | 1.061 |
| | 120 | 82 | 18 | 100 | 1.614 | 1.063 |
| 144 | 5 | 55 | 22 | 77 | 1.386 | 1.084 |
| | 10 | 80 | 14 | 94 | 1.600 | 1.059 |
| | 20 | 81 | 16 | 97 | 1.616 | 1.058 |
| | 30 | 82 | 14 | 96 | 1.589 | 1.058 |
| | 60 | 81 | 16 | 97 | 1.569 | 1.057 |
| | 120 | 82 | 14 | 96 | 1.575 | 1.046 |

results are shown in Tables VII—XII.

**The Property of Polymer.** — *i) Melting Point.*— The melting point of water-soluble and water-insoluble polymer was determined in the nitrogen atomosphere in an electric heater, which was 330°~335°C.

*ii) Infrared Spectrum.*—The infrared spectrum of water-soluble and water-insoluble polymer was determined with KBr disc. by Hitachi spectrophotometer IR II. The characteristic absorption band (Amide II band) of a monosubstituted amide appears at 6.5 $\mu$ and no absorptions due to ethylenic double bond appear in comparison with the spectrum of polyacrylamide, which is shown in Figs. 2—5.

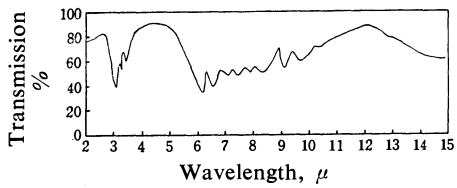



Fig. 2. The infrared spectrum of water-insoluble poly-$\beta$-alanine, which is obtained in chlorobenzene at 115°C for 30 min. (KBr disc).

TABLE XII. THE RATE OF POLYMERIZATION IN ANILINE AND ITS DERIVATIVES

| Solvent | Temp. °C | Time hr. | Water-insoluble polymer % | Water-soluble polymer % | Total polymer % | $\eta_{rel}$ of water-insoluble polymer | $\eta_{rel}$ of water-soluble polymer |
|---|---|---|---|---|---|---|---|
| Aniline | 115 | 0.5 | 16 | 21 | 37 | 1.541 | 1.229 |
| | | 1 | 17 | 11 | 28 | 1.508 | 1.224 |
| | | 1.5 | 22 | 15 | 37 | 1.497 | 1.234 |
| | | 2 | 23 | 15 | 38 | 1.410 | 1.206 |
| | | 4 | 26 | 15 | 41 | 1.435 | 1.176 |
| | | 7 | 23 | 19 | 42 | 1.405 | 1.185 |
| Monomethylaniline | 115 | 0.5 | 8 | 50 | 58 | — | 1.388 |
| | | 1 | 40 | 34 | 74 | 1.670 | 1.243 |
| | | 1.5 | 38 | 37 | 75 | 1.709 | 1.248 |
| | | 2 | 37 | 30 | 67 | 1.719 | 1.239 |
| | | 4 | 40 | 34 | 74 | 1.670 | 1.243 |
| | | 7 | 48 | 32 | 80 | 1.625 | 1.227 |
| Dimethylaniline | 115 | 0.5 | 3 | 80 | 83 | — | 1.354 |
| | | 1 | 40 | 52 | 92 | 1.802 | 1.322 |
| | | 1.5 | 61 | 37 | 98 | 1.810 | 1.296 |
| | | 2 | 60 | 23 | 83 | 1.835 | 1.256 |
| | | 4 | 64 | 32 | 96 | 1.805 | 1.254 |
| | | 7 | 67 | 18 | 85 | 1.705 | 1.220 |

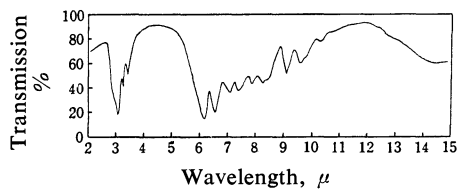



Fig. 3. The infrared spectrum of water-soluble poly-β-alanine, which is obtained in chlorobenzene at 115°C for 30 min. (KBr disc).

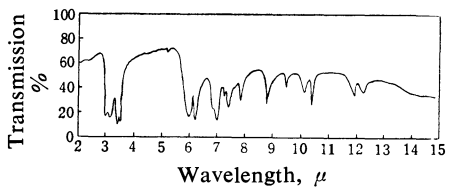



Fig. 4. The infrared spectrum of acrylamide. (KBr disc).

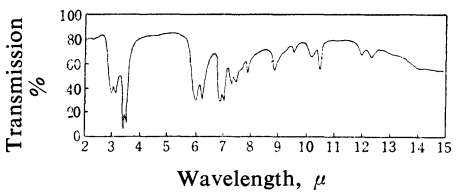



Fig. 5. The infrared spectrum of polyacrylamide. (Film).

TABLE XIII. SOLUBILITY OF POLY-β-ALANINE

| Solvent | Concentration of polymer % | Solubility |
|---|---|---|
| 1,1-Dichloroethanol-1 | 10 | Insoluble |
| 1,1-Dichloroethanol-2 | 10 | 〃 |
| 1,1-Dichloropropanol-2 | 10 | 〃 |
| Trichloroethanol | 10 | 〃 |
| α-Dichlorohydrin | 10 | 〃 |
| 1,1,1-Trichloroisopropanol | 10 | 〃 |
| *m*-Cresol | 10 | 〃 |
| Resorcinol | 30 | 〃 |
| 52% Aqueous $SnCl_2$ solution | 30 | 〃 |
| 50% Aqueous $CaCl_2$ solution | 30 | 〃 |
| Alkaline cupro-glycerol solution | 30 | 〃 |
| Cupro-ethylenediamine solution | 30 | 〃 |
| Cupro-ammonium solution | 30 | 〃 |
| Phosphoric acid | 30 | 〃 |
| ε-Caprolactam | 10 | 〃 |
| α-Pyrrolidone | 10 | 〃 |
| α-Pyperidone | 10 | 〃 |
| Acetamide | 10 | 〃 |
| Dimethylformamide | 10 | 〃 |
| Urea | 10 | Swelling |
| 70% Aqueous $CaCl_2$ solution | 30 | 〃 |
| Anhydrous formic acid | 30 | 〃 |
| Phenol | 30 | 〃 |
| 98% Sulfuric acid | 10 | Soluble |
| Aqua regia | 30 | 〃 |
| 60% Nitric acid | 30 | 〃 |
| Anhydrous formic acid (containing 5% $CaCl_2$) | 30 | 〃 |
| Methanol saturated with $ZnBr_2$ | 10 | 〃 |
| Methanol saturated with $CaCl_2$ | 10 | 〃 |

*iii) Moisture Absorption.* — The moisture content of the polymer ($\eta_{rel}=1.9-2.1$) at various relative humidities is shown in Fig. 6.

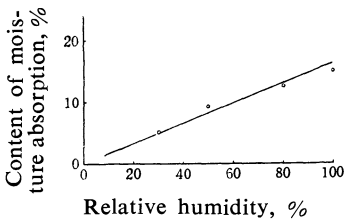



Fig. 6. The moisture content of poly-β-alanine.

*iv) Solubility of polymer.*—The solubility of the polymer in various solvents at 25°C is shown in Table XIII. Anhydrous formic acid containing 5% of calcium chloride is a good solvent for poly-β-alanine.

## Discussion

The conversion curve of acrylamide to water-soluble poly-β-alanine shows a maximum, while the yield of water-insoluble polymer increases with time after a short induction period. The total yield of water-soluble and insoluble polymer is not affected so much with time. The final yield of water-insoluble polymer increases as the reaction temperature becomes higher. Therefore, it is expected that the transition reaction of acrylamide to poly-β-alanine occurs very rapidly as soon as a catalyst is added and then the growth of polymer follows slowly.

It is assumed that the transition of an amide hydrogen may be hindered in the solvents with active hydrogen, as the yield of polymer decreases with the amount of active hydrogen of the solvents. The alkoxide ion may decompose in the solvents with active hydrogen, as follows:

$$RO\text{–}Na+H\text{–}X \rightleftarrows ROH+Na\text{–}X$$

It is expected that the transition polymerization may proceed at first through the addition of alkoxide ion to acrylamide, because no absorptions due to double bond appear in the infrared spectrum of water-soluble polymer which is obtainded at the initial stage of the reaction.

The reaction mechanism will be proposed in a later paper, and the further investigation on the property of polymer and the application to fiber or plastics is now being carried out.

## Summary

The polymerization condition for the transition polymerization of acrylamide to poly-β-alanine has been investigated in the presence of alkali catalyst. The catalytic effect of alkali catalysts is largest for tertiary alkoxide and that of alkali metals is in the order as K>Na>Li. The yield of polymer is larger in the solvents of lower dielectric constant and in aromatic solvents than in aliphatic solvents. The polymerization seldom occurs in the solvents with active hydrogen. The property of the polymer has also been investigated.

The author wishes to express his gratitude to Dr. K. Hoshino and Dr. H. Kobayashi for their instructions and permissions to publish this study, and he also thanks Mr. K. Sugii for his assistance in experiments.

*Nylon Laboratory, Research Department*
*Toyo Rayon Co. Ltd.*
*Minato-ku, Nagoya*

# *Absorption Spectra of Dyes. VI.*[1] *Steric Effects in Conjugated Systems of Benzidine Disazo Dyes and their Copper Derivatives*

By Teruaki KOBAYASHI, Yoshié TANIZAKI and Noboru ANDO

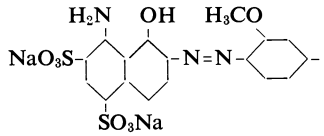
(Received December 25, 1959)

The first absorption bands of dyes are considered to be due to the longest conjugated systems connected with auxochromes, and as is well known, their intensities are the highest when these systems are coplanar. For examples, $\varepsilon_{max}$ of the first absorption band of Benzopurpurine 4B in methanol is 55,000, compared with 42,000 for that of meta-Benzopurpurine[2]. The case is the same with Congo Red. The corresponding value of it in ethanol is 54,000, while there can always be seen remarkable reductions in those of its dimethyl, dichloro and dibromo derivatives, which are prepared with the substituents introduced into the 2- and the 2'-positions of the diphenyl nucleus[3]. Such a decrease in intensity should apparently be caused by steric effects of the substituents. The same phenomena are also found for other dyes: Chlorazol Sky Blue FF has $\varepsilon_{max}$ of 100,000, compared with 74,000 for Direct Sky Blue 5B which is different from the former only in positions of sulfonic groups. Further, their copper derivatives have weaker intensities. Such difference in intensity also seems to be caused by steric effects.

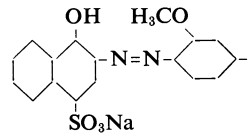
In previous works of this series, absorption spectra of dyes under various conditions have been studied mainly with respect to their first absorption bands, in order to see how they vary with aggregation or formation of complexes. In this paper, absorption spectra in aqueous solutions of both benzidine disazo dyes such as Chlorazol Sky Blue FF and their copper derivatives have been studied in connection with their stereochemical forms and steric hindrances.

## Experimental

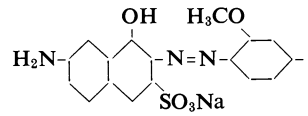
**Preparation of Samples.**—The following dyes were used in the present work. They will be called the abbreviations shown in the parentheses.



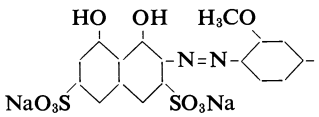

(Dye I)



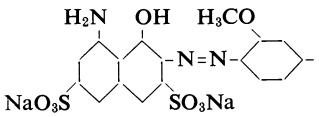

(Dye II)




(Dye III)

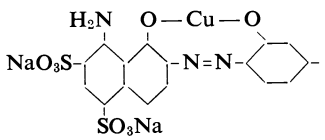



(Dye IV)




(Dye V)

Where the halves of their structures are shown. Their copper derivatives will be called Dye I', Dye II', etc., corresponding to each of them. These copper derivatives are known to have the following structures[4]; e. g., Dye I' is




(Dye I')

Dye I—Dye V were purified by Robinson and Mills' method[5]. The copper derivatives were prepared from these dyes by a method reported elsewhere.[4],*1 The purification of them followed the above method. Found values of copper contents of Dye III' and Dye V' were 90% and 86%, respectively*2. The concentrations of dye solutions were $(1\sim130)\times10^{-6}$ mol./l., which were determined by weight.

**Absorption Spectra.**—All the absorption spectra were measured in 0.2 to 10 cm. cells by a Shimadzu QR-50 spectrophotometer at room temperature (ca. 20°C).

## Results

The absorption spectra of Dye I and Dye I' and of Dye V and Dye V' are illustrated as

1) Part V of this series, This Bulletin, **33**, 661 (1960).
2) H. A. Standing aud M. Stein, *J. Text. Inst.*, **44**, T224 (1953).
3) F. H. Holmes, *Trans. Faraday Soc.*, **54**, 1166 (1958).
4) U. S. Pat., 2,036,159 (1935).
5) C. Robinson and H. A. T. Mills, *Proc. Roy. Soc. (London)*, **A131**, 576 (1931).

* Some of the dyes were presented by Mr. Yoshiji Ishii of the Faculty of Technology, the Gumma University.

*2 For the other dyes see the reference, Y. Ishii, *J. Soc. Tex. Cell. Ind. Japan*, **14**, 718 (1958).

TABLE I. COMPARISON OF THE FIRST ABSORPTION BANDS OF THE DYES

| Dyes | Concn. mol./l×10⁶ | Temp. °C | $\lambda_{max}$ mμ | $\varepsilon_{max}\times10^{-4}$ | | | Oscillator strength | | |
|---|---|---|---|---|---|---|---|---|---|
| | | | | $\varepsilon$ | $\varepsilon_c$ | $\frac{\varepsilon-\varepsilon_c}{\varepsilon}\times100$ | $f$ | $f_c$ | $\frac{f-f_c}{f}\times100$ |
| I | 0.946 | 18~19 | 620 | 10.1 | | 50 | 1.44 | | 30 |
| I′ | 1.000 | 〃 | 596 | | 5.1 | | | 1.01 | |
| II | 1.008 | 〃 | 568 | 6.7 | | 39 | 1.14 | | 34 |
| II′ | 1.006 | 〃 | 555 | | 4.1 | | | 0.75 | |
| III | 15.62 | 15~16 | 562 | 6.2 | | 26 | 1.22 | | 21 |
| III′* | 19.65 | 〃 | 548 | | 4.6 | | | 0.96 | |
| IV | 1.003 | 18~19 | 612 | 7.6 | | 21 | 1.20 | | 13 |
| IV′ | 0.997 | 〃 | 588 | | 6.0 | | | 1.04 | |
| V | 1.509 | 〃 | 612 | 7.4 | | 12 | 1.21 | | 10 |
| V′ | 1.275 | 〃 | 611 | | 6.5 | | | 1.09 | |

* See foot note 3.

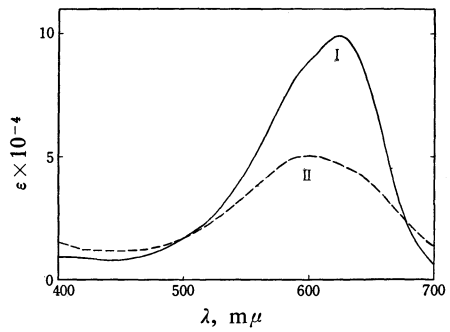



Fig. 1. Absorption spectra of Chlorazol Sky Blue FF (Dye I) and its copper derivative (Dye I′) in aqueous solution at room temperature.
I: Dye I, $1.03\times10^{-5}$ mol./l.; II: Dye I′, $1.01\times10^{-5}$ mol./l.

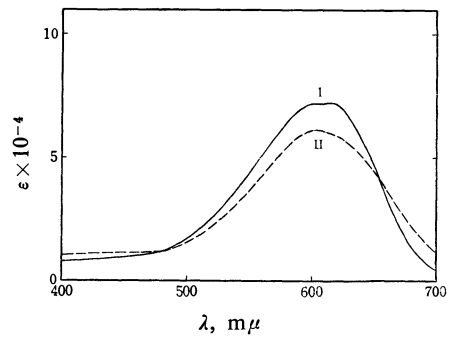



Fig. 2. Absorption spectra of Direct Sky Blue 5B (Dye V) and its copper derivative (Dye V′) in aqueous solution at room temperature.
I: Dye V, $1.13\times10^{-5}$ mol./l.; II: Dye V′, $0.946\times10^{-5}$ mol./l.

examples in Figs. 1 and 2 respectively, in which the full lines mean the results of Dye I and Dye V and the dotted lines those of Dye I′ and Dye V′. Inspection of them shows that the absorption intensity of Dye I is high compared with that of Dye V, and the copper derivatives have remarkably decreased intensities. The same phenomena are observed for the other dyes. In order to investigate these changes in spectra in more detail, $\lambda_{max}$, $\varepsilon_{max}$ and oscillator strengths of the first absorption bands of the dyes are shown in Table I. Variation of the concentrations of these dyes over a wide range revealed that $\lambda_{max}$, $\varepsilon_{max}$ and the shapes of their first bands all vary with concentrations: e. g., results of Dye IV′ are shown in Fig. 3. Therefore, the values in Table I correspond only with the respective concentrations shown in the same table and

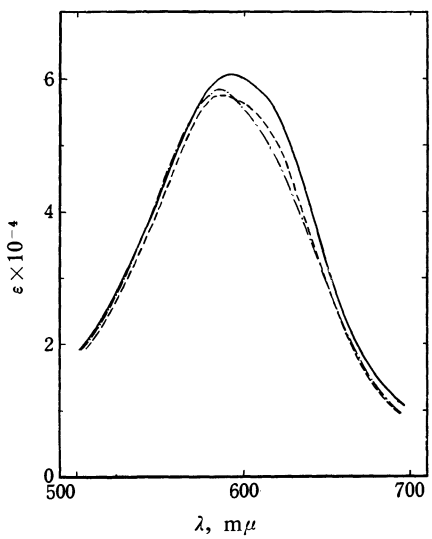



Fig. 3. Absorption spectra of Dye IV′ in aqueous solution at room temperature.
—— $1.01\times10^{-6}$ mol./l.
---- $1.01\times10^{-5}$ 〃
-·-· $0.87\times10^{-4}$ 〃

will somewhat vary with concentrations*3. Oscillator strengths $f$ were calculated by[6]

$$f=4.31\times10^{-9}\int\varepsilon_\nu d\nu$$

As the calculation was carried out for the absorptions longer than 460 m$\mu$ because their train in short wavelengths were obscure, the values are not true ones. However, they will at least satisfy the purpose of mere mutual comparisons. The molecular extinction coefficients and the oscillator strengths of the copper derivatives were distinguished by the suffix c as $\varepsilon_c$ and $f_c$ from those of the non-copper dyes. The table shows that

1. The absorption intensity of Dye I is the highest of all.
2. All the intensities of the dyes are decreased by the introduction of copper into them. The relative order of the percentage decrease in intensity is

Dye I$\approx$Dye II$>$Dye III$>$Dye IV$>$Dye V

The copper derivatives have nearly equal intensities to one another, except Dye II'

3. $\lambda_{max}$ of each dye shifts somewhat to shorter wavelengths by the introduction of copper*4.

## Discussion

As shown in the previous section, the intensities of the first absorption bands of Dye I—Dye V all decrease by the introduction of copper. Comparison of the intensities of Dye I, Dye IV and Dye V which have similar structures to one another shows that while Dye IV and Dye V have nearly equal values, Dye I has a very large one relative to them. If the first absorption bands of these dyes are due to the conjugated double bond chains connecting their auxochromes, they should be the same with one another, because they have the same conjugated chains and auxochromes. The difference in the structures of the dyes is found in positions of sulfonic groups. It should reasonably be considered that the difference in intensity was caused not by the difference in auxochromic effects of the sulfonic groups due to their positions on the naphthalene rings, but rather by their steric effects. On the other hand, the strain in a conjugated system generally causes a decrease in absorption intensity*5. Some of the present results seem to be the case: the intensity of Dye IV or Dye V, which has sulfonic groups in the positions adjacent to the azo groups is remarkably weak compared with that of Dye I which has sulfonic groups in the positions far from the azo groups. Consequently, it would be proper to discuss the experimental results with respect to the positions of sulfonic groups from the stand point of steric effects.

If the dyes are of coplanar structures, scale drawings give conformations as in Fig. 4, in which the halves of the structures of Dye I, Dye II and Dye V are shown. The figure clearly shows that a repulsion between the sulfonic group and the unshared electrons of N may be anticipated in Dye V, but not in

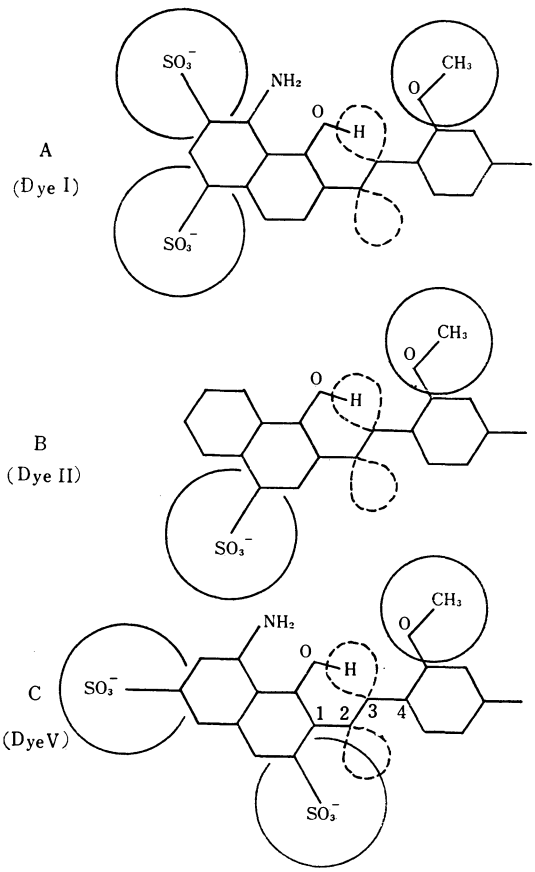



Fig. 4. Models of Dye I, Dye II and Dye V.

*3 The first absorption band of Dye III' varied remarkably with changes in outside conditions and time from preparation of its solutions till measurements. Hence, its values in Table I are less valid.

6) W. West, "Technique of Organic Chemistry", Interscience Publisher, New York (1956), Vol. IX, p. 66.

*4 The first absorption bands of these dyes are considered to be composed of two bands [Y. Tanizaki, T. Kobayashi and N. Ando, This Bulletin, 32, 119 (1959)]. In fact, their behaviors are complicated, apart from variations owing to changes in concentrations. This leads us to difficulty in our exact investigation of their behaviors.

*5 It is not always easy to predict whether absorption bands are shifted to red or blue by steric hindrances. Recently Dewar has discussed the relationship between noncoplanarity of cyanine dyes and shifts of wavelengths of their absorption (M. J. S. Dewar, "Steric Effects in Conjugated Systems", Proceedings of a Symposium held at the University, Hull, 1958, by the Chemical Society (Butterworths, London, 1958), p. 46).

Dye I and Dye II*6. Hence, Dye V (also Dye III and Dye IV) seems to be less planar relative to Dye I (or Dye II) because of the repulsion owing to the sulfonic group. Propriety of this expectation is proved by the fact that $\varepsilon_{max}$ of Dye I is 100,000, compared with 74,000 for that of Dye V which has the same structure as Dye I except the positions of the sulfonic groups.

Now, let us suppose simply that in such a dye as Dye V the repulsion by the sulfonic group only results in twist of the 1–2 bond (see Fig. 4C). Then, owing to the bond twist, the repulsion between the sulfonic group and the unshared electrons of N in position 2 (N(2)) will decrease, whereas the one by the unshared electrons of N(3) will increase. The exchange integral of the 1–2 bond also changes. Hydrogen of the auxochrome OH is generally considered to form a hydrogen bond with N(3), hence the energy of the bond will also change with the twist. On the basis of such consideration, an approximate calculation of the change in energy of the molecule with the twist will be performed.

The change of the exchange integral of a bond with twist has already been studied[7]. According to this procedure, the exchange integral of the 1–2 bond is expressed by

$$V_1(\theta)=\beta S(R)\cos\theta/S(1.39) \quad (1)$$

$$\frac{S(R)-S(1.47)}{S(1.40)-S(1.47)}=\cos\theta \quad (2)$$

where $S(1.39)$, $S(1.47)$, $S(1.40)$ and $S(R)$ are the $\pi$–$\pi$ overlap integrals of the C–C bond of benzene, the normal C–N single bond, the conjugated C–N bond of azobenzene and the 1–2 bond when its length is $R$ corresponding to the angle of twist $\theta$, respectively. These values can be obtained from Mulliken's Table[8].

The repulsion between the charges on the sulfonic group and of the unshared electrons may roughly be estimated, if the center of the charge on the sulfonic group is approximately taken at the point where the extension of the C–S bond crosses the plane decided by the three oxygen atoms, and the distance between this point and the center of the unshared electrons (1.2 Å from the nitrogen nucleus) is taken as that between the two charges, though the effective charges spread widely. Let us put $a_S e$ and $a_N e$ (where $a_S$ and $a_N$ are numerical constants) as the effective charges, with $a_S a_N = a$, and the repulsive energy is expressed by

$$V_2(\theta)=ae^2\{1/r_2(\theta)+1/r_3(\theta)\} \quad (3)$$

where $r_2(\theta)$ and $r_3(\theta)$ are the distances between the sulfonic group and the unshared electrons of N(2) and N(3) respectively.

As mentioned above, the auxochrome OH is considered to form a hydrogen bond with N(3). If the energy of the hydrogen bond O–H···N is approximately estimated to be −5 kcal. and is assumed to be electrostatic, it becomes

$$V_3(\theta)=-2.45/r(\theta) \quad (4)$$

where $r(\theta)$ means the distance between hydrogen and the unshared electrons.

On putting $V(\theta)=V_1(\theta)+V_2(\theta)+V_3(\theta)$ (5)

the change in energy of the molecule becomes

$$\Delta V(\theta)=V(\theta)-V(0)$$

Fig. 5 illustrates $\Delta V(\theta)$-$\theta$ curves, which were drawn by use of various values of $a$ appeared in Eq. 3. As $a$ relates mainly to the effective charges of the sulfonic group and the unshared electrons, it would not exceed two. Although the above calculation is quite simple, the appearance of minima in the curves in a certain range of $a$ suggests that the molecule becomes stable when the 1–2 bond was twisted by 50° to 60° on account of the repulsion. This coincides with the result that the absorption intensity of the dyes in which a sulfonic group is adjacent to the C–N bond is remarkably weak compared with that of the dye which has no such sulfonic group.

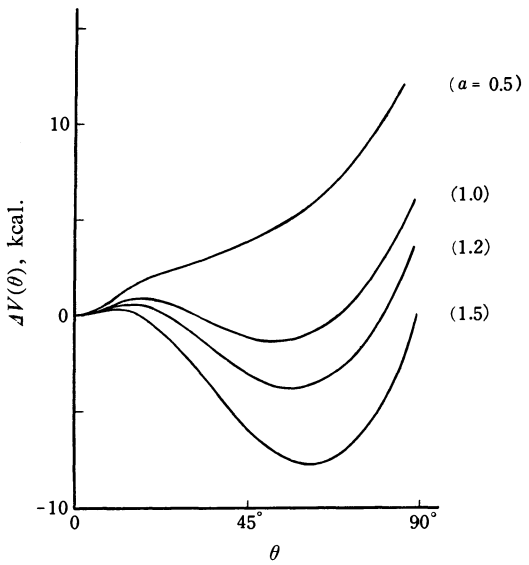



Fig. 5. The change in energy of the sterically hindered dyes with the angle of twist.

*6 The steric effect of unshared electrons of N has been discussed concerning phenyl-azo-azulene, and a reasonable result has been obtained [F. Gerson, T. Gäumann und E. Heilbronner, *Helv. Chim. Acta*, **41**, 1481 (1958)].

7) H. Suzuki, This Bulletin, **25**, 145 (1952); **27**, 597 (1954).

8) R. S. Mulliken, C. A. Lieke, D. Orloff and H. Orloff, *J. Chem. Phys.*, **17**, 1248 (1949).

Copper derivatives of *o*, *o'*-dihydroxy-azo-compounds or of similar compounds have been studied by many workers[9-11], but little is known about their stereochemical forms. In general, coplanar structures seem to be adopted[9], whereas a structure in which a copper atom is centralized on the –N=N– double bond is also considered[11]. Consequently, the stereochemical forms of the dyes studied in the present work are not yet clear.

Absorption spectra of copper derivatives of this kind have also been measured. Inspection of them reveals that intensities of their first bands are generally weak or equal as compared with those of the non-copper substances, without showing any tendency to increase. All of the present copper derivatives have decreased intensities, as mentioned in the previous section, and further a certain tendency was observed in the decrease in intensity: the decrease in intensity of the copper derivative of Dye V (or Dye IV or Dye III) which seems to have a strained conformation was slight, compared with the very remarkable one of the copper derivative of Dye I (or Dye II) which is considered to have a relatively planar conformation. Further the absorption intensities of the copper derivatives are nearly equal to one another. These results prove a great possibility that copper derivatives may have strained conformations.

9) H. D. K. Drew and J. K. Landquist, *J. Chem. Soc.*, **1938**, 292.
10) M. Elkins and L. Hunter, ibid., **1935**, 1598; F. A. Snavely and W. C. Fernelius, *Science*, **117**, 15 (1953); H. B. Jonassen, M. M. Cook and J. S. Wilson, *J. Am. Chem. Soc.*, **73**, 4683 (1951); H. B. Jonassen and J. S. Wilson, ibid., **75**, 4201 (1953).
11) L. G. Van Uitert and W. C. Fernelius, *J. Am. Chem. Soc.*, **76**, 379 (1954).

## Summary

1. Absorption spectra of benzidine disazo dyes and their copper derivatives in aqueous solution were measured at room temperature, and they are compared with one another.

2. It was shown by a simple calculation that the dyes, each of which has sulfonic groups adjacent to the azo groups, have strained conformations caused by the repulsion between the sulfonic groups and the unshared electrons of nitrogen. It was also shown that the relationship between the relative positions of sulfonic groups to the azo groups and the relative absorption intensities could well be explained.

3. The absorption intensities of the copper derivatives were nearly equal, having no relation to the positions of the sulfonic groups, and in addition they were near to those of the non-copper dyes which have the sulfonic groups adjacent to the azo groups. Hence, it was pointed out that the introduction of copper caused the same extent of strain in conjugated systems as sulfonic groups did.

The authors wish to express their thanks to Mr. Yoshiji Ishii of the Gumma University for his kind present of some of the dyes.

*Department of Physical Chemistry*
*Tokyo Institute of Technology*
*Meguro-ku, Tokyo*

# $\pi$-Electronic Structure of Diphenoquinone

By Akira KUBOYAMA

(Received January 11, 1960)

In previous papers the $\pi$-electronic structures of *p*-quinones[1] (*p*-benzoquinone, $\alpha$-naphthoquinone and anthraquinone) and *o*-quinones[2] (*o*-benzoquinone, $\beta$-naphthoquinone and phenanthrenequinone) were studied by the aid of the simple LCAO MO method, with good agreement between the calculated and experimental results concerning the near UV absorption bands of these quinones. In the present paper, it is undertaken to carry out a similar study on the $\pi$-electronic structure of diphenoquinone*, the spectroscopic feature of which has never been theoretically studied.

## Method of Calculation

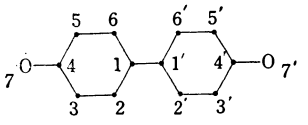
As the molecular dimension of diphenoquinone(DQ) has never been known, it is

1) A. Kuboyama, This Bulletin, 31, 752 (1958).
2) A. Kuboyama, ibid., 32, 1226 (1959).

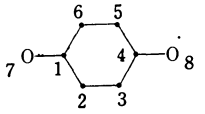
* C. A. Coulson has studied the bond orders of diphenoquinone [*Trans. Faraday Soc.*, 42, 106 (1946)].

impossible to calculate the overlap integrals necessary for the evaluation of exchange integrals ($\beta_{ij}$). Therefore, the values of exchange integrals as well as of Coulomb integrals ($\alpha_i$) were determined by referring to the corresponding values for *p*-benzoquinone(BQ)[1]. The values of these integrals eventually used for the present calculation are shown in Chart I. As it was expected that owing to the steric hindrance between hydrogen atoms at the 2, 6-positions and at the 2′, 6′-positions, two six-membered rings of DQ are somewhat twisted together around the $C_1$–$C_{1'}$ bond, the adopted value for $\beta_{11'}$ was a little smaller than that for $\beta_{23}$.

Chart I. Values of exchange and Coulomb integrals




$\alpha_7=\alpha+1.3\beta$,
$\alpha_4=\alpha+0.2\beta$,
$\alpha_1=\alpha_2=\alpha_3=\alpha$,
$\beta_{47}=\beta_{23}=\beta$,
$\beta_{11'}=0.9\beta$,
$\beta_{12}=\beta_{34}=0.8\beta$




$\alpha_7=\alpha+1.3\beta$,
$\alpha_1=\alpha+0.2\beta$,
$\alpha_2=\alpha$,
$\beta_{17}=\beta$,
$\beta_{12}=0.8\beta$,
$\beta_{23}=1.1\beta$

## Results

The molecular diagrams are given in Charts II and III, together with those of BQ.

Chart II. Charge densities and bond orders

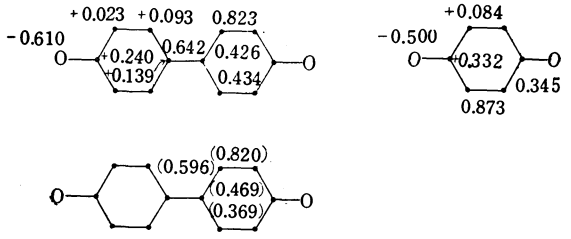
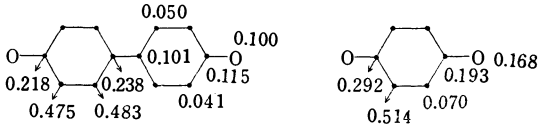



Chart III. Free valences and unpaired electron densities




In these diagrams, the unpaired electron densities are the squares of the coefficients of atomic orbitals in the lowest unfilled orbital. The bond order values of DQ in parentheses are those obtained by Coulson**. The orbital

** In the calculation*, the adopted integral values are as follows. $\alpha_7$ and $\beta_{47}$ are respectively $\alpha+2\beta$, $2\beta$ and the other Coulomb and exchange integrals are all $\alpha$ and $\beta$, respectively.

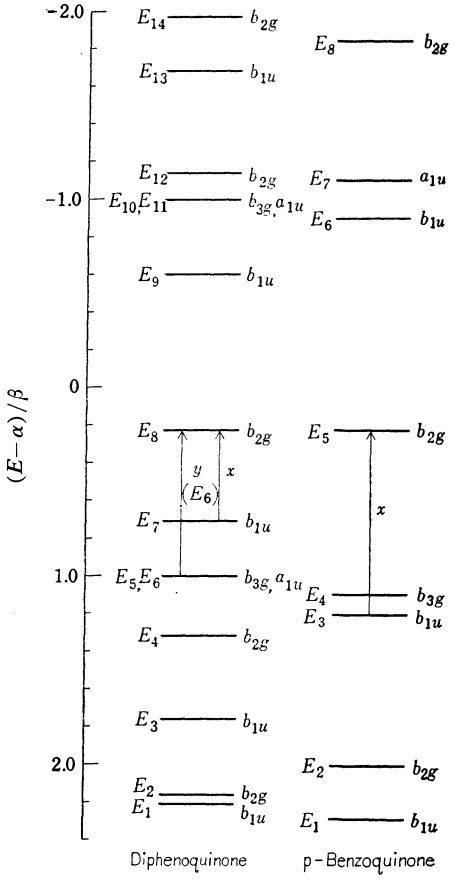



Fig. 1.

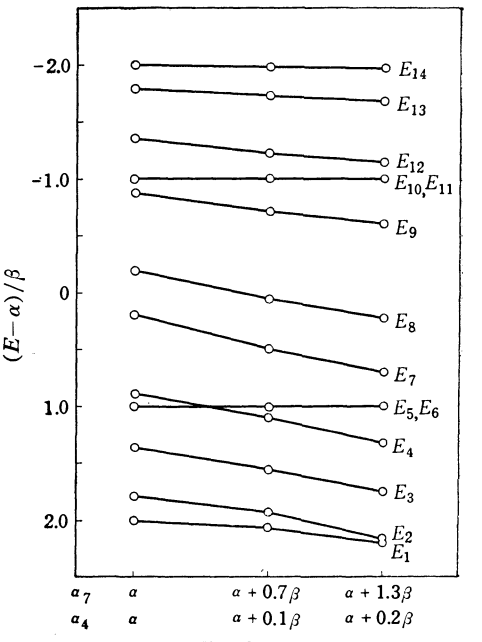



Fig. 2.

energies of DQ are given in Fig. 1, together with those of BQ. The dependence of the orbital energies upon the Coulomb integral of the oxygen atoms of DQ is shown in Fig. 2. the molecular orbitals are classified according to their symmetry properties in the symmetry group ($D_{2h}$), the O–O direction being taken as the $x$-axis and the molecular plane as the $xy$ plane. The $E_5$ and $E_6$ orbitals as well as the $E_{10}$ and $E_{11}$ orbitals are accidentally degenerate. The letter "$x$" or "$y$" attached to the arrow showing a transition denotes the direction of polarization in an allowed transition. The filled and the lowest unfilled molecular orbitals of DQ are given below with their energy values. $\chi_i$ denotes the $2p\pi$ atomic orbital of the $i$th atom.

$$E_1\ 0.2100(\chi_1+\chi_{1'})+0.1721(\chi_2+\chi_6+\chi_{2'}+\chi_{6'})+0.2127(\chi_3+\chi_5+\chi_{3'}+\chi_{5'})+0.3726(\chi_4+\chi_{4'})+0.4091(\chi_7+\chi_{7'})$$

$$E_2\ 0.0611(\chi_1-\chi_{1'})+0.1169(\chi_2+\chi_6-\chi_{2'}-\chi_{6'})+0.2041(\chi_3+\chi_5-\chi_{3'}-\chi_{5'})+0.4058(\chi_4-\chi_{4'})+0.4701(\chi_7-\chi_{7'})$$

$$E_3\ 0.4604(\chi_1+\chi_{1'})+0.2465(\chi_2+\chi_6+\chi_{2'}+\chi_{6'})+0.0650(\chi_3+\chi_5+\chi_{3'}+\chi_{5'})-0.1654(\chi_4+\chi_{4'})-0.3616(\chi_7+\chi_{7'})$$

$$E_4\ 0.2255(\chi_1-\chi_{1'})+0.3128(\chi_2+\chi_6-\chi_{2'}-\chi_{6'})+0.2325(\chi_3+\chi_5-\chi_{3'}-\chi_{5'})-0.0075(\chi_4-\chi_{4'})-0.3804(\chi_7-\chi_{7'})$$

$$E_5\ 0.3535(\chi_2+\chi_3-\chi_5-\chi_6+\chi_{2'}+\chi_{3'}-\chi_{5'}-\chi_{6'})$$

$$E_6\ 0.3535(\chi_2+\chi_3-\chi_5-\chi_6-\chi_{2'}-\chi_{3'}+\chi_{5'}+\chi_{6'})$$

$$E_7\ 0.3459(\chi_1+\chi_{1'})-0.0406(\chi_2+\chi_6+\chi_{2'}+\chi_{6'})-0.3056(\chi_3+\chi_5+\chi_{3'}+\chi_{5'})-0.2211(\chi_4+\chi_{4'})+0.3759(\chi_7+\chi_{7'})$$

$$E_8\ 0.3185(\chi_1-\chi_{1'})+0.2246(\chi_2+\chi_6-\chi_{2'}-\chi_{6'})-0.2015(\chi_3+\chi_5-\chi_{3'}-\chi_{5'})-0.3388(\chi_4-\chi_{4'})+0.3161(\chi_7-\chi_{7'})$$

| | | | |
|---|---|---|---|
| $E_1(b_{1u})$ | $\alpha+2.21098\beta$ | $E_8(b_{2g})$ | $\alpha+0.22822\beta$ |
| $E_2(b_{2g})$ | $\alpha+2.16326\beta$ | $E_9(b_{1u})$ | $\alpha-0.60266\beta$ |
| $E_3(b_{1u})$ | $\alpha+1.75738\beta$ | $E_{10}(b_{3g})$ | $\alpha-\beta$ |
| $E_4(b_{2g})$ | $\alpha+1.31977\beta$ | $E_{11}(a_{1u})$ | $\alpha-\beta$ |
| $E_5(b_{3g})$ | $\alpha+\beta$ | $E_{12}(b_{2g})$ | $\alpha-1.13941\beta$ |
| $E_6(a_{1u})$ | $\alpha+\beta$ | $E_{13}(b_{1u})$ | $\alpha-1.67736\beta$ |
| $E_7(b_{1u})$ | $\alpha+0.71165\beta$ | $E_{14}(b_{2g})$ | $\alpha-1.97184\beta$ |

## Discussion

**Molecular Diagram.**—As for charge distribution, the negative charge of the oxygen atom of DQ is a little larger than that of BQ and of anthraquinone (0.567 $e$). As for bond orders, the general feature of DQ is in qualitative agreement with the one obtained by Coulson. The bond order of the $C_2$–$C_3$ bond of DQ is nearly as large as that of the $C_2$–$C_3$ bond of BQ, and the bond orders of the $C_1$–$C_2$ and $C_3$–$C_4$ bonds of DQ are nearly equal. The bond order obtained by Coulson is considerably smaller in the $C_3$–$C_4$ bond than in the $C_1$–$C_2$ bond. The free valences of DQ are in general nearly equal to those of BQ. In DQ the free valency value of the $C_1$ atom is almost the same as that of the $C_4$ atom. As for the unpaired electron densities, in $o$- and $p$-quinones previously studied, the part larger than sixty percent of the total unpaired electron density exists at the two carbonyl groups, while in DQ the part smaller than fifty percent of the total unpaired electron density exists at the two carbonyl groups. The relatively large unpaired electron density value for the $C_1$ atom of DQ is noticeable. Unfortunately, in DQ the hfs of the electron paramagnetic resonance absorption of the semiquinone ion has never been measured due to the unstability of the ion, but for 3, 5, 3′, 5′-tetramethyl-DQ Matsunaga*** obtained the splitting constant (0.78 gauss) of the hfs due to ring protons. This value is considerably smaller than the one (1.39 gauss) calculated from the combination of the obtained unpaired electron density with McConnell's formula[3].

**Energy Levels.**—Concerning the energy levels given above, two points should be mentioned. First, the lowest unfilled orbital ($E_8$) is far lower than the other unfilled orbitals, as was previously obtained with $o$- and $p$-quinones, and is near the orbital ($E_5$) of BQ. Second, the highest filled orbital ($E_7$) is considerably higher than the ones of the $p$-quinones. The electronic spectrum of DQ in dioxanë obtained by Hartmann and Lorenz[4] is given in Fig. 3. As is seen in Fig. 3, DQ has three adsorption bands at about 500, 390 and 260 mμ. Now these absorption bands are reasonably attributed to the transitions from the rather higher filled

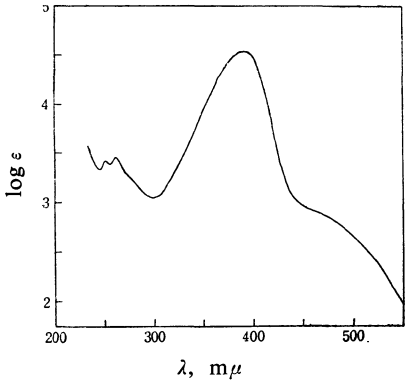



Fig. 3[4]. Electronic spectrum of diphenoquinone, solvent dioxane.

*** Unpublished data.

3) H. M. McConnell, *J. Chem. Phys.*, **24**, 632 (1956).

4) H. Hartmann and E. Lorenz, *Z. Naturforsch.*, **7a**, 360 (1952).

orbitals to the lowest unfilled orbital($E_8$) of DQ. The transitions $E_4 \rightarrow E_8$, $E_5 \rightarrow E_8$ are forbidden. The dipole strengths, calculated with Mulliken's approximation[5], are 0.0014 ($Å^2$) and 5.97 ($Å^2$) for the transitions $E_6 \rightarrow E_8$ and $E_7 \rightarrow E_8$, respectively. Thus, the strong band near 390 m$\mu$ is unambiguously assigned to the transition $E_7 \rightarrow E_8 (A_{1g} \rightarrow B_{3u})$. This transition corresponds to the transition $E_3 \rightarrow E_5 (A_{1g} \rightarrow B_{3u})$ of BQ. For the $A_{1g} \rightarrow B_{3u}$ transition bands, the calculated transition energies ($0.979\beta$ for BQ, $0.483\beta$ for DQ) are reasonable in comparison with the observed ones (ca. 5.0 e. V. for BQ, ca. 3.2 e. V. for DQ). The weak band near 500 m$\mu$ may be assigned to the transition $E_6 \rightarrow E_8 (A_{1g} \rightarrow B_{2u})$ or $E_5 \rightarrow E_8 (A_{1g} \rightarrow B_{1g})$, but the transition energy ($0.772\beta$) seems too great for this assignment. This band may tentatively be due to the $n$-$\pi^*$ transition. The intensity of this band seems considerably great compared with the $n$-$\pi^*$ transition band of other quinones but is nearly equal to that of the $n$-$\pi^*$ transition band of *trans*-azobenzene[6]. The band near 260 m$\mu$ is tentatively assigned to the transition $E_4 \rightarrow E_g (A_{1g} \rightarrow A_{1g})$.

## Summary

The electronic structure of diphenoquinone was studied with the simple MO method using the similar integral values as adopted in our previous work on *p*-quinones. The obtained result was discussed in comparison with the previously obtained one for *p*-benzoquinone. As for energy levels, the lowest unfilled orbital ($b_{2g}$) of diphenoquinone is far lower than the other unfilled orbitals as was obtained with the *p*-quinones The highest filled orbital ($b_{1u}$) of diphenoquinone is considerably higher than the ones of the *p*-quinones. From the calculated result the intense absorption band near 390 m$\mu$ was unambiguously assigned to the $A_{1g} \rightarrow B_{3u}$ transition.

The author wishes to express his sincere thanks to Professor S. Nagakura of the University of Tokyo for his kind guidance and to Dr. Y. Mashiko of this Institute for his kind offices. The author's thanks are also due to Dr. Y. Matsunaga of the University of Tokyo for his kindness in giving valuable information on the EPR data of semiquinone ions prior to publication.

*Government Chemical Industrial Research Institute, Tokyo*
*Shibuya-ku, Tokyo*

5) R. S. Mulliken, *J. Chem. Phys.*, 7, 20 (1939).
6) P. P. Birnbaum, J. H. Linford and D. W. G. Style, *Trans. Faraday Soc.*, **49**, 735 (1953).

# *Harmonic Oscillator Model for the Analysis of NMR Spectra of Di-substituted Benzenes*

By Hiroshi SHIMIZU* and Shizuo FUJIWARA*

(Received December 28, 1959)

Since the experiments of the high-resolution spectrum of the proton magnetic resonance in organic compounds showed very fruitful results, many efforts have been made to continue the measurements and to analyze the spectra of many compounds[1]. During these measurements, one encountered spectra so complicated that they can not be analyzed by the simple inspection of the chemical formula of the samples. These complicated spectra arise in the systems where the differences of the chemical shift values, $\Delta\sigma_{ij}$, and the spin-spin coupling constants, $J_{ij}$, are comparable to each other, where $i$ and $j$ refer to the resonating nuclei, and they can be analyzed by quantum-mechanical procedures. Two methods have so far been proposed for the analysis of these complicated spectra; one was shown by Banerjee, Das, and Saha[2] in the treatments of the two- and three-proton systems and the other, which is more general than the former, was shown by McConnell, McLean and Reilley[3].

This paper concerns the analyses of such

* Present address: Department of Chemistry, Faculty of Science, The University of Tokyo, Hongo, Tokyo.

1) See, for example, Pople, Schneider and Bernstein, "High Resolution Nuclear Magnetic Resonance," McGraw Hill Book Co. Inc., New York (1959).

2) N. K. Banerjee, T. P. Das and A. K. Saha, *Proc. Roy. Soc.* (*London*), A, **226**, 490 (1954).

3) H. M. McConnell, A. D. McLean and C. A. Reilley, *J. Chem. Phys.*, **23**, 1152 (1955).

complicated spectra, using di-substituted benzenes of the type X-  -Y as an example. The method to be shown here is based on the classical treatment of the nuclear magnetic resonance (NMR) phenomena, and is assumed to be helpful for chemists who are not familiar with the quantum-mechanical procedures to obtain the necessary understanding of the analysis of the NMR spectrum.

## Analysis of NMR Spectrum by a Harmonic Oscillator Model

First, the nuclear magnetic resonance of a molecule which has only one hydrogen atom is considered. As there is no interest in the time-dependent phenomena, the equation of the classical or macroscopic vector $\vec{M}$ placed in a static magnetic field $\vec{H}_0$ may be written as

$$d\vec{M}/dt = \gamma\vec{M}\times\vec{H}_0 \qquad (1)$$

where, $\gamma$ is the gyromagnetic ratio of proton. Eq. 1 is the formula given by Bloch[4]. The intensity of the signal due to the nuclear magnetic resonance can be measured by the $x$-component $\vec{M}(z//H_0)$ when $\vec{M}$ is forced to flip down onto the $x$-$y$ plane by the interaction of the nucleus with the oscillating magnetic field $\vec{H}_1(t)$ which rotates in the $x$-$y$ plane with the angular frequency $\omega_0$. Thus, the resonance angular frequency is defined as that of $\vec{H}_1$ which flips $\vec{M}$ most effectively, called as the angular frequency of the Larmor precessional motion of $\vec{M}$ in the field of $\vec{H}_0$. Hence, we can calculate the resonant frequency and the relative intensity of the spectrum, even if we omit the effect of $\vec{H}_1$, and the contribution of $\vec{H}_1$ is taken into account in the considerations of the amplitude of the precession.

From (1), it is easily seen that $M_x$ behaves as a simple harmonic oscillator which obeys Eq. 2 at resonance:

$$d^2M_x/dt^2+\omega_0^2M_x=0 \qquad (2)$$

On the other hand, the equation of the motion of a simple harmonic oscillator may be written as

$$m(d^2X/dt^2)+fX=0 \qquad (3)$$

where $m$ and $f$ are the mass and the force constant of the oscillator. Eq. 3 will become equal to Fig. 2 by making the following interpretation:

$$X=M_x,\quad f=\gamma H_0=\omega_0 \text{ and } m=1/\omega \ (=1/\omega_0 \text{ at resonance}) \qquad (4)$$

4) F. Bloch, *Phys. Rev.*, **70**, 460 (1946).

These relations can be extended to any many-spin system by slight modification of the definition of the force constants. For example, the straightforward extension to a two-spin system composed of two protons, A and B, may be made by additional replacement of the force constant, $f$, by the spin-spin coupling constant $J$ as

$$f_{AB}=\pm J_{AB}/2 \qquad (4a)$$

A positive sign is used when $\vec{M}_A$ and $\vec{M}_B$ are parallel, and the negative sign antiparallel. The situation of this model of the interacting oscillators is illustrated in Fig. 1. The interaction energies of these oscillators refer the off-diagonal terms of secular equations, where the sign of eac term his taken to be positive as well as that of J. Justification of this choice of the sign will be given later.

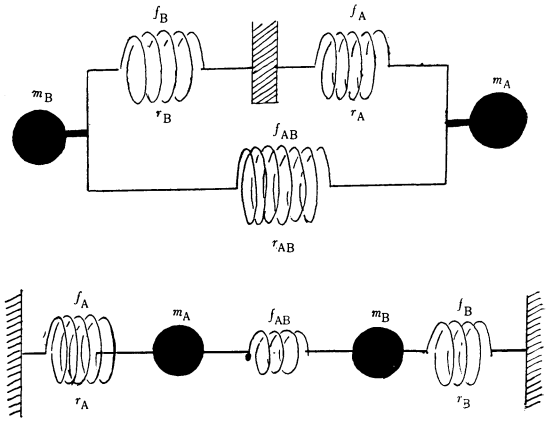



Fig. 1. Explanation of the oscillator model.
(a) $f_{AB}=J_{AB}/2$
(b) $f_{AB}=J_{AB}/2$

The potential energy of the system may be written as Eq. 5,

$$V=1/2\cdot[f_A(\Delta r_A)^2+f_{AB}(\Delta r_{AB})^2+f_B(\Delta r_B)^2] \qquad (5)$$

where $r_A$, $r_B$ and $r_{AB}$ are the elongations of the springs, A, B and C, whose force constants are $f_A$, $f_B$, and $f_{AB}$, respectively. The expression (5) may be rewritten by the Cartesian coordinate $x$ as

$$\begin{aligned} V&=1/2\cdot[(f_A+f_{AB})x^2{}_A+2f_{AB}x_Ax_B \\ &\quad+(f_B+f_{AB})x^2{}_B] \\ &=1/2\cdot[(\omega_A+J_{AB}/2)M^2{}_{Ax}+J_{AB}M_{Ax}M_{Bx} \\ &\quad+(\omega_B+J_{AB}/2)M^2{}_{Bx}] \end{aligned} \qquad (6)$$

In Eq. 6 we used the relations, $\Delta r_A=x_A$, $\Delta r_B=-x_B$ and $\Delta r_{AB}=x_A+x_B$.

The kinetic energy of the system, $T$, is as shown by

$$T=m[\dot{x}^2_A+\dot{x}^2_B]/2 \tag{7}$$

$$=[\dot{M}^2_{Ax}+\dot{M}^2_{Bx}]/2\omega \tag{7a}$$

As the $x$-$y$ components of the magnetic vectors, $\vec{M}_{Axy}$ and $\vec{M}_{Bxy}$ rotate about the $z$-axis, the $x$-components of these vectors may be written as

$$\left.\begin{aligned} M_{Ax}&=M_{Axy}\cos\omega t \\ M_{Bx}&=M_{Bxy}\cos\omega t \end{aligned}\right\} \tag{8}$$

Substituting Eq. 8 into Eqs. 6a and 7a, the motion of $M_{Ax}$ and $M_{Bx}$ are given by the classical equation of motion,

$$\frac{d}{dt}\left(\frac{\partial T}{\partial \dot{M}_{ix}}\right)+\frac{\partial V}{\partial M_{ix}}=0 \quad (i=A, B)$$

which leads a set of two homogeneous equations,

$$(\omega_A+J_{AB}/2-\omega)M_{Ax}+J_{AB}M_{Bx}/2=0 \tag{10}$$

$$J_{AB}M_{Ax}/2+(\omega_B+J_{AB}/2-\omega)M_{Bx}=0 \tag{10a}$$

These equations have a non-vanishing solution only when the determinant of the coefficients of $M_{Ax}$ and $M_{Bx}$ is zero, i. e.,

$$\begin{vmatrix} \omega_A+J_{AB}/2-\omega, & J_{AB}/2 \\ J_{AB}/2, & \omega_B+J_{AB}/2-\omega \end{vmatrix}=0 \tag{11}$$

and from the secular equation (11), we obtain the relation,

$$\omega_0=1/2\cdot[(\omega_A+\omega_B)+J_{AB}\pm(\sigma^2_{AB}+J^2_{AB})^{1/2}] \tag{12}$$

where $\sigma_{AB}=\delta_A-\delta_B$ is the chemical shift between the protons of A and B. Similar treatment of model 2b gives the resonant frequency,

$$\omega_0=1/2\cdot[(\omega_A+\omega_B)-J_{AB}\pm(\sigma^2_{AB}+J^2_{AB})^{1/2}] \tag{12a}$$

It is reasonable to assume that the energy absorbed by the system at resonance is proportional to the magnitude of the mean kinetic energy of the oscillator, i. e., to the square of the vector $\vec{M}_{xy}=\vec{M}_{Axy}+\vec{M}_{Bxy}$. Hence, the relative intensity of the spectrum at the frequency $\omega_0$, $I(\omega_0)$, is calculated from Eq. 10 or 10a with the normalization condition of the magnetic vector, (13),

$$M_{Axy}(\omega_0)^2+M_{Bxy}(\omega_0)^2=1 \tag{13}$$

as

$$I(\omega_0)=[M_{Axy}(\omega_0)+M_{Bxy}(\omega_0)]^2 \tag{14}$$

$$=1-2\frac{(\omega_A-\omega_0)(\omega_B-\omega_0)}{(\omega_A-\omega_0)^2+(\omega_B-\omega_0)^2} \tag{15}$$

The calculated spectrum is shown in Fig. 2.

Although the present method of analysis is based on the classical treatment of an oscillator model, it is shown that the results of this analysis are in accordance with those to be obtained quantum-mechanically.

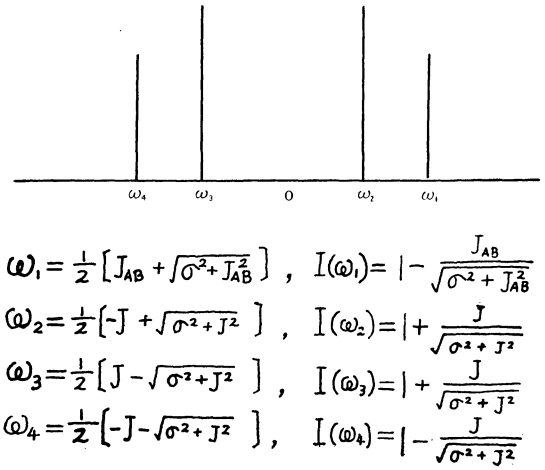



Fig. 2. Calculated spectrum.

The quantum-mechanical Hamiltonian of a two-spin system in a laboratory coordinate system may be expressed as

$$\mathcal{H}=-\gamma_A\vec{I}_A\cdot\vec{H}_A-\gamma_B\vec{I}_B\cdot\vec{H}_B+J_{AB}\vec{I}_A\cdot\vec{I}_B \tag{16}$$

The time-dependent Schroedinger equation is given by Eq. 17 in a rotating coordinate system which rotates with angular velocity, $\vec{\omega}$, as

$$i\hbar\dot{\Psi}_r=[-\gamma_A\vec{I}_A(\vec{H}_A+\omega/\gamma_A)-\gamma_B\vec{I}_B(\vec{H}_B+\omega/\gamma_B)+J\vec{I}_A\vec{I}_B]\Psi_r \tag{17}$$

The fields at $I_A$ and $I_B$ are effectively reduced to zero, provided that the angular velocities of the coordinates are given by

$$\vec{\omega}_A=-\gamma_A(\vec{H}_A-J_{AB}\vec{I}_B/\gamma_A) \tag{18}$$

and

$$\vec{\omega}_B=-\gamma_B(\vec{H}_B-J_{AB}\vec{I}_A/\gamma_B) \tag{18a}$$

If we return to the laboratory coordinate system, the effective fields at $\vec{I}_A$ and $\vec{I}_B$ are written as

$$\vec{H}_A-J_{AB}\vec{M}_B/2\gamma_A \tag{19}$$

and

$$\vec{H}_B-J_{AB}\vec{M}_A/2\gamma_B \tag{19a}$$

respectively.

By assuming the macroscopic equations which have the same form as Eq. 1, we obtain the equations,

$$d\vec{M}_A/dt=\gamma_A\vec{M}_A\times(\vec{H}_A-J_{AB}\vec{M}_B/2\gamma_A) \tag{20}$$

and

$$d\vec{M}_B/dt=\gamma_B\vec{M}_B\times(\vec{H}_B-J_{AB}\vec{M}_A/2\gamma_B) \tag{20a}$$

By taking the time-independence of the components of $M_{Az}$ and $M_{Bz}$ into consideration,

Eqs. 22 and 22a are substituted into Eqs. 21 and 21a, respectively.

The equations for the $x$-components of Eqs. 20 and 20a are

$$dM_{Ax}/dt=(\gamma_A-J_{AB}M_{Bz}/2)M_{Ay}+J_{AB}M_{By}M_{Az}/2 \quad (21)$$

and

$$dM_{Bx}/dt=(\gamma_B-J_{AB}M_{Az}/2)M_{By}+J_{AB}M_{Ay}M_{Bz}/2 \quad (21a)$$

where

$$\left.\begin{aligned}M_{Ax}&=M_{Axy}\cos\omega t\\ M_{Ay}&=-M_{Axy}\sin\omega t\end{aligned}\right\} \quad (22)$$

and

$$\left.\begin{aligned}M_{Bx}&=M_{Bxy}\cos\omega t\\ M_{By}&=-M_{Bxy}\sin\omega t\end{aligned}\right\} \quad (22a)$$

## Experimental

Calculations and measurements of the NMR spectra were performed for the di-substituted benzenes of the type of X-  -Y: $p$-aminobenzoic acid was dissolved in a concentrated aqueous solution of potassium hydroxide, and $p$-toluidine, $p$-nitrophenol, and $p$-nitrobenzaldehyde were dissolved in carbon tetrachloride, methanol and acetone, respectively. These solutions were saturated at 28°C and sealed in the glass tubes with the diameter of 3.5~3.8 mm.

The apparatus of the NMR measurements is the one constructed in this laboratory having the same structure as the one reported by Gutowsky et al. before[5], and operated at the frequency of 27.030 Mc. The samples were spinned during the measurements. The separations of each component of the spectra were measured on the recorded charts using the records of ethanol as the standard reference: the $J$ value of the coupling between the methyl and methylene groups in ethanol was taken as 6.90 cps.[5]

## Discussion

In Fig. 3, the spectrum for the anisaldehyde is shown as an example of NMR measurements. The values of the chemical shift and the spin-spin couplings were calculated from Eqs. 12 and 12a as listed in Table I. The maximum error in the results of Table I is about 10%, which is assumed to be mainly due to the fluctuations in the chart speed of the recorder. Rigorously speaking, the compounds used here are not the two-spin system, but belong to four-spin system, and the values listed in Table I contain some error due to this approximation. But, this error is assumed to be quite small.

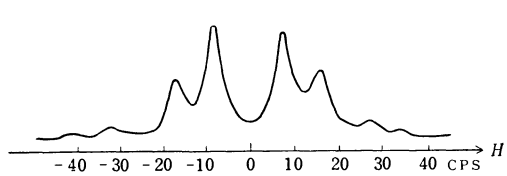



Fig. 3. The spectrum of anisaldehyde. Resonance frequency=27 Mc.

Table I. $J$ and $\sigma$ values of the ring protons of X-  -Y type molecules

Res. freq.=27 Mc.

| X | Y | $J$ cps. | $\sigma$ cps. |
|---|---|---|---|
| -CHO | $CH_3O$- | 8.62 | 24.2 |
| -COOH | $NH_2$- | 8.21 | 30.1 |
| $-CH_3$ | $NH_2$- | 8.70 | 13.54 |
| $-NO_2$ | HO- | 9.06 | 31.1 |
| $-NO_2$ | OHC- | 9.24 | 6.6 |

It is seen in Table I that the $\sigma$'s are dependent on the species of the substituents of X and Y, whereas $J$'s are not dependent with a constant value of about 8.7($\pm$0.5) cps. If we can assume that an additive law holds with the chemical shifts of the ring protons, $\delta$, of monosubstituted benzenes, the magnitudes of $\sigma$'s could be related by the relation,

$$|\sigma|=|(\delta_X{}^o-\delta_Y{}^m)-(\delta_Y{}^o+\delta_X{}^m)| \quad (23)$$

where, for example, $\delta_X{}^o$ and $\delta_Y{}^m$ refer to the chemical shifs of *ortho*-proton of X and the meta-proton of Y, respectively.

We calculated the magnitudes of $\sigma$ by using the values of $\delta$'s for the monosubstituted benzenes reported by Corio and Dailey[7], and compared the calculated results with those obtained experimentally. Agreements are not good between the $\sigma$'s of calculation and of observation whereas the observed values of $\sigma$'s showed good proportionality to $|\delta_x{}^o-\delta_y{}^o|$. This seems to suggest that the additivity does not hold with the $\delta$'s for the ring protons of di-substituted benzenes.

The authors are indebted to Professor Shōji Shibata and Professor Tyūnoshin Ukita and to Miss Motoko Nakahara of the University of Tokyo for their help in the preparation of the samples. Thanks are also due to Mr. Ichiro Yamaguchi of the Japan Atomic Energy Research Institute, who kindly sent us the preprint of his work on the substituted benzenes.

*University of Electro-Communications*
*Chofu, Tokyo*

5) H. S. Gutowsky, L. Meyer and R. E. McClure, *Rev. Sci. Inst.*, **24**, 644 (1953).
6) J. T. Arnold, *Phys. Rev.*, **102**, 136 (1956).
7) P. L. Corio and B. P. Dailey, *J. Am. Chem. Soc.*, **78**, 3043 (1956).

# *Polyethers. III. Polymerizations and Polymers of Some Substituted Ethylene Oxides**

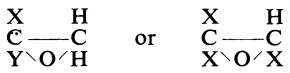
By Shin'ichi ISHIDA**

(Received December 18, 1959)

A variety of polyethers has been prepared by ring-opening polymerization of cyclic ethers, for example from ethylene oxide[1], propylene oxide[2], fluorine-containing olefine oxides[3], oxacyclobutanes[4] and from tetrahydrofuran[5].

A systematic survey in this field will offer an interesting new field for studies both on stereospecific polymerization and on structure of crystalline polyethers.

In the light of this consideration, polymerizations of some substituted ethylene oxides were tried with attempts to obtain crystalline polymers by a stereospecific polymerization for some oxides of the types.



The present paper is in the nature of a survey and a tentative report on some oxides involved.

## Experimental

**Materials.**—*1-Chloro-2-methyl-2-propanol.*— It was prepared by Burgin's method[6]. After the treatment of 90 g. of methallyl chloride with molar proportion of 80% sulfuric acid at 5~10°C for 2.5 hr. with vigorous stirring, the reaction mixture was hydrated on cracked ice. The chlorohydrin was distilled as a constant boiling mixture which, after being salted out, redistilled, b. p. 126~129°C. The yield was about 40~50% (63~66% reported).

*1,1-Dimethyl Ethylene Oxide.*— The preceding chlorohydrin (50 g.) was slowly added to powdered potassium hydroxide (120 g.) with stirring at such a rate that the temperature of the distillate did not exceed 55°C. When the reaction ceased the remaining volatile matter was distilled off under water pump vacuum at room temperature to a trap cooled at −70°C. The total condensate was dried with potassium hydroxide and fractionated to yield the desired oxide; 25 g., 63% of theory, b. p. 50.2~50.5°C. $n_D^{20}$ 1.3730 (reported b. p. 53°C, $n_D^{20}$ 1.3730)[7].

*2-Methyl-3-chloro-2-butanol.*—It was prepared from 3-chlorobutanone-2 (b. p. 114°C) obtained by chlorination of methylethylketone in the presence of marbel and methyl magnesium bromide by Fourneau's method[8]. 20% yield of light yellow liquid boiled at 140°C (reported b. p. 141~142°C). This chlorohydrin was also prepared by the action of hypochlorous acid on trimethyl ethylene in some runs but the yield and the purity were rather poor.

*1,1,2-Trimethyl Ethylene Oxide.*—It was prepared by dehydrochlorination of trimethyl ethylene chlorohydrin. Dehydrochlorination was carried out in all cases by adding the chlorohydrin slowly on to solid potassium hydroxide with stirring. The yield was about 30% based on the chlorohydrin.

*Tetramethyl Ethylene Oxide.* — Anhydrous pinacol (115 g.) obtained from acetone was treated with molar proportion of anhydrous hydrogen chloride (41 g.) at 35~45°C and the resulting chlorohydrin was recrystallized (melted at 63°C) and treated as above with solid potassium hydroxide to produce the epoxide (35 g.), b. p. 90~93°C, $n_D^{20}$ 1.3985 (lit. b. p. as reported[9], $n_D^{20}$ 1.3986). The yield was 13% based on anhydrous pinacol.

*1-Methyl-1-phenyl-2-chloro Ethanol.*—It was prepared by King's procedure[10] from monochloroacetone and phenylmagnesium bromide.

The reaction mixture was stirred at −10°C during the addition of Grignard reagent under the protection of dry nitrogen and then allowed to warm slowly to room temperature after being kept standing overnight. To the cold reaction mixture was then added dropwise with stirring a solution of ammonium chloride (100 g.) in water (400 ml.). The ether layer was separated and the aqueous layer was extracted with ether. The combined ether extracts were washed once with 250 ml. of water and dried over anhydrous sodium sulfate. Removal of the ether by distillation gave a crude residue (50 g.) which was fractionated under reduced pressure. Eighty grams (72.7%) of the product distilled at 109~112°C/12 mmHg were obtained (lit. b. p. 129~132°C/21 mmHg).

*1-Methyl-1-phenyl Ethylene Oxide.*—The chlorohydrin was decomposed with sodium ethoxide to give methylphenyl ethylene oxide. A colorless liquid

* Presented at the 8th Annual Meeting of the Society of the Polymer Science of Japan, Tokyo, May, 1959. Part I and II; This Bulletin, 33, 727, 731 (1960).

** Present address; The Textile Research Laboratory, Asahi Chemical Industry, Co. Ltd., 118 Ama, Takatsuki, Osaka.

1) H. Staudinger, "Hochmolekularen Organischen Verbindungen", Springer (1932), p. 287.

2) For example; C. C. Price et al., *J. Am. Chem. Soc.*, 78, 690, 4787 (1956).

3) D. D. Smith et al., *Ind. Eng. Chem.*, 49, 1241 (1957).

4) A. C. Farthing et al., *J. Chem. Soc.*, 1955, 3648.

5) K. Hamnan, *Angew. Chem.*, 63, 231 (1951).

6) J. Burgin and G. Hearne, *Ind. Eng. Chem.*, 33, 385 (1941).

7) W. T. Somerville, *J. Am. Chem. Soc.*, 72, 737, 2185 (1950).

8) M. M. Fourneau and M. Tiffeneau, *Compt. rend.*, 145, 437 (1907).

9) F. H. Norton, *J. Am. Chem. Soc.*, 58, 2147 (1936).

10) L. F. King, ibid., 61, 2383 (1959); W. J. Hickinbottom et al., *J. Chem. Soc.*, 1954, 4200.

b. p. 75～76°C/12 mmHg (lit.[10] b. p. 72～75°C/11 mmHg).

*1, 1-Diphenyl-2-chloroethanol.* — To a stirred solution of ethyl chloroacetate (84 g.) in dry ether (300 ml.) was added dropwise over a period of 4.5 hr. a solution of phenylmagnesium bromide previously prepared from magnesium (36.5 g.) and bromobenzene (252 g.) in dry ether (650 ml.). The reaction mixture was maintained at 0 to −5°C and then treated according to the procedure similar to the synthesis of 1-methyl-1-phenyl-2-chloroethanol. The product was isolated by distillation under reduced pressure and purified by recrystallization from ligroin. A yield 46 g. (26%), m. p. 53～56°C (lit. m. p. 52～57°C).

*1,1-Diphenyl Ethylene Oxide.*—A yield of an almost quantitative amount of crude oxide (m. p. 42～45°C) was obtained by action of the chlorohydrin on the aqueous solution of sodium hydroxide by Zaugg's method[11]. Twice recrystallization from absolute ethanol gave a pure oxide, m. p. 55～56°C (reported m. p. 56～57°C).

*1, 1-Diethyl-2-chloroethanol.* — It was prepared by the same procedure used in the synthesis of 1,1-diphenyl-2-chloroethanol. To a stirred solution of ethylchloroacetate (65 g.) in dry ether (300 ml.) was added a solution of ethylmagnesium bromide previously prepared from magnesium (24 g.) and ethyl bromide (109 g.) in dry ether (200 ml.). Resulting chlorohydrin was obtained in a yield of 44%, b. p. 66～67°C/16～18 mmHg (lit.[12] b. p. 70°C/20 mmHg).

*1, 1-Diethyl Ethylene Oxide.*—It was prepared by the conversion of the chlorohydrin by the same procedure as in the synthesis of 1,1-dimethyl ethylene oxide mentioned above. Thirty grams of the chlorohydrin gave 15 g. of the raw epoxide, which gave by the fractional distillation a distillate boiling at 105～106°C (lit. b. p. 107°C).

**General Procedure of Polymerization.**—A catalyst was added to a monomer or a monomer solution in a glass tube which was flashed by nitrogen previously and then cooled in dry ice-acetone.

The tube was sealed and placed in a constant temperature bath. At the end of the reaction time, the tube was recooled and opened. To the reaction mixture, a small quantity of methanol or some appropriate agents for stopping the reaction were added and the resulting polymer was washed thoroughly with methanol so as to remove the catalyst residue. In the case when the reaction product was an oil it was dissolved in acetone and precipitated with a large volume of methanol.

## Results and Discussion

**1, 1-Dimethyl Ethylene Oxide (D. M. E. O.).**— 1,1-Dimethyl ethylene oxide was attempted to polymerize by different catalysts and some details were given in Table I. The polymer was found to consist of two fractions; fraction I was insoluble in acetone, benzene, methanol and ether and soluble in hot tetrahydrofuran, dioxane and dimethylformamide, except in some cases, where a small quantity of the insoluble part in these solvents was contained. Fraction II was soluble in acetone but insoluble in methanol.

Fraction I, a white and nontacky powder, was shown by X-ray examination to be crystalline. The melting points of these materials obtained from the different catalysts varied from 127 to 155°C. Fraction II was usually a white solid, melting at about 90～100°C, but in the case, where diethyl zinc and $FeCl_3$–PO was used as catalyst, it was a tacky semi-solid or a pasty mass.

As may be seen in Table I, the polymerization with the catalysts borontrifluoride etherate ($BF_3$-$Et_2O$) and triethyl aluminum ($AlEt_3$) and diethyl zinc ($ZnEt_2$) respectively proceeded very rapidly at low temperatures;

Table I. Polymerization of 1,1-dimethyl ethylene oxide with different catalysts

| Catalyst | wt. % | Reaction temp. °C | Time hr. | Yield, % | Fraction, % | | m. p. of I, °C |
|---|---|---|---|---|---|---|---|
| | | | | | I | II | |
| $FeCl_3$-PO | 5 | 70 | 64 | 15.0 | 42 | 58 | — |
| $FeCl_3$[a] | 5 | 80 | 20 | 15.6 | major | minor | — |
| $BF_3Et_2O$ | 5 | r. t. | 24 | considerable | major | minor | 159～160 |
| $TiCl_4$ | 3.5 | −78-r. t. | 48 | 28.5 | 68.0 | 32.0 | — |
| $TiCl_4$ | 3.0 | r. t. | 3 days | 25.9 | 83.0 | 17.0 | 127 |
| AIP[b] | 2 | 80 | 20 days | nil | — | — | — |
| AIP-$ZnCl_2$[c] | 2 | 80 | 6 days | nil | — | — | — |
| $AlEt_3$[d] | 3.5 | −78-r. t. | 6 days | 57.2 | 91.4 | 8.6 | 155 |
| $AlEt_3$ | 5 | r. t. | 5 | — | 27.2 | — | 152 |
| $ZnEt_2$[e] | 5 | r. t. | 4 days | 46.8 | 83.4 | 16.6 | 151～152 |
| $ZnEt_2$-$Al_2O_3$[f] | 2 | r. t. | 20 days | nil | — | — | — |

a) anhydrous ferric chloride, b) aluminum isopropoxide, c) aluminum isoproxide-zinc chloride, d) trimethyl aluminum in *n*-hexane, e) diethyl zinc in diethyl ether, f) diethyl zinc on alumina.

11) H. E. Zaugg et al., *J. Am. Chem. Soc.*, **80**, 2770 (1958).

12) R. Dalebroux and H. Wuyps, *Chem. Zentr.*, **1906 II**, 1179.

TABLE II. COPOLYMERIZATION OF 1,1-DIMETHYL ETHYLENE OXIDE ($M_1$) WITH EPICHLOROHYDRIN ($M_2$) USING $AlEt_3$ AS CATALYST IN *n*-HEXANE AT LOW TEMPERATURE

| $M_1$ in comonomer | | Total conversion | Fraction, % | | Chlorine content in I, % | m. p. of I °C | X-ray pattern of I |
|---|---|---|---|---|---|---|---|
| wt. % | mol. % | % | I | II | | | |
| 100 | 100 | 57.2 | 91.0 | 9.0 | — | 155 | DMEO |
| 68.0 | 74.0 | 22.6 | 36.6 | 63.4 | 8.66 | 125 | DMEO |
| 41.3 | 47.0 | 34.3 | 8.5 | 91.5 | 37.37 | 117 | EpCl |
| 19.0 | 23.0 | 39.1 | 84.9 | 15.1 | — | — | EpCl |
| 0 | 0 | 72.7 | 73.7 | 26.3 | — | 117 | EpCl |

Fraction I: methanol-insoluble part, Fraction II: methanol-soluble part

TABLE III. COPOLYMERIZATION OF 1,1-DIMETHYL ETHYLENE OXIDE ($M_1$) WITH EPICHLOROHYDRIN ($M_2$) BY 4% OF $AlEt_3$ IN *n*-HEXANE AT 80±0.5°C

| $M_1$ in comonomer | | Total conversion | Fraction | | | Chlorine content in I, % | m. p. of I °C | X-ray pattern of I |
|---|---|---|---|---|---|---|---|---|
| wt. % | mol. % | % | I | II | III | | | |
| 86.4 | 89.8 | 80.8 | 16.7 | 83.3 | | 2.44 | 140 | DMEO |
| 68.0 | 74.0 | 47.0 | 13.4 | 54.3 | 32.3 | 2.22 | 140 | DMEO |
| 41.3 | 47.0 | 76.6 | 4.3 | 3.2 | 92.5 | 36.45 | 117 | EpCl |
| 19.0 | 23.0 | 83.8 | 9.5 | 11.5 | 79.0 | 32.07 | 117 | EpCl |

the reaction mixture was solidified as soon as the catalyst was added. Aluminum isopropoxide (AIP) and the one in conjunction with zinc chloride (AIP-$ZnCl_2$)[13] as well as diethyl zinc-alumina system[14] were completely inactive for this monomer in contrast to the fact of their being active for propylene oxide.

Copolymerizations of 1,1-dimethyl ethylene oxide with epichlorohydrin (EpCl) were also studied. Epichlorohydrin was chosen for the convenience of its analysis and $AlEt_3$ was used as catalyst because of the feasibility of its purification from resulting polymer compared with those from $FeCl_3$-PO catalyst. Some runs of polymerization were carried out at a low temperature. (The catalyst was added to the monomer solution in a glass tube cooled in dry ice-acetone, the reaction started and the reaction mixture was solidified immediately, and then the glass ampoule was placed in a water bath and kept at room temperature for further promotion of polymerization.) The other runs were done in an oil bath at 80°C from the beginning. The resulting products were in both cases fractionated by the precipitation method. In the case at low temperature, the products were divided into two fractions; methanol-insoluble fraction (I) and methanol-soluble fraction (II). In the latter case at the higher temperature, the product was separated into three fractions; acetone-soluble fraction (I'), acetone-soluble but methanol-insoluble fraction (II') and methanol-soluble fraction (III). These results were shown in Tables II and III.

In both the cases, there existed a minimum of conversion versus monomer composition fed in the range of monomer composition of about 70% of 1,1-dimethyl ethylene oxide ($M_1$) in comonomer, and this corresponded also with a minimum yield of fractions I, I' and II' at about 40% of $M_1$. Of these fractions, fractions I and I' were white powders and these two were examined in some details. Melting points, chlorine contents and X-ray patterns of these fractions showed that these fractions were either homopolymer of D. M. E. O. or that of EpCl depending upon the preference of one monomer in the monomer composition.

The critical monomer composition coincided with the composition corresponding to a minimum percent of fraction I and I'.

From the results mentioned above, it may be seen, in this comonomer system, that a crystalline copolymer had not been obtained and fractions I and I' are both of the pure homopolymers.

**1,1,2-Trimethyl Ethylene Oxide (tri-M.E.O.).** —This oxide was polymerized neither with $FeCl_3$-PO nor with AIP-$ZnCl_2$ as catalyst but with $BF_3Et_2O$ it was rapidly polymerized at low temperature to a viscous liquid (Table IV). A tacky solid or an elastic mass could be obtained only with $AlEt_3$ at room temperature. The polymer was soluble in ether and acetone but insoluble in methanol.

**1,1,2,2-Tetramethyl Ethylene Oxide (tetra-M. E. O.).** — Both the catalysts $AlEt_3$ and AIP-$ZnCl_2$ were inactive for the polymerization

13) M. Osgan and C. Price, *J. Polymer Sci.*, 34, 153 (1959).
14) J. Furukawa et al., ibid., 36, 541 (1959).

Table IV. Polymerization of 1,1,2-trimethyl ethylene oxide

| Catalyst | % | Temp., °C | Time, hr. | Conversion, % | Remarks |
|---|---|---|---|---|---|
| $BF_3Et_2O$ | 0.5 | −68-r. t. | 24 | ca. 98 | viscous liquid |
| $FeCl_3$-PO | ca. 2 | 80 | 20 days | none | |
| AIP-$ZnCl_2$ | 2 | 80 | 1 month | none | |
| $AlEt_3$ | 2 | r. t. | 68 | 57.0 | tacky solid |

Table V. Polymerization of tetramethyl ethylene oxide

| Catalyst | wt. % | Solvent | Temp., °C | Time, hr. | Conversion, % |
|---|---|---|---|---|---|
| $BF_3Et_2O$ | 2 | $CH_2Cl_2$ | r. t. | 72 | 51.3 |
| AIP-$ZnCl_2$ | 2 | benzene | 80 | 5 days | none |
| $AlEt_3$ | 5 | benzene | r. t. | 〃 | trace |
| 〃 | 5 | none | r. t. | 〃 | trace |

of this monomer but $BF_3Et_2O$ gave a crystalline polymer (Table V). The polymer neither melted and nor decomposed even at 300°C. No usual organic solvents could be found for this polymer but the polymer was swollen by decalin or tetralin at 80~90°C. An attempt to copolymerize this monomer with 1,1-dimethyl ethylene oxide by $BF_3Et_2O$ was failed and gave only polymer of tetra-M. E. O. which was proved by X-ray examination, melting point and solubility (Table VI).

Table VI. Attempted copolymerization of tetramethyl ethylene oxide ($M_1$) with 1,1-dimethyl ethylene oxide
catalyst: $BF_3$-$Et_2O$ 2% wt.,
solvent: methylene chloride,
temp.: r. t., reaction time: 4 days

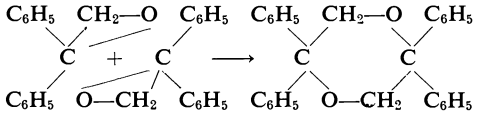
| $M_1$ in comonomer mol. % | Total conversion wt % | Remarks |
|---|---|---|
| 100 | 51.3 | Poly-tetra-M. E. O. |
| 90 | 20.6 | 〃 |
| 75 | 5.9 | 〃 |
| 50 | 3.9 | 〃 |
| 25 | trace | 〃 |
| 10 | 1.8 | 〃 |
| 0 | 36.7 | Poly-D.M.E.O. |

**1-Methyl-1-phenyl Ethylene Oxide (M.P.E.O.)**—$BF_3Et_2O$, $AlEt_3$ and $ZnEt_2$ were active to polymerize this epoxide which was converted into viscous liquid polymers which were insoluble in methanol. $BF_3Et_2O$ gave a reddish brown oily polymer, while the others gave colorless polymers.

No polymer could be obtained with AIP-$ZnCl_2$ system even after prolonged heating at 80°C for two days. $FeCl_3$-PO catalyst gave a colored oily product accompanied by a small quantity of needle crystals whose structure has not yet been determined in this work.

**1.1-Diphenyl Ethylene Oxide (D.P.E.O.).**—$AlEt_3$ and AIP–$ZnCl_2$ were inactive for this monomer while both $BF_3Et_2O$ and $TiCl_4$ were active catalysts. To a cooled solution of the oxide in methylene dichloride, the catalyst, for instance $BF_3Et_2O$ 3% by weight was added slowly and the reaction mixture was sealed and placed in a dry ice-acetone bath for two days. The glass ampoule was then opened and an ammoniacal methanol was poured into the ampule and the product was washed thoroughly with methanol.

The product (38.5% yield) was needle crystals and did not melt at 300°C but was found to sublime slightly. This material was believed to be a ring dimer of the epoxide



and was shown from the elemental analysis and the molecular weight determination, both of which were demonstrated in good accordance with a calculated value for the ring dimer (Table VII).

Table VII. Some analysis of the reaction product

| | C | H | O | Mol. wt* |
|---|---|---|---|---|
| Obs. | 87.75 | 6.24 | 8.01 | 383 |
| Calc. for ring dimer | 85.68 | 6.16 | 8.15 | 392.3 |

* by cryoscopic method using camphor

Infrared spectra of the product showed the absence of the characteristic absorption band of hydroxyl group at near 3500 $cm^{-1}$ and disappearance of bands of epoxy ring observed in the monomer at 825 and 925 $cm^{-1}$. Bands associated with an epoxy ring of monomer epoxide were estimated to be at 825 and 925 $cm^{-1}$ by comparative method of spectra of 1, 1-diphenyl ethylene, its polymer[15] and 1.4-

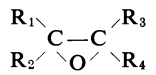
15) K. Kuwata et al., *J. Chem. Soc. Japan, Pure Chem. Section (Nippon Kagaku Zasshi)*, **80**, 25 (1959).

TABLE VIII. INFRARED SPECTRA OF THE POLYMERS FROM FOUR METHYL-SUBSTITUTED ETHYLENE OXIDES

| Propylene oxide (cryst.) | | D.M.E.O. | | Tri-M.E.O. | | Tetra-M.E.O. | |
|---|---|---|---|---|---|---|---|
| $cm^{-1}$ | Relative intensity | $cm^{-1}$ | Relative intensity | $cm^{-1}$ | Relative intensity | $cm^{-1}$ | Relative intensity |
| 2980 | 7 | 2970 | 6 | 2975 | 8 | 2990 | 6 |
| 2910 | sh 8 | 2920 | 5 | 2940 | 7 | 2960 | sh 6 |
| 2880 | sh 8 | 2880 | 4.5 | 2885 | sh 5 | 2880 | sh 2 |
| 1480 | 8 cr | 1465 | 3.5 | 1465 | 4.5 | 1477 | 3.5 |
| 1453 | 9 | | | | | | |
| 1375 | 10 | 1386 | 4 | 1370 | 6.5 | 1377 | 6 |
| 1342 | 8 | 1354 | 6 | 1360 | 6.5 | 1361 | 6 |
| 1330 | 8 cr | | | | | | |
| 1293 | 9 | 1266 | 2 | | | | |
| 1240 | 8 cr | 1245 | b 2 | 1235 | b 1 | | |
| 1140 | 8 cr | 1163 | 8.5 | 1160 | 7.5 | 1163 | 9 |
| 1105 | 9 | 1115 | 8 | 1105 | 9 | 1120 | 10 |
| | | | | 1090 | 9 | | |
| 1038 | 8.5 cr | | | 1044 | | | |
| 1010 | 8 | 1013 | 3.5 | 1020 | b 4 | | |
| | | | | 993 | 4 | 985 | b 5 |
| | | | | 970 | b 2 | 975 | 4.5 |
| 932 | 9 cr | | | 930 | b 2 | 944 | b 2 |
| 917 | 8.5 | 890 | 5.5 | | | 905 | b 2 |
| 905 | sh 6 | | | | | | |
| 866 | 4.5 | | | | | 714 | 1 |
| 831 | 6 | | | | | | |

sh : shoulder absorption band, b : broad band, cr : crystalline sensitive band*.

TABLE IX. SOME PHYSICAL PROPERTIES OF POLYMERS OF SUBSTITUTED ETHYLENE OXIDES



| | $R_1$ | $R_2$ | $R_3$ | $R_4$ | m. p., °C | Remarks |
|---|---|---|---|---|---|---|
| PO | $CH_3$ | H | H | H | 72 | crystalline |
| D.M.E.O. | $CH_3$ | $CH_3$ | H | H | 155 | crystalline |
| Tri-M.E.O. | $CH_3$ | $CH_3$ | $CH_3$ | H | — | amorphous, pasty |
| Tetra-M.E.O. | $CH_3$ | $CH_3$ | $CH_3$ | $CH_3$ | <300 | crystalline |
| M.P.E.O. | $CH_3$ | $C_6H_5$ | H | H | — | amorphous, liquid |
| D.P.E.O. | $C_6H_5$ | $C_6H_5$ | H | H | — | ring dimer |

TABLE X. X-RAY DIFFRACTION SPECTRA OF CRYSTALLINE POLYMER

| Propylene oxide | | D.M.E.O. | | tetra-M.E.O. | |
|---|---|---|---|---|---|
| Spacing, Å | Relative intensity | Spacing, Å | Relative intensity | Spacing, Å | Relative intensity |
| 5.17 | s | 5.20 | vs | 6.04 | vs |
| | | 4.58 | w | 4.61 | w |
| 4.23 | s | 4.12 | s | | |
| 4.05 | w | 3.53 | m | 3.43 | s |
| 3.63 | w | 3.03 | s | 2.96 | vw |
| 3.46 | w | 2.79 | m | 2.68 | w |
| 3.10 | w | 2.54 | m | 2.31 | m |
| 2.78 | w | 2.23 | w | | |
| 2.61 | w | 2.12 | m | | |
| | | 1.96 | w | | |

* Part I. This Bulletin, 33, 727 (1960).

dioxane and these bands were in agreement with 877 (11.40 $\mu$), 812 (12.3 $\mu$) $cm^{-1}$ of styrene oxide and 863 (11.85 $\mu$), 786 (12.72 $\mu$) $cm^{-1}$ of $\alpha$-methyl styrene oxide oberved by Patterson[16] (Fig. 1).

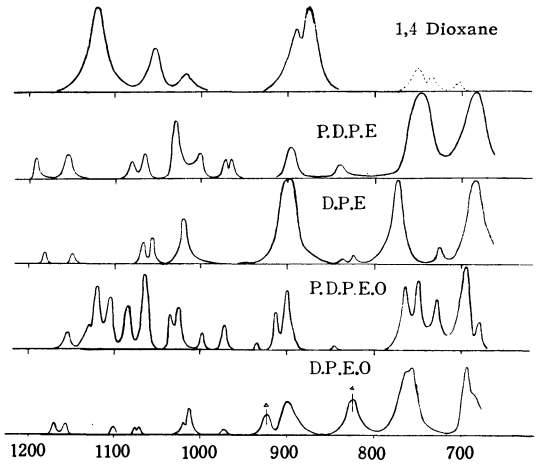



Fig. 1. Infrared spectra of diphenyl ethylene oxide and related compounds ; D.P.E.O. ; diphenyl ethylene oxide P.D.P.E.O. ; polymer of D.P.E.O., D.P.E. : diphenyl ethylene, P.D.P.E. : polymer of D.P.E. Epoxy bands were marked by triangle.

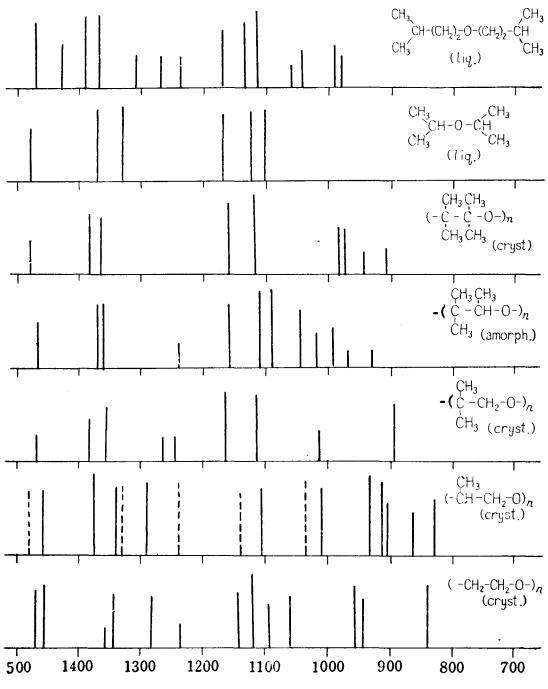



Fig. 2. Infrared spectra of polymers of methyl-substituted ethylene oxides and some related ethers (dotted line : crystalline sensitive bands).

Since absorption bands characteristic of 6-membered carbon oxygen ring had been noted to occur at near 11 $\mu$ and in the range 1124~1030 $cm^{-1}$ by Shreve[17], bands at near 1100 $cm^{-1}$ and 912 $cm^{-1}$ which appeared in the spectra of the dimer, would be bands characteristic of ring ether.

**1,1-Diethyl Ethylene Oxide.**—Using both $BF_3Et_2O$ and $TiCl_4$ as catalyst, no polymer-like substance could be obtained while a resin-like material was produced by $AlEt_3$ as catalyst. But no further experiments could proceed because of paucity of the material.

Infrared spectra of polymers from four methyl-substituted ethylene oxides together with some related ethers for comparison were shown in Fig. 2 and their characteristic bands were tabulated for comparison in Table VIII.

Some properties of polymers were summarized in Table IX and X-ray spectra of crystalline polymers were shown in Table X and Figs. 3 and 4.

The action of $AlEt_3$ as polymerization catalyst for epoxides used in this experiment might well be compared with those of cationic

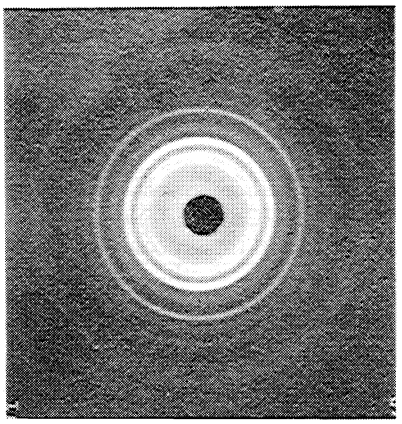


Fig. 3. X-ray pattern of the polymer of 1,1-dimethyl ethylene oxide.

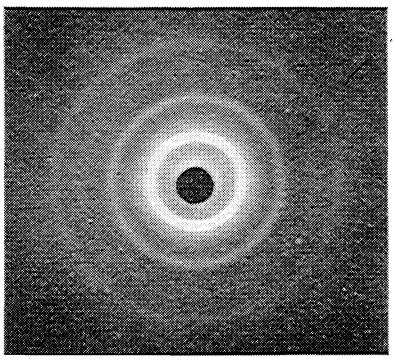


Fig. 4. X-ray pattern of the polymer of tetramethyl ethylene oxide.

16) W. A. Patterson, *Anal. Chem.*, 26, 823 (1954).

17) O. D. Shreve et al., *Anal. Chem.*, 23, 382 (1951).

catalysts. These epoxides were polymerized by $AlEt_3$ as well as $BF_3Et_2O$ and $TiCl_4$ at low temperature. The similar feature was illustrated in the case of four and five membered cyclic oxides[18], that is, ring ethers such as oxacyclobutanes, tetrahydrofuran were polymerized by $AlEt_3$ as well as $BF_3Et_2O$. While catalyst $ZnEt_2$ seemed to act in a manner unlike that of $AlEt_3$.

"Coordinated complex catalyst" such as $FeCl_3$-PO and AIP-$ZnCl_2$ could be applied to polymerization of limited kinds of epoxides and the polymerization by these catalysts proceeded much slower in the rate than that both by some cationic catalysts and some organometallic compounds such as $AlEt_3$ and $EnEt_2$.

The author offers sincere thanks to Professor Dr. S. Murahashi for his kind guidance and encouragement throughout this work and he is indebted to Dr. H. Tani, Dr. T. Takizawa and Dr. S. Nozakura for their valuable discussions and helpful suggestions in the experiments and to Mr. K. Katayama (Textile Res. Lab., Asahi Chem. Ind. Co. Ltd.) for X-ray examinations.

*Department of Polymer Science*
*Faculty of Science*
*Osaka University*
*Nakanoshima, Osaka*

18) S. Kambara et al., *J. Polymer Sci.*, 27, 586 (1958).

# *Spectrochemical Study of Microscopic Crystals. XXI*[1]. *The Structure and Absorption Spectra of the Red and the Black Form of Nitrosopentammine-cobalt Salts*[2]

By Shoichiro YAMADA, Hiroaki NISHIKAWA and Ryutaro TSUCHIDA

(Received December 16, 1959)

Two series of compounds with the same composition of $[Co(NH_3)_5NO]X_2$, have been known for a long time[3], one of them being colored black and the other red. The marked difference in the color and other properties between the two series of compounds has attracted a number of investigators[4-10], but rather conflicting conclusion have so far been drawn about the configuration and the electronic structure of the two compounds. It seems, therefore, to be of significance to examine the compounds using some new sorts of materials which have neither been much discussed nor obtained before. This paper presents ultraviolet absorption spectra of the black and the red salt in the crystalline state, and discusses their structure on the basis of the present measurement.

## Experimental

**Materials.** — Red nitrosopentammine-cobalt(III) nitrate, $[Co(NH_3)_5NO](NO_3)_2$, was prepared in rectangular, thin plates by the method of Asmussen and others[9]. The compound is comparatively stable, and may be recrystallized from water.

Black nitrosopentammine-cobalt chloride, $[Co(NH_3)_5NO]Cl_2$ was prepared according to the direction of Asmussen and others[9]. The compound is unstable, undergoing decomposition by water, acid or alkali. On exposure to the air, the compound gradually changes into a red material. The decomposition, however, seemed to be so slow that no change of the crystal surface was observed under the microscope after the dichroism measurement. The compound is often contaminated with the $[Co(NH_3)_6]^{2+}$, which is very sensitive with respect to magnetic susceptibility, but not to ultraviolet spectra of the salt.

**Measurements.** — Visible and ultraviolet spectra of both the red and the black compound in the crystalline state have been quantitatively determined

1) Part XX of this series, S. Yamada and R. Tsuchida, This Bulletin, **33**, 98 (1960).
2) Presented before the 12th Annual Meeting of Japan Chemical Society, Kyoto, April, 1959.
3) J. Sand and O. Gennsler, *Ann.*, **123**, 43 (1862); ibid., **329**, 194 (1903); *Ber.*, **36**, 2083 (1903).
4) A. Werner and P. Karrer, *Helv. Chim. Acta*, **1**, 54 (1918).
5) D. P. Mellor and D. P. Craig, *J. Proc. Roy. Soc. N. S. Wales*, **78**, 25 (1944): L. N. Short, *Rev. Pure Appl. Chem.*, **4**, 41 (1954).
6) S. P. Ghosh and P. Rây, *J. Indian Chem. Soc.*, **20**, 409 (1943).
7) J. L. Milward, W. Wardlaw and W. J. R. Way, *J. Chem. Soc.*, **1938**, 233; N.V. Sidgwick and R. Bailey, *Proc. Roy. Soc. (London)*, **A144**, 521 (1934).
8) W. P. Griffith, J. Lewis and G. Wilkinson, *J. Inorg. Nuclear Chem.*, **7**, 38 (1958).
9) R. W. Asmussen, O. Bostrup and J. P. Jensen, *Acta Chem. Scand.*, **12**, 24 (1958).
10) E. P. Bertin, S. Mizushima, T. J. Lane and J. V. Quagliano, *J. Am. Chem. Soc.*, **81**, 3821 (1959).

at room temperature on well-developed planes by Tsuchida and Kobayashi's microscopic method[11] using linearly polarized light. The A- and the B-absorption refer to the direction shown in the figures.

Visible and ultraviolet absorption spectrum of the red salt in an aqueous solution was measured by a Beckman DU spectrophotometer.

The symbols used in the present paper are the same as those in the former reports of this series.

In the analysis of the absorption curve in Fig. 4, it is assumed that the second absorption band has a molar extinction coefficient almost equal to that of the first band, the distance between the maxima of the first and the second bands being almost equal for complexes of cobalt(III).

## Results and Discussion

**Structure of Black Nitrosopentammine-cobalt Salt.** — Uninuclear and binuclear structures have been given to the black nitrosopentammine-cobalt salt. Contrary to the result by former investigators that the "black salts" were paramagnetic, Asmussen and others[9] found that the "black salts", when carefully purified, actually showed diamagnetism. The structures, as suggested formerly on the erroneous magnetic data, need not be given serious consideration. The black series of the salts were regarded by Asmussen and others as a co-ordination compound of cobalt(III), the lowest energy level being very close to the level of the bivalent cobalt.

Bertin and others[10] concluded on the basis of the infrared spectra of these compounds that the isomerism of the black and the red series is dependent upon the nature of the linkages of the co-ordinated NO-group and not upon difference in the oxidation state of the central metal. However, they did not discuss the structure of the salts in detail. Griffith and others[8] discussed the same problem on the basis of the chemical reactions, and finally favored the binuclear structure for the "black salt". Most of their discussion, however, seems to be rather speculative, and reexamination from materials of different kinds might be desirable.

Dichroism in the visible and ultraviolet region of the "black salt" is shown in Fig. 1. It seems fortunate that the impurity, $[Co(NH_3)_6]^{2+}$, often appearing in the "black salt" is not important in the UV-absorption spectra of the compound, in contrast to magnetic susceptibility which is affected seriously by a small amount of the impurity. The absorption spectra, as shown in Fig. 1, seem to be so complicated that they would not be understandable on the assumption of the uninuclear

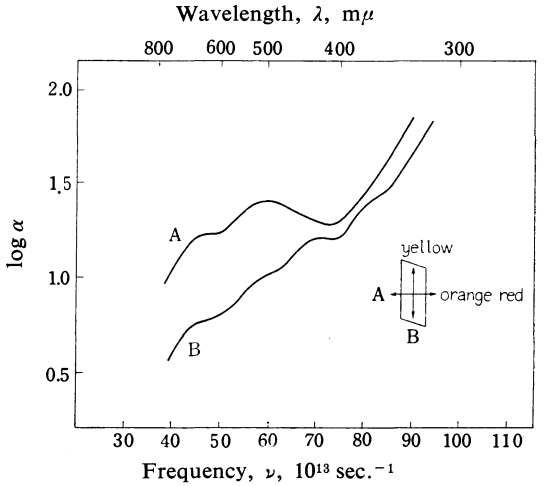


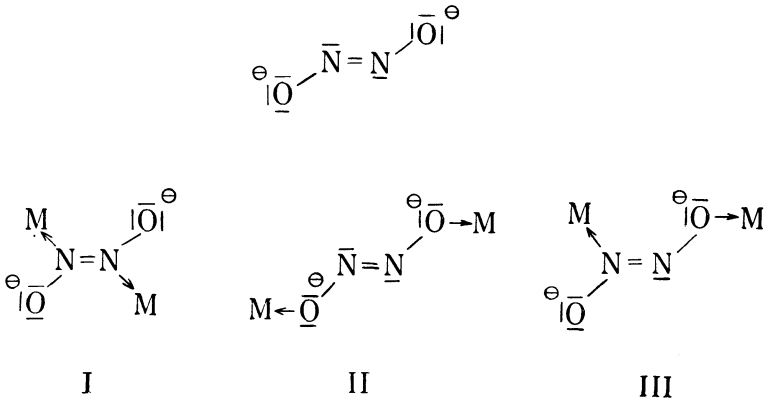

Fig. 1. Absorption spectra of black nitrosopentammine-cobalt chloride, $[Co(NH_3)_5NO]Cl_2$, in the crystalline state.

model of the "black salt". Thus the "black salt" exhibits an absorption band at about $46\times10^{13}\,sec^{-1}$, the wavelength region which is much longer than would be expected for the uninuclear nitrosopentammine-cobalt(III) complex. There might be a possibility that the band at about $46\times10^{13}\,sec^{-1}$ would originate from a nitroso-group. In fact, a number of nitroso-derivatives, such as nitroso-benzene and its derivatives, are known to show a rather special type of an absorption band characteristic of a nitroso-group in the long wavelength region. It may be difficult, however, to assume that the NO-group in the "black salt" should be isolated electronically from the cobalt ion to such an extent that the band of this sort may appear in this wavelength region. The band at about $46\times10^{13}\,sec^{-1}$ of the "black salt", therefore, may not be regarded as due to a nitroso-group which is rather isolated in the cobalt-complex. Moreover, the absorption curve of the "black salt" appears to be too complicated for a uninuclear complex of cobalt(III).

On the contrary, the absorption curve of the "black salt" may be understood much more readily as that of a binuclear complex than as that of a uninuclear complex. Possible structures for a binuclear form are shown in Fig. 2, the $\pi$-bonding between the metal and the $NO^-$ ion being neglected for the present. It is to be noted that the dichroism of the "black salt" is markedly similar to that of $\mu$-peroxo-dicobalt complexes with an $O^{2-}$ group which connects two cobalt ions together[12]. Moreover, just as the peroxo-dicobalt compound

11) R. Tsuchida and M. Kobayashi, "The Color and the Structure of Metallic Compounds", Zoshindo, Osaka (1944), p. 180 (in Japanese), This Bulletin, 13, 619 (1938).

12) S. Yamada, Y. Shimura and R. Tsuchida, This Bulletin, 26, 72 (1953).



I II III

Fig. 2.

has an absorption band in the very long wavelength region, so the "black salt" shows an absorption band at about $46\times10^{13}\,sec^{-1}$. The band of the peroxo-dicobalt compound in the longer wavelength region, with maximum at about $46\times10^{13}\,sec^{-1}$, was ascribed to a group of Co–$O_2$–Co with a special electronic structure which gives rise to a special absorption band due to the interaction between the two cobalt ions through the peroxide group[12]. The band in question of the "black salt", therefore, may be a special type of the interaction band due to a group of atoms having an electronic structure of Co–X–Co somewhat similar to that of Co–$O_2$–Co, originating from the interaction between the two cobalt ions through $N_2$ group. A-absorption in Fig. 1 may be regarded as representing the main features of the component absorption which is richer with the interaction absorption due to the Co–$N_2$–Co group than is the other component absorption.

Since it is difficult to expect the interaction band with structure II and structure III, structure I having a group of Co–N–N–Co may be favored best as a model of the "black salt" by the ultraviolet absorption spectra with the interaction band. The conclusion obtained here by the present authors about the structure of the "black salt" is found to be in agreement with the view of Griffith and others[8], who regarded it as most likely that the "black salt" has a binuclear structure with a hyponitrite-group as a bridge, on the ground that the "black salt" undergoes decomposition by acid or carbon dioxide to give nitrous oxide and that the salt can be prepared, though in a low yield, from sodium hyponitrite and a cobalt salt.

It may also be noteworthy that an infrared absorption band at 1620 to 1640 $cm^{-1}$ due to the NO part of the "black salt"[10] is very close to the frequency of the –N=N– group in ordinary azo-compounds. This to beseems consistent with structure I, having a kind of interaction between the two cobalt ions through the $N_2$ group, as has been concluded to be most probable in the present work. The order of the N–N bond may be almost equal to the bond order in ordinary azo-groups of organic azo-compounds.

In summary, it may be concluded that *the "black salt" has structure I with the Co–N=N–Co group, displaying the special band due to the interaction between the two cobalt ions through the –N=N– group.*

**Polarized Absorption Spectra of Red Nitroso-pentammine-cobalt(III) Nitrate.** — Ultraviolet absorption spectra of the "red salt" in the crystalline state are shown in Fig. 3 and Table I. The crystal structure analysis has not been

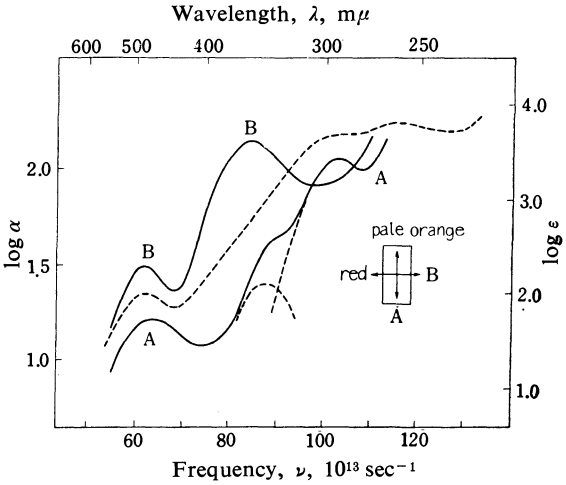



Fig. 3. Absorption spectra of red nitroso-pentammine-cobalt nitrate, $[Co(NH_3)_5ON](NO_3)_2$, in the crystalline state (——) and in aqueous solution (----).

TABLE I. UV ABSORPTION SPECTRA OF RED NITROSOPENTAMMINE-COBALT(III) NITRATE $[Co(NH_3)_5NO](NO_3)_2$ IN THE CRYSTALLINE STATE AND IN SOLUTION

| Absorption band | Spin-forbidden | I | NO-spec. | II | III | IV |
|---|---|---|---|---|---|---|
| | | $\nu$, log $\alpha$ | $\nu$, log $\alpha$ | $\nu$, log $\alpha$ | $\nu$, log $\alpha$ | |
| In crystalline state | | | | | | |
| B-abs. | | 62, 1.5 | 84, 2.3 | (covered) | — — | |
| A-abs. | | 1.15 | 1.2 | 87, 1.5 | 102, 2.1 | |
| Stronger component[a] | | Z | Z | (X, Y) | X, Y | |
| In aqueous solution | | | | | | |
| | $\nu$, log $\varepsilon$ | $\nu$, log $\varepsilon$ | $\nu$, log $\varepsilon$ | | $\nu$, log $\varepsilon$ | $\nu$, log $\varepsilon$ |
| | 38.5, 1.85 | 62.1, 1.98 | 83.5, 2.6 | (covered) | 100, 3.6 | 114.5, 3.83 |

$\nu$: $10^{13}\,sec^{-1}$

a) Z refers to the direction combining the cobalt ion with the ON-group in the complex-ion.

reported with the compound as yet. However, the dichroism, as has been determined in the present work, may be regarded to represent the main characteristics of the component absorptions of the complex-ion itself under slight perturbation from the surrounding ions.

A striking dichroism is observed with the first absorption band. It may be assumed that A-absorption in Fig. 3, having the stronger absorption band at about $62\times10^{13}\,sec^{-1}$ represents characteristics of the component absorption of the complex-ion with electric vector along the direction connecting the cobalt(III) ion and the nitroso-group.

The specific band due to the NO-group in co-ordination is observed as a distinct maximum at about $84\times10^{13}\,sec^{-1}$ in Fig. 3, whereas the band is obscured by neighboring stronger absorption in the absorption curve of the compound in solution. The present measurement shows that the specific band is greatly polarized along the Co–ON direction. This is readily understandable if it is assumed that the band is due to electron transfer, possibly from the ON-group to the central metal-ion.

The band at about $102\times10^{13}\,sec^{-1}$ is seen to be polarized in the direction perpendicular to the Co–ON direction. The absorption band due to nitrate ions is expected to appear at about $100\times10^{13}\,sec^{-1}$, but the band of the nitrate ion is so low that the band at about $102\times10^{13}\,sec^{-1}$, as observed with the "red salt" in the present work, may be due to another origin. This band may be a sort of charge transfer band, but its origin is not quite clear for the present.

The second ligand field band is covered under greater specific band in A-absorption, but appears as inflation at about $87\times10^{13}\,sec^{-1}$ in B-absorption. This may be consistent with the frequency difference of about $25\times10^{13}\,sec^{-1}$ between the first and the second band, which was reported with numerous cobalt(III)-complexes.

**Structure of Red Nitrosopentammine-cobalt Salts.**—Both the uni- and the bi-nuclear structure have been proposed for the "red salt". Very recently Asmussen et al.[9] regarded, mostly from magnetic measurements, that the "red salt" may be either a uninuclear or a binuclear complex of cobalt(III). Griffith et al.[8] concluded from examination of its chemical property that the "red salt" may be uninuclear. Bertin et al.[10] concluded, from its infrared spectrum, the oxidation state of the cobalt to be tervalent, but presented no detailed discussion about the structure of the "red salt". Thus the "red salt" may be a uninuclear or a binuclear complex of cobalt(III). In the following, we shall discuss about the structure of the "red salt" on the basis of the present measurements with consideration to the former results.

Possible structures of the binuclear ions for the "red salt" are shown in Fig. 2. Structure I is assigned to the "black salt", as discussed above. Structure II and structure III may be rejected on the ground of the chemical reactions of the "red salt", since the compound with structure II or structure III would be expected to give nitrous oxide in acidic solution, just like the hyponitrite ion. In fact, the "red salt" is stable in water, whereas the "black salt" is readily decomposed to give nitrous oxide. Moreover, the fact that the "red salt" in solution or in the crystalline state shows a definite maximum for the first absorption band seems to be inconsistent with structure III, which would show two "first ligand field absorption bands" originating from the two kinds of cobalt ions. Therefore, the "red salt" can not be assigned to a binuclear form. Thus the present authors are inclined to assume that the "red salt" be uninuclear.

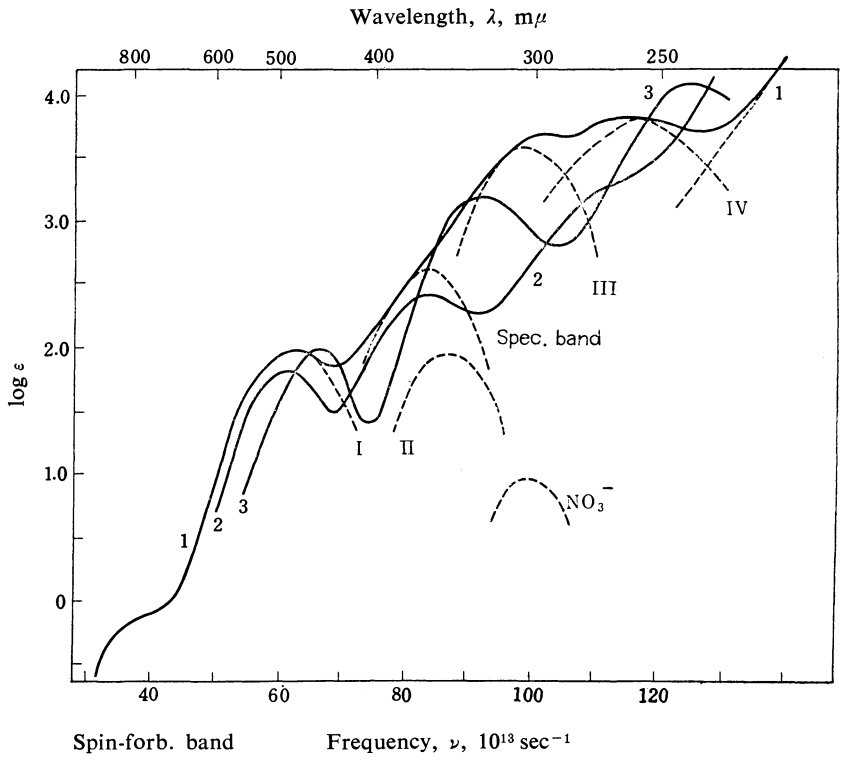



Fig. 4. Absorption spectra of $[Co(NH_3)_5X]^{2+}$ in aqueous solution: 1, $X=NO^-$; 2, $X=ONO^-$ (nitrito); 3, $X=NO_2^-$ (nitro-). Dotted curves represent absorption bands obtained by analysis of the absorption curve 1. The curves 1 and 2 are taken from Ref. 13 in the text.

In addition, the absorption spectra of the "red salt" may be consistent with the assumption of the uninuclear model of the "red salt", as shown in the succeeding paragraph of the present discussion.

Ultraviolet absorption spectra of the "red salt" in solution and in the crystalline state have been determined in the present work, and are shown in Figs. 3 and 4 and Table I. The absorption curve of the compound in solution, as determined in the present work, shows absorption maxima which generally agree with those reported by the former investigators with the compound in solution[9]. Asmussen and others[9] pointed out vague similarity of its absorption spectrum to spectra of most cobaltic compounds, but gave no further discussion about the spectrum. After all, they seemed to conclude that the "red salt" may be either uninuclear or binuclear. It is seen in Fig. 3 and Table I that the "red salt" shows a well-defined maximum for the first band at about 61 to $62\times10^{13}\,sec^{-1}$. The second band, which is characteristic of most complexes of cobalt(III), is covered under strong neighboring absorption bands in the curve of the salt in aqueous solution. Analysis of the absorption curve reveals that there appears a band at about $84\times10^{13}\,sec^{-1}$ which may be regarded as a specific band due mainly to an NO-group in combination with the cobalt(III)-ion. The intensity of the specific band is found to be much smaller than the intensity of the specific band due to a nitro-, an isothiocyanato- or an azide group in the pentammine-cobalt(III) complex. As is evident from inspection of the data in Table II, it is difficult to assume that the band at about $100\times10^{13}\,sec^{-1}$ in the curve of the "red salt"

TABLE II. ABSORPTION MAXIMA OF COMPLEXES OF A TYPE, $[Co(NH_3)_5X]^{2+}$, IN SOLUTION

| X | 1st band | | Specific band | | Ref. |
|---|---|---|---|---|---|
| | ν | log ε | ν | log ε | |
| $NO_2^-$ | 65.8 | 2.00 | 92.4 | 3.22 | a |
| $NH_3$ | 63.2 | 1.78 | — | — | b |
| $ONO^-$ | 61.2 | 1.86 | 82.9 | 2.44 | a |
| $ON^-$ | 62.1 | 1.98 | 84 | 2.5 | c |

ν: $10^{13}\,sec^{-1}$.

a) M. Linhard, H. Siebert and M. Weigel, *Z. anorg. allgem. Chem.*, **278**, 287 (1955).
b) M. Linhard, *Z. Elektrochem.*, **50**, 224 (1944).
c) Present measurement.

may correspond to the specific band due to the NO-group in the complex-ion. On the contrary, it is noteworthy that the band at about $84\times10^{13}$ sec$^{-1}$ of the "red salt" is almost as intense as the specific band of a nitrite-group in the pentammine-cobalt(III) in which a nitrite group is co-ordinated to the cobalt-(III) ion through its oxygen atom.

It also is to be noted that the absorption curve of the "red salt", $[Co(NH_3)_5ON](NO_3)_2$ in solution bears a resemblance to the curve[13] of the $[Co(NH_3)_5ONO]^{2+}$ ion in which a nitrite ion is co-ordinated to the cobalt(III) ion through its oxygen atom. This seems to indicate that the NO-group in the "red salt" is co-ordinated to the cobalt(III) ion through its oxygen atom, as will be described in more detail in the later part of the present discussion.

It is known from existing data that substitution of a nitro-group for ammonia in the hexammine-cobalt(III) ion gives rise to a hypsochromic shift of the first absorption band, whereas the substitution of a nitrite group for ammonia yields a bathochromic shift of the first band. In the case of a nitrate-group, an even greater bathochromic shift is observed. It is found in Fig. 4 and Table II that the first absorption band of the "red salt" lies at a longer wavelength than the first band of the hexammine-cobalt(III) ion. Therefore, it may be concluded, from comparison of the wavelength of the first absorption band of the "red salt" with those of the relevant complexes, that *the NO-group in the "red salt" is co-ordinated to the cobalt(III) ion throuh its oxygen atom, and not through the nitrogen atom*, as is customarily assumed for this compound.

Inspection of existing data, summarized in Table II and Fig. 4, also reveals that the specific band due to a nitrite-group lies at about 83 to $84\times10^{13}$ sec$^{-1}$ and the band due to a nitro-group lies at about $92\times10^{13}$ sec$^{-1}$ in the pentammine-cobalt(III) complex. It is seen that the nitrite-group with its oxygen co-ordinated to the cobalt(III) ion shows its specific absorption band at a longer wavelength than does the nitro-group with its nitrogen co-ordinated to the cobalt(III) ion. The present measurement shows that the "red salt" has its specific band at about $84\times10^{13}$ sec$^{-1}$ with log $\varepsilon$ of about 2.6. Thus it is concluded also from examination of the specific band that the NO-group in the "red salt" is co-ordinated to the cobalt(III) ion through its oxygen atom.

The intensity of the specific band due to the nitroso-group in the "red nitroso-pentammine complex" is found to be smaller than the intensity of the specific band due to a nitro-group in the metallic complex, but is almost equal to the intensity of the specific band due to the nitrite group in the pentammine-cobalt(III) complex. This fact also may be consistent with the conclusion that the nitroso-group is co-ordinated to the cobalt(III) ion through the oxygen atom in the "red salt".

In this connection, the close similarity of the absorption curve of the "red salt" to the curve of the nitritopentammine-cobalt(III) complex is noteworthy. In the case of the "red salt", band III and band IV are seen to be displaced to a little longer wavelength than the corresponding bands of the nitritopentammine-cobalt(III) complex, as is seen in Fig. 4, but the correspondence of the absorption bands between the "red salt" and the nitritopentammine-cobalt(III) complex may be evident. This fact also may be taken as indicating that the absorption spectrum of the "red salt" is understood on the assumption of the mononuclear model with the cobalt-to-oxygen bond.

It is interesting to find that a very weak absorption system appears at about $39\times10^{13}$ sec$^{-1}$ in the absorption curve of the "red salt" in solution, as shown in Fig. 4. This absorption band is regarded as being due to electronic transitions between levels with different multiplicities. This spin-forbidden band of the "red salt" is found to lie in the longer wavelength region than $[Co(NH_3)_6]Cl_3$ which shows the band at about $40\times10^{13}$ sec$^{-1}$. This fact is also compatible with the conclusion in the present article that the NO-group is bound to the cobalt ion through its oxygen atom, since the band of this kind would appear in the shorter wavelength region if the NO-group were bound to the cobalt(III) ion through its nitrogen atom.

Summarizing the above discussion, mainly on the basis of the absorption spectra, it is concluded that *the "red salt" is uninuclear, with the nitroso-group co-ordinated to the cobalt-(III) ion through the oxygen atom.*

## Summary

In order to examine the structure of the red and the black nitrosopentammine-cobalt salts, their dichroism in the visible and near-ultraviolet region has been quantitatively determined at room temperature by the microscopic method.

The absorption spectrum of the "black salt" is found to be understandable best on the assumption that the "black salt" has binuclear complexes of cobalt(III), showing a special kind of absorption band due to the interaction between the two cobalt(III) ions through the $N_2$ group.

13) M. Weigel, H. Siebert and M. Linhard, *Z. anorg. allgem. Chem.*, **278**, 287 (1955).

The absorption spectrum of the "red salt" is concluded to be consistent with the model of the uninuclear complex of cobalt(III) with the NO-group co-ordinated to the cobalt(III) ion through its oxygen atom.

*Department of Chemistry*
*Faculty of Science*
*Osaka University*
*Nakanoshima, Osaka*

# *Chemisorption of Hydrogen on Zinc Oxide. III. The Effect of Additions of Foreign Ions to Zinc Oxide*

By Yutaka KUBOKAWA

(Received January 20, 1960)

Since the electron barrier theory was suggested for the chemisorption on semiconductors by Hauffe, Weisz, and others[1], the importance of the electronic structure of oxides in catalysis has been emphasized by various workers. As an approach along this line, the following method has often been adopted. The electronic structure of a given oxide is modified by the addition of small amounts of foreign ions, and the resulting changes in catalytic activity are then studied. As regards the hydrogen-deuterium exchange reaction on zinc oxide, Parravano et al.[2] found that the addition of $Al^{3+}$ or $Ga^{3+}$, which should increase its electrical conductivity, increased the activity and lowered the activation energy, while the addition of $Li^+$ showed a reverse effect. On the basis of these results, Hauffe[3] suggested that the rate-determining step in this case was the electron transfer from zinc oxide to adsorbed hydrogen ions to allow it to desorb, closely correlating the catalytic activity of zinc oxide with its properties as a semiconductor.

Whatever mechanism may be operative in the hydrogen-deuterium exchange reaction, it is obvious that the hydrogen chemisorption on zinc oxide samples containing these foreign ions must be studied before any conclusive explanation of the activity changes caused by such additions can be given. Apart from the exchange reaction, such a study may be of considerable interest concerning the relation between the electronic structure of oxide and its hydrogen chemisorption. At present the only work along this line seems to be that of Cimino et al.[4] In this work, as described in previous papers,[5,6] hydrogen chemisorption has been investigated by measuring the rates of adsorption and desorption, and the adsorption equilibrium, with zinc oxide modified by the addition of foreign ions such as $Li^+$, $Al^{3+}$ and $Ga^{3+}$.

## Fxperimental

**Materials.**—Zinc oxide without foreign ions was prepared by sintering at 800°C for 5 hr. of non-sintered zinc oxide, which was obtained from zinc oxalate as described previously.[5] ZnO+1 mole % $Al_2O_3$, ZnO+1 mole% $Ga_2O_3$, and ZnO+0.5 mole% $Li_2O$: Non-sintered zinc oxide was impregnated with a solution containing a desired amount of aluminum, gallium, or lithium nitrate, dried at 110°C, and sintered at 800°C for 5 hr. Hydrogen and other gases used were prepared and purified as described in the previous work[5,7].

The weight of adsorbent and the surface area determined by the B. E. T. method using nitrogen adsorption are shown in Table I.

TABLE I.

| Adsorbent | Weight, g. | Surface area, $m^2/g.$ |
|---|---|---|
| ZnO | 19.6 | 1.0 |
| ZnO+1 mole% $Al_2O_3$ | 20.6 | 1.7 |
| ZnO+1 mole% $Ga_2O_3$ | 22.7 | 3.6 |
| ZnO+0.5 mole% $Li_2O$ | 27.5 | 0.40 |

**Apparatus and Procedure.** — Details of the apparatus and procedure were already described in the previous paper[5]. Prior to a series of experiments, all the adsorbents used in the present work

1) K. Hauffe and H. J. Engell, *Z. Elektrochem.*, **56**, 366 (1952); **57**, 763, 773 (1953); P. Aigrain and C. Dugas, ibid., **56**, 363 (1952); P. B. Weisz, *J. Chem. Phys.*, **21**, 1531 (1953).
2) E. Molinari and G. Parravano, *J. Am. Chem. Soc.*, **75**, 5233 (1953).
3) K. Hauffe, *Angew. Chem.*, 67, 189 (1955).
4) A. Cimino, E. Cipollini and E. Molinari, *Naturwissenschaften*, **43**, 58 (1956).
5) Y. Kubokawa, This Bulletin, **33**, 546(1960).
6) Y. Kubokawa, ibid., **33**, 550 (1960).
7) Y. Kubokawa, ibid., **33**, 555 (1960).

were subjected to repeated pretreatments with hydrogen at 450°C followed by evacuation at the same temperature.

## Results

**The Variation in the Adsorbed Amount on Raising Temperature During Adsorption.** — Hydrogen was allowed to be chemisorbed by the adsorbent at room temperature and the temperature of the whole system was raised up to a higher temperature in stages, at each of which, in most cases, a rapid desorption followed by a slow uptake was observed. The activation energy of adsorption was determined by comparison of the rates at different temperatures corresponding to equal amount of the slow chemisorption as described in the previous paper[6]. As an example, a run between 215 and 266°C on ZnO+1 mole% $Ga_2O_3$ is shown in Fig. 1. The activation energies thus obtained in various temperature ranges with ZnO, ZnO+1 mole% $Ga_2O_3$, and ZnO+0.5 mole% $Li_2O$ are shown in Table II. Here, the activation energies in similar temperature ranges are almost of the same order of magnitude throughout all the adsorbents, suggesting that the activation energy of adsorption is not affected seriously by the addition of foreign ions. However, the proportion of the amount rapidly desorbed on an abrupt temperature rise to the total amount adsorbed is clearly affected by the addition of foreign ions. The amount of such rapid desorption at each stage is shown in Figs. 2—4, together with the amount adsorbed in a certain constant time period at each temperature. Comparison between Figs. 2 and 3 shows that for ZnO+1 mole% $Ga_2O_3$ the rapid desorption occurs to a much less extent than for ZnO.

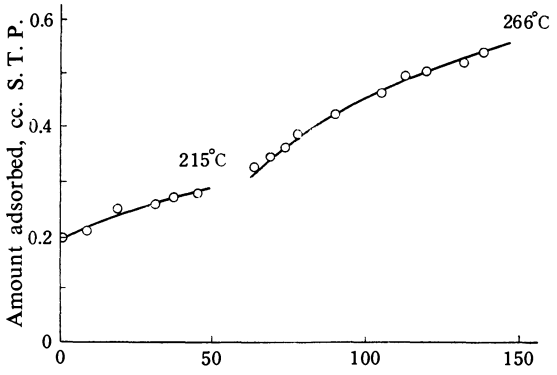



Fig. 1. Rate of hydrogen chemisorption on ZnO+1 mole% $Ga_2O_3$ in case of temp. change during adsorption ; Pressure, 50~60 mmHg.

TABLE II. ACTIVATION ENERGY OF ADSORPTION*

| Adsorbent | Temp. range, °C | Activation energy of adsorption, kcal./mole |
|---|---|---|
| ZnO | 72~143 | — |
| | 143~203 | 12 |
| | 203~254 | 15 |
| ZnO+0.5 mole% $Li_2O$ | 98~146 | 7.5 |
| | 146~196 | 11 |
| | 196~244 | 14.5 |
| ZnO+1 mole% $Ga_2O_3$ | 124~171 | 8.5 |
| | 171~215 | 11.5 |
| | 215~266 | 16 |

* The upper limit of the experimental error was ±10%.

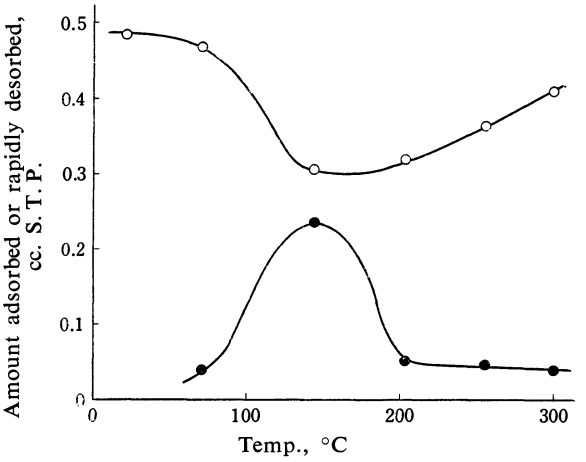



Fig. 2. Variation in the amount adsorbed on ZnO on raising temp. ; Hydrogen pressure, 80~90 mmHg ; -○-, the amount adsorbed after 3 hr. ; -●-, the amount rapidly desorbed.

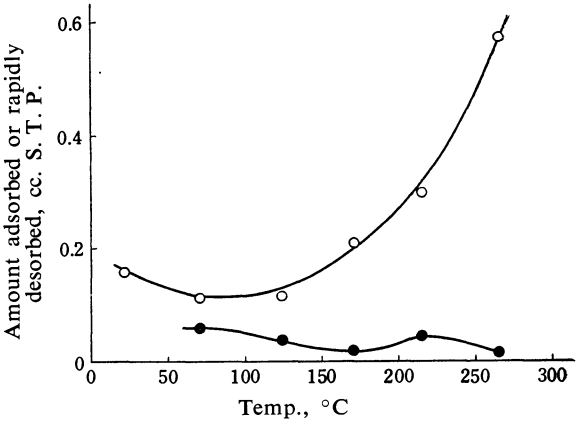



Fig. 3. Variation in the amount adsorbed on ZnO+1 mole% $Ga_2O_3$ on raising temp. ; Hydrogen pressure, 50~60 mmHg ; -○-, the amount adsorbed after 1.5 hr. -●-, the amount rapidly desorbed.

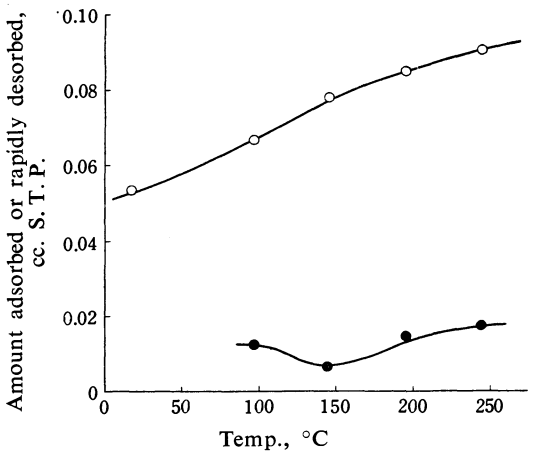



Fig. 4. Variation in the amount adsorbed on ZnO+0.5 mole% $Li_2O$; on raising temp.; Hydrogen pressure, 0.2~0.3 mmHg; -○-, the amount adsorbed after 1 hr.; -●-, the amount rapidly desorbed.

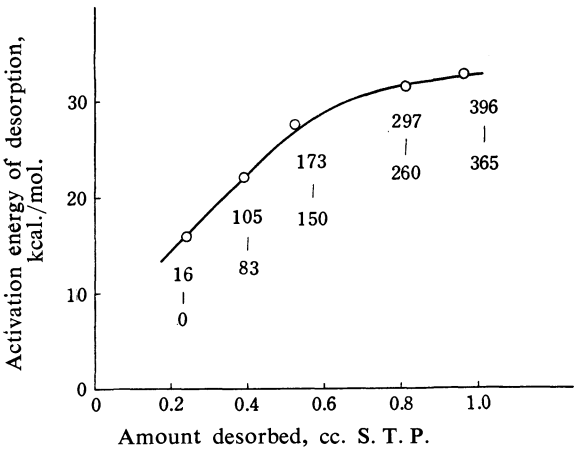



Fig. 5. Activation energies of desorption of hydrogen chemisorbed on ZnO. The amount adsorbed and equilibrium pressure at room temp. before desorption were 1.10 cc. and 42.2 mmHg, respectively. Numerical values in Figs. 5, 6, and 7 refer to the temp. interval where the activation energies were determined.

The results with ZnO+0.5 mole% $Li_2O$ can not be compared directly with the others owing to different pressure conditions.

**The Activation Energies of Desorption at Various Coverages.**—After hydrogen was allowed to be adsorbed at about 400°C, the temperature of the specimen was raised from 0 to 400°C in stages, at each of which the activation energy of desorption was determined from comparison between the rates of desorption at different temperatures corresponding to equal amounts left adsorbed as stated

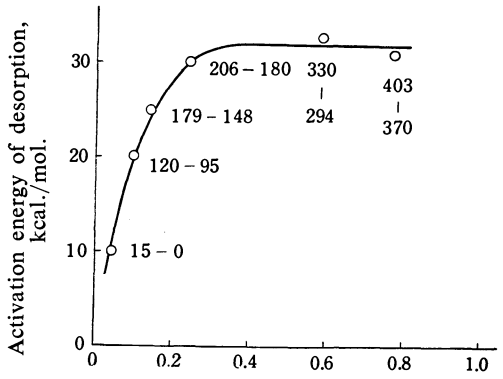



Fig. 6. Activation energies of desorption of hydrogen chemisorbed on ZnO+1 mole% $Ga_2O_3$. The amount adsorbed and equilibrium pressure at room temp. before desorption were 0.98 cc. and 52.3 mmHg, respectively.

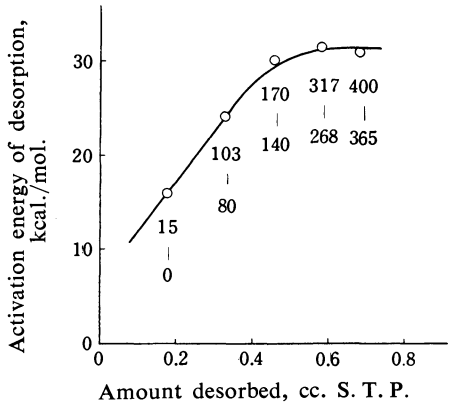



Fig. 7. Activation energies of desorption of hydrogen chemisorbed on ZnO+0.5 mole% $Li_2O$. The amount adsorbed and equilibrium pressure at room temp. before desorption were 0.78 cc. and 41.0 mmHg, respectively.

in the previous paper[5]. The results obtained with ZnO, ZnO+1 mole% $Ga_2O_3$ and ZnO+0.5 mole% $Li_2O$ are shown in Figs. 5—7. Here, it was confirmed, in the same manner as described previously, that the rate of adsorption was negligible during the desorption experiment for all the adsorbents studied. From these figures the following picture would be obtained. For all the adsorbents with and without foreign ions, the activation energy increases with decreasing amount adsorbed up to almost the same value of 30~33 kcal./mol., although the proportions of the amounts desorbed with a lower activation energy (<20 kcal./mol.) to the total amount desorbed are different from one another, the smallest value being found with ZnO+1 mole% $Ga_2O_3$ in accordance with the results of adsorption experiment above mentioned.

**Adsorption Isotherms.** — Adsorption equilibrium measurements were carried out only with ZnO and ZnO+1 mole% $Al_2O_3$ in the same manner as described previously[5]: After hydrogen was allowed to be adsorbed at about 350°C, the isotherms were determined by successive withdrawals of the gas. The isotherms thus obtained were found to be reproduced on increasing or decreasing pressure subsequently. For both systems the Langmuir plot was applicable in the pressure range

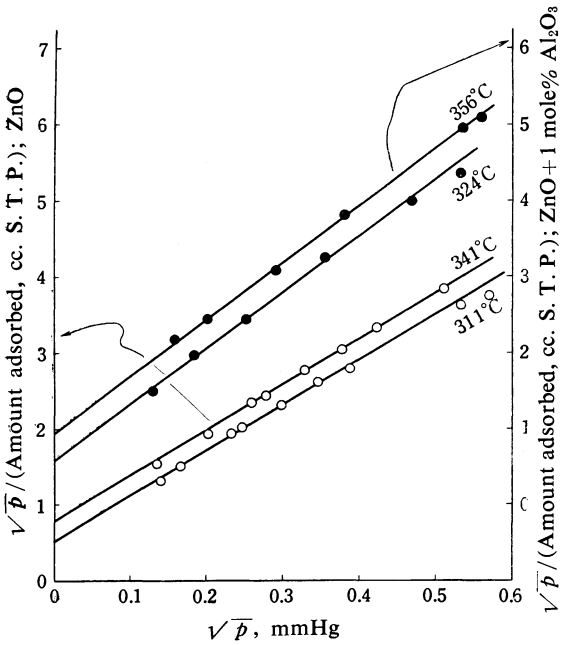



Fig. 8. Langmuir plots for ZnO and ZnO +1 mole% $Al_2O_3$; -○-, ZnO; -●-, ZnO+1 mole% $Al_2O_3$.

studied as seen in Fig. 8. It follows from this figure that the heat of adsorption is unaffected by the addition and is equal to 18 kcal./mol. Although such applicability of the Langmuir plot probably results from a limited range of coverage, the slopes of the lines in Fig. 8 may be utilized to estimate the magnitude of the surface available for the chemisorption under the given experimental conditions; (Reciprocal of the slope per unit area) is 0.0039 cc. for ZnO+1 mole% $Al_2O_3$ and 0.0085 cc. for ZnO.

**The Effect of Additions of Foreign Ions on Carbon Monoxide Chemisorption.** — According to the previous work[7] on carbon monoxide chemisorption on zinc oxide, there are two types of chemisorption, one predominating at low and the other at high temperatures. The effect of foreign ions was studied only for the adsorption of the former type. Because of a small amount adsorbed on ZnO+0.5 mole% $Li_2O$, the adsorption isotherms were determined only with ZnO and ZnO+1 mole% $Al_2O_3$ in similar way to that given previously. The heats of adsorption thus obtained for the two adsorbents proved to be almost the same, i. e., 10~12 kcal./mol.

## Discussion

In view of the low temperature used in preparing the samples, it seems unlikely that the added foreign ions are distributed uniformly throughout. As seen in Table I, however, surface area of the adsorbents is increased by the addition of $Ga_2O_3$ or $Al_2O_3$ and decreased by that of $Li_2O$. According to Hauffe[8] and Parravano[3], such variation in surface area suggests a decrease in the concentration of interstitial zinc ions, i. e., an increase in the concentration of free electrons in the former case, and the reverse change in the latter case. It may therefore be supposed that at least in a qualitative sense the electronic structure of the adsorbents in this work has been modified by such addition in the manner predicted by the theory of Hauffe and others.

As for the interpretation of the effect of the addition of foreign ions in the present work, it should be taken into consideration that such addition will change the heterogeneity of the surface as well as the electronic state of zinc oxide, both affecting the features of its hydrogen chemisorption. Although it is difficult to separate these two effects, the results obtained in this work, however, may be interpreted as follows: The identical heat of adsorption of 18 kcal./mol. for ZnO and ZnO +1 mole% $Al_2O_3$ is in agreement with the maximum heat of adsorption for non-sintered zinc oxide given in the previous work[5], suggesting that the maximum heat of adsorption is probably unaffected by the additions of foreign ions. This result together with the identical maximum activation energy of desorption throughout all the adsorbents with and without foreign ions would be unexpected, if the electronic state of zinc oxide played a large part in determining the features of hydrogen chemisorption. In addition, the activation energies of adsorption in similar temperature ranges are almost the same throughout all the adsorbents. Moreover, as described in the previous paper[9], the oxygen pretreatment at a high temperature which should change the electronic state of zinc oxide, gives little effect on its hydrogen chemisorption. Thus, taking account of the existence of surface heterogeneity in this system, the following tentative conclusion may be drawn:

8) K. Hauffe and A. L. Vierk, *Z. physik. Chem.*, **196**, 160 (1950).
9) Y. Kubokawa, This Bulletin, **33**, 743 (1960).

The heat of adsorption and the activation energy of adsorption associated with each set of sites may not be affected seriously by the addition of foreign ions; the variation in the features of the hydrogen chemisorption caused by such addition can probably be attributed to the change in the distribution function of sites rather than to that in the electronic structure of the adsorbents.

According to Cimino et al.[4], the adsorption isobars obtained with ZnO and ZnO+0.5 mole% $Li_2O$ show one or two maxima, while on ZnO+0.3 mole% $Ga_2O_3$ the amount adsorbed increases steadily with temperature, in qualitative agreement with the results mentioned above; the addition of $Ga_2O_3$ reduces the amount adsorbed over the whole range of temperature in an analogous way to that of $Al_2O_3$ (Fig. 8). This is reflected in the change of the amount adsorbed before desorption experiments (Figs. 5—7); the amount adsorbed on unit surface area is 0.056 cc. for ZnO, 0.012 cc. for ZnO+1 mol% $Ga_2O_3$, and 0.071 cc. for ZnO+0.5 mole% $Li_2O$. Although the true nature of such change in the amount adsorbed is not yet clear, there seems to be little or no doubt that such behavior can not be explained in terms of the change in the electronic structure of zinc oxide alone.

As regards the change in activity towards the hydrogen-deuterium exchange reaction caused by the addition of foreign ions, the considerations given above seem to indicate that it is doubtful that such an effect is attributed to the change in the electronic structure of zinc oxide. In fact, according to Heckelsberg et al.[10], although the activity is higher on ZnO+1 mole% $Al_2O_3$ than on ZnO, the activation energy is essentially the same for the two adsorbents, in contradiction with the results of Parravano. Such an identical activation energy is, however, what would rather be expected from the results in the present work. Further study of the hydrogen chemisorption and the exchange reaction with one and the same specimen of zinc oxide will probably lead us to a more consistent picture of all the related phenomena.

10) L. F. Heckelsberg, A. Clark and G. C. Bailey, *J. Phys. Chem.*, **60**, 559 (1956).

## Summary

The hydrogen chemisorption on zinc oxide samples modified by the addition of foreign ions such as $Li^+$, $Al^{3+}$, and $Ga^{3+}$ was investigated by measuring the rates of adsorption and desorption, and the adsorption equilibrium. The addition of foreign ions gave little or no effect on the maximum values of the activation energy for desorption and of the heat of adsorption, and the activation energies of adsorption in similar temperature ranges. On the basis of these results combined with the effect of oxygen treatment on this chemisorption on zinc oxide described previously, it was tentatively concluded that the variation in the features of hydrogen chemisorption caused by the addition of foreign ions is probably attributable to the change in a heterogeneity of the surface rather than that in the electronic state of zinc oxide. Finally, it was mentioned that the heat of adsorption of carbon monoxide at room temperature was also unaffected by such additions.

The author wishes to express his sincere thanks to Professor O. Toyama for his guidance and encouragement throughout the course of this study.

*Department of Applied Chemistry*
*College of Engineering*
*University of Osaka Prefecture*
*Sakai-shi, Osaka*

# *Zur Darstellung von 3-Methylpolymethoxyphthaliden*

Von Eturô MAEKAWA und Yukiko SUMIMOTO

(Eingegangen am 23. Januar, 1960)

3-Methylpolymethoxyphthalide erweckten unser Interesse, weil sie durch Grignardreaktion mit Alkylmagnesiumbromiden und durch anschließende Oxydation mit Kaliumpermanganat Polymethoxy-*o*-acyl-acetophenon ergeben, die dann durch Oxydation mit Selendioxyd in Polymethoxynaphthochinone übergehen[1]. Aus *o*-Phthalaldehydsäure wurde 3-Methylphthalid durch Grignardreaktion mit Methylmagnesiumjodid in guter Ausbeute[2] dargestellt. Auf diese Weise wurden auch 3-Methyl-6. 7-dimethoxy-[2,3], 3-Methyl-4. 5. 6-trimethoxy-[4] und 3-Methyl-4. 5. 6. 7-tetramethoxyphthalid[1] aus den entsprechenden polymethoxylierten *o*-Phthalaldehydsäuren gewonnen. Bei den polymethoxylierten Derivaten, besonders bei Opiansäure nimmt die Ausbeute der Grignardreaktion jedoch stark ab, offenbar weil die Löslichkeit der Polymethoxyphthalaldehydsäuren in Äther viel geringer ist. Obwohl die Ausbeute dadurch einigermaßen verbessert werden konnte[5], daß man die Dosis des Äthers als Lösungsmittels bei der Grignardreaktion erhöhte, oder, daß man einer ätherischen Suspension der Polymethoxyphthalaldehydsäuren des vorher hergestellten Grignardreagens zutropft, und obwohl es uns weiter gelingt, drei in der Literatur noch nicht beschriebene Produkte, nämlich 3-Methyl-5. 6-dimethoxy-, 3-Methyl-5. 6. 7-trimethoxy- und 3. 7-Dimethyl-4. 5. 6-trimethoxyphthalid, auf diese Weise darzustellen, erscheint diese Methode der Darstellung nicht sehr praktisch.

Andererseits stellten Gabriel und Michael aus *o*-Acetylbenzoesäure, die aus Phthalsäureanhydrid und Malonsäure in Pyridin leicht zugänglich ist[6], durch Reduktion mit Natriumamalgam 3-Methylphthalid in einer fast quantitativen Ausbeute dar[7]. Es wurde von uns fesgestellt[4], daß sich aus Polymethoxyphthaliden durch Behandeln mit doppeltermolekularer Menge *N*-Bromsuccinimid (abgekürzt NBS) unter Bestrahlung und durch anschließende Hydrolyse des bromierten Produktes neben den Polymethoxyphthalaldehydsäuren die entsprechenden Polymethoxy-*o*-phthalsäuren bilden. Um eine praktische Darstellungsmethode der Polymethoxyphthalsäure zu finden, wurde nun die Reaktion des NBS auf Polymethoxyphthalaldehydsäuren, die aus den entsprechenden Phthaliden durch Versetzen mit NBS leicht hergestellt werden können[1,4,8], ausführlich untersucht. Yamaguchi stellte fest, daß Piperonal beim Versetzen mit NBS 3. 4-Methylendioxybenzoesäure und daneben noch Protocatechualdehyd sowie 6-Brom-3. 4-methylendioxybenzoesäure ergab[9], während Vanilin keine Carbonsäuren sondern 5-Bromvanilin und daneben wenig Dehydrodivanilin lieferte[10], und nahm an, daß die Aldehydgruppe über Bromcarbonyl-in die Carboxylgruppe übergeht[11].

Erhitzt man *o*-Phthalaldehydsäure oder deren

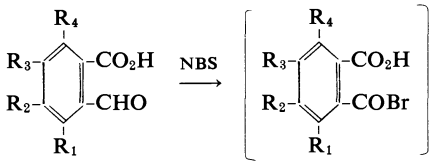
TABELLE I. DARSTELLUNG VON POLYMETHOXYPHTHALSÄUREANHYDRIDEN AUS POLYMETHOXYPHTHALALDEHYDSÄUREN MIT NBS

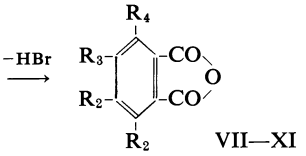
| Phthalaldehydsäure | Phthalsäureanhydrid[a] (°C, aus Benzol umkristallisiert) |
|---|---|
| I | VII, Fp. 127~128[b] (96,4%)[c] |
| II | VIII, Fp. 172~174[d] (90,0%) |
| III | IX, Fp. 166~167[e] (96,3%) |
| IV | X, Fp. 143~144[f] (95,0%) |
| V | X, Fp. 143~144 (96,7%) |
| VI | XI, Fp. 137~138[g] (93,7%) |

a) Die Produkte wurden sowohl durch Mikroanalysen als auch durch Mischschmelzpunkt der freien Phthalsäuren mit den durch in der Literatur beschriebenen Methoden hergestellten Produkten identifiziert;
b) Lit. 12, Fp. 130, 8°C;
c) in Klammern Ausbeute;
d) R. G. Fargher u. a., *J. Chem. Soc.*, **119**, 1724 (1921), Fp. 179°C;
e) W. H. Perkin u. a., ebenda, **1925**, 127, Fp. 167°C;
f) G. Bergellini u. a., *Atti Acad. Lincei*, **21** II, 146 (1912), Fp. 143°C;
g) Lit. 4, Ep. 137, 5~138°C.

1) F. Weygand, H. Weber und E. Maekawa, *Chem. Ber.*, **90**, 1879 (1957),
2) H. Simonis, E. Marben und E. Mermod, *Ber.* **38**, 3981 (1905).
3) E. Mermod und H. Simonis, ebenda, **41**, 982 (1907).
4) E. Maekawa und S. Nan'ya, dieses Bulletin, **32**, 1311 (1959).
5) E. Maekawa, Dissertation, Berlin-Charlottenburg (1956).
6) S. Gabriel und A. Michael, *Ber.* **10**, 2205 (1877).
7) H. L. Yale, *J. Am. Chem. Soc.*, **69**, 1547 (1947).
8) J, J. Brown und G. T. Newbold, *J. Chem. Soc.*, **1952**, 4397.
9) M. Yamaguchi, *J. Chem. Soc. Japan, Pure Chem. Sect.* (*Nippon Kagaku Zasshi*), **77**, 515 (1956).
10) M. Yamaguchi, ebenda, **77**, 593 (1956).
11) M. Yamaguchi, ebenda, 77, 591 (1956).

polymethoxylierte Derivate in Tetrachlorkohlenstoff in Gegenwart von Dibenzoylperoxyd (abgekürzt BPO), so entwickelt sich Bromwasserstoff und aus dem Reaktionsgemisch können die entsprechenden Phthalsäureanhydride in guter Ausbeute leicht isoliert werden. Da die Reaktion unter Bromwasserstoffentwicklung zu Phthalsäureanhydriden führt, scheint sie gemäß folgendem Schema zu verlaufen:




I: $R_1=R_2=R_3=R_4=H$
II: $R_1=R_4=H$, $R_2=R_3=OCH_3$
III: $R_1=R_2=H$, $R_3=R=OCH_3$
IV: $R_1=R_2=R_3=OCH_3$, $R_4=H$
V: $R_1=H$, $R_2=R_3=R_4=OCH_3$
VI: $R_1=R_2=R_3=R_4=OCH_3$
VII: $R_1=R_2=R_3=R_4=H$
VIII: $R_1=R_4=H$, $R_2=R_3=OCH_3$
IX: $R_1=R_2=H$, $R_3=R_4=OCH_3$
X: $R_1=R_2=R_3=OCH_3$, $R_4=H$
XI: $R_1=R_2=R_3=R_4=OCH_3$

Die Ergebnisse sind zusammenfassend in der Tabelle I angegeben. Weder kernbromierte noch dimerisierte Produkte wurden in den Reaktionsgemischen gefunden; Bildung von Substanzen, die mit Eisenchlorid eine violette Farbreaktion zeigen, wurde auch nicht festgestellt.

Da die Ausbeute an den Phthalsäuren bei der Reaktion der Polymethoxyphthalide mit doppelter molekularer Menge NBS von der Feuchtigkeit der Reaktionssysteme abhängig ist, scheinen die Phthalsäuren zum Teil über die freien *o*-Phthalaldehydsäuren, die sich durch die Wirkung der Feuchtigkeit auf die 3-Bromphthalide bilden, durch deren Reaktion mit NBS über die Phthalsäuremonobromide zu entsehen. Die Entstehung von Phthalsäuren muß jedoch aus Polymethoxyphthaliden auch anders, als über die freien *o*-Phthalaldehydsäuren möglich sein, da sich Phthalsäuren auch unter Feuchtigkeitsausschluß ohne Entwicklung von Bromwasserstoff bilden, man kann sie erst nach der Hydrolyse des Produktes isolieren.

Die gebildeten Polymethoxyphthalsäuren werden durch Erhitzen zu ihren Anhydriden geführt, welche dann mit Malonsäure in Pyridin erwärmt werden. Da es im allgemeinen schwierig war, aus den Reaktionsgemischen die erwarteten Polymethoxy-*o*-acetylbenzoesäuren rein zu isolieren, werden sie in rohem Zustand mit Natriumamalgam oder Zink und Essigsäure versetzt und 3-Methylpolymethoxyphthalide aus den schwach angesäuerten Reaktionsgemischen ausgeäthert (Tabelle II). Hemipinsäure- bzw. 3. 4. 5-Trimethoxyphthalsäureanhydrid ergibt 3-Methylmekonin bzw. 3-Methyl-5. 6. 7-trimethoxyphthalid, wobei 3-Methyl-4. 5-dimethoxy- bzw. 3-Methyl-4. 5. 6-trimethoxyphthalid im Reaktionsgemisch nicht gefunden wurden, was vermutlich auf die sterische Behinderung durch die *o*-stehende Methoxygruppe zurückzuführen ist. Bei der Reduktion des rohen Reaktionsproduktes aus 4. 5-Dimethoxyphthalsäureanhydrid und Malonsäure, das noch die entsprechende freie Phthalsäure zu erheblicher Menge enthält, bildete sich auch daneben durch deren Reduktion 5. 6-Dimethoxyphthalid. Die Kondensation der Polymethoxyphthalsäureanhydride, die in Pyridin als Phthalsäureanhydrid viel weniger löslich sind, verlief mit Malonsäure nur in sehr schlechten Ausbeuten, und ihre präparative Bedeutung blieb noch zweifelhaft, obgleich wir noch nicht versucht haben, optimale Bedingungen zu suchen.

TABELLE II. 3-METHYLPOLYMETHOXYPHTHALIDE AUS POLYMETHOXYPHTHALSÄUREANHYDRIDEN

| Phthalsäureanhydrid | Produkt (°C) |
|---|---|
| VIII | 3-Methyl-5. 6-dimethoxyphthalid, Fp. 109~110 (35%)[a] u. daneben 5. 6-Dimethoxyphthalid, Fp. 154~155[b] (1%) |
| IX | 3-Methyl-6. 7-dimethoxyphthalid, Fp. 100~101[c] (17%) |
| X | 3-Methyl-5. 6. 7-trimethoxyphthalid, Fp. 103,5~104,5 (12%) |
| XI | kein Phthalid erhalten |

a) In Klammern die auf das umgesetzte Anhydrid bezogene Ausbeute;
b) J. A. McRae u. a., *Can. J. Chem.*, **29**, 482 (1951), Fp. 155°C;
c) Lit. 2, Fp. 101°C.

## Beschreibung der Versuche

**1. *o*-Phthalaldehydsäuren.**—Wurden aus den entsprechenden Phthaliden durch Versetzen mit NBS und durch anschließende Hydrolyse der bromierten Produkte hergestellt[1].

**2. Phthalsäureanhydrid.**—5 g (1/30 mol) *o*-Phthalaldehydsäure wurden in 200 ccm Benzol gelöst, ca. 20 ccm des Benzols abdestilliert, um die Feuchtigkeit des Systems azeotropisch zu beseitigen, dann mit 200 ccm Tetrachlorkohlenstoff und 5,9 g (1/30 mol) NBS in Gegenwart von wenig BPO und unter Bestrahlung mit einer 500 W-Wolframlampe

1 Std. am Rückfluß erhitzt. Das beim Erkalten ausgeschiedene Succinimid (ca. 3,3 g) wurde abgesaugt, das Filtrat eingeengt, der Rückstand vorsichtig mit wenig kaltem Wasser zum Beseitigen des Succinimids gewaschen und aus Benzol umkristallisiert, 4,66 g (94,5%) farblose Nadeln, Fp. 127~128°C* (Lit.[12] 130, 8°C).

**3. Polymethoxyphthalsäureanhydride.**—Die entsprechenden Polymethoxyphthalaldehydsäuren wurden wie vorstehend mit NBS versetzt: die besten Ergebnisse sind in der Tabelle I zusammenfassend angegeben.

**4. 3-Methyl-5. 6-dimethoxyphthalid (*α*-Methyl-*m*-mekonin).**—(a) Einer gut umgerührten Suspension von 3,7 g 4. 5-Dimethoxyphthalaldehydsäure (*m*-Opiansäure) in 500 ccm Äther wurde ein Grignardreagens aus 9,5 g Methyljodid und 1,7 g Magnesiumspänen unter Eiskühlung langsam zugetropft. Das Gemisch wurde 1 Std. unter Eiskühlung und noch 1 Std unter Erwärmen am Rückfluß umgerührt, dann mit 2 N Schwefelsäure angesäuert und mit Äther ausgezogen, wobei aus der wässerigen Schicht 3,1 g nicht umgesetzte *m*-Opiansäure zurückgewonnen wurden. Die ätherische Lösung wurde mit Sodalösung und anschließend mit Wasser gewaschen, mit Natriumsulfat getrocknet und eingeengt. Der Rückstand wurde aus ca. 250 ccm Wasser kristallisieren gelassen, 160 mg farblose Prismen oder Nadeln, Fp. 108~110°C.

Gef.**: C 63,20; H 5,62. Ber. für $C_{11}H_{11}O_4$ (208,2): C 63,50; H 5,81.

Es fiel unter Umständen aus den Wasser in durchsichtigen Nadeln aus, die bei 118,5~120°C schmelzen; sie scheinen kristallwasserhaltig zu sein, reichten jedoch zu einer Elementaranalyse nicht.

(b) 4 g 4. 5-Dimethoxyphthalsäureanhydrid wurden 3 Std mit 2,3 g Malonsäure und 3 ccm Pyridin in 10 ccm Xylol auf dem Wasserbad unter Feuchtigkeitsausschluß erwärmt. Beim Erkalten des Reaktionsgemisches fielen 3,3 g des Anhydrids aus. Das Gemisch wurde abfiltriert, das Filtrat mit 80 ccm Wasser gemischt, mit Salzsäure angesäuert und mit Äther ausgezogen. Der ätherische Ausznng wurde mit Wasser gewaschen und einge engt, der Rückstand mit Wasser zum Sieden erhitzt, um das Xylol azeotropisch zu entfernen, und die wässerige Lösung eingeengt. Der Rückstand (0,45 g) wurde 2 Std. mit 1 g Zinkstaub in einem Gemisch aus 1 ccm Wasser und 4 ccm Essigsäure am Rückfluß erhitzt, das Gemisch im Vakuum eingeengt, der Rückstand in Äther gelöst und die ätherische Lösung mit Sodalösung gewaschen und eingeengt. Aus Wasser umkristallisiert ergab der Rückstand wenig *m*-Mekonin (Fp. 154~155°C) und daneben 185 mg 3-Methyl-5. 6-dimethoxyphthalid (Fp. 109~110°C), der beim Mischschmelzpunkt mit dem obenerwähnten Produkt keine Depression zeigte.

**5. 2. 7 - Dimethyl - 4. 5. 6 - trimethoxyphthalid.** — Einem Geignardreagens aus 0,8 g Magnesiumspänen und 5,5 g Methyljodid wurde eine Lösung von 2 g 3. 4. 5-Trimethoxy-6-methylphthalaldehydsäure (Fp. 109~113°C) in 320 ccm Äther unter kräftigem Umrühren und Eiskühlung langsam zugetropft und das Gemisch wie üblich aufgearbeitet. Aus der ätherischen Lösung wurden durch Waschen mit Sodalösung 0,2 g Ausgangsprodukt und durch anschließendes Einengen ein fettartiger Rückstand gewonnen, der aus alkoholhaltigem Wasser in farblosen Nadeln ausfiel, 0,76 g, Fp. 80~81,5°C.

Gef.: C 62,16; H 6,33. Ber. für $C_{13}H_{16}O$ (252,2): C 61,89; H 6,39.

**6. 3 - Methyl - 5. 6. 7 - trimethoxyphthalid.** — (a) Einem Grignardreagens aus 0,5 g Magnesiumspänen und 3,0 g Methyljodid wurde eine Suspension von 1,5 g 4. 5. 6-Trimethoxyphthalaldehydsäure in 500 ccm Äther unter Eiskühlung zugetropft. Es wurde wie üblich aufgearbeitet und das Produkt aus Wasser umkristallisiert, 0,80 g farblose Nadeln, Fp. 103, 5~104,5°C.

Gef. C 60,53; H 6,00. Ber. für $C_{12}H_{14}O_5$ (238,2): C 60,50; H 5,92.

(b) 3,5 g 3. 4. 5-Trimethoxyphthalsäureanhydrid wurden 3 Std in 4,5 ccm Pyridin mit 1,8 g Malonsäure auf dem Wasserbad unter Feuchtigkeitsausschluß erwärmt. Das Reaktionsgemisch wurde in 25 ccm Wasser gelöst, die Lösung mit Salzsäure angesäuert und mit Äther ausgezogen. Die ätherische Lösung wurde nach dem Waschen mit Wasser eingeengt, der Rückstand in wenig Wasser gelöst und die wässerige Lösung bei Zimmertemperatur eindunsten gelassen, wobei 2,3 g 3. 4. 5-Trimethoxyphthalsäure zurückgewonnen wurden. Die Mutterlauge wurde eingeengt und der Rückstand (1 g) in einer Natronlauge aus 2 g Natriumhydroxyd und 150 ccm Wasser gelöst, mit einem Natriumamalgam aus 0,65 g Natrium und 30 g Quecksilber 24 Std. bei Raumtemperatur stehengelassen und anschließend 8 Std. unter Zusatz von 50 ccm Wasser auf dem Wasserbad erwärmt. Die wässerige Schicht wurde mit Salzsäure angesäuert, auf 50 ccm eingeengt und ausgeäthert. Die ätherische Lösung wurde mit Wasser, mit Natriumhydrogencarbonatlösung und mit Wasser gewaschen und eingeengt. Der Rückstand wurde aus Wasser mit Aktivkohle kristallisieren gelassen, 150 mg farblose Nadeln, Fp. 103,5~104,5°C, die beim Mischschmelzpunkt mit dem oberen Produkt keine Depression zeigte.

**7. 3-Methyl-6. 7-dimethoxyphthalid (*α*-Methyl-mekonin).**—4 g 3. 4-Dimethoxyphthalsäureanhydrid (Hemipinsäureanhydrid) wurden 3 Std mit 5 ccm Pyridin und 2,3 g Malonsäure auf dem Wasserbad in Abwesenheit von Feuchtigkeit erwärmt. Das Reaktionsgemisch wurde wie bei Darstellung der von 3-Methyl-5. 6. 7-trimethoxyphthalid nach der Methode (b) aufgearbeite, wobei 2,67 g 3. 4-Dimethoxyphthalsäure zurückgewonnen und 230 mg des Produktes erhalten wurden. Das Produkt zeigte aus Wasser umkristallisiert einen Fp. von 100~101°C (Lit.[2] 101°C).

## Zusammenfassung

Polymethoxy-*o*-phthalaldehydsäuren wurden mit *N*-Bromsuccinimid zu den entsprechenden Phthalsäureanhydriden unter Bromwasserstoffentwicklung in guter Ausbeute oxydiert, wobei kernbromierte bzw. dimerisierte Produkte oder

* Schmelzpunkte wurden mikroskopisch bestimmt, aber nicht korrigiert.

12) K. P. Monroe, *Ind. Eng. Chem.*, **11**, 1116 (1919).

** Für Mikroanalyse der Verbindungen sind wir der Zentralen Mikroanalysenstelle Univ. Kyoto sehr dankbar.

phenolische Verbindungen nicht nachgewiesen wurden. Aus den Polymethoxyphthalsäureanhydriden wurden durch Versetzen mit Malonsäure in Pyridin die *o*-Acetylpolymethoxybenzoesäuren hergestellt, die zu den 3-Methylpolymethoxyphthaliden reduziert wurden, obwohl die erste Stufe der Reaktion, nämlich die Kondensation mit Malonsäure, nur in sehr schlechter Ausbeute verlief. Bei dieser Kondensation wurde eine sterische Behinderung durch die *o*-ständige Methoxygruppe beobachtet, wie sich aus 3. 4. 5-Trimethoxyphthalsäureanhydrid nur 3-Methyl-5. 6. 7-trimethoxyphthalid bildet. 3-Methyl-5. 6-dimethoxy-, 3-Methyl-5. 6. 7-trimethoxy- und 3. 7-Dimethyl-4. 5. 6-trimethoxyphthalid wurden aus den entsprechenden *o*-Phthalaldehydsäuren durch die Grignardreaktion unter Verwendung von großer Dosis des Äthers, oder durch eine umgekehrte Grignardreaktion dargestellt.

Herrn Prof. Dr. F. Weygand, München, sind wir für seine Anregung und Anleitung zu vorstehender Arbeit zum aufrichtigsten Dank verpflichtet. Auch Doktor der Technology, Frau Seiko Nan'ya danken wir für ihre intensive Mitwirkung bestens.

*Organisch-Chemisches Laboratorium*
*der Technischen Hochschule Nagoya*
*Syôwa-ku, Nagoya*

# *The Ultraviolet Absorption Spectra of Stilbene and Some Related Compounds in the Solid State Measured by the Pressed KCl Disk Technique*

By Hiroshi SUZUKI

(Received December 15, 1959)

Molecular structures are, needless to say, not rigid. Even the equilibrium or most probable conformation of a compound can vary, depending on, above all, the aggregation state and the temperature. Thus, the equilibrium conformation of a compound determined by the X-ray crystal analysis, for example, is not necessarily maintained in a state other than the crystalline state. A typical example is biphenyl. This compound is planar in the crystalline state, non-planar in the gaseous state, and probably slightly non-planar in solution[1-1)].

If the most probable conformation of a compound is appreciably different in various states, the electronic absorption spectra of the compound in the various states must be correspondingly different from each other. The author has shown in a series of papers[1)] that the most probable conformations of many conjugated componds in various states, especially in solution, can be inferred with almost complete satisfaction from the electronic absorption spectra. The principle of the inference consists in comparison of the spectrum of a given compound under a given condition with that of a suitable reference compound under a suitable condition, whose conformation is already known, or else, can be presumed reasonably. Since the conformation of the reference compound is determined by the X-ray crystal analysis in most cases, it is frequently necessary to compare the concerned spectrum with the spectrum of the reference compound in the crystalline state.

The spectra of compounds in the crystalline state have been measured so far by various methods and for various purposes. Thus, they have been measured often with single crystals and with polarized light[2)]. This method is useful particularly for the assignment of absorption bands. Alternatively, they have been measured also with solid films prepared on quartz, silica, or glass plates by sublimation of crystals, by evaporation of thin layers of solutions, or by solidification of melted substances[3)]. These methods have been used sometimes for the purpose of studying the crystal spectra themselves, and sometimes simply for the reason that the spectra can not be measured in solutions because of the low solubilities of the substances.

In the crystal spectra measured by these

1) H. Suzuki This Bulletin, (I) **32**, 1340, (II) 1350, (III) 1357 (1959), (IV) **33**, 109, (V) 379, (VI) 389, (VII) 396, (VIII) 406, (IX) 410, (X) 613, (XI) 619 (1960).

2) See, for example, A. C. Albrecht and W. T. Simpson, *J. Chem. Phys.*, **23**, 1480 (1955).

3) See, for example; J. W. Weigl, ibid., **24**, 364 (1956).

methods the effect of the orientation of molecules in crystals reveals itself markedly[4]. This marked orientation effect is, of course, essential to the purpose of assignment of bands. However, this effect makes the spectra measured by these methods unsuitable for direct comparison with the spectra of solutions where molecules are oriented at random.

For this reason, in the foregoing series of papers the spectra measured by the "pressed KCl disk technique" were used as the crystal spectra of the reference compounds. The pressed KCl disk technique is quite analogous to the well-known pressed KBr disk technique developed for infrared spectroscopy, and was applied to electronic absorption spectroscopy first by Dale[4] in 1957. It may be somewhat doubtful whether or not the state of molecules in pressed KCl disks is quite the same as that in the crystals. Thus, there may be a possibility that the state is near to that of solid solutions. It seems, however, to be more probable that micro-crystals are oriented at random in disks. If it is so, it seems reasonable to consider that the spectra measured by this method are most suitable, as the spectra of the compounds in the crystalline state, to be directly compared with the solution spectra.

An additional advantage of this method over the others is that the influence of reflection at the disk surface can approximately be eliminated by using a pressed disk of pure potassium chloride as the reference in measurement of the spectra. In contrast, in spectra measured by the other methods the influence of reflection at the crystal surface, at the surface of the plate, or at the crystal-plate interface is frequently sufficiently great to cause serious distortion of the absorption spectra[5], and consequently it is necessary to correct for this influence of reflection. In addition, the pressed KCl disk technique will be very useful to measure the spectra of compounds of low solubility in usual solvents, and particularly of crystalline molecular complexes, whose spectra are difficult in general to measure by other methods.

It is to be noted here that the difference between the spectrum of a compound in the crystalline state and that in solution may be due partly at least to the effect of intermolecular interactions in crystals, besides the possible difference of the most probable conformation in both the states. In general, molecules in crystals can not be treated simply by a so-called oriented gas model. Forces between molecules in aromatic crystals are small compared with intramolecular forces, but they frequently exert appreciable effects on the electronic states of molecules and consequently affect the electronic absorption spectra. In a spectrum measured with a single crystal and with polarized light, the most important effect of a crystal field appears to reveal itself as a so-called Davydov splitting[6]. It seems to be of interest to notice how the effect of a crystal field manifests itself in the spectrum measured by the pressed KCl disk technique, if the spectrum is the one of micro-crystals oriented at random.

At any rate, in view of the possible usefulness of the pressed KCl disk technique in electronic absorption spectroscopy, it seems to be not only interesting but also desirable to study general characteristic features, if any, of the spectra measured by this technique as compared with the corresponding solution spectra.

The author has measured the spectra of stilbene and its related compounds by this technique, of which the spectra of *trans*-stilbene and tolan were already reported in previous papers (Refs. 1-V and VI), and he has found that some generalizations can be drawn from comparison of the spectra with the corresponding spectra of solutions in *n*-heptane, although their theoretical interpretation has not yet been attained. In the present paper, the results of the measurement are summarized and discussed mainly from a phenomenological standpoint.

## Experimental

**Materials.**—The compounds used in this study were prepared as reported previously[1-V-IX]. Potassium chloride was precipitated from water solution with hydrochloric acid to obtain small particle size and dried at 400~450°C for about 6 hr., according to the procedure described by Hales and Kynaston[7].

**Measurements of the Solid State Spectra.**—The general procedure of measurements of the solid state spectra by the pressed KCl disk technique is quite analogous to the procedure for *trans*-stilbene and tolan described in the previous papers. Thus, 1 to 10 mg. of the pure organic compound was thoroughly ground in an agate mortar (for about 15~20 min.) with about 200 mg. of the pure potassium chloride. About 10 mg. of the mixture was then ground with about 350 mg. of new potassium chloride. The concentration of the substance in the final mixture, from which a disk was prepared, was adjusted in order that the disk might show suitable absorbances (about 0.8~1.9 at the most intense absorption maximum). For example, in

4) J. Dale, *Acta Chem. Scand.*, **11**, 650 (1957).
5) J. W. Weigl, *J. Chem. Phys.*, **24**, 577 (1956).
6) See, for example, D. P. Craig and P. C. Hobbins, *J. Chem. Soc.*, 1955, 539; D. P. Craig, ibid., 1955, 2302; D. P. Craig and P. C. Hobbins, ibid., 1955, 2309.
7) J. L. Hales and W. Kynaston, *Analyst*, **79**, 702 (1954).

the case of *trans-p*-phenylstilbene, the mixing was carried out as follows; 2.35 mg. of the substance was ground with about 200 mg. of KCl, and about 10 mg. of the first mixture was ground with about 350 mg. of KCl to get the final mixture. II the case of triphenylethylene, 8.35 mg. of the compound was ground with 200 mg. of KCl, 10 mg. of the first mixture was ground with 350 mg. of KCl, and finally 80 mg. of the second mixture was ground with 177 mg. of KCl. As will be described later, the apparent molecular extinction coefficients in the spectra measured by this technique were generally lower than the corresponding values in the solution spectra, and furthermore, were not reproducible. Therefore, the adjustment of the concentrations in the final mixtures was not straightforward and frequently had to be carried out by the method of trial and error.

In most cases except for the cases of *trans*-stilbene and tolan, about 150 mg. (146~148 mg.) of each final mixture was pressed under vacuum in the usual manner into a transparent disk (pressure: about 12 tons per sq. cm.). The ultraviolet absorption spectrum of the disk was measured with a Cary recording spectrophotometer Model 14 by using a disk prepared of about 150 mg. (146 and 148 mg.) of pure potassium chloride as the reference. The transmission spectrum of one of the reference disks used (weight: 146.25 mg.) is shown in Fig. 1. It is characteristic that the spectrum exhibits a feeble absorption band at near 270.5 mμ. This band was observed similarly in all the spectra of the reference disks used.

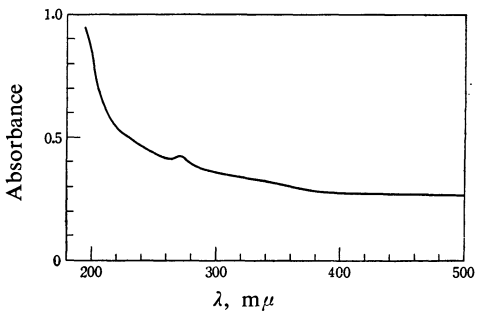



Fig. 1. The transmission spectrum of a reference KCl disk (weight: 146.25 mg.).

**Calculations of Thicknesses of Disks, Concentrations, and Molecular Extinction Coefficients.**— The radius of a disk is 0.65 cm. Since the weights of the disks used are 146~148 mg. in most cases, the thicknesses of the disks are calculated to be 0.055~0.056 cm, when it is assumed that the density of the disks is 1.988. These values of the thicknesses are in fairly good agreement with the rough values obtained by direct measurement. The concentrations of the organic substances in the disks can be calculated easily, on the basis of an assumption that micro-crystals or molecules are evenly dispersed in each mixture. Then, the molecular extinction coefficients (ε) are evaluated in the usual manner as the values of absorbance divided by the thickness of the disk and the molar concentration of the substance in the disk.

## Discussion

In the ensuing discussion, the spectra measured by the pressed KCl disk technique are referred to as the solid state spectra. The solution spectra refer to the spectra of solutions in *n*-heptane, except where indicated otherwise.

The newly measured solid state spectra are shown in Figs. 2—6, together with the corresponding solution spectra reported in previous

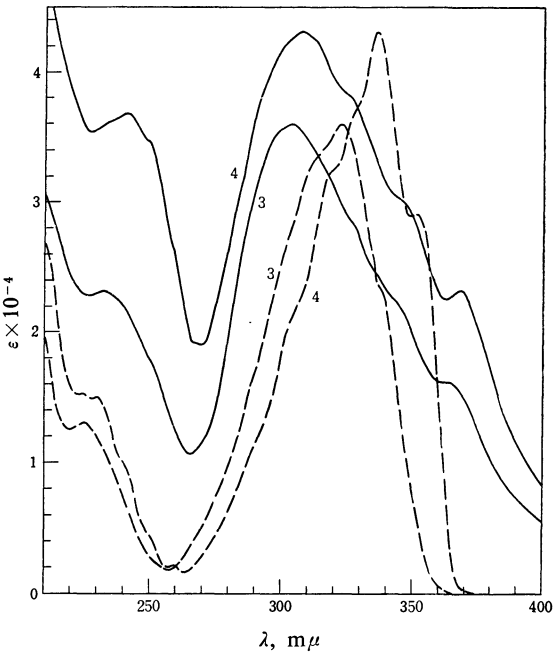



Fig. 2. Ultraviolet absorption spectra: 3, *trans-p*-phenylstilbene; 4, *trans*-1-phenyl-2-(2-fluorenyl)-ethylene.

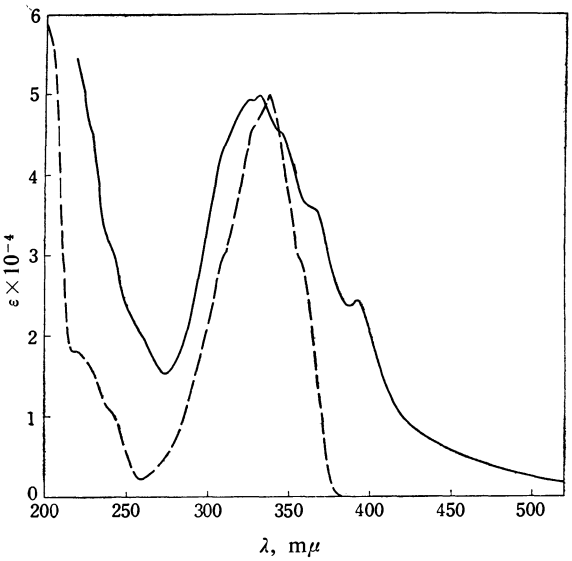



Fig. 3. Ultraviolet absorption spectra: *trans-p, p'*-diphenylstilbene.

papers (Refs. 1-VI—IX). The solid lines represent the solid state spectra and the broken lines the solution spectra. In these figures, the extinction of the most intense maximum of the conjugation band in each solid state spectrum has been arbitrarily set equal to the extinction of the most intense maximum of the conjugation band in the corresponding solution spectrum, because reliable solute extinction values for the solid state spectra could not be obtained. In addition, in Fig. 3 the extinction of the maximum of the conjugation band in the spectrum of *n*-heptane solution has been

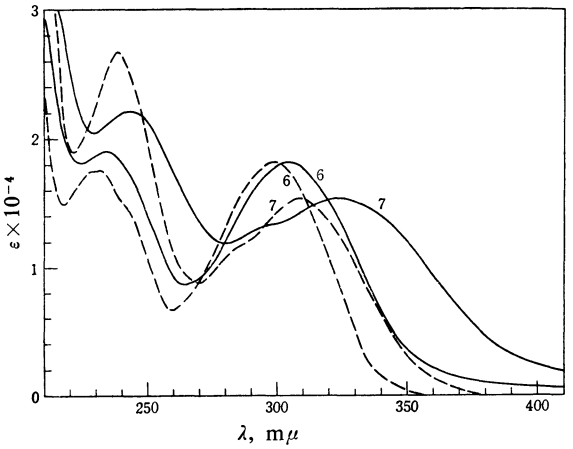



Fig. 4. Ultraviolet absorption spectra: 6, triphenylethylene; 7, tetraphenylethylene.

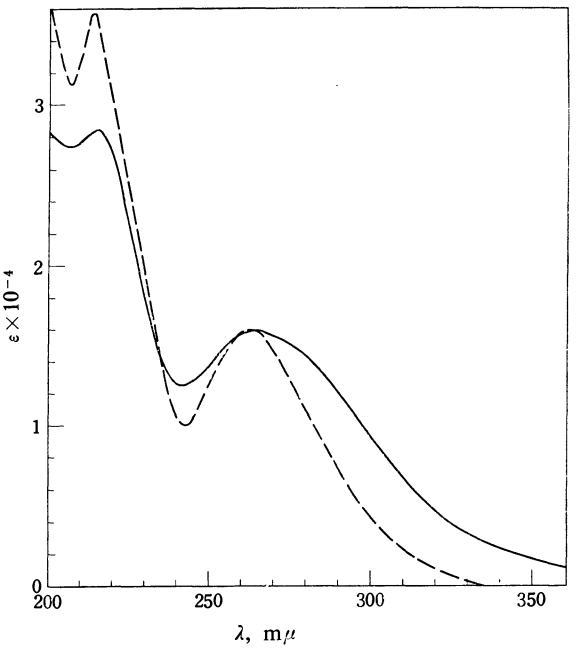



Fig. 5. Ultraviolet absorption spectra: *trans*-1, 2-dimesitylethylene.

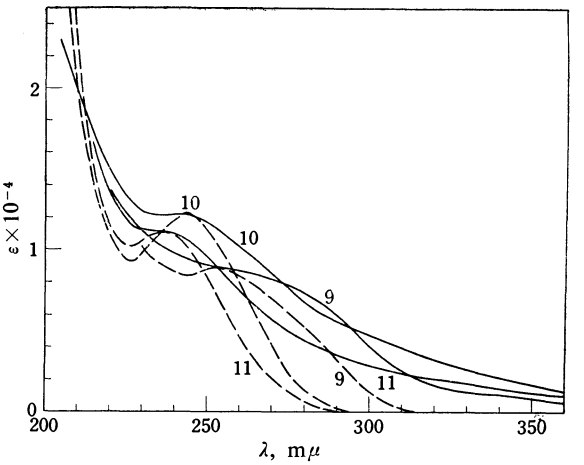



Fig. 6. Ultraviolet absorption spectra: 9, *cis*-$\alpha$, $\alpha'$-dimethylstilbene; 10, *trans*-$\alpha$, $\alpha'$-dimethylstilbene; 11, *trans*-$\alpha$, $\alpha'$-diethylstilbene.

arbitrarily set equal to that in the spectrum of benzene solution (cf. Ref. 1-IX). It is seen that the solid state spectra resemble considerably the corresponding solution spectra on the whole.

The data of the maxima and the inflections in these spectra as well as in the spectra of *trans*-stilbene and tolan are summarized in Table I. In this table, A refers to the A-band, i. e. the conjugation band due to transitions from the highest occupied orbital to the lowest vacant orbital, and B refers to the B-band, i. e. the band probably due to transitions from the highest occupied orbital to the vacant orbitals localized in the benzene nuclei or from the occupied orbitals localized in the benzene nuclei to the lowest vacant orbital (cf. Ref. 1-V). The symbol △ denotes the most intense maximum of fine structure of the conjugation band in each spectrum. Wavelengths (in m$\mu$) in parentheses denotes inflections, and those in double parentheses denote very indistinct inflections. $\Delta\lambda$ represents the wavelength difference (in m$\mu$) between the band in the solid state spectrum and the probably corresponding band in the solution spectrum. Values of $\Delta\lambda$ in parentheses are values for the cases in which either or both of the bands to be compared are inflections. $\varepsilon_K/\varepsilon_H$ represents the ratio of the apparent value of the molecular extinction coefficient of the band in the solid state spectrum to the value of the corresponding band in the solution spectrum.

**Absorption Intensities.**—The molecular extinction coefficients in the solid state spectra, calculated by the above mentioned procedure, were not reproducible. Not withstanding, it may be said that they are generally considerably

TABLE I. THE SOLID STATE SPECTRA (BY THE PRESSED KCl DISK TECHNIQUE) AND THE SOLUTION SPECTRA (IN *n*-HEPTANE) OF STILBENE AND RELATED COMPOUNDS

| Entry No. | Compound | | Solid state spectrum $\lambda_{max}$, mμ | Solid state spectrum $\varepsilon(\varepsilon_K)$ | Solution spectrum $\lambda_{max}$, mμ | Solution spectrum $\varepsilon(\varepsilon_H)$ | $\Delta\lambda$, mμ | $\varepsilon_K/\varepsilon_H$ |
|---|---|---|---|---|---|---|---|---|
| 1 | Tolan | | | | | | | |
| | | A | 301.6 | 1920 | 297.2 | 27500 | 4.4 | 0.070 |
| | | | 292.4 | 1680 | 288.5 | 20800 | 3.9 | 0.081 |
| | | | △ 283.3 | 2380 | △ 279.9 | 30800 | 3.4 | 0.077 |
| | | | (275.8) | 1960 | 272.7 | 22400 | (3.1) | 0.088 |
| | | | 268.0 | 1760 | 265.3 | 20600 | 2.7 | 0.085 |
| | | B | (239.0) | 680 | 237.2 | 6930 | (1.8) | 0.098 |
| | | | | | 232.2 | 6520 | | |
| | | | (223.5) | 1540 | 222.0 | 16500 | (1.5) | 0.093 |
| | | | (218.5) | 1790 | 217.2 | 19000 | (1.3) | 0.094 |
| 2 | *trans*-Stilbene | | | | | | | |
| | | A | (327.5) | 960 | (320.5) | 16000 | (7.0) | 0.060 |
| | | | (312.5) | 1500 | 306.9 | 26500 | (5.6) | 0.057 |
| | | | (298.5) | 1750 | △ 294.1 | 27950 | (4.4) | 0.063 |
| | | | △ 287.0 | 1790 | (283) | 24500 | (4.0) | 0.073 |
| | | | (276) | 1610 | | | | |
| | | B | (241.5) | 1420 | (236) | 10400 | (5.5) | 0.137 |
| | | | 233.0 | 1670 | 228.5 | 16200 | 4.5 | 0.103 |
| | | | (225.5) | 1640 | (222) | 15500 | (3.5) | 0.106 |
| 3 | *trans-p*-Phenylstilbene | | | | | | | |
| | | A | (364.4) | 6850 | | | | |
| | | | ((343)) | 9540 | ((338)) | 23200 | (5.0) | 0.411 |
| | | | ((328)) | 11880 | △ 322.5 | 36000 | (5.5) | 0.330 |
| | | | | | (311.5) | 33200 | | |
| | | | △ 303.6 | 15240 | | | | |
| | | B | 232.3 | 9810 | 225.5 | 13100 | 6.8 | 0.749 |
| 4 | *trans*-1-Phenyl-2-(2-fluorenyl)-ethylene | | | | | | | |
| | | A | 368.0 | 5370 | | | | |
| | | | | | 351.2 | 29100 | | |
| | | | (345) | 6980 | △ 335.8 | 43100 | (9.2) | 0.162 |
| | | | (325) | 8820 | (318.5) | 32450 | (6.5) | 0.272 |
| | | | (313) | 9750 | | | | |
| | | | △ 307.0 | 9920 | ((303.5)) | 21000 | (3.5) | 0.472 |
| | | | ((299)) | 9580 | | | | |
| | | B | (249.5) | 7970 | ((237.5)) | 10900 | (12.0) | 0.731 |
| | | | 241.0 | 8470 | 230.0 | 15230 | 11.0 | 0.556 |
| | | | (233.5) | 8290 | 223.7 | 15420 | (9.8) | 0.538 |
| 5 | *trans-p, p'*-Diphenylstilbene | | | | | | | |
| | | A | 391.8 | 12260 | | | | |
| | | | (366.0) | 17980 | ((357)) | 29400* | (9.0) | 0.612 |
| | | | (345.2) | 22970 | △ 337.4 | 49900* | (7.8) | 0.460 |
| | | | △ 331.6 | 25130 | (327.5) | 46200* | (4.1) | 0.544 |
| | | | (324) | 24820 | | | | |
| | | B | ((229)) | 18640 | (220.5) | 18200* | (8.5) | 1.024 |
| 6 | Triphenylethylene | | | | | | | |
| | | A | ((308)) | 8090 | | | | |
| | | | 303.8 | 8180 | 298.5 | 18220 | 5.3 | 0.449 |
| | | B | | | (242.5) | 14570 | | |
| | | | 233.9 | 8550 | 232.0 | 17580 | 1.9 | 0.486 |
| | | | ((230)) | 8500 | (228) | 17540 | (2.0) | 0.485 |

TABLE I (continued)

| | | | | | | | |
|---|---|---|---|---|---|---|---|
| 7 | Tetraphenylethylene | | | | | | |
| | A | 322.9 | 10970 | 308.7 | 15300 | 14.2 | 0.717 |
| | | (296) | 9480 | (285.8) | 11700 | (10.2) | 0.810 |
| | B | 243.3 | 15940 | 238.5 | 26800 | 4.8 | 0.595 |
| 8 | *trans*-1,2-Dimesitylethylene | | | | | | |
| | A | 264.4 | 9170 | 262.7 | 16000 | 1.7 | 0.573 |
| | B | 215.0 | 16340 | 214.0 | 35700 | 1.0 | 0.458 |
| 9 | *cis*-$\alpha$, $\alpha'$-Dimethylstilbene | | | | | | |
| | A | 252.4 | 570 | 252.0 | 8880 | 0.4 | 0.064 |
| 10 | *trans*-$\alpha$, $\alpha'$-Dimethylstilbene | | | | | | |
| | A | (240.6) | 2250 | 243.3 | 12270 | (−2.7) | 0.183 |
| 11 | *trans*-$\alpha$, $\alpha'$-Diethylstilbene | | | | | | |
| | A | (236.9) | 2220 | 236.6 | 11090 | (0.3) | 0.200 |

* Values estimated by taking the value for the maximum of the conjugation band in the spectrum of the *n*-heptane solution to be equal to the value in the spectrum of the benzene solution.

smaller than the values in the corresponding solution spectra. Thus, as is seen in Table I, the values of $\varepsilon_K/\varepsilon_H$ are about 1/3∼2/3 for the compounds of the numbers 3—8, and are only about 1/20∼1/5 for the compounds of the entry numbers 1, 2, 9, 10 and 11.

These depressions of intensities seem to be partly at least intrinsic ones. As is seen in Figs. 2—6, the bands, especially the A-bands, are markedly more broad in the solid state spectra than in the solution spectra. Therefore, it is believed that the intensities of especially the A-bands are actually considerably smaller in the former spectra than in the latter. This presumption is supported also by the fact that in the figures the intensities of the B-bands are apparently much larger in the solid state spectra than in the solution spectra in most cases. If it is assumed that the actual intensities of the B-bands are not markedly different in both spectra, this fact is, of course, considered to indicate the actual depressions of intensities of the A-bands in the solid state spectra.

In addition to the actual or intrinsic depressions, the intensities may be apparently depressed by contribution of other factors. As the factor contributing to the apparent depressions, the following possibilities may be considered. (1) A part of the organic substance weighed in may be lost during grinding and evacuation of the press, as pointed out already by Dale[4]. (2) Mixing may be imperfect in each process of grinding. That is, the substance may be unevenly dispersed in each mixture, and consequently, the actual concentration in the final mixture may be more or less different from the culculated value. (3) The absorption intensities in the solid state spectra may essentially depend on the condition of dispersion of the micro-crystals or the sizes of the micro-crystals, as suggested by the somewhat similar phenomenon observed by Weigl[3] in his study on the absorption spectra of some crystalline cationic dyes. Especially in the cases where the values of $\varepsilon_K/\varepsilon_H$ are extraordinarily small, the contribution of factor 1 may be predominant.

**Shapes of Absorption Curves and Wavelengths of Bands.**—Although the shape of the absorption curve of the solid state spectrum of a compound varies slightly from disk to disk in some cases, the reproducibility of the wavelength positions of the absorption maxima and the inflections was almost always fairly good.

Comparison of the solid state spectra with the solution spectra seems to suggest that it is convenient to divide the compounds into the following four groups with respect to the shapes of the absorption curves as well as the magnitudes of the wavelength displacements $\Delta\lambda$: (I) entry 1 in Table I, (II) entries 2—5, (III) entries 6 and 7, and (IV) entries 8—11.

**Group I.**—Tolan. The solid state spectrum it not significantly different from the solution spectrum, except for the bathochromic displacement of the normal magnitude (see below) of each band (cf. Fig. 2 in Ref. 1-VI). *trans*-Azobenzene also belongs to this group, whose spectra will be reported and discussed in a

later publication.

**Group II.—Redistribution of Intensity among the Vibrational Sub-bands.**—*trans*-Stilbene, *trans*-*p*-phenylstilbene, *trans*-1-phenyl-2-(2-fluorenyl)-ethylene, and *trans*-*p*,*p*'-diphenylstilbene. All these compounds are *trans*-stilbene-type compounds which have no substituent at sterically hindering positions and consequently are probably planar. It is a common distinctive feature of the spectra of these compounds that the bands, especially the conjugation bands, exhibit more or less well-resolved fine structures. With these compounds, a marked redistribution of intensity among the vibrational fine structure bands of the conjugation band occurs, that is, the relative intensities of the vibrational bands change markedly, when the state is changed from solution to solid. Thus, the band which appears as the most intense maximum in the solution spectrum, appears as the inflection at a longer wavelength than the most intense maximum in the solid state spectrum. On the other and the band which appears as the inflection at a shorter wavelength than the most intense maximum in the solution spectrum, appears as the most intense maximum in the solid state spectrum.

A typical example is *trans*-stilbene. As described in Ref. 1-V, when the vibrational sub-bands of the conjugation band of this compound are called $\alpha$, $\beta$, $\gamma$, $\delta$, ..... in the order from longer-wavelength-side, the most intense maximum is the $\gamma$-band in the solution spectrum, and is the $\delta$-band in the solid state spectrum. In this connection, it has been known that the temperature affects markedly the relative intensities of the vibrational sub-bands. Thus, in the spectrum of *trans*-stilbene in mixed alcohols at $-130°C$ measured by Beale and Roe[8], the fine structure is much more sharply resolved, the intensities of the $\alpha$- and the $\beta$-bands are much greater, and the intensity of the $\gamma$-band is much smaller than in the solution spectrum measured at room temperature. In this low temperature spectrum, the most intense maximum is the $\beta$-band. To illustrate the situation, the three spectra of *trans*-stilbene are shown in Fig. 7.

In the present case, both the solution spectra and the solid state spectra are the ones measured at room temperature. Therefore, the fact that the marked redistribution of intensity among the vibrational sub-bands occurs between them may be said to be rather surprising. Further investigation seems to be necessary to interpret satisfactorily this interesting phenomenon.

8) R. N. Beale and E. M. F. Roe, *J. Chem. Soc.*, 1953, 2755.

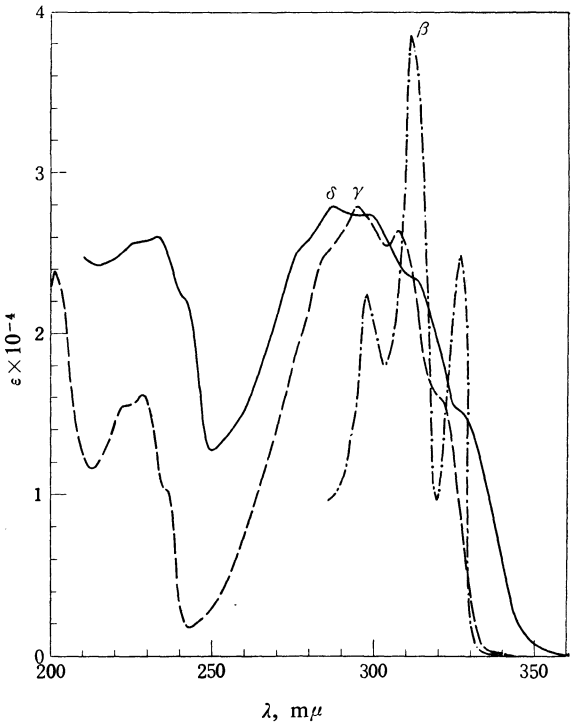



Fig. 7. Ultraviolet absorption spectra of *trans*-stilbene: ——, the solid state spectrum; ----, the solution spectrum; -·--·, the low temperature spectrum (in mixed alcohols at $-130°C$, redrawn from Beale and Roe's paper[8]).

**Wavelength Shifts of Bands.**—In Fig. 8, the values of $\Delta\lambda$ for the compounds belonging to Groups I and II are plotted against the wavelengths $\lambda$ of the corresponding maxima or inflections in the solution spectra. As mentioned already, $\Delta\lambda$ represents the magnitude of the wavelength shift of the band associated with the change of the state from *n*-heptane solution to solid.

A positive value of $\Delta\lambda$ indicates that the shift is bathochromic. As is seen in Table I, all the shifts, except for that in the case of *trans*-$\alpha$, $\alpha'$-dimethylstilbene, are bathochromic. Of course, the individual numerical values of $\Delta\lambda$ may not be decisive because of inevitable uncertainty in determination of the wavelength positions of the absorption maxima and especially of the inflections. Notwithstanding, it may be said that a rough correlation exists between $\lambda$ and $\Delta\lambda$. Thus, in Fig. 8, almost all the points for the A-bands of all the compounds as well as the B-band of tolan are nearly on a correlation line, which has been drawn as the solid line in the figure. This means that $\Delta\lambda$ for these increases fairly regularly with $\lambda$ from about 1.5 m$\mu$ at 220 m$\mu$ to about 5 m$\mu$ at 300 m$\mu$, and to about 9.5 m$\mu$

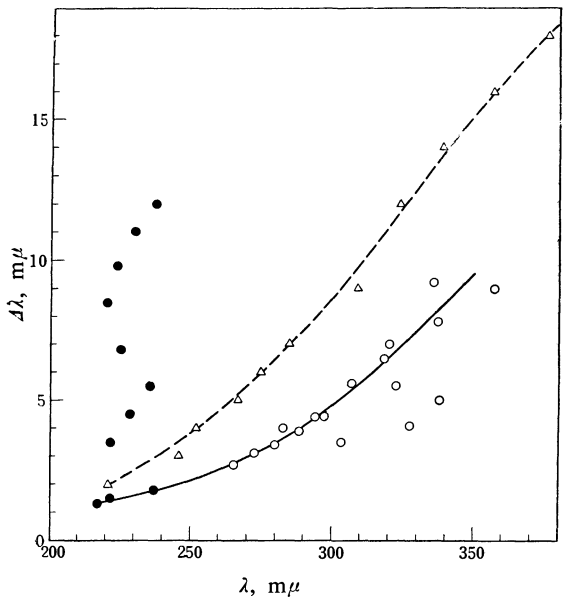



Fig. 8. Correlations between the magnitudes of wavelength shifts of bands (from solution to the solid state) and the wavelengths of the bands in the solution spectra.
○, for the A-bands of tolan and the stilbenes.
●, for the B-bands of tolan and the stilbenes.
△, for the bands of naphthalene and anthracene (according to Dale's data[4]).

at 350 mμ. On the other hand, most of the points for the B-bands, the bands which appear in the region about 220~250 mμ, are markedly deviating from the correlation line. There appears to be a very rough relation that the longer the conjugated system is, or in other words, the longer the wavelength of the A-band is, the value of $\Delta\lambda$ for the corresponding B-band is the larger.

What is the cause of such bathochromic shifts of bands? This problem is unsettled. If the solid state spectra can be considered to be the spectra of micro-crystals oriented at random directions, the shifts are probably due to the intermolecular interactions in the crystals. Alternatively, if the solid state spectra are to be considered as the spectra of solid solutions, the shifts are probably due to a sort of solvent effect. Furthermore, the shifts may be due to other unknown causes. At any rate, whatever the mechanism of the shifts may be, the fact that there is a regular relation between the magnitudes of the shifts and the wavelengths of the bands is very interesting.

A similar regular relation has been found already by Dale[4] for the spectra of naphthalene and anthracene. According to him, the magnitude of the wavelength shift of a band of these "rigid" molecules due to the change of the state from hexane solution to solid, viz. the "normal red-shift", increases regularly with the wavelength of the band, from about 2 mμ at 220 mμ to about 8 mμ at 300 mμ, and to about 19 mμ at 400 mμ. As discussed in a previous paper (Ref. 1–I), this regular relation appears to hold good regardless of kinds of compounds, of characters of bands, and of intensities of bands. In Fig. 8, the values of the "normal red-shifts" are also plotted against the wavelengths of the bands in the spectra of hexane solutions according to Dale's data. A correlation line for these points is shown as the broken line.

It may be noteworthy that the correlation line obtained in the present work for stilbenes, which is subsequently referred to as the present correlation line, is located considerably lower than Dale's correlation line. That is, it may be said that the *trans*-stilbene-type compounds show the red-shifts of the normal magnitudes in themselves, which are smaller than the magnitudes of the normal red-shifts of naphthalene and anthracene. The latter compounds are, to use Dale's words, the "rigid" compounds which obviously can not assume other conformations in solution thanin the crystal lattice. Therefore, the above mentioned fact may be considered as an evidence indicating that the most probable conformationsof these stilbenes in solution are not significantly different from those in the solid, probably crystalline state, and accordingly, are probably planar.

While the probably planar compounds show the red-shifts of normal magnitudes, some compounds, which are discussed in the succeeding paragraphs as belonging to Groups III and IV, show the shifts of more or less abnormal magnitudes. It may be significant that the latter compounds are evidently non-planar. The conjugation bands of these compounds have no distinct fine structure, in contrast with the foregoing sterically unhindered compounds, and as a matter of fact, the shapes of the solid state spectra of these compounds are apparently not markedly different from those of the solution spectra.

**Group III.**—Triphenylethylene and tetraphenylethylene. The values of $\Delta\lambda$ for triphenylethylene are very slightly greater, and the values for tetraphenylethylene are much greater than those anticipated from the present correlation line in Fig. 8. The extraordinarily large shifts especially in the case of tetraphenylethylene may be considered to indicate that the most

probable conformation of this compound in the solid state is considerably different from that in solution. That is, it may be inferred that the interplanar angles between the phenyl groups and the ethylenic bond are appreciably smaller in the most probable conformation in the solid, probably crystalline state, than in that in solution (cf. Ref. 1–VI).

**Group IV.**—*trans*-2, 4, 6, 2′, 4′, 6′-Hexamethylstilbene (*trans*-1, 2-dimesitylethylene), *cis*- and *trans*-$\alpha$, $\alpha'$-dimethylstilbenes, and *trans*-$\alpha$, $\alpha'$-diethylstilbene. The values of $\Delta\lambda$ for these compounds are smaller than anticipated from the present correlation line. Thus, the value for dimesitylethylene is slightly smaller, and the values for $\alpha$, $\alpha'$-dialkylstilbenes are much smaller than anticipated from the correlation line. The value for *trans*-$\alpha$, $\alpha'$-dimethylstilbene is apparently even negative.

The most probable conformations of these compounds are undoubtedly non-planar, owing to the steric effects of the alkyl substituents (cf. Refs. 1–VII and VIII). Therefore, it seems quite reasonable to correlate the smallness of the shifts with the non-planarity of the molecular structures. It may be presumed that with these non-planar compounds the intermolecular interactions in the crystals (or the interactions of the molecules with potassium chloride) are smaller than in the case of the foregoing planar compounds.

The author desires to thank Mr. Akira Kuboyama of Government Chemical Industrial Research Institute, Tokyo, for the use of the spectrophotometer.

*Department of Chemistry*
*College of General Education*
*The University of Tokyo*
*Meguro-ku, Tokyo*

# *Paramagnetic Resonance of Radicals of Some Aromatic Vinyl Compounds. I*

By Kazuo MORIGAGI, Keiji KUWATA and Kozo HIROTA

(Received January 20, 1960)

Free radicals produced by the reaction of aromatic hydrocarbons with alkali metals have been investigated by the paramagnetic resonance method for several years by Weissman[1] and others. Usually the paramagnetic resonance spectra of these radicals consist of many lines which are coming from the hyperfine interaction of the unpaired electron with protons in these radicals. We have observed the paramagnetic resonance of radicals. We have obtained from the following aromatic vinyl compounds: styrene, $\alpha$-methyl styrene, $p$-methyl styrene, 1, 1-diphenylethylene, stilbene and 1, 4-diphenylbutadiene. A part of the experimental results has been already reported briefly[2]. The paramagnetic resonance of the above radicals, except that of stilbene, shows many absorption lines, which are attributed to the hyperfine structure arising from the hyperfine interaction of the unpaired electron with protons in the radicals.

The results obtained by the analysis of these spectra contribute not only to the determination of the unpaired electron density in the radicals, but also give some information about the mechanism of polymerization of these aromatic hydrocarbons, because some of the above compounds polymerize easily by the reaction with monomer, turning into so called "living polymers".

The experimental results and discussion in the case of styrene, $\alpha$-methyl styrene and $p$-methyl styrene will de described in the present paper, and the forthcoming paper will describe the results in the case of 1, 1-diphenyl-ethylene, stilbene and 1, 4-diphenylbutadiene.

## Experimental

**1) Paramagnetic Resonance Spectrometer and Experimental arrangement.**—The measurements of paramagnetic resonance of the above radicals were performed at room temperature, except that of styrene radicals which were measured at about $-100$°C and $-40$°C besides room temperature. The spectrometer used for the paramagnetic resonance measurements was a transmission type operating at 9300 Mc. The rectangular cavity, which has a

1) S. I. Weissman, T. R. Tuttle, Jr. and E. De Boer, *J. Phys. Chem.*, **61**, 28 (1957); T. R. Tuttle, Jr., R. L. Ward and S. I. Weissman, *J. Chem. Phys.*, **25**, 189 (1956).

2) K. Hirota, K. Kuwata and K. Morigaki, This Bulletin, **31**, 538 (1958); **32**, 100 (1959).

hole at the half-point of the narrow side, was excited at the mode of $TE_{012}$. The sample, being enclosed in a glass tube, was put into the cavity through the hole. By modulating the applied magnetic field at the frequency of 315 c/s, the resonance signal was detected with a phase sensitive detector, and was recorded on a milliampere recorder. The cavity system and the Dewar arrangement for measurement at low temperatures were designed as shown in Fig. 1. The sample enclosed in a

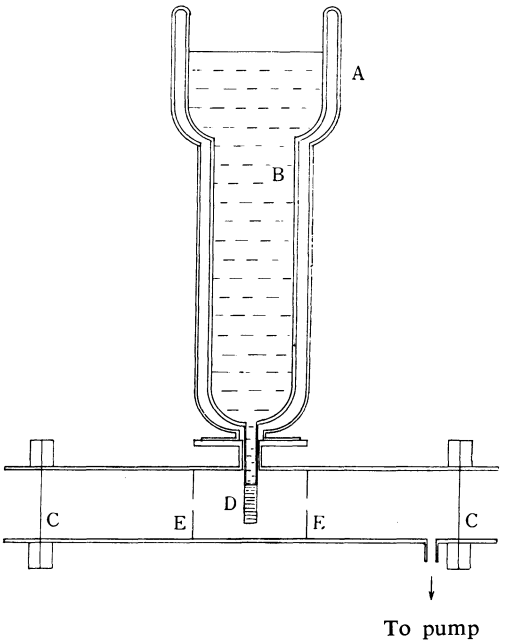



Fig. 1. Cryostat and cavity assembly

(A) Glass Dewar (D) Sample
(B) Liquid nitrogen (E) Iris
(C) Mica

small glass-tube was attached with some cement to the end-plane of the inner glass tube of the Dewar inserted into the cavity. The temperature at the position of the sample was measured by a copper-constantan thermocouple, which indicated a temperature of $-100$°C or $-40$°C when liquid nitrogen or methanol mixed with dry-ice was filled in the Dewar, respectively, As the outer part of the Dewar was jointed on a copper-head standing out of the cavity on its narrow side, removal of the entire assembly from the cavity for cleaning or using the cavity for measurements at room temperature was done easily. The space between the inner and outer parts of the Dewar and the inside part of the cavity were pumped out to get vacuum by closing the waveguide with thin mica foils in front of and behind the cavity.

2) **Preparation of Samples.**—The samples used in our experiment were prepared by two ways. One of them may be called the method I, while the other the method II. The latter will be described in details. As shown in Fig. 2, the apparatus for preparing the samples consists of several reaction vessels, all of which can be kept at high vacuum.

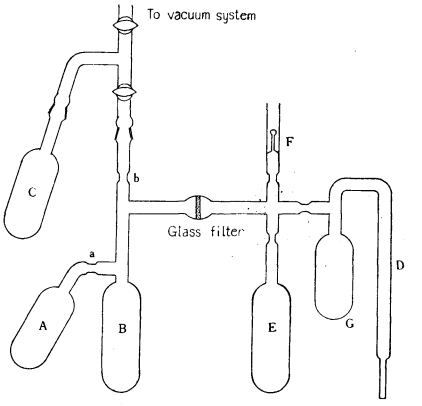



Fig. 2. Apparatus for preparation of sample.

The samples were prepared using this apparatus as follows. Connecting the entire vessel to the vacuum system, water and oxygen adsorbed on the wall of the glass vessels were excluded by heating and discharging the tube with a tesla coil. The sodium metal contained inside the glass vessel A was distilled into the reaction vessel B under reduced pressure, and the vessel A was sealed off from the system at the part "a". Then the aromatice hydrocarbons and toluene contained in the vessel were distilled into the vessel B under reduced pressure, and the vessels B, D, E and G were taken off from the vacuum system at the part of "b". The reaction vessel B was kept at about 100°C for a long time, in order to change the high-polymerized adduct of the aromatic hydrocarbon, formed inside the reaction vessel B before the heat-treatment, to a low-polymerized one. After the precipitate* inside the reaction vessel B was separated from the solvent, was transfered into the vessel E and was distilled under reduced pressure through the breakable joint, the precipitate was dissolved into the tetrahydrofuran or dioxane which was stored in the vessel G through the breakable joint F. Tetrahydrofuran and dioxane were used here as the solvent in which paramagnetic free radicals were contained as a diluted state. For the measurement of paramagnetic resonance the sample thus prepared was used in the glass tube D, the end part of which was inserted into the cavity. The method II described above was applied to the production of radicals of styrene, $\alpha$-methyl styrene, $p$-methyl styrene and 1, 1-diphenylethylene.

In the method I the aromatic hydrocarbon whose radical was to be produced was reacted directly with sodium metal in tetrahydrofuran or dioxane in a way similar to that of the method II without using toluene. The radicals of styrene, $\alpha$-methylstyrene, $p$-methylstyrene, 1, 1-diphenylethylene, stilbene, 1, 4-diphenylbutadiene and isoprene** could be produced by this method.

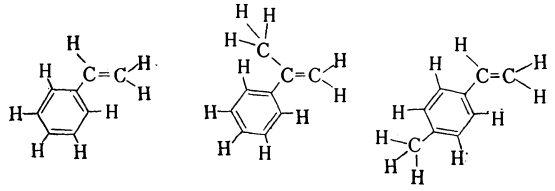
Determining the concentration of sodium ion in

* A strong paramagnetic resonance line was observed in the precipitate of the sodium adducts of styrene. The line width and $g$-factor were about 2 gauss and 2.002 respectively, and the line shape was Lorentzian.

** Reported briefly: K. Kuwata, K. Morigaki and K. Hirota, This Bulletin, 32, 895 (1959).

sample of styrene by flame spectroscopy, the ratio of radical part to an ionic part was estimated. It was of the order of one tenth. All measurements were carried out in the concentration range of about $10^{-3}$ to $10^{-4}$ spin per liter.

In the preparation of radicals described above precautions are taken against contamination of the reaction vessel used, because a trace of water and oxygen, if left in the vessel, may react easily with the adduct of the aromatic hydrocarbon and make the concentration of radicals decrease. Purification of aromatic hydrocarbons, sodium metal and solvents was performed in the following way. The aromatic hydrocarbons purified by the usual method were put in contact with sodium metal so as to remove the remaining water and were purified by vaccum distillation. The solvent purified in the usual way was reacted with stilbene anions or naphthalene anions by utilizing the reactive properties of these anions with the water and oxygen, and then the stilbene or the naphthalene was removed from the solvent by distillation. Naphthalene was used only in the preparation of the first samples of styrene radical. In the other samples, stilbene was used in most cases including the preparation of the styrene radical, because the stilbene anion gave no more than a broad resonance line without any structure even if it remained in the solvent.



Styrene α-Methyl styrene p-Methyl styrene

Fig. 3

## Results and Discussion

**Styrene.**—We have observed three kinds of paramagnetic resonance spectra in the styrene radical*. They were i) four lines, ii) nine lines and iii) many complex lines respectively.

i) Four lines.—The four-lines spectrum has been observed in many samples of dilute solution of the styrene adduct with sodium metal, when the solvent is tetrahydrofuran or dioxane. Even if either solvent is used and potassium metal is used in place of sodium metal, almost identical spectra of four lines were given. The above samples were prepared by the methods I and II described in the section 2. The spectrum consists of almost equally spaced four lines of which the intensities of each components are 1 : 3.2 : 3.3 : 1.2 in ratio in order of the strength of the magnetic field corresponding to the resonance lines. From the above results the hyperfine splitting is considered to arise from the hyperfine interaction between the unpaired electron and three equivalent protons. The hyperfine splitting is 4.3±0.5 gauss and the $g$-factor is 2.0031±0.0006.

The line-shape of each components is almost Gaussian with the half-width of about 3.9 gauss as shown in Fig. 5 (B).

The spectra observed at low temperatures, −40°C and −100°C, were almost identical with those observed at room temperature. From these results the width of each component is attributed to the unresolved hyperfine interaction with protons.

Three equivalent protons contributing to the

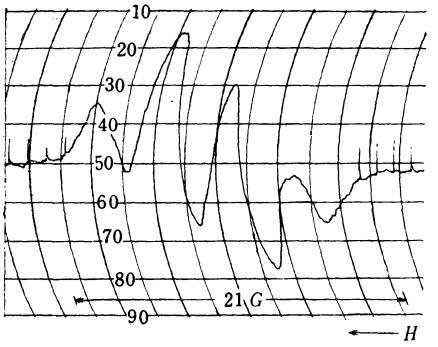



Fig. 4. Paramagnetic resonance spectrum of styrene radical.

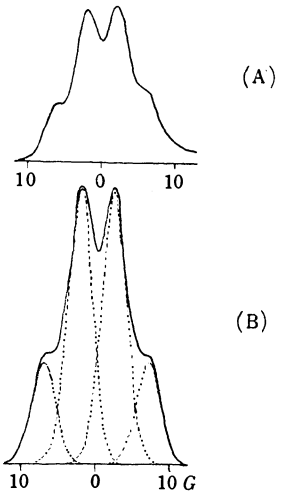



Fig. 5. Paramagnetic resonance spectra of styrene radical.

(A) The observed spectrum obtained by numerical integration.

(B) The calculated spectrum constructed from four Gaussian shaped lines with relative intensities of 1 : 3 : 3 : 1.

* Besides the three kinds of spectra, the other spectrum similar to that of the naphthalene anion was observed in the styrene radical in the tetrahydrofuran solution prepared by the methods I and II with sodium metal at the first stage of our experiment, which has been already reported briefly[2]. As it has not been reproducible, it will not be described here.

hyperfine splitting and some protons constructing the line-width of each components have not been able to be given a definite correspondence to the protons of the styrene anion.

ii) Nine lines.—The spectrum consisting of equally spaced nine lines has been observed in the styrene radical in the tetrahydrofuran solution prepared by the method I with sodium metal. The spacing between each components was 2.2±0.2 gauss.

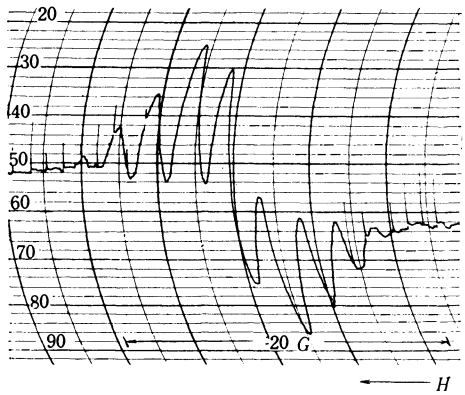



Fig. 6. Paramagnetic resonance spectrum of styrene radical

iii) Many complex lines.—The complex spectrum has been observed in the styrene radical in the tetrahydrofuran solution prepared by the method I with sodium metal. The spectrum extends to the length of 24±3 gauss on the scale of the magnetic field. The *g*-factor is 2.0028±0.0005.

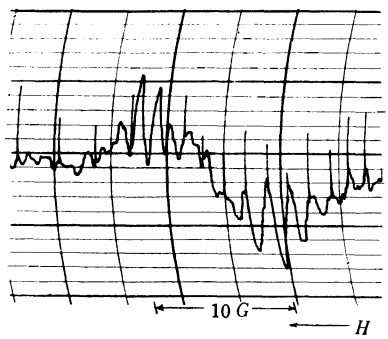



Fig. 7. Paramagnetic resonance spectrum of styrene radical.

The relation among the above three spectra on the point of the preparation of the styrene radical and the magnetic centers corresponding to the spectra have not been found in the present stage, so further experiments will be required to obtain some information about this problem.

On the other hand, we tried to observe the paramagnetic resonance of the styrene radical formed on the film of the vaporized sodium metal, but it gave a negative result*.

**α-Methylstyrene.**—We have observed the paramagnetic resonance spectrum, as shown in Fig. 8, of the α-methylstyrene radical in the tetrahydrofuran solution prepared by the method I with sodium metal. This spectrum extends to the length of about 32 gauss on the scale of the magnetic field. It may be explained by assuming that the hyperfine splitting is mainly attributed to the hyperfine interaction with three equivalent protons and another two equivalent protons with the coupling constant of 4.2 gauss and 2.5 gauss respectively and some protons contribute to construct the line shape of each components. If the magnetic center corresponding to the above spectrum is assumed to be the unpaired electron being localized on the α-methylstyrene anion, the following assignment might be reasonable on the basis of the unpaired electron density calculated by using the simple LCAO-MO theory: the three equivalent protons and two equivalent protons in the above analysis correspond to the *ortho*, *para*-protons and β-protons respectively, and the *meta*-protons

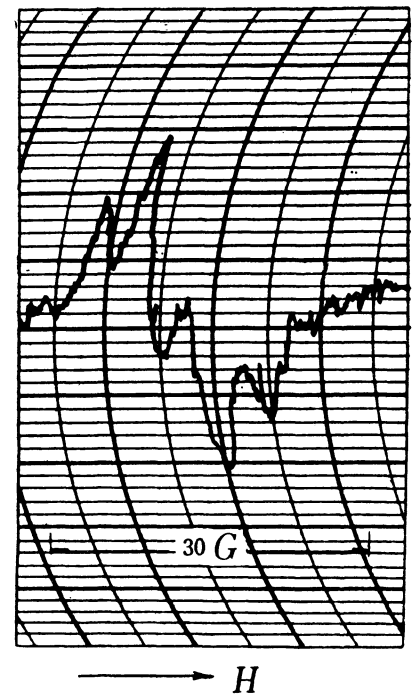



Fig. 8. Paramagnetic resonance spectrum of α-methylstyrene radical.

* It might be necessary to refer to the Weissman's answer in discussion [*J. Phys. Chem.*, 57, 507 (1953)], that "the paramagnetic resonance absorption in styrene as it is undergoing polymerization initiated by metallic sodium is not reproducible".

and the protons belonging to the methyl-group construct the line width of each components. The simple LCAO-MO calculation gives the following unpaired electron densities on the carbon atom of *ortho*, *meta*, *para*, $H_3$ and $\beta$ positions respectively.

$$\rho_o=0.091, \quad \rho_m=0.016, \quad \rho_p=0.149,$$
$$\rho_{H_3}=0.026, \quad \rho_\beta=0.355.$$

***p*-Methylstyrene.**—The observed spectrum of the *p*-methylstyrene radical is shown in Fig. 9. This sample consists of *p*-methylstyrene and *ortho*-methylstyrene with concentration of 60% and 40% respectively. This situation complicates the spectrum. Besides, the proton of the methyl group seems to contribute to the observed spectrum much more than in the case of the $\alpha$-methylstyrene radical. We have not been able to analyze the observed spectrum.

A few months later than the time of preparation of the samples during which the sample was kept at room temperature, the spectrum became simpler and weaker than that observed immediately after the preparation of the samples. This changes of the spectrum is shown in Fig. 10. No change of the color and viscosity accompained with that of the spectrum were observed. The hyperfine structure of the spectrum exists in the region of the length of about 25 ($\pm$5) gauss on the scale of the magnetic field. After this change, the samples always showed the same patterns of the spectrum as the above one, but the intensity of the resonance lines has decreased gradually with time.

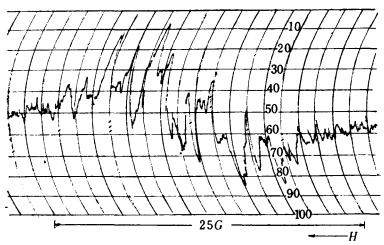



Fig. 9. Paramagnetic resonance spectrum of *p*-methylstyrene radical.

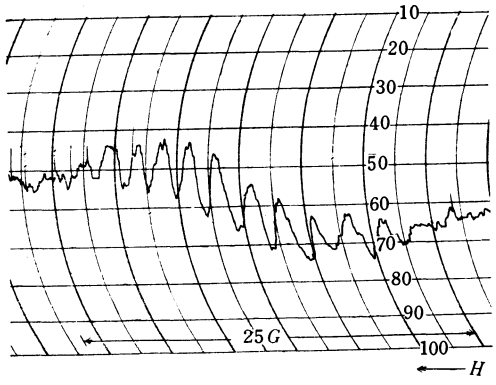



Fig. 10. Paramagnetic resonance spectrum of *p*-methylstyrene radical

### Reaction of the Aromatic Hydrocarbons with Alkali Metals

As described briefly in the section 1, the aromatic vinyl compounds, especially styrene, are initiated to polymerize with alkali metal. This property of styrene adducts with sodium metal as chain initiators was found independently by Szwarc et al.[3] and by Meshitsuka et al.[4] When the monomers of styrene exist in some suitable solvents (toluene, tetrahydrofuran, dioxane etc.), polymerization of them proceeds under existence of the adducts which produce the living polymer. The styrene adducts similar to that in the above case are produced by Scott's method in which naphthalene anions are used as a substitute of alkali metal. In this case, according to Szwarc, the living polymers consist of the dimerized styrene anions with both ends "living",

$$[:\mathrm{CH}(\phi)-\mathrm{CH_2}-\mathrm{CH_2}-\ddot{\mathrm{C}}\mathrm{H}(\phi)]^{2-} \quad (\phi=\mathrm{C_6H_5})$$

which is formed by dimerization of univalent monomer anions

$$[:\mathrm{CH}(\phi)-\dot{\mathrm{C}}\mathrm{H_2}] \quad \text{or} \quad [\dot{\mathrm{C}}\mathrm{H}(\phi)-\ddot{\mathrm{C}}\mathrm{H_2}]^-$$

being produced through the following process of electron transfer,

$$\text{naphthalene}^- + \text{styrene} \rightarrow \text{naphtharene} + \text{stylene}^-$$

The above situation in the case of polymerization of styrene initiated by the styrene adduct formed through electron transfer which takes place between naphthalene anions and the monomers of styrene will be applied to our cases in which the styrene adducts with sodium metal form the living polymers. Then, the existence of the radical anions will not be detected because dimerization of univalent monomer anions is performed in a very short time in the above process.

On the other hand, two of the present authors found that if the styrene adduct with a high degree of polymerization formed at the first stage of the reaction of styrene with sodium metal reacts with sodium metal still

3) M. Szwarc, M. Levy and R. Milkovich, *J. Am. Chem. Soc.*, **78**, 2656 (1958); M. Szwarc, *Nature*, **178**, 1168 (1956).
4) G. Meshitsuka and Y. Okada, *Chem. High Polymers (Tokyo)*, (*Kobunshi Kagaku*) 14, 33, 37, 123 (1957).

more, the dark red precipitates are formed in the solution of toluene as a result of dissociation of the styrene polymer. These precipitates showed a strong paramagnetic resonance line, of which the line width and $g$-factor were about 2 gauss and 2.002 and the line shape was Lorentzian, and when they were diluted into the tetrahydrofuran, the hyperfine splitting in the paramagnetic resonance spectra was observed as described in the former sections. These spectra were attributed to be coming from monomer anions of styrene or polymer radicals with the low degree of polymerization.

The observations of the paramagnetic resonance of radicals of the aromatic vinyl compounds may be considered to become possible for the following reasons. Under non-existence of the monomer of aromatic vinyl compounds radical anions will exist stably in the polar solvents*, as tetrahydrofuran and dioxane, because they are electrically repulsed by each other in the polar solvent to be obstructed to dimerize.

In the case of the radicals with a high degree of polymerization, it will be difficult to observe their paramagnetic resonance owing to the following two reasons; one of the reasons is that the concentration of radicals in the solution becomes small, and the other is that the motion of such radicals becomes slower than that of monomer radicals or radicals with a low degree of polymerization to extend the linewidth of each components of the hyperfine structure by contribution of the anisotropic hyperfine interaction of the unpaired electron with the protons. Indeed, no paramagnetic resonance of the radicals of a highly polymerized styrene diluted in the tetrahydrofuran was observed and the intensity of the resonance lines which were observed in most of the other samples of the aromatic vinyl compounds, described in the present paper, decreased gradually with time in accordance with the progress of polymerization. In some cases the change of patterns of the paramagnetic resonance spectrum was accompanied by decrease of intensity. As an example of such a change of spectrum we can see clearly the tendency in the case of $p$-methylstyrene as described in the section 3.

In the forthcoming paper, which will describe the results of the paramagnetic resonance of radicals of 1, 1-diphenylethylene, stilbene and 1, 4-diphenylbutadiene, a formulation which describes the process of polymerization will be presented.

* We could not observe paramagnetic resonance of the styrene radicals diluted in the solution of toluene which was a non-polar solvent.

## Summary

Paramagnetic resonance of radicals of the aromatic vinyl compounds in the tetrahydrofuran and dioxane solutions was observed: styrene, $\alpha$-methyl styrene and $p$-methyl styrene. By analyzing the observed spectra the structure of the radicals is discussed. From these results it may be concluded that the reaction of the aromtic vinyl compounds with alkali metal proceeds through two steps; formation of their radical anions, and successive addition of the monomers to this radical anion turning into "living polymers".

The authors wish to express their sincere thanks to Professor Junkichi Itoh of Osaka University for his continuous encouragement and his helpful discussions throughout this work.

*Physics Department (K. M.)*
*Chemistry Department*
*(K. K. and K. H.)*
*Osaka University*
*Nakanoshima, Osaka*

# *Paramagnetic Resonance of Radicals of Some Aromatic Vinyl Compounds. II*

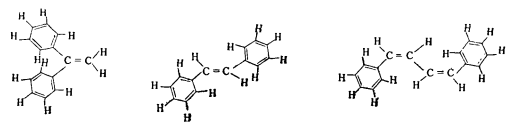
By Kazuo MORIGAKI, Keiji KUWATA and Kozo HIROTA

(Received January 20, 1960)

In the preceding paper[1] the results of the paramagnetic resonance of radicals of styrene, $\alpha$-methylstyrene and *p*-methylstyrene were described. Here the results of the paramagnetic resonance of radicals of 1, 1-diphenylethylene, stilbene and 1, 4-diphenylbutadiene will be described and will be discussed in connection with the problem of the process of the polymerization of these compounds.

## Experimental

The measurements of paramagnetic resonance of the above radicals were performed at room temperature by using the same apparatus as that being described in the preceding paper and the samples were also prepared by the same method as that described in the preceding paper.



1-1 Diphenylethylene Stilbene 1-4 Diphenylbutadiene

Fig. 1.

## Results and Discussion

**1,1-Diphenylethylene (DPE).** — Two spectra have been observed in the 1, 1-diphenylethylene (DPE) radical in the tetrahydrofuran solution with its concentration of $10^{-3}\sim10^{-4}$ M under different conditions of the sample. In the DPE radical produced by method I described in section 2 of the preceding paper, many lines were observed as shown in Fig. 2.

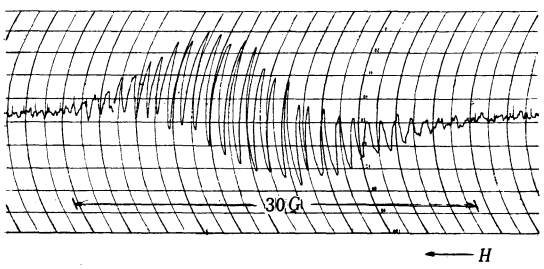



Fig. 2. Paramagnetic resonance spectrum of 1-1 diphenylethylene radical.

We tried to explain the observed spectrum through the following spin Hamiltonian,

$$\mathcal{H}=g\beta \boldsymbol{H}\boldsymbol{S}+\sum_{i=1}^{4} A_o \boldsymbol{I}_{o_i}\boldsymbol{S}+\sum_{i=1}^{4} A_m \boldsymbol{I}_{m_i}\boldsymbol{S} + \sum_{i=1}^{2} A_p \boldsymbol{I}_{p_i}\boldsymbol{S}+\sum_{i=1}^{2} A_\beta \boldsymbol{I}_{\beta_i}\boldsymbol{S} \qquad (1)$$

where the first term describes the Zeeman energy and $\boldsymbol{I}_o$, $\boldsymbol{I}_m$, $\boldsymbol{I}_p$ and $\boldsymbol{I}_\beta$ describe the spin of the proton in the *ortho*-, *meta*-, *para*- and $\beta$ position respectively, and the suffix $i$ given under the spins of the proton $\boldsymbol{I}$ shows a different position in the same site with respect to the symmetry of the molecule. Although the observed spectrum is so complicated that we can not analyze it definitely, the following values of the parameters, $g$, $A_o$, $A_m$, $A_p$ and $A_\beta$, in the above spin Hamiltonian seem to fit best with the observed spectrum: $g=2.002$ $A_p=A_p\sim6$ gauss, $A_m\sim1$ gauss, $A_\beta\sim3$ gauss. However, some ambiguities are left in these values except in the case of $g$. The calculated spectrum is shown in Fig. 3, where several lines at both sides apart from the center are assumed not to be observed owing to their weak intensities. The above analysis indicates that the magnetic center corresponding to the observed spectrum is the unpaired electron in the DPE monomer anion.

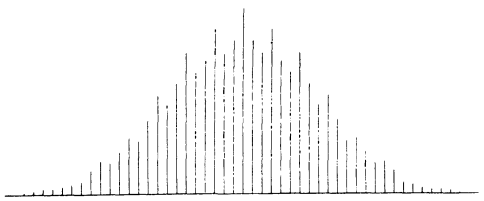


Fig. 3. The calculated spectrum of 1-1 diphenylethylene anion.

According to McConnell[2] the hyperfine splitting constant is proportional to the unpaired electron density on the carbon atom adjacent to the proton in the aromatic hydrocarbon. From the above hyperfine splitting

1) K. Morigaki, K. Kuwata and K. Hirota, This Bulletin, 33, 952 (1960).

2) H. M. McConnell, *J. Chem. Phys.*, **24**, 764 (1956); H. M. McConnell and D. B. Chesnut, ibid., **28**, 107 (1958).

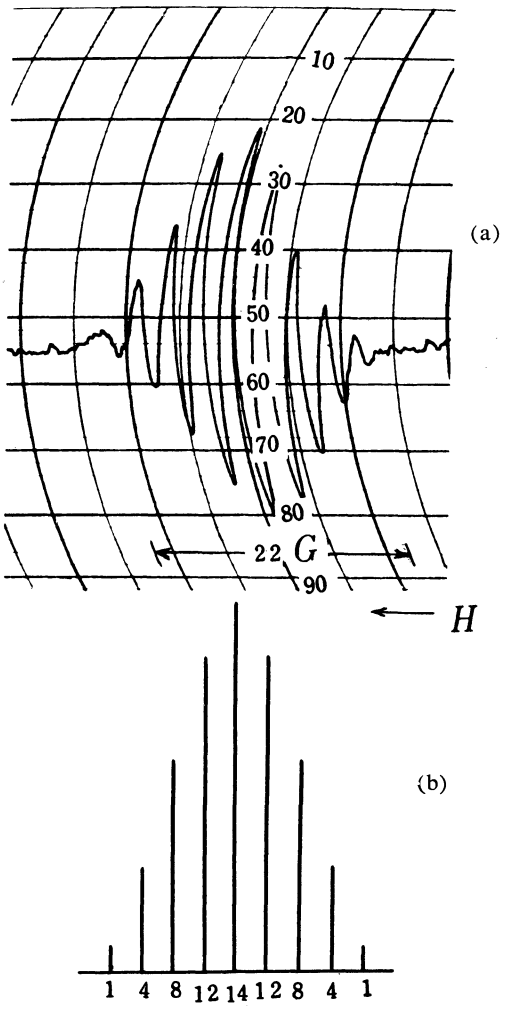



Fig. 4. (a) Paramagnetic resonance spectrum of 1-1 diphenylethylene radical.
(b) The calculated spectrum of 1-1 diphenylethylene radical.

constant in Eq. (1) the unpaired electron densities of the DPE monomer anion at each carbon atom in the aromatic ring can be derived, i. e., they are given in ratio as follows:

$$\rho_o : \rho_p : \rho_m = 6 : 6 : 1$$

where $\rho_o$, $\rho_p$ and $\rho_m$ give the unpaired electron densities on the carbon atom adjacent to the *ortho*-, *para*- and *meta*-hydrogen atom respectively.

On the other hand, the simple LCAO-MO calculation gives the normalized unpaired electron densities the following values,

$$\rho_o = 0.05521, \quad \rho_p = 0.07813, \quad \rho_m = 0.00622$$

or

$$\rho_o : \rho_p : \rho_m = 8.9 : 12 : 1$$

The observed spin densities on the *ortho*- and *para*-carbon atoms are smaller than those expected from the simple LCAO-MO calculation. The normalized unpaired electron density on the $\beta$-carbon atom given by the simple LCAO-MO calculation is given by $\rho_\beta = 0.3856$. In spite of the large value of the electron density on the $\beta$ carbon atom, the observed hyperfine splitting is half as much as that corresponding to the unpaired electron densities on the *para*- and *ortho*- carbon atoms. This means that there is a marked difference between the cases of the $\beta$-proton and the ring proton in the proportionality constants connecting the unpaired electron density to the hyperfine splitting. However, the origin of the small proportionality constant for the hyperfine splitting at the $\beta$-proton has not been found.

Another spectrum, as shown in Fig. 4 (a), was observed in the sample of DPE which has been kept at 110°C for two days after the observation of the first spectrum shown in Fig. 2. The change of the spectrum coming from the heat-treatment of the sample is drastic and is accompanied with that of its color from dark yellow to green. This indicates that the DPE radical was changed into another kind of radical through the heat-treatment. From the following analysis of the observed spectrum the magnetic center corresponding to the second spectrum seems to be identified with the unpaired electron being localized around the end of the anion of the DPE polymer as shown in Fig. 5.

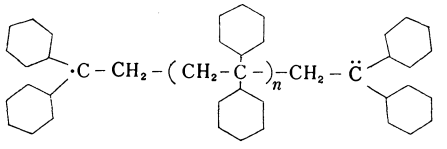


Fig. 5. Structural formula for 1-1 diphenyl polymer anion.

The observed spectrum can be explained by the following spin Hamiltonian,

$$\mathcal{H} = g\beta \boldsymbol{H}\boldsymbol{S} + \sum_{i=1}^{4} A_o \boldsymbol{I}_{oi}\boldsymbol{S} + \sum_{i=1}^{4} A_m \boldsymbol{I}_{mi}\boldsymbol{S} + \sum_{i=1}^{2} A_p \boldsymbol{I}_{pi}\boldsymbol{S} \qquad (2)$$

with $g = 2.0026 \pm 0.0005$, $A_p = 5.4 \pm 0.5$ gauss, $A_o = 2.7 \pm 0.3$ gauss and $A_m \sim 0$ gauss. Although two kinds of hyperfine interaction with four equivalent protons are indistinguishable from each other in the resonance experiment, it is assumed in the above assignment from the theoretical point of view that the hyperfine interaction with the *ortho*-protons will be stronger than that with the *meta*-protons. A pattern of the spectrum is constructed from the above spin Hamiltonian with the parameters given above

as shown in Fig. 4 (b). This spectrum consists of nine lines with relative intensities of 1 : 4 : 8 : 12 : 14 : 12 : 8 : 4 : 1. The relative intensities of each component in the calculated spectrum are in good agreement with the observed ones of 1 : 4 : 8 : 12.5 : 14 : 12.5 : 7.5 : 3.8 : 1. If the line widths of each component are attributed to the unresolved hyperfine interaction due to the four *meta*-protons, the coupling constant $A_m$ is given by the value of about 0.7 gauss.

The above model of the magnetic center is similar to the diphenylmethyl radical concerned with the part on which the unpaired electron is localized. The calculation of the spin densities of the $\pi$-electrons on the carbon atoms in the diphenylmethyl radical performed by using the Pauling-Wheland valence-bond theory shows that the spin densities of the $\pi$-electrons on the *para*-, *ortho*- and *meta*-carbon atoms are given as follows (See Appendix):

$$\rho_p = 0.2790, \quad \rho_o = 0.2732, \quad \rho_m = -0.1483.$$

The spectrum constructed on the basis of the above spin densities, as shown in the appendix, is slightly different from the observed spectrum. The relative spin densities obtained from the above analysis of the observed spectrum are not in agreement with the calculated ones. The actual situation of distribution of the $\pi$-electrons in the DPE polymer radical will not be so simple as the case of diphenylmethyl. Indeed the DPE polymer forms a bending chain, so the two benzene rings in which the unpaired electron is to be localized may not be on the co-plane. However, it has not been clear at the present stage whether the above difference between the observed spectrum and the calculated one shows that the magnetic center corresponding to the observed paramagnetic resonance may not be the unpaired electron in the DPE polymer radical.

**Stilbene.** — A resonance line without any structures was observed in the stilbene radical in tetrahydrofuran solution with its concentration of $10^{-3}\sim10^{-4}$ M (Fig. 6). It has the maximum separation of thirteen gauss in the derivatives of the absorption line and the *g*-factor of 2.002. This result indicates that the hyperfine structure can not be resolved because many protons contribute to the hyperfine splitting. This situation is consistent with the simple LCAO–MO calculation of the unpaired electron density in the stilbene anion. The stilbene radical in tetrahydrofuran with its concentration of $10^{-1}$ M showed a Lorentzian-shaped line with the line width of 1.8 gauss.

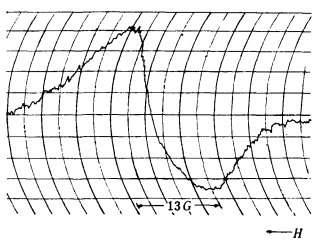



Fig. 6. Paramagnetic resonance spectrum of stylbene radical.

**1,4-Diphenylbutadiene.**—In a sample including the radical of 1,4-diphenylbutadiene prepared by method I, a resonance spectrum with unresolved h. f. s., which extends in the region of the magnetic field of about thirty-four gauss with $g=2.00$, has been observed as shown in Fig. 7. But it has not been investigated in detail.

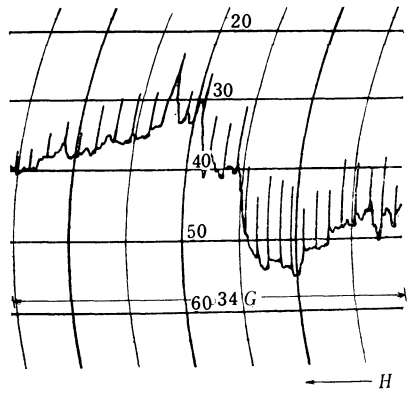



Fig. 7. Paramagnetic resonance spectrum of 1,4-diphenylbutadiene radical.

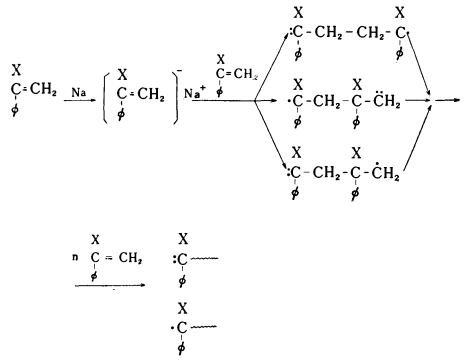
## Discussions on the Process of Polymerization

As described in the preceding paper, the pattern of the paramagnetic resonance spectra of radicals of styrene and *p*-methylstyrene depends sensitively on the degree of polymerization. In the latter substance changes of pattern and intensity of the paramagnetic resonance with time have been clearly observed. In the former samples three kinds of spectra have been observed, according to the conditions of preparation of the radicals. In the preceding paper the situations under which the polymerization of styrene and its derivatives proceeds were discussed by considering the above results.

In the case of DPE radicals, when a renewed reaction of DPE adducts, which had shown many resonance lines, with the sodium metal was performed by keeping the sample at 100°C for two days, another new spectrum was observed, which was considered to be coming from the hyperfine interaction of the unpaired electron being localized around the end molecule of DPE polymer, probably with a

low degree of polymerization, with its protons.

From these results it may be considered that polymerization is initiated through the process in which the monomer of the aromatic vinyl compound forms a bond between itself and the $\alpha$- or $\beta$-carbon atoms of the radical anion to grow into the polymer. This situation can be described in the following formula.



where X means H, $CH_3$ or $\phi(=C_6H_5)$.

The process of polymerization of the aromatic vinyl compounds has been studied through the optical absorption spectroscopy[3]. In order to confirm the above model of the process of polymerization, further experiments will be necessary.

## Summary

Paramagnetic resonance absorption of the radicals of 1, 1-diphenylethylene, stilbene and 1, 4-diphenylbutadiene in tetrahydrofuran solution was investigated at room temperature. In diphenylethylene (DPE) radicals two kinds of spectra were observed corresponding to two states of the radicals; one is the DPE monomer anion and the other the DPE polymer anion. In connection with the experimental results in the case of styrene, $\alpha$-methylstyrene and *p*-methylstyrene described in the preceding paper, the process of polymerization of some aromatic vinyl compounds was discussed.

The authors wish to express their sincere thanks to Professor Junkichi Itoh of Osaka University for his continuous encouragement and his helpful discussions throughout this work.

*Physics Department (K. M.)*
*Chemistry Department*
*(K. K. and K. H.)*
*Osaka University*
*Nakanoshima, Osaka*

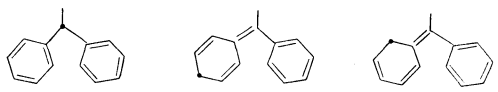
3) K. Hirota, K. Kuwata, H. Togawa and S. Ishida, *J. Chem. Soc. Japan, Pure Chem. Sec. (Nippon Kagaku Zasshi)*, **79**, 602 (1958); K. Kuwata, to be published in This Bulletin.

## Appendix

### Spin Densities in the Diphenylmethyl Radical

Spin densities of $\pi$-electrons on carbon atoms in the diphenylmethyl radical are calculated by using valence-bond theory. Valence-bond theory has been so far applied also to calculations of spin densities on carbon atoms in the triphenylmethyl radical by Brovetto and Ferroni[4] and in the perinaphthenyl radical by McConnell and Dearman[5] in good agreements with the experimental results. Therefore, valencebond theory is adequate to calculate the spin densities of $\pi$-electrons in these odd-alternant hydrocarbon radicals.

Valence-bond structures for calculation of the spin densities of $\pi$-electrons on carbon atoms in the diphenylmethyl radical can be divided into three groups shown in Fig. 8. To these three groups belong the 4, 4, 8 independent wave functions for the unpaired electron on the methylic carbon atom, and the *para*- and the *ortho*-carbon atoms of the benzene ring respectively. All functions related to Dewar structures will be neglected.



$\varphi_1$ $\varphi_2$ $\varphi_3$

Fig. 8.

With a linear combination for the $\varphi_{ik}$ the wave function $\Psi$ in the ground state can be constructed in such a way as to minimize the total energy of electrons. Then, $\Psi$ is given by the following equation,

$$\Psi = \sum_i C_i \sum_k \varphi_{ik} \qquad \text{(A1)}$$

The total Hamiltonian fo the $\pi$-electrons under the existence of the external magnetic field is:

$$\mathcal{H} = \mathcal{H}_0 + \mathcal{H}_1 + \mathcal{H}_2 \qquad \text{(A2)}$$
$$\mathcal{H}_1 = g\beta \boldsymbol{HS}$$
$$\mathcal{H}_2 = -(8\pi/3) g\beta g_N \beta_N \sum_k \boldsymbol{I}_k \boldsymbol{S} \delta(\boldsymbol{r}_e - \boldsymbol{r}_k)$$

where $\mathcal{H}_0$ means the kinetic energy and the Coulomb potential energy of the electrons; $\mathcal{H}_1$ is Zeeman energy in which the external magnetic field and the electronic spin are described by $\boldsymbol{H}$ and $\boldsymbol{S}$ respectively, $\mathcal{H}_2$ is the hyperfine interaction energy coming from the Fermi type contact hyperfine interaction between the electron and the $k$th-proton with

4) P. Brovetto and S. Ferroni, *Nuovo Cimento*, **5**, 142 (1957).

5) H. M. McConnell and H. H. Dearman, *J. Chem. Phys.*, **28**, 51 (1958).

the nuclear spin $I_k$, $\beta$ and $\beta_N$ are the electronic and nuclear Bohr magnetrons respectively, and $g$ and $g_N$ are the electronic and nuclear $g$-factors and $\delta(\boldsymbol{r}_e-\boldsymbol{r}_k)$ means the Dirac delta function for the distance between the electron and the $k$th-proton. In the above Hamiltonian the dipolar interaction between the electron and the proton is neglected, because it is averaged out not to contribute to the paramagnetic resonance spectrum by a tumbling motion of the molecule in the solution.

After some computations the minimum energy $W$ of the Hamiltonian $\mathcal{H}_0$ is given in the following equation,

$$W=Q+4.7046\alpha \qquad \text{(A3)}$$

where $Q$ means the Coulomb integral and $\alpha$ the single exchange integral.

Corresponding to the state with the minimum energy, the wave function in the ground state is given as follows:

$$\Psi=0.1572\varphi_1+0.1341\varphi_2+0.1312\varphi_3 \qquad \text{(A4)}$$

The matrix element of the hyperfine interaction $\mathcal{H}_2$ is calculated by using the Brovetto-Ferroni method as applied to triphenylmethyl. By using Eq. (A1) the matrix element $\langle\Psi|\mathcal{H}_2|\Psi\rangle$ is given in the following equation,

$$\langle\Psi|\mathcal{H}_2|\Psi\rangle=\sum_{ij} c_i c_j \sum_{kl}\langle\varphi_{ik}|\mathcal{H}_2|\varphi_{il}\rangle \qquad \text{(A5)}$$

The matrix elements $\langle\varphi_{ik}|\mathcal{H}_2|\varphi_{il}\rangle$ can be calculated in a similar way to the case of triphenylmethyl.

$$\langle\Psi|\mathcal{H}_2|\Psi\rangle=-(8\pi/3)g\beta g_N\beta_N A \times[0.2790I_{zp}-0.1483I_{zm}+0.2732I_{zo}]\cdot S_z \qquad \text{(A6)}$$

where $I_{zp}$, $I_{zm}$ and $I_{zo}$ mean the component along the external magnetic field of the total spin of the protons in the *para*, *ortho* and *meta* position of the benzene ring respectively, and $A$ is the factor which depends on the strength of the $\sigma-\pi$ interaction.

The magnetic field $H$ corresponding to the transition $\Delta S_z=\pm1$, $\Delta I_z=0$ in the experiment using the microwave with the frequency $\nu$ is given by the following equation

$$H=h\nu/g\beta+(8\pi/3)g_N\beta_N A \times[0.2790I_{zp}-0.1483I_{zm}+0.2732I_{zo}] \qquad \text{(A7)}$$

Then, the paramagnetic resonance spectrum can be constructed by Eq. (A7) as shown in Fig. 9, where only the upper part of the spectrum corresponding to the value of $H$ larger than $h\nu/g\beta$ is given, because the spectrum is symmetrical with respect to the value of the magnetic field $H=h\nu/g\beta$.

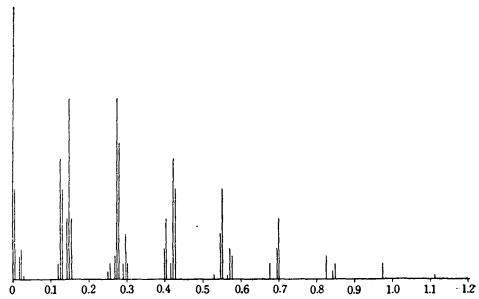



Fig. 9. The calculated spectrum of diphenylmethyl radical.

A comparison of the above calculated spectrum with the observed one in the DPE radical shows some differences as shown in Fig. 9. Though the observed spectrum consists of nine lines, more lines should be expected from the results of the calculation. Especially, the fifth line from the central one, which has about half the intensity in comparison with the fourth line in the calculated spectrum, should be observed from the experimental condition of our spectrometer. The origin of the above differences between the theoretical spectrum and experimental one is discussed in the text.

# *A Further Study of Simple LCAO MO Perturbation Treatment of Conjugated Molecules*

By Kenichi FUKUI, Keiji MOROKUMA, Teijiro YONEZAWA and Chikayoshi NAGATA

(Received December 19, 1959)

The perturbation theory in the simple LCAO MO method has been studied by many authors, for instance, by Coulson and Longuet-Higgins[1] and by Dewar[2]. Recently, by the present authors[3], a new mathematical method of perturbation theory, named the method of perturbed secular determinant, has been developed and several useful equations have been derived which give the orbital energy, the electron density and the bond order of the perturbed system.

The only system involved in these works, however, was the one which suffered only one perturbation, that is, a small change of a Coulomb integral or of a resonance integral, or a weak bonding to another system. There could be seen no systematic perturbation treatment of the system which was affected by two or more perturbations, for instance, changes of two Coulomb integrals, changes of a Coulomb integral and of a resonance integral, and a weak bonding with a change of a Coulomb integral. To deal with such a system would be of practical interest in discussing the chemical reactivity, absorption spectrum, dipole moment and other electronic properties of large conjugated molecules.

In the present paper are derived several equations or relations which give the molecular orbital, its orbital energy, the electron density and the bond order of systems affected by two perturbations, and lastly they are extended to a more general case of many perturbations.

## Non-degenerate System

**1. Summary of Results for Single Perturbation.**—In order to simplify the expression of various equations appearing in the treatment of multiple-perturbed systems, it would be convenient to summarize the results for single perturbation. The following formulae, obtained by the method of perturbed secular determinant and also by the existing method of perturbation, were given in the previous paper, though some of them not explicitly.

In this section it is assumed that the system to be treated is not degenerate in itself, nor has it any degenerate level between another system to conjugate with.

First, if the Coulomb integral, $\alpha_r$, of the $r$th atom in a conjugated system, $\Delta(\varepsilon)$,* is increased by $\alpha_r'$ (Case A of Ref. 3), then, as its consequence, the $j$th orbital energy, $\varepsilon_j$, will increase by $(\delta\varepsilon_j)_r$, the separate bond order, $p_{uv}{}^j$, by $(\delta p_{uv}{}^j)_r$, the separate electron density, $p_{uu}{}^j$, by $(\delta p_{uu}{}^j)_r$, the total $\pi$ electronic energy, $\varepsilon$, by $(\delta\varepsilon)_r$, the bond order, $p_{uv}$, by $(\delta p_{uv})_r$, the electron density, $p_{uu}$, by $(\delta p_{uu})_r$ and the $j$th molecular orbital, $\Psi_j$, by $(\delta\Psi_j)_r$, in such a way that**

$$(\delta\varepsilon_j)_r=(c_r{}^j)^2\alpha_r'+\sum_{k(\neq j)}^{\text{all}}\frac{(c_r{}^jc_r{}^k)^2}{\varepsilon_j-\varepsilon_k}(\alpha_r')^2+\cdots\cdots \tag{1}$$

$$\begin{aligned}(\delta p_{uv}{}^j)_r=&\sum_{k(\neq j)}^{\text{all}}\frac{c_r{}^jc_r{}^k(c_u{}^jc_v{}^k+c_v{}^jc_u{}^k)}{\varepsilon_j-\varepsilon_k}\alpha_r'\\&+\sum_{k(\neq j)}^{\text{all}}\frac{c_r{}^jc_r{}^k}{\varepsilon_j-\varepsilon_k}\left[\sum_{m(\neq j)}^{\text{all}}\frac{c_r{}^m\{c_r{}^jc_u{}^kc_v{}^m+c_r{}^m(c_u{}^jc_v{}^k+c_v{}^jc_u{}^k)\}}{\varepsilon_j-\varepsilon_m}\right.\\&\left.-\frac{c_r{}^j\{c_r{}^kc_u{}^jc_v{}^j+c_r{}^j(c_u{}^jc_v{}^k+c_v{}^jc_u{}^k)\}}{\varepsilon_j-\varepsilon_k}\right](\alpha_r')^2+\cdots\cdots\qquad(u=v\text{ or }u\neq v)\end{aligned} \tag{2}$$

1) C. A. Coulson and H. C. Longuet-Higgins, *Proc. Roy. Soc. (London)*, **A191**, 39 (1947); **A192**, 16 (1947): **A193**, 447, 456 (1948); **A195**, 188 (1948).
2) M. J. S. Dewar, *J. Am. Chem. Soc.*, **74**, 3341 (1952).
3) K. Fukui, C. Nagata, T. Yonezawa, H. Kato and K. Morokuma, *J. Chem. Phys.*, **31**, 287 (1959).

* $\Delta(\varepsilon)$ is the secular determinant of the system and will be used also to characterize a conjugated system.

** As for the nomenclature, see Ref. 3. Electron density will be looked upon as a special case ($u=v$) of bond order in the further discussion.

$$(\delta\varepsilon)_r = p_{rr}\alpha_r' + 2\sum_j^{\text{occ}}\sum_k^{\text{unocc}} \frac{(c_r{}^j c_r{}^k)^2}{\varepsilon_j - \varepsilon_k}(\alpha_r')^2 + \cdots\cdots \tag{3}$$

$$(\delta p_{uv})_r = 2\sum_j^{\text{occ}}\sum_k^{\text{unocc}} \frac{c_r{}^j c^{\ k}(c_u{}^j c_v{}^k + c_v{}^j c_u{}^k)}{\varepsilon_j - \varepsilon_k}\alpha_r' + 2\sum_j^{\text{occ}}\{\text{the second order term in}(\delta p_{uv}{}^j)_r\} + \cdots\cdots \quad (u=v \text{ or } u\neq v) \tag{4}$$

$$(\delta\Psi_j)_r = \sum_{k(\neq j)}^{\text{all}} \frac{c_r{}^j c_r{}^k}{\varepsilon_j - \varepsilon_k}\alpha_r'\Psi_k - \frac{1}{2}\left\{\sum_{k(\neq j)}^{\text{all}} \frac{(c_r{}^j c_r{}^k)^2}{(\varepsilon_j - \varepsilon_k)^2}\right\}(\alpha_r')^2\Psi_j + \sum_{k(\neq j)}^{\text{all}} \frac{c_r{}^j c_r{}^k}{\varepsilon_j - \varepsilon_m}\left\{\sum_{m(\neq j)}^{\text{all}} \frac{(c_r{}^m)^2}{\varepsilon_j - \varepsilon_m} - \frac{(c_r{}^j)^2}{\varepsilon_j - \varepsilon_k}\right\}(\alpha_r')^2\Psi_k + \cdots\cdots \tag{5}$$

Secondly, when the resonance integral, $\beta_{st}$, of the bond $(st)$ in the system $\Delta(\varepsilon)$ is increased by $\beta_{st}'$ (Case B of Ref. 3), increases of those quantities are written as follows:

$$(\delta\varepsilon_j)_{st} = 2c_s{}^j c_t{}^j\beta_{st}' + \sum_{k(\neq j)}^{\text{all}} \frac{(c_s{}^j c_t{}^k + c_t{}^j c_s{}^k)^2}{\varepsilon_j - \varepsilon_k}(\beta_{st}')^2 + \cdots\cdots \tag{6}$$

$$(\delta p_{uv}{}^j)_{st} = \sum_{k(\neq j)}^{\text{all}} \frac{(c_s{}^j c_t{}^k + c_t{}^j c_s{}^k)(c_u{}^j c_v{}^k + c_v{}^j c_u{}^k)}{\varepsilon_j - \varepsilon_k}\beta_{st}' + \sum_{k(\neq j)}^{\text{all}} \frac{(c_s{}^j c_t{}^k + c_t{}^j c_s{}^k)}{\varepsilon_j - \varepsilon_k}\left\{\sum_{m(\neq j)}^{\text{all}} \frac{(c_s{}^j c_t{}^m + c_t{}^j c_s{}^m)c_u{}^k c_v{}^m + (c_s{}^k c_t{}^m + c_t{}^k c_s{}^m)(c_u{}^j c_v{}^m + c_v{}^j c_u{}^m)}{\varepsilon_j - \varepsilon_m} - \frac{(c_s{}^j c_t{}^k + c_t{}^j c_s{}^k)c_u{}^j c_v{}^j + 2c_s{}^j c_t{}^j(c_u{}^j c_v{}^k + c_v{}^j c_u{}^k)}{\varepsilon_j - \varepsilon_k}\right\}(\beta_{st}')^2 + \cdots\cdots \quad (u=v \text{ or } u\neq v) \tag{7}$$

$$(\delta\varepsilon)_{st} = 2p_{st}\beta_{st}' + 2\sum_j^{\text{occ}}\sum_k^{\text{unocc}} \frac{(c_s{}^j c_t{}^k + c_t{}^j c_s{}^k)^2}{\varepsilon_j - \varepsilon_k}(\beta_{st}')^2 + \cdots\cdots \tag{8}$$

$$(\delta p_{uv})_{st} = 2\sum_j^{\text{occ}}\sum_k^{\text{unocc}} \frac{(c_s{}^j c_t{}^k + c_t{}^j c_s{}^k)(c_u{}^j c_v{}^k + c_v{}^j c_u{}^k)}{\varepsilon_j - \varepsilon_k}\beta_{st}' + 2\sum_j^{\text{occ}}\{\text{the second order term in}(\delta p_{uv}{}^j)_{st}\} + \cdots\cdots \quad (u=v \text{ or } u\neq v) \tag{9}$$

$$(\delta\Psi_j)_{st} = \sum_{k(\neq j)}^{\text{all}} \frac{(c_s{}^j c_t{}^k + c_t{}^j c_s{}^k)}{\varepsilon_j - \varepsilon_k}\beta_{st}'\Psi_k - \frac{1}{2}\sum_{k(\neq j)}^{\text{all}} \frac{(c_s{}^j c_t{}^k + c_t{}^j c_s{}^k)^2}{(\varepsilon_j - \varepsilon_k)^2}(\beta_{st}')^2\Psi_j + \sum_{k(\neq j)}^{\text{all}} \frac{c_s{}^j c_t{}^k + c_t{}^j c_s{}^k}{\varepsilon_j - \varepsilon_k}\left\{\sum_{m(\neq j)}^{\text{all}} \frac{c_s{}^k c_t{}^m + c_t{}^k c_s{}^m}{\varepsilon_j - \varepsilon_m} - \frac{2c_s{}^j c_t{}^j}{\varepsilon_j - \varepsilon_k}\right\}\Big](\beta_{st}')^2\Psi_k + \cdots\cdots \tag{10}$$

Thirdly, when a conjugated system, $\Delta(\varepsilon)$, conjugates at the $r$th atom through a weak bonding, whose resonance integral is $\gamma_r$, with another conjugated system, whose secular determinant is $\Delta_1(\varepsilon)$, (Case C of Ref. 3), then the increases of molecular quantities by this perturbation are given by the following formulae. The orbital energy of the $k$th orbital $\phi_{1k}$ of the system $\Delta_1(\varepsilon)$ is $\eta_{1k}$ and the coefficient of the $\xi$th atomic orbital in that molecular orbital is written as $d_\xi{}^{1k}$.

$$(\delta\varepsilon_j)_{r\xi} = \sum_k^{\text{all}} \frac{(c_r{}^j d_\xi{}^{1k})^2}{\varepsilon_j - \eta_{1k}}(\gamma_r)^2 + \left\{\sum_k^{\text{all}} \frac{(c_r{}^j d_\xi{}^{1k})^2}{\varepsilon_j - \eta_{1k}}\right\}\left[\sum_k^{\text{all}} \frac{(d_\xi{}^{1k})^2}{\varepsilon_j - \eta_{1k}}\left\{\sum_{m(\neq j)}^{\text{all}} \frac{(c_r{}^m)^2}{\varepsilon_j - \varepsilon_m} - \frac{(c_r{}^j)^2}{\varepsilon_j - \eta_{1k}}\right\}\right](\gamma_r)^4 + \cdots\cdots \tag{11}$$

$$(\delta p_{uv}{}^j)_{r\xi} = \sum_k^{\text{all}} \frac{c_r{}^j d_\xi{}^{1k}}{\varepsilon_j - \eta_{1k}}\left\{\sum_{m(\neq j)}^{\text{all}} \frac{c_r{}^m d_\xi{}^{1k}(c_u{}^j c_v{}^m + c_v{}^j c_u{}^m)}{\varepsilon_j - \varepsilon_m} - \frac{c_r{}^j d_\xi{}^{1k} c_u{}^j c_v{}^j}{\varepsilon_j - \eta_{1k}}\right\}(\gamma_r)^2 + \cdots\cdots \quad (u=v \text{ or } u\neq v) \tag{12}$$

$$(\delta p_{r\xi}{}^j)_{r\xi} = \sum_k^{\text{all}} \frac{(c_r{}^j d_\xi{}^{1k})^2}{\varepsilon_j - \eta_{1k}}\gamma_r + 2\sum_k^{\text{all}}\sum_n^{\text{all}} \frac{(c_r{}^j d_\xi{}^{1k} d_\xi{}^{1n})^2}{(\varepsilon_j - \eta_{1k})(\varepsilon_j - \eta_{1n})}\left\{\sum_{m(\neq j)}^{\text{all}} \frac{(c_r{}^m)^2}{\varepsilon_j - \varepsilon_m} - \frac{(c_r{}^j)^2}{\varepsilon_j - \eta_{1k}}\right\}(\gamma_r)^3 + \cdots \tag{12'}$$

$$(\delta p_{uv}{}^{1k})_{r\xi} = \sum_j^{\text{all}}\sum_m^{\text{all}} \frac{c_r{}^j c_r{}^m (d_\xi{}^{1k})^2 c_u{}^j c_v{}^m}{(\eta_{1k} - \varepsilon_j)(\eta_{1k} - \varepsilon_m)}(\gamma_r)^2 + \cdots\cdots \quad (u=v \text{ or } u\neq v) \tag{13}$$

$$(\delta\Psi_j)_{r\xi}=\sum_k^{\text{all}}\frac{c_r{}^j d_\xi{}^{1k}}{\varepsilon_j-\eta_{1k}}\gamma_r\psi_k-\frac{1}{2}\sum_k^{\text{all}}\frac{(c_r{}^j d_\xi{}^{1k})^2}{(\varepsilon_j-\eta_{1k})^2}(\gamma_r)^2\Psi_j+\sum_{m(\neq j)}^{\text{all}}\frac{c_r{}^j c_r{}^m}{\varepsilon_j-\varepsilon_m}\sum_k^{\text{all}}\frac{(d_\xi{}^{1k})^2}{\varepsilon_j-\eta_{1k}}(\gamma_r)^2\Psi_m+\cdots\cdots \quad (14)$$

where the atom $u$ and the bond $(uv)$ are in the system $\Delta(\varepsilon)$, and $\xi$ is the position of weak conjugation in the system $\Delta_1(\varepsilon)$. Similar formulae would be obtained for the system $\Delta_1(\varepsilon)$. Thus the change of bond order and that of electron density and total $\pi$ electronic energy change of the combined system are obtained as follows:

$$\begin{aligned}(\delta\varepsilon)_{r\xi}&=2\sum_j^{\text{occ}}(\delta\varepsilon_j)_{r\xi}+2\sum_k^{\text{occ}}(\delta\eta_{1k})_{r\xi}\\&=2\Big(\sum_j^{\text{occ}}\sum_k^{\text{unocc}}-\sum_j^{\text{unocc}}\sum_k^{\text{occ}}\Big)\frac{(c_r{}^j d_\xi{}^{1k})^2}{\varepsilon_j-\eta_{1k}}(\gamma_r)^2+2\sum_j^{\text{occ}}\{\text{the fourth order term in}(\delta\varepsilon_j)_{r\xi}\}\\&\quad+2\sum_k^{\text{occ}}\{\text{the fourth order term in}(\delta\eta_{1k})_{r\xi}\}+\cdots\cdots\end{aligned} \quad (15)$$

$$\begin{aligned}(\delta p_{uv})_{r\xi}&=2\sum_j^{\text{occ}}(\delta p_{uv}{}^j)_{r\xi}+2\sum_k^{\text{occ}}(\delta p_{uv}{}^{1k})_{r\xi}\\&=2\Big(\sum_k^{\text{occ}}\sum_j^{\text{unocc}}-\sum_k^{\text{unocc}}\sum_j^{\text{occ}}\Big)\Big[\frac{(d_\xi{}^{1k})^2}{\varepsilon_j-\eta_{1k}}\Big\{\frac{(c_r{}^j)^2c_u{}^jc_v{}^j}{\varepsilon_j-\eta_{1k}}\\&\quad-\sum_{m(\neq j)}^{\text{all}}\frac{c_r{}^jc_r{}^m(c_u{}^jc_v{}^m+c_v{}^jc_u{}^m)}{\varepsilon_j-\varepsilon_m}\Big\}\Big](\gamma_r)^2+\cdots\cdots\end{aligned} \quad (u=v \text{ or } u\neq v) \quad (16)$$

$$(\delta p_{r\xi})_{r\xi}=2\Big(\sum_j^{\text{occ}}\sum_k^{\text{unocc}}-\sum_j^{\text{unocc}}\sum_k^{\text{occ}}\Big)\frac{(c_r{}^j d_\xi{}^{1k})^2}{\varepsilon_j-\eta_{1k}}\gamma_r+2\sum_j^{\text{occ}}\{\text{the third order term in}(\delta p_{r\xi}{}^j)_{r\xi}\}$$

$$+2\sum_k^{\text{occ}}\{\text{the third order term in}(\delta p_{r\xi}{}^{1k})_{r\xi}\}+\cdots\cdots \quad (16')$$

Here it was assumed that the highest occupied orbitals of the systems $\Delta(\varepsilon)$ and $\Delta_1(\varepsilon)$ are lower than the lowest unoccupied orbitals of the systems $\Delta_1(\varepsilon)$ and $\Delta(\varepsilon)$, respectively. The total charge transfer, $\delta Q$, from the system $\Delta_1(\varepsilon)$ to the system $\Delta(\varepsilon)$ is defined by

$$\delta Q=\sum_{u=1}^{n}\delta p_{uu} \quad (17)$$

where $n$ is the number of atomic orbitals in the system $\Delta(\varepsilon)$.

For this case $\delta Q$ is given by the following equation.

$$(\delta Q)_{r\xi}=2\Big(\sum_k^{\text{occ}}\sum_j^{\text{unocc}}-\sum_k^{\text{unocc}}\sum_j^{\text{occ}}\Big)\frac{(c_r{}^j d_\xi{}^{1k})^2}{(\varepsilon_j-\eta_{1k})^2}(\gamma_r)^2+\cdots\cdots \quad (18)$$

As a special case involved in the Case C, when the system $\Delta_1(\varepsilon)$ is an atom or a mesomeric group, X, Eqs. 11 to 16 and 18 become

$$(\delta\varepsilon_j)_{rX}=\frac{(c_r{}^j)^2}{\varepsilon_j-\alpha_X}(\gamma_r)^2+\frac{(c_r{}^j)^2}{\varepsilon_j-\alpha_X}\Big\{-\frac{(c_r{}^j)^2}{(\varepsilon_j-\alpha_X)^2}+\sum_{m(\neq j)}^{\text{all}}\frac{(c_r{}^m)^2}{(\varepsilon_j-\alpha_X)(\varepsilon_j-\varepsilon_m)}\Big\}(\gamma_r)^4+\cdots\cdots \quad (11\text{-a})$$

$$(\delta\alpha_X)_{rX}=\sum_j^{\text{all}}\frac{(c_r{}^j)^2}{\alpha_X-\varepsilon_j}(\gamma_r)^2+\Big\{\sum_j^{\text{all}}\frac{(c_r{}^j)^2}{\alpha_X-\varepsilon_j}\Big\}\Big\{-\sum_j^{\text{all}}\frac{(c_r{}^j)^2}{(\alpha_X-\varepsilon_j)^2}\Big\}(\gamma_r)^4+\cdots\cdots \quad (11\text{-b})$$

$$(\delta p_{uv}{}^j)_{rX}=\Big\{\sum_{m(\neq j)}^{\text{all}}\frac{c_r{}^jc_r{}^m(c_u{}^jc_v{}^m+c_v{}^jc_u{}^m)}{(\varepsilon_j-\varepsilon_m)(\varepsilon_j-\alpha_X)}-\frac{(c_r{}^j)^2c_u{}^jc_v{}^j}{(\varepsilon_j-\alpha_X)^2}\Big\}(\gamma_r)^2+\cdots\cdots \quad (12\text{-a})$$

$$(\delta p_{rX}{}^j)_{rX}=\frac{(c_r{}^j)^2}{\varepsilon_j-\alpha_X}\gamma_r+\frac{2(c_r{}^j)^2}{(\varepsilon_j-\alpha_X)^2}\Big\{\sum_{m(\neq j)}^{\text{all}}\frac{(c_r{}^m)^2}{\varepsilon_j-\varepsilon_m}-\frac{(c_r{}^j)^2}{\varepsilon_j-\alpha_X}\Big\}(\gamma_r)^3+\cdots\cdots \quad (12'\text{-a})$$

$$(\delta p_{uv}{}^X)_{rX}=\Big\{\sum_j^{\text{all}}\sum_m^{\text{all}}\frac{c_r{}^jc_r{}^mc_u{}^jc_v{}^m}{(\varepsilon_j-\alpha_X)(\varepsilon_m-\alpha_X)}\Big\}(\gamma_r)^2+\cdots \quad (13\text{-a})$$

$$(\delta p_{rX}{}^X)_{rX}=\sum_j^{\text{all}}\frac{(c_r{}^j)^2}{\alpha_X-\varepsilon_j}\gamma_r-2\Big\{\sum_j^{\text{all}}\sum_m^{\text{all}}\frac{(c_r{}^jc_r{}^m)^2}{(\alpha_X-\varepsilon_j)^2(\alpha_X-\varepsilon_m)}\Big\}(\gamma_r)^3+\cdots\cdots \quad (13'\text{-a})$$

$$(\delta p_{XX}{}^{j})_{rX}=\frac{(c_r{}^{j})^2}{(\varepsilon_j-\alpha_X)^2}(\gamma_r)^2+\cdots\cdots \tag{12-b}$$

$$(\delta p_{XX}{}^{X})_{rX}=-\sum_{j}^{\text{all}}\frac{(c_r{}^{j})^2}{(\alpha_X-\varepsilon_j)^2}(\gamma_r)^2+\cdots\cdots \tag{13-b}$$

$$(\delta p_{uv})_{rX}=(\nu\sum_{j}^{\text{all}}-2\sum_{j}^{\text{occ}})\left\{\frac{(c_r{}^{j})^2c_u{}^{j}c_v{}^{j}}{(\varepsilon_j-\alpha_X)^2}+\sum_{m(\neq j)}^{\text{all}}\frac{c_r{}^{j}c_r{}^{m}(c_u{}^{j}c_v{}^{m}+c_v{}^{j}c_u{}^{m})}{(\alpha_X-\varepsilon_j)(\varepsilon_j-\varepsilon_m)}\right\}(\gamma_r)^2+\cdots\cdots \tag{16-a}$$

$$(\delta p_{XX})_{rX}=(2\sum_{j}^{\text{occ}}-\nu\sum_{j}^{\text{all}})\frac{(c_v{}^{j})^2}{(\alpha_X-\varepsilon_j)^2}(\gamma_r)^2+\cdots\cdots \tag{16-b}$$

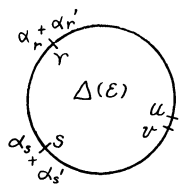
$$(\delta p_{rX})_{rX}=(2\sum_{j}^{\text{occ}}-\nu\sum_{j}^{\text{all}})\frac{(c_r{}^{j})^2}{\varepsilon_j-\alpha_X}\gamma_r+2\sum_{j}^{\text{occ}}\{\text{the third order term in}(\delta p_{rX}{}^{j})_{rX}\}$$
$$+\nu\{\text{the third order term in}(\delta p_{rX}{}^{X})_{rX}\}+\cdots\cdots \tag{16'-a}$$

$$(\delta Q)_{rX}=(\nu\sum_{j}^{\text{all}}-2\sum_{j}^{\text{occ}})\frac{(c_r{}^{j})^2}{(\alpha_X-\varepsilon_j)^2}(\gamma_r)^2+\cdots\cdots \tag{18-a}$$

where $\nu$ is the number of electrons in the atom X. The equations corresponding to Eqs. 14 and 15 are omitted for simplicity.

In the following paragraphs some important cases of doubly perturbed systems will be treated.

**2. Case I. Changes of Two Coulomb Integrals.**—If two atoms, say the $r$th and the $s$th atoms, in a conjugated molecule, $\Delta(\varepsilon)$, are replaced by two heteroatoms, the Coulomb integrals of these atoms will become $\alpha_r+\alpha_r'$ and $\alpha_s+\alpha_s'$, respectively. Then the perturbed secular determinant of the system will be written




$$D(\varepsilon)=\Delta(\varepsilon)+\alpha_r'\Delta_{rr}(\varepsilon)+\alpha_s'\Delta_{ss}(\varepsilon)+\alpha_r'\alpha_s'\Delta_{rrss}(\varepsilon) \tag{19}$$

where $\Delta_{rr}(\varepsilon)$ and $\Delta_{rrss}(\varepsilon)$ are the $(rr)$ minor and the $(rr, ss)$ minor of $\Delta(\varepsilon)$, respectively. Regarding these changes, $\alpha_r'$ and $\alpha_s'$, as perturbations, one can easily obtain the perturbed orbital energy, of the $j$th molecular orbital, the perturbed bond order and the perturbed electron density by the use of the method of perturbed secular determinant, as will be briefly explained in the following.

First if one intermediately considers a system where $\alpha_s'$ is zero, the intermediate perturbed secular determinant is given as:

$$\square(\varepsilon)=\Delta(\varepsilon)+\alpha_r'\Delta_{rr}(\varepsilon) \tag{20}$$

According to the procedure utilized in the previous paper, the intermediate perturbed orbital energy, $\tilde{\varepsilon}_j$, and the intermediate perturbed separate bond order, $\tilde{p}_{uv}{}^{j}$, are expanded in powers of $\alpha_r'$:

$$\left.\begin{aligned}\tilde{\varepsilon}_j&=\sum_{m=0}^{\infty}a_r{}^{j(m)}(\alpha_r')^m\\ \tilde{p}_{uv}{}^{j}&=\sum_{m=0}^{\infty}a_{r,uv}{}^{j(m)}(\alpha_r')^m\end{aligned}\right\} \tag{21}$$

and the coefficients, $a_r{}^{j(m)}$ and $a_{r,uv}{}^{j(m)}$, are given by the following formulae.

$$\left.\begin{aligned}a_r{}^{j(m)}&=\frac{(-1)^m}{m!}\left[\frac{\mathrm{d}^m}{\mathrm{d}z^m}\frac{z\{\Delta_{rr}(z)\}^{m-1}\{\Delta'(z)\Delta_{rr}(z)-\Delta(z)\Delta_{rr}'(z)\}}{\{\Delta(z)/(z-\varepsilon_j)\}^{m+1}}\right]_{z=\varepsilon_j}\\ &\qquad(m=0,1,2,\cdots\cdots)\\ a_{r,uv}{}^{j(m)}&=\frac{(-1)^{m+1}}{m!}\left[\frac{\mathrm{d}^m}{\mathrm{d}z^m}\frac{\{\Delta_{rr}(z)\}^m\Delta_{ur}(z)\Delta_{rv}(z)}{\{\Delta(z)/(z-\varepsilon_j)\}^{m+1}}\right]_{z=\varepsilon_j}\\ &\qquad(m=0,1,2,\cdots\cdots)\end{aligned}\right\} \tag{22}$$

Directly from these formulae the following expressions are obtained

$$\left.\begin{aligned}\tilde{\varepsilon}_j &= \varepsilon_j + (\delta\varepsilon_j)_r \\ \tilde{p}_{uv}{}^j &= p_{uv}{}^j + (\delta p_{uv}{}^j)_r\end{aligned}\right\} \tag{23}$$

where $(\delta\varepsilon_j)_r$ and $(\delta p_{uv}{}^j)_r$ are given by Eqs. 1 and 2.

Then the second perturbation, $\alpha_s'$, is to be taken into account. The perturbed secular determinant of the system in question is expressed with the aid of the secular determinant of the intermediate system,

$$D(\varepsilon) = \square(\varepsilon) + \alpha_s' \square_{ss}(\varepsilon) \tag{24}$$

A similar procedure leads to the expansion formulae

$$\left.\begin{aligned}\varepsilon_j' &= \sum_{m=0}^{\infty} b_s{}^{j(m)} (\alpha_s')^m \\ P_{uv}{}^j &= \sum_{m=0}^{\infty} b_{s,uv}{}^{j(m)} (\alpha_s')^m\end{aligned}\right\} \tag{25}$$

where the coefficients, $b_s{}^{j(m)}$ and $b_{s,uv}{}^{j(m)}$, are the functions of $\alpha_r'$ and are given by

$$\left.\begin{aligned}b_s{}^{j(m)} &= \frac{(-1)^m}{m!}\left[\frac{\mathrm{d}^m}{\mathrm{d}z^m}\frac{z\{\square_{ss}(z)\}^{m-1}\{\square'(z)\square_{ss}(z) - \square(z)\square_{ss}'(z)\}}{\{\square(z)/(z-\tilde{\varepsilon}_j)\}^{m+1}}\right]_{z=\tilde{\varepsilon}_j} \\ &\qquad (m=0, 1, 2, \cdots\cdots) \\ b_{s,uv}{}^{j(m)} &= \frac{(-1)^{m+1}}{m!}\left[\frac{\mathrm{d}^m}{\mathrm{d}z^m}\frac{\{\square_{ss}(z)\}^m \square_{us}(z)\square_{sv}(z)}{\{\square(z)/(z-\tilde{\varepsilon}_j)\}^{m+1}}\right]_{z=\tilde{\varepsilon}_j} \\ &\qquad (m=0, 1, 2, \cdots\cdots)\end{aligned}\right\} \tag{26}$$

Thus we finally reach the following results for this perturbed system.

$$\varepsilon_j' = \varepsilon_j + (\delta\varepsilon_j)_r + (\delta\varepsilon_j)_s + 2\sum_{k(\neq j)}^{\text{all}} \frac{c_r{}^j c_r{}^k c_s{}^j c_s{}^k}{\varepsilon_j - \varepsilon_k}\alpha_r'\alpha_s' + \cdots\cdots \tag{27}$$

$$\begin{aligned}P_{uv}{}^j = p_{uv}{}^j &+ (\delta p_{uv}{}^j)_r + (\delta p_{uv}{}^j)_s \\ &+ \Bigg[\sum_{k(\neq j)}^{\text{all}}\sum_{m(\neq j)}^{\text{all}} \frac{c_r{}^j c_s{}^j (c_r{}^k c_s{}^m + c_s{}^k c_r{}^m) c_u{}^k c_v{}^m + c_r{}^m c_s{}^m (c_r{}^j c_s{}^k + c_s{}^j c_r{}^k)(c_u{}^j c_v{}^k + c_v{}^j c_u{}^k)}{(\varepsilon_j - \varepsilon_k)(\varepsilon_j - \varepsilon_m)} \\ &- \sum_{k(\neq j)}^{\text{all}} \frac{c_r{}^j c_s{}^j\{(c_r{}^j c_s{}^k + c_s{}^j c_r{}^k)(c_u{}^j c_v{}^k + c_v{}^j c_u{}^k) + 2c_r{}^k c_s{}^k c_u{}^j c_v{}^j\}}{(\varepsilon_j - \varepsilon_k)^2}\Bigg]\alpha_r'\alpha_s' + \cdots\cdots\end{aligned} \tag{28}$$

where $(\delta\varepsilon_j)_r$ and $(\delta p_{uv}{}^j)_r$ are the change of the orbital energy and the separate bond order (or the separate electron density) respectively, of the $j$th molecular orbital caused by the perturbation $\alpha_r'$, as were given in Eqs, 1 and 2.

On inspection of Eqs. 27 and 28 it is clearly seen that, as concerns the first order terms, two perturbations have no effect upon each other and, therefore, the so-called "additivity rule" comes into being. That is to say, the change of the orbital energy, the bond order or the electron density caused by two perturbations is expressed by the mathematical sum of its changes caused by each perturbation. In the second order a cross term appears, which may become comparable in magnitude with the non-cross term and cannot be neglected. Also as for the total $\pi$ electronic energy, the bond order and the electron density, which are expressed by the sum of corresponding separate quantity, the circumstances are the same, as follows:

$$\varepsilon' = \varepsilon + (\delta\varepsilon)_r + (\delta\varepsilon)_s + 2\sum_{j}^{\text{occ}}\sum_{k}^{\text{unocc}} \frac{c_r{}^j c_r{}^k c_s{}^j c_s{}^k}{\varepsilon_j - \varepsilon_k}\alpha_r'\alpha_s' + \cdots\cdots \tag{29}$$

$$P_{uv} = p_{uv} + (\delta p_{uv})_r + (\delta p_{uv})_s + \sum_{j}^{\text{occ}}\{\text{cross term of the order } \alpha_r'\alpha_s' \text{ in } P_{uv}{}^j\} + \cdots\cdots \tag{30}$$

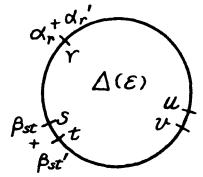
where $(\delta\varepsilon)_r$ and $(\delta p_{uv})_r$, given by Eqs. 3 and 4, are the changes of total $\pi$ electronic energy and the bond order (or the electron density) respectively, caused by the perturbation $\alpha_r'$. Eqs. 27 to 30 can also be derived by the existing method of perturbation.

The explicit expression of perturbed molecular orbital would be useful for some purposes. It is

$$\Psi_j' = \Psi_j + (\delta\Psi_j)_r + (\delta\Psi_j)_s - \sum_{k(\neq j)}^{\text{all}} \frac{c_r^j c_r^k c_s^j c_s^k}{(\varepsilon_j - \varepsilon_k)^2} \alpha_r' \alpha_s' \Psi_j$$
$$+ \sum_{k(\neq j)}^{\text{all}} \frac{(c_r^j c_s^k + c_s^j c_r^k)}{\varepsilon_j - \varepsilon_k} \left\{ \sum_{m(\neq j)}^{\text{all}} \frac{c_r^m c_s^m}{\varepsilon_j - \varepsilon_m} - \frac{c_r^j c_s^j}{\varepsilon_j - \varepsilon_k} \right\} \alpha_r' \alpha_s' \Psi_k + \cdots\cdots \quad (31)$$

where $(\delta\Psi_j)_r$ is given by Eq. 5.

**3. Case II. Changes of a Coulomb Integral and a Resonance Integral.**—When at the same time the Coulomb integral of the $r$th atom is increased by $\alpha_r'$ and the resonance integral of the bond $(st)$, $\beta_{st}$, by $\beta_{st}'$, then the perturbed secular determinant of the system is expressed* by




$$D(\varepsilon) = \Delta(\varepsilon) + \alpha_r' \Delta_{rr}(\varepsilon) + (-1)^{s+t} 2\beta_{st}' \Delta_{st}(\varepsilon) - (\beta_{st}')^2 \Delta_{sstt}(\varepsilon)$$
$$+ (-1)^{s+t} \alpha_r' \beta_{st}' \Delta_{rrst}(\varepsilon) - \alpha_r' (\beta_{st}')^2 \Delta_{rrsstt}(\varepsilon) \quad (32)$$

As well as in Case I, the following expressions of the orbital energy, the separate bond order and the separate electron density are obtained.

$$\varepsilon_j' = \varepsilon_j + (\delta\varepsilon_j)_r + (\delta\varepsilon_j)_{st} + 2 \sum_{k(\neq j)}^{\text{all}} \frac{c_r^j c_r^k (c_s^j c_t^k + c_t^j c_s^k)}{\varepsilon_j - \varepsilon_k} \alpha_r' \beta_{st}' + \cdots\cdots \quad (33)$$

$$P_{uv}^j = p_{uv}^j + (\delta p_{uv}^j)_r + (\delta p_{uv}^j)_{st}$$
$$+ \left[ \sum_{k(\neq j)}^{\text{all}} \sum_{m(\neq j)}^{\text{all}} \frac{c_r^j c_r^k (c_s^j c_t^m + c_t^j c_s^m)(c_u^k c_v^m + c_v^k c_u^m)}{(\varepsilon_j - \varepsilon_k)} \right.$$
$$\times \frac{\{c_r^k c_r^m (c_s^j c_t^m + c_t^j c_s^m) + c_r^m c_r^j (c_s^k c_t^m + c_t^k c_s^m)\}(c_u^j c_v^k + c_v^j c_u^k)}{(\varepsilon_j - \varepsilon_m)}$$
$$\left. - \sum_{k(\neq j)}^{\text{all}} \frac{2\{2c_r^j c_r^k c_s^j c_t^j + (c_r^j)^2 (c_s^j c_t^k + c_t^j c_s^k)\}(c_u^j c_v^k + c_v^j c_u^k) c_r^j c_r^k (c_s^j c_t^k + c_t^j c_s^k) c_u^j c_v^j}{(\varepsilon_j - \varepsilon_k)^2} \right] \alpha_r' \beta_{st}'$$
$$+ \cdots\cdots \quad (34)$$

where $(\delta\varepsilon_j)_r$, $(\delta\varepsilon_j)_{st}$, $(\delta p_{uv}^j)_r$ and $(\delta p_{uv}^j)_{st}$ are given by Eqs. 1, 6, 2 and 7, respectively. Also in this case a cross term between the two perturbations, both in the orbital energy and in the bond order (and the density), first arises in the second order, and therefore the additivity rule is correct in the first order. The circumtances are the same for the total energy, the bond order and the electron density.

$$\left.\begin{aligned} \varepsilon' &= \varepsilon + (\delta\varepsilon)_r + (\delta\varepsilon)_{st} + 2 \sum_j^{\text{occ}} \{\text{cross term of the order } \alpha_r' \beta_{st}' \text{ in } \varepsilon_j'\} + \cdots\cdots \\ P_{uv} &= p_{uv} + (\delta p_{uv})_r + (\delta p_{uv})_{st} + 2 \sum_j^{\text{occ}} \{\text{cross term of the order } \alpha_r' \beta_{st}' \text{ in } P_{uv}^j\} \\ &+ \cdots\cdots \end{aligned}\right\} \quad (35)$$

where $(\delta\varepsilon)_{st}$ and $(\delta p_{uv})_{st}$ are given by Eqs. 8 and 9. The perturbed molecular orbital is obtained as follows:

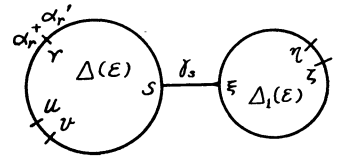
$$\Psi_j' = \Psi_j + (\delta\Psi_j)_r + (\delta\Psi_j)_{st} + \sum_{k(\neq j)}^{\text{all}} \left\{ \sum_{m(\neq j)}^{\text{all}} \frac{c_r^k c_r^m (c_s^j c_t^m + c_t^j c_s^m) + c_r^j c_r^m (c_s^k c_t^m + c_t^k c_s^m)}{(\varepsilon_j - \varepsilon_k)(\varepsilon_j - \varepsilon_m)} \right.$$
$$\left. - \frac{2c_r^j c_r^k c_s^j c_t^j + (c_r^j)^2 (c_s^j c_t^k + c_t^j c_s^k)}{(\varepsilon_j - \varepsilon_k)^2} \right\} \alpha_r' \beta_{st}' \Psi_k$$
$$- \sum_{m(\neq j)}^{\text{all}} \frac{c_r^j c_r^k (c_s^j c_t^k + c_t^j c_s^k)}{(\varepsilon_j - \varepsilon_k)^2} \alpha_r' \beta_{sr}' \Psi_k + \cdots\cdots \quad (36)$$

where $(\delta\Psi_j)_{st}$ is given by Eq. 10.

**4. Case III. A Weak Bonding with a Change of a Coulomb Integral.** — When a conjugated system, $\Delta(\varepsilon)$, conjugates at the $s$th atom through a weak bonding, whose

* When $r=t$, though the perturbed secular determinant becomes $D(\varepsilon) = \Delta(\varepsilon) + \alpha_r' \Delta_{rr}(\varepsilon) + (-1)^{s+r} 2\beta_{sr}' \Delta_{sr}(\varepsilon) - (\beta_{sr}')^2 \Delta_{ssrr}(\varepsilon)$, Eqs. 33 to 36 are valid.

resonance integral is $\gamma_s$, with another conjugated system $\Delta_1(\varepsilon)$, and at the same time the Coulomb integral of the $r$th atom is increased by $\alpha_r'$, as illustrated in the figure, then the following formulae are obtained.




$$D(\varepsilon)=\Delta(\varepsilon)\Delta_1(\varepsilon)+\alpha_r'\Delta_{rr}(\varepsilon)\Delta_1(\varepsilon)-(\gamma_s)^2\Delta_{ss}(\varepsilon)\Delta_{1\xi\xi}(\varepsilon)-\alpha_r'(\gamma_s)^2\Delta_{rrss}(\varepsilon)\Delta_{1\xi\xi}(\varepsilon) \tag{37}$$

$$\varepsilon_j'=\varepsilon_j+(\delta\varepsilon_j)_r+(\delta\varepsilon_j)_{s\xi}+\sum_k^{\text{all}}\frac{c_r^jc_s^j(d_\xi^{1k})^2}{\varepsilon_j-\eta_{1k}}\left\{2\sum_{m(\neq j)}^{\text{all}}\frac{c_r^mc_s^m}{\varepsilon_j-\varepsilon_m}-\frac{c_r^jc_s^j}{\varepsilon_j-\eta_{1k}}\right\}\alpha_r'(\gamma_s)^2+\cdots\cdots \tag{38}$$

$$\eta_{1k}'=\eta_{1k}+(\delta\eta_{1k})_{s\xi}+\sum_j^{\text{all}}\frac{c_r^jc_s^j(d_\xi^{1k})^2}{\eta_{1k}-\varepsilon_j}\left\{2\sum_{m(\neq j)}^{\text{all}}\frac{c_r^mc_s^m}{\varepsilon_j-\varepsilon_m}-\frac{c_r^jc_s^j}{\varepsilon_j-\eta_{1k}}\right\}\alpha_r'(\gamma_s)^2+\cdots\cdots \tag{39}$$

$$P_{uv}{}^j=p_{uv}{}^j+(\delta p_{uv}{}^j)_r+(\delta p_{uv}{}^j)_{s\xi}+\{\text{cross term of the order }\alpha_r'(\gamma_s)^2\}+\cdots\cdots \tag{40}$$

$$P_{s\xi}{}^j=(\delta p_{s\xi}{}^j)_{s\xi}+\sum_k^{\text{all}}\frac{c_r^jc_s^j(d_\xi^{1k})^2}{\varepsilon_j-\eta_{1k}}\left\{2\sum_{m(\neq j)}^{\text{all}}\frac{c_r^mc_s^m}{\varepsilon_j-\varepsilon_m}-\frac{c_r^jc_s^j}{\varepsilon_j-\eta_{1k}}\right\}\alpha_r'\gamma_s+\cdots\cdots \tag{40'}$$

$$P_{uv}{}^{1k}=(\delta p_{uv}{}^{1k})_{s\xi}+\{\text{cross term of the order }\alpha_r'(\gamma_s)^2\}+\cdots \tag{41}$$

$$P_{\eta\zeta}{}^{1k}=p_{\eta\zeta}{}^{1k}+(\delta p_{\eta\zeta}{}^{1k})_{s\xi}+\{\text{cross term of the order }\alpha_r'(\gamma_s)^2\}+\cdots \tag{42}$$

$$P_{s\xi}{}^{1k}=(\delta p_{s\xi}{}^{1k})_{s\xi}+\sum_j^{\text{all}}\frac{c_r^jc_s^j(d_\xi^{1k})^2}{\eta_{1k}-\varepsilon_j}\left\{2\sum_{m(\neq j)}^{\text{all}}\frac{c_r^mc_s^m}{\varepsilon_j-\varepsilon_m}-\frac{c_r^jc_s^j}{\varepsilon_j-\eta_{1k}}\right\}\alpha_r'\gamma_s+\cdots\cdots \tag{42'}$$

$$P_{\eta\zeta}{}^j=(\delta p_{\eta\zeta}{}^j)_{s\xi}+\{\text{cross term of the order }\alpha_r'(\gamma_s)^2\}+\cdots \tag{43}$$

where $\xi$ is the position of weak conjugation in the system $\Delta_1(\varepsilon)$, the bond $(\eta\zeta)$ is in the system $\Delta_1(\varepsilon)$; and $(\delta\varepsilon_j)_{s\xi}$, $(\delta p_{uv}{}^j)_{s\xi}$, $(\delta p_{s\xi}{}^j)_{s\xi}$ and $(\delta p_{uv}{}^{1k})_{s\xi}$ are given by Eqs. 11, 12, 12′ and 13, from which $(\delta\eta_{1k})_{s\xi}$, $(\delta p_{\eta\zeta}{}^j)_{s\xi}$, $(\delta p_{\eta\zeta}{}^{1k})_{s\xi}$ and $(\delta p_{s\xi}{}^{1k})_{s\xi}$ will easily be formulated. Therefore the total $\pi$ electronic energy of the combined system is

$$\varepsilon'=\varepsilon+(\delta\varepsilon)_r+(\delta\varepsilon)_{s\xi}+2\Big(\sum_j^{\text{occ}}\sum_k^{\text{unocc}}-\sum_j^{\text{unocc}}\sum_k^{\text{occ}}\Big)\times\left[\frac{c_r^jc_s^j(d_\xi^{1k})^2}{\varepsilon_j-\eta_{1k}}\left\{2\sum_{m(\neq j)}^{\text{all}}\frac{c_r^mc_s^m}{\varepsilon_j-\varepsilon_m}-\frac{c_r^jc_s^j}{\varepsilon_j-\eta_{1k}}\right\}\right]\alpha_r'(\gamma_s)^2+\cdots\cdots \tag{44}$$

And

$$P_{uv}=p_{uv}+(\delta p_{uv})_r+(\delta p_{uv})_{s\xi}+\{\text{cross term of the order }\alpha_r'(\gamma_s)^2\}+\cdots \tag{45}$$

$$P_{s\xi}=(\delta p_{s\xi})_{s\xi}+2\Big(\sum_j^{\text{occ}}\sum_k^{\text{unocc}}-\sum_j^{\text{unocc}}\sum_k^{\text{occ}}\Big)\left[\frac{c_r^jc_s^j(d_\xi^{1k})^2}{\varepsilon_j-\eta_{1k}}\left\{2\sum_{m(\neq j)}^{\text{all}}\frac{c_r^mc_s^m}{\varepsilon_j-\varepsilon_m}-\frac{c_r^jc_s^j}{\varepsilon_j-\eta_{1k}}\right\}\right]\alpha_r'\gamma_s+\cdots\cdots \tag{45'}$$

$$P_{\eta\zeta}=p_{\eta\zeta}+(\delta p_{\eta\zeta})_{s\xi}+\{\text{cross term of the order }\alpha_r'(\gamma_s)^2\}+\cdots \tag{46}$$

$$\delta Q=(\delta Q)_{s\xi}+\{\text{cross term of the order }\alpha_r'(\gamma_s)^2\}+\cdots \tag{47}$$

where $(\delta\varepsilon)_{s\xi}$, $(\delta p_{uv})_{s\xi}$, $(\delta p_{s\xi})_{s\xi}$ and $(\delta Q)_{s\xi}$ are given by Eqs. 15, 16, 16′ and 18. $(\delta p_{\eta\zeta})_{s\xi}$ is easily written on inspection of Eq. 16. As is seen in Eqs. 45 to 47, a cross term first appears in the third order, that is, the order of $\alpha_r'(\gamma_s)^2$, and the additivity rule is valid up to the second order perturbation.

The wave functions of this perturbed system are represented by

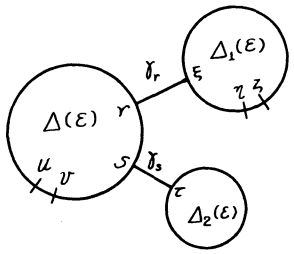
$$\Psi_j'=\Psi_j+(\delta\Psi_j)_r+(\delta\Psi_j)_{s\xi}+\sum_k^{\text{all}}\frac{c_r^jd_\xi^{1k}}{\varepsilon_j-\eta_{1k}}\left\{\sum_{m(\neq j)}^{\text{all}}\frac{c_r^mc_s^m}{\varepsilon_j-\varepsilon_m}-\frac{c_r^jc_s^j}{\varepsilon_j-\eta_{1k}}\right\}\alpha_r'\gamma_s\phi_{1k}+\cdots\cdots \tag{48}$$

$$\phi_{1k}'=\phi_{1k}+(\delta\phi_{1k})_{s\xi}+\sum_j^{\text{all}}\frac{c_r^jd_\xi^{1k}}{\eta_{1k}-\varepsilon_j}\sum_{m(\neq j)}^{\text{all}}\frac{c_r^mc_s^m}{\eta_{1k}-\varepsilon_m}\alpha_r'\gamma_s\Psi_j+\cdots \tag{49}$$

where $(\delta\Psi_j)_{s\xi}$ is given by Eq. 14, from which also $(\delta\phi_{1k})_{s\xi}$ may easily be written.

**5. Case IV. Weak Bondings to Two Conjugated Systems.**—Here we consider a case in which a conjugated system, $\Delta(\varepsilon)$, conjugates at the $r$th and the $s$th atoms with two other

conjugated systems, $\Delta_1(\varepsilon)$ and $\Delta_2(\varepsilon)$, respectively, making weak bondings whose resonance integrals are $\gamma_r$ and $\gamma_s$, respectively. The molecular orbital, its orbital energy and the coefficient of atomic orbital in the non-perturbed $\Delta_1(\varepsilon)$ system are designated by $\psi_{1k}$, $\eta_{1k}$ and $d_\mu{}^{1k}$, respectively, and in the system $\Delta_2(\varepsilon)$ by $\psi_{2k}$, $\eta_{2k}$ and $d_\nu{}^{2k}$. Then the following expressions are easily obtained for the perturbed combined system.




$$D(\varepsilon)=\Delta(\varepsilon)\Delta_1(\varepsilon)\Delta_2(\varepsilon)-(\gamma_r)^2\Delta_{rr}(\varepsilon)\Delta_{1\xi\xi}(\varepsilon)\Delta_2(\varepsilon)$$
$$-(\gamma_s)^2\Delta_{ss}(\varepsilon)\Delta_1(\varepsilon)\Delta_{2\tau\tau}(\varepsilon)+(\gamma_r\gamma_s)^2\Delta_{rrss}(\varepsilon)\Delta_{1\xi\xi}(\varepsilon)\Delta_{2\tau\tau}(\varepsilon) \tag{50}$$

$$\varepsilon_j'=\varepsilon_j+(\delta\varepsilon_j)_{r\xi}+(\delta\varepsilon_j)_{s\tau}+\sum_k^{\text{all}}\frac{c_r{}^j(d_\xi{}^{1k})^2}{\varepsilon_j-\eta_{1k}}U_{jk}(\gamma_r\gamma_s)^2+\cdots\cdots \tag{51}$$

$$U_{jk}=\sum_l^{\text{all}}\frac{c_s{}^j(d_\tau{}^{2l})^2}{\varepsilon_j-\eta_{2l}}\left\{2\sum_{m(\neq j)}^{\text{all}}\frac{c_r{}^mc_s{}^m}{\varepsilon_j-\varepsilon_m}-\frac{c_r{}^jc_s{}^j}{\varepsilon_j-\eta_{1k}}-\frac{c_r{}^jc_s{}^j}{\varepsilon_j-\eta_{2l}}\right\} \tag{51-a}$$

$$\eta_{1k}'=\eta_{1k}+(\delta\eta_{1k})_{r\xi}+\sum_j^{\text{all}}\frac{c_r{}^j(d_\xi{}^{1k})^2}{\eta_{1k}-\varepsilon_j}U_{jk}(\gamma_r\gamma_s)^2+\cdots\cdots \tag{52}$$

$$P_{uv}{}^j=p_{uv}{}^j+(\delta p_{uv}{}^j)_{r\xi}+(\delta p_{uv}{}^j)_{s\tau}+\{\text{cross term of the order }(\gamma_r\gamma_s)^2\}+\cdots\cdots \tag{53}$$

$$P_{r\xi}{}^j=(\delta p_{r\xi}{}^j)_{r\xi}+\sum_k^{\text{all}}\frac{c_r{}^j(d_\xi{}^{1k})^2}{\varepsilon_j-\eta_{1k}}U_{jk}\gamma_r(\gamma_s)^2+\cdots\cdots \tag{53'}$$

$$P_{uv}{}^{1k}=(\delta p_{uv}{}^{1k})_{r\xi}+\{\text{cross term of the order }(\gamma_r\gamma_s)^2\}+\cdots\cdots \tag{54}$$

$$P_{r\xi}{}^{1k}=(\delta p_{r\xi}{}^{1k})_{r\xi}+\sum_j^{\text{all}}\frac{c_r{}^j(d_\xi{}^{1k})^2}{\eta_{1k}-\varepsilon_j}U_{jk}\gamma_r(\gamma_s)^2+\cdots\cdots \tag{54'}$$

$$P_{uv}{}^{2l}=(\delta p_{uv}{}^{2l})_{s\tau}+\{\text{cross term of the order }(\gamma_r\gamma_s)^2\}+\cdots\cdots \tag{55}$$

$$P_{r\xi}{}^{2k}=\sum_k^{\text{all}}\frac{(d_\xi{}^{1k})^2}{\eta_{2l}-\eta_{1k}}\sum_j^{\text{all}}\sum_m^{\text{all}}\frac{c_r{}^jc_r{}^mc_s{}^jc_s{}^m(d_\tau{}^{2l})^2}{(\eta_{2l}-\varepsilon_j)(\eta_{2l}-\varepsilon_m)}\gamma_r(\gamma_s)^2+\cdots\cdots \tag{55'}$$

$$P_{\eta\zeta}{}^{1k}=p_{\eta\zeta}{}^{1k}+(\delta p_{\eta\zeta}{}^{1k})_{r\xi}+\{\text{cross term of the order }(\gamma_r\gamma_s)^2\}+\cdots\cdots \tag{56}$$

$$P_{\eta\zeta}{}^j=(\delta p_{\eta\zeta}{}^j)_{r\xi}+\{\text{cross term of the order}(\gamma_r\gamma_s)^2\}+\cdots\cdots \tag{57}$$

$$P_{\eta\zeta}{}^{2l}=\{\text{cross term of the order}(\gamma_r\gamma_s)^2\}+\cdots\cdots \tag{58}$$

where $\xi$ and $\tau$ are the positions of the weak conjugation in the systems $\Delta_1(\varepsilon)$ and $\Delta_2(\varepsilon)$, respectively, and the bond $(uv)$ or the atom $u$ is assumed to be in the system $\Delta(\varepsilon)$, and the bond $(\eta\zeta)$ or the atom $\eta$ in the system $\Delta_1(\varepsilon)$. Similar expressions as above may be written for the system $\Delta_2(\varepsilon)$. Thus the total $\pi$ electronic energy and the bond order of this perturbed system are given as follows:

$$\varepsilon'=2\sum_j^{\text{occ}}\varepsilon_j'+2\sum_k^{\text{occ}}\eta_{1k}'+2\sum_l^{\text{occ}}\eta_{2l}'$$
$$=\varepsilon+(\delta\varepsilon)_{r\xi}+(\delta\varepsilon)_{st}$$
$$+\left\{\sum_j^{\text{occ}}\left(\sum_k^{\text{unocc}}\sum_l^{\text{unocc}}-\sum_k^{\text{occ}}\sum_l^{\text{occ}}\right)-\sum_j^{\text{unocc}}\left(\sum_k^{\text{occ}}\sum_l^{\text{all}}+\sum_k^{\text{all}}\sum_l^{\text{occ}}\right)\right\}\frac{c_r{}^jc_s{}^j(d_\xi{}^{1k})^2(d_\tau{}^{2l})^2}{(\varepsilon_j-\eta_{1k})(\varepsilon_j-\eta_{2l})}$$
$$\times\left(2\sum_{m(\neq j)}^{\text{all}}\frac{c_r{}^mc_s{}^m}{\varepsilon_j-\varepsilon_m}-\frac{c_r{}^jc_s{}^j}{\varepsilon_j-\eta_{1k}}-\frac{c_r{}^jc_s{}^j}{\varepsilon_j-\eta_{2l}}\right)(\gamma_r\gamma_s)^2+\cdots\cdots \tag{59}$$

$$P_{uv}=p_{uv}+(\delta p_{uv})_{r\xi}+(\delta p_{uv})_{s\tau}+\{\text{cross term of the order }(\gamma_r\gamma_s)^2\}+\cdots\cdots \tag{60}$$

$$P_{r\xi}=(\delta p_{r\xi})_{r\xi}+\left[2\left(\sum_j^{\text{occ}}\sum_k^{\text{unocc}}-\sum_j^{\text{unocc}}\sum_k^{\text{occ}}\right)\frac{c_r{}^j(d_\xi{}^{1k})^2}{\varepsilon_j-\eta_{1k}}U_{jk}\right.$$
$$\left.+2\sum_l^{\text{occ}}\sum_k^{\text{all}}\frac{(d_\xi{}^{1k})^2}{\eta_{2l}-\eta_{1k}}\sum_j^{\text{all}}\sum_m^{\text{all}}\frac{c_r{}^jc_r{}^mc_s{}^jc_s{}^m(d_\tau{}^{2l})^2}{(\eta_{2l}-\varepsilon_j)(\eta_{2l}-\varepsilon_m)}\right]\gamma_r(\gamma_s)^2+\cdots \tag{60'}$$

$$P_{\eta\zeta}=p_{\eta\zeta}+(\delta p_{\eta\zeta})_{r\xi}+\{\text{cross term of the order } (\gamma_r\gamma_s)^2\}+\cdots\cdots \tag{61}$$

The changes of total charge involved in the systems $\Delta(\varepsilon)$ and $\Delta_1(\varepsilon)$ are designated as $\delta Q$ and $\delta Q_1$, respectively, which are written as follows:

$$\delta Q=(\delta Q)_{r\xi}+(\delta Q)_{s\tau}+\{\text{cross term of the order } (\gamma_r\gamma_s)^2\}+\cdots\cdots \tag{62}$$

$$\delta Q_1=(\delta Q)_{r\xi}+\{\text{cross term of the order } (\gamma_r\gamma_s)^2\}+\cdots\cdots \tag{63}$$

A similar equation may be written also for the system $\Delta_2(\varepsilon)$.

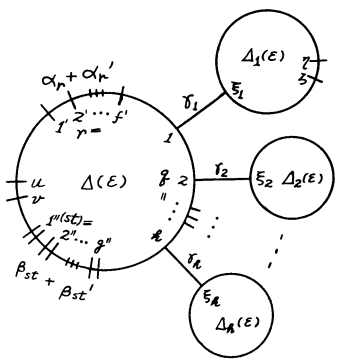
The molecular orbitals of this perturbed system are

$$\Psi_j'=\Psi_j+(\delta\Psi_j)_{r\xi}+(\delta\Psi_j)_{s\tau}+\{\text{cross term of the orders } \gamma_r(\gamma_s)^2 \text{ and } (\gamma_r)^2\gamma_s\}+\cdots\cdots \tag{64}$$

$$\psi_{1k}'=\psi_{1k}+(\delta\Psi_{1k})_{r\xi}+\sum_{j}^{\text{all}}\sum_{l}^{\text{all}}\frac{c_r{}^j c_s{}^j d_\xi{}^{1k} d_\eta{}^{2l}}{(\eta_{1k}-\eta_{2l})(\eta_{1k}-\varepsilon_j)}\gamma_r\gamma_s\psi_{2k}+\cdots\cdots \tag{65}$$

As to special cases in which either or both of the systems $\Delta_1(\varepsilon)$ and $\Delta_2(\varepsilon)$ are single atoms, one may simplify the results of Cases III and IV by using Eqs. 11-a to 18-a instead of Eqs. 11 to 18 for non-cross terms and by abridging cross terms.

**6. More General Case of Many Perturbations.** — Perturbation treatment of systems affected by two perturbations stated above may be extended to a more general case of many perturbations. As illustrated in the figure, we consider a conjugated system, $\Delta(\varepsilon)$, and increase the Coulomb integrals of the $r$th atoms in it ($r=1', 2', \cdots\cdots, f'$) by $\alpha_r'$ and the resonance integrals of the bonds $(st)$ ($st=1'', 2'', \cdots\cdots, g''$) by $\beta_{st}'$, and make weak bondings, whose resonance integral is $\gamma_q$, between the $q$th atoms ($q=1, 2, \cdots\cdots, h$) in the system and the $\xi_q$th atoms in other conjugated systems $\Delta_q(\varepsilon)$. Here some of the $r$'s, $s$'s and $q$'s may be the identical atoms.




Then the perturbed $j$th orbital energy of the system $\Delta(\varepsilon)$ is

$$\begin{aligned}\varepsilon_j'=\varepsilon_j&+\sum_{r=1'}^{f'}(\delta\varepsilon_j)_r+\sum_{(st)=1''}^{g''}(\delta\varepsilon_j)_{st}+\sum_{q=1}^{h}(\delta\varepsilon_j)_{q\xi}\\&+C(\alpha^2,\alpha\beta,\beta^2)+C(\alpha^3,\alpha^2\beta,\alpha\beta^2,\beta^3,\alpha\gamma^2,\beta\gamma^2)\\&+C(\alpha^4,\alpha^3\beta,\alpha^2\beta^2,\alpha\beta^3,\beta^4,\alpha^2\gamma^2,\alpha\beta\gamma^2,\beta^2\gamma^2,\gamma^4)+\cdots\cdots\end{aligned} \tag{66}$$

where $(\delta\varepsilon_j)_r$, $(\delta\varepsilon_j)_{st}$ and $(\delta\varepsilon_j)_{q\xi}$ are energy changes caused by perturbations $\alpha_r'$, $\beta_{st}'$ and $\gamma_q$, respectively, and are given by Eqs. 1, 6 and 11. and $C$ means the cross term among perturbations. For instance $C(\alpha^2,\alpha\beta,\beta^2)$ consists of cross terms of orders $\alpha_1'\alpha_2'$, $\alpha_1'\alpha_3'$, $\cdots\cdots$, $\alpha_2'\alpha_3'$, $\cdots\cdots$, $\alpha_1'\beta_1'$, $\alpha_1'\beta_2'$, $\cdots\cdots$, $\alpha_2'\beta_1'$, $\cdots\cdots$, $\beta_1'\beta_2'$, $\beta_1'\beta_3'$, $\cdots\cdots$, $\beta_2'\beta_3'$, $\cdots\cdots$; and $C(\alpha^3,\alpha^2\beta,\alpha\beta^2,\beta^3,\alpha\gamma^2,\beta\gamma^2)$ of orders $(\alpha_1')^2\alpha_2'$, $\cdots\cdots$, $\alpha_1'\alpha_2'\alpha_3'$, $\cdots\cdots$, $(\alpha_1')^2\beta_1'$, $\cdots\cdots$, $\alpha_1'\alpha_2'\beta_1'$, $\cdots\cdots$, $\alpha_1'(\beta_1')^2$, $\cdots\cdots$, $\alpha_1'\beta_1'\beta_2'$, $\cdots\cdots$, $(\beta_1')^2\beta_2'$, $\cdots\cdots$, $\beta_1'\beta_2'\beta_3'$, $\cdots\cdots$, $\alpha_1'(\gamma_1)^2$, $\cdots\cdots$, $\beta_1'(\gamma_1)^2$, $\cdots\cdots$. The perturbed separate bond order by this orbital of the bond $(uv)$ in the system $\Delta(\varepsilon)$ is

$$\begin{aligned}P_{uv}{}^j=p_{uv}{}^j&+\sum_{r=1'}^{f'}(\delta p_{uv}{}^j)_r+\sum_{(st)=1''}^{g''}(\delta p_{uv}{}^j)_{st}+\sum_{q=1}^{h}(\delta p_{uv}{}^j)_{q\xi}\\&+C(\alpha^2,\alpha\beta,\beta^2)+C(\alpha^3,\alpha^2\beta,\alpha\beta^2,\beta^3,\alpha\gamma^2,\beta\gamma^2)\\&+C(\alpha^4,\alpha^3\beta,\alpha^2\beta^2,\alpha\beta^3,\beta^4,\alpha^2\gamma^2,\alpha\beta\gamma^2,\beta^2\gamma^2,\gamma^4)+\cdots\cdots\end{aligned} \tag{67}$$

where $(\delta p_{uv}{}^j)_r$, $(\delta p_{uv}{}^j)_{st}$ and $(\delta p_{uv}{}^j)_{q\xi}$ are the changes caused by $\alpha_r'$, $\beta_{st}'$ and $\gamma_q$, respectively, and are given by Eqs. 2, 7 and 12. The perturbed separate bond order by this orbital of the bond $(\eta\zeta)$ in another system, say, the system $\Delta_1(\varepsilon)$, is

$$\begin{aligned}P_{\eta\zeta}{}^j=&(\delta p_{\eta\zeta}{}^j)_{1\xi}+C\{\alpha(\gamma_1)^2,\beta(\gamma_1)^2\}\\&+C\{\alpha^2(\gamma_1)^2,\alpha\beta(\gamma_1)^2,\beta^2(\gamma_1)^2,\gamma^2(\gamma_1)^2\}+\cdots\cdots\end{aligned} \tag{68}$$

The perturbed $k$th orbital energy of a system, say, the system $\Delta_1(\varepsilon)$, is

$$\eta_{1k}'=\eta_{1k}+(\delta\eta_{1k})_{1\xi}+C\{\alpha(\gamma_1)^2,\beta(\gamma)_1)^2\}$$
$$+C\{\alpha^2(\gamma_1)^2,\alpha\beta(\gamma_1)^2,\beta^2(\gamma_1)^2,\gamma^2(\gamma_1)^2\}+\cdots\cdots \quad (69)$$

The perturbed separate bond orders by this orbital of bonds $(\eta\zeta)$ and $(\mu\nu)$ are

$$P_{\eta\zeta}{}^{1k}=p_{\eta\zeta}{}^{1k}+(\delta p_{\eta\zeta}{}^{1k})_{1\xi}+C\{\alpha(\gamma_1)^2,\beta(\gamma_1)^2\}$$
$$+C\{\alpha^2(\gamma_1)^2,\alpha\beta(\gamma_1)^2,\beta^2(\gamma_1)^2,\gamma^2(\gamma_1)^2\}+\cdots\cdots \quad (70)$$
$$P_{\mu\nu}{}^{1k}=(\delta p_{\mu\nu}{}^{1k})_{1\xi}+C\{\alpha(\gamma_1)^2,\beta(\gamma_1)^2\}$$
$$+C\{\alpha^2(\gamma_1)^2,\alpha\beta(\gamma_1)^2,\beta^2(\gamma_1)^2,\gamma^2(\gamma_1)^2\}+\cdots\cdots \quad (71)$$

Also this bond order by this orbital of the bond $(\mu\nu)$, which is located in another system, say, the system $\Delta_h(\varepsilon)$, is given by

$$P_{\mu\nu}{}^{1k}=C\{(\gamma_1)^2(\gamma_h)^2\}+\cdots\cdots \quad (72)$$

The perturbed separate bond order of the bond which is made anew by perturbation between conjugated systems, say, the bond $(1\xi_1)$ between the systems $\Delta(\varepsilon)$ and $\Delta_1(\varepsilon)$, may be written as

$$P_{1\xi}{}^{j}=(\delta p_{1\xi}{}^{j})_{1\xi}+C\{\alpha\gamma_1,\beta\gamma_1\}+C\{\alpha^2\gamma_1,\alpha\beta\gamma_1,\beta^2\gamma_1,\gamma^2\gamma_1\}$$
$$+C\{\alpha^3\gamma_1,\alpha^2\beta\gamma_1,\alpha\beta^2\gamma_1,\beta^3\gamma_1,\alpha\gamma^2\gamma_1,\beta\gamma^2\gamma_1,\alpha(\gamma_1)^3,\beta(\gamma_1)^3\}+\cdots\cdots \quad (73)$$
$$P_{1\xi}{}^{1k}=(\delta p_{1\xi}{}^{1k})_{1\xi}+C\{\alpha\gamma_1,\beta\gamma_1\}+C\{\alpha^2\gamma_1,a\beta\gamma_1,\beta^2\gamma_1,\gamma^2\gamma_1\}$$
$$+C\{\alpha^3\gamma_1,\alpha^2\beta\gamma_1,\alpha\beta^2\gamma_1,\beta^3\gamma_1,\alpha\gamma^2\gamma_1,\beta\gamma^2\gamma_1,\alpha(\gamma_1)^3,\beta(\gamma_1)^3\}+\cdots\cdots \quad (74)$$
$$P_{1\xi}{}^{ql}=C\{(\gamma_q)^2\gamma_1\}+C\{\alpha(\gamma_q)^2\gamma_1,\beta(\gamma_q)^2\gamma_1\}+\cdots\cdots \qquad (q=2,3,\cdots\cdots,h) \quad (75)$$

As for the total $\pi$ electronic energy an equation similar to Eq. 66, as for the total bond order (and the electron density) one similar to Eq. 67, and as for the total bond order of a newly formed bond one similar to Eq. 75 may be obtained.

Thus it has become clear to what order of perturbation terms the additivity rule applies, and what kinds of terms appear in several molecular quantities. If it is necessary, one could formulate cross terms in reference to the results of two perturbations.

## Degenerate System

In the previous section it was assumed that no molecular orbital is degenerate with any other molecular orbital in the same molecule, not with molecular orbitals in any other system to be subjected to conjugation.

Even if some levels in the non-perturbed systems are degenerate, so far as they are chosen mutually orthogonal, the perturbed orbital energy and the perturbed separate bond order (and electron density) corresponding to non-degenerate orbitals are not affected at all, that is, equations derived in the preceding section, giving separate quantities, are valid also in this case.

As for degenerate levels, on the other hand, the sum of the perturbed orbital energies or of the perturbed bond orders over all the degenerate levels is easily obtained by taking a limit of the corresponding sum which is derived as if they were not degenerate. For instance, in Case I, when the $l$th and the $(l+1)$th levels are degenerate,

$$\varepsilon_l'+\varepsilon_{l+1}'=\lim_{\varepsilon_{l+1}\to\varepsilon_l}[\varepsilon_l',_{\text{nondeg}}+\varepsilon_{l+1}',_{\text{nondeg}}]$$
$$=2\varepsilon_l+[\delta(\varepsilon_l+\varepsilon_{l+1})]_r+[\delta(\varepsilon_l+\varepsilon_{l+1})]_s$$
$$+2\sum_{(\neq l,l+1)}^{k,\text{all}}\frac{c_r{}^k c_s{}^k(c_r{}^l c_s{}^l+c_r{}^{l+1}c_s{}^{l+1})}{\varepsilon_l-\varepsilon_k}(\alpha_r'\alpha_s')+\cdots\cdots \quad (76)$$

where

$$[\delta(\varepsilon_l+\varepsilon_{l+1})]_r=[(c_r{}^l)^2+(c_r{}^{l+1})^2]\alpha_r'$$
$$+\sum_{(\neq l,l+1)}^{k,\text{all}}\frac{(c_r{}^k)^2[(c_r{}^l)^2+(c_r{}^{l+1})^2]}{\varepsilon_l-\varepsilon_k}(\alpha_r')^2+\cdots\cdots \quad (77)$$

and $\varepsilon_l',_{\text{nondeg}}$ is given by Eq. 27, which is derived for non-degenerate system. Explicit formulae for other various degenerate cases are omitted here for the sake of brevity, but one

might write them down without difficulty according to the above principle. The total $\pi$ electronic energy and the bond order (or the electron density) being represented as the sums of orbital energies and separate orders (or densities) over the occupied orbitals, it is concluded that, even in the degenerate cases, if all the degenerate levels are occupied, the degeneracy does not affect the additivity rule, though concrete formulae involved may differ from the case of no degeneracy.

## Discussion

By the results obtained in the preceding sections the additivity rule concerning multiple perturbations and its limits of use have been clarified.

When a hetero-substitution of an atom in a conjugated system causes changes of the Coulomb integral of the atom and of the resonance integrals between neighboring atoms, their effects as a whole may be additively estimated in the first order perturbation treatment. When introduction of a conjugable group into a conjugated system at its certain atom gives rise simultaneously to a change of the Coulomb integral of the atom, the additivity rule applies to the first order terms.

Further, for the introduction of many substituents and hetero-substitutions, the additivity of these effects are materialized, and various examples are seen in experiments. The additivity of shift of absorption sprctra would be explained by the additivity in the orbital energy. The vector additivity of dipole moment would be understood as the additivity in the electron density or in the amount of charge transfer. Aono and Higuchi[4] interpreted the additivity of hyperfine splitting in the electron spin resonance spectrum of substituted semiquinones in terms of the additivity in the unpaired electron density.

Speaking of reactivity indices, i. g. the frontier electron density, $P_{uu}{}^{f}$, localization energy, $\varepsilon'$(localized state)$-\varepsilon'$(non-localized state), total $\pi$ electron density, $P_{uu}$, free valence, $\sqrt{3}-\sum_{v}{}'P_{uv}$, and most other indices, the additivity rule is applicable to a certain order of perturbation terms. Superdelocalizability is also proved to fulfil the additivity rule.

If one practically evaluates the cross terms appearing in the formulae, one would be able to discuss the deviation from the additivity rule, which is also often realized in experiments.

The authors are much indebted to Mr. Shigeyuki Aono for his helpful suggestions.

*Faculty of Engineering*
*Kyoto University*
*Sakyo-ku, Kyoto*

4) S. Aono, J. Higuchi, *Busseiron Kenkyu*, 7, 197 (1960).

# *The Adsorption of Dye Mixtures by Cellophane Sheet. II*[1]. *A Quantitative Discussion of the Adsorption of Dyes*

By Yukio HORIKI

(Received November 27, 1959)

In the previous work[1], a method of quantitative discussion of the interaction between dyes in a binary mixture dyebath has been discussed on the assumption that the decrease in adsorption of dyes from mixture dyeing is due to interaction. Further, the behavior of dyes in mixture dyeing has been qualitatively explained from those of single dyeings, taking account of the interaction obtained by the above method.

In this paper, the single dyeings of Chlorazol Sky Blue FF and Chrysophenine G and their mixture dyeing have been carried out in detail, to discuss quantitatively their behavior in mixture dyeing. In the single dyeing, the surface layer volume in Vickerstaff's theoretical equation for adsorption[2] has been discussed to obtain constant values of the standard affinity. In the mixture dyeing, the observed amounts of adsorption of the dyes have been compared with those calculated on the basis of the information both about the single dyeing particularly discussed and about the interaction obtained from the single and the mixture dyeings by the method reported before[1].

## Experimental and Results

The single dyeings of Chlorazol Sky Blue FF (shortly called Blue dye) and Chrysophenine G (Yellow dye) and the mixture dyeing of them follow a method quite similar to that in the previous work[1].

In the single dyeings, the initial concentration ranged from $1\times10^{-6}$ to $1.5\times10^{-5}$ mol./l. for Blue dye and $1.25\times10^{-6}$ to $1\times10^{-4}$ mol./l. for Yellow dye, and in the mixture dyeing, that of Blue dye was fixed at about $1\times10^{-5}$ mol./l. and that of Yellow dye varied from $2.5\times10^{-6}$ to $1\times10^{-4}$ mol./l.

Each dyeing was carried out for three, two and one day* at 50°, 70° and 90°C, respectively. The concentration of sodium chloride (2 g./l.) was the same as that in the previous work.

Results for single dyeings are shown in Figs. 1 (Blue dye) and 2 (Yellow dye) in terms of the relation between logarithms of the final dyebath concentration (Blue dye, $F_\sigma$ mol./l.; Yellow dye, $G_\sigma$ mol./l.) and those of the amount of adsorption (Blue dye, $F_\phi$ mol./kg.; Yellow dye, $G_\phi$ mol./kg.) of the dyes. The affinities of Blue dye and Yellow dye ($-\Delta\mu^0_F$ cal./mol.; $-\Delta\mu^0_G$ cal./mol.) were calculated by Vickerstaff's equation with $V=0.45$ l./kg. These results are shown in Figs. 3 (Blue dye) and 4 (Yellow dye) in terms of the relation between

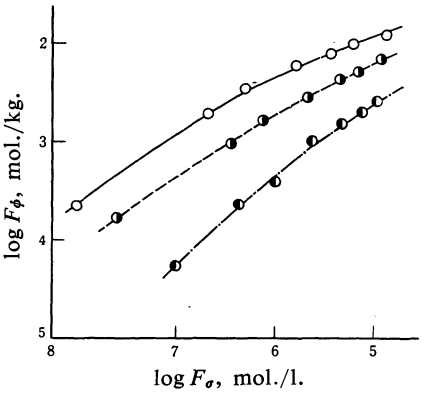



Fig. 1. Adsorption isotherms of Chlorazol Sky Blue FF on 'Cellophane' sheet at various temperatures: logarithmic plot of dyebath concentration and adsorption on the fiber.
—○— 50°C --◑-- 70°C -·-◐-·- 90°C

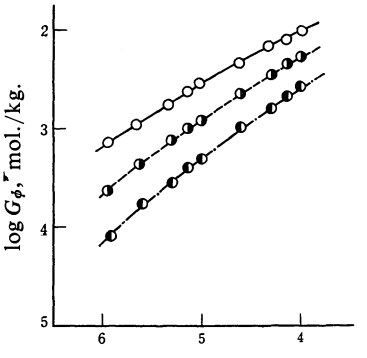



Fig. 2. Adsorption isotherms of Chrysophenine G on 'Cellophane' sheet at various temperatures: logarithmic plot of dyebath concentration and adsorption on the fiber.
—○— 50°C --◑-- 70°C -·-◐-·- 90°C

1) Part I of this series, Y. Horiki, Y. Tanizaki and N. Ando, This Bulletin, 33, 163 (1960).
2) R. H. Peters and T. Vickerstaff, *Proc. Roy. Soc.* (*London*) A192, 292 (1948).
* The dyeing time was ascertained to be sufficient to reach equilibrium at each temperature.

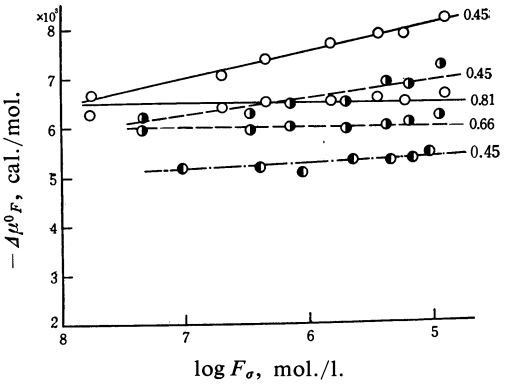



Fig. 3. Dependence of the standard affinity on dyebath concentration of Chlorazol Sky Blue FF at each temperature: plot of the standard affinity for logarithm of final dyebath concentration. The figures on each line indicate the surface layer volume (l./kg.) used in calculation.
—○— 50°C --◑-- 70°C -·-◐-·- 90°C

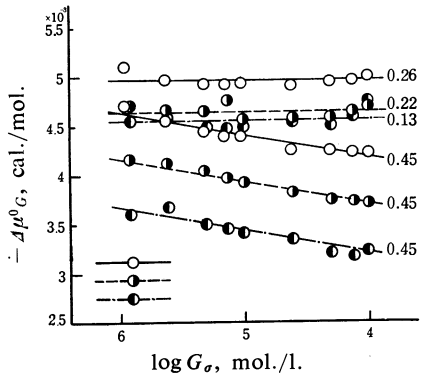



Fig. 4. Dependence of the standard affinity on dyebath concentration of Chrysophenine G at each temperature: plot of the standard affinity for logarithm of final dyebath concentration. The figure on each line indicates the surface layer volume (l./kg.) used in calculation.

the affinity and the logarithm of the final dyebath concentration. The relations of ($\log F_\phi\ Na^4_\phi - \log F_\sigma\ Na^4_\sigma$) and of ($\log G_\phi\ Na^2_\phi - \log G_\sigma\ Na^2_\sigma$) are shown in Figs. 5 and 6, respectively. It is recognized that they are nearly linear. Results of mixture dyeing, that is, the adsorptions of Blue dye ($F_\phi$ mol./kg.) and Yellow dye ($G_\phi$ mol./kg.), their effective dyebath concentrations obtained by the method reported before[1] ($F_\sigma'$ mol./l.; $G_\sigma'$ mol./l.), their dyebath concentrations which contributed to the interaction ($F_c$ mol./l.; $G_c$ mol./l.), and the ratios $G_\sigma/F_\sigma$ and $G_c/F_c$ are shown in Table I, together with the instability constant $K$ (mol./l.) calculated in the region where $G_\sigma/F_\sigma = 0.8 \sim 1.1$, according to

$$K = \frac{\frac{F_\sigma' \cdot G_\sigma'}{F_c + G_c}}{2} = \frac{2F_\sigma' \cdot G_\sigma'}{F_c + G_c} = \frac{2(F_\sigma - F_c)(G_\sigma - G_c)}{F_c + G_c} \quad (1)$$

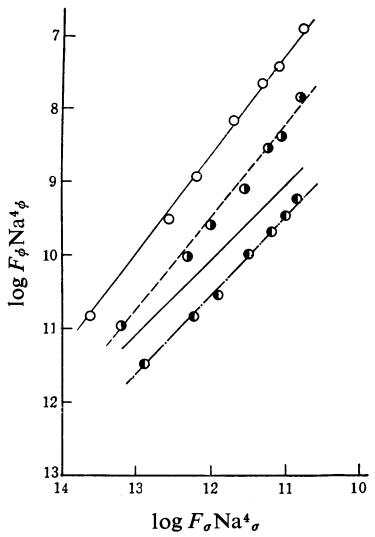



Fig. 5. Adsorption of Chlorazol Sky Blue FF on 'Cellophane' sheet at each temperature: plot of logarithm of ionic products in the fiber and in dyebath.

| | | $\alpha$ |
|---|---|---|
| ——— | | 1.00 |
| —○— | 50°C | 1.32 |
| ---◑--- | 70°C | 1.20 |
| -·-◐-·- | 90°C | 1.05 |

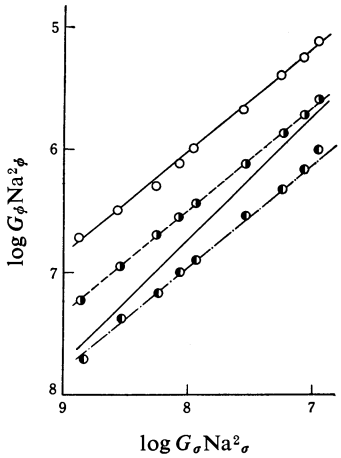



Fig. 6. Adsorption of Chrysophenine G on 'Cellophane' sheet at each temperature: Plot of logarithm of ionic products in the fiber and in dyebath.

| | | $\alpha$ |
|---|---|---|
| ——— | | 1.00 |
| —○— | 50°C | 0.85 |
| ---◑--- | 70°C | 0.84 |
| -·-◐-·- | 90°C | 0.82 |

Table I

| T°C | Exp. No. | $F_\phi$ mol./kg. $\times10^3$ | $F_\sigma$ mol./l. $\times10^6$ | $F_\sigma'$ mol./l. $\times10^6$ | $F_c$ mol./l. $\times10^6$ | $G_\phi$ mol./kg. $\times10^3$ | $G_\sigma$ mol./l. $\times10^6$ | $G_\sigma'$ mol./l. $\times10^6$ | $G_c$ mol./l. $\times10^6$ | $G_\sigma/F_\sigma$ | $G_c/F_c$ | $K$ mol./l. |
|---|---|---|---|---|---|---|---|---|---|---|---|---|
| | 1 | 10.36 | 9.46 | 7.5 | 2.0 | 0.03 | 2.53 | ? | ? | 0.27 | ? | |
| | 2 | 8.98 | 9.30 | 4.9 | 4.4 | 0.25 | 4.94 | ? | ? | 0.53 | ? | |
| | 3 | 7.76 | 9.64 | 3.2 | 6.4 | 0.45 | 6.91 | ? | ? | 0.72 | ? | |
| | 4 | 6.37 | 9.72 | 1.8 | 7.9 | 0.78 | 8.88 | 1.1 | 7.9 | 0.91 | 1.0 | $2.5\times10^{-7}$ |
| 50 | 5 | 4.87 | 9.78 | 0.91 | 8.9 | 1.00 | 10.92 | 1.8 | 9.1 | 1.12 | 1.0 | $1.8\times$ 〃 |
| | 6 | 1.82 | 9.74 | 0.19 | 9.6 | 2.36 | 19.79 | 7 | 12.8 | 2.03 | 1.3 | |
| | 7 | 0.56 | 10.01 | 0.04 | 10.0 | 4.46 | 39.66 | 23 | 16.7 | 3.96 | 1.7 | |
| | 8 | 0.27 | 10.04 | 0.01 | 10.0 | 5.96 | 59.10 | 36 | 23.1 | 5.89 | 2.3 | |
| | 9 | 0.14 | 10.11 | 0.01 | 10.0 | 7.47 | 79.21 | 56 | 23.2 | 7.83 | 2.3 | |
| | 10 | 0.05 | 10.09 | ? | ≒10 | 9.33 | 98.90 | 83 | 15.9 | 9.80 | 1.6 | |
| | 1 | 5.33 | 9.82 | 6.8 | 3.0 | 0.07 | 2.53 | ? | ? | 0.26 | ? | |
| | 2 | 4.53 | 9.83 | 4.8 | 5.0 | 0.19 | 5.05 | 0.9 | 4.2 | 0.51 | 0.8 | $9.4\times10^{-7}$ |
| | 3 | 3.94 | 9.73 | 3.7 | 6.0 | 0.25 | 6.96 | 1.3 | 5.7 | 0.72 | 1.0 | $8.2\times$ 〃 |
| | 4 | 3.40 | 9.78 | 2.9 | 6.9 | 0.40 | 8.90 | 2.2 | 6.7 | 0.91 | 1.0 | $9.4\times$ 〃 |
| 70 | 5 | 2.87 | 9.91 | 2.0 | 7.9 | 0.51 | 10.91 | 2.9 | 8.0 | 1.10 | 1.0 | $7.3\times$ 〃 |
| | 6 | 1.56 | 9.75 | 0.66 | 9.1 | 1.32 | 19.95 | 10 | 10.0 | 2.05 | 1.1 | $6.9\times$ 〃 |
| | 7 | 0.72 | 9.92 | 0.25 | 9.7 | 2.34 | 39.61 | 25 | 14.6 | 3.99 | 1.5 | |
| | 8 | 0.44 | 9.92 | 0.14 | 9.8 | 3.18 | 59.77 | 43 | 16.8 | 6.02 | 1.7 | |
| | 9 | 0.29 | 10.01 | 0.09 | 9.9 | 3.92 | 79.75 | 61 | 18.8 | 7.97 | 1.9 | |
| | 10 | 0.20 | 9.97 | 0.06 | 9.9 | 5.47 | 99.33 | 100 | ? | 9.96 | ? | |
| | 1 | 1.96 | 9.64 | 6.8 | 2.8 | 0.09 | 2.51 | 1.3 | 1.2 | 0.26 | 0.4 | |
| | 2 | 1.87 | 9.74 | 6.2 | 3.5 | 0.10 | 4.98 | 1.5 | 3.5 | 0.51 | 1.0 | $2.7\times10^{-6}$ |
| | 3 | 1.72 | 9.77 | 5.4 | 4.4 | 0.18 | 7.48 | 2.8 | 4.7 | 0.77 | 1.1 | $3.3\times$ 〃 |
| | 4 | 1.63 | 9.64 | 4.9 | 4.7 | 0.30 | 10.02 | 5.2 | 4.8 | 1.04 | 1.0 | $5.4\times$ 〃 |
| 90 | 5 | 1.14 | 9.79 | 2.8 | 7.0 | 0.52 | 20.08 | 10.5 | 9.6 | 2.05 | 1.4 | |
| | 6 | 0.71 | 10.01 | 1.3 | 8.7 | 1.02 | 39.83 | 25 | 14.8 | 3.98 | 1.7 | |
| | 7 | 0.51 | 9.94 | 0.87 | 9.1 | 1.53 | 59.63 | 45 | 14.6 | 6.00 | 1.6 | |
| | 8 | 0.37 | 9.90 | 0.58 | 9.3 | 1.94 | 79.60 | 64 | 15.6 | 8.04 | 1.7 | |
| | 9 | 0.30 | 10.05 | 0.45 | 9.6 | 2.35 | 99.11 | 86 | 13.1 | 9.86 | 1.4 | |

## Discussion

The standard affinity of dye anions for the fiber in the single dyeing can be calculated theoretically by[2]

$$\log \frac{D_\phi \mathrm{Na}^z{}_\phi}{V^{z+1}} = \log D_\sigma \mathrm{Na}^z{}_\sigma + \left(\frac{-\Delta\mu^0}{RT}\right) \quad (2)$$

$$\mathrm{Na}_\phi = D_\phi \left\{\frac{z}{2} + \left(\frac{z^2}{4} + \frac{V^2 \mathrm{Na}_\sigma \cdot \mathrm{Cl}_\sigma}{D^2_\phi}\right)^{1/2}\right\} \quad (2')$$

where $D_\phi$ is the amount of adsorbed dye anions on the fiber at equilibrium (mol./kg.), $D_\sigma$, the dyebath concentration of dye anions at equilibrium (mol./l.), $\mathrm{Na}_\phi$, the concentration of the sodium ion in the fibre phase at equilibrium (mol./kg.), $\mathrm{Na}_\sigma$, $\mathrm{Cl}_\sigma$, the concentrations of the sodium and the chloride ions in the dyebath at equilibrium (mol./l.), $-\Delta\mu^0$, the standard affinity of dye anions for the fiber (cal./mol.), $z$, the valency of dye anions, $R$, $T$, the gas constant and the absolute temperature, and $V$, the surface layer volume of the fiber (l./kg.). However, the relation of Eq. 2 does not always come into being, depending on values employed as the surface layer volume, and it forms the following relations usually:

$$\log \frac{D_\phi \mathrm{Na}^z{}_\phi}{V^{z+1}} = \alpha \log D_\sigma \mathrm{Na}^z{}_\sigma + \left(\frac{-\Delta\mu^{0\prime}}{RT}\right) \quad (3)$$

Hence, $-\Delta\mu^{0\prime}$ corresponding to the affinity in this equation does not show a constant value. This was also seen in the present results; the value of $\alpha$ obtained from the results of the single dyeing of Blue dye or Yellow dye by using $V=0.45$ l./kg. does not become unity, as is shown clearly by the relations of $\log F_\phi \mathrm{Na}^4_\phi - \log F_\sigma \mathrm{Na}^4_\sigma$ and of $\log G_\phi \mathrm{Na}^2_\phi - \log G_\sigma \mathrm{Na}^2_\sigma$ in Figs. 5 and 6. Consequently, $-\Delta\mu^{0\prime}$ does not show constant values as shown in Figs. 3 and 4. Theoretically the affinity should remain constant. In order to discuss quantitatively the behavior of dyes in the mixture dyeing, it is desirable that $-\Delta\mu^{0\prime}$ obtained from the single dyeing should be constant. Now, let us assume simply that the reason why $\alpha$ is not unity is due to the improper value of $V$. If

$V'$ is put as the surface layer volume corresponding to $\alpha=1$, $V$ should be replaced by $V'$ in Eq. 2, and then $Na_\phi$ by $Na_\phi'$ (mol./kg.) corresponding to $V'$. Thus we obtain

$$\frac{1}{\alpha}\log\frac{D_\phi Na^z{}_\phi}{V^{z+1}}=\log\frac{D_\phi Na_\phi{}'^z}{V'^{z+1}} \tag{4}$$

Then, Eq. 3 becomes

$$\log\frac{D_\phi Na_\phi{}'^z}{V'^{z+1}}=\log D_\sigma Na_\sigma{}^z+\frac{1}{\alpha}\left(\frac{-\Delta\mu^0}{RT}\right) \tag{5}$$

Thus we shall obtain constant affinities by putting

$$\frac{1}{\alpha}\left(\frac{-\Delta\mu^{0\prime}}{RT}\right)=\frac{-\Delta\mu^0}{RT} \tag{6}$$

Such a surface layer volume $V'$ can be calculated as follows: from a graph of $\log D_\phi Na^z{}_\phi-\log D_\sigma Na^z{}_\sigma$ drawn by using any seemingly adequate value of $V$ (e. g. 0.45 l./kg.), we obtain a value of $\alpha$, and then putting it into Eq. 4 together with any two pairs of the results of single dyeing $(D_{\phi_1}, Na_{\phi_1})$ $(D_{\phi_2}, Na_{\phi_2})$, we have

$$\frac{1}{\alpha}\log\frac{D_{\phi_1}Na^z{}_{\phi_1}}{V^{z+1}}=\log\frac{D_{\phi_1}Na'^z{}_{\phi_1}}{V'^{z+1}} \tag{7}$$

$$\frac{1}{\alpha}\log\frac{D_{\phi_2}Na^z{}_{\phi_2}}{V^{z+1}}=\log\frac{D_{\phi_2}Na'^z{}_{\phi_2}}{V'^{z+1}} \tag{7'}$$

Thus the following equation is obtained,

$$\frac{Na'_{\phi_1}}{Na'_{\phi_2}}=\left(\frac{D_{\phi_1}}{D_{\phi_2}}\right)^{\left(\frac{1}{\alpha}-1\right)/z}\cdot\left(\frac{Na_{\phi_1}}{Na_{\phi_2}}\right)^{\frac{1}{\alpha}} \tag{8}$$

On the other hand, if each of $(D_{\phi_1}, Na'_{\phi_1})$ and $(D_{\phi_2}, Na'_{\phi_2})$ satisfies Eq. 2', we obtain from Eqs. 8 and 2'

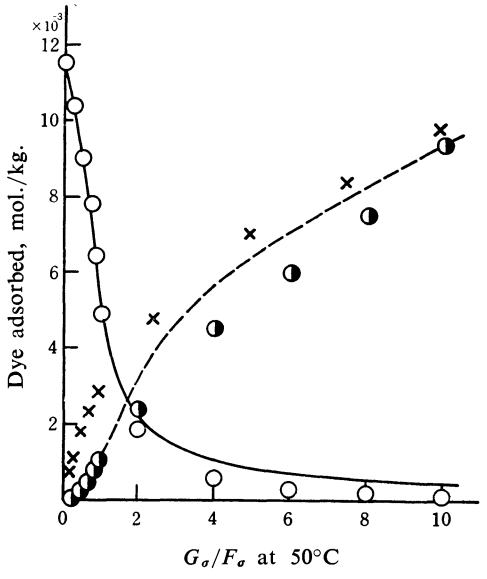



Fig. 7.

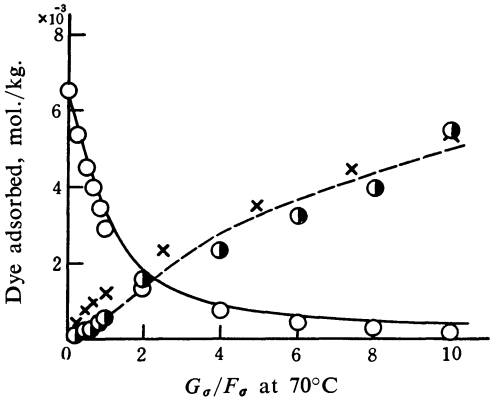



Fig. 8.

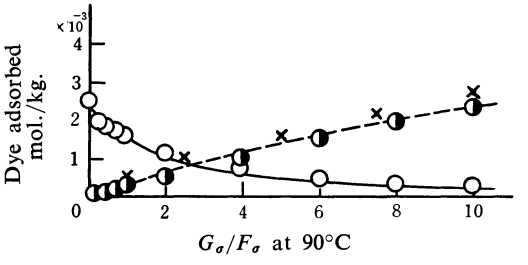



Fig. 9.

Figs. 7, 8 and 9. Adsorption isotherms of Chlorazol Sky Blue FF and Chrysophenine G in mixture dyeing at various temperatures: plot of adsorption on the fibre and ratio $G_\sigma/F_\sigma$; solid line, the curve of adsorption predicted theoretically of Chlorazol Sky Blue FF in mixture dyeing; broken line, the curve of adsorption predicted theoretically of Chrysophenine G in mixture dyeing.
○: The adsorption observed of Chlorazol Sky Blue FF in mixture dyeing.
◑: The adsorption observed of Chrysophenine G in mixture dyeing.
×: The adsorption observed of Chrysophenine G in single dyeing.

$$\frac{Na'_{\phi_1}}{Na'_{\phi_2}}=\frac{D_{\phi_1}\left\{\frac{z}{2}+\left(\frac{z^2}{4}+\frac{V'^2Na_{\sigma_1}\cdot Cl_{\sigma_1}}{D^2{}_{\phi_1}}\right)^{1/2}\right\}}{D_{\phi_2}\left\{\frac{z}{2}+\left(\frac{z^2}{4}+\frac{V'^2Na_{\sigma_2}\cdot Cl_{\sigma_2}}{D^2{}_{\phi_2}}\right)^{1/2}\right\}} \tag{9}$$

where $Na_{\sigma_1}$, $Cl_{\sigma_1}$, etc. denote the concentrations of the sodium and the chloride ion in the dyebath at equilibrium (mol./l.) respectively. When we solve Eq. 9 with respect to $V'$ and put it into Eq. 5, we may be able to obtain constant values of the standard affinity.

Now in practice, values of the surface layer volume $V'$ for the single dyeings of Blue dye and Yellow dye are obtained by use of $\alpha$ resulting from $V=0.45$ l./kg. and the affinities

are calculated from Eqs. 5 and 6 by use of this $V'$. These results are shown in Table II, Figs. 3 and 4. "$-\Delta\mu^0_{mean}$" in the table denotes the mean values of adjusted affinities of Blue dye and Yellow dye. They give rather constant values**. Such adjustment of the surface layer volume so as to obtain a constant affinity means to treat $V$ as a parameter.

The observed amounts of adsorption of the dyes from the mixture dyeing are compared with those calculated by using the adjusted $-\Delta\mu^0_{mean}$ (Table II) and the instability constant $K$ (Table I), which was obtained from the results of the single and the mixture dyeings as mentioned before[1], on the assumption

TABLE II

| Dye | $T$°C | $\alpha$ | $V'$ l./kg. | $-\Delta\mu^0_{mean}$ cal./mol. |
|---|---|---|---|---|
| Blue dye | 50 | 1.32 | 0.81 | 6500 |
| | 70 | 1.20 | 0.66 | 6000 |
| | 90 | 1.05 | 0.45 | 5300 |
| Yellow dye | 50 | 0.85 | 0.26 | 4970 |
| | 70 | 0.84 | 0.22 | 4640 |
| | 90 | 0.82 | 0.13 | 4550 |

that the reduction in amounts of adsorption from mixture dyeing is mainly due to an interaction between both dyes in the dyebath. These results are shown in Figs 7, 8 and 9. However, on the supposition that only a one to one complex is formed over the whole concentration region of the dyes and that dye molecules which contribute to the complex formation have no relation to adsorption, the effective dyebath concentration of Blue dye $F'_{\sigma cal}$ (hereafter "cal" is suffixed to calculated values) is obtained from Eq. 10

$$F'_{\sigma cal}=1/2\{(G_\sigma-a)^2+(b^2-a^2)\}^{1/2}+1/2(a-G_\sigma) \quad (10)$$

where $a=F_\sigma-K$ and $b=F_\sigma+K$, and the mean value of the instability constant shown in Table I is used as $K$, i. e. $2\times10^{-7}$, $8\times10^{-7}$ and $4\times10^{-6}$ (mol./l.) at 50°, 70° and 90°C, respectively. The final dyebath concentration of Blue dye and Yellow dye in Table I are used as $F_\sigma$ and $G_\sigma$ in Eq. 10.

The effective dyebath concentration of Yellow dye $G'_{\sigma cal}$ is obtained from

$$G'_{\sigma cal}=G_\sigma-G_{c cal}=G_\sigma-(F_\sigma-F'_{\sigma cal})=G_\sigma-F_{c cal} \quad (11)$$

** Standing has discussed the value of $V$ for Chrysophenine G ($z=2$) using the so-called $p$-$q$ equation (*J. Text. Inst.*, **45**, T 21 (1954)). With his method, however, the calculation for Chlorazol Sky Blue FF ($z=4$) becomes complicated. Hence in this work, $V$ was adjusted as above. The results for Chrysophenine G are considerably approximated to his result.

The amount of adsorption of both dyes are calculated by the following equations, on the assumption that the affinity of each dye does not change in the mixture dyeing.

$$F_{\phi cal}=F'_{\sigma cal}Na^{-4}_{F\phi cal}Na^4{}_\sigma V_F{}'^5\times\exp\left(\frac{-\Delta\mu^0_{F mean}}{RT}\right) \quad (12)$$

$$G_{\phi cal}=G'_{\sigma cal}Na^{-2}{}_{G\phi cal}Na^2{}_\sigma V_G{}'^3\times\exp\left(\frac{-\Delta\mu^0_{G mean}}{RT}\right) \quad (12')$$

where the values for $Na_{F\phi cal}$ and $Na_{G\phi cal}$ are approximately obtained from the equations derived by eliminating $D_\phi$ in Eqs. 2 and 2′,

$$Na^3_{F\phi cal}(Na^2_{F\phi cal}-V_F{}'^2Na_\sigma\cdot Cl_\sigma)=4Na_\sigma{}^{-4}F'_{\sigma cal}V_F{}'^5\exp\left(\frac{-\Delta\mu^0_{F mean}}{RT}\right) \quad (13)$$

$$Na_{G\phi cal}(Na^2_{G\phi cal}-V_G{}'^2Na_\sigma\cdot Cl_\sigma)=2Na_\sigma{}^{-2}G'_{\sigma cal}V_G{}'^3\exp\left(\frac{-\Delta\mu^0_{G mean}}{RT}\right) \quad (13')$$

where the values of $V_F'$, $V_G'$, $-\Delta\mu^0_{F mean}$ and $-\Delta\mu^0_{G mean}$ are obtained from the respective values at the various temperatures shown in Table II.

It is brought out from these results that the observed amounts of adsorption of the dyes agree well with those calculated over the whole range of concentration at 90°C (Fig. 9); this means that the behavior of the dyes in mixture may be explained quantitatively by the formation of a 1 : 1 complex in the dyebath. Though both values calculated and observed show considerably good agreement at 70 and 50°C, too, some deviation is recognized at these temperatures in the range where $2\lesssim G_\sigma/F_\sigma\lesssim 8$. It may be due to the fact that where $G_\sigma/F_\sigma\geqq 2$, the dyes form not only one to one complex, but higher complexes richer in Yellow dye (may be one to two), which promote the reduction of adsorption***. In the region $G_\sigma/F_\sigma\approx 10$, the observed adsorption of Yellow dye tends to approach that in the single dyeing. This will be explained by the thought that even if the composition of complexes becomes completely one to two, Yellow dye may behave as in the single dyeing, because of its comparatively higher concentration than

*** It has been recognized by spectral measurements that a 1:2 complex richer in Yellow dye is also formed in the mixture of Blue and Yellow dye at room temperature (T. Kobayashi, Y. Tanizaki and N. Ando., This Bulletin, **33**, 661 (1960)). On the other hand, it has been concluded that only a one to one complex is formed at 60°C (A. N. Derbyshire and R. H. Peters, *J. Soc. Dyers Col.*, **72**, 268 (1956)).

However, the spectral measurements for the mixture solution in the presence of sodium chloride at high temperature has not yet been carried out, so the composition of complexes may be open to discussion.

that of Blue dye. On the other hand, since $F_a$ is almost constant, the formation of complexes and their compositions may have considerable influence on the adsorption of Blue dye with an increase of Yellow dye. In fact, the observed values of adsorption of Blue dye shown in Figs. 7 and 8 are small compared with those calculated on the basis of the formation of only a one to one complex.

Thus the behavior of dyes in the mixture dyeing may be well explained quantitatively by the method mentioned above if both dyes interact with each other (complex formation) in the dyebath. If further information on these matters, i. e. on the single dyeing and the interaction, is obtained hereafter, this problem will be treated more clearly.

## Summary

1. The single dyeings of Chlorazol Sky Blue FF and Chrysophenine G and the mixture dyeing of them were carried out at 50, 70 and 90°C.

2. In the single dyeing, the surface layer volume in Vickerstaff's equation was adjusted so as to obtain constant values of the standard affinity.

3. In the mixture dyeing, the behavior of dyes was explained quantitatively on the basis of the information of the single dyeing and the interaction between both dyes in the dyebath.

The author is greatly indebted to Professor Noboru Ando and Mr. Yoshié Tanizaki for their valuable advice and encouragement throughout this work.

*Laboratory of Physical Chemistry*
*Tokyo Institute of Technology*
*Meguro-ku, Tokyo*

# *Dichroism of Dyes in the Stretched PVA Sheet. III*[1]. *Direction of Absorption of Pinacyanol Iodide*[*1]

By Yoshié TANIZAKI

(Received December 18, 1959)

In the previous paper[1], a theoretical expression was derived concerning the relation between the optical density ratio $R_d(=D_{\parallel}/D_{\perp})$ and the stretch ratio $R_s$ of the sample sheet, for the analysis of the relative absorption direction of dye molecules in the stretched PVA (polyvinyl alcohol) sheet. It was also proved experimentally that the adopted assumption in the derivation of the distribution function and accordingly the above $R_d$ expression are adequate[2]. A parameter $r$ in the $R_d$ expression, which determines the $R_d-R_s$ curve practically, is a particular one to each absorption band. Also this $r$-value determines the angle between the transition direction and the orientation axis of the molecule. Therefore, the greater the number of the absorption band in the observable region, the easier would be the discussion on the correspondence between the relative transition direction and the molecular structure.

In this paper, turning our attention to the fact that the pinacyanol cation reveals a number of absorption bands from the visible to the near ultraviolet region, we determined the relative transition direction of some absorptions from the quantitative analysis. We also deduced the directions of other absorptions.

## Experimental

The pinacyanol iodide used was synthesised and purified in the Laboratory of Fuji Photo Film Co., Ltd.

The experiment was carried out in the same way as before[1,3]. When a quantitative test is required, the correction of absorption and reflection by the substrate of the sheet becomes important, especially in the ultraviolet region.

Resultant optical density $D$ from the absorption and/or the reflection of the PVA sheet itself in the visible region is as small as less than 0.05, almost

1) Part II of this series, Y. Tanizaki, This Bulletin, 32, 75 (1959).

*1 Presented at the 12th Annual Meeting of the Chemical Society of Japan, Kyoto, April, 1959.

2) Y. Tanizaki, T. Kobayashi and N. Ando, This Bulletin, 32, 1362 (1959).

3) Y. Tanizaki and N. Ando, *J. Chem. Soc. Japan, Pure Chem. Sec. (Nippon Kagaku Zasshi)*, 78, 542 (1957).

independent of the stretch ratio $R_s$, and the difference of $D_{\parallel}$ and $D_{\perp}$ is negligible because it is of the order of 0.001. In the near ultraviolet region, however, with decrease in wavelength, not only $D_{\parallel}$ and $D_{\perp}$ but their differences increases gradually, and these are all dependent on $R_s$. Accordingly, in the dichroic measurement the error arising from the incongruity in the stretch directions of the sample sheet and the correction sheet with each other (in ihe same $R_s$-value) becomes considerably large in general in the ultraviolet region. For this reason, the correction in the ultraviolet region, especially for the comparatively small density absorption, is of importance. So it was taken into consideration that the specific directions—the stretch directions—of the stained and the unstained sheet must be kept parallel with each other. An example of the observed relation between angle $\theta$ and optical density $D_\theta$ is illustrated in Fig. 1, in which $\theta$

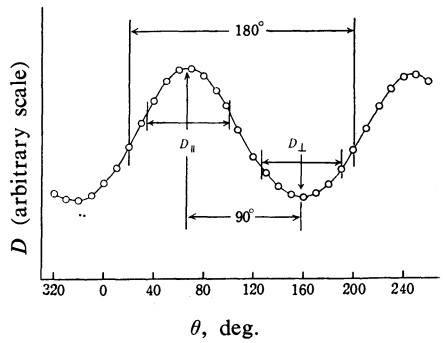



Fig. 1. Relation of optical density of pinacyanol in the stretched PVA sheet to the angle $\theta$ graduated on the disk of the sheet rotation apparatus. $R_s=5.4$, $\lambda=284$ m$\mu$.

means the angle graduated on the disk of the sheet-rotation apparatus (see Figure 1 of Ref. 1). In Fig. 1, $D_\theta$ for a given angle $\theta$ coincides with $D_{(\theta+180°)}$ for $(\theta+180°)$. When the angle of the middle point of equivalent densities on both sides of the maximum is denoted as $\parallel$ and that for the minimum as $\perp$, the angle scale difference between $\parallel$ and $\perp$ is equal to just 90°. The optical densities for $\parallel$ and $\perp$ are indicated by $D_{\parallel}$ and $D_{\perp}$, respectively. A revolution of the disk gives two $D_{\parallel}$'s and two $D_{\perp}$'s. Two $D_{\parallel}$'s ought to be equivalent to each other, and the same must be said with two $D_{\perp}$'s, but sometimes they were not. These differences, however, were small, so that the mean value of each was used for the purpose of analysis.

## Results

Absorption spectra of pinacyanol in the non-stretched PVA sheet are shown by solid lines in Figs. 2 and 3. In these figures, spectra in ethanol are also shown by broken lines for the comparison. Pinacyanol reveals absolutely corresponding absorption bands in both media, where every band in the sheet only shifts more or less to the longer side (200~300 cm$^{-1}$) compared with that in ethanol.

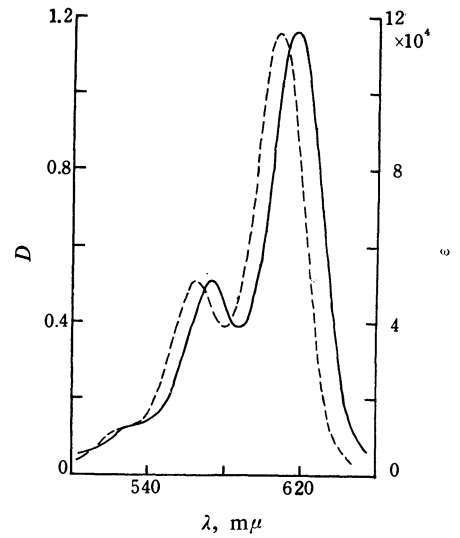



Fig. 2. Absorption spectra both in visible region of pinacyanol in the non-stretched ($R_s=1.0$) PVA sheet (solid line) and in an ethanolic solution of $2.79\times10^{-5}$ mol./kg. (broken line).

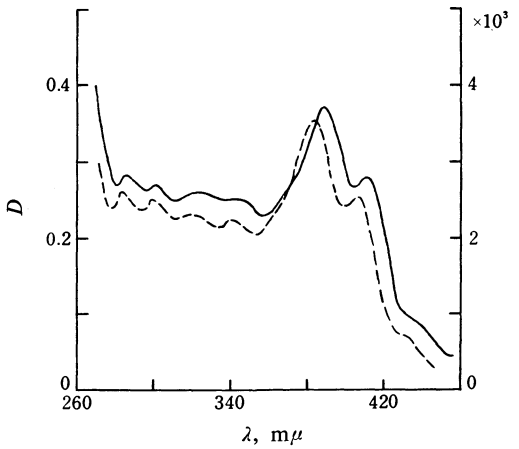



Fig. 3. Absorption spectra both in the near ultraviolet region of pinacyanol in the non-stretched ($R_s=1.0_4$) PVA sheet (solid line) and in ethanolic solution of $2.79\times10^{-5}$ mol./kg. (broken line).

Curves indicated in Figs. 4 and 5 corresponding to respective ones of Figs. 2 and 3 are obtained by stretching the sheet and then observing it with polarized light. None of the bands in Fig. 4 nor those around 400 m$\mu$ in Fig. 5 have any change either in shape or in maximum position, with the change of angle $\theta$, and they have the same order of the optical density ratio $R_d$, with a considerably large value compared with the rest of the bands.

The rest, on the other hand, change in shape and maximum position, together with $\theta$. The behavior with $\theta$ of the absorption curves near

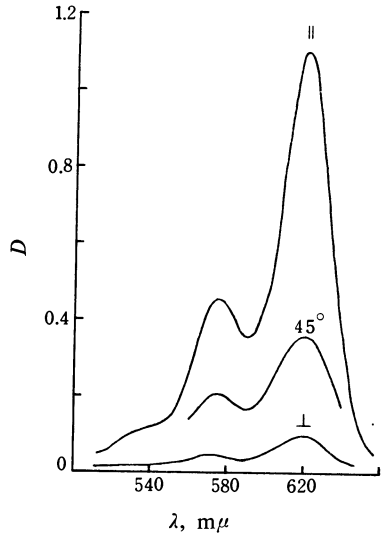



Fig. 4. Dichroism of pinacyanol in the stretched sheet at $R_s=8.2$, corresponding to Fig. 2. The sheet reflection is already corrected. ∥, 45° and ⊥ mean the absorptions for the polarized light of which the direction of the electric vector is parallel, 45° and right angles to the stretch direction of the sheet, respectively.

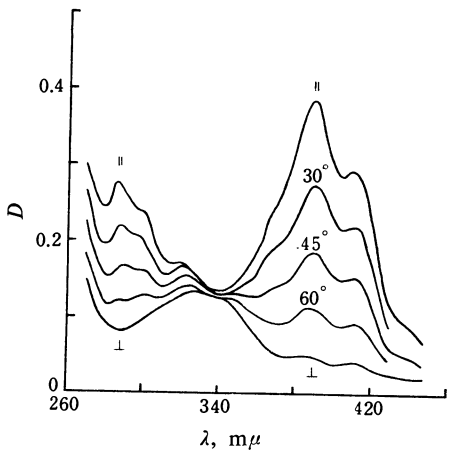



Fig. 5. Dichroism of pinacyanol in the stretched sheet at $R_s=8.0$, corresponding to Fig. 3. Corrected as for the absorption and reflection of the sheet. ∥, 30°, 45°, etc. have the same meaning as these in Fig. 4.

340 mμ is especially noticeable in the point that the absorption intensity has no great change with $\theta$.

Expansion of observation from the first bands to the long wavelength found out a weak but single band at 700 mμ. This is as shown in Fig. 6 and has similar behavior as other visible bands. Moreover, there were noticed weak absorptions at about 470 mμ and at 440 mμ,

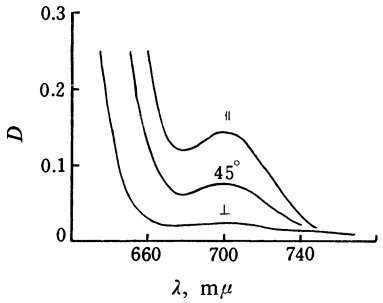



Fig. 6. Dichroism of the pinacyanol weak band at 700 mμ. $R_s=11$.

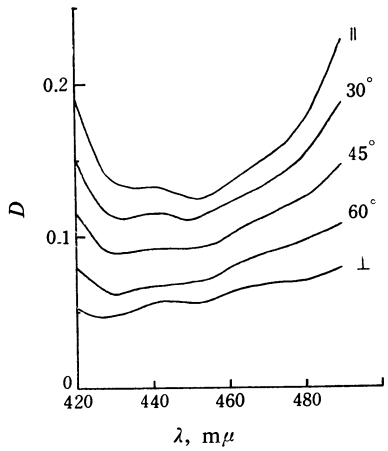



Fig. 7. Dichroism of the Pinacyanol weak band at about 470 mμ and at 440 mμ. $R_s=6.0$.

but their properties could not be judged owing to the nearby strong absorptions (Fig. 7).

The polarization degree of the polaroid used decreases in short region of 300 mμ and follows a curve as shown in Fig. 8. That is to say, the incident light in this region is a partially polarized light. Absorption spectra by this light are indicated by solid lines in Fig. 8. Curves in this figure show an obvious absorption band at 240 mμ and a shoulder at 260 mμ. The absorption at 240 mμ becomes more indistinct as it moves from $D_{\parallel}$ to $D_{\perp}$ curve, and that of 260 mμ stands just on the reverse.

All the absorption bands that could be recognized by the measurement are summarized in Table I, being numbered in order from high to low wavelength. These bands in Table I were distinguished by their shape in this way as follows. The number, wavelength and wavenumber of a band have no mark when it indicated a distinct maximum at least in one of $D_{\parallel}$ and $D_{\perp}$ (in general $D_{\theta}$) curve, are put in parentheses when it indicated distinct shoulder, and are put in brackets when it showed indistinct shoulder or curvature.

Experimental relations between each $R_d$ and

TABLE I. *r*-VALUES, DIRECTIONS AND CLASSIFICATION OF THE ABSORPTION BANDS OF PINACYANOL RECOGNIZED IN THE PVA SHEET BY DICHROIC MEASUREMENTS

| Band No. | $\lambda$ m$\mu$ | $\nu$ cm$^{-1}$ | *r*-Value | Angle | Direction | Classification |
|---|---|---|---|---|---|---|
| I | 700 | 14280 | | | longi. | |
| II | 620 | 16120 | 2.60~2.00 | 21.0~26.5 | longi. | First group |
| III | 575 | 17380 | 2.60~2.00 | 21.0~26.5 | longi. | (strong) |
| (IV) | (530) | (18860) | | | longi. | |
| [V] | [470] | [21270] | | | longi. ? | |
| (VI) | (440) | (22710) | | | longi. | Second group |
| VII | 410 | 24380 | 2.60~2.00 | 21.0~26.5 | longi. | (weak) |
| VIII | 388 | 25760 | 2.60~2.00 | 21.0~26.5 | longi. | |
| [IX] | [365] | [27400] | | | longi. ? | |
| (X) | (345) | (29000) | 0.75 | 53.1 | $\perp$ | |
| XI | 328 | 30500 | 0.85 | 49.6 | $\perp$ | Third group |
| (XII) | (300) | (33300) | 1.15 | 41.0 | $\parallel$ | (weak) |
| XIII | 286 | 35000 | 1.30 | 37.6 | $\parallel$ | |
| (XIV) | (275) | (38900) | | | $\perp$ | Fourth group |
| XV | 240 | 41650 | | | $\parallel$ | (strong) |
| [XVI] | [230] | [43500] | | | $\perp$ | |

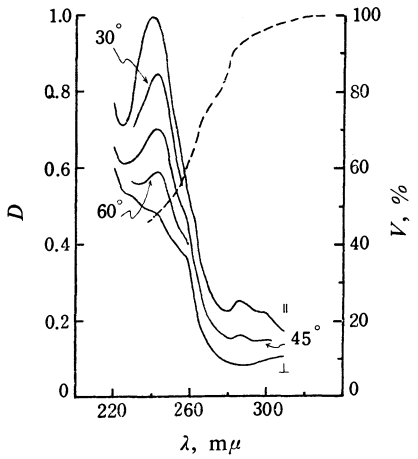



Fig. 8. Dichroism in the ultraviolet region of pinacyanol at $R_s$=5.4. The broken line represents the polarization degree of the polaroid used. Taken from Y. Tanizaki, This Bulletin, **30**, 935 (1957).

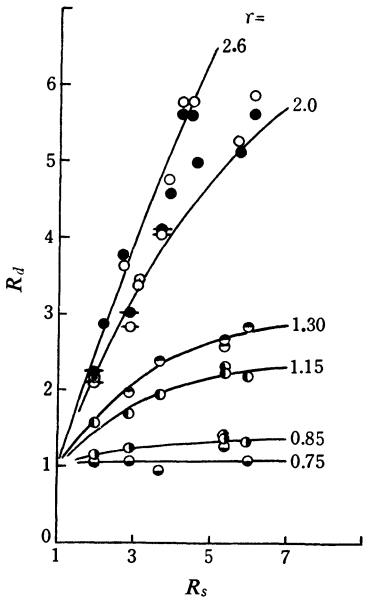



Fig. 9. Relations of $R_d$ to $R_s$ of absorption bands. Circles represent the observed values; ○: 620 m$\mu$ (Band II), ●: 570 m$\mu$ (III), -○-: 410 m$\mu$ (VII), -●-: 388 m$\mu$ (VIII), ◓: 286 m$\mu$ (XIII), ◒: 344 m$\mu$ (X), ◐: 300 m$\mu$ (XII), ◑: 328 m$\mu$ (XI). Curves are the calculated ones for respective *r*-value from the $R_d$ expression of Ref. 1.

$R_s$ of Bands II, III, VII, VIII and X—XIII are shown in Fig. 9. Curves in the figure are theoretical ones corresponding to respective *r*-values[1),*2]. Observed values of each Band II, III, VII and VIII approximately fall between these curves which have peculiar *r*-values. Angles between transition directions and an orientation axis of the molecule are evaluated from the *r*-values and indicated in Table I.

**Assignment of Transition Direction.**—As shown in Figs. 2—8, all the absorption bands in visible region and around 400 m$\mu$ had so large $R_d$ values that they were distinguished from others. It is considered that the double bond system which runs through over the molecular axis responsible for the first band of cyanines of this kind (here Band II)[4]. If

*2 Cot$^{-1}r$ gives the angle between the direction of orientation and that of transition of the absorption.

4) For example, H. Kuhn, *J. Chem. Phys.*, 17, 1198 (1949); G. S. Levinson, W. T. Simpson and W. Curtis, *J. Am. Chem. Soc.*, 79, 4314 (1957).

this is the case, it must be expected that such an absorption band gives the maximum $R_d$ when the longitudinal axis of the molecule meets the stretching direction of the sheet. In effects, the fact that the $R_d$-value of the first band is always larger than that of any band in the region below 360 m$\mu$, means that this molecular axis approaches most completely its orientation axis. Accordingly, it is concluded that a group of bands, of which $r$-values fall between 2.0~2.6, as indicated in Fig. 9, is all due to transitions parallel to the long axis of molecule.

When two transition directions are at right angles to each other in a molecule, a product of these $r$-values must be unity. Namely,

$$r_{\parallel} \times r_{\perp} = 1 \quad (1)$$

According to Table I, the following two pairs are approximately unity*3.

$$r_{\mathrm{X}} \times r_{\mathrm{XIII}} = 0.975 \quad (2)$$

$$r_{\mathrm{XI}} \times r_{\mathrm{XII}} = 0.978 \quad (3)$$

Moreover, Table I indicates $r_{\mathrm{X}} < r_{\mathrm{XI}}$ and $r_{\mathrm{XIII}} > r_{\mathrm{XII}}$. If they lie in a common absorption plane[1] (made of an orientation axis and a transition direction) and if Relation 1 is held, relations $r_{\perp} = r_{\mathrm{X}} = r_{\mathrm{XI}}$ and $r_{\parallel} = r_{\mathrm{XIII}} = r_{\mathrm{XII}}$ must be kept. These disagreements would be due to the following reason. Because there are two bands XI and XII of opposite character existing close to each other, as is clarified in Fig. 5, $R_d$ of Band XI might be elevated by might be elevated by XII, while that of XII might be lowered by XI. For this reason, concerning $r$-values in this case, $r_{\mathrm{X}}$ and $r_{\mathrm{XIII}}$ are believed to be a most reliable $r_{\perp}$ and $r_{\parallel}$ respectively. From the above discussion, it may be concluded that the product of each pair of $r$-values in Relations 2 and 3 is in fact unity and therefore satisfies Relation 1 in itself, and that the relations $r_{\perp} = r_{\mathrm{X}} = r_{\mathrm{XI}}$ and $r_{\parallel} = r_{\mathrm{XII}} = r_{\mathrm{XIII}}$ should come into existence.

If Bands XV (240 m$\mu$) and XIV (260 m$\mu$) in Fig. 8 were measured by perfect polarized light*4, $R_d$ for XV would perhaps be found to be larger and for XIV smaller. Consequently, it can be expected that $r$-values for these bands approach $r_{\mathrm{XIII}}$ and $r_{\mathrm{X}}$, respectively. In this case, therefore, $r_{\mathrm{XV}}$ presumably corresponds to $r_{\parallel}$ and $r_{\mathrm{XIV}}$ to $r_{\perp}$. Moreover, the weak band XVI (230 m$\mu$) is not thought of conclusively.

According to the above discussion, the absorptions of Pinacyanol will be distinguished into the following three groups. One of these groups is such that the transition direction runs along the molecular axis. And to this groups Bands I—IX belong, although it is not certain regarding Bands V and IX. The other two groups contain the bands of which any two transition directions taken from each group separately are orthogonal. Let us decide to make "$\parallel$" represent those near to the molecular axis and make "$\perp$" represent the others; then Bands XII, XIII and XV become "$\parallel$" and X, XI, XIV and XVI become "$\perp$".

The transition direction assigned above was based on an analysis of the observed $R_d$—$R_s$ relation. However, when we compare again the dichroic behavior of the band in the curves of Figs. 4—8 with their transition directions indicated in Table I, we see that the direction can well be decided only by an inspection of the dichroic behavior without the help of the $R_d$—$R_s$ relation: for instance, absorption bands which have the maximum $R_d$ for the same $R_s$ in the whole region with no change in shape and in $\lambda_{\max}$ can be decided as "longi." (bands shown in Fig. 2 and around 400 m$\mu$ in Fig. 3). Others in general change in their shape of absorption and in $\lambda_{\max}$ for $D_\theta$: this fact suggests the superposition of absorptions with different directions. $R_d$-values of these bands are so small as to be easily distinguished from "longi.". This absorption group is considered to be formed of $\parallel$ $\perp$ absorptions. Accordingly, of these absorptions the ones with the larger $R_d$ may be decided as $\parallel$ and the others with the smaller $R_d$ as $\perp$.

## Discussion

It is evident from Figs. 2 and 3 that pinacyanol shows the identical absorption both in PVA sheet and in ethanol. Therefore, the following discussion on the light absorption in PVA sheet may be thought to apply to that in ethanol.

In the last section, the absorption bands have been classified only from the standpoint of their transition directions. Now, turning attention to the absorption position and intensity, we can roughly divide them again into four groups (Table I and Figs. 2—8): the first group includes Bands I—IV, the second group Bands V*5—IX, the third group Bands X—XIII,

*3 In fact, however, these products are slightly smaller than unity. This may be interpreted by the following reason. From the polarization degree curve in Fig. 8, it is noticed that Bands XIII and XII were observed by the light of 93% and 97% polarization respectively. In this case, therefore, $R_d$ becomes smaller than when observed by 100% polarization light, and $r$-value might be estimated to be exceedingly small.

*4 From Fig. 8, it is estimated, $R_d$(XV)=2.0 and $R_d$(XIV)=1.5 at $R_s$=5.4. As for $r$-values, $r_{\mathrm{XV}}$=1.1 and $r_{\mathrm{XIV}}$=0.9, and the former is smaller than 1.3 of $r_{\mathrm{XIII}}$ and latter is larger than 0.75 of $r_{\mathrm{X}}$. But the product is again approximately unity.

*5 According to the apparent shape of the curve in Fig. 7, it seems plausible that Band V belongs to the 1st group. But, from the standpoint of band distance, as will be seen later, it will reasonably be put into the 2nd group.

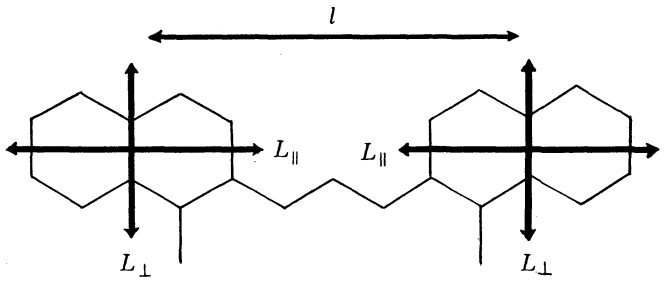



Fig. 10. The molecular skeleton of pinacyanol.

and the fourth groups Band XIV—XVI.

As already mentioned, the absorptions of the first and the second group lie on the long axis of the molecule. Accordingly, if the molecular skeleton of Pinacyanol cation is just as shown in Fig. 10, the direction of these absorptions may correspond to *l*-direction of the figure. And again as mentioned, the ∥ and the ⊥ transition are normal to each other in the same plane. This is visually understood from the fact that the sum of angles between the transition direction and orientation axis in Table I, for example, Band X(⊥) and XIII (∥), is approximately 90 degrees. Thus, it may conclusively be said that the ∥ and the ⊥ transition coinside with the long and the short axis of the quinoline nucleus, respectively.

The absorption bands of the 3rd and the 4th groups, therefore, are attributed to the localized $\pi$ electron system in the quinoline nuclei: those of the 3rd group would be derived, for example, from the weak 320 and 310 m$\mu$ absorption of 2-methyl-*N*-ethyl-quinolinium cation, and those of the 4th group from the strong 240 and 220 m$\mu$ absorption.

Now, if the molecule is planar in the shape of Fig. 10, the direction of the long axis ($L_{\parallel}$) of quinoline nucleus and *l*-direction become parallel, hence these two directions must take any identical angle toward the orientation axis of the molecule. Table I actually shows, however, rather great difference between the two angles*[6]. This means that two quinolines are to a large extent off the common plane*[7].

Absorptions of the 1st and the 2nd group apparently resemble each other in shape (cf. Figs. 2 and 3). Further, the fact that the latter is weaker than the former in intensity and that their directions are the same suggests that the 2nd goup corresponds to an overtone of the 1st group. In this connection, the following fact is of interest: the distances of the adjacent bands in the 1st group are $1500\pm300\,cm^{-1}$ and those in the 2nd group are also $1500\pm200\,cm^{-1}$, indicating a constant space of band-distribution. It is from the standpoint of band distance that we have put Band V into the 2nd group, in the above group classification.

As is already well known, the first group absorption is very sensitive to the solvent nature[5,6]. A correspondence of complexes of monomer, dimer, etc. with absorptions were attempted[6], with the help of the fact that the pinacyanol cation is easily aggregated. At the present stage, however, it can not be decided whether respective absorption bands correspond to those intrinsic to respective complexes possibly considered, e. g. such new absorptions as revealed by a Davidov splitting[7], or transitions originally existing are intensified by coupling with vibration[8] on some account involving complex formation.

## Summary

1. Dichroism of pinacyanol iodide in the PVA sheet was observed in the region higher than 220 m$\mu$, and at least sixteen absorption bands were recognized.

2. The relation of $R_d$ to $R_s$ was analyzed concerning some absorption bands, and it was verified that there are two groups of transitions,

*[6] Namely, if two absorption planes of "longi". and "∥" (Band XIII) were coincident, the angle between these transitions would be about 64 degrees. The difference is about 14 degrees, indicating that the molecule is almost planar. That this is not correct would be shown by constructing the structural model corresponding to Fig. 10. Besides, the assumption that the absorption planes coincide with each other has no grounds.

*[7] Concerning the double bond character, this is not inconsistent with the concept of the usual planar molecule. Because, if the rotation of quinoline planes is equally shared by the polymethine bonds (here 4 bonds) the double bond character of each bond will be roughly lowered only by about 10 percent of that in case of planar, even though the inclined angle of the planes is 80 degrees.

5) I. M. Klotz, *Chem. Revs.*, **41**, 382 (1947); S. E. Sheppard and A. L. Geddes, *J. Chem. Rhys.*, 13, 63 (1945).

6) R. C. Merrill and R. W. Spencer, *J. Am. Chem. Soc.*, **72**, 2894 (1950).

7) For instance, J. W. Weigl, *J. Chem. Rhys.*, **24**, 364 (1956).

8) S. E. Sheppard and G. R. Brigham, *J. Am. Chem. Soc.*, **66**, 380 (1944); S. E. Sheppard and A. L. Geddes, ibid., **66**, 2003 (1944).

one existing along the long axis of the molecule, the other being at right angles to one another in geometry.

3. The absorption group at right angles to one another appears in the shorter wavelength region than about 340 m$\mu$, and it was shown that this is due to the two orthogonal electronic transitions localized in the quinoline nuclei of the molecule.

4. The absorptions of the long axis of the pinacyanol molecule consist of two groups, each involving several bands and it was pointed out that the bands are distributed with nearly constant distance of 1500 $cm^{-1}$ between adjacent one.

5. It was deduced that the molecule is not a planar and both quinoline planes are far from planar.

6. Sixteen absorptions mentioned above were reasonably classified in their relation to the transition direction or in their correspondence to the molecular structure.

The author wishes to express his thanks to Professor N. Ando and I. Tana kain this laboratory for their encouragement throughout this work, also to Mr. Y. Mori in our laboratory for his useful discussion and helpful advice, and to Mr. H. Ono of the Laboratory of Fuji Photo Film Co. for his kind supply of the dye sample used in this investigation.

*Laboratory of Physical Chemistry*
*Tokyo Institute of Technology*
*Meguro-ku, Tokyo*

# *On Some Dark-colored Chlorocuprates(I, II) and Related Compounds. I. The Method of Preparation and Some Properties**

By Masayasu MORI

(Received September 14, 1959)

A considerable amount of data has now been accumulated concerning the characteristic properties of "mixed valence" compounds, i. e. compounds containing atoms of the same element in different valence states. Mixed valence compounds having a comparatively covalent character have been fairly well studied and are now utilized in the field of semiconductors. One of the most characteristic features of such mixed valence semiconductors is that the ratio of atoms in two valence states can often be changed arbitrarily, thus resulting in a change in the properties of the substance, as if the valence of the metal could take a continuous non-integral number. Such a technique of preparing semiconductors, termed *valence control*, is often useful for giving desired electrical properties to these substances[1]. On the other hand the properties of the mixed valence compounds of ionic character containing halometallate ions have scarcely ever been elucidated. Most of these mixed valence halometallates show an "interaction color" due to an abnormal light absorption[2].

The interaction color of copper(I) and copper(II) chlorides in hydrochloric acid solution has been known from an early date. Doehlemann and Fromherz measured the absorption spectrum of this system and found a broad interaction absorption in the visible region[3]. However, the present-day knowledge of the structure of chlorocuprate ions is very meager, and it is not known what kinds of chlorocuprate ion are responsible for the interaction color. This is mainly due to the fact that the phenomenon has hitherto been observed only in aqueous solution. It occurred, therefore, to the present author that an investigation on crystalline compounds showing an interaction color of copper(I) and copper(II) might be helpful in throwing light on the nature of this problem and he succeeded in obtaining dark brown chlorocuprates(I, II) of hexamminechromium(III) and hexamminecobalt(III) cations. For comparison the chlorocuprates(I) and chlorocuprates(II) of these

1) E. J. W. Verwey, *Philips Research Repts.*, 5, 173 (1950).

* A part of this study was presented at the Symposium on Coordination Chemistry, Tokyo, November, 1958.

2) The paper of J. E. Whitney and N. Davidson [*J. Am. Chem. Soc.*, 71, 3809 (1949)] contains a survey of the literature up to that time.

3) E. Doehlemann and H. Fromherz, *Z. physik. Chem.*, 171A, 353 (1934).

complex cations were also prepared and they were found to form yellow or orange crystals. In the following paragraphs the methods of preparation and some properties of these compounds will be described.

## Experimental

**Methods of Preparation.**—*Hexamminechromium(III) Chlorocuprate(I, II) and Hexamminecobalt(III) Chlorocuprate(I, II).*—Five tenths grams of copper(I) chloride was dissolved in 100 ml. of hot water containing 15 g. of ammonium chloride and 40 ml. of concentrated hydrochloric acid. When the color of the solution was found to be greenish yellow, a dilute solution of titanium(III) chloride was added dropwise, until the very moment when the yellow color disappeared. The solution was quickly filtered and the filtrate was poured into a solution of 2.7g. of hexamminechromium(III) chloride mono-hydrate and 3 g. of copper(II) chloride di-hydrate in 100 ml. of water. The same amount of hexamminecobalt-(III) chloride was used in preparing the corresponding cobalt compound. It seemed preferable to heat both solutions to about 60°C before mixing, for the precipitate formed in the cold solution was very fine and liable to decomposition. The mixture was cooled in a cold water bath for 30 min. with occasional stirring. The dark brown or almost black crystalline precipitate thus formed was filtered off, washed with 2 N hydrochloric acid and then with ethanol, and dried in air. (Samples No. 3 and 8 in Table I.)

Found for the chromium compound: Cr, 14.2, 13.8, 13.6; N, 21.5, 21.7, 21.8; total Cu, 16.8, 15.7; Cl, 42.3; loss in wt. at 110°C, 1.05, 1.23. Calcd. for $[Cr(NH_3)_6]_2Cu_2Cl_9(H_2O)_{1/2}$: Cr, 13.6; N, 22.0; Cu, 16.6; Cl, 41.8; $H_2O$, 1.14%.

Found for the cobalt compound: Cu, 15.2; N, 21.3; total Cu, 16.5, 16.9; Cl, 41.1; loss in wt. at 110°C, 1.15. Calcd. for $[Co(NH_3)_6]_2Cu_2Cl_9(H_2O)_{1/2}$: Co, 15.2; N, 21.6; Cu, 16.4; Cl, 41.1; $H_2O$, 1.13%.

The total copper content in the above analytical data was determined gravimetrically. The content of bivalent copper was determined iodometrically in 3 N acetic acid using finely powdered sample. The chromium compound gave a fairly sharp end point of titration and it was found to contain about a half of the total copper in the bivalent state (Found, 8.4; calcd., 8.3). In the cobalt compound the end point of the iodometric titration was very obscure, and the results were less reproducible (Found, 8.7, 9.0, 9.1, 9.3. Calcd., 8.2). It was found, however, that the composition of the chlorocuprate(I, II) depends on the quantity of copper(I) and copper(II) chlorides and used in the preparation. An outline of this relationship is given in Table I. Samples Nos. 1—6 are chromium compounds and Nos. 7—11 cobalt compounds. The procedure adopted in preparing these samples was the same as that given above except the difference in the quantities of the copper chlorides used.

*Hexamminechromium(III) Chlorocuprate(I) and Hexamminecobalt(III)Chlorocuprate(I).*—One gram of copper(I) chloride and 15 g. of ammonium chloride were dissolved in a mixture of 100 ml. of hot water, 20 ml. of 15% titanium(III) chloride solution in hydrochloric acid and 40 ml. of concentrated hydrochloric acid. The solution was quickly filtered and the filtrate was poured into a solution at 60°C of 2.7 g. of hexamminechromium(III) chloride mono-hydrate in 100 ml. of water. The same amount of hexamminecobalt(III) chloride was used in preparing the corresponding cobalt compound. The mixture was cooled in a cold water bath for 30 min. with occasional stirring. The yellow or orange precipitate was filtered off and washed with 2 N hydrochloric acid and ethanol, and then it was

TABLE I. THE RELATIONSHIP BETWEEN THE QUANTITIES OF THE STARTING MATERIALS AND THE CHEMICAL COMPOSITION OF THE CHLOROCUPRATE

| Sample No. | Starting Material[a] | | Product | | |
|---|---|---|---|---|---|
| | CuCl (in g.) | $CuCl_2 \cdot 2H_2O$ (in g.) | Total Cu (in %) | Bivalent Cu (in %) | Color |
| 1 | 0 | 3 | 16.1 | 16.1 | yellow |
| 2 | 0.2 | 3 | 17.0 | 12.7 | brownish black |
| 3 | 0.5 | 3 | 16.8 | 8.4 | black |
| 4 | 1 | 3 | 19.5 | 2.0 | grayish brown |
| 5 | 1 | 1 | 20.0 | 1.0 | brown |
| 6 | 1 | 0 | 20.4 | 0 | yellow |
| 7 | 0 | 3 | 15.8 | 16.8[b] | orange |
| 8 | 0.5 | 3 | 16.4 | 9.2[b] | black |
| 9 | 1 | 3 | 19.0 | 2.3[b] | dark brown |
| 10 | 1 | 1 | 19.8 | 1.6[b] | brown |
| 11 | 1 | 0 | 19.8 | 0 | orange |

a) For samples Nos. 1—6 the complex cation used was hexamminechromium(III) ion and for samples Nos. 7—11 hexamminecobalt(III) ion.

b) The end point of the iodometry of the cobalt compound is very obscure.

dried in vacuo over potassium hydroxide. (Samples No. 6 and No. 11 in Table I.)

Found for the chromium compound: Cr, 13.6; N, 21.7; Cu, 20.4; Cl, 39.2. Calcd. for $[Cr(NH_3)_6]_4 \cdot Cu_5Cl_{17}$: Cr, 13.5; N, 21.9; Cu, 20.7; Cl, 39.2%.

Found for the cobalt compound: Co, 15.4; N, 20.8; Cu, 19.8; Cl, 38.5. Calcd. for $[Co(NH_3)_6]_4 \cdot Cu_5Cl_{17}$: Co, 15.1; N, 21.5; Cu, 20.3; Cl, 38.5%.

*Hexamminechromium(III) Chlorocuprate(II).*—Two grams of hexamminechromium(III) chloride monohydrate and 2 g. of copper(II) chloride di-hydrate were dissolved in 60 ml. of water. The solution was filtered and the filtrate was heated to 60°C and mixed with 20 ml. of concentrated hydrochloric acid. The mixture was cooled in a cold water bath for 30 min. with occasional stirring and the precipitated complex was filtered and washed with ethanol. (Sample No. 1, Table I.)

Found: Cr, 13.8; N, 21.5; Cu, 16.1; Cl, 44.9. Calcd. for $[Cr(NH_3)_6]CuCl_5$: Cr, 13.2; N, 21.3; Cu, 16.1; Cl, 44.5%.

The corresponding cobalt compound had already been prepared by Levi[4]. (Sample No. 7, Table I).

*Hexamminechromium(III) Bromocuprate(II).*—Two grams of hexamminechromium(III) bromide, 2.4 g. of copper(II) sulfate penta-hydrate, 10 g. of sodium bromide, 20 ml. of water and 20 ml. of 48% hydrobromic acid were mixed and the mixture was occasionally stirred. After 1 hour the resulting black crystals were filtered off through a glass filter under strong suction, washed quickly with fuming hydrobromic acid (ca. 66%) and dried in vacuo over sulfuric acid.

Found: Cr, 9.0; N, 13.9; Cu, 9.6; Br, 65.1. Cacld. for $[Cr(NH_3)_6]CuBr_5$; Cr, 8.4; N, 13.6; Cu, 10.3; Br, 64.7%.

An attempt to prepare the corresponding cobalt compound was unsuccessful.

**Absorption Spectrum Measurement.**—The absorption spectrum of copper sulfate dissolved in 48% hydrobromic acid was measured with a Beckman spectrophotometer, model DU. The result is given in Fig. 1. The concentration of copper sulfate was 0.0000870 M and the extinction coefficient is expressed on the basis of g. ion of copper.

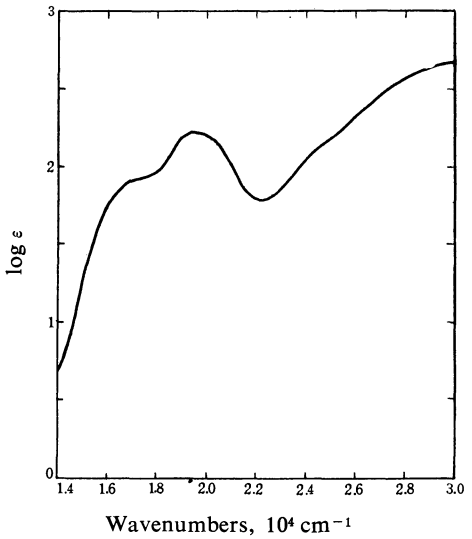



Fig. 1. Absorption spectrum of copper(II) sulfate in 48% hydrobromic acid.

**Measurement of Magnetic Susceptibility.**—Dr. Saburo Fujii* of the Tokyo Institute of Technology kindly measured the magnetic susceptibility of hexamminecobalt(III) chlorocuprate(I, II) by Weiss-Foex's zero point compensation method.

## Results and Discussion

All the foregoing chlorocuprates crystallize in regular octahedra. As has been pointed out in the preceding section, the composition of the chlorocuprate(I, II) depends on the quantities of copper(I) and copper(II) chlorides used in the preparation (Table I). Observation under a microscope as well as with the naked eye shows that the color changes from sample to sample as the chemical composition changes, although it is uniform in a given sample. This fact indicates that the product is not a mixture of two chemical species, but a nearly uniform chemical compound whose composition can change continuously. As far as is known to the present author, this series of chlorocuprates form the only known typical ionic crystals consisting of well-defined cations and anions in which the valence control is possible.

From the total copper content given in Table I it will be seen that the atomic ratio of chromium to copper is 1 : 1 when more than a half of the total copper is bivalent, and that this ratio gradually decreases to the limiting value of 4 : 5 when the bivalent copper is less than a half. In this extreme case the product is a pure chlorocuprate(I) (samples No. 6 and No. 11 in Table 1). The reason why compounds having such different chemical formulae belong to one series of compounds would be made clear only by a crystallographic investigation with X-rays. A research along this line is now in progress and the results will be published shortly.

An interesting phenomenon is observed when crystals of hexamminecobalt(III) chlorocuprate-(I, II) are digested in the mother liquor at 30~40°C for many hours. The crystals reach 0.1~1 mm. in size and often present a tortoise-shell appearance. The black or dark brown crystals are spotted with yellow transparent portions although the crystals as a whole are well developed octahedra. This may be explained as follows. By the oxidation of the mother liquor in the air the quantity of univalent copper therein is gradually decreased. The portions of the crystals that grow at later stages, therefore, have a poorer content of

4) G. R. Levi, *Atti Accad. Lincei*, (5) 32 I, 633 (1923).

* The present address: Toho Rayon Co., Ltd., Kitajima-cho, Itano-gun, Tokushima-ken.

univalent copper and consequently the interaction color is feeble in these portions.

Hexamminechromium(III) bromocuprate(II) is black in contrast to yellow chlorocuprate(II). This difference of color is probably due to the strong absorption band of bromocuprate(II) ion with a peak at $1.95\times10^4\,cm^{-1}$ as is observed in the spectrum of copper(II) sulfate in hydrobromic acid in Fig. 1. An investigation of hexamminechromium(III) bromocuprate(II) may give some information about the ionic species to which this absorption band belongs.

Magnetic study on $[Co(NH_3)_6]_2Cu_2Cl_9(H_2O)_{1/2}$ showed, after a correction being made for the presence of diamagnetic groups, a magnetic moment of 1.9 Bohr magnetons per each formula unit. This value may be considered quite reasonable as the magnetic moment ascribed to the bivalent copper atom present in the crystals. The magnetic moment of the bivalent copper atom, therefore, seems to be little affected even when an interaction color is observed.

**Summary**

A series of dark-colored chlorocuprates(I, II) of hexamminechromium(III) and hexamminecobalt(III) have been prepared. The chemical composition and the color of these compounds have been found to change continuously with the composition of the mother liquor in which they were crystallized.

The author wishes to express his sincere thanks to Professor Yuichi Nakatsuka under whose kind guidance the present work was carried out. He is also grateful to Dr. Saburo Fujii for the magnetic measurement. A part of the expenses of the present study was defrayed by a grant-in-aid of the Ministry of Education.

*Institute of Polytechnics*
*Osaka City University*
*Kita-ku, Osaka*

# *Diffusion Coefficients for Amorphous Polymer and Water Systems*

By Akira KISHIMOTO, Etsuji MAEKAWA and Hiroshi FUJITA

(Received December 29, 1959)

Recent studies of absorption and desorption of low-molecular-weight substances in amorphous polymers olids have demonstrated a sharp distinction between organic solvents and water. In systems of amorphous polymer + organic vapor the processes are of the Fickian type[1-4], usually with a diffusion coefficient which depends appreciably on penetrant concentration, when the systems are well above the glass transition temperatures, $T_g$, of respective polymers. At temperatures below $T_g$ they exhibit various non-Fickian features[5-8]. No definite information has as yet been obtained about the behavior at temperatures slightly above $T_g$[9]. On the other hand, the processes of water are Fickian both above and below $T_g$, if in the latter region the system is not greatly removed from $T_g$[10]. In addition, the diffusion coefficients for amorphous polymer +water systems are practically independent of water concentration at any given temperature in the region mentioned above[10-13]. It is also reported that while the apparent activation energies, $\Delta H_d$, for diffusion of organic solvents in amorphous polymers increase as the temperature is lowered toward $T_g$[3,4], the $\Delta H_d$ for aqueous systems are constant in the corresponding temperature region[10-12]. Furthermore, there are some experimental data[13] which show that plots of $\log D$ vs. $1/T$ for a water system

1) S. Prager and F. A. Long, *J. Am. Chem. Soc.*, **73**, 4072 (1951).
2) S. Prager, E. Bagley and F. A. Long, ibid., **75**, 1255 (1953).
3) M. J. Hayes and G. S. Park, *Trans. Faraday Soc.*, **51**, 1134 (1955).
H. Fujita, A. Kishimoto and K. Matsumoto, ibid. **56**,, 438 (1960).
5) R. J. Kokes, F. A. Long and J. L. Hoard, *J. Chem. Phys.*, **20**, 1711 (1952).
6) F. A. Long and R. J. Kokes, *J. Am. Chem. Soc.*, **75**, 2232 (1953).
7) G. S. Park, *J. Polymer Sci.*, **11**, 97 (1953).
8) A. Kishimoto, H. Fujita, H. Odani, M. Kurata and M. Tamura, *J. Phys. Chem.*, **64**, 594 (1960).
9) A. Kishimoto and K. Matsumoto, ibid., **63**, 1529 (1959); A. Kishimoto and K. Matsumoto, unpublished results.
10) F. A. Long and L. J. Thompson, *J. Polymer Sci.*, **15**, 413 (1955).
11) A. M. Thomas, *J. Appl. Chem.*, **1**, 141 (1951).
12) F. Bueche, *J. Polymer Sci.*, **14**, 414 (1954).
13) K. Kawasaki and Y. Sekita, *J. Appl. Phys. Japan, (Oyo Butsuri Gakkaishi)*, **26**, 678 (1957).

are represented by two straight lines intersecting at $T_g$, where $D$ is the mutual diffusion coefficient of the system and $T$ is the absolute temperature. This implies that the $\Delta H_d$ of such a system changes discontinuously to another constant value when the temperature is lowered through $T_g$. These features suggest that the molecular mechanism responsible for the diffusion of water in amorphous polymers must be different from that for the diffusion of organic solvents in the same polymers. No adequate explanation has yet been presented concerning this problem.

In a recent publication[4] we have shown that the dependence on temperature and also on concentration of diffusion coefficients for systems of amorphous polymer+organic solvent above $T_g$ can be interpreted quite satisfactorily in terms of a simple theory based on the free volume model of polymer network. One will find it natural that in view of this previous success we were interested in examining the extent to which our free volume theory can account for data of diffusion coefficients for polymer + water systems. One of the purposes of the study reported in this paper is to obtain experimental data pertinent to this problem. The other purpose is concerned with the re-examination of the previously reported variation of $D$ for polymer + water systems with temperature. This arose from a close inspection of existing data and also from the prediction that if the free volume of the polymer network is the controlling factor for the diffusion of water, the linear relation between $\log D$ and $1/T$ should be only approximate.

## Experimental

**Materials.**—Two amorphous polymers, polyvinyl acetate (PVAc) and polymethyl acrylate (PMA), were chosen for the present study. These were purified, unfractionated materials obtained from the Institute for Chemical Research, University of Kyoto. The number-average molecular weight of the PVAc, determined osmotically in a mixture of methanol (80) and ethanol (20) at 17°C, was $8.3\times10^4$. According to Naito[14], this is a thata solvent for PVAc. In fact, our osmotic measurements gave a second virial coefficient which was zero within the accuracy of the experiment. The films for sorption experiments were prepared in the same manner as described previously[15]. Their thicknesses were varied from $1.0\times10^{-2}$ to $4.1\times10^{-2}$ cm., depending upon the rate of absorption or desorption in respective cases.

The PMA used was identical to that used for obtaining the data reported in reference (4) and had a number-average molecular weight of $3.1\times10^5$ (determined osmotically in acetone at 25°C). Films of this polymer prepared for sorption measurements were $1.1\times10^{-2}$ to $4.9\times10^{-2}$ cm. thick.

**Apparatus and Procedure.** — Our sorption apparatus has been described previously[15]. Integral absorption from and integral desorption to zero pressure were measured for several external pressures of water vapor at a number of temperatures in the range 10 to 60°C for PMA and in the range 5 to 60°C for PVAc. In each experiment the temperature of the system was controlled to within ±0.1°C. According to the literature[16], the glass transition temperatures, $T_g$, of dry PMA and PVAc are about 3°C and about 28°C, respectively. Thus the present study for PVAc covered the temperature range both above and below $T_g$, and that for PMA treated the range above $T_g$ only. Pressures of water vapor in the sorption tube were measured to ±1 mm. on a dioctyl phthalate manometer. This corresponded to an accuracy of ±0.07 mmHg. At every temperature studied, especially at temperatures below $T_g$, it was essential to use well-annealed specimens in order to obtain reproducible results.

For PVAc we performed steady-state permeation measurements at three temperatures, 10, 30 and 40°C, by using the cup method.

## Results and Discussion

**Diffusion Coefficients.**—It was found that for both PVAc and PMA the equilibrium water concentrations, $Q_\infty$ (grams of water sorbed per gram of dry polymer), at given relative humidities are independent of the temperature, over the ranges studied, within the accuracy of the present measurements. Those isotherm data are not shown here.

All the absorption and desorption data obtained were plotted in the form of $Q_t/Q_\infty$ against $(t)^{1/2}$, where $Q_t$ denotes the amount (in grams) of water absorbed or desorbed per gram of dry polymer for a time $t$ from the start of a particular run. For all the external pressure and temperature measured, these plots had shapes expected from the normal Fickian diffusion mechanism. Furthermore, in each case, the absorption curve and the corresponding desorption curve coincided with each other over the entire range of time-scale of the experiment. According to theory[17], these features indicate that the mutual diffusion coefficient, $D$, of such a system should be independent of the penetrant concentration and may be evaluated from the initial slope, $I$, of the coincident absorption-desorption plot by means of the equation:

$$D=\pi I^2X^2/16 \qquad (1)$$

where $X$ is the thickness of the sample film.

14) R. Naito, *Chem. High Polymers (Tokyo)* (*Kobunshi Kagaku*), **16**, 7 (1959).
15) H. Fujita and A. Kishimoto, *J. Polymer Sci.*, **28**, 547 (1958).
16) M. L. Williams, R. F. Landel and J. D. Ferry, *J. Am. Chem. Soc.*, 77, 3701 (1955).
17) J. Crank, "The Mathematics of Diffusion", Oxford Univ. Press, Oxford (1956).

Fig. 1 illustrates how well a pair of absorption and desorption curves coincided with each other. The solid line in the figure represents the curve which has been calculated from the Fick diffusion equation by using for $D$ the value determined by Eq. 1. A similar agreement between observed and calculated values was found for almost all the experimental data obtained. In Fig. 2 the values of $D$ calculated by Eq. 1 from the data for the PVAc system are semi-logarithmically plotted against the equilibrium water concentration $Q_\infty$. It is seen that the $D$ values for each temperature are independent of $Q_\infty$, and hence of the penetrant concentration, within errors of experiment. In the figure the filled circles give results from the steady-state permeation measurements. There are good agreements between the $D$ values from the two different types of measurement at all temperatures where comparison can be made. It is of interest to note that this agreement was obtained even at 10°C, a tempetature about 20°C below $T_g$ of PVAc. The indication from these results is that the diffusion of water into PVAc is controlled by the purely Fickian mechanism not only above $T_g$ but also below $T_g$, provided that in the latter region the temperature is not too low from $T_g$. In this connection it is of significance to recall that the sorption processes of organic vapors in amorphous polymers generally exhibit marked deviations from the behavior expected from the normal Fickian mechanism when the systems are studied at temperatures below $T_g$ of respective polymers.

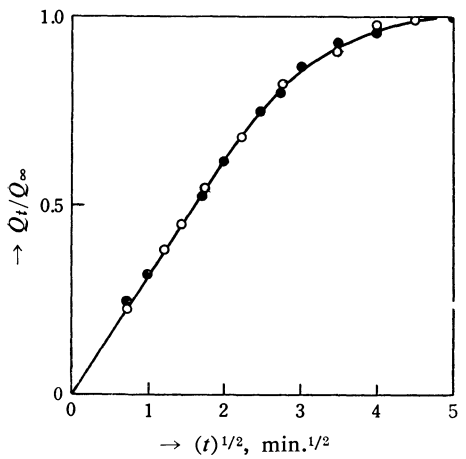



Fig. 1. Absorption and desorption curves for water in PMA. Water vapor pressure =17.2 mmHg; thickness of film=$1.83\times10^{-2}$ cm; temperature=30°C; concentration of water at sorption equilibrium=$0.99\times10^{-2}$ g./g. Open circles, absorption; filled circles, desorption; solid line, theoretical.

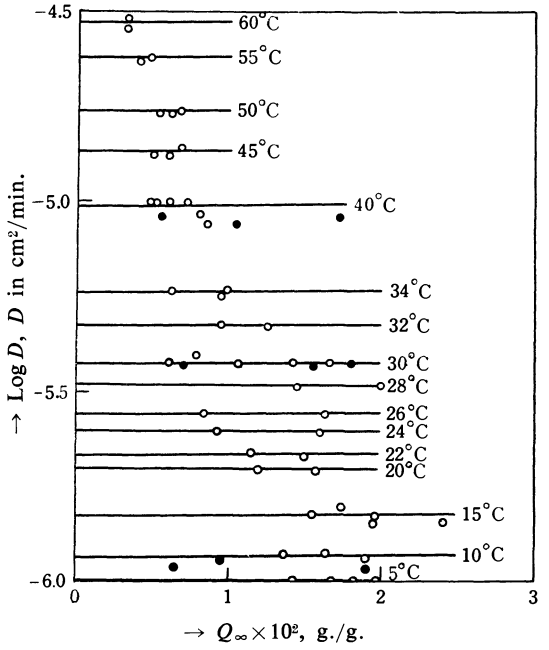



Fig. 2. Mutual diffusion coefficient vs. concentration relations on the system PVAc+water.
○ sorption studies;
● steady-state permeation studies.

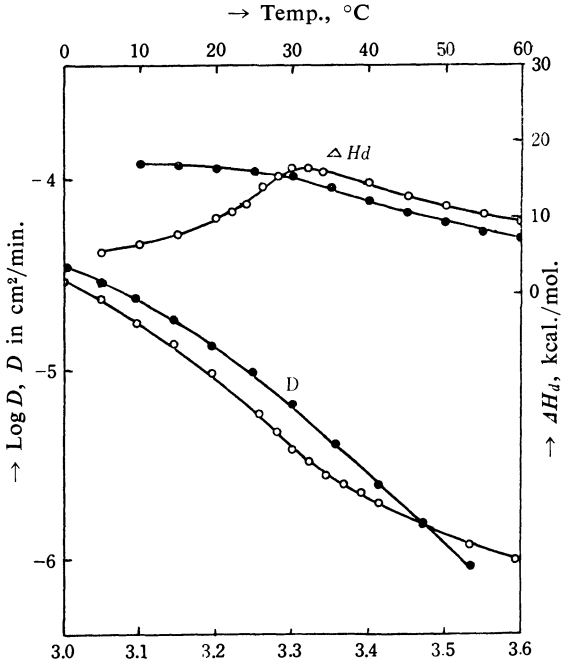



Fig. 3. Mutual diffusion coefficient vs. reciprocal absolute temperature (lower part); Apparent activation energies for diffusion, $\Delta H_d$, vs. temperature (upper part).
○ PVAc; ● PMA.

The data for the PMA system were exactly similar to those for the PVAc system described above, although the behavior below $T_g$ could not be studied on this polymer in the present work.

In Fig. 3 the values of $D$ for the two systems are semi-logarithmically plotted against the reciprocal of absolute temperature $T$. First it will be seen that the plots for the two systems are not linear but curved. Of special interest is the inflection point which appeared on the plot for PVAc at a temperature near $T_g$ of the polymer. Values of $\Delta H_d$, the activation energy for diffusion of water in a polymer, were calculated from the smooth $\log D$ vs. $1/T$ curves drawn in Fig. 3, and are plotted against $T$ in the upper part of the same figure. One finds that for both systems $\Delta H_d$ increases as the temperature is lowered toward $T_g$ of respective polymers, and for PVAc it reaches a maximum at a temperature near $T_g$ and then decreases gradually with further decrease in temperature. This appearance of a maximum $\Delta H_d$ is the reflection of the fact that the corresponding $\log D$ vs. $1/T$ plot has an inflection point. We wish to emphasize that this is the first experimental demonstration of a $\Delta H_d$ vs. $T$ curve which goes through a maximum at a temperature in the vicinity of which the system undergoes glass transition. It should also be mentioned that our data for PVAc do not conform to the previous finding[13] for the system polymethyl methacrylate+water where the plots for $\log D$ vs. $1/T$ were represented by two straight lines intersecting at a temperature near $T_g$.

By employing the steady-state permeation method Meares[18,19] measured diffusion coefficients of several gases in PVAc and found that the slope of the plots for $\log D$ vs. $1/T$ showed distinct discontinuities at two temperatures, about 10°C apart from one another, in the region encompassing $T_g$ of the polymer. Then he suggested that the glass transition of PVAc must take place over a range of temperature, rather than at a particular temperature. Although our PVAc data do not show any break in the temperature region studied, it appears that the occurrence of a broad maximum in $\Delta H_d$ has some correlation with Meares' suggestion on the "glass transition region". Recently, there are similar arguments from measurements of viscoelastic properties of dry polymers[20].

**Comparison with Amorphous Polymer+Organic Solvent Systems.**—Fig. 4 compares the

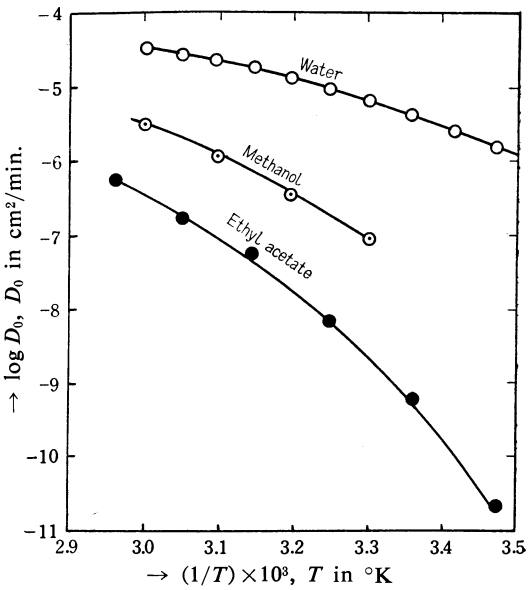



Fig. 4. Mutual diffusion coefficients at the limit of zero penetrant concentration as a function of reciprocal absolute temperature.

temperature dependence of $D_0$ (the value of $D$ at the limit of zero penetrant concentration) for systems PMA+ethyl acetate, PMA+methanol, and PMA+water. The data for the first two systems were taken from our previous publication[4]. The graph shows that with increasing molecular size as well as chemical affinity to PMA of the penetrant the values of $\log D_0$ at fixed temperatures decrease and their temperature dependence becomes more pronounced. This latter fact implies that more activation energy for diffusion into PMA is required at any given temperature (above $T_g$) for organic solvents than for water.

As noted in the introduction to this article, we have recently shown that the dependence on temperature and also on penetrant concentration of diffusions coefficients for amorphous polymer+organic solvent systems (above $T_g$ of respective polymers) can be accounted for satisfactorily by a simple free volume theory[4]. According to this theory, the thermodynamic diffusion coefficient, $\mathfrak{D}_T$, of a penetrant in an amorphous polymer at a temperature $T$ is represented by the equation:

$$\ln\ (\mathfrak{D}_T/\mathfrak{D}_0) = B_d\beta'(T)/[f(T,0)^2 + \beta'(T)f(T,0)v_1] \qquad (2)$$

Here $\mathfrak{D}_0$ is the value of $\mathfrak{D}_T$ at the limit of zero penetrant concentration, $f(T,0)$ is the average fractional free volume in the dry polymer at temperature $T$, $v_1$ is the volume fraction of the penetrant in the mixture, $B_d$ is

18) P. Meares, *J. Am. Chem. Soc.*, 76, 3415 (1957).
19) P. Meares, *Trans. Faraday Soc.*, 53, 101 (1957).
20) e. g. T. Hideshima, *Sci. Pap. Inst. Phys. & Chem. Research (Tokyo)*, 53, 36 (1959).

a constant characteristic of the system, and $\beta'(T)$ is a parameter representing the plasticizing effect of the penetrant. The value of $\mathfrak{D}_T$ can be calculated from $D$ when the corrections for the volume expansion of the polymer by the addition of penetrant and for the thermodynamic non-ideality of the mixture are applied. The former correction can be made under the assumption that no volume change on mixing occurs and the latter correction may be derived from the analysis of the isotherm curve of the system.

We examined the applicability of Eq. 2 to the present data, by assigning to $\beta'(T)$ the values which we had previously deduced from measurements of stress-relaxation on these systems[15]. It was found that in order that Eq. 2 may fit the concentration dependence data obtained, the values of $B_d$ have to be chosen as almost equal to zero for both PVAc and PMA systems. On the other hand, as shown previously[4], the constant $B_d$ may also be determined from the ratio of $\Delta H_d$ to $\Delta H_v$, where $\Delta H_v$ is the apparent activation energy for the steady-flow viscosity of the pure polymer. Comparison of the $\Delta H_d$ data given in Fig. 3 with the $\Delta H_v$ values calculated from the equation of Williams, Landel and Ferry[16] yielded $B_d=0.16$ for PVAc and 0.25 for PMA. These $B_d$ values are inconsistent with those derived above from the analysis of concentration dependence data, indicating that Eq. 2 is no longer applicable to the polymer+water systems investigated here. This result leads us to the conjecture that the amount of free volume must not be a major controlling factor for the diffusion of small molecules, such as water, through amorphous polymers. Previously we have inferred[4] that for penetrants very small in size and less soluble in the given polymer only a very local cooperation of the solid-like vibrations of two or three monomer units on the polymer chain would be sufficient to give a cross-section for the penetrant molecules to pass. This cooperative motion is so local that the probability of its occurrence, and hence the rate of diffusion of the penetrant molecule in the mixture, may be, in a first approximation, independent of how large the free volume in the mixture is. This will explain why the $D$ values for the polymer+water systems studied did not exhibit measurable variation with water content. If the above is the case, then we would have to ascribe the observed temperature dependence of $D$ for these systems to a temperature variation of solid-like vibration of monomer units, rather than to the temperature dependence of the free volume which is thought to be associated with larger-scale cooperative motions of several polymer segments.

We wish to thank Mr. Kinya Matsumoto of this Laboratory who carried out the steady-state permeation experiments on PVAc.

*Physical Chemistry Laboratory*
*Department of Fisheries*
*University of Kyoto*
*Maizuru, Kyoto-fu*

# *On the Assignment of a Band at 727 cm$^{-1}$ in Polyethylene Terephthalate*

By Akihisa MIYAKE

(Received December 17, 1959)

Some controversy surrounds the assignment of a strong band at 727 cm$^{-1}$ in polyethylene terephthalate. It was first assigned to a C–O–C bending mode[1]. This assignment is now believed to be incorrect[2,3] because it seems much too high for a C–O–C bending mode. The most generally favored explanation is that the band arises from an aromatic C–H out-of-plane bending mode[4-6] and therefore that it is similar in origin to a band at 875 cm$^{-1}$. The removal of the band in question, on going from polyethylene terephthalate to polyethylene deuteroterephthalate[2,5], has been considered as strong evidence for this explanation. On the other hand, the present author has proposed an alternative interpretation that two bands at

1) R. G. J. Miller and H. A. Willis, *Trans. Faraday Soc.*, **49**, 433 (1953).
2) D. Grime and I. M. Ward, ibid., **54**, 959 (1958).
3) A. Miyake, *J. Polymer Sci.*, **38**, 497 (1959).
4) C. Y. Liang and S. Krimm, *J. Chem. Phys.*, **27**, 327 (1957).
5) W. W. Daniels and R. E. Kitson, *J. Polymer Sci.*, **33**, 161 (1958).
6) M. C. Tobin, *J. Phys. Chem.*, **61**, 1392 (954).

875 $cm^{-1}$ and 727 $cm^{-1}$ arise from coupled C–H out-of-plane bending and $CO_2$ out-of-plane bending vibrations[3].

This problem is of interest because the band mentioned above is in close relation with the so-called extra-bands[7] present in aromatic acids, esters, amides and nitro compounds, the origin of which has yet been unexplained. In order to ascertain whether the author's interpretation is correct or not, some additional observations have been carried out, infrared investigations of polyethylene terephthalate below NaCl region and examinations of thiol esters as model compounds.

## Experimental

**Material.** — 1) *Polyethylene Terephthalate, Polyethylene-$d_4$ Terephthalate.*—The film samples used are the same as those used in previous researches[3,8].

2) *1,2-Ethanedithiol Dibenzoate.* — Benzoyl chloride (20 g.) was added dropwise with agitation to an ice-cooled solution of 1,2-ethanedithiol (7.5 g.) in pyridine (40 g.). The reaction mixture was allowed to stand overnight and poured into cold dilute sulfuric acid. The solid resulted was collected by filtration and washed successively with aqueous sodium carbonate and water. Repeated recrystallization from ethanol gave white crystals, m. p. 94.5°.

Found: C, 63.18; H, 4.61; O, 10.72. Calcd. for $C_{16}H_{14}O_2S_2$: C, 63.59; H, 4.64; O, 10.59%.

3) *1,2-Ethanedithiol Bis-(4-methoxycarbonylbenzoate).* — A solution of 4-methoxycarbonylbenzoyl chloride (10 g.) in chloroform (50 ml.) was added dropwise with agitation to an ice-cooled solution of 1,2-ethanedithiol (3 g.) in pyridine (40 g.). The reaction mixture, after standing overnight, was poured into cold dilute sulfuric acid with stirring. The solid product obtained as a suspension in the chloroform layer was recrystallized after the addition of ethanol. The resulting crystals were collected by filtration and washed with aqueous sodium hydroxide. Recrystallization from a mixture of ethanol and benzene (1 : 2) gave white crystals, m. p. 208~210°.

Found: C, 57.20; H, 4.35; O, 22.68. Calcd. for $C_{20}H_{18}O_6S_2$: C, 57.40; H, 4.33; O, 22.94%.

**Infrared Spectra*.** — The infrared spectra were obtained by means of Perkin-Elmer spectrometers model 21, 13 and 321 with NaCl, KBr and CsBr prisms respecively.

The polymer films were investigated in the KBr and CsBr regions. The two thiol esters were investigated in the NaCl and KBr regions as Nujol mulls and KBr disks. Dichroic measurements for the polymer were made in the KBr region on drawn films. Dichroic measurements for 1,2-ethanedithiol dibenzoate were made in the NaCl region on oriented crystal film obtained by differential cooling of a melt between rock-salt plates.

## Results

**Polyethylene Terephthalate.**—Infrared spectra of polyethylene terephthalate and polyethylene-$d_4$ terephthalate in the range 10~32 $\mu$ are shown in Fig. 1. The frequencies of the bands observed below 750 $cm^{-1}$ together with those reported by Tobin[6] are listed in Table I. Two bands at 575 and 422 $cm^{-1}$ reported by Tobin were not observed though a band at 631 $cm^{-1}$ which was reported as a weaker band than the above two was detected. None of the bands between 700~400 $cm^{-1}$ showed perpendicular dichroism. Tentative assignments for some of the bands are given in the last column of Table I. The assignment of the $CO_2$ rocking vibrations is supported by the fact that corresponding bands are found in ethylene glycol dibenzoate (480 $cm^{-1}$) and 1,2-ethanedithiol bis-(4-methoxycarbonylbenzoate) (488 $cm^{-1}$) but not in 1,2-ethanedithiol dibenzoate.

TABLE I. INFRARED FREQUENCIES ($cm^{-1}$) OF POLYETHYLENE TEREPHTHALATE

| P. E. T. | | P. E.-$d_4$. T. | Mode |
|---|---|---|---|
| Tobin | This work | | |
| 727(s) $\sigma$ | 727(s) $\sigma$ | 725(s) $\sigma$ | |
| 670(m) | 680(w) | | |
| 628(w)[c] | 631(w) $\pi$ | 631(w) $\pi$ | aromatic vibration |
| 575(m) | | | |
| 508(s)[a] $\pi$ | 506(m)[c] $\pi$ | 502(m)[c] $\pi$ | $CO_2$ rocking |
| 500(s)[a] | 500(m)[a] | 530(m)[a] | |
| 437(c) $\pi$ | 437(m)[c] $\pi$ | | C-C-O deformation |
| 422(s)[a] | | | |
| 382(s)[c] | 379(s)[c] | 364(s)[c] | C-O-C deformation |

s: strong, m: medium, w: weak, a: amorphous band, c: crystalline band,
$\sigma$: perpendicular dichroism, $\pi$: parallel dichroism.

7) M. Margoshes and V. A. Fassel, *Spectrochim. Acta*, 7, 14 (1955).
8) A. Miyake, *J. Polymer Sci.*, 38, 479 (1959).
* The author is indebted to Dr. Y. Mashiko et al. of the Government Chemical Industrial Research Institute, Tokyo, for the measurement in the CsBr region and to Dr. H. Tadokoro of Osaka University for the dichroic measurement for 1,2-ethanedithiol dibenzoate.

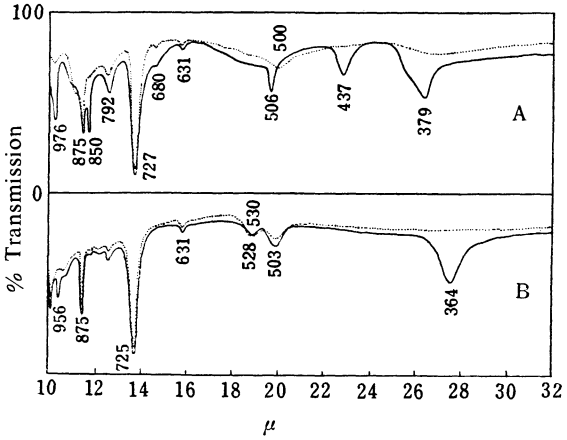



Fig. 1. Infrared spectra of polyethylene terephthalate (A) and polyethylene-$d_4$ terephthalate (B). ····· quenched sample; —— annealed sample.

**Thiol Esters.** — Infrared spectra of the two thiol esters in the NaCl region are shown in Fig. 2 together with that of ethylene glycol bis-(4-methoxycarbonylbenzoate) previously reported[8]. It is apparent that the strong band at 727 $cm^{-1}$ observed in ethylene glycol bis-(4-methoxycarbonylbenzoate) disappears in 1,2-ethanedithiol bis-(4-methoxycarbonylbenzoate), while the bands at 1502, 1408 and 1021 $cm^{-1}$ in the former which are attributable to the vibrations of *p*-phenylene group by analogy with polyethylene terephthalate[3] also appear in the latter at substantially the same frequencies (1502, 1403, and 1016 $cm^{-1}$). Most of the strong bands observed in the latter can be attributed to the ester or thiol ester groups (Table II). The bands which arise from the thiol ester group are easily identified by their distinguished intensities in 1,2-ethanedithiol dibenzoate. The assignments for the vibrations of the thiol ester group given in Table II are consistent with the results of dichroic measurement which will be described next.

**Dichroic Measurement for 1,2-Ethanedithiol Dibenzoate.** — Fig. 3 shows the spectra of an oriented crystalline film of 1,2-ethanedithiol dibenzoate. The solid curve was run with the polarizer setting so that the electric vector of the polarized beam was perpendicular to the direction of the crystal growth of the sample.

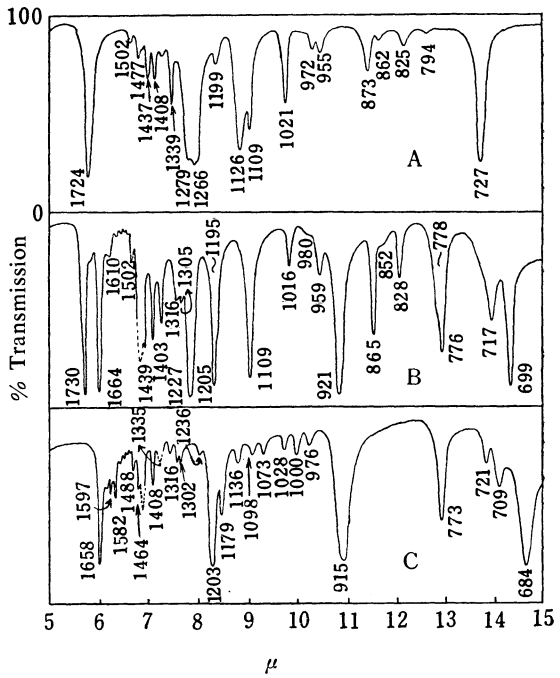



Fig. 2. Infrared spectra of ethylene glycol bis-(4-methoxycarbonylbenzoate) (A), 1,2-ethanedithiol bis-(4-methoxycarbonylbenzoate) (B) and 1,2-ethanedithiol dibenzoate (C).

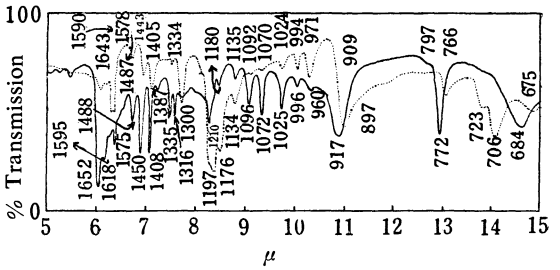



Fig. 3. Polarized infrared spectra of 1,2-ethanedithiol dibenzoate.

TABLE II. VIBRATION OF ESTER AND THIOL ESTER GROUPS ($cm^{-1}$)

| $(CH_3O_2CC_6H_4CO_2CH_2-)_2$ | $(CH_3O_2CC_6H_4COSCH_2-)_2$ | $(C_6H_5COSCH_2-)_2$ | Assignment |
|---|---|---|---|
| 1724 | 1730 | | C=O stretching |
| | 1664 | 1658 | C=O stretching |
| 1279, 1266 | 1277 | | C-O-C asym. stretching |
| | 1205 | 1203 | C-S-C asym. stretching |
| 972 | 1109 | | C-O-C sym. stretching |
| | 921 | 915 | C-S-C sym. stretching |
| | 776 | 773 | COS out-of-plane bending |
| | 717 | | $CO_2$ in-plane bending |
| | 699 | 684 | COS in-plane bending |

The dotted curve was run with the sample in the same position but with the polarizer rotated 90° from the first position. The C=O stretching (1652 cm$^{-1}$) and C–S–C antisymmetric stretching (1197 cm$^{-1}$) bands whose assignments are certain, show perpendicular and parallel dichroisms respectively. Further, a band at 1450 cm$^{-1}$ attributable to $CH_2$ bending vibrations shows perpendicular dichroism and a band at 1300 cm$^{-1}$ attributable to $CH_2$ wagging vibrations shows parallel dichroism. From these facts, it follows that the chain CO–S–$CH_2$–$CH_2$–S–CO is essentially parallel to the direction of crystal growth. On the other hand, bands attributable to in-plane vibrations of the phenyl group by analogy with toluene and monodeutero benzene show perpendicular dichroism, while bands attributable to out-of-plane vibrations show parallel dichroism (Table III). This indicates that the plane of the phenyl group is approximately normal to the direction of crystal growth. Based on these results, the probable configuration and arrangement of the molecule** are shown in Fig. 4. The dichroisms observed for the three strong bands at 917, 772 and 684 cm$^{-1}$ which were assigned, respectively, to the C–S–C symmetric stretching, COS out-of-plane bending, and COS in-plane bending vibrations are in agreement with those expected from the above arrangement.

TABLE III. VIBRATION OF PHENYL GROUP (cm$^{-1}$)

| Mode[a] | | $C_6H_5D$[9] | $C_6H_5CH_3$[10] | $(C_6H_5COSCH_2-)_2$ |
|---|---|---|---|---|
| In-plane | 8 b | 1574 | 1586 | 1575 ($\sigma$) |
| | 19 a | 1480 | 1483 | 1488 ($\sigma$) |
| | 19 b | 1450 | 1310 | 1316 ($\sigma$) |
| | 15 | 1076 | 1070 | 1072 ($\sigma$) |
| | 18 a | 1031 | 1030 | 1025 ($\sigma$) |
| Out-of-plane | 5 | 995 | 943 | 994 ($\pi$) |
| | 17 a | 970 | (985) | 971 ($\pi$) |
| | 17 b | 922 | 890 | 890 ($\pi$) |
| | 10 b | 850 | 730 | 723 ($\pi$) |
| | 4 | 698 | 695 | 706 ($\pi$) |

a) We owe the numbering of vibrational modes to Wilson [E. B. Wilson, Jr., *Phys. Rev.*, **45**, 706 (1934)].

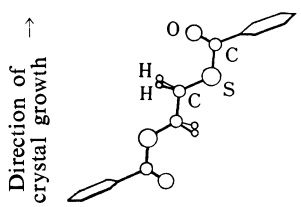



Fig. 4. Probable configuration of 1,2-ethane dithiol dibenzoate.

## Discussion

Although a good deal of work has been done on the characteristic stretching frequencies of the ester group, no systematic study of the deformation frequencies has been carried out. Our knowledge of the factors influencing the frequency and intensity of the deformation vibrations is still relatively meager. Nevertheless, it is possible to predict the approximate position for some of them. Thompson and Torkington[11] have found two characteristic bands of fair intensities at about 600 cm$^{-1}$ for acetates and propionates (612 and 640 cm$^{-1}$ for acetates and 590 and 610 cm$^{-1}$ for propionates). Later, Wilmshurst[12] has assigned the bands at 639 and 615 cm$^{-1}$ in methyl acetate to $CO_2$ in-plane bending and $CO_2$ out-of-plane bending vibrations, respectively. In a number of $\alpha,\beta$-unsaturated esters, Walton and Hughes[13] have found strong bands at 850~750 cm$^{-1}$, which have been reasonably assigned to the $CO_2$ out-of-plane vibration by their dichroic behaviors. A band of similar nature falls at 781 cm$^{-1}$ in methyl oxalate[13]. In the light of these results, the $CO_2$ out-of-plane bending vibration of aromatic esters is reasonably expected to appear above 600 cm$^{-1}$.

In either polyethylene terephthalate or polyethylene-$d_4$ terephthalate, however, no band attributable to the $CO_2$ out-of-plane bending vibration is observed in the range 700~550 cm$^{-1}$. The bands at 680 and 631 cm$^{-1}$ are too weak to be assigned to a $CO_2$ out-of-plane vibration, and moreover their dichroisms are inconsistent with that expected for an out-of-plane vibration. The polymer chain in a drawn sample of polyethylene terephthalate has been known to orient parallel to the direction of drawing[1,4,14] and hence an out-of-plane vibration is expected to exhibit perpendicular dichroism. Since the absorption bands above 750 cm$^{-1}$ in this polymer have been assigned with fair certainty[3] to vibrations other than the $CO_2$ out-of-plane bending vibration, the only band left assignable to it is the strong and perpendicular band at 727 cm$^{-1}$.

There are three infrared-active out-of-plane

9) C. K. Ingold et al., *J. Chem. Soc.*, **1946**, 299, 316.
10) K. S. Pitzer and D. W. Scott, *J. Am. Chem. Soc.*, 65, 817 (1943).
** The crystal structure of this compound is not known. It is assumed that all the molecules take the same arrangement with respect to the direction of crystal growth. Configurations obtained from that shown in Fig. 4 by rotating the S-CO bond are also possible, but this does not affect the following discussions.
11) H. W. Thompson and P. Torkington, *J. Chem. Soc.*, **1945**, 640.
12) J. K. Wilmshurst, *J. Mol. Spectroscopy*, **1**, 201 (1957).
13) W. L. Walton and R. B. Hughes, *J. Am. Chem. Soc.*, **79**, 3985 (1957).
14) W. J. Dulmage and A. L. Geddes, *J. Polymer Sci.*, **31**, 499 (1958).

TABLE IV. INFRARED-ACTIVE OUT-OF-PLANE VIBRATIONS ($cm^{-1}$)

| Mode | $C_6H_6$[15] | $p$-$C_6H_4D_2$[16] | $p$-$C_6H_2D_4$[16] | $C_6D_6$[15] | $p$-$C_6H_4(CH_3)_2$[10] |
|---|---|---|---|---|---|
| 16 b | 405 | 367 | 383 | 350 | 389 |
| 11 | 673 | 597 | 548 | 496 | (170) |
| 17 b | 975 | 876 | 925 | 793 | 796 |

vibrations for $p$-disubstituted benzenes (point group $V_h$). Some authentic frequencies for these vibrations are listed in Table IV together with those of benzene. Based on these frequencies, modes 16b and 11 in polyethylene terephthalate can be reasonably assumed to appear below 500 $cm^{-1}$. Hence, the only aromatic out-of-plane vibration expected to appear above 700 $cm^{-1}$ is the mode 17b. It is unlikely that both the perpendicular bands (875 and 727 $cm^{-1}$) observed in polyethylene terephthalate can be assigned to aromatic out-of-plane vibrations.

It thus seems logical to consider that the band at 727 $cm^{-1}$ is related to the $CO_2$ out-of-plane bending vibration. It should be noted that similar bands called the extra bands[7] are found in aromatic esters, acids, amides, and nitro compounds, all of which have out-of-plane bending vibrations of the substituents.

The band at 727 $cm^{-1}$, however, cannot be described as a pure $CO_2$ out-of-plane bending vibration, because it is removed by the deuteration of terephthalic acid residue[2,5]. This removal can be explained by assuming that the $CO_2$ out-of-plane bending mode and the 17b mode referred to above couple between each other. These two modes are similar in their frequencies and symmetry types. Therefore it is very probable that the perpendicular band at 875 and 727 $cm^{-1}$ in polyethylene terephthalate arise from these coupled vibrations. The assumption of the coupling between the $CO_2$ and aromatic C–H out-of-plane bending vibration can also explain the anomalous shift of the latter in certain aromatic esters[7]. For example, the appearance of two bands at 809 and 711 $cm^{-1}$ in methyl benzoate[8] may be explained as a consequence of this coupling, considering that pure frequencies for phenyl C–H and ester $CO_2$ out-of-plane bending vibrations fall at 770～730 $cm^{-1}$ and 800～750 $cm^{-1}$, respectively. Furthermore, similar anomalies of C–H out-of-plane bending frequencies in some $\alpha, \beta$-unsaturated esters seem also to result from an analogous coupling. The ethylenic C–H out-of-plane bending frequencies of acrylates and methacrylates fall outside the normal range, while those of crotonates lie close to the normal range (Table V). Based on the assumption that the ethylenic C–H and ester $CO_2$ out-of-plane bending vibrations in crotonates are substantially free of coupling and hence that the frequency of a pure out-of-plane vibration of an ester group attached to an ethylenic bond falls at about 840 $cm^{-1}$, the shifts in acrylates and methacrylates can be easily explained as the result of coupling between the ethylenic C–H and ester $CO_2$ out-of-plane bending vibrations. The frequency difference between the two pure modes is about 50 $cm^{-1}$ in acrylates and methacrylates, while it amounts to about 120 $cm^{-1}$ in crotonates.

TABLE V. C–H AND $CO_2$ OUT-OF-PLANE BENDING FREQUENCIES ($cm^{-1}$) FOR $\alpha, \beta$-UNSATURATED ESTERS

| Compound | $\pi$(C–H) | $\pi$($CO_2$) | Normal position[17] for $\pi$(C–H) |
|---|---|---|---|
| Crotonates[13] | 982～970 | 842～833 | 970～960 |
| Acrylates[13,18] | 988～981<br>967～960 | 813～808 | 995～985<br>915～905 |
| Methacrylates[13,18] | 943～935 | 817～813 | 895～885 |

All these facts indicate the general occurrence of the coupling between $CO_2$ and C–H out-of-plane bending vibrations in aromatic esters. This coupling is, of course, destroyed when any one of the following conditions is not satisfied; first, similarity of frequencies of pure vibrations for the two modes, and second, coplanarity of the aromatic ring and the ester group.

1, 2-Ethanedithiol dibenzoate and 1, 2-ethanedithiol bis-(4-methoxycarbonylbenzoate) investigated in the present work provide further evidence for the interpretation developed above. As was shown in the section of experimental results, phenyl and thiol ester groups of the former compound are not present in the same plane, and hence no coupling is expected between the out-of-plane vibrations of the two groups. Therefore the perpendicular band at 773 $cm^{-1}$ can be considered as an essentially pure COS out-of-plane bending vibration. Since the out-of-plane bending frequency of an ester group is expected not to be very different from that of a thiol ester group, the appearance of the latter at 773 $cm^{-1}$ supports

15) F. A. Miller, *J. Chem. Phys.*, **24**, 996 (1956).
16) S. C. Carson, R. R. Gordon and C. K. Ingold, *J. Chem. Soc.*, **1946**, 288.
17) L. J. Bellamy, "The Infrared Spectra of Complex Molecules", 2nd Ed., Methuen, London (1958), p. 34.
18) W. H. T. Davison and G. R. Bates, *J. Chem. Soc.*, **1953**, 2607.

the assumption adopted in the foregoing discussion that a pure out-of-plane bending vibration of an aromatic ester group falls at about 800 $cm^{-1}$. The aromatic out-of-plane vibration of this compound (721 and 709 $cm^{-1}$) falls close to the normal positions for phenyl groups (see Table III). In ethylene glycol dibenzoate[8], however, three bands were observed at 804, 695 and 683 $cm^{-1}$, but no band was observed in the normal range (770~720 $cm^{-1}$) for the mode 10b. This difference between the thiol ester and the ester can be again explained by the coupling between the out-of-plane vibrations. If one assumes that the $CO_2$ vibration couples with phenyl vibration, the lowering of the phenyl out-of-plane frequency in ethylene glycol dibenzoate is readily explained.

Two bands at 873 and 727 $cm^{-1}$ in ethylene glycol bis-(4-methoxycarbonylbenzoate) undoubtedly correspond to the two perpendicular bands at 875 and 727 $cm^{-1}$ in polyethylene terephthalate. The latter disappears and the former shifts to 865 $cm^{-1}$ on going from ethylene glycol bis-(4-methoxycarbonylbenzoate) to 1, 2-ethanedithiol bis-(4-methoxycarbonylbenzoate). This change seems also to be accounted for by assuming that the aromatic ring and thiol ester group in the latter are not coplanar. The C–H out-of-plane vibration of the *p*-phenylene group and the $CO_2$ out-of-plane vibrations of the two ester groups in the former compound couple amoung each other giving rise to two bands at 873 and 727 $cm^{-1}$. On the other hand, in the latter compound, at least the vibration of the thiol ester group may not be coupled with the aromatic vibration, and hence their frequencies are different from those of the former compound. It is not known whether the ester and *p*-phenylene groups in 1, 2-ethanedithiol bis-(4-methoxycarbonylbenzoate) are coplanar or not, but in any case the bands at 865 and 778 $cm^{-1}$ (shoulder) are attributable to the out-of-plane vibrations of these two groups. It is difficult to explain the spectral difference between the two model compounds on the basis of assigning both the bands at 873 and 727 $cm^{-1}$ cited above to aromatic out-of-plane vibrations.

In conclusion, the bands at 875 and 727 $cm^{-1}$ in polyethylene terephthalate can be reasonably assigned to coupled vibrations of aromatic C–H and ester $CO_2$ out-of-plane bending modes which provide a consistent explanation for several aromatic esters and thiol esters.

Finally, mention should be made of the $CO_2$ in-plane bending frequency. Since this is expected not to be very different from that of the COS in-plane bending vibration, that band at 717 $cm^{-1}$ in 1, 2-ethanedithiol bis-(4-methoxycarbonylbenzoate) can probably be assigned to this mode. It is possible that this vibration in polyethylene terephthalate lies buried under the band at 727 $cm^{-1}$.

## Summary

Infrared spectra of polyethylene terephthalate and polyethylene-$d_4$ terephthalate were investigated in the KBr and CsBr regions. No band attributable to a $CO_2$ out-of-plane bending vibration was found below 700 $cm^{-1}$. The only band assignable to this mode is a strong and perpendicular band at 727 $cm^{-1}$. This fact together with the disappearance of the 727 $cm^{-1}$ band in polyethylene deuteroterephthalate, indicates that two bands at 875 and 727 $cm^{-1}$ in polyethylene terephthalate can be assigned to coupled vibrations of aromatic C–H and ester $CO_2$ out-of-plane bending modes. This interpretation provides a consistent explanation for the spectral differences between ethylene glycol dibenzoate and 1, 2-ethanedithiol dibenzoate and between ethylene glycol bis-(4-methoxycarbonylbenzoate) and 1, 2-ethanedithiol bis-(4-methoxycarbonylbenzoate) as well as for the anomalous shifts of C–H out-of-plane frequencies and the appearances of " extra bands " in several aromatic esters.

*Central Research Laboratories*
*Toyo Rayon Co.*
*Otsu, Shiga*

*Note Added in Proof*:

Recently, perpendicular bands at about 820 $cm^{-1}$ have been found in polyethylene terephthalate-$d_4$ and polyethylene $d_4$ terephthalate-$d_4$ [C. Y. Liang and S. Krimm, *J. Mol. Spectroscopy*, 3, 554 (1959).]. These bands can be assigned to the $CO_2$ out-of-plane vibration in these deuteroterephthalates. If this assingnment is correct, it seems better to consider that the 17b vibration of the terephthalates has a lower frequency than the $CO_2$ out-of-plane vibration. Then, for the band at 727 $cm^{-1}$ in polyethylene terephthalate, the contribution of the 17b vibration may exceed that of the $CO_2$ vibration, and vice versa for the band at 875 $cm^{-1}$[9].

# *Application of the Theory of Regular Solutions to Binary Phase Equilibria. I. Method of Application to Binary Liquid Equilibria*

By Kiyoharu ISHIDA

(Received January 7, 1960)

Accurate prediction of phase relationships over a wide range of temperatures from some data determined at several temperatures is difficult in general. It seems that if the theory of strictly regular solutions developed by Guggenheim[1] is applicable to mixtures for most binary systems, the behavior of solutions may be more satisfactorily interpreted by the theory than by the semi-empirical equations according to van Laar or Margules. However, exceedingly few systems satisfy all the conditions for forming regular mixtures in which the molecules are assumed to be sufficiently alike in size and shape to be interchangeable on a lattice or quasi-lattice.

The author has shown that the theory of regular solutions can apply to a much wider class of mixtures by assuming the formation of stable 'clusters' consisting of each component in its liquid phases[2]. This paper will be concerned with the derivation of the relationship between the compositions in two conjugate liquid phases on which the application of the theory of regular solutions is based and with the method of representing the solubility curves for most binary systems symmetrically. Detailed consideration referring to the estimation of interchange energy from mutual solubility data and its dependency upon temperature will be given in a subsequent paper.

## 1. Thermodynamic Aspects on the Coexistence Curve of Binary Liquid Mixtures

The rigorous thermodynamic equations of the form

$$\ln(a_{\mathrm{I}}/a_{\mathrm{II}}) = \ln(x_{\mathrm{I}}/x_{\mathrm{II}}) + \ln(\gamma_{\mathrm{I}}/\gamma_{\mathrm{II}}) \qquad (1,1)$$

are applicable to any binary mixtures, where $a$'s, $x$'s and $\gamma$'s denote activities, mole fractions and activity coefficients of the component designated by subscripts I and II at a given temperature, respectively. (The pure component is taken as standard state). When the solution is separated into two liquid phases by the increase of the deviation from Raoult's law, designating the I-component rich phase by one prime and the II-component rich phase by two primes,

$$a_{\mathrm{I}}' = a_{\mathrm{I}}'', \quad a_{\mathrm{II}}' = a_{\mathrm{II}}'' \text{ and } x_{\mathrm{I}}' = 1 - x_{\mathrm{II}}'.$$

It therefore follows

$$\ln\{(1-x_{\mathrm{II}}')/x_{\mathrm{II}}'\} - \ln\{(1-x_{\mathrm{II}}'')/x_{\mathrm{II}}''\} = \ln(\gamma_{\mathrm{I}}''\gamma_{\mathrm{II}}'/\gamma_{\mathrm{I}}'\gamma_{\mathrm{II}}'') \qquad (1,2)$$

In cases where mutual solubilities are not so great, both values of $\gamma_{\mathrm{I}}'$ and $\gamma_{\mathrm{II}}''$ are near unity.

The temperature dependence of the activity coefficient can be related to the heat of mixing by the following equation

$$\frac{\mathrm{d}\ln\gamma_{\mathrm{I}}}{\mathrm{d}T} = -\frac{\Delta\bar{H}_{\mathrm{I}}}{\boldsymbol{R}T^2} \qquad (1,3)$$

where $\Delta\bar{H}_{\mathrm{I}}$ is the partial molal heat of solution of component I, $\boldsymbol{R}$ the gas constant and $T$ the absolute temperature. Then, Eq. 1,2 may be transformed into

$$\frac{\mathrm{d}\ln\{(1-x')/x'\}}{\mathrm{d}T} - \frac{\mathrm{d}\ln\{(1-x'')/x''\}}{\mathrm{d}T} = -\frac{\Delta H}{\boldsymbol{R}T^2} \qquad (1,4)$$

where

$$\Delta H = \Delta\bar{H}_{\mathrm{I}}'' - \Delta\bar{H}_{\mathrm{II}}'' - (\Delta\bar{H}_{\mathrm{I}}' - \Delta\bar{H}_{\mathrm{II}}') \qquad (1,5)$$

In Eq. 1,4 $x_{\mathrm{II}}$ is represented as $x$ for the sake of simplicity.

For most binary liquid mixtures with a few exceptions, it is observed that the solubilities of one component in one phase increase as the corresponding values in the other conjugate phase decrease with changing temperatures, and then the signs of $(\Delta\bar{H}_{\mathrm{I}}'' - \Delta\bar{H}_{\mathrm{II}}'')$ and $(\Delta\bar{H}_{\mathrm{I}}' - \Delta\bar{H}_{\mathrm{II}}')$ are opposite. The absolute values of these two quantities are equal in particular systems where the solubility curves are symmetrical with respect to the mole fraction as it is for a regular mixture. If the absolute value of the latter of these two quantities is $m$ times the former and $m$ is assumed to be independent of temperature, then

$$\Delta\bar{H}_{\mathrm{I}}' - \Delta\bar{H}_{\mathrm{II}}' = -m(\Delta\bar{H}_{\mathrm{I}}'' - \Delta\bar{H}_{\mathrm{II}}'') \qquad (1,6)$$

1) E. A. Guggenheim, "Mixtures", Oxford University Press, London (1952).
2) K. Ishida, *Nature*, **184**, 814 (1959).

Using these assumptions, Eq. 1, 4 may be written in the form

$$\frac{d\ln\{(1-x')/x'\}}{dT} - \frac{d\ln\{(1-x'')/x''\}}{dT} = (1+m)\frac{d\ln(\gamma_I''/\gamma_{II}'')}{dT} \qquad (1,7)$$

In the following Eq. 1, 8, which is obtained by setting the value of the first derivative of the molal free energy of mixing at a given temperature and pressure, $g(x)$, with respect to $x$ equal to zero,

$$\ln(\gamma_I/\gamma_{II}) = -\ln\{(1-x)/x\} \qquad (1,8)$$

values of $x$ represent the mole fractions of component II along the coexistence curve in cases of symmetrical systems. However, in cases of ordinary unsymmetrical systems, values of $x$ do not represent the mole fractions along the consolute curve, but they represent those at the extreme values on the $g(x)$ curve in the neighborhood of the compositions in mutual equilibrium of two phases such as $x'$ and $x''$, which are the two points of contact of the common tangent on the $g(x)$ curve. If the dependency of the logarithms of mole ratio of two components at the compositions in two coexisting phases upon temperature is assumed to be scarcely different from that at the compositions corresponding to the extreme values on the $g(x)$ curve, the following simple relation can be obtained

$$\ln\{(1-x')/x'\} = -m\ln\{(1-x'')/x''\} + B \qquad (1,9)$$

for the values of $x'$ and $x''$ on the coexistence curves, where $B$ is a constant independent of temperature.

As will be clear from Figs. 1—3* in which plots are made of the logarithms of the mole ratios of two components in one phase against the corresponding values in the other conjugate phase for several systems described in the literature, fair straight lines whose slopes are near minus unity are obtained from these plots over the considerably wide range of temperatures not only for systems with virtually symmetrical solubility curves, but also for systems with extremely unsymmetrical ones. Even for the systems showing the closed solubility curve, the linear relationships between the functions $\log\{(1-x')/x'\}$ and $\log\{(1-x'')/x''\}$ hold for temperatures within 30° of a critical solution temperature, $T_c$. This fact indicates that the value of $m$ is near unity for most systems and the deviations due to two assumptions involved in the derivation of Eq. 1, 9 from actual behavior of solutions are almost cancelled, and that when the logarithm of the mole ratio of two components in one phase increases with the change in temperature, the corresponding value in the other phase decreases in proportion to the increase of that in the former phase and the proportional factor is a constant over a wide range of temperature. It is clear that the form of Eq. 1, 9 is independent of whether weight, mole or volume fractions are used for the unit of concentration.

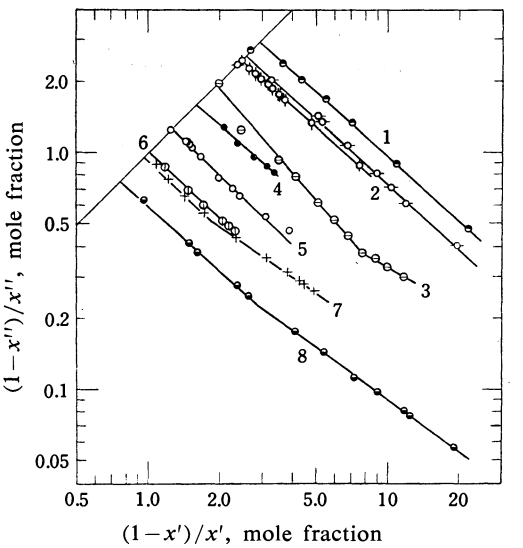



Fig. 1. Plot on double logarithmic coordinates of $(1-x'')/x''$ against $(1-x')/x'$.

| No. | Symbol | Component I | Component II | Ref. |
|---|---|---|---|---|
| 1 | ◓ | Benzene— | Perfluoromethylcyclohexane | 3 |
| 2 | -○- | Carbon tetrachloride— | Perfluoromethylcyclohexane | 3 |
| | ○ | 〃 | 〃 | 4 |
| 3 | ⊖ | *n*-Butane— | Perfluoro-*n*-butane | 5 |
| 4 | ● | Silicon tetrachloride— | Stannic iodide | 6 |
| 5 | ○ | Cyclohexane— | Aniline | 7 |
| 6 | ① | Isooctane— | Stannic iodide | 8 |
| 7 | + | Cyclohexane— | Methanol | 9 |
| 8 | ◒ | *n*-Heptane— | Furfural | 10 |

* Estimated values of the compositions in coexisting phases from solubility curves are also included as points in these figures.

3) J. H. Hildebrand and D. R. F. Cochran, *J. Am. Chem. Soc.*, 71, 22 (1949).
4) B. H. Zimm, *J. Phys. & Colloid Chem.*, 54, 1306 (1950).
5) J. H. Simons and J. W. Mansteller, *J. Chem. Phys.*, 20, 1516 (1952).
6) J. H. Hildebrand and G. R. Negishi, *J. Am. Chem. Soc.*, 59, 339 (1937).
7) D. Atack and O. K. Rice, *J. Chem. Phys.*, 22, 382 (1954); *Disc. Faraday Soc.*, 15, 210 (1953).
8) M. E. Dice and J. H. Hildebrand, *J. Am. Chem. Soc.*, 50, 3023 (1928).
9) E. L. Eckfeldt and W. W. Lucasse, *J. Phys. Chem.*, 47, 164 (1934).
10) E. N. Pennington and S. J. Marwil, *Ind. Eng. Chem.*, 45, 1371 (1953).

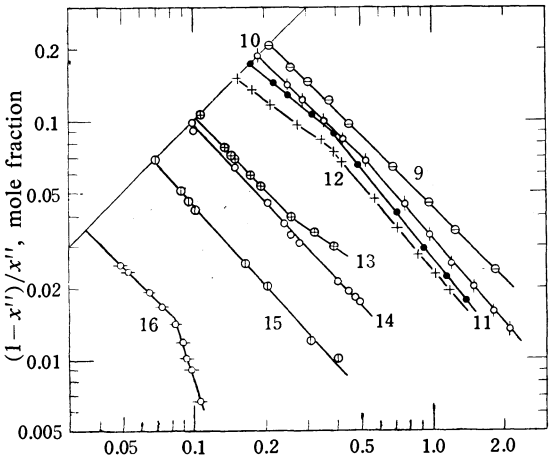



Fig. 2. Plot on double logarithmic coordinates of $(1-x'')/x''$ against $(1-x')/x'$.

| No. | Symbol | Component I | Component II | Ref. |
|---|---|---|---|---|
| 9 | ⊖ | Ethylbenzene— | Liquid ammonia | 11 |
| 10 | ○ | Mesitylene— | Liquid ammonia | 11 |
| 11 | ● | Propylbenzene— | Liquid ammonia | 11 |
| 12 | + | 1-Methylnaphthalene— | Liquid ammonia | 11 |
| 13 | ⊕ | Methyldiethylamine— | Water | 12 |
| 14 | ○ | Phenol— | Water | 13 |
| 15 | ⓘ | 2,6-Dimethylpyridine— | Water | 14 |
| 16 | -○- | Palmitic acid— | Liquid propane | 15 |

It is reasonable that Eq. 1, 9 holds for temperatures within 30°C of a critical solution temperature for most binary liquid systems, since this formula is immediately derived from the empirical relations 1, 10 shown by Cox and Herington[14].

$$T-T_c=[A'\log\{(1-x')/x'\}+B']^3 \qquad (1, 10a)$$

$$T-T_c=[A''\log\{(1-x'')/x''\}+B'']^3 \qquad (1, 10b)$$

## 2. Method of Representing the Solubility Curve Symmetrically

At the critical solution temperature $T_c$, the two coexisting phases become identical having the composition $x'=x''=x_c$. Eq. 1, 9 may be transformed into

$$\frac{1-x'}{x'}\cdot\frac{x_c}{1-x_c}=\left[\frac{1-x''}{x''}\cdot\frac{x_c}{1-x_c}\right]^{-m} \qquad (2, 1)$$

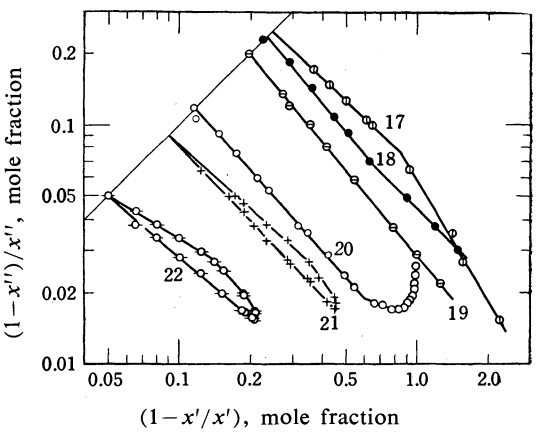



Fig. 3. Plot on double logarithmic coordinates of $(1-x'')/x''$ against $(1-x')/x'$.

| No. | Symbol | Component I | Component II | Ref. |
|---|---|---|---|---|
| 17 | ⓘ | Octene— | Liquid sulfur dioxide | 16 |
| 18 | ● | *m*-Xylene— | Liquid ammonia | 11 |
| 19 | ⊖ | Isopropylbenzene— | Liquid ammonia | 11 |
| 20 | ○ | *n*-Butanol— | Water | 13 |
| 21 | + | 1-Propoxypropane-2-ol— | Water | 17 |
| 22 | -○- | Ethylene glycol *n*-butyl ether— | Water | 18 |

It is possible to represent the solubility curve for a binary liquid system symmetrically with respect to the composition by plotting properly selected units. When the following units $\varphi$, which are the variation of volume fractions, are used for the concentrations, the resulting solubility curve will be symmetrical with respect to $\varphi$ as for regular binary mixtures, since $\varphi'+\varphi''=1$.

$$\varphi'=\frac{x'/x_c}{x'/x_c+(1-x')/(1-x_c)}$$

$$\varphi''=\frac{(x''/x_c)^m}{(x''/x_c)^m+\{(1-x'')/(1-x_c)\}^m} \qquad (2, 2)$$

Therefore, the interchange energy $w$ between two kinds of cluster may be obtained from the theory of regular solutions by assuming that each component forms clusters consisting of each component in its liquid phase, the number of moles being $(1-x')x_c$ and $x'(1-x_c)$ respectively, and that two kinds of cluster are stable and sufficiently alike in size and shape to satisfy all the conditions for forming strictly regular solutions on mixing[2]. In this case, by the definition of Eq. 2, 2 the molecular

11) K. Ishida, This Bulletin, **31**, 143 (1958).
12) J. L. Copp, *Trans. Faraday Soc.*, **51**, 1056 (1955).
13) A. E. Hill and W. M. Malisoff, *J. Am. Chem. Soc.*, **48**, 918 (1926).
14) J. D. Cox and E. F. G. Herington, *Trans. Faraday Soc.*, **52**, 926 (1956).
15) D. A. Drew and A. N. Hixson, *Trans. Am. Inst. Chem. Engrs.*, **40**, 675 (1944).
16) W. F. Seyer and L. Hodnett, *J. Am. Chem. Soc.*, **58**, 996 (1936).
17) H. L. Cox, W. L. Nelson and L. H. Cretcher, ibid., **49**, 1080 (1927).
18) H. L. Cox and L. H. Cretcher, ibid., **48**, 451 (1926).

ratio, $r'$, becomes

$$r'=\frac{1-\varphi'}{\varphi'}=\frac{1-x'}{x'}\cdot\frac{x_c}{1-x_c} \qquad (2,3)$$

Sometimes values of the interchange energy estimated from the compositions in one phase, $x'$, differ a little from those estimated by the use of the compositions in the other phase, $x''$, since a constant $m$ is not always exactly equal to unity as shown in Figs. 1—3. Of course, both values should coincide with each other when they are calculated by $\varphi'$ and $\varphi''$ using the value of $m$ estimated from the mutual solubility data determined at two temperatures by Eq. 1, 9, but calculations are considerably tedious.

It is convenient to introduce a variable $x_k$ defined by

$$\frac{x_k}{1-x_k}=\left(\frac{x'}{1-x'}\cdot\frac{x''}{1-x''}\right)^{1/2} \qquad (2,4)$$

and to use the variable $x_k$ instead of critical composition $x_c$ setting the value of $m$ equal to unity. Then,

$$\varphi'=\frac{\{x'/(1-x')\}^{1/2}}{\{x'/(1-x')\}^{1/2}+\{x''/(1-x'')\}^{1/2}}$$
$$=\frac{\{(1-x'')/x''\}^{1/2}}{\{(1-x')/x'\}^{1/2}+\{(1-x'')/x''\}^{1/2}}\equiv\varphi$$

and Eq. 2, 3 is replaced by Eq. 2, 6

$$r=\frac{1-\varphi}{\varphi}=\left(\frac{x''}{1-x''}\cdot\frac{1-x'}{x'}\right)^{1/2} \qquad (2,6)$$

Thus, by using $x_k$ instead of $x_c$ and putting $m=1$, the solubility curve can always be represented symmetrically with respect to $\varphi$ and the molecular ratio and the interchange energy at a given temperature can be evaluated by simpler calculation.

The value of $x_k$ may be dependent of the temperature and different from $x_c$ to a certain extent when $m$ is not unity, but $x_k$ corresponds to $x_c$ at the critical solution temperature. It may be easily proved by further algebraic arguments that there are straight line relationships between the functions $\log\{x_k/(1-x_k)\}$ and $\log\{x'/(1-x')\}$ and between the functions $\log\{x_k/(1-x_k)\}$ and $\log\{x''/(1-x'')\}$, and that $x_c$ is given by the following equation

$$\log\frac{x_c}{1-x_c}=\left[\log\frac{1-x_2'}{x_2'}\log\frac{x_1''}{1-x_1''}-\log\frac{1-x_1'}{x_1'}\log\frac{x_2''}{1-x_2''}\right]\Big/\left[\log\left(\frac{x_1'}{1-x_1'}\cdot\frac{1-x_2'}{x_2'}\right)-\log\left(\frac{x_1''}{1-x_1''}\cdot\frac{1-x_2''}{x_2''}\right)\right] \qquad (2,7)$$

where subscripts 1 and 2 denote the values at temperatures $T_1$ and $T_2$, respectively.

Thus it should be possible to predict the solubility relationships of the system from mutual solubility data, determined at more than one temperature, when the dependence of the interchange energy estimated from mutual solubility data in terms of $\varphi$-fractions upon temperature is known.

## Summary

The same expression for the correlation of compositions in mutual equilibrium of two liquid phases as that which is immediately obtained from the empirical relations used by Cox and Herington was derived thermodynamically. The method has been given in such a manner as to represent the solubility curve for a binary liquid system symmetrically and to estimate the interchange energy from the mutual solubility data by applying the theory of regular solutions.

*The Chemical Research Institute of Non-Aqueous Solutions*
*Tohoku University*
*Katahira-cho, Sendai*

# *Application of the Theory of Regular Solutions to Binary Phase Equilibria. II. Dependency of the Interchange Energy upon Temperature*

By Kiyoharu ISHIDA

(Received January 7, 1960)

A few examples[1] have been shown for the comparison of the theories of strictly regular solutions with experiments, since there are few suitable systems for which measurements necessary to adequate comparison have been made. In cases of many systems in which mixtures of two components show so great deviations from Raoult's law that the solutions separate into two liquid phases, the solutions are generally formed from chemically dissimilar constituents which are different in molecular size, chemical structure, polarity and so on, these conditions being far from those for forming regular mixtures. It, therefore, was impossible that the comparisons of the theories with experimental results obtained for such mixtures with great deviations from ideal behavior were made in order to verify the validity of theories and to extend their application to the field of the chemical engineering design, but now the application of the theories of strictly regular solutions to most partially miscible liquid systems and the estimation of the interchange energy from the mutual solubility data have become possible as described in the previous paper[2]. It is interesting and desirable from a practical viewpoint to study what relations are obtained between the interchange energy or the co-operative energy and the temperature for such systems.

## 3. Theoretical Expressions for Estimating Co-operative Energy from Compositions in Two Coexisting Phases

It has been shown that the problem of the phase transition for the regular mixtures of two components is mathematically identical with that of the so-called Ising model of ferromagnetism and that there is an equivalent relation between the compositions in mutual equilibrium of two liquid phases and the intensity of spontaneous magnetization in the absence of a magnetic field[3,4]. No exact results for the three-dimensional problems are available at present that could be applied to phase equilibria, but exact closed form expressions of the free energy in the absence of a magnetic field[5], which corresponds to the theory of regular solutions with equal ratio of constituents, and of the spontaneous magnetization[6] are available for the two-dimensional model, particularly the square net, though it has been found that there is a marked difference in behavior between two- and more realistic three-dimensional model[7].

The intensity of spontaneous magnetization per spin at zero magnetic field for a two-dimensional ferromagnetic Ising square lattice is given by

$$I=\left[\frac{1+\zeta^2}{(1-\zeta^2)^2}(1-6\zeta^2+\zeta^4)^{1/2}\right]^{1/4} \quad \text{for } \zeta\leqq\sqrt{2}-1 \tag{3,1}$$

$$\zeta=\exp(-\varepsilon/\boldsymbol{k}T) \tag{3,2}$$

where $\varepsilon$ is the interaction energy between each pair of nearest neighbor antiparallel spins assuming the interaction energy between pairs of parallel spins to be zero, and $\boldsymbol{k}$ is the Boltzmann constant.

By the correspondence of the theory of regular solutions to the Ising model, the interchange energy or one half of the energy increase of the whole system when a pair of two molecules of type I and a pair of two molecules of type II are converted into two pairs of a molecule of type I and a molecule of type II, $w$, will be obtained in terms of the mole fractions of component II in two coexisting phases, $x$, by the relation

$$\exp(w/\boldsymbol{k}T)=\left[\frac{1+[1+\{1-(1-2x)^8\}^{1/2}]^{1,2}}{\{1-(1-2x)^8\}^{1\,4}}\right]^4 \tag{3,3}$$

for the square lattice. At the critical solution temperature,

1) E. A. Guggenheim, "Mixtures", Oxford Press, (1952).
2) K. Ishida, *Nature*, **184**, 814 (1959). See also the preceding paper.
3) R. Peierls, *Proc. Cambridge Phil. Soc.*, **32**, 477 (1936). G. F. Newell and E. W. Montroll, *Rev. Mod. Phys.*, **25**, 353 (1953).
4) C. Domb, *Proc. Roy. Soc.*, A **199**, 199 (1949).
5) L. Onsager, *Phys. Rev.*, **65**, 117 (1944).
6) C. N. Yang, ibid., **85**, 808 (1952).
7) C. Domb and M. F. Sykes, *Proc. Roy. Soc.*, A**235**, 247 (1956).

$$x=1/2, \qquad \exp(w/\boldsymbol{kT})_c=[1+\sqrt{2}]^4 \quad (3,4)$$

The information on the behavior of the model has been provided by exact series expansion of the partition function to any desired degree of accuracy[4,7-9]. In the rigorous expansion of the partition function by Bethe-Kirkwood's method of moments[8], the molar free energy of mixing in the notation used by Guggenheim[1] is given by

$$\frac{\Delta mF}{\boldsymbol{RT}}=(1-x)\ln(1-x)+x\ln x+x(1-x)\frac{w}{\boldsymbol{kT}} -\frac{z}{2}\left[\frac{l_2}{2!}\left(\frac{2w}{z\boldsymbol{kT}}\right)^2+\frac{l_3}{3!}\left(\frac{2w}{z\boldsymbol{kT}}\right)^3+\frac{l_4}{4!}\left(\frac{2w}{z\boldsymbol{kT}}\right)^4+\cdots\right] \quad (3,5)$$

where $z$ is the coordination number and

$$l_2=x^2(1-x)^2 \quad (3,6)$$

$$l_3=x^2(1-x)^2(1-2x)^2 \quad (3,7)$$

$$l_4=x^2(1-x)^2(1-6x+6x^2)^2 +6\left(\frac{y}{z}-1\right)x^4(1-x)^4 \quad (3,8)$$

$$l_5=x^2(1-x)^2(1-2x)^2(1-12x+12x^2)^2 +60\left(\frac{y}{z}-1\right)x^4(1-x)^4(1-2x)^2 \quad (3,9)$$

$$l_6=x^2(1-x)^2\{1-60x(1-x)(1-2x)^2\} +30\left(13\frac{y}{z}+17\right)x^4(1-x)^4 +120\left(\frac{\gamma_1}{z}-30\frac{y}{z}-28\right)x^5(1-x)^5 +120\left(\frac{\gamma_2}{z}-4\frac{\gamma_1}{z}+66\frac{y}{z}+42\right)x^6(1-x)^6 \quad (3,10)$$

$y$, $\gamma_1$ and $\gamma_2$ are parameters depending on the lattice and defined by

$$y=\sum_{a'} z^2_{aa'}-z(z-1) \quad (3,11)$$

$$\gamma_1=\sum_{a'} z^3_{aa'}-3\sum_{a'} z^2_{aa'}+2z(z-1) \quad (3,12)$$

$$\gamma_2=\sum_{a'a''} z_{aa'}z_{a'a''}z_{a''a}-3(z-2)\sum_{a'} z^2_{aa'} +2z(z-1)(z-2) \quad (3,13)$$

where $z_{aa'}$ is another coordination number denoting the number of first neighbors common to the sites $a$ and $a'$.

The compositions in two coexisting phases are given by the points where the value of the first derivative of the free energy of mixing is zero, owing to the symmetry of the solubility curve. To obtain the value of $w/\boldsymbol{kT}$ it is convenient to introduce an abbreviation $u$ defined by

$$u=\ln\frac{1-x}{x}\Big/(1-2x) \quad (3,14)$$

Differentiating Eq. 3, 5 with respect to $x$ and setting $\mathrm{d}(\Delta_m F/\boldsymbol{RT})/\mathrm{d}x$ equal to zero, the expression for $u/z$ as a power series in $2w/z\boldsymbol{kT}$ is obtained, which can be inverted into an expression for $2w/z\boldsymbol{kT}$ as a power series in $u/z$ as follows:

$$\frac{w}{\boldsymbol{kT}}=u\left[1+x(1-x)\frac{2u}{z}+\frac{x(1-x)}{3}\left(\frac{2u}{z}\right)^2 +\frac{x(1-x)}{12}\left\{1+2x(1-x) +12x^2(1-x)^2\frac{y}{z}\right\}\left(\frac{2u}{z}\right)^3 +\frac{x(1-x)}{60}\left\{1+8x(1-x) +120x^2(1-x)^2(1-2x+2x^2)\frac{y}{z}\right\}\left(\frac{2u}{z}\right)^4 +\frac{x(1-x)}{360}\left\{1+22x(1-x) +4x^2(1-x)^2\left(4+195\frac{y}{z}\right) +30x^3(1-x)^3\left(10\frac{\gamma_1}{z}-104\frac{y}{z}\right) +360x^4(1-x)^4\left(\frac{\gamma_2}{z}-4\frac{\gamma_1}{z} +10\frac{y}{z}\right)\right\}\left(\frac{2u}{z}\right)^5+\cdots\cdots\right] \quad (3,15)$$

And

$$(w/\boldsymbol{kT})_c=2\left[1+\frac{1}{z}+\frac{4}{3}\frac{1}{z^2}+\left(2+\frac{y}{z}\right)\frac{1}{z^3} +\left(\frac{16}{5}+4\frac{y}{z}\right)\frac{1}{z^4} +\left(\frac{16}{3}+10\frac{y}{z}-\frac{2}{3}\frac{\gamma_1}{z}+\frac{\gamma_2}{z}\right)\frac{1}{z^5}+\cdots\cdots\right] \quad (3,16)$$

The evaluation of the series of coefficients is increasingly tedious and complicated as the series is ascended.

Since the series converges to the exact value extremely slowly, and the presence of a magnetic field, which corresponds to regular solutions of varying concentrations, is difficult to deal with by an exact method even in

8) J. G. Kirkwood, *J. Chem. Phys.*, 6, 70 (1938); *J. Phys. Chem.*, 43, 97 (1939); H. A. Bethe and J. G. Kirkwood, *J. Chem. Phys.*, 7, 578 (1939); T. S. Chang, ibid., 9, 169 (1941).

9) G. S. Rushbrooke, *Nuovo cimento*, 6, (suppl. 2), 251 (1949); A. J. Wakefield, *Proc. Cambridge Phil. Soc.*, 47, 419, 799 (1951); C. Domb, *Proc. Roy. Soc.*, A196, 36 (1949); J. E. Brooks and C. Domb, ibid., A207, 343 (1951); T. Tanaka, H. Katsumori and S. Toshima, *Prog. Theoret. Phys.*, 6, 17 (1951); etc.

two-dimensions, several approximate solutions have been derived in closed form[1,10,11].

In the first (pairs) approximation[1] treated according to the quasi-chemical equilibrium conditions which is equivalent to Bethe approximation, $w$ is given by

$$\exp(w/zkT)=(1-r)/(r^{1/z}-r^{(z-1)/z}) \qquad (3,17)$$

where $r$ is the molecular ratio. At the critical solution temperature

$$\exp(w/zkT)_c=\frac{z}{z-2} \qquad (3,18)$$

In the zeroth approximation[1] which corresponds to the limiting form taken by the first approximation when the coordination number is made infinite, and is equivalent to Bragg-Williams approximation,

$$\frac{w}{kT}=\ln\frac{1-x}{x}\Big/(1-2x)=u \qquad (3,19)$$

Eq. 3,19 is only the first term in the Eq. 3,15 of rigorous series expansion. At the critical solution temperature

$$(w/kT)_c=2 \qquad (3,20)$$

Several methods which are capable of yielding successively higher approximations in the quasi-chemical method have been developed[1,10,12], but the use of a large group introduces troublesome calculations in practical applications of these higher approximations. In the higher approximation for the case of the simple square lattice with the tetrahedra as basic figure[1,10], which is the simplest case treated by the method of a logical extention to larger groups of the quasi-chemical approximation for pairs, the method being equivalent to an approximation developed by Kikuchi, $w/kT$ is obtained from

$$\exp\left(\frac{w}{kT}\right)=\left[\frac{(\sqrt{r}+1)^2+\{(\sqrt{r}+1)^4+4r\}^{1/2}}{2\sqrt{r}}\right]^2 \qquad (3,21)$$

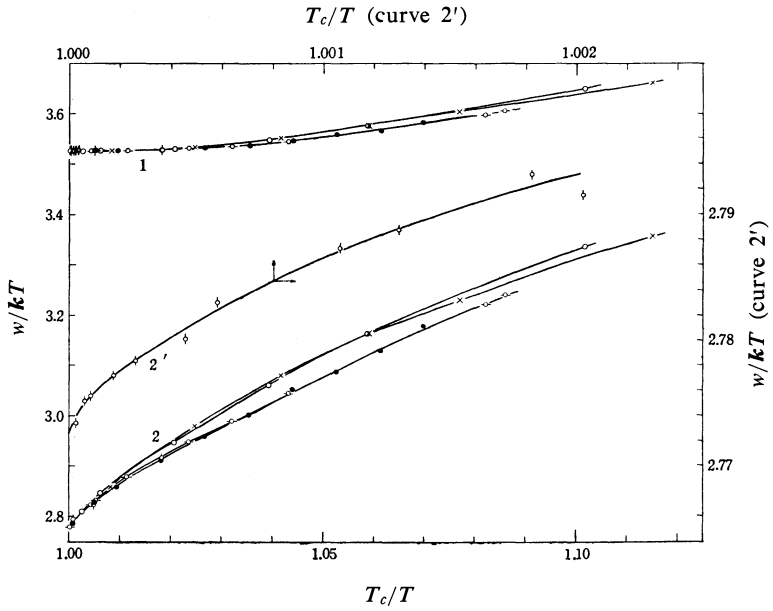



Fig. 4. Relations between $w/kT$ and $T_c/T$ for several systems. Values of $w/kT$ along curve 1 are obtained from Eq. 3,3. Corresponding values along curves 2 and 2' are obtained from Eq. 3,17 assuming $z=4$.

| Symbol | System | Ref. |
|---|---|---|
| ○ | Ethylbenzene—Liquid ammonia | 13 |
| -○- | Carbon tetrachloride—Perfluoromethylcyclohexane | 14 |
| ○ | 〃 — 〃 | 15 |
| ● | *n*-Butane—Perfluoro-*n*-butane | 16 |
| × | *n*-Hexane—Methanol | 17 |

10) J. A. Barker, *Proc. Roy. Soc.*, A216, 45 (1953).
11) I. Prigogine, L. S. Mathot and L. van Hove. *Trans. Faraday Soc.*, **48**, 485 (1952).
12) Y. Y. Li, *Phys. Rev.*, 76, 972 (1949); C. N. Yang, *J. Chem. Phys.*, **13**, 66 (1945).
13) K. Ishida, This Bulletin, **31**, 143 (1958).
14) J. H. Hildebrand and D. R. F. Cochran, *J. Am. Chem. Soc.*, **71**, 22 (1949),
15) B. H. Zimm, *J. Phys. & Colloid Chem.*, **54**, 1306 (1950).
16) J. H. Simons and J. W. Mansteller, *J. Chem. Phys.*, **20**, 1516 (1952).
17) "International Critical Tables", III, McGraw-Hill Book Company, Inc., New York (1928), p. 386.

At the critical solution temperature

$$\exp(w/kT)_c = (2+\sqrt{5})^2 \qquad (3,22)$$

When the value of $w/kT$ is less than the value given by Eqs. 3,4, 3,16, 3,18, 3,20 or 3,22, the separation into two liquid phases does not occur.

## 4. Dependency of $w/kT$ upon Temperature

All formulae described in the above section contain the co-operative energy $w$ in the form of the ratio $w/kT$ or in particular $\exp(w/kT)$. It is convenient to compare the theories with the experiment, regarding either of these quantities as a single parameter whose value determines all the thermodynamic properties at a given temperature. Using $\varphi$ defined by Eq. 2,5 in the preceding paper instead of $x$, similar results between the functions $w/kT$ according to each theoretical formula and $T_c/T$ were obtained from the mutual solubility data for most binary liquid systems described in the literature as shown in Fig. 4. Accordingly, it may be sufficiently shown by the results for some representative systems how values of $w/kT$ are affected by such various theoretical

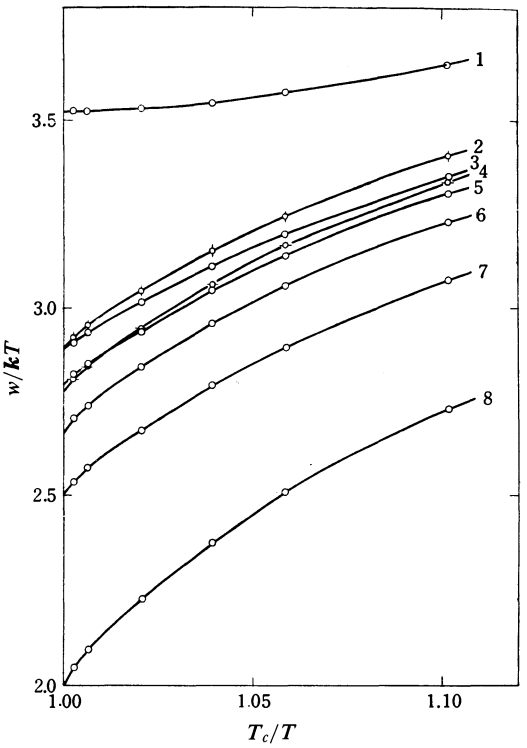



Fig. 5. Plot of values of $w/kT$ obtained from several theoretical expressions against $T_c/T$ for the system ethylbenzene—liquid ammonia.

Curve 1 is obtained from Eq. 3,3; curve 2 is obtained from Eq. 3,21; curve 3 is the expansion to terms of order $(2u/z)^4$ as given by Eq. 3,15 assuming $z=4$; curve 4 corresponds to Eq. 3,17 assuming $z=4$; curves 5, 6 and 7 are the expansions to terms of order $(2u/z)^3$, $(2u/z)^2$ and $(2u/z)$ as given by Eq. 3,15 assuming $z=4$, respectively; curve 8 is obtained from Eq. 3,19.

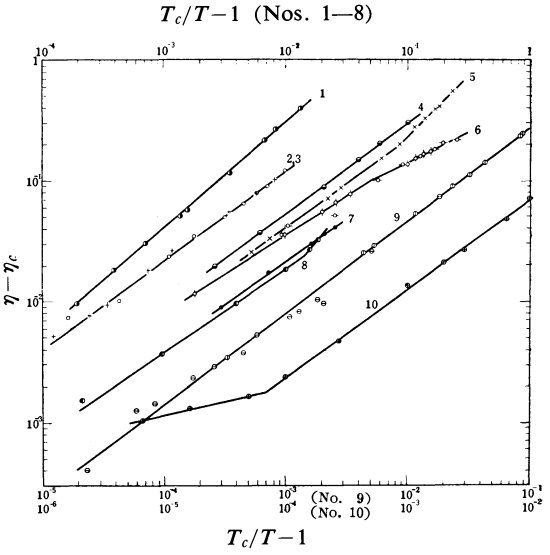



Fig. 6. Plot on logarithmic coordinates $\eta-\eta_c$ against $|T_c/T-1|$ for several systems.

| No. | Symbol | System | Ref. |
|---|---|---|---|
| 1 | ◑ | Octene—Liquid sulfur dioxide | 18 |
| 2 | + | Methyldiethylamine—Water | 19 |
| 3 | ○ | Palmitic acid—Liquid propane | 20 |
| 4 | ◒ | Ethylbenzene—Liquid ammonia | 13 |
| 5 | × | *n*-Heptane—Furfural | 21 |
| 6 | ○ | Phenol—Water | 22 |
| | -○- | Phenol—Water | 17 |
| 7 | ● | Isooctane—Stannic iodide | 23 |
| 8 | ◐ | Silicon tetrachloride—Stannic iodide | 24 |
| 9 | ⊕ | Carbon tetrachloride—Perfluoromethylcyclohexane | 14 |
| | ⊖ | Carbon tetrachloride—Perfluoromethylcyclohexane | 15 |
| 10 | ⊕ | Cyclohexane—Aniline | 25 |

18) W. F. Seyer and L. Hodnett, *J. Am. Chem. Soc.*, **58**, 996 (1936).
19) J. L. Copp, *Trans. Faraday Soc.*, **51**, 1056 (1955).
20) D. A. Drew and A. N. Hixson, *Trans. Am. Inst. Chem. Engrs.*, **40**, 675 (1944).
21) E. N. Pennington and S. J. Marwil, *Ind. Eng. Chem.*, **45**, 1371 (1953).
22) A. E. Hill and W. M. Malisoff, *J. Am. Chem. Soc.*, **48**, 918 (1926).
23) M. E. Dice and J. H. Hildebrand, ibid., **50**, 3023 (1928).
24) J. H. Hildebrand and G. R. Negishi, ibid., **59**, 339 (1937).
25) D. Atack and O. K. Rice, *J. Chem. Phys.*, **22**, 382 (1954); Idem., *Disc. Faraday Soc.*, **15**, 210 (1953).

TABLE I. COMPARISON OF ESTIMATED VALUES FOR CRITICAL SOLUTION POINT WITH OBSERVED VALUES

| System | | $T_1$ | $T_2$ | Observed value | | Eq. 2,7 | Eq. 5,1 | Eq. 1,10 | Ref. |
|---|---|---|---|---|---|---|---|---|---|
| | | | | $T_c$ | $x_c$ | $x_c$ | $\Delta T_c$ | $\Delta T_c$ | |
| Component I | Component II | °C | °C | °C | Mole fraction | Mole fraction | °C | °C | |
| Cyclohexane | Methanol | 31.30 | 39.05 | 45.14 | 0.507 | 0.537 | 0.46 | 1.18 | 26 |
| Cyclohexane | Aniline | 27.459 | 29.339 | 29.422 | 0.447 | 0.445 | 0.007 | 0.023 | 25 |
| *n*-Heptane | Furfural | 37.4 | 48.8 | 93.7 | 0.56 | 0.596 | 11.7 | 17.2 | 21 |
| *n*-Butane | Perfluoro-*n*-butane | −53.2 | −45.2 | −41.0 | 0.37 | 0.365 | 0.5 | 1.0 | 16 |
| Methyldiethylamine | Water* | 51.28 | 50.52 | 49.42 | 0.902 | 0.922 | 0.10 | −0.01 | 19 |
| Carbon tetrachloride | Perfluoromethylcyclohexane | 4.0 | 14.4 | 26.8 | 0.30 | 0.301 | 2.3 | 3.7 | 14 |
| 〃 | 〃 | 27.92 | 28.232 | 28.310 | 0.290 | 0.289 | −0.010 | 0.000 | 15 |
| Benzene | Perfluoromethylcyclohexane | 61.1 | 81.6 | 85.3 | 0.27 | 0.255 | 1.3 | 1.8 | 14 |
| Phenol | Water | 25.0 | 35.0 | 65.85 | 0.910 | 0.924 | −2.75 | 3.39 | 22 |
| Octene | Liquid sulfur dioxide | −47.1 | −32.8 | −16.4 | 0.801 | 0·749 | 4.0 | 6.0 | 18 |
| Butanol | Water | 80.0 | 90.0 | 125.15 | 0.895 | 0.915 | −4.23 | 4.64 | 17 |
| Isooctane | Stannic iodide | 185.4 | 191.6 | 195.4 | 0.501 | 0.506 | 0.2 | 0.6 | 23 |
| Silicon tetrachloride | Stannic iodide | 133.4 | 138.2 | 139.8 | 0.432 | 0.389 | 0.1 | 0.3 | 24 |
| Cetylstearate | Liquid propane* | 99.5 | 97.0 | 95.2 | 0.979 | 0.972 | −0.4 | −1.2 | 20 |
| Palmitic acid | Liquid propane* | 100.5 | 98.5 | 96.9 | 0.966 | 0.936 | −0.2 | −0.4 | 20 |
| *n*-Hexane | Methanol | 25.0 | 30.0 | 42.6 | 0.548 | 0.573 | 0.2 | 1.6 | 17 |
| Ethylbenzene | Liquid ammonia | 0.0 | 10.0 | 10.7 | 0.827 | 0.823 | 0.1 | 0.2 | 13 |
| Isopropylbenzene | Liquid ammonia | 0.0 | 10.0 | 20.0 | 0.835 | 0.839 | 1.9 | 3.0 | 13 |
| Mesitylene | Liquid ammonia | 0.0 | 20.0 | 33.9 | 0.841 | 0.826 | 3.6 | 5.4 | 13 |
| 1-Methylnaphthalene | Liquid ammonia | 0.0 | 20.0 | 28.8 | 0.861 | 0.846 | 1.8 | 3.1 | 13 |
| Aniline | Water | 80.0 | 100.0 | 167.5 | 0.844 | 0.862 | 0.8 | 15.9 | 17 |

$\Delta T_c$ indicates the difference between observed and calculated values.
* These are systems which show a lower critical solution temperature.

expressions. Fig. 4. shows the relations between $w/kT$ by Eqs. 3, 3 and 3, 17 in which $z$ is assumed to be 4 and $T_c/T$ for systems of ethylbenzene—liquid ammonia[13], carbon tetrachloride—perfluoromethylcyclohexane[14,15], *n*-butane—perfluoro-*n*-butane[16] and *n*-hexane—methanol[17]. Plots are made of values of $w/kT$ obtained from formulae according to several approximations for square lattice against $T_c/T$ for the system ethylbenzene—liquid ammonia in Fig. 5, compared with results obtained from Eq. 3, 3. As will be clear from these figures, simple uninflected curves convex downward are obtained by exact solution for the two dimensional model, while similar curves convex upward by several approximate solutions, and it is observed that $w$ can be represented by neither a linear function of $T$ nor a constant since no linear relationships are observed in these figures.

Inspection of literature data on partially miscible binary liquid systems reveals that $w/kT$ is satisfactorily expressed by the following exponential functions

$$w/kT-(w/kT)_c=K(|T_c/T-1|)^n \qquad (4,1)$$

where $K$ and $n$ are constants. When values of $|T_c/T-1|$ are small, using the abbreviation $\eta$ for the quantity $\exp(w/zkT)$, this formula may be transformed into

$$\eta-\eta_c=K\eta_c(|T_c/T-1|)^n/z \qquad (4,2)$$

by expanding $\eta/\eta_c$ in terms of $K(T_c/T-1)^n/z$ and neglecting higher than square.

Plots of $\log(\eta-\eta_c)$ against $\log(|T_c/T-1|)$ for several binary liquid systems are shown in Fig. 6 where values of $\eta$ are evaluated from the mutual solubility data described in the literature according to Eqs. 3, 17 and 3, 18 assuming $z=4$. It will be seen from Fig. 6 that fair straight lines are obtained from these plots over a wide range of temperatures.

26) E. L. Eckfeldt and W. W. Lucasse, *J. Phys. Chem.*, 47, 164 (1943).

## 5. Prediction of the Critical Solution Temperature

It has been observed that the quasi-chemical approximation is considerably more accurate than the zeroth approximation and the results given by the first approximation differ little from those given by the higher approximations. Considering the possibility of the application of the theory of regular solutions to the vapor-liquid equilibria, it will be convenient at present to estimate $w/\boldsymbol{kT}$ by the Eqs. 3, 17 and 3, 18 according to the first approximation.

Since two empirical constants $K$ and $n$, besides the critical solution temperature $T_c$, are involved in Eqs. 4, 1 or 4, 2, three pairs of data are required for the estimation of the critical solution temperature. However, it is observed in Fig. 6 that the average value of $n$ for many systems is about 5/7 in the first approximation when $z$ is assumed to be 4. When the approximate value of five seventh is used for $n$ in Eq. 4, 2, it is possible to estimate the critical solution temperature and the solubility relationships at any other temperature from two pairs of the mutual solubility data.

In Table I are given critical compositions estimated by Eq. 2, 7 from the solubility data at temperatures $T_1$ and $T_2$ and critical solution temperatures calculated according to the expression

$$T_c=\frac{T_1T_2\{(\eta_1-\eta_c)^{7/5}-(\eta_2-\eta_c)^{7/5}\}}{T_1(\eta_1-\eta_c)^{7/5}-T_2(\eta_2-\eta_c)^{7/5}} \qquad (5,1)$$

which is derived from Eq. 4, 2 by the use of approximate value of five seventh for $n$ and the notation of $\eta_1$ and $\eta_2$ for the respective values of $\exp(w/z\boldsymbol{kT})$ at temperatures $T_1$ and $T_2$, compared with experimental values and the calculated values of critical solution temperature according to Eq. 1, 10.

It will be seen that with few exceptions in which $m$ in Eq. 1, 9 is not a constant over a wide range of temperatures, showing two straight lines having different slopes on plots of $\log\{(1-x')/x'\}$ against $\log\{(1-x'')/x''\}$ such as shown in Figs. 1—3 in the preceding paper, the agreement between the experimental and calculated values of $T_c$ by Eq. 5, 1 is about as good as the experimental accuracy even though the approximation of $n=5/7$ is used, better than the results given by Eq. 1, 10 which has been proposed by Cox and Herington[27].

## Summary

Theoretical expressions for estimating the interchange energy $w$ were given in such form as to be obtained from the mutual solubility data. It has been found that the dependency of the interchange energy estimated from mutual solubility data in terms of $\varphi$-fractions upon temperature is satisfactorily expressed by the form of equations $w/\boldsymbol{kT}-(w/\boldsymbol{kT})_c=K(|T_c/T-1|)^n$. The method of predicting the critical solution point was described as an example of the application of the theory of regular solutions.

*The Chemical Research Institute of Non-Aqueous Solutions*
*Tohoku University*
*Katahira-cho, Sendai*

27) J. D. Cox and E. F. G. Herington, *Trans. Faraday Soc.*, **52**, 926 (1956).

# *Normal Vibrations and Thermodynamic Properties of Chromium and Molybdenum Hexacarbonyls*

By Kiyoyasu KAWAI and Hiromu MURATA

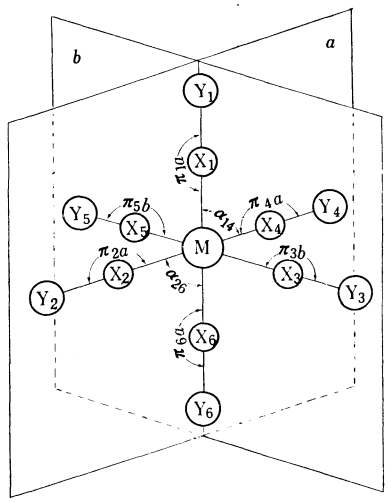
(Received December 4, 1959)

Hawkins, Mattraw, Sabol and Carpenter[1] have observed successfully infrared spectra of chromium and molybdenum hexacarbonyls in gaseous state and have made an attempt to obtain Raman spectra of molybdenum hexacarbonyl. Recently, Danti and Cotton[2] have reported Raman spectra of those and tungsten hexacarbonyls using chloroform as solvent. The molecular structure by electron diffraction has been reported by Brockway, Evens and Lister[3], and by X-ray diffraction by Rudorf and Fofmann[4], and it has been clear for the molecule to have $O_h$-symmetry. The assignments of the observed frequencies have been made by these investigators and the thermodynamic properties have been calculated by Hawkins, Mattraw, Sabor and Carpenter[1].

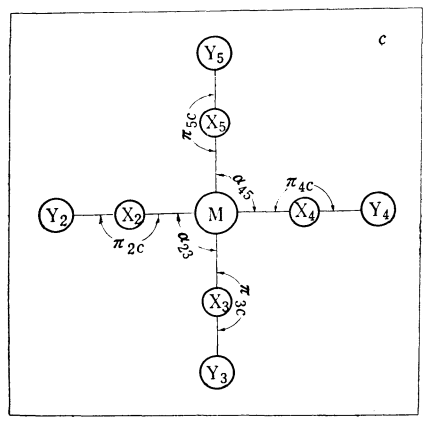
Out of thirteen fundamental vibrations resulting from the $O_h$-symmetry of the $M(XY)_6$ type of molecule only four fundamental vibrations are infrared active, and the lowest frequency of them, which has considerably great contribution to thermodynamic properties is out of the region of the observation by a usual spectrometer. In connection with the other metal carbonyls previously reported[5] and now proceeding*, the present paper** deals with a normal coordinate analysis for chromium and molybdenum hexacarbonyls to establish the more reliable assignments of vibrational frequencies and to compute the potential constants which may afford some information concerning the nature of the metal-carbonyl and carbonyl bonds in those compounds. The thermodynamic properties based on these assignments were calculated.

## Normal Coordinate Treatment

The method of group theory shows that, as explained by Hawkins, Mattraw, Sabol and Carpenter[1], thirty-three normal modes of vibration of the octahedral $M(XY)_6$ type molecule are reduced to two of $a_{1g}$, two of $e_g$, one of $f_{1g}$, four of $f_{1u}$, two of $f_{2g}$ and two of $f_{2u}$, and $a_{1g}$, $e_g$ and $f_{2g}$ species are active in Raman and $f_{1u}$ species in infrared. The $f_{1g}$ and $f_{2u}$ species are inactive in both.




Side view




End view

Fig. 1. Internal coordinates of $M(XY)_6$ molecule.

1) N. J. Hawkins, H. C. Mattraw, W. W. Sabol and D. R. Carpenter, *J. Chem. Phys.*, **23**, 2422 (1955).
2) A. Danti and F. A. Cotton, ibid., **28**, 736 (1958).
3) L. O. Brockway, R. V. G. Evens and M. W. Lister, *Trans. Faraday Soc.*, **34**, 1350 (1938).
4) W. Rudorf and U. Fofmann, *Z. physik Chem.*, **B28**, 351 (1935).
5) H. Murata and K. Kawai, *J. Chem. Phys.*, **26**, 1355 (1957); K. Kawai and H. Murata, *J. Chem. Soc. Japan, Pure Chem. Sec. (Nippon Kagaku Zasshi)*, **78**, 496 (1957).

* A normal coordinate treatment of iron pentacarbonyl is being carried out in our laboratory. A part of the study has already been reported by H. Murata and K. Kawai, *J. Chem. Phys.*, **28**, 516 (1958).

** A part of this work has been reported by H. Murata and K. Kawai, *J. Chem. Phys.*, **27**, 605 (1957).

The general secular equation may be obtained by means of the Wilson's method[6]. The internal coordinates of $M(XY)_6$ molecule of this type are as follows:

$$d(M-X_i)=x_i \qquad d(X_i-Y_i)=y_i$$
$$\angle(M-X_i-Y_i)_{\text{lying in } j\text{th plane}}=\pi_{ij}$$
$$\angle(X_i-M-X_j)=\alpha_{ij}$$

Fig. 1 illustrates the above internal coordinates.

The symmetry coordinates were set up from these internal coordinates as follows:

For $a_{1g}$ species:

$$R_1=1/\sqrt{6}\,(\Delta y_1+\Delta y_2+\Delta y_3+\Delta y_4+\Delta y_5+\Delta y_6)$$
$$R_2=1/\sqrt{6}\,(\Delta x_1+\Delta x_2+\Delta x_3+\Delta x_4+\Delta x_5+\Delta x_6)$$

For $e_g$ species:

$$R_{3a}=1/\sqrt{12}(2\Delta y_1-\Delta y_2-\Delta y_3-\Delta y_4-\Delta y_5+2\Delta y_6)$$
$$R_{4a}=1/\sqrt{12}(2\Delta x_1-\Delta x_2-\Delta x_3-\Delta x_4-\Delta x_5+2\Delta x_6)$$

For $f_{1g}$ species:

$$R_{5a}=1/2(\Delta\pi_{1a}-\Delta\pi_{2a}+\Delta\pi_{4a}-\Delta\pi_{6a})$$

For $f_{1u}$ species:

$$R_{6a}=1/2(\Delta y_1+\Delta y_2-\Delta y_4-\Delta y_6)$$
$$R_{7a}=1/\sqrt{8}\,(\Delta\pi_{1a}+\Delta\pi_{2a}+\Delta\pi_{3b}-\Delta\pi_{3c}+\Delta\pi_{4a}+\Delta\pi_{5b}+\Delta\pi_{5c}+\Delta\pi_{6a})$$
$$R_{8a}=1/2(\Delta x_1+\Delta x_2-\Delta x_4-\Delta x_6)$$
$$R_{9a}=1/4(2\Delta\alpha_{12}+\Delta\alpha_{13}+\Delta\alpha_{15}+\Delta\alpha_{23}+\Delta\alpha_{25}-\Delta\alpha_{34}-\Delta\alpha_{36}-\Delta\alpha_{45}-\Delta\alpha_{56}-2\Delta\alpha_{46})$$

For $f_{2g}$ species:

$$R_{10a}=1/2(\Delta\pi_{1a}+\Delta\pi_{2a}-\Delta\pi_{4a}-\Delta\pi_{6a})$$
$$R_{11a}=1/2(\Delta\alpha_{12}-\Delta\alpha_{14}-\Delta\alpha_{26}+\Delta\alpha_{46})$$

For $f_{2ua}$ species:

$$R_{12a}=1/\sqrt{8}\,(\Delta\pi_{1a}+\Delta\pi_{2a}-\Delta\pi_{3b}+\Delta\pi_{3c}+\Delta\pi_{4a}-\Delta\pi_{5b}-\Delta\pi_{5c}+\Delta\pi_{6a})$$
$$R_{13a}=1/4\,(2\Delta\alpha_{12}-\Delta\alpha_{13}-\Delta\alpha_{15}-\Delta\alpha_{23}-\Delta\alpha_{25}+\Delta\alpha_{34}+\Delta\alpha_{36}+\Delta\alpha_{45}+\Delta\alpha_{56}-2\Delta\alpha_{46})$$

Using the table of Decius[7] and for the M−X−Y bending the method by Ferigle and Meister[8] **G** matrices were evaluated. In therms of the abbreviations $\rho$ and $\tau$ for reciprocal of the bond lengths $x$ and $y$, respectively, and $\mu_M$, $\mu_X$ and $\mu_Y$ for the reciprocals of the atomic masses, the following **G** matrix elements were obtained***:

For $a_{1g}$ species:

$$G_{11}=\mu_X+\mu_Y,\quad G_{12}=-\mu_X,\quad G_{22}=\mu_X$$

For $e_g$ species:

$$G_{33}=G_{11}(a_{1g}),\quad G_{34}=G_{12}(a_{1g}),\quad G_{44}=G_{22}(a_{1g})$$

For $f_{1g}$ species:

$$G_{55}=(\rho+\tau)^2\mu_X+\tau^2\mu_Y$$

For $f_{1u}$ species:

$$G_{66}=G_{11}(a_{1g}),\quad G_{67}=G_{69}=0,$$
$$G_{68}=G_{12}(a_{1g}),$$
$$G_{77}=4\rho^2\mu_M+(\rho+\tau)^2\mu_X+\tau^2\mu_Y,$$
$$G_{78}=\sqrt{8}\,\rho\mu_M,$$
$$G_{79}=-\sqrt{2}\{4\rho^2\mu_M+(\rho^2+\rho\tau)\mu_X\},$$
$$G_{88}=2\mu_M+\mu_X,\quad G_{89}=-4\rho\mu_M,$$
$$G_{99}=2\rho^2(4\mu_M+\mu_X)$$

For $f_{2g}$ species:

$$G_{1010}=G_{55}(f_{1g}),$$
$$G_{1011}=-2(\rho^2+\rho\tau)\mu_X,\quad G_{1111}=4\rho^2\mu_X$$

For $f_{2u}$ species:

$$G_{1212}=G_{55}(f_{1g}),$$
$$G_{1213}=-\sqrt{2}\,(\rho^2+\rho\tau)\mu_X,$$
$$G_{1313}=2\rho^2\mu_x$$

Following the method of Shimanouchi[9], the Urey-Bradley type quadratic potential energy function for octahedral $M(XY)_6$ molecule may be written as:

$$2V=\sum_{i=1}^{6}\{K(M-X)+2[F(X\cdots X)+F'(X\cdots X)]\}(\Delta x_i)^2$$
$$+\sum_{i=1}^{6}K(X-Y)(\Delta y_i)^2$$
$$+\sum_{i<j=1}^{6}\{H(X-M-X)+1/2[F(X\cdots X)-F'(X\cdots X)]\}(x_0\Delta\alpha_{ij})^2$$
$$+\sum_{i=1}^{6}\sum_{l=a}^{c}H(M-X-Y)(\sqrt{x_0y_0}\Delta\pi_{il})^2$$
$$+2\sum_{i<j=1}^{6}1/2[F(X\cdots X)$$

6) E. B. Wilson, Jr., *J. Chem. Phys.*, 7, 1047 (1939), **9**, 76 (1941).
7) J. C. Decius, ibid., **16**, 1025 (1948).
8) S. M. Ferigle and A. G. Meister, ibid., **19**, 982 (1951).

*** There is one misprint in the G matrix elements presented by H. Murata and K. Kawai, *J. Chem. Phys.*, **26**, 605 (1957), *viz* $G_{24}$ in $f_{1u}$ species which corresponds to $G_{79}$ of this paper.
9) T. Shimanouchi, *J. Chem. Phys.*, **17**, 245, 734, 848 (1949).

$$-F'(\mathrm{X}\cdots\mathrm{X})]\,(\Delta x_i)(\Delta x_j)$$
$$+2\sum_{i<j=1}^{6} 1/2\,[F(\mathrm{X}\cdots\mathrm{X})$$
$$+F'(\mathrm{Y}\cdots\mathrm{X})]\,(\Delta x_i)(x_0\Delta\alpha_{ij})$$
$$+2\sum_{i\neq j\neq k=1}^{6} 1/(2x_0^2)\kappa(x_0\Delta\alpha_{ij})(x_0\Delta\alpha_{ik})$$

where $x_0$ and $y_0$ are the equilibrium M−X and X−Y bond distances respectively; $K$, $H$, $F$ and $F'$ are the potential constants and $\kappa$ the intramolecular tension whose definition and physical meaning were expressed by Shimanouchi[9].

The intra-molecular tension for the octahedral $MX_6$ type molecule can easily be derived from the following relation obtained for the octahedral geometrical structure

$$\Sigma(\Delta\alpha_{ij})+1/2\Sigma(\Delta\alpha_{ij})(\Delta\alpha_{ik})=0$$

where the first summation extends for all of the twelve angles and the second for all the forty-eight sets of adjacent angles.

The potential energy matrix elements evaluated from the above potential function are as follows:

For $a_{1g}$ species:

$$\boldsymbol{F}_{11}=K(\mathrm{X}-\mathrm{Y}),\quad \boldsymbol{F}_{12}=0,$$
$$\boldsymbol{F}_{22}=K(\mathrm{M}-\mathrm{X})+4F(\mathrm{X}\cdots\mathrm{X})$$

For $e_g$ species:

$$\boldsymbol{F}_{33}=\boldsymbol{F}_{11}(\mathrm{a_{1g}}),\quad \boldsymbol{F}_{34}=0,$$
$$\boldsymbol{F}_{44}=K(\mathrm{M}-\mathrm{X})+0.7F(\mathrm{X}\cdots\mathrm{X})$$

For $f_{1g}$ species:

$$\boldsymbol{F}_{55}=x_0y_0H(\mathrm{M}-\mathrm{X}-\mathrm{Y})$$

For $f_{1u}$ species:

$$\boldsymbol{F}_{66}=\boldsymbol{F}_{11}(\mathrm{a_{1g}}),\quad \boldsymbol{F}_{77}=\boldsymbol{F}_{55}(\mathrm{f_{1g}}),$$
$$\boldsymbol{F}_{88}=K(\mathrm{M}-\mathrm{X})+1.8F(\mathrm{X}\cdots\mathrm{X}),$$
$$\boldsymbol{F}_{89}=0.9x_0F(\mathrm{X}\cdots\mathrm{X}),$$
$$\boldsymbol{F}_{99}=x_0^2\,[H(\mathrm{X}-\mathrm{M}-\mathrm{X})+0.55F(\mathrm{X}\cdots\mathrm{X})]+\kappa,$$
$$\boldsymbol{F}_{67}=\boldsymbol{F}_{68}=\boldsymbol{F}_{69}=\boldsymbol{F}_{78}=\boldsymbol{F}_{79}=0$$

For $f_{2g}$ species:

$$\boldsymbol{F}_{1010}=\boldsymbol{F}_{55}(\mathrm{f_{1g}}),\quad \boldsymbol{F}_{1011}=0,$$
$$\boldsymbol{F}_{1111}=x_0^2\,[H(\mathrm{X}-\mathrm{M}-\mathrm{X})+0.55F(\mathrm{X}\cdots\mathrm{X})]$$

For $f_{2u}$ species:

$$\boldsymbol{F}_{1212}=\boldsymbol{F}_{55}(\mathrm{f_{1g}}),\quad \boldsymbol{F}_{1213}=0,$$
$$\boldsymbol{F}_{1313}=x_0^2\,[H(\mathrm{X}-\mathrm{M}-\mathrm{X})+0.55F(\mathrm{X}\cdots\mathrm{X})]-\kappa$$

In the above elements it was assumed experimentally that $F'=-1/10F$, and consequently six potential constants are used here.

TABLE I. MOLECULAR CONSTANTS FOR $Cr(CO)_6$ AND $Mo(CO)_6$[a]

| Bond | $Cr(CO)_6$ | $Mo(CO)_6$ |
|---|---|---|
| M[b]—C | 1.92 Å | 2.08 Å |
| C—O | 1.16 Å | 1.15 Å |

Symmetry number……24 for all fundamentals

a From Ref. 3.
b M denotes Cr or Mo.

TABLE II. POTENTIAL CONSTANTS FOR $Cr(CO)_6$ AND $Mo(CO)_6$ (mdyn./Å)

| Type | $Cr(CO)_6$ | $Mo(CO)_6$ |
|---|---|---|
| $K$(C—O) | 16.2 | 16.02 |
| $K$(M—C) | 1.83 | 1.77 |
| $H$(M—C—O) | 0.41 | 0.34 |
| $H$(C—M—C) | 0.03 | 0.02 |
| $F$(C···C) | 0.15 | 0.12 |
| $\kappa(MC_6)$ | 0.02 Å$^2$ | 0.02 Å$^2$ |

TABLE III. COMPARISON OF OBSERVED AND CALCULATED FUNDAMENTALS FOR $Cr(CO)_6$ AND $Mo(CO)_6$

| Assignment | | | $Cr(CO)_6$ | | $Mo(CO)_6$ | |
|---|---|---|---|---|---|---|
| Type | Fundamental | Description | Calc. | Obs. | Calc. | Obs. |
| $a_{1g}$: | $\sigma_1$ | $\nu$(C—O) | 2042 | 2108 | 2037 | 2131 |
| | $\sigma_2$ | $\nu$(M—C) | 374 | 393 | 361 | 379 |
| $e_g$: | $\sigma_3$ | $\nu$(C—O) | 2031 | 2019 | 2029 | 2022 |
| | $\sigma_4$ | $\nu$(M—C) | 336 | 373 | 329 | 334 |
| $f_{1g}$: | $\sigma_5$ | $\delta$(M—C—O) | 564 | 539 | 524 | 477 |
| $f_{1u}$: | $\sigma_6$ | $\nu$(C—O) | 1992[c] | 2000 | 1992[c] | 2000 |
| | $\sigma_7$ | $\delta$(M—C—O) | 636 | 661 | 560 | 595 |
| | $\sigma_8$ | $\nu$(M—C) | 475 | 436 | 422 | 368 |
| | $\sigma_9$ | $\delta$(C—M—C) | 113 | 102 | 95 | 80 |
| $f_{2g}$: | $\sigma_{10}$ | $\delta$(M—C—O) | 608 | 598[b] | 560 | 557[b] |
| | $\sigma_{11}$ | $\delta$(C—M—C) | 111 | 90 | 101 | 80 |
| $f_{2u}$: | $\sigma_{12}$ | $\delta$(M—C—O) | 586 | 570[b] | 541 | 517[b] |
| | $\sigma_{13}$ | $\delta$(C—M—C) | 81 | 80 | 72 | 70 |

a Obtained from the values of the L matrix elements.
b Inferred from combination or overtone bands.
c Obtained by the method of high-frequency separation.

To evaluate numerically the above elements, the bond lengths listed in Table I and the atomic masses on a physical scale were used.

## Discussion

A comparison of the normal frequencies calculated from the set of potential constants in Table II with those observed by Hawkins, Mattraw, Sabol and Carpenter[1] are summarized in Table III. The numbering of the frequencies is the same as that used by Hawkins et al.[1]

The agreement between the calculated and the observed frequencies is satisfactory except for the M—C—O bending vibrations. The present results from the Urey-Bradley type potential function in which all the M—C—O bending interaction constants are not included indicated that 213 and 310 $cm^{-1}$ bands assigned to $\sigma_{10}$ and $\sigma_{12}$ respectively by Hawkins, Matraw, Sabol and Carpenter[1] and 137.1 $cm^{-1}$ band to $\sigma_{10}$ by Danti and Cotton[2] for chromium hexacarbonyl and 230 and 327 $cm^{-1}$ bands by the former[1] and 135.7 $cm^{-1}$ band by the latter[2] for molybdenum hexacarbonyl are too small for M—C—O bending vibrational frequencies. Based on this point of view, all of the observed bands by Hawkins, Matraw, Sabol and Carpenter[1] except for only three strong bands which may be designated as fundamentals, were reassigned as shown in Table IV for chromium hexacarbonyl and Table V for molybdenum hexacarbonyl.

In order to obtain better agreement with the observed frequencies of $a_{1g}$ and $e_g$ species some other sets of values of diagonal terms in **F** matrix were used, but as long as proper values with physical meaning were used the calculated values were not close to the observed ones. This, therefore, may suggest that the

Table IV. Infrared bands of gaseous $Cr(CO)_6$

| Frequency ($cm^{-1}$) | Intensity | Assignment | Calc. ($cm^{-1}$) |
|---|---|---|---|
| 4098 | m | $\sigma_1+\sigma_6$ | 4108 |
| 4000 | m | $\sigma_3+\sigma_6$ | 4019 |
| 2688 | w | $\sigma_3+\sigma_7$ | 2680 |
| 2554 | w | $\sigma_1+\sigma_8$, $\sigma_5+\sigma_6$ | 2544, 2539 |
| 2466 | m | $\sigma_3+\sigma_8$ | 2455 |
| 2393 | s | $\sigma_2+\sigma_6$ | 2393 |
| 2336 | sh | q | |
| 2212 | w | $\sigma_1+\sigma_9$ | 2210 |
| 2174 | w | q | |
| 2121 | s | $\sigma_3+\sigma_9$ | 2121 |
| 2090 | s | $\sigma_6+\sigma_{11}$, $\sigma_3+\sigma_{13}$ | 2090, 2099 |
| 2033 | sh | q | |
| 2000 | vs | $\sigma_6$ | |
| 1970 | sh | q | |
| 1912 | m | $\sigma_3-\sigma_9$, $\sigma_6-\sigma_{11}$ | 1917, 1910 |
| 1631 | w | $\sigma_6-\sigma_4$ | 1627 |
| 1196 | s | $\sigma_5+\sigma_7$ | 1200 |
| 1055 | sh | $\sigma_2+\sigma_7$ | 1054 |
| 1032 | s | $\sigma_4+\sigma_7$, $\sigma_8+\sigma_{10}$ | 1034, 1034 |
| 963 | m | $\sigma_5+\sigma_8$ | 975 |
| 875 | s | q | |
| 811 | s | $\sigma_4+\sigma_8$ | 809 |
| 755 | m | $\sigma_7+\sigma_{11}$ | 751 |
| 673 | sh | $\sigma_{10}+\sigma_{13}$ | 678 |
| 661 | vs | $\sigma_7$ | |
| 635 | s (sh) | $\sigma_5+\sigma_9$ | 641 |
| 595 | sh | q | |
| 522 | mb | $\sigma_8+\sigma_{11}$, $\sigma_{10}-\sigma_{13}$ | 526, 518 |
| 513 | mb | $\sigma_{10}-\sigma_{13}$, $\sigma_2+\sigma_9$ | 518, 495 |
| 477 | mb | $\sigma_4+\sigma_9$, $\sigma_{12}-\sigma_{11}$ | 475, 480 |
| 465 | wb | q | |
| 449 | wb | $\sigma_4+\sigma_{13}$ | 453 |
| 436 | s | $\sigma_8$ | |

vs Very strong; s Strong; m Medium; w Weak; b Broad; sh Shoulder; q More than binary combination or questionable band.

Table V. Infrared bands of gaseous $Mo(CO)_6$

| Frequency ($cm^{-1}$) | Intensity | Assignment | Calc. ($cm^{-1}$) |
|---|---|---|---|
| 4150 | m | $\sigma_1+\sigma_6$ | 4131 |
| 4050 | m | $\sigma_3+\sigma_6$ | 4022 |
| 2600 | w | $\sigma_3+\sigma_7$ | 2617 |
| 2480 | w | $\sigma_1+\sigma_8$, $\sigma_5+\sigma_6$ | 2499, 2477 |
| 2380 | s | $\sigma_3+\sigma_8$, $\sigma_2+\sigma_6$ | 2390, 2379 |
| 2330 | w | $\sigma_4+\sigma_6$ | 2334 |
| 2210 | m | $\sigma_1+\sigma_9$ | 2211 |
| 2115 | s | $\sigma_3+\sigma_9$ | 2102 |
| 2085 | s | $\sigma_6+\sigma_{11}$, $\sigma_3+\sigma_{13}$ | 2080, 2092 |
| 2000 | vs | $\sigma_6$ | |
| 1985 | sh | q | |
| 1955 | m (sh) | $\sigma_3-\sigma_{13}$ | 1952 |
| 1925 | m (sh) | $\sigma_6-\sigma_{11}$ | 1920 |
| 1650 | w | $\sigma_3-\sigma_8$ | 1654 |
| 1615 | w | $\sigma_6-\sigma_2$ | 1621 |
| 1070 | s | $\sigma_5+\rho_7$, $\sigma_{10}+\sigma_{12}$ | 1072, 1074 |
| 980 | s | $\sigma_2+\sigma_7$ | 974 |
| 927 | s | $\sigma_4+\sigma_7$, $\sigma_8+\sigma_{10}$ | 929, 925 |
| 905 | w | q | |
| 845 | s | $\sigma_5+\sigma_8$, $\sigma_4+\sigma_{12}$ | 845, 851 |
| 740 | m | $\sigma_2+\sigma_8$ | 747 |
| 705 | m | $\sigma_4+\sigma_8$ | 702 |
| 670 | m | $\sigma_7+\sigma_{11}$ | 675 |
| 661 | w | q | |
| 595 | vs | $\sigma_7$ | |
| 563 | s | $\sigma_5+\sigma_9$ | 557 |
| 386 | s | $\sigma_8$ | |

vs Very strong; s Strong; m Medium; w Weak; b Broad; sh Shoulder; q More than binary combination or questionable band.

TABLE VI. L MATRICES FOR $Cr(CO)_6$

| | | $Q_1$ | $Q_2$ | $Q_3$ | $Q_4$ | $Q_7$ | $Q_8$ | $Q_9$ | $Q_{10}$ | $Q_{11}$ | $Q_{12}$ | $Q_{13}$ |
|---|---|---|---|---|---|---|---|---|---|---|---|---|
| $a_{1g}$: | $R_1$ | 0.381 | 0.017 | | | | | | | | | |
| | $R_2$ | −0.226 | 0.187 | | | | | | | | | |
| $e_g$: | $R_3$ | | | 0.380 | 0.012 | | | | | | | |
| | $R_4$ | | | −0.224 | 0.169 | | | | | | | |
| $f_{1u}$: | $R_7$ | | | | | 0.453 | −0.113 | 0.028 | | | | |
| | $R_8$ | | | | | 0.120 | 0.242 | −0.007 | | | | |
| | $R_9$ | | | | | −0.258 | −0.029 | 0.128 | | | | |
| $f_{2g}$: | $R_{10}$ | | | | | | | | 0.452 | 0.034 | | |
| | $R_{11}$ | | | | | | | | −0.274 | 0.123 | | |
| $f_{2u}$: | $R_{12}$ | | | | | | | | | | 0.453 | 0.017 |
| | $R_{13}$ | | | | | | | | | | −0·191 | 0.094 |

TABLE VII. L MATRICES FOR $Mo(CO)_6$

| | | $Q_1$ | $Q_2$ | $Q_3$ | $Q_4$ | $Q_7$ | $Q_8$ | $Q_9$ | $Q_{10}$ | $Q_{11}$ | $Q_{12}$ | $Q_{13}$ |
|---|---|---|---|---|---|---|---|---|---|---|---|---|
| $a_{1g}$: | $R_1$ | 0.382 | 0.015 | | | | | | | | | |
| | $R_2$ | −0.225 | 0.180 | | | | | | | | | |
| $e_g$: | $R_3$ | | | 0.382 | 0.012 | | | | | | | |
| | $R_4$ | | | −0.224 | 0.182 | | | | | | | |
| $f_{1u}$: | $R_7$ | | | | | 0.451 | −0.044 | −0.021 | | | | |
| | $R_8$ | | | | | 0.054 | 0.229 | 0.008 | | | | |
| | $R_9$ | | | | | −0.021 | −0.034 | 0.110 | | | | |
| $f_{2g}$: | $R_{10}$ | | | | | | | | 0.445 | 0.031 | | |
| | $R_{11}$ | | | | | | | | −0.251 | 0.118 | | |
| $f_{2u}$: | $R_{12}$ | | | | | | | | | | 0.446 | 0.016 |
| | $R_{13}$ | | | | | | | | | | −0.175 | 0.090 |

TABLE VIII. HEAT CONTENT, FREE ENERGY, AND HEAT CAPACITY OF $Cr(CO)_6$ AND $Mo(CO)_6$ FOR THE IDEAL GASEOUS STATE AT 1 ATOMOS PRESSURE (cal. $deg^{-1}$ $mol^{-1}$)

| | $Cr(CO)_6$ | | | | $MO(CO)_6$ | | | |
|---|---|---|---|---|---|---|---|---|
| $T$(°K) | $(H^0-E_0^0)/T$ | $-(F^0-E_0^0)/T$ | $S^0$ | $C_p^0$ | $(H^0-E_0^0)/T$ | $-(F-E_0^0)/T$ | $S^0$ | $C_p^0$ |
| 273.15 | 28.99 | 78.68 | 107.67 | 45.01 | 30.77 | 82.65 | 113.42 | 48.24 |
| 298.15 | 30.48 | 81.16 | 111.64 | 46.94 | 32.28 | 85.43 | 117.71 | 49.08 |
| 300 | 30.58 | 81.35 | 111.93 | 47.06 | 32.38 | 85.65 | 118.00 | 49.20 |
| 400 | 35.52 | 90.76 | 126.28 | 52.65 | 37.25 | 95.63 | 132.88 | 54.17 |
| 600 | 42.48 | 106.49 | 148.97 | 59.20 | 43.95 | 112.12 | 156.07 | 60.00 |
| 800 | 47.24 | 119.34 | 166.58 | 63.26 | 48.49 | 125.45 | 173.94 | 63.74 |
| 1000 | 50.73 | 130.36 | 181.09 | 65.98 | 51.78 | 136.77 | 188.55 | 66.28 |

interaction terms between X−Y and M−X or X—Y stretching internal coordinates in the Urey-Bradley type potential function are not negligibly small.

Though, as explained above, there are contained a few quetionable points and the limits of error are uncertain, we may be allowed to conclude that the assignments in Table III and the potential constants in Table II are reasonable.

As the carbon-oxygen stretching potential constant $K$(C−O), that of nickel carbonyl[5], 16.02 mdyn./Å, was employed. For this selection the metal-carbon stretching potential constants $K$(M−X) were obtained to be 1.83 and 1.77 mdyn./Å for chromium and molybdenum hexacarbonyls respectively. These metal-carbon stretching potential constants are a little smaller than that of nickel carbonyl[5], 2.12 mdyn./Å, and this fact is in agreement with the study by Giacometti[10] who suggested that the shortening of chromium-carbon bond is smaller than that of nickel-carbon bond in the metal carbonyls. The values of the metal-carbon stretching potential constant, although many authors[10,11] have discussed the evidence of partial double bond caracter in such coordination compounds of various symmetry as these metal carbonyls, are nearly equal to those of Si—C and Cr—Cl bonds of tetramethylsilane[12] and chromyl

10) G. Giacometti, ibid., 23, 2068 (1955).
11) See e. g., L. Pauling, "The Nature of the Chemical Bond", Cornell University Press. Ithaca. New York (1939), p, 251.
12) K. Shimizu and H. Murata, private communication.

chloride[13] (2.72 and 2.56 mdyn./Å respectively), which are considered as single bonds.

The **L** matrices, whose components give the transformation from normal to symmetry coordinates, were calculated and listed in Table VI for chromium hexacarbonyl and Table VII for molybdenum hexacarbonyl.

## Thermodynamic Properties

The heat content, free energy, entropy and heat capacity at constant pressure were calculated for seven temperatures from 273.15 to 1000°K in the rigid rotator-harmonic oscillator approximation using the probable values of the observed wave numbers listed in Table III. The molecular constants used in these computation and the symmetry number are given in Table I, while Table VIII lists the thermodynamic properties.

The authors express their sincere appreciation to Professor R. Tsuchida of Osaka University for helpful suggestions and valuable advice.

*Osaka Municipal*
*Technical Research Institute*
*Kita-ku, Osaka*

13) H. Stammreich, K. Kawai and Y. Tavares, *Spectrochim. Acta*, **1959**, 438.

# SHORT COMMUNICATIONS

## *Glumamycin, A New Peptide-type Antibiotic**

By Michitaka INOUE, Hiroshi HITOMI, Komei MIZUNO, Masahiko FUJINO, Akira MIYAKE, Koiti NAKAZAWA, Motoo SHIBATA and Toshihiko KANZAKI

(Received May 13, 1960)

A Streptomyces strain isolated in March, 1954 from a sample collected in Osaka Prefecture resembled the Zaomycin producing strain, S. zaomyceticus[1], in morphological and cultural characteristics and the utilization of carbon source, and therefore it was named S. zaomyceticus No. 7548 tentatively. The strain, when cultivated on a medium containing 3.0% of starch, 1.0% of polypepton, 0.2% of potassium phosphate 0.3% of soybean oil, and 2.0% of rice bran for 96 hr., produced an antibiotic, but the potency lowered abruptly thereafter.

The antibiotic inhibited the growth of Gram-positive bacteria such as Micrococcus aureus 209p and B. subtilis and was especially active against the bacteria resistant to known antibiotics. Although this antibiotic was similar to Amphomycin[2,3], Zaomycin[1] and Crystallomycin[4,5], it differed from them clearly. The authors, having found it to be a new antibiotic, named it Glumamycin and investigated its constituents.

The antibiotic was isolated pure from the broth by Craig's counter current distribution method 300 plates; chloroform- methanol-0.02 N hydrochloric acid (2 : 2 : 1), and it gave only one spot in paper chromatography and paper ionophoresis at various pH's. M. p. 230°C (decomp.). Found: C, 51.71; H, 7.20; N, 12.99%. From its dissociation constant, the molecular weight was estimated to be about 1800. The antibiotic had its isoelectric point at pH 3.4, and though it showed the typical infrared-spectrum characteristic of peptides, it exhibited no peculiar absorption in the ultraviolet-region.

The antibiotic was not hydrolized by any hydrolyrase such as pepsin, trypsin and carboxypeptidase, but it was completely hydrolized by heating with 6 N hydrochloric acid at 110°C for 20 hr. When the hydrolysate was subjected to two dimensional paper chromatography *n*-butanol-acetic acid-water (4 : 1 : 5) or 80% phenol containing 0.5 N ammonia, six amino acids were detected, four of which were aspartic acid, glycine, valine and proline and the other were unknown. Of the two unknown amino acids, one was a basic amino acid differing from lysine, histidine and arginine on paper chromatogram, and the other was a neutral amino acid which was characterized by a violet blue color with ninhydrin and a blue color with isatin. The six amino acids were separated from each other in crystalline form when chromatographed first on ion-exchange resin (IR-4B, Dowex 50×8) and then on cellulose powder.

After recrystallization from 75% methanol, the unknown basic amino acid showed m. p. 202°C (decomp.), $[\alpha]_D^{22} = +16°$ (c, 1 : $H_2O$), Pk <2, 6.6, 9.6, and gave the values of 1.0 mol. of C-$CH_3$ (Kuhn-Roth) and 1.8 mol. of amino nitrogen (Van Slyke), and it was different from authentic $\alpha,\gamma$-diaminobutyric acid on paper chromatogram. From these facts it was presumed to be $\alpha,\beta$-diaminobutyric acid. On the other hand, the unknown neutral amino acid, when recrystallized from methanol·ether, melted at 240°C (decomp.), showed $[\alpha]_D^{21} = +10°$ (c, 1 : $H_2O$) and accorded with $C_6H_{11}O_2N$·HCl, but no amino nitrogen (Van Slyke) and C-$CH_3$ (Kuhn-Roth) were detected. This compound was in complete agreement with synthetic DL-pipecolic acid in paper chromatography with various solvent systems, and the optical rotations of its hydrochloride and tartarate were $[\alpha]_D^{25} = +10°$ (c, 1 : $H_2O$) and $[\alpha]_D^{25} = +20°$ (c, 1 : $H_2O$), respectively. As the sign of optical activity of the neutral amino acid was opposite to that of the natural pipecolic acid it belongs to the D-series; the aspartic acid, valine, and proline derived from the antibiotic belong to the L-series.

The hydrolysate mentioned before contained about 10% of a substance soluble in ether, which was found to ba a monobasic unsaturated fatty acid, b. p. 139°C (1 mmHg), $[\alpha]_D^{21} = +4°$

* Presented at the 119th Monthyl Meeting of Japan Antibiotic Association, March 25, 1960.

1) Y. Hinuma, *J. Antibiotics*, ser. A 7, 134 (1954).
2) B. Heinemann, M. A. Kaplan, et al., *Antib. & Chemoth.*, 3, 1239 (1953).
3) G. Giolitti, G. Corti et al., *Giorn. Microbiol.*, 3, 70 (1957).
4) G. F. Game et al., *Antibiotiki*, 2, (6) 14 (1957).
5) N. N. Lomakina and M. G. Branzhnikova, *Biokhimiya* **24**, 425 (1959).

(c, 1 : $C_2H_5OH$), $C_{13}H_{24}O_2$. Oxidation of the substance with ozone afforded a compound $C_9H_{18}O_2$, b. p. 154°C (25 mmHg), $[\alpha]_D^{21} = +12°$ (c. 1 : $C_2H_5OH$), and from this and other results, a 4-isotridecenoic acid structure, $C_8H_{17}CH=CHC_2H_4$–COOH, was assigned to the unsaturated fatty acid.

Thus Glumamycin was assumed to be composed of 4-isotridecenoic acid, L-aspartic acid, glycine, L-valine, L-proline, D-pipecolic acid, and $\alpha$, $\beta$-diaminobutyric acid combined through peptide linkages. Full details of this work will be reported shortly.

The authors are grateful to Dr. Satoru Kuwada, Dr. Kikiti Sato and Dr. Sueo Tatsuoka for their guidance and encouragement in this work.

*Research Laboratories, Takeda Pharmaceutical Industries, Ltd.*
*Juso, Higashiyodogawa-ku, Osaka*
*(M.I., H.H., K.M., M.F. and A.M.)*
*Institute for Fermentation*
*Juso, Higashiyodogawa-ku, Osaka*
*(K. N., M. S. and T. K.)*

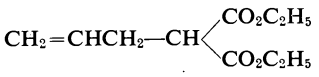
# *Eine Neue Synthese des cis- und trans D, L-Desmethylmuscarins*

Von Takeshi MATSUMOTO
und Akitami ICHIHARA

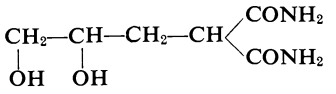
(Eingegangen am 4. Juni, 1960)

In früheren Mitteilungen[1,2] haben wir die Synthese und pharmakologische Wirkung von stereoisomeren Muscarinen beschrieben. Hier soll nun über die Synthese der einfacher gebauten Desmethylmuscarine berichtet werden. Zu ihrer Herstellung haben wir die Reaktionsfolge, die bei der Durcharbeitung der Muscarinsynthesen erprobt wurde, übertragen.

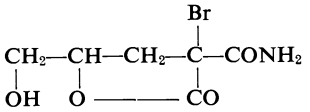
Als Ausgangsmaterial bot sich Allylmalonsäure-äthylester (I). Durch Hydroxylierung dieses Esters mittels Perameisensäure und darauf folgende Ammonolyse wurde Dihydroxydiamid (II)[3] erhalten. Das letztere wurde dann nach der bekannten Methode von W. Traube[3] über Bromlacton (III) in Tetrahydrofurandicarbonsäure (IV) übergeführt. Erhitzte man die wässrige Lösung von Dicarbonsäure (IV) auf 150～160°C, so entstanden erwartungsgemäss zwei stereoisomere Monocarbonsäuren (V) ($\alpha$, Schmp. 143.5°C, Ber. C 45.45 H 6.10 Gef. C 45.59 H 5.99%; $\beta$, Schmp. 129°C, Ber. C 45.45 H 6.10 Gef. C 45.50 H 6.10, die sich durch Chromatographie an Alumina-Säule



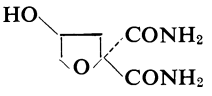
I

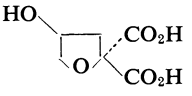


II

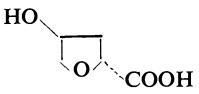


III

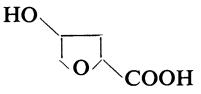




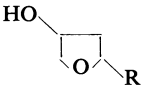
IV



V



V



VI $\alpha$ R = ···$CO_2CH_3$; $\beta$ R = —$CO_2CH_3$

VII $\alpha$ R = ···$CON(CH_3)_2$; $\beta$ R = —$CON(CH_3)_2$

VIII $\alpha$ R = ···$CH_2N(CH_3)_2$; $\beta$ R = —$CH_2N(CH_3)_2$

IX $\alpha$ R = ···$CH_2\overset{+}{N}(CH_3)_3\ I^-$; $\beta$ R = —$CH_2\overset{+}{N}(CH_3)_3\ I^-$

1) T. Matsumoto und H. Maekawa, *Angew. Chem.*, **70** 507, (1958).

2) T. Matsumoto und A. Ichihara, *Biochem. Z.*, **331**, 580 (1959).

3) W. Traube, *Ber.*, **37**, 4540 (1904).

trennen liessen, in Mengenverhältnisse von um 1 : 1. Veresterung dieser beiden Säuren mittels Diazomethans ergab Methylester (VI) ($\alpha$, Sdp. 115°C/7 Torr. IR. 3410 (OH) 1735 ($-COOCH_3$) 1075 $cm^{-1}$ (tetrahydrofuran) ohne Lösungsmittel; $\beta$, Sdp. 110°C/7 Torr. IR. 3420 (OH) 1740 ($-COOCH_3$) 1080 $cm^{-1}$ (Tetrahydrofuran) ohne Lösungsmittel), die mittels Dimethylamin in Dimethylamide VII ($\alpha$, IR. 3400 (OH) 1635 ($CONMe_2$) 1077 $cm^{-1}$ (Tetrahydrofuran) ohne Lösungsmittel; $\beta$, IR. 3400 (OH) 1640 ($CONMe_2$) 1075 $cm^{-1}$ (Tetrahydrofuran) ohne Lösungsmittel) umgesetzt wurden. Aus diesen Amiden erhielt man mit Hilfe von Lithium Alanat D, L-Nordesmethylmuscarine (VIII) ($\alpha$, IR. 3410 (OH) 1066 $cm^{-1}$ (Tetrahydrofuran) in Tetrachlorkohlenstoff; $\beta$, IR. 3194 (OH) 1085 $cm^{-1}$ (Tetrahydrofuran) in Tetrachlorkohlenstoff). Die OH Valenzschwingung der $\beta$-Norbase in Tetrachlorkohlenstoff bleibt beim genügenden Verdünnen (0.0072 Mol) konstant. Es liegt also bei der $\beta$-Norbase die Wasserstoffbrücke vor. Es kommt daher den Verbindungen der $\beta$-Reihe cis- Konfiguration zu. Die quarternären Ammonium Iodide IX wurden kristallisiert erhalten ($\alpha$, Schmp. 120°C $\beta$, Schmp. 117°C, Ber. C 33.47 H 6.32 Gef. C 33.70 H 6.59). Die IR. Spektren der beiden Desmethylmuscarine stimmen mit denjenigen der Eugsters Präparate[4] gut überein. Gegen Krötenherzen zeigen Desmethylmuscarine schwächere, aber charakteristische Muscarin wirkung. Von den beiden Isomeren wirkte *trans*-Desmethylmuscarin stärker[5].

*Chemische Abteilung*
*Naturwissenschaftliche Fakultät*
*Universität Hokkaido*
*Sapporo*

4) C. H. Eugster, *Helv. Chim. Acta*, 42, 1177 (1959).

5) Herrn Prof. Dr. Akira Ooga an dem Pharmakologischen Institut der Universität Hokkaido möchten wir fur seine Prüfung bestens danken.

# *Formation of Isoxazolecarboxylic Acids from α, β-Unsaturated α-Nitroesters*[1]

By Sumio UMEZAWA and Shōnosuke ZEN

(Received April 15, 1960)

We wish to report the synthesis of new members of isoxazolecarboxylic acids. When treated with *n*-butylamine (2.0 g.) in ligroin at room temperature overnight, diethyl α-nitroglutaconate[2] (I) (1.0 g.) produced 3, 5-bis(*n*-butylcarbamoyl) - 4 - (*n*-butylcarbamoylmethyl)-isoxazole (III) (crude product 0.6 g.). We have found that the cyclization is generally applicable to the synthesis of 4-substituted isoxazole-3, 5-dicarboxylic acids. Thus, 4-phenyl-3, 5-bis(*n*-butylcarbamoyl)isoxazole (VI) (crude product 0.22 g.) and 4-methyl-3, 5-bis (*n*-butylcarbamoyl)isoxazole (IX) have been obtained from ethyl α-nitrocinnamate[3] (V) (1.0 g.) and ethyl α-nitrocrotonate[4] (VIII) by refluxing with *n*-butylamine in absolute ethanol for three hours, respectively (Tables I and II).

By mild alkaline hydrolysis with 10% sodium hydroxide in 50% aqueous ethanol at about 60°C for two hours, III (1.12 g.) and VI (1.0 g.) were converted into isoxazole-3, 5-dicarboxylic-4-acetic acid (IV) (crude product 0.56 g.) and 4-phenylisoxazole-3, 5-dicarboxylic acid (VII) (crude product 0.45 g.), respectively (Table I).

Drastic alkaline hydrolysis of VI by refluxing with 28% potassium hydroxide in 50% aqueous ethanol resulted in the formation of phenylacetic acid and oxalic acid, the fact indicating that the above-mentioned cyclization forms a 4-substituted isoxazole-3, 5-dicarboxylic acid derivative.

It seems reasonable to suggest that the initial step involves base-catalyzed cleavage of α, β-unsaturated α-nitroester to liberate nitroacetic ester moiety which may be in equilibrium

1) Presented in part at the Division of Organic Chemistry of the Annual Meeting of the Chemical Society of Japan, Kyoto, April 2, 1959.

2) Prepared by the condensation of sodium salt of ethyl formylacetate with ethyl nitroacetate in the presence of diethylamine or *n*-butylamine; b. p. 125~130°C/0.2 mmHg.

3) Prepared by the method of A. Dornow and H. Menzel, [*Ann.*, **580**, 43 (1952)]. They obtained carbethoxy-diethylcarbamoyl-4-phenylisoxazoline *N*-oxide by refluxing an ethanol solution of diethylamine and diethylamine salt of ethyl 1,3-dinitro-2,3-diphenylbutyrate which was prepared from ethyl α-nitrocinnamate and phenylnitromethane. This result is closely related to the method reported in the present paper, whereby, however, isoxazole derivatives are obtained.

4) Prepared from ethyl α-nitro-β-acetoxybutyrate by heating with anhydrous sodium carbonate in dry benzene by a variation of the method of H. B. Hass, A. G. Susie and R. L. Heider, (*J. Org. Chem.*, **15**, 8 (1950)).

TABLE I. 4-SUBSTITUTED 3,5-BIS(*n*-BUTYLCARBAMOYL)ISOXAZOLES AND ISOXAZOLE-3,5-DICARBOXYLIC ACIDS

| Compounds | M.p. °C | Formula | Analyses Calcd. C,% | H,% | N,% | Found C,% | H,% | N,% | Neutralization equivalent Calcd. | Found |
|---|---|---|---|---|---|---|---|---|---|---|
| III | 179~179.5[a] | $C_{19}H_{32}O_4N_4$ | 59.97 | 8.48 | 14.73 | 60.41 | 8.22 | 15.15 | — | — |
| VI | 160~162[a] | $C_{19}H_{25}O_3N_3$ | 66.45 | 7.34 | 12.24 | 66.86 | 6.90 | 12.55 | — | — |
| IX | 84~ 86[b] | $C_{14}H_{23}O_3N_3$ | 59.76 | 8.24 | 14.94 | 60.32 | 7.95 | 15.18 | — | — |
| IV | 108~110 (hydrate)[c] | $C_7H_5O_7N$ | 39.08 | 2.34 | 6.51 | 39.02 | 2.42 | 6.57 | 71.7 | 72.3 |
| VII | 183~183.5[d] (decomp.) | $C_{11}H_7O_5N$ | 56.66 | 3.03 | 6.01 | 56.87 | 2.97 | 6.08 | 116.6 | 115.7 |

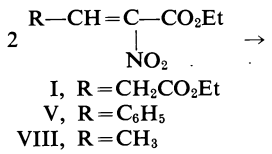
a) Recrystallized from ethanol.
b) Recrystallized from ligroin.
c) Recrystallized from dioxane-chloroform; the anhydrous sample melted at 177~178°C (decomp.).
d) Recrystallized from a mixture of dioxane and ethylenedichloride-ligroin.

TABLE II. ABSORPTION SPECTRA OF 4-SUBSTITUTED 3,5-BIS(*n*-BUTYLCARBAMOYL)ISOXAZOLES

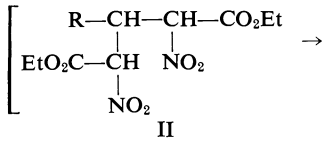
| Compounds | U.V. absorption $\lambda_{max}$, m$\mu$ ($\varepsilon$) | Infrared absorption $\gamma_{max}^{Nujol}$, cm$^{-1}$ | | |
|---|---|---|---|---|
| III | 245 (10500)[a] | 3299 (NH), | 1682 (CO), | 1537 (secondary, non-cyclic amide) |
| VI | —[b] | 3338, | 1678, | 1535 |
| IX | 246 (10100)[c] | 3290, | 1664, | 1555 |

a) Methanol solution.
b) No characteristic maximum in the range of 220~340 m$\mu$.
c) Ethanol solution.

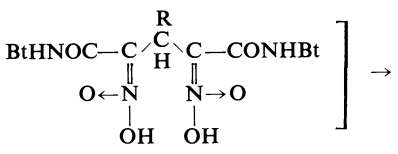
with the original unsaturated nitroester, followed by the addition of the former to the latter to give a key intermediate II, which may cyclize by elimination of water and nitrous acid to form isoxazole derivatives, as outlined in the following scheme:



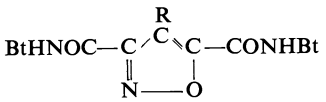
I, R=$CH_2CO_2Et$
V, R=$C_6H_5$
VIII, R=$CH_3$



II



Bt=*n*-Butyl



III, R=$CH_2CONHBt$
VI, R=$C_6H_5$
IX, R=$CH_3$

The validity of the above mechanism has been supported by the experimental observation that, if ethyl nitroacetate is added to the above-mentioned reaction system as an external source of nitroacetate moiety, the yield of isoxazole derivative is significantly increased. As a typical result: When a mixture of ethyl $\alpha$-nitrocinnamate (5.0 g.) and ethyl nitroacetate (3.0 g.) was caused to react with *n*-butylamine (10 g.) under similar conditions, VI (crude product 4.7 g.) was obtained in a 60% yield.

Further studies on the related reactions are in progress.

The authors are grateful to Mr. S. Nakada and Miss S. Taguchi for helping their experiments.

*Department of Applied Chemistry*
*Faculty of Engineering*
*Keio University, Tokyo*

## *Genesis of Sulfate in Acid Hot Spring*

By Iwaji IWASAKI and Takejiro OZAWA

(Received March 18, 1960)

Acid hot springs contain generally large amounts of sulfate ion, and it has been usually considered that most of them are formed by the oxidation of hydrogen sulfide or other sulfides with oxygen from the air at or near the ground surface[1].

However, this explanation is not always acceptable, when their high discharges and the chemical composition of gases accompanied with the acid hot springs are taken into consideration.

Fumarolic gases from active volcanoes contain usually hydrogen sulfide, sulfur dioxide,

1) E. T. Allen and A. L. Day, "Hot Springs of the Yellowstone National Park" Carnegie Inst. Washington Pub. (1935); D. E. White, *Bull. Geol. Soc. Am.*, **68**, 1637 (1957) etc.

TABLE I

| Silicate rock | Condition | $H_2SO_3$(mM) Residual | $H_2SO_4$(mM) Found | S(mM) Found | $H_2SO_4$/S |
|---|---|---|---|---|---|
| None | A | 6.51 | 2.36 | 1.10 | 2.1 |
| | B | 3.43 | 3.79 | 1.80 | 2.1 |
| Basalt | A | 0.69 | 5.96 | 2.38 | 2.5 |
| | B | 0.36 | 5.68 | 2.69 | 2.1 |
| Andesite | A | 0.26 | 5.89 | 2.75 | 2.1 |
| | B | 0.14 | 5.25 | 2.95 | 2.1 |
| Granite | A | 1.03 | 5.60 | 2.70 | 2.1 |
| | B | 2.68 | 3.89 | 1.72 | 2.3 |

hydrogen chloride and carbon dioxide in the same order of amounts, and nitrogen in a smaller amount, but scarcely any oxygen and sulfur trioxide.

On the other hand, gases from region of the acid hot springs consist of carbon dioxide and hydrogen sulfide as the major components, and of nitrogen as the minor components, and of sulfur dioxide, hydrogen chloride and oxygen as the trace components. Therefore, the most important chemical species for the formation of sulfate would not be hydrogen sulfide, but sulfur dioxide.

When volcanic gases are condensed by cooling under the ground, hydrogen chloride and sulfur dioxide would dissolve into the condensed water to form hydrochloric and sulfurous acids. Then sulfuric acid may be formed from this sulfurous acid, liberating sulfur by the following self oxidation-reduction reaction.

$$3H_2SO_3 = 2H_2SO_4 + S + H_2O \qquad (1)$$

In order to confirm this new hypothesis, some experiments were carried out as follows. Two grams of the powdered silicate rock were taken into an ampoule (50 ml.) and 20 ml. of 0.5 M sulfurous acid solution (condition A) or 20 ml. of the mixed solution consisting of 0.5 M sulfurous acid and 0.5 M hydrochloric acid (condition B) were added. Then each ampoule was sealed in the atmosphere of carbon dioxide and kept at 105°C. After about three days, some droplets of sulfur were observed on the surface of the solution into which andesite or granite was added. After a week, all ampoules were cooled to room temperature and the amount of each reaction product was determined (Table I).

It is clear that, as shown in Table I, the self oxidation-reduction reaction of sulfurous acid is mainly based on Eq. 1 under these conditions and this reaction proceeds easily in the presence of hydrochloric acid or silicate rock. Under natural circumstances where higher pressure and temperature are expected, this reaction would proceed more easily and the sulfur formed may contribute to the formation of some ores such as pyrite and native sulfur impregnated with wall rocks.

It is concluded that the principal source of sulfate in the acid hot spring may be sulfur dioxide from volcanic gas and the formation of sulfate may be based on the self oxidation-reduction of sulfurous acid.

*Laboratory of Analytical Chemistry and Geochemistry*
*Tokyo Institute of Technology*
*Ookayama, Meguro-ku, Tokyo*

# *A Research on Isotopic Composition of Evolved Hydrogen Molecules with Special Reference to the Mechanism of Nickel Cathode*

By Kozo HIROTA and Takeo HISANO*

(Received May 2, 1960)

Although a number of research has been published on the separation factor of hydrogen evolved at the electrolysis of aqueous solutions, no attention has been paid on the composition of isotopically different molecules, i.e., $H_2$ HD and $D_2$. However, by the following reasoning, it seems very important to investigate if the composition coincides with the one expected by the gaseous equilibrium:

$$H_2 + D_2 \rightleftarrows 2HD \qquad (1)$$

In the case of the discharge mechanism (A), evolved hydrogen must be equilibrated by the practical equilibrium of the recombination step of statistically independent hydrogen atoms formed by the rate-determining step $H^+ + e \rightarrow H$ of this mechanism. On the other hand, in the case of the catalytic (B) or the electrochemical (C) mechanism the evolved hydrogen need not be equilibrated, inasmuch

* Research fellow from the Engineering Faculty, Tokushima University (1959-1960).

TABLE I. SEPARATION FACTOR AND ISOTOPIC COMPOSITION EVOLVED AT THE NICKEL ELECTRODE AT 0°C

| Exp. no. | Current density mA/cm² | D atom% | Separation factor $\alpha$ | $K(\text{obs}) = \frac{[HD]^2}{[H_2][D_2]}$ |
|---|---|---|---|---|
| 41 | 25.3 | 30.3 | 4.3 | 2.8 |
| 42 | 50.6 | 25.1 | 5.6 | 2.7 |
| 43 | 84.3 | 21.6 | 6.6 | 2.7 |
| 44 | 147.3 | 20.5 | 7.3 | 2.7 |
| 45 | 190 | 21.4 | 7.4 | 2.8 |

* a) All the data of the columns 3,4 and 5 are the means of two measurements except for No. 41.
b) D atom% of the original solution: 65.2%.

as the rate is governed in either case by the step of formation of the hydrogen molecule itself, which is not of course in equilibrium.

It is interesting therefore to demonstrate the above consideration experimentally on some cathode. As the first example, nickel electrode has been taken up, because the mechanism of this electrode is not yet determined in spite of the effort of many researchers. The electrolysis was carried out on 1 N sodium carbonate solution with the cathode of nickel plate (surface area, 0.48 cm²) and the anode of platinum wire. Deuterium content in the original solution was 65.2% (atom%). The ratio $H_2$ : HD : $D_2$ of the hydrogen evolved at the cathode as well as the separation factor $\alpha$, defined by $(H/D)_{gas}/(H/D)_{sol}$, were determined mass-spectrometrically.

The result obtained at 0°C is summarized in Table I. It is shown that $\alpha$ increases with current density and approaches to the value of 7.4 which is nearly equal to that hitherto obtained by the electrolysis of aqueous solution of low deuterium concentration in the case of nickel cathode[1]. It is noteworthy on the other hand that the factor $K(\text{obs.}) = [HD]^2/[H_2][D_2]$ is 2.7 or 2.8 which is less than the $K$ (equil.), i. e., 3.25 at 0°C[2].

Such being the situation, the discharge mechanism (A) can not be accepted so far as nickel cathode is concerned. Although the mechanism (B) or (C) is reasonable, some other experimental fact must be resorted to for the discussion between the mechanisms. From the reason that no positive proof for the mechanism (C) has been found until now, the catalytic mechanism (B)[1,3] may be accepted.

Detailed research on other electrodes is now in progress.

We express sincere thanks to Professor J. Horiuti, Hokkaido University, for his kind advice and discussions on this research.

*Department of Chemistry*
*Faculty of Science*
*Osaka University*
*Nakanoshima, Osaka*

1) G. Okamoto and J. Horiuti, *Sci. Pap. Inst. Phys. Chem. Res.* (Tokyo), **28**, 231 (1936).
2) H. Urey, *J. Chem. Soc.*, **1947**, 562.
3) J. Horiuti, G. Okamoto and K. Hirota, *Sci. Pap. Inst. Phys. Chem. Res.* (Tokyo), **29**, 223 (1936).

# *The Assignment of Infrared Absorption Bands of p-Dichlorobenzene*

By Shinnosuke SAËKI*

(Received December 27, 1959)

Many works have been published by a number of investigators concerning the vibrational spectra of *p*-dichlorobenzene (for example Ref. 1 and 2). But all of these measurements were done in solid state or in solution, and we have not yet any molecular spectrum of this substance in gaseous state. Since the spectrum of *p*-dichlorobenzene in solid or solution shows many strong overtones and combination liable to lead to an erroneous assignment, we have measured the gaseous spectra of deuterated and non-deuterated *p*-dichlorobenzenes to obtain the correct assignment.

## Experimental

The measurements were carried out using Perkin-Elmer model 112 spectrometer, for the region from 5,000 to 2,000 $cm^{-1}$ with a LiF prism, from 2,000 to 700 $cm^{-1}$ with an NaCl prism and from 700 to 400 $cm^{-1}$ with a KBr prism.

As the boiling points of these substances are considerably high (173.4°C for $C_6H_4Cl_2$), it was necessary to use a high temperature cell to obtain their gaseous spectra. An ordinary gas cell 85 mm. thick with pyrex bracelets of 15 mm. height on the KBr windows was coiled by a fine nichrome wire, then covered by a thick layer of asbestos for the sake of thermal insulation. The bracelets prevented the sample gas from condensing on the KBr windows and made sure to obtain the real gas phase spectra. This cell was usable at any temperature below 300°C by the aid of a slide wire resistor. We did not use any binding agent either to fix the KBr windows to the cell body, or to attach the pyrex rings to the windows, in order to avoid introduction of any impurity which might result from the thermal decomposition of the binding agent. The design of the cell is shown in Fig. 1. The inequality of the diameters at both ends of the cell might cause an inhomogeneity of the temperature in the cell to some extent, but it was not considered to have any effect on the spectra obtained.

The powder of the substance was put in the cell which was previously heated to a temperature sufficiently higher than its boiling point, and the measurement was carried out for the mixture of the vapor and the air at one atmospheric pressure.

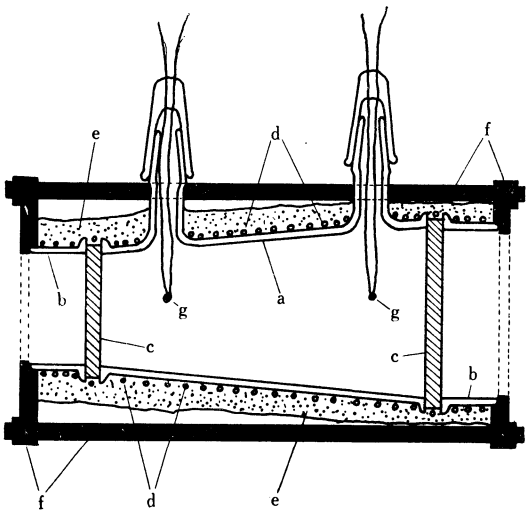



Fig. 1. Description of the high temperature cell

a: cell body
b: bracelets
c: KBr windows
d: nichrome wire
e: asbestos
f: supporting frame work
g: thermocouples

## Results

The spectra obtained are shown in Fig. 2, and the observed frequencies of the absorption bands are shown in Table I. The spectra of deuterated *p*-dichlorobenzene were not so clear as those of ordinary *p*-dichlorobenzene because of the small available quantity of the substance. Thus we could detect no overtone nor combination band of deuterated *p*-dichlorobenzene

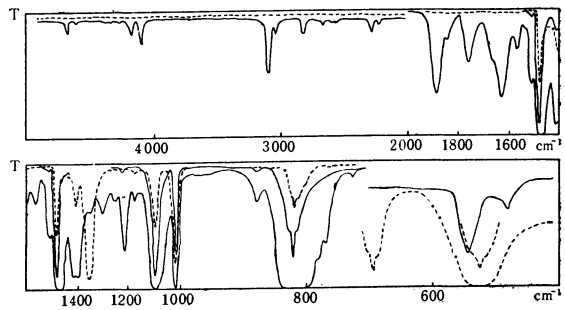



Fig. 2. Infrared absorption spectra of *p*-dichlorobenzene
—— non-deuterated
---- deuterated

* Present address: Government Chemical Industrial Research Institute, Tokyo, Hatagaya, Shibuya-ku, Tokyo.

1) D. H. Whiffen, *Spectrochim. Acta*, 7, 253 (1955).
2) E. K. Plyler, H. C. Allen, Jr. and E. D. Tidwell, *J. Research Natl. Bur. Standards*, **58**, 255 (1957).

TABLE I. OBSERVED FREQUENCIES ($cm^{-1}$)

| Non-deuterated | | Deuterated | Non-deuterated | | Deuterated | |
|---|---|---|---|---|---|---|
| 4675 | m | | 1626 | s | 1479 | s |
| 4605 | w | | 1567 | m | | |
| 4384 | w | | 1509 | m | | |
| 4328 | w | | 1478 | s | 1404 | m |
| 4258 | w | | 1417 | s | | |
| 4170 | m | | 1395 | s | 1357 | s |
| 4095 | m | | 1348 | w | | |
| 3094 | s | (2290) | 1301 | m | | |
| 3035 | m | (2283) | 1251 | w | 1174 | w |
| 2816 | m | | 1217 | m | 1090 | s |
| 2665 | w | | 1175 | w | | |
| 2590 | w | | 1091 | s | 1020 | s |
| 2556 | w | | 1014 | s | 800?* | m |
| 2273 | w | | 878 | w | | |
| 2220 | w | | 819 | s | 695 | s |
| 1882 | s | | 725 | w | | |
| 1837 | w | | 544 | s | 526 | s |
| 1758 | m | | 483 | s | (436) | |
| 1664 | w | | | | (414) | |

N. B. The values in the brackets are the frequencies observed in solid state by other author (J. Lecomte, unpublished).
The indication of the intensities are not very precise.

* This band was covered by the strong band at 819 $cm^{-1}$ of ordinary *p*-dichlorobenzene, and observed as a shoulder.

in the LiF region, and further it is necessary to mention here that the shapes of bands of deuterated *p*-dichlorobenzene in the figure are not so precise as those of ordinary *p*-dichlorobenzene.

Several measurements were repeated for non-deuterated *p*-dichlorobenzene to observe the correct shapes of the absorption bands, but were not successful except for those in the lower frequency part of NaCl region, that is, for the bands at 1013 $cm^{-1}$ and at 819 $cm^{-1}$ which were found to be type B and type C (or A) bands respectively. The other bands did not show any definite feature of the envelopes by which the types of the bands might be decided.

## Assignment

The molecular structure of *p*-dichlorobenzene has the $V_h$ symmetry, and we can expect for the molecule thirteen infrared active fundamental vibrations which are shown in Table II. Among those vibrations the frequencies of the C–Cl deformation vibrations are obviously too low to be measured under our experimental conditions, and it is possible that the frequencies of the ring deformation vibrations are also too low to be observed. Consequently only from nine to eleven bands are expected to be observed by our measurements.

TABLE II. INFRARED ACTIVE NORMAL VIBRATIONS OF *p*-DICHLOROBENZENE

Species $B_{1u}$ (in-plane)
- C–H stretching
- C–H bending
- C–C stretching
- ring deformation
- C–Cl stretching

Species $B_{2u}$ (in-plane)
- C–H stretching
- C–H bending
- C–C stretching
- ring deformation
- C–Cl deformation

Species $B_{3u}$ (out-of-plane)
- C–H bending
- ring deformation
- C–Cl deformation

TABLE III. ASSIGNMENT OF INFRARED FUNDAMENTAL BANDS OF *p*-DICHLOROBENZENE

| Species | Non-deuterated $cm^{-1}$ | Deuterated $cm^{-1}$ | Mode |
|---|---|---|---|
| $B_{1u}$ | 3094 | 2290 | C–H stretching |
| | 1478 | 1404 | ring stretching |
| | 1217 | 1090 | C–H deformation |
| | 1091 | 1020 | skeletal vibration |
| | 483 | 414 | skeletal vibration |
| $B_{2u}$ | 3035 | 2283 | C–H stretching |
| | 1626 | 1479 | ring stretching |
| | 1405* | 1357 | C–H deformation |
| | 1014 | 800 | ring deformation |
| | — | — | C–Cl deformation |
| $B_{3u}$ | 819 | 695 | C–H deformation |
| | 544 | 526 | ring deformation |
| | — | — | C–Cl deformation |

N. B. Concerning the notations for symmetry species, we remark that we have chosen x-axis to be perpendicular to the plane of molecule and z-axis in the direction of the line combining two chlorine atoms.

* The mean value of 1395 and 1417 $cm^{-1}$ in Table I.

We can easily assign the absorption bands at 3094 $cm^{-1}$ (2290 $cm^{-1}$ for $C_6D_4Cl_2$) and 3035 $cm^{-1}$ (2283 $cm^{-1}$ for $C_6D_4Cl_2$) to the two C–H (or C–D) stretching frequencies. The absorption band at 819 $cm^{-1}$ of $C_6H_4Cl_2$ (695 $cm^{-1}$ for $C_6D_4Cl_2$) is assigned to the out-of-plane vibration of C–H (or C–D) by many authors (for example, by D. H. Whiffen[1] and Y. Kakiuchi[3]). We have assigned a strong band at 544 $cm^{-1}$ of $C_6H_4Cl_2$ (526 $cm^{-1}$ for $C_6D_4Cl_2$) to the out-of-plane vibration of benzene ring. This band might be assigned to the in-plane deformation vibration of the ring,

3) Y. Kakiuchi, *J. Chem. Soc. Japan, Pure Chem. Sec.* (*Nippon Kagaku Zasshi*), 77, 1572 (1956).

but, as shown later, this assignment does not satisfy the product rule.

As for the other normal frequencies, we measured seven strong bands between 1000 and 2000 $cm^{-1}$ in the spectrum of $C_6H_4Cl_2$ (six bands for $C_6D_4Cl_2$), while there remain six normal vibrations to assign them. As there were too many absorption bands in the spectrum of $C_6H_4Cl_2$, we assumed that the two bands at 1417 and at 1395 $cm^{-1}$ are caused by a Fermi resonance between a fundamental and a combination* near by it. Taking into account of the fact that the intensities of these two bands were nearly equal, we estimated that the position of the fundamental would be 1405 $cm^{-1}$ (mean value of these two observed frequencies) if it were not for the Fermi resonance. We assigned the highest two of these six bands to the stretching vibrations of the ring, and the next two frequencies (one of which is the above-mentioned 1405 $cm^{-1}$) to the in-plane bending vibrations of C–H, and 1015 $cm^{-1}$ and 1091 $cm^{-1}$ to the deformation vibration of the ring and the stretching vibration of C–Cl respectively. As for the C–Cl stretching vibration, we could easily imagine from its abnormal frequency that this mode might be extremely mixed with some other modes. Although assignments of the last two frequencies seem to be mutually exchangeable, the exchange would result the larger deviation from the product rule.

In addition to the above-mentioned bands, we observed a strong band at 483 $cm^{-1}$ in the spectrum of the $C_6H_4Cl_2$. This band corresponds to the band at 414 $cm^{-1}$ in the spectrum of the $C_6D_4Cl_2$. We assigned these bands to the skeletal vibration of the molecule, i. e., the mixed vibration of ring deformation and C-Cl stretching.

Thus we assigned eleven of thirteen fundamental vibrations, and the remaining two fundamentals are the vibrations of C-Cl deformation, the frequencies of which are expected to be too low to be measured. The present assignments are shown in Table III.

## Discussion

According to the product rule, the ratio of the products of the frequencies of non-deuterated and deuterated *p*-dichlorobenzene is 1.972 for the species $B_{1u}$ and $B_{2u}$, and 1.388 for the species $B_{3u}$. In the case of the species $B_{1u}$ we found that the ratio calculated from the observed frequencies was 1.970 which is in good accordance with the theoretical value. But in the case of the other species, the unobserved bands of low frequencies prevented us from applying the product rule perfectly, and all that we were able to do was to verify that the ratios calculated from the observed frequencies alone did not exceed the theoretical value. Actually these ratios were calculated as 1.917 and 1.219 for species $B_{2u}$ and $B_{3u}$ respectively, and these were quite plausible values.

As for the band envelopes, as mentioned in the previous chapter, for non-deuterated *p*-dichlorobenzene the band at 1014 $cm^{-1}$ was found to be a type B band showing an apparent absorption minimum at the center of the band, while the band at 819 $cm^{-1}$ was found to be type A or C band showing a prominent Q branch accompanied by P and R branches at its both sides. Considering that the axis of the largest moment of inertia of this molecule is perpendicular to the molecular plane, and that the axis of the smallest moment of inertia combines the two chlorine atoms, it would be easily shown that the type A, B and C bands belong to the species $B_{1u}$, $B_{2u}$ and $B_{3u}$ respectively, and that the band at 1014 $cm^{-1}$ belongs to species $B_{2u}$ and the band at 819 $cm^{-1}$ belongs to the species $B_{1u}$ or $B_{3u}$. The assignment shown in Table III is in good accordance with these results. The observed envelopes of the other bands were not adequately clear to give some suggestions for their assignments. Further for the spectra of deuterated *p*-dichlorobenzene we could not find any absorption band which showed a clear band envelope. The band at 819 $cm^{-1}$ the envelope of which showed a clear feature of type A or C band was apparently to be considered as the extremely strong band of ordinary *p*-dichlorobenzene contained in deuterated *p*-dichlorobenzene as a slight impurity.

We had tried many other assignments which seemed to be compatible with the empirical knowledge. But they did not satisfy the product rule so well as the one shown in Table III.

The present assignment is different at some points from those given by other authors for their spectra in solid state or in solution. Comparing our gaseous spectra with those spectra of solid or solution, we saw that many strong bands in the latter spectra disappeared entirely or partially in the former. Thus we believe that the spectrum measured in solid state or in solution is not suitable for the assignment of the absorption bands.

## Summary

The infrared absorption spectra of deuterated and non-deuterated *p*-dichlorobenzene were measured in the vapor state using a high

* We observed a strong Raman line at 331 $cm^{-1}$. The combination of this vibration with the infrared active vibration at 1090 $cm^{-1}$ would appear in the neighborhood of 1405 $cm^{-1}$. We shall present a paper on the Raman spectra of *p*-dichlorobenzene in near future.

temperature cell. The results obtained by the measurements permitted us the assignment of the observed fundamental bands with the aid of the product rule. For some frequencies which we could not measure under our experimental conditions, we used the frequencies observed by other workers in the solid state which enabled us to apply the product rule.

This work was done at the laboratory of Professor J. Lecomte of the Laboratoire des Recherches Physiques, Faculté des Sciences de Paris. The author acknowledges gratefully his encouragement and advice. He also wishes to thank Dr. Leitch of the National Research Council at Ottawa for kindly sending us deuterated *p*-dichlorobenzene prepared by him.

*Laboratoire des Recherches Physiques*
*Faculté des Sciences de Paris*

# The Assignment of Infrared Absorption Bands of 1, 3, 5-Trichlorobenzene

By Shinnosuke SAËKI*

(Received January 23, 1960)

Several works have been published concerning the infrared spectra of 1, 3, 5-trichlorobenzene (for example, Ref. 1 and 2). However, all of these spectra were measured in solid state or in solution and we have no spectrum of this substance in vapor state. As we pointed out in our previous paper[3] chlorobenzenes show strong bands of overtones and combinations in solid state or in solution. So, one must be very cautious in trying the assignment of infrared bands of these substances using the spectra in these states. For this reason, we measured the infrared absorption spectra of deuterated and non-deuterated 1, 3, 5-trichlorobenzenes in vapor state to make the assignment of the absorption bands of these substances.

## Experimental and Results

Spectral data were obtained by means of a Perkin-Elmer 112 spectrometer equipped with LiF, NaCl and KBr prisms. The measurements were carried out under ordinary pressure at high temperature. In these measurements we used the high temperatures cell which we described in detail in our previous paper[3]. The non-deuterated 1, 3, 5-trichlorobenzene used in our experiments was the "extra pure" one on the market, and the deuterated one was kindly provided by Dr. Leitch in Canada.

For the non-deuterated substance we made several measurements in various concentrations to obtain the correct frequencies and shapes of the strong bands and also to ascertain the existence of very weak bands. But, for the deuterated substance, we could not measure its spectra so attentively because of the smallness of the quantity, and it is possible that some weak bands were missed in our measurements. However, as we are going to assign only the fundamental bands of these spectra, this missing would not be very serious.

The spectra obtained by our measurements are shown in Fig. 1, and the frequencies of the observed bands are shown in Table I.

TABLE I. THE INFRARED ABSORPTION BANDS OF 1, 3, 5-TRICHLOROBENZENE ($cm^{-1}$)

| Non-deuterated | | Deuterated | | Non-deuterated | | Deuterated | |
|---|---|---|---|---|---|---|---|
| 4650 | w | 4550 | w | 1565 | s | 1549 | s |
| 4365 | w | 3256 | w | 1464 | w | | |
| 4236 | w | 3105 | w | 1419 | s | 1333 | s |
| 4085 | m | 2800 | w | 1380 | m | 1257 | m |
| 3132 | w | 2687 | w | | | 1206 | m |
| | | 2600 | w | 1261 | w | 1066 | w |
| 3089 | m | (2310) | | | | 1024 | w |
| 2951 | w | 2274 | w | | | 950 | w |
| 2928 | w | | | | | 896 | w |
| 2838 | w | | | 1100 | s | | |
| 2712 | w | | | 1055 | m | | |
| 2632 | w | | | 889 | w | | |
| 2592 | m | | | 853 | s | 843 | s |
| 2197 | w | | | 813 | s | 795 | s |
| 1944 | w | | | | | 769 | w |
| 1722 | m | | | 719 | w | | |
| 1606 | w | | | 662 | s | 532 | s |

N. B. The value in the bracket is the frequencies observed in solid state by other authors. The indication of the intensities are not very precise.

* Present address: Government Chemical Industrial Research Institute, Tokyo. Hatagaya, Shibuya-ku, Tokyo.

1) E. Herz, K. W. F. Kohlrausch and R. Vogel, *Monatsh.* 76, 200 (1947).

2) E. K. Plyler, H. C. Allen, Jr. and E. D. Tidwell, *J. Research Nat. Bur. Standards* 58, 255 (1957).

3) S. Saëki, This Bulletin, 33, 1021 (1960).

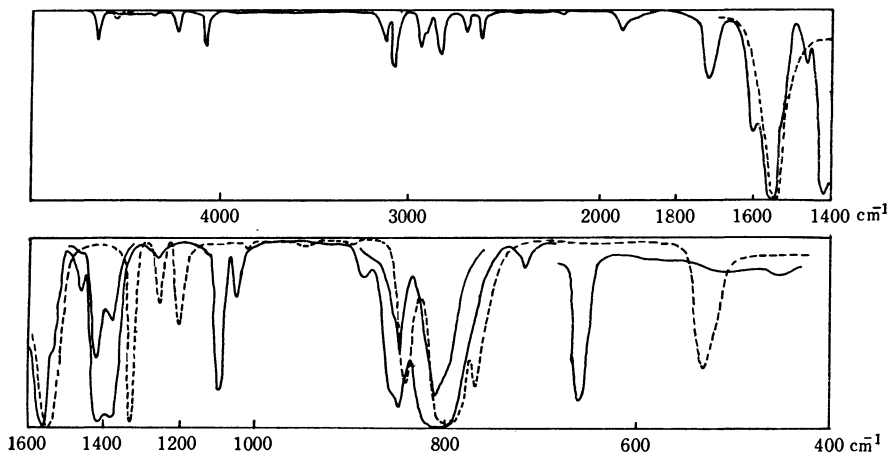



Fig. 1. Infrared absorption spectra of 1,3,5-trichlorobenzene.
—— non-deuterated ---- deuterated

## Assignments

Assuming the molecular structure of 1,3,5-trichlorobenzene to be of $D_{3h}$ form, it has ten infrared active fundamental frequencies, of which seven are doubly degenerate (species E′, in-plane) and three are non-degenerate (species $A_2''$, out-of-plane). The modes of these vibrations are shown in Table II. Of course we can not expect to observe all of these ten normal frequencies under our experimental conditions, because two C–Cl deformation frequencies (E′ and $A_2''$) are evidently too low to be measured, and two ring deformation frequencies might also exist below the observable region. Thus only from six to eight fundamental frequencies might be observed by our experiments. However, as is shown in Fig. 1 and Table I, there were too many strong bands in the spectra, but we could eliminate some of them by comparing the spectrum of non-deuterated substance with that of deuterated one.

Table II. Normal vibrations of 1,3,5-trichlorobenzene

| E′ (in-plane) | $A_2''$ (out-of-plane) |
|---|---|
| C–H stretching | C–H deformation |
| ring stretching | ring deformation |
| ring stretching | C–Cl deformation |
| C–H deformation | |
| ring deformation | |
| C–Cl stretching | |
| C–Cl deformation | |

We could easily assign the band at 3089 $cm^{-1}$ of $C_6H_3Cl_3$ to the C–H stretching vibration (E′). The C–D stretching vibration of $C_6D_3Cl_3$ was not observed. It might be because of the unfortunate overlapping with the strong band of carbon dioxide near 2200 $cm^{-1}$. In solid state, it was observed at 2310 $cm^{-1}$ [4].

We assigned two strong bands at 1565 and 1419 $cm^{-1}$ of $C_6H_3Cl_3$ (1549 and 1333 $cm^{-1}$ of $C_6D_3Cl$) to the ring stretching fundamental vibrations of species E′, and the strong band at 1380 $cm^{-1}$ of $C_6H_3Cl_3$ to the C–H deformation vibration of E′ (in-plane). However, for the corresponding band of $C_6D_3Cl_3$, we observed two bands of considerable intensity at 1257 and 1206 $cm^{-1}$. These two bands were considered to be brought about by a Fermi resonance between a fundamental and an overtone or combination of species E′, and their nearly equal relative intensities suggested to us that the proper frequency of the concerned fundamental band might be about 1230 $cm^{-1}$. As for the overtone or combination band which interacts with the fundamental, we can say little of it because of the lack of data in the low frequency region and also of the lack of the Raman spectrum* of this substance.

We observed another strong band at 1100 $cm^{-1}$ in the spectrum of $C_6H_3Cl_3$ but in the spectrum of $C_6D_3Cl_3$ we did not find any strong band corresponding to it. Although the intensity of the band at 1100 $cm^{-1}$ of $C_6H_3Cl_3$ was very remarkable, this lack of corresponding band in the spectrum of $C_6D_3Cl_3$ kept us from assigning the band to a fundamental one.

The band at 853 $cm^{-1}$ of $C_6H_3Cl_3$, was hitherto pointed out by many investigators[5] as an out-of-plane fundamental vibration band of C–H

4) J. Lecomte, unpublished.

* We have not yet succeeded in observing the Raman lines of this substance. For, when this substance was resolved in the solvents, the solution was slightly colored, and it prevented us from measuring the Raman spectrum.

5) For example, Y. Kakiuchi, *J. Chem. Soc. Japan, Pure Chem. Sec.* (*Nippon Kagaku Zasshi*), **80**, 356 (1959) and A. R. H. Cole and H. W. Thompson, *Trans. Faraday Soc.*, **46** 103 (1950).

bond. But, as is shown in our spectrum of Fig. 1, this band corresponds to the band at 843 $cm^{-1}$ of $C_6D_3Cl_3$. That means, the frequency shift caused by the substitution of hydrogen atoms by deuterium atoms was only 10 $cm^{-1}$. If this is a band principally concerning the vibration of C–H bond, the frequency shift might be much greater than 10 $cm^{-1}$. Even if we dare to consider that it is the band at 769 $cm^{-1}$ of $C_6D_3Cl_3$ that corresponds to 853 $cm^{-1}$ of $C_6H_3Cl_3$, another difficulty would be caused. As we shall show later, we have a band in a lower frequency region which showed a large frequency shift by the substitution of hydrogen atoms, that is, the band at 662 $cm^{-1}$ of $C_6H_3$ (532 $cm^{-1}$ of $C_6D_3Cl_3$). If we assign the band at 853 $cm^{-1}$ to the out-of-plane C–H vibration, there should be no way to explain the band at 662 $cm^{-1}$ which was shifted widely to 532 $cm^{-1}$ by the introduction of deuterium atoms. Therefore we did not assign this band at 853 $cm^{-1}$ (at 843 $cm^{-1}$ in the case of $C_6D_3Cl_3$) to the out-of-plane C–H (or C–D) vibration. One might also assign it to the in-plane ring deformation fundamental vibration (E′). But it is generally known that the frequency of this mode is very variable over a wide region, especially when there is a large possibility of coupling with other modes. So we are not sure that we could assign this band to the ring deformation fundamental vibration. After all we assigned it to no normal vibraton. After all we assigned it to no normal vibration, considering it as an overtone or combination band which was brought about by the Fermi resonances with a fundamental band at 813 $cm^{-1}$ and which borrowed the intensity from the fundamental band. Thus we could get over the superabundance of the strong bands in the observed spectra.

We assigned the very strong bands at 813 $cm^{-1}$ of $C_6H_3Cl_3$ and at 795 $cm^{-1}$ of $C_6D_3Cl_3$ to the C–Cl stretching vibration. But it should be mentioned here that this designation of the vibrational mode is used just as a convention. For, as we showed in our previous paper[3], the mixing of the vibrational modes is extreme in this region of frequency, and it might not be very correct to designate the modes of these normal vibrations by simple terms as C–Cl stretching vibration and so forth.

We observed only one strong band in KBr region in each spectrum of $C_6H_3Cl_3$ and $C_6D_3Cl_3$, that is, the bands at 662 $cm^{-1}$ and at 532 $cm^{-1}$ respectively. As there was no other strong absorption band, it is quite certain that these two bands correspond to each other. Further, the fact that the ratio of their frequencies is considerably apart from 1 (1.24) suggests to us that these vibrational bands are concerned with the hydrogen and deuterium atoms respectively. For the spectrum of mesitylene Whiffen[6] assigned the band at 928 $cm^{-1}$ to the out-of-plane vibration of C–H bond. In the case 1, 3, 5-trichlorobenzene, since no appropriate strong band was found in the neighbourhood of 900 $cm^{-1}$, we assigned the band at 662 $cm^{-1}$ (at 532 $cm^{-1}$ for $C_6D_3Cl_3$) to the C–H (C–D) out-of-plane vibration. The above-mentioned assignment is shown in Table III.

TABLE III. THE ASSIGNMENT OF THE INFRARED BANDS OF 1,3,5-TRICHLOROBENZENE

| Type | $C_6H_3Cl_3$ | $C_6D_3Cl_3$ | Mode |
|---|---|---|---|
| E′ | 3089 | (2310) | C–H stretching |
| | 1565 | 1549 | ring stretching |
| | 1419 | 1333 | ring stretching |
| | 1380 | 1230* | C–H deformation |
| | 813 | 795 | C–Cl stretching |
| | — | — | ring deformation |
| | — | — | C–Cl deformation |
| $A_2''$ | 662 | 532 | C–H deformation |
| | — | — | ring deformation |
| | — | — | C–Cl deformation |

* This is the average value of the two observed frequencies, i.e., 1257 and 1206 $cm^{-1}$.

## Discussion

The theoretical values of the ratios of products of normal frequencies of each substance (deuterated and non-deuterated) are 1.972 for the species E′ and 1.402 for the species $A_2''$. For the species $A_2''$ we could observe only one frequency of each substance, and it was impossible to apply the product rule to this species. The only one observed frequency of species $A_2''$ was 662 $cm^{-1}$ of $C_6H_3Cl_3$ (532 $cm^{-1}$ of $C_6D_3Cl_3$) which we assigned to the out-of-plane C–H (or C–D) fundamental vibration by reason of the large shift of frequency accompanying the substitution of hydrogen atoms by deuterium atoms. As was mentioned in the previous section, this assignment is quite different from that which is generally admitted now. We can not get to a definite conclusion on this point at present, but if we succeed in measuring the spectra of these substances in the far infrared region, and if we observe the other two out-of-plane fundamental bands, we shall be able to determine the correct assignment.

For the species E′ too, there were some frequencies that were left unobservable under our experimental conditions, and it is also impossible to apply the product rule perfectly. But, in this case, five or six normal frequencies (seven in all) were observed, so it is not

6) D. H. Whiffen, *Spectrochim. Acta*, 7, 253 (1955–6).

completely meaningless to calculate the ratio of products of observed frequencies alone. This calculated ratio was 1.650, when we excluded the pair of frequencies at 853 $cm^{-1}$ (for $C_6H_3Cl_3$) and at 843 $cm^{-1}$ (for $C_6D_3Cl_3$) from this calculation. It means that the ratio of products by the other two unobserved frequencies is to be about 1.19, and this is quite an appropriate value. But if we include the above-mentioned pair of frequencies into this calculation, the ratio increases only a little and becomes 1.670. It requires that the ratio of the last unobserved frequency of each substance is 1.18. This value seems to be too great to attribute to the ratio of only one pair of frequency. This is another reason why we have not dared to assign this pair of bands to the fundamental ones.

## Summary

The infrared absorption spectra of deuterated nd non-deuterated 1,3,5-trichlorobenzenes were measured in the vapor state from 5,000 to 400 $cm^{-1}$. The results of our measurements allowed us the assignment of the fundamental bands of this substance by the aid of the product rule. As we could not observe all of the fundamental bands of this substance, the perfect application of the product rule was not possible. But we proved that our assignment did not conflict with the product rule.

This work was done at the laboratory of Professor J. Lecomte of the laboratoire des Recherches Physiques, Faculté des Sciences de Paris. The author acknowledges gratefully Professor Lecomte's encouragement and advice. He also wishes to thank Dr. Leitch of the National Research Council at Ottawa for kindly sending deuterated 1, 3, 5-trichlorobenzene prepared by him.

*Laboratoire des Recherches Physiques*
*Faculté des Sciences de Paris*

# *The $n$—$\pi^*$ Transition Band of Acenaphthenequinone*

By Akira KUBOYAMA

(Received January 26, 1960)

In a previous paper[1], Nagakura and the present author measured the weak visible bands of *o*- and *p*-quinones in various solvents. From the result on the solvent effect these bands were ascribed to an $n-\pi^*$ transition, namely, the transition from the non-bonding electron orbital of oxygen atom to the excited $\pi$-electron orbital. However, the $n-\pi^*$ transition band of acenaphthenequinone has never been studied. Thus, the present author measures the $n-\pi^*$ transition band of acenaphthenequinone in various solvents. Further, for the purpose of comparison, the absorption spectra of various *o*- and *p*-quinones are newly measured. The obtained results are now reported.

## Experimental

**Measurements.** — The absorption spectra were measured with a Cary recording spectrophotometer 14 M. Quartz cylindrical cells with path lengths of 1, 2 and 5 cm. were used. A thermostated cell jacket was used for measurements at 35°C.

**Materials.** — Acenaphthenequinone[2] (AQ) was prepared through the oxidation of acenaphthene with potassium bichromate and was recrystallized from benzene, m. p. 256°C. *p*-Benzoquinone[3] was prepared through the oxidation of hydroquinone with potassium bichromate and was purified by sublimation, m.p. 114°C. $\alpha$- And $\beta$-naphthoquinones and phenanthrenequinone were prepared according to L. F. Fieser's method[4]. $\alpha$-Naphthoquinone was purified by charcoal treatment in ether solution, m. p. 124°C. $\beta$-Naphthoquinone was used without further purification, according to Fieser's note[4], m. p. with decomp. 145~147°C. Phenanthrenequinone was recrystallized from ethanol, m. p. 208°C. All the solvents used in the present study were of special grade. Benzene and ethyl ether were distilled after being dried over sodium metal. Dioxane was distilled from sodium metal, after being dried with it. Carbon disulfide was distilled after being dried over calcium chloride, and was

1) S. Nagakura and A. Kuboyama, *J. Chem. Soc. Japan, Pure Chem. Sec. (Nippon Kagaku Zasshi)*, 74, 499 (1953); S. Nagakura and A. Kuboyama, *J. Am. Chem. Soc.*, 76, 1003 (1954).

2) "Organic Syntheses", Vol. XXIV, p. 1.

3) "Organic Syntheses", Col. Vol. I, p. 469.

4) L. F. Fieser, "Experiments in Organic Chemistry", D. C. Heath and Co., Boston (1941), pp. 230, 232 and 233.

kept in the dark. Chloroform was washed successively with concentrated sulfuric acid and with aqueous sodium hydroxide, and was distilled after being dried over calcium chloride. *n*-Heptane was distilled after being treated as in the case of chloroform and being dried over sodium metal.

## Results

The obtained absorption spectra are given in Figs. 1—6. The spectra of AQ in various solvents are given in Figs. 1* and 2 and those of β-naphthoquinone, phenanthrenequinone, *p*-benzoquinone, and α-naphthoquinone are given in Figs. 3**, 4, 5 and 6, respectively.

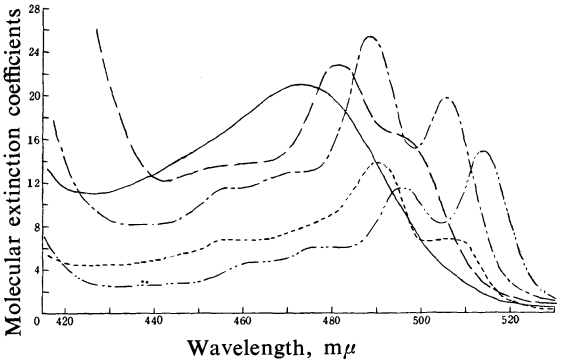



Fig. 1. Absorption spectra of acenaphthenequinone, solvent, —— benzene, —— chloroform, —— dioxane, —— carbon disulfide, ---- ethyl ether (in case of the latter two*, the scale of the ordinate is arbitrary).

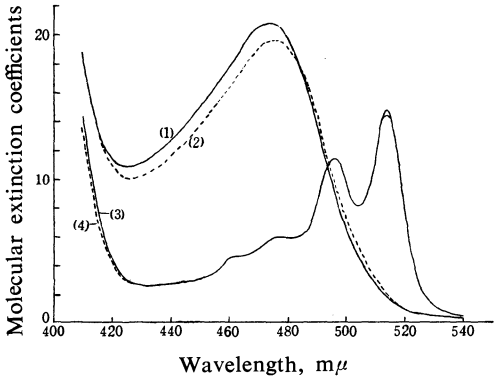



Fig. 2. Absorption spectra of acenaphthenequinone, solvent, (1), (2) dioxane, (3), (4) carbon disulfide; temperature, (1), (3) room temperature (17°C), (2), (4) 37°C (in case of carbon disulfide, the scale of the ordinate is arbitrary).

*1 AQ is sparingly soluble in carbon disulfide and ethyl ether. Thus, the molecular extinction coefficient of the α-band in these solvents could not be determined.

*2 The longest wavelength π-π* transition band of β-naphthoquinone in chloroform largely shifts towards longer wavelengths as in AQ.

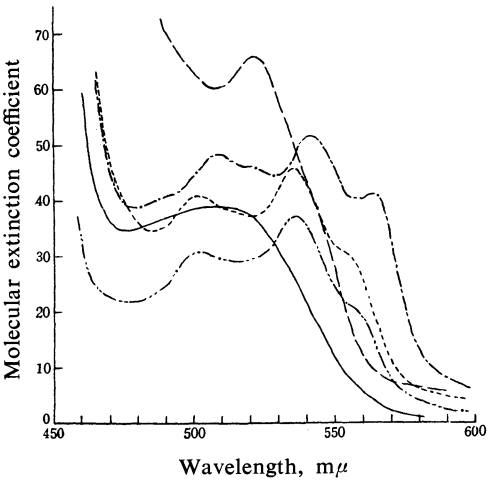



Fig. 3. Absorption spectra of β-naphthoquinone, solvent; —— carbon disulfide, ---- benzene, —— ethyl ether, —— chloroform, —— dioxane.

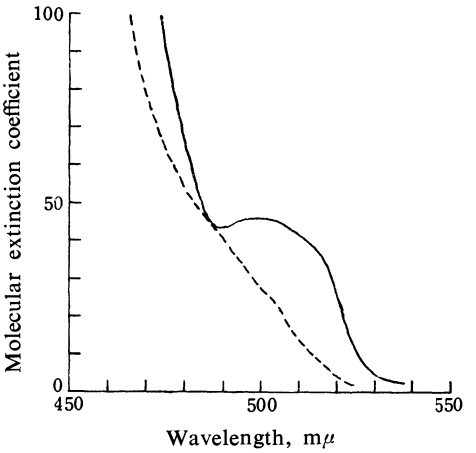



Fig. 4. Absorption spectra of phenanthrenequinone, solvent; —— benzene, ---- dioxane.

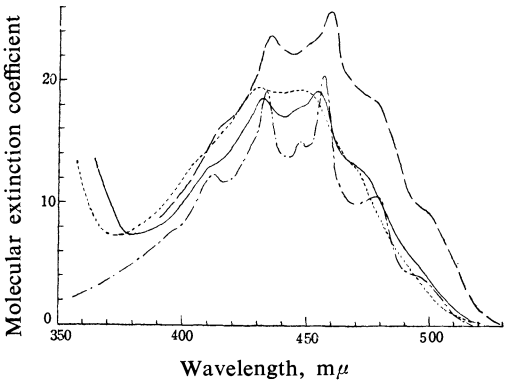



Fig. 5. Absorption spectra of *p*-benzoquinone, solvent; —— carbon disulfide, —— *n*-heptane, —— benzene, ---- dioxane.

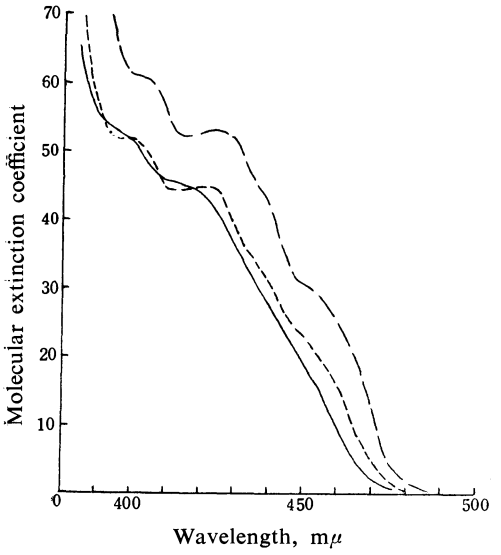



Fig. 6. Absorption spectra of α-naphthoquinone, solvent; —— carbon disulfide, ---- benzene, —— dioxane.

## Discussion

In the visible and near UV regions, AQ has three main peaks at 225 mμ, 300 mμ, and 500 mμ. It is thought that strong peaks at 225 mμ and 300 mμ correspond to the $\beta$ and the $p$ bands of naphthalene[5], respectively, while a weak peak at 500 mμ which is given in Fig. 1 is assumed to be an $n-\pi^*$ transition band from the consideration of its intensity and position. Hereafter, this band will be called the α-band. As for the solvent effect on the α-band, which is shown in Fig. 1, two points are noticeable. First, the α-band in dioxane and chloroform largely shifts towards shorter wavelengths and almost completely loses vibrational structures. Secondly, the relative height of the two main peaks of the α-band markedly depends upon solvents such as carbon disulfide, benzene, ethyl ether etc. As for the first point, the blue-shift of the α-band in chloroform is attributed to hydrogen bond formation[6]. This fact verifies the assignment of the α-band to the $n-\pi^*$ transition band. The large blue-shift of the α-band in dioxane may be attributable to molecular complex formation. Here, dioxane is an $n$-type donor[7]. The blue-shift of an $n-\pi^*$ transition band due to molecular complex formation has never been pointed out. The mechanism of this blue-shift is thought to be similar to the one[8] due to the substitutions of electron-donating groups to a $\pi$-electronic system containing carbonyl groups. The fact that such a large blue-shift of the α-band as in dioxane is not seen in ethyl ether, may be attributable to the large steric hindrance caused by the side chains of ethyl ether in the molecular complex formation. As is seen from Figs. 1, 3, 4, 5 and 6, the blue-shift of the α-band in dioxane is much larger in the ortho-type quinones than in the para-type quinones***. This fact may be explained as follows. The oxygen atoms of dioxane are expected to coordinate themselves to carbon atoms of carbonyl groups of the quinones by the electrostatic interaction as well as by the charge transfer interaction. The electrostatic interaction is thought to be caused by the interaction between the atomic dipoles of the oxygen atoms of dioxane and the positive charges of the carbon atoms of the carbonyl groups. Hence, the magnitude of the electrostatic interaction is determined by the amount of the positive charges of the carbon atoms. The charge transfer interaction can be approximately represented by the interaction between the lowest unfilled orbitals of the quinones and the lone pair orbitals of the oxygen atoms of dioxane. Therefore, the magnitude of the charge transfer interaction is roughly determined by the coefficients of the atomic orbitals of the carbonyl carbon atoms in the lowest unfilled orbitals of the quinones. The greater those coefficients are, the greater is the charge transfer interaction. From our previous calculations[9] for $o$- and $p$-quinones, it is seen that the above two requirements are best fulfilled by the carbon atoms of the carbonyl groups of the quinones. The above requirements are also expected to be satisfied for AQ, which may be regarded as one of the $o$-quinones. Since in $o$-quinones the two carbon atoms of the two carbonyl groups are jointed with each other, the interaction between the oxygen atoms of dioxane and the carbonyl carbon atoms of $o$-quinones**** is expected to be larger than that of $p$-quinones. It is naturally expected that the above fact is ascribed to this point.

As for the second point previously described, there occurs a question whether the two main peaks of the α-band are ascribed to the vibrational structure of the one $n-\pi^*$ transition

5) E. Clar, "Aromatische Kohlenwasserstoffe" 1st Edn., Springer, Berlin (1941).
6) G. J. Brealey and M. Kasha, *J. Am. Chem. Soc.*, 77, 4462 (1955).
7) R. S. Mulliken, *J. Chem. Phys.*, 56, 801 (1952).
8) H. Baba, *J. Chem. Soc. Japan, Pure Chem. Sec.* (*Nippon Kagaku Zasshi*), 72. 341 (1951); S. Nagakura, This Bulletin, 25, 164 (1952).
*3 Previously, L. S. Forster found that the weak visible absorption band of biacetyl in dioxane shows relatively large shift towards shorter wavelengths (*J. Am. Chem. Soc.*, 77, 1417 (1955)). But this blue-shift is not so large as the ones of ortho-type quinones, here found.
9) a) A. Kuboyama, This Bulletin, 31, 752 (1958); b) A. Kuboyama, ibid., 32, 1226 (1959).

band, to the two different $n-\pi^*$ transition bands of the one form of AQ or to the two different $n-\pi^*$ transition bands belonging to the two different forms of AQ. As is seen in Fig. 2, the $\alpha$-band in dioxane and in carbon disulfide are almost independent of temperature. Thus, the third possibility is probably denied. As is seen in Fig. 3, the behaviors of the two peaks in the longer wavelength side of $\beta$-naphthoquinone are, though less marked, similar to the ones of the two main peaks of the $\alpha$-band of AQ and the distance (ca. 700 $cm^{-1}$) between the two peaks of $\beta$-naphthoquinone is almost equal to that of the $\alpha$-band*****. Previously, J. W. Sidman[10] experimentally concluded that *p*-benzoquinone in crystalline state has two distinct singlet-singlet $n-\pi^*$ transition bands in the wave number region of 20000 $cm^{-1}$ to 25000 $cm^{-1}$. In that case, the wave number difference between the two 0—0 bands corresponding to these two transitions was determined to be 797 $cm^{-1}$. In connection with Sidman's conclusion mentioned above, it[11] may safely be assumed that the two main peaks of the $\alpha$-band may be due to the two $n-\pi^*$ transitions whose energy difference is ca. 700 $cm^{-1}$.

As is seen in Figs. 3, 5 and 6, in carbon disulfide the intensities of the $n-\pi^*$ transition bands of the quinones, especially of *p*-benzoquinone, are considerably larger than the ones in the other solvents. This fact is probably attributed to the large refractive index of carbon disulfide[12].

*4 The signs of the two atomic orbitals of the two carbonyl carbon atoms in the lowest unfilled orbitals of *o*-quinones[9b] are equal.

*5 Forster*[3] found the fact, similar to the one of $\beta$-naphthoquinone, for the $n$-$\pi^*$ transition band of biacetyl, where the distance between the two peaks is ca. 1300 $cm^{-1}$. He thought that these two peaks respectively result from two electronic transitions.

10) J. W. Sidman *J. Am. Chem. Soc.* **78**, 2363 (1956).
11) H. L. McMurry, *J. Chem. Phys.*, **9**, 245 (1941).
12) N. Q. Chako, *J. Chem. Phys.*, **2**, 644 (1934).

**Summary**

The weak absorption band ($\alpha$-band) ($\varepsilon_{max}\sim$ 20) near 500 m$\mu$ of acenaphthenequinone was measured in various solvents. This band was determined as the $n-\pi^*$ transition band on the basis of the observed results on intensity and solvent effect. In dioxane, the $n-\pi^*$ transition bands of the *o*-quinones, including the $\alpha$-band, largely shift towards shorter wavelengths. This fact, which is thought to be due to molecular complex formation, was discussed from the qualitative point of view. The relative height of the two main peaks of the $\alpha$-band markedly depends upon solvents. The similar, though less marked, fact is seen in $\beta$-naphthoquinone. The two main peaks of the $\alpha$-band were assumed to be due to the two $n-\pi^*$ transitions, whose transition energy difference is ca. 700 $cm^{-1}$. It was found that the $n-\pi^*$ transition bands of the quinones, especially of *p*-benzoquinone, are markedly intensified in carbon disulfide. This fact is probably attributed to the large refractive index of this solvent.

The author wishes to express his sincere thanks to Professor S. Nagakura of the University of Tokyo for his kind guidance and to Dr. Y. Mashiko of this Institute for his kind offices. The author's thanks are also due to Mr. H. Takaya for his kind cooperation in this research.

*Government Chemical Industrial Research Institute, Tokyo*
*Shibuya-ku, Tokyo*

# *The Stochastic Model for Unimolecular Gas Reaction*

By Kenji ISHIDA

(Received July 13, 1959)

According to the probabilistic representation for the deterministic theory of the "true" unimolecular gas reaction[1], in which it is assumed that the reactant molecules are independent of the coexisting resultant molecules, i. e., the distribution of each reactant molecule is not correlated to the distribution of each resultant molecule, and that the reverse reaction is not taking place, the fraction of the reactant molecules which react during time $dt$ can be set equal to the probability $k_1 dt$;

$$-\frac{dn}{n}=k_1 dt \tag{1}$$

1) Jen-Yuan Chien, *J. Chem. Phys.*, **16**, 426 (1948). See, e. g., A. A. Frost and R. G. Pearson, "Kinetics and Mechanism", John Wiley & Sons, Inc., New York (1953), p. 67.

where the rate constant $k_1$ denotes the probability that one molecule reacts during unit time, $n$ is the number of reactant molecules at time $t$ and $-dn$ the number reacting during time $dt$. It should be emphasized, however, that in Eq. 1 the probabilistic notions are not manifested in a precise form, and that the number of molecules predicted for various times is not precise, but the reaction proceeds at random at an average rate[2]. In order to formulate this on the basis of the mathematically exact laws of the theory of probability, Bartholomay[3] has recently presented a method to construct the stochastic model for the true unimolecular gas reaction by starting from the deterministic theory as represented by Eq. 1. But the chemical and mathematical foundations on which the theory of the stochastic process can be applied to this chemical reaction do not appear to have been exactly mentioned. Therefore it is instructive to formulate definitely the probabilistic properties of the chemical reaction.

If the number of resultant molecules produced during the time interval $(0, t)$ is denoted by $n_p(t)$, the function $n_p(t)$ itself is a random variable for all arbitrary but fixed periods of duration $t$. Since the function $n_p(t)$ which assumes only the integers and is nondecreasing becomes the aggregate of random variables with continuous parameter when $t$ varies, this represents a possible development of the chemical reaction. Consequently the course of the chemical reaction is a stochastic process. It has been acknowledged, in general, that under the given temperature and external parameters the rate of a chemical reaction is determined only by the composition of the reaction system at the time and does not depend on its previous history, so that it is concluded that the course of chemical reaction is a Markov process[4]. It has been recognized for many years that by its very nature a chemical reaction must disturb the equilibrium distribution of the reactant species[5]. If, however, we assume that the rate of the chemical reaction is sufficiently small compared with the rate of energy exchange and the disturbance of the equilibrium distribution of energy during the course of the chemical reaction can be approximately neglected, the reaction system can be discussed on the assumption that it is at thermal equilibrium. By "temporally homogeneous"[6] for the course of chemical reaction we mean that the thermal equilibrium remains absolutely unchanged throughout the process. Accordingly, we obtain the conclusion that *the theory of temporally homogeneous Markov process can be applied to the course of chemical reaction* for such reaction systems at thermal equilibrium that the reactant molecules do not interact mutually with the coexisting resultant molecules and the reverse reaction does not occur, and such conditions permit us to calculated the average rate of the chemical reaction at a time.

Although the one-dimensional stochastic process for the total number of reactant molecules has been studied by Bartholomay who, from the macroscopic point of view, has given a rate constant to the whole reaction, we shall be able to calculate the average rate constant by constructing microscopically the multi-dimensional stochastic process[7] for the number of reactant molecules in various states of energy, on the assumption that the stochastic model is conformable also to the "true" unimolecular reaction concerning the reactant molecules in each state of energy.

## One-dimensional Stochastic Model

In general the Chapman-Kolmogorov equation for temporally homogeneous Markov processes[8] is given by

$$P_{i,n}(t+\tau)=\sum_{\nu}P_{i,\nu}(t)\cdot P_{\nu,n}(\tau) \qquad (2)$$

where $P_{i,\nu}(t)$ is the transition probability from any state $E_i$ to any other state $E_\nu$ during the time interval of length $t$ and for the process of chemical reaction $i$, $\nu$ and $n$ represent the numbers of reactant molecules, respectively. If the initial probability $P_i(0)$ is known, then the probability $P_n(t)$ of finding the system at time $t$ in the state $E_n$ is set equal to the quantity $\sum_{i=0}^{n_0}P_i(0)P_{i,n}(t)$ according to the theorem of total probability[9], that is, $P_n(t)=\sum_{i=0}^{n_0}P_i(0)P_{i,n}(t)$, where $n_0$ is the total number of reactant molecules at time $t=0$. Hence this probability $P_n(t)$ is related to both $t$ and $P_i(0)$. In our case, however, it may be provided that one of the probabilities $P_i(0)$ $(i=0, 1, 2, \cdots\cdots, n_0)$ is equal to one, and the others to zero;

$$\text{if} \qquad i=n_0, \quad P_i(0)=1 \qquad (3)$$

2) L. Pauling, "General Chemistry", W. H. Freeman and Co. (1949), p. 335.
3) G. F. Bartholomay, *Bull. Math. Biophys.*, 20, 175 (1958).
4) W. Feller, "An Introduction to Probability Theory and its Applications", John Wiley & Sons, Inc., New York (1950), p. 337.
5) R. H. Fowler and E. A. Guggenheim, "Statistical Thermodynamics". Cambridge University Press (1939), p. 490.
6) W. Feller, Ref. 4, p. 386.
7) N. Arley, "On the Theory of Stochastic Process and their Application to the Theory of Cosmic Radiation", John Wiley & Sons, Inc., New York (1948), p. 73.
8) W. Feller's book, p. 388.
9) A. N. Kolmogorov. "Foundations of the Theory of Probability" (Translation edited by Nathan Morrison), Chelsea Publishing Co., New York (1950). p. 7.

otherwise, $P_i(0)=0$

Multiplying both sides of Eq. 2 by $P_i(0)$ and summing over all values of $i$, we get

$$\sum_{i=0}^{n_0} P_i(0)P_{i,n}(t+\tau)=\sum_{\nu}\left(\sum_{i=0}^{n_0} P_i(0)P_{i,\nu}(t)\right)P_{\nu,n}(\tau)$$

which is reduced to, according to the theorem of total probability,

$$P_n(t+\tau)=\sum_{\nu} P_\nu(t)P_{\nu,n}(\tau) \qquad (4)$$

where $P_\nu(t)$ denotes the probability of finding $\nu$ reactant molecules at time $t$ in the reaction system. This is the fundamental equation for the application of the stochastic process to the chemical reaction.

If at time $t$ the reaction system is in the state $E_n$, the probability that any one of $n$ reactant molecules will undergo a reaction during the infinitely small time interval of length $(t, t+\tau)$ is equal to $P_{n,n-1}(\tau)=k_1 n\tau+o(\tau)$, where $k_1$ is a constant and $o(\tau)$ denotes the probability that more than one reaction occurs is of smaller order of magnitude than $\tau$. Similarly the transition probability $P_{n+1,n}(\tau)$ from the state $E_{n+1}$ to the adjacent state $E_n$ is equal to $k_1(n+1)\tau+o(\tau)$, and the probability of staying in the state $E_n$ is given by $P_{n,n}(\tau)=1-P_{n,n-1}(\tau)=1-(k_1 n\tau+o(\tau))$. Rewriting $P_\nu(t)$ in the alternative form $P(\nu, t)$, we have, according to Eq. 4,

$$\begin{aligned}P(n, t+\tau)&=P(n+1, t)P_{n+1,n}(\tau)+P(n, t)P_{n,n}(\tau)\\&=k_1(n+1)\tau P(n+1, t)\\&\quad+(1-k_1 n\tau)P(n, t)+o(\tau)\end{aligned}$$

From this we obtain

$$\begin{aligned}\frac{P(n, t+\tau)-P(n, t)}{\tau}&=-k_1 nP(n, t)\\&\quad+k_1(n+1)P(n+1, t)+o(1)\end{aligned}$$

Thus if we let $\tau\to 0$ for fixed $t$, we have

$$\frac{\mathrm{d}}{\mathrm{d}t}P(n, t)=-k_1 nP(n, t)+k_1(n+1)P(n+1, t) \qquad (5)$$

In particular, by assuming $P(n+1, t)=0$ for $n=n_0$, we obtain $\frac{\mathrm{d}}{\mathrm{d}t}P(n_0, t)=-k_1 n_0 P(n_0, t)$ in place of Eq. 5, and for $n=0$, Eq. 5 is reduced to $\frac{\mathrm{d}}{\mathrm{d}t}P(0, t)=k_1 P(1, t)$. Hence Eq. 5 holds for all values of $n$. Solving Eq. 5 under the conditions (3), we obtain the binomial distribution

$$P(n, t)=\binom{n_0}{n}\{\exp(-k_1 t)\}^n\{1-\exp(-k_1 t)\}^{n_0-n} \qquad (6)$$

whose derivation will be shown later. Of course, the equation $\sum_{n=0}^{n_0} P(n, t)=1$ holds certainly.

In order to reduce Eq. 5 to the equation of the mean value for the number of reactant molecules, if we multiply both sides of Eq. 5 by $n$ and summing over all values of $n$, we get

$$\begin{aligned}\frac{\mathrm{d}}{\mathrm{d}t}\sum_{n=0}^{n_0} nP(n, t)&=-k_1\sum_{n=0}^{n_0} n^2P(n, t)\\&\quad+k_1\sum_{n=0}^{n_0} n(n-1)P(n, t)\end{aligned}$$

that is,

$$\frac{\mathrm{d}\langle n\rangle}{\mathrm{d}t}=-k_1\langle n\rangle \qquad (7)$$

where $\sum_{n=0}^{n_0} nP(n, t)=\langle n\rangle$ denotes the mean value for the number of reactant molecules at time $t$. This equation is consistent "in the mean" with the deterministic rate equation $\frac{\mathrm{d}n}{\mathrm{d}t}=-k_1 n$, excepting the chance fluctuations* which arise inherently in the reaction itself and are not associated with random experimental errors.

We have so far discussed the stochastic model for such a true unimolecular reaction as the rate constant $k_1$ is invariable with time, but we can easily extend this to the more general cases in which the rate constants are variable with time. Using in place of $k_1$ the "instantaneous" value $k(t)$ of the rate constant which is able to take different values at different points on the time axis, we have, instaed of Eq. 5,

$$\begin{aligned}\frac{\mathrm{d}}{\mathrm{d}t}P(n, t)&=-k(t)nP(n, t)\\&\quad+k(t)(n+1)P(n+1, t) \qquad (8)^*\end{aligned}$$

In order to solve this equation, we introduce the generating function $\varphi(t, x)=\sum_{n=0}^{n_0} x^n P(n, t)$, which is convergent for $|x|\leq 1$ and defined so that the coefficient of $x^n$ is the probability of finding $n$ reactant molecules at time $t$ in the reaction system. Multiplying both sides of Eq. 8 by $x^n$ and summing from $n=0$ to $n=n_0$, we have

$$\begin{aligned}\frac{\mathrm{d}}{\mathrm{d}t}\sum_{n=0}^{n_0} x^n P(n, t)&=-k(t)\sum_{n=0}^{n_0} nx^n P(n, t)\\&\quad+k(t)\sum_{n=0}^{n_0} nx^{n-1}P(n, t)\end{aligned}$$

Substituting $\frac{\partial\varphi}{\partial t}=\frac{\mathrm{d}}{\mathrm{d}t}\sum_{n=0}^{n_0} x^n P(n, t)$ and $x\frac{\partial\varphi}{\partial x}=\sum_{n=0}^{n_0} nx^n P(n, t)$ into this equation, we obtain the first-order partial differential equation

* cf. Eq. 22.

** This equation refers to non-stationary process with $k(t)$ depending on time. Since, however, Eq. 5 has the purely "localized" property, the method by which we have derived Eq. (5) is completely applicable to such Markov processes as are not temporally homogeneous.

$$\frac{\partial\varphi}{\partial t}=k(t)(1-x)\frac{\partial\varphi}{\partial x} \tag{9}$$

The auxiliary differential equation of Eq. 9 is given by

$$\frac{dx}{k(t)(1-x)}=\frac{\mathrm{d}t}{-1}$$

Solving this, we obtain

$$(1-x)\exp\left(-\int_0^t k(t)\mathrm{d}t\right)=\text{constant}$$

According to the theory of partial differential equation the general solution of Eq. 9 is then given by

$$\varphi(t,x)=f\left((1-x)\exp\left(-\int_0^t k(t)\mathrm{d}t\right)\right) \tag{10}$$

where $f$ is an arbitrary function which is to be determined by the initial condition; the function $f$ is led to the form $f(1-x)=x^{n_0}$ by $\varphi(0,x)=f(1-x)$ and $\varphi(0,x)=\sum_{n=0}^{n_0}x^nP(n,0)=x^{n_0}$, where the initial condition (3) has been used. If we replace $1-x$ by $\xi$, we obtain the relation $f(\xi)=(1-\xi)^{n_0}$. Again, replacing $\xi$ by $(1-x)\exp\left(-\int_0^t k(t)\mathrm{d}t\right)$, we can transform Eq. 10 into the form

$$\varphi(t,x)=\left\{\left(1-\exp\left(-\int_0^t k(t)\mathrm{d}t\right)\right)+x\exp\left(-\int_0^t k(t)\mathrm{d}t\right)\right\}^{n_0} \tag{11}$$

which satisfies the condition $\varphi(t,1)=1$, i. e., $\sum_{n=0}^{n_0}P(n,t)=1$. Hence expanding the r. h. s. of Eq. (11), we obtain the binomial distribution by the definition of the generating function,

$$P(n,t)=\binom{n_0}{n}\left(\exp\left(-\int_0^t k(t)\mathrm{d}t\right)\right)^n\times\left(1-\exp\left(-\int_0^t k(t)\mathrm{d}t\right)\right)^{n_0-n} \tag{12}$$

Since the mean value for the number of reactant molecules at time $t$ is given by $\langle n\rangle=\left(x\frac{\partial\varphi}{\partial x}\right)_{x=1}$, we can easily find

$$\langle n\rangle=n_0\exp\left(-\int_0^t k(t)\mathrm{d}t\right) \tag{13}$$

If $k(t)$ is set equal to $k_1$ invariable with time, the above equation becomes $\langle n\rangle=n_0\exp(-k_1t)$, which agrees with the integral of Eq. 7. Such stochastic processes with the variable parameter $k(t)$ can be applied to such various cases as will be described below.

**Example 1. Bimolecular Reaction.** — The deterministic rate of the bimolecular reaction $2A\rightarrow A_2$ is expressed in the form

$$\frac{\mathrm{d}(2n)}{\mathrm{d}t}=-k_2(2n)^2 \tag{1, 1}$$

where $2n$ denotes the number of reactant molecules at time $t$ and $k_2$ the rate constant. Solving Eq. 1, 1 under the initial condition that $2n=2n_0$ at $t=0$, we obtain

$$2n=\frac{2n_0}{1+k_2(2n_0)t} \tag{1, 2}$$

or if we set $2n=N$, this becomes

$$N=\frac{N_0}{1+k_2N_0t} \tag{1, 3}$$

From Eq. 1, 2 the probability that any one of $n$ reactant molecules undergoes a chemical transformation during the time interval $(t, t+\Delta t)$ is given by

$$\frac{|\Delta n|}{n}=\frac{k_2N_0}{1+k_2N_0t}\Delta t+o(\Delta t) \tag{1, 4}$$

If we set $\frac{k_2N_0}{1+k_2N_0t}=k(t)$, then we have according to Eq. 8

$$\frac{\mathrm{d}}{\mathrm{d}t}P(n,t)=-\frac{k_2N_0}{1+k_2N_0t}nP(n,t)+\frac{k_2N_0}{1+k_2N_0t}(n+1)P(n+1,t) \tag{1, 5}$$

Multiplying both sides of Eq. 1, 5 by $n$ and summing over all values of $n$, we obtain as the differential equation concerning the mean value for the number of reactant molecules

$$\frac{\mathrm{d}\langle n\rangle}{\mathrm{d}t}=-\frac{k_2N_0}{1+k_2N_0t}\langle n\rangle \tag{1, 6}$$

or

$$\frac{\mathrm{d}\langle N\rangle}{\mathrm{d}t}=-\frac{k_2N_0}{1+k_2N_0t}\langle N\rangle \tag{1, 7}$$

whose solution is given by

$$\langle N\rangle=\frac{N_0}{1+k_2N_0t} \tag{1, 8}$$*

---

* In general we have as the stochastic model for the bimolecular reaction $2A\rightarrow A_2$

$$\frac{\mathrm{d}}{dt}P(2n,t)=-k_2\frac{(2n)(2n-1)}{2}P(2n,t)+k_2\frac{\{2(n+1)\}\{2n+1)-1\}}{2}P(2(n+1),t) \tag{1}$$

Transforming this into the differential equation of the mean value, we obtain

$$\frac{\mathrm{d}\langle 2n\rangle}{\mathrm{d}t}=-k_2(\langle(2n)^2\rangle-\langle 2n\rangle) \tag{2}$$

If we set $2n=N$, we have in place of Eq. 2

$$\frac{\mathrm{d}\langle N\rangle}{\mathrm{d}t}=-k_2(\langle N^2\rangle-\langle N\rangle) \tag{2}'$$

Solving this under the initial condition that $N=N_0$ at $t=0$, we obtain

$$\langle N\rangle=\frac{N_0}{1+k_1N_0t+k_2N_0\int_0^t\frac{\sigma^2(t)-\langle N\rangle}{\langle N\rangle^2}\mathrm{d}t} \tag{3}$$

where $N_0$ is the initial number of reactant molecules and $\sigma^2(t)=\langle N^2\rangle-\langle N^2\rangle$ denotes the variance.

for the initial condition that $N=N_0$ at $t=0$. It should be here noted that Eq. 1, 8 agrees "in the mean" with the result derived by the deterministic theory. If we multiply both sides of Eq. 1, 5 by $n^2$ and sum over all values of $n$, we obtain as the differential equation for the second moment $\langle n^2\rangle$

$$\frac{d\langle n^2\rangle}{dt}=-2\frac{k_2N_0}{1+k_2N_0t}\langle n^2\rangle+\frac{k_2N_0}{1+k_2N_0t}\langle n\rangle \tag{1, 9}$$

which is transformed into the form, according to $2n=N$ and Eq. 1, 8,

$$\frac{d\langle N^2\rangle}{dt}+2\frac{k_2N_0}{1+k_2N_0t}\langle N^2\rangle=2k_2\left(\frac{N_0}{1+k_2N_0t}\right)^2 \tag{1, 10}$$

Solving Eq. 1, 10 under the initial condition that $N=N_0$ at $t=0$, we obtain

$$\langle N^2\rangle=\left(\frac{N_0}{1+k_2N_0t}\right)^2+2k_2t\left(\frac{N_0}{1+k_2N_0t}\right)^2 \tag{1, 11}$$

Substituting Eq. 1, 8 into this equation, we have as the variance $\sigma^2(t)=\langle N^2\rangle-\langle N\rangle^2$

$$\sigma^2(t)=2k_2t\langle N\rangle^2 \tag{1, 12}$$

and consequently the coefficient of variation $\delta(t)=\frac{\sigma(t)}{\langle N\rangle}$ is expressed in the form

$$\delta(t)=\sqrt{2k_2t} \tag{1, 13}$$

For sufficiently large values of $t$, the coefficient of variation, which is independent of the initial number of reactant molecules, is considerably large, so that the statistical fluctuation arising inherently in the bimolecular reaction itself may become large compared with the random experimental errors incidental to the observed value $\langle N\rangle$.

**Example 2. Lindemann's Mechanism.** — Let us consider the collision theory for the unimolecular reaction which is usually associated with the name of Lindemann[10].

$$\begin{array}{ccc} A+A & \rightleftarrows & A^*+A \\ & & \downarrow \\ & & B \end{array}$$

The reaction $A+A\rightarrow A^*+A$ is the activation process by the collision between two inert reactant molecules, the reverse reaction $A+A^*\rightarrow A+A$ is the deactivation process by the collision between an inert reactant molecule and an activated molecule and the spontaneous reaction $A^*\rightarrow B$ is the "true" unimolecular reaction. If we denote by $P(n_a, n_a^*, n_b, t)$ the probability that $n_a$ inert reactant molecules, $n_a^*$ activated molecules and $n_b$ resultant molecules coexist in the reaction system at time $t$, then we have

$$\begin{aligned}\frac{d}{dt}P(n_a, n_a^*, n_b, t)&=-k^*(t)n_aP(n_a, n_a^*, n_b, t)\\&\quad+k^*(t)(n_a+1)P(n_a+1, n_a^*-1, n_b, t)\\&\quad-k'(t)n_a^*P(n_a, n_a^*, n_b, t)\\&\quad+k'(t)(n_a^*+1)P(n_a-1, n_a^*+1, n_b, t)\\&\quad-kn_a^*P(n_a, n_a^*, n_b, t)\\&\quad+k(n_a^*+1)P(n_a, n_a^*+1, n_b-1, t)\end{aligned} \tag{2, 1}$$

where $k^*(t)$ and $k'(t)$ denote the instantaneous values of the rate constants for the reactions $A+A\rightarrow A^*+A$ and $A+A^*\rightarrow A+A$ respectively and $k$ the rate constant for the true unimolecular reaction $A^*\rightarrow B$. Thus the differential equations for the mean values $\langle n_a\rangle$ and $\langle n_a^*\rangle$ are given by

$$\frac{d\langle n_a\rangle}{dt}=-k^*(t)\langle n_a\rangle+k'(t)\langle n_a^*\rangle \tag{2, 2}$$

and

$$\frac{d\langle n_a^*\rangle}{dt}=k^*(t)\langle n_a\rangle-(k'(t)+k)\langle n_a^*\rangle \tag{2, 3}$$

respectively, which are consistent "in the mean" with Fowler's equations[11].

## Multitdimensional Stochastic Model

In comparing the probabilistic theory with the deterministic theory, we have so far considered the one-dimensional stochastic process for the "true" unimolecular gas reaction on the macroscopic point of view. Now consider microscopically the multi-dimensional stochastic process for a reaction system, such that at time $t$ the numbers of reactant molecules in the states of internal energies $\varepsilon_1, \varepsilon_2, \cdots\cdots, \varepsilon_i, \cdots\cdots$ are $n_1, n_2, \cdots\cdots, n_i, \cdots\cdots$, respectively, under the same conditions as in the previous section. Then if we denote the probability for this reaction system by $P(n_1, n_2, \cdots\cdots, n_i, \cdots\cdots, t)=P(\{n_i\}, t)$, we have

10) F. A. Lindemann, *Trans. Faraday. Soc.*, 17, 599 (1921).

11) R. H. Fowler, "Statistical Mechanics", Cambridge University Press (1936), p. 712.

* The internal energy $\varepsilon_i$ of reactant molecule changes continually into the enregy $\varepsilon$ with various values by the random energy transfer between molecules. Expressing the distribution of such energy $\varepsilon$ by $F_i(\varepsilon)$, we have as the averaged specific reaction rate $\langle k_1(\varepsilon_i)\rangle$

$$\langle k_1(\varepsilon_i)\rangle=\int_0^\infty k_1(\varepsilon/\varepsilon_i)dF_i(\varepsilon),$$

where we may take such distribution function that $F_i(0)=0$ and $F_i(\infty)=1$, and $k_1(\varepsilon/\varepsilon_i)=0$ if $\varepsilon$ is smaller then the value necessary for a chemical reaction to occur. The $k_1^{(\varepsilon)}$ in Eq. 14 denotes such $\langle k_1(\varepsilon_i)\rangle$.

$$\begin{aligned}
&\frac{d}{dt}P(n_1, n_2, \cdots\cdots, n_i, \cdots\cdots, t)\\
&= -k_1^{(1)}n_1P(n_1, n_2, \cdots\cdots, n_i, \cdots\cdots, t)\\
&\quad +k_1^{(1)}(n_1+1)P(n_1+1, n_2, \cdots\cdots, n_i, \cdots\cdots, t)\\
&\quad -k_1^{(2)}n_2P(n_1, n_2, \cdots\cdots, n_i, \cdots\cdots, t)\\
&\quad +k_1^{(2)}(n_2+1)P(n_1, n_2+1, \cdots\cdots, n_i, \cdots\cdots, t)\\
&\quad \vdots\\
&\quad -k_1^{(i)}n_iP(n_1, n_2, \cdots\cdots, n_i, \cdots\cdots, t)\\
&\quad +k_1^{(i)}(n_i+1)P(n_1, n_2, \cdots\cdots, n_i+1, \cdots\cdots, t)\\
&\quad \vdots
\end{aligned} \tag{14}$$

or

$$\begin{aligned}
\frac{d}{dt}P(\{n_i\}, t) &= -\sum_i k_1^{(i)}n_iP(\{n_j\}_{j\neq i}, n_i, t)\\
&\quad +\sum_i k_1^{(i)}(n_i+1)P(\{n_j\}_{j\neq i}, n_i+1, t)
\end{aligned} \tag{14}'$$

where $P(\{n_j\}_{j\neq i}, n_i+1, t) = P(n_1, n_2, \cdots\cdots, n_{i-1}, n_i+1, n_{i+1}, \cdots\cdots, t)$ and the rate constant $k_1^{(i)}$* which is the function of energy $\varepsilon_i$ denotes the transition probability that a molecule in the internal state with an energy $\varepsilon_i$ is transformed into a resultant molecule during unit time. Let the total number of reactant molecules at time $t$ be $n=\sum_i n_i$ and the initial number of reactant molecules with the internal energy $\varepsilon_i$ be $n_i^0$. If we multiply both sides of Eq. 14 by $\sum n_i$ and sum from 0 to $n_i^0$ $(i=1, 2, \cdots\cdots)$ with respect to each energy state, we obtain

$$\begin{aligned}
\frac{d}{dt}\langle\sum_i n_i\rangle &= -\langle k_1^{(1)}n_1\sum_i n_i\rangle + \langle k_1^{(1)}n_1(\sum_i n_i - 1)\rangle\\
&\quad -\langle k_1^{(2)}n_2\sum_i n_i\rangle + \langle k_1^{(2)}n_2(\sum_i n_i - 1)\rangle\\
&\quad \vdots\\
&\quad -\langle k_1^{(i)}n_i\sum_i n_i\rangle + \langle k_1^{(i)}n_i(\sum_i n_i - 1)\rangle\\
&\quad \vdots\\
&= -\langle\sum_i k_1^{(i)}n_i\rangle
\end{aligned}$$

that is,

$$\frac{d\langle n\rangle}{dt} = -\langle\sum_i k_1^{(i)}n_i\rangle \tag{15}$$

Here if we set

$$\frac{\sum_i k_1^{(i)}n_i}{\sum_i n_i} = \bar{k}_1 \tag{16}$$

Eq. 15 becomes, according to $\sum_i k_1^{(i)}n_i = \bar{k}_1 n$,

$$\frac{d\langle n\rangle}{dt} = -\bar{k}_1\langle n\rangle \tag{17}$$

which formally agrees with Eq. 7. The rate constant $\bar{k}_1$ denotes the "average" probability that one molecule undergoes a chemical transformation during unit time. On comparing Eq. 17 with the conventional rate equation

$$\frac{dn}{dt} = -\bar{k}_1 n, \tag{18}$$

which is statistical only with respect to the rate constant but deterministic with respect to the number of reactant molecules, it should be noticed that the application of the multi-dimensional stochastic model to the "true" unimolecular gas reaction presents us with an excellent method for calculating statistically the rate constant together with the number of reactant molecules.

In order to calculate the variance of the total number of reactant molecules, if we multiply both sides of Eq. 14′ by $(\sum_i n_i)^2$ and sum over all values of each $n_i$ we obtain as the differential equation of the mean value for $(\sum_i n_i)^2$

$$\begin{aligned}
\frac{d}{dt}\langle(\sum_i n_i)^2\rangle &= -2\langle(\sum_i k_1^{(i)}n_i)(\sum_i n_i)\rangle\\
&\quad +\langle\sum_i k_1^{(i)}n_i\rangle
\end{aligned}$$

Using $\sum_i n_i = n$ and $\sum_i k_1^{(i)}n_i = \bar{k}_1 n$, we can transform this to

$$\frac{d\langle n^2\rangle}{dt} = -2\bar{k}_1\langle n^2\rangle + \bar{k}_1\langle n\rangle \tag{19}$$

When we rewrite Eq. 17 by the alternative equation

$$\frac{d\langle n\rangle^2}{dt} = -2\bar{k}_1\langle n\rangle^2 \tag{20}$$

and subtract Eq. 20 from Eq. 19, we obtain, using $\langle n\rangle = n_0\exp(-\bar{k}_1 t)$,

$$\begin{aligned}
&\frac{d}{dt}(\langle n^2\rangle - \langle n\rangle^2) + 2\bar{k}_1(\langle n^2\rangle - \langle n\rangle^2)\\
&\quad = \bar{k}_1 n_0\exp(-\bar{k}_1 t)
\end{aligned} \tag{21}$$

Solving Eq. 21 with respect to the variance $\langle n^2\rangle - \langle n\rangle^2$, we obtain

$$\langle n^2\rangle - \langle n^2\rangle = n_0\exp(-\bar{k}_1 t)\{1-\exp(-\bar{k}_1 t)\} \tag{22}$$

which agrees with the variance in Bartholomay's macroscopic treatment if we use $k_1$ in place of $\bar{k}_1$. We observe, however, that $\bar{k}_1$ is estimated by the method to be shown below.

In the reaction system at thermal equilibrium the equilibrium fraction of reactant molecules in the energy state $\varepsilon_i$ is given by

$$n_i = n\frac{g(\varepsilon_i)\exp(-\varepsilon_i/\boldsymbol{kT})}{\sum_i g(\varepsilon_i)\exp(-\varepsilon_i/\boldsymbol{kT})} \tag{23}$$

where $g(\varepsilon_i)$ denotes the quantum statistical weight for the state of energy $\varepsilon_i$. Substituting Eq. 23 into Eq. 16, we find

$$\bar{k}_1=\frac{\sum_i k_1^{(i)}(\varepsilon_i)g(\varepsilon_i)\exp(-\varepsilon_i/\boldsymbol{kT})}{\sum_i g(\varepsilon_i)\exp(-\varepsilon_i/\boldsymbol{kT})} \tag{24}$$

If we differentiate logarithmically with respect to $T$, we obtain

$$kT^2\frac{\partial \ln \bar{k}_1}{\partial T}=\frac{\sum_i \varepsilon_i k_1^{(i)}(\varepsilon_i)g(\varepsilon_i)\exp(-\varepsilon_i/\boldsymbol{kT})}{\sum_i k_1^{(i)}(\varepsilon_i)g(\varepsilon_i)\exp(-\varepsilon_i/\boldsymbol{kT})}$$
$$-\frac{\sum_i \varepsilon_i g(\varepsilon_i)\exp(-\varepsilon_i/\boldsymbol{kT})}{\sum_i g(\varepsilon_i)\exp(-\varepsilon_i/\boldsymbol{kT})} \tag{25}$$

where the first term on the r. h. s. is the average internal energy, not of the existing energized molecules, but of those which react during unit time and the second term is the average internal energy for all molecules[12]. If all reacting molecules that possess energy exceeding $\varepsilon_0$ have the same probability $\lambda_0$ for the "true" unimolecular reaction during unit time, then we have the following relations;

$$k_1^{(i)}=0 \quad \text{for} \quad \varepsilon_i<\varepsilon_0,$$
$$k_1^{(i)}=\lambda_0 \quad \text{for} \quad \varepsilon_i\geq\varepsilon_0.$$

Eq. 24 is therefore transformed into

$$\bar{k}_1=\frac{\lambda_0\sum_{\varepsilon_i\geq\varepsilon_0} g(\varepsilon_i)\exp(\varepsilon_i/\boldsymbol{kT})}{\sum_i g(\varepsilon_i)\exp(-\varepsilon_i/\boldsymbol{kT})} \tag{26}$$

If we treat the internal vibration of molecule as consisting of linear harmonic oscillators whose energy levels are continuous, we have $g(\varepsilon)\propto\varepsilon^{s-1}\Delta\varepsilon$ within a certain range of $\Delta\varepsilon$ and can approximate the r. h. s. of Eq. 26 by the distribution function of $\Gamma$-type

$$\frac{\lambda_0}{\Gamma(s)}\int_{\varepsilon_0}^{\infty}\left(\frac{\varepsilon}{\boldsymbol{kT}}\right)^{s-1}\exp(-\varepsilon/kT)\frac{d\varepsilon}{\boldsymbol{kT}}$$

where $\Gamma(s)=(s-1)!$. Hence we have in place of Eq. 26

$$\bar{k}_1\simeq\lambda_0\exp(-\xi_0/\boldsymbol{kT})\sum_{r=0}^{s-1}\frac{1}{r!}\left(\frac{\varepsilon_0}{\boldsymbol{kT}}\right)^r \tag{27}$$

where $\varepsilon_0$ denotes the minimum energy required for reaction. But if $\varepsilon_0\gg s\boldsymbol{kT}$, the overall rate constant $\bar{k}_1$ is approximately given by

$$\bar{k}_1\simeq\frac{\lambda_0}{\Gamma(s)}\left(\frac{\varepsilon_0}{\boldsymbol{kT}}\right)^{s-1}\exp(-\varepsilon_0/\boldsymbol{kT}) \tag{27}'$$

And more generally, if we denote the probability for the distribution of higher energy levels than $\varepsilon_0$ by $g(\varepsilon_i-\varepsilon_0)/g(\varepsilon_i)$, $k_1^{(i)}$, the specific reaction rate for molecules of energy $\varepsilon_i\geq\varepsilon_0$, is proportional to this probability. We then have the relations

$$k_1^{(i)}=0 \quad \text{for} \quad \varepsilon_i<\varepsilon_0$$
$$k_1^{(i)}=Ag(\varepsilon_i-\varepsilon_0)/g(\varepsilon_i) \quad \text{for} \quad \varepsilon_i\geq\varepsilon \tag{28}$$

where $A$ is the proportional coefficient and we define $g(\varepsilon_i-\varepsilon_0)=0$ for $\varepsilon_i\leq\varepsilon_0$. Thus substituting Eq. 28 into Eq. 24, we obtain

$$\bar{k}_1=A\exp(-\varepsilon_0/\boldsymbol{kT})$$
$$\times\frac{\sum_{\varepsilon_i\geq\varepsilon_0} g(\varepsilon_i-\varepsilon_0)\exp\{-(\varepsilon_i-\varepsilon_0)\boldsymbol{kT}\}}{\sum_i g(\varepsilon_i)\exp(-\varepsilon_i/\boldsymbol{kT})}$$
$$=A\exp(-\varepsilon_0/\boldsymbol{kT})\frac{\sum_{\varepsilon_i'} g(\varepsilon_i')\exp(-\varepsilon_i'/\boldsymbol{kT})}{\sum_i g(\varepsilon_i)\exp(-\varepsilon_i/\boldsymbol{kT})}$$

where $\varepsilon_i'=\varepsilon_i-\varepsilon_0$. If, however, we use the same model molecule composed of a set of simple harmonic oscillators of equal frequency as in Kassel's theory[13], $\sum_{\varepsilon_i'} g(\varepsilon_i')\exp(-\varepsilon_i'/\boldsymbol{kT})$ is equal to $\sum_i g(\varepsilon_i)\exp(-\varepsilon_i/\boldsymbol{kT})$, and consequently we obtain the Arrhenius' equation

$$\bar{k}_1=A\exp(-\varepsilon_0/\boldsymbol{kT}) \tag{29}$$

And from Eqs. 28 and 29 $k_1^{(i)}$ is given by

$$k_1^{(i)}=\bar{k}_1\exp(-\varepsilon_0/\boldsymbol{kT})\frac{g(\varepsilon_i-\varepsilon_0)}{g(\varepsilon_i)} \tag{30}$$

where $\varepsilon_i\geq\varepsilon_0$.

## Conclusions

We have clarified the probabilistic foundations for the application of the theory of the stochastic process to the "true" unimolecular reaction. By extending Bartholomay's method to the more general stochastic process having the parameter $k(t)$ variable with time, we have shown that the theory of stochastic process can be applied to any chemical reaction other than the unimolecular reaction. We have also noticed that the averaged rate constant $\bar{k}_1$ of the "true" unimolecular reaction is legitimately calculated by the application of the multi-dimensional stochastic process to the chemical reaction.

*Laboratory of Industrial Inorganic Chemistry*
*Tokyo Institute of Technology*
*Meguro-ku, Tokyo*

12) R. H. Fowler and E. A. Guggenheim, Ref. 5, p. 522.

13) L. Kassel, *J. Phys. Chem.*, 32, 225, 1065 (1928).

# *The Functional Groups of Sachaconitine*

By Nobukatsu KATSUI and Gen HASEGAWA

(Received December 25, 1959)

In a previous paper[1] the extended formula of sachaconitine (I) ($C_{23}H_{37}O_4N$), one of the alkaloids of *Aconitium miyabei* Nakai, was given as follows:

$$C_{19}H_{24}\begin{cases}(OH)_2\\(OCH_3)_2\\N\text{-}C_2H_5\end{cases}$$

Experiments for characterizing the functional groups of "compound I" have been carried out, and the results are here comunicated.

Oxidation of "compound I" with potassium permanganate in acetone gave a mixture of (a) a neutral compound (II), m. p. 194~196°C, $[\alpha]_D$ −37.8 (EtOH) (Found: C, 67.92; H, 8.71; N, 3.51. Calcd. for $C_{23}H_{35}O_5N$: C, 68.12; H, 8.70; N, 3.45%), and (b) a basic compound (III), m. p. 230~231°C, $[\alpha]_D$ +17.1° (EtOH), p$K_a$ 9.8, $\nu_{max}$ 3545, 3447 $cm^{-1}$ (OH), 3230 $cm^{-1}$ (NH) (Found: C, 69.30; H, 8.97; N, 4.04. Calcd. for $C_{21}H_{33}O_4N$: C, 69.39; H, 9.15; N, 3.85%).

"Compound II" was characterized as the lactam, oxosachaconitine, by its infrared spectrum, $\nu_{max}$ 3537, 3447 $cm^{-1}$ (OH), 1635 $cm^{-1}$ (lactam), and by treatment with lithium aluminum hydride, which converted it into "compound I".

"Base III" was shown to be *N*-desethylsachaconitine by treatment with ethyl iodide, which also reverted to "compound I", thus firmly establishing the presence of an *N*-ethyl group in the alkaloid. Treatment of "compound II" with acetylchloride gave diacetyloxosachaconitine, m. p. 149~151°C, $\nu_{max}$ 1725 $cm^{-1}$ (ester carbonyl), 1625 $cm^{-1}$ (lactam) (Found: C, 64.15; H, 8.00; N, 3.01. Calcd. for $C_{27}H_{39}O_7N$: C, 64.49; H, 8.44; N, 3.01%). On the same treatment, "compound III" gave a neutral product in very poor yield, which could not be purified. Hence "compound III" was treated with acetic anhydride in pyridine at room temperature, and then a neutral product, m. p. 175~176°C, was yielded. In the infrared spectrum this product showed an amide band at 1635 $cm^{-1}$, hydroxyl bands at 3487 and 3331 $cm^{-1}$, but no ester carbonyl band. With the same reagent "compound I" or "II" were recovered without change, and thus it was suggested that the hydroxyls of the alkaloid resisted acetylation with acetic anhydride at room temperature. Oxidation of "compound I" with chromic acid—pyridine complex or with potassium permanganate in acetone-acetic acid produced again two products: one was a neutral compound (IV), m. p. 237~239°C, $[\alpha]_D$ +35.7° (EtOH), $\lambda_{max}$ 290 m$\mu$ ($\varepsilon$ 40) (Found: C, 68.46; H, 8.25; N, 3.62. Calcd. for $C_{23}H_{35}O_5N$: C, 68.46; H, 8.24; N, 3.47%), the second was a base (V), m. p. 275~277°C, $[\alpha]_D$ +107° (EtOH), p$K_a$ 8.3 (Found: C, 70.35; H, 8.00; N, 4.04. Calcd. for $C_{21}H_{29}O_4N$: C, 70.17; N, 8.13; N, 3.90%). "Compound IV", also obtainable from "compound II" by oxidation with chromic acid in acetone, showed a hydroxyl band at 3470 $cm^{-1}$ a lactam band at 1619 $cm^{-1}$ and a five-membered carbonyl band at 1745 $cm^{-1}$ in infrared. Reduction of "compound IV" with sodium borohydride produced "compound II", and with lithium aluminium hydride gave back "compound I". Thus "compound IV" is a keto-lactam, oxosachaconitinone, and also it is indicated, that one of the two hydroxyls in "compound I" or "II" is a secondary one in a five-membered ring.

"Base V" showed a band at 1741 $cm^{-1}$ due to the five-membered ketone carbonyl, a band at 3300 $cm^{-1}$ and no double bond band in infrared, and in ultraviolet spectrum this base contained two maxima at 290 m$\mu$ ($\varepsilon$ 70) and 250m$\mu$ ($\varepsilon$ 210) due to ketone carbonyl respectively. Confirmation of base V as a *N*-desethyl base was supported by the facts that the base gave "compound III" on reduction with sodium borohydride and was obtained also from "compound III" by oxidation with chromic acid in acetone; accordingly the above noted band at 3300 $cm^{-1}$ may be due to N–H group. Thus the results of ultraviolet and infrared absorptions give the assumption, that in "base V" two hydroxyls of "compound III" were oxidized to diketo groups both being five-membered cyclic ketones without more free hydroxyl present.

This consideration was further tested by treatment of "base V" with acetic anhydride in pyridine at room temperature, which as above mentioned, is not capable of acetylating the hydroxyls of the alkaloid. The neutral product obtained, m. p. 222~224°C, showed

1) H. Suginome, N. Katsui and G. Hasegawa, This Bulletin 32, 604 (1959).

a band at 1755 $cm^{-1}$ (carbonyl) and 1616 $cm^{-1}$ (amide), but no hydroxyl band in infrared. On the other hand, one maximum(290 m$\mu$, $\varepsilon$ 70) in ultraviolet of "base V" is normal and may be caused by the same carbonyl as that of "compound IV", but the second (250 m$\mu$, $\varepsilon$ 210) is abnormal. The same abnormality in ultraviolet has been already shown in dehydrodelpheline[2] (250 m$\mu$, $\varepsilon$ 200), obtainable by oxidation of the delphinium alkaloid, delpheline, having the same skeletal formula ($C_{21}H_{33}N$) as sachaconitine.

Furthermore the decrease of p$K_a$ in the conversion from "compound I" (p$K_a$ 9.7) or "compound III" (p$K_a$ 9.8) to "compound V" (p$K_a$ 8.3) has been also observed analogously in the change of parent alkaloid to a dehydroderivative. Then it may be assumed, that in "compound V" a carbonyl is present at the analogous position with dehydrodelpheline. Thus "compound V" is assigned the name, *N*-desethyldehydrosachaconitinone; the environment of the ring containing nitrogen in "compound I" is considered to resemble that of delcosine[3], one of the delphinum alkaloids, because the *N*-ethyl group of the former is more readily oxidized as well as the latter to a *N*-desethyl derivative than the other delphinum or aconitum alkaloids.

But it may be more plausible to assume, that the position of a carbonyl in "compound V" is not the same with didehydrodelcosine[4] but with dehydrodelpheline[5], since the carbonyl is a five-membered ring ketone.

Investigation concerning the methoxyl functions of the alkaloid is in progress and will be reported later.

The authors are grateful to Professor Harusada Suginome, President of Hokkaido University, for his exceedingly kind direction throughout this work.

*Department of Chemistry*
*Faculty of Science*
*Hokkaido University*
*Sapporo*

2) R. C. Cookson and M. E. Trevett, *Chem. and Ind.*, 1324 (1954), *J. Chem. Soc.*, **1956**, 2689.
3) R. Anet, D. W. Clayton and L. Marion, *Can. J. Chem.*, **35**, 397 (1957).
4) V. Skaric and L. Marion, *J. Am. Chem. Soc.*, **80**, 4434 (1958).
5) R. C. Cookson and M. E. Trevett, *J. Chem. Soc.*, **1956**, 3121.

# *Inorganic Extraction Studies on the System between Bis(2-ethyl hexyl)-orthophosphoric Acid and Hydrochloric Acid (I)*

By Kan KIMURA

(Received January 26, 1960)

During the last decade, alkyl esters of orthophosphoric acid as liquid-liquid solvent extraction reagents have been investigated widely for both chemical and chemical engineering purposes. A number of review articles on this subject[1,2] have been published. Among the esters, tributyl phosphate is beneficially used in several processes of the recovery of uranium and plutonium as well as in many other chemical separation techniques.

Bis(2-ethyl hexyl)-orthophosphoric acid, commonly abbreviated as HDEHP or D2EHPA, has been employed as a liquid-liquid extraction reagent primarily for uranium by Blake et al.[3] at Oak Ridge National Laboratory, and furthermore by Peppard et al. for berkelium-(IV)[4] and lanthanides[5]. Some physicochemical studies have also been performed by Peppard[6,7], Baes and others[8]. Recently, some metal complexes of this reagent were prepared by Peppard and Ferraro[9] and their infrared spectra were also surveyed.

However, no comprehensive study on the

1) C. A. Blake, Jr., C. F. Baes, Jr., K. B. Brown, C. F. Coleman and J. C. White, "Proceeding of the Second International Conference on the Peaceful Uses of Atomic Energy", A/Conf. 15/P/1550 (1958).

2) G. H. Morrison and H. Freiser, "Solvent Extraction in Analytical Chemistry", John Wiley & Sons. Inc., New York (1957), p. 146.

3) C. A. Blake, D. J. Crouse, C. E. Coleman, K. B. Brown and A. D. Klemers, USAEC ORNL-2172 (1956).

4) D. F. Peppard, S. W. Moline and G. W. Mason, *J. Inorg. Nucl. Chem.*, **4**, 344 (1957).

5) D. F. Peppard, G. W. Mason and S. W. Moline, ibid., **5**, 141 (1957).

6) D. F. Peppard, G. W. Mason, W. J. Driscoll and R. J. Sironen, ibid., **7**, 276 (1958).

7) D. F. Peppard, G. W. Mason, J. L. Maier and W. J. Driscoll, ibid., **4**, 334 (1957).

8) C. F. Baes, Jr., R. A. Zingaro and C. F. Coleman, *J. Phys. Chem.*, **62**, 129 (1958).

9) D. F. Peppard and J. R. Ferraro, *J. Inorg. Nucl. Chem.*, **10**, 275 (1959).

extraction from a given mineral acid solution has been reported. In the present paper, the influence of acid concentration is presented and discussed when the extraction is carried out from hydrochloric acid solution containing each of about fifty elements.

## Experimental

**Solvent.**—The bis(2-ethyl hexyl)-orthophosphoric acid received from Virginia Chemicals, Co. was purified according to the method of Peppard[7,10]. All treatments were manually performed using two separatory funnels. The purity of the solvent was checked by the determination of the distribution ratio, $K_d$, for lanthanum and iron[1,6]. The work reported here was carried out using HDEHP diluted to 50 volume percent with toluene of chemically pure grade.

**Determination of Distribution Ratios.** — The distribution ratio, $K_d$, of a given nuclide (or nuclides), defined as the concentration of nuclide in the organic layer divided by that in the aqueous layer, was determined radiometrically. In the determination, a portion of an aqueous acid solution of a given concentration containing the radioactive tracer was shaken with a portion of the solvent which had been previously equilibrated with the corresponding barren aqueous acid.

Details of the method of the determination were as follows. Two millilitres each of aqueous acid and pre-equilibrated HDEHP were placed in a 5 ml. glass-stoppered measuring-cylinder, and shaken vigorously. After the two layers were transferred together into a centrifuge tube, the content was centrifuged at 4000 rpm for 1 min. Nearly all of the aqueous layer was transferred with a transfer pipette to a new centrifuge tube. Both tubes were centrifuged for 1 min. again. Aliquots of each layer were taken into two glass-stoppered tubes for the radioassay. The quantity of the aliquots taken was usually 1 ml.

In several cases, a portion of the organic extract obtained was transferred to a new 5-ml. cylinder, shaken with an equal volume of fresh aqueous acid, and treated again as mentioned above. Further scrubbings were made in a few cases. By these scrubbings and the following redetermination of $K_d$ values, difficulties caused by the undesired metal hydrates were obviated.

The greater part of the data was obtained by $\gamma$-ray scintillation counting. The counter was a Philips Model PW 4022-52-32 counting unit and the scintillator was a well-type Na(Tl)I crystal "7F8" made by Harshow Chemicals Co. In cases of $\beta$- and $\alpha$-ray emitters aliquot portions from both layers were carefully dried up on small stainless steel or platinum disks, under an infrared lamp or in an induction furnace avoiding any loss of activity and dissolution of stainless steel in hydrochloric acid. $\beta$-Counting was performed with a G-M counter having a mica window of 2.1 mg./cm$^2$ thick made by Rikagaku Kenkyujo, and $\alpha$-rays with a proportional counter of Nuclear Measurement Corp. or with an $\alpha$-ray scintillation counter of Nihon-Musen Irigaku Kenkyujo.

**Remarks on the Determination.**—Almost all data in this experiment were obtained after shaking the two layers for two minutes. According to Peppard and his co-workers[7], the equilibrium of extraction of $^{147}$Pm was attainable in a mixing period of less than 30 sec. Thus the equilibrium might be attained within two minutes for almost all elements. The $K_d$ values for magnesium, aluminum, titanium, vanadium and silver were obtained by one minute shaking, because their half-lives are short.

The range of acidity of the aqueous hydrochloric acid solution covered mainly from 0.01 to 2 N. In some cases, it was extended to 12 N. The acidity was determined volumetrically, when necessary. Although the amount of the elements in the initial 2 ml. of the hydrochloric acid solutions was made as small as possible, it varied from tracer amount to about 1 mg. Details are shown in Table I. In all cases, the specific activity was higher than $10^4$ cpm/mg. under a given condition of measurement.

All experiments were carried out at $21\pm3$°C. Within this range, the variations in $K_d$ values have been shown to be within experimental error.

**Radioisotopes Used.** — The radioactive isotopes used in this experiment were mainly prepared by irradiation of high purity targets in a water-boiler type reactor (Japan Research Reactor I, (neutron flux: $5\times10^{11}$ n/sec. cm$^2$), whereas some of the isotopes were imported from Oak Ridge National Laboratory, U.S.A. or Radiochemical Centre, U.K.

The radiochemical purity of the isotopes was checked by their half-lives, $\gamma$-ray spectra, and/or $\beta$-ray absorption curves with aluminum foils. The $\gamma$-ray spectrograms were obtained with an RCL 256 channel $\gamma$-ray spectrometer or a single channel spectrometer made by Tokyo Shibaura Denki Co.

Table I[14-21] shows the radio-isotopes used[11], together with their half-lives and mass numbers, the target materials or sources, the method of checking the radiochemical purity, and the weight of the materials added in the initial 2 ml. of hydrochloric acid solutions.

Usually the irradiated targets were dissolved in hydrochloric acid and used without further treatment. For example, lanthanum oxide, magnesium

10) D. C. Stewart and H. W. Crandall, *J. Am. Chem. Soc.*, 73, 1377 (1951).

11) K. Kimura, "Hoshasen Data Book", Chijin Shokan, Tokyo (1958), p. 92.

12) N. Shibata and K. Yoshihara, This Bulletin, 32, 422 (1959).

13) H. Ebihara and K. Yoshihara, ibid., in press.

14) K. A. Kraus and F. Nelson," Proceeding of the International Conference on the Peaceful Uses of Atomic Energy", Geneva, A/Conf. 8/p/837 (1955); Vol. VII, United Nations Publication, New York (1956), p. 118.

15) Green and Kafalas, *J. Chem. Phys.*, 22, 760 (1954).

16) T. Ishimori, E. Nakamura and K. Watanabe, This Bulletin, in press.

17) T. Nakai and S. Yajima, *J. Chem. Soc. Japan, Pure Chem. Sec. (Nippon Kagaku Zasshi)*, 79, 1267 (1958).

18) T. Ishimori, H. Umezawa and K. Watanabe, *J. Atomic Energy Soc. Japan*, 1, 299 (1959).

19) S. Yajima, This Bulletin, 31, 699 (1958).

20) K. A. Kraus and G. E. Moore, *J. Chem. Soc.*, 72, 4293 (1950).

21) C. J. Rodden, editor in chief, "Analytical Chemistry of the Manhattan Project", McGraw Hill, New York (1950), p. 83.

TABLE I. RADIOISOTOPES USED

| Nuclide | Target material or source | Radiochemical purity was checked by | Weight | Remarks |
|---|---|---|---|---|
| 15.0 hr. Na-24 | $NaNO_3$, G. R. | $\gamma$-spec., $\gamma$-decay | 100 $\gamma$ | |
| 9.45 min. Mg-27 | Mg metal, 99.99% | $\gamma$-decay | 250 $\gamma$ | |
| 2.27 min. Al-28 | Al metal, 99.99% | $\gamma$-decay, $\gamma$-spec. | 250 $\gamma$ | |
| 37.3 min. Cl-38 | $NH_4Cl$, G. R. | $\gamma$-decay | 250 $\gamma$ | |
| 12.51 hr. K-42 | $KNO_3$, G. R. | $\gamma$-spec., $\gamma$-decay | 100 $\gamma$ | |
| 164 d. Ca-45 | imported | | 60 $\gamma$ | $CaCl_2$ in HCl soln. |
| 85 d. Sc-46 | imported | | 60 $\gamma$ | $ScOl_3$ in HCl soln. |
| 5.80 min. Ti | Ti-hydroxide | $\gamma$-decay | 250 $\gamma$ | |
| 3.76 min. V-52 | $NH_4VO_3$, G. R. | $\gamma$-decay | 5 $\gamma$ | |
| 27.8 d. Cr-51 | Cr-dye, R. I. | | ~tracer | |
| 2.58 hr. Mn-58 | $MnO_2$, G. R. | $\gamma$-decay | 250 $\gamma$ | |
| 3.0 y. Fe-55<br>45.1 d. Fe-59 | imported | | 10 $\gamma$ | $FeCl_3$ in HCl soln. |
| 5.2 y. Co-60 | imported | | | $CoCl_2$ in HCl soln. |
| 2.56 hr. Ni-65 | Ni metal | $\gamma$-decay | 0.5 mg. | Co-58 was removed by ion exchange[14]. |
| 12.8 hr. Cu-64 | Cu metal, 99.9% | $\gamma$-decay | 100 $\gamma$ | |
| 245 d. Zn-65 | imported | | 5 $\gamma$ | $ZnCl_2$ in HCl soln. |
| 14.2 hr. Ga-72 | $Ga_2O_3$, J. M. | $\gamma$-spec., $\gamma$-decay | 100 $\gamma$ | |
| 11.4 d. Ge-71 | Ge metal, 99.9% | $\gamma$-decay | 500 $\gamma$ | Separated from As-77 by benzene extraction[15]. |
| 26.5 hr. As-76 | $As_2O_3$, G. R. | $\gamma$-decay | 500 $\gamma$ | |
| 127 d. Se-75 | Se metal, G. R. | $\gamma$-decay, $\gamma$-spec. | 300 $\gamma$ | |
| 4.5 hr. Br-80 m<br>35.9 hr. Br-82 | $NH_4Br$, G. R. | $\gamma$-decay | 250 $\gamma$ | |
| 19 d. Rb-86. | RbCl, G. R. | $\gamma$-decay | 1 mg. | Cooled for five hours. |
| 28 y. Sr-90 | imported | | tracer | $SrCl_2$ in HCl soln. |
| 64 hr. Y-90 | imported Sr-90 | $\beta$-abs., $\beta$-decay | tracer | |
| 65 d. Zr-95 | imported | | tracer | Oxalate, $\beta$-activity of Nb-95 was eliminated with a 17.6 mg./cm$^2$ Al absorber. |
| 17.0 hr. Zr-97 | $UO_2$-Oxalic acid | $\gamma$-spec. | tracer | Separated by method 17) and 18). Counted at 0.65~0.8 MeV. |
| 35 d. Nb-95 | imported Zr-95 | $\beta$-decay, $\beta$-abs. | | Oxalate; separated by Yajima's method[19]. |
| 67 hr. Mo-99 | $(NH_4)MoO_4$, G. R. | $\gamma$-spec., $\beta$-decay | | |
| $2.12\times10^5$ y. Tc-99 | imported | | tracer | Sodium pertechnetate in KOH soln. |
| 1.0 y. Ru-106 | imported | | | $RuCl_3$ in HCl soln. |
| 17 d. Pd-103<br>13.6 d. Pd-109 | Pd metal, J. M. | $\gamma$-decay | 250 $\gamma$ | |
| 2.3 min. Ag-108 | Ag metal, 99.9% | $\gamma$-decay | 50 $\gamma$ | |
| 53 hr. Cd-115<br>43 d. Cd-115 m | Cd metal, J. M. | $\gamma$-spec. | 210 $\gamma$ | |
| 54.0 min. In-116 m | $In(OH)_3$, R. I. | $\gamma$-spec, $\beta$-decay | 100 $\gamma$ | |
| 112 d. Sn-113 | Sn metal, 99.997% | $\gamma$-spec. | 750 $\gamma$ | |
| 2.75 d. Sb-122 | Sb metal, 99.99% | $\gamma$-decay | 750 $\gamma$ | |
| 33.5 d. Te-129 m, etc. | Te metal, G. R. | | 1 mg. | |
| 8.06 d. I-131 | imported | | tracer | |
| 30 y. Cs-137 | imported | | tracer | CsCl in HCl soln. |
| 85 min. Ba-139 | $BaCO_3$, J. M. | $\gamma$-decay | 50 $\gamma$ | |
| 40.2 hr. La-140 | $La_2O_3$, J. M. | $\gamma$-decay | 100 $\gamma$ | |
| 46 d. Hf-181 | imported | | ~tracer | $HfOCl_2$ in HCl soln. |
| 111 d. Ta-182 | imported | | | Potassium tantalate in KOH soln. |

TABLE I (Continued)

| | | | | |
|---|---|---|---|---|
| 23.9 hr. W-187 | W oxinate, R.I. | $\gamma$-decay | ~tracer | |
| 3.87 d. Re-186<br>17 hr. Re-188 | Re metal, J.M. | $\gamma$-decay | 500 $\gamma$ | |
| 15 d. Os-191<br>31 hr. Os-193 | Os metal, J.M.<br>or imported Os-191 | $\gamma$-decay | 250 $\gamma$ | $Na_2CO_3$-$NaNO_3$ fusion<br>Osmate in NaOH soln. |
| 74.4 d. Ir-192<br>19 hr. Ir-194 | Ir metal, J.M. | $\gamma$-decay | 50 $\gamma$ | $Na_2O_2$ fusion. |
| 4.5 d. Pt-193<br>18 hr. Pt-197 | Pt metal, 99.9% | $\beta$, $\gamma$-decay | 50 $\gamma$ | |
| 2.69 d. Au-198 | Au metal, 99.9% | $\gamma$-decay | 10 $\gamma$ | |
| 48 d. Hg-203 | imported | | 5 $\gamma$ | $Hg(NO_3)_2$ in $HNO_3$ soln. |
| 4.0 y. Tl-204 | imported | | tracer | |
| 3.64 d. Ra-224 | imported Th-228 | $\alpha$-decay | tracer | Separated by TBP extraction[16]. |
| 24.1 d. Th-234 | uranyl chloride | $\gamma$-spec. $\gamma$-decay | tracer | Separated by TBP extraction[16]. |
| 27.4 d. Pa-233 | $ThO_2$ | $\gamma$-spec. $\gamma$-decay | tracer | Separated by ion exchange[20]. |

G.R.: Guaranteed reagent.
J.M.: "Spec-pure" standard source produced by Johnson-Matthey Chemicals Co.
R.I.: High purity target produced by the Radioisototope Production Group, JAERI.

metal, sodium nitrate and barium carbonate were simply dissolved in hydrochloric acid after irradiation. Some of the irradiated targets were dissolved in nitric acid, aqua regia or sodium hydroxide solution and converted into hydrochloric acid solution. For example, rhenium and silver were primarily dissolved in nitric acid, platinum and gold in aqua regia, and arsenous oxide was dissolved in sodium hydroxide solution.

It is likely that the $K_d$ values for arsenic were not largely affected by sodium chloride resulting from sodium hydroxide, for only one drop of tracer solution was added into 2 ml. of the aqueous phase.

Chromium and tungsten tracers were prepared by Yoshihara and Ebihara[12,13], Radioisotope Production Group, Japan Atomic Energy Research Institute. Both were of a high specific activity. On the other hand, most of the imported tracers were used as received.

Some special precautions taken both for the preparation of tracers and for the measurement of distribution ratios are given below in detail:

*Vanadium.*—Irradiated ammonium metavanadate was dissolved in hot 5 N hydrochloric acid and used without any further treatment. Hence, the chemical form of the vanadium tracer was not clearly known. It might have remained in the V(V) state. *Selenium.*—Irradiated selenium was dissolved in nitric acid containing bromine water, and then converted into a hydrochloric acid solution. The resultant solution was used without heating, as selenic tracer, whereas selenous tracer was obtained by heating the solution in 3 N hydrochloric acid. *Molybdenum.*—Irradiated ammonium molybdate showed a pale purple tint, and the hydrochloric acid solution colored blue-green. It was likely that this color came from a certain reduced chemical form. However, the solution was used without any further treatment, e.g., oxidation. *Antimony.*—Irradiated antimony was dissolved in hydrochloric acid containing a small volume of nitric acid. In an acid range below 2 N, obvious hydrolysis occurred. As the $K_d$ values for 3 N acid is fairly high, being as high as 0.2, the HDEHP solution of antimony that had been prepared by extracting antimony(III) from 3 N hydrochloric acid solution was used as the organic phase. *Tantalum.*—Tantalum-182 solution was acidified with hydrochloric acid, and hydrated tantalum precipitate was centrifuged off. The supernatant solution was used as the tracer solution. *Iridium.*—Fusion with sodium peroxide was more rapid and complete than sodium nitrate-carbonate fusion. *Mercury.*—A dilute nitric acid solution of imported mercury tracer was dropped into hydrochloric acid of known concentration, and used without any further treatment. Both phases were clear after the contact. *Thallium.*—Thallic chloride solution was prepared by oxidation of Tl(I) solution with ceric ammonium nitrate or potassium bromate. *Uranium.*—$K_d$ values for uranium were obtained photometrically[21].

## Results and Discussion

The results are summarized in Fig. 1 as a series of graphs of $\log K_d$ vs. $\log N$, where $K_d$ is the distribution ratio and $N$ the acidity in normality. Fig. 1 was compiled from some published and unpublished results. Data for lead, bismuth and americium were taken from the observation of Ishimori[22]. Data for neptunium were taken from the work of Nakamura[23].

Peppard and his coworkers reported that the $K_d$ values for selected lanthanide and actinide cations (III) in the system of HDEHP—perchloric acid are inverse third power dependent on the hydrogen ion concentration in the aqueous phase (0.15 M HDEHP—toluene solution) and direct third power dependent on

22) T. Ishimori, unpublished.
23) E. Nakamura, unpublished.

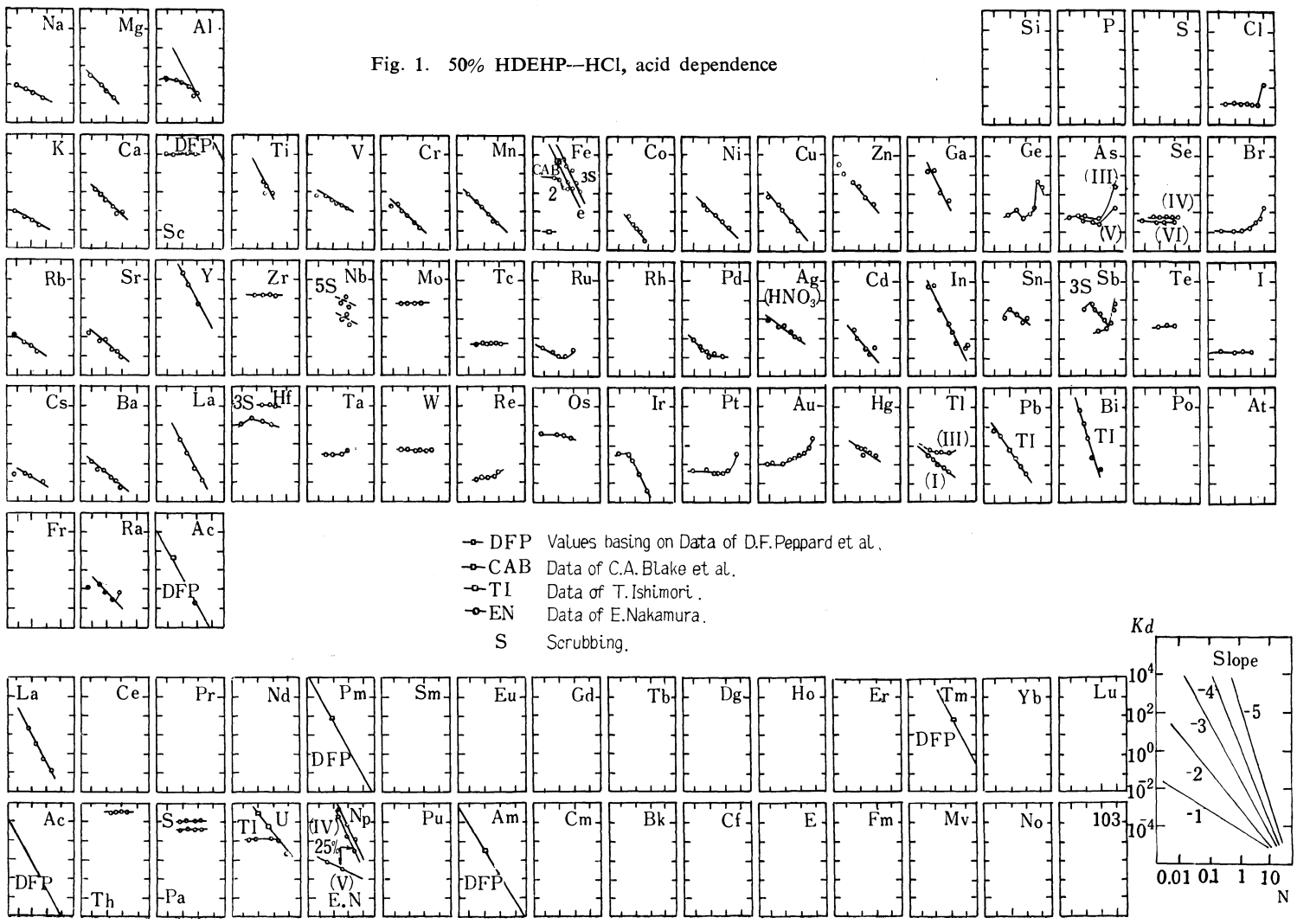



Fig. 1. 50% HDEHP–HCl, acid dependence

the solvent concentration. The results for yttrium and lanthanum of the present author agree with those of Peppard in $K_d$ values. Therefore, $K_d$ values for thulium, promethium, actinium and americium were taken from their data corrected for 50% HDEHP (1.5 M) assuming that the solvent dependence remains unchanged at this high concentration.

According to Peppard and his coworkers[6,9] and Baes et al.[8], the $K_d$ values for scandium, thorium and uranium for diluted HDEHP solution are inverse third, fourth and second power dependent on the hydrogen ion concentration in the aqueous phase, respectively. However, the concentration of HDEHP is so high in this experiment that the $K_d$ values for these elements show almost horizontal curves. It is caused by the limitation of the method of determination. The fact that the horizontal $K_d$ curve for uranium is lower than those for thorium and scandium is mainly brought about by the difference in the method of $K_d$ determinations. The same can be said for protactinium, zirconium and hafnium, whereas the fourth power acid dependence of $K_d$ values is obtained for titanium. Ishimori's data for uranium in the system of 0.75 M HDEHP solution and hydrochloric acid solution are also added after correction for the concentration of HDEHP. The $K_d$ values show inverse second power dependence on the hydrogen ion concentration in the aqueous phase.

As Fig. 1 shows, the shape of the curves is roughly divided into two types. The first type consists of those in which the absolute figures of the slope are identical with the ionic charges or at least the figures are below minus one. On the other hand, the $K_d$ values of the second type are unaffected by the hydrogen ion concentration in the aqueous phase in the acid range below about 2 N.

The $K_d$ values for alkali metals, alkaline earth metals and lanthanide elements are characteristic of the first type, showing first, second and third power dependence on the hydrogen ion concentration in the aqueous phase, respectively. A similar relationship holds for the elements of Ib, IIb and IIIb group in the periodic table except in the case of gold.

The extraction of metal cation with HDEHP is expressed generally in the following equation[1,6]:

$$M^{m+}_{(aq)} + m(HDEHP)_{2\,(org)} \rightleftarrows MH_m(DEHP)_{2m\,(org)} + mH^+_{(aq.)}$$

$$K_d = K \cdot [(HDEHP)_{2\,(org)}]^m \cdot [H^+_{(aq)}]^{-m} \quad (1)$$

where, $K$ is the constant of the above equilibrium. In this equation, $(HDEHP)_{2\,(org)}$ represents the dimer of HDEHP in the organic phase[24]. Eq. 1 indicates that an ion with $+m$ charge shows a curve of $-m$ slope. It appears as if an element giving a $K_d$ curve of the first type behaves as a cation in the given system.

On the other hand, the $K_d$ curves for chlorine, bromine and iodine are typical of the second type. Germanium, arsenic, platinum and gold give curves of a similar shape. Almost all of these elements give higher $K_d$ values in an acid solution over 2 N than in 1 N. It is likely that the extraction of these elements is not based on the chelation mentioned above, but on partition, as is found in the case of extraction with TBP[25].

Although the three light elements of Va, VIa and VIIa group, vanadium, chromium and manganese, show the characteristic curves of the first type, the heavy elements of the groups, niobium, molybdenum, technetium, tantalum, tungsten and rhenium, show those of the second type. This appears to be in accord with the fact that Cr(III) and Mn(II) are apt to behave in cationic state in hydrochloric acid media, whilst niobium, molybdenum, technetium, tantalum, tangsten and rhenium are not. The present $K_d$ values for vanadium were relatively low. Vanadinyl(IV) ion in the system HDEHP-sulfate solution, however, shows high $K_d$ values which depend on the hydrogen ion concentration with a slope of ca. $-2$[1].

Chromium resembles manganese more than it does molybdenum or tungsten as regards the type of acid concentration-$K_d$ value relation. Besides, the slope of ca. $-2$ for chromium gives a suggestion that chromium exists as a mixture of hydrated chloro-complexes. $K_d$ values for molybdenum and niobium are relatively high, while those for technetium and rhenium are very low.

In contrast with the Va, VIa and VIIa groups, the light elements of IVb, Vb and VIb group, germanium, arsenic and selenium, show $K_d$ curves of the second type, while heavy elements, lead and bismuth, show that of the first type.

It is known that iron(III) and aluminum require a long time to attain extraction equilibrium[1]. In graph "Fe" in Fig. 1, curve 2 shows $K_d$ values for 2 min. shaking, line 3s those for three times scrubbing, line e those for thirty hours shaking. Line e has a slope of $-3$. In all three cases, iron gives high $K_d$ values, while cobalt and nickel give low values throughout the acidity range. For aluminum,

24) D. F. Peppard, J. R. Ferraro and G. W. Mason, *J. Inorg. Nucl. Chem.*, **4**, 371 (1957).
25) D. Dyrssen and F. Krasovec, *Acta Chem. Scand.*, **13**, 568 (1959).

the $K_d$ values for the equilibrium were not obtained, because the aluminum tracer used was short-lived.

It is difficult to account for the difference in the behavior of the platinum elements because the methods used in preparing the tracers were quite different. The $K_d$ values for osmium are relatively high, those for iridium show $-4$th power acid dependence, and those for others are low.

Indium gives a straight line of slope ca. $-3$ over the acidity range from 0.05 to 10 N. Copper, silver, zinc, cadmium and gallium also behave similarly giving the slope of $-m$. It is generally accepted that these elements form chloro-complexes easily. However, the absolute figures of the slopes for these are nearly equal to those of ionic charges in such condition that the elements do not form chloro-complexes.

As was mentioned by Peppard and his coworkers[6], Eq. 1 is principally analogous to that of the equilibrium found for the extraction of metals with thenoyl trifluoroacetone, HTTA. Figs. 2 and 3 show the comparison between HDEHP and HTTA extraction for

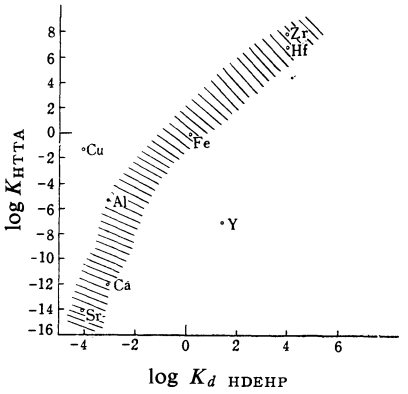



Fig. 2. Relation between $K_{d\ HDEHP}$ and $K_{HTTA}$ values.

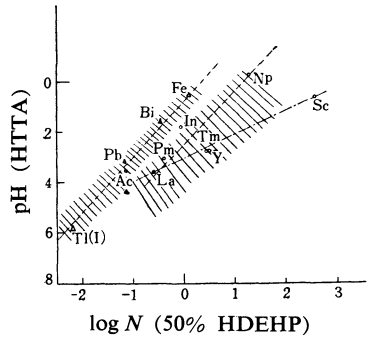



Fig. 3. Relation between $\log N_{1/2}$ for HDEHP system and $pH_{1/2}$ for HTTA system.
○ 0.5 M HTTA; △ 0.25 M HTTA

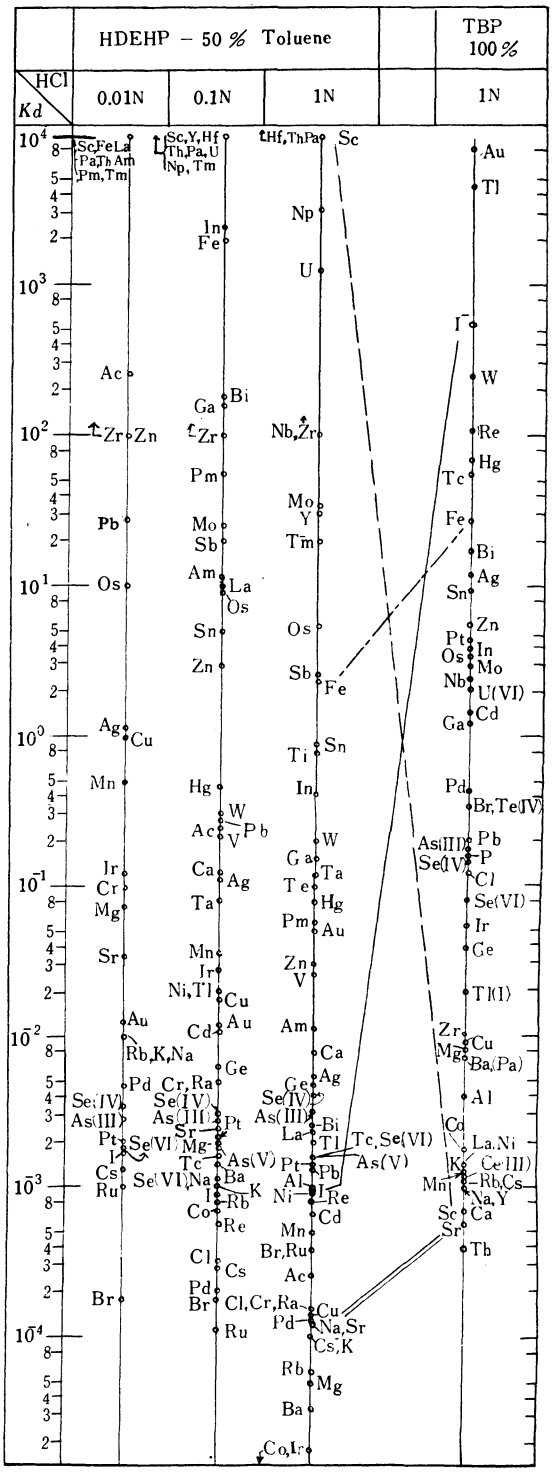



Fig. 4. $K_d$ values in 50% HDEHP—0.01 ~1 N HCl and comparison with 100% TBP—1 N HCl.

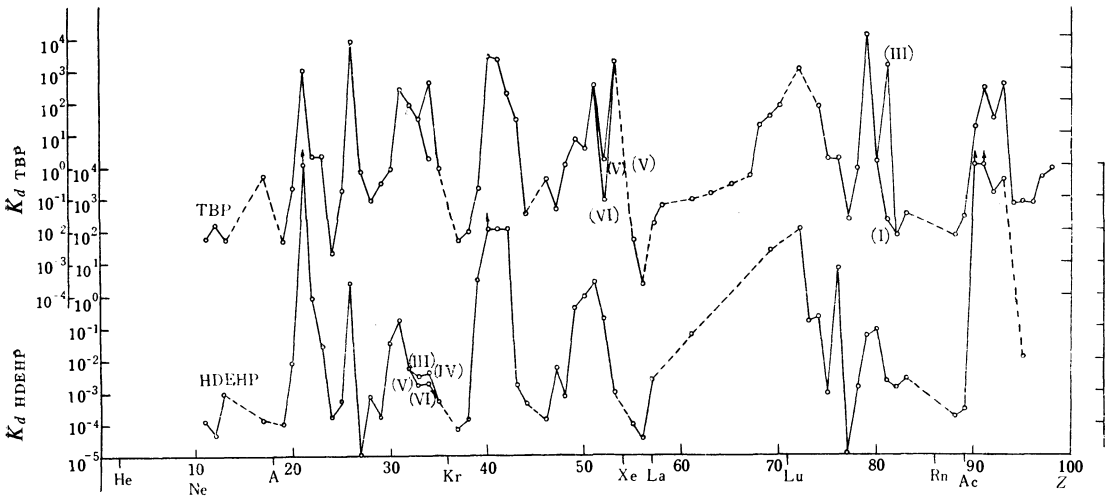



Fig. 5. Relation between $K_d$ values and $Z$.

some cations. The $K_d$ values for 50% HDEHP at 1 N hydrochloric acid are plotted against $K_{HTTA}$ values*[26,27]. In Fig. 3, the acidity given by $\log K_d = 0$ with HDEHP are plotted against the pH values giving 50% extraction with HTTA[27-29]. As Fig. 2 shows, the plots for zirconium, hafnium, iron, aluminum, calcium and strontium appear in the hatched band. Besides, as seen in Fig. 3, Fe-Bi-Pb-Tl and Np-In-La-lines show a straight line of slope ca. +2, showing that mutual difference of the values for these elements are larger in the HTTA system rather than in the HDEHP system. The Sc-Y-Tm-Pm-La-Ac-line of Fig. 3, however, gives a slope of +1. In all cases, it is found that these cations extractable into HTTA phase are also readily extracted into HDEHP.

Fig. 4 gives $K_d$ values in 50% HDEHP (toluene) vs. 1, 0.1 and 0.01 N HCl systems together with $K_d$ values in 100% TBP—1 N hydrochloric acid system. Alkali and alkaline earth metals are situated in a range of low $K_d$ values both for the systems of HDEHP and TBP—1 N hydrochloric acid. It is very interestingthat $K_d$ values for scandium, thorium and protactinium are very high for HDEHP, but very low for TBP. In contrast with this fact $K_d$ values for zinc, cadmium and gold are very high for TBP, but relatively low for HDEHP. However, it is found that iron and indium have relatively high $K_d$ values both for HDEHP and TBP.

$K_d$ values between 50% HDEHP and 1N hydrochloric acid are plotted against the atomic number, $Z$, in Fig. 5. The figure shows that the $K_d$ values vary regularly to some extent, giving two peaks in a given long period of the periodic table. A similar regularity is also found in the system of 50% HDEHP vs. 0.1 N and 0.01 N hydrochloric acid. Although an obvious exception for this regularity is the peak for iron(III), this peak may become low by adopting the $K_d$ value for iron(II) which is more suitable for this consideration from the viewpoint of the electron configuration. Blake et al.[1] mentioned that iron(II) is less extractable. In Fig. 5, $K_d$ values at 12 N hydrochloric acid and 100% TBP are also plotted on the same scale for comparison. It is clear and somewhat noticeable that the readily extractable ions are almost common for systems 100% TBP-12 N hydrochloric acid and 50% HDEHP-1 N hydrochloric acid. It appears as if the extraction of ions with HDEHP is not only based on chelation, but also based on partition as in the extraction with TBP. A notable exception is the case of iodine. Iodine shows remarkably high $K_d$ values for TBP, but low for HDEHP.

As can be seen in Figs. 1 and 5, the $K_d$ values for Ia, IIa and IIIa groups in low acidity region decrease according to the following sequence: Sc > Ca > K, Y > Sr > Rb and La > Ba > Cs. These are analogous to the sequence of relative affinity $K^*$ for cation exchange resin Dowex 50 or Diaion SK:

$$M^{4+} > M^{3+} > M^{2+} > M^{+}$$

However, the order of the extractability with HDEHP for cations of the same valence is

* $K_{HTTA} = (MT_m)_{org} \cdot (H^+)^m_{aq} \cdot (M^{m+})^{-1}_{org} \cdot (HT)^{-m}_{org}$.

* $K = [MR_m]_{resin} \cdot [H^+]^m_{aq.} \cdot [HR]^{-m}_{resin} \cdot [M^{m+}]^{-1}_{aq.}$

26) E. H. Huffman and L. J. Beaufait, *J. Am. Chem. Soc.*, 71, 3179 (1949).
27) R. A. Bolomy and L. Wish, ibid., 72, 4483 (1950).
28) F. Hageman, ibid., 72, 768 (1950).
29) W. W. Meinke, Progress Report 7, Univ. of Michigan, No. 1 (1958).

Table II. Comparison of the order of selectivity

| | |
|---|---|
| Cation(III) | |
| HDEHQ | Sc>Tm>Y>In>Ga>Pm>Am>La>Ac, (Al) |
| Resin | Ac>La>·····>Dy>Y>Ho>·····>La>Sc>Al |
| TBP(max) | Fe, Tl>Sc>Ga>In>Yb>Tm>Er>Ho>Y>Tb>Eu,Pm,Am>Ce>La>Al |
| TBP | Tl>Fe>In>Ga>Al>La>Ce>Y |
| Cation(II) | |
| HDEHP | $UO_2$, Zn>Ga>Pb>Mn, Cu>Cd, Ni>Mg, (Ra)>Ba, Sr, Co |
| Resin | Ra>Ba>Pb>(Sr, $Be_2O$)>Ca>(Mg, Zn, Cu, Ni, Co, Mn, $UO_2$, Cd)>Be |
| TBP(max) | $UO_2$, Zn>Cd>Cu, Pb>Ca, Co>Mn, Mg>Ra>Ni>Ba, Sr |
| TBP | Zn>Cd>$UO_2$>Pb>Cu, Mg, Ba>Co>Mn, Ni |
| Cation(I) | |
| HDEHP | Ag>Tl>Na>K>Rb>Cs |
| Resin | Tl>Ag>Cs>Rb>K=$NH_4$>Na>H>Li |
| TBP(max) | Ag>Tl>Alkali metals |
| TBP | Ag>Tl>(K>Rb, Cs>Na) |

reverse to that of the relative affinity for cation exchange resin. A similar reversal had been found in the pairs of mono(2-ethyl hexyl)-orthophosphoric acid and sulfonated cation exchange resin for selected lanthanides and actinides[30], of HDEHP and mono(heptadecyl) sulfuric acid for K, Na, and Li[30] and of phosphonic resin and sulfonic resin for K, Na and Li[31].

Table II shows the comparison of the orders of selectivity. In the table, the heading HDEHP and TBP stand for the values in the systems of 100% TBP-1 N hydrochloric acid and of 50% HDEHP-1 N hydrochloric acid, respectively. The TBP(max) for the maximum $K_d$ values.

The author wishes to express his thanks to Dr. Tomitaro Ishimori for helpful suggestions and guidance in the course of this work. Thanks are also due to Dr. Kenjiro Kimura and Dr. Toshio Nakai for their advice and encouragemement, and to Mr. Ikuo Suzuki for his valuable assistance.

*Chemistry Division*
*Japan Atomic Energy Research Institute*
*Tokai, Ibaraki-ken*

30) D. F. Peppard, G. W. Mason and R. J. Sironen, *J. Inorg. Nucl. Chem.*, **10**, 117 (1959).
31) J. I. Bregman and Y. Murata, *J. Am. Chem. Soc.*, **74**, 1867 (1952).

# *Coloration and Decarboxylation of the Aniline Salts of 2, 4, 6-Trinitrobenzoic Acid in Ketones and Other Solvents*

By Minoru HIROTA

(Received February 15, 1960)

Molecular compounds of aromatic polynitro compounds with aromatic hydrocarbons and with aromatic amines have been reported by many authors[1] and a number of molecular compounds of 1, 3, 5-trinitrobenzene[2-4], 2, 4, 6-trinitrotoluene[5], 2, 4, 6-trinitroanisole[6], picric acid[7,8], etc., have been investigated, but little has been known of 2, 4, 6-trinitrobenzoic acid (TNBA) complexes. So the present author studied TNBA complexes and found that, while several aromatic hydrocarbons and phenols form normal molecular complexes with TNBA, aniline, as expected, forms salts when one mole of aniline is added to one mole of TNBA.

The TNBA salts of anilines decompose into the complexes of 1, 3, 5-trinitrobenzene (TNB) with anilines and carbon dioxide on heating in solution or in the crystalline state, and the decarboxylation is extremely fast in ketonic solvents even at low temperatures. Moreover, a striking dark red color is produced in ketonic solvents. From the investigation of the relation

1) Extensively reviewed by L. J. Andrews, *Chem. Revs.*, **54**, 713 (1954).
2) H. Kronberger and J. Weiss, *J. Chem. Soc.*, **1948**, 464.
3) B. R. Brown and D. L. Hammick, *J. Chem. Soc.*, **1948**, 1395.
4) H. M. Powell and G. Huse, *J. Chem. Soc.*, **1943**, 435.
5) J. Landauer and H. McConnel. *J. Am. Chem. Soc.*, **74**, 1221 (1952).
6) E. Hertel et al., *Ber.*, **61**, 1545 (1928); **63**, 2446 (1930).
7) O. L. Baril and E. S. Hauber, *J. Am. Chem. Soc.*, **53**, 1087 (1931).
8) R. Kuhn and A. Winterstein, *Helv. Chim. Acta*, **11**, 144 (1938).

between the coloration and the rates of decarboxylation in various solvents it has been found that there are two types of coloration. The color of the first type occurs immediately after the dissolution of a salt in a pure ketone, accompanying very rapid decarboxylation, its intensity decreasing rather rapidly. The color of the other type occurs some time after the dissolution of the salt in an alcohol or in a mixed solvent containing an alcohol, when the decarboxylation is completed and almost all the TNBA has decomposed, its intensity increasing gradually. The spectra of the colors of both types resemble each other in shapes but differ in the locations of the absorption maxima. The measurments of the rates of the decarboxylation of the complexes of TNBA with anilines also showed that the decarboxylation in ketones is extremely rapid.

**2, 4, 6-Trinitrobenzoates of Aniline and Substituted Anilines and their Decomposition into Corresponding Trinitrobenzene Complexes on Fusion.** — A colorless crystalline substance was obtained when one mole of aniline and one mole of TNBA, both in cold acetone solution, were mixed, while a red mass was obtained from one mole of TNBA and two moles of aniline. The colorless substance was proved to be a 1 : 1 compound by analysis (Found: N, 18.09%, Calcd: N, 18.30%). The infrared absorption spectrum indicated that this compound is a salt[9]; namely it showed no absorption near 1725 $cm^{-1}$ (carbonyl stretching frequency of the carboxyl group), and 1270 $cm^{-1}$, but absorption bands at 1600 $cm^{-1}$ and 1380 $cm^{-1}$ (antisymmetric and symmetric stretching frequencies of the carboxylate ion). (See Fig. 1 for the infrared spectra of the TNBA salts of aniline and pyridine.) The molecular compounds[10] of TNBA with benzene, naphthalene and chrysene have acid type carbonyl absorptions near 1730 and 1270 $cm^{-1}$. The 2 : 1 compound also showed no absorption near 1730 $cm^{-1}$ but more experiments are required for further information.

TABLE I. INFRARED SPECTRA OF TNBA AND ITS SALTS

| Compound | Infrared absorption by carboxyl group, $cm^{-1}$ | | |
|---|---|---|---|
| | $\nu_{C=O}$ | $\nu_{CO_2^-}$ | $\nu_{C-O}$ or $\delta_{O-H}$ |
| TNBA | 1737 | | 1272 |
| Sodium salt | | 1603 1310 | |
| Aniline salt | | 1603 1370 | |
| *N*-Methylaniline salt | | 1600 1348 | |
| *N*, *N*-Dimethylaniline salt | | 1600 1326 | |
| *p*-Toluidine salt | | 1597 1366 | |
| *p*-Anisidine salt | | 1605 1366 | |
| *p*-Bromoaniline salt | | 1603 1372 | |
| Pyridine salt | | 1602 1353 | |

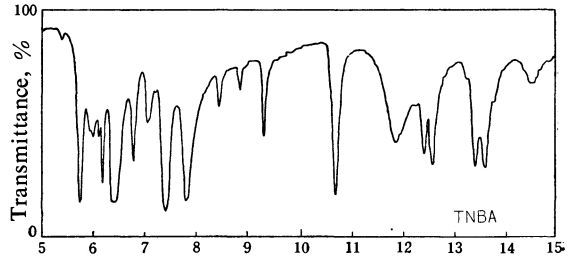


Fig. 1a.

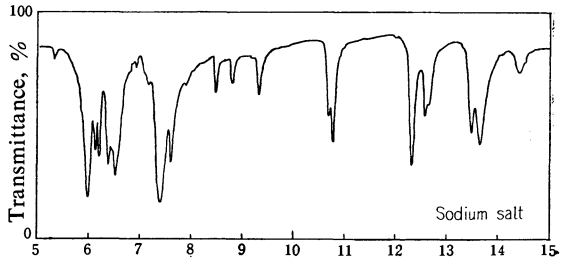


Fig. 1b.

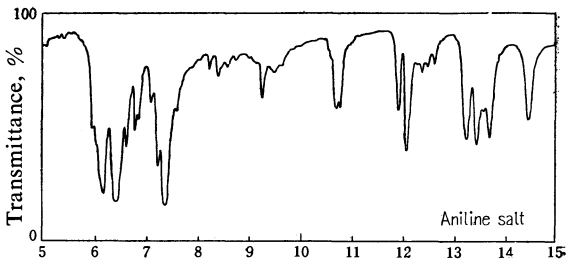


Fig. 1c.

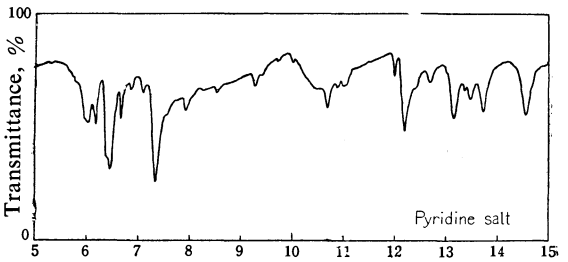


Fig. 1d.

Fig. 1. Infrared spectra of 2, 4, 6-trinitrobenzoates.

9) The salt form is proved mainly by the absence of the bands at 1730 and 1270 $cm^{-1}$, because the bands at 1600 and 1360 $cm^{-1}$ overlap with the strong bands of the nitro group.

10) These molecular compounds will be described later.

2, 4, 6-Trinitrobenzoates of substituted anilines were also prepared and compared in the infrared spectra with the sodium and ammonium salts of TNBA (Table I and Fig. 1), which showed that all of these colorless 1 : 1 compounds are salts.

The 2, 4, 6-trinitrobenzoates decomposed at their melting points and changed into an orange-yellow or red liquid. The orange-yellow crystalline substance melting at 127°C, obtained from the melt of the aniline salt, was identified with the TNB-aniline complex. Other salts also gave the corresponding TNB complexes.

TABLE II. COLORATION OF ANILINE SALTS OF TNBA IN VARIOUS SOLVENTS

| Solvents | 2, 4, 6-Trinitrobenzoate of | | |
|---|---|---|---|
| | Aniline | *N*-Monoethyl-aniline | *N*, *N*-Diethyl-aniline |
| Acetone | + | + | + |
| Methyl ethyl ketone | + | + | + |
| Acetophenone | + | + | + |
| Benzophenone | + | + | + |
| Cyclohexanone | + | + | + |
| Ethyl acetoacetate | + | + | + |
| Benzaldehyde | + | + | + |
| Acetaldehyde* | − | − | |
| Pinacolone | + | + | + |
| *p*-Ethylacetophenone | + | + | + |
| Ethanol | − | − | − |
| Amyl alcohol | − | − | − |
| Ethylene chlorohydrin | | − | |
| Allyl alcohol | − | − | |
| Triethylene glycol | ± | ± | ± |
| Glycerol | − | − | − |
| Diethylene glycol monoethyl ether | ± | ± | ± |
| Ethylene bromide | − | − | − |
| Chloroform | − | − | − |
| Benzyl chloride | − | − | |
| Chlorobenzene | − | − | |
| Nitrobenzene | + | + | + |
| Nitromethane | + | + | + |
| Ether | − | − | − |
| Dioxane** | + | + | + |
| Anisole | − | − | − |
| Petroleum ether | − | − | − |
| Benzene | − | − | − |
| Acetic anhydride | − | − | − |
| Carbon disulfide | − | − | − |

* 50% aqueous solution

** The color is much paler than in ketonic solvents.

The sign + is for rapid coloration, the sign ± is for slow coloration (about one hour after heating) and the sign − is for no coloration.

**Coloration and Decarboxylation of the Aniline Salts of TNBA in Various Solvents.** — The aniline salt of TNBA could be recrystallized from boiling benzene without coloration, but a dark red color appeared when boiling acetone was used as the solvent for recrystallization, an orange crystalline substance being obtained from the colored solution after spontaneous evaporation of acetone and was again identified with the TNB-aniline complex by the melting point and by the X-ray diffraction pattern (Table IV). On the other hand, the free TNBA could be recrystallized from boiling acetone without decomposition; and, therefore, the aniline salt form is essential for the unusual

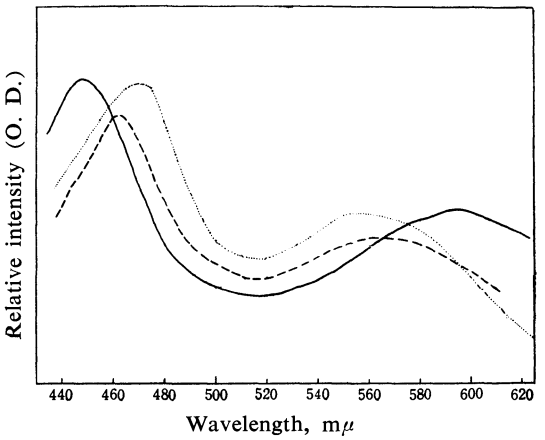



Fig. 2a.

Aniline salt of TNBA { in acetone ——; in triethylene glycol ·····; in a mixture of 60% acetone and 40% ethanol ----

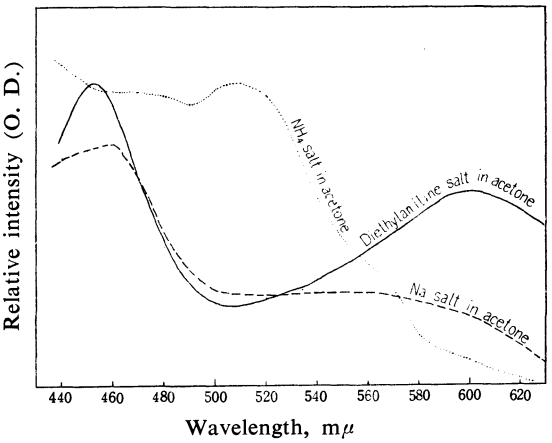



Fig. 2b.

Dimethylaniline salt ——
Ammonium salt ·····
Sodium salt ----
} in acetone.

Fig. 2. The visible spectra of TNBA salt in various solvents.

TABLE III. ABSORPTION SPECTRA OF THE ANILINE SALTS OF TNBA

| Compound | Solvent* | Absorption maxima, mμ | | |
|---|---|---|---|---|
| TNBA-aniline | A | 447.5 | 595 | |
| | MEK | 450 | 595 | |
| | Dioxane | 442.5 | 595 | |
| | Triethylene glycol | 470 | 552 | |
| | Nitromethane | 448 | 590 | |
| | Ethanol | 475 | 550(sh) | |
| | A90%-E10% | 464 | 570 | |
| | A80%-E20% | 463 | 565 | |
| | A40%-E60% | 465 | 560 | |
| TNBA-*N*-monomethylaniline | MEK | 447 | 598 | |
| | Ethanol | 465 | 555(sh) | |
| | MEK75%-E25% | 464 | 560 | |
| TNBA-*N*, *N*-diethylaniline | MEK | 452 | 605 | |
| Na salt of TNBA | MEK | 456 | 560(sh) | |
| $NH_4$ salt of TNBA | MEK | 470 | 505 | 520(sh) |
| | | 560(sh) | | |

* "A" is for acetone, "MEK" for methyl ethyl ketone and "E" for ethanol.

TABLE IV. X-RAY DIFFRACTION PATTERNS OF THE DECARBOXYLATION PRODUCTS

| Compounds | Diffraction angles, 2θ (Relative intensities)* |
|---|---|
| TNB-Aniline : | 13.10(1.00), 14.26(0.22), 14.96(0.17), 18.54(0.55), 22.02(0.13), 22.75(0.11), 24.43(0.17), 25.48(0.28), 27.82(9.34), 30.55(0.15) |
| The decarboxylation products of TNBA salt of aniline | 13.60(1.00), 14.30(0.29), 14.95(0.19), 18.60(0.82), 22.05(0.26), 22.40(0.25), 24.54(0.35), 25.52(0.50), 27.82(0.58), 30.58(0.30) |

* Relative intensities to the strongest diffracted beams are in parentheses.

TABLE V. RESULTS OF THE ELEMENTARY ANALYSES OF 2, 4, 6-TRINITROBENZOATES

| Compounds | m. p. °C | N calcd. | N found |
|---|---|---|---|
| Aniline salt | 156 | 16.00 | 16.19 |
| *p*-Anisidine salt | 155~6 | 14.73 | 14.88 |
| *p*-Bromoaniline salt | 129 | 13.43 | 13.2 |
| *p*-Toluidine salt | 158 | 15.38 | 15.22 |
| *N*-Methylaniline salt | 148 | 15.38 | 15.33 |
| *N*, *N*-Dimethylaniline salt | 158 | 14.81 | 14.75 |
| Pyridine salt | 174 | 16.67 | 16.95 |

facility of decarboxylation of TNBA in ketones.

In order to investigate what kind of solvent produces the particular red color, 5 mg. of a salt was added in 2 ml. of a solvent (if insoluble, the salt was suspended in the solvent), and then the whole was heated for 5 sec. on a water bath of 60°C. If the red did not appear markedly immediately after heating, the

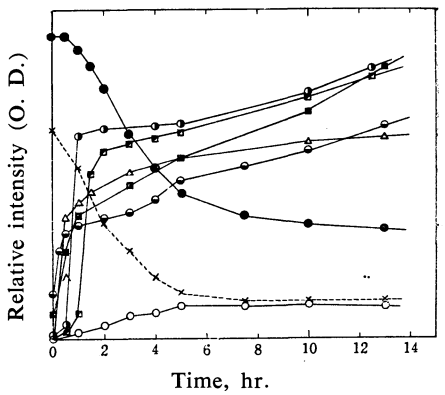



Fig. 3. Intensity change of the color produced by dissolving the aniline salt of TNBA in acetone-ethanol mixture. (at 38°C) *

—◒— {90% {460 mμ
—◩— {20% {460 mμ
—■— {80% {460 mμ
—○— {0% (ethanol) {460 mμ
—△— {60% {460 mμ
—●— {100% {450 mμ
—◐— {40% {460 mμ
---×--- {100% {600 mμ

* This figure shows the changes of the absorption intensities of the solutions. Time after dissolution of the salt is plotted on the horizontal axis; while the relative intensity at constant wavelength (mostly at 460 mμ) on the vertical axis. The percentages in this figure indicate volume percentages of acetone in ethanol: for example, "90%, 460 mμ" means that a mixed solvent consists of 90% of acetone and of 10% of ethanol is used for the measurement of the intensity change, and the measurement is done at 460 mμ.

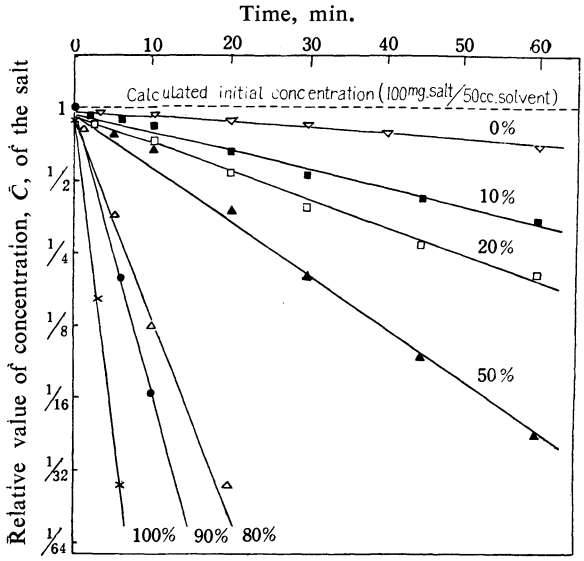



Fig. 4. Rates of decarboxylation of aniline salt of TNBA in acetone-ethanol mixed solvent.*

* The logarithmic value of relative concentration referred to the calculated initial concentration is plotted on the vertical axis. The percentages on the figure indicated acetone content in the mixture, the remainder is ethanol only.

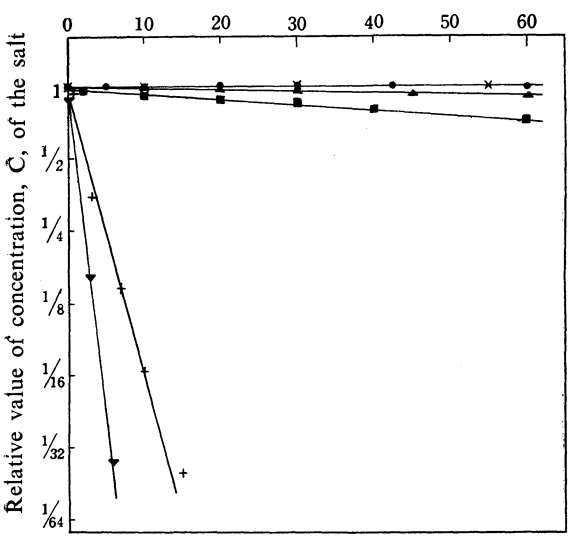



Fig. 5. Rates of decarboxylation of aniline salt of TNBA in various solvents.

—×— in water —■— in ethanol
—●— in dioxane —+— in methyl ethyl ketone
—▲— in methanol —▼— in acetone

color was observed after heating at 50°C for 3 up to 60 min.

Dark red coloration was instantly observed when a carbonyl or nitro compound was used

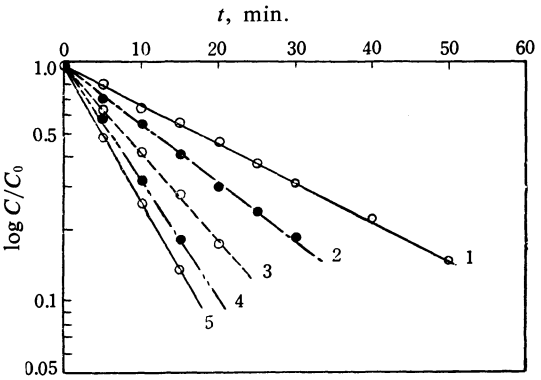



Fig. 6. The rates of decarboxylation of *p*-substituted aniline of TNBA in acetone 30°C.

$C_0$: intial concentration (about 0.004 mol./l.)
$C$: concentration at time $t$.
$t$: time after the beginning of the reaction.
1: *p*-Br, 2: *p*-$NO_2$, 3: *p*-Me,
4: H, 5: *p*-MeO

as the solvent. Some alcohols and ethers also produced a red color on longer heating. The color in ketones is so intense immediately after heating that very small amounts of a ketone and the aniline salts are needed for the color reaction and it gives a method for the qualitative detection of ketones. Nevertheless, this method requires ketones of high purity, so the utilization is limited. Some nitro compounds, ethers and alcohols also produced coloration, but the greenish red color in ketones and nitro compounds seemed to be different from the red color in alcohols. Results of the color reaction in various solvents are summarized in Table II.

Then, the absorption spectra of the aniline salts in various solvents were measured. Some of the spectra are illustrated in Fig. 2 and the locations of the absorption maxima are given in Table III. The spectra of the aniline salt of TNBA in a pure ketone or nitromethane, measured immediately after dissolution and warming, had absorption maxima at 447.5 and 595 m$\mu$, and their intensities (extinction coefficients) decreased as time passed. On the other hand, the spectra of the salt in alcohols had absorption maxima at 465 and 565 m$\mu$ and their intensities gradually increased as time passed. From these experimental results it was certain that there were two types of coloration, so the time dependence of the absorption intensity was measured with the results given below.

**Relation between the Rate of Decarboxylation and Coloration of the Aniline Salts of TNBA in Various Solvents.**—The relation between the decarboxylation and the coloration of the TNBA salt of aniline was investigated by measuring the rate of decarboxylation and the change of

absorption intensity. The decarboxylation is extremely fast in ketones (Fig. 5). The rate of decarboxylation is in the order: acetone> methyl ethyl ketone>ethanol>methanol> dioxane. Measurements of the change of absorption intensity revealed that the intensity in pure ketones is reduced fast, while the color in the acetone-ethanol mixture, though not very intense at the beginning, becomes intense gradually. The more acetone the mixed solvent contains, the more promptly the coloration occurs, while, the more ethanol is present in the solvent, the more intense the absorption of the solution becomes. However the coloration is hardly observed in pure ethanol. On the other hand, since the decarboxylation of the aniline salt proceeds without any coloration in many other solvents at higher temperatures, the color is not essential for the decarboxylation, but the unusual facility of decarboxylation with simultaneous coloration in ketones suggests different mechanisms of the two types of decarboxylation.

The decarboxylation of the TNBA salts of substituted anilines were also examined with the results shown in Fig. 6.

To examine the nature of the intermediate compounds of the decarboxylation, the TNBA salts of some *p*-substituted anilines were prepared and the rates of decarboxylation were measured. The order of the decarboxylation rates is almost parallel to that of the coloration rates. Namely, ammonium salt $\ll$*p*-nitroaniline salt $<$*p*-bromoaniline salt $<$ aniline salt $<$*p*-anisidine salt for the coloration, and *p*-bromoaniline salt $<$*N*, *N*-dimethylaniline salt $<$*p*-nitroaniline salt $<$*N*-methylaniline salt $<$*p*-toluidine salt $<$ aniline salt $<$*p*-anisidine salt for the decarboxylation.

The order of the decarboxylation rates is not simply in the order of basicity of the anilines.

## Experimental

**Qualitative Tests for the Coloration.** — To examine a solvent in the coloration, about 5 mg. of the aniline salt of TNBA was dissolved in 2 ml. of the solvent and the solution was heated for 30 seconds in a water bath of 60°C. If the salt was not completely dissolved, a suspension was used. All solutions in ketones produced dark red color instantly on heating. When no coloration occurred, the solution was examined after heating at 50°C for 3 minutes and 60 minutes. To test a solution in ether or other volatile solvents, the solution was heated under reflux on a water bath.

**Visible Spectra of the Color.** — Visible spectra were measured in the range of wavelength from 420 to 625 m$\mu$. with a Beckman DU type quartz spectrophotometer. Determination of the band envelopes and locations of the absorption maxima were the main purpose of the spectral measurements, while the exact determination of the absolute values of intensities was less important and only relative intensities were needed for the present discussions, since the intensities of the absorption bands changed rather rapidly.

**Infrared Spectra of the Salt.** — The infrared spectra were determined with an Infracord infrared spectrophotometer or with a Baird Model B infrared spectrophotometer. All measurements were made in solid state; the potassium bromide pellet method was employed in most measurements, and the mull method in a few measurements. Nujol and hexachlorobutadiene were used as mulling agents, because they compensate each other, the whole wavelength region between 2.5 and 15 $\mu$ thus being covered without interference of the absorption bands of the mulling agents.

**Preparation of the Materials and Determination of the Rates.**—All salts were prepared by the following procedure: TNBA[12] in acetone and an equivalent amount of a base in the same solvent were mixed in an ice bath and the precipitated salt was collected by filtration as rapidly as possible, washed first with a small amount of cold acetone and then with benzene, and dried in a vacuum desiccator. The salts prepared in this way were analytically pure (Table V) and can be used in the spectral and other measurements. The rate of decarboxylation was determined by titrating the unchanged acid with a standard alkali in aqueous solution, methyl red being used as the indicator without interference by the anilines.

**X-ray Diffraction Measurements.**—Powder X-ray diffraction patterns were obtained with a Norelco X-ray diffractometer. Diffraction angles and relative intensities of the diffracted beams are listed in Table IV.

The author wishes to express his hearty thanks to Professor Y. Urushibara, and to Professor M. Ōki for their helpful advice and to Mr. Masuda for elementary analyses.

*Department of Chemistry*
*Faculty of Science*
*The University of Tokyo*
*Hongo, Tokyo*

11) Similar spectra are observed with TNB and 2, 4, 6-trinitroanisole in ethanol solution containing sodium ethoxide. R. Foster, *Nature*, **176**, 746 (1955); **183**, 1042 (1959).

12) 2, 4, 6-Trinitrobenzoic acid is prepared by the method described in "Organic Syntheses" [H. T. Clarke and W. W. Hartman, "Org. Syntheses", Col. Vol. I, p. 543 (1941)].

# *Sur la Dissolution des Minerais Sulfurés en Divers Milieux. II. Dissolution de la Pyrite et de la Chalcopyrite*

Par Masami ICHIKUNI

(Reçu le 22 octobre 1959)

La décomposition ou l'altération des minerais sulfurés dépend, d'une part, de leur propre caractère, composition chimique, propriété minéralogique, structure cristalline, et d'autre part, des facteurs du milieu, température, pression, pH, potentiel d'oxydo-réduction, présence d'autres substances. Ayant exécuté des essais préliminaires, on a déjà signalé dans le rapport précédent[1] des rôles importants que jouent le pH et l'air dans la dissolution des minerais. Dans le but d'élargir et de généraliser ce résultat, on reprend l'expérience de la dissolution de la pyrite et de la chalcopyrite, classées parmi les plus importants des minéraux sulfurés primaires. L'expérience s'effectue sous les conditions oxydantes et non-oxydantes à divers pH. Les premières conditions sont caractérisées par la présence de l'air, les dernières par l'absence de l'oxygène. On met en évidence le mécanisme de la dissolution des minerais et montre sa signification géochimique. L'application du résultat du présent rapport aux phénomènes naturels sera utile pour l'éclaircissement de ces derniers.

## Expérience

**Généralité.** — Le dispositif et les conditions de l'expérience sont les mêmes que ceux décrits dans le rapport précédent. On prend 200 ml. d'acide chlorhydrique de concentration connue ou la même quantité d'eau bidistillée dans un ballon à 300 ml., l'apporte sur un bain-marie, chauffe la liqueur à la température de 80 à 85°C, y ajoute 1 g. de minéral pulvérisé et traite pendant quatre heures, en y introduisant l'air ou l'azote avec un débit constant de 1,5 l./min. Chaque prélèvement de portion de 10 ml. doit être effectué avec l'interval d'une heure. Le dosage du fer divalent, du cuivre et du sulfate sont fait sur la liqueur filtrée.

L'interféromètre ayant indiqué 0,05% comme teneur en oxygène de l'azote, celui-ci est lavé à une solution de pyrogallol, afin d'éliminer l'oxygène.

**Echantillons.**—La pyrite s'est produite à la mine de Kanaborizawa, département d'Aomori, la chalcopyrite, à la mine d'Ani, department d'Akita. La dernière a été examinée par voie diffractométrique à rayons X pour qu'on vérifie qu'elle est exempte d'autres impuretés minéralogiques. Le résultat d'analyse chimique est porté sur le Tableau I. La composition chimque des échantillons se conforme approximativement à la formule chimique idéale des minéraux, $FeS_2$ et $CuFeS_2$. Une petite quantité d'impuretés qu'on a décelées par la spectrographie ne présentera aucun inconvénient pour l'expérience.

TABLEAU I. RÉSULTAT D'ANALYSE DES MINÉRAUX

| Elément | Pyrite | Chalcopyrite |
|---|---|---|
| Fe | 46,50% | 30,40% |
| Cu | — | 34,35 |
| S | 53,36 | 34,86 |
| Total | 99,86 | 99,61 |

Tout en évitant l'oxydation provoquée par la pulvérisation, on arrête cette opération lorsque toutes les poudres passent par un tamis à nombre de maille de 100.

**Considérations.** — (1) *Diminution du Volume de Liqueur par l'Evaporation.* — Entraînée par l'air ou l'azote introduit dans la liqueur, une portion de liqueur s'évapore. L'augmentation apparente de quantité dissoute de composants, si elle était calculée par la différence des concentrations trouvées tout en négligeant la diminution du volume, doit être supérieure à son augmentation véritable. Cela nécessite donc une correction pour la diminution du volume causée par l'évaporation. Cette correction a une importance particulière dans le cas d'un composant qui ne se dissout que très peu. Elle s'effectue par la division des concentrations trouvées par le taux de concentration, rapport du volume initial sur la somme du volume final et du volume prélevé. Toutes les concentrations trouveées ont été ainsi recalculées pour qu'on puisse éliminer l'influence de l'évaporation. Si le minéral pulvérisé contient une certaine quantité de sulfate ou d'oxyde, qui dépasse la quantité dissoute par le traitement, cela empêchera de déterminer précisément la quantité véritable de dissolution, car la correction ne se fait pas très rigoureusement. On est obligé de prendre une grande précaution pour la préparation des échantillons. On peut effectuer la correction avec une erreur inférieure à 5%.

(2) *Variation du pH.*—Lorsqu'on traite les minerais sulfurés en présence de l'oxygène, il se produit toujours une certaine quantité d'acide sulfurique et le pH de la liqueur diminue. L'effet de l'évaporation qui concentre la liqueur, par conséquent l'ion hydrogène, participe également à l'abaissement du pH. Il n'est que de 0,2, en milieu acide, avant et après le traitement, tandis que le pH descend de 6 à 3 environ par le traitement effectué avec de l'eau bidistillée. Lorsqu'on examine la relation

1) M. Ichikuni et H. Kamiya, Ce Bulletin, 32. 1368 (1959).

entre la dissolution et le pH, on prend la valeur moyenne de pH au cours du traitement, et elle est de 3,2 et de 4,2 pour le traitement effectué avec l'eau de la pyrite et de la chalcopyrite, respectivement. Pour maintenir le pH du milieu à une valeur donnée, on pourrait utiliser une solution tampon, mais son emploi offre en même temps un inconvénient, car la présence des sels étrangers exerce une influence considérable sur la dissolution des minéraux; on aura donc de la difficulté à interpréter le résultat obtenu.

(3) *Efficacité de l'Agitation.*—La réaction ayant lieu entre la phase solide et la phase liquide, l'agitation donne une influence considérable sur la vitesse de réaction. On maintient le débit du gaz à une valeur constante de 1,5 l./min., afin d'égaliser, pour toute la série d'expériences, l'efficacité de l'agitation.

(4) *Suppression du Dosage du Fer Trivalent.*—Comme la concentration de fer trivalent ne dépasse que très rarement 1% de celle de fer divalent, on a supprimé le dosage de celui-là.

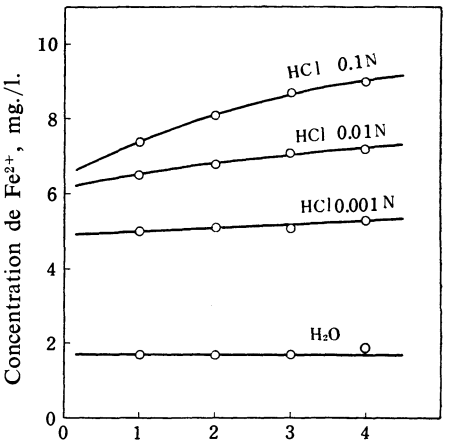



Fig. 1 Dissolution du fer à partir de la pyrite en milieu exempt d'oxygène

## Résultats et Discussion

**Expérience de Dissolution de la Pyrite Effectuée à l'Exclusion de l'Oxygène.**—L'exclusion de l'oxygène a été réalisée par l'introduction de l'azote dans le dispositif.

Le Tableau II montre la concentration de composants qui a été correctionnée pour la diminution du volume, et qui correspond à l'heure du prélèvement et aux conditions d'expérience. L'absence de l'oxygène ne provoque presque pas la formation du sulfate, tandis que celle-ci est remarquée légèrement lors du traitement avec l'eau. Comme la pyrite est très sensible à l'oxydation en milieu à pH élevé, la formation du sulfate est attribuable à des traces d'oxygène contenu dans l'azote. Comme l'indique la Figure 1, la dissolution du fer s'accélère à mesure que le pH s'abaisse. Toutefois la courbe de concentration a une tendance à s'aplanir.

Par ces résultats, on peut exprimer la décomposition de la pyrite en milieu acide et en l'absence de l'oxygène par l'équation (1)

$$(1) \quad FeS_2 + 2H^+ \rightarrow Fe^{2+} + H_2S + S$$

L'hydrogène sulfuré étant chassé par le barbotage de l'azote, la réaction peut avancer.

Tableau II. Variation de concentration de fer divalent et de sulfate au cours de la dissolution de la pyrite

| Milieu | Durée du traitement | Expérience effectuée en l'absence de l'oxygène | | Expérience effectuée en présence de l'air | |
|---|---|---|---|---|---|
| | | $Fe^{2+}$ | $SO_4^{2-}$ | $Fe^{2+}$ | $SO_4^{2-}$ |
| | hr. | mg./l. | mg./l. | mg./l. | mg./l. |
| | 1 | 7,4 | 8 | 15,1 | 21 |
| HCl | 2 | 8,1 | 7 | 21,0 | 26 |
| 0,1 N | 3 | 8,7 | 6 | 25,6 | 30 |
| | 4 | 9,0 | 6 | 29,6 | 39 |
| | 1 | 6,5 | 6 | 14,4 | 29 |
| HCl | 2 | 6,8 | 4 | 20,2 | 46 |
| 0,01 N | 3 | 7,1 | 5 | 25,4 | 60 |
| | 4 | 7,2 | 5 | 28,3 | 72 |
| | 1 | 5,0 | 9 | 12,7 | 36 |
| HCl | 2 | 5,1 | 10 | 19,6 | 59 |
| 0,001 N | 3 | 5,1 | 9 | 24,4 | 80 |
| | 4 | 5,3 | 9 | 28,8 | 102 |
| | 1 | 1,7 | 10 | 11,9 | 48 |
| | 2 | 1,7 | 13 | 18,2 | 78 |
| $H_2O$ | 3 | 1,7 | 14 | 21,6 | 104 |
| | 4 | 1,9 | 19 | 24,7 | 129 |

TABLEAU III. VITESSE DE DISSOLUTION DU FER DIVALENT ET DU SULFATE À PARTIR DE 1 g. DE PYÉITE EN PRÉSENCE DE L'AIR

| Milieu | Valeur moyenne de pH | $Fe^{2+}$ m mol./hr. ($\times 10^{-2}$) | $SO_4^{2-}$ m mol./hr. ($\times 10^{-2}$) | $SO_4^{2-}/Fe^{2+}$ |
|---|---|---|---|---|
| HCl 0,1 N | 1,1 | 1,53 | 1,03 | 0,67 |
| HCl 0,01 N | 2,0 | 1,78 | 2,80 | 1,57 |
| HCl 0,001 N | 2,9 | 1,70 | 4,58 | 2,70 |
| $H_2O$ | 3,2 | 1,12 | 5,35 | 4,78 |

La présence de l'hydrogène sulfuré, au contraire, empêche la réaction. Pour cette raison, la pyrite reste stable en milieu acide, si le milieu est caractérisé par la présence de l'hydrogène sulfuré. Ainsi s'expliquent la stabilité et la formation de la pyrite dans la nature.

**Expérience de Dissolution de la Pyrite Effectuée en Présence de l'Air.**—Dans le Tableau II, on trouve que la présence de l'air favorise une dissolution considérable du fer divalent et du sulfate, et on peut constater que le potentiel d'oxydo-réduction est un facteur important pour la décomposition de la pyrite. La vitesse de dissolution du fer et du soufre dépend du pH et du potentiel d'oxydo-réduction du milieu. Il est bien connu que l'oxydation de l'hydrogène sulfuré par l'oxygène libre donne génénralement le soufre libre et non l'acide sulfurique en milieu acide[2].

En partant de l'équation (1), on a deux équations suivantes:

$$(2)\quad FeS_2 + 2H^+ + O \rightarrow Fe^{2+} + H_2O + 2S$$

où la pyrite se décompose en fer divalent et soufre libre,

$$(3)\quad FeS_2 + H_2O + 7O \rightarrow Fe^{2+} + 2H^+ + 2SO_4^{2-}$$

où tous les soufres sont oxydés en sulfate. Ces deux équations correspondent aux deux cas extrêmes de la décomposition de la pyrite, et le rapport de $SO_4^{2-}/Fe$ peut varier de 0 à 2. Cependant au-dessus de pH 3, le fer trivalent, formé par oxydation du fer divalent, précipitant sous forme de l'hydroxyde, le rapport de $SO_4^{2-}/Fe$ est toujours suppérieur à 2. Dans le Tableau III, on montre la vitesse de formation du fer divalent et du sulfate par la dissolution de la pyrite.

La Figure 2 montre la relation entre le pH et le rapport de $SO_4^{2-}/Fe^{2+}$. A un petit pH, la réaction exprimée par l'équation (2) est prédominante. Au-dessus de pH 2,5, on remarque déjà l'hydrolyse du fer trivalent, et la précipitation de l'hydroxyde devient très rapide au delà du pH 3.

Que la vitesse de formation du fer divalent et du sulfate soit variable selon le pH du milieu

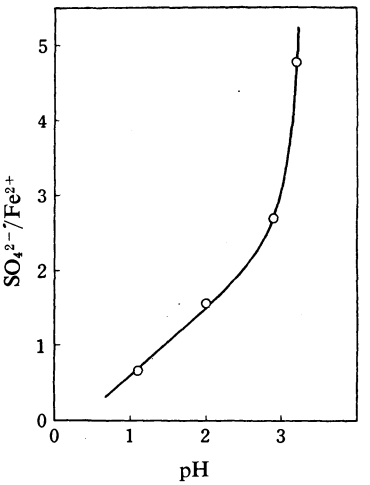



Fig. 2 Relation entre le pH et le rapport de $SO_4^{2-}/Fe^{2+}$, qui se trouve dans la dissolution de la pyrite.

a une signification très importante au point de vue géochimique. La variation du rapport de $SO_4^{2-}/Fe$ en fonction du pH est influencée par les conditions d'expérience, toutefois elle garderait toujours la même tendance. Dans la nature, l'acidité forte à pH inférieur à 1 étant exceptionnelle, la désagrégation de la pyrite donne simplement l'acide sulfurique et le sulfate de fer(II). La neutralisation de la solution ainsi formée provoque la précipitation du fer, notamment l'hydroxyde de fer(III) par l'intervention de l'oxygène. L'oxydation du sulfure en sulfate se produit d'autant plus vite que le pH est plus élevé.

**Expérience de Dissolution de la Chalcopyrite Effectuée à l'Exclusion de l'Oxygène.** — Le Tableau IV montre le résultat de la dissolution du minéral dont l'expérience est effectuée en présence de l'azote et de l'air. Le traitement du minéral, effectué en milieu exempt d'oxygène et avec l'acide chlorhydrique, ne donne que du fer divalent et rien d'autres composants. La décomposition proposée par l'équation (4) explique bien l'indissolution du cuivre:

$$(4)\quad CuFeS_2 + 2H^+ \rightarrow CuS + Fe^{2+} + H_2S$$

On comprend que la dissolution du fer divalent est d'autant plus rapide que le pH du milieu est plus petit. D'après le Tableau

2) H. Miura, *J. Chem. Soc. Japan, Pure Chem. Sec.* (*Nippon Kagaku Zasshi*), 77, 417 (1956).

TABLEAU IV. VARIATION DE CONCENTRATION DE FER DIVALENT, DE CUIVRE ET DE SULFATE AU COURS DE LA DISSOLUTION DE LA CHALCOPYRITE

| Milieu | Durée du traitement | Expérience effectuée en l'absence de l'oxygène | | | Expérience effectuée en présence de l'air | | |
|---|---|---|---|---|---|---|---|
| | | $Fe^{2+}$ | Cu | $SO_4^{2-}$ | $Fe^{2+}$ | Cu | $SO_4^{2-}$ |
| | hr. | mg./l. | mg./l. | mg./l. | mg./l. | mg./l. | mg./l. |
| | 1 | 6,8 | 0,36 | 5 | 47 | 99 | 9 |
| HCl | 2 | 9,2 | 0,15 | 4 | 95 | 119 | 11 |
| 0,1 N | 3 | 10,5 | 0,11 | 4 | 145 | 136 | 13 |
| | 4 | 11,9 | <0,10 | 4 | 183 | 150 | 15 |
| | 1 | 6,8 | <0,10 | 5 | 6,1 | 0,19 | 10 |
| HCl | 2 | 9,4 | <0,10 | 6 | 8,2 | 0,16 | 11 |
| 0.01 N | 3 | 10,1 | <0,10 | 5 | 10,4 | 1,11 | 11 |
| | 4 | 10,7 | <0,10 | 4 | 12,6 | 3,11 | 13 |
| | 1 | 4,3 | <0,10 | 6 | 5,3 | <0,10 | 12 |
| HCl | 2 | 5,3 | <0,10 | 7 | 5,9 | <0,10 | 13 |
| 0,001 N | 3 | 6,4 | <0,10 | 7 | 6,9 | <0,10 | 13 |
| | 4 | 7,3 | <0,10 | 7 | 8,0 | <0,10 | 15 |
| | 1 | <0,5 | <0,10 | 8 | <0,5 | <0,10 | 12 |
| $H_2O$ | 2 | <0,5 | <0,10 | 9 | 0,6 | <0,10 | 14 |
| | 3 | <0,5 | <0,10 | 9 | 0,9 | <0,10 | 14 |
| | 4 | <0,5 | <0,10 | 14 ? | 1,2 | <0,10 | 14 |

TABLEAU V. VITESSE DE DISSOLUTION DU FER DIVALENT, DU CUIVRE ET DU SULFATE À PARTIR DE 1 g. DE CHALCOPYRITE EN PRÉSENCE DE L'AIR

| Milieu | Valeur moyenne de pH | $Fe^{2+}$ m mol./hr. ($\times 10^{-2}$) | Cu m mol./hr. ($\times 10^{-2}$) | $SO_4^{2-}$ m mol./hr. ($\times 10^{-2}$) | $Cu/Fe^{2+}$ |
|---|---|---|---|---|---|
| HCl 0,1 N | 1,1 | 16,3 | 5,31 | 0,4 | 0,33 |
| HCl 0,01 N | 2,0 | 0,80 | <0,63 | 0,2 | $\leq$0,79 |
| HCl 0,001 N | 3,0 | 0,37 | 0 | 0,2 | 0 |
| $H_2O$ | 4,2 | 0,11 | 0 | 0 | 0 |

IV, la vitesse de dissolution du fer est de 0,26 mg. à l'heure, dans l'acide 0,1 N, et de 0,13 mg. à l'heure, dans l'acide 0,01 N. Le fer ne se dissout aucunement dans l'eau.

**Expérience de Dissolution de la Chalcopyrite Effectuée en Présence de l'Air.** — Dans le Tableau IV, on voit que l'expérience effectuée en présence de l'air donne approximativement le même résultat que celle qui a été effectuée en milieu exempt d'oxygène, d'autant que le pH soit supérieur à 2. A un pH supérieur à 3, aucune dissolution du cuivre n'est remarquée, et celle du sulfate est très limitée. De ce fait on peut conclure que l'oxygène n'exerce pas une grande influence sur la dissolution de la chalcopyrite à un pH supérieur à 2. Cela se conforme au résultat du rapport précédent que la dissolution du cuivre est soumise à l'influence du pH et non du débit de l'air qu'on introduit dans la liqueur contenant du minerai pulvérisé.

Une vitesse très limitée de formation du sulfate en milieux neutre et faiblement acide attire notre attention. Pour cette raison, le traitement de la chalcopyrite avec l'eau ne diminue que modérément le pH de la liqueur. La pyrite, au contraire, diminue considérablement le pH de la liqueur, lorsqu'elle est traitée avec de l'eau, d'ailleurs chez la pyrite, la vitesse de formation du sulfate est d'autant plus grande que le pH du milieu est plus élevé. Cependant la dissolution de la chalcopyrite augmente énormément en milieu acide 0,1 N, ce qui n'est pas pareil au cas de la pyrite.

Le Tableau V montre la vitesse de formation du fer divalent, du cuivre et du sulfate par la dissolution de la chalcopyrite.

Dans le Tableau V, on trouve que la quantité dissoute de cuivre est toujours inférieure à celle de fer, quoique le rapport de Cu/Fe soit de l'unité dans le minéral. La dissolution du soufre, sous forme du sulfate, est très faible par rapport à celle du fer et du cuivre. Alors on remarque que le soufre libre se forme abondamment au cours de l'expérience effectuée en milieu acide 0,1 N. On présente donc les équations (5) et (6) qui conviendront à l'explication de ce résultat :

(5) $CuFeS_2 + 2H^+ + O \rightarrow CuS + Fe^{2+} + H_2O + S$

(6) $CuFeS_2 + 4H^+ + 2O \rightarrow Cu^{2+} + Fe^{2+} + 2H_2O + 2S$

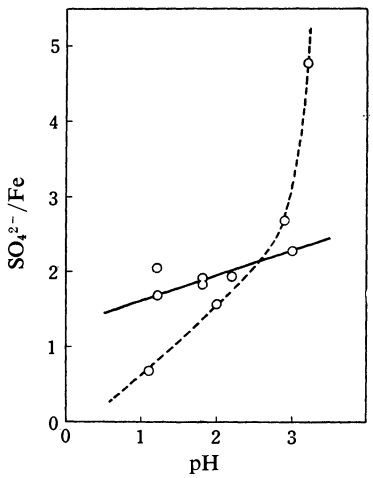
D'après ce résultat, on peut déduire qu'une grande dissolution du cuivre à partir de la chalcopyrite est peu possible, d'autant que le minéral se trouve indépendamment des autres minéraux, et que le milieu en question ne soit pas très acide et oxydant. Cependant on trouve souvent une dissolution rapide du cuivre à partir du gisement des minerais sulfurés. On ne pourra pas éclaircir ce phénomène sans avoir recours aux effets de la co-présence d'autres minéraux, notamment de la pyrite, et de l'action de l'acide sulfurique ou du fer, qui sont produits par la désagrégation des minerais sulfurés. D'après Ohashi[3], la présence de la pyrite ne favorise pas particulièrement la dissolution du cuivre à partir de la chalcopyrite, toutefois le fer trivalent contribue à sa dissolution, en réagissant sur le minéral.

Les effets de la co-présence d'autres minéraux sur la dissolution de la chalcopyrite présentent un problème intéressant, car on a déjà désigné la présence d'autres substances comme un des facteurs importants déterminant le milieu géochimique.

### Désagrégation de la Pyrite dans la Nature

L'acide sulfurique et le sulfate de fer se forment en grande quantité par la désagrégation des minerais sulfurés. C'est ainsi que les eaux d'une forte acidité, souvent de pH inférieur à 3, jaillissent au fond de mine. Ces eaux se jettent dans une rivière, et abaissent dans une grande mesure le pH des eaux de rivière. Il est d'un intérêt particulier de comparer le résultat de ces expériences avec celui d'analyse des eaux de mine.

On a choisi donc à partir des résultats d'analyses des eaux de mine de Kamikita, département d'Aomori,[4] les eaux contenant simplement de l'acide sulfurique et du sulfate de fer. Le résultat d'analyse des dernières est indiqué par le Tableau VI.




Fig, 3 Relation entre le pH et le rapport de $SO_4^{2-}/Fe$, qui se trouve dans les eaux de mine de Kamikita (courbe discontinue correspondant à celle de la Fig. 2).

Avec les chiffres du Tableau VI, on examine la relation entre le pH et le rapport de $SO_4^{2-}/Fe$, et la compare avec celle obtenue par les expériences décrites ci-dessus. La Figure 3 montre cette comparaison. On en a constaté que:

1. A mesure que le pH s'abaisse, le rapport de $SO_4^{2-}/Fe$ a une tendance à diminuer, mais il n'est pas très inférieur à 2, même à pH 1.
2. Cela souligne que la réaction exprimée par l'équation (3) est toujours prédominante dans la nature, même à un petit pH, par conséquent la formation abondante du soufre libre par la désagrégation de la pyrite serait peu possible.

La relation entre le pH et le rapport de $SO_4^{2-}/Fe$, qui se trouve dans les données du Tableau VI, ne se conforme pas à celle obtenue par les expériences. Cette discordance peut s'expliquer par le fait que dans la nature, la manière de contact des minerais avec l'air est entièrement différente de celle effectuée au laboratoire, et que la dissolution des minerais est soumise à l'influence des substances

TABLEAU VI. QUELQUES RELEVÉS DES DONNÉES D'ANALYSE DES EAUX DE MINE DE KAMIKITA, DÉPARTEMENT D'AOMORI (D'APRÈS T. HAMACHI ET H. GOTO)

| pH | $Fe^{2+}$ m mol./l. | $Fe^{3+}$ m mol./l. | $SO_4^{2-}$ m mol./l. | $SO_4^{2-}/Fe$ total |
|---|---|---|---|---|
| 1,2 | 107 | 95,8 | 340 | 1,68 |
| 1,2 | 182 | 80 | 535 | 2,04 |
| 1,8 | 15,0 | 9,5 | 46,4 | 1,89 |
| 1,8 | 22,7 | 0 | 42,2 | 1,86 |
| 2,2 | 9,3 | 0,7 | 19,4 | 1,94 |
| 3,0 | 5,0 | 3,8 | 20,1 | 2,28 |

3) S. Ohashi, *J. Chem. Soc. Japan, Pure Chem. Sec.* (*Nippon Kagaku Zasshi*), **74**, 845 (1953).

4) T. Hamachi et H. Goto, *Bull. Geol. Survey Japan*, **6**, 265 (1955).

co-existantes. Au laboratoire on effectue le barbotage de l'air, mais une agitation violente de solution est plutôt rare dans la nature, par conséquent l'hydrogène sulfuré ne sera pas chassé hors de solution, même s'il s'est formé. D'ailleurs la relation entre le pH et le rapport de $SO_4^{2-}$/Fe peut varier selon la manière d'introduction de l'air.

Dans le Tableau VI, on trouve qu'il y a une quantité considérable de fer trivalent dans les eaux, et que l'acidité des eaux consiste en acide sulfurique, ce qui n'est pas pareil aux conditions d'expérience où l'acidité consiste en acide chlorhydrique. Il faut qu'on tienne compte de la présence du fer trivalent et de l'acide sulfurique pour l'explication complète du phénomène de désagrégation des minerais sulfurés. Toutefois il est d'une signification particulière qu'on a pu ici reproduire d'une façon réduite le phénomène de désagrégation.

L'auteur exprime ses remerciements sincères à Monsieur le professeur K. Noguchi qui a bien voulu lire cet essai et lui donner des conseils utiles, et particulièrement à Monsieur H. Kamiya dont le concours aimable et l'encouragement étaient indispensables pour la réalisation de ce travail. Il remercie également Monsieur le professeur T. Watanabe et Monsieur le docteur A. Kato, à l'Université de Tokyo, pour l'examen diffractométrique à rayons X de la chalcopyrite.

*Faculté des Sciences*
*Université Métropolitaine de Tokyo*
*Sétagaya, Tokyo*

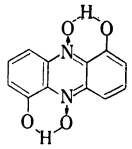
# *The Constitution of the Pigments of Brevibacterium Crystalloiodinum, Sasaki, Yoshida et Sasaki*

By Tosi Irie, Etsuro Kurosawa and Iwao Nagaoka

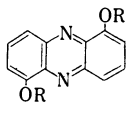
(Received January 14, 1960)

Sasaki, Yoshida and Sasaki[1] isolated a deep purple, antibiotic pigment and a yellow pigment from the culture medium of *Brevibacterium crystalloiodinum*, Sasaki, Yoshida et Sasaki*, and named them crystalloiodinine A and B, respectively. The name of crystalloiodinine was proposed on account of the purple pigment resembling to iodinine[2].

The present paper is concerned with the study on the structure of these pigments, which were sent by Professor Yuji Sasaki, to whom the authors' thanks are due. It has been established that crystalloiodinine A is identical with iodinine, *i.e.*, 1, 6-dihydroxyphenazine di-*N*-oxide (I), and crystalloiodinine B is 1, 6-dihydroxyphenazine (II: R=H).



(I)



(II)

The purple pigment, isolated from the culture medium, was purified by repeated recrystallizations from chloroform or dioxane; its homogeneity was indicated by the fact, that it gives a single blue band on alumina chromatogram. Crystalloiodinine A, $C_{12}H_8O_4N_2$, was thus obtained in deep purple prisms with coppery lustre, m. p. 230°C (decomp.). It dissolves in aqueous sodium hydroxide to a blue solution, and separates in purple crystals when the alkaline solution is acidified. It shows greenish coloration in ethanol with ferric chloride. The ultraviolet spectrum in chloroform shows maxima at 291 m$\mu$ ($\log \varepsilon = 5.1$) and 355 m$\mu$ ($\log \varepsilon = 3.9$) (Fig. 1); and the infrared spectrum exhibits absorptions due to a bonded hydroxyl group at 3400 $cm^{-1}$ and that of *N*-oxide group at 1285, 1160 and 1025 $cm^{-1}$ (Fig. 2). The infrared spectrum and certain chemical properties[1] indicated, that the pigment closely resembles iodinine[2-6]. Accordingly, crystalloiodinine A

1) Y. Sasaki, T. Yoshida and H. Sasaki, presented at the Meetings of the Society of Agricultural Chemistry of Japan, Sapporo, Nov. 21, 1957 and Tokyo, April 4, 1959.

2) G. R. Clemo and H. McIlwain, *J. Chem. Soc.*, **1938**, 479.

* This new species of *Brevibacterium* was isolated at the Faculty of Agritculture of Hokkaido University by Prof. Y. Sasaki and his collaborators[1].

3) G. R. Clemo and A. F. Daglish, *J. Chem. Soc.*, **1950**, 1481.

4) A. I. Kiprianov, S. B. Serebryanyi and V. P. Chernernetskii, *Doklady Akad. Nauk. S. S. S. R.*, **69**, 651 (1949); *Chem. Abstr.*, **46**, 4010 (1952).

5) S. B. Serebryanyi, V. P. Chernetskii and A. I. Kiprianov, ibid., **70**, 645 (1950); *Chem. Abstr.*, **45**, 4249 (1951).

6) I. Yoshioka and Y. Kidani, *J. Pharm. Soc. Japan*, **72**, 1301 (1952).

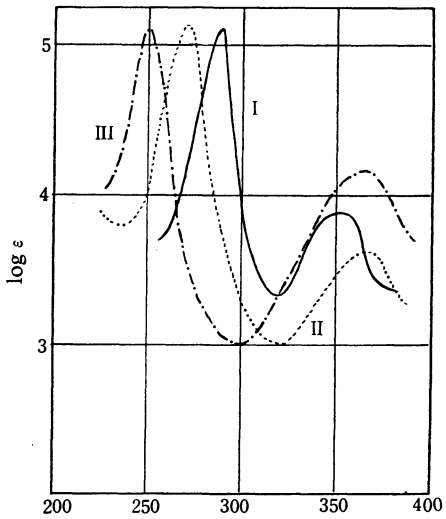



Fig. 1. Absorption spectra of:
I. crystalloiodinine A and 1, 6-dihydroxyphenazine di-*N*-oxide (in chloroform),
II. crystalloiodinine B (in ethanol),
III. acetate of crystalloiodinine B (in ethanol).

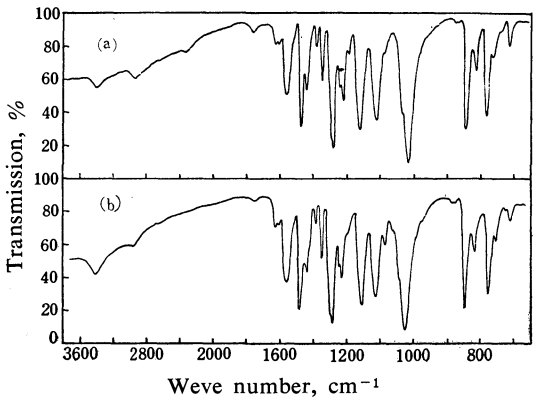



Fig. 2. IR spectra in KBr of (a) crystalloiodinine A and (b) 1, 6-dihydroxyphenazine di-*N*-oxide.

has been found to be identical with 1, 6-dihydroxyphenazine di-*N*-oxide, which was synthesized after Yoshioka and Kidani[6], by the mixed melting point method and by comparison of ultraviolet** and infrared spectra (Figs. 1 and 2).

On hydrogenating the pigment over Adams platinum catalyst, golden yellow plates, $C_{12}H_8O_2N_2$, m. p. 273~4°C (diacetate: pale yellow needles, m. p. 234°C) were yielded. This

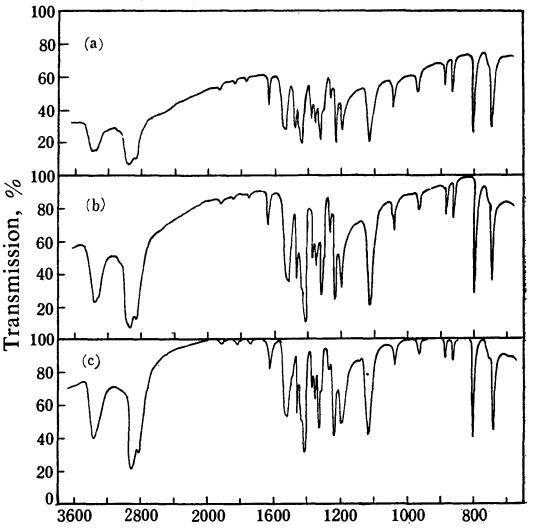



Fig. 3. IR spectra in nujol of (a) reduction product of crystalloiodinine A, (b) crystalloiodinine B, and (c) 1, 6-dihydroxyphenazine.

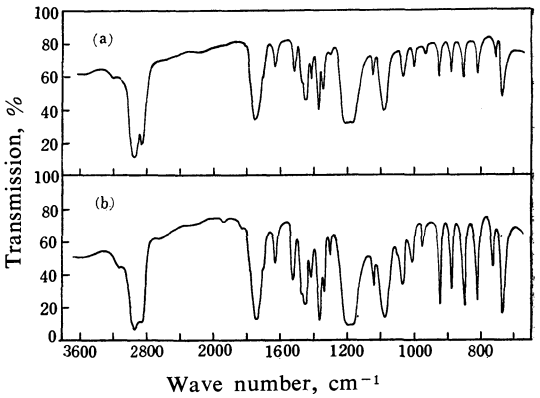



Fig. 4. IR spectra in nujol of (a) diacetate of crystalloiodinine B and (b) 1, 6-diacetoxyphenazine.

material has been identified as 1, 6-dihydroxyphenazine[7] as described below.

The yellow pigment, isolated from the culture medium, was also purified by the chromatographical method and recrystallization from benzene or sublimation under reduced pressure. Crystalloiodinine B, $C_{12}H_8O_2N_2$, was obtained in golden yellow plates, m. p. 273~4°C. It dissolves in aqueous sodium hydroxide to a purplish-red solution and separates in yellow crystals on acidification of the alkaline solution. It shows greenish coloration in ethanol with ferric chloride. The ultraviolet spectrum in ethanol shows maxima at 274 mμ (log ε=5.1) and 370 mμ (log ε=3.6) (Fig. 1); and the infrared spectrum exhibits absorption due to a

** The ultraviolet spectrum does not agree with that shown in the literature.[2]

7) I. Yoshioka and Y. Kidani, ibid., 72, 847 (1952).

hydroxyl group at 3390 $cm^{-1}$, but does not exhibit an *N*-oxide band (Fig. 3). Diacetate of this pigment, $C_{16}H_{12}O_4N_2$, was obtained in pale yellow needles, m. p. 234°C (the ultraviolet and infrared spectra are shown in Figs. 1 and 4, respectively). Thus, by the mixed melting point method and by comparison of the absorption spectra of the pigments and of their diacetates, it has been established that crystalloiodinine B is identical with the above reduction product of crystalloiodinine A and with 1, 6-dihydroxyphenazine.

It is possible to assume that 1, 6-dihydroxyphenazine, which has not hitherto been isolated from any natural source, plays the role of a precursor of iodinine[1].

## Experimental

**Isolation of the Pigments. (1) Purple Pigment, Crystalloiodinine A.**—The bacteria were incubated in the broth containing 1% glycerine. The cultures were shaken at 30°C for 5 days, during which deep purple crystals developed. Water was added to the cultures and shaken, and the washings were allowed to stand. After 24 hr. the suspension of bacteria was decanted from precipitated pigment. Several treatments were sufficient to remove the pigment. The crude pigments were filtered and extracted in a Soxhlet apparatus with chloroform. On concentration, the pigment separated as purple prisms with coppery lustre; it was recrystallized from chloroform or dioxane, m. p. 230°C (decomp.). Qualitative tests showed the pigment to contain nitrogen; sulfur and metals were absent.

Found: C, 58.61; H, 3.43; N, 11.42. Calcd. for $C_{12}H_8O_4N_2$: C, 59.02; H, 3.30; N, 11.48%.

It was slightly soluble in chloroform, carbon disulfide, petroleum ether, glacial acetic acid, acetone, dioxane and benzene, but not soluble in water, ethenol, nor ether. It was soluble in concentrated sulfuric acid with blue-greenish coloration, and also in aqueous sodium hydroxide with blue coloration. It showed greenish coloration in ethanol with ferric chloride. It dissolved in glacial acetic acid to give a red solution, which on warming with the addition of 10% potassium iodide liberated iodine.

This compound was found to be identical with 1,6-dihydroxyphenazine di-*N*-oxide, which was synthesized after Yoshioka and Kidani[6], by the mixed melting point method and by comparison of their absorption spectra.

(2) **Yellow Pigment, Crystalloiodinine B.**—The water layer obtained by decantation to remove crystalloiodinine A, was acidified by hydrochloric acid and extracted with ether. After evaporation of the ether, black gruel was obtained. This was treated with a small amount of chloroform and filtered. Dark brown crystals were boiled with benzene and filtered. Evaporation of the solvent afforded yellow crystals, which were recrystallized from benzene or sublimated under reduced pressure. Golden yellow plates were obtained, m. p. 273~4°C.

Found: C, 67.98; H, 3.53; N, 13.12. Calcd. for $C_{12}H_8O_2N_2$: C, 67.97; H, 3.80; N, 13.28%.

This material was soluble in benzene, alcohol, and ether. It was soluble in concentrated sulfuric acid with greenish coloration and also in aqueous sodium hydroxide with purplish-red coloration. It showed greenish coloration in ethanol with ferric chloride.

This compound was identified as 1,6-dihydroxyphenazine[7] by the mixed melting point method and by comparison of absorption spectra with an authentic specimen.

**Reduction of Crystalloiodinine A.**—The pigment (0.6 g.), platinum oxide (0.6 g.) and absolute ethanol (50 cc.) were shaken in hydrogen (1 atm.) for 24 hr., during which the pigment completely dissolved. Catalysts were then filtered off. On being exposed to air, the color of the filtrate changed soon from pale orange to yellow. This meant, that the hydrogenation yielded the dihydrophenazine compound and it was oxidized by air to the corresponding phenazine derivative. After evaporation of the solvent under reduced pressure, dark brown crystals were obtained. On purification by recrystallization from benzene or sublimation under reduced pressure, golden yellow plates were yielded, m. p. 273~4°C. This material was found to be identical with 1,6-dihydroxyphenazine and crystalloiodinine B, by the mixed melting point method and by comparison of the absorption spectra.

Found: C, 67.48; H, 3.45; N, 13.08. Calcd. for $C_{12}H_8O_2N_2$: C, 67.97; H, 3.80; N, 13.28%.

**Acetylations of the Reduction Product and Crystalloiodinine B.**—The compound (50 mg.), pyridine (5 cc.), and acetic anhydride (1 cc.) were refluxed for 2 hr. The solvent was removed under reduced pressure and the residue was recrystallized from ethanol. Pale yellow needles were obtained, m. p. 234°C. This compound was found to be identical with an authentic specimen of 1,6-diacetoxyphenazine (II: $R=COCH_3$) by the mixed melting point method and by comparison of the absorption spectra.

Found: C, 64.58; H, 3.86; N, 9.50. Calcd. for $C_{16}H_{12}O_4N_2$: C, 64.86; H, 4.06; N, 9.46%.

The authors are indebted to Mr. Y. Ichinoe for measurements of absorption spectra and to Mr. H. Homma of the Institute of Physical and Chemical Research, Tokyo, for microanalyses.

*Department of Chemistry*
*Faculty of Science*
*Hokkaido Uuiversity*
*Sapporo*

# *Dilatometric Study on Transition Phenomena of Various Polyethylenes with Different Degree of Chain Branching*

By Kōji TANAKA

(Received January 26, 1960)

Much interesting work has been done about the effect of chain branching of polyethylene on its physical and chemical properties. It is well known that branches in ordinary high-pressure polyethylene are of two types, short chain and long chain branchings. According to Roedel[1] short chain branching has the most marked effect on such properties as melting point, yield point, bending modulus, hardness, and vapour permeability, while long chain branching has a marked effect on melt flow and viscoelastic properties. Richards[2] presented data on the relation between the degree of crystallinity and the degree of short chain branching in a series of polyethylenes, and Sperati et al.[3] gave quantitative relations between density, degree of chain branching, and degree of crystallinity, and also between density and many other physical properties.

An early study of polyethylene by volume dilatometry was carried out by Boyer and Spencer[4]. They found melting points at 103°C and in the neighborhood of 115°C for different polyethylenes. Hunter and Oakes[5] reported from the volume measurement of a number of polyethylenes in the range from 0° to 170°C that the percentage of crystalline part did not change up to about 70°C, but thereafter fell more and more rapidly until the substances became wholly amorphous at a temperature depending on the nature of the specimen and that density of molten polyethylene showed little dependence on average molecular weight, but the temperature at which crystalline material first appeared on cooling was raised by increase in molecular weight. Mandelkern and his co-workers[6] presented the results of a study of volume-temperature behavior and melting temperatures of linear polymethylene and highly branched polyethylene. For polymethylene a well defined first order transition or melting temperature was found at 136.5±0.5°C and 70% of melting occurred in only a three to four degree interval, while for branched polyethylene the melting temperature was 115°C and the melting range considerably extended in comparison with the linear polymethylene. Similar results were reported by Nielsen[7] and recently by Marker[8] as for the melting of polyethylene. Grams and Gaube[9] showed that melting temperature existed between 124° and 133°C for low-pressure polyethylene and between 104° and 111°C for high-pressure polyethylene. According to the results by Hunter and Oakes, and by Nielsen, specific volumes above melting point were equal for various polyethylenes at the same temperature, but according to Grams and Gaube high-pressure polyethylene had higher specific volume than low-pressure polyethylene. Gubler and Kovacs[10] determined the specific volume of three samples (high-pressure, Ziegler and Marlex) dilatometrically between −38.8° and 170°C after various heat treatments, and showed the variation of the degree of crystallinity with temperature, the size of the polyethylene crystal and the state of the distribution of the crystal. About the specific volume above melting point they also showed that all the polyethylenes had the equal specific volumes at the same temperature regardless of the properties of polyethylenes. Moreover they showed that the cubic expansion coefficient changed at the temperature between −20° and −25°C for high-pressure polyethylene and Ziegler polyethylene, which was well consistent with the result presented by Danusso et al.[11]

Now, according to Hunter and Oakes as is mentioned already, molecular weight is given as a factor affecting the properties such as melting point, crystallizing temperature, that is, the temperature at which crystalline material first appears on cooling, and premelting phenomenon. However, by the appearance of polyethylene made by the low-pressure process and from the

1) M. J. Roedel, *J. Am. Chem. Soc.*, **75**, 6110 (1953).
2) R. B. Richards, *J. Appl. Chem.*, **1**, 370 (1951).
3) C. A. Sperati, W. A. Franta and H. W. Starkweather, Jr., *J. Am. Chem. Soc.*, **75**, 6127 (1953).
4) R. F. Boyer and R. S. Spencer, *J. Appl. Phys.*, **15**, 398 (1944).
5) E. Hunter and W. G. Oakes, *Trans. Faraday Soc.*, **41**, 49 (1945).
6) L. Mandelkern et al., *J. Am. Chem. Soc.*, **75**, 4093 (1953).
7) L. E. Nielsen, *J. Appl. Phys.*, **25**, 1209 (1954).
8) L. Marker, R. Early and S. L. Aggarwal, *J. Polymer Sci.*, **38**, 369 (1959).
9) E. Grams and E. Gaube, *Angew. Chem.*, **67**, 548 (1955).
10) M. G. Gubler and A. J. Kovacs, *J. Polymer Sci.*, **34**, 551 (1959).
11) F. Danusso, G. Moraglio and G. Talamini, ibid., **21**, 139 (1956).

several reports above quoted, it seems that chain branching must be regarded as a more significant factor affecting those properties. But at present detailed data about this point are not yet available.

Therefore a series of measurements were performed in the present paper about melting point, crystallizing temperature, premelting phenomenon, glass transition temperature, and degree of crystallinity at 25°C for various polyethylenes with different degrees of short chain and of long chain branchings. The results obtained showed that the temperature and degree crystallinity were raised with the increase of short chain branching. About the effect of long chain branching, no remarkable result could be found, since the amount of long chain branching contained in the sample used was very small.

**Sample.**—Samples used in this investigation were Marlex 50-9, Ziegler polyethylenes, and eight kinds of high-pressure polyethylenes. These high-pressure samples were provided by the courtesy of Dr. Hammer of E. I. du Pont de Nemours and Company. These samples, the molecular parameters of which are listed in Table I, were different in molecular weight, melt index, degree of short chain branching and that of long chain branching. Marlex 50-9 and Ziegler polyethylene were commercially available polymers made by Phillips Petroleum Company and The Dow Chemical Company, respectively. As the molecular parameters for these samples were not available, the degree of short chain branching was determined by the infrared method by using the 1370 and 1378 $cm^{-1}$ bands according to Slowinski[12]. It was found to be 0.25 for Marlex 50-9 and 0.4 for Ziegler polyethylene.

TABLE I. THE MOLECULAR PARAMETERS[a] FOR POLYETHYLENE SAMPLES

| Sample | Melt index | $M_n \times 10^{-3}$ | $N_c$[b] | $N_w$[c] |
|---|---|---|---|---|
| A[d] | 0.2 | 34 | 1.6 | 20 |
| B | 2.1 | 32 | 1.6 | 18 |
| C | 2.1 | 21 | 2.2 | 27 |
| D | 2.1 | 18 | 3.0 | 34 |
| E | 3.8 | 20 | 1.6 | 13 |
| F | 2.0 | 50 | 2.0 | 18 |
| G | 1.8 | 27 | 0.6 | 10 |
| H | 16.0 | 12 | 3.2 | 29 |
| Marlex 50-9 | | | 0.25[e] | |
| Ziegler | | | 0.4[e] | |

a) These were determined in E. I. du Pont de Nemours and Company by the methods described in J. Am. Chem. Soc., **75**, 6110 (1953).
b) Short chain branching index in $CH_3$ groups per 100 $CH_2$ groups.
c) Long chain weight average number of branch points per molecule. According to Bunn*, polyethylene has generally a relatively small number of long chain branches, 8-10 per molecule on a weight average basis and this is equivalent to less than one per molecule on a number average basis.
* C. W. Bunn, Polythene, A. Renfrew and P. Morgan, eds., Iliffe, London, Interscience, New York, 1957, Ch. 7.
d) These (A to H) are high-pressure polyethylenes.
e) This was determined here by the infrared method.

## Experimental

An experiment was carried out by volume dilatometry on which there was detailed description by Bekkedahl[13].

The dilatometer used in this experiment was made of Pyrex glass (as the volume expansion coefficient 0.00001/deg. was used) and consisted of three parts (Fig. 1, a). They were connected together tightly

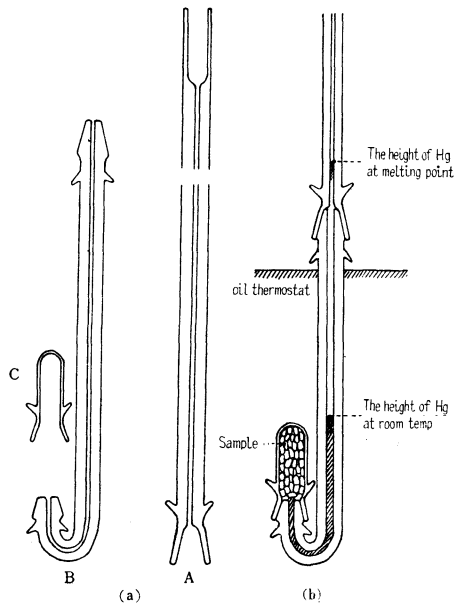



Fig. 1. Dilatometers: (a) for the measurements from about −40° to 150°C. (b) for the measurements above melting point.

with springs and in the case of measurement the dilatometer was immersed into the bath up to the height a little below the ground joint connecting the parts A and B. Prior to the experiment the capillary of part A was calibrated. After the dried and weighed sample was put in part C and this part was combined with part B, they were weighed, and then they were connected to the apparatus shown in

12) E. J. Slowinski, Jr., H. Walter and R. L. Miller, ibid., **19**, 353 (1956).
13) N. Bekkedahl, *J. Research Natl. Bur. Standards*, **42**, 145 (1949).

Fig. 2 and all the ground parts greased with silicone grease. Mercury as the confining liquid was inserted by distillation under vacuum of $10^{-3}$ mmHg and finally the total weight was weighed again in order to known the amount of mercury. As this amount of mercury was insufficient for the measurement, the adequate amount of mercury was weighed and added after parts A and B were combined together. The specific volume of the sample at the fixed temperature was calculated from the weights of the sample and of mercury and the total volume of parts B and C of the dilatometer which had been determined by using mercury in advance. In the case of calculation, corrections for the emergent stem and the expansion or contraction of the glass of the dilatometer were made according to Bekkedahl.

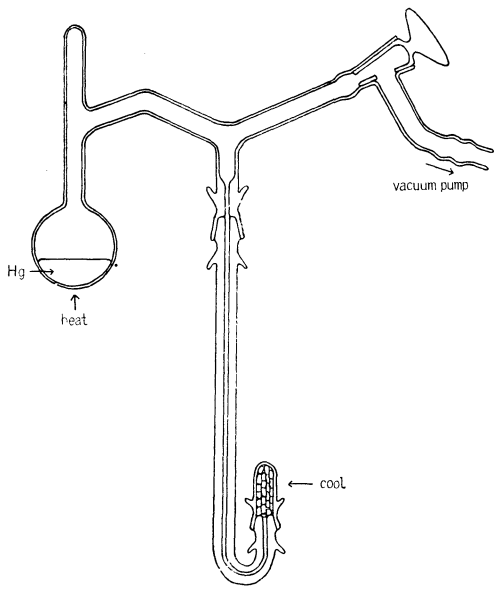



Fig. 2. The apparatus for insertion of Hg by vacuum distillation.

As is well known, the specific volume of polyethylene is dependent on temperature, as well as on its crystallinity and the amorphous region may have the possibility of further crystallization at temperature above its glass transition temperature, if the sample is not sufficiently crystallized. Therefore it is naturally expected that the volume-temperature curve above the glass transition temperature obtained by heating such a specimen contains both effects of the increase of volume by thermal expansion and the decrease of volume by further crystallization, which will obstruct the reproducibility of the curve and complicate the analysis of it. In order to eliminate such disadvantages, volume-temperature curves were taken for sufficiently crystallized samples. Sufficient crystallization of samples was carried out as follows. (1) The height of mercury in the capillary of the dilatometer containing the untreated polyethylene and mercury was recorded at 25°C exactly to 0.001 cm. (2) The dilatometer was gradually heated in the oil thermostat up to 150°C and kept at that temperature for about three hours to melt the sample in the dilatometer. (3) It was then cooled down slowly at the rate of 1/5°C per min. to 25°C. (4) The height of the mercury column was again recorded at 25°C. In this case the height was lower than that in the former case, which showed that the volume of the sample decreased by further crystallization by this treatment. Similar operations were performed, the time of melting being lengthened or shortened and the cooling rate being slower or faster, and also the dilatometer being kept for several hours at the temperature where crystallization occurred, on the way back to 25°C from 150°C at the rate of 1/5°C per min. The height of the mercury column thus obtained at 25° was equal to or higher than that obtained by the already mentioned way. As the result it is considered that the polyethylene sample can be crystallized to the highest degree by this procedure, and all the most highly crystallized specimens of polyethylene used for this investigation were obtained in this way. Volume temperature measurements were repeatedly performed in two temperature ranges, from 40°C to around freezing point of mercury and from 20° to 150°C. For measurements below 40°C a Dewar vessel containing toluene was used as a bath. The bath temperature was lowered about 5°C at a time by throwing pieces of dry-ice into the bath and it was kept at constant temperature for 15 min. by controlling the fluctuation of temperature $\pm 0.05$°C. After that the bath temperature and the height of mercury column which corresponded to the volume change by cooling of the dilatometer contents, polyethylene and mercury, were recorded. It was confirmed that 15 min. was sufficient for polyethylene to attain the equilibrium temperature within the experimental error. Similar operations were taken down to the melting point of mercury. After the measurement at the lowest temperature was finished, the bath temperature was raised by inserting nichrom wire into the bath and measurements were performed in quite the same way up to 40°C. The temperature control of the bath was carried out by letting toluene chilled below the bath temperature run through the cooling pipe immersed in the bath. The current of chilled toluene was regulated so that it might be turned off or on automatically according to the change of the bath temperature.

The measurements from 20° to 150°C were performed in the oil thermostat which was used for thermal treatment of the sample and carried out in the same way as the measurements below 40°C except in the case of the temperature range around melting point of polyethylene. In the vicinity of the melting point of the specimen the height of mercury column abruptly increased owing to the expansion of the sample by premelting or melting, so the bath temperature was raised 1°C at a time and a sufficiently long time was taken until the sample ceased to expand. When the measurement was finished at 150°C, the dilatometer was kept at the temperature for three hours, and then cooled slowly down to 25°C at the rate of 1/5°C per min. to crystallize sufficiently the sample again, and the experiment was repeated. In this case the measurements were carried out around the melting point of the sample at a one degree intervals, in order to

know exactly the crystallizing temperature. Experiments of these kinds were repeated two or three times for each sample.

## Result and Discussion

The specific volume-temperature curves from around −40° to 150°C for the most highly crystallized polyethylenes are shown in Fig. 3.

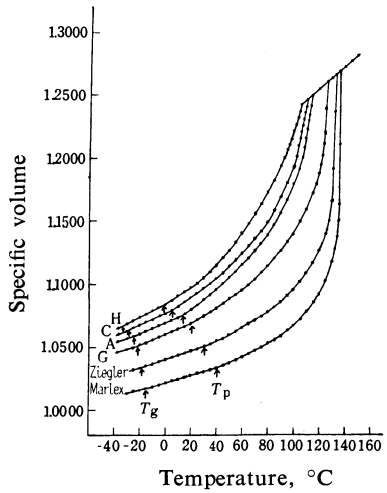



Fig. 3. Specific volume-temperature curves of the most highly crystallized polyethylenes from about −40° to 150°C. Those of samples B, D, E and F are omitted to avoid confusion.

As was mentioned already, the volume-temperature measurements were performed separately, covering two temperature ranges, below 40°C and above 20°C. The two curves obtained in these temperature ranges coincided perfectly between 20° and 40°C.

As is shown in the figure, the sample having the higher degree of short chain branching has the higher specific volume in the temperature range below melting point. Samples A, B and E which are equal in degree of short chain branching have almost equal values of specific volume at each measured temperature. This results shows that the highest degree of crystallinity of polyethylene is dependent upon the degree of short chain branching as was reported already by Richards. By inferring from the fact that when they are annealed, the unbranched linear polymethylene gets a considerably high degree of crystallinity and the more or less branched polyethylene has a lower one, it is considered that most of the amorphous regions of the most highly crytsallized polyethylene arises from the existence of short chain branching and branch point of long chain branching which disturb the regularity of molecules and keep the molecules from being

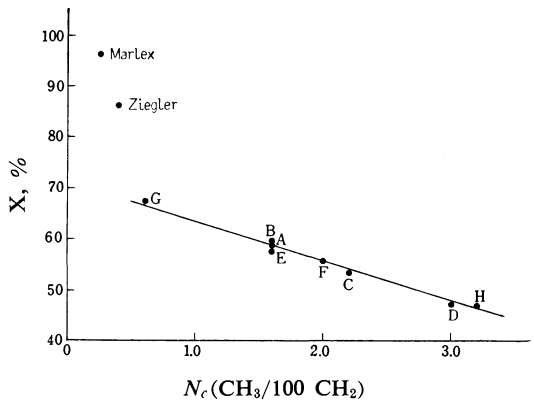



Fig. 4. The relation between degree of short chain branching and degree of crystallinity.

arranged in good order in proportion to their number. Therefore polyethylene containing the larger amount of chain branching is considered to have the poorer degree of crystallinity, even if it has the highest degree of crytallinity.

The highest degree of crystallinity of polyethylene samples at 25°C are illustrated in Fig. 4 as a function of short chain branching. They were obtained transforming the following equation, as was done by Kuroda et al.[14],

$$X=\frac{V-V_l}{V_c-V_l} \qquad (1)$$

where $V$ was the specific volume of the sample directly obtained from the volume-temperature measurement, $V_l$ the specific volume of purely amorphous region, and $V_c$ that of the entirely crystalline region. According to Gubler and Kovacs, $V_l$ and $V_c$ are expressed as follows;

$$V_l=1.170+9\times10^{-4}(T-25) \qquad (2)$$

and

$$V_c=1.0255+3\times10^{-4}(T-25) \qquad (3),$$

where $T$ shows temperature in °C. The relation between $V$ and $T$ at any degree of crystallinity is shown by a straight line by putting $V_l$, $V_c$ above presented and optional value for $X$ into the equation (1). For the values 0.0, 0.1, 0.2, ..... 0.9 and 1.0 of $X$, a series of $V$—$T$ line was obtained (Fig. 5) and from these straight lines and specific volume-temperature curve of polyethylene the degree of crystallinity was estimated.

A curve similar to that shown by Richards was obtained as a whole between the degree of crystallinity and the degree of short chain branching. According to the equations presented by Sperati et al. which showed the relation

14) T. Kuroda et al., given out in the symposium on polyethylene in Tokyo, November 1959.

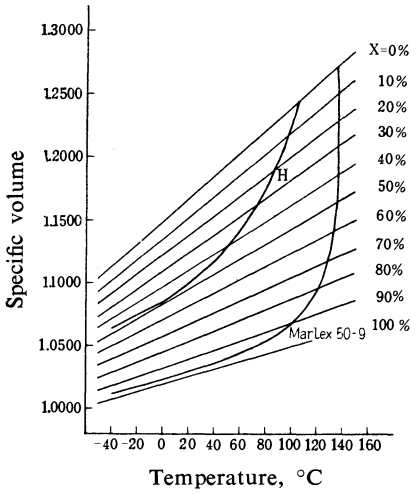



Fig. 5. The relationship between specific volume and temperature in various degree of crystallinity from which the degree of crystallinity of polyethylene was estimated.

between the density and the degree of crystallinity and that between the density and short chain branching, the linear relation is formed between the degree of crystallinity and the degree of short chain branching in the range of $CH_3$/100C from 0.4 to 5.0 and within the accuracy of $\pm 1.0\%$. In this experiment the linear relation was also obtained in the range of degree of short chain branching within the same accuracy shown by Sperati et al., though the slope of the straight line differed from that obtained by them. Marlex and Ziegler polyethylenes have a remarkably high degree of crystallinity in comparison with high-pressure polyethylene, which is probably due to the difference in the nature of their short chain branching reported by Willbourn[15]; that is, according to him short chain branches of high-pressure polyethylene are ethyl and butyl branches and those of Marlex and Ziegler polyethylene are methyl, and methyl and ethyl, respectively, which are shorter than butyl. Therefore these low-pressure polyethylenes are considered to have a higher degree of crystallinity. As is mentioned already it is expected that the increasing amount of branch point of long chain branching lowers the degree of crystallinity. In this experiment, however, no appreciable result was obtained in this respect. This is probably due to the very small amount of long chain branching.

Above the melting point the values of specific volume of all samples at each temperature were equal within the experimental error. The calculation of specific volume by volume dilatometry is accompanied by a larger error as the difference between bath temperature and room temperature becomes larger. In order to reduce the error, volume-temperature measurements were performed in the temperature range from the melting point to 150°C by using a larger amount of the sample than that previously used. For this experiment the bulb (part C in Fig. 1, a) and the inside diameter of the capillary in part B were made large. As part A, the capillary of the equal diameter as previous was used, so as not to reduce the accuracy of the measurement. The amount of mercury inserted was adjusted so that its top might be at the middle part of part B at room temperature, and measurements were started after the bath temperature was raised and the top of the mercury column reached a height a little above the joint connecting parts A and B at around the melting point of the sample (Fig. 1, b). The total volume up to a height a little above the joint was measured by using mercury in advance and in the case of calculation, corrections were made in quite the same way as previously. Results thus obtained for low-pressure and high-pressure polyethylenes were almost equal and well consistent with the result shown by Gubler and Kovacs in specific volume and the degree of cubic expansion, and also with those by Danusso et al.[16] for a polyethylene and a polypropylene which has methyl branch every second carbon. From these results it was confirmed that the volume-temperature relation above melting point was equal regardless of the kind of polyethylene. These results

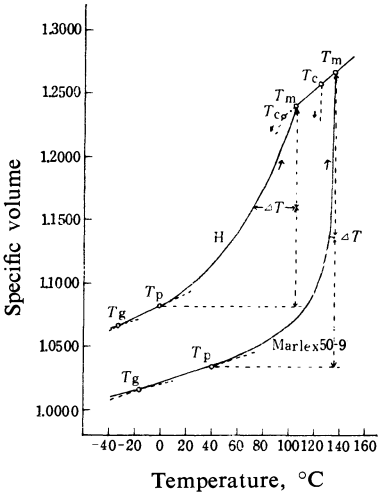



Fig. 6. Specific volume-temperature curves for Marlex 50-9 and high-pressure polyethylene H, in which the points of $T_m$, $T_c$, $T_p$ and $T_g$ and $\Delta T$ are shown.

15) A. H. Willbourn, *J. Polymer Sci.*, **34**, 569 (1959).

16) F. Danusso, G. Moraglio and G. Natta, *Ind. Plastiques Mod. (Paris)*, **10**, 40 (1958).

TABLE II. TEMPERATURES OF VARIOUS TRANSITIONS OF POLYETHYLENES IN °C

| Sample | $N_c$ | $T_m$ | $T_c$ | $T_p$ | $T_g$ | $\Delta T$ |
|---|---|---|---|---|---|---|
| Marlex 50-9 | 0.25 | 135.5 | 125.0 | 40.5 | −16.0 | 2.5 |
| Ziegler | 0.4 | 132.1 | 122.0 | 30.8 | −19.0 | 6.1 |
| G | 0.6 | 122.8 | 113.7 | 21.5 | −22.2 | 11.8 |
| A | 1.6 | 113.2 | 106.8 | 13.3 | −25.2 | 19.3 |
| B | 1.6 | 113.5 | 108.5 | 10.9 | −25.8 | 21.0 |
| E | 1.6 | 113.5 | 105.6 | 11.7 | −26.3 | 19.8 |
| F | 2.0 | 111.6 | 102.9 | 4.5 | −27.3 | 22.1 |
| C | 2.2 | 109.8 | 103.2 | 5.5 | −28.8 | 22.8 |
| D | 3.0 | 108.1 | 100.8 | −1.8 | −32.5 | 30.7 |
| H | 3.2 | 105.1 | 94.1 | −2.0 | −34.0 | 32.1 |

led to the following equation by using the method of least square;

$$V_{sp}=9\times10^{-4}T+1.1480$$

As is shown in Fig. 6 for Marlex 50-9 and high-pressure polyethylene H as examples, the specific volume-temperature curve of polyethylene has several transition points peculiar to the kind of polyethylene, that is, a melting point $T_m$, a crystallizing point $T_c$, a glass transition temperature $T_g$, and a premelting point $T_p$, at which the volume-temperature relation above $T_g$ deviates from the straight line and polyethylene crystals are considered to begin to melt. Their temperatures became higher with the decrease of degree of short chain branching. They are listed in Table II in the order of degree of short chain branching. The curvature of the curve between premelting point and melting point which showed the premelting process grew larger and the curve came to show almost typical first order transition as the amount of short chain branching became smaller. The premelting phenomenon is considered to be due to the variety of the size of crystalline regions in polyethylene which have different melting points according to their size. According to Gubler and Kovacs the crystalline region of low-pressure polyethylene is on the whole considerably larger than that of high-pressure polyethylene. Therefore it is considered that low-pressure polyethylene begins and finishes melting at the higher temperature and sharply at that. In order to show quantitatively the difference of curvature of these curves, $\Delta T$ was given in Table II for each sample. Here, $\Delta T$ represents the temperature difference beween the melting point and the point at which half of the difference between specific volume at the premelting point and that at the melting point is shown (Fig. 6). The values of $\Delta T$ were plotted as a function of short chain branching in Fig. 7. Among high-pressure polyethylenes it seems that these values increase with the increasing amount of short chain branching and between these two quantities

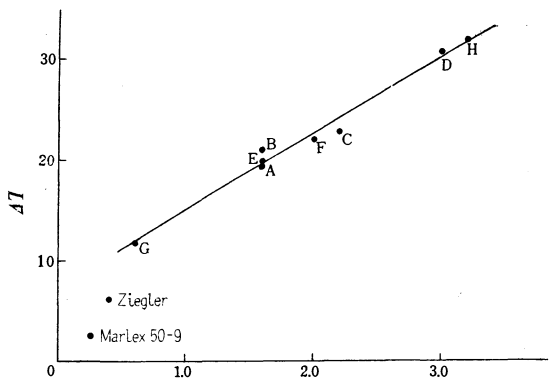



Fig. 7. The relation between short chain branching and the temperature difference between $T_m$ and the point where half of the difference in specific volumes at $T_p$ and $T_m$ are shown.

the following linear relationship is obtained approximately;

$$\Delta T=7.7N_c+7.3$$

According to Hunter and Oakes, melting point, crystallizing temperature and premelting phenomenon were dependent upon the molecular weight of the sample. In this experiment the values of $T_m$, $T_c$, $T_p$ and $T_g$ apparently rose with the increase of molecular weight on the whole. But sample E showed almost equal values of these temperatures to those of samples A and B, though it had lower molecular weight by about 10,000 than samples A and B, and it was the same with samples C and F, that is, sample F which is almost equal in the amount of short chain branching to sample C and in molecular weight more than double that of sample C, showed almost equal values of these temperatures to those of sample C. Therefore it seems that molecular weight has almost no or a very small effect on these temperatures in comparison with short chain branching.

The glass transition temperature appears at

present to be considered −21°C regardless of molecular weight, degree of crystallinity and degree of chain branching from the experimental results by Danusso et al., though there had been presented different values by other researchers previously. The results obtained in this experiment, however, showed that the glass transition temperature of polyethylene was dependent upon the degree of short chain branching. The details about this will be presented later.

As quenched polyethylene has a very low degree of crystallinity and crystalline regions of rather small size are considered to be distributed in it, it is expected that quenched low-branched polyethylene melts in the process similar to that of highly-branched polyethylene. Therefore volume temperature measurements were carried out by using quenched Marlex 50–9. Quenching of the sample was performed by immersing the dilatometer containing the sample and mercury into the toluene-bath cooled at −40°C after it was kept at 150°C for about three hours. The volume-temperature curve for Marlex 50–9 treated in this way is shown in Fig. 8 with the curve for the most highly crystallized Marlex 50–9. This quenched sample had a low degree of crystallinity of 38.6% at 25°C. The result as expected, however, was not obtained, but the curve showing sharp melting phenomenon was obtained, which is probably due to further crystallization which is occurring slowly on raising temperature. Similar

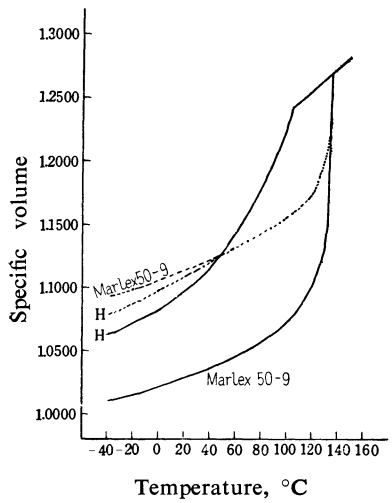



Fig. 8. Volume-temperature curves of Marlex 50–9 and high-pressure polyethylene H obtained for the most highly crystallized and quenched samples.

measurements were performed by using sample H quenched in the same way. The volume-temperature curve was also illustrated in Fig. 8 with the curve for the most highly crystallized sample H. The degree of crystallinity of this quenched sample was 40.0% at 25°C. The curve for quenched and the most highly crystallized Marlex 50–9 do not overlap with each other up to just below melting point, while the curve for quenched sample H falls on the curve for the most highly crystallized sample at around 50°C. From these results it is considered that further crystallization of the quenched sample occurs at a lower temperature and more easily in highly-branched polyethylene than in low-branched polyethylene. Probably short chain branchings of polyethylene expand the average intermolecular distances in the amorphous regions and weaken the intermolecular interaction, and as a result the molecules can begin to move easily at low temperature.

## Summary

The specific volumes of various kinds of polyethylenes with the different degrees of short chain and long chain branchings were measured by volume dilatometry in the temperature range from −40° to 150°C, and volume-temperature curves were determined. Polyethylene having the higher degree of short chain branching had the higher specific volume at any temperature below the melting point. Above the melting point specific volumes of all the polyethylenes were equal at the same temperature. Melting point, crystallizing temperature, premelting point, and glass transition temperature were raised with the decrease of degree of short chain branching. The curvature of the curve showing premelting process grew large as the amount of short chain branching contained in the sample became small, and came to show the typical first order transition phenomenon.

The author is indebted to Professor Masatami Takeda for his helpful suggestions and discussion. He also thanks Dr. C. F. Hammer of E. I. du Pont de Nemours and Company for providing the samples of polyethylene. It is also a pleasure to aknowledge the assistance in experimental work given by Miss Masako Yoshida.

*Department of Chemistry*
*Faculty of Science*
*Tokyo College of Science*
*Kagurazaka, Shinjuku-ku*
*Tokyo*

# *Stability of Complexes of Several Carboxylic Acids Formed with Bivalent Metals**

By Motoo YASUDA, Kazuo YAMASAKI and Hitoshi OHTAKI**

(Received February 4, 1960)

Numerous reports have been published on the stability of various complexes formed between bivalent metals and carboxylic acids; however, no extensive study regarding these complexes has ever been performed in any one laboratory under identical experimental conditions. Experiments under identical conditions are of primary importance because the respective values of the stability of these complexes and the differences between these values are quite small; therefore, a precise comparison of these stability constants is possible only when the values determined under the same conditions are available.

In this report the stability of various complexes formed between carboxylic acids and bivalent metals having the ratio of 1 : 1 was determined by using the pH titration method. The monobasic and dibasic acids containing the COOH groups alone were studied, i. e. the acids containing the OH groups in addition to the COOH group were excluded. Thus tartaric acid or similar acids were not studied because of their rather complicated bahavior in a solution.

## Experimental

**Materials.**—The nitrates of lead, copper, cadmium, zinc and nickel were chemicals of the analytical grade. The carboxylic acids used are listed in Table I. They were reagents of the analytical or highest grade available.

**Procedure.**—The pH values were measured with a pH meter having a glass electrode made by Horiba and Co. The temperature of the measurement was 25°C and the ionic strength of the solution was maintained at 0.1 by the addition of sodium perchlorate; however, in some cases where the stability of the complex was small such as in the nickel benzoate complex the ionic strength of the solution was kept at 0.1 by nickel nitrate itself without the addition of sodium perchlorate.

The concentration of the metal nitrate was kept generally higher than that of the carboxylic acid to prevent the formation of a complex having the metal to ligand ratio of 1 : 2. The concentrations used were as follows:

Monobasic acids

| | | | |
|---|---|---|---|
| Lead nitrate | 0.004~0.02M | Acid | 0.004~0.009M |
| Copper nitrate | 0.006~0.015 | 〃 | 0.004~0.009 |
| Cadmium nitrate | 0.03 | 〃 | 0.012 |
| Zinc nitrate | 0.034 | 〃 | 0.012 |
| Nickel nitrate | 0.026 | 〃 | 0.009~0.012 |

Dibasic acids except diglycolic and thiodiglycolic acids

| | | | |
|---|---|---|---|
| Lead nitrate | 0.004M | Acid | 0.002M |
| Copper nitrate | 0.003 | 〃 | 0.002 |
| Cadmium nitrate | 0.006 | 〃 | 0.01 |
| Zinc nitrate | 0.007 | 〃 | 0.01 |
| Nickel nitrate | 0.01 | 〃 | 0.01 |

Diglycolic and thiodiglycolic acids

| | | | |
|---|---|---|---|
| Lead nitrate | 0.002M | Acid | 0.001M |
| Cadmium nitrate | 0.002 | 〃 | 0.001 |
| Zinc nitrate | 0.002 | 〃 | 0.001 |
| Copper nitrate | 0.0015 | 〃 | 0.001 |
| Nickel nitrate | 0.0026 | 〃 | 0.001 |

To convert the hydrogen ion activity into its concentration in the solution, the value 0.83 suggested by Kielland[1] was used.

## Results

**Acid Dissociation Constant.**—If the dibasic acid is represented as $H_2A$, the acid dissociation constants to be determined may be expressed as

$$K_1 = \frac{[H^+]\,[HA^-]}{[H_2A]} \qquad (1)$$

and

$$K_2 = \frac{[H^+]\,[A^{2-}]}{[HA^-]} \qquad (2)$$

where [ ] expresses the concentration in mole per litre. The values of the dissociation constant were determined by titration with alkali and they are given in Table I[2]. For some dicarboxylic acids such as succinic, itaconic, glutaric, adipic, diglycolic and thiodiglycolic acids the first and second dissociation occurred simultaneously and the method of successive approximation was used to calculate their dissociation constants.

**Stability Constant.**—The values of the stability constant of the complexes formed are expressed by

* Presented at the XVIIth International Congress of Pure and Applied Chemistry held at Munich in 1959.

** Present address of H. Ohtaki: Tokyo Institute of Technology, Ookayama, Meguro-ku, Tokyo.

1) J. Kielland, *J. Am. Chem. Soc.*, **59**, 1675 (1937).

2) The results for phthalic acid were taken from the report by M. Yasuda, K. Suzuki and K. Yamasaki, *J. Phys. Chem.*, **60**, 1649 (1956).

TABLE I. ACID DISSOCIATION CONSTANTS
25°C, $\mu=0.1$

| | Acids | p$K_1$ | p$K_2$ |
|---|---|---|---|
| 1 | Acetic acid | 4.53 | |
| 2 | Benzoic acid | 4.01 | |
| 3 | *o*-Methoxybenzoic acid | 3.90 | |
| 4 | Succinic acid | 4.00 | 5.21 |
| 5 | Itaconic acid | 3.68 | 5.14 |
| 6 | Glutaric acid | 4.14 | 5.01 |
| 7 | Adipic acid | 4.28 | 5.00 |
| 8 | Phthalic acid | 2.76 | 4.92 |
| 9 | Malonic acid | 2.76 | 5.29 |
| 10 | Maleic acid | <2 | 5.79 |
| 11 | Citraconic acid | 2.2 | 5.60 |
| 12 | Diglycolic acid | 2.77 | 3.92 |
| 13 | Thiodiglycoic acid | 3.15 | 4.13 |

$$k_1=\frac{[MA]}{[M^{2+}]\,[A^{2-}]} \tag{3}$$

Under the conditions in the present experiments, the formation of complexes having a metal to ligand ratio of 1:2 is negligible. Therefore the species present in the solutions are $H^+$, $M^{2+}$, MA, $A^{2-}$, $HA^-$, $H_2A$ and $OH^-$ except in the case of sodium and perchlorate ions which were added in order to keep the ionic strength of the solution constant. Then the following relations exist between the total concentrations of acidic hydrogen, acid and metal for which the symbols $C_H$, $C_A$ and $C_M$ are used respectively.

The concentration of $OH^-$ is negligible in acid solutions.

Thus

$$C_H=[H^+]+[HA^-]+2[H_2A] \tag{4}$$

$$C_A=[A^{2-}]+[HA^-]+[H_2A]+[MA] \tag{5}$$

$$C_M=[M^{2+}]+[MA] \tag{6}$$

By substituting Eqs. 1 and 2 into 4, Eq. 7 may be obtained

$$C_H-[H^+]=\frac{[H^+]\,[A^{2-}]}{K_2}+\frac{2[H^+]^2[A^{2-}]}{K_1K_2} \tag{7}$$

From the pH measurements of the solutions $[H^+]$ was calculated. By substituting $[H^+]$ into 7 $[A^{2-}]$ was found and then [MA] and $[M^{2+}]$ were obtained from 5 and 6 combined with 1 and 2 and finally $k_1=[MA]/[M^{2+}]\,[A^{2-}]$ was found. The logarithmic values of the stability constant thus obtained are given in Table II. For monobasic acids the calculations are more simple than for dibasic acids shown above.

The stability of these complexes under somewhat different experimental conditions of temperature and ionic strength have been previously determined by several other authors, as listed in Table III:

If the differences in temperature and ionic strength of the solution are taken into consideration, their results agree fairly well with the results of the present study.

From the results shown in Table II the acids studied are divided into three groups:

1) Dibasic acids forming a seven membered or a larger chelate ring and having no double bonds in the chelate ring. Monobasic acids also belong to this group.

2) Dibasic acids forming a six membered ring such as malonic acid and those having double bonds in the chelate ring such as maleic and citraconic acids.

3) Dibasic acids seeming to act as tridentate chelating agent. Diglycolic and thiodiglycolic acids belong to this group.

It is obvious from Table II that the acids of the first group form complexes whose stability constants follow the order

$$Pb>Cu>Cd>Zn>Ni$$

and that lead shows the highest stability. The values for monobasic acids are nearly

TABLE II. STABILITY CONSTANTS ($\log k_1$)

| | Acids | Pb | Cu | Cd | Zn | Ni |
|---|---|---|---|---|---|---|
| 1 | Acetic acid | 2.1 | 1.8 | 1.5 | 1.0 | 1.0 |
| 2 | Benzoic acid | 2.0 | 1.6 | 1.4 | 0.9 | 0.9 |
| 3 | *o*-Methoxybenzoic acid | 1.9 | 1.6 | 1.3 | 0.9 | 0.8 |
| 4 | Succinic acid | 2.8 | 2.6 | 2.1 | 1.6 | 1.6 |
| 5 | Itaconic acid | 3.1 | 2.8 | 2.3 | 1.9 | 1.8 |
| 6 | Glutaric acid | 2.8 | 2.4 | 2.0 | 1.6 | 1.6 |
| 7 | Adipic acid | 2.8 | 2.3 | 2.1 | 1.8 | 1.6 |
| 8 | Phthalic acid[2] | ppt. | 3.1 | 2.5 | 2.2 | 2.1 |
| 9 | Malonic acid | 3.1 | 5.0 | 2.3 | 2.7 | 3.2 |
| 10 | Maleic acid | 3.2 | 3.4 | 2.4 | 2.0 | 2.0 |
| 11 | Citraconic acid | 3.3 | 3.4 | 2.2 | 1.8 | 1.8 |
| 12 | Diglycolic acid | 4.4 | 3.9 | 3.3 | 3.6 | 2.6 |
| 13 | Thiodiglycolic acid | 3.6 | 4.3 | 2.6 | 2.9 | 4.0 |

TABLE III

| Acids | References |
|---|---|
| Acetic | Cannan and Kibrick[3] |
| | Lloyd, Wycherley and Monk[4] |
| | Edmonds and Birnbaum[5] |
| | Fronaeus[6] |
| | Tanaka et al.[7] |
| Succinic | Cannan and Kibrick[3] |
| | Peacock and James[8] |
| Glutaric | Cannan and Kibrick[3] |
| | Peacock and James[8] |
| Adipic, phthalic and maleic | Peacock and James[8] |
| Malonic | Riley[9] |
| | Stock and Davies[10] |
| | Money and Davies[11] |
| Diglycolic and thiodiglycolic | Tichane and Bennett[12] |

the same and show only small differences between them. The dibasic acids show higher values than monobasic acids. Both succinic and itaconic acids form seven membered rings, but the stability constants are a little larger for the latter, which has a double bond in the side chain.

The empirical stability order for bivalent metals was proposed by various authors and the order

$$Cu > Ni > Pb > Co,\ Zn$$

found by Mellor and Maley[13] holds with some variations for many O and N type ligands. Irving and Williams[14] pointed out that the order

$$Zn < Cu > Ni > Co > Fe > Mn$$

for the metals of the first transition series held irrespective of the nature of the ligands involved. However, generally the order of stability depends on the nature of ligands, especially when metals of non-transition series are concerned.

The stability constants of more than five hundred ligands have so far been determined, but no example of a ligand showing a high stability for lead has been found except in the case of $\beta$-(*S*-ethyl)mercaptopropionic acid as determined by Irving and Fernelius[15] in a water-dioxane mixture. The order of stability found by them is the same as the present one, i. e. lead showed the highest stability. The highest stability found in the lead complexes of carboxylic acids is, therefore, quite remarkable. The exact reason for the large stability of lead is rather difficult to explain at present.

The above mentioned order in the first group does not hold for the acids in the second group. The complexes of malonic acid which form six membered chelate rings follow the stability order

$$Cu > Ni > Pb > Zn > Cd$$

However, with the other two acids, maleic and citraconic acids which form seven membered chelate rings, copper is the highest in the stability order,

$$Cu > Pb > Cd > Zn > Ni$$

Citraconic acid has a methyl group and its effect seems to decrease somewhat the stability, perhaps due to steric hindrance.

If the size of the chelate ring for one metal is compared, for example, for copper, the stability is highest for malonic acid and it decreases in the following order as the size of the chelate ring increases,

| | |
|---|---|
| malonic acid | six membered ring, |
| succinic acid | seven membered ring, |
| glutaric acid | eight membered ring, |
| adipic acid | nine membered ring. |

If we could determine the stability of oxalic acid complexes which form a five membered ring, it might be interesting. However, under the experimental conditions of the present study, precipitation occurred instantaneously. The stability of oxalic acid complexes given in the literature are few and no data for lead are available.

For the acids in the third group the order of metals are

$Pb > Cu > Zn > Cd > Ni$ for diglycolic acid

and

$Cu > Ni > Pb > Zn > Cd$ for thiodiglycolic acid.

These two acids have rather small values for their acid dissociation constants. On the other hand, the values of their stability constant are large and it seems that they form tridentate complexes with O and S atoms participating in the chelation as Tichane and Bennett[12] pointed out.

3) R. K. Cannan and A. Kibrick, *J. Am. Chem. Soc.*, **60**, 2314 (1938).
4) M. Lloyd, V. Wycherley and C. B. Monk, *J. Chem. Soc.*, **1951**, 1786.
5) S. M. Edmonds and N. Birnbaum, *J. Am. Chem. Soc.*, **62**, 2367 (1940).
6) S. Fronaeus, *Acta Chem. Scand.*, 6, 1200 (1952).
7) N. Tanaka et al., This Bulletin, **32**, 516 (1959); **33**, 417 (1960).
8) J. M. Peacock and J. C. James, *J. Chem. Soc.*, **1951**, 2233.
9) H. L. Riley, ibid., **1930**, 1642.
10) D. I. Stock and C. W. Davies, ibid., **1949**, 1371.
11) R. W. Money and C. W. Davies, *Trans. Faraday Soc.*, **28**, 609 (1932).
12) R. M. Tichane and W. E. Bennett, *J. Am. Chem. Soc.*, **79**, 1293 (1957).
13) L. E. Maley and D. P. Mellor, *Austhal. J. Sci. Res.*, A2, 92, 579 (1949).
14) H. Irving and R. J. P. Williams, *J. Chem. Soc.*, **1953**, 3192.
15) R. J. Irving and W. C. Fernelius, *J. Phys. Chem.*, **60**, 1427 (1956).

In connection with this point, *o*-methoxybenzoic acid was studied to ascertain whether the O atom of the methoxy group participates in the chelation. The values for *o*-methoxybenzoic acid complexes were nearly the same as those of the benzoic acid complexes. This appears to mean that the O atom of the methoxy group has very little relation to the chelation.

Concerning the chelating tendency of various bivalent metals for O and S atoms of similar ligands, several studies have been made on *o*-aminobenzenethiol[16], *β*-mercaptopropionic acid[17], *β*-(*S*-ethyl)mercaptopropionic acid[15] and purine derivatives[18], and zinc was found to form a stronger complex than nickel when sulfur is involved in the metal-ligand bond. However, this is not the case for thiodiglycolic acid, and a more detailed study on ligands containing sulfur is desirable to elucidate this problem.

Finally the use of these dicarboxylic acids as the eluting agent of the metal ions adsorbed on ion exchange resins was investigated. As the acid, adipic acid was chosen, as it showed suitable differences of stability for various metals.

Metal ions were adsorbed on the resin Dowex 50, H-form. Sodium adipate solution of pH 5.2 (0.1 molar solution) was poured into the column. Lead was omitted as it formed a precipitate in the 0.1 molar solution of sodium adipate. The metals in the eluted solution were determined by titration with ethylenediaminetetraacetate. The vertical axis of the graph (Fig. 1) indicates the values proportional to the metal concentration in each fraction (5 ml.) and the horizontal axis the fraction number. The separation between copper, cadmium and zinc is complete, but the separation between zinc and nickel is not. Diglycolic acid was also tested for the eluting agent, but in this case the tailing of each metal was remarkable and the complete separation was difficult.

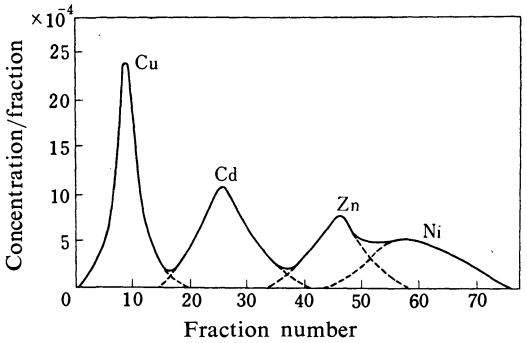



Fig. 1. Elution of Cu, Cd, Zn and Ni ions by adipic acid.

Resin: Dowex 50×−4
Column: dia. 1 cm.×5 cm.
Flow rate: 0.5 ml. per min.
Adipic acid: 0.1 M pH 5.2
One fraction: 5 ml.

## Summary

Stability constants of the bivalent metal complexes formed with several mono- and dicarboxylic acids were determined at 25°C and ionic strength of 0.1. For monocarboxylic acids and several dicarboxylic acids having no double bond or forming larger chelate rings than six membered rings the following stability order held: Pb>Cu>Cd>Zn>Ni. It is very remarkable that lead showed the highest stability among bivalent metals.

A part of the expense of the present study was defrayed by a Grant-in-aid for Fundamental Scientific Research from the Ministry of Education.

*Chemical Institute*
*Nagoya University*
*Chikusa, Nagoya*

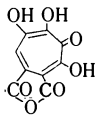
16) R. G. Charles and H. Freiser, *J. Am. Chem. Soc.*, **74**, 1385 (1952).
17) Q. Fernando and H. Freiser, ibid., **80**, 4928 (1958).
18) G. E. Cheney, H. Freiser and Q. Fernando, ibid., **81**, 2611 (1959).

# *Synthesis of Puberulonic Acid*[1]

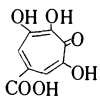
By Tetsuo NOZOE, Kozo DOI* and Tokuro HASHIMOTO**

(Received January 16, 1960)

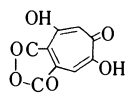
Puberulonic acid (I) was first isolated, together with puberulic acid (II), by Birkinshaw and Raistrick[2] from cultures of the moulds *Penicillium puberulum* Bainer and *P. aurentio-virens* Biourge. These mould tropolones (I and II) have been reported to have a significant antibiotic activity against various Gram-positive organisms[3]. The structure I for puberulonic acid has been accepted reasonably by the presence of a dicarboxylic anhydride grouping evidenced from the data of the infrared spectrum[4], ultraviolet spectrum[5] and titration[6], and by the decarboxylation of it to puberulic acid[6,7] (II). As other mould tropolones, stipitatonic acid[8] (III) and stipitatic acid[9] (IV) have been isolated from culture of *P. stipitatum* Thom. Of the above four mould tropolones, puberulic acid[10] (II) and stipitatic acid[11,12] (IV) have already been synthesized by Johnson and his collaborators from 1, 2, 4-trimethoxybenzene and diazoacetate.



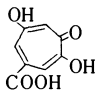
I



II



III



IV

The present authors have been able to synthesize puberulonic acid (I), the details of which will be reported in this communication.

The starting material used was tropolone-3, 4-dicarboxylic anhydride[13] (V), which had been obtained in a poor yield by alkaline hydrogen peroxide oxidation[14] of purpurogallin, of which synthesis[15] had been completed by Haworth and his co-workers. The structure of the anhydride V had been proved by the conversion of it to benzene-1, 2, 3-tricarboxylic acid with alkali-fusion.

As an approach to the synthesis of puberulonic acid (I), it was adopted, that an introduction of bromine, followed by replacing of the bromine with the hydroxyl group, into the anhydride V, was carried out and that a further brominationhydroxylation process were repeated in the resulted hydroxytropolone-dicarboxylic anhydride (XIII). To the reaction for replacing bromine atom with the hydroxyl group, the Rosenmund method[16], in which *o*-bromobenzoic acid was converted into salicylic acid, was satisfactorily applied.

When 3-bromotropolone (VI) was heated with sodium $\beta$-naphthalenesulfonate in dilute alkaline solution, 3-hydroxytropolone (VII) was obtained in a 40% yield. This fact proves that a normal nucleophilic substitution of the bromine into the hydroxyl group took place in the above reaction, contrary to formation of 4-hydroxytropolone, a *ciné* (abnormal) substitution product, in high temperature hydrolysis of 3-bromotropolone (VI) with 75% potassium hydroxide[17]. Application of similar reaction to 3, 7-dibromotropolone (VIII) afforded in less yield 3, 4-dihydroxytropolone (IX), which was proved to be identical with the compound known as "decarboxylated puberulic acid"[6,18].

Bromination of tropolone-3, 4-dicarboxylic anhydride (V) in acetic acid gave easily 7-bromotropolone-3, 4-dicarboxylic anhydride (X) in a good yield. Heating of the anhydride X in

* Present address, The Chemical Research Institute of Non-Aqueous Solutions, Tohoku University, Sendai.

** Present address, No. 3-1 Kanda-Jimbo-cho, Chiyoda, Tokyo.

1) This article was read at the 11th Annual Meeting of the Chemical Society of Japan, April, 1957; partly read by T. Nozoe at the 16th International Congress of IUPAC in Paris, July 18, 1957.

2) J. H. Birkinshaw and H. Raistrick, *Biochem. J.*, **26**, 441 (1932).

3) A. E. Oxford, H. Raistrick and G. Smith, *Chem. & Ind.*, **61**, 485 (1942).

4) A. W. Johnson, N. Sheppard and A. R. Todd, *J. Chem. Soc.*, **1951**, 1139.

5) G. Aulin-Erdtman, *Acta Chem. Scand.*, **4**, 1325 (1950); **5**, 301 (1951).

6) R. E. Corbett, C. Hassal, A. W. Johnson and A. R. Todd, *J. Chem. Soc.*, **1950**, 1.

7) R. E. Corbett, A. W. Johnson and A. R. Todd, ibid.. **1950**, 6.

8) a) W. Segal, *Chem. & Ind.*, **1957**, 1040. b) K. Doi and Y. Kitahara have corrected the earlier formulation of stipitatonic acid by W. Segal to that of III. This Bulletin, **31**, 788 (1958).

9) J. H. Birkinshaw, A. R. Chambers and H. Raistrick, *Biochem. J.*, **36**, 242 (1942).

10) R. B. Johns, A. W. Johnson and J. Murray, *J. Chem. Soc.*, **1954**, 198.

11) J. R. Bartels-Keith, A. W. Johnson and W. I. Taylor, ibid., **1951**, 2352.

12) R. B. Johns, A. W. Johnson and M. Tisler, ibid., **1954**, 4605.

13) T. Nozoe et al.. *Science Repts. Tohoku Univ., Ser.* I, **38**, 257 (1954).

14) W. D. Crow, R. D. Haworth and P. R. Jefferies, *J. Chem. Soc.*, **1952**, 3705.

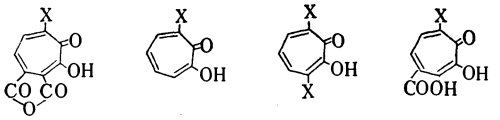
15) D. Caunt, W. D. Crow, R. D. Haworth and C. A. Vodoz, ibid., **1950**, 1631.

16) K. W. Rosenmund and H. Harms, *Ber.*, **53**, 2226 (1920).

17) Y. Kitahara, *Science Repts. Tohoku Univ., Ser.* I, **39**, 258 (1956).

18) G. Barger and O. Dorrer, *Biochem. J.*, **28**, 11 (1934).

water at 180°C afforded 3-bromo-6-carboxytropolone[19] (XI), a bromination product of 4-carboxytropolone (XII). This fact, together with derivation of 3-hydroxytropolone (VII) from the compound XIII described below, appears to determine the position of the bromine-atom in the molecule X.



V : X=H X : X=Br XIII : X=OH



VI : X=Br VII : X=OH



VIII : X=Br IX : X=OH

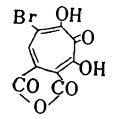


XI : X=Br XII : X=H XIV : X=OH

Reaction of the bromo derivative X with sodium β-naphthalenesulfonate in weak alkaline solution for four hours gave 3-hydroxytropolone-4, 5-dicarboxylic anhydride (XIII) in a good yield. The replacement of the bromine-atom in the compound X with hydroxyl group appeared to be more facile than in the cases of 3-bromotropolone (VI) and 3, 7-dibromotropolone (IX), the fact of which indicates probably, that the bromine-atom in the former X is activated by the dicarboxylic anhydride grouping situated at the *p*-position.

It was found, that stipitatonic acid[8a] (III) gives stipitatic acid (IV) under the same condition as that[6] of formation of puberulic acid (II) from puberulonic acid (I). On the contrary, 3-hydroxytropolone derivative XIII did not decarboxylate under the same condition, but caused decarboxylation under heating with water in a sealed tube at 180°C to 5-carboxy-3-hydroxytropolone (XIV), which corresponds to "isostipitatic acid"[10,12], synthesized already by Johnson and others. Subsequent heating of the compound (XIV) at its melting point gave 3-hydroxytropolone (VII). 3-Hydroxytropolone-4, 5-dicarboxylic anhydride (XIII) was also obtained by treatment of the corresponding bromo derivative X with 75% potassium hydroxide or by persulfate oxidation of the anhydride V, the details of which will be reported elsewhere.

It was found, that the monobromination of the hydroxy compound XIII was unexpectedly difficult. Addition of bromine to XIII in acetic acid appeared to result in consumption of about one-half of the calculated amount of bromine, and the successive isolation procedure of the product left only charred matter. This fact recalls an observation of Johnson and others on bromination of isostipitatic acid[10] (XIV). In this series of experiments, however, 7-bromo-3-hydroxytropolone-4, 5-dicarboxylic anhydride (XV) could be obtained by the bromination of XIII in the presence of sodium hydrogen sulfite in a 50% yield.



XV

Fig. 1 shows the ultraviolet absorption spectra of the foregoing four intermediates (V, X, XIII and XV). The absorption maximum near 350 mμ in curves (1) and (2) is respectively split into three absorption peaks in curves (3) and (4), the fact of which is probably characteristic of those of 3-hydroxytropolones[20].

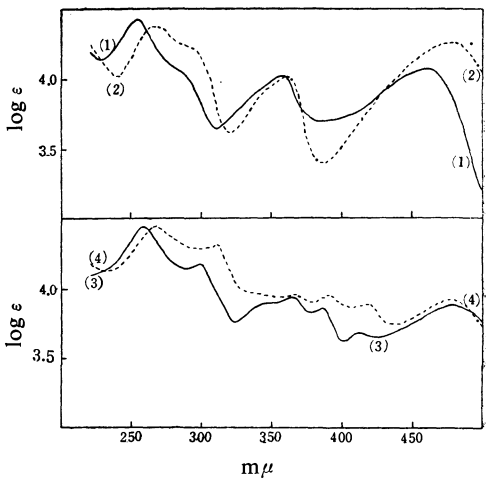



Fig. 1. Ultraviolet absorption spectra in methanol.
(1) : Tropolone-3, 4-dicarboxylic anhydride (V)
(2) : 7-Bromotropolone-3, 4-dicarboxylic anhydride (X)
(3) : 3-Hydroxytropolone-4, 5-dicarboxylic anhydride (XIII)
(4) : 7-Bromo-3-hydroxytropolone-4, 5-dicarboxylic anhydride (XV)

Treatment of the bromo derivative XV with sodium β-naphthalenesulfonate in slightly alkaline solution resulted in formation of puberulonic acid (I) in a 35% yield. The nucleophilic reactivity of the bromine atom in XV seemed to be distinctly smaller than that of the bromine in X. Puberulonic acid (I) synthesized as above did not show any depression of the melting point on admixture with a natural one[21].

19) Y. Kitahara, *Science Repts. Tohoku Univ., Ser.* I, **40**, 74 (1956).

20) T. Nozoe et al., ibid., **37**, 191 (1953); **40**, 121 (1957).

21) It was separated from a mixture of puberulonic and puberulic acids, m. p. 275°C (decomp.), which Professor J. H. Birkinshaw had kindly sent to us.

Puberulic acid (II), obtained by decarboxylation of the synthesized puberulonic acid, also showed no depression of the melting point on admixture with a natural one[21].

In Fig. 2 are shown the comparisons of the ultraviolet absorption spectra of synthetic puberulonic and puberulic acids with natural ones, and in Table I is shown, that of the infrared absorptions (6 $\mu$ bands) of synthetic and natural puberulonic acid.

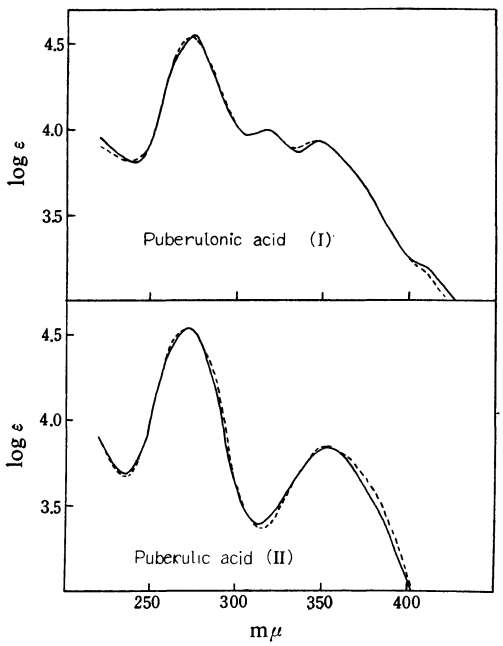



Fig. 2. Ultraviolet absorption spectra in water.
(——) : Synthetic products
(------) : Natural products

TABLE I. COMPARISON OF THE INFRARED ABSORPTION OF SYNTHETIC AND NATURAL PUBERULONIC ACID

| Puberulonic acid | M.p. | Main strong bands $cm^{-1}$ | | | | |
|---|---|---|---|---|---|---|
| Synthetic[22] | 293°C | 1830 | 1765 | 1618 | 1545 | KBr |
| Natural[22] | 293°C | 1830 | 1765 | 1618 | 1545 | KBr |
| Johnson et al.[4] | 298°C | 1830 | 1770 | 1615 | 1544 | Nujol |

## Experimental[23]

**3-Hydroxytropolone (VII).**—A mixture of 3-bromotropolone (VI, 0.60 g.), sodium $\beta$-naphthalenesulfonate (0.76 g.), sodium hydroxide (0.4 g.), copper bronze (60 mg.) and water (45 cc.) was heated under reflux for 4 hr. The filtrate, from which copper was removed, was acidified with dilute sulfuric acid to Congo-red and extracted with ethyl acetate (100 cc.). The evaporated residue of the extract, after sublimation in vacuo followed by crystallization from cyclohexane, gave 3-hydroxytropolone (VII, 0.14 g., 44%), m. p. 136°C, undepressed on admixture with an authentic specimen[20].

**3, 4-Dihydroxytropolone (IX).**—A mixture of 3, 7-dibromotropolone (VIII, 0.28 g.), sodium $\beta$-naphthalenesulfonate (0.7 g.), sodium hydroxide (0.2 g.), copper powder (10 mg.) and water (30 cc.) was heated under reflux for 8 hr. The similar procedure as above described, after sublimation in vacuo and subsequent crystallization from ethyl acetate, yielded 3, 4-dihydroxytropolone (IX, 35 mg., 22%), colorless prisms, m. p. 237°C (reported 233~235°C[18], 237~238°C[6]).

Found : C, 54.58 ; H, 4.00. Calcd. for $C_7H_6O_4$ : C, 54.55 ; H, 3.92%.

The ultraviolet absorption, having maxima at 272 m$\mu$ (log $\varepsilon$ 4.64) and 355 (3.95) in water, was identical with that of the reported decarboxylated puberulic acid[6].

**7-Bromotropolone-3, 4-dicarboxylic Anhydride (X).**—To a stirred mixture of the dicarboxylic anhydride (V, 2.5 g.), sodium acetate trihydrate (1.8 g.) and acetic acid (40 cc.) was added, dropwise, bromine (2.1 g.) in acetic acid (5 cc.). After being stirred for 2 hr. at room temperature, the mixture was diluted with water, acidified with dilute sulfuric acid to Congo-red, and then extracted with methyl ethyl ketone. The concentrated residue of the extract was crystallized from acetic acid to form 7-bromotropolone-3,4-dicarboxylic anhydride (X, 3.0 g., 86%), yellow needles, m. p. 197~198°C. The analytical sample, m. p. 198°C, was obtained after sublimation in vacuo following recrystallization from acetic acid.

Found : C, 39.73 ; H, 1.42. Calcd. for $C_9H_3O_5Br$ : C, 39.85 ; H, 1.11%.

$\lambda_{max}^{MeOH}$ m$\mu$ (log $\varepsilon$) : 265 (4.38), 362 (4.03), 480 (4.27).

**Decarboxylation of X.**—A mixture of the bromotropolonedicarboxylic anhydride (X, 70 mg.) and water (3 cc.) was heated in a sealed tube at 180°C for 2 hr. The evaporated residue, after sublimation in vacuo and successive crystallization from methanol, afforded 3-bromo-6-carboxytropolone (XI, 20 mg.), pale yellow prisms, m. p. 233~234°C, alone or mixed on admixture with an authentic specimen[17].

**3-Hydroxytropolone-4, 5-dicarboxylic Anhydride (XIII).**—A mixture of the bromo derivative (X, 0.5 g.), sodium $\beta$-naphthalenesulfonate (0.42 g.), sodium hydroxide (0.3 g.), copper powder (10 mg.) and water (6 cc.) was heated on a boiling water bath for 4 hr. The filtrate, after copper was removed from the mixture, was acidified with dilute sulfuric acid to Congo-red and extracted with ether for 48 hr. continuously. The evaporated residue of the extract, after being washed with a small volume of methanol, gave 3-hydroxytropolone-4, 5-dicarboxylic anhydride (XIII), yellow prisms, m. p. 254~255°C. Yield, 0.32 g. (83%). The analytical sample melted at 258°C was obtained by sublimation in vacuo and by successive recrystallization from acetic acid.

22) The infrared spectra were measured by a Perkin-Elmer Model 21 Infrared Spectrometer with a rock salt prism.
23) All melting points are uncorrected.

Found: C, 51.74; H, 2.02. Calcd. for $C_9H_6O_6$: C, 51.93; H, 1.94%.

$\lambda_{max}^{MeOH}$ mμ (log ε): 258 (4.44), 300 (4.14), 365 (3.94), 385 (3.88), 410 (3.69), 475 (3.90).

**Decarboxylation of XIII.** — A mixture of XIII (100 mg.) and water (4 cc.) was heated in a sealed tube at 180°C for 2 hr. The reaction mixture was evaporated and the residual solid was washed with ethyl acetate. The soluble part in the same solvent afforded 3-hydroxytropolone (VII, 15 mg.), undepressed on admixture with an authentic specimen[20]. The less soluble part, after crystallization from water, gave 5-carboxy-3-hydroxytropolone (XIV, 40 mg.), m. p. 279°C (decomp.), of which further heating at its decomposition point yielded 3-hydroxytropolone. The product XIV is assumed to correspond to impure "isostipitatic acid"[10,12], having m. p. of 282°C.

**7-Bromo-3-hydroxytropolone-4, 5-dicarboxylic Anhydride (XV).**—To astirred mixture of the hydroxytropolone-dicarboxylic anhydride (XIII, 0.21 g.), sodium acetate trihydrate (0.14 g.) and acetic acid (4 cc.), was added dropwise a solution of bromine (0.16 g.) in acetic acid (1 cc.) at room temperature. At the point of dropping of about one-half volume of bromine, sodium hydrogen sulfite (20 mg.) was added, further bromination being followed. Then, the reaction proceeded smoothly and the reaction mixture became a transparent solution, which was allowed to evaporate in vacuo over an alkali-desiccator. The residue was diluted with water, acidified with dilute sulfuric acid to Congo-red, and extracted with methyl ethyl ketone. The residue obtained after removal of the solvent crystallized from acetic acid to give the bromo derivative (XV, 0.16 g.), yellow needles, m. p. 236~237°C (decomp). The analytical sample melted at 240°C (decomp.) was obtained by sublimation in vacuo followed by recrystallization from acetic acid.

Found: C, 38.00; H, 1.27. Calcd. for $C_9H_3O_6Br$: C, 37.66; H, 1.05%.

$\lambda_{max}^{MeOH}$ mμ (log ε): 266 (4.44), 310 (4.31), 365 (3.96), 390 (3.96), 420 (3.89), 480 (3.92).

**Puberulonic Acid (I).**—A mixture of the above bromo compound (XV, 0.57 g.), sodium β-naphthalenesulfonate (0.7 g.), sodium hydroxide (0.56 g.), copper powder (20 mg.) and water (7 cc.) was heated on a boiling water-bath for 8 hr. The solution obtained by removal of copper was acidified with dilute sulfuric acid to Congo-red and extracted wih ether for 48 hr. continuously. The evaporated residue of the extract crystallized to give yellow solids, m. p. 265~270°C (decomp.), of which washing with a small volume of methanol, sublimation in vacuo and subsequent recrystallization from methanol gave puberulonic acid (I, 15 mg., 35%), yellow crystals, m. p. 293°C (decomp.), undepressed on admixture with natural puberulonic acid[21].

Found: C, 48.04; H, 1.62. Calcd. for $C_9H_4O_7$: C, 48.23; H, 1.80%.

The ultraviolet absorption (in water) of the synthesized puberulonic acid (I) has maxima at 275 (4.54), 317 (4.00) and 447 mμ (log ε 3.94), identical with those of the authentic specimen[6].

**Puberulic Acid (II).**—A mixture of the above synthesized puberulonic acid (I, 80 mg.) and water (2 cc.) was heated under reflux for one hour. The evaporated residue of the mixture was dissolved in sodium hydrogen carbonate solution and treated with active charcoal. The solution obtained by removal of the charcoal crystallized by acidification with dilute sulfuric acid to give puberulic acid (II, 45 mg.), colorless crystals, m. p. 317~318°C, not depressed on admixture with natural puberulic acid[21].

Found: C, 48.37; H, 2.96. Calcd. for $C_8H_6O_6$: C, 48.49; H, 3.05%.

The ultraviolet absorption spectrum (in water), having maxima at 274 (4.54) and 352 mμ (log ε 3.84), was identical with that of the authentic specimen[6]. Heating of the synthesized puberulic acid (II) at 350°C and subsequent sublimation in vacuo afforded 3,4-dihydroxytropolone (IX), undepressed on admixture with an authentic specimen.

The authors express their sincere thanks to the Ministry of Education for a monetary assistance from the Grant in Aid for Scientific Research, to Professor J. H. Birkinshaw for his kind gift of natural puberulonic and puberulic acids, to Mr. Yusaku Ikegami for the infrared spectral measurements and to Messrs. Ohyama, Kato, Iwanaga and Azumi for microanalyses.

*Department of Chemistry*
*Faculty of Science*
*Tohoku University*
*Katahira-cho, Sendai*

# *Studies on Antibiotics and Related Substances. X. Syntheses of Some Unsaturated Ketocarboxylic Acids, Anti-tumor Substances**

By Mitsuhiro KINOSHITA and Sumio UMEZAWA

(Received December 26, 1959)

The anti-tumor activities of sarkomycin[1] (2-methylenecyclopentanone-3-carboxylic acid), 5-methylenecyclopentanone-3-carboxylic acid[2] and its esters prompted us to investigate some related aliphatic compounds. The present paper presents the syntheses of two isomeric methylenelevulinic acids, 4-keto-5-hexene-1-carboxylic acid and 4-keto-3-methylenepentane-1-carboxylc acid, which have been found to possess significant anti-tumor and antibacterial activities. In addition, we have described here two rare illustrations of the Mannich reaction where the formation of two isomers respecting to the methylene groups at either side of the ketone-group has been demonstrated.

**δ-Methylene- and β-Methylene-levulinic Acid.** —Ethyl 5-dimethylamino-3-keto-pentane-1-carboxylate hydrochloride (II) was prepared by the esterification of 5-dimethylamino-3-keto-pentane-1-carboxylic acid hydrochloride (I) which was synthesized from levulinic acid as reported by Mannich[3]. Thermal degradation of II afforded a 61% yield of ethyl δ-methylene-levulinate (III). Structural proof of II was obtained by hydrogenation of III with platinum catalyst to give a 83% yield of ethyl γ-keto-*n*-caproate (V). Mild hydrolysis of the ester III with dilute sulfuric acid afforded a crude product of δ-methylenelevulinic acid (IV), which resisted attempts to purify it. The analytically pure product of IV has been prepared by thermal degradation of 5-dimethylamino-3-keto-pentane-1-carboxylic acid hydrochloride I.

The ultraviolet absorption of III in methanol solution showed peaks at 211 and 315 mμ, suggesting the presence of an α, β-unsaturated ketone group. The absorption of IV prepared directly from I also showed peaks at 212 and 305 mμ in aqueous solution (Fig. 1). The infrared absorption characteristics of IV was just as expected, showing the presence of double bond, conjugated carbonyl and carboxyl groups

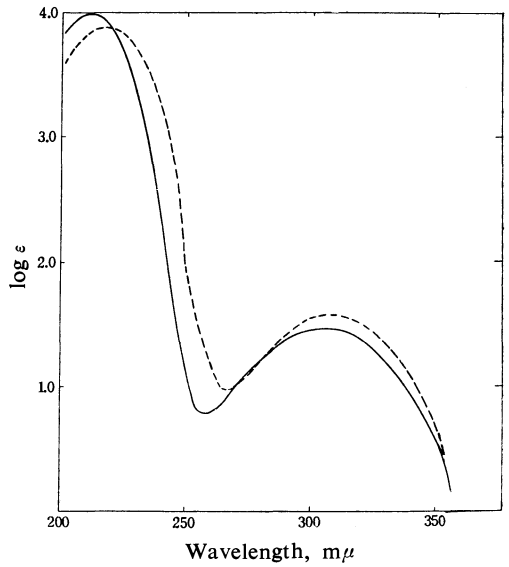



Fig. 1. Ultraviolet absorption spectra of δ-methylenelevulinic acid (——) and β-methylenelevulinic acid (----) in water.

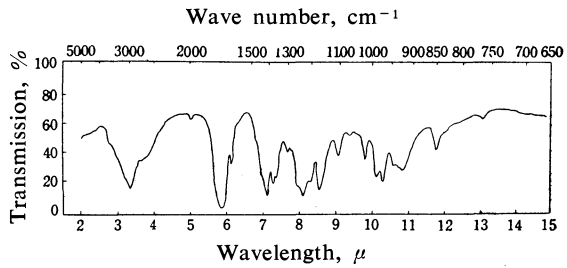



Fig. 2. Infrared absorption spectrum of δ-methylenelevulinic acid in Nujol.

(Fig. 2).

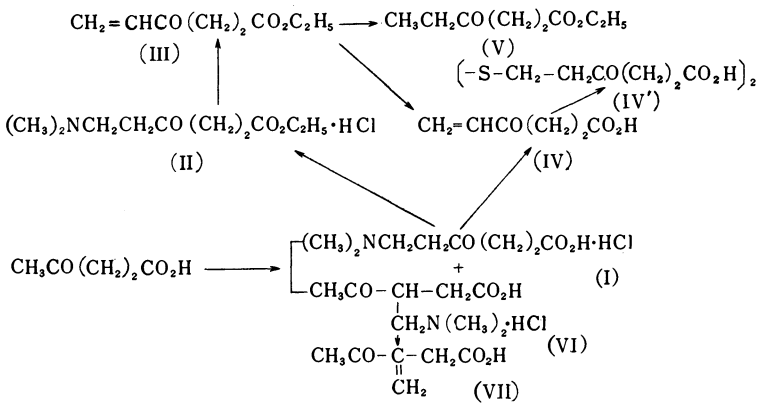
By adding a large quantity of acetone to the mother-liquor which was separated from I, the hydrochloride (VI) of 2-(dimethylamino-methyl)-3-ketobutane-1-carboxylic acid, a Mannich base isomer of I, has been obtained. Thermal degradation of VI afforded β-methyl-enelevulinic acid (VII), an isomer of IV. β-Methylenelevulinic acid (VII) has been found to be stable, while, δ-methylene isomer (IV) polymerized gradually on standing.

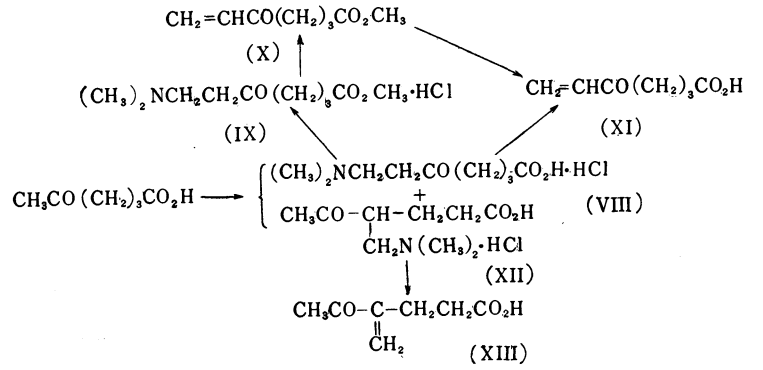
* Presented at the Division of Organic Chemistry of the Annual Meeting of the Chemical Society of Japan, Kyoto, April 2, 1959.

1) H. Umezawa, T. Yamamoto, T. Takeuchi, T. Osato, Y. Okami, S. Yamaoka, T. Okuda, K. Nitta, K. Yagishita, R. Utahara and S. Umezawa, *Antibiotics a. Chemotherapy*, **4**, 514 (1954).

2) S. Umezawa and M. Kinoshita, This Bulletin, **30**, 268 (1957).

3) C. Mannich and M. Bauroth, *Ber.*, **57**, 1108 (1924).




Addition of hydrogen sulfide to IV afforded ε, ε-dithio-di-γ-keto-*n*-caproic acid (IV'), which has been found to have a strongly inhibitory effect only for the growth of *Micrococcus flavus*.

**4-Keto-5-hexene-1-carboxylic Acid and 4-Keto-3-methylenepentane-1-carboxylic Acid.**—Methyl 4-keto-5-hexene-1-carboxylate (X) has been prepared from δ-ketocaproic acid by an analogous series of reactions as described above in the synthesis of ethyl δ-methylenelevulinate (III).

Structural proof for 6-dimethylamino-4-keto-hexane-1-carboxylic acid hydrochloride (VIII) was obtained by paper chromatographic confirmation of the spot of glutaric acid as well as that of succinic acid as the oxidation products of VIII with nitric acid[3]. VIII was esterified to yield methyl ester hydrochloride IX, which was degraded by pyrolysis to yield a crude product of methyl 4-keto-5-hexene-1-carboxylate (X). Mild hydrolysis of X with dilute sulfuric acid afforded a crude product of 4-keto-5-hexene-1-carboxylic acid (XI) in a low yield, while thermal degradation of VIII gave better result, yielding XI in a 31% yield. Unexpectedly, XI was very hygroscopic and easily crystallized as its monohydrate which was stable, showing almost no tendency to polymerize.

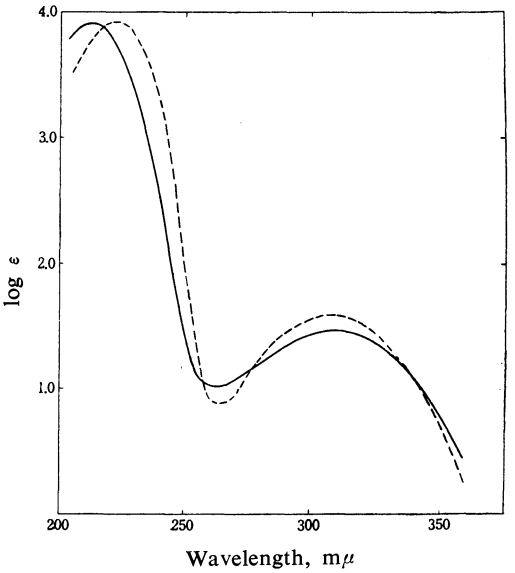



Fig. 3. Ultraviolet absorption spectra of 4-keto-5-hexene-1-carboxylic acid (——) and 4-keto-3-methylenepentane-1-carboxylic acid (----) in water.

Ozonolysis of XI gave formaldehyde as one of the products, indicating the presence of a terminal methylene group. The ultraviolet and

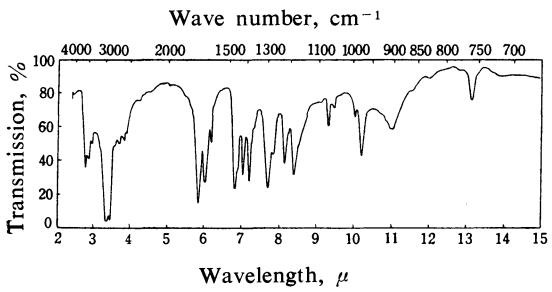



Fig. 4. Infrared absorption spectrum of 4-keto-5-hexene-1-carboxylic acid in Nujol.

infrared absorption spectra of XI presented in Fig. 3 and 4 indicated that XI is an $\alpha,\beta$-unsaturated ketocarboxylic acid.

When the mother liquor separated from VIII was stored in a refrigerator for two weeks, the hydrochloride (XII) of 3-(dimethylaminomethyl)-4-ketopentane-1-carboxylic acid separated in a crystalline mass. The product showed a positive test for iodoform reaction, suggesting that the product still contained a terminal acetyl group. Thermal degradation of XII afforded 4-keto-3-methylenepentane-1-carboxylic acid (XIII) in 71% yield. From the fact that ozonolysis of XIII yielded formaldehyde and succinic acid in reasonable yields, the structure of XIII has been confirmed and it has been further concluded that the structure of XII is 3-(dimethylaminomethyl)-4-ketopentane-1-carboxylic acid. The ultraviolet spectrum of XIII presented in Fig. 3 indicated that XIII is an $\alpha,\beta$-unsaturated ketocarboxylic acid.

## Experimental

**Separation of 5-Dimethylamino-3-ketopentane-1-carboxylic Acid Hydrochloride (I) and 2-(Dimethylaminomethyl)-3-ketobutane-1-carboxylic Acid Hydrochloride (VI) from Mannich Reaction Product.**—A mixture of levulinic acid (25 g.) and dimethylamine hydrochloride (17.6 g.) was heated to 105°C in an oil bath. To the resulting melt was added paraformaldehyde (6.45 g.) and then the mixture was stirred at 105~110°C for 30 min. After evaporation under reduced pressure, the resulting syrup was dissolved in absolute ethanol (22 cc.) by warming. To the cooled solution was added acetone (93 cc.) and the mixture was allowed to stand overnight in a refrigerator to precipitate a first crystalline crop (17.5 g.); m. p. 94~104°C. Recrystallization from ethanol gave a pure sample of I (12.9 g.), m. p. 119.5~120.5°C. An additional crop (0.9 g.) of I was obtained from the recrystallization mother liquor. The total yield of I was 31%.

Acetone (135 cc.) was added to the mother liquor of the above mentioned first crop and the mixture was stored in a refrigerator for several days to give the second crystalline crop, which was collected and washed with absolute ethanol (15 cc.); yield 7.3 g., m. p. 102~115°C. Recrystallization from ethanol gave colorless short prisms of VI, yield 3.3 g., m. p. 121~122°C. By the treatment of the recrystallization mother liquor of the second crop, additional crystals (0.5 g.) of VI (m. p. 121~122°C) were recovered. Further storage of the mother liquor of the second crop at room temperature for 3 months afforded the third crop which was recrystallized from ethanol to yield short prisms of VI (1.9 g.), m. p. 121~122°C. The total yield of VI was 12.6%. On admixing with a sample of I, the m. p. of VI was depressed.

Found: C, 45.77; H, 7.50; N, 6.42. Calcd. for $C_8H_{16}O_3NCl$: C, 45.82; H, 7.69; N, 6.68%.

**Ethyl 5-Dimethylamino-3-ketopentane-1-carboxylate Hydrochloride (II).**—A mixture of I (2.0 g.) and absolute ethanol (80 cc.) was saturated with dry hydrogen chloride and allowed to stand overnight. The ethanol was removed by distillation at about 40°C under reduced pressure and the residue was dried in a desiccator over phosphorous pentoxide. The resulting crystals were dissolved in a small quantity of ethanol by gentle warming and the solution was diluted with absolute ether, whereupon there separated a crystalline precipitate of ethyl 5-dimethylamino-3-ketopentane-1-carboxylate hydrochloride (II); yield 1.8 g. (80%). On recrystallization from absolute ethanol-absolute ether, colorless plates of m. p. 105~107°C were obtained and found to be hygroscopic.

Found: N, 6.02. Calcd. for $C_{10}H_{20}O_3NCl$: N, 5.89%.

**Ethyl δ-Methylenelevulinate (III)*.**—A sample of 1.5 g. of II was placed in a round-bottom flask and heated at 150°C in an oil bath under highly reduced pressure (0.002 mmHg). Colorless liquid with the characteristic smell of III was obtained in a receiver cooled in a dry ice-methanol bath; yield 0.6 g. (61%), $\lambda_{max}^{MeOH}$ 210 (ε 10650) and 315 mμ (ε 27).

Found: C, 61.58; H, 7.14. Calcd. for $C_8H_{12}O_3$: C, 61.52; H, 7.75%.

**Hydrogenation of III to Ethyl γ-Keto-*n*-caproate (V).**—A sample (III) (440 mg.) in ethanol (3 cc.) absorbed hydrogen (75 cc. at 11°C, 753.7 mmHg) in the presence of platinum oxide (40 mg.). The reduced product was purified by fractional distillation in vacuo to give 370 mg. of ethyl γ-keto-*n*-caproate (V), b. p. (bath temp.) 122~126°C/18 mmHg This was identified by formation of semicarbazone and 2, 4-dinitrophenylhydrazone by the usual procedure. Semicarbazone was recrystallized from ethyl acetate-petroleum ether; m. p. 105~106.5°C. The reported m. p. 106°C[4].

Found: N, 19.25. Calcd. for $C_9H_{17}O_3N_3$: N, 19.52%. 2,4-Dinitrophenylhydrazone was recrystallized twice from ethanol; long, orange-yellow needles, m. p. 69.5~71.0°C.

Found; N, 16.67. Calcd. for $C_{14}H_{18}O_6N_4$: N, 16.56%.

**δ-Methylenelevulinic Acid (IV).**—A mixture of

* Methyl ester of the same acid was reported by I. N. Nazarov and S. I. Zavyalov, *Izvest, Akad, Nauk S. S. S. R., Otdel. Khim. Nauk*, **1952**, 289; *Chem. Abstr.*, **47**, 5364 (1953) and by C. Grundmann and W. Ruske, *Chem. Ber.*, **86**, 939 (1953).

4) M. Maire, *Bull. Soc. chim. France*, [4] 3, 285 (1908).

370 mg. of III and 7.5 cc. of 1.5 N sulfuric acid was stirred at 30°C for 3 hr. The reaction mixture was cooled with ice and adjusted to pH 8 with a saturated solution of sodium bicarbonate and washed with three 5 cc. portions of ethyl acetate. The water-layer was adjusted to pH 2.0 and extracted with three 6 cc. portions of ethyl acetate. After the extract has been dried over sodium sulfate, the ethyl acetate was removed by distillation under reduced pressure at 30°C to yield crude $\delta$-methylenelevulinic acid, a colorless viscous liquid which is soluble in water; yield 50 mg. (17%). Ultraviolet spectrum of this compound in water showed the presence of a $\alpha,\beta$-unsaturated ketone group at 212 m$\mu$. However, purification of the product was unsuccessful. The analytically pure sample of IV has been obtained directly by thermal degradation of 5-dimethylamino-3-ketopentane-1-carboxylic acid hydrochloride (I) as described below.

A sample of 5 g. of I was heated (bath temp. 185°C/0.0075 mmHg) as described in the preparation of III to give a solid mass of crystals intermixed with oil in a receiver cooled in a dry ice-methanol bath. The crystals were drained on porous porcelain to remove the oily part; yield 1.26 g. (41.2%), m. p. 34.0~42.5°C*. The product was soluble in methanol, ether and water. Recrystallization from ether gave an analytical sample of $\delta$-methylenelevulinic acid (IV), m. p. 44.0~45.5°C, $\lambda_{max}^{H_2O}$ 212 m$\mu$ ($\varepsilon$ 9870) and 305 m$\mu$ ($\varepsilon$ 30.3), $\nu_{max}^{Nujol}$ 1701 (conjugated carbonyl), 1644 (C=C), 2700~2500 (carboxyl OH) and 1724 cm$^{-1}$ (carboxyl C=O).

Found: C, 55.97; H, 6.24. Calcd. for $C_6H_8O_3$: C, 56.24; H, 6.29%.

**Semicarbazone.** — m. p. 152~153°C (decomp.), $\lambda_{max}^{MeOH}$ 262 m$\mu$ ($\varepsilon$ 16200).

Found: C, 45.27; H, 5.98; N, 22.67. Calcd. for $C_{17}H_{11}O_3N_3$: C, 45.40; H, 5.99; N, 22.69%.

**$\varepsilon,\varepsilon'$-Dithio-di-$\gamma$-keto-*n*-caproic Acid (IV').**—$\delta$-Methylenelevulinic acid (IV) (760 mg.) was added to a 4.12 M aqueous solution (1.45 cc.) of sodium tetrasulfide with stirring. The reaction was exothermic and the resulting orange-red solution was allowed to stand overnight at room temperature, and then adjusted to pH 7.4 with concentrated hydrochloric acid. After removal of the separated sulfur, the filtrate was shaken with three 10 cc. portions of ethyl acetate. The water-layer was adjusted to pH 4.0 and extracted with five 10 cc. portions of ethyl acetate. The dried extract was concentrated in vacuo to afford a crystalline mass (820 mg.). A mixture of the crude product and water was adjusted to pH 7.0 with sodium bicarbonate, filtered off the precipitated sulfur and then acidified to pH 4.0. The resulting precipitate was collected and washed with water, yield 429 mg. (45%). Recrystallization from ethyl acetate and then absolute ethanol resulted pure $\varepsilon,\varepsilon'$-dithio-di-$\gamma$-keto-*n*-caproic acid; yield 180 mg., m. p. 131~131.5°C.

Found: C, 44.50; H, 5.48. Calcd. for $C_{12}H_{18}O_6S_2$: C, 44.73; H, 5.60%.

**Ozonolysis of IV.** — (a) A solution of IV (200 mg.) in ethyl acetate (10 cc.) was treated with an approximately 3% by weight ozone-oxygen mixture at 0°C at a rate of 500 cc./min. for 30 min. To the resulting solution was added water (10 cc.) and zinc dust (300 mg.). The mixture was refluxed on a water bath for 30 min. The reaction mixture was filtered, while hot, into a solution of methone (300 mg.) in 10 cc. of ethanol. Dilution with water (20 cc.) afforded needless of (200 mg., 44%), m. p. 185~187°C. Recrystallization from aqueous methanol gave pure crystals of m. p. 188~189.5°C. The m. p. was undepressed on admixing with an authentic sample of formaldehyde methone. This established the presence of the terminal methylene group in IV. (b) A solution of IV (300 mg.) in ethyl acetate (15 cc.) was treated with 3% ozone-oxygen at −20°C at a rate of 400 cc./min. for 2 hr. The resulting yellow solution was concentrated to about 0.8 cc. in vacuo below 10°C, then 30% hydrogen peroxide (1.7 cc.) was added. After gentle warming of the mixture at 60°C for a little while, the resulting solution was kept at room temperature overnight. The colorless solution was evaporated under reduced pressure. Addition of water to the residue followed by evaporation was repeated to remove exess of hydrogen peroxide as much as possible. The final crystalline residue (320 mg.) gave only the distinct spot of succinic acid on paper chromatography[5] using xylene-phenol-85% formic acid (7:3:1) as a solvent. Recrystallization from ethanol gave 194 mg. (70%) of a pure sample of succinic acid, m. p. 183~184°C; mixed m. p. determination showed no depression.

**$\beta$-Methylenelevulinic Acid (VII).**—A sample of 4 g. of VI was heated (bath temp. 180°C/0.002 mmHg) as described in the preparation of III to give a crystalline product in a receiver cooled in a dry ice-methanol bath. A small amount of oily material was removed by treatment on a porous porcelain; yield 1.7 g. (69.5%), m. p. 62~66°C. Recrystallization from ether followed by fractional vacuum sublimation (60°C/0.06 mmHg) afforded an analytical pure sample; m. p. 67.0~68.5°C; $\lambda_{max}^{H_2O}$ 218~219 ($\varepsilon$ 7520) and 309 m$\mu$ ($\varepsilon$ 38.5); $\nu_{max}^{Nujol}$ 1682 (conjugated carbonyl), 1640 (C=C), 2800~2500 (carboxyl OH), and 1715 cm$^{-1}$, (carboxyl C=O).

Found: C, 56.29; H, 6.11. Calcd. for $C_6H_8O_3$: C, 56.24; H, 6.29%.

**Ca Salt.**—Found: C, 48.70; H, 4.72; Ca, 13.83. Calcd. for $C_{12}H_{14}O_8Ca$: C, 48.91; H, 4.80; Ca, 13.62%.

**Semicarbazone.**—M. p. 184°C (decomp.). Found: C, 45.38; H, 5.71; N, 22.44. Calcd. for $C_7H_{11}O_3N_3$: C, 45.40; H, 5.99; N, 22.69%.

**2, 4-Dinitrophenylhydrazone.** — M. p. 210°C (decomp.)[6]. Found: C, 46.66; H, 4.15; N, 18.25. Calcd. for $C_{12}H_{12}O_6N_4$: C, 46.76; H, 3.92; N, 18.18%.

Ozonolysis of VII was carried out in the same manner as described in the ozonolysis of IV: (a) The compound VII (99 mg.) gave formaldehyde methone (96 mg., 42.5%), indicating the presence

* B. p. of this compound was reported by H. T. Taylor, *J. Chem. Soc.*, 1958, 3922.

5) N. F. Holyer and B. C. L. Weedon, *Chem. and Industry*, (1955), 1219. H. Kalbe, *Z. physiol. Chem.*, 297, 19 (1954).

6) The same m. p. was reported by L. Birkofer and L. Storch, *Chem. Ber.*, 87, 571 (1954).

of terminal methylene group. (b) The compound (346 mg.) gave a crude crystalline product (250 mg.) which gave only the distinct spot of malonic acid on paper chromatography. Pure malonic acid was obtained by fractional vacuum sublimation, m. p. and mixed m. p. 134~135°C (decomp.).

**Separation of 6-Dimethylamino-4-ketohexane-1-carboxylic Acid Hydrochloride (VIII) and 3-(Dimethylaminomethyl)-4-ketopentane-1-carboxylic Acid Hydrochloride (XII) from Mannich Reaction Product.**—A mixture of 5-ketocaproic acid[7] (30 g.) and dimethylamine hydrochloride (20.2 g.) was heated to 114°C in an oil bath. To the resulting melt was added paraformaldehyde (7 g.) and then the mixture was stirred at 114°C for 1.5 hr. After evaporation under reduced pressure, the resulting syrup was dissolved in absolute ethanol (35 cc.) by warming. To the cooled solution was added acetone (100 cc.) and some seeds of pure VIII, and the mixture was allowed to stand in a refrigerator for 3 days to give the first crystalline crop, which was separated and washed with a mixture of acetone-ethanol (14 : 5); yield 15.8 g., m. p. 98~108°C. Recrystallization from ethanol (18 cc.) gave a pure sample of VIII; yield 13.9 g. (27%), m. p. 116~117°C.

Found: C, 48.49; H, 7.90; N, 6.18. Calcd. for $C_9H_{18}O_3NCl$: C, 48.32; H, 8.11; N, 6.26%.

A sample of VIII (50 mg.) was added by bits to 1 cc. of fuming nitric acid. The reaction mixture was heated on a water bath until the evolution of nitrogen oxide ceased. After concentration, the reaction mixture was diluted with water and evaporated to dryness. The residue was dissolved in water. Aliquots of the solution were used for paper chromatography in the same manner as described above to give the spots of glutaric acid and succinic acid.

The mother liquor of the above mentioned first crop was stored in a refrigerator for 2 weeks to afford the second crop, which was collected and washed with acetone-ethanol and dried; yield 7.6 g. Recrystallization from ethanol gave a pure sample of XII; yield 6.6 g. (11.3%), m. p. 131~132°C. Iodoform test was positive.

Found: C, 48.53; H, 8.00; N, 6.44. Calcd. for $C_9H_{18}O_3NCl$: C, 48.32; H, 8.11; N, 6.26%.

**4-Keto-5-hexene-1-carboxylic Acid (XI).**—A sample of 5 g. of VIII was heated (bath temp. 185~190°C/0.005 mmHg) in the same manner as described in the preparation of III to give a crystalline product (2 g.) in a receiver in a dry ice-methanol bath. The product melted at room temperature into a colorless viscous liquid which was very hygroscopic and, on standing in atmosphere, formed a crystalline monohydrate. To the liquid product (2 g.) was added water (0.27 cc.) and the resulting crystalline monohydrate of XI was collected by filtration under ice-cooling, dried on a porous sheet; yield 1.4 g. (39%), m. p. 43~45°C. Cautious recrystallization from water gave a pure sample of monohydrate of XI; yield 1.2 g. (31%), m. p. 45.0~46.5°C. $\lambda_{max}^{H_2O}$ 212~3 ($\varepsilon$ 8190) and 310~3 m$\mu$ ($\varepsilon$ 29.6), $\nu_{max}^{Nujol}$ 1692 (conjugated carbonyl), 1617 (C=C), 2700~2500 (carboxyl OH), 1746 (carboxyl C=O) and 3600~3350 $cm^{-1}$ (crystalline water).

(a) Crystalline monohydrate; Found: C, 52.46; H, 7.52. Calcd. for $C_7H_{10}O_3 \cdot H_2O$: C, 52.49; H, 7.55%. (b) Anhydrous acid (dried at 100°C/10 mmHg for 4 hr.); Found: C, 59.57; H, 7.35. Calcd. for $C_7H_{10}O_3$: C, 59.14; H, 7.09%. (c) Calcium salt* (dried at 125~130°C/10 mmHg for 4 hr.); Found: C, 51.71; 5.87; Ca, 12.42. Calcd. for $C_{14}H_{18}O_6Ca$: C, 52.16; H, 5.62; Ca, 12.43%.

**Semicarbazone.**—M. p. 156~157°C (decomp.), $\lambda_{max}^{MeOH}$ 260 m$\mu$ ($\varepsilon$ 17100).

Found: C, 47.62; H, 6.33; N, 21.18. Calcd. for $C_8H_{13}O_3N_3$: C, 48.23; H, 6.58; N, 21.09%.

Ozonolysis of XI was carried out in the same manner as described in the ozonolysis of IV: (a) The monohydrate (200 mg.) gave formaldehyde methone (148 mg., 40.5%). (b) The monohydrate (426 mg.) gave a crude crystalline product (245 mg., 70%) which gave only the distinct spot of glutaric acid on paper chromatography. Recrystallization from benzene gave pure glutaric acid; m. p. and mixed m. p. 95~96°C.

**4-Keto-3-methylenepentane-1-carboxylic Acid (XIII).**—A sample of 2 g. of XII was heated (bath temp. 175~180°C/0.002 mmHg) as described in the preparation of III to give a crystalline product; yield 0.9 g. (71%), m. p. 56~62°C. Three recrystallizations from ether gave a pure sample of XIII, m. p. 66~67°C, $\lambda_{max}^{H_2O}$ 222 ($\varepsilon$ 8270) and 308 m$\mu$ ($\varepsilon$ 39.5), $\nu_{max}^{Nujol}$ 1648 (conjugated carbonyl), 1631 (C=C), 2800~2500 (carboxyl OH) and 1738 $cm^{-1}$ (carboxyl C=O).

Found: C, 59.22; H, 6.92. Calcd. for $C_7H_{10}O_3$: C, 59.14; H, 7.09%.

**Semicarbazone.**—M. p. 164~165°C (decomp.), long needles.

Found: C, 48.30; H, 6.38; N, 21.13. Calcd. for $C_8H_{13}O_3N_3$: C, 48.23; H, 6.58; N, 21.10%.

Ozonolysis of XIII was carried out in the same manner as described in the ozonolysis of IV: (a) The compound (100 mg.) gave formaldehyde methone (84 mg., 46%). (b) The compound (300 mg.) gave a crude crystalline product (295 mg.) which gave only the distinct spot of succinic acid on paper chromatography. Recrystallization from ethanol afforded 150 mg. (65%) of pure succinic acid, m. p. and mixed 183~184°C.

**Methyl 6-Dimethylamino-4-ketohexane-1-carboxylate Hydrochloride (IX).**—A mixture of VIII (3 g.) and absolute methanol (75 cc.) was saturated with dry hydrogen chloride and after-treatment was carried out just as described in the preparation of II. Recrystallization from absolute methanol-absolute ether gave long needles of IX (3 g., 95%), m. p. 91~93°C, very hygroscopic.

Found: N, 5.73. Calcd. for $C_{10}H_{20}O_3NCl$: N, 5.90%.

**Methyl 4-Keto-5-hexene-1-carboxylate (X).**—A sample of 2 g. of IX was heated (bath temp. 140~148°C/0.001 mmHg) in the same manner as described in the preparation of III. Yield 0.34 g. (26%), b. p.

7) H. Fittig and L. Wolff, *Ann.*, **216**, 129 (1883); W. H. Bentley and W. H. Perkin, *J. Chem. Soc.*, **69**, 1510 (1896).

* Prepared by Mr. T. Soga of Nikken Kagaku Co.

(bath temp.) 36~38°C/0.002 mmHg, $\lambda_{max}^{MeOH}$ 209 mμ (ε 9570) and 320 mμ (ε 27.2), $\nu_{max}^{CCl_4}$ 1692 (conjugated carbonyl), 1617 (C=C) and 1746 $cm^{-1}$ (ester C=O).

Found: C, 61.04; H, 7.56. Calcd. for $C_8H_{12}O_3$: C, 61.52; H, 7.75%.

Hydrolysis of X with dilute sulfuric acid in the same manner as described in the preparation of IV resulted a low yield of oily product, the ultraviolet absorption of which showed the presence of α,β-unsaturated ketone at 213 mμ in water. However, the product resisted an attempt to obtain a pure sample of 4-keto-5-hexene-1-carboxylic acid (XI).

**Biological Activities.**—δ-Methylenelevulinic acid (IV), β-methylenelevulinic acid (VII), 4-keto-5-hexene-1-carboxylic acid (XI) and 4-keto-3-methylenepentane-1-carboxylic acid (XIII) showed a potency of 0.6, 0.9, 0.4 and 1.3 units/mg. (in terms of sarkomycin potency) against *M. pyogenes var. aureus* 209-P, respectively. The ethyl ester III of IV and the methyl ester X of XI showed much higher potency than the original acids, but had higher toxicity than the original acid. $LD_{50}$ of IV, VII, XI, XIII and III were 1.0, 3.7, 2.0, 4.7 and 0.78 mg./mouse, respectively. ε,ε'-dithio-di-γ-keto-*n*-caproic acid (IV') exhibited a curious activity; it inhibited strongly the growth of *Micrococcus flavus*, but had almost no activity against tested bacteria and fungi.

It is very interesting to find, that all these compounds possess antitumor activities against Ehrlich cells and HeLa cells[9]. The minimum necessary concentrations of IV, VII, XI and XIII for anti-HeLa cell effect were 62.5, 62.5, 12.5 and 62.5 mcg./cc. Against cells of Ehrlich carcinoma, IV, VII, XI and XIII had a potency of 1.56, 3.8, 2.2 and 3.4 units/mg. (in terms of sarkomycin potency) by cylinder plate method. The daily intraperitoneal injection of 0.5 mg./mouse/day of IV inhibited the ascites increase and prolonged the survival period of mice (highly inbred) bearing ascites type of Ehrlich carcinoma by intraperitoneal route. Especially, calcium salt of 4-keto-5-hexene-1-carboxylic acid (XI) showed an excellent results; daily intraperitoneal injection of 0.125, 0.25 or 0.5 mg./mouse/day which was continued for 52 days showed significant inhibition. The control mice all died in 14~22 days. Mice of the group treated with 0.5 mg. daily all survived 52 days. Moreover, toxicity of the calcium salt of XI was $LD_{50}$=4.0 mg./mouse.

A detailed report on the biological activities of the above-mentioned compounds will be published elswhere.

9) Private communicaiton from Professor H. Umezawa of National Institute of Health, Tokyo.

## Summary

1) 2-(Dimethylaminomethyl)-3-ketobutane-1-carboxylic acid hydrochloride (VI) as well as 5-dimethylamino-3-ketopentane-1-carboxylic acid hydrochloride (I) has been obtained from levulinic acid, paraformaldehyde and dimethylamine hydrochloride by means of the Mannich reaction. Thermal degradation of I and VI afforded δ-methylenelevulinic acid (IV) and β-methylenelevulinic acid (VII), respectively.

2) 3-(Dimethylaminomethyl)-4-ketopentane-1-carboxylic acid hydrochloride (XII) as well as 6-dimethylamino-4-ketohexane-1-carboxylic acid hydrochloride (VIII) has been obtained from 5-ketocaproic acid, paraformaldehyde and dimethylamine hydrochloride by means of the Mannich reaction. Thermal degradation of XII and VIII afforded 4-keto-5-hexene-1-carboxylic acid (XI) and 4-keto-3-methylenepentane-1-carboxylic acid (XIII), respectively.

3) The structures of IV, VII, XI and XIII have been proven.

4) Some derivatives of above-mentioned carboxylic acids have been described.

5) It has been found that IV, VII, XI and XIII possess significant antitumor and antibacterial activites; especially calcium salt of 4-keto-5-hexene-1-carboxylic acid (XI) gave an excellent result in animal experiments.

A part of expenses for this work was defrayed by the Grant-in-Aid for Scientific Research from the Ministry of Education, which is gratefully acknowledged. The authors are indebted to Professor H. Umezawa, National Institute of Health, Tokyo, for antitumor assays.

*Department of Applied Chemistry*
*Engineering Faculty of*
*Keio University, Tokyo*

# *The Reaction of Tropoids and Quinone Derivatives. I. Reaction of Several Tropolones and p-Benzoquinone-dibenzenesulfonimide**

By Shuichi SETO, Hiromi YAMAZAKI and Yukio NISHIYAMA

(Received January 28, 1960)

Several processes have been reported for the synthesis of tropolones having an aryl group[1]. For example, as a method of introducing an aryl group into the 5-position of the tropolone ring, one by the decomposition of the diazonium salt obtained from 5-aminotropolone in benzene, anisole or allied compounds has been described, but the yield is generally not good.

Based on the work of Admas and others[2] that aryl phenylenediamide derivatives are obtained in good yields from quinonimide derivatives by their reactions with aromatic compounds, an attempt was made to apply this reaction to tropolones.

This reaction appears to be the action of quinonimide, acting as a kind of a cationoid reagent, on the aromatic compounds and it seems possible to apply this to tropoids other than tropolones.

Mixing of the chloroform solutions of tropolone and *p*-benzoquinonedibenzenesulfonimide (I) results in orange red solution. Addition of a small amount of triethylamine to this solution results in change of color of the solution to yellow and after some time, a colorless solid (II) separates.

This behavior is similar to the formation of 2-(4′-hydroxyphenyl)-*p*-phenylenedibenzenesulfonamide from phenol and I[3].

It is clear from its ultraviolet absorption spectrum, and coloration with ferric chloride that II possesses a tropolone ring, and its analytical values agree with those calculated for 2′,5′-dibenzenesulfonamidophenyltropolone.

From an analogy, to the reaction of phenol, the 2′, 5′-dibenzenesulfonamidophenyl-group is considered to have entered the *para*- or 5-position of the tropolone ring and the experimental results described below supports this assumption.

The same reaction carried out with 3-bromotropolone and 3, 7-dibromotropolone in place of tropolone respectively affords colorless crystals (III) and pale yellow crystals (IV), although the reaction velocity is somewhat slower than that in the case of tropolone itself. The analytical values of III and IV agree respectively with those for the monobromo and dibromo derivatives of II.

Hydrogenolysis of III and IV in the presence of palladium-charcoal affords II, and bromination of II and III in chloroform affords IV. These fact can be understood by assuming that the 2′, 5′-dibenzenesulfonamidophenyl group in II, III and IV is situated in the 5-position of the tropolone ring.

The reaction of I and 4-isopropyltropolone (hinokitiol) is likely to be affected by steric hindrance of the isopropyl group in the 4-position, but the reaction actually progressed smoothly, giving colorless crystals (V). Further, reaction of I with 3-bromo-6-isopropyltropolone and 3, 7-dibromo-4-isopropyltropolone respectively afforded colorless crystals (VI) and pale yellow crystals (VII).

Hydrogenolysis of VI and VII gave V.

From the foregoing experimental facts, and from analytical values and ultraviolet absorption spectra of V, VI and VII, it is clear, that V is 4-isopropyl-5-(2′, 5′-dibenzenesulfonamidophenyl)tropolone, and VI and VII are respectively its monobromo and dibromo derivatives. The fact, that the aryl group enters the 5-position without interference of such a bulky group in 4-position suggests, that this reaction might be applied to the syntheses of tricyclic tropolone derivatives.

3-Isopropyltropolone ($\alpha$-thujaplicin) also reacts easily with I to form 3-isopropyl-5-(2′, 5′-dibenzenesulfonamidophenyl)tropolone (VIII).

The reaction of tropolone derivatives with a substituent in the 5-position with I was then carried out. Addition of triethylamine to the chloroform solution of 5-methyltropolone and I resulted in gradual blackening of the solution. This color change is different from that observed, when the reaction is progressing as anticipated.

Colorless crystals separated on standing this reaction mixture and this substance was found to be the reduction product of I, i. e. *p*-phenylenedibenzenesulfonamide.

A part of the starting 5-methyltropolone was recovered from the filtrate.

*) Presented at the 49th Tohoku Local Meeting of the Chemical Society of Japan, Yamagata, June, 1959.

1) Cf. T. Nozoe, Festschrift Arthur Stoll, Birkhäuser A. G., Basel (1957) p. 746.

2) R. Adams and W. Reifschneider, *Bull. Soc. chim. France*, **1958**, 23.

3) R. Adams and D. C. Blomstrom, *J. Am. Chem. Soc.*, **75**, 3405 (1953).

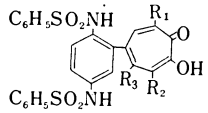


TABLE I. SOME PROPERTIES OF THE REACTION PRODUCTS

| | $R_1$ | $R_2$ | $R_3$ | M. p. °C (decomp.) | UV $\lambda_{max}^{MeOH}$ m$\mu$(log $\varepsilon$) |
|---|---|---|---|---|---|
| II | H | H | H | 233~235 | 241(4.49), 345(4.15), 390(3.79) |
| III | Br | H | H | 210~213 | 257(4.65), 351(4.29), 418(3.99) |
| IV | Br | Br | H | 211~213 | 272(4.60), 356(4.31), 435(4.18) |
| V | H | H | isoPr | 254~256 | 250(4.60), 344(4.24) |
| VI | Br | H | isoPr | 242~243 | 263(4.58), 349(4.24), 413(3.93) |
| VII | Br | Br | isoPr | 195~197 | 265(4.44), 355(4.06), 430(3.84) |
| VIII | isoPr | H | H | 207~215 | 243(4.58), 340(4.28), 390(3.84) |

The reaction of 5-bromotropolone and I also took the same course. It is known, that when the *para* position of phenol is blocked, as in *p*-cresol, the same reaction affords the reduction product, *p*-phenylenedibenzenesulfonamide[3,4].

I specifically attacks the *para* position of phenols and it is interesting, that it also attacks the 5-position of tropolones, corresponding to the *para* position, showing the similarity of phenols and tropolones.

## Experimental[5]

**5-(2′, 5′-Dibenzenesulfonamidophenyl) tropolone (II).**—To a solution of 1 g. of *p*-benzoquinonedibenzenesulfonimide (I) dissolved in 25 ml. of chloroform, a solution of 0.8 g. of tropolone in 2 ml. of chloroform was added, by which the color of the solution changed to orange red. Addition of 3 drops of triethylamine to it further changed the color of the solution to yellow and colorless crystals began to separate after a few minutes. The mixture was allowed to stand for 1 hr. and the crystals were collected by filtration to 1.27 g. of the first crop of crystals, m. p. 228~232°C (decomp.). The filtrate was evaporated under a reduced pressure, 5 ml. of benzene and 2 ml. of 1 N sulfuric acid were added to the residue, and the crystals that separated out were collected by filtration. The crystals were washed with benzene and water, and amounted to 70 mg. of the second crop of m. p. 228~230°C (decomp.). The combined first and second crops of crystals were recrystallized from a mixture of chloroform and benzene to yield 1.30 g. of II of m. p. 233~235°C (decomp.).

Found: C, 59.20; H, 3.64; N, 5.30. Calcd. for $C_{25}H_{20}O_6N_2S_2$: C, 59.02; H, 3.97; N, 5.51%.

The filtrate left after separation of the second crop of crystals was combined with the washings, the benzene layer was separated, and evaporated under a reduced pressure. The residue was sublimed at 1 mmHg in a bath of 60°C, and 0.46 g. of tropolone was recovered.

II was dissolved in ethyl acetate and aqueous solution of ferric chloride was added by which the organic layer colored red.

**2-Acetoxy-5-(2′, 5′-dibenzenesulfonamidophenyl)-tropone.**—A mixture of 100 mg. of II and 0.5 ml. of acetic anhydride was heated at 140°C for 20 min., by which II dissolved completely. The mixture was evaporated under a reduced pressure and the crystalline residue was recrystallized from chloroform to 60 mg. of crystals melting at 200~201°C.

Found: C, 58.85; H, 4.18; N, 5.03. Calcd. for $C_{27}H_{22}O_7N_2S_2$: C, 58.87; H, 4.03; N, 5.09%.

U. V. $\lambda_{max}^{MeOH}$ m$\mu$ (log $\varepsilon$): 231(4.56), 330(4.11).

**2-Methoxy-5-(2′, 5′-dibenzenesulfonamidophenyl)-tropone.**—An ether solution of diazomethane was added to 100 mg. of II suspended in 4 ml. of methanol by which an active reaction set in with evolution of nitrogen. After standing the mixture over night, the crystals were collected and recrystallized from methanol, affording 70 mg. of colorless needles, m. p. 190~191°C.

Found: C, 60.36; H, 4.36; N, 5.27. Calcd. for $C_{26}H_{22}O_6N_2S_2$: C, 59.73; H, 4.24; N, 5.36%.

U. V. $\lambda_{max}^{MeOH}$ m$\mu$ (log $\varepsilon$): 226(4.47), 330(4.11).

**3-Bromo-5-(2′, 5′-dibenzenesulfonamidophenyl)-tropolone (III).**—One drop of triethylamine was added to the solution of 130 mg. of 3-bromotropolone and 100 mg. of I dissolved in 5 ml. of chloroform and the mixture was allowed to stand for 2 days. The first crop of crystals that separated was collected by filtration to 50 mg. of crystals of m. p. 210~213°C (decomp.). The filtrate was evaporated under a reduced pressure, 2 ml. of benzene and 1 ml. of 1 N sulfuric acid were added and 90 mg. of the second crop of crystals, m. p. 205~212°C (decomp.), was obtained. The first and second crops of crystals were combined and recrystallized from chloroform-ethanol mixture to 135 mg. of crystals of m. p. 210~213°C (decomp.).

Found: C, 50.76; H, 3.26; N, 4.70. Calcd. for $C_{25}H_{19}O_6N_2BrS_2$: C, 51.08; H, 3.26; N, 4.77%.

The benzene layer was separated from the filtrate left after removal of the second crop of crystals, the solvent was evaporated, and the residue was sublimed at 1 mmHg in a bath of 100°C, by which 70 mg. of 3-bromotropolone was recovered.

4) R. Adams and K. R. Eilar, ibid., 73, 1149 (1951).

5) All melting points are uncorrected. The microanalyses were carried out by Mr. S. Ohyama and Miss Y. Endo of this Institute.

**3, 7-Dibromo-5-(2′, 5′-dibenzenesulfonamidophenyl)tropolone (IV).**—One drop of triethylamine was added to the solution of 180 mg. of 3,7-dibromotropolone and 100 mg. of I dissolved in 5 ml. of chloroform and the mixture was allowed to stand for 5 days. The first crop of 160 mg. of crystals, m. p. 207~210°C (decomp.), was collected by filtration, the filtrate was evaporated, and 5 ml. of benzene and 1 ml. of 1 N sulfuric acid were added to its residue. The second crop of 10 mg. of crystals, m. p. 206~210°C (decomp.), thereby obtained was collected by filtration, combined with the first crop, and recrystallized from ethanol-chloroform mixture, affording 165 mg. of pale yellow crystals, m. p. 211~213°C (decomp.).

Found: C, 45.48; H, 2.71; N, 3.97. Calcd. for $C_{25}H_{18}O_6N_2Br_2S_2$: C, 45.03; H, 2.72; N, 4.20%.

The benzene layer was separated from the filtrate left after removal of the second crop of crystals, the solvent was evaporated, and the residue was sublimed at 1 mmHg and 120°C, from which 85 mg. of 3,7-dibromotropolone was recovered.

**Hydrogenolysis of III.**—A solution of 90 mg. of III dissolved in 20 ml. of 0.1 N sodium hydroxide, added with 200 mg. of 5% palladium-charcoal, was shaken in hydrogen atomsphere at ordinary temperature. After the absorption of hydrogen ended, the catalyst was filtered off, the filtrate was acidified, and the precipitate thereby formed was crystallized from a mixture of ethanol and chloroform to 25 mg. of crystals, m. p. 230~233°C (decomp.), undepressed on admixture with II. The ultraviolet absorption spectra of these two substances were also in complete agreement.

**Hydrogenolysis of IV.**—A solution of 50 mg. of IV dissolved in 20 ml. of 0.1 N sodium hydroxide was added with palladium-charcoal. The mixture was treated as in the foregoing example. Recrystallization of the precipitate gave 15 mg. of crystals of m. p. 233~234°C (decomp.), undepressed on admixture with II. The ultraviolet absorption of this product was also in agreement with that of II.

**Bromination of II.**—A mixture of 60 mg. of bromine added to a suspension of 70 mg. of II in 5 ml. of chloroform was allowed to stand for 2 days and crystals were collected. This substance was found to be the unreacted II. The filtrate was evaporated under a reduced pressure and the oily residue solidified on being added with methanol. This solid was recrystallized from a chloroform-ethanol mixture to 10 mg. of pale yellow crystals, m. p. 207~210°C (decomp.), undepressed on admixture with IV. The ultraviolet absorption spectra of these two substances were also in good agreement. Admixture of this product with III melted at 195~200°C.

**Bromination of III.**—A suspension of 50 mg. of III in 5 ml. of chloroform, added by 60 mg. of bromine, was allowed to stand for 2 days. The reaction mixture was filtered to collect 30 mg. of crystals which was proved to be the unreacted III. The filtrate was treated as in the foregoing example and 10 mg. of pale yellow crystals, m. p. 207~209°C (decomp.), was obtained. This showed no depression of m. p. on admixture with IV.

**4-Isopropyl-5-(2′,5′-dibenzenesulfonamidophenyl)-tropolone (V).**—One drop of triethylamine was added to the reddish orange solution formed by dissolving 110 mg. of 4-isopropyltropolone and 100 mg. of I in 4 ml. of chloroform and the color of the solution changed immediately to yellow, gradually separating colorless crystals. After allowing the mixture to stand for 30 minutes, the crystals were collected by filtration, affording 130 mg. of colorless crystals, m. p. 253~256°C (decomp.). The filtrate was evaporated under a reduced pressure, 5 ml. of benzene and 1 ml. of 1 N sulfuric acid were added to the residue, and 10 mg. of the second crop of crystals, m. p. 247~251°C (decomp.), was collected. The first and second crops of crystals were combined and recrystallized from a chloroform-ethanol mixture to 135 mg. of crystals, m. p. 254~256°C (decomp.).

Found: C, 60.36; H, 4.67; N, 4.90. Calcd. for $C_{25}H_{26}O_6N_2S_2$: C, 61.06; H, 4.76; N, 5.09%.

The benzene layer was separated from the filtrate left after removal of the second crop of crystals, the solvent was evaporated from it, and the residue was sublimed under a reduced pressure, from which 60 mg. of 4-isopropyltropolone was recovered.

**3-Bromo-6-isopropyl-5-(2′, 5′-dibenzenesulfonamidophenyl)tropolone (VI).**—An orange solution formed on dissolving 170 mg. of 3-bromo-6-isopropyltropolone and 100 mg. of I in 4 ml. of chloroform was added with one drop of triethylamine and the solution turned yellow but there was no precipitation of crystals. After allowing this mixture to stand for 7 days, the solvent was evaporated under a reduced pressure, leaving a mixture of crystals and oil. To this residue, 5 ml. of benzene and 1 ml. of 1 N sulfuric acid were added and crystals that separated out were collected to 150 mg. of colorless crystals, m. p. 242~243°C (decomp.).

Found: C, 53.21; H, 3.67; N, 4.10. Calcd. for $C_{28}H_{25}O_6N_2BrS_2$: C, 53.39; H, 4.00; N, 4.45%.

The benzene layer was separated from the filtrate left after removal of crystals, the solvent was evaporated from this layer, and sublimation of the residue under a reduced pressure gave 85 mg. of the recovered 3-bromo-6-isopropyltropolone.

**3,7-Dibromo-4-isopropyl-5-(2′,5′-dibenzenesulfonamidophenyl)tropolone (VII).**—To the yellow solution formed on dissolving of 400 mg. of 3,7-dibromo-4-isopropyltropolone and 200 mg. of I in 8 ml. of chloroform, one drop of triethylamine was added and the solution changed transitrally red but returned immediately to the original yellow color. There was no precipitation of crystals after standing the mixture for 10 days. The solvent was evaporated under a reduced pressure from this mixture, 6 ml. of benzene and 1 ml. of 1 N sulfuric acid were added to the residue, and the crystallized residue was recrystallized from a chloroform-ethanol mixture to 330 mg. of pale yellow crystals, m. p. 195~197°C (decomp.).

Found: C, 47.62; H, 3.26; N, 3.73. Calcd. for $C_{28}H_{24}O_6N_2Br_2S_2$: C, 47.44; H, 3.42; N, 3.96%.

Evaporation of the benzene layer separated from the filtrate and low-pressure sublimation of its residue afforded 210 mg. of recovered 3,7-dibromo-4-isopropyltropolone.

**Hydrogenolysis of VI.**—Hydrogenolysis of 50 mg. of VI in the same manner as for III afforded 30

mg. of crystals, m. p. 251~253°C (decomp.), undepressed on admixture with V.

**Hydrogenolysis of VII.**—Treatment of 100 mg. of VII as in the foregoing examples afforded 50 mg. of crystals of m. p. 251~253°C (decomp.), undepressed on admixture with V.

**3-Isopropyl-5-(2',5'-dibenzenesulfonamidophenyl)-tropolone (VIII).**—Treatment of 110 mg. of 3-isopropyltropolone and 100 mg. of I in the same manner as for V afforded 140 mg. of crystals of m. p. 207~215°C (decomp.).

Found: C, 61.92; H, 4.59; N, 4.84. Calcd. for $C_{28}H_{26}O_6N_2S_2$: C, 61.05; H, 4.76; N, 5.09%.

There was recovered 60 mg. of 3-isopropyltropolone.

**Reaction of 5-Methyltropolone and I.**—One drop of triethylamine was added to the solution of 40 mg. of 5-methyltropolone and 50 mg. of I dissolved in 2 ml. of chloroform by which the solution turned dark brown and crystals began to form after some time. The mixture was allowed to stand for 2 hr. and 20 mg. of colorless crystals, m. p. 240~241°C, were obtained. This showed no depression of m. p. on admixture with *p*-phenylenedibenzenesulfonamide and the ultraviolet absorption spectra of the two substances were identical.

Evaporation of the filtrate left an oily substance to which benzene and 1 N sulfuric acid were added, and the benzene layer was separated. The benzene solution was chromatographed over silica gel and 20 mg. of 5-methyltropolone was recovered from it.

**Reaction of 5-Bromotropolone and I.**—One drop of triethylamine was added to the solution of 30 mg. of 5-bromotropolone and 20 mg. of I dissolved in 2 ml. of chloroform by which the color of the solution changed through dark green to dark brown. The reaction mixture was treated as above, and 15 mg. of *p*-phenylenedibenzenesulfonamide and 15 mg. of 5-bromotropolone were obtained.

## Summary

The reaction of tropolones with *p*-benzoquinonedibenzenesulfonimide was carried out and the following points were observed.

1) The 2', 5'-dibenzenesulfonamidophenyl group enters the 5-position of the tropolone ring, similar to the case of phenol.

2) The reaction proceeds in the same way in the case of 4-isopropyltropolone, without interference of the isopropyl group.

3) In the case of tropolones with a substituent in 5-position, reduction of *p*-benzoquinonedibenzenesulfonimide takes place.

A part of the expenses for the present work was supported by a fund from the Sankyo Co., Ltd., which is gratefully acknowledged.

*The Chemical Research Institute of Non-Aqueous Solutions*
*Tohoku University*
*Katahira-cho, Sendai*

# *The Mannich Base of Troponoid and its Application. IV. The Synthesis of Tropolon-5-ylalanine*

By Shuichi SETO and Kyozo OGURA

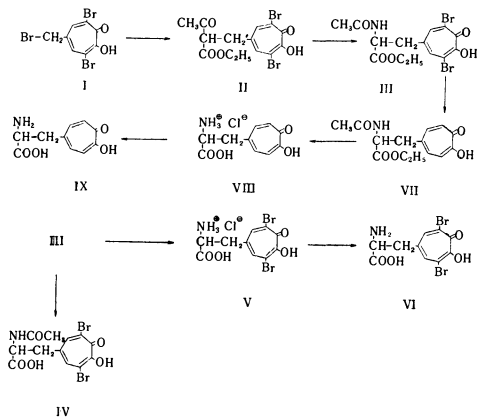
(Received February 13, 1960)

It was shown in previous reports[1,2] that 5-hydroxymethyl-, 5-formyl- and 5-bromomethyl-tropolone derivatives were derived from 3, 7-dibromo-5-morpholinomethyltropolone and that 3, 7-dibromo-5-formyltropolone and 3, 7-dibromo-5-bromomethyltropolone (I) were important starting materials for the synthesis of various tropolone derivatives possessing a substituent in the 5-position of the tropolone ring. The present paper describes the synthesis of tropolone derivative possessing an amino acid residue in the 5-position of tropolone ring, i. e. tropolon-5-ylalanine, and related compounds from I.

Application of a large excess of ethyl potassioacetoacetate to I affords 3, 7-dibromo-5-(β-acetyl-β-ethoxycarbonylethyl)tropolone (II)[2] whose Schmidt reaction gives 3, 7-dibromo-5-(β-acetamido-β-ethoxycarbonylethyl)tropolone (III), m. p. 198°C. Hydrolysis of III with dilute alkali produces 3, 7-dibromo-5-(β-acetamido-β-carboxyethyl)tropolone (IV), m. p. 217°C (decomp.), but the treatment of III with concentrated hydrochloric acid with boiling gives 3, 7-dibromotropolon-5-ylalanine hydrochloride (V), m. p. 223~230°C (decomp.). Neutralization of V liberates 3, 7-dibromotropolon-5-ylalanine (VI), m. p. 216°C (decomp.). Hydrogenolysis of III over palladium-carbon as a catalyst, in methanol affords 5-(β-acetamido-β-ethoxycarbonylethyl)tropolone (VII), m. p. 176°C. Treatment of VII with concentrated hydrochloric acid by boiling produces

1) S. Seto and K. Ogura, This Bulletin, 32, 493 (1959).
2) S. Seto and K. Ogura, ibid., 32. 1118 (1959).

tropolon-5-ylalanine hydrochloride (VIII), m. p. 215~220°C (decomp.), which liberates tropolon-5-ylalanine (IX), m. p. 240°C (decomp.), by neutralization. The amino acids so obtained, VI and IX, color reddish violet to ninhydrin and the aqueous layer turns green with ferric chloride. The infrared spectra of these compounds show absorption bands[3] originating in the zwitter ion structure characteristic of amino acid[4], by the presence of marked absorption at 3030, 1631 and 1575 $cm^{-1}$ in VI and at 3020 and 1640 $cm^{-1}$ in IX.



## Experimental[5]

**3, 7-Dibromo-5-(β-acetamido-β-ethoxycarbonylethyl)tropolone (III).**— To a solution of 500 mg. of II dissolved in 25 ml. of benzene, 10 ml. of conc. sulfuric acid was added and the mixture was stirred under ice-cooling. To this mixture, 180 mg. of sodium azide was added and the stirring was continued for a further 1 hr. period, during which vigorous evolution of nitrogen gas occurred and the reaction product transited to the conc. sulfuric acid layer. The benzene layer was discarded, ca. 20 g. of cracked ice was added to the sulfuric acid layer, and the colorless precipitate thereby formed was collected by filtration. After washing the precipitate with water and drying, it was recrystallized from methanol and III was obtained as colorless needles, m. p. 197~198°C. Yield, 500 mg. The aqueous layer colored green to ferric chloride.

Found: C, 38.46; H, 3.62; N, 3.41. Calcd. for $C_{14}H_{15}O_5NBr_2$: C, 38.44; H, 3.43; N, 3.20%.

U. V. $\lambda_{max}^{MeOH}$ mμ (log ε): 268 (4.50), 345 (3.99), 430 (3.88).

**3, 7-Dibromo-5-(β-acetamido-β-carboxyethyl)tropolone (IV).** — A solution of 50 mg. of III dissolved in 0.5 ml. of 10% sodium hydroxide solution was heated on a water bath for about 10 min. and cooled to room temperature when yellow crystals of the sodium salt separated out. The salt was neutralized with 6 N hydrochloric acid, the colorless crystals that formed were collected, and recrystallized from ethanol. Yield, 20 mg. of m. p. 216~217°C (decomp.).

Found: C, 35.10; H, 2.61; N, 3.44. Calcd. for $C_{12}H_{11}O_5NBr_2$: C, 35.21; H, 2.69; N, 3.42%.

U. V. $\lambda_{max}^{MeOH}$ mμ (log ε): 268 (4.48), 345 (4.00), 425 (3.80).

**3, 7-Dibromotropolon-5-ylalanine Hydrochloride (V).** — A mixture of 150 mg. of III and 5 ml. of conc. hydrochloric acid was heated on a water bath for 2 hr. when the crystals dissolved completely. The solution was evaporated to dryness and residual colorless prismatic crystals were collected after addition of ethanol. Yield, 100 mg. of m. p. 223~230°C (decomp.).

Found: C, 30.11; H, 2.59; N, 3.38. Calcd. for $C_{10}H_{10}O_4NBr_2Cl$: C, 29.78; H, 2.48; N, 3.46%.

U. V. $\lambda_{max}^{MeOH}$ mμ (log ε): 267 (4.47), 340 (3.88), 425 (3.66).

**3, 7-Dibromotropolon-5-ylalanine (VI).** — Adjustment of 50 mg. of V to pH 6 by addition of diluted ammonia water produced a pale yellow precipitate which was collected, washed with water, and recrystallized from ethanol to colorless crystals, m. p. 215~216°C (decomp.). Yield, 30 mg.

Found: C, 32.70; H, 2.45; N, 3.82. Calcd. for $C_{10}H_9O_4NBr_2$: C, 32.91; H, 2.76; N, 3.25%.

U. V. $\lambda_{max}^{MeOH}$ mμ (log ε): 270 (4.85), 348 (4.09), 435 (4.90).

**5-(β-Acetamido-β-ethoxycarbonylethyl)tropolone (VII).**—A suspension of 1.5 g. of III in a solution of 0.6 g. of potassium hydroxide in 200 ml. of ethanol was shaken in hydrogen atmosphere after the addition of palladium-carbon catalyst. After absorption of 2 molar equivalents of hydrogen, the catalyst was filtered off and ethanol was evaporated completely from the filtrate. The residual, yellow potassium salt was dissolved in a small quantity of water and neutralized with 6 N hydrochloric acid, by which a yellow precipitate was produced. The mother liquor left after removal of the precipitate also afforded a small quantity of VII, m. p. 171~173°C, by extraction with ethyl acetate. Yield, 0.6 g.

Found: C, 59.42; H, 5.90; N, 5.01. Calcd. for $C_{14}H_{17}O_5N$: C, 60.20; H, 6.14; N, 5.02%.

U. V. $\lambda_{max}^{MeOH}$ mμ (log ε): 231 (4.37), 228 (4.05).

**Tropolon-5-ylalanine Hydrochloride (VIII).**—A solution of 100 mg. of VII dissolved in 0.5 ml. of conc. hydrochloric acid was heated on a water bath for 1 hr. and the solution was evaporated to dryness, leaving a syrupy residue. The addition of ethanol to this residue resulted in crystallization, the crystals were collected, and recrystallized from ethanol. Yield, 50 mg. of m. p. 220°C (decomp.).

Found: C, 48.76; H, 5.27; N, 5.45. Calcd. for $C_{10}H_{12}O_4NCl$: C, 48.40; H, 4.84; N, 5.70%.

U. V. $\lambda_{max}^{MeOH}$ (log ε): 229 (4.37), 326 (4.01).

**Tropolon-5-ylalanine (IX).** — A solution of 100 mg. of VIII dissolved in a small quantity of water was adjusted to pH 6 by addition of dilute ammonia water, the precipitate formed was collected, and recrystallized from ethanol. Yield, 40 mg. of m. p. 240°C (decomp.).

Found: C, 52.20; H, 5.77; N, 5.83. Calcd. for $C_{10}H_{11}O_4N \cdot H_2O$: C, 52.86; H, 5.77; N, 6.17%.

U. V. $\lambda_{max}^{MeOH}$ mμ (log ε): 230 (4.31), 330 (4.00).

3) L. J. Bellamy, "The Infrared Spectra of Complex Molecules", Methuen. London (1958), p. 234.

4) K. Ogura and Y. Ikegami, *Bull. Chem. Research Inst. Non-Aqueous Solutions, Tohoku Univ.*, **9**, 23 (1959).

5) All melting points are uncorrected. The microanalyses were carried out by Mr. S. Oyama and Miss Y. Endo of this Institute.

A part of the expense for the present research was defrayed by Sankyo Co., Ltd. The authors wish to express their sincere gratitude to Mr. S. Aono who carried out the measurement of infrared spectra.

*The Chemical Research Institute of Non-Aqueous Solutions*
*Tohoku University*
*Katahira-cho, Sendai*

# *Infrared Spectra of Diacetyl Monoxime and Isonitrosoacetone*

By Masao KIMURA, Yoko KURODA, Hitoshi TAKAGI*
and Masaji KUBO

(Received February 17, 1960)

Oximes are known to be subject to association, which has hampered the elucidation of the molecular structures of this type of compounds by means of physical methods such as dipole moment measurement, etc. The association through hydrogen bonding is an interesting problem in its own right and extensive studies have been made on these compounds by means of infrared spectroscopy[1] and Raman effect and also by the freezing point depression[2] of solutions, X-ray analysis[3-6] on crystals, etc. For this purpose, it is desirable and even necessary to carry out as complete assignments as possible of observed frequencies to various modes of vibrations of characteristic groups. Two oximes having conjugated double bonds were chosen in the present study anticipating the possible increase of the effect of hydrogen bonding due to conjugation.

## Materials

**Diacetyl Monoxime.**—A commerical preparation was purified by recrystallization from an aqueous solution (m. p. 74.5°C).

**Isonitrosoacetone.**—A commercial sample was purified by extraction from an ether solution with petroleum ether (m. p. 64.5°C).

## Experimental

The infrared spectra were recorded with a Hilger H-800 infrared spectrophotometer equipped with a rock-salt prism as well as with a fluorite prism. Both these compounds were studied in carbon tetrachloride and in carbon bisulfide, no appreciable dependence of frequencies upon the kind of solvents being observed. For isonitrosoacetone, which was sparingly soluble in carbon tetrachloride and carbon bisulfide, also chloroform solutions were employed. The results are shown in Tables I and II.

The spectra of solutions of various concentrations, solid samples, and some of the deuterated compounds, $CH_3$-CO-CR-NOD ($R=CH_3$ or H), were also studied whenever they were required for carrying out assignments.

## Discussion

The spectra of diacetyl monoxime and isonitrosoacetone in the wave number range from 3200 to 3600 $cm^{-1}$ are reproduced in Figs. 1 and 2. They show a very strong sharp band at about 3570 $cm^{-1}$ and a broad band at about 3330 $cm^{-1}$. The intensity of the former decreases, whereas that of the latter increases with increasing concentration. The former disappears completely in the solid state. These bands are absent in the spectra of the corresponding deuterated compounds, which display a new strong sharp band at about 2620 $cm^{-1}$ along with a broad band at about 2470 $cm^{-1}$. These facts indicate that the band of diacetyl monoxime at 3577 $cm^{-1}$ and that of isonitrosoacetone at 3574 $cm^{-1}$ can be unequivocally assigned to the OH stretching vibration of free OH groups, while the band of the former compound at about 3345 $cm^{-1}$ and that of the latter at about 3325 $cm^{-1}$ can be assigned to the OH stretching vibration of hydrogen-bonded OH groups. These wave numbers suggest that

* Present address: Shin Nippon Chisso Hiryo Co. Ltd., Moriyamashi, Shigaken.

1) A. M. Buswell, W. H. Rodebush and M. F. Roy, *J. Am. Chem. Soc.*, **60**, 2444 (1938).
2) A. Reiser, Symposium on Hydrogen Bonding held in Ljubljana, 1957. See also D. Hadži and H. W. Thompson, "Hydrogen Bonding", Pergamon Press, London (1959), p. 443.
3) T. K. Bierlein and E. C. Lingafelter, *Acta Cryst.*, **4**, 450 (1951).
4) Y. Okaya, A. Shimada and I. Nitta, This Bulletin, **29**, 210 (1956).
5) D. E. Williams, G. Wohlauer and R. E. Rundle, *J. Am. Chem. Soc.*, **81**, 755 (1959).
6) L. E. Godycki and R. E. Rundle, *Acta Cryst.*, **6**, 487 (1953).

TABLE I. INFRARED ABSORPTION OF DIACETYL MONOXIME

| Wave number $cm^{-1}$ | Intensity | Assignment |
|---|---|---|
| 3577 | strong | OH stretching (free) |
| 3345 | strong, very broad | OH stretching (assoc.) |
| 3065 | weak, broad | $CH_3$ degenerate stretching |
| 2945 | weak, broad | $CH_3$ symmetric stretching |
| 1698 | strong | CO stretching (free) |
| 1686 | shoulder | CO stretching (assoc.) |
| 1630 | weak | CN stretching |
| 1424 | medium, broad | $CH_3$ degenerate deformation |
| 1365 | strong | $CH_3$ symmetric deformation |
| 1355 | strong | OH in-plane bending (free) |
| 1304 | weak | CC(central) stretching (assoc.) |
| 1298 | weak | CC(central) stretching (free) |
| 1124 | strong | $CH_3$ in-plane rocking |
| 1022 | strong | $CH_3$ in-plane rocking |
| 970 | weak | NO stretching (assoc.) |
| 963 | weak | NO stretching (free) |
| 933 | weak | C-$CH_3$ stretching |

TABLE II. INFRARED ABSORPTIONS OF ISONITROSOACETONE

| Wave number $cm^{-1}$ | Intensity | Assignment |
|---|---|---|
| 3574 | strong | OH stretching (free) |
| 3325 | strong, broad | OH stretching (assoc.) |
| 1703 | strong | CO stretching (free) |
| 1674 | strong | CO stretching (assoc.) |
| 1614 | medium | CN stretching |
| 1450 | medium | $CH_3$ degenerate deformation |
| 1398 | strong | OH bending (free) |
| 1366 | strong | $CH_3$ symmetric deformation |
| 1320 | very weak | CC(central) stretching |
| 1226 | strong | CH in-plane bending |
| 1016 | strong | $CH_3$ in-plane rocking |
| 990 | strong | NO stretching (assoc.) |
| 972 | strong | NO stretching (free) |
| 920 | medium | C-$CH_3$ stretching |
| 835 | weak | CH out-of-plane bending |

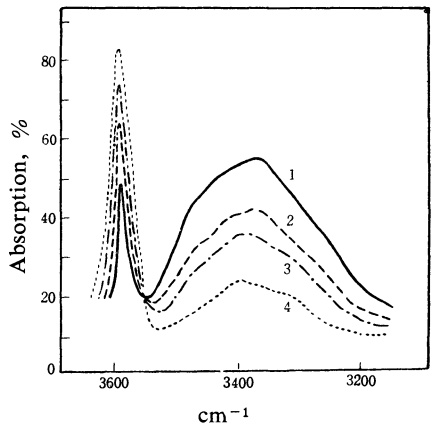



Fig. 1. Diacetyl monoxime in carbon tetrachloride.
1) 0.312 mol./l., 0.010 cm. cell. 2) 0.078 mol./l., 0.040 cm. cell. 3) 0.039 mol./l., 0.080 cm. cell. 4) 0.010 mol./l., 0.320 cm. cell.

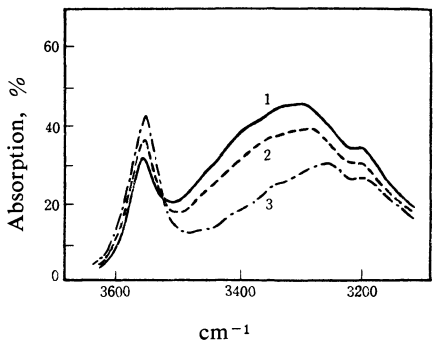



Fig. 2. Isonitrosoacetone in chloroform.
1) 0.901 mol./l., 0.002 cm. cell. 2) 0.340 mol./l., 0.004 cm. cell. 3) 0.021 mol./l., 0.064 cm. cell.

intermolecular hydrogen bondings are involved in association, because the stretching vibration of OH groups forming a chelate ring is known[7] to absorb at a frequency much lower than 3300 $cm^{-1}$.

The value of about 3570 $cm^{-1}$ for the wave number of stretching vibration of free OH groups is fairly low compared with those of alcohols ranging in 3600~3650 $cm^{-1}$ and is rather close to those of carboxylic acids at about 3600 $cm^{-1}$. Oximes having no conjugate double bonds, such as acetaldoxime, acetoxime, cyclohexanoxime, etc.[8] absorb at about 3600 $cm^{-1}$ in solutions, while those containing conjugate double bonds show absorptions at lower frequencies. For instance, benzaldoxime and its derivatives absorb in the wave number range 3500~3560 $cm^{-1}$ in solutions,* and quinone monoxime[10] at 3540 $cm^{-1}$. The present results are consistent with this relation. On the other hand, the values of 3345 $cm^{-1}$ and 3325 $cm^{-1}$ for the wave numbers of stretching vibrations of hydrogen-bonded OH groups of the two compounds under investigation are higher than those of the oximes mentioned above, most of which absorb at a wave number lower than 3300 $cm^{-1}$**.

Three types of hydrogen bonds can be presumed, namely –OH···N=C, –OH···O–N= and –OH···O=C–. The type of association will be discussed below in connection with other absorption bands. As can be anticipated, Raman spectra show no line corresponding to OH stretching vibration or only a very weak line[11,12].

The weak broad bands at 3065 and 2945 $cm^{-1}$ of diacetyl monoxime were assigned to the degenerate and symmetric stretching vibrations of methyl groups, respectively. The appearance of these bands observed in solutions were not altered appreciably on solidification or on deuteration. The corresponding bands and the CH stretching vibration of isonitrosoacetone were too weak to be observed with certainty. Therefore, they are not listed in Table II.

The spectra in the wave number range covering 1600~1700 $cm^{-1}$ are shown in Figs. 3 and 4. Diacetyl monoxime has a very strong band at 1698 $cm^{-1}$ with a shoulder at 1686 $cm^{-1}$. The corresponding band of isonitrosoacetone split into two peaks, a main peak being found at 1703 $cm^{-1}$ and a subsidiary one at 1674 $cm^{-1}$. Besides, a relatively weak band appeared at 1630 $cm^{-1}$ in the spectrum of diacetyl monoxime and at 1614 $cm^{-1}$ in that of isonitrosoacetone. The general features of these bands were not affected by deuteration, except for slight changes taking place in the

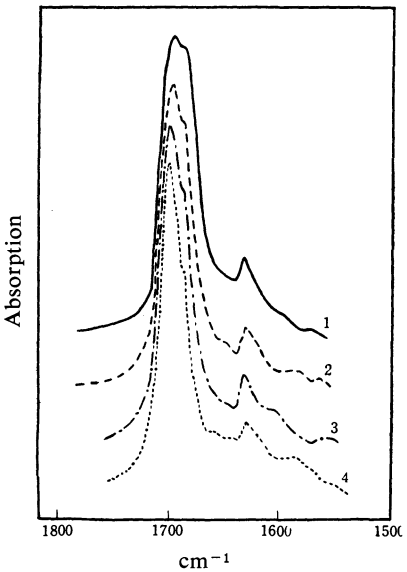



Fig. 3. Diacetyl monoxime in carbon tetrachloride.
1) 0.312 mol./1., 0.010 cm. cell. 2) 0.078 mol./1., 0.040 cm. cell. 3) 0.039 mol./1., 0.080 cm. cell. 4) 0.020 mol./1., 0.160 cm. cell. In this and subsequent figures, the ordinates of curves are shifted from one another for the sake of clarity.

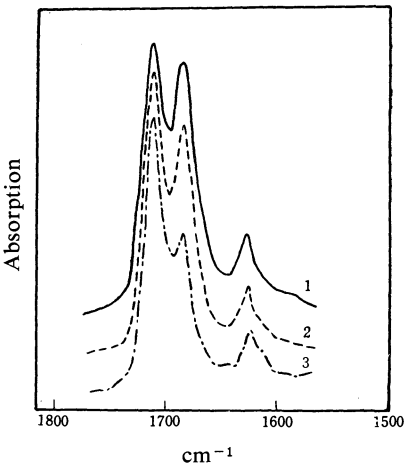



Fig. 4. Isonitrosoacetone in chloroform.
1) 0.901 mol./1., 0.002 cm. cell. 2) 0.340 mol./1., 0.004 cm. cell. 3) 0.021 mol./1., 0.064 cm. cell.

7) L. J. Bellamay, "The Infrared Spectra of Complex Molecules", 2nd Ed., Methuen, London (1958).
8) S. Califano and W. Lüttke, *Z. physik. Chem.* (neue Folge), 5, 240 (1956).
9) A. Palm and H. Werbin, *Can. J. Chem.*, 31, 1004 (1953).
10) D. Hadži, *J. Chem. Soc.*, 1956, 2725.
* The values of wave numbers observed by Palm and Werbin[9] are distributed over a wide range, no characteristic tendency being found for the present.
** Califano and Lüttke[8] reported a value of 3315 $cm^{-1}$ for *syn*-benzaldoxime, while Palm and Werbin[9] observed a band at 3270 $cm^{-1}$ for *β(anti)*-benzaldoxime in a chloroform solution.
11) M. Milone, *Gazz. chim. ital.*, 67, 527 (1937).
12) L. Kahovec and K. W. F. Kohlrausch, *Ber.*, 75, 1541 (1942).

position of absorption bands. In general, saturated open chain ketones absorb in the range of 1705~1725 $cm^{-1}$, while compounds having a C=N bond show an absorption in the range of 1640~1690 $cm^{-1}$, provied that the compounds have an open chain or that they have a ring system involving no conjugation. Although the frequencies of CO and CN stretching vibrations may shift to some extent in conjugate systems, it is still reasonable to presume that the CO stretching vibration has a higher frequency than that of the CN stretching vibration. In addition, a band due to the CO stretching vibration is, in general, very strong, whereas a band due to the CN stretching is not always so. For these reasons, the bands at about 1700 $cm^{-1}$ were assigned to the CO stretching vibration and those at about 1620 $cm^{-1}$ to the CN stretching mode.

Kahovec and Kohlrausch[12] observed two Raman frequencies, 1679 and 1632 $cm^{-1}$, of diacetyl monoxime in the crystalline state. They tentatively assigned these frequencies to the CO stretching and the CN stretching vibration, respectively, with due precaution to the low value of the latter frequency compared with those of acetaldoxime, etc.[11,13,14] at about 1670 $cm^{-1}$. Their assignments seem to be adequate, because strong conjugation in a molecule will lower the characteristic frequency associated with a double bond. In fact, Hadži[10] observed the CO band of 1, 4-benzoquinone monoxime at 1628 $cm^{-1}$ in the solid state and at 1648 $cm^{-1}$ in solutions and also the CN band at 1555 $cm^{-1}$ in the solid state. Palm and Werbin[9] have made observations on the CN frequencies of benzaldoxime and its derivatives in the solid state, the observed values ranging from 1614 to 1650 $cm^{-1}$.

The CO bands mentioned above showed a decrease in intensity of the main peak and an increase in that of the subsidiary peak or the shoulder with increasing concentration. The effect of association on the CO stretching frequency is presumed to cause a shift towards a lower frequency owing to the increased single bond character of the C=O bond due to hydrogen bond formation. Accordingly, the main peaks were assigned to the stretching vibration of free CO groups while the subsidiary peak and the shoulder were assigned to that of hydrogen-bonded CO groups. This suggests that hydrogen bonds of the -OH··· O=C- type are present in solutions.

The absorption spectrum of diacetyl monoxime in the wave number range 1300~1500 $cm^{-1}$ is shown in Fig. 5. A band at about

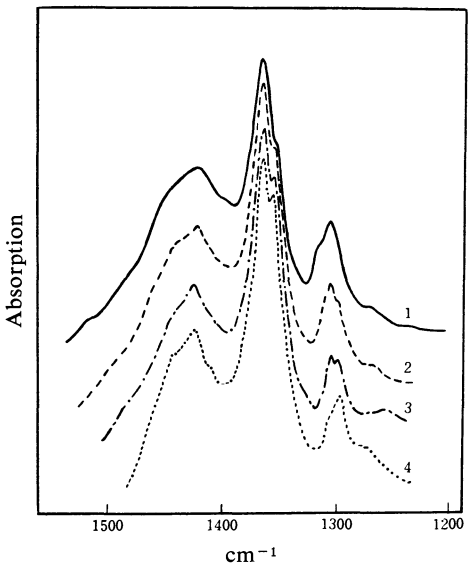



Fig. 5. Diacetyl monoxime in carbon tetrachloride.

The concentrations and the cell lengths are the same as given in Fig. 3.

1424 $cm^{-1}$ is a broad one of medium intensity. A strong band 1365 $cm^{-1}$ had a shoulder, which changed into a distinct maximum at 1355 $cm^{-1}$ with increasing dilution. The same compound in the solid state showed a broad band at about 1430 $cm^{-1}$ and a sharp one at 1365 $cm^{-1}$, no peak or shoulder being observed at about 1355 $cm^{-1}$. The change of spectral features taking place on deuteration was inappreciable, except that the band at 1355 $cm^{-1}$ disappeared and a new band appeared at about 1000 $cm^{-1}$, although it overlapped with other bands. Based on these experimental facts, the band at 1355 $cm^{-1}$ was assigned to the bending vibration of free OH groups. Palm and Werbin[15] proposed to assign a band of $\alpha$(*syn*)-benzaldoxime at 1265 $cm^{-1}$ to the OH in-plane bending vibration, Hadži[10] assigned a band of quinone oxime near 1450 $cm^{-1}$ to the OH bending vibration, and Bratož et al.[16] found the values of 1460 and 1078 $cm^{-1}$ for the OH and OD bending vibrations, respectively. These results suggest the adequacy of the present assignments.

Two bands at 1424 and 1365 $cm^{-1}$ mentioned above were assigned to the $CH_3$ degenerate and symmetric deformation vibrations, respectively, because they showed no concentration change and also because they were not affected by deuteration. The slight decrease of these frequencies below those of hydrocarbons is presumed to be a result of the presence of a C=O or C=N group in the molecule. In fact,

13) J. Goubeau, ibid., 68, 912 (1935).
14) H. J. Bernstein and W. H. Martin, *Trans. Roy. Soc. Canada*, Sect. III, 31, 105 (1937).
15) A. Palm and H. Werbin, *Can. J. Chem.*, 32, 858 (1954).
16) S. Bratož, D. Hadži and G. Rossmy, *Trans. Faraday Soc.*, 52, 464 (1956).

acetone[17] shows absorptions at 1430 and 1363 $cm^{-1}$ and diacetyl at 1426 and 1362 $cm^{-1}$ in the vapor state and at 1420 and 1352 $cm^{-1}$ in the liquid state[18,19]. The Raman frequencies of diacetyl monoxime observed by Kahovec and Kohlrausch[12] correspond to these vibrational modes. The OH bending frequency of hydrogen-bonded OH groups was not observed clearly but, as suggested also by Califano and Lüttke[20] in their studies on formaldoxime and acetoxime, is expected to be masked by the band at 1424 $cm^{-1}$. In fact, this band became relatively weak and sharp with decreasing concentration as well as on deuteration.

Another band at about 1300 $cm^{-1}$ appeared to consist of two component peaks at 1304 and 1298 $cm^{-1}$. The former was stronger than the latter in concentrated solutions, whereas the intensity relation was reversed in dilute solutions. Accordingly, by taking into account the weak intensity of the band and the value of the wave number, the former was assigned to the C–C(central) stretching vibration of associated molecules, while the latter was assigned to that of unassociated ones. The increase of frequency displayed by associated molecules over that of unassociated ones can be readily explained, since the C–C bond in an associated molecule has a greater double bond character than the bond has in an unassociated molecule. This rather weak band due to the C–C stretching vibration has its counterpart in the Raman spectra observed by Kahovec and Kohlrausch[12], who observed a very strong Raman band at 1310 $cm^{-1}$ in a chloroform solution and at 1315 $cm^{-1}$ in the crystalline state. The value of 1300 $cm^{-1}$ is fairly large for a C–C stretching vibration, but is nearly equal to 1284 $cm^{-1}$ observed in the Raman spectra of diacetyl involving also the conjugation of double bonds[18,19].

In this wave number range, isonitrosoacetone absorbed in much the same way as diacetyl monoxime did. The spectra of the former differed from that of the latter only in that the absorption frequency due to the OH bending vibration at 1398 $cm^{-1}$ and that due to the $CH_3$ degenerate deformation vibration overlapped each other. Accordingly, the latter was evaluated from the spectra of the solid or of the deuterated sample. The same precaution was also taken for the C–C stretching vibration, because it was very weak.

The vibrational modes expected to appear in the wave number range 800~1250 $cm^{-1}$ are $CH_3$ in-plane and out-of-plane rocking vibrations, an NO stretching vibration, a C–$CH_3$ stretching vibration and an OH out-of-plane bending vibration. Isonitrosoacetone will show additional bands due to the CH in-plane and out-of-plane bending motions. Only a band arising from the NO stretching vibrations is possibly subject to an intensity change with concentration. A band having such a character was observed at 963~970 $cm^{-1}$ for diacetyl monoxime (See Fig. 6.) and at 972~990 $cm^{-1}$ for isonitrosoacetone.

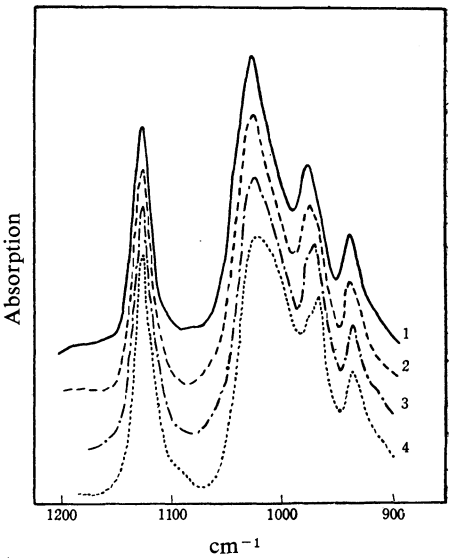



Fig. 6. Diacetyl monoxime in carbon tetrachloride.
1) 0.397 mol./1., 0.008 cm. cell. 2) 0.198 mol./1., 0.016 cm. cell. 3) 0.099 mol./1., 0.032 cm. cell. 4) 0.060 mol./1., 0.053 cm. cell.

The double bond character of the N–O bond will be greater in associated molecules than in unassociated ones. Accordingly, the increase in the amount of associated molecules with increasing concentration will give rise to an increase in the intensity of the component peak of higher frequency. This explains adequately the results of observations that with increasing dilution the maximum of these composite bands shifted towards the longer wavelength side. Hadži[10] assigned a band of 1, 4-benzoquinone monoxime at 1025 $cm^{-1}$ while Palm and Werbin[15] assigned the bands of various oximes at about 940 $cm^{-1}$ to the NO stretching vibration. The present assignment is in agreement with theirs.

A weak band of diacetyl monoxime at 933 $cm^{-1}$ and that of isonitrosoacetone at 920 $cm^{-1}$ were assigned to the C–$CH_3$ stretching vibration, reference being directed to a similar band of diacetyl at 945 $cm^{-1}$.

17) D. Price, *J. Chem. Phys.*, **9**, 725 (1941).
18) T. Miyazawa, *J. Chem. Soc. Japan, Pure Chem. Sec.* (*Nippon Kagaku Zasshi*), **74**, 743 (1953).
19) J. W. Sidman and D. S. McClure, *J. Am. Chem. Soc.*, **77**, 6471 (1955).
20) S. Califano and W. Lüttke, *Z. physik. Chem.* (neue Folge), **6**, 83 (1956).

Isonitrosoacetone showed an absorption at 833 $cm^{-1}$, which had no counterpart in the spectrum of diacetyl monoxime. For this reason and also because the frequencies of out-of-plane vibrations are known to be lower than those of in-plane vibrations, this band was assigned to the CH out-of-plane bending vibration.

Bands still left to be assigned are those of diacetyl monoxime at 1124 and 1022 $cm^{-1}$ and of isonitrosoacetone at 1226 and 1016 $cm^{-1}$. Since CH in-plane bending vibrations usually absorb at higher frequencies than $CH_3$ in-plane rocking vibrations do, the band at 1226 $cm^{-1}$ was assigned to the CH in-plane bending mode and others to the $CH_3$ rocking modes.

For both diacetyl monoxime and isonitrosoacetone, the band near 1020 $cm^{-1}$, which was sharp in the solid state, showed a hump on the lower frequency side especially in dilute solutions. This suggests the presence of another band capable of being assigned to the OH out-of-plane bending vibration of unassociated molecules.

In this way, all major observed bands have been interpreted in terms of the molecular form of an oxime type, $CH_3$–CO–CR=NOH (R=$CH_3$ or H). If the molecules exist in a nitroso form, $CH_3$–CO–CHR–NO, bands ascribed to hydroxyl groups in the present investigation could hardly be explained adequately. In addition, the presence of a C–N bond and an N=O bond in a molecule of the nitroso form in place of a C=N bond and an N–O bond as in that of the oxime form will render proper assignments almost impossible. The coexistence of the two forms is also ruled out, because the spectra are simpler than might be expected for the presence of the two forms. This conclusion affords at least an element of simplification in dealing with these molecules by means of other physical methods of attack.

## Summary

The infrared absorption spectra of diacetyl monoxime and isonitrosoacetone in solutions were recorded in the rock-salt region. The assignment of observed bands was carried out, taking into account the concentration dependence of the spectra, the effect of deuteration, and the absorptions in the solid state. All the observed frequencies could be interpreted in terms of the molecular form of an oxime type, the presence of molecules in a nitroso form being presumed to be unlikely.

*Chemistry Department*
*Nagoya University*
*Chikusa, Nagoya*

# *Spectroscopic Study on the Living Polymers of Styrene, Butadiene and their Derivatives*

By Keiji KUWATA

(Received October 29, 1959)

Recently the living polymers of styrene[1-3,5-7], its derivatives, butadiene[4] and isoprene have been an object of investigation, in view of their interesting property as an initiator of polymerization of vinyl monomers.

Their structure which seems to be the origin of the red color and the reactivity has been the subject of considerable discussion[1,2,5]. For the living polymer of styrene Szwarc proposed a structure of polymer anion having two groups of benzyl anion type at both ends of the polymer chain[2]. However, no direct evidence has been shown for this structure.

In the present paper, comparing the spectra of the living polymers of styrene and its derivatives with that of alkali benzyl, the

1) G. Meshitsuka and Y. Okada, *Chemistry of High Polymers (Kobunshi-kagaku)*, **14**, 33, 37, 123 (1957).
2) M. Szwarc, M. Levy and R. Milkovitch, *J. Am. Chem. Soc.*, **78**, 2655 (1956); M. Szwarc, *Nature*, **178**, 1168 (1956).
3) R. Wack, A. Rembaum, J. D. Coombes and M. Szwarc, *J. Am. Chem. Soc.*, **79**, 2026 (1957).
4) H. Brody, M. Ladacki, R. Milkovitch and M. Szwarc, *J. Polymer Sci.*, **25**, 221 (1957).
5) K. Hirota, K. Kuwata, H. Togawa and S. Ishida, *J. Chem. Soc. Japan, Pure Chem. Sec. (Nippon Kagaku Zasshi)*, **79**, 602 (1958).
6) K. Hirota, K. Kuwata and K. Morigaki, This Bulletin, **31**, 538 (1958); **32**, 100 (1959).
7) K. Hirota and K. Kuwata, *J. Chem. Soc. Japan, Pure Chem. Sec. (Nippon Kagaku Zasshi)*, **78**, 1421 (1957); K. Kuwata and K. Hirota, *Annual Reports of the Institute for Fibre Research (Sen-i Kagaku Kenkyu-jo Nen-po)*, **11**, 20 (1958).

author is to report that their structure is a polymer anion with the end of benzyl anion type.

The existence of the living polymers of butadiene and isoprene was asserted by Szwarc et al.[4] In this paper, their structure and reactivity are to be discussed from the spectroscopic data on the living polymers prepared by the direct reaction of butadiene and isoprene with metallic sodium, and on the block polymerization of isoprene with the living polymers of styrene.

## Experimental

**Materials Used.**—Since the living polymers have an extreme reactivity toward water, oxygen, and carbon dioxide, special precautions on purifications of the starting materials are required[5,7]. In addition to the ordinary method of purification the monomers (styrene, $\alpha$-methyl styrene, *p*-methyl styrene and *p*-divinyl benzene) were dried over metallic sodium for several hours and then distilled into storage vessels under reduced pressure. The solvents, tetrahydrofuran (THF), dioxane and toluene, were refluxed over metallic sodium or potassium for several hours, and also distilled under reduced pressure into a glass ampoul containing a piece of sodium and a small amount of anthracene. The blue color appeared instantly and stayed permanently. The solvents were distilled under reduced pressure into the reaction vessel as required. For toluene, however, styrene was used instead of anthracene, since toluene is a poor solvent for sodium adduct of anthracene. Mercury dibenzyl, prepared by the Grignard reaction[8] between benzylmagnesium chloride with mercuric chloride, was purified by recrystallization from toluene. Diallyl ether of GR grade, dried over metallic sodium for a short time, was purified by distillation under reduced pressure.

**Preparation of the Samples.**—All the processes of preparations and measurements were carried out in the glass vessels which were previously degassed as much as possible. A typical method of preparation was as follows: Alkali metal was distilled under reduced pressure from an ampoul A into an ampoul B (see Fig. 1). Monomer or solvent was distilled into B from an ampoul C. Then the vessel was sealed off from the vacuum system. The reaction proceeded gradually and an intensely colored solution of the living polymer formed. This solution was filtered through a glass filter G and stored in an ampoul D. The solution of the living polymer or the anion formed was poured into the measuring cell E and was diluted by the solvent distilled from D until an appropriate concentration was obtained. The concentration of the living polymers of styrene and isoprene were determined by the flame spectroscopy of alkali metal contained in the solutions, and the molar extinction coefficients of the living polymers were estimated.

8) P. Wolff, *Ber.*, **46**, 64 (1913).

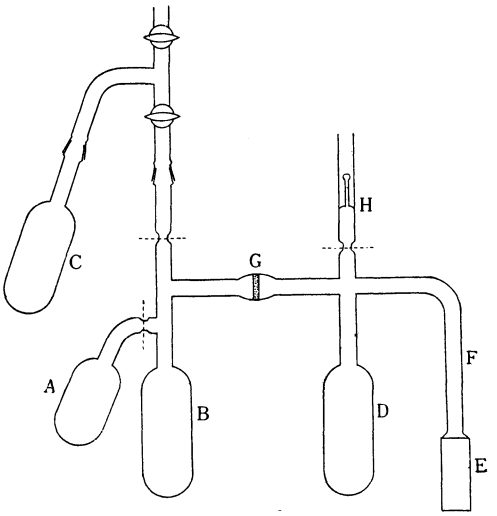



Fig. 1. Apparatus for preparation of the living polymers.
A, B, C and D: Glass ampoul, E: quartz cell, F: Gradual joint, G: Glass filter, H: Breakable joint.

**Measurement of Absorption Spectra.** — Absorption spectra of the living polymers and the anions were measured from 300 m$\mu$ to 2 $\mu$ with a Beckman DU type spectrophotometer equipped with an additional cover on the cell holder. After the measurement of the spectra, the vacuum was broken off and the spectra of the product were again measured.

## Experimental Results

A spectrum between 300 m$\mu$ and 2 $\mu$ for the toluene solution of the living polymer of styrene is shown in Fig. 2. In addition to the characteristic absorption at 510 m$\mu$ which had already been reported[1,5] another absorption at 450 m$\mu$ and an end absorption at longer wavelength were also observed. On the THF and dioxane solutions the absorptions were observed at 520 and 535 m$\mu$ respectively, shifting

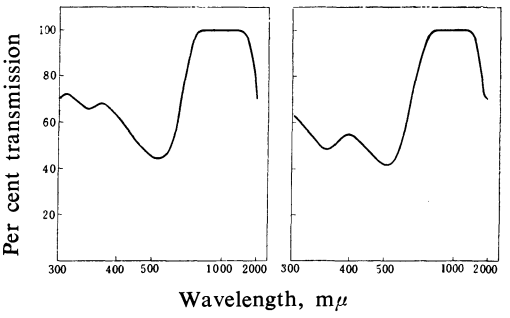



Fig. 2. Spectrum of the toluene solution of the living polymer of styrene.

Fig. 3. Spectrum of the THF solution of benzyl anion sodium.

toward longer wavelength according as the solutions were diluted.

The near infrared spectrum for the filmy state of the living polymer of styrene from 2 to 3.5 $\mu$ was the same as that of polystyrene, but its intensity was stronger than that of "dead polymer"* throughout this region. Therefore a very broad absorption in this region may exist. In the cases of the living polymers of styrene with potassium, rubidium and cesium in toluene solution, the corresponding absorptions were observed at 518, 525 and 535 m$\mu$ respectively.

For the living polymer of 1, 1-diphenyl ethylene in THF solution, the absorption at 525 m$\mu$ and two other absorption at 450 m$\mu$ and the end one at longer wavelength were also observed.

In cases of $\alpha$-methyl styrene and $p$-methyl styrene of toluene solution the absorption at 515 m$\mu$ was observed in addition to two other absorptions.

The absorptions at 550 and 1650 m$\mu$ were observed in case of divinyl benzene, and the latter seems to correspond to the end absorptions at longer wavelength for the living polymers of styrene etc.

A spectrum of the red THF solution of alkali benzyl is shown in Fig. 3. A maximum absorption which is characteristic of alkali benzyl at 505 m$\mu$ was observed in addition to two other absorptions. The shift of the maximum absorption at 505 m$\mu$ which originated from the alteration of alkali metal was very small. This absorption obeyed the law of Beer-Lambert within a concentration range of $10^{-2}\sim10^{-3}$ moles per litre.

Isoprene and butadiene reacted with sodium film, forming yellow adducts of high molecular weight. Dissolving these adducts into THF, slightly yellow and very reactive solutions were obtained. These solutions showed the maximum absorptions at 375 and 357 m$\mu$ respectively, and could initiate the polymerization of styrene and isoprene. These absorptions quickly disappeared upon exposure to air. A spectrum for the living polymer of isoprene in THF solution is shown in Fig. 4.

A yellow solution of allyl sodium containing sodium allylate, which was a byproduct[9] of the reaction, had a maximum absorption at 375 m$\mu$ and an end absorption at longer wavelength as shown in Fig. 5. The maximum absorption at 375 m$\mu$ was unaltered on dilution within the concentration range of $10^{-2}\sim10^{-3}$ moles per litre.

* The reaction product of the living polymer with air, and such product has no more reactivity to initiate the polymerization of styrene etc.

9) R. L. Letsinger and J. G. Traynham, *J. Am. Chem. Soc.*, **70**, 3342 (1948).

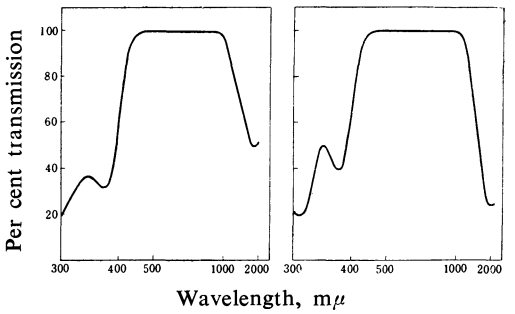



Fig. 4. Spectrum of the THF solution of the living polymer of isoprene.

Fig. 5. Spectrum of the THF solution of allyl sodium.

Block polymerization of isoprene with styrene was carried out, by use of the living polymer of styrene as the initiator, as follows: A constant amount of purified isoprene monomer was added by distillation through a breakable joint into the THF solution of styrene living polymer contained in ampoul D (Fig. 1). The absorption at 510 m$\mu$ of the living polymer of styrene (Fig. 6a) decreased by addition of isoprene and the absorption at 375 m$\mu$ of the living polymer of isoprene appeared as shown in Fig. 6b. The latter increased by further addition of isoprene as shown in Fig. 6c.

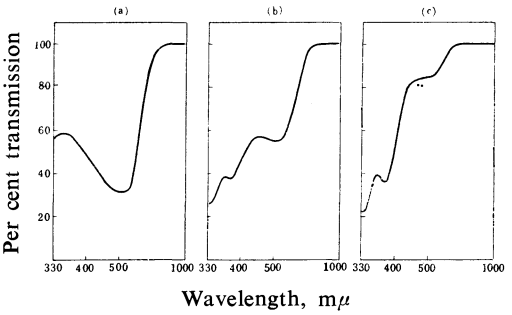



Fig. 6. Change of spectrum in the block polymerization of isoprene by the living polymer of styrene.

## Discussion

**Absorption Spectra of Benzyl Anion Type.**— Since the two maximum absorptions and the end absorption observed for the living polymer of styrene disappeared quickly upon exposure to air, they seem to be characteristic of the living polymer. However, when the starting materials used were not perfectly purified, yellow solutions were obtained. They had the maximum absorption only at 430 m$\mu$ besides the end absorption, and could not initiate polymerization. These two absorptions, therefore, may have originated from the decomposition product of the living polymer.

It seems that the temperature dependence of the absorption at 510 mμ of the living polymer of styrene may indicate the behaviour of association, but further study is necessary to confirm the conjecture.

The other absorption at 510 mμ, which may be a characteristic measure of the living polymer of styrene varied according as the kind of alkali metal was altered. The intermolecular charge-transfer spectra shown by a large number of molecular complexes in solution were found to exhibit certain regularities in regard to wavelength[10]. The wavelength of these transitions shows an excellent correlation i.e. a linear relation between frequency $\nu$ and ionization potential $I_p$ of the electron donor partners of the complexes :

$$h\nu = 0.61 I_p - 1.8 \text{ (in eV.)}$$

In case of the living polymer of styrene, the similar relation seems to exist as shown in Fig. 7, but the decrease of wavelength with the increase of ionization potential was small as compared with those of the molecular complexes, and also no donor-acceptor complexes such as a type containing alkali metal as the donor or aromatic hydrocarbon as the acceptor has been known. The change of absorption, therefore, would be caused by the change of solvation or dissociation of the polymer anion.

Considering the facts that the position of the maximum absorption near 505 mμ of THF solution of benzyl sodium is constant on dilution and that ether solution of benzyl sodium is conductive as shown by previous investigators[11], it is believed that alkali benzyl

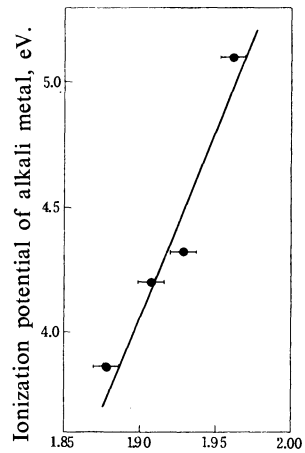



Fig. 7. Ionization potential of alkali metal versus the frequency of the absorption maximum.

in dilute THF solution is completely ionized. The absorption curve of alkali benzyl is the same as that of the living polymer of styrene. It seems evident, therefore, that the end group of benzyl anion type exists in the solution.

The theoretical investigations on the electronic states of benzyl anion and allyl anion were already carried out by several researchers[12-14]. Theoretically calculated wavelength of absorption for benzyl anion, shown in Table I are shorter than that of the observed absorption. The cause of this difference is partly due to the solvation of anion, but this effect may not be so much. Therefore,

TABLE I. MAXIMUM ABSORPTION OF THE LIVING POLYMERS, ALKALI BENZYL AND ALLYL SODIUM

| | Living polymer of styrene with sodium | Alkali benzyl | | | Living polymer of butadiene with sodium | Living polymer of isoprene with sodium | Allyl sodium |
|---|---|---|---|---|---|---|---|
| | | Sodium | Potassium | Rubidium | | | |
| Wavelength(mμ) obs. | 510(530) | 510 | 512 | 515 | 357 | 375 | 375 |
| Wavelength(mμ) theor. | 464 (transition $^1A_1 - {}^1B_1$)[b] | | | | 326[c], 250[a] | (transition $^1A_1 - {}^1B_1$) | |
| Extinction coeff. obs. | $1.9\times10^3$ | — | — | — | — | $3.2\times10^2$ | |
| Oscilator strength theor. | 0.43 | | | | 0.036 | | |

a) Chalvet[16], b) Longuet-Higgins and Pople[15], c) corrected value.

TABLE II. MAXIMUM ABSORPTIONS OF THE LIVING POLYMERS OF STYRENE AND ITS DERIVATIVES

| | Styrene | α-Methyl styrene | p-Methyl styrene | Divinyl benzene | 1,1-Diphenyl ethylene |
|---|---|---|---|---|---|
| Wavelength(mμ) ($\lambda$) obs. | 510($=\lambda_s$) | 515 | 515 | 550 | 525 |
| $\lambda/\lambda_s$ obs. | 1.00 | 1.01 | 1.01 | 1.08 | 1.03 |
| $\lambda/\lambda_s$ theor. | 1.00 | 1.01 | 1.01 | 1.04 | 1.00 |

10) H. McConnell, J. S. Ham and J. R. Platt, *J. Chem. Phys.*, **21**, 66 (1953).
11) W. Schlenk, *Ber.*, **50**, 262 (1917).
12) W. Bingel, *Z. für Naturforschung*, **10a**, 463 (1955).
13) H. G. Longuet-Higgins and J. A. Pople, *Proc. Phys. Soc., (London)*, **A68**, 591 (1955).
14) O. Chalvet, *Comt. rend.*, **234**, 2369 (1952).

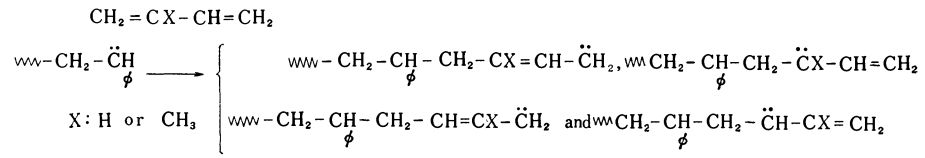
it may be attributed to oversimplification of the theory or to inadequate estimation of the electron interaction integrals used, as will be discussed later in the case of allyl anion.

The small difference of the absorption maximum between the solution of alkali benzyl and the living polymer of styrene may be ascribed to the effect of substitution of $\alpha$-hydrogen of benzyl anion by the polymer chain of polystyrene, since no difference was observed between the solution of alkali benzyl-polystyrene mixture and that of alkali benzyl.

As an effect of substitutions in anionic group of the living polymer of styrene, it was observed that the maximum absorption shifted toward a longer wavelength as the $\pi$-electronic conjugation in anionic group became larger. This effect was approximately interpreted by the Hückel treatment on the $\pi$-electronic structure of the anions as shown in Table II.

**Absorption Spectra of Allyl Anion Type.**—By comparing the maximum absorptions of the living polymers of butadiene and isoprene at 375 and 357 m$\mu$ with that of allyl sodium, they seem to be characteristic of allyl anion. Extinction coefficient of the absorption for the living polymer of isoprene was the order of $3\times10^3$ corresponding to the calculated oscillator strength of the order of 0.036 for allyl anion. Two other absorptions for the solution of the living polymers and that of anion may be attributed to the decomposition product or the byproduct. A typical value[14] of the longest wavelength calculated semi-empirically for allyl anion is shown in Table I, where considerable discrepancies between calculated and experimental values exist. This may be ascribed to the solvation of the anion in solution to some extent, but should rather be attributed to other causes: for example, rough approximation in the theory or inadequate estimation of the integrals used. If the Coulomb electronic repulsion integral for the two electrons on adjacent two carbon atoms in the method of Pople or of Pariser and Parr is decreased, a better approach to the observed value will be obtained*. Such a correction seems to be reasonable since the abnormally partial distribution of electronic charge, which resulted from the calculation, diminishes at the same time. A value corrected on this line is listed in Table I, showing that the partial distribution of charge diminishes to that of the Hückel method. It may be reasonable to consider that the structure of the living polymers of butadiene and isoprene are the polymer anion having the group of allyl anion type at the end of a polymer chain.

Both benzyl sodium and allyl sodium were known to have a reactivity as the initiators of polymerization of styrene[15] etc. Therefore, it may be plausible to attribute the reactivity of the living polymers to their anionic groups. Such a presumption was justified by the change of spectrum for the living polymer of styrene to that for isoprene, in the block polymerization of isoprene by the use of the living polymer of styrene as the initiator; the alteration of end group of benzyl anion type with that of allyl anion type may occur as follows:



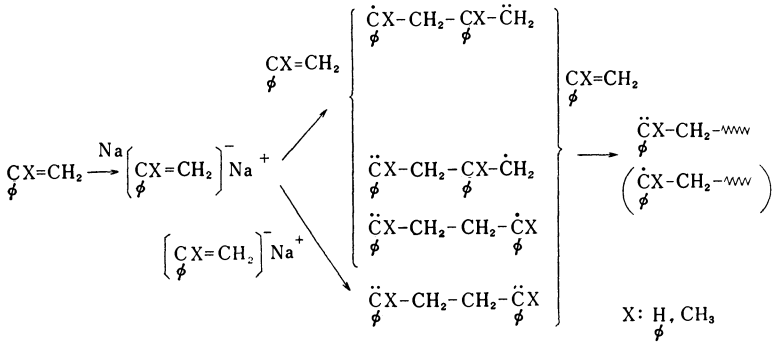

**Mechanism of Polymerization.**—The existence of the radical anion of styrene and its derivatives in the living polymers of low molecular weight was shown by the paramagnetic resonance absorption measurements[6,17]. Then the first step of the polymerization of styrene and its derivatives may be the formation of the radical anion which can play the role of the initiator of polymerization. The next step is the successive addition of monomers to the radical anion which will convert into the polymer anion making the polymerization reaction proceed. The end groups of radical type did not remain in the solution of the living polymers except the relatively stable diphenylmethyl radical type formed from the radical anion of 1, 1-diphenyl ethylene[16,17]. The general reaction scheme may be as follows:

* Since the electronegativities of the carbon atoms of the anions should be different from these of the neutral molecule, the correction on this line is also necessary.

15) A. A. Morton, *J. Am. Chem. Soc.*, **68**, 93 (1946).

16) K. Kuwata, K. Morigaki, K. Hirota and J. Itoh, *Annual Reports of the Institute for Fibre Research (Sen-i Kagaku Kenkyu-jo Nen-po)*, **12**, 9 (1959).

17) K. Kuwata, S. Ishida and K. Hirota, *J. Chem. Soc. Japan Pure Chem. Sec. (Nippon Kagaku Zasshi)*, **80**, 25 (1959).



This scheme is more general than that of Szwarc, because the formation of radical anions is considered in addition to the bivalent dimer anion proposed by Szwarc.

In cases of butadiene and isoprene the situation is the same, but the existence of monomer radical anion has been confirmed experimentally only with isoprene[18].

## Summary

The absorption spectra of the living polymers of styrene and its derivatives as well as of alkali benzyl have been measured from near infrared region to near ultra violet region, and they were compared. It has been concluded that these living polymers are the polymer anions having the groups of benzyl anion type at the end of a polymer chain.

The living polymers of butadiene and isoprene have been separated as the intermediates of polymerization by metallic sodium, and their spectra have been measured. Comparing these spectra with that of allyl sodium, it has been concluded that the living polymer of butadiene and isoprene are the polymer anions having the groups of allyl anion type at the end of a polymer chain. The spectroscopic study on the block polymerization of isoprene with the living polymer of styrene has been carried out. The mechanism of polymerization has been discussed.

The author wishes to express his sincere thanks to Professor Kozo Hirota of Osaka University for his guidance and encouragement throughout this work, and is also indebted to Professor Saburo Nagakura of Tokyo University for his helpful discussions.

*Department of Chemistry*
*Faculty of Science*
*Osaka University*
*Kita-ku, Osaka*

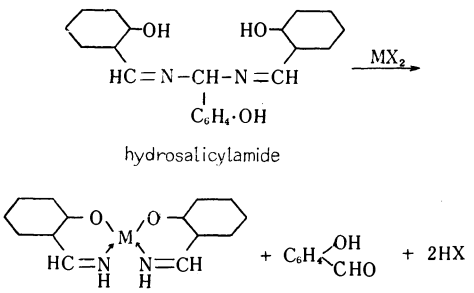
18) K. Kuwata, K. Morigaki and K. Hirota, This Bulletin, 32, 895 (1959).

# *Coördinate Valency Rings. XXIV.*[1] *On Some Inner Complex Ferric Salts of Hydrosalicylamide and its Derivatives**

By Tokuichi TSUMAKI, Shigetoshi ANTOKU and Michio SHITO

(Received February 12, 1960)

It is well known that salicylaldehyde reacts readily with ammonia in an alcoholic solution to form hydrosalicylamide, which consists of 3 molecules of salicylaldehyde and 2 molecules of ammonia, involving elimination of 3 molecules of water. When hydrosalicylamide is treated with divalent metallic salts, such as




(1)

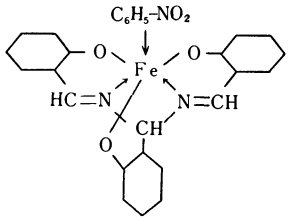
1) Part XXIII: T. Tsumaki, K. Katsuta and S. Okada, *J. Chem. Soc. Japan, Pure Chem. Sec.* (*Nippon Kagaku Zasshi*), **78**, 1086 (1957).

* Presented at the Joint Meeting of the Chugoku-Shikoku Branch and Kyushu Branch of the Chemical Society of Japan, Matsuyama, June 7, 1958.

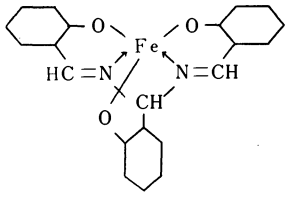
copper or nickel salts, metal chelates of salicylaldimine (formula 1) instead of those of hydrosalicylamide are obtained[2].

In the chelate-forming reactions, therefore, hydrosalicylamide splits by metallic salts giving one molecule of salicylaldehyde.

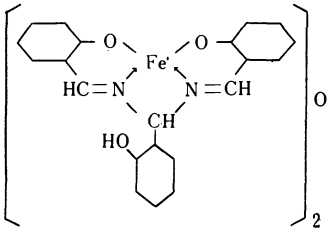
An attempt was made in 1934, by one of the authors[3], to obtain an analogous ferrous complex salt, that is, bis-salicylaldimine-iron-(II) by the reaction between hydrosalicylamide and ferrous sulfate. But the obtained chelate recrystallized from nitrobenzene was trisalicylaldehyde-diimine-iron(III), which contained one molecule of nitrobenzene coördinated to iron atom (formula 2). During the reaction, therefore, ferrous complex salt was oxidized to ferric by atmospheric oxygen.




(2)




(3)




(4)

Later, by using ammonium ferric sulfate, instead of ferrous sulfate, the same product was obtained as had been expected[4].

In the above-mentioned reactions, the main product, before recrystallization from nitrobenzene, consists of reddish brown powder. In the present paper are described the method of preparation of this compound in pure state and the comfirmation of its chemical structure. The structure of the compound, in recognition of the structure of nitrobenzene-containing chelate indicated by formula 2, is considered as a rarely known penta-coördinated ferric complex (formula 3). Besides formula 3, another formula, 4, may be taken into consideration for the ferric complex, on the basis of the results of elementary analysis and of the route of preparation of the complex. Of these two formulae, the latter should be excluded for reasons described below.

1) The complex salt does not react with diazomethane. The presence of a phenolic hydroxyl group must be denied.

2) It is known that the ferric complexes of oxide-form, for example, bis-salicylaldehyde-ethylenediimine-ferric oxide, react with a number of weak organic acids to give their salts (formula 5)[5]. Our complex, however, does not show such behavior.

3) If the hydroxyl group of the central salicylidene group does not take part in the complex formation as in the case of formula 4, the synthesis of a complex salt having formula 6, which has a benzylidene group in place of a salicylidene group in formula 4, may be possible by the action of a ferric salt on 2, 2′-dihydroxyhydrobenzamide. The complex salt of formula 6, however, could not be obtained by such attempts, and only a complex salt of hydrosalicylamide having formula 3 was obtained. Therefore, it can be considered that benzaldehyde splits off from the ligand and salicylaldehyde takes its place in the course of the reaction. This fact indicates that three hydroxyl groups of hydrosalicylamide may all be used for the complex formation.

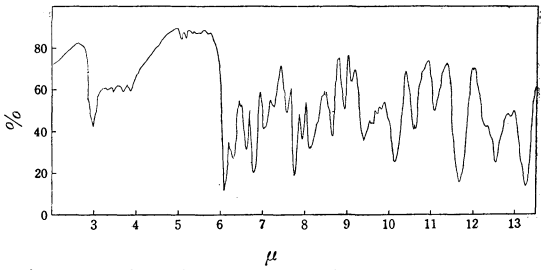



Fig. 1. Infrared spectrum of hydrosalicylamide.

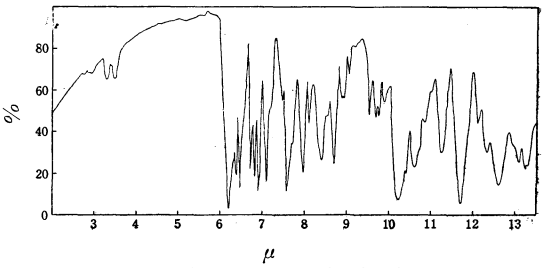



Fig. 2. Infrared spectrum of trisalicylaldehyd-diimine-iron(III).

2) P. Pfeiffer, E. Buchholz and O. Bauer, *J. prakt. Chem.*, **129**, 163 (1931).

3) T. Tsumaki, *J. Chem. Soc. Japan (Nippon Kwagaku Kwaishi)*, **55**, 1245 (1934).

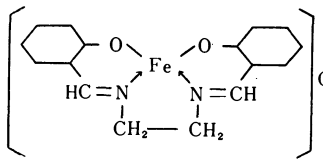
4) T. Tsumaki, ibid., **56**, 1329 (1935).

5) P. Pfeiffer, E. Breith, E. Lübbe and T. Tsumaki, *Ann.* **503**, 84 (1933). T. Tsumaki, M. Kuramoto, Y. Nakaishi and S. Suzuki, *Reports of Faculty of Science, Kyushu Univ., Chem. Sec.*, **1**, 63 (1950).

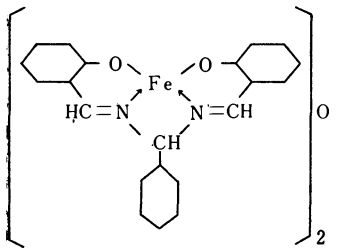
4) The infrared spectra indicate the absence of phenolic hydroxyl groups (Figs. 1 and 2).

Because of the above-mentioned experimental facts, the pentadentate formula 3 should be given to the ferric complex in question and the structure (formula 2) of its nitrobenzene-containing adduct has been proved to be correct.

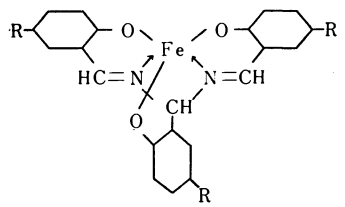
For some of the so-called tri-coördinated copper complexes, the presence of dimeric molecules has been suggested because of their abnormally low magnetic moments[6]. In the case of our pentadentate ferric complex, it has been shown by the measurement of magnetic susceptibilities that it has a normal magnetic moment (5.82 B. M.) and O–Fe bonds are essentially ionic. Therefore, the complex does not exist in the form of dimers.




(5)




(6)




(7)

As the penta-coördinated complex is coördinatively unsaturated, it will be expected that the complex will have a strong tendency to become a hexa-coördinated one, by the addition of a ligand molecule. The nitrobenzene adduct is a good example. Further, we succeeded in obtaining some such adducts, which contain pyridine, quinoline, bromobenzene, $\alpha$-chloronaphthalene, ethylene chloride and methyl benzoate. Each of the ligand molecules, except ethylene chloride, is bound firmly to the complex. The expelling of them is completed only by heating the adducts at 150~170°C for 8~10 hr. under 10 mmHg. It is well known that tertiary amines such as pyridine or quinoline enter very often into the complexes as ligands, but the examples of adducts which contain nitro-compounds or halogenated hydrocarbons have been rarely known.

Starting from benzene-substituted methyl-, chloro-, bromo- and nitro-derivatives of hydrosalicylamide, corresponding penta-coördinated iron complexes and their hexa-coödinated adducts were obtained (formula 7). In the case of methyl derivative, however, it formed no addition compound.

All these complexes decompose hydrogen peroxide catalytically and for that reason show strong chemi-luminescence in the presence of luminol in an alkaline solution.

## Experimental

**Trisalicylaldehyde - diimine - iron(III).** — Hydrosalicylamide (2 g.) is dissolved in absolute alcohol (300 cc.) in a three necked round-bottomed flask (500 cc.) fitted with a glass filter, a stirrer and a reflux condenser protected by calcium chloride. The solution is stirred and heated to 70~75°C on a water bath. A solution of anhydrous ferric chloride (0.6 g.) in absolute alcohol (50 cc.) is allowed to flow into the flask through a glass filter. The solution changes at once from yellow to orange red. After about two hours the reaction product is filtered off, washed with hot alcohol several times and dried at 90°C. Yield 1.5 g., black needles.

Found: C. 62.71; H, 4.18; N, 6.76; Fe, 13.78. Calcd. for $C_{21}H_{15}N_2O_3Fe$: C, 63.18; H, 3.78; N, 7.02; Fe, 13.99%.

**Reaction between 2,2'-Dihydroxyhydrobenzamide and Ferric Chloride.**—The reaction is carried out by essentially the same method as described above, using 2,2'-dihydroxyhydrobenzamide and ferric chloride. The resulting black crystals are recrystallized from nitrobenzene.

Found: N, 8.25; Fe, 10.52; drying loss, 23.66. Calcd. for $C_{21}H_{15}N_2O_3Fe \cdot C_6H_5NO_2$: N, 8.05; Fe, 10.69; nitrobenzene, 23.57%.

Since the description in the literature regarding 2,2'-dihydroxyhydrobenzamide had been only briefly given in the U. S. patent[7], a sample synthesized by the authors was ascertained by elementary analysis. m. p. 117°C. Pale yellow needles.

Found: C, 76.48; H, 5.52; N, 8.35. Calcd. for $C_{21}H_{18}N_2O_2$: C, 76.34; H, 5.49; N, 8.48%.

**Magnetic Susceptibility.**—The magnetic susceptibilities of trisalicylaldehyde-diimine-iron(III) and its nitrobenzene adduct were measured by the Curie method at room temperature (17°C). Cupric sulfate pentahydrate (further purified by the recrystallization of an extra pure reagent thrice from water) was used as the standard sample. The results are presented in Table I, where $\chi$ is the magnetic susceptibility per gram of the complex.

Neglecting the diamagnetic contribution of the ligand and assuming the validity of Curie-Langevin's law, the effective magnetic moments $\mu$ per one mole of the complex were calculated (see also Table I).

6) M. Kishita, Y. Muto and M. Kubo, *Austral. J. Chem.*, **10**, 386 (1957).

7) J. A. Chenicek, U. S. Pat. 2,533,205 (1950).

TABLE I.

| | $\chi$ (c. g. s., e. m. u.) | $\mu$ (B. M.) |
|---|---|---|
| Trisalicylaldehyde-diimine-iron(III) + nitrobenzene | $28.5\times10^{-6}$ | 5.90 |
| Trisalicylaldehyde-diimine-iron(III) | $36.3\times10^{-6}$ | 5.82 |

The theoretical moment of iron(III) (calculated from "spin-only" formula) is 1.73 B. M. for covalent bonds and 5.92 for the ionic ones.

**Infrared Spectra.**—They were taken in a hexachlorobutadiene mull, with an Oyo-Koken double beam instrument equipped with a sodium chloride prism (Figs. 1 and 2).

**Addition Compounds of Trisalicylaldehyde-diimine-iron(III).**—These compounds were prepared by the recrystallization of trisalicylaldehyde-diimine-iron (III) from various organic solvents. They are dried in a vacuum desiccator, because the coördinated solvent molecules are partially removed on heating or by washing with alcohol. All of them form black plates and their appearance or colors are almost unaltered by desolvation.

**Trisalicylaldehyde-diimine-iron(III)+Pyridine.** Found: N, 8.88; Fe, 11.51; drying loss, 16.90. Calcd. for $C_{21}H_{15}N_2O_3Fe\cdot C_5H_5N$: N, 8.79; Fe, 11.68; pyridine, 16.54%.

**Trisalicylaldehyde-diimine-iron(III)+Quinoline.** Found: C, 67.94; H, 4.46; N, 7.82; Fe, 10.42; drying loss, 24.63. Calcd. for $C_{21}H_{15}N_2O_3Fe\cdot C_9H_7N$: C, 68.18; H, 4.17; N, 7.95; Fe, 10.57; quinoline, 24.43%.

**Trisalicylaldehyde-diimine-iron(III)+α-Chloronaphthalene.** Found: C, 65.95; H, 4.26; N, 4.78; Fe, 9.60. Calcd. for $C_{21}H_{15}N_2O_3Fe\cdot C_{10}H_7Cl$: C, 66.27; H, 3.95; N, 4.99; Fe, 9.33%.

**Trisalicylaldehyde-diimine-iron(III)+Ethylene Chloride.** Found: C, 57.35; H, 4.13; N, 5.72; Cl, 12.35; Fe, 11.65; drying loss, 16.40. Calcd. for $C_{21}H_{15}N_2O_3Fe\cdot 0.8\ C_2H_4Cl_2$: C, 57.12; H, 3.86; N, 5.90; Cl, 11.94; ethylene chloride, 16.00%. The complex salt desolvates at room temperature. The analytical results shown above are the average values of several analyses.

**Trisalicylaldehyde-diimine-iron(III)+Methyl Benzoate.** Found: Fe, 10.32; drying loss, 25.92. Calcd. for $C_{21}H_{15}N_2O_3Fe\cdot C_8H_8O_2$: Fe, 10.43; methyl benzoate, 25.43%.

**Tri(5-substituted-salicylaldehyde)-diimine-iron-(III).**

**Tri(5-methylsalicylaldehyde)-diimine-iron(III).**—By a method similar to that mentioned above for the synthesis of trisalicylaldehyde-diimine-iron(III), a solution of ferric chloride (0.4 g.) in absolute alcohol (10 cc.) is added to a solution of 5, 5′, 5″-trimethylhydrosalicylamide (1 g.) in absolute alcohol (70 cc.). But in this case, in order to avoid the decomposition of the ligand at high temperature, the reaction is carried out at 45~50°C. The product was purified by reprecipitation from pyridine with water. Black needles.

Found: C, 64.87; H, 4.98; N, 6.36; Fe, 12.40. Calcd. for $C_{24}H_{21}N_2O_3Fe$: C, 65.32; H, 4.80; N, 6.35; Fe, 12.66%.

**Tri(5-bromosalicylaldehyde)-diimine-iron(III)+Nitrobenzene.**—A solution of 5, 5′, 5″-tribromohydrosalicylamide (1 g.) (or 5-bromosalicyladehyde and ammonia) in alcohol (30 cc.) is warmed on a water bath and a solution of ammonium ferric sulfate (dodecahydrate; 0.7 g.) in water (7 cc.) is added to it. After about half an hour, the black brown precipitates are filtered off, washed with hot alcohol and dried on a tone plate. Yield 0.7 g.

The powder is recrystallized from nitrobenzene to give the black plates which are dried in vacuo.

Found: C, 42.87; H, 2.48; N, 5.37; Fe, 7.27; drying loss, 16.17. Calcd. for $C_{21}H_{12}N_2O_3Br_3Fe\cdot C_6H_5NO_2$: C, 42.67; H, 2.25; N, 5.37; Fe, 7.36: nitrobenzene, 16.20%.

**Tri(5-bromosalicylaldehyde)-diimine-iron(III)+Bromobenzene.**—The black brown powder obtained above is recrystallized from bromobenzene. Dark violet needles.

Found: N, 3.64; Fe, 6.90; drying loss, 19.81. Calcd. for $C_{21}H_{12}N_2O_3Br_3Fe\cdot C_6H_5Br$: N, 3.54; Fe, 7.05; bromobenzene, 19.81%.

**Tri(5-chlorosalicylaldehyde)-diimine-iron(III)+Nitrobenzene.**—The reddish brown powder is obtained by the same treatment as in the case of the bromoderivative, using a solution of 5, 5′, 5″-trichlorohydrosalicylamide (3.5 g.) (or 5-chlorosalicylaldehyde and ammonia) in alcohol (60 cc.) and a solution of ammonium ferric sulfate (dodecahydrate; 4 g.) in water (20 cc.). Yield 3 g. This powder is recrystallized from nitrobenzene. Black plates.

Found: N, 6.88; Fe, 9.05; drying loss, 19.49. Calcd. for $C_{21}H_{12}N_2O_3Cl_3Fe\cdot C_6H_5NO_2$: N, 6.72; Fe, 8.93; nitrobenzene, 19.67%.

**Tri(5-chlorosalicylaldehyde)-diimine-iron(III)+Bromobenzene.**—This is prepared by the recrystallization of the powder from bromobenzene. Dark violet needles.

Found: N, 4.01; Fe, 8.64; drying loss, 23.55. Calcd. for $C_{21}H_{12}N_2O_3Cl_3Fe\cdot C_6H_5Br$: N, 4.24; Fe, 8.47; bromobenzene, 23.80%.

**Tri(5-nitrosalicylaldehyde)-diimine-iron(III)+Nitrobenzene.**—A Solution of 5, 5′, 5″-trinitrohydrosalicylamide (1 g.) in alcohol (50 cc.) is warmed on a water bath and a solution of ammonium ferric sulfate (dodecahydrate: 0.7 g.) in water (10 cc.) is added to it. The resulting reddish brown precipitates are treated as before. This powder is insoluble in common organic solvents and slightly soluble in nitrobenzene. When the powder is recrystallized from nitrobenzene, a small amount of crystals is obtained after about two days.

Found: N, 12.41; Fe, 8.43; drying loss, 18.48. Calcd. for $C_{21}H_{12}N_5O_9Fe\cdot C_6H_5NO_2$: N, 12.79; Fe, 8.50; nitrobenzene, 18.70%.

The authors wish to express their thanks to Miss S. Indo for N-analysis, to Dr. K. Hirakawa (Department of Physics) for the measurement

of magnetic susceptibilities, and to Assistant Professor Dr. Y. Ueda, Dr. H. Yoshimura and Mr. H. Yano (Department of Pharmacy, Faculty of Medicine) who kindly took the infrared spectra.

*Department of Chemistry*
*Faculty of Science*
*Kyushu University*
*Fukuoka*

# *Studies on Leucomycin. II. Preparative Chromatography of Macrolides on Amberlite IRC-50**

By Tetsuo WATANABE

(Received January 16, 1960)

As shown in the previous paper[1], leucomycin, a basic antibiotic produced by *Streptomyces kitasatoensis* Hata[2-4], was proved by the paper-chromatographic and -electrophoretic analysis, to be a mixture composed of at least six biologically active components, $A_1$, $A_2$, $B_1$, $B_2$, $B_3$ and $B_4$. Preliminary experiments on the chromatographic separation of these components in a preparative scale showed, that both leucomycin groups, A and B, were able to be absorbed on a column of alumina or silisic acid from the benzene solution and to be separately eluted with the same solvent containing methanol in this order. Using this or similar chromatographic systems, however, recoveries of the antibiotics was markedly low (50~70 per cent in weight, less than 40 per cent in biological activity; presumably accompanied with decomposition) and a more minute resolution into each component, was unsuccessful.

In course of our studies, it was found that leucomycin absorbed on a column of carboxylic resin, such as Amberlite IRC-50 in H-cycle, could be eluted quantitatively with sodium citrate buffer, and that all six components in the leucomycin complex were separately eluted with a mixture of citrate buffer and ethanol, in such a high concentration as the chromatographic system could be used for a preparative separation of these components. Using this method, not only leucomycin complex, but also some derivatives of leucomycin $A_1$ and other macrolides such as erythromycin[5], magnamycin[6] and spiramycin[7], having dimethylamino sugar as the basic moiety[8], could be purified from the contaminated minor components, which had been separated only with difficulties by counter current distribution. In this paper, we propose to report these results. In addition some properties of purified leucomycin components $B_1$, $B_2$, $B_3$ and $B_4$ and the composition of these components in leucomycin complex will be reported.

## Experimental

**Materials.**—Leucomycin complex (I)** and the fractionated antibiotics (II, III, IV) were kindly prepared for this study by J. Abe et al., at the Research Institute, Toyo Jozo Co. Ltd., according to the methods summarized in Table I. Erythromycin, magnamycin and spiramycin were the samples furnished as "standard antibiotics" through the National Institute for Preventive Medicine, Tokyo. Diacetylleucomycin $A_1$ ($C_{50}H_{85}O_{19}N$, m. p. 127~129°C)[9], propionylleucomycin $A_1$ ($C_{49}H_{85}O_{18}N$, m. p. 123~126°C)[10], tetrahydroleucomycin $A_1$ ($C_{46}H_{85}O_{17}N$, m. p. 162~164°C)[11], and a basic moiety derived from leucomycin $A_1$ with the methanolysis ($C_{34}H_{59}O_{13}N$, m. p. 154~155°C; corresponding to carimbose fragment in magnamycin)[12], were prepared from leucomycin $A_1$ by the present author, according to the methods which will be published soon.

* Pat., Application No. 13908 (1959).

1) J. Abe, Y. Suzuki, T. Watanabe and K. Satake, *J. Chem. Soc. Japan, Pure Chem. Sec. (Nippon Kagaku Zasshi)*, 81, 969 (1960).

2) T. Hata, Y. Sano, N. Ohki et al., *J. Antibiotics*, Ser. A6, No. 2, 87 (1953).

3) T. Hata, F. Koga and H. Kanamori, *J. Antibiotics*, Ser. A6 No. 3, 109 (1953).

4) Y. Sano, *J. Antibiotics*, Ser. A7, No. 3, 93 (1953).

5) J. M. McGuire, R. L. Bunch, R. C. Anderson, H. E. Boaz et al., *Antibiot. Chemoth.*, 2, 281 (1952).

6) W. Tanner, A. R. Englisb, T. M. Less and J. B. Routen, *Antibiot. Chemoth.*, 2, 441 (1952).

7) S. Pinnert-Sindico. L. Ninet, S. Preud'homme and C. Coser, *Antibiot. Annual.*, 724 (1954—1955).

8) R. K. Darke, *Antibiot. Chemoth.*, 3, 663 (1953); R. B. Hasbrouck and F. C. Garben, *Antibiot. Chemoth.*, 3, 1040 (1953); F. A. Hochstein and P. R. Regar, *J. Am. Chem. Soc.*, 77, 3353 (1955).

** Corresponded to "Commercial bulk".

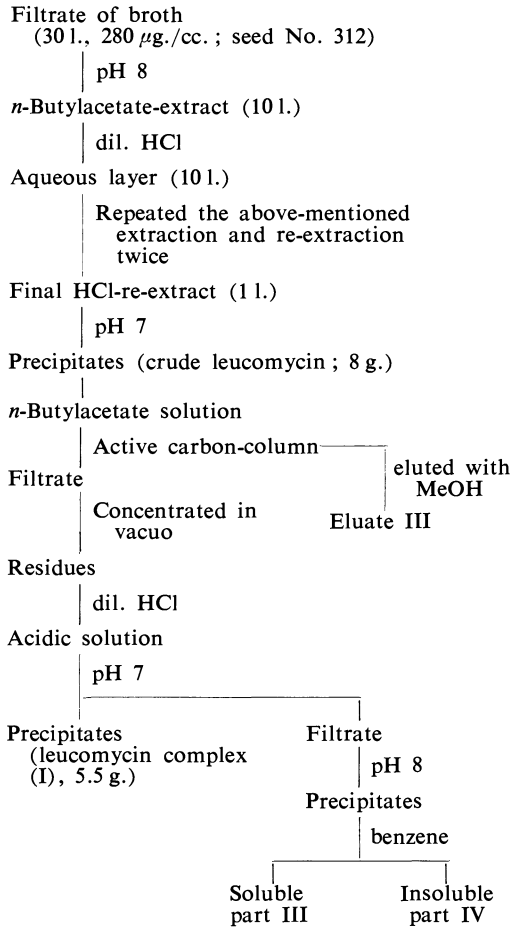
9) C. L. Ogg, W. L. Porter and C. D. Willits, *Ind. Eng. Chem., Anal. Ed.*, 17, 394 (1945).

10) V. C. Stephens, B. J. S. Conine, *Antibiotic. Annual*, 346 (1958—1959).

11) T. Watanabe, will be published.

12) R. B. Woodward, *Angew. Chem.*, 68, 133 (1956).

TABLE I. FRACTIONATION OF LEUCOMYCIN




**Chromatography on Amberlite IRC-50.** — One hundred grams of the resin (XE-64) of approximately 150 mesh, was suspended in 500 cc. of 1 N sodium hydroxide and the suspensions were heated on a water bath at 60°C for 3 hours under occasional stirring. After the decantation of brown colored supernatant, the resin of the Na-cycle was washed with distilled water thoroughly, then suspended in 1 N hydrochloric acid at room temperature. After 30 minutes, the resin was washed with distilled water until the washing became free from acid. Forty grams of so purified resin of H-cycle, was added as thick suspension in water to a column of 1 cm. in the diameter, to a hight of 45 cm. To the column, 10 mg. of sample to be analyzed was added as 1 per cent solution in N/100 hydrochloric acid. As soon as the applied sample solution had been allowed to flow into the column, washing with 150 ml. of distilled water, then elution with a mixture of 96 per cent ethanol and M/5 sodium citrate buffer ($Na^+$ 1.6 g. ion per liter, pH 5.0) in an equal volume, was initiated at a flow rate of 9 cc. per $cm^2$ per hour at 15°C. The effluent was collected in 4.5 cc. fraction by means of automatic fraction collector. For the chromatography in a preparative scale (15 g. of sample), a column of 3×180 cm. was used.

**Chemical Assay of Leucomycin in the Effluent.** —The concentration of leucomycin in each effluent fraction was determined photocolorimetrically with sulfuric acid as follows. An aliquot of sample solution was mixed with an equal volume of concentrated sulfuric acid under adequate shaking, and the resulting red brown color was measured between 10 and 30 minutes after the addition of sulfuric acid, with Kotaki photometer Model D2 using filter 470. Experiments showed, that the readings were strictly proportional to leucomycin concentration up to an optical density of about 1.1 equivalent to approximately 500 μg per cc. of leucomycin complex (I) and they were not affected by the presence or absence of M/5 citrate and of 50 per cent ethanol. As the color developed per unit weight of leucomycin components, were not just the same, the correction was made for the calculation of weight composition of each component. This method could be also applied with success for the assay of leucomycin derivatives and other macrolides, except erythromycin which with sulfuric acid colored only slightly. The fact, however, did not prevent the determination of an approximate elution position of erythromycin with this coloration.

**Paper Chromatography of Leucomycin.**—Leucomycin components contained in each fraction of chromatographic effluent, were identified from the chromatographic $R_f$ values, A and B groups could be easily distinguished from the $R_f$ developed with *n*-butyl acetate containing M/15 sodium phosphate (pH 6) ; while $A_1$ and $A_2$ ; $B_1$, $B_2$, $B_3$ and $B_4$ from the $R_f$ developed with M/15 sodium phosphate containing *n*-butyl acetate (pH 8) on a liquid paraffin-treated filter paper. The position of the leucomycin component migrated on the filter paper, was detected as a growth-inhibited zone of *Bacillus subtilis* on the bioautogram[1].

**Isolation of Leucomycin Components.**—Fractions corresponding to each peak on the elution diagram, were combined and cocentrated to about one third volume under reduced pressure. The basic antibiotics in the aqueous concentrates, after adjusting the pH to 8, were extracted with *n*-butyl acetate. From the acid re-extract of the ester layer, leucomycin was crystallized by adjusting the pH to 7. For the recrystallization benzene-cyclohexane solvent for A group and hot benzene for the B group were used.

**Assay of Antibacterial Activity.**—The assay of the antibacterial activity of the so purified components, was kindly done by the Bioassay Division, Toyo Jozo Co. Ltd., according to the usual cup method against *Bacillus subtilis* No. 209 as the test organism.

## Results

**Chromatography of Leucomycin.**—Fig. 1-A represents a typical elution diagram of a leucomycin complex (I) from a column of Amberlite XE-64 (H-cycle) with a mixture of ethanol and M/5 sodium citrate buffer (pH 5.0) in an equal volume. Fig. 1-B illustrates the paper-chromatograms of the above-mentioned effluent fractions detected by the growth-inhibition of

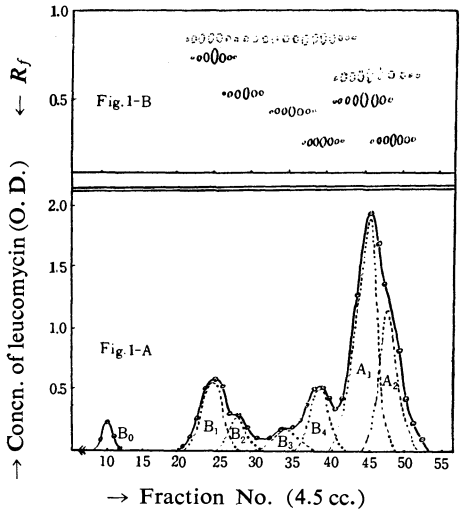



Fig. 1-A. Chromatography of leucomycin complex (I) on 1×40 cm. column of Amberlite XE-64, eluted with a mixture of 96 per cent ethanol and M/5 citrate buffer in an equal valume, at a flow rate of 9 cc. per $cm^2$ per hour at 15°C. -⊙- concentration (uncorr.) assayed photocolorimetrically. ---- concentration of each component presumed from paper chromatographic analysis (Fig. 1-B).

Fig. 1-B. Composite paper chromatograms of each effluent fraction. ○ developed with *n*-butyl acetate containing phosphate buffer (pH 6). ○ developed with phosphate buffer (pH 8) containing *n*-butyl acetate.

*Bacillus sabtilis*. These results indicated that leucomycin components, $B_1$, $B_2$, $B_3$, $B_4$, $A_1$ and $A_2$ were eluted from the column in this order and these components could be separated from each other under the conditions used, except the last two components $A_1$ and $A_2$, which could be only partially separated***. A minor component $B_0$ eluted at the hold-up volume, colored with concentrated sulfuric acid but showed no antibacterial activity (less than 10 unit per mg.). Some discrepancies occasionally observed between both of the amounts of leucomycin complexes, assayed photocolorimetrically and biologically, might be due in part to the presence of this component. The recovery of leucomycin from the column assayed both photocolorimetrically and biologically, was more than 90 per cent and the rechromatography of each component showed an elution of only one component at the same position, indicating that no appreciable degradation occurred for this antibiotic.

*** Recently, however, both of the components were found to be completely separated on a longer column (1.5~2.0 m.), if the amount of the sample added to the column was limited.

The reproducibility of this chromatography was fairly good and the position of the elution of each component varied only within 5 per cent, so far as the chromatographic conditions mentioned rather in detail in the experimental part were exactly maintained. The flow rate of 9 cc./$cm^2$/hr. seemed to be an upper limit for the elution without any broadening of each peak. The pH of buffer should be selected between 4 and 8, as the more acidic or alkaline pH caused slight degradation of leucomycin even at room temperature. In this region, the higher the pH, the less the spreading of the elution peak but also lesser than the separation of the components among each other. Most important in this chromatographic method is the temperature. At higher temperature than 25°C, all components were eluted very rapidly, while at a lower than 10°C very slowly, and both of the extremes resulted into a poor resolution. For a precise analysis, a device to maintain the temperature of the column at a constant (15~20°C) might be profitable.

**Leucomycin Components.**—From the elution diagram as shown in Fig. 1, the composition of the leucomycin complex (I) was estimated to be composed of 11 per cent of $B_1$, 7 per cent of $B_2$, 8 per cent of $B_3$, 13 per cent of $B_4$, 32 per cent of $A_1$ and 24 per cent of $A_2$, in weight respectively. These values were by no means inconsistent with those estimated from the counter current distribution diagram of the same sample[13].

Using the same chromatographic technique, another sample of leucomycin complex (I) produced by a new strain (seed No. L 149-373) and some fractionated leucomycin samples (II, III and IV) from the original strain, were analyzed. The results indicated, that a new strain of *Streptmyces kitasatoensis* produced mainly A components; B components produced by the original strain were much more absorbed on a column of active carbon from the *n*-butyl acetate solution and were precipitated at higher pH from the aqueous solution than A components did; and the crystallization of B components from benzene was effective for the separation of $B_2$ and $B_4$ from less active components $B_1$ and $B_3$. Four leucomycin components, $B_1$, $B_2$, $B_3$ and $B_4$ and partially purified $A_1$ (contaminated small amount of $A_2$) were actually isolated from the preparations which had been previously fractionated (see Table I) according to the above mentioned method by the use of preparative column (3×180 cm.).

The antibacterial activity of $A_1$, though still contaminated with a small amount of $A_2$, was as much as 1000 unit per mg. This value was

13) T. Watanabe, H. Nishida, J. Abe and K. Satake, This Bulletin, 33, 347 (1960).

TABLE II. YIELDS, PROPERTIES AND ANTIBACTERIAL ACTIVITY OF LEUCOMYCIN COMPONENTS

| Component | Yield (%) from I | II | III | IV | m. p. °C | Molecular formula | Antibacterial activity (unit/mg.)* |
|---|---|---|---|---|---|---|---|
| $A_1$ | 32 | 12 | 10 | 0 | 132.0~137.0 | — | 1000 |
| $A_2$ | 24 | 6 | 3 | 0 | — | — | — |
| $B_0$ | 5 | 1 | 0 | 0 | — | — | 10 |
| $B_1$ | 11 | 16 | 53 | 25 | 214.5~216.5 | $C_{35}H_{59}NO_{13}$ | 100 |
| $B_2$ | 7 | 28 | 1 | 31 | 214.0~216.0 | $C_{38}H_{65}NO_{16}$ | 215 |
| $B_3$ | 8 | 29 | 28 | 12 | 216.0~217.0 | $C_{34}H_{53}NO_{13}$ | 570 |
| $B_4$ | 13 | 8 | 5 | 32 | 221.0~223.8 | $C_{35}H_{59}NO_{16}$ | 700 |

* Leucomycin complex (I) ; 560 unit/mg.

approximately 1.8~1.9 times as much as that of leucomycin complex (I) produced by the original strain, and was the highest one as far as known on leucomycin samples. These facts will be explained by the contamination of less active B components. It may be of interest that the activity of B components varied from 700 units to 100 units. According to J. Abe slight undesirable properties observed in the leucomycin complex (produced by the original strain) was mainly due to the presence of B components and their action increased in the following order; $B_4$, $B_3$, $B_2$ and $B_1$, thus with the decrease of the antibacterial activity. These results are summarized in Table II, together with some analytical data of purified B components.

**Chromatography of Leucomycin Derivatives.**—Under the same condition as used for the separation of leucomycin complex, some leucomycin derivatives, acetyl-[9], propionyl-[10], tetrahydroleucomycin $A_1$[11], and a basic moiety derived from $A_1$ by methanolysis[12], were also eluted quantitatively, but at a different position, which are summarized in Table III. The results indicated that this chromatography was effective for the purification of these derivatives from the unreacted leucomycin $A_1$. Less-retardation of the basic moiety derived from $A_1$ by methanolysis and more retardation of the two acyl derivatives on a column of carboxylic acid resin, will be related to their different $pK'_a$ values ($pK'_a$ 5.0 for acyl derivatives; $pK'_a$ 8.1 for basic moiety derived from $A_1$ by methanolysis) from the original leucomycin $A_1$ ($pK'_a$ 7.1)****, but the different chromatographic behaviors of $A_1$ and of the tetrahydro-derivative and of other leucomycin components ($pK'_a$ 6.8~7.1) indicated that " Weiss's effect " would play a predominant rôle in these separations.

**Chromatography of Other Macrolides.**—Table III lists the elution position of several macrolides, including erythromycin, magnamycin, and spiramycin, from a column of Amberlite XE-64 (H-cycle) with an equi-volume mixture of ethanol and M/5 sodium citrate buffer (pH 5.0). These results, together with the results of the paper-chromatographic and -electrophoretic analysis[1], indicated that all six antibiotics contained in leucomycin complex different from one another well-known macrolides, namely: erythromycin, magnamycin and spiramycin. As reported already by the other authors, antibiotics belonging to macrolides were usually produced as a complex composed of a main and a few minor components, the latter of which could be fairly separated with some difficulties. In these experiments,

TABLE III. THE ELUTION POSITION OF SOME LEUCOMYCIN DERIVATIVES AND MACROLIDES UNDER THE SAME CONDITIONS AS USED FOR THE SEPARATION OF LEUCOMYCIN COMPLEX (I)

| Antibiotics | | | Volume cc. |
|---|---|---|---|
| Leucomycin | Main component | $A_1$ | 180~225 |
| | Minor component | $B_1$ | 90~120 |
| | | $B_2$ | 112~144 |
| | | $B_3$ | 144~166 |
| | | $B_4$ | 157~189 |
| | | $A_2$ | 198~238 |
| | Derivatives of $A_1$ | Des-sugar | 50~ 76 |
| | | Tetrahydro- | 71~126 |
| | | Acetyl- | 201~255 |
| | | Propionyl- | 197~259 |
| Erythromycin | Main component | | 126~193 |
| | Minor component | | 99~144<br>189~250 |
| Magnamycin | Main component | | 76~126 |
| | Minor component | | 67~ 90<br>98~148 |
| Spiramycin | Main component | | 234~292 |
| | Minor component | | 126~157<br>211~270 |

**** Basicity of leucomycin is due to the presence of 3-dimethylamino sugar, so the $pK'_a$ was fairly affected by the 2, 4-*O*-substitution.

too, some commercial samples of the above-mentioned antibiotics, though considered to be fairly purified, showed the presence of these minor antibiotics. Such minor components of usual macrolides, however, had been limited to only two or three kinds. The presence of many minor components, as much as five in leucomycin seemed to belong to the first case.

*Department of Chemistry*
*Faculty of Science*
*Tokyo Metropolitan University*
*Setagaya-ku, Tokyo*

# *Studies on Leucomycin. III. Isolation*[1] *and Properties of Six Antibacterial Components in Leucomycin Complex*

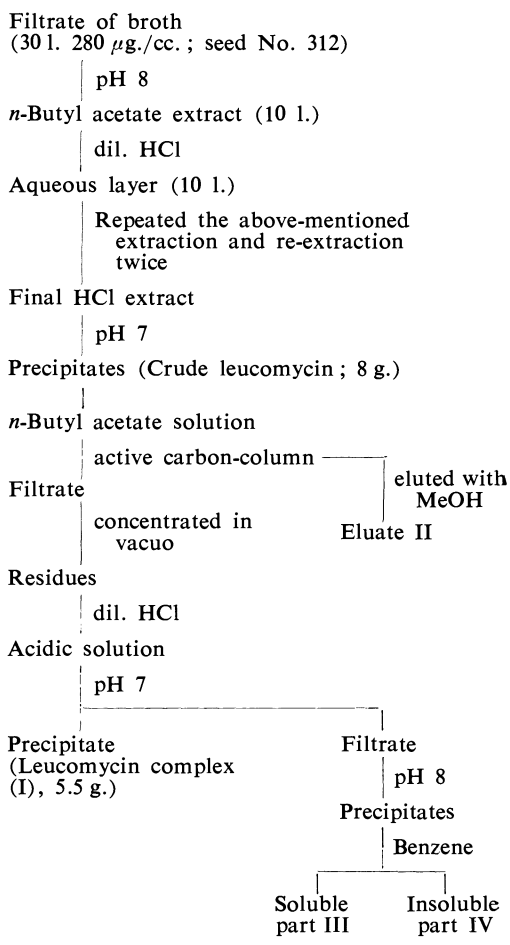
By Tetsuo WATANABE, Hisao NISHIDA, Jinnosuke ABE and Kazuo SATAKE

(Received February 4, 1960)

Leucomycin[2], a basic antibiotic obtained from the broth-filtrate of *Streptomyces kitasatoensis* Hata[3,4], has been presumed to be a macrolides on its physical, chemical[3,5] and antibacterial[3,6] properties. In the previous papers of this series[7,8] it was reported that the antibiotic was a mixture of six biologically active components, $A_1$, $A_2$, $B_1$, $B_2$, $B_3$ and $B_4$ and that the last four minor components, though in a minute amount, could be purified by fractional precipitation[8] of the mixture from aqueous and from benzene solutions (see Table I), followed by the further minute resolution of the resulting fractions by chromatography on a column of Amberlite IRC-50[8]. The main component $A_1$ which seemed to have the highest activity[8], however, had been scarcely separated from $B_4$ and another minor component $A_2$, by this method.

For the resolution of macrolides complex in preparative scale, counter current distribution has been reported to be effective[9-12]. Using this technique, leucomycin complex was also

TABLE I. FRACTIONATION OF LEUCOMYCIN




1) Japanese Pat., Application No. 13909 (1958).

2) Leucomycin used in this study, was obtained from the broth of *S. kitasatoensis* Hata No. 312, in 1956 and had a similar component composition to that of the original preparation by Hata[3,6]. Recent preparation from No. L-149-373, a mutant of the original strain, was almost free from B components.

3) T. Hata, Y. Sano, M. Ohki, Y. Yokohama A. Matsumae and S. Ito, *J. Antibiotics, Ser.* A6, (2), 87 (1953).

4) T. Hata, F. Koga and H. Kanamori, ibid., Ser, A, 6 (3), 109 (1953).

5) Y. Sano, ibid., Ser. A7 (3), 93 (1954).

6) T. Hata, Y. Sano, Y. Yokohama, S. Ito, S. Okazaki, K. Takeno, H. Ito, Y. Owada, Y. Saito and M. Soekawa, ibid., Ser. A6 (4), 163 (1953).

7) J. Abe, Y. Suzuki, T. Watanabe and K. Satake, *J. Chem. Soc. Japan, Pure Chem. Sec.* (*Nippon Kagaku Zasshi*), 81, 969 (1960).

8) T. Watanabe et al., This Bulletin, 33, 1100 (1960).

9) J. M. McGuire, L. Bunch, R. C. Anderson, H. E. Boaz, E. H. Flynn, H. M. Powell and T. W. Smith, *Antibiot. Chemoth.* 2, 281 (1952).

10) R. L. Sagner, F. A. Hochstein and K. Murai, *J. Am. Chem. Soc.*, 75, 4684 (1953).

11) S. P. Sindico, L. Ninet, S. Preud'homme and C. Coser, *Antibiotics Annual*, 724 (1955-1956).

12) H. Schmitz, M. Misick, B. Heinemann and I. R. Hooper, *Antibiot. Chemoth.*, 7, 37 (1957).

analyzed[13]. The distribution diagram, though after only 30 transfers, seemed to suggest a partial resolution. These facts prompted us to study the counter current distribution of leucomycin complex (I) (see Table I) in more detail. In this paper we wish to report on these results. In addition, some properties of such purified antibacterial components as $A_1$, $A_2$, $B_1$, $B_2$, $B_3$ and $B_4$, will be described.

**Solvent System for the Distribution of Leucomycin Complex.** — The marked difference observed among the solubilities of each of the components of leucomycin complex in aqueous solution at pH 7~8 and in benzene[8], seemed to suggest the use of both solvents for the counter current distribution. Preliminary experiments showed that the addition of methanol to this binary system further improved the resolution. Fig. 1 presents the distribution diagram of leucomycin complex (I), after 150 transfers between the two layers which resulted from a mixture of five parts of benzene, two parts of M/15 sodium phosphate buffer at pH 6.5, and five parts of methanol (Solvent system 1); together with a composite paper chromatogram of leucomycin components in each distribution tube. The results suggested that system 1 could be used for the isolation of $A_1$, $A_2$ and $B_1$.

A solvent system which gave a more minute resolution of leucomycin complex, could be obtained by using much more acid citrate buffer and by adding a sufficient amount of choroform to the triple-system composed of benzene, citrate buffer and methanol. Differing from solvent system 1, the quartet-system separated into two layers very rapidly, though the volume-ratio of these two layers differed to some extent by a slight change of temperature. Fig. 2 illustrates the distribution diagram

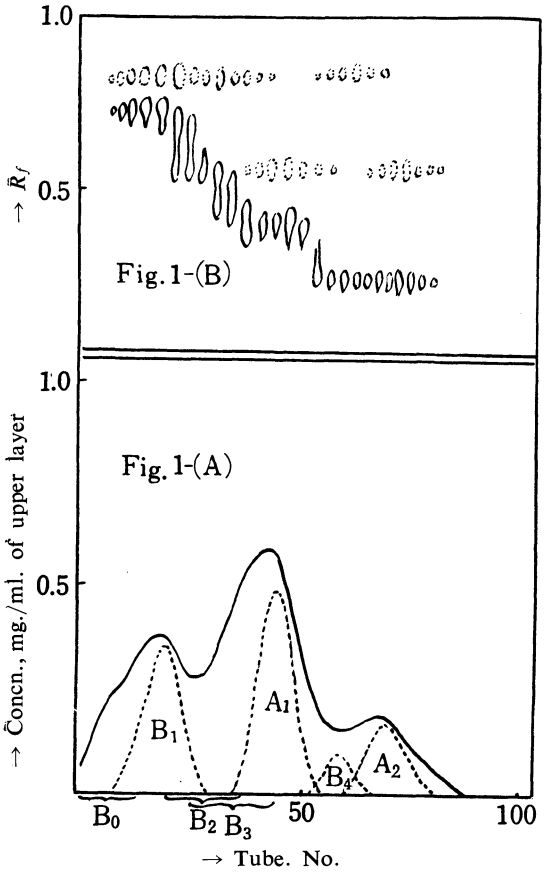



Fig. 1—(A). ---- Counter current distribution of luecomycin complex (I) using "Solvent system 1".

Fig. 1—(B). ---- Composite paper chromatogram of luecomycin components in each distribution tube. ○ developed with *n*-butyl acetate containing phosphate buffer (pH 6). ○ developed with phosphate buffer (pH 8) containing *n*-butyl acetate.

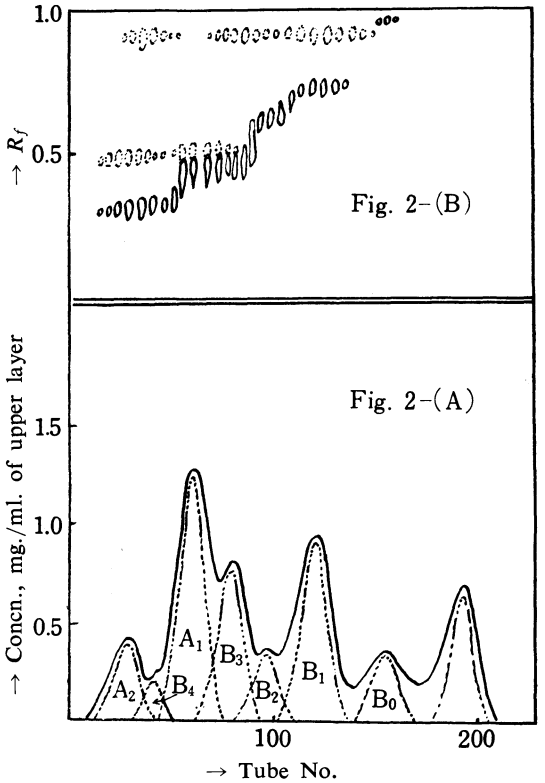



Fig. 2—(A). ---- Counter current distribution of leucomycin complex (I) using "Solvent system 2".

Fig. 2—(B). ---- Composite paper chromatogram of leucomycin components in each distribution tube; ○ developed with *n*-butyl acetate containing phosphate buffer (pH 8) containing *n*-butyl acetate.

13) Y. Sano. T. Hoshi and T. Hata, *J. Antibiotics*, Ser. A7, (3) 88 (1954).

of leucomycin complex (I), after 210 transfers between the two layers which resulted from a mixture of ten parts of benzene, nine parts of M/15 sodium citrate buffer of pH 4.9, eight parts of chloroform and twenty parts of methanol (Solvent system 2); together with a composite paper chromatogram of leucomycin components in each distribution tube. From the appropriate tubes after this distribution, five kinds of antibacterial component could be isolated completely free from other components though the yields of $B_2$ and of $B_3$ were not so excellent as that of $A_1$ $A_2$ or $B_1$ due to the partial resolution of the former two.

For the resolution of B components, especially of $B_2$ and $B_4$ which were only slightly soluble in benzene, another system composed of chloroform and acid buffer seemed to be promising, as B components showed a moderate solubility in both solvents. In this case, too, the resolution was improved by adding an appropriate amount of a third solvent which could be mixed with upper and lower layers at any ratio, and the effect of acetone seemed to be superior to that of methanol in this solvent system. Fig. 3 shows the distribution diagram of antibiotic IV (see Table I) present in the filtrate fraction from leucomycin complex (I) precipitated at pH 7, after 250 transfers between the two layers which resulted from a mixture of one part of chloroform, two parts of M/15 sodium acetate buffer of pH 4.5, and two parts of acetone (Solvent system 3), together with a composite paper chromatogram of leucomycin components in each distribution tube. From the appropriate fractions after this distribution, all B components, $B_1$, $B_2$, $B_3$ and $B_4$, could be isolated in a good yield, respectively. The results suggested that the counter current distribution with "Solvent system 3" was the most suitable method for the isolation of four B components; if the most part of $A_1$ which was the main component of leucomycin complex, had been previously removed.

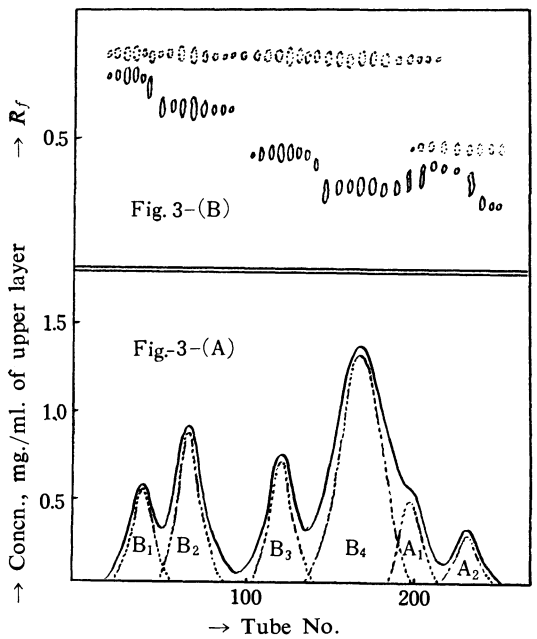



Fig. 3—(A). ---- Counter current distribution of fraction IV (See Table I, B components rich fraction) using "Solvent system 3".

Fig. 3—(B). ---- Composite paper chromatogram in each distribution tube; ○ developed with *n*-butyl acetate containing phosphate buffer (pH 6). ○ developed with phosphate buffer (pH 8) containing *n*-butyl acetate.

**Leucomycin $A_1$ and $A_2$.**—As shown in Fig. 2, the observed distribution curves of $A_1$ and of $A_2$, showed no serious disagreement with the theoretical ones calculated from the maximum peak position[14], nor with the distribution of $A_1$ and $A_2$ estimated by paper chromatography. The facts seemed to indicate the homogeneity of both the components resolved by counter current distribution. The presumption was verified by the identity of the observed and the calculated re-distribution

TABLE II. PROPERTIES OF LEUCOMYCIN $A_1$ AND $A_2$

| | $A_1$ | $A_2$ |
|---|---|---|
| Partition coefficient $K$ | | |
| Solvent system 1 | 0.92 | 2.33 |
| Solvent system 2 | 0.33 | 0.14 |
| Solvent system 3 | 1.86 | 3.00 |
| $\lambda_{max}^{N/1000\ HCl}(\varepsilon_{max})$ | 233 mμ ($2.45\times10^4$) | 231 mμ ($1.98\times10^4$) |
| $pK'_a$ | 7.1 | 7.1 |
| Equivalent as base | | |
| Found. | 920~950 | 1220~1250 |
| (Calcd.) | (918)[a] | (1265)[b] |
| C%; Found. (Calcd.) | 60.99 (60.13) | 62.13 (61.66) |
| H%: Found. (Calcd.) | 8.72 (8.75) | 8.61 (8.70) |
| N%; Found. (Calcd.) | 1.52 (1.54) | 1.10 (1.11) |
| Antibacterial activity (unit/mg.) | 1000 | 910 |
| Content (%) in I | 33 | 19 |
| II | — | — |
| III | 8 | 4 |
| IV | 3 | 1 |

a) as $C_{46}H_{81}NO_{17}$
b) as $C_{65}H_{111}NO_{22}$

14) L. C. Craig and O. Cost, *Anal. Chem.*, 21, 508 (1949).

curves (using "Solvent system 1 or 2" for the samples isolated with "Solvent system 2 or 1", respectively).

In Table II, are summarized the analytical data and some properties of leucomycin $A_1$ and $A_2$. There have been reported several macrolides, from picromycin ($C_{25}H_{43}NO_7$)[15] up to magnamycin ($C_{42}H_{67}NO_{16}$)[16]. Minor components $A_2$ ($C_{65}H_{111}NO_{22}$) seemed to be a macrolide of highest molecular weight, as far as we know. Main component $A_1$ ($C_{46}H_{81}NO_{17}$), on the other hand, was similar to magnamycin in the molecular weight and $pK'_a$, though the former had an antibacterial activity higher than that of the latter. In Table II, are also presented the contents of $A_1$ and $A_2$, in leucomycin complex and in several fractions derived during the preparation of fraction I. These values calculated from the distribution diagram with "Solvent system 2" were not inconsistent with the $A_1$- and $A_2$-content estimated from the elution diagram from a column of Amberlite IRC-50 with a mixture of ethanol and M/15 sodium citrate buffer at pH 5[8]. The results also indicated that both the components were less soluble in aqueous solution at pH 7, less absorbed on a column of active carbon, and more soluble in benzene than B components. Fig. 4 represents infrared spectra of $A_1$. The presence of OH, C=O (ester) and C=C was presumed from the characteristic absorption at 3450 $cm^{-1}$, 1750 $cm^{-1}$ and 1680 $cm^{-1}$, respectively. A shoulder at 1710 $cm^{-1}$ seemed to be due to the presence of the second C=O (lactone).

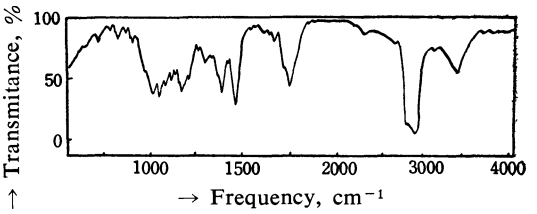



Fig. 4. Infrared spectrum of leucomycin $A_1$. (in Nujol)

Infrared spectrum of $A_2$ was extremely close to that of $A_1$.

**Leucomycin $B_1$, $B_2$, $B_3$ and $B_4$.** — Four components, $B_1$, $B_2$, $B_3$ and $B_4$, found in leucomycin complex as minor components, could be isolated by counter current distribution using "Solvent system 3" from the filtrates III and IV of leucomycin complex (I) precipitated at pH 7[8], from the mother liquid of the recrystallization of leucomycin complex (I); and from the methanol-eluate II of the carbon-column previously treated with *n*-butyl acetate solution of leucomycin[7,8]. As shown in Fig. 3, the distribution curves of these components agreed with the corresponding theoretical curve. The homogeneity of the component so isolated was further verified by analytical chromatography on a column of Amberlite IRC-50[8].

Leucomycin B components ($C_{34}$—$C_{38}$) had a molecular weight similar to that of erythromycin A[18], but the $pK'_a$ value (6.8) was similar to those of leucomycin A and magnamycin. The antibacterial activity was considerably lower than that of $A_1$. In Table III,

Table III. Yields, properties and antibacterial activity of leucomycin components

| Component | *K* Solvent system 1 | 2 | 3 | m.p. °C | C % Found (Calcd.) | H % Found (Calcd.) | N % Found (Calcd.) |
|---|---|---|---|---|---|---|---|
| $B_0$ | 0.1 | 2.3 | — | — | — | — | — |
| $B_1$ | 0.19 | 1.3 | 0.15 | 214.5~216.5 | 60.30(60.00) | 8.22(8.20) | 1.99(2.00)[a] |
| $B_2$ | 0.37 | 0.91 | 0.28 | 214.0~216.0 | 56.85(56.50) | 8.14(8.05) | 1.66(1.63)[b] |
| $B_3$ | 0.54 | 0.50 | 0.67 | 216.0~217.0 | 59.39(59.73) | 7.65(7.72) | 2.05(2.05)[c] |
| $B_4$ | 1.50 | 0.19 | 1.22 | 221.0~223.8 | 56.27(56.81) | 7.59(7.64) | 1.81(1.78)[d] |

| | Antibacterial activity (unit/mg.)* | $\lambda_{max}^{N/1000\ HCl}$ ($\varepsilon_{max}$) | Yield (%) from I* | II** | III** | IV*** |
|---|---|---|---|---|---|---|
| $B_0$ | <10 | — | 2 | 8 | 0 | 0 |
| $B_1$ | 100 | 234 mμ(2.24×10⁴) | 11 | 23 | 50 | 24 |
| $B_2$ | 215 | 234 mμ(2.47×10⁴) | 6 | 12 | 20 | 29 |
| $B_3$ | 570 | 234 mμ(2.32×10⁴) | 19 | 38 | 27 | 13 |
| $B_4$ | 700 | 233 mμ(2.45×10⁴) | 8 | 20 | 9 | 30 |

* Leucomycin complex (I); 560 unit/mg. ** Using "Solvent system 2".
*** Using "Solvent system 3".
a) as $C_{35}H_{59}NO_{13}$ b) as $C_{38}H_{65}NO_{16}$ c) as $C_{34}H_{53}NO_{13}$ d) as $C_{38}H_{59}NO_{16}$

15) H. Brockmann et al., *Ber*, **84**, 284 (1951).
16) R. L. Wagner, F. A. Hochstein and K. Murai, *J. Am. Chem. Soc.*, **75**, 4684 (1953).
17) E. H. Flynn, M. V. Sigal and F. R. Wiley, ibid., **76**, 3121 (1954).

are summarized the analytical data, some properties and the content in leucomycin complex (I) and in several fractions II, III and IV. The last data indicated that B components could be fractionated, and that the fractions thus obtained could be further separated into two groups, $B_1$ and $B_3$ rich III, and $B_2$ and $B_4$ rich group IV. It seems to be interesting that the original strain of *Streptomyces kitasatoensis* produced as many as six kinds of macrolide, while the mutant (strain No. L-149-373) gave only $A_1$ and $A_2$ without any decrease of the weight of total antibiotics. The elucidation and comparison of the structure of these components might give valuable information on the biosynthesis of macrolides.

## Experimental

**Materials.**—Leucomycin complex (I) and the fractionated antibiotics II, III, IV were prepared by the methods summarized in Table I.

**Counter Current Distribution.** — The procedure was achieved at 15~20°C in an automatic "Craig-type" apparatus having 300 transfer tubes No. 555 F, Mitamura Shoten, Tokyo). The sample (1~10 g.) was added as a concentrated solution in the lower solvent layer (5~10%) into the first few tubes. The volume of the upper and the lower layer in each distribution tube was 10 cc. each. The partition coefficient of distributed components was calculated from the peak position on the distribution diagram and the total transfer-number. The theoretical distribution curve was calculated from the partition coefficient so obtained, according to Craig's method[14].

**Determination of the Concentration of Leucomycin.** — The concentration was assayed by the photometry of red brown color which was produced by mixing 0.5 cc. of the sample (aqueous layer in the distribution tube) with 2.0 cc. of concentrated sulfuric acid[8]. The concentration in organic-solvent rich layer, was calculated from the above-mentioned concentration in aqueous layer and the calculated partition coefficient.

**Paper Chromatography of Leucomycin Components.**—Paper chromatography of leucomycin in each distribution tube was achieved by the method already reported[7], using 0.02 cc. of the organic-solvent rich phase as the sample.

**Crystallization of Each Component.**—The leucomycin components separated by counter current distribution, was crystallized from the aqueous solution by adjusting the pH to 8 according to the method reported already[8].

**Antibacterial Activity.** — The assay of the antibacterial activity of the components so purified, was done by the Bio-assay Division, Toyo Jozo Co. Ltd., according to the usual cup assay method with the use of *Baccillus subtilis* No. 209 as the test organism.

**Absorption Specta.** — Absorption spectra were measured by Hitachi Spectrophotometer Model DUP-2.

**p$K'_a$.**—p$K'_a$ was measured on the sample solution in a dimethylformamide (60%) at a concentration of 0.05 per cent, by titrating with 1 N hydrochloric acid with the use of Toa-denpa pH meter HM-5.

We are greatly indebted to Mr. S. Suda for his assistance in paper chromatographic analysis of the distributed fractions.

*Research Institute*
*Toyo Jozo Co. Ltd.*
*Ohito, Shizuoka-ken*
*(T. W., J. A.)*

*Department of Chemistry*
*Faculty of Science*
*Tokyo Metropolitan University*
*Setagaya, Tokyo*
*(H. N., K. S.)*

# *Studies on Seven-Membered Heterocyclic Compounds Containing Nitrogen. IV. Hexahydro-1, 2, 5-Triazazulene*

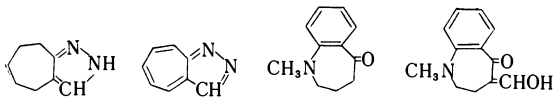
By Shiro MOROSAWA

(Received February 6, 1960)

It has been found that hexahydro-1, 2-diazazulene (I)[1-3] was prepared from 2-hydroxymethylenecycloheptanone. Buchta[4] has made only a simple statement that W. Treibs succeeded in dehydrogenation of the hydroazazulene by chloranil to yield 1, 2-diazazulene (II), but no further detailed report was given. The present author has synthesized hitherto unknown hexahydro-1, 2, 5 (or 1, 2, 6)-triazazulene (XIa or XIb), having one nitrogen atom in the seven-membered ring in satisfying yield. Spectral studies have shown that the former

1) O. Wallach, *Ann.*, **329**, 109 (1903).
2) W. Treibs and H. J. Neupert, ibid., **595**, 219 (1955).
3) E. Buchta and J. Kranz, ibid., **601**, 170 (1956).
4) E. Buchta et al., *Angew. Chem.*, **67**, 77 (1955).

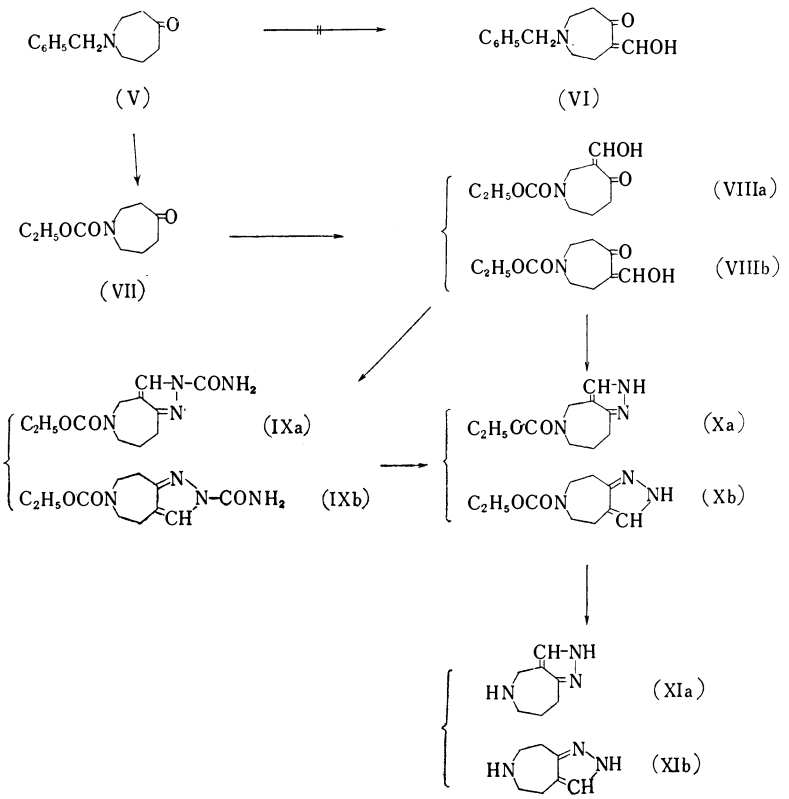
structure is more reasonable. A preliminary test of dehydrogenation was quite unsuccessful, but further attempts are in progress.



(I) (II) (III) (IV)

*N*-Methyl type azasuberenone, 1-methyl-2, 3, 4, 5-tetrahydro-5-keto-1-benzazepine (III)[5] has been reported to afford 4-hydroxymethylene derivative (IV) in 72% yield by the reaction with ethyl formate in the presence of sodium methoxide in benzene. Under the same condition, however, *N*-benzyl type azasuberone, 1-benzyl-1-azacycloheptan-4-one (V)[6] gave only a trace of hydroxymethylene compound, which certified as bis-2, 4-dinitrophenylhydrazone, leaving much residue on distillation. 1-Ethoxycarbonyl-1-azacycloheptan-4-one (VII) derived from V was subjected to the similar treatment and 1-ethoxycarbonyl-3 (or 5)-hydroxymethylene-1-azacycloheptan-4-one (VIIIa or VIIIb)*, b. p. 127~130°C/0.7 mmHg was obtained in 72.5% yield as a colorless oil. Reaction of hydrazine hydrate with VIII in ether gave a stable pyrazole derivative (Xa or Xb), b. p. 183~185°C/0.3 mmHg in 87.6% yield. X was also derived from VIII cyclic semicarbazone (IXa or IXb), m. p. 159~159.5°C by hydrolysis. X afforded a picrate of m. p. 136.5~137.5°C and a chloroplatinate of m. p. 184°C (decomp.) respectively. Deethoxycarbonylation of X by hydrogen bromide in glacial acetic acid gave hydrobromide of XIa or XIb in 84% yield as hygroscopic colorless long prisms which softened at above 260°C. Free base, XIa or XIb, was liberated almost quantitatively from the hydrobromide with alkali as hygroscopic, colorless hexagonal prisms of m. p. 155.5~156.5°C. XI formed a picrate of m. p. 220~221°C (decomp.), which was unstable to light and turned brown on standing.

As a preliminary examination of dehydrogenation 4, 5-cyclohepteno-7-methylthiazole (XIV), b. p. 109~111°C/15 mmHg which was prepared from cycloheptanone** (XII) by NBS bromination and condensation with thioacetamide was subjected to the dehydrogenation

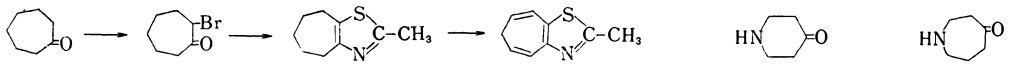


5) B. D. Astill and V. Beokelheide, *J. Am. Chem. Soc.*, 77, 4079 (1955).

6) (a) A. Yokoo and S. Morosawa, This Bulletin, 29, 631 (1956); (b) S. Morosawa, ibid., 31, 418 (1958).

* Degradative studies will be reported later.

** The author wishes to thank Professor Tetsuo Nozoe (Tohoku University) for donating the sample.



(XII) (XIII) (XIV) (XV) (XVI) (XVII)

with 10% palladium on carbon at elevated temperature. Thus 4, 5-cycloheptatrieno-7-methylthiazole (XV) was obtained as a colorless oil, b. p. 104°C/12 mmHg, XV gave a picrate of m. p. 147~148°C. XI, however, was decomposed under the same condition with evolution of hydrogen. Ultraviolet absorption spectra of XI, XIV and XV are given in Fig. 1, together with that of the condensation product of XIV ethiodide with *p*-dimethylaminobenzaldehyde.

It appeared of interest to obtain a unique product in the formation of the hydroxymethylene compound (VIII) from the asymmetrical ring ketone (VII). The structure of the pyrazole derivative (XI) was estimated by the following spectral studies. It has already been recognized[7] that the band arising from the hydrogen bending vibrations of methylene appeared near the 1450 $cm^{-1}$ region and shifted in some degree higher when attached to the nitrogen atom and somewhat lower to carbon-carbon or carbon-oxygen double bond. As shown in Fig. 2, 1-azacyclohexane-4-one (XVI)[8],* gave rise to only two bands near the region at 1469 and 1428 $cm^{-1}$, presumably arising from 2 (or 6)- and 3 (or 5)-methylene of the ring respectively. 1-Azacycloheptan-4-one (XVII)**, on the other hand, indicated at least three bands at 1464, 1452 and 1431 $cm^{-1}$, probably due to 2 (or 7)-, 6- and 3 (or 5)-methylene respectively. Hydrochlorides of XVI and XVII also gave rise to two and three bands respectively, corresponding to the above absorption bands. XV was expected to show two bands near the region arising from methyl*** at 2-position of the thiazole ring and methylene in the seven-membered ring, and in fact two bands at 1457 and 1437 $cm^{-1}$ were observed. From a consideration of these facts it became clear that the methylenes in the nitrogen containing ring ketone were distinguishable from each other in the infrared

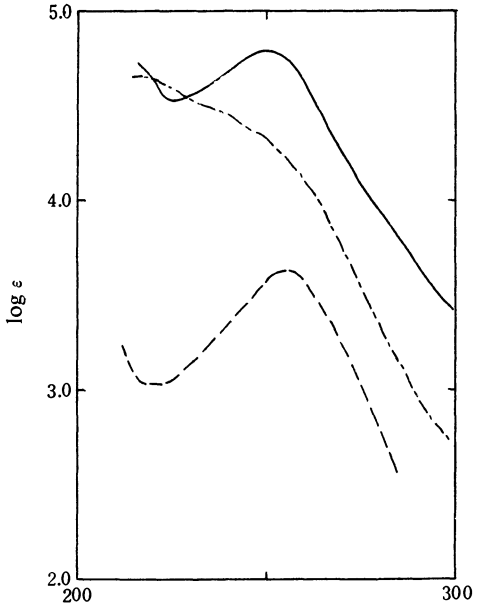



Fig. 1. (in methanol)
—— XI, ——— XIV, ———— XV

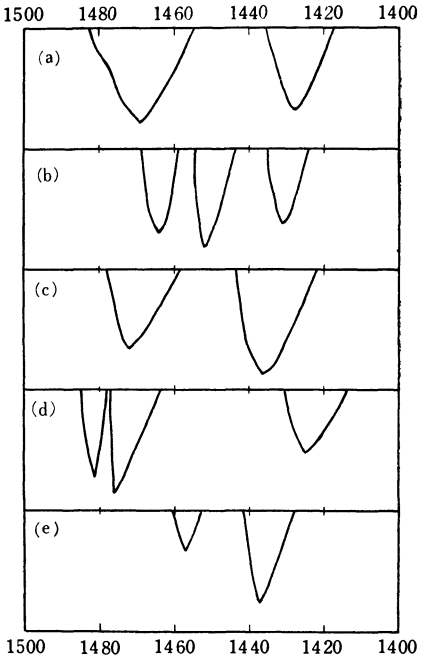



Fig. 2.
(a) XVI; (b) XVII; (c) XVI hydrochloride; (d) XVII hydrochloride; (e) XV

7) L. J. Bellamy, "The Infra-red Spectra of Complex Molecules", Methuen & Co. Ltd., London (1958), p. 20.
8) E. Königs and L. Neumann, *Ber.*, **48**, 956 (1915).

* Prepared from 1-benzyl-1-azacyclohexan-4-one[6b] by catalytic reduction in the presence of palladous oxide, b. p. 56~57°C/6 mmHg. It began to polymerize into a white solid within an hour after distillation.

** Liberated by potassium carbonate from its hydrochloride[6a], b. p. 95~96°C/15 mmHg.

*** According to Bellamy[7], the band arising from the methyl group adjacent to the carbon atom appeared near 1450 $cm^{-1}$ in relatively low intensity.

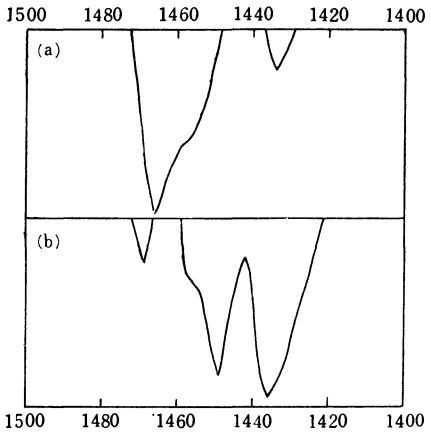



Fig. 3.
(a) XI; (b) XI hydrobromide

absorption spectra. The pyrazole derivative (XI) indicated, as seen in Fig. 3, three bands at 1466, 1458 (shoulder) and 1434 $cm^{-1}$. It may be assumed that the former band is due to 6-methylene and the latter to 8, the shoulder being due to overlapping of bands arising from 4- and 7-methylene. Hydrobromide of XI distinctly showed three principal bands at 1469, 1449 and 1436 $cm^{-1}$ together with a shoulder at 1456 $cm^{-1}$ which probably arose from 4-methylene. From these spectral data it may be concluded that XI has an angular form (XIa) rather than a linear one (XIb) and therefore the hydroxymethylene compound is in the form of VIIIa.

## Experimental

**1-Ethoxycarbony-1-azacycloheptan-4-one (VII).**—A solution of 15 g. of V hydrochloride[6a,b] in 200 cc. of water was shaken with hydrogen in the presence of 0.2 g. of palladous oxide under normal temperature and pressure. After the theoretical amount of hydrogen was consumed the catalyst was filtered off and evaporated to a smaller volume under reduced pressure. To this were added a solution of 2.7 g. of sodium hydroxide in 5 cc. of water and 14.7 g. of anhydrous potassium carbonate. The mixture was kept at 10°C and 15 g. of ethyl chlorocarbonate was added dropwise during 45 minutes with stirring, followed by further stirring for 1 hour at the same temperature. Precipitates were collected and washed well with ether, and the filtrate was thoroughly extracted with ether. The water layer was evaporated under reduced pressure until precipitation began and treated as before. The ethereal solutions were combined and dried over anhydrous potassium carbonate. Evaporation of ether and vacuum distillation gave 11.5 g. (99.1%) of a colorless oil, b. p. 117°C/1 mmHg The oil was fairly soluble in water and did not give a bisulfite addition compound.

Found: N, 7.66. Calcd. for $C_9H_{15}O_3N$: N, 7.56%.

**1-Ethoxycarbonyl-3(or 5)-hydroxymethylene-1-azacycloheptan-4-one (VIIIa or VIIIb).**—A solution of 6 g. of VII and 9.5 g. of ethyl formate in 50 cc. of dry benzene was added with swirling to an ice cold suspension of crushed methanol-free sodium methoxide[9] (from 1.6 g. of sodium) in 50 cc. of dry benzene, and the whole was evacuated and filled with nitrogen. After the mixture had been allowed to stand at room temperature for 3 hours, it was boiled under gentle reflux for 1 hour. After cooling, 10 cc. of water was added and the aqueous layer was separated. The benzene solution was washed twice with 10% sodium hydroxide solution. The combined water layer was washed with ether and adjusted to pH 3.4 by adding hydrochloric acid. A reddish orange oil deposited was extracted three times with benzene. The acidic water layer was evaporated to a smaller volume under reduced pressure and nitrogen atmosphere and extracted with benzene. The benzene extracts were united, washed three times with small portions of saturated sodium chloride solution and dried over anhydrous magnesium sulfate. Evaporation of benzene and vacuum distillation of the residue under nitrogen gave 5 g. of a colorless oil, b.p. 127~130°C/0.7 mmHg in 72.5% yield. It gave a deep purple coloration with ferric chloride solution.

Found: N, 6.80. Calcd. for $C_{10}H_{15}O_4N$: N, 67.5%.

**2, 4-Dinitrophenylhydrazone,** orange prisms, m.p. 172°C (from methanol).

Found: N, 19.24. Calcd. for $C_{15}H_{19}O_6N_5$: N, 19.17%.

**VIII Cyclic Semicarbazone (IXa or IXb).**—A solution of 2.2 g. of VIII in 9 cc. of glacial acetic acid was added to a separately prepared solution of 1.7 g. of semicarbazide hydrochloride and 1.7 g. of anhydrous sodium acetate in as small an amount of water as possible. After the mixture was allowed to stand for a few days with 1 cc. of concentrated sulfuric acid, 50 cc. of water was added to deposit gradually 1.0 g. of cyclic semicarbazone in colorless needles, m. p. 155°C. Recrystallization from ethanol raised the m. p. to 159~159.5°C.

Found: N, 22.16. Calcd. for $C_{11}H_{16}O_3N_4$: N, 22.21%.

**5(or 6)-Ethoxycarbonyl-1, 2, 5(or 1, 2, 6)-triazazulene (Xa or Xb).**—(a) To a solution of 5 g. of VIII in 50 cc. of ether was added dropwise under stirring and ice-water cooling 1.2 g. of hydrazine hydrate (100%), followed by an additional stirring for 1 hour. After decantation of the ethereal solution, a large excess of anhydrous potassium carbonate was added to the viscous water layer in order to remove the water completely. Ether was added, agitated well and decanted repeatedly. The combined ethereal solution was dried over anhydrous potassium carbonate and the ether was removed by distillation. Vacuum distillation of the residue gave 4.3 g. of a colorless viscous oil, b. p. 183~185°C/0.3 mmHg in 87.6% yield.

9) W. S. Johnson and H. Posvic, *J. Am. Chem. Soc.*, 69, 1361 (1947).

Found: N, 20.15. Calcd. for $C_{10}H_{15}N_2O_3$: N, 20.08%.

A **picrate** derived from the above oil showed, after several recrystallizations from ethanol, m. p. 136.5~137.5°C with sintering at about 80°C.

Found: N, 17.53. Calcd. for $C_{10}H_{15}O_2N_3 \cdot C_6H_3O_7N_3 \cdot C_2H_6O$: N, 17.35%.

After drying at 100°C for 1 hour the nitrogen content varied to 19.38%. (Calcd. for $C_{10}H_{15}O_2N_3 \cdot C_6H_3O_7N_3$: N, 19.17%).

The oil also afforded a cream yellow **chloroplatinate,** m. p. 184°C (decomp.) (from aqueous ethanol containing 1 drop of concentrated hydrochloric acid).

Found: N, 10.50. Calcd. for $(C_{10}H_{15}O_2N_3)_2 \cdot H_2PtCl_6$: N, 10.14%.

(b) A mixture of 1.35 g. of IX, 1.7 cc. of concentrated sulfuric acid and 5.1 cc. of water was heated under reflux for 15 minutes. After cooling it was made alkaline by adding aqueous ammonia, extracted with benzene and dried over anhydrous potassium carbonate. Benzene was removed and the residue was distilled in vacuo to give 1.0 g. of colorless viscous oil, b.p. 201°C/0.7 mmHg in 89.3% yield. (Found: N, 19.79%). The **picrate** formed was not depressed on admixture with that described above, m. p. and mixed m. p. 137°C. (Found: N, 17.61%).

**Hexahydro-1, 2, 5 (or 1, 2, 6)-triazazulene (XIa or XIb).**—A solution of 1.5 g. of X in 15 cc. of glacial acetic acid was saturated with dry hydrogen bromide under ice-water cooling. After standing overnight at room temperature, the solution was heated slowly to 90°C and kept for 2 hours at the same temperature, followed by refluxing for 1 hour. The hydrobromide deposited during the refluxing was separated by decantation, washed twice with a small amount of ethanol and recrystallized from methanol and ether to yield 1.4 g. of hygroscopic, colorless long prisms, which softened at above 260°C, and the second crop of the crystal, 0.4 g. was obtained from the filtrate. The total yield was 84%.

Found: N, 13.83. Calcd. for $C_7H_{11}N_3 \cdot 2HBr$: N, 14.05%.

To a solution of 7.5 g. of the hydrobromide in a small amount of water anhydrous potassium carbonate was added to make it sufficiently alkaline and the mixture was evaporated to dryness under reduced pressure. The residual mass was dried in a desiccator and extracted in the Soxhlet apparatus with isopropyl ether for 15 hours to give 3.4 g. of somewhat hygroscopic, hexagonal **free base,** m. p. 155.5~156.5°C in 99% yield. An analytical specimen was recrystallized from benzene and ethanol.

Found: C, 61.40; H, 8.22; N, 30.75. Calcd. for $C_7H_{11}N_3$: C, 61.29; H, 8.08; N, 30.63%.

The free base and a saturated ethanolic solution of picric acid formed a picrate, which was recrystallized from ethanol to yellow rhombo prisms, m. p. 220~221°C (decomp.). These gradually turned brown on standing.

Found: N, 23.04. Calcd. for $C_7H_{11}N_3 \cdot C_6H_3O_7N_3$: N, 22.94%.

**NBS Bromination of Cycloheptanone.**—A mixture of 12.4 g. of cycloheptanone (b. p. 174~181°C), 25 g. of NBS and 1.5 g. of benzoyl peroxide in 600 cc. of carbon tetrachloride was boiled under reflux for 5 hours on a water bath. Initially the mixture was gradually colored, and reaction suddenly started to make it colorless with the evolution of much hydrogen bromide. After cooling in ice-water succinimide was separated, and the filtrate was washed with 50 cc. of 40% potassium carbonate solution and with 10 cc. of water and finally dried over anhydrous potassium carbonate. The solvent was removed and the residue was distilled in vacuo to yield 11 g. of 2-bromocycloheptanone (XIII) as a colorless oil, b. p. 90~130°C/5 mmHg. This was fractionated into three parts, b. p. 90~101°C/5 mmHg, 101~111°C/5 mmHg and 111~128°C/5 mmHg. These, however, gave the same thiazole derivative as described below.

**Condensation of XIII with Thioacetamide.**—A solution of 11 g. of XIII and 6 g. of thioacetamide in 20 cc. of ethanol was refluxed on a water bath for 5 hours. After removing ethanol and heating the residue for 5 hours in an oil bath kept at 160°C, 40 cc. of 4 N hydrochloric acid was added and extracted three times with each 20 cc. portion of ether. The combined ethereal solution was washed with 10 cc. of 4N hydrochloric acid. Acidic solutions were united, made alkaline by adding anhydrous potassium carbonate and 5 cc. of 5N sodium hydroxide solution, and extracted three times with each 20 cc. portion of ether. After drying over anhydrous potassium carbonate, the ether was expelled and the residue was distilled in vacuo to yield 1.4 g. of **4, 5-cyclohepteno-2-methylthiazole (XIV)** as a colorless oil, b. p. 109~111°C/15 mmHg.

Found: N, 8.06. Calcd. for $C_9H_{13}NS$: N, 8.38%.

Ethanolic solution of XIV was boiled with an excessive picric acid to form a **picrate,** which was recrystallized three times from ethanol to yellow crystals, m. p. 129~131°C.

Found: N, 13.84. Calcd. for $C_9H_{13}NS \cdot C_6H_3O_7N_3$: N, 14.15%.

**Ethiodide** of XIV was obtained as an oily substance by refluxing an ethanolic solution of 0.2 g. of XIV with an excessive ethyl iodide for 8 hours, followed by the addition of ether. This, however, gave a crystalline condensation product assumed to be **4, 5-cyclohepteno-2-(*p*-dimethylaminostyryl)-3-ethylthiazolium iodide** by refluxing with *p*-dimethylaminobenzaldehyde for 8 hours in the presence of a small amount of piperidine and adding ether. The condensation product was recrystallized from ethanol to afford 50 mg. of red crystals, m. p. 219~220°C (decomp.).

Found: N, 5.88. Calcd. for $C_{20}H_{27}N_2SI$: N, 6.17%.

The red crystals showed absorption maximum at 480 mμ.

**Dehydrogenation of XIV.**—In a 25 cc. hard ground glass flask jointed with an air condenser, the top of which was connected to a measuring bottle, were placed 1.5 g. of XIV, 1.5 g. of 10% palladium on carbon and 1 g. of roughly crushed boiling stone, and heated in an electric oven. Hydrogen began to evolve when the temperature of the oven indicated about 390°C. About 450 cc. of hydrogen had been collected

after heating for 6 hours at 440~460°C. The reaction mixture was first washed out with hot benzene and then with ether. After drying the combined organic solution over anhydrous magnesium sulfate, the solvent was removed and the residue was distilled in vacuo to yield 0.7 g. of **4, 5-cyclohepta-trieno-2-methylthiazole** (XV) as a colorless liquid, b. p. 104°C/12 mmHg.

Found: C, 65.95; H, 5.66; N, 8.70. Calcd. for $C_9H_9NS$: C, 66. 24; H, 5.56; N, 8.58%.

A **picrate** derived from the liquid was recrystallized three times from ethanol in yellow crystals, m. p. 147~148°C.

Found: N, 14.50. Calcd. for $C_9H_9NS \cdot C_6H_3O_7N_3$: N, 14.27%.

The author wishes to thank Professor A. Yokoo (this laboratory) for his frequent helpful advice and Mr. K. Kurosaki (Research Laboratory of Fuji Photo Film Company) for the infrared measurements and valuable suggestions. Thanks are also due to Mr. A. Kondo (the Department of Organic Chemistry, Tokyo Institute of Technology) for carrying out the carbon and hydrogen micro-analyses.

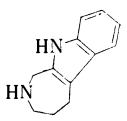
*Chemical Institute*
*Faculty of Science*
*Okayama University*
*Tsushima, Okayama*

# *Studies on Seven-Membered Heterocyclic Compounds Containing Nitrogen. V. 2, 3, 4, 5-Tetrahydro-1(H)-indolo[2, 3-c]azepine*

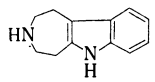
By Shiro MOROSAWA

(Received February 6, 1960)

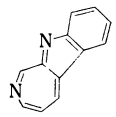
The initial purpose of the present investigation was to prepare 2, 3, 4, 5-tetrahydro-1(H)-indolo[2, 3-c]azepine (Ia) or 1, 2, 4, 5-tetrahydro-3(H)-indolo[3, 2-d]azepine (Ib) which suggests a possibility of dehydrogenation into 2, 3-benzo-1, 7-diazazulene (IIa) or 2, 3-benzo-1, 6-diazazulene (IIb). As similar compounds of this type, 4-ethyl-5, 6, 7, 12-tetrahydro-2-methylindolo[3,2-d] [1]-benzazepine (III)[1], 6,7-dihydro-1-methyl-2, 3-benzindolo[2′ : 3′-4 : 5]-azepine (IV)[2] and 1, 2, 3, 4, 5, 10-hexahydro-7-hydroxy-3-methylazep[4, 5-b]indole (V)[3] have been known. These are, however, compounds of *N*-alkyl or condensed type of phenyl and seven-membered ring, and it may be impossible to bring them into an azulene system by dehydrogenation. After several attempts the author synthesized 2-ethoxycarbonyl-2, 3, 4, 5-tetrahydro-1(H)-indolo[2, 3-c]azepine (XXII), 2-ethoxycarbonyl-7-methoxy-2, 3, 4, 5-tetrahydro-1(H)-indolo[2, 3-c]azepine (XXIII) (as picrate only) and Ia (as picrate only), each of which was assumed to have an angular structure as written from spectral data.



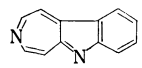

(Ia)



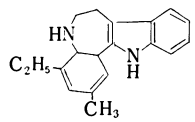

(Ib)



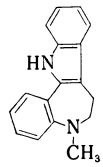

(IIa)



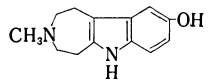

(IIb)




(III)




(IV)

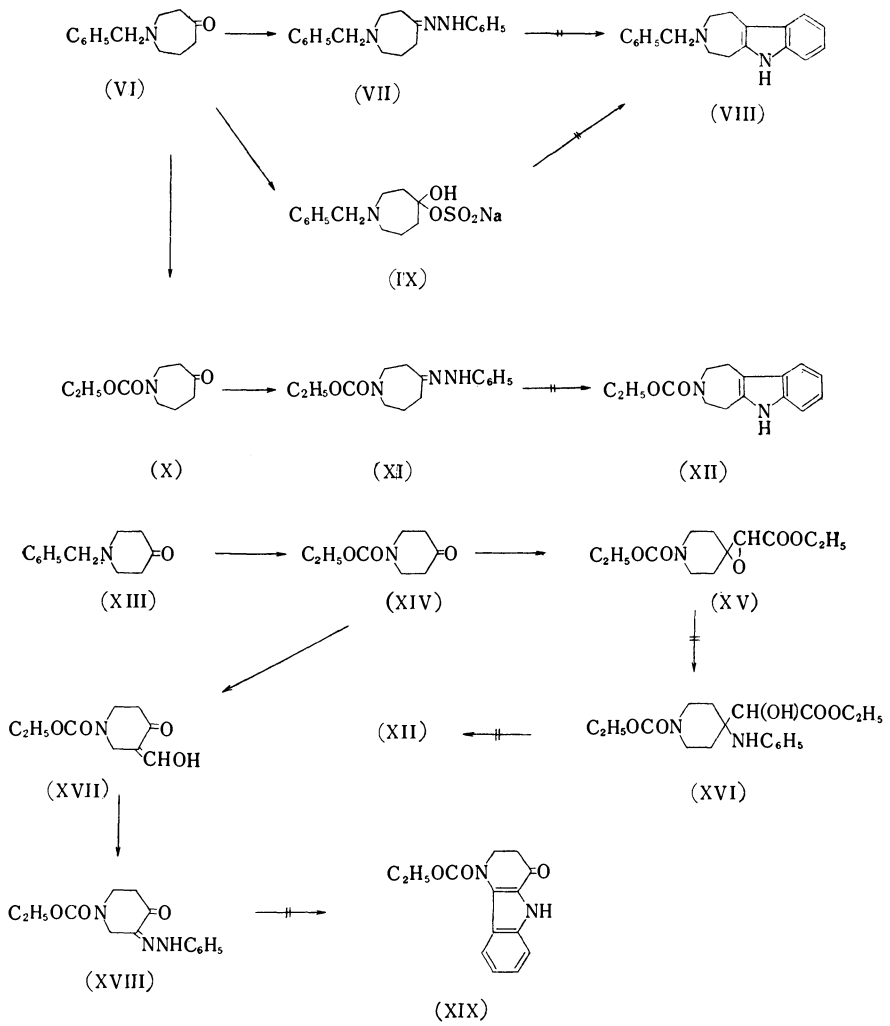



(V)

1) H. B. MacPhillamy et al., *J. Am. Chem. Soc.*, **80**, 2172 (1958).

2) J. T. Braunholtz and F. G. Mann, *J. Chem. Soc.*, **1958**, 3377.

3) J. Harley-Mason and A. H. Jackson, ibid., **1955**, 374.



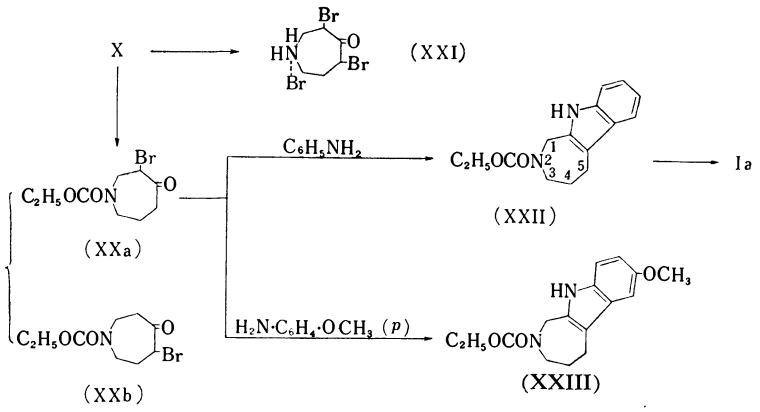
First of all the author attempted cyclization of phenylhydrazone (VII) and of its hydrochloride of 1-benzyl-1-azacycloheptan-4-one (VI)[4] under the condition of Fischer indole synthesis and under other similar conditions. They have shown a considerable resistance in the cyclizations and were recovered unchanged. In some cases, only a slight indole-like odor and a positive pine-splinter test were observed. Phenylhydrazone (XI) of 1-ethoxycarbonyl-1-azacycloheptan-4-one (X)[5] was also not cyclized with hydrogen chloride in ethanol. An application of the carbazole synthesis to bisulfite compound (IX)[6] of VI resulted in the recovery of VII.

Martynov's method[7], which has obtained 2, 3-pentamethyleneindole in good yield from cyclohexanone via glycidic acid derivative, was applied to 1-ethoxycarbonyl-1-azacyclohexan-4-one (XIV), but the addition reaction of glycidic acid derivative (XV) with aniline failed.

Mühlstädt and Treibs[8] have synthesized 1-keto-2, 3, 4, 5-tetrahydroheptiadole from monophenylhydrazone of cycloheptane-1, 2-dione, and Kent[9] has also obtained 1-keto-1, 2, 3, 4-tetrahydrocarbazole from cyclohexane-1, 2-dione monophenylhydrazone. As a preliminary experiment 1-ethoxycarbonyl-1-azacyclohexane-3, 4-dione monophenylhydrazone (XVIII) derived from XIV was treated under the above conditions, but no expected compound was obtained.

Campbell and McCall[10] have obtained some tetrahydrocarbazoles by heating 2-chlorocyclohexanone with arylamines. In a similar manner, a bromoketone (XXa or XXb)*, which

4) S. Morosawa, This Bulletin, **31**, 418 (1958).
5) S. Morosawa, ibid., **33**, 1108 (1960).
6) S. Morosawa, ibid., **33**, 575 (1960).
7) V. F. Martynov, *Chem. Abstr.*, **49**, 3124 (1955).
8) M. Mühlstädt and W. Treibs, *Ann.*, **608**, 38 (1957).
9) A. Kent, *J. Chem. Soc.*, **1935**, 976.
10) N. Campbell and E. B. McCall, ibid., **1950**, 2870.
* Situation of bromine atom is now under investigation by degradative method.




derived from X by NBS bromination, with aniline and *p*-anisidine gave rise to the desired compounds, XXII and XXIII (as picrate) respectively. The elimination of ethoxycarbonyl groupe of XXII gave Ia as a picrate. According to the same procedure of the formation of 3, 5, 7-tribromotropone[11], X was brominated in glacial acetic acid with bromine. But it resulted in elimination of the ethoxycarbonyl group, yielding 3, 5-dibromo-1-azacycloheptan-4-one hydrobromide (XXI). Ultraviolet absorption spectrum of XXII is given in Fig. 1, being compared with that of indole.

In the NBS bromination of X two kinds of bromide, 3-bromo (XXa) and 5-bromo (XXb) derivatives were expected. But only one kind of bromide was obtained. Sprague[12] has reported that NBS bromination of tetrahydro-1, 3-thiapyrone yielded 2-bromo compound exclusively. Similarly one might assume in the 1-azacycloheptan-4-one ring that activated 3-position by neighboring carbonyl, though weak, would be further affected more by the inductive effect of the nitrogen atom than 5-position, making the bromine attack on the position to give 3-bromo compound. Consequently XXII and XXIII may be assumed to be angular structures as shown. This accorded with the spectral data as follows:

The picrate of I indicated four bands near the region due to the hydrogen bending vibration of methylene at 1495, 1486, 1466 and 1430 $cm^{-1}$. The band at 1495 $cm^{-1}$ was due to stretching vibration of the double bond in benzene ring and the other three to 3-, 1-(overlapping with 4-) and 5-methylene in the seven-membered ring as mentioned in the foregoing paper[5]. XXII, on the other hand, gave a broad absorption band in the region owing to overlapping of the above three bands with that arising

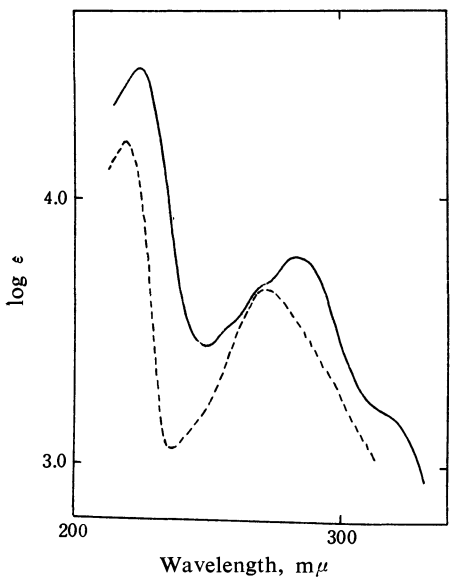



Fig. 1. (in methanol).
—— XXII; ---- indole.

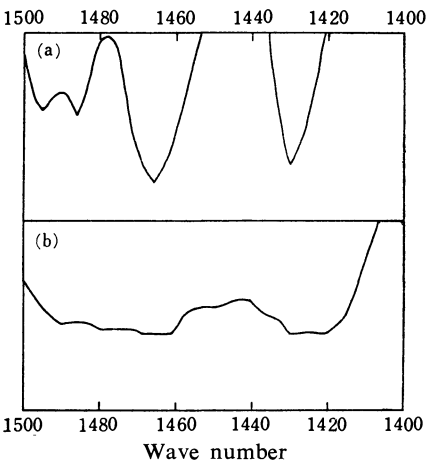



Fig. 2. (a) I picrate; (b) XXII.

11) T. Nozoe, Y. Kitahara, T. Ando and S. Masamune, *Proc. Japan Acad.*, 27, 415 (1951).
12) R. H. Sprague, *J. Am. Chem. Soc.*, 79, 2275 (1957).

from methyl and methylene in the ethoxycarbonyl group. Infrared absorption spectra of these two compounds are given in Fig. 2.

## Experimental

**1-Benzyl-1-azacycloheptan-4-one Phenylhydrazone (VII).**—To a solution of 1 g. of recrystallized phenylhydrazine hydrochloride and 1.6 g. of anhydrous sodium acetate in 10 cc. of water was added 0.8 g. of VI. Ethanol was added to the mixture until a clear solution was obtained and heated on a water bath for 30 minutes. Crystals formed on cooling were recrystallized from diluted ethanol to give 1.1 g. (80%) of **VII hydrochloride** in light greenish yellow needles, m. p. 225°C (decomp.).

Found: N, 12.39. Calcd. for $C_{19}H_{23}N_3 \cdot HCl$: N, 12.74%.

The hydrochloride was mixed with an excessive diluted potassium carbonate solution and evaporated to dryness under reduced pressure. The residual mass was treated with benzene, and benzene was expelled to leave **free phenylhydrazone** as an oil which crystallized on standing. It was recrystallized from diluted ethanol in light yellow needles, m. p. 75°C.

Found: N, 14.98. Calcd. for $C_{19}H_{23}N_3$: N, 14.32%.

**1-Ethoxycarbonyl-1-azacycloheptan-4-one Phenylhydrazone (XI).**—A mixture of 1.6 cc. of phenylhydrazine, 1.6 cc. of glacial acetic acid and 0.8 g. of X was treated as above. Crude product 1.2 g. (100%), m. p. 130°C (decomp.), was recrystallized from diluted ethanol to give 0.9 g. of XI as yellow needles, m. p. 130°C (decomp.).

**1-Ethoxycarbonyl-1-azacyclohexan-4-one (XIV).**—According to the same procedure as that of the formation of X, 15 g. of 1-benzyl-1-azacyclohexan-4-one (XIII)[4] yielded 12.3 g. (90.8%) of XIV, boiling at 93~94°C/1 mmHg as a colorless oil.

Found: N, 8.12. Calcd. for $C_8H_{13}O_3N$: N, 8.18%.

**2, 5-Diethoxycarbonyl-1-oxa-5-azaspiro (5, 2) octane (XV).**—To a mixture of 3.5g. of XIV and 2.4g. of ethyl monochloroacetate was added a solution of 0.74 g. of metallic potassium in 25 cc. of tertiary butanol under stirring and ice-water cooling during 30 minutes in the nitrogen atmosphere. After an additional stirring for 1 hour the butanol was expelled under reduced pressure and the residue was dissolved in 15 cc. of water. The solution was adjusted to pH 2.0 with hydrochloric acid and extracted with ether. The ethereal solution was washed once with water and dried over anhydrous sodium sulfate. The ether was removed and the residue was distilled in vacuo to give 2.5 g. (47.7%) of a colorless viscous oil, b.p. 146~150°C/1.5 mmHg.

Found: N, 5.21. Calcd. for $C_{12}H_{19}O_5N$: N, 5.44%.

**1-Ethoxycarbonyl-3-hydroxymethylene-1-azacyclohexan-4-one (XVII).**—A solution of 12.3 g. of XIV and 10.6 g. of ethyl formate in 150 cc. of dry benzene was added with swirling to an ice cold suspension of crushed methanol-free sodium methoxide[13] (from 3.3 g. of sodium) in 150 cc. of dry benzene. The system was evacuated and filled with nitrogen, and allowed to stand at room temperature overnight. Precipitates were dissolved by adding 60 cc. of water. The benzene layer was separated and washed four times with each 10 cc. of 5% solution of sodium hydroxide. The water layer and the washings were united, washed once with ether and acidified with concentrated hydrochloric acid to deposit an orange oil. The oil was taken up in benzene and the water layer was concentrated under reduced pressure, and extracted further with benzene. Benzene extracts were united, washed five times with a small volume of saturated sodium chloride solution and dried over anhydrous magnesium sulfate. After removal of benzene, the vacuum distillation gave 3.5 g. (24.5%) of a colorless viscous oil, boiling at 130~131°C/2 mmHg.

Found: N, 7.06. Calcd. for $C_9H_{13}O_4N$: N, 7.03%.

The oil gave a **monosemicarbazone**, m. p. 156.5°C (Found: N, 22.09%) and a **cyclic semicarbazone**, m. p. 128.5°C (Found: N, 23.28%).

**1-Ethoxycarbonyl-1-azacyclohexan-3, 4-dione Monophenylhydrazone (XVIII).**—To a mixture of 0.63 g. of redistilled aniline, 0.67 cc. of concentrated sulfuric acid and 5 cc. of water was added dropwise a solution of 0.47 g. of sodium nitrite in 1.8 cc. of water under stirring and ice-water cooling, followed by the addition of a saturated solution of 1.1 g. of anhydrous sodium acetate. Then a solution of 1 g. of XVII in 3 cc. of ether was added dropwise and the resultant mixture was stirred for 15 minutes while cold and for 30 minutes at room temperature. The orange crystals which separated were collected and recrystallized five times from methanol to give 0.6 g. (43.5%) of XVIII, m. p. 116~117°C.

Found: N, 15.07. Calcd. for $C_{14}H_{17}O_3N_3$: N, 15.26%.

**3(or 5)-Bromo-1-ethoxycarbonyl-1-azacycloheptan-4-one (XXa or XXb).**—A mixture of 7.4 g. of X, 0.3 g. of benozyl peroxide and 8 g. of NBS in 400 cc. of carbon tetrachloride was heated on a water bath, protected from moisture. As soon as the boiling took place, the mixture turned red and suddenly the color disappeared. After the boiling was further continued gently for 3 minutes the mixture was cooled under the tap and allowed to stand for 2 hours in a refrigerator. Succinimide was removed and washed with carbon tetrachloride. Carbon tetrachloride solutions were united, washed with 20 cc. of 20% sodium carbonate solution and then with water, and finally dried over anhydrous potassium carbonate. After removal of the solvent, residual oil was distilled in vacuo to yield 5.3 g. (50%) of a slightly colored oil, boiling at 140~145°C/1 mmHg.

Found: N, 5.85. Calcd. for $C_9H_{14}O_3NBr$: N, 5.31%.

A mixture of 0.1 g. of the above oil, 0.1 g. of 2,4-dinitrophenylhydrazine, 3 cc. of ethanol and 0.1 cc. of concentrated hydrochloric acid was boiled on a water bath for 2 minutes and let stand overnight. Crystals formed were recrystallized twice

13) W. S. Johnson and H. Posvic, *J. Am. Chem. Soc.*, 69, 1361 (1947).

from methanol to yield yellow **2, 4-dinitrophenylhydrazone**, m. p. 149~152°C (decomp.).

Found: N, 15.86. Calcd. for $C_{15}H_{18}O_6N_5Br$: N, 15.75%.

**3, 5-Dibromo-1-azacycloheptan-4-one Hydrobromide (XXI).**—A solution of 3 g. of X and 15 g. of bromine dissolved in 5 cc. of glacial acetic acid was allowed to stand overnight. The solution was heated on a water bath for 50 hours and evaporated under reduced preseure. The residue was taken up in ethanol, which was evaporated to leave an oil with some crystals. To this was added a small amount of ethanol to bring the oil into solution and isopropyl ether was added in small portions until precipitation occurred. After standing overnight in a refrigerator, the crystals were collected and charcoaled in 200 cc. of ethanol. Charcoal was separated and the ethanolic solution was concentrated to a smaller volume under reduced pressure. The crystals which were deposited during the evaporation were collected and washed with ethanol to yield 0.8 g. of XXI. Another crop, 0.4 g. was obtained from the filtrate. Crude crystals were recrystallized together from a small amount of water to give 0.7 g. of XXI as slightly colored microneedles, m. p. 186°C (decomp.).

Found: C, 20.33; H, 2.89; N, 3.68. Calcd. for $C_6H_9ONBr_2 \cdot HBr$: C, 20.45; H, 2.84; N, 3.97%.

**2-Ethoxycarbonyl-2, 3, 4, 5-tetrahydro-1(H)-indolo-[2, 3-c]azepine (XXII).**—A mixture of 5.3 g. of XX and 10.6 g. of redistilled aniline was boiled in an oil bath for 3 hours. The reaction mixture was treated with diluted potassium carbonate solution and taken up in ether. Ether was removed and aniline was thoroughly driven off by distillation in an oil bath maintained at 180°C under diminished pressure (0.8 mmHg). The residual tarry oil was dissolved in 70 cc. of benzene and washed once with 5 cc. of 2 N hydrochloric acid, thrice with a small portion of saturated sodium chloride solution and dried over anhydrous potassium carbonate. To the residue left on evaporation of benzene were added ethanol and picric acid, boiled for a while and allowed to stand overnight. Crystals formed were collected, washed with ether and recrystallized from ethanol to yield 1.5 g. (15.3%) of **picrate** as tan needles (indol odor), m. p. 156°C.

Found: N, 14.46. Calcd. for $C_{15}H_{18}O_2N_2 \cdot C_6H_3O_7N_3$: N, 14.37%.

**Free base**, though in poor yield, was obtained by treating the picrate with a saturated sodium bicarbonate solution and extracting with benzene as extremely viscous yellow oil (indole odor), boiling at 216°C/0.4 mmHg. This did not crystallize on standing.

Found: N, 10.75. Calcd. for $C_{15}H_{18}O_2N_2$: N, 10.85%.

The free base again formed a **picrate** which was found to be the same as that mentioned above, giving no m. p. depression.

**2-Ethoxycarbonyl-7-methoxy-2, 3, 4, 5-tetrahydro-1(H)-indolo[2, 3-c]azepine (XXIII) Picrate.**—A mixture of 2.8 g. of XX and 3.3 g. of redistilled *p*-anisidine was treated as before and 0.5 g. (9.1%) of picrate (indole odor) was obtained as deep tan needles, m. p. 164.5°C.

Found: N, 13.66. Calcd. for $C_{16}H_{20}O_3N_2 \cdot C_6H_3O_7N_3$: N, 13.54%.

Free base was distilled in vacuo at 220~228°C/0.5 mmHg with decomposition, and for lack of the distillate it could not be studied further.

**Deethoxycarbonylation of XXII.**—The picrate of XXII, 1 g. was treated with a saturated sodium bicarbonate solution and taken up in benzene. The residual oil which was left on evaporation of benzene was dissolved in 8 cc. of glacial acetic acid and saturated with dry hydrogen bromide under cooling. After standing overnight the solution was boiled under reflux for 2 hours. Acetic acid was removed under reduced pressure and the residue was heated in ethanol with an excessive picric acid. Crystals deposited on standing were recrystallized twice from ethanol to give 0.2 g. of Ia picrate as tan yellow prisms, m. p. 254°C (decomp.).

Found: C, 51.80; H, 4.43; N, 16.65. Calcd. for $C_{12}H_{14}N_2 \cdot C_6H_3O_7N_3$: C, 52.05; H, 4.13; N, 16.86%.

The author wishes to acknowledge the helpful advice of Professor A. Yokoo (this laboratory), and to thank Mr. A. Kondo (the Department of Organic Chemistry, Tokyo Institute of Technology) for carrying out the carbon and hydrogen micro-analyses and Mr. K. Kurosaki (Research Laboratory of Fuji-Photo Film Company) for the infrared measurements and valuable suggestions.

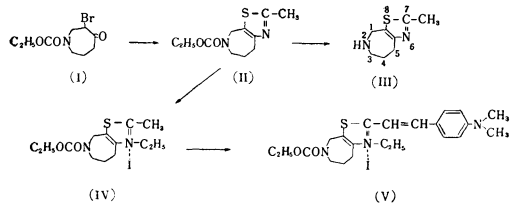
*Chemical Institute*
*Faculty of Science*
*Okayama University*
*Tsushima, Okayama*

# *Studies on Seven-Membered Heterocyclic Compounds Containing Nitrogen. VI. 7-Methyl-2,3,4,5-tetrahydro-1(H)-thiazolo[5,4-c]azepine*

By Akira YOKOO and Shiro MOROSAWA

(Received February 6, 1960)

The present authors have synthesized 7-methyl-2,3,4,5-tetrahydro-1-(H)-thiazolo[5,4-c]-azepine (III). Spectral studies also supported the structure.



3-Bromo-1-ethoxycarbonyl-1-azacycloheptan-4-one (I)[1] yielded 2-ethoxycarbonyl-7-methyl-2, 3, 4, 5-tetrahydro-1(H)-thiazolo[5,4-c]azepine (II), b. p. 160~164°C/1 mmHg, by condensation with thioacetamide. II gave a chloroaurate of m. p. 180°C (decomp.). On deethoxycarbonylation of II by hydrogen bromide in glacial acetic acid, III was obtained as an oil of b. p. 101~102°C/4 mmHg, which gave a hydrochloride of m. p. 207~212°C (decomp.) and a chloroaurate of m. p. 179°C (decomp.) respectively. Ethiodide (IV) of II condensed with *p*-dimethylaminobenzaldehyde to afford 2-ethoxycarbonyl-7-(*p*-dimethylaminostyryl)-6-ethyl-2, 3, 4, 5-tetrahydro-1(H)-thiazolo[5,4-c]azepinium iodide (V), m. p. 203°C (decomp.). Dehydrogenation of III by heating with 10% palladium on carbon at elevated temperature evolved hydrogen, but led to decomposition of III.

It has already been reported[1] that bromine atom entered the 3-position by NBS bromination of 1-ethoxycarbonyl-1-azacycloheptan-4-one and that the indole compounds derived from the consequent bromoketone by the condensation with some arylamines might have angular structures. As shown in Fig. 1, III gave four bands at 1478, 1468, 1455 and 1430 $cm^{-1}$ near the region due to the hydrogen bending vibration of methylene. These bands were assumed, as stated in the former paper[2], to be ascribed to 3-, 1-, 4- and 5-methylenes respectively. It was considered that the intensity of the band at 1455 $cm^{-1}$ was too strong for the methyl group in the thiazole ring and therefore it

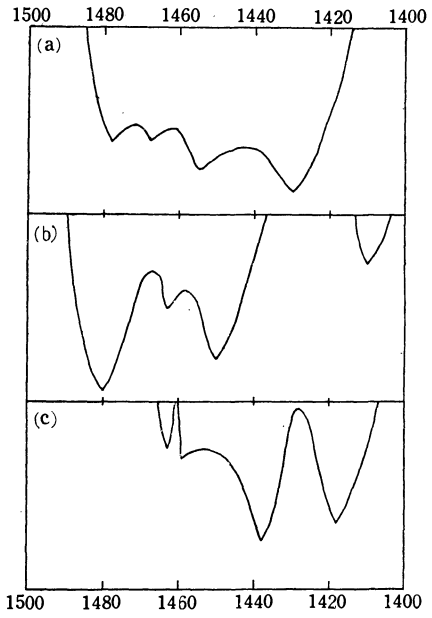



Fig. 1.

(a) III; (b) III hydrochloride; (c) III hydrobromide

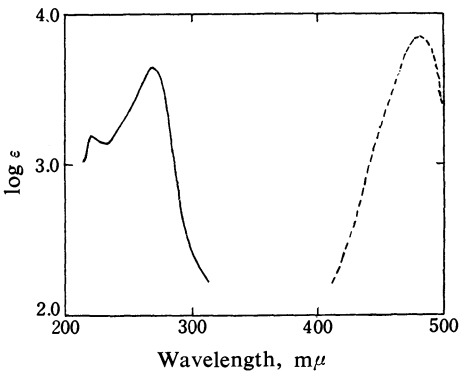



Fig. 2. (in methanol)

—— II, ---- V (concn. unknown)

appeared as an overlapping with 4-methylene. Both hydrochloride and hydrobromide of III gave also four bands, corresponding to the above absorptions. From these facts it may be reasonable to assume that III also had an angular

1) S. Morosawa, This Bulletin, 33, 1113 (1960).
2) S. Morosawa, ibid., 33, 1108 (1960).

form like the compounds reported before[1,2]. Ultraviolet absorption spectra of II and V are also given in Fig. 2.

## Experimental

**2-Ethoxycarbonyl-7-methyl-2, 3, 4, 5-tetrahydro-1 (H)-thiazolo[5, 4-c]azepine (II).**—A solution of 5 g. of I and 2 g. of thioacetamide in 15 cc. of ethanol was boiled under reflux on a water bath for 5 hours. The ethanol was removed and the residue was heated in an oil bath kept at 160~165°C under reduced pressure (water pump) for 5 hours. After cooling, 10 cc. of 4 N hydrochloric acid was added and taken up three times in ether. The ether was washed twice with each 5 cc. portion of 4 N hydrochloric acid. Acidic solutions were united and made alkaline with anhydrous potassium carbonate, followed by adding 5 cc. of 5 N sodium hydroxide solution. The alkaline solution was shaken three times with each 20 cc. portion of ether. After drying over anhydrous potassium carbonate, the ethereal solution was concentrated and the residue was distilled in vacuo to give 1.6 g. of a light yellow viscous oil, b. p. 160~164°C/1 mmHg.

Found: C, 54.53; H, 6.74; N, 11.20. Calcd. for $C_{11}H_{16}O_2N_2S$: C, 54.99; H, 6.71; N, 11.65%.

The nitrogen content showed a slightly low value even after several repetitions, and the inclination was also observed in the following compounds of this series.

Ethanolic solution of the oil was mixed with an excessive chloroauric acid, heated for a while and allowed to cool. The **chloroaurate** formed was recrystallized twice from ethanol to yellow crystals, melting at 180°C with decomposition.

Found: C, 22.20; H, 3.33; Au, 32.50. Calcd. for $C_{11}H_{16}O_2N_2S \cdot HAuCl_4$: C, 22.60; H, 2.94; Au, 33.80%.

The oil and an excessive amount of ethyl iodide were allowed to stand for one day. The mixture was then refluxed for 8 hours to form an **ethiodide IV.** It was filtered and recrystallized from ethanol and ether to colorless crystals, m. p. 155~156.5°C.

Found: C, 39.05; H, 5.32; N, 6.39. Calcd. for $C_{11}H_{16}O_2N_2S \cdot C_2H_5I$: C, 39.40; H, 5.34; N, 7.07%.

**7-Methyl-2,3,4,5-tetrahydro-1(H)-thiazolo[5,4-c]-azepine (III).**—A solution of 0.8 g. of II in 20 cc. of glacial acetic acid was saturated with hydrogen bromide under ice-water cooling. After standing for 2 hours the solution was heated gradually in an oil bath and refluxed for 5 hours. The Hydrobromide which remained as a crystalline residue on evaporation of acetic acid was recrystallized from a mixture of ethanol and methanol to colorless crystals, m. p. 248~252°C (decomp.). These were dissolved in a small amount of water, made alkaline by adding concentrated sodium hydroxide solution and taken up in ether. After drying over anhydrous potassium carbonate, the ether was expelled and the residue was distilled in vacuo to yield 0.4 g. of a colorless, strongly hygroscopic oily substance, b. p. 101~102°C/4 mmHg.

Found: C, 56.60; H, 7.40; N, 16.29. Calcd. for $C_8H_{12}N_2S$: C, 57.14; H, 7.19; N, 16.65%.

The above oil was dissolved in concentrated hydrochloric acid and evaporated to dryness under reduced pressure to afford a **hydrochloride.** This was recrystallized twice from ethanol to extremely hygroscopic colorless plates, m. p. 207~212°C (decomp.).

Found: N, 11.16. Calcd. for $C_8H_{12}N_2S \cdot 2HCl$: N, 11.62%.

The **chloroaurate** which formed by mixing the oil with an excessive amount of chloroauric acid in ethanol containing one drop of concentrated hydrochloric acid was collected and washed with ethanol. This was dissolved in an ethanol-methanol mixed solvent with heating, the methanol was expelled and the solution was allowed to stand with one drop of concentrated hydrochloric acid to yield yellow crystals, which decomposed at about 179°C.

Found: N, 5.06. Calcd. for $C_8H_{12}N_2S \cdot HAuCl_4$: N, 5.50%.

**2-Ethoxycarbonyl-7-(*p*-dimethylaminostyryl)-6-ethyl-2, 3, 4, 5-tetrahydro-1(H)-thiazolo[5, 4-c]azepinium Iodide (V).**—A solution of 0.1 g. of IV and 0.1 g. of *p*-dimethylaminobenzaldehyde in 2 cc. of ethanol containing a small amount of piperidine was boiled under reflux for 10 hours. The ethanol was expelled and water was added to the residue to deposit crystals, which were collected and washed well with ether. The crystals were dissolved in a small volume of ethanol with heating and ether was added until the solution became turbid. The red crystals which formed were treated repeatedly like the above to give 40 mg. of V, m. p. 203°C (decomp.). The nitrogen content showed some deviation from the theoretical value even after several recrystallizations.

Found: N, 7.01. Calcd. for $C_{22}H_{30}O_2N_3SI$: N, 7.97%.

The authors wish to thank Mr. K. Kurosaki (Research Laboratory of Fuji Photo Film Company) for the infrared measurements and Mr. A. Kondo (the Department of Organic Chemistry, Tokyo Institute Technology) for the carbon and hydrogen micro-analyses.

*Chemical Institute*
*Faculty of Science*
*Okayama University*
*Tsushima, Okayama*

# *The Photolysis of Acetaldehyde in the Presence of Hydrogen Sulfide*

By Naomi IMAI and Osamu TOYAMA

(Received February 17, 1960)

The present authors have recently studied the photolysis of acetone in the presence of hydrogen sulfide in order to obtain information on the hydrogen abstraction from hydrogen sulfide molecules by methyl radicals[1]. The activation energy of the abstraction reaction thus obtained is of such small value that it seems desirable to check it in another way. The present work presents such an attempt on the basis of an investigation on the photolysis of acetaldehyde in the presence of hydrogen sulfide.

We have been interested in this abstraction reaction in conjunction with the mechanism of the thermal decomposition of acetaldehyde in the presence of hydrogen sulfide. The present study is therefore expected to give valuable information also on other elementary reactions involved in common in both kinds of decomposition, photochemical and thermal, in the system consisting of acetaldehyde and hydrogen sulfide.

## Experimental

**Materials.**—Acetaldehyde was prepared by distillation of paraldehyde containing a little quantity of sulfuric acid, and stored in a bulb at 0°C. When the acetaldehyde thus stored was not used at once, it was again purified by distillation befroe use. Hydrogen sulfide was prepared by dropping water on aluminum sulfide in an evacuated vessel, dried by passing through a trap at −78°C and purified by bulb to bulb distillation.

**Apparatus.** — Photolysis was carried out in a cylindrical quartz vessel of about 110 cc. placed in an electric furnace with a thin glass window which cuts off the light of a wavelength region shorter than 2800 Å to prevent absorption by hydrogen sulfide. The reaction vessel was connected to a mercury manometer, to an analytical system, to storage bulbs and to a bulb in which acetaldehyde and hydrogen sulfide were mixed before they were admitted to the reaction vessel. The full light from a medium pressure mercury arc was used in the present study, and its intensity was kept constant for a series of runs by using a voltage stabilizer. For experiments with varied intensity, the distance between the light source and the reaction vessel was changed. The reaction vessel, the manometer, the bulbs for storage and mixing and the analytical system were all attached to a conventional vacuum line.

**Procedure.**—Required quantities of acetaldehyde and hydrogen sulfide were admitted into the mixing bulb at room temperature and left for about 30 minutes to allow them to mix thoroughly. The mixed gases were then introduced into the reaction vessel which had already been irradiated, and the change in the total pressure with time was followed on a manometer.

The analytical technique employed was the same as that described previously[1]. In this work the hydrogen sulfide added initially was found by analysis to remain almost unconsumed even after a prolonged photolysis.

## Results and Discussion

It has been established by many workers[2] that the products of the photolysis of acetaldehyde above 100°C under normal conditions are almost exclusively methane and carbon monoxide. Similarly in this work, i. e., in the presence of hydrogen sulfide, it has been confirmed by analysis that the rate of formation of methane is identical with that of carbon monoxide, and the pressure of either one of these products corresponds to the total pressure increase within the experimental error. Thus, irrespective of the presence of hydrogen sulfide, the total pressure increase is always equal to the decrease in the pressure of acetaldehyde

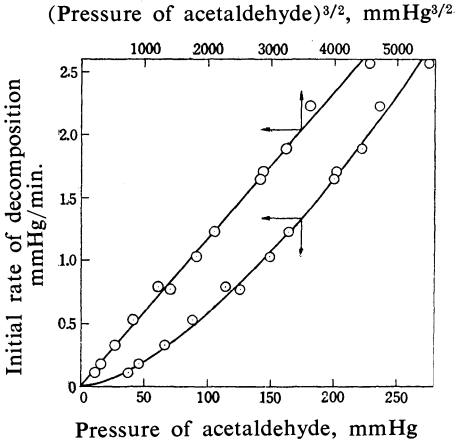



Fig. 1. Rate of decomposition of acetaldehyde alone at 250°C.

1) N. Imai and O. Toyama, This Bulletin, 33, 652 (1960).

2) F. E. Blacet and D. Volman, *J. Am. Chem. Soc.*, **60**, 1243 (1938); F. E. Blacet and W. J. Blaedel, ibid., **62**, 3374 (1940); R. E. Dodd and J. D. Waldron, *Nature*, **167**, 655 (1951).

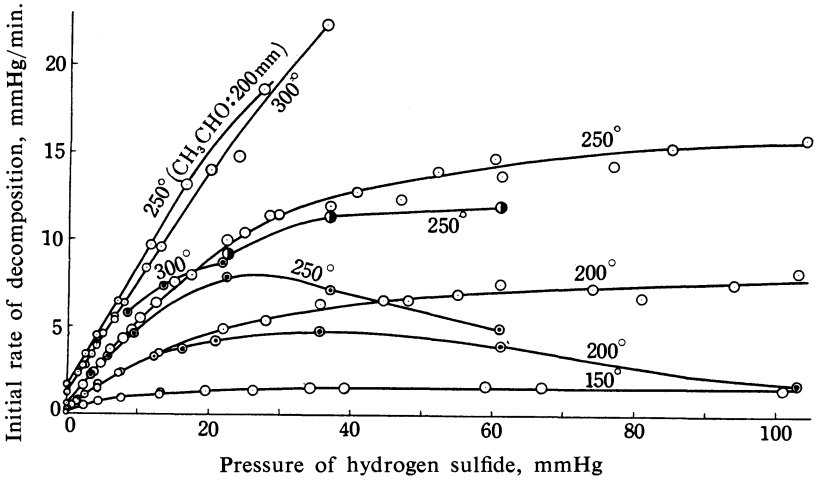



Fig. 2. Dependence of the rate of decomposition in the presence of hydrogen sulfide on its pressure. Relative light intensity : 1. $CH_3CHO$ : 100 mmHg unless otherwise described. ○, without preheating; ◑, with preheating for 1 min.; ⊙, with preheating for 5 min.

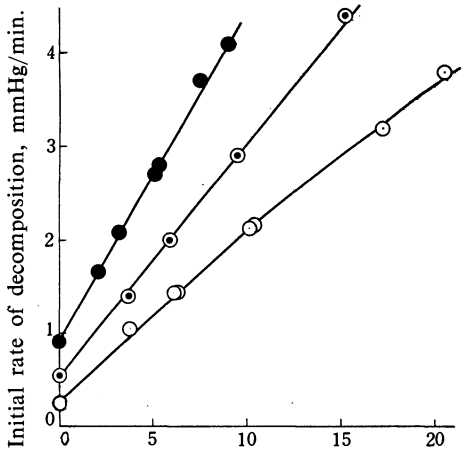



Fig. 3. Dependence of the rate of decomposition in the presence of hydrogen sulfide on its pressure. Relative light intensity : 1/4. $CH_3CHO$ : 100 mmHg, ○, 250°; ⊙, 300°; ●, 360°C. All the data were obtained without preheating.

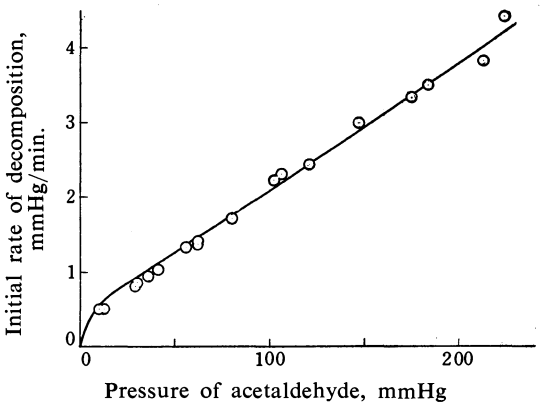



Fig. 4. Dependence of the rate of decomposition in the presence of hydrogen sulfide on acetaldehyde pressure. Temperature : 250°C. $H_2S$ : 3.16 mmHg. Circles and full line represent observed and calculated rates respectively.

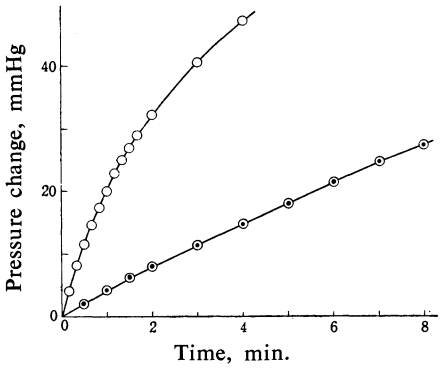



Fig. 5. Pressure-time curves at 300°C. Initial pressure : $CH_3CHO$, 100 mmHg. $H_2S$, ⊙, 3.5; ○, 36.2 mmHg.

due to decomposition. Accordingly, the initial rate of decomposition was determined from the initial slope of a total pressure-time curve with the results shown in Figs. 1—4. Fig. 1 shows the dependence of the rate of decomposition on the pressure of acetaldehyde in the experiments with acetaldehyde alone. Figs. 2 and 3 show the dependence of the rate of decomposition in the presence of hydrogen sulfide on its pressure under various experimental conditions. The relative light intensity intensity for the experiments shown in Fig. 2 is four times as great as that in Fig. 3. Fig.

4 shows the dependence of the rate on acetaldehyde pressure in the presence of hydrogen sulfide.

It should be noted that, at a high temperature, in a run with a high concentration of hydrogen sulfide, the rate of decomposition falls off very rapidly, as seen in Fig. 5, compared to the results obtained with low concentrations of hydrogen sulfide. Similar reduction in the rate was observed, as seen in Fig. 2, when the acetaldehyde mixed with a large quantity of hydrogen sulfide was preheated for a few minutes at the experimental temperature prior to irradiation. Although the exact nature of these phenomena has not yet been fully elucidated, it is obvious from these findings that at still higher concentrations of hydrogen sulfide than those given in Fig. 2, determination of the initial rate of decomposition becomes considerably unreliable.

It is generally agreed that the main features of the photochemical decomposition of acetaldehyde can be explained by the following mechanism[3]:

$$CH_3CHO + h\nu = CH_3 + CHO \quad (0)$$

$$CHO = CO + H \quad (1)$$

$$H + CH_3CHO = H_2 + CH_3CO \quad (2)$$

$$CH_3CO = CH_3 + CO \quad (3)$$

$$CH_3 + CH_3CHO = CH_4 + CH_3CO \quad (4)$$

$$CH_3 + CH_3 = C_2H_6 \quad (5)$$

Solution of the steady state equations derived from this scheme yields the rate equation ($I_a$ = the rate of absorption of light quanta)

$$-\mathrm{d}[CH_3CHO]/\mathrm{d}t = k_4 k_5^{-1/2} I_a^{1/2} [CH_3CHO] \quad (I)$$

in general agreement with experimental results obtained by various workers. The existence of a primary reaction other than reaction (0) is well known[4]. This, however, gives no substantial alteration in Eq. I. From the plot given in Fig. 1 it is seen that the rate of decomposition of acetaldehyde alone is proportional to the 3/2 power of its pressure. This simply means that under the present experimental conditions the rate of absorption of light quanta is proportional to the acetaldehyde pressure.

Now in the presence of hydrogen sulfide, the possible additional reactions may be[5]

$$CH_3 + H_2S = CH_4 + HS \quad (6)$$

$$HS + CH_3CHO = H_2S + CH_3CO \quad (7)$$

$$HS + HS = \text{products} \quad (8)$$

If reaction (8) can be neglected and consequently the chain terminates still by reaction (5),

$$-\mathrm{d}[CH_3CHO]/\mathrm{d}t = k_4 k_5^{-1/2} I_a^{1/2} [CH_3CHO] + k_6 k_5^{-1/2} I_a^{1/2} [H_2S] \quad (II)$$

while, if the chain terminates now by reaction (8), the result is

$$-\mathrm{d}[CH_3CHO]/\mathrm{d}t = k_7 k_8^{-1/2} I_a^{1/2} [CH_3CHO] \quad (III)$$

It is readily shown that in the steady state,

$$k_6 [CH_3] [H_2S] = k_7 [HS] [CH_3CHO]$$

or

$$[HS]/[CH_3] = (k_6/k_7)([H_2S]/[CH_3CHO])$$

Therefore, when the value of $(k_6/k_7)([H_2S]/[CH_3CHO])$ is very small, i. e., the concentration of methyl radical is much higher than that of hydrosulfide radical, the rate of decomposition will be represented by Eq. II. On the contrary, when the value of $(k_6/k_7)([H_2S]/[CH_3CHO])$ is very large, Eq. III will hold.

In Figs. 2 and 3 where the rates of decomposition are plotted against pressures of hydrogen sulfide, it is seen that, in the low pressure range of hydrogen sulfide, except for the experiments with preheating, the rate of decomposition increases linearly with the pressure of hydrogen sulfide in agreement with Eq. II. The fact that the intercept on the ordinate is always equal to the rate of decomposition in the absence of hydrogen sulfide also conforms to Eq. II. According to the equation the slope of the linear part divided by the intercept gives the ratio $k_6/k_4$. The values of $k_6/k_4$ thus

TABLE I. VALUES OF $k_6/k_4$

Initial pressure of $CH_3CHO$: 100 mmHg

| Temp. °C | Relative light intensity=1 | Relative light intensity=1/4 |
|---|---|---|
| 200 | 115 | |
| 250 | 78.7 | 75.5 |
| | 82.0[a] | |
| 300 | 55.2 | 54.1 |
| 360 | | 38.6 |

a) Initial pressure of $CH_3CHO$: 200 mmHg.

3) E. I. Akeroyd and R. G. W. Norrish, *J. Chem. Soc.*, **1936**, 890; J. A. Leemakers, *J. Am. Chem. Soc.*, **56**, 1537 (1934); D. C. Grahame and G. K. Rollefson, *J. Chem. Phys.*, **8**, 98 (1940); C. J. Darby, A. S. Buchanan and I. H. S. Henderson, *J. Chem. Soc.*, **1951**, 1426.

4) (a) F. E. Blacet and D. E. Loeffler, *J. Am. Chem. Soc.*, **64**, 893 (1942). (b) M. A. Khan, R. G. W. Norrish and G. Porter, *Proc. Roy. Soc. (London)*, **A219**, 312 (1953). (c) P. P. Manning, *J. Am. Chem. Soc.*, **79**, 5151 (1957). (d) R. E. Dodd, *Can. J. Chem.*, **33**, 699 (1955).

5) Similar reactions have been proposed by the following workers: (a) E. F. P. Harris and W. A. Waters, *Nature*, **170**, 212 (1952); (b) K. E. J. Banett and W. A. Waters, *Disc. Faraday Soc.*, **14**, 221 (1953); (c) R. N. Birrell, R. F. Smith, A. F. Trotman-Dickenson and H. Wilkie, *J. Chem. Soc.*, **1957**, 2087.

determined are listed in Table I[6]. The fact that neither a two-fold increase in the pressure of acetaldehyde, nor the variation in light intensity by a factor of four, yields any significant change in the values of $k_6/k_4$ may be taken as additional evidence for the validity of Eq. II.

A further check in favor of Eq. II is provided by Fig. 4, where the plot of the rates of decomposition observed at a constant pressure of hydrogen sulfide against acetaldehyde pressures is shown together with the curve predicted from Eq. II as follows: Since the rate of absorption of radiation in the present investigation is proportional to the concentration of acetaldehyde as mentioned above, the values of $k_4k_5^{-1/2}I_a^{1/2}$ and $k_6k_5^{-1/2}I_a^{1/2}$ required for the calculation of the rate of decomposition by means of Eq. II can be obtained from the data given in Figs. 1 and 2. As seen in Fig. 4, the curve representing the rate thus calculated as a function of acetaldehyde pressure is in satisfactory agreement with the experimental plot over a wide range of acetaldehyde pressure.

The Arrhenius plots of the values of $k_6/k_4$ given in the two series in Table I yielded two parallel straight lines lying close to each other from which the values $E_4-E_6=4.0\pm0.3$ kcal./mol. and $A_6/A_4=1.7\pm0.5$ were obtained, where $E$ denotes the activation energy and $A$ the pre-exponential factor. The ratio $A_6/A_4=1.7$ seems to be reasonable since $A$ factors for most hydrogen abstraction reactions by methyl radicals are of the same order of magnitude. The activation energy difference $E_4-E_6=4.0$ kcal./mol., when combined with $E_4=6.8$ kcal./mol. given by Ausloos and Steacie[7], yields 2.8 kcal./mol. for $E_6$ which compares satisfactorily with our previous value of 2.6 kcal./mol. obtained in the photolysis of acetone in the presence of hydrogen sulfide[1]. If, instead, $E_4=7.5\sim8.0$ kcal./mol. reported by Brinton and Volman[8] and Dodd[4d] is accepted, the result is $E_6=3.5\sim4.0$ kcal./mol. which is now clearly higher than the previous value but still lower than 5.6 kcal./mol.[9] estimated for the activation energy of hydrogen abstraction from methane thiol by methyl radical, in agreement with our previous conclusion[1].

It is evident from Figs. 2 and 3 that, for the experiments without preheating, the lower the temperature, the lower is the pressure of hydrogen sulfide at which a plot of the rate of the decomposition against the pressure of hydrogen sulfide shows a departure from a straight line. At a temperature as low as 150°C, the plot (Fig. 2) shows a curvature from the very beginning and, in the range of pressure of hydrogen sulfide higher than about 30 mmHg the rate of decomposition attains an almost constant value in agreement with Eq. III.

Presumably, these fact indicate that the ratio $k_6/k_7$ increases with lowering of temperature, for, with the increase in the ratio $k_6/k_7$, $[CH_3]/[HS]$ and hence the ratio of the rate of reaction (8) to that of reaction (5) increases, provided the ratio $[H_2S]/[CH_3CHO]$ is constant. Such dependence of the ratio $k_6/k_7$ on temperature seems to be reasonable since the activation energy for reaction (6) is very low as estimated above so that it is probably lower than that of reaction (7).

The afore-mentioned observation that, in the presence of a large concentration of hydrogen sulfide, the rate of photolysis suffered considerable reduction not only by preheating the reaction mixture, but also during the photolysis at a high temperature, cannot fully be explained at present. It may, however, be possible that a small quantity of a yet unidentified compound produced in the thermal reaction between acetaldehyde and hydrogen sulfide gives rise to the observed phenomena. Birrell et al.[5c] found that the rate of decomposition of acetaldehyde is reduced appreciably by large quantities of isopropanethiol and tertiary-butanethiol below 300°C, and to almost negligible values by small quantities of tertiary-butanethiol and isopropanethiol above 300°C and 340°C respectively. We have also found[10] that the presence of a little quantity of methanethiol lowers remarkably the rates of photolyses of acetone, acetaldehyde and a mixture of acetaldehyde and hydrogen sulfide. In view of the similarity of the phenomena cited, it seems probable that all of these resulted from similar causes which, however, are to be clarified by further studies of these phenomena in future.

## Summary

Acetaldehyde has been photolyzed in the presence of hydrogen sulfide over the temperature range from 150 to 360°C. The initial rates of decomposition obtained under various experimental conditions are consistent with a mechanism which involves the reactions $CH_3+H_2S=CH_4+HS$ (6) and $HS+CH_3CHO=H_2S+CH_3CO$ (7) in addition to those established already for the photolysis of acetaldehyde alone. Analysis of the data on this basis gives

6) The value of the intercept was actually determined from several repeated runs of the photolysis of 100 mmHg acetaldehyde in the absence of hydrogen sulfide at the same temperature.

7) P. Ausloos and E. W. R. Steacie, *Can. J. Chem.*, **33**, 31 (1955).

8) D. H. Volman and R. K. Brinton, *J. Chem. Phys.*, **20**, 1764 (1952).

9) T. A. Kerr and A. F. Trotman-Dickenson, *J. Chem. Soc.*, **1957**, 3322.

10) N. Imai and O. Toyama, unpublished work.

a value of 4.0 kcal./mol. for the difference in activation energy $E_4-E_6$, where $E_4$ refers to the reaction $CH_3+CH_3CHO=CH_4+CH_3CO$ (4). This result, when combined with $E_4=6.8$ kcal./mol. found by Ausloos and Steacie, gives $E_6=2.8$ kcal./mol. in excellent agreement with our previous value of 2.6 kcal./mol. obtained in the photolysis of acetone in the presence of hydrogen sulfide. As the temperature is lowered and the ratio $[H_2S]/[CH_3CHO]$ increased, the importance of the combination of methyl radicals to ethane as the chain terminating step decreases, until it is replaced by the combination of hydrosulfide radicals. This is explained in terms of the relationship $E_7>E_6$.

The present study was partly supported by financial aid from the Ministry of Education, to which the authors' thanks are due.

*Department of Applied Chemistry*
*College of Engineering*
*University of Osaka Prefecture*
*Sakai, Osaka*

# *Alternating Current Polarization Titration with Two Hanging Mercury Drop Electrodes—Application to Chelatometric Titration of Cadmium*

By Toyokichi KITAGAWA

(Received March 3, 1960)

Both potentiometry at a constant current and amperometry at a small constant applied voltage with two polarized platinum electrodes are widely used for the determination of the equivalent point in a large number of titrations. The relation between the two methods of titration mentioned above has been recently discussed by several authors on the basis of voltammetry[1-4].

On the other hand, conductometric titration using low frequency of 200~1000 c/sec. has been applied to the determination of the equivalent point in titrations involving acid-base neutralization reaction or precipitation reaction. However, alternating current polarization titration, which corresponds to the alternating current analogs of the two direct current method, situated between direct current polarization titration and conductometric titration has not been studied systematically. Recently Franck[5], Laitinen[6] and the present author[7] studied these methods, and applied them to redox, precipitation and complex formation reaction.

The present author studied polarization titration fundamentally, applying to a pair of platinum microelectrodes a square wave or sine wave signal of constant current and measuring the alternating voltage (polarization voltage) in the course of a titration.

This is a suitable method which can be applied in redox reaction, complex formation reaction and neutralization reaction. It is impossible, however, that metal ion concentration is indicated by the platinum electrode, except in the case of some reversible system; for example, ferric-ferrous system. Hence when the chelatometric titration of metal ion is carried out by the polarization titration method, an excess of ethylenediaminetetraacetate (EDTA) solution of a known concentration is added, and the excess of EDTA is back-titrated with standard ferric solution. However, when the stability constant of metal ion titrated is much smaller than that of ferric ion, this titration method can not be used. Accordingly, only a few kinds of metal ion, ferric, indium and nickel, are titrated by this method[8]. For this reason, it seemed desirable and worth while to investigate the chelatometric titration of most metal ions by alternating current polarization titration with two mercury drop electrodes.

In this paper, the experimental results of the application to the cheltometric titration of the cadmium ion are presented, and the factors which affect this titration method are discussed.

1) R. Gauguin, *Anal. Chim. Acta*, **5**, 200 (1951): **7**, 172, 360, 408 (1952).
2) I. M. Kolthoff, *Anal. Chem.*, **26**, 1685 (1954).
3) M. Ishibashi and T. Fujinaga, *J. Electrochem. Soc. Japan (Denkikagaku)*, **23**, 494 (1955).
4) N. Tanaka, *Japan Analyst (Bunseki Kagaku)*, **4**, 640 (1955).
5) U. F. Franck, *Z. Elektrochem.*, **58**, (1954).
6) H. A. Laitinen and L. C. Hall, *Anal. Chem.*, **29**, 1390 (1957).
7) T. Kitagawa, *Bulletin of the Faculty of Education, Kobe University (Kobedaigaku Kyōikugakubu Kenkyushūroku)*, **21**, 29 (1959).
8) T. Kitagawa, *Bulletin of the Faculty of Education, Kobe Univrsity (Kobedaigaku Kyōikugakubu Kenkyushuroku)*, **21**, 39 (1959).

## Experimental

**Reagents.** — A standard EDTA solution was obtained by dissolving the pure disodium ethylenediaminetetraacetate dihydrate (Wako Junyaku Co. Ltd.) in distilled water. The concentration was standardized against a standard copper solution by photometric titration using Murexide as indicator. The concentration was 0.100 M. A 0.01 M EDTA solution was prepared by dilution. Standard cadmium solution was prepared by dissolving cadmium nitrate in distilled water. The concentration was determined gravimetrically as cadmium oxinate. Standard mercuric ethylenediaminetetraacetate was prepared by mixing equivalent amounts of mercuric nitrate solution and EDTA solution. The concentration was 0.05 M.

All other chemicals were of analytical reagent grades. Redistilled water was used for the preparation of the solutions.

**Apparatus.**—Alternating current polarization titration apparatus is shown in Fig. 1. Kikusui Type CR oscillator was used for sine wave or square wave generator (20～2000 c/sec.). The circuit of measuring polarization voltage is shown in Fig. 2.

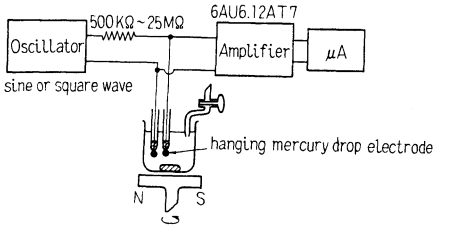



Fig. 1. Alternating current polarization titration apparatus.

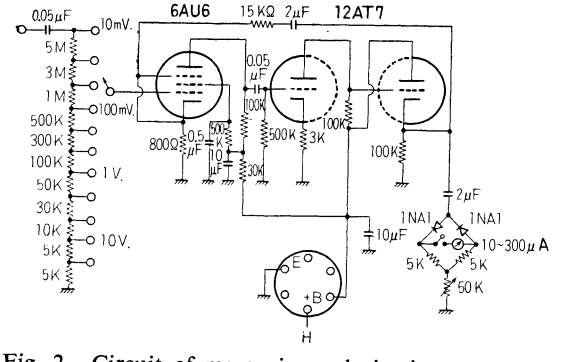



Fig. 2. Circuit of measuring polarization voltage.

The measurement was made at a small current using a large resistor in series with the electrolytic cell and an output voltage (12 volt) from the sine wave or square wave generator. The alternating voltage (polarization voltage) between two electrodes was measured as a function of the volume of reagent added.

The mercury drop electrode was prepared by fixing the mercury drop on the top of amalgamated platinum electrodes. Mercury can be deposited on the platinum electrode out of 1 M mercuric nitrate solution by the impression of an electromotive force of about 2 V. The surface area of the mercury drop was about 0.021 $cm^2$. A calibrated semimicroburet 5 ml. was used for all titrations.

**Procedure.**—About 50 ml. of the solution, which contained definite amounts of cadmium nitrate solution, 50 ml. of 1 M ammoium acetate-acetic acid buffer solution (pH 4.3～5.0), 1 ml. of 0.1% gelatine and 10 ml. of 0.05 M mercury (II) EDTA solution, was titrated with $10^{-1}$ or $10^{-2}$ M standard solution of EDTA. The frequency of square wave or sine wave was 25 c/sec. and the alternating current was 20～25 μA*. The polarization voltage was recorded at every 0.01 ml. of added titrant in the neighborhood of the equivalence point of this titration.

An example of this titration curve is shown in Fig. 3. In the course of this titration, the solution was stirred at a constant speed by a magnetic stirrer.

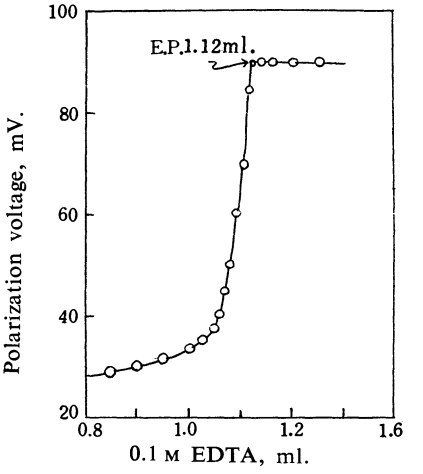



Fig. 3. Titration curve. $Cd^{2+}$ 12.5 mg.

## Results

In the procedure described above, the following factors were specially considered.

*1) Relation between Polarization Voltage and Frequency.*—Polarization voltage was measured at the equivalence point by the procedure described above. As shown in Fig. 4, a plot of polarization voltage against the reciprocal of square root of frequency gives a straight line at frequency 20～200 c/sec. Therefore, the frequency 20 c/sec. was used as a suitable frequency in this titration. In a frequency above 500 c/sec. it was impossible to apply this end point detection method, because the polarization voltage became very small.

*2) Relation between Polarization Voltage and Alternating Current.*—In the potentiometry at a constant direct current, the difference in potential between two identical indicator

* Calculated value $12(V) \div 500(K\Omega) = 24(\mu A)$

electrodes becomes more extended with the increase of the current[2-4]. On the other hand, polarization voltage at alternating current polarization titration is proportional to the alternating current as shown in Fig. 4. Therefore, 25 $\mu$A was used for the suitable alternating current in this titration. If the alternating current becomes very small, it is impossible to use this titration method owing to the decrease of the polarization voltage.

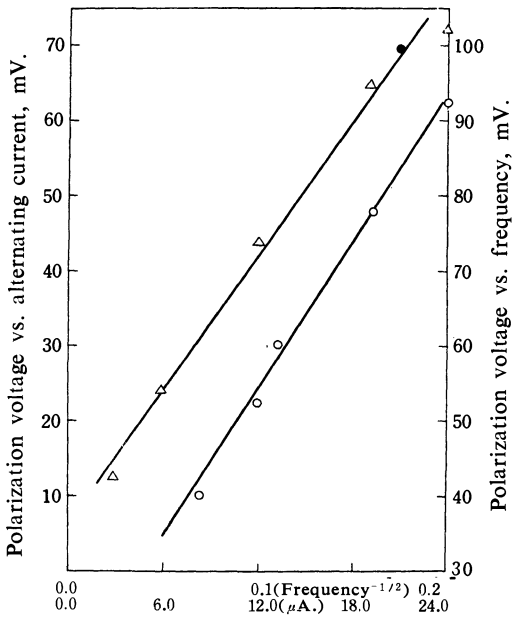



Fig. 4. A) Relation between polarization voltage and frequency (-○-).
B) Relation between polarization voltage and alternating current (-△-).

*3) Effect of Surface Area of Mercury Drop.* —The polarization voltage became smaller with the increase of the surface area of mercury drop as shown in Fig. 5. However, the area of the mercury electrode gave no effect on the experimental result. The pretreatment of the mercury electrode had also little effect on the shape of this titration curve and on the experimental results. Therefore, alternating current polarization titration has advantages in this point over the direct current polarization titration.

*4) Effect of Gelatine.* — In chelatometric titration of cadmium using potentiometry at a constant current and amperometry at a constant potential, the addition of gelatine was necessary[9] in order to suppress the kinetic current due to the dissociation of Cd-EDTA. Experimental results in the presence or the absence

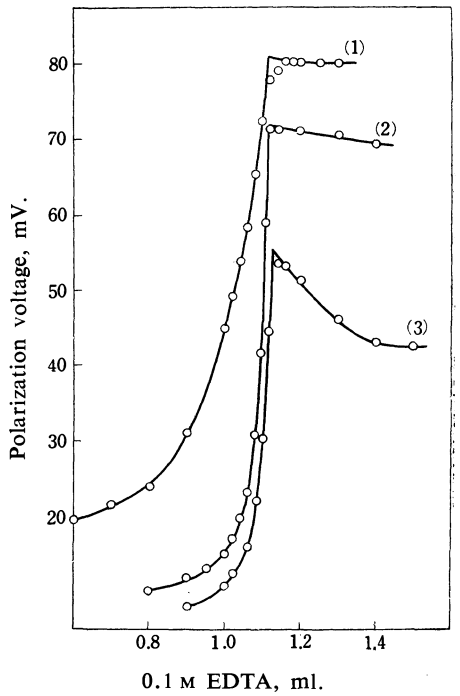



Fig. 5. Effect of surface area of mercury drop.
(1) surface area about 0.02 cm$^2$
(2) 〃 0.03 cm$^2$
(3) 〃 0.05 cm$^2$

of gelatine in this method are shown in Table I. Although experimental results are not reproducible in the absence of gelatine, it is clear that the reproducible and precise results are obtained in the presence of gelatine. Therefore, the addition of 1 ml. of 0.1% gelatine is indispensable in this titration.

TABLE I. EFFECT OF GELATINE ADDED

| Cd taken mg. | 0.1% Gelatine added ml. | Volume of $10^{-1}$M EDTA titrated ml. | Cd found mg. |
|---|---|---|---|
| 6.29 | 0 | $0.55_0$ | 6.18 |
| 6.29 | 0 | $0.53_5$ | 6.01 |
| 6.29 | 0 | $0.55_5$ | 6.18 |
| 6.29 | 0.2 | $0.55_5$ | 6.24 |
| 6.29 | 0.5 | $0.56_0$ | 6.28 |
| 6.29 | 1.0 | $0.56_0$ | 6.28 |
| 6.29 | 2.0 | $0.56_0$ | 6.28 |

*5) Effect of Wave Form.*—The Effect of wave form to this titration (sine wave or square wave) was examined. Although polarization voltage was greater in the case of using sine wave than square wave, it was recognized that the wave form gave little effect on the experimental results.

*6) Effect of Hg-EDTA Added.*—To determine the optimum amount of Hg-EDTA to be added,

9) N. Tanaka et al., *Japan Analyst (Bunseki Kagaku)*, 6, 86 (1957).

various volumes of the Hg-EDTA solution were added to a constant volume of cadmium nitrate solution. In this case, all other conditions were kept constant according to the procedure described above. The results are shown in Table II. It was found that the amount of the reagent did not affect the determination of cadmium provided that it ranged from 5 to 15 ml.

Table II. Effect of Hg-EDTA added

| Cd taken mg. | 0.05 M Hg-EDTA added ml. | Volume of $10^{-1}$ M EDTA titrated ml. | Cd found mg. |
|---|---|---|---|
| 12.58 | 0 | $1.11_0$ | 12.48 |
| 12.58 | 1 | $1.12_0$ | 12.56 |
| 12.58 | 2 | $1.12_5$ | 12.60 |
| 12.58 | 3 | $1.12_0$ | 12.56 |
| 12.58 | 4 | $1.12_5$ | 12.60 |
| 12.58 | 5 | $1.12_5$ | 12.60 |
| 12.58 | 10 | $1.12_0$ | 12.56 |
| 12.58 | 15 | $1.12_5$ | 12.60 |

7) *The Optimum Conditions for the Above-mentioned Procedure.*—They have been concluded as follows: frequency, 20~50 c/sec.; alternating current, 20~25 $\mu$A., gelatine, 0.1% 1 ml.; pH of titration solution, 4.3~5.0; the amounts of Hg-EDTA, 10 ml.

8) *Determination of Various Concentrations of Cadmium under the Optimum Conditions.*—Various concentrations of cadmium ions were determined by the procedure described above under the optimum conditions and the results are shown in Table III.

Table III. Determination of various concentrations of $Cd^{2+}$ at the optimum conditions

| Cd taken mg. | Volume of EDTA titrated ml. | Cd found mg. | error % |
|---|---|---|---|
| | $10^{-1}$ M EDTA | | |
| 12.58 | $1.12_0$ | 12.56 | −0.2 |
| | $1.12_5$ | 12.60 | +0.2 |
| | $1.12_5$ | 12.60 | +0.2 |
| 6.29 | $0.56_0$ | 6.28 | −0.2 |
| | $0.55_5$ | 6.24 | −0.9 |
| | $0.55_5$ | 6.24 | −0.9 |
| | $10^{-2}$ M EDTA | | |
| 0.62 | $0.55_5$ | 0.62 | −0.9 |
| | $0.55_5$ | 0.62 | −0.9 |
| | $0.55_5$ | 0.62 | −0.9 |

## Discussion

Before the titration is initiated, some of the mercury(II) is displaced from its Hg-EDTA complex by the cadmium ion. The following substitution reaction occurs in the solution[10]

$$HgY^{2-} + Cd \text{ acetate} \rightarrow Hg \text{ acetate} + CdY^{2-}$$

In this case, complete substitution of the Hg-EDTA by the cadmium ion to be titrated is not necessary for successful titration. The end point of chelatometric titration of the cadmium ion in this procedure will be indicated by the change of polarization voltage based on the change of the mercuric ion concentration in the neighborhood of the end point. Accordingly, most metal ions will be titratid by this titration method using suitable solution conditions.

The principle on which alternating current polarization titration is based is the same as that of the direct current method. However, this is a more suitable method than the direct current polarization method in the point that the pretreatment of the mercury drop electrode is not necessary.

## Summary

Cadmium was titrated with the EDTA by the alternating current polarization titration with two hanging mercury electrodes and the factors which affect this titration were examined. As a result, it is clear that the end point is indicated by the change of the mercuric ion con centration in the neighborhood of equivalence point. Pretreatment of the mercury drop electrode is not necessary. By this method, cadmium of $10^{-2}$~$10^{-3}$ M were titrated with a relative error of 0.9%.

The author wishes to express his hearty thanks to Professor M. Ishibashi, Assistant Professor T. Fujinaga, University of Kyoto, and Assistant Professor H. Hayakawa, University of Kobe, for their encouragement throughout this investigation.

*Department of Chemistry*
*Faculty of Education*
*Kobe University*
*Kobe*

10) A. E. Martin and C. N. Reilly, *Anal. Chem.*, **31**, 993 (1959).

# *High Resolution Nuclear Magnetic Resonance Spectra of Ring Protons in Substituted Benzenes*

By Ichiro YAMAGUCHI and Naohiro HAYAKAWA

(Received February 16, 1960)

The electron distribution on the benzene ring has been considered to be a very interesting object by many organic chemists, especially with respect to the correlation with the reactivity of the molecule. An experiment of approach to this problem was carried out by Gutowsky and his coworkers[1]. They measured the fluorine nuclear magnetic resonance in a number of fluorobenzenes and investigated the effect of substituents on the fluorine resonance shift and found the correlations between the values of the Hammett $\sigma$ constant and of the resonance shift. Recently, Bothner-By and Glick[2] and also Corio and Dailey[3] observed the proton resonance spectra of benzene derivatives and discussed the electron densities on the *o*-, *m*- and *p*- protons. The patterns of the proton resonance spectra obtained by them are simple and not adequate for the precise examination of the electron distribution in the benzene derivative molecules. Patterns simpler than the expected ones are mainly due to the fact that the resonance frequency of the experiments was as low as 30 Mc.

Hence, we planned to investigate the proton resonance spectra of the benzene ring protons of a variety of benzene derivatives at 56.4 Mc. This paper reports the results of the analysis of their spectra, and the spectra of disubstituted benzenes are discussed with correlation to the substituents.

## Experimental

The Varian High Resolution NMR Spectrometer was operated at 56.4 Mc. The resolution of the apparatus was higher than $10^{-8}$ when the sample was spun.

The samples measured were of commercial guaranteed grade, and these were used without further purification. The spectra of the liquid samples were taken in pure liquid state. Most of the solid samples were dissolved in acetone to make saturated solutions, and the spectra were taken. The others were dissolved in ethanol or ether.

All of the NMR measurements were carried out at 20°C for the samples sealed in glass tubes with the outer diameter of 5 mm. The spectra were recorded by the Sanborn Recorder and the separations of the resonance peaks were measured on the recorded charts. The magnetic field was swept in both decreasing and increasing directions and the measurements were made by taking the average of the records of both directions of the sweep. The calibration of the sweep rate was made by recording the spectrum of the methylene group of ethanol and by reading the separation of the two highest peaks as 7.0 cps[4]. The sweep rate was about 1 cps/sec.

The chemical shift of the ring proton resonance referred to benzene ring proton was determined for several compounds by adding a small amount of benzene to the sample liquid as an internal standard. This method was found to be inadequate for the precise determination of the shift value, because it was noticed that an additive shift arose by the addition of benzene. Therefore the observed values of the shift referred to benzene, $\delta_B$, include an error of about $\pm 0.05$ p.p.m.

The experimental error over the entire measurements was about 3%. This arose mainly from the instability of the field sweeping of the spectrometer.

## Analysis of the Spectra

The systems of the ring protons of benzene derivatives are represented as in Table I, according to the notation proposed by Bernstein et al.[5]. In these systems, the spectra with simple structure may be analyzed by solving the equations of the Hamiltonian of the nuclear spin system and the assignment of the spectral lines can be made. The ratio $J/\nu_0\delta$, where $J$ and $\nu_0\delta$ are respectively the spin coupling constant and the chemical shift in cps between the two resonating nuclei, ranges from 0.2 to more than 1 in the case of benzene ring protons, and in some cases the chemical shift is very small compared with the values of the spin coupling constant. This should be noted when the analysis is made by any approximate method which neglects higher order perturbation terms or some coupling constants.

For each system of ring protons the appropriate approximation method was adopted to

1) H. S. Gutowsky, D. W. McCall, B. R. McGarvey and L. H. Meyer, *J. Am. Chem. Soc.*, **74**, 4809 (1952).
2) A. A. Bothner-By and R. E. Glick, ibid., **78**, 1071 (1956).
3) P. L. Corio and B. P. Dailey, ibid., **78**, 3043 (1956).
4) Varian Assoc., "Technical Information Bulletin", No. II-2.
5) H. J. Bernstein, J. A. Pople and W. G. Schneider, *Can. J. Chem.*, **35**, 65 (1957).

TABLE I. PROTON GROUPINGS IN SUBSTITUTED BENZENES

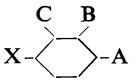
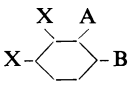
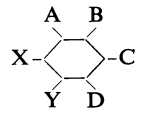
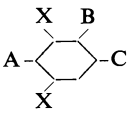
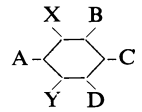
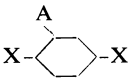
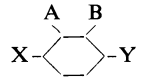
| | | | | | |
|---|---|---|---|---|---|
| Mono-X benzene | $AB_2C_2$ |  | | | |
| *o*-Di-X benzene | $A_2B_2$ |  | *o*-XY benzene | ABCD |  |
| *m*-Di-X benzene | $AB_2C$ |  | *m*-XY benzene | ABCD |  |
| *p*-Di-X benzene | $A_4$ |  | *p*-XY benzene | $A_2B_2$ |  |

TABLE II. SPREADING RANGE OF PROTON RESONANCE LINES OF MONO-SUBSTITUTED BENZENES (in cps at 56.4 Mc)

| | | | |
|---|---|---|---|
| Nitrobenzene | 55 | Bromobenzene | 35 |
| Benzaldehyde | 40 | Iodobenzene | 50 |
| Toluene | Single peak | Aniline | 55 |
| Chlorobenzene | 22 | | |

analyze the spectrum. In the system of *o*-di-X benzene, the result of the analysis of *o*-dichlorobenzene, obtained by solving the secular equation by Pople et al.[6] was adopted. In *m*-di-X benzene the calculation based on the second order perturbation theory could be adopted for molecules where the ratios $J/\nu_0\delta$ in the molecule are comparatively small. In *p*-XY benzene, the secular equation of the system was solved by neglecting the spin couplings between the protons in *m*-position and in *p*-position to each other[7]. In each case of analysis, the coupling constants between protons are assumed to have positive sign.

## Results and Discussion

**Monosubstituted Benzene.** — The spectra of monosubstituted benzenes are generally very complicated ones and none of the spectral lines can be assigned completely by a simple glance of the structure of the spectra. The preliminary analysis of the spectrum of this system shows that the line groups of *o*-, *m*- and *p*-protons have many lines and each of these spreads over a wide range. In most cases, the *m*- and *p*-protons are overlapping each other as the result of the couplings of protons where the chemical shifts are very small. This chemical shift is, in certain cases, much smaller than the coupling constant between the protons concerned. In addition to this, the spreading range of the resonance lines of *p*-protons is generally wide compared to that of *m*-protons. This makes the assignment of the ring proton spectral lines of monosubstituted benzene very difficult

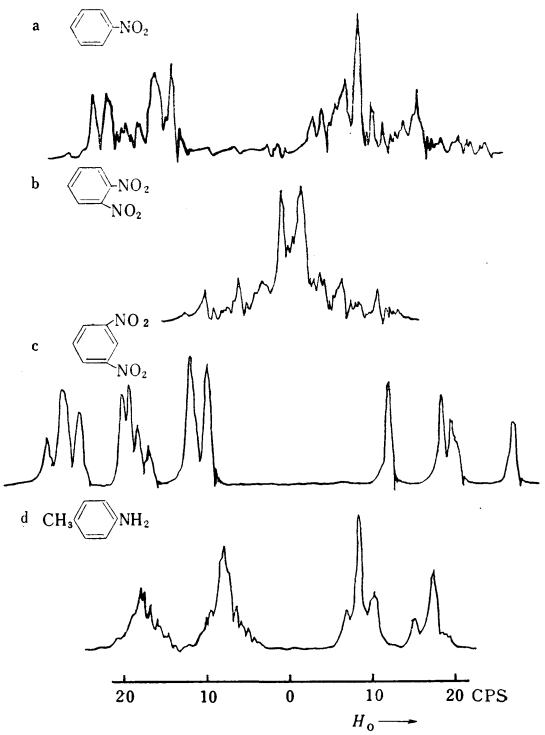



Fig. 1. NMR spectra of ring protons in mono- and di-substituted benzenes.

6) J. A. Pople, W. G. Schneider and H. J. Bernstein "High Resolution Nuclear Magnetic Resonance", McGraw-Hill Book Co., New York (1959), pp. 145-149.

7) R. E. Richards and T. P. Schaefer, *J. Mol. Spectroscopy*, **2**, 1280 (1958).

compared with the other symmetrical systems. Though the spectra of the system reported by Corio and Dailey[3] are relatively simple, the simple spectra are due to the low resonance frequency of their experiment. It seems that the values of chemical shift reported by them may have errors as the result of the fact that the spectral patterns are not well resolved. An example of the spectrum of monosubstituted benzene is shown in Fig. 1a. The range of the spreading of the spectral lines is also shown in Table II. The spreading electron-range of the spectrum is wider as the releasing or withdrawing power of the substituent is stronger.

**Disubstituted Benzene.**—*o-Di-X Benzene.*—An example of the spectrum of the system is is shown in Fig. 1b. The spectrum spreads in a rather narrow range showing a symmetrical pattern. The magnitudes of the chemical shift and the spin coupling constants are listed in Table III. Generally, the chemical shift between A and B groups of protons is very small and this shows that the difference of the resultant electronic effects of the substituent on the protons of A and B groups is very small.

The chemical shift of the ring proton resonance referred to the benzene ring proton may be considered to arise from two origins. One is variation in the ring current and the other that in the electronic shielding of the protons affected by the substituent. The ring current variation might cause the shift of the whole spectrum in either direction according to whether the ring current density increases or decreases. On the other hand, electronic effects of the substituent would affect the protons at different positions separately by its inductive and resonance effects and the scectral figure would vary according to the difference in the effect on different protons.

For all *o*-di-X benzenes observed, the spectral lines spread almost in similar magnitude while the variety in $\delta_B$ is rather remarkable. This result would lead to the conclusion that the ring current is considerably affected by the substituent. The same consideration will be held for the other proton systems.

*m-Di-X Benzene.*—The spectrum of this system is characterized by its three-group pattern as illustrated in Fig. 1c. The last column in Table IV shows the arrangement of spectral line groups in increasing field direction. The order of arrangement of these groups in the spectrum is understood mainly in terms of the electron-releasing and withdrawing power of the substituent X. The resonance position of the A proton is greatly influenced by the electronic nature of the substituent because the position of the proton is between two X's,

TABLE III. CHEMICAL SHIFT AND COUPLING CONSTANT IN *o*-di-X BENZENES
(in cps at 56.4 Mc)

| Compound | Solvent | $\nu_0\delta_{AB}$ | $J_{AB}$ | $J_{AB'}$ | $J_{BB'}$ | $\delta_B$ (in p.p.m.) |
|---|---|---|---|---|---|---|
| *o*-Dinitrobenzene | Acetone | 7.1 | 8.4 | 0.9 | 3.1 | −0.74 |
| Phthalic acid | Acetone | 9.3 | 7.8 | 0.5 | 4.1 | −0.35 |
| *o*-Xylene | — | 0.0 | | | | |
| *o*-Dichlorobenzene | — | 13.8 | 8.4 | 1.9 | 6.9 | +0.24 |
| Catechol | Acetone | 11.2 | 8.1 | 1.3 | 5.0 | +0.43 |

TABLE IV. CHEMICAL SHIFT AND COUPLING CONSTANT IN *m*-di-X BENZENES
(in cps at 56.4 Mc)

| Compound | Solvent | $\nu_0\delta_{AB}$ | $\nu_0\delta_{BC}$ | $J_{BC}$ | $J_{AB}$ | $J_{AC}$ | Spectrum |
|---|---|---|---|---|---|---|---|
| *m*-Dinitrobenzene | Acetone | 12.6 | 33.0 | 7.6 | 2.0 | 0.5 | A-B-C |
| Isophthalic acid | $(CH_3)_2SO$ | 23.4 | 30.2 | 8.0 | 1.6 | 1.0 | A-B-C |
| *m*-Xylene | — | | | | | | C-A-B |
| *m*-Dichlorobenzene | — | | | | | | C-A-B |
| Resorcinol | Acetone | | 36 | 8.5 | 2 | 1 | C-A-B |
| *m*-Phenylenediamine | Acetone | 4.8 | 45.2 | 8.4 | 2 | 1 | C-B-A |

TABLE V. CHEMICAL SHIFT IN *p*-di-X BENZENES

| Compound | Solvent | $\delta_B$ (in p.p.m.) |
|---|---|---|
| *p*-Dinitrobenzene | Acetone | −1.17 |
| Terephthalaldehyde | Acetone | −0.77 |
| *p*-Xylene | — | +0.29 |
| *p*-Dichlorobenzene | Acetone | −0.05 |
| *p*-Dibromobenzene | Acetone | +0.30 |
| *p*-Phenylenediamine | Acetone | +0.85 |

TABLE VI. CHEMICAL SHIFT AND COUPLING CONSTANT IN *p*-XY BENZENES (in cps at 56.4 Mc)

| Compound | Solvent | $\nu_0\delta_{AB}$ | $J_{AB}$ | $\delta_B$ (in p.p.m.) |
|---|---|---|---|---|
| *p*-Nitrobenzaldehyde | Acetone | 12.3 | 9.3 | −0.87 |
| *p*-Nitrobenzoic acid | Acetone | 23.1 | 8.4 | |
| *p*-Nitrotoluene | — | 38.1 | 9.5 | −0.32 |
| *p*-Nitrochlorobenzene | Acetone | 31.7 | 9.0 | −0.53 |
| *p*-Nitrobromobenzene | Acetone | 22.1 | 9.8 | −0.71 |
| *p*-Nitrophenol | Acetone | 68.0 | 9.5 | −0.23 |
| *p*-Nitroaniline | Acetone | 64.7 | 8.9 | −0.05 |
| *p*-Hydroxybenzaldehyde | Ethanol | 46.7 | 9.5 | |
| *p*-Aminobenzaldehyde | Acetone | 45.8 | 8.2 | +0.02 |
| *p*-Toluic acid | Acetone | 37.0 | 8.1 | |
| *p*-Chlorotoluene | — | 12.1 | 8.3 | +0.27 |
| *p*-Bromotoluene | — | 22.9 | 8.2 | +0.22 |
| *p*-Cresol | — | 0.0 | | |
| *p*-Toluidine | Ether | 23.7 | 9.0 | +0.69 |
| *p*-Bromochlorobenzene | Acetone | 11.6 | 8.8 | |
| *p*-Chlorophenol | — | 14.1 | | |
| *p*-Chloroaniline | Acetone | 26.1 | 9.0 | +0.51 |
| *p*-Bromophenol | Ether | 31.4 | 9.7 | |
| *p*-Iodoaniline | Acetone | 48.4 | 8.8 | +0.41 |

while the C proton is not so much influenced.

The analyzed results are tabulated in Table IV. The perturbation treatment of the second order could be applied to two compounds (*m*-dinitrobenzene and *m*-dichlorobenzene) well, but not to the others where the resonance positions of A and B protons are closely located. For these compounds, the analysis of the spectrum should be accomplished with the higher order approximation.

*p-Di-X Benzene.*—The spectra are single line as expected from the symmetry consideration of this system. The chemical shift referred to benzene is shown in Table V.

*p-XY Benzene.*—This system has two different substituents and the different electronic effect is given on the proton neighboring to each of them. In addition to this, the spectrum of this system is comparatively simple and can be analyzed easily Therefore, the investigation of the spectrum of this system is interesting to show the overlapping extent of the effects of both substituents on the ring. An example of the spectrum of this system is shown in Fig. 1d. This consists of two groups A and B, which correspond to the protons A and B in the molecule.

This system has been analyzed for several compounds with appropriate approximation by Richards and Schaefer[7]. The present spectra were analyzed according to their method. The values of the chemical shift and the coupling constant obtained are listed in Table VI, where the $J_{AB}$ is the coupling constant between A and B protons when the $J_{AB'}$ (coupling constant between A and B′ protons which one *p*-position to each other) is neglected.

Qualitatively, the shift between the two groups A and B is large when the electronic effects of the two substituents X and Y upon the ring protons are greatly different and vice versa. For example, $\delta_{AB}$ of *p*-nitroaniline is very large where the electronic nature of $NO_2$ and $NH_2$ group are greatly different to each other as is well known by the evidence of their effect on the substitution reaction of ring protons, whereas the one of bromochloro-benzene is very small as is expected.

*Other Systems.*—The spectral figures of the other systems are generally more complicated than the systems described above. *o*-XY- and *m*-XY-benzenes are of this sort. These systems have no symmetry, therefore their analyses are of course very cumbersome. These systems will not be dealt with further in this paper.

The values of the coupling constant between two protons on the benzene ring are approximately definite with respect to their mutual *o*-, *m*- or *p*-positions. The values deduced from the results of the analyses may be summarized as follows;

$J$ between two protons located at

| | |
|---|---|
| *o*-position mutually | 7∼9 cps |
| *m*-position mutually | 1∼3 cps |
| *p*-position mutually | 0∼1 cps |

The values indicated that the coupling is attenuated in proportion to the exponent of about −5 to the direct bond length between the two protons concerned. The values listed above

coincide well with the description which appeared in the book of Pople et al.[8]

The resonance position of a benzene ring proton is closely related to the relative location of the proton to the substituent on the benzene ring. The same evidence was discussed by Gutowsky et al.[1] with the fluorobenzene derivatives. They showed also that the shift values for the ring fluorine of polysubstituted fluorobenzenes may be calculated from the shift values of monosubstituted fluorobenzenes with the assumption of an additive law of shift. Their calculated results with this law coincide with the experimental values with deviations less than 10%. We applied the law to the samples investigated. The values for the disubstituted benzenes were calculated with the shift values of the monosubstituted benzenes reported by Corio and Dailey[3]. The results of the calculation showed that the shift values do not necessarily coincide well, but showed a close relation with the experimental values. The explanation of the shift values with the additive law may of course be oversimplified by neglecting to take into account all the interactions in the molecule, and further consideration of the results will be postponed until more experimental data with monosubstituted benzenes become available.

The resonance lines for the protons just adjacent to the methyl group on the ring generally show fine structure. This splitting is illustrated in Fig. 1d for the ring proton resonance of *p*-toluidine. Hoffman[9] reported that the ring proton resonance line of mesitylene showed broadening, and he assumed that this broadening arose from the coupling between the ring proton and the methyl protons by hyperconjugation mechanism. Although the observed fine structure reported here may be a similar one to the case of mesitylene, further experimental verification seems necessary for deciding the true origin of the splitting.

The present work is carried out with saturated acetone solutions in almost all cases, however; the solvent effect on the shift between ring protons appears to be noticeable. Thus the shift values may differ from one another among solutions with different concentrations. This intramolecular shift may be assumed to arise from the selective interaction between the proton located at the specific position on the ring and the solvent molecule. The nature of this interaction is at present unexplained.

8) Ref. 6, p 193, Table 8-1.
9) R. A. Hoffman, *Mol. Phys*,, 1, 326 (1958).

## Summary

High resolution proton magnetic resonance spectra of a variety of mono- and di-substituted benzenes were observed at 56.4 Mc. The spectra of molecules with higher symmetry were analyzed, and the values of chemical shifts among the ring protons and those referred to benzene were obtained as well as spin coupling constants. The spectra were discussed with correlation to the substituents.

The authors wish to express their thanks to Professor S. Fujiwara for his encouragement and guidance of this work and also to Mr. H. Shimizu for his helpful discussions on this subject.

*Division of Radiation Applications*
*Japan Atomic Energy Research Institute, Tokai, Ibaraki-ken*

# *The Effect of Chain Branching and Molecular Weight of Polyethylene on its Glass Transition Temperature*

By Kōji TANAKA

(Received February 16, 1960)

In the previous paper[1] the effects of chain branching, mainly short chain branching, on such properties as the melting point, the crystallizing temperature and the premelting phenomenon were reported and discussed. In this paper the effect of chain branching on the glass transition temperature and the degree of cubic expansion above and below the glass transition temperature are described.

Regarding the glass transition temperature, a sort of second-order transition temperature, of polyethylene, a number of reports have been presented. Hunter and Oakes[2] showed from the measurement of linear expansion that there was a sign of transition occurring at about $-45°C$. Later Danusso et al.[3] reported from the volume expansion measurement that the second-order transition temperature of polyethylene existed arround $-20°C$ regardless of molecular weight, degree of chain branching or degree of crystallinity. According to the paper of Gubler and Kovacs[4] the cubic expansion coefficient changes between $-20$ and $-25°C$ for both a high-pressure and a Ziegler polyethylene. It has also been confirmed by some other methods that a transition occurs at about $-20°C$ or at a still lower temperature[5-10]. By considering the change of mechanical properties of polyethylene at about $-50°C$, reported by Carey et al.[11], and the brittle point of $-68°C$ reported by Boyer and Spencer[12], this second-order transition at arround $-20°C$ seems to be the glass transition, though the existence of another transition at the temperature below $-100°C$ was reported by Schmieder and Wolf[13], Oakes and Robinson[14] and Dannis[15]. As for the effect of the degree of chain branchig on the glass transition temperature, it may be inferred from the results reported hitherto that the degree of chain branching has no effect on the glass transition temperature. Such a conclusion, however, can not be reached so hastily, as only a few kinds of samples were used in each experiment.

The glass transition temperature is generally defined as the point at which the main chain in an amorphous region of a polymer acquires large scale mobility. It is therefore expected that short chain branching and the branch point of long chain branching, which are contained in the amorphous region, disturb the regularity of molecules and keep the molecules from arranging themselves in good order in proportion to the number of them, and consequently the molecular mobility of the amorphous region is affected not a little by them; that is, the more branches the amorphous region contains, the more easily it initiates the large scale molecular motion and as a result the glass transition of polyethylene having the higher degree of chain branching occurs at the lower temperature.

From this point of view, a series of measurements have been taken by using various polyethylenes. From the results obtained it appears that short chain branching has a large effect on the glass transition temperature, independent of the degree of crystallinity. Long chain branching scarcely exists in low-pressure polyethylene, and in high-pressure polyethylene only a few long chain branching are contained in comparison with short one. It is therefore considered that its effect is not noticeable, even if each branch point has some effect on the glass transition temperature.

1) K. Tanaka, This Bulletin, **33**, 1060 (1960).
2) E. Hunter and W. G. Oakes, *Trans. Faraday Soc.*, **41**, 49 (1945).
3) F. Danusso, G. Moraglio and G. Talamini, *J. Polymer Sci.*, **21**, 139 (1956).
4) M. G. Gubler and A. J. Kovacs, *J. Polymer Sci.*, **34**, 551 (1959).
5) E. Butta and A. Charlesby, *J. Polymer Sci.*, **33**, 119 (1958).
6) C. W. Deeley, D. E. Kline, J. A. Sauer and A. E. Woodward, *J. Polymer Sci.*, **28**, 109 (1958).
7) N. Fuschillo, E. Rhian and J. A. Sauer, *J. Polymer Sci.*, **25**, 381 (1957).
8) A. H. Willbourn, *Trans. Faraday Soc.*, **54**, 717 (1958).
9) W. P. Slichter and D. W. McCall, *J. Polymer Sci.*, **25**, 230 (1957); **26**, 171 (1957).
10) P. W. Jensen, *J. Polymer Sci.*, **28**, 635 (1958).
11) R. H. Carey, E. F. Schultz and G. J. Dienes, *Ind. Eng. Chem.*, **42**, 842 (1950).
12) R. F. Boyer and R. S. Spencer, *J. Appl. Phys.*, **15**, 398 (1944).
13) K. Schmieder and K. Wolf, *Kolloid-Z.*, **134**, Sonderausgabe 2, Marburger Diskussionstagung: Das Relaxationsverhalten der Materie, 157 (1953).
14) W. G. Oakes and B. W. Robinson, *J. Polymer Sci.*, **14**, 505 (1954).
15) M. L. Dannis, *J. Appl. Polymer Sci.*, **1**, 121 (1959).

## Samples

Samples used were Marlex 50-9, Ziegler polyethylene, and eight kinds of high-pressure polyethylenes with the different molecular parameters which were provided by courtesy of Dr. Hammer of E. I. du Pont de Nemours and Company. The molecular parameters are shown in Table I. Marlex 50-9 and Ziegler polyethylene were commercially available polymers made by Phillips Petroleum Company and Dow Chemical Company, respectively. As the molecular parameters for these two samples were not available, the degree of short chain branching was determined by the infra-red method according to Slowinski[16]. It was found to be 0.25 for Marlex 50-9 and 0.4 for Ziegler polyethylene.

TABLE I. THE MOLECULAR PARAMETERS FOR POLYETHYLENE SAMPLES

| Sample | Melt index | $M_n \times 10^{-3}$ | $N_c$* | $N_w$** |
|---|---|---|---|---|
| A*** | 0.2 | 34 | 1.6 | 20 |
| B | 2.1 | 32 | 1.6 | 18 |
| C | 2.1 | 21 | 2.2 | 27 |
| D | 2.1 | 18 | 3.0 | 34 |
| E | 3.8 | 20 | 1.6 | 13 |
| F | 2.0 | 50 | 2.0 | 18 |
| G | 1.8 | 27 | 0.6 | 10 |
| H | 16.0 | 12 | 3.2 | 29 |
| Marlex 50-9 | | | 0.25 | |
| Ziegler | | | 0.4 | |

* Short chain branching index in $CH_3$ groups per 100 $CH_2$ groups.
** Long chain weight average number of branch points per molecule.
*** These (A to H) are high-pressure samples.

## Experimental

Dilatometric measurements were at first taken in the temperature range from −40 to 150°C by using mercury as the confining liquid. However, it seemed to be undesirable to determine the glass transition point merely from the measurements in which mercury was used as the confining liquid, as the temperature range below the glass transition temperature was small. Therefore 99.5% ethanol being used as the confining liquid, measurements were carried out over the temperature range from room temperature to −70°C. In this measurement Bekkedahl's straight type dilatometer[17] was used and the preparation of the most highly crystallized sample was performed by following the way mentioned in the previous paper in the sufficiently evaluated glass tube in order to protect the sample from oxidation before it was enclosed in the dilatometer. A Dewar vessel containing toluene was used as a bath. The details about the experimental procedure were omitted in this paper, as they were described in the previous paper.

The glass transition temperature, $T_g$, was determined by extrapolation of two straight lines connected by a curved section, consisting of the volume-temperature curve of high polymer. As polyethylene is a semi-crystalline polymer and the difference between cubic expansion coefficients above and below $T_g$ is small, an error is apt to be made. In order to eliminate such an error $T_g$ was also determined from the discontinuity of the curve obtained by plotting the volume temperature derivatives, $\Delta V/\Delta t$, as a function of temperature as was done by Hoffmann and Weeks[18].

## Results and Discussion

The specific volume-temperature curves of the most highly crystallized polyethylenes ranging from above to below the glass transition temperature are shown in Fig. 1. The volume temperature derivatives are plotted as a function of temperature in Fig. 2. In these two figures only a few curves were shown to avoid confusion.

The average value of the glass transition temperature obtained for each sample is given in Table II. These values are plotted in Fig. 3 as a function of the degree of short chain branching. As is shown in the figure, the glass transition temperature lowered with the increasing amount of short chain branching

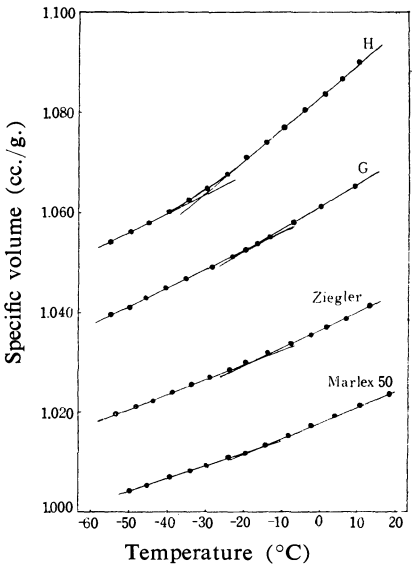



Fig. 1. Specific volume-temperature curves of the most highly crystallized polyethylene ranging from above to below $T_g$.

16) E. J. Slowinski, Jr., H. Walter and R. L. Miller. *J. Polymer Sci.*, **19**, 353 (1956).
17) N. Bekkedahl, *J. Research Natl. Bur. Standards*, **42**, 145 (1949).
18) J. D. Hoffmann and J. J. Weeks, *J. Research Natl. Bur. Standards*, **61**, 465 (1958).

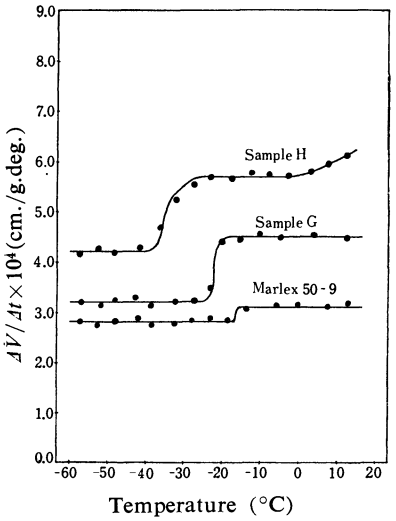



Fig. 2. Volume-temperature derivatives of some of the most highly crystallized samples as a function of temperature.

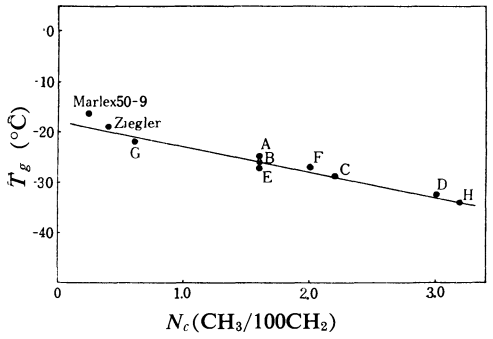



Fig. 3. $T_g$ as a function of degree of short chain branching

and there seems to be a linear relation between the glass transition temperature and the degree of short chain branching.

The degree of cubic expansion above and below the glass transition temperature, which are presented by the gradients of the straight lines above and below the temperature, are also listed in Table II. These values generally increased as the amount of short chain branching became larger and those above the glass transition point increased in a greater extent than did those below the point, which fact is probably because the large-scale segmental motion in the amorphous region is excited at the temperature above the glass transition point and the more the sample of polyethylene branched, the greater is the scale of the motion. As regards the degree of cubic expansion below the glass transition point there is a view by Price[19] and Danusso et al.[20]

Table II. The glass transition temperatures and degrees of cubic expansion above and below that temperature

| Sample | $N_c$ | $T_g$ | $\alpha_1$*$\times 10^4$ | $\alpha_2$**$\times 10^4$ |
|---|---|---|---|---|
| Marlex 50-9 | 0.25 | −16.0 | 2.8 | 3.1 |
| Ziegler | 0.4 | −19.1 | 2.8 | 3.4 |
| G | 0.6 | −22.2 | 3.2 | 4.5 |
| A | 1.6 | −25.2 | 3.9 | 5.1 |
| B | 1.6 | −25.8 | 3.5 | 5.0 |
| E | 1.6 | −26.3 | 3.7 | 5.3 |
| F | 2.0 | −27.3 | 4.0 | 5.3 |
| C | 2.2 | −28.8 | 3.9 | 5.2 |
| D | 3.0 | −32.5 | 4.1 | 5.9 |
| H | 3.2 | −34.0 | 4.2 | 5.7 |

* Degree of expansion below $T_g$.
** Degree of expansion above $T_g$.

that it is considered to be equal for all the polyethylene, but in this experiment the result as above was obtained, that is, the degree of cubic expansion below the glass transition point increased as a whole with the increase of the degree of short chain branching.

Since short chain branching affects the degree of crystallinity of polyethylene as was mentioned in the previous paper, it is expected that the lowering of the transition temperature by the increase of short chain branching shown in Fig. 3 is attributable to the decrease of the degree of crystallinity. However, glass transition temperatures of the quenched samples of these polyethylenes, which showed a low degree of crystallinity about 40% at 25°C, were found at nearly equal temperatures to those of crystallized samples. Therefore the lowering of the glass transition temperature is probably due to the direct effect of short chain branching itself and not to the decrease of the degree of crystallinity. According to the recent result of linear expansion measurements by Saito[21], a transition was found at around −32°C for a low-branched polyethylene and at about −45°C for a highly-branched polyethylene. The difference between these temperatures was almost equal to that found by the author, though each temperature was lower by about 10 degrees than that obtained here.

Considering the results mentioned above, short chain branching of polyethylene appears to affect the glass transition temperature independent of such factors as degree of crystallinity and molecular weight. Moreover, according to Gubler and Kovacs[4] the number of $CH_2$ groups constituting the main chain in amorphous regions of polyethylene thermally

19) F. P. Price, *J. Chem. Phys.*, **19**, 973 (1951).
20) F. Danusso, G. Moraglio and G. Natta, *Ind. Plastiques Mod. (Paris)*, **10**, 40 (1958).
21) S. Saito, private communication.

treated in the same way are almost equal regardless of its kind. Therefore the polyethylene having the higher degree of short chain branching will contain more branches in one amorphous region, provided that short chain branching is distributed equally in all the amorphous regions. It is considered that the shorter the branches which are contained in the amorphous regions equal in size, the smaller is the intermolecular interaction between the segments in those regions in the temperature range below the glass transition temperature, and as a result the Macro-Brownian motion in amorphous regions starts at the lower temperature, that is, the glass transition occurs at the lower temperature.

The relation between the glass transition temperature and degree of short chain branching in high pressure polyethylene shown in Fig. 3 is led to the following expression by using the method of least square,

$$T_g = -4.6N_c - 18.7$$

Marlex 50-9 and Ziegler polyethylene deviate somewhat from this expression. According to Willbourn[22] short chain branches of high-pressure polyethylene are ethyl and butyl branches and those of Marlex and Ziegler polyethylene are methyl, and methyl and ethyl, respectively. Therefore in the amorphous region of Marlex 50-9 and Ziegler polyethylene molecules possess a greater intermolecular interaction than expected from the case of high-pressure polyethylene.

As in short chain branching, so in long chain branching, it is expected that the increasing amount of long chain branching lowers the glass transition temperature. In this experiment, however, no appreciable result was produced. This is probably attributable to the very small amount of long chain branching, that is, the effect of long chain branching on the glass transition temperature is covered by the effect of short chain branching and of molecular weight. For example, as to the samples A, B and E which were equal in degree of short chain branching but different in degree of long chain branching, even the reverse phenomenon was observed that the sample having the larger amount of long chain branching showed a higher glass transition temperature. It is perhaps due to the effect of molecular weight of the sample as is discussed below.

It is generally said that the glass transition temperature is affected by molecular weight. Molecular weights of the samples used cover a wide range, so transition temperaturs are illustrated in Fig. 4 as a function of molecular weight. In the figure the glass transition temperature apparently rises with the increase of molecular weight, but short chain branching considerably affects the glass transition temperature as was stated above. A definite conclusion cannot be deduced without eliminating the effect of short chain branching. In order to remove this effect, the difference between the glass transition temperature obtained from practical measurement and that from the expression already presented is illustrated in Fig. 5 as a function of molecular weight. As is shown in the figure the rise of the glass transition temperature is only less than 2°C as molecular weights increase from 10,000 to 50,000. Therefore it will be evident that molecular weight has a smaller effect on this transition temperature compared with that of short chain branching. According to Fox and Flory[23], however, the glass transition temperature of atactic polystyrene rose by 14°C as the molecular weight increases from 10,000 to 50,000 as is shown in Fig. 5. This difference in polyethylene and polystyrene is probably due to the fact that the former is a crystalline polymer and the latter an amorphous polymer.

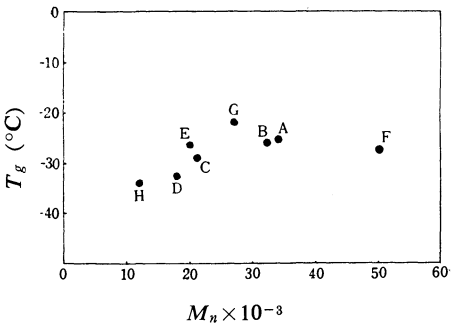



Fig. 4. $T_g$ as a function of molecular weight.

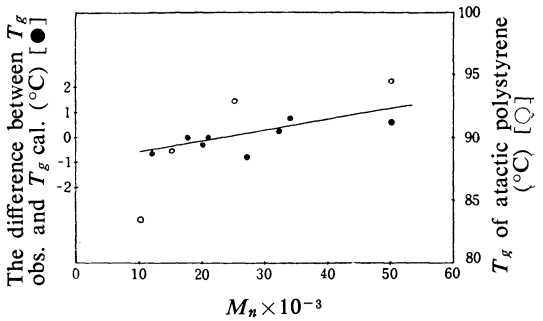



Fig. 5. The difference between $T_g$ from the practical measurement and that from the expression presented in this paper, and $T_g$ of atactic polystyrene are illustrated as a function of molecular weight.

22) A. H. Willbourn, *J. Polymer Sci.*, **34**, 569 (1959).

23) T. G. Fox, Jr. and P. J. Flory, *J. Appl. Phys.*, **21**, 581 (1950).

that is, this contains very large amorphous regions, whose size is greatly affected by molecular weight, while that includes alternately crystalline and amorphous regions. According to Gubler and Kovacs the size of the individual amorphous region in the samples thermally treated in the same way is almost equal regardless of the kind of polyethylene, as was mentioned already. From this point of view, it is considered that the effect of molecular weight on the glass transition temperature is essentially very small in polyethylene.

In addition it is reported by Smith[24] that polyethylene contains double bonds in it and most of them belong to the terminal of the main chain for Marlex and to the side chain for high-pressure polyethylene. But, as the amount of double bonds is very small, the effect on the glass transition temperature and degree of crystallinity will not be worth discussing in this paper.

## Summary

A series of measurements by volume dilatometry were performed in order to know whether short chain and long chain branchings, and molecular weight of polyethylene affected the glass transition temperature or not. The glass transition temperature, $T_g$, was obtained from the intersection of two straight lines of volume-temperature curve and from the discontinuity of the curve obtained by plotting the volume temperature derivatives as a function of temperature. $T_g$ lowered with the increasing amount of short chain branching and there seems to be a linear relationship between $T_g$ and the degree of short chain branching. No appreciable effect of long chain branching on $T_g$ was observed. $T_g$ rose apparently with the increase of molecular weight, but the true rise of $T_g$ was only less than 2°C as molecular weight increased from 10,000 to 50,000. The degree of cubic expansion above and below $T_g$ increased generally as the amount of short chain branching increased.

The author wishes to express his gratitude to Professor Masatami Takeda for his valuable suggestion and discussion, and his thanks to Dr. C. F. Hammer of E. I. du Pont de Nemours and Company for the gift of polyethylene samples. He is also indebted to Miss M. Yoshida for her assistance in experimental work.

*Department of Chemistry*
*Faculty of Science*
*Tokyo College of Science*
*Kagurazaka, Shinjuku-ku*
*Tokyo*

24) D. C. Smith, *Ind. Eng. Chem.*, **48**, 1161 (1956).

# *On the Thermal Dissociation of Organic Compounds*[1]. *XIV. The Effects of the Solvents and of the Substituents on the Thermal Dissociation of Urethans in Amines*

By Teruaki MUKAIYAMA, Toyohiko AKIBA and Tamio ASAHI

(Received February 17, 1960)

In previous papers[2,3] of this series the kinetic studies of the dissociation of *N*-phenyl-alkyl carbamates in basic solvents were described. *N*-phenyl-alkyl carbamates dissociate in the presence of 10 molar excess of an amine at above 120°C; however, *N*-phenyl-phenyl carbamates dissociate instantly under the same condition.

In the case of *N*-phenyl-phenyl carbamates, the addition reaction of isocyanates with phenols to form urethans, which is the reversal of the dissociations, reaction do not proceed under the experimental conditions. Therefore, the dissociation proceeds to essentially 100% completion in the presence of an equimolar amount of an amine.

$$RHNCOOR \rightleftharpoons R\text{-}N{=}C{=}O + HO\text{-}R \quad (1)$$

$$R\text{-}N{=}C{=}O + HNR'R' \rightleftharpoons RHNCONR'R' \quad (2)$$

As described in the previous papers, reaction 1 is the rate-determining step in the above

1) This investigation was performed at the Gakushuin University.
2) T. Mukaiyama and Y. Hoshino, *J. Am. Chem. Soc.*, **78**, 1946 (1956).
3) T. Mukaiyama and M. Iwanami, ibid., **79**, 73 (1957).

sequence and the rate constants for the dissociation of urethans can be measured by determining the amount of the remaining amine.

The kinetic order of the dissociation of urethans was studied by the effect of change of initial concentration of both urethan and amine and it was shown that the dissociation is of the first order with respect to urethan and to amine respectively.

In order to study the effects of amines and solvents on the rate of dissociation of urethans, eight amines such as di-*n*-butyl amine and benzyl amine and ten inert solvents such as nitrobenzene and cumene were used. It was observed that the rates of the dissociation increased as the base strength of amines increased and the rates increased also as the dielectric properties of solvents increased.

The rates of dissociation of *N*-phenyl-phenyl carbamates substituted with methyl, methoxyl, chloro and nitro groups in the ortho, meta and para positions were determined to clarify the effects of substituents on the dissociation of urethans in amines. The results show that meta and para substituted *N*-phenyl-tolyl carbamates, N-phenyl-anisyl carbamates and unsubstituted urethans follow the Hammett equation with a positive $\rho$ value, but *N*-phenyl-chlorophenyl carbamates and *N*-phenyl-nitrophenyl carbamates dissociate rapidly and deviate from the linear relationship of the Hammett equation. Except in the case of the methyl derivative, ortho-substituted urethans dissociate faster than the corresponding meta and para substituted urethans; this may be attributed to steric effects.

It can be concluded that, in amine, the dissociation proceeds via the concerted mechanism involving both urethan and amine.

TABLE I. MELTING POINTS AND ANALYSES FOR $C_6H_5NHCOOC_6H_4R$

| R | M. p. °C | Nitrogen, % Calcd. | Found |
|---|---|---|---|
| *o*-Methoxy | 151～152 (136)[a] | 5.71 | 5.94 |
| *m*-Methoxy | 119 | 5.71 | 5.93 |
| *p*-Methoxy | 133 | 5.71 | 5.83 |
| *o*-Methyl | 143 (144)[b] | | |
| *m*-Methyl | 123～123.5 (125)[b] | | |
| *p*-Methyl | 114～115 (115)[b] | | |
| H | 126 (124)[c] | | |
| *o*-Chloro | 122～122.5 (120～121)[d] | | |
| *m*-Chloro | 124～125 | 5.65 | 5.95 |
| *p*-Chloro | 140～141 (138)[e] | | |
| *m*-Nitro | 129～129.5 (129)[f] | | |
| *p*-Nitro | 145～146 (147～148)[g] | | |

a) A. Morel, *Bull. soc. chim. France*, (3) **21**, 827 (1899).
b) E. Fromm and H. Eckhard, *Ber.*, **56**, 953 (1923).
c) R. Leuckart, *J. prakt. Chem.*, (2) **41**, 318 (1890).
d) A. Michael and P. Cobb, *Ann.*, **363**, 92 (1908).
e) A. Hantzsch and L. Mai, *Ber.*, **28**, 979(1895).
f) O. Brady and J. Harris, *J. Chem. Soc.*, **127**, 2176 (1925).
g) M. Busch, G. Blume and E. Pungs, *J. prakt. Chem.*, [2] **79**, 534 (1909).

## Experimental

**Procedure.** — The experimental procedure was essentially that used in the earlier investigation[2,3]. The amount of the amine remaining was determined by titrating with 0.025 N hydrochloric acid, using Bromocresol Green as indicator.

**Materials.** — N-phenyl-phenly carbamates were prepared from phenyl isocyanate and the purified corresponding phenols according to the procedure of Leuckart[4]. Amines and solvents were purified by distillation. The boiling points for these substances are listed in Table I and II.

TABLE II

| Amines | B. p. °C/mmHg | Solvents | B. p. °C/mmHg |
|---|---|---|---|
| Di-benzyl | 187/18 | Anisole | 153～154 |
| Benzyl | 89～90/12 | Tetralin | 92/18 |
| Cyclohexyl | 130.5～131 | Decarlin | 192 |
| Di-isobutyl | 139 | Nitrobenzene | 93/11 |
| 2-Ethylhexyl | 165～165.5 | Phenetole | 167～168 |
| Di-*n*-butyl | 158～159 | Triethyl-benzene | 104～155/20 |
| Lauryl | 133～134/15 | Cumene | 150～151 |
| *n*-Hexyl | 129 | Cymene | 174～176 |
| | | *o*-Xylene | 141.5～142 |
| | | *p*-Xylene | 137.5 |

## Results

The second order rate constant $k_2$ was calculated by Eq. 3

$$k_2 = 1/t \cdot x/a\ (a-x) \qquad (3)$$

where $t$, the time in second; $x$, the amount of reacted amine at time $t$; $a$, the initial concentration of both urethan and amine.

The values of the second order coefficient $k_2$ remained constant until the 60% of the dissociation with a tendency to drift upward in the later stage of the dissociation. It can be considered that the upward drift of $k_2$ might result from weak catalysis of the dissociation by urea or phenol produced. This was confirmed by the demonstration of the catalytic effect of added urea. The results are shown in Table III and Fig. 1. The addition of phenol to the reaction showed no effect on the rate of dissociation.

4) R. Leuckart, *J. prakt. Chem.*, [2] **41**, 318 (1890).

TABLE III. CATALYTIC EFFECT OF ADDED 1-PHENYL-3,3-DIBENZYLUREA ON THE DISSOCIATION OF *N*-PHENYL-PHENYL CARBAMATE IN BENZYL AMINE, BOTH 0.0535 mol./l. IN NITROBENZENE SOLVENT AT 94°C

| Urethan mol. | Urea mol. | $k_2\times10^3$ l. mol$^{-1}$ sec$^{-1}$ |
|---|---|---|
| 1 | 0 | 2.20 |
| 1 | 1 | 2.85 |
| 1 | 2 | 3.40 |

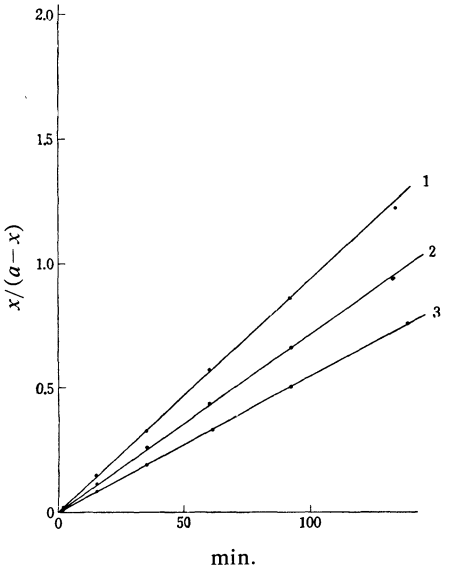



Fig. 1. Second-order plots of the thermal dissociation of *N*-phenyl-phenyl carbamate in benzyl amine and nitrobenzene in the presence or absence of 1-phenyl-3,3-dibenzylurea at 94°C.

| | Urethan, mol. | Urea, mol. |
|---|---|---|
| 1) | 1 | 2 |
| 2) | 1 | 1 |
| 3) | 1 | 0 |

The kinetic order of the dissociation of urethans in amines were examined further by changing the initial concentration of both the urethan and the amine. The second order rate constants are nearly constant when the initial concentration of the reactants are changed from 1/2 : 1/2 to 2 : 2. When the molar ratio of the initial concentration of urethan to amine are changed from 1 : 1 to 1 : 10, the rates of dissociation increase as the amine concentration increases. When the molar ratio of urethan to amine is less than 2.5, the rate did not conform to the second order kinetics, but a first order plot fits the data well. The $k_2$ values calculated by dividing the $k_1$ value thus obtained by the concentration of the amine are nearly equal as shown in Table IV.

TABLE IV. EFFECT OF VARIATION OF THE RELATIVE CONCENTRATION OF *N*-PHENYL-PHENYL CARBAMATE AND DI-*n*-BUTYL AMINE, BOTH 0.0535 mol./l. IN NITROBENZENE SOLVENT AT 25°C AND 45°C

| Temp. °C | Urethan mol. | Amine mol. | $k_1\times10^6$ sec$^{-1}$ | $k_2\times10^4$ l. mol$^{-1}$ sec$^{-1}$ |
|---|---|---|---|---|
| 25 | 1 | 1 | | 5.93 |
| | 2 | 2 | | 6.80 |
| | 1 | 2.5 | 8.24 | 6.16 |
| | 1 | 5 | 16.3 | 6.09 |
| | 1 | 7.5 | 23.5 | 5.85 |
| | 1 | 10 | 27.4 | 5.12 |
| 45 | 1/2 | 1/2 | | 31.2 |
| | 1 | 1 | | 27.0 |
| | 2 | 2 | | 35.6 |

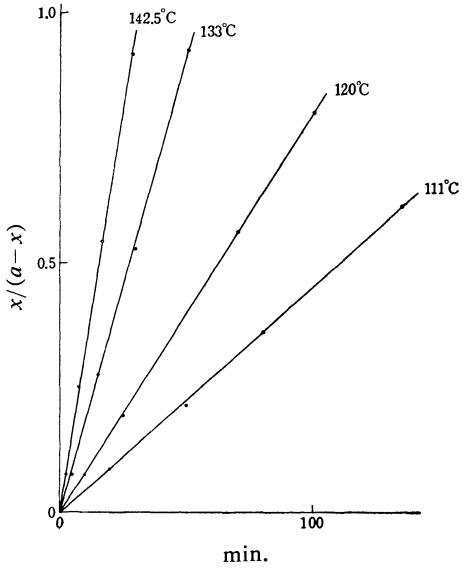



Fig. 2. Second-order plots of the thermal dissociation of N-phenyl-phenyl carbamate in dibenzyl amine and nitrobenzene.

The second order rate constants of various substituted urethans in amines and various inert solvents were obtained. As a typical run, the dissociation of *N*-phenyl-phenyl carbamate in dibenzyl amine and nitrobenzene at temperature betewen 111~142.5°C is shown in Fig. 2. The rate constants of the dissociation of *N*-phenyl-phenyl carbamates in amines were calculated by the method of least squares and are shown in Tables V—VII.

The plot of the logarithm of the rate constants vs. reciprocal absolute temperature gave satisfactory straight lines from which the activation energies and the entropies of activation were calculated by the method of least squares (Tables V—VII).

TABLE V. THE RATE CONSTANTS AND THE THERMODYNAMIC QUANTITIES FOR THE DISSOCIATION OF *N*-PHENYL-PHENYL CARBAMATE AND VARIOUS AMINES, BOTH 0.0535 mol./l. IN NITROBENZENE SOLVENT

| Amines | Temp. °C | $k_2\times10^3$ l. mol$^{-1}$ sec$^{-1}$ | $E$ kcal. | $\Delta S^{\neq}$ e. u. |
|---|---|---|---|---|
| Dibenzyl | 111 | 1.45 ±0.01 | 21.0±0.2 | −17.3±1.2 |
| | 120 | 2.52 ±0.02 | | |
| | 133 | 5.89 ±0.09 | | |
| | 142.5 | 11.2 ±0.03 | | |
| Benzyl | 94 | 2.21 ±0.03 | 19.2±0.4 | −18.6±2.5 |
| | 103 | 4.33 ±0.11 | | |
| | 113 | 8.04 ±0.00 | | |
| | 133 | 23.7 ±0.09 | | |
| *n*-Hexyl | 61 | 2.83 ±0.07 | 13.8±0.08 | −29.5±0.5 |
| | 70 | 5.08 ±0.01 | | |
| | 80 | 8.61 ±0.05 | | |
| | 89 | 14.3 ±0.13 | | |
| Cyclohexyl | 61 | 1.99 ±0.04 | 15.3±0.45 | −25.4±2.5 |
| | 70 | 3.53 ±0.01 | | |
| | 80 | 6.28 ±0.06 | | |
| | 89 | 12.1 ±0.09 | | |
| 2-Ethylhexyl | 61 | 1.37 ±0.03 | 15.2±0.16 | −26.6±0.9 |
| | 70 | 2.28 ±0.02 | | |
| | 80 | 4.30 ±0.06 | | |
| | 89 | 7.36 ±0.09 | | |
| Di-isobutyl | 61 | 1.05 ±0.00 | 15.6±0.33 | −25.6±1.9 |
| | 70 | 2.06 ±0.00 | | |
| | 80 | 4.04 ±0.02 | | |
| | 89 | 6.86 ±0.05 | | |
| Lauryl | 35 | 0.611±0.00 | 14.6±0.7 | −26.2±4.0 |
| | 45 | 1.05 ±0.08 | | |
| | 55 | 2.92 ±0.00 | | |
| | 80 | 12.2 ±0.00 | | |
| Di-*n*-butyl | 25 | 0.593±0.00 | 15.1±0.3 | −20.6±1.4 |
| | 35 | 1.36 ±0.00 | | |
| | 45 | 2.73 ±0.00 | | |
| | 60 | 8.75 ±0.00 | | |

## Discussion

The rate constants of the dissociation of urethans in various amines increase in the following order,

di-*n*-butyl ≫ lauryl > *n*-hexyl,

cyclohexyl > 2-ethylhexyl,

di-isobutyl > benzyl ≫ dibenzyl.

As noted in the above sequence, urethans dissociate rapidly in di-*n*-butyl amine ($K_b=2.05\times10^3$, at 25°C), moderately in cyclohexyl amine ($K_b=4.39\times10^4$, at 25°C) and slowly in benzyl amine ($K_b=2.4\times10^5$, at 25°C).

The activation energies of the dissociation of urethans in weak bases such as benzyl amine and dibenzyl amine are greater than those in strong bases such as di-*n*-butyl amine.

The results show that, in amines the rates of dissociation increase as the basicities of the amines increase and it can be concluded that the dissociation proceeds via the base catalyzed mechanism in which the process of deprotonation of urethans by a base is a predominant factor.

The rates of dissociation are also affected by the nature of inert solvents. The rate constant of dissociation in a polar solvent such as nitrobenzene is much larger than that in a non-polar solvent such as tetralin and *m*-xylene. As shown in the following sequence, the rates increase as the dielectric properties of solvent increase.

Nitrobenzene ≫ anisole, phenetole >

tetralin, decalin, *o*-xylene, cumene,

triethylbenzene, *m*-xylene, cymene

The results suggest an important solvent interaction in the dissociation process which may stabilize the forming phenoxyl ion and facilitate the cleavage of the carbon-oxygen bond in the activated state.

The results of the rate measurement given in Table VII show that for substitution in the *meta* and *para* position, the greater the electron-attracting power of the substituents, the greater

TABLE VI. THE RATE CONSTANTS AND THE THERMODYNAMIC QUANTITIES FOR THE DISSOCIATION OF *N*-PHENYL-PHENYL CARBAMATE AND DI-*n*-BUTYL AMINE, BOTH 0.0535 mol./l. IN VARIOUS SOLVENTS

| Solvent | Temp. °C | $k_2 \times 10^3$ l. mol$^{-1}$ sec$^{-1}$ | $E$ kcal. | $\Delta S^{\neq}$ e. u. |
|---|---|---|---|---|
| Decalin | 70 | 0.767±0.06 | 14.6±0.5 | −30.5±2.61 |
| | 80 | 1.30 ±0.01 | | |
| | 90 | 1.86 ±0.02 | | |
| | 100 | 4.24 ±0.01 | | |
| Tetralin | 70 | 0.900±0.00 | 15.2±0.1 | −28.5±0.53 |
| | 80 | 1.67 ±0.01 | | |
| | 90 | 3.06 ±0.76 | | |
| | 100 | 5.85 ±0.03 | | |
| Anisole | 70 | 1.96 ±0.01 | 15.0±0.5 | −27.6±2.95 |
| | 80 | 3.27 ±0.00 | | |
| | 90 | 6.01 ±0.00 | | |
| | 100 | 11.4 ±0.27 | | |
| Nitrobenzene | 25 | 0.593±0.00 | 15.1±0.25 | −20.6±1.4 |
| | 45 | 1.36 ±0.00 | | |
| | 60 | 2.73 ±0.00 | | |
| | 80 | 8.75 ±0.00 | | |
| Cumene | 80 | 1.31 ±0.06 | 17.4±1.6 | −22.6±8.8 |
| | 90 | 2.61 ±0.01 | | |
| | 100 | 5.09 ±0.00 | | |
| | 110 | 8.88 ±0.24 | | |
| Cymene | 80 | 1.01 ±0.01 | 17.3±0.3 | −23.5±1.0 |
| | 90 | 2.03 ±0.00 | | |
| | 100 | 3.93 ±0.06 | | |
| | 110 | 7.09 ±0.02 | | |
| Phenetole | 80 | 2.09 ±0.00 | 19.0±0.2 | −17.3±1.1 |
| | 90 | 4.28 ±0.02 | | |
| | 100 | 9.45 ±0.12 | | |
| | 110 | 17.3 ±0.27 | | |
| Triethylbenzene | 80 | 1.24 ±0.02 | 17.1±0.1 | −23.7±0.3 |
| | 90 | 2.45 ±0.02 | | |
| | 100 | 4.60 ±0.16 | | |
| | 110 | 8.42 ±0.19 | | |
| *o*-Xylene | 80 | 1.34 ±0.01 | 16.7±0.3 | −24.7±0.5 |
| | 90 | 2.62 ±0.04 | | |
| | 100 | 4.81 ±0.07 | | |
| | 110 | 8.36 ±0.12 | | |
| *m*-Xylene | 80 | 1.13 ±0.01 | 17.2±0.7 | −23.6±1.9 |
| | 90 | 2.17 ±0.02 | | |
| | 110 | 7.71 ±0.07 | | |

are the rate constants and the lower the activation energy; the greater the electron-donating power of the substituents, the lower are the rate constants and the greater the activation energy. The logarithm of the $k$ of the dissociation of methyl and methoxy substituted urethans and unsubstituted urethan is a linear function of the substituent constants given by Hammett and the gradient of the plot gave values for the reaction constant, $\rho$, of 1.72 in di-*n*-butyl amine and of 1.90 in benzyl amine, respectively. *N*-phenyl-chlorophenyl carbamate and *N*-phenyl-nitrophenyl carbamate dissociate very rapidly and deviate from the linear relationship of the Hammett equation.

The rates of dissociation of various substituted urethans in di-*n*-butyl amine are greater than those in benzyl amine and the activation energies and the entropies of activation in di-*n*-butyl amine are lower than those in benzyl amine. As mentioned above, the rates of dissociation depend on the basic strength of amine and the results might be attributed to the basicity of the amines which participate in the deprotonation of urethans in the dissociation process.

The higher rates with lower activation energies for the dissociation of urethans with electron-attracting substituents such as chloro and nitro groups may be ascribed to the stability of the phenoxyl ion dissociated. The phenoxyl ion with electron-attracting groups is

TABLE VII. THE RATE CONSTANTS AND THE THERMODYNAMIC QUANTITIES FOR THE DISSOCIATION OF *N*-PHENYL-PHENYL CARBAMATES AND AMINES, BOTH 0.044 mol./l. IN NITROBENZENE SOLVENT

a) In di-*n*-butyl amine:

| Substituents | Temp. °C | $k_2 \times 10^3$ l. mol$^{-1}$ sec$^{-1}$ | $E$ kcal. | $\Delta S^{\neq}$ e. u. |
|---|---|---|---|---|
| *o*-Methyl | 60 | 1.50 ±0.13 | 16.6±0.4 | −21.5±2.7 |
| | 70 | 3.48 ±0.18 | | |
| | 80 | 6.26 ±0.21 | | |
| | 90 | 12.2 ±0.53 | | |
| *m*-Methyl | 50 | 2.07 ±0.20 | 16.4±0.3 | −20.2±1.8 |
| | 60 | 3.48 ±0.17 | | |
| | 70 | 8.07 ±0.24 | | |
| | 80 | 17.7 ±0.00 | | |
| *p*-Methyl | 60 | 2.64 ±0.01 | 16.2±0.1 | −23.2±0.4 |
| | 70 | 6.42 ±0.13 | | |
| | 80 | 10.6 ±0.29 | | |
| | 90 | 20.1 ±0.92 | | |
| *o*-Methoxy | 40 | 5.27 ±0.14 | 13.1±0.2 | −21.1±1.1 |
| | 50 | 10.64 ±0.00 | | |
| | 60 | 19.3 ±0.51 | | |
| *m*-Methoxy | 70 | 1.95 ±0.20 | 15.8±0.2 | −20.3±1.4 |
| | 80 | 4.1 ±0.96 | | |
| | 90 | 6.76 ±0.43 | | |
| | 100 | 12.4 ±0.12 | | |
| *p*-Methoxy | 60 | 1.90 ±0.00 | 14.5±0.0 | −27.4±0.2 |
| | 70 | 3.60 ±0.15 | | |
| | 80 | 7.51 ±0.26 | | |
| | 90 | 11.65 ±0.28 | | |
| *o*-Chloro | 0 | 3.62 ±0.27 | 11.6±0.0 | −26.4±0.1 |
| | 15 | 17.8 ±1.3 | | |
| | 25 | 36.1 ±0.0 | | |
| | 35 | 66.0 ±0.22 | | |
| *m*-Chloro | 0 | 1.47 ±0.02 | 12.4±0.3 | −26.1±1.6 |
| | 15 | 4.50 ±0.82 | | |
| | 25 | 12.8 ±0.82 | | |
| | 35 | 19.6 ±0.02 | | |
| *p*-Chloro | 0 | 0.455±0.01 | 13.3±0.2 | −25.2±1.4 |
| | 15 | 1.02 ±0.08 | | |
| | 25 | 3.37 ±0.00 | | |
| | 35 | 7.45 ±0.07 | | |
| *m*-Nitro | | fast | | |
| *p*-Nitro | | very fast | | |

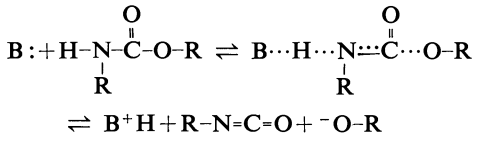
b) In benzyl amine:

| | | | | |
|---|---|---|---|---|
| *o*-Methyl | 110 | 2.40 ±0.32 | 21.4±0.91 | −15.4±4.5 |
| | 120 | 5.10 ±0.14 | | |
| | 140 | 21.5 ±1.03 | | |
| *m*-Methyl | 110 | 4.33 ±0.03 | 17.1±0.3 | −25.3±1.6 |
| | 120 | 7.97 ±0.02 | | |
| | 130 | 12.9 ±0.00 | | |
| | 140 | 22.7 ±0.01 | | |
| *p*-Methyl | 110 | 2.56 ±0.01 | 17.7±0.6 | −24.7±0.0 |
| | 120 | 4.20 ±0.02 | | |
| | 130 | 8.39 ±0.00 | | |
| | 140 | 13.2 ±0.02 | | |
| *o*-Methoxy | 100 | 8.70 ±0.06 | 19.1±1.4 | −15.5±7.2 |
| | 110 | 14.9 ±0.71 | | |
| | 120 | 37.5 ±0.85 | | |
| | 130 | 55.2 ±0.50 | | |

TABLE VII (continued)

| Substituents | Temp. °C | $k_2 \times 10^3$ l. mol$^{-1}$ sec$^{-1}$ | $E$ kcal. | $\Delta S^{\neq}$ e. u. |
|---|---|---|---|---|
| *m*-Methoxy | 100 | 7.3 ±0.64 | 16.8±0.5 | −24.2±2.3 |
| | 110 | 11.0 ±0.29 | | |
| | 120 | 18.5 ±0.65 | | |
| *p*-Methoxy | 110 | 2.72 ±0.17 | 20.7±0.7 | −16.8±3.8 |
| | 120 | 4.73 ±0.36 | | |
| | 130 | 9.60 ±0.28 | | |
| *o*-Chloro | 50 | 5.43 ±0.07 | 14.0±1.3 | −24.7±6.7 |
| | 60 | 12.7 ±0.41 | | |
| | 70 | 21.8 ±1.31 | | |
| | 80 | 49.8 ±0.98 | | |
| *m*-Chloro | 60 | 7.67 ±0.00 | 15.3±0.0 | −22.6±0.2 |
| | 70 | 15.2 ±0.00 | | |
| | 80 | 28.5 ±0.03 | | |
| | 90 | 71.9 ±1.11 | | |

more stable than that with electron-donating groups and this ion stabilizing effect may be the chemical driving force in the following dissociation mechanism.



The above one step mechanism involving urethan and amine can be confirmed by the rate dependency on both factors. In the strong bases, such as aliphatic amines, the dissociation proceeds by bimolecular concerted mechanism and not by termolecular mechanism as proposed in the previous reports[2,3].

## Summary

*N*-phenyl-phenyl carbamates dissociate into their component compounds very readily in the presence of a base. Unlike the case of *N*-phenyl-alkyl carbamates, *N*-phenyl-phenyl carbamates dissociate in the presence of an equimolar amount of an amine at lower temperature. The kinetics of the dissociation of *N*-phenyl-phenyl carbamates were of the first order with respect to carbamates and of the first order with respect to base.

The rate constants, the activation energies and the entropies of activation of the dissociation of *N*-phenyl-phenyl carbamates in various amines and solvents were measured throughout temperature interval 0～140°C.

The effects of amines, solvents and substituents on the dissociation of urethans in amines were studied.

The authors wish to express their hearty thanks to Professor Toshio Hoshino for his encouragement throughout the course of this experiment.

*Tokyo Institute of Technology*
*Meguro-ku, Tokyo*

# *Rates of Solvolysis of 2-Hydroxycyclohexyl Brosylates*

By Nobuo MORI

(Received February 10, 1960)

In the present paper there will be reported the preparation and the solvolysis rates of *cis*- and *trans*-2-hydroxycyclohexyl brosylates. The *cis* isomer used for solvolysis is a new substance and could not be prepared by the usual method[1]. The *cis* isomer has now been obtained in a good yield by the reaction of *cis*-cyclohexane-1, 2-diol with 2 to 3 equivalent quantities of *p*-bromobenzenesulfonyl chloride in dry pyridine.

The solvolysis rates were measured at 99.8°C in ethanol (98.5% by weight) and also in acetic acid containing a slight excess of acetic anhydride. In all cases, the observed rates, especially in ethanol, were of the first order and the error of the measurements was always lower than 5%. In acetolysis, one free hydroxyl group in each of the isomers will react with acetic acid to form 2-acetoxycyclohexyl brosylate, especially in the presence of *p*-bromobenzenesulfonic acid liberated during the solvolysis. Therefore, a calculated first order rate constant in a run in acetic acid will change continuously and gradually. However, the rates were nearly of the first order. Table I lists the data for a run with *trans*-2-hydroxycyclohexyl brosylate in acetic acid. It is seen that in the run the first order rate constant is almost constant. The slight increase of the rate the during run is probably attributed to the accompanying acetolysis of the corresponding acetoxy cyclohexyl brosylate formed.

TABLE I. ACETOLYSIS OF *trans*-2-HYDROXYCYCLOHEXYL BROSYLATE IN ACETIC ACID AT 99.8°C

| Time (min.) | Brosylate (mol./l.) | $k_1 \times 10^2$ ($min^{-1}$) |
|---|---|---|
| 0.0 | $6.16 \times 10^{-3}$ | |
| 30 | 3.36 | 2.02 |
| 50 | 2.20 | 2.06 |
| 70 | 1.49 | 2.02 |
| 90 | 0.91 | 2.12 |
| 110 | 0.051 | 2.26 |
| 150 | 0.016 | 2.44 |
| | Mean | 2.15 |

The rate constants and the relative rates for the isomeric brosylates are summarized in Table II.

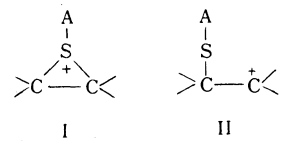
TABLE II. RATE CONSTANTS AND RELATIVE RATES FOR BROSYLATES AT 99.8°C

| 2-Substituent | $k_1 \times 10^2$, $min^{-1}$ EtOH | AcOH | $k_{cis}/k_{trans}$ EtOH | AcOH |
|---|---|---|---|---|
| *cis*-OH | 9.5 | 2.23 | 1.1 | 1.03 |
| *trans*-OH | 8.5 | 2.15 | | |
| *cis*-OAc | | 0.0058* | | |
| *trans*-OAc | | 3.1* | | |
| H | | ca. 11** | | |

* From data in Ref. 1

** Calculated from data at lower temperatures in Ref. 1

Generally, in solvolysis of 2-functionally substituted cyclohexyl brosylates and tosylates, the reaction rate of the *trans*-forms is larger than that of the *cis*-form. For example, the relative rates of acetolysis (at 75°C) of 2-acetoxycyclohexyl *p*-brosylates are in the following sequence[1]: unsubstituted(1.0) > *trans* (0.3) ≪ *cis*($1.31 \times 10^{-4}$). In those cases, with the *trans*-group, the reaction proceeds substantially by way of cyclic ion I, and with the *cis*-group, probably carbonium ion II.



I II

However, unlike those compounds, the reactivity of *cis*-2-hydroxycyclohexyl brosylate is slightly greater than that of the *trans*-isomer. Further, the rate constants for the brosylates are in the same order as that for unsubstituted cyclohexyl *p*-brosylate (see Table II). The slightly higher reactivity of the *cis*-isomer and the very small difference in reactivity between the *cis*- and *trans*-isomers can not be explained on the basis of the participation of hydroxyl group alone. The high reactivity of the isomers is probably due to the participation of the hydrogen atom in β-position similar to unsubstituted cyclohexyl brosylate, rather than due to that of hydroxyl group. The fact that the reactivity of the *cis*-isomer is higher than that of the *trans*-isomer is mainly due to steric acceleration based on 1*a*, 3*a*-interaction (or B-strain). Those facts are in good agreement

1) S. Winstein, E. Grundwald and L. L. Ingraham, *J. Am. Chem. Soc.*, **70**, 821 (1948).

with the behavior in solvolysis of 2-*tert*.-butylcyclohexyl *p*-tosylate[2].

## Experimental

**Samples and Solvents. *cis*-2-Hydroxycyclohexyl *p*-Brosylate.**—A solution of 0.5g. of *cis*-cyclohexane-1,2-diol (m. p. 97°C., prepared from cyclohexene in *tert*.-butanol with $OsO_4$[3]) in 2 cc. of dry pyridine was treated with 2.5 g. of *p*-bromobenzenesulfonyl chloride at 5 to 10°C. After 30 to 40 min. the mixture was diluted with cold 6N HCl and the oily product precipitated was triturated with dil. HCl repeatedly to solidify. After recrystallization from benzene and ligroin (b. p. 75~120°C), 0.7 g. of the *cis*-brosylate was obtained as brittle needles, m. p. 110.6°C.

Found: C, 42.93; H, 4.80. Calcd. for $C_{12}H_{15}O_4SBr$: C, 42.99; H, 4.51%.

***trans*-2-Hydroxycyclohexyl *p*-Brosylate** was obtained with a good yield from *trans*-cyclohexane-1,2-diol (m. p. 102~104°C., prepared from cyclohexene and hydrogen peroxide in formic acid[4]) in an analogous way to the *cis*-isomer. After recrystallization from benzene and ligroin, the *trans*-brosylate was obtained as needles, m. p. 108°C (reported 106.9~108.8°C[1]).

**Ethanol** (98.5% by weight).—Commercial reagent grade absolute ethanol was fractionally distilled.

**Acetic Acid.**—Reagent grade glacial acetic acid was crystallized twice by the freezing method, refluxed with 2% by weight of acetic anhydride and 1% by weight of anhydrous sodium acetate for 3 hr., and distilled.

**Procedure for Rate Measurements**[5].—The sample was weighed out and made up to volume in the solvent at 15~20°C. About 6~7 cc. portions were sealed in tubes and immersed in vapor over boiling water (99.8°C). Time was counted from immersion of the tube to its removal and quenching in ice-water. After being cooled the tube was allowed to come to room temperature and then opened, a 5 cc. aliquot was pippetted out and titrated with standard base from a 2 cc. microburet. Concentrations of brosylates (all given at room temperature) were in the range from 0.02 to 0.07 mol./1. and titrations in acetic acid were carried out with a 0.05 N standard solution of AcONa in acetic acid with Bromophenol Blue as indicator, and in ethanol, a 0.05 N standard aquous solution of NaOH was used for titration with phenolphthalein as indicator. Rate constants were calculated from the formula

$$k_1 = 1/t \cdot \ln a/(a-x)$$

in which $a$ was the initial concentration of brosylate and $x$ was the concentration of sulfonic acid at time $t$.

The author expresses his sincere thanks to Professor Y. Tsuzuki for his advice and to Mr. M. Watanabe who prepared the diols used as starting materials.

*Department of Chemistry*
*Tokyo College of Science*
*Kagurazaka, Shinjuku-ku*
*Tokyo*

2) H. L. Goering and R. L. Reeves, *J. Am. Chem. Soc.*, **78**, 4931 (1956).
3) N. A. Milas and S. Sussman, ibid., **59**, 2345 (1937).
4) Organic Synthesis, Vol. 28, p. 35 (1948).
5) N. Mori, *J. Chem. Soc. Japan, Pure Chem. Sec. (Nippon Kagaku Zasshi)*, **80**, 1458 (1959).

# SHORT COMMUNICATIONS

## *Reaction of* DL-*Threonine with Recoil Tritium Atoms*

By Yoshishige SATO, Teruhiko MESHI and Tadao TAKAHASHI

(Received April 28, 1960)

Using recoil tritium atoms from the $^{6}Li(n, \alpha)$ $^{3}H$ reaction, the studies on preparation of tritium labeled organic compounds have been carried out by Wolfgang[1], Rowland[2,3] and other investigators. In 1959, Kay, Malson and Rowland[4] investigated recoil tritium reaction with L-alanine having asymmetric carbon atom. They described that the tritium activity which is found on the $\alpha$-carbon is, within error, all in the L(+) form—the substitution reaction proceeds with retention of configuration, and no racemization or inversion occurs. This result is in accord with the essential absence of labeled galactose in irradiated crystalline glucose[5]. We have carried out the same experiments using DL-threonine and found the isomer (allo form) of it. The procedure is as follows.

A mixture of 2 g. DL-threonine and 1 g. lithium carbonate was irradiated with thermal neutron for 17 hr. at flux $2.5 \times 10^{11}$ n/cm$^2$ sec. After irradiation the mixture was somewhat brownish. It was dissolved in water. To the aqueous solution was added basic copper carbonate. After filtering off the unchanged basic copper carbonate, the filtrate was concentrated in vacuo. Alcohol was added and thus crystals of amino acid copper salt were obtained. This amino acid copper salt was dissolved in water and to the solution an aqueous solution of hydrogen sulfide was added until the blue color disappeared. The precipitated cupric sulfide was removed by filtration, and the filtrate was concentrated. By the addition of alcohol to the concentrated solution, white crystals were obtained with yield of 800 mg. (sp. act. 0.113 $\mu$c/mg.).

Paper chromatography of the crystal using *n* - butanol - acetone - concentrated ammonium hydroxide-water (50 : 6.3 : 6.2 : 37.5, upper phase) as developing solvent showed three spots on spraying with ninhydrine. $R_f$ values of three spots were identical with those obtained by pure DL-threonine (0.24), allo-threonine (0.17) and glycine (0.05), respectively. The product (120 $\mu$g.) was employed as sample of paper chromatography, and DL-threonine, allo-threonine and glycine were obtained in the amounts and with activity values as shown in Table I.

TABLE I. SPECIFIC ACTIVITY OF VARIOUS AMINO ACIDS SEPARATED FROM IRRADIATED DL-THREONINE

| | Activity (cpm) | Amount ($\mu$g.)* | Sp. act. $\mu$c/mg. |
|---|---|---|---|
| DL-Threonine | 961 | 65 | 0.082 |
| allo-Threonine | 138 | 7 | 0.108 |
| Glycine | 80 | 40 | 0.011 |

* Paper chromatographic yield from 120 $\mu$g. of the irradiated product.
** Approximate calculation.

In order to determine whether or not the inversion occurs at neutron irradiation, the blank test of the chemical purification described above was carried out, but allo-threonine was not detected. Under the consideration that DL-threonine is heated in the atomic reactor, the mixture of DL-threonine and lithium carbonate was heated at about 70°C for 17 hr. in an electric oven. However, in this experiment, allo-threonine could not be discovered.

*Osaka Research Laboratory*
*Tanabe Seiyaku Co., Ltd.*
*Kashima, Higashiyodogawa-ku*
*Osaka*

1) D. S. Urch and R. Wolfgang, *J. Am. Chem. Soc.*, 81, 2025 (1959).
2) F. S. Rowland and R. Wolfgang, *Nucleonics*, 14, (8) 58 (1956).
3) J. K. Lee, B. Musgrave and F. S. Rowland, *J. Am. Chem. Soc.*, 81, 3803 (1959).
4) J. G. Kay, R. P. Malsan and F. S. Rowland, *J. Am. Chem. Soc.*, 81, 5050 (1959).
5) H. Keller and F. S. Rowland, *J. Phys. Chem.*, 62, 1373 (1958).

# *Estrogenic Biphenyls. IX*[1]. *Optical Resolution and Estrogenic Activity of 4'-(1-Hydroxypropyl)-4-methoxybiphenyl*

By Takeo SATO, Ken-ichi SASAMORI and Michinori ŌKI*

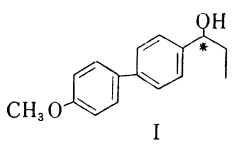
(Received July 5, 1960)

As reported in the preceding paper of this series[1], (4'-1-hydroxypropyl)-4-methoxybiphenyl (I) was moderately estrogenic when injected subcutaneously to ovariectomized mice. Since the location of the hydroxyl group attached to the asymmetric carbon atom in compound I corresponds to that of $C_{17}$-OH of estradiol (II) when the former is regarded as an aromatized BD-ring-lacking model of the latter, it has become of particular interest to examine the estrogenic activity of optically active form of compound I in comparison with the activities of epimeric estradiols, of which 17-$\beta$ isomer represents more active form, being about 40 times more active than 17-$\alpha$ isomer.

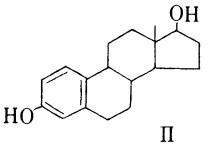
* Present address: Department of Chemistry, Faculty of Science, The University of Tokyo, Hongo, Tokyo.

1) Part VIII: T. Sato, This Bulletin, 33, 5 (1960).

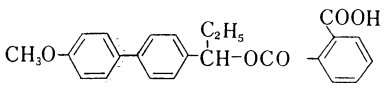
(±)-4′-(1-Hydroxypropyl)-4-methoxybiphenyl (I)[1] was treated with phthalic anhydride in pyridine to produce (±)-4′-(1-hydroxypropyl)-4-methoxybiphenyl hydrogen phthalate (III), m. p. 164~165°C (Found: C, 76.64; H, 5.50. Calcd. for $C_{24}H_{21}O_5$: C, 76.58; H, 5.44%). It was converted into strychnine salt, which afforded a well crystallized optically active salt, m. p. 187~188.5°C (Found: N, 3.86. Calcd. for $C_{45}H_{44}N_2O_7$: N, 3.86%) with $[\alpha]_D^{18}$ −69.0° (*C*=2, 95% ethanol) through several recrystallization from ethanol. Combined mother liquors contained an oil which resisted attempts to induce crystallization.




I




II




III

The crystalline strychnine salt was treated with dilute hydrochloric acid to produce (+)-III, m. p. 149~153°C (Found: C, 76.10; H, 5.45. Calcd. for $C_{24}H_{21}O_5$: C, 76.58; H, 5.44%) having $[\alpha]_D^{17}$ +24.9° (*C*=2, 95% ethanol). Levorotatory alcohol (−)-I, m. p. 99~101.5°C (Found: C, 79.42; H, 7.65. Calcd. for $C_{16}H_{18}O_2$: C, 79.31; H, 7.49%) with $[\alpha]_D^{14}$ −23.7° (*C*=2, 95% ethanol) was thus produced by the alkaline hydrolysis of (+)-III.

An attempt to obtain another alcohol with the opposite sign of rotation through cinchonine salt of the hydrogen phthalate III, m. p. 153~155.5°C, obtained by the hydrolysis of the oily strychnine salt mentioned above, failed owing to the unfavorable crystallizability of the salt.

Compound (−)-I, which was found to be active only in 20% of the test animals (ovariectomized mice) at the does of 200 $\gamma$, had weaker estrogenic activity than (±)-I as the latter was active in 80% of the animals at the same level[1]. Although the reason why dextro- and levorotatory 3,4-bis-(*p*-hydroxyphenyl)-hexanes show different estrogenic potencies[2] is still obsure, the present finding which suggests that the levorotatory isomer is the poorer estrogen may be attributed to the absolute configuration about the carbon atom which carries the hydroxyl group.

*Department of Chemistry*
*Faculty of Science*
*Tokyo Metropolitan University*
*Setagaya-ku, Tokyo*

2) F. v. Wessely and H. Welleba, *Ber.*, **74**, 777 (1941).

# *Absorption Spectra of Methylene Blue Adsorbed on Homoionic Bentonites Suspended in Water*

By Choei SATO

(Received June 18, 1960)

The changes of the spectra of dyes added to some colloidal solutions are well-known as metachromasy. When some powdered materials usually used as adsorbents are suspended in water and dye solutions are added to them, color changes of the dye are also frequently observed if the dyes have the possibility ready to be adsorbed by those materials. In order to investigate if any relations exist between the trend of color changes of the dyes adsorbed and the surface structures of powdered materials used, the experiments have been carried out by using some kinds of clay minerals and silica gel, etc.[1] An interesting phenomenon has been observed in montmorillonite-methylene blue system; that is, the spectrum of the dye adsorbed on montmorillonite changes gradually with lapse of time after mixing of them. Furthermore this color change is influenced remarkably according to the kinds of added cation[2]. In order to clarify this phenomenon more thoroughly, the absorption

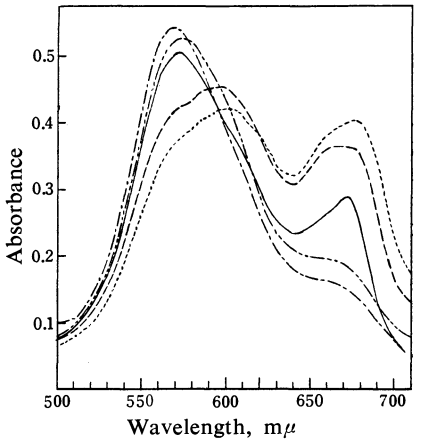



Fig. 1. Absorption spectra of methylene blue adsorbed on homoionic bentonites, after an hour from mixing.

—— Na-; -·-·- Ca-; -··- H-; ---- K-; ------ $NH_4$-bentonite

1) C. Sato, "Advances in Clay Science" Vol. 2, Edited by the Clay Research Group of Japan, Gihodo, Tokyo (1960), p. 69.

2) C. Sato, ibid. Vol., 3, in press; N. E. Vedeneeva, *Chem. Abstr.*, **49**, 4405$^b$ (1955).

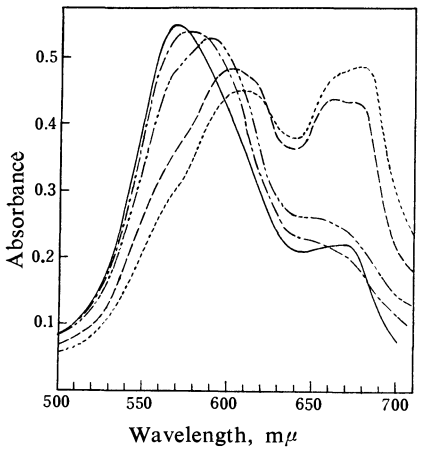



Fig. 2. Absorption spectra of methylene blue adsorbed on homoionic bentonites, after 2 days from mixing.

—— Na-; -·-·- Ca-; -·-· H-; ---- K-; ------ $NH_4$-bentonite

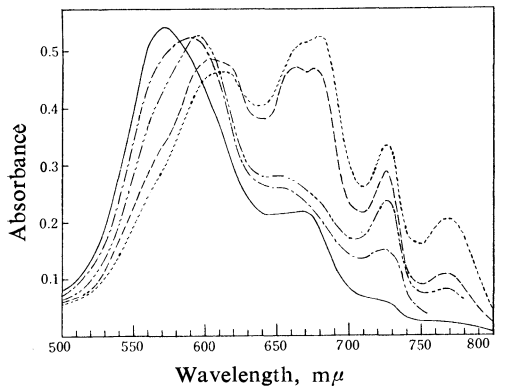



Fig. 3. Absorption spectra of methylene blue adsorbed on homoionic bentonites, after 7 days from mixing.

—— Na-; -·-·- Ca-; -·-· H-; ---- K-; ------ $NH_4$-bentonite

spectra of methylene blue adsorbed on homoionic bentonites suspended in water and having exchangeable cations of hydrogen, sodium, potassium, ammonium and calcium, have been observed.

Homoionic bentonite suspensions were prepared according to the method of Slabaugh, etc.[3] In each run 10 ml. of this suspension (0.13%) was divided into two equivalent parts, to one of which was added 0.5 ml. of the dye solution of a definite concentration, $1.74 \times 10^{-4}$ mol./l., and to the other was added the equivalent amount of distilled water. Then the absorption spectrum of the former was measured with reference to the latter with a spectrophotometer, after about an hour from the addition of dye. Furthermore, the change of spectrum of the above system with longer lapse of time was also examined. The results obtained are indicated in Figs. 1, 2 and 3.

As seen in the figures, in potassium and ammonium bentonites, the band at 570 mμ decreases its intensity remarkably, and the broad bands at 600~620 mμ and 660~680 mμ, especially the latter, increase their absorbance markedly, with lapse of time. The bands at 725 mμ and 770 mμ become also apparent gradually. But in hydrogen and calcium bentonites the above change appears considerably slowly and in sodium one any change is scarcely observed in the spectrum which shows a strong band at 570 mμ and a weak one at 670 mμ. According to the view reported in literature[4] for the interpretation of absorption spectrum of methylene blue dissolved in water, it may be presumed that in ammonium and potassium clays a greater part of dye adsorbed initially in associated form on the outer surface of clay particle migrates easily to the firm binding of the unassociated dye ion on the interlayer surface, but in sodium, calcium and hydrogen clays, especially in sodium type, this migration is impeded. It is also assumed that these differences by the kinds of exchangeable cations may result from the correlation between the arrangement of water molecules adsorbed on interlayer surface and surrounding the hydrated cation, and the size of methylene blue ion. But any quantitative interpretation has not been attempted yet. The interpretation of appearance of the bands at 725 and 770 mμ has also been left unsolved.

*Department of Chemistry*
*Faculty of Literature and Science*
*Hirosaki University*
*Hirosaki*

3) W. H. Slabaugh and R. H. Siegel, *J. Phys. Chem.*, 60, 1105 (1956).

4) M. Schubert and A. Levine, *J. Am. Chem. Soc.*, 77, 4197 (1955).

## *Synthesen von N-(4-Pyridyl)glycine*

Von Masaki OHTA und Mitsuo MASAKI

(Eingegangen am 6. Juli, 1960)

Bei der Umsetzung von 3-Aminopyridin und 2-Aminopyridin mit Bisulfitverbindungen von Aldehyden und Alkalicyanid wurden die entsprechenden Glycine, *N*-(3-Pyridyl)glycine[1] und *N*-(2-Pyridyl)glycine[2] erhalten.

Weiter durch diesen Methode haben wir aus 4-Aminopyridin *N*-(4-Pyridyl)glycin und seine Derivate erhalten können.

Bei der Einwirkung von Bisulfitverbindung von Formaldehyd und Kaliumcyanid auf 4-Aminopyridin erhält man ein rotes Öl, das 4-Pyridylglycinnitril zu sein schient und beim Kochen mit Salzsäure *N*-(4-Pyridyl)glycin ergibt. Das letztere wird durch Einwirkung von Natriumnitrit in *N*-nitroso-*N*-(4-Pyridyl) glycin umgewandelt. Um 3-(4-Pyridyl)-sydnon darzustellen, versuchten wir Cyclisierung-Reaktion von der Nitrosoverbindung.

Wenn man die Nitrosoverbindung in Essigsäureanhydrid erwarmt, so erhält man farblose Nadeln von Schmp. 144~145°C, die aber nicht Sydnon, $C_7H_5O_2N_3$, sind. Sondern das Produkt zeigt sich durch Elementaranalyse eine Bruttoformel, $C_{10}H_{13}O_2N_3$, dessen Konstitution wir noch jetzt untersuchen.

In ähnlicher Weise reagiert 4-Aminopyridin mit Bisulfitverbindung von Benzaldehyd und Kaliumcyanid, und ergibt ein rotes Öl, woraus *N*-(4-Pyridyl)-phenylglycine durch Kochen mit Salzsäure dargestellt werden kann.

### Beschreibung der Versuche

**Salzsaures *N*-(4-Pyridyl)glycin.** — Man versetzt 4 g von 37 proz. Formalin mit einer Lösung von 5.2 g Natriumbisulfit in 10 ccm Wasser, erhitzt 0.5 Std auf dem Wasserbad und darauf versetzt mit 4.7 g 4-Aminopyridin. Nach 1.5 std. Erhitzen und Umrühren setzt man dazu 3.5 g Kaliumcyanid in wenigem Wasser zu. Das Gemisch wird unter mechanischem Rühren 2 Std auf dem Wasserbad erhitzt, noch 1 Std bei Raumtemperatur umrührt und dann unter vermindertem Druck eingedampft. Der Rückstand wird mit Äthanol ausgezogen, nach dem Abdampfen des Äthanol ergibt die Lösung ein rotes Öl. Man löst das Öl in 30 ccm von 1 : 1 HCl, erhitzt auf dem Wasserbad und nach 3 std. Erhitzen läßt bei Raumtemperatur stehen, bald scheiden sich 2.8 g Nadeln ab. Aus die Mutterlauge erhält man noch 1.6 g Salzsäuresalz. Farblose Nädelchen von Schmp. 255~256°C (aus Wasser).

$C_7H_8O_2N_2 \cdot HCl$

Ber. C 44.56 H 4.77 N 14.85
Gef. C 44.28 H 4.94 N 14.86

***N*-Nitroso-*N*-(4-pyridyl)glycin.** — Man löst 3.7 g salzsaures *N*-(4-Pyridyl)glycin in 40 ccm Wasser, fügt langsam 1.6 g Natriumnitrit unter Eiskühlung und Umrühren hinzu und läßt im Eisschrank stehen. Nach 30 std. Stehen wird der ausgefallene farblose Niederschlag abfiltriert. Ausb. 3 g. Farblose Nädelchen vom Schmp. 202°C (aus Wasser) zeigen Liebermannsche Reaktion.

$C_7H_7O_3N_3$

Ber. C 46.41 H 3.90 N 23.20
Gef. C 46.56 H 4.14 N 23.22

***N*-(4-Pyridyl)phenylglycin.**—Zur Lösung von 10.4 g Natriumbisulfit in 40 ccm Wasser gibt man 10.6 g Benzaldehyd, erhitzt 1 Std auf dem Wasserbad und dann fügt 9.4 g 4-Aminopyridin hinzu. Nach 2 std. Erhitzen setzt man dazu 7 g Kaliumcyanid gelöst in 20 ccm Wasser zu und rührt 2 Std bei Raumtemperatur und dann 0.5 Std auf siedendem Wasserbad. Das abgeschiedene gelbrote Öl wird mit Chloroform ausgeschüttelt und mit Natriumsulfat getrocknet. Das nach dem Abdampfen des Chloroforms zurückbleibende rote Öl löst man in 70 ccm von 1 : 1 HCl, erhitzt 4 Std auf dem Wasserbad und dann läßt die Lösung bei Raumtemperatur stehen. Nach einer Nacht wird der ausgefallene Niederschlag abfiltriert, im Wasser gelöst und dann mit Natriumbicarbonat neutralisiert. Bald fällt ein farblose Niederschlag aus, der zusammen mit dem durch Neutralisierung von die erste Mutterlauge erhaltenen Niederschlag aus Wasser in Nadeln vom Schmp. 240°C umkristallisiert wird, die zur Analyse 4 Std bei 100°C in Vakuum getrocknet wird.

$C_{13}H_{12}O_2N_2$

Ber. C 68.41 H 5.30 N 12.27
Gef. C 68.71 H 5.57 N 12.44

Herrn Asaji Kondo danken wir bestens für seine Ausführung der Mikro-analyse.

*Organisch-Chemisches Laboratrium*
*Technische Hochschule zu Tokyo*
*Meguro-ku, Tokyo*

1) M. Ohta und M. Masaki, Dieses Bulletin, **33**, 649 (1960).
2) M. Ohta und M. Masaki, ebenda, **33**, im Druck.

# *Oxidation of Terpene Compounds with tert-Butyl Chromate. VI. Oxidation of Terpinolene*

By Tamon MATSUURA, Kozo SAITO and Yasuo SHIMAKAWA

(Received February 4, 1960)

On oxidation of terpene hydrocarbons with *tert*-butyl chromate[1-5] it was recognized that the active methylene group adjacent to a double bond in a molecule was mainly oxidized to $\alpha, \beta$-unsaturated carbonyl. Among diene terpene hydrocarbons, only D-limonene has been researched and the oxidation products were rather more complicated than in the cases of $\alpha$-pinene[1,5], D-carvomenthene[2,5] and D, L-$\alpha$-terpinyl acetate[4]; D-limonene was oxidized to D, L-carvone, D-isopiperitenone, piperitenone and carvacrol. This report is concerned with the oxidation of terpinolene (I) which has an active methylene group at $C_{(3)}$ position situated between two double bonds.

## Results and Discussion

The oxidizing agent was prepared in a manner similar to that in the previous reports[3,4] from chromic anhydride and *tert*-butyl alcohol, glacial acetic acid and acetic anhydride being added.

Experiment 1.—The mole ratio of sample to chromic anhydride was 1 to 2. After the reaction was carried out at 10°C during 15 hr., the reaction mixture which resulted was treated with water and oxalic acid under ice-cooling to decompose the excess of the oxidant. Then the mixture was separated into a benzene and an aqueous layer. From the benzene layer was obtained a neutral brown oil which was fractionated and the constituents of which were identified.

Experiment 2.—The mole ratio of sample to chromic anhydride was 1 to 2, and the reaction was carried out at 10°C during 45 hr. The reaction mixture was treated in the same manner as in Experiment 1.

Experiment 3. — In this experiment glacial acetic acid and acetic anhydride were excluded from the oxidant. This is not the case in Experiments 1 and 2. When the oxidant was added to the sample solution at 0°C during 2 hr., the reaction was stopped and the reaction products were examined.

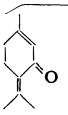
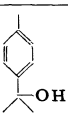
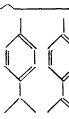
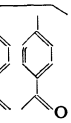
In the case of each of the above three experiments, piperitenone (II), 8-hydroxy-*p*-cymene (III), *p*-cymene (IV) and $\alpha$,*p*-dimethylstyrene (V) were identified as constituents of the reaction products, and an unidentified carbonyl compound was also recognized.

Experiment 4.—*p*-Cymene was treated with *tert*-butyl chromate under the same condition as in Experiment 1, and small amounts of 8-hydroxy-*p*-cymene and *p*-methylacetophenone were identified as reaction products.

The above results are summarized in Table I.

In the oxidation of terpinolene with *tert*-butyl chromate, the point different from the oxidation of the other cyclic terpene compounds already reported is the aromatization of the hydroaromatic ring by dehydrogenation in addition to the oxidation of the active methylene group adjacent to a double bond. On oxidation of D-limonene and D, L-$\alpha$-terpineol it has been clarified that among two active methylene

TABLE I

| No. of Experiment | Sample | Reaction condition: Sample : $CrO_3$ mole ratio | $CH_3COOH$ wt. % to sample | $(CH_3CO)_2O$ wt. % to sample | Temp. °C | Time hr. | Reaction product wt. % to sample:  |  |  |  |  |
|---|---|---|---|---|---|---|---|---|---|---|---|
| 1 | Terpinolene | 1 : 2 | 17 | 17 | 10 | 15 | 6 | 8 | 1 | 2 | 0 |
| 2 | Terpinolene | 1 : 2 | 50 | 50 | 10 | 45 | 11 | 6 | 2 | 3 | 0 |
| 3 | Terpinolene | 1 : 2 | 0 | 0 | 0 | 2 | 4 | 4 | 2 | 1 | 0 |
| 4 | *p*-Cymene | 1 : 2 | 17 | 17 | 25 | 15 | 0 | 0.8 | — | 0 | 0.2 |

1) T. Matsuura and K. Fujita, *J. Sci. Hiroshima Univ.*, **A16**, 173 (1952).
2) K. Fujita and T. Matsuura, ibid., **18**, 455 (1955).
3) K. Fujita, *J. Chem. Soc. Japan, Pure Chem. Sec.* (*Nippon Kagaku Zasshi*), **78**, 1112 (1957).
4) T. Matsuura, T. Suga and K. Suga, ibid., **78**, 1122 (1957).
5) G. Dupont, R. Dulou and O. Mondou, *Bull. soc. chim. France*, **1953**, 60.

groups adjacent to a double bond in the carbon ring the $C_{(6)}$ active methylene is predominantly oxidized in comparison with the $C_{(3)}$ active methylene. In the case of terpinolene, however, it was found that the oxidation of the $C_{(3)}$ active methylene has proceeded in exclusion of the oxidation of the $C_{(6)}$ active methylene, owing to the existence of a double bond between $C_{(4)}$ and $C_{(8)}$ atoms.

The formation of piperitenone II from terpinolene I by the oxidation of the $C_{(3)}$ active methylene is an analogous reaction to the formation of $\alpha,\beta$-unsaturated ketone from cyclic terpene compounds such as $\alpha$-pinene, limonene, carvomenthene and $\alpha$-terpinyl acetate reported already. However the formation of 8-hydroxy-*p*-cymene III and *p*-cymene IV from terpinolene is due to oxidation of the $C_{(8)}$ position and dehydrogenation, which was found for the first time in the oxidation of terpinolene. An exocyclic double bond between $C_{(4)}$ and $C_{(8)}$ carbons in terpinolene seems to migrate into the carbon ring in the presence of acid to form $\alpha$-terpinene[6]. It has been reported that menthene-4(8) is rearranged into menthene-3 by the action of dilute sulfuric acid solution[7]. Thus it may be considered that an exocyclic double bond of terpinolene molecule migrates into the ring to form a conjugated diene ($\alpha$-terpinene) by acid reagent. Although $\alpha$-terpinene was not found in the reaction products, it has reacted easily with *tert*-butyl chromate to produce a large amount of *p*-cymene*[1]. Therefore *p*-cymene in the reaction products is considered to be produced by dehydrogenation of $\alpha$-terpinene which results from isomerization of terpinolene.

It would seem that 8-hydroxy-*p*-cymene has been formed from *p*-cymene by the oxidation of an active methine group at $C_{(8)}$. But this is not the case, because the result of the oxidation of *p*-cymene with *tert*-butyl chromate in the same conditions as in Experiment 1 (sample, terpinolene) has shown that *p*-cymene is virtually stable against *tert*-butyl chromate, giving only a small amount (1% to the sample) of 8-hydroxy-*p*-cymene and of *p*-methylacetophenone.

Accordingly it can not be considered that 8-hydroxy-*p*-cymene is formed via *p*-cymene.

It has been recognized that on distillation of 8-hydroxy-*p*-cymene in presence of acid (a small amount) $\alpha,p$-dimethylstyrene is produced by dehydration[8], so $\alpha,p$-dimethylstyrene is considered to be a secondary product formed by dehydration during the oxidation reaction or distillation of the reaction products.

On the basis of the above results and discussion the reaction course is summarized as shown in Fig. 1.

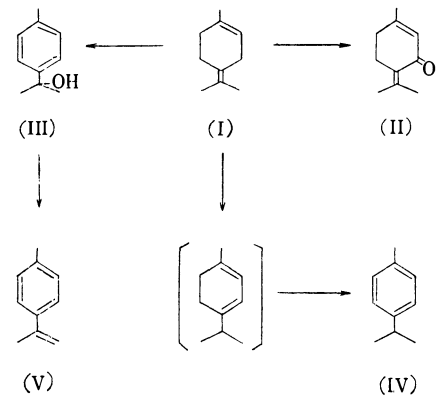



Fig. 1

## Experimental

### 1. Oxidation of Terpinolene

#### 1.1. Preparation of Terpinolene

Terpinolene (b. p.$_{21}$ 78.0°C, $n_D^{25}$ 1.4859, $d_4^{25}$ 0.8577, tetrabromide m. p. 116°C) was prepared, according to Charalton and Day's method[9] by treating $\alpha$-pinene (b. p.$_{28}$ 58~59°C, $n_D^{25}$ 1.4628, $d_4^{25}$ 0.8548, $[\alpha]_D$ +40.62°) with 50% alcoholic solution of sulfuric acid, and by rectifying the crude product.

#### 1.2. Oxidation and Identification of Reaction Products

##### 1.2.1. Experiment 1

*tert*-Butyl chromate was prepared by adding 88 g. of chromic anhydride in small portions to 163 g. of *tert*-butyl alcohol under ice-cooling, diluting the resultant with 650 g. of benzene, and drying the resulting benzene solution on anhydrous sodium sulfate. To the solution were added 10 g. of glacial acetic acid and 10 g. of acetic anhydride just prior to the oxidation. This oxidant was added dropwise with stirring at 10°C to 60 g. of terpinolene in 60 g. of dry benzene during 1 hr., and the mixture was left to stand at 10°C for 15 hr. Then 700 cc. of water and 160 g. of oxalic acid were added under ice-cooling to the viscous reaction mixture and shaken to decompose the excess of the oxidant. The mixture was separated into a benzene layer and an aqueous one, and the latter was extracted with benzene. The combined benzene solution was washed with 10% aqueous solution of sodium carbonate and with water successively, and dried (anhydrous sodium sulfate). After removal of the solvent, 28.1 g. of a neutral brown oil was obtained.

The aqueous solution was neutralized with a sodium carbonate solution and extracted with chloroform. From the extract 7.9 g. of a dark-brown viscous oil was obtained. The sodium carbonate solution was acidified with 10% sulfuric acid solution and

6) O. Wallach, *Ann.*, **275**, 103 (1893).
7) O. Wallach, *Ber.*, **39**, 2504 (1906); *Ann.*, **360**, 70 (1908).
*1 T. Matsuura, unpublished.
8) J. N. Borglin, D. A. Lister, E. J. Lorand and J. E. Reese, *J. Am. Chem. Soc.*, **72**, 4591 (1950).
9) R. W. Charalton and A. R. Day, *Ind. Eng. Chem.*, **29**, 92 (1937).

extracted with chloroform, giving 18.9 g. of a dark-brown viscous oil. As neither of the above dark-brown viscous oils could be distilled under reduced pressure and also could not be crystallized, they seemed to be polymer, the further test of which was not undertaken.

The neutral oil was fractionated, giving the physical properties of Fig. 2, and then the constituents of fractions were identified.

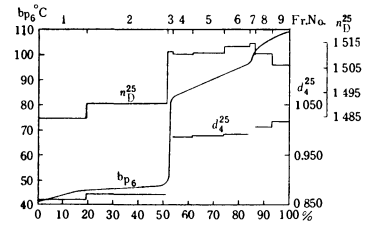



Fig. 2

(i) *p*-Cymene and $\alpha,p$-Dimethylstyrene. Fractions 1 and 2 gave a tetrabromide of m. p. 116°C which was identified as terpinolene tetrabromide by admixture with an authentic sample. On the other hand, the ultraviolet absorption spectra of these two fractions showed the absorption maxima at 247 and 273 m$\mu$ which coincide with those of $\alpha,p$-dimethylstyrene (247 m$\mu$)[10] and *p*-cymene (273 m$\mu$)[11].

Ozone was passed in a solution of 5 g. of the combined fractions 1 and 2 dissolved in 20 cc. of ethyl acetate-glacial acetic acid (6 : 2) under ice-cooling. The ozonized solution, after the solvent having been driven off under reduced pressure and 50 cc. of water being added, was steam-distilled to decompose the ozonide. The distillate was extracted with ether, and the ether extract was washed with 10% aqueous sodium carbonate solution and dried. From the ether extract thus treated, 2.1 g. of an oily product was obtained, after the solvent was driven off. The oily product was eluted through a silica gel column with petroleum benzine and ether successively, and the following two fractions, A and B, were obtained.

| Fraction | Yield (g.) | $\lambda_{max}$ (m$\mu$) (absorptivity $a$*2) |
|---|---|---|
| A | 1.20 | 254(1.42), 260(2.35), 265(2.86), 267(2.95), 273(3.34) |
| B | 0.67 | 252(68.90) |

Fraction A (b. p.$_{15}$ 62~64°C, $n_D^{25}$ 1.4795, $d_4^{25}$ 0.8552) was confirmed to be *p*-cymene from its ultraviolet spectrum. Ultraviolet absorption spectrum of fraction B coincided with that of *p*-methylacetophenone ($\lambda_{max}$; 252 m$\mu$)[12]. 2,4-Dinitrophenylhydrazone m. p. 256.5~257.0°C and semicarbazone m. p. 205~206°C of fraction B were identified to be those of *p*-methylacetophenone by mixing with authentic samples. The formation of *p*-methylacetophenone by ozonolysis of fractions 1 and 2 shows the existence of $\alpha,p$-dimethylstyrene. From the result of ozonolysis the amounts of *p*-cymene and $\alpha,p$-dimethylstyrene in fractions 1 and 2 (unified) were calculated to be 24% and 13% respectively.

(ii) 8-Hydroxy-*p*-cymene. Infrared absorption spectra of fractions 4 and 5 showed a hydroxy band in a region of 3400 cm$^{-1}$, and from these fractions a phenylurethane of m. p. 118~119°C was obtained, which was identified as that of 8-hydroxy-*p*-cymene*3 by the mixed melting point determination.

Three grams of the combined fractions 4 and 5 was heated with 3 g. of powdered potassium hydrogen sulfate at 190~200°C and distilled. The distillate was extracted with petroleum benzine, and the extract was washed with 10% aqueous sodium carbonate solution, dried and eluted through a silica gel column. From the extract thus treated 0.72 g. of an oily product was obtained after the solvent was driven off. Its infrared spectrum showed absorption bands at 1630 cm$^{-1}$ (conjugated double bond), 883 cm$^{-1}$ (end methylene) and 816 cm$^{-1}$ (aromatic *para* substitution), and its ultraviolet spectrum had an absorption maximum at 246 m$\mu$. Thus the dehydration product was confirmed to be $\alpha,p$-dimethylstyrene, and therefore the original alcohol to be 8-hydroxy-*p*-cymene.

(iii) Piperitenone. Ultraviolet absorption spectra of fractions 6 and 7 showed $\lambda_{max}$ 242 m$\mu$ ($\varepsilon$ : 10140) and 276 m$\mu$ ($\varepsilon$ : 7640) which coincide with absorption maxima of piperitenone, 242 m$\mu$ ($\varepsilon$ : 12500) and 278 m$\mu$ ($\varepsilon$ : 7920)[13]. 2,4-Dinitrophenylhydrazone of the above fractions melted at 183.5~184°C. This was identified as that of piperitenone by mixing with a known sample.

Fractions 8 and 9 were unified and eluted through a silica gel—plaster of paris (4 : 1) column with ether-petroleum benzine (3 : 7), and it was verified that 37% of the above unified two fractions was piperitenone.

(iv) Unidentified Carbonyl Compound. By column chromatography of fractions 8 and 9 mentioned above, a carbonyl compound was separated, which gave a 2,4-dinitrophenylhydrazone of m. p. 216.5~217°C and ultraviolet absorption spectrum which had $\lambda_{max}$ 244 m$\mu$ and 257 m$\mu$, but it was not identified.

**1.2.2. Experiment 2**

*tert*-Butyl chromate solution was prepared, in the same way as in Experiment 1, from chromic anhydride (147 g.), *tert*-butyl alcohol (274 g.), benzene (1000 g.), glacial acetic acid (50 g.), and acetic anhydride (50 g.). This oxidant was added dropwise to 100 g. of terpinolene in 100 g. of dry benzene, and the reaction was carried out for 45 hr. at 10°C. Then the reaction mixture was treated as in Experiment 1, and 56.1 g. of a neutral oil was obtained. Piperitenone, 8-hydroxy-*p*-cymene, $\alpha,p$-dimethylstyrene and *p*-cymene were found in the neutral oil*4 (cf. Table I).

10) M. J. Murray and W. S. Gallaway, *J. Am. Chem. Soc.*, **70**, 3867 (1948).
11) R. T. O'Connor and L. A. Goldblatt, *Anal. Chem.*, **26**, 1726 (1954).
12) J. Tanaka, S. Nagakura and M. Kobayashi, *J. Chem. Phys.*, **24**, 311 (1956).
*2 The concentration is in g./l. and the cell length in cm.
*3 8-Hydroxy-*p*-cymene was prepared from *p*-bromotoluene and acetone by Grignard reaction (V. N. Ipatieff, H. Pines and R. C. Obberg, *J. Am. Chem. Soc.*, **70**, 2123 (1948)).
13) R. Y. Naves, *Bull. soc. chim. France*, **1951**, 370.
*4 Identification of the constituents in the neutral oils in 1. 2. 2 and 1. 2. 3 was carried out by the similar methods as in 1. 2. 1.

**1.2.3. Experiment 3**

*tert*-Butyl chromate solution was prepared from the same amounts of chromic anhydride, *tert*-butyl alcohol and benzene as in Experiment 1, but glacial acetic acid and acetic anhydride were excluded. Sixty grams of terpinolene in 60 g. of dry benzene was stirred with the above oxidant for 2 hr. at 0°C. Then the reaction mixture was treated as in Experiment 1, and 28.5 g. of a neutral oil was obtained. The same compounds as in Experiment 2 were confirmed to exist in the neutral oil (cf. Table I).

**2. Oxidation of *p*-Cymene (Experiment 4)**

To 60 g. of *p*-cymene (b.p.$_{22}$ 70.5°C, $n_D^{25}$ 1.4860, $d_4^{25}$ 0.8519) dissolved in benzene (60 g.) was added dropwise an oxidant solution consisting of chromic anhydride (89 g.), *tert*-butyl alcohol (166 g.), benzene (650 g.), glacial acetic acid (10 g.) and acetic anhydride (10 g.), and the reaction was carried out for 15 hr. at 25°C. Then the reaction mixture, after being treated as in the preceding experiments, gave 56.4 g. of a neutral oil which was fractionated as follows: fraction 1 (53 g., b.p.$_{25}$ 73～74°C, $n_D^{25}$ 1.4876, $d_4^{25}$ 0.8645), fraction 2 (0.6 g., b.p.$_4$ 46～70°C, $n_D^{25}$ 1.5017) and residue (0.4 g.).

It was confirmed that fraction 1 was unchanged *p*-cymene by its ultraviolet spectrum measurement. Fraction 2 gave 2,4-dinitrophenylhydrazone m.p. 256°C of *p*-methylacetophenone and phenylurethane m. p. 120°C of 8-hydroxy-*p*-cymene, both of which were identified by mixing with authentic samples. An ultraviolet absorption spectrum of fraction 2 have $\lambda_{max}$ 250 m$\mu$ ($a$: 20) which agrees virtually with $\lambda_{max}$ 252 m$\mu$ ($a$: 117) of *p*-methylacetophenone.

## Summary

Oxidation of terpinolene with *tert*-butyl chromate was carried out, and piperitenone, 8-hydroxy-*p*-cymene, *p*-cymene and $\alpha$, *p*-dimethylstyrene were obtained as reaction products. In this oxidation it was found that the active methylene group at $C_{(3)}$ position in terpinolene was oxidized to a carbonyl group, and that the aromatization of carbon ring in terpinolene molecule took place. This could not be recognized in the oxidation of terpene compounds already reported by this oxidant.

This research was aided by a grant from the Ministry of Education.

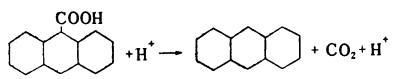
*Department of Chemistry*
*Faculty of Science*
*Hiroshima University*
*Hiroshima*

# *Thermal Decarboxylation of p-Chlorobenzoic Acid*

By S. S. MUHAMMAD

(Received February 13, 1960)

Though Fieser and Fieser[1a] had suggested in 1944 the probability of an electrophilic bimolecular ($S_E2$) mechanism for the decarboxylation of *o*- and *p*-hydroxybenzoic acids, no experimental evidence was available for this till 1948, when Schenkel and Schenkel-Rudin[2] recognized this as likely for the decomposition of anthracene-9-carboxylic acid:




since Schenkel[3] had established the fact that this acid underwent decarboxylation more readily in acidic solvents such as sulfuric or dichloroacetic acid than in basic solvents such as 7:8 benzoquinoline. Schubert[4] tried to establish a relation between the rate of decarboxylation and hydrogen ion concentration of the medium, by studying the decomposition of mesitoic acid in aqueous sulfuric acid of 80 to 100%. Johnson and Heinz[5] obtained evidence for the $S_E2$ mechanism by studying the rates of decarboxylation, under identical conditions, of different substituted cinnamic acids, $PhCR'=CR''COOH$. The order of rates found by them agreed with the electronic effects of the substituents R′ and R″ on the basis of the following bimolecular mechanism:

$$PhCR'=CR''COOH + HA \rightleftharpoons Ph\overset{+}{C}R'CHR''COOH + A'$$

followed by a comparatively fast step:

$$Ph\overset{+}{C}R'CHR''COOH \rightarrow PhCR'=CHR''CO_2 + H^+$$

1) L. Fieser and M. Fieser, "Organic Chemistry", Heath & Co., Boston 1944; a p. 674, b 568.
2) H. Schenkel and M. Schenkel-Rudin, *Helv. Chim. Acta*, **31**, 514 (1948).
3) H. Schenkel, ibid., **29**, 436 (1946).
4) W. M. Schubert, *J. Am. Chem. Soc.*, **71**, 2639 (1949).
5) W. S. Johnson and W. E. Heinz, ibid., **71**, 2913 (1949).

Then Brown, Hammick and Scholefield[6] showed that the decarboxylation of salicylic, 2, 4-dihydroxy- and 2, 4, 6-trihydroxybenzoic acids occurs by an $S_E2$ mechanism. These studies were extended by S. S. Muhammad and Mrs. Aziz Mirza on benzoic acid[8], *o*-chloro- and 2, 4-dichlorobenzoic acids[9,10]. The technique employed was primarily to collect the carbon dioxide evolved in a gas burette. But in the present study a slightly different technique has been adopted. The results reported pertain to *p*-chlorobenzoic acid and these will be shortly extended to other acids.

## Experimental and Results

**Materials.** — All the chemicals were of analar grade, and were used without further purification. The solvents, resorcinol, glycerol and aniline were of extra pure quality and when heated alone did not emit carbon dioxide.

**Apparatus.**—The heating device consisted of an oil bath heated electrically, the temperature control being achieved by means of a Sunvic energy regulator and a Sunvic relay. Temperatures were recorded with a 300°C thermometer having an accuracy of ±0.5°C. The bath liquid was a local sweet oil which, on heating for 24 hr. at 300°C, emitted volatile vapours and then behaved as a nonvolatile liquid below this temperature.

The reaction vessel was a modified Walton's[11] apparatus, the mouth of which was made of ground glass joint with stopper to which a glass tube was attached and this served as delivery tube for carbon dioxide liberated. The side tube had also a neck made of glass joint. The stopper for this had a spoon device where a weighed amount of the acid could be kept in a small test tube, which could be dropped by a slight turn of the stopper. Both the stoppers were lubricated with the least quantity of Silicone grease.

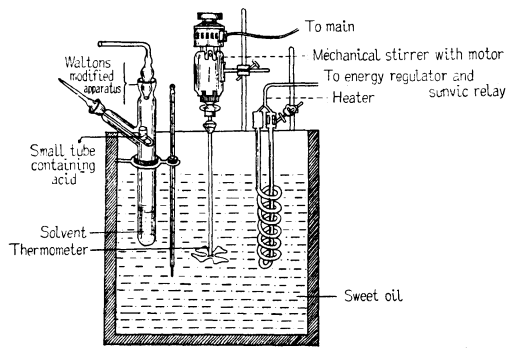



Fig. 1.

The carbon dioxide was absorbed in baryta solution kept in an Erlenmeyer flask.

The oil thermostat with the modified Walton apparatus is shown in Fig. 1.

**Procedure.**—In order to find the order of reaction, different amounts of *p*-chlorobenzoic acid were taken with 20 g. of resorcinol in the Walton tube and heated for a definite interval. The liberated carbon dioxide was absorbed in baryta solution of approximately N/10 strength. Its exact titre value was determined by standardized N/10 oxalic acid before and after the absorption of carbon dioxide. The amount of acid decomposed, $x$, was calculated by the relation: $\Delta v \times 10^{-4}$ g. mol., where $\Delta v$ is the difference in the titre values '$v_0$' initially and '$v$' after absorption. Since the amount of acid initially taken, '$a$', is known, the amount of acid remaining at any interval, '$a-x$', can be found.

In the first series of experiments, the initial amounts '$a$' were converted into relative concentrations, '$c$', and the corresponding amounts '$x$' decomposed in the same interval were converted into relative rates '$r$' (Table I).

The plot of log $c$ against log $r$ yields a slope of 1, indicating the order to be one.

In the second series of experiments, the same initial amount of the acid '$a$', was heated. The carbon dioxide evolved was absorbed in the same volume of the baryta solution of the same concentration. The latter solution was titrated by N/10 oxalic acid after a desired interval. The same operation being repeated for different desired intervals. Table II contains these data.

The plot of log $(a-x)$ against time $t$ gives straight line proving the first order character of the reaction.

The rate constants can be obtained by the equation $k=2.303/t \cdot \log a/a-x$. Thus using the data of Expt. 4, we get $k=2.303/12 \log 29.4/19.6 = 3.378\times10^{-2}\,\mathrm{min}^{-1} = 5.63\times10^{-4}\,\mathrm{sec}^{-1}$. Alternatively the rate constant can be derived by the relation

$$k' = \frac{x}{t} \times \frac{1}{\bar{a}}$$

where $x$ is the amount decomposed in the interval $t$ and $\bar{a}$ is the average concentration during this interval i. e. $\{a+(a-x)\}/2$. Thus the data of Expt. 4, give

$$k' = \frac{9.8\times10^{-4}}{12} \times \frac{1}{(29.4+19.6)\times10^{-4}/2}$$
$$= \frac{9.8\times10^{-4}}{12\times24.5\times10^{-4}} = 3.33\times10^{-2}\,\mathrm{min}^{-1}$$
$$= 5.56\times10^{-4}\,\mathrm{sec}^{-1}$$

In subsequent experiments, the latter method of deriving the rate constant has been used.

In the third series of experiments, different initial amounts of the acid, '$a$', were heated at constant temperature, $T$, and the amounts '$x$', decomposed in 12 minutes were determined in each case. The rate constants were calculated as above. At each temperature, 5 observations were made and the mean of these was taken as the rate constant at that temperature. These results are presented in Table III.

6) B. R. Brown, D. LL. Hammick and A. J. B. Scholefield, *J. Chem. Soc.*, **1950**, 778.
7) B. R. Brown, W. W. Elliott and D. LL. Hammick, ibid., **1951**, 1384.
8) S. S. Muhammad and Aziz Siddiqui, *J. Indian Chem. Soc.*, **31**, 726 (1954).
9) S. S. Muhammad and Aziz Siddiqui, ibid., **33**, 570 (1956).
10) Aziz Mirza, Ph. D. thesis approved by the Osmania University, 1957 pp. 100—106.
11) J. H. Walton, *Physik. Chem.*, **47**, 185 (1904).

TABLE I. SOLVENT RESORCINOL, $T=235°C$

| Weight of acid, g. | Weight, g., decomposed per sec. | Relative concentration $c$ | Relative rate $r$ | log $c$ | log $r$ |
|---|---|---|---|---|---|
| 0.12 | $5.83\times10^{-5}$ | 1 | 1 | 0 | 0 |
| 0.16 | 8.00 | 1.33 | 1.37 | 0.1239 | 0.1367 |
| 0.20 | 10.00 | 1.67 | 1.72 | 0.2227 | 0.2355 |
| 0.25 | 12.17 | 2.08 | 2.09 | 0.3181 | 0.3201 |
| 0.35 | 17.5 | 2.92 | 3.00 | 0.4654 | 0.4771 |
| 0.40 | 20.33 | 3.33 | 3.49 | 0.5224 | 0.5428 |
| 0.50 | 25.67 | 4.17 | 4.40 | 0.6201 | 0.6435 |
| 0.60 | 29.67 | 5.00 | 5.09 | 0.6990 | 0.7067 |

TABLE II.

A 0.460 g. portion of acid was taken in each experiment (i.e. $a=29.4\times10^{-4}$ g. mol.). The carbon dioxide formed was absorbed in 40 cc. of baryta solution which was titrated with N/10 oxalic acid.

| Expt. No. | Time, $t$ min. | Titre value of N/10 Oxalic acid, $T$ | Amount of acid decomposed, $x$ ($x=T\times10^4$ g. mol.) | $(a-x)\times10^4$ | log$(a-x)$ |
|---|---|---|---|---|---|
| 1 | 0 | 33.4 | — | 29.4 | 1.4683 |
| 2 | 4 | 29.8 | 3.6 | 25.8 | 1.4116 |
| 3 | 8 | 26.4 | 7.0 | 22.4 | 1.3502 |
| 4 | 12 | 23.6 | 9.8 | 19.6 | 1.2923 |
| 5 | 15 | 21.4 | 12.0 | 17.4 | 1.2405 |
| 6 | 20 | 19.0 | 14.4 | 15.0 | 1.1761 |
| 7 | 26 | 16.5 | 16.9 | 12.5 | 1.0969 |
| 8 | 32 | 15.0 | 18.4 | 11.0 | 1.0414 |

In order to examine the above results, it was desirable to derive the activation energy $E$, frequency factor $A$, free energy of activation $\Delta F°$ and entropy of activation $\Delta S°$.

The plot of log $k$ vs. $1/T$ (Fig. 2) gave the activation energy $E$.

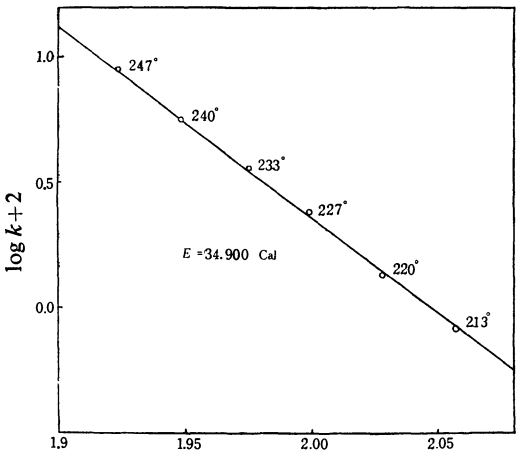



Fig. 2.

The Arrhenius equation $k=Ae^{-E/RT}$ was used to calculate the frequency factor $A$ and the Eyring equations[12]

$$\Delta F°=2.303\ RT\ \log\ (RT/Nhk)$$

$$\Delta S°=(\Delta H°-\Delta F°)/T$$

yielded the free energy and entropy of activation. The term $\Delta H°$ is the enthalpy of activation, taken equal to $E-RT$, where $E$ is the observed activation energy and $T$ the temperature at which entropy and free energy are being calculated. The values of the constants used are[13]: $R=1.987$ cal. and $8.31439\times10^7$ erg, $N=6.02308\times10^{23}$, $h=6.6252\times10^{-27}$ erg, $T°=$ °C+273.15. The results of these calculations are shown in Table IV.

**Effect of Other Solvents.**—The solvent glycerol is also effective in bringing about decarboxylation of *p*-chlorobenzoic acid, but the rate of decarboxylation is less in glycerol than in resorcinol. Thus, while at 233°C in resorcinol 2.5% of the acid decomposed per minute, in glycerol under identical conditions the rate of decarboxylation is 1.9% per minute. Besides, the rate constants for decarboxylation in glycerol calculated from the first and the second order rate equations show large trends.

Addition of a small quantity of aniline to glycerol solution retards the rate of decarboxylation and when enough of aniline is added, the reaction completely stops. When the acid was dissolved in pure aniline, it did not decompose at 247°C, which was the highest temperature employed in the present investigation.

12) S. Glasstone, K. J. Laidler and H. Eyring, "The Theory of Rate Processes", McGraw Hill Book Co., (1941).

13) G. W. C. Kaye and T. H. Laby, "Tables of Physical and Chemical Constants", Longmans (1956).

TABLE III.

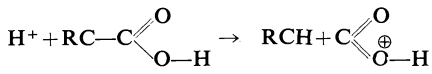
| Expt. No. | $a\times10^4$ g. mol. | $x\times10^4$ g. mol. | $a\times10^4$ g. mol. | $k=\left(\frac{x}{a}\times\frac{1}{12}\right)\text{min}^{-1}$ |
|---|---|---|---|---|
| | | (a) $T=213°C$ | | |
| 1 | 58.8 | 5.6 | 56.0 | $0.83\times10^{-2}$ |
| 2 | 44.1 | 4.3 | 41.95 | 0.85 |
| 3 | 39.2 | 3.6 | 37.4 | 0.80 |
| 4 | 35.3 | 3.4 | 33.6 | 0.84 |
| 5 | 29.4 | 2.9 | 27.95 | 0.86 |
| | | | | Mean……0.84 |
| | | (b) $T=220°C$ | | |
| 1 | 58.8 | 8.6 | 54.5 | 1.32 |
| 2 | 44.1 | 6.6 | 40.8 | 1.35 |
| 3 | 39.2 | 6.0 | 36.2 | 1.38 |
| 4 | 35.3 | 5.2 | 32.7 | 1.33 |
| 5 | 29.4 | 4.6 | 27.1 | 1.42 |
| | | | | Mean……1.36 |
| | | (c) $T=227°C$ | | |
| 1 | 73.5 | 18.2 | 64.4 | 2.36 |
| 2 | 58.8 | 14.3 | 51.4 | 2.40 |
| 3 | 44.1 | 11.2 | 38.5 | 2.42 |
| 4 | 35.3 | 8.6 | 31.0 | 2.31 |
| 5 | 23.5 | 6.0 | 20.5 | 2.44 |
| | | | | Mean……2.39 |
| | | (d) $T=233°C$ | | |
| 1 | 73.5 | 25.6 | 60.7 | 3.51 |
| 2 | 58.8 | 20.8 | 48.4 | 3.58 |
| 3 | 44.1 | 16.0 | 36.1 | 3.69 |
| 4 | 35.3 | 12.2 | 29.2 | 3.48 |
| 5 | 23.5 | 8.4 | 19.3 | 3.63 |
| | | | | Mean……3.58 |
| | | (e) $T=240°C$ | | |
| 1 | 88.2 | 43.8 | 66.3 | 5.51 |
| 2 | 70.6 | 35.0 | 53.1 | 5.49 |
| 3 | 58.8 | 29.4 | 44.1 | 5.55 |
| 4 | 44.1 | 22.1 | 33.05 | 5.57 |
| 5 | 29.4 | 14.8 | 22.0 | 5.61 |
| | | | | Mean……5.55 |
| | | (f) $T=247°C$ | | |
| 1 | 88.2 | 61.6 | 57.4 | 8.94 |
| 2 | 70.6 | 49.4 | 45.9 | 8.97 |
| 3 | 58.8 | 42.0 | 37.8 | 9.26 |
| 4 | 44.1 | 30.8 | 29.0 | 8.68 |
| 5 | 29.4 | 20.4 | 19.2 | 8.86 |
| | | | | Mean……8.94 |

TABLE IV.

| Property | $k$, 220°C | $E$ | $\log A$ | $\Delta H_{220°C}$ | $\Delta F°$ | $\Delta S°_{220°C}$ |
|---|---|---|---|---|---|---|
| Value | $2.25\times10^{-4}\,\text{sec}^{-1}$ | 34900 cal. | 11.81 | 33900 cal. | 37600 cal. | $-7.5$ cal. deg$^{-1}$ |

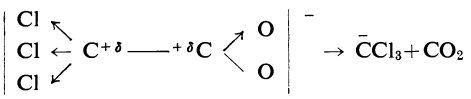
## Discussion

The data presented above show that *p*-chlorobenzoic acid is stable in basic solvents and is unstable in acidic solvents. In this respect, it is analogous with salicylic acid[6] and orthochlorobenzoic acid[9] which undergo decomposition through an electrophilic bimolecular ($S_E2$) mechanism, involving the replacement of the carboxyl:

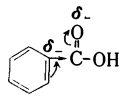


or $RCH + CO_2 + H^+$

In *p*-chlorobenzoic acid, the inductive effect of chlorine in the para position is likely to cause electron deficiency on the $\alpha$-cabon. The result of this would be that decarboxylation would not occur in acid medium and would be facilitated in neutral and basic media. This would be in harmony with the view of Fairclough[14], according to whom in trichloroacetic and tribromoacetic acids the $\alpha$-carbon is attached to strongly electron attracting chloro and bromo groups which weakens the carbon-carboxy bond and facilitates its unimolecular rupture:



According to Fieser and Fieser[16], the inductive effect estimated from dipole moments accounts well for the activating or deactivating influence of different groups, but does not explain the orientation and it is seen that although the majority of electron attracting groups orient an entering group to the meta position, halogen substituents, like the electron repelling amino and hydroxyl groups are ortho, para directing. This is due to the resonance effect. Thus in chlorobenzene resonance leads to development of electron density at the ortho and para positions (with reference to chlorine atom). In *p*-chlorobenzoic acid, structures in which carboxyl also partakes of the resonance are possible. But according to Schubert[4], in the presence of substituents, the resonance interaction of the carboxyl with the benzene nucleus is inhibited. This leads to the weakening of the bond between the carboxyl and $\alpha$-carbon and to its easy rupture. Another interesting explanation is that of Royals[15], according to whom the presence of meta orienting groups like carboxyl produces an electromeric effect indicated in the accompanying structure, due to which nucleophilic reactivity is developed at the $\alpha$-carbon atom adjacent to meta orienting group. Hence an electrophilic reagent attacks this position and displaces the meta orienting group:

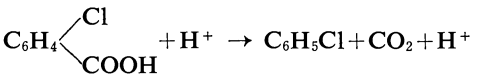


This also accounts satisfactorily the decarboxylation of benzoic acid[8] in the solvent resorcinol.

The bimolecular electrophilic substitution ($S_E2$) mechanism also accounts for the behavior of *p*-chlorobenzoic acid in the solvent glycerol which has been recently used by Clark[16] in decarboxylations. Glycerol being a polyhydric compound may act as a protophilic solvent and facilitate the ionization of *p*-chlorobenzoic acid to a limited extent.

$$\underset{\text{acid}}{HA} + \underset{\text{solvent}}{ROH} \rightleftharpoons (ROH_2)^+ + A^-$$

where $(ROH_2)^+$ is solvated hydrogen ion. The "hydrogen ions" so formed will facilitate the decarboxylation:



The trends in the rate constants during decarboxylation in glycerol may be due to the fact that along with decarboxylation, the ester formation between glycerol and the acid takes place and the ester so formed decomposes decarboxylatively introducing complications in the interpretation of rate data. The retarding effect of aniline on decarboxylation in glycerol is also consistent with the $S_E2$ mechanism proposed, since aniline removes the hydrogen ions present and thus causes retardation in their attack on the carboxylic acid. On the contrary if decarboxylation were to occur via the first order decomposition of the carboxylate anion by the $S_E1$ mechanism, the rate should have increased due to the carboxylate anions being formed in abundance:

$$C_6H_5NH_2 + HA = (C_6H_5NH_3)^+ + A^-$$

## Summary

The decarboxylation of *p*-chlorobenzoic acid has been studied in the solvent resorcinol. The activation energy, frequency factor and free energy and entropy of activation have been calculated. It is shown that the reaction follows the $S_E2$ mechanism.

*Department of Chemistry*
*University College of Science*
*Osmania University*
*Hyderabad, India*

14) R. A. Fairclough, *J. Chem. Soc.*, **1938**, 1186.
15) E. Royals, "Advanced Organic Chemistry" Constable & Co., p. 450.
16) L. W. Clark, *J. Am. Chem. Soc.*, **77**, 3130 (1955).

# *Sur la Dissolution des Minerais Sulfurés en Divers Milieux. III. Facteurs Intervenant à la Dissolution de la Chalcopyrite*

Par Masami ICHIKUNI

(Reçu le 1er Novembre 1959)

On a examiné dans le rapport précédent[1] les influences du pH et de l'oxygène sur la dissolution de la chalcopyrite qui existe indépendamment des autres minéraux. Cependant tous les minerais produits dans la nature sont d'un système complexe de plusieurs minéraux. On ne peut pas supposer que chaque minéral se comporte indépendamment des autres au cours de la dissolution du minerai; il doit y avoir évidemment les actions réciproques entre les minéraux ainsi que celles des ions en solution. Ohashi[2] a déjà traité l'aspect général de ce problème; toutefois, à ce sujet, notre connaissance reste encore peu satisfaisante.

## Expérience

On examine ici les effets de la présence de la pyrite, qui se trouve associée très souvent à la chalcopyrite, et ceux des ions de fer divalent, qui se forment par la désagrégation. Le dispositif destiné à l'expérience est le même que précédemment décrit[1].

**Effets de la Présence de la Pyrite.**—On mélange bien la pyrite et la chalcopyrite, en proportion connue; les deux ont été utilisées dans les expériences du rapport précédent. De ce mélange bien pulvérisé, on met 1 g. dans 200 ml. d'acide chlorhydrique 0,01 N et traite pendant deux heures à la température de 80°C. Le prélèvement de 10 ml. de liqueur s'effectue avec l'interval d'une demi-heure après l'addition du mélange. L'air est introduit dans un ballon contenant de la liqueur et de la poudre des minéraux avec un débit de 1,5 l./min. Quant aux conditions d'expériences, voir le rapport précédent.

**Effets des Ions de Fer Divalent en Solution.**—On dissout une quantité connue de sulfate de fer-(II), $FeSO_4 \cdot 7H_2O$, dans l'acide chlorhydrique 0,01 N, prend 200 ml. de cette solution, y ajoute 1 g. de chalcopyrite pulvérisée, et traite pendant deux heures. Le prélèvement de liqueur s'effectue de la même façon que l'expérience décrite ci-dessus. Dans la liqueur on introduit de l'air ou de l'azote avec un débit de 1,5 l./min., l'introduction de ce dernier ayant pour but de réaliser une condition non-oxydante.

## Résultats et Discussion

**Co-présence de la Pyrite.** — On a préparé quatre mélanges de proportions différentes de ces deux minéraux. La composition des mélanges est donnée dans le Tableau I. Les concentrations de fer divalent, de cuivre et de sulfate, qu'on a calculées en tenant compte de la diminution du volume de liqueur par l'évaporation, sont portées sur le Tableau II.

TABLEAU I. COMPOSITION DES MÉLANGES CONSISTANT EN PYRITE ET EN CHALCOPYRITE

| No. du mélange | Pyrite % | Chalcopyrite % | Cu % | Fe % | $(Cu/Fe)_{min.}$ $\times 10^{-2}$ |
|---|---|---|---|---|---|
| 1 | 95,5 | 4,5 | 1,56 | 45,8 | 3,71 |
| 2 | 84,6 | 15,4 | 5,34 | 44,0 | 12,1 |
| 3 | 62,1 | 37,9 | 13,1 | 40,4 | 32,4 |
| 4 | 51,4 | 48,6 | 16,8 | 38,6 | 43,6 |

Remarque: Les teneurs en cuivre et en fer des mélanges sont calculées d'après les résultats d'analyse des minéraux. La valeur $(Cu/Fe)_{min.}$ représente le rapport de teneur en cuivre sur celle en fer du mélange.

TABLEAU II. VARIATION DE CONCENTRATIONS DE FER DIVALENT, DE CUIVRE ET DE SULFATE AU COURS DE LA DISSOLUTION DE 1 g. DE CHAQUE MÉLANGE

| No. du mélange | Durée du traitement hr. | Cu mg./l. | $Fe^{2+}$ mg./l. | $SO_4^{2-}$ mg./l. |
|---|---|---|---|---|
| 1 | 0,5 | 3,92 | 16,3 | 29 |
| | 1 | 6,05 | 19,2 | 39 |
| | 1,5 | 9,89 | 23,6 | 49 |
| | 2 | 12,0 | 27,1 | 59 |
| 2 | 0,5 | 4,39 | 18,4 | 23 |
| | 1 | 6,89 | 22,5 | 30 |
| | 1,5 | 10,5 | 26,4 | 42 |
| | 2 | 14,4 | 31,0 | 53 |
| 3 | 0,5 | 4,13 | 19,4 | 17 |
| | 1 | 6,06 | 25,8 | 25 |
| | 1,5 | 8,12 | 31,8 | 32 |
| | 2 | 8,85 | 38,1 | 41 |
| 4 | 0,5 | 3,38 | 17,5 | 19,5 |
| | 1 | 4,00 | 23,6 | 24 |
| | 1,5 | 4,95 | 31,0 | 28 |
| | 2 | 5,95 | 37,6 | 36 |

Avec les données du Tableau II, on calcule la vitesse de dissolution à partir de la pente de la droite représentant la concentration de composants en fonction de durée du traitement. Sa vitesse est considérablement grande au

1) M. Ichikuni, Ce Bulletin, 33, 1052 (1960).
2) S. Ohashi, *J. Chem. Soc. Japan, Pure Chem. Sec.* (*Nippon Kagaku Zasshi*), 74, 845 (1953).

Tableau III. Vitesse de dissolution du cuivre, du fer divalent et du sulfate à partir de 1 g. de mélange

| No. du mélange | Cu mg./hr. | $Fe^{2+}$ mg./hr. | $SO_4^{2-}$ mg./hr | $(Cu/Fe)_{soln.}$ $(\times 10^{-2})$ | $\frac{(Cu/Fe)_{soln.}}{(Cu/Fe)_{min.}}$ |
|---|---|---|---|---|---|
| 1 | 1,10 | 1,47 | 4,0 | 74,9 | 20,2 |
| 2 | 1,35 | 1,66 | 4,05 | 81,4 | 6,73 |
| 3 | 0,76 | 2,41 | 3,2 | 31,5 | 0,973 |
| 4 | 0,41 | 2,70 | 2,2 | 15,2 | 0,349 |

début, et après elle prend une valeur constante. Cette irrégularité de dissolution fait supposer la présence des parties facilement solubles du minéral, mais dont l'essentiel reste encore peu clair.

En examinant la vitesse de dissolution des composants sur les quatre échantillons de mélanges, on a trouvé des faits suivants: avec l'augmentation de proportion de chalcopyrite dans les mélanges,

1° la vitesse de dissolution du fer augmente,

2° celle du cuivre va d'abord montant, atteint le maximum, et après, descend graduellement.

3° celle du sulfate ne fait que diminuer.

Cela signifie que la pyrite et la chalcopyrite ne se dissolvent pas indépendamment l'une de l'autre et qu'il existe les influences réciproques sur la dissolution de leur mélange. D'où vient que la vitesse de dissolution des composants à partir du mélange est toujours différente de celle prévue d'après les résultats de la dissolution de chacun des deux minéraux purs.

La vitesse de dissolution des composants est montrée dans le Tableau III, où $(Cu/Fe)_{soln.}$ et $(Cu/Fe)_{min.}$ représentent respectivement le rapport de vitesse de dissolution du cuivre sur celle du fer, et le rapport de teneur en cuivre sur celle en fer du mélange.

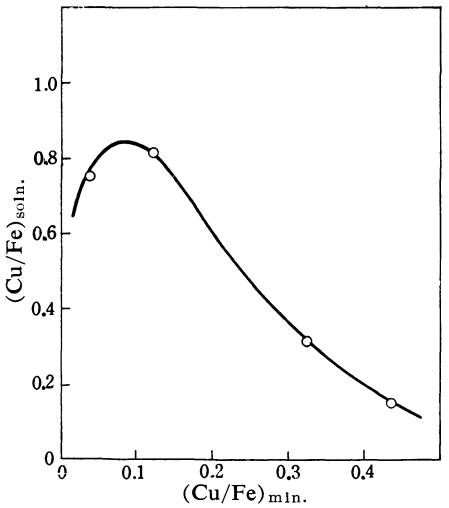



Fig. 1. Relation entre la valeur de $(Cu/Fe)_{min.}$ et la valeur de $(Cu/Fe)_{soln.}$

L'augmentation de teneur en cuivre du mélange, c'est-à-dire celle de valeur de $(Cu/Fe)_{min.}$, diminue la valeur de $(Cu/Fe)_{soln.}$. La Fig. 1 montre cette relation où la valeur de $(Cu/Fe)_{soln.}$ atteint le maximum au moment où la valeur de $(Cu/Fe)_{min.}$ est de 0,1 environ. La diminution de la valeur de $(Cu/Fe)_{min.}$ au-dessous de 0,1 abaisse également la valeur de $(Cu/Fe)_{soln.}$; mais le rapport de $(Cu/Fe)_{soln.}$ sur $(Cu/Fe)_{min.}$ a une signification particulière au point de vue géochimique et pratique.

Ce rapport soit $r$,

$$r=\frac{(Cu/Fe)_{soln.}}{(Cu/Fe)_{min.}}$$

Si $r>1$, le minerai résiduel s'appauvrit en cuivre. Si $r<1$, le minerai résiduel devient riche en cuivre. On a déjà remarqué cette possibilité d'enrichissement du cuivre dans certaines discussions concernant la dissolution de la chalcopyrite. Le point où $r=1$ se trouve à la valeur de $(Cu/Fe)_{min.}$ de 0,32. Supposons que le minerai consiste simplement en pyrite et en chalcopyrite, alors la teneur en cuivre du minerai est de 13%. Comme la plupart des minerais sulfurés cuprifères sont moins riches en cuivre que ce minerai en supposition, l'enrichissement en cuivre du minerai résiduel n'aura pas lieu en réalité au cours de la désagrégation, et l'extraction du cuivre s'effectue efficacement par l'action des eaux.

Le rapport $r$ représente l'efficacité d'extraction du cuivre à partir du minerai, ou le coefficient de concentration du cuivre de la phase solide en phase liquide; la valeur $r$ est d'autant plus grande que la teneur en cuivre du minerai est plus petite (voir le Tableau III). Il est donc avantageux d'extraire du cuivre d'un minerai pauvre en cuivre par l'action des eaux. Ce procédé est exécuté dans certain nombre de mines. A titre d'exemple, on calcule ici la valeur $r$ sur le minerai siliceux (kéi-kô), qui a été utilisé comme échantillon dans le premier rapport relatif à la dissolution des minerais sulfurés[3], où

$$(Cu/Fe)_{min.}=0{,}361\times10^{-2}$$
$$(Cu/Fe)_{soln.}=9{,}83\times10^{-2}$$

3) M. Ichikuni et H. Kamiya, Ce Bulletin, 32, 1368 (1959).

on a donc $r=27,2$, qui est exceptionnellement grand; on notera d'ailleurs que la teneur en cuivre du minerai n'est que de 0,048%.

**Effets des Ions de Fer Divalent en Solution.** —Le Tableau IV donne les concentrations de composants dissous, correspondant à l'heure du prélèvement de liqueur et à la quantité additionnée de fer divalent. La quantité dissoute de fer et de sulfate est très limitée et reste inférieure à l'erreur du dosage de ces composants, lorsque la concentration de fer est plus de 500 mg./l. Notons que le fer est ajouté sous forme du sulfate de fer(II), $FeSO_4 \cdot 7H_2O$. Cela gêne de vérifier l'augmentation de concentration de sulfate.

Le dosage du fer divalent et du sulfate s'est donc effectué, lorsque la concentration initiale de fer était inférieure à 100 mg./l. On montre dans le Tableau V la vitesse de dissolution du fer divalent, du cuivre et du sulfate calculée d'après le Tableau IV.

TABLEAU IV. VARIATION DE CONCENTRATIONS DE CUIVRE, DE FER DIVALENT ET DE SULFATE AU COURS DE LA DISSOLUTION DE 1 g. DE CHALCOPYRITE, EN PRÉSENCE DU FER DIVALENT

| Conc. initiale de $Fe^{2+}$ mg./l. | Durée du traitement hr. | Cu mg./l. | $Fe^{2+}$ mg./l. | $SO_4^{2-}$ mg./l. |
|---|---|---|---|---|
| 30 | 0,5 | 0,16 | 32,0 | 37 |
| | 1 | 0,45 | 35,0 | 37 |
| | 1,5 | 0,45 | 38,5 | 37 |
| | 2 | 0,43 | 40,5 | 38 |
| 55 | 0,5 | <0,10 | 57,5 | 78 |
| | 1 | 0,15 | 61,2 | 80 |
| | 1,5 | 0,59 | 63,6 | 82 |
| | 2 | 0,40 | 67,2 | 84 |
| 100 | 0,5 | 0,15 | 102 | 150 |
| | 1 | 0,32 | 104 | 150 |
| | 1,5 | 0,69 | 106 | 155 |
| | 2 | 0,95 | 112 | 157 |
| 500 | 0,5 | 3,74 | — | — |
| | 1 | 8,10 | — | — |
| | 1,5 | 11,6 | — | — |
| | 2 | 15,3 | — | — |
| 1000 | 0,5 | 5.81 | — | — |
| | 1 | 10,6 | — | — |
| | 1,5 | 16,6 | — | — |
| | 2 | 23,2 | — | — |
| 1000 | 0,5 | 0,34 | — | — |
| | 1 | <0,10 | — | — |
| | 1,5 | <0,10 | — | — |
| | 2 | <0,10 | — | — |

Remarque: Ces expériences ont été effectuées en présence de l'air, à l'exception de la dernière qui a été exécutée en milieu exempt d'oxygène.

TABLEAU V. VITESSE DE DISSOLUTION DU CUIVRE, DU FER DIVALENT ET DU SULFATE À PARTIR DE 1 g. DE CHALCOPYRITE EN PRÉSENCE DU FER DIVALENT

| Conc. initiale de $Fe^{2+}$ mg./l. | Cu mg./hr. | $Fe^{2+}$ mg./hr. | $SO_4^{2-}$ mg./hr. |
|---|---|---|---|
| 30 | <0,05 | 1,05 | 0,15 |
| 55 | <0,05 | 1,28 | 0,80 |
| 100 | 0,11 | 1,33 | 0,90 |
| 500 | 1,55 | — | — |
| 1000 | 2,28 | — | — |
| 1000 | 0 | — | — |

Remarque: Le dernier rang correspond à l'expérience effectuée en milieu exempt d'oxygène.

*Dissolution du Fer.*—A mesure que la concentration de fer divalent augmente, la quantité dissoute de fer à partir de la chalcopyrite augmente. Cette tendance existerait même en présence du fer dont la concentration est plus de 100 mg./l. D'autre part, sous les conditions où la concentration de fer est moins de 100 mg./l., il n'y a presque pas de dissolution du cuivre. On peut donc admettre que la dissolution du fer s'effectue plus facilement que celle du cuivre. L'accélération de dissolution du fer serait attribuable à des ions de fer trivalent. On a donc:

$$(1)\quad CuFeS_2 + 2Fe^{3+} \rightarrow CuS + S + 3Fe^{2+}$$

et on en déduit, en tenant compte de l'augmentation de concentration de sulfate:

$$(2)\quad CuFeS_2 + 8Fe^{3+} + 4H_2O \rightarrow CuS + SO_4^{2-} + 8H^+ + 9Fe^{2+}$$

Toutefois l'augmentation de concentration de sulfate est toujours inférieure à celle de fer,

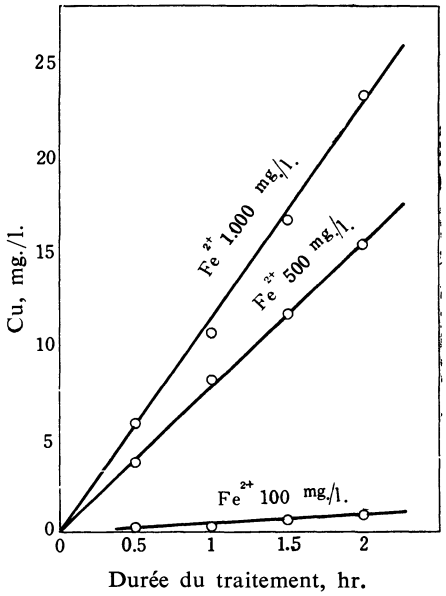



Fig. 2. Dissolution du cuivre à partir de la chalcopyrite en présence du fer divalent et de l'air.

par conséquent la réaction exprimée par l'équation (1) est prédominante dans le cas d'expériences.

*Dissolution du Cuivre.*—Elle n'est presque pas remarquée en présence du fer dont la concentration est inférieure à 100 mg./l. Au delà de 100 mg./l., pourtant, le cuivre se dissout considérablement. La Fig. 2 est dessinée avec les chiffres du Tableau IV. On y voit bien la dissolution du cuivre en présence du fer dont la concentration est supérieure à 100 mg./l. D'après Ohashi[2], la dissolution du cuivre à partir de la chalcopyrite est favorisée par l'action des ions de fer trivalent, ce qui est à comparer avec le résultat décrit ci-dessus. Un mécanisme de dissolution du cuivre, semblable à celui du fer, peut être admis :

$$(3)\quad CuFeS_2 + 4Fe^{3+} \rightarrow Cu^{2+} + 5Fe^{2+} + 2S$$

La quantité de fer trivalent est d'autant plus grande que celle de fer divalent en solution est plus grande, car le fer trivalent est formé par l'oxydation du fer divalent par l'oxygène. Ce phénomène favorise la dissolution de la chalcopyrite dans une mesure considérable.

Ce résultat est soutenu par le fait que la présence d'une quantité importante de fer divalent n'accélère pas la dissolution du cuivre en milieu exempt d'oxygène.

La majeure partie de fer en solution se trouve à l'état divalent, et la quantité de fer trivalent n'est au maximum que de 1% de celle de fer divalent, si la solution est en contact avec un minerai. Cela s'explique bien par le fait que la réaction de l'attaque du fer trivalent sur le minéral s'effectue rapide par rapport à celle de l'oxydation du fer divalent en fer trivalent.

On n'a pas de chiffres en ce qui concerne le soufre, mais il est probable que le fer trivalent intervient à la formation du sulfate. Comme les eaux en contact avec le gisement des minerais sulfurés contiennent généralement une quantité considérable de fer, la dissolution de la chalcopyrite ne peut pas s'expliquer par un mécanisme simple, mais elle est soumise à des influences de plusieurs facteurs, dont dépend la quantité dissoute de cuivre, de fer et de soufre.

## Résumé

La dissolution du cuivre à partir de la chalcopyrite est influencée par le fer en solution qui est en contact avec le minéral, mais plus remarquable est l'effet de la co-présence de la pyrite. L'influence du fer en solution devient considérable, si la concentration de fer dépasse 100 mg./l.

L'auteur exprime ses remerciements profonds à Monsieur le professeur Noguchi qui a bien voulu lire ce rapport et lui donner des conseils utiles, et particulièrement à Monsieur H. Kamiya qui a participé aux expériences et à la discussion sur l'interprétation des résultats.

*Faculté des Sciences*
*Université Métropolitaine de Tokyo*
*Sétagaya, Tokyo*

# *Sur la Dissolution des Minerais Sulfurés en Divers Milieux. IV. Dissolution du Minerai Jaune*

Par Masami ICHIKUNI

(Reçu le 19 Novembre 1959)

La dissolution des minerais sulfurés, notamment celle de la pyrite et de la chalcopyrite, a été systématiquement étudiée, et le résultat des expériences a été réuni dans le 2ème rapport[1] des travaux de la présente série. L'action réciproque des deux minéraux lors de la dissolution de leur mélange était le sujet du rapport précédent[2]. Il serait donc intéressant de vérifier que la dissolution d'un certain minerai peut être expliquée complètement par l'application des résultats obtenus jusqu'ici. Comme les minerais sont d'une association de nombreux minéraux, leur dissolution est influencée à la fois par les facteurs de milieu et par l'action réciproque existant entre les minéraux. Il n'y aurait pas de manière générale d'interpréter le résultat d'expériences concernant la dissolution des minerais. L'état actuel des

1) M. Ichikuni, Ce Bulletin, 33, 1052 (1960).
2) M. Ichikuni, Ce Bulletin, 33, 1159 (1960).

recherches ne permet que d'appliquer les résultats obtenus sur les minéraux ou leur mélange à l'interprétation de la dissolution d'un minerai sulfuré qui a une composition minéralogique simple. On prend donc comme échantillon le minerai jaune, ou *ô-kô*, qui est constitué généralement par le quartz, la pyrite et la chalcopyrite, sans parler des composants mineurs.

## Expérience

On suit la méthode d'expériences qui est déjà mise au point et dont la description détaillée est donnée dans le 2ème rapport.

L'échantillon utilisé dans cette étude est le minerai jaune qui s'est produit à la mine de Kosaka, département d'Akita. Le résultat d'analyse chimique en est montré par le Tableau I. On a décelé par voie spectrographique des traces d'aluminium, d'argent et d'arsenic. Les minéraux arsénifères existent en quantité négligeable. On a soumis ensuite le minerai à l'examen diffractométrique à rayons X, et a décelé le quartz, la pyrite et la chalcopyrite. La présence de la blende est incertaine, car la teneur en zinc est trop petite pour qu'on identifie précisément l'espèce de minéral de zinc. Toutefois il est probable que le zinc se trouve sous forme de blende. En admettant que chaque minéral a une composition correspondant à la formule chimique idéale, on a calculé la composition minéralogique du minerai en question, dont le résultat est porté sur le Tableau II. La présence d'une seule espèce de minéral de cuivre simplifie l'analyse des résultats d'expériences.

Pour chaque expérience, on a utilisé 1 g. de minerai pulvérisé.

Tableau I. Composition chimique du minerai jaune

| Composant | Teneur % |
|---|---|
| Fe | 31,17 |
| Cu | 2,41 |
| Zn | 0,14 |
| S | 35,25 |
| $SiO_2$ | 29,13 |
| Total | 98,10 |

Tableau II. Composition minéralogique du minerai jaune

| Minéral | Formule chimique | Teneur % |
|---|---|---|
| Pyrite | $FeS_2$ | 62,4 |
| Chalcopyrite | $CuFeS_2$ | 7,0 |
| Blende | ZnS | 0,2 |
| Quartz | $SiO_2$ | 29,1 |
| Total | | 98,7 |

## Résultats et Discussion

**Expérience de Dissolution Effectuée en Présence de l'Air.**—Le Tableau III rassemble les résultats obtenus. La vitesse de dissolution du fer, de cuivre, du zinc et de soufre a été calculée en traçant la droite de concentration de chaque composant en fonction de la durée du traitement. On envisage ici le soufre qui se dissout sous forme de sulfate. Le résultat du calcul est montré dans le Tableau IV. A mesure que le pH du milieu diminue, la vitesse de dissolution du cuivre et du zinc augmente, tandis que celle du sulfate ne fait que diminuer. La vitesse de dissolution du fer est approximativement constante en milieu à pH inférieur à 3. A partir de ces résultats, on conclut que la dissolution du minerai jaune ressemble à celle de la pyrite que l'on a étudiée sous la même condition. On notera que ce

Tableau III. Variation de concentration de fer divalent, de cuivre, de zinc et de sulfate au cours de la dissolution du minerai jaune en présence de l'air

| Milieu | Valeur moyenne de pH | Durée du traitement hr. | $Fe^{2+}$ mg./l. | Cu mg./l. | Zn mg./l. | $SO_4^{2-}$ mg./l. |
|---|---|---|---|---|---|---|
| HCl 0,1 N | 1,1 | 1 | 62,5 | 31,4 | 4,6 | 111 |
| | | 2 | 66,8 | 34,3 | 5,9 | 111 |
| | | 3 | 68,0 | 35,7 | 6,2 | 114 |
| | | 4 | 70,0 | 36,4 | 6,1 | 113 |
| HCl 0,01 N | 2,05 | 1 | 37,7 | 14,2 | 3,0 | 97 |
| | | 2 | 40,7 | 15,2 | 3,5 | 104 |
| | | 3 | 41,8 | 16,2 | 3,5 | 110 |
| | | 4 | 42,9 | 17,0 | 3,6 | 116 |
| HCl 0,001 N | 3,0 | 1 | 36,7 | 9,7 | 3,2 | 87,5 |
| | | 2 | 38,1 | 9,8 | 3,3 | 98 |
| | | 3 | 42,0 | 9,8 | 3,3 | 116 |
| | | 4 | 43,7 | 9,7 | 3,5 | 133 |
| $H_2O$ | 3,0* | 1 | 16,7 | 5,4 | 2,8 | 77 |
| | | 2 | 16,5 | 6,2 | 2,3 | 97 |
| | | 3 | 16,6 | 6,6 | 4,5? | 113 |
| | | 4 | 16,7 | 6,8 | 2,8 | 169 |

* L'abaissement du pH est dû à la formation de l'acide sulfurique par l'oxydation.

TABLEAU IV. VITESSE DE DISSOLUTION DU FER DIVALENT, DU CUIVRE, DU ZINC ET DU SULFATE À PARTIR DE 1 g. DE MINERAI JAUNE EN PRÉSENCE DE L'AIR

| Milieu | $Fe^{2+}$ mg./hr. | Cu mg./hr. | Zn mg./hr. | $SO_4^{2-}$ mg./hr. | $Cu/Fe^{2+}$ | $Zn/Fe^{2+}$ |
|---|---|---|---|---|---|---|
| HCl 0,1 N | 0,34 | 0,24 | >0,26 | 0,14 | 0,71 | >0,89 |
| HCl 0,01 N | 0,39 | 0,20 | >0,10 | 1,24 | 0,51 | >0,26 |
| HCl 0,001 N | 0,44 | 0 | 0,03 | 3,0 | 0 | 0,07 |
| $H_2O$ | 0 | 0 | 0 | 3,6 | — | — |

minéral constitue la plus grande partie (62,4%) du minerai.

*Fer.*—Lors du traitement du minerai avec de l'eau, la dissolution du fer n'a pas lieu, bien que le pH de la liqueur s'abaisse à 3 près. Cependant sous la même condition, une quantité appréciable de fer s'est dissoute à partir de la pyrite. On envisage maintenant le problème du comportement de la pyrite qui se trouve associée à d'autres minéraux. Ce problème pourrait être résolu par l'examen des influences des minéraux co-existants. D'ailleurs il est bien connu que la présence de la blende empêche la dissolution de la pyrite et de la chalcopyrite[3]. Pourtant cette raison n'est pas très convaincante pour la résolution totale du problème.

*Cuivre.*—La dissolution du cuivre est évidemment influencée par le pH du milieu, mais d'une façon différente du cas de dissolution du cuivre à partir de la chalcopyrite qui se trouve indépendamment des autres minéraux. Dans le cas de la chalcopyrite, la vitesse de dissolution du cuivre ainsi que du fer augmente brusquement au moment où l'acidité du milieu atteint 0,1 N, tandis que celle du cuivre à partir du minerai jaune n'augmente que légèrement par l'abaissement du pH de 2 à 1. La dissolution sélective de la chalcopyrite ne se produit pas même à pH 1. La valeur de $(Cu/Fe)_{soln.}$, rapport de vitesse de dissolution du cuivre sur celle du fer, était de 0,38 à pH 1 pour la chalcopyrite. Elle est de 0,71 au même pH pour le minerai, et dépasse le chiffre trouvé pour la chalcopyrite.

On constate ainsi que la dissolution du cuivre à partir de la chalcopyrite est certainement favorisée par la présence de la pyrite, ce qui conforme au résultat du rapport précédent[2]. Les effets de la pyrite sur la dissolution de la chalcopyrite qui ont été trouvés en milieu à pH 2 continuent à exister même à pH 1. Le coefficient de concentration du cuivre par rapport au fer, au cours de la dissolution du minerai, est exprimé par la relation suivante et calculé d'après le résultat d'expériences effectuées en milieu acide 0,01 N. Le coefficient soit $r$, et on a:

$$r=\frac{(Cu/Fe)_{soln.}}{(Cu/Fe)_{min.}}=\frac{51\times10^{-2}}{7{,}75\times10^{-2}}=6{,}6$$

où $(Cu/Fe)_{soln.}$ est le rapport de vitesse de dissolution du cuivre sur celle du fer, et $(Cu/Fe)_{min.}$ est le rapport de teneur en cuivre du minerai sur celle en fer. Ce chiffre n'est pas très éloigné de 10,6, chiffre prévu d'après les expériences effectuées sur le mélange de la pyrite et de la chalcopyrite. Toutefois il n'est pas facile à dire par quelle raison cet écart peut être expliqué. Comme cet écart peut être attribué, d'une part, aux effets des substances co-existantes, telles que la blende, et d'autre part, à l'individualité du minerai, une étude plus approfondie est exigée pour la mise en évidence de la cause de l'écart. Il est probable que les impuretés contenues dans le minerai détermine son individualité, par conséquent on ne peut pas passer des études des composants mineurs.

D'après le Tableau IV, la valeur de $(Cu/Fe)_{soln.}$ est d'autant plus grande que le pH du milieu est plus petit, d'où on désigne comme facteurs intervenant à la dissolution du cuivre à partir de la chalcopyrite située dans la zone d'oxydation les suivants: pH, co-présence de la pyrite et concentration de fer en solution. Comme il a été signalé dans le rapport précédent,[2] l'influence de fer en solution devient remarquable, lorsque sa concentration dépasse 100 mg./l. Il faut qu'on tienne compte de la température, de la pression et de la co-présence des autres substances que la pyrite, mais l'état actuel des recherches ne permet pas de discuter davantage sur ces facteurs de milieu.

*Zinc.*—Le travail effectué par Ohashi a montré que la dissolution de la blende est accélérée par la présence de la pyrite et de la chalcopyrite[3]. Les effets du pH se joignant à ceux de la présence de ces minéraux, le phénomène de la dissolution du zinc a un aspect très compliqué, par conséquent la formation de l'acide par la désagrégation des minerais sulfurés est un facteur non-négligeable, tant qu'on traite la dissolution de ce métal.

**Expérience de Dissolution Effectuée en Milieu Exempt d'Oxygène.** — Le résultat obtenu est porté sur le Tableau V. Comme on a prévu d'après les résultats d'expériences concernant

3) S. Ohashi, *J. Chem. Soc. Japan, Pure Chem. Sec.* (*Nippon Kagaku Zasshi*), **74**, 845 (1953).

TABLEAU V. VARIATION DE CONCENTRATION DE FER DIVALENT, DE CUIVRE, DE ZINC ET DE SULFATE AU COURS DE LA DISSOLUTION DU MINERAI JAUNE EN MILIEU EXEMPT D'OXYGÈNE

| Milieu | Valeur moyenne de pH | Durée du traitement hr. | $Fe^{2+}$ mg./l. | Cu mg./l. | Zn mg./l. | $SO_4^{2-}$ mg./l. |
|---|---|---|---|---|---|---|
| HCl 0,1 N | 1,2 | 1 | 37,1 | 6,75 | 2,9 | 74 |
| | | 2 | 36,7 | 6,30 | 3,4? | 76 |
| | | 3 | 36,9 | 5,10 | 2,8 | 76 |
| | | 4 | 36,3 | 4,58 | 2,6 | 74 |
| HCl 0,01 N | 2,05 | 1 | 37,8 | 2,25 | 2,2 | 77 |
| | | 2 | 39,7 | 0,90 | 2,0 | 78 |
| | | 3 | 40,1 | 0,44 | 2,0 | 81 |
| | | 4 | 40,0 | 0,36 | 1,6 | 81 |
| HCl 0,001 N | 3,0 | 1 | 37,0 | 0,61 | 2,6 | 78 |
| | | 2 | 37,8 | 0,59 | 2,5 | 79 |
| | | 3 | 38,1 | 0,50 | 2,4 | 79 |
| | | 4 | 38,3 | 0,26 | 2,2 | 81 |
| $H_2O$ | 4,0 | 1 | 32,4 | 0,2 | 2,4 | 81 |
| | | 2 | 33,2 | 0,2 | 1,9 | 82 |
| | | 3 | 33,0 | 0,2 | 1,7 | 83 |
| | | 4 | 33,6 | 0,2 | 1,6 | 84 |

la dissolution de la pyrite et de la chalcopyrite, la formation du sulfate n'a pas lieu. Au reste, l'indissolution du fer attire notre attention. Il peut y avoir là les influences de la co-présence des minéraux. On remarque encore que sous les conditions acides et non-oxydantes le comportement du cuivre est différent de celui du zinc.

*Cuivre.*—L'échantillon utilisé étant partiellement oxydé par la pulvérisation, une petite quantité de cuivre se dissout au début du traitement, même en milieu exempt d'oxygène. La concentration de cuivre diminue, pourtant, avec la durée du traitement. De ces expériences on ne peut tirer les matières suffisantes pour avoir des idées claires sur le mécanisme de la fixation du cuivre. Il se peut que l'hydrogène sulfuré, formé par l'action de l'acide sur le minerai sulfuré, cause la précipitation ou l'adsorption du cuivre sous forme de sulfure. Ce phénomène se produit même à pH 1, ce qui souligne que la dissolution du cuivre à partir des minerais sulfurés est peu possible dans les conditions acides et non-oxydantes, et que le contact des eaux contenant des ions de cuivre avec un minerai sulfuré conduit à la fixation du cuivre, si le milieu est caractérisé par l'absence de l'oxygène. On reconnaît la fixation de ce métal dans le phénomène de l'enrichissement secondaire du minerai cuprifère. Bien que cette fixation est réalisée par l'expérience, il est difficile d'éclaircir par le moyen de laboratoire les réactions qui prennent part à l'enrichissement secondaire du cuivre.

*Zinc.*—Le comportement du zinc en milieu à pH 1 n'a pas de ressemblance avec celui du cuivre: le zinc n'a pas de tendance à être fixé au cours du traitement. A pH supérieur à 2, la concentration de zinc commence à diminuer avec la durée du traitement. On en déduit la précipitation ou l'adsorption du zinc sous forme de sulfure, analogue à celle du cuivre. Toutefois la vitesse de fixation du zinc est moins grande que celle du cuivre. Ce fait est expliqué par la différence de la propriété chimique des deux métaux.

L'explication des réactions chimiques participant à l'enrichissement secondaire et l'examen des facteurs de milieu intervenant à ce phénomène composeront la suite des études de cette série.

**Résumé**

Les facteurs favorisant la dissolution du cuivre à partir de la chalcopyrite sont les suivants: condition acide et oxydante, co-présence de la pyrite et contact avec l'ion de fer. Ils favoriseraient également la dissolution du zinc à partir de la blende. On peut bien expliquer la dissolution du minerai jaune, en prenant ces facteurs en considération.

L'auteur se permet d'adresser ses remerciements sincères à Monsieur le professeur Noguchi qui a bien voulu lire le manuscrit de ce rapport et aux chercheurs du laboratoire qui lui ont conseillé au cours de l'exécution de ce travail. Il remercie particulièrement Monsieur H. Kamiya pour la collaboration précieuse. Il remercie aussi Monsieur le professeur T. Watanabé et Monsieur le docteur A. Kato, à l'Université de Tokyo, pour l'examen diffractométrique à rayons X de l'échantillon ainsi que les renseignements utiles sur les propriétés des minerais sulfurés.

*Faculté des Sciences*
*Université Métropolitaine de Tokyo*
*Sétagaya, Tokyo*

# *Synthesis of 2-Phenyltropone and its Bromo-derivatives from 2-Phenylsuberone*[1]

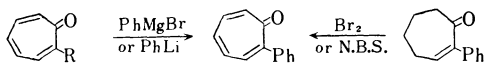
By Tadashi MUROI*

(Received December 22, 1959)

Nozoe, Mukai and their collaborators[2,3] have already reported that 2-phenyltropone (I) is obtained by the reaction of tropolone methyl ether and phenylmagnesium bromide in a good yield. Doering and others[4,5] have also obtained I by the treatment of tropolone and its derivatives with phenylmagnesium bromide or phenyllithium. On the other hand, it is well known that[6-9] various troponoid compounds are derived from cycloheptanons by their direct bromination-dehydrobromination. Nozoe and Ito[10,11] have obtained bromo-derivatives of I by the reaction of bromine and 2-phenylcyclohept-2-enone derived from cycloheptanone. Ginsburg and others[12] have also obtained I by the application of *N*-bromosuccinimide to 2-phenylcycloheptenone.

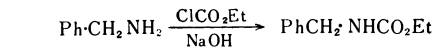
The present author has examined the reaction of 2-phenylsuberone (II) and bromine, and obtained I and its bromo-derivatives in a good yield. This paper describes these results.

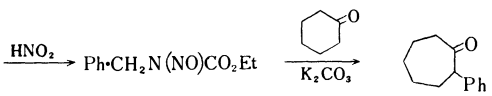
2-Phenylsuberone (II) was prepared by the treatment of cyclohexanone with phenyldiazomethane derived from benzylamine according to Gutsche's method[13].



(I)

R=-OH, -OCH$_3$, -O 1/2 Cu or -Cl



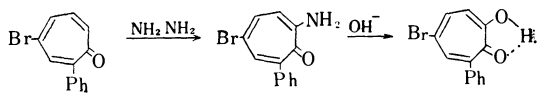


(II)

Scheme 1

When three molar equivalents of bromine were added dropwise into a solution of II dissolved in glacial acetic acid, the reaction of bromine proceeded smoothly with the liberation of hydrogen bromide, and yellow needles (III), decomp. p. 185~187°C, were yielded. By the treatment with water, III was decomposed to give yellow needles (IV) m. p. 91~92°C. The yield of IV is about 30% calculated from II. From the mother liquor, a small amount of I was obtained.

Previously, Nozoe and others[10] confirmed the structure of 4-bromo-2-phenyltropone (IV) by deriving from it 5-bromo-3-phenyltropolone (V) through 7-amino-4-bromo-2-phenyltropone (VI). The present author has also obtained V from IV by the same treatment, and the melting point and the ultraviolet spectrum of IV (Fig. 1) are also identical with those of 4-bromo-2-phenyltropone[10]. It is obvious, therefore, that III is a hydrogen bromide adduct of 4-bromo-2-phenyltropone.



(IV) (VI) (V)

Scheme 2

In some cases, especially, when the reaction was carried out at a lower temperature, a small amount of colorless needles (VII), m. p. 155~156°C and colorless needles (VIII), m. p. 128~129°C were obtained besides IV and I. Though the details of the structure of VII and VIII are not clarified yet, each of them has been proved to be a dibromo-derivative of II from their analytical value.

When four molar equivalents of bromine

1) Presented at the Local Meeting of Tohoku District of the Chemical Society of Japan, held at Kōriyama, Oct. 5. 1957.

* Present address, Hitachi Research Laboratory, Hitachi, Ltd. Sukekawa-machi, Hitachi-shi.

2) T. Nozoe, T. Mukai and J. Minegishi, *Proc. Japan Acad.*, **27**, 419 (1951).

3) T. Nozoe, T. Mukai, J. Minegishi and T. Fujisawa, Science Repts., *Tohoku Univ.*, **I**, 388 (1953).

4) W. von E. Doering and C. H. Hyskey, *J. Am. Chem. Soc.*, **74**, 5688 (1952).

5) W. von E. Doering and J. R. Mayer, ibid., **75**, 2387 (1953).

6) H. J. Dauben and H. J. Ringold, ibid., 73, 876 (1951).

7) T. Nozoe, Y. Kitahara, T. Ando and S. Masamune, *Proc. Japan Acad.*, **27**. 415 (1951).

8) T. Nozoe, Y. Kitahara, T. Ando, S. Masamune and H. Abe, *Science Repts. Tohoku Univ.*, **I**, **36**, 166 (1952).

9) P. L. Pauson, *Chem. Revs.*, **55**, 9, (1955).

10) T. Nozoe, S. Ito and K. Sonobe, *Science Repts, Tohoku Univ.*, **I**, **38**, 141 (1954).

11) T. Nozoe, S. Ito and K. Sonobe, *Proc. Japan Acad.*, **29**, 101 (1953).

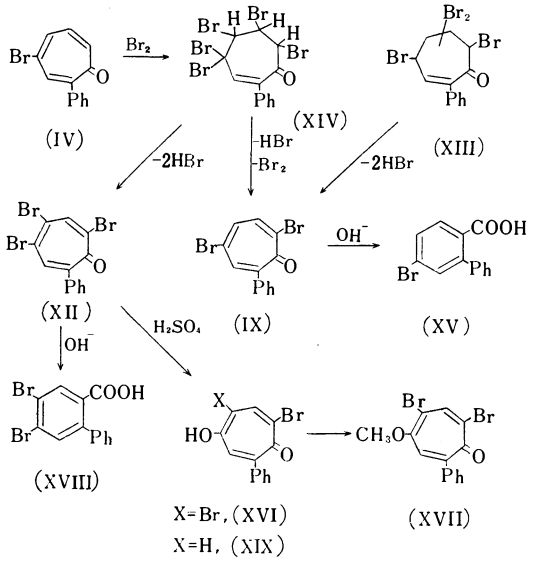
12) D. Elead and D. Ginsburg, *J. Chem. Soc.*, **1954**, 471.

13) D. Gutsche, "Organic Syntheses", **35**, 91 (1955).

were applied to II, it was found that the yield of IV increased remarkablly to about 80%. In this case, moreover, yellow needles (IX), m. p. 117~118°C, and yellow acid crystals (X), decomp. p. ca 200°C, were obtained, though in a small amount.

The reaction of five molar equivalents of bromine and II was found to be somewhat complicated. In this case, prolonged heating and stirring were required to complete the reaction, and the yield of IX was increased to about 78%. From the neutral portion of the mother liquor, besides IX and IV, the following compounds were obtained: pale yellow plates (XI) m. p. 79~80°C pale yellow needles (XII) m. p. 112~113°C and colorless needles (XIII) m. p. 149~150°C. From the acidic portion, a fair amount of X was obtained.

Previously, Mukai[14] reported that a dibromo-derivative of I was obtained by the decomposition of 4, 4, 5, 6, 7-pentabromo-2-phenyl-2-cyclohepten-1-one (XIV) which was derived from IV, and that its structure was assumed to be 4, 7-dibromo-2-phenyltropone.




Scheme 3

The author also obtained IX by the bromination of IV as Mukai reported, and moreover found that, when IX was treated with dilute alkali, it easily rearranged itself to give 4-bromo-2-phenylbenzoic acid (XV)[15]. Therefore, IX seems to be 4, 7-dibromo-2-phenyltropone as Mukai assumed.

The crystal (XI) was proved to be identical with the authentic sample of 7-bromo-2-phenyltropone[12] by the mixed melting point.

The crystal (XII) was found to be a tribromo-derivative of I from its analytical value and U. V. spectrum, (Fig. 1) and it was also obtained from XIV by treating with pyridine. When XII was heated for a long period with 75% sulfuric acid, it gave 5, 7-dibromo-4-hydroxy-2-phenyltropone (XVI)[16], whose structure was confirmed by deriving from it 5, 7-dibromo-4-methoxy-2-phenyltropone (XVII)[16]. It was also found that, by heating with dilute alkali, XII was easily rearranged to give colorless needles of m. p. 180~181°C of 4, 5-dibromo-2-phenylbenzoic acid (XVIII). These facts, therefore, indicated that XII was 4, 5, 7-tribromo-2-phenyltropone.

The crystal (XIII) was a tetrabromo-derivative of 2-phenylsuberenone. When XIII was heated to effect dehydrobromination, it gave IX. It is, therefore, found that two of four bromine atoms of XIII, at least, are presented in the C-4 and C-7 position, and XIII is probably one of the intermediate products in the formation of IX from II.

Though the detailed studies on the acidic product (X) will be described in the near future, it will be noted here that X is a mixture of 7-bromo-4-hydroxy-2-phenyltropone-(XIX) and XVI, and that they are isolated from each other with difficulty.

Even when five molar equivalents of bromine were applied to II, the formation of X was very small, if the addition of bromine was carried out at 30~60°C and the duration of heating was shortened. In this case,. the yield of IX was about 30% and that of XIII proved to be increased.

In order to prevent the formation of X completely, II was treated with five moles of bromine in a mixture of acetic acid and acetic anhydride but a considerable amount of X was still found in the acidic portion. In this case, IV was obtained mainly in about 30% yield but IX was in poor yield and, moreover, a trace of yellow needles (XX) m. p. 144~145°C was obtained. This compound XX was proved to be a monobromo-derivative of I from its analytical value and U. V. spectrum (Fig. 1) and gave by the further bromination a dibromo compound XXI as pale yellow needles m. p. 141~142°C.

As it is known that, on the bromination of tropone derivatives, the bromine atom enters at the carbon atoms adjacent to the carbonyl carbon (i. e., C-2 and C-7) preferentially[14,17], at least the one of bromine atoms of XXI was assumed to be in the C-7 position. It was proved, however, that XXI was identical

14) T. Mukai, *Science Repts. Tohoku Univ.*, I, 38, 280 (1954).
15) I. M. Heilbron et al., *J. Chem. Soc.*, 1938, 115.
16) T. Muroi, to be published.
17) T. Mukai, This Bulletin, 31, 846 (1958).

with neither 3, 7-[18], 4, 7-, 5, 7-[14] and 6, 7-dibromo-derivative[14] of I. Therefore, the other bromine atom of XXI, i.e., that of XX is assumed not to be in the tropone nucleus but in the phenyl group.

In the above reactions, the yield of I was poor but, as it is known that IV is easily debrominated to give I, this reaction is considered to be a useful synthetic method for the preparation of I. As the mechanism of this reaction is not clarified yet this is considered to be an interesting question in future.

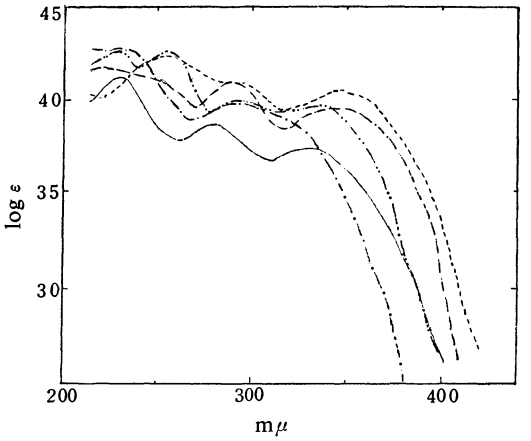



Fig. 1. U. V. Absorption spectra of IV, IX, XII, XX and XXI in methanol.
——— (IV) – – – (IX) ------ (XII)
–·–· (XX) –··–·· (XXI)

## Experimental[19]

**Action of Bromine on 2-Phenylsuberone (II).**—II was prepared according to the description of "Organic Syntheses"[13], and the fraction of b. p. 110~111°C/0.3~0.4 mmHg; $n_D^{27}$: 1.5390, was used[20].

**a) Application of 3 Molar Equivalents of Bromine.**—i) To a solution of 4.7 g. of II in 7.5 cc. of acetic acid, a mixture of 12 g. of bromine and 2 cc. of acetic acid was added dropwise with stirring for a period of 1 hr. at 30~40°C. After the addition, the reaction mixture was heated on a water bath to about 80°C and kept at the same temperature for 30 min. and then yellow crystals were separated out. Additional heating and stirring were continued until there was no liberation of hydrogen bromide. After cooling, the crystals were collected by filtration and washed with a small amount of acetic acid and benzene, successively. Yellow crystals (III) decomp. p. 185~187°C, 3.7 g. were obtained. On standing overnight, the filtrate gave the second crop of III, 0.28 g. When III was treated with about 50 cc. of water, 2.3 g. of pale yellow crystals were obtained. Recrystallization from alcohol or methanol gave yellow needles (IV) m. p. 91~92°C.

Found: C, 60.06; H, 3.63. Calcd. for $C_{13}H_9OBr$: C, 59.74; H, 3.74%.

The mother liquor was evaporated under reduced pressure and the residue, treated with water, was extracted with chloroform. The extract was washed with 10% sodium carbonate solution. After the removal of the solvent, the residual oil, dissolved in a mixture of benzene and petroleum ether (1 : 1), was chromatographed through a silica-gel column. It was eluted successively with a mixture of benzene and petroleum ether, benzene, chloroform and alcohol. From the chloroform eluent, 0.2 g. of raw crystals of I was obtained but the other eluent gave no crystals.

Acidification of the sodium carbonate solution gave no crystalline products.

ii) As in the above case, 4.7 g. of II in 7.5 cc. of acetic acid was treated with 12 g. of bromine dissolved in 2 cc. of acetic acid. In this case, however, heating was stopped at ones when the separation of III occurred. After cooling, III was collected by filtration and treated with water to give 2.0 g. of IV. The filtrate, after standing for a few days, gave 0.22 g. of pale yellow crystals, m. p. 115~120°C. This was decomposed with water to give colorless crystals m. p. 175~180°C. Recrystallization from alcohol or benzene gave sparingly soluble colorless needles (VII) m. p. 155~156°C and comparatively soluble colorless needles (VIII) m. p. 128~129°C, respectively.

Found for VII: C, 45.41; H, 3.95. Calcd. for $C_{13}H_{14}OBr_2$: C, 45.12; H, 4.08%.

Found for VIII: C, 45.23; H, 3.97. Calcd. for $C_{13}H_{14}OBr_2$: C. 45.12; H, 4.08%.

After being treated as in i), the mother liquor gave 0.5 g. of I.

**b) Application of 4 Molar Equivalents of Bromine.**—To a solution of 4.7 g. of II in 7.5 cc. of acetic acid, 16 g. of bromine dissolved in 2.7 cc. of acetic acid was added dropwise during about 1.5 hr. at 30~60°C. In this case, when treated as in a), it gave three kinds of crystals from the neutral portion as follows: 5.2 g. of IV, 0.28 g. of IX and a small amount of I. Recrystallization of IX from alcohol gave yellow needles, m. p. 117~118°C.

Found: C, 45.68; 2.38. Calcd. for $C_{13}H_9OBr_2$: C, 45.93; H, 2.36%.

The acidic portion gave yellow crystals (X) decomp. p. 185~190°C, 0.02 g.

**c) Application of 5 Molar Equivalents of Bromine.**—i) To a solution of 4.7 g. of II in 7.5 cc. of acetic acid, 20 g. of bromine dissolved in 3.5 cc. of acetic acid was added dropwise over a period of 2.5 hr. at 30~65°C. After the addition, the mixture was heated on a water bath for 4 hr., until there was no liberation of hydrogen bromide. By chilling with ice no crystals were separated out, then the solvent was distilled off under reduced

18) T. Nozoe, T. Mukai and I. Murata, *Proc. Japan Acad.*, **28**, 142 (1952).

19) M. p. are uncorrected. The microanalyses and the measurement of U. V. spectra were carried out by Mrs. K. Kodaira of Tohoku University, to whom the author's deep gratitude is hereby expressed.

20) The fractional distillation of II was carried out at Kitahara's Laboratory in the Chemical Research Institute of Non-aqueous Solution, Tohoku University, using the Stedtmann type fractional column (40 plates). The author expresses hereby his deep gratitude to Professor Yoshio Kitahara for his kindness.

pressure. The residue, decomposed with water, was extracted with chloroform. After washing the extract with 10% sodium carbonate solution, the solvent was evaporated off. The residual oil (10 g.), digested with alcohol or ether, gave 0.9 g. of IX m. p. 113~115°C. After being treated as in a) i), the mother liquor was chromatographed through a silica-gel column. The benzene-petroleum ether eluent gave 1.0 g. of XIII, 0.8 g. of XII and 1.0 g. of IX, successively.

Recrystallization of XIII from alcohol gave colorless needles m. p. 149~150°C.

Found: C, 31.49; H, 2.13. Calcd. for $C_{13}H_{10}OBr_4$: C, 31.11; H, 2.00%.

Recrystallization of XII from alcohol gave pale yellow needles m. p. 113~114°C.

Found: C, 37.41; H, 1.19. Calcd. for $C_{13}H_7OBr_3$: C, 37.28; H, 1.99%.

The benzene eluent gave 0.6 g. of IX, 0.7 g. of IV and 0.1 g. of XI, successively. From the chloroform eluent, 0.1 g. of I was obtained, acompanied with a resinous substance. Alcohol eluent did not give any crystals.

In this case, the alkaline washing solution gave no crystals by acidification.

ii) To a solution of 4.7 g. of II in 7.5 cc. of acetic acid, 20 g. of bromine dissolved in 3.5 cc. of acetic acid was added. About 3/4 vols. of bromine solution was added at 40~75°C for a period of 1.5 hrs., then yellow crystals were separated out. These were dissolved again in a dark red solution when the rest of the bromine was added at 85°C. The mixture was further heated for 6 hr. until there was no liberation of hydrogen bromide. After cooling, the yellow crystals (a) thereby separated were collected by filtration. There were digested with benzene and an insoluble portion (b) was filtered off. The filtrate was shaken with 10% sodium carbonate solution and the aqueous layer was combined with (b). This alkaline solution, after being treated with active carbon, was acidified to give 0.27 g. of X, m. p. 200~205°C. The benzene layer, after removal of the solvent, left a crystalline residue which was recrystalized from alcohol or ether to give 4.5 g. of IX.

The mother liquor of (a), treated as in a, i), gave the following crystals: 1.0 g. of IX, 0.44 g. of X, 0.1 g. of XI, 0.2 g. of XII and 0.15 g. of XIII.

iii) To a solution of 4.7 g. of II in 7.5 cc. of acetic acid and 2.5 cc. of acetic anhydride, 20 g. of bromine dissolved in 3.5 cc. of acetic acid was added as in the above case. In this case, no crystals were separated during the reaction. On cooling, 5.3 g. of III was obtained and this was decomposed to 3.1 g. of IV. After being treated as in a, i), 0.2 g. of X was obtained from the 10% sodium carbonate soluble part of the mother liquor. The chromatographic separation of the neutral substance gave successively the following crystals: 0.35 g. of IX, 0.40 g. of IV, 0.15 g. of XX and 0.1 g. of I.

The recrystallization of XX from methanol gave yellow needless of m. p. 144~145°C.

Found: C, 60.29; H, 3.58. Calcd. for $C_{13}H_9OBr$: C, 59.79; H, 3.47%.

**Action of Hydrazine on 4-Bromo-2-phenyltropone (IV).** — A mixture of 0.2 g. of IV, 0.2 cc. of 80% hydrazine hydrate and 2 cc. of alcohol was refluxed on a water bath for 30 min., and the crystals that separated out were collected by filtration. Recrystallization from alcohol gave orange yellow needles of VI, m. p. 210°C.

A mixture of 0.08 g. of VI, 0.3 cc. of 6 N sodium hydroxide solution and 1.6 cc. of alcohol was refluxed for 3 hr. The alcohol was distilled off, the residue was acidified, and the precipitate thereby formed was recrystallized from methanol to give yellow needles of m. p. 135~136°C. This was found to be identical by mixed fusion with the authentic sample of 5-bromo-3-phenyltropolone (V)[10].

**Bromination of 4-Bromo-2-phenyltropone (IV).** — To a solution of 2.6 g. of IV in 40 cc. of acetic acid, 4.8 g. of bromine in 5 cc. of acetic acid was added and this mixture was allowed to stand over night. The crystals that separated out were collected and recrystallized from alcohol and benzene to give colorless prisms of XIV, m. p. 121~122°C (decomp.). Yield, 4.7 g.

Found: C, 27.26; H, 1.68. Calcd. for $C_{13}H_9OBr_5$: C, 26.89; H, 1.56%.

The filtrate was evaporated under reduced pressure and the residue, after being treated with water, was extracted with benzene. After removal of solvent, the extract left a crystalline residue which was recrystallized from alcohol to give yellow crystals of m. p. 110~113°C. This showed no depression of melting point on admixture with IX obtained in the above cases.

**Decomposition of 4,4,5,6,7-Pentabromo-2-phenyl-2-cyclohepten-1-one (XIV).** — i) By heating 0.15 g. of XIV in an oil bath at 120~130°C for 10 min., XIV melted with effervescence and underwent decomposition to an oil. After cooling, this was dissolved in benzene and washed with a diluted sodium hyposulfate solution. The benzene layer, after the removal of solvent, left a crystalline residue that was recrystallized from alcohol to give yellow crystals of m. p. 116~117°C, undepressed on admixture with IX. Yield, 0.05 g.

ii) A mixture of 0.58 g. of XIV, 0.6 cc. of pyridine and 0.3 g. of benzene was heated for 15 min. at 55~60°C. This was diluted with water and extracted with benzene. The extract after evaporation, left yellow crystals. Recrystallization from alcohol gave yellow needles of m. p. 112~113°C, undepressed on admixture with XII obtained above.

**Action of Alkali on 4,7-Dibromo-2-phenyltropone (IX).**—A mixture of 0.06 g. of IX, 1.5 cc. of alcohol and 1 cc. of 2 N sodium hydroxide solution was refluxed on a water bath for 30 min. After the removal of solvent it was acidified and extracted with benzene. The benzene layer gave colorless crystals that were recrystallized from cyclohexane to give XV as colorless needles of m. p. 173~175°C.

Found: C, 56.75; H, 3.47. Calcd. for $C_{13}H_9OBr$: C, 56.34; H, 3.27%.

**Action of Alkali on 4,5,7-Tribromo-2-phenyltropone (XII).**—A mixture of 0.05 g. of XII, 0.7 cc. of alcohol and 0.5 cc. of 2 N sodium hydroxide was refluxed on a water bath for 15 min. This, treated as in the above case, gave colorless needles of XVIII, m. p. 180~181°C.

Found : C, 43.76 ; H, 2.15. Calcd. for $C_{13}H_8O_2Br_2$ : C, 43.76 ; H, 2.26%.

**Action of Sulfuric Acid on 4, 5, 7-Tribromo-2-phenyltropone(XII).**—A solution of 0.25 g. of XII and 2.5 cc. of 75% sulfuric acid was heated for 10 hr. at 170~180°C. This was poured into about 20 cc. of ice water, and thereby precipitated crystals were collected. The crystals, after being dried, were washed with benzene and dissolved in 10% sodium carbonate solution. After being treated with active carbon, the solution was acidified and 0.1 g. of yellow crystals of d. p. ca 190°C were obtained. This was treated with a 2.8% diazomethane-ether solution and the thereby obtained oily product was dissolved in a mixture of benzene and petroleum ether. This was chromatographed on a silica-gel column and gave yellow crystals of m. p. 128~129°C. Recrystallization from methanol gave yellow needles of m. p. 131~132°C, which showed no depression with authentic sample of XVI.

**Thermal Decomposition of 4, 7, *x*, *x*-Tetrabromo-2-phenylsuberenone(XIII).** — By heating 0.12 g. of XIII on an oil bath for 20 min. at 150~160°C, it melted and underwent decomposition. The fused mass, dissolved in benzene, was washed sufficiently with water. The benzene solution was passed through a silica-gel column and yellow needles of m. p. 117~118°C were obtained. These showed no depression on admixture with IX obtained above.

**Bromination of *x*-Bromo-2-phenyltropone(XX).** —To a solution of 0.06 g. of XX in 1 cc. of acetic acid, 0.06 g. of bromine was added and the whole was heated on a water bath for 30 min. Then this was diluted with water and extracted with chloroform. After the removal of solvent, this gave colorless crystals of m. p. 135~140°C, which were recrystallized from benzene or alcohol to give pale yellow needles, m. p. 141~142°C.

Found : C, 45.94 ; H, 2.36. Calcd. for $C_{13}H_8OBr_2$ : C, 45.93 ; H, 2. 36%.

The author takes this opportunity to express his sincere gratitude to professor Tetsuo Nozoe of Tohoku University for his guidance and encouragement throughout the course of this work, to Professor Shuichi Seto, Professor Yoshio Kitahara and Assistant Professor Toshio Mukai for much helpful advice, and to assistant Professor Katsuo Kikuchi of Yamagata University for his kind discussion and helpful advice.

*Department of Chemistry*
*Faculty of Liberal Arts and Science*
*Yamagata University*
*Koshirakawa-machi, Yamagata*

# *Stereoregular Polymers. VI. Copolymerization with the Ziegler Catalysts**

By Shunsuke MURAHASHI, Shun'ichi NOZAKURA and Masao SUMI

(Received January 5, 1960)

Binary copolymerizations of $\alpha$-olefins, which are known individually to form isotactic polymers with the Ziegler catalyst, were investigated to see if stereospecific copolymerization could be seen to yield crystalline copolymers.

Although there are a number of reports by Natta and his collaborators on copolymerization of propylene and ethylene with complex catalysts of the Ziegler type[1], one of the comonomers was always ethylene and this has substantially no concern with the assymmetricity on the polymer. Besides, ethylene has markedly higher activity towards the anionic polymerization as compared to propylene, and their efforts were apparently directed towards the study of amorphous copolymers.

In the present work, the situation was distinctly different from that in the case of Natta. Particular attention was directed to the formation of crystalline copolymers, because it was believed that crystalline copolymers could be produced if the isotactic orientation had been held during copolymerization**.

The monomers chosen here are styrene, allyl- and 3-butenyl-trimethylsilane, which are known by the present authors to yield the corresponding isotactic polymers by themselves and to have the similar reactivity towards the Ziegler catalyst[3,4].

The following abreviations will be used in

* Presented at the 8th. Annual Meeting of Society of Polymer Science (Japan), May 30, 1959.

1) G. Natta et al., *Chim. e ind.*, **39**, 733, 743, 825 (1957); **40**, 717, 896 (1958).

** In the course of our study, Reding has reported in a brief note the cocrystalline copolymers of 3-methyl-1-butene and 4-methyl-1-pentene, which were found to be surprisingly highly crystalline over the entire range of compositions.[2]

2) F. P. Reding and E. R. Walter, *J. Polymer Sci.*, **37**, 555 (1959).

3) S. Murahashi, S. Nozakura and M. Sumi, This Bulletin, **32**, 670 (1959).

4) G. Natta, G. Mazzanti, P. Longi and F. Bernardini, *J. Polymer Sci.*, **31**, 181 (1958).

TABLE I. COPOLYMERIZATION OF STYRENE AND ALKENYLTRIMETHYLSILANES WITH $AlEt_3$-$TiCl_4$ CATALYST AT 70°C

| Combination of monomers | Monomer, mole | | Catalyst, millimole | | | *n*-Heptane ml. | Time hr. | Polymer yield, % | Composition, mole % of silane* | |
|---|---|---|---|---|---|---|---|---|---|---|
| | Silane | St | $AlEt_3$ | $TiCl_4$ | Al/Ti ratio | | | | Monomer | Polymer |
| St-VSi | 0.0298 | 0.0290 | 4.30 | 1.79 | 2.40 | 20 | 7 | 16.0 | 50.48 | 1.94 |
| St-ASi | 0.0176 | 0.0724 | 5.61 | 2.26 | 2.48 | 20 | 3.5 | 13.2 | 19.56 | 6.19 |
| | 0.0166 | 0.0173 | 3.77 | 1.42 | 2.65 | 15 | 6 | 23.3 | 48.97 | 18.87 |
| | 0.0615 | 0.0165 | 5.87 | 2.21 | 2.66 | 20 | 2 | 10.1 | 78.85 | 66.62 |
| St-BSi | 0.0146 | 0.0624 | 5.70 | 2.21 | 2.58 | 20 | 3 | 15.3 | 18.96 | 10.64 |
| | 0.0378 | 0.0379 | 5.87 | 2.32 | 2.53 | 20 | 3 | 20.5 | 49.93 | 42.71 |
| | 0.0650 | 0.0170 | 6.87 | 2.63 | 2.60 | 20 | 4 | 27.4 | 79.27 | 70.21 |

* Copolymer composition was determined by the gravimetric analysis of silicon.

TABLE II. COPOLYMERIZATION OF ASi AND BSi WITH $AlEt_3$-$TiCl_4$ CATALYST AT 70°C

| Monomer, mole | | Catalyst, millimole | | | *n*-Heptane ml. | Time hr. | Polymer yield, % | Composition, mole % of silane | |
|---|---|---|---|---|---|---|---|---|---|
| ASi | BSi | $AlEt_3$ | $TiCl_4$ | Al/Ti ratio | | | | Monomer | Polymer |
| 0.0306 | 0.0289 | 5.35 | 2.21 | 2.42 | 20 | 3.5 | 22.1 | 51.43 | 8.74 |
| 0.0735 | 0.0192 | 6.58* | 2.63 | 2.50 | 25 | 3.5 | 9.9 | 79.29 | 48.72 |

* A solution of $AlEt_3$(3.86 millimole) was added to a boiling *n*-heptane solution of $TiCl_4$ (2.63 millimole) and after cooling it the precipitated mass was washed with *n*-heptane, and then $AlEt_3$(2.72 millimole) was added.

this paper for convenience:

| | |
|---|---|
| Vinyltrimethylsilane | VSi |
| Allyltrimethylsilane | ASi |
| 3-Butenyltrimethylsilane | BSi |
| Styrene | St |

## Results and Discussion

**Polymerization.** — Binary copolymerizations were carried out using these monomers with $AlEt_3$-$TiCl_4$ catalyst at 70°C. The results were summarized in Tables I and II.

VSi, the first member of alkenyltrimethylsilane, was found to enter into copolymerization with great difficulty as anticipated from the case of its homopolymerization with the same catalyst, and hence a further study was omitted from our program.

As is shown in Tables I and II, the compositions of the crude polymers varied with monomer compositions and copolymerization appeared at first to have been realized. The apparent monomer reactivities towards the Ziegler catalyst was found to be in the order of St > BSi > ASi ≫ VSi.

**Fractionation of the Crude Polymers.** — As these copolymers showed some degree of crystallinity on X-ray diffraction patterns, fractionations were carried out with a series of solvents selected from the knowledge of the solubility characteristics of the individual crystalline homopolymers. (Table III).

TABLE III. SOLUBILITY CHARACTERISTICS OF ISOTACTIC POLYMERS OF St, ASi AND BSi

| | *n*-Heptane | Toluene | Decalin |
|---|---|---|---|
| Poly(BSi) | Sol. in hot | Sol. | Sol. |
| Poly(St) | Insol. | Sol. in hot | Sol. |
| Poly(ASi) | Insol. | Insol. | Sol. in hot |

Thus, a St–BSi copolymer was fractionally extracted with a series of solvents: acetone, ether, methylethylketone, *n*-heptane and toluene under reflux in this order. The results are shown in Table IV in which was included, for reference, the results of model fractional extractions of an artificial mixture of two homopolymers, showing practically a complete separation of the crystalline parts into the original components. The acetone-, ether- and methylethylketone-soluble fractions of the copolymer are all found to give almost amorphous X-ray diffraction patterns, while both the *n*-heptane- and the toluene-fraction are found to give crystalline patterns. Analytical data of the last two fractions show that the *n*-heptane-fraction is closely similar to isotactic poly(BSi) with a minor amount of St, while the toluene-fraction is similar to isotactic poly(St) with a minor amount of BSi. The amount of the minor ingredient (St) in the former fraction showed no appreciable change even after repeated purification, that is, extraction with methylethylketone followed by dissolution of the residue into hot *n*-heptane and reprecipitation by cooling the solution. Therefore, it

Table IV. Fractionation of St-BSi copolymers

| Polymers | Composition of the crude polymer | Acetone-extract | | | | Ether extract | | M. E. K extract | | *n*-Heptane extract | | Toluene extract | |
|---|---|---|---|---|---|---|---|---|---|---|---|---|---|
| | | Sol. in cold | | Sol. in hot | | | | | | | | | |
| | mole % of silane | % | mole % of silane | % | mole % of silane | % | mole % of silane | % | mole % of silane | % | mole % of silane | % | mole % of silane |
| Copolymer | 10.64 | 23.1 | 7.35 | 5.5 | 35.03 | 3.3 | 49.59 | 1.8 | — | 3.3 | 76.72 | 53.7 | 2.76 |
| Copolymer | 42.25 | 19.9 | 18.68 | 10.1 | 49.23 | 18.6 | 67.62 | 3.1 | 14.48 | 19.6 | 89.57 | 22.4 | 3.81 |
| Copolymer | 70.21 | 5.4 | 40.73 | 8.9 | 67.22 | 13.2 | 76.46 | 0.8 | — | 53.0 | 90.61 | 4.6 | 13.53 |
| Mixture | 40.64 | 5.8 | 22.75 | 1.2 | — | 6.2 | 94.60 | 0.7 | — | 29.4 | 92.79 | 43.7 | 0.19 |
| X-ray evidence | | amorph. | | amorph. | | amorph. | | amorph. | | cryst. | | cryst. | |

Table V. Fractionation of St-ASi copolymers

| Polymers | Composition of the crude polymer | Acetone extract | | Ether extract | | *n*-Heptane extract | | M. E. K. extract | | Toluene extract | | Toluene residue | | Decalin extract | |
|---|---|---|---|---|---|---|---|---|---|---|---|---|---|---|---|
| | mole % of ASi | % | mole % of ASi | % | mole % of ASi | % | mole % of ASi | % | mole % of ASi | % | mole % of ASi | % | mole % of ASi | % | mole % of ASi |
| Copolymer | 6.19 | 9.0 | 19.84 | 1.3 | — | 1.4 | — | 2.5 | — | 78.1 | 1.52 | 1.2 | — | | |
| Copolymer | 18.89 | 13.3 | 33.76 | 4.8 | 51.57 | 1.2 | 53.91 | 0.9 | 18.02 | 63.4 | 2.48 | 10.6 | 77.44 | | |
| Copolymer | 66.62 | 16.1 | — | 11.5 | — | 4.2 | — | 0.9 | — | 17.9 | 9.19 | | | 0.79 | 85.07 |
| Micture | 19.39 | 6.4 | 52.14 | 2.4 | — | 1.0 | — | 0.5 | — | 68.8 | 0.22 | 11.8 | 95.50 | | |
| X-ray evidence | | amorph. | | amorph. | | amorph. | | amorph. | | cryst. | | cryst. | | | |

Table VI. Fractionation of ASi-BSi copolymers

| Polymers | Crude polymers Si, %* | Acetone extract % | Ether extract % | *n*-Heptane extract | | Decalin extract | |
|---|---|---|---|---|---|---|---|
| | | | | % | Si, %* | % | Si, %* |
| Copolymer | 22.13 | 20.3 | 45.7 | 18.6 | — | 6.6 | — |
| Copolymer | 23.13 | 15.9 | 29.3 | 14.7 | 21.0 | 31.0 | 24.0 |
| X-ray evidence | | amorph. | amorph. | cryst. | | cryst. | |

* The theoretical Si content of BSi and ASi are 21.90 and 24.59%, respectively. The analysis of the fractions was carried out on a microscale.

was concluded that the *n*-heptane-fraction might not be a mixture but a genuine copolymer. It was also found that the same was held to be the case by the latter fraction.

An additional evidence for the copolymeric character of the two crystalline fractions is the change of their compositions with the fed monomer compositions. By increasing the silane content in monomer composition, the silane content of both the *n*-heptane- and the toluene-fraction increased.

Thus, it was confirmed that the crystalline portion of the St–BSi polymer consisted of two kinds of crystalline copolymers of quite different compositions, that is, both a crystalline copolymer with a predominant portion of one component and another crystalline copolymer of another predominant component were produced side by side.

Similar results hold in the copolymerization with the combinations of St–ASi and ASi–BSi (Tables V and VI), though in the latter case the pair selected was of very similar monomers.

From these results, one might postulate that the catalyst surface might possess two kinds of isotactically active sites for each monomer. One kind of the sites is more favorable to polymerize one monomer than other monomers and this is true of other site. More generally, one might say that the catalytic surface possesses several different kinds of active sites suitable for some kinds of monomers. Copolymerization would have taken place on such sites, leading to the crystalline copolymers of different compositions.

An alternative interpretation might also be possible where the nature of an active site may not have been set specifically beforehand at the time when the catalyst is formed, and may become specific after the first attack of a monomer molecule on the catalyst site.

It may not be easy to distinguish which of the two alternative mechanisms is more favorable in our case, but the following experimental results seems to show that the former mechanism might be more favorable. It was demonstrated in one experiment where a small amount of one monomer (about 1millimole) was added preliminarily to the catalyst at 70°C, and after 20 minutes of polymerization a mixture of two monomers St and ASi (20 millimole : 20 millimole) was then added. Two runs that were carried out by the preliminary addition of St in one case and ASi in another case resulted in practically the same distribution of fractions in the extraction experiment.

**X-Ray Examination of the Crystalline Fractions.**—In the case of the copolymerization of St and BSi, for instance, the *n*-heptane- and the toluene-fraction showed some degree of

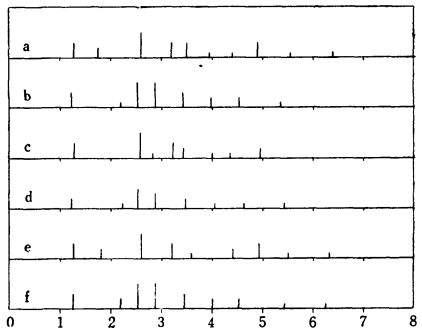



Fig. 1. X-Ray spectra of ASi-St copolymers. ($R$=4.45 cm.)
a) Copolymer : silane, 77.4 mole %.
b) Copolymer : silane, 9.1 mole %.
c) Artificial mixture : silane, 77 mole %.
d) Artificial mixture : silane, 9.2 mole %.
e) Isotactic poly(allylsilane).
f) Isotactic polystyrene.

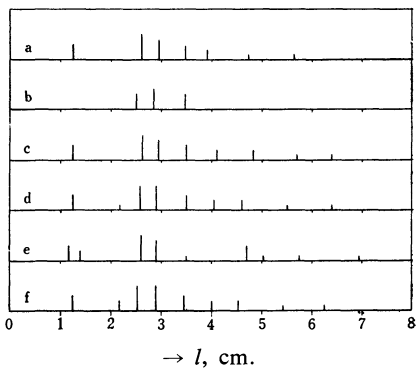



Fig. 2. X-Ray spectra of BSi-St copolymers. ($R$=4.45 cm.)
a) Copolymer : silane, 89.6 mole %.
b) Copolymer : silane, 13.5 mole %.
c) Artificial mixture : silane, 73 mole %.
d) Artificial mixture : silane, 23 mole %.
e) Isotactic poly(3-butenylsilane).
f) Isotactic polystyrene.

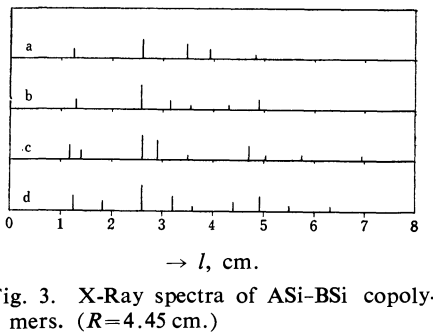



Fig. 3. X-Ray spectra of ASi-BSi copolymers. ($R$=4.45 cm.)
a) Copolymer : the *n*-heptane-fraction.
b) Copolymer : the decalin-fraction.
c) Isotactic poly(3-butenylsilane).
d) Isotactic poly(allylsilane).

crystalline patterns on X-ray diagrams. X-Ray powder patterns of these two fractions were compared with those of two homopolymers and of the artificial mixtures of similar compositions. The same comparison was also made in other cases. X-Ray spectra of St–ASi copolymers, St–BSi copolymers, and ASi–BSi copolymers were shown in Figs. 1, 2 and 3, respectively***.

From the close inspection of these results, it was found that in some cases the patterns closely resemble those of artificial mixtures of the similar compositions (Figs. 1a and 1b), some had a new kind of additional reflections over those of artificial mixtures or a superposition of homopolymers (Figs. 2a and 3a), and others showed only very diffuse reflections of one homopolymer (Figs. 2b and 3b). These facts might suggest the possible existence of constitutional varieties in copolymers with the change of monomer species, that is, one copolymer might have a structure of block copolymer and another might have a structure of random copolymer. For instance, the decalin-fraction (Fig. 1a) of St–ASi copolymer has a rather high crystallinity which is comparable to that of poly(ASi) and shows a diffraction pattern that is closely similar to an artificial mixture of the same composition, suggesting a block structure. If it were a random copolymer, incorporation of about 20% of St units, as is the case, would almost destroy the crystallinity of the copolymer.

## Experimental

**Materials.**—A commercial styrene was purified according to the usual method[5].

Vinyl-, allyl, and 3-butenyl-trimethylsilane are prepared and purified just as described in the previous paper[3].

$AlEt_3$ and $TiCl_4$ are the products of Mitsui Chem. Ind. Co. and Osaka Titanium Co., respectively and were used as about 30 and 21% solutions in *n*-heptane.

**Polymerization.**—Polymerization was carried out without agitation in an apparatus described in the previous paper[6]. The solution of $AlEt_3$ was added first to *n*-heptane in the apparatus under nitrogen, and mixed, and then the solution of $TiCl_4$ was dropped slowly along the wall of the vessel. After ten minutes, the mixed monomers were added and polymerization was carried out without agitation.

Polymerization was stopped by the addition of methanol (2 ml.) and concentrated hydrochloric acid (0.3 ml.), and the mixture was poured into a large amount of methanol. After being kept overnight, the polymer was collected, washed with methanol and dried.

**Fractionation of the Crude Copolymers.** — Hot extraction was carried out at the boiling temperature of the solvents, using a modified Soxhlet extraction apparatus. Complete extraction with one solvent generally took about seven to ten hours. After the completion of one extraction, the extraction cup with the residual polymer in it was dried, and was subjected to the next extraction. Each extract was concentrated to about 50 ml. and poured into a large amount of methanol, and the precipitate was collected, washed and dried.

Purification of the crystalline fraction, for example, the *n*-heptane fraction of St–BSi copolymer was carried out as follows: the fraction (Si, 20.08%) was extracted with methyl ethyl ketone, and dissolved in hot *n*-heptane. The hot solution, after being filtered through a glass filter, was poured into a large amount of methanol. The precipitated polymer was collected, washed and dried in vacuum at about 100°C (Si, 19.92%). The toluene fraction (Si, 1.80%) of the polymer was also purified by extraction with *n*-heptane followed by dissolution in toluene and reprecipitation with methanol, giving the silicon content of 1.40 and 1.48%, successively.

**Preparation of Artificial Mixture of Homopolymers.** — Generally, a mechanical mixture of two kinds of polymers was dissolved in a hot solvent common to them and poured quickly into a large amount of methanol and then the precipitate was collected.

**Determination of Copolymer Composition.**—The composition of copolymers was determined by the gravimetric analysis of silicon. Analysis was carried out by wet digestion with fuming sulfuric acid in a platinum crucible. The ignited silica was ascertained by treating it with 60% hydrofluoric acid.

**X-Ray Study.** — All samples were annealed at 150~160°C for 2 hr. The diffraction patterns were taken using nickel filtered Cu$K\alpha$ radiation. The film distance was 4.45 cm.

## Summary

Binary copolymerization of styrene, allyltrimethylsilane and 3-butenyltrimethylsilane was investigated using the Ziegler catalyst at 70°C. It was found to be possible to separate the crystalline part of copolymers by fractional extraction into two kinds of genuine crystalline copolymers, each of which has an extremely different composition from the other.

The nature of the active sites on the catalytic surface was discussed in order to elucidate the above fact.

The constitution of the individual crystalline fractions appeared to vary case by case, i. e., the structure of blockcopolymer might be assigned to some cases and random copolymers to some other cases.

*Department of Polymer Science*
*Faculty of Science*
*Osaka University*
*Nakanoshima, Kita-ku, Osaka*

*** Since the exact copolymer composition was not obvious in the case of ASi-BSi copolymer because of the small difference of silicon content between ASi and BSi units, comparison with artificial mixtures was not indicated in the list.

5) E. R. Blout and H. Mark, "Monomers", Interscience Publisher (1944).

6) S. Murahashi, S. Nozakura, M. Sumi and K. Hatada, This Bulletin, 32, 1094 (1959).

# *The Aconite Alkaloids. XXXIV*[1]*. On Lucidusculine. Part IV*[2]

By Takashi AMIYA

(Received January 6, 1960)

In previous reports[3,4] the partial formula of lucidusculine (I), $C_{24}H_{35}O_4N$, has been summarized as[5],

$C_{16}H_{20}$ { $CH_2OH$, $OCOCH_3$, $>CH(OH)$ (six-membered ring), $>NC_2H_5$, $>C=CH_2$ }

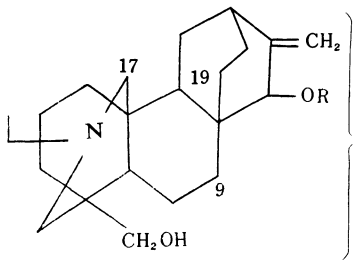
(I)

Moreover, luciculine (II), $C_{22}H_{33}O_3N \cdot H_2O$, which is yielded from compound I by hydrolysis and hence is a sort of trihydric amino alcohol, has been shown to possess an allyl alcohol moiety in its six-membered ring[6].

On the other hand, on dehydrogenation of compound I, phenanthrene and its homologues were obtained by Suginome and Kakimoto[7] in this laboratory.

Under the same conditions as in the case of isomerization of compound II to isoluciculine (III)[6], compound I was found not to isomerize. Instead, a certain compound IV was formed. This compound did not crystallize. It seemed to be a dihydro compound. In the infrared spectrum, compound IV gave no band characteristic of a ketone carbonyl group in a six-membered ring near 5.8 $\mu$ but it did give a band characteristic of an ester carbonyl group. No absorption band near 11 $\mu$, indicative of a terminal methylene group, was observed in the spectrum. On hydrolysis of compound IV by alcoholic potassium hydroxide, an amorphous base V was obtained. In the infrared region, this base showed no band near 5.7~5.8 $\mu$, indicating that carbonyl group, either ester or ketone, was quite absent. The spectrum also showed that no band characteristic of a terminal methylene group near 11 $\mu$ existed. This fact may show that the acetylated hydroxyl group in compound I is the secondary one involved in the allyl alcohol moiety mentioned above. The above hydrogenation seems to proceed similarly to that of Shimoburo base I diacetate[8].

On the basis of these experimental results as well as in view of the structures of other aconite alkaloids, the partial formula of compounds I and II is now represented in Fig. 1.




(I) R=Ac
(II) R=H

Fig. 1.

Lucidusculine has been assumed to have a hexacyclic structure[9]. Considering the structures of hypogenavine[10], kobusine[11], ignavine[12], hetisine[13] and songorine[14], the existence of the C-17—C-19 or C-17—C-9 bond seems to be reasonable. Moreover, to complete the structure of compound I, it is necessary to confirm the position of an indefinite secondary hydroxyl group (see Fig. 1).

## Experimental

**Hydrogenation of Lucidusculine (I) with Pd-C.** —Lucidusculine (0.3 g.) was dissolved in 15 cc. of methanol and hydrogenated with 10% palladium-carbon (0.2 g.) at room temperature for 4.5 hr. After removal of palladium-carbon, the solution was evaporated to dryness. On treatment with methanol, the residue was not crystallized. The infrared absorption spectrum in nujol had no peak attributable to a terminal methylene group but

1) This constitues a part of a series entitled "The Aconite Alkaloids" by H. Suginome. Part XXXIII: cf. Ref. 4).
2) XXXIII of this series corresponds to part III of "On Lucidusculine".
3) T. Amiya, This Bulletin, 30, 677 (1957).
4) T. Amiya, ibid., 33, 644 (1960)..
5) The partial formula of I was presented in a previous report[3], as $C_{17}H_{20}$ erroneously, but this should be corrected.
6) T. Amiya, This Bulletin, 32, 421 (1959).
7) H. Suginome and S. Kakimoto, ibid., 32, 352 (1959).
8) T. Sugasawa, *Pharm. Bull.*, 4, 6 (1956).
9) H. Suginome, T. Amiya and T. Shima, This Bulletin, 32, 824 (1959).
10) S. Sakai, *Chem. Pharm. Bull.*, 6, 448 (1958).
11) M. Natsume, ibid., 7, 539 (1959).
12) E. Ochiai and T. Okamoto, ibid., 7, 556 (1959).
13) A. J. Solo and S. W. Pelletier, *J. Am. Chem. Soc.*, 81, 4439 (1959).
14) E. Ochiai, T. Okamoto, S. Sakai, T. Sugasawa and T. Onouchi, *Chem. Pharm. Bull.*, 7, 542 (1959).

showed the presence of hydroxyl groups (2.92~2.94 $\mu$) and an acetoxyl group (5.80 and 8.10 $\mu$).

**Hydrolysis of Compound IV.** — A solution of compound IV (0.05 g.) and potassium hydroxide (0.15 g.), dissolved in 2 cc. of ethanol and a drop of water, was heated for 1.5 hr. After removal of the solvents, the residue was washed with water. On treatment with methanol, it was not crystallized. The infrared absorption spectrum in nujol had no peak attributable to a terminal methylene group but showed the presence of hydroxyl groups (2.97 $\mu$).

The author wishes to express his sincere thanks to Professor Harusada Suginome, President of Hokkaido University, for his unfailing kindness in encouraging this work.

*Department of Chemistry*
*Faculty of Science*
*Hokkaido University*
*Sapporo*

# *Halogen Substitution in Liquid Sulfur Dioxide. I. Formation of Alkyl Halides from Alcohols and Halogens*

By Niichiro TOKURA, Ritsuro TADA and Ryoichi IGARASHI

(Received December 28, 1959)

The writers clarified the point previously[1] that ketoximes undergo rearrangement by the action of a halogen in liquid sulfur dioxide at room temperature. Scheme 1 was tentatively assigned to the mechanism of the rearrangement. The solvation by the solvent (liq. $SO_2$) may favor the ionization of the bromine molecule.

Sheme 1

$$Br_2 \overset{\text{liq. } SO_2}{\rightleftharpoons} Br^+ + Br^- \quad (1)$$

$$\begin{matrix} R \\ R' \end{matrix}\!\!>\!C{=}N{-}OH \xrightarrow{Br^+} \begin{matrix} R \\ R' \end{matrix}\!\!>\!C{=}N^+ + BrOH \quad (2)$$

$$\begin{matrix} R \\ R' \end{matrix}\!\!>\!C{=}N^+ + Br^- \longrightarrow \begin{matrix} R \\ Br \end{matrix}\!\!>\!C{=}N{-}R' \xrightarrow{H_2O} R{-}\underset{\underset{O}{\|}}{C}{-}NHR' \quad (3)$$

$$BrOH + SO_2 \longrightarrow HBr + SO_3 \quad (3)$$

From the structural similarity between alcohols R–C–OH and oximes R–C=H–OH, it is expected that all alcohols have a similar behavior towards bromine in liquid sulfur dioxide and, consequently, the reaction will proceed to form the corresponding alkyl halides. (Scheme 2).

Scheme 2

$$ROH + Br^+ \longrightarrow R^+ + BrOH \quad (5)$$

$$R^+ + Br^- \longrightarrow RBr \quad (6)$$

$$BrOH + SO_2 \longrightarrow HBr + SO_3 \quad (7)$$

1) N. Tokura, R. Asami and R. Tada, *J. Am. Chem. Soc.*, **76**, 3135 (1957).

The borderline nature[2] of liquid sulfur dioxide as a solvent was first recognized by Ingold[2] and, if the reaction follows the SNl mechanism, Eq. 5 being a slow step, the ease of the reaction of alcohols will be in the order of just tertiary, then, secondary, and finally, primary.[3]

A direct substitution of an alcoholic hydroxyl by a bromine atom has been reported to be the case, though only in tertiary alcohols, but this method[4] is not used because of its low yield. Substitution of the hydroxyl in liquid sulfur dioxide by a halogen has already been carried out[5], but with such halogenating reagents as thionyl halides, phosphorus trihalides and pentahalides, liquid sulfur dioxide being used as a solvent because of its excellence.

In expectation of obtaining alkyl halides by direct application of a halogen in liquid sulfur dioxide at room temperature, the lower members of aliphatic and alicyclic alcohols were submitted to the reaction with bromine with the results summarized in Table I.

The total amount of the products increased in the order of primary, secondary and tertiary alcohols. Only small amounts of alkyl halides were obtained from primary alcohols. Higher boiling halides were produced by further

2) C. K. Ingold, *Proc. Chem. Soc.*, 279 (1957).

3) C. K. Ingold, "Structure and Mechanism in Org. Chem.", Cornell Univ. Press, Ithaca, N.Y. (1955), p. 317.

4) C. Hell and F. Urech, *Ber.*, **15**, 1249 (1882).

5) For example, R. B. Woodward et al., *J. Am. Chem. Soc.*, **76**, 5256 (1954), used thionyl chloride in liq. $SO_2$ for the substitution of hydroxyl with chlorine in their synthetic course to lysergic acid, one of the ergot alkaloids.

Table I. Reaction of bromine and alchlols in liq. $SO_2$

Alcohol : 0.4 mol., Bromine : 0.4 mol. (64 g.)

Liq. $SO_2$ : 100 mol., Time : 5 hr. at room temperature

| Alcohol ROH | R | Ethyl | *n*-Propyl | Iso-propyl | *n*-Butyl | Iso-butyl | *sec*-Butyl | *tert*-Butyl | Iso-amyl. |
|---|---|---|---|---|---|---|---|---|---|
| | g. | 18.4 | 24.0 | 24.0 | 30.0 | 30.0 | 30.0 | 30.0 | 35.0 |
| Product: Total | g. | 3.0 | 3.0 | 30.0 | 8.0 | 17.0 | 60.0 | 69.0 | 4.0 |
| Product: Total | Yield weight % | 3.6 | 3.4 | 34.1 | 8.5 | 18.1 | 63.9 | 73.3 | 4.0 |
| Product: Alkyl bromide RBr | b.p., °C | 37~38 | 68~70 | 59~60 | 99~101 | 88~91 | 90~92 | 71~73 | 120~121 |
| Product: Alkyl bromide RBr | g. | 2.0 | 2.5 | 19.0 | 5.0 | 1.5 | 18.0 | 13.0 | 3.0 |
| Product: Alkyl bromide RBr | Yield, % | 5.3 | 5.1 | 38.6 | 7.2 | 2.7 | 32.5 | 23.4 | 6.7 |
| Product: Alkyl bromide RBr | $n_D^{26}$ | 1.425 | 1.435 | 1.423 | 1.440 | 1.438 | 1.438 | 1.430 | 1.443 |
| Product: Alkyl bromide RBr | Br % found. | 71.5 | 63.0 | 62.5 | 57.9 | 58.1 | 56.1 | 57.3 | 53.0 |
| Product: Alkyl bromide RBr | Br % calcd. | 73.0 | 64.9 | 64.9 | 58.3 | 58.3 | 58.3 | 58.3 | 52.9 |
| Product: Alkyl bromide RBr | $RCONHC_6H_5$ m.p., °C | 104 | 91~92 | 101~10 | 62~63 | 108~109 | 107~108 | 127~128 | 107~108 |
| Product: Higher boiling fractions | | | | b.p. 42~43 (20 mmHg) 7.0 g. | | b.p. 41~44 (10 mmHg) 9.0 g. | b.p. 41~44 (12 mmHg) 30.0 g. | b.p. 46~51 (20 mmHg) 31.0 g. | |
| | | | | | | b.p. 90~99 (10 mmHg) 5.0 g. | b.p. 90~100 (10 mmHg) 2.0 g. | b.p. 80~110 (20 mmHg) 4.0 g. | |

elimination, dimerization and bromination. In all experimants sulfuric acid separated out on the bottom of the reaction vessel. The highest yield was 38.6% of isopropyl bromide, but it was accompanied by a hexyl bromide with a carbon number twice as large as the original alkyl, and most of the butyl bromides were contaminated with butylene dibromides. (Scheme 3)

Scheme 3

$$R_1R_2\cdot(R_3CH_2)\cdot C{-}OH \xrightarrow{Br^+} A^+ + BrOH \quad (8)$$

$$A^+ ;\ R_1R_2\cdot(R_3CH_2)\cdot C^+$$

$$A^+ + Br^- \longrightarrow R_1R_2(R_3CH_2)\cdot C\cdot Br \quad (9)$$

$$A^+ \longrightarrow R_1R_2(R_3CH_2)\cdot C{=}CH\cdot R_3\ (B) + H^+ \quad (10)$$

$$BrOH + SO_2 \longrightarrow HBr + SO_3 \quad (11)$$

$$R_1R_2(R_3CH_2)\cdot C{-}OH + SO_3 \longrightarrow A^+ + HSO_4^- \quad (12)$$

$$H^+ + HSO_4^- \longrightarrow H_2SO_4 \quad (13)$$

$$B + A^+ \longrightarrow R_1R_2\cdot C{-}R_3CH{-}C\cdot R_1R_2\cdot(CH_2R_3)$$

$$\xrightarrow{Br^-} R_1R_2{-}C{-}R_3CH{-}CR_1R_2(CH_2R_3)^* \quad (14)$$

$$B + Br_2 \longrightarrow R_1R_2C{-}\underset{\displaystyle Br}{\underset{|}{CH}}\cdot R_3 \quad (15)$$

where $R_1$, $R_2$, $R_3$=H or $CH_3$

* more isomers are possible.

Thus, as might be expected, elimination reaction prevails to a considerable extent in liquid sulfur dioxide. The rather complicated feature of the reaction will be understood if the sulfur trioxide produced by the secondary step is assumed to play an important role in the elimination reaction and the dimerization.

$$RBr \rightleftharpoons R^+ + Br^- \longrightarrow \text{Olefin} + H^+\,Br^- \xrightarrow{+Br_2} \text{dibromide}$$

The equilibrium tends to the formation of the dibromide. It is further supported by the fact that phenethyl chloride and bromine in liquid sulfur dioxide afford styrene, polystyrene and styrene dibromide[6].

As the reaction proceeds, sulfur trioxide, formed according to Eq. 7, will favor the formation of the alkyl cation followed by elimination to olefin and sulfuric acid thus produced separates out owing to its slight solubility in liquid sulfur dioxide. Since this is an irreversible reaction, the reaction reaches a final state when the whole acid is precipitated.

In the case of the Beckmann rearrangement, the formation of a nitrogen cation or its ion-pair is the main reaction and no elimination occurs, the secondarily formed sulfur trioxide bearing a lesser meaning.

In the bromination of alcohols by bromine in liquid sulfur dioxide, the decisive factor is the SNl tendency of both alcohols and the solvent. The larger amounts of reaction products from secondary and tertiary alcohols are well consistent with the above consideration.

The writers have no evidence to rule out the participation of hydrogen bromide afforded by Eq. 7 in the bromine substitution reaction. An exact elucidation of the reaction needs further examination.

6) E. D. Hughes, C. K. Ingold and A. D. Scott, *J. Chem. Soc.*, **1937**, 1271.

TABLE II. EFFECT OF THE AMOUNT OF BROMINE ON THE YIELD AND ACTION OF HYDROGEN BROMIDE ON ISOPROPYL ALCOHOL

Isopropyl alcohol: 24 g. (0.4 mol.).
Liq. $SO_2$: 100 ml., Time 5 hr., at room temperature.

| Bromine g. | Mol. ratio Alcohol : Bromine | Isopropyl bromide g. | Isopropyl bromide yield, % | Higher boiling fraction 42~43°C(20 mmHg) |
|---|---|---|---|---|
| 32 | 1 : 0.5 | 8.0 | 16.2 | 5.1 |
| 48 | 1 : 0.75 | 18.5 | 38.0 | 7.0 |
| 64 | 1 : 1.0 | 19.0 | 38.6 | 7.4 |
| 77 | 1 : 1.2 | 18.8 | 38.1 | 8.3 |
| 32 (with $H_2O$ 7.2 g.) | 1 : 0.5 : ($H_2O$) 1, | 0.5 | 2.0 | trace |

TABLE III. ACTION OF CHLORINE AND OF CHLORINE WITH A CATALYTIC AMOUNT OF BROMINE

Alcohol: 0.4 mol., Chlorine: 0.4 mol.
Liq. $SO_2$: 100 ml., Time: 5 hr. at room temperature.

| Alcohol | Reagent | Mole ratio of alcohol to halogen | Alkyl chloride b.p., °C | Alkyl chloride Yield, % |
|---|---|---|---|---|
| *n*-Butyl | $Cl_2$ | 1 : 1 | 77~79 | 11.6 |
| | $Cl_2+Br_2$ | 1 : 1 : 0.02 | 77~79 | 11.6 |
| Isobuyl | $Cl_2$ | 1 : 1 | 60~65 | trace |
| | $Cl_2+Br_2$ | 1 : 1 : 0.02 | 60~65 | 2.4 |
| *sec*-Butyl | $Cl_2$ | 1 : 1 | 67~69 | 6.2 |
| | $Cl_2+Br_2$ | 1 : 1 : 0.02 | 67~69 | 3.5 |
| *tert*-Butyl | $Cl_2$ | 1 : 1 | 49~53 | 18.6 |
| | $Cl_2+Br_2$ | 1 : 1 : 0.02 | 49~53 | 17.2 |
| Cyclohexyl | $Cl_2$ | 1 : 1 | 98~102 | 6.5 |
| | $Cl_2+Br_2$ | 1 : 1 : 0.02 | 98~102 | 9.4 |

A considerable isomerization is also expected in the alkyl cation, but the writers are not yet in a position to discuss the structures of the carbon skeletons of the dimeric alkyl bromides produced.

In the bromine substitution of isopropyl alcohol, besides 38.6% of isopropyl bromide, a hexyl bromide, (probably 2-bromo-4-methylpentane) b. p. 42~43°C (20 mmHg) was formed in a yield of 21.2% of the theoretical. This substance afforded a hexyl acetate of b. p. 135~140°C with potassium acetate in glacial acetic acid. Its hydrolysis gave a hexene, $C_6H_{12}$, b. p. 70~73°C, possessing a comphor-like aroma, and a small amount of a hexyl alcohol, b. p. 125~130°C.

Similar phenomena were observed in the reactions of secondary or tertiary butyl alcohols with bromine, large amounts of octyl bromides being formed besides butyl bromides. Further, formation of dibromobutanes were also observed, which are assumed to have been formed by the addition of bromine to butenes produced from butyl cations.

In the alicyclic alcohols, it was observed that the formation of the cycloalkylene dibromides predominated over the cyclohexyl bromides. Thus, cyclohexyl alcohol afforded dibromocyclohexane in a yield of 64.2% and *d*-borneol afforded 71.2% of 2,10-dibromocamphane, indicating that a path through the Wagner-Meerwein rearrangement was followed.

The relation between the yield of the alkyl bromide vs. the amount of bromine was examined with isopropyl alcohol, the results being listed in Table II.

Only a small yield of the products was obtained with hydrogen bromide formed in the liquid sulfur dioxide[7] according to the formula:

$$Br_2 + 2H_2O + SO_2 \longrightarrow 2HBr + H_2SO_4 \quad (16)$$

In the next place, the action of chlorine on aliphatic alcohols was examined. The results shown in Table III indicate that chlorine is not so reactive as bromine, the yields being depressed. Subsequently, a small amount of bromine was added to chlorine (0.02 mol. of bromine to one mol. of chlorine) in expectation of a better result as in the case of the Beckmann rearrangement by chlorine[1] in liquid sulfur dioxide, but it proved ineffective.

## Experimental

**Materials.**—*1. Liquid Sulfur Dioxide.*—Liquid sulfur dioxide, dehydrated and purified in the plant and filled in an iron cylinder, was used. The water content measured in accordance with the principle of the Karl Fischer method

7) J. Ross, T. H. Percy, R. L. Brandt, A. I. Gebhart, J. E. Mitchell and S. Yolles, *Ind. Eng. Chem.*, 34, 924 (1942).

was 0.05~0.2%. This was further dehydrated with concentrated sulfuric acid and then with phosphorus pentoxide to bring the water content below 0.01%. However, practically no difference was found between these two kinds of liquid sulfur dioxide with respect to the reaction,

*2. Alcohols.* — All the alcohols were commercial products of the purest grade, which were dehydrated by the known method and redistilled.

*3. Bromine.* — Commercial bromine was washed with water and with concentrated sulfuric acid, dehydrated, and distilled once.

*4. Chlorine.*—Commercial chlorine was dehydrated with concentrated sulfuric acid and distilled.

*5. Reaction Vessel.*—A glass pressure bottle of 200 ml. capacity was used.

**Experimental Method.**—The amount of alcohols was 0.4 mol. each and that of bromine 0.4 mol. The solution of bromine in 50 ml. of liquid sulfur dioxide was added gradually to 50 ml. of liquid sulfur dioxide containing the alcohol at room temperature (20°C). The mixture was allowed to stand for a definite time. The reaction of secondary and tertiary alcohols occurred at once, the bromine color disappeared immediately, and the liquid sulfur dioxide solution became turbid. Sulfuric acid separated out as a colorless, translucent liquid on the bottom of the pressure bottle. After a definite time (usually 5 hr.), liquid sulfur dioxide was distilled off and the residual liquid was poured into ice water. The unchanged alcohols, especially butyl alcohols and lower aliphatic alcohols, dissolved out in water. The oily layer, after repeatedly being washed with water and with 1 N sodium carbonate solution and again with water, was dried over calcium chloride, and distilled to examine the amount of the lakyl halide formed.

**Results.**—*(A) Reaction of Alcohols with Bromine.*—1. Ethyl alcohol: From the reaction of 18.4 g. (0.4 mol.) of ethyl alcohol and 64 g. (0.4 mol.) of bromine in 100 ml. of liquid sulfur dioxide for 5 hours, 3.0 g. of a bromide was obtained. B. p. 37~38°C. Yield, 2.0 g. (5.3%). $n_D^{26}=1.425$. The bromide was identified with ethyl bromide by deriving propioanilide from it. Namely, the bromide was changed into a Grignard reagent and the latter was treated with phenyl isocyanate, and propionanilide (m. p. 104°C)[8] was obtained, which showed no depression of the melting point on admixture with an authentic specimen.

2. *n*-Propyl alcohol: A mixture of 24.0 g. (0.4 mol.) of *n*-propyl alcohol, 64 g. of bromine, and 100 ml. of liquid sulfur dioxide was kept at 20°C for 5 hr. and 3.0 g. of a crude halide was obtained. Redistillation afforded 2.5 g. (5.1%) of colorless, translucent liquid, b. p. 68~70°C, $n_D^{26}=1.435$. The bromide was identified with *n*-propyl bromide by deriving butyranilide, m. p. and mixed m. p. 91~92°C.[8]

3. Isopropyl alcohol: A mixture of 24 g. (0.4 mol.) of isopropyl alcohol, 64 g. (0.4 mol.) of bromine, and 100 ml. of liquid sulfur dioxide was kept at 20°C for 5 hr. The bromine color disappeared immediately after the starting of the reaction, the whole liquid became orange-colored and turbid, and ca. 10 ml. of a colorless, translucent liquid was deposited on the bottom. After 5 hr. this liquid was collected and titration gave a value corresponding to 13.2 g. of sulfuric acid. Liquid sulfur dioxide was then evaporated, the residual liquid was poured into ice water, and the oily layer was repeatedly washed with water and with 1 N sodium carbonate as described above. The crude halide thus obtained (30.0 g.) was fractionally distilled into the following fractions:

1) b. p. 59~60°C (760 mmHg), $n_D^{26}=1.425$, 19.0 g. (38.6%).

2) b. p. 42~43°C (20 mmHg), $n_D^{26}=1.525$, 7.0 g. (21.2%).

3) Residue, 0.3 g.

Fraction 1 was isopropyl bromide, forming isobutyranilide,[8] m. p. and mixed m. p. 101~102°C. Fraction 2 was a hexyl bromide (Found: Br, 47.9. Calcd for $C_6H_{13}Br$: Br, 48.41). Five grams of Fraction 2 was refluxed with 30 ml. of glacial acetic acid and 5 g. of potassium acetate, and 3.8 g. of a hexyl acetate, b. p. 135~140°C. (Found: $CH_3CO$, 30.11. Calcd. for $CH_3COOC_6H_{13}$; $CH_3CO$, 29.82), was obtained. Hydrolysis of this hexyl acetate by warming with ethanolic potassium hydroxide for 1 hr. afforded an olefin with camphor-like aroma, a hexene, $C_6H_{12}$, b. p. 70~73°C (Found: C, 85.98, H, 14.02, bromine number, 188.0. Calcd. for $C_6H_{12}$: C, 85.63, H, 14.37%, bromine number, 190.5).

Further, 0.3 g. of an oil, b. p. 125~130°C, assumed to be a hexyl alcohol, was obtained. This hexyl bromide may be assumed to be 2-bromo-4-methylpentane.

4. *n*-Butyl alcohol: A mixture of 30.0 g. (0.4 mol.) of *n*-butyl alcohol, 64 g. (0.4 mol.) of bromine, and 100 ml. of liquid sulfur dioxide was similarly treated and 8.0 g. of the product was fractionated, affording 5 g. (7.2%) of *n*-butyl bromide, b. p. 99~101°C, $n_D^{26}=1.440$ (Found: Br, 57.9. Calcd. for $C_4H_9Br$: Br, 58.33%). Valeranilide[8], m. p. and mixed m. p. 62~63°C. Further distillation of the residual

8) R. L. Shriner and R. C. Fuson, "Sstematic Identification of Organic Compounds", John Wiley & Sons, Inc., New York (1948), p. 255.

liquid afforded about 2.5 g. of an oil which boiled over a wide range of 40~90°C at 10 mmHg.

5. Isobutyl alcohol: Thirty grams of isobutyl alcohol was treated with bromine as above and 17.0 g. of the reaction product was obtained. This liquid was fractionated into three components.

1) b. p. 88~91°C, 1.5 g. (2.7%).
2) b. p. 32~38°C (10 mmHg), 9.0 g. (8.6%).
3) b. p. 90~99°C (10 mmHg), 5.0 g. (5.7%).

Fraction 1, $n_D^{26}=1.438$, was isobutyl bromide, affording isovaleranilide[8], m. p. and mixed m. p. 108~109°C. Fraction 2 was an octyl bromide, (Found: Br, 40.25, Calcd. for $C_8H_{17}Br$: Br, 41.38%). Fraction 3 corresponded to dibromo-isobutane (Found: Br, 72.56. Calcd. for $C_4H_8Br_2$: Br, 73.61%).

6. *sec*-Butyl alcohol: Thirty grams (0.4 mol.) of *sec*-butyl alcohol was similarly treated and 60.0 g. of the reaction product was obtained and fractionated.

1) b. p. 90~92°C, 18.0 g. (32.5%).
2) b. p. 41~44°C (12 mmHg), 25.0 g. (51.8%).
3) b. p. 90~110°C (10 mmHg), 2.0 g. (2.3%).
4) Residue, 3.1 g.

Fraction 1, $n_D^{26}=1.438$, was *sec*-butyl bromide (Found: Br, 57.60. Calcd. for $C_4H_9Br$, 58.3%), forming $\alpha$-methylbutyranilide[8], m. p. and mixed m. p. 107~108°C. Fraction 2 was an octyl bromide (Found: Br, 40.59. Calcd. for $C_8H_{17}Br$; Br, 41.38%), and Fraction 3 was assumed to be a dibromobutane with some impurity (Found: Br, 70.56. Calcd. for $C_4H_8Br_2$: Br, 73.61%).

7. *tert*-Butyl alcohol: Thirty grams (0.4 mol.) of *tert*-butyl alcohol was similarly treated and 69.0 g. of the oil formed was fractions.

1) b. p. 71~73°C, 13.0 g. (23.4%).
2) b. p. 46~51°C (20 mmHg), 31.5 g. (65.1%).
3) b. p. 80~110°C (20 mmHg), 4.0 g. (4.5%).
4) Residue, 7.0 g.

Fraction 1 was *tert*-butyl bromide, $n_D^{26}=1.655$, (Found: Br, 41.96. Calcd. for $C_4H_9Br$: Br, 41.38%). Trimethylacetanilide, m. p. and mixed m. p. 127~128°C. Fraction 2 was an octylbromide, $n_D^{26}=1.655$ (Found: Br, 41.96. Calcd. for $C_8H_{17}Br$: Br, 41.38%). Ten grams of Fraction 2 was refluxed with 10 g. of potassium acetate and 30 g. of glacial acetic acid for 1 hr. and 60 g. of an octyl acetate, with characteristic sweet aroma, was obtained, b. p. 120~126°C, $n_D^{26}=1.644$ (Found: $CH_3CO$, 20.5. Calcd. for $C_{10}H_6O_2$: $CH_3CO$, 21.04%). Hydrolysis of this substance with ethanolic potassium hydroxide afforded 3 g. of a colorless, translucent oil, b. p. 118~121°C, with camphor-like odor (Found: bromine number, 139.0. Calcd. for $C_8H_{16}$ ($F_1$); bromine number, 142.3). Fraction 3 was assumed to be a dibromobutane with some impurity (Found: Br, 71.74. Calcd. for $C_4H_8Br_2$: Br, 73.61%).

The amount of sulfuric acid formed during this reaction was 13.0 g. (titrated as $H_2SO_4$).

8. Isoamyl alcohol: A similar treatment of 35.0 g. (0.4 mol.) of isoamyl alcohol afforded 4.0 g. of a product which was distilled to give 3.0 g. (6.6%) of isoamyl bromide, b. p. 120~121°C, $n_D^{26}=1.443$. Isohexananilide[8], m. p. and mixed m. p. 107~108°C.

9. Cyclohexyl alcohol: Forty grams (0.4 mol.) of cyclohexyl alcohol was treated with 0.4 mol. of bromine in 100 ml. of liquid sulfur dioxide at room temperature for 5 hr. to give 72.2 g. of an oily product, which was fractionated into two fractions:

1) cyclohexyl bromide, b. p. 55~61°C (20 mmHg), 9.2 g. (14.1%), $n_D^{23}=1.496$ (Found: Br, 50.4. Calcd. for $C_6H_{11}Br$; Br, 49.0%).
2) dibromocyclohexane, b. p. 97~108°C (20 mmHg), 62.2 g. (64.2%).

The dibromocyclohexane was redistilled, b. p. 98~101°C (17 mmHg), $n_D^{24}=1.549$ (literature[9]: b. p. 100°C (13 mmHg), $n_D^{25}=1.5506$) (Found: Br, 65.0. Calcd. for $C_6H_{10}Br_2$: Br, 66.0%).

10. *d*-Borneol: *d*-Borneol, m. p. 201~204°C, $[\alpha]_D^{21.5}=+31.88°$, was prepared, according to the procedure of Amagasa et al., by reduction of *d*-camphor with sodium in liquid ammonia followed by rectification and recrystallization. A similar treatment of 15.5 g. (0.1 mol.) of *d*-borneol and 17.6 g. (0.11 mol.) of bromine in 140 ml. of liquid sulfur dioxide at room temperature for 18 hours afforded 26.0 g. of products, from which 11.6 g. of dark crystals were separated and recrystallized from ethyl alcohol in white crystals of m. p. 90~91°C. From the filtrate, 9.7 g. of an oil was distilled at 120~134°C (4.5 mmHg) which after recrystallization showed m.p. 90~91°C, alone and in admixture with the above specimen. Total yield, 71.2%. $[\alpha]_D^{16}=-15.0°$. This was identified with 2, 10-dibromocamphane[11] by a mixed melting point. The small amount of the forerun of the filtrate, b. p. 70~75°C (3 mmHg), 1.8 g. and b. p. 110~122°C (4 mmHg), is yet unidentified. (The optical rotations were measured in 95% ethyl alcohol in a tube of 2 cm. length.)

*(B) The Mole Ratios of Bromine to Alcohols and Yields of Alkyl Bromides.*—Similar treatments were carried out with various mole ratios of bromine to isopropyl and to *tert*-butyl alcohols.

*(C) The Preparation of Alkyl Bromides with 1 mol. of Bromine and 2 mol. of Water in Liquid Sulfur Dioxide.*—The procedures were

9) S. Winstein, *J. Am. Chem. Soc.*, **64**, 2792 (1942).
10) M. Amagasa and K. Yamaguchi, presented at the 6th Annual Meeting of the Chemical Society of Japan, April, (1953), Tokyo.
11) P. Lipp and F. Lausberg, *Ann.*, **436**, 274 (1924).

similar to those described above but two mol. of water was added to liquid sulfur dioxide to produce hydrogen bromide[7].

*(D) Action of Chlorine with a Small Amount of Bromine on Alcohols in Liquid Sulfur Dioxide.* —In these experiments, chlorine or chlorine with 0.1 mol. of bromine to improve the yield of the chlorides was applied to aliphatic alcohols, the procedures being essentially similar as in the case of bromine.

## Summary

The reaction between aliphatic alcohols and bromine in liquid sulfur dioxide at room temperature was investigated in order to obtain further information concerning the behavior of bromine in liquid sulfur dioxide. The reactivity of the alcohols increased in the order of primary <secondary<tertiary.

In addition to alkyl bromides, higher boiling bromides were also produced. The latter resulted from further elimination, dimerization and bromine addition. The rather complicated feature of the bromination is attributable to the presence of sulfur trioxide secondarily formed in the reaction mixture.

The microanalysis was performed by Miss Yoko Endo. A part of the expenses for the present work was defrayed from the Grant in Aid for Scientific Research from the Ministry of Education. The liquid sulfur dioxide was kindly donated by the Befu Chemical Industries, Ltd. All this help is gratefully acknowledged.

*Chemical Research Institute*
*of Non-aqueous Solutions*
*Tohoku University*
*Katahiracho, Sendai*

# *On the Oxidation of β-Aminopropionitrile. I*

By Toshihisa TACHIKAWA

(Received January 18, 1960)

It is known that β-aminopropionitrile which can easily be synthesized from acrylonitrile and ammonia, turns to a viscous liquid and finally to a resinous solid, when it is stored in the air for a prolonged period. However, very little has been investigated on the polymerization of aminonitriles.

Akabori[1] proposed in his interesting theory of protein formation, that the protein-like polyamide would result from the polymerization of α-aminonitrile, $NH_2CH_2CN \rightarrow (-CH_2-CO-NH-)_x$. However he gave no experimental proof on his theory.

Whitmore and Mosher[2] have studied the polymerization of β-aminopropionitrile, and stated that the reaction proceeds according to the following scheme,

$$NH_2CH_2CH_2CN \rightarrow CH_2=CHCN+NH_3$$

$$CH_2=CHCN \rightarrow \left[-CH_2-\underset{CN}{CH}-CH_2-\underset{CN}{CH}-\right]_x$$

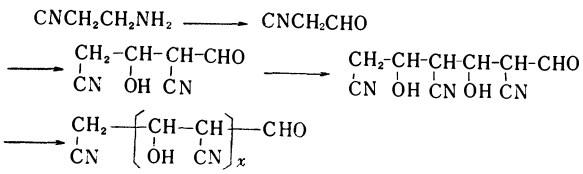
where the reaction was initiated by the decomposition of β-aminopropionitrile into acrylonitrile and ammonia, then followed by the polymerization of acrylonitrile. However, it does not seem probable that the polymerization of acrylonitrile will occur in the presence of ammonia, since ammonia is known as a polymerization inhibitor. It is also unlikely that polymerization proceeded through a viscous product because polyacrylonitrile should precipitate from the reaction mixture, as it is not soluble in acrylonitrile, water and ammonia.

As our resinous product obtained from β-aminopropionitrile was found to be easily soluble in methanol, glacial acetic acid and formic acid, this material must be quite different from the polyacrylonitrile obtained by Whitmore and his co-worker.

This paper is to report on the result of our detailed investigation on the reaction products and the mechanism of polymerization reaction of β-aminopropionitrile.

It is well known, that the aliphatic amino group is easily oxidized to aldehyde. So that β-aminopropionitrile could be oxidized in an analogous manner and the resulting aldehyde may polymerize by aldol condensation according to the following reaction scheme;

1) S. Akabori, *Kagaku*, **25**, 54, (1955).
2) F. C. Whitmore and H. S. Mosher, *J. Am. Chem. Soc.*, **66**, 725 (1944).



If this is the case, the resulting polymer may be acetylated and may give rise to the characteristic infrared absorption bands due to -OH and -CN groups. However, it was not successful to acetylate the polymer with various reagents, and no evidence for -OH or -CN was found from the infrared absorption spectrum of this compound as shown in Fig. 1. From these findings, it is believed that the polymerization reaction proceeds in a different way.

The colorless amorphous solid, obtained by treating the resinous polymer with anhydrous acetone to remove water and unreacted β-aminopropionitrile, was found to be very hygroscopic and to decompose at 120°C, resulting in the yellow mass which did not melt even above 250°C. The results of the molecular weight determination and the elementary analysis of this compound indicated the formular of $C_{12}H_{22}N_6O_5$ and the infrared absorption spectrum is shown in Fig. 1. As is clear from the spectrum, some differences were observed between the monomeric aminonitrile and the polymeric product.

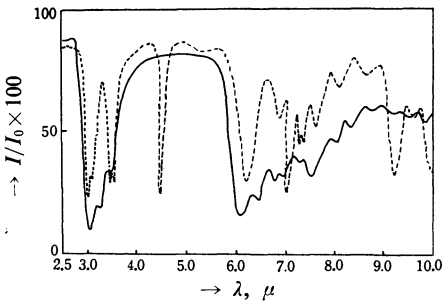



Fig. 1. Infrared absorption spectra.
---- β-Aminopropionitrile
—— Polymerization product

Two bands of N-H stretching vibration at 3.0 and 3.05 μ, splitted into three bands and shifted to 3.1, 3.3 and 3.4 μ. A band due to N-H bending vibration at 6.25 μ shifted to 6.45 μ, and a new band at 6.05 μ due to C=O stretching vibration appeared. These characteristic absorptions resembled very much those of the secondary amide such as *N*-methylacetamide which was investigated by Davis, Evans and Jones[3] as a model compound for polypeptides, and those of 6,6-Nylon. Therefore, it is very likely that this compound has a -CONH- linkage in its structure.

Regarding a new band at 6.70 μ, it is probable, that this band is due to the azoxy group. The reason for this assignment is that the position of this band coincided with that of the band arising from the stretching vibration of the azoxy group which was confirmed by Langley and others[4] in their infrared absorption study on azoxy compounds, such as 2-azoxy-2 : 5-dimethylhexane and ethyl 2-azoxybutylate.

Ultraviolet absorption spectra of these two compounds were also observed by the same authors, and their absorption maxima were reported as having two maxima at 223 and 280 mμ. The ultraviolet absorption spectrum of the polymer is also found to show two maxima at 215 and 275 mμ as shown in Fig. 2, and the locations of maxima are in good agreement with those of azoxy compounds if one considers the hypsochromic shift due to the use of water as a solvent.

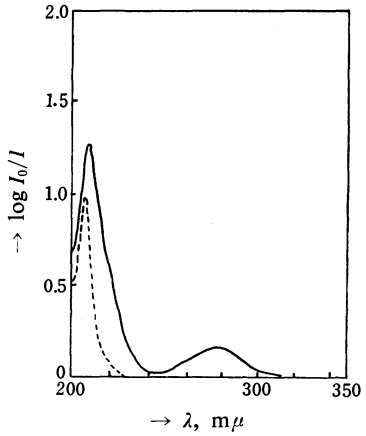



Fig. 2. Ultraviolet absorption spectra.
---- β-Aminopropionitrile
—— Polymerization product

In order to confirm the evidences of the azoxy group and -CONH- linkage in the polymer, the reduction of this compound was carried out, using concentrated hydrochloric acid and tin. The infrared absorption spectrum of the reaction product, which was obtained as colorless crystals, showed five bands at 5.85, 6.30, 6.70, 7.15 and 7.55 μ, as shown in Fig. 3, indicating the presence of amino acid, because these bands are characteristic of the hydrochloride of amino acid. And this supports the evidence of -CONH- linkage in the mother compound.

3) M. Davis, J. C. Evans and R. L. Jones., *Trans. Faraday Soc.*, **51**, 761 (1955).

4) B. W. Langley, B. Lythgoe and N. V. Riggs, *J. Chem. Soc.*, **1951**, 2309.

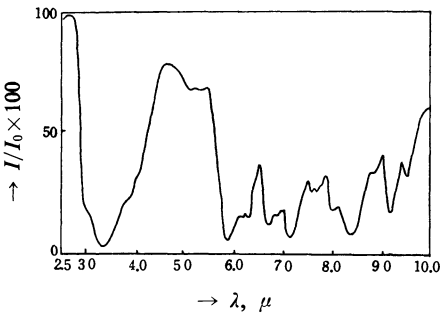



Fig. 3. Infrared absorption spectrum of reduction product of polymerization product.

Further investigation on the reduction product showed that the product was β-alanine and that this was obtained quantitatively by the reduction of the polymer. The presence of $-CONH_2$ group was also proved by the fact that ammonium chloride was found in the reduction products, and it was further confirmed that the nitrile group did not hydrolyze to -COOH group during the reaction, because no metallic salt can be precipitated from the aqueous polymer solution.

The presence of an azoxy group was also confirmed by the rapid evolution of gaseous nitrogen when the aqueous solution of the polymer was decomposed with sulfuric acid at room temperature. The fact that the aqueous solution of polymer was neutral, in contrast to the strong basicity of β-aminopropionitrile, indicated the polymer did not have a free amino group.

After considering above findings, the structure of resinous polymer obtained by standing β-aminopropionitrile in the air, is proposed as below;

$$\begin{array}{l} \bar{O}\text{-}\overset{+}{N}\text{-}CH_2CH_2CONHCH_2CH_2CONH_2 \\ \quad \| \\ \quad N\text{-}CH_2CH_2CONHCH_2CH_2CONH_2 \end{array}$$

And the scheme of decomposition to yield β-alanine during the reduction may be shown as follows;

$$\begin{array}{lll} & \overset{+OH}{\vdots} \; \overset{+H}{\vdots} & \overset{+OH}{\vdots} \; \overset{+H}{\vdots} \\ O\text{-}N\text{-}CH_2CH_2CO & \vdots \; NHCH_2CH_2CO & \vdots \; NH_2 \\ \quad \| \; {}^{+H_2} & \vdots & \vdots \\ \cdots\cdots \| \; \cdots\cdots & \vdots & \vdots \\ \quad \| \; {}^{+H_2} & \vdots & \vdots \\ N\text{-}CH_2CH_2CO & \vdots \; NHCH_2CH_2CO & \vdots \; NH_2 \\ & \underset{+OH}{\vdots} \; \underset{+H}{\vdots} & \underset{+OH}{\vdots} \; \underset{+H}{\vdots} \end{array}$$

The rate of polymerization of β-aminopropionitrile was accelerated by adding small amounts of water and bubbling the air into the reaction mixture. The polymer thus obtained was found to be exactly identical to that obtained by standing the monomer in the air, and since one mole of ammonia and a small amount of hydrogen peroxide were formed from two moles of β-aminopropionitrile, the mechanism of this polymerization can be considered as the oxidation reaction accompanied by the evolution of ammonia in the presence of water as shown in Table I.

Table I. The air oxidation reaction

| Nitrile g. | $H_2O$ g. | Gas used | Gas blown l. | Product g. | $NH_3$ generated g. |
|---|---|---|---|---|---|
| 15 | 0 | Air | 2800 | No change | None |
| 15 | 1.0 | Air | 560 | White solid 15.0 | 1.80 |
| 15 | 3.8 | Air | 560 | White solid 15.8 | 1.91 |
| 15 | 6.0 | Air | 720 | White solid 15.1 | 1.87 |
| 15 | 1.0 | $N_2$ | 2020 | No change | None |

## Experimentals

**1. Raw Material and Sample.**—β-Aminopropionitrile was synthesized from acrylonitrile and aqueous ammonia according to Buc, Ford and Wise[5], and the fraction boiling at 86.3~87.0°C/21 mmHg was collected.

A polymeric sample was prepared by standing β-aminopropionitrile for two months in the air, followed by washing the resulting solid mass with anhydrous acetone to remove unreacted aminonitrile and water. A white amorphous and very hygroscopic solid was thus obtained, and dried in a vacuum. This sample decomposed at 120°C, yielding a product which did not melt above 250°C.

Found: C, 43.27; H, 6.69; N, 25.04%; mol. wt., detd. by freezing point depression using acetic acid. 311.1. Calcd. for $C_{12}H_{22}N_6O_5$: C, 43.63; H, 6.71; N; 24.22%; mol. wt., 330.4.

Ultraviolet absorption spectra were measured for the aqueous solution of 0.0651 g./l. A Shimadzu Model QR 51 spectrophotometer with 1 cm. quart celles was employed. Infrared absorption spectra were recorded with a Perkin Elmer Model 21 spectrophotometer on the sample film which was prepared by evaporating 2—3 drops of 3% methanolic solution on the sodium chloride window.

**2. Reduction of Polymer.**—Twelve grams sample was dissolved into 15 g. of water, and the solution was treated with 19.1 g. of metallic tin and 75 g. of 35% hydrochloric acid at 95~100°C for 10 hr. under stirring until the tin dissolved completely.

The resulting solution was diluted with four volumes of water and stannous ion was precipitated with hydrogen sulfide. The filtrate was concentrated under reduced pressure to get a crystalline product I which was found to be ammonium chloride.

After filtering it, the filtrate was subjected to further evaporation until one could get 16.5 g. of the second crystalline product II. The infrared absorption spectrum was measured on this material II using the potassium bromide pellet method.

The product II was then dissolved in a small amount of water and after neutralizing the solution with 1 N sodium hydroxide solution, it was boiled

5) S. R. Buc, J. H. Ford and E. C. Wise, *J. Am. Chem. Soc.*, 67, 92 (1945).

with an excess amount of freshly prepared cupric hydroxide. The hot filtrate was concentrated and cooled to get dark blue crystals. This was re-dissolved in water, and cupric ion was precipitated with hydrogen sulfide. When the filtrate was evaporated almost to dryness, a crystalline product III was obtained.

Found: C, 40.27; H, 7.86; N, 15.81. Calcd. for $C_3H_7NO_2$: C, 40.44; H, 7.92; N, 15.72%.

**3. Decomposition with Sulfuric Acid.**—According to Curtius procedure, 0.0818 g. of the sample was dissolved in 1.0 ml. of water and 1.5 ml. of 98% sulfuric acid was dropped into this solution with gentle heating. The evolving gas, collected over a 10% potassium hydroxide solution, measured 5.34 ml. As this gas was not absorbed by the alkaline pyrogallol solution, ammoniacal cuprous chloride solution or barium hydroxide solution, it was found to be pure nitrogen. The amount of nitrogen evolved was 8.17% per mole of the sample.

**4. Determination of Neutralization Equivalent.**—A solution of 0.0999 g. sample in 50 ml. of water was titrated with 0.1 N hydrochloric acid using methyl orange as an indicator. Neutralization equivalent was calculated as 951.4 from the titre of 1.05 ml. This value is considerably larger than that of β-aminopropionitrile (69.5), and the sample can be considered as almost neutral material.

**5. Formation of Metallic Salts.**—No precipitation was observed when barium hydroxide, cupric nitrate or silver nitrate solution was added to the aqueous sample solution.

**6. Air Oxidation.**—Decarbonated air or nitrogen was bubbled into β-aminopropionitrile in a 100 ml. reaction flask at the rate of 20 l./hr. The increase of viscosity and the rapid evolution of gas were observed during she introduction of air, which was continued until the content rapidly increased its viscosity, resulting in a resinous material. This product was treated with anhydrous acetone to remove unreacted β-aminopropionitrile and water, then it was dried under reduced pressure. The product was obtained as a very hygroscopic white amorphous mass.

Amount of ammonia evolved during the reaction, was determined by passing the gas into sulfuric acid, and the presence of hydrogen peroxide in the gas was detected by passing it into barium hydroxide solution, followed by the dissolution of the resulting white precipitate into hydrochloric acid, which turned to red with an addition of potassium iodide.

The author wishes to express his sincere thanks to Professor Ryozo Goto of Kyoto University for his kind advice, and also to Mr. Murataro Nakashima, President of Kunoshima Chemical Co., for his permission to publish this paper.

*Research Laboratory of Kunoshima Chemical Industry Co., Ltd.*
*En-ichi-cho, Mihara*

# *The Self-diffusion of Surface Active Agents in Nylon*

By Makoto HAYASHI

(Received January 20, 1960)

Adsorption of surface active agents on various solid surfaces such as metal, carbon, wool, cotton, acetate and polyamide fibers has been studied by many workers[1-5] as the fundamental contributions to the study of the physicochemical properties of detergents or as the first step to study the mechanism of detergency. However, the process of adsorption of detergents by the solid is rather complicated and there are a number of problems to be solved by further investigation.

We have studied[6] the adsorption of the surface active agents such as sodium dodecyl sulfate, sodium tetradecyl sulfate as well as inorganic ions such as sulfate, chloride, phosphate and calcium ions on the surface of nylon plate. The quantities of these substances taken up by nylon are very great and a very long time is required to reach an adsorption equilibrium. From these facts, it seems that the penetration of the adsorbed substances into the solid body plays an important role in the process of sorption and so the measurement of diffusion in solid is considered to be significant in a study of the adsorption of these substances to polymer solid.

In this paper, the self-diffusion rates in nylon

1) A. L. Meader and B. A. Fries, *Ind. Eng. Chem.*, **44**, 1636 (1952).
2) L. Hsiao and H. N. Dunning, *J. Phys. Chem.*, **59**, 362 (1955).
3) A. Fava and H. Eyring, ibid., **60**, 890 (1956).
4) H. C. Evans, *J. Colloid Sci.*, **13**, 537 (1958).
5) R. D. Vold and N. H. Sivaramakrishnan, *J. Phys. Chem.*, **62**, 984 (1958).
6) M. Hayashi and Y Nakazawa, *Radioisotopes*, **8**, 149 (1959).

of sodium dodecyl sulfate and sodium tetradecyl sulfate, and also of sulfuric acid and hydrochloric acid were studied, using the nylon plates and the radioactive tracers.

## Experimental Method

The measurement was carried out by the surface radioactivity decrease method, which consists in measuring the decrease in radioactivity of the surface with the time due to the diffusion of the radioactive tracer into nylon. This method has the following advantages: the measurement is accomplished in a short diffusion time when the suitable $\beta$-ray energy such as that of $^{35}S$ is used and it is not necessary to use any particular arrangements.

A nylon plate was 2.5 mm. in thickness, 2.5 cm. $\times$2.5 cm. in size. It was cleaned by washing with ether, acetone and hot water before use.

The surface active agents used in this experiment were sodium dodecyl surfate (SDS) and sodium tetradecyl sulfate (STS). They were prepared from pure dodecyl alcohol and tetradecyl alcohol, respectively, and their purity was confirmed surface-chemically. The radioactive SDS and STS, both tagged with $^{35}S$, were prepared from corresponding alcohols and radioactive sulfuric acid ($H_2{}^{35}SO_4$). Radioactive sulfuric acid ($H_2{}^{35}SO_4$) and hydrochloric acid ($H^{36}Cl$) were used for the measurement of diffusion of the sulfate ion and the chloride ion, respectively. The absorption coefficients of the $\beta$-rays of $^{35}S$ and $^{36}Cl$ in nylon were estimated using the sufficiently swollen nylon film (25$\mu$ in thickness), and the values, 321 $cm^{-1}$ for $^{35}S$ and 12.7 $cm^{-1}$ for $^{36}Cl$ were obtained.

Diffusion experiments were accomplished as follows: the nylon plates are immersed in various concentrations of each non-radioactive solution at 33°C for about two weeks in order that the nylon might sorb the solute by a complete equilibrium amount corresponding to each concentration. (It has been shown that the sorption equilibrium is accomplished completely under these circumstances.) They are taken up from the solution, blotted by filter paper, then immersed instantly in each radioactive solution of the same concentrations as the non-radioactive solution used, for the purpose of making a surface radioactive layer, probably, by surface exchange. They are stirred sufficiently for about 0.5~2 min., then the nylon plates are taken up, washed with a large amount of water for a few seconds, blotted with filter paper and counted instantly under the G-M tube. They are then fitted in a closed glass vessel of saturated humidity which is then kept in a thermostat. When the diffusion has progressed appropriately (about 20 hr. for SDS and STS, 4 hr. for $H_2SO_4$, 48 hr. for HCl at 33°C, respectively), the nylon plates are removed from the vessel and their radioactivity is counted in the same manner as before, and the ratio $A/A_0$ ($A_0$: initial counts of the surface of nylon, $A$: its counts at time $t$) is estimated. $A/A_0$ is given by the following equation[7,8]

$$A/A_0=[1-\mathrm{erf}\{(\mu^2Dt)^{1/2}\}]\exp(\mu^2Dt) \quad (1)$$

where $D$ is the self-diffusion coefficient of the diffusing ion, and $\mu$ is the absorption coefficient of the $\beta$-ray in nylon. $A/A_0$ can be plotted as a function of $\mu^2Dt$ and by using this graph $D$ can be obtained from the measured value of $A/A_0$ since $\mu$ and $t$ are known.

The quantity of each solute sorbed by nylon was measured by the same method as in the previous paper[6] and expressed as millimoles per kilogram of nylon, which was calculated by calibrating the decrease of counts owing to the absorption of radiation by nylon.

Radioactivity measurements carried out by means of a thin mica window G-M tube (1.4 mg./$cm^2$) and the conventional scaler. For the purpose of establishing the counting area and avoiding the edge effect on counting, a brass ring 1 mm. think and 22 mm. in inner diameter was placed on the plate when it was counted.

The change of the efficiency of the counting equipment was always checked by a radioactive standard prepared on a nylon plate. Counting times were made so long that the standard counting error was less than 1%.

## Results

To confirm the compatibility of the above diffusion equation (1) in these measurements the values of $A/A_0$ at various diffusing time were measured at 33°C with SDS and $H_2SO_4$ (Figs. 1 and 2). In these figures, the curves of solid line show the calculated values obtained by the above equation and the value of $D$ at $A/A_0=0.5$. The points are the measured ones. It is seen that this equation can be applied to calculate the diffusion coefficient in these systems.

The sorption isotherms of each substance by nylon plate were measured by the radiotracers to estimate the quantities sorbed in nylon.

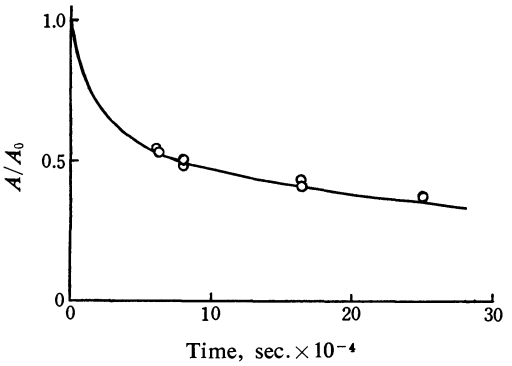



Fig. 1. The check of compatibility of the Eq. 1 by the diffusion of SDS at the concentration of 34 millimol./kg. in nylon at 33°C. The solid line is the calculated values and the points are the measured ones.

7) V. Linnenbom, M. Tetenbaum and C. Cheek, *J. Appl. Phys.*, 26, 932 (1955).
8) F. Bueche, W. M. Cashin and P. Debye, *J. Chem. Phys.*, 20, 1956 (1952).

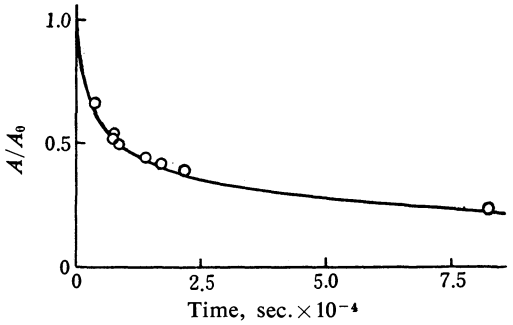



Fig. 2. The check of compatibility of the Eq. 1 by the diffusion of $H_2SO_4$ at the concentration of 63 millimol./kg. in nylon at 33°C. The solid line is the calculated values and the points are the measured ones.

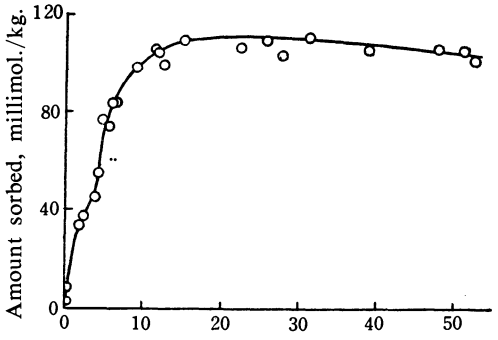



Fig. 3. The isotherm of the sorption of SDS by nylon plate at 33°C.

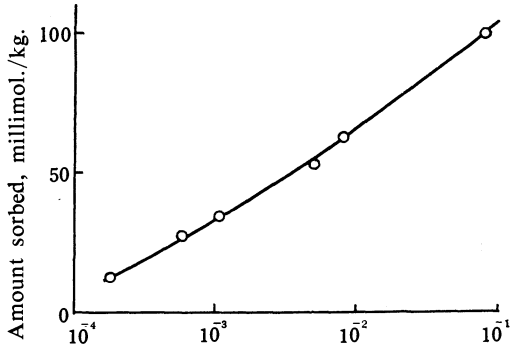



Fig. 4. The isotherm of the sorption of $H_2SO_4$ by nylon plate at 33°C.

The results for SDS and $H_2SO_4$ as examples are shown in Figs. 3 and 4, respectively.

The diffusion coefficients of SDS, STS, $H_2SO_4$ and HCl were measured at various concentrations of every solute in nylon. The results are shown in Figs. 5 and 6 and in Table I.

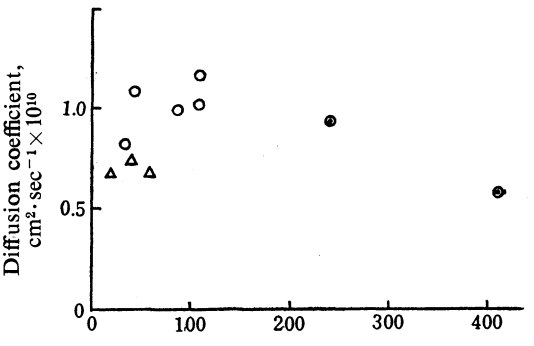



Fig. 5. Diffusion coefficient of SDS and STS at 33°C.

○ SDS
△ STS
⊙ The values of SDS obtained by the nylon plate which contained the large quantity of SDS by the lowering of the medium pH with HCl and KCl.

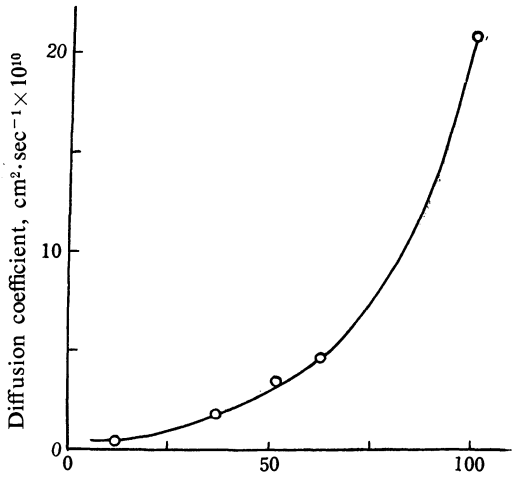



Fig. 6. Diffusion coefficient of $H_2SO_4$ at 33°C.

Table I. Self-diffusion coefficients of HCl at 33°C

| Concentration of HCl* mol./l. | Diffusion coefficient $cm^2 \cdot sec^{-1} \times 10^9$ |
|---|---|
| $10^{-1}$ | 6.46 |
| $10^{-2}$ | 0.120 |
| $10^{-3}$ | 0.176 |

* The concentration of the solution described here is that which is in sorption equilibrium.

The diffusion coefficients of SDS and $H_2SO_4$ at various temperatures were measured to observe the effect of temperature on the diffusion and are shown in Table II. When $\log D$ is plotted against $1/T$, the straight lines are obtained as shown in Fig. 7, from which the

TABLE II. TEMPERATURE DEPENDENCE OF DIFFUSION COEFFICIENTS

| Diffusing substance | Concentration in nylon (millimol./kg) | Diffusion coefficient $cm^2 \cdot sec^{-1} \times 10^{10}$ | | | | | Activation energy, $E$ cal./mol. |
|---|---|---|---|---|---|---|---|
| | | −4°C | 5°C | 10°C | 19°C | 33°C | |
| SDS | 102 | 0.00012 | 0.0053 | 0.0177 | 0.182 | 1.10 | 33400 |
| $H_2SO_4$ | 63 | 0.0209 | 0.102 | 0.241 | 0.927 | 4.69 | 23200 |

activation energy $E$ in the equation $D=D_0 \exp(-E/RT)$ was estimated and shown in the last column of Table II.

If the nylon sample is dried before or after the dipping in radioactive solution, the diffusion is little observed by this method at the room temperature.

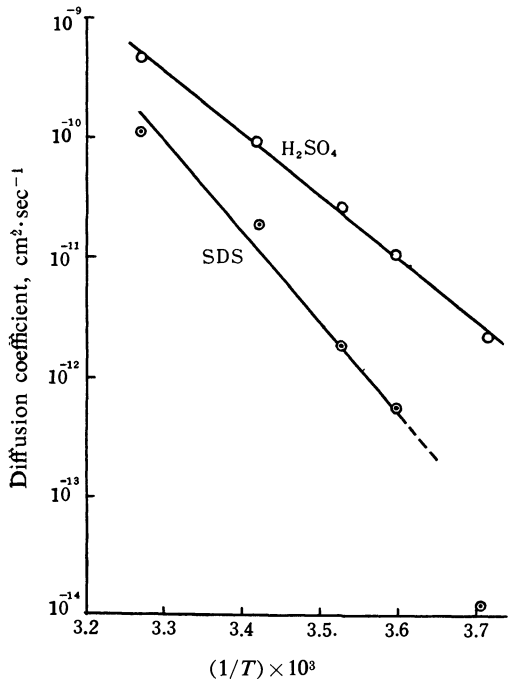



Fig. 7. Temperature dependence of diffusion coefficients of SDS (102 millimol./kg.) and $H_2SO_4$ (63 millimol./kg.).

## Discussion

In this experiment the measurements of the self-diffusion rate were always carried out using sufficiently swollen nylon plates and it has been confirmed by weight that the swelling of each sample under the condition of the present experiment is constant throughout the whole diffusion process. The self-diffusion of the surface active agents or inorganic acids became remarkably slower as a nylon plate was dried and could not be observed at the room temperature in the completely dried state of nylon. It is evident, therefore, that these substances diffuse with the aid of water in nylon.

It is clear from the results of the present experiment that in the sorption of surface active agents and also of inorganic acids from their aqueous solutions by nylon, not only the surface phenomenon but also the diffusion into the solid body is responsible for its process towards equilibrium.

The self-diffusion coefficients of SDS and STS in nylon at 33°C are dependent, though not remarkably, on the concentration of each detergent in nylon as shown in Fig. 5. The values are comparable with those of several dyes reported by some workers[9,10], but they are much smaller than the values[11] in aqueous solutions. We suppose that the internal body of nylon is a gel of extremely close-packed network structures, water being included and forming fine canals among them. The molecules of detergent will penetrate along these canals into the internal structures of nylon, but they are immobilized by the adsorption sites to a large extent and so the rate of diffusion is reduced considerably compared with the free diffusion in aqueous systems. It is considered that the jumping of the adsorbed molecules from site to site occurs just as in the diffusion of ions in their crystals. Indeed the activation energies for diffusion of SDS and sulfuric acid are 33.4 and 23.2 kcal. per mole respectively as shown in Table II. These values are much greater than the values of many substances in aqueous systems, rather resembling these in solid crystals[12].

We suppose that the interaction of ionic detergents and nylon takes place not only by ionic force but also by van der Waals force, since the amount of detergents sorbed by nylon is much larger than that of simple inorganic ions which are considered to be bound to nylon mainly by ionic interaction[6]. This is confirmed by the fact that the amount of detergents taken up is also much larger than the value corresponding to the amine content of nylon[13,14]. The sorption of sulfuric acid

9) T. Vickerstaff, "The Physical Chemistry of Dyeing", 2nd ed. Olyver and Boyd, London (1954), pp. 152, 449.
10) M. Yoshida and H. Morita, *Sen-i-gakkaishi*, **12**, 662 (1956).
11) D. Stigter, R. J. Williams and K. J. Mysels, *J. Phys. Chem.*, **59**, 330 (1955).
12) G. E. Boyd and B. A. Soldano, *J. Am. Chem. Soc.*, **75**, 6091 (1954).
13) J. E. Waltz and G. B. Taylor, *Anal. Chem.*, **19**, 448 (1947).
14) F. C. McGrew and A. K. Schneider, *J. Am. Chem. Soc.*, **72**, 2547 (1950).

and hydrochloric acid will be caused mainly by the attachment of these substances to the amino groups or to the amide groups in the molecule of nylon. From this point of view, therefore, it is supposed that there is also a difference between detergent and inorganic acid in the mechanism of diffusion. Indeed as shown in Figs. 5 and 6, the diffusion coefficient of the detergent does not change markedly with concentration of the detergent in nylon, while that of the inorganic acid increases remarkably with its concentration. At present, however, it is difficult to give a precise mechanism for the diffusion of the detergent and inorganic acid in nylon. This will be discussed after further investigation has been performed.

## Summary

The self-diffusion rates of sodium dodecyl sulfate, sodium tetradecyl sulfate, sulfuric acid and hydrochloric acid in nylon containing various amounts of each solute and their temperature dependence were measured by the surface radioactivity decrease method using $^{35}S$ and $^{36}Cl$.

From the experimental results, it has become clear that the diffusion of the solute in nylon is important in the process towards the attainment of sorption equilibrium of these substances by nylon, and in this case the presence of water in nylon is necessary for the diffusion to take place appreciably. The diffusion coefficients were much smaller than those in their aqueous solutions.

The diffusion rates of the surface active agents depended little on the concentration in nylon compared with those of the inorganic acids. The diffusion rates of sulfuric acid and hydrochloric acid depended largely on their concentration in nylon. This will be due to a difference of the mechanism of diffusion between the former and the latter.

The activation energies of SDS and sulfuric acid for diffusion were considerably great and approximated to those of many substances in solid.

The author wishes to express his gratitude to Professor R. Matuura of Kyushu University for his kind guidance and for supplying the radioisotopic samples, and also to Toyo Rayon Co. for its supply of nylon samples.

*Department of Pharmacology*
*Nagasaki University*
*School of Medicine, Nagasaki*

# *Estimation of the Energy of Hydrogen Bonds Formed in Crystals. III. Amides*

By Ariyuki AIHARA

(Received January 20, 1960)

A study of the NH···O bonding bears a particular significance in relation to the basic structure and behavior of proteins, and a fairly large amount of data of the bond have been accumulated up to now. Nevertheless, it cannot be said that the strength of the NH···O bonding has been fully examined so as to allow us to decide definitely whether this type of hydrogen bond is weaker than the OH···O bonding or not, especially in the crystalline state. Thus we find a considerable divergence in the data of the energy of NH···O bondings already published by several investigators. For instance, Coulson cites, in his well-known publication[1], 2~3 kcal./mol. for the energy of the NH···O bond, while the following data are available in the literature: 3.0 kcal./mol. (acetamide, *N*-methylacetamide)[2], (diacetylhydrazine)[3], 3.5 kcal./mol. (urea)[4], 4.2 kcal./mol. (oxamide)[5], 4.7 kcal./mol. (sulfamide)[3], 5.3 kcal./mol. (diketopiperazine)[6], ~6.0 kcal./mol.

* Present address; University of Electro-Communications, Chofu-shi, Tokyo.

1) C. A. Coulson, "Valence", Clarendon Press, Oxford (1952), p. 301.
2) A. Aihara, *J. Chem. Soc. Japan, Pure Chem. Sec.* (*Nippon Kagaku Zasshi*), **73**, 855 (1952).
3) S. Takagi, R. Shintani, H. Chihara and S. Seki, This Bulletin, 32, 137 (1959).
4) K. Suzuki, S. Onishi, T. Koide and S. Seki, ibid., **29**, 127 (1956).
5) R. S. Bradley and A. D. Care, *J. Chem. Soc.*, **1953**, 1681.
6) S. Seki, K. Suzuki and T. Koide, *J. Chem. Soc. Japan, Pure Chem. Sec.* (*Nippon Kagaku Zasshi*), **77**, 346 (1956).

(δ-valerolactam and ε-caprolactam)[7], 6.1 kcal./mol. (diformylhydrazine)[4].

In this connection, the author has tried to get more knowledge on the strength of the NH···O bond, and has estimated the energy of the bond with thirteen amides in the crystalline state, following the procedure proposed in previous papers[8]. The obtained values of the energy range from 3.5 to 7.0 kcal./mol., showing that the NH···O bond is not always weaker than the OH···O bond as has hitherto been presumed.

## Experimental

The measurement of the sublimation pressures was done with the same apparatus as that used before[3]. Of the materials dealt with in this investigation, formanilide and *N*-methylbenzamide were prepared in this laboratory following the usual procedure (the former from aniline and formaldehyde, the latter from methylamine and benzoylchloride). δ-Valerolactam and ε-caprolactam were kindly sent by Dr. Tsuboi, the University of Tokyo The result of the measurement of their sublimation pressures was reported before by the author[7], but, for the sake of comparison, it will be included here. 1-Phenyl-3pyrazolidone (phenydone) was sent by Dr. Kurosaki, Fuji Photo Film Co., Ltd., to whom author's thanks are due. Others were all commercial products and were purified by repeated fractional sublimation under high vacuum pressure before use.

## Results and Discussion

**Sublimation Pressures.**—The results of measurements of sublimation pressure of thirteen amides are shown in the following tables (from Table I to Table XIII) together with their

Table I. Sublimation pressure of formanilide

| $T$°K | $P$(mmHg)$\times 10^4$ | $T$°K | $P$(mmHg)$\times 10^4$ |
|---|---|---|---|
| 297.7 | 6.86 | 311.9 | 28.7 |
| 301.6 | 10.3 | 313.6 | 34.2 |
| 308.4 | 20.3 | 314.6 | 37.2 |
| 309.3 | 22.0 | 316.8 | 45.9 |
| 310.7 | 25.9 | 317.8 | 49.4 |

$\log P(\text{mmHg}) = 10.511 - 4071.0/T$: m. p. 48.7°C.

Table II. Sublimation pressure of acetanilide

| $T$°K | $P$(mmHg)$\times 10^4$ | $T$°K | $P$(mmHg)$\times 10^4$ |
|---|---|---|---|
| 317.7 | 8.03 | 327.7 | 21.2 |
| 320.0 | 10.2 | 330.1 | 26.8 |
| 322.7 | 12.9 | 333.2 | 36.2 |
| 325.4 | 16.4 | 335.8 | 48.1 |

$\log P(\text{mmHg}) = 11.166 - 4533.6/T$: m. p. 115.0°C.

Table III. Sublimation pressure of *o*-acetoluidine

| $T$°K | $P$(mmHg)$\times 10^4$ | $T$°K | $P$(mmHg)$\times 10^4$ |
|---|---|---|---|
| 315.2 | 4.20 | 330.8 | 23.6 |
| 318.5 | 6.31 | 334.2 | 35.3 |
| 321.2 | 8.80 | 337.5 | 48.6 |
| 324.2 | 11.8 | 340.0 | 65.6 |
| 327.3 | 16.5 | | |

$\log P(\text{mmHg}) = 12.717 - 5070.8/T$: m. p. 111.5°C.

Table IV. Sublimation pressure of *p*-acetotoluidine

| $T$°K | $P$(mmHg)$\times 10^4$ | $T$°K | $P$(mmHg)$\times 10^4$ |
|---|---|---|---|
| 330.7 | 6.20 | 337.9 | 13.0 |
| 332.1 | 7.23 | 340.6 | 17.5 |
| 333.1 | 7.93 | 343.4 | 23.2 |
| 334.0 | 8.98 | 346.5 | 31.6 |
| 335.2 | 10.1 | 350.1 | 46.6 |

$\log P(\text{mmHg}) = 12.437 - 5172.9/T$: m. p. 149°C.

Table V. Sublimation pressure of *p*-acetaminobenzaldehyde

| $T$°K | $P$(mmHg)$\times 10^4$ | $T$°K | $P$(mmHg)$\times 10^4$ |
|---|---|---|---|
| 328.3 | 5.59 | 337.4 | 14.9 |
| 330.1 | 6.73 | 339.9 | 19.4 |
| 332.6 | 8.82 | 342.4 | 25.2 |
| 335.1 | 11.5 | 345.4 | 32.8 |

$\log P(\text{mmHg}) = 12.516 - 5177.7/T$: m. p. 155.5°C.

Table VI. Sublimation pressure of benzanilide

| $T$°K | $P$(mmHg)$\times 10^4$ | $T$°K | $P$(mmHg)$\times 10^4$ |
|---|---|---|---|
| 353.0 | 3.93 | 363.7 | 10.6 |
| 355.4 | 4.73 | 366.7 | 13.7 |
| 357.0 | 5.64 | 368.9 | 16.4 |
| 360.2 | 7.53 | | |

$\log P(\text{mmHg}) = 11.264 - 5181.2/T$: m. p. 163.5°C.

Table VII. Sublimation pressure of benzamide

| $T$°K | $P$(mmHg)$\times 10^3$ | $T$°K | $P$(mmHg)$\times 10^3$ |
|---|---|---|---|
| 325.3 | 1.04 | 334.3 | 2.67 |
| 327.4 | 1.31 | 335.4 | 3.00 |
| 328.4 | 1.39 | 337.0 | 3.49 |
| 330.0 | 1.70 | 338.9 | 4.37 |
| 332.9 | 2.33 | 341.9 | 5.86 |

$\log P(\text{mmHg}) = 12.579 - 5063.6/T$: m. p. 130.5°C.

Table VIII. Sublimation pressure of *N*-methylbenzamide

| $T$°K | $P$(mmHg)$\times 10^4$ | $T$°K | $P$(mmHg)$\times 10^4$ |
|---|---|---|---|
| 308.0 | 7.06 | 320.9 | 27.3 |
| 310.6 | 9.16 | 323.7 | 35.3 |
| 313.0 | 11.9 | 326.8 | 47.8 |
| 315.7 | 15.7 | 329.3 | 60.9 |
| 318.5 | 21.0 | | |

$\log P(\text{mmHg}) = 11.358 - 4469.8/T$: m. p. 79.8°C.

7) A. Aihara, ibid., 74, 631, 634 (1953).
8) A. Aihara, This Bulletin, 32, 1242 (1959); 33, 194 (1960).

TABLE IX. SUBLIMATION PRESSURE OF α-PHENYLACETAMIDE

| $T$°K | $P$(mmHg)$\times 10^4$ | $T$°K | $P$(mmHg)$\times 10^4$ |
|---|---|---|---|
| 330.0 | 5.18 | 340.9 | 16.4 |
| 332.9 | 7.12 | 344.0 | 21.9 |
| 335.2 | 9.09 | 348.0 | 31.7 |
| 338.2 | 12.4 | 351.8 | 46.5 |

$\log P(\text{mmHg}) = 12.242 - 5123.7/T$: m. p. 158.5°C.

TABLE X. SUBLIMATION PRESSURE OF N-ACETYL-α-NAPHTHYLAMINE

| $T$°K | $P$(mmHg)$\times 10^4$ | $T$°K | $P$(mmHg)$\times 10^4$ |
|---|---|---|---|
| 337.9 | 2.66 | 348.0 | 6.93 |
| 341.0 | 3.56 | 350.6 | 8.80 |
| 342.3 | 4.18 | 354.5 | 12.2 |
| 345.5 | 5.47 | 359.7 | 20.8 |

$\log P(\text{mmHg}) = 10.959 - 4912.2/T$: m. p. 159°C.

TABLE XI. SUBLIMATION PRESSURE OF 1-PHENYL-3-PYRAZOLIDONE

| $T$°K | $P$(mmHg)$\times 10^4$ | $T$°K | $P$(mmHg)$\times 10^4$ |
|---|---|---|---|
| 327.8 | 4.18 | 340.4 | 13.2 |
| 331.0 | 5.46 | 343.9 | 17.5 |
| 333.9 | 6.85 | 348.2 | 24.6 |
| 336.8 | 9.09 | | |

$\log P(\text{mmHg}) = 10.025 - 4397.5/T$: m. p. 120.8°C.

TABLE XII. SUBLIMATION PRESSURE OF δ-VALEROLACTAM

| $T$°K | $P$(mmHg)$\times 10^3$ | $T$°K | $P$(mmHg)$\times 10^3$ |
|---|---|---|---|
| 293.9 | 2.81 | 304.7 | 8.35 |
| 294.7 | 3.09 | 306.7 | 10.35 |
| 297.0 | 3.96 | 308.4 | 11.66 |
| 298.9 | 4.67 | 310.6 | 13.84 |
| 300.7 | 5.65 | 312.5 | 15.70 |
| 302.5 | 6.63 | | |

$\log P(\text{mmHg}) = 10.692 - 3891.0/T$: m. p. 39.3°C.

TABLE XIII. SUBLIMATION PRESSURE OF ε-CAPROLACTAM

| $T$°K | $P$(mmHg)$\times 10^3$ | $T$°K | $P$(mmHg)$\times 10^3$ |
|---|---|---|---|
| 294.0 | 1.18 | 305.2 | 4.21 |
| 295.2 | 1.38 | 306.9 | 5.03 |
| 297.1 | 1.72 | 308.7 | 6.02 |
| 298.3 | 1.93 | 310.6 | 7.43 |
| 300.4 | 2.44 | 312.2 | 8.70 |
| 301.9 | 2.92 | 313.9 | 10.03 |
| 303.7 | 3.56 | | |

$\log P(\text{mmHg}) = 11.839 - 4339.8/T$: m. p. 69.8°C.

vapor pressure equations obtained by the method of least squares. The linear relation between $\log p$ and $1/T$ is found to be quite satisfactory for all the measurements here mentioned.

In addition to the sublimation pressure of the amides listed above, that of *p*-aminoacetophenone, which should be classified as an amine in the usual sense, is also shown in Table XIV. Since the molecular structure of *p*-aminoacetophenone bears some resemblance to that of acetamide, except that the amino group is separated from the carbonyl group by a phenyl nucleus, it might be expected to form NH···O bonds with neighboring molecules in the crystal.

TABLE XIV. SUBLIMATION PRESSURE OF p-AMINOACETOPHENONE

| $T$°K | $P$(mmHg)$\times 10^4$ | $T$°K | $P$(mmHg)$\times 10^4$ |
|---|---|---|---|
| 314.2 | 3.32 | 326.0 | 11.9 |
| 315.6 | 3.78 | 329.2 | 16.5 |
| 318.6 | 5.47 | 332.3 | 22.5 |
| 320.1 | 6.42 | 335.2 | 30.2 |
| 323.8 | 9.47 | 338.2 | 41.7 |

$\log P(\text{mmHg}) = 11.900 - 4832.6/T$: m. p. 106.2°C.

The values of the heat of sublimation ($\Delta H$), the change of free energy at 298.2°K ($\Delta G^{298.2°}$) and of entropy ($\Delta S$) on sublimation are shown in Table XV.

**Energy of Hydrogen Bond.**—Table XV shows the estimated energies ($E$) of hydrogen bonds (NH···O) in the fourth column, together with the hypothetical lattice energies ($\Delta H'$) obtained conventionally, assuming the additivity rule of the lattice energy, without taking into account the formation of hydrogen bonds in the crystalline state[8]. The values of $E$ were obtained by subtracting $\Delta H'$ from $\Delta H$.

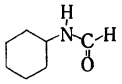
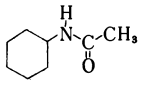
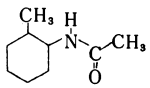
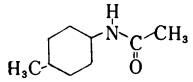
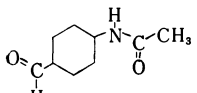
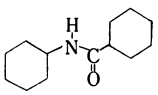
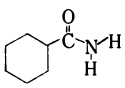
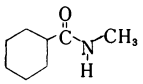
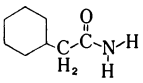
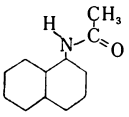
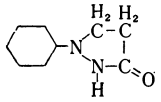
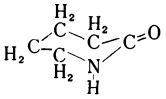
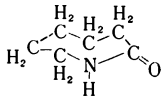
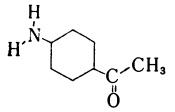
Because the crystal structures of the majority of compounds listed in Table XV are not analyzed as yet except for those of acetanilide[9] and benzamide[10], the formation of the NH···O bond is implicitly assumed for the rest of the compounds. considering the similarity of their molecular structures, this assumption would not be unreasonable.

It is clear, from the values of $E$ in the table, that the compounds dealt with in this investigation can be classified into three categories: the first showing little or no tendency to associate mutually by NH···O bondings (benzanilide, *N*-acetyl-α-naphthylamine and 1-phenyl-3-pyrazolidone); the second forming NH···O bondings of the order of $4\pm1$ kcal./mol. (formanilide, acetanilide, *o*- and *p*-acetotoluidine, *p*-acetaminobenzaldehyde, benzamide, *N*-methylbenzamide and α-phenylacetamide), and the third capable of making hydrogen bondings as strong as 6~7 kcal./mol. (δ-valerolactam and ε-caprolactam).

Let us first examine those which belong to category I. An alternative nomenclature of

9) C. J. Brown and D. E. Corbridge, *Nature*, **162**, 72 (1948); *Acta Cryst.*, **7**, 711 (1954).
10) B. R. Penfold and J. C. B. White, ibid., **12**, 130 (1959).

TABLE XV. VALUES OF THERMODYNAMIC FUNCTIONS AND ENERGIES OF HYDROGEN BOND

| Compounds | $\Delta H$ kcal./mol. | $\Delta H'$ kcal./mol. | $E$ kcal./mol. | $\Delta G^{298.2°}$ kcal./mol. | $\Delta S$ cal./deg. mol. |
|---|---|---|---|---|---|
|  | 18.63±0.11 | 14.5 | 4.1 | 8.22±0.21 | 34.9±0.3 |
|  | 20.75±0.37 | 16.5 | 4.3 | 9.44±0.70 | 37.9±1.1 |
|  | 23.20±0.22 | 18.5 | 4.7 | 9.78±0.40 | 45.0±0.6 |
|  | 23.67±0.23 | 18.5 | 5.2 | 10.63±0.43 | 43.7±0.7 |
|  | 23.69±0.23 | 20.0 | 3.7 | 10.54±0.44 | 44.1±0.7 |
|  | 23.71±0.29 | 23.5 | 0.2 | 12.27±0.53 | 38.4±0.8 |
|  | 23.17±0.27 | 14.5 | 8.7×(1/2) | 9.94±0.51 | 44.4±0.8 |
|  | 20.45±0.08 | 16.5 | 4.0 | 8.85±0.15 | 38.9±0.2 |
|  | 23.45±0.21 | 16.5 | 7.0×(1/2) | 10.67±0.46 | 42.8±0.8 |
|  | 22.48±0.30 | 23.0 | −0.5 | 11.46±0.86 | 37.0±0.6 |
|  | 20.12±0.40 | 20.5 | −0.4 | 10.37±0.75 | 32.7±1.2 |
|  | 17.81±0.12 | 11.5* | 6.3 | 7.15±0.16 | 35.7±0.4 |
|  | 19.86±0.11 | 13.0* | 6.9 | 7.64±0.22 | 41.0±0.4 |
|  | 22.11±0.13 | 16.5 | 5.6×(1/2) | 9.80±0.25 | 41.3±0.4 |

* In these cases, the increment of the lattice energy due to a $CH_2$ group was taken as 1.5 kcal./mol., taking into consideration the volume effect due to ring formation: the value was estimated from the heat of sublimation of cyclohexane, ~8.5 kcal./mol. (the sum of the heats of vaporization and fusion).

benzanilide is *N*-phenylbenzamide and the molecule consists of two large phenyl groups attached to both sides of a peptide linkage. These phenyl groups will inevitablly prevent the molecules from approaching each other closely to make association by the NH···O bonding. The infrared absorption data[11] prove also that the NH···O bond in the crystal of benzanilide is rather weak, if it is formed to any extent: the wavelength of the N-H absorption band in the crystalline state is 2.99 $\mu$ compared with 3.08 $\mu$ in the case of acetanilide, which is known to form NH···O bonds in the crystals[9]. *N*-acetyl-$\alpha$-naphthylamine is also known to show little tendency to form hydrogen bonds with dioxane and cyclohexanone as revealed from the study of ultraviolet absorption of this substance by Baba and Suzuki[12]. The small negative value of $E$ for this compound implies that there would be no hydrogen bond formed in the crystalline state in accordance with the result of ultraviolet absorption. This may be due to the blocking effect of a phenyl nucleus located very close to the N-H group at the $\alpha$-position.

As to 1-phenyl-3-pyrazolidone, Kurosaki[13] has observed the formation of associated dimers in its $CCl_4$ and $CHCl_3$ solutions by the infrared and dielectric technique. But, at the same time, he noticed that its tendency to associate was much decreased in $CHCl_3$ solution due to the high polarity of the solvent which interacts with the solute molecules. Therefore, if an extrapolation is allowed to be made to the extreme case where the solute is surrounded completely by the same substance as a solvent (that is, a pure liquid or solid), we may assume that the molecule should exist as a monomer in the crystalline state without making any association, because the dipole moment of 1-phenyl-3-pyrazolidone 3.5~3.6 D[13] is much greater than that of chloroform 1.05 D[14]. The result obtained by the author shown in Table XV confirms this conclusion.

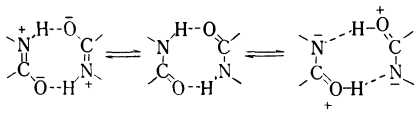
Those in category II may be regarded as forming "normal" hydrogen bonds of NH···O type, the energy of the bond being about 4 kcal./mol. The small differences between the values of these compounds might have some meaning concerning the strength of the bond formed, but, considering the approximate nature of the method of estimation, a further discussion on the difference of the strength of the bond cannot be made. It is interesting, however, to see that the methyl groups substituted to the phenyl nucleus seem to incsease the strength of the NH···O bond in the case of *o*- and *p*-acetotoluidine, while the formyl group in the para position of *p*-acetaminobenzaldehyde tends to decrease the NH···O bond-forming-power of the molecule: the weakly electron-releasing inductive and hyperconjugative effects of the methyl group might cause an increase of the negative charge on the oxygen atom of the carbonyl group, thereby reinforcing the strength of the hydrogen bond, while the strong electron-withdrawing inductive effect of the formyl group might result in the reverse way. In the case of benzamide and $\alpha$-phenylacetamide, the $E$ values in Table XV were obtained by dividing the difference of $\Delta H$ and $\Delta H'$ by two, because these molecules are connected to each other by two NH···O bonds per molecule in the crystalline state, as is revealed by Penfold and White[10].

The value of $E$ for *p*-aminoacetophenone, 2.8 kcal./mol. (=5.6/2 kcal./mol.), is somewhat smaller than those of the compounds in the second category. This is probably due to the separation of the amino and carbonyl groups by a phenyl nucleus which might prevent the mutual approach of molecules to some extent, although the positive charge on the NH group as well as negative charge on the C=O group are presumably increased to favor the formation of a strong NH···O bond due to the existence of a phenyl nucleus. An alternative way of explaining the smaller value of the energy of hydrogen bond in this compound is that it may behave as an amine forming hydrogen bonds of NH···N type in the crystalline state. This problem must be solved either by infrared absorption measurement or by crystallographic analysis.

The energies of an NH···O bond estimated for $\delta$-valerolactam and $\varepsilon$-caprolactam amount to 6~7 kcal./mol. and can be favorably compared with those observed for carboxylic acids[15] which are known to form dimers in the crystalline state as well as in liquid and in solutions. Here, it would be reasonable to assume that the two lactams exist as dimers in the crystalline state, because their molecular structures are such as to favor the formation of dimers (N-H is located in the *cis* position to C=O), just like those of carboxylic acids, although the crystal structures of the lactams are not analyzed as yet. Thus, the appreciable increase in the strength of NH···O bonds in

11) H. M. Randall et al., "Infrared Determination of Organic Structures", D. Van Nostrand Co., Inc., New York (1949), pp. 82, 147.
12) H. Baba and T. Suzuki, *J. Chem. Soc. Japan, Pure Chem. Sec.* (*Nippon Kagaku Zasshi*), **81**, 366 (1960).
13) K. Kurosaki, ibid., **79**, 1339, 1362 (1958).
14) C. P. Smyth, "Dielectric Behavior and Structure", McGraw-Hill Book Co., Inc., New York (1955), p. 237.
15) F. H. McDougall, *J. Am. Chem. Soc.*, **58**, 2585 (1936); E. W. Johnson and L. K. Nash, ibid., **72**, 547 (1950); R. E. Lundin, F. E. Harris and L. K. Nash, ibid., **74**, 743, 4654, (1952).

these cases, compared with a "normal" NH···O bond, can be understood as due to the conjugation of $\pi$-electrons in the ring system formed by two molecules:



A simple treatment of this problem based on the assumption of a dipole-dipole interaction between hydrogen-bond-forming molecules is mentioned in a previous paper[7]. It should be mentioned that the estimated value of the energy of an NH···O bond for $\delta$-valerolactam, 6.3 kcal./mol., is consistent with Tsuboi's value, 5.2 kcal./mol., obtained by the infrared spectroscopy on the association of the molecules in a $CCl_4$ solution[16].

In relation to the formation of ring dimers by the lactams mentioned above, a comment will be made on the molecular configuration of formanilide which is regarded as forming a "normal" hydrogen bond in this paper. Here it was implicitly assumed that the configurational position of the NH group was *trans* to the C=O group in this molecule, following the experimental result on the molecular structure of acetanilide[9]. Recently, however, Suzuki[17] has observed the existence of a *cis* form of this molecule in a $CCl_4$ solution in the study of its infrared absorptions and dipole moment: *cis* and *trans* forms exist in equilibrium, the energy difference being 600 cal./mol. The problem is whether the two forms should be found even in the crystalline state or not. Considering the "normal" value of the energy of hydrogen bond for formanilide, 4.1 kcal./mol., estimated in this study, the author is inclined to conclude that the molecule exists in the crystalline state as a *trans* form, because, if there is an appreciable amount of *cis* form, forming ring dimers, the energy of the hydrogen bond should be much higher, as can be seen from the values estimated for $\delta$-valero- and $\varepsilon$-caprolactam.

**Comparison of the Energies of Hydrogen Bonds in Crystalline State between the Types NH···O and OH···O.**—In order to get a general view on the strength of NH···O and OH···O bondings in the crystalline state, a comparison was made between the two types of the hydrogen bonds using the energy values of the bonds estimated by the author in series of studies[8], together with those published already by other investigators (recalculated by the author). The result is shown in Fig. 1. In this figure, numbers of the compounds which show particular values of the energy of the hydrogen bond are plotted against the energy values: for the sake of simplicity the values are rounded off to integers approximating to the original values. The following compounds and energy values are picked up mostly from the publications by Seki and his collaborators[18]: $CH_3OH$ 5.9 (6.0), $C_2H_5OH$ 6.5 (5.8), $n$-$C_3H_7OH$ 6.4 (5.6), $n$-$C_4H_9OH$ 6.0 (5.1), $n$-$C_6H_{13}OH$ 6.5 (5.5), cyclohexanol 5.8 (3.5), pentaerythritol 5.4 (4.0), $i$-erythritol 5.4[19] (4.0), phenol 4.5 (5.2), hydroquinone 4.7 (4.2), ice 4.4 (4.7), hydrogen peroxide 4.5 (5.1), diformylhydrazine 6.0[4] (6.6), diacetylhydrazine 3.1[3] (4.8), diketopiperazine 5.3[6] (4.9), urea 3.5[4] (3.4), oxamide 4.2[5] (4.0), sulphamide 4.7[3] kcal./mol., respectively. The figures in parentheses are the energy values estimated by the procedure proposed by the author[2]. Acetamide 3.1, *N*-methylacetamide 3.4[2], acetylglycine-*N*-methylamide 3.2[20] and acetylglycine-anilide 2.5[20] kcal./mol., respectively, are also included in Fig. 1.

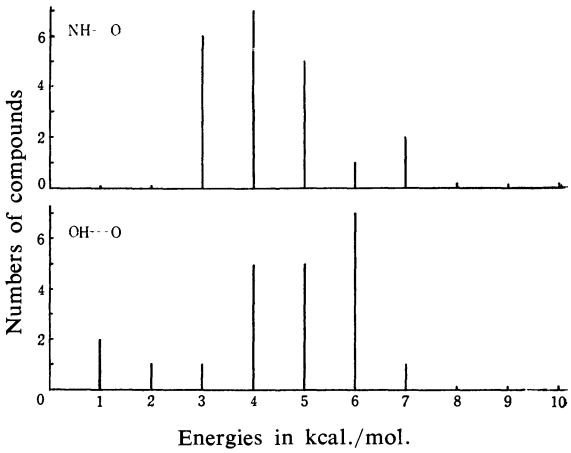



Fig. 1. Comparison of the energy of hydrogen bond between the type NH···O and OH···O.

It may be concluded from the distribution of the energy of hydrogen bonds as is seen in the figure, that the "normal" value of the energy of the NH···O bond can be 4±1 kcal./mol., while that of the OH···O bond amounts to 5±1 kcal./mol., and that a higher value both for NH···O and OH···O bonds can be ascribed to a favorable effect of conjugation in the $\pi$ electron systems as is seen in the formation of ring dimers by lactams and carboxylic acids. The lower values observed in the case of

16) M. Tsuboi, This Bulletin, 24, 75 (1951).
17) I. Suzuki, *J. Chem. Soc. Japan, Pure Chem. Sec.* (*Nippon Kagaku Zasshi*), **80**, 353 (1959).
18) S. Seki et al., "Hydrogen Bond", Iwanami, Tokyo (1956), p. 41.
19) A. Shimada, This Bulletin, 32, 330 (1959).
20) A. Aihara, *J. Chem. Soc. Japan, Prue Chem. Sec.* (*Nippon Kagaku Zasshi*), **76**, 495 (1955).

OH···O bonding are due to the steric hindrance by substituted groups which prevent the mutual approach of hydroxyl groups.

**Summary**

The energies of hydrogen bonds formed in the crystalline state of thirteen amides and one amine have been estimated following the procedure proposed in a previous paper. The values of the energy of an NH···O bond can be estimated at about 4±1 kcal./mol. for the majority of compounds treated in this paper, except two lactams which show energy values as large as 6~7 kcal./mol. A comparison was made between the energy values of NH···O and OH···O bonding using the data obtained by the author and other investigators.

*Department of Chemistry*
*Faculty of Liberal Arts and Science*
*Shinshu University*
*Agata-machi, Matsumoto*

# *Effect of Compacting and Grinding on the Hydrogen Reduction of Nickel Oxide*

By Yoshio IIDA and Kenzo SHIMADA

(Received February 10, 1960)

It has long been known that metal is hardened as a result of plastic deformation when it is pressed or rolled. Recently, it has been reported that the physical or chemical properties of non-metallic substances such as oxide[1], ionic crystal[2] and mineral[3] also vary when they are ground or pressed. Although these phenomena are not explained completely at present, increasing interest is being shown in the plastic deformation of ionic crystal.

In the previous paper[4] dealing with the hydrogen reduction of nickel oxide, it was shown that the rate of reduction was affected by the crystal distortion induced by the dissolution of minor additives. It is thought to be desirable to see how the reduction of nickel oxide is affected by grinding or compacting. In the present paper the isothermal reduction of nickel oxide, in a single crystal form or in powder form, subjected to grinding or compacting has been studied, consideration being given to the surface area of the specimens.

## Experimental

Chemical pure nickel sulfate recrystallized four times was heated at 850°C for 10 hr. to obtain nickel oxide powder. The average unit-particle size of nickel oxide was about 0.5 $\mu$ according to its electron micrograph. Nickel oxide was compacted into tablets at various pressures of 0 to 2000 kg./cm$^2$. A single crystal of nickel oxide was prepared by the method similar to that described by Verneuil[5].

The rate of reduction by hydrogen was determined by a thermobalance with a sensitivity of 0.5 mg. and could be used in hydrogen and in vacuo. Since the rate of reduction of nickel oxide by hydrogen at 200°C was a suitable magnitude for a comparison of the rates of specimens subjected to various treatments, the isothermal reduction was carried out at 200°C in the present study. In all cases of this experiment, nickel oxide of a constant weight of 500 mg. was heated up to 200°C in a vacuum of $10^{-3}$ mmHg and reduced at a constant temperature of 200°C by hydrogen whose flowing velocity was 100 cc./min.

Hydrogen from a commercially available cylinder was used after being purified with concentrated sulfuric acid, hot platinum asbestos, potassium hydroxide and phosphorus pentoxide.

The surface area of nickel oxide powder was determined by the B. E. T. method[6] in which nitrogen was the absorbent.

## Results and Discussion

**Effect of Compacting Pressure.**—The bulk density of nickel oxide pressed at various pressures of 0 to 2000 kg./cm$^2$ was measured from the ratio of weight of dimension. Table I shows that the bulk density increases and the calculated porosity decreases with an increase

1) J. B. Wachtman, *J. Am. Ceram. Soc.*, **37**, 291 (1954). A. S. Keh et al., *Acta Metallurgica*, **7**, 694 (1959).
2) S. Sonoike and T. Ninomiya, *Metal Physics* (*Kinzoku-Buturi*), **1**, 67 (1955); H. Kanzaki, ibid., **1**, 108 (1955).
3) H. Takahashi, This Bulletin, **32**, 235, 245, 252 (1958).
4) Y. Iida and K. Shimada, ibid., **33**, 8 (1960).
5) J. Nakazumi, *J. Chem. Soc. Japan. Ind. Chem. Sec.* (*Kogyo Kagaku Zasshi*), **59**, 1304 (1956).
6) S. Brunauer, P. H. Emmett and E. Teller, *J. Am. Chem. Soc.*, **60**, 309 (1938).

TABLE I. BULK DENSITY, POROCITY AND SURFACE AREA OF NICKEL OXIDE PRESSED AT VARIOUS PRESSURES

| Compacting pressure, kg./cm² | 0 | 200 | 500 | 1000 | 2000 |
|---|---|---|---|---|---|
| Bulk density, g./cc. | 1.7 | 2.1 | 2.5 | 3.0 | 3.4 |
| Surface area, m²/g. | 1.60 | — | 1.54 | 1.67 | 1.50 |
| Porosity, % | 75 | 69 | 63 | 56 | 50 |

in the compacting pressure. Although the surface area could be thought to decrease with an increase in the pressure, it does not vary with the pressure as shown in Table I. From these data it is found that a contact point which is formed by an atomic distance between nickel oxide particles and which prevents the adsorption of nitrogen, does not decrease with the pressure in spite of the decreasing porosity. In the previous paper[7] dealing with the oxidation of nickel powders it was shown that a surface area of nickel powders with a ductile property did not vary with the compacting pressure in the range of 0 to 1000 kg./cm². In view of the results concerning nickel powders, the results shown in Table I can be accepted as correct.

The effect of compacting pressure on the isothermal reduction of nickel oxide is shown in Fig. 1. It is seen that the rate of reduction increases with an increase in the compacting pressure below 1000 kg./cm². It should be noted that the amount of reduced nickel oxide in 5 hr. at 200°C is only 50% for an unpressed nickel oxide whereas it is 100% for nickel oxide pressed at 1000 kg./cm². Inasmuch as the surface area does not vary with the compacting pressure as shown in Table I, the accelerated reduction by compacting can be attributed to the crystal distortion which may be induced by compacting. Although the mechanism of hydrogen reduction of nickel oxide compact is very complicated[8] and not yet understood clearly, the porosity of the compact is thought to play an important role in the reduction which is a chemical reaction of solid with gas. The rate is lower at 2000 kg./cm² than at 1000 kg./cm². It is found that the effect of porosity on the reduction exceeds that of compacting when the pressure is relatively high and the porosity is small.

From these data it is expected that the rate becomes higher when nickel oxide compact pressed at a high pressure is ground into fine powders and its porosity becomes larger. Fig. 2 shows that the reduction is promoted further when the compact pressed at 1000 kg./cm² is ground into powders. It is seen that the rate of reduction of nickel oxide powder prepared by compacting and grinding is obviously higher than that of the nickel oxide powder subjected to no mechanical treatment and having the same porosity. This means that the effect of mechanical treatment on the hydrogen reduction is large and the effect of the porosity is small.

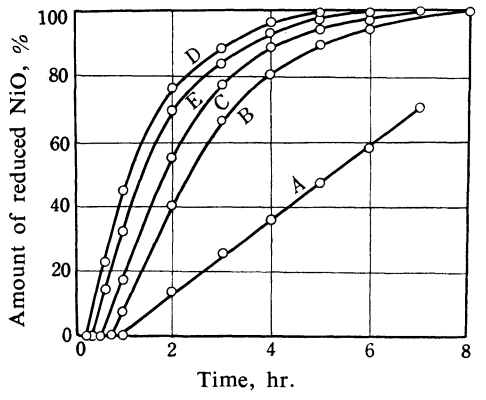



Fig. 1. Isothermal reduction of nickel oxide pressed at various pressures. The reduction temperature is 200°C. A is for nickel oxide unpressed, B, for nickel oxide pressed at 200 kg./cm², C, at 500 kg./cm², D, at 1000 kg./cm², and E, at 2000 kg./cm², respectively.

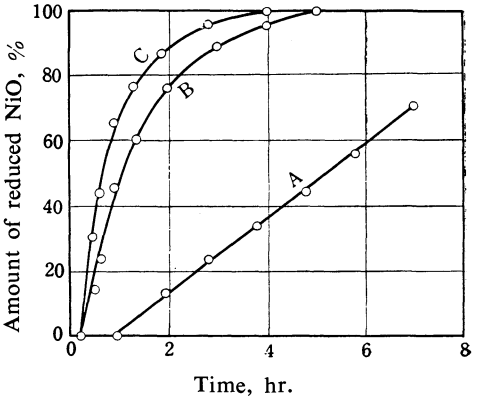



Fig. 2. Effect of compacting and grinding on the hydrogen reduction of nickel oxide at 200°C. A is for nickel oxide without compacting, B, nickel oxide compacted at 1000 kg./cm², and C, nickel oxide ground after compacting at 1000 kg/cm².

7) Y. Iida, S. Ozaki and K. Shimada, *Reports of the Government Industrial Research Institute, Nagoya (Nagoya Kogyo Gijitsu Shikenjo Hokoku)*, **10**, 569 (1957).

8) Y. Iida and K. Shimada, This Bulletin, to be published.

**Effect of Grinding.**—Isothermal reductions of a single crystal of nickel oxide and of nickel oxide powders prepared by grinding of the crystal were compared with that of nickel oxide prepared by ignition of nickel sulfate. The results in Fig. 3 show that the rate of

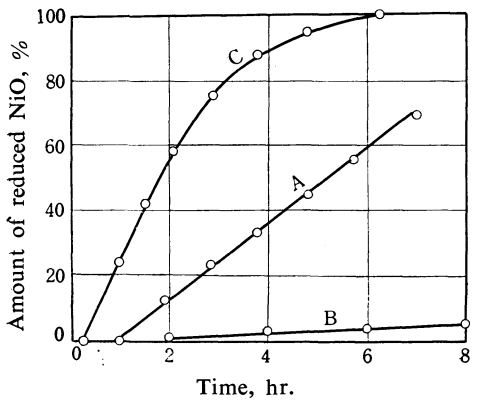



Fig. 3. Effect of grinding of a single crystal on the hydrogen reduction of nickel oxide at 200°C. A is for nickel oxide powders from ignition of nickel sulfate, B, a single crystal of nickel oxide and C, nickel oxide powders from grinding of the single crystal.

reduction of nickel oxide prepared by grinding of the single crystal is larger than those of a single crystal and nickel oxide prepared by ignition of nickel sulfate. It is a natural result from the consideration of the surface area that the rate of reduction of nickel oxide powders prepared by grinding of the single crystal exceeds that of the single crystal. The particles size of nickel oxide prepared by grinding of the single crystal is about 50 $\mu$ by a microphotograph and its surface area is too small to be determined by the B. E. T. method. The particle size of nickel oxide prepared by ignition of nickel sulfate is about 0.5 $\mu$ and is evidently smaller than that of nickel oxide prepared by grinding of the single crystal. The rate of reduction of nickel oxide prepared by ignition, however, is lower than that of nickel oxide prepared by grinding. As the single crystal was prepared from nickel oxide by igniting C. P. nickel sulfate, the purity of both nickel oxides is thought to be essentially the same. From the viewpoint of the surface area of nickel oxides, these facts cannot be understood reasonably.

Recently, it was reported that a change in physical properties of sodium chloride[2], zinc oxide* and kaoline[3] by grinding or compressing might be attributed to the crystal distortion which was caused by the plastic deformation. From these considerations it is concluded that the accelerated reduction of nickel oxide prepared by grinding of the single crystal results from the crystal distortion induced by grinding. On the basis of these data, it seems reasonable to assume that nickel oxide, either in powder form or single crystal form, shows plastic deformation which results in the accelerated hydrogen reduction, when it is compacted or ground.

## Summary

The rate of hydrogen reduction of nickel oxide increases with an increase in the compacting pressure although the bulk density of nickel oxide increases and the surface area does not vary with the pressure. The rate of reduction of nickel oxide which is prepared by the grinding of a single crystal and has a large particle size of 50 $\mu$ is higher than that of nickel oxide which is prepared by ignition of nickel sulfate and has small particle size of 0.5 $\mu$. It seems reasonable to conclude that the accelerated reduction is attributed to the crystal distortion which may result from plastic deformation by grinding or compacting.

The authors wish to express their sincere thanks to Tochigi Kagaku Kogyo Co. for the presentation of the single crystal.

*Government Industrial Research Institute*
*Kitaku, Nagoya*

* It is easily observed that zinc oxide turns yellow when it is ground after sintering.

# *A Molecular Orbital Theory of Saturated Compounds. I. Ionization Potential and Bond Dissociation Energy*

By Kenichi FUKUI, Hiroshi KATO and Teijiro YONEZAWA

(Received February 10, 1960)

Recently, several simple quantum-mechanical methods have been proposed to discuss physical properties of saturated compounds. That is to say, the bond energy and the heat of formation have been studied by Brown's bond orbital method[1] and by Dewar's perturbation treatment[2]. The ionization potential and the electron affinity have been investigated by the equivalent orbital method of Lennard-Jones and Hall, Franklin's united atom treatment[4], and Higuchi's UAO method[5].

In the present paper, the aliphatic and alicyclic compounds will essentially be treated by the use of the method previously presented by Yoshizumi[6], in which the skeleton consisting of carbon chain in an aliphatic molecule was exclusively taken into consideration. Thus, the ionization potential, heat of formation and bond energy of various saturated compounds are calculated according to this procedure, and the results obtained are in good agreement with experiments.

## Theoretical

Yoshizumi applied the strategy which was usual for treating the $\pi$-electron system to attacking the $\sigma$ electron system. Namely, in treating aliphatic molecules the $sp^3$-hybridized orbital of a carbon atom appeared in place of the $2p\pi$ atomic orbital in the treatment of conjugated molecules. He neglected the C–H bond of paraffin hydrocarbons for the sake of simplicity. Thus the molecular orbital was represented by a linear combination of $sp^3$ hydridized orbitals of carbon atoms, as follows:

$$\phi_j = \sum_j C_{rj}\phi_r \qquad (1)$$

where $C_{rj}$ is the coefficient of the $r$th atomic $sp^3$ hybridized orbital of carbon, $\phi_r$, in the $j$th molecular orbital, $\phi_j$. All the overlap integrals were neglected as in the simple LCAO MO theory in $\pi$-electron system. The resonance integrals in C–C bond and that between the orbitals attached to the same carbon atom were assumed as

$$\int \phi_i H \phi_{i+1} d\tau = \beta$$

and

$$\int \phi_i H \phi_{i+1} d\tau = m\beta$$

respectively, where $m$ was a small quantity which was determined by Yoshizumi as $m^2 = 0.12$ referring to the value of dipole moment of halogen-substituted hydrocarbons. The resonance integrals between non-neighboring atomic orbitals were neglected. In Fig. 1, it will be seen that when the number of an orbital $i$ is odd, the integral corresponds to that between two adjacent carbon atoms, and when $i$ is even, the resonance integral between two atomic orbitals of one and the same carbon atom.

In Yoshizumi's paper only linear paraffins were treated. In treating the other saturated compounds, it is necessary to introduce some emprical parameters besides.

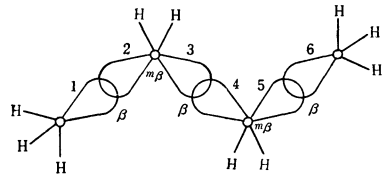



Fig. 1. Carbon $sp^3$ hybridized orbitals in *n*-butane.

## Parameters

For tertiary and quaternary carbon atoms in branched chain hydrocarbons, the Coulomb integral is tentatively taken as $\alpha_C = \alpha - \delta\beta$ in common according to their electronegativity, where $\alpha$ is the Coulomb integral of $sp^3$ hybridized orbital of primary and secondary carbon atoms. The value of $\delta$ is determined as equal to 0.3 considering the value of ionization potential of *i*-butane.

For alkyl halides (R–X), the Coulomb integral, $\alpha_X$, is taken as $\alpha + a\beta$ and the resonance integral, $\beta_{C-X}$ as equal to $b\beta$, where $b$ is determined by the formula $\frac{\beta_{C-X}}{\beta_{C-C}} = \frac{S_{C-X}}{S_{C-C}}$ ($S$ is

1) R. D. Brown, *J. Chem. Soc.*, **1953**, 2615.
2) M. J. S. Dewar and R. Pettit, *J. Chem. Soc.*, **1954**, 1625.
3) J. Lennard-Jones and G. G. Hall, *Disc. Faraday Soc.*, **10**, 18 (1951); G. G. Hall, *Proc. Soc.*, **A213**, 102 (1952), *Trans. Faraday Soc.*, **49**, 113 (1953).
4) J. L. Franklin, *J. Chem. Phys.*, **22**, 1304 (1954).
5) J. Higuchi, *Summary of Electronic Structure Symposium*, 23 (1958).
6) H. Yoshizumi, *Trans. Faraday Soc.*, **53**, 125 (1957).

obtainable from Mulliken's table[7]*) and $a$ is determined referring to the values of ionization potential of C-X bonding electron of methyl halides assigned by McDowell[8]. The values of $a$ and $b$ used in the present paper are listed in the following table.

| X | $a$ | $b$ |
|---|---|---|
| F | 0.91 | 0.51 |
| Cl | 0.56 | 0.65 |
| Br | 0.54 | 0.58 |
| I | 0.50 | 0.53 |

For alkyl alcohols, the Coulomb integral of alcoholic oxygen, $\alpha_{OH}$, is taken as $\alpha+0.5\beta$ and the resonance integral, $\beta_{C-OH}$, as $0.5\beta$, where $\beta_{C-OH}$ is determined by using the formula stated above (the value of $S_{C-OH}$ is put nearly equal to that of $S_{C-O}$). Since the value of the ionization potential of C-OH bonding electron of methyl alcohol has never been known, the value of $\alpha_{OH}$ is tentatively assumed as above.

## Results and Discussion

**a) Ionization Potential.**—(1) It was pointed out[8,9] that in normal parraffins their first ionization could be attributed to the removal of one electron localized in C-C bonds. This was supported by the difference between observed C-H and C-C bond energies, and also by the result of Hall's calculation[3]. Namely, he elucidated the theory that in the highest occupied orbital of normal paraffins the electron density of C-C bond was larger than that of C-H bond. Therefore, the ionization potential may safely be considered to be equal to the negative of the highest occupied orbital energy obtained by solving the secular determinant. The calculated results are listed in Table I, and the plot of calculated energy values versus observed ionization potentials is shown in Fig. 2. From the linear relation between the calculated and the observed, the values of $\alpha$ and $\beta$ are estimated as $-5.850$ eV. and $-6.364$ eV., respectively. With these values, the recalculated ionization potentials of paraffins are listed in the third column of Table I which are in good agreement with the observed, except in ethane.

TABLE I. CALCULATED ENERGIES OF THE HIGHEST OCCUPIED ORBITAL AND OBSERVED IONIZATION POTENTIALS OF NORMAL PARAFFINS

| Compound | Calcd. energy[a] $\lambda_{ho}$ | $\varepsilon_{ho}$ eV. | Obsd. I. P.[9] eV. |
|---|---|---|---|
| Ethane | 1.0000 | 12.21 | 11.76 |
| Propane | 0.8444 | 11.22 | 11.21 |
| *n*-Butane | 0.7752 | 10.77 | 10.80 |
| *n*-Pentane | 0.7388 | 10.55 | 10.55 |
| *n*-Hexane | 0.7170 | 10.41 | 10.43 |
| *n*-Heptane | 0.7034 | 10.33 | 10.35 |
| *n*-Octane | 0.6921 | 10.25 | 10.24 |
| *n*-Decane | 0.6820 | 10.19 | 10.19 |

a) $\lambda_{ho}$ is the coefficient in $\varepsilon_{ho}=\alpha+\lambda_{ho}\beta$, where $\varepsilon_{ho}$ is the highest occupied orbital energy.

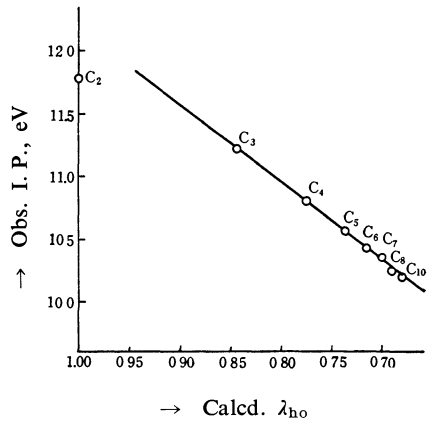



Fig. 2. Ionization potential of normal paraffins vs. $\lambda_{ho}$.

(2) In the calculation of cycloparaffins the steric configuration is left out of consideration, all the C-C-C angles being assumed equal to that of linear molecules. Therefore, no parameter is introduced anew. The results are listed in Table II, together with observed and Franklin's values[4] for the sake of comparison. It is seen that the smaller the deviation of an actual C-C-C angle from the normal one, the better agreement between the observed and the calculated results is found. This suggests that there is some room for improvement in future.

(3) For branched chain paraffins, the calculated values of ionization potentials are listed in the third column of Table III.

(4) It is considered that the first ionization potential of alkyl alcohols is due to removal of one of the lone pair electrons of the oxygen atom. The correlation of calculated values of the highest occupied orbital energies with observed ionization potentials is examined and an apparent linear relation between them is shown in Table IV, and it may result from the following cause. In general, the inductive effect of alkyl group may exert an influence

* The evaluation of the overlap integral, $S_{C-X}$, for bromine using the Slater orbital can not be carried out in the usual way. Therefore, the nearest integral power of $r$ in Slater orbital is adopted in our calculation.

7) R. S. Mulliken, C. A. Rieke, D. Orloff and H Orloff, *J. Chem. Phys.*, **17**, 1248 (1949).

8) D. C. Frost and C. A. McDowell, *Proc. Roy. Soc.*, **A241**, 194 (1957).

9) R. E. Hornig, *J. Chem. Phys.*, **16**, 105 (1948).

TABLE II. CALCULATED ENERGIES OF THE HIGHEST OCCUPIED ORBITAL AND OBSERVED IONIZATION POTENTIALS OF CYCLOPARAFFINS

| Compounds | Calcd. energy $\lambda_{ho}$ | Calcd. energy $\varepsilon_{ho}$ eV. | Calcd. I. P.[a] by Franklin eV. | Obsd. I. P. eV. | Deviation[b] from normal C-C-C angle |
|---|---|---|---|---|---|
| Cyclopropane | 0.8806 | 11.45 | 11.76 | 10.23[a] | +24°44′ |
| Methylcyclopropane | 0.7050 | 10.34 | 10.98 | 9.88[a] | — |
| Cyclobutane | 0.6600 | 10.05 | 10.21 | | + 9°44′ |
| Cyclopentane | 0.7520 | 10.64 | 10.80 | 11.10[a] | + 0°44′ |
| Cyclohexane | 0.6600 | 10.05 | 10.21 | 10.40[a] | − 5°16′ |

a) J. Hissel, *Bull. Soc. Roy. Sci. Liege*, **21**, 4576 (1952).
b) L. F. Fieser and M. Fieser, "Textbook of Organic Chemistry", D. C. Heath Co., Boston (1950).

TABLE III. CALCULATED ENERGIES OF THE HIGHEST OCCUPIED ORBITAL AND OBSERVED IONIZATION POTENTIALS OF BRANCHED PARAFFINS

| Compounds | Calcd. energy $\lambda_{ho}$ | Calcd. energy $\varepsilon_{ho}$ eV. | Obsd. I. P. eV. |
|---|---|---|---|
| Methylpropane | (0.6995) | (10.30) | 10.40[a] |
| Tetramethylmethane | 0.6995 | 10.30 | 10.30[b] |
| Ethylpropane | 0.6469 | 9.96 | 10.19[c] |
| 2,2-Dimethylbutane | 0.6378 | 9.93 | 9.90[c] |
| 3-Methylpentane | 0.6222 | 9.81 | 9.81[c] |

a) D. P. Stevenson, *J. Am. Chem. Soc.*, **64**, 2766 (1942).
b) D. P. Stevenson, *Disc. Faraday Soc.*, **10**, 35 (1951).
c) M. B. Koffel, *J. Chem. Phys.*, **17**, 44 (1948).

TABLE IV. CALCULATED ENERGIES OF THE HIGHEST OCCUPIED ORBITAL AND TOTAL ELECTRON DENSITIES AT OXYGEN AND OBSERVED IONIZATION POTENTIALS OF ALKYL ALCOHOLS

| Compounds | Calcd. energy $\lambda_{ho}$ | Calcd. total dens. at oxy. | Obsd. I. P. eV. |
|---|---|---|---|
| Methyl alcohol | (0.8090) | 1.4472 | 10.95[a] |
| Ethyl alcohol | 0.7589 | 1.4618 | 10.60[a] |
| Propyl alcohol | 0.7350 | 1.4643 | 10.46[a] |
| Butyl alcohol | 0.7180 | 1.4712 | 10.30[b] |
| *i*-Propyl alcohol | 0.6807 | 1.4784 | 10.27[b] |

a) J. D. Morrison and A. J. C. Nicholson, *J. Chem. Phys.*, **20**, 1021 (1952).
b) Reference 10).

on the electronegativity of oxygen lone pairs[10]. Therefore, the parallelism may be more directly understood by comparing the observed ionization potential with the magnitude of total $\sigma$ electron density the oxygen atom which is also given in the same table.

10) I. Omura, H. Baba and K. Higashi, This Bulletin, **28**, 147 (1955).

**b) Total Electronic Energy and Bond Dissociation Energy.**—The calculated total electronic energies are compared with observed values of heat of formation of several normal paraffins. The results indicate a good parallelism between them. For each increase of one $CH_2$-group the increment in the calculated energy lies between $2\alpha+2.057\beta$ and $2\alpha+2.059\beta$, while the observed difference in energy is in the range $-4.6\sim-5.2$ kcal./mol.[1] as shown in Table V. For cycloparaffins, the calculated total electronic energies are compared with observed heats of combustion and both the values per $CH_2$ are listed in Table VI*. Thus we can conclude that a simple additivity rule may approximately hold in normal paraffins and cycloparaffins.

In order to calculate the bond dissociation energy, we assume that it can be obtained by the following formula**.

$$D(R_1-R_2)=\{E(R_1\cdot)+E(R_2\cdot)\}-E(R_1-R_2) \quad (2)$$

where $D(R_1-R_2)$ denotes the dissociation energy of the bond between $R_1$ and $R_2$ in the compound $R_1-R_2$, $E$ is the total electronic energy, and $R_1$ and $R_2$ are two alkyl groups. For simplicity, the energy of an odd electron in alkyl radical, which is localized on one carbon atom, is assumed equal to $\alpha$. The results are listed in Table VII, where the numbers in parentheses are the observed values of bond energy and the numbers below them are the calculated values of bond energy in units of $(-\beta)$. In lower paraffins, the values obtained by Eq. (2) are shown to be a good measure for bond energy value. In hexane, a slight disagreement is observed. No internuclear repulsion is involved in the present treatment, and hence this discrepancy may, at

* The failure seen in the case of cyclobutane may probably be attributed to the approximation adopted in which steric circumstances are entirely disregarded.
** In the calculation of energy of alkyl radicals, the effect of hyperconjugation of alkyl group is left out of account.

TABLE V. CALCULATED TOTAL ELECTRONIC ENERGIES AND OBSERVED HEATS OF FORMATION OF NORMAL PARAFFINS

| Compounds | Calcd. total energy | Obsd. heat of formation[a] kcal./mol. | Difference Calcd. | Difference Obsd. kcal./mol. |
|---|---|---|---|---|
| Ethane | $4\alpha+2.000\beta$ | −20.2 | | |
| | | | $2\alpha+2.057\beta$ | −4.6 |
| Propane | $6\alpha+4.057\beta$ | −24.8 | | |
| | | | $2\alpha+2.058\beta$ | −5.0 |
| *n*-Butane | $8\alpha+6.115\beta$ | −29.8 | | |
| | | | $2\alpha+2.058\beta$ | −5.2 |
| *n*-Pentane | $10\alpha+8.157\beta$ | −35.0 | | |
| | | | $2\alpha+2.058\beta$ | −5.0 |
| *n*-Hexane | $12\alpha+10.231\beta$ | −40.0 | | |
| | | | $2\alpha+2.059\beta$ | — |
| *n*-Heptane | $14\alpha+12.290\beta$ | — | | |

a) F. D. Rossini et al., "Selected Values of Physical and Thermodynamic Properties of Hydrocarbons and Related Compounds", Carnegie Press, Pittsburgh (1953).

TABLE VI. CALCULATED TOTAL ELECTRONIC ENERGIES AND OBSERVED HEATS OF COMBUSTION OF CYCLOPARAFFINS

| Compounds | Calcd. energy Total | Calcd. energy per $CH_2$ | Obsd. heat of combustion[a] Total kcal./mol. | Obsd. heat of combustion[a] per $CH_2$ kcal./mol. |
|---|---|---|---|---|
| Cyclopropane | $6\alpha+6.203\beta$ | $2\alpha+2.067\beta$ | 505.5 | 168.5 |
| Cyclobutane | $8\alpha+8.225\beta$ | $2\alpha+2.056\beta$ | 662.5 | 165.5 |
| Cyclopentane | $10\alpha+10.293\beta$ | $2\alpha+2.059\beta$ | 797 | 159 |
| Cyclohexane | $12\alpha+12.348\beta$ | $2\alpha+2.058\beta$ | 939 | 157 |

a) Reference b) in Table II.

TABLE VII. DISSOCIATION ENERGIES OF C-C BONDS

| $R_1$ | $R_2$ Methyl | Ethyl | Propyl | Butyl |
|---|---|---|---|---|
| Methyl | (82) 2.000 | (82) 2.057 | (79) 2.058 | (78) 2.058 |
| Ethyl | — | (82) 2.115 | (79) 2.116 | (78) 2.116 |
| Propyl | — | — | (76) 2.117 | — |

Ethane $C\overset{(82)}{\underset{2.000}{}}C$

Propane $C\overset{(82)}{\underset{2.057}{}}C-C$

*n*-Butane $C\overset{(78)}{\underset{2.058}{}}C\overset{(82)}{\underset{2.115}{}}C-C$

*n*-Pentane $C\overset{(78)}{\underset{2.058}{}}C\overset{(79)}{\underset{2.116}{}}C-C\cdots C$

*n*-Hexane $C\overset{?}{\underset{2.058}{}}C\overset{(78)}{\underset{2.116}{}}C\overset{(76)}{\underset{2.117}{}}C-C\cdots C$

TABLE VIII. CALCULATED AND OBSERVED BOND DISSOCIATION ENERGIES OF ETHYL HALIDES

| X in $C_2H_5X$ | C-X bond diss. energy Calcd. $(-\beta)$ | Obsd.[a] (kcal./mol.) |
|---|---|---|
| F | 2.690 | 107.0 |
| Cl | 2.049 | 66.5 |
| Br | 1.896 | 54·0 |
| I | 1.749 | 45.5 |

a) Reference b) in Table II.

least partly, be ascribed to such a rough approximation adopted. Further improvement should be made on this point.

With regard to ethyl halides, the bond dissociation energies of C-X bond are obtained and compared with experimental values in Table VIII. Compounds are arranged in decreasing order of bond energies. It is seen that the result coincides well with experiments.

## Summary

The ionization potential and the bond dissociation energy of saturated compounds are calculated by Yoshizumi's C-C bond skeleton method. With regard to ionization potentials, the calculated results are parallel to the observed values. In particular, for normal paraffins the parallelism is almost complete. For total electronic energies, the calculated results indicate a simple additivity rule in normal and cycloparaffins, and for bond dissociation energies an approximate agreement is obtained between the calculated and the observed values.

In spite of the rough approximation involved in the present treatment, it may be said that the results obtained are rather satisfactory.

*Faculty of Engineering*
*Kyoto University*
*Sakyo-ku, Kyoto*

# *A Molecular Orbital Theory of Saturated Compounds. II. Chemical Reactivity in Nucleophilic Substitution*

By Kenichi FUKUI, Hiroshi KATO and Teijiro YONEZAWA

(Received February 26, 1960)

It is well known that a nucleophilic substitution of aliphatic compounds has available two reaction mechanisms, one being the unimolecular ($S_N1$) and the other the bimolecular mechanism ($S_N2$)[1]. The explanation of reactivity in aliphatic substitution has hitherto been carried out only by means of empirical electronic theory. No quantum-mechanical treatment of chemical reactivity in nucleophilic aliphatic substitution has ever been put into practice though some theoretical studies have been made with regard to the Walden inversion by Jaffé[2] and others[3,4].

In Part I[5] of this series of papers the ionization potential and the bond dissociation energy of several aliphatic compounds were calculated by the use of the C–C skeleton method proposed by Yoshizumi[6], resulting in a good agreement with the experiments.

In the present paper, an attempt is made to elucidate the reactivity in nucleophilic substitution of some alkyl halides, following the same quantum-mechanical procedure as used in Part I[5]. Also by the use of the procedure of simple LCAO MO method of conjugated molecules the stability of some aliphatic ions is discussed, in which the hyperconjugative effect is thought to be prevailing.

## $S_N2$ Reaction

The reaction of this type is expressed by the equation[1]

$$A^- + R-X \rightarrow [A\cdots R\cdots X]^- \rightarrow A-R + X^-$$

where $A^-$ is a nucleophilic reagent, R is an alkyl group, X is the group to be expelled, and the compound in brackets, stands for the activated complex.

The structure of activated complex is schematically written in Fig. 1. In this state, R′, R″, R‴ and C-atom lie all in one plane, and also A, C-atom and X lie on one straight line perpendicular to the plane. Four $sp^3$ orbitals of the central carbon atom may change to three $sp^2$ orbitals and one $p$ orbital which binds both A and X to C-atom. However, for the sake of simplicity, we neglect the influence of altered hybridization at the central C-atom and adopt the same values for Coulomb and exchange integrals as $sp^3$ hybridization. The overlap integral between $sp^2$ orbital and $p$ orbital is put equal to zero. The contribution of the reagent A to the energy of the total system is regarded as the same in all the reactions of the same type. We assume that in the transition state two $\sigma$ electrons in the C–X bond to be broken are localized at X-atom*. According to the present model, the difference in the energy between the transition state and the initial state, $\Delta E$, is calculated as

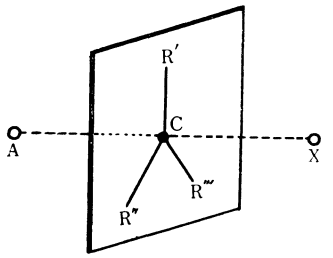



Fig. 1. Transition state in $S_N2$ reaction.

$$\Delta E = \{E[R^+] + E[X^-]\} - E[R-X] \qquad (1)$$

where $E[A]$ is the calculated total energy of the molecule or ion A. This procedure corresponds to the localization method in the theory of aromatic substitution. This energy, $\Delta E$, is considered to be a measure of the activation energy of the reaction.

Calculations are made with respect to some alkyl bromides, chlorides and iodides. The second order reactions of ethoxide anion and

1) C. K. Ingold, "Structure and Mechanism in Organic Chemistry", Cornell University Press, Ithaca, N. Y. (1953), Chapter VII.
2) H. H. Jaffé, *J. Chem. Phys.*, **22**, 1618 (1953).
3) I. Dostrovsky, E. D. Hughes and C. K. Ingold, *J. Chem. Soc.*, **1946**, 173.
4) S. Glasstone K. J. Laidlar and H. Eyring, "The Theory of Rate Processes", McGraw-Hill Book Co., New York, London (1941), pp. 135, 400.
5) U. Fukui, H. Kato and T. Yonezawa, This Bulletin, **33**, 1197 (1960).
6) H. Yoshizumi, *Trans. Faraday Soc.*, **53**, 123 (1957).

* Two alternative models may be possible. The one is the model in which the two $\sigma$ electrons are localized in the C-X bond, and the other is that in which the two electrons move in A···C and C···X bonds. Whichever of these two models one may adopt, only a constant term will be added to the energy difference obtained in the present treatment and no serious alteration arises with regard to the results.

chloride anion with alkyl bromides are investigated and the calculated results are compared with the ovserved activation energy and reaction rate in Table I. The agreement with this experiment is found satisfactory. In the present calculation, the energetic contribution of the attacking anion is not taken into account, since the anion is regarded as having the same energy in all the reactions of the same type.

In Table I, $\Delta E$ values of several alkyl bromides are listed for two types of nucleophilic reaction. In Table II, the experimental activation energies of alkyl iodides in the Menschutkin type reaction and in the substitution with the chloride anion are compared with the calculated values of $\Delta E$. Table III indicates the results of calculation with regard to the reaction of alkyl chloride with iodide anion. It is observed that the value of $\Delta E$ increases according as the reaction rate decreases.

TABLE I

(1) $RBr+C_2H_5O^- \rightarrow C_2H_5OR+Br^-$ [1]

| RBr | $\Delta E$ calc. $(-\beta)$ | Activation energy obs. (kcal./mol.) | Rate constant obs. $10^8k$ at 55°C ($sec^{-1}mol^{-1}l.$) |
|---|---|---|---|
| C-Br | 0.7420 | 20.0 | 34.4 |
| C-C-Br | 0.8156 | 21.0 | 1.95 |
| C-C-C-Br | 0.8174 | — | 0.55 |
|  | 0.8215 | 22.8 | 0.05 |
|  | 0.9215 | 26.2 | 0.000008 |

(2) $RBr+Cl^- \rightarrow RCl+Br^-$ [1]

| RBr | $\Delta E$ calc. $(-\beta)$ | Activation energy obs. (kcal./mol.) | Relative rate obs. |
|---|---|---|---|
| C-Br | 0.7420 | 15.8 | 100 |
| C-C-Br | 0.8156 | 17.9 | 1.97 |
| C-C-C-Br | 0.8174 | 18.1 | 1.29 |
| C-C-C-C-Br | 0.8174 | — | 1.29 |
|  | 0.8911 | 18.7 | 0.040 |
|  | 0.9580 | 21.2 | 0.009 |

The calculated results in these tables indicate that the rate of $S_N2$ reaction decreases in the order methyl>ethyl>higher *n*-alkyl>*i*-propyl >*t*-butyl, in accordance with experience.

The absolute rate of $S_N2$ substitution is strongly affected by an exchange of the group to be displaced. The observed rate of hydrolysis or alcoholysis decreases in the order R–I >R–Br>R–Cl. Calculated values in brackets exhibit a similar tendency as follows:

C–C–I (0.7494($-\beta$))>C–C–Br(0.8156($-\beta$))
>C–C–Cl(0.9288($-\beta$)).
C–C–C–I (0.7524($-\beta$))
>C–C–C–Br(0.8174($-\beta$))
>C–C–C–Cl(0.9305($-\beta$))

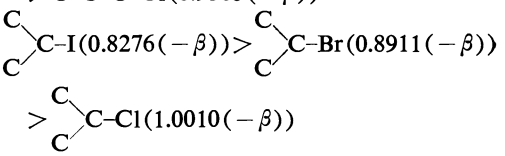



TABLE II

(3) $RI+Cl^- \rightarrow RCl+I^-$ [1]

| RI | $\Delta E$ calc. $(-\beta)$ | Activation energy obs. (kcal./mol.) | Relative rate Obs. |
|---|---|---|---|
| C-I | 0.6880 | 16.0 | 100 |
| C-C-I | 0.7494 | 17.3 | 8.9 |
| C-C-C-I | 0.7524 | 17.3 | 5.2 |
| C-C-C-C-I | 0.7520 | — | — |
|  | 0.8276 | 18.0 | 0.26 |

(4) $RI+(CH_3)_3N \rightarrow (CH_3)_3N^+R+I^-$ [1]

| RI | $\Delta E$ calc. $(-\beta)$ | Activation energy obs. (kcal./mol.) | Relative rate obs. |
|---|---|---|---|
| C-I | 0.6880 | 9.7 | 100 |
| C-C-I | 0.7494 | 11.4 | 0.58 |
|  | 0.8276 | 17.1 | 0.003 |

$RI+Et_3N \rightarrow RN^+Et_3+I^-$ [a]

| RI | $\Delta E$ calc. $(-\beta)$ | Activation energy obs. (kcal./mol.) | Relative rate obs. |
|---|---|---|---|
| C-I | 0.6880 | 9.7 | 100 |
| C-C-I | 0.7494 | 12.5 | 8.8 |
| C-C-C-I | 0.7524 | — | 1.7 |
| C-C-C-C-I | 0.7520 | 16.0 | 1.2 |
|  | 0.8276 | — | 0.18 |

a) M. S. Newman, "Steric Effects in Organic Chemistry", John Wiley & Sons, Inc., New York (1956), p. 75.

TABLE III

$RCl+I^- \rightarrow RI+Cl^-$ [1]

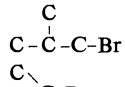
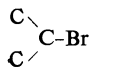
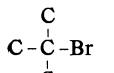
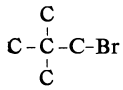
| RCl | $\Delta E$ calc. $(-\beta)$ | Activation energy obs. (kcal./mol.) | Relative rate obs. |
|---|---|---|---|
| C-Cl | 0.8480 | — | 93 |
| C-C-Cl | 0.9288 | — | 1.0 |
| C-C-C-Cl | 0.9305 | — | 0.37 |
| C-C-C-C-Cl | 0.9324 | — | 0.57 |
|  | 1.0010 | — | 0.0076 |
|  | 1.0942 | — | — |

### $S_N1$ Reaction

The rate determining step in this type of reaction is the ionic dissociation represented by the formula $RX \rightarrow R^+ + X^-$. Dewar[7] proposed a model for this transition state which may be written as S···R···X···S, where S stands for a solvent molecule, R is the alkyl group, and X is the group to be expelled. The factors affecting the rate of $S_N1$ reactions are considered to be (1) the rate of ionic dissociation of the molecule R–X, (2) the solvent effect, and so on. Refering to this we adopt as reactivity indexes the electron densities at the central C-atom ($q_C$) and at the X-atom ($q_X$) in the C–X bond. The larger $q_C$ is, the faster is the rate of ionic dissociation of the molecule R–X. Furthermore, the larger $q_X$ is, the stronger is the X···S binding.

TABLE IV

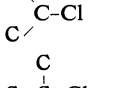
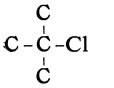
$RBr + OH^- \rightarrow ROH + Br^-$ [1]

| RBr | Calc. total density $q_C$ | Calc. total density $q_{Br}$ | Relative rate obs. |
|---|---|---|---|
| C-Br | 0.5768 | 1.4231 | 1.00 |
| C-C-Br | 0.5979 | 1.4359 | 1.71 |
| C-C-C-Br | 0.6000 | 1.4401 | — |
|  | 0.6005 | 1.4437 | — |
|  | 0.6063 | 1.4511 | 44.7 |
|  | 0.6056 | 1.4667 | $10^8$ |
|  | 0.6091 | 1.4874 | — |

Calculated values of $q_C$ and $q_{Br}$ are listed together with the rate of hydrolysis of alkyl bromide in Table IV in which a parallelism between them is found. Since there exist, however, no sufficient data available for comparison, the heat of reaction, $Q$, i. e. the approximate activation energy in $S_N1$ solvolysis of alkyl halides, computed by Evans[8,9] is used in Table V for this purpose. The magnitudes of $q_C$ and $q_X$ are seen to be parallel with the value of $Q$. Therefore, we conclude that $q_C$ and $q_X$ are useful reactivity indexes in $S_N1$ reaction.

TABLE V

(1) $R-X\ aq \rightarrow R^+\ aq + X^-\ aq$[7]

| R-Cl | Calc. total density $q_C$ | Calc. total density $q_{Cl}$ | Heat of reaction by Evans, $Q$ (kcal./mol.) |
|---|---|---|---|
| C-Cl | 0.6076 | 1.3924 | 89 |
| C-C-Cl | 0.6219 | 1.4085 | 59 |
|  | 0.6289 | 1.4223 | 37 |
|  | 0.6257 | 1.4358 | 26 |

(2)

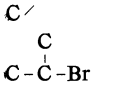
| R-Br | Calc. total density $q_C$ | Calc. total density $q_{Br}$ | Heat of reaction by Evans, $Q$ (kcal./mol.) |
|---|---|---|---|
| C-Br | 0.5768 | 1.4231 | 86.5 |
| C-C-Br | 0.5979 | 1.4359 | 56.5 |
|  | 0.6063 | 1.4511 | 34.5 |
|  | 0.6056 | 1.4667 | 23.5 |

TABLE VI

| Ions | Resonance energy calc. $(-\beta_0)$ | Stabilization energy[10] obs. (kcal./mol.) |
|---|---|---|
| $CH_3^+$ | 0 | 0 |
| $C_2H_5^+$ | 0.3350 | 36 |
| $n$-$C_3H_7^+$ | 0.5081 | — |
| $i$-$C_3H_7^+$ | 0.6462 | 66 |
| $t$-$C_4H_9^+$ | 0.9043 | 84 |

Furthermore, it has been shown that the rates of some $S_N1$ reactions can be connected with stabilites of alkyl ions formed by dissociation[10,12]. These stabilities can be represented by the resonance energy. In order to calculate the resonance energy in these saturated molecules, we may apply the simple LCAO MO treatment of conjugated molecules[10]. The following parameters are adopted in this calculation:

Coulomb integrals:

$\alpha_{H_3} = \alpha_0 - 0.3\,\beta_0$, $\alpha_{H_2} = \alpha_0 - 0.5\,\beta_0$,

Resonance integrals:

$\beta_{H_3 \equiv C} = 2.5\beta_0$, $\beta_{H_2 = C} = 2.0\beta_0$,

$\beta_{C-C} = 0.88\beta_0$ (in a C–C bond adjacent to the central C-atom),

$\beta_{C-C} = 0.50\beta_0$ (in other C–C bonds),

where $\alpha_0$ and $\beta_0$ are the Coulomb and resonance integrals in benzene, respectively. The latter two parameters $\beta_{C-C}$ are evaluated by considering the degree of localization in hyperconjugation[11].

The result of calculation with respect to several alkyl ions is indicated in Table VI. In $S_N1$ reaction the rate decreases along the series methyl < ethyl < higher $n$-alkyl < $i$-propyl < $t$-butyl, and the extremely large stability of the

7) M. J. S. Dewar, "Electronic Theory of Organic Chemistry," Clarendon Press, Oxford (1949), p. 64.
8) A. G. Evans, *Trans. Faraday Soc.*, **42**, 719 (1946).
9) J. L. Franklin, ibid., **48**, 443 (1952).
10) N. Muller and R. S. Mulliken, *J. Am. Chem. Soc.*, **80**, 3489 (1958).
11) Y. I'haya, This Bulletin, **28**, 369, 376 (1955).
12) A. Stretwieser, *Chem. Revs.*, **56**, 570 (1956).

tertiary carbonium ion was also reflected in the solvolysis rates of alkyl halides[12]. These facts are explained by our results.

*Faculty of Engineering*
*Kyoto University*
*Sakyo-ku, Kyoto*

# *Investigation on Mixed Complexes. IV. The Formation of a Mixed Complex by Reaction of Tetracyanoniccolate(II) with Bis-(dithiooxalato)-niccolate(II)*

By Sigeo KIDA

(Received August 31, 1959)

In the preceding paper of this series[1], it was demonstrated that the chlorocyano- and bromocyano- platinum(II) complex could not be formed in solution. However, one can not say that the formation of any mixed cyano complexes must be ruled out. Since it is commonly known that bis-(dithiooxalato)-niccolate(II) and tetracyanoniccolate(II) ions have the planar configuration, one should expect that a reaction between these reactants in solution might produce a complex containing both cyano and dithiooxalato as ligand. The purpose of the present paper is to present spectrophotometric evidence for the formation of a mixed cyano complex of the type, $[Ni(C_2S_2O_2)(CN)_2]^{2-}$, in solution.

Equivalent quantities of potassium bis-(dithiooxalato)-niccolate(II) and potassium tetracyanoniccolate(II) were mixed in solution. At first, the dark red color of the bis-(dithiooxalato)-niccolate(II) ion was predominant in the solution, then the color slowly changed to orange, the reaction being complete in two hours at room temperature (15°C). This change was followed spectrophotometrically, and the results are shown in Fig. 1. The intensity of the absorption band at 501 m$\mu$ of the bis-(dithiooxalato)-niccolate(II) ion decreases remarkably with time, while a new band appears at 380 m$\mu$, the intensity of which increases in nearly reciprocal proporation to that of the band at 541 m$\mu$. This implies that a reaction such as,

$$[Ni(C_2S_2O_2)_2]^{2-} + [Ni(CN)_4]^{2-} \rightleftarrows 2[Ni(C_2S_2O_2)(CN)_2]^{2-},$$

might be taking place in solution. The reasons are: 1) the blue shift of the band from 501 m$\mu$ to 380 m$\mu$ is indicative of the replacement of the dithiooxalate ion by cyanide ions, since the former is placed behind the latter in the spectrochemical series[2], and 2) the frequency of the new band is nearly equal to the mean of frequencies of the bands of the parent complexes, $[Ni(C_2S_2O_2)_2]^{2-}$ and $[Ni(CN)_4]^{2-}$, as shown in Table I. This is the relationship which can always be seen between the mixed complex and its parent complexes[3,4].

Previously[5], polarographic measurements were carried out on a mixed solution of potassium bis-(dithiooxalato)-niccolate(II) by Maki, Kida and Tsuchida, and it was reported that a new compound, perhaps the mixed complex, $[Ni(C_2S_2O_2)(CN)_2]^{2-}$, must be formed in the solution. Thus, the present result is not in consistent with the previous one.

Similar spectrophotometric observations were made also on the bis-dithiooxalato- and the tetracyano- platinum(II) and palladium(II) complexes. Unfortunately, no indication of the expected reactions, such as

$$[Pt(C_2S_2O_2)_2]^{2-} + [Pt(CN)_4]^{2-} \rightleftharpoons 2[Pt(C_2S_2O_2)(CN)_2]^{2-} \text{ and}$$

$$[Pd(C_2S_2O_2)_2]^{2-} + [Pd(CN)_4]^{2-} \rightleftharpoons 2[Pd(C_2S_2O_2)(CN)_2]^{2-},$$

could be detected. At present, however, it is quite uncertain whether this is due to the total inertness of these parent complexes or to the extreme instability of the ligand-mixed complexes.

Therefore, another attempt was made as follows: in order to obtain some information on the possible reaction between the bis-(dithiooxalato)-platinate(II) ion and the cyanide ion, a potassium cyanide solution and a potassium

1) Part III of this series; S. Kida, This Bulletin, 33, 587 (1960).

2) Y. Shimura and R. Tsuchida, This Bulletin, 29, 311 (1956); R. Tsuchida, ibid., 13, 388 (1938).

3) S. Kida, ibid., 29, 805 (1956).

4) Y. Shimura and R. Tsuchida, ibid., 28, 572 (1955).

5) N. Maki, S. Kida and R. Tsuchida, ibid., 32, 573 (1959).

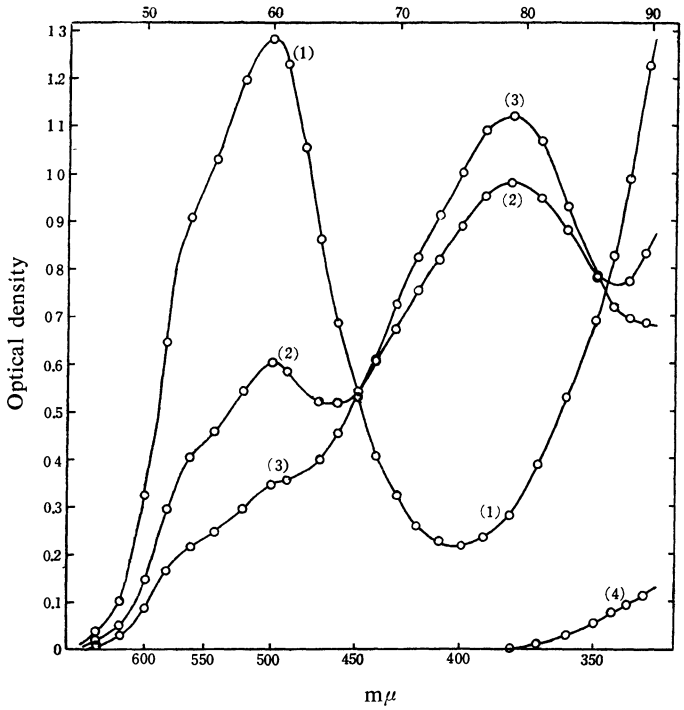



Fig. 1.

(1) $1/3\times10^{-3}$ F $K_2[Ni(C_2S_2O_2)_2]$ solution
(2) $1/3\times10^{-3}$ F $K_2[Ni(C_2S_2O_2)_2]$ and $1/3\times10^{-3}$ F $K_2[Ni(CN)_4]$ solution, (1/2 hr. after mixing)
(3) The same as solution (2), (2 hr. after mixing)
(4) $1/3\times10^{-3}$ F $K_2[Ni(CN)_4]$ solution

Table I. Frequencies of absorption bands of the complexes

| $K_2[Ni(C_2S_2O_2)_2]$ | $K_2[Ni(CN)_4]$ | New band | $(\nu_1+\nu_2)/2$ |
|---|---|---|---|
| 59.7 (501 mμ) | 96.9 (310 mμ) | 78.9 (380 mμ) | 78.3 |

$\nu\times10^{13}$: the frequency of the absorption maximum ($sec^{-1}$)

bis-(dithiooxalato)-platinate(II) solution were mixed in the ratio 2 : 1. The intensity of the absorption band due to the bis-(dithiooxalato)-platinate(II) ion at 430 mμ was appreciably reduced, while in a shorter wavelength region, the absorption showed a uniform increase in intensity. No distinct new band was formed, as shown in Fig. 2.

This uniform increase in absorption intensity in the shorter wavelength region may be regarded as being due to the decomposition of the bis-(dithiooxalato)-platinate(II) ion, since it can be demonstrated spectrophotometrically that, in an alkaline solution, this ion is subject to a slow decomposition which results in increased absorption at the shorter wavelength[6]. Accordingly, a mixed complex, such as $[Pt(C_2S_2O_2)(CN)_2]^{2-}$, is unlikely to be present in the solution, though it is better not to draw a decisive conclusion until more experimental data are obtained. On the other hand, there is no doubt that some quantity of the tetracyanoplatinate(II) ion has been produced in this solution, because the characteristic band, of this ion, at 279 mμ, is evidently found in the absorption curve 6 in Fig. 2.

## Experimental

Solutions of the following concentrations were mixed, $(2/3)\times10^{-3}$ F potassium bis-(dithiooxalato)-niccolate(II) and $(2/3)\times10^{-3}$ F potassium tetracyano-niccolate(II), and the mixed solution was placed in the dark at room temperature (15°C). The reaction was almost complete in two hours. It was ascertained by extinction measurements that the decomposition of bis-(dithiooxalato)-niccolate(II) ion was small during the experiment.

6) This was verified by extinction measurements on a weakly alkaline solution of this complex.
The bis-(dithiooxalato)-palladate (II) ion so rapidly decomposed in an alkaline solution that extinction measurements of this complex could not be carried out in a solution containing potassium cyanide.

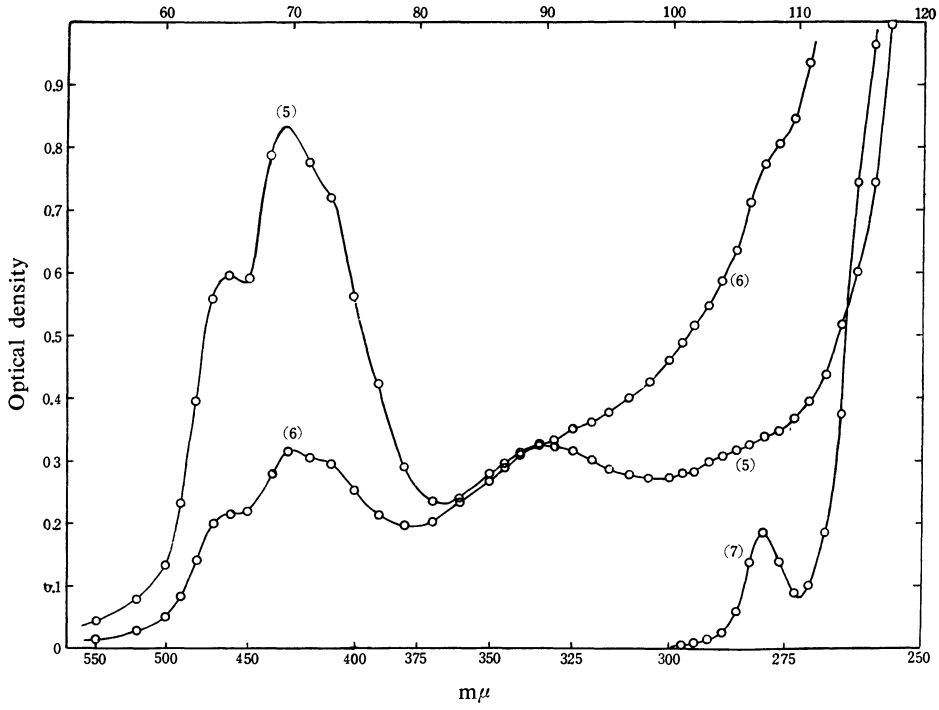



Fig. 2.

(5) $10^{-4}$ F $K_2[Pt(C_2S_2O_2)_2]$ solution
(6) $10^{-4}$ F $K_2[Pt(C_2S_2O_2)_2]$ and $2\times10^{-4}$ KCN solution, (2 days after mixising)
(7) $10^{-4}$ F $K_2[Pt(CN)_4]$

Solutions of potassium cyanide (0.1 F) and of potassium bis-(dithiooxalato)-platinate(II) (0.2 F) were mixed and placed in the dark at room temperature (15°C). For extinction measurements, 5 ml. of the solution was diluted to 500 ml. The extinction measurements were carried out with a Beckman model DU spectrophotometer.

The complexes, $K_2[Ni(C_2S_2O_2)_2]$[7], $K_2Pd(C_2S_2O_2)_2]$[7], $K_2[Pt(C_2S_2O_2)_2]$[7], $K_2[Ni(CN)_4]\cdot H_2O$[8], $K_2[Pd(CN)_4]\cdot 3H_2O$[8], and $K_2[Pt(CN)_4]\cdot 3H_2O$[9], were prepared according to the literature cited.

## Summary

It has been concluded, by the spectrophotometric method, that 1) potassium bis-(dithiooxalato)-niccolate(II) and potassium tetracyanoniccolate(II) react in solution to form a mixed complex, $[Ni(C_2S_2O_2)(CN)_2]^{2-}$, 2) in the case of palladium(II) and platinum(II), bis-(dithiooxalato)- and tetracyano- complexes do not react in solution, unlike the case of nickel(II), and 3) the dithiooxalate ion in the complex, $[Pt(C_2S_2O_2)_2]^{2-}$, is replaced by the cyanide ion in solution, the tetracyanoplatinate(II) ion being formed, but the formation of the mixed complex, such as $[Pt(C_2S_2O_2)(CN)_2]^{2-}$, is not certain.

The author wishes to express his heartfelt thanks to Professor R. Tsuchida for his kind instruction and advice throughout this work.

*Department of Chemistry*
*Wakayama University*
*Masagocho, Wakayama*

7) H. O. Jones and H. S. Tasker, *J. Chem. Soc.*, **1905**, 95.
8) W. C. Fernelius, "Inorganic Syntheses", vol. II. McGraw-Hill Book Co. Inc., 1946, pp. 243, 227.
9) G. Brauer, "Handbuch der präparativen anorganishe Chemie", F. Enke Verlag, Stuttgart, 1954, p. 1179.

# *Dichroism of Dyes in the Stretched PVA Sheet. IV.*[1] *Absorption Spectra of Carbocyanines and Note on the Chemical Structures**

By Yoshié TANIZAKI and Hisataké ONO

(Received February 9, 1960)

In the previous paper[1], the dichroic behavior of Pinacyanol in the stretched polyvinylalcohol (PVA) sheet was discussed in detail. It was pointed out that the directions of absorptions, which were judged by an inspection of the dichroic curves observed at a high stretch ratio, are in agreement with those obtained from a quantitative analysis of the relation between the density ratio $R_d$ and the stretch ratio $R_s$[1].

The purpose of this paper is to analyze the dichroism of carbocyanines by this method of inspection, to confirm the fact that the result thus obtained can be explained consistently by the conclusion derived from Pinacyanol[1], and to add some new information about the visible absorption phenomena after the inclusive discussion on the further experimental facts obtained here.

## Experimental

Here were used the following four dyes, which were prepared by the known methods:

1, 1'-Diethyl-2, 2'-cyanine iodide, — m. p. 274°C (277°C in literature[2]). Found: C, 59.92; H, 5.04; N, 6.32. Calcd. for $C_{23}H_{23}N_2I$: C, 60.79; H, 5.07; N, 6.18%.

1, 1'-Diethyl-2, 2'-dicarbocyanine iodide, — m. p. 268~9°C (270°C in literature[4]).

1, 1'-Diethyl-2, 2'-tricarbocyanine iodide, — m. p. 222~3°C (225°C in literature[4]). Found: C, 61.30; H, 5.75; N, 4.80. Calcd. for $C_{29}H_{29}N_2I \cdot 2H_2O$: C, 61.30; H, 5.81; N, 4.93%.

1, 1'-Diethyl-4, 4'-cyanine iodide, — m. p. 282°C (271~3°C in literature[5]). Found: C, 60.96; H, 5.35; N, 6.37. Calcd. for $C_{23}H_{23}N_2I$: C, 60.79; H, 5.07; N, 6.18%.

Let us use the notations, $j=0(2,2')$, $j=2(2,2')$, $j=3(2,2')$ and $j=0(4,4')$, for the respective dyes described above. At the same time, the Pinacyanol used in the previous paper[1] will be denoted by $j=1(2,2')$.

The preparation of the sample sheet, the measurement, etc. followed the manner reported before[1,6]. Here, the dyeing bath of the dye which failed to dissolve in water at the necessary concentration was prepared by adding a calculated amount of water to the hot ethanol solution of the dye concentrated as much as possible.

## Results

Let us number the absorption bands of each dye in the order of wavelength, for the convenience of the following description (see figures and tables).

Figs. 1 and 2 show, the interpretation of the dichroism of $j=0(4,4')$ in the near ultraviolet and in the visible regions, respectively. In Fig. 1, it is seen as a distinctive feature that the $D_{\parallel}$ and $D_{\perp}$ curves cross in the neighborhood of Band VII, that $D_{\perp}$ of Band VIII is apparently higher than $D_{\parallel}$, and that $D_{\theta}$ of Band V does not change much with increasing $\theta$.

Figs. 3 and 4 indicate the dichroism of $j=0$ $(2,2')$ in the ultraviolet and visible regions respectively. Their special feature is that $\lambda_{max}$'s in the region longer than 300 m$\mu$ are

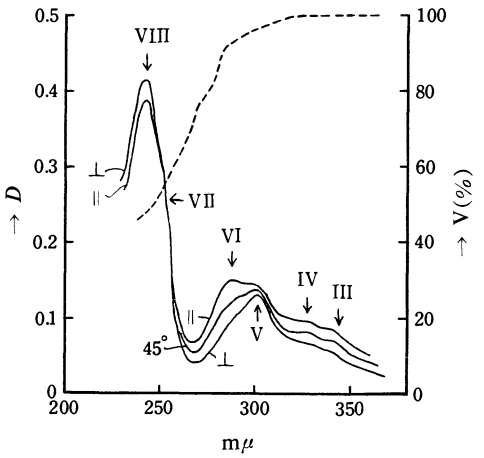



Fig. 1. The dichroism of 1,1'-diethyl-4,4'-cyanine iodide, $j=0(4,4')$, in the stretched PVA sheet. $R_s=5.7$. The broken line indicates the polarization degree curve of the polaroid used, taken from Y. Tanizaki, This Bulletin, **30**, 935 (1957).

* Presented at the Electronic Structure, Symposium, Tokyo, Sep. 1959.

1) Part III of this series, Y. Tanizaki, This Bulletin, **33**, 979 (1960).

2) F. M. Hamer, *J. Chem. Soc.*, **1928**, 208.

3) F. Kimura, F. Homma and F. Kobayashi, *Japan*, **228**, 529 (1957).

4) T. Ogata and T. Shiozaki, *Bull. Iust. Phys. Chem. Res.* (*Tokyo*), **13**, 511 (1934).

5) T. Ogata and S. Sakurai, *Bull. Inst. Phys. Chem. Res.* (*Tokyo*), **3**, 77 (1924).

6) Y. Tanizaki, This Bulletin, **32**, 75 (1959); Y. Tanizaki and N. Ando, *J. Chem. Soc. Japan, Pure Chem. Sec.* (*Nippon Kagaku Zasshi*), **78**, 542 (1957).

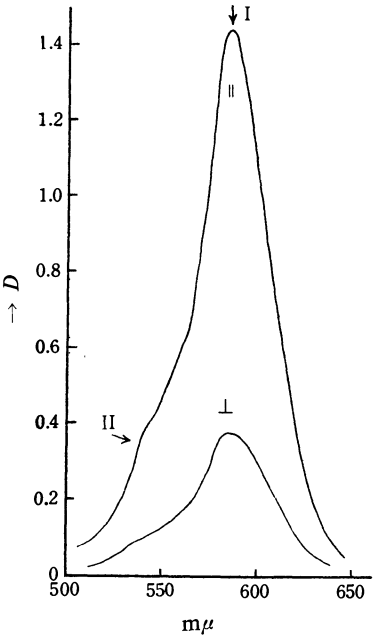



Fig. 2. The dichroism of 1,1'-diethyl-4,4'-cyanine iodide, $j=0(4,4')$, in the stretched PVA sheet. $R_s=10$.

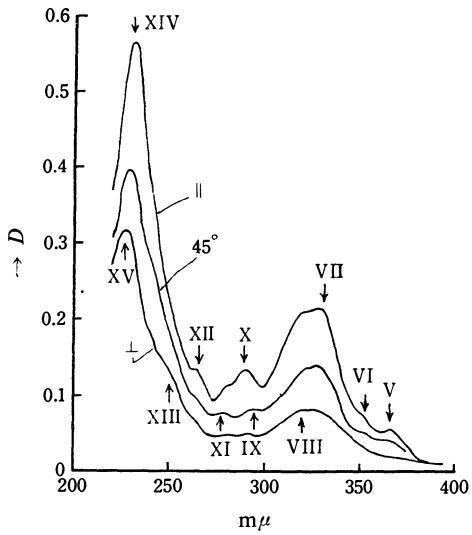



Fig. 3. The dichroism of 1,1'-diethyl-2,2'-cyanine iodide, $j=0(2,2')$, $R_s=9.0$.

almost independent of $\theta$**, while those in the region thereunder show an apparent change. It is also an interesting fact that the shapes of absorption bands in the visible and 300~400 mμ regions resemble each other considerably (see Figs. 3 and 4), though not so closely as in the case of Pinacyanol, $j=1(2,2')$[1].

** A detailed inspection revealed a slight shift of $\lambda_{max}$ with $\theta$ in the visible region. This we will discuss later.

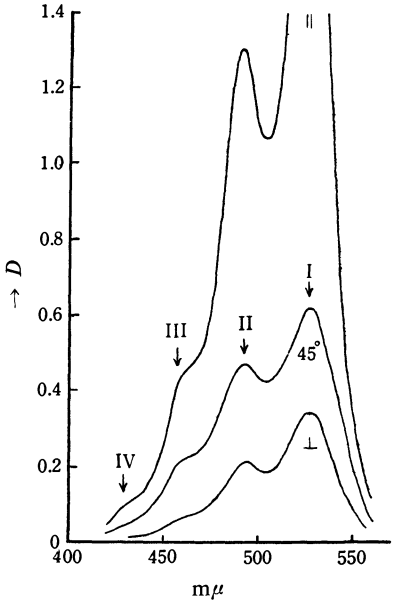



Fig. 4. The dichroism of 1,1'-diethyl-2,2'-cyanine iodide, $j=0(2,2')$, $R_s=9.0$.

Figs. 5 and 6 show the dichroism of $j=2$ $(2,2')$ at 220~500 mμ and 500~850 mμ, respectively. In this case, too, $\lambda_{max}$'s as above 400 mμ show little change with $\theta$**, while those below 400 mμ show a clear change.

Figs. 7 and 8 show the dichroism of $j=3$ $(2,2')$. Here is found the important fact that $\lambda_{max}$'s of $D_\theta$ in Fig. 8, which shows the absorptions supposedly along the long axis of the molecule[1], apparently shift with $\theta$. Similar behavior was also recognized in the case of $j=0$ (Fig. 4) and $j=2$ (Fig. 6), though very slightly. Band II (493 mμ) in Fig. 4, for example, shows a slight shift in $\lambda_{max}$ towards shorter wavelengths with a change from $D_\perp$ to $D_\parallel$ curve. Such a tendency may be due principally to the following fact: small directional differences originally existing between the absorptions along the molecular axis come to be appreciable owing to a sharpening in the

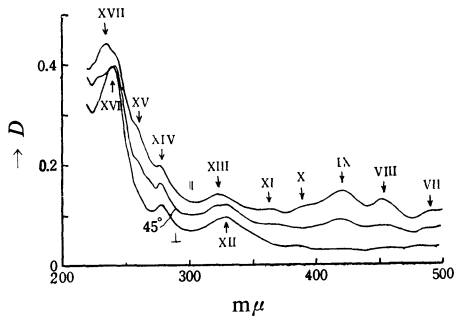



Fig. 5. The dichroism of 1,1'-diethyl-2,2'-dicarbocyanine iodide, $j=2(2,2')$. $R_s=8.1$.

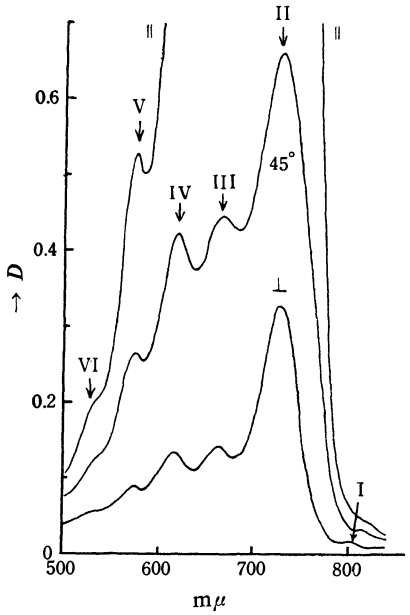



Fig. 6. The dichroism of 1,1'-diethyl-2,2'-dicarbocyanine iodide, $j=2(2,2')$. $R_S=8.1$.

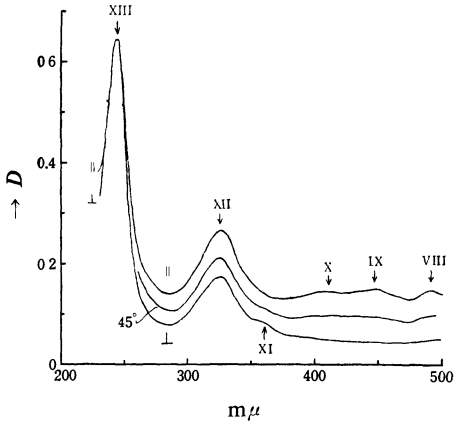



Fig. 7. The dichroism of 1,1'-diethyl-2,2'-tricarbocyanine iodide, $j=3(2,2')$. $R_S=6.1$.

distribution for the direction of the statistic orientation axis attendant on the molecule with the increase of its length. On the other hand, the directional properties of the short wavelength absorptions show a tendency to become indistinct with the increase of $j$. They are most indistinct in the case of $j=3$. It should be noticed that even the absorptions below 350 mμ have no change in $\lambda_{max}$ with $\theta$. Moreover, $D_{\parallel}$ and $D_{\perp}$ of Band XIII coincide with each other (Fig. 7), with the incident light of 50% polarization in this region (cf. Fig. 1).

Tables I—V involve the transition directions, the classification of band-groups, etc., as in the previous paper[1], judged from the data mentioned above. Here, table III shows again the data of Pinacyanol obtained previously[1]. Band-groups in tables have the following meaning: the absorptions in the first and the second group are both due to the transitions along the long axis of the molecule, and the absorption intensities of the second group are considerably

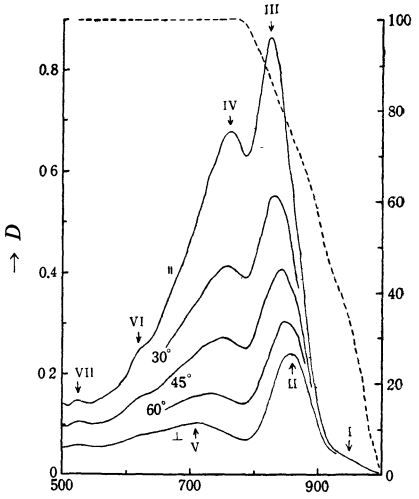



Fig. 8. The dichroism of 1,1'-diethyl-2,2'-tricarbocyanine iodide, $j=3(2,2')$. $R_S=6.9$. The broken line indicates the polarization degree curve of polaroid used, taken from Y. Tanizaki, This Bulletin, **30**, 935 (1957).

Table I. The absorption bands of 1,1'-diethyl-4,4'-cyanine iodide, $j=0(4,4')$, in the stretched PVA sheet

| Band No. | $\lambda$ mμ | $\nu$ cm$^{-1}$ | $\Delta\nu$ cm$^{-1}$ | Direction | Group | $\Delta\tilde{\nu}$ cm$^{-1}$ |
|---|---|---|---|---|---|---|
| I | 585 | 17100 | 1480 | $l$ | 1st | 1480 |
| II | 538 | 18580 | 10640 | $l$ | | |
| III | 342 | 29220 | 1440 | ? | 2nd | 1440 |
| IV | 326 | 30660 | 2540 | ? | | |
| V | 301 | 33200 | 1500 | $\perp(L_{\parallel})$ | 3rd | |
| VI | 288 | 34700 | 4980 | $\parallel(L_{\perp})$ | | |
| VII | 252 | 39680 | 1620 | $\parallel$ ?$(L_{\perp}$?) | 4th | |
| VIII | 242 | 41300 | | $\perp(L_{\parallel})$ | | |

Note: $\Delta\nu$ and $\Delta\tilde{\nu}$ indicate the distance between the adjacent bands and the mean of the band distance among the group, respectively. The notation "$l$" means the longitudinal direction of the molecule, and "$\parallel$" or "$\perp$" means the direction more parallel or more normal to the $l$-direction, respectively, among transitions in the quinoline parts. In this table, $\parallel$ corresponds to $L_{\perp}$, the short axis of the quinoline nucleus, and $\perp$ to $L_{\parallel}$. In the following tables, $\parallel$ corresponds to $L_{\parallel}$ and $\perp$ to $L_{\perp}$.

TABLE II. THE ABSORPTION BANDS OF 1,1'-DIETHYL-2,2'-CYANINE IODIDE IN THE STRETCHED PVA SHEET

| Band No. | $\lambda$ mμ | $\nu$ cm$^{-1}$ | $\Delta\nu$ cm$^{-1}$ | Direction | Group | $\tilde{\Delta\nu}$ cm$^{-1}$ |
|---|---|---|---|---|---|---|
| I | 527 | 18960 | | $l$ | | |
| | | | 1320 | | | |
| II | 493 | 20280 | | $l$ | | 1450 |
| | | | 1600 | | 1st | ±150 |
| III | 457 | 21880 | | $l$ | | |
| | | | 1380 | | | |
| IV | 430 | 23260 | | $l$ | | |
| | | | 4040 | | | |
| V | 366 | 27300 | | $l$ | | |
| | | | 1180 | | | |
| VI | 351 | 28480 | | $l$ | | 1050 |
| | | | 950 | | 2nd | ±100 |
| VII | 330 | 30300 | | ? | | |
| | | | 950 | | | |
| VIII | 320 | 31250 | | ? | | |
| | | | 2650 | | | |
| IX | 295 | 33900 | | ? | | |
| | | | 500 | | | |
| X | 290 | 34480 | | ∥ | | |
| | | | 1470 | | 3rd | |
| XI | 278 | 35950 | | ⊥? | | |
| | | | 1630 | | | |
| XII | 266 | 37580 | | ∥ | | |
| | | | 2240 | | | |
| XIII | 251 | 39820 | | ⊥ | | |
| | | | 3280 | | | |
| XIV | 232 | 43100 | | ∥ | 4th | |
| | | | 950 | | | |
| XV | 227 | 44050 | | ⊥ | | |

Note: See the note of Table I.

TABLE III. THE ABSORPTION BANDS OF 1,1'-IODIDE DIETHYL-2,2'-CARBOCYANINE IN THE STRETCHED PVA SHEET

| Band No. | $\lambda$ mμ | $\nu$ cm$^{-1}$ | $\Delta\nu$ cm$^{-1}$ | Direction | Group | $\tilde{\Delta\nu}$ cm$^{-1}$ |
|---|---|---|---|---|---|---|
| I | 700 | 14280 | | $l$ | | |
| | | | 1840 | | | |
| II | 620 | 16120 | | $l$ | | 1500 |
| | | | 1260 | | 1st | ±300 |
| III | 575 | 17380 | | $l$ | | |
| | | | 1480 | | | |
| IV | 530 | 18860 | | $l$ | | |
| | | | 2410 | | | |
| V | 470 | 21270 | | $l$ ? | | |
| | | | 1440 | | | |
| VI | 440 | 22710 | | $l$ | | 1500 |
| | | | 1670 | | 2nd | ±200 |
| VII | 410 | 24380 | | $l$ | | |
| | | | 1380 | | | |
| VIII | 388 | 25760 | | $l$ | | |
| | | | 1640 | | | |
| IX | 365 | 27400 | | $l$ ? | | |
| | | | 1600 | | | |
| X | 345 | 29000 | | ⊥ | | |
| | | | 1500 | | | |
| XI | 328 | 30500 | | ⊥ | 3rd | |
| | | | 2800 | | | |
| XII | 300 | 33300 | | ∥ | | |
| | | | 1700 | | | |
| XIII | 286 | 35000 | | ∥ | | |
| | | | 3900 | | | |
| XIV | 257 | 38900 | | ⊥ | | |
| | | | 2750 | | | |
| XV | 240 | 41650 | | ∥ | 4th | |
| | | | 1850 | | | |
| XVI | 230 | 43500 | | ⊥ | | |

Note: See the note of Table I. Cited from Ref. 1.

TABLE IV. THE ABSORPTION BANDS OF 1,1'-DIETHYL-2,2'-DICARBOCYANINE IODIDE IN THE STRETCHED PVA SHEET

| Band No. | $\lambda$ mμ | $\nu$ cm$^{-1}$ | $\Delta\nu$ cm$^{-1}$ | Direction | Group | $\tilde{\Delta\nu}$ cm$^{-1}$ |
|---|---|---|---|---|---|---|
| I | 804 | 12440 | | $l$ | | |
| | | | 1400 | | | |
| II | 725 | 13790 | | $l$ | | |
| | | | 1240 | | | |
| III | 665 | 15030 | | $l$ | | |
| | | | 1090 | | | |
| IV | 620 | 16120 | | $l$ | 1st | 1300 |
| | | | 1270 | | | ±200 |
| V | 575 | 17390 | | $l$ | | |
| | | | 1470 | | | |
| VI | 530 | 18860 | | $l$ ? | | |
| | | | 1340 | | | |
| VII | 495 | 20200 | | $l$ ? | | |
| | | | 1880 | | | |
| VIII | 453 | 22080 | | $l$ | | |
| | | | 1720 | | | |
| IX | 420 | 23800 | | $l$ | 2nd | 1800 |
| | | | 1980 | | | ±100 |
| X | 388 | 25780 | | ? | | |
| | | | 1820 | | | |
| XI | 362 | 27600 | | ? | | |
| | | | 2880 | | | |
| XII | 328 | 30480 | | ⊥ | 3rd | |
| | | | 570 | | | |
| XIII | 322 | 31050 | | ∥ | | |
| | | | 3900 | | | |
| XIV | 278 | 35950 | | ⊥? | | |
| | | | 2480 | | | |
| XV | 260 | 38430 | | ∥ | 4th | |
| | | | 3390 | | | |
| XVI | 239 | 41820 | | ⊥ | | |
| | | | 900 | | | |
| XVII | 234 | 42720 | | ∥ | | |

Note: See the note of Table I.

TABLE V. THE ABSORPTION BANDS OF 1,1'-DIETHYL-2,2'-TRICARBOCYANINE IODIDE IN THE STRETCHED PVA SHEET

| Band No. | $\lambda$ mμ | $\nu$ cm$^{-1}$ | $\Delta\nu$ cm$^{-1}$ | Direction | Group | $\tilde{\Delta\nu}$ cm$^{-1}$ |
|---|---|---|---|---|---|---|
| I | 950 | 10520 | | $l$ | | |
| | | | 1110 | | | |
| II | 860 | 11630 | | $l$ | | ca. |
| | | | 530 | | | 1000 |
| III | 825 | 12120 | | $l$ | 1st | |
| | | | 980 | | | |
| IV | 763 | 13100 | | $l$ | | |
| | | | 980 | | | |
| V | 710 | 14080 | | $l$ | | |
| | | | 2050 | | | |
| VI | 620 | 16130 | | $l$ | | |
| | | | 2830 | | | |
| VII | 527 | 18960 | | $l$ | 2nd | ca. |
| | | | 2150 | | | 2400 |
| VIII | 492 | 20320 | | $l$ | | |
| | | | 2150 | | | |
| IX | 445 | 22470 | | $l$ ? | | |
| | | | 1330 | | | |
| X | 420 | 23800 | | ∥ | | |
| | | | 3810 | | | |
| XI | 362 | 27610 | | ⊥ | 3rd | |
| | | | 3150 | | | |
| XII | 325 | 30760 | | ∥ | | |
| | | | 10370 | | | |
| XIII | 243 | 41130 | | ⊥ | 4th | |

Note: See the note of Table I.

weak compared with those of the first one. There is a clear boundary between these two groups, as seen in their band distances, e.g. the separation of Bands IV and V in Table II is 4040 cm$^{-1}$. Consequently the first and the second groups can be distinguished from each other. The third and the fourth groups consist of the ∥ ⊥ character-absorptions. The third group bands are weak and the fourth strong.

According to the polarization degree curve indicated in Fig. 8, the polarization degree of incident light begins to fall precipitously at about 800 mμ, becomes about 50% at 900 mμ,

Table VI. Average wavenumber of the absorption bands in the first and the second group, difference and ratio

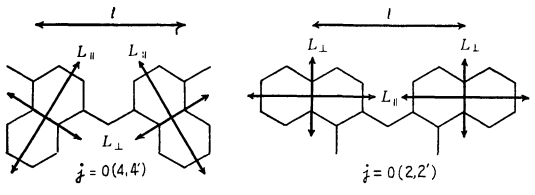
| Dyes | $\tilde{\nu}$ cm$^{-1}$ 1st group | $\tilde{\nu}$ cm$^{-1}$ 2nd group | $\Delta\tilde{\nu}$ cm$^{-1}$ | Ratio (2nd/1st) |
|---|---|---|---|---|
| $j$=0 (4,4′) | 17840 | 29940 | 12100 | 1.68 |
| $j$=0 (2,2′) | 21100 | 29330 | 8230 | 1.39 |
| $j$=1 ( 〃 ) | 16660 | 24300 | 7640 | 1.46 |
| $j$=2 ( 〃 ) | 16260 | 24820 | 8560 | 1.53 |
| $j$=3 ( 〃 ) | 12290 | 19470 | 7180 | 1.58 |

and then vanishes at 1000 m$\mu$. For this reason, it will be expected that when the absorption of 860 m$\mu$ (Band II) in Fig. 8, $j$=3(2, 2′), is measured with the perfect polarized light, the band maximum will be shifted towards the longer wavelength side. Consequently, the distance between Bands I and II in Table V becomes smaller, while the distance between Bands II and III becomes greater. As a result, it will be expected that the two band distances approach the mean value of the first group in Table V.

Table VI includes the mean wave numbers of the absorption bands in the first and the second group, the difference and the ratio between these wavenumbers having been derived from Tables I—V. The ratio is approximately constant at about 1.5, except for the case of $j$=0 (4, 4′) dye.

## Discussion

**Absorptions in the Short Wavelength Region.**— It has already been clarified from a detailed analysis of Pinacyanol that the absorption bands in the third and the fourth group are originated from the electronic transitions, in two directions at right angles, localized in the quinoline nucleus parts[1]. If this is the case with these absorptions, and if both (4, 4′) and (2, 2′) dye of $j$=0 have the planar structures indicated in Figs. 9(a) and (b) as respective possible ones, the dichroism similar to Pinacyanol should be expected for the latter rather than for the former. Nevertheless, according to Figs. 1 and 3, the distinct differences in direction among $l$, $L_{\parallel}$ and $L_{\perp}$ indicated in Fig. 9 are obviously recognized in (4, 4′) but not in (2, 2′) dye. This may be due to the steric hindrance; these molecules ($j$=0), as is well known, can not keep the planar structure. Both quinoline planes are inclined to each other, and this may be contributed mostly by the twisting of the central methine bonds. In Fig. 9(a), therefore, two $L_{\parallel}$ directions through the twisting of the methine bonds approach to being parallel with each other and normal to the $l$-direction. But the relative directions of $L_{\perp}$ are not altered by the twisting just mentioned. On the other hand, in Fig. 9(b), the twisting of methine bonds makes two $L_{\parallel}$'s and two $L_{\perp}$'s oblique to each other, respectively, and it may possibly occur that their oblique angles against $l$-direction become the same in their degree. Owing to this situation, (4, 4′) dye might reveal such dichroic behavior as that shown in for Fig. 1: instance the 288 m$\mu$ band (VI) has the similar tendency as the absorptions parallel with $l$-direction (Fig. 2), and the 301 m$\mu$ (V) and the 242 m$\mu$ band (VIII) have a tendency to be considered almost normal to $l$-direction. As for (2, 2′) dye (Fig. 9(b)), on the other hand, on account of certain resultant inclinations of $L_{\perp}$ and $L_{\parallel}$ against $l$-direction produced by steric hindrance, it has the dichroism indistinctive in $\parallel$ $\perp$ character as shown in Fig. 3. In contrast with this, in case of $j$=1(2, 2′) (Pinacyanol) in which a steric hindrance is considered to be not so great as in $j$=0, the dichroism similar to that in Fig. 1 in appearance was observed with distinct difference in direction among $L_{\parallel}$, $L_{\perp}$ and $l$. This dichroism was already illustrated in the previous paper[1]. Thus, at least concerning $j$=0 dyes, the dichroism is reasonably understood by regarding the third and the fourth group absorptions as being caused by the transition at right angles to one another.




a b

Fig. 9. Molecular skeleton diagrams of (a) 1,1′-diethyl-4,4′-cyanine cation, $j$=0 (4,4′), and (b) 1,1′-diethyl-2,2′-cyanine cation, $j$=0(2,2′).

According to the conventional consideration, the dye molecule becomes more planar with an increase in the number of methine bond, namely $j$. From this point of view, the $\parallel$ and $\perp$ character of absorptions of the third and fourth groups ought to be much more manifest with the increase of $j$. As for the (2, 2′) dyes, however, there is found a tendency to the contrary: the increase of $j$ obscures the $\parallel$ $\perp$ character in dichroism. This character is observed typically in the case of Pinacyanol[1] with small $j$. This fact suggests that the whole strain angle of the molecule in the case of $j>1$ results from the successive summing up of the twisting angle peculiar to one methine bond. That this consideration is correct will

also be supported by the discussion in the following section.

**Absorptions in the Long Wavelength Region.**— It was considered previously that the second group absorptions correspond to an overtone of those of the first group[1]. One of the reasons for such consideration is also found in the dyes used here. That is to say, the second group resembles generally the first group in shape and the former is much weaker in intensity than the latter. Moreover, the ratios of their transition energies lie between 1.4 and 1.7 This fact can be interpreted in quite the same way by *second order absorption* theory on the absorptions with the same direction, proposed by Lewis et al.[7]. For this reason, there seems now no room for doubt that the absorptions of the first group and those of the second group are associated with each other as the first and the second order absorption, respectively.

It is clear from many experimental facts that the absorption phenomena of the first group of Pinacyanol is subject to remarkable change on account of its complex formation[8]. When these absorptions correspond to particular ones of respective complexes, the phenomena could be interpreted by the Davidov splitting. If so, in a case when a band in the first group is split by the formation of a complex, a corresponding absorption band in the second group with the same direction should be split in the same way. The fact that the absorptions of the first and the second group are distributed in respective groups, as shown in the tables, may suggest the very occurrence of the Davidov effect***. According to tables I—V, however, the separation of bands in the first and the second group does not change with the same tendency but with different behaviors with an increase of $j$ (see Fig. 10) : when $j=0$, the band distance in the first group is greater than that in the second, while for $j \geqq 1$ the former becomes smaller and the latter greater with the increase of $j$. These relations are illustrated in Fig. 10. These obvious phenomena do not seem to be explained simply by the consideration of the Davidov effect. One possible interpretation may be given, as below, taking into account the vibrational states whose contribution might be induced by the complex formation.

Interatomic distances, usually, are lengthened by excitation to the upper state unless the ground state is forced to be strained by a particular steric hindrance. In case the molecule is already hindered in the ground state,

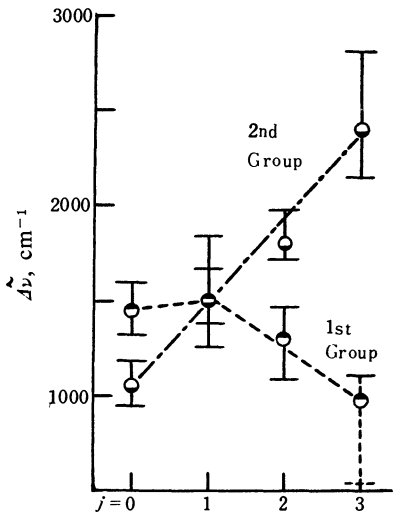



Fig. 10. Relation between $\tilde{\Delta\nu}$ and the number $j$ of the 1st and the 2nd group absorption.

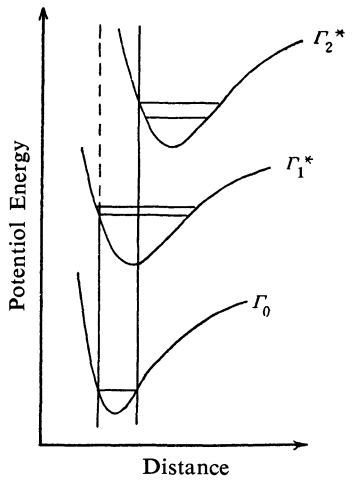



Fig. 11. Schematic potential curves for $j>1$. $\Gamma_0$ for the ground state, $\Gamma_1$* and $\Gamma_2$* for the first and the second excited state, respectively. The minimum parts of the respective curves shift to the right hand successively in the order of $\Gamma_0$, $\Gamma_1$* and $\Gamma_2$*.

7) G. N. Lewis and J. Bigeleisen, *J. Am. Chem. Soc.*, 65, 2107 (1943).

8) I. M. Klotz, *Chem. Revs.*, **41**, 373 (1947); H. B. Klevens, *J. Phys. Chem.*, **51**, 1143 (1947); R. C. Merrill, R. W. Spencer and R. Getty, *J. Am. Chem. Soc.*, **70**, 2460 (1948); R. C. Merrill and R. W. Spencer, ibid., **70**, 3683 (1948); **72**, 2894 (1950).

*** Davidov splitting of Pinacyanol under a certain condition was found for the electronic transition to the first excited state but not decidedly for the second excited state. In this case the absorption spectrum in acetone was thought to be due to the monomer, though it indicated the $\alpha$ and $\beta$ bands. See, J. W. Weigl, *J. Chem. Phys.*, 24, 364 (1956).

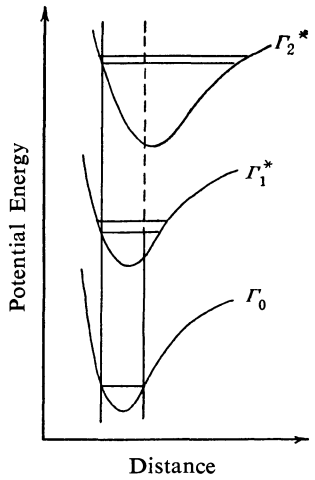



Fig. 12. Schematic potential curves for $j=0$. In this case, the minimum parts of the $\Gamma_0$ and $\Gamma_1^*$ curve do not shift, but only that of the $\Gamma_2^*$ curve deviates to the right side.

it may happen that the interatomic distances are not changed by excitation. Relative configurations of the potential curves in such cases would be represented schematically by Figs. 11 and 12. Fig. 11 corresponds to $j>1$, and Fig. 12 to $j=0$. In the case of Fig. 11, the minimum positions of the ground state ($\Gamma_0$), the first ($\Gamma_1^*$) and the second excited state curve ($\Gamma_2^*$) may shift towards the right hand, usually in this order. Then, if the configurational relations of $\Gamma_1^*$ and $\Gamma_2^*$ to $\Gamma_0$ are such as shown in Fig. 11, the band distances of the first group become smaller than those of the second group, for the higher the vibrational states are along the curve the narrower the space between the two adjacent states becomes. On the other hand, in Fig. 12 the band distances of the first group would become greater than those of the second group, if the correlation of $\Gamma_0$ and $\Gamma_2^*$ curves is like that of $\Gamma_0$ and $\Gamma_1^*$ curves in Fig. 11, because there is no shift between the minimum positions of $\Gamma_0$ and $\Gamma_1^*$ curves as presumed above. Thus, we have one plausible interpretation of the experimental facts, according to the above consideration. At the present stage, however, there is no theoretical base for the diagrams in Figs. 11 and 12. Nevertheless, it has an instructive meaning that the phenomena shown in Fig. 10 can be explained qualitatively only by admitting such a possibility as mentioned above for the potential curves of molecules in a complex formed.

It has already been described that the absorption bands of the first group have the tendency to reveal their directional difference in dichroism with an increase of $j$. This does not seem to agree with conventional consideration that the increase of $j$ makes the molecules approach to planar configurations. The reason is as follows: the better the planarity of the molecule, the better should be the parallelism of any vector in the $l$-direction, regardless of terminated points on both quinoline planes of a transition vector, on account of the symmetry of the molecule as seen from the structure in Fig. 9(b). That is to say, the larger the number $j$, the smaller must become the directional difference in dichroism. This is just opposite to the experimental facts. Thus, applying over again the consideration that the peculiar twisting angle per methine bond is added successively with an increase of $j$ as mentioned in the last section, it stands to reason that the angles against $l$-direction differ in respective absorptions, so far as $j$ is not so large and the terminals of the different transition vectors do not agree with one another; and further taking into account the sharpening of the orientation axis of the molecule, the behavior in dichroism of the first group-bands can be reasonably understood.

## Summary

1. Dichroism of the electronic spectra over 220 m$\mu$ was measured for 1, 1'-diethyl-2, 2'-cyanine, -dicarbocyanine, and -tricarbocyanine iodide, and -4, 4'-cyanine iodide, respectively, in the stretched polyvinylalcohol sheets under the stretch ratio of about 6~10.

2. The correspondence of the transition directions of absorptions and the chemical structures, and the classification of the absorption bands were made into tables.

3. All the dichroic behaviors of the absorption bands could be interpreted by the transitions along the longitudinal axis of the molecule and by those, localized in the quinoline nuclei, of two directions at right angles.

4. It was confirmed that the second group absorptions correspond to the overtone of the first group ones. It was shown by the schematical potential curves that the systematic changes in the band distances in these groups with the variation of the methine bond number may be plausibly explained in connection with the vibrational states.

5. It was pointed out that a reasonable understanding for certain experimental facts in dichroism is given by regarding the molecular structures as follows; 1, 1'-diethyl-2, 2'-cyanine and -4, 4'-cyanine are far from planar because of their particular great steric hindrance, and the other cyanines are strained by the succes-

sive addition of a peculiar twisting angle per methine bond.

The authors wish to express their thanks to Professor N. Ando and Professor I. Tanaka of Tokyo Institute of Technology for their encouragement throughout this work, to Mr. Y. Mori of this Institute for his useful discussion and helpful advice, and also to Mr. Y. Hamada of the Research Laboratory of Fuji Photo Film Co., Ltd. for his help in the preparation of the dyes used.

*Laboratory of Physical Chemistry*
*Tokyo Institute of Technology*
*Meguro-ku, Tokyo (Y. T.)*

*Research Laboratory*
*Fuji Film Co., Ltd.*
*Minami-Ashigaramachi*
*Kanagawa-Ken (H. O.)*

# *A Molecular Orbital Treatment of Phosphate Bonds of Biochemical Interest. I. Simple LCAO MO Treatment*

By Kenichi FUKUI, Keiji MOROKUMA and Chikayoshi NAGATA

(Received January 18, 1960)

It is well known that adenosine triphosphate (ATP) is used as a catalyst in varions kinds of in vivo chemical processes. Kalckar[1] and Lipman[2] for the first time pointed out that the energy change of hydrolysis of phosphate P–O bond of ATP was much greater than that of ordinary phosphate bonds and that this energy liberated by hydrolysis might promote endergonic reactions. Thus P–O bonds of ATP were named "high energy phosphate bonds" characterized by the sign "P~O". Further, adenosine diphosphate (ADP), phosphoenol pyruvate (PEP) and acetyl phosphate (AcP) are some of the phosphates which were believed to have high energy phosphate bonds[1-4,5]; but they can hardly be used in in vivo reactions. In this they are different from ATP[5].

Recently it has been found in calorimetrical measurements by Podolsky and Morales[6] that the enthalpy change in hydrolysis of ATP is considerably smaller than the value hitherto reported and is parallel with those of simple polyphosphates. This finding has been supported by Benzinger and Kitzinger[7], and by Burton[8]. These results suggested that there might be a revision of our understanding with respect to the role of ATP[6-8].

Kalckar[1] and Lipman[2] studied the high energy phosphate bond on the basis of the mesomeric theory. Lately Ooshika[9] assumed in their quantum-chemical discussions that the phosphate bonds of ATP were of high energy. Grabe[10] calculated the charge density of the system $-\overset{|}{\underset{\|}{C}}-O-\overset{|}{\underset{\|}{P}}-$ (O, O), and discussed at which side of the bridge oxygen the bond dissociation occurred. Gillespie et al.[11] stressed the necessity of studies on this problem from the point of view of reaction kinetics.

In this paper the authors have carried out a systematic computation on the electronic energy changes, the reactivity indexes and charge distributions of four organic phosphates, ATP, ADP, PEP and AcP, with so-called "high energy" bonds and, for comparison's sake, two phosphates lacking such bonds, adenosine monophosphate (AMP) and glycerol 1-phosphate (GLP), by a simple molecular orbital approximation. From these calculated results they have concluded that, so far as the phosphate parts only are considered, the difference, if it might exist, in the energy of

1) H. M. Kalckar, *Chem. Revs.*, **28**, 71 (1941).
2) F. Lipman, *Advances in Enzymol.*, **1**, 99 (1941).
3) P. Oesper, *Arch. Biochem.*, **27**, 255 (1950).
4) T. L. Hill and M. F. Morales, *J. Am. Chem. Soc.*, **73**, 1656 (1951).
5) E. Baldwin, "Dynamic Aspects of Biochemistry", Cambridge Univ. Press, New York, 1951.
6) R. L. Podolsky and M. F. Morales, *J. Biol. Chem.*, **218**, 945 (1956).
7) T. B. Benzinger and C. Kitzinger, *Z. Naturforsch.*, **10b**, 375 (1955).
8) K. Burton, *Nature*, **181**, 1594 (1958).
9) Y. Ooshika, *Seitai-no-kagaku*, **7**, 322 (1955).
10) B. Grabe, *Biochim. Biophys. Acta*, **30**, 560 (1958); *Archiv Fysik*, **15**, 207 (1959).
11) R. J. Gillespie, G. Maw and C. A. Vernon, *Nature*, **171**, 1147 (1953).

hydrolysis between two kinds of phosphates can not be attributed to the difference of $\pi$ electronic energy change, though their reactivity is somewhat different.

## Method of Calculation

The calculation is carried out in the approximation of the simple LCAO MO (linear-combination-of-atomic-orbitals molecular orbital) treatment neglecting overlap. For AcP and PEP the conjugation is spreading throughout the molecule. For ATP, ADP and AMP, on the other hand, phosphate parts only are taken into account, i.e., the adenine part, which is separated from the phosphate part by the non-conjugating ribose, is assumed not to be interacting with the phosphate part. On this assumption a few essential discussions will be given in the following section. AMP, GLP and other low energy phosphates come to have the same conjugated system in this approximation. Phosphorus atoms in the phosphates have a nearly tetrahedral, $sp^3$-hybridized configuration, with one electron jumping up into one of $3d$ orbitals. Strictly speaking, $2p$ $\pi$ electrons on the neighboring oxygen atoms can interact not only with these $d$ orbitals but also, though presumably only slightly, with the $sp^3$-hybridized orbitals[12,13]. Taking into account all of these interactions, however, complicates the problems extremely and makes it practically impossible to treat large molecules of interest. We conveniently assume, therefore, that only one hybridized $d$ orbital on a phosphorus atom, say e.g. $d^3s$ hybridized orbital which can afford to give a directed valence of tetrahedral symmetry, conjugates with $2p\pi$ orbitals of the neighboring oxygens in this simple treatment. Accordingly ATP, for instance, is regarded as a system consisting of 13 orbitals and 20 electrons.

The Coulomb integral of the atom or group X, that of the carbon atom attached to X and the resonance integral between that carbon atom and X are written as $\alpha+a_X\beta$, $\alpha+a_r\beta$ and $l\beta$, respectively, where $\alpha$ and $\beta$ are the Coulomb and the resonance integrals of a carbon atom and a C-C bond in benzene, respectively. Since the precise value of $a_{-O-}$ seems unsettled, two parallel computations are carried out for two $a_{-O-}$ values. In Table I, together with $a_X$'s of oxygen atoms in the phosphate part, are listed the numerical values of $a_X$, $a_r$ and $l$ adopted by us, which do not differ so much from those which were previously used by the present authors[21,22] and others[15,16]. If some oxygen atoms assigned to different $a_X$'s should be considered to be equivalent, the mean value of their $a_X$'s is employed; for instance, $a_X$ of each oxygen atom in the $-PO_3^{2-}$ group is regarded as 1.0 and that in the $-PO_2^-$ group as 1.25.

Table I. Parameters used in the calculation

1. Phosphate part

| X | $a_X$ |
|---|---|
| =O | 2.0 |
| $-O^-$ | 0.5 |
| -O- | 0.5, 2.0 |

2. Others

| X | $a_X$ | $a_r$ | $l$ |
|---|---|---|---|
| =O | 2.0 | 0.2 | $\sqrt{2}$ |
| -OH | 0.5 | 0 | 0.6 |
| $-CH_3$ | 3.0 | −0.1 | 1 |

The resonance integral between a phosphorus atom and an oxygen atom, $\beta_{P-O}$, is tentatively taken 0.6 $\beta$, regardless of the bonding states of the oxygen atom (-O- type, O=type or $-O^-$ type) from a rather simple theoretical consideration on the overlap integral[13], but the numerical value itself is not essential to our results of calculation, as will be stated below. Furthermore, it is hardly possible to decide semiempirically the Coulomb integral of the phosphorus atom in the valence state in question, $\alpha_P=\alpha+a_P\beta$, because of the lack of sufficient experimental data and knowledge on the $d$ electron phenomena. Therefore in order to avoid the unreliability of the results caused by a rather arbitrary choice of $a_P$, we vary the $a_P$ value as widely as possible, as 0, −0.2, −0.4, −0.6, −1.0, −1.5, −2.0, −3.0 and $-\infty$. It should be stressed concerning this point that by means of this sliding of $a_P$ values we can practically afford to evade not only the ambiguity of the $a_P$ value but also the arbitrariness of the $\beta_{P-O}$ value and moreover, partly, the error due to the above-stated conventional choice of the orbitals on a phosphorus atom, at least for ATP, ADP and AMP where conjugated systems are consisting of only phosphorus and oxygen atoms. In this sense the present treatment has a very general character. Judging from the ionization potential of a $3p$ electron (I=10.98 eV.)[10] and from Pauling's electronegativity scale ($\chi_P=2.1$), −0.6 or smaller would be appropriate for the real $a_P$ value of a hybridized $d$ electron.

The present authors have previously presented the frontier electron theory and have succeeded in interpreting theoretically the experience on

12) R. S. Mulliken, C. A. Rieke, D. Orloff and H. Orloff, *J. Chem. Phys.*, **17**, 1248 (1949).
13) H. H. Jaffé, *J. Phys. Chem.*, **58**, 185 (1954).
14) C. Nagata, K. Fukui, T. Yonezawa and Y. Tagashira, *Cancer Resarch*, **15**, 233 (1955).
15) H. H. Jaffé, *J. Chem. Phys.*, **20**, 279 (1952).
16) L. E. Orgel et al., *Trans. Faraday Soc.*, **47**, 113 (1951).

the chemical reactivity of $\pi$ electron system[17-21]. Here we do not repeat the details of the theory but we mention only the fact that the superdelocalizability, $S_r$, has been known as a good intermolecular reactivity index for the substitution and the addition reactions. Also for hydrolysis of phosphates $S_r$ is expected to remain a good measure of reactivity and is used in the present paper for discussing the ease of hydrolysis of phosphates.

## Results and Discussion

**The $\pi$ Electronic Energy Change of Hydrolysis.**—The results of calculation of the $\pi$ electronic energy change of hydrolysis for two $a_{-O-}$ values and various $a_P$ values are listed in Table II. The listed value, $-\Delta E$, is expressed as the difference of $\pi$ electronic energy between the hydrolysis products and the original reactant excepting water. For ATP, for instance, it becomes

$$-\Delta E = E(\mathrm{ADP})^{3-} + E(\mathrm{PO_4}^{3-}) - E(\mathrm{ATP})^{4-}$$

The electronic energy of water is not included in this expression because it is a constant and can not precisely be evaluated. Therefore, not the absolute value of $\Delta E$ but its difference between the two kinds of phosphate or between ATP and other phosphates has practical meaning in further discussions.

As clearly seen in Table II, $\Delta E$ of each compound does not vary so much according to $a_P$ values. Furthermore it should be noticed that its difference between the two kinds of phosphate bonds does not exceed $-0.2\beta$ for any pair of $a_P$ and $a_{-O-}$ values. This maximum value corresponds to ATP when $a_P$ is zero and $a_{-O-}=2.0$. The difference for $a_P=-1.0$, a most probable value of $a_P$, is about $-0.12\ \beta$. Putting $\beta$ as $-20$ kcal./mol., it corresponds to ca. 2.5 kcal./mol. If $\beta_{P-O}$ is taken to be $0.8\ \beta$, it becomes ca. 3 kcal./mol. by changing the energy value of $\beta$. Thus it might be said that in the difference of the free energy change of hydrolysis between the two kinds of phosphate only 2.5 to 3 kcal./mol. at most can be ascribed to the $\pi$ electronic energy.

Consequently it is concluded that, so far as phosphate parts only are taken into account, the peculiarity of ATP in several in vivo reactions cannot be attributed to the electronic energy.

**Superdelocalizability for a Nucleophilic Attack and the Reactivity of Phosphate Bond.**—By this time most contributions to the problem of these organic phosphate bonds of biochemical interest have been carried out from the

TABLE II. $\pi$-ELECTRONIC ENERGY CHANGE OF HYDROLYSIS

1) $a_{-O-}=0.5$.

| Class | Compound | $-\Delta E$ | | | | | | | | |
|---|---|---|---|---|---|---|---|---|---|---|
| | $a_P=$ | 0 | −0.2 | −0.4 | −0.6 | −1.0 | −1.5 | −2.0 | −3.0 | $-\infty$ |
| Low energy | AMP, GLP etc. | $2\alpha+1.143\beta$ | $2\alpha+1.168\beta$ | $2\alpha+1.173\beta$ | $2\alpha+1.176\beta$ | $2\alpha+1.182\beta$ | $2\alpha+1.187\beta$ | $2\alpha+1.191\beta$ | $2\alpha+1.195\beta$ | $2\alpha+1.200\beta$ |
| High energy | ATP (I)[a] | 1.176 | 1.198 | 1.199 | 1.199 | 1.199 | 1.199 | 1.199 | 1.199 | 1.200 |
| | ATP (II)[b] | 0.976 | 0.999 | 1.000 | 1.001 | 1.002 | 1.002 | 1.001 | 1.001 | 1.000 |
| | ADP | 1.174 | 1.196 | 1.197 | 1.198 | 1.199 | 1.199 | 1.199 | 1.199 | 1.200 |
| | AcP | 1.181 | 1.201 | 1.201 | 1.201 | 1.200 | 1.197 | 1.195 | 1.192 | 1.175 |
| | PEP | 1.163 | — | 1.193 | — | 1.201 | — | 1.206 | 1.207 | 1.200 |

2) $a_{-O-}=2.0$.

| Class | Compound | $-\Delta E$ | | |
|---|---|---|---|---|
| | $a_P=$ | 0 | −1.0 | −2.0 |
| Low energy | AMP, GLP etc. | $2\alpha-1.654\beta$ | $2\alpha-1.697\beta$ | $2\alpha-1.735\beta$ |
| High energy | ATP (I)[a] | −1.446 | −1.575 | −1.659 |
| | ATP (II)[b] | −1.614 | −1.763 | −1.854 |
| | ADP | −1.449 | −1.576 | −1.659 |

[a] The end "high energy" phosphate bond.
[b] The central "high energy" phosphate bond.

17) K. Fukui, T. Yonezawa and H. Shingu, *J. Chem. Phys.*, **20**, 722 (1952).
18) K. Fukui, T. Yonezawa, C. Nagata and H. Shingu, ibid., **22**, 1433 (1954).
19) K. Fukui, T. Yonezawa and C. Nagata, This Bulletin, **27**, 423 (1954).
20) K. Fukui, T. Yonezawa and C. Nagata, *J. Chem. Phys.*, **26**, 831 (1957).
21) K. Fukui, T. Yonezawa and C. Nagata, *J. Am. Chem. Soc.*, **80**, 2268 (1958).

TABLE III. SUPERDELOCALIZABILITY OF THE PHOSPHORUS ATOM FOR NUCLEOPHILIC ATTACK

1) $a_{-O-}=0.5$.

| Class | Compound | $a_P=$ | $S_P^{(N)}$ 0 | −0.2 | −0.4 | −0.6 | −1.0 | −1.5 | −2.0 | −3.0 | −∞ |
|---|---|---|---|---|---|---|---|---|---|---|---|
| Low energy | AMP, GLP etc. | | 1.555 | 1.412 | 1.290 | 1.185 | 1.012 | 0.848 | 0.724 | 0.553 | 0.000 |
| High energy | ATP (I)[a] | | 1.733 | 1.525 | 1.362 | 1.236 | 1.037 | 0.860 | 0.730 | 0.555 | 0.000 |
| | ATP (II)[b] | | 1.810 | 1.576 | 1.401 | 1.259 | 1.049 | 0.865 | 0.732 | 0.556 | 0.000 |
| | ADP | | 1.708 | 1.513 | 1.359 | 1.233 | 1.036 | 0.858 | 0.730 | 0.555 | 0.000 |
| | AcP | | 1.696 | — | 1.371 | — | 1.054 | — | 0.728 | 0.561 | 0.000 |
| | PEP | | 1.600 | — | 1.322 | — | 1.031 | — | 0.734 | 0.559 | 0.000 |

2) $a_{-O-}=2.0$.

| Class | Compound | $a_P=$ | $S_P^{(N)}$ 0 | −1.0 | −2.0 |
|---|---|---|---|---|---|
| Low energy | AMP, GLP etc. | | 1.907 | 1.092 | 0.749 |
| High energy | ATP (I)[a] | | 1.956 | 1.099 | 0.751 |
| | ATP (II)[b] | | 2.511 | 1.191 | 0.778 |
| | ADP | | 1.954 | 1.099 | 0.751 |

[a] The end "high energy" phosphate bond.
[b] The central "high energy" phosphate bond.

energetical point of view. But it seems important and interesting at this juncture for us to discuss the reactivity or the ease of hydrolysis of phosphate bonds. Hydrolysis of phosphates would be initiated by the attack of a hydroxyl anion to the phosphorus atom in vivo or of some nucleophilic group or site of tissue in vivo. So the superdelocalizability, $S_P^{(N)}$, of the phosphorus atom for a nucleophilic attack is expected to represent a theoretical index to the ease of hydrolysis. In Table III are collected the results of the calculation of superdelocalizability for a nucleophilic attack for various $a_P$ values. The larger the $S_P^{(N)}$ is, the more reactive for a nucleophilic attack is the phosphorus atom.

As is seen in Table III, the value of $S_P^{(N)}$ of each compound is reduced markedly with the decrease of $a_P$ values; but it is noticed that comparison of $S_P^{(N)}$ of various compounds at the same $a_P$ value shows us some difference between the two kinds of phosphate bond, which decreases with the decrease of $a_P$, as 0.05 to 0.2 when $a_P=0$, 0.04 to 0.1 when $a_P=-0.4$, 0.02 to 0.04 when $a_P=-1.0$, and less than 0.01 when $a_P=-2$ and $a_P=-3$. Even larger differences of the superdelocalizability, which are realized for larger values of $a_P$ (smaller in the absolute value), would not be sufficient to cause a casual difference of actual ease of hydrolysis. Nor could the conspicuous role of ATP be attributed to this difference, for the difference for ATP is not at all markedly greater than that for other "high energy" phosphates*. So far as phosphate parts only are considered, it would be concluded that, though some distinction can be seen in the reactivity for hydrolysis between the "high energy" bond and the ordinary one, it does not seem great enough to cause a serious difference in the role in biochemical processes.

**Total $\pi$ Electron Density of Oxygen Atoms.** —In some biochemical problems of reactivity of conjugated molecules, effects of subsidiary atoms and bonds in the compounds were often noticed to play an essential part as well as some steric factors. A few examples of this can be seen in the carcinogenic activity of condensed aromatic hydrocarbons[14] and dimethylaminoazobenzene derivatives[22] and also in auxin activity of benzoic acid derivatives[21]. In this sense the total $\pi$ electron density of oxygen atoms ($q_{-O-}$ and $q_{-O^-}$) attached to a phosphorus atom may be expected to prevent electrostatically a nucleophilic reagent from approaching the phosphorus atom, where –O– and $-O^-$ stand for an oxygen atom on the phosphate bond to be broken and an oxygen anion attached to the phosphorus atom on that bond, respectively. The calculation of them has been carried out only when $a_P$ is

* Of the two so-called high energy bonds in an ATP molecule, the inner one seems to be of very low energy (about 4 kcal. lower than the outer) from an energetic point of view, whereas the value of $S_P^{(N)}$ shows that the inner is the more reactive. It would not be possible to decide from this calculation, therefore, which bond is the easier to break.

22) C. Nagata, K. Fukui, T. Yonezawa, H. Kitano, Y. Inamoto, K. Kanai and Y. Tagashira, *Gann*, **46**, 346 (1955).

TABLE IV. TOTAL $\pi$ ELECTRON DENSITY AND SUPERDELOCALIZABILITY OF OXYGEN ATOMS FOR ELECTROPHILIC ATTACK[a]

1) $a_{-O-}=0.5$.

| Class | Compound | $S_{-O-}^{(E)}$ | $q_{-O-}$ | $S_{-O^-}^{(E)}$ | $q_{-O^-}$ |
|---|---|---|---|---|---|
| Low energy | AMP, GLP etc. | 3.055 | 1.868 | 1.797 | 1.914 |
| High energy | ATP (I)[b] | 2.508 | 1.773 | 1.783 | 1.912 |
| | ATP (II)[c] | 2.550 | 1.773 | 1.475 | 1.925 |
| | ADP | 2.546 | 1.783 | 1.818 | 1.963 |

2) $a_{-O-}=2.0$.

| Class | Compound | $S_{-O-}^{(E)}$ | $q_{-O-}$ | $S_{-O^-}^{(E)}$ | $q_{-O^-}$ |
|---|---|---|---|---|---|
| Low energy | AMP, GLP etc. | 0.952 | 1.952 | 1.743 | 1.991 |
| High energy | ATP (I)[b] | 0.900 | 1.906 | 1.742 | 1.990 |
| | ATP (II)[c] | 0.878 | 1.903 | 1.417 | 1.991 |
| | ADP | 0.900 | 1.906 | 1.742 | 1.991 |

[a] $O^-$ stands for the three or the two equivalent oxygens in $-PO_3^{2-}$ or $-PO_2^-$ ; -O- stands for the bridge oxygen in phosphate bonds.
[b] The end "high energy" phosphate bond.
[c] The central "high energy" phosphate bond.

$-1$, since the choice of the value of $a_P$ was proved in the previous paragraph not to affect the results so seriously.

On inspection of the fourth and the sixth columns of Table IV, ATP and ADP would be understood to be to a small extent preferential in hydrolysis, since the interference by the electron density in it must be smaller than in AMP.

**Superdelocalizability of the Oxygen Atom for Electrophilic Attack.**—In this case assuming, as was not done in the preceding paragraphs, that the initial stage of hydrolysis is the attack of proton or an electrophilic group upon the bridge oxygen atom of the phosphate bond, the superdelocalizability of the oxygen atom, $S_O^{(E)}$, for an electrophilic attack was calculated and listed in the third column of Table IV. The order of $S_{-O-}^{(E)}$ cannot explain the singularity of ATP in biochemical reactions. Nor can the order of the superdelocalizability of oxygen, $S_{-O^-}^{(E)}$, do so as clearly seen in the fifth column of Table IV.

In the foregoing discussion we found that the "high energy" phosphate bonds are not of electronically high energy, though to some extent they are more reactive, and that the conspicuous role which ATP exclusively plays in in vivo chemical reactions cannot be explained by these simple models of phosphates.

Two things must be investigated prior to the ascertainment of this conclusion. One of them is that the calculations in the present paper have been performed in the simple LCAO MO approximation: that is to say, no electron interaction has been explicitly taken into account. Interactions to be considered would occur also among $2p\pi$ electrons on a phosphorus atom. As stated in the previous section, however, since the wide sliding of $a_P$ values from zero to minus infinity would considerably diminish the unreliability of this approximation, no serious alteration of results could be expected even in a more precise treatment.

The other is more essential. In the present paper AMP, ADP and ATP have been treated as if they were composed of only polyphosphate parts. No attention has been paid to the other conjugated part of the molecule, the adenine part, which is intervened and separated by the non-conjugated ribose group from the polyphosphate parts. This large conjugated system, however, would have some interaction with the polyphosphate part. Levendahl and James[23] found in their study on the rotatory dispersion of AMP, ADP and ATP that in ATP the last two phosphate groups and the amino group of adenine part were interacting, whereas no such interaction was noticed in the others, and suggested that this stabilized structure would an important significance in the peculiarity of the function of ATP. Szent-Györgyi[24] surmised that, as for ATP, among the 6-amino group and the 7-nitrogen of adenine parts and the two oxygens of the last two phosphate parts, the magnesium cation might intervene, through which the conjugation would spread over the molecule.

From the above calculations and discussions

23) B. H. Levendahl and J. W. James, *Biochim. Biophys. Acta*, **21**, 298 (1956).
24) A. Szent-Gyorgyi, "Biogenetics", Academic Press, New York, 1957.

we might say that the peculiar in vivo behavior of ATP must not be attributed to the polyphosphate part itself, but to the whole system including the polyphosphate part and the adenine part, interacting with each other directly or through a metal cation.

In the latter case the interaction of the polyphosphate part with a metal cation would considerably enhance the reactivity of its phosphorus atoms for a nucleophilic attack. Forming a weak bonding, metal cation will help them to interact. Calculation under the explicit consideration of these interactions is now going to be carried out with respect to several models for different interacting positions, extents of interaction and roles of metal cations. This will be published elsewhere.

*Faculty of Engineering*
*Kyoto University*
*Sakyo-ku, Kyoto*

# *Studies on the Configuration and Conformation of Polystyrene*

By Masatami TAKEDA, Kazuyoshi IIMURA, Akira YAMADA and Yoshio IMAMURA

(Received February 13, 1960)

This work was undertaken to investigate the relationship between the chemical configuration of vinyl-type polymer determined by the process of polymerization reaction and the conformation of vinyl-type polymer determined by the physical state of a polymer.

Natta[1] showed that the polystyrene prepared by the Ziegler catalyst contains higher isotactic sequences in its chain configuration and that the crystallizability of this polystyrene is due to the helical conformation[2] of the isotactic chain which makes up the crystalline region of crystallized polystyrene.

Williams et al.[3] also found that the polystyrene prepared by the Alfin catalyst has the same tendency of crystallizability but at a lower degree.

These findings led to two different types of problems. One of them is the existence of configurational isomers, and the concept of isotactic or syndiotactic configurations. The concept of tacticity or stereoregularity is developed in this direction. The distribution of configurational isomers in each sample will be determined by the process of polymerization and solvent extraction.

The other is the existence of conformational isomers for each configurational isomer; and the distribution of conformational isomers for each configuration will be determined by the physical state of the sample and its history such as heat treatment. The dominant existence of the helical conformation of the isotactic chain in the crystalline parts of crystallized polystyrene was the only available information about polystyrene in this direction.

In the present work, the infrared spectra have been measured with four different types of polystyrenes which have been prepared by Ziegler, Natta, Alfin and Radical catalysts and by following extraction processes with cold MEK (methyl ethyl ketone). Measurements of spectra were carried out in various physical states such as quenched solid, crystallized solid, molten state and solution. The differences among spectra of the four polystyrenes in each physical state, and the differences among spectra in the physical state of each polystyrene were interpreted in the terms of configuration and conformation. Crystalline contents of samples were determined by infrared and X-ray methods. The quantitative measure of isotactic configuration has been obtained from the analysis of infrared spectra of sample solutions. The relation between the maximum content of crystallization and the measure of isotactic configuration has been studied.

## Experimental

a) **Sample.**—Crystalline polystyrene I (CPS-I) prepared by polymerization with $AlEt_3$-$TiCl_3$ catalyst and crystalline polystyrene II (CPS-II) prepared by polymerization with $AlEt_3$-$TiCl_4$ catalyst and crystalline polystypene III (CPS-III) prepared by polymerization with Alfin Catalyst were used. Each sample of CPS was prepared from the parts insoluble in cold MEK after treating with *n*-heptane. As

1) G. Natta, *Makromol. Chem.*, **16**, 213, (1955).
2) C. W. Bunn and E. R. Howelles, *J. Polymer Sci.*, **18**, 307 (1955).
3) J. L. R. Williams, J. Vandenberche, K. R. Dunham and W. J. Dulmage, *J. Am. Chem. Soc.*, **79**, 1716 (1957).

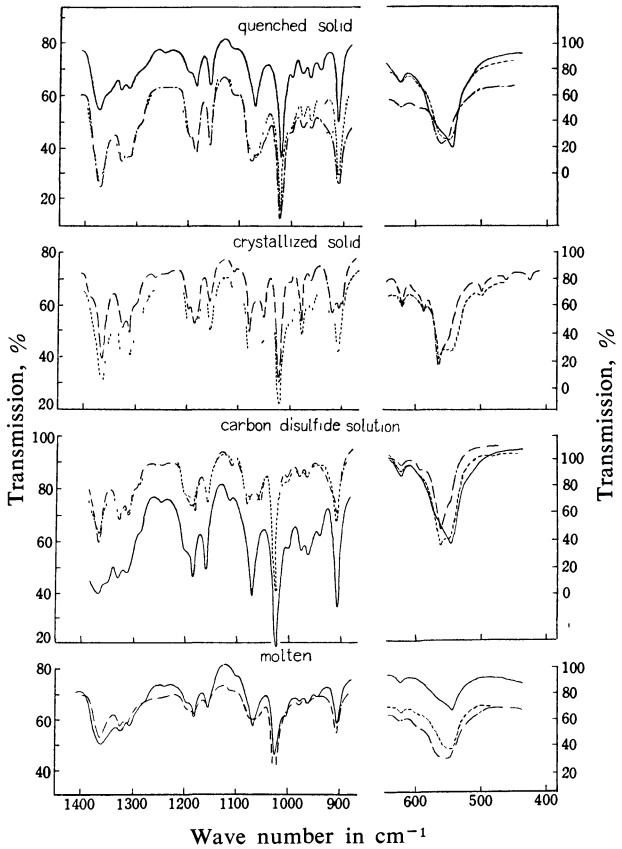



Fig. 1. Spectra of CPS-II, CPS-III and APS in various physical states.
——— APS ····· CPS-III —·—·— CPS-II

the sample of amorphous polystyrene (APS), Styron-666 of Asahi-Dow Company in Japan was used.

Film specimens for the measurement of infrared spectra were prepared by casting from carbon disulfide solution. Solution of polymers were prepared by dissolving the samples in hot carbon disulfide and the undissolved parts of CPS-I and CPS-II were filtered out.

**b) Measurement of Spectra.**—For measurement of the infrared absorption spectra, a Hitachi EPI-2 infrared spectrophotometer equipped with NaCl and KBr prisms was used. Spectra at the molten state of the samples were observed between 240 and 250°C by using the heating cell. Spectra of carbon disulfide solutions were observed at 2~5% concentration contained in a cell with 0.5~1.0 mm. thickness.

**c) Density and X-ray Measurements.**—A flotation method with NaCl solution was used for the measurement of the density at 30°C. X-ray diffraction diagrams were taken by using a Geigerflex made by Rigaku-Denki Co., Ltd.

## Results and Discussion

**1. Comparison of Infrared Spectra in Crystallized Solid, Quenched Solid, Solution and Molten State**[4].—The infrared spectra of the four different samples have been measured in crystallized solid, quenched solid, solution and molten state. The spectra of these samples in various states are shown in Figs. 1 and 2.

In the molten state, the spectra of the four samples are almost the same. However, there

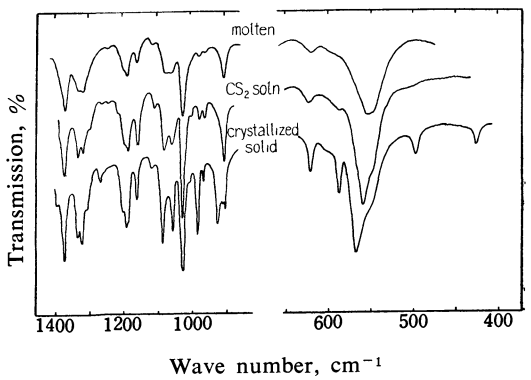



Fig. 2. Spectra of CPS-I in various physical states.

4) M. Takeda, A. Iimura, A. Yamada and Y. Imamura This Bulletin 32, 1151 (1959).

TABLE I. CLASSIFICATION OF FREQUENCIES

| CPS-I | | | CPS-II | | | CPS-III | | | APS | Classification of the band |
|---|---|---|---|---|---|---|---|---|---|---|
| Cryst. solid | Soln. | Molten | Cryst. solid | Soln. | Molten | Cryst. solid | Soln. | Quenched | | |
| 1385 | 1385 | | 1385 | | | | | | | |
| 1364 | 1364 | 1364 | 1364 | 1364 | 1370 | 1365 | 1367 | 1367 | 1370 | B |
| 1314 | 1314 | 1314 | 1314 | 1314 | 1314 | 1314 | 1314 | 1313 | 1312 | B |
| 1297 | 1297 | | 1297 | 1297 | 1295 | 1297 | 1297 | 1295 | 1295 | B |
| 1258 | | | 1258 | | | | | | | |
| 1185 | 1190 | | 1185 | 1190 | | 1185 | 1190 | | | B |
| 1085 | 1080 | | 1085 | 1080 | | 1080 | 1080 | 1079 | | $C_1$ |
| | | 1065 b | | | 1063 b | 1065 | 1068 | 1068 | 1070 | $C_2$ |
| 1054 | 1054 | | 1054 | 1057 | | 1053 | 1056 | | | $C_1$ |
| 984 | 978 | 978w | 984 | 978w | 978w | 982 | 978w | 979w | 980w | A |
| 923 | | | 923 | | | 921 | | | | A |
| 910 | 908 | 905 | 910 | 908 | 905 | 908 | 908 | 908 | 905 | |
| 901 | | | 901 | | | | | | | A |
| 620 s | 620 b | 620 b | 620 s | 620 b | 620 b | 620 s | 620 b | 620 b | 620 b | A |
| 587 | 588w, b | | 587 | 590w, b | | 587 | 590w, b | 590w, b | | A |
| 568 | | | 567 | | | 567 | | | | $C_1$ |
| | 560 | | | 560 | | | 560 | | | $C_1$ |
| | | 555 b | | | 552 b | | | | | $C_1$ |
| | | | | | | 543 | 544 | 546 b | 543 | $C_2$ |
| 499 | | | 499 | | | 499 | | | | A |
| | | | 465 | | | | | | | A |
| 428 | | | 426 | | | 426 | | | | A |

Note. (1) Only the bands which show remarkable change are listed in Table I.
(2) Remarkable change of frequencies of APS is not found with varying state.
(3) w: weak band, b: broad band, s: sharp band.

are definite differences between the band at 555 (symmetrical broad band) of CPS-I and the band at 543 $cm^{-1}$ (asymmetrical broad band) of APS. The band at 546 $cm^{-1}$ (asymmetrical broad band) of CPS-III appeared as the superposition of the above two bands. The rather flat and broad band at 1063 $cm^{-1}$ of CPS-I is different from the sharp band at 1070 $cm^{-1}$ of APS. The spectrum of molten CPS-II is similar to that of molten CPS-I.

The difference of spectra among the samples in quenched solid was very similar to the difference of those in the molten state and became larger in the crystallized solid state.

In the spectra of crystallized CPS-I and CPS-II, a new sharp band appeared at 567 $cm^{-1}$ and the form became an asymmetric one. The broad band at 1063 $cm^{-1}$ of molten CPS-I and CPS-II became a sharp doublet with the maxima at 1085 and 1054 $cm^{-1}$. In the spectrum of crystallized CPS-III, the intensity of the band increased with maximum at 567 $cm^{-1}$. The band around 1070 $cm^{-1}$ of CPS-III has shown a very complicated form and probably it has three maxima at 1080, 1065 and 1053 $cm^{-1}$. It is also recognized that the intensity of the band at 1365, 1314, 1297 and 1185 $cm^{-1}$ increased more in the spectra of crystallized CPS-I, CPS-II and CPS-III than in the spectra of the quenched solids as found by Tadokoro et al.[5] They suggested that these bands may be assigned to CH or $CH_2$ deformation vibrations and are closely related to the intramolecular interactions in the helical chain having the three fold screw axis (alternate sequences of *trans* and *gauche* conformation along the C–C chain). Other new bands with maxima at 984, 923, 901, 620, 587, 499, 465 and 426 $cm^{-1}$ appeared in the crystallized CPS-I and CPS-II, and also the bands with maxima at 982, 921, 620, 587, 499 and 426 $cm^{-1}$ appeared in the crystallized CPS-III. These bands are probably ascribable to the usual crystalline bands. Several heat treatments for crystallization gave no remarkable change in the spectra of APS. This fact suggests that APS does not crystallize appreciably.

The difference of spectrum became very simple in carbon disulfide solution compared to that of the crystallized solid. The bands at 1085, 1054 and 567 $cm^{-1}$ of the crystallized CPS-I, CPS-II and CPS-III still persist in the spectra of the solution, even though slight shifts of absorbance maximum are observed. The bands at 1070 and 543 $cm^{-1}$ of APS remain in the spectra of the solution

5) H. Tadokoro, S. Nozakura, T. Kitazawa, Y. Yasuhara and S. Murahashi, This Bulletin, 32, 313 (1959).

with no change from those of the solid. The bands at 1364, 1314, 1297 and 1185 $cm^{-1}$ of CPS-I and CPS-II also persist in the spectra of the solution, but a slight decrease of their intensity is noted. Other bands ascribable to the crystalline band disappear or are very much weakened in the spectra of the solutions.

According to the above mentioned observation, it is possible to classify the spectra which differ from sample to sample, into three groups, A, B and C as shown in Table I.

The A group bands are characteristic in the crystallized solid and dissappear instantly or are very much weakened when the crystallized solid is dissolved in solution or is melted. These bands, which are not observed in the spectra of APS, may be assigned to the crystalline bands caused by the perturbation due to rather long range intra- and intermolecular interaction in the microcrystals of polystyrene. The assignment of A group bands to the crystalline bands makes it possible to use them for the quantitative estimation of crystalline contents of the crystallized polystyrene. The maximum crystalline content $X_{max}$ in polystyrene might be associated with the contents of isotactic configuration in polystyrene, since only the polystyrene which has isotactic configuration can form crystalline regions with its helical conformation. This problem is studied in the 2nd part of this paper.

The B group bands are stronger in the crystallized polystyrene than in the quenched solid or the molten state, and they persist in the spectra of CPS-I, CPS-II and CPS-III even in their solutions, and are not found in that of APS. Our observations are consistent with the assignment[5] of these bands to the CH or $CH_2$ deformation vibration which are due to the intramolecular interaction in the helical chain conformation having a three-fold screw axis.

The $C_1$ and $C_2$ groups have shown different spectra among four samples in all physical states such as crstallized solid, quenched solid, solution and molten states. The band with maximum at 543 $cm^{-1}$ of APS has been assigned to $\nu_4(B_2)$ vibration mode of mono-substituted benzene by Liang and Krimm[6]. According to this assignment, it can be assumed that the origin of the absorption bands which belong to the C group is the phenyl group vibration which is sensitive to the short range intramolecular interaction along the C–C main chain conformation. It is possible to subclassify the C group bands into $C_1$ and $C_2$ based on the differences of samples as shown in Table I. The $C_1$ group bands then become the characteristic vibrations of the C–C chain, which has the helical conformation or *trans-gauche* alternate conformation along the C–C chain from isotactic configuration. The $C_2$ group bands may be due to the characteristic vibration of the C–C chain which has mainly *trans* confomation along the C–C chain from syndiotactic configuration. Morton and Taylor[7] have used the new IR rating method of isotacticity based on the absorption in the 1070 $cm^{-1}$ region of KBr disk samples. The pattern of their spectra in this region is very similar to the pettern of our spectra in the same region which are observed using the sample of crystallized film and solution.

On the basis of the above empirical classification of the characteristic bands of polystyrenes and a possible interpretation of the origin of these absorption bands, the following conclusions are tentatively drawn.

Based on the behaviors of the C class bands, the conformation of the C–C chain of a few monomer units seems to differ among the samples even in their molten states. The intensity of bands in the $C_1$ group will be related with the content of helical conformation of polystyrene, because its intensity becomes strong in the crystallized state. In the solution, the helical conformation of crystallizable polystyrene is partly preserved, because the persistence of the $C_1$ and B class bands in the spectra of CPS-I, CPS-II and CPS-III is well recognized and their intensities are stronger than these in the quenched solids. It may be suggested that the intensity ratio D560 to D543 (D560/D543) in the spectra of the solution can be used to measure the content of isotactic configuration of the same polystyrene, as well as the band around 1070 $cm^{-1}$. In that case the equilibrium content of helical conformation of polystyrene is determined only by its isotactic content of chain configuration, and not by its previous history like heat treatment in the solid state. The observed values of D560/D543 in solution are shown in Table II.

**2. Behavior of the Crystalline Bands and the Estimation of Crystalline Content.**—Based on the conclusions in part 1, among several crystalline bands of the A group, the intensity of the bands at 984 and 587 $cm^{-1}$ have been used to measure the crystalline content in various polystyrene samples. The possibility of measuring the crystalline content using the intensity of the band at 984 $cm^{-1}$ has also been pointed out by Braun et al.[8] from their investigation on the temperature dependence of the band.

6) C. Y. Liang and S. Krimm, *J. Polymer Sci.*, **27**, 241 (1958).

7) A. A. Morton and L. D. Taylor, ibid., **38**, 7 (1959).

8) D. Braun, W. Betz and W. Kern, *Naturwissenschaften*, **46**, 344 (1959).

For avoiding the difficulty of measurement of film thickness, the band at 1030 $cm^{-1}$ has been used as a reference, since the optical densities of this band had a linear relationship with thickness for each sample and were independent of the crystal content of samples as shown in Fig. 3.

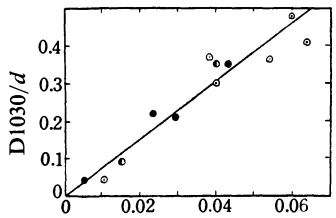



Fig. 3. Linear relation between optical density of 1030 $cm^{-1}$ and thickness.

○ : CPS-I ⊙ : CPS-III
● : CPS-II ◐ : APS

The measured values of D984/D1030 and D587/D1030 are listed in Table II. The linearity between both values suggests that the origin of these bands is the same crystalline band as shown in Fig. 4. The specific volumes of samples were calculated from the measured densities, and are also listed in Table II. From the specific volume, the crystalline content of polystyrene $X_{sv}$ can be calculated by the following equation:

$$X_{sv}=(V_a-V)/(V_a-V_c) \quad (1)$$

where, $V_a$ is the specific volume of the amorphous part and $V_c$ is the specific volume of the crystalline part.

If the intensities of D587 and D984 are proportional to the crystalline content, the following equation can be proved:

TABLE II. NUMERICAL DATA FOR EACH SAMPLE

| Sample | Density (30°C) | Specific volume | D587/D1030 | D984/D1030 | Crystalline content (%) $X_i$ (587) | $X_i$ (984) | $X_{sv}$ | $X_x$ | D560/D543 in $CS_2$ soln. |
|---|---|---|---|---|---|---|---|---|---|
| (CPS-I) | | | | | | | | | |
| Q-2 | 1.0529 | 0.950 | 0.042 | 0.082 | 8 | 5 | 0 | 11.5 | |
| Q-2 | 1.0582 | 0.945 | 0.023 | 0.067 | 4 | 2 | 8 | 9.5 | |
| Q-2 | 1.0582 | 0.945 | 0.026 | 0.060 | 5 | 0 | 8 | | |
| Q-2 | 1.0650 | 0.939 | 0.122 | 0.178 | 23 | 23 | 18 | | |
| Q-1 | 1.0652 | 0.939 | 0.122 | 0.172 | 23 | 22 | 18 | | |
| Q-1 | 1.0683 | 0.936 | 0.157 | 0.201 | 29 | 28 | 23 | | 2.85 |
| Q-1 | 1.0692 | 0.935 | 0.186 | 0.232 | 34 | 34 | 24 | 26.6 | |
| Q-190-10 | 1.0742 | 0.931 | 0.204 | 0.248 | 38 | 37 | 31 | | |
| Q-205～175-310 | 1.0815 | 0.925 | 0.271 | 0.310 | 50 | 49 | 40 | | |
| A-220～170-480 | 1.0873 | 0.920 | 0.313 | 0.353 | 58 | 58 | 48 | | |
| A-220～160-480 | 1.0898 | 0.918 | 0.292 | 0.329 | 54 | 53 | 52 | | |
| A-220～160-750 | 1.0915 | 0.916 | 0.336 | 0.393 | 62 | 66 | 55 | 73.3* | |
| (CPS-II) | | | | | | | | | |
| Q-160-30 | 1.085 | 0.922 | 0.167 | 0.189 | 31 | 26 | 45 | 24.6 | |
| Q-180-120 | 1.088 | 0.919 | 0.210 | 0.244 | 39 | 36 | 50 | | 2.26 |
| A-205-60 | 1.089 | 0.918 | 0.236 | 0.277 | 44 | 43 | 52 | 51.4* | |
| (CPS-III) | | | | | | | | | |
| Q-1 | 1.056 | 0.947 | 0.012 | 0.059 | 2 | 0 | 5 | | |
| Q-160-30 | 1.062 | 0.942 | 0·022 | 0.085 | 4 | 6 | 13 | | 1.10 |
| Q-185-120 | 1.068 | 0.936 | 0.078 | 0.132 | 14 | 14 | 23 | 16.4 | |
| A-205-60 | 1.065 | 0.939 | 0.087 | 0.168 | 16 | 22 | 18 | 17.1* | |
| (APS) | | | | | | | | | |
| Q-1 | 1.052 | 0.951 | 0 | 0.066 | 0 | 2 | — | 0* | |
| Q-160-30 | 1.054 | 0.949 | 0 | 0.057 | 0 | — | 2 | | 0.54 |
| A-180-120 | 1.055 | 0.948 | 0 | 0.060 | 0 | 0 | 3 | | |

Note. Q-1: Quenched in ice water after keeping the sample at 245～248°C.
Q-2: Quenched at −70°C after keeping the samples at 270°C.
Q-160-30: Means that the quenched solid was kept at 160°C during 30 minutes and after that, the temperature was lowered slowly.
A-205-60: Means that annealing was made, keeping the sample at 205°C for 60 minutes.
* These values are chosen as the maximum crystalline content $X_{max}$.

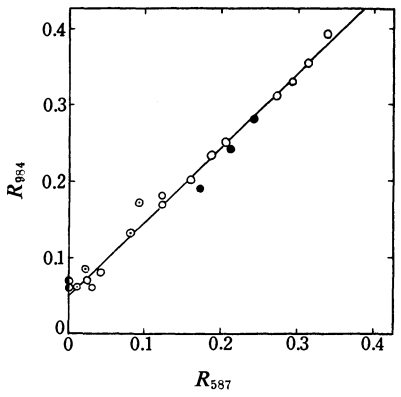



Fig. 4. Linear relation between $R_{984}$ and $R_{587}$.
○ : CPS-I ⊙ : CPS-III
● : CPS-II ◐ : APS

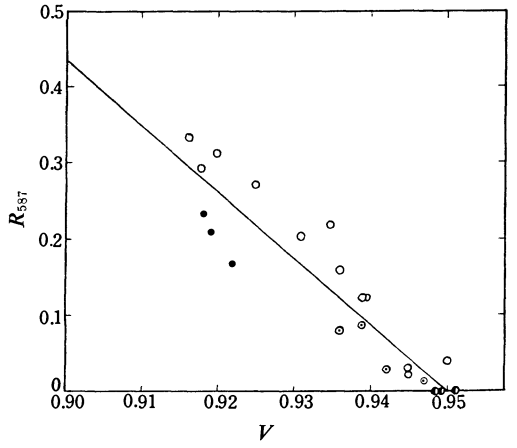



Fig. 5. Relation between $R_{587}$ and specific volume.
○ : CPS-I ⊙ : CPS-III
● : CPS-II ◐ : APS

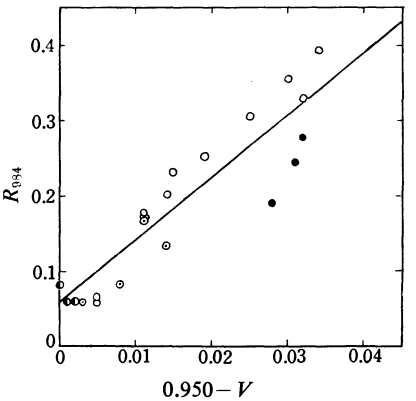



Fig. 6. Relation between $R_{984}$ and $(V_a-V)$.
○ : CPS-I ⊙ : CPS-III
● : CPS-II ◐ : APS

$$R_{587}=\mathrm{D587/D1030}=K_1(V_a-V) \quad (2)$$

$$R_{984}=\mathrm{D984/D1030}=K_2(V_a-V)+A \quad (3)$$

where, $K_1$ and $K_2$ are constant, and $A$ is added because the band at 984 $cm^{-1}$ has some intensity even in the amorphous state. From the linear relation between $R_{587}$ and $V$, and $R_{984}$ and $(V_a-V)$, as shown in Figs. 5 and 6, $K_1$, $K_2$ and $A$ were determined experimentally as follows.

$$K_1=8.729,\ K_2=8.242 \text{ and } A=0.058.$$

The value of $V_a$ is determined, from Fig. 5, as 0.950 from the value of $V$ at $R_{587}=0$. The value of $V_c$ is estimated as 0.888 from the results of Natta's X-ray analysis[9].

Combining the equations (1), (2) and (3), the following relationships are obtained:

$$X_{sv}=16.13(0.950-V) \quad (4)$$

$$X_i(587)=1.85(R_{587}) \quad (5)$$

$$X_i(984)=1.96(R_{984}-0.058) \quad (6)$$

where $X_i(587)$ and $X_i(984)$ are the crystalline content by the infrared method from the 587 $cm^{-1}$ and 984 $cm^{-1}$ bands, respectively. The determined values of crystalline content for each sample are shown in Table II, and the agreement among $X_{sv}$, $X_i(587)$ and $X_i(984)$ is satisfactory considering the difference of methods. Another approximate estimation[10]

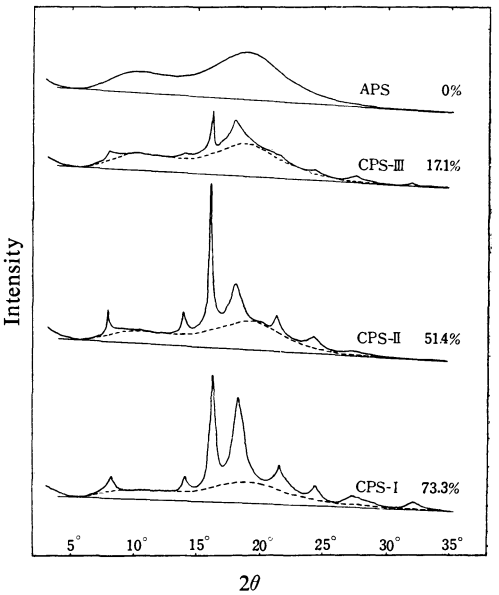



Fig. 7. X-ray diffraction diagrams of each polystyrene at maximum crystallinity and their crystalline contents.

9) G. Natta and P. Corradini, *Makromol. Chem.*, **16**, 77 (1955).
10) G. Natta et al., Atti. *accad. nazl. Lincei, Rend., Classe sci. fis., mat. e nat.*, **22**, 11 (1957).

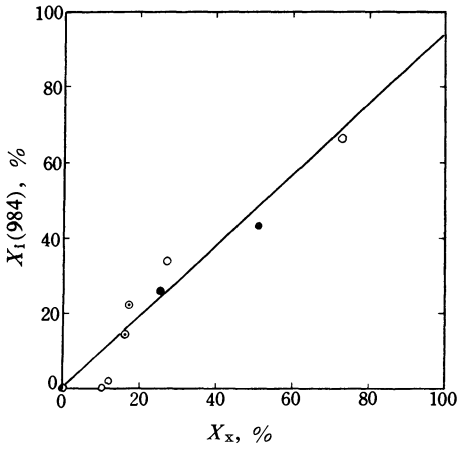



Fig. 8. Linear relation between $X_i(984)$ and $X_x$.

○ : CPS-I ⊙ : CPS-III
● : CPS-II ◐ : APS

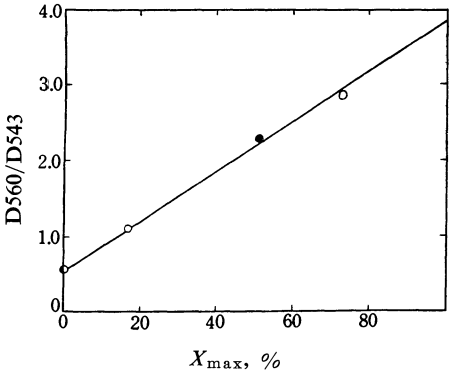



Fig. 9. Linear relation between D560/D543 and maximum crystallinity for each sample.

○ : CPS-I ⊙ : CPS-III
● : CPS-II ◐ : APS

of the crystalline content, $X_x$, by X-ray diffraction curve has been tried, and the values are also shown in Table II. The diffraction curve of APS in Fig. 7 has been used as the standard curve of amorphous parts. The estimated curve of amorphous parts was drawn through the point ($2\theta=12.5°$) on the experimental curve of the crystallized polystyrene making it similar to the standard curve in the direction of intensity. The intensity at $2\theta=12.5°$ was little influenced from the scattering of the crystalline parts which had the strong peaks at $2\theta=8.1°$ and $2\theta=16.2°$. The ratio of crystalline region to total area is taken as the agreement between $X_x$ and $X_i(984)$ was satisfactory as shown in Fig. 8. The determined values of $X_x$ for the most crystallized state of the four polystyrenes, CPS-I, CPS-II, CPS-III and APS, are taken as the maximum crystalline content, $X_{max}$, of each polystyrene. A strong correlation was found between $X_{max}$ and the ratio D560/D543 in the solution, as shown in Fig. 9. This will suggest that both the maximum crystalline content, $X_{max}$, and D560/D543 in the solution can be used to measure the content of isotactic configuration of polystyrene from the quantitative point of view. The same treatment of the band at around 1070 $cm^{-1}$ in the solution may be possible for the determination of the isotactic content of polystyrene, but is not considered in this paper.

We are very grateful to Mr. N. Yamazaki of the Tokyo Institute of Technology for his kind donation of the sample of CPS-I, and to Mr. S. Kondo of the Tokyo College of Science for his assistance in making the X-ray measurement.

*Department of Chemistry*
*Tokyo College of Science*
*Kagurazaka, Shinjuku-ku*
*Tokyo*

# *Rate of Desorption from a Heterogeneous Surface*

By Yutaka KUBOKAWA

(Received February 15, 1960)

The previous studies of chemisorption of hydrogen and carbon monoxide on zinc oxide and other catalysts[1], particularly of the rates of desorption at a constant temperature, showed that, although the Elovich equation was approximately obeyed in a limited range of coverage, a slight decrease in the adsorbed amount caused a marked increase in the value of $\mathrm{d}\ln R_{\mathrm{dep}}/\mathrm{d}q$ where $R_{\mathrm{dep}}$ is the rate of desorption and $q$ the adsorbed amount. A typical example is shown in Fig. 1. As was pointed out previously, such a phenomenon cannot be explained in terms of the concept that the decrease in the heat of adsorption is due to interaction between adsorbed species or to the induction effect emphasized by Boudart[2]. The concept of an a priort heterogeneity alone seems therefore to offer a satisfactory explanation of the experimental results.

Rate expressions for adsorption on such a heterogeneous surface were already derived in the previous work[3], whereby the physical meaning of $\mathrm{d}\ln R_{\mathrm{adp}}/dq$ ($R_{\mathrm{adp}}$=rate of adsorption) was also given. This paper presents an attempt to formulate the rate of desorption from a heterogeneous surface in a similar manner, and to explain the variation in $\mathrm{d}\ln R_{\mathrm{dep}}/\mathrm{d}q$ mentioned above on the basis of the surface heterogeneity.

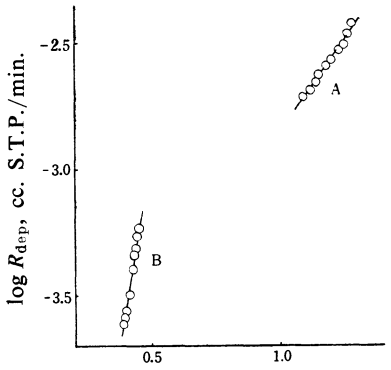



Fig. 1. Rates of desorption of carbon monoxide chemisorbed on zinc oxide. (Reproduced from "Carbon Monoxide Chemisorption on Zinc oxide" by the present author.) Temp., 192°C; The adsorbed amount at saturation is about 10 cc.; the time allowed for adsorption in run A is different from that in run B.

As described previously, the measured rate of desorption is, in most cases, unaffected by the reverse reaction, i.e., the re-adsorption. Consequently, the rate of desorption from any set of sites of the same kind on a heterogeneous surface may be

$$R=N\theta_i k\mathrm{e}^{-kt}=\alpha k\mathrm{e}^{-kt},\quad \alpha=N\theta_i$$

where $\theta_i$ is the coverage at $t=0$ and $N$ is the distribution function of sites, both of which may usually have different values for a different set of sites. At any moment during a desorption experiment, as was found for adsorption, there is always a certain set of sites for which the rate passes through a maximum. The condition for the maximum, can be written as

$$\mathrm{d}R/\mathrm{d}k=\alpha\mathrm{e}^{-kt}(1+\beta-kt)=0,\quad \beta=\mathrm{d}\ln\alpha/\mathrm{d}\ln k$$

or
$$kt=1+\beta \qquad (1)$$

Thus the maximum rate is

$$R_m=\alpha k\mathrm{e}^{-(1+\beta)} \qquad (2)$$

Such a maximum rate may be assumed, as a first approximation, to be proportional to the overall rate on a similar ground to that given previously. Then, from the same argument as that given for the rate of adsorption, the following expression can be derived for the overall rate of desorption $R_{\mathrm{dep}}$ by using Eqs. 1 and 2:

$$\mathrm{d}\ln R_{\mathrm{dep}}/\mathrm{d}q=-(\mathrm{e}^{\beta}/RT\alpha) \qquad (3)$$

In the course of desorption, $k$ and $\alpha$ will vary as the set of sites for which the rate passes through a maximum is replaced by others successively. Hence, the left-hand side of Eq. 3 will generally vary as the desorption proceeds. In a limited range of coverage, however, an approximately constant value of $\mathrm{d}\ln R_{\mathrm{dep}}/\mathrm{d}q$ will be expected. The behavior of desorption such as that shown in Fig. 1 is thus in agreement with what would be expected on a heterogenous surface, although its quantitative discussion is not feasible without complete information on the site distribution function etc.

1) Y. Kubokawa, This Bulletin, 33, 546, 550, 555, 739, 743, 747 (1960).
2) M. Boudart, *J. Am. Chem. Soc.*, 74, 3556 (1952).
3) Y. Kubokawa, This Bulletin, 33, 734 (1960).

The author wishes to express his sincere thanks to Professor O. Toyama for his guidance and encouragement throughout the course of this study.

*Department of Applied Chemistry*
*College of Engineering*
*University of Osaka Prefecture*
*Sakai-shi, Osaka*

# *Rate of Adsorption on a Heterogeneous Surface. Determination of the Distribution Function of Sites from Adsorption Rate Curves*

By Yutaka KUBOKAWA

(Received February 24, 1960)

In view of the importance of surface heterogeneity in the chemisorption on oxide catalysts as revealed by desorption experiments[1], the present author has derived in a recent paper[2] the rate of adsorption on a heterogeneous surface for the cases where the distribution function of sites is variable and/or desorption can not be neglected. The rate formula thus obtained has led to an interpretation of the Elovich equation

$$dq/dt = ae^{-bq}$$

where $q$ is the adsorbed amount and $a$ and $b$ are constants. Thus, explicit expressions and hence a physical meaning have been given to the constant $b$ in the Elovich equation on the basis of the surface heterogeneity. The frequently observed variation in the constant $b$ with pressure or temperature has been shown to be explained since the Elovich equation is usually applied only in a limited range of coverage. It is rather customary to use the integrated form of the Elovich equation for its actual application. Nevertheless, as has been pointed out in the previous paper, the constant $b$ obtained from the integrated form of the equation, in most cases, can not be given any such physical meaning as that mentioned above, and consequently can not be related to the surface heterogeneity in a quantitative way. It has therefore been undertaken in the present work to devise a method of obtaining quantitative information on the surface heterogeneity, i. e, the distribution function of sites, directly from the adsorption rate curves.

**Analysis of Adsorption Rate Curves.** — As described in the previous work[2], the rate of adsorption on a heterogeneous surface can be represented by the following equation when desorption is negligibly small during the adsorption rate measurement:

$$v = Kf(p)RTNe^{-\beta} \tag{1}$$

where $K$ and $N$ are the rate constant of adsorption and the distribution function of sites respectively, both referring to the set of sites mainly responsible for adsorption at a given time; the value of $K$ in Eq. 1 varies with time according to

$$Kf(p)t = 1 + \beta \tag{2}$$

where $\beta = d\ln N/d\ln K$. Thus the rate as a function of time becomes

$$v = (RTN/t)(1+\beta)e^{-\beta} \tag{3}$$

Using Eq. 1—3, the constant $b$ of the Elovich equation, $d\ln v/dq$, is given by[3]

$$d\ln v/dq = -(1/RTN)e^{\beta} \tag{4}$$

Transposing Eq. 3,

$$d\ln t/dq = (1/RTN)(1/1+\beta)e^{\beta} \tag{5}$$

Combining Eq. 4 and 5,

$$1+\beta = -(d\ln v/dq)/(d\ln t/dq) \tag{6}$$

The right hand side of Eq. 6 is determined from the adsorption rate curves by graphical differentiation, and consequently the value of $\beta$ at a given adsorbed amount, $q$, is obtained. Substituting $\beta$ thus obtained into Eq. 1 and 4, the values of $N$ and $K$ are determined as a function of the adsorbed amount.

As described previously[3], the chemisorption of hydrogen on chromic oxide gel investigated by Burwell and Taylor[4] belongs to the case where desorption is negligibly small above 457°K. The data at 457°K and 1 atm. have been treated in the manner mentioned above

1) Y. Kubokawa, This Bulletin, 33, 546, 550, 555, 739, 743, 747 (1960).
2) Y. Kubokawa, This Bulletin, 33, 734 (1960).
3) The pressure term in the rate expression, $f(p)$, is assumed to be constant during adsorption.
4) R. L. Burwell and H. S. Taylor, *J. Am. Chem. Soc.*, 58, 697 (1936).

TABLE I. HYDROGEN CHEMISORPTION ON $Cr_2O_3$ GEL AT 457°K AND 1 atm.

| $q$ | $-\mathrm{d}\ln v/\mathrm{d}q$ | $\mathrm{d}\ln t/\mathrm{d}q$ | $-\beta$ | $-\ln N$ | $-\ln K$ |
|---|---|---|---|---|---|
| 3 | 0.163 | 0.495 | 0.67 | 5.66 | 2.02 |
| 5 | 0.131 | 0.333 | 0.61 | 5.38 | 2.51 |
| 7 | 0.092 | 0.244 | 0.62 | 5.04 | 3.06 |
| 10 | 0.072 | 0.172 | 0.58 | 4.74 | 3.55 |
| 12 | 0.064 | 0.142 | 0.55 | 4.60 | 3.79 |
| 15 | 0.059 | 0.115 | 0.49 | 4.46 | 4.07 |
| 20 | 0.053 | 0.092 | 0.43 | 4.30 | 4.45 |
| 25 | 0.051 | 0.082 | 0.38 | 4.21 | 4.75 |
| 30 | 0.047 | 0.075 | 0.37 | 4.12 | 5.07 |

$q$ is in cc. (S. T. P.), $v$ in cc./min., $N$ in cc./cal., and $K$ in $\mathrm{min}^{-1}$.

with the results listed in Table I[5]. Here, as adsorption proceeds, the value of $\ln N$ increases with decreasing value of $\ln K$. The relationship of $\ln N$ against $\ln K$ is also obtained from a similar treatment for the data at other pressures at 457°K; the plots $\ln N - \ln K$ at different pressures at 457°K thus obtained were found to lie on the same curve, as would be expected.

By assuming that the variation in $\ln K$ arises only from that in activation energy of adsorption $E$, the following expression results:

$$RT \ln K = RT \ln C - E$$

where $C$ is a constant. Plots of $\ln N$ against $\ln K$ at various temperatures combined with the above expression give those of $\ln N$ against

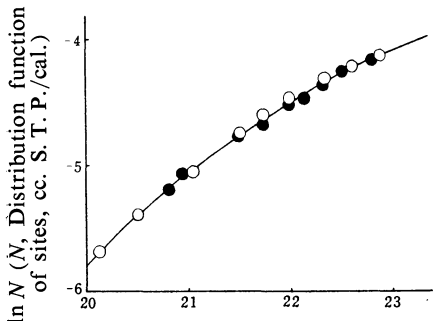



Fig. 1. Hydrogen chemisorption on $Cr_2O_3$ gel (Burwell and Taylor).
-○-, 457°K; -●-, 491°K; $\ln C = 20.1$.

5) $f(p) = p^{0.8}$ ($p$ in atm.) was used, since Burwell and Taylor state that the rate of adsorption is proportional to $p^{0.8}$.

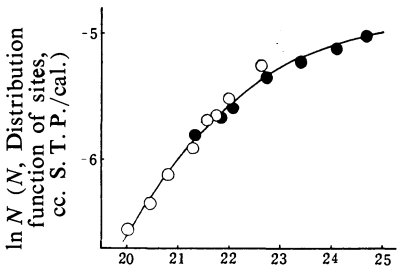



Fig. 2. Hydrogen chemisorption on $ZnO \cdot MoO_3$ (Taylor and Ogden).
-○-, 527°K; -●-, 577°K; $\ln C = 15.5$.

$E$ all of which should lie on the same curve since $N$ has been assumed to be a function of $E$ alone. This requirement is fulfilled by adjusting the parameter $C$ as shown in Fig. 1 where $\ln C = 20.1$. The figure shows that, as adsorption proceeds, the value of $E$ increases with that of $\ln N$ from 20 to 23 kcal./mol. Values of $E$ in this range seem to be reasonable, judging by the temperature dependence of the rate.

Fig. 2 represents the result of a similar treatment of the data of Taylor and Ogden[6] on the chemisorption of hydrogen on $ZnO \cdot MoO_3$, where desorption is negligible as described in the previous paper[1]. It is seen that the sites with a lower value of $E$ are mainly occupied at a lower temperature.

## Summary

A device to obtain the distribution function of sites from adsorption rate curves was worked out for the chemisorption for which desorption is negligible. It was then applied to the rate data of hydrogen chemisorption on chromic oxide gel and on $ZnO \cdot MoO_3$ with reasonable results.

The author wishes to express his sincere thanks to Professor O. Toyama for his guidance and encouragement throughout this work.

*Department of Applied Chemistry*
*College of Engineering*
*University of Osaka Prefecture*
*Sakai-shi Osaka*

6) G. Ogden and H. S. Taylor, *Trans. Faraday Soc.*, **30**, 1178 (1934).

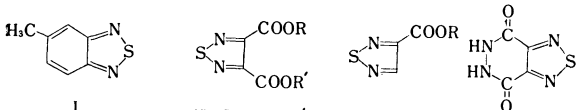
# *Oxidation of 5-Methyl-2, 1, 3-benzothiadiazole with Potassium Permanganate**

By Isao SEKIKAWA

(Received February 4, 1960)

As one of the series of studies on the relation between the antitubercular activity and the molecular structure, 2, 1, 3-benzothiadiazole-5-carboxylic acid was synthesized from 5-methyl-2, 1, 3-benzothiadiazole (I) by conversion via the corresponding 5-bromomethyl- into a formyl-derivative, followed by oxidation with silver oxide.[1]

For the purpose of preparing this acid, I was oxidized with potassium permanganate at 60°C but in vain; an acid of different structure (II) was formed.[2] This new acid was finally found to be in its structure a potassium 3-carboxy-1,-2, 5-thiadiazole-4-carboxylate.



I

II R=H, R'=K
III R=R'=$C_2H_5$
V R=R'=H

VI R=H
VII R=$C_2H_5$

X

Product II was an acidic potassium salt, m. p. 278°C decomp., extremely insoluble in organic solvent, with an empirical formula of $C_4HO_4 \cdot N_2SK$ or $C_4H_3O_4N_2SK$ as measured by microanalysis. This salt was recrystallized unchanged from dilute hydrochloric acid and was not hydrogenated over palladium-charcoal at room temperature.

Esterification of product II yielded a colorless diethylester (III), b. p. 140~142°C (10 mmHg). The molecular formula of product III was $C_8H_{10}O_4N_2S$, as measured by microanalysis and molecular weight determination. The diethylester was converted into a diamide (IV), $C_4H_4O_2N_4S$, m. p. 234~235°C decomp., with aqueous ammonia at room temperature. Hydrolysis of the diethylester together with the diamide in boiling aqueous potassium hydroxide, followed by acidification with acetic acid, regenerated product II. From these observations the molecular formula of product II was assumed to be $C_4HO_4N_2SK$. When the diethylester was hydrolyzed with diluted hydrochloric acid, a free diacid (V) was obtained, m. p. 154~155°C, $C_4H_2O_4N_2S \cdot 2H_2O$.

On decarboxylation of diacid V in the presence of quinoline and copper powder, no definite product was obtained, but when heated at 180~190°C in vacuo, the diacid evolved carbon dioxide and was converted into a white mono acid (VI), m. p. 167°C. Acid VI was purified by sublimation, and its molecular formula was formed to be $C_3H_2O_2N_2S$, as measured by microanalysis and molecular weight determination. Mono acid VI formed

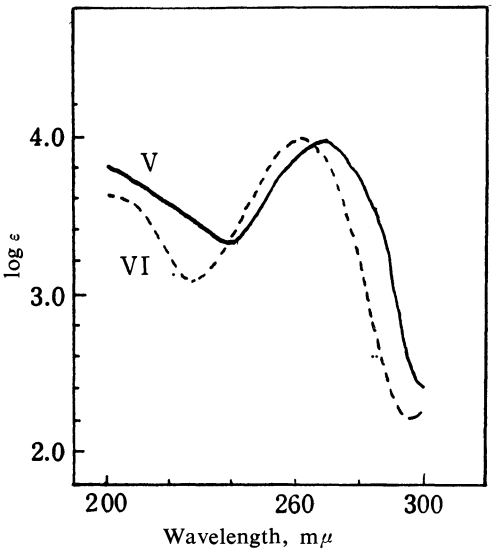



Fig. 1. Ultraviolet spectra of V and VI in water.

an ester (VII), b. p. 72°C (6 mmHg) and an acidhydrazide (VIII), m. p. 150~151°C, $C_3H_4 \cdot ON_4S$. This indicates that the partial structure of mono acid VI may be $C_2HN_2S \cdot COOH$. Mono acid VI was not hydrogenated over palladium-charcoal at room temperature, being stable in boiling concentrated hydrochloric acid.

The ultraviolet spectrum (Fig. 1) of diacid V showed a pattern identical to that of acid VI. The diethylester of diacid V assigned the structure of product III, since the infrared spectra (Fig. 2) of both products VII and III showed a S–N band at 890 $cm^{-1}$ [3].

* A part of this study was presented at the Annual Meeting of the Chemical Society of Japan, Kyoto, April 2, 1959.

1) I. Sekikawa, This Bulletin, **32**, 551 (1959).

2) I. Sekikawa, This Bulletin, **31**, 252 (1958).

3) The seven kinds of 1, 2, 5-thiadiazole compounds, showed a weak absorption band in the region of 900~880 $cm^{-1}$. D. H. Hadzi, *J. Chem. Soc.*, 1957, 847; T. Momose et al., *Chem. Parm. Bull.*, **7**, 734 (1959).

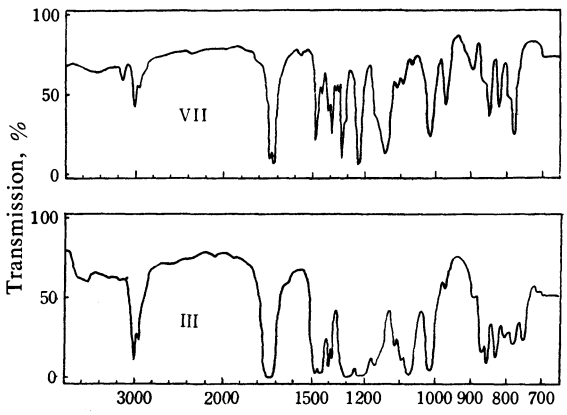



Fig. 2. Infrared spectra of VII and III.

Since the $C_2N_2S$-skeleton exists in sample I, it is almost certain that the white mono acid VI is 1, 2, 5,-thiadiazole-3-carboxylic acid. The presence of the 1, 2, 5-thiadiazole nucleus has been hitherto unknown.

Treatment of diethylester III with excess hydrazine hydrate in alcohol yielded almost quantitatively an orange-yellow dihydrazide (IX), m. p. 245°C decomp. with sintering from 170°C on, $C_4H_6O_2N_4S$. By hydrolysis with boiling dilute hydrochloric acid for 8 hr., one mole hydrazine was split off, from product IX and facile ring closure occurred, giving yellow 4, 5, 6, 7-tetrahydro-4, 7-dioxopyridazino-(4, 5-d)-2, 1, 3-thiadiazole (X), m. p. 333°C decomp., $C_4H_2O_2N_2S \cdot H_2O$. On the contrary, although one mole hydrazine was likewise split off, alkaline hydrolysis of product IX did not lead to product X, but to another product, which contained no sulfur atom and showed an empirical formula of $C_4H_6O_2N_4$, m. p. 331°C decomp. The determination of the structure of this compound is now in progress.

Recently, A. M. Khalexskiĭ et al. reported that acid V was obtained by ozonolysis of 2, 1, 3-benzothiadiazole and that on the contrary alkaline permanganate oxidation gave a 2, 1, 3-thiadiazole-4, 5-dicarboxylic acid *S*, *S*-dioxide.[4] The oxidation of sample I to product II with potassium permanganate was a reaction similar to the oxidation of quinoline to quinolinic acid.[5]

## Experimental[6]

**Oxidation of I with Potassium Permanganate.**—To a suspension of 10 g. of 5-methyl-2, 1, 3-benzothiadiazole in 200 ml. of water, 53 g. of potassium permanganate dissolved in 1300 ml. of water was added during 8 hr. at 60°C with vigorous stirring. After the last addition, the mixture was heated for 30 min. to complete the oxidation and then unchanged 5-methyl-2, 1, 3-benzothiadiazole was removed by steam distillation. The separated manganese dioxide was removed by filtration and washed with 500 ml. of water. The filtrates were combined, acidified with glacial acetic acid and evaporated to dryness. The residue was recrystallized from water to give 8.0 g. of white needles (II), m. p. 276~277°C (decomp.)[7]. The ultraviolet absorption bands at 270 mμ (log ε=3.94).

Found: C, 22.34; H, 0.94; N, 13.05; K, 18.58. C, 22.29; H, 0.99; N, 12.76; K, 18.34. C, 22.32; H, 0.71; N, 13.27.

Calcd. for $C_4HO_4N_2SK$: C, 22.64; H, 0.47; N, 13.20; K, 18.42. $C_4H_3O_4N_2SK$: C, 22.42; H, 1.41; N, 13.08; K, 18.25%.

**III.**—A mixture of 1.3 g. of II, 100 ml. of absolute ethanol and 1 ml. of concentrated sulfuric acid was refluxed for 24 hr. The separated potassium sulfate was filtered off and the filtrate was concentrated in vacuo. The residue was treated with 100 ml. of water and neutralized with sodium hydrogen carbonate. The mixture was extracted with 50 ml. of ether (twice), and the ether extract was dried and evaporated. The pale yellow oil was then distilled in vacuo, and a fraction boiling at 140~142°C (10 mmHg) was collected. The analytical sample distilled at 133°C (8 mmHg).

Found: C, 41.91; H, 4.61; N, 11.55; mol. wt. 235 (Rast mol. wt. determination).

Calcd. for $C_8H_{10}O_4N_2S$ (230.3): C, 41.74; H, 4.38; N, 12.17%.

**IV.**—To a solution of 5 g. of III in 50 ml. of ethanol, 10 ml. of aquous ammonium hydroxide ($d$ =0.8) was added. After about 1 hr. a white precipitate separated. After the solution was kept overnight at room temperature, the white crystalline solid was collected by filtration and washed with cold ethanol; yield; 3 g. Recrystallization from ethanol yielded white needles, m. p. 234~235°C (decomp.).

Found: C, 28.21; H, 2.60; N, 32.38.

Calcd. for $C_4H_4O_2N_4S$: C, 27.90; H, 2.34; N, 32.54%.

**Hydrolysis of III.**—A mixture of 1 g. of III and 25 ml. of 15% hydrochloric acid was heated under reflux for 5 hr. The reaction mixture was filtered to remove a small amount of suspended solid and evaporated under reduced pressure. The residual solid was recrystallized from water to give 0.5 g. of white sandy crystals (V).

It softened at 97°C, melted at 154~155°C with effervescence and was decomposed at 160°C. The ultraviolet absorption bands at 270 mμ (log ε=3.97).

Found: C, 22.71; H, 3.05; $H_2O$, 16.91.

Calcd. for $C_4H_2O_4N_2S \cdot 2H_2O$; C, 22.86; H, 2.88; $H_2O$, 17.14%.

**Pyrolysis of V.**—One gram of V was placed in a sublimation tube and heated for 5 min. at 180~190°C. Under this condition the material rapidly

4) A. M. Khalexskiĭ, V. G. Pesin and Tsin Chou, *Doklady Akad. Nauk. S. S. S. R.*, **114**, 811 (1957); *Chem. Abstr.*, **52**, 4605 (1958).

5) S. Hoogewerff und W. A. van Dorp, *Ber.*, **12**, 747 (1879).

6) All the melting points are uncorrected.

7) The m. p. of 281°C (decomp.) was recorded in the previous paper[2].

melted with evolution of carbon dioxide. The tube was then connected to a vacuum-pump and the decarboxylated product was sublimed at 190°C to give 0.5 g. of white crystals (VI), m. p. 164~165°C. The ultraviolet absorption bands at 260 mμ (log ε = 3.98).

Found: C, 27.51; H, 1.42; N, 21.50.

Calcd. for $C_3H_2O_2N_2S$: C, 27.69; H, 1.55; N, 21.53%.

Rast mol. wt. detn. gave value of 135.8, $C_3H_2O_2N_2S$ requires 130.1.

**VII and VIII.**—The esterification was carried out by gently refluxing for 10 hr. a mixtur of 0.9 g. of VI, 10 ml. of absolute ethanol and 0.5 ml. of concentrated sulfuric acid. After removal of the excess of ethanol, the residue was treated with water and neutralized with sodium hydrogen carbonate. The mixture was extracted with ether (twice), and the ether extract was dried, evaporated, and the residual oil was distilled to give 0.6 g. of ester (VII), b. p. 72°C (6 mmHg).

A mixture of 6.2 g. of VII, 0.2 ml. of hydrazine hydrate (80%), and 2 ml. of ethanol was heated on a water bath for 5 hr. After removing the ethanol, the solidified residue was recrystallized from ethanol, affording 0.1 g. of acid hydrazide (VIII) in the form of white needles. It softened at 140°C and melted at 150~151°C.

Found: C, 25.13; H, 3.00; N, 38.53.

Calcd. for $C_3H_4ON_4S$: C, 24.99; H, 2.80; N, 38.87%.

**IX.**—To a solution of 4.2 g. of diethylester III in 20 ml. of ethanol, 3.7 ml. of 80% hydrazine hydrate was added. An orange-red solid immediately separated from the reaction mixture, which was set aside overnight at room temperature and then filtered to give 3.6 g. of product. Recrystallization from water yielded yellow needles.

It softened at 150°C, reddened at 180°C and was decomposed at 248°C.

Found: C, 23.57; H, 3.20; N, 41.33.

Calcd. for $C_4H_6O_2N_6S$: C, 23.76; H, 2.99; N, 41.57%.

**Hydrolysis of IX with Diluted Hydrochloric Acid.**—A mixture of 2 g. of dihydrazide IX, 3 ml. of concentrated hydrochloric acid and 100 ml. of water was heated under reflux for 8 hr. Cooling and filtering yielded 1.3 g. of white crystals, which were recrystallized from water to give light yellow plates. m. p. 333°C (decomp.) (monohydrate). The ultraviolet absorption bands at 265 mμ (log ε = 4.20).

Found: C, 25.63; H, 2.35; N, 29.94; $H_2O$, 9.35.

Calcd. for $C_4H_2O_2N_4S \cdot H_2O$: C, 25.53; H, 2.14; N, 29.78; $H_2O$, 9.57%.

The filtrate from the above reaction mixture was evaporated to dryness. The residue was recrystallized from water to give white needles, m. p. 198°C (decomp.).

This material was identical with a hydrazine hydrochloride..

**Hydrolysis of IV and III with Potassium Hydroxide.**—A mixture of 0.5 g. of diamide IV, 0.3 g. of potassium hydroxide and 20 ml. of water was heated for 2 hr., after which time ammonia evolution had ceased. The reaction mixture was evaporated to dryness under reduced pressure. The residue was dissolved in a small amount of water, acidified with acetic acid and the precipitated solid was collected by filtration. The product was recrystallized from water to give white needles. m. p. 274°C (decomp.).

Hydrolysis of diethylester III with dilute potassium hydroxide for 1 hr., followed by isolation of the product as described above, afforded I in 60% yield.

The products from diamide and diethylester were shown to be identical with I by a microanalysis and by comparison of infrared spectra.

The author wishes to express his gratitude to Professor S. Kakimoto for his kind encouragement and advice.

*The Research Institute for Tuberculosis*
*Hokkaido University*
*Sapporo*

# *Decay of Free Radicals in γ-Irradiated Polymethyl Methacrylate*

By Jiro HIGUCHI, Shōji SHIDA, Riichiro KUSAKA* and Teruo MIYAMAE

(Received February 16, 1960)

Recently, many investigations have been carried out for polymers by using the electron spin resonance (ESR) technique. Especially the polymethyl methacrylate (PMMA) is one of the most comprehensively investigated ones, and the properties of the radicals produced by γ-irradiation have been clarified fairly well[1,2]. In the present communication, a preliminary work on the decay of radicals in γ-irradiated PMMA above and below the transition point by the ESR spectrometer will be reported, while a similar work by Ohnishi and Nitta was recently carried out independently of ours only below the transition point[3].

The samples used were PMMA plates (a section $0.2\times0.2$ cm$^2$ : columnar-shaped ; Acrylite, Mitsubishi Rayon Co., Ltd.) and the irradiations were carried out $3\times10^6$ r. at room temperature with γ-ray from a $^{60}$Co source (dose rate $2.2\times10^5$ r./hr.). The radicals produced were detected by the ESR spectrometer (JEP-1 E.P.R. Spectroscope; Japan Electron Optics Laboratory Co., Ltd., X-band, bridge-type). The resonance pattern thus obtained is the same as in the case of fine powdered samples sealed in vacuo, and also similar to those by Schneider[1] and by Abraham et al.[2], and no appreciable change by the influence of oxygen was detected in the present experiment, in spite of a considerable change observed in the powdered sample exposed to air. So the experiments were carried out by using plated samples only, to avoid color centers resulting from irradiation in the glass which was used to seal the samples in vacuo.

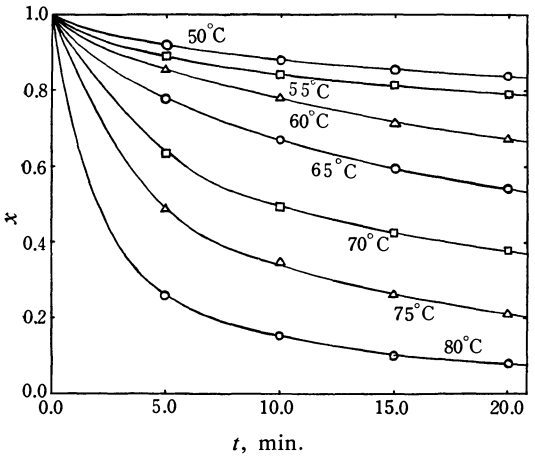



Fig. 1. Relative concentration of free radicals $x$ aginst time $t$.

Decay of the free radicals was investigated at temperatures between 50 and 80°C. In detection, the samples (stored in dry ice after irradiation) kept at the reaction temperature were taken out every five minutes and suddenly cooled to the room temperature by dry ice in order to interrupt the reaction rapidly, because

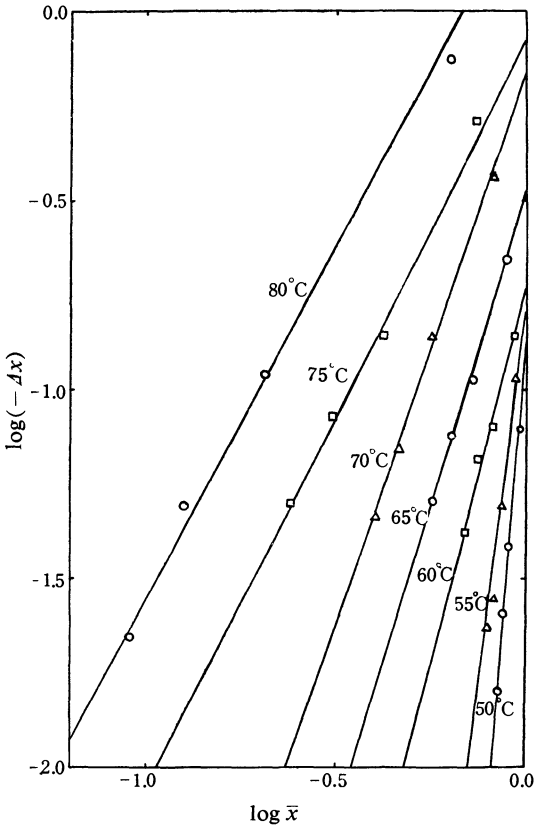



Fig. 2. Logarithm of the change of the relative concentration in five minutes $\log(-\Delta x)$ against logarithm of the mean value of the relative concentration $\log \bar{x}$.

* Present address, Yahata Iron and Steel Co., Ltd., Tokyo Research Institute.

1) E. E. Schnider, *Disc. Faraday Soc.*, **19**, 158 (1955).
2) R. J. Abraham, H. W. Melville, D. W. Overnall, and D. H. Whiffen, *Trans. Farady Soc.*, **54**, 1133 (1958).
3) S. Ohnishi and I. Nitta, *J. Polymer Sci.*, **38**, 451 (1959). In this paper, our result quoted should be corrected.

the change in the room temperature is very slow. Thus the relative concentrations in these samples were obtained by the ESR spectra at the room temperature comparing with the reference sample which was irradiated under the same condition and stored in dry ice. Under these circumstances, no appreciable change of the resonance pattern was observed.

The variation of the radical concentration so obtained is given in Fig. 1. To determine the order of the reaction, the logarithm of the change of the relative concentration in five minutes $\Delta t$, $\log(-\Delta x)$, was plotted against the logarithm of the mean value of the relative concentration, $\log \bar{x}$, as shown in Fig. 2, since the order $n$ is obtainable from the slope by using the following relation:

$$\log(-\Delta x) = n \log \bar{x} + (\log k + \log \Delta t)$$

From Fig. 2, one can easily find the interesting feature that above 70°C the reaction is of the second order while below 70°C the apparent order is greater than the second and increases with decreasing temperature. Since the PMMA is amorphous and its transition point is considered to be about 70°C, the mechanism of the decay of the radical is considered to be different above and below the transition point taken as the border. That is, above the transition point the motion of the chain segment is rather unrestricted so that the reaction rate is proportional to the concentrations of each radical recombined, because the radicals are considered to be independent for the dose rate used, whereas below the point, the decaying process becomes complicated because of relaxation. This is also consistent with the result by Ohnishi and Nitta[3] in which below the transition point the reaction was the second order except in the beginning range (several hours). The activation energy obtained in the present work is $3 \times 10$ kcal./mol., which is also consistent with their result, although it is rather difficult to obtain accurately because of the aforementioned mechanism.

The present work is preliminary and includes many points requiring improvements as follows: (1) The error due to the fact that the samples were taken out from the reaction temperature and the ESR spectrum was observed at the room temperature. (The decay at the room temperature could not be absolutely negligible. This can be improved by the use of a cavity which can be used at various temperatures in question.) (2) A little influence of oxygen because of the experiment carried out in air. (This can be improved by sealing the sample in vacuo.) (3) The inconsistency of the experimental conditions; i. e. the $\gamma$-irradiation due to the $^{60}$Co irradiation apparatus, and in the change of temperatures.

Although the present experiment encounters the above-mentioned problems, the result gives the following interesting suggestion: investigation of the decay of radicals in the $\gamma$-irradiated polymer gives information concerning the knowledge of the motion of polymers. Although it is not a direct method and the change of the mechanism bordering the transition point has already been observed in the crosslinking of polyethylene and of polyvinyl chloride[4], the present phenomenon is rather simple and favorable to the investigation of the motion of polymers. Though the present PMMA is amorphous, similar investigations can also be carried out for partially crystalline polymers. In this case, it is possible to observe separately the motion of polymers in the crystalline and amorphous regions since the resonance patterns for these regions can not always be the same because of the steric effect of the radical produced. In fact, including the case of PMMA, a more precise investigation is absolutely necessary, especially for the points aforementioned, in order to obtain more conclusive result.

The authors wish to thank Dr. M. Kurata for his helpful advice.

*Tokyo Institute of Technology*
*Ookayama, Meguro-ku, Tokyo*
*(J. H. & S. S.)*

*Japan Electron Optics Laboratory Co., Ltd.*
*Kamirenjaku, Mitaka, Tokyo*
*(R. K. & T. M.)*

4) A. N. Pravednikov, Y. S. Kan, and S. S. Medvedev, *Proc. United Nations International Conference on the Peaceful Uses of Atomic Energy*, No. 2294, 192 (1958); See, S. Okamura, *Chemistry (Kagaku)*, 5, 7 (1960).

# *Structure of Namakochrome. II**

By Toshihiko MUKAI**

(Received February 12, 1960)

Previous paper[1] has reported that namakochrome which is a new pigment isolated from *polycheira rufescens*, should be either 2-hydroxymethyl-3, 6, 7-trihydroxy-naphthazarin (I or II) or 2-methoxy-3, 6, 7-trihydroxy-naphthazarin (III or IV). Thus, for the complete elucidation of the namakochrome structure there remains to be established the form of the functional group in 2-position of the naphthalene nucleus.



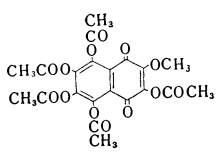
I II



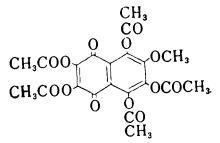
III IV

Although, in the preceding work[1], a qualitative detection of the quinone group in namakochrome by reductive acetylation has been also described, the isolation of crystalline products from the resulting solution was unsuccessful. Namakochrome-trimethyl ether was then acetylated in the presence of zinc dust, and a benzene solution of the reaction products was filtrated through an alumina column, and afforded a leuco-acetyl derivative, $C_{11}H_3O_5\cdot(OCH_3)_3(COCH_3)_4$, as colorless prisms, m. p. 226~227°C.

Now, in order to characterize the unascertained oxygen atom in 2-position of namakochrome, the 3, 5-dinitrobenzoate was prepared by the action of 3, 5-dinitrobenzoyl chloride on namakochrome-trimethyl ether. By carrying out this process in the presence of pyridine, there were obtained lemon yellow prisms, melting at 218~220°C. Its analytical composition is in agreement with a formula $C_{11}H_3O_3\cdot(OCH_3)_3[C_6H_3(NO_2)_2(COO)]_2$. The fact that namakochrome-trimethyl ether reacted with two molecular equivalents of 3, 5-dinitrobenzoyl chloride suggests, that the positions for the 3, 5-dinitrobenzoyl groups in the naphthalene nucleus should be at 5 and 8. The functional group at 2-position of the naphthalene nucleus might be a methoxyl group because of its resistance to both of the acetylation[1] and the 3, 5-dinitrobenzoylation. A qualitative detection of the methoxyl group in namakochrome was then made. In the alkoxyl microapparatus of Zeisel, namakochrome was treated with hydriodic acid as usual. The resulting vapor was passed through a bubbler which contained a mixed aqueous solution of sodium thiosulfate and cadmium sulfate, and then swept into a 10% alcoholic solution of dimethylaniline. Thus, it was possible to isolate trimethyl phenyl ammonium iodide, colorless plates, subliming at 216°C. This showed a methoxyl group to be present in namakochrome. The quantitative determination was then carried out by the same method, and namakochrome had shown an average value of 9.26% for the methoxyl group content (calcd. for III or IV: $CH_3O$, 11.6%). Similarly the determination was effected on a few derivatives of namakochrome described in the previous paper[1] and in this paper. A pentaacetyl-derivative[1] was found to show the methoxyl group content of 4.42% (calcd. for V and VI: $CH_3O$, 6.5%).

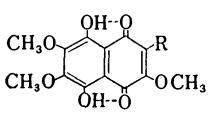


V



VI

The result for trimethyl ether of namakochrome was 37.38% of the methoxyl group content (calcd. for VII: $4CH_3O$, 40.0%, and for VIII: $3CH_3O$, 30.0%), and then for the leuco-acetyl derivative was found the methoxyl group content of 23.38% (calcd. for IX: $4CH_3O$, 25.81%, and for X: $3CH_3O$, 19.24%).

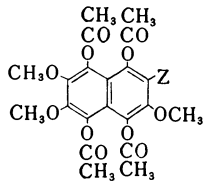


VII, R=-$OCH_3$,
VIII, R=-$CH_2OH$.

* "Pigments of Marine Animals", X. IX of this series; This Bulletin, 33, 453 (1960).

** Present address, Yoshitomi Pharmaceutical Industries, Ltd. Yoshitomi Factory, Yoshitomi-cho, Chikujo-gun, Fukuoka-ken.

1) This Bulletin, 33, 453 (1960).



IX, Z=-$OCH_3$,

X, Z=-$CH_2OH$.

From these experimental results, it is considered to be very likely that the structure of namakochrome is 2-methoxy-3, 6, 7-trihydroxy-naphthazarin (beta-position in I or II : methoxyl group)***. Although many compounds which contain methoxyl groups have been known as plant components, the author has been unable to find in the literature any reports on the marine-animal pigments, especially on naphthoquinone-derivatives, which contain methoxyl groups. This must be, therefore, the first time, that the pigment containing a methoxyl group is isolated from the marine animal.

## Experimental

**Reductive Acetylation of Namakochrome-trimethyl Ether.**—To a solution of 55 mg. of namakochrome-trimethyl ether in 1 g. of acetic anhydride and 1.5 g. of anhydrous pyridine was added 500 mg. of zinc dust, and shaken at room temperature until the solution becomes colorless. But the colorless solution soon acquired a yellow color and finally an orange yellow color. The colored reaction mixture, after setting overnight and removal of zinc dust, was poured into ice-water and extracted with several portions of benzene. The yellow benzene layer was washed with dilute hydrochloric acid solution and with water. The resulting colorless benzene solution was then dried with sodium sulfate. Removal of all solvent under the diminished pressure left 72 mg. of a pale yellow colored residue. It was purified by recrystallization from ethanol ; colorless prisms, m. p. 226~227°C.

Found : C, 55.26 ; H, 5.22 ; $CH_3O$-, 23.38 ; $CH_3CO$-, 35.27. Calcd. for $C_{22}H_{24}O_{12}$ : C, 55.00 ; H, 5.01 ; $CH_3O$-, 25.81 ; $CH_3CO$-, 35.87%.

**5, 8-Di-(3', 5'-dinitrobenzoyl)-namakochrome-trimethyl Ether.**—40 mg. of namakochrome was dissolved in 10 ml. of hot anhydrous pyridine. To the crimson-colored solution, about 55 mg. of finely pulverized 3, 5-dinitrobenzoyl chloride was added at room temperature, and the reaction mixture was gently shaken. The color changed through yellow to orange red. After an hour, the mixture was poured into ice-water and extracted with benzene. The orange red benzene layer was washed with dilute hydrochloric acid solution, followed by dilute sodium carbonate solution and water. The orange red benzene solution was dried with sodium sulfate, and concentrated to a small volume under reduced pressure. The concentrate was filtered through a calcium carbonate column (3×15 cm.). The orange eluate was evaporated to dryness under reduced pressure, and there was obtained an orange-yellow pasty product which was recrystallized (acetone-ethanol=2 : 1) to afford 66 mg. of the 3, 5-dinitrobenzoate, lemon yellow prisms, m. p. 218~220°C.

Found : C, 48.41 ; H, 3.09 ; N, 7.70. Calcd. for $C_{28}H_{18}O_{18}N_4$ : C, 48.15 ;H, 2.60 ; N, 8.02%.

I am deeply indebted to Professor Dr. Tokuichi Tsumaki for his continuing interest in this work and particularly for his suggestions. The microanalyses were carried out under Mr. Michio Shido and Miss. Sachiko Indo, to whom I extend my thanks. The expenses of the work were partially covered by a scientific Research Grant of the Ministry of Education.

*Department of Chemistry*
*Faculty of Science*
*Kyushu University*
*Hakozaki, Fukuoka*

*** That tautomerisation of this type readily occurs had been synthetically demonstrated[2] in the case of methyl-naphthazarin, which was prepared (a) by condensing maleic anhydride with toluquinol and (b) by condensing citraconic anhydride with quinol, and the two products were identical.

2) A. K. Macbeth et al., *J. Chem. Soc.*, 1935, 333.

# *The Kinetics of Substitution Reactions Involving Metal Complexes. IV. Reaction between Lead and Zinc-Ethylenediaminetetraacetate Complexes in Aqueous Solutions*

By Nobuyuki TANAKA and Kiyoko KATO*

(Received February 22, 1960)

The substitution reaction of lead ions and zinc-ethylenediaminetetraacetate (EDTA) complexes was investigated by Bril, Bril and Krumholz[1]. The rate of the reaction was followed by measuring the change of the polarographic diffusion current of lead ions with time in acetate buffer solutions using the streaming mercury electrode. The reaction was found to proceed, under the experimental conditions, through three different reaction paths simultaneously, and the rate constants of several reactions were determined.

Although Bril et al.[1] measured the reaction rate in acetate buffer solutions, they did not take consideration of the effect of acetate ions on the reaction rate. Recently, the present authors[2,3] dealt with the substitution reaction of copper ions and lead-EDTA complexes and that of copper ions and zinc-EDTA complexes, and explained the decrease of the reaction rate with increasing concentration of acetate by assuming that the substitution reaction proceeds only through the hydrated metal ions.

In this situation it seems worth while to reinvestigate the substitution reaction of lead ions and zinc-EDTA complexs from the same viewpoint as given in the previous papers[2,3].

## Experimental

The preparation of the solutions of lead nitrate, zinc nitrate and disodium ethylenediaminetetraacetate was described in the previous papers[3,4].

The rate of the reaction between lead ions and zinc-EDTA complexes was followed by measuring the change of the polarographic diffusion current of lead ions with time in acetate buffer solutions. Current-time curves were obtained with a Shimadzu RP-2 pen-recording polarograph and a dropping mercury electrode. The latter was the same as described in the previous papers[2-4] and had an $m$ value of 1.27 mg./sec. and a drop time of 3.69 sec. in an air-free 0.1 M potassium chloride solution at 25°C with open circuit.

Measurements were made at 15 and 25°C in acetate buffers of pH 4.8 to 5.7 which contained 0.1 M of sodium acetate. The ionic strength was adjusted to be 0.2 with potassium nitrate, unless otherwise stated. Gelatin was added as a maximum suppressor by 0.01% in concentration.

## Results and Discussion

In the solution containing acetate ions less than 0.2 M in concentration, lead(II) forms mono- and diacetato complexes, whereas zinc(II) forms only a monoacetato complex[5]. Therefore, the overall substitution reaction of lead ions and zinc-EDTA complexes in acetate buffer solutions is represented with the equations

$$\begin{aligned} Pb^{2+} + 2\,OAc^- &\rightleftharpoons PbOAc^+ + OAc^- \\ &\rightleftharpoons Pb(OAc)_2 \end{aligned} \quad (1)$$

$$Pb^{2+} + ZnY^{2-} \rightleftharpoons PbY^{2-} + Zn^{2+} \quad (2)$$

$$Zn^{2+} + OAc^- \rightleftharpoons ZnOAc^+ \quad (3)$$

where $Y^{4-}$ means a completely dissociated EDTA anion. Under the condition that both zinc ions and zinc-EDTA complexes are present in a large excess over lead ions, the substitution reaction 2 can be treated simply as

$$Pb^{2+} \underset{k^-}{\overset{k^+}{\rightleftharpoons}} PbY^{2-} \quad (4)$$

The rate equation for the reaction 4 is expressed as[2]

$$-\frac{d[Pb^{2+}]_{app}}{dt} = k^+[Pb^{2+}]_{app} - k^-[PbY^{2-}] \quad (5)$$

where $[Pb^{2+}]_{app}$ is the concentration of lead ions that can be determined polarographically, and given by the equation

$$\begin{aligned} [Pb^{2+}]_{app} = {} & [Pb^{2+}] + [PbOAc^+] \\ & + [Pb(OAc)_2] \end{aligned} \quad (6)$$

Integrating Eq. 5,

$$\begin{aligned} \ln\{[Pb^{2+}]_{app} - [Pb^{2+}]_{e,app}\} &= -(k^+ + k^-)t \\ &+ \ln\{[Pb^{2+}]_{0,app} - [Pb^{2+}]_{e,app}\} \end{aligned}$$

is obtained, where subscripts o and e denote

* Present addess; The Women's Department, Tokyo College of Pharmacy, 31, Uenosakuragi-cho, Taito-ku, Tokyo.

1) K. Bril, S. Bril and P. Krumholz, *J. Phys. Chem.*, **59**, 596 (1955); **60**, 251 (1956).

2) N. Tanaka and K. Kato, This Bulletin, **32**, 1376 (1959).

3) K. Kato, ibid., **33**, 600 (1960).

4) N. Tanaka, K. Kato and R. Tamamushi, ibid., **31**, 283 (1958).

5) N. Tanaka and K. Kato, This Bulletin, **33**, 417 (1960).

the initial and the equilibrium condition, respectively. At the equilibrium of the reaction, the relation

$$\frac{k^+}{k^-}=\frac{[PbY^{2-}]_e}{[Pb^{2+}]_{e,app}}\doteqdot K^{Pb}_{Zn,app}\frac{[ZnY^{2-}]_0}{[Zn^{2+}]_{0,app}}$$

may be satisfied, where $K^{Pb}_{Zn,app}$ represents the apparent equilibrium constant expressed as

$$K^{Pb}_{Zn,app}=\frac{[Zn^{2+}]_{e,app}[PbY^{2-}]_e}{[Pb^{2+}]_{e,app}[ZnY^{2-}]_e}$$

The values of $K^{Pb}_{Zn,app}$ were determined polarographically to be 9.0 at 15°C and 5.4 at 25°C in acetate buffer solutions which contained 0.1 M of sodium acetate.

The apparent rate constant, $k^+/[ZnY^{2-}]_0$, was obtained at varied pH's at two different concentrations of zinc ions but at the same concentrations of other species. The values obtained were plotted against the hydrogen ion concentration. The plots obtained for 15°C are given in Fig. 1, which clearly indicate linear relations existing between $k^+/[ZnY^{2-}]_0$ and $[H^+]$. Similar relations were also found at 25°C.

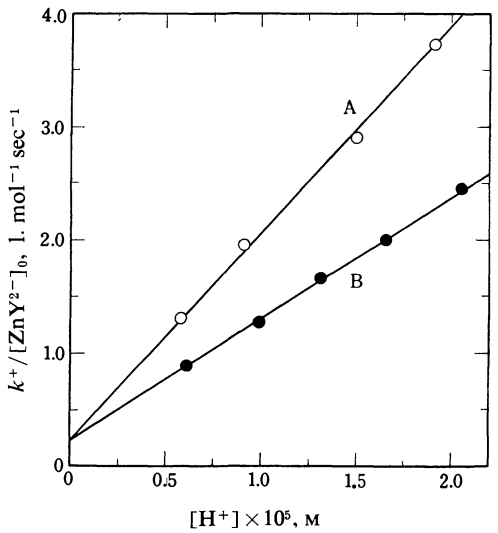



Fig. 1. $k^+/[ZnY^{2-}]_0$ as a function of the hydrogen ion concentration in acetate buffer-potassium nitrate solutions of ionic strength 0.2 at 15°C. Initial concentrations are: $[Pb^{2+}]_{0,app}=1.60\times10^{-4}$ M; $[ZnY^{2-}]_0=5.04\times10^{-3}$ M; $[Zn^{2+}]_{0,app}=5.10\times10^{-3}$ M (curve A) and $1.02\times10^{-2}$ M (curve B). Concentrations of free acetate are: 0.098 M (A) and 0.096 M (B).

According to Bril, Bril and Krumholz[1], the substitution reaction between lead ions and zinc-EDTA complexes is supposed to proceed simultaneously through the following three reaction paths:

$$\text{(i)}\quad Pb^{2+}+ZnY^{2-}\rightleftharpoons PbY^{2-}+Zn^{2+} \quad (7)$$

$$\text{(ii)}\quad ZnY^{2-}+H^+\rightleftharpoons ZnHY^- \quad (8a)$$

$$Pb^{2+}+ZnHY^-\rightleftharpoons PbHY^-+Zn^{2+} \quad (8b)$$

$$PbHY^-\rightleftharpoons PbY^{2-}+H^+ \quad (8c)$$

$$\text{(iii)}\quad ZnY^{2-}+H^+\rightleftharpoons Zn^{2+}+HY^{3-} \quad (9a)$$

$$Pb^{2+}+HY^{3-}\rightleftharpoons PbY^{2-}+H^+ \quad (9b)$$

In the polarographic measurement in acetate media, the concentration of lead ions that is actually measured polarogrphically is not the concentration of hydrated lead ions but the sum of the concentrations of hydrated ions and acetato complexes[2]. Therefore, if it is assumed that the substitution reaction proceeds only through the hydrated ions which are in equilibrium with the acetato complexes, the apparent rate of the forward reaction ($v^+=k^+[Pb^{2+}]_{app}$) determined polarographically is represented by Eq. 10[2,3].

$$v^+=k^+[Pb^{2+}]_{app}=\left\{\frac{k_1^++k_2^+[H^+]+k_3^+[H^+]\dfrac{1+K_{ZnOAc}[OAc^-]}{[Zn^{2+}]_{app}}}{1+\sum_{n=1}^{2}K_{Pb(OAc)_n}[OAc^-]^n}\right\}\times[Pb^{2+}]_{app}[ZnY^{2-}] \quad (10)$$

In Eq. 10

$$\left.\begin{aligned}k_2^+&=k_{II}^+K^H_{ZnHY}\\k_3^+&=k_{III}^+/K_{ZnY}K_{HY}\end{aligned}\right\} \quad (11)$$

where $K^H_{ZnHY}$ represents the equilibrium constant of the reaction 8a, $K_{ZnY}$, the formation constant of $ZnY^{2-}$ and $K_{HY}$, the fourth dissociation constant of ethylenediaminetetraacetic acid. $K_{Pb(OAc)_n}$ and $K_{ZnOAc}$ represent the overall formation constants of acetatolead(II) and acetatozinc(II) complexes, respectively.

From Eq. 10, Eq. 12 is obtained, where the initial concentrations, $[Zn^{2+}]_0$ and $[ZnY^{2-}]_0$, are substituted for $[Zn^{2+}]$ and $[ZnY^{2-}]$,

$$\frac{k^+}{[ZnY^{2-}]_0}=\frac{k_1^++k_2^+[H^+]+k_3^+[H^+]\dfrac{1+K_{ZnOAc}[OAc^-]}{[Zn^{2+}]_{0,app}}}{1+\sum_{n=1}^{2}K_{Pb(OAc)_n}[OAc^-]^n} \quad (12)$$

respectively. Since both $Zn^{2+}$ and $ZnY^{2-}$ are present in the reaction mixture in a large excess over concentration of lead ions, the change of their concentrations during the reaction can be neglected.

The rate constants in Eq. 10 were calculated from the plots of $k^+/[ZnY^{2-}]_0$ against the hydrogen ion concentration, which are tabulated in Table I. The formation constants of acetatolead(II) and acetatozinc(II) complexes which were used in the calculation are those that were determined polarographically at ionic strength 0.2 at 15 and 25°C[5]. The concentration of uncomplexed acetate in the solution was calculated by successive approximation.

The rate constants of both elementary reactions 8b and 9b were calculated from the relations given in Eqs. 11, using the values of $K^{H}_{ZnHY}$, $K_{ZnY}$ and $K_{HY}$ which were obtained with the same procedure as described previously[3,4] and are given in Table II. The rate constants of three elementary reactions 7, 8b and 9b thus calculated are summarized in Table III.

TABLE I. RATE CONSTANTS IN EQ. 10 OBTAINED EXPERIMENTALLY AT IONIC STRENGTH 0.2 AT VARIOUS TEMPERATURES

| Temp., °C | Rate constant, l. mol$^{-1}$ sec$^{-1}$ | | |
|---|---|---|---|
| | $k_1^+$ | $k_2^+$ | $k_3^+$ |
| 15 | 4.6 | $6\times10^5$ | $1.1\times10^4$ |
| 25 | 8.9 | $9\times10^5$ | $2.4\times10^4$ |

TABLE II. EQUILIBRIUM CONSTANTS AT IONIC STRENGTH 0.2 AT VARIUS TEMPERATURES

| Temp., °C | log $K_{ZnY}$ | p$K_{HY}$ | log $K^{H}_{ZnHY}$ |
|---|---|---|---|
| 15 | 16.17 | 10.20 | — |
| 20 | — | — | 2.9 |
| 25 | 15.94 | 10.04 | — |

TABLE III. RATE CONSTANTS FOR REACTIONS 7, 8b AND 9b AT IONIC STRENGTH 0.2 AT VARIOUS TEMPERATURES

| Temp., °C | Rate constant, l. mol$^{-1}$ sec$^{-1}$ | | |
|---|---|---|---|
| | $k_1^+$ | $k_{II}^+$ | $k_{III}^+$ |
| 15 | 4.6 | $8\times10^2$ | $1.0\times10^{10}$ |
| 25 | 8.9 | $1\times10^3$ | $1.9\times10^{10}$ |

From these results, the rate constants expressed in the form of the Arrhenius equation were derived and the heats of activation and entropies of activation were calculated for three elementary reactions 7, 8b and 9b. The results are given in Table IV.

Bril et al. determined the rate constants of this substitution reaction in acetate buffer solutions of ionic strength 1.0 containing 0.1 M acetate at 25°C[1], but they took no account of the effect of acetate ion on the reaction rate. Therefore, the rate constants reported by Bril et al., $R_1$, $R_2$ and $R_3$[6], correspond to those given by the equations,

$$R_1=\frac{k_1^+}{1+\sum_{n=1}^{2}K_{Pb(OAc)_n}[OAc^-]^n}$$

$$R_2=\frac{k_2^+}{f_H\{1+\sum_{n=1}^{2}K_{Pb(OAc)_n}[OAc^-]^n\}} \qquad (13)$$

$$R_3=\frac{k_3^+\{1+K_{ZnOAc}[OAc^-]\}}{f_H\{1+\sum_{n=1}^{2}K_{Pb(OAc)_n}[OAc^-]^n\}}$$

where $f_H$ means the activity coefficient of hydrogen ions. Since the values of $K_{PbOAc}$, $K_{Pb(OAc)_2}$, $K_{ZnOAc}$, $K^{H}_{ZnHY}$, $K_{ZnY}$ and $K_{HY}$ and $f_H$ are all unknown at ionic strength 1.0 at 25°C, it seems impossible to calculate the rate constants $R_1$, $R_2$ and $R_3$ in Eq. 13, using the values of $k_1^+$, $k_2^+$ and $k_3^+$ obtained in this study.

In the measurement of the reaction rate, Bril et al. employed the streaming mercury electrode. They stated that the streaming electrode had an advantage over the conventional dropping mercury electrode when used as an indicator electrode for kinetic measurements. However, the diffusion current obtained with the streaming mercury electrode was considered less accurate and less reproducible than that obtained with the dropping mercury electrode. For comparison, therefore, the measurements were made under the same condition as Bril et al.'s but with the dropping mercury electrode, and the values of $R_1$, $R_2$ and $R_3$ were determined with the same procedure as mentioned above. The results are given in Table V and compared with the values reported by Bril et al. An agreement between both results seems to indicate no significant discrepancy between the two methods[7].

TABLE IV. RATE CONSTANTS, HEATS OF ACTIVATION AND ENTROPIES OF ACTIVATION FOR REACTIONS 7, 8b AND 9b

| Reaction | Rate constant, expressed in l. mol$^{-1}$ sec$^{-1}$ | $\Delta H^{\ddagger}$, kcal. mol$^{-1}$ | $\Delta S^{\ddagger}$, e. u. |
|---|---|---|---|
| $Pb^{2+} + ZnY^{2-} \rightarrow PbY^{2-} + Zn^{2+}$ | $k_1^+ = 1.1\times10^9 \exp(-11,000/RT)$ | 10 | −19 |
| $Pb^{2+} + ZnHY^{-} \rightarrow PbHY^{-} + Zn^{2+}$ | $k_{II}^+ = 9.3\times10^7 \exp(-6,700/RT)$ | 6.1 | −24 |
| $Pb^{2+} + HY^{3-} \rightarrow PbY^{2-} + H^+$ | $k_{III}^+ = 1.2\times10^{18} \exp(-11,000/RT)$ | 10 | 22 |

6) $R_1$, $R_2$ and $R_3$ correspond to $k_0^+$, $k_1^+$ and $k_2^+$, respectively, given in the first paper of Bril, Bril and Krumholz[1].

7) The values of $R_2$ are considerably less accurate than those of $R_1$ and $R_3$[4].

TABLE V. RATE CONSTANTS EXPRESSED IN EQS. 13 OBTAINED EXPERIMENTALLY AT IONIC STRENGTH 1.0 AT 25°C

| | Rate constant, l. $mol^{-1}$ $sec^{-1}$, obtained | |
|---|---|---|
| | by Bril et al. | by the present authors |
| $R_1$ | 0.34 | 0.30 |
| $R_2$ | $2\times10^4$ | $8\times10^4$ |
| $R_3$ | $1.1\times10^3$ | $1.5\times10^3$ |

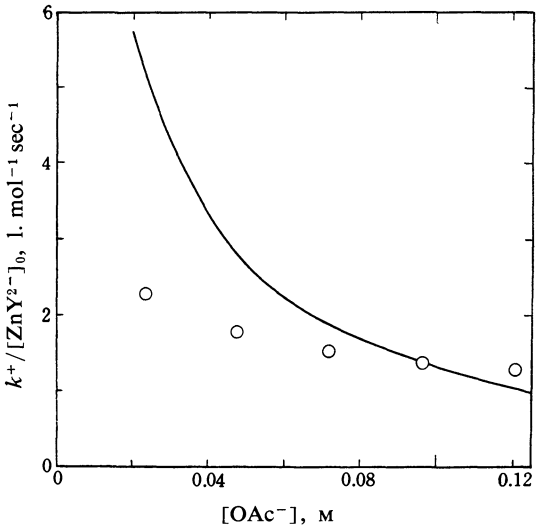



Fig. 2. $k^+/[ZnY^{2-}]_0$ as a function of the acetate concentration in acetate buffer-potassium nitrate solutions of pH 5.09 and ionic strength 0.2 at 15°C. Initial concentrations are: $[Pb^{2+}]_{0,app}=1.65\times10^{-4}$ M; $[ZnY^{2-}]_0=5.00\times10^{-3}$ M; $[Zn^{2+}]_{0,app}=1.00\times10^{-2}$ M. —— indicates the theoretical curve and ○, the experimental value.

From Eq. 10, it is predicted that the reaction rate decreases with increasing concentrations of acetate ions. Using Eq. 12, the values of $k^+/[ZnY^{2-}]_0$ were calculated at various acetate concentrations with the rate constants given in Table I and the formation constants of the acetato complexes. They are plotted against the acetate ion concentration as shown in Fig. 2. The overall rate constants ($k^+/[ZnY^{2-}]_0$) were actually measured at varied acetate concentrations under the conditions in which the theoretical values were calculated. They are also given in Fig. 2. Both the calculated and the experimental values increase with decreasing concentrations of aetate. The discrepancy existing between the calculated and experimental values is considered probably to be due to the contribution of the reaction in which acetato complexes participate.

## Summary

The kinetic study of the substitution reaction of lead ions and zinc-EDTA complexs in acetate buffer solutions has been carried out with the same procedure as that reported previously[2-4]. Under the experimental conditions, the reaction is found to proceed simultaneously through three different reaction paths, and the rate constants for three elementary reactions of those reaction paths are determined at ionic strength 0.2 at 15 and 25°C. The heats of activation and the entropies of activation for the three elementary reactions are calculated.

The authors thank the Ministry of Education for the financial support granted for this research. Part of the experimental work has been carried out with the assistance of Dr. Gen Satô.

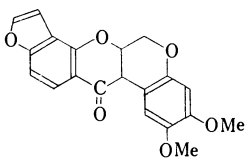
*Department of Chemistry*
*Faculty of Science*
*Tohoku University*
*Katahira-cho, Sendai*

# *Synthetic Studies on the Benzofuran Derivatives. VI. Synthesis of Furano(2'', 3'' : 7, 8)-2'-methoxy-isoflavone Derivatives*

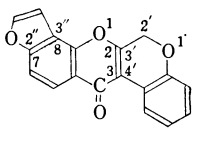
By Yoshiyuki KAWASE, Kiyomi OGAWA, Setsuko MIYOSHI and Kenji FUKUI*

(Received February 15, 1960)

The structure of elliptone, the simplest member of rotenoids, has been established[1] to be a dimethoxy derivative of furano-chromano-chromanone (I), but the synthesis of it and other rotenoids** is not yet achieved. Many efforts have hitherto been made on the synthesis of rotenoids, and recently the total synthesis of dihydrorotenone has been accomplished by Miyano and Matsui[2], who succeeded in the reduction of the chromenochromone system to give the chromanochromanone system. Therefore, it seems desirable for the synthesis of elliptone to prepare the furano-chromenochromone system, from which the furano-chromanochromanone system may be derived by reduction. For the preparation of chromenochromones, two methods are available



I

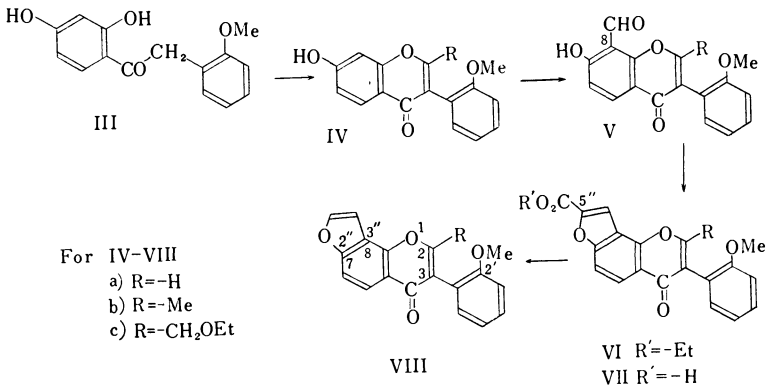


II

—those are (a) by chromenochromone-ring formation of phenoxyacetic acid-2-(*o*-hydroxy)-acetophenones[3] and (b) by chromen-ring formation of 2-methyl[4] or 2-ethoxymethyl[5] derivatives of 2'-methoxy-isoflavones.

Following the latter method, the authors attempted to synthesize furano(2'', 3'' : 7, 8)-chromeno(3', 4' : 2, 3)chromone (II), and in this paper describe the preparation of three intermediate derivatives (VIIIa, b, c) of furano (2'', 3'' : 7, 8)-2'-methoxy-isoflavone.

Starting from three isoflavones (IVa, b, c), furan-ring was built up on the 7, 8-position of them smoothly by a similar method reported in the previous papers[6] as follows : the isoflavones IVa, b, c were formulated by the hexamine method to give 8-formyl derivatives (Va, b, c), which were converted into $\alpha$-ethoxycarbonyl-furano derivatives (VIa, b, c) by the action of ethyl bromomalonate and potassium carbonate in acetone. Hydrolysis of the esters VIa, b, c under mild alkaline condition (aqueous sodium carbonate in acetone) furnished the corresponding acids VIIa, b, c which were decarboxylated in quinoline with the aid of copper catalyst



For IV-VIII
a) R=-H
b) R=-Me
c) R=-$CH_2OEt$

III IV V VI R'=-Et VII R'=-H VIII

* Present adress: Faculty of Science, Hiroshima University, Hiroshima.

1) S. H. Harper, *J. Chem. Soc.*, **1939**, 1099, 1424; ibid., **1942**, 587.

** Recentry, total synthesis of *dl*-deguelin has been reported by H. Fukami, J. Oda, G. Sakata and M. Nakajima (*Bull. Agr. Chem. Soc. Japan*, **24**, 327 (1960)). (added in proof).

2) M. Miyano und M. Matsui, *Chem. Ber.*, **91**, 2044 (1958); ibid., **92**, 2487 (1959); M. Matsui und M. Miyano, *Proc. Japan Acad.*, **35**, 175 (1959).

3) A. Robertson, *J. Chem. Soc.*, **1933**, 489, 1163.

4) T. R. Seshadri and S. Varadarajan, *Proc. Indian Acad. Sci.*, **37A**, 784 (1953).

5) A. C. Mehta and T. R. Seshadri, ibid., **42A**, 192 (1955).

6) T. Matsumoto, Y. Kawase, M. Nanbu and K. Fukui, This Bulletin, **31**, 688 (1958); K. Fukui and Y. Kawase, ibid., **31**, 693 (1958).

to give furano(2'', 3'' : 7, 8)-2'-methoxy-isoflavone*** (VIIIa), furano(2'', 3'' : 7, 8)-2'-methoxy-2-methylisoflavone (VIIIb) and furano-(2'', 3'' : 7, 8)-2'-methoxy-2-ethoxymethylisoflavone (VIIIc) respectively. Attempts to prepare II from VIIIb or VIIIc are now in progress.

## Experimental[7]

**2, 4-Dihydroxyphenyl 2-Methoxybenzyl Ketone (III).**—This ketone was prepared from resorcinol and *o*-methoxyphenylacetonitrile by the Hoesch reaction[4] or more conveniently from resorcinol and *o*-methoxy-phenylacetic acid by means of boron trifluoride[8]. M. p. 158~159°C (reported m. p. 159~160°C[4]).

**7-Hydroxy-2'-methoxy-isoflavone (IVa).**—A mixture of the ketone III (10 g.), ethyl orthoformate (20 ml.), piperidine (4 ml.) and pyridine (80 ml.) was refluxed for 8 hr. in an oil-bath. The resulting solution was cooled and acidified with dilute hydrochloric acid. The crystals formed were recrystallized from ethanol to give IVa, m. p. 226.5~227.5°C (reported m. p. 230~232°C[9]), having negative ferric reaction in ethanol; yield 6.6 g.

**7-Hydroxy-2'-methoxy-8-formyl-isoflavone (Va).**—A mixture of the isoflavone IVa (6 g.), hexamine (32 g.) and acetic acid (100 ml.) was heated in an oil bath (100°C) for 6 hr. The resulting hot solution was treated with hot dilute hydrochloric acid (1 : 1, 100 ml.) and again heated for 10 min., then allowed to stand overnight. The precipitates were collected, washed with water and dissolved in benzene, and the benzene solution was extracted with dilute aqueous sodium hydroxide. The product obtained by acidifying the alkaline solution was recrystallized from ethanol to give Va in faintly yellow colored microcrystals, m. p. 187~189°C, having a red ferric reaction in ethanol; yield 2.1 g.

Found: C, 68.40; H, 4.25. Calcd. for $C_{17}H_{12}O_5$: C, 68.92; H, 4.05%.

**7-Hydroxy-2'-methoxy-8-formyl-2-methylisoflavone (Vb).**—By the similar method as described for Va, 1.3 g. of Vb was obtained from 7-hydroxy-2'-methoxy-2-methylisoflavone[4] (IVb, m. p. 222~223°C, 3 g.), hexamine (16 g.) and acetic acid (50 ml.); m. p. 165.5~166.5°C (from ethanol) faintly yellow colored microcrystals, having a red ferric reaction in ethanol.

Found: C, 69.18; H, 4.67. Calcd. for $C_{18}H_{14}O_5$: C, 69.68; H, 4.52%.

**7-Hydroxy-2'-methoxy-8-formyl-2-ethoxymethyl-isoflavone (Vc).**—By the similar method, 1 g. of Vc was obtained from 7-hydroxy-2'-methoxy-2-ethoxymethylisoflavone[5] (IVc, m. p. 163~164°C, 1.5 g.), hexamine (8 g.) and acetic acid (25 ml.); m. p. 129~130°C (from 80% ethanol) faintly yellow colored microcrystals, having a red ferric reaction in ethanol.

Found: C, 68.04; H, 5.24. Calcd. for $C_{20}H_{18}O_6$: C, 67.79; H, 5.12%.

**5''-Ethoxycarbonyl-furano(2'',3'':7,8)-2'-methoxy-isoflavone (VIa).**—To a solution of the formyl-isoflavone Va (2 g.) and ethyl bromomalonate (2.2 g.) in anhydrous acetone (65 ml.) was added anhydrous potassium carbonate (7.8 g.), and the mixture was refluxed for 8 hr. in a steam bath. The resulting solution was filtered from precipitates and the solvent was distilled off. The residual oily product was recrystallized from ethanol to give VIa, m. p. 164.5°C, having a negative ferric reaction; yield 1.1 g.

Found: C, 69.12; H, 4.50. Calcd. for $C_{21}H_{16}O_6$: C, 69.23; H, 4.40%.

**5''-Ethoxycarbonyl-furano(2'',3'':7,8)-2'-methoxy-2-methylisoflavone (VIb).**—By the similar method as described for VIa, 1.2 g. of VIb was obtained from the formyl-isoflavone Vb (2 g.), ethyl bromomalonate (2.2 g.) and potassium carbonate (7.8 g.); m. p. 161.5~162.5°C (from ethanol), having a negative ferric reaction.

Found: C, 69.97; H, 4.96. Calcd. for $C_{22}H_{18}O_6$: C, 69.84; H, 4.76%.

**5''-Ethoxycarbonyl-furano(2'',3'':7,8)-2'-methoxy-2-ethoxymethylisoflavone (VIc).**—By the similar method, 1 g. of VIc was obtained from the formyl-isoflavone Vc (1.5 g.), ethyl bromomalonate (1.7 g.) and potassium carbonate (6 g.); m. p. 177.5~178.5°C (from ethanol), having a negative ferric reaction.

Found: C, 68.55; H, 5.33. Calcd. for $C_{24}H_{22}O_7$: C, 68.24; H, 5.25%.

**5''-Carboxy-furano(2'', 3'' : 7, 8)-2'-methoxy-isoflavone (VIIa).**—A mixture of the ester VIa (0.8 g.), acetone (40 ml.) and 5% aqueous sodium carbonate (30 ml.) was refluxed for 3 hr. Dilute hydrochloric acid (20 ml.) was added to the resulting mixture, and acetone was distilled off. The precipitates were collected and recrystallized from ethanol; m. p. 273.5~274°C, having a negative ferric reaction; yield 0.6 g.

Found: C, 67.83; H, 3.65. Calcd. for $C_{19}H_{12}O_6$: C, 67.86; H, 3.57%.

**5''-Carboxy-furano(2'', 3'' : 7, 8)-2'-methoxy-2-methylisoflavone (VIIb).**—By the similar method as described for VIIa, 1.1 g. of VIIb was obtained from the ester VIb (1.2 g.), acetone (50 ml.) and 5% aqueous sodium carbonate (50 ml.); m. p. 294°C (from ethanol), having a negative ferric reaction.

Found: C, 68.41; H, 4.02. Calcd. for $C_{20}H_{14}O_6$: C, 68.57; H, 4.00%.

**5''-Carboxy-furano(2'', 3'' : 7, 8)-2'-methoxy-2-ethoxymethylisoflavone (VIIc).**—By the similar method, 0.3 g. of VIIc was obtained from the ester VIc (0.5 g.), acetone (20 ml.) and 5% aqueous sodium carbonate (20 ml.); m. p. 233~234°C (from ethanol), having a negative ferric reaction.

Found: C, 67.21; H, 4.57. Calcd. for $C_{22}H_{18}O_7$: C, 67.00; H, 4.60%.

**Furano(2'',3'' : 7,8)-2'-methoxy-isoflavone (VIIIa).**—A mixture of the acid VIIa (0.5 g.), copper powder (0.3 g.) and quinoline (20 ml.) was heated while stirring in an atmosphere of nitrogen for 20 min.

*** It has recently been reported that munetone is 5''-isopropyl derivative of VIIIa by N. L. Dutta (*J. Indian Chem. Soc.*, 36, 165 (1959)).

7) Melting points are uncorrected, and the products are colorless microcrystals unless otherwise noted.

8) Private communication from H. Fukami of the Agricultural Department of Kyoto University.

9) P. K. Grover and T. R. Seshadri, *Proc. Indian Acad. Sci.*, 38A, 122 (1953).

at 190~200°C until evolution of carbon dioxide ceased. Quinoline was distilled off by steam-distillation, and the residual product was dissolved in ethyl acetate, filtered from copper, and washed with dilute sulfuric acid and dilute aqueous sodium hydroxide. Evaporation of ethyl acetate gave VIIIa, m. p. 182°C (from ethyl acetate and then from ethanol), having a negative ferric reaction; yield 0.3 g.

Found: C, 74.04; H, 4.20. Calcd. for $C_{18}H_{12}O_4$: C, 73.97; H, 4.11%.

**Furano(2'',3'':7,8)-2'-methoxy-2-methylisoflavone (VIIIb).**—By the similar method as described for VIIIa, 0.6 g. of VIIIb was obtained from the acid VIIb (1 g.), copper powder (0.5 g.) and quinoline (35 ml.); m. p. 168°C (from ethyl acetate and then from ethanol), having a negative ferric reaction.

Found: C, 74.33; H, 4.64. Calcd. for $C_{19}H_{14}O_4$: C, 74.51; H, 4.58%.

**Furano(2'', 3'' : 7, 8)-2'-methoxy-2-ethoxymethylisoflavone (VIIIc).**—By the similar method, 0.5 g. of VIIIc was obtained from the acid VIIc (1 g.), copper powder (0.5 g.) and quinoline (35 ml.); m. p. 119~120°C (from ethyl acetate and then from ethanol), having a negative ferric reaction.

Found: C, 72.18; H, 5.21. Calcd. for $C_{21}H_{18}O_5$: C, 71.99; H, 5.18%.

The authors are grateful to the Faculty of Pharmacy of this University for microanalyses, and the cost of this research was partly defrayed from the Research Grant of the Ministry of Education, to which the author's thanks are also due.

*Faculty of Literature and Science*
*Toyama University*
*Hasumachi, Toyama*

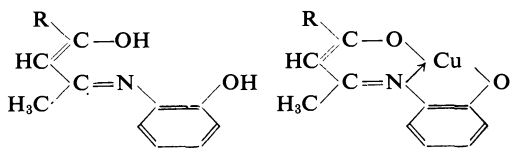
# *Metal Complexes with Terdentate Ligands. II*[1]. *Synthesis and Properties of Tri-coordinated Copper(II) Complexes*[2]

By Yoneichiro MUTO

(Received February 13, 1960)

So-called tri-coordinated copper(II) complexes have been reported by several investigators. For instance, Pfeiffer et al.[3] have prepared salicylaldehyde-2-hydroxyanil copper(II), while Yamaguchi[4], Dikmen et al.[5] and the present author[6] have synthesized salicylaldehyde-2-hydroxybenzylimine copper(II). Although it is presumed that the copper atoms in these chelates have an unusual coordination number, three, it is desirable to study extensively tri-coordinated copper(II) complexes having different types of ligand molecules in order to obtain more definite information about the tri-coordination of the copper atoms. This paper presents the synthesis and properties of some tri-coordinated copper(II) complexes.

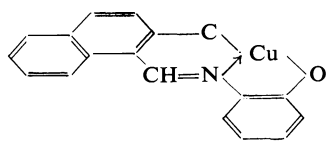
**I. Copper(II) Complexes having Schiff Bases of 2-Aminophenol.**—In order to obtain terdentate ligands of similar type to salicylaldehyde-2-hydroxyanil, the present author prepared acetylacetone-mono-(2-hydroxyanil) and benzoylacetone-mono-(2-hydroxyanil) by the condensation of 2-aminophenol with acetylacetone and benzoylacetone, respectively. It is expected that they act as terdentate ligands in their enol forms shown in A′ and B′. That is to say, they have two hydrogen atoms capable of being replaced by metal atoms (i. e., hydrogen



A′ R: $CH_3$
B′ R: $C_6H_5$*



A R: $CH_3$
B R: $C_6H_5$



C

1) Y. Muto, This Bulletin, **31**, 1017 (1958).
2) This was presented partly in a previous paper (Y. Muto, *J. Chem. Soc. Japan, Pure Chem. Sec.* (*Nippon Kagaku Zasshi*), **76**, 1405 (1955).), and partly at the Symposium on Co-ordination Compounds held by the Chemical Society of Japan in Fukuoka on October 21, 1959.
3) P. Pfeiffer, Th. Hesse, G. Pfizner, W. Scholl and H. Thielert, *J. prakt. Chem.*, **149**, 217 (1937).
4) M. Yamaguchi, *J. Chem. Soc. Japan, Pure Chem. Sec.* (*Nippon Kagaku Zasshi*), **74**, 261 (1954).
5) C. Dikmen and T. Günduz, *Ber.*, **89**, 2637 (1956).
6) Y. Muto, *J. Chem. Soc. Japan, Pure Chem. Sec.* (*Nippon Kagaku Zasshi*), **74**, 274 (1953).

* It is known that primary amines condense with benzoylacetone to form Schiff bases having a general formula $C_6H_5CO\cdot CH_2C(=N-R)\cdot CH_3$. Therefore, benzoylacetone-mono-(2-hydroxyanil) must have the structure shown in B′, althogh it may be presumed that the anil has the structure, $C_6H_5C(=N-C_6H_4OH)\cdot CH_2CO\cdot CH_3$.

of the phenolic and enolic hydroxyl groups) as well as a nitrogen atom capable of being coordinated to a metal atom (i. e., nitrogen of an azomethine group). Therefore, they will react with copper(II) ion to form chelates having a five-membered ring and a six-membered one, which are very common. On being treated with copper(II) acetate, they yielded complexes having the compositions expected for the formulae A and B. Similarly, 2-hydroxynaphthaldehyde-(1)-[*o*-hydroxyanil] yielded a copper(II) complex having the composition shown in C.

These complexes were readily soluble in pyridine, slightly soluble in nitrobenzene, and soluble with difficulty in other common organic solvents. When these complexes were recrystallized from pyridine, the corresponding monopyridinates were formed. The pyridinates liberated pyridine gradually at 70°C and completely at 120°C. The decrease in weight corresponded to one molecule of pyridine per one atom of copper. From these facts, it seems very likely that these pyridine-free complexes have two interlocked chelate rings shown in A, B and C, although their structures might not be so simple as is implied by the ordinary chemical formulae. This conclusion has been suggested further by magnetochemical studies[7,8]. As the present author et al. have already reported in previous papers[7,8], these pyridine-free complexes show magnetic moments considerably smaller than the theoretical value predicted from the presence of one odd electron, and the subnormal moments suggest the presence of dimeric molecules, in which two copper atoms are very close to each other as in copper(II) acetate monohydrate crystals, whereas the pyridinates have the normal moments expected for tetra-coordinated copper(II) complexes (Table I).

It has been presumed by the method of ligand-exchange[9] that these tri-coordinated complexes are more stable than the tetra-coordinated complexes having ligands similar to A′ or B′ from the structural point of view, but that they are less stable than bis-8-oxyquinolin copper(II) or salicylaldehyde-ethylenediimine copper(II) (Table II). For instance, when an alcoholic solution of benzoylacetone-mono-(2-hydroxyanil) was mixed with an alcoholic solution of bis-salicylaldehydeanil copper(II), benzoylacetone-mono-(2-hydroxyanil) copper(II) was formed, whereas the reverse reaction of this exchange did not take place.

**II. Copper(II) Complexes Having Schiff Bases of Anthranilic Acid.** — These complexes were synthesized by essentially the same method as that described in I. Namely, anthranilic acid was subjected to condensation with 5-*X*-salicylaldehyde (*X*-: chloro-, bromo- or nitro-), and the resulting Schiff bases (Formula D′) were treated with copper(II) acetate. In this

TABLE I. THE MAGNETIC MOMENTS OF TRI-COORDINATED COPPER(II) COMPLEXES AND THEIR PYRIDINATES

| Chelates | $\mu$ (B. M.) | Reference |
|---|---|---|
| Salicylaldehyde-2-hydroxybenzylimine Cu(II) | 0.87 | 7 |
| Monopyridino-salicylaldehyde-2-hydroxybenzylimine Cu(II) | 1.83 | 7 |
| Salicylaldehyde-2-hydroxyanil Cu(II) | 1.34 | 7 |
| Monopyridino-salicylaldehyde-2-hydroxyanil Cu(II) | 1.84 | 7 |
| Acetylacetone-mono-(2-hydroxyanil) Cu(II) | 1.37 | 7 |
| Monopyridino-acetylacetone-mono-(2-hydroxyanil) Cu(II) | 1.81 | 7 |
| Benzoylacetone-mono-(2-hydroxyanil) Cu(II) | 1.11 | 7 |
| Monopyridino-benzoylacetone-mono-(2-hydroxyanil) Cu(II) | 1.84 | 7 |
| 2-Hydroxynaphthaldehyde-(1)-[*o*-hydroxyanil] Cu(II) | 1.39 | 8 |
| Monopyridino-2-hydroxynaphthaldehyde-(1)-[*o*-hydroxyanil] Cu(II) | 1.77 | 8 |
| 5-Bromosalicylalanthranilic acid Cu(II) | 1.87 | 8 |
| Monopyridino-5-bromosalicylalanthranilic acid Cu(II) | 1.86 | 8 |
| 5-Nitrosalicylalanthranilic acid Cu(II) | 1.87 | 8 |
| Monopyridino-5-nitrosalicylalanthranilic acid Cu(II) | 1.84 | 8 |
| Salicylaldehyde-2-mercaptoanil Cu(II) | 1.82* | |
| 2-Hydroxy-5-methylbenzaldehyde-*o*-mercaptoanil Cu(II) | 1.93* | |
| 5-Bromosalicylaldehyde-*o*-mercaptoanil Cu(II) | 1.76* | |

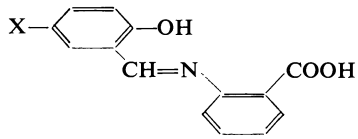
* The magnetic susceptibilities were determined by the Gouy method at room temperature (28~31°C).

7) M. Kishita, Y. Muto and M. Kubo, *Naturwissenschaften*, **44**, 372 (1957); *Australian J. Chem.*, **10**, 386 (1957).
8) M. Kishita, Y. Muto and M. Kubo, *Naturwissenschaften*, **44**, 612 (1957); *Australian J. Chem.*, **11**, 309 (1958).
9) Y. Muto, *J. Chem. Soc. Japan, Pure Chem. Sec.* (*Nippon Kagaku Zasshi*), **76**, 252 (1955).

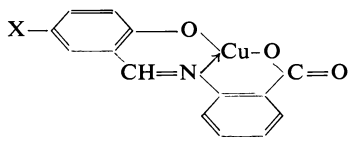
TABLE II. THE LIGAND-EXCHANGE REACTIONS

| Chelates | Replacing agents | Resulting chelates | Analysis Cu % Calcd. | Cu % Found | N % Calcd. | N % Found |
|---|---|---|---|---|---|---|
| Bis-acetylacetone Cu(II) | Acetylacetone-mono-(2-hydroxyanil) | Acetylacetone-mono-(2-hydroxyanil) Cu(II) | 25.14 | 25.08 | 5.54 | 5.71 |
| Bis-benzoylacetone Cu(II) | Benzoylacetone-mono-(2-hydroxyanil) | Benzoylacetone-mono-(2-hydroxyanil) Cu(II) | 20.18 | 20.15 | 4.45 | 4.49 |
| Bis-2-hydroxynaphthaldehyde-(1) Cu(II) | 2-Hydroxynaphthaldehyde-(1)-[*o*-hydroxyanil] | 2-Hydroxynaphthaldehyde-(1)-[*o*-hydroxyanil] Cu(II) | 19.52 | 19.38 | 4.40 | 4.54 |
| Bis-salicylaldimine Cu(II) | Benzoylacetone-mono-(2-hydroxyanil) | Benzoylacetone-mono-(2-hydroxyanil) Cu(II) | 20.18 | 20.09 | 4.45 | 4.54 |
| Bis-salicylaldehyde-anil Cu(II) | Acetylacetone-mono-(2-hydroxyanil) | Acetylacetone-mono-(2-hydroxyanil) Cu(II) | 25.14 | 25.16 | 5.54 | 5.64 |
| Bis-dimethylglyoxime Cu(II) | Benzoylacetone-mono-(2-hydroxyanil) | Benzoylacetone-mono-(2-hydroxyanil) Cu(II) | 20.18 | 20.23 | 4.45 | 4.57 |
| Bis-ethylacetoacetate Cu(II) | Acetylacetone-mono-(2-hydroxyanil) | Acetylacetone-mono-(2-hydroxyanil) Cu(II) | 25.14 | 25.13 | 5.54 | 5.67 |
| Benzoylacetone-mono-(2-hydroxyanil) Cu(II) | 8-Oxyquinoline | Bis-8-oxyquinoline Cu(II) | 18.06 | 18.11 | 7.96 | 8.02 |
| Acetylacetone-mono-(2-hydroxyanil) Cu(II) | Salicylaldehyde-ethylene-diimine | Salicylaldehyde-ethylene-diimine Cu(II) | 19.27 | 19.20 | 8.49 | 8.61 |

way the complexes having the compositions shown in D were obtained. These complexes were soluble with difficulty in common organic solvents such as ethanol or benzene, while their monopyridinates were soluble in ethanol to a certain extent. Pyridine could be removed from the pyridinates by heating at about 150~200°C in air or boiling in ethanol.



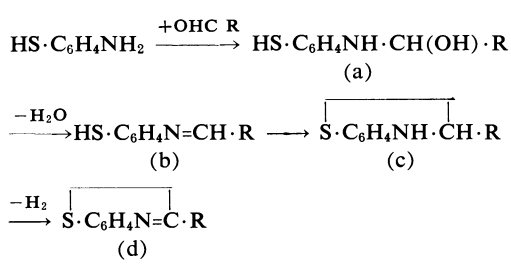
D'



D

X: Cl, Br, $NO_2$

**III. Copper(II) Complexes Having Schiff Bases of 2-Aminothiophenol.**—Unlike the case of 2-aminophenol or anthranilic acid, 2-aminothiophenol condenses with aldehydes to form benzothiazoles. It seems probable from the results of several investigators[10] that the mechanism of the reaction can be represented as follows:



(a) (b) (c) (d)

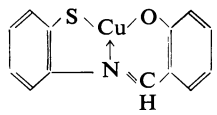
Although the thiazolines (c) were isolated as intermediates in the formation of the thiazoles (d) from 2-aminothiophenol and aldehydes, neither the aldols (a) nor the anils (b) have been isolated.

Claasz[10] obtained 2-(*o*-hydroxyphenyl)benzothiazol (m. p. 130°C) by the reaction of 2-aminothiophenol with salicylaldehyde. Recently, Charles and Freiser[11] have obtained 2-(*o*-hydroxyphenyl)benzothiazoline (m.p. 136~137°C). However, in the course of this study, the present author has mixed 2-aminothiophenol and salicylaldehyde in ethanol and obtained a product of m. p. 148~148.5°C. This compound was converted into 2-(*o*-hydroxyphenyl)benzothiazol when it was recrystallized from ethanol containing a small amount of hydrogen chloride. On oxidation with hydrogen peroxide, this compound yielded 2-salicylaminophenyldisulfide, $(HO\cdot C_6H_4CH{=}N\cdot C_6H_4S{-})_2$, indicating the presence of a mercapto group. The elementary analysis of this compound agreed with the formula $HO\cdot C_6H_4CH{=}N\cdot C_6H_4SH$. On treating this compound with

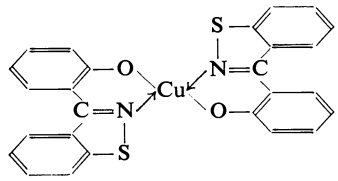
10) M. Claasz, *Ber.*, **45**, 1031 (1912); **49**, 1141 (1916); M. T. Bogert and A. Stull, *J. Am. Chem. Soc.*, **47**, 3038 (1925); H. P. Lankelma and P. X. Sharnoff, ibid., **53**, 2654 (1931); M. T. Bogert and B. Naiman, ibid., **57**, 1529 (1935).

11) R. G. Charles and H. Freiser, *J. Org. Chem.*, **18**, 422 (1953).

copper(II) acetate, it yielded a complex having a composition agreeing with the formula E.



E



F

This complex was also prepared by the condensation of bis-salicylaldehyde copper(II) with 2-aminothiophenol. This formula was suggested further by the following observations. First, when this complex was decomposed by dilute sulfuric acid, salicylaldehyde was liberated. If this complex had had a thiazol or thiazoline link, salicylaldehyde would not have been liberated from it. Secondly, when this complex was recrystallized from pyridine, its monopyridinate was formed in the same manner as the tri-coordinated copper(II) complexes described in I and II. This shows that the composition of the complex has the molar ratio 1 : 1 of copper(II) to the ligand molecule.

As an example of metal complexes having the Schiff base of 2-aminothiophenol, only the following zinc complex has been reported. Bogert and Naiman[10] have shown that zinc 2-aminothiophenolate could be condensed directly with aromatic aldehydes to form zinc complexes having a general formula $(R\cdot CH=N\cdot C_6H_4S-)_2Zn$, which yielded 2-R-benzothiazoles when they were boiled in glacial acetic acid. The present author has also found that the corresponding 2-R-benzothiazoline does not form zinc or copper(II) complexes, while 2-(*o*-hydroxyphenyl)benzothiazol forms a copper(II) complex having the molar ratio 1 : 2 of copper(II) to the ligand molecule as shown in F. This result suggests that the thiazolines (c) cannot be converted into anils (b) by the action of metal ions. Therefore, the fact that reaction product of 2-aminothiophenol with salicylaldehyde (m. p. 148~148.5°C) yielded a complex having the composition shown in E gives support to the conclusion that the product must be salicylaldehyde-2-mercaptoanil.

2-Hydroxy-5-methylbenzaldehyde-*o*-mercaptoanil copper(II), 5-bromosalicylaldehyde-*o*-mercaptoanil copper(II) and their monopyridinates could be prepared in an analogous way.

12) W. Suida, *J. prakt. Chem.*, [2] **83**, 241 (1911).

## Experimental

**Preparation of Copper(II) Complexes.**—Appropriate amines were subjected to condensation with suitable ketones or aldehydes in ethanol. The resulting Schiff bases were separated and were treated with copper(II) acetate in the mixture of ethanol and water. The crude products which precipitated were separated, dissolved in pyridine and filtered. When water was added to the filtrates, the monopyridinates of the complexes were formed as crystals. On heating to an appropriate temperature (100~200°C), almost all the pyridine was removed. To ensure the complete removal, the residue were boiled in ethanol on a water bath for about half an hour. After being allowed to cool, the precipitates were filtered and dried at about 90°C. In this way pyridine-free copper(II) complexes were prepared. None of them melted below 300°C.

**(1) Acetylacetone-mono-(2-hydroxyanil) Copper(II).**—This was prepared from copper(II) acetate and acetylacetone-mono-(2-hydroxyanil)[12] (m. p. 187°C, yellow prismatic crystals. Found: N, 7.48. Calcd. for $C_{11}H_{13}O_2N$: N, 7.33%). The copper(II) chelate formed green prismatic crystals, while its pyridinate crystallized as deep green plates.

Found: N, 5.78; Cu, 25.32. Calcd. for $C_{11}H_{11}\cdot O_2NCu$: N, 5.54; Cu, 25.14%. Found: N, 8.69; Cu, 19.34; py., 23.73. Calcd. for $C_{11}H_{11}O_2NCu\cdot C_5H_5N$, N, 8.44; Cu, 19.15; py., 23.84%.

**(2) Benzoylacetone-mono-(2-hydroxyanil) Copper(II).**—Benzoylacetone-mono-(2-hydroxyanil) was prepared by the condensation of benzoylacetone (1.7 g.) with 2-aminophenol (1.1 g.) in ethanol (30 ml.). It was isolated in the form of yellow prismatic crystals; m. p. 169~170°C, yield 2 g.

Found: C, 75.76; H, 6.02; N, 5.81. Calcd. for $C_{16}H_{15}O_2N$: C, 75.87; H, 5.97; N, 5.53%.

The copper(II) chelate formed yellow-green needles, while its pyridinate crystallized as deep green plates.

Found: N, 4.49; Cu, 20.19. Calcd. for $C_{16}H_{13}\cdot O_2NCu$: N, 4.45; Cu, 20.18%. Found: N, 7.01; Cu, 16.23; py., 19.69. Calcd. for $C_{16}H_{13}O_2NCu\cdot C_5H_5N$: N, 7.09; Cu, 16.09; py., 20.03%.

**(3) 2-Hydroxynaphthaldehyde-(1)-[*o*-hydroxyanil] Copper(II).**—This was prepared from copper(II) acetate and 2-hydroxynaphthaldehyde-(1)-[*o*-hydroxyanil][13] (m.p. 248~249°C, brown-red needles, Found: N, 5.41. Calcd. for $C_{17}H_{13}O_2N$: N, 5.32%). The copper(II) chelate was yellow-green, while its pyridinate was brown. Both crystallized as needles.

Found: N, 4.40; Cu, 19.52. Calcd. for $C_{17}H_{11}\cdot O_2NCu$: N, 4.31; Cu, 19.56%. Found: N, 6.99; Cu, 15.71; py., 19.39. Calcd. for $C_{17}H_{11}O_2NCu\cdot C_5H_5N$: N, 6.94; Cu, 15.73; py., 19.59%.

**(4) 5-Chlorosalicylalanthranilic Acid Copper(II).**—5-Chlorosalicylalanthranilic acid was prepared by the condensation of 5-chlorosalicylaldehyde (1.6 g.) with anthranilic acid (1.4 g.) in ethanol (50 ml.). It was isolated in the form of orange prismatic crystals; m. p. 200°C, yield 2 g.

13) A. Senier and R. Clarke, *J. Chem. Soc.*, **99**, 2082 (1911—2).

Found: C, 61.10; H, 3.63; N, 5.39. Calcd. for $C_{14}H_{10}O_3NCl$: C, 60.99; H, 3.66; N, 5.08%.

The copper(II) chelate formed greenish brown needles, while its pyridinate crystallized as bright green plates.

Found: N, 4.29; Cu, 18.63. Calcd. for $C_{14}H_8O_3NClCu$: N, 4.15; Cu, 18.84%. Found: N, 6.83; Cu, 14.98; py., 19.24. Calcd. for $C_{14}H_8O_3NClCu \cdot C_5H_5N$: N, 6.73; Cu, 15.26; py., 19.00%.

(5) **5-Bromosalicylalanthranilic Acid Copper(II).**—5-Bromosalicylalanthranilic acid was prepared by the condensation of 5-bromosalicylaldehyde (2 g.) with anthranilic acid (1.5 g.) in ethanol (50 ml.). It was isolated in the form of orange prismatic crystals; m. p. 202°C, yield 3 g.

Found: C, 52.47; H, 3.12; N, 4.48. Calcd. for $C_{14}H_{10}O_3NBr$: C, 52.52; H, 3.15; N, 4.38%.

The copper(II) chelate formed greenish brown needles, while its pyridinate crystallized as bright green plates.

Found: N, 3.96; Cu, 16.87. Calcd. for $C_{14}H_8O_3NBrCu$: N, 3.71; Cu, 16.82%. Found: N, 6.30; Cu, 13.86; py., 17.36. Calcd. for $C_{14}H_8O_3NBrCu \cdot C_5H_5N$; N, 6.08; Cu, 13.79; py., 17.17%.

(6) **5-Nitrosalicylalanthranilic Acid Copper(II).**—5-Nitrosalicylalanthranilic acid was prepared by the condensation of 5-nitrosalicylaldehyde (1.7 g.) with anthranilic acid (1.4 g.) in ethanol (50 ml.). It was isolated in the form of red prismatic crystals; m. p. 271°C, yield 2.2 g.

Found: C, 58.67; H, 3.48; N, 10.04. Calcd. for $C_{14}H_{10}O_5N_2$: C, 58.74; H, 3.52; N, 9.79%.

The copper(II) chelate was greenish brown, while its pyridinate was bright green. Both formed prismatic crystals.

Found: N, 7.80; Cu, 18.43. Calcd. for $C_{14}H_8O_5N_2Cu$: N, 8.06; Cu, 18.27%. Found: N, 10.12; Cu, 15.15; py., 18.31. Calcd. for $C_{14}H_8O_5N_2Cu \cdot C_5H_5N$: N, 9.85; Cu, 14.89; py., 18.53%.

(7) **Salicylaldehyde-2-mercaptoanil Copper(II).** — *a) Salicylaldehyde-2-mercaptoanil.* — Equimolar amounts (0.01 mol.) of 2-aminothiophenol and salicylaldehyde were dissolved in ethanol (30 ml.). The resulting solution was kept below 30°C by means of a cold water bath for about two hours; meanwhile the crude product precipitated. Recrystallization from ether gave colorless prismatic crystals; m. p. 148~148.5°C, yield 1.5 g.

Found: C, 68.27; H, 5.11; N, 6.08. Calcd. for $C_{13}H_{11}NOS$: C, 68.10; H, 4.84; N, 6.11%.

*b)* The copper(II) chelate was prepared by the reaction of salicylaldehyde-2-mercaptoanil described above with copper(II) acetate. This chelate was also obtained by the condensation of bis-salicylaldehyde copper(II) with 2-aminothiophenol in the same way as that described in (9). The pyridine-free complex was deep green, while the pyridinate was brown. Both crystallized as needles.

Found: C, 53.74; H, 3.41; N, 4.67; Cu, 21.80. Calcd. for $C_{13}H_9NOSCu$: C, 53.69; H, 3.12; N, 4.82; Cu, 21.85%. Found: N, 7.70; Cu, 17.31; py., 21.39. Calcd. for $C_{13}H_9NOSCu \cdot C_5H_5N$: N, 7.57; Cu, 17.18; py., 21.38%.

*c) Oxidation of Salicylaldehyde-2-mercaptoanil.*— Salicylaldehyde-2-mercaptoanil (0.5 g.) was dissolved in a mixture of ethanol (20 ml.) and aqueous hydrogen peroxide (30%, 5 ml.). After being heated gently on a water bath for ten minutes, the solution was allowed to stand overnight in air at room temperature; meanwhile yellow crystals precipitated. Recrystallization from benzene gave yellow needles; m. p. 171°C, yield 0.3 g. When this product was mixed with 2-salicylaminophenyldisulfide, the melting point was unaltered.

Found: N, 6.26. Calcd. for $C_{26}H_{16}O_2N_2S_2$: N, 6.19%.

(8) **5-Bromosalicylaldehyde-*o*-mercaptoanil Copper(II).**—5-Bromosalicylaldehyde-*o*-mercaptoanil was prepared by the condensation of 5-bromosalicylaldehyde (2 g.) with 2-aminothiophenol (1.3 g.) in the same way as that described in (7). It was isolated in the form of colorless prismatic crystals; m. p. 147°C, yield 2 g.

Found: C, 50.90; H, 3.60; N, 4.31. Calcd. for $C_{13}H_{10}NOSBr$: C, 50.66; H, 3.27; N, 4.54%.

The copper(II) chelate was deep green, while its pyridinate was brown-red. Both crystallized as needles.

Found: C, 41.89; H, 2.42; N, 3.84; Cu, 17.25. Calcd. for $C_{13}H_8NOSBrCu$: C, 42.23; H, 2.18; N, 3.79; Cu, 17.19%. Found: N, 6.42; Cu, 14.30; py., 17.66. Calcd. for $C_{13}H_8NOSBrCu \cdot C_5H_5N$: N, 6.24; Cu, 14.16; py., 17.62%.

(9) **2-Hydroxy-5-methylbenzaldehyde-*o*-mercaptoanil Copper(II).**—A solution of 2-aminothiophenol (0.7 g.) in ethanol (10 ml.) was added to a boiling solution of bis-2-hydroxy-5-methylbenzaldehyde copper(II) (1.7 g.) in ethanol (50 ml.). Deep green micro-crystals immediately precipitated. It was purified by recrystallization from pyridine. The copper(II) chelate was deep green, while its pyridinate was brown-red. Both crystallized as needles.

Found: C, 55.10; H, 3.87; N, 4.47; Cu, 20.85. Calcd. for $C_{14}H_{11}NOSCu$: C, 55.16; H, 3.64; N, 4.59; Cu, 20.84%. Found: N, 7.45; Cu, 16.59; py., 20.63. Calcd. for $C_{14}H_{11}NOSCu \cdot C_5H_5N$: N, 7.30; Cu, 16.55; py., 20.60%.

(10) **Bis-2-(*o*-hydroxyphenyl)benzothiazol Copper(II).**—A solution of copper(II) acetate monohydrate (0.5 g.) in water (30 ml.) was added to a boiling solution of 2-(*o*-hydroxyphenyl)benzothiazol (0.6 g.) in ethanol (30 ml.). Dark green microcrystals immediately precipitated. Recrystallization from pyridine gave dark green plates. Yield 0.7 g.

Found: N, 5.40; Cu, 12.38. Calcd. for $C_{26}H_{16}O_2N_2S_2Cu$: N, 5.31; Cu, 12.31%.

Bis-2-(*o*-hydroxy-*m*-bromophenyl)benzothiazol copper(II) could be prepared in a similar manner. It was isolated in the form of dark green plates.

Found: N, 4.21; Cu, 9.52. Calcd. for $C_{26}H_{14}O_2N_2S_2Br_2Cu$: N, 4.16; Cu, 9.43%.

**Decomposition of Complexes (7), (8) and (9).**— The complexes described in (7), (8) and (9) were decomposed by dilute sulfuric acid and then subjected to steam distillation. Salicylaldehyde, 5-bromosalicylaldehyde and 2-hydroxy-5-methylbenzaldehyde in the distillates were identified by their phenylhydrazones which melted at 143°C, 151°C and 149°C respectively.

**Reaction of 2-R-benzothiazolines with Zinc or Copper(II) Acetate.** — The reaction of 2-phenylbenzothiazoline with zinc or copper(II) acetate was

attempted in organic solvents such as ethanol, pyridine or acetic acid, but the product isolated was only 2-phenylbenzothiazol. Similarly, 5-chloro-2-phenylbenzothiazoline did not form zinc or copper-(II) complex.

**Exchange Experiments.**—Calculated amounts of appropriate reagents and suitable complexes were dissolved or suspended in ethanol. The mixtures were heated on a water bath for about five minutes. The resulting complexes were separated, washed with hot ethanol repeatedly and then dried at 80°C. The elementary analysis of the resulting complexes is presented in Table II.

The author is grateful to Mr. Michihiko Kishita of Nagoya University for measurements of magnetic susceptibilities and to Mr. Michio Shido of Kyushu University for elementary analyses.

*Chemical Laboratory, Faculty of Liberal Arts, Saga University*
*Honjo-machi, Saga*

# *Tropones. V.* Addition Reaction of Tropone and Maleic Anhydride***

By Tetsuo NOZOE, Toshio MUKAI, Tsuneyuki NAGASE and Yasuo TOYOOKA

(Received March 15, 1960)

Troponoid compounds were at first considered to be resistant to the Diels-Alder type addition reactions because of their high aromaticity[1,2] but later, Sebe and others[3] found that hinokitiol underwent an addition reaction with maleic anhydride. Since then, the Diels-Alder reactions of tropolone, its methyl ether[4], 4-methyltropone[4], and 2-phenyltropone[5] have been reported. There still remained many points to be examined regarding the configuration of these adducts.

The present series of works was at first undertaken in order to examine the unsaturation characteristics of tropone and during the course of this work, some observations were gained regarding the configuration of the addition compound, which are described herein.

It has been pointed out[6] that the unsaturation characteristics of a tropone is greater than that of a tropolone and, as anticipated, the heating of tropone with two molar equivalents of maleic anhydride in xylene for a few hours easily effected reaction, affording the adduct I, m. p. 181.5~182.5°C, in a good yield of around 95%.

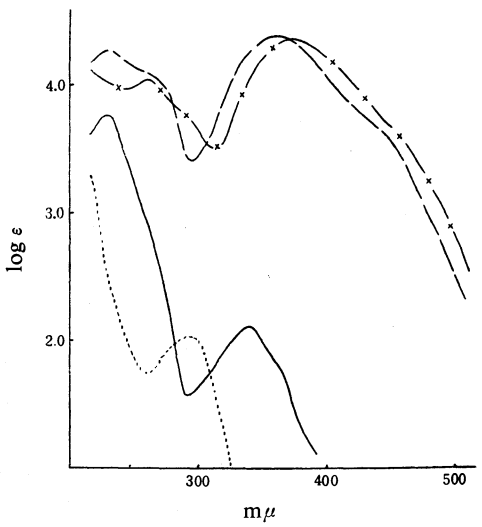



Fig. 1. —— I ----- II
-×- 2.4 DNP of V
—— 2.4 DNP of VI

Catalytic reduction of the adduct I in ethyl acetate or acetone with palladium-carbon as a catalyst, results in absorption of 2 molar equivalents of hydrogen to form a tetrahydro compound II. This shows the presence of two ethylenic linkages in I. The ultraviolet absorption spectra of I and II are shown in Fig. 1 and the spectrum of (I) exhibits a typical absorption of $\alpha\beta$-unsaturated ketone[7].

* Part IV. T. Mukai, This Bulletin, 33, 238 (1960).

** A part of this work was presented as a paper at the 6th Annual Meeting of the Chemical Society of Japan, Kyoto, April 5, 1953. Cf T. Nozoe, T. Mukai, K. Takase and T. Nagase, *Proc. Japan Acad.*, **28**, 477 (1952).

1) R. D. Brown, *J. Chem. Soc.*, **1951**, 2670.

2) J. W. Cook, A. R. Gibb, R. A. Raphael and A. R. Somerville, ibid., **1951**, 503.

3) E. Sebe and C. Ôsako: Paper read before the 4th Annual Meeting of the Chemical Society of Japan in April, 1951. cf. *Proc. Japan Acad.*, **28**, 282.

4) T. Nozoe, S. Seto and T. Ikemi, *Proc. Japan Acad.*, **27**, 10 (1951).

5) T. Nozoe, T. Mukai, J. Minegishi and T. Fujisawa, *Sci. Repts. Tohoku Univ.*, Ser. I, **37**, 388 (1953).

6) T. Mukai, This Bulletin, **31**, 846 (1958).

7) R. B. Woodward, *J. Am. Chem. Soc.*, **63**, 1123 (1941); **64**, 72, 76 (1942).

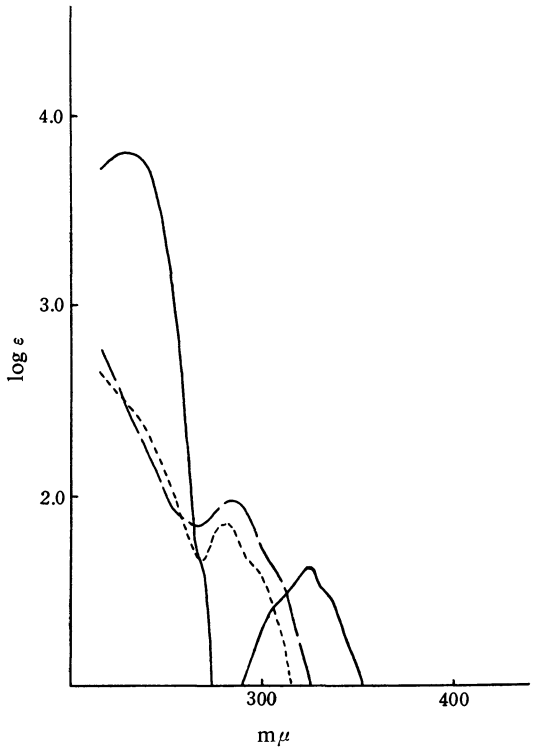



Fig. 2. —— VIII ------ X
—— XI

The infrared spectra of I and II are shown in Table I. The absorption of a carbonyl in the acid anhydride of a five-membered ring is common to I and II, but while the absorption of an $\alpha\beta$-unsaturated ketone appears at 1665 $cm^{-1}$ in the spectrum of I, absorption of a saturated ketone is present at 1700 $cm^{-1}$ in that of II.

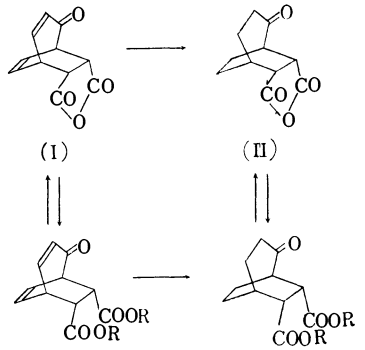
The presence of an $\alpha\beta$-unsaturated ketone in I not only offers an important clue to the structure of I but also proves the addition occurring at C-2 and C-5 positions in the tropone ring.

Treatment of the adduct I with hot water or sodium bicarbonate solution results in facile hydrolysis and a dibasic acid III is formed. The acid III is known to be dibasic from its analytical values and titration, as well as from its infrared spectrum (Table I) which shows the presence of two carbonyls.

TABLE I.

| | $\nu_{OH}$ $cm^{-1}$ | $\nu_{C=O}$ $cm^{-1}$ | $\nu_{C=C}$ $cm^{-1}$ |
|---|---|---|---|
| I | | 1840, 1780 | 1665, 1625 |
| II | | 1840, 1775, 1700 | |
| III | 3250, 2960 | 1740, 1710 | 1650, 1625 |
| V | | 1730 | 1670, 1633 |
| VIII | 3320 | 1770, 1730 | 1675 |
| XI | | 1780, 1726, 1706 | |

Determination of the melting point of III indicates decomposition at 167.5°C but solidification of the melt and reexamination of the melting point shows it melting at 182.5°C, the same as that of I. This is considered to be due to the facile dehydration of III to form the anhydride.




III, R=H IV, R=H
V, R=$CH_3$ VI, R=$CH_3$

Actually, drying of III at 100°C under a reduced pressure results in the formation of I and such a fact naturally indicates that the two carboxyls are in *cis* configuration.

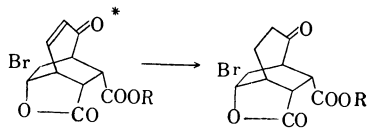
The tetrahydro compound II is also easily hydrolyzed and forms a dibasic acid (IV) which undergoes facile dehydration as in the case of III. Catalytic reduction of the unsaturated dibasic acid III in acetone, with palladium-carbon as a catalyst, results in absorption of two molar equivalents of hydrogen to form IV. Methylation of these two dibasic acids (III and IV) with diazomethane affords respective dimethyl esters (V and VI). It has been found, however, that reaction of III and excess of diazomethane also affords a compound (VII) of $C_{14}H_{16}O_5N_2$, besides V. In general, it is known that a reaction of $\alpha\beta$-unsaturated ketone and diazomethane results in formation of a pyrazole ring[8] and VII is considered to be this kind of product.

Both the methyl esters (V and VI) easily form crystalline 2, 4-dinitrophenylhydrazones whose ultraviolet absorption spectra are indicated in Fig, 1. The absorption of the 2, 4-dinitrophenylhydrazone of V shows a shift of 13 mμ to the longer wavelength region than that of VI and this fact indicates the presence of $\alpha\beta$-unsaturated ketone in V.[9] Catalytic reduction of V in ethyl acetate over palladium-carbon gives an oily product whose derivation to 2,4-dinitrophenylhydrazone proved that the oily product is VI.

8) H. Gilman, "Org. Chem.", Vol. IV, John Wiley & Sons., Inc., London, (1953), p. 780.
9) E. A. Braude and E. R. H. Jones, *J. Chem. Soc.*, 1945, 498.

Bromination of the adduct I in aqueous solution by the method of Alder-Stein[10] results in addition to the double bond and a bromo-lactone VIII is obtained in a good yield. Titration of VIII shows it to be a monobasic acid and the presence of a carboxyl (3320 and 1730 $cm^{-1}$) and a $\gamma$-lactone (1770 $cm^{-1}$) is also indicated from the infrared spectral values listed in Table I. In addition, there is an absorption of $\alpha\beta$-unsaturated carbonyl at 1675 $cm^{-1}$ in the spectrum of VIII. This fact is also certain from the ultraviolet spectrum of V shown in Fig. 2. These facts indicate that the addition of BrOH occurs at the non-conjugated double bond of the two ethylenic linkages present in I. It is therefore concluded that VIII has the configuration shown in Fig. 2 and that the structure of I to VI is in *endo-cis* form.

The unsaturated bromo-lactone VIII forms a monomethyl ester IX on methylation with diazomethane and IX easily forms a 2, 4-dinitrophenylhydrazone. The ultraviolet spectrum of 2, 4-dinitrophenylhydrazone of IX exhibits absorption maximum at 371 m$\mu$ and



VIII, R=H IX, R=$CH_3$ X, R=H XI, R=$CH_3$

this corresponds to that of 2, 4-dinitrophenylhydrazone of an $\alpha\beta$-unsaturated ketone.

Catalytic reduction of VIII over palladium-carbon in ethyl acetate results in absorption of one mole equivalent of hydrogen and saturated bromo-lactone (X) is produced. The structure of X was confirmed by the derivation of a monomethyl ester (XI) by reaction with diazomethane since it failed to undergo crystallization.

## Experimental

**Diels-Alder Reaction of Tropone and Maleic Anhydride; Formation of Tropone-Maleic Anhydride Adduct (I).**—A mixture of 8.36 g. (0.079 mol.) of tropone and 15.70 g. (0.16 mol.) of maleic anhydride in 60 cc. of dry xylene was refluxed in an oil bath for 2 hr. by which pale yellow crystals began to be deposited on the wall of the vessel. After refluxing for 4.5 hr, the mixture was allowed to stand overnight in a cool place and 16.6 g. (95%) of pale yellow crystals, m. p. 175~179°C, that precipitated out were collected by filtration. Several recrystallizations from acetone afforded I as colorless prismatic crystals, m. p. 181.5~182.5°C.

Found: C, 64.77; H, 4.14%. Cald. for $C_{11}H_8O_4$: C, 64.70; H, 3.95%.

I is easily soluble in acetone, ethyl acetate, ethanol, methanol and chloroform, and sparingly soluble in ether, petroleum ether, carbon tetrachloride and benzene.

**Catalytic Reduction of I; Formation of the Tetrahydro Compound (II) of the Adduct.**—A solution of 500 mg. of I dissolved in 20 cc. of ethyl acetate, to which 20 mg. of 5% palladium-carbon had been added, was submitted to catalytic reduction at ordinary pressure. After absorption of 2.05 mole equivalent (109 cc.) of hydrogen, the product (500 mg.) was obtained as colorless crystals of m. p. 168~181°C and several recrystallizations from acetone-ether mixture afforded II as colorless leaflets, m. p. 191~192°C.

Found: C, 63.67; H, 5.39%. Calcd. for $C_{11}H_{12}O_4$: C, 63.45; H, 5.81%.

The use of acetone in place of ethyl acetate as a solvent in this reduction also results in absorption of two mole equivalent of hydrogen and the same product is obtained.

**Hydrolysis of I; Formation of the Dicarboxylic Acid (III) of the Adduct.**—*a) Hydrolysis with Water:* A solution of 1 g. of I dissolved in 30 cc. of hot water was allowed to stand overnight and 530 mg. of a colorless prismatic crystals, m. p. 162.5°C (decomp.), was obtained. Concentration of its filtrate on a water bath afforded a second crop of colorless crystals, m. p. 160°C (decomp.). The two kinds of crystals were combined and washed with acetone, affording (III) as colorless crystals, m. p. 167.5°C.

Found: C, 59.34; H, 4.35%. Calcd. for $C_{11}H_{10}O_5$: C, 59.46; H, 4.54%.

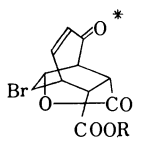
*b) Hydrolysis with Sodium Bicarbonate Solution:* To a solution of 420 mg. (0.005 mol.) of sodium bicarbonate dissolved in 4 cc. of water, 500 mg. of I was added and warmed on a water bath to dissolve all the crystals. The reaction mixture was concentrated acidified with hydrochloric acid while cooling with water and 400 mg. of colorless microneedles, m. p. 164~165°C (decomp.). The crystals were collected and washed several times with hot acetone, giving III as colorless microneedles, m. p. 167.5°C.

Ultraviolet spectrum: $\lambda_{max}^{MeOH}$ m$\mu$ (log $\varepsilon$): 228 (3.87), 337 (2.49).

The acid III obtained by both the foregoing methods (a) and (b) showed no depression of the melting point on admixture with I. The melted III, upon solidification, melted at 181.5~182.5°C, same as I.

**Dehydration of III; Formation of I.**—The Acid III obtained from the both methods (a) and (b) as above was each kept in a vacuum (10 mmHg) desiccator over phosphorus pentoxide

10) K. Alder und G. Stein, *Anal. Chem.*, 514, 4 (1934).



In this case there are two possible structures to VIII. Detailed reports on the structure of VIII will be made elsewhere.

11) All m. p. are uncorrected. The microanalyses were carried out by Miss Ayako Iwanaga of this laboratory to whom the authors are indebted.

at 100°C for 2 days. Determination of the melting point of resultant product showed formation of 45 mg. of a product of m. p. 181.5~182.5°C from 50 mg. of III. No depression of the melting point was observed on admixture with I.

Found : C, 64.59 ; H, 4.00%. Calcd. for $C_{11}H_8O_4$ : C, 64.70 ; H, 3.95%.

**Hydrolysis of II; Formation of Dicarboxylic Acid (IV) of the Tetrahydro Derivative of the Adduct.**—A solution of 150 mg. of II dissolved in 3 cc. of hot water was allowed to cool and colorless crystals that separated out were collected to 100 mg. of IV as colorless microneedles, m. p. 173°C (decomp.).

Found : C, 58.33; H, 5.80%. Calcd. for $C_{11}H_{14}O_5$ : C, 58.40 ; H, 6.24%.

The filtrate was concentrated at room temperature under a reduced pressure and a second crop of crystals was obtained as 80 mg. of colorless crystals, m. p. 169~170°C (decomp.).

Ultraviolet spectrum : $\lambda_{max}^{MeOH}$ mμ (log ε) : 285 (1.84).

Admixture of IV and II showed no depression of the melting point. Determination of the melting point after solidification of melted II showed m. p. 191~192°C.

**Dehydration of IV ; Formation of the Tetrahydro Compound (II) of the Adduct.**—Thirty milligrams of IV was kept over phosphorus pentoxide in a vacuum (10 mmHg) desiccator at 100°C for two days and 28 mg. of the resultant product melted at 171~172°C, alone and in admixture with II.

Found : C, 58.43 ; H, 6.30%. Calcd. for $C_{11}H_{12}O_4$ : C, 58.40 ; H, 6.24%.

**Catalytic Reduction of III; Formation of IV.**—A solution of 500 mg. of III dissolved in 70 cc. of acetone, added with 20 mg. of 5% palladium-carbon, was submitted to catalytic reduction at ordinary pressure and 2.08 mole equivalents of hydrogen (105 cc.) was absorbed. The catalyst was removed by filtration and the filtrate was concentrated, affording 460 mg. of colorless crystals, m. p. 154~155.5°C. The crystals were washed several times with warm acetone and (IV) was obtained as colorless crystals of m. p. 173°C (decomp.).

Found : C, 58.30 ; H, 5.93%. Calcd. for $C_{11}H_{14}O_5$ : C, 58.40; H, 6.24%.

The compound (IV) obtained by this means easily lost one mole of water to form II, as was the case with IV obtained by the hydrolysis of II.

**Raction of (III) and Diazomethane.**—*a) Formation of the Dimethyl ester (V) of III*: To a suspension of 220 mg. (ca. 0.001 mol.) of finely pulverized III in 10 cc. of ethyl acetate, 3.6 cc. (0.002 mol.) of ether solution of diazomethane was added dropwise at room temperature by which a vigorous reaction set in and III dissolved almost completely. The solution was evaporated on a water bath, the concentrated solution was cooled in ice, and 20 mg. of colorless crystals VII, m. p. 212°C, separated out.

Concentration of the mother liquor left 200 mg. of yellow oil which solidified gradually upon standing. Recrystallization from a small volume of methanol afforded V as yellow microneedles, m. p. 83~88°C.

Found : C, 62.42 ; H, 5.52%. Calcd. for $C_{13}H_{14}O_5$ : C, 62.39 ; H, 5.64%.

Ultraviolet spectrum : $\lambda_{max}^{MeOH}$ mμ (log ε) : 227 (3.90), 337(2.40).

*b) Formation of VII*: To a suspension of 300 mg. (0.0014 mol.) of III in 20 cc. of ethyl acetate, 9 cc. (0.0042 mol.) of ether solution of diazomethane was added in drops at room temperature by which III dissolved to form a uniform yellow solution. On standing, colorless crystals separated out which were collected and recrystallized from water to 340 mg. of colorless needles (VII), m. p. 212°C (decomp.).

Found : C, 57.19; H, 5.13%. Calcd. for $C_{13}H_{14}O_5 \cdot CH_2N_2$ : C, 57.53 ; H, 5.52%.

Ultraviolet spectrum : $\lambda_{max}^{MeOH}$ mμ (log ε) : 235 (3.36), 307(3.68).

*c) 2,4-Dinitrophenylhydrazone of V*: A solution (conc. sulfuric acid, 1.3 cc., methanol, 6.5 cc.) of 250 mg. (0.0013 mol.) of 2,4-dinitrophenylhydrazine was added to a solution of 250 mg. (0.001 mol.) of V dissolved in 2.5 cc. of methanol by which a fine orange powder precipitated out immediately. The mixture was stirred and allowed to stand overnight at room temperature. The solid was collected and recrystallized several times from acetone-methanol mixture to 230 mg. of VII as lustrous orange powder, m. p. 221.5~222°C.

Found : C, 52.80 ; H, 3.96 ; N, 13.07%. Calcd. for $C_{19}H_{18}O_8N_4$ : C, 53.02 ; H, 4.22 ; N, 13.02.

**Formation of the Dimethyl Ester (VI) of IV.**—(a) The calculated amount (0.004 mol.) of the ether solution of diazomethane was added dropwise at room temperature into a solution of 450 mg. (0.002 mol.) of IV dissolved in 20 cc. of ethyl acetate by which a vigorous effervescence set in. After standing at room temperature for a few hours, the solvent was distilled off and left 480 mg. of pale yellow oil. This oily residue was dissolved in acetone and purified by passage through alumina layer, from which 420 mg. of pale yellow oil (VI) was obtained.

Ultraviolet spectrum : $\lambda_{max}^{MeOH}$ mμ (log ε): 284(1.19).

b) Catalytic reduction of 50 mg. of V dissolved in 10 cc. of ethyl acetate, with 5% palladium-carbon as a catalyst, resulted in absorption of 2 mol. equivalents (5 cc., calcd. 4.5 cc.) and 50 mg. of pale yellow oil (VI) was obtained.

Ultraviolet spectrum : $\lambda_{max}^{MeOH}$ mμ (log ε): 284(1.20).

*c) Formation of 2,4-Dinitrophenylhydrazone of VI:* The hydrazone was prepared as in the case of V and recrystallized from methanol to fine orange needles, m. p. 89°C (decomp.).

Found : C, 52.50 ; H, 4.90 ; N, 12.87%. Calcd. for $C_{19}H_{22}O_8N_4$ : C, 52.53 ; H, 5.10 ; N, 12.90%.

**Formation of Bromolactone-monocarboxylic Acid (VIII).**—To a solution of 500 mg. (0.0025 mol.) of I dissolved in 30 cc. of water, 500 mg. (0.0031 mol.) of bromine was dropped in under ice-cooling and stirring. After some time, pale yellow crystals began to precipitate out. The mixture was stirred under ice-cooling for a further 4 hr., the excess of bromine was removed by addition of sodium bisulfite, and the mixture was filtered, affording 570 mg. of fine colorless crystals, m. p. 185°C

(decomp.). After drying over phosphorus pentoxide in a vacuum desiccator, the crystals were recrystallized from acetone to 500 mg. of colorless plates (VIII), m. p. 219°C (decomp.). VIII dissolved in cold, saturated solution of sodium bicarbonate with effervescence and colors green to the Beilstein test.

Found: C, 43.81; H, 2.99%. Calcd. for $C_{11}H_9O_5Br$: C, 43.87; H, 3.01%.

**Formation of the Methyl Ester (IX) of the Bromo-lactone VIII.**—To a solution of 300 mg. (0.001 mol.) of VIII dissolved in 10 cc. of ethyl acetate, 1.9 cc. (0.001 mol.) of the ether solution of diazomethane was added in drops and the mixture was allowed to stand for a few days from which 150 mg. of colorless scaly crystals of m. p. 213~215°C separated out. These crystals were collected by filtration, the filtrate was concentrated, and a second crop of crystals were obtained as 150 mg. of pale yellow crystals, m. p. 178~195°C. The two crops of crystals were combined and recrystallized from acetone-methanol mixture to IX as colorless scales, m. p. 216~217°C.

Found: C, 45.69; H, 3.25%. Calcd. for $C_{12}H_{11}O_5Br$: C, 45.73; H, 3.52%.

Ultraviolet spectrum: $\lambda_{max}^{MeOH}$ m$\mu$ (log $\varepsilon$): 232 (3.82), 320(2.37).

*2,4-Dinitrophenylhydrazone of IX:* A mixture of 200 mg. of IX dissolved in 20 cc. of methanol and methanolic solution (3.5 cc. of methanol and 0.9 cc. of conc. sulfuric acid) of 150 mg. of 2,4-dinitrophenylhydrazine was refluxed on a water bath for 3.5 hr. Concentration of this solution until only a part of the solvent remained left 220 mg. of dark brown crystals which were collected and recrystallized repeatedly from methanol to dark brown, fine needles, m. p. 146~147°C (decomp.).

Found: C, 43.50; H, 3.00; N, 11.02%. Calcd. for $C_{18}H_{15}O_8N_4Br$; C, 43.65; H, 3.05; N, 11.31%.

Ultraviolet spectrum: $\lambda_{max}^{MeOH}$ m$\mu$ (log $\varepsilon$): 255 (4.13), 371(4.43).

**Catalytic Reduction of VIII; Formation of Dihydro-bromo-lactone (X) and Methyl Ester (XI). of X,**—A solution of 240 mg. of VIII dissolved in 20 cc. of ethyl acetate, to which 20 mg. of palladium-carbon was added, was submitted to reduction at ordinary pressure and 0.95 mole equivalent (24.5 cc.) of hydrogen was absorbed. The product obtained therefrom was 220 mg. of yellowish brown oil (X) which failed to crystallize.

A calculated amount of ether solution of diazomethane was added to a solution of 120 mg. of above oil dissolved in 1 cc. of ethyl acetate and the mixture was allowed to stand overnight, from which 100 mg. of colorless crystals precipitated out. This was recrystallized from methanol-acetone mixture to colorless fine powder (XI), m. p. 167.5°C.

Found: C, 45.46; H, 4.02%. Calcd. for $C_{12}H_{13}O_5Br$: C, 45.44; H, 4.13%.

*Chemical Institute*
*Faculty of Science*
*Tohoku University*
*Katahira-cho, Sendai*

# *Theory of the Influence of the Dielectric Constant on the Rate of Reaction in Solution with Application to Enzyme Reactions. I. Development of the Theory and its Application to Some Simple Systems**

By Keitaro HIROMI

(Received December 18, 1959)

The rate of the reaction in solution involving ions or dipolar molecules is generally influenced by the dielectric constant of the medium, and this effect, termed the solvent effect, has been quantitatively interpreted by various authors in conformity to the electrostatic theories[1-5]. There is, however, marked inconsistency between the prediction of Amis-Jaffé's theory and that of Laidler-Eyring's for reactions between a negative ion and a dipolar molecule[2]. Recently Laidler and Landskroener developed a more general theory of the solvent effect[6] based on Kirkwood's model for a spherical solute molecule having an arbitrary charge

* Presented in part at the 11th Annual Meeting of Chem. Soc. Japan, Tokyo, April 1958, and at the Symposium on Enzyme Chem., Sapporo, July, 1958.

1) S. Glasstone, K. J. Laidler and H. Eyring, "The Theory of Rate Processes", McGraw-Hill, New York (1954), p. 400.

2) E. S. Amis, "Kinetics of Chemical Change in Solution", MacMillan Co., New York (1949), p. 153.

3) E. S. Amis, *J. Chem. Educ.*, **28**, 635 (1951); **29**, 337 (1952); **30**, 351 (1953).

4) E. A. Moelwyn-Hughes, "The Kinetics of Reactions in Solution", Oxford University Press, London (1947), p. 90, 120, 202.

5) G. Scatchard, *J. Am. Chem. Soc.*, **52**, 52 (1930).

6) K. J. Laidler and P. A. Landskroener, *Trans. Faraday Soc.*, **52**, 200 (1956).

distribution[7,8], considering the microscopic distribution of charges in the reactants and the activated complexes, which had not been taken into account explicitly in the previous treatments[1-5]. Their theory was applied to the interpretation of the effect of solvent on the rates of the acid and base hydrolyses of esters, amides and anilides, and the results were considered to be successful[6].

The influence of the dielectric constant upon the rates of several enzyme reactions have been treated quantitatively on the basis of simple models[9,10], which seem evidently inadequate to a large complex ion such as protein. The Kirkwood's model may be a suitable one for the treatment of the electrostatic properties of protein molecules[11-13]. Although Laidler-Landskroener's theory is based on this model, it is not applicable to enzyme reactions, because of the approximation made in its derivation, which is not adequate for the large molecules with their charges near the surface of the sphere.

In this paper, a theory of the solvent effect which is applicable to enzyme reactions as well as to reactions involving small ions or molecules is developed, based on the Kirkwood's model. The theory is applied to the interpretation of the effect of solvent on the dissociation constants of carboxylic acids and on the rate constants of unimolecular and bimolecular reactions of simple organic compounds. Application of the theory to enzyme reactions will be treated in the following paper.

## Theoretical

Kirkwood[7] obtained an expression for the work of charging, or the electrostatic free energy, of a spherical solute molecule of radius $b$, having a low dielectric constant $D_i$, within which are situated $M$ discrete point charges $e_1 \cdots e_M$, and which is immersed in a solvent of dielectric constant $D$, as illustrated in Fig. 1. For zero ionic strength, the work of charging, $W_0$, with respect to the energy zero for the completely discharged state, is expressed as follows[7,8,12,14]:

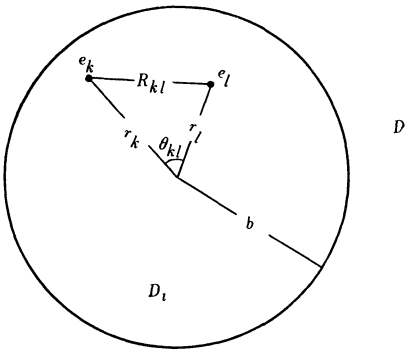



Fig. 1. Kirkwood's model for a spherical solute species having an arbitrary charge distribution.

$$W_0 = \frac{1}{2D_i}\sum_{k=1}^{M}\sum_{l=1}^{M} e_k e_l / R_{kl} + \frac{1}{2}\left(\frac{1}{D} - \frac{1}{D_i}\right)\sum_{n=0}^{\infty} \frac{(n+1)Q_n}{b^{2n+1}[(n+1)+nD_i/D]} \quad (1)$$

$$Q_n = \sum_{k=1}^{M}\sum_{l=1}^{M} e_k e_l r_k{}^n r_l{}^n P_n(\cos\theta_{kl}) \quad (2)$$

where $R_{kl}$ is the distance between the charges $e_k$ and $e_l$, $r_k$ and $r_l$ the distances of charges $e_k$ and $e_l$ from the center of the sphere, $\theta_{kl}$ the angle between $r_k$ and $r_l$, and $P_n(\cos\theta_{kl})$ is the Legendre polynomial. $Q_0$ is simply the square of the total net charge of the ion, and $Q_1$ is equal to the square of the dipole moment of the molecule. The succeeding $Q_n$'s involve the higher multipole moments, and depend not only upon the relative position of the charges, but also upon the distance of the charges from the surface of the sphere.

When the charges are situated not so near to the surface of the sphere, i. e., $r_k/b$ is not so close to unity, the summation in Eq. 1 converges rapidly, and the terms beyond $n=1$ can be dropped without serious error. This is the case in Laidler and Landskroener's treatment[6]. However, this approximation is not a reasonable one, especially when $b$ is large and the charges are situated near the surface, as is the case of a large complex ion such as protein. Now it is necessary to take the sum of the infinite series in Eq. 1. Since $D_i \ll D$ ($D_i$ was taken by Kirkwood to be 2), in a similar manner to Kirkwood's treatment[8], the sum is obtained by expanding the second term of Eq. 1 in increasing powers of $D_i/D$, and dropping all terms

7) J. G. Kirkwood, *J. Chem. Phys.*, **2**, 351 (1934).
8) J. G. Kirkwood and F. H. Westheimer, ibid., **6**, 506 (1938).
9) Y. Ogura et al., *Symposia on Enzyme Chem.* (*Kôso Kagaku Shimpojiumu*), **5**, 28 (1950); Y. Tonomura, *J. Japan. Biochem. Soc.*, (*Seikagaku*), **25**, 157 (1953).
10) M. L. Barnard and K. J. Laidler, *J. Am. Chem. Soc.*, **74**, 6099 (1952); K. J. Laidler and M. C. Ethier, *Arch. Biochem. Biophys.*, **44**, 338 (1953).
11) T. L. Hill, *J. Phys. Chem.*, **60**, 253 (1956); *J. Am. Chem. Soc.*, **78**, 3330 (1956); ibid., **78**, 5527 (1956).
12) C. Tanford and J. G. Kirkwood, ibid. **79**, 5333 (1957).
13) C. Tanford, ibid., **79**, 5340 (1957).
14) The first term in Eq. 1 represents the work of charging in an unbounded medium of dielectric constant $D_i$, and is independent of the solvent. It contains self-energy terms (i. e., $k=l$), which are infinite because of the assumption of point charges. But this term does not appear in the final expression for the activity coefficient (Eq. 8 below). The second term represents the mutual electrostatic energy of the molecule and the solvent medium, and is the important term in the present treatment.

higher than the first. Finally we have[15]

$$W_0=\frac{1}{2D_i}\left[\sum_{k=1}^{M}\sum_{l=1}^{M}\frac{e_ke_l}{R_{kl}}-\frac{1}{b}\left(\sum_{k=1}^{M}e_k^2f'_{kk}+\sum_{k=1}^{M}\sum_{l\neq k}e_ke_lg'_{kl}\right)\right]+\frac{1}{2Db}\left[\sum_{k=1}^{M}e_k^2f_{kk}+\sum_{k=1}^{M}\sum_{l\neq k}e_ke_lg_{kl}\right] \quad (3)$$

where

$$\left.\begin{aligned} f_{kk}&=\frac{2}{1-x_{kk}}+\frac{1}{x_{kk}}\ln(1-x_{kk})\\ g_{kl}&=\frac{2}{(1-2\alpha_{kl}x_{kl}+x_{kl}^2)^{1/2}}\\ &+\frac{1}{x_{kl}}\ln\frac{1-\alpha_{kl}}{(1-2\alpha_{kl}x_{kl}+x_{kl}^2)^{1/2}+x_{kl}-\alpha_{kl}}\end{aligned}\right\} \quad (4)$$

$$\left.\begin{aligned} f'_{kk}&=\frac{1}{1-x_{kk}}\\ g'_{kl}&=\frac{1}{(1-2\alpha_{kl}x_{kl}+x_{kl}^2)^{1/2}}\end{aligned}\right\} \quad (5)$$

where

$$x_{kl}=r_kr_l/b^2;\quad x_{kk}=(r_k/b)^2;\quad \alpha_{kl}=\cos\theta_{kl} \quad (6)$$

For zero ionic strength, the activity coefficient $\gamma$ of a solute species in the solvent of dielectric constant $D$ with respect to a standard solvent of dielectric constant $D_0$ ($D_0\gg D_i$) is related to the work of charging $W_0$ and $W_0^0$ in each solvent, respectively, in the following manner

$$\ln\gamma=(W_0-W_0^0)/\boldsymbol{k}T \quad (7)$$

where $\boldsymbol{k}$ is the Boltzmann constant and $T$ the absolute temperature. Insertion of Eq. 3 into Eq. 7 gives rise to

$$\ln\gamma=\frac{\varepsilon^2L}{2b\boldsymbol{k}T}\left(\frac{1}{D}-\frac{1}{D_0}\right) \quad (8)$$

where $\varepsilon$ is the protonic charge and $L$ is a new dimensionless parameter defined as

$$L=\sum_{k=1}^{M}\xi_k^2f_{kk}+\sum_{k=1}^{M}\sum_{l\neq k}\xi_k\xi_lg_{kl} \quad (9)$$

where $\xi_k$ is the valence of the charge $e_k$, i. e., $\xi_k=e_k/\varepsilon$. The value of $L$ is determined by the charge configuration of the species, i. e., $L$ is a function of $\xi$'s, $r$'s, $\theta$'s of the charges and the radius $b$. Thus $L$ will be conveniently termed "charge configuration function". $L/b$ represents the susceptibility of the electrostatic free energy of the solute species to the change in dielectric constant of the medium.

By the use of this new parameter $L$, a relationship between the rate or the equilibrium constant of a chemical change in solution and the dielectric constant of the solvent can readily be obtained. For example, let us consider the reaction

$$A+B\rightleftarrows X_{\neq}\rightarrow \text{Products}$$

where the reactants A, B and the activated complex $X_{\neq}$ may be either ions or molecules with particular charge configuration. Let $k_0$ denote the rate constant in the standard solvent of dielectric constant $D_0$ ($D_0\gg D_i$), then the rate constant $k$ in a solvent of dielectric constant $D$ is[1]

$$k=k_0\gamma_A\gamma_B/\gamma_{\neq} \quad (10)$$

where the $\gamma$'s are the activity coefficients of the corresponding species. Using Eq. 8 we have

$$\ln k=\ln k_0+\frac{\varepsilon^2}{2\boldsymbol{k}T}\left(\frac{1}{D}-\frac{1}{D_0}\right)\left(\frac{L_A}{b_A}+\frac{L_B}{b_B}-\frac{L_{\neq}}{b_{\neq}}\right) \quad (11)$$

where $L$'s and $b$'s are the charge configuration functions and the radii of the species, respectively. This equation indicates that the plot of $\log k$ against $1/D$ gives a straight line and that the slope is

$$\frac{\mathrm{d}\log k}{\mathrm{d}(1/D)}=\frac{\varepsilon^2}{2.303\,(2\boldsymbol{k}T)}\left(\frac{L_A}{b_A}+\frac{L_B}{b_B}-\frac{L_{\neq}}{b_{\neq}}\right) \quad (12)$$

Thus the slope is determined by the charge configuration functions and the radii of the species.

In a similar manner, the relationship between the equilibrium constant $K$ and the dielectric constant of the medium, $D$, can be obtained. For the equilibrium

TABLE I. VALUES OF $f$ FOR VARIOUS VALUES OF $x$

| $x$ | $f$ | $x$ | $f$ |
|---|---|---|---|
| 0 | 1.000 | 0.925 | 23.866 |
| 0.05 | 1.079 | 0.930 | 25.712 |
| 0.1 | 1.169 | 0.935 | 27.846 |
| 0.2 | 1.384 | 0.940 | 30.340 |
| 0.3 | 1.668 | 0.945 | 33.294 |
| 0.4 | 2.056 | 0.950 | 36.847 |
| 0.5 | 2.614 | 0.955 | 41.197 |
| 0.6 | 3.473 | 0.960 | 46.647 |
| 0.7 | 4.947 | 0.965 | 53.669 |
| 0.8 | 7.988 | 0.970 | 63.052 |
| 0.83 | 9.630 | 0.975 | 76.217 |
| 0.85 | 11.101 | 0.980 | 96.008 |
| 0.88 | 14.257 | 0.985 | 129.070 |
| 0.90 | 17.442 | 0.990 | 195.348 |
| 0.91 | 19.576 | 0.995 | 394.675 |
| 0.92 | 22.255 | 1 | $\infty$ |

15) Eq. 2 can be written as

$$Q_n=\sum_{k=1}^{M}e_k^2r_k^{2n}+\sum_{k=1}^{M}\sum_{l\neq k}e_ke_lr_k^nr_l^nP_n(\cos\theta_{kl})$$

When this is inserted into Eq. 1 and the summation is performed, the first term gives the $f$ and $f'$ terms and the second term gives the $g$ and $g'$ terms in Eq. 3.

TABLE II. VALUES OF $g$ FOR

| $\alpha \setminus x$ | 0.1 | 0.2 | 0.3 | 0.4 | 0.5 | 0.6 | 0.7 | 0.8 | 0.85 | 0.90 |
|---|---|---|---|---|---|---|---|---|---|---|
| −1 | 0.865 | 0.755 | 0.664 | 0.587 | 0.522 | 0.467 | 0.418 | 0.376 | 0.357 | 0.339 |
| −0.9 | 0.876 | 0.772 | 0.683 | 0.607 | 0.542 | 0.485 | 0.436 | 0.392 | 0.372 | 0.354 |
| −0.8 | 0.887 | 0.789 | 0.703 | 0.628 | 0.563 | 0.505 | 0.454 | 0.409 | 0.389 | 0.370 |
| −0.7 | 0.899 | 0.807 | 0.725 | 0.651 | 0.585 | 0.527 | 0.475 | 0.428 | 0.407 | 0.387 |
| −0.6 | 0.911 | 0.827 | 0.748 | 0.676 | 0.610 | 0.551 | 0.497 | 0.449 | 0.427 | 0.406 |
| −0.5 | 0.924 | 0.847 | 0.773 | 0.702 | 0.637 | 0.577 | 0.522 | 0.473 | 0.450 | 0.428 |
| −0.4 | 0.936 | 0.868 | 0.799 | 0.732 | 0.667 | 0.607 | 0.551 | 0.499 | 0.475 | 0.452 |
| −0.3 | 0.950 | 0.891 | 0.828 | 0.764 | 0.700 | 0.639 | 0.582 | 0.528 | 0.503 | 0.479 |
| −0.2 | 0.963 | 0.915 | 0.859 | 0.799 | 0.737 | 0.677 | 0.618 | 0.562 | 0.536 | 0.510 |
| −0.1 | 0.977 | 0.941 | 0.893 | 0.838 | 0.779 | 0.719 | 0.659 | 0.601 | 0.573 | 0.546 |
| 0 | 0.992 | 0.968 | 0.930 | 0.882 | 0.826 | 0.767 | 0.706 | 0.646 | 0.617 | 0.588 |
| 0.1 | 1.007 | 0.997 | 0.971 | 0.931 | 0.881 | 0.823 | 0.762 | 0.699 | 0.668 | 0.637 |
| 0.2 | 1.022 | 1.028 | 1.015 | 0.986 | 0.943 | 0.889 | 0.828 | 0.763 | 0.730 | 0.697 |
| 0.3 | 1.038 | 1.061 | 1.065 | 1.050 | 1.017 | 0.968 | 0.909 | 0.842 | 0.807 | 0.771 |
| 0.4 | 1.055 | 1.096 | 1.120 | 1.123 | 1.104 | 1.065 | 1.009 | 0.941 | 0.904 | 0.865 |
| 0.5 | 1.072 | 1.135 | 1.182 | 1.209 | 1.211 | 1.187 | 1.138 | 1.071 | 1.032 | 0.990 |
| 0.6 | 1.090 | 1.176 | 1.253 | 1.311 | 1.344 | 1.345 | 1.312 | 1.250 | 1.209 | 1.163 |
| 0.7 | 1.108 | 1.222 | 1.333 | 1.435 | 1.515 | 1.561 | 1.562 | 1.515 | 1.475 | 1.426 |
| 0.8 | 1.128 | 1.271 | 1.427 | 1.590 | 1.747 | 1.877 | 1.956 | 1.960 | 1.931 | 1.883 |
| 0.9 | 1.148 | 1.325 | 1.537 | 1.789 | 2.080 | 2.398 | 2.702 | 2.916 | 2.961 | 2.953 |
| 0.92 | 1.152 | 1.336 | 1.561 | 1.836 | 2.166 | 2.547 | 2.945 | 3.270 | 3.363 | 3.388 |
| 0.94 | 1.156 | 1.348 | 1.586 | 1.886 | 2.260 | 2.720 | 3.248 | 3.750 | 3.930 | 4.021 |
| 0.96 | 1.160 | 1.360 | 1.613 | 1.939 | 2.365 | 2.925 | 3.640 | 4.450 | 4.810 | 5.058 |
| 0.98 | 1.164 | 1.372 | 1.640 | 1.995 | 2.482 | 3.171 | 4.172 | 5.597 | 6.433 | 7.208 |
| 0.99 | 1.166 | 1.378 | 1.654 | 2.025 | 2.546 | 3.313 | 4.518 | 6.527 | 7.980 | 9.679 |
| 0.995 | 1.168 | 1.381 | 1.661 | 2.041 | 2.579 | 3.391 | 4.720 | 7.163 | 9.210 | 12.123 |
| 0.997 | 1.168 | 1.382 | 1.664 | 2.047 | 2.593 | 3.423 | 4.808 | 7.466 | 9.859 | 13.671 |
| 0.998 | 1.168 | 1.383 | 1.665 | 2.050 | 2.600 | 3.439 | 4.853 | 7.630 | 10.231 | 14.671 |
| 0.999 | 1.168 | 1.384 | 1.667 | 2.053 | 2.607 | 3.456 | 4.899 | 7.804 | 10.643 | 15.895 |
| 1 | 1.169 | 1.384 | 1.668 | 2.056 | 2.614 | 3.473 | 4.947 | 7.988 | 11.101 | 17.442 |

* When $x$ is zero, the value of $g$ is equal to unity for any value of $\alpha$.

$$A+B \rightleftharpoons C+D$$

the final expression is

$$\frac{d \log K}{d(1/D)}=\frac{\varepsilon^2}{2.303(2kT)}\left[\left(\frac{L_A}{b_A}+\frac{L_B}{b_B}\right)-\left(\frac{L_C}{b_C}+\frac{L_D}{b_D}\right)\right] \quad (13)$$

Assuming that the molecule or ion is a sphere within which each point charge is located at the center of each constituting atom, the value of $L$ of the molecule or ion with known charge configuration can be calculated using Eqs. 4, 6 and 9. For convenience of calculation, the values of $f$ and $g$ for various values of $x$ and $\alpha$ are tabulated in Tables I and II. For $x=0$, $f$ and $g$ are both equal to unity. The value of $g$ for $\alpha=1$ is equal to that of $f$ for the corresponding value of $x$. The value of $L$ is dependent on the position of the center to be chosen. It may be most reasonable to choose the center at the geometrical center of the

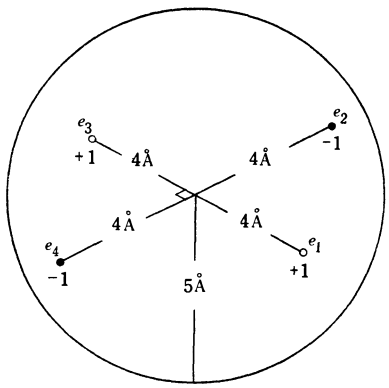



Fig. 2. A hypothetical dipolar ion. Two sets of charges, unit positive charges, $e_1$ anp $e_3$, and unit negative charges $e_2$ and $e_4$, are situated at equal distance 4 Å from the center, on the two diameters which are perpendicular to each other. The radius of the sphere is 5 Å.

VARIOUS VALUES OF $x$ AND $\alpha$*

| 0.91 | 0.92 | 0.93 | 0.94 | 0.95 | 0.96 | 0.97 | 0.98 | 0.99 | 1 | $x/\alpha$ |
|---|---|---|---|---|---|---|---|---|---|---|
| 0.336 | 0.333 | 0.329 | 0.326 | 0.323 | 0.319 | 0.316 | 0.313 | 0.310 | 0.307 | −1 |
| 0.350 | 0.347 | 0.343 | 0.340 | 0.336 | 0.333 | 0.330 | 0.326 | 0.323 | 0.320 | −0.9 |
| 0.366 | 0.362 | 0.359 | 0.355 | 0.351 | 0.348 | 0.344 | 0.341 | 0.338 | 0.334 | −0.8 |
| 0.383 | 0.379 | 0.376 | 0.372 | 0.368 | 0.364 | 0.361 | 0.357 | 0.354 | 0.350 | −0.7 |
| 0.402 | 0.398 | 0.394 | 0.390 | 0.386 | 0.383 | 0.379 | 0.375 | 0.371 | 0.368 | −0.6 |
| 0.424 | 0.419 | 0.415 | 0.411 | 0.407 | 0.403 | 0.399 | 0.395 | 0.391 | 0.387 | −0.5 |
| 0.447 | 0.443 | 0.439 | 0.434 | 0.430 | 0.426 | 0.422 | 0.417 | 0.413 | 0.409 | −0.4 |
| 0.474 | 0.470 | 0.465 | 0.460 | 0.456 | 0.451 | 0.447 | 0.442 | 0.438 | 0.434 | −0.3 |
| 0.505 | 0.500 | 0.495 | 0.490 | 0.486 | 0.481 | 0.477 | 0.471 | 0.467 | 0.462 | −0.2 |
| 0.541 | 0.535 | 0.530 | 0.525 | 0.520 | 0.515 | 0.510 | 0.505 | 0.500 | 0.495 | −0.1 |
| 0.582 | 0.576 | 0.571 | 0.565 | 0.560 | 0.554 | 0.549 | 0.544 | 0.538 | 0.533 | 0 |
| 0.631 | 0.625 | 0.619 | 0.613 | 0.607 | 0.602 | 0.596 | 0.590 | 0.584 | 0.578 | 0.1 |
| 0.691 | 0.684 | 0.678 | 0.671 | 0.665 | 0.658 | 0.652 | 0.646 | 0.639 | 0.633 | 0.2 |
| 0.764 | 0.757 | 0.750 | 0.743 | 0.736 | 0.729 | 0.722 | 0.714 | 0.708 | 0.701 | 0.3 |
| 0.858 | 0.850 | 0.842 | 0.834 | 0.826 | 0.818 | 0.810 | 0.803 | 0.795 | 0.787 | 0.4 |
| 0.981 | 0.972 | 0.964 | 0.955 | 0.946 | 0.937 | 0.928 | 0.919 | 0.910 | 0.901 | 0.5 |
| 1.154 | 1.144 | 1.134 | 1.124 | 1.114 | 1.104 | 1.093 | 1.083 | 1.072 | 1.062 | 0.6 |
| 1.415 | 1.404 | 1.393 | 1.381 | 1.369 | 1.357 | 1.344 | 1.332 | 1.319 | 1.306 | 0.7 |
| 1.871 | 1.858 | 1.845 | 1.831 | 1.817 | 1.802 | 1.786 | 1.770 | 1.753 | 1.736 | 0.8 |
| 2.944 | 2.933 | 2.921 | 2.905 | 2.888 | 2.869 | 2.848 | 2.824 | 2.799 | 2.772 | 0.9 |
| 3.383 | 3.376 | 3.365 | 3.352 | 3.335 | 3.315 | 3.293 | 3.267 | 3.239 | 3.208 | 0.92 |
| 4.026 | 4.027 | 4.022 | 4.013 | 3.999 | 3.981 | 3.957 | 3.929 | 3.897 | 3.860 | 0.94 |
| 5.088 | 5.111 | 5.125 | 5.131 | 5.128 | 5.116 | 5.095 | 5.066 | 5.029 | 4.983 | 0.96 |
| 7.335 | 7.448 | 7.544 | 7.622 | 7.678 | 7.711 | 7.720 | 7.706 | 7.666 | 7.602 | 0.98 |
| 10.018 | 10.343 | 10.645 | 10.917 | 11.149 | 11.330 | 11.454 | 11.514 | 11.504 | 11.425 | 0.99 |
| 12.808 | 13.512 | 14.222 | 14.915 | 15.565 | 16.137 | 16.594 | 16.900 | 17.026 | 16.955 | 0.995 |
| 14.665 | 15.740 | 16.884 | 18.074 | 19.270 | 20.407 | 21.399 | 22.143 | 22.542 | 22.531 | 0.997 |
| 15.909 | 17.295 | 18.832 | 20.513 | 22.300 | 24.113 | 25.811 | 27.192 | 28.027 | 28.138 | 0.998 |
| 17.486 | 19.352 | 21.549 | 24.134 | 27.148 | 30.572 | 34.241 | 37.713 | 40.216 | 40.899 | 0.999 |
| 19.576 | 22.255 | 25.712 | 30.340 | 36.847 | 46.647 | 63.052 | 96.008 | 195.348 | ∞ | 1 |

molecule or ion concerned. As an example, $L$ of a hypothetical dipolar ion such as that depicted in Fig. 2 is calculated to be 11.8. The procedure of the calculation is illustrated in Appendix I.

For a spherical ion including a charge $Z\varepsilon$ at its center, $L$ is simply $Z^2$ (since $x=0$ and $f$ is unity). Thus for a reaction between such unipolar ions Eq. 12 reduces to the familiar expression of Laidler-Eyring for reactions between ions[1].

For the purpose of comparison, Laidler-Landskroener's equation[6], which corresponds to Eq. 12, is cited below;

$$\frac{\mathrm{d}\log k}{\mathrm{d}(1/D)}=\frac{\varepsilon^2}{2.303(2kT)}\left[\left(\frac{Z_A{}^2}{b_A}+\frac{Z_B{}^2}{b_B}-\frac{(Z_A+Z_B)^2}{b_\ddagger}\right)+\frac{3}{2}\left(\frac{G_A}{b_A{}^3}+\frac{G_B}{b_B{}^3}-\frac{G_\ddagger}{b_\ddagger{}^3}\right)\right] \quad (14)$$

where $b$ and $Z$ represent the radius and the net charge of the species, respectively, and $G$ is a quantity determined by the given charge distribution in the species, which is proportional to the square of the dipole moment.

## Application of the Theory to Some Simple Systems

Before applying the theory to enzyme reactions, it is desirable to test its applicability to some simple systems, for which the structure and the charge distribution in the species concerned can be visualized with considerable certainty. Three examples will be treated here; first, the dissociation equilibria of carboxylic acids; second, the $S_N1$ solvolysis; and third, the acid and base catalyzed hydrolyses of esters, amides and anilides.

**Dissociation of Carboxylic Acids.** — The dissociation constants of some carboxylic acids have been measured by several authors in

TABLE III. THE INFLUENCE OF THE DIELECTRIC CONSTANT UPON THE DISSOCIATION CONSTANTS OF CARBOXYLIC ACIDS

| Acid | Temp. °C | Solvent[a] | Dissociation constant | $\frac{d(pK)}{d(1/D)}$ | $b$(Å)[b] I | $b$(Å)[b] II | $d$(Å)[b] I | $d$(Å)[b] II |
|---|---|---|---|---|---|---|---|---|
| Acetic | 25 | (W, W-E / W-D) | $K$ | 118 | 2.97 | | 1.33 | |
| Benzoic | 20 | (W, W-E / W-D) | $K$ | 170 | 3.75 | | 0.65 | |
| Succinic | 20 | (W, W-E / W-M, W-D) | $K_1$ | 133 | 4.30 | 4.40 | 1.09 | 1.19 |
| | | | | 150 | 4.07 | 4.10 | 0.86 | 0.89 |
| | | | $K_2$ | 178 | 3.73 | 3.80 | 1.01 | 1.08 |
| | | | | 200 | 3.48 | 3.50 | 0.76 | 0.78 |
| Adipic | 20 | (W, W-E / W-D) | $K_1$ | 147 | | 4.84 (all *trans*) | | 0.99 |
| | | | | | | 3.95 (di-*cis*) | | 0.94 |
| | | | $K_2$ | 164 | | 4.88 (all *trans*) | | 1.03 |
| | | | | | | 4.06 (di-*cis*) | | 1.05 |
| Azelaic | 20 | (W, W-E / W-M, W-D) | $K_1$ | 135 | | 6.84 (all *trans*) | | 1.23 |
| | | | | | | 5.84 (tri-*cis*) | | 1.21 |
| | | | $K_2$ | 140 | | 6.98 (all *trans*) | | 1.37 |
| | | | | | | 6.03 (tri-*cis*) | | 1.40 |

a) W: water, E: ethanol, M: methanol, D: dioxane.
b) $b$ (or $d$) indicates the radius (or the depth of the charge on the oxygen atom in $COO^-$) of $A^-$, $AH^-$ or $A^=$ corresponding to the dissociation constant $K$, $K_1$ or $K_2$, respectively. I: Calculated by Method I. II: Calculated by Method II.

various mixed aqueous solvents. The apparent dissociation constant $K_a$ of an acid AH ($K_a = [H^+][A^-]/[AH]$) in various mixed solvents having equal dielectric constants does not give the same value in different media having different water concentrations[16,17]. Yasuda[18] proposed that the dissociation constant $K$ of an acid in aqueous mixed solvents should be given by the following equation:

$$K = [A^-][H_3O^+]/[AH][H_2O]$$

corresponding to the equilibrium

$$AH + H_2O \rightleftharpoons H_3O^+ + A^-$$

He found that the plot of p$K$, instead of p$K_a$, of an acid against $1/D$ becomes a single straight line, irrespective of the sort of mixed solvent used, unless $1/D$ exceeds ca. 0.02[18]. Therefore, it may be reasonable to conclude that the variation in p$K$ is essentially due to the change in the dielectric constant of the medium, at least in the range stated above. The slope $d(pK)/d(1/D)$ is written as follows;

$$-\frac{d(pK)}{d(1/D)} = \frac{\varepsilon^2}{2.303(2kT)}\left(\frac{L_{AH}}{b_{AH}} + \frac{L_{H_2O}}{b_{H_2O}} - \frac{L_{A^-}}{b_{A^-}} - \frac{L_{H_3O^+}}{b_{H_3O^+}}\right) \quad (15)$$

Values of the slopes obtained from Yasuda's results for several carboxylic acids are summarized in Table III, where $K_1$ and $K_2$ are the first and the second dissociation constants of dibasic acids, respectively.

$$K_1 = [AH^-][H_3O^+]/[AH_2][H_2O]$$

$$K_2 = [A^=][H_3O^+]/[AH^-][H_2O]$$

Procedure of testing the theory is as follows; first, for the three species, $H_2O$, $H_3O^+$ and AH (or $AH_2$ for the dibasic acid), $L/b$'s are calculated from the charge configurations and the radii of these species; insertion of these values together with the value of the slope into Eq. 15 leads to an equation for $L_{A^-}/b_{A^-}$; if the magnitudes and the relative positions of the charges in $A^-$ are known, $L_{A^-}$ and $L_{A^-}/b_{A^-}$ are the functions of $b_{A^-}$ only; then the equation can be solved for $b_{A^-}$[19]. If the theory is correct, $b_{A^-}$ thus obtained should be of reasonable magnitude as is expected from the structure of $A^-$. The geometry and the charge distribution of the species which are necessary for the calculation of $L$'s are summarized in Appendix II.

Succinic acid was treated by the following two methods. In Method I, the charge distribution in the COOH group was considered explicitly in the evaluation of $L_{AH_2}$ and $L_{AH^-}$ as in the case of acetic acid and benzoic acid. Since $L_{AH_2}$ was found to be appreciably small,

16) J. C. Speakman, *J. Chem. Soc.*, **1943**, 270.
17) M. L. Dondon. *J chim. phys.*, **54**, 290, 304 (1957).
18) M. Yasuda, This Bulletin, **32**, 429 (1959).
19) Practically $b_{A^-}$ is obtained in the following manner. For several fixed values of $b_{A^-}$ suitably chosen, $L_{A^-}$'s are calculated and $L_{A^-}/b_{A^-}$ is plotted against $b_{A^-}$. By graphical interpolation $b_{A^-}$ to be solved is readily found.

TABLE IV. THE INFLUENCE OF SOLVENT UPON THE RATE CONSTANTS OF $S_N1$ SOLVOLYSIS

| Compound | Temp. °C | Solvent[a] | $\frac{d \log k_1}{d(1/D)}$ | Model | Type | Present theory $b_{\ddagger}$(Å) | Present theory $d$(Å)[b] | L-L theory $b_{\ddagger}$(Å)[c] |
|---|---|---|---|---|---|---|---|---|
| *tert*-Butyl chloride | 25 | (W-E, W-M / W-A, HCOOH) | −179 | I | (1) | 3.12 | 0.48 | |
| | | | | | (2) | 3.10 | 0.46 | 1.92 |
| | | | | II | (1) | 2.41 | 0.47 | |
| | | | | | (2) | 2.36 | 0.42 | |
| *tert*-Butyl bromide | 25 | (W-E, W-A) | −127 | I | (1) | 3.50 | 0.64 | |
| | | | | | (2) | 3.46 | 0.60 | 2.27 |
| | | | | II | (1) | 2.72 | 0.62 | |
| | | | | | (2) | 2.65 | 0.55 | |
| Benzhydryl chloride | 25 | W-E | −122 | I | (2) | 3.84 | 0.60 | 2.19 |
| | | W-A | −137 | I | (2) | 3.79 | 0.55 | 2.10 |
| α-Phenethyl chloride | 50 | W-E | −166 | I | (2) | 3.92 | 0.45 | 1.99 |
| | | W-A | −150 | I | (2) | 3.96 | 0.49 | 1.92 |
| Neopentyl bromide | 95 | (W-E / HCOOH) | −162 | I | (2) | 3.62 | 0.42 | 1.96 |
| Pinacolyl-*p*-bromobenzene sulfonate | 70 | (W-E, W-A / $Ac_2O$-AcOH) | −103 | I | (2) | 8.05 | 0.60 | 2.34 |
| α-Methylallyl chloride | 25 | (W, W-E) | −161 | I | (2) | 3.48 | 0.49 | 1.99 |

a) W: water, E: ethanol. M: methanol, A: acetone.
b) The depth of the charge on the halogen atom from the surface.
c) $b_{\ddagger}$ calculated by the present author with Laidler-Landskroener's equation (Eq. 14).

in Method II, $L_{AH_2}$ and $L_{AH^-}$ were evaluated assuming that the charge on every atom in the COOH group is zero. This greatly simplifies the calculation, without affecting the results seriously (compare $b$'s for I and II in Table III). Hence, adipic acid and azelaic acid were treated by Method II. For these two acids calculations were made for the all *trans* form and the di-*cis* or tri-*cis* form (see Appendix II).

The results of the calculations are summarized in Table III. In the last two columns are presented the values of $d$, the depth of the charge on the oxygen atom in the $COO^-$ group from the surface of the sphere[20]. It is noted that $d$'s are nearly constant for the acids in spite of the wide variation in $b$'s.

**$S_N1$ Solvolysis.** — The influence of the dielectric constant of the medium upon the rate constant $k_1$ of $S_N1$ solvolysis has been discussed by Shingu and Okamoto[21]. The linear relationship between $\log k_1$ and $1/D$ was interpreted quantitatively on the basis of an ion-pair model for the activated complex. In the present study, the activated complex itself is treated as a sphere, within which positive and negative charges are assumed to be located at the centers of the carbon and halogen atoms, respectively. The equation to be used is as follows;

$$\frac{d \log k_1}{d(1/D)} = \frac{\varepsilon^2}{2.303\,(2kT)}\left(\frac{L_A}{b_A} - \frac{L_{\ddagger}}{b_{\ddagger}}\right) \qquad (16)$$

where $L_A/b_A$ and $L_{\ddagger}/b_{\ddagger}$ are concerned with the reactant molecule and the activated complex, respectively. In the manner similar to that of the preceding example, the radius of the activated complex $b_{\ddagger}$ was determined to fit the experimentally obtained slope.

For *tert*-butyl chloride and *tert*-butyl bromide the charge distributions were calculated from the observed dipole moments[22,23] considering the inductive effect[24], and the $L_A$'s were estimated. Since it was found that they are sufficiently small (see Appendix II), and the final values of $b_{\ddagger}$ are only slightly affected by ignoring them (by 0.01 Å or less), $L_A/b_A$ in Eq. 16 was approximated to zero for the present example. In the activated complexes the carbon-halogen bond lengths were assumed to be increased 50% (Model I) or 10% (Model II) over the normal bond lengths. In calculating $L$, two types of charge distribution were assumed for the activated complexes. Type 1

20) $d$ is equal to $b$ minus $r$ for the oxygen atom.
21) H. Shingu and K. Okamoto, *J. Chem. Soc. Japan, Pure Chem. Sec.* (*Nippon Kagaku Zasshi*), **78**, 558 (1957).
22) L. E. Sutton, "Determination of Organic Structures by Physical Methods", edited by E. A. Braud and F. C. Nachod, Academic Press, New York (1955), p. 392.
23) C. P. Smyth, "Dielectric Behavior and Structure", McGraw-Hill, New York (1955).
24) R. P. Smith, T. Ree, J. L. Magee and H. Eyring, *J. Am. Chem. Soc.*, **73**, 2263 (1951); R. P. Smith and H. Eyring, ibid., **74**, 229 (1952).

consists of a unit negative charge on the halogen atom, and compensating positive charges distributed on the remaining atoms in the same proportion to those in the normal molecules. In Type 2, simplification was made, so that a unit positive charge is localized solely on the $\alpha$-carbon atom, neglecting the charges on the remaining atoms except for a unit negative charge on the halogen atom. Calculation showed that the solved $b_{\ddagger}$'s are somewhat smaller in Type 2. Since the difference in $b_{\ddagger}$'s is not serious, the other five compounds were treated with the simplified models (Type 2), assuming that the carbon-halogen bond lengths in the activated complexes are increased 50% over the normal ones (Model I).

The results are listed in Table IV, where $b_{\ddagger}$'s calculated with Laidler-Landskroener's equation (Eq. 14) are also included. $d$ indicates the depth of the charge on the halogen atom from the surface of the sphere. It is noticed that $d$'s, in contrast to $b_{\ddagger}$'s, are not affected appreciably by the choice between Models I and II.

**III. Acid and Base Catalyzed Hydrolyses of Esters, Amides and Anilides.**—As an example of bimolecular reactions, and for the purpose of comparing the applicability of the present theory with that of Laidler-Landskroener's, the acid and base hydrolyses of certain esters, amides and anilides are treated along the same line and on exactly the same models for the activated complexes as those they proposed[6]. The relevant equation is

$$\frac{\mathrm{d}\log k}{\mathrm{d}(1/D)} = \frac{\varepsilon^2}{2.303(2kT)}\left(\frac{1}{b_{\mathrm{A}}} - \frac{L_{\ddagger}}{b_{\ddagger}}\right) \qquad (17)$$

where $k$ denotes the bimolecular rate constant, $b_{\mathrm{A}}$ the radius of a hydronium or hydroxyl ion, and $L_{\ddagger}$ and $b_{\ddagger}$ refer to the activated complex. In accordance with Laidler-Landskroener's treatment, it was assumed that the hydronium and the hydroxyl ions are unipolar ions (the charge is located at the center of the ion) with the radii of 1.70 Å[25] and 1.40 Å[26],

TABLE V. THE INFLUENCE OF SOLVENT UPON THE RATE CONSTANTS OF THE ACID AND BASE HYDROLYSES OF ESTERS, AMIDES AND ANILIDES

| Compound | Catalyst | Temp. °C | Solvent[a] | $\frac{\mathrm{d}\log k}{\mathrm{d}(1/D)}$ | $b_{\ddagger}$(Å) | | |
|---|---|---|---|---|---|---|---|
| | | | | | L-L theory[b] | Present theory C[c] | Present theory P[d] |
| Ethyl acetate | $H_3O^+$ | 35 | W-D | −11 | 4.6 | 5.39 | 4.29 |
| | | 35 | W-A | −34 | 4.1 | 5.08 | 3.97 |
| Methyl propionate | $H_3O^+$ | 35.3 | W-A | −31 | 4.2 | 5.11 | 4.00 |
| Ethyl acetate | $OH^-$ | 25 | W-D | −24 | 1.9 | 4.47 | 3.56 |
| | | | W-A | −32 | 1.8 | 4.45 | 3.51 |
| | | | W-*i*Pr | −50 | 1.7 | 4.41 | 3.42 |
| | | | W-*t*Bu | −61 | 1.7 | 4.39 | 3.38 |
| | | | W-*n*Pr | −74 | 1.6 | 4.37 | 3.34 |
| | | | W-E | −96 | 1.5 | 4.35 | 3.29 |
| | | | W-M | −155 | 1.3 | 4.31 | 3.20 |
| Formanilide | $H_3O^+$ | 30 | W-E | −13.8 | 3.7 | 4.33 | 3.65 |
| Form-*o*-toluidide | $H_3O^+$ | 30 | W-E | −14.5 | 3.7 | 4.32 | 3.64 |
| Form-*p*-toluidide | $H_3O^+$ | 40 | W-E | −13.8 | 3.7 | 4.32 | 3.65 |
| *o*-Nitro-acetanilide | $H_3O^+$ | 80 | W-E | − 5.5 | 3.9 | 4.42 | 3.76 |
| Acetanilide | $H^3O^+$ | 80 | W-E | − 5.4 | 3.9 | 4.42 | 3.76 |
| Aceto-*m*-toluidide | $H_3O^+$ | 80 | W-E | − 7.8 | 3.8 | 4.38 | 3.72 |
| Acetamide | $H_3O^+$ | 80 | W-E | −42.1 | 3.2 | 4.09 | 3.37 |
| Propionamide | $H_3O^+$ | 80 | W-E | −39.7 | 3.2 | 4.10 | 3.38 |
| Acetamide | $OH^-$ | 80 | W-E | −71.3 | 1.6 | 4.39 | 3.34 |
| Propionamide | $OH^-$ | 80 | W-E | −68.4 | 1.6 | 4.39 | 3.35 |

a) W: water, E: ethanol, M: methanol, D: dioxane, *i*Pr: isopropanol, *n*Pr: *n*-propanol, *t*Bu: *tert*-butanol.
b) Values calculated by Laidler and Landskroener[6].
c) Center: Carbonyl carbon atom.
d) Center: Point P depicted in Fig. A-5 in Appendix II.

25) J. D. Bernal and R. H. Fowler, *J. Chem. Phys.*, **1**, 515 (1933).
26) J. Buchanan and S. D. Hamann, *Trans. Faraday Soc.*, **49**, 1425 (1953).

respectively. Hence their $L$'s are unity. $L$'s of the substrate molecules were also approximated to zero. By Eq. 17, $b_{\pm}$'s were determined to fit the observed slopes using their models for the activated complexes (see Fig. A-5 in Appendix II). The results are listed in Table V. In the column of $b_{\pm}$, L-L indicates Laidler-Landskroener's values[6], and C or P denotes the results of the present study when the center of the activated complex is taken at the carbonyl carbon atom as in Laidler-Landskroener's calculation, or at the point P depicted in the models, respectively.

## Discussion

In the previous theories of the solvent effect[1-5], an ion or a molecule was treated as a uniformly charged sphere or a dipole, respectively, disregarding the actual distribution of charges within them. It is more reasonable to treat the reactants and the activated complex as those having the particular distribution of charges. In this sense, Laidler-Landskroener's treatment[6] and the present one may be said to be more accurate and general than the previous treatments.

However, as seen from Tables IV and V, the radii of the activated complexes calculated according to Laidler-Landskroener's formula are unreasonably too small for the $S_N1$ solvolysis and the base hydrolysis of esters and amides. These values of radii would lead to an improbable situation where some of the charges are extruded out of the sphere, which is obviously inconsistent with the Kirkwood's model on which the theory is based. On the other hand, the application of the present theory to the above three examples has revealed that the radii of the species concerned are of quite reasonable magnitude as are to be expected from the structures of the species. It is evident from Example III that this discrepancy has come from the approximation made in the derivation of Laidler-Landskroener's equation in which the higher terms were dropped in the sum in Eq. 1, the other circumstances being equal in both treatmnets. The difference between the two theories may be most clearly illustrated in the following example. Suppose a unimolecular reaction in which the reactant is a neutral molecule having no distribution of charge and the activated complex is such as is shown in Fig. 2. Since both the net charge and the dipole moment are zero, the slope $\mathrm{d}\log k/\mathrm{d}(1/D)$ predicted by Laidler-Lands-kroener's equation (Eq. 14) is zero. On the other hand, the slope predicted by the present theory at 25°C is

$$\frac{\mathrm{d}\log k}{\mathrm{d}(1/D)} = -\frac{\varepsilon^2}{2.303(2kT)}\left(\frac{L}{b}\right) = -121.7 \times \frac{11.8}{5}$$

$$= -286 \qquad (18)$$

The value of $L$ depends sensitively upon the depth of the charge, $d$, at which the charge is located within the sphere. It is worthwhile to examine the values of $d$ determined to fit the observed slopes in the above examples, since they serve as a more rigorous check for the validity of the theory than the radii do.

In treating the interaction energies between charges on organic ions, as reflected in p$K$'s of dibasic acids and amino acids, based on the Kirkwood's model, Tanford[27] showed that the interaction energies critically depend upon the depth, $d$, of the charges, and it is necessary that $d$ be assigned a value close to 1.0 Å to account for experimentally observed interaction energies. He also found[13] that in calculating titration curves for simple protein model molecules using the Kirkwood model, merely by placing charges about 1 Å below the surfaces the titration curves can be obtained with a slope whose order of magnitude is in the best agreement with that observed experimentally.

Application of the present theory to the dissociation of carboxylic acids showed, as seen from Table III, that $d$'s of the charge on the oxygen atom in the carboxylate group are of nearly constant value around 1.0 Å within the error of the slope[28]. It is of interest to see that these values of $d$ are in good agreement with Tanford's value obtained from the calculation of interaction energies stated above, although different lines of approach have been made. These values of $d$ are comparable to the van der Waals radius (1.40 Å) or the ionic radius (1.4 Å) of oxygen atom[29]. Considering the simplicity of the Kirkwood model, the agreement may be considered to be satisfactory.

The depths, $d$'s calculated for the $S_N1$ solvolysis are also nearly constant for the series of compounds, but are considerably smaller compared with the van der Waals or ionic radii of the halogen atoms[29]. However, we have good reasons to accept the first example (variation of p$K$ of carboxylic acids with $D$) as the most reliable one, for in the remaining two examples the structures and the charge configurations of the activated complexes are essentially speculative in nature and are not so definitely established. In addition there is

27) C. Tanford, *J. Am. Chem. Soc.*, **79**, 5348 (1957).
28) The error in the slope may amount to ca. 10%, which leads to an uncertainty of 0.2 Å in $b$ or $d$.
29) L. Pauling, "The Nature of the Chemical Bond", Cornell University Press, New York (1940).

some possibility that an influence other than that of the dielectric constant might be included in the experimentally determined slopes. In fact, for the $S_N1$ solvolysis of *tert*-butyl chloride, Okamoto and Shingu[30] have pointed out that the solvent molecules containing one or more hydroxyl groups have some specific effect in accelerating the solvolytic reaction, and this effect is to be distinguished from the dielectric constant effect. Therefore, the observed slopes may be, at least in part, attributed to this specific effect caused by changing the composition of mixed solvents. The true slopes may be less negative, which may lead to larger values of $d$ in the above calculations.

Since the present theory has been developed for zero ionic strength, a comment will be needed about the influence of ionic strength, $\mu$, on the theoretical expressions. According to Kirkwood, the work of charging $W$ of the spherical molecule stated above in the presence of external ions in the solvent is[7]

$$W = W_0 + W_{\text{ion}} \tag{19}$$

where $W_0$ is a work of charging at zero ionic strength which was already expressed in Eq. 1, and $W_{\text{ion}}$ is a term arising from the presence of external ions and is given in the following formula[7,12]

$$W_{\text{ion}} = -\frac{\varepsilon^2}{2a}\sum_{k=1}^{M}\sum_{l=1}^{M}\xi_k\xi_l\, C_{kl} \tag{20}$$

where $a$ is the mean distance of closest approach of ions in the solvent to the solute species and $C_{kl}$ is a complex function of $D$, $D_i$, $a$, $\mu$ and the charge configuration of the species, and is difficult to manage in a simple manner. However, at low ionic strength[31] it is a good approximation to write $C_{kl}$ as

$$C_{kl} \simeq \frac{1}{D}\cdot\frac{\kappa a}{1+\kappa a} \tag{21}$$

where $\kappa$ is the Debye-Hückel parameter

$$\kappa = \sqrt{8\pi N\varepsilon^2\mu/1000DkT} \tag{22}$$

and is also a function of $D$. In a manner similar to that of Eq. 7 through Eq. 13, an expression for $\mathrm{d}\log k/\mathrm{d}(1/D)$ in the presence of ions, corresponding to, e. g., Eq. 12, is obtained as follows;

$$\frac{\mathrm{d}\log k}{\mathrm{d}(1/D)} = \frac{\varepsilon^2}{2.303(2kT)}\left[\left(\frac{L_A}{b_A}+\frac{L_B}{b_B}-\frac{L_\pm}{b_\pm}\right) - \frac{\mathrm{d}}{\mathrm{d}(1/D)}\left(\frac{\Phi_A}{a_A}+\frac{\Phi_B}{a_B}-\frac{\Phi_\pm}{a_\pm}\right)\right] \tag{23}$$

where

$$\Phi = \sum_{k=1}^{M}\sum_{l=1}^{M}\xi_k\xi_l C_{kl} \simeq \frac{Z^2}{D}\cdot\frac{\kappa a}{1+\kappa a} \tag{24}$$

since $\sum_{k=1}^{M}\sum_{l=1}^{M}\xi_k\xi_l$ is equal to the square of the total net charge $Z^2$ of the species. The second term in the right hand side in Eq. 23 represents a contribution of the term dependent on ionic strength to the slope. The contribution at various ionic strengths was estimated for the reaction

$$A + B \rightleftarrows X_\pm \rightarrow \text{Products}$$

for which $a_A = a_B = 5$ Å and $a_\pm = 6$ Å, at 25°C and $D$=78.5. The results are summarized in Table VI, where $\varphi$ designates the contribution of the term dependent on ionic strength to the slope.

$$\varphi \equiv \frac{\varepsilon^2}{2.303(2kT)}\cdot\frac{\mathrm{d}}{\mathrm{d}(1/D)}\left(\frac{\Phi_A}{a_A}+\frac{\Phi_B}{a_B}-\frac{\Phi_\pm}{a_\pm}\right) \tag{25}$$

TABLE VI. THE CONTRIBUTION OF THE TERM DEPENDENT ON IONIC STRENGTH TO THE SLOPE

| | $\varphi$ | | |
|---|---|---|---|
| $\mu$ | $Z_A=+1$ $Z_B=+1$ | $Z_A=+1$ $Z_B=-1$ | $Z_A=\pm1$ $Z_B=0$ |
| 0.01 | − 9.2 | 9.9 | 0.17 |
| 0.04 | −14.7 | 16.7 | 0.49 |
| 0.09 | −18.2 | 21.6 | 0.83 |
| 0.25 | −23.1 | 28.1 | 1.26 |
| 0.49 | −24.9 | 32.2 | 1.83 |
| 1.0 | −26.0 | 37.0 | 2.75 |

$\varphi$ is seen to be positive or negative according as the charges of the reactant ions are of opposite or like sign, and to be small if one of the reactants has no net charge. Although the $\varphi$ is only approximate especially at high ionic strengths, it may serve as a rough estimate of the contribution of the term dependent on ionic strength to the slope.

## Summary

A theory has been developed on the relationship between the equilibrium constant or the rate constant of a reaction and the dielectric constant of the solvent based on the Kirkwood's model. It is applicable to equilibrium states or reaction processes in which ions or molecules having arbitrary charge distributions are involved, including enzyme reactions. The theory predicts that there is a linear relationship between the logarithm of the equilibrium or rate constant and the reciprocal of the dielectric constant of the solvent. The slope is determined by the new parameter $L$, termed the charge

30) K. Okamoto and H. Shingu, reported at the Symposium on Mechanisms of Organic Reactions, Tokyo, 1959.

31) Ionic strength up to $\kappa a$=0.5 with charges near the surface, and to even higher values of $\kappa a$ for charges appreciably below the surface[12].

configuration function, and the radius of each species involved. $L$ of a species is a function of the magnitudes and the relative positions of charges in it and its radius. Tables have been presented in order to facilitate the evaluation of $L$.

The applicability of the theory has been tested for the dissociation of carboxylic acids, the $S_N1$ solvolysis of organic halides, and the acid and base hydrolyses of esters, amides and anilides, and the results are found to be satisfactory.

The influence of ionic strength on the theoretical expressions has also been discussed.

The author is deeply grateful to Professor Sôzaburo Ono for his kind guidance and discussion throughout this work. He is also indebted to Dr. Kunio Okamoto of Kyoto University and to Dr. Ichiro Moritani and Dr. Tsutomu Ishimura of Osaka University for their helpful discussions. He thanks Professor Wasaburo Jôno of Kyoto University for his interest and encouragement.

*Laboratory of Biophysical Chemistry*
*College of Agriculture*
*University of Osaka Prefecture*
*Sakai, Osaka*

## Appendix I

**Evaluation of $L$.** — The charge configuration function $L$ of the hypothetical dipolar ion depicted in Fig. 2 is evaluated as follows; $L$ is written as

$$L=\xi_1^2f_{11}+\xi_2^2f_{22}+\xi_3^2f_{33}+\xi_4^2f_{44}+2\xi_1\xi_2g_{12}+2\xi_1\xi_3g_{13}+2\xi_1\xi_4g_{14}+2\xi_2\xi_3g_{23}+2\xi_2\xi_4g_{24}+2\xi_3\xi_4g_{34}$$

where

$$\xi_1=\xi_3=-\xi_2=-\xi_4=1$$

And

$$b=5\text{ Å}$$

$$r_1=r_2=r_3=r_4=4\text{ Å}$$

$$x_{11}=x_{22}=\cdots\cdots=x_{12}=\cdots\cdots=x_{34}=(r/b)^2=0.64$$

$$\alpha_{12}=\alpha_{14}=\alpha_{23}=\alpha_{34}=\cos 90^\circ=0$$

$$\alpha_{13}=\alpha_{24}=\cos 180^\circ=-1$$

The values of $f(x)$ and $g(x,\alpha)$ are given from Tables I and II as follows;

$$f_{11}=f_{22}=f_{33}=f_{44}=3.98$$

$$g_{12}=g_{14}=g_{23}=g_{34}=0.743$$

$$g_{13}=g_{24}=0.447$$

Hence $L$ is evaluated to be

$$L=4\times3.98-2\times4\times0.743+2\times2\times0.447=11.76$$

## Appendix II

The geometry and the charge distribution necessary for the calculation of $L$'s in the above three examples are summarized here. $r$'s and $\theta$'s are readily computed from them with trigonometry. A-B designates the distance between atoms A and B, $\xi_A$ the valence of the charge on A. The positions of the centers of the species are also shown. The procedure of determining $b$ to fit the observed slope is illustrated for the acetate ion.

### Dissociation of Carboxylic Acids.

1) $H_2O$ :— O-H=0.96 Å, ∠HOH=105°[29]. $\xi_0=-0.66$, $\xi_H=0.33$ (calculated from the dipole moment[23]). Center: Oxygen atom. $b=1.40$ Å[32]. $L$ calculated=0.263.

2) $H_3O^+$ :— O-H=1.01 Å, ∠HOH=117°[33] (pyramidal structure with equivalent H). $\xi_H=0.50$, $\xi_0=-0.50$. Center: Oxygen atom. $b=1.70$ Å. $L$ calculated=1.266.

3) Carboxyl group :—The structure of the carboxyl group[23] for acetic acid, benzoic acid and succinic acid (Method I) is shown in Fig. A-1. All the atoms are assumed to lie on the same plane[34]. The charge distribution is shown in the individual articles below.

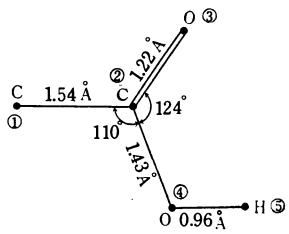



Fig. A-1. The structure of the carboxyl group. The atoms are numbered as indicated.

4) Carboxylate group :—The structure[35] and the charge distribution of the carboxylate group is depicted in Fig. A-2. This was used as the carboxylate model in every acid anion throughout this

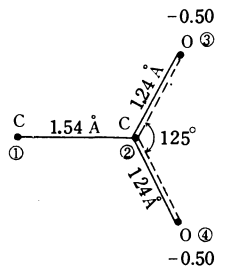



Fig. A-2. The structure of the carboxylate group. The atoms are numbered as indicated. The valences of the charges on the oxygen atoms are also shown.

32) R. W. Gurney, "Ionic Processes in Solution", McGraw-Hill, New York (1953), p. 16.
33) S. Seki et al., "Gendai Kagaku", VIG, Iwanami, Tokyo (1956), p. 51.
34) R. F. Curl, *J. Chem. Phys.*, **30**, 1529 (1959).
35) G. A. Jeffrey and G. S. Parry, *J. Chem. Soc.*, **1952**, 4864.

example. The two oxygen atoms are equivalent[36]. It was assumed that the four atoms are coplanar, and $\xi_1=\xi_2=0$, $\xi_3=\xi_4=-0.50$.

5) Acetic acid (AH):—The charge distribution was calculated from the bond moments[23] and the dipole moment[23] considering the inductive effect[24]. $\xi_1=0.110$, $\xi_2=0.409$, $\xi_3=-0.412$, $\xi_4=-0.435$, $\xi_5=0.325$. Center: Carboxyl C atom. $b=3.00$ Å. $L$ calculated $=0.097$.

6) Acetate ion ($A^-$) : — Center: Point on the $C_1$-$C_2$ line at 0.64 Å apart from $C_2$ atom. $L_{A^-}/b_{A^-}$ calculated for various values of $b_{A^-}$ are as follows;

| $b_{A^-}$(Å) | 2.40 | 2.70 | 3.00 | 3.30 |
|---|---|---|---|---|
| $L_{A^-}/b_{A^-}$(Å$^{-1}$) | 0.689 | 0.529 | 0.437 | 0.376 |

Insertion of the observed slope $d(pK)/d(1/D)$, $L$'s and $b$'s for $H_2O$, $H_3O^+$ and HA into Eq. 15 gives

$$\frac{L_{A^-}}{b_{A^-}}=\frac{118}{121.7}+\frac{0.263}{1.40}+\frac{0.097}{3.00}-\frac{1.266}{1.70}=0.445\ (\text{Å}^{-1}) \qquad \text{(A-1)}$$

$L_{A^-}/b_{A^-}$ is plotted against $b_{A^-}$, and the value of $b_{A^-}$ which fulfils Eq. A-1 can be obtained graphically. $b_{A^-}$ thus obtained is 2.97 Å.

7) Benzoic acid (AH) :—The charge distribution was determined to fit the observed dipole moment[23] assuming that $\xi_3$, $\xi_4$ and $\xi_5$ are the same as those in acetic acid and the remaining charges are shared by the $C_2$ atom and the center of the ring, Q. $\xi_2=0.455$, $\xi_3=-0.412$, $\xi_4=-0.435$, $\xi_5=0.328$, $\xi_Q=0.064$. Center: Point on the $C_2$-Q line at 1.88 Å apart from $C_2$. $b=4.60$ Å. $L$ calculated $=0.102$.

8) Benzoate ion ($A^-$) : — Center: Point on the $C_2$-Q line at 2.32 Å apart from $C_2$ atom.

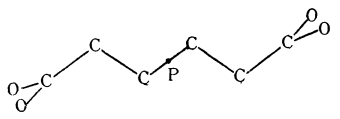
9) Succinic acid ($AH_2$) (Method I) :—*trans* Form, symmetric with respect to the middle point of the C-C bond in $CH_2$-$CH_2$ group, was assumed. The four carbon atoms lie on the same plane, to which the planes including each carboxyl group are perpendicular. $\xi_1=0$, $\xi_2=0.519$, $\xi_3=-0.412$, $\xi_4=-0.435$, $\xi_5=0.328$. The charge distribution in the two carboxyl groups are the same. Center: Center of symmetry. $b=4.60$ Å. $L$ calculated $=0.210$.

10) Bisuccinate ion ($AH^-$) (Method I) :—*trans* Form similar to $AH_2$ except that one of the carboxyl groups is replaced by carboxylate group. Center: C atom adjacent to the carboxyl C atom. The charge distribution in the carboxyl group is the same as that in $AH_2$.

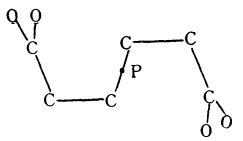
11) Succinate ion ($A^=$) (Method I) :—Symmetric *trans* form similar to $AH_2$ except that the carboxyl groups are replaced by the carboxylate groups. Center: Center of symmetry.

12) Succinic acid ($AH_2$, $AH^-$, $A^=$)(Method II): —The geometry of each species is the same as that of the corresponding species treated in Method I. The charges on all the atoms in COOH group were assumed to be zero.

13) Adipic acid ($AH_2$, $AH^-$, $A^=$) (Method II) : —The structures assumed are schematically depicted in Fig. A-3. In both forms, all the carbon atoms lie on the same plane, to which the two planes including each carboxyl group are perpendicular.

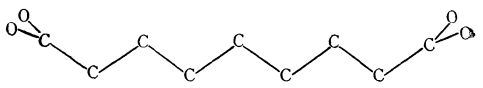


all *trans* form

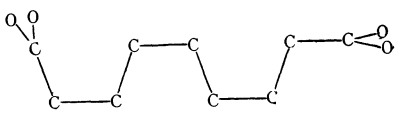


di-*cis* form

Fig. A-3. Schematic representation of the structures of adipic acid.



all *trans* form



tri-*cis* form

Fig. A-4. Schematic representation of the structures of azelaic acid.

Center: Middle point of C-C bond, P, as shown in Fig. A-3.

14) Azelaic acid ($AH_2$, $AH^-$, $A^=$) (Method II): The structures assumed are depicted in Fig. A-4. All the carbon atoms were assumed to lie on the same plane, to which the two COOH planes are perpendicular. Center: Center of the rectangle formed by the four oxygen atoms in $A^=$ form.

### SN1 Solvolysis.

In *tert*-butyl chloride and *tert*-butyl bromide, the atoms are numbered as follows; methyl carbon atom 1, $\alpha$-carbon atom 2, and halogen atom (X) 3. The carbon atoms were all assumed to be tetrahedral. The center was chosen at $C_2$ atom in both normal state and activated state.

1) *tert*-Butyl chloride.

Normal state : — C-X=1.76 Å, C-C=1.54 Å. $\xi_1=0.0417$, $\xi_2=0.0882$, $\xi_3=-0.213$. (The small charges

36) L. J. Bellamy, "The Infra-red Spectra of Complex Molecules", Methuen & Co., London (1958), p. 161.

on the methyl hydrogen atoms were included in $\xi_1$). $b=3.00$ Å. $L$ calculated $=0.048$.

Activated state :— C-X $=2.64$ Å (Model I) ; C-X $=1.94$ Å (Model II). $\xi_1=0.196$, $\xi_2=0.414$, $\xi_3=-1.0$ (Type 1), $\xi_1=0$, $\xi_2=1.0$, $\xi_3=-1.0$ (Type 2).

2) *tert*-Butyl bromide.

Normal state :— C-X $=1.91$ Å, C-C $=1.54$ Å. $\xi_1=0.0403$, $\xi_2=0.085$, $\xi_3=-0.206$. $b=3.00$ Å. $L$ calculated $=0.057$.

Activated state :— C-X $=2.86$ Å (Model I) ; C-X $=2.10$ Å (Model II). $\xi_1=0.195$, $\xi_2=0.414$, $\xi_3=-1.0$ (Type 1); $\xi_1=0$, $\xi_2=1.0$, $\xi_3=-1.0$ (Type 2).

The following five compounds were treated by the simplified type of charge distribution for the activated complexes (Type 2), $\xi_2=1$, $\xi_3=-1$, ignoring every small charge on the remaining atoms. The C-X bond distance in the activated complex was taken as 2.86 Å for bromide, and 2.64 Å for chloride (Model I).

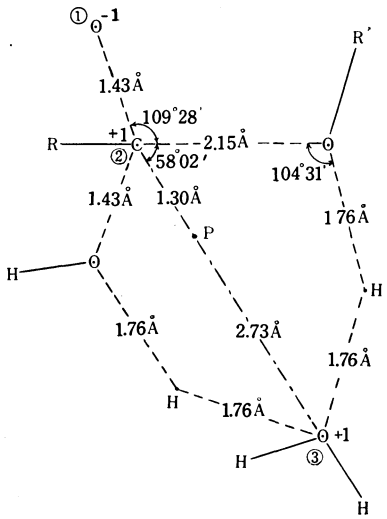
3) Neopentyl bromide :—Center : Middle point between $\alpha$-C and $\beta$-C atoms.

4) Benzhydryl chloride :—Center : Middle point between the two aromatic C atoms to which the $\alpha$-C atom is attached.

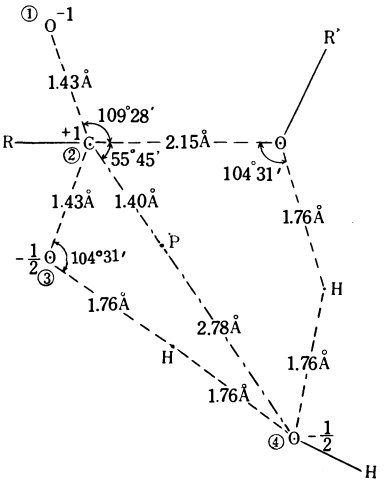
5) $\alpha$-Phenethyl chloride :—Center : $C_1$ atom of phenyl group.

6) Pinacolyl-*p*-bromobenzenesulfonate :—Center : Sulfur atom.

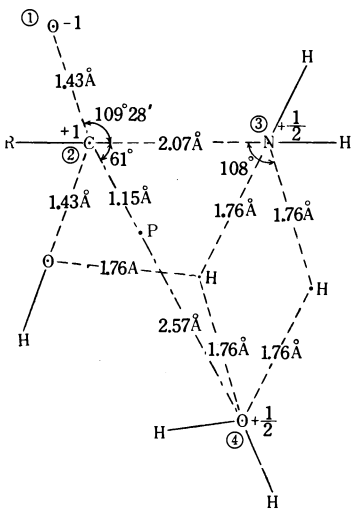
7) $\alpha$-Methylallyl chloride:—Center : Middle point between the $\alpha$-C atom and the adjacent double bonded C atom.



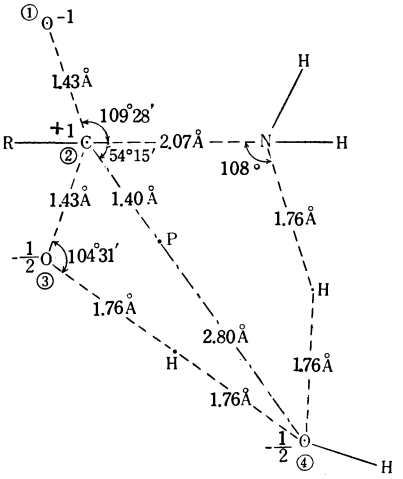

(1) Acid hydrolysis of an ester




(2) Base hydrolysis of an ester




(3) Acid hydrolysis of an amide or anilide




(4) Base hydrolysis of an amide or anilide

Fig. A-5. Laidler-Landskroener's models for the activated complexes in the acid and base hydrolyses of esters, amides and anilides.

**III. Acid and Base Hydrolyses of Esters, Amides and Anilides.**

Laidler-Landskroener's models for the activated complexes are shown in Fig. A-5. It was assumed that the $C_2$ atoms are tetrahedral, and the following four atoms lie on the same plane;

$O_1$, $C_2$, $O_3$ and O(esteric) in Model (1)
$O_1$, $C_2$, $O_4$ and O(esteric) in Model (2)
$O_1$, $C_2$, $N_3$ and $O_4$ in Model (3)
$O_1$, $C_2$, N and $O_4$ in Model (4).

The center was chosen at $C_2$ atom or at point **P** depicted in the models (cf. Table V).

# *Theory of the Influence of the Dielectric Constant on the Rate of Reaction in Solution with Application to Enzyme Reactions. II. Application of the Theory to Enzyme Reactions**

By Keitaro HIROMI

(Received December 18, 1959)

The enzyme molecule in solution has a number of charged groups, some of which play an essential role in the catalytic reactions. Rates of enzyme reactions, therefore, may be expected to be influenced by the dielectric constant of a medium as are generally observed in reactions involving simple ions or dipolar molecules. From this viewpoint, rates of several enzyme reactions have been measured in aqueous mixed solvents, and the results have been discussed in relation to the dielectric constant of the medium[1-8]. In treating catalase and peroxidase reactions, Ogura et al.[1] and Tonomura[3] considered the enzyme or the enzyme-substrate complex as a dipole, to which the expression for the reaction between dipolar molecules[9] was applied. On the other hand, for $\alpha$-chymotrypsin[2] and myosin[4] catalyzed reactions, Laidler and his coworkers applied the coulombic law to the interaction between the charges of the substrate and the essential groups of the enzyme. However, since it is supposed that the reaction may occur in a local region near the surface of a large cavity of low dielectric constant formed by the enzyme molecule in solution, these treatments may be said to be over-simplified, and the validity of the conclusions deduced from them may be subject to criticism.

The Kirkwood's model for a spherical solute molecule having an arbitrary charge distribution, on which a general theory of the solvent effect has been developed in the preceding paper[10], seems to be appropriate as a model for a protein in solution. In this paper, the theory will be extended to include the solvent effect upon enzyme reactions.

## Theoretical

Enzyme reactions in general consist of two stages, formation of an intermediate enzyme-substrate complex, and its breakdown into products and free enzyme.

$$E + S \underset{k_{-1}}{\overset{k_1}{\rightleftharpoons}} ES \overset{k_2}{\rightarrow} E + P$$

The Michaelis constant $K_m$ and the rate constant of breakdown $k_2$ can be obtained in the usual manner[11]. In certain cases in which $k_{-1} \gg k_2$, $K_m$ may be identified with the reciprocal of the equilibrium constant $K$ for the formation of ES complex[12]. In some instances, $k_1$ or $k_{-1}$ can be measured directly[13], or may

* Presented in part at the Symposium on Enzyme Chem., Sapporo, July, 1958.

1) Y. Ogura, A. Hattori, Y. Tonomura and S. Hino, *Symposia on Enzyme Chem.* (*Kôso Kagaku Shimpojiumu*), **5**, 28 (1950); Y. Ogura and H. Hasegawa, ibid., **7**, 79 (1952).

2) M. L. Barnard and K. J. Laidler, *J. Am. Chem. Soc.*, **74**, 6099 (1952).

3) Y. Tonomura, *J. Japan Biochem. Soc.*, (*Seikagaku*), **25**, 175 (1953).

4) K. J. Laidler and M. C. Ethier, *Arch. Biochem. Biophys.*, **44**, 338 (1953).

5) R. Lumry and E. L. Smith, *Discussions Faraday Soc.*, **20**, 105 (1955).

6) S. Ono, K. Hiromi and Y. Sano, Presented as a lecture at the 8th Annual Meeting of Chem. Soc. Japan, Tokyo (1955); S. Ono, K. Hiromi and Y. Sano, to be published.

7) A. Stockell and E. L. Smith, *J. Biol. Chem.*, **227**, 1 (1957).

8) T. Hosoya, *J. Biochem.* (Tokyo) in press.

9) S. Glasstone, K. J. Laidler and H. Eyring, "The Theory of Rate Processes", McGraw-Hill New York (1941), p. 419.

10) K. Hiromi, This Bulletin, **33**, 1251 (1960).

11) For example, H. Lineweaver and D. Burk, *J. Am. Chem. Soc.*, **56**, 658 (1934).

12) M. F. Morales, ibid., **77**, 4169 (1955); K. J. Laidler, *Trans. Faraday* Soc., **51**, 540 (1955).

13) B. Chance, "Investigation of Rates and Mechanisms of Reactions", in "Technique of Organic Chemistry", edited by A. Weissberger, Interscience Publishers, New York (1953), Vol. VIII, p. 627.

be obtained from the analysis of overall reaction rates[14]. These kinetic parameters, $k$'s and $K$, may be influenced by the dielectric constant $D$ of the solvent, and equations similar to Eqs. 12 and 13 in the preceding paper[10] may be available. They involve the charge configuration functions $L$'s of the substrate, enzyme, ES complex and/or $ES_{\neq}$, the activated complex of ES. The $L$'s of the last three species involve the contribution of all the charges of the enzyme molecule, which we cannot evaluate explicitly because of our lack of knowledge about their spatial distribution over the enzyme molecule. However, as will be seen shortly, the following treatment may be allowable. Instead of $L$, the complete charge configuration function involving all the charges in the enzyme, we may use $L^0$, the effective charge configuration function concerned only with the small number of charges of special interest belonging to a limited reaction region, disregarding all the remaining charges in the enzyme which are considered to be kept fixed and not to come into play during the reaction process.

Consider the equilibrium, for example,

$$E + S \underset{k_{-1}}{\overset{k_1}{\rightleftharpoons}} ES$$

The variation of the equilibrium constant $K(=k_1/k_{-1})$ with $D$ can be written as[10]

$$\frac{d \log K}{d(1/D)} = \frac{\varepsilon^2}{2.303(2kT)}\left(\frac{L_S}{b_S} + \frac{L_E}{b_E} - \frac{L_{ES}}{b_{ES}}\right) \tag{1}$$

where $b$'s are the radii of the substrate, enzyme and ES complex, as indicated by the suffixes, $L$'s are the corresponding complete charge configuration functions which contain the contribution of all the charges in E and ES, and the other symbols have the same meaning as those in the preceding paper[10]. For small substrates $b_E$ and $b_{ES}$ may be equated. Let E and ES have in the total $M$ and $M'$ charges, respectively, and let $n$ of them be kept fixed in position and free from any change during the process. Thus

$$\left.\begin{aligned} M &= n+m \\ M' &= n+m' \end{aligned}\right\} \tag{2}$$

where $m$ and $m'$ are the number of charges of special interest which belong to the local reaction region in E and ES, respectively. $L_E$ and $L_{ES}$ are written as follows[10];

$$\begin{aligned} L_E &= \sum_{k=1}^{M} \xi_k^2 f_{kk} + \sum_{k=1}^{M} \sum_{l\neq k} \xi_k \xi_l g_{kl} \\ &= \sum_{i=1}^{m} \xi_i^2 f_{ii} + \sum_{s=1}^{n} \xi_s^2 f_{ss} + \sum_{i=1}^{m} \sum_{s=1}^{n} \xi_i \xi_s g_{is} \\ &\quad + \sum_{i=1}^{m} \sum_{j\neq i} \xi_i \xi_j g_{ij} + \sum_{s=1}^{n} \sum_{t\neq s} \xi_s \xi_t g_{st} \end{aligned} \tag{3}$$

$$\begin{aligned} L_{ES} &= \sum_{k=1}^{M'} \xi_k^2 f_{kk} + \sum_{k=1}^{M'} \sum_{l\neq k} \xi_k \xi_l g_{kl} \\ &= \sum_{i=1}^{m'} \xi_i^2 f_{ii} + \sum_{s=1}^{n} \xi_s^2 f_{ss} + \sum_{i=1}^{m'} \sum_{s=1}^{n} \xi_i \xi_s g_{is} \\ &\quad + \sum_{i=1}^{m'} \sum_{j\neq i} \xi_i \xi_j g_{ij} + \sum_{i=1}^{n} \sum_{t\neq s} \xi_s \xi_t g_{st} \end{aligned} \tag{4}$$

where the suffixes $i$ and $j$ refer to the charge number of the charges belonging to the $m$ or $m'$ group, $s$ and $t$ the $n$ group, and $f$ and $g$ are the functions of the positions of charges as were defined by Eq. 4 in the preceding paper[10].

Hence we have

$$\begin{aligned} L_E - L_{ES} &= \Big(\sum_{i=1}^{m} \xi_i^2 f_{ii} + \sum_{i=1}^{m} \sum_{j\neq i} \xi_i \xi_j g_{ij}\Big)_E \\ &\quad - \Big(\sum_{i=1}^{m'} \xi_i^2 f_{ii} + \sum_{i=1}^{m'} \sum_{j\neq i} \xi_i \xi_j g_{ij}\Big)_{ES} \\ &\quad + \Big(\sum_{i=1}^{m} \sum_{s=1}^{n} \xi_i \xi_s g_{is}\Big)_E - \Big(\sum_{i=1}^{m'} \sum_{s=1}^{n} \xi_i \xi_s g_{is}\Big)_{ES} \end{aligned} \tag{5}$$

The last two terms of the right hand side in Eq. 5 are those from the pair-wise contribution between the $m$ or $m'$ charges of special interest and the $n$ remaining fixed charges in E and ES. If the $n$ charges consist of approximately equal numbers of positive and negative charges, and they are distributed at random over the enzyme molecule, these terms may be appreciably small and may be dropped without serious error. Hence

$$\left.\begin{aligned} L_E - L_{ES} &= L^0{}_E - L^0{}_{ES} \\ L^0{}_E &= \Big(\sum_{i=1}^{m} \xi_i^2 f_{ii} + \sum_{i=1}^{m} \sum_{j\neq i} \xi_i \xi_j g_{ij}\Big)_E \\ L^0{}_{ES} &= \Big(\sum_{i=1}^{m'} \xi_i^2 f_{ii} + \sum_{i=1}^{m'} \sum_{j\neq i} \xi_i \xi_j g_{ij}\Big)_{ES} \end{aligned}\right\} \tag{6}$$

where $L^0{}_E$ and $L^0{}_{ES}$ are the effective charge configuration functions of E and ES, concerned only with the charges of special interest. Eq. 1 becomes, therefore,

$$\frac{d \log K}{d(1/D)} = \frac{\varepsilon^2}{2.303(2kT)} \times \left[\frac{L_S}{b_S} + \frac{1}{b_E}(L^0{}_E - L^0{}_{ES})\right] \tag{7}$$

Similarly for the breakdown process of ES, we have

$$\frac{d \log k_2}{d(1/D)} = \frac{\varepsilon^2}{2.303(2kT)}\left(\frac{L^0{}_{ES}}{b_{ES}} - \frac{L^0{}_{ES\neq}}{b_{ES\neq}}\right) \tag{8}$$

14) H. Gutfreund, *Discussions Faraday Soc.*, **20**, 167 (1955); E. C. Slater, ibid., **20**, 231 (1955).

where $L^0_{ES\neq}$ is the effective charge configuration function of $ES_{\neq}$. Similar equations for $k_1$ or $k_{-1}$ if necessary, may readily be obtained.

### Application to Some Typical Models

In Table I are summarized the data of the solvent effect upon the kinetic parameter $\mathfrak{R}$ which have been obtained for various enzyme reactions[1-8]. $\mathfrak{R}$ represents the rate constant or equilibrium constant specified in each item. The slopes $d \log \mathfrak{R}/d(1/D)$ have been calculated under the assumption that the observed changes in $\mathfrak{R}$ are due entirely to the variation in dielectric constant of the mixed solvent. The radii of the enzymes are computed from the molecular weight and the specific volume[15] assuming the spherical shape of the enzymes. In many cases, the slopes have considerably large negative values of the order of $-200$.

It is worthwhile to see whether the present theory can reasonably account for the slopes of the observed order of magnitude, considering only the electrostatic rearrangement in the local reaction region.

For the present, let us confine our attention to the breakdown process of ES complex in which the bond X–Y of a substrate molecule is to be split. During the activation process a change in charge state may occur in the local reaction region which involves the bound substrate molecule and the catalytic center of the enzyme. We may assume that ES and $ES_{\neq}$ are spheres of equal radii $b_{ES}$, and that the substrate molecule is situated near the surface of the sphere. It is reasonable to suppose that in the activated complex the bond to be split is polarized so that a positive charge and a negative charge will be produced on the atoms X and Y forming the bond, as a preliminary stage of bond splitting[2]. It may lead to a change in $L^0$ by which the slope $d \log k_2/d(1/D)$ will be determined. The increment in $L^0$, and hence the slope, may depend on the magnitude of the charges produced, their position in the sphere (or the depth of the charges from the surface), and the situation of the neighboring charges. Two typical models for $ES_{\neq}$ are shown in Fig. 1. $e_3$ and $e_4$ are the charges produced on the atoms X and Y in $ES_{\neq}$ at a depth $d$ from the surface of the sphere. $e_1$ and $e_2$ are the neighboring charges which represent, for example, the charges of the active site of the enzyme, or the other charges the substrate may bear. In both models, the distance between $e_3$ and $e_4$ is taken as 2 Å, which is nearly equal to 50% stretched bond length of C–O or C–N

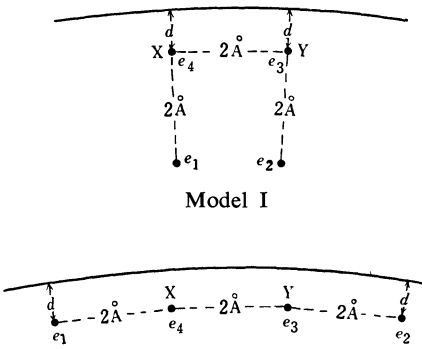



Fig. 1. Models of $ES_{\neq}$.
$e_1$ and $e_2$ represent the neighboring charges, and $e_3$ and $e_4$ the charges produced on the atoms X and Y in the activated state.

bond over their normal ones. In Model I, $e_1$ and $e_2$ are assumed to be situated by 2 Å inside on the lines drawn from the center to the charges $e_4$ and $e_3$, respectively. In Model II, $e_1$ and $e_2$ are situated on both sides of $e_4$ and $e_3$, 2 Å apart from them, respectively, at a depth $d$ from the surface. $\xi$'s denote the valences of the charges. The increment in the effective charge configuration function, $\Delta L^0_{\neq}$ $(=L^0_{ES\neq} - L^0_{ES})$, accompanied with the activation of ES complex, can be calculated from Eq. 6, using Tables I and II in the preceding paper[10], and the slope $d \log k_2/d(1/D)$ from Eq. 8. In the present case, calculations were made under the following conditions; i) the charges $e_3$ and $e_4$ are both zero in ES, ii) $-\xi_3=\xi_4=1$ or 1/2 in $ES_{\neq}$, iii) $e_1$ and $e_2$ are either positive or negative unit charges and are fixed during the activation process, iv) $d$ is taken as 0.5 Å or 1.0 Å, and v) $b_{ES}=b_{ES\neq}=21$ Å and the temperature is 25°C. The results are summarized in Table II. It is seen that the slope is determined primarily by the magnitude of the charges produced and by the depth of the charges below the surface, $d$, and is also dependent upon the situation of the neighboring charges especially in Model II. The slope of the observed order of magnitude is reasonably accounted for, if a pair of charges of opposite sign whose valence is close to unity are produced in the activated complex at the depth of 0.5~1.0 Å below the surface. These values for depth of charges are in reasonable agreement with those determined for the simple systems in the preceding paper[10]. On the other hand, Laidler-Landskroener's equation[16] applied to the above models, yields a slope, at the greatest, of about

15) E. J. Cohn and J. T. Edsall, "Proteins, Amino Acids and Peptides", Reinhold Publishing Co., New York (1943), p. 370.

16) K. J. Laidler and P. A. Landskroener, *Trans. Faraday Soc.*, **52**, 200 (1956). (cf. Eq. 14 in the preceding paper).

TABLE I. SOLVENT EFFECTS UPON VARIOUS ENZYME REACTIONS

| Substrate | Enzyme | Radius $b_E$, Å | Temp. °C | $\mathfrak{R}$ | Solvent[a] | $\frac{d \log \mathfrak{R}}{d(1/D)}$ | Reference No. |
|---|---|---|---|---|---|---|---|
| Carbobenzoxy-glycyl-L-tryptophan | Carboxy-peptidase | 21 | 25 | $k_2$ | W-M | −200 | |
| | | | | | W-E | −180 | 5 |
| | | | | | W-D | − 30 | |
| Methyl hydrocinnamate | α-chymo-trypsin | 20 | 25 | $k_2$ | W-M | −260 | 2 |
| | | | | $K$ | W-M | −240 | |
| α-Benzoyl-L-argininamide | Papain | 18 | 38 | $k_1$ | W-M | −160 | |
| | | | 38 | $k_1$ | W-*i*Pr | −160 | 7 |
| | | | 5 | $k_1$ | W-M | −180 | |
| Soluble starch | Bacterial α-amylase | 23 | 25 | $k_2$ | W-M | −210 | 6 |
| | | | | $K$ | W-M | 0 | |
| ATP | Myosin | — | 25 | $k_2$ | W-M | 80 | 4 |
| | | | | $K$ | W-M | 330 | |
| $H_2O_2$ | Catalase | 42 | 0 | $k_3$[b] | W-E | −160 | 1 |
| $H_2O_2$+guaiacol | Peroxidase (Japanese radish) | 22 | 25 | $k$[c] | (W-E, W-A) W-D | −200 | 3 |
| $H_2O_2$+guaiacol | Peroxidase (Turnip) $A_1$ | 23 | 20 | $k_4$[d] | (W-M, W-A) | −210 | |
| | $A_2$ | 23 | 20 | $k_4$ | W-M | −220 | 8 |
| | D | 23 | 20 | $k_4$ | W-M | −250 | |

a) W: water, M: methanol, E: ethanol, D: dioxane, *i*Pr: *iso*-propanol, A: Acetone.

b) $ES \xrightarrow{s\ k_3} E + P$ (s: $H_2O_2$)

c) $ES \xrightarrow{a\ k} E + P$ (a: guaiacol)

d) The apparent rate constant of the reaction between complex II and guaiacol.

TABLE II. PREDICTION OF THE THEORY FOR TYPICAL MODEL REACTIONS

| Charges produced | Model | Neighboring charges $\xi_1$ | Neighboring charges $\xi_2$ | Charge configuration in $ES_{\neq}$[a] | $\Delta L^0_{\neq}$ $d=$ 0.5 Å | $\Delta L^0_{\neq}$ $d=$ 1.0 Å | $-d \log k_2/d(1/D)$ $d=$ 0.5 Å | $-d \log k_2/d(1/D)$ $d=$ 1.0 Å |
|---|---|---|---|---|---|---|---|---|
| | I, II | 0 | 0 | (○ ●) | 46.3 | 12.8 | 269 | 74.2 |
| | I | +1 | +1 | (○ ● / ○ ○) | 46.3 | 12.8 | 269 | 74.2 |
| $\xi_3=-1$ | I | +1 | −1 | (○ ● / ○ ●) | 55.1 | 16.8 | 320 | 97.4 |
| $\xi_4=+1$ | I | −1 | +1 | (○ ● / ◕ ○) | 37.5 | 8.8 | 218 | 51.0 |
| | II | +1 | +1 | (○ ○ ● ○) | 46.3 | 12.8 | 269 | 74.2 |
| | II | +1 | −1 | (○ ○ ● ●) | 80.4 | 34.1 | 466 | 198 |
| | II | −1 | +1 | (◕ ○ ● ○) | 13.0 | −8.4 | 75.4 | −48.7 |
| | I, II | 0 | 0 | (◦ •) | 11.6 | 3.2 | 67.3 | 18.6 |
| | I | +1 | +1 | (◦ • / ○ ○) | 11.6 | 3.2 | 67.3 | 18.6 |
| $\xi_3=-1/2$ | I | +1 | −1 | (◦ • / ○ ●) | 16.0 | 5.2 | 92.8 | 30.2 |
| $\xi_4=+1/2$ | I | −1 | +1 | (◦ • / ● ○) | 7.2 | 1.2 | 41.8 | 7.0 |
| | II | +1 | +1 | (○ ◦ • ○) | 11.6 | 3.2 | 67.3 | 18.6 |
| | II | +1 | −1 | (○ ◦ • ●) | 28.6 | 13.8 | 169 | 80.0 |
| | II | −1 | +1 | (● ◦ • ○) | −5.4 | −7.4 | −31.3 | −42.9 |

a) The charge configurations in $ES_{\neq}$ (Models I and II) are schematically illustrated with the white and the black circles. The large white or black circle represents a positive or a negative unit charge, and the small white or black circle a positive or a negative half unit charge, respectively.

$-0.8$, by a factor of $10^2$ less than the observed values.

## Discussion

The present theory which is based on the Kirkwood's model may be more suited for treating the solvent effect upon enzyme reactions than the previous ones[1-4], although some simplifications inevitable in dealing with the complex enzyme molecule have still been made. The application of the theory to the typical models has shown that it successfully accounts for the experimentally obtained slopes, considering only the local rearrangement of charges in the enzyme-substrate complex. An advantage of the present theory over the existing theories is that it can deal with any microscopic change in charge state in any position in the spherical solute. It eliminates the disadvantage of the treatment which regards the enzyme or the enzyme-substrate complex as a dipole[1,3], according to which an extraordinarily large dipole moment had to be assigned to the activated complex in order to account for the slope of the observed order of magnitude[17].

At present we shall have to be content with the successful results of the application of the theory to the typical examples stated above. However, when our knowledge has accumulated about the value of $d$ to be assigned in the individual cases, we may reasonably hope that we can have an insight into the microscopic charge configuration in the activated state from the slope obtained by the study of the solvent effect on the reaction rate, which may serve as a tool for elucidating the mechanism of the reaction.

However, in interpreting the experimental data of solvent effect, attention must be paid to the possibility that the observed effects may involve contributions of various factors other than the purely electrostatic effect of dielectric constant on the rate. The factors that may possibly influence the rate by changing the composition of mixed solvents are enumerated as follows; 1) decrease in water concentration which might result in reduction of rates, if the rate determining step involves participation of the water molecules especially for hydrolytic enzymes, 2) shift of the activity-pH curve which may decrease or increase the rate when the experiments are carried out at constant pH[6], 3) possible inhibition by some component of the mixed solvent, 4) irreversible or reversible denatuation of the enzyme caused by the addition of organic solvents, 5) change in viscosity which may influence the rate if the reaction is diffusion controlled[18-20]. In most cases, the addition of organic solvents may lead to a decrease in rates due to these factors, in addition to a decrease in the dielectric constant of the medium. If this is the case, the observed slopes may possibly have been over-estimated in the negative direction, which would lead to larger values of $d$ in the above calculation.

For non-zero values of ionic strength, the slope may be affected by the inclusion of the term dependent on ionic strength as already discussed in the preceding paper[10]. The contribution of this term may be small except for bimolecular processes in which both of the reactants have non-zero net charges. Of course, the contribution is greater at higher ionic strength. A rough estimate reveals that for ionic strength of 0.02 and the radius of the enzyme taken as 20 Å[21], the contribution to the slope may be less than about $\pm 40$ for a bimolecular process between reactants having univalent net charge. It is desirable that the reaction should be carried out at an ionic strength as low as possible, in order to elucidate the effect of dielectric constant on the rate.

The theory may also be applied to the influence of solvent on binding of substrates or inhibitors to the enzyme, although there are restrictions inherent to the Kirkwood's model.

## Summary

The theory of solvent effect developed in the preceding paper has been extended to include the enzyme reactions. The application to some typical model reactions which resemble the breakdown of enzyme-substrate complex has shown that the order of magnitude of experimentally observed effects can reasonably be accounted for by the theory.

Factors which may possibly influence rates of enzyme reactions by changing the composition of mixed solvents have also been discussed.

The author expresses his hearty thanks to Professor Sôzaburo Ono for his kind guidance

17) For example, if the slope d log $k_2$/d(1/$D$) of the order of $-200$ is interpreted by the equation for dipolar molecules[1,3,9]

$$\frac{\mathrm{d}\log k_2}{\mathrm{d}[(D-1)/(2D+1)]} = \frac{1}{2.303\,kTb_{ES}{}^3}(\mu_{ES^\ddagger}{}^2 - \mu_{ES}{}^2)$$

where $\mu$'s are the dipole moments, it is necessary that $\mu_{ES^\ddagger}{}^2$ be larger than $\mu_{ES}{}^2$ by ca. $2.4\times10^5$ Debye$^2$, for $b_{ES}$ = 21 Å at 25°C. Accepting this large increase in $\mu$, one might be forcibly led to the conclusion that a profound change in shape or charge distribution in the whole body of the enzyme molecule had been brought about during the activation process.

18) E. Ackerman, G. K. Strother and R. L. Berger, "The Influence of Temperature on Biological Systems", Papers Symposium, Storrs, Conn. (1956), p. 25.

19) R. A. Alberty and G. G. Hammes, *J. Phys. Chem.*, 62, 154 (1958).

20) H. Mitsuda et al., *Symposia on Enzyme Chem.*, (*Kôso Kagaku Shimpojiumu*), in press.

21) Accordingly $\kappa a$ (cf. Eq. 21 in the preceding paper) at room temperature is about unity.

and discussion throughout this work. The author is also indebted to Professor Wasaburo Jôno of Kyoto University for his interest and encouragement.

*Laboratory of Biophysical Chemistry*
*College of Agriculture*
*University of Osaka Prefecture*
*Sakai, Osaka*

Note: The present theory was recently applied by Hosoya to the interpretation of his data of solvent effect upon the peroxidase reactions. (See Ref. 8.)

# *Amylose-Iodine Complex. II*[1]. *Effects of Inorganic Salts*

By Takashi KUGE and Sôzaburo ONO

(Received March 21, 1960)

The starch-iodine reaction in solution is markedly affected by some conditions (i. e. temperature, history of amylose solution and concentrations of reactants, etc.) under which the reaction takes place. However, the effect of salts on starch-iodine reaction has scarcely been investigated except in the case of studies[2] made at the beginning of this century at which time starch chemistry had not yet been established. The authors have found that certain salts strongly aid the formation of the amylose-iodine complex in a solution containing small amount of iodide ion. Referring these results to the helical theory[3], the authors intend to elucidate the structure of the amylose-iodine complex in solution.

## Experimental

**Materials.**—Amylose was obtained from potato starch by a selective precipitation method with *n*-butyl alcohol and isoamyl alcohol[4]. This amylose was recrystallized twice from boiling water in the presence of excess butanol. All other reagents were of the purest grade commercially available and used without further purification.

**Procedure.**—Hot water was poured on the recrystallized dry amylose of known amount and the suspension was heated on a water bath, being stirred for one hour in order to complete the dispersion of amylose. After being cooled, the solution was filtered with a glass filter and the filtrate was diluted to a desired volume with water. The above prepared solution, aqueous iodine solution, iodide solution and salt solution were used to make the final solutions which were composed of 0.005~0.015% amylose, $10^{-5}$~$2\times10^{-5}$ M iodine, $10^{-6}$~$10^{-5}$ M potassium iodide and $10^{-5}$~$10^{-1}$ M salt. In these compositions the amount of iodine was less than one third of that sufficient to saturate the amylose, and the ratio of iodide to iodine was unusually small, compared with that in a usual case. After being stood for more than one hour, the final colored solutions were used for spectrophotometric measurements.

A nearly saturated solution of iodine which was used to prepare the final solutions was made by shaking iodine crystals in water at room temperature. The concentrations of iodine and iodide ion in this solution were determined immediately before use by measuring their absorbances at wavelengths 288, 350 and 460 mμ[5], since iodide ion is formed by the hydrolysis of iodine.

The spectrophotometric measurements were carried out at room temperature by a Shimadzu type QB-50 spectrophotometer with 1.00 cm. thick silica cells.

## Results and Discussion

Iodide ion plays an important role in the amylose-iodine reaction but it remains uncertain whether or not amylose can form an iodide-free iodine complex in solution[6]. To solve this question, an aqueous iodine solution, in which iodic acid, perchloric acid or sulfuric acid was contained to repress any iodide ion due to the hydrolysis of iodine, was added to the amylose solution. Absorption at 350 mμ

1) S. Ono, S. Tsuchihashi and T. Kuge, *J. Am. Chem. Soc.*, **75**, 3601 (1953) is the Part I of this series.

2) For a review, see "Chemistry and Industry of Starch", edited by R. W. Kerr, Academic Press, Inc., New York, (1950), Chapter XVII, p. 455.

3) R. E. Rundle and D. French, *J. Am. Chem. Soc.*, **65**, 554 (1943); R. E. Rundle and R. R. Baldwin, ibid., **65**, 558 (1943); R. E. Rundle, ibid., **69**, 1769 (1957); R. S. Stein and R. E. Rundle, *J. Chem. Phys.*, **16**, 195 (1948).

4) E. J. Wilson, T. J. Schoch and C. S. Hadson, *J. Am. Chem. Soc.*, **65**, 1380 (1943).

5) A. D. Awtrey and R. E. Connick, ibid., **73**, 1842 (1951).

6) E. O. Forster, Ph. D. Thesis, Columbia University, (1951), through J. A. Thoma and D. French, *J. Am. Chem. Soc.*, **80**, 6142 (1958).

due to triiodide ion was not observed in 0.2 M iodic acid solution and the blue coloration due to complex formation did not occur with the amylose solution. On the contrary, when the other acid solutions were used, the absorption due to a small amount of triiodide ion was always observed and the coloration took place. Therefore, the blue amylose-iodine complex seems to be formed only when iodide is in solution.

Gilbert and Marriot[7] have suggested that the constitution of the complex is ($3I_2 \cdot 2I^-$) or ($I_8^{2-}$) and this resonating ion is thought to be responsible for the blue color. However, as mentioned in the previous paper[1], the amount of iodide ions necessary for the coloration may be very small compared with that concluded by the above authors. Rundle and French[8] have demonstrated the formation of colored complex by absorption of iodine vapors by helical amylose in solid state[9]. It was, hence, inferred that a large amount of iodide ions is not necessary for the coloration. Recently, Holló and Szejtli[10] have agreed with our opinion concerning the constitution of the complex from amperometric studies. Although there are some evidences[7,11,12] indicating that iodide ions are adsorbed as well as iodine molecules by amylose in solution, it is still in doubt whether they all take part in the resonating polyiodine chains which are responsible for the blue color. The authors are inclined to think that the iodide ions indispensable for the resonating chain are only small fractions of adsorbed iodide ions. The triiodide ion adsorbed on the surface of amylose will be discussed in the following paper[13].

From Fig. 1 it is seen that the amylose-iodine complex has a spectrum having two absorption maxima, each of which is in the visible and ultraviolet region, respectively. The absorption is small in the low concentration of potassium iodide and it increases considerably with increasing iodide concentration until $5\times10^{-3}$ M iodide is reached, after which the blue shift of the spectrum takes place, accompanying the decrease of the visible absorption.

Fig. 2 shows the changes of the spectra with the increase of potassium chloride at constant iodide concentration ($10^{-5}$ M). It is seen that

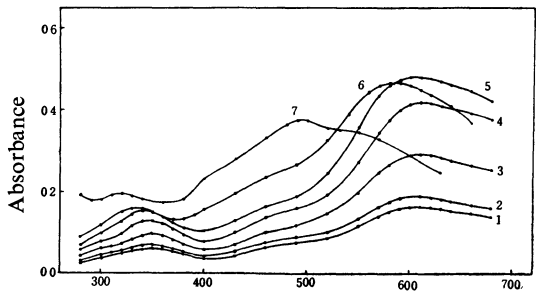



Fig. 1. The absorption spectra of amylose-iodine complexes formed under the various concentrations of potassium iodide: amylose 0.005%, total iodine $1.5\times10^{-5}$ M, potassium iodide (1) $1.3\times10^{-5}$ M, (2) $1.8\times10^{-5}$ M, (3) $6.3\times10^{-5}$ M, (4) $5\times10^{-4}$ M, (5) $5\times10^{-3}$ M, (6) $5\times10^{-2}$ M, (7) $5\times10^{-1}$ M.

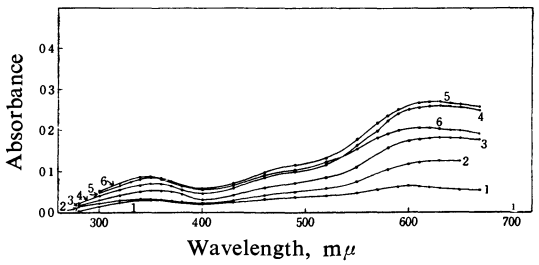



Fig. 2. The absorption spectra of amylose-iodine complexes formed under the various concentrations of potassium chloride: amylose 0.008%, total iodine $1.3\times10^{-5}$ M, potassium iodide $1\times10^{-5}$ M, potassium chloride (1) zero, (2) $5\times10^{-4}$ M, (3) $2.5\times10^{-3}$ M, (4) $1.3\times10^{-2}$ M, (5) $6\times10^{-2}$ M, (6) $1.2\times10^{-1}$ M.

the increase in the concentration of potassium chloride causes the shift of the wavelength of maximum absorption $\lambda_{max}$, to a longer wavelength in the visible region, accompanying the considerable increase of absorption.

Certain other salts[14] also aid the complex formation in a manner similar to that of potassium chloride. These results are collected in Fig. 3. Fig. 3 (a) shows the relationship between $\lambda_{max}$ and the salt concentration and (b) the dependence of absorbance at $\lambda_{max}$ on the salt concentration, in the visible region. The amylose-iodine complexes formed in the solution, which contains 0.005~0.015% amylose, $10^{-5}\sim2\times10^{-5}$ M iodine and $10^{-6}\sim10^{-5}$ M iodide but no any other salt, has $\lambda_{max}$ at 600 mμ, and its absorbance $E_{max}$, is very small. It is seen

7) G. A. Gilbert and J. V. R. Marriott, *Trans. Faraday Soc.*, **44**, 84 (1948).
8) R. E. Rundle and D. French, *J. Am. Chem. Soc.*, **65**, 1707 (1943).
9) Even with dry amylose, traces of iodide ions appeared to be produced by reduction of iodine by impurities (remaining water etc.).
10) J. Holló and J. Szejtli, *Die Stärke*, **10**, 248 (1958).
11) R. S. Higginbotham, *Shirley Institute Memoris*, **23**, 159 (1949).
12) D. L. Molud, *Biochem. J.*, **58**, 593 (1954).
13) T. Kuge and S. Ono, This Bulletin,**33**, 1273 (1960).
14) Salts, whose aqueous solutions show alkaline pH, for example, sodium carbonate, potassium carbonate and disodium hydrogen phosphate, etc., inhibited the coloration. It can be ascribed to the reduction of iodine by hydroxyl ions.

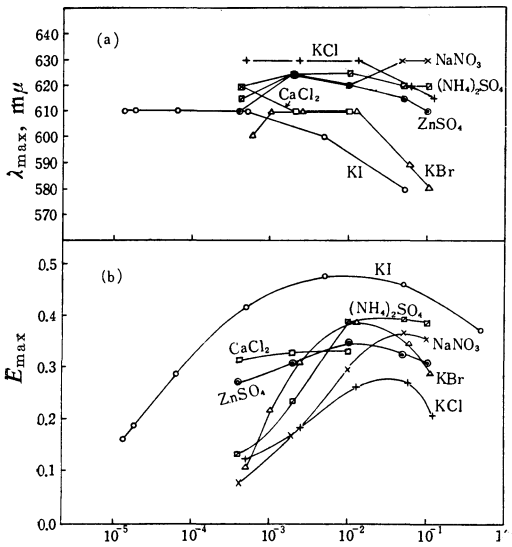



Fig. 3. The effects of various salts on the formation of amylose-iodine complex.

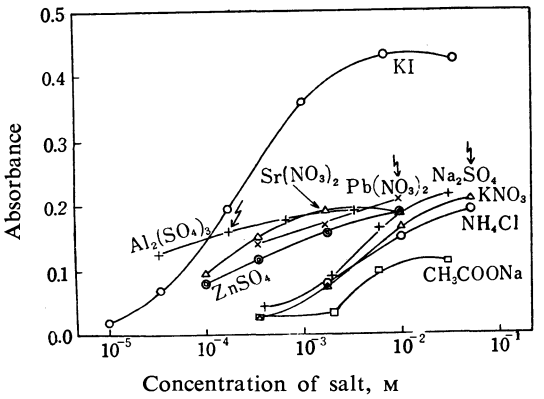



Fig. 4. The changes of absorbance at 610 mμ with increasing concentrations of various salts: amylose 0.007%, total iodine $1.25\times10^{-5}$ M, potassium iodide $1\times10^{-5}$ M.

that $E_{max}$ shows a maximum value at $5\times10^{-3}$ M iodide. The maximum value seems to be determined by the iodine concentration in the solution, while the maximum values caused by the additions of the other salts seem to be mainly determined by the iodide concentration. The addition of more iodide than $10^{-3}$ M causes the large shift of $\lambda_{max}$ to a shorter wavelength as described in the previous paper[1]. The blue shifts due to additions of an excess of the other salts are small and $\lambda_{max}$ are always more than 600 mμ. Only bromide is exceptionally similar to iodide in respect of the blue shift. This seems to be caused by the formation of the iodine-bromide ion[15] that would enter the polyiodine chain and shorten the resonating length as iodide ions do[1], but it may not be the case with other ions.

As described above, the complex formation seems to be influenced to a great extent by iodide and the other salts. Iodide, however, has a different role in the complex formation from the other salts; that is, iodide is essential for the reaction, while the other salts aid strongly the formation of the complex from amylose, iodine and iodide ion when the concentration of iodide is as low as $10^{-5}$ M. Since the decrease of $E_{max}$ observed with the addition of salts over 0.01 M seems to be partly owing to the precipitation of the complexes, this phenomenon will not be further discussed.

Fig. 4 shows another series of experiments carried out. It can be seen that the investigated salts are divided into three groups according to their valency. The higher the valency which the cation has, the lower becomes the concentration of the salt efficient for the completion of the amylose-iodine reaction. The arrows in Fig. 4 indicate the concentrations at which the precipitant of the complex becomes apparent to the naked eye. This concentration also changes in a regular fashion with the valency of cation. These facts may be connected with the Schulze-Hardy rule. Thus it seems quite natural to correlate the increase in absorbance of the complex by added salts with the increase of the aggregation of amylose through the neutralization of the charge on amylose. It is, hence, plausible that the aggregation of amylose caused by the addition of salts would play an important role in the formation of the stable amylose-iodine complex.

Since amylose has been known to have few ionized groups (about one phosphate group per three thousand glucose residues, calculated from the data obtained by Kerr et al.[16]), adsorbed iodide ions would mainly be the source of the charges that prevent the aggregation of amylose.

Although the nature of the amylose-iodine interaction remains controversial[17], Stein and Rundle[3] have presented a theory for the dipolar attraction between amylose and iodine in solid state on the basis of the helical model of amylose. It should be noted that, according to them, the dipolar field provided from the helical amylose in aqueous solution may be

15) A marked change of the absorption spectrum of aqueous iodine solution was observed by the addition of bromide or chloride, indicating the strong interaction between iodine and bromide or chloride ion. The other salts hardly altered the spectrum.

16) R. W. Kerr and G. M. Severson, *J. Am. Chem. Soc.*, 65, 193 (1943).

17) H. Murakami, *J. Chem. Phys.*, 22, 367 (1954); C. T. Greenwood and H. Rossotti, *J. Polymer Sci.*, 27, 481 (1958).

materially reduced by polarization of water, and no strong interaction between amylose and iodine may occur if the helical amylose is surrounded by water molecules with a higher macroscopic dielectric constant.

It is not unreasonable to thnik that since the complexes consisting of amylose, iodine and iodide ion are negatively charged, they can be kept separated without aggregation owing to their Coulombic repulsive force, if the concentration of cation is largely insufficient to repress the force. The complex thus formed may be supposed to be meta-stable since amylose-iodine interaction may not be strong for the reason described above, and may be called intermediate complex. The intermediate complex may not have well-shaped helical structure because of the charges due to adsorbed iodide ion.

By addition of salts these intermediate complexes may tend to gather to aggregates through which water may be excluded from the interstices among them. Moreover, if the aggregates contain helical amylose molecules in close packing, it may be expected that the dipolar field in a given helix would be enhanced by surrounding amylose chains. Then the amylose-iodine complexes formed in aqueous solution would be stabilized by the formation of the aggregates in which the helical complexes would probably be refined on shape and oriented parallel to one another.

Foster and Paschall[18] found that the disaggregation of amylose aggregates results in a decrease in iodine binding capacity and a decrease in the wavelength of maximum absorption of the complex. They also suggested the significance of crystalline order in the complex formation. This seems to support the authors' opinion concerning the nature of the complex as above described. Mayer and Bernfeld[19] considered that the adsorption of iodine occurs on colloidal micells of amylose molecules. Although their conclusion may not be accepted without modification from the helical theory generally accepted at present, their experimental results also indicate that the state of the aggregate of amylose may be closely related to the formation of the blue complex.

In conclusion, it may be said that the blue complex can hardly be formed in solution where ionic strength is so low that the aggregation of the complex takes place with difficulty. The stable state of the blue amylose-iodine complexes formed in solution may be parallel-oriented aggregates composed of helical complexes.

## Summary

The relations between the light absorptions of the amylose-iodine complex and the concentrations of various added salts have been investigated. The iodide ion appears to be indispensable for the formation of the blue complex. The complex formation can be greatly aided by certain salts when the concentration of iodide is low. This salt effect suggests that the parallel-oriented aggregation of amylose-iodine helical complex is essential for the formation of the stable blue complex.

The authors wish to thank Miss Setsuko Sugawara for her technical assistance in this study.

*Laboratory of Biophysical Chemistry*
*College of Agriculture*
*University of Osaka Prefecture*
*Sakai, Osaka*

18) J. F. Foster and E. F. Paschall, *J. Am. Chem. Soc.*, **75**, 1181 (1953).

19) K. H. Meyer and P. Bernfeld, *Helv. Chim. Acta*, **24**, 389 (1941).

# *Amylose-Iodine Complex. III. Potentiometric and Spectrophotometric Studies*

By Takashi KUGE and Sôzaburo ONO

(Received March 21, 1960)

Potentiometric titrations and spectrophotometric measurements have been used as methods of studying the starch-iodine reaction by many authors. Most of these investigations, however, were carried out at room temperature. When the temperature of amylose solution is raised, it may be expected that the amylose molecule enormously increases its flexibility and takes a more random configuration[1]. In parallel with this, it becomes difficult to form amylose-iodine complex with increasing temperature. Hence, it seems interesting to investigate the temperature dependence of the amylose-iodine reaction.

In the present paper, the authors describe the enthalpy change of the amylose-iodine reaction obtained by the potentiometric and/or the spectrophotometric method at wider temperature range than previously reported, and some information concerning the nature of the complex which is deduced from the results obtained.

## Experimental

**Potentiometric Titrations with Iodine.**—The amyloses used for potentiometric titrations were those obtained from potato (white potato), corn and sweet potato starch by hot water extraction[2] at 60°, 69° and 72°C, respectively.

The technique of potentiometric titration was essentially similar to that described by Bates et al.[3]: In our procedure about 0.015 g. of amylose was dispersed in 10 ml. of 0.5 M potassium hydroxide. When dispersal was complete, the mixture was made neutral to methyl orange by the addition of hydrochloric acid, added 10 ml. of 0.5 M potassium iodide, and then filled up to 100 ml. The solution thus prepared was titrated with 0.0005 M iodine in 0.05 M potassium iodide solution. A control solution which contains the same components as that described above but no amylose, was also titrated in the same way.

Titration was carried out in a cell immersed in a thermostat.

For the potential measurements, a Yokogawa high precision potentiometer was used in conjunction with a normal calomel electrode and a bright platinum electrode.

**Spectrophotometric Measurements.**—The amylose used was obtained from potato starch by a selective precipitation method with *n*-butyl alcohol and isoamyl alcohol[4].

Spectrophotometric titration was carried out as follows: 100 mg. of amylose was dispersed in 100 ml. of 0.5 M potassium hydroxide and diluted to 500 ml. with distilled water after neutralization with hydrochloric acid. Each 25 ml. of the solution was diluted to 100 ml., a requisite amount of 0.1 M potassium iodide being added to make the final solution 0.01 M in iodide after the addition of 1 to 22 ml. of a solution of 0.0005 M iodine in 0.001 M potassium iodide. Although the absorptions of the sample in which 6.5 ml. or less of 0.0005 M iodine solution was contained, were directly measured, those of the sample in which 8.0 ml. or more of the iodine solution was contained, were measured after twofold dilution with water. The absorptions were measured at 15°C at wavelengths of 288, 350 and 640 m$\mu$, respectively.

The change of the absorption with temperature change was measured in the following way: The solution (0.005% amylose, $2.5\times10^{-5}$ M iodine), in which the amount of iodine was nearly half of the amount to saturated amylose, was prepared in the same way as that for the spectrophotometric titrations. This solution was placed in a 250 ml. colored volumetric flask and kept in a thermostat at each given temperature for 20 min. and then aliquots of the solution were used to measure the absorption at wavelengths of 288, 350 and 640 m$\mu$, respectively.

A Shimadzu type QB-50 spectrophotometer with thermo-regulating device was used with 1 cm. thick silica cell throughout this investigation.

## Results and Discussion

**Potentiometric Titrations.**—Titration curves of potato amylose and control solution (0.05 M in potassium iodide) at various temperatures are shown in Fig. 1. It can be seen that the potential of these systems becomes high with increasing temperature. At a given temperature the potential is determined by the concentration of free iodine which is in equilibrium with amylose-iodine complex, since the concentration of iodide ion is kept practically constant.

Referring to the results of Dube[5] and Gilbert et al.[6], it may be considered that the ratio of

1) S. Ono, T. Kuge and Y. Yoshikawa, presented at the 11th Symposium on Colloid Chemistry held in Sendai, September, 1958.

2) K. G. Krishnaswamy and A. Sreenivasan, *J. Biol. Chem.*, **176**, 1253 (1948).

3) F. L. Bates, D. French and R. E. Rundle, *J. Am. Chem. Soc.*, **65**, 142 (1943).

4) E. J. Wilson, T. J. Schoch and C. S. Hadson, ibid., **65**, 1380 (1943).

5) H. A. Dube, Dissertation, Iowa State College, (1947), through "Chemistry and Industry of Starch", edited by R. W. Kerr, Academic Press, Inc., New York, (1950), Chapter XVII, p. 461.

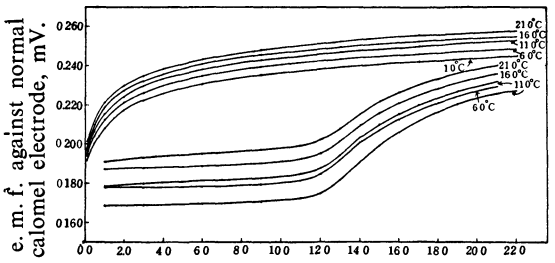



Fig. 1. Potentiometric titration curves: 100 ml. of 0.012% potato amylose solution (the lower five curves), 100 ml. of 0.05 M potassium iodide (the upper five curves).

adsorbed iodide ions to adsorbed iodine molecules on amylose is unity in the present experimental conditions (0.05 M in potassium iodide). Therefore, the amylose-iodine reaction can be expressed as

$$\mathrm{Am} + n\mathrm{I}_2 + n\mathrm{I}^- \rightleftarrows \mathrm{Com} \qquad (1)$$

where Am and Com represent amylose and amylose-iodine complex, respectively.

The equilibrium constant $K$, which is constant for the amylose of a given chain length, is then

$$K = [\mathrm{Com}] / [\mathrm{Am}]\,[\mathrm{I}_2]^n\,[\mathrm{I}^-]^n$$

hence

$$K^{1/n} = [\mathrm{Com}]^{1/n} / [\mathrm{Am}]^{1/n}\,[\mathrm{I}_2]\,[\mathrm{I}^-] \qquad (2)$$

In the amylose-iodine reaction, the activities of the complex and amylose can be regarded as unity, in the manner of a heterogeneous reaction. Eq. 2, therefore, may be written as

$$K^{1/n} = 1/[\mathrm{I}_2]\,[\mathrm{I}^-] \qquad (3)$$

Since the potential of the horizontal part of the titration curve is lower than the lowest potential obtained with the control solution in a given temperature, as can be seen in Fig. 1, direct calculation of free iodine from the potential, which was made by Bates et al.[3], is impossible in the present case. Accordingly, the calculation of $K^{1/n}$ was carried out as follows. The potential difference, $E_d$, between the potential of the sample at the mid-point of the titration (i. e. characteristic potential[7]) and that of the control solution at the corresponding titration point, can be written as

$$E_d = (\boldsymbol{RT}/2\boldsymbol{F}) \ln ([\mathrm{I}_2]_c / [\mathrm{I}_2]_s) \qquad (4)$$

where $[\mathrm{I}_2]_c$ is the concentration of free iodine in the control solution and $[\mathrm{I}_2]_s$ corresponds to that of the sample, and $\boldsymbol{R}$ and $T$ are gas constant and absolute temperature, respectively, and $\boldsymbol{F}$ is Faraday constant. From Eqs. 3 and 4

$$E_d = (\boldsymbol{RT}/2\boldsymbol{F}) \ln [\mathrm{I}_2]_c\,[\mathrm{I}^-]_s\,K^{1/n} \qquad (5)$$

or

$$E_d = (\boldsymbol{RT}/2\boldsymbol{F}) \ln ([\mathrm{I}_3^-]_c\,K^{1/n}/K_1) \qquad (6)$$

where $[\mathrm{I}^-]_s$ is the concentration of iodide ion in the sample, $[\mathrm{I}_3^-]_c$ is the concentration of triiodide ion in the control solution and $K_1$ is the equiliblium constant of the following reaction

$$\mathrm{I}_2 + \mathrm{I}^- = \mathrm{I}_3^-$$

Therefore, $K^{1/n}$ can be calculated from $E_d$, $[\mathrm{I}_3^-]_c$ and $K_1$ which is given in literature[8], using Eq. 6.

In Table I are listed observed $K^{1/n}$, the enthalpy change of the reaction obtained from the temperature dependence of $K^{1/n}$, characteristic potentials, intrinsic viscosities of amylose in 1 M potassium hydroxide by Ostwald viscometer[9] and the temperature of water extraction of amylose. As the temperature of the water extraction is raised, the mean length of the extracted amylose chain may be expected to become longer. This is inferred from their characteristic potentials[7] and intrinsic viscosities, though the contamination of amylopectin may increase. The enthalpy changes of the reaction with amyloses from different sources agree within experimental error in spite of the difference of the size of molecule among these amyloses. Similar values have also been obtained with amyloses partially degraded by bacterial $\alpha$-amylase.

Since the results obtained at temperatures higher than those described above are confused owing to the vaporization of iodine during the procedure, the analysis of the results is not made as those obtained at a lower temperature. However, it seems worth while to mention that the end-point of titration shifted to higher concentration of iodine and became obscure with increasing temperature, from which the occurrence of a complex having a short polyiodine-chain (also suggested in the following spectrophotometric studies) at a higher temperature might be supposed.

**Spectrophotometric Studies.**—Fig. 2 shows the results obtained from spectrophotometric titrations at 15°C. At the beginning of the titration, the curve for 640 m$\mu$ has a small lag and thereafter increases linearly with the amount of iodine added until the vicinity of end-point.

6) G. A. Gilbert and J. V. R. Marriott, *Trans. Faraday Soc.*, 44, 84 (1948).

7) J. F. Foster, Dissertation, Iowa State College, Ames, Iowa (1943), through "Chemistry and Industry of Starch", edited by R. W. Kerr, Academic Press, Inc., New York, (1950), Chapter XVII, p. 460.

8) M. Davies and E. Gwynne, *J. Am. Chem. Soc.*, 74, 2748 (1952).

9) Viscometric studies were carried out in a way similar to that described by S. Lansky et al., *J. Am. Chem. Soc.*, 71, 4066 (1949).

TABLE I. SOME CONSTANTS OBTAINED WITH AMYLOSES FROM DIFFERENT SOURCES

| Amylose | Temp. of water extraction | Equilibrium constant $K^{1/n}$ at 16°C | Enthalpy change kcal./mol. iodine | Charact. potential v.s. N. C. E. at 16°C | Intrinsic viscosity |
|---|---|---|---|---|---|
| Potato | 60°C | $2.2\times10^{9}$ | −15.5 | 0.1890 | 0.80 |
| Corn | 69°C | $2.4\times10^{9}$ | −15.8 | 0.1878 | 1.20 |
| Sweet potato | 72°C | $3.0\times10^{9}$ | −15.3 | 0.1856 | 2.15 |

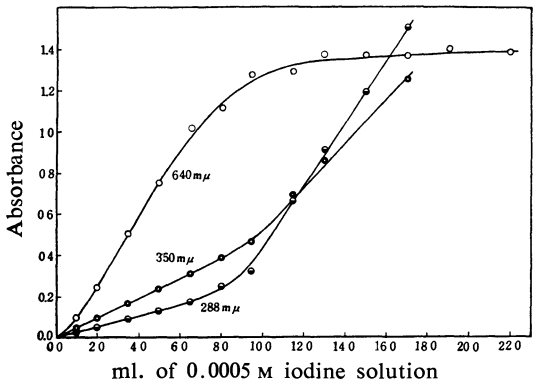



Fig. 2. Spectrophotometric titration curves: 100 ml. of 0.005% potato amylose solution.

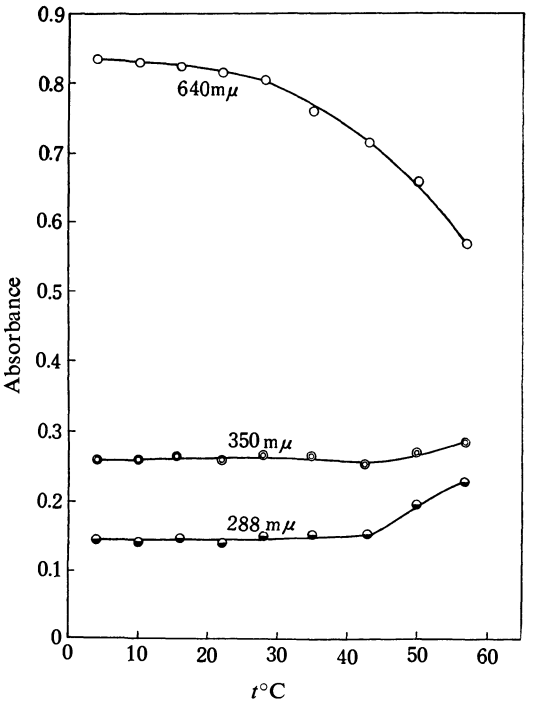



Fig. 3. Temperature dependences of absorptions at wavelengths of 640, 350 and 288 mμ.

The absorptions of ultraviolet region (at 288, 350 mμ) appear to have no such lag and their sharp increases due to free triiodide ion are seen after the end-point. Using the slopes of the initial linear parts of the titration curves, the molecular extinction coefficients of iodine in the complex were estimated to be 36300, 10500 and 5230 at wavelengths of 640, 350 and 288 mμ, respectively. The latter two values are in good agreement with that calculated from Mould's report[10] by the present authors.

The temperature dependences of absorptions are shown in Fig. 3, in which it can be seen that the absorption at 640 mμ decreases in a regular fashion with increasing temperature, while the absorption of the ultraviolet region (at 288 and 350 mμ) remains almost unchanged and has rather a tendency to increase at temperature higher than 40°C.

Free triiodide ion in an aqueous solution exhibits two ultraviolet absorption bands whose maxima are at 288 and 353 mμ[11], respectively. Since the concentration of free iodine molecules which are in equilibrium with the complexes may increase with increasing temperature and consequently the concentration of free triiodide ions may increase, the above described temperature dependence of absorption in the ultraviolet region may be principally ascribed to the increase of the free triiodide ions.

The absorption at 640 mμ may be considered to be due to the complex alone, since free iodine concentration is low enough that its contribution to the absorption can be neglected. Assuming that the absorption of the ultraviolet region is determined by the concentrations of the complex and free triiodide ion, as a first approximation, the following equations can be derived.

$$E_{640}=C_c\varepsilon_{c640} \tag{7}$$

$$E_{288}=C_c\varepsilon_{c288}+C_i\varepsilon_{i288} \tag{8}$$

$$E_{350}=C_c\varepsilon_{c350}+C_i\varepsilon_{i350} \tag{8'}$$

where $E$ represents the absorbance observed, $C_c$ and $C_i$ are the concentrations of the complex and free triiodide ion, respectively, $\varepsilon_c$ and $\varepsilon_i$ are the molecular extinction coefficients of the complex and free triiodide ion, respectively, and the numerical suffixes represent their corresponding wavelengths in mμ. The concentrations of the complex, for the sake of convenience, are expressed as moles of iodine bound.

10) D. L. Mould, *Biochem. J.*, **58**, 593 (1954).
11) A. D. Awtrey and R. E. Connick, *J. Am. Chem. Soc.*, **73**, 1842 (1951).

TABLE II. TEMPERATURE DEPENDENCE OF SOME PROPERTIES OF POTATO AMYLOSE

| Temp. $t$°C | Concn. of complex $C_c$ mol./l. | Concentration of free triiodide ion $C_{1288}$ mol./l. | $C_{1350}$ mol./l. | $C_{1c}$ mol./l. | Concn. of short polyiodine $C_u$ mol./l. | Equilibrium constant $K_s^{1/n}$ | $K^{1/n}$ a) | Enthalpy change kcal./mol. iodine |
|---|---|---|---|---|---|---|---|---|
| 1.0 | — | — | — | — | — | — | $9.2\times10^{9}$ | |
| 4.0 | $2.29\times10^{-5}$ | $5.8\times10^{-7}$ | $6.2\times10^{-7}$ | $5.6\times10^{-7}$ | $1.5\times10^{-7}$ | $2.4\times10^{9}$ | — | |
| 6.0 | — | — | — | — | — | — | 4.8 | |
| 10.0 | 2.28 | 5.6 | 6.9 | 4.9 | 5.2 | 2.3 | — | |
| 11.0 | — | — | — | — | — | — | 4.2 | |
| 16.0 | 2.27 | 6.1 | 9.2 | 4.6 | $1.1\times10^{-6}$ | 2.1 | 2.2 | −15.5[a)] |
| 21.0 | — | — | — | — | — | — | 1.3 | |
| 22.0 | 2.24 | 5.3 | 9.2 | 3.4 | 1.4 | 2.4 | — | |
| 28.0 | 2.22 | 8.1 | $1.31\times10^{-6}$ | 5.6 | 1.8 | 1.3 | — | |
| 35.0 | 2.09 | $1.06\times10^{-6}$ | 1.81 | 6.9 | 2.8 | $9.1\times10^{8}$ | — | |
| 43.0 | 1.97 | 1.24 | 1.88 | 9.2 | 2.4 | 6.0 | — | |
| 50.0 | 1.81 | 2.51 | 3.12 | $2.21\times10^{-6}$ | 2.3 | 2.2 | — | −20.8 |
| 57.0 | 1.57 | 3.65 | 4.62 | 3.17 | 3.6 | 1.4 | — | |

a) This value was obtained by potentiometric titration.

Assuming that these molecular extinction coefficients are independent of temperature, the concentration of the free triiodide ion at each temperature may be found, using Eqs. 7 and 8 or 8′ [12]. The values obtained are shown in Table II, in which $C_{1288}$ and $C_{1350}$ are the concentrations of free triiodide ion estimated by using the absorbance observed at wavelengths of 288 and 350 mμ, respectively. It can be seen that $C_{1288}$ and $C_{1350}$ do not agree with each other and that the former is smaller than the latter at any temperatures. This seems to suggest that Eq. 8 or 8′ would not be an adequate expression for the observed absorbance. A more favorable equation than Eq. 8 or 8′ is seemed to be written as

$$E=C_c\varepsilon_c+C_i\varepsilon_i+C_u\varepsilon_u+C_a\varepsilon_a \qquad (9)$$

where $C_u$ represents the concentration of the polyiodine of short length and is also expressed as moles of single iodine molecule, $\varepsilon_u$ is the molecular extinction coefficient of iodine in the polyiodine, $C_a$ and $\varepsilon_a$ represent the concentration and molecular extinction coefficient of the triiodide ion loosely adsorbed on the surface of amylose, respectively. It would appear that little attention has been given to the ultraviolet absorption of the amylose-iodine complex and an investigation of the ultraviolet absorption has been inconclusive[10,13]. However, the fact that the titration curve at 640 mμ has a small lag may reasonably suggest the existence of polyiodine of short length which exhibits no appreciable absorption at 640 mμ but ultraviolet absorption similar to that of the complex. It may be assumed that the absorption spectrum of the triiodide ion is unchanged whether in the adsorbed state described above or in an aqueous solution.

The use of Eq. 8 or 8′ instead of Eq. 9 would cause an error $\Delta C_i$ being always positive, in the estimation of the concentration of the free triiodide ion. The error can be expressed as follows.

$$\Delta C_i=C_u\varepsilon_u/\varepsilon_i+C_a\varepsilon_a/\varepsilon_i \qquad (10)$$

Since, $\varepsilon_u$ may be roughly assumed to be not appreciably different from $\varepsilon_c$ and $\varepsilon_a$ may be considered as equal to $\varepsilon_i$, the ratio of $\varepsilon_u$ to $\varepsilon_i$ depends on wavelength while that of $\varepsilon_a$ to $\varepsilon_i$ seems to be unity, independent of wavelength. The smaller the ratio of $\varepsilon_u$ to $\varepsilon_i$, the smaller the error becomes. Therefore, $C_{1288}$ should be smaller than $C_{1350}$, and the experimental results given in Table II satisfy this requirement.

The true concentration of free triiodide ion, $C_{it}$, would be written as

$$C_{it}=C_{1288}-C_u\varepsilon_{u288}/\varepsilon_{i288}-C_a\varepsilon_{a288}/\varepsilon_{i288} \qquad (11)$$

or

$$C_{it}=C_{1350}-C_u\varepsilon_{u350}/\varepsilon_{i350}-C_a\varepsilon_{a350}/\varepsilon_{i350} \qquad (11')$$

Therefore, $C_u$ can be obtained by subtraction of Eq. 11 from Eq. 11′. $C_u$ obtained thus is shown in Table II, and the increase of $C_u$ with increasing temperature is seen. $C_{1c}$ listed in Table II is the corrected concentration of free triiodide ion in respect to $C_u$. It should be noted that $C_{1c}$ is not free from the error due to $C_a$. $C_{1c}$ was used to calculate $K^{1/n}$, and the

12) $\varepsilon_{1288}$ and $\varepsilon_{1350}$ used in the calculation were 40000 and 26000, respectively, which were obtained from our experiments and have no essential difference from the values in reference 11.

13) Y. Tanizaki, T. Kobayashi and N. Andô, *J. Chem. Soc. Japan, Pure Chem. Sec.* (*Nippon Kagaku Zasshi*), **80**, 445 (1959).

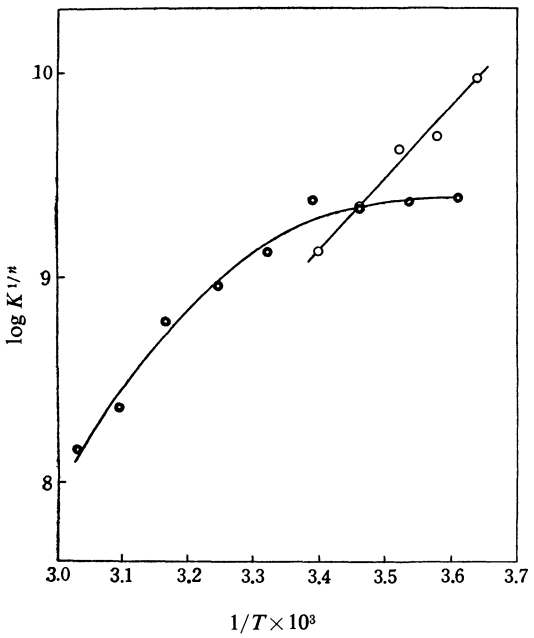



Fig. 4. $\log K^{1/n} \sim 1/T$ plot for potato amylose: —◎—◎—, $\log K_s^{1/n}$, obtained from spectrophotometric method; —○—○—, $\log K^{1/n}$, obtained from potentiometric titration.

value obtained is given in Table II expressed as $K_s^{1/n}$. In Fig. 4, $\log K_s^{1/n}$ is plotted against reciprocal absolute temperature, and it can be seen that the slope of the curve becomes steeper with increasing temperature. Comparing $K_s^{1/n}$ with $K^{1/n}$ obtained by the potentiometric titrations, it can be found that they have similar values at about 16°C, but the slopes as above described, from which the enthalpy change of the reaction would be calculated, are quite different from each other in the neighborhood of the temperature. Such difference may be reasonably explained in terms of the error in the spectrophotometric estimation of free triiodide ion concentration at low temperature region. Considering the data obtained by the potentiometric titrations, it can be seen that free iodine concentration in equilibrium with the complex should decrease with decreasing temperature. However, $C_{ic}$ rather increases with decreasing temperature in the temperature region lower than 22°C. This fact suggests that the amount of the triiodide ion adsorbed on the surface of amylose may be comparable with that of free triiodide ion in the temperature region below 22°C, and a serious error is caused in the estimation of free triiodide ion concentration. It may also be supposed that the lower the temperature, the more the contribution of $C_a$ to $C_{ic}$ becomes. Therefore, it can be inferred that $\log K_s^{1/n} \sim 1/T$ plot should be steeper than that seen in Fig. 4, especially in the lower temperature region. Consequently, the equilibrium constant obtained spectrophotometrically should be larger than that obtained potentiometrically. This result may not be unreasonable, since $K^{1/n}$ is considered as a function of chain length of amylose, being larger with increasing chain length of amylose[9,14], and amylose used in the spectrophotometric study is thought to be longer than that used in potentiometric titration. The selective precipitation method of amylose seems to give amylose with longer chain length than that obtained by the hot water extraction.

For the reason described above, the spectrophotometric method may not be applicable for the estimation of free iodine concentration at room temperature, at which potentiometric titrations are adequate. However, with increasing temperature, when the concentration of free iodine in equilibrium with the amylose-iodine complex increases, the concentration of the free iodine appears to be reasonably estimated by the spectrophotometric method, since, at the higher temperature, $C_a$ can be neglected without a serious error, compared with the free iodine concentration. Even when the vaporization of iodine takes place, free iodine concentration may remain approximately constant as far as amylose-iodine complex exists in solution. Therefore, the present results obtained at a relatively high temperature region may be available for the discussion of the temperature dependence of the amylose-iodine reaction.

From the inspection of the slope of $\log K_s^{1/n} \sim 1/T$ plot in Fig. 4, the enthalpy change of the reaction appears to increase with increasing temperature. The enthalpy change obtained at 50°C is −20.8 kcal. Comparing this value with that obtained potentiometrically at 16°C, −15.5 kcal., it seems certain that the enthalpy change increases as the temperature is raised. This may also be checked with the fact that all the enthalpy changes of the reaction hitherto obtained at different temperatures below 35°C by other authors[5,6,15,16] are −11 to −19 kcal.

At the temperature at which the color of the complex disappears, the free energy change of the reaction should be nearly zero so that the entropy change should have a large value almost corresponding to the enthalpy change at the temperature. This seems to indicate that the amylose, which is free from iodine, would come to take more random configurations

14) Also seen in Table I.

15) Presented at the 12th Symposium on Structural Chemistry held in Fukuoka, November, 1957, by H. Azumi et. al.

16) J. Holló and J. Szejtli, *Periodica Polytechnica*, **1**, 223 (1957).

with increasing temperature through the rupture of both inter- and intramolecular hydrogen bonding. This thought is also supported by the results obtained from the studies in viscosity and optical rotatory power[1].

## Summary

The amylose-iodine reaction has been studied in a wider temperature range than hitherto reported by both potentiometric and spectrophotometric methods.

The enthalpy change of the reaction obtained potentiometrically is $-15.5$ kcal. at 16°C, and appears to be independent of the chain length and the kind of parent starch of amylose.

The change of the absorptions of the amylose-iodine complex with temperature has been pursued at wavelengths of 650, 288 and 350 m$\mu$, respectively.

The triiodide ion adsorbed on the surface of amylose causes an error in the spectrophotometric estimation of free iodine concentration. At the higher temperature, however, this error may be neglected, and the results obtained seem to be reliable.

The enthalpy change appears to increase with increasing temperature and $-20.8$ kcal. has been obtained at 50°C.

*Laboratory of Biophysical Chemistry*
*College of Agriculture, University of*
*Osaka Prefecture, Sakai, Osaka*

# *Spectrochemical Study of Microscopic Crystals. XXII.*[1] *The Structure of Cupric Mono-, Di- and Trichloroacetate*[2]

By Shoichiro YAMADA, Hiroaki NISHIKAWA and Ryutaro TSUCHIDA

(Received April 27, 1960)

Previously the present authors[3,4] studied the structure of cupric *n*- and *iso*-alkanoates, anhydrous and hydrated, and showed mostly on the basis of the polarized absorption spectra that these carboxylates, in the crystalline state and in non-coordinating organic solvents, consist of binuclear molecules which are similar to that of cupric acetate and have a sort of copper-to-copper linkage within the molecules. In continuation of the former study, the structure of cupric mono-, di- and trichloroacetate has now been examined, and the effect of replacement by chlorine atoms discussed in relation to the dimer formation of the cupric carboxylates. A brief account of a part of this study was formerly presented as a short communication[5], the details of which are given below.

1) Part XXI of this series, S. Yamada, H. Nishikawa and R. Tsuchida, This Bulletin, 33, 930 (1960).
2) Presented in part at the Symposium on Co-ordination Copounds, Nagoya, November, 1958.
3) R. Tsuchida and S. Yamada, *Nature*, 176, 1171 (1955). R. Tsuchida, S. Yamada and H. Nakamura, ibid., 178, 1192 (1956).
4) S. Yamada, H. Nakamura and R. Tsuchida, This Bulletin, 30, 953 (1957); ibid., 31, 303 (1958).
5) R. Tsuchida, S. Yamada and H. Nakamura, *Nature*, 181, 479 (1958).
6) W. G. Bateman and A. B. Hoel, *J. Am. Chem. Soc.*, 36, 2517 (1914).
7) W. G. Bateman and D. B. Conrad, ibid., 37, 2553 (1915).

## Experimental

**Materials.** — All the cupric chloroacetates were prepared according to the method of Bateman et al.[6,7] from cupric carbonate and the corresponding chloroacetic acid or from sodium carboxylate and cupric sulfate. All the compounds were identified by elemental analysis. Crystals of the anhydrous forms of the compounds were obtained by recrystallization using non-aqueous solvents after dehydrating the hydrated crystals. The absence of the water of crystallization was confirmed by infrared spectra and elemental analysis.

Anhydrous and hydrated cupric monochloroacetate were obtained in green crystals. The hydrated monochloroacetate corresponds to the formula, $Cu(ClCH_2COO)_2 \cdot 2.5H_2O$. Calcd.: Cu, 21.5; Cl, 30.6; C, 20.7; H, 2.61. Found: Cu, 21.5; Cl, 30.4; C, 20.4; H, 2.55%. A blue form has also been prepared besides the green form. Thus the blue crystals of the anhydrous monocloroacetate were obtained, when ethanol was added to an aqueous solution of the monochloroacetate.

Anhydrous cupric dichloroacetate was prepared in green crystals. Hydrated crystals, which are colored blue, were also obtained together with the anhydrous crystals, when recrystatallization was made from water. The result with the hydrated crystal is reported elsewhere.

Cupric trichloroacetate was obtained in blue crystals after recrystallization from water. The

elemental analysis by the present authors indicates that the blue crystals correspond to the formula, $Cu(Cl_3C\cdot COO)_2\cdot 3H_2O$, in agreement with the analysis by Bateman et al.[6]

**Measurements.**—Quantitative dichroism measurements in the visible and ultraviolet regions were carried out at room temperature by Tsuchida and Kobayashi's microscopic method[8].

Absorption spectra of the compounds in solution were determined by a Beckman DU spectrophotometer. It was confirmed in all the measurements that Beer's law was obeyed in the presence of the free carboxylic acid.

The notations in the present paper are the same as close used in the former papers of this series. Extinction coefficients, $\varepsilon$, are calculated on the basis of a formula-weight instead of a molecular weight.

## Results and Discussion

**Structure of Cupric Chloroacetates in the Crystalline State.** — Previously the present authors[3-5] reported about the structure of cupric formate, acetate and higher carboxylates on the basis of their polarized absorption spectra. A similar treatment will be made in the present article concerning the structure of cupric chloroacetates. Since some of the results and the discussions in the former papers are used in the present work, it would be appropriate to give a brief account of the conclusions obtained formerly.

Cupric salts of acetic acid and higher fatty acids in the crystalline state and in non-coordinating organic solvents show in the visible and the near-ultraviolet region a band at about $80\times10^{13}\,sec^{-1}$(band II) besides a band at about $43\times10^{13}\,sec^{-1}$(band I), whereas most cupric compounds of an ordinary type show in this wavelength region only one band which may be considered as corresponding to the band at about $43\times10^{13}\,sec^{-1}$ of cupric alkanoates. With the cupric carboxylates consisting of binuclear molecules, the following features characteristic of these compounds were observed in the dichroism. "For the band I, the electric vector is more strongly absorbed along the complex plane than along the *Z*-direction of the binuclear molecule, the *Z*-direction being the direction connecting the two copper ions in the binuclear molecule. For the band II, the electric vector is more strongly absorbed along the *Z*-direction. The polarization for the band II is thus seen to be the reverse of the polarization for the band I". These facts are considered to show that the compounds involve along the *Z*-direction a sort of copper-to-copper linkage characteristic of the binuclear molecules of the cupric alkanoates. On the contrary, cupric formate tetrahydrate[3,4], which is known from examination with X-rays[9] to have no copper-to-copper linkage[10], shows no absorption band at about $80\times10^{13}\,sec^{-1}$. Thus the appearance of the band at about $80\times10^{13}\,sec^{-1}$, combined with the polarization property of the band, may be regarded as showing the existence of the binuclear molecule similar to that of cupric acetate hydrate involving the copper-to-copper linkage.

The results of the present dichroism measurements are shown in Figs. 1 to 4. The components of the cupric compounds in the crystalline state may be under rather weak perturbation owing to the crystalline field, but the polarized absorption spectra as determined on a suitable plane are regarded as representing the main features of the dichroism of the component molecule. The exact arrangement of the molecules in the crystals is unknown for all the cupric compounds reported in the present work. It is easy, however, to find the principal characteristics of the dichroism of the molecules themselves by comparing their polarized absorption spectra with those of cupric acetate monohydrate, whose crystal structure was accurately determined, and also with those of cupric alkanoates, which were extensively studied on the basis of the comparison with cupric acetate.

The present measurement, as seen in Fig. 1, indicates that the green anhydrous cupric monochloroacetate in the crystalline state shows an absorption band at about $80\times10^{13}\,sec^{-1}$, in

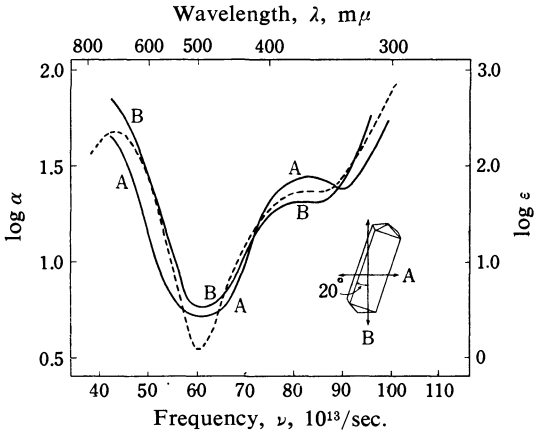



Fig. 1. Absorption spectra of anhydrous $Cu(Cl\cdot CH_2COO)_2$ in the crystalline state (——) and in dioxane (----).

8) R. Tsuchida and M. Kobayashi, "*The Color and the Structure of Metallic Compounds*", (*Kinzokukagōbutsu no Iro to Kōzō*), Zoshindo, Osaka, 1944, p. 180 (in Japanese).

9) R. Kiriyama, H. Ibamoto and K. Matsuo, *Acta Cryst.*, 7, 482 (1954).

10) Cupric formate in dioxan exists mostly as binuclear molecules of the acetate-type, and crystals of the formate consisting of the binuclear molecules were isolated. Cf. R. L. Martin and H. Waterman, *J. Chem. Soc.*, 1959, 1359.

addition to a band at about $40\times10^{13}\,sec^{-1}$. Moreover, it is recognizable that the polarization for the former band is found to be the reverse of the polarization for the latter. This relationship, which closely resembles that encountered in the case of the acetate monohydrate and higher alkanoates[3,4], may suggest that the green anhydrous cupric monochloroacetate in the crystaline state consists of the binuclear molecules of the acetate-type, since the dichroism of the anhydrous monochloroacetate may be readily understandable when it is assumed that A- and B-absorption in Fig. 1 represent the main characteristics of the *Z*- and *X*, *Y*-absorption of the binuclear molecule, respectively.

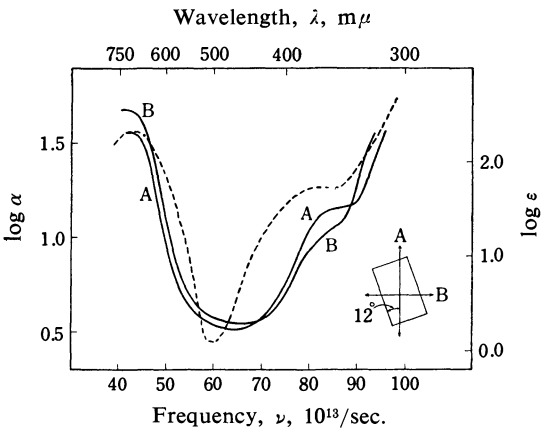



Fig. 2. Absorption spectra of $Cu(Cl\cdot CH_2COO)_2\cdot 2.5H_2O$ in the crystalline state (——) and in dioxane (----).

The present measurement also indicates that cupric monochloroacetate hydrate in the crystalline state shows dichroism with characteristics similar to those of cupric acetate, as is readily seen in Fig. 2. Thus the monochloroacetate hydrate shows an absorption band at about $80\times10^{13}\,sec^{-1}$ in addition to a band at about $40\times10^{13}\,sec^{-1}$. The main characteristics of the dichroism with the component molecule may be recognized, although the dichroism is not very remarkable. It is, therefore, concluded that cupric monochloroacetate hydrate consists of the binuclear molecule of the acetate-type. As comparison of the dichroism of the green anhydrous monochloroacetate with the dichroism of the green monochloroacetate hydrate shows, the presence of the water molecules of crystallization is expected to have a more or less remarkable effect upon the copper-to-copper linkage, but no marked difference was observed in the absorption maxima in the visible and the near-ultraviolet regions between the anhydrous and the hydrated form.

The blue form of anhydrous cupric monochloroacetate is also obtained when ethanol is added to an aqueous solution of the monochloroacetate. The blue crystal is found in the present work to show an absorption band in the near-infrared region, but no absorption band at about $80\times10^{13}\,sec^{-1}$. It is, therefore, concluded that the blue form of the monochloroacetate contains no binuclear molecule.

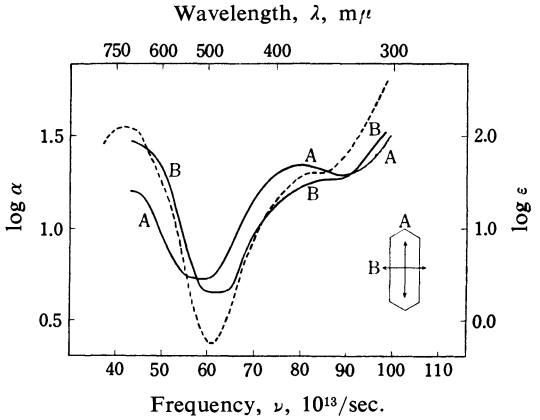



Fig. 3. Absorption spectra of anhydrous $Cu(Cl_2\cdot CHCOO)_2$ in the crystalline state (——) and in dioxane (----).

The present measurement, as seen in Fig. 3, indicates that the green crystal of anhydrous cupric dichloroacetate shows a band at about $80\times10^{13}\,sec^{-1}$ besides a band at about $40\times10^{-13}\,sec^{-1}$, the polarization of the former band being the reverse of the polarization of the latter. This relationship, which is similar to the relationship with cupric acetate hydrate, indicates that anhydorus cupric dichloroacetate in the crystalline state consists of binuclear molecules.

Cupric dichloroacetate is known to exist in a tetrahydrate as well. The dichroism of this form, which is colored blue, is not identical with that of the anhydrous form. The structure of the tetrahydrate will be discussed separately in a later communication.

Cupric trichloroacetate is obtained in the tetrahydrate, when recrystallized from water, ethanol-water, or dioxane-water. The trichloroacetate tetrahydrate shows the dichroism which is quite different from the dichroism of the green form of the mono- or the dichloroacetate. Thus the trichloroacetate tetrahydrate shows only one absorption band at about $40\times10^{13}\,sec^{-1}$, but no absorption band in the neighborhood of the wavelength region around $80\times10^{13}\,sec^{-1}$, as seen in Fig. 4. The absorption spectrum of the trichloroacetate, which is similar to the absorption spectra of ordinary cupric complexes such as cupric sulfate, indicates clearly that cupric trichloroacetate

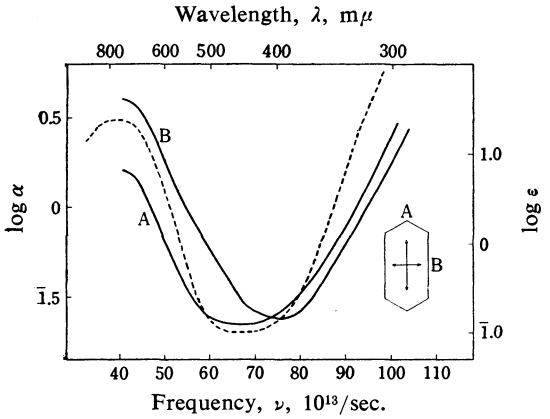



Fig. 4. Absorption spectra of $Cu(Cl_3C\cdot COO)_2\cdot 4H_2O$ in the crystalline state (——) and in dioxane (----).

tetrahydrate contains no binuclear molecule of the acetate-type in the crystalline state.

Anhydrous cupric trichloroacetate, which is obtained in green crystals when recrystallized from ethyl ether after dehydration of the tetrahydrate, may probably consist of the binuclear molecule of the acetate-type, but the dichroism measurement with the crystal has not been performed in the present work. As discussed in a later paragraph of the present article, the ultraviolet spectrum shows that the anhydrous trichloroacetate exists as the binuclear molecules in ethyl ether.

Magnetic susceptibility at room temperature was reported with cupric mono-, di- and trichloroacetates in the solid state[11]. The results seem to be compatible with the conclusions from the present study about the structure of these compounds.

**Structure of Cupric Chloroacetates in Solution.**—The binuclear cupric carboxylates in water are found to undergo dissociation most readily. Even cupric acetate exists in this solvent mostly as the monomer in equilibrium with the binuclear form in a smaller proportion, although the degree of dissociation depends upon the concentration of the solution. All the cupric monocarboxylates so far examined have been found to exist in water as their monomers to a considerable extent if they are soluble in water at all. This may evidently be due to the great tendency of water molecules to be co-ordinated with the cupric ion. On the contrary, dissociation into the monomeric complex-ion has been found to be quite small in non-co-ordinating organic solvents, such as ethanol, dioxane, ethyl ether and chloroform. Needless to say, cupric carboxylates in co-ordinating solvents such as pyridine undergo decomposition to form cupric complexes with the solvent molecules. In the present work, comparison of the absorption spectra is made with the cupric carboxylates in these solvents in almost the same concentration.

It was found in the former investigations that the cupric monocarboxylates having the binuclear molecules of the acetate-type show in non-co-ordinating organic solvents the characteristic absorption spectra with the following features[4].

(1) A band at about $40\times10^{13}\,sec^{-1}$ of the binuclear cupric carboxylate is much stronger than the corresponding band of the mononuclear cupric compounds. (2) Besides the absorption at about $40\times10^{13}\,sec^{-1}$ of the binuclear, cupric carboxylate shows another band at about $80\times10^{13}\,sec^{-1}$, which is about four times less in intensity than the band in the longer wave-length region of the same compound. As reported in the former papers[3,4], these features may be used as criteria in telling whether a cupric carboxylate exists mostly as binuclear molecules of the acetate-type or not.

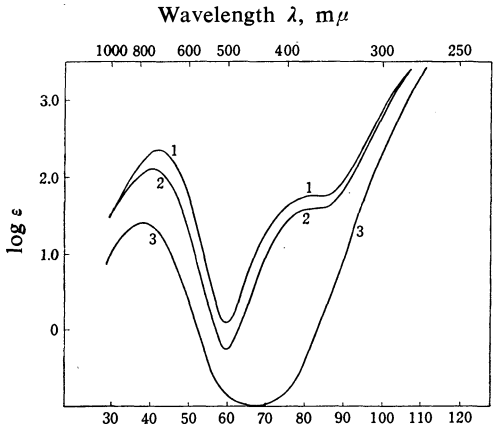



Fig. 5. Absorption spectra of $Cu(Cl_nH_{3-n}C\cdot COO)_2$ in dioxane: 1, $n=1$; 2, $n=2$; 3, $n=3$.

Absorption spectra of cupric chloroacetates in dioxane are shown in Fig. 5. The absorption spectra characteristic of the cupric carboxylates having binuclear structure of the acetate-type are observed with the mono- and the dichloroacetate. Thus the two chloroacetates in dioxan show an absorption band at about $80\times10^{13}\,sec^{-1}$, in addition to a band at about $40\times10^{13}\,sec^{-1}$ which has an extinction coefficient about nine times higher than the corresponding band of an ordinary type of cupric complex such as an aquated ion of copper. This fact indicates, on the basis of the criteria formerly obtained, that the mono- and the

11) M. Kondo and M. Kubo, *J. Phys. Chem.*, 62, 1558 (1958).

dichloroacetate in dioxane exist, at least in most part, as binuclear molecules.

On the contrary, cupric trichloroacetate in dioxane shows an absorption band at about $40\times10^{13}\,sec^{-1}$, but no absorption band at about $80\times10^{13}\,sec^{-1}$. The spectrum shows the main features of the spectrum of ordinary cupric complexes without specific metal-to-metal linkage. It may be concluded, therefore, that cupric trichloroacetate does not contain the binuclear molecule of the acetate-type in dioxan. It is noteworthy that even anhydrous cupric trichloroacetate in dioxane shows no band at about $80\times10^{13}\,sec^{-1}$, having no binuclear molecule in this solvent. It is most probable that two trichloroacetate ions are coordinated as bidentate ligands with a single cupric ion to form a planar complex-ion.

The present work shows that the maximum for the band I of the cupric carboxylate is displaced bathochromically, when the hydrogen atom is replaced by the chlorine atom in the series from the acetate to the trichloroacetate, as seen in Table I. The fact that this order

TABLE I. VISIBLE AND ULTRAVIOLET ABSORPTION SPECTRA OF CUPRIC MONOCARBOXYLATES WITH AN EMPIRICAL FORMULA OF $Cu(R\cdot COO)_2$

| R | Solvent | Band I | | Band II | |
|---|---|---|---|---|---|
| | | $\nu$ | log $\varepsilon$ | $\nu$ | log $\varepsilon$ |
| $CH_3$ | ethanol | 42.8 | 2.25 | 82.0 | 1.65 |
| | dioxane | 45.2 | 2.25 | 81.1 | 1.81 |
| $Cl\cdot CH_2$ | ethanol | 40.2 | 1.82 | 82 | 1.1 |
| | dioxane | 42.9 | 2.34 | 82 | 1.74 |
| $Cl_2\cdot CH$ | ethanol | 38.5 | 1.58 | 83 | 0.5 |
| | dioxane | 41.1 | 2.12 | 83 | 1.60 |
| $Cl_3\cdot C$ | ethanol | 38.0 | 1.47 | none | |
| | dioxane | 38.4 | 1.44 | none | |
| | ethyl ether | 38.3 | 2.18 | ca. 84 | 1.50 |

$\nu$: $10^{13}\,sec^{-1}$.

seems to be parallel with the stability of the binuclear molecule may be readily understandable in terms of the ligand field theory, since the band I corresponds to the electronic transitions between the terms formed by splitting from the cupric ion under the ligand field, which is expected to be stronger, as the cupric carboxylates become more stable.

From the above-mentioned observation with the cupric chloroacetates both in the crystalline state and in dioxane, it may be concluded that the tendency of the cupric carboxylates to form binuclear molecules of the acetate-type seems to decrease in the following order: $CH_3-$ $>Cl\cdot CH_2->Cl_2\cdot CH->Cl_3\cdot C-$ for a series of compounds with an empirical formula of $Cu(R\cdot COO)_2$, R being the afore-mentioned radical. This trend may be understood as due primarily to the accumulation of the inductive effect of the chlorine. Thus, as the hydrogen atom in the $CH_3-$ group is replaced by the chlorine atom, the electron-withdrawing power of group R becomes greater to the effect that the electron density on the oxygen atom of the carboxylate group becomes smaller and consequently the electron on the copper atom would be withdrawn more strongly toward the oxygen atom. If it is assumed that the increase in the electronic density on the copper atom means increase of the electronic charge available for the additional linkage between the two copper atoms, the copper-to-copper linkage might become weaker as the electronic charge on the copper decreases on going from the trichloroacetate to the acetate.

**Dimer Formation of Cupric Chloroacetates in Different Solvents.**—The tendency to the dimer formation of cupric carboxylates in solution is found to depend greatly upon the solvent used. In the present work, water, ethanol, dioxane and ethyl ether as a solvent were compared with one another in respect of the dimer formation of the cupric carboxylates. Examinations were made about the structure of the cupric chloroacetates in these solvents in almost equal concentration. Examinations were also made about the structure of the component molecules in the crystals obtained after recrystallization from these solvents.

Absorption spectra of cupric mono-, di- and trichloroacetates in ethanol are shown in Fig. 6. From the above-mentioned criteria, it may be readily concluded that cupric monochloroacetate in ethanol exists mostly as the binuclear molecules, since the compound shows an absorption band at about $80\times10^{13}\,sec^{-1}$ in addition to a band at about $40\times10^{13}\,sec^{-1}$, the intensity of these bands being characteristic of

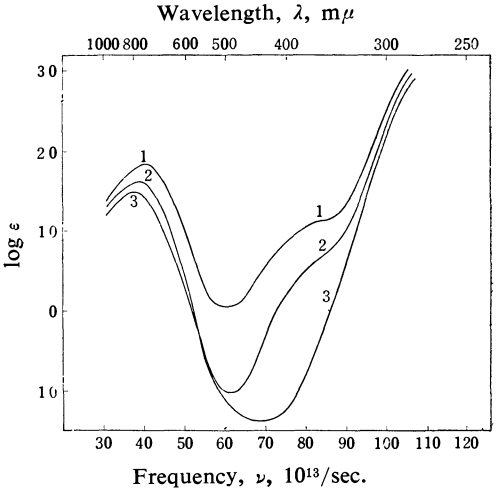



Fig. 6. Absorption spectra of $Cu(Cl_nH_{3-n}C\cdot COO)_2$ in ethanol: 1, $n=1$; 2, $n=2$; 3, $n=3$.

the binuclear cupric carboxylates. On the contrary, the dichloroacetate in ethanol shows only one band at about $40\times10^{13}\,sec^{-1}$ which is much weaker than the corresponding band of cupric monochloroacetate. Moreover, the compound shows no band at about $80\times10^{13}\,sec^{-1}$, although only a very small inflation was observed in this wavelength region. Judging from the criteria mentioned above, the dichloroacetate in ethanol exists mostly in the mononuclear form, although the binuclear molecule might be present in a very minor proportion. The trichloroacetate in ethanol is also seen to show an absorption spectrum, quite similar to the spectrum of the dichloroacetate in ethanol. It is, therefore, concluded that the trichloroacetate exists in the mononuclear form in this solvent. It is to be noted that the band at about $40\times10^{13}\,sec^{-1}$ of the monochloroacetate in ethanol seems to be a little weaker than the corresponding band of the same compound in dioxane, where it exists as binuclear molecules. Therefore, even the monochloroacetate in ethanol contains mononuclear complexes in a very small amount, which is in equilibrium with the binuclear molecules in most part.

In a similar way, the ultraviolet spectra indicate that cupric mono- and dichloroacetate in ethyl ether exist mostly as their binuclear molecules. It is to be noted that anhydrous cupric trichloroacetate shows an absorption spectrum in ethyl ether which is quite different from its spectrum in dioxan, ethanol or water. The spectrum of anhydrous trichloroacetate in ethyl ether was determined in the present work and is shown in Fig. 7. It is seen from the figure that anhydrous cupric trichloroacetate in ethyl ether shows the two absorption bands at about 38 and $80\times10^{13}\,sec^{-1}$, with the

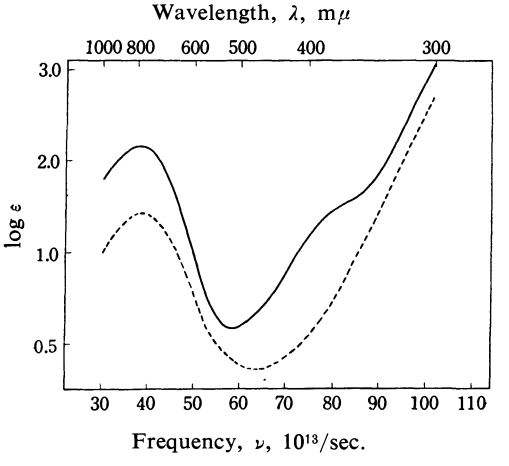



Fig. 7. Absorption spectra of anhydrous $Cu(Cl_3C\cdot COO)_2$ in ethyl ether (——) and in dioxane (----).

principal characteristics of the binuclear cupric carboxylates.

It is seen again that the band I of the cupric chloroacetates is displaced bathochromically, as the hydrogen atom is replaced by the chlorine atom in the series from the acetate to the trichloroacetate. This is in agreement with the relationship, which was derived in the case of dioxane as a solvent, and may be understood in a similar way. It is clearly seen that the cupric chloroacetates exist as binuclear molecules most readily in ethyl ether, of the solvents examined.

Thus the presentd work indicates that cupric trichloroacetate exists as mononuclear complexes in ethanol and in dioxane as well as in water, but that anhydrous cupric trichloroacetate exists in ethyl ether mostly as the binuclear molecules with the metal-to-metal linkage. Similarly it is found that cupric dichloroacetate exists as its binuclear form in dioxane and ether, but as the mononuclear form in ethanol and water. The monochloroacetate is found to exist mostly as binuclear molecules in ethyl ether, dioxane and ethanol, but as mononuclear molecules in water.

The dissociation of the dimer into the monomers takes place most readily in water. Even cupric acetate exists in this solvent mostly as monomeric complexes in equilibrium with the binuclear molecules in a small proportion, although the degree of dissociation depends upon the concentration of the solution. All the cupric monocarboxylates so far examined are found to exist in water as their monomers to a considerable extent if they are soluble in water at all.

Inspection of the data, which are summarized in Table II, reveals that the dimer formation of the cupric carboxylates in different solvents seems to become more difficult in the following order of the solvents: ethyl ether, dioxane, ethanol and water.

The order of the solvents, as presented above, is seen to agree with the increasing order of the electronic charge on the oxygen atom which also represents an increasing order of the co-ordinating capacity of the oxygen to

Table II. Structure of cupric chloroacetates in solution

| | Water | Ethanol | Dioxane | Ethyl ether |
|---|---|---|---|---|
| Acetate | m | d | d | insoluble |
| Monochloro-〃 | m | d | d | d |
| Dichloro- 〃 | m | m | d | d |
| Trichloro- 〃 | m | m | m | d |

d: The compound exists mostly as binuclear molecules.
m: The compound exists mostly as mononuclear complexes.

the cupric ion. It is likely that the stronger co-ordination of the solvent molecules at the residual co-ordination position of the copper ion may break the binuclear molecules into the mononuclear complexes more easily. The present examinations also indicate that the mono- and the dichloroacetate give crystals consisting of the binuclear molecules, when recrystallized from water, ethanol or dioxane. On the contrary, the trichloroacetate gives from the same solvents no crystals of the binuclear molecules. The trichloroacetate, however, gives crystals of the binuclear molecules on recrystallization from ethyl ether after careful dehydration of the hydrated crystals. These observations, which are summarized in Table III, seem to be compatible with the above-mentioned order of the solvents concerning the dimer formation of the cupric monocarboxylates.

TABLE III. STRUCTURE OF THE COMPLEXES CONSTITUTING THE CRYSTALS OBTAINED BY RECRYSTALLIZATION OF CUPRIC CHLOROACETATES FROM VARIOUS SOLVENTS

| | Water | Ethanol | Dioxane | Ethyl ether |
|---|---|---|---|---|
| Acetate | D | D | D | Insoluble |
| Monochloro-〃 | D | D | D | D |
| Dichloro-〃 | D | D | D | D |
| Trichloro-〃 | M | M | M | D |

D : Crystals consisting of dimeric molecules are obtained, aside from the question whether crystals of the monomeric complexes may be obtained or not.

M : Only crystals consisting of the monomeric complexes are obtained.

All these results are found to be in agreement with the conclusion that the trichloroacetate is the cupric chloroacetate which forms the binuclear molecule of the acetate-type with the greatest difficulty, the dichloroacetate being the next. Such a tendency may be understood as due primarily to the accumulation of the inductive effect of the chlorine, which seems to be in parallelism with the decrease in electronic density on the oxygen atom and with the decrease of dissociation constant of the free carboxylic acid. Among cupric carboxylates which are closely related with one another, the dissociation constant of the free carboxylic acid may be regarded as a measure of the formation of the binuclear molecule of the acetate-type.

## Summary

In order to examine the structure of cupric chloroacetates, the dichroism in the visible and the ultraviolet region has been determined at room temperature by the microscopic method with mono-, di- and trichloroacetate. Visible and ultraviolet absorption spectra have also been determined with the above compounds in organic solvents.

The monochloroacetate consists of the binuclear molecules of the acetate-type in the crystalline state and in solution. It has been found that there is another form of the anhydrous monochloroacetate, which is colored blue and contains no binuclear molecule.

The dichloroacetate exists as binuclear molecules in ethyl ether and dioxane, but as mononuclear complexes in ethanol. The anhydrous dichloroacetate in the crystalline state consists of binuclear molecules of the acetate-type.

The trichloroacetate exists as mononuclear complexes in ethanol and in dioxane, and in the crystalline state. The compound exists as binuclear molecules in ethyl ether. Crystals of another form have also been obtained. These possibly consist of binuclear molecules.

The present authors wish to thank the Ministry of Education for a grant-in-aid, and Mr, H. Nakamura for experimental assistance at the earlier stage of this work.

*Department of Chemistry*
*Faculty of Science*
*Osaka University*
*Nakanoshima Kita-ku, Osaka*

# *The Reaction Products of 2, 4, 7-Tribromotropone and Anilines*

By Tetsuo NOZOE, Kozo DOI* and Shigetaka ENDO**

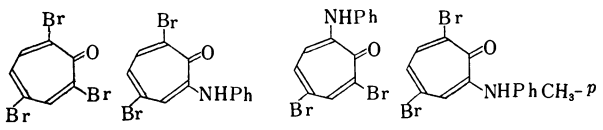
(Received March 11, 1960)

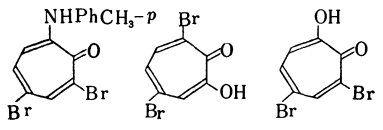
Nozoe and his co-workers[1] have revealed that the treatment of 2, 4, 7-tribromotropone (I) with aniline or *p*-toluidine affords a mixture of 2-anilino-4, 7-dibromotropone (II) and 7-anilino-2, 4-dibromotropone (III), or 4, 7-dibromo-2-*p*-toluidinotropone (IV) and 2, 4-dibromo-7-*p*-toluidinotropone (V); however, the respective components were not separated.

S. Iseda[2], in 1955, reported that the reaction of tribromotropone and aniline or *p*-toluidine resulted in the selective formation of 2-anilinotropone (II) or 2-*p*-toluidinotropone (IV), hydrolyses of which with ethanolic potassium hydroxide easily gave 3, 6-dibromotropolone (VI).

The present authors have re-examined these reactions in order to prepare the dibromotropolone and have been able to isolate some reaction products besides the ones described above.

Heating of the tribromotropone (I) and aniline in benzene afforded 7-anilino-2, 4-dibromotropone (III) in 21% yield, besides known 2-anilino-4, 7-dibromotropone (II) in 66% yield. Separation of both products was easily effected by the application of the difference in their solubilities in chloroform. The structure of the former (III) was clarified through the formation of known 3, 5-dibromotropolone (VII) on hydrolysis with alcoholic potassium hydroxide.




It had been found that the reaction of the tribromotropone and sodium acetate in acetic acid affords 3, 6- (VI) and 3, 5-dibromotropolones[1] (VII). In a similar manner, the above reaction of the tribromotropone and aniline was proved to give not only a 2-substituted but also a 7-substituted product, unlike that observed by Iseda[2].

The reaction of the tribromotropone and *p*-toluidine appeared to result in the formation of more complicated reaction products. Heating of the two compounds in benzene under the same condition as the above gave the 2-*p*-toluidinotropone (IV) in 55% yield and the 7-*p*-toluidinotropone (V) too in 5% yield, as was expected from the reaction in the case of aniline. The structure of the latter V was proved by the formation of known 3, 5-dibromotropolone (VII) on its hydrolysis with alcoholic potassium hydroxide.

The ultraviolet absorption spectra of the above four kinds of anilinotropone are shown in Figs. 1 and 2. In general, the 7-anilinotropones (III and V) have absorption maxima in the longer wavelength region than the 2-anilinotropones (II and IV); this fact appears

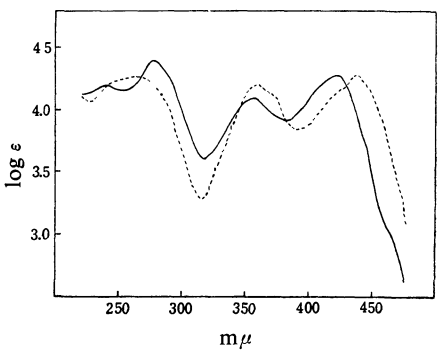



Fig. 1. Ultraviolet absorption spectra.
(——): 2-Anilino-4, 7-dibromotropone (II)
(------): 7-Anilino-2, 4-dibromotropone (III)

to be probably due to a stronger resonance effect of the bromine atom in the 4-position of the former (III and V) than that in the same position of the latter (II and IV) on the respective mesomeric interaction between the tropone ring and the benzene ring involving a nitrogen atom.

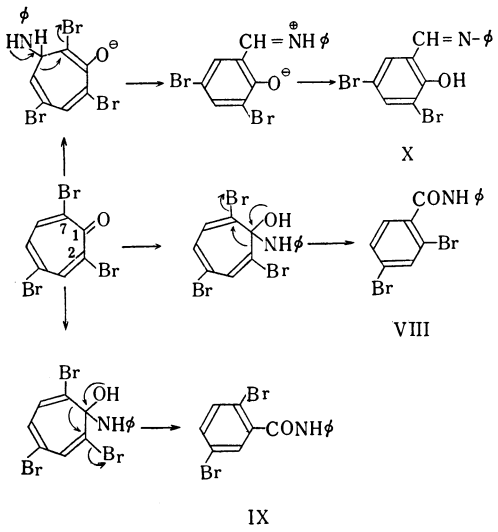
* Present address: The Chemical Research Institute of Non-Aqueous Solutions, Tohoku University, Katahira-cho, Sendai.
** Present address: Tokyo Research Laboratory, Dai-Nippon Celluloid Co. Ltd., Itabashi-ku, Tokyo.

1) T. Nozoe, Y. Kitahara, T. Ando, S. Masamune and H. Abe, *Sci. Repts. Tohoku Univ., Ser. I*, **36**, 166 (1952).
2) S. Iseda, This Bulletin, **28**, 617 (1955).

The reaction mixture, from which the foregoing toluidinotropones (IV and V) were removed, afforded furthermore four kinds of reaction product not isolated to date: 2, 4-dibromobenz-*p*-toluidide (VIII), 2, 5-dibromobenz-*p*-toluidide (IX), 3, 5-dibromosalicylidene-*p*-toluidine (X), and an unidentified substance XI of m. p. 158°C.

The toluidide (VIII and IX) was easily converted into the known dibromobenzoic acid, respectively, on treatment with 75% sulfuric acid. The azomethine compound X was identified with a condensation product of 3, 5-dibromosalicylaldehyde and *p*-toluidine. Another reaction product XI has the composition of $C_{14}H_{12}O_2NBr$, the structure of which will be elucidated in future.

It has been found that the tribromotropone (I) converts into benzoic acid derivatives by the action of bases such as dilute alkali or ammonia[1]. Formations of the dibromobenz-*p*-toluidides (VIII and IX) from the tribromotropone may be taken as the products of the benzilic acid type of rearrangement due to a nucleophilic attack of *p*-toluidine on the 1-position of the molecule. Formation of a Schiff's base X recalls that of 3-bromosalicylaldehyde from 2, 7-dibromotropone by the action of alkali[3,4], and the mechanisms of the above reaction can be illustrated as follows:



## Experimental

The ultraviolet absorption spectra were measured in methanol with a Beckman model DU spectrophotometer.

**Reaction of 2, 4, 7-Tribromotropone (I) and Aniline.**—A mixture of the tribromotropone (I, 70 g.), anhydrous sodium acetate (21 g.), aniline (28 g.) and benzene (1400 ml.) was heated under reflux for 3 hr. The residue obtained by the evaporation of the solvent was washed with water and subsequently extracted with chloroform (100 ml). Crystallization of the part less soluble in chloroform gave 2-anilino-4, 7-dibromotropone (II) as yellow needles from benzene, m. p. 197~198°C (reported[2] m. p. 196~197°C) (47.4 g., 66%). The part more soluble in chloroform, after evaporation of the solvent followed by crystallization from benzene, afforded 7-anilino-2, 4-dibromotropone (III) as yellow needles, m. p. 179.5°C (15 g., 21%).

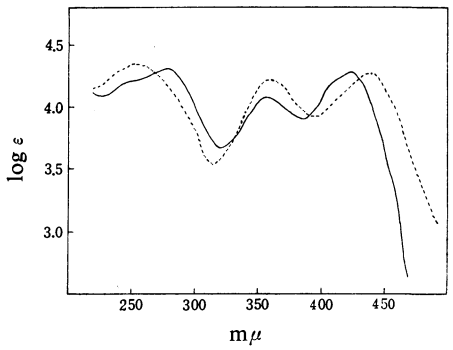



Fig. 2. Ultraviolet absorption spectra.
(——): 4, 7-Dibromo-2-*p*-toluidinotropone (IV)
(------): 2, 4-Dibromo-7-*p*-toluidinotropone (V)

Found: C, 43.52; H, 2.46; N, 4.10. Calcd. for $C_{13}H_9ONBr_2$: C, 43.96; H, 2.56; N, 3.95%. $\lambda_{max}^{MeOH}$ mμ (log ε): 265 (4.25), 361 (4.18), 438 (4.27).

**Hydrolysis of 7-Anilino-2, 4-dibromotropone (III).**—A mixture of III (280 mg.), ethanol (10 ml.), potassium hydroxide (440 mg.) and water (4 ml.) was heated under reflux for 20 min. It was then diluted with water, acidified with concentrated hydrochloric acid to Congo-red and extracted with chloroform. The extract, after evaporation of the solvent followed by crystallization from methanol, gave 3, 5-dibromotropolone (VII), m. p. 154~155°C, undepressed on admixture with an authentic specimen[5].

**Reaction of Tribromotropone (I) and *p*-Toluidine.**—A mixture of the tribromotropone (40 g.), anhydrous sodium acetate (11.6 g.), *p*-toluidine (13 g.) and benzene (700 ml.) was heated under reflux for 3 hr. The residue obtained by evaporation of the solvent was washed with water and extracted with acetone to separate into the less soluble A and the more soluble B portion. The fraction A, 37.3 g., after two recrystallizations from benzene, afforded 4, 7-dibromo-2-*p*-toluidinotropone (IV) as yellow needles, m. p. 194.5°C (reported[2] m. p. 196°C) (24 g., 55%). The benzene mother-liquor, after chromatographic purification (benzene—alumina) followed by two fractional recrystallizations from the same solvent, gave a more soluble product, 2, 4-dibromo-7-*p*-toluidinotropone (V) as yellow needles, m. p. 177°C (2.4 g., 5.6%).

Found: C, 45.68; H, 3.08; N, 3.67. Calcd. for

3) S. Seto, *Sci. Repts. Tohoku Univ., Ser. I*, **37**, 377 (1953).
4) Y. Kitahara, ibid., **39**, 250 (1956).
5) T. Nozoe, Y. Kitahara, K. Doi and T. Arai, *Bull. Chem. Research Inst. Non-Aqueous Solns., Tohoku Univ.*, **7**, 13 (1957).

$C_{14}H_{11}ONBr_2$: C, 45.54; H, 3.01; N, 3.79%. $\lambda_{max}^{MeOH}$ mμ (log ε): 250 (4.35), 361 (4.22), 440 (4.28).

From the same source a less soluble product XI was obtained as yellow plates, m.p. 157.5～158°C (2.3 g).

Found: C, 55.38; H, 4.02; N, 4.58. Calcd. for $C_{14}H_{12}O_2NBr$: C, 54.92; H, 3.95; N, 4.58%. $\lambda_{max}^{MeOH}$ mμ (log ε): 240 (4.17), 283 (4.37), 345 (3.99), 350 (4.01), 400 (4.20).

The fraction B, after evaporation of the solvent, crystallization from ethyl acetate and chromatographic purification (benzene—alumina) followed by several recrystallizations from benzene, yielded the following three products in the order of decreasing of solubilities in the solvent:

2,5-Dibromobenz-*p*-toluidide (IX), colorless needles, m. p. 155～155.5°C (0.25 g.),

Found: C, 45.64; H, 2.85; N, 3.80. Calcd. for $C_{14}H_{11}ONBr_2$: C, 45.54; H, 3.01; N, 3.79%.

2,4-Dibromobenz-*p*-toluidide (VIII), colorless needles, m.p. 174°C (0.2 g.),

Found: C, 45.27; H, 2.70; N, 3.89%.

3,5-Dibromosalicylidene-*p*-toluidine (X), orange needles, m.p. 129.5°C (0.44 g.).

Found: C, 45.58; H, 2.92; N, 4.00%.

**Hydrolysis of 2,4-Dibromo-7-*p*-toluidinotropone (V).**—A mixture of the tropone (V, 90 mg), ethanol (5 ml.), potassium hydroxide (200 mg.), and water (3 ml.) was heated under reflux for 30 min., then acidified with dilute hydrochloric acid to Congo-red, and extracted with chloroform. The extract gave 3,5-dibromotropolone (VII, 40 mg.), m.p. 154～155°C, undepressed on admixture with an authentic sample[5].

**Hydrolysis of 2,4-Dibromobenz-*p*-toluidide (VIII).**—A mixture of the toluidide (VIII, 70 mg.) and 75% sulfuric acid (5 ml.) was heated at 130°C for 30 min. The solid obtained by pouring the reaction mixture onto crushed ice gave 2,4-dibromobenzoic acid, m.p. 166～169°C, undepressed on admixture with an authentic specimen[6].

**Hydrolysis of 2,5-Dibromobenz-*p*-toluidide (IX).**—Hydrolysis of IX under the same condition as the above yielded 2,5-dibromobenzoic acid, m.p. 151～153°C, undepressed on admixture with an authentic sample[7].

**3,5-Dibromosalicylidene-*p*-toluidine (X).**—A mixture of 3,5-dibromosalicylaldehyde[8] (30 mg.), *p*-toluidine (20 mg.) and ethanol (2 ml.) was heated under reflux for one hour. The reaction mixture, when cooled, afforded Schiff's base X as orange needles, m.p. 129～129.5°C, undepressed on admixture with the reaction product X of the tribromotropone and *p*-toluidine.

We gratefully acknowledge our debt to the Ministry of Education for the Grant in Aid for Fundamental Scientific Research and to Messrs. S. Ohyama, K. Kato, A. Iwanaga and S. Azumi for the microanalyses.

*Department of Chemistry*
*Faculty of Science*
*Tohoku University*
*Katahira-cho, Sendai*

6) A. K. Miller, *J. Chem. Soc.*, **61**, 1033 (1892).
7) H.Hubner, *Ber.*, **10**, 1705 (1877).
8) E. Tummeley, *Ann.*, **251**, 179 (1889).

# *Further Studies on the Intramolecular Cyclization of o, o'-Dihydroxydiphenyldiacetylene*

By Fumio TODA and Masazumi NAKAGAWA

(Received February 27, 1960)

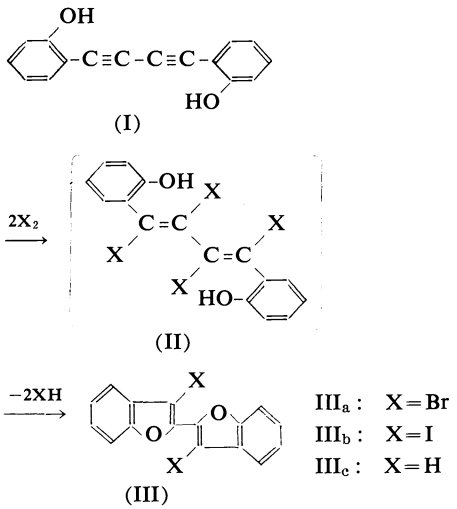
In the previous paper, the present authors reported the formation of 2, 2'-dibenzofuranyl ($III_c$) from *o*, *o'*-dihydroxydiphenyldiacetylene (I) in alkaline madia[1]. The present paper deals with the same type of intramolecular cyclization of I and its silver salt IV in a neutral or an acidic medium.

Treatment of I in carbon tetrachloride with bromine yielded colorless needles in a 37% yield with evolution of hydrogen bromide. The structure of $III_a$ was assigned to the substance from the analytical data, ultraviolet and infrared spectroscopic evidences (Figs. 1, 2 and Table I). The cyclization of I to $III_a$ presumably involves the addition of bromine to the triple bands followed by the elimination of hydrogen bromide as indicated in the following scheme. The formation of diindole from *o*, *o'*-dinitrotolan which was reported by Ruggli and his associate seems to involve an essentially similar reaction[2]. In the case of the reaction of iodine with I under the same

1) F. Toda and M. Nakagawa, This Bulletin, **32**, 514 (1959).

2) P. Ruggli, *Ber.*, **50**, 883 (1917); P. Ruggli and O. Schmid, *Helv. Chim. Acta*, **18**, 1215 (1935).

condition, compounds $III_b$ and $III_c$ were isolated in a 10% and a 29% yield respectively.




When the reaction was carried out in the presence of finely powdered calcium carbonate in order to remove the evolved hydrogen iodide, the only product was found to be $III_b$. Treatment of $III_b$ with hydroiodic acid resulted in the formation of $III_c$, therefore, the formation of $III_c$ in the reaction of I with iodine is attributable to the reduction of $III_b$ by

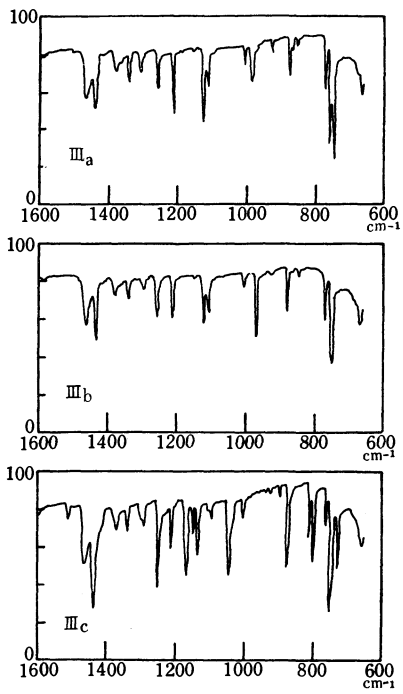



Fig. 1. The infrared spectra of 2,2'-dibenzofuranyl derivatives (Nujol mull)
$III_a$: 3,3'-Dibromo-2,2'-dibenzofuranyl
$III_b$: 3,3'-Diiodo-2,2'-dibenzofuranyl
$III_c$: 2,2'-Dibenzofuranyl

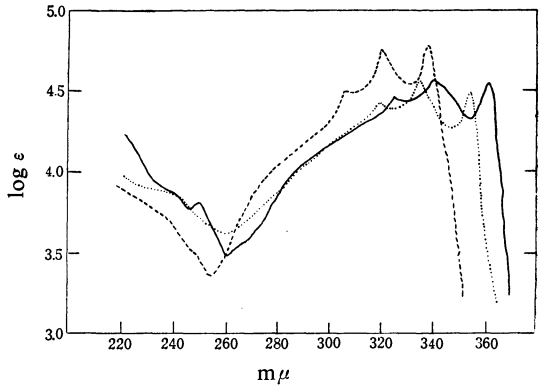



Fig. 2. The ultraviolet spectra of 2,2'-dibenzofuranyl derivatives.
·····: 3,3'-Dibromo-2,2'-dibenzofuranyl ($III_a$)
——: 3,3'-Diiodo-2,2'-dibenzofuranyl ($III_b$)
----: 2,2'-Dibenzofuranyl ($III_c$)

hydrogen iodide. The infrared and ultraviolet spectrum of $III_b$ are shown in Figs. 1, 2 and Table I together with its mother substance and analogues. As illustrated in Fig. 1, the infrared spectra of $III_a$ and $III_b$ lack absorption at 800 and 812 $cm^{-1}$ which exsists in the spectra of $III_c$ and related 2-substituted benzofurans. Therefore, the absorption at ca. 800 $cm^{-1}$ may be ascribed to the out-of-plane deformation of the hydrogen atom at the 3-position of the benzofuran ring.

A quantitative formation of $III_c$ was observed when the silver salt IV was exposed to light for a few days. The reaction of methyl iodide with IV which was kept in a brown desiccator for a day gave 2-(*o*-methoxyphenylethynyl)-benzofuran (VI) together with $III_c$. The structure of VI was inferred from the close resemblance of its ultraviolet and infrared spectrum with those of 2-(*o*-hydroxyphenylethynyl)-benzofuran (VII)[1] as shown in Fig. 3 and Table I.

It is the most interesting result that the silver salt IV was converted into $III_c$ and

TABLE I. ULTRAVIOLET SPECTRA OF 3,3'-DISUBSTITUTED 2,2'-DIBENZOFURANYL AND RELATED COMPOUNDS

| Compound | Absorption ($\lambda_{max}$ in mμ in 95% ethanol) | | | | |
|---|---|---|---|---|---|
| $III_a$ | | | 319 (253) | 335 (352) | 354 (299) |
| $III_b$ | 250 (63) | | 325 (276) | 342 (395) | 361 (338) |
| $III_c$ | | 306 (316) | 320 (589) | 338 (601) | |
| VI | 250 (75) | 299 (251) | 318 (305) | 340 (294) | |
| VII | 250 (79) | 298 (265) | 319 (297) | 340 (284) | |

The figures in parentheses are $\varepsilon_{max} \times 10^{-2}$.

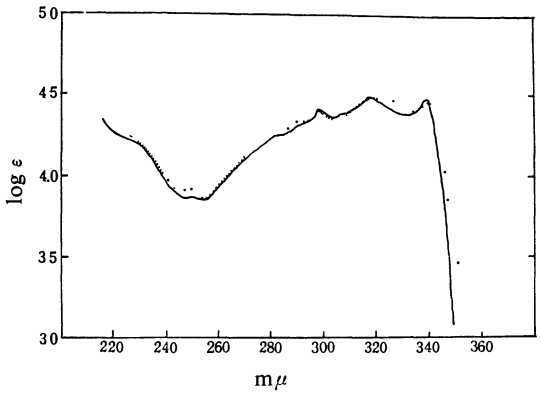



Fig. 3. The ultraviolet spectra of 2-substituted benzofurane derivatives.
——: 2-(*o*-Methoxyphenylethynyl)-benzofuran (VI).
……: 2-(*o*-Hydroxyphenylethynyl)-benzofuran (VII).

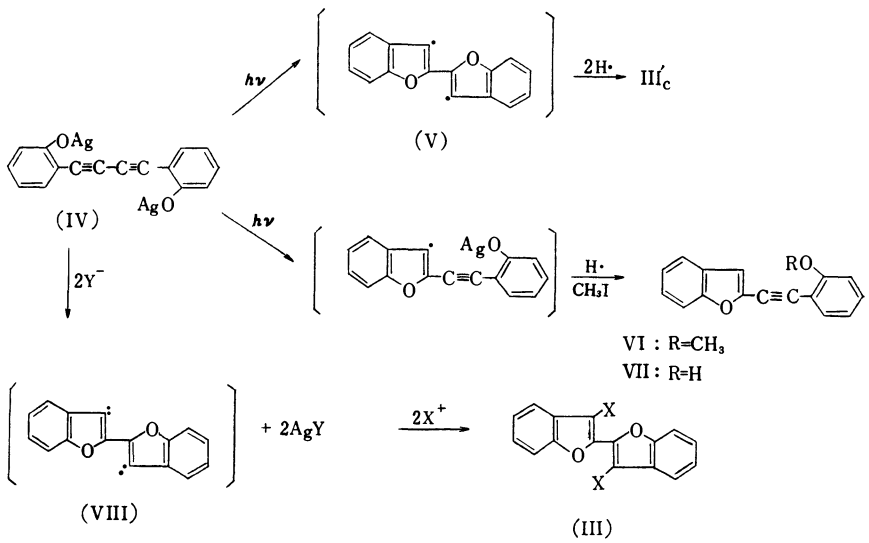
its derivatives in good yield by the reaction with various kind of reagents X-Y, such as hydrogen chloride, hydrogen iodide, acetic acid, potassium iodide, ammonium bromide, bromine, iodine and iodine chloride. The results are summarized in Table II.

The photochemical transformation of IV into $III_c$ proceeds probably through a radical mechanism. The photodecomposition of IV may produce a phenoxy radical, and the intramolecular addition of the oxygen radical to the triple bonds would yield an intermediate dibenzofuranyl radical (V) as illustrated in the following scheme. The radical may be stabilized

Table II. Reaction of the silver salt IV with X-Y

| Reagent X | Reagent Y | Medium | Product |
|---|---|---|---|
| H | Cl | Water | 2,2'-Dibenzofuranyl ($III_c$) |
| H | I | 〃 | 〃 |
| H | $CH_3CO_2$ | Acetic acid | 〃 |
| K | I | Water | 〃 |
| $NH_4$ | Br | 〃 | 〃 |
| Br | Br | 〃 | 3,3'-Dibromo-2,2'-dibenzofuranyl($III_a$) |
| I | I | Carbon tetrachloride | 3,3'-Diiodo-2,2'-dibenzofuranyl($III_b$) |
| I | Cl | Water | 〃 |

by the substruction of hydrogen atoms from water or ethanol molecule yielding $III_c$*. Also the formation of VI is quite understandable assuming that the light induced half ring closure of IV is followed or is preceded by the ionic displacement of the silver atom by the methyl group. A same type of photochemical reaction of an acetylenic compound has been reported by Prey[3]. He found that the silver acetylide of *o*-hydroxyphenylacetylene yields benzofuran when irradiated with a quarz lamp. On the other hand, the above mentioned reactions of IV with various kinds of argentphilic reagents presumably proceed through an ionic mechanism. The substruction of silver cation from IV by the attack of the anionic moiety of the reagent $Y^-$ should result in the formation of 2,2'-dibenzofuranyl anion (VIII). The combination of the cationic moiety of the reagent $X^+$ or proton of the




3) V. Prey and G. Pieh, *Monatsh.*, **80**, 790 (1949).
* The silver salt was prepared as a pasty mass by the addition of an aqueous silver nitrate to a solution of I in ammoniacal ethanol.

solvent with VIII gives dibenzofuranyl ($III_c$) or its 3, 3'-disubstituted derivatives.

The bathochromic shifts of the spectrum of $III_a$, $III_b$ and $III_c$ are found to be in the expected sequence of H < Br < I with respect to the substituents at the position of 3 and 3'. On the other hand, the hyperchromic effect of the substituents is in the sequence of H < I < Br. The low $\varepsilon$-values of the K-band of $III_a$ and $III_b$ as compared with that of $III_c$ may be attributable to an increase of twist of the molecule around the 2, 2'-single bond caused by the presence of bulky halogen atoms at 3- and 3'-position. Similar phenomena have already been observed in several instances[4], and were explained in terms of the diminished probability of excitation of the molecule to a coplanar excitation state.

## Experimental*

**Formation of 3, 3'-Dibromo-2,2'-dibenzofuranyl ($III_a$) from *o*,*o*'-Dihydroxydiphenyldiacetylene (I).**—Bromine (3.2 g.) was added to a suspension of finely powdered I (2.4 g.) in dry carbon tetrachloride (40 cc.). An evolution of hydrogen bromide under an exothermic reaction was observed. The mixture was shaken for one hour with occasional cooling with water. The crystals separated were filtered, and the solvent was evaporated. The remaining solid was combined with the crystals, washed with hot ethanol. Recrystallization from benzene yielded $III_a$ as colorless needles, 1.5 g. (37%), m. p. 225°C.

Found: C, 48.58; H, 2.03; Br, 41.02. Calcd. for $C_{16}H_8O_2Br_2$: C, 49.02; H, 2.05; Br, 40.77%.

I. R. max., 1255 (=C-O-), 875(furan ring)$cm^{-1}$.

**Formation of 3, 3'-Diiodo-2, 2'-dibenzofuranyl ($III_b$) and 2, 2'-Dibenzofuranyl ($III_c$) from *o*, *o*'-Dihydroxydiphenyldiacetylene (I).**—A mixture of I (1.2 g.), dry carbon tetrachloride (25 cc.) and iodine (2.6 g.) was allowed to stand for 3 days at room temperature. The solvent was removed by distillation, and the careful fractional recrystallization of the residual solid from ethanol resulted in the separation of two substances. The less soluble substance was found to be $III_b$, 0.25 g. (10%), m. p. 212°C.

Found: C, 39.59; H, 1.59; I, 52.58. Calcd. for $C_{16}H_8O_2I_2$: C, 39.54; H, 1.64; I, 52.22%.

I. R. max., 1252 (=C-O-), 875 (furan ring)$cm^{-1}$.

The more soluble substance, 0.35 g. (29%), m. p. 193~194.5°C was identified as $III_c$ by a mixed melting point determination with an authentic specimen.

A mixture of I (0.95 g.), dry carbon tetrachloride (30 cc.), iodine (2.06 g.) and finely powdered calcium carbonate (1.6 g.) was kept at room temperature for 2 days. The inorganic salt was removed by filtration and extracted with hot benzene. The extract was combined with the filtrate and the solvent was removed under reduced pressure. The residue thus obtained was digested with hot benzene. The crude crystals obtained by the evaporation of the solvent in vacuo was recrystallized from ethanol yielding 0.32 g,. (16%) of $III_b$, m. p. 212°C as colorless needles.

**Reduction of $III_b$ with Hydrogen Iodide.**—Hydroiodic acid (57% aqueous solution, 4 g.) was added to a solution of $III_b$ (50 mg.) in carbon tetrachloride (30 cc.), and the mixture was shaken for 2 days at room temperature. Treatment of the reaction mixture afforded crystalline solid. Fractional recrystallization of the crude solid gave recovered $III_a$, 30 mg., m. p., 211~212°C and a small amount of III, m. p. 190~194°C.

**Preparation of the Silver Salt of *o*, *o*'-Dihydroxydiphenyldiacetylene (IV).**—Silver nitrate (2.8 g.) in water (5.0 cc.) was added to the solution of I (1.8 g.) in a mixture of concentrated ammonia (1.2 cc.) and ethanol (15 cc.). The light yellow precipitate formed was collected by filtration and washed with ethanol, yielding 2.8 g. (ca. 80%) of the silver salt (IV). The attempt to determine the melting point of the saltfailed. A gradual decomposition was observed, when the salt (IV) was heated in a capillary tube, and the substance in the tube fused at 194.5~195.5C showing the melting point of $III_c$.

**Photodecomposition of the Silver Salt (IV).**—Finely powdered IV was exposed to a diffused light in the laboratory for a few days. The resulted greyish powder was digested with benzene. The solvent was removed by distillation, and the residue was recrystallized from benzene or ethanol yielding colorless needles, m. p. 194.5~195.5°C in an almost quantitative yield. This substance was identified as $III_c$ by a mixed melting point determination with an authentic specimen.

**Formation of 2, 2'-Dibenzofuranyl ($III_c$) from the Silver Salt IV.**—A mixture of freshly prepared IV and aqueous hydroiodic acid (57%) was shaken for 5 min. The precipitate formed was collected and washed with water and ethanol, successively. The residue was digested with hot benzene. Concentration of the benzene solution afforded crude crystals. Recrystallization of the crude product from ethanol resulted in colorless needles, m. p. 194.5~195.5°C in good yield. The mixed melting point of this substance with authentic $III_c$ showed no depression. Similar treatment of IV with concentrated hydrochloric acid, acetic acid, aqueous solution of potassium iodide (30%) and aqueous solution of ammonium bromide (30%) also yielded $III_c$ in good yield.

**Formation of 3, 3'-Dibromo-2, 2'-dibenzofuranyl ($III_a$) from the Silver Salt IV.**—To a suspension of a freshly prepared IV in water, bromine was added drop by drop with shaking until the color of bromine persists. The insoluble material was collected by filtration, and washed with water and ethanol successively. The residue was digested with hot benzene and the solvent was evaporated. The crude crystals thus obtained were recrystallized from ethanol yielding colorless needles, m. p. 220~223°C, which showed no depression of the melting point on admixture with previously obtained $III_a$.

4) E. A. Braude, F. Sondheimer and W. F. Forbes, *Nature*, 173, 117 (1954); F. Toda and M. Nakagawa, This Bulletin, 33, 223 (1960).

* No melting points are corrected.

**Formation of 3,3'-Diiodo-2,2'-dibenzofuranyl ($III_b$) from the Silver Salt IV.** — A mixture of freshly prepared IV, iodine and dry carbon tetrachloride was shaken for 5 min. Silver iodide formed was removed by filtration. The crude crystals obtained by the evaporation of the solvent were recrystallized from ethanol resulting in colorless needles, m. p. 211~212°C. This substance showed no depression of the melting point on admixture with authentic $III_b$.

The reaction of iodine chloride with IV under the same condition also gave $III_b$ in good yield.

**Formation of 2-(*o*-Methoxyphenylethynyl)-benzofuran (VI) from the Silver Salt IV.**—The silver (IV, 2.8 g.) which was kept in a brown desiccator for a day was mixed with methyl iodide (1.5 g.) and dry benzene (5.0 cc.). The mixture was refluxed for 1.5 hr. The precipitate formed was collected by filtration, and extracted with hot benzene (30 cc.). The crude crystals obtained by the evaporation of the solvent was digested with cold ethanol (15 cc.). The insoluble material was recrystallized from benzene resulting in colorless needles, 1.08 g. (78%), m. p. 194.5~195.5°C. The mixed melting point of this substance with 2,2'-dibenzofuranyl ($III_c$) showed no depression. The alcoholic solution was diluted with water, and the crude crystals formed were recrystallized from a diluted ethanol resulting in VI, colorless needles, 100 mg. (6%), m. p. 72°C.

Found: C, 82.33; H, 4.94. Calcd. for $C_{17}H_{12}O_2$: C, 82.24; H, 4.87%.

I. R. max., 1246, 1265, 1040 (=C-O-), 2200 (-C≡C-), 884 (furan ring), 807, 792 ($\delta$ CH of 3-position of furan ring) $cm^{-1}$.

The present authors wish to thank the Ministry of Education for a grant-in-aid. The authors are also grateful to Dr. T. Shiba, Mr. M. Okumiya and Miss K. Koike for the microanalyses.

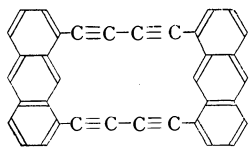
*Department of Chemistry*
*Faculty of Science*
*Osaka University*
*Nakanoshima, Osaka*

# *Cyclic Acetylenes. III.* Synthesis of 1, 1'-Dianthryldiacetylene. A Model Substance of a Cyclic Tetraacetylene Containing Anthracene Nuclei*

By Shuzo AKIYAMA and Masazumi NAKAGAWA

(Received March 24, 1960)

In the course of the synthetical studies on the cyclic tetraacetylene containing two anthracene nuclei (I)[1], the authors have studied the synthesis of 1, 1'-dianthryldiacetylene (X) as a model substance of I.



(I)

After several experimentations, the following route to X was developed. 1-Carboxyanthraquinone (III)[2] which was derived from 1, 9-benz-10-anthrone (II) by chromic acid oxidation was converted to 1-carboxyanthracene (IV)[3] by reduction with zinc dust in aqueous ammonia. The acid chloride V[4] which was obtained on treatment of IV with thionyl chloride was caused to react with diethyl ethoxymagnesiomalonate in toluene. The ketomalonate VI thus obtained was treated without further purification with a mixture of propionic acid and sulfuric acid to cause ester exchange and decarboxylation. The over-all yield of 1-acetylanthracene (VII)[5] from II was found to be 52%. The attempt to prepare VII by the reaction of dimethyl cadmium with V was found to be unsatisfactory.

The ketone VII was treated with phosphorus pentachloride in phosphorus oxychloride, and the crude chloride VIII was dehydrochlorinated with sodium amide in liquid ammonia yielding 1-ethynylanthracene (IX) as light yellow cubes. This substance decomposed gradually on standing at room temperature. The presence of a terminal acetylene was confirmed by the formation of yellow cuprous

* For Part II, see F. Toda and M. Nakagawa, This Bulletin, 33, 230 (1960).

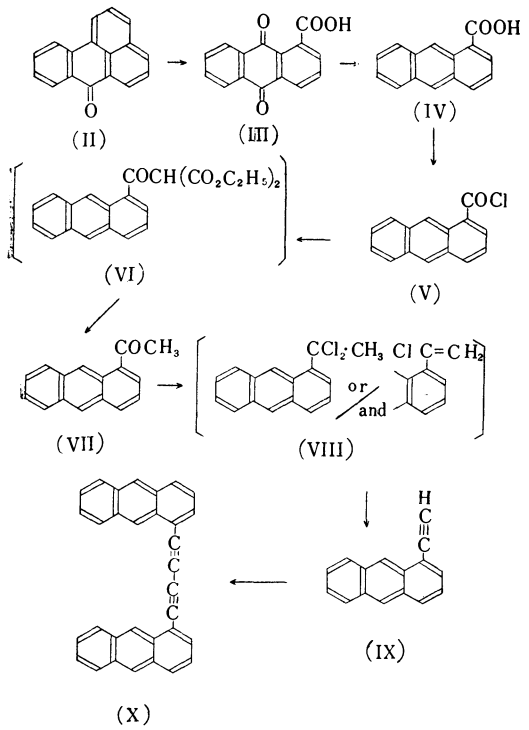
1) The following paper.

2) E. B. Barnett and J. W. Cook, *Ber.*, 57, 1777 (1924).

3) C. Graebe and S. Blumenfeld, ibid., 30, 1118 (1897).

4) J. W. Cook, *J. Chem. Soc.*, 1931, 566; R. Scholl and J. Donat, *Ber.*, 62, 1297 (1929).

5) VII can be obtained by the fractional recrystallization of a mixture with the 2-isomer which is the product of the direct acetylation of anthracene by the Friedel-Crafts reaction. The authors are grateful to Professor P. H. Gore for private communication suggesting the details of the above mentioned process. cf., P. H. Gore, *J. Org. Chem.*, 22, 135 (1957).




and silver acetylides. Also the infrared spectrum of IX showed an absorption at 3270 $cm^{-1}$ indicating the presence of the ethynyl group as illustrated in Fig. 1.

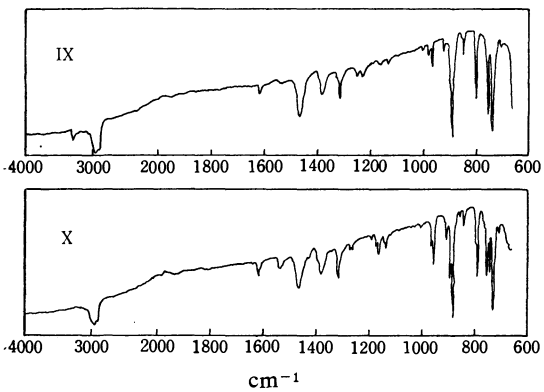



Fig. 1. The infrared spectra of 1-Ethynylanthracene (IX) and 1,1'-dianthryldiacetylene (X). (Nujol mull)

The oxidative coupling of IX according to the procedure of Eglinton[6] afforded fine yellow needles in almost quantitative yield. This was identified as X from its analytical data and the absence of free ethynyl absorption in the infrared spectrum (Fig. 1). X was found to be a stable substance and could be kept unchanged for a long time. X is slightly soluble in benzene and gives a greenish yellow solution with intense blue fluorescence. The diyne X is almost insoluble in common organic solvents such as ethanol and petroleum benzine.

The ultraviolet spectra of IX and X will be discussed in the following paper comparing them with those of the analogous compounds.

## Experimental**

**1-Carboxyanthraquinone (III).**—The acid (III) was prepared by the chromic acid oxidation of 1,9-benz-10-anthrone (II) according to the method of J. W. Cook[2].

**1-Carboxyanthracene (IV).**—III was reduced by means of zinc dust and aqueous ammonia[3], m. p. 245°C, yellow rods (the reported value, m.p. 245°C[3]).

Found: C, 80.83; H, 4.63. Calcd. for $C_{15}H_{10}O_2$: C, 81.06; H, 4.54%.

**1-Acetylanthracene (VII).**—IV was converted to the corresponding acid chloride V by the reaction with thionyl chloride. Diethyl ethoxymagnesiomalonate was prepared from diethyl malonate (48 g., 0.3 mol.), magnesium (7.3 g., 0.3 gram atom) and absolute ethanol (27.6 g., 0.6 mol.) in dry toluene (150 ml.). The excess of ethanol was removed by the azeotropic distillation with toluene. To the refluxed solution of the malonate a solution of crude V (24 g., 0.1 mol.) in dry toluene (400 ml.) was added in 30 min., and the stirring was continued for 3 hr. also under reflux. The reaction mixture was chilled with ice, and decomposed by the addition of 6 N sulfuric acid (100 ml.). The organic layer separated was washed thoroughly with water and dried over anhydrous sodium sulfate. The solvent was removed under reduced pressure. The crude ketomalonate VI was obtained as an orange-yellow oil. The crude product was mixed with propionic acid (80 ml.) and concentrated sulfuric acid (0.5 ml.), and the mixture was refluxed. After 3 hr., 4 N sulfuric acid (50 ml.) was added and the refluxing was further continued for 8 hr. to complete decarboxylation. A small amount of toluene was co-distilled out with water from the reaction mixture. The residue was diluted with water (300 ml.), and the mixture was extracted with benzene (100 ml.×6). The extract was washed with dilute sodium hydroxide and water, successively. The dried benzene solution was concentrated to 200 ml. and filtered through a short column of alumina (20 g.). Light yellow cubes, (15 g., 68%), m. p. 103~106°C were obtained on concentrating the filtrate. Recrystallization of the crude crystals from benzene afforded pure VII as light yellow cubes, m. p. 106~107°C (the reported value, m. p. 105~106°C[5]).

Found: C, 87.52; H, 5.50. Calcd. for $C_{16}H_{12}O$: C, 87.24; H, 5.49%.

I. R. max., 1670 $cm^{-1}$ (C=O).

**1-Ethynylanthracene (IX).**—The acetyl compound VII (10 g., 0.046 mol.) and phosphorus pentachloride (9.8 g., 0.068 mol.) was added to

6) G. Eglinton and A. R. Galbraith, *Chem. & Ind.*, **1956**, 737; *J. Chem. Soc.*, **1959**, 889.

** All melting points are uncorrected. The infrared spectra were measured by the Nujol mull method.

phosphorus oxychloride (70 ml.) and the mixture was refluxed for 1 hr. The mixture changed to a homogeneous dark red solution with an evolution of hydrogen chloride. Phosphorus oxychloride was removed completely under reduced pressure and the residual dark brown viscous oil was kept for several hours in an evacuated desiccator containing phosphorus pentoxide and potassium hydroxide.

The solution of the crude chloride in dry tetrahydrofuran (20 ml.) was added in 1 hr. to a solution of sodium amide (prepared from 11.5 g. of sodium) in liquid ammonia (500 ml.). After evaporation of ammonia, water (100 ml.) was added to the reaction product and extracted with ligh petroleum (b. p. 60~80°C, 1000 ml.). The extract was washed with water and dried over anhydrous sodium sulfate. The dried solution was filtered through a thin layer of alumina (40 g.). Concentration of the filtrate resulted in IX as light yellow cubes, 5.1 g. (55%), m. p. 88~90°C. This material was recrystallized from light petroleum or sublimed under high vacuum ($0.5\times10^{-4}$ mmHg) to yield pure IX, m. p. 90°C.

Found: C, 95.04; H, 5.10. Calcd. for $C_{16}H_{10}$: C, 95.02; H, 4.98%.

I. R. max., 3270cm$^{-1}$ (-C≡C-H).

U. V. max. (in cyclohexane), $\lambda_{max}$ 255 m$\mu$, (log $\varepsilon$ =5.05), 274.5 (4.04), 305 (2.60), 322 (3.03), 333.5 (3.44), 352 (3.78), 371 (4.04), 386 (3.68)* and 391 (4.06). Asterisk indicates shoulder.

**Oxidative Coupling of 1-Ethynylanthracene (IX).**—Cupric acetate monohydrate (40 g.) was added to the mixture of IX (1.89 g., 0.0094 mol.), dry pyridine (300 ml.) and methanol (20 ml.), and the mixture was stirred for 9 hr. at 55°C. The reaction mixture was filtered and the solid obtained was washed thoroughly with water. Yellow powder almost free from inorganic material was obtained, 1.45 g. (85%), m. p. 287~290°C (decomp.). The residue which was obtained by the concentration of the filtrate under a reduced pressure was digested with benzene. The benzene solution was passed through a short column of alumina and the filtrate was evaporated to yield yellow powder, 0.17 g. (10%), m. p. 289~291°C (decomp.). This was combined with the first crop and recrystallized from benzene to give pure X, yellow fine needles, m. p. 289~291°C (decomp.).

Found: C, 95.61; H, 4.47. Calcd. for $C_{32}H_{18}$: C, 95.49; H, 4.51%.

X gave no precipitate with an alcoholic silver nitrate solution.

U. V. max. (in cyclohexane), $\lambda_{max}$ 259 m$\mu$ (log $\varepsilon$ =5.16), 283 (4.27), 295 (4.35), 315.5 (3.52), 329 (3.66), 346 (3.64)*, 365 (3.99), 386 (4.26), 407 (4.42) and 428 (4.39). Asterisk indicates shoulder.

The authors are indebted to Mr. M. Okumiya and Miss K. Koike for the microanalyses. A part of the expenses of this research was defrayed from the grant-in-aid of the Ministry of Education to which the authors' thanks are also due.

*Department of Chemistry*
*Faculty of Science*
*Osaka University*
*Nakanoshima, Osaka*

# *Cyclic Acetylenes. IV. Synthesis of a Cyclic Tetraacetylene Containing Anthracene Nuclei**

By Shuzo AKIYAMA, Soichi MISUMI and Masazumi NAKAGAWA

(Received March 24, 1960)

There has already been discussion concerning the fact that a conjugated planar cyclic en-yne system may form a continuous molecular $\pi$-orbital overlapping the *p*-orbitals of the carbon atoms of the unsaturated linkages in the cycle[1]. It is of interest to synthesize such a cyclic acetylene in order to establish experimentally the validity of the theoretical prediction, but the only member of this series known up to now is the completely conjugated planar eighteen membered monocyclic hexaene-triyne which was reported recently by Sondheimer and Wolovsky[2]. They synthesized the hexaene-triyne by a prototropic rearrangement of the corresponding cyclic hexa acetylene which was prepared by the oxidative coupling of 1,5-hexadiyne. Another promising approach to the synthesis of a planar cyclic en-yne system is the oxidative coupling of a diethynyl aromatic compound in which the two ethynyl groups are directly attached to the proper positions of the aromatic nucleus. The rigid geometry of this type of molecule may be favorable to the ring formation by oxidative coupling as pointed out by W. Baker[3]. The

* For a preliminary report of a part of this work, see *Chem. & Ind.*, **1960**, 346.

1) T. J. Sworski, *J. Chem. Phys.*, **16**, 550 (1948).

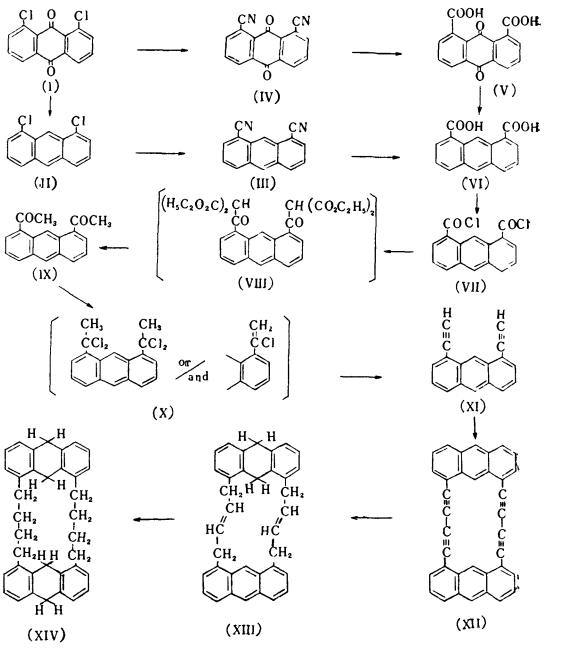
2) F. Sondheimer and R. Wolovsky, *J. Am. Chem. Soc.*, **81**, 1771 (1959).

first attempt according to this principle has been reported by Eglinton and his coworker. They carried out the oxidative coupling of *o*-diethynylbenzene expecting the formation of a fully conjugated strainless cyclic trimer, the tribenzo derivative of cyclo-octadeca-triene-hexayne[4]. But unexpectedly the product was identified to be a highly strained cyclic dimer of *o*-diethynylbenzene[5].

We have synthesized a planar conjugated cyclic tetraacetylene containing two anthracene nuclei (XII) according to the following scheme. The starting material for our work was 1, 8-dichloroanthraquinone (I). The dichloroquinone I was reduced to 1, 8-dichloroanthracene (II)[6], and the reaction of II with cuprous cyanide in quinoline gave 1, 8-dicyanoanthracene (III). The attempt to obtain 1, 8-diacetylanthracene (IX) by the reaction of III with methylmagnesium iodide in anisol failed on account of the poor solubility and inert reactivity of III. Therefore, according to the results of the preliminary experiments[7], the route to the diacetyl compound IX via dicarboxylic acid VI was chosen. 1, 8-Dicarboxyanthracene (VI) was synthesized by the alkaline hydrolysis of the dinitrile III in ethylene glycol. The diacid VI was also prepared according to the procedure of Waldmann[8] by the reduction of 1,8-dicarboxyanthraquinone (V) which was derived from I via IV.

Treatment of VI with thionyl chloride in chlorobenzene afforded the diacid dichloride VII. VII was caused to react with diethyl ethoxymagnesiomalonate in xylene to yield the ketomalonate VIII. The curde VIII was heated without further purification with the mixture of propionic and sulfuric acid. Treatment of the reaction mixture resulted in 1, 8-diacetylanthracene (IX) as light yellow cubes.

The crude chloride X which was obtained by the reaction of the diacetyl compound IX with phosphorus pentachloride in phosphorus oxychloride was dehydrochlorinated with sodium amide in liquid ammonia. 1, 8-Diethynylanthracene (XI) was obtained as yellow cubic crystals which melted at 150~151°C with decomposition. XI was found to be a fairly unstable substance and could not be kept without de-composition for a long time. The in-



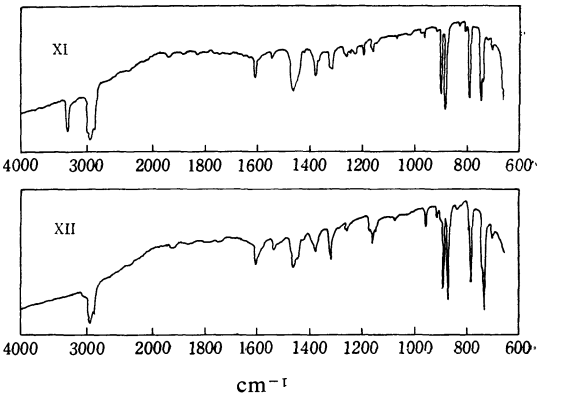



Fig. 1. The infrared spectra of 1,8-diethynylanthracene (XI) and the cyclic tetraacetylene (XII). (Nujol mull)

frared spectrum of XI shows an absorption at 3260 $cm^{-1}$ indicating the presence of terminal acetylene as illustrated in Fig. 1. XI gives also red cuprous and yellow silver acetylides.

The oxidative coupling of the diethynyl compound XI, conducted according to the procedure of Eglinton[9], yielded orange crystals in a high yield. The structure of the cyclic tetraacetylene (XII) was assigned to the substance from the method of preparation and from the following evidences. The cyclic nature of XII was confirmed by the absence of free ethynyl absorption in the infrared spectrum (Fig. 1) and by the negative test against alcoholic silver nitrate solution. Various

3) W. Baker, J. F. W. McOmie and W. D. Ollis, *J. Chem. Soc.*, **1951**, 200.
4) G. Eglinton and A. R. Galbraith, *Proc. Chem. Soc.*, **1957**, 350.
5) O. M. Behr, G. Eglinton and R. A. Raphael, *Chem. & Ind.*, **1959**, 699; W. K. Grant and J. C. Speakmann, *Proc. Chem. Soc.*, **1959**, 231.
6) H. Schilling, *Ber.*, **46**, 1066 (1913).
7) The preceding paper.
8) a) H. Waldmann and A. Oblath, *Ber.*, **71**, 366 (1938). b) H. Waldmann and R. Stengl, *Chem. Ber.*, **83**, 167 (1950).
9) G. Eglinton and A. R. Galbraith, *Chem. & Ind.*, **1956**, 737; *J. Chem. Soc.*, **1959**, 886.

methods for determining the molecular weight of XII were tried unsuccessfully as a result of the poor solubility of this substance in organic solvents. Reduction of XII with an excess of sodium in liquid ammonia yielded a substance with a composition $C_{36}H_{30}$ as a main product.

The infrared spectroscopy of this material revealed the presene of a methylene group ($\nu_{as}$: 2860, $\nu_s$: 2920 $cm^{-1}$), unconjugated *trans*-ethylenic bond ($\delta_{CH}$: 952 $cm^{-1}$) and 1,2,4,5-tetrasubstituted benzene ($\delta_{CH}$: 875 $cm^{-1}$) as illustrated in Fig. 1. From these evidences,

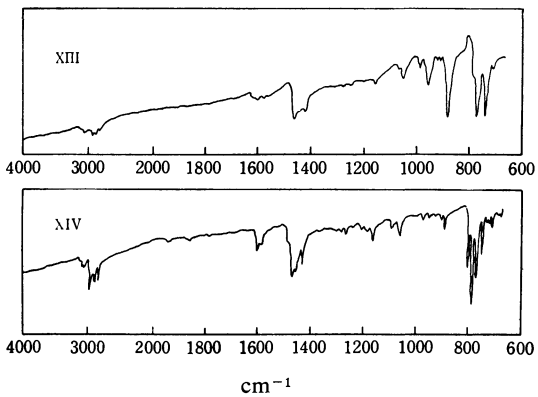



Fig. 2. The infrared spectra of $C_{36}H_{30}$ (XIII) and the hydrogenated product (XIV). (KBr-disk)

the structure of XIII was assigned tentatively to the reduction product. Further hydrogenation of XIII in benzene over palladium on charcoal gave tiny colorless cubes with the empirical formula $(C_9H_9)_n$. The molecular weight of this substance could be determined accurately by Rast's method in camphor. The molecular weight thus determined (450; Calcd. for $C_{36}H_{36}$: 469) provided an unequivocal evidence regarding the dimeric cyclic acetylene for XII. The fully hydrogenated product shows no absorption at 875 $cm^{-1}$ in the infrared spectrum, indicating the absence of the anthracene nucleus in the molecule. The infrared spectrum of this substance was illustrated in Fig. 2 together with that of XIII. The ultraviolet spectrum of the hydrogenated product also indicates the destruction of anthracene chromophor. From these observations structure XIV was given to the reduction product.

The high yield of the oxidative cyclic dimerization of XI to XII seems to reflect the favorable orientation of the ethynyl groups in XI. Examination of the bond angles of the compound XII readily verifies its planar and strainless nature. XII was found to be a very stable compound and can be kept without change for a long time in air and light. In

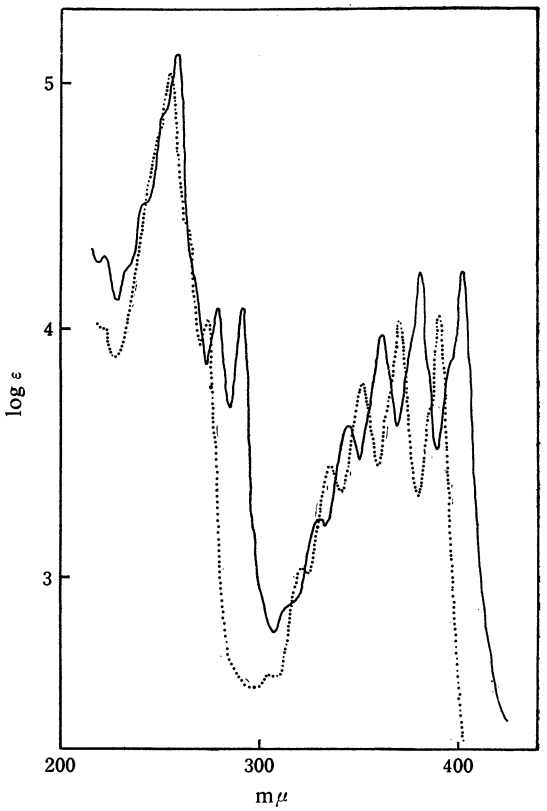



Fig. 3. The ultraviolet spectra of 1-ethynylanthracene (XVI, ·····) and 1,8-diethnylanthracene (XI, ——).

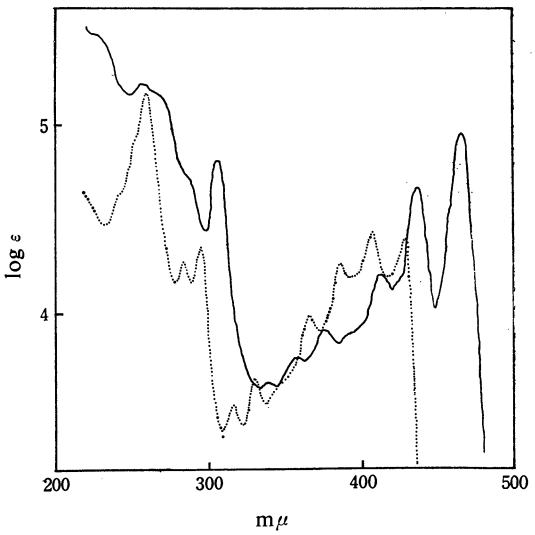



Fig. 4. The ultraviolet spectra of 1,1'-dianthryldiacetylene (XVIII, ·····) and the cyclic tetraacetylene (XII, ——).

an evacuated capillary tube, XII turned to black at a temperature over 370°C without the change of crystal form. XII is sparingly soluble in common organic solvents. The

TABLE I. THE BATHOCHROMIC SHIFTS OF THE ULTRAVIOLET SPECTRA OF THE ACETYLENES

| Compound | $\lambda_{max}$ | $\varepsilon$ | Solvent | Shifts in mμ from XV | XVI | XI | XVII |
|---|---|---|---|---|---|---|---|
| Anthracene (XV) | 374 | 7,460 | C | — | — | — | — |
| 1-Ethynylanthracene (XVI) | 391 | 11,500 | C | 17 | — | — | — |
| 1,8-Diethynylanthracene (XI) | 402 | 17,400 | C | 28 | 11 | — | — |
| 1,1'-Dianthryldiacetylene (XVII) | 428 | 24,600 | C | 54 | 37 | 26 | — |
| Cyclic tetraacetylene (XII) | 465 | 91,200 | B | 91 | 74 | 63 | 37 |

C: cyclohexane, B: benzene.

solution in dimethylformamide, in which XII is slightly soluble, exhibits an orange yellow color with intense and characteristic green fluorescence.

The ultraviolet spectra of 1-ethynylanthracene (XVI)[7], 1,8-diethynylanthracene (XI), 1,1'-dianthryldiacetylene (XVII)[7] and the cyclic tetraacetylene (XII) are illustrated in Figs. 3 and 4. The bathochromic shifts of the absorption maxima at the longest wavelength and the $\varepsilon$-values of these acetylenes as compared with anthracene are tabulated in Table I. The $\varepsilon$-value of XVII reduced to per acetylene-unit ($0.5\times24,600=12,300$) is approximately the same as that of XVI (11,500), whereas the $\varepsilon$-value of XII reduced per diyne-unit ($0.5\times91,200=45,600$) is much greater than those of XVII (24,600) and XI (17,400). The marked increase in the absorption intensities and the remarkable red-shift of the spectrum of XII indicate that the cyclic tetraacetylene can not be regarded as a simple derivative of anthracene. These ultraviolet spectroscopic properties and, at least to some extent, the unusual stability of XII seem to be attributable to an enhanced interaction of $\pi$-electrons of the acetylenic bonds with those of the aromatic system.

The syntheses of the same type of higher cyclic acetylenes are now being investigated.

## Experimental**

**1,8-Dichloroanthracene (II).**—The reduction of I with zinc dust in aqueous ammonia[6] yielded a product consisting of mainly 1,8-dichloro-9,10-dihydroanthranol[10]. The reduction product was extracted with ethanol. The solvent was removed and the light yellow crystalline residue was recrystallized from carbon tetrachloride to give the pure anthranol, white needles, m.p. 136~136.5°C.

Found: C, 63.52; H, 4.03; Cl, 27.27. Calcd. for $C_{14}H_{10}OCl_2$: C, 63.41; H, 3.78; Cl, 26.80%.

I.R. max., Broad absorption near 3200 (-OH); 1180 $cm^{-1}$ (C-O).

A catalytic amount of concentrated sulfuric acid was added to a solution of the anthranol in hot ethanol. Immediate precipitation of practically pure II, light yellow needles, m.p. 157~158°C, (values in literature, 156°C[6]; 160°C[11]) was observed.

Found: C, 68.04; H, 3.28; Cl, 28.96. Calcd. for $C_{14}H_8Cl_2$: C, 68.05; H, 3.26; Cl, 28.69%.

In practice it was found more convenient to treat the ethanol extract of the reduction product with a small amount of sulfuric acid without the isolation of the anthranol.

**1,8-Dicyanoanthracene (III).**—A mixture of II (50 g., 0.19 mol.), cuprous cyanide (60 g.) and quinoline (500 ml.) was stirred for 24 hr. under reflux. The cooled reaction mixture was filtered and the solid was washed with dilute hydrochloric acid, then treated with dilute aqueous sodium cyanide to dissolve cuprous cyanide, and was washed with water. The dried light brown powder was digested with nitromethane (250 ml.) to remove the resinous material on the powder. Recrystallization of the powder from acetic acid using active charcoal yielded III, long yellow needles, m.p. 299~304°C, 22 g. (48%). Further recrystallization of this material from acetic acid gave pure III, m.p. 304~306°C, (value in literature, m.p. 300.5°C[8]). III is soluble in concentrated sulfuric acid giving a greenish yellow solution.

Found: C, 83.69; H, 3.47; N, 12.13. Calcd. for $C_{16}H_8N_2$: C, 84.19; H, 3.53; N, 12.28%.

I.R. max., 2225 $cm^{-1}$ (-C≡N).

**1,8-Dicarboxyanthracene (VI).**—*a) Hydrolysis of 1,8-Dicyanoanthracene (II).*—A mixture of II (10 g., 0.044 mol.), potassium hydroxide (125 g.) and ethylene glycol (270 ml.) was heated to 150~155°C under stirring until the evolution of ammonia ceased (ca. 70 hr.). The reaction mixture was neutralized with hydrochloric acid resulting in formation of a yellow precipitate. The precipitate was filtered, washed with water and dried, yielding yellow powder, 11 g. (94%), m.p. 341~345°C (decomp.). Recrystallization of this material from 95% ethanol resulted in pure VI, yellow needles, m.p. 347°C (decomp.). (value in literature, 345°C (decomp.)[8]).

Found: C, 71.84; H, 3.77. Calcd. for $C_{16}H_{10}O_4$: C, 72.18; H, 3.79%.

*b) Reduction of 1,8-Dicarboxyanthraquinone (V).*—1,8-Dicyanoanthraquinone (IV) which was obtained by the reaction of I with cuprous cyanide in benzyl cyanide[8a] was hydrolyzed to V by the reaction with sulfuric acid[8]. The reduction of V by means of zinc dust in aqueous ammonia yielded

** All melting points are uncorrected. The infrared spectra were measured by the Nujol mull method otherwise special indication is given.

10) It has been reported that the reduction of anthracene with zinc dust in aqueous ammonia yields anthranol. Cf., H. R. von Perger, *J. prakt. Chem.*, **23**, 137 (1881).

11) E. B. Barnett and M. A. Matthews, *J. Chem. Soc.*, **123**, 2549 (1923).

VI, m. p. 347°C (decomp.). This substance showed no depression of the melting point on admixture with the specimen prepared by route *a*).

**Anthracene-1, 8-dicarboxylic Acid Chloride (VII).**—The acid chloride (VII) was prepared according to the procedure of Waldmann[8b]. Recrystallization of the crude product from toluene gave pure VII, orange needles, m. p. 255~257°C (decomp., in a sealed capillary tube). (value in literature, m. p. lower than 220°C (decomp.)[8b]). VII gives yellow solution in concentrated sulfuric acid.

Found: C, 63.15; H, 2.80; Cl, 23.37. Calcd. for $C_{16}H_8O_2Cl_2$: C, 63.39; H, 2.66; Cl, 23.39%.

**1, 8-Diacetylanthracene (IX).**—1) *Malonation of the Acid Chloride (VII.)*—Diethyl ethoxymagnesiomalonate was prepared from magnesium (11 g., 0.46 gram atom), diethylmalonate (73.5 g., 0.46 mol.) and absolute ethanol (27.6 g., 0.6 mol.) in dry xylene (100 ml.). The excess of ethanol was removed by the azeotropic distillation with xylene. The solution of the malonate was added to the hot solution of VII (17 g., 0.057 mol.) in dry xylene (1.8 l.) in 30 min. under stirring. The mixture was refluxed for 1 hr. and decomposed with the addition of crushed ice (100 g.) and 4 N sulfuric acid (300 ml.). The organic layer was washed with water, and dried over anhydrous sodium sulfate. Evaporation of the solvent under reduced pressure resulted in the crude ketomalonate (VIII) as an orange red oil.

2). *Ester Exchange and Decarboxylation of the Ketomalonate (VIII).*—The crude VIII was mixed with propionic acid (320 ml.) and concentrated sulfuric acid (4 ml.), and the mixture was refluxed for 4 hr. with a vigorous evolution of carbon dioxide. Sulfuric acid (4 N, 250 ml.) was added to the reaction mixture and the reflux was continued until no more evolution of carbon dioxide was observed. The mixture was distilled to remove a small amount of xylene with water, and poured onto ice-water (1 l.). The ice cooled mixture was filtered. The solid thus obtained was washed with water, and dissolved in benzene. The benzene solution was washed with dilute sodium hydroxide solution and water, successively. The dried solution was filtered through a short column of aluminum oxide, and the concentration of the filtrate resulted in IX, light yellow cubes, 7.4 g. (50%.), m. p. 176~179°C (Kofler block). Recrystallization of this substance from benzene resulted in pure IX, light yellow cubic crystals, m. p. 179~180°C. IX gives an orange red solution with concentrated sulfuric acid.

Found: C, 82.49; H, 5.49. Calcd. for $C_{18}H_{14}O_2$: C, 82.43; H, 5.38%.

I. R. max., 1675 $cm^{-1}$ (C=O).

**1, 8-Diethynylanthracene (IX).**—*1) Chlorination of the Diacetylanthracene (IX).*—IX (5.25 g., 0.02 mol.) was mixed with phosphorus pentachloride (12.5 g., 0.06mol.) and phosphorus oxychloride (50 ml.), and the mixture was heated under reflux for 1.5 hr. With an evolution of hydrogen chloride, the mixture changed to a homogeneous dark red solution. The oxychloride was removed completely under reduced pressure. The dark red viscous oil was kept for several hours in a desiccator containing phosphorus pentoxide and potassium hydroxide.

*2). Dehydrochlorination of the Chloride (X).*—The crude chloride (X) in absolute ether (30 ml.) was added in 40 min. to a solution of sodium amide (prepared from sodium, 11.5 g., 0.5 gram atom) in liquid ammonia (500 ml.). The mixture was stirred for 2 hr. at the temperature of dry ice-ethanol bath. After evaporation of ammonia, water (250 ml.) was added cautiously to the reaction mixture and filtered to collect insoluble material. The dark brown solid obtained was digested with light petroleum (b. p. 60~80°C, 1.5 l.). The solution was washed with water and dried over anhydrous sodium sulfate. The solution was passed through a short column of alumina, and the filtrate was evaporated to yield XI, 1.65 g. (37%), m. p. 150~151°C (decomp., Kofler block). XI gave red cuprous, yellow silver and mercuric acetylides.

Found: C, 95.49; H, 4.45. Calcd. for $C_{18}H_{10}$: C, 95.54; H, 4.46%.

I. R. max., 3260 $cm^{-1}$ (-C≡CH).

U. V. max. (in cyclohexane), $\lambda_{max}$ 258 mμ (log ε =5.13), 279 (4.08), 291 (4.08), 312 (2.87)*, 330 (3.22), 345 (3.60), 362 (3.98), 381 (4.22) and 402 (4.24). Asterisk indicates shoulder.

**Oxidative Coupling of 1, 8-Diethynylanthracene (XI).**—To the solution of XI (0.600 g., 0.0027 mol.) in pyridine (100 ml.) and methanol (8 ml.) was added cupric acetate monohydrate (12 g.), and the mixture was vigorously stirred for 4 hr. at 55°C. Stirring was continued for a further 3 hr. period at room temperature. The reaction mixture was filtered and the solid obtained was washed thoroughly with water, a small amount of benzene and ethanol, successively. The cyclic tetrayne XII almost free from inorganic contaminate was obtained as orange powder, 0.562 g. (95%). This substance decomposed over 370°C. A minor amount of XII of poor purity was obtained from the pyridine solution.

The crude XII was recrystallized 3 times from xylene and once from dimethylformamide yielding tiny orange cubes. These crystals decomposed over 370°C in an evacuated capillary tube without any change of the crystal form.

Found: C, 95.72; H, 3.61. Calcd. for $C_{36}H_{16}$: C, 96.40; H, 3.60%.

The unsatisfactory result in the analysis of carbon may be due to explosive decomposition of XII in the combustion tube forming a carbonaceous material difficult to burn.

U. V. max., $\lambda_{max}$ 258 mμ (log ε=5.22) (in *n*-hexane), 307 (4.82), 340 (3.66), 358 (3.79), 376 (3.93), 413 (4.22), 437 (4.67) and 465 (4.96) (in benzene).

**Reduction of the Cyclic Tetraacetylene (XII) with Sodium in Liquid Ammonia.**—The mixture of XII (0.42 g., 0.0009 mol.), sodium (0.9 g., 0.039 gram atom) and liquid ammonia (150 ml.) was stirred for 7 hr. at the temperature of dry ice-ethanol bath. Ammonium nitrate was added to the reaction mixture, and ammonia was evaporated. Water was added to the residue and the light yellow powder formed was collected by filtration. The powder was digested with benzene to remove the insoluble material. The benzene solution was filtered

through a thin layer of alumina (10 g.). Evaporation of the solvent afforded XIII, yellow needles, 0.20 g. (48%), m. p. 365~368°C (decomp., in an evacuated capillary tube, metal block).

Found: C, 93.24; H, 6.67. Calcd. for $C_{36}H_{30}$: C, 93.46; H, 6.54%.

I. R. max. (KBr-disk method), 2920, 2860 ($-CH_2-$), 952 (isolated trans-ethylenic bond), 875 $cm^{-1}$ (tetra-substituted benzene).

U. V. max., $\lambda_{max}$ 257 m$\mu$ ($\log \varepsilon = 4.91$) (in *n*-hexane), 318 (3.71), 332 (3.72), 348 (3.73), 368 (3.84) and 387 (3.89) (in benzene).

**Catalytic Reduction of $C_{36}H_{30}$ (XIII).**—The solution of XII (0.19 g.) in benzene (300 ml.) was shaken in hydrogen with palladium (5%) on charcoal (0.5 g.). The color and the fluorescence of the solution gradually disappeared in the course of the hydrogenation. The catalyst was filtered and washed with benzene. The filtrate was combined with the washing, and the evaporation of the solvent yielded XIV as fine colorless needles in almost quantitative yield. This was recrystallized from benzene to give pure XIV, m. p. 316~318°C, (in an evacuated capillary tube; metal block).

Found: C, 92.10; H, 7.67; Mol. wt. (Rast, camphor), 450. Calcd. for $C_{36}H_{36}$: C, 92.26; H, 7.74%; Mol. wt., 469.

I. R. max. (KBr-disk method), 2935, 2870 ($-CH_2-$), 735 $cm^{-1}$ ($-(CH_2)_4-$).

U. V. max. (in ethanol), $\lambda_{max}$ 256 m$\mu$; $\lambda_{min}$ 248 m$\mu$.

The financial support of this research was granted by the Ministry of Education. The starting material was donated by the Mitsui Chemical Industries Co., Ltd. The elementary analyses were performed by Mr. M. Okumiya and Miss K. Koike. The authors wish to express their sincere thanks for these donation and for the help received.

*Department of Chemistry*
*Faculty of Science*
*Osaka University*
*Nakanoshima, Osaka*

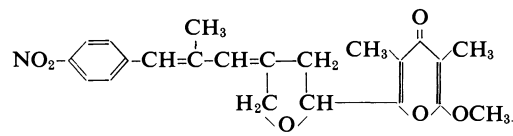
# *The Structure of Aureothin. X*[1]. *Aza Derivatives of Aureothin, Isoaureothin and Desmethylisoaureothin*

By Kiyoyuki YAMADA, Hisao NAKATA and Yoshimasa HIRATA

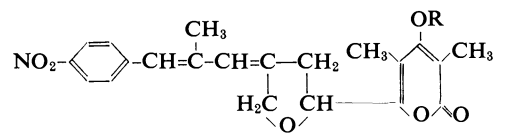
(Received April 2, 1960)

A recent publication[2] from our laboratory has indicated that the structure of aureothin was shown to be I, on a firm basis of a quantity of chemical and spectroscopic evidence. Aureothin undergoes demethylation with various acids, followed by isomerization, to give desmethylisoaureothin (II, R=H), the methylation of which, in turn leads to isoaureothin (II, $R=CH_3$) as a major product[1].

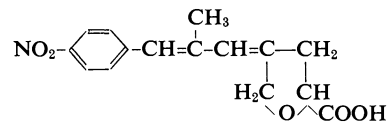
During the course of the structural investigation, it was found that I, II ($R=CH_3$) and II (R=H) reacted with ammonia and were transformed to aza-aureothin (IV), aza-isoaureothin (V) and aza-desmethylisoaureothin (VI), respectively. In the present paper, the properties of these aza-derivatives are described, being compared with those of other model compounds. Each of these aza-derivatives contains one more nitrogen, besides an original one (nitro group), and is sparingly soluble both in organic solvents and water.



(I)



(II)



(III)

**Aza-aureothin (IV).**—The elemental analysis of IV was incompatible with the molecular formula, expected for γ-pyrone—γ-pyridone

1) For Part IX of this series, see, H. Nakata, This Bulletin, in press.

2) K. Yamada, H. Nakata and Y. Hirata, *J. Chem. Soc. Japan, Pure Chem. Sec.* (*Nippon Kagaku Zasshi*), **81**, 340 (1960).

3) Y. Hirata, K. Okuhara, H. Nakata, T. Naito and K. Iwadare, ibid., **78**, 1700 (1957).

transformation; there remained no methoxyl group in IV. Thus, somewhat complicated reactions must take place during the formation of IV from I. It is apparent from the ultraviolet spectrum that $\gamma$-pyrone moiety is involved in the reaction, and the conjugated *p*-nitrophenyl system remains intact. Subtraction of the ultraviolet spectrum of aureothinic acid (III) from that of aza-aureothin (IV) gave an absorption spectrum due to the chromophore in question—presumably, a nitrogen-containing ring; the subtraction curves, taken in neutral and acid solutions, were different, as shown in Fig. 1.

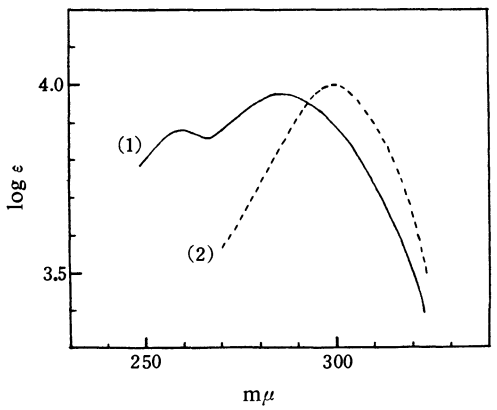



Fig. 1. Substraction curves obtained by aza-aureothin (IV)—aureothinic acid (III) in ethanol.
(1): Neutral and alkaline (0.1 N EtONa) solutions.
(2): Acidic (0.1 N HCl) solution.

The infrared spectrum showed bands at 1666(s), 1643(m), 1583(s), 1529(s), 1509(s) $cm^{-1}$ and at 3385, 3285 and 3175 $cm^{-1}$, the latter group of bands suggesting the presence of N-H and/or O-H. Treatment of IV with acetic anhydride and pyridine yielded an amorphous substance, the infrared spectrum of which showed bands at 1731(s), 1666(s), 1623(s), 1596(s) and 1516(s) $cm^{-1}$ (in chloroform). This must be an ester. The insolubility of IV in various solvents prevented us from attempting further studies on this substance, and the details of the structure are still uncertain.

**Aza-isoaureothin (V).**—Analytical data of V agreed with a molecular formula $C_{21}H_{22}O_5N_2$, identical with that of aza-desmethylisoaureothin (VI), but the chemical behavior, as described below, is quite different from those expected for aza-desmethylisoaureothin (VI). In this case, again, some other reaction might occur concomitantly with the pyrone—pyridone transformation. This compound is not an acidic substance but a neutral one, and an attempted acetylation only resulted in the complete recovery of the starting material. The same procedure used for IV was applied for the measurement of the ultraviolet spectrum; the results obtained by the subtraction method of the ultraviolet curves are shown in Fig. 2. In this case also, the absorption maximum in an acidic medium is situated at somewhat longer wavelength than that in neutral solution.

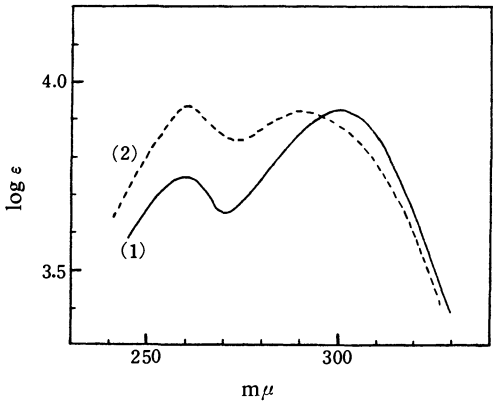



Fig. 2. Subtraction curves obtained by aza-isoaureothin (V) — aureothinic acid (III) in ethanol.
(1): Neutral and alkaline (0.1 N EtONa) solutions.
(2): Acidic (0.1 N HCl) solution.

Remarkable differences were observed in the infrared spectra between isoaureothin (II, R=$CH_3$) and aza-isoaureothin (V), as illustrated in Fig. 3. The following points are worth noticing; the shift of carbonyl band (1716 $cm^{-1}$ for isoaureothin, 1660 $cm^{-1}$ for aza-isoaureothin), and the appearance of a new band at 1554 $cm^{-1}$ and of a series of bands at 3225, 3322, 3434 $cm^{-1}$.

From these spectroscopic data, it is seen that an $\alpha$-pyridone ring is likely to be present in V, but the whole structural aspect of V could not yet be disclosed, owing to the same reason, as that encountered in the case of aza-aureothin (IV).

**Aza-desmethylisoaureothin (VI).** — Aza-desmethylisoaureothin $C_{21}H_{22}O_5N_2$, was prepared via two routes; one is based on a reaction of desmethylisoaureothin (II, R=H) with ammonia, and the other is due to the treatment of aureothin with ammonium acetate in acetic acid. Chemical and spectroscopic behavior of VI, described below, substantiates a simple pyrone-pyridone transformation. VI dissolved in aqueous alkali, although no reaction took place between VI and ethereal diazomethane (under heterogeneous condition). Acetylation of VI with acetic anhydride-pyridine gave aza-desmethylisoaureothin acetate, $C_{23}H_{24}O_6N_2$ (VII), which showed an enol acetate band at 1767 $cm^{-1}$ (KBr).

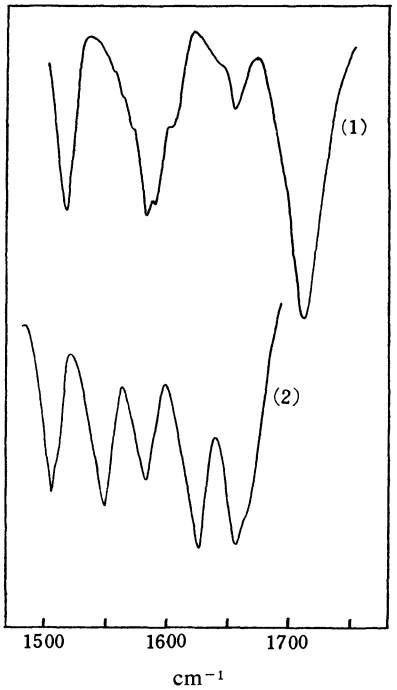



Fig. 3. Infrared spectra (KBr)
(1): Isoaureothin. (II, R=$CH_3$).
(2): Aza-isoaureothin. (V).

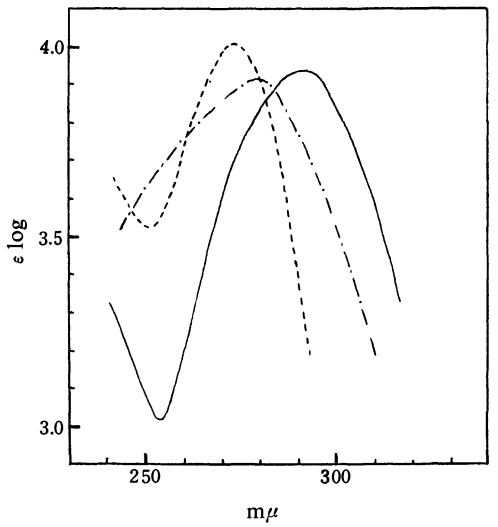
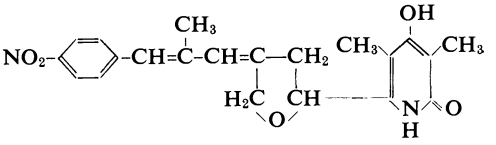



Fig. 4. Subtraction curves obtained by aza-desmethylisoaureothin (VI)—aureothinic acid (III) in ethanol.
(1): Neutral solution.
(2): Acidic (0.1 N HCl) solution.
(3): Alkaline (0.1 N EtONa) solution.

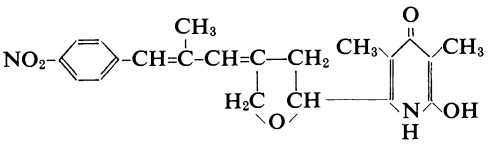
In the infrared spectrum of VI, there appeared bands at 1643(s), 1605(v. s), 1585(v. s), 1564(m) and 1510(s) $cm^{-1}$ in 1800~1500 $cm^{-1}$ region and a broad band ranging from 2500 $cm^{-1}$ to 3000 $cm^{-1}$, which indicates the occurrence of hydrogen bonding. The position of pyridone-carbonyl band unaffected by hydrogen bonding is available from aza-desmethylisoaureothin acetate (VII); i. e., in this case, $\nu_{C=O}$ appeared at 1654 $cm^{-1}$ (KBr).

In the ultraviolet region, the absorption due to the pyridone ring of VI had its maximum at 291 mμ in neutral solution, while acidic and alkaline conditions caused the hypsochromic displacement of the absorption (Fig. 4). The moderate solubility in chloroform made possible the ozonization of VII, which afforded aza-desmethylisoaureonone acetate, $C_{13}H_{15}O_5N$ (VIII). This product VIII, now free from the conjugated *p*-nitrophenyl system, showed an absorption maximum at 304 mμ in the ultraviolet region, and bands at 1762(s), 1658(s), 1640(sh.) and 1577(w) $cm^{-1}$ in the infrared region.

**Structure of Aza-desmethylisoaureothin.** — Both types VIa and VIb would be possible for VI, since enolization can occur in two directions[4].




(VIa)




(VIb)

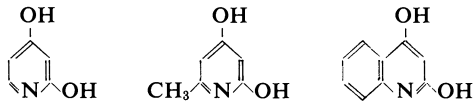
A considerable amount of data[5] concerning the infrared spectra of various α-pyridones is now at hand. The condition of the measurement (solid or solution) has a fairly large influence on the position of carbonyl absorption. The ranges quoted for carbonyl absorption in the solid state are rather wide (1630~1680 $cm^{-1}$)[5], whereas in solution, it has been reported that carbonyl frequencies fell into a somewhat narrow range (1654~1687 $cm^{-1}$)[6].

As to γ- pyridones, the data so far are not sufficient to obtain the detailed information about $\nu_{C=O}$; in general, $\nu_{C=O}$ is expected to appear in

4) One more possibilty, the diketo-form, is excluded on the ground of its relation to the ultraviolet spectrum.
5) (a) W. F. Cockburn and L. Marion, *Can. J. Chem.*, **29**, 13 (1951). (b) F. Ramirez and A. P. Paul, *J. Org. Chem.*, **19**, 183 (1954); *J. Am. Chem. Soc.*, **77**, 1035, 3377 (1955). (c) J. A. Gibson, W. Kynaston and A. S. Lindsey, *J. Chem. Soc.*, **1955**, 4340. (d) F. Bohlman, A. Englisch, N. Ottawa, H. Sander and W. Weise, *Chem. Ber.*, **89**, 792 (1956). (e) K. Hoegerle and H. Erlenmeyer, *Helv. Chim. Acta*, **39**, 1203 (1956). (f) R. H. Wiley and S. C. Slaymaker, *J. Am. Chem. Soc.*, **78**, 2393 (1956).
6) S. F. Mason, *J. Chem. Soc.*, **1957**, 4874.

the region 1630~1650 $cm^{-1}$ (solid and solution)[7]. According to Mason, the C=O band of the $\alpha$-pyridones is located at higher frequency than that of $\gamma$-isomers, whilst the reverse relation is observed regarding the N-H band[6]. Further, it was noticed[7d] that in $\alpha$-pyridones, the intensity of $\nu_{C=O}$ is usually stronger than that of $\nu_{C=C}$, whereas in $\gamma$-pyridones carbonyl absorption appears as a relatively weak band.

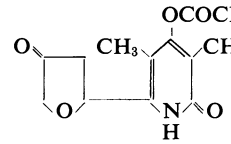
The following compounds may serve as good models of aza-desmethylisoaureothin (VI), in relation to the problem of tautomerism; 2, 4-dihydroxypyridine (IX)[6], 6-methyl-2, 4-dihydroxypyridine (X) and 2, 4-dihydroxyquinoline (XI)[6].



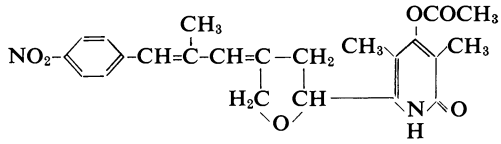
(IX) (X) (XI)

As to dihydroxypyridine (IX) it was believed that an $\alpha$-pyridone form was predominant in aqueous solution[8] on the ground of the ultraviolet evidence, while the possible coexistence of $\alpha, \gamma$-forms was suggested for IX in the solid state[9]. As for 6-methyl-2, 4-dihydroxypyridine (X), it is insufficiently soluble in chloroform to give an infrared spectrum in solution, but in the solid state (KBr), there appeared bands at 1658(s), 1639(s) and 1607(s) $cm^{-1}$ and a broad band near 3000 $cm^{-1}$ indicating a hydrogen bond. With the information about the diagnosis of $\alpha, \gamma$-tautomers at hand, it is concluded that the tautomer of $\alpha$-pyridone form occurs in X. An $\alpha$-pyridone structure was inferred[7d] for XI itself and its acetate, but not established firmly as yet.

With the help of the generalization described above, the structural examination of aza-desmethylisoaureothin (VI) will be made. The structure VIII is assigned to aza-desmethylisoaureonone acetate, the ozonisation product, on the basis of the position (1658 $cm^{-1}$) and the strong intensity of the pyridone carbonyl band. A strong band at 1762 $cm^{-1}$ in VIII is due to two carbonyls of enol acetate and five-membered ketone of tetrahydrofuran ring; two bands at 1640 and 1557 $cm^{-1}$ are ascribed to the unsaturation of the pyridone ring[10]. Establishment of VIII for the ozonisation product leads to structure VII for aza-desmethylisoaureothin acetate.



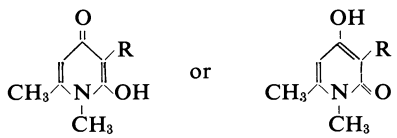
(VIII)



(VII)

The disagreement in the position of the carbonyl band of aza-desmethylisoaureothin (1643 $cm^{-1}$) with that of the model compound (X, 1658 $cm^{-1}$), taken in conjunction with the weak intensity in the former $\nu_{C=O}$, might be in favor of the $\gamma$-pyridone structure VIb for this derivative of the natural product. However, in aza-desmethylisoaureothin, the intermolecular (or intramolecular) interaction would be more complicated than in a simple molecule, and the overlappings of the bands due to benzene ring with those of the pyridone ring make it difficult to compare exactly the intensities between $\nu_{C=O}$ and $\nu_{C=C}$ in the pyridone ring. Such circumstances give rise to difficulty in making the discrimination between (Va) and Vb, solely on the basis of the infrared spectrum.

The unusual hypsochromic shift of the ultraviolet absorption maximum in alkaline solution was recognized as a characteristic feature of the hydroxypyridones (A), distinguishing the type (A) from other types of hydroxypyridone[11]. As is expected, the model compound IX behaves similarly (see Fig. 4).



(A): R=H or $C_2H_5$

A good paralellism of the ultraviolet spectra between the pyridone part of VI and the model X was observed, in regard to the magnitudes

7) (a) R. Adams, V. V. Jones and J. L. Johnson, *J. Am. Chem. Soc.*, **69** 1810 (1947); (b) N. J. Leonard and D. M. Locke, ibid., **77**, 1852 (1955); (c) P. I. Ittyeran and F. G. Mann, *J. Chem. Soc.*, **1958**, 467; (d) H. Shindo, "Infrared Absorption Spectrum Series No. 3" Nankodo, Tokyo, (1957), p. 186.

8) H. J. den Hertog and D. J. Buurman, *Rec. trav. chim.*, **75**, 257 (1956). Cf. H. M. Woodburn and M. Hellman, ibid.. **70**, 813 (1951).

9) There was recorded in the solid state, a pair of bands, 1661 and 1635 $cm^{-1}$ for IX (1662 and 1628 $cm^{-1}$ for (XI)), upon which the presumption of the coexistence of $\alpha, \gamma$-tautomers was based. Alternative interpretation of the spectrum, however, seems to be more reasonable; both IX and XI exist simply as an $\alpha$-pyridone form on the assumption that bands, 1635 and 1628 $cm^{-1}$ are respectively, associated with the unsaturated bonds of the ring.

10) The positions of bands associated with the unsaturated bonds of the ring are very sensitive to the substituents[5f]; therefore, these bands are not so useful for the identification of the pyridone ring.

11) J. A. Berson, W. M. Jones and S. L. F. O'callaghan, C. S. J., *J. Am. Chem. Soc.*, **78**, 622 (1956).

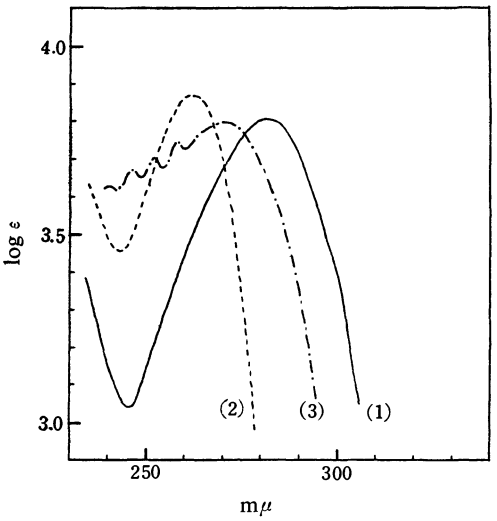



Fig. 5. Ultraviolet spectra of 6-methyl-4-hydroxy-2-pyridone (X) in ethanol.
(1): Neutral solution.
(2): Acidic (0.1 N HCl) solution.
(3): Alkaline (0.1 N EtONa) solution.

of the hypsochromic shifts and of the relative intensities. It is inferred that α-pyridone form VIa predominates in aza-desmethylisoaureothin in solution, on the analogy of the preferential α-tautomer in the cases of the models IX and X. Furthermore, the absorption at 292 mμ due to the pyridone part of VI is regarded as a reasonable position of α-pyridone ring[12].

## Experimental

**Aza-aureothin (IV).**—One gram of aureothin was added in a mixture of ethanol (40 ml.) and aqueous ammonia (10 ml.), and the suspension was kept at 90~95°C in a sealed tube for 10~12 hr. Aureothin gradually dissolved with heating, and after several hours a small number of crystals began to appear. The solution on cooling to room temperature deposited yellow crystals, which were filtered and recrystallized from a large amount of ethanol, m. p. 230~231°C. No methoxyl group was detected by Zeisel's method; the ultraviolet spectrum was measured in neutral ethanol, by assuming 380 for its molecular weight: $\lambda_{max}$ 345 mμ (log ε 4.25), 290 mμ (log ε 4.15).

Found: C, 64.75; H, 5.68%.

A suspension of 20 mg. of aza-aureothin was heated in acetic anhydride (5 ml.) and pyridine (1 ml.) at 80~90°C for thirty minutes. Water was added, to give the yellow precipitate, easily soluble in chloroform and ethanol.

**Aza-isoaureothin (V).**—A suspension of 1 g. of isoaureothin in 50 ml. of ethanol-aqueous ammonia (4 : 1) was heated at 90~95°C in a sealed tube for 18 hr. Complete dissolution of isoaureothin was observed within the initial five hours, and then crystallization of V slowly began to take place. As the heating was continued, the solution became dark red. The product was collected and treated with 20 ml. of hot ethanol, in order to remove remaining isoaureothin. Recrystallization from a fairly large amount of dioxane gave 360 mg. of V in yellow prisms, m. p. 228~229°C. The ultraviolet spectrum was measured in neutral ethanol with the assumption of 380 of molecular weight: $\lambda_{max}$ 343 mμ (log ε 4.25), 253 mμ (log ε 4.25).

Found: C, 65.84, 65.62; H, 5.99, 5.97; N, 7.33%.

A mixture, which consisted of 20 mg. of V, 8 ml. of acetic anhydride and 1 ml. of pyridine, was heated at 80~90°C for 1 hr. to give a clear solution. Upon cooling, the yellow needles separated. These were identified as starting material V.

**Aza-desmethylisoaureothin (VI).**—Though aza-desmethylisoaureothin was obtained by a procedure similar to that used for the preparation of IV and V, an efficient method, starting from aureothin, was developed, to give an excellent yield of (VI). A suspension of 1 g. of aureothin in 10 ml. of acetic acid containing 3 g. of ammonium acetate was gently refluxed for 4 hr. To the cooled solution, 200 ml. of water was added, when a brown oily layer at once separated and solidified. The liquid layer was removed by decantation, and the residue turned to a crystalline substance by the addition of 50ml. of hot ethanol. Washed with hot ethanol three times, the product was recrystallized from dimethylformamide and weighed 250 mg., m. p. 238~239°C; ultraviolet spectrum: $\lambda_{max}$ 341 mμ (log ε 4.25), 296 mμ (log ε 4.16), 245 mμ (log ε 4.18) (ethanol as solvent).

Found: C, 65.76, 65.48; H, 5.95, 6.19; N, 7.63. Calcd. for $C_{21}H_{22}O_5N_2$: C, 65.95; H, 5.80; N, 7.33%.

To a solution of 1 ml. of pyridine and 5 ml. of acetic anhydride, 20 mg. of VI was suspended. The mixture became a clear solution when kept at 70~80°C for 30 min. Yellow precipitates were obtained from the cooled solution, by the addition of 20 ml. of water. They were recrystallized from ethanol whereupon yellow needles of VII with m. p. 211~213°C were obtained (15 mg.): ultraviolet spectrum: $\lambda_{max}$ 325 mμ (log ε 4.32), 238 mμ (log ε 4.30); infrared spectrum: 1767(v. s), 1652(s), 1610(m), 1591(s) and 1516(s)cm$^{-1}$ (KBr).

**Aza-desmethylisoaureonone Acetate (VIII).**—A solution of 350 mg. (0.83 m. mol.) of aza-desmethylisoaureothin acetate (VII) in 15 ml. of chloroform was cooled to −5~−10°C and ozone was passed through this solution, until about one equivalent amount (0.95 m. mol.) of ozone was absorbed. On removal of solvent under reduced pressure, a gummy residue was obtained, which was treated with 10 ml. of water in a flask provided by a reflux condenser at 60°C. The aqueous layer in the flask was separated from the solid residue by decantation and the aqueous fraction was distilled under reduced pressure to afford a slightly yellow residue, which on recrystallization from methanol, weighed 10 mg.

12) The ultraviolet technique is not necessarily reliable for the discrimination of α-pyridones from their γ-isomers, in spite of the fact that α-pyridone itself absorbs at a much higher wave length (297 mμ) than γ-isomer (256 mμ); the substitution of the ring often causes an outstanding change in the spectrum.

with m. p. 208~209°C. No volatile carbonyl compound could be detected by distilling the aqueous fraction into a 2, 4-dinitrophenylhydrazine solution. The solid residue, obtained from the decomposition of ozonide, consisted of two components; one was easily soluble in methanol, whereas the other was sparingly soluble. The former was identified as *p*-nitro-$\alpha$-methylcinnamaldehyde by its melting point and infrared spectrum. The latter, sparingly soluble in methanol, was recrystallized from methanol and gave 70 mg. of colorless needles, which turned out to be identical with the crystals obtained from the water soluble fraction, as described before. The total amount was 80 mg., m. p. 209~210°C; ultraviolet spectrum: $\lambda_{max}$ 304 m$\mu$ (log $\varepsilon$ 3.85), 233 m$\mu$ (log $\varepsilon$ 3.81).

Found: C, 58.76, 58.86; H, 5.84, 5.98; N, 5.66, 5.45. Calcd. for $C_{13}H_{15}O_5N$: C, 58.83; H, 5.70; N, 5.28%.

## Summary

Aureothin (I), isoaureothin (II, R=$CH_3$) and desmethylisoaureothin (II, R=H) reacted with ammonia in a somewhat drastic way, and gave aza-derivatives respectively, some properties of which are described. Of these, aza-desmethyl-isoaureothin was shown to be VI containing tautomeric $\alpha, \gamma$-dihydroxypridine, on a basis of chemical and spectroscopic evidence.

The authors are indebted to Dr. Koichi Iwadare, Banyu Pharmaceutical Co. for his generous supply of aureothin used in this research, and to Mr. Takayuki Naito, Banyu Pharmaceutical Co., and Mr. Kunio Okuhara, Government Industrial Research Institute of Nagoya, for their helpful discussion throughout this work. The authors also wish to thank the Ministry of Education for a grant-in-aid.

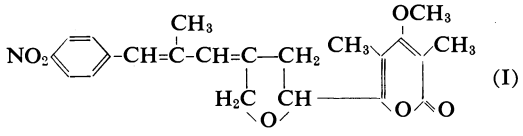
*Chemical Institute*
*Faculty of Science*
*Nagoya University*
*Chikusa-ku, Nagoya*

# *The Structure of Aureothin. XI*[1]. *On the Structure of Some of the Isoaureothin Derivatives*

By Kiyoyuki YAMADA, Takayuki NAITO, Kunio OKUHARA, Hisao NAKATA and Yoshimasa HIRATA

(Received April 2, 1960)

Among many derivatives obtained from isoaureothin (I)[2], there are several, the structures of which has not yet been disclosed. These derivatives, owing to their unexpected behavior, made the investigation of isoaureothin rather complicated. In this paper, the structures of these derivatives are put forward. They are well related to isoaureothin (I) and, of course account for all their properties. Further, the aspect of these reactions is briefly discussed. Of these derivatives, some descriptions were already made as to the nature of the products obtained by complex metal hydride reduction[3].




(I)

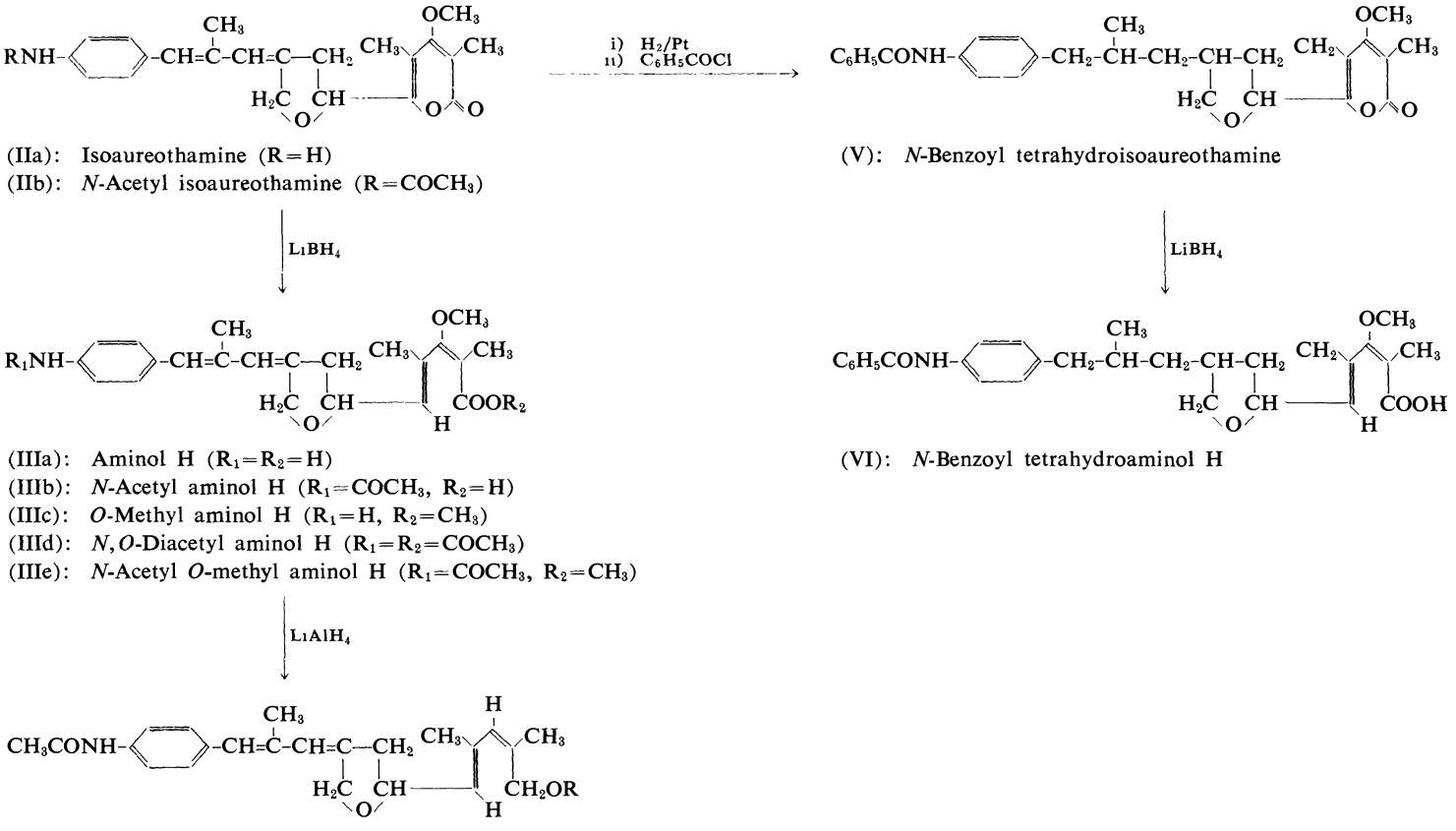
1) Part X. K. Yamada. H. Nakata and Y. Hirata, This Bulletin, 33, 1298 (1960).
2) K. Yamada, H. Nakata and Y. Hirata, *J. Chem. Soc. Japan, Pure Chem. Sec.* (*Nippon Kagaku Zasshi*), **81**, 340 (1960).
3) K. Yamada, Y. Hirata, K. Okuhara, H. Nakata, T. Naito and K. Iwadare, ibid., **79**, 384 (1958).

## On the Structures of Aminol Compounds

*Structure of Aminol H (IIIa).*—The reduction of the nitro group in isoaureothin (I) by ferrous hydroxide afforded a corresponding amino derivative $C_{22}H_{25}O_4N$ (IIa), which in turn was treated with lithium borohydride in tetrahydrofuran to give an acidic compound named "aminol H", $C_{22}H_{27}O_4N$[3]. As regards the acidic nature of aminol H, the infrared evidence (broad band at 2600~2700 $cm^{-1}$ in aminol H: bands at 1795, 1712 $cm^{-1}$ in *N, O*-diacetyl aminol H (IIId)), coupled with the result of the methoxyl analysis[4], showed that it might be due to a carboxyl group. *p*-Bromophenacyl ester of aminol H (m. p. 85~87°C) was obtained. Taking account of the fact that aminol H is optically active and has two more hydrogen atoms than isoaureothamine (IIa), it seems reasonable to deduce the occurrence of the hydrogenolytic cleavage in $\alpha$-pyrone ring,

4) Aminol H (IIIa) contains one methoxyl group, whereas two such groups present in the methylated product, *O*-methyl aminol H (IIIc).

Chart 1. Derivatives of isoaureothin.




(IIa): Isoaureothamine (R=H)
(IIb): *N*-Acetyl isoaureothamine (R=$COCH_3$)

(V): *N*-Benzoyl tetrahydroisoaureothamine

(IIIa): Aminol H ($R_1=R_2=H$)
(IIIb): *N*-Acetyl aminol H ($R_1=COCH_3$, $R_2=H$)
(IIIc): *O*-Methyl aminol H ($R_1=H$, $R_2=CH_3$)
(IIId): *N*,*O*-Diacetyl aminol H ($R_1=R_2=COCH_3$)
(IIIe): *N*-Acetyl *O*-methyl aminol H ($R_1=COCH_3$, $R_2=CH_3$)

(VI): *N*-Benzoyl tetrahydroaminol H

(IVa): *N*-Acetyl aminol A (R=H)
(IVb): *N*,*O*-Diacetyl aminol A (R=$COCH_3$)

Table I. Yield of methyl pyruvate

| Compound | Sample mg. | $CH_3COCOOCH_3$[a] mg. | Equiv. mol. |
|---|---|---|---|
| Isoaureothin (I) | 940 | 130 | 0.19 |
| *N*-Acetyl isoaureothamine (IIb) | 300 | 40 | 0.21 |
| *N*-Benzoyl tetrahydroisoaureothamine (V) | 470 | 32 | 0.15 |
| *N*-Acetyl aminol H (IIIb) | 250 | 38 | 0.22 |
| *N*-Benzoyl tetrahydroaminol H (VI)[b] | 620 | 80 | 0.22 |
| *N*-Acetyl *O*-methyl aminol H (IIIe) | 450 | 311 | 1.05 |

a) Determined as 2,4-dinitrophenylhydrazone.
b) Crude sample (m. p. 78~83°C) was used without recrystallisation.

to produce a carboxyl group[5]. The various properties previously described[3] (infrared and ultraviolet spectra etc.), thus can best be accounted for by assigning the structure IIIa to aminol H. Furthermore, the following experiment supports the correctness of formula IIIa; ozonisation of compounds belonging to the isoaureothin- and aminol-series always afforded methyl pyruvate, the yield of which in each case is listed in Table I. An essentially equal amount of methyl pyruvate (ca., 0.2 equivalent mole) was produced in every case[6], except the largely enhanced amount (1.05 equivalent moles) in the case of *N*-acetyl *O*-methyl aminol H (IIIe). Therefore, in *N*-acetyl *O*-methyl aminol H (IIIe), it becomes evident that there exist in one molecule two such units, from which methyl pyruvate is formed: in addition, one of such units should originate from the newly formed carbomethoxyl group by complex metal hydride reduction and subsequent methylation (cf. methoxyl analysis[4]).

*Structure of N-Acetyl Aminol A (IVa).*—Reduction of *N*-acetyl *O*-methyl aminol H (IIIe) with lithium aluminum hydride gave a neutral product, *N*-acetyl aminol A, $C_{23}H_{28}O_3N$ in poor yield[3]; no other crystalline products than this were isolated. Elemental and methoxyl analysis showed, during the reduction of IIIe, the occurrence of unusual hydrogenolysis of methoxyl group (enol ether), originally present in isoaureothin (I), in addition to the expected transformation of the ester group into alcohol.

*Aspect of Complex Metal Hydride Reduction.*—As described above, plausible structural assignments were made to the reduction products, aminol H (IIIa) and *N*-acetyl aminol A (IVa), on a basis of their chemical and spectroscopic properties. These would, at first sight, be regarded as unusual reduction products.

In the case of aminol H, however, it is expected that $\alpha$-pyrone shows peculiar reactivity far different from that of lactone toward hydride reagents, owing to the high conjugation of $\alpha$-pyrone and a possible effect of substituents of the ring. So far, very little is known about the reduction of $\alpha$- and $\gamma$-pyrones with various complex metal hydrides, except for limited examples of xanthone[7], benzo-$\alpha$-[8] and benzo-$\gamma$-pyrones[9], where not unexpected results were recorded. In contrast to the reduction of such benzopyrones, a situation, however, would be unique in the case of pyrones if no aromatic ring was fused to them. Investigation on the reactivity of pyrones toward complex metal hydrides is desirable.

Of particular interest is a hydrogenolytic cleavage of enol-ether (methoxyl group), during the formation of *N*-acetyl aminol A (IVa). In general, enol ethers are inert to complex metal hydride reduction[10], and so is a $\beta$-alkoxy-$\alpha$, $\beta$-unsaturated ester[11]. An exception[12] was reported; reduction of dihydrocorynantheine (A) with lithium aluminum hydride led to demethoxylated products B and C. Sarett and his coworkers reported a similar exception[13], found in $\beta$-alkoxy-$\alpha$, $\beta$-unsaturated

5) On catalytic hydrogenation, aminol H absorbed quantitatively two moles of hydrogen, with which the double bonds conjugated with aminophenyl group were saturated[3]. From this result, it is tempting to consider the possibility of the existence of an $\alpha$-pyrone ring in aminol H. However, this view is untenable on the ground that a band near 1575 $cm^{-1}$, characteristic of $\alpha$-pyrone, is absent in all of the aminol compounds studied.

6) Ozonisation was carried out repeatedly, in order to ascertain the reproducible yield of methyl pyruvate in each case.

7) A. Mustafa and M. K. Hilmy, *J. Chem. Soc.*, 1952, 1343.

8) (a) F. A. Hochstein, *J. Am. Chem. Soc.*, **71**, 305 (1949); (b) P. Karrer and P. Banerjea, *Helv. Chim. Acta*, **32**, 1692 (1949). (c) S. Siegel and S. Coburn, *J. Am. Chem. Soc.*, **73**, 5494 (1951); (d) J. P. Freeman and M. F. Hawthorne, ibid., **78**, 3366 (1956).

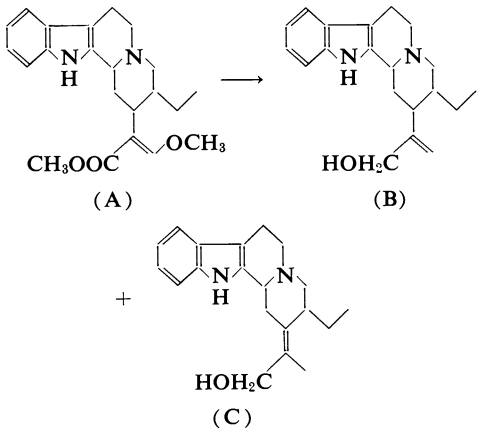
9) (a) R. Robinson and R. Mirza, *Nature*, **166**, 929 (1950); (b) R. Mirza and R. Robinson, ibid., **166**, 997 (1950); (c) M. Miyano and M. Matsui, *Chem. Ber.*, **91**, 2044 (1958).

10) N. G. Gaylord, "Reduction with Complex Metal Hydrides", Interscience Publishers, Inc., New York (1956), p. 695.

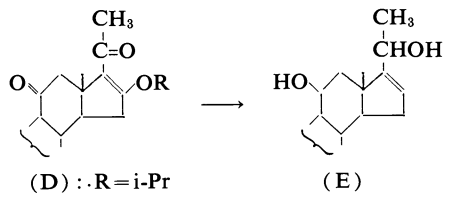
11) (a) J. C. Seaton and LeoMarion, *Can. J. Chem.*, **35**, 1102 (1957); (b) J. C. Seaton, R. Tondeur and LeoMarion, ibid., **36**, 1031 (1958).

12) P. Karrer, R. Schwyzer and A. Flam, *Helv. Chim. Acta*, **35**, 851 (1952); cf. A. Chatterjee and P. Karrer, ibid., **33**, 802 (1950).

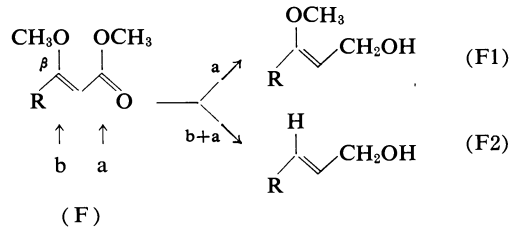
13) G. E. Arth, G. I. Poos and L. H. Sarett, *J. Am. Chem. Soc.*, **77**, 3834 (1955).




ketone (D), which afforded product E lacking in alkoxyl group. Such an apparent anomaly




of $\beta$-alkoxyl group in $\alpha$, $\beta$-unsaturated carbonyl system, encountered in the exceptions, can be interpreted in terms of vinylogy in reaction (see F); since $\beta$-carbon is regarded as a vinylogous position of carbonyl carbon, the reactivity of two methoxyl groups would be expected to be comparable.




Therefore, the mode of attack of the hydride reagent would be possible in two directions, as indicated by arrows in F, to give a normal product F1 and/or anomalous product F2. The subtle difference of the reactivity between two such positions would be influenced by structural variations and experimental conditions, neither of which, however, have yet been examined systematically.

## Structure of "Lactol"

*Property of Lactol (VIII).* — *N*-Acetyl isoaureothamine (IIb) was converted to Lactol $C_{24}H_{29}O_6N$ (VIII), by the action of aqueous alkali[14]. The product, Lactol, is soluble in alkali and optically inactive, while the starting material IIb shows remarkable optical activity, $[\alpha]_D^{28°}$ +140°.

The ultraviolet spectrum of Lactol shows the absence of $\alpha$-pyrone chromophore (Fig. 1); the subtraction of ultraviolet spectrum of conjugated *p*-acetylaminophenyl group from that of Lactol gives a curve, which shows its maximum near 248 m$\mu$ and should correspond to that of $\alpha$-pyrone ring ($\lambda_{max}$ 295 m$\mu$) of *N*-acetyl isoaureothamine (IIb). This outstanding hypsochromic shift, observed in the transformation of IIb to Lactol proves the destruction of $\alpha$-pyrone chromophore in the latter[15]. There were observed bands at 1708(sh.), 1675 (s), 1645(s), 1599(s), 1530(s) and 1516(s)cm$^{-1}$ in the 1800~1500cm$^{-1}$ range of the infrared spectrum (KBr). The presence of a hydroxyl

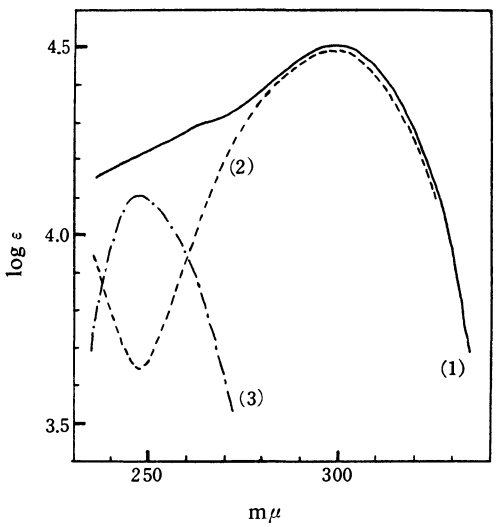
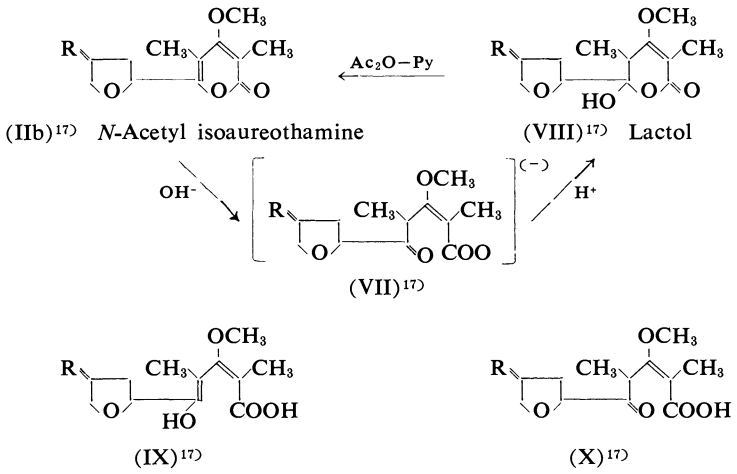



Fig. 1. Ultraviolet spectra (in ethanol)
(1): Lactol
(2): $CH_3CONH-C_6H_4-CH=C(CH_3)-CH=CH-CH(CH_3)-OH$
(3): Subtraction curve, (1) — (2)

group in Lactol was detected from a broad band near 3200 cm$^{-1}$ and a band at 1150 cm$^{-1}$. Lactol was neutralized by sodium hydroxide[16], to afford its sodium salt with bands located at 1717, 1672, 1640, 1595(s. and br.), 1530 and 1510 cm$^{-1}$ (KBr). In order to clarify the nature of this hydroxyl group, acetylation with pyridine-acetic anhydride was carried out; an unexpected product, racemic *N*-acetyl isoaureothamine (IIb) was obtained. Methylation

14) In the same treatment of isoaureothin (I) and isoaureothamine (IIa), amorphous products were obtained showing properties similar to that of Lactol.
15) This view was also supported by the lack of the characteristic band of $\alpha$-pyrone at 1575 cm$^{-1}$ in Lactol.
16) The addition of excessive sodium hydroxide did not significantly after the infrared spectrum of the salt.



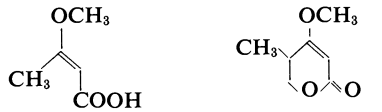

(IIb)[17] *N*-Acetyl isoaureothamine (VIII)[17] Lactol

(VII)[17]

(IX)[17] (X)[17]

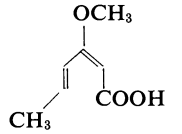
with diazomethane brought out the same result obtained in acetylation. In spite of careful scrutiny of the reaction products, no methylated substance was obtained in crystalline state. Since the formation of sodium salt suggests an acidic nature of Lactol, measurement of acidity constant ($pK_a$) by titration method was undertaken. No consumption of alkali by sample was observed below pH 10.5, implying the absence or masked state of carboxyl group under the conditions studied.

*Structure of Lactol.*—By comparison of the molecular formula between Lactol $C_{24}H_{29}O_6N$ and *N*-acetyl isoaureothamine $C_{24}H_{27}O_5N$, it is at once evident that hydrolysis of $\alpha$-pyrone took place, leading to a product soluble in alkali. Since alcoholic part formed is an enol, it would exist enolate under strongly alkaline condition. Assuming the anion in alkaline solution to be expressed approximately as VII, disappearance of optical activity would naturally result. Examination of the properties of Lactol secures structure VIII for this product and excludes another possibility such as tautomeric $\alpha,\beta$-$\gamma,\delta$-unsaturated carboxylic acid IX and $\alpha,\beta$-unsaturated ketocarboxylic acid X. Thinking of the result on the titration of Lactol, carboxylic acid structures are clearly ruled out and the structure VIII is assigned to Lactol in solution. The use of ultraviolet spectrum is not reliable for the discrimination between lactol structure (VIII) and carboxylic acid structure X[18]; an absorption maximum in question is located near 245 m$\mu$ (Fig. 1), which would be reasonable both for Lactol (VIII) and $\alpha,\beta$-unsaturated carboxylic acid (IX), considering the spectra of models G[19] and H[20].




$\lambda_{max}$ 234 m$\mu$ (G) $\lambda_{max}$ 234 m$\mu$ (H)

From the position and the shape of hydroxyl stretching vibration which appeared in 3000 $cm^{-1}$ region of the infrared spectrum, it becomes highly probable that there is no hydroxyl group of carboxylic nature. There was observed a band at 1708 $cm^{-1}$, the overlapping of which with a strong amide I band (1675 $cm^{-1}$) rendered the former to be a shoulder band of the latter. Utilizing this shoulder band, in conjunction with bands which appeared in sodium salt, it is possible to discriminate a structure VIII from IX and X. First, form IX is taken into account. Considering the infrared spectrum of model J, >C=O vibration of IX is expected to occur near 1660 $cm^{-1}$, which is not an actual case (band observed is at 1708 $cm^{-1}$).




$\nu_{C=O}$: 1665 $cm^{-1}$ (J)

Secondly, if Lactol took form X, it should, in addition to a band due to carboxylic acid, exhibit a band of isolated ketone at 1717 $cm^{-1}$ (observed in sodium salt), which is absent in Lactol itself. Carboxylic acid structures are, in any event, inconsistent with the observation about $\nu_{O-H}$ region as described before.

Structure VIII can, in every respect, be re-

17) R=*p*-acetylamino-$\alpha$-methyl cinnamylidene.
18) The possibility of IX is clearly excluded, since this should show an absorption at much longer wavelengths.
19) K. Bowden, E. A. Braude and E. R. H. Jones, *J. Chem. Soc.*, **1946**, 948.
20) E. R. H. Jones and M. C. Whiting, ibid., **1949**, 1419.

conciled with the infrared spectra of Lactol and of its sodium salt. Looking upon $\alpha,\beta$-unsaturated lactone ($\nu_{C=O}$: 1717~1730 $cm^{-1}$) as the fundamental system, the structure VIII is constructed by attaching hydroxyl and methoxyl group to the fundamental system. These two substituents, in this case, cause opposite effects on the position of carbonyl absorption in the $\alpha,\beta$-unsaturated ester system; i. e., carbonyl frequency tends to be lowered by the mesomeric effect due to the methoxyl group and to be raised by the inductive effect of the hydroxyl group. A slight lowering of carbonyl frequency would be expected as a net result, according to the estimation of two such effects based on the data[21] so far available. Thus, it is reasonable to ascribe a band at 1708 $cm^{-1}$ to the lactonic carbonyl group in structure VIII. Furthermore, the appearance of a band at 1717 $cm^{-1}$ in sodium salt is quite consonant with structure VIII.

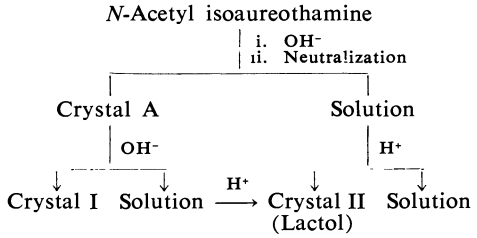
Chemical and spectral evidence now substantiates lactol structure VIII and rules out other possibilities, both in solution and solid state.

## Experimental

**Ozonization of Isoaureothin Derivatives.** — In order to estimate the amount of methyl pyruvate produced by ozonization, the following procedure was applied in each run. Through a solution of ca. 500 mg. of sample in 10~15 ml. of chloroform, ozone was passed at −5~−10°C, until the uptake of ozone by sample ceased. On removal of the solvent at reduced pressure, a viscous syrup was obtained which was then treated at 60°C with 10~15 ml. of water in a flask equipped with a condenser. The aqueous fraction was separated, and a solution of 2,4-dinitrophenylhydrazine in 2 N hydrochloric acid was added to it. The crude hydrazone was collected, dried, dissolved in benzene and chromatographed on alumina. 2,4-Dinitrophenylhydrazone of methyl pyruvate, eluted with benzene-ether was collected and weighed, m. p. above 140°C, m. p. 145~147°C after recrystallization from benzene. Formaldehyde was also detected in every sample, except in the cases of *N*-acetyl aminol H (IIIb) and *N*-acetyl *O*-methyl aminol H (IIIe).

**Lactol (VIII).** — To a mixture of 110 ml. of ethanol and 55 ml. of 3 N aqueous sodium hydroxide, 2 g. of *N*-acetyl isoaureothamine was added. The flask was equipped with a reflux condenser and the suspension was warmed on a water bath at about 80°C for ten min., when the mixture became clear and of an orange color. After rapid cooling, the solution was neutralized with dilute hydrochloric acid; the solution turned yellow immediately at the neutralization point (pH 7). The solution was concentrated to 50 ml. under reduced pressure to yield fine crystals ("crystal A"). The yellow filtrate from "crystal A" was acidified gradually with dilute hydrochloric acid and the resultant precipitates (in part oily material) were collected and recrystallized from ethanol to yield almost colorless needles ("crystal II"), named Lactol, m. p. 170~171°C, 500 mg. When "crystal A" was dissolved in aqueous sodium hydroxide solution, a small part was insoluble in alkali. The alkali-insoluble crystals ("crystal I") were collected and recrystallized from ethanol repeatedly, m. p. 223~225°C. 40 mg.

The filtrate from "crystal I" was acidified and the resulting crystals were identified as "crystal II"; yield 250 mg., combined amount of "crystal II", 750 mg. The ultraviolet spectrum of "crystal II" showed $\lambda_{max}$ 299 m$\mu$ (log $\varepsilon$ 4.52) (in ethanol). $[\alpha]_D^{27}$, 0±1.5° (methanol, c=0.75). Titration was carried out in 66% aqueous ethanol solution.




Analysis was carried out on "crystal II" (Lactol):
Found: C, 67.06; H, 7.19; N, 3.63. Calcd. for $C_{24}H_{29}O_6N$: C, 67.43; H, 6.84; N, 3.28%.

**Action of Diazomethane on Lactol.**—Crystalline Lactol was added to ethereal diazomethane, but no reaction took place under the heterogeneous condition and the starting material was recovered. To 20 ml. of ethereal diazomethane was added 100 mg. of Lactol, dissolved in 20 ml. of methanol and the mixture was allowed to stand overnight. After removal of about two-thirds of the volume of solvent at reduced pressure, the precipitated crystals were filtered and recrystallized from ethanol to give colorless needles, m. p. 191~193°C, 25 mg., $[\alpha]_D^{28}$, 0±2° (c=0.8 in a mixture of chloroform and methanol (1:2)). The infrared spectrum taken in solid state (KBr) was identical with that of *N*-acetyl isoaureothamine (m. p. 209~211°C; $[\alpha]_D^{28}$ +140 ±1.5° in a mixture of chloroform and methanol (1:2)), the starting material of Lactol. Mixing two species of *N*-acetyl isoaureothamine (optical active and inactive species), no depression of the melting point was observed; mixted melting point, 193~200°C. Further concentration of filtrate gave a small amount of oily material, the infrared spectrum of which included bands at 1701(sh), 1690(s), 1606(m), 1592(m) and 1512(s) $cm^{-1}$ (in chloroform). The main portion of the product might be an ester.

21) Literatures for the estimation of mesomeric effect of methoxyl group; (a) R. N. Jones and F. Herling, *J. Org. Chem.*, **19**, 1252 (1954); (b) R. S. Rasmussen and R. R. Brattain, *J. Am. Chem. Soc.*, **71**, 1073 (1949); (c) H. Heyman, S. S. Bhatnagar and L. F. Fieser, ibid., **76**, 3689 (1954).
Literatures as to inductive effect of hydroxyl (and alkoxyl) group: (d) R. B. Woodward and E. G. Kovach, *J. Am. Chem. Soc.*, **72**, 1009 (1950); (e) J. F. Grove and G. A. Willis, *J. Chem. Soc.*, **1951**, 877; (f) J. F. Grove ibid., **1952**, 3345; (g) L. A. Duncanson, J. F. Grove and J. Zealley, ibid., **1953**, 1331, 3637.

**Action of Acetic Anhydride on Lactol.**—To a mixture of 1 ml. of pyridine and 5 ml. of acetic anhydride was added 50 mg. of Lactol. It was kept at 70°C for ten minutes and after cooling, water was added to the solution, the resultant crystals were collected, recrystallized from ethanol and identified as the starting material, Lactol. Again, the same procedure was applied with prolonged heating (one hour); the resultant crystals, differing from Lactol, were recrystallized from ethanol and were identified as *N*-acetyl isoaureothamine by the comparison of the infrared spectra, m.p. 193~194°C.

Found: C, 70.59; H, 6.50. Calcd. for $C_{24}H_{27}O_5N$: C, 70.40; H, 6.50%.

All melting points were uncorrected. The ultraviolet spectra were measured with a Hitachi spectrophotometer and the infrared spectra with a Hilger H 800 spectrometer, equipped with rock-salt prisms. The optical rotations were measured with a Rudolf polarimeter.

## Summary

During the course of the investigation of isoaureothin (I), several derivatives were obtained, the structure of which still remains unknown. The structure of these derivatives is presented in this paper on a basis of spectral and chemical evidence. The reduction of isoaureothamine (IIa) with lithium borohydride yielded an unexpected acidic substance, aminol H (IIIa) the formation of which, taken in conjunction with that of *N*-acetyl aminol A (IVa), provides an unusual type of reduction by complex metal hydride. Treatment of *N*-acetyl isoaureothamine (IIb) with alkali yielded an optically inactive substance, Lactol, which was formulated as VIII. The action of acetic anhydride on Lactol resulted in the formation of racemate of *N*-acetyl isoaureothamine (IIb).

This stuty was supported by a grant from the Ministry of Education, to which the authors are indebted.

*Chemical Institute*
*Faculty of Science*
*Nagoya University*
*Chikusa-ku, Nagoya*

*Banyu Pharmaceutical Co.*
*Okazaki, Aichi-ken (T. N.)*

# SHORT COMMUNICATIONS

## *NMR Spectra of the Metabolites of Monascus. I. NMR Spectra of Several Authentic Pyrones**

By Akira TERAHARA, Mamoru OHASHI, Koji NAKANISHI, Ichiro YAMAGUCHI and Naohiro HAYAKAWA

(Received July 15, 1960)

As with the C–2 and C–5 protons of furans[1] it may be expected that the protons alpha to the pyronoid oxygen will absorb at characteristically low frequencies and thus assist in the identification of the substitution pattern, which is not so facile by other physico-chemical methods. A Varian model V-4300 spectrometer was employedat 56.4 Mc; the band separations were estimated from the toluene peaks and chloroform was used as internal reference. The measurements were carried out in 10~20 percent solutions of 1 : 1 mixtures of chloroform and carbon tetrachloride. The results are summarized in Table I[2]. It can be seen qualitatively that the $\alpha$-protons of both $\alpha$- and $\gamma$-pyrones absorb at lower fields than the chloroform proton, and that they can be clearly differentiated from the other unsaturated protons. The coupling constant of the $\alpha$- and $\beta$-protons, ca. 6 cps, is larger than the 1.3 cps value reported for furans[3]. The C–2 and C–6 methyl groups absorb in the range of 280~300 cps (II, III and VII). One of the nuclear protons of the extended pyronoid compound VII had its peak at an exceptionally low field, and this interesting phenomenon is presumably caused by the strong long range shielding effect of the nearby nitrile group. It is to be noted that this shift is opposite to that encountered in the well-known acetylenic protons[4] and this can be attributed to the directional difference of the triple bond[5]. Citrinin has been chosen

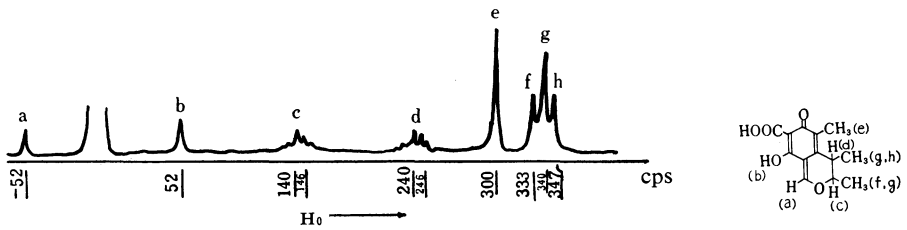
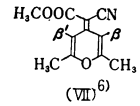



Fig. 1. NMR spectra of citrinin.

TABLE I. NMR SPECTRA OF PYRONES

| Compound | $\alpha$-H | $\beta$-H | Other H |
|---|---|---|---|
| $\gamma$-Pyrone(I) | −15, −9 | 71, 76 | |
| 2,6-Dimethyl-$\gamma$-pyrone(II) | | 73 | 289 ($CH_3$) |
| 2-Methoxy-6-methyl-$\gamma$-pyrone(III) | | 87, 116 | 205 ($OCH_3$), 294 ($CH_3$) |
| 2,6-Dimethoxycarbonyl-$\gamma$-pyrone(IV) | | 12 | 188 ($OCH_3$) |
| $\alpha$-Pyrone(V) | −15 | 53, 60 | |
| 6-Methoxycarbonyl-$\alpha$-pyrone(VI) | | 12 | 194 ($OCH_3$) |
|  (VII)[6] | | −42, 52 | 200 ($OCH_3$), 284 ($CH_3$) |



* Presented at the 13th Annual Meeting of the Chemical Society of Japan, Tokyo, April, 1960.

1) R. J. Abraham and H. J. Bernstein, *Can. J. Chem.*, **37**, 1056 (1959).

2) No corrections for the bulk susceptibilities were carried out.

3) J. A. Pople, W. G. Schneider and H. J. Bernstein, "High-resolution Nuclear Magnetic Resonance", McGraw-Hill Book Company, New York (1959), p. 193.

4) We are grateful to Dr. N. Nakagawa, University of Electro-Communications, for this explanation.

5) L. M. Jackman, "Applications of NMR Spectroscopy in Organic Chemistry", Pergamon Press, London (1959), p. 114.

6) M. Ohta and H. Kato, This Bulletin, **32**, 707 (1959).

as an appropriate model to clarify the spectra of the more complicated natural products, and its spectrum is analyzed in Fig. 1. The qualitative results obtained from the spectra of the pyrones are hoped to assist in handling related compounds.

We are grateful to Professor S. Fujiwara, the University of Tokyo for valuable suggestions.

*Department of Chemistry*
*Faculty of Science*
*Tokyo University of Education*
*Bunkyo-ku, Tokyo*
*(A. T., M. O. & K. N.)*

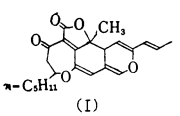
*Division of Radiation Applications*
*Japan Atomic Energy Research Institute*
*Tokai, Ibaraki-ken*
*(I. Y. & N. H.)*

## *NMR Spectra of the Metabolites of Monascus. II. Monascorubrin**

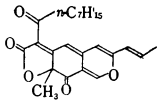
Mamoru OHASHI, Akira TERAHARA and Koji NAKANISHI

(Received July 15, 1960)

Structures I[1] and II[2] have been tentatively proposed for monascorubrin[3], $C_{23}H_{26}O_5$, the orange pigment produced by *Monascus purpureus Wentii*. The NMR spectra of monascorubrin and dihydromonascorubrin have been measured in order to check the gross character of this complicated pigment, and if possible to differentiate between the two structures.




(I)




(II)

The measurements were carried out with a Varian V-4300 High Resolution Spectrometer operating at 40 Mc; chloroform was chosen as the inner reference and the band positions were read by the side-band method. It is seen in Fig. 1 that instead of the doublet "d" and "e" (propenyl methyl) and multiplet around "g", the spectrum of the dihydro-compound (Fig. 2) shows a triplet "j" which corresponds to the $\alpha$-methylene of the propyl chain. Signals "a" and "b" are due to the *n*-alkyl chain and "c" arises from an uncoupled methyl group. Signal "i" corresponds in position to a proton adjacent to the pyronoid oxygen[4] and this is supported by chemical evidence[1]. The other two low-field signals, "g" and "h", undoubtedly arise from the remaining two nuclear protons. The shape and intensity of signal "f" is similar to "j" which has been assigned to a methylene group, and therefore in structure II it could be correlated with the $-CH_2CO-$ protons of the $n$-$C_7H_{15}CO-$ side-chain. On the other hand, in structure I the $-CH_2CO-$protons belong to the ABX type and thus a complicated pattern would be expected. The signal for the bridgehead proton of the ethereal ring in I can not be detected in the expected 100~200 cps region, but this could be due to extensive coupling with adjacent protons. The coupling of signals "h" and "i" (ca. 1.2 cps) presumably correspond to that observed between meta-oriented protons on benzene nuclei[5]. Thus, although no clear-cut differentiation between structures I and II is possible, the present measurements appear to be slightly in favor for the latter; however, chemical and ultraviolet spectroscopic evidence can be accounted for more smoothly

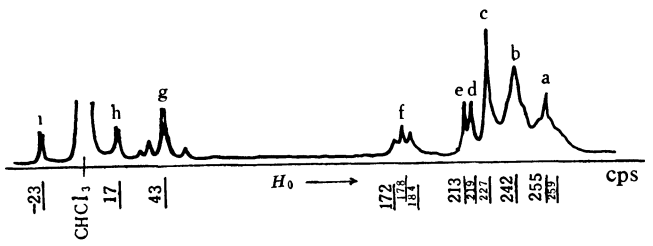



Fig. 1. Monascorubrin.

* Presented at the 13th Annual Meeting of the Chemical Society of Japan, Tokyo, April, 1960.

1) K. Nakanishi, M. Ohashi, S. Kumasaki and S. Yamamura, *J. Am. Chem. Soc.*, **81**, 6339 (1959).
2) B. C. Fielding, F. J. Haws, J. S. E. Holker, A. D. G. Powell, A. Robertson, D. N. Stanway and W. B. Whalley, *Tetrahedron Letters*, No. 5, 24 (1960).
3) A. Nishikawa, *J. Agr. Chem. Soc., Japan*, **8**, 1007 (1932).
4) Preceding paper.
5) J. A. Pople, W. G. Schneider and H. J. Bernstein, "High-resolution Nuclear Magnetic Resonance", McGraw-Hill Book Company, New York (1959), p. 193.

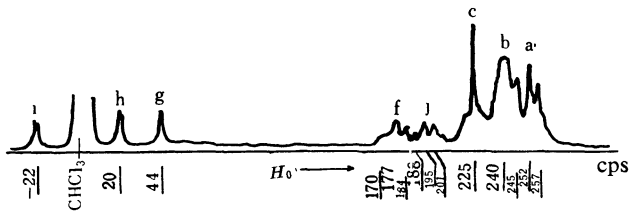



Fig. 2. Dihydromonascorubrin.

by structure I and this point will be reported shortly.

The authors are grateful to Professor Y. Yukawa, Osaka University, for measurement of the spectra and suggestions.

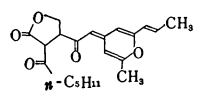
*Department of Chemistry*
*Faculty of Science*
*Tokyo University of Education*
*Bunkyo-ku, Tokyo*

## *NMR Spectra of the Metabolites of Monascus. III. Monascoflavin and Reduction Products**

Mamoru OHASHI, Akira TERAHARA, Koji NAKANISHI, Ichiro YAMAGUCHI and Naohiro HAYAKAWA

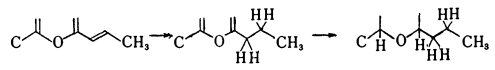
(Received July 15, 1960)

The structure of monascoflavin[1], $C_{21}H_{26}O_5$, m. p. 143°C, the yellow metabolite of *Monascus purpureus Wentii* has still not been elucidated. Its chemical properties showed that it was related to γ-pyrones[2], and the close relationship with monascorubrin has also been suggested[3]; structure I was provisionally proposed in 1959 as



(I)

a working hypothesis[4]. The NMR spectra of I, dihydro-I, hexahydro-I, and octahydro-I[5] have been measured with a Varian V-4300 model Spectrometer at 56.4 Mc, in order to correlate the chemical transformations with appropriate changes in the spectra (Figs. 1—4) and thus gain an insight into its structure. Chloroform was employed as an inner reference, and toluene was used for calculating line separation. Unlike monascorubrin[6], the present monascoflavin showed no peak in the −30 cps region corresponding to the α-hydrogen of γ-pyrones[7]. Instead of the "d" doublet ($J$: 6 cps, area for three protons) and the weak "k" multiplet in Fig. 1, the spectrum of II revealed a triplet "1" ($J$: 8 cps); this can be ascribed to the hydrogenation of the propenyl side-chain. The "a" and "b" peaks arise from the methyl and methylene groups, respectively, of the *n*-$C_5H_{11}$ side-chain. The peaks at "c" is due to an uncoupled methyl group, and peaks "i" and "j" (Figs. 1 and 2) suggest that three protons attached to an unsaturated system are present besides the propenyl group. In Fig. 3, only a diffuse absorption "i" is left in this region; instead there appears two ill-defined peaks "m" and "n" which could be assigned to protons attached to α-carbons of an ethereal linkage. The hydrogenation stages can be represented by the following scheme:



(I) (II) (III)

Peaks "g" and "h" seem to originate from the γ-methylene of γ-lactone ring[8]; however, the coupling is not clear. The quadraplet "i" (Figs. 1 and 2) seems to arise from an AB type of coupling ($J$: 10 cps) and is absent in Fig. 3. Although it is apparent that the quadraplet is

* Presented at the 13th Annual Meeting of the Chemical Society of Japan, Tokyo, April, 1960.

1) A. Nishikawa, *J. Agr. Chem. Soc., Japan*, **8**, 1007 (1932); H. Salomon and P. Karrer, *Helv. Chim. Acta*, **15**, 18 (1931).

2) P. Karrer and A. Geiger, *Helv. Chim. Acta*, **25**, 289 (1941).

3) A. D. G. Powell, A. Robertson and W. B. Whalley, *Chem. Soc. Special Publ.*, No. 5, 27 (1956).

4) K. Nakanishi, M. Ohashi, A. Terahara, S. Kumasaki, S. Yamamura, Y. Hirata and H. Koike, the 3rd Symposium on the Organic Chemistry of Natural Products, Tokyo, 1959, Abstract, p. 55.

5) Chemical and spectroscopic results indicate that this is not a straight-forward reduction product. Accordingly, the spectrum will not be discussed at present.

6) Part II of this series.

7) Part I of this series.

8) L. M. Jackman, "Applications of NMR Spectroscopy in Organic Chemistry", Pergamon Press, London (1959), p. 55.

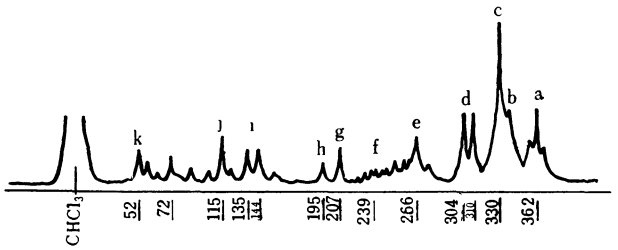



Fig. 1. Monascoflavin.

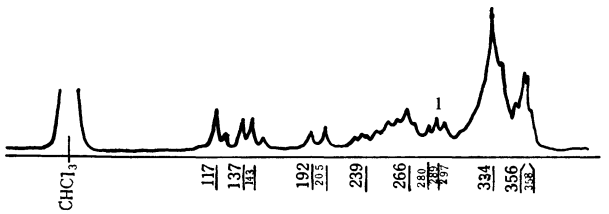



Fig. 2. Dihydromonascoflavin.

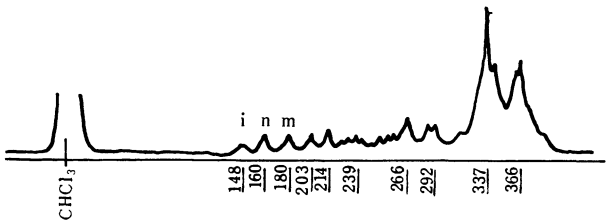



Fig. 3. Hexahydromonascoflavin.

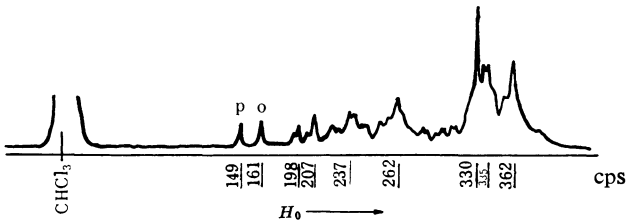
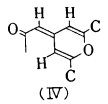
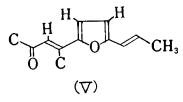



Fig. 4. "Octahydromonascoflavin".

due to protons on an unsaturated system, it is questionable that any two protons shown in the partial structure IV should couple so extensively.



(IV)



(V)

Structure V appears to be more appropriate to account for the coupling but this, in turn, can not be reconciled with ultraviolet spectral data[4]. Model compounds are being synthesized in order to check this point further. Peak "e" is presumably due to the $-COCH_2-$ protons but the reason that it is not split into a triplet is not clear. The diffuse "f" signal could arise from the bridgehead proton(s) of the $\beta$-keto-$\gamma$-lactone moiety.

*Department of Chemistry*
*Faculty of Science*
*Tokyo University of Education*
*Bunkyo-ku, Tokyo*
*(M. O., A. T. & K. N.)*

*Division of Radiation Applications*
*Japan Atomic Energy Research Institute*
*Tokai, Ibaraki-ken*
*(I. Y. & N. H.)*

## *On the Unusual Premelting Phenomenon of Potassium Thiocyanate Crystal*

By Takako SHINODA, Hiroshi SUGA and Syûzô SEKI

(Received July 30, 1960)

Recently, Ubbelohde et al.[1] have published a series of papers on the unusual premelting effect of potassium thiocyanate crystal and concluded the rapid homophase increase of lattice defects as the melting point is approached. Quite independently,we have studied the transition phenomenon of this crystal in relation to that found in ammonium thiocyanate[2]. During the course of the differential thermal analysis of potassium thiocyanate we can not detect any such a tendency of premelting found by them, so we have reexamined the existence of the effect by use of the methods of dilatometric and d. c. conductivity measurements.

The sample (special grade, Wakō Pharmaceutical Co.) used were purified three times by fractional recrystallization from aqueous solution and then dried at 150°C under high vacuum ($10^{-5}$ mmHg) for several hours after packing the sample in the glass-made dilatometer. Mercury was employed as a confining liquid, since it was confirmed that the mercury did not react with the sample even above the melting point. The results obtained are shown in Fig. 1 and in Table I in which the data by Ubbelohde and others are also given for comparison. For the d. c. conductivity measurement the specimen purified in the same way

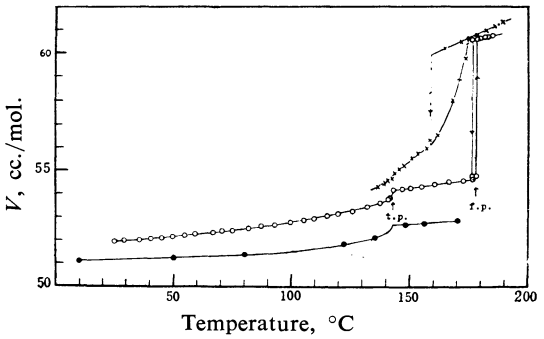



Fig. 1. The molar volume versus temperature curves of KSCN.
× Ubbelohde et al.
○ Present authors
● Yamada et al. (by X-ray method)

1) D. W. Plester, S. E. Rogers and A. R. Ubbelohde, *Proc. Roy. Soc.*, A235, 469 (1956); E. Rhodes and A. R. Ubbelohde, ibid., A251, 156 (1959); Idem, *Trans. Faraday Soc.*, 55, 1705 (1959).

2) M. Sakiyama, H. Suga and S. Seki, presented at the 13th Annual Meeting of the Chemical Society of Japan, Tokyo, April, 1960.

TABLE I. VOLUME PARAMETERS OF KSCN

| | Present authors | Ubbelohde and others |
|---|---|---|
| $V_L$ | 60.6 | 60.6±0.1 |
| $V_S$ | 54.7 | 57.5 |
| $\Delta V_f$ | 5.9 | 3.1 |
| $\Delta V_f/V_S$ (%) | 10.8 | 5.4 |
| $V_t$ | 54.13 | 54.7 |
| $\Delta V_t/V_t$ (%) | 1.53 | 0.36 |
| $\Delta V_t$ | 0.83 | — |
| $V_{25°}$ (by flotation) | 51.92*(51.3**) | 51.92 |
| t. p. | 142.7°C | 141.4°C |
| f. p. | 178.45°C | 175.1°C |
| $\alpha_S$ (high temp. phase) | $2.6\times10^{-4}$ | $1.27\times10^{-3}$ |
| $\alpha_L$ (low temp. phase) | $3.91\times10^{-4}$ | $4.86\times10^{-4}$ |

$V_L$=molar volume of liquid at freezing point.
$V_S$=molar volume of solid at freezing point.
$V_t$=molar volume of solid at transition point.
$\Delta V_f$=change in volume on melting.
$\Delta V_t$=change in volume at transition point.
$V_{25°}$*=molar volume measured at 25°C by Ubbelohde et al.
** molar volume at ca. 10°C calculated from the dimensions of the unit cell[3].
(molar volumes are in cc./g. formula weight)

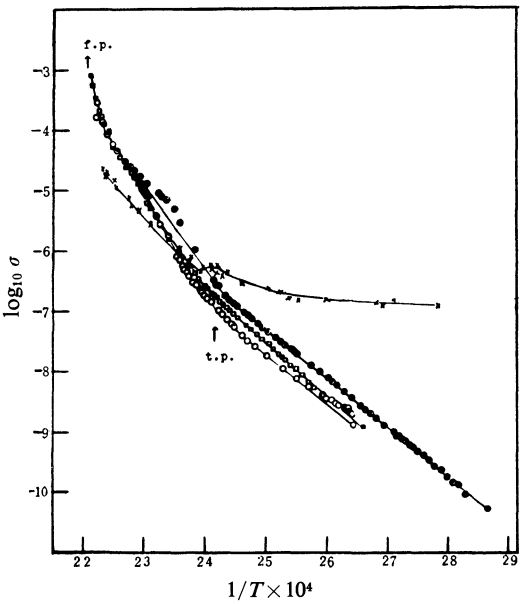



Fig. 2. The d. c. conductivity versus $1/T$ curves and their empirical equations of KSCN.
× Ubbelohde et al.
$\sigma_L=1\times10^{-3}\times\exp(-6.6/RT)$
$\sigma_H=3\times10^{14}\times\exp(-47.2/RT)$
⊙ Our results
$\sigma_L=2\times10^{12}\times\exp(-36.1/RT)$
$\sigma_H=1\times10^{25}\times\exp(-59.5/RT)$
○ $\sigma_L=3\times10^{10}\times\exp(-33.3/RT)$
$\sigma_H=6\times10^{16}\times\exp(-44.0/RT)$
□ $\sigma_L=2\times10^{11}\times\exp(-34.3/RT)$
$\sigma_H=3\times10^{19}\times\exp(-49.2/RT)$
$\sigma_L$: d. c. conductivity for low temperature phase
$\sigma_H$: d. c. conductivity for high temperature phase

as mentioned above was used in the shape of disk tablet (weight : 100 mg. ; diameter : 13 mm. ; thickness : 1 mm.). The conductivity versus $1/T$ relationships and empirical equations derived are shown in Fig. 2 together with the results by Ubbelohde et al.

From the results of our dilatometric study it is found that the volume changes abruptly at the melting point with almost no hysteresis effect in the cooling direction, standing in remarkable contrast to the case by Ubbelohde et al., and that our data are in good harmony with the thermal expansion determined with the X-ray method by Yamada et al[3]. who kindly measured the temperature dependence of the unit cell dimensions in accordance with our request. The fact that we obtained much larger activation energy ($\sim$35 kcal./mol.) for the d. c. conductivity at lower temperature region seems to indicate that our sample involves less impurities and is also in parallel with the dilatometric data. Detailed descriptions of the experimental procedures and discussion will be published in due course.

*Faculty of Science*
*Osaka University*
*Nakanoshima, Osaka*

3) Y. Yamada, H. Suga and T. Watanabe, presented at the 7th Annual Meeting of the Society of Applied Physics, Japan, 1960.

## *Isotopic Exchange of Gallium between the Gallium(III) Ion and its Ethylenediamine-N, N, N', N'-tetraacetate and N-2-Hydroxyethylethylenediamine-N, N', N'-triacetate in an Aqueous Solution*

By Kazuo Saito and Michiko Tsuchimoto (née Tamura)

(Received July 11, 1960)

As an extention of the present authors' study of the isotopic exchange of metal chelate compounds having $d^{10}$ structure[1,2], they have examined the kinetics of exchange of gallium between the gallium(III) ion and its ethylenediamine-*N*, *N*, *N'*, *N'*-tetraacetate (EDTA) and *N*-2-hydroxyethylethylenediamine-*N*, *N'*, *N'*-triacetate (EDTA-OH) in water by the use of gallium-67. The radioisotope was produced by the irradiation of zinc with $\alpha$-particles in a cyclotron and the $\gamma$-activity was measured with a scintillation counter having a sodium iodide crystal as scintillator. A gallium nitrate solution of a given pH was mixed with radioactive gallium EDTA or EDTA-OH complex solution of the same pH value and a part of the gallium ion was precipitated with 8-quinolinol at a certain lapse of time. The precipitate was filtered off, with a sintered glass filter plate, washed, dried, weighed and submitted to $\gamma$-ray counting.

The result is quite different from that for the corresponding exchange of indium[2]. The rate is very small in a neutral or an acid solution of pH more than 2, and is very great in a basic medium. In the pH range from 7 to 9, the exchange proceeds at a measurable rate. Since the exchange constant $R$ expressed according to McKay's formula[3] is proportional to the concentration of the chelate $b$ and is independent of that of the gallium ion $a$, the rate constant $k$ is shown as $R/b$. Dependence of $R$ upon various factors is shown in the Table together with other constants of the reaction. It is rather marked that the energy of activation $E_A$ is very great as compared with that for the exchange of indium in an acid solution (10 kcal. per mol.). The present authors tend to suggest that the attack of the hydroxyl ion upon the central gallium in the co-ordination compound might play an important role in determining the exchange rate. Detail of the result and discussion on the reaction mechanism will be published later.

Table. Dependence of $R$ upon various factors and some constants for the exchange in an aqueous solution of pH 7 to 9

| | Ga-EDTA-OH | Ga-EDTA |
|---|---|---|
| $[OH^-]$ | Proportional | Proportional |
| $[a]$ | Independent | Independent |
| $[b]$ | Proportional | Proportional |
| Ionic strength | Dependent to a less extent | Dependent to a less extent |
| Concn. of buffer | Almost independent | Almost independent |
| $k/[OH^-]_{25°C}$ ($sec^{-1}$) | 32 | 12 |
| $E_A$ (kcal./mol.) | 27 | 25 |
| $A$ ($sec^{-1}$) | $3\times10^{15}$ | $2\times10^{13}$ |
| $\Delta S$ (cal./mol./deg.) | +11 | +1 |

At an ionic strength $\mu=0.2$ ($KNO_3$). $A$, frequency factor for $k$; $\Delta S$, entropy of activation for $k$ on the assumption $\kappa=1$ ($\kappa$, transmission coeff.), at pH 8.0.

1) K. Saito and M. Tamura, This Bulletin, **32**, 533 (1959).
2) K. Saito and M. Tamura, *J. Inorg. Nur. Chem.*, **13**, 334 (1960).
3) H. A. C. McKay, *Nature*, **142**, 997 (1938).

*Institute for Nuclear Study*
*The University of Tokyo*
*Tanashi, Tokyo*

## *The Polymerization of α-Methylstyrene by Iodine Catalyst*

By Kozo HIROTA, Gisuke MESHITSUKA*, Fukuo TAKEMURA and Tatsuto TANAKA

(Received May 19, 1960)

Although it is well known that iodine is an inhibitor for radical polymerization, its power of polymerizing some vinyl monomers has been reported by several investigators[1-4]. We have also found that iodine plays a role as an initiator for the polymerization of α-methylstyrene (αMS) at room temperature. Since it seems interesting that the reaction proceeds under the presence of lower concentration of iodine (0.1~0.3%) as compared with the case of polymerization of styrene by iodine (10~20%) recently reported[4], preliminary results are reported as follows.

It was found that the reaction proceeded even in the atmosphere but reproducible results were not obtained. The sample, therefore, was dehydrated in vacuo with metallic sodium or calcium hydride and was distilled into a reaction vessel without exposing to the air. The extent of polymerization of the monomer for a week reached maximum when the concentration of iodine added was ca. 0.1~0.3%. When more iodine than 1% was added to the monomer, the temperature of the reactant rose markedly high, as soon as iodine was allowed to contact wiih the monomer. In such cases the reactant became very viscous but the high polymers could not be obtained.

In Fig. 1, the yield of polymer for the reaction at 25°C vs. time are plotted. All the samples were enclosed at the same time and polymerized for different intervals of time, and the polymers were precipitated with excess of methanol. It is shown that the initial rate of polymerization in higher concentration of iodine (0.2%) is larger than that in lower one (0.1%), but in the former case the conversion did not become more than about 25%, while it increased up to more than 50% for an interval of 160 hr. in the latter case.

The color of iodine disappeared in both cases after a long period of reaction. The

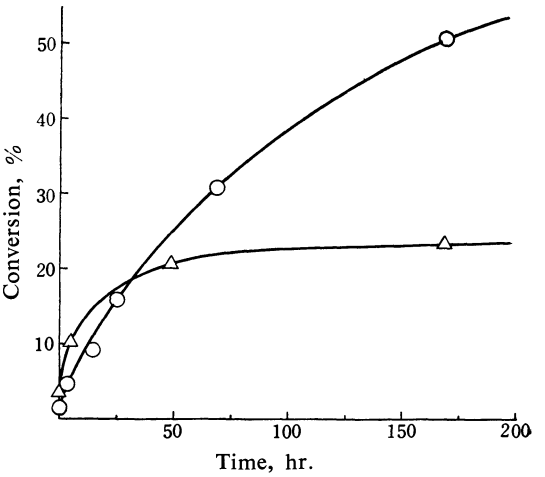



Fig. 1. Conversion of αMS vs. time.
Concn. of iodine: ○ 0.1%; △ 0.2%.

intrinsic viscosity of the polymers was independent of the time of polymerization, i. e., ca. 0.1** dl./g. and slightly larger in the case of lower concentration of iodine.

It is clear from the inhibitory power of iodine for polymerization by free radical mechanisms that this polymerization must be of non-radical and presumably of ionic character. It may be natural to assume that this reaction proceeds by a cationic mechanism as concluded in the polymerization of vinyloctylether[2] and of styrene[4] by iodine in view of the following experimental fact:—The polymer which is obtained from the mixture of αMS and methyl methacrylate (1 : 1 in volume ratio) in the presence of iodine showed essentially the same infrared absorption spectra as that of the polymer obtained from the similar mixture by stannic chloride.

Details of the experiment will be published in *J. Chem. Soc. Japan, Pure Chem. Sec. (Nippon Kagaku Zasshi)*.

*Department of Chemistry*
*Faculty of Science*
*Osaka University*
*Nakanoshima, Osaka*
*(K. H., G. M. & T. T.)*

*Department of Chemistry*
*Faculty of Science*
*Nara Women's University*
*Nara (F. T.)*

* Present address: Tokyo Metropolitan Isotope Center, Setagaya-ku, Tokyo.

1) W. Chalmer, *Can. J. Research*, **7**, 472 (1932).
2) D. D. Eley and A. W. Richard, *Trans. Faraday Soc.*, **45**, 425 (1949).
3) P. D. Bartlett and H. Kwart, *J. Am. Chem. Soc.*, **72**, 1056 (1950).
4) D. S. Trifan and P. D. Bartlett, ibid., **81**, 5573 (1959).

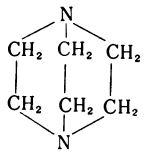
** This intrinsic viscosity corresponds to the molecular weight of ca. 3,000 (cf. C. P. Brown and A. R. Matheson, *J. Chem. Soc.*, 1958, 3507).

## *Crystal Structure and Thermodynamical Investigations of Triethylenediamine, $C_6H_{12}N_2$*

By Tadayoshi WADA*, Etsuko KISHIDA, Yujiro TOMIIE, Hiroshi SUGA, Syûzô SEKI and Isamu NITTA

(Received August 11, 1960)

Triethylenediamine, or 1, 4-diazabicyclo-(2, 2, 2)-octane, is considered to be a typical globular cage molecule with high symmetry. In order to amplify our knowledge on the thermal behavior of molecules in crystals, we have studied the crystal structure and some thermodynamical properties of this material.



The sample used for the present research was kindly offered us by Dr. Oae and by Houdry Process Corporation, Pa., U. S. A.

Small single crystals for the X-ray investigation, obtained from a saturated ethereal solution, were kept in glass capillaries to avoid humidity since the material has strong tendency of forming monohydrate. Useful X-ray data were obtained from Weissenberg photographs around $a$ and $c$ axes respectively taken with Ni-filtered Cu $K_\alpha$ radiation. The crystallographic data are: hexagonal system; $a=6.20 \pm 0.01$, $c=9.58 \pm 0.02$ Å; $Z=2$; $D_X=1.17$, $D_{obs}=1.14$ g. cm$^{-3}$ [1]; space group $C_{6h}^2-P6_3/m$.

After seven and six successive calculations of the $(F_0-F_c)$-syntheses along [001] and [100] respectively, the final atomic parameters (Table I) and temperature factors were obtained. The interatomic distances thus calculated are given in Table II together with their standard deviations. Fig. 1 shows the molecular arrangement in a unit cell projected on (001).

TABLE I. ATOMIC PARAMETERS

| | $x$ | $y$ | $z$ |
|---|---|---|---|
| N | 2/3 | 1/3 | 0.612 |
| C | 0.870 | 0.571 | 0.667 |
| $H_1$ | 0.024 | 0.593 | 0.632 |
| $H_2$ | 0.848 | 0.703 | 0.632 |

TABLE II. INTERATOMIC DISTANCES AND BOND ANGLES WITH STANDARD DEVIATIONS (Å UNIT)

| | | | |
|---|---|---|---|
| C-C | 1.590 (0.034) | C-C-N | 110°53′ |
| C-N | 1.477 (0.017) | C-N-C | 108°1′ |
| C-H | 0.96 | | |
| N···N | 2.643 (0.020) | (in a molecule) | |
| | 4.276, 6.932 | (between molecules) | |
| C···N | 3.748 | | |
| C···C | 3.876, 3.977 | | |

Molecules are approximately closest packed in the hexagonal lattice. The molecule in crystal has nearly $D_{3h}-\bar{6}m2$. The linkage of N-C-C-N shows a cis configuration. The crystal does not show any disordered structure in the room temperature phase.

In connection with the crystal analysis, differential thermal analysis was carried out up to 180°C. (Fig. 2). The sample, recrystallized from ethereal solution and sublimed repeatedly under high vacuum ($10^{-5}$ mmHg), evacuated sufficiently at an elevated temperature prior to the measurement. The curve shows the presence of a phase transition at 79.8°C**, the entropy change of which is larger than that at the m. p. 161.1°C. These temperatures are more or less higher than those reported hitherto[1]. Measurements of vapor pressures have also been carried out below and above the transition point. The data are summarized in Table III.

The relatively small entropy of fusion shows that the high temperature phase of the crystal might belong to the category of the so-called

TABLE III. VAPOR PRESSURE DATA

Low temperature phase (51.3~78.6°C)

$\log p(\text{mmHg}) = -3233.6_3/T + 10.473_2$

$\Delta H = 14.8$ kcal./mol.

$\Delta S = 34.8$ e. u.

$\Delta G = 14.80_6 - 0.0347_6 T$ kcal./mol.

High temperature phase (80.0~96.3°C)

$\log p(\text{mmHg}) = -2722.1_8/T + 9.026_9$

$\Delta H = 12.5$ kcal./mol.

$\Delta S = 28.1$ e. u.

$\Delta G = 12.46_4 - 0.0281_4 T$ kcal./mol.

Transition (79.8°C)

$\Delta H = 2.3_4$ kcal./mol.

$\Delta S = 6.6_2$ e. u.

Fusion (161.1°C)

$\Delta H = 1.4_5$ kcal./mol.*

$\Delta S = 3.3$ e. u.

* This value was estimated from the differential thermal analysis curve.

* Present address: Yahata Iron and Steel Co., Ltd., Yahata.

1) A. Farkas, G. A. Mills, W. E. Erner and J. B. Maerker *J. Chem. Engineering Data*, **4**, 334 (1959).

** According to the private communication from Dr. E. F. Westrum the transition temperature is found to be about 353°K.

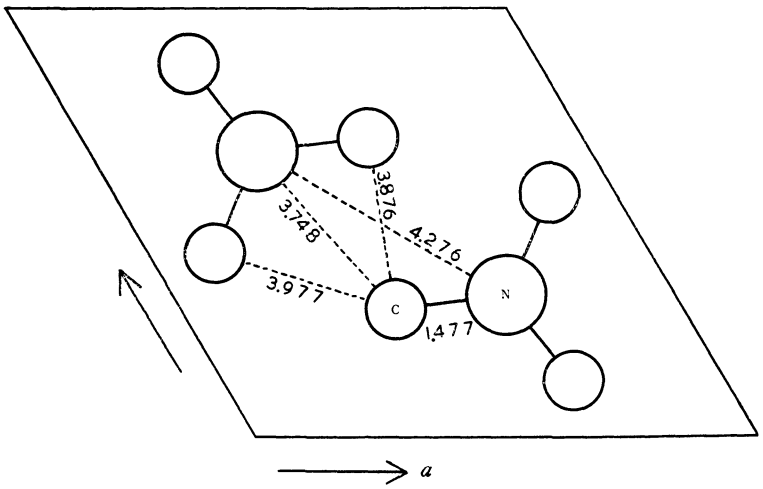



Fig. 1. The molecular arrangement in a unit cell projected on (001).

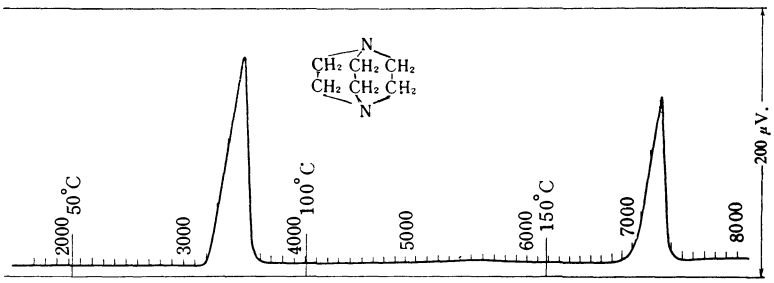



Fig. 2. Automatic recording curve of differential thermal analysis.

" plastic crystals " in the sense as suggested by Timmermans[2]. Accompanied with the large increase of entropy at the transition point, the molecule will gain some orientational, rotational or even translational freedom. Detailed analysis of the crystal structure in the high temperature phase is now going on. The heat capacities near the transition and melting points and the NMR measurement are currently under study in our laboratory. These studies may provide further informations on the mechanism of the phase transition and on the thermal motions in the high temperature phase.

*Department of Chemistry*
*Faculty of Science*
*Osaka University*
*Nakanoshima, Osaka*

2) J. Timmermans, *J. chim. phys.*, **35**, 331 (1938).

# *Isomerization of Unsaturated Fatty Acids and their Esters with Acetic or Inorganic Acid*

By Yutaka WATANABE

(Received January 18, 1960)

It is generally accepted, that the isomerization of fatty materials includes the following events:

i) Formation of conjugated double bonds in the fatty molecule by heating with alkali; that gives rise to cis → trans isomerization[1].

ii) Shifting of double bonds during catalytic hydrogenation[2].

iii) Elaidinization with selenium or nitrous acid[3].

There are many literatures which describe the reaction of unsaturated fatty materials with concentrated sulfuric acid[4], and a synthesis of hydroxy acids or production of sulfated or sulfonated oils and of "iso-oleic" acid was also given. But no detailed description of analysis of "iso-oleic" acid was shown in previous literatures. Furthermore, it is not possible to find any information which refers to the reaction of unsaturated fatty materials with aqueous sulfuric acid solution at moderate temperatures.

Besides these matters the author[5] found the isomerization of oleate or palmitoleate of the following scheme, followed by oxidative fission with *tert*-butyl chromate (type C)*:

$$CH_3(CH_2)_mCH : CH(CH_2)_7C\overset{O}{\diagdown\!\!\diagup}OCH_3$$

$$\longrightarrow CH_3(CH_2)_nCH : CHC\overset{O}{\diagdown\!\!\diagup}OCH_3$$

$m=7$ or 5; $n=14$ or 12

In this experiment, when methyl oleate in benzene was oxidized with *tert*-butyl chromate (type C) at 40°C for 30 hr., nonanoic, azelaic and palmitic acids were obtained as oxidation products. On the other hand, it was found, that oleate in benzene/acetic acid or benzene/acetic acid/sulfuric acid was isomerized partly into 2-octadecenoate. In the oxidation of palmitoleate under almost the same condition as that of oleate, the author recognized the formation of myristic, lauric, capric, heptanoic and azelaic acid. From these experimental results, he proposed the $\beta$-oxidative action of *tert*-butyl chromate, accompanied by the isomerization shown in the above scheme.

It seems very noticeable that the isomerization of unsaturated fatty materials in acid medium proceeds even at moderate temperature. From this point of view, the action of acetic acid and inorganic acids, including aqueous sulfuric, phosphoric and boric acids, towards sesame oil fatty acid was studied. It was observed that the isomerization (conjugation) of triethylenic fatty acids of sesame oil constituents occurs by the treatment of above reagents except boric acid. The examination of ultraviolet absorption spectra of fatty acid was convenient for this purpose.

## Experimental

**Sample.**—*Methyl Oleate*[6].—Commercial olive oil was saponified with alcoholic potash, and the mixed fatty acids obtained were treated by means of lead salt-alcohol method. The resulted liquid acid had an iodine value of 93.1, and a 10% solution of this acid in acetone was cooled to −20°C and filtered. The cake of oleic acid was collected after maintaining the filtrate at −60°C. This acid (I. V. 90.1) was esterified in the usual manner, and the ester obtained was distilled under reduced pressure. Methyl oleate thus prepared had the following properties: b. p.$_5$ 180°C; $d_4^{25}$ 0.8712; $n_D^{25}$ 1.4469; acid value 0.17; saponification value 183.9; I. V. 86.4.

Ozonization of this oleate in chloroform gave no palmitic acid. This indicates the absence of 2-octadecenoate in the specimen.

*Methyl Palmitoleate.*—Sperm oil fatty acid was fractionated into solid and liquid acid by means of lead salt-alcohol method. The liquid acid obtained was esterified and the ester was distilled in vacuo. Methyl palmitoleate thus obtained had the following properties: b. p.$_4$ 160∼165°C; $d_4^{25}$ 0.8748; $n_D^{25}$ 1.4481; A. V. 3.45; S. V. 201.5; I. V. 86.1. Ozonolysis of this palmitoleate gave a complex mixture

1) R. T. Holman, W. O. Lundberg and T. Malkin ed., "Progress in the Chemistry of Fats and Other Lipids", Vol. 4, Pergamon Press, London (1957), p. 227.

2) A. E. Bailey, "Industrial Oil and Fat Products", 2nd ed., Interscience Publishers, New York (1951), p. 687.

3) A. E. Bailey, ibid., p. 910.

4) For instance, R. M. Koppenhoefer, *J. Am. Leather Chem. Assoc.*, **34**, 622 (1939); T. N. Mehta et al., *J. Indian Chem. Soc. Ind. & News Ed.*, **15**, 111 (1952); **16**, 81 (1953); **18**, 195 (1955); K. Nishizawa et al., *J. Chem. Soc. Japan, Ind. Chem. Sec.* (*Kogyo Kagaku Zasshi*), **34**, 836 (1927); **49**, 12 (1946).

5) Y. Watanabe, *J. Chem. Soc. Japan, Pure Chem. Sec.* (*Nippon Kagaku Zasshi*), **80**, 310 (1959); ibid., **80**, 1187 (1959).

* *tert*-Butyl chromate (type C) was prepared according to the method of Oppenauer and Oberrauch (*Anal. asoc. quim. Argentina*, **37**, 247 (1949)).

6) E. G. Ball ed., "Biochemical Preparations", Vol. 2, Wiley, New York (1952), p. 100.

of saturated monocarboxylic acids. Paper chromatographic analysis of the mixed acids, according to the method of Inouye et al.[7] gave the result that the major components of this mixture were nonanoic and heptanoic acids, and the minor were myristic and capric (trace) acids. This means, therefore, that palmitoleate contains a small amount of oleate and a trace of myristate and caprate as contaminants. Ultraviolet and infrared absorption spectra of palmitoleate revealed, that there is neither conjugated diethylenic and more highly conjugated polyethylenic acid esters nor trans type acid esters in the sample.

*Sesame Oil Fatty Acid.* — Saponification of commercial sesame oil ($d_4^{25}$ 0.9097; $n_D^{25}$ 1.4718; A. V. 0.14; S. V. 187.7; I. V. 118.9; unsaponifiable matter 1.11%) with alcoholic potash, gave the mixed fatty acids. This had the following properties: $d_4^{25}$ 0.8983; $n_D^{25}$ 1.4627; A. V. 185.0; I. V. 120.0; content of conjugated diene 0.55%; conjugated triene 0%. Ultraviolet absorption spectrum of this mixed acids is shown in Fig. 1. The content of linoleic and linolenic acids in this sesame oil fatty acid, estimated by the A. O. C. S. standard method[8], was 20.0 and 14.2%, respectively.

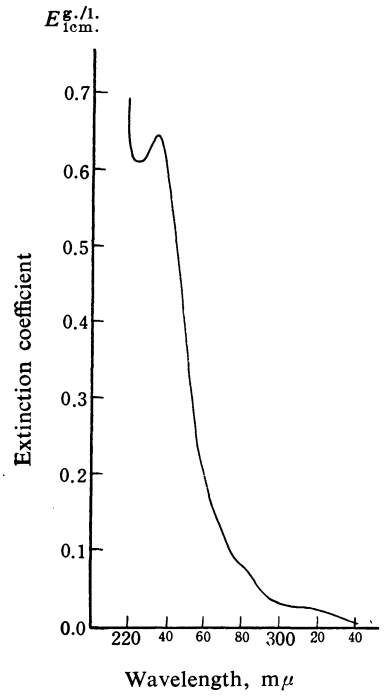



Fig. 1. U. V. absorption spectrum of sesame oil fatty acid.

**Ultraviolet and Infrared Absorption Spectrum.**— All ultraviolet and infrared absorption spectra mentioned in the present paper were measured by using Hilger's UVISPEK and H-800 spectrophotometer, respectively.

Purified ethyl alcohol was used as a solvent for ultraviolet spectroscopy instead of isoöctane.

**Isomerization of Double Bond to α,β-Conjugated Position to Ester Carbonyl Group**[5].—*Methyl Oleate.* — Twenty grams of methyl oleate were added to the mixture of 90 g. of benzene, 36 g. of *tert*-butyl alcohol, 15 g. of acetic acid, and 3.0 g. of acetic anhydride, and the whole was kept at 40°C for 30 hr. with stirring. On the other hand, the mixture of 8 g. of oleate, 26 g. of benzene, 12 g. of acetic acid and 0.1 g. of concentrated sulfuric acid was kept at 70°C for 20 hr. with stirring. After each reaction time mentioned above was over, the reaction mixture was washed with water, 3% aqueous sodium bicarbonate solution, and finally again, water successively dried over anhydrous sodium sulfate, and a mixture of fatty esters was recovered after distilling off the volatile materials.

The fatty esters thus obtained were ozonized at 0°C using chloroform as a solvent. A mixture of monocarboxylic acids was obtained after the oxidative decomposition of the ozonized material, followed by extraction with petroleum ether. Paper chromatographic analyses of samples, derived from different isomerization condition were carried out using the same method as mentioned above. It was recognized that the chromatogram showed the presence of two kinds of fatty acid, namely nonanoic (major) and palmitic (minor) acids. When the mixtures of both of the monocarboxylic acids were fractionally crystallized from methyl alcohol at 0°C, an acid (m. p. 60~63°C) was precipitated in each case. This acid was identified as palmitic acid by the preparation of its *p*-bromophenacyl ester (m. p. 84~84.5°C) and mixed melting point determination with the known specimen.

*Methyl Palmitoleate.* — Eight grams of methyl palmitoleate were added to the mixture of 32 g. of benzene and 5.4 g. of acetic acid, and the whole was kept at 70°C for 30 hr. with stirring. The reaction product was treated in a similar way as in the case of oleate, and the result obtained was as follows. Monocarboxylic acids obtained were heptanoic, nonanoic, capric (trace) and myristic acids. The amount of myristic acid in this case seemed to be larger than that of the sample derived from the starting material (palmitoleate itself); because, the larger and more intense spot of myristic acid on the paper chromatogram was observed in the case of isomerized sample than in the case of the starting material although almost the same quantity of each sample was analyzed by means of paper chromatography mentioned above. However, the conclusive evidence, that the amount of myristic acid increased after isomerization followed by ozonization was not so remarkable.

**Formation of Conjugated Triethylenic Acid in Sesame Oil Fatty Acid.** — *Blank Test.* — Fifteen grams of sesame oil fatty acid and 80 g. of water in a flask provided with a gas-inlet tube, a stirrer, and a reflux condenser, were maintained at 90°C with constant stirring, under nitrogen atmosphere, for 3~30 hr. Contents of conjugated diene and triene in samples calculated from the equation shown in standard method were shown in Table I.

7) Y. Inouye, O. Hirayama and M. Noda, *Bull. Agr. Chem. Soc. Japan*, **20**, 200 (1956); *J. Agr. Chem. Soc. Japan (Nippon Nogei-kagaku Kaishi)*, **31**, 568 (1957).

8) American Oil Chemists' Soc., Tentative Method Cd 7-48; *J. Am. Oil Chemists' Soc.*, **35**, 593 (1958).

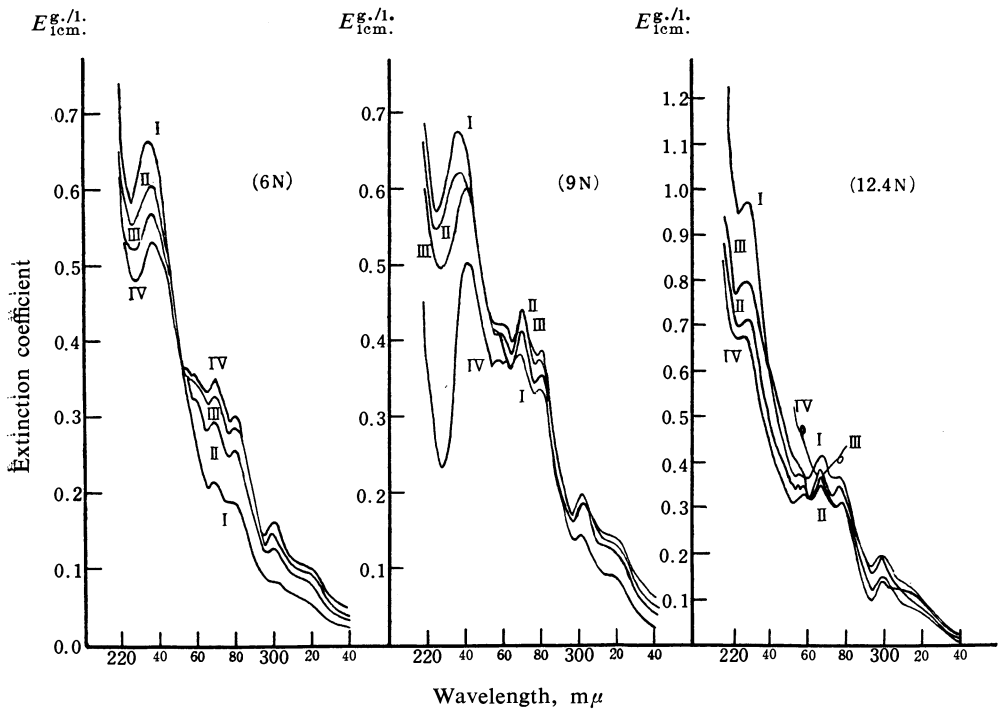



Fig. 2. U. V. absorption spectra of sesame oil fatty acid isomerized with aqueous sulfuric acid solutions. I 3 hr., II 10 hr., III 20 hr., IV 30 hr.

Table I. Conts. of conjugated diene and triene (blank test)

| Time, hr. | 3 | 10 | 20 | 30 |
|---|---|---|---|---|
| Diene, % | 0.70 | 0.89 | 1.17 | 1.79 |
| Triene, % | 0 | 0 | 0.0026 | 0.0026 |

*Aqueous Sulfuric Acid Solution.*—The concentrations of sulfuric acid solutions used for isomerization were 6 N ($d$=1.18), 9 N ($d$=1.26) and 12.4 N ($d$=1.35), respectively. Each time, 30 g. of sesame oil fatty acid and 300 g. of aqueous sulfuric acid solution were treated similarly as in the case of the blank test. These isomerization experiments were carried out at 90°C. After each reaction time (Table II), fatty acid was taken out from the reaction vessel, and washed thoroughly with water and dried, and the ultraviolet absorption spectrum (Fig. 2) was measured, and the contents of diene and triene in it were calculated. The results were shown in Table II.

Table II. Conts. of conjugated diene and triene (treatment with sulfuric acid solution)

| Time, hr. | | 3 | 10 | 20 | 30 |
|---|---|---|---|---|---|
| | Concn. of aq. $H_2SO_4$ | | | | |
| Diene, % | 6 N | 0.54 | 0.48 | 0.45 | 0.42 |
| | 9 N | 0.55 | 0.50 | — | — |
| Triene, % | 6 N | 0.010 | 0.056 | 0.039 | 0.052 |
| | 9 N | 0.053 | 0.062 | 0.086 | 0.085 |
| | 12.4 N | 0.062 | 0.062 | 0.072 | 0.084 |

When sesame oil fatty acid was treated with 6 N sulfuric acid at room temperature for 30 hr., no remarkable change of the ultraviolet absorption spectrogram was observed.

*Phosphoric Acid.* — Phosphoric acid (300 g.) and sesame oil fatty acid (60 g.) were treated quite similarly as in the case of sulfuric acid solution at 90°C. In this case, remarkable coloration of phosphoric acid was observed during the reaction. After the reaction, the fatty acid was recovered similarly as in the case of sulfuric acid solution. The results obtained were shown in Table III. Ultraviolet absorption spectra of isomerized acids were shown in Fig. 3. Physical properties of recovered fatty acids were shown in Table IV.

Table III. Conts. of conjugated diene and triene (treatment with phosphoric acid)

| Time, hr. | 3 | 6 | 10 | 15 | 20 | 30 |
|---|---|---|---|---|---|---|
| Diene, % | 0.61 | 0.65 | 0.62 | 0.76 | 0.61 | 0.71 |
| Triene, % | 0.0619 | 0.0711 | 0.0776 | 0.1066 | 0.0882 | 0.1040 |

Table IV. Physical properties of isomerized sesame oil fatty acid after treatment with phosphoric acid at 90°C

| Time, hr. | $d_4^{25}$ | $n_D^{25}$ | A. V. | I. V. |
|---|---|---|---|---|
| 3 | 0.8924 | 1.4636 | 185.1 | 117.2 |
| 15 | 0.8920 | 1.4632 | 186.6 | 118.9 |
| 30 | 0.8936 | 1.4630 | 188.8 | 117.3 |

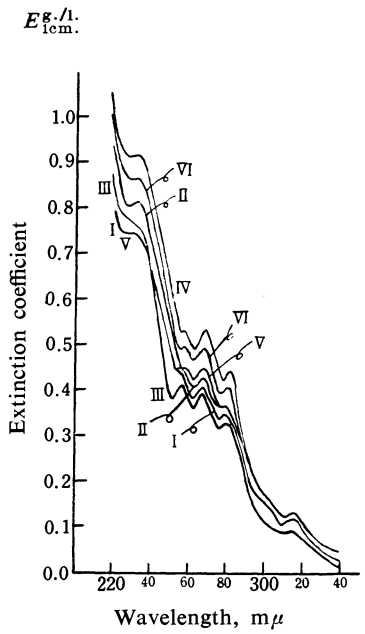



Fig. 3. U. V. absorption spectra of sesame oil fatty acid isomerized with phosphoric acid.
I 3 hr., II 6 hr., III 10 hr., IV 15 hr., V 20 hr., VI 30 hr.

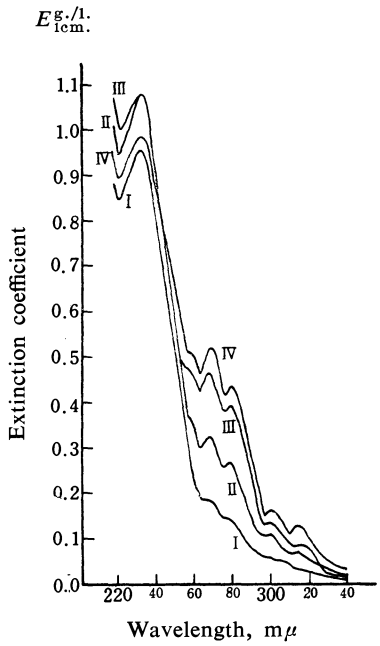



Fig. 4. U. V. absorption spectra of sesame oil fatty acid isomerized with acetic acid.
I 3 hr., II 10 hr., III 20 hr., IV 30 hr.

*Glacial Acetic Acid.* — Glacial acetic acid (300 g.) and sesame oil fatty acid (30 g.) were mixed and the solution was maintained at 90°C under nitrogen atmosphere, with stirring, for 30 hr. In the course of the reaction, 30 cc. portion of the solution was taken out, poured into water, extracted with ether and the ethereal solution was washed thoroughly with water, and dried over anhydrous sodium sulfate. After evaporation of the solvent, isomerized material was recovered, and its ultraviolet absorption spectrum was measured (Fig. 4). The contents of conjugated diene and triene calculated were shown in Table V.

TABLE V. CONTS. OF CONJUGATED DIENE AND TRIENE (TREATMENT WITH GLACIAL ACETIC ACID)

| Time, hr. | 3 | 10 | 20 | 30 |
|---|---|---|---|---|
| Diene, % | 0.78 | 0.88 | 0.88 | 0.81 |
| Triene, % | 0.0066 | 0.054 | 0.096 | 0.112 |

*Treatment with Boric Acid.* — At 90°C, sesame oil fatty acid (30 g.), boric acid (90 g.) and water (410 g.) were treated similarly as in the case of the blank test. Even after 30 hr., the fatty acid was so stable that the contents of conjugated diene and triene in it were essentially the same as in the case of the blank test.

## Discussion

It will be noticeably demonstrated that the isomerization of unsaturated fatty materials occurs at moderate temperature (30~90°C) in the acid medium mentioned above. In the case of monoethylenic fatty esters, namely methyl oleate and palmitoleate, the double bond migrates to $\alpha,\beta$-conjugated position to ester carbonyl group. Although the isolation of isoöleate or isopalmitoleate was unsuccessful, the formation of $\alpha,\beta$-unsaturated esters was definitely supported by the identification of a shorter-chain saturated fatty acid, which was obtained after ozonolysis of isomerized products. The identification of palmitic and myristic acids has important meaning in this aspect. These facts support the $\beta$-oxidation mechanism of oleate and palmitoleate with *tert*-butyl chromate (type C).

In the case of sesame oil fatty acid, it is sure, that conjugation of triethylenic system in fatty acid molecule proceeds, when it was treated with acetic, phosphoric or aqueous sulfuric acid solution at 90°C. But there was no appreciable formation of a conjugated diethylenic system in such treatment, because the contents of conjugated diene of sesame oil fatty acid were almost constant throughout the whole various conditions. It is certain that the formation of conjugated triethylenic acid proceeds neither in the experiment of the blank test nor with the treatment with boric acid at 90°C. Also, the same result was obtained in the case of the treatment with 6 N sulfuric acid at room temperature. The smallest content found (0.0066%) of conjugated

triene was obtained in the treatment of the fatty acid with acetic acid at 90°C for 3 hr. The highest content observed (0.112%) was obtained in the isomerization with acetic acid at 90°C for 30 hr. This value (0.112%) corresponded to 0.784% for linolenic acid present in sesame oil fatty acid.

According to Privett and Quackenbush[9], no phosphorylation occurred, when ethyl linoleate was treated with a catalytic amount of phosphoric acid (below 1%) in a sealed tube, under vacuum at 100°C for 36 hr. They have refered nothing to the isomerization of linoleate. However, in the case of the treatment of fatty acid with a large amount of phosphoric acid at 90°C described in the present paper, the author recognized the isomerization of fatty acid as above. But the physical properties of the isomerized products shown in Table IV seemed to be virtually constant, the same interpretation as for no phosphorylation can be relied on.

The author wishes to express his gratefulness to Professor T. Matsuura for his suggestions and encouragement, and also to Messrs. H. Tanimoto and A. Ohtawa for their assistance.

*Department of Chemistry*
*Faculty of Science*
*Hiroshima University*
*Hiroshima*

9) O. S. Privett and F. W. Quackenbush, *J. Am. Oil Chemists' Soc.*, **31**, 225 (1954).

# *Studies on Organic Peroxides. VI. Thermal Analysis of the Decomposition of Benzoyl Peroxide by Ferrous Ion**

By Shigeo HASEGAWA, Norio NISHIMURA and Kimpei MIURA

(Received February 11, 1960)

In the previous paper[1], the analytical method was applied to follow the rate of the decomposition of benzoyl peroxide catalyzed by ferrous ion and it was found that the apparent decomposition rate was of the first order with respect to the concentration of benzoyl peroxide and that the activation energy of the decomposition was about 14 kcal./mol. This was much less than that of the spontaneous decomposition. In this report, similar reactions were carried out in methanol, ethanol, *n*-propanol and *n*-butanol and the reaction was followed by means of the method of thermal analysis[2].

## Experimental

**Reagents.**—Benzoyl peroxide and ferrous chloride were prepared by the methods reported earlier[3]. Other chemicals used were of reagent grade and repeatedly distilled.

**Apparatus and Procedure.**—The reaction was carried out in a glass calorimeter shown in Fig. 1. In this figure, A is a Dewar vessel, the capacity of which is about 200 cc., B a glass stirrer sealed by mercury, C a Beckmann thermometer, D a platinum wire heater, E a glass vessel of about 30 cc. and F and F' glass tubes.

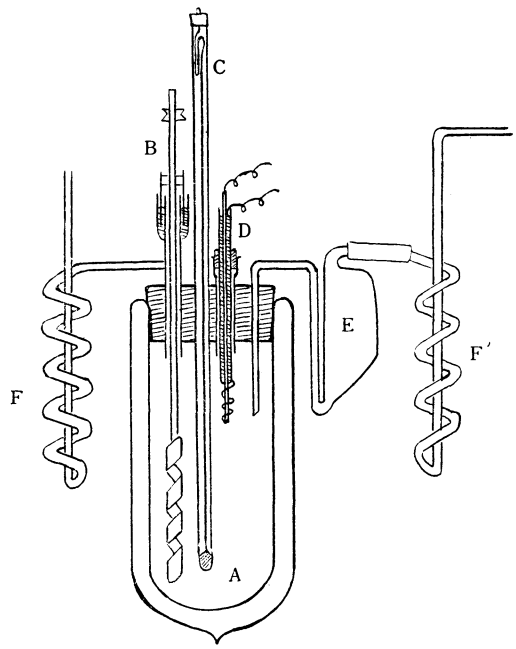



Fig. 1. Reaction vessel.

* Presented in part at the Chugoku-Shikoku and Kinki Local Meeting of the Chemical Society of Japan, Tokushima, August 29 (1958).

1) S. Hasegawa and N. Nishimura, This Bulletin, 33, 775 (1960).

2) S. Horiba and T. Ichikawa, *Rev. Phys. Chem. Japan*, 1, 145 (1927); Ichikawa, *Z. Physik. Chem.*, (B) 10, 299 (1930).

3) S. Hasegawa et al., This Bulletin, 31, 696 (1958).

The atomosphere of the vessel was previously substituted by carbon dioxide. Oxygen-free benzoyl peroxide and ferrous chloride solutions were introduced into A and E, respectively. The calorimeter was held in a thermostat. The temperature in A was adjusted to that of the thermostat by the heater D. After thermal equilibrium was attained, the ferrous chloride solution in E was siphoned into A. As soon as they were mixed, the reaction started and the rise of the temperature was recorded as the time passed.

The initial concentration of benzoyl peroxide was 0.01 mol./l. for all runs.

**The Method of Thermal Analysis.**—The fundamental equation of thermal analysis is given by Eq. 1[2,4],

$$\frac{dT}{dt}+K\Delta T=\frac{Q}{W}\cdot\frac{dx}{dt} \qquad (1)$$

where $dT/dt$ is the velocity of temperature change in solution, and $K\Delta T$ is a correction term for Newtonian cooling due to the temperature difference $\Delta T$ between the system and its surroundings and hence the rise in the temperature of reaction solution, $K$ being the cooling constant. $Q$ and $W$ denote the heat of the reaction and the water equivalent of the reaction vessel, respectively, and $dx/dt$ the rate of the reaction.

The cooling constant $K$ can easily be determined by plotting the temperature difference between the reaction vessel and the thermostat against time.

When a reaction is of the first order, the rate of the reaction may be expressed as:

$$dx/dt=kae^{-kt} \qquad (2)$$

where $k$ is the specific reaction rate and $a$ is the initial concentration of the reactant. From Eqs. 1 and 2, it follows,

$$\log(dT/dt+K\Delta T)=\log\frac{Q}{W}\cdot ka-\frac{kt}{2.303} \qquad (3)$$

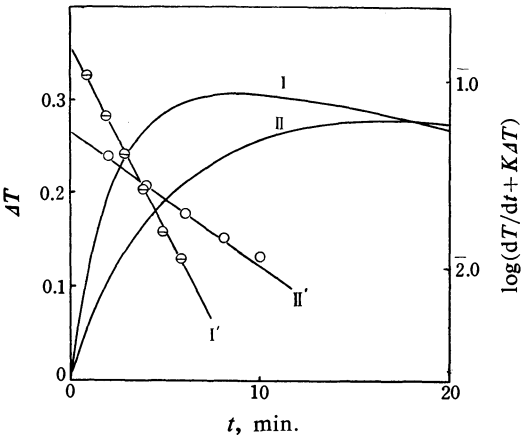



Fig. 2. Curves I and II: $\Delta T$ vs. $t$; curves I′ and II′: $\log(dT/dt+K\Delta T)$ vs. $t$ in ethanol at 15°C; $[FeCl_2]_0$: 0.0038 mol./l. for I and 0.0012 mol./l. for II, respectively; $[BPO]_0$: 0.01 mol./l.

4) E. Suito, *Rev. Phys. Chem. Japan*, **13**, 74 (1939).

Accordingly, the plot of the left hand side of Eq. 3 against time $t$ will give a straight line, the slope of which is $k/2.303$.

## Results

The ferrous ion catalyzed decomposition of benzoyl peroxide is a exothermal reaction and an example is shown in Fig. 2 in which curves I and II show the dependence of $\Delta T$ upon

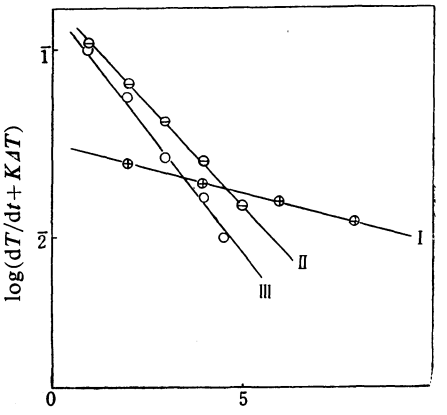



Fig. 3. $\log(dT/dt+K\Delta T)$ against $t$.
I: methanol, 40°C, $[FeCl_2]_0$: 0.0050 mol./l.
II: butanol, 15°C, $[FeCl_2]_0$: 0.0030 mol./l.
III: propanol, 15°C, $[FeCl_2]_0$: 0.0030 mol./l.
$[BPO]_0$: 0.01 mol./l.

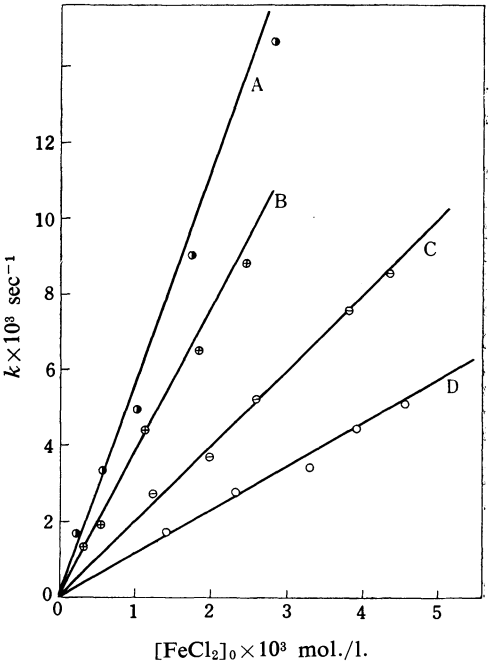



Fig. 4. Dependence of $k$ upon $[FeCl_2]_0$ in ethanol at various temperatures: A, 30; B, 25; C, 15; D, 10°C, respectively; $[BPO]_0$: 0.01 mol./l.

TABLE I. THE RATE CONSTANTS FOR THE DECOMPOSITION OF BENZOYL PEROXIDE BY FERROUS ION

| Temp. °C | $[FeCl_2]_0 \times 10^3$ mol. $l^{-1}$ | $k \times 10^3$ $sec^{-1}$ | $k'$ l. $mol^{-1}$ $sec^{-1}$ | $k'_{av}$ |
|---|---|---|---|---|
| | | Methanol | | |
| 25 | 2.00 | 0.18 | 0.09 | |
| | 3.00 | 0.29 | 0.10 | $0.10 \pm 0.00^3$ |
| | 4.00 | 0.43 | 0.11 | |
| | 5.00 | 0.48 | 0.10 | |
| 30 | 1.90 | 0.54 | 0.28 | |
| | 3.00 | 0.69 | 0.23 | |
| | 4.66 | 0.92 | 0.20 | $0.23 \pm 0.01^4$ |
| | 4.90 | 0.92 | 0.19 | |
| 35 | 1.50 | 0.48 | 0.32 | |
| | 2.50 | 0.84 | 0.34 | $0.29 \pm 0.02$ |
| | 3.50 | 0.98 | 0.28 | |
| | 4.50 | 1.04 | 0.23 | |
| 40 | 1.50 | 1.00 | 0.67 | |
| | 2.74 | 1.38 | 0.50 | $0.54 \pm 0.03$ |
| | 3.50 | 1.80 | 0.51 | |
| | 5.00 | 2.34 | 0.47 | |
| | | Ethanol | | |
| 10 | 1.38 | 1.77 | 1.28 | |
| | 2.31 | 2.80 | 1.21 | |
| | 3.30 | 3.45 | 1.05 | $1.16 \pm 0.03$ |
| | 3.92 | 4.49 | 1.15 | |
| | 4.54 | 5.14 | 1.13 | |
| 15 | 1.22 | 2.76 | 2.26 | |
| | 1.99 | 3.76 | 1.89 | |
| | 2.59 | 5.26 | 2.03 | $2.03 \pm 0.04$ |
| | 3.81 | 7.60 | 1.99 | |
| | 4.35 | 8.56 | 1.97 | |
| 25 | 0.29 | 1.34 | 4.62 | |
| | 0.53 | 1.92 | 3.62 | |
| | 1.11 | 4.41 | 3.97 | $3.87 \pm 0.13$ |
| | 1.83 | 6.52 | 3.56 | |
| | 2.45 | 8.83 | 3.60 | |
| 30 | 0.23 | 1.65 | 7.08 | |
| | 0.55 | 3.34 | 6.07 | |
| | 1.00 | 4.91 | 4.91 | $5.70 \pm 0.27$ |
| | 1.71 | 8.98 | 5.25 | |
| | 2.82 | 14.66 | 5.20 | |
| | | *n*-Propanol | | |
| 5 | 0.96 | 1.42 | 1.48 | |
| | 2.39 | 3.30 | 1.38 | |
| | 3.08 | 3.65 | 1.18 | $1.34 \pm 0.05$ |
| | 3.82 | 5.76 | 1.51 | |
| | 5.00 | 5.83 | 1.17 | |
| 10 | 1.28 | 3.22 | 2.52 | |
| | 2.17 | 5.37 | 2.48 | |
| | 2.92 | 6.72 | 2.30 | $2.44 \pm 0.04$ |
| | 4.00 | 10.48 | 2.62 | |
| | 5.04 | 11.55 | 2.29 | |
| 15 | 1.00 | 3.84 | 3.84 | |
| | 2.00 | 7.22 | 3.61 | |
| | 3.00 | 10.36 | 3.45 | $3.44 \pm 0.10$ |
| | 4.00 | 13.43 | 3.36 | |
| | 5.00 | 14.58 | 2.92 | |
| | | *n*-Butanol | | |
| 5 | 1.04 | 1.80 | 1.73 | |
| | 2.10 | 2.92 | 1.39 | |
| | 3.08 | 3.88 | 1.26 | $1.38 \pm 0.06$ |
| | 3.98 | 5.07 | 1.27 | |
| | 5.20 | 6.49 | 1.25 | |
| 10 | 1.00 | 2.23 | 2.23 | |
| | 2.00 | 3.84 | 1.92 | |
| | 3.00 | 5.53 | 1.84 | $2.02 \pm 0.05$ |
| | 4.00 | 7.98 | 2.00 | |
| | 5.00 | 10.75 | 2.15 | |
| 15 | 1.00 | 2.92 | 2.92 | |
| | 2.00 | 6.64 | 3.32 | |
| | 3.00 | 8.83 | 2.94 | $3.01 \pm 0.08$ |
| | 3.52 | 10.94 | 3.13 | |
| | 4.00 | 12.47 | 3.11 | |
| | 5.00 | 13.05 | 2.61 | |

time $t$ in ethanol at 15°C. The slope $dT/dt$ of the curve at any time $t$ can be obtained from the figure. Curves I′ and II′ which are obtained by plotting the left hand side term in Eq. 3 against time give straight lines, therefore, it may be concluded that this reaction is apparently of the first order. Reactions in methyl, *n*-propyl and *n*-butyl alcohols were also the case, as shown in Fig. 3.

It was also found that the slope of the $\log (dT/dt + K\Delta T)$ vs. $t$ curve was independent of the initial concentration of benzoyl peroxide.

According to Eq. 3, the slope of the line should give $k/2.303$. However, the specific rate constant $k$ thus obtained in this reaction can not be considered as the true rate constants, because the ferrous ion may be considered to take part in the reaction. The discussion will be undertaken shortly.

The initial concentrations of the ferrous ion, alcohols and the values of $k$ at various temperatures are listed in Table I. From the table, it may be concluded that the values of $k$ seem directly proportional to the initial concentration of the ferrous ion. For example, $k$ vs. $[FeCl_2]_0$ was plotted at temperatures between 10 and 30°C in ethanolic solution as shown in Fig. 4. It seems that each of the values falls on a straight line and converges to the origin. If this conclusion is correct, it follows:

$$k = k' [FeCl_2]_0 \qquad (4)$$

where $k'$ is a constant. In the fourth and fifth columns in Table I are listed the values of $k'$ calculated from Eq. 4. The slopes in Fig. 4 represent the average values of $k'$ for each temperature.

It may be seen that the differences in the reaction rates among ethanol, *n*-propanol and

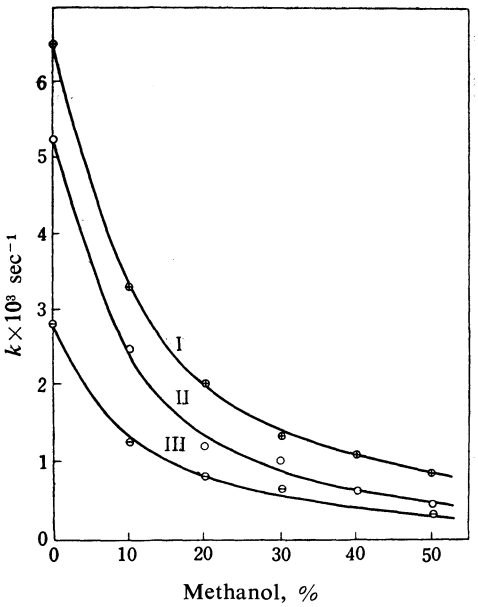



Fig. 5. Values of $k$ for methanol-ethanol mixture : I, 20 ; II, 15 ; III, 10°C ; $[BPO]_0$ : 0.01 mol./l., $[FeCl_2]_0$ : 0.0025 mol./l.

*n*-butanol are not particularly appreciable, but in methanol, the rate is appreciably smaller than in the three other alcohols. In the mixture of methanol and ethanol, $k$ values were rapidly decreased by increasing the proportion of methanol as seen in Fig. 5. Above 50% of methanol, the reaction rates became too small to determine over the experimental temperature range.

## Reaction Mechanism

As suggested in the previous paper[1], the overall reactions in this system will take place as follows:

First of all, reaction between benzoyl peroxide and ferrous ion will occur:

$$Fe^{2+}+P \xrightarrow{k_1} RCOO\cdot+RCOO^-+Fe^{3+} \quad (5)$$

The benzoxy radical thus produced will attack a solvent molecule and abstract a hydrogen atom on $\alpha$-carbon atom.

$$RCOO\cdot+R'CH_2OH \xrightarrow{k_2} RCOOH+R'\dot{C}HOH \quad (6)$$

In addition, the reduction of ferrous to ferric ion is assumed:

$$R'\dot{C}HOH+Fe^{3+} \xrightarrow{k_3} RCHO+Fe^{2+}+H^+ \quad (7)$$

Therefore, the heat evolved in this reaction may be the sum of the contribution from these reactions. Hence, the apparent rate constant $k$ may be considered to include some specific rate constants.

In the previous paper, it was also mentioned that the rate of the decomposition of benzoyl peroxide might well be expressed as

$$-d[P]/dt=k_1[P][Fe^{2+}] \quad (8)$$

In addition, the apparent overall decomposition rate was approximately of the first order, that is

$$-d[P]/dt=k_0[P] \quad (9)$$

where $k_0$ is a constant. Therefore, the ferrous ion concentration should be constant during the reactions, if Eqs. 8 and 9 are not inconsistent with each other. From Eqs. 8 and 9, it follows,

$$k_0=k_1[Fe^{2+}] \quad (10)$$

As was assumed, if the rate of reduction of ferric to ferrous ions are equal or almost equal to that of oxidation, the equilibrium between ferrous and ferric ions would be attained. Then, ferrous ion concentration may be expressed in terms of its initial concentration and the equilibrium constant $K_0$, i. e.,

$$[Fe^{2+}]=\frac{K_0}{1+K_0}[Fe^{2+}]_0 \quad (11)$$

Inserting this value into Eq. 10, it follows,

$$k_0=k_1\cdot\frac{K_0}{1+K_0}\cdot[Fe^{2+}]_0 \quad (12)$$

Thus, as was suggested, in the previous paper, $k_0$ should be a linear function of $[Fe^{2+}]_0$. Eq. 9 shows that $k_0$ can be obtained from the slope of the $\log[P]$ vs. $t$ curve. If Eq. 12 is compared with Eq. 4, the conclusion that the rate constant $k$ obtained from the thermal analysis is a linear function of the initial ferrous ion concentration, agrees formally with the conclusion that the apparent first order rate constant $k_0$ obtained from the analytical data, would be a linear function of the initial ferrous concentration. Each value of $k$ and $k'$ could, therefore, be referred as a measure of $k_0$ and $k_1$, respectively. Thus, it may be concluded that though the data from the thermal analysis in this reaction do not offer true rate constants, they still offer a means for studying the mechanism of this reaction in alcohols.

## Solvent Effect

Since $k'$ corresponds to the true rate constant $k_1$ as mentioned above, it is of interest to calculate the apparent activation energy by plotting $\log k'$ against $1/T$. The Arrhenius plots may be seen in Fig. 6. By applying the least squares method, the activation energies and the frequency factors for each alcohol were calculated and listed in Table II.

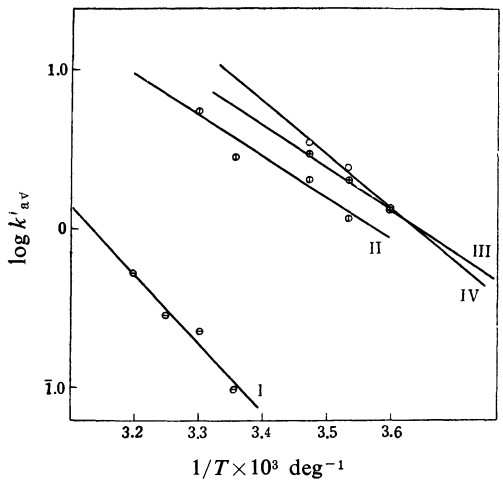



Fig. 6. Plots of $\log k'_{av}$ against $1/T$, solvent, I, methanol; II, ethanol; III, *n*-propanol; IV, *n*-butanol.

TABLE II. ACTIVATION ENERGIES AND FREQUENCY FACTORS

| Solvent | $E$(kcal./mol.) | $A$ | $S^*$(e. u.) 300°K |
|---|---|---|---|
| Methanol | 19.8 | $3.3\times10^{13}$ | 1.3 |
| Ethanol | 12.0 | $2.3\times10^{9}$ | −17.7 |
| *n*-Propanol | 15.0 | $8.7\times10^{11}$ | −5.9 |
| *n*-Butanol | 12.4 | $7.5\times10^{9}$ | −15.3 |
| Methanol (10%)-Ethanol (90%) | 15.2 | $3.2\times10^{11}$ | −7.9 |
| Methanol (20%)-Ethanol (80%) | 16.7 | $2.3\times10^{12}$ | −4.0 |

The influence of the solvent on chemical reaction rate would be partly due to its physical properties such as dielectric constant or molecular size. In reactions between ions and molecules, the solvent will play an important role and the increase in the dielectric constant of the solvent will cause a decrease in the free energy of the system, and hence will result in a decrease in their reaction rates. Since ferrous ions in alcohol are solvated, the reaction rates between ferrous ion and benzoyl peroxide will depend partly on the dielectric constants of the solvents. The dielectric constants of methanol, ethanol, *n*-propanol at 20°C and *n*-butanol at 25°C are 33.7, 25.7, 21.8 and 17.8, respectively[5].

It may be seen from the table that the $k'$ values are increased in the order of methanol, ethanol, *n*-butanol and *n*-propanol, in agreement with the order of decreasing dielectric constants except that the order of *n*-propanol and *n*-butanol is reversed. But the difference in the rates between these alcohols is not so appreciable.

5) International Critical Table, VI, p. 83.

It was pointed out[6] that abstraction of the hydrogen atom from the alcohol molecule took place on the $\alpha$-carbon atom exclusively.

In reaction 6, methylenic hydrogen atoms will exclusively be abstracted in ethanol, *n*-propanol and *n*-butanol, whereas methyl hydrogen atoms will be abstracted in methanol. This will suggest the exceptionally slow reaction rates in methanol.

### Enthalpy-Entropy Relationship

Mention may be made about the relation between activation energy and frequency factor.

There are cases when a linear relationship between $\Delta S^*$ and $E$ can be observed. Especially, it was pointed out that in a series of reactions, $\log A$ was a linear function of $E$ when the Hammett equation held[7].

According to the theory of the absolute reaction rates[8], the specific rate constant $k$ of a reaction is related to the standard free energy of activation $\Delta F^*$ by Eq. 13:

$$k=\kappa\frac{kT}{h}\exp\left(-\frac{\Delta F^*}{RT}\right) \tag{13}$$

The free energy of activation may be a function of the intensity factors such as steric, resonance, or solvent effects. In a series of reactions, all such intensity factors are assumed to remain constant except that there is a change in one of these intensity factors, and $\Delta F^*$ is assumed to be linearly related to it.

Any reaction in the series may be chosen as standard and its specific rate constant may be denoted by $k_0$. If the difference in the intensity factor between any reaction and the standard one is expressed by $\Delta\chi$, then from the assumption mentioned above, the specific rate constant $k$ can be derived from Eq. 13:

$$\ln k/k_0=-\frac{\Delta\Delta F^*}{RT}=-\frac{1}{RT}\left(\frac{\partial\Delta F^*}{\partial\chi}\right)_T\Delta\chi$$
$$=-\frac{1}{RT}\left\{\left(\frac{\partial\Delta H^*}{\partial\chi}\right)_T-T\left(\frac{\partial\Delta S^*}{\partial\chi}\right)_T\right\}\Delta\chi \tag{14}$$

where $\Delta\Delta F^*$ represents the difference in the standard free energy of activation between the reaction and the standard one; $\Delta H^*$ and $\Delta S^*$ denote the standard activation enthalpy and entropy, respectively.

In a case when the intensity factor $\chi$ represents a substituent effect, the reaction constant

6) M. S. Kharasch, J. L. Rowe and W. H. Urry, *J. Org. Chem.*, **16**, 905 (1951).

7) J. E. Leffler and Shih-Kung Liu, *J. Am. Chem. Soc.*, **78**, 1949 (1956); I. Meloche and K. J. Laidler, ibid., **73**, 1712 (1951); D. A. Brown and R. F. Hudson, *J. Chem. Soc.*, **1953**, 883.

8) S. Glasstone, K. J. Laidler and H. Eyring, "The Theory of Rate Processes", McGraw-Hill, New York (1941), p. 195.

$\rho$ in the Hammett equation[9] may be expressed as

$$-\frac{1}{RT}\left\{\left(\frac{\partial \Delta H^{\ddagger}}{\partial \chi}\right)_T - T\left(\frac{\partial \Delta S^{\ddagger}}{\partial \chi}\right)_T\right\} = \rho \times \text{const} \quad (15)$$

Jaffé[10] has pointed out, quoting many examples, that in a series of reactions where the Hammett equation held, $\rho$ was linearly related to $1/T$. This fact can successfully be explained by Eq. 15 if $(\partial \Delta H^{\ddagger}/\partial \chi)_T$ and $(\partial \Delta S^{\ddagger}/\partial \chi)_T$ are both independent of temperature.

In a series of related reactions, changes in polarity of a substituted group may be associated with the change in the electrostatic field strength at the reaction center.

Hence it may be reasonable to expect that the greater the enthalpy of activation, the greater will become the entropy of activation, because formation of a more rigid activated complex will need fewer entropy and enthalpy changes and vice versa.

In case of solvent changes, the linear relationship between enthalpy and entropy of activation is also observed[11,12]. If reactants are solvated, solvation will cause the decrease in the potential energy and entropy of the system, and hence both the enthalpy and entropy of activation will be increased. Thus, it may be reasonable to assume that the sign of $(\partial \Delta H^{\ddagger}/\partial \chi)_T$ is the same as that of $(\partial \Delta S^{\ddagger}/\partial \chi)_T$ and that neither of them is zero. Then, there must be a temperature, denoted by $\beta$, at which the left hand side of Eq. 14 becomes zero and it must be characteristic in the reaction series. From the discussion mentioned above, it is concluded that at the temperature $\beta$, which has been called "isokinetic temperature"[12], all the reaction rates should become identical.

From Eq. 14, it follows:

$$\left(\frac{\partial \Delta H^{\ddagger}}{\partial \chi}\right)_T \Delta \chi = \beta \left(\frac{\partial \Delta S^{\ddagger}}{\partial \chi}\right)_T \Delta \chi \quad (16)$$

or

$$\Delta \Delta H^{\ddagger} = \beta \Delta \Delta S^{\ddagger} \quad (17)$$

where $\Delta\Delta H^{\ddagger}$ and $\Delta\Delta S^{\ddagger}$ denote the difference in the activation enthalpy and entropy between a reaction and the standard one, respectively. Hence, $\Delta\Delta H^{\ddagger}$ is a linear function of $\Delta\Delta S^{\ddagger}$, in agreement with experimental facts.

In this study, the apparent activation energy

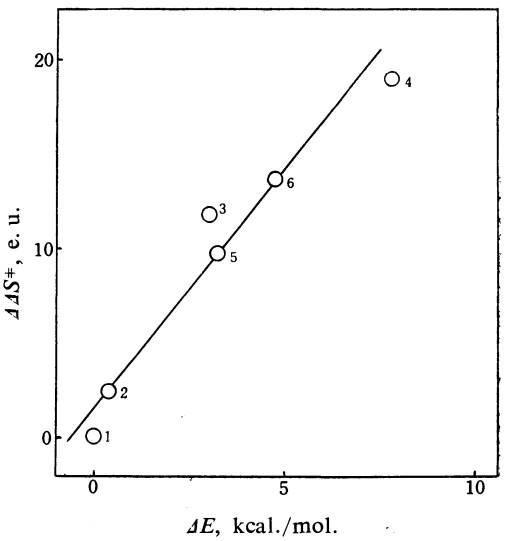



Fig. 7. Relationship between $\Delta E$ and $\Delta\Delta S^{\ddagger}$. 1, ethanol; 2, butanol; 3 propanol; 4, methanol; 5, methanol (10%)-ethanol (90%); 6, methanol (20%)-ethanol (80%).

$E$ was also proportional to the activation entropy. In Fig, 7, the reaction in ethanol was chosen as standard, and the differences in activation energies were plotted against the differences in the activation entropies. A straight line was obtained as shown in the figure. From the slope, the isokinetic temperature was calculated to be 400°K.

## Summary

The thermal analysis method was applied to follow the rate of the decomposition of benzoyl peroxide catalysed by ferrous ion in methanol, ethanol, *n*-propanol and *n*-butanol.

The apparent rates were of the first order and no fundamental difference in the reaction mechanism was observed among these alcohols. However, the reaction rates in methanol were much slower than in three other alcohols. Solvent effects on the reaction rate were discussed.

Linear enthalpy-entropy relationship was deduced, assuming that the free energy of activation is the linear function of an intensity factor in a series of reactions. This was found to be true in our case.

*Department of Chemistry*
*Faculty of Science*
*Okayama University*
*Tsushima, Okayama*

9) L. P. Hammett, *J. Am. Chem. Soc.*, **59**, 96 (1937).
10) H. H. Jaffé, *Chem. Revs.*, **53**, 191 (1953).
11) E. A. Moelwyn-Hughes, "The Kinetics of Reactions in Solution", Second Ed., Oxford Univ. Press (1947), p. 278.
12) J. E. Leffler, *J. Org. Chem.*, **20**, 1202 (1955).

# *Synthesis and Purification of Sexiphenyl for Scintillator*

By Tadashi NOZAKI, Michiko TAMURA, Yuhei HARADA* and Kazuo SAITO

(Received March 21, 1960)

It has been believed that sexiphenyl is an interesting organic semi-conductor and a promising scintillator for charged particles[1]. However its preparation was made only on a small scale[2-4], and an attempt to obtain this compound in sufficient quality and quantity for scintillator met with little success[1]. The present authors have found a favorable condition for the production of 4-nitroterphenyl from *p*-terphenyl (1, 4-diphenylbenzene) and succeeded in obtaining several tens of grams of sexiphenyl in a moderate yield. Although its purification involved a great difficulty, repeated vacuum sublimation and zone refining followed by recrystallization from tetralin afforded this compound in high purity. Its almost colorless single crystal gives an intense violet fluorescence and is satisfactorily used as a scintillator and wavelength shifter for Čerenkov radiation.

**Preparation of Sexiphenyl.**—The process is shown in Table I. Two methods have so far been presented for the synthesis: 1) the Ullmann condensation of 4-iodoterphenyl with the aid of silver powder at 320°C[2]; 2) the same condensation of a mixture of 4-iodobiphenyl and 4, 4'-diiodobiphenyl with copper powder[3]. According to the present authors' re-examination, both gave a very poor yield. Especially the latter provided a product containing as much as 0.7% iodine, after repeated vacuum sublimation and recrystallization from tetralin and dibutylphthalate. Contrary to the description in the literature, the Ullmann condensation of 4-iodoterphenyl with copper gave a good yield (more than 40%), provided that the iodoterphenyl was sufficiently pure and the condensation was carried out on a small scale. It appears as if the exothermic reaction, when carried out on a large scale, raises the temperature so remarkably that both the yield and the purity of the product were lowered.

4-Iodoterphenyl was obtained from 4-aminoterphenyl hydrochloride by diazotization and Sandmeyer's reaction, made free from phenols and the remaining amines by extraction with xylene and further purified by vacuum distillation and recrystallization from isoamyl acetate. Although both the amine and the diazonium salt are sparingly soluble in dilute hydrochloric acid, the diazotization proceeds in a good yield in suspension. This process compares favorably with that in concentrated sulfuric acid[2].

For obtaining pure 4-aminoterphenyl, preparation of pure 4-nitroterphenyl is essential. Nitration of terphenyl usually gives polynitro

TABLE I. SYNTHESIS OF SEXIPHENYL

| Raw material | Product | Process | Remarks |
|---|---|---|---|
| *p*-terphenyl (I) | 4-nitroterphenyl (II) (ca. 60%)<br>2-nitroterphenyl (15 to 20%)<br>2'-nitroterphenyl (15 to 25%) | $HNO_3$ in acetic acid and acetic anhydride | new process |
| 4-nitroterphenyl (II) | 4-aminoterphenyl hydrochloride (III) (almost 100%) | $SnCl_2$ in ethanol and HCl | Ref. 2 (slightly modified) |
| 4-aminoterphenyl hydrochloride (III) | 4-iodoterphenyl (IV) (ca. 40%) | $NaNO_2$ in HCl suspension; urea and KI | Ref. 2 (modified) |
| 4-iodoterphenyl | sexiphenyl (V) (40 to 80%) | Cu at 280°C | Ref. 2 (modified) |

* Present address, Kitazono High School, Itabashi-ku, Tokyo.

1) R. C. Sangstar et al., *J. Chem. Phys.*, **24**, 713 (1956).
2) R. Pummerer and K. Bittner, *Ber.*, **57**, 84 (1924).
3) R. Pummerer and L. Selingsberger, ibid., **64**, 2477 (1931).
4) A. E. Gillam and D. H. Hey, *J. Chem. Soc.*, **1939**, 1170.

compounds[5]. Allen et al. obtained 4-nitroterphenyl in 72% yield in glacial acetic acid in the presence of a small excess of nitric acid[6]; they gave, however, no information on the other 28% portion. The present authors have found that at temperatures exceeding 100°C and in glacial acetic acid containing about 10% of acetic anhydride and a trace of sulfuric acid, the rate of mono-nitration of *p*-terphenyl is significantly greater than the decomposition of nitric acid, which is in turn much greater than the rate of nitration of mononitroterphenyls. Higher temperature and greater concentration of acetic anhydride and sulfuric acid increase the solubility of *p*-terphenyl, but facilitates the decomposition of nitric acid, resulting in incomplete nitration of *p*-terphenyl. On the other hand, the amount and the concentration of nitric acid affected the result to a less extent. When the reaction mixture was cooled, fairly pure 4-nitroterphenyl separated as light yellow needles. Column chromatography of the mother liquor gave pure 2-nitro- and 2'-nitroterphenyl.

**Purification of Sexiphenyl.**—Crude sexiphenyl obtained by vacuum sublimation from the condensation product was yellow in color and contained significant amounts of copper and iodine. Most copper was removed by digesting the sublimate in aqueous potassium cyanide solution. Extremely low solubility of sexiphenyl in any organic solvent (e. g. less than 0.1 g. in one litre of boiling tetralin) makes recrystallization and chromatographic purification very laborious or even impracticable. It was further disclosed by neutron activation analysis that vacuum sublimation and recrystallization from various organic solvents were less effective for the removal of iodine-containing compounds. On the other hand, a cycle consisting of zone refining and vacuum sublimation was very useful for this purpose. (Table II) It appears as if the iodine-containing substance suffers thermal decomposition during zone refining to give compounds that are more easily removed through these processes. However, too high a temperature caused considerable decomposition of sexiphenyl itself, especially when the purity was low. Since the thermal decomposition of sexiphenyl becomes marked over 480°C, the zone refining was best effected at a maximum temperature between 440 and 450°C.

After a vacuum sublimation and a recrystallization from tetralin, the crystalline product gave the correct carbon and hydrogen content. Nevertheless the melting point rose with repeated zone refining and vacuum sublimation, until it reached a constant value after four times' repetition of the cycle, a recrystallization from tetralin and a vacuum sublimation. The final product becomes a translucent fluid at 428~429°C; it appears to be present in a liquid crystalline state until the translucent phase becomes transparent sharply at 543°C. Further purification brought about no change in these constants. Formation of a nematic or a smectic state is quite probable for such a long molecule. The melting point seems to be very sensitive toward impurity and the low values (465°C[3] and 475°C[2]) given by former authors appear to be due to insufficient purity.

TABLE II. IODINE CONTENT OF SEXIPHENYL PURIFIED BY ZONE REFINING AND VACUUM SUBLIMATION

| Repetition of the cycle | Location of sample piece (cm. from the bottom) | I content (p.p.m.) |
|---|---|---|
| 2 | 0 | 6.5 |
| | 2 | 3.0 |
| | 4 | 1.6 |
| | 6 | 5.2 |
| | 7.5 (top) | 2.0 |
| | residue on sublimation | 2.5 |
| 4 | 0 | <0.15 |
| | 2 | <0.08 |
| | 4 | <0.3 |
| | 6 | <0.05 |
| | 7 (top) | <0.06 |
| 5 | after recrystaln. and sublimation (final product) | <0.04 |

The quantity decreased to one sixth of that of the crude compound through the purification process, but the purity was so high that no impurity element was detected by chemical and neutron activation analysis. The low iodine content (less than 0.04 p.p.m.) compares with that of silicon for semi-conductor, which is regarded as one of the purest substance available. The final product is evaporated onto the window of a photomultiplier tube in vacuo and used as wavelength shifter. It is also converted into a large single crystal (10×5×2 mm.) and used as scintillator for alpha- and beta-rays. The photomultiplier pulse obtained with this scintillator is higher than that with quaterphenyl or anthracene, which has been regarded the best organic scintillator. The result will be reported elsewhere together with the optical properties of sexiphenyl.

## Experimental

**Preparation of Sexiphenyl.** — *Mono-nitration of p-Terphenyl.*—Chemically pure *p*-terphenyl (I) (m. p.

5) H. France, I. M. Heilbron and D. H. Hey, *J. Chem. Soc.*, **1938**, 1364.
6) C. F. A. Allen and D. M. J. Burness, *J. Org. Chem.*, **14**, 177 (1949).

205~210°C, 500 g.) was dissolved in a boiling mixture of glacial acetic acid (18 l.) and acetic anhydride (2 l.) containing 6 N sulfuric acid (1 ml.). The solution was cooled to 105°C and treated with small portions of nitric acid (*d*, 1.42; total 200 ml.) with good stirring, the temperature being kept below 110°C. When the evolution of brown gas ceased, the solution was heated to boiling and then cooled to give small pale yellow needles of 4-nitroterphenyl (II), which were recrystallized from isoamyl acetate. M. p. 213°C, yield 290 g., corresponding to 60% of I.

Found: C, 78.46; H, 4.71; N, 5.02. Calcd. for $C_{18}H_{13}O_2N$: C, 78.53; H, 4.76; N, 5.01%.

The mother liquor was evaporated to remove most of the acetic acid and acetic anhydride, the orange residue dissolved in a mixture of benzene and petroleum benzine and submitted to column chromatography by the use of activated alumina (10 g.). Only a small amount of dark resinous substance remained on the column and further chromatographic separation of the effluent afforded two sorts of crystalline compound.

1) Colorless small plates melting at 129~130°C gave 4, 2', 4'-trinitroterphenyl and thus was identified as 2'-nitroterphenyl. Yield ca. 20%.

Found: N, 5.03, 5.15. Calcd. for $C_{18}H_{13}O_2N$: N, 5.01%.

2) Clear yellow plates melting at 126~127°C were identified as 2-nitroterphenyl. The corresponding amine, and acetylated amine gave the same melting points with those in the literature. Yield, 15 to 20%.

Found: N, 5.00, 5.12. Calcd. for $C_{18}H_{13}O_2N$: N, 5.01%.

*Reduction of 4-Nitroterphenyl.*—II (250 g.) in hot isoamyl acetate (8 l.) was gradually added to a warm mixture of ethanol (8 l.) and 11 N hydrochloric acid (2 l.) containing stannous chloride (dihydrate, 2 kg.) with a good stirring. The mixture was boiled for 30 min.; the almost colorless 4-aminoterphenyl hydrochloride (III) was filtered off, washed with ethanol, suspended in 0.1 N hydrochloric acid. boiled to remove ethanol and filtered off. The reduction was almost quantitative.

*Diazotization and the Sandmeyer Decomposition.*—To a freshly prepared suspension of III in water (20 l.) containing 11 N hydrochloric acid (250 ml.) and zinc chloride (dihydrate 50 g.), was dripped sodium nitrite (80 g.) in water (1 l.) with good stirring. This was continued for 3 hr. after the addition of nitrite, the temperature being kept at 10°C. No apparent change was observed. The excess of nitrite having been decomposed with urea, the suspension was treated with potassium iodide (200 g.) solution and heated to nearly boiling. When the suspension became colorless and the evolution of nitrogen ceased, the precipitate was filtered off, washed with sodium sulfite solution and dried. Powder of crude 4-iodoterphenyl (IV) was dissolved in hot xylene filtered and shaken first with hot 6 N sodium hydroxide solution and then with hot 6 N sulfuric acid containing stannous chloride and filtered. The filtrate was evaporated to remove most of the xylene and treated with ethanol to give pure IV, which was further distilled in vacuo (240°C, $10^{-2}$ mmHg) and recrystallized from isoamyl acetate. Yield, 40% based on II, m.p. 247~248°C.

Found: C, 60.74, 60.60; H, 3.67, 3.62; I, 35.64, 35.60. Calcd. for $C_{18}H_{13}I$: C, 60.69; H, 3.68; I, 35.63%.

*The Ullmann Condensation.*—In a small test tube, the powder of IV was mixed with copper (1 to 4 by weight), freshly prepared from copper sulfate and zinc dust and dried in vacuo, and placed in a potassium hydrogen sulfate bath at 280°C for 15 min. The reaction mixture was extracted with xylene and the residue sublimed in vacuo (400°C, $10^{-3}$ mmHg) to give crude sexiphenyl (V). The yield of this crude product was 0.25 g. from 1 g. of IV, corresponding to 10% based on I.

**Purification of Sexiphenyl.**—The crude V (12 g.) was boiled in potassium cyanide solution (10%, 500 ml.) for 30 min., sublimed in vacuo and further purified by recrystallization or by zone refining.

*Recrystallization.*—Since V is very sparingly soluble in organic solvents, only those with high boiling points are useful. Tetralin and dibutyl phthalate were passed through a column (diameter, 25 mm.; length, 600 mm.) of activated alumina, distilled in vacuo and used for recrystallization in a nitrogen atmosphere. Sublimed V (0.1 g.) was dissolved in boiling tetralin (1 l.), filtered, and the filtrate gradually cooled to give fluorescent platelets, which were filtered off, washed with ethanol, and dried. The product melted to a translucent fluid at 420°C.

Found: C, 94.04, 93.96; H, 5.75, 5.74. Calcd. for $C_{36}H_{26}$: C, 94.29; H, 5.71%.

*Zone Refining.*—A Bridgemann type furnace (diameter, 35 mm.) was set up to give a narrow region (ca. 2 cm.) of the maximum temperature (450°C) and have a suitable temperature gradient. A Telex tube containing V in vacuo ($10^{-4}$ mmHg) was caused to move downward at a rate of 3 cm. per hr. in the furnace. After this process a pale yellow mass with many dark brown stripes was obtained with a brown segregate on the top. The solid was taken out of the tube, the separable colored part removed and the yellowish mass was sublimed in vacuo. Almost colorless V came out, preceded by a small amount of yellowish substance, and a small amount of dark yellow residue remained. The sublimate consisted of almost pure V.

Since organic iodine compounds quench the fluorescence of organic scintillators to a marked extent[7], the removal of iodine was studied by repeated zone refining and vacuum sublimation. The sublimed V was submitted to zone refining and the iodine content of the solid determined by neutron activation analysis at various locations. The solid was then sublimed in vacuo and a similar cycle repeated. The results are summarized in Table II. It is seen that the difference in iodine content at varying locations in one lot is not marked but there appears to be an overall trend toward a lower iodine content with repetition of the cycle.

**Examination of the Purity of Sexiphenyl.**—The purity of V was examined by the usual chemical analysis and the neutron activation analysis.

*Neutron Activation Analysis.*—This is suitable for the determination of more than 0.005 $\mu$g. of iodine.

7) W. H. Helhuish and W. S. Metcalf, *J. Chem. Soc.*, 1958, 480.

The sample (10 mg.) was sealed in a polyethylene envelope and irradiated with thermal neutrons in a water-boiler type reactor for 1 hr. under a neutron flux $6\times10^{11}$ neutrons per $cm^2$ per sec., together with a standard potassium iodide. The irradiated sample was swiftly taken out of the reactor and the counting rate due to iodine-128 (half life, 25 min.) was determined with a G. M. counter. A known portion of the standard was converted into silver iodide together with a known amount of carrier iodine and the counting rate similarly measured under the same condition. The radioisotope was identified by the measurement of the half life; carbon, hydrogen, oxygen and nitrogen give no appreciable amount of radioisotope.

A similar method was also useful for the determination of copper (more than 0.02 $\mu$g.) by the use of copper acetate as a standard. The irradiated sample was set aside until radioactive iodine decayed and submitted to scintillation spectrometry for the counting rate due to 0.51 MeV annihilation peak of copper-64 (half life, 12.8 hr.) to be measured. No appreciable amount of copper was found in sublimed V.

*Measurement of the Melting Point.*—This involved some experimental difficulty, because V melts at a very high temperature and sublimes to a significant extent at more than 350°C. The sample was sealed in a glass capillary in vacuo and placed in a quartz tube together with an Almel-Chromel thermocouple. The tube was heated from outside with nichrom wire and the temperature was read on a calibrated millivoltmeter. A fused sodium nitrate bath was also useful for the same purpose.

**Summary**

1) Mononitration of *p*-terphenyl is satisfactorily effected at 100 to 110°C in glacial acetic acid containing about 10% acetic anhydride and a trace of sulfuric acid, and 4-nitro- (ca. 60%), 2'-nitro- (20 to 25%) and 2-nitroterphenyl (15 to 20%) are obtained.

2) Sexiphenyl is formed in a fairly good yield (more than 40%) by the Ullmann condensation of 4-iodoterphenyl and copper.

3) Sexiphenyl is satisfactorily purified by repeated zone refining and vacuum sublimation. The final product melts at 428~429°C to form an apparent liquid crystalline state and becomes tranparent at 543°C (475°C in literature). It contains an appreciable amount of neither iodine nor copper and can be converted into a fairly large single crystal to be used as scintillator.

A part of the expenses was defrayed by a grant from the Ministry of Education, to which the authors' thanks are due.

*Institute for Nuclear Study*
*The University of Tokyo*
*Tanashi, Tokyo*
*(M. T. and K. S.)*

*The Electrical Communication Laboratory, Musashino, Tokyo*
*(T. N.)*

# *On the Reactivity of 4-Hydroxycyclohexyl p-Tosylates*

By Nobuo MORI

(Received March 3, 1960)

The effect of a conformation on the reactivity in cyclohexane systems is very important*, and especially the difference in reactivity between *cis*- and *trans*-cyclohexane compounds serves generally for the study on their configurations.

The present paper describes the unexpected result that *trans*-4-hydroxy or -4-acetoxycyclohexyl *p*-tosylate was solvolyzed more rapidly than the corresponding cis isomer.

## Results and Discussion

The solvolysis rates of 4-hydroxycyclohexyl *p*-tosylates were measured at 99.8°C in ethanol (98.5% by weight), and that of 4-acetoxycyclohexyl *p*-tosylates measured in acetic acid containing a slight excess of acetic anhydride. In all cases, except alkaline ethanolysis, the observed rates were of the first order and the error of the measurements was always lower than 3%. Since the mean rate constants of the acetolysis of the *cis*- and *trans*-4-acetoxylcyclohexyl *p*-tosylates were not substantially affected by addition of a small quantity of anhydrous sodium acetate, the acetolysis is probably of the unimolecular type. On the other hand, a calculated first order rate constant decreased gradually during the solvolysis of the isomeric hydroxycyclohexyl *p*-tosylates in ethanol containing sodium ethoxide in 0.02 mol./l., in agreement with the behavior of 3-methyl

* The importance was first pointed out by D. H. R. Barton (*Experientia*, **6**, 316 (1950)).

cyclohexyl *p*-tosylate described previously[1], and the mean rate constants were about 3 times of that in neutral ethanol. This fact suggests that a part of the alkaline ethanolysis consists of a bimolecular reaction based on the back-side attack of the ethoxide ion. Table I lists the data for a run with *cis*-4-acetoxycyclohexyl *p*-tosylate in acetic acid containing sodium acetate in 0.029 mol./l., while a run with *cis*-4-hydroxycyclohexyl *p*-tosylate in ethanol containing sodium ethoxide in 0.02 mol./l. is given in Table II. It is seen that in the former run a first order rate constant is satisfactorily constant and in the latter run a rate constant decreases gradually during the solvolysis.

Table I. Acetolysis of *cis*-4-acetoxycyclohexyl *p*-tosylate in acetic acid containing AcONa in 0.029 mol./l. at 99.8°C

| Time, min. | Tosylate, mol./l. | $k_1\times10^3$, $min^{-1}$ |
|---|---|---|
| 0.0 | 0.0282 | |
| 30 | 0.0250 | 4.07 |
| 60 | 0.0220 | 4.14 |
| 90 | 0.0192 | 4.25 |
| 120 | 0.0173 | 4.03 |
| 150 | 0.0150 | 4.19 |
| 210 | 0.0122 | 4.03 |
| | Mean | 4.12 |

Table II. Ethanolysis of *cis*-4-hydroxycyclohexyl *p*-tosylate in ethanol containing EtONa in 0.02 mol./l. at 99.8°C

| Time, min. | Tosylate, mol./l. | $k_1\times10^2$, $min^{-1}$ |
|---|---|---|
| 0.0 | 0.0180 | |
| 20 | $0.0094_5$ | 3.68 |
| 30 | 0.0072 | 3.24 |
| 40 | 0.0058 | 3.01 |
| 50 | 0.0050 | 2.76 |
| 80 | 0.0031 | 2.30 |
| | Mean | 3.0 |

The rate constants and the relative rates for the isomeric tosylates are summarized in Tables III and IV, respectively.

Table III. Rate constants of solvolysis of 4-substituted cyclohexyl *p*-tosylates at 99.8°C

| 4-Substituent | Tosylate mol./l. | Solvent | Alkali mol./l. | $k_1\times10^2$ $min^{-1}$ |
|---|---|---|---|---|
| *cis*-OH | 0.018 | a | 0.020 c | 3.0 |
| | 0.020 | a | | 0.835 |
| *trans*-OH | 0.018 | a | 0.020 c | 10 |
| | 0.020 | a | | 2.97 |
| *cis*-OAc | 0.0282 | b | 0.0290 d | 0.412 |
| | 0.0284 | b | | 0.400 |
| *trans*-OAc | 0.0283 | b | 0.0292 d | 1.10 |
| | 0.0284 | b | | 1.00 |

a, ethanol; b, acetic acid; c, sodium ethoxide; d, sodium acetate.

Table IV. Relative rates of solvolysis of 4-substituted cyclohexyl *p*-tosylates

| | 4-OH | | 4-OAc | |
|---|---|---|---|---|
| Solvent | a | containing c | a | b containing d b |
| $k_{trans}/k_{cis}$ | 3.3 | 3.5 | 2.6 | 2.5 |

Generally, in solvolysis of rigid cyclohexane systems for example *t*-butylcyclohexyl *p*-tosylate, the compound where the departing group is axial is solvolyzed in ethanol, acetic acid or formic acid at a rate 3~4 times as fast as that of the corresponding isomer where the departing group is equatorial, and also in a mobile substituted cyclohexane system, as that shown in Fig. 1, where that two possible chair conformations are readily interconvertible, for example as 3-methoxycarbonylcyclohexyl *p*-tosylate[3] or 1, 3-di-*p*-toluenesulfoxycyclohexane[1], the solvolysis leads to an essencially similar result.

The possible conformations of 4-substituted cyclohexyl *p*-tosylates are as follows:

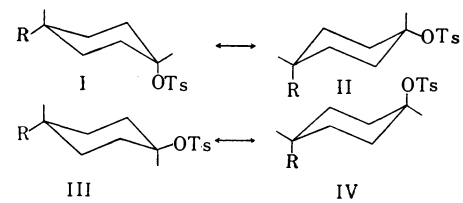



Fig. 1

where R is a substituent and Ts is the tosyl group. The conformation III of the trans form is probably more stable than the conformation IV, while the difference in stability between the conformation I and II of the cis form is probably very small or negligible, when R is not so large a group as *t*-butyl group. Thus, it is expected that the cis form is more reactive than the trans form, as described above.

However, in the present work, the *trans*-4-hydroxycyclohexyl *p*-tosylate was ethanolyzed at a rate 3.5 times as fast as that of the corresponding cis isomer, and also the *trans*-4-acetoxycyclohexyl *p*-tosylate was acetolyzed at a rate 2.5 times as fast as that of the corresponding cis isomer. These facts can not be explained on the basis of the general rule described above.

Further, the configuration of the isomeric cyclohexane-1, 4-diols, which was first established by Bayer[4], is in agreement with the chemical fact that, by direct dehydration of

1) N. Mori, *J. Chem. Soc. Japan, Pure Chem. Sec.* (*Nippon Kagaku Zasshi*), **80**, 1458 (1959).
2) S. Winstein and H. J. Holmess, *J. Am. Chem. Soc.*, **77**, 5562 (1955).
3) D. S. Noyce and H. J. Weingarten, ibid., **79**, 3103 (1957).
4) A. Bayer, *Ann.*, **278**, 92 (1894).

diol over alumina, the yield of 1, 4-epoxycyclohexane from the *trans*-diol was much higher than that from the *cis*-diol[5], and it is probably right.

A further study concerning this problem will be reported shortly.

## Experimental

**Samples*: *cis*- and *trans*-Cyclohexane-1, 4-diol.**—Quinol (25 g.) in methanol (30 cc.) in an autoclave was hydrogenated at 120°C under 80 initial atm. in the presence of Raney nickel (10 g.) for about 3 hr. until no more hydrogen was absorbed. The filtered solution was evaporated under reduced pressure and the residue was acetylated by refluxing with acetic anhydride (70 cc.) for 3 hr. and the crude diacetate crystallized from hot acetone (30 cc.), to give prisms of the *trans*-diacetate which melted at 100.5 ~102°C after one recrystallization from ligroin (b. p. 75~120°C). The yield was 13.5 g. The acetone filtrate was concentrated, diluted with benzene (5 cc.) and then ligroin, and seeded with the *trans*-diacetate in a refrigerator, to give a small amount of this material. The residual solution was concentrated and placed with occasional stirring in a refrigerator for several days until it crystallized, to give the *cis*-diacetate which melted at 34~35°C after recrystallization from a small volume of ligroin. The yield was 12 g.

A solution of the *trans*-diacetate in absolute methanol (30 cc.) treated with a very small piece of metal sodium was refluxed for 30~60 min., concentrated to a small volume under reduced pressure, dissolved in hot dry ether and cooled to 0°C, to give as prisms the *trans*-diol, m. p. 144°C.

The *cis*-diacetate was similarly treated and the residue obtained by concentration of the reaction mixture was crystallized from hot acetone, to give as needles the *cis*-diol, m. p. 110°C.

The *trans*-diol (4.9 g.) in dry pyridine (25 cc.) was treated under stirring and cooling to 0~5°C with *p*-toluenesulfonyl chloride (7.52 g.) in chloroform (25 cc.). After stirring for 3 hr. at room temperature, the mixture was poured into excess of dilute hydrochloric acid cooled with ice, the resulting chloroform solution was washed with dilute hydrochloric acid, water and then a 10% solution of sodium carbonate, dried over sodium sulfate and evaporated under reduced pressure. The residue was dissolved in hot benzene, treated with hot ligroin and cooled to room temperature, to give the *trans*-monotosylate in needles, m. p. 112.5°C after recrystallization from benzene-ligroin.

When the reaction mixture, treated with *p*-toluenesulfonyl chloride as described above, was further treated with one equivalent quantity of acetyl chloride in chloroform, it gave the *trans*-acetoxy cyclohexyl *p*-tosylate in needles, m. p. 81~81.5°C after crystallization from benzene-ligroin.

When the *cis*-diol was similarly treated and recrystallized, the *cis*-hydroxycyclohexyl tosylate (m.p. 94~95°C) and the *cis*-acetoxycyclohexyl tosylate (m. p. 105°C) were obtained.

**Solvents.**—*Ethanol* (98.5% by weight).—Reagent grade absolute ethanol was fractionally distilled.

*Acetic Acid.* — Reagent grade glacial acetic acid was crystallized twice by the freezing method, refluxed with 2% by weight of acetic anhydride and 1% by weight of anhydrous sodium acetate for 3 hr. and distilled.

**Procedure.**—Rates were measured by the usual ampoule technique[7]. Concentrations are given at room temperature and the reaction was followed by the titration at intervals for the sulfonic acid liberated or the base consumed during the solvolysis. Titrations in acetic acid were carried out with a 0.05 N solution of AcONa or *p*-toluenesulfonic acid in acetic acid with bromophenol blue as indicator, and in ethanol a 0.05 N solution of sodium hydroxide or hydrochloric acid in water was used for titration with phenolphthalein as indicator. Rate constants were calculated from the formula

$$k_1 = 1/t \ln a/(a-x)$$

in which $a$ was the initial concentration of tosylate and $x$ was the concentration of sulfonic acid liberated or base consumed at time $t$.

The author expresses his sincere thanks to Professor Y. Tsuzuki for his advice during the investigation.

*Department of Chemistry*
*Tokyo College of Science*
*Shinjuku-ku, Tokyo*

5) R. C. Olberg, H. Pines and U. N. Ipatieff, *J. Am. Chem. Soc.*, **66**, 1096 (1944).

* All samples were prepared by the methods described in Ref. 6 with some modifications.

6) L. N. Owen and P. A. Robins, *J. Chem. Soc.*, **1959** 320.

7) N. Mori, This Bulletin, **33**, 1144 (1960).

# *Ultraviolet Absorption Spectra of Substituted Phenylureas. Part II*[1]. *Solvent Effect and Structure of Carbamide Group*

By Yojiro TSUZUKI, Shinichi MOTOKI and Ritsuko TANESE

(Received April 11, 1960)

In the previous paper dealing with the ultraviolet absorption spectra of substituted phenylureas it was suggested that the carbamide group $-NHCONH_2$ behaves electronically as a peculiar substituent[1].

With disubstituted benzenes in general Doub and Vandenbelt found some semiquantitative relationships[2], which exist between the absorption displacement $\Delta\lambda$ and the electronic properties of the two substituents. Applying these empirical rules to the previous results, it has now been confirmed that the substituent $-NHCONH_2$ behaves as an electron-attracting or releasing group according as the other substituent is electron-releasing or attracting. During the course of an investigation of the unusual property of this group, attention has been drawn to the data given by Schroeder[3] of the spectra of ethyl phenylureas.

As is shown in Table I, *N*-ethyl phenylureas show markedly decreased intensity of absorption, whereas *N'*-ethyl derivatives exhibit strong

TABLE I. ULTRAVIOLET ABSORPTION SPECTRA OF ETHYL PHENYLUREAS (IN ETHANOL)

| | $\lambda_{1\,max}$ | $\varepsilon_{1\,max}$ | $\lambda_{2\,max}$ | $\varepsilon_{2\,max}$ |
|---|---|---|---|---|
| $C_6H_5NHCON'H_2$ | 237 | 17,700 | 268～275 | 1,100 |
| $C_6H_5NC_2H_5CON'H_2$ | 235～237 | 3,480 | no absorption | |
| $C_6H_5NC_2H_5CON'HC_2H_5$ | 243 | 3,630 | no absorption | |
| $C_6H_5NHCON'HC_2H_5$ | 240～241 | 19,800 | 275～277 | 1,000 |
| $C_6H_5NHCON'(C_2H_5)_2$ | 239～241 | 18,300 | 270～273 | 1,100 |

TABLE II. ABSORPTION SPECTRA OF PARA-SUBSTITUTED PHENYLUREAS IN AQUEOUS, ALCOHOLIC AND ETHEREAL SOLUTION

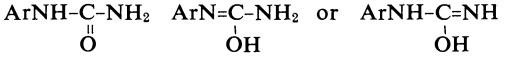
| Compounds | Absorption bands | Solvent | | |
|---|---|---|---|---|
| | | Water | Ethanol | Ether |
| $C_6H_5NHCONH_2$ | $\lambda_1$ | 234 | 287 | 237.5 |
| | $\varepsilon_1$ | 6,420 | 18,800 | 19,000 |
| | $\lambda_2$ | no absorption | 274 | 275 |
| | $\varepsilon_2$ | 〃 | 1,200 | 1,160 |
| *p*-$C_2H_5OC_6H_4NHCONH_2$ | $\lambda_1$ | 236.5 | 242 | 243.5 |
| | $\varepsilon_1$ | 12,800 | 18,200 | 19,300 |
| | $\lambda_2$ | 280 | 290 | 293.5 |
| | $\varepsilon_2$ | 1,860 | 1,980 | 2,180 |
| *p*-$CH_3C_6H_4NHCONH_2$ | $\lambda_1$ | 236 | 240 | 241.5 |
| | $\varepsilon_1$ | 12,400 | 18,400 | 20,100 |
| | $\lambda_2$ | 272～276 | 281 | 281 |
| | $\varepsilon_2$ | 650 | 1,090 | 1,290 |
| *p*-$NO_2C_6H_4NHCONH_2$ | $\lambda_1$ | 325～329 | 322 | 321.5 |
| | $\varepsilon_1$ | 10,700 | 13,200 | 14,500 |
| | $\lambda_2$ | no absorpt. | no absorpt. | no absorpt. |
| | $\varepsilon_2$ | 〃 | 〃 | 〃 |
| *p*-$CH_3OC_6H_4NHCONH_2$ | $\lambda_1$ | 235 | 237 | 242 |
| | $\varepsilon_1$ | 12,900 | 17,700 | 18,200 |
| | $\lambda_2$ | 279 | 284.5 | 293.5 |
| | $\varepsilon_2$ | 1,990 | 1,870 | 2,700 |

1) Part I. Y. Tsuzuki, S. Motoki and K. Migita, This Bulletin, **32**, 1189 (1959).

2) L. Doub and J. M. Vandenbelt, *J. Am. Chem. Soc.*, **69**, 2714 (1947).

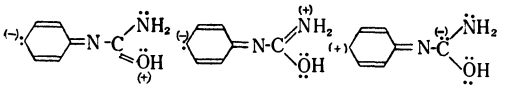
3) W. A. Schroeder, *Anal. Chem.*, **23**, 1740 (1951).

absorption, as is observable in phenylurea itself. Since this effect of the alkyl group is likely to be observed in general when prototropy is set up in the systems[4], the following tautomerism (I, II, and III form) may be possible, and hence aryl ureas may, at least partly, be present in the pseudo form II. This form is impossible for *N*-alkyl phenylureas, which exhibit less intense absorptions.



(I) (II) (III)

The electronically amphoteric property of the carbamide group is thus clearly shown with the following resonance structures of the isomer.



(IV) (V) (VI)

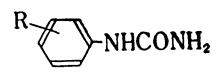
The presence of an acidic, enolizable hydrogen atom in the carbamide group is also supported by the fact that phenylureas are more soluble in aqueous alkalis than in water. From these considerations it becomes a theme of some interest to study the solvent effect on the spectra of these compounds for the purpose of getting further information on the nature of the group. In the present study were used some solvents of different polarity, such as water, ethanol and ethyl ether.

## Results and Discussions

The experimental results are given in Tables II and III. It is clearly seen that the absorption intensity of the compounds increases markedly, as the polarity of the solvent decreases.

Now the remarkable solvent effect seen in Tables II and III should be considered. With common substances the extinction coefficient is, however, only slightly (5~7%) affected by the solvent, whereas the above cases are entirely different, namely $\varepsilon_1$ and $\varepsilon_2$ radically change on the whole according to the solvent. These remarkable solvent effects are occasionally observed by dissolving substances in such solvents as bring about some very mild chemical changes, as complex formation or displacement of tautomeric equilibrium[5]. Thus the data of the absorption spectrum are reasonably interpreted by assuming that in less polar solvents the equilibrium of tautomerism of aryl ureas moves towards the acidic pseudo form II which absorbs more intensely than the normal form I.

Table III. Absorption spectra in solution of ethoxyl and methoxyl phenylureas



| Absorption | Solvent: Water | Ethanol | Ether |
|---|---|---|---|
| (a) R=*p*-$C_2H_5O$ | | | |
| $\lambda_1$ | 236.5 | 242 | 243.5 |
| $\varepsilon_1$ | 12,800 | 18,200 | 19,300 |
| $\lambda_2$ | 279 | 290 | 293.5 |
| $\varepsilon_2$ | 1,860 | 1,980 | 2,180 |
| (b) R=*m*-$C_2H_5O$ | | | |
| $\lambda_1$ | 238 | 240.5 | 242 |
| $\varepsilon_1$ | 10,400 | 13,500 | 14,800 |
| $\lambda_2$ | 278 | 280 | 280 |
| $\varepsilon_2$ | 2,360 | 2,550 | 3,000 |
| (c) R=*o*-$C_2H_5O$ | | | |
| $\lambda_1$ | 236 | 241 | 242 |
| $\varepsilon_1$ | 8,820 | 15,400 | 16,300 |
| $\lambda_2$ | 278 | 281 | 281 |
| $\varepsilon_2$ | 2,860 | 3,830 | 3,600 |
| (d) R=*p*-$CH_3O$ | | | |
| $\lambda_1$ | 235 | 237 | 242 |
| $\varepsilon_1$ | 12,900 | 17,700 | 18,200 |
| $\lambda_2$ | 279 | 284.5 | 293.5 |
| $\varepsilon_2$ | 1,990 | 1,870 | 2,700 |
| (e) R=*m*-$CH_3O$ | | | |
| $\lambda_1$ | 238 | 236 | 241.5 |
| $\varepsilon_1$ | 11,600 | 13,700 | 16,500 |
| $\lambda_2$ | 277.5 | 275 | 280 |
| $\varepsilon_2$ | 3,280 | 2,570 | 2,800 |
| (f) R=*o*-$CH_3O$ | | | |
| $\lambda_1$ | 237 | 236 | 241.5 |
| $\varepsilon_1$ | 8,810 | 15,500 | 16,500 |
| $\lambda_2$ | 277.5 | 275.5 | 281 |
| $\varepsilon_2$ | 3,210 | 4,050 | 3,900 |

Another outstanding feature noticeable in Tables II and III is the blue shift of the absorption bands which shift further as the polarity of the solvent increases, however, with a few exceptions of *p*-nitro-, *m*-methoxy- and *o*-methoxy-phenylureas. This feature is peculiar, for increasing polarity of the solvent usually causes on the contrary a red shift of the absorption band[6].

To see clearly the effect of orientation (*o*, *m* and *p*-RO) on the red shift in ethoxy- and methoxy-phenylureas, the data in Table III were analyzed and the results are shown in Table IV.

4) See A. E. Gillam and E. S. Stern, " Introduction to Electronic Absorption Spectroscopy in Organic Chemistry", 2nd Ed., Edward Arnold Publishers, London (1957), p. 259.

5) A. E. Gillam and E. S. Stern, loc. cit., pp. 301—2. Cf. L. N. Ferguson, *Chem. Revs.*, **43**, 394 (1948).

6) A. E. Gillam and E. S. Stern, loc. cit., p. 303.

TABLE IV. ORIENTATION EFFECT ON BATHOCHROMIC SHIFT IN ETHOXYL AND METHOXYL PHENYLUREAS (ANALYSIS OF THE ABSORPTION DATA IN TABLE III)

| Solvent | Compound | Relation | |
|---|---|---|---|
| | | K-band | B-band |
| Ether | $C_2H_5OC_6H_4NHCONH_2$ | $p>o=m$ | $p\gg o>m$ |
| Ether | $CH_3OC_6H_4NHCONH_2$ | $p>o=m$ | $p\gg o>m$ |
| Ethanol | $C_2H_5OC_6H_4NHCONH_2$ | $p>o>m$ | $p\gg o>m$ |
| Ethanol | $CH_3OC_6H_4NHCONH_2$ | $p>o=m$ | $p\gg o>m$ |
| Water | $C_2H_5OC_6H_4NHCONH_2$ | $m>p>o$ | $p>o=m$ |
| Water | $CH_3OC_6H_4NHCONH_2$ | $m>o>p$ | $p>o=m$ |

From Tables III and IV is noticed a third interesting phenomenon, namely, for B-band the absorption maximum of the alkoxy-phenylureas is in the order $p\gg o>m$ in both ethanol and ether, while in aqueous solution the three nuclear isomers absorb nearly the same wave length region; for the K-band, *m*-compounds absorb in aqueous solution the region of the longest wavelength ($m>p=o$), although the former relation $p>o>m$ nearly holds in ethanolic and ethereal solution.

These somewhat peculiar relations may be interpreted, at least partly, by the idea that in aqueous solution the carbamide group mainly takes the urea form, so that it loses the electron-attracting property as the result of the absence of resonance with the alkoxyl group, but in non-aqueous solutions the carbamide group assumes a greater part of the pseudo form, making the resonance possible with the alkoxyl group.

Thus the pseudo form of phenylureas is assumed and may be confirmed from various angles. For this purpose it is desirable to synthesize some of the pseudo derivatives, and to make a special study of the spectrum[7]. The result of this study will be reported in the next paper.

## Experimental

**Preparation of Compounds.**—Substituted phenylureas were prepared from potassium cyanate and the corresponding nuclear substituted anilines by the methods described in "Organic Syntheses"[8], *o*-Methoxyl phenylurea, m. p. 146.5°C, *m*-isomer, m. p. 130°C, *p*-isomer, m. p. 164~5°C. The solvents were purified by distillation. Ethanol was tested to be free from benzene.

**Absorption Spectra.**—The absorption spectra were measured in the region of 200~350 mμ by means of a Beckmann Model DU Quartz spectrophotometer with the solutions of concentration about 1/10,000 M.

*Tokyo College of Science*
*Kagurazaka, Shinjuku-ku, Tokyo*

7) See A. E. Gillam and E. S. Stern, loc. cit., p. 257.
8) F. Kurzer, "Organic Syntheses", Vol. 31, John Wiley & Sons, Inc. New York (1951), p. 8.

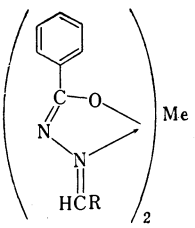
# *Über die Kupfer(II)- und Nickel(II)-komplexsalze der Benzoylhydrazone einiger aliphatischen Carbonylverbindungen**

Von Hiroshi OHTA

(Eingegangen am 18. Februar, 1960)

Als Carbonylreagens bildet das Benzoylhydrazin mit den Aldehyden Benzoylhydrazone. Die Benzoylhydrazone der aromatischen Aldehyde sind in den organischen Lösungsmitteln ziemlich schwer löslich, diejenigen der aliphatischen Reihe sind aber spielend löslich. Im vorliegenden Experiment ist gezeigt worden, daß die ersteren mit zweiwertigem Kupfer- oder Nickel-Ion keine charakterisierbaren Komplexsalze geben, während die letzteren gut gebildete Komplexsalze liefern.

Zuerst sollen die Kupfer(II)- und Nickel-(II)-komplexsalze einiger aliphatischen Monoaldehyde beschrieben werden. Als Aldehydkomponente wurden Acetaldehyd (Äthanal), *n*-Butyraldehyd (*n*-Butanal), *n*-Önanthaldehyd



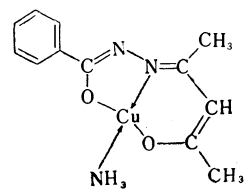

I

Me=Cu oder Ni.
R=1) $CH_3$, 2) $(CH_2)_2CH_3$, 3) $(CH_2)_5CH_3$, 4) $(CH_2)_8CH_3$.

* Organische Metallkomplexsalze IV. III. Mitteilung: H. Ohta, Dieses Bull., 33, 202 (1960).

(*n*-Heptanal) und *n*-Caprinaldehyd (*n*-Dekanal) ausgewählt. Die komplexsalze wurden aus dem Benzoylhydrazin, den Aldehyden und den Metallacetaten in Äthanol leicht dargestellt und in schönen Kristallen erhalten. Die Kupfersalze sind rötlich violett, die Nickelsalze gelbrot. Sie würden mit der Formel I formuliert werden können. Alle diese Komplexsalze, besonders diejenigen des *n*-Heptanal-benzoylhydrazons und des *n*-Dekanal-benzoylhydrozons sind in den meisten organischen Lösungsmitteln leicht löslich und die letzteren zwei zeigen ziemlich niedrige Schmelzpunkte kraft der längeren aliphatischen Ketten[1].

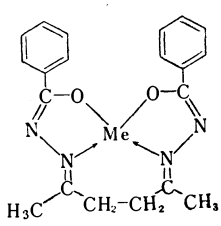
Dann werden die Kupfer(II)- und Nickel-(II)-komplexsalze der Benzoylhydrazone von den aliphatischen 1, 3- und 1, 4-Diketonen, dem Acetylaceton (2, 4-Pentandion) und dem Acetonylaceton (2, 5-Hexandion) beschrieben. Aus Benzoylhydrazin, 2, 4-Pentandion und Kupferacetat in alkoholischem Ammoniak wurde nur 2, 4-Pentandion-monobenzoylhydrazono-monoammin-kupfer(II) (Formel II), nicht 2, 4-Pentandion-dibenzoylhydrazono-kupfer(II) noch 1-Benzoyl-3, 5-dimethyl-pyrazol erhalten. Das entsprechende Nickelkomplexsalz konnte nicht erhalten werden, weil es so sehr leicht löslich war.



II

Die Komplexsalze vom 2, 3-Butandion-dibenzoylhydrazon waren schon von Sacconi[2] berichtet worden. Es ist klar, daß sie beständig sind, weil sie durch den Chelat- und Resonanzeffekt stabilisiert sind.

Um zu entscheiden, welche Komplexsalze das 2, 5-Hexandion-dibenzoylhydrazon gibt, welches zwei mehr Methylen-Gruppen enthält als 2, 3-Butandion-dibenzoylhydrazon, wurde die Synthese seiner Kupfer(II)- und Nickel(II)-komplexsalze versucht. Ein schwärzlich-braunes Kupfersalz und ein rotes Nickelsalz wurden erhalten, die nach den analytischen Daten mit der Formel III formuliert werden können, denn sie sind kristallinisch erhalten und in den organischen Lösungsmitteln leicht löslich.



III

Me=Cu oder Ni

Nach den Farben dieser Komplexsalze (Kupfersalze: rötlich-violett bzw. schwärzlich-braun, Nickelsalze: gelbrot bzw. rot) besitzen sie alle wohl quadratische, ebene Konfiguration. Die Struktur der Nickelkomplexsalze konnte sich aus der magnetischen Suszeptibilität erschließen**. Nach den magnetischen Messungen sind beide Bis-(Äthanal-benzoylhydrazono)-nickel(II) und 2, 5-Hexandion-dibenzoylhydrazono-nickel(II) diamagnetisch, was auf planen Bau hindeutet***.

## Beschreibung der Versuche

Die magnetischen Messungen wurden mit der Gouyschen Waage ausgeführt.

*Bis-(Äthanal-benzoylhydrazono)-kupfer(II).* — Man gibt zur Lösung von 324 mg Äthanal-benzoylhydrazon[3] in 10 ccm Äthanol, 200 mg Kupferacetat (Monohydrat) in 5 ccm Wasser. Die Farbe der Lösung verändert sich zu Dunkelgrün und ein Niederschlag entsteht. Erwärmt man das Gemisch auf dem Wasserbade, so verwandelt sich der Niederschlag nach und nach in hell rötlich-violette Nadeln, die man aus 1, 4-Dioxan umkristallisiert. Hell rötlich-violette Nadeln.

Gef.: C, 56.08; H, 4.72; N, 14.57; Cu, 16.42. Ber. für $C_{18}H_{18}O_2N_4Cu$: C, 56.02; H, 4.70; N, 14.52; Cu, 16.46.

*Bis-(Äthanal-benzoylhydrazono)-nickel(II).* — Man gibt zur Lösung von 342 mg Äthanal-benzoylhydrazon in 10 ccm Äthanol, 250 mg Nickelacetat (Tetrahydrat) gelöst in 5 ccm Wasser. Es entsteht eine klare, dunkelblaue lösung, die sich durch kurzes Erwärmen auf dem Wasserbade in eine bräunlich-grüne verwandelt, aus der sich rötlich-gelbe Nadeln ausscheiden. Man kristallisiert sie aus dem Gemische von 1, 4-Dioxan und Äthylenglykol-monoäthyläther um. Rötlich-gelbe Nadeln.

Gef.: C, 56.70; H, 4.84; N, 14.70; Ni, 15.23. Ber. für $C_{18}H_{18}O_2N_4Ni$: C, 56.73; H, 4.76; N, 14.70; Ni, 15.41.

*Bis-(n-Butanal-benzoylhydrazono)-kupfer(II).* — Man gibt zur Lösung von 272 mg Benzoylhydrazin in 10 ccm Äthanol, 200 mg Kupferacetat (Monohydrat) in 5 ccm Wasser und darauf 144 mg *n*-Butanal. Es

1) Bezüglich der anderen Beispiele, siehe, T. Tsumaki und Mitarbb., *J. Chem. Soc. Japan Pure Chem. Sec.* (*Nippon Kagaku Zasshi*), **78**, 1086 (1957).

2) L. Sacconi, *Z. anorg. u. allgem. Chem.*, **275**, 249 (1954). *Chem. Abstr.*, **48**, 8105$^g$ (1954).

** Verschieden von der Konfiguration der Nickelkomplexsalze, kann diejenige der Kupferkomplexsalze allein nur aus der magnetischen Suszeptibilität nicht eindeutig entschieden werden, weil die Kupfer(II)komplexe unabhängig von allen, möglichen Konfigurationen immer ein ungepaartes Elektron besitzen.

*** Die Beispiele sind sehr viel; s. z. B., A. E. Martell & M. Calvin, „Chemistry of the Metal Chelate Compounds", Prentice-Hall, Inc., New York (1952), S. 279, 283.

3) R. Stollé und E. Münch, *J. prakt. Chem.*, [2] **70**, 400 (1904).

entsteht sofort unter Selbsterwärmung eine dunkelblaue Lösung, die sich nach einigen Minuten trübt. Erwärmt man die Lösung auf dem Wasserbade, so verschwindet die Trübung und eine dunkel grünlichblaue Lösung entsteht, aus der nach dem Erkalten (wenn nötig, durch Reiben der Gefäßwand mit dem Glasstab) graülich rotviolette Kristalle auskristallisieren, die man aus Äthanol umkristallisiert. Rötlich-violette Nadeln, die bei 173~174°C (unkorr.) unter Zersetzung schmelzen. Ziemlich löslich in warmem Äthanol.

Gef.: C, 59.71; H, 5.97; N, 12.54; Cu, 14.20. Ber. für $C_{22}H_{26}O_2N_4Cu$: C, 59.78; H, 5.93; N, 12.68; Cu, 14.37.

*Bis-(n-Butanal-benzoylhydrazono)-nickel(II).* — Man fügt zur Lösung von 272 mg Benzoylhydrazin in 10 ccm Äthanol, 250 mg Nickelacetat (Tetrahydrat) in 5 ccm Wasser und darauf 144 mg *n*-Butanal zu. Es entsteht sofort eine dunkelblaue Lösung, die sich durch Erwärmen auf dem Wasserbade in eine bräunlich-grüne verwandelt, aus der sich rötlich-gelbe Nadeln ausscheiden, welche man aus dem Gemische von 1,4-Dioxan und Äthylenglykol-monoäthyläther umkristallisiert. Rötlich-gelbe Nadeln, die bei 207~208°C (unkorr.) unter Zersetzung schmelzen.

Gef.: C, 60.65; H, 5.91; N, 12.98; Ni, 13.11. Ber. für $C_{22}H_{26}O_2N_4Ni$: C, 60.44; H, 5.99; N, 12.82; Ni, 13.43.

*Bis-(n-Heptanal-benzoylhydrazono)-kupfer(II).* — Man gibt zur Lösung von 272 mg Benzoylhydrazin in 2 ccm Äthanol, 200 mg Kupferacetat (Monohydrat) in 10 ccm Äthanol, und darauf 228 mg *n*-Heptanal. Es entsteht sofort eine schwärzlich-blaue Lösung, die eine kurze Weile auf dem Wasserbade erwärmt wird. Beim Erkalten scheiden sich hell rötlich-violette Kristalle aus (wenn nötig, muß man die Gefäßwand mit dem Glasstab reiben, oder die Lösung etwas konzentrieren), die man aus Äthanol umkristallisiert. Hell rötlich-violette, zarte Nadeln, welche bei 118~119°C (unkorr.) schmelzen. Ziemlich löslich in warmem Äthanol.

Gef.: C, 63.84; H, 7.26; N, 10.71; Cu, 12.44. Ber. für $C_{28}H_{38}O_2N_4Cu$: C, 63.91; H, 7.28; N, 10.65; Cu, 12.07.

*Bis-(n-Heptanal-benzoylhydrazono)-nickel(II).*—Man gibt zur Lösung von 272 mg Benzoylhydrazin in 10 ccm Äthanol, 250 mg Nickelacetat (Tetrahydrat) in 7 ccm Wasser und darauf 228 mg *n*-Heptanal. Es entsteht anfangs eine dunkelblaue, klare Lösung, die sich aber nach einigen Sekunden unter Trübung in eine schmutzig gelbgrüne verwandelt, aus der gelbrote Kristalle auszufallen beginnen. Nach der beinahe vollkommenen Ausscheidung der Kristalle, fügt man noch 3 ccm Wasser hinzu. Die Lösung trübt sich, welche aber durch Umrühren unter Abscheidung von noch einer kleinen Menge Kristalle klar wird. Man kristallisiert das Salz aus Äthylenglykol-monoäthyläther um. Gelbrote Blättchen, die bei 120~121.5°C (unkorr.) schmelzen.

Gef.: C, 64.56; H, 7.48; N, 10.58; Ni, 11.11. Ber. für $C_{28}H_{38}O_2N_4Ni$: C, 64.51; H, 7.35; N, 10.75; Ni, 11.26.

*Bis-(n-Dekanal-benzoylhydrazono)-kupfer(II).*—Man stellt es in derselben Weise wie beim Bis-(*n*-Heptanal-benzoylhydrazono)-kupfer(II) aus 272 mg Benzoylhydrazin in 2 ccm Äthanol, 200 mg Kupferacetat (Monohydrat) in 10 ccm Äthanol und 313 mg *n*-Dekanal dar und kristallisiert aus Äthanol um. Rötlich-violette, zarte Nadeln, die bei 106~107°C (unkorr.) schmelzen. Ziemlich löslich in warmem Äthanol.

Gef.: C, 66.98; H, 8.25; N, 9.24; Cu, 10.35. Ber. für $C_{34}H_{50}O_2N_4Cu$: C, 66.91; H, 8.26; N, 9.18; Cu, 10.41.

*Bis-(n-Dekanal-benzoylhydrazono)-nickel(II).*—Man fügt zur Lösung von 272 mg Benzoylhydrazin in 10 ccm Äthanol, 250 mg Nickelacetat (Tetrahydrat) in 5 ccm Wasser und darauf 313 mg *n*-Dekanal hinzu. Es entsteht sofort eine dunkelblaue, klare Lösung, die sich bald trübt; aus der getrübten Lösung scheiden sich schöne, gelbrote Kristalle aus, welche man aus 1,4-Dioxan umkristallisiert. Rötlich-gelbe Säulchen, die bei 108~109°C (unkorr.) schmelzen.

Gef.: C, 67.33; H, 8.23; N, 9.30; Ni, 9.55. Ber. für $C_{34}H_{50}O_2N_4Ni$: C, 67.44; H, 8.32; N, 9.25; Ni, 9.69.

*2,4-Pentandion-monobenzoylhydrazono-monoammin-kupfer(II).*—Man löst 272 mg Benzoylhydrazin in 200 mg 2,4-Pentandion durch Erwärmen, und darauf fügt man 5 ccm Äthanol zur Lösung zu. Gibt man zu dieser Lösung eine Lösung von 400 mg Kupferacetat (Monohydrat) in 10 ccm wässrigem Ammoniak (ca. 28%), so entsteht sofort eine schwärzlich-grüne, klare Lösung, die man auf dem Wasserbade so lange erwärmt, bis eine kleine Menge Kristalle auf der Oberfläche schwimmt. Beim Erkalten scheiden sich sehr langsam glänzende, schwärzlich-grüne Nadeln aus.

Gef.: C, 48.25; H, 5.19; N, 14.12; Cu, 21.11. Ber. für $C_{12}H_{12}O_2N_2 \cdot NH_3 \cdot Cu$: C, 48.56; H, 5.09; N, 14.16; Cu, 21.41.

*2,5-Hexandion-dibenzoylhydrazono-kupfer(II).* — Man gibt zur Lösung von 272 mg Benzoylhydrazin in 15 ccm Äthanol, 114 mg 2,5-Hxandion und darauf 200 mg Kupferacetat (Monohydrat) in 5 ccm Wasser. Es entsteht sofort eine dunkelgrüne Lösung, aus der sich beim kurzen Erwärmen glänzende, schwärzlich-braune Kristalle ausscheiden. Man kristallisiert sie aus 1,4-Dioxan um. Schwärzlich-braune, glänzende Rauten. Etwas löslich in Dioxan; Lösungsfarbe: dunkelgrün.

Gef.: C, 58.35; H, 4.97; N, 13.67; Cu, 15.41. Ber. für $C_{20}H_{20}O_2N_4Cu$: C, 58.31; H, 4.89; N, 13.60; Cu, 15.42.

*2,5-Hexandion-dibenzoylhydrazono-nickel(II).*—Man gibt zur Lösung von 272 mg Benzoylhydrazin in 20 ccm Äthanol, 114 mg 2,5-Hexandion und darauf 250 mg Nickelacetat (Tetrahydrat) in 5 ccm wässrigem Ammoniak (ca. 28%). Eine hellviolette Lösung entsteht, die sich durch Erwärmen auf dem Wasserbade in eine dunkelgrüne, dann in eine bräunlich-grüne verwandelt. Engt man diese Lösung auf dem Wasserbade stark ein, so scheiden sich rote Kristalle aus, die man aus 1,4-Dioxan umkristallisiert. Rote, glänzende Rauten.

Gef.: C, 59.10; H, 5.07; N, 13.84; Ni, 14.32. Ber. für $C_{20}H_{20}O_2N_4Ni$: C, 59.00; H, 4.95; N, 13.76; Ni, 14.42.

Zum Schluß möchte ich meinem Lehrer, Herrn Prof. Dr. Tokuichi Tsumaki für die Unterstützung und Forderung dieser Arbeit

meinen herzlichen Dank aussprechen. Herrn Professor Dr. Ryohei Matsuura und Herrn Dr. Yasushi Koga (Physikalisch-chemisches Laboratorium) für die magnetischen Messungen danke ich auch herzlichst. Herrn Michio Shido und Frl. Sachiko Indo (Laboratorium der Elementaranalyse, Kyushu Universität) verdanke ich die Durchführung der C-, H- und N-Bestimmungen.

*Chemisches Institut*
*Naturwissenschaftliche Fakultät*
*Kyushu Universität*
*Hakozaki, Fukuoka*

# *Determination of Oxygen in Some Minerals Using Pyrite*

By Iwaji IWASAKI, Takashi KATSURA and Minoru YOSHIDA

(Received February 26, 1960)

A few years ago some experiments on the reactions among various kinds of sulfides, sulfates and oxides which occur in volcanic and hot spring districts were carried out by the present authors to ascertain the relations of their formation and occurrence[1]. The results of the experiments indicated that the amount of oxygen in some minerals can be easily determined with pyrite.

It has been pointed out that pyrite is easily oxidized during the process of grinding in the air and that a remarkable error may be introduced into the result of chemical analysis of pyrite from this oxidation[2]. While no method has yet been found to determine the minute amount of oxygen in pyrite, some reports described oxidation products of pyrite. From those reports, it would be concluded that iron sulfates may be formed by the oxidation[3,4]. In addition to these products, fine powder of pyrite may absorb moisture and oxygen from the air, and it should also be considered that the sample of pyrite may be contaminated with the small amount of oxides or sulfates contained originally in the raw minerals. Thus iron oxides, absorbed oxygen and absorbed water could be the sources of oxygen in pyrite samples, even if the samples, were almost pure under microscopic observation. And it should be pointed out that the oxygen in the samples reacts with the pyrite and is liberated as sulfur dioxide on heating the samples at a high temperature in vacuo. If the liberation of sulfur dioxide is quantitative, the amount of oxygen in the samples can be estimated from that of the sulfur dioxide evolved.

When moisture exists, hydrogen sulfide may also be formed, and the situation may be somewhat complicated because of the equilibrium among hydrogen sulfide, sulfur dioxide and water vapour. The nature of these reactions should be carefully investigated to establish an accurate method for the determination of oxygen in pyrite and other minerals. There are some reports on the reactions between pyrites and iron oxides[5], iron sulfates[6,7] and water[8], but the results are insufficient for the present purpose. In the present paper, the results obtained on these reactions and the method for the determination of a minute amount of oxygen in pyrite and the amount of oxygen in other minerals by using pyrite are given.

## Experimental

**Materials.**—Natural pyrites used in the present study had a chemical composition* nearly equal to the ideal chemical formula, $FeS_2$, and the values obtained for the lattice constant of crystals agreed well with the data described by Parker and Whitehouse[9], and also by Hiemstra[10] (5.416~5.417Å). Iron monosulfide was obtained by thermal decomposition of the pyrites at about 900°C in vacuo. The chemical composition of the artifical

1) I. Iwasaki, T. Katsura and M. Yoshida, read before the 10th Annual Meeting of the Chemical Society of Japan, Tokyo, 1957.
2) E. A. Hontoir, *Bull. Inst. Mining. Met.*, No. 553, 95 (1952).
3) A. Wurm, *Z. prakt. Geol.*, **35**, 130 (1927).
4) G. E. Mapstone, *Chemistry & Industry*, **1954**, 577.
5) F. Martin and O. Fuchs, *Z. anorg. Chem.*, **125**, 307 (1922).
6) Kothny, *Met.*, **8**, 392 (1911) (cited by Gmelin's Handbook).
7) Gorgew, *Compt. rend.*, **104**, 1174 (1887) (cited by Gmelin's Handbook).
8) E. Grünnert, *J. prakt. Chem.*, [2], **122**, 91 (1929).
* The accurate chemical composition of these pyrites will be reported in another paper.
9) H. M. Parker and W. J. Whitehouse, *Phil. Mag.*, **14**, 939 (1932).
10) S. A. Hiemstra, *Am. Mineralogist*, **41**, 519 (1956).

iron monosulfide was somewhat richer in sulfur, and its chemical formula was $FeS_{1.03}$. It was not ferromagnetic and its properties agreed well with those of troilite under microscopic observation. Magnetite was obtained by thermal decomposition of reagent grade $\alpha$-ferric oxide in a quartz tube at about 1200°C and below $1\times10^{-4}$ mmHg of oxygen pressure achieved by pumping it out. The magnetite obtained as above had almost the ideal chemical composition, 49.9% FeO and 50.1% $Fe_2O_3$ in molar ratio. Other chemicals, such as $\alpha$-ferric oxide, ferrous sulfate $FeSO_4\cdot7H_2O$, and ferric sulfate $Fe_2(SO_4)_3\cdot nH_2O$ [78% $Fe_2(SO_4)_3$] employed were all of reagent grade. The reagents were used after removing the water by heating in vacuo.

**Apparatus and Procedure.** — The apparatus employed is shown in Fig. 1. The maximum temperature attained is about 1000°C.

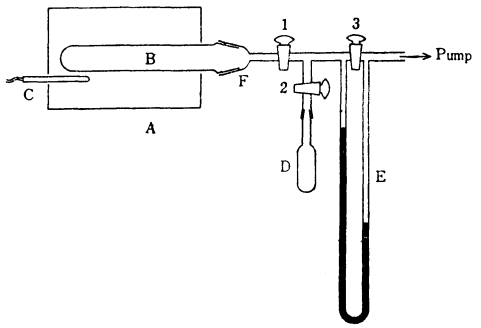



Fig. 1. Apparatus
A. Electric furnace
B. Quartz tube
C. Thermocouple
D. Absorption tube
E. Manometer
1,2,3 Cock

The finely powdered mixture of the sample with the pyrite was packed in a small quartz tube, and then placed at the bottom of a quartz combustion tube B (Fig. 1). Then all of the apparatus was evacuated to a pressure of $10^{-2}\sim10^{-3}$ mmHg. To analyse the gas evolved from the sample, potassium hydroxide was placed in tube D. After evacuation, cocks 2 and 3 were closed, then the temperature was raised at a rate of about 200°C per hr. The pressure of the evolved gas was continuously measured. The correction of the pressure for the temperature change was experimentally determined, and the volume of the evolved gas was calculated in N. T. P. When the reaction came to the end, cock 2 was opened, and the pressure of the unabsorbed gas was determined. This was usually very low in all of the present experiments. Potassium hydroxide which absorbed the acid gas was then dissolved in water and was poured into a suspension of freshly precipitated basic cadmium carbonate. By this procedure hydrogen sulfide is fixed in the precipitate as cadmium sulfide and sulfur dioxide remains in the filtrate as sulfite ions. The amount of hydrogen sulfide from the precipitate and the amount of sulfur dioxide from the filtrate were determined by iodometric titration. As the gas evolved from the reactions of the oxide and the sulfate with the pyrite contained only a negligible amount of hydrogen sulfide, the amount of sulfur dioxide could be determined directly by the manometric method. The nature of the solid products was also examined by chemical, X-ray and microscopic methods.

## Results and Discussion

When the powdered pyrite alone was heated in the apparatus, a dissociated sulfur was deposited inside F the silica tube, and in some cases the evolution of a small amount of a gas which was stable at room temperature was observed. The analysis of the gas showed that it consists mainly of sulfur dioxide, hydrogen sulfide and water vapor, and that its amount is influenced to some extent by the degree of pulverization or other conditions. Therefore, a correction must be made for each kind of pyrite, when the volume of the sulfur dioxide evolved by the reaction between pyrites and iron oxides or iron sulfates is measured. From the repeated blank experiments, the blank values for the pyrite used in the present experiments were obtained as shown in Table I:

TABLE I

| Temp. range | Correction ml. per 1 g. pyrite |
|---|---|
| Below 450°C | Almost negligible |
| 450~550°C | 2.5 |
| 550~650°C | 3.0 |

**(1) The Reaction between Pyrite and Ferric Oxide.**—As will be seen in Fig. 2, the reaction between pyrite and ferric oxide begins at about 500°C and comes to the end at about 600°C. When an excess of pyrite exists, the solid product of the reaction is only troilite, and the reaction may be regarded as follows:

$$7FeS_2+2Fe_2O_3=11FeS+3SO_2 \qquad (1)$$

The amount of sulfur dioxide evolved from

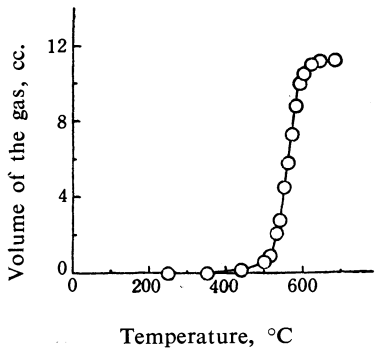



Fig. 2. Reaction between pyrite and $\alpha$-ferric oxide (I).
Pyrite 200 mg.
$Fe_2O_3$ 50 mg.

the mixture of 200 mg. of pyrite and 50 mg. of ferric oxide was 10 ml. (0°C, 1 atm.) in the range 500~600°C, and the value calculated from Eq. 1 is 10.5 ml.

When the amount of pyrite was insufficient to reduce all ferric oxide to troilite, the reaction was likely to proceed through two stages as shown in Fig. 3. The first stage of the reaction would correspond to Eq. 1, and the second to Eq. 2, which shows the reaction between the troilite and the remainder of the ferric oxide.

$$FeS + 10Fe_2O_3 = SO_2 + 7Fe_3O_4 \quad (2)$$

All the results such as the amount of gas evolved through each stage, the range of the reaction temperature, and the properties of the solid products observed by X-ray and microscopic method support the assumption described above. Martin and Fuchs[5] studied the reaction of similar mixtures of pyrite and

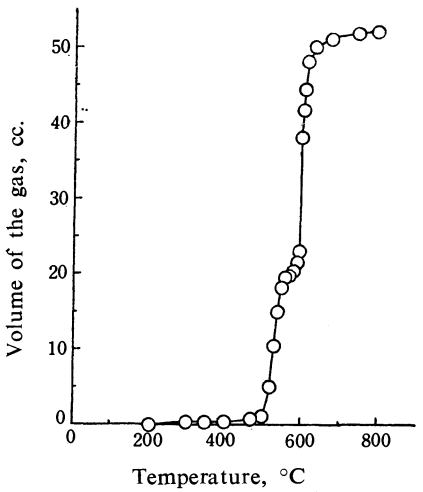



Fig. 3. Reaction between pyrite and α-ferric oxide (II).
Pyrite 250 mg.
$Fe_2O_3$ 2.0 g.

ferric oxide (weight ratio 1 : 2.25 or 1 : 3) and obtained a mixture of troilite and magnetite as solid products. The co-existence of these solid phases can be interpreted by the results obtained by our experiments, but according to theirs, the reaction began at 570°C, came to the end at 870°C, and the range of the reaction temperature was higher than that obtained by the present authors.

As the ferric oxide reacts completely with the pyrite to liberate sulfur dioxide at about 600°C as shown in Fig. 2, the amount of the ferric oxide in the iron sulfides can be determined by measuring the amount of sulfur dioxide evolved from the samples with a sufficient amount of pyrite.

**(2) The Reaction between Pyrite and Magnetite.** — Magnetite ($Fe_3O_4$) also reacts with pyrite to form troilite and sulfur dioxide at a high temperature as shown in Eq. 3.

$$5FeS_2 + Fe_3O_4 = 8FeS + 2SO_2 \quad (3)$$

The amount of the gas evolved was in good agreement with Eq. 3. The reaction began at about 550°C, and came to the end at about 650°C as shown in Fig. 4. The temperature range of the reaction overlapped with that of the reaction between pyrite and ferric oxide. Magnetite did not react practically with troilite below 1000°C.

As magnetite reacts completely with the pyrite to liberate sulfur dioxide at about 650°C as shown in Fig. 4, the amount of the magnetite in the iron sulfides can be determined by measuring the amount of sulfur dioxide evolved from the samples with a sufficient amount of pyrite.

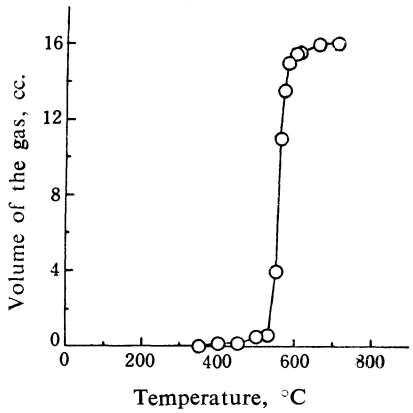



Fig. 4. Reaction between pyrite and magnetite.
Pyrite 200 mg.
$Fe_3O_4$ 100 mg.

**(3) The Reaction between Pyrite and Ferric Sulfate.**—When sufficient amount of pyrite is present, the reaction between pyrite and ferric sulfate began at about 300°C and came to an end at about 650°C proceeding through three stages as shown in Fig. 5. The final product was only troilite, and the equation of the reaction in each stage can be considered as follows:

The first stage (about 300~420°C)

$$FeS_2 + 3Fe_2(SO_4)_3 = 7FeSO_4 + 4SO_2 \quad (4)$$

the second stage (about 450~520°C)

$$FeS_2 + 8FeSO_4 = 3Fe_3O_4 + 10SO_2 \quad (5)$$

the third stage (about 550~650°C)

$$5FeS_2 + Fe_3O_4 = 8FeS + 2SO_2 \quad (3)$$

The volumes of sulfur dioxide calculated from

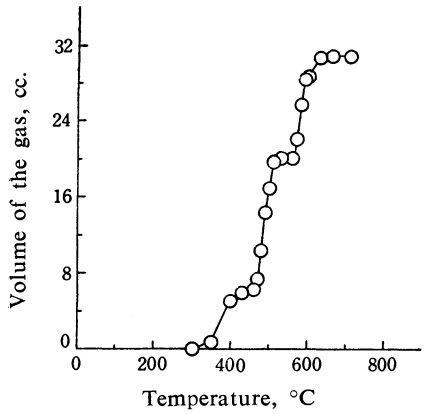



Fig. 5. Reaction between pyrite and ferric sulfate.

| | |
|---|---|
| Pyrite | 200 mg. |
| $Fe_2(SO_4)_3 \cdot nH_2O$ | 100 mg. |

TABLE II

Example 1 $Fe_2(SO_4)_3 \cdot nH_2O$ 0.1 g., $FeS_2$ 0.2 g.

| | $SO_2$ found, ml. | $SO_2$ calcd., ml. |
|---|---|---|
| First stage | 6.0 | 5.8 |
| Second stage | 13 | 12.7 |
| Third stage | 10 | 9.7 |

Example 2 $Fe_2(SO_4)_3 \cdot nH_2O$ 0.2 g., $FeS_2$ 0.4 g.

| | $SO_2$ found, ml. | $SO_2$ calcd., ml. |
|---|---|---|
| First stage | 12 | 11.6 |
| Second stage | 26 | 25.4 |
| Third stage | 20 | 19.4 |

the Eqs. 4, 5 and 3 agreed fairly well with the experimental data for each stage as is seen in Table II. The range of the reaction temperature of the third stage agrees with that of the reaction described in section 2. To ascertain these equations, the reactions were cut off at the end of cach stage by a rapid cooling and the solid products were examined. The product of the first stage was extracted by water, and the ferrous ion in the aqueous solution was titrated by a standard potassium permanganate solution. The value for ferrous sulfate in the solution was 56 mg. which agrees well with the value 54 mg. calculated by Eq. 4. The product of the second stage was strongly ferromagnetic with black color, and its X-ray diagram showed the diffraction lines of magnetite. These results showed that the reaction could be adequately expressed by Eqs. 4, 5 and 3. When the amount of pyrite was reduced, the product was changed as was expected from the Eqs. 3—5.

As ferric sulfate also reacts completely with pyrite to liberate sulfur dioxide around 650°C as shown in Fig. 5, the amount of ferric sulfate in the iron sulfides can be determined by measuring the amount of the sulfur dioxide liberated with a sufficient amount of pyrite.

**(4) The Reaction between Pyrite and Ferrous Sulfate.**—Remembering the three stages of the reaction between pyrite and ferric sulfate described above, the reaction between pyrite and ferrous sulfate would be considered to proceed similarly to the second and the third stage. As will be seen in Fig. 6, the reaction proceeds actually as was expected. Thus, the determination of ferrous sulfate in the mixture of ferrous sulfate and iron sulfides is possible from the amount of sulfur dioxide liberated when they are heated with a sufficient amount of pyrite at about 650°C in vacuo.

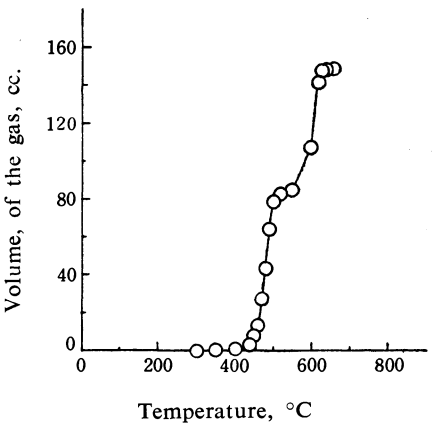



Fig. 6. Reaction between pyrite and ferrous sulfate.

| | |
|---|---|
| Pyrite | 1.0 g. |
| $FeSO_4 \cdot 7H_2O$ | 450 mg. |

When the amount of pyrite was insufficient, hematite was formed as a final product.

$$FeS_2 + 11FeSO_4 = 6Fe_2O_3 + 13SO_2 \qquad (6)$$

When the amount of pyrite was less than that of the stoichiometric ratio of Eq. 6, sulfur trioxide and oxygen were also liberated by the decomposition of the remainder of the ferrous sulfate.

**(5) The Determination of Ferric Sulfate, Ferrous Sulfate and Magnetite in their Mixture.**—When a sufficient amount of pyrite is present, the reaction between ferric sulfate and pyrite proceeds through three stages as stated above. The second stage of the reaction corresponds to the reaction between pyrite and ferrous sulfate, and the third stage to the reaction between pyrite and magnetite. Consequently when a mixture of ferric sulfate, ferrous sulfate and magnetite is heated with a sufficient amount of pyrite, all the gas liberated at the first stage may be attributed to ferric sulfate, and that at the end of the second stage to ferric sulfate and ferrous sulfate, and that at

the end of the third stage to ferric sulfate, ferrous sulfate and magnetite. Therefore, the amount of each substance in the mixture can be determined from the amount of sulfur dioxide liberated at each stage of the reaction. Some results of these determinations of the amount of each substance by this procedure are shown in Table III. As will be seen in Table III, the accuracy of this procedure is sufficient for the present study.

TABLE III

| | Example 1 | | Example 2 | |
|---|---|---|---|---|
| | Added mg. | Found mg. | Added mg. | Found mg. |
| $Fe_2(SO_4)_3 \cdot nH_2O$ | 70 | 70 | 50 | 55 |
| $FeSO_4 \cdot 7H_2O$ | 50 | 54 | 50 | 48 |
| $Fe_3O_4$ | 30 | 33 | 50 | 54 |

**(6) The Determination of a Very Small Amount of Oxygen in Pyrite.** — The results of the experiments on the reactions between pyrite and iron oxides or sulfates show that the oxygen contained in iron oxides or sulfates are completely liberated as sulfur dioxide, when the samples are heated at 650°C in vacuo with a sufficient amount of pyrite. Therefore, when the powdered pyrite contains a small amount of oxygen-iron compounds such as $Fe_2O_3$ and $FeSO_4$, the total amount of oxygen in the pyrite sample can be determined by the present method. But, as already mentioned above, absorbed oxygen and absorbed water which can not be removed by pumping at a low temperature may be conceivable as another source of oxygen.

The absorbed oxygen will be evolved as sulfur dioxide at 650°C, because the vapor pressure of sulfur in equilibrium with pyrite is fairly high in this condition[11-13] and oxygen is readily converted into sulfur dioxide. Minden[14] reported that the evaporated film of lead sulfide chemisorbs oxygen and evolves it as sulfur dioxide above 200°C. His results may support the view that oxygen absorbed on the surface of pyrite is evolved as sulfur dioxide on heating.

On the reaction between pyrite and water at a high temperature, Grünnert[8] concluded that the reaction proceeds as follows:

$$\text{(I)} \quad 2FeS_2 = 2FeS + S_2$$

$$\text{(II)} \quad 3S_2 + 4H_2O = 4H_2S + 2SO_2$$

$$\text{(III)} \quad FeS + H_2O = FeO + H_2S$$

$$\text{(IV)} \quad 3FeO + H_2O = Fe_3O_4 + H_2$$

These equations may explain the results of his experiments using a large amount of water. However, the amount of water absorbed on the surface of pyrite may be too small to follow the reactions III and IV. Therefore, in our case the reaction between pyrite and water may proceed as the following Eq. 7.

$$3FeS_2 + 2H_2O = 3FeS + 2H_2S + SO_2 \qquad (7)$$

in which water vapor, sulfur dioxide and hydrogen sulfide are equilibrated with pyrite and troilite. From these facts, the amount of oxygen in pyrite can readily be determined by that of sulfur dioxide, hydrogen sulfide and water vapor.

When a small crystal of pyrite was heated without being pulverized, a small amount of gas was liberated and the pyrite was completely decomposed to troilite and sulfur. But, when the same sample was pulverized and heated, a larger amount of gas was liberated as will be seen in Fig. 7. From this fact, it is obvious that as a result of pulverization of pyrite, oxidation occurs or absorption of oxygen or water. The evolved gas was completely absorbed by potassium hydroxide, and about two thirds of the absorbed gas was sulfur dioxide and hydrogen sulfide, and the remainder seems to be water vapor as will be shown in the following experiments. Phosphorus pentoxide was placed in tube D in Fig. 1 and cock 2 was

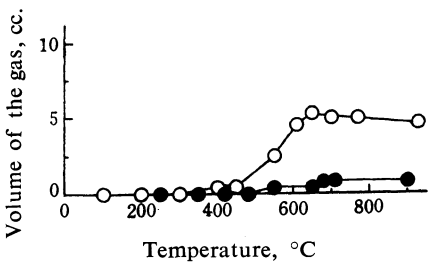



Fig. 7. Evolution of the gas from pyrite (1 g.)
● crystal ○ powder

TABLE IV

| | Experiment 1 | Experiment 2 |
|---|---|---|
| Sample weight | 3.0 g. | 2.0 g. |
| Total volume of the gas evolved | 3.0 ml. | 1.7 ml. |
| $SO_2$ | 0.85 ml. (2.9 mg.) | 0.70 ml. (2.0 mg.) |
| $H_2S$ | 0.98 ml. (1.5 mg.) | 0.52 ml. (0.79 mg.) |
| $H_2O$ | 1.17 ml. (0.94 mg.) | 0.48 ml. (0.39 mg.) |
| O attributed to $SO_2$ | 1.4 mg. | 1.0 mg. |
| O attributed to $H_2O$ | 0.8 mg. | 0.34 mg. |
| Total amount of O | 2.2 mg. | 1.34 mg. |
| O content | 0.073% | 0.067% |

11) R. Juza and W. Biltz, *Z. anorg. allg. Chem.*, **205**, 273 (1932).
12) L. D'or, *J. Chim. Phys.*, **28**, 377 (1931).
13) G. M. Schwab and J. Philinis, *J. Am. Chem. Soc.*, **69**, 2588 (1947).
14) H. T. Minden, *J. Chem. Phys.*, **23**, 1948 (1955).

kept open through the experiment. The amount of gas evolved was fairly small and it consists of only sulfur dioxide.

The results of the experiments for the determination of oxygen content of powder pyrite are shown in Table IV. As will be seen in the analytical results, the precision is sufficient for the present study.

## Summary

In the present paper a method for the determination of a very small amount of oxygen in an almost pure pyrite was proposed. From the results of the fundamental experiments on the reactions between the pyrite and the other minerals containing oxygen, it was ascertained that oxygen is completely liberated as sulfur dioxide and water vapor by heating in vacuo. The reproducibility of this method is fairly satisfactory, but there are no standard samples to examine the accuracy of this method. The results of the experiments indicate that this method could be used as a method for estimating the degree of oxidation of almost pure pyrites, for determining the amount of oxygen in some minerals, and in some cases for calculating the ratio of the oxygen containing compounds in their mixtures. Moreover, it seems possible to use this method for the determination of oxygen in a mixture of sulfides and oxides or sulfates of other metals than iron, and also oxygen in the metals. After the work reported herein had been almost completed, the authors were informed of the work, "The Sulfur Method of Oxygen Determination in Metals", of Babko et al.[15,16] who reported a somewhat similar study on the determination of oxygen in metals by using elementary sulfur instead of pyrite.

The authors are much indebted to Professor T. Watanabe and Mr. A. Sasaki, Department of Geology, The University of Tokyo for kindly supplying the samples of pyrite and for the microscopic study. We also express our hearty thanks to Dr. S. Akimoto, Geophysical Institute, the University of Tokyo, for his great help and valuable advice in X-ray study.

*Laboratory of Analytical Chemistry*
*and Geochemistry*
*Tokyo Institute of Technology*
*Ookayama Meguro-ku, Tokyo*

15) A. K. Babko, K. E. Kleiner and L. V. Markova, *Zavodskaya Lab.*, **22**, 640 (1956); *Chem. Abstr.*, **50**, 15339g (1956).

16) A. K. Babko, A. I. Volkava and O. F. Drako, *Zavodskaya Lab.*, **23**, 136 (1957); *Chem. Abstr.*, **51**, 17591c (1957).

# *Vapor Pressure of Zinc in Tin-Zinc Binary Liquid Alloy*

By Kichizo NIWA, Toshio YOKOKAWA and Harue WADA

(Received April 7, 1960)

For the development of the theory of metallic solution, systematic studies on thermodynamics of multi-component systems are required as well as those on electric and magnetic properties. Vapor pressure measurements directly provide the activity or the partial molar free energy of mixing of vaporizing components, though their temperature coefficients or heat terms are not so reliable as those determined by the calorimetric method. In the present work the applicability of Knudsen's effusion method was examined for the measurement of low vapor pressure of liquid alloy. This method is convenient for a measurement of this kind because small quantities of samples are enough to determine the vapor pressures. Also the concentration change of alloys with measuring time does not bring big error on account of low values of vapor pressure. In Knudsen's method, two conditions must be fulfilled. Firstly, vaporization velocity from alloy surface is so great that the vapor phase in the crucible may be maintained at equilibrium pressure. Secondly, diffusion through bulk phase of the alloy to surface is so rapid as to compensate for the decrease in the concentration of the vaporizing component. In relation to the above conditions, the effect of an oxide film and diffusivity in alloy phase as compared with the vaporization velocity must be taken into consideration. In order to make these points clear the vapor pressure of zinc in tin-zinc

liquid alloy was measured. Further, thermodynamic excess functions of this system were discussed.

## Experimental

**Experimental Method.**—In the effusion method vapor pressure is calculated from effusion velocity by an equation

$$P=\sqrt{\frac{2\pi RT}{M}}\cdot\frac{1}{KA}\cdot\frac{G}{\tau}\left(1+\frac{KA}{\alpha B}\right) \qquad (1)$$

where $A$ is the geometric area of the effusion orifice and $KA$ is the effective area. $K$ is the Clausing factor, a correction for the inevitable thickness of the orifice. $\alpha$ is the accomodation coefficient and $B$ is the effective vaporization area in the crucible. $KA/\alpha B$ is a correction term for deviation of pressure in the crucible from saturation. $G$ is the weight (in grams) of effused molecule within time interval $\tau$ (sec.). $M$ is the molecular weight of the effusing molecule. Other symbols mean ordinary quantities. In the temperature interval of this experiment, vapor pressure of tin may be neglected and besides zinc vapor is taken as monatomic, so $M$ in this case becomes the atomic weight of zinc. As $K$ cannot be precisely determined by experiment, the effective area $KA$ has been determined by combining the effusion velocity of solid zinc and its vapor pressure, presented by Barrow[1]. The correction term $KA/\alpha B$ is negligible compared with unity, provided that $\alpha$ is not very small. As will be shown later, this correction was proved not necessary.

**Apparatus.**—The apparatus, which had been previously used in the authors' laboratory[2], was modified in the reading of thermobalance. The latter is shown in Fig. 1. The beam A is of

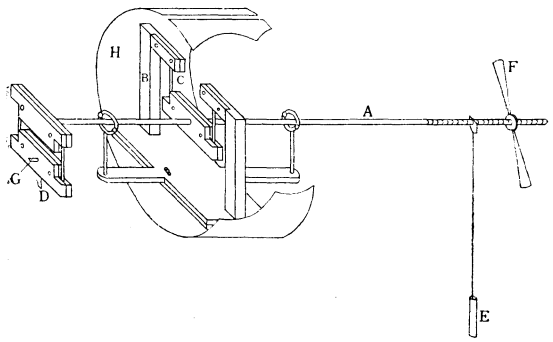



Fig. 1. Schematic diagram of the thermobalance.

aluminum and hung with a phosphorus bronze ribbon C from a frame of brass B, which is held in a brass vessel with a brass ring H. The effusion crucible is hung from D with a platinum wire. E is a dust core of 3 mm. in diameter and 1 cm. in length, and is used to convert the inclination of the balance into a change of electric current by means of a linear differential transformer. F is a counter weight of soft iron which can be shifted at a proper position along the beam by a magnet from the outside of the glass tube. A crucible of pyrex glass is 1 cm. in diameter and 1 cm. in height including its lid. An effusion orifice is bored at the center of the lid which is ground with the crucible. The orifice is ground as thin as possible (0.1 mm.) from both the up and down sides of the lid. The furnace consists of a porcelain tube wound by a nichrome resistance wire. The temperature was manually controlled at a constancy of $\pm 1$°C during each measurement (20 min. to 2 hr.). Temperature was measured by a platinum vs. platinum-rhodium thermocouple, the end of which was nearly in contact with the crucible through a quartz tube. The thermocouple was calibrated at the melting points of zinc, tin, bismuth, lead and antimony.

**Procedure.**—About one gram of metal or alloy sample is placed in the crucible, which is hung from the thermobalance by a platinum wire of 0.2 mm. in diameter, then the counter weight is properly adjusted. Sensitivity of the balance is determined at each run by loading riders of known weight on G in Fig. 1 (about 0.1 mg./$\mu$A). Then a rider of the right weight is again loaded on the same position in order that the balance may be settled through the measuring time within the inclination range where the sensitivity has been measured. After that the system is evacuated to a pressure of $10^{-5}$ mmHg and the furnace is heated up to the desired temperature and the rate of weight loss is measured by way of the current in the transformer circuit.

**Sample.**—Purities of metals used are 99.9% (zinc), chemical pure (tin), 99.9% (bismuth), and 99.999% (indium). Zinc ribbon was used for the measurement in pure solid state. Alloys were prepared in the following way; pure metals of desired amount were sealed in a small pyrex tube in vacuo and kept at about 450°C for ten hr., followed by quenching.

**Experimental Error.**—As the sources of error of this measurement, temperature, area of the orifice, sensitivity of the balance and rate of change of current should be taken into account. Relative errors of these contents are 0.08, 2.7, 1.5 and 1% respectively. Then the fractional average deviation may amount to 3.2%. Next, the error of activity, calculated from the vapor pressure of pure liquid and alloys, amounts to 4%. The decrease in concentration of zinc with vaporization affects the activity coefficient by decreases of 6 and 3% at mole fractions of 0.05 and 0.1, respectively.

**Measurement of Liquid Alloy.**—The applicability of Knudsen's effusion method to alloy of liquid state was examined in the following points.

*(A) Saturation of Vapor Phase.*—In order to make certain that the vapor phase was saturated, vaporization velocity was measured, when the lid of the crucible was removed and the vapor freely escaped from the surface (nearly Langmuir-like). This velocity was about $1\times10^{-2}$ mg./sec., while the ordinary effusion velocity was at most $6\times10^{-4}$ mg./sec. Then, one can assume that zinc vapor is saturated in the crucible even in the case of liquid

1) R. F. Barrow et al., *Trans. Faraday Soc.*, **51**, 1354 (1955).
2) Z. Shibata and K. Niwa, *J. Fac. Sci. Hokkaido Imp. Univ.* Ser. III, Vol. II, 183 (1938).

solution, where a thin film of zinc oxide may cover and disturb vaporization, or may reduce the accommodation coefficient.

*(B) Concentration Difference between the Surface and the Bulk Phase of Liquid Alloy.*—The surface concentration of zinc decreases with its vaporization, while the concentration recovers by diffusion through the bulk phase. The following calculation has been made for the sake of estimation of this concentration gradient in the steady state. Assuming (a) that there exists a linear concentration gradient between the surface and a position, $\Delta L$ cm. distant under the surface, and (b) that there is no convection in the bulk phase, flow of zinc to the surface is given by

$$J(\text{g./sec.}) = -BD\Delta C/\Delta L$$

where $B$ is the surface area and $D$, the diffusion coefficient of zinc in the solution and $C$, the concentration in g. per cc. This flow should be equal to effusion velocity at the steady state. The latter being at most $6\times10^{-7}$ g./sec. at a vapor pressure of $10^{-2}$ mmHg, $\Delta C/\Delta L$ becomes 0.15, if $B$ is 0.42 cm$^2$ and $D$ is $10^{-5}$ cm$^2$/sec. Then $\Delta C$ becomes 0.0045 g./cc., when $\Delta L$ is 0.3 cm., the same length as the depth of the solution. This value of $\Delta C$ corresponds to about 0.01 mol. fraction. At the practical condition the supplement of zinc would be faster, as there may occur convection and the concentration gradient is not linear.

*(C) Concentration Change due to Vaporization.*—In one run 1 to 2 mg. of zinc effuses out. This affects the concentration by 0.003 at 0.05 and 0.0015 at 0.1 respectively in mole fraction. Then this effect is not so severe except in a composition of high dilution, where the effusion time of one run is desirable to be short.

## Results and Discussion

**Vapor Pressure of Pure Zinc.**—For the purpose of determining the effective area of the effusion orifice, effusion velocity was measured with pure solid zinc. An example of the results is shown in Table I. By means of

Table I. Effusion velocity of solid pure zinc

| $T$, °K | $P\times KA$* mmHg×cm$^2$ | $T$, °K | $P\times KA$ mmHg×cm$^2$ |
|---|---|---|---|
| 613 | $4.663\times10^{-6}$ | 646 | $17.15\times10^{-6}$ |
| 621 | 6.678 〃 | 649 | 18.58 〃 |
| 625 | 9.575 〃 | 658 | 25.88 〃 |
| 635 | 11.71 〃 | 661 | 34.46 〃 |
| 636 | 12.27 〃 | | |

* The geometrical area $A$ is $7.566\times10^{-3}$ cm$^2$.

the least square method, these values are expressed as a linear function of $1/T$ by

$$\log P\times(KA) = -6716/T + 5.649 \qquad (2)$$

The vapor pressure of solid zinc has been investigated by many workers. The most reliable value, which Barrow and his coworkers derived[1], is

$$\log P = 9.8253 - 0.1923\log T - 0.2623\times10^{-3}T - 6862.5/T \qquad (3)$$

Comparing Eq. 2 with Eq. 3, the effective area $KA$ of the orifice is calculated as 0.5735 mm$^2$. The geometrical area ($A$) was 0.7566 by microscopic measurement. The ratio of these figures leads to 0.758 as the Clausing factor, which corresponds to 0.099 mm. of thickness of the orifice. Substituting the effective area in Eq. 2, it can be rewritten as

$$\log P = -6716/T + 8.891 \qquad (4)$$

The vapor pressure of liquid zinc can be calculated from Eq. 4 and the free energy change of solidification of zinc[3] as a function of temperature. Thus the vapor pressure at 625°K is $1.603\times10^{-2}$ mmHg, which is used as the reference in derivation of activity of zinc in alloys.

**Vapor Pressure of Zinc in Liquid Alloy.**—At the range of high content of zinc, zinc separates as solid matter over the temperature range where vapor pressure is appropriate in magnitude for the effusion method. The present measurement has covered up to 0.4 of mole fraction of zinc. Measured values are summarized in Table II, and plotted against reciprocal temperature in Fig. 2. The activity of zinc at 625°K, calculated from the above-mentioned values and $1.603\times10^{-2}$ mmHg of

Table II. Vapor pressure of zinc in liquid tin-zinc system

| $X_{Zn}$ | $T$, °K | $P_{Zn}$ mmHg $\times10^3$ | $X_{Zn}$ | $T$, °K | $P_{Zn}$ mmHg $\times10^3$ |
|---|---|---|---|---|---|
| 0.027 | 645 | 2.99 | | 659 | 18.1 |
| | 650 | 3.50 | | 671 | 25.4 |
| | 660 | 4.31 | | 686 | 40.5 |
| | 665 | 5.67 | $\log P = -5976/T + 7.312$ | | |
| | 675 | 6.09 | 0.252 | 615 | 6.08 |
| | 681 | 8.43 | | 625 | 8.62 |
| | 685 | 8.90 | | 636 | 11.9 |
| $\log P = -5206/T + 5.546$ | | | | 650 | 20.1 |
| 0.104 | 645 | 7.44 | $\log P = -5822/T + 7.249$ | | |
| | 655 | 10.1 | 0.364 | 597 | 4.11 |
| | 665 | 12.2 | | 604 | 5.57 |
| | 670 | 15.0 | | 606 | 5.74 |
| | 688 | 25.9 | | 613 | 6.77 |
| $\log P = -5432/T + 6.286$ | | | | 621 | 9.15 |
| 0.150 | 616 | 4.34 | | 625 | 12.2 |
| | 621 | 4.78 | | 627 | 11.5 |
| | 626 | 5.83 | | 635 | 13.9 |
| | 640 | 8.77 | | 651 | 26.6 |
| | 640 | 9.95 | | 659 | 34.8 |
| | 650 | 12.8 | $\log P = -5769/T + 7.273$ | | |
| | 652 | 13.5 | | | |

3) J. Lumsden, "Thermodynamics of Alloys", Institute of Metals, London (1952), p. 140.

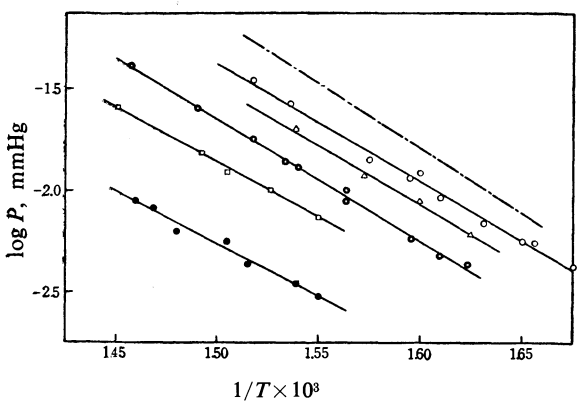



Fig. 2. Relation between logarithm of vapor pressure and reciprocal temperature.
—— liquid pure zinc ◎ $X_{Zn}=0.150$
○ $X_{Zn}=0.027$ □ 〃 0.252
△ 〃 0.104 ● 〃 0.364

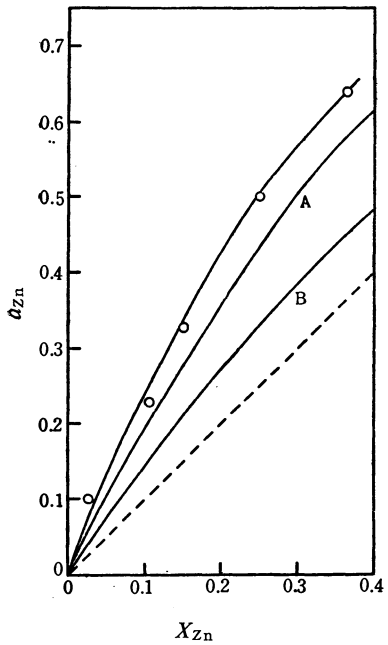



Fig. 3. Activity of zinc: open circle, present work at 625°K, line A, Taylor's value at 650°C, and line B, Jellinek's value at 700°C.

pure liquid zinc, is shown in Fig. 3. On this system Taylor[4] determined activity by e. m. f. method at 400 to 600°C, and Burmeister and Jellinek[5] measured vapor pressure of zinc by the transpiration method at a temperature range of 684 to 785°C. Their results are also shown in Fig. 3.

The thermodynamic property of alloys can be appropriately given in terms of excess function, where solutions are classified as ideal,

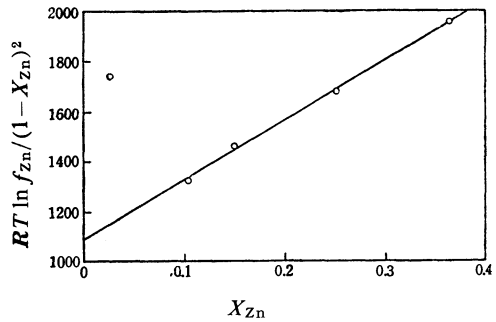



Fig. 4. Relation between $RT\ln f_{Zn}/(1-X_{Zn})^2$ and $X_{Zn}$.

regular or sub-regular ones. Wittig and his coworkers[6] have found that the heat of solution of this system behaves as a sub-regular solution as far as enthalpy is concerned. In Fig. 4 $RT\ln f_{Zn}/(1-X_{Zn})^2$ is plotted against concentration of zinc. All points are on a straight line

$$\frac{RT\ln f_{Zn}}{(1-X_{Zn})^2}=2370\,X_{Zn}+1090 \qquad (5)$$

One point at $X=0.027$ deviates from this line, probably because of the uncertainty of concentration. It would be worth while to find what these figures mean when this system is regarded as a sub-regular solution. By definition[7] excess free energy of solution is related to concentration by

$$\frac{G^e}{X_{Zn}X_{Sn}}=A^0+(X_{Sn}-X_{Zn})A^1 \qquad (6)$$

where $A^0$ and $A^1$ are constants. From this equation one can derive a formula for the excess chemical potential, defined as a difference between partial molar free energy of solution and ideal partial molar free energy of solution,

$$\mu^e{}_{Zn}/X^2{}_{Sn}=RT\ln f_{Zn}\times 1/X^2{}_{Sn}=A^0 +(1-4X_{Zn})A^1 \qquad (7)$$

Comparing Eq. 7 with Eq. 5, values of $A$s are given,

$$A^0=1680 \quad \text{and} \quad A^1=-590$$

Taylor's data at equal range of concentration lead to $A^0=1660$ and $A^1=-430$. Accounting for the temperature dependence of these quantities, two sets of data are in good agreement within experimental error.

This sub-regular behavior has not yet been completely interpreted. In the case of molecular liquid solutions, Hildebrand[8] succeeded in explaining energetic asymmetry by using

4) N. W. Taylor, *J. Am. Chem. Soc.*, **45**, 2865 (1923).
5) E. Burmeister and K. Jellinek, *Z. phys. Chem.*, **A165**. 121 (1933).
6) F. E. Wittig, *Z. Electrochem.*, **63**, 327 (1959).
7) H. Hardy, *Acta Met.*, **1**, 202 (1952).
8) J. H. Hildebrand and R. L. Scott, "The Solubility of Nonelectrolytes", Reinhold, New York (1952), p. 109.

volume fraction in place of mole fraction. In the present case this correction is not enough. Kleppa[9] and Wittig[6] pointed out the correlation of the energetic asymmetry with valence electron concentration from the experimental data of many alloy systems. Recently some investigators[10] paid attention to the cohesive energy of metals in light of metallic characteristics and considered what happened on mixing. Shimoji[11] discussed the excess energy of binary alloys by using the cellular approximation for metals and explained energetic asymmetry on mixing, not by the simple volume effect, but by the changes of the energy due to the boundary correction, Fermi energy, interelectronic energy, closed shell repulsive energy, polarization energy etc. It is interesting to compare the calculation with the present data. In the moderately dilute range, integral heats of mixing can be expanded in a power series of the mole fraction of the solute,

$$\Delta H^{M} = P_1 x_2 + P_2 x_2^2 + \cdots\cdots \quad (8)$$

According to Shimoji the ratio $-P_2/P_1$ is 0.4 in the zinc dilute portion of tin-zinc system. From Eq. 8 one obtains the relative partial molar enthalpy as

$$\overline{\Delta H}_2 = P_1 + 2P_2 x_2 + \cdots\cdots \quad (9)$$

The corresponding equation can be derived from the present data by the following equation, provided that the partial molar excess entropy is known,

$$\overline{\Delta H}_{Zn} = \mu^e{}_{Zn} + T\overline{\Delta S}^e{}_{Zn} \quad (10)$$

Assuming that the excess entropy is mainly due to volume difference, partial molar excess entropy of solution of zinc can be calculated by free volume model[8]:

$$\overline{\Delta S}^e{}_{Zn} = -R\left[\ln \varphi_{Zn} + \varphi\left(1 - \frac{V_{Zn}}{V_{Sn}}\right) - \ln X_{Zn}\right] \quad (11)$$

where $\varphi$ is the volume fraction and $V$ is the molar volume. Replacing $\varphi$ by the mole fraction and molar volumes, one obtains

$$\overline{\Delta S}^e{}_{Zn} = 1.05 - 1.31\, X_{Zn} + \cdots\cdots \quad (12)$$

where 16.9 and 9.9 is used as molar volumes of tin and zinc. On the other hand, Eq. 5 is rewritten as

$$\mu^e{}_{Zn} = 1090 + 190 X_{Zn} + \cdots\cdots \quad (13)$$

From Eqs. 12 and 13 the partial molar enthalpy of zinc at 625°K is

$$\overline{\Delta H}_{Zn} = 1750 - 630 X_{Zn} + \cdots\cdots \quad (14)$$

giving 1750 and $-315$ cal./mol. for $P_1$ and $P_2$ respectively. Then the present value 0.18 for $-P_2/P_1$ seems to agree with 0.4 (Shimoji's value) in deviation from $P_2/P_1 = -1$ (regular solution). The experimental results about ternary solutions will be reported in the next paper.

## Summary

The vapor pressure of zinc in liquid tin-zinc alloys has been measured by Knudsen's effusion method. Application of this method to liquid alloys has been found to be successful. Observed activity coefficients of zinc are discussed in relation to theoretical calculations. The deviation from the regular solution model has been interpreted in terms of the cellular approximation as well as the volume difference effect.

The authors are indebted to Dr. M. Shimoji for his valuable discussion.

*Department of Chemistry*
*Faculty of Science*
*Hokkaido University, Sapporo*

9) O. J. Kleppa, *Acta Met.*, 6, 225 (1958).
10) J. Friedel, *Phil. Mag.*, 43, 153 (1952); J. H. O. Varley, ibid., 45, 887 (1954).
11) M. Shimoji, *J. Phys. Soc. Japan*, 14, 1525 (1959).

# *Studies on the Decomposition of Ammonia and Hydrazine by High Frequency Discharge*

By Saku TAKAHASHI

(Received February 20, 1960)

The chemical reaction under high frequency discharge has been studied and it has been found that the energy consumed in the reaction is roughly proportional to the frequency of the applied electric current[1]. However, from the standpoint of reaction rate, it is highly questionable whether the rate of reaction under high frequency discharge would be affected by the frequency of the applied electric current or not. In order to obtain information concerning the reactions under high frequency discharge, the selectivities of frequencies to the reactions in the decomposition of both ammonia and hydrazine vapour have been studied.

## Experimental Procedures

The decomposition of ammonia and also of hydrazine under high frequency discharge were carried out in a closed vessel shown in Fig. 1. The volume of the glass vessel, cylindrical in shape, of which the diameter was 7 cm., was approximately 1000 cc. A single electrode was inserted into this vessel at the bottom and high frequency electric current was applied to this electrode. The electric discharge occurred at the top of this electrode.

The frequencies of electric current used in these experiments were 100 and 250 MC. For the purpose of keeping their power applied on these reactions at a definite value, all the electric conditions of a generator were constantly fixed in every case.

The ammonia, hydrazine, nitrogen and hydrogen used in these experiments were purified by ordinary methods. The quantities of ammonia and hydrazine in the reaction vessel were expressed by the partial pressures in the reaction vessel at 25°C. The initial pressure of ammonia was from 50 to 250 mmHg and that of hydrazine was from 3 to 10 mmHg.

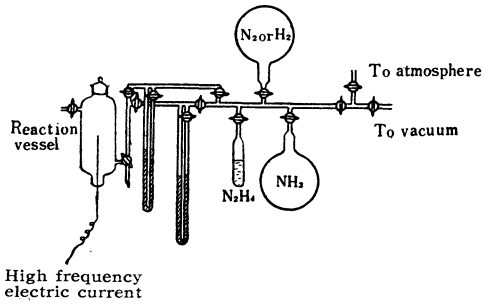



Fig. 1. Apparatus

## Results and Discussion

In these experiments, the amounts of reactant were plotted against the reaction time. Several experiments with additional hydrogen or nitrogen were also carried out. From these results, the rate of the reaction was expressed with the amount of the reactant decomposed in a certain reaction time.

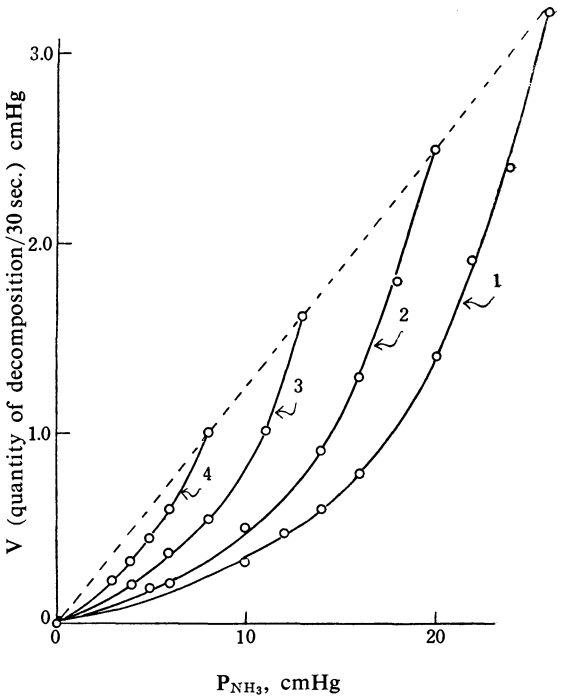



Fig. 2. Influence of initial pressure on reaction rate under 100 MC frequency discharge. Showing that the initial reaction rate is proportional to the amount of ammonia and the decomposition products retard the reaction.

| NO. | $[P_{NH_3}]_0$, cmHg |
|---|---|
| 1 | 26.0 |
| 2 | 20.0 |
| 3 | 13.0 |
| 4 | 8.0 |

1) E. Briner et al., *Helv. Chim. Acta*, **14**, 534 (1931); **18**, 1468 (1935); **19**, 287 (1936); **28**, 714 (1945); **30**, 105 (1947).

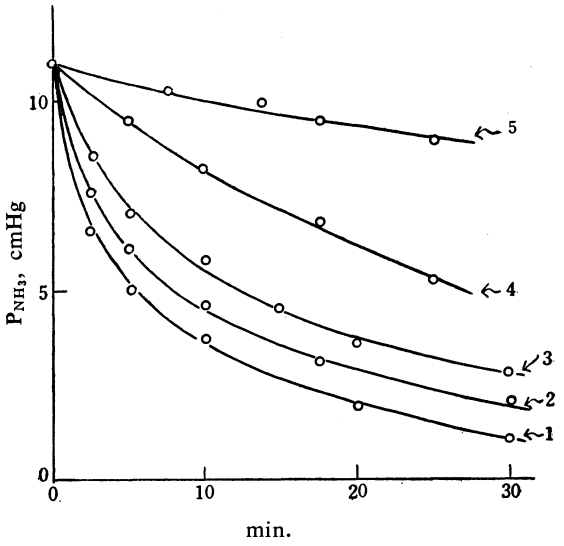



Fig. 3. Effect of hydrogen on decomposition of ammonia under 100 MC frequency discharge. Plots of amount of ammonia against reaction time.

$[P_{NH_3}]_0$; 11.0 cmHg

| NO. | $[H_2]_0$, cmHg |
|---|---|
| 1 | 0 |
| 2 | 3.50 |
| 3 | 14.30 |
| 4 | 25.80 |
| 5 | 32.80 |

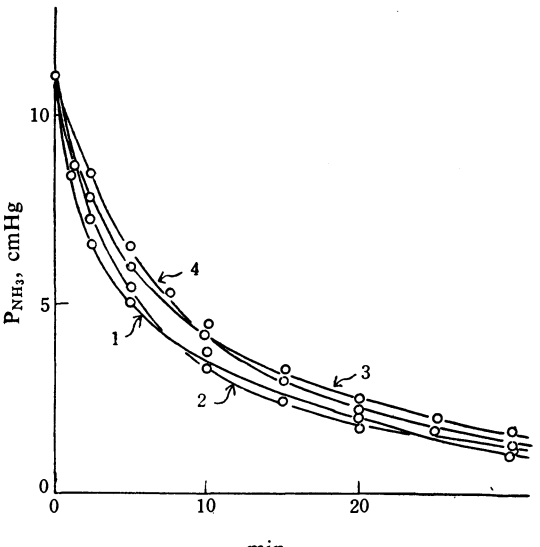



Fig. 4. Effect of nitrogen on decomposition of ammonia under 100 MC frequency discharge. Plots of amount of ammonia against reaction time.

$[P_{NH_3}]_0$; 11.0 cmHg

| NO. | $[N_2]_0$, cmHg |
|---|---|
| 1 | 0 |
| 2 | 3.10 |
| 3 | 11.80 |
| 4 | 33.80 |

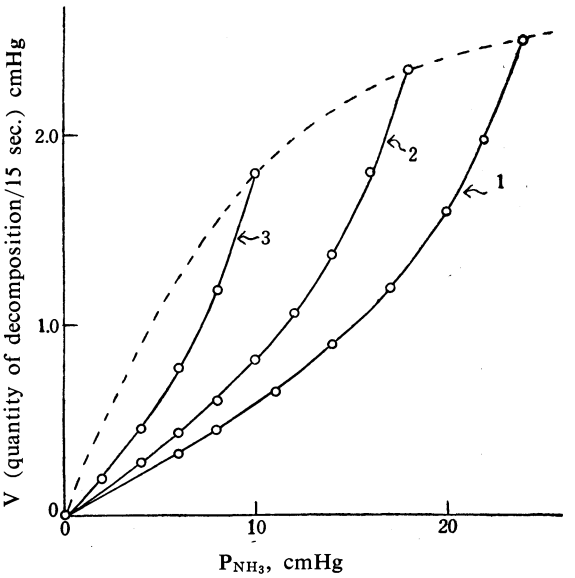



Fig. 5. Influence of initial pressure on reaction rate under 250 MC frequency discharge. Showing that the initial reaction is an intermediate type between the zero and the 1st order reaction and the reaction is retarded by the decomposition products.

| NO. | $[P_{NH_3}]_0$, cmHg |
|---|---|
| 1 | 24.0 |
| 2 | 18.0 |
| 3 | 10.0 |

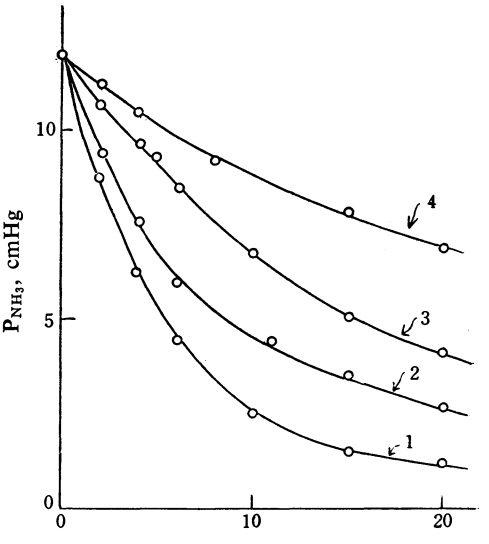



Fig. 6. Effect of hydrogen on decomposition of ammonia under 250 MC frequency discharge. Plots of amount of ammonia against reaction time.

$[P_{NH_3}]_0$; 12.0 cmHg

| NO. | $[P_{H_2}]_0$, cmHg |
|---|---|
| 1 | 0 |
| 2 | 3.0 |
| 3 | 9.0 |
| 4 | 12.0 |

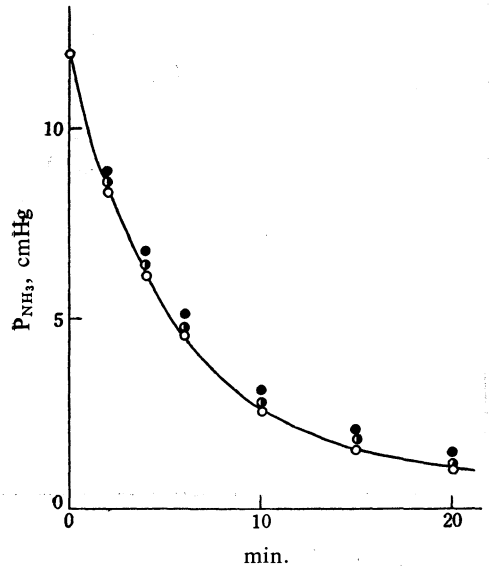



Fig. 7. Effect of nitrogen on decomposition of ammonia under 250 MC frequency discharge. Plots of amount of ammonia against reaction time.
$[P_{NH_3}]_0$; 12.0 cmHg
$[P_{N_2}]_0$, cmHg
○····· 0
◑····· 6.00
●·····10.50

**Decomposition of Ammonia.**—The decomposition products were analysed by gas chromatography. They were nitrogen, hydrogen and hydrazine. The main products were nitrogen and hydrogen. The amount of hydrazine produced was so small that the effect caused by the hydrazine on this reaction may be ignored.

On the decomposition under 100 MC frequency discharge, it is shown in Fig. 2 that the initial stage of the reaction was of the 1st order and that the retardation by both nitrogen and hydrogen was observed. Comparing Fig. 3 with Fig. 4, it is seen that the amount of ammonia decomposed in a definite time decreases according to the quantity of hydrogen added, while the nitrogen added exhibits no effects on the rate of ammonia decomposition. Under 250 MC frequency discharge, it is known from Fig. 5 that the initial reaction is not of the 1st order, but it is an intermediate type between the zero and 1st order reactions, and comparing Fig. 6 with Fig. 7, it may be seen that the overall reaction is retarded by hydrogen.

The molecules in electric discharge are excited by a collision with an impacting electron and change to an excited molecule or a positive ion. It is considered that both a positive ion and an excited molecule are possible agents in the chemical reaction. If excited molecules were responsible, the reaction should be pressure sensitive, for it may be expected that the concentration of excited molecules would decrease with pressure. The outstanding feature of the experiment in electric discharge is that the reaction is directly proportional to the discharge current and it is independent of pressure over a large range of values. Furthermore, it has been observed in the studies[2] with electrons of controlled speed that the reaction hardly occurs below the ionization potential of the gas. These experimental results favor an ionic reaction in electric discharge. Upon neutralization of a positive ion, the entire energy of ionization available may serve as activation energy for chemical processes or else the molecule will return to the normal state after a short average life with the emission of radiation[3]. In a spectroscopic investigation[4], on high frequency discharge, it has been noticed that, in a discharge tube, a molecule with one charge comes to be clearly observed as the frequency of electric current increases. This phenomenon shows one of the specific properties of high frequency discharge and from this fact it is presumed that the life-time and number of positive charge moleculs produced in a discharge tube tend to increase with the frequency of the electric current.

Thus, one accounts for the kinetics of reactions by the following series of reactions:

$$NH_3 \xrightarrow{k_1} NH_3^+ \quad \text{(in electric discharge)}$$

$$NH_3^+ \xrightarrow{k_2} NH_3^*$$

$$NH_3^* \xrightarrow{k_3} \frac{1}{2}N_2 + \frac{3}{2}H_2$$

$$NH_3^+ \xrightarrow{k_4} NH_3 + E$$

$$NH_3^+ + H_2 \xrightarrow{k_5} [NH_3^+ \cdot H_2] \longrightarrow NH_3 + H_2 + E_1$$

$$NH_3^+ + NH_3 \xrightarrow{k_6} [NH_3^+ \cdot NH_3] \longrightarrow NH_3 + NH_3 + E_2$$

In these reactions, it is difficult to understand strictly the behaviour of hydrogen molecules, but from the results obtained in this experiment it is supposed that hydrogen has the greatest probability of deactivation of all ionized molecules. If the life-time of $NH_3^+$ is long, it is known that, as the results of several collisions between hydrogen and the ionized

2) C. H. Kunsman, *Phys. Rev.*, **31**, 307 (1928).
3) G. Glockler, "The Electrochemistry of Gases and other Dielectrics", John Wiley & Sons, Inc., New York (1939), p. 430.
4) W. Jones, *Proc. Roy. Soc.*, **A127**, 511 (1930); L. Henry, *J. Phys. Chem.*, **34**, 2792 (1930).

molecule, the ionized molecule loses its excessive energy and becomes a normal molecule, while hydrogen becomes an activated molecule. Applying the steady state assumption, one arrives at expression 1 for the rate of decomposition.

$$\frac{d[NH_3^+]}{dt}=k_1[NH_3]-k_2[NH_3^+]-k_4[NH_3^+]$$
$$-k_5[NH_3^+][H_2]-k_6[NH_3^+][NH_3]=0$$
$$[NH_3^+]=\frac{k_1[NH_3]}{k_2+k_4+k_5[H_2]+k_6[NH_3]}$$
$$\frac{d[NH_3^*]}{dt}=k_2[NH_3^+]-k_3[NH_3^*]=0$$
$$[NH_3^*]=\frac{k_2}{k_3}[NH_3^+]$$
$$V=k_3[NH_3^*]=k_2[NH_3^+]$$
$$=\frac{k_1k_2[NH_3]}{k_2+k_4+k_5[H_2]+k_6[NH_3]} \quad (1)$$

When a hydrogen molecule does not exist in a reaction vessel, the rate of reaction is expressed as follows and this formula expresses the relation between the initial rate $V_0$ and the concentration of ammonia.

$$V_0=k_3[NH_3^*]=k_2[NH_3^+]$$
$$=\frac{k_1k_2[NH_3]}{k_2+k_4+k_6[NH_3]} \quad (2)$$

Using expressions 1 and 2, the following relations are obtained.

$$\frac{V_0-V}{V}=\frac{k_5[H_2]}{k_2+k_4+k_6[NH_3]}=\Theta$$
$$\frac{k_2+k_4}{k_5}+\frac{k_6}{k_5}[NH_3]=\frac{[H_2]}{\Theta} \quad (3)$$

If the life-time of $NH_3^+$ is short, the $k_6$ process may be neglected and the rate of decomposition is approximated as follows:

$$V=\frac{k_1k_2[NH_3]}{k_2+k_4+k_5[H_2]} \quad (4)$$
$$\frac{k_2+k_4}{k_1k_2}+\frac{k_5}{k_1k_2}[H_2]=\frac{[NH_3]}{V} \quad (5)$$

Using the results shown in Figs. 2 and 5, the plots of $NH_3/V$ vs. $H_2$ and $H_2/\Theta$ vs. $NH_3$ are shown in Figs. 12 and 13, respectively. A linear relation between $NH_3/V$ and $H_2$ or $H_2/\Theta$ and $NH_3$ is clearly shown in these figures, being independent of the initial concentration of ammonia, and the agreement between the experiment and the calculation is reasonable.

**Decomposition of Hydrazine.**—The decomposition products of this reaction are nitrogen and hydrogen and ammonia is not produced. In this reaction, comparing Fig. 8 with Fig. 9

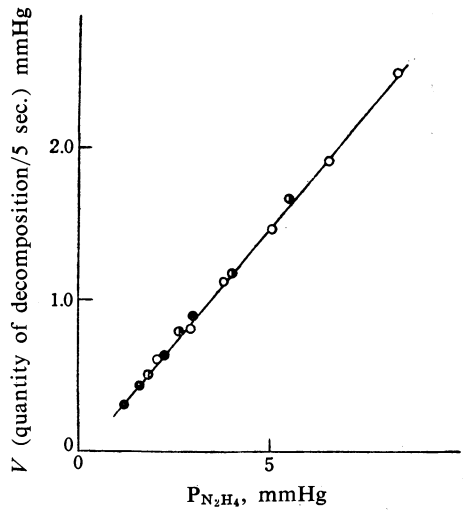



Fig. 8. Decomposition of hydrazine under 100 MC frequency discharge. Plots of reaction rate against hydrazine concentration.

$[P_{N_2H_4}]_0$, mmHg
○……8.40
◑……5.50
●……3.00

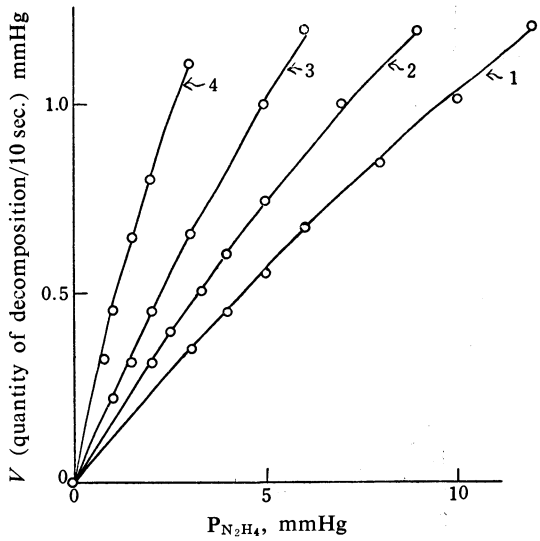



Fig. 9. Influence of initial pressure on reaction rate under 250 MC frequency discharge. Showing that the initial reaction is zero order and the reaction is retarded by the decomposition products.

| NO. | $[P_{N_2H_4}]_0$, mmHg |
|---|---|
| 1 | 12.0 |
| 2 | 9.0 |
| 3 | 6.0 |
| 4 | 3.0 |

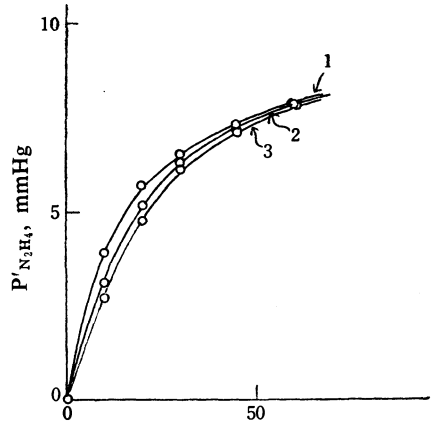



Fig. 10. Effect of nitrogen and hydrogen on decomposition of hydrazine under 100 MC frequency discharge. Plots of amount of hydrazine decomposed against reaction time.

$[P_{N_2H_4}]_0$; 8.40 mmHg

| NO. | $[P_{H_2}]_0$, mmHg | $[P_{N_2}]_0$, mmHg |
|---|---|---|
| 1 | 0 | 0 |
| 2 | 15.0 | 0 |
| 3 | 0 | 15.0 |

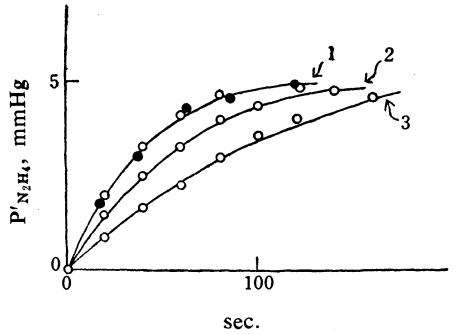



Fig. 11. Effect of nitrogen and hydrogen on decomposition of hydrazine under 250 MC frequency discharge. Plots of amount of hydrazine decomposed against reaction time.

$[P_{N_2H_4}]_0$; 5.0 mmHg

| NO. | $[P_{N_2}]_0$, mmHg | $[P_{H_2}]_0$, mmHg |
|---|---|---|
| 1 ○ | 0 | 0 |
| 1 ● | 0 | 6.0 |
| 2 | 6.0 | 0 |
| 3 | 9.0 | 0 |

it can be shown that the rate of decomposition under high frequency discharge varies with the values of frequencies of the applied electric current. The reaction under the frequency 100 MC is a 1st order reaction, but under the frequency 250 MC the initial rate of decomposition is of zero order. Moreover, as is seen in Figs. 10 and 11, the hydrogen produced in the course of the decomposition does not retard the rate of decomposition

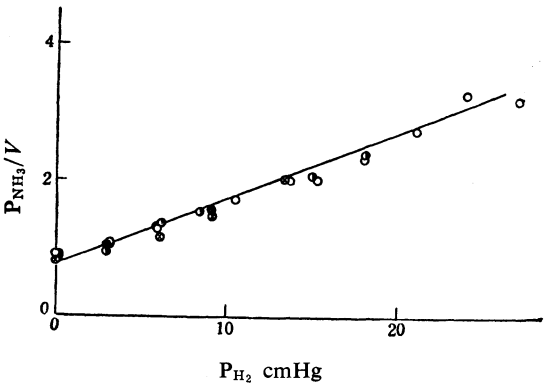



Fig. 12. Plots of $P_{NH_3}/V$ vs. $P_{H_2}$.

| $[P_{NH_3}]_0$, cmHg | $[P_{NH_3}]_0$, cmHg |
|---|---|
| ○……26.0 | ◑……20.0 |
| ⊗……13.0 | ●…… 8.0 |

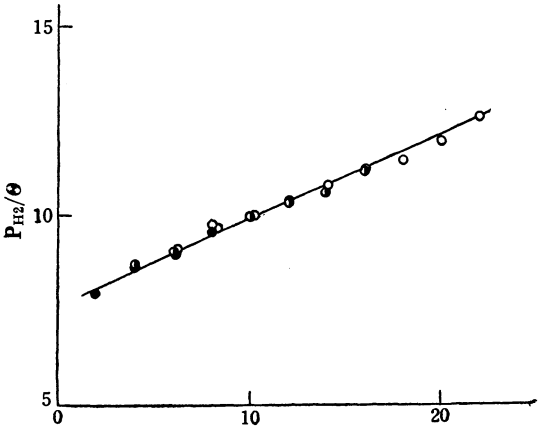



Fig. 13. Plots of $P_{H_2}/\theta$ vs. $P_{NH_3}$.

| $[P_{NH_3}]_0$, cmHg | $[P_{NH_3}]_0$, cmHg |
|---|---|
| ○……24.0 | ◑……18.0 |
| ●……10.0 | |

under the former condition, but it moderately retards the rate of reaction under the latter condition. From these results, it is possible to explain the reaction processes as follows:

$$N_2H_4 \xrightarrow{k_1} N_2H_4^+ \text{ (in electric discharge)}$$

$$N_2H_4^+ \xrightarrow{k_2} N_2H_4^*$$

$$N_2H_4^* \xrightarrow{k_3} N_2+2H_2$$

$$N_2H_4^+ \xrightarrow{k_4} N_2H_4+E$$

$$N_2H_4^+ + H_2 \xrightarrow{k_5} [N_2H_4^+ \cdot H_2] \longrightarrow N_2H_4+H_2+E_1$$

$$N_2H_4^+ + N_2H_4 \xrightarrow{k_6} [N_2H_4^+ \cdot N_2H_4] \longrightarrow N_2H_4+N_2H_4+E_2$$

Under the frequency 100 MC, if the lifetime of $N_2H_4^+$ is short, it is supposed that $N_2H_4^+$ cannot be deactivated by the collision with $H_2$ or $N_2H_4$. In this case, applying the usual steady state assumption, expression 6 for the rate of decomposition is obtained.

$$\frac{d[N_2H_4^+]}{dt}=k_1[N_2H_4]-k_2[N_2H_4^+]-k_4[N_2H_4^+]=0$$

$$[N_2H_4^+]=\frac{k_1[N_2H_4]}{k_2+k_4}$$

$$\frac{d[N_2H_4^*]}{dt}=k_2[N_2H_4^+]-k_3[N_2H_4^*]=0$$

$$[N_2H_4^*]=\frac{k_2}{k_3}[N_2H_4^+]$$

$$V=k_3[N_2H_4^*]=\frac{k_1k_2}{k_2+k_4}[N_2H_4] \qquad (6)$$

Under the frequency 250 MC, if the lifetime of $N_2H_4^+$ becomes longer with the increase of frequency of electric current, it is supposed that $N_2H_4^+$ comes to be deactivated by each molecule of hydrogen and hydrazine. In this case, the following equations are obtained:

$$\frac{d[N_2H_4^+]}{dt}=k_1[N_2H_4]-k_2[N_2H_4^+]-k_4[N_2H_4^+]-k_5[N_2H_4^+][H_2]-k_6[N_2H_4^+][N_2H_4]=0$$

$$[N_2H_4^+]=\frac{k_1[N_2H_4]}{k_2+k_4+k_5[H_2]+k_6[N_2H_4]}$$

$$\frac{d[N_2H_4^*]}{dt}=k_2[N_2H_4^+]-k_3[N_2H_4^*]=0$$

$$[N_2H_4^*]=\frac{k_2}{k_3}[N_2H_4^+]$$

$$V=k_3[N_2H_4^+]=\frac{k_1k_2[N_2H_4]}{k_2+k_4+k_5[H_2]+k_6[N_2H_4]} \qquad (7)$$

In this decomposition, as the value of hydrogen produced in the course of the decomposition is equal to $2([N_2H_4]_0-[N_2H_4])$ the following equations are derived.

$$V=\frac{k_1k_2[N_2H_4]}{k_2+k_4+2k_5[N_2H_4]_0+(k_6-2k_5)[N_2H_4]}$$

$$\frac{[N_2H_4]}{V}=\frac{1}{k_1k_2}\{(k_2+k_4+2k_5[N_2H_4]_0)+(k_6-2k_5)[N_2H_4]\} \qquad (8)$$

where, $[N_2H_4]_0$ is the initial concentration of hydrazine. Using the results shown in Fig. 9, $N_2H_4/V$ is plotted against $N_2H_4$ as shown in Fig. 14. As is obvious from these figures, the agreement between the experiment and the calculation is satisfactory.

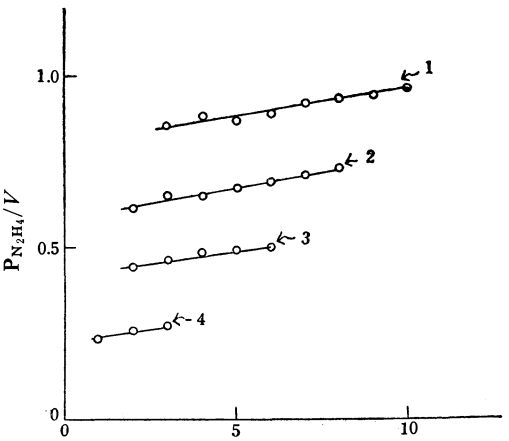



Fig. 14. Plots of $P_{N_2H_4}/V$ vs. $P_{N_2H_4}$.

| NO. | $[P_{N_2H_4}]_0$, mmHg |
|---|---|
| 1 | 12.0 |
| 2 | 9.0 |
| 3 | 6.0 |
| 4 | 3.0 |

## Summary

1) The decomposition of both ammonia and hydrazine were carried out under high frequency discharge and the effects of frequency on the chemical reactions were investigated. The frequencies of electric current were 100 and 250 MC.

2) The effects of frequency appeared clearly on the decomposition of hydrazine: under 100 MC frequency discharge the decomposition was a 1st order reaction, while under 250 MC it was approximately zero order reaction, and the overall reaction was retarded moderately by the hydrogen produced in the course of the reaction.

3) As for the decomposition of ammonia, in any case, the reactions were retarded by hydrogen. Under 100 MC frequency discharge the reaction was 1st order, while under 250 MC it was a fractional order reaction.

The author wishes to express her thanks to Professor M. Suzuki for his exceedingly kind direction throughout this work. The author also thanks Professor K. Tamaru of the University of Yokohama for his helpful advice.

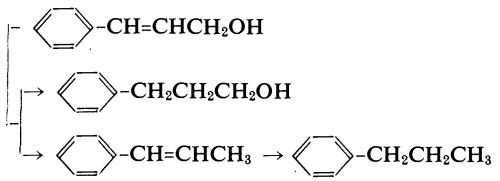
*Department of Chemistry*
*Defense Academy*
*Yokosuka*

# *Hydrogenation and Hydrogenolysis. IV*[1]*. Catalytic Reductions of Cinnamyl Alcohols and 3-Phenylpropargyl Alcohol**

By Shigeo NISHIMURA, Takeru ONODA and Akiya NAKAMURA

(Received May 9, 1960)

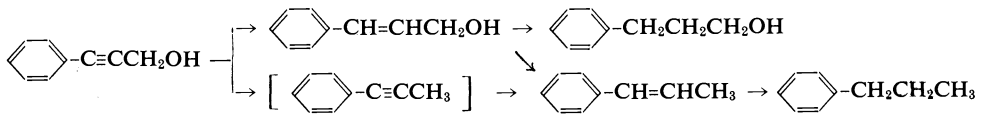
Cinnamyl alcohol may be catalytically reduced either to 3-phenyl-1-propanol, absorbing 1 mole of hydrogen, or to propylbenzene through propenylbenzene, absorbing 2 moles of hydrogen, as far as the hydrogenation is concerned with the side chain:



The reduction with nickel[2,3], cobalt[2] and copper[4] catalysts of Raney type gives phenylpropanol exclusively. Straus and Grindel[5] reduced cinnamyl alcohol with a palladium catalyst prepared by reducing palladium chloride with hydrogen in acetone, and obtained a mixture of propylbenzene (18%) and phenylpropanol (55%) with the absorption 1.38 moles of hydrogen. Baltzly and Buck[6] obtained about equal moles of the two compounds with the use of palladized charcoal in ethanol. Waser[7] obtained cyclohexylpropanol quantitatively by the reduction with a platinum black without using any solvent. Tuley and Adams[8] hydrogenated cinnamyl alcohol to phenylpropanol quantitatively in ethanol in the presence of platinum oxide and a small amount of ferrous chloride.

Different results of previous works on the hydrogenation of cinnamyl alcohol seem to be closely related to solvents and to metals and the methods of preparation of the catalysts. As reported previously[9,10], with platinum oxide as the catalyst, the hydrogenolysis of the C–O linkage with a bouble bond in $\beta,\gamma$- or $\alpha,\beta$-position is much more favored than the hydrogenation of the double bond in acidic media. On the other hand, the double bond can be hydrogenated with little hydrogenolysis or none under neutral or slightly acidic conditions. In the present investigation, the influence of solvents on the hydrogenation and hydrogenolysis of cinnamyl alcohol was re-examined in detail with platinum, palladium, rhodium and rhodium-platinum catalysts.

3-Phenylpropargyl alcohol may be catalytically reduced either to 3-phenyl-1-propanol through *cis*-cinnamyl alcohol, absorbing 2 moles of hydrogen, or to propylbenzene, through *cis*-cinnamyl alcohol or through propynylbenzene, absorbing 3 moles of hydrogen:



In order to know whether the hydrogenolysis would occur or not before the reduction of the triple bond to the double bond, the catalytic reduction of 3-phenylpropargyl alcohol and of the intermediate *cis*-cinnamyl alcohol was investigated with Adams platinum oxide as a catalyst.

## Experimental

**Substrates.**—*Cinnamyl Alcohol* (*trans*). —A commercial preparation was treated with aluminum ethoxide and absolute ethanol followed by hydrolysis with sodium hydroxide solution and extraction with ether[11], and then fractionally distilled twice under reduced pressure. B. p. 139.5~140.5°C/16 mmHg; $n_D^{21}$ 1.5820.

1) Part III of this series: S. Nishimura, This Bulletin, **33**, 566 (1960).

* Presented at the 13th Annual Meeting of the Chemical Society of Japan, Tokyo, April, 1960.

2) B. V. Aller, *J. Appl. Chem.*, **8**, 492 (1958).

3) Cinnamyl alcohol absorbed 0.98 mole of hydrogen in ethanol under ordinary conditions with T-4 Raney nickel (S. Nishimura, This Bulletin, **32**, 61 (1959)).

4) J. Jadot and R. Braine, *Bull. soc. roy. sci. Liége*, **25**, 62 (1956); *Chem. Abstr.*, **50**, 16651h (1956).

5) F. Straus and H. Grindel, *Ann.*, **439**, 276 (1924).

6) R. Baltzly and J. S. Buck, *J. Am. Chem. Soc.*, **65**, 1984 (1943).

7) E. Waser, *Helv. Chim. Acta*, **8**, 117 (1925).

8) W. F. Tuley and R. Adams, *J. Am. Chem. Soc.*, **47**, 3061 (1925).

9) S. Nishimura and K. Mori, This Bulletin, **32**, 103 (1959). Also cf. C. W. Shoppee et al., *J. Chem. Soc.*, **1957**, 3107.

10) S. Nishimura, This Bulletin, **32**, 1155 (1959).

TABLE I. MOLES OF HYDROGEN ABSORBED BY CINNAMYL ALCOHOL AT ORDINARY TEMPERATURE AND PRESSURE[a)]

| Catalyst* | Solvent | | | |
|---|---|---|---|---|
| | EtOH, 20 cc. | AcOH, 20 cc. | EtOH, 20 cc.+ 3N HCl, 0.1 cc. | AcOH, 20 cc.+ 3N HCl, 0.1 cc. |
| Pt oxide | 1.03 | 1.31 | 1.60 | 1.79 |
| Pd oxide | 1.02 | 1.10 | 1.21 | 1.63 |
| Rh-Pt (1 : 1) oxide | | 1.10 | | 1.73** |
| Rh-Pt (2 : 1) oxide | | 1.07 | | 1.71** |
| Rh-Pt (3 : 1) oxide | 0.94 | 1.04 | 1.25 | 1.66** |
| Pd-on-carbon (I) | 0.99 | | 1.22 | |
| Pd-on-carbon (II) | 1.10 | 1.07 | 1.23 | 1.57 |
| Rh-on-carbon (II) | 1.24 | 1.14 | 1.33 | 1.45 |

a) 1.342 g. (0.01 mol.) of cinnamyl alcohol was hydrogenated with 50 mg. of the oxide or 600 mg. of the supported catalysts each time.

* For the notations attached to the catalysts, see the experimental part.

** These are approximate values, because the further hydrogenation of the benzene nucleus made obscure the completion of the reduction of the side chain.

*Cinnamyl Acetate* (*trans*).—Cinnamyl alcohol was refluxed with acetic anhydride and the product was fractionated twice under reduced pressure. B. p. 140~141°C/16 mmHg ; $n_D^{21}$ 1.5439.

*3-Phenylpropargyl Alcohol.*—This compound was prepared by passing mixed nitrogen and formaldehyde gases into an ethereal solution of phenylethynylmagnesium bromide prepared from phenylacetylene and ethylmagnesium bromide[12]. The product was distilled twice under reduced pressure. B. p. 150°C/30 mmHg ; $n_D^{20}$ 1.5845.

*cis-Cinnamyl Alcohol.*—3-Phenylpropargyl alcohol was partially hydrogenated in ethyl acetate with 5% palladium-on-barium sulfate[13] poisoned with a few drops of quinoline. The rate of the hydrogenation became markedly slow after the absorption of 0.97 mole of hydrogen. The product was distilled twice under reduced pressure. B. p. 125°C/14 mmHg (lit.[13] 125.5°C/13 mmHg); $n_D^{16}$ 1.5745 (lit.[13] $n_D^{14}$ 1.573). It was confirmed by the infrared adsorption that the alcohol thus prepared contained, if any, less than 10% of its trans isomer and less than 3% of 3-phenylpropargyl alcohol*.

**Catalysts.** — Platinum oxide was prepared by fusion of ammonium chloroplatinate with sodium nitrate according to the method of Bruce[14].

Palladous oxide was prepared by the fusion of palladium chloride with sodium nitrate according to the method of Shriner and Adams[15].

Rhodium-platinum oxide catalysts were prepared by fusion of the mixtures of rhodium chloride and chloroplatinic acid or ammonium chloroplatinate with sodium nitrate as reported previously[1]. The figures in parentheses in Table I indicate the ratios of rhodium to platinum by the weights of the metals.

Palladium-on-carbon (I) (5% Pd) was prepared by reducing a palladium chloride solution with aqueous formaldehyde and sodium hydroxide[16].

Palladium-on-carbon (II) and rhodium-on-carbon (II) (5% Pd or Rh) were prepared by reducing palladium and rhodium chloride solutions with hydrogen with the addition of sodium acetate[17].

**Solvents.**—*Acetic Acid.* — Glacial acetic acid of Wakō Pure Chemical Industries G. R. grade was used without further purification.

*Ethanol.*—Commercial 95% ethanol was used after distillation.

**Hydrogenation.**—Hydrogenation was carried out at room temperature (20~25°C) and atmospheric pressure. After the catalyst was shaken with hydrogen in 15 cc. of the solvent until no more hydrogen was absorbed, the substance, dissolved in 5 cc. of the solvent, was added. The mixture was shaken with hydrogen at about 350~400 oscillations per minute. In using rhodium-platinum oxide catalysts, hydrochloric acid was added after the oxide was reduced to the metal, since the presence of hydrochloric acid greatly retarded the reduction of the oxide.

## Results and Discussion

**Catalytic Reduction of Cinnamyl Alcohol (trans).**—The effects of solvents on the hydrogenation of cinnamyl alcohol are summarized in Table I in the moles of hydrogen absorbed per mole of cinnamyl alcohol. As expected from previous results, little hydrogenolysis or none occurred in neutral ethanolic solution[18]

11) H. Meerwein and R. Schmidt, *Ann.*, **444**, 221 (1925).
12) H. H. Guest, *J. Am. Chem. Soc.*, **47**, 860 (1925).
13) Cf. M. Bourguel, *Bull. soc. chim. France*, [4], **45**, 1083 (1929).
* The authors wish to thank Dr. H. Iwamura of this laboratory for his kind help in the measurement of infrared spectra.
14) W. F. Bruce, *J. Am. Chem. Soc.*, **58**, 687 (1936); R. Adams, V. Voorhees and R. L. Shriner, "Organic Syntheses", Col. Vol. 1, 2nd Ed., John Wiley & Sons, Inc., New York (1941), p. 463.
15) R. L. Shriner and R. Adams, *J. Am. Chem. Soc.*, **46**, 1683 (1924).
16) R. Mozingo, "Organic Syntheses", Col. Vol. 3, John Wiley & Sons, Inc., New York (1955), p. 685 (Method B).
17) Method D in Ref. 16.
18) The hydrogen uptake less than 1 mole with rhodium-platium (3 : 1) oxide in ethanol may be due to dimerization though it has not been investigated further.

TABLE II. EFFECT OF VARYING AMOUNTS OF ADDED HYDROCHLORIC ACID ON THE HYDROGEN UPTAKE BY CINNAMYL ALCOHOL[a]

| Solvent | Hydrogen uptake mol./mol. |
|---|---|
| AcOH, 20 cc.+3N HCl, 0.025 cc. | 1.72 |
| 〃 , 0.05 cc. | 1.78 |
| 〃 , 0.10 cc. | 1.78 |
| 〃 , 0.15 cc. | 1.79 |
| 〃 , 0.20 cc. | 1.79 |

a) 1.342 g. (0.01 mol.) of cinnamyl alcohol was hydrogenated with 50 mg. of platinum oxide each time.

TABLE III. CATALYTIC REDUCTIONS OF CINNAMYL ACETATE AND CINNAMYL ALCOHOL[a]

| Solvent | Hydrogen uptake mol./mol. | |
|---|---|---|
| | Cinnamyl acetate | Cinnamyl alcohol |
| AcOH, 20 cc. | 1.30 | 1.31 |
| EtOH, 20 cc. +3N HCl, 0.1 cc. | 1.50 | 1.60 |
| AcOH, 20 cc. +3N HCl, 0.1 cc. | 1.80 | 1.79 |

a) 0.01 mol. of the substrate was hydrogenated with 50 mg. of platinum oxide each time.

except in hydrogenation with palladium-on-carbon (II) and rhodium-on-carbon (II), which were prepared from acidic media though washed with water many times and dried before use. Generally, the absorption of hydrogen increased in the following order with respect to the solvents; ethanol, acetic acid, ethanol with hydrochloric acid, and acetic acid with hydrochloric acid. This may be interpreted as the order of the abilities of the solvents as proton donors, which may become clearer by considering their conjugate acids, namely, $EtOH < AcOH < EtOH_2^+ < AcOH_2^+$[19], indicating that the hydrogenolysis is acid-catalyzed[20]. With respect to the catalysts, platinum oxide causes the greatest absorption of hydrogen[21], and rhodium added to platinum decreases the hydrogenolysis markedly. For instance, in acetic acid with hydrochloric acid, as much as 79% of cinnamyl alcohol is reduced to propylbenzene with platinum oxide. On the other hand, with rhodium-platinum (3 : 1) oxide only 4% is hydrogenolyzed in acetic acid, compared with 31% with platinum oxide in the same solvent.

Table II shows the effect of varying amounts of added hydrochloric acid on the hydrogen uptake by cinnamyl alcohol in acetic acid with platinum oxide as a catalyst. It is seen that a very small amount of hydrochloric acid is sufficient for the maximum absorption of hydrogen and further addition has little effect. It seems improbable that the greater absorption of hydrogen would result from the intermediate formation of cinnamyl acetate, because cinnamyl acetate absorbed no more hydrogen than cinnamyl alcohol in hydrogenation with platinum oxide as shown in Table III.

With respect to the activities of the three oxide catalysts, it may be said that the order was as follows; rhodium-platinum (3 : 1) oxide > palladous oxide > platinum oxide, though an accurate comparison was not possible because of the different amounts of hydrogen absorbed. For example, with 50 mg. of each catalyst, 1.342 g. (0.01 mol.) of cinnamyl alcohol was reduced in 11 min. with rhodium-platinum (3:1) oxide, in 14 min. with palladous oxide, and in 26 min. with platinum oxide, in 20 cc. of acetic acid at 25°C and under atmospheric pressure.

**Catalytic Reduction of 3-Phenylpropargyl Alcohol and *cis*-Cinnamyl Alcohol.**—Table IV summarizes the results of the hydrogenation of 3-phenylpropargyl alcohol and *cis*-cinnamyl alcohol in various solvents with the use of platinum oxide as a catalyst together with those of the trans isomer. It is seen from the table that 3-phenylpropargyl alcohol absorbs nearly one mole of hydrogen more than *cis*-cinnamyl alcohol in any solvent used. This means that little hydrogenolysis or none occurred before the reduction of the triple bond to the double bond. The result may be explained by the strong affinity of the triple bond for the catalyst surface, which may prevent the C–O linkage from being adsorbed

TABLE IV. CATALYTIC REDUCTIONS OF 3-PHENYLPROPARGYL ALCOHOL AND CINNAMYL ALCOHOL[a]

| Solvent | Hydrogen uptake mol./mol. | | |
|---|---|---|---|
| | 3-Phenylpropargyl alcohol | Cinnamyl alcohol *cis*- | *trans*- |
| EtOH, 20 cc. | 2.01 | 1.04 | 1.03 |
| AcOH, 20 cc. | 2.29 | 1.24 | 1.31 |
| EtOH, 20 cc. +3N HCl, 0.1 cc. | 2.64 | 1.64 | 1.60 |
| AcOH, 20 cc. +3N HCl, 0.1 cc. | 2.79 | 1.77 | 1.79 |

a) 0.01 mol. of the substrate was hydrogenated with 50 mg. of platinum oxide each time.

19) For the superacidic character of hydrochloric acid in acetic acid, see for instance; G. Schwarzenbach and P. Stensby, *Helv. Chim. Acta*, **42**, 2342 (1959).

20) This does not mean that the hydrogenation of the double bond is unaffected by acid, but does mean that the hydrogenolysis is much more promoted by acid than the hydrogenation.

21) This does not mean necessarily that platinum oxide has the highest activity for the hydrogenolysis. The lower values for palladous oxide may probably result from its greater activity for the hydrogenation of the double bond.

on the surface of the catalyst, just as the triple bond is more tightly adsorbed than the double bond. Though the fact that *cis*-cinnamyl alcohol absorbed almost as much hydrogen as its trans isomer seems to suggest isomerization to a large extent in the course of the reduction, it will be difficult to say whether or not this is the case from the data now available[22].

## Summary

1. The hydrogenation and hydrogenolysis of cinnamyl alcohol was studied with platinum, palladium, rhodium, and rhodium-platinum catalysts. The following results were obtained:

(i) The absorption of hydrogen increases with respect to the solvents in the following order; ethanol, acetic acid, ethanol with hydrochloric acid, and acetic acid with hydrochloric acid. The order was interpreted as that of the abilities of the solvents as proton donors.

(ii) With respect to the catalysts, platinum oxide causes the maximum absorption of hydrogen, and rhodium added to platinum decreases the hydrogenolysis markedly.

(iii) With respect to the activities of the three oxide catalysts in acetic acid, the order was; rhodium-platinum (3 : 1) oxide > palladous oxide > platinum oxide.

2. From the comparison of the hydrogen uptakes by 3-phenylpropargyl alcohol and by *cis*-cinnamyl alcohol, it was shown that little hydrogenolysis or none occurs before the reduction of the triple bond of the phenylpropargyl alcohol to the double bond.

The authors wish to express their hearty thanks to Professor Yoshiyuki Urushibara for his valuable suggestions and encouragement. The authors are also indebted to the Ministry of Education for a Grant-in-Aid for Scientific Research.

*Department of Chemistry*
*Faculty of Science*
*The University of Tokyo*
*Hongo, Tokyo*

22) Cf. R. L. Burwell, Jr., *Chem. Revs.*, **57**, 895 (1957).

# *Infrared Spectra and Normal Vibrations of Formamide; $HCONH_2$, $HCOND_2$, $DCONH_2$ and $DCOND_2$*

By Isao SUZUKI

(Received May 7, 1960)

A number of investigations have been made on the molecular structure of formamide. The geometrical structure of the molecule was precisely determined by the studies of the microwave spectrum[1-3], X-ray diffraction[4], and nuclear magnetic resonance[5]. It was indicated that the formamide molecule is planar in the solid state and is nearly planar and of very shallow pyramidal configuration as to the C-$NH_2$ group in the gaseous state. The Raman and infrared spectra of $HCONH_2$ were observed by a number of investigators in the gaseous, liquid, and solid states and in solutions[6-13]. The infrared spectra of *N*-deuterated formamide, $HCOND_2$, were also observed in the liquid state and in solutions[11,13]. A normal coordinate treatment of the molecule as a three-body problem was made by Miyazawa[13]. However, a full analysis of the normal vibrations of the formamide molecule has never been attempted, and the assignments of the observed frequencies are not yet complete.

In order to clarify the nature of the normal vibrations of the formamide molecule, the present writer observed the infrared spectra of *C*-deuterated formamides; $DCONH_2$ and $DCOND_2$. The infrared spectra of undeuterated

1) R. J. Kurland, *J. Chem. Phys.*, **23**, 2202 (1955).
2) R. J. Kurland and E. B. Wilson Jr., ibid., **27**, 585 (1957).
3) C. C. Costain and J. M. Dowling, ibid., **32**, 158 (1960).
4) C. Post and J. Ladell, *Acta Cryst.*, **7**, 559 (1954).
5) R. A. Krombrout and G. B. Moulton, *J. Chem. Phys.*, **25**, 35 (1956).
6) B. D. Saksena, *Proc. Indian Acad. Sci.*, **11**, 53 (1940).
7) A. L. SunderRao, *J. Indian Chem. Soc.*, **18**, 337 (1941),
8) L. Kohovec and H. Wasmuth, *Z. Physik. Chem.*, **48B**, 70 (1941).
9) P. G. Puranik and K. Venkata Raman, *J. Mol. Spectroscopy*, **3**, 486 (1959).
10) J. Lecomte and R. Freymann, *Bull. Soc. Chim.*, **8**, 612 (1941).
11) J. C. Evans, *J. Chem. Phys.*, **22**, 1228 (1954); **31**, 1435 (1959).
12) M. Davies and J. C. Evans, ibid., **20**, 342 (1952).
13) T. Miyazawa, *J. Chem. Soc. Japan, Pure Chem. Sec.* (*Nippon Kagaku Zasshi*), **76**, 821 (1955); **77**, 366 (1956).

formamide ($HCONH_2$) and *N*-deuterated formamide ($HCOND_2$) have been remeasured.

A normal coordinate treatment has been made for all of these four molecules as a six-body problem. Fourteen force constants have been determined so that all the thirty-six observed frequencies are thereby explained. With these force constants, the vibrational mode and the potential energy distribution among the symmetry coordinates have been calculated for each normal vibration.

The purpose of this paper is to give the results of these observations and calculations and to present a complete assignment of the observed frequencies and a detailed discussion on the nature of each normal vibration of the formamide molecule.

## Experimental

**Formamide $HCONH_2$.** — The sample used was obtained from a commercial source, and was purified several times by vacuum distillation; b. p. 86°C (5 mmHg).

***C*-Deuterated Formamide $DCONH_2$.**—This compound was prepared from DCOOD and urea by the following procedures. First, DCOOD was prepared by the thermal decomposition of anhidrous heavy oxalic acid $(COOD)_2$ which was obtained by the exchange reaction of $(COOH)_2$ and $D_2O$[14]. DCOOD was then mixed with urea and heated at about 150°C for 4 hr.[15] Ammonia, carbon dioxide and water produced by the reaction were pumped out in vacuum. From the residual, $DCONH_2$ was distilled out. It was treated with a small amount of aqueous solution of potassium hydroxide to neutralize the remaining free acid and distilled in vacuum again.

Replacement of the amide hydrogen by deuterium was accomplished by adding an excess of $D_2O$, evaporating the heavy water in vacuum, and repeating this procedure three times.

**Infrared Spectra.**—Infrared spectra were measured in the region from 3600 to 525 $cm^{-1}$ with a Perkin-Elmer grating spectrometer model 112G equipped with a KBr foreprism[16], and in the region from 700 to 300 $cm^{-1}$ with a Perkin-Elmer spectrometer model 21, equipped with a CsBr prism. All the measurements were made in the liquid state.

## Infrared Spectra

Infrared spectra of $HCONH_2$ and $DCONH_2$ are shown in Figs. 1 (a)–(c), and those of $HCOND_2$ and $DCOND_2$ in Figs. 2 (a)–(c). As may be expected, the bands at 2882, 1391 and 1056 $cm^{-1}$ of $HCONH_2$ which are assigned respectively to the CH stretching, CH in-plane and out-of-plane deformation vibrations, completely disappear on the *C*-deuteration, and

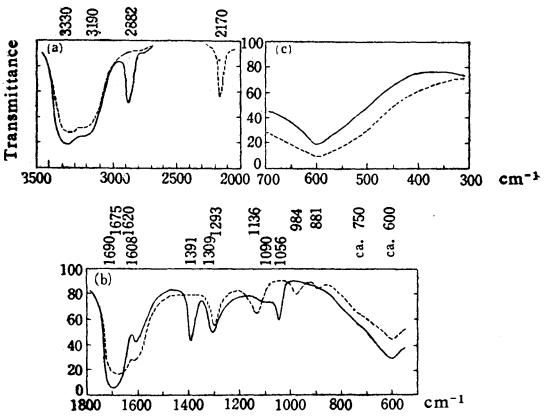



Fig. 1. Infrared spectra of $HCONH_2$ and $DCONH_2$.
(a) 3600~2000 $cm^{-1}$ (b) 1800~525 $cm^{-1}$
(c) 700~300 $cm^{-1}$;
—— $HCONH_2$ and ---- $DCONH_2$.

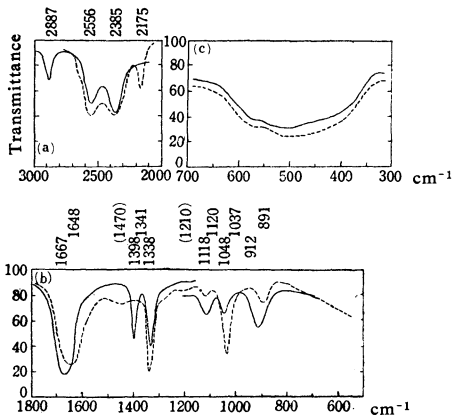



Fig. 2. Infrared spectra of $HCOND_2$ and $DCOND_2$.
(a) 3000~2000 $cm^{-1}$ (b) 1800~525 $cm^{-1}$
(c) 700~300 $cm^{-1}$;
—— $HCOND_2$ and ---- $DCOND_2$.

new bands appear at 2170, 984 and 881 $cm^{-1}$. These are assigned to the CD stretching, CD in-plane and out-of-plane deformation vibrations respectively. Besides these, every band below 1700 $cm^{-1}$ is more or less affected by the *C*-deuteration as well as by the *N*-deuteration. This fact suggests that, in almost every normal mode, the CH, $NH_2$, CD and/or $ND_2$ deformation motions more or less take place.

When $HCOND_2$ or $DCOND_2$ was exposed in the atomopheric air for a while, several weak bands appeared besides the absorption bands illustrated in Figs. 2 (a)–(c). These bands are supposed to be arising from *N*-monosubstituted amides, which were produced by the partial hydrogenation due to the atomospheric water vapour. The positions of these bands were also determined; 3300, 2460, 1470, 1212 and about 700 $cm^{-1}$ for HCONHD (both cis and

14) R. F. Curl, Jr., *J. Chem. Phys.*, **30**, 1529 (1959).
15) E. Cherabliez and F. Landolt, *Helv. Chim. Acta*, **29**, 1438 (1946).
16) S. Mizushima et al., A Report on the Perkin-Elmer Grating Spectrophotometer Model 112G, The Perkin-Elmer Corp. (1959).

TABLE I. THE SYMMETRY COORDINATES

| Symmetry coordinate | | Vibrational mode | Abr. |
|---|---|---|---|
| $S_1$ | $(\Delta r_{NHa}-\Delta r_{NHb})/\sqrt{2}$ | $NH_2$ antisym. stretching | $\nu_a(NH_2)$ |
| $S_2$ | $(\Delta r_{NHa}+\Delta r_{NHb})/\sqrt{2}$ | $NH_2$ symm. stretching | $\nu_s(NH_2)$ |
| $S_3$ | $\Delta r_{CH}$ | CH stretching | $\nu$(CH) |
| $S_4$ | $\Delta r_{CO}$ | CO stretching | $\nu$(CO) |
| $S_5$ | $\Delta r_{CN}$ | CN stretching | $\nu$(CN) |
| $S_6$ | $(2\Delta\alpha_{HNH}-\Delta\alpha_{CNHa}-\Delta\alpha_{CNHb})/\sqrt{6}$ | $NH_2$ bending | $b(NH_2)$ |
| $S_7$ | $(\Delta\alpha_{NCH}-\Delta\alpha_{HCO})/\sqrt{2}$ | CH deformation | $\delta$(CH) |
| $S_8$ | $(\Delta\alpha_{CNHa}-\Delta\alpha_{CNHb})/\sqrt{2}$ | $NH_2$ rocking | $r(NH_2)$ |
| $S_9$ | $(2\Delta\alpha_{OCN}-\Delta\alpha_{NCH}-\Delta\alpha_{HCO})/\sqrt{6}$ | NCO deformation | $\delta$(NCO) |
| $S_{10}$ | $(\Delta\alpha_{CNHa}+\Delta\alpha_{CNHb}+\Delta\alpha_{HNH})/\sqrt{3}$ | redundant | — |
| $S_{11}$ | $(\Delta\alpha_{NCH}+\Delta\alpha_{HCO}+\Delta\alpha_{OCN})/\sqrt{3}$ | redundant | — |

TABLE II. THE FINAL SET OF FORCE CONSTANTS (md/A)

| | | | | | |
|---|---|---|---|---|---|
| $K_{NH}$ | 5.80 | $H_{HNH}$ | 0.40 | $F_{H\cdots H}$ | 0 |
| $K_{CH}$ | 3.74 | $H_{HNC}$ | 0.32 | $F_{H\cdots C}$ | 0.46 |
| $K_{CO}$ | 8.80 | $H_{HCN}$ | 0.18 | $F_{H\cdots N}$ | 0.70 |
| $K_{CN}$ | 6.15 | $H_{HCO}$ | 0.20 | $F_{H\cdots O}$ | 0.92 |
| $F'=-F/10$ | | $H_{NCO}$ | 0.34 | $F_{O\cdots N}$ | 1.50 |

trans forms), and 3300, 2460, 1470, 1290, 1053 and about 700 $cm^{-1}$ for DCONHD.

The values of the observed frequencies are given in the first column of Table III.

## Calculation of Normal Vibrations

The calculation of normal vibrations was made by the method presented by Wilson[17], according to which the secular equation was set in the form $|\boldsymbol{GF}-\lambda\boldsymbol{E}|=0$, where $\boldsymbol{F}$ and $\boldsymbol{G}$ are the potential and reciprocal kinetic energy matrices respectively. It was assumed that the molecule has a planar configuration ($C_s$), the normal vibrations are classified into 9 in-plane (A′) and 3 out-of-plane (A″) vibrations. In the present paper, only the in-plane vibrations were treated. The structural parameters used in this calculation are as follows; the bond lengths of $r$(NH) = 1.04, $r$(CN) = 1.30, $r$(CH) = 1.07 and $r$(C=O) = 1.225 A[4,5], all the bond angles are assumed to be 120°. The symmetry coordinates $\boldsymbol{S}$ obtained from the internal coordinates $\boldsymbol{R}$ by a linear transformation;

$$\boldsymbol{S}=\boldsymbol{UR}$$

are given in Table I.

**Force Constants.** — The potential function employed in the calculation is of the Urey-Bradley type[18];

$$2V=\sum K_i(\Delta r_i)^2+\sum H_{ij}r^0{}_i r^0{}_j(\Delta\alpha_{ij})^2 + \sum F_{ij}(\Delta q_{ij})^2+\text{linear terms}$$

where $r_i$ and $r_j$ are bond lengths with equilibrium values $r^0{}_i$ and $r^0{}_j$; $\alpha_{ij}$ are bond angles and $q_{ij}$ distances betweeen nonbonded atoms. $K$, $H$ and $F$ are stretching, bending and repulsive force constants respectively.

The values of the force constants were first transferred from diformylhydrazine, *N*-methylacetamide[19] and urea[20]. A refinement of the values of the force constants was made by the method developed by Miyazawa[21]. The final set of their values is given in Table II, and the calculated frequencies with these values are shown in the second column of Table III.

The calculated frequencies are in excellent agreement with the observed ones, the maximum deviation being 3.0% and the average deviation 1.3%. Therefore, the values of the force constants obtained in this calculation may be used for the normal vibration calculations of the molecules which are closely related with formamide[22].

***L* Matrix and Potential Energy Distribution.** —In order to clarify the nature of the observed frequencies precisely, it is desirable to calculate the relative amplitude of each symmetry coordinate in a given normal mode of vibration. The symmetry coordinates $\boldsymbol{S}$ are related linearly to the normal coordinates $\boldsymbol{Q}$ through the matrix expression;

$$\boldsymbol{S}=\boldsymbol{LQ}$$

The relative amplitude for each symmetry coordinate in a given normal vibration is given

17) E. B. Wilson, *J. Chem. Phys.*, **7**, 1047 (1939); **9**, 96 (1941).
18) T. Shimanouchi, ibid., **17**, 245, 734, 848 (1949).
19) T. Miyazawa, T. Shimanouchi and S. Mizushima, ibid., **29**, 611 (1959).
20) A. Yamaguchi, T. Miyazawa, T. Shimanouchi and S. Mizushima, *Spectrochim. Acta*, **10**, 170 (1957).
21) T. Miyazawa, *J. Chem. Soc. Japan, Pure Chem. Sec.* (*Nippon Kagaku Zasshi*), **76**, 1132 (1955).
22) I. Suzuki, to be published.

TABLE III. THE OBSERVED AND CALCULATED FREQUENCIES, AND POTENTIAL ENERGY DISTRIBUTIONS

| | | Frequency | | | P. E. D. $(F_{ii}L^2_{is}/\lambda_s)\times 100$ | | | | | | | | |
|---|---|---|---|---|---|---|---|---|---|---|---|---|---|
| | | $\nu_{obs}$ | $\nu_{calc}$ | $\Delta$ | $S_1$ | $S_2$ | $S_3$ | $S_4$ | $S_5$ | $S_6$ | $S_7$ | $S_8$ | $S_9$ |
| $HCONH_2$ | $\nu_1$ | 3330 | 3367 | −1.1 | 100 | 0 | 0 | 0 | 0 | 0 | 0 | 0 | 0 |
| | $\nu_2$ | 3190 | 3268 | −2.5 | 0 | 99 | 0 | 0 | 0 | 0 | 0 | 0 | 0 |
| | $\nu_3$ | 2882 | 2935 | −1.8 | 0 | 0 | 102 | 0 | 0 | 0 | 0 | 0 | 0 |
| | $\nu_4$ | 1690 | 1681 | +0.5 | 0 | 1 | 0 | 64 | 33 | 8 | 19 | 3 | 0 |
| | $\nu_5$ | 1608 | 1606 | +0.1 | 0 | 0 | 0 | 11 | 3 | 85 | 3 | 1 | 1 |
| | $\nu_6$ | 1391 | 1398 | −0.5 | 0 | 0 | 1 | 19 | 7 | 0 | 65 | 2 | 4 |
| | $\nu_7$ | 1309 | 1304 | +0.4 | 0 | 0 | 0 | 1 | 57 | 6 | 13 | 13 | 9 |
| | $\nu_8$ | 1090 | 1103 | −1.2 | 0 | 0 | 0 | 11 | 8 | 1 | 1 | 73 | 1 |
| | $\nu_9$ | 608 | 617 | −1.5 | 0 | 0 | 1 | 0 | 0 | 0 | 0 | 8 | 90 |
| $HCOND_2$ | $\nu_1$ | 2556 | 2494 | +2.4 | 100 | 0 | 0 | 0 | 0 | 0 | 0 | 1 | 0 |
| | $\nu_2$ | 2385 | 2361 | +1.0 | 0 | 98 | 0 | 0 | 2 | 1 | 0 | 0 | 0 |
| | $\nu_3$ | 2887 | 2936 | −1.7 | 0 | 0 | 102 | 0 | 0 | 0 | 0 | 0 | 0 |
| | $\nu_4$ | 1667 | 1672 | −0.3 | 0 | 0 | 0 | 73 | 29 | 1 | 22 | 2 | 0 |
| | $\nu_5$ | 1398 | 1400 | −0.1 | 0 | 0 | 1 | 25 | 16 | 3 | 49 | 1 | 5 |
| | $\nu_6$ | 1338 | 1362 | +1.8 | 0 | 2 | 0 | 1 | 43 | 22 | 30 | 1 | 3 |
| | $\nu_7$ | 1118 | 1098 | +1.8 | 0 | 1 | 0 | 0 | 14 | 69 | 1 | 6 | 9 |
| | $\nu_8$ | 912 | 905 | +0.8 | 0 | 0 | 0 | 6 | 4 | 4 | 0 | 66 | 13 |
| | $\nu_9$ | 570 | 554 | +2.7 | 0 | 0 | 1 | 0 | 0 | 1 | 0 | 24 | 74 |
| $DCONH_2$ | $\nu_1$ | 3330 | 3366 | −1.1 | 100 | 0 | 0 | 0 | 0 | 0 | 0 | 0 | 0 |
| | $\nu_2$ | 3190 | 3266 | −2.5 | 0 | 100 | 0 | 0 | 0 | 0 | 0 | 0 | 0 |
| | $\nu_3$ | 2170 | 2146 | +1.1 | 0 | 0 | 103 | 2 | 1 | 0 | 0 | 0 | 1 |
| | $\nu_4$ | 1675 | 1669 | +0.4 | 0 | 0 | 0 | 62 | 37 | 14 | 9 | 3 | 0 |
| | $\nu_5$ | 1620 | 1609 | +1.2 | 0 | 1 | 0 | 18 | 1 | 80 | 2 | 1 | 1 |
| | $\nu_6$ | 1293 | 1313 | −1.6 | 0 | 0 | 0 | 11 | 60 | 6 | 3 | 11 | 12 |
| | $\nu_7$ | 1136 | 1120 | −1.4 | 0 | 0 | 0 | 13 | 2 | 0 | 8 | 71 | 2 |
| | $\nu_8$ | 984 | 998 | −1.4 | 0 | 0 | 0 | 0 | 7 | 1 | 80 | 6 | 0 |
| | $\nu_9$ | 600 | 610 | −1.5 | 0 | 0 | 0 | 0 | 0 | 0 | 1 | 8 | 90 |
| $DCOND_2$ | $\nu_1$ | 2556 | 2498 | +2.4 | 100 | 0 | 0 | 0 | 0 | 0 | 0 | 1 | 0 |
| | $\nu_2$ | 2383 | 2362 | +0.9 | 0 | 98 | 0 | 0 | 2 | 1 | 0 | 0 | 0 |
| | $\nu_3$ | 2175 | 2146 | +1.3 | 0 | 0 | 103 | 2 | 1 | 0 | 0 | 0 | 0 |
| | $\nu_4$ | 1648 | 1654 | −0.4 | 0 | 0 | 0 | 78 | 32 | 1 | 11 | 2 | 0 |
| | $\nu_5$ | 1341 | 1366 | −1.9 | 0 | 2 | 0 | 18 | 56 | 23 | 0 | 2 | 7 |
| | $\nu_6$ | 1120 | 1123 | −0.3 | 0 | 1 | 0 | 2 | 8 | 63 | 19 | 1 | 6 |
| | $\nu_7$ | 1037 | 1006 | +3.0 | 0 | 0 | 0 | 2 | 5 | 8 | 62 | 14 | 4 |
| | $\nu_8$ | 891 | 891 | 0 | 0 | 0 | 0 | 4 | 5 | 5 | 10 | 56 | 12 |
| | $\nu_9$ | 560 | 548 | +2.4 | 0 | 0 | 0 | 0 | 0 | 0 | 1 | 24 | 76 |

$\Delta = [\nu_{obs} - \nu_{calc}/\nu_{obs}] \times 100$

by the corresponding element of the $L$ matrix. The elements of the $L$ matrix computed for each species of formamide are given in Table IV. (The $L$ matrix is normalized to $G$; $LL' = G$[23])

It has been shown that the ratios of the potential energy distribution (P. E. D.) among the symmetry coordinates ($S_i$) for a given normal coordinate ($Q_s$) can approximately be expressed as $F_{ii}L^2_{is}/\lambda_s$,[24] where $F_{ii}$ is a diagonal element of the $F$ matrix, $\lambda_s$ is $s$th frequency parameter. These are also computed and the results are shown in Table III.

**Numerical Computations.**—All the numerical computations were carried out with a parametron computor PC 1, which was designed and constructed by Professor H. Takahashi and his collaborators in the Department of Physics, Faculty of Science, University of Tokyo. The routines used in the computations have been programmed by Shimanouchi, Takeda and the present writer. The details will be published elsewhere[23].

## The Nature of the Observed Bands

Based on the calculated values of vibrational amplitudes and potential energy distributions

23) T. Shimanouchi and I. Suzuki, to be published.
24) Y. Morino and K. Kuchitsu, *J. Chem. Phys.*, **20**, 1809 (1953). I. Nakagawa, *J. Chem. Soc. Japan, Pure Chem. Sec. (Nippon Kagaku Zasshi)*, **74**, 243 (1953).

TABLE IV. THE ELEMENTS OF THE $L$ MATRICES

| | $S_1$ | $S_2$ | $S_3$ | $S_4$ | $S_5$ | $S_6$ | $S_7$ | $S_8$ | $S_9$ | |
|---|---|---|---|---|---|---|---|---|---|---|
| $Q_1$ | 1.048 | −0.001 | −0.013 | 0.002 | 0.000 | 0.001 | −0.051 | 0.128 | 0.076 | |
| $Q_2$ | 0.001 | 1.012 | −0.028 | −0.002 | −0.049 | −0.196 | −0.009 | −0.001 | −0.005 | |
| $Q_3$ | 0.013 | 0.028 | 1.035 | −0.031 | −0.031 | 0.010 | −0.031 | 0.075 | 0.114 | |
| $Q_4$ | 0.003 | 0.007 | −0.001 | −0.316 | 0.254 | 0.530 | −0.724 | 0.297 | 0.079 | |
| $Q_5$ | −0.002 | 0.053 | −0.017 | 0.126 | 0.069 | 1.606 | 0.284 | −0.158 | −0.090 | $HCONH_2$ |
| $Q_6$ | 0.008 | 0.007 | 0.043 | −0.142 | −0.094 | 0.094 | 1.106 | 0.185 | 0.208 | |
| $Q_7$ | −0.004 | −0.015 | −0.018 | 0.033 | 0.258 | −0.359 | 0.466 | −0.453 | −0.288 | |
| $Q_8$ | 0.014 | −0.002 | −0.015 | 0.087 | 0.081 | −0.097 | 0.129 | 0.914 | 0.105 | |
| $Q_9$ | −0.009 | 0.001 | 0.017 | 0.004 | 0.010 | −0.028 | −0.037 | −0.170 | 0.427 | |
| $Q_1$ | 0.776 | −0.007 | 0.013 | −0.002 | 0.001 | 0.004 | −0.088 | 0.204 | 0.115 | |
| $Q_2$ | 0.008 | 0.726 | 0.022 | −0.001 | −0.090 | −0.250 | −0.008 | 0.004 | 0.009 | |
| $Q_3$ | −0.010 | −0.014 | 1.035 | −0.031 | −0.028 | 0.016 | −0.029 | 0.067 | 0.112 | |
| $Q_4$ | 0.007 | −0.014 | −0.003 | 0.336 | −0.237 | −0.149 | 0.770 | −0.238 | −0.082 | |
| $Q_5$ | 0.008 | −0.019 | 0.048 | −0.165 | −0.146 | −0.272 | 0.959 | 0.148 | 0.239 | $HCOND_2$ |
| $Q_6$ | 0.009 | 0.052 | −0.013 | 0.039 | 0.234 | 0.699 | 0.725 | −0.156 | −0.170 | |
| $Q_7$ | −0.006 | 0.035 | 0.011 | −0.011 | −0.106 | 0.992 | −0.122 | 0.249 | 0.237 | |
| $Q_8$ | −0.003 | −0.002 | −0.003 | 0.053 | 0.046 | −0.205 | 0.060 | 0.708 | 0.237 | |
| $Q_9$ | −0.011 | 0.001 | 0.015 | −0.001 | 0.008 | −0.044 | −0.036 | −0.261 | 0.347 | |
| $Q_1$ | 1.048 | −0.003 | −0.003 | 0.001 | 0.000 | 0.001 | −0.047 | 0.128 | 0.077 | |
| $Q_2$ | 0.004 | 1.012 | −0.006 | −0.002 | −0.050 | −0.196 | −0.007 | 0.000 | −0.003 | |
| $Q_3$ | 0.005 | 0.008 | 0.770 | −0.064 | −0.047 | 0.018 | −0.035 | 0.145 | 0.184 | |
| $Q_4$ | 0.004 | 0.012 | −0.028 | −0.310 | 0.266 | 0.680 | −0.486 | 0.274 | 0.065 | |
| $Q_5$ | −0.003 | 0.052 | 0.003 | 0.162 | 0.038 | 1.553 | 0.198 | −0.176 | −0.091 | $DCONH_2$ |
| $Q_6$ | 0.006 | 0.017 | −0.004 | −0.101 | −0.268 | 0.351 | 0.228 | 0.423 | 0.328 | |
| $Q_7$ | 0.013 | −0.001 | −0.024 | 0.095 | 0.043 | −0.053 | −0.316 | 0.912 | 0.107 | |
| $Q_8$ | 0.006 | −0.001 | 0.009 | 0.003 | 0.067 | −0.087 | 0.876 | 0.239 | 0.051 | |
| $Q_9$ | −0.009 | 0.001 | 0.011 | 0.003 | 0.009 | −0.026 | −0.056 | −0.166 | 0.423 | |
| $Q_1$ | 0.777 | −0.004 | −0.006 | −0.001 | 0.001 | 0.004 | −0.073 | 0.202 | 0.112 | |
| $Q_2$ | 0.004 | 0.726 | −0.028 | 0.003 | −0.088 | −0.251 | 0.004 | −0.004 | −0.001 | |
| $Q_3$ | 0.006 | 0.027 | 0.760 | −0.064 | −0.051 | −0.002 | −0.033 | 0.126 | 0.183 | |
| $Q_4$ | 0.004 | −0.017 | 0.023 | 0.344 | −0.245 | −0.165 | 0.525 | −0.231 | −0.077 | |
| $Q_5$ | 0.001 | 0.052 | −0.001 | 0.135 | 0.268 | 0.711 | −0.104 | −0.194 | −0.261 | $DCOND_2$ |
| $Q_6$ | 0.001 | 0.038 | 0.004 | −0.041 | −0.081 | 0.965 | 0.478 | 0.124 | 0.202 | |
| $Q_7$ | 0.009 | −0.007 | 0.018 | −0.035 | 0.056 | −0.307 | 0.773 | −0.371 | −0.143 | |
| $Q_8$ | −0.002 | −0.002 | −0.004 | 0.043 | 0.052 | −0.226 | 0.282 | 0.643 | 0.226 | |
| $Q_9$ | −0.010 | 0.001 | 0.011 | −0.001 | 0.007 | −0.042 | −0.056 | −0.257 | 0.347 | |

shown in Tables III and IV, the nature of the observed bands will be discussed.

**The Bands above 2000 cm$^{-1}$.**—The 3330, 3190 and 2882 cm$^{-1}$ bands of $HCONH_2$ are undoubtedly assigned respectively to the $NH_2$ antisymmetric, $NH_2$ symmetric stretching and the CH stretching vibrations. As may be seen from Table III, each of the normal vibrations corresponding to these frequencies takes place along one of these symmetry coordinates, and practically no other vibrations are coupled with it. The bands at 3330, 3190 and 2170 cm$^{-1}$ of $DCONH_2$ are likewise shown to be almost pure $NH_2$ antisymmetric, $NH_2$ symmetric stretching and CD stretching vibrations respectively. In a similar way, each of the three high frequencies of $HCOND_2$ and $DCOND_2$ is assigned to almost pure $ND_2$ antisymmetric, $ND_2$ symmetric, CH or CD stretching vibration.

The calculated frequencies of these $NH_2$, $ND_2$, CH and CD stretching vibrations are in agreement with the observed ones with the maximum deviation of 2.5%. In detail, however, there are systematic deviations found between the calculated and observed frequencies. Namely, the frequency difference $\Delta\nu = \nu_{obs} - \nu_{calc}$ is always negative for the $NH_2$ and CH stretching vibrations and always positive for the $ND_2$ and CD stretching vibrations. This may be interpreted as due to the anharmonicity in the internal potential in which the hydrogen or deuterium atoms are placed, which is neglected in the present calculation.

**The Band at 1690 cm$^{-1}$.**—To this band there

are considerable contributions of both the $\nu$(C=O) and $\nu$(CN) vibrations. The energy associated with the $\nu$(C=O) vibration is 50% of the total and that associated with the $\nu$(CN) is 25%, while the amplitude ratio of the $\nu$(CN) to the $\nu$(C=O) is computed to be $-0.73$. Therefore, this band may well be called "N–C=O antisymmetric vibration" rather than "C=O stretching vibration". In addition, the contribution of the $\delta$(CH) motion to this band is not negligible as it is in the case of *N*-methylformamide[22] and diformylhydrazine[19].

This band at 1690 $cm^{-1}$ shifts towards lower frequency both on *N*-deuteration and *C*-deuteration the amount of shift being 23 and 15 $cm^{-1}$ respectively. For $DCOND_2$, it is found at 1648 $cm^{-1}$. On the *C*-deuteration the contribution of the $\delta$(CH) vibration is removed, and on the *N*-deuteration the interaction from the b($NH_2$) vibration is removed. This may be the cause of the shifts of the band in question. The way of coupling of the $\nu$(C=O) and $\nu$(CN) vibrations in this normal mode seems to be unaffected by any deuteration.

**The Band at 1608 $cm^{-1}$.**—The band at 1608 $cm^{-1}$ of $HCONH_2$ corresponds to almost pure b($NH_2$) vibration. This band is not sensitive to the *C*-deuteration and is found at 1620 $cm^{-1}$ in $DCONH_2$. The band corresponding to the b($ND_2$) vibration is found at 1118 $cm^{-1}$ in $HCOND_2$. The position of the band is hardly affected by *C*-deuteration, but its intensity becomes weaker.

**The Band at 1391 $cm^{-1}$.**—The band at 1391 $cm^{-1}$ of $HCONH_2$ can be assigned to the $\delta$(CH) vibration. However, contributions of both the $\nu$(CN) and $\nu$(C=O) vibrations are not negligible. In the normal vibration, the C–N and C=O bonds stretch and contract in phase with an amplitude ratio of $+0.66$. This band is not sensitive to *N*-deuteration and is found at 1398 $cm^{-1}$ in $HCOND_2$. The band at 984 $cm^{-1}$ in $DCONH_2$ corresponds to almost pure $\delta$(CD) vibration. It shifts towards higher frequency on *N*-deuteration by 53 $cm^{-1}$. As is seen from Tables III and IV the shift can be explained as due to the interaction between $\delta$(CD) and r($ND_2$) vibrations.

**The Band at 1309 $cm^{-1}$.**—This band is mainly due to the $\nu$(CN) vibration, although there are energetically small contributions of $\delta$(CH) and r($NH_2$) vibrations. The contribution of the $\nu$(C=O) motion is shown to be quite negligible by the present calculation, in contradiction to some previous authors' expectation[12,13]. On *N*-deuteration the band moves to higher frequency by 29 $cm^{-1}$. The nature of the normal mode corresponding to this band is more complex. Here, the contributions of the $\delta$(CH) and b($ND_2$) vibrations are as important as the $\nu$(CN) vibration.

It is noted that the contribution of the $\nu$(C=O) vibration increases on *C*-deuteration, while that of the $\delta$(CH) becomes negligible. In the corresponding normal vibration at 1341 $cm^{-1}$ of $DCOND_2$ the energy associated with the $\nu$(C=O) vibration is 16% of the total.

**The Bands at 1090 and ca. 600 $cm^{-1}$.**—The band which occurs at about 1090 $cm^{-1}$ in $HCONH_2$ can be assigned to the r($NH_2$) vibration, although there is a small contribution of the $\nu$(C=O) vibration. On *C*-deuteration it shifts towards higher frequency by about 40 $cm^{-1}$. The broad band at about 600 $cm^{-1}$ of $HCONH_2$ corresponds to almost pure $\delta$(NCO) vibration. (It is overlapped with another broad band arising from the $NH_2$ wagging vibration.) The band is insensitive to *C*-deuteration. In *N*-deuterated formamides, an interaction between the r($ND_2$) and $\delta$(NCO) vibrations takes place, and this gives rise to two obserbed bands at 912 and about 570 $cm^{-1}$ in $HCOND_2$ and those at 891 and about 560 $cm^{-1}$ in $DCOND_2$. In addition, there is a small contribution of the $\delta$(CD) vibration to the band at 891 $cm^{-1}$ of $DCOND_2$.

**The Out-of-plane Vibrations**—Of three out-of-plane vibrations, two can easily be identified. They are the CH out-of-plane deformation and $NH_2$ wagging vibrations; $\pi$(CH) and w($NH_2$).

Of $HCONH_2$, the $\pi$(CH) vibration is assigned to a band at 1056 $cm^{-1}$. On *N*-deuteration it is a little shifted, while on *C*-deuteration it disappears as is expected from the assignment. The band at 881 $cm^{-1}$ in $DCONH_2$ can be assigned to the $\pi$(CD) vibration, although its intensity is comparatively weak. In $DCOND_2$ it is probably overlapped by the r($ND_2$) band at 891 $cm^{-1}$ and cannot be distinguished. The above assignment is consistent with the result given by a study on the infrared spectra of $DCONHCH_3$ and $DCONDCH_3$[22]. Both of them show a band at 864 $cm^{-1}$, the intensity of which is as weak as that of the 881 $cm^{-1}$ band of $DCONH_2$.

A broad band found at about 750 $cm^{-1}$ in both $HCONH_2$ and $DCONH_2$ is assigned to the w($NH_2$) vibration. On *N*-deuteration it moves to lower frequency up to about 450 $cm^{-1}$.

Another out-of-plane vibration, the $NH_2$ twisting or torsional vibration, is expected to occur at a lower frequency than 300 $cm^{-1}$. The Raman line found at 200 $cm^{-1}$ of $HCONH_2$[9] may be assigned to this vibration.

Thus, a complete assignment has been made of the infrared absorption bands of the four isotopic species of formamide observed in the 3600~300 $cm^{-1}$ region. The present assignment for $HCONH_2$ and $HCOND_2$ is in comformity

with that proposed by Miyazawa[13] except for a few minor points, but considerably different from others' assignments.

The present writer wishes to express his gratitude to Professor Takehiko Shimanouchi for his kind guidance and encouragement throughout this work and to Professor Hidetoshi Takahashi for allowing to use the PC-1 computor. His thanks are also due to Dr. Michiro Kawano for the infrared measurements in the CsBr region.

*Department of Chemistry*
*Faculty of Science*
*University of Tokyo*
*Hongo, Tokyo*

# *Investigation on Mixed Complexes. V. A Conductometric Study of Cyano-ethylenediamine Complexes*

By Sigeo KIDA

(Received February 15, 1960)

In the preceding papers of this series[1-3], the present author has dealt with the formation of mixed cyano complexes in solution. It was indicated spectrophotometrically that the octahedral nickel(II) complex ion, such as the hexaquo nickel(II) ion or the bis-(ethylenediamine)-nickel(II) ion, does not react with planar nickel(II) complexes, for example tetracyano niccolate(II) or bis-(dithio-oxalato)-niccolate(II) ion, to form a mixed complex. However, nickel(II) complexes have a tendency to react with each other, when they are of similar configuration, to produce mixed complexes as shown in the following expression:

$$[Ni(C_2S_2O_2)]^{2-} + [Ni(CN)_4]^{2-} \rightleftarrows 2[Ni(C_2S_2O_2)(CN)_2]^{2-}$$

where $C_2S_2O_2$ indicates dithio-oxalate. However, in the case of platinum(II) complex ions such as tetrachloro platinate(II), tetrabromo platinate(II) and tetracyano platinate(II) ions, all of which are of similar configuration, no tendency of forming any mixed cyano-halogeno complex has been observed in solution.

In order to ascertain the exact conditions under which a cyano mixed complex is formed, one needs to carry out further experiments, but unfortunately it is not always easy to find substances which are suitable for the examination by spectrophotometric methods as previously reported. In the present investigation therefore, the conductometric method has been applied to the complexes of platinum(II), palladium(II), zinc(II) and cadmium(II), which are all colorless and hence can not be studied by the spectrophotometric method[4].

## Results and Discussion

It is known that the conductivity of a solution has no linear relationship to the concentration of the dissolved salt in the range of $10^{-2}$ F, used in the present study. A linear relationship, however, is required by the method of continuous variation[5]. However, the data reported in the present work show that, so far as only the detection of a mixed complex formation is desired, the conductometric continuous variation method can be applied satisfactory for this purpose.

Eight solutions were prepared for the respective metals by mixing a solution of the ethylenediamine complex with the potassium cyanide solution in the ratios as shown in Table I. The conductivity was measured at 25°C.

TABLE I. COMPOSITION OF MIXED SOLUTIONS USED IN THE CONDUCTOMETRIC MEASUREMENTS

| | | | | | | | | | |
|---|---|---|---|---|---|---|---|---|---|
| 0.01 F $[M\,en_n]X_2$ | 20 | 10 | 10 | 10 | 10 | 10 | 5 | 5 | ml. |
| 0.02 F KCN | 10 | 7.5 | 10 | 12.5 | 15 | 20 | 12.5 | 15 | |
| [CN]/[M] | 1 | 1.5 | 2 | 2.5 | 3 | 4 | 5 | 6 | |

X=Cl, $NO_3$, $1/2(SO_4)$

1) Part IV of this series: S. Kida, This Bulletin, 33, 1204 (1960).
2) S. Kida, ibid., 33, 587 (1960).
3) S. Kida, ibid., 32, 981 (1959).
4) The absorption of these complexes in the ultraviolet region are irregular and complicated, probably owing to the presence of association bands resulting from the complex and simple ions in the solution.
5) R. C. Brasted and W. E. Cooley, "Physical Methods in Coordination Chemistry", Ch. 18 in J. C. Bailar and D. H. Busch, ed., "The Chemistry of the Coordination Compounds", Reinhold Pub. Co., New York, (1956), pp. 569-572 and references therein.

The reaction proceeds to decrease the total ionic charge in the solution as follows:

$$[M\,en_n]^{2+} + 4CN^- \rightarrow [M(CN)_4]^{2-} + n\,en \quad (1)$$

or $$[M\,en_n]^{2+} + 2CN^- \rightarrow [M\,en(CN)_2] + (n-1)en \quad (2)$$

(M=Ni, Pd, Pt, Zn and Cd; $n$=2 for Pd and Pt; $n$=3 for Ni, Zn and Cd).

Therefore, if a reaction of type 1 took place in solution the curves in Figs. 1 and 2 should have minimum points at [M]/[CN]=1:4, while that of type 2 should give a minimum point at [M]/[CN]=1:2. In fact, as can be seen in Figs. 1 and 2, minimum points are found at [M]/[CN]=1:4 on curves A and E, and at [M]/[CN]=1:2 on curves B, C and D. This shows that, in the former cases, mixed complexes, such as $[Ni\,en(CN)_2]$ and $[Pt\,en(CN)_2]$, are not formed, but the following reactions take place:

$$[Ni\,en_3]^{2+} + 4CN^- \rightarrow [Ni(CN)_4]^{2-} + 3\,en$$

and

$$[Pt\,en_2]^{2+} + 4CN^- \rightarrow [Pt(CN)_4]^{2-} + 2\,en$$

while in the latter cases the mixed complexes

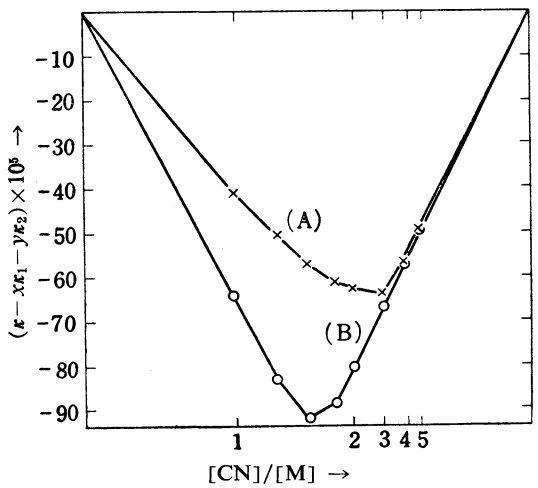



Fig. 1. The curves, (A) and (B), are referred to the complexes of Pd(II) and Pt(II), respectively.
[M]=Concentration of metal in F.
[CN]=Concentration of cyanide ion in F.
$\kappa$=Specific conductivity of a mixed solution ($\Omega^{-1}\times cm^{-1}$).
$\kappa_1$=Specific conductivity of a 0.01 F $[M\,en_n]X_2$ solution ($\Omega^{-1}\times cm^{-1}$).
$\kappa_2$=Specific conductivity of a 0.02 F KCN solution ($\Omega^{-1}\times cm^{-1}$).
$x$=Volume of the complex solution/Volume of the mixed solution.
$y$=Volume of the cyanide solution/Volume of the mixed solution.

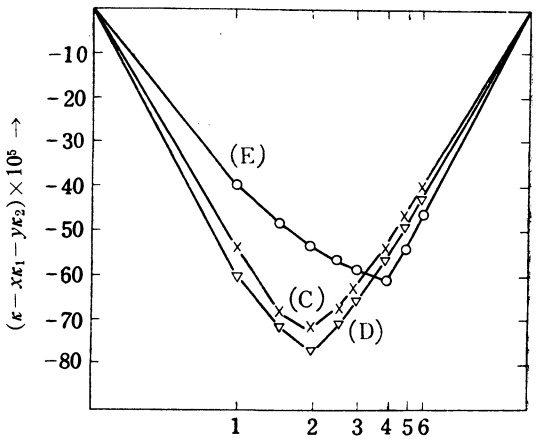



Fig. 2. Curves, (C), (D) and (E), are referred to the complexes of Zn(II), Cd (II) and Ni(II), respectively.

of zinc(II), cadmium(II) and palladium(II) were formed in the solutions through the following reactions:

$$[Zn\,en_3]^{2+} + 2CN^- \rightarrow [Zn\,en(CN)_2] + 2\,en^{6)}$$
$$[Cd\,en_3]^{2+} + 2CN^- \rightarrow [Cd\,en(CN)_2] + 2\,en^{6)}$$
$$[Pd\,en_2]^{2+} + 2CN^- \rightarrow [Pd\,en(CN)_2] + en$$

The result obtained for the nickel complex is in accord with that in the spectrophotometric investigation[3], showing that this conductometric method can be used for the purpose above mentioned. In the cases of zinc, cadmium and palladium complexes, minimum points are found only at [M]/[CN]=1:2 and not at [M]/[CN]=1:4. Neverthless, it should be noted that the formation of tetracyano complexes can not be neglected, since the reaction, $[M\,en(CN)_2] + 2CN^- \rightarrow [M(CN)_4]^{2-} + en$, does not give rise to any decrease in ionic charge in the solution, and accordingly the formation of dicyano complex succeeded by that of tetracyano complex does not always give a minimum point at [M]/[CN]=1:4.

It should also be noted that the curve of the platinum complex is in sharp contrast to that of palladium as a result of their different behavior; the formation of mixed cyano complexes was verified in all the cases of the other metallic ions, but no mixed cyano complex of platinum(II) has ever been observed.

6) It is known that $[Zn\,en_3]^{2+}$ and $[Cd\,en_3]^{2+}$ have octahedral configuration, while $[Zn(CN)_4]^{2-}$ and $[Cd(CN)_4]^{2-}$ are tetrahedral in configuration. However, J. Bjerrum (*Chem. Revs.*, 46, 381 (1950)) has pointed out that tetrammine or bis-ethylenediamine zinc(II) and cadmium(II) complexes tend to be four-co-ordinated and have a tetrahedral configuration as in $[Zn\,en_2]^{2+}$ and $[Cd\,en_2]^{2+}$, but do not tend to have an octahedral one as in $[Zn\,en_2(OH_2)_2]^{2+}$ or $[Cd\,en_2(OH_2)_2]^{2+}$. Therefore, the mixed complexes present in the solution may possibly have tetrahedral configurations of the formulae, $[Cd\,en(CN)_2]$ and $[Zn\,en(CN)_2]$.

The cause of this fact will be the subject of the next investigation.

## Experimental

**Conductometric Measurement.**—The conductivities of the solutions were measured at 25°±0.1°C with Kohlrausch's bridge. The cell constant was determined by using a standard potassium chloride solution of 0.01 F. In the cases of platinum(II) and palladium(II) complexes, the substitution reaction of the cyanide ion for the ethylenediamine molecule was slow, and accordingly the mixed solution was allowed to stand in a thermostat until the conductivity came to show a constant value in each case.

**Materials.** — $[Pt\,en_2]Cl_2$[7], $[Ni\,en_3](NO_3)_2$[8], $[Zn\,en_3]SO_4$[9] and $[Cd\,en_3]Cl_2$[10] were prepared according to the methods described in the references. $[Pd\,en_2]Cl_2$[11] was prepared in a way similar to that for $[Pt\,en_2]Cl_2$. The purity was checked by determining the chloride with silver nitrate.

7) F. Basolo, J. C. Bailar and B. R. Tarr, *J. Am. Chem. Soc.*, **72**, 2433 (1950).
8) A. Werner, *Z. anorg. Chem.*, **21**, 212 (1899).
9) A. Grünberg, ibid., **157**, 201 (1926).
10) A. Werner, ibid., **21**, 226 (1899).
11) H. D. K. Drew, F. W. Pinkard, G. H. Prester and W. Wardlaw, *J. Chem. Soc.*, **1932**, 1906.


## Summary

The conductometric method was applied to the determination of the formation of mixed complexes in solution, using the method of continuous variation. It was shown that

1) $[Ni\,en_3]^{2+}$ reacts with $CN^-$ and forms $[Ni(CN)_4]^{2-}$ only, leading to the same conclusion as in the spectrophotometric investigation carried out previously.

2) $[Pt\,en_2]^{2+}$ forms only a tetracyano complex, but no mixed dicyano complex.

3) $[Pd\,en_2]^{2+}$, $[Zn\,en_3]^{2+}$ and $[Cd\,en_3]^{2+}$ form dicyano-ethylenediamine complexes in solution.


The author wishes to express his sincere thanks to Professor R. Tsuchida of Osaka University for his kind advice and encouragement during this work. His appreciation is also expressed to Dr. H. Yoneda for his helpful discussion.

*Department of Chemistry*
*Wakayama University*
*Masagocho, Wakayama*

# 2-Carboxymethylthio- and 2-Hydrazino-1, 3-diazaazulenes

By Ichiro MURATA

(Received March 1, 1960)

2-Mercapto-1, 3-diazaazulene[1] (I) easily undergoes condensation with monochloroacetic acid to form 2-carboxymethylthio-1, 3-diazaazulene[2] (II), as has already been reported, and various properties of II, and 2-hydrazino-1, 3-diazaazulene[3] derived from I and II, are described in this paper.

II forms a pale yellow, crystalline powder only sparingly soluble in water and organic solvents, and has a melting point exceeding 300°C. Its esterification by the Fischer method affords methyl ester IV of m. p. 118~118.5°C and the ethyl ester V of m. p. 89°C. V is also obtained upon reaction of ethyl monochloroacetate on the sodium salt of I. These esters easily undergo hydrolysis to regenerate II and are converted into an amide (VI) of m. p. 207~208°C by the action of 40% ammonia water.

It is known, that pyridines[4] and quinolines[5] possessing a carboxymethylthio group in the $\alpha$-position generally form a cyclized product, called meso-ionic compound, on heating with acetic anhydride. On refluxing II in acetic anhydride, it is converted into an extremely sparingly soluble substance* of violet color. The analytical values of this substance suggest an intermolecular dehydrated product but no detailed examination has been made on it.

* A part of this work was presented as a paper at the 10th Annual Meeting of the Chemical Society of Japan, Tokyo, April, 1957.

1) T. Nozoe, T. Mukai and I. Murata, *J. Am. Chem. Soc.*, **76**, 3352 (1954).

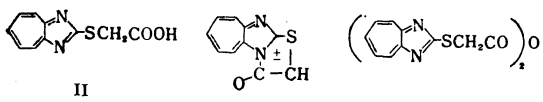
2) I. Murata, This Bulletin, **33**, 56 (1960).

3) T. Nozoe, T. Mukai and I. Murata, *Proc. Japan Acad.*, **30**, 482 (1954).

4) E. Koenigs and H. Geisler, *Ber.*, **57**, 2076 (1924); G. F. Duffin and J. D. Kendall, *J. Chem. Soc.*, **1951**, 734.

5) E. B. Knott, ibid., **1955**, 937.

* Duffin and Kendall[4] reported that the use of phosphorus pentoxide or thionyl chloride in place of acetic anhydride as the dehydration agent afforded structurally unkonwn substance as a brown powder.

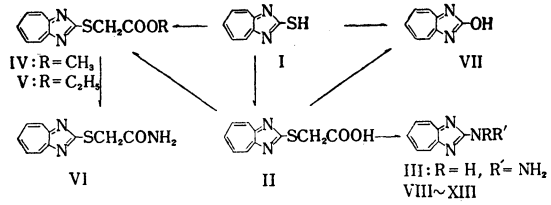


II

Refluxing of II in concentrated hydrochloric acid results in its conversion to 2-hydroxy-1, 3-diazaazulene (VII) in good yield. Such comparatively facile hydrolysis of II suggests the possibility of I being desulfurized by the action of monochloroacetic acid.

Desulfurization of heterocyclic compounds with a mercapto group by the action of monochloroacetic acid has been reported by numerous workers on thiopyrimidines[6], thioquinoline[7], thiohydantoin[8], thiouracil[9] and thiooxazole and thiothiazole[10]. On heating I in aqueous solution of excess of monochloroacetic acid, II is first formed after 15~20 min. When this mixture is heated for a longer period, such as further 25 hr., without isolation of II, the separated II dissolves gradually and changes almost quantitatively into VII.

Oxidation of the ethyl ester V with hydrogen peroxide in glacial acetic acid, in an attempt to obtain the ethoxycarbonylsulfonyl derivative, invariably gives VII as the product, whether the reaction is carried out at 60~70°C with an excess of the reagent or at room temperature with an equivalent amount of the reagent, and the sulfone is not isolated. Ohta[10] obtained the sulfone by oxidation of carboxymethylthio derivatives of thiazole and thiadiazole under the same conditions but found that the same oxidation of oxadiazole had changed it into the hydroxy derivatives and the sulfone was not obtained. II also undergoes oxidation by hydrogen peroxide to form VII.



IV: R=$CH_3$
V: R=$C_2H_5$

VI II III: R=H, R'=$NH_2$
VIII~XIII

The carboxymethylthio group present in 2-position of pyrimidine is known to be substituted by amino and benzylamino groups[11]. II also reacts comparatively easily with various amines to form derivatives listed in Table I.

In the foregoing reaction, II reacts most readily with hydrazine and III is formed in a good yield only by letting stand their mixture at room temperature.

III has already been obtained by the application of hydrazine to 2-chloro-1, 3-diazaazulene but its properties are almost unknown. As has already been mentioned, III can now be prepared easily from II but it can also be obtained easily from I by refluxing it with hydrazine hydrate in butanol, generating hydrogen sulfide gas.

III easily undergoes condensation with various ketones and aldehydes in alcohol to form the corresponding hydrazones (Table II). The ultraviolet absorption maxima of these hydrazones are indicated in Table III.

In general, six-membered, heterocyclic aromatic compounds of nitrogen possessing a hydrazino group in the $\alpha$-position undergoes cyclization between the ring nitrogen and the hydrazino group by the action of formic acid, ethyl orthoformate, or acetic anhydride and form triazole derivatives. They also undergo

TABLE I. 2-SUBSTITUTED DERIVATIVES OBTAINED FROM 2-CARBOXYMETHYLTHIO COMPOUND

| Compd. No. | R | R' | Cryst. form* | m.p., °C | Yield % | N Analysis Calcd. | N Analysis Found | Ref. |
|---|---|---|---|---|---|---|---|---|
| III | H | $NH_2$ | y. N. | 189 | 89 | — | — | 3 |
| VIII | H | H | y. N. | 295(d.) | 43 | — | — | 12 |
| IX | H | $CH_3$ | y. P. | 172~173 | 90 | — | — | 3 |
| X | $CH_3$ | $CH_3$ | y. P. | 133~134 | 92 | — | — | 3 |
| XI | H | $C_6H_5$ | o. P. | 239~240 | 80 | — | — | 2 |
| XII | H | $CH_2C_6H_5$ | y. P. | 173 | 75 | 17.86 | 17.92 | — |
| XIII | H | $NHC_6H_5$ | y. P. | 222 | 30 | 23.72 | 23.40 | — |

* y, yellow; o, orange; N, needles; P, prisms.

6) T. B. Johnson and A. W. Joyce, *J. Am. Chem. Soc.*, **38**, 1385 (1916); A. R. Todd, *J. Chem. Soc.*, **1946**, 357; D. J. Brown, *J. Soc. Chem. Ind. (London)*, **69**, 353 (1950).
7) R. V. Jones and H. R. Henze, *J. Am. Chem. Soc.*, **64**, 1669 (1942).
8) T. B. Johnson, G. M. Pfau and W. W. Hodge, ibid., **34**, 1041 (1912); T. B. Johnson and S. E. Hadley, ibid., **37**, 171 (1915); T. B. Johnson and R. Wrenshall, ibid., **37**, 2133 (1915); T. B. Johnson, A. J. Hill and E. B. Kelsey, ibid., **42**, 1711 (1920).
9) H. L. Wheeler and L. M. Liddle, *Am. Chem. J.*, **40**, 547 (1908); T. B. Johnson and E. H. Hemingway, *J. Am. Chem. Soc.*, **37**, 378 (1915).
10) H. Ohta and M. Ohta, *J. Chem. Soc. Japan, Pure Chem. Sec. (Nippon Kagaku Zasshi)*, **78**, 700 (1957); W. J. Croxall, Chien-Pen Lo and E. Y. Shropshire, *J. Am. Chem. Soc.*, **75**, 5419 (1953).
11) G. H. Hitchings and P. B. Russel, *J. Chem. Soc.*, **1949**, 2454; P. B. Russel, G. B. Elion, E. A. Falco and G. H. Hitchings, *J. Am. Chem. Soc.*, **71**, 2279 (1949).
12) T. Nozoe, T. Mukai, K. Takase, I. Murata and K. Matsumoto, *Proc. Japan Acad.*, **29**, 452 (1953).

TABLE II. REACTION PRODUCTS OF III WITH VARIOUS KETONES AND ALDEHYDES

| $R_1$ | $R_2$ | Cryst. form* | m.p. °C | Mol. form | Analysis Calcd. C | Calcd. H | Calcd. N | Found C | Found H | Found N |
|---|---|---|---|---|---|---|---|---|---|---|
| $CH_3$ | $CH_3$ | y. N. | 201(d.) | $C_{11}H_{12}N_4$ | 65.98 | 6.04 | 27.98 | 67.05 | 5.72 | 27.67 |
| H | $C_6H_5$ | y. N. | 235(d.) | $C_{15}H_{12}N_4$ | 72.56 | 4.89 | 22.57 | 72.51 | 4.59 | 22.56 |
| H | $C_6H_4Br$ | y. N. | 274(d.) | $C_{15}H_{11}N_4Br$ | 55.06 | 3.38 | 17.12 | 55.63 | 3.48 | 17.11 |
| H | $C_6H_4N(CH_3)_2$ | r. P. | 247(d.) | $C_{17}H_{17}N_5 \cdot H_2O$ | 66.00 | 6.19 | 22.64 | 66.18 | 6.21 | 22.81 |
| H | $C_6H_4OCH_3$ | o. P. | 241(d.) | $C_{16}H_{14}ON_4 \cdot 1/2H_2O$ | 66.88 | 5.26 | 19.50 | 66.80 | 4.78 | 19.52 |
| H | $C_6H_4NO_2$ | y. N. | 290 | $C_{15}H_{11}O_2N_5 \cdot 3/2H_2O$ | 56.24 | 4.45 | 21.86 | 55.87 | 4.39 | 21.86 |
| H | $C_6H_4O_2CH_2$ | o. P. | 262(d.) | $C_{16}H_{12}O_2N_4 \cdot H_2O$ | 61.93 | 4.55 | 18.06 | 62.12 | 4.05 | 18.55 |

* y, yellow; r, red; o, orange; N, needles; P, prisms.

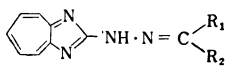


TABLE III. ULTRAVIOLET MAXIMA OF 1,3-DIAZAAZULENYL-2-HYDRAZONES

| $R_1$ | $R_2$ | $\lambda_{max}^{MeOH}$ mμ (log ε) | | | | |
|---|---|---|---|---|---|---|
| $CH_3$ | $CH_3$ | — | 248(4.46) | 264(4.46) | 295(*) | 370(4.35) |
| H | $C_6H_5$ | — | 243(4.46) | 285(4.38) | 305(*) | 389(4.50) |
| H | $C_6H_4Br$-*p* | — | 242(4.48) | 286(4.37) | 305(*) | 391(4.55) |
| H | $C_6H_3O_2CH_2$-3,4 | 219(4.33) | 245(4.46) | 287(4.30) | 312(4.22) | 400(4.46) |
| H | $C_6H_4OCH_3$-*p* | — | 245(4.46) | 289(4.26) | 310(4.21) | 408(4.41) |
| H | $C_6H_4NO_2$-*p* | — | 240(4.42) | 268(*) | 300(*) | 410(4.57) |
| H | $C_6H_4N(CH_3)_2$-*p* | — | 242(4.43) | 265(*) | 317(4.35) | 428(4.47) |

* shoulder

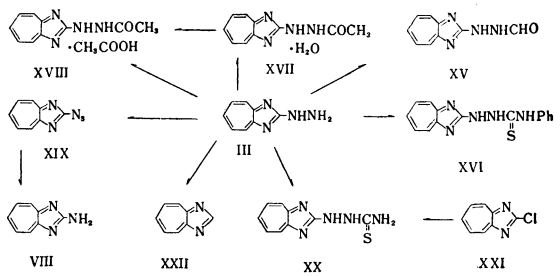
cyclization by the action of nitrous acid to form tetrazole derivatives[13].

III does not cyclize by the reaction of these reagents, even under a rather drastic conditions. The reaction of III with formic acid gives the formate XV of m. p. 249°C (decomp.) and that with phenyl-mustard oil gives the phenylthiosemicarbazide compound XVI. Application of acetic anhydride to III affords two kinds of crystals, m. p. 248°C (decomp.) (XVII) and m. p. 189°C (decomp.) (XVIII). Further application of acetic anhydride to XVII converts it to XVIII. It is therefore known that XVII is an acetylhydrazino compound with one molecule of water of crystallization while XVIII is an acetate of the acetylhydrazino compound.

Application of sodium nitrite in 2 N hydrochloric acid or in acetic acid to III gives extremely labile yellow needles (XIX) of m. p. 135°C (decomp.). The ultraviolet absorption maxima of XIX appear at 228 mμ (log ε 4.03), 262 (4.41), and 337 (4.15), and this makes it impossible to assume any skeletal change in 1,3-diazaazulene molecule. The infrared spectrum of XIX shows distinct absorption of an azide at 2150 $cm^{-1}$ [14] and XIX should therefore be 2-azido-1,3-diazaazulene and not the anticipated tetrazole compound. Actually, reduction of XIX with hydrogen sulfide results in quantitative formation of 2-amino-1,3-diazaazulene[12] and this also endorses above assumption.

Reaction of potassium thiocyanate on III in the presence of hydrochloric acid affords reddish brown prisms XX, m. p. 179.5°C, which is also obtained upon reaction of thiosemicarbazide on 2-chloro-1,3-diazaazulene (XXI), and this shows that XX is 2-thiosemicarbazido-1,3-diazaazulene.

III was decomposed by the Stephens-McFadyen method[15] to 1,3-diazaazulene (XXII).



13) A. A. Morton, "The Chemistry of Heterocyclic Compounds", McGraw-Hill Book Company, Inc., New York (1946).

14) E. H. Eyster, *J. Chem. Phys.*, **8**, 369 (1940); E. Lieber, D. R. Levering and L. J. Patterson, *Anal. Chem.*, **23**, 1594 (1951).

15) H. E. Baumgarten and H. Chien-Fan Su, *J. Am. Chem. Soc.*, **74**, 3830 (1952).

## Experimental

**2-Carboxymethylthio-1, 3-diazaazulene (II).** — Prepared by the method given in the literature[2].

**2-Methoxycarbonylmethylthio-1, 3-diazaazulene (IV).** — A mixture of II (100 mg.) suspended in methanol (2 ml.) and added with concentrated hydrochloric acid (0.05 ml.) was refluxed on a water bath for 45 min. This mixture was diluted with water and extracted with chloroform. The chloroform extract was washed with water, dried, and the solvent was evaporated. The residue was dissolved in benzene and the solution was purified by passage through an alumina layer. The yellow crystals (100 mg.), m. p. 120~122°C, was recrystallized from benzenepetroleum ether mixture to pale yellow needles (IV), m. p. 121~122°C.

Found: C, 56.71; H, 4.08; N, 12.12. Calcd. for $C_{11}H_{10}O_2N_2S$: C, 56.41; H, 4.30; N, 11.96%. Ultraviolet $\lambda_{max}^{MeOH}$ m$\mu$ (log $\varepsilon$): 238(4.35), 269(4.28), 355(4.19).

**2-Ethoxycarbonylmethylthio-1, 3-diazaazulene (V).**—a) Obtained by a method similar to that for IV, as pale yellow needles, m. p. 89~89.5°C.

b) A solution of the sodium salt (200 mg.) of I dissolved in ethanol (2 ml.) and added with ethyl monochloroacetate (150 mg.) was refluxed on a water bath for 50 min. Sodium chloride formed by the reaction was filtered off, ethanol was evaporated from the filtrate and benzene soluble portion of the residue afforded 230 mg. of V, m. p. 89~89.5°C.

Found: C, 58.11; H, 4.39; N, 11.56. Calcd. for $C_{12}H_{12}O_2N_2S$: C, 58.06; H, 4.87; N, 11.29%. Ultraviolet $\lambda_{max}^{MeOH}$ m$\mu$ (log $\varepsilon$): 238(4.46), 269(4.37), 355(4.29).

**2-Carbamoylmethylthio-1, 3-diazaazulene (VI).**— A mixture of V (70 mg.) and 40% ammonia water (2 ml.) was stirred for 10 hr. at room temperature. After allowing this to stand over night, the crystals (60 mg.) of m. p. 202~205°C (decomp.) were collected and recrystallized from ethanol to pale yellow needles (VI), m. p. 207~208°C (decomp.).

Found: C, 55.15; H, 3.82; N, 19.57. Calcd. for $C_{10}H_9ON_3S$: C, 54.79; H, 4.14; N, 19.17%. Ultraviolet $\lambda_{max}^{MeOH}$ m$\mu$ (log $\varepsilon$): 239(4.49), 270(4.36), 355(4.29).

**Action of Acetic Anhydride on II.**—A suspension of II (40 mg.) in acetic anhydride (1 ml.) was refluxed for 10 min. in an oil bath. The cooled reaction mixture was thoroughly washed with water and ethanol, and brownish violet powder (30 mg.) which turns black from around 220°C, was obtained.

Found: N, 12.83. Calcd. for $C_{20}H_{14}O_3N_4S_2$: N, 12.54%.

**Hydrolysis of II.** — A solution of II (50 mg.) dissolved in concentrated hydrochloric acid (0.5 ml.) was refluxed for 2 hr. in an oil bath, hydrochloric acid was evaporated to dryness, and the residue was neutralized with sodium hydrogen carbonate, and crystals (30 mg.) melting at 225~228°C were obtained. Recrystallization from ethanol after treatment with activated carbon afforded crystals of m. p. 244~245°C, undepressed on admixture with VII.

**Reaction of I and Monochloroacetic Acid.**—a) A suspension of I (100 mg.) in a mixture of monochloroacetic acid (100 mg.) and water (10 ml.) was refluxed for 20 min. in an oil bath, cooled, and the crystals that separated out were collected by filtration to 80 mg. of II, m. p. over 300°C.

b) The reaction was carried out as above but the refluxing was continued for 25 hr. by which the crystals of II dissolved completely. The reaction mixture was evaporated to dryness, ethanol was added to the residue, and this was filtered. The crystals (100 mg.) of m. p. over 300°C so obtained were neutralized with sodium hydrogen carbonate and recrystallized from ethanol to VII, m. p. 244~245°C.

**Oxidation of II with Hydrogen Peroxide.** — To a suspension of II (80 mg.) in glacial acetic acid (0.5 ml.), 30% hydrogen peroxide (0.2 ml.) was added and the mixture was heated with stirring at 75~80°C for 2 hr. The pale yellow solution so obtained was concentrated under a reduced pressure and neutralized with saturated solution of sodium hydrogen carbonate. The crude crystals (40 mg.) of m. p. 229°C were recrystallized from ethanol to VII, m. p. 244~245°C.

**Reaction of II and Ammonia or Amines.**—a) A solution of II (100 mg.) dissolved in 40% ammonia water (1.5 ml.) was sealed in a tube and heated at 100°C for 6 hr. The reaction mixture was allowed to stand over night and the crystals (30 mg.) of m. p. 270°C (decomp.) were collected and recrystallized from water to pale yellow needles (VIII), m. p. 294°C (decomp.). The mother liquor left after separation of VIII afforded the recovered II (55 mg.).

b) A solution of II (150 mg.) dissolved in 40% aqueous solution (2 ml.) of methylamine or dimethylamine was sealed in a tube and heated at 100°C for 20 hr. The reaction mixture was evaporated to dryness over sulfuric acid in a vacuum desiccator and the benzene soluble portion of this residue afforded IX, m. p. 173~174°C, and X, m. p. 133~134°C.

c) A mixture of II (150 mg.) in ethanol (2 ml.) and aniline or benzylamine (1 ml.) was heated in a sealed tube at 165~170°C for 7 hr., cooled over night, and crystals that separated out were collected, afforded 120 mg. of XI, m. p. 239°C, and XII, m. p. 173°C.

**2-Phenylhydrazino-1, 3-diazaazulene (VIII).**—A mixture of II (100 mg.) in ethanol (4 ml.) and added with phenylhydrazine (100 mg.) was heated in a sealed tube at 155~160°C for 6 hr. The crystals that separated out on allowing the reaction mixture to cool were collected (30 mg.) melting with decomposition at 200°C. This was recrystallized from dilute ethanol to orange prisms, XIII, m. p. 222°C (decomp.).

Found: C, 70.64; H, 5.25; N, 23.40. Calcd. for $C_{14}H_{12}N_4$: C, 71.16; H, 5.12; N, 23.72%. Ultraviolet $\lambda_{max}^{MeOH}$ m$\mu$ (log $\varepsilon$): 238(4.18), 260(4.56), 354(4.22).

**2-Hydrazino-1, 3-diazaazulene (III).**—a) II (1 g.) was dissolved in hydrazine hydrate (10 ml.) with warming and the solution was allowed to cool to room temperature by which brown needles, m. p.

187°C (decomp.), separated out. This was recrystallized from ethanol to III (650 mg.), m. p. 188～189°C (decomp.).

b) To a suspension of I (250 mg.) in *n*-butanol (6 ml.), 80% hydrazine hydrate (0.5 ml.) was added and the mixture was refluxed in an oil bath for 4 hr., until there was no longer evolution of hydrogen sulfide. The solvent was evaporated under a reduced pressure, ethanol was added to the residue, and filtration afforded III (220 mg.), m. p. 184～185°C (decomp.).

**Reaction of III and Carbonyl Compounds.**—A mixture of III and a carbonyl compound (1.1 mol. equiv.) in ethanol was heated for 5～10 min., cooled, and the crystals so formed or obtained by evaporation of ethanol was recrystallized from ethanol or a mixed solvent of ethanol and dioxane. The hydrazones listed in Table II were thereby obtained in a quantitative yield.

**Reaction of III and Formic Acid.**—A solution of III (100 mg.) dissolved in 80% formic acid (1 ml.) was heated at 90°C for 4 hr. Formic acid was then evaporated under a reduced pressure, the residue was washed with ethanol, and crystals (85 mg.) of m. p. 245°C (decomp.) were obtained. Recrystallization from ethanol afforded XV, m. p. 249°C (decomp.).

Found: C, 57.36; H, 3.90; N, 30.41. Calcd. for $C_9H_8ON_4$: C, 57.44; H, 4.29; N, 29.77%. Ultraviolet $\lambda_{max}^{MeOH}$ m$\mu$ (log $\varepsilon$): 257(4.42), 347(4.09).

**Reaction of III and Phenyl-mustard Oil.**—Phenyl-mustard oil (90 mg.) was added to the solution of III (100 mg.) dissolved in ethanol (6 ml.) and the mixture was refluxed for 15 min. The crystals that separated out on cooling this reaction mixture were collected by filtration and recrystallized from ethanol to XVI (90 mg.) as reddish violet prisms, which does not indicate any definite melting point, gradually turning black by heating.

Found: C, 59.62; H, 4.00; N, 23.28. Calcd. for $C_{15}H_{13}N_5S$: C, 61.01; H, 4.44; N, 23.72%. Ultraviolet $\lambda_{max}^{MeOH}$ m$\mu$ (log $\varepsilon$): 257(4.61), 347(4.13), 460 (3.50).

**Reaction of III and Acetic Anhydride.**—A mixture of III (50 mg.) and acetic anhydride (0.2 ml.) was allowed to stand at room temperature by which III dissolved once and crystals (30 mg.) of m. p. 210°C separated out. These crystals were recrystallized from ethanol to XVII, m. p. 248°C (decomp.).

Found: C, 54.38; H, 5.34; N, 25.22; $H_2O$, 7.72. Calcd. for $C_{10}H_{10}ON_4 \cdot H_2O$: C, 54.54; H, 5.49; N, 25.44; $H_2O$, 8.18%. Ultraviolet $\lambda_{max}^{MeOH}$ m$\mu$ (log $\varepsilon$): 259(4.48), 350(4.18).

The filtrate left after separation of XVII was concentrated and the crystalline residue was recrystallized from ethanol to XVIII (10 mg.), m. p. 189°C (decomp.).

Found: C, 55.18; H, 5.10; N, 21.34. Calcd. for $C_{10}H_{10}ON_4 \cdot CH_3COOH$: C, 54.95; H, 5.38; N, 21.37%.

**Reaction of III and Nitrous Acid.**—A solution of sodium nitrite (95 mg.) in water (0.3 ml.) was added dropwise into a solution of III (200 mg.) dissolved in 2 N acetic acid (2 ml.) at room temperature. The mixture was then heated for a few minutes at 80°C, diluted with water, and extracted with benzene. The benzene layer was treated with activated carbon and crystals, m. p. 133～134°C (170 mg.), were obtained. This was recrystallized from benzene-petroleum ether mixture to pale yellow prisms XIX, m. p. 134～135°C (decomp.). Ultraviolet $\lambda_{max}^{MeOH}$ m$\mu$ (log $\varepsilon$): 228(4.03), 262(4.41), 337(4.15), 370(shoulder).

Picrate: Yellow needles from ethanol, m. p. 273～274°C (decomp.).

Found: N, 15.68. Calcd. for $C_8H_5N_5 \cdot C_6H_3O_7N_3$: N, 15.79%.

Hydrogen sulfide gas was passed through a solution of XIX (100 mg.) dissolved in water (8 ml.) by which the solution gradually turbid. After thoroughly saturating hydrogen sulfide, the white precipitate so formed was collected by filtration, the portion of the precipitate soluble in hydrochloric acid was combined with the filtrate, and the solution was evaporated. The residue was neutralized with sodium hydrogen carbonate and yellow crystals (60 mg.), m. p. 289°C (decomp.), were obtained. This was recrystallized from water to yellow needles, m. p. 294°C (decomp.), whose ultraviolet and infrared spectra agreed completely with those of 2-amino-1,3-diazaazulene.

**Reaction of III and Potassium Thiocyanate.**—To a solution of III (400 mg.) dissolved in water (2.5 ml.) and added with 4 drops of concentrated hydrochloric acid, aqueous solution of potassium thiocyanate (260 mg.) was added and the mixture was heated on a water bath for 15 min. The crystals formed on coolling this solution were collected (460 mg.) and recrystallized from diluted ethanol to brown prisms, XXI, m. p. 179～179.5°C (decomp.).

Found: C, 49.43; H, 3.92; N, 31.45. Calcd. for $C_9H_9N_5S$: C, 49.31; H, 4.14; N, 31.95%. Ultraviolet $\lambda_{max}^{MeOH}$ m$\mu$ (log $\varepsilon$): 265(4.50), 300(3.75), 367 (4.34).

**Stephens-McFadyen Decomposition of III.**—III (50 mg.) was dissolved in 50% acetic acid (4 ml.), to which 10% copper sulfate solution (1.2 ml.) was added. The mixture was then warmed on a water bath, the solution turned yellowish green and nitrogen gas evolved. After 10 min., the reaction mixture was filtered, and the filtrate was neutralized with a solid sodium hydrogen carbonate, extracted with chloroform. The chloroform extracts were evaporated, and the residue was dissolved in benzene and purified through a short column of alumina. The elute gave yellow needles, m. p. 115～118°C, and no depression with authentic 1,3-diazaazulene on mixed fusion.

The author expresses his deep gratitude to Professor Tetsuo Nozoe of the Faculty of Science of this University for kind and unfailing guidance throughout the course of this work. The elementary analyses were performed by Mr. Shinichi Oyama and Miss Ayako Iwanaga. The author wishs to express his thanks to these helps and donations.

*The Chemical Research Institute of Non-Aqueous Solutions*
*Tohoku University*
*Katahira-cho, Sendai*

# *Non-stoichiometry of Nickel Oxide*

By Yoshio IIDA, Kenzo SHIMADA and Shunro OZAKI

(Received March 9, 1960)

The physical and chemical properties of nickel oxide have been studied extensively by many investigators[1]. Gray[2] and Iida[3] reported that the electrical properties of nickel oxide varied with the preparation method. Since nickel oxide is a *p*-type semiconductor containing an excess of oxygen, the change in the electrical properties are thought to be attributed to a concentration of an excess of oxygen which produces cation vacancy in nickel oxide. From the electrical neutrality of the crystal, $2x$ $Ni^{3+}$ ions must be formed when there are $x$ vacancies of $Ni^{2+}$ in the crystal.

In the present experiment, the concentrations of $Ni^{3+}$ ion in nickel oxide crystals prepared from various methods have been determined by chemical analysis and a concentration of cation vacancy has been calculated. The concentration of cation vacancy thus obtained has been compared with that obtained by the density and lattice parameter of nickel oxide.

## Experimental

Recrystallized nickel nitrate was prepared by dissolving electro-deposited nickel of 99.9% purity in c. p. nitric acid. Nickel carbonate and nickel hydroxide were precipitated in an aqueous solution of nickel nitrate by ammonium carbonate and ammonium hydroxide. These nickel salts were heated for 3 hr. in air in the temperature range of 400 to 1300°C to obtain nickel oxide.

Electrical resistance was measured in the air from room temperature to 300°C by a method similar to that described by Griffith[4].

The density measurement was the same as that described by Culbertson[5] except that a weighing glass bulb sealed under evacuation was broken off in distilled water containing 0.001% of surface active reagent.

Powder diffraction patterns were recorded by a diffractometer with copper-target radiation. The lattice parameter of nickel oxide was determined by the diffraction peak of (420).

The chemical analysis of $Ni^{3+}$ was made according to the directions of Verwey[6].

The composition ratio of Ni/O was determined by hydrogen reduction of samples at 700°C for 5 hr.

## Results and Discussion

**Non-stoichiometry of Nickel Oxide Prepared from Nickel Nitrate.**—Nickel oxide was prepared by heating nickel nitrate for 3 hr. at temperatures of 400 to 1200°C. Experimental results are shown in Table I. It is seen from electron photographs that particle size increases with an increase in the heating temperature (Fig. 1). At low temperatures of 400 and 500°C, unit particle size can not be determined by an electron photograph because nickel oxide is in the form of very small particles or their aggregates. At 600°C it is about 0.2 $\mu$ and grows to 1 $\mu$ at 1000°C. Inasmuch as the width of diffraction peak (200) at half intensity did not vary with the heating temperature in the range of 400 to 1200°C, the crystallization of nickel oxide heated at 400 and 500°C is thought to be completed.

The composition ratio of O/Ni is larger than 1 below 600°C and is nearly 1 above 600°C. It is seen that nickel oxide prepared by heating the nitrate below 600°C has obviously an excess of oxygen. The lattice parameter of nickel oxide does not vary with the heating temperature within the experimental error. The density of nickel oxide increases with an increase in the heating temperature as shown in Table I. The change in the lattice parameter is more strongly dependent on the oxygen ion which has a larger ion radius than the nickel ion. From the consideration of a constant lattice parameter and the decreasing densities of nickel oxide with an excess of oxygen, it seems to be reasonable to assume that nickel oxide has a cation vacancy as mentioned previously[7].

It has been known[8] that the $Ni^{3+}$ ion is not present in pure and dry nickel oxide. Chemical analysis, however, shows that the $Ni^{3+}$ ion is evidently present in pure and dry nickel

1) Y. Shimomura, *J. Phys. Soc. Japan*, **9**, 521 (1954): F. J. Morin, *Phys. Rev.*, **93**, 1199 (1954); K. Igaki, *Bull. Naniwa Univ.*, 3A, 113 (1955); A. Cimino et al., *Z. physik. Chem.* [*N.F.*], **16**, 101 (1958); Y. Iida, *J. Am. Ceram. Soc.*, **41**, 397 (1958).
2) T. G. Gray, *J. Phys. Chem.*, **60**, 201 (1956).
3) Y. Iida and S. Ozaki, *J. Am. Ceram. Soc.*, **42**, 219 (1959).
4) R. H. Griffith, *Discuss. Faraday Soc.*, **8**, 258 (1950).
5) J. L. Culberston, *J. Am. Chem. Soc.*, **59**, 306 (1937).
6) E. J. W. Verwey et al., *Philips Res. Rep.*, **5**, 173 (1950).
7) N. F. Mott and P. W. Gurney, "Electronic Process in Ionic Crystals", Second Ed., Oxford Prees, Oxford (1948) p. 152.
8) O. Glemser and J. Einhand, *Z. anorg. u. allgem. Chem.*, **261**, 43 (1950).

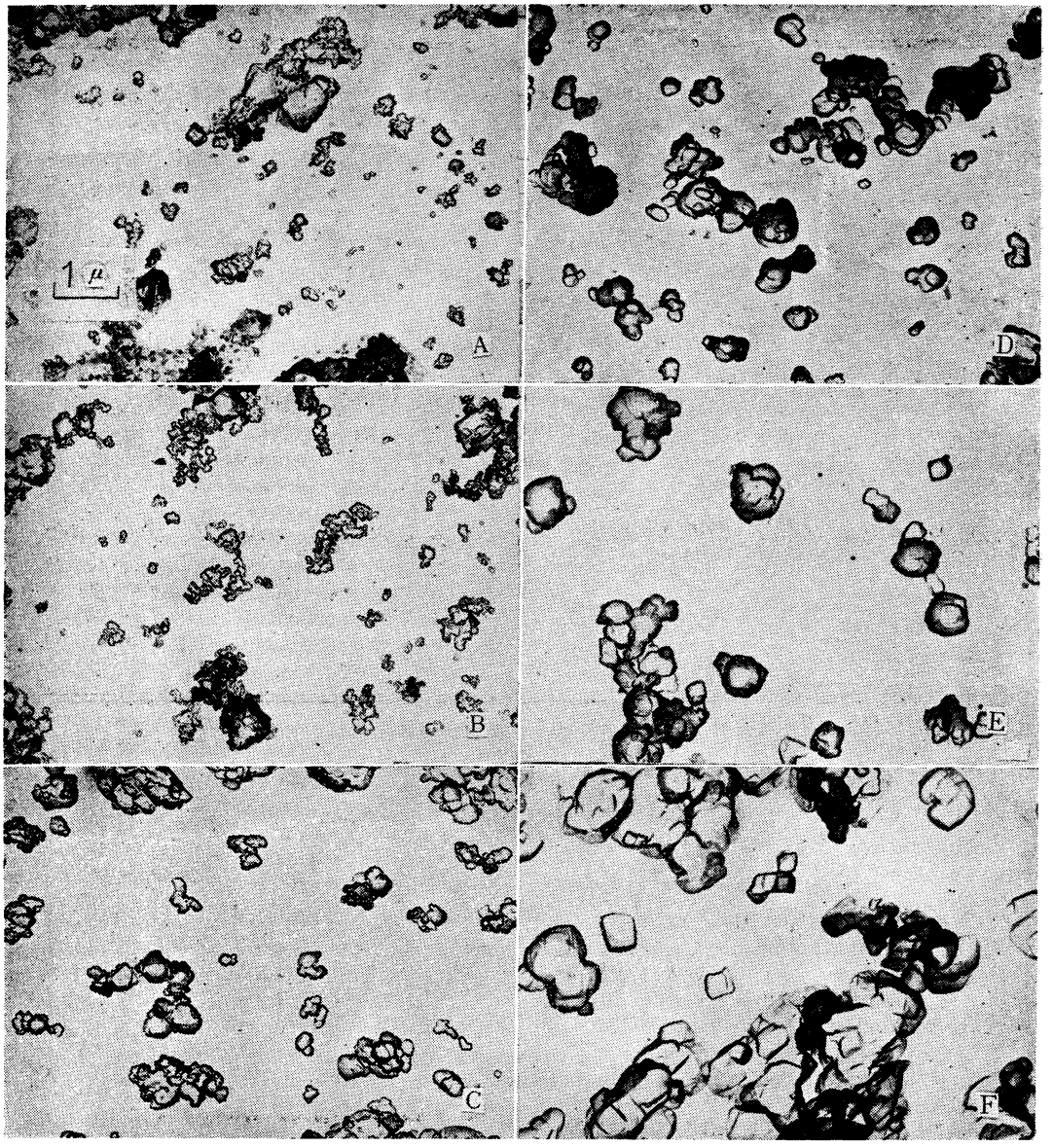



Fig. 1. Electron photographs of nickel oxides prepared by decomposition of nickel nitrate at (A) 400°C, (B) 600°C, (C) 700°C, (D) 800°C, (E) 900°C and (F) 1000°C.

oxide and decreases with the calcining temperature of nickel nitrate. From the reason mentioned above, a concentration of cation vacancy can be calculated as shown in Table I.

From the viewpoint of a semiconducting mechanism, electrical conductivity of nickel oxide should increase with an increase in an excess of oxygen or in a concentration of cation vacancy. The experimental resuls show that the conductivity increases with the cation vacancy. As nickel oxide calcined at low temperatures has a small particle size, the conductivity is thought to increase with an increase in the particle size in view of the contacting resistance of the powder. The conductivity of nickel oxide calcined at low temperatures, however, is high in spite of its small particle size according to the experimental results. Furthermore, Table I shows that the activation energy of the conductivity of nickel oxide decreases with an increase in the cation vacancy. From these facts it is concluded that nickel oxide calcined at low temperatures is obviously a non-stoichiometric compound and has $Ni^{3+}$ ions and cation vacancies, consequently.

Table I shows that the concentration of vacancies calculated from the densities is higher than that from chemical analysis of the

TABLE I. PHYSICAL AND CHEMICAL ANALYSIS OF NICKEL OXIDE PREPARED FROM DECOMPOSITION OF NICKEL NITRATE

| Calcining temp., °C | 400 | 500 | 600 | 700 | 800 | 900 | 1000 | 1200 |
|---|---|---|---|---|---|---|---|---|
| Ratio of O/Ni | 1.10 | 1.04 | 1.01 | 0.995 | 0.995 | 0.995 | 0.993 | 0.995 |
| Density observed, g./cc. | 5.74 | 6.28 | 6.40 | 6.48 | 6.53 | 6.62 | 6.65 | 6.80 |
| Lattice parameter, Å | 4.1798 | 4.1801 | 4.1792 | 4.1788 | 4.1788 | 4.1788 | 4.1788 | 4.1756 |
| Electrical conductivity at 300°C, Ω cm. | $6.8\times10^{-4}$ | $4.9\times10^{-4}$ | $4.1\times10^{-4}$ | $2.1\times10^{-4}$ | $1.0\times10^{-4}$ | | | |
| Activation energy of the conductivity, kcal./mol. | 8.5 | 9.5 | 10.0 | 10.3 | 10.5 | 11.0 | 11.4 | |
| $Ni^{3+}$, at. % | 1.07 | 0.41 | 0.31 | 0.27 | 0.11 | 0.040 | 0 | 0 |
| Density calculated, g./cc. | 6.789 | 6.787 | 6.792 | 6.794 | 6.794 | 6.794 | 6.794 | 6.809 |
| Number* of vacancy per cc. | $1.71\times10^{21}$ | $1.30\times10^{21}$ | $1.00\times10^{21}$ | $8.01\times10^{20}$ | $6.73\times10^{20}$ | $4.42\times10^{20}$ | $3.65\times10^{20}$ | $2.10\times10^{19}$ |
| Number** of vacancy per cc. | $2.79\times10^{20}$ | $1.24\times10^{20}$ | $8.62\times10^{19}$ | $7.40\times10^{19}$ | $3.02\times10^{19}$ | $1.09\times10^{19}$ | | |

* Values calculated from the densities.
** Values calculated from $Ni^{3+}$ atomic per cent.

TABLE II. COMPOSITION RATIO OF O/Ni OF NICKEL OXIDE PREPARED VARIOUS NICKEL SALTS

| Calcining temp., °C | 400 | 500 | 600 | 700 | 800 | 900 | 1000 |
|---|---|---|---|---|---|---|---|
| Nitrate | 1.10 | 1.04 | 1.01 | 0.995 | 0.995 | 0.995 | 0.993 |
| Hydroxide | 1.12 | 1.07 | | 1.02 | | 1.00 | 0.997 |
| Carbonate | 1.21 | 1.09 | | 1.02 | | 1.00 | 0.991 |

TABLE III. ACTIVATION ENERGY OF ELECTRICAL CONDUCTIVITY OF NICKEL OXIDE PREPARED FROM VARIOUS SALTS (kcal./mol.)

| Calcining temp., °C | 400 | 500 | 600 | 700 | 800 | 900 | 1000 |
|---|---|---|---|---|---|---|---|
| Nitrate | 8.5 | 9.5 | 10.0 | 10.3 | 10.5 | 11.0 | 11.4 |
| Hydroxide | 7.7 | 8.3 | — | 10.3 | — | — | — |
| Carbonate | 5.3 | 6.3 | — | 7.4 | — | 8.2 | 9.3 |

$Ni^{3+}$ ion. As a measurement is liable to give too low density values to small particles because of the incomplete desorption of gases even under the cautious density measurement, the disagreement may be attributed to the lowering of observed density. Further experiment, however, is necessary to determine which method is better to obtain the concentration of vacancy in nickel oxide.

**Effect of Starting Material.** — As nitrogen peroxide which may be responsible for an excess of oxygen in nickel oxide may be formed when nickel nitrate is decomposed, it is of interest to know whether the excess of oxygen in nickel oxide can be formed when nickel carbonate or nickel hydroxide is decomposed. Table II shows that the excess of oxygen is formed in the nickel oxides prepared from nickel carbonate and hydroxide as well as from nitrate. It is seen that the excess of oxygen is higher in nickel oxide from carbonate than in nickel oxides from nitrate and hydroxide. Electrical conductivity measurement shows that the activation energy of electrical conductivity decreases with an increase in the excess of oxygen for all nickel oxides and is the lowest for nickel oxide obtained from carbonate. It is confirmed that the excess of oxygen can be formd in nickel oxide prepared from other salts which are different from the nitrate. No reasonable explanation, however, has yet been found to make clear why the excess of oxygen is the highest in nickel oxide from carbonate, although nickel carbonate, hydroxide and nitrate start to decompose at about 250°C and their purity is essentially the same.

**Isothermal Change in Electrical Conductivity.** —From the above experiments, it has been evident that the nickel oxide obtained by heating nickel salts at low temperatures exhibits a vacant cation structure and its electrical properties vary with the cation vacancy and the concentration of cation vacancy decreases with the increasing heating temperature. It seems to be desirable to determine the isothermal change in electrical conductivity of the nickel oxide. Nickel nitrate was heated at 300°C for 3 hr. to obtain nickel oxide with a high concentration of the vacancy whose ratio of O/Ni

is 1.36. The isothermal change in the electrical conductivity at 300, 400 and 500°C is shown in Fig. 2. It is seen that the behavior of electrical conductivity varies with heating temperature. At 300°C, the electrical conductivity increases with the heating time while it

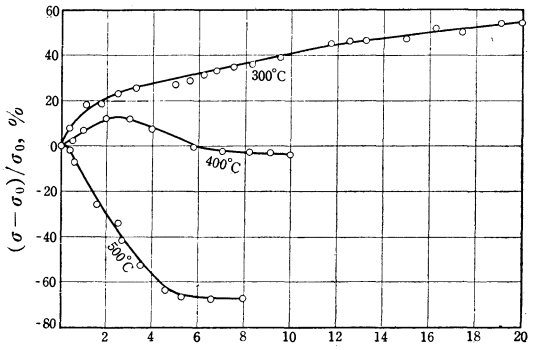



Fig. 2. The isothermal change in electrical conductivity of nickel oxide at various temperatures. Nickel oxide was made by decomposition of nickel nitrate at 300°C for 3 hr.

decreases with the heating time at 500°C. At 400°C, the conductivity increases initially in a heating period of 2 hr. and then decreases with the time. Since the cation deficient structure of nickel oxide is thought to be formed during the decomposition process of nickel nitrate and to be uncompleted in 3 hr. at 300°C, the conductivity increases with the time when it is reheated at 300°C. At 400°C, the uncompleted cation deficient structure is completed in an initial heating period. This may be the result in the initial inrease in the conductivity at 400°C.

The cation deficient structure of nickel oxide is expressed by the following equation according to Hauffe[9]

$$NiO+2\oplus+\square'' \rightleftharpoons \frac{1}{2}O_2$$

where $\square''$ represents the vacancy of nickel site and $\oplus$, a positive hole of the electron. There are equilibrium states at various temperatures between the concentration of the vacancy and oxygen pressure following the above equation. Since nickel oxide calcined at 300°C has a higher concentration of vacancy than the equilibrium state at 400°C, the vacancies greater than the equilibrium value diffuse to the surface of the crystal and disappear. The decreasing conductivity at 400°C in Fig. 2 can be explained by the diffusion of vacancy.

## Summary

Nickel oxide obtained by heating nickel nitrate, carbonate and hydroxide at low temperatures exhibits a non-stoichiometric structure. An excess of oxygen decreases with an increase in the heating temperature of nickel salts. Concentration of $Ni^{3+}$ determined by chemical analysis increases with the excess of oxygen. Densities of nickel oxide or activation energy of electrical conductivity decrease with an increase in the excess of oxygen, whereas lattice parameter does not vary. Isothermal change in electrical conductivity of nickel oxide shows that the decrease in vacancies may be attributed to the diffusion of vacancies to the crystal surface. The concentration of vacancies calculated from the density is higher than that from the concentration of $Ni^{3+}$ ion. The disagreement may be attributed to the density measurement technique.

*Government Industrial Research Institute*
*Kita-ku, Nagoya*

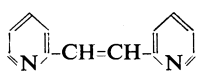
9) K. Hauffe und J. Bloch, *Z. physik. Chem.*, **198**, 232 (1951).

# *Geometrical Isomers of 1,2-Bis-(4-pyridyl)-ethylene*

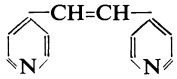
By Takumi KATSUMOTO

(Received March 11, 1960)

In the preceding paper[1] the author reported the geometrical isomers of 1,2-bis-(2-pyridyl)-ethylene. Regarding 1,2-bis-(4-pyridyl)-ethylene, it is also expected that it will be able to exhibit geometrical isomerism and then to prove its existence in a cis and a trans form. Hitherto, however only one species[2,3] which melts at 151~152°C has been known. The author condensed 4-picoline and 4-pyridylaldehyde into 1,2-bis-(4-pyridyl)-ethylene and then separated two isomers from the ethylene, one corresponding to the known species and the other to the unknown one. The elementary analyses, molecular weight, melting points and ultraviolet and infrared absorptions, all prove that the former is a trans isomer and the latter a cis isomer of 1,2-bis-(4-pyridyl)ethylene.



1,2-Bis-(2-pyridyl)-ethylene



1,2-Bis-(4-pyridyl)-ethylene

## Experimental

**Synthesis of 1,2-Bis-(4-pyridyl)-ethylene.**—The ethylene was synthesized from 4-pyridylaldehyde, 4-picoline and anhydrous zinc chloride according to Thayer and Corson's method[2]. 4-Pyridylaldehyde from the Aldrich Chemicals was distilled under 16 mmHg pressure and the fraction boiling at 85.5°C was used; the phenylhydrazone, m. p. 177.0~178.5°C (lit., 178~179°C[4]). 4-Picoline was separated from the "β-picoline", b. p. 140~148°C, according to the following method[5]. The "β-picoline" contains 3-picoline, 4-picoline and 2,6-lutidine. 2,6-Lutidine was first removed as the urea adduct[6], and then the mixture of the unchanged 3- and 4-picoline was converted into their oxalates[7]. 4-Picoline oxalate was separated by the fractional crystallization from the absolute alcohol solution, as it is less soluble in absolute ethanol than 3-picoline oxalate; 4-picoline oxalate, m. p. 138~139°C. 4-Picoline was recovered by the decomposition of the oxalate with sodium hydroxide and distilled; b. p. 145.0~146.0°C; picrate, m. p. 165.5~166.5C. The infrared absorption spectra of the 4-pyridylaldehyde and the 4-picoline showed the complete absence of the 2- and the 3-isomer, respectively in them. 4-Pyridylaldehyde (0.022 mol.), was heated with the equivaleat moles of 4-picoline and anhydrous zinc chloride in a sealed tube at 200~215°C for 16 hr. The reaction mixture was cooled, dissolved in 40 cc. of 3 N sulfuric acid, and basified with sodium hydroxide. The cooled alkaline solution was extracted twice with 30 cc. portion of ether and four times with 30 cc. portions of chloroform. The chloroform extract was dried over anhydrous potassium carbonate. After the greater part of the solvent was removed, the concentrated chloroform extract was chromatographed on a column (2×40 cm.) of alumina and the column was eluted with chloroform. The chromatograph afforded a satisfactory fractionation. One (**A**), eluted first, formed colorless, long needles, which melted at 151.5~152.5°C after three additional recrystallizations from water and corresponds to the known species of the ethylene. Yield, 17% theoretical. The other (**B**), contained in the next eluate, formed colorless, viscid oil and crystallized by being scratched with a sharp glass rod. The repeated recrystallizations of the crystals from cyclohexane-benzene (1:1) gave colorless, small needles, m. p. 110~111°C. Yield, 17.5% theoretical.

**Measurements.**—Molecular weight was determined by Rast's method. The ultraviolet absorption spectra (in absolute ethanol) were made with a Shimadzu QB-50 quartz spectrophotometer. The wavelengths of the photometer were calibrated with the absorption band at 301 mμ of an aqueous potassium nitrate solution. The infrared absorption spectra were obtained with a Shimadzu IR spectrophotometer equipped with a rock-salt prism. Readings were taken in the range 2000~670 $cm^{-1}$ and calibrated with the absorption bands of polystyrene.

## Results and Discussion

As described above, **A** is colorless, long needles and melts at 151.5~152.5°C, while **B** is colorless, small needles and melts at 110.0~111.0°C. **A** is identified with the known species of 1,2-bis-(4-pyridyl)-ethylene, as the melting point is in good agreement with the published value of the ethylene (lit., 151~152°C[2]) and the result of the elementary analyses is consistent with the calculated value for the ethylene $C_{12}H_{10}N_2$ (Table I). Furthermore, the assignment of the infrared

1) T. Katsumoto, This Bulletin, **32**, 1019 (1948).
2) H. I. Thayer and B. B. Corson, *J. Am. Chem. Soc.*, **70**, 2330 (1948).
3) E. D. Bergmann et al., ibid., **74**, 5979 (1952).
4) J. P. Wibaut et al., *Rec. trav. chim.* **64**, 30 (1945).
5) T. Katsumoto et al., *Coaltar (Japan)*, **3**, 368 (1951).
6) F. Othmer, *Ind. Eng. Chem.*, **40**, 168 (1948).
7) A. G. Lidstone, *J. Chem. Soc.*, **1940**, 243.

TABLE I. COMPARISON OF THE TWO ISOMERS OF 1,2-BIS-(4-PYRIDYL)-ETHYLENE

| Compound | A long needles | B small needles |
|---|---|---|
| M.p. | 151.5~152.5°C | 110.0~111.0°C |
| Elementary analyses | | |
| Found | C: 78.9 %<br>H: 5.75<br>N: 15.60 | C: 79.0 %<br>H: 5.83<br>N: 15.20 |
| Calcd. for $C_{12}H_{10}N_2$ | C: 79.1 %<br>H: 5.53<br>N: 15.40 | |
| Molecular weight | | |
| Found | — | 188 |
| Calcd. for $C_{12}H_{10}N_2$ | | 182 |

spectrum makes sure of the above determination, as is described later. The elementary analyses and molecular weight of B are also consistent with the calculated values for the ethylene (Table II); thus **B** is an isomer of **A**. Thayer et al. reported that 1,2-bis-(4-pyridyl)-ethane melted at 110~111°C, which is the same temperature at which **B** melts. Although there is little possibility of producing the ethane in our experimentation, the author has proved that **B** is quite different from the ethane by the mixed examination and the infrared absorption spectra in carbon disulfide as follows; the ethane from the Aldrich Chemicals (m. p. 111~112°C) depresses largely the melting point of **B** in the mixed examination and it shows no absorption in the range 830~670 $cm^{-1}$, while **B** absorbs strongly at 763 $cm^{-1}$.

The infrared absorption spectra of the two isomers, **A** and **B**, are shown in Table II and Fig. 1. They resemble each other very closely except for a few absorptions. **A** and **B** give the following common absorptions; four absorptions in the range 1630~1430 $cm^{-1}$ due to the double bond stretching vibrations of the pyridine ring, three absorptions in the range 1250~950 $cm^{-1}$ due to the C-H in-plane bending vibrations of the 4-substituted pyridine ring and one strong absorption in the range 790~830 $cm^{-1}$ due to the C-H out-of-plane bending vibration of the 4-substituted pyridine ring, respectively[8,9,10]. These absorptions lie always in the range indicated by Shindo[8] and Katritzky[9] for the above vibration modes of the 4-substituted pyridine, as shown in the last column of Table II. A few absorptions that are not common to them arise from the disubstituted ethylene as will be discussed later. No other significant absorptions are found in the spectra. Thus, it is certain that **A** and **B** are the disubstituted ethylenes with 4-pyridyl radicals, i. e. 1,2-bis-(4-pyridyl)-ethylenes and the geometrical isomers with each other.

The geometrical arrangements of **A** and **B** are determined by the infrared and ultraviolet absorption spectra, the melting points, and the solubilities in organic solvents.

TABLE II. INFRARED ABSORPTION BANDS OF 1,2-BIS-(4-PYRIDYL)-ETHYLENE

| A (trans) $cm^{-1}$ | A (trans) $\varepsilon$ | B (cis) $cm^{-1}$ | B (cis) $\varepsilon$ | Assignment* | Reference range |
|---|---|---|---|---|---|
| 1595 | 234 | 1603 | 206 | PR-1 | |
| 1560 | 51 | 1567 | 57 | PR-2 | four bands in the range |
| 1504 | 24 | 1508 | 17 | PR-3 | 1630~1430 $cm^{-1}$ |
| | | 1458 | 24 | | |
| 1418 | 106 | 1420 | 111 | PR-4 | |
| 1289 | 29 | | | EHI (*trans*) | 1310~1290[13] |
| 1242 | 51 | 1242 | 38 | PHI-1 | 1232~1211[8] |
| 1070 | 24 | 1070 | 34 | PHI-2 | 1070~1053[8] |
| | | | | | 1072~1055[9] |
| 995 | 94 | 997 | 66 | PHI-3 | 1003~ 990[8] |
| | | | | | 997~ 985[9] |
| 966 | 145 | | | EHO (*trans*) | 990~ 965[12] |
| 951 | 61 | | | | |
| 837 | 104 | | | | |
| 821 | 182 | 819 | 103 | PHO | 790~ 830[11] |
| | | 805 | 66 | | |
| | | 763 | 190 | EHO (*cis*) | 800~ 650[11] |

* PR means the stretching vibration of a pyridine ring; EHI and PHI mean the in-plane bending vibrations and EHO and PHO mean the out-of-plane bending vibrations of the hydrogen atoms remaining on an ethylene and a pyridine ring, respectively.

8) H. Shindo, *Pharm. Bull. (Japan)*, **5**, 472 (1957).
9) A. R. Katritzky and J. N. Gardner, *J. Chem. Soc.*, **1958**, 2198.
10) T. Katsumoto, This Bulletin, **33**, 242 (1960).

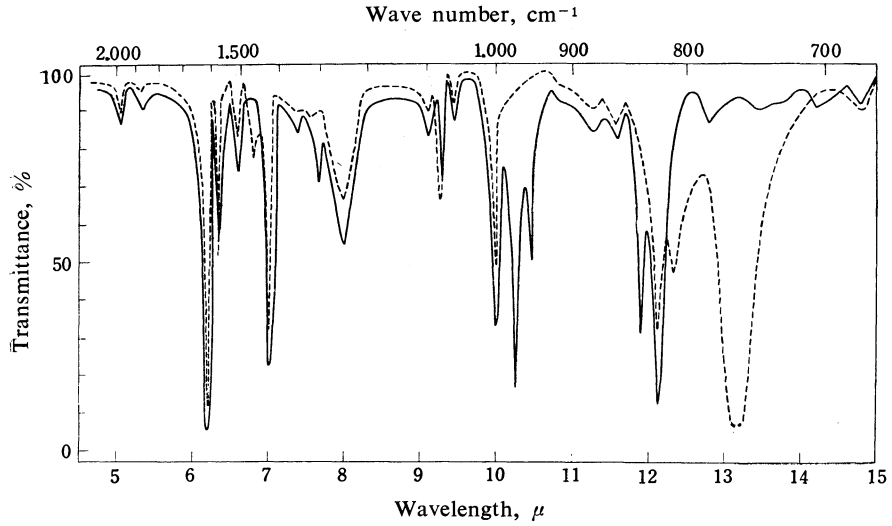



Fig. 1. Infrared absorption spectra of 1,2-bis-(4-pyridyl)-ethylene.
A 5 μ~12.5 μ (chloroform), 12.5~15 μ (acetone).
B 5 μ~12.5 μ (chloroform), 12.5~15 μ (carbon disulfide).
—— A (trans), ------ B (cis)

TABLE III. ULTRAVIOLET ABSORPTION BANDS OF 1,2-BIS-(4-PYRIDYL)-ETHYLENE (in absolute ethanol)

| | E-band | | K-band | |
|---|---|---|---|---|
| | $\lambda_{max}$ | $\varepsilon_{max}$ | $\lambda_{max}$ | $\varepsilon_{max}$ |
| cis Form (**B**) | 212 mμ | 8,390 | 257 mμ | 4,210 |
| trans Form (**A**) | 218 mμ | 11,460 | 288 mμ | 32,490 |
| | 223 | 11,990 | 299 | 33,380 |
| | | | 312 | 19,470 |

The infrared absorptions due to the cis- and the trans form are quite different[11]. trans isomers absorb strongly close to 965 $cm^{-1}$ and weakly in the range 1310~1290 $cm^{-1}$. Rasmussen and Brattain showed that the former absorptions appear only with the trans double bond[12]. This absorption is attributed to the =C-H out-of-plane bending vibration, and the latter to the in-plane bending vibration, of the *trans*-disubstituted ethylene[13]. Cis isomers give no absorptions in this range. **A** gives the two absorptions at 966 $cm^{-1}$ and 1298 $cm^{-1}$, but the absorptions corresponding to them cannot be found in the spectrum of **B**. While, Zechmeister[14] suggested the *cis*-disubstituted ethylenes conjugated with double bonds on both sides give an absorption near 780 $cm^{-1}$. **B** absorbs strongly at 763 $cm^{-1}$ as described above and **A** gives no absorptions in the regions. These absorptions suggest that **A** is a trans isomer and **B** is a cis isomer.

The melting point of **B** is lower by about forty degrees than that of **A**, as shown in

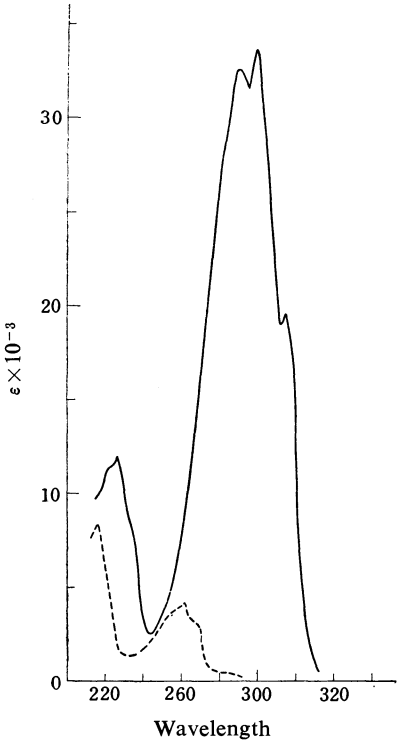



Fig. 2. Ultraviolet absorption spectra of 1,2-bis-(4-pyridyl)-ethylene.
—— **A** (trans), ---- **B** (cis)

11) L. J. Bellamy, "The Infrared Spectra of Complex Molecule", 2nd Ed., Methuen, London (1958), p. 45.
12) R. S. Rasmussen and R. R. Brattain, *J. Chem. Phys.*, 15, 131, 135 (1947).
13) N. Sheppard and G. Sutherland, *Proc. Roy. Soc.* A196, 195 (1949).
14) L. Zechmeister et al., *Acta Chem. Scand.*, 8, 1421 (1954).

Table I. As the cis isomer always melts at a very much lower temperature than trans isomer does, **B** and **A** seem to be a cis and a trans isomer, respectively. The polar substance like a cis isomer is not easily dissolved in the non-polar solvents. **B** is insoluble in cyclohexane, while **A** is readily soluble in it. **B** seems to be a cis isomer.

Regarding the conjugation band of the ultraviolet absorption spectra, a cis isomer gives the spectrum similar to the sum of the spectrum of the component parts of the molecule on the either side of the double bond. The bathochromic displacement and much increase of the absorption intensity of the conjugation band always occur on passing from the cis structure to the trans structure. The ultraviolet absorption spectra of **A** and **B** are shown in Table III and Fig. 2. The conjugation band of 4-picoline has the intensity of some 2,000 at 255 m$\mu$ and that of **B** has about two times as much intensity of 4,210 as the former at 257 m$\mu$. While **A** gives the band at 299 m$\mu$ with intensity 33,380. The ultraviolet absorption spectra of **A** and **B** are typical of the trans and the cis structure.

The conclusion is that the known species of 1, 2-bis-(4-pyridyl)-ethylene (**A**) is the trans isomer and another species (**B**) which was separated by the present author is the cis isomer.

The author wishes to thank Professor S. Kimura of Kyoto University for encouragement, Professor T. Matsu'ura of Hiroshima University for recording infrared spectra and Mr. Yamaguchi of this laboratory for his helpful assistance.

*Chemical Laboratory*
*Kwansei Gakuin University*
*Nishinomiya, Hyogo*

# γ-Hydroxyarginine, a New Guanidino Compound from a Sea-cucumber II. Determination of the Configuration

By Yoshimasa FUJITA

(Received March 21, 1960)

A new guanidino compound was first discovered in a sea-cucumber, *polycheira rufescence*[1], and then isolated purely and identified as γ-hydroxy-L-arginine (I)[2]. The compound contains two asymmetric carbon atoms (α and γ) and should, therefore, exist theoretically in four stereoisomeric forms. In the preceding paper[2] it was concluded that the configuration on the α-carbon is the L$_S$-form[3] in view of the susceptibility to arginase[4] and L-amino acid oxidase[5], whereas that on the γ-carbon was not yet decided. The conclusion was further supported by Makisumi[6] in our laboratory. He observed that I was quantitatively decarboxylated by the action of L-arginine decarboxylase from *E. coli* 7020[7].

In contrast with γ-hydroxyarginine, γ-hydroxyornithine was studied in detail with regard to its stereoisomers by Witkop et al.[8,9]. They proved that *erythro*- and *threo*-γ-hydroxy-L-ornithine were stereochemically equivalent to hydroxy-L-proline and allohydroxy-L-proline, respectively.

In the present study, the configuration on the γ-carbon was established according to the method of Witkop et al.[8] with a slight modification. γ-Hydroxy-L-ornithine (II) produced from I by the action of arginase was treated first with nitrosyl chloride, and then with barium hydroxide. From this reaction mixture, a product which gave a yellow spot with ninhydrin reagent on a paper chromatogram was isolated by fractionation on a column of Amberlite CG-120. The product was identified

1) H. Sasaki, Y. Fujita, S. Makisumi and S. Shibuya, *J. Japanese Biochem. Soc.* (*Seikagaku*), **30**, 642 (1958).
2) Y. Fujita, This Bulletin, **32**, 439 (1959).
3) E. J. Crane, *Chem. Eng. News*, **25**, 1363 (1947).
4) D. M. Greenberg, "The Enzymes", Vol. 1, edited by J. B. Sumner and K. Myrbäck, Academic Press Inc., New York (1951), p. 894.
5) Y. Robin, *Bull. Soc. Chim. Biol.*, **35**, 285 (1953). H. Blashko and D. B. Hope, *Biochem. J.*, **62**, 335 (1956).
6) S. Makisumi, unpublished data.
7) E. F. Gale, *Biochem. J.*, **41**, vii (1947). S. M. Birnbaum and J. P. Greenstein, *Arch. Biochem. Biophys.*, **39**, 108 (1952).
8) B. Witkop and T. Beiler, *J. Am. Chem. Soc.*, **78**, 2882 (1956).
9) B. Witkop, *Special Publication No. 3.*, The Chemical Society, Burlington House, W. 1, London, (1955), p. 60.

as allohydroxy-D-proline (III). The optical purity of III was assured with the aid of column chromatography (Fig. 2).

The fact that a compound having the $L_S$ configuration as to the $\alpha$-carbon atom converts by the action of a certain reagent into a product having the $D_S$ configuration, suggests that it is a result of the Walden inversion. According to the extensive studies by Izumiya et al.[10] on the Walden inversion of $\alpha$-amino acid, it is generally accepted that in an $\alpha$-amino acid possessing a secondary carbon atom at $\beta$-position the inversion does not occur by the halogenation with nitrosyl halide, but takes place on treating the resulting $\alpha$-halogeno acid with basic reagents such as ammonia.

When, as in the case of the present experiment, nitrosyl chloride acts on II, there is a possibility that three chlorinated acids ($\alpha$-chloro-$\delta$-amino-$\gamma$-hydroxyvaleric, $\delta$-chloro-$\alpha$-amino-$\gamma$-hydroxyvaleric, and $\alpha,\delta$-dichloro-$\gamma$-hydroxyvaleric acids) are produced therefrom. Of the three acids, $\alpha$-chloroacid and $\delta$-chloroacid are concerned in the formation of hydroxyproline after cyclization. The composition of the reaction mixture was, therefore, examined by means of determination of the total nitrogen, carbon dioxide liberated with Chloramine T and chloride ions (Table I). The results indicated that the amount of $\alpha$-chloroacid was much grater than that of $\delta$-chloroacid, showing a preferential reactivity of the $\alpha$-amino group of II. It is reasonable, as in the cases of chain compound, that the inversion should also occur in the stage of a base-catalyzed cyclization of $\alpha$-chloro-$\delta$-amino-$\gamma$-hydroxyvaleric acid. Accordingly, the allohydroxy-D-proline obtained by the inversion can be established as originating from *erythro*-$\gamma$-hydroxy-L-ornithine. The latter compound, if the inversion did not occur, would convert into hydroxy-L-proline (IV). Therefore, the whole configuration of I should, as a matter of course, be concluded to be *erythro*-$\gamma$-hydroxy-L-arginine.

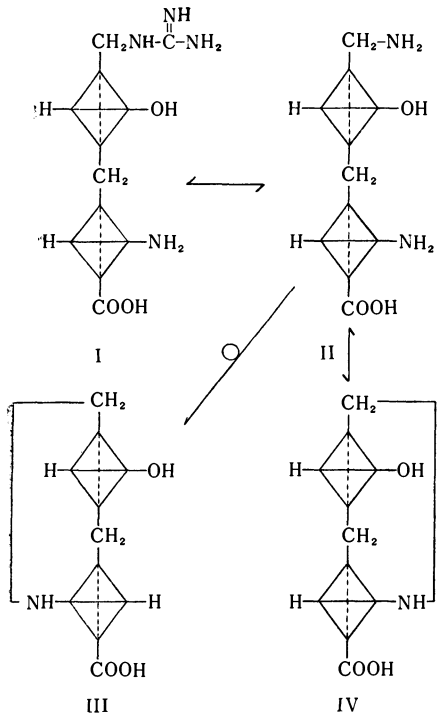



Fig. 1. Stereochemical correlation between $\gamma$-hydroxyarginine, $\gamma$-hydroxyornithine and (allo)hydroxyproline.
⟷ Stereochemical equivalence
⟲ Walden inversion

## Experimental

**Material.** — The $\gamma$-hydroxy-L-ornithine hydrochloride used in the present study was prepared from $\gamma$-hydroxy-L-arginine hydrochloride by the action of arginase[2]: m. p. 182~183°C (decomp.), $[\alpha]_D^{20}$ +10.6° (*c* 5, in water)[11].

According to Witkop et al.[8], in the conversion of $\gamma$-hydroxyornithine to (allo)hydroxyproline different results are obtained by using either the open acid or the lactone as the starting material. Therefore, whether or not contaminated with lactonized $\gamma$-hydroxyornithine, the material was checked by determining the carbon dioxide evolved with Chloramine T at pH 4.7 and 25°C. On mixing $\gamma$-hydroxyornithine with the reagent, a brisk evolution of the gas was observed. This amounted to 90% after 5 min. and to 100% after 15 min. The observation was in good accordance with that of Witkop on the open acid.

**Conversion of $\gamma$-Hydroxy-L-ornithine to Allohydroxy-D-proline.** — A nitrosyl chloride solution (6 ml.) prepared according to Witkop et al.[8] was added drop by drop to an ice-cold solution of $\gamma$-hydroxy-L-ornithine hydrochloride (185 mg.) dissolved in 9 N hydrochloric acid (10 ml.). The reaction mixture was stirred for 10 min. in the cold and then heated at 55°C for 20 min., followed by evaporation to dryness in vacuo. The residue was dissolved in water (2 ml.), and heated with 0.2 N barium hydroxide solution (10 ml.) in a boiling water bath for 10 min. The solution was freed from barium by neutralizing with sulfuric acid and centrifugation. The supernatant solution was passed through a column of Amberlite CG-120 (H-form, 1×18 cm.). The adsorbed substances were eluted with 0.2 N hydrochloric acid (15 ml./hr.), and collected in 5 ml. fractions. Each fraction was analyzed by paper chromatography and only the fractions (31st to 40th tubes) which gave a single yellow spot with ninhydrin were united. The resulting solution was evaporated up to dryness in

10) N. Izumiya et al., *J. Chem. Soc. Japan, Pure Chem. Sec.* (*Nippon Kagaku Zasshi*), **72**, 26, 149, 445, 550, 1050 (1951); This Bulletin, **25**, 265 (1952); **26**, 53 (1953).

11) The author wishes to correct the erroneous figure for the specific rotation described in Ref. 2.

vacuo. The crystalline residue was dissolved in a small volume of water and the solution was passed through a column of Amberlite IR-4B (OH-form). The effluent freed from chloride by this treatment was again concentrated in vacuo and the crystalline residue was triturated with methanol (2 ml.), filtration and washing with methanol and ether being followed. The product was recrystallized from water-ethanol. Yield 31 mg.; m. p. 237~239°C (decomp.); $[\alpha]_D^{15}$ +57.0° (*c* 1, in water).

Found: C, 45.87; H, 6.78; N, 10.86. Calcd. for $C_5H_9NO_3$: C, 45.80; H, 6.92; N, 10.68%.

The above product (1 mg.) dissolved in citrate buffer pH 3.20 (1 ml.) was passed through a column of Dowex 50-X8 (0.9×50 cm.)[12,13] maintained at 37°C, and eluted (4 ml./hr.) with the same buffer. The effluent was collected in 1 ml. fractions and each fraction was analyzed by ninhydrin colorimetry[14]. The elution pattern of the product had a single peak which corresponded to allohydroxyproline and no other peak was observed, while the authentic mixture of hydroxyproline and allohydroxyproline[15] was completely resolved into two peaks under the same condition (Fig. 2).

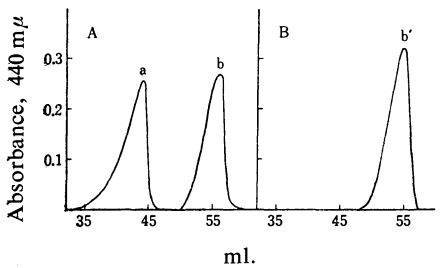



Fig. 2. The elution pattern of hydroxyproline (HP) and allohydroxyproline (AHP) from a column of Dowex-50 (0.9×50 cm.) at pH 3.20 and 37°C.
A: Authentic mixture of L-HP (a) and D-AHP (b)
B: D-AHP (b') prepared by cyclization from γ-hydroxy-L-ornithine

12) S. Moore and W. H. Stein, *J. Biol. Chem.*, **192**, 663 (1951).
13) K. A. Piez, *J. Biol. Chem.*, **207**, 77 (1954).
14) E. W. Yemm and E. C. Cocking, *Analyst*, **80**, 209 (1955); *Biochem. J.*, **58**, xii (1954).
15) The author is indebted to Dr. S. M. Birnbaum and Dr. M. Winitz for a generous supply of the sample of hydroxy-L-proline and allohydroxy-D-proline, respectively.

**Composition of the Reaction Mixture with Nitrosyl Chloride.** — A solution of γ-hydroxy-L-ornithine hydrochloride (100 mg.) was treated with a nitrosyl chloride solution (3 ml.) as described above. The reaction mixture was evaporated up to dryness in vacuo and further dried in a vacuum desiccator on potassium hydroxide until it reached a constant weight. It was analyzed for total nitrogen by the micro Kieldahl method, for the liberation of carbon dioxide with Chloramine T at 25°C in a Warburg manometer and for chloride by the titration with silver nitrate[16]. The following values were obtained: 5.32% total nitrogen, 4.12% $CO_2$ and 13.43% $Cl^-$. The results were summarized in Table I.

TABLE I. COMPOSITION OF THE REACTION MIXTURE WITH NITROSYL CHLORIDE

| Symbol* | Mol. wt. | Theory, % $N_2$ | $CO_2$ | $Cl^-$ | Composition of the reaction mixture, % |
|---|---|---|---|---|---|
| W | 221.09 | 12.7 | 19.9 | 32.1 | 20 |
| X | 204.06 | 6.9 | 0 | 17.4 | 39 |
| Y | 204.06 | 6.9 | 21.6 | 17.4 | 1 |
| Z | 187.03 | 0 | 0 | 0 | 40 |

* W: γ-Hydroxyornithine·2HCl
X: α-Chloro-δ-amino acid·HCl
Y: δ-Chloro-α-amino acid·HCl
Z: α,δ-Dichloro acid

The figures for W, X, Y and Z in Table I were calculated from the following equations: 12.7W+6.9X+6.9Y=5.32; 19.9W+21.6Y=4.12; 32.1W+17.4X+17.4Y=13.43; W+X+Y+Z=1.

The author wishes to express his cordial thanks to Professor S. Shibuya for his guidance and encouragement, and to Assistant Professor N. Izumiya for his advice. His thanks are also due to the Ministry of Education for financial support of this research.

*Laboratory of Biochemistry*
*Faculty of Science*
*Kyushu University*
*Fukuoka*

16) S. Ueo and S. Sakamoto, *J. Pharm. Soc. Japan* (*Yakugaku Zasshi*), **58**, 711 (1938).

# *The Dehydration Reactions of Nitroparaffins and Aldoximes*

By Teruaki MUKAIYAMA and Tsujiaki HATA

(Received May 4, 1960)

The preceding paper[1] describes the reaction of primary nitroparaffin with isocyanate which gives *sym*-disubstituted urea, furoxane and carbon dioxide in excellent yields in the presence of a catalytic amount of tertiary amine.

$$4R\text{-}N{=}C{=}O + 2R'CH_2NO_2 \xrightarrow{R_3N} 2RHNCONHR + 2CO_2 + R'C(=N\text{-}O)C(=N\text{-}O)R' \quad (1)$$

This reaction proceeds to the formation of disubstituted urea and furoxane through intermediates or amine and nitrile oxide which are formed by the decomposition of the addition compound of isocyanate and *aci*-nitroparaffin with spontaneous evolution of carbon dioxide. The reaction of the amine with isocyanate yields di-substituted urea and furoxane is formed by the dimerization of nitrile oxide.

Nitrile oxide, one of the two intermediates, was confirmed by the formation of isoxazoline when isocyanate, nitroparaffin and tertiary amine are reacted in the presence of unsaturated compound as shown in the following equation.

$$RCH_2NO_2 + CH_2{=}CH\text{-}OAc + 2R'\text{-}N{=}C{=}O \xrightarrow{R_3N} CO_2 + R'HNCONHR' + CH_2\text{-}CH(\text{-}OAc)\text{-}C(=O)\text{-}N{=}R \quad (2)$$

These two reactions 1 and 2 involve initial formation of nitrile oxide by the dehydration of nitroparaffiin with isocyanate and this suggests an interesting study of the dehydration of nitroparaffin with the other organic reagents. Three organic reagents were used to check the dehydration process of nitroparaffins. Firstly, the reaction of primary nitroparaffin with carbodiimide[2] is studied because of its similar behavior to isocyanate. When di-*p*-tolyl carbodiimide and phenylnitromethane are reacted in the presence of tertiary alkyl amine, *sym*-di-*p*-tolylurea and 3-phenyl-4-*p*-tolyl-5-*p*-tolylimino-oxadiazole are obtained (Eq. 3).

$$2CH_3C_6H_4N{=}C{=}N\text{-}C_6H_4CH_3 + C_6H_5CH_2NO_2 \xrightarrow{R_3N} CH_3C_6H_4NHCONHC_6H_4CH_3 + CH_3C_6H_4N{=}C(\text{-}O\text{-}C_6H_5)\text{-}N{=}C_6H_4CH_3 \quad (3)$$

The reaction is satisfactorily explained by the same consideration described in the case of isocyanate which involves the initial formation of nitronate ion by the interaction of nitroparaffin with tertiary amine. One of the oxygen atoms of the nitro group combines in turn with the positively charged carbon of carbodiimide, forming the addition compound I shown in the next scheme.

$$R''_3N + RCH_2NO_2 \rightleftharpoons R''_3\overset{+}{N}H + \left[R\text{-}C(=N\text{-}O^-)\text{-}H \longleftrightarrow R\text{-}C(=N\text{-}O)\text{-}H\right] \xrightarrow{R'N=C=N-R'} R'\text{-}N(H)\text{-}C(=N\text{-}R')\text{-}O\text{-}N{=}C(H)\text{-}R \quad (I)$$

By transferring the hydrogen atom attached to the carbon as a proton, the adduct I decomposes to nitrile oxide and isourea. The latter readily isomerizes to urea and the nitrile oxide adds to carbodiimide, forming oxadiazolone-anil.

$$(I) \rightarrow \begin{cases} CH_3C_6H_4\text{-}N(H)\text{-}C(=N\text{-}C_6H_4\text{-}CH_3)\text{-}OH \longrightarrow CH_3\text{-}C_6H_4N(H)\text{-}C(=O)\text{-}N(H)\text{-}C_6H_4CH_3 \\ C_6H_5C{\equiv}N{\rightarrow}O \xrightarrow{CH_3C_6H_4N=C=NC_6H_4CH_3} CH_3C_6H_4\text{-}N(\text{-}C(=O)\text{-}C_6H_5)\text{-}C(=N\text{-}C_6H_4CH_3)\text{-}O\text{-}N \end{cases}$$

1) T. Mukaiyama and T. Hoshino, *J. Am. Chem. Soc.*, in press.

2) H. G. Khorana, *Chem. Revs.*, 53, 145 (1953).

From the above result it appears interesting to extend the dehydration reaction to aldoxime which has a structure similar to that of *aci*-nitroparaffin. When aldoximes and carbodiimide react with each other, *sym*-disubstituted urea and corresponding nitriles result in high yields either in the absence or the presence of tertiary amine according to the Eq. 4.

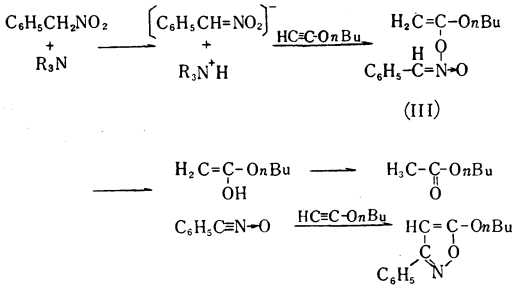
$$\begin{aligned} &R\text{-}CH{=}NOH + R'\text{-}N{=}C{=}N\text{-}R' \\ &\longrightarrow R'HNC(=NR')\text{-}ON{=}HC\text{-}R \quad (II) \\ &\longrightarrow R\text{-}C{\equiv}N + R'HNCONHR' \end{aligned} \tag{4}$$

Unlike the case of nitroparaffin, the dehydration of aldoxime is carried out even in the absence of catalyst. This would be rationalized if the intermediate II is considered to be formed by the addition of aldoxime, which contains a reactive hydroxyl group in itself, to carbodiimide.

Secondly, the reactions of nitroparaffin and aldoxime with acetylenic ether which is known as a strong dehydrating agent were tested, and the similar results were obtained[3,4]. When *n*-butyl acetylenic ether and phenylnitromethane are reacted in the presence of tertiary alkyl amine, *n*-butyl acetate and 3-phenyl-5-*n*-butoxyisoxazole are obtained along with by-product, i. e. 3, 4, 5-triphenylisoxazole, formed by the self-condensation of phenylnitromethane[5].

$$\begin{aligned} &HC{\equiv}C\text{-}O\text{-}n\text{-}Bu + C_6H_5CH_2NO_2 \\ &\longrightarrow CH_3COO\text{-}n\text{-}Bu + HC(C_6H_5)(O)=C\text{-}O\text{-}n\text{-}Bu \\ &+ C_6H_5C(C_6H_5)(O)=C\text{-}C_6H_5 \end{aligned} \tag{5}$$

The reaction can be understood by considering the addition compound III formed by the addition of the nitronate ion of nitroparaffin to acetylenic ether. By transferring a hydrogen atom, this decomposes to nitrile oxide and enolic derivative of ester. The latter readily isomerizes to ester, and the nitrile oxide adds to acetylenic ether to form isoxazole.



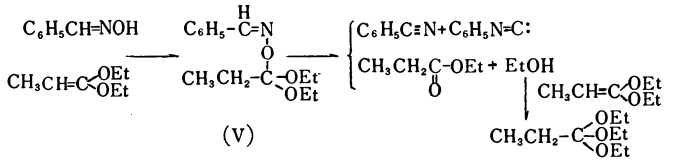
(III)

Aldoxime reacts with acetylenic ether to give ester and nitrile in high yields at room temperature in the absence of tertiary amine probably through intermediate IV.

$$\begin{aligned} &HC{\equiv}C\text{-}OR + R'CH{=}NOH \\ &\longrightarrow H_2C{=}C(ON{=}CHR')\text{-}OR \longrightarrow CH_3COOR + R'C{\equiv}N \end{aligned} \tag{6}$$

(IV)

Thirdly, further study on the dehydration of aldoxime with ketene acetal[6] which reacts with water to form ester and alcohol was tested. In the presence of a catalytic amount of boron trifluoride and yellow mercuric oxide, the reaction of benzaldoxime and methyl ketene diethyl acetal gives two dehydrated products, benzonitrile and benzoisonitrile, in nearly the same amount, along with ethyl propionate and ethyl orthopropionate. The unexpected formation of benzoisonitrile is of much interesting and this rearrangement found in this reaction is considered to be the simplest model of the Beckmann rearrangement.



(V)

Although the addition compound V can not be isolated when benzaldoxime and the ketene acetal are reacted in the presence of the said catalysts, it can be produced in good yield by reacting them either in the presence of triethylamine or in the absence of a catalyst. When the addition compound thus obtained is decomposed in the presence of boron trifluoride and mercuric oxide, both benzoisonitrile and benzonitrile are obtained. But when the adduct is decomposed in the presence of boron trifluoride alone, benzoisonitrile is not obtained

3) J. F. Arens and T. Doornbos, *Rec. trav. chim.* **74**, 79 (1955).
4) T. L. Jacobs, R. Cramer and J. E. Hanson, *J. Am. Chem. Soc.*, **64**, 223 (1942).
5) W. R. Dunstan and T. S. Dymond, *J. Chem. Soc.*, **59**, 410 (1891); S. B. Lippincott, *J. Am. Chem. Soc.*, **62**, 2604 (1940).
6) S. M. McElvain, *Chem. Revs.*, **45**, 453 (1949).

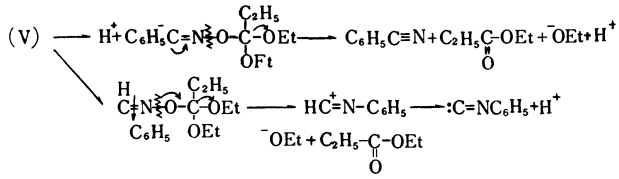
and benzonitrile is exclusively obtained. And no reaction is observed when only mercuric oxide is used. This gives the conclusion that the coexistence of boron trifluoride and mercuric oxide is a necessary condition for the formation of isonitrile.

$$V \xrightarrow{BF_3} C_6H_5C{\equiv}N + CH_3CH_2COOC_2H_5$$

$$V \xrightarrow{HgO} \text{no reaction}$$

Since it has been confirmed that the reaction of aliphatic aldoxime or *n*-heptanaldoxime and ketene acetal gives only nitrile under the same condition, the above-mentioned rearrangement is surely one of the characteristics of aromatic aldoximes.

The course of the rearrangement can be shown by the following scheme.



The addition compound V containing three oxygen atoms attached to one carbon atom has two pathways of decomposition, namely the decomposition with oxygen-carbon bond fission and that with nitrogen-carbon bond fission. The analogous reaction is already known in the decomposition of orthoester[4] to form ester and ether. In the compound V, the decomposition with oxygen-carbon bond fission to form alkyl cation is considered to be more difficult than that with nitrogen-carbon bond to form nitrile or isonitrile cations shown in the above scheme. By direct deprotonation from V, nitrile and orthoester anions are formed. On the other hand, with the migration of phenyl group, the isonitrile cation is formed along with simultaneous formation of the orthoester anion. The former deprotonates to form isonitrile and the orthoester anion loses the alkoxyl anion by the shift of an electron pair and forms ethyl propionate. Further work on this rearrangement of aldoximes and ketoximes is now in progress and will be reported in a later paper.

It is worth while reconsider the above-discussed dehydration reactions carried out with carbodiimide, acetylenic ether and ketene acetal. It is known that these compounds react readily with water to form urea, ester, and ester and alcohol according to the Eqs. 7, 8 and 9, respectively.

$$R\text{-}N{=}C{=}N\text{-}R + H_2O \longrightarrow R\text{-}NHC(OH){=}N\text{-}R \longrightarrow RHNCONHR \quad (7)$$

$$HC{\equiv}C\text{-}OR + H_2O \longrightarrow CH_2{=}C(OH)\text{-}OR \longrightarrow CH_3COOR \quad (8)$$

$$CH_2{=}C(OR)_2 + H_2O \longrightarrow CH_3C(OH)(OR)_2 \longrightarrow CH_3COOR + R\text{-}OH \quad (9)$$

Finding a compound reactive with water would accordingly provide a method of looking for a dehydrating agent. If compounds with carbon-carbon or carbon-nitrogen bond are considered, allene with a twinned double bond and nitrile with a triple bond may also be used as an effective dehydrating agent.

$$R\text{-}CH{=}C{=}CH\text{-}R + H_2O \longrightarrow RCH_2C(OH){=}CH\text{-}R \longrightarrow RCH_2COCH_2R \quad (10)$$

$$R\text{-}C{\equiv}N + H_2O \longrightarrow R\text{-}C(OH){=}NH \longrightarrow RCONH_2 \quad (11)$$

The hydration reactions of Eqs. 10 and 11 have already been studied[7,8]. These compounds may be added to the agents of the intramolecular dehydration reactions of the here-discussed type.

## Experimental

**Reaction of Phenylnitromethane with Di-*p*-tolylcarbodiimide.**—To a solution of phenylnitromethane (6.1 g., 0.045 mol.) and di-*p*-tolylcarbodiimide (10 g., 0.045 mol.) in 25 ml. dry benzene were added 10 drops of triethylamine. Then the mixture was heated under reflux for 2.5 hr. and *sym*-di-*p*-tolylurea precipitated. It was filtered and washed with benzene and weighed 5.2 g., (48% of theoretical), m. p. 257~9°C. 3-Phenyl-4-*p*-tolyl-5-*p*-tolylimino-oxadiazole was separated as a white crystal on standing the filtrate overnight at room temperature. It was recrystallized from 95% ethanol, 1.5 g., (10% of theoretical), m. p. 171~2°C.

Found: C, 77.42; H, 5.57; N, 12.30. Calcd. for $C_{22}H_{19}ON_3$: C, 77.75; H, 5.56; N, 12.24%.

7) G. Gustavson and N. Demjanow, *J. prak. Chem.*, [2], **38**, 202 (1888).

8) J. J. Sudborough, *J. Chem. Soc.*, **67**, 601 (1895).

**Reactions of Aldoximes with Di-*p*-tolylcarbodiimide.**—A solution of α-benzaldoxime (4.4 g., 0.036 mol.) and di-*p*-tolylcarbodiimide (8 g., 0.036 mol.) in 35 ml. dry ether was heated under reflux for 11 hr. and *sym*-di-*p*-tolylurea precipitated. It was filtered and washed with ether and weighed 5.5 g., (63% of theoretical), m. p. 258~259°C. The filtrate was evaporated and distilled. Benzonitrile, b. p. 70~2°C (21 mmHg), 2.4 g., (65% of theoretical) was obtained. The same result was obtained when α-benzaldoxime and di-*p*-tolylcarbodiimide were reacted in the presence of tertiary alkyl amine.

When *n*-heptanaldoxime (4.7 g., 0.036 mol.) in place of α-benzaldoxime in the above experiment was used, di-*p*-tolylurea, 7.3 g., (67% of theoretical) and *n*-heptanneitrile, 2.3 g., (57% of theoretical) were obtained.

**Reactions of Aldoximes with Dicyclohexylcarbodiimide.**—To a solution of dicyclohexylcarbodiimide (10 g., 0.049 mol.) in 50 ml. dry benzene was added α-benzaldoxime (5.9 g., 0.049 mol.). Then the reaction started soon with the liberation of heat and *sym*-dicyclohexylurea began to precipitate. After the mixture was refluxed for 7 hr., it was cooled and filtered. The precipitate of *sym*-dicyclohexylurea was weighed 11 g., (92% of theoretical), m. p. 226~228°C. The filtrate was worked up in the usual manner, benzonitrile 5.1 g., (77% of theoretical), b. p. 83~84°C (21 mmHg), was obtained.

With *n*-heptanaldoxime (6.3 g., 0.049 mol.) in place of α-benzaldoxime in the above experiment, dicyclohexylurea 8.9 g., (81% of theoretical) and *n*-heptaennitrile 3.3 g., (62% of theoretical) were obtained.

**Reaction of Phenylnitromethane with *n*-Butyl Acetylenic Ether.** — To a solution of phenylnitromethane (2.8 g., 0.02 mol.) and *n*-butyl acetylenic ether (4.0 g., 0.04 mol.) in 10 ml. dry benzene were added 20 drops of triethylamine and the mixture was refluxed for 10 hr. After removing benzene and triethylamine in vacuo, *n*-butyl acetate 1.5 g., (32% of theoretical), b.p. 123~126°C and 3-phenyl-5-*n*-butoxyisoxazole 0.8 g., (18% of theoretical), b. p. 120~125°C (0.1 mmHg) were obtained. The latter solidified on cooling and melted at 59~61°C (recrystallized from ethanol-water).

Found: C, 71.8; H, 6.94; N, 6.63. Calcd. for $C_{13}H_{15}NO_2$: C, 71.8; H, 6.93; N, 6.46%.

The residual oil crystallized by the addition of 95% ethanol and melted at 209~210°C (recrystallized from 95% ethanol), (0.2 g.). It was 3,4,5-triphenylisoxazole.

**Reaction of Benzaldoxime with Methyl Acetylenic Ether.** — To a solution of α-benzaldoxime (6.1 g., 0.05 mol.) and methyl acetylenic ether (2.8 g., 0.05 mol.) in 10 ml. dry ether were added 20 drops of triethylamine and the mixture was allowed to stand for 43 hr. at room temperature. Then it was worked up in the usual manner, methyl acetate 1.5 g., (41% of theoretical), b. p. 57°C and benzonitrile 3.6 g., (69% of theoretical), b. p. 187~189°C, were obtained.

**Reaction of α-Benzaldoxime with Methyl Ketene Diethyl Acetal in the Presence of Boron Trifluoride and Mercuric Oxide.** — To a solution of methyl ketene diethyl acetal (3 g., 0.023 mol.) and α-benzaldoxime (2.8 g., 0.023 mol.) in 10 ml. dry ether were added 2 drops of boron trifluoride (40% ether solution) and 0.1 g. of mercuric oxide. After the mixture was refluxed for 6 hr., ether was removed and distilled. Ethyl propionate 0.8 g., (68% of theoretical), b. p. 45°C (108 mmHg), benzonitrile 0.9 g., (38% of theoretical), b.p. 57~59°C(4 mmHg), benzoisonitrile 0.5 g., (21% of theoretical), b. p. 38~42°C (3 mmHg), and ethyl orthopropionate 0.6 g., (30% of theoretical), b. p. 89°C (75 mmHg) were obtained.

**Reaction of α-Benzaldoxime with Methyl Ketene Diethyl Acetal in the Presence of Triethylamine.** —To a solution of methyl ketene diethyl acetal (3 g., 0.023 mol.) and α-benzaldoxime (2.8 g., 0.023 mol.) in 10 ml. dry ether was added 2 drops of triethylamine. After refluxing the mixture for 7 hr., it was worked up in the usual manner, the addition compound of α-benzaldoxime and methyl ketene diethyl acetal 4.8 g., (83% of theoretical), b. p. 157~158°C (18 mmHg), was obtained.

Found: C, 66.75; H, 8.25; N, 5.57. Calcd. for $C_{14}H_{21}NO_3$: C, 66.90; H, 8.42; N, 5.57%.

The same result was observed when α-benzaldoxime and methyl ketene diethyl acetal were reacted in the absence of catalyst.

**Decomposition of the Addition Compound in the Presence of Boron Trifluoride and Mercuric Oxide.**—To a solution of the above addition compound (2.5 g., 0.01 mol.) in 5 ml. dry ether were added 2 drops of boron trifluoride (40% ether solution) and 0.1 g. of mercuric oxide. After refluxing the mixture for 6 hr., it was treated in the usual manner and ethanol 0.1 g. (22% of theoretical), ethyl propionate 0.6 g. (59% of theoretical), b.p. 38°C (120 mmHg), benzonitrile 0.5 g. (40% of theoretical), b. p. 52°C (2 mmHg), and benzoisonitrile 0.6 g. (50%. of theoretical), b. p. 54°C (12 mmHg) were obtained.

**Decomposition of the Addition Compound in the Presence of Boron Trifluoride.**—With 2 drops of boron trifluoride (40% ether solution) in place of the said two catalysts in the above experiment, ethanol 0.1 g. (22% of theoretical), ethyl propionate 0.5 g. (49% of theoretical), b. p. 42°C (96 mmHg) and benzonitrile 0.5 g. (41% of theoretical), b. p. 68.5°C (10 mmHg) were obtained.

Decomposition reaction of the addition compound in the presence of mercuric oxide could not be observed and the starting material was recovered.

**Reaction of *n*-Heptanaldoxime with Methyl Ketene Diethyl Acetal in the Presence of Boron Trifluoride and Mercuric Oxide.**—To a solution of *n*-heptanaldoxime (2.8 g., 0.022 mol.) and methyl ketene diethyl acetal (2.8 g., 0.022 mol.) in 10 ml. dry ether were added 2 drops of boron trifluoride (40% ether solution) and 0.1 g. of mercuric oxide. After the mixture was refluxed for 7 hr., it was treated in the usual manner and ethanol 0.7 g. (78% of theoretical), ethyl propionate 0.2 g. (10% of theoretical), b. p. 44~47°C (89 mmHg) and *n*-heptanitrile 1.3 g. (54% of theoretical), b. p. 67~67.5°C (13 mmHg) were obtained.

The authors wish to express their hearty thanks to Professor Toshio Hoshino for his encouragement and to Mr. Norio Shibata

for his help throughout the course of this experiment. Thanks are also due to Mr. Asaji Kondo for the microanalyses.

*Department of Chemistry*
*Tokyo Institute Technology*
*Meguro-ku, Tokyo*

# *On Solvolysis of α-Phosphorus(V) Oxide*

By Masako SHIMA, Kazue HAMAMOTO* and Seiichiro UTSUMI

(Received April 11, 1960)

It has been well-known[1-3] since 1940 that phosphorus(V) oxide exists in three crystalline modifications ($\alpha$, $\beta$, $\gamma$)[4] and that the crystal of the $\alpha$-modification is composed of $P_4O_{10}$ molecules in which four phosphorus atoms are at the apices of a tetrahedron and are bonded to one another with six P-O-P linkages[1,2,5], as is shown in Fig. 1. Water reacts violently

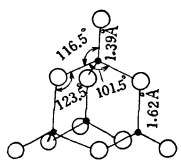



Fig. 1. The structure of the molecule $P_4O_{10}$.
○ Oxygen atoms • Phosphorus atoms

with it, and organic solvents such as alcohols and acetone[6] also indicate some chemical action. As regards the reaction process of $\alpha$-phosphorus(V) oxide with water and the resulting products thereof, much information is available[7-11], but little is known about the reactions with organic solvents.

The present authors attempted to clarify the general reaction mechaniem of $\alpha$-phosphorus (V) oxide to which special attention was given to the solvolytic opening of the P-O-P linkages in this molecule and the accompanying condensation processes of phosphate radicals. Experiments were conducted along three lines: (a) direct hydrolysis with a large quantity of pure water, (b) solvolysis with organic solvents (e.g. ethanol and acetone) which are miscible with water and have some reaction with the oxide and (c) hydrolysis of the oxide dispersed in organic solvents which are non-reactive and able to hold a limited amount of water.

## Experimental

**Materials.**—Purification by subliming guaranteed reagent of $\alpha$-phosphorus(V) oxide with simple

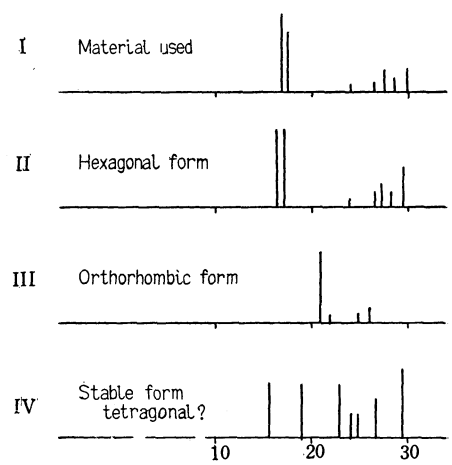



Fig. 2. The experimental X-ray diagram (I) of reagent $\alpha$-phosphorus(V) oxide compared with those data (II~IV) of polymorphic forms of phosphorus oxide by Hill et al.[2].
Experimental conditions:
Cu $K_\alpha$ (Ni filter)
35 KVP—15 mA
Slit 0.2-2½-2½, 16-1-2
Scan. sp. 4°/min.
Ch. sp. 1 cm./min.

* Present address, Japan Atomic Energy Research Institute, Tokai, Ibaraki-ken.

1) H. C. J. deDeker and C. H. MacGillavry, *Rec. trav. chim.*, **60**, 153 (1941); H. C. J. deDeker, ibid., 413.
2) W. L. Hill, G. T. Faust and S. B. Hendricks, *J. Am. Chem. Soc.*, **65**, 794 (1943).
3) C. H. MacGillavry, H. C. J. deDeker and L. M. Nijland, *Nature*, **164**, 448 (1949).
4) The three crystalline modifications of phosphorus-(V) oxide were designated by deDeker et al. as $S_1$, $S_2$ and $S_3$, and by Thilo et al., as M., R. and S.
5) G. C. Hampson and A. J. Stosick, *J. Am. Chem. Soc.*, **60**, 1814 (1938).
6) T. Kuwata, "Yozai", Maruzen Co. (1951), p. 256.
7) R. N. Bell, L. F. Audrieth and O. F. Hill, *Ind. Eng. Chem., Anal. Ed.*, **44**, 568 (1952).
8) E. Thilo and W. Widker, *Z. anorg. allgem. Chem.*, 277, 27 (1954).
9) A. E. R. Westman, A. E. Scott and J. T. Pedley, *Chemistry in Canada*, Oct. 1 (1952).
10) A. Travers and Yu Kwong Chu, *Compt. rend.*, **198**, 2169 (1934).
11) S. Glixelli and K. Borantynsky, *Z. anorg. allgem. Chem.*, **235**, 225 (1938).

equipment proved to be unsuitable because of the extraordinarily strong absorptive power of the sublimate against traces of moisture remaining in dried vessels. However, as this material was confirmed to be very pure by X-ray examination (as shown in Fig. 2) it was used without further purification.

**Organic Solvents.** — Diethyl ether and benzene were dried with sodium metal, acetone with anhydrous sodium sulfate and ethanol with calcium oxide. The diethyl ether, benzene and acetone were of reagent grade and ethanol was of guaranteed grade. They were distilled at least twice and used dry or after a definite weight or volume of water had been added.

**Reaction Procedure.**—Each solvent was weighed in a beaker or in a large weighing bottle[12], kept at 0°C and agitated vigorously with a magnetic stirrer. Then 0.5 g. of α-phosphorus(V) oxide was added to the solvent in small portions using a special vessel equipped with a closely fitting lid worked by a spring so as to cause complete dispersion[13].

When water or any solvent miscible with water, for example, acetone or ethanol with or without added water, was used, stirring was continued until the added oxide thoroughly dissolved, the resulting solution was still kept at 0°C and neutralized with 1 N sodium hydroxide[14] (indicator; litmus test paper). In the case of pure water 10 ml. was used each time. Since α-phosphorus(V) oxide went almost completely into solution[15], no treatment was necessary before spotting 0.01 ml. or 0.02 ml. of the sample with a micropipette on a chromatographic paper along a starting line. Different species of the condensed phosphates in this solution were successfully separated. At the same time, a 2 ml. aliquot of the sample solution was taken in order to determine the total phosphorus-(V) concentration by colorimetric analysis. In the case of acetone or ethanol with or without added water (20 ml. in total volume), α-phosphorus(V) oxide dissolved only to a limited extent, and the remaining precipitate had to be separated from the solution with decantation and dissolved in 20 ml. of pure water. After the volume had been adjusted, the contents of the various condensed phosphates, and the total phosphate concentration were determined for these two solutions. On the other hand, in the case of diethyl ether (13 ml.) or benzene (10 ml.), α-phosphorus(V) oxide was dispersed in it as perfectly as possible, and, the mixture being kept in vigorous agitation with a magnetic stirrer, 10 ml. of water was added, and the resulting solution was neutralized with 1 N sodium hydroxide, and then transferred to a separating funnel. The organic phase was removed from the aqueous phase and washed with 2 ml. of water; it was discarded, for no trace of phosphorus(V) was found in it. The aqueous phase was added to the above wash water, and was subjected to analysis for the various condensed phosphates and the total phosphate concentration.

**The Separation of Various Species of Condensed Phosphates by Filter Paper Chromatography.**— Various condensed phosphates differing in degree and mode of polymerization were separated by ascending chromatography on filter paper. The method has been studied by many workers[9,16-21]. In the present work, eleven kinds of acidic solvent and six kinds of basic solvent already reported were tested with Toyo Roshi No. 5B for quantitative analysis[22], and the two following solvents were chosen for their most effective separating ability. Acidic solvent: a mixture of propan-2-ol (70 ml.), water (30 ml.), trichloroacetic acid (5 g.) and concentrated aqueous ammonia (0.3 ml.). Basic solvent: a mixture of isobutanol (30 ml.), ethanol (30 ml.), water (39 ml.) and concentrated aqueous ammonia (1 ml.). $R_f$ values are given in Table I. For further work, experimental conditions were made as follows; length of the filter paper, 40 cm.; width, 2.5 cm.; time of chromatographic development, about 20 hr.; temperature, 10~20°C (room temperature). Lower ends of filter papers were narrowed after the method of Thilo et al.[19a]. The chromatographic separation seemed to improved by this cutting. Each condensed phosphate distributed in bands on a chromatogram was identified by Crowther's method[17c].

**Colorimetric Estimation of Each Condensed Phosphate.** — The condensed phosphates separated in bands on each chromatogram were determined by Crowther's method[17c] by the following procedure. Bands were cut out, soaked with 10 ml. of 1 N aqueous ammonia and eluted by warming on a

12) When dry or volatile solvent was used, reaction was performed in a large weighing bottle with a fitted stopper to prevent moist air from entering or the solvent from evaporating.

13) α-Phosphorus(V) oxide must be kept moisture-tight during the operation. The above-mentioned vessel, originally designed as a receptacle of "Ajinomoto powder", was obtained from the Ajinomoto Co., and was found to be very suitable for this purpose.

14) In the case of solvolysis with a large amount of water, the resulting solution was almost clear. This solution was subjected to moderate neutralization with Amberlite IRC-50, Na-form resin, or with sodium carbonate, so that the hydrolysis that might otherwise proceed during this procedure could be prevented. But these three neutralizing procedures with respective agents did not show any difference in results, as is shown in Table II.

15) A slight turbidity may appear in the solution, but it can be dispersed uniformly in a colloidal form and made to disappear when the solution is stirred sufficiently.

16) a) J. P. Ebel and Y. Volmar, *Compt. rend.*, **233**, 415 (1951); b) Y. Volmar, J. P. Ebel and Y. F. Bassili, *Bull. soc. chim. France*, **20**, 1085 (1953); c) J. P. Ebel, ibid., 991; d) 998; e) 1089; f) 1096.

17) a) A. E. R. Westman and A. E. Scott, *Nature*, **168**, 740 (1951); b) A. E. R. Westman and J. Crowther, *J. Am. Cer. Soc.*, **37**, 420 (1954); c) J. Crowther, *Anal. Chem.*, **26**, 1383 (1954).

18) a) H. Grunze and E. Thilo, *Mathematik allgem. Naturwiss.*, **1953**, No. 5, 1 (1953); b) H. Roux, E. Thilo, H. Grunze and M. Viscontini, *Helv. Chim. Acta*, **38**, 15 (1955); c) H. Grunze and E. Thilo, *Z. Silikattechnik*, **7**, 134 (1956).

19) E. Karl-Kroupa, *Anal. Chem.*, **28**, 1091 (1956).

20) A. L. Huhti and P. A. Gartaganis, *Can. J. Chem.*, **34**, 785 (1956).

21) G. G. Berg, *Anal. Chem.*, **30**, 213 (1958).

22) Filter papers often contain phosphorus(V) which can be detected by a qualitative method or with colorimetric analysis of eluted solution. Toyo Roshi No. 52 for chromatography contains substances which reduce ammonium molybdate during the procedure of phosphorus(V) detection. In Toyo Roshi No. 53 or No. 54 for chromatography, this was not noticed, but by the use of No. 54 paper, separation of various species of condensed phosphates was notably poor. In this work, No. 53 paper was also used.

TABLE I. SEPARATION OF VARIOUS CONDENSED PHOSPHATES BY ASCENDING CHROMATOGRAPHY WITH THE USE OF TWO KINDS OF SOLVENT

Filter paper; TOYO ROSHI No. 5B for quantitative analysis.

| Solvents | pH | Distances from base to front cm. | Time of development hr. | $R_f$ | | | | | | Reference |
|---|---|---|---|---|---|---|---|---|---|---|
| | | | | Ortho- | Pyro- | Tripoly- | Trimeta- | Tetra-meta- | Highpoly- | |
| Acidic | 1.65 | 20.6 | 9.67 | 0.75 | 0.52 | 0.38 | 0.26 | 0.12 | 0 | 18b, 20 |
| Basic | 11.35 | 19.2 | 8.5 | 0.37 | 0.28 | 0.25 | 0.59 | 0.47 | 0 | 18b |

* All phosphates were used in the form of sodium salts. Standard substances were sodium salts. Test samples were neutralized with sodium hydroxide, sodium carbonate or sodium-form resin. But as the hydrogen ion concentration of chromatographic solvents was adjusted with aqueous ammonia, sodium may have been replaced by ammonium during the development process. In our experiments, the appearance of a spot of another phosphate species was very often noticed, especially in a basic solvent. This additional spot was confirmed to correspond to amomnium salt, for when the sodium in the phosphate had been replaced by ammonium through ion exchange resin column of Amberlite IR-120 ammonium-form, this spot alone was observed.

** The composition of the solvents are described in the text.

TABLE II. DISTRIBUTION OF PHOSPHORUS AMONG THE SOLVOLYSIS PRODUCT OF PHOSPHORUS(V) OXIDE BY A LARGE AMOUNT OF ICE WATER

| No. | Neutralizing agent | $PO_4^{3-}$ | $P_2O_7^{4-}$ | $P_3O_{10}^{5-}$ | $(PO_3)_3^{3-}$ | $(PO_3)_4^{4-}$ | Highpoly | Chromatographic solvent |
|---|---|---|---|---|---|---|---|---|
| 1 | NaOH | 2.0 | 2.1 | 2.7 | 14.1 | 60.1 | 19.0 | Acidic |
| 2 | $Na_2CO_3$ | 1.5 | 1.8 | 2.2 | 12.9 | 48.0 | 33.7 | Acidic |
| 3 | Resin | | 7.1 | | 15.2 | 60.2 | 17.4 | Acidic |
| 4 | Resin | | 26.7*** | | | 64.5 | 8.9*** | Basic |
| 5 | Resin | 2.0 | 1.5 | 4.6 | 16.0 | 66.0 | 10.3 | Acidic |
| 6 | Resin | 2.2 | 3.5*** | 9.1*** | 14.0 | 66.0 | 6.0*** | Basic |
| (Average of the above 2 lines) | | 2.1 | 2.5 | 6.8 | 15.0 | 66.0 | 8.2 | |
| 7 | NaOH | 2.3 | 1.5 | 4.5 | 12.9 | 61.3 | 17.4 | Acidic |
| 8 | NaOH | 2.6 | 2.0 | 2.3 | 16.2 | 58.5 | 18.3 | Acidic |
| (Total average) | | 2.1 | 2.1 | 4.2 | 14.5 | 60.0 | 16.4 | |

* Data from No. 5 to No. 8: Average of two determinations.

** Figures in this Table are the values of percentage distribution of phosphorus among respective phosphates.

*** During separation by filter paper chromatography, hydrolysis of the condensed phosphates seemed to advance more by the use of basic solvent than by the use of the acidic solvent. Accordingly, use of the basic solvent was avoided except in the experiment with a large amount of water.

water bath for 1 hr. The eluted sample solutions were treated with the molybdenum reagent in the ordinary way. The absorbance due to molybdenum blue was measured by a Hitachi EPU-2A type spectrophotometer at 830 m$\mu$ in glass cells with a 1 cm. light path using distilled water as the reference.

## Results

**Solvolysis (or Direct Hydrolysis) by a Large Quantity of Water.**—The main product in this case was tetrametaphosphoric acid mounting up to ca. 60% of phosphorus in agreement with the results of Bell et al.[7], Thilo et al.[8] and Westman et al.[9]. The detailed numerical records of contents of each condensed phosphate produced by this direct action are given in Table II.

**Solvolysis by Acetone.**—The ratio of acetone to water was varied as follows: 10 : 0, 9.5 : 0.5, 9.0 : 1.0, 5.0 : 5.0, 0 : 10 by volume. The solvolysis by pure acetone gave 28.5% of tetrametaphosphoric acid and 42% of highpolyphosphoric acid as the major product. The percentage of tetrametaphosphoric acid increased with the water content of the solvent. The results are illustrated in Fig. 3.

**Solvolysis by Ethanol.**—The ratio of ethanol to water was varied in the same way as for acetone and water. $\alpha$-Phosphorus(V) oxide reacted with anhydrous ethanol and most of phosphorus(V) changed into pyrophosphoric acid, less than 5% of it becoming highpolyphosphoric acid and none turning into tetrametaphosphoric acid. Up to 50% of water

TABLE III. DISTRIBUTION OF PHOSPHORUS AMONG THE HYDROLYSIS PRODUCT OF PHOSPHORUS(V) OXIDE WITH ETHYL ETHER AND BENZENE AS DISPERSING AGENT

| $P_4O_{10}$ : $H_2O$ | Dispersing agent | $PO_4^{3-}$ | $P_2O_7^{4-}$ | $P_3O_{10}^{5-}$ | $(PO_3)_3^{3-}$ | $(PO_3)_4^{4-}$ | Highpoly | Number of highpoly spot |
|---|---|---|---|---|---|---|---|---|
| Dehydrated | Ether | 1.76 | 1.02 | 0 | 14.4 | 68.3 | 14.4 | 2 |
| 1 : 2 | Ether | 2.42 | 2.42 | 0 | 12.4 | 50.3 | 32.2 | 2 |
| 1 : 10 | Ether | 1.88 | 1.07 | 3.44 | 10.2 | 55.3 | 28.9 | 3 |
| Dehydrated | Benzene | 1.56 | 0.96 | 1.66 | 11.4 | 65.7 | 18.6 | 2 |
| 1 : 1 | Benzene | 2.06 | 1.13 | 1.68 | 10.6 | 57.5 | 27.1 | 1 |
| 1 : 2 | Benzene | 1.93 | 0.99 | 1.86 | 11.4 | 58.5 | 25.6 | 1 |

* Data with ether: Average of four determinations.
Data with benzene: Average of two determinations.

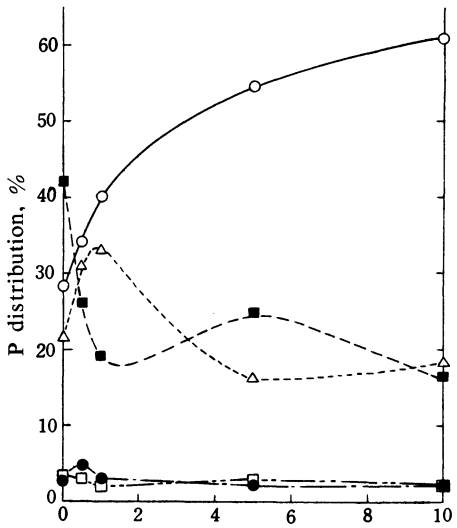



Fig. 3. Distribution of phosphorus among the solvolysis product of phosphorus(V) oxide by acetone and water-in-acetone system as solvent.
● Orthophosphate
□ Pyrophosphate
△ Tripoly- and trimetaphosphates
○ Tetrametaphosphate
■ Highpolyphosphate

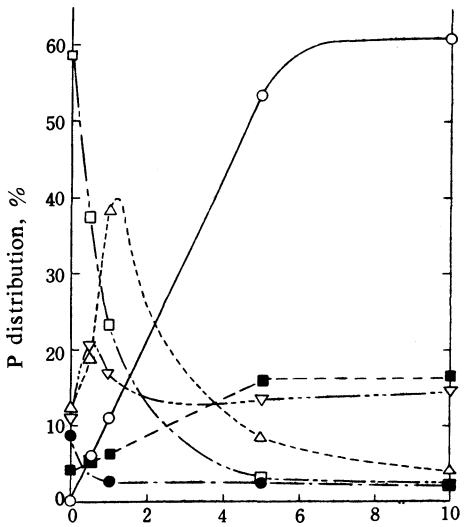



Fig. 4. Distribution of phosphorus among the solvolysis product of phosphorus(V) oxide by ethanol and water-in-ethanol system as solvent.
● Orthophosphate
□ Pyrophosphate
△ Tripolyphosphate
▽ Trimetaphosphate
○ Tetrametaphosphate
■ Highpolyphosphate

content, the yield of tetrameta- and highpoly-phosphoric acid is linerly related to the water content, the yield of pyrophosphoric acid being rapidly decreased with increase in water content. The entire result is shown in Fig. 4.

**Hydrolysis with Diethyl Ether and Benzene as Dispersing Agents.**—It was considered that when these solvents were used in a completely anhydrous state, results might differ essentially from what would be the case when they contained initially a minute amount of water. However, results did not show the expected tendency distinctly, as may be seen in Table III.

## Discussion

The molecular structure of α-phosphorus(V) oxide can be conveniently represented by a square formula I in Fig. 5, in which four P=O bonds are at the four corners and six P-O-P linkages are shown by four sides and two diagonals.

The P=O bonds are very stable as indicated by the short distances shown in Fig. 1, and they remain unaffected throughout the reactions dealt with in this study. Only the P-O-P linkages are attacked by reactive solvent molecules. Reaction of α-phosphorus(V) oxide

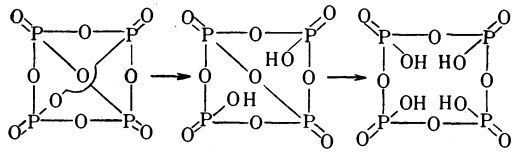



Fig. 5. Formulation of the process of tetrametaphosphoric acid formation.

with a large quantity of water, yielding tetrametaphosphoric acid as a principal product, can be formulated as shown in Fig. 5. The first water molecule approaching the oxide molecule opens any one of the six P-O-P linkages and produces an intermediate hydrolyzate (II), which is attacked by the second water molecule in succession. The fact that the main product is III can be explained by assuming that the weakest P-O-P linkage in II is the one situated diagonally opposite. This is quite easy to understand because only this P-O-P linkage is left to be strained owing to the bond angles of phosphorus atoms. Moreover, as the molecule of tetrametaphosphoric acid (III) has a fairly symmetrical structure, it is sufficiently stable and resists further attack of water molecules; it can be detected practically intact after the hydrolysis experiment. When the oxide reacts with alcohol, reaction proceeds I-IV-V-VI as shown in Fig. 6, yielding pyrophosphoric acid by the hydrolysis of the rather unstable ester formed. The reason why V receives further attack is attributable to its asymmetrical structure.

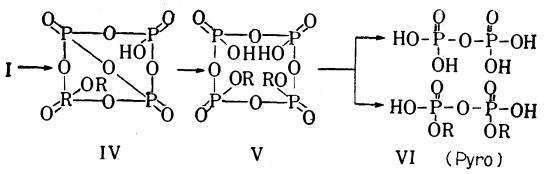



Fig. 6. Formulation of the process of pyrophosphoric acid formation.

A small quantity of trimeta- and tripolyphosphoric acids together with a still smaller quantity of orthophosphoric acid appearing in this case is explained as owing to the simultaneous reaction occurring along the schemes shown in Fig. 7. The reason why this branch reaction is possible in the case of alcoholic solvolysis must lie in the fact that the weak linkages in the intermediate IV are not restricted to the one diagonally opposite, because the ethyl radical is very large as compared with hydrogen atom and does not become ionized while hydrogen does. Other P-O-P linkages

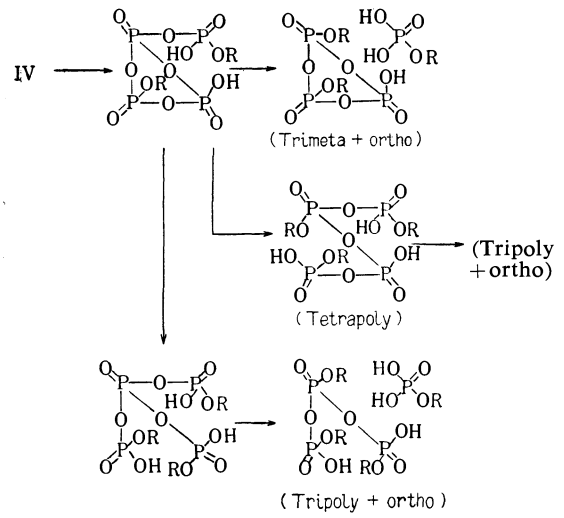



Fig. 7. Formulation of the process of tripoly-, tetrapoly- and orthophosphoric acid formation.

represented by sides of the square in IV may rupture though to a less extent. The phosphorus atom quota found in trimeta- and tripolyphosphoric acids and that found in orthophosphoric acid are in the ratio of three to one, which is quite consistent with the above-mentioned postulation.

When alcohol mixed with a small quantity of water is the reacting solvent against the oxide, tripoly- and trimetaphosphoric acids appear in a conspicuous amount in place of pyrophosphoric acid. As the water content further increases, these tri- species are very rapidly replaced by tetrametaphosphoric acid. It must, however, be noted that the above-mentioned transient increase in tripoly- and trimetaphosphoric acid is not accompanied by the production of a corresponding amount of orthophosphoric acid.

The branch reaction mentioned above does not explain the missing of orthophosphoric acid in this case, and for that same reason, it can explain the increase neither in tripoly- nor in trimetaphosphoric acid. These tri-species can not originate from highpolyphosphoric acid as precursor, because the production of the latter increases only gradually and without a maximum with the increase of water content in the solvent.

Involvement of condensation mechanism of phosphate radicals is the only conceivable explanation for the above. Condensation of phosphate radicals is an endothermic reaction, and does not occur under usual conditions in solution. It is here postulated that it does occur when a solvolytic opening of the P-O-P

linkages gives rise to the excitation of phosphate radicals and when they are close to one another. The same argument will explain the ever increasing formation of highpolyphosphoric acid in hydrolysis. The maximum yield of tripoly- and trimetaphosphoric acid with 90% ethanol may be attributable to the condensation between a pyrophosphoric acid radical and free orthophosphate radical.

Vigorous reaction between the oxide and water evolves much heat, and even under a cooling condition, some local heating can not be avoided. This must undoubtedly promote the condensation process.

Thorough dispersion of the oxide in dry ether or benzene was attempted to ensure synchronized contact with a large amount of water. Similar experiments, using ether and benzene containing trace quantities of water were carried out as well. In the former case, one would expect complete transformation to 100% tetrametaphosphoric acid, whereas in the latter case, one would expect 100% highpolyphosphoric acid. Difficulty in pulverizing the oxide crystals and the reacted mass prevented us from obtaining clear-cut results, but the expected tendency was observed.

Acetone may behave as a solvent having -OH radicals, as is explicable by its enol form, forming $-P-O-C\diagdown\begin{matrix}CH_3\\CH_2\end{matrix}$ on solvolytic opening of a P-O-P linkage. This must be an intermediate very liable to undergo subsequent decomposition giving rise to a fairly large amount of highpolyphosphoric acid as the final hydrolysis product. Tetrametaphosphoric acid can be detected right from the beginning of the reaction, as well as tripoly- and trimetaphosphoric acid. In this case too, almost no orthophosphoric acid is produced.

Orthophosphoric acid is the most easily detectable species among various phosphates; it is inconceivable for us to have missed it in the analysis.

## Summary

1. α-Phosphorus(V) oxide was allowed to react with water, with ethanol or acetone, both dry or mixed with water by adding the powder crystal directly into these liquids. The oxide was also brought in contact with water after being dispersed in diethyl ether or benzene mechanically.

2. The main final hydrolysis products formed in the following cases were tetrametaphosphoric acid by direct action of a large quantity of water, pyrophosphoric acid by anhydrous ethanol, tripolyphosphoric acid by ethanol with a low water content, and highpolyphosphoric acid by anhydrous acetone. Quick contact with water after the oxide has been dispersed in ether or benzene leads to the formation of a larger amount of tetrametaphosphoric acid when these solvents were dry, while the formation of an increased amount of highpolyphosphoric acid was the result when they contained trace quantities of water initially.

3. Separation, identification and estimation of various condensed phosphate species were executed by paper chromatography and colorimetric analysis.

4. Reaction mechanisms were postulated to explain these results. Special attention was given to the solvolytic opening of P-O-P linkages and the accompanying condensation process of phosphate radicals.

*Department of Chemistry*
*Faculty of Science*
*Ochanomizu University*
*Otsuka, Tokyo*

# *Untersuchungen über Meso-ionischen Verbindungen. XI. Versuche zur Darstellung von 3-(2'-Pyridyl)sydnon*

Von Masaki OHTA und Mitsuo MASAKI

(Eingegangen am 11. März, 1960)

In der X. Mitteilung[1] dieser Reihe wurde gezeigt, daß bei der Einwirkung von Bisulfitverbindungen der Aldehyde und Alkalicyanid auf 3-Aminopyridin $\alpha$-substituierte 3-Pyridylglycinnitrile bzw. 3-Pyridylglycinnitril selbst entstehen, und daß diese Nitrile sich durch Hydrolyse in die entsprechenden Glycine umsetzen, die weiter bei der Einwirkung von Natriumnitrit in *N*-Nitrosokörper umgewandelt werden und aus den letzteren 4-substituierte 3-(3'-Pyridyl) sydnone durch Cyclisierung-Reaktion mit Essigsäureanhydrid dargestellt werden können.

Nach dieser Methode haben wir eine Reihe von Untersuchungen ausgeführt, die das Ziel hatten, 2-Pyridylglycin, 3-(2'-Pyridyl)sydnon und dessen derivate darzustellen.

Schon ist von Bristow u. a.[2] die Darstellung von 2-Pyridylglycinnitril nach der oben erwähnten Methode berichtet worden. Andererseits wurde von Reynaud u. a.[3] beschrieben, daß sie nach dieser Methode nur ein dunkelfarbiges Produkt und kein Nitril erharten konnten. Sie erhielten dabei das Nitril durch einen anderen Weg, nähmlich bei der Einwirkung von Bromdiäthylacetal auf 2-Aminopyridin in der Gegenwart von Natriumamid erhielten sie Pyridylaminodiäthylacetal, das durch Hydrolyse in das entsprechende Aldehyd umgewandelt wurde, dessen Oxim beim Versetzen mit Essigsäureanhydrid den *N*-Acetylkör per des Nitrils lieferte.

Durch die Einwirkung von Bisulfitverbindung des Formaldehyds und Natriumcyanid auf 2-Aminopyridin erhalten wir das Nitril (I), das durch Kochen mit Salzsäure salzsaures *N*-(2-Pyridyl)glycin[3](II) ergibt.

Bei der Einwirkung von Natriumnitrit auf II in Kälte, entsteht eine kristalline Substanz von Schmp. 119°C, die nicht *N*-Nitroso-*N*-(2-pyridyl)glycin (III), sondern $\alpha$-Nitroso-*N*-(2-pyridyl)glycin (IV) ist, dessen Konstitution durch Elementaranalyse und durch Reaction mit Essigsäureanhydrid festgestellt wurde.

Wenn man die Nitrosoverbindung in Essigsäureanhydrid löst und bei Raumtemperatur stehen läßt, so fällt langsam der farblose Niederschlag vom Schmp. 196~8°C aus, dessen Molekularformel, $C_7H_6O_3N_2$, durch Elementaranalyse festgestellt wurde. Unsere Vermutung, daß dieses Produkt *N*-(2-Pyridyl)-oxamidsäure (V) sei, wurde durch IR-Absorptionen bei 1300, 1540 und 1655 $cm^{-1}$ als dem sekundären Amid typische Banden und durch die Bildung von *N*, *N'*-Di-(2-pyridyl)oxamid (VII) bei der Pyrolyse bestätigt.

Beim Erhitzen auf 200~220°C ergibt V in guter Ausbeute VII, das durch die Mischprobe mit dem authentischen[4] Präparat bestätigt wurde. Laurent u. a.[5] beobachteten beim Erhitzen von Oxanilsäure auf höheren Temperaturen die Bildung von Oxanilid. Man kann sich die Bildung von VII aus V so denken, daß zunächst aus V durch Pyrolyse 2-Aminopyridin entsteht, und das letztere durch weitere Einwirkung von V in VII umgewandelt wird. In der Tat kann man Aminopyridiniumsalz vom V als Zwischenverbinding erhalten.

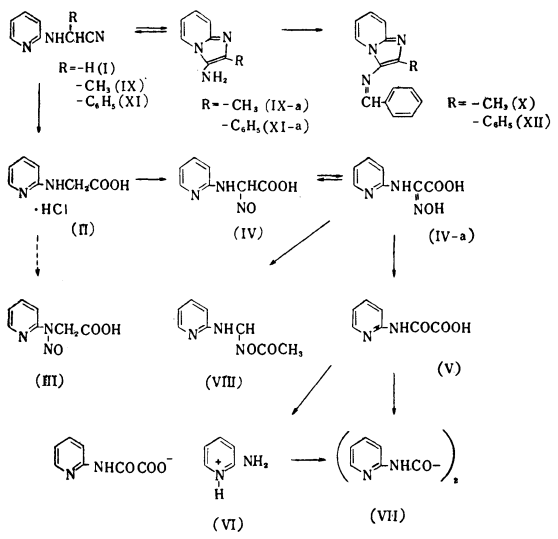
Wenn man IV mit Essigsäureanhydrid erhitzt, so erhält man *N*-(2-Pyridyl)acetylformamidoxim (VIII), dessen Bildung man sich so vorstellen kann, daß zunächst in der tautomeren Form (IV-a) des IV Acetylierung erfolgt, darauf dieses sich unter Decarboxylierung in VIII überführen läßt.

Wie oben erwähnt, ist die bei Nitrosierung auf 2-Pyridylglycin erhaltene Verbindung nicht *N*-Nitroso- (III), sondern $\alpha$-Nitroso-körper (IV), so versuchten wir die substituierten 2-Pyridylglycine, die $CH_3$- oder $C_6H_5$- Gruppe am $\alpha$-Kohlenstoffatom tragen, darzustellen, um *N*-Nitroso-(2-pyridyl)glycin zu erhalten, das durch Cyclisierung 3-(2'-Pyridyl)sydnon ergeben sollte.

Im Wasser reagiert 2-Aminopyridin mit Bisulfitverbindung des Acetaldehyds oder des Benzaldehyds und Natrium cyanid, wobei $\alpha$-(2-Pyridylamino)propionitril (IX) oder $\alpha$-(2-Pyridylamino)phenylacetnitril (XI) entsteht.

Unter verschiedenen Bedingungen versuchten wir die Hydrolyse des XI, doch konnten wir kein entsprechendes Glycin erhalten, z. B. beim Erhitzen von XI mit Mineralsäuren entsteht

1) M. Ohta und M. Masaki, Dieses Bulletin, 33, 649 (1960).
2) N. W. Bristow, P. T. Charlton, D. A. Peak und W. F. Short, *J. Chem. Soc.*, **1954**, 616.
3) P. Reynaud, T. Tupin und R. Delaby, *Bull. soc. chim.*, **1957**, 718.
4) A. E. Tschitschibabin, *Ber.*, **57**, 1172 (1924).
5) A. Laurent und C. Gerhardt, *Ann.*, **68**, 20 (1848).




nur sein stabiles Salz. Diese Tatsache scheint zu zeigen, daß bei XI Ringschluß eintritt[2] und ein Imidazol-Kern sich bildet, nähmlich, XI befindet sich in der tautomeren Form (XI-a). In der Tat läßt sich XI mit Benzaldehyd in nah-quantitativer Ausbeute in Benzal-Derivat (XII) überführen.

Es gelang uns auch nicht aus IX das entsprechende Glycin darzustellen. In ähnlicher Weise ergibt IX bei Einwirkung von Benzaldehyd Benzal-Derivat (X) in guter Ausbeute.

## Beschreibung der Versuche

**2-Pyridylaminoacetnitril (I).**—Man versetzt 4.1 g von 37 proz. Formalin mit einer Lösung von 5.4 g Natriumbisulfit in 8 ccm Wasser, erhitzt 0.5 Std und versetzt daraufhin mit 4.7 g 2-Aminopyridin. Nach ein stdg. Erhitzen und Umrühren setzt man 5 g Natriumcyanid in wenigem Wasser zu. Das Gemisch wird unter mechanischem Rühren noch 4 Std auf dem siedendem Wasserbad erwärmt, und der ausgefallene Niederschlag abfiltriert. Das Filtrat schüttelt man 5 mal mit je 30~50 ccm Chloroform aus. Das vereinigte Chloroformextract wird mit Natriumsulfat getrocknet und im Vakuum eingedampft. Es hinterbleibt schwarzes Öl, wozu 30~40 ccm Äther hinzugefügt wird und läßt es stehen. Dabei fallen braune Prismen aus. Ausbeute 2~3 g (30~45%). Schmp. 126~7°C (aus Benzol).

**Salzsaures 2-Pyridylglycin (II).**—Man löst 2.1 g I in 20 proz. Salzsäure, erhitzt 3~4 Std auf dem Wasserbad und dampft das Reaktionsgemisch im Vakuum ein. Der Rückstand wird mit Äthanol ausgezogen, die Lösung mit Aceton versetzt und bei Raumtemperatur stehen gelassen. Dabei fallen farblose Kristalle aus. Ausbeute 2.7 g (70%). Schmp. 206°C (aus Äthanol).

Gef.: N 14.71. Ber. für $C_7H_9O_2N_2Cl$: N 14.85.

*Pikrat.* Gelbliche Nadeln vom Schmp. 199°C (aus Methanol)

Gef.: N 18.59. Ber. für $C_{13}H_{11}O_9N_5$: N 18.37.

**α-Nitroso-(2-pyridyl)glycin (IV).**—Man löst 1.9 g II in 20 ccm Wasser und fügt 0.7 g Natriumnitrit unter Eiskühlung hinzu, wobei sich langsam ein farbloser Niederschlag abscheidet. Nach 3~4 std. Stehen unter Eiskühlung wird er abfiltriert. Ausbeute 1.5 g. Gelbliche Nadeln vom Schmp. 119°C (aus Wasser).

Gef.: C 46.61; H 3.90; N 23.20. Ber. für $C_7H_7O_3N_3$: C 46.31; H 4.02; N 23.32.

Diese Subtanz zeigt Liebermannsche Reaktion.

***N*-(2-Pyridyl)oxamidsäure (V).**—Man löst 1 g IV in 35 ccm Essigsäureanhydrid auf, wobei fast augenblicklich Farbumschlag von grün nach gelb erfolgt, und läßt dies bei Raumtemperatur stehen. Bald fing sich ein farbloser amorpher Niederschlag auszuscheiden an. Nach eintägigem Stehen wird der Niederschlag abfiltriert, und das Filtrat läßt sich bei Raumtemperatur untergehalten. Nach noch zwei Tagen filtriert man den aufs neue abgeschiedenen Niederschlag ab, der zusammen mit dem oben erhaltenen Produkt umkristallisiert wird. Farblose Naldeln vom Schmp. 196~8°C (aus Äthanol oder Essigsäure). Ausbeute 0.8 g (87%).

Gef.: C 50.71; H 4.13; N 16.95. Ber. für $C_7H_6O_3N_2$: C 50.60; H 3.61; N 16.87.

IR-Spektrum in KBr: 1300, 1540 und 1655 $cm^{-1}$ (-NHCO-).

***N*,*N'*-Di-(2-pyridyl)oxamid (VII).**—Beim Erhitzen auf 200~220°C in Ölbad schmilzt V unter heftiger Zersetzung, und nach 2~3 min. Erhitzen wird das erhaltene, ölige Produkt abgekühlt, das bald kristallinish erstarrt Aus äthanol umkristallisiert, farblose Nadeln oder Prismen zeigen den Schmp. 161°C.

Gef.: C 59.30; H 4.19; N 23.19. Ber. für $C_{12}H_{10}N_4O_2$: C 59.50; H 4.16; N 23.13.

Mischprobe mit dem authentischen[4] Präparat zeigt keine Depresion.

***N*-(2-Pyridyl)oxamidsäure-Aminopyridiniumsalz (VI).**—Man erhitzt V in einem Kolben im Ölbad vorsichtig auf 200~210°C, und wenn V unter der Zersetzung kaum anfängt zu schmelzen, da kühlt man den Kolben ab. Bald erstarrt die erhaltene, ölige Substanz kristallinisch. Aus Äthanol umkristallisiert, erzeugen sich grünliche Blättchen vom Schmp. 206°C.

Gef.: C 55.08; H 4.98; N 21.40. Ber. für $C_{12}H_{12}O_3N_4$: C 55.39; H 4.62; N 21.54.

Die Substanz läßt sich durch nochmaliges Erhitzen unter Wasserabspaltung in VII umwandeln.

***N*-(2-Pyridyl)acetylfomamidoxim (VIII).**—Man löst 2 g IV in 25 ccm Essigsäureanhydrid und erhitzt auf siedendem Wasserbad. Nach einer Stunde wird die schwarze Lösung in $N_2$ unter vermindertem Druck eingedampft. Es hinterbleibt ein braunrotes Öl, das mit Äther ausgeschüttelt wird. Die ätherische Lösung wird mit Natriumsulfat getrocknet und eingeengt, wobei ein roter Rückstand erhalten wird, der aus Benzol umkristallisiert wird. Ausbeute 0.2 g. Bräunliche Nadeln vom Schmp. 192~5°C.

Gef.: C 53.87; H 5.15; N 23.50. Ber. für $C_8H_9O_2N_3$: C 53.62; H 5.06; N 23.45.

**α-(2-Pyridylamino)phenylacetnitril (XI).**—Man versetzt 10.6 g Benzaldehyd mit einer Lösung von 10.4 g Natriumbisulfit in 25 ccm Wasser, erhitzt 1

Std und dann versetzt man es mit 9.4 g 2-Aminopyridin. Nach 3 stdg. Erhitzen setzt man dazu 6.5 g Kaliumcyanid in wenigem Wasser zu, rührt 2～3 Std bei Raumtemperatur um und filtriert den gebildeten gelben Niederschlag ab. Gelbe Nadeln vom Schmp. 210～211°C (aus Äthanol). Ausbeute 8.5 g (40%).

Gef.: N 20.15. Ber. für $C_{13}H_{11}N_3$: N 20.08.

**4-Phenyl-5-benzylidenaminopyrimidazol (II).**—Eine Lösung von 2 g XI und 1 g Benzaldehyd in 10 ccm Äthanol wird 2 Std am Rückfluß erhizt und dann eingeengt. Es hinterbleibt ein gelbes Fett, das aus Ligroin umkristallisiert wird. Gelbe Nadeln vom Schmp. 137°C. Ausbeute nah-quantitativ.

Gef.: C 80.86; H 5.37; N 13.94. Ber. für $C_{20}H_{15}N_3$: C 80.80; H 5.05; N 14.14.

**α-(2-Pyridylamino)propionitril** (IX).—Man versetzt eine Lösung von 10.5 g Natriumbisulfit in 20 ccm Wasser mit 10 g. von 44 proz. Acetaldehyd, erhitzt 1 Std auf dem Wasserbad und dann fügt man 9.4 g 2-Aminopyridin hinzu. Nach 2 stdg. Erhitzen setzt man 7 g Natliumcyanid, in 10 ccm von heissem Wasser gelöst zu, und erhitzt es unter mechanischem Rühren 2 Std auf dem Wasserbad. Das abgeschiedene Öl kristallisiert beim Abkühlen bis Raumtemperatur. Ausbeute 8 g. Gelbliche Nadeln vom Schmp. 133～135°C (aus Benzol).

Gef.: N 28.33. Ber. für $C_8H_9N_3$: N 28.57.

**4-Methyl-5-benzylidenaminopyrimidazol (X).**—Eine Lösung von 1 g IX und 1 g Benzaldehyd in 10 ccm Äthanol wird 2 Std am Rückfluß erhitzt und das Gemisch wird wie vorstehend aufgearbeitet, wobei 1.5 g X erhalten wird. Gelbe Schuppen vom Schmp. 52～56°C (aus Ligroin).

Gef.: N 17.59. Ber. für $C_{15}H_{13}H_3$: N 17.86.

Herrn Asaji Kondo für die Ausführung der Mikroanalysen und Dr. Tadashi Sato (Waseda Universität) für die Aufnahme der IR-Spektren danken wir bestens.

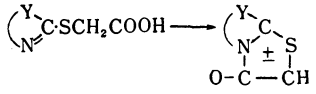
*Organisch-Chemisches Laboratrium*
*Technische Hochschule zu Tokyo*
*Meguro-ku, Tokyo*

# *Studies on Meso-ionic Compounds. XII*[1]*. Reaction between Acetic Anhydride and Azoles having Carboxymethylmercapto-group**

By Mutsuko HASHIMOTO and Masaki OHTA

(Received April 14, 1960)

Duffin et al.[2,3] already reported that when a heterocyclic compound of the type I was subjected to the action of acetic anhydride, water was eliminated and a ring closure followed to give a meso-ionic compound of the type II.



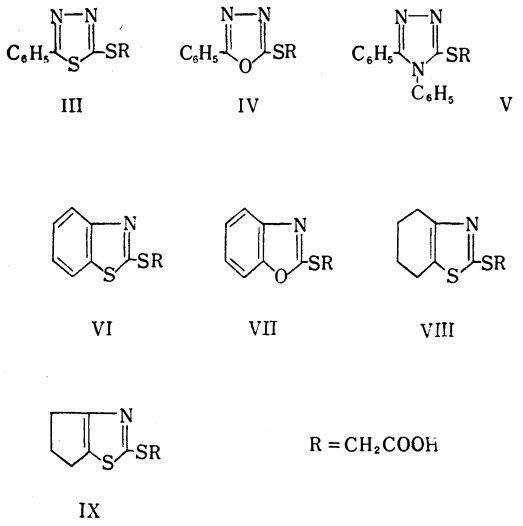
I II

Y=Remainder of heterocyclic nucleus.

Fig. 1

The heterocyclic nuclei used by them were pyridine, quinoline, imidazole and benzimidazole.

In the present paper, this reaction is extended further to several kinds of azoles containing oxygen or sulfur (III–IX), and their behavior to acetic anhydride is investigated in detail.



III IV V

VI VII VIII

IX

R = $CH_2COOH$

Fig. 2

**Action of Acetic Anhydride on the Azoles.**— 5-Phenyl-1, 3, 4-thiadiazolyl-2-thioglycollic acid (III) is sparingly soluble in acetic anhydride at room temperature, while being heated on a

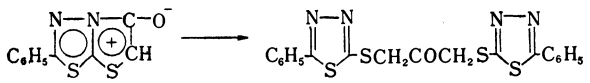
1) Part XI. M. Masaki and M. Ohta, This Bulletin, 33, 1392 (1960).

* Presented at the 12th Annual Meeting of the Chemical Society of Japan, Kyoto, April 2, 1959.

2) G. F. Duffin and J. D. Kendall, *J. Chem. Soc.*, **1951**, 734.

3) G. F. Duffin and J. D. Kendall. ibid., **1956**, 361.

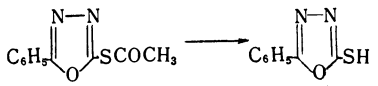
water bath, it dissolves in acetic anhydride and the solution quickly turns from yellow to dark red, and after 5 min. yellow crystals separate, which can be recrystallized unchanged from acetic anhydride. Elemental analysis indicates the compound to be an anhydro-compound of the structure X**, which is also supported by infrared analysis described below. When refluxed gently with 50% aqueous sulfuric acid or pyridine, the anhydro-compound X gives bis-5-phenyl-1, 3, 4-thiadiazolyl-2-thioacetone (XI).



X XI

Fig. 3

When 5-phenyl-1, 3, 4-oxadiazolyl-2-thioglycollic acid (IV) is boiled in acetic anhydride, no intense color develops, but 5-phenyl-1, 3, 4-oxadiazolyl-2-thioacetate (XII) is obtained. The product XII is hydrolyzed to 2-mercapto-5-phenyl-1, 3, 4-oxadiazole (XIII) with 10% aqueous sodium hydroxide.

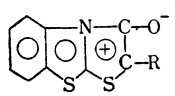


XII XIII

Fig. 4

Under similar conditions, 1, 5-diphenyl-1, 3, 4-triazolyl-2-thioglycollic acid (V) gives no pure reaction product.

When benzothiazolyl-2-thioglycollic acid (VI) is dissolved in acetic anhydride and the solution is warmed, it rapidly becomes dark red, and lustrous red-purple crystals separate. The compound is sparingly soluble in organic solvents and so difficult to burn that its elemental analysis corresponds to $C_{11}H_7O_2NS_2$ for the acetyl derivative of an anhydro-compound (XIVa ; R=$COCH_3$) with a difference of 1% or so in the carbon content. However, the same colored crystals are obtained by the action of propionic anhydride instead of acetic anhydride on the acid VI, and consequently the assignment of the structure XIVa for the colored compound would not be correct.

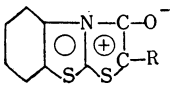


XIV

Fig. 5

On being treated with acetic anhydride, benzoxazolyl-2-thioglycollic acid (VII) gives only a yellow gummy material.

When cyclohexenothiazolyl-2-thioglycollic acid (VIII) is warmed in acetic anhydride, an orange color quickly develops which gradually changes to intense blue-violet, and black-violet crystals separate. The compound is as sparingly soluble in organic solvents and as difficult to burn as that obtained from the acid VI. Elemental analysis of the compound corresponds to $C_{11}H_{11}O_2NS_2$ with a difference of 1% or so in the carbon content. Although the formula $C_{11}H_{11}O_2NS_2$ suggests the structure of the acetyl derivateve of an anhydro-compound derived from the acid VIII (XVa ; R=$COCH_3$), this structure should be excluded by the fact that the same compound is also obtained on treating with propionic anhydride.



XV

Fig. 6

The infrared spectra of the compounds $C_{11}H_7O_2NS_2$ and $C_{11}H_{11}O_2NS_2$ are similar to each other and show that there is great resemblance between structures of both compounds, and these structures are under investigation.

**Action of Acetic Anhydride and Pyridine or Triethylamine on the Azoles.**—When 5-phenyl-1, 3, 4-thiadiazolyl-2-thioglycollic acid (III) is added to a mixture of acetic anhydride and dry pyridine (volume ratio of 1 : 2), a yellow color immediately develops and the color changes to orange as the acid III dissolves. After several minutes yellow crystals separate, which are identical with the anhydro-compound X described above.

Under similar conditions, 5-phenyl-1, 3, 4-oxadiazolyl-2-thioglycollic acid (IV) affords 5-phenyl-1, 3, 4-oxadiazolyl-2-thioacetate (XII) which is obtained from IV by treating with acetic anhydride only, while 1, 5-diphenyl-1, 3, 4-triazolyl-2-thioglycollic acid (V) is recovered unchanged.

When benzothiazolyl-2-thioglycollic acid (VI) is added to acetic anhydride and dry pyridine (volume ratio of 1 : 2), the mixture immediately turns yellow as the acid VI dissolves, and the color finally becomes dark green. After a few minutes blue-green crystals separate, from which yellow needles are obtained by extraction with benzene. Elemental analysis shows

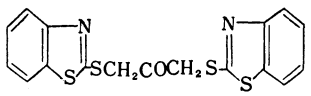
** The formulation adopted is that put forward by Baker and Ollis. W. Baker and W. D. Ollis, *Quart. Rev.*, **11**, 15 (1957); W. Baker, *Proc. Chem. Soc.*, **1959**, 75.

the compound to be an anhydro-compound of the structure (XIVb; R=H), which is also supported by infrared analysis described below.

Besides the anhydro-compound XIVb, the lustrous red-purple crystals are obtained from the benzene-insoluble portion in a considerable yield.

When the acid VI is dissolved in a mixture of acetic anhydride and triethylamine (volume ratio of 1 : 2), a yellow color develops and yellowish-brown crystals separate, which are recrystallized from benzene to yield the anhydro-compound XIVb.

On refluxing gently with pyridine the anhydro-compound XIVb affords bisbenzothiazolyl-2-thioacetone (XVI), which is identical with a specimen prepared from sym-dichloroacetone and 2-mercaptobenzothiazole. With hot 50% aqueous sulfuric acid the compound XIVb affords the compound XVI and the parent acid VI.



XVI

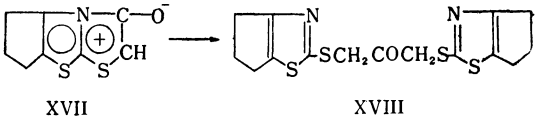
Fig. 7

When benzoxazolyl-2-thioglycollic acid (VII) is treated with acetic anhydride in pyridine or triethylamine, no anhydro-compound can be obtained but the starting material is recovered.

When cyclohexenothiazolyl-2-thioglycollic acid (VIII) is dissolved in a mixture of acetic anhydride and dry pyridine (volume ratio of 1 : 2), a deep yellow color quickly develops which gradually changes to blue-green, and light blue crystals separate. Extraction of the crystals with benzene gives benzene-soluble light green needles and the benzene-insoluble black-violet crystals. The former compound is also obtained exclusively on treating the acid VIII with acetic anhydride and triethylamine. Elemental analysis of the compound indicates that it is not an anhydro-compound of the structure (XVb; R=H), but a compound of the formula $C_{10}H_9ONS_2$.

With hot 50% aqueous sulfuric acid the compound $C_{10}H_9ONS_2$ is hydrated to the parent acid VIII, and with boiling pyridine it affords a compound of the formula $C_8H_{11}ONS_2$. The structures of both compounds $C_{10}H_9ONS_2$ and $C_8H_{11}ONS_2$ await further investigation.

When cyclopentenothiazolyl-2-thioglycollic acid (IX) is dissolved in a mixture of acetic anhydride and triethylamine (volume ratio of 1 : 2), deep yellow crystals immediately separate, which are shown to be an anhydro-compound of the structure XVII by elemental and infrared analyses. The compound XVII is hydrated to the parent acid IX with hot 50% aqueous sulfuric acid, and with boiling pyridine it affords monohydrate of biscyclopentenothiazolyl-2-thioacetone (XVIII).



XVII XVIII

Fig. 8

It seems very interesting that the behavior of the acid VIII to acetic anhydride and triethylamine differs greatly from that of the acid IX; nevertheless, the structures of two acids nearly the same. However, the question what factor of the acids can give rise to such a significant difference remains obscure.

The results presented in this paper speak for themselves. Several points deserve further comment, however.

In the first place, it is clear that the azoles free from sulfur in their nuclei; IV, V and VII give no intensely colored compounds like the compounds $C_{11}H_{11}O_2NS_2$ and $C_{11}H_9O_2NS_2$ on treating with acetic anhydride. Duffin et al., on the other hand, did not report that such a colored compound was obtained. Consequently, it is considered that the reaction center in formation of the colored compounds might be at the ring-sulfur of heterocycle.

It is also clear that the azoles containing sulfur in their nuclei; III, VI and IX can be subjected to two different types of reactions to give the colored compound and the anhydro-compound like X, XIVb and XVII, respectively.

The mechanism of formation of the anhydro-compounds is obscure, but in this case the reaction center seems to be at the ring-nitrogen of heterocycle.

**Infrared Analyses of the Anhydro-compounds X, XIVb and XVII.**—The infrared spectra of the anhydro-compounds, their parent acids and decomposition products were taken.

When the spectra of the anhydro-compounds are compared with those of their parent acids, three remarkable changes can be observed. Firstly, the disappearance of the band at 1720～1708 $cm^{-1}$ due to the C=O vibration of carboxylic group and the appearance of a band at 1645 $cm^{-1}$, which is probably due to the amide I band of tertiary amide. Secondly, the appearance of a new strong band near 1600 $cm^{-1}$, which disappears again in the spectrum of the decomposition product. Consequently, this band seems to be produced by formation of a meso-ionic ring, but the assignment of the band is still unknown. Lastly, the red

shift of 35 $cm^{-1}$ or so of the band at 1180± 10 $cm^{-1}$.

The three remarkable changes mentioned above can be also observed in the spectra of the anhydro-compound derived from (2-pyridylthio)acetic acid, whose structure has been confirmed synthetically.[2]

## Experimental

**5-Phenyl-1, 3, 4-thiadiazolyl-2-thioglycollic Acid (III).**—This acid was prepared by Sato's method[4].

**Anhydro-compound X from III.** — (a) A solution of the acid III (5.0 g.) in acetic anhydride (100 ml.) was heated on a boiling water bath for 5 min., quickly turning from yellow to red. Yellow crystals which separated were filtered off and recrystallized from acetic anhydride to give the anhydro-compound as small yellow needles (1.9 g.), m. p. 231°C (decomp.).

Found: C, 51.54; H, 2.80; N, 11.71. Calcd. for $C_{10}H_6ON_2S_2$: C, 51·29; H, 2.58; N, 11.96%.

(b) III (1.0 g.) was dissolved with stirring at room temperature in a mixture of acetic anhydride (3 ml.) and dry pyridine (6 ml.). A yellow color immediately developed and the color changed to orange. After several minutes yellow crystals separated, which were filtered off after 0.5 hr., washed with water, and dried to give deep yellow crystals (0.6 g.), m. p. 229~230°C (decomp.). Recrystallization from acetic anhydride gave small yellow needles, m. p. 231°C (decomp.).

Found: N, 11.70. Calcd. for $C_{10}H_6ON_2S_2$: N, 11.96%.

**Action of Aqueous Sulfuric Acid on the Anhydro-compound X.**—X (1.0 g.) was refluxed gently with 50% aqueous sulfuric acid (10 ml.) for 10 min. The cooled solution was diluted with water (50 ml.) to give a crystalline precipitate which was filtered off and recrystallized from ethanol, affording small colorless needles of bis-5-phenyl-1, 3, 4-thiadiazolyl-2-thioacetone (XI) (0.69 g.), m. p. 148°C.

Found: C, 51.36; H, 3.42; N, 12.75; S, 29.06; mol. wt. (Rast), 455. Calcd. for $C_{19}H_{14}ON_4S_4$: C, 51.58; H, 3.17; N, 12.67; S, 28.96%; mol. wt., 442.

**Action of Pyridine on X.**—X (0.3 g.) was refluxed gently with pyridine (10 ml.) for 5 min. After cooling, the solution was diluted with water (50 ml.) to give a crystalline precipitate (0.24 g.), m. p. 146 ~147°C. Recrystallization from ethanol yielded small colorless needles, m. p. 148°C, undepressed by admixture with XI.

**5-Phenyl-1, 3, 4-oxadiazolyl-2-thioglycollic Acid (IV).**—A solution of chloroacetic acid (2.0 g.) and sodium carbonate (1.1 g.) in water (20 ml.) was added to a solution of crude 2-mercapto-5-phenyl-1, 3, 4-oxadiazole (3.0 g.) and potassium hydroxide (1.0 g.) in water (30 ml.). The solution was kept to stand at room temperature overnight, neutralized with dilute hydrochloric acid. The resulting precipitate was filtered off, dissolved in aqueous sodium bicarbonate to remove insoluble impurities and neutralized with dilute hydrochloric acid. After filtration and drying 5-phenyl-1, 3, 4-oxadiazolyl-2-thioglycollic acid was obtained (5.0 g.), m. p. 157~ 162°C. Recrystallization from hot water gave white needles, m. p. 168~169°C.

Found: N, 12.15. Calcd. for $C_{10}H_8O_3N_2S$: N, 12.86%.

**Action of Acetic Anhydride on IV.** — The acid IV (1.0 g.) and acetic anhydride (10 ml.) were boiled under reflux for 0.5 hr. The anhydride was evaporated under reduced pressure and the residue was recrystallized from ethanol to give 5-phenyl-1, 3, 4-oxadiazolyl-2-thioacetate (XII) as colorless needles (0.22 g.), m. p. 152.5~153°C.

Found: C, 54.33; H, 3.63; N, 12.74. Calcd. for $C_{10}H_8O_2N_2S$: C, 54.54; H, 3.64; N, 12.73%.

XII was dissolved in 10% aqueous sodium hydroxide and then neutralized with 10% aqueous sulfuric acid to give colorless needles, m. p. 217°C, undepressed by admixture with authentic 2-mercapto-5-phenyl-1, 3, 4-oxadiazole.

**1, 5-Diphenyl-1, 3, 4-triazolyl-2-thioglycollic Acid (V).**—This acid was prepared by Ueda's method[5].

**Action of Acetic Anhydride on V.**—The acid V (0.5 g.) and acetic anhydride (10 ml.) were boiled under reflux for 0.5 hr., affording a yellow solution. On addition of water (100 ml.) the solution yielded a pale brown gummy material from which no pure compound could be isolated.

**Benzothiazolyl-2-thioglycollic Acid (VI).**—This acid was prepared by Ohta's method[6].

**Action of Acetic Anhydride on VI.**—The acid VI (1.0 g.) was added to acetic anhydride (20 ml.) and warmed on a water bath. The solution rapidly became dark red and at the same time crystals separated, which were filtered off and washed with hot ethanol, giving lustrous red-purple crystals (0.57 g.), m. p. 297°C.

The anhydride filtrate was diluted with water (100 ml.) and washed with hot ethanol to give lustrous red-purple crystals (0.35 g.), m. p. 297°C. Total yield, 0.92 g.

Found: C, 51.80; H, 3.00; N, 5.85. Calcd. for $C_{11}H_7O_2NS_2$: C, 53.01; H, 2.81; N, 5.62%.

The above experiment was repeated but with propionic anhydride instead of acetic anhydride, the same product being obtained.

**Benzoxazolyl-2-thioglycollic Acid (VII).**—A solution of chloroacetic acid (1.9 g.) and sodium carbonate (1.06 g.) in water (20 ml.) was added to a solution of 2-mercaptobenzoxazole (3.0 g.) and sodium hydroxide (0.8 g.) in water (20 ml.). The solution was warmed on a water bath for 0.5 hr. and kept standing at room temperature overnight. After neutralization with dilute hydrochloric acid, the resulting precipitate was filtered off, washed with water and recrystallized from dilute ethanol to give colorless plates of VII (3.85 g.), m. p. 160~ 161°C.

Found: N, 6.27. Calcd. for $C_9H_7O_3NS \cdot H_2O$; N, 6.17%.

**Action of Acetic Anhydride on VII.**—The acid VII (1.0 g.) was refluxed gently with acetic anhydride (10 ml.) for 0.5 hr., affording a deep yellow

4) T. Sato and M. Ohta, *J. Pharm. Soc. Japan*, **77**, 771 (1957).

5) H. Ueda, unpublished work.

6) H. Ohta and M. Ohta, *J. Chem. Soc. Japan, Pure Chem. Sec. (Nippon Kagaku Zasshi)*, **78**, 700 (1957).

solution. The anhydride was evaporated under reduced pressure, the residue of violet gum extracted with ether and the extract evaporated to dryness to give yellowish gummy material which could not be purified.

**Cyclohexenothiazolyl-2-thioglycollic Acid (VIII).**—This acid was prepared by the same process as used for benzothiazolyl-2-thioglycollic acid (VI)[6]. Colorless lancets, m. p. 124~125°C. Yield, 80.4%.

**Action of Acetic Anhydride on VIII.**—The acid VIII (1.0 g.) was added to acetic anhydride (2 ml.) and warmed on a water bath. An orange color quickly developed which gradually changed to intense blue-violet, and black-violet crystals separated. The crystals were filtered off and washed with hot ethanol to give black-violet crystals (0.7 g.), m. p. 254.5~255°C (decomp.).

The anhydride filtrate was diluted with water (200 ml.), and the resulting precipitate was filtered off and washed with hot ethanol to give black-violet crystals (0.02 g.), m. p. 254.5~255°C (decomp.). Total yield, 0.76 g.

Found: C, 50.84; H, 4.35; N, 5.72. Calcd. for $C_{11}H_{11}O_2NS_2$: C, 52.17; H, 4.35; N, 5.53%.

The above experiment was repeated but with propionic anhydride instead of acetic anhydride, the same product being obtained.

**Action of Acetic Anhydride and Pyridine on IV.**—The acid IV (1.0 g.) was refluxed in a mixture of acetic anhydride (5 ml.) and dry pyridine (5 ml.) for 0.5 hr. and the solvent was removed in vacuo to give a black oil, which was solidified by addition of a small amount of ethanol. Recrystallization from ethanol gave XII as colorless needles (0.12 g.), m. p. 149~150°C, undepressed by admixture with authentic sample.

**Action of Acetic Anhydride and Pyridine on V.**—The acid V (0.5 g.) was refluxed in a mixture of acetic anhydride (3 ml.) and dry pyridine (6 ml.) for 5 min., the solvent removed in vacuo and the residue recrystallized from ethanol to give colorless needles, m. p. 238°C, undepressed by admixture with the acid V.

Found: N, 13.65. Calcd. for $C_{16}H_{13}O_2N_3S$: N, 13.50%.

**Anhydro-compound XIVb from VI.**—(a) The acid VI (1.0 g.) was dissolved with stirring at room temperature in a mixture of acetic anhydride (3 ml.) and dry pyridine (6 ml.). The solution immediately turned yellow and the color finally became dark green. After a few minutes crystals separated, which were filtered off, washed thoroughly with water, dried and then extracted with hot benzene. The extract was evaporated to dryness giving yellow crystals (0.3 g.), m. p. 209~212°C (decomp.). Recrystallization from benzene yielded the anhydro-compound as bright yellow leaflets, m. p. 215~216°C (decomp.).

Found: C, 51.94; H, 2.58; N, 6.89. Calcd. for $C_9H_5ONS_2$: C, 52.18; H, 2.43; N, 6.76%.

From the benzene-insoluble portion, the lustrous red-purple crystals were obtained (0.33 g.).

(b) VI (1.0 g.) was dissolved with stirring at room temperature in a mixture of acetic anhydride (3 ml.) and triethylamine (6 ml.), a yellow color quickly developing. After a few minutes yellowish brown crystals separated, which were filtered off, washed thoroughly with water, dried and extracted with hot benzene. The extract was evaporated to dryness to give yellow crystals (0.47 g.), m. p. 210~212°C (decomp.). Recrystallization from benzene yielded the anhydro-compound as bright yellow leaflets, m. p. 216~216.5°C (decomp.).

Found: N, 6.55. Calcd. for $C_9H_5ONS_2$: N, 6.76%.

**Action of Pyridine on the Anhydro-compound XIVb.**—XIVb (0.3 g.) was refluxed gently with pyridine (10 ml.) for 5 min. After cooling, the solution was diluted which water (50 ml.) to give a crystalline precipitate with was filtered off and recrystallized from ethanol, affording bisbenzothiazolyl-2-thioacetone (XVI) as colorless needles (0.18 g.), m. p. 127°C, undepressed by admixture with authentic sample.

Found: N, 7.36. Calcd. for $C_{17}H_{12}ON_2S_4$: N, 7.21%.

**Bisbenzothiazolyl-2-thioacetone.**—To a solution of 2-mercaptobenzothiazole (5.5 g.) in absolute ethanol (50 ml.) containing metallic sodium (0.8 g.) was added *sym*-dichloroacetone (2.0 g.). After 5 min. crystals separated at a time. The crystals were filtered off, washed with water and recrystallized twice from ethanol to give colorless needles (8.0 g.), m. p. 127°C.

Found: C, 52.83; H, 3.37; N, 7.18. Calcd. for $C_{17}H_{12}ON_2S_4$: C, 52.56; H, 3.09; N, 7.21%.

**Action of Aqueous Sulfuric Acid on XIVb.**—XIVb (0.3 g.) was refluxed gently with 50% aqueous sulfuric acid (10 ml.) for 10 min. and the cooled solution was diluted with water (50 ml.) to give a crystalline precipitate which was filtered off and recrystallized from ethanol, affording colorless needles (0.05 g.), m. p. 124°C, undepressed by admixture with authentic sample of XVI. Addition of water to the mother-liquor precipitated pale yellow prisms (0.06 g.), m. p. 157~158°C, undepressed by admixture with the acid VI.

**Action of Acetic Anhydride and Pyridine on VII.**—The acid VII (1.0 g.), acetic anhydride (1 ml.) and dry pyridine (3 ml.) were heated on a boiling water bath for 0.5 hr. and after cooling, the solution was concentrated under reduced pressure to give colorless leaflets (0.9 g.), m. p. 160~162°C, undepressed by admixture with the acid VII.

**Action of Acetic Anhydride and Triethylamine on VII.**—The acid VII (1.0 g.) was dissolved in a mixture of acetic anhydride (1 ml.) and triethylamine (3 ml.) and the solution kept to stand at room temperature for 3 hr. The solution was concentrated under reduced pressure to give an orange oily material, which rapidly solidified by addition of water. Colorless leaflets (0.91 g.), m. p. 163°C, undepressed by admixture with the acid VII.

**Action of Acetic Anhydride and Pyridine on VIII.**—The acid VIII (1.0 g.) was dissolved with stirring at room temperature in a mixture of acetic anhydride (3 ml.) and dry pyridine (6 ml.). A deep yellow color quickly developed which gradually changed to blue-green and light blue crystals separated. After 0.5 hr., the crystals were filtered off, washed thoroughly with water, dried and then

extracted with hot benzene and the extract was evaporated to dryness to give light green needles (0.52 g.), m. p. 198~199°C (decomp.). Recrystallization from benzene gave m. p. 198~199°C (decomp.).

Found: C, 53.51; H, 4.60; N, 6.08. Calcd. for $C_{10}H_9ONS_2$: C, 53.81; H, 4.06; N, 6.28%.

From the benzene-insoluble portion, the black-violet crystals were obtained (0.17 g.).

**Action of Acetic Anhydride and Triethylamine on VIII.**—The acid VIII (1.0 g.) was dissolved with stirring at room temperature in a mixture of acetic anhydride (3 ml.) and triethylamine (6 ml.). Light brown crystals rapidly separated, which were filtered off, washed thoroughly with water, dried and extracted with hot benzene. The extract was evaporated to dryness to give light yellow crystals (0.68 g.), m. p. 197~199°C (decomp.). Recrystallization from benzene yielded light yellow needles, m. p. 198°C (decomp.).

Found: N, 6.26. Calcd. for $C_{10}H_9ONS_2$: N, 6.28%.

**Action of Aqueous Sulfuric Acid on the Compound $C_{10}H_9ONS_2$.**—The compound (0.5 g.) was refluxed gently with 50% aqueous sulfuric acid (12 ml.) for 0.5 hr. The cooled solution was diluted with water (50 ml.) and extracted with ether. The ether extract was evaporated and the residue recrystallized from ethanol to give colorless prisms, m. p. 125~126°C, undepressed with the acid VIII.

Found: N, 5.94. Calcd. for $C_9H_{11}O_2NS_2$: N, 6.11%.

**Action of Pyridine on the Compound $C_{10}H_9ONS_2$.**—The compound (1.0 g.) was refluxed gently with pyridine (20 ml.) for 20 min. After cooling, the solution was diluted with water (150 ml.) and colorless needles which separated were filtered off and dried. M. p. 94.5°C, 1.0 g. Recrystallization from dilute pyridine gave colorless silky needles, m p. 98.5~99.5°C.

Found: C, 47.60; H, 5.35; N, 6.86; S, 31.1. Calcd. for $C_8H_{11}ONS_2$: C, 47.76; H, 5.47; N, 6.97; S, 31.84%.

**Cyclopentenothiazolyl-2-thioglycollic Acid (IX).**—This acid was prepared by the same process as used for benzothiazolyl-2-thioglycollic acid (VI)[6]. Colorless needles, m. p. 126°C, yield, 45.6%.

**Anhydro-compound XVII from IX.**—The acid IX (1.0 g.) was dissolved with stirring at room temperature in a mixture of acetic anhydride (3 ml.) and triethylamine (6 ml.). After one minute crystals separated, which were filtered off, washed thoroughly with water and dried. M. p. 198~201°C, 0.67 g. Recrystallization from benzene gave the anhydro-compound as deep yellow crystals, m. p. 213.5~214°C (decomp.).

Found: C, 48.65; H, 3.97; N, 7.20. Calcd. for $C_8H_7ONS_2$: C, 48.74; H, 3.58; N, 7.11%.

**Action of Aqueous Sulfuric Acid on the Anhydro-compound XVII.**—XVII (0.5 g.) was dissolved in 50% aqueous sulfurid acid (12 ml.) and the resultant yellow solution refluxed gently for 10 min., the yellow color disappearing. The solution was diluted with water (150 ml.), neutralized with sodium carbonate, extracted with ether and the extract evaporated to give colorless needles (0.38 g.), m. p. 117°C. Recrystallization from dilute ethanol gave colorless needles, m. p. 124~126°C, undepressed by admixture with the acid IX.

Found: N, 6.41. Calcd. for $C_9H_9O_2NS_2$: N, 6.51%.

**Action of Pyridine on XVII.**—XVII (0.3 g.) was refluxed gently with pyridine (10 ml.) for 5 min. The solution was diluted with water (50 ml.) and a crystalline precipitate filtered off, washed with water and dried. M. p. 81.5°C, 0.27 g. Recrystallization from dilute ethanol afforded colorless silky needles, m. p. 81~82°C.

Found: C, 46.39; H, 4.83; N, 7.53. Calcd. for $C_{15}H_{16}ON_2S_4 \cdot H_2O$: C, 46.63; H, 4.66; N, 7.25%.

The authors are indebted to Mr. Asaji Kondo for performing the microanalyses and to Dr. Tadashi Sato for assistance in the infrared determinations.

*Laboratory of Organic Chemistry*
*Tokyo Institute of Technology*
*Meguro-ku, Tokyo*

# *Polyaddition Reaction of Diphenylsilane to Difunctional Unsaturated Compounds. II*

By Kuniharu KOJIMA

(Received March 22, 1960)

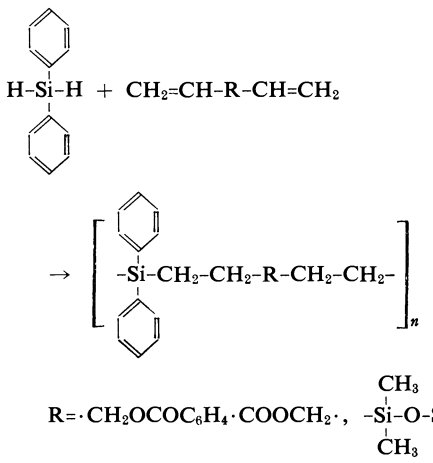
Several literatures have been published on the addition reaction of silicon hydrides to a number of olefines using peroxide, ultraviolet light, $\gamma$-rays or platinum catalysts.

In 1947, L. H Sommer reported that *n*-octyltrichlorosilane was prepared by the addition reaction of 1-octene with trichlorosilane in the presence of a small amount of diacetyl peroxide catalysts at 50~63°C[1,2]. This addition reaction was also carried out using $\gamma$-rays from a 30 kilocurie $Co^{60}$ source at room temperature in an almost quantitative yield[3].

The addition reaction of trichlorosilane to styrene was first carried out by C. A. Burkhard in the presence of peroxide catalysts, resulting in the formation of only non-volatile telomeric products[4]. W. S. Wagner and coworkers succeeded in the preparation of $\beta$-phenylethyltrichlorosilane by the above mentioned addition reaction using platinized charcoal as the catalyst at 200°C[5]. S. Nozakura reported the formation of $\alpha$- and $\beta$-trichlorosilylethylbenzene by the same reaction using tetrapyridine nickel chloride as the catalyst at 160°C[6]. The platinum catalyzed addition reaction of methyldichlorosilane with methyl methacrylate was carried out by L. H. Sommer and coworkers in the preparation of $\alpha$-methyl-$\beta$-methyldichlorosilyl propionate[7].

The addition reaction of methyldichlorosilane with vinyl acetate was studied by J. L. Speier and coworkers in the preparation of 2-methyldichlorosilylethyl acetate[8]. L. Goodman reported similar reactions of various silanes (phenylsilane, methyldiethoxysilane, trichlorosilane or methyldichlorosilane to allyl acetate[9]. J. W. Curry and coworkers have recently described the polymerization of certain silanes having an unsaturated organic group and a hydrogen on the same silicon atom[10,11].

In the previous paper, we have reported the result of the polyaddition reaction of diphenylsilane with diallyl phthalate or methyldisiloxane in the presence of a small amount of platinum black[12].




By these reactions carried out in sealed glass tubes, new polymers containing silicon were obtained in good yield. As a continuation of the experiment, the present paper deals with a new synthetic method of polymers which can be generally applied to the polyaddition reaction of diphenylsilane with various difunctional unsaturated compound (diallyl adipate, divinyl adipate, tetramethylene dimethacrylate, divinylbenzene and hexadiene).

Our first work was to examine the polyaddition reaction of diphenylsilane with diallyl phthalate using platinum black as the catalyst. As the extension of this work, the effect of various catalysts (i. e. platinum black, chloroplatinic acid, benzoyl peroxide, *tert*-butyl hydroperoxide, and azobisisobyturonitrile) has been studied. The results are shown in Table I.

Platinum catalysts were more effective than other catalysts. The effect of the irradiation of $\gamma$-ray or ultraviolet light in this reaction was hardly recognized at room temperature.

Similarly, by the polyaddition reaction of diphenylsilane with diallyl adipate was also prepared a linear polyaddition product in a

1) L. H. Sommer et al., *J. Am. Chem. Soc.*, **69**, 188 (1947).
2) L. H. Sommer et al., ibid., **70**, 484 (1948).
3) L. C. Anderson et al., ibid., **80**, 1737 (1958).
4) C. A. Burkhard et al., ibid., **69**, 2687 (1947).
5) W. S. Wagner et al., *Ind. Eng. Chem.*, **45**, 367 (1953).
6) S. Nozakura., This Bulletin, **29**, 784 (1956).
7) L. H. Sommer et al., *J. Am. Chem. Soc.*, **79**. 2764 (1957).
8) J. L. Speier et al., ibid., **79**, 974 (1957).
9) L. Goodman et al., ibid., **79**, 3073 (1957).
10) J. W. Curry, ibid., **78**, 1689 (1956).
11) J. W. Curry et al., *J. Org. Chem.*, **23**, 1219 (1958).
12) K. Kojima, This Bulletin, **31**, 663 (1958).

TABLE I. POLYADDITION OF DIPHENYLSILANE WITH DIALLYL PHTHALATE

| Catalyst (mol.) | React. time (hr.) | Temp. (°C) | Yield (%) | Mol. wt. |
|---|---|---|---|---|
| Pt-black, $2 \cdot 10^{-4}$ | 50 | 110~20 | 76 | 2390 |
| Chloroplatinic acid, $2 \cdot 10^{-6}$ | 〃 | 〃 | 73 | 2060 |
| Benzoyl peroxide, $2 \cdot 10^{-4}$ | 〃 | 〃 | 60 | 955 |
| *tert*-Butyl hydroperoxide, $2 \cdot 10^{-4}$ | 〃 | 〃 | 67 | 765 |
| Azobisisobutyronitrile, $2 \cdot 10^{-4}$ | 〃 | 〃 | 69 | 775 |

In these experiments, 0.02 mol. of diphenylsilane and 0.02 mol. of diallyl phthalate were used.

76% yield. The molecular weight of this polyadduct was 1400.

In the polyaddition reaction of diphenylsilane with divinyl adipate using platinum black as catalyst, however, the linear polyaddition product was obtained in 34% yield and the other polyadduct was a highly branched (or a cross-linked) polymer. The molecular weight of the linear polymer was 1660. The combination ratio of divinyl adipate and diphenylsilane of the branched polymer was 4 : 1.

The reaction of diphenylsilane with tetramethylene dimethacrylate did not produce a linear high polymer, but gave a low molecular weight adduct (mol. wt. 460) in 37% yield and a branched polymer (combination ratio, tetramethylene dimethacrylate 2 moles : diphenylsilane 1 mole).

When diphenylsilane and divinylbenzene were heated at 120°C in the presence of Pt-black, the highly branched polymer and low molecular weight adducts were obtained. The molecular weight of this low-adduct was 440. The combination ratio of branched polymer was diphenylsilane 1 mol. : divinylbenzene 18 mol.

In the addition reaction of diphenylsilane with hexadiene using platinum black catalyst, the low molecular weight adduct (mol. wt. 685) was only obtained in a 43% yield.

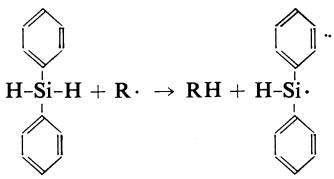
The mechanism of the addition reaction of silicon hydride to olefinic compounds catalyzed by platinum is not clear yet. But it has been asserted, that the addition reaction of silicon hydride to alkene using peroxide catalyst is a free radical chain reaction[1]. The proposed mechanism for the reaction is

$$R\cdot + HSi\equiv \rightarrow RH + \equiv Si\cdot$$

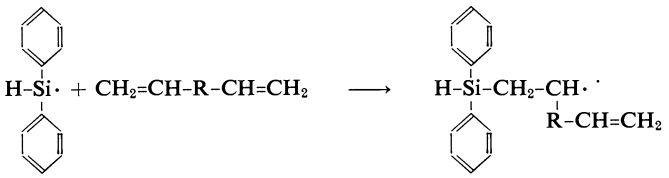
$$RCH{=}CH_2 + \equiv Si\cdot \rightarrow R\dot{C}H{-}CH_2Si\equiv$$

$$R\dot{C}HCH_2Si\equiv + HSi\equiv \rightarrow RCH_2CH_2Si\equiv + \equiv Si\cdot$$

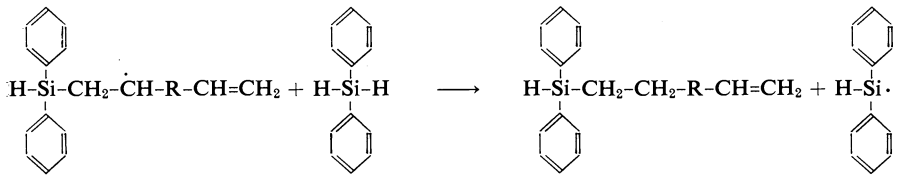
In this paper, the reaction of diphenylsilane with difunctional unsaturated compound to form the linear high molecular weight polymer was predominant.



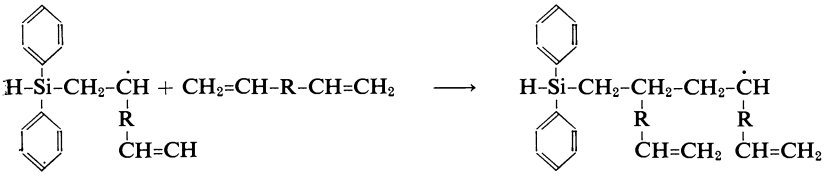
(1)



(2)



(3)



(4)

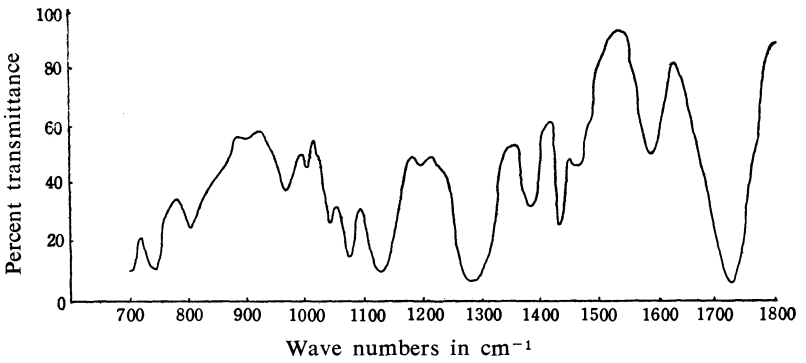



Fig. 1. Infrared spectrum of adduct of diphenylsilane with diallyl phthalate.

But in some cases, it was found that the second reaction shown in Eq. 4 also took place.

This reaction is responsible for the formation of branched polymer and a strong competitor for the normal addition reaction 3. In case of diallyl phthalate, diallyl adipate and hexadiene, only the reaction 3 can proceed. Theerfore it gave linear products only. But, in the case of divinyl adipate, tetramethylene dimethacrylate and divinylbenzene, branched polymers were obtained together with linear polymers.

The addition reaction of silicon hydrides to some unsaturated compounds has been shown to yield two isomers by other investigators[9,13,14]. The addition compound of trichlorosilane to acrylonitrile could be either $NCCH_2CH_2SiCl_3$ ($\alpha$-adduct) or $NCCH(CH_3)SiCl_3$ ($\beta$-adduct).

But, in the case of platinum catalyzed reaction, the addition reactions of silicon hydrides to vinyl acetate and to methyl methacrylate have been shown to yield $\beta$-adducts, and the addition to allyl acetate has been shown to yield $\gamma$-adducts.

By analogy, the addition compounds of diphenylsilane with each of divinyl adipate, and tetramethylene dimethacylate are presumed to be mainly $\beta$-adducts, and the adduct of diallyl phthalate are $\gamma$-adduct. But, it was shown, that the infrared absorption spectra of the addition compounds obtained in this work were identical in all important respects with that of the mixture of them.

In the isolation of the polymer, it was found, thats ome volatile by-products are also obtained from the reaction mixture. In the case of tetramethylene dimethacrylate, the volatile product was obtained in considerable quantities, and the yielded gas was identified as propylene and propane by gas-chromatography. But the mechanism of the production of propylene and propane is indistinct.

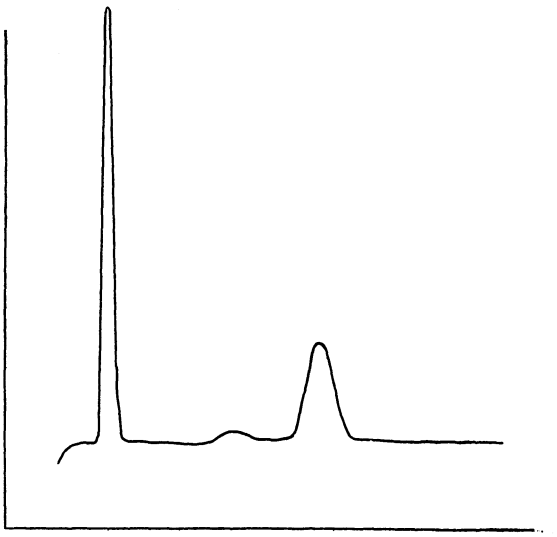


Fig. 2. Gas-chromatograph of the reaction by-products of diphenylsilane with tetramethylene dimethacrylate. Carrier gas, hydrogen; column dimethyl formamid-active charcoal.

## Experimental

**Materials.**—Diallyl adipate[15] and divinyl adipate[16] were prepared by the published methods. Tetramethylene dimethacrylate was prepared by the ester interchange reaction of methyl methacrylate with 1,4-butanediol in the presence of sulfuric acid and hydroquinone[17]. Diallyl phthalate and divinylbenzene were commercial products. Hexadiene was prepared by the reaction of allyl bromide with metallic magnesium in ether[18]. Diphenylsilane was prepared from diphenyldichlorosilane by lithium

13) S. Nozakura et al., ibid., **29**, 322 (1956).
14) S. Nozakura et al., ibid., **29**, 326 (1956).
15) K. Kojima et al., *Reports of the Research Institute of Dental Materials, Japan.*, 8, 136, (1957).
16) K. Kojima et al., ibid., **9**, 38 (1958).
17) K. Kojima et al., ibid., **8**, 144 (1957).
18) L. Vanino, "Handbuch der Präparativen Chemie", Bd. 2, 7 (1937).

aluminum hydride by ordinary method[19]. Diphenyldichlorosilane was supplied by Shin-etu Chem. Co. and redistilled before being used.

**Polyaddition of Diphenylsilane with Diallyl Phthalate.**—*Method 1—Pt Black Initiation.*—Diallyl phthalate (4.92 g., 0.02 mol.), diphenylsilane (3.68 g., 0.02 mol.) and platinum black (0.03 g.) as catalyst were placed in a glass tube and the tube was sealed in nitrogen stream, and then heated at 110~120°C in an air oven for 50 hr. The reaction product was dissolved in 100 ml. benzene and reprecipitated by 200 ml. methanol. The precipitated material was separated and dried in a vacuum desiccator at 50°C for 7 days. Yield, 76%.

Found: Si, 5.34. Calcd. for $C_{26}H_{26}O_4Si$: Si, 5.83% mol. wt., 2390.

*Method 2—Chloroplatinic Acid Initiation.*—Under similar condition as described for Pt black initiation, chloroplatinic acid ($2\cdot10^{-5}$ mol.) in methanol solution, diphenylsilane (3.65 g.) and dially phthalate (4.92 g.) were heated and the product was reprecipitated. The average molecular weight of this polymer was found to be 2060. Yield 73%.

*Method 3—Benzoyl Peroxide Initiation.*—The mixture of diphenylsilane (3.68 g.), diallyl phthalate (4.92 g.) and benzoyl peroxide (0.005 g.) were heated in an air oven for 50 hr. at 110~20°C. The reaction gave a linear polymer of mol. wt. 954. Yield 60%.

*Method 4—tert-Butyl Hydroperoxide Initiation.*—Under similar condition as described above, 0.002 g. of *tert*-butyl hydroperoxide was used as the catalyst. The reaction gave a linear polymer of mol. wt. 765. Yield 67%.

*Method 5—Azobisisobutyronitrile Initiation.*—Under similar condition as employed in the preceding experiment, diphenylsilane (3.68 g.), diallyl phthalate (4.92 g.), and azobisisobutyronitril (0.003 g.) were traced to produce 5.81 g. of the linear polymer with 69% of theoretical yield. mol. wt. 774.

*Method 6—*$^{60}$Co *Initiation.*—Diphenylsilane (3.68 g.) and diallyl phthalate (4.92 g.) were charged in a glass tube. The tube was sealed in dry nitrogen atmosphere, and then exposed to $^{60}$Co irradiation at room temperature for 150 hr. at a rate of $2.1\cdot10^{-5}$ r.e.p./hr. The molecular weight of this product was 600. Yield 9.8%.

*Method 7—Ultraviolet Light Initiation.*—The same mixture employed in the preceding experiment was exposed to ultraviolet light irradiation at room temperature for 150 hr. at 10170 c. d. by merucric lamp but the unreacted diphenylsilane and diallyl phthalate were recovered.

**Polyaddition of Diphenylsilane with Diallyl Adipate.**—A mixture of diphenylsilane (3.68 g.) and diallyl adipate (4.52 g., 0.02 mole) with 0.03 g. platinum black were heated for 50 hrs. at 120°C in a sealed glass tube. The product was dissolved in benzene and reprecipitated by methanol. The average molecular weight of this polymer was found to be 1400. Yield 68%.

Found: Si, 6.69. Calcd for $C_{24}H_{28}OSi$: Si, 6.84%.

**Polyaddition of Diphenylsilane with Divinyl Adipate.**—Divinyl adipate (3.96 g., 0.02 mole), diphenylsilane (3.68 g., 0.02 mole) and 0.03 g. platinum black as the catalyst were heated at 120°C for 50 hr. in a sealed glass tube. The product was dissolved in benzene and reprecipitated in methanol. The molecular weight of benzene-soluble polymer was 1660.

Found: Si, 7.12. Calcd. for $C_{22}H_{24}O_4Si$: Si, 7.38%. Yield 39%.

The benzene-insoluble polymer was found to be an adduct of diphenylsilane and divinyl adipate at the mole ratio of 1 : 4.

Found: Si, 3.32. Calcd. for 1 : 4 adduct: Si, 3.59%.

**Polyaddition of Diphenylsilane with Tetramethylene Dimethacrylate.**—Tetramethylene dimethacrylate (4.52 g., 0.02 mol.), diphenylsilane (3.68 g., 0.02 mol.) and 0.03 g. platinum black were heated for 50 hr. at 120°C in a sealed glass tube. The product was dissolved in benzene and reprecipitated by methanol. The low molecular weight addition product (benzene-soluble part) was obtained in a 37% yield. The average molecular weight of this polymer was found to be 460. A branched (or cross-linked) polymer was also formed and it has been cleared by Si analysis, that it was the addition product of diphenylsilane and tetramethylene dimethacrylate at the mole ratio of 1 : 2.

Found: Si, 4.18, Calcd. for 1 : 2 adduct: Si, 4.18%.

**Polyaddition of Diphenylsilane with Divinylbenzene.**—Divinylbenzene (2.60 g., 0.02 mol.), diphenylsilane (3.68 g., 0.02 mol.) and platinum black (0.03 g.) were charged in a glass tube. The tube was sealed under the atmosphere of nitrogen and heated in an air oven for 50 hr. at 125~130°C. The product was dissolved in benzene. The average molecular weight of the soluble product was 440. Yield 65%. The insoluble product was an addition product of diphenylsilane 1 mol. and divinylbenzene 18 mol.

Found: Si, 1.11. Calcd. for 1 : 18 adduct: Si, 1.10%.

**Polyaddition of Diphenylsilane with Hexadiene.** Hexadiene (1.64 g., 0.02 mol.), diphenylsilane (3.68 g. 0.02 mol.) and platinum black (0.03 g.) were charged in a glass tube, and the tube was sealed under the nitrogen atmosphere and heated in an air oven for 50 hr. at 110~120°C. Only the low molecular weight product (mol. wt. 685) was obtained in a 43% yield.

Found: Si, 9.87. Calcd for $C_{18}H_{22}Si$: Si, 10.78%.

The author is much indebted to Prof. Yoshio Iwakura for his many useful suggestions and to Mr. Niro Tarumi for his help in the experiments. Appreciation is also due to Shin-etu Chem. Co. for their kindness in supplying the diphenyldichlorosilane.

*Tokyo Medical and Dental University*
*Yushima, Bunkyo-ku, Tokyo*

19) R. A. Benkeser et al., *J. Am. Chem. Soc.*, **74**, 648 (1952).

# *Studies on D-Glucosamine Derivatives. V. Some Derivatives of N-Phenyl-D- and L-glucosaminonitrile*

By Juji YOSHIMURA

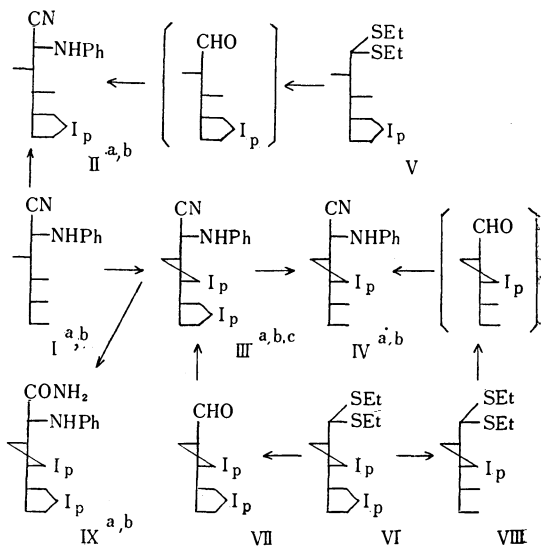
(Received April 22, 1960)

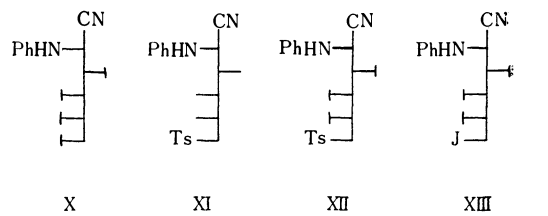
In the preceding paper of this series[1], syntheses of isopropylidene and some other derivatives of D-glucosamine diethylmercaptals were described. In the present paper, the corresponding derivatives of *N*-phenyl-D- and L-glucosaminonitrile were synthesized, and the structure of isopropylidene derivatives were unambiguously confirmed by different derivations.

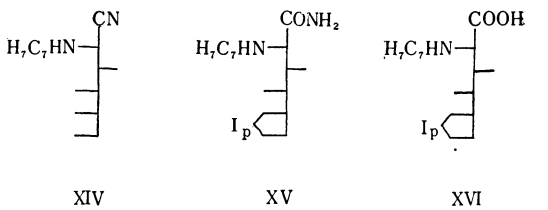
Warming of *N*-phenyl-D- ($I^a$) or L-glucosaminonitril ($I^b$), prepared from anhydrous hydrogen cyanide, aniline and D- or L-arabinose by Kuhn's method[2], with anhydrous cupric sulfate in acetone afford the corresponding 5, 6-*O*-isopropylidene derivatives ($II^a$ or $II^b$) respectively, whilst these are converted into the corresponding 3, 4 ; 5, 6-di-*O*-isopropylidene derivatives ($III^a$ or $III^b$) by treating with acetone in the presence of concentrated sulfuric acid. $III^a$ and $III^b$ are partially hydrolyzed to the corresponding 3, 4-*O*-isopropylidene derivatives ($IV^a$ and $IV^b$) under an acidic condition.

All these derivations of isopropylidene derivatives are very similar to that of D-glucosamine diethylmercaptals described in Part IV. To determine the position of isopropylidene groups, these were synthesized from isopropylidene *aldehydo*-arabinose, aniline and anhydrous hydrogen cyanide in ethanol. Thus, 2,3 ; 4,5-di-*O*-isopropylidene-*aldehyde*-D-arabinose (VII)[3] was converted in good yield into a mixture of $III^a$ and its epimer ; 3, 4 ; 5, 6-di-*O*-isopropylidene-*N*-phenyl-D-mannosaminonitrile ($III^c$). Meanwhile, the unpurified 5, 6- and 2, 3-*O*-isopropylidene-D-arabinose obtained from the corresponding diethylmercaptal (V)[3] and (VIII) which is the partial hydrolyzed product of 2, 3 ; 4, 5-di-*O*-isopropylidene-D-arabinose diethylmercaptal (VI)[3] were converted into $II^a$ and $IV^a$ in poor yield.

Aldonic acidamides known as an intermediate of Weerman's degradation for shortening the carbon chain of sugars are generally synthesized from aldonic acids or lactones and alcoholic[4] or liquid[5] ammonia. Partial




1) J. Yoshimura and T. Sata, *J. Chem. Soc. Japan, Pure Chem. Sec.* (*Nippon Kagaku Zasshi*), **80**, 1479 (1959).
2) R. Kuhn and W. Kirschenlohr, *Ann.*, **600**, 115 (1956).
3) K. Gätzi and V. T. Reichstein, *Helv. Chim. Acta.*, **21**, 914 (1938) ; J. English, Jr. and P. H. Griswold,Jr., *J. Am. Chem. Soc.*, **67**, 2039 (1945).
4) C. S. Hudson, **41**, 1141 (1919).
5) W. E. Glattfeld and D. Macmillan, **56**, 2481 (1934).

TABLE I. RESULTS OF PERIODATE OXIDATION EXPERIMENTS

| Compounds | Mol. of periodate consumed/mol. of compds. | | | | Mol. of formaldehyde liberated |
|---|---|---|---|---|---|
| | 1 hr. | 2 hr. | 3 hr. | 9 hr. | |
| $I^a$ | 3.50 | 3.53 | 3.69 | 3.80 | 1.07 |
| $II^a$ | 1.70 | 1.70 | 1.92 | 2.20 | 0.02 |
| $III^b$ | 0.00 | 0.00 | 0.00 | 0.00 | — |
| $IV^b$ | 0.85 | 0·89 | 0.93 | 1.09 | 1.02 |
| IX | 0.00 | 0.00 | 0.00 | 0.26 | — |
| X | 0.00 | 0.00 | 0.00 | 0.00 | — |
| XV | 1.82 | 1.85 | 1.90 | 2.13 | 0.03 |
| XVI | 1.93 | 1.97 | 2.15 | 2.35 | — |

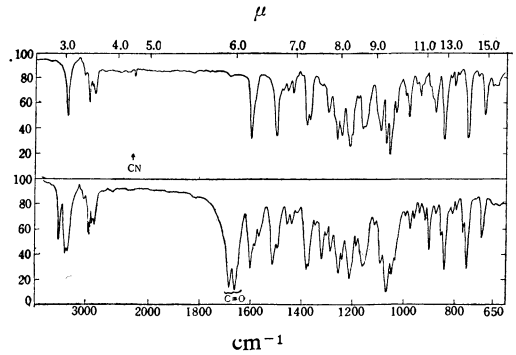



Fig. 1. The infrared specta of $III^a$ and $IX^b$.

hydrolysis of organic nitriles[6] to acidamides in alkalline hydrogen peroxide was applied to the above isopropylidene glucosaminonitriles. $III^a$ and $III^b$ are successfuly hydrolyzed to the corresponding glucosaminic acidamide ($IX^a$ and $IX^b$) in good yield, though $II^a$ or $IV^a$ does not afford a crystalline product. The infrared spectra (Fig. 1) show the absorption peak of nitrile (4.5 $\mu$) in $III^a$ but not in $IX^b$, while as for the carbonyl peaks (5.94, 6.01 $\mu$) the condition is vice versa.

Different from the corresponding *N*-methyl[7] and *N*-benzyl[2] derivatives, acetylation of $I^b$ with acetic anhydride in pyridine affords the corresponding tetra-*O*-acetate (X) in which the hydrogen atom attached to nitrogen is not being replaced by an acetyl group. Tosylation of $I^b$ in pyridine led to the crystalline 6-*O*-*p*-toluenesulfonyl derivative (XI), which is acetylated to the corresponding 3, 4, 5-tri-*O*-acetyl derivative (XII), and the position of *p*-toluenesulfonyl group was confirmed by conversion to the 6-iodo derivative (XIII).

Periodate oxidation of these derivatives (Table I) shows that a nitrile group does not consume the periodate as a mercaptal group[1,8] does, and nitriles having the unprotected hydroxyl group at carbon 3 (adjacent to amino group) are over-oxidized similarly to that of mercaptals[1].

There are a few examples[2,9] in which the reactivity of glucosaminonitrils are different with *N*-substituted groups. Thus, the reaction of *N*-benzyl-L-glucosaminonitrile (XIV) with acetone in the presence of concentrated sulfuric acid does not lead to the corresponding isopropylidine derivative, but crystalline 5, 6-*O*-isopropylidene-*N*-bynzyl-L-glucosaminic acid amide (XV) and 5, 6-*O*-isopropylidene-*N*-benzyl-L-glucosaminic acid, (XVI) in which the position of these isopropylidene groups was deduced from the results of periodate oxidation in Table I, were separated by chromatography of the reaction product on a magnesol-celite column. These aspects are now under investigation.

## Experimental

**5, 6-*O*-Isopropylidene-*N*-phenyl-D-glucosaminonitrile ($II^a$).**—(i) A mixture of 1 g. of *N*-phenyl-D-glucosaminonitrile ($I^a$), 30 ml. of anhydrous acetone and 4 g. of anhydrous cupric sulfate was stirred at 37~40°C for 6 hr., and the acetone solution separated from solids was concentrated in vacuo. The residual sirup crystallized on scratching with a little amount of ether was recrystallized twice from ethanol-petrolum ether; m. p. 124~5°C. Yield, 0.8 g. $[\alpha]_D^{26}+141°$ (*c* 0.82, methanol).

Found: C, 61.55; H, 7.02; N, 9.54. Calcd. for $C_{15}H_{20}O_4N_2$ (292.3): C, 61.63; H, 6.90; N, 9.58%.

(ii) To a mixture of 9.0 g. of 5,6-*O*-isopropylidene-D-arabinose diethylmercaptal (V) in 50 ml. of acetone and 70 g. of moist cadmium carbonate was added a solution of 30 g. of mercuric chloride in 40 ml. of acetone and the mixture was vigorously stirred for 4 hr. at room temperature. 20 g. of moist cadmium carbonate was again added, and then heated at 50°C for 1 hr. The reaction mixture was cooled, diluted with acetone, filtered and the solid was washed with the same solvent. After complete removal of acetone from the combined filtrate and washings at room temperature in the presence of cadmium carbonate, the mixture was extracted with chloroform and the extract dried with sodium

6) R. H. Wiley and H. S. Morgan, Jr., *J. Org. Chem.*, **15**, 800 (1950); J. V. Murray and J. B. Cloke, *J. Am. Chem. Soc.*, **56**, 2749 (1934).
7) M. L. Wofrom, A. Thompson and I. R. Hooper, *J. Am. Chem. Soc.*, **68**, 2343 (1946).
8) L. Hough and M. I. Taha, *J. Chem. Soc.*, **1956**, 2042.
9) R. Kuhn and W. Bister, *Ann.*, **602**, 217 (1957).

sulfate. A pale yellow sirup (2.5 g.) remained by evaporation of the solvent was dissolved in 4 ml. of ethanol, and 1 ml. of aniline and 1.5 ml. of ethanol, and 1 ml. of aniline and 1.5 ml. of hydrogen cyanide was added. After being kept in the refrigerator for 3 hr., the mixture was concentrated to dryness in vacuo, and the residual syrup was dissolved in ethanol-petroleum ether. The solution was seeded with II[a] and stored in the refrigerator overnight and 0.8 g. of crystals, m. p. 123~5°C, was yielded. These showed no depression on admixture with II[a].

**5, 6-*O*-Isopropylidene-*N*-phenyl-L-glucosaminonitrile (II[b]).**—0.8 g. of *N*-phenyl-L-glucosaminonitrile (I[b]) was treated in exactly the same manner as in the case of II[a], and 0.6 g. of colorless needles was obtained, m. p. 124~5°C. $[\alpha]_D^{25}-138°$ (*c* 0.70, methanol).

Found: C, 61.66; H, 7.05; N, 9.60. Calcd. for $C_{15}H_{20}O_4N_2$ (292.3); C, 61.63; H, 6.90; N, 9.58%.

**3, 4; 5, 6-Di-*O*-isopropylidene-*N*-phenyl-D-glucosaminonitrile (III[a]).**—To a mixture of 3 g. of I[a] and 60 ml. of anhydrous acetone, 1.6 ml. of concentrated sulfuric acid was added dropwise. After standing at room temperature for 4 hr., the slightly colored clear solution was poured into an excess amount of saturated aqueous solution of sodium carbonate in cooling, and filtered. The filtrate was extracted with chloroform used for washing the filtered sodium sulfate, and the extract was washed with water and dried with anhydrous sodium sulfate. The colorless crystals obtained by evaporation of the chloroform extract were recrystallized twice from ethanol: m. p. 106~8°C, Yield 2.5 g., $[\alpha]_D^{26}$ +140° (*c* 0.37, methanol.)

Found: C, 64.74; H, 7.27; N, 8.50. Calcd. for $C_{18}H_{24}O_4N_2$ (332.4): C, 65.04; H, 7.28; N, 8.43%.

**Reaction of 2, 3; 4, 5-Di-*O*-isopropylidene-aldehydo-D-arabinose (VII), Aniline and Hydrogen Cyanide.**—To a solution of 15 ml. of absolute ethanol and 9 g. of VII (b. p. 182~3°C/0.35 mmHg) were added 5 ml. of aniline and 10 ml. of anhydrous hydrogen cyanide. After being kept overnight in the refrigerator, the solution was concentrated in vacuo to a sirup, which was crystallized on scratching with a small amount of petroleum ether, and recrystallized from ethanol; yield 9 g., m. p. 106~8°C. $[\alpha]_D^{25}$+138° (*c* 2.0, methanol). These showed no depression on admixture with III[a]. 3,4; 5,6-Di-*O*-isopropylidene-*N*-phenyl-D-mannosaminonitrile obtained from the above mother liquor by concentration was recrystallized twice from ether-petrolum ether; yield 3 g., m. p. 93~5°C. $[\alpha]_D^{26}$ +12.8° (*c* 0.35, methanol).

Found: C, 64.97; H, 7.50; N, 8.36. Calcd. for $C_{18}H_{24}O_4N_2$ (332.4): C, 65.04; H, 7.28; N, 8.43%.

**3, 4-*O*-Isopropylidene-*N*-phenyl-D-glucosaminonitrile (IV[a]).**—(i) A mixture of 2 g. of III[a] in acetone (65%, 50 ml.) and aqueous sulfuric acid (6 N, 10 ml.) was warmed at 45~55°C for 40 min., and then poured into an excess amount of saturated sodium bicarbonate solution under cooling; it was then filtered. The residue was washed with chloroform, and the filtrate was extracted with the washings. The chloroform extract was washed with water and dried with anhydrous sodium sulfate, and evaporated in vacuo. The residual syrup was crystallized from ether-petroleum ether; m. p. 97~9°C. Yield 1.2 g. $[\alpha]_D^{24}$+75.6° (*c* 0.79, methanol).

Found: C, 61.46; H, 7.38; N, 9.52. Calcd. for $C_{15}H_{20}O_4N_2$ (292.3): C, 61.63; H, 6.90; N, 9.58%.

(ii) Freshly precipitated moist cadmium carbonate, 90 g. was heated rapidly to 50°C in a solution of 10.5 g. of 2,3-*O*-isopropylidene-D-arabinose diethylmercaptal in 55 ml. of acetone with vigorous stirring in nitrogen atmosphere. As soon as 50°C was reached 40 g. of mercuric chloride in 50 ml. of acetone was added over a period of 10 min. and stirring continued at 50°C for further 5 min. The mixiure was immediately cooled, diluted with acetone, centrifuged and washed on the centrifuge with the same solvent. After complete removal of acetone from the combined filtrate and washings at room temperature in the presence of fresh cadmium carbonate, the mixture was extracted with chloroform and the extract dried with sodium sulfate. Evaporation of the solvents gave 2 g. of pale yellow sirup. This syrup was dissolved in 5 ml. of ethanol with 1 g. of aniline and 1 ml. of anhydrous hydrogen cyanide, and left to stand for 3 hr. at room temperature. The mixture was concentrated in vacuo to a sirup, again dissolved in 5 ml. of ethanol, and water was added just before clouding took place at 40°C. A little amount of syrup separated was decanted at room temperature and the clear solution was stored in the refrigerator overnight. The crystals separated were collected and recrystallized from ethanol-water, m. p. 97~9°C. Yield 0.6 g. These showed no depression on admixture with IV[a].

**3, 4-*O*-Isopropylidene-*N*-phenyl-L-glucosaminonitrile (IV[b]).**—In exactly the same manner in the case of IV[a], 1.3 g. of crystals was obtained from 2 g. of III[b]. It was recrystallized from aqueous ethanol, m. p. 97~9°C, $[\alpha]_D^{26}-78.3°$ (*c* 0.97, methanol).

Found: C, 61.34; H, 7.28; N, 9.54. Calcd. for $C_{15}H_{20}O_4N_2$ (292.3): C, 61.63; H, 6.90; N. 9.58%.

**2, 3-*O*-Isopropylidene-D-arabinose Diethylmercaptal (VIII).**—A mixture of 16 g. of 2, 3; 4, 5-di-*O*-isopropylidene-D-arabinose diethylmercaptal in acetone (90 ml.) and aqueous sulfuric acid (6 N, 18 ml.) was heated at 45~50°C for 20 min. The solution was poured into an excess amount of cold saturated sodium bicarbonate solution and filtered. The residue was washed with chloroform, and the filtrate was extracted with washings. The chloroform extract was washed, dried and concentrated in the usual manner. By fractional distillation of the residue was obtained 10.4 g. of colorless syrup; b. p. 140°C/0.07 mmHg, 150~1°C/0.3 mmHg. $[\alpha]_D^{26}$ +86.2° (*c* 0.44, methanol).

Found: C, 48.94; H, 8.39; S, 21.23. Calcd. for $C_{12}H_{24}O_4S_2$ (296.4): C, 48.62; H, 8.16; S. 21.63%.

**2, 3; 4, 5-Di-*O*-isopropylidene-*N*-phenyl-D-glucosaminic Acidamide (IX[a]).**—A mixture of 2 g. of III[a], 35 ml. of acetone, hydrogen peroxide (30%, 7 ml.), sodium carbonate (10%, 3 ml.) and 18 ml. of water was refluxed 80 min. on a steam bath, and acetone was then removed in vacuo. The remained mixture of crystalline substances and water was extracted with chloroform in the usual

manner. The crystals obtained by evaporation of solvents in vacuo were recrystallized from ethanol; yield, 1.4 g., m. p. 147~8°C. $[\alpha]_D^{25}$ −5.1° (*c* 0.33, methanol).

Found: C, 61.40; H, 7.56; N, 8.00. Calcd. for $C_{18}H_{26}O_5N_2$ (350.4): C, 61.70; H, 7.48; N, 8.00%.

**2, 3, 4, 5-Di-*O*-isopropylidene-*N*-phenyl-L-glucosaminic Acidamide (IX[b]).**—In exactly the same manner in the case of IX[a], 3.5 g. of crystals was obtained from 5 g. of III[b]. It was recrystallized from ethanol-petroleum ether, m. p. 146~8C. $[\alpha]_D^{26}$ −4.5° (*c* 1.81, methanol).

Found: C, 61.80; H, 7.66; N, 7.17. Calcd. for $C_{18}H_{26}O_5N_2$ (350.4): C, 61.70; H, 7.48; N, 8.00%.

**3, 4, 5, 6-Tetra-*O*-acetyl-*N*-phenyl-L-glucosaminonitrile (X).**—To a solution of 3 g. of I[b] in 16 ml. of dry pyridine, 15 ml. of acetic anhydride was added under cooling, and the mixed solution was left to stand for 24 hr. at room temperature. The reaction mixture was then poured into ice-water and extracted with chloroform in the usual manner. The extract was evaporated to dryness, and the residue was crystallized from ethanol. Yield 3.2 g., m. p. 127~8°C. $[\alpha]_D^{25}$ −83.5° (*c* 0.55, methanol).

Found: C, 56.59; H, 5.99; N, 6.82. Calcd. for $C_{20}H_{24}O_8N_2$ (420.6): C, 57.13; H, 5.75; N, 6.66%.

**6-*O*-(*p*-Toluenesulfonyl)-*N*-phenyl-L-glucosaminonitrile (XI).**—To a solution of 2 g. of I[b] in 10 ml. of dry pyridine, a solution of 1 g. of *p*-toluenesulfonylchloride in 5 ml. of dry pyridine was added under cooling. After standing overnight at room temperature, the reaction mixture was poured into ice-water and extracted with chloroform. In the course of washing the extracts with 1 N sulfuric acid crystalls precipitated, and these were collected and recrystallized from ethanol. Yield, 1.5 g., m. p. 131~4°C, $[\alpha]_D^{25}$ −96.5° (*c* 0.96, methanol).

Found: C, 56.48; H, 5.71, N, 6.87; S, 7.55. Calcd. for $C_{19}H_{22}O_6N_2S$ (406.5): C, 56.15; H, 5.46; N, 6.89; S, 7.89%.

**3, 4, 5-Tri-*O*-acetyl-6-*O*-(*p*-toluenesulfonyl)-*N*-phenyl-L-glucosaminonitrile (XII).**—A mixture of 3 g. of XI, 20 ml. of acetic anhydride and 20 ml. of dry pyridine was left to stand overnight at room temperature and then poured into ice-water. The solution was extracted with chloroform in the usual manner. The crystals obtained by evaporation of the solvent was recrystallized from ethanol; yield. 2.9 g., m. p. 132~4°C., $[\alpha]_D^{25}$ −62.5° (*c* 0.28, methanol).

Found: C, 56.54; H, 5.50; N, 5.26; S, 5.85. Calcd. for $C_{25}H_{28}O_9N_2S$ (532.6): C, 56.38; H, 5.30; N, 5.26; S, 6.02%.

**3, 4, 5-Tri-*O*-acetyl-6-iodo-*N*-phenyl-L-glucosaminonitrile (XIII).**—In a glass tube 2 g. of XII. 0.56 g. of sodium iodide and 40 ml. of dry acetone were sealed and heated in a steam bath for 1 hr. Sodium *p*-toluenesulfonate separated (0.69 g., 95% of the theoretical amount) was filtered off. The filtrate was evaporated to dryness in vacuo, and the residue was extracted with chloroform in the usual manner. Evaporation of the extracts afford 1.6 g. of pale yellow syrup, which could not crystallize or distill for purification. $[\alpha]_D^{25}$ −51.5° (*c* 0.55, methanol).

Found: C, 44.73; H, 4.68; N, 6.06; I, 25.18. Calcd. for $C_{18}H_{21}O_6N_2I$ (488.3): C, 44.27; H, 4.33; N, 5.74; J, 25.99%.

**Reaction of *N*-benzyl-L-glucosaminonitrile (XV) and Acetone in the Presence of Concentrated Sulfuric Acid.**—A mixture of 10 g. of XV, 200 ml. of anhydrous acetone and 5 ml. of conc. sulfuric acid was stirred at room temperature for 4 hr. The brown reaction mixture was treated similarly to that the case of III[a]. The crude syrup (9 g.) was fractionated on a magesol-celite column (25 g. of 1 : 5 mixture) with every 100 ml. of the solvent; (1) benzene-petroleum ether (1 : 1), (2) benzene-petroleum ether (2 : 1), (3) benzene, (4) benzene-ethanol (2 : 1), (5) benzene-ethanol (1 : 2) as mobile phase.

Fraction 3 gave needles of 5,6-*O*-isopropylidene-*N*-benzyl-L-glucosaminic acid (0.5 g.) which were recrystallized from ethanol, m. p. 192~3°C decomp., $[\alpha]_D^{25}$ −165° (*c* 0.2, methanol).

Found: C, 59.10; H, 7.36; N, 4.35. Calcd. for $C_{16}H_{23}O_6N$ (325.3): C, 59.06; H, 7.13; N, 4.31%.

Fraction 4 gave crystals of 5,6-*O*-isopropylidene-*N*-benzyl-L-glucosaminic acidamide (2.0 g.) which were recrystallized from ethanol-ether, m. p. 163~4°C, $[\alpha]_D^{24}$ −42.5° (*c* 0.65, methanol).

Found: C, 58.89; H, 7.35; N, 8.70. Calcd. for $C_{16}H_{24}O_5N_2$ (324.4): C, 59.24; H, 7.46; N, 8.64%.

**Periodate Oxidation Experiments.**—In each case, a mixture of 0.2 M-sodium periodate (5 ml.) and the compound (25~30 mg. accurately weighed) and 4 ml. of ethanol was made up to 25 ml. with water and stored in a refrigerator. A blank containing none of the compound was worked concurrently. At intervals, the periodate uptake was estimated by transferring sample (2 ml.) from the oxidation mixture and the blank into mixtures of phosphate buffer (pH 6.98; 25 ml.) and 20% potassium iodate solution (1 ml.), and the liberated iodine titrated with 0.01 N sodium thiosulfate solution, starch being used as indicator[10]. Formaldehyde was determined colorimetrically with chromotropic acid according to O'Dea and Gibbon's method[11], D-glucose being used as standard.

The author wishes to express his hearty thanks to Professor T. Sato, Tokyo Institute of Technology, for his encouragement throughout this work.

*Laboratory of Organic Chemistry*
*Tokyo Institute of Technology*
*Meguro-ku, Tokyo*

10) G. Neumüller and E. Vasseur, *Arkiv Kemi.*, **5**, 235 (1953).
11) J. F. O'Dea and R. A. Gibbons, *Biochem. J.*, **55**, 580 (1953).

# *The Thermal Decomposition of Acetaldehyde in the Presence of Methanethiol*

By Naomi IMAI and Osamu TOYAMA

(Receiced April 16, 1960)

It is well known that reactions between thiols and free redicals, and between organic compounds and thiol radicals occur easily compared to other radical-molecule reactions. But only a few kinetic studies about these reactions are found in the literature[1,2]. The present authors have recently studied the photochemical[3] as well as the thermal[4] decomposition of acetaldehyde in the presence of hydrogen sulfide. These studies have shown that the chain decomposition of acetaldehyde is catalyzed by hydrogen sulfide, and this catalytic effect has been attributed to a chain mechanism involving reactions between methyl radical and hydrogen sulfide and between hydrosulfide radical and acetaldehyde. In a mixture of acetaldehyde and a thiol, a similar catalysis may be expected to take place. In this work a kinetic study of the thermal decomposition of acetaldehyde in the presence of methanethiol has been carried out to obtain information on elementary reactions involving methanethiol or its radical.

## Experimental

**Materials.**—Acetaldehyde was prepared by distillation of paraldehyde containing a small quantity of sulfuric acid and purified by bulb-to-bulb distillation. Methanthiol was obtained[5] by adding a sodium hydroxide solution to *S*-methyl isothiourea sulfate, which was prepared by the reaction between dimethyl sulfate and thiourea. It was then passed through a trap containing concentrated sulfuric acid and through a tower containing dry calcium chloride, and finally purified by bulb-to-bulb distillation.

**Apparatus.**—The thermal decomposition was carried out in a cylindrical glass vessel of 137 cc. placed in an electric furnace. The reaction vessel was connected to a mercury manometer, to an analytical system, to storage bulbs and to a bulb in which acetaldehyde and methanethiol were mixed before they were admitted to the reaction vessel. The reaction vessel, the manometer, the bulbs for storage and mixing and the analytical system were all attached to a conventional vacuum line.

**Procedure.**—Required quantities of acetaldehyde and methanethiol were admitted into the mixing bulb at room temperature and left for about 30 minutes to allow them to mix thoroughly. The mixed reactant gases were then introduced into the reaction vessel, which had already been kept at the experimental temperature, and the change in the total pressure with time was followed on a manometer. The products of decomposition in several runs were analyzed quantitatively in the same way as described previously[6].

## Results

It has been established by many workers that the products of the thermal decomposition of acetaldehyde are almost exclusively equal quantities of methane and carbon monoxide[7]. Similarly in this work, i. e., in the presence of methanethiol, it has been confirmed by analysis that the rate of formation of methane is identical with that of carbon monoxide, and the pressure of either one of these products corresponds to the total pressure increase within the experimental error. Thus, irrespective of the presence of methanethiol, the total pressure increase is always equal to the decrease in the pressure of acetaldehyde due to decomposition. Accordingly, the initial rate of decomposition was determined from the initial slope of a total pressure-time curve with the results shown in Figs. 1 and 3 and Table I. Fig. 1 shows the dependence of the rate of decomposition on the pressure of acetaldehyde in the experiments with acetaldehyde alone. Table I and Fig. 3 show the dependence of the rate of decomposition in the presence of methanethiol on the pressures of methanethiol and of acetaldehyde, respectively.

## Discussion

It is generally agreed that the main feature of thermal decomposition of acetaldehyde can

1) R. N. Birrell, R. F. Smith, A. F. Trotman-Dickenson and H. Wilkie, *J. Chem. Soc.*, **1957**, 2807.
2) J. A. Kerr and A. F. Trotman-Dickenson, ibid., **1957**, 3322.
3) N. Imai and O. Toyama, This Bulletin, 33, 1120 (1960).
4) Unpublished work.
5) F. Arndt, *Ber.*, **54**, 2236 (1921).
6) N. Imai and O. Toyama, This Bulletin, 33, 652 (1960).
7) C. J. M. Fletcher and C. N. Hinshelwood, *Proc. Roy. Soc.* (London), **A141**, 41 (1933); C. A. Winkler and C. N. Hinshelwood, ibid., **A149**, 355 (1935); R. V. Seddon and M. W. Travers, ibid., **A156**, 234 (1936); E. Leifer and H. C. Urey, *J. Am. Chem. Soc.*, **64**, 994 (1942).

TABLE I. EFFECT OF METHANETHIOL ON THE PYROLYSIS OF ACETALDEHYDE
Initial pressure of $CH_3CHO$, 100 mmHg

| 400°C | | 420°C | | 440°C | |
|---|---|---|---|---|---|
| Initial press. of $CH_3SH$ (mmHg) | Initial rate of decomp. (mmHg/min.) | Initial press. of $CH_3SH$ (mmHg) | Initial rate of decomp. (mmHg/min.) | Initial press. of $CH_3SH$ (mmHg) | Initial press. of decomp. (mmHg/min.) |
| 0.63 | 0.40 | 5.8 | 2.1 | 5.8 | 4.7 |
| 1.0 | 0.50 | 9.2 | 2.5 | 6.9 | 4.8 |
| 3.3 | 0.64 | 10.5 | 2.6 | 9.5 | 5.1 |
| 3.5 | 0.77 | 11.8 | 2.8 | 11.1 | 5.6 |
| 5.3 | 0.88 | 14.6 | 2.9 | 12.3 | 5.6 |
| 8.4 | 1.04 | 14.8 | 3.2 | 13.6 | 6.1 |
| 13.3 | 1.32 | 23.0 | 3.4 | 14.8 | 6.4 |
| 15.0 | 1.4 | 25.5 | 3.6 | 20.0 | 6.7 |
| 20.0 | 1.6 | 29 | 3.9 | 22.1 | 7.2 |
| 21.3 | 1.7 | 33 | 4.0 | 24 | 7.5 |
| 21.4 | 1.7 | 36 | 4.4 | 26 | 8.0 |
| 34 | 2.0 | 58 | 5.4 | 35 | 8.2 |
| 42 | 2.3 | 71 | 6.0 | 47 | 9.8 |
| 67 | 2.7 | 85 | 6.7 | 55 | 10.4 |
| 88 | 3.1 | | | | |

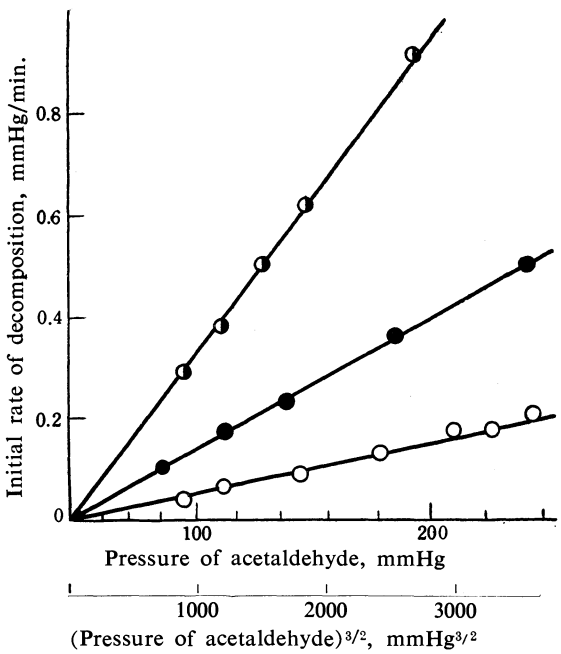



Fig. 1. Rate of decomposition of acetaldehyde alone. ○, 400; ●, 420; ◑, 440°C.

be explained by the following mechanism[8]

$$CH_3CHO = CH_3 + CHO \quad (1)$$

$$CHO = CO + H \quad (2)$$

$$H + CH_3CHO = H_2 + CH_3CO \quad (3)$$

$$CH_3CO = CH_3 + CO \quad (4)$$

$$CH_3 + CH_3CHO = CH_4 + CH_3CO \quad (5)$$

$$CH_3 + CH_3 = C_2H_6 \quad (6)$$

The steady state equations derived from this scheme yield the rate equation

$$-d[CH_3CHO]/dt = k_1^{1/2}k_5\ k_6^{-1/2}[CH_3CHO]^{3/2} \quad (I)$$

in general agreement with experimental results obtained by various workers. Also in this work, the rate of decomposition was found to be proportional to the 3/2 power of the pressure of acetaldehyde as seen in Fig. 1. From the slopes of the straight lines in the figure, the value of $k_1^{1/2}k_5\ k_6^{-1/2}$ at each temperature was obtained and listed in Table II.

TABLE II. VALUES OF $k_1^{1/2}k_5k_6^{-1/2}$, $k_1k_{11}^2k_{12}^{-1}$ AND $k_7k_{11}^2k_{12}^{-1}$

| Temp. (°C) | $k_1^{1/2}k_5k_6^{-1/2}$ ($mol^{-1/2}$ $cc^{1/2}$ $sec^{-1/2}$) | $k_1k_{11}^2k_{12}^{-1}$ ($mol^{-1}$ cc $sec^{-1}$) | $k_7k_{11}^2k_{12}^{-1}$ ($mol^{-1}$ cc $sec^{-1}$) |
|---|---|---|---|
| 400 | 0.045 | 0.245 | 7.4 |
| 420 | 0.116 | 1.40 | 33 |
| 440 | 0.28 | 7.4 | 141 |

Now in the presence of methanethiol, the additional possibilities may be[9]

$$CH_3SH = CH_3 + SH \quad (7)$$

$$SH + CH_3SH = H_2S + CH_3S \quad (8)$$

8) F. O. Rice and K. F. Herzfeld, *J. Am. Chem. Soc.*, **56**, 284 (1934); E. W. R. Steacie, "Atomic and Free Radical Reaction", 2nd Ed., Reinhold Publ. Corp., New York, (1954), p. 206.

9) Reactions similar to 10, 11 and 12 have been proposed by the following workers: E. F. P. Harris and W. A. Waters, *Nature*, **170**, 212 (1952); K. E. J. Banett and W. A. Waters, *Discussions Faraday Soc.*, **14**, 221 (1953); Ref. 1.

$$SH + CH_3CHO = H_2S + CH_3CO \quad (9)$$

$$CH_3 + CH_3SH = CH_3S + CH_4 \quad (10)$$

$$CH_3S + CH_3CHO = CH_3SH + CH_3CO \quad (11)$$

$$CH_3S + CH_3S = \text{Product} \quad (12)$$

Sehon and Darwent[10] suggest that in the thermal decomposition of methanethiol the split of C–S bond, and not that of S–H, takes place, in view of the fact that major products found by using toluene as a carrier are methane, hydrogen sulfide and dibenzyl. Their suggestion seems reasonable judging from the dissociation energies of C–S and S–H bonds of methanethiol which have been estimated as 74.2 and 88.8 kcal./mol., respectively[11]. Skerrett and Thompson[12] have shown that the product of reaction 12 is mainly methyl disulfide $(CH_3)_2S_2$ by analysis of the products obtained in the photolysis of methanethiol, where the primary reaction is the split of S–H bond of the methanethiol molecule that absorbed light.

When reactions 10 and 11 are much faster than reaction 5, acetaldehyde decomposes mostly by a chain mechanism consisting of reactions 10, 11 and 4. If, in addition, reaction 10 is faster than reaction 11, the concentration of methylthio radicals will be greater than that of methyl radicals and reaction 12. These assumptions lead to the following rate equation.

$$-d[CH_3CHO]/dt = k_{11}k_{12}^{-1/2}(k_1[CH_3CHO] + k_7[CH_3SH])1/2[CH_3CHO] \quad (II)$$

or

$$(-d[CH_3CHO]/dt)^2 = k_{11}^2k_{12}^{-1}(k_1[CH_3CHO]^3 + k_7[CH_3CHO]^2[CH_3SH]) \quad (III)$$

As seen in Fig. 2, except in a low pressure range of methanethiol, the square of the rate of decomposition increases linearly with the pressure of methanethiol in agreement with equation III. At lower pressures of methanethiol, the relative concentration of methylthio radicals to that of methyl radicals falls off and consequently the importance of the recombination of methyl radicals becomes greater. This explains the deviation from equation III at

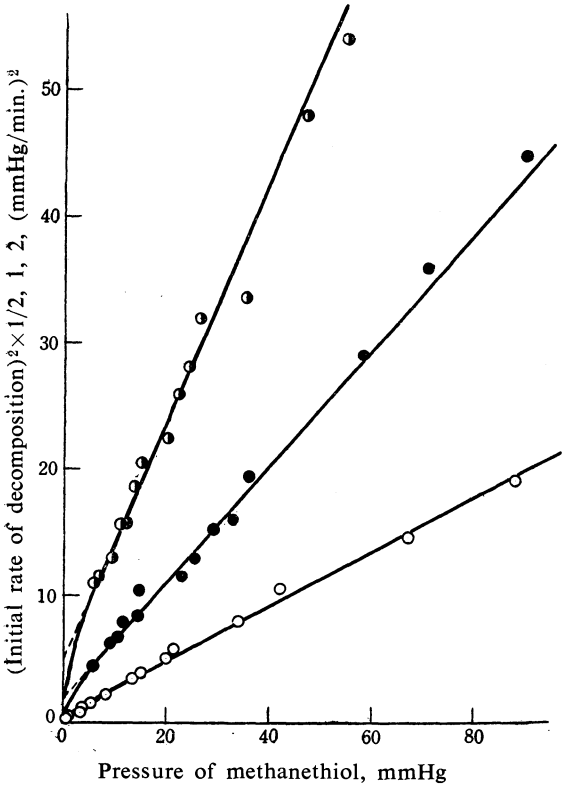



Fig. 2. Dependence of the rate of decomposition in the presence of methanethiol on its pressure. $CH_3CHO$ : 100 mmHg. ○, (Rate)²×2, 400°C; ●, (Rate)²×1, 420°C; ◑, (Rate)²×1/2, 440°C.

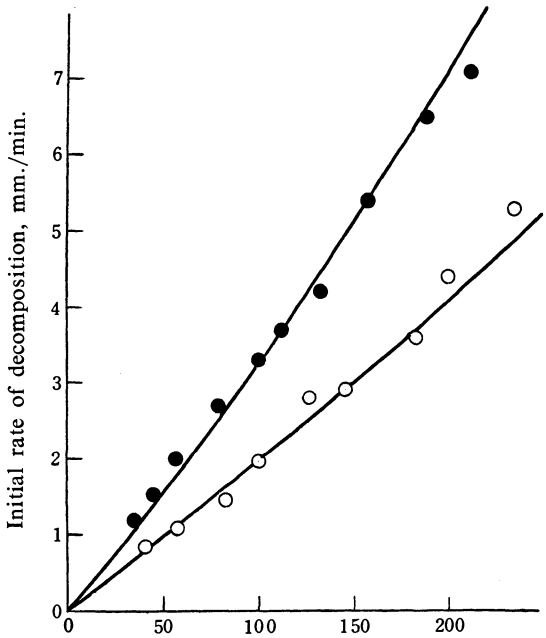



Fig. 3. Dependence of the rate of decomposition in the presence of methanethiol on acetaldehyde pressure. ○, $CH_3SH$: 33 mmHg, 400°C; ●, $CH_3SH$ : 19 mmHg, 420°C. Circles and full lines represent observed and calculated rates, respectively.

10) A. H. Sehon and B. Darwent, *J. Am. Chem. Soc.*, 76, 4806 (1954).
11) J. L. Franklin and H. E. Lumpkin, ibid., 74, 1023 (1952).
12) N. D. Skerrett and N. W. Thompson. *Trans. Faraday Soc.*, 37, 81 (1941).

low pressures of methanethiol. From the intercepts and slopes of the straight lines in Fig. 2 values of $k_1k_{11}^2k_{12}^{-1}$ and $k_7k_{11}^2k_{12}^{-1}$ are obtained, which are listed in Table II together with values of $k_1^{1/2}k_5k_6^{-1/2}$ already mentioned above.

Fig. 3 shows the plots of the rate of decomposition observed at a constant pressure of methanethiol against the pressure of acetaldehyde, together with the curves representing the rate calculated as a function of acetaldehyde pressure by equation II using the values of $k_1k_{11}^2k_{12}^{-1}$ and $k_7k_{11}^2k_{12}^{-1}$ given in Table II. The fact that the calculated curves are in satisfactory agreement with the experimental plots over a wide range of acetaldehyde pressure may be taken as an additional evidence for the validity of equation II.

The values given in Table II lead to the following Arrhenius expressions:

$$k_1^{1/2}k_5k_6^{-1/2}=10^{12.8}\exp(-43{,}500/\boldsymbol{RT})$$
$$(\mathrm{mol}^{-1/2}\ \mathrm{cc}^{1.2}\ \mathrm{sec}^{-1/2})$$
$$k_1k_{11}^2k_{12}^{-1}=10^{25.8}\exp(-81{,}300/\boldsymbol{RT})$$
$$(\mathrm{mol}^{-1}\ \mathrm{cc.}\ \mathrm{sec}^{-1})$$
$$k_7k_{11}^2k_{12}^{-1}=10^{23.7}\exp(-70{,}200/\boldsymbol{RT})$$
$$(\mathrm{mol}^{-1}\ \mathrm{cc.}\ \mathrm{sec}^{-1})$$

The expression for $k_1^{1/2}k_5k_6^{-1/2}$ agrees with those reported previously by various workers. Combining the expression for $k_1^{1/2}k_5k_6^{-1/2}$ with that for $k_1k_{11}^2k_{12}^{-1}$, we obtain

$$(k_5/k_{11})\,(k_{12}/k_6)^{1/2}=0.8\exp(-2{,}800/\boldsymbol{RT})$$

If we assume that $k_{12}$ has zero activation energy and a pre-exponential factor of the same value as that of $k_6$, the left-hand side of the equation becomes equal to $k_5/k_{11}$. The difference in activation energies $E_5-E_{11}=2.8$ kcal./mol. thus obtained compares with 1.6 kcal./mol. obtained by Birrel et al.[1] in the photolysis of mixtures of acetaldehyde and methanethiol. The value of the ratio $A_5/A_{11}=0.8$ also seems reasonable, as pre-exponential factors of these two reactions are expected to be of the same order of magnitude.

From the expressions for $k_1k_{11}^2k_{12}^{-1}$ and $k_7k_{11}^2k_{12}^{-1}$ given above, it follows that

$$k_1/k_7=130\exp(-11{,}100/\boldsymbol{RT})$$

The difference in activation energies $E_1-E_7=11$ kcal./mol., when combined with $E_1=75$ kcal./mol., yields a value of 64 kcal./mol. for $E_7$. Franklin and Lumpkin[11] estimated the dissociation energy of C-S bond in methanethiol to be 74.2 kcal./mol. by an electron impact method. Sehon and Darwent[10] obtained a lower dissociation energy of 67 kcal./mol. from the rates of decomposition of methanethiol in the presence of toluene as a carrier, assuming a pre-exponential factor of $3\times10^{13}$ $\mathrm{sec}^{-1}$. The value of 64 kcal./mol. obtained above in the present work is still lower than that of Sehon and Darwent. As can be seen in Fig. 2, the straight lines representing the square of the rate of decomposition as a function of acetaldehyde pressure cut the ordinate axis very close to the origin. Hence the values of the intercept and consequently the expression for $k_1/k_7$ given above must be accepted with some reserve. In fact, a value of the ratio $A_1/A_7$ amounting to $1.3\times10^2$ may be too large. If this ratio has really a smaller value, $E_7$ is greater than the value estimated above; if $A_1/A_7$ is put equal to unity, $E_7$ becomes as large as 70 kcal./mol.

As has been shown above, the results obtained in the present work comform to equation II based upon a mechanism in which the reaction chain terminates by the combination of methylthio radicals, while, in the photochemical[3] and thermal[3] decomposition of acetaldehyde in the presence of hydrogen sulfide, the experimental results indicate that the chain terminates by the combination of methyl radicals and not of hydrosulfide radicals. In these decomposition reactions, factors determining the chain-ending step may be the concentration ratio $[RS]/[CH_3]$, where R represents $CH_3$ or H, and the relative abilities of radicals to recombine. The former quantity in the steady state is given by $k_A[RSH]/k_B[CH_3CHO]$ where $k_A$ and $k_B$ are respectively the specific rates of the following reactions:

$$CH_3 + RSH = CH_4 + RS \qquad (A)$$
$$RS + CH_3CHO = RSH + CH_3CO \qquad (B)$$

Although our experimental results indicate that the activation energy of reaction A, $E_A$, is lower than $E_B$ for hydrogen sulfide, and that $k_A=10^{11.4}\exp(-2{,}600/\boldsymbol{RT})$ $\mathrm{mol}^{-1}$[6] cc. $\mathrm{sec}^{-1}$ for hydrogen sulfide and $E_B$ is around 4 kcal./mol. methanethiol, we are yet given no complete expressions for all the $k_A$'s and $k_B$'s at present and accordingly cannot compare the value of the ratio $[RS]/[CH_3]$ for methanethiol with that for hydrogen sulfide. If, however, these values were of comparable magnitudes in these experiments, the difference between the chain-ending steps in the experiments with methanethiol and with hydrogen sulfide would mean the lower ability of hydrosulfide radicals to recombine, compared to that of methylthio radicals.

It has been found in the present work that the rate of decomposition falls off during a run faster than can be expected from the rate equation. The higher are the pressure of methanethiol and the temperature, the greater is the extent of this reduction in the rate. Similar

phenomena have been observed in the photolysis of acetaldehyde in the presence of hydrogen sulfide[3]. The exact nature of these phenomena are not clear at present.

## Summary

Acetaldehyde has been decomposed thermally in the presence of methanethiol over the temperature range from 400° to 440°C. The presence of methanethiol markedly enhances the rate of decomposition. Analysis of the initial rates of decomposition obtained under various experimental conditions suggests: a) one of the chain-carrying steps $CH_3+CH_3CHO=CH_4+CH_3CO$ (5) in the decomposition of acetaldehyde alone is replaced by $CH_3+CH_3SH=CH_4+CH_3S$ (10) and $CH_3S+CH_3CHO=CH_3SH+CH_3CO$ (11) in the presence of methanethiol; b) the reaction $CH_3SH=CH_3+SH$ (7), in addition to $CH_3CHO=CH_3+CHO$ (1), contributes to the chain initiation; c) the chain terminates by the combination of methylthio radicals in contrast to the decomposition in the presence of hydrogen sulfide where the chain-ending step is the combination of methyl radicals under similar experimental conditions; d) $k_5/k_{11}=0.8\exp(-2{,}800/\boldsymbol{RT})$ and $k_1/k_7=130\exp(-11{,}000/\boldsymbol{RT})$, the latter expression being less certain.

The present study was partly supported by the finantial aid of the Ministry of Education, to which the authors' thanks are due.

*Department of Applied Chemistry*
*College of Engineering*
*University of Osaka Prefecture*
*Sakai, Osaka*

# *The Formation Constants of Metal Acetate Complexes. III. Polarographic Determination of the Formation Constants of Acetatocadmium(II) and Acetatocobalt(II) Complexes*

By Nobuyuki TANAKA, MINORU KAMADA, Hisao OSAWA and Gen SATÔ

(Received May 18, 1960)

In the previous papers[1,2], the formation constants of acetato complexes of nickel(II), copper(II), lead(II) and zinc(II) were reported. They were determined by the newly devised methods, which are based on the polarographic measurement of the sum of the equilibrium concentrations of hydrated metal ions and metal acetate complexes. In the case of acetatocopper(II), acetatolead(II) and acetatozinc(II) complexes, the substitution reaction of the type,

$$M^{m+} + M'Y^{(m'-4)+} \rightleftarrows MY^{(m-4)+} + M'^{m'+} \quad (1)$$

where $Y^{4-}$ means a completely dissociated ethylenediaminetetraacetate(EDTA) anion, was used for the determination of the formation constants. This was based on the fact that, in acetate buffers, the substitution reaction (Eq. 1) was considered to be

$$\left\{\begin{matrix} M^{m+} \\ \uparrow\downarrow \\ M(OAc)_n^{(m-n)+} \end{matrix}\right\} + \left\{\begin{matrix} M'Y^{(m'-4)+} \\ \uparrow\downarrow \\ M'HY^{(m'-3)+} \end{matrix}\right\} \rightleftarrows \left\{\begin{matrix} MY^{(m-4)+} \\ \uparrow\downarrow \\ MHY^{(m-3)+} \end{matrix}\right\} + \left\{\begin{matrix} M'^{m'+} \\ \uparrow\downarrow \\ M'(OAc)_{n'}^{(m'-n')+} \end{matrix}\right\} \quad (2)$$

In this paper are presented the formation constants of acetatocadmium(II) and acetatocobalt(II) complexes which have been determined by the same procedure as used for the acetato complexes of copper(II), lead(II) and zinc(II).

## Experimental

**Reagent.**—Standard solutions of copper(II) nitrate and cadmium(II) nitrate were prepared by dissolving known amounts of pure copper and pure cadmium metals (Merck Co. Ltd.), respectively, in reagent-grade nitric acid. In the case of cadmium metal, the oxide layer on the metal surface was removed with hydrochloric acid. This cadmium metal was found by the a. c. polarographic method to contain 0.08% of lead as impurity. The careful examination, however, showed that this minute quantity of lead would give no appreciable effect on the equilibrium determination, and therefore no further purification was carried out. The solution of disodium ethylenediaminetetraacetate (EDTA) was standardized against the standard solution of copper(II) nitrate by amperometric titration with the dropping mercury electrode[3]. A standard solution of cobalt(II) nitrate was prepared by dissolving an appropriate

1) N. Tanaka and K. Kato, This Bulletin, **32**, 516 (1959).
2) N. Tanaka and K. Kato, ibid., **33**, 417 (1960).
3) N. Tanaka, M. Kodama, M. Sasaki and M. Sugino, *Japan Analyst (Bunseki Kagaku)*, **6**, 86 (1957).

amount of cobalt metal in reagent-grade nitric acid. Its concentration was determined with the standardized EDTA solution volumetrically using murexide as an indicator[4] and also amperometrically using the dropping mercury electrode as an indicator electrode[3]. The polarographic analysis showed that the cobalt metal contained 0.2% of nickel as impurity. Therefore, the equilibrium study of the reaction involving cobalt(II) ions or cobalt(II)-EDTA complexes was carried out, taking into consideration the substitution reaction involving nickel(II)-EDTA complexes (see below).

Sodium acetate-acetic acid buffers were prepared by mixing the solutions of sodium carbonate and acetic acid. Sodium carbonate, acetic acid and other reagents used for the supporting electrolyte were of guaranteed reagent grade and used without further purification.

**Apparatus and procedure.** — A Shimadzu RP-2 pen-recording polarograph and a manual apparatus similar to that of Kolthoff and Lingane[5] were used for the measurement of current-voltage curves. Two dropping mercury electrodes were used. One had an $m$ value of 2.57 mg./sec. and a drop time $\tau$ of 3.52 sec. in an air-free acetate buffer of pH 4.7 containing 0.1 M acetate, 0.1 M potassium nitrate and 0.01% gelatin at 25°C with open circuit. The other had an $m$ value of 2.93 mg./sec. and a drop time $\tau$ of 3.16 sec. in an air-free 0.1 M potassium nitrate solution at 25°C with open circuit. A saturated calomel electrode with a large area was used as the anode, which was connected to the electrolytic solution by a Hume and Harris-type agar bridge[6]. A Hitachi Model EHP-1 pH meter was used for the pH measurement. Dissolved oxygen in the solution was removed by bubbling pure tank nitrogen through the solution.

The measurements of the diffusion current of copper(II) in acetate buffer solutions were carried out with the following two reaction mixtures:

(a) copper(II)—cadmium(II)—EDTA

(b) copper(II)—cobalt(II)—EDTA.

The measurements were made at 15, 25 and 35°C in acetate buffers of pH 4.75 (for cadmium(II)) and pH 4.70 (for cobalt(II)) of which the acetate concentrations were varied from 0.02 M to 0.10 M (for cobalt(II)) or to 0.15 M (for cadmium(II)). The ionic strength was adjusted to be 0.2 with potassium nitrate. Gelatin was added as a maximum suppressor by 0.01% in concentration.

In the preliminary experiments, it was found that the substitution reactions between copper(II) ions and cadmium(II)-EDTA complexes and those between copper(II) ions and cobalt(II)-EDTA complexes proceeded at considerable reaction rates. The reaction mixtures of the copper(II)-cadmium-(II)-EDTA system were kept standing at the given temperature for ten to twenty hours after the preparation and were subjected to the measurement, though they were found to reach nearly the equilibrium within 60 minutes. In the case of the copper(II)-cobalt(II)-EDTA system, the diffusion currents of the copper(II) in the reaction mixtures were measured 45 min. after the preparation at 15°C, 30 min. at 25°C and 25 min. at 35°C. This was decided from the consideration of the effect of the reaction between copper(II) and nickel(II)-EDTA complexes on the equilibrium under consideration, because the cobalt(II) solution used in this experiment contained a small amount of nickel as impurity. It was found in the preliminary experiments that the reaction between copper(II) and nickel(II)-EDTA complexes affect more or less the equilibrium concentration of copper(II) in the substitution reaction between copper(II) and cobalt-(II)-EDTA complexes after the above-mentioned period, though the former reaction proceeds at much slower rate than the latter[7].

## Results

The apparent diffusion current constants[2] of copper(II) were determined by measuring the diffusion current at various acetate concentrations. The values of $[Cu^{2+}]_{app}$ which is given by[2]

$$[Cu^{2+}]_{app} = [Cu^{2+}] + \sum_{1}^{n} [Cu(OAc)_n^{(2-n)+}] \tag{3}$$

were determined with the aid of those apparent diffusion current constants from the diffusion currents obtained with the reaction mixtures of systems a and b. Then, the apparent equilibrium constants ($K^{M}_{M',app}$) for Eq. 2, expressed as[2]

$$K^{M}_{M',\,app} = \frac{[M'^{m'+}]_{app}\{[MY^{(m-4)+}] + [MHY^{(m-3)+}]\}}{[M^{m+}]_{app}\{[M'Y^{(m'-4)+}] + [M'HY^{(m'-3)+}]\}} \tag{4}$$

were culculated. The $F_n$ functions expressed as[2]

$$F_0 \equiv K^{M}_{M',\,app}\left\{1 + \sum_{1}^{n} K_{M(OAc)}[OAc^-]^n\right\} = K^{M}_{M'}\frac{\beta}{\beta'}\left\{1 + \sum_{1}^{n'} K_{M'(OAc)_{n'}}[OAc^-]^{n'}\right\} \tag{5}$$

$$F_1 = \frac{F_0 - \frac{\beta}{\beta'}K^{M}_{M'}}{\frac{\beta}{\beta'}K^{M}_{M'}[OAc^-]} = K_{M'OAc} + K_{M'(OAc)_2}[OAc^-] + \cdots\cdots \tag{6}$$

$$F_2 \equiv \frac{F_1 - K_{M'OAc}}{[OAc^-]} = K_{M'(OAc)_2} + K_{M'(OAc)_3}[OAc^-] + \cdots\cdots \tag{7}$$

.....

4) G. Schwarzenbach, "Complexometric Titrations" translated by H. Irving, Methuen & Co. Ltd., London (1957), p. 78.

5) I. M. Kolthoff and J. J. Lingane, "Polarography," Vol. I, Interscience Publishers, New York (1952), p. 297.

6) D. N. Hume and W. E. Harris, *Ind. Eng. Chem., Anal. Ed.*, **15**, 465 (1943).

7) unpublished work.

$$F_{n'} \equiv \frac{F_{n'-1} - K_{M'(OAc)_{n'-1}}}{[OAc^-]} = K_{M'(OAc)n'} \qquad (8)$$

were successively obtained, where $K^{M}_{M'}$ means the true equilibrium constant given by

$$K^{M}_{M'} = \frac{[M'^{m'+}]\,[MY^{(m-4)+}]}{[M^{m+}]\,[M'Y^{(m'-4)+}]} \qquad (9)$$

and $\beta$ and $\beta'$ are

$$\beta = 1 + K^{H}_{MHY}[H^+]$$

$$\beta' = 1 + K^{H}_{M'HY}[H^+]$$

The results obtained for systems a and b are given below. The values of $\beta/\beta'$ were calculated to be approximately unity for both a and b systems at the pH's in the present experiments, using the equilibrium constants $K^{H}_{MHY}$ and $K^{H}_{M'HY}$ given by Schwarzenbach, Gut and Anderegg[8].

**(a) Copper(II)-Cadmium(II)-EDTA System.** —The formation constants of acetatocadmium (II) complexes were determined by the measurement of $K^{Cu}_{Cd,app}$ at various acetate concentrations with the aid of the formation constants of $CuOAc^+$ and $Cu(OAc)_2$ obtained in the previous paper[2], where, under the experimental condition, $K^{Cu}_{Cd,app}$ is given by the equation

$$K^{Cu}_{Cd,app} = \frac{[Cd^{2+}]_{app}\{[CuY^{2-}] + [CuHY^-]\}}{[Cu^{2+}]_{app}\{[CdY^{2-}] + [CdHY^-]\}}$$

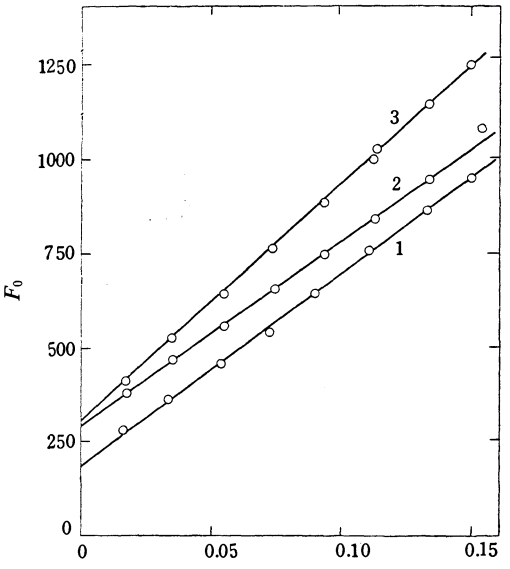



Fig. 1. $F_0$ (Eq. 5) as a function of the acetate ion concentration in copper(II)-cadmium(II)-EDTA system: 1, at 15°C; 2, at 25°C; 3, at 35°C.

8) G. Schwarzenbach, R. Gut and G. Anderegg, *Helv. Chim. Acta*, **37**, 937 (1954).

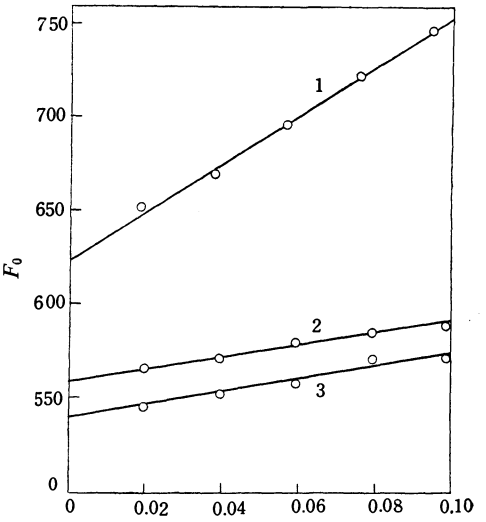



Fig. 2. $F_0$ (Eq. 5) as a function of the acetate ion concentration in copper(II)-cobalt(II)-EDTA system: 1, at 15°C; 2, at 25°C; 3, at 35°C.

The values of $F_0$ given by Eq. 5 were calculated and plotted against the acetate ion concentration. These plots for 15, 25 and 35°C are shown in Fig. 1, in which all $F_0$ plots give straight lines indicating that at acetate concentrations up to 0.15 M $CdOAc^+$ is only species of acetatocadmium(II) complex which exists in the solution at an appreciable concentration. The formation constants of $CdOAc^+$ are listed in Table I.

**(b) Copper(II)-Cobalt(II)-EDTA System.** —The formation constants of acetatocobalt(II) complexes were determined with the same procedure as for the acetatocadmium(II) complexes. $K^{Cu}_{Co,app}$ which is given by the equation

$$K^{Cu}_{Co,apq} = \frac{[Co^{2+}]_{app}\{[CuY^{2-}] + [CuHY^-]\}}{[Cu^{2+}]_{app}\{[CoY^{2-}] + [CoHY^-]\}}$$

was determined at various acetate concentrations. In this case also, the $F_0$ plots gave straight lines as shown in Fig. 2. From these plots the formation constants of $CoOAc^+$ were determined, which are given in Table I.

TABLE I. FORMATION CONSTANTS OF ACETATOCADMIUM(II) AND ACETATOCOBALT(II) COMPLEXES AT VARIOUS TEMPERATURES

| Metal ions | Temp., °C | $K_{MOAc}$ ($\mu$=0.2) |
|---|---|---|
| Cadmium(II) | 15 | 27 |
| | 25 | 16 |
| | 35 | 20 |
| Cobalt(II) | 15 | 2.1 |
| | 25 | 0.6 |
| | 35 | 0.6 |

TABLE II. SOME EXAMPLES OF THE REPORTED VALUES OF FORMATION CONSTANTS OF ACETATOCADMIUM(II) AND ACETATOCOBALT(II) COMPLEXES

| Metal ion | Investigator | Method | Temp., °C | Ionic strength | $K_{MOAc}$ | $K_{M(OAc)_2}$ | Ref. |
|---|---|---|---|---|---|---|---|
| Cadmium(II) | I. Leden et al. | Potentiometric | 25 | 3 | 20 | 190 | 9,10 |
| | A. Jacques | 〃 | 25 | ≃0.5 | 100 | ~150 | 11 |
| | E. Ferrell et al. | 〃 | 20 | ≦0.55 | 50 | — | 9,12 |
| Cobalt(II) | S. Bardhan et al. | Potentiometric | 35 | 0 | 23 | — | 13 |
| | | | | 0.2 | 7.6* | | (13) |
| | S. K. Siddhanta et al. | 〃 | 30~35 | 0 | 33 | 127 | 14 |
| | | | | 0.2 | 11* | 22* | (14) |

* Those values are the formation constants which were calculated by the present authors with the values reported in the literature referred to. In the calculation, the activity coefficients of cadmium(II), cobalt(II) and acetate ions were estimated to be 0.30, 0.33 and 0.73, respectively, and the activity coefficient of monoacetato complexes was assumed to be equal to that of acetate ions[2,15].

## Discussion

The formatiom constants of the acetato complexes of cadmium(II) and cobalt(II) have been reported by several researchers. In Table II some of them are given, which are compared with the formation constants listed in Table I.

Recently, Yasuda and Yamasaki[16] determined the formation constants of acetato complexes of some bivalent metal ions and found that the stabilities of those complexes decreased in the order of Pb > Cu > Cd > Zn > Ni. The formation constants of $K_{MOAc}$ obtained in the previous[1,2] and present investigations agree with the above order.

The equilibria of the substitution reaction represented by Eq. 1 have been studied with the same procedure as that reported previously[2]. The equilibrium constants, $K_{Cd}^{Cu}$ and $K_{Co}^{Cu}$, are given in Table III. Schwarzenbach and his co-workers[8] studied the substitution reaction of copper(II) ions and cadmium(II)-EDTA complexes at 20°C in the solution of ionic strength 0.1 with $8\times10^{-3}$ M sodium acetate. The equilibrium constant which was reported by those researchers was corrected for the acetato complex formation using the formation constants $K_{CuOAc}$, $K_{Cu(OAc)_2}$ and $K_{CdOAc}$. The resulting constant is also given in Table III. On the other hand, no investigation had been reported on the substitution reaction between copper(II) ions and cobalt(II)-EDTA complexes. Therefore, the equilibrium constant of the reaction was calculated with the formation constants of copper(II)-EDTA and cobalt(II)-EDTA complexes[8]. This is also shown in Table III. It is seen that the $K_{M'}^{M}$ values obtained in this study are in satisfactory agreement with those calculated from the equilibrium or the formation constants reported by Schwarzenbach et al.

TABLE III. EQUILIBRIUM CONSTANTS FOR THE SUBSTITUTION REACTION (EQ. 1) AT IONIC STRENGTH 0.2 COMPARED WITH SCHWARZENBACH'S VALUES

| Temp., °C | $K_{Cd}^{Cu}\times10^{-2}$ | | $K_{Co}^{Cu}\times10^{-2}$ | |
|---|---|---|---|---|
| | I | II | I | III |
| 15 | 1.9 | — | 6.2 | — |
| 20 | — | 2.6±0.5 | — | 4.4±2.0 |
| 25 | 3.0 | — | 5.6 | — |
| 35 | 3.1 | — | 5.4 | — |

I. Values obtained in the present investigation.
II. Values calcuated from the Schwarzenbach's $K_{Cd,app}^{Cu}$[8].
III. Values calculated from the formation constants[8].

## Summary

The formation constants of acetatocadmium-(II) and acetatocobalt(II) complexes were determined at ionic strength of 0.2 at 15, 25 and 35°C with the procedure that is based on the polarographic measurement of the sum of the equilibrium concentrations of the hydrated metal ions and the metal acetate complexes in the substitution reaction involving EDTA complexes. The resulting formation constants $K_{CdOAc}$ and $K_{CoOAc}$ are 27 and 2.1 at 15°C, 16 and 0.6 at 25°C and 20 and 0.6 at 35°C, respectively.

9) J. Bjerrum, G. Schwarzenbach and L. G. Sillén, "Stability Constants of Metal Ion Complexes, Part I, Organic Ligands," the Chemical Society, London (1957), Special Publ. No. 6, p. 3.
10) I. Leden, *Svensk Kem. Tidskr.*, **58**, 129 (1946); Doctoral Diss., Lund, **1943**, 89.
11) A. Jacques, *Trans, Faraday Soc.*, **5**, 225 (1910).
12) E. Ferrell, J. M. Ridgion and H. L. Riley, *J. Chem. Soc.*, **1934**, 1440.
13) S. Bardhan and S. Aditya, *J. Indian. Chem. Soc.*, **32**, 109 (1955).
14) S. K. Siddhanta and S. N. Banerjee, *Ibid.*, **35**, 343 (1958).
15) J. Kielland, *J. Am. Chem. Soc.*, **59**, 1675 (1937).
16) M. Yasuda and K. Yamasaki, presented at the Symposium on Metal Complexes, Fukuoka, October, 1959.

The authors thank the Ministry of Education for the financial support granted for this research.

*Department of Chemistry*
*Faculty of Science*
*Tohoku University*
*Katahira-cho, Sendai*

# *Infrared Spectrum of Some Deuterated Crystalline Polystyrenes. I. Isotactic Poly-$\alpha d_1$-styrene*

By Masamichi KOBAYASHI

(Received April 14, 1960)

During these a few years many studies have been made on the molecular structure of the stereospecific vinyl polymer, and it has been found that most of isotactic polymers have the helical structure in their crystalline regions mainly because of steric hindrances of side groups.

To makë clear the helical structure of the polymer molecule, infrared spectroscopy is one of the most powerful methods as well as X-ray analysis.

Recently, Tadokoro et al[1]. reported the studies on the infrared spectra of isotactic polystyrene and its $\alpha, \beta, \beta$-tri-deuterated derivative and detected that in the spectrum of the polystyrene the absorption bands appearing in region of 1400~1180 $cm^{-1}$, such as the bands at 1364, 1314, 1297 and 1185 $cm^{-1}$, are characteristic of the three-fold helical structure of the polystyrene molecule and assumed to be associated with the vibrations of $CH_2$, CH and the carbon skeletal chain.

To make the assignments of these bands more clearly it is desirable to study the spectra of several other deuterated derivatives. For this purpose, isotactic poly-$\alpha d_1$-styrene was prepared and its infrared spectrum was studied.

## Experimental

**1. Preparation of $\alpha d_1$-Styrene.**—$\alpha d_1$-Styrene was prepared by hydrolysis with deuterium oxide of the Grignard reagent of $\alpha$-bromostyrene. From the massspectroscopic data, it was proved that the monomer prepared contained 99.5% of $d_1$-styrene. The infrared spectrum of this monomer is shown in Fig. 1 (solid line) in comparison with that of styrene (dotted line). It is justifiable to regard the sample as $\alpha d_1$-styrene from a few spectroscopic evidences ; the appearance of the band at 2230 $cm^{-1}$ corresponding to the stretching vibration of CD group, the shift of the band corresponding to the C=C stretching from 1628 to 1614 $cm^{-1}$ on deuteration and appearances of the bands corresponding to the bending vibration (at near 1400 $cm^{-1}$) and the rocking vibration (at near 1160 $cm^{-1}$) of $CH_2$ group in the spectra of both monomers.

To determine more precisely the position of the

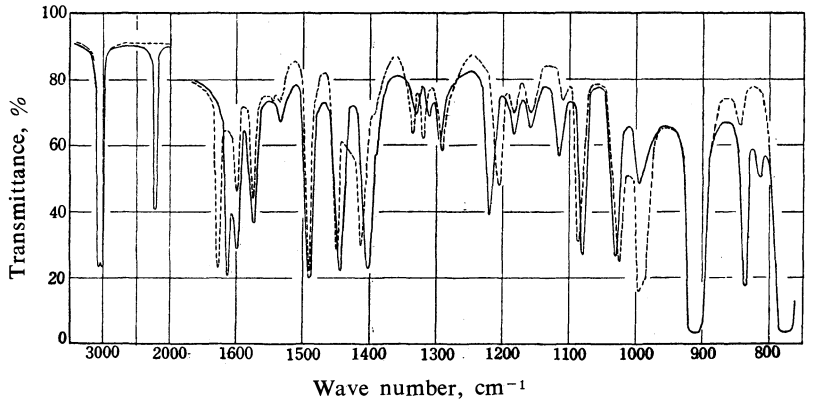



Fig. 1. Infrared spectra of $\alpha d_1$-styrene (——) and styrene (——).

1) H. Tadokoro, N. Nishiyama, S. Nozakura and S. Murahashi, *J. Polymer Sci.*, **36**, 553 (1959).

deuterium atom in this monomer, the proton magnetic resonance spectrum of this monomer was compared with that of styrene. The spectra were measured using a Nihon Denshi Kogaku N. M. R. spectrometer.

Proton signals of the spectrum of styrene, from lower to higher field, are assigned[2] to $H_1$, $H_2$, $H_4$ and $H_3$ respectively as shown in Fig. 2. While the signals due to $H_3$ and $H_4$ of styrene both split into quartets by spin coupling with $H_2$ and with each other, the spectrum of the ethylenic protons of the deuterated styrene is doublet with some closely spaced fine structure. If a small coupling constant between $H_3$ and $H_4$ is taken into account, this deuterated styrene can be identified as $\alpha d_1$-styrene.

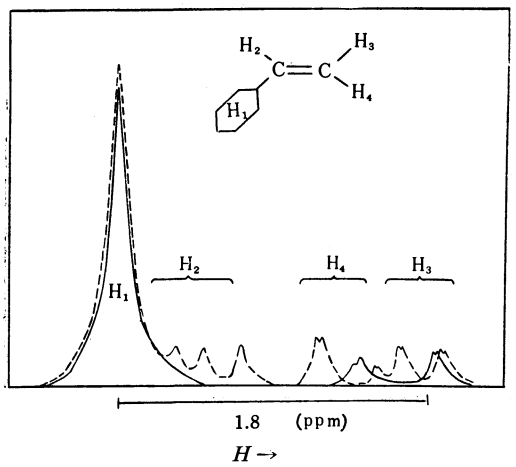



Fig. 2. Proton magnetic resonance spectra of $\alpha d_1$-styrene (——) and styrene (----) at 40 Mc/sec.

**2. Polymerization and Preparation of the Samples for I. R. Measurements.**—The monomer was polymerized with Ziegler catalyst ($AlEt_3+TiCl_4$) in *n*-heptane and the polymer prepared was purified by the usual method. The films cast from the toluene solution were oriented by drawing them to about five times their original lengths in boiling water and were crystallized by heating at 60°C for 10 minutes in glycerol.

The I. R. spectra were measured in the region of 3500~400 $cm^{-1}$ using a Hilger H800 I. R. spectrometer and the polarized spectra were measured in the region of 3500~650 $cm^{-1}$ using a selenium polarizer.

## Experimental Results

In Fig. 3a and 3b are shown the polarized spectra of isotactic poly-$\alpha d_1$-styrene in the region of 3500~2000 $cm^{-1}$ and 1600~650 $cm^{-1}$ respectively. The wave numbers, the dichroisms and the relative intensities of the absorption bands are given in Table I in comparison with those of isotactic polystyrene.

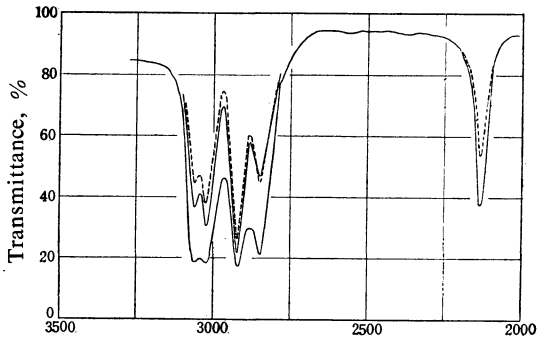



Fig. 3a. Infrared dichroisms of isotactic poly-$\alpha d_1$-styrene.
—— electric vector perpendicular to elongation
---- electric vector parallel to elongation

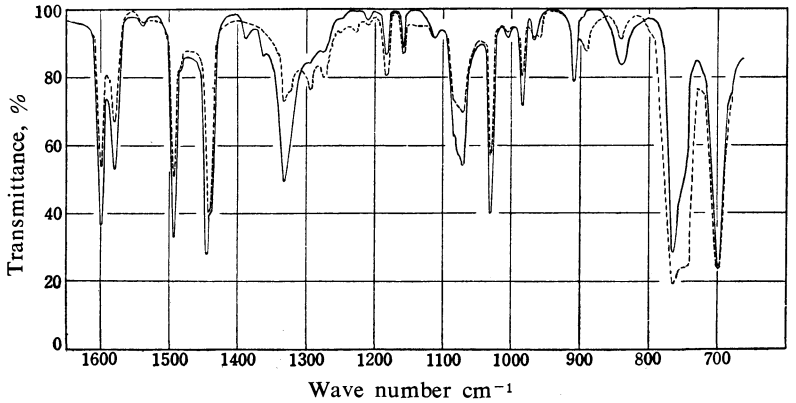



Fig. 3b. Infrared dichroisms isotactic poly-$\alpha d_1$-styrene.
—— electric vector perpendicular to elongation
---- electric vector parallel to elongation

2) J. A. Pople, W. G. Schneider and H. J. Bernstein, "High-resolution Nuclear Magnetic Resonance", McGraw-Hill Book Company, Inc., New York (1959), p. 238.

TABLE I. INFRARED SPECTRA OF ISOTACTIC POLYSTYRENE AND ISOTACTIC POLY-$\alpha d_1$-STYRENE AND VIBRATIONAL ASSIGNMENTS

| Polystyrene | | | Poly-$\alpha$ $d_1$-styrene | | | Assignments |
|---|---|---|---|---|---|---|
| Freq. ($cm^{-1}$) | Dichr. | R. I. | Freq. ($cm^{-1}$) | Dichr. | R. I. | |
| 3082 | $\sigma$ | mw | 3082 | $\sigma$ | mw | |
| 3060 | $\sigma$ | s | 3060 | $\sigma$ | s | $\nu$(CH) phenyl |
| 3025 | $\sigma$ | s | 3025 | $\sigma$ | s | |
| 2923 | $\sigma$ | vs | 2923 | $\sigma$ | vs | $\nu(CH_2)$ asym |
| 2849 | — | s | 2849 | — | s | $\nu(CH_2)$ sym. |
| | | | 2134 | $\sigma$ | m | $\nu$(CD) |
| 1602 | $\sigma$ | s | 1600 | $\sigma$ | s | k* mode $A_1$ |
| 1580 | $\sigma$ | ms | 1580 | $\sigma$ | ms | l* mode $B_1$ |
| 1493 | $\sigma$ | s | 1495 | $\sigma$ | s | m* mode $A_1$ |
| 1452 | $\sigma$ | vs | 1447 | $\sigma$ | vs | n* mode $B_1$ |
| 1444 | — | ssh | 1440 | — | ssh | $\delta(CH_2)$ A+E |
| 1389 | $\sigma$ | vw | 1388 | $\sigma$ | vw | |
| 1364 | $\sigma$ | ms | | | | $\delta$(CH)E |
| | | | 1334 | $\sigma$ | ms | $\delta$(CD)E ? |
| 1314 | $\sigma$ | m | | | | |
| 1297 | $\pi$ | mw | 1295 | $\pi$ | mw | w$(CH_2)$A |
| | | | 1275 | $\pi$ | w | $\delta$(CD) |
| 1261** | $\sigma$ | w | | | | |
| | | | 1227 | $\pi$ | vw | |
| | | | 1210 | $\sigma$ | vw | |
| 1195 | $\pi$ | mw | | | | w(CH)A |
| 1185 | $\pi$ | mw | 1183 | $\pi$ | mw | $\nu$(CC)A |
| 1180 | ? | mw | (1180)** | | | $\delta$(CH) phenyl |
| 1154 | — | mw | 1158 | — | mw | c* mode $B_1$ |
| 1110 | $\sigma$ | w | 1115 | $\sigma$ | w | |
| 1080 | $\sigma$ | m | 1084 | $\sigma$ | m | CH (or CD), $CH_2$+ |
| | | | 1072 | $\sigma$ | msh | phenyl |
| 1048 | $\sigma$ | m | | | | |
| 1028 | $\sigma$ | ms | 1031 | $\sigma$ | ms | b* mode $A_1$ |
| 1005 | $\sigma$ | w | 1005 | $\sigma$ | w | p* mode $A_1$ |
| 985 | $\sigma$ | m | 985 | $\sigma$ | m | cryst. sensitive |
| 964 | — | w | 968 | — | w | h* mode $A_2$ |
| | | | 960 | $\pi$ | w | w(CD)A |
| 920 | $\sigma$ | m | | | | |
| 906 | $\pi$ | m | 910 | — | m | i* mode $B_2$ |
| 898 | $\pi$ | mw | 891 | $\pi$ | mw | |
| 842 | $\sigma$ | mw | 842 | $\sigma$ | w | g* mode $A_2$ |
| 783 | $\pi$ | ssh | | | | |
| 755 | $\pi$ | vs | 765 | $\pi$ | vs | f* mode $B_2$ |
| | | | 748 | $\pi$ | ssh | |
| | | | 705 | $\pi$ | vs | |
| 700 | $\pi$ | vs | 700 | $\pi$ | vs | |
| 615 | | w | 615 | | w | s* mode $B_1$ |
| 579 | | mw | 570 | | mwsh | skeletal |
| 557 | | s | 557 | | s | v* mode+skeletal |
| 489 | | vw | 489 | | vw | skeletal |

* Assignments of the normal mode of monosubstituted benzene according to Whiffen's notation.
** This band is assumed to overlap the band at 1183 $cm^{-1}$.

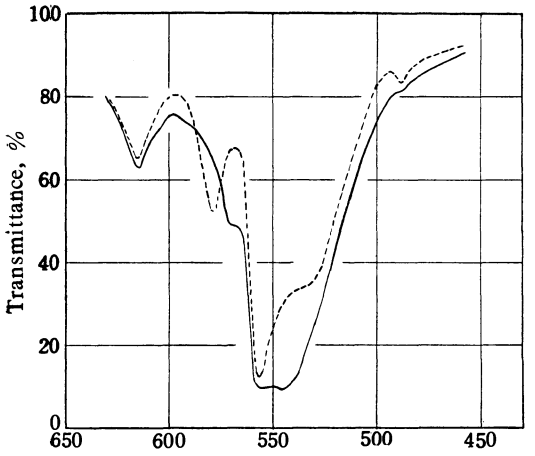



Fig. 3c. Infrared spectra of isotactic poly-$\alpha d_1$-styrene (——) and isotactic polystyrene (----).

## Discussions

**1. General Discussions.**—In the crystalline region, the molecule of isotactic polymer consists of a sequence of repeating units with a regular spatial arrangement. Strictly speaking, therefore, the molecular vibrations of the whole polymer molecule should be considered for the analysis of the absorption bands. Nevertheless, the normal modes of the phenyl group and the skeletal chain may be analyzed separately for the sake of simplicity. Comparing the spectrum of the isotactic polystyrene with that of the atactic one, most of the absorption bands associated with the phenyl group differ from each other by a small amount and, hence, this approximation seems reasonable for our case.

Since the molecular vibrations of the phenyl groups of polystyrene and its deuterated derivatives in which the deuterium is substituted in the skeletal chain may be regarded as those of monosubstituted benzene having a point symmetry $C_{2v}$[3], the assignments of some bands of these polymers immediately can be made from the well-known results on the molecular vibrations of monosubstituted benzene. In our case, the assignments are made according to Whiffen's notaion[4]. The results are given in the last column of Table I. These bands are common to polystrene and the deutero-derivatives in wave number and dichroism. The bands assignable to the modes belonging to $A_1$ species, e. g., 1600, 1495, 1031 $cm^{-1}$ bands, and $B_1$ species, e. g., 1580, 1462 $cm^{-1}$ bands have $\sigma$ nature, and, on the other hand, $B_2$ species, e. g., 765 $cm^{-1}$ band, have $\pi$ nature. These polarization properties may be interpreted by the molecular structure determined by Natta and Corradini[5].

The $\sigma$ band which is crystallization-sensitive appears at the same wave number, 985 $cm^{-1}$, as those of polystyrene and poly-$\alpha, \beta, \beta$ $d_3$-styrene. This may be due to interactions between the phenyl groups of the neighboring molecules in the crystalline lattice.

In Fig. 3c are shown the spectra of isotactic poly-$\alpha d_1$-styrene (solid line) and isotactic polystyrene (dotted line) in the region of 650~450 $cm^{-1}$. The band at 557 $cm^{-1}$ which has been detected[6] as characteristic of the isotactic configuration of the polystyrene molecule also appears in isotactic poly-$\alpha d_1$-styrene. This band might be assigned to the v-mode coupling with the skeletal vibration.

The molecular vibrations of the skeletal chain (consisting of CH (or CD) and $CH_2$ groups) of isotactic polystyrene or isotactic poly-$\alpha d_1$-styrene may be considered as those of a one-dimensional three-fold helical chain having a point symmetry C $(2\pi/3)$[7]. From the factor group analysis it is concluded that the normal vibrations of this chain are divided into two symmetry species; A (non-degenerate) and E (doubly degenerate), and the fundamentals of the former should have $\pi$ nature and those of the latter $\sigma$ nature. In physical meanings, the symmetry species correspond to the phase differences between the vibrations of the neighboring monomer units. Therefore, the normal modes of the helix can be considered as ones composed of the basic modes of the monomer units.

As for the stretching vibrations of $CH_2$ and CH (or CD) groups and the $CH_2$ bending vibration, the normal modes under the symmetry species A have almost the same frequencies as those under E species. The observed absorption band due to each of such modes, therefore, may be considered as that consisting of two overlapping bands, one being assigned to the mode under A and another to that under E.

The polarization properties of these bands depend on the chain conformation of the polymer molecule. In the spectrum of poly-$\alpha d_1$-styrene, the band at 2923 $cm^{-1}$ (antisymmetric $CH_2$ stretching) has $\sigma$ nature and the band at 2849 $cm^{-1}$ (symmetric $CH_2$ stretching)

3) C. Y. Liang and S. Krimm, *J. Polymer Sci.*, **27**, 241 (1958).
4) D. C. Whiffen, *J. Chem. Soc.* **1956**, 1350.
5) G. Natta and P. Corradini, *Makromol. Chem.*, **16**, 77 (1955).
6) M. Kobayashi, presented at the 12th Annual Meeting of the Chemical Society of Japan, Kyoto, April, 1959.
7) C. Y. Liang and S. Krim, *J. Chem. Phys.*, **25**, 563 (1956).

shows almost no dichroism. These results coincide whih Tadokoro et al.'s results on isotactic polystyrene and its several derivatives[8]. The band at 2134 $cm^{-1}$ (CD stretching) has $\sigma$ nature, and the band at 1440 $cm^{-1}$ ($CH_2$ bending) shows almost no dichroism. Dichroic ratio is expressed for a uniaxial orientation as

$$(A_{\parallel}/A_{\perp}) = 2 \cot^2 \psi$$

where $\psi$ is the angle between the transition moment accompanied with the vibration and the fiber axis.

The dichroic ratios calculated on the basis of the predicted molecular conformation are as follows; zero for $\nu_{asym}(CH_2)$, 0.78 for $\nu_{sym}(CH_2)$ and $\delta(CH_2)$, and 0.27 for $\nu$(CD). The results well fit the polarization properties of these bands.

As for the deformation vibrations of $CH_2$ and CH (or CD) groups except $\delta(CH_2)$, the frequencies of the normal modes under A species, in general, differ from those under E. Since the relative intensity of each fundamental of these modes depends on the chain conformation of the polymer molecule, the assignments of some bands, therefore, may be made from the polarization properties and the relative intensities of the bands. Further, the changes in spectrum on deuteration give us some additional information for this purpose. On the basis of the molecular structure of isotactic polystyrene, it seems reasonable that relatively large intensities are expected for the banbs assignable to the deformation of CH (or CD) under E, $\delta$(CH)E ($\delta$(CD)E), the wagging of CH (or CD) under A, w(CH)A (w(CD)A), the rocking of $CH_2$ under E, r($CH_2$)E, the wagging of $CH_2$ under A, w($CH_2$)A, and the stretching of the skeletal carbon atoms under A, $\nu$(CC)A.

**2. Bands in the Region of 1400~1180 $cm^{-1}$.** —In this region appear the bands which have been considered by Tadokoro et al. as characteristic to the helical structure of polystrene.

The $\sigma$ band at 1364 $cm^{-1}$ of isotactic polystyrene disappears on deuteration, and the corresponding $\sigma$ band of similar intensity appears at 1334 $cm^{-1}$ in poly-$\alpha d_1$-styrene. This fact may support the assumption that the band at 1364 $cm^{-1}$ is mainly due to $\delta$(CH)E. Whether the 1334 $cm^{-1}$ band may be assigned to $\delta$(CD)E is still in question, for there is a possibility of the appearance of the band associated with the phenyl group at this position.

The 1297 $cm^{-1}$ band of isotactic polystyrene appears also in isotactic poly-$\alpha d_1$-styrene, but not in the trideutero-derivative. Therefore, this band may be assigned to w($CH_2$)A.

In the spectrum of isotactic polystyrene, there are three bands, i. e., 1195 ($\pi$), 1185 ($\pi$) and 1180 $cm^{-1}$ ( ? ) bands in the vicinity of 1180 $cm^{-1}$. The two $\pi$ bands disappear in isotactic poly-$\alpha d_1$-styrene. Since the CC stretching band and the CH wagging band are expected to be observed in this region, it seems reasonable to presume that one of them is due to $\nu$(CC)A and another is to w(CH)A. The following facts may be cited to support the assignments of $\nu$(CC)A to the 1185 $cm^{-1}$ band and w(CH)A to the 1195 $cm^{-1}$ band. (1) The 1195 $cm^{-1}$ band appears in isotactic poly-$\beta d_1$-styrene.[9] (2) The 1183 $cm^{-1}$ band of poly-$\alpha d_1$-styrene shows a remarkable $\pi$ nature. Although a band assignable to the a-mode ($A_1$) of the phenyl group is expected to appear in the vicinity of 1180 $cm^{-1}$, the 1183 $cm^{-1}$ band could not be assigned to this mode because of its polarization property. Therefore, this may be due to the overlapping of the CC stretching mode and the a-mode.

The weak $\pi$ band appears at 1275 $cm^{-1}$ on deuteration. This may be due to the CD deformation. The weak $\pi$ band at 960 $cm^{-1}$ which appears on deuteration may be assigned to w(CD)A.

**3. Other Bands.** — Remarkable changes in the spectrum on deuteration are observed in the regions of 1085~1040 $cm^{-1}$ and 920~810 $cm^{-1}$. While the atactic polystyrene band at 1070 $cm^{-1}$ splits into two $\sigma$ bands at 1080 and 1048 $cm^{-1}$, the corresponding bands of isotactic poly-$\alpha d_1$-styrene appear at 1084 $cm^{-1}$ and 1072 $cm^{-1}$. It seems reasonable to assume these bands as associated rather with the characteristics of the helical polymer chain themselves than with the interaction between the neighboring molecules in the crystalline lattice, for these bands do not disappear even at molten state. From the fact that the bands corresponding to them do not appear in some ring-substituted derivatives, e. g., poly-*p*-deutero-styrene[8] or poly-*p*-halogeno-styrenes[10], these may be due to the coupling of a vibrational mode of the phenyl group and that of $CH_2$ or CH (or CD).

Corresponding to the bands of isotactic polystyrene at 920 ($\sigma$), 910 (no dichroism) and 898 ($\pi$) $cm^{-1}$ which are very sensitive to the crystallization degree of the sample, the $\pi$ band and the band showing almost no dichroism appear at 891 $cm^{-1}$ and 910 $cm^{-1}$

8) H. Tadokoro, S. Nozakura, T. Kitazawa, Y. Yasuhara and S. Murahashi, This Bulletin, 32, 313 (1951); S. Murahashi, S. Nozakura and H. Tadokoro, ibid., 32, 534 (1959).

9) M. Kobayashi, presented at the 13th Annual Meeting of the Chemical Society of Japan, Tokyo, April, 1960.

10) K. Nagai, M. Kobayashi and E. Nagai, presented at the 8th Annual Meeting of the Society of Polymer Science of Japan, Tokyo, May, 1959.

respectively in isotactic poly-$\alpha d_1$-styrene. The band at near 910 $cm^{-1}$ of both polymers may be assigned to an out-of-plane deformation of CH of the phenyl group (probably i-mode) since the corresponding band appears also in poly-$\alpha$, $\beta$, $\beta d_3$-styrene. The assignments of the other two bands are left uncertain for the present.

## Summary

In Table I are given the results of discussions described above on the assignments of the absorption bands.

The bands characteristic to the isotactic polymers, i. e. the bands appearing in the region of 1400~1180 $cm^{-1}$ or in the vicinity of 1070 and 900 $cm^{-1}$, are proved as associated with the $CH_2$ and CH groups.

To make assignments of the bands more precisely, the studies are in progress on the infrared spectra of the other several deuterated derivatives, such as poly-$\beta d_1$-, poly-$\alpha$, $\beta d_2$ and poly-$\beta$, $\beta$ $d_2$-styrenes.

The author is indebted to Mr. Seiichi Mima for mass spectroscopic measurements and to Mr. Hiroshi Shima for measurements of proton magnetic resonance spectra.

*Osaka Industrial Research Institute*
*Oyodo-ku, Osaka*

# *On the Infrared Spectra of Crystalline Poly-p-fluorostyrene*

By Masamichi KOBAYASHI, Kazuo NAGAI and Eiichi NAGAI*

(Received April 30, 1960)

During the last few years, many isotactic vinyl polymers have been obtained from various ring-substituted styrene monomers with Ziegler type catalysts[1]. Most of them crystallize with helical molecular conformation similar to that of isotactic polystyrene, but the pitches of the helixes are different from each other depending on the size, the site and the number of substituents. For instances, while poly-*o*-fluorostyrene crystallizes in three-fold helix with the identity period of 6.65 Å, but poly-*p*-fluorostyrene in four-fold helix with the period of approximately 8.3 Å[1]. Further, it has been noticed by Murahashi et al.[2] that the polymers of *p*-methyl, *m*-methyl and *p*-trimethylsilyl styrene prepared with Ziegler catalyst have larger fiber periods of 12.9, 57 and 60.4 Å, respectively.

Recently, from the infrared spectroscopic studies on several isotactic polymers, Tadokoro et al.[3] found that the characteristics of helical structure of the polymers would be indicated in common by the infrared dichroisms of the several absorption bands, especially of the stretching vibrations of the $CH_2$ groups. Keeping in mind their findings, we measured the infrared spectra of crystalline poly-*p*-fluorostyrene with an aim to find in what respects they would reflect the characteristics of the helical structure of its own.

As a result, it was found that the dichroic ratios of the bands, especially those assigned to the stretching vibrations of $CH_2$ groups differed from those of polystyrene.

To obtain a theoretical ground for this fact, we calculated the dichroic ratios of the bands associated with $CH_2$ and CH groups, assuming the polymer chain to have a four-fold helical structure allowed for the observed fiber period.

On the other hand, we analyzed the infrared spectrum of the polymer under the assumption that they, in an approximation, may be divided into two parts, one being associated with the side group and another with the skeletal chain. The molecular vibrations of the former were analyzed in terms of $D_{2h}$ symmetry and those of the latter in terms of $C(\pi/2)$ symmetry.

## Experimental

*p*-Fluorostyrene (4 g.) prepared by an usual method was polymerized in *n*-heptane at 70°C for 10 hr. using triethyl aluminum (0.53 g.)+titanium tetrachloride (0.18 g.) as a catalyst in a sealed tube. The solid product was washed with hot methanol and then boiled in water to change the organometallic compounds contaminated in the polymer into insoluble oxides. The white polymeric substance was dissolved in boiling xylene and the

* Present address: Takatsuki Laboratory, Kureha Boseki Co. Ltd., Takatsuki, Osaka.

1) G. Natta, F. Danusso and D. Sianesi, *Makromol. Chem.*, **28**, 253 (1958).

2) S. Murahashi. S. Nozakura, and H. Tadokoro, This Bulletin. **32**, 534 (1959).

3) H. Tadokoro, S. Nozakura, T. Kitazawa, Y. Yasuhara and S. Murahashi, This Bulletin, **32**, 313 (1959).

solution was filtered. The gelatinous precipitate separated from the filterate kept at room temperature was dried after centrifugation.

To gain a high degree of crystallinity, the polymer film cast from the toluene solution was subjected to heat-treatment at 160°C for 1 hr. in glycerol. It had the density of 1.23 and melting point of 240°C. The oriented film for measurements of the polarized spectrum was made by drawing it to five times the length of the original in boiling water.

The infrared measurements were made in the region of 3500~400 $cm^{-1}$ using Hilger H 800 and Perkin Elmer Model 21 I. R. spectrometers; the former was equipped with the polarizer consisting of a set of six selenium films, each approximetely 5 $\mu$. thick. The amorphous polymer for comparison was prepared with benzoyl peroxide as a catalyst.

## Experimental Results

**X-ray Diagram.** — In Fig. 1 is illustrated the X-ray fiber diagram of the stretched film of crystalline poly-*p*-fluorostyrene (abbreviated to PFS). The measured identity period along the fiber axis was 8.31 Å being similar value reported by Natta et al.[1] This value assumes that the polymer chain is of isotactic configuration and takes four-fold helix in the crystalline regions. The calculated angles

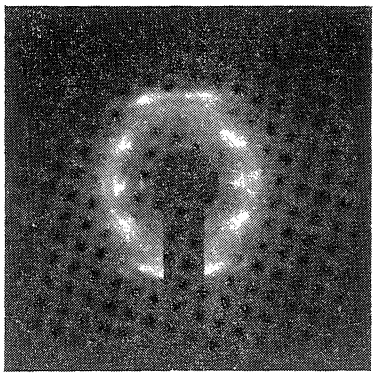


Fig. 1.

of internal rotation of the chain about the C–C bonds with which the helix is formed will be presented later.

**Infrared Spectra.**—In Fig. 2 are shown the spectra infrared in the region of 3500~400 $cm^{-1}$ of atactic and isotactic PFS together with that of the latter measured at molten state.

In Fig. 3 are shown the polarized spectra of isotactic PFS in the region of 3500~650 $cm^{-1}$.

The wave numbers, the dichroisms and the relative intensities of the absorption bands are given in Table I.

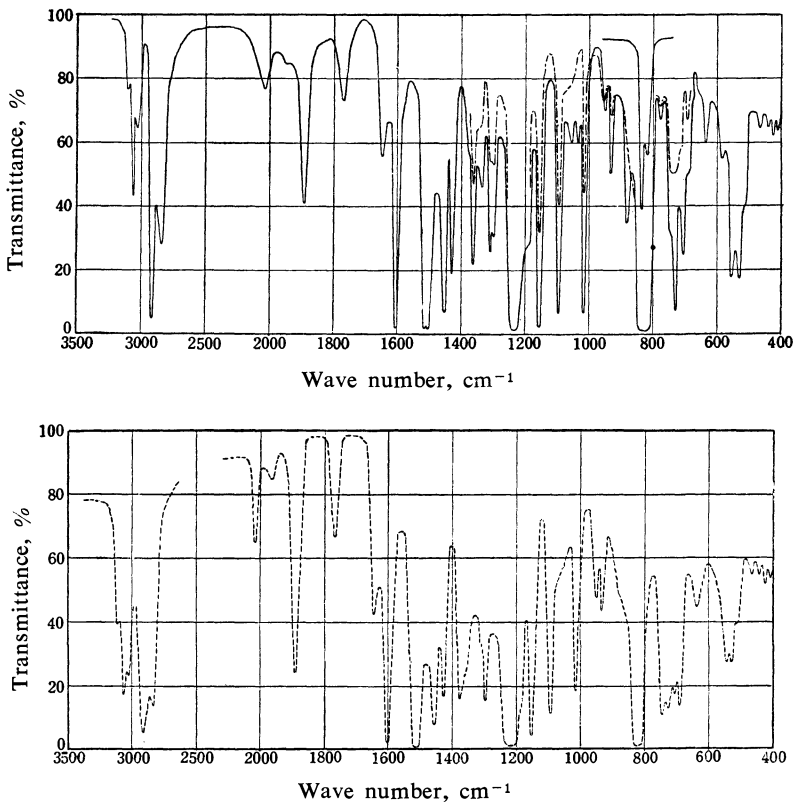



Fig. 2. Infrared spectra of PFS; isotactic at crystalline state ——, isotactic at molten state – – –, atactic – – – –.

TABLE I. BAND ASSIGNMENTS OF THE SPECTRA OF ISOTACTIC AND ATACTIC PFS

| Isotactic cryst. | | | Isotactic molt. | | Atactic | | Assignment |
|---|---|---|---|---|---|---|---|
| Freq. ($cm^{-1}$) | Dichr. | R. I. | Freq. ($cm^{-1}$) | R. I. | Freq. ($cm^{-1}$) | R. I. | |
| 3112 | $\sigma$ | vw | 3112 | vw | 3112 | vw | $A_g+B_{2g}$ |
| 3060 | $\sigma$ | m | 3060 | m | 3060 | m | $B_{3u}$ |
| 3026 | $\sigma$ | w | 3026 | w | 3026 | w | $B_{1u}$ |
| 2924 | $\sigma$ | s | 2924 | s | 2924 | s | $\nu_{asym}$ $(CH_2)$ |
| 2849 | $\pi$ | m | 2849 | m | 2849 | m | $\nu_{sym}$ $(CH_2)$ |
| 2047 | $\sigma$ | w | 2047 | w | 2047 | w | 530+1515=2045 |
| 1891 | $\sigma$ | m | 1891 | m | 1891 | m | 819+1096=1915 |
| 1770 | $\sigma$ | w | 1770 | w | 1770 | w | |
| 1647 | $\sigma$ | w | 1647 | w | 1647 | w | $B_{3u}$ |
| 1603 | — | s | 1603 | s | 1603 | s | $A_g$ |
| 1515 | $\sigma$ | s | 1515 | s | 1515 | s | $B_{1u}$ |
| 1503 | — | s | | | | | |
| 1454 | ($\sigma$) | s | 1454 | s | 1457 | s | $\delta$ $(CH_2)$ |
| 1448 | ($\pi$) | s | 1448 | s | 1448 | s | |
| 1428 | $\sigma$ | ms | 1428 | ms | 1428 | ms | |
| 1377 | — | sh | 1377 | sh | 1377 | m | |
| 1361 | $\sigma$ | m | 1361 | m | | | $\delta$ (CH)E |
| 1336 | $\pi$ | w | 1336 | sh | | | |
| 1309 | $\sigma$ | m | 1309 | m | 1309 | sh | |
| 1300 | $\pi$ | m | 1300 | m | 1300 | m | $w$ $(CH_2)A$ |
| 1234 | — | vs | 1234 | vs | 1234 | vs | $\nu$ $(CF)A_g$ |
| 1191 | $\pi$ | sh | 1191 | sh | | | $\nu$ (CC)A |
| 1154 | $\sigma$ | s | 1154 | s | 1154 | s | $\nu$ $(CF)B_{1u}$ |
| 1096 | $\sigma$ | s | 1096 | s | 1096 | s | $B_{3u}$ |
| 1056 | $\sigma$ | w | 1056 | sh | 1056 | sh | $B_{3u}$ |
| 1035 | $\sigma$ | w | | | | | |
| 1015 | $\sigma$ | s | 1015 | s | 1015 | s | $B_{1u}$ |
| 950 | — | w | 950 | w | 950 | w | $A_u$ |
| 932 | — | m | 932 | w | 932 | w | $B_{3g}$ |
| 881 | $\sigma$ | m | 881 | sh | 881 | sh | |
| 832 | — | vs | 832 | vs | 832 | vs | $B_{2u}$ |
| 819 | $\pi$ | vs | 819 | vs | 819 | vs | $A_g$ |
| 738 | — | sh | 738 | sh | 748 | s | |
| 730 | — | s | 725 | s | 725 | ms | $B_{1u}$ |
| 708 | $\sigma$ | m | 708 | sh | 708 | mw | $r$ $(CH_2)$E ? |
| 694 | $\sigma$ | s | 694 | w | 694 | m | |
| 634 | | w | 634 | w | 634 | w | $\delta$ $(CF)B_{2g}$ |
| 583 | | msh | 583 | msh | | | |
| 555 | | s | 553 | s | 545 | s | |
| 530 | | s | 530 | s | 530 | s | $\delta$ $(CF)B_{2u}$ |
| 515 | | wsh | 515 | sh | 515 | sh | |
| 464 | | vw | 464 | vw | 464 | vw | $A_g$ |
| 444 | | vw | 444 | vw | 444 | vw | |
| 425 | | vw | 425 | vw | 425 | vw | $\delta$ $(CF)B_{3u}$ |
| 410 | | vw | 410 | vw | 410 | vw | |

## Discussions

In this paper the molecular vibractions of the polymer molecule with four-fold helical structure are analyzed following the same way as described in the previous paper[4] on isotactic poly-$\alpha d_1$-styrene; the vibrations of the side group and the skeletal chain are considered separately.

**Vibrational Modes of the Side Group.** — The molecular vibrations of the side group of PFS correspond to those of *p*-disubstituted benzene. The data useful for our study have

4) M. Kobayashi, to be published in this Bulletin.

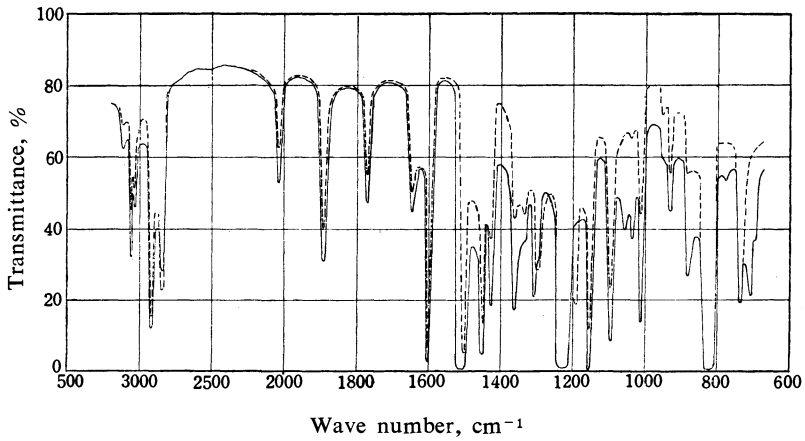



Fig. 3. Infrared dichroism of isotactic PFS. —— Electric vector perpendicular to elongation. ---- Electric vector parallel to elongation.

TABLE II. CHARACTER TABLE, NUMBER OF NORMAL MODES AND SELECTION RULES FOR POINT GROUP $D_{2h}$

| | E | $\sigma$(xy) | $\sigma$(xz) | $\sigma$(yz) | i | $C_2$(z) | $C_2$(y) | $C_2$(x) | Zero fr. | $n$ | Selec. rule |
|---|---|---|---|---|---|---|---|---|---|---|---|
| $A_g$ | +1 | +1 | +1 | +1 | +1 | +1 | +1 | +1 | | 6 | R. |
| $A_u$ | +1 | −1 | −1 | −1 | −1 | +1 | +1 | +1 | | 2 | — |
| $B_{1g}$ | +1 | +1 | −1 | −1 | +1 | +1 | −1 | −1 | $R_z$ | 1 | R. |
| $B_{1u}$ | +1 | −1 | +1 | +1 | −1 | +1 | −1 | −1 | $T_z$ | 5 | I.R. |
| $B_{2g}$ | +1 | −1 | +1 | −1 | +1 | −1 | +1 | −1 | $R_y$ | 5 | R. |
| $B_{2u}$ | +1 | +1 | −1 | +1 | −1 | −1 | +1 | −1 | $T_y$ | 3 | I.R. |
| $B_{3g}$ | +1 | −1 | −1 | +1 | +1 | −1 | −1 | +1 | $R_x$ | 3 | R. |
| $B_{3u}$ | +1 | +1 | +1 | −1 | −1 | −1 | −1 | +1 | $T_x$ | 5 | I.R. |

already been published. Freguson et al.[5] and Tobin[6] have made assignments of the absorption bands of *p*-fluorotoluene and *p*-dichlorobenzene respectively. In applying their results to our aim, it is assumed that the analysis using a point group of $D_{2h}$ woluld be preferable, if it is taken into account that fluorine atom and CH group attached to the para position of benzene nucleus are similar in mass.

Symmetry species, irreducible representations, numbers of normal modes and selection rules for the point group $D_{2h}$ are given in Table II. The selection rules can not be applied rigorously in our case, since the two substituents at the para positions will not suffer the same transition moment. As a result, the fundamentals under all species would become Raman active and those except $A_u$ and $B_{1g}$ infrared active. Referring to the assignments of the bands of *p*-fluorotoluene given by Freguson, we selected out from the spectrum of PFS the bands which might be assigned to the vibrational modes of the side group. They are given in Table III.

It is, of course, anticipated that they will be more or less under the influences of the crystalline field. In fact, considerable differences are observed in some of the bands before and after crystallization or on melting. For example, the band at 1056 $cm^{-1}$ assigned to CH in-plane deformation ($B_{3u}$) becomes sharper and the intensity of the band at 932 $cm^{-1}$ assigned to CH out-of-plane deformation ($B_{3g}$) increases on crystallization.

**Vibrations of the Skeletal Chain.** — Since the molecule of isotactic PFS has four-fold helical structure in the crystalline region, the molecular vibrations of the skeletal chain may be accounted for by using the factor group $C(\pi/2)$[7]. From the result of the factor group analysis, the normal modes are divided into three symmetry species; A (non-degenerate), B (non-degenerate) and E (doubly degenerate) species. Symmetry species, irreducible representations, selection rules and numbers of the normal modes are given in Table IV. In the calculation of the numbers of the normal modes, the side group attached to the skeletal chain is taken as a mass point. The modes under A and E are infrared active and ones under B are inactive. The fundamentals under

5) E. E. Freguson, R. L. Hudson, J. Rud Nielsen and D. C. Smith, *J. Chem. Phys.*, 21, 1736 (1953).
6) M. C. Tobin, *J. Phys. Chem.*, **61**, 1392 (1957).
7) C. Y. Liang and S. Krimm. *J. Chem. Phys.*, **25**, 563 (1956).

TABLE III. ASSIGNMENTS OF THE BANDS DUE TO THE SIDE GROUP

| *p*-FT | PFS | | *p*-FT | PFS | |
|---|---|---|---|---|---|
| $\nu$ (CH) | | | $\delta$ $(C\text{-}C\text{-}C)_{in}$ | | |
| 3071 | 3112 | $A_g$ | 1099 | 1096 | $B_{3u}$ |
| 3071 | 3112 | $B_{2g}$ | 728 | 730 | $B_{1u}$ |
| 3069 | 3060 | $B_{3u}$ | 455 | 464 | $A_g$ |
| 3043 | 3026 | $B_{1u}$ | 313 | | $B_{2g}$ |
| $\delta$ (CH) | | | ring | | |
| 1222 | (1211) | $B_{2g}$ | 842 | | $A_g$ |
| 1044 | 1056 | $B_{3u}$ | | | |
| 1017 | 1015 | $B_{1u}$ | $\delta$ $(C\text{-}C\text{-}C)_{out}$ | | |
| 825 | 819 | $A_g$ | 695 | 694 | $B_{3g}$ |
| | | | 390 | | $A_u$ |
| $\gamma$ (CH) | | | 152 | | $B_{2u}$ |
| 956 | 950 | $A_u$ | | | |
| 929 | 932 | $B_{3g}$ | $\nu$ (CF) | | |
| 817 | 832 | $B_{2u}$ | 1214 | 1234 | $A_g$ |
| (810) | | $B_{1g}$ | 1157 | 1154 | $B_{1u}$ |
| $\nu$ (CC) | | | $\delta$ (CF) | | |
| 1614 | 1647 | $B_{3u}$ | 638 | 634 | $B_{2g}$ |
| 1602 | 1603 | $A_g$ | 503 | 530 | $B_{2u}$ |
| 1512 | 1515 | $B_{1u}$ | 422 | 425 | $B_{3u}$ |
| 1299 | (1300)* | $B_{2g}$ | 341 | | $B_{3g}$ |

$\nu$ (CH); CH stretching, $\delta$ (CH); CH in-plane deformation, $\gamma$ (CH); CH out-of-plane deformation, $\nu$(CC); CC stretching, $\delta$ $(C\text{-}C\text{-}C)_{in}$; CC in-plane deformation, $\delta$ $(C\text{-}C\text{-}C)_{out}$; CC out-of-plane deformation, $\nu$ (CF); CF stretching, $\delta$ (CF); CF deformation.

* The 1300 $cm^{-1}$ band observed may be due mainly to $w$ ($CH_2$).

A and E should exhibit parallel ($\pi$) and perpendicular ($\sigma$) dichroisms respectively. Physically, the symmetry species A, E and B mean that the neighboring monomer units constituting the helix vibrate with a definite phase difference of 0, $\pm\pi/2$ and $\pi$, respectively.

**Infrared Dichroism.** — Bearing in mind the fact noted in the introduction that infrared dichroisms of several bands, especially of those due to the $CH_2$ stretching vibrations, have been detected as reflecting helical structures of the isotactic polymers, the infrared dichroisms of the stretched film of isotactic PFS were measured (see Fig. 3). It was demonstrated that the 2849 $cm^{-1}$ band assigned to the $CH_2$ symmetric stretching exhibited a considerable $\pi$ nature and the 2924 $cm^{-1}$ band assignable to the $CH_2$ antisymmetric stretching showed a slight $\sigma$ nature. These facts do not coincide with Tadokoro et al.'s results on isotactic polystyrene and others; the former band shows almost no dichroism and the latter a considerable $\sigma$ nature.

This discrepancy may be attributed to the reason that the plane of the methylene group in the helix of PFS is inclined to the fiber axis in a different way from that of isotactic polystyrene. In other words, this is attributed to the difference in conformation of the skeletal carbon chain between them.

To gain a concrete ground for this, we calculated the theoretical dichroic ratios ($A_{\parallel}/A_{\perp}$) of the absorption bands. In doing this, however, precise knowledge about the conformation of the molecule of PFS is needed. For this purpose, the data available at present is the observed fiber period of the polymer. A helical structure of an isotactic polymer which gives a definite identity period is determined by the angles of internal rotation of the chain elements about the C–C bonds, provided that the length of C–C bond and the bond angle are kept at constant.

From the mathematical calculations presented in the appendix, we can search for the angles of internal rotation which will fulfill the conditions that the helix of PFS has the observed identity period of 8.31 Å and contains four monomer units in one pitch. In Table V is given the relation between the angles of internal rotation ($\theta_1$ and $\theta_2$) and the calculated identity period, $R$. In this table $\nu_x$, $\nu_y$ and $\nu_z$ are the components of the unit vector of the fiber axis in an internal Cartesian coordinate. Using them, calculation of the dichroic ratio may be made.

$\theta_1$ (or $\theta_2$) is the angle with which a given bond is rotated from the trans position with the clockwise direction taken as plus when seen from the lower indexed carbon atom (see Fig. 4). If $\theta_1=0°$ and $\theta_2=120°$, $R$ will give an identity period 6.65 Å of the three-fold helix (isotactic polystyrene).

The most reasonable values of $\theta_1$ and $\theta_2$ for PFS will be present between $-10°$ and $-12°$ and between 94° and 95° respectively, provided

TABLE IV. SYMMETRY SPECIES, IRREDUCIBLE REPRESENTATIONS, NUMBER OF NORMAL MODES AND SELECTION RULES FOR POINT GROUP $C(\pi/2)$

| | E | $C^1$ | $C^2$ | $C^3$ | $N$ | Zero fr. | $n$ | I.R. | R. |
|---|---|---|---|---|---|---|---|---|---|
| A | +1 | +1 | +1 | +1 | 18 | $T_\pi$, $R_\pi$ | 16 | A | A |
| B | +1 | −1 | +1 | −1 | 18 | | 18 | F | A |
| E | +1 | +i | −1 | −i | 18 | ($T_\sigma$, $R_\sigma$) | (16) | A | A |
| | +1 | −i | −1 | +i | 18 | | | A | A |

TABLE V. ANGLES OF INTERNAL ROTATION AND FIBER PERIOD FOR FOUR-FOLD HELIX

| $\theta_1$ | $\theta_2$ | $\nu_x$ | $\nu_y$ | $\nu_z$ | $R$*,** |
|---|---|---|---|---|---|
| 0 | 90 | 0.438 | 0.899 | 0 | 8.86 Å |
| −10 | 94 | 0.368 | 0.926 | −0.081 | 8.39 |
| −12 | 95 | 0.354 | 0.930 | −0.098 | 8.29 |

* Assuming C-C bond length of 1.54 Å and C-C-C bond angle of 116°.
** The observed fiber period of PFS is 8.31 Å.

that the C-C-C bond angle takes the same value as that of polystyrene, 116°.

Dichroic ratio is expressed for a uniaxial orientation as follows;

$$A_{\parallel}/A_{\perp}=2\cot^2\varphi$$

where $\varphi$ is the angle between the transition moment and the fiber axis. If a unit vector $\boldsymbol{m}$ of a transition moment accompanied with a vibrational mode of the $CH_2$ group is defined by the components $m_x$, $m_y$ and $m_z$ in the Cartesian system ($x_i$, $y_i$, $z_i$), it follows that

$$\cos\varphi=\boldsymbol{\nu}^{\top}\cdot\boldsymbol{m}=\nu_x m_x+\nu_y m_y+\nu_z m_z$$

On the other hand, if a unit vector $\boldsymbol{m}'$ of a transition moment accompanied with a vibrational mode of the CH or the phenyl group is defined by the components $m'_x$, $m'_y$ and $m'_z$ in the Cartesian coordinate ($x_{i+1}$, $y_{i+1}$, $z_{i+1}$), the corresponding expression is

$$\begin{aligned}\cos\varphi&=\boldsymbol{\nu}^{\top}\cdot\boldsymbol{A}_1\boldsymbol{m}'\\&=\nu_x(m'_x\cos\omega+m'_y\sin\omega)\\&+\nu_y(m'_x\sin\omega\cos\theta_1\\&-m'_y\cos\omega\cos\theta_1+m'_z\sin\theta_1)\\&+\nu_z(m'_x\sin\omega\sin\theta_1\\&-m'_y\cos\omega\sin\theta_1+m'_z\cos\theta_1)\end{aligned}$$

where $\boldsymbol{A}_1$ is the matrix of the orthogonal transformation defined in the appendix.

Using the values of $\nu_x$, $\nu_y$ and $\nu_z$, the dichroic ratios of the absorption bands due to the vibrational modes of the $CH_2$ and CH groups were calculated. The results are given in Table VI.

It is shown as expected that they depend on the angles of internal rotation, $\theta_1$ and $\theta_2$. The changes in dichroic ratio of the bands due to the $CH_2$ stretching vibrations are of importance by reason of that described above. The dichroic ratios of the $\nu_{sym}$ ($CH_2$) band and the $\nu_{asym}$ ($CH_2$) band increase with $\theta_2$.

TABLE VI. THE CALCULATED DICHROIC RATIOS FOR FOUR-FOLD HELICAL POLYMER

| Vibrational mode | $\theta_1=0°$ | $\theta_1=-10°$ | $\theta_1=-12°$ |
|---|---|---|---|
| $\nu_{sym}$ ($CH_2$), $\delta$ ($CH_2$) | 0.781 | 1.073 | 1.132 |
| $\nu_{asym}$ ($CH_2$), $r$ ($CH_2$) | 0 | 0.013 | 0.019 |
| $w$ ($CH_2$) | 5.122 | 3.626 | 3.422 |
| $\delta$ (CH) | 0 | 0.013 | 0.019 |
| $w$ (CH) | 5.122 | 3.626 | 3.422 |

Since when $\theta_1=0$, the calculated values do not depend on the number of monomer unit in one pitch provided that the bond angle is kept at constant ($\theta_2=120°$ for three-fold helix, $\theta_2=90°$ for four-fold helix), the values for $\theta_1=0°$ may be regarded as those of isotactic polystyrene. Therefore, the results well explain the differences between PFS and polystyrene in polarization property of the bands due to the $CH_2$ stretching vibrations.

Although the coincidence between the observed property and the predicted value of dichroism of the $\nu_{asym}$ ($CH_2$) is yet qualitative, it would be accepted as correct if we take into account of the contribution from the chain segments randomly oriented in the amorphous regions.

**Absorption Bands Characteristic to the Helical Structure of PFS.** —As in the cases of polystyrene and its several derivatives, the bands characteristic of the helical structure (alternate sequence of trans and gauche conformations) of the polymer molecule are observed in the spectrum of isotactic PFS. They do not disappear even at molten state and are assumed to be associated mainly with the deformational vibrations of the $CH_2$ or CH group or the skeletal modes.

The band at near 1450 $cm^{-1}$ may be ascribed to the $CH_2$ bending ($\delta(CH_2)$). Using the differential method it was made clear that this band consisted of two bands at 1454 and 1448 $cm^{-1}$, having $\sigma$ and $\pi$ nature respectively, and the former might be assigned to $\delta(CH_2)E$ and the latter to $\delta(CH_2)A$.

The five bands at 1361 ($\sigma$), 1336 ($\pi$), 1309 ($\sigma$), 1300 ($\pi$) and 1191 ($\pi$)$cm^{-1}$ of isotactic PFS may correspond to the bands which have been detected by Tadokoro et al. as characteristic of the helical structure of isotactic polystyrene and others. Measurements of the dependence of the spectrum on temperature showed that with increasing temperature the band at 1336 $cm^{-1}$ decreased its relative intensity and disappeared at molten state, on the other hand, the other four bands were hardly affected by temperature change. Then, the four bands may be considered as indicating rather the characteristics of the polymer molecule itself than the interactions of neighboring molecules in the crystalline lattice.

On the basis of the results on the assignments of the bands characteristic of isotactic polystyrene[4], the assignments of these bands may be made as follows; the 1361 $cm^{-1}$ band is assigned to the CH deformation under the E species ($\delta$ (CH)E), the 1300 $cm^{-1}$ band to the $CH_2$ wagging under the A species (w

$(CH_2)A$), the 1191 $cm^{-1}$ band to the CC stretching under the A species ($\nu$ (CC)A). The 1309 $cm^{-1}$ band is still unassigned.

The difference between isotactic PFS and atactic one in spectrum are observed also in the region of 690~750 $cm^{-1}$. The band at 738 $cm^{-1}$ of isotactic PFS has smaller intensity than the corresponding band at 748 $cm^{-1}$ of atactic one. This fact remains even at molten state. The $\sigma$ band at 708 $cm^{-1}$ of isotactic PFS decreases its intensity with increasing temperature, on the other hand, the band at 694 $cm^{-1}$ shows the reverse change. Although the $CH_2$ rocking mode is anticipated to be ovserved in this region and, from polarization property, the 708 $cm^{-1}$ bond is assumed to be assigned to it, the precise assignment to date is open to question.

The results of the discussions on the assignments of the absorption bands are given in the last column of Table I.

## Appendix

**The Geometrical Structures of Polymers with Helical Structure.** — Spatial configuration of a vinyl polymer is determined primarily by angles of internal rotation of C-C bonds. If the spatial position of each monomer unit in the helix is equivalent, the conformation of the polymer chain is defined by two angles of internal rotation as described below. The internal Cartesian coordinates are defined as shown in Fig. 4. The matrix which transforms the coordinate from $(x_{i+1}, y_{i+1}, z_{i+1})$ to $(x_i, y_i, z_i)$ system, or from $(x_{i+2}, y_{i+2}, z_{i+2})$ to $(x_{i+1}, y_{i+1}, z_{i+1})$ system is represented by $\boldsymbol{A}_1$ (or $\boldsymbol{A}_2$);

$$\boldsymbol{A}=\begin{pmatrix}\cos\omega & \sin\omega & 0\\ \sin\omega\cos\theta & -\cos\omega\cos\theta & \sin\theta\\ \sin\omega\sin\theta & -\cos\omega\sin\theta & -\cos\theta\end{pmatrix}$$

where $\theta=\theta_1(\boldsymbol{A}_1)$ or $\theta=\theta_2(\boldsymbol{A}_2)$, and $\omega$ is the supplement angle of C-C-C and angle.

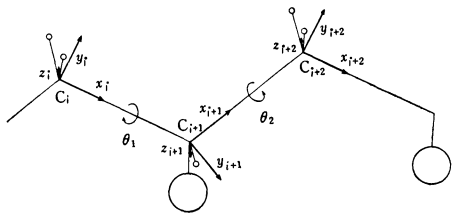



Fig. 4. Internal coordinates for vinyl polymer.

If the unit vector of the fiber axis in $(x_i, y_i, z_i)$ system is defined by $\boldsymbol{\nu}$ $(\nu_x, \nu_y, \nu_z)^\top$, the following relation is introduced;

$$\boldsymbol{\nu} = \boldsymbol{A}_1\boldsymbol{A}_2\boldsymbol{\nu}$$

Since $\boldsymbol{A}$'s are matrixes of orthogonal transformation,

$$(\boldsymbol{A}_1{}^\top-\boldsymbol{A}_2)\boldsymbol{\nu} = \boldsymbol{0}$$

Then, it follows that

$$(\cos\theta_1-1)\nu_y+(\sin\theta_1)\nu_z = 0 \quad (1)$$

$$\sin\omega(1-\cos\theta_2)\nu_x+\cos\omega(\cos\theta_2-\cos\theta_1)\nu_y - (\cos\omega\sin\theta_1+\sin\theta_2)\nu_z = 0 \quad (2)$$

$$-(\sin\omega\sin\theta_2)\nu_x+(\sin\theta_1+\cos\omega\sin\theta_2)\nu_y + (\cos\theta_2-\cos\theta_1)\nu_z = 0 \quad (3)$$

As $\boldsymbol{\nu}$ is unit vector

$$\nu_x{}^2+\nu_y{}^2+\nu_z{}^2 = 1 \quad (4)$$

If the fiber period of $n$-fold helix is $R$,

$$R/n = \boldsymbol{\nu}^\top\cdot(\boldsymbol{b}+\boldsymbol{A}_1\boldsymbol{b})$$

where

$$\boldsymbol{b} = (b, 0, 0)^\top$$

$b$ is the CC bond length. Therefore,

$$R/n = b\{(1+\cos\omega)\nu_x+(\sin\omega\cos\theta_1)\nu_y + (\sin\omega\sin\theta_1)\nu_z\} \quad (5)$$

To construct $n$-fold helix, the following condition must be satisfied; the angle between the projection of $\overline{C_iC_{i+1}}$ to the plane perpendicular to the fiber axis and the one of $\overline{C_{i+2}C_{i+3}}$ to the same plane must be $2\pi/n$. Then,

$$(\boldsymbol{A}_1\boldsymbol{A}_2\boldsymbol{1}\times\boldsymbol{\nu})\cdot(\boldsymbol{1}\times\boldsymbol{\nu}) = \cos(\pi-2\pi/n)$$

Then,

$$\cos^2\omega+\sin^2\omega\cos\theta_2 -\{\nu_x{}^2+\nu_x\nu_y\sin\omega\sin\theta_1\sin\theta_2 -\nu_x\nu_z(1+\cos\theta_1)\sin\omega\sin\theta_2\} = \cos(n-2)\pi/n \quad (6)$$

Provided that fiber period, C-C-C bond angle, C-C bond length and number of monomer units in one pitch of the helix are known, it is possible to calculate the angles of internal rotation, $\theta_1$ and $\theta_2$, using the Eqs. 1—6.

In Table V are given the results of the calculation for four-fold helix. In this calculation, the C-C bond length of 1.54 Å and the C-C-C bond angle of 116° are assumed.

*Osaka Industrial Research Institute*
*Oyodo-ku, Osaka*

# *Neutron Activation Analysis of Halogens in High-Purity Silicon*

By Tadashi NOZAKI, Toshi KAWASHIMA, Hideo BABA and Hidemaro ARAKI

(Received May 6, 1960)

Extreme purification is of vital importance when silicon is used as a semiconductor material, and many papers treating many kinds of trace impurity in high-purity silicon have been published. However, neither the method of the determination nor the behavior of halogens in a given material has been studied enough. Previously, we reported[1] on the neutron activation analysis of iodine in silicon. In this paper, a method for simultaneous determination of chlorine, bromine and iodine in one sample is presented with some results.

Fusion of the neutron-irradiated silicon with potassium hydroxide containing potassium iodide as carrier was proved suitable for decomposing the sample in the determination of iodine. A similar fusion with alkali chloride, bromide and iodide as carrier should serve satisfactorily for their simultaneous determination. On such fusion under a reducing atmosphere, both chlorine and bromine in the sample will be converted into chloride and bromide respectively. Even if they were present in other forms than halide ions, they would be converted into chloride and bromide, when the basic cake is dissolved in an aqueous sulfuric acid in the presence of a large excess of iodide. Although perchlorate is not readily reduced to chloride on such a treatment, the formation of perchlorate under the given condition is least probable. Thus the carriers should work satisfactorily.

When a sulfuric acid solution containing the three halides was distilled in the presence of chromium(VI) oxide, the following three fractions of the distillate were successively obtained: (1) light brown solution containing bromine, (2) almost colorless solution containing only a small amount of halogen, (3) faintly yellow solution containing chlorine and hydrogen chloride. Addition of a sufficient quantity of oxalic acid and some water into the residual solution resulted in the reduction of the iodate to iodine. This was easily distilled, purified and converted into silver iodide for $\beta$-ray counting.

The bromine must be carefully purified. This is because after neutron irradiation of natural bromine, three radioactive nuclides of bromine are present as shown in Table I. The radiochemical purity of the bromine sample, however, can be checked precisely neither from its decay curve nor from the $\gamma$-ray spectrum. The first fraction, containing some chlorine and perhaps a trace of iodine too, was submitted, before being converted into silver bromide for counting, to a further purification, whose usefulness was checked by a tracer technique using $^{36}Cl$ and $^{131}I$. On the

TABLE I. RADIOACTIVE NUCLIDES OF THE HALOGENS FORMED BY THE NEUTRON IRRADIATION

| Nuclide | Half-life | $\beta$-Ray energy (MeV.) | $\gamma$-Ray energy (MeV.) | *Activity formed (dpm) |
|---|---|---|---|---|
| $^{36}Cl$ | $3\times10^5$y | $\beta^-$0.704 (98%) | none | negligible |
| $^{38}Cl$ | 37.3m | $\beta^-$4.81 (53%)<br>2.77 (16%)<br>1.11 (31%) | 2.15 (31+16%)<br>1.60 (31%) | $5.4\times10^{10}$ |
| $^{80m}Br$ | 4.4h | | 0.049<br>0.037 | $5\times10^{10}$ |
| $^{80}Br$ | 17.6m | $\beta^-$1.99 (72%) etc.<br>$\beta^+$0.87 (3%) | 0.62 (13%) | $1.1\times10^{12}$ |
| $^{82}Br$ | 35.9h | $\beta^-$0.444 (100%) | 0.55, 1.47<br>eight $\gamma$-rays | $9\times10^7$ |
| $^{128}I$ | 25.0m | $\beta^-$2.12 (76%) etc. | 0.46 (17%)<br>others (weak) | $8\times10^{11}$ |

* Just after 1 hr's irradiation of 1 g. of a natural halogen under a thermal neutron flux of $6\times10^{11}$ $n/cm^2$ sec.

1) T. Nozaki et al., This Bulletin, 33, 320 (1960).

other hand, chlorine in the third fraction was converted into silver chloride for counting without further purification, for it involves some difficulty and is time-consuming, and there is no possible nuclide that enters the silver chloride and decays with a similar half-life emitting an energetic $\gamma$-ray. The silver chloride was proved to be radiochemically pure, as far as the distillation was carried out with care to prevent contamination with radioactive silica.

When the sample contains by far the least amount of iodine amidst the three halogens, there is another preferable process, which consists of the distillation of iodine after the treatment of the fused cake as reported previously and the separation of bromine and chlorine by the method indicated above. The two complete processes require nearly equal time, with a good yield and radiochemical purity.

Unfortunately, fluorine can not be determined by a similar technique because of the lack of a suitable radioactive nuclide formed by neutron irradiation.

## Experimental

*Sample.*—All of the silicon samples were of transistor grade, purified by the chloride process (in U. S. A.), by the iodide process (in the Electrical Communication Laboratory) or by an unknown method (in Europe). Many other impurities in them were determined by emission spectroscopy or by neutron activation analysis with an irradiation under a higher flux and for a longer period, the results indicating their high purity. In most cases, two portions of the same sample were analyzed, each being 0.5 to 1 g.

*Irradiation.*—The samples enveloped in thick polyethylene sheets were irradiated in a water boiler type reactor, (Japan Research Reactor 1) for an hour under a neutron flux of about $6\times10^{11}$ $n/cm^2$ sec., placed side by side with the radioactivation standard of ammonium chloride, ammonium bromide and potassium iodide, and taken out swiftly through a neumatic tube.

*Chemical Separation.*—The irradiated samples were etched with a mixture of hydrofluoric and nitric acid, to avoid possible surface contamination pulverized, weighed and fused with potassium hydroxide (10 to 15 g.) kept just above its melting point and containing a known ammount of sodium chloride, potassium bromide and potassium iodide (each 5 to 10 mg.) as carriers. The fused cake was dissolved in sulfuric acid (2 : 3, 100 ml.) containing a small quantity of sodium sulfite (about 0.01g.). The solution was transferred into a crooked neck distillation flask (in order to protect the distillate from contamination by the radioactive silicon) and distilled after the addition of chromium(VI) oxide (10 g.).

The bromine distilled out in the first few minutes. The colored distillate was caught in an aqueous sodium sulfite (25 ml. of 10 g./l. solution) containing sodium chloride and potassium iodide (each a few mg.), oxidized by adding concentrated phosphoric acid (10 ml.) and potassium permanganate (20 ml. of 10 g./l. solution), and the bromine was extracted with carbon tetrachloride (20 ml.), back-extracted with hydroxylamine (0.1 g.) in nitric acid (1 : 100, 20 ml.) and converted into silver bromide.

A tracer study to prove the usefulness of this purification was carried out preliminarily by the use of $^{36}Cl$ and $^{131}I$. On oxidation with permanganate, no detectable $^{36}Cl$ (less than 1/5,000) entered the organic phase, but a trace of iodine did when the treatment was performed with less care. However, the iodine was removed completely (to less than 1/5,000) by back-extraction, for a solution of hydroxylamine in dilute nitric acid reduces molecular bromine to bromide and oxidizes iodide to iodine.

The distillation was continued, and after several minutes from the disappearence of the bromine color when a faint color of chlorine became recognizable by a careful observation, the distillate was introduced into an aqueous sodium sulfite (10 g./l. 25 ml.). When the color of chlorine in the distillate disappeared, the chloride was converted into silver chloride without further purification. It was somewhat preferable to carry out the distillation of bromine with a smaller amount (1 g.) of chromium(VI) oxide and to add a larger amount (10 g.) before the distillation of chlorine.

When the determination of iodine was necessary, it was attained by adding a sufficient quantity (more than 30 g.) of oxalic acid and some water (30 ml.) into the residual solution, distilling the liberated iodine and converting it into silver iodide after the purification as mentioned previously[1].

Each silver halide was filtered off with a glass filter (No. 3), washed with nitric acid (1 : 100, 50 ml.), water, ethanol and ether, and submitted to counting and weighing. The time required for the chemical process was less than an hour for bromine, about one hour for chlorine and 1.2 hr. for iodine, with a yield exceeding 50%.

*Radioactivation Standard.*—Each of the irradiated bromide and iodide was dissolved in water containing a known amount of the same halide as carrier, and converted into silver bromide and iodide after being purified by the oxidation, extraction and back-extraction. On the other hand, silver chloride was precipitated without purification.

*Counting.*—A simple G-M counter of an end window type was used in all cases. For chlorine, a scintillation counter with a large sodium iodide crystal ($4''\times4''$) and a single channel analyzer was also used (the region between 1.8 MeV. and 3.5 MeV.). More precise determination could be done by the latter, but the efficiency of the former was somewhat higher. The decay curve of the chlorine measured by a G-M counter agreed well with that of the standard sample and the theoretical curve. The agreement of the decay curve of the bromine and iodine with that of the corresponding standard was complete. For lowering the detection limit, use of a $2\pi$ counter was also examined, and its efficiency was found to be about five times higher

than that of the G-M counter with the sample kept as near as possible.

## Results and Discussion

Some of the results are shown in Tables II and III. It is natural that a silicon purified by the chloride method contains a trace of chlorine and that purified by the iodide method contains iodine. On the other hand, it should be an interesting fact that most of the high-purity silicons contain two other halogens too, indicating a tendency that the less the concentration of a halogen becomes, the greater the persistency with which it remains in the silicon. Silicon powder obtained by the thermal decomposition of silicon tetraiodide usually contained several ppm of iodine. The iodine content could be lowered down to about 0.3 ppm by a simple technique (i. e. fusion under an argon flow or segregation). Table III indicates the segregation of iodine in a single crystal of silicon about 7 cm. long prepared by pulling it from the melt at a rate of 1 cm. per min. Here, it is also shown tha the iodine content decreased fairly rapidly down to 0.3 to 0.2 ppm. However, a high-purity silicon prepared by the iodide process and purified by 30 times' zone refining still contained nearly the same amount of iodine. On the other hand, a determination showed that heating in a hydrogen atmosphere seems to be effective to reduce the iodine as low as several hundredths ppm.

TABLE II. HALOGEN CONTENT OF HIGH-PURITY SILICONS

| Method of purification | Halogen content (ppm) | | |
|---|---|---|---|
| | Cl | Br | I |
| Chloride method | 2.2 | 0.18 | 0.15 |
| Iodide method | 0.2 | 0.05 | 0.38 |
| (Unknown) | <0.15 | <0.02 | 0.17 |

TABLE III. SEGREGATION OF IODINE

| Location (centimeter from the tail) | 0.3 | 1.6 | 2.9 | 4.8 | 6.2 |
|---|---|---|---|---|---|
| Iodine content (ppm) | 1.5 | 0.94 | 0.83 | 0.32 | 0.22 |

As the result, a trace of any of the three halogens remains in a high-purity silicon quite persistently after many physical purifications, and the persistency increases with the decrease of its concentration. The authors are wishing to elucidate this reason.

When it is assumed that an activity of 150 cpm at the initiation of counting is essential for precise identification of the nuclide, the detection limit is $1.5\times10^{-7}$ g., $1.5\times10^{-8}$ g. and $3.0\times10^{-8}$ g. for chlorine, bromine and iodine respectively by the use of a G-M counter and under the conditions described above. Use of a $2\pi$ counter could lower the limit down to one-fifth of the above values.

## Summary

A trace quantity of chlorine, bromine and iodine was determined simultaneously by neutron activation analysis. By careful distillation of a solution containing the alkali-fused silicon, chromium(VI) oxide and sulfuric acid, bromine and chlorine were distilled out separately, leaving iodine in the residual solution, which was then distilled out after adding oxalic acid.

Most kinds of high-purity silicon contained more than 0.1 ppm of a halogen, which was used in the course of its purification process, and also two other halogens, though of a smaller quantity.

The authors acknowledge with thanks the help given by the Staff Members of the Japan. Atomic Energy Research Institute.

*The Electrical Communication Laboratory*
*Musashino, Tokyo*

# *Long-chain Phosphates. I. Reactions of Solid Potassium Kurrol Salt with Solutions of Various Metal Salts*

By Shigeru OHASHI and Kazuo YAMAGISHI

(Received May 12, 1960)

Long-chain potassium metaphosphate, $(KPO_3)_n$, which is called potassium Kurrol salt, can be readily prepared by dehydrating potassium dihydrogen orthophosphate. It is a well-known fact[1] that potassium Kurrol salt is not easily soluble in pure water, but dissolution takes place in dilute solutions of salts of alkali metals other than potassium to give a highly viscous solution which is characteristic of a linear polymer of a high molecular weight. Thilo et al.[2,3], investigated the reactions between solutions of potassium Kurrol salt and those of various metal ions. It is the purpose of this paper to present some information on the behavior of potassium Kurrol salt in a solid state toward solutions of various metal ions. Solid potassium Kurrol salt reacts with solutions of certain multivalent cations to give gummy substances. The authors investigated particularly in details a reaction of potassium Kurrol salt with nickel ion, since the colored substance produced allowed easy observation upon the process of the reaction. The results indicated that the potassium ion in solid potassium Kurrol salt can be replaced by the nickel ion in a solution through a cation-exchange process. In the course of this investigation Weiss and Michel[4] found that reactions of solid potassium Kurrol salt with solutions of various alkylammonium ions can be regarded as a cation-exchange process.

## Experimental

**Preparation of Potassium Kurrol Salt.**—Potassium Kurrol salt is usually prepared by dehydrating potassium dihydrogen orthophosphate. Pfanstiel and Iler[5] investigated the effect of minute variations in the original K/P ratio on the viscosity of the solution of potassium Kurrol salt and indicated that when there is a deficiency of potassium in a starting material, cross-linking occurs between phosphate polymer chains in the resulting potassium Kurrol salt crystal. An excess of potassium in a starting material forms potassium tripolyphosphate as a separate phase. Pfanstiel and Iler[5] gave the relationship between pH of a 0.1 M solution of potassium dihydrogen orthophosphate and its K/P ratio. A 0.1M solution of potassium dihydrogen orthophosphate of Wako special grade (lot 1335) was prepared in carbon dioxide-free distilled water. The pH of the solution was 4.50. According to Pfanstiel and Iler's data the K/P ratio of the potassium dihydrogen orthophosphate was calculated to be $0.9998 \pm 0.0008$. This value means that no further adjustment of the K/P ratio is necessary for the present purpose.

In a platinum dish 156.4 g. of the potassium dihydrogen orthophosphate was dehydrated at a lower temperature than the melting point, 807°C, of potassium Kurrol salt. Then it was melted in an electric furnace at 870°C. After being kept at this temperature for 30 min., it was gradually cooled to 775°C in 3 hr. After being kept at 775°C for 25 hr., the sample was removed from the furnace and chilled by holding the lower part of the dish in water. A transparent crystalline product was prepared. According to Malmgren and Lamm's study[6,7] the molecular weight of the potassium Kurrol salt prepared in this work was presumed to be about $10^6$.

**X-ray Diffractometry.**—X-ray patterns of the potassium Kurrol salt as well as hydrated metaphosphate containing potassium and nickel and its dehydrated products were taken with Copper $K_\alpha$ radiation and a nickel filter by means of an automatic recording X-ray diffractometer, "Geigerflex", of Rigaku Denki Co., Ltd. For the potassium Kurrol salt a rotating mount was used to avoid the preferred Crientation.

**Paper Chromatography.**—Two-dimensional paper chromatography was carried out according to Karl-Kroupa's procedure[8]. Acid solvent was made by mixing 735 ml. of isopropyl alcohol, a solution of 50 g. of trichloroacetic acid in 265 ml. of water, and 2.5 ml. of concentrated aqueous ammonia. Basic solvent was made by mixing 387 ml. of isopropyl alcohol, 200 ml. of isobutyl alcohol, 408 ml. of water, and 5 ml. of concentrated aqueous ammonia. Filter papers used in this work were Toyo No. 53.

**Analytical Methods for the Determination of Phosphate, Potassium, Nickel and Other Metal Ions.**—For the determenation of phosphate, potassium, and nickel ions in a solid and an aqueous

1) J. R. Van Wazer, "Phosphorus and its Compounds", Vol. I, Interscience Publishers, New York (1958), p. 665.
2) E. Thilo, G. Schulz and E. M. Wickmann, *Z. anorg. allgem. Chem.*, **272**, 182 (1953).
3) E. Thilo and A. Winkler, *J. prakt. Chem.*, **7**, 46 (1958).
4) A. Weiss and E. Michel, *Z. anorg. allgem. Chem.*, **296**, 313 (1958).
5) R. Pfanstiel and R. K. Iler, *J. Am. Chem. Soc.*, 74, 6059 (1952).
6) H. Malmgren and O. Lamm, *Z. anorg. allgem. Chem.*, **252**, 256 (1944).
7) H. Malmgren, *Acta Chem. Scand.*, 6, 1 (1952).
8) E. Karl-Kroupa, *Anal. Chem.*, **28**, 1091 (1956) and her private publication.

phase obtained by the reaction of the potassium Kurrol salt with an aqueous solution of nickel sulfate, the following method was used. An aliquot of the solution was charged into an ion-exchange column of Dowex 1-X4 of chloride form and the column was washed with water. From the solution which passed through the column, the nickel ion was precipitated with dimethylglyoxime and aqueous ammonia and determined gravimetrically. After the separation of nickel the filtrate containing the potassium ion was evaporated to dryness in a platinum dish and the residue was heated at a temperature 300~320°C. Ammonium chloride and the excess of dimethylglyoxime were sublimed and the potassium was determined gravimetrically as potassium chloride. The phosphate absorbed on the column was eluted with 3N hydrochloric acid, hydrolyzed to orthophosphate by boiling, precipitated with a magnesia mixture, and determined gravimetrically as magnesium pyrophosphate. The solid phase was dissolved in 1N hydrochloric acid, evaporated to dryness, dissolved in water, and neutralized with a dilute solution of sodium hydroxide. The solution thus obtained was treated using the same procedure as in the case of the aqueous phase.

In the process of the reaction with the potassium Kurrol salt, variation of nickel ion concentration was followed by a direct colorimetric method for the nickel ion with a filter of 390 mμ. Various metal ions in aqueous phases were determined as follows: the cobalt(II) ion was determined by the tricarbonato cobalt(III) method[9], the calcium, the magnesium, and the zinc ion were by the chelatometric titration with ethylenediaminetetraacetate, the iron(II) ion was by the permanganometric titration, and copper ion by the iodometric titration. The manganese(II) ion was oxidized with silver nitrate and ammonium persulfate to permanganate, a solution of ammonium iron(II) sulfate, of a known concentration was added, and the excess of iron-(II) was titrated with a standard solution of permanganate. The iron(III) ion was reduced with zinc amalgam to iron(II) and determined by the permanganometric titration. A minute amount of condensed phosphate dissolved in the aqueous solution was determined by the colorimetry[10], after being hydolyzed to orthophosphate.

## Results and Discussion

**1. X-ray Diffraction Data of the Potassium Kurrol Salt.**—Klement and Schmid[11] took the X-ray powder diffraction photographs of potassium Kurrol salt used in his study. Both results in Klement and Schmid's and the present work indicated a good coincidence as shown in Table I. The X-ray pattern of potassium Kurrol salt was not changed by any of the following treatments: Drying at 100° to 110°C for 1 hr., washing with ethanol and ether, and drying in air after being immersed in water for 50 hr.

TABLE I. X-RAY DIFFRACTION DATA OF POTASSIUM KURROL SALT

| This work | | Klement and Schmid[11] | |
|---|---|---|---|
| Spacing Å | Intensity | Spacing Å | Intensity |
| 6.28 | 100 | 6.40 | 3 |
| 5.24 | 15 | 5.18 | 2 |
| 5.06 | 28 | | |
| 4.50 | 30 | 4.54 | 2 |
| 3.75 | 18 | 3.92 | 2 |
| 3.45 | 60 | 3.42 | 5 |
| 3.35 | 21 | | |
| 3.29 | 30 | — | — |
| 3.14 | 79 | 3.13 | 3 |
| 3.08 | 15 | | |
| 2.83 | 14 | 2.82 | 2 |
| 2.74 | 9 | 2.74 | 2 |
| 2.68 | 37 | 2.64 | 2 |
| 2.58 | 6 | 2.55 | 1 |
| 2.26 | 35 | 2.25 | 4 |
| 2.21 | 12 | 2.20 | 3 |
| 2.10 | 5 | — | — |
| 2.05 | 3 | 2.02 | 2 |
| 2.03 | 3 | | |
| 1.89 | 6 | 1.88 | 3 |
| 1.88 | 6 | | |
| 1.80 | 3 | — | — |
| 1.74 | 5 | 1.72 | 2 |
| 1.69 | 3 | — | — |
| 1.67 | 5 | — | — |
| 1.64 | 3 | — | — |
| 1.61 | 3 | 1.61 | 2 |
| 1.57 | 5 | 1.57 | 2 |
| 1.50 | 4 | — | — |

**2. Non-existence of Tripolyphosphate in the Potassium Kurrol Salt.**—About 0.9 g. of the pulverized potassium Kurrol salt was further ground in 100 ml. of ice-water and the suspension was filtered. By this treatment potassium tripolyphosphate, if present, can be washed out of the sample and at the same time the hydrolysis of condensed phosphate may be reduced to a negligible extent. After the filtrate was dried by the use of a freeze-drying machine, the residue was brought into a solution with 0.5 ml. of water. In a two-dimensional paper chromatogram of this solution, there was only a non-moving spot at the original point. This means that the potassium Kurrol salt did not contain any tripolyphosphate or any other shorter chain or ring phosphates and that a minute amount of the potassium Kurrol salt was brought into the solution without intense hydrolysis.

**3. Solubility of the Potassium Kurrol Salt.**—About 1 g. of the potassium Kurrol salt was

9) M. Mori and M. Shibata, *J. Chem. Soc. Japan, Pure Chem. Soc.* (*Nippon Kagaku Zasshi*), **75**, 1044 (1954).
10) M. Nakamura, *J. Agr. Chem. Soc. Japan* (*Nippon Nogei Kagaku Kai-shi*), **24**, 1 (1950).
11) R. Klement and J. Schmid, *Z. anorg. allgem. Chem.*, **290**, 113 (1957).

put into 1 l. of water and stirred at room temperature (20~23°C). After 1, 2, 3, and 25 hr. the phosphorus content of the phosphate in the solution were determined to be 19, 17, 20, and 23 $\gamma$ P per ml., respectively. From these values the solubility was calculated to be 0.007 ~0.009 per cent.

**4. Qualitative Observation on the Behavior of the Potassium Kurrol Salt toward Aqueous Solutions of Various Metal Ions.**—As mentioned previously, potassium Kurrol salt is dissolved in aqueous solutions of sodium salts. To 0.1 g. of the potassium Kurrol salt 10 ml. of a 0.1 M solution of each of the following sodium salts was added; acetate, bromide, carbonate, chloride, cyanate, dihydrogen orthophosphate, monohydrogen carbonate, monohydrogen orthophosphate, nitrate, orthophosphate (normal), oxalate, pyrophosphate, sulfate, and tripolyphosphate. In every case a greater part of the potassium Kurrol salt was dissolved. However, it appeared that the potassium Kurrol salt was more rapidly dissolved in the solutions of ortho-, pyro- and tripolyphosphate in comparison with the other salts.

To 0.1 g. of the potassium Kurrol salt, 10 ml. of 1, 0.5, 0.1, or 0.01 M solution of sodium chloride was added, respectively, where the ratio Na/K was 10, 5, 1, or 0.1. When the ratio was 5, the sample was most easily dissolved. When the ratio was 10, a part of the sample was converted into a gelatinous substance. Probably it was due to salting-out effect.

The results of the qualitative observation on the behavior of the potassium Kurrol salt toward solutions of various metal ions are summarized in Table II. These results were obtained when 0.1 g. of the potassium Kurrol salt was added to 10 ml. of a 0.1 M solution of the metal ion.

Table II. Reactions of potassium Kurrol salt with solutions of metal ions

| Metal ion | Reaction |
|---|---|
| $Na^+$, $NH_4^+$ | Potassium Kurrol salt is gradually dissolved. |
| $Ca^{2+}$, $Cr^{3+}$, $Ag^+$ | Potassium Kurrol salt forms a lump which has not plasticity. |
| $Mg^{2+}$, $Mn^{2+}$, $Fe^{2+}$, $Co^{2+}$, $Ni^{2+}$, $Cu^{2+}$, $Sn^{2+}$ | Potassium Kurrol salt forms a gummy substance. |
| $Al^{3+}$, $Fe^{3+}$, $Ce^{3+}$, $Hg^{2+}$, $Bi^{3+}$, $Pb^{2+}$ | Potassium Kurol salt reacts with them very slowly. |

**5. Reaction between the Potassium Kurrol Salt and Solutions of Nickel Sulfate.**—When the potassium Kurrol salt was added to a solution of nickel sulfate, the white crystalline potassium Kurrol salt was gradually converted into a green gummy substance. The absorption of nickel ion was investigated as follows. At a bottom of an Erlenmeyer flask of 300 ml., 1 g. of the ground potassium Kurrol salt was flatly placed and 200 ml. of a 0.0984 M solution of nickel sulfate was added to it. The mixture was kept at 20°C without agitation. The variation of the amounts of the nickel ion absorbed with time was determined by measuring the decrease of the nickel ion concentration in the solution. As shown by the curve A in Fig. 1,

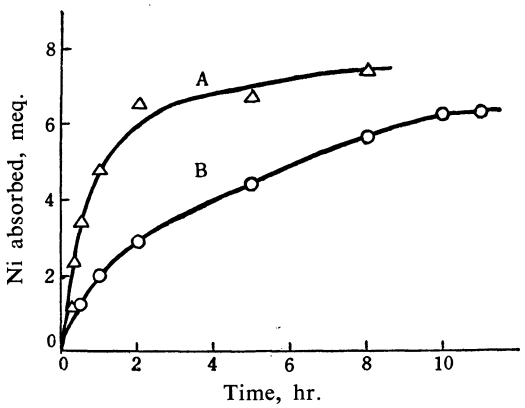



Fig. 1. The variation of the amounts of ion absorbed with time. The initial concentrations of nickel sulfate are 0.0984 M in Curve A and 0.0366 M in Curve B.

after about 8 hr. the reaction reached the equilibrium. When a 0.0366 M solution of nickel sulfate was used, the curve B in Fig. 1 was obtained by a similar experiment. In this case the reaction reached the equilibrium after about 11 hr. After the reaction was equilibrated, the solid phase was removed from the solution, washed quickly with water, and analyzed for potassium, nickel and phosphorus. The amounts of sulfate ion absorbed by the solid phase were negligibly small. The phosphorus contents in the solid phases were 8.50 mg. atom in both cases in comparison with 8.47 mg. atom which was the calculated value of phosphorus content in the initial potassium Kurrol salt. Therefore, all of the phosphorus in the initial sample were assumed to remain in the solid phase in the process of the reaction. As shown in Table III the quantity of the potassium ion which came out of the solid phase was equivalent to the quantity of the nickel ion which went into the solid phase. It was concluded that the reaction mentioned above is a kind of cation-exchange reaction. In the systems of 1 g. of the potassium Kurrol salt and 200 ml. of the 0.0984 M and 0.0366 M solution of nickel sulfate 91 and 74 per cent of potassium ion was exchanged with nickel

TABLE III. CATION-EXCHANGE REACTION BETWEEN POTASSIUM KURROL SALT AND SOLUTIONS OF NICKEL SULFATE

| No. | Initial quantity of $K^+$ ion in the solid phase meq. | Final quantity of $K^+$ ion in the solid phase meq. | Quantity of $K^+$ ion which came out of the solid phase | | Quantity of $Ni^{2+}$ ion which went into the solid phase | |
|---|---|---|---|---|---|---|
| | | | meq. | % exchange | meq. | % exchange |
| A* | 8.47 | 0.81 | 7.66 | 90.4 | 7.68 | 90.8 |
| B** | 8.47 | 2.16 | 6.31 | 74.5 | 6.24 | 73.7 |

*A A reaction between 1 g. of potassium Kurrol salt and 200 ml. of a 0.0984 M solution of $NiSO_4$ for 8 hr. at 20°C.

**B A reaction between 1 g. of potassium Kurrol salt and 200 ml. of a 0.0366 M solution of $NiSO_4$ for 11 hr. at at 20°C.

TABLE IV. PROPERTIES OF THE NICKEL-SUBSTITUTED PRODUCTS HEATED AT VARIOUS TEMPERATURES

| Product | Heated at, °C | Appearance | For X-rays | Two-dimensional paper chromatographic information |
|---|---|---|---|---|
| A | 100~110 | green, transparent | amorphous | — |
| B | 300 | dark brown, powder | amorphous slightly crystalline | — |
| C | 600 | light yellow, powder | crystalline | non-moving spot indicating long-chain phosphate |
| D | 1000 | yellowish green, powder | crystalline | chain series containing ortho-, pyro-, tripolyphosphate, etc., ring series containing trimeta-, tetrameta,, pentametaphosphate, etc. and non-moving spot |
| E | 1200 | dark yellow, powder | crystalline | chain series containing ortho-, pyro-, tripolyphosphate, etc. and non-moving spot |

ions in 8 and 11 hr., respectively.

In order to confirm the reversibility of the cation-exchange reaction, a green product obtained by the reaction between 1 g. of the potassium Kurrol salt and 200 ml. of a 0.1052 M solution of nickel sulfate for 8 hr. at 20°C was subjected to react with 50 ml. of a 0.2 M solution of potassium chloride for 40 hr. at 20°C. Before and after the reverse reaction, the solid phase was analyzed for potassium, nickel and phosphorus. Phosphate was not dissolved in the process of this reaction. The quantity of the potassium ion which went into the solid phase was 1.48 meq. and the quantity of the nickel ion which came out of the solid phase was 1.47 meq. This fact indicates that the reaction is reversible. The rate of the reverse reaction was slower than that of the ordinary reaction, since the surface area of the primary product was smaller than that of the initial potassium Kurrol salt. The equilibration of the reverse reactoin was attained after about 40 hr.

**6. Properties of the Nickel-substituted Product.**—The nickel-substituted product in which about 90 per cent of the initial amount of the potassium ion is replaced by the nickel ion is green-colored and gummy. It is quite similar to chewed chewing-gum. The green product is gradually dissolved into a large amount of water. A similar product can be made in a short time by dissolving potassium Kurrol salt in a dilute solution of sodium chloride or sodium tripolyphosphate and adding a concentrated solution of nickel sulfate. This fact may be due to salting-out effect.

The variation in the properties of the green product by heating was investigated and the results are summarized in Tablle IV. The green primary product and the product A were completely amorphous for X-rays. The product B was practically amorphous for X-rays, but it contained a small amount of crystalline substance. The products C, D and E were all crystalline for X-rays and their X-ray patterns were different from one another. The products A and B were soluble in mineral acids, but the products C, D, and E were soluble in mineral acids only with difficulty. The product E was not dissolved even by heating it with 6 N hydrochloric acid, 6 N nitric acid, aqua regia, or 3 N sodium hydroxide. Each 0.1 g. of the products C, D and E was well mixed with 1 g. of Amberlite IR-120 resin in sodium form (100~200 mesh) in 8 ml. of water. After centrifugation the supernatant was concentrated

TABLE V. CATION-EXCHANGE REACTION BETWEEN POTASSIUM KURROL SALT AND SOLUTIONS OF VARIOUS METAL IONS

| Metal salt | Concn. | pH, initial | Quantity of metal ion exchanged | Exchange capacity at the end of the reaction | % exchange |
|---|---|---|---|---|---|
| | M | | meq. | meq. | |
| $MgCl_2$ | 0.0946 | 5.6 | 7.08 | 8.45 | 83.8 |
| $CaCl_2$ | 0.0981 | 3.9 | 6.95 | 8.43 | 82.4 |
| $MnCl_2$ | 0.1300 | 3.0 | 7.84 | 8.32 | 94.2 |
| $FeSO_4$ | 0.0928 | 1.3 | 7.59 | 8.39 | 90.5 |
| $Fe_2(SO_4)_3$ | 0.1568 | 0.8 | 3.80 | 7.35 | 51.7 |
| $CoCl_2$ | 0.0987 | 4.7 | 7.39 | 8.46 | 87.3 |
| $NiSO_4$ | 0.0984 | 5.6 | 7.68 | 8.47 | 90.8 |
| $CuSO_4$ | 0.1006 | 4.3 | 5.03 | 5.77 | 87.2 |
| $ZnCl_2$ | 0.0910 | 2.1 | 7.92 | 8.46 | 93.7 |

at room temperature. Two-dimensional paper chromatography for the solution was carried out. The results are shown in Table IV. Although only minute parts of the products C, D and E were brought into the solutions, the paper chromatographic data suggested the difference of the chemical compositions of these products.

**7. Exchange-reactions of Various Metal Ions.** —In conformity to the procedure used for the nickel ion, 1 g. of the potassium Kurrol salt was subjected to react with 200 ml. of about 0.09~0.16 M solution of each of the following metal ions for 8 hr. at 20°C: magnesium, calcium, manganese(II), iron(II), iron(III), cobalt(II), copper(II) and zinc. After the exchange reactions, the amounts of phosphate dissolved in the solution and the decreases in the metal ion concentrations were measured. With the aid of these measurements, percentages of exchange based on millieqivalent of cations were calculated as shown in Table V. Only in the case of copper(II) sulfate a large amount of the initial potassium Kurrol salt was dissolved in the course of the reaction. Except for iron(III), percentages of exchange for all cations investigated in the present work were in the range 82 to 94.

## Summary

Pure crystalline potassium Kurrol salt was prepared and its X-ray pattern was compared with that obtained by Klement et al. The solubility of the potassium Kurrol salt in water was 0.007~0.009 per cent at room temperature. Qualitative observation was made for the reactions of the potassium Kurrol salt with various metal ions. Therefore was an optimum concentration of sodium chloride to dissolve the potassium Kurrol salt. The investigation of reactions of the potassium Kurrol salt in a solid state with solutions of nickel sulfate indicated that the reaction is a cation-exchange reaction between potassium and nickel ions. It was also found that the reaction is reverssible. The nickel-substituted product is green-colored and gummy. Some properties of the substances obtained by heating the above green product were studied. Exchange reactions of potassium Kurrol salt with various metal ions were investigated. Percentages of exchange for magnesium, calcium, manganese(II), iron(II), cobalt(II), nickel(II), copper(II) and zinc were all in the range 82 to 94 under the conditions used in the present work.

The authors are indebted to Professor T. Kiba for his continued encouragement.

*Department of Chemistry*
*Faculty of Science*
*Kanazawa University*
*Kanazawa*

# *Distribution of Unpaired π-Electron in Some Semiquinone Ions*

By Yoshio MATSUNAGA

(Received May 2, 1960)

The hyperfine structure (hfs) of the electron spin resonance (ESR) spectra of free radicals in the dissolved state arises from the interaction between the magnetic moment of the unpaired π-electron and the magnetic moments of the protons and some other magnetic nuclei in the molecule. Based on the spectra of *o*- and *p*-benzosemiquinone ions McConnell has suggested that the magnitude of ring proton splitting constant $a_j$ is approximately proportional to the density of unpaired π-electron $\rho_j$ on the adjacent aromatic carbon atom $j$ given by a simple MO treatment, and proposed the relation $a_j=34\rho_j$[1]. Later he has developed a theoretical study in terms of configurational interaction and concluded that the above-mentioned empirical relation can be used for practical calculation[2]. This approximation has been applied successfully to the interpretation of hfs of ESR spectra of a number of alternant aromatic hydrocarbon monopositive and mononegative ions[3,4].

McConnell has used a set of parameters $\alpha_O=\alpha+\beta$ and $\beta_{CO}=\beta$ in his simple MO treatment of benzosemiquinone ions[1]. These values have been originally proposed for the oxygen atoms and the carbon-oxygen bonds in neutral quinone molecule[5], and the effect of negative charge on the magnitude of these parameters has not been taken into consideration in the treatment of semiquinone ions. Therefore, it seemed to be desirable to find a correct set of parameters for the extension of theoretical work to the semiquinone ions with more complicated molecular structure. The MO treatment with such a set of parameters might be very helpful to the analysis of hfs of ESR spectra of semiquinone ions. In the previous paper the author has attempted to estimate the required parameters based on the frequencies of the C-O stretching vibration in alkali salts of *p*-benzo- and *p*-biphenosemiquinones and obtained a set of $\alpha_O=\alpha+(1/3\sim1/2)\beta$ and $\beta_{CO}=\beta$[6]. Here we wish to present the results of simple MO treatment with the suggested parameters and compare with the experimental results for several semiquinone ions.

## Method of Calculation

The calculations in the present paper were carried out by the simple LCAO MO method. The density of unpaired π-electron at each carbon atom was approximated by the square of the coefficient of its $2p$ function in the singly occupied MO. The coulomb integrals for carbon atoms were assumed to be $\alpha$, and the exchange integrals were taken as $\beta$ including that for C-O bonds. The coulomb integral for the oxygen atoms was assumed to be $\alpha+(1/2)\beta$ or $\alpha+(2/3)\beta$. The former value was taken from the previous paper[6] and the latter was estimated by the following method. Naphthosemiquinone ion gives a spectrum of three quintets, therefore the density of unpaired π-electron on the aromatic carbon atoms 5 and 5′ is practically equal to that on the carbon atoms 6 and 6′ (see structural formula). The singly occupied MO of this semiquinone ion is antisymmetric. Accordingly, if we assume $\beta_{CO}=\beta$, the magnitude of the coulomb integral for the oxygen atoms $\alpha_O=\alpha+\delta\beta$ can be determined by the system of equations for the coefficient $c_j$ of $2p$ function at carbon atom $j$;

$$
\begin{aligned}
&(y+\delta)c_1+c_3=0\\
&(y-1)c_2+c_3=0\\
&c_1+c_2+yc_3+c_4=0\\
&c_3+(y-1)c_4+c_5=0\\
&c_4+yc_5+c_6=0\\
&c_5+(y-1)c_6=0,
\end{aligned}
$$

where $y=(\alpha-E)/\beta$, and the normalizing condition $\sum c_j^2=1$. If the coefficients of $2p$ function at the carbon atoms 5 and 6 are supposed to be exactly equal to each other, we obtain $\alpha_O=\alpha+(2/3)\beta$. We used $a_j=32\rho_j$ throughout this paper instead of $a_j=34\rho_j$ proposed by McConnell for semiquinone ions simply by the reason that the former seems to fit better with the experimental results. The structural formula and the numbering of oxygen and carbon atoms chosen for convenience are summarized in Fig. 1.

1) H. M. McConnell, *J. Chem. Phys.*, **24**, 632 (1956).
2) M. M. McConnell, ibid., **28**, 1188 (1958).
3) E. de Boer and S. I. Weissman, *J. Am. Chem. Soc.*, **80**, 4549 (1958).
4) A. Carrington, F. Dravnieks and M. C. R. Symons, *J. Chem. Soc.*, **1959**, 947.
5) M. G. Evans, J. Gergely and J. de Heer, *Trans. Faraday Soc.*, **45**, 312 (1949).
6) Y. Matsunaga, *Can. J. Chem.*, to be published,

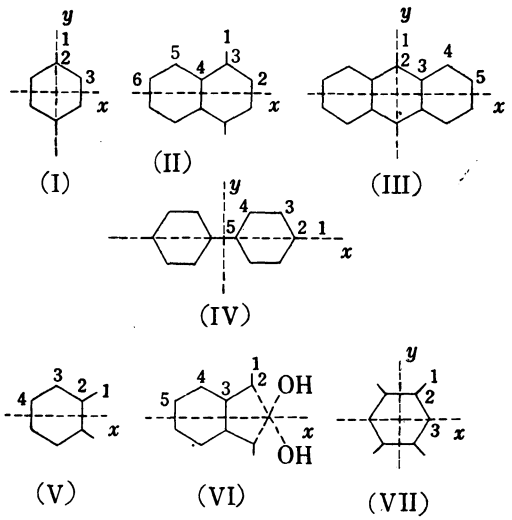



Fig. 1. Structural formula and numbering of oxygen and carbon atoms.

## Results and Discussion

***p*-Benzosemiquinone Ion (I).**—This free radical ion has four equivalent protons and gives a predicted quintet with intensity ratios 1 : 4 : 6 : 4 : 1. The splitting constant has been reported as 2.37±0.01 oersteds by Adams, Blois, and Sands[7]. The densities of unpaired π-electron given by a simple MO treatment and the predicted splitting constant are presented in Table I for various values of $\delta=(\alpha_O-\alpha)/\beta$. Since the magnitude of splitting constant depends only slightly on the value of $\delta$, it is hard to tell which value of $\delta$ gives the best result.

Table I. Unpaired electron densities ($\rho_j$) and splitting constant ($a_3$ in oersted) for *p*-benzosemiquinone ion

| $\delta$ | $\rho_1$ | $\rho_2$ | $\rho_3$ | $a_3$ |
|---|---|---|---|---|
| 0 | 0.332 | 0.032 | 0.068 | 2.18 |
| 1/2 | 0.286 | 0.071 | 0.071 | 2.27 |
| 2/3 | 0.264 | 0.088 | 0.074 | 2.37 |
| 1 | 0.221 | 0.123 | 0.078 | 2.50 |

**Naphthosemiquinone Ion (II).**—The splitting constants have been reported as 3.22±0.03 oersteds for the ring protons attached to the positions 2 and 2′ and 0.57±0.03 oersteds for those 5, 5′, 6 and 6′. The results of calculation are given in Table II. With a difference of 0.1 oersted it is difficult to distinguish experimentally the splittings due to $a_5$ and $a_6$, therefore both of the results obtained assuming $\delta=1/2$ and 2/3 may be considered to be in good agreement with the observed values.

It has been shown that the hf splitting constant for a methyl proton is related to the unpaired π-electron density on the carbon atom, to which the methyl group is attached, by a formula of the same type as for a ring proton[8,9]. Besides the proportional constants for these two kinds of protons seem to be nearly the same. As the unpaired electron density in a methyl group is only in the order of 0.01, we may expect the distribution of unpaired π-electron is not much modified by methyl substitution. Therefore, the magnitude of a methyl proton splitting may be close to that of the ring proton attached to the corresponding carbon atom in the unsubstituted free radical ion. The following splitting constants could be assigned for monomethylnaphthosemiquinone ion; 3.2 oersteds for the methyl group attached to the position 2, 2.6 oersteds for the ring proton attached to the position 2′, and 0.6 oersteds for the remaining four ring protons. The spectrum consists of twenty-four lines as shown in Fig. 2. For dimethyl-derivative 2.3 oersteds for the six protons in the methyl groups attached to the positions 2 and 2′ and 0.57 oersteds for the ring protons have been assigned by Vivo[10]. Contrary to Vivo's result, an expected quintet with a spacing of

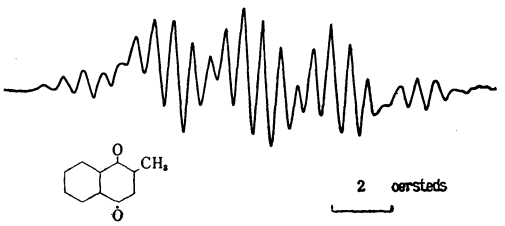



Fig. 2. Electron spin resonance spectrum of monomethylnaphthosemiquinone ion.

Table II. Unpaired electron densities ($\rho_j$) and splitting constants ($a_j$ in oersted) for naphthosemiquinone ion

| $\delta$ | $\rho_1$ | $\rho_2$ | $\rho_3$ | $\rho_4$ | $\rho_5$ | $\rho_6$ | $a_2$ | $a_5$ | $a_6$ |
|---|---|---|---|---|---|---|---|---|---|
| 0 | 0.307 | 0.097 | 0.040 | 0.029 | 0.008 | 0.019 | 3.10 | 0.26 | 0.61 |
| 1/2 | 0.249 | 0.099 | 0.083 | 0.026 | 0.019 | 0.023 | 3.17 | 0.61 | 0.74 |
| 2/3 | 0.225 | 0.100 | 0.100 | 0.025 | 0.025 | 0.025 | 3.20 | 0.80 | 0.80 |
| 1 | 0.175 | 0.103 | 0.132 | 0.022 | 0.039 | 0.030 | 3.30 | 1.25 | 0.96 |

7) M. Adams, M. S. Blois, Jr. and R. H. Sands, *J. Chem. Phys.*, **28**, 774 (1958).
8) C. B. Chesnut, ibid., **29**, 43 (1958).
9) A. C. McLachlan, *Mol. Phys.*, **1**, 233 (1958).
10) J. L. Vivo, Dissertation, University of Minnesota, 1956.

0.6 oersteds was found in the case of dichloronaphthosemiquinone ion. We may conclude that the ring protons at 5 and 6 are nearly equivalent in all of the examined derivatives.

The semiquinone ion formed on reduction of hydroxynaphthoquinone in alkaline medium has an ionized oxygen atom attached to the position 2. The effect of this substituent is so strong that the distribution of unpaired $\pi$-electron in naphthosemiquinone ion is completely changed. The spectrum consists of partially resolved two doublets (1.6 and 1.8 oersteds) instead of two quintets. By comparison with the well-resolved two doublets with 1.5 and 1.9 oersteds given by the semiquinone ion from hydroxychloronaphthoquinone, in which the chlorine atom can be considered inactive to hf splitting, it appears that the observed hfs is entirely due to the interaction between unpaired electron and two protons among four attached to the positions 5, 5′, 6 and 6′ (see Fig. 3).

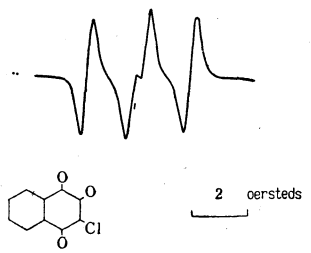



Fig. 3. Electron spin resonance spectrum of the semiquinone ion from hydroxychloronaphthoquinone.

**Anthrasemiquinone Ion (III).**—This semiquinone ion gives a spectrum of thirteen lines resulting from one set of four equivalent protons and another of four. The splitting constant for one set must be 1.0 oersted and for the other 0.5 oersteds. However, without further information we cannot determine which of the two possible assignments is responsible. The results by simple MO treatment with the proposed parameters suggest that the proton at 5 and its three equivalents give the larger splitting.

TABLE III. UNPAIRED ELECTRON DENSITIES ($\rho_j$) AND SPLITTING CONSTANTS ($a_j$ IN OERSTED) FOR ANTHRASEMIQUINONE ION

| $\delta$ | $\rho_1$ | $\rho_2$ | $\rho_3$ | $\rho_4$ | $\rho_5$ | $a_4$ | $a_5$ |
|---|---|---|---|---|---|---|---|
| 0 | 0.277 | 0.050 | 0.046 | 0.010 | 0.030 | 0.32 | 0.96 |
| 1/2 | 0.214 | 0.098 | 0.042 | 0.021 | 0.031 | 0.67 | 0.99 |
| 2/3 | 0.191 | 0.115 | 0.040 | 0.026 | 0.031 | 0.83 | 0.99 |
| 1 | 0.143 | 0.143 | 0.036 | 0.036 | 0.036 | 1.15 | 1.15 |

**Biphenosemiquinone Ion (IV).**—As shown in Table IV, the splitting due to the proton at 3 is expected to be twice or a little more larger than that due to the proton at 4. Unfortunately this free radical ion was found too unstable to be examined by our spectrometer. Tetramethylbiphenosemiquinone ion has four methyl groups attached to the position 3 and its equivalents and gives a spectrum of twenty-one lines with a spacing of 0.78 oersteds[11]. This pattern could be explained using the splitting constants 2.34 oersteds for the ring protons and 0.78 oersteds for the methyl protons as well as using 0.78 oersteds for the ring protons and 1.56 oersteds for the methyl protons. The theoretical results given in Table IV are definitely favorable to the latter assignment.

TABLE IV. UNPAIRED ELECTRON DENSITIES ($\rho_j$) AND SPLITTING CONSTANTS ($a_j$ IN OERSTED) FOR BIPHENOSEMIQUINONE ION

| $\delta$ | $\rho_1$ | $\rho_2$ | $\rho_3$ | $\rho_4$ | $\rho_5$ | $a_3$ | $a_4$ |
|---|---|---|---|---|---|---|---|
| 0 | 0.278 | 0.005 | 0.067 | 0.011 | 0.060 | 2.14 | 0.35 |
| 1/2 | 0.227 | 0.033 | 0.062 | 0.023 | 0.071 | 1.98 | 0.74 |
| 2/3 | 0.202 | 0.045 | 0.060 | 0.028 | 0.077 | 1.92 | 0.90 |
| 1 | 0.152 | 0.072 | 0.056 | 0.038 | 0.088 | 1.79 | 1.22 |

***o*-Benzosemiquinone Ion (V).** — The three triplets observed in the ESR spectrum of this radical ion have been analyzed by Hoskins[12]. The major splitting has been attributed to the protons attached positions 4 and 4′ and the minor one to those at 3 and 3′. The values have been estimated as $3.65\pm0.04$ and $0.95\pm0.04$ oersteds by Adams et al.[7] Both of the splitting constants calculated using $\delta=1/2$ and 2/3 were found in serious disagreement with the experimetnal ones. Since our parameters seemed not applicable to *o*-semiquinone ions, we attempted to estimate a new one which gives a ratio of $c_4^2/c_3^2=4$ in the present case. Although the value thus estimated as high as 1.611 might suggest that a more refined model is required for the MO treatment of *o*-semiquinone ion, it must be noted that the calculated splitting constants are in good agreement with the observed ones. The unpaired $\pi$-electron distribution cited in the last line of Table V is taken from Kuboyama's work on *o*-quinones[13]. As we may expect for the reasons discussed above, his results obtained with the following parameters for neutral quinone molecule predict the splitting constants not far from the experimental ones; $\alpha_O=\alpha+1.3\beta$, $\alpha_2=\alpha+0.2\beta$, $\beta_{22'}=0.8\beta$, $\beta_{23}=\beta_{44'}=0.9\beta$, $\alpha_3=\alpha_4=\alpha$ and $\beta_{12}=\beta_{34}=\beta$.

11) Y. Matsunaga and C. A. McDowell, *Can. J. Chem.*, to be published.
12) R. H. Hoskins, *J. Chem. Phys.*, **23**, 1975 (1955).
13) A. Kuboyama, This Bulletin, **32**, 1226 (1959).

Table V. Unpaired electron densities ($\rho_j$) and splitting constants ($a_j$ in oersted) for *o*-benzosemiquinone ion

| $\delta$ | $\rho_1$ | $\rho_2$ | $\rho_3$ | $\rho_4$ | $a_3$ | $a_4$ |
|---|---|---|---|---|---|---|
| 0 | 0.295 | 0.026 | 0.113 | 0.067 | 3.62 | 2.14 |
| 1/2 | 0.286 | 0.071 | 0.071 | 0.071 | 2.27 | 2.27 |
| 2/3 | 0.272 | 0.090 | 0.062 | 0.076 | 1.98 | 2.43 |
| 1 | 0.234 | 0.128 | 0.049 | 0.089 | 1.57 | 2.85 |
| 1.611 | 0.155 | 0.192 | 0.031 | 0.123 | 0.99 | 3.94 |
| Kuboyama* | 0.191 | 0.176 | 0.032 | 0.101 | 1.02 | 3.23 |

* See Ref. 13.

**Semiquinone Ion from Ninhydrin (VI).** — Adams et al. have observed that ninhydrin on reduction gives a spectrum of three triplets due to the two pairs of equivalent protons on the aromatic ring, and estimated the splitting constants to be 1.95±0.04 and 1.59±0.04 oersteds[7]. The conjugated system of this radical ion was considered to be similar to that of *o*-divinylbenzene and examined by the simple MO method changing the magnitude of $\delta$. The results suggest that the larger splitting is attributed to the protons attached to the positions 5 and 5', and the value of $\delta$ close to 1.6 is again required for quantitative agreement with the experimental results.

Table VI. Unpaired electron densities ($\rho_j$) and splitting constants ($a_j$ in oersted) for the semiquinone ion from ninhydrin

| $\delta$ | $\rho_1$ | $\rho_2$ | $\rho_3$ | $\rho_4$ | $\rho_5$ | $a_4$ | $a_5$ |
|---|---|---|---|---|---|---|---|
| 0 | 0.232 | 0.071 | 0.111 | 0.014 | 0.071 | 0.45 | 2.27 |
| 1/2 | 0.185 | 0.132 | 0.093 | 0.027 | 0.063 | 0.86 | 2.02 |
| 2/3 | 0.167 | 0.152 | 0.089 | 0.031 | 0.061 | 0.99 | 1.95 |
| 1 | 0.132 | 0.186 | 0.080 | 0.041 | 0.061 | 1.31 | 1.95 |
| 1.6 | 0.084 | 0.231 | 0.069 | 0.055 | 0.061 | 1.76 | 1.95 |

**Semiquinone Ion from Dihydroxy-*p*-benzoquinone (VII).** — It has been found that the ring proton splitting changes from 1.83 oersteds in dimethyl-*p*-benzosemiquinone ion to 0.30 oersteds in dimethoxy-derivative[11]. This considerable decrease suggests the localization of unpaired π-electron on the oxygen atoms in the methoxyl groups. We extended here our measurements to the highly symmetric semiquinone ion formed on reduction of dihydroxy-*p*-benzoquinone. Although we do not know the correct value of $\delta$ for this triply charged semiquinone ion, the value must be in the range from −1 for negatively charged oxygen to +1 for the oxygen atom in carbonyl group[14]. The singly occupied level predicted by a simple MO treatment for this semiquinone ion is antisymmetric with respect to the *x*-plane. Therefore, no unpaired π-electron density is found on the carbon atoms to which the ring protons are attached and we may expect no hfs in the ESR spectrum of the present radical ion. The small splitting due to the ring protons observed in the case of dimethoxy-*p*-benzosemiquinone ion may be correlated with the difference between the electronegativities for two kinds of oxygen atoms.

Contrary to the expectation, on reduction with sodium dithionate dihydroxy-*p*-benzoquinone dissolved in a mixture of pyridine, ethylene glycol, and 2 N pottasium hydroxide (1 : 2 : 1 by volume) shows a triplet with a spacing of 0.78 oersteds. If we substitute the two ring protons with chlorine or bromine atoms, the semiquinone ion gives an expected single line spectrum. Apparently there is the ring proton splitting in the ESR spectrum of the radical ion formed by reduction of dihydroxy-*p*-benzoquinone. The unpaired π-electron density on the adjacent carbon atoms must be as high as 0.02. Therefore, we may conclude that a single configuration MO treatment does give neither the correct symmetyr of energy level nor the correct distribution of unpaired π-electron for the present radical. A similalr disagreement as to the symmetry of energy level has been reported by de Boer and Weissman in the case of pyrene negative ion[3].

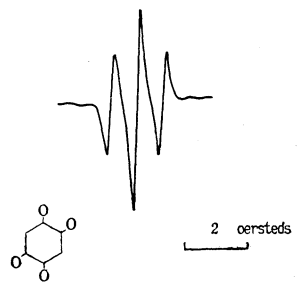



Fig. 4. Electron spin resonance spectrum of the semiquinone ion from dihydroxy-*p*-benzoquinone.

## Summary

The distribution of unpaired π-electron was calculated by the simple MO method using the proposed parameters $\alpha_O = \alpha + (1/2)\beta$ and $\alpha + (2/3)\beta$ for six semiquinone ions. The calculated splitting constants for the ring protons in *p*-benzo- and naphtho-semiquinone ions were found in good agreement with the experimental ones and the MO treatment with the proposed parameters seemed to be very helpful to the analysis of the hfs of ESR spectra of anthra- and bipheno-semiquinone ions. In the case of *o*-semiquinone ion, a much higher value of $\alpha_O$ was required to obtain quantitative agreement. The assignment of splitting constants was

14) H. H. Jaffe, *J. Am. Chem. Soc.*, 77, 4448 (1955).

attempted for the semiquinone ion from ninhydrin. It was found that the simple MO method fails to predict the symmetry of the singly occupied MO in the semiquinone ion formed on reduction of dihydroxy-*p*-benzoquinone. In addition the ESR spectra of the semiquinone ions from methyl- and hydroxynaphthoquinones etc. were described.

The spectra quoted in this paper were obtained at the University of British Columbia during the tenure of a National Research Council of Canada Postdoctorate Fellowship. The author wishes to express his sincere thanks to Professor C. A. McDowell for his generous keep and hospitality.

*Department of Chemistry*
*Faculty of Science*
*The University of Tokyo*
*Hongo, Tokyo*

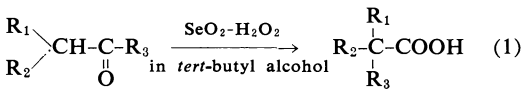
# *Hydrogen Peroxide Oxidation. IV. A New Rearrangement Reaction of Phenyl Alkyl Ketones by Selenium Dioxide Catalyst*[1]

By Noboru SONODA and Shigeru TSUTSUMI

(Received May 10, 1960)

In the previous papers[2,3] we reported the rearrangement reactions of dialkyl ketones by selenium dioxide catalyzed oxidation with hydrogen peroxide, and now the present paper deals with a similar study using several phenyl alkyl ketones.

The rearrangement reaction mode of a dialkyl ketone is shown generally as below;

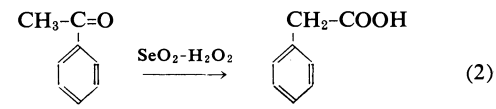



(1)

$R_1, R_2$=H or alkyl, $R_3$=alkyl

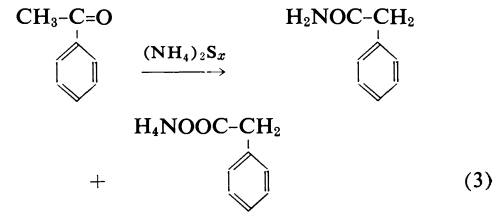
where either of the two alkyl groups $R_1R_2CH$- and $R_3$, can migrate onto the $\alpha$-carbon atom of the other alkyl group so that the two isomeric acids containing the same number of carbon atoms as original ketone are produced when unsymmetrical ketone is used. In the case of phenyl alkyl ketone, only the rearrangement of the phenyl group is possible, because the phenyl group does not possess an $\alpha$-hydrogen atom which may be substituted by the migrating alkyl group. Thus, the $\alpha$-phenyl carboxylic acids are synthesized from phenyl alkyl ketones by the oxidation with selenium dioxide-hydrogen peroxide reagent.

For example, when acetophenone was treated with hydrogen peroxide in *tert*-butyl alcohol in the presence of a small amount of selenium dioxide as catalyst at about 80~82°C, phenyl acetic acid was isolated from the reaction products as well as some cleavaged products.




(2)

Synthesis of phenyl acetic acid derivatives from acetophenone had also been undertaken by Willgerodt[4] showing that phenyl acetamide and ammonium phenyl acetate were obtained by the oxidation of acetophenone with ammonium polysulfide. But in the Willgerodt reaction[5] no change of carbon skeleton was observed because of the reduction of the carbonyl group to the methylene group and the oxidation of the methyl group to carbonamide or salt of carboxylic acid.

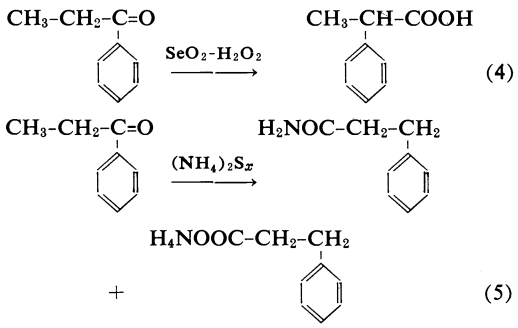



(3)

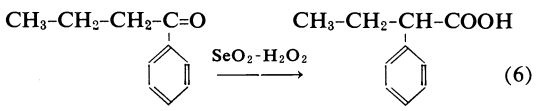
On the other hand the production of phenyl acetic acid from acetophenone by selenium

1) Presented at the 12th Annual Meeting of the Chemical Society of Japan, Kyoto, April 2, 1959.
2) N. Sonoda and S. Tsutsumi, This Bulletin, **32**, 505 (1959).
3) N. Sonoda, T. Yamaguchi and S. Tsutsumi, *J. Chem. Soc. Japan, Ind. Chem. Sec.* (*Kogyo Kagaku Zasshi*), **63**, 737 (1960).
4) C. Willgerodt, *Ber.*, **21**, 534 (1888); C. Willgerodt and F. H. Merk, *J. prakt. Chem.*, **80**, 192 (1909).
5) For a review of the Willgerodt reaction, see (a) M. Carmack, "Organic Reactions", Vol. III, John Wiley & Sons, Inc., New York, N. Y. (1946), pp. 83-107; (b) R. Wegler, E. Kühle and W. Schäfer, *Angew. Chem.*, **70**, 351 (1958).

dioxide catalyzed hydrogen peroxide oxidation is clearly based on the migration of the phenyl group to the methyl carbon atom. An evidence of the rearrangement was shown by the fact that $\alpha$-phenyl propionic acid was produced by the phenyl migration when phenyl ethyl ketone was treated under the reaction condition similar to that of acetophenone, whereas $\beta$-phenyl propionic acid derivatives were formed from phenyl ethyl ketone under the Willgerodt reaction condition[4].




In a similar manner, phenyl *n*-propyl ketone was oxidized with selenium dioxide-hydrogen peroxide reagent to give $\alpha$-phenyl butyric acid.




These facts suggest that similar treatment may be generally applicable to the other aryl alkyl ketones.

The reactivity of phenyl alkyl ketones was apparently lower than that of dialkyl ketones[2,3]. The yield of the rearrangement products was only about 10 per cent based on the treated ketones in spite of using an excess amount of hydrogen peroxide, and fairly good recovery of starting ketones was observed in all the cases.

On the other hand, oxidative cleavage was also observed. Benzoic acid was isolated as a main cleavage product in a comparable yield to the rearrangement product and phenol was identified as its tribromide in all cases. Aliphatic acids derived from the aliphatic fragments of the ketones or oxidative decomposition product[6] of *tert*-butyl alcohol used as solvent were also detected by gaschromatography. These products are listed in Table I.

We have proposed the probable mechanism[2] of these rearrangement reactions, which comprise the enol formation of the ketones

Table I. Cleavage products from oxidative reaction of phenyl alkyl ketones

| Reactants | Products confirmed | Yield % |
|---|---|---|
| Acetophenone | Benzoic acid | 12.3 |
| | Phenol | trace |
| | Acetic acid[a] | — |
| | Propionic acid[b] | — |
| Phenyl ethyl ketone | Benzoic acid | 4.1 |
| | Phenol | trace |
| | Acetic acid | — |
| | Propionic acid | — |
| Phenyl *n*-propyl ketone | Benzoic acid | 4.9 |
| | Phenol | trace |
| | Propionic acid | — |
| | *n*-Butyric acid | — |

a) Formic acid was assumed to be present, but was not detected.
b) This propionic acid was supplied from the solvent.

followed by the attack of peroxyselenious acid as the most possible active species. Since peroxyselenious acid is a kind of peracid, it is reasonable to believe that the Baeyer-Villiger oxidation[7] may be accompanied in this reaction system. Formation of phenol and aliphatic acid from the corresponding ketone may be interpreted as results of hydrolysis of the phenyl ester produced by the Baeyer-Villiger reaction. In addition, the other cleavage path is assumed to be present, because alkyl benzoate will not be formed from phenyl alkyl ketone[7] under the Baeyer-Villiger reaction condition so that benzoic acid may not be the reaction product via the Baeyer-Villiger oxidation.

## Experimental[8]

**Oxidative Reagent.**—Selenium dioxide-hydrogen peroxide reagent was prepared in the same manner as previously described[2]. This reagent includes 2.0 g. of selenium dioxide and 1.0 mol. of hydrogen peroxide in about 500 ml. of *tert*-butyl alcohol solution.

**Oxidation of Acetophenone.**—To a 100 ml. of the selenium dioxide-hydrogen peroxide reagent (0.4 g. of selenium dioxide and 0.2 mol. of hydrogen peroxide) was added 12.0 g. (0.1 mol.) of acetophenone, and the resulting mixture was heated to 80~82°C for 17 hr. The reaction mixture turned red during the oxidation. The mixture was distilled to remove the solvent and the small amount of metallic selenium deposited was filtered off. The filtrate was poured into 200 ml. of ether, and the ethereal solution was extracted first with saturated sodium bicarbonate solusion (A) and then with 8% sodium hydroxide solution (B). After the ethereal solution was dried over anhydrous sodium sulfate,

6) Propionic acid was partly produced from acetone which was formed by the decomposition of *tert*-butyl hydroperoxide or di-*tert*-butyl peroxide being furnished by the oxidation of *tert*-butyl alcohol used as solvent. This reaction path was already confirmed (see Ref. 2).

7) C. H. Hassall, "Organic Reactions", Vol. IX, John Wiley & Sons, Inc., New York, N. Y. (1957), p. 73-106.

8) The boiling and melting points are uncorrected.

the ether was removed and the residue was distilled under reduced pressure; 6.6 g. of neutral substance, consisting mainly of unreacted acetophenone, was obtained, b. p. 62~65°C (4 mmHg), 2,4-dinitrophenyl-hydrazone of this fraction melted at 245~246°C (lit.[9] m. p. 247~248°C) and mixed melting point with an authentic sample (m. p. 245~246°C) showed no depression.

The sodium bicarbonate solution A was acidified with 3 N hydrochloric acid and was extracted with ether. After the ethereal solution was dried over anhydrous sodium sulfate, the ether was removed by distillation and the residue was distilled under reduced pressure. Acetic acid and propionic acid were identified in the low boiling products by gaschromatography: column, tricresylphosphate; column temperature, 140°C; carrier gas, $H_2$; flow rate of $H_2$, 40 ml./min. The fraction boiling between 112~122°C (4 mmHg), which solidified at once, was collected. This gave 2.8 g. of a mixture of acids. A small portion of the mixture was recrystallized from hot water, and a mixture of two kinds of crystalline solids was obtained. One of them was white plate, phenyl acetic acid, which was separated as floats over the surface of water by shaking. After further recrystallization from petroleum ether, a sample (m. p. 75.5~76°C) was obtained (lit.[10] m. p. 76°C), mixed melting point with an authentic sample was not depressed. The yield of phenyl acetic acid was 9.6% based on the used ketone calculated from ultraviolet spectrum of the mixture of acids.

Found: C, 70.65; H, 6.02. Calcd. for $C_8H_8O_2$: C, 70.57; H, 5.92%.

Benzoic acid, white needle crystals from hot water, was obtained as residue after removal of phenyl acetic acid; the melting point and mixed melting point with an authentic sample was 121°C (lit.[10] m. p. 121°C); the yield was 12.3% calculated from the ultraviolet spectrum.

The sodium hydroxide solution B was acidified and extracted with ether. After the ethereal solution was dried over anhydrous sodium sulfate, the ether was removed by distillation. On distillation of the residual brown oil under reduced pressure, 0.15 g. of phenol was isolated; the tribromide was prepared which melted at 94°C (lit.[10] m. p. 95°C), mixed melting point with an authentic sample showed no depression.

**Oxidation of Phenyl Ethyl Ketone.**—To a 100 ml. of the selenium dioxide-hydrogen peroxide reagent (0.4 g. of selenium dioxide and 0.2 mol. of hydrogen peroxide) was added 13.4 g. (0.1 mol.) of phenyl ethyl ketone, and the reaction was carried out at 80~82°C for 20 hr. The reaction products were separated in the same manner as described for the oxidation of acetophenone.

Uureacted phenyl ethyl ketone (9.1 g.) was recovered from the neutral part; b. p. 70~73°C (5 mmHg); 2.4-dinitrophenylhydrazone of this fraction melted at 191~192°C (lit.[10] 191°C), mixed melting point with an authentic sample showed no depression.

Acetic acid and propionic acid were identified in the acidic part by the gaschromatography. A mixture of acids, 2.2 g. of oily product of b. p. 115~120°C (3 mmHg), was obtained. After a portion of this product was cooled to 0°C, a crystalline solid deposited was collected on a filter and was purified by recrystallization from petroleum ether to give benzoic acid. The melting point and mixed melting point with an authentic sample was 120~121°C (4.1% yield calculated from ultraviolet spectrum of the mixture of acids). The filtrate was an oily product, which was proved to be $\alpha$-phenyl propionic acid (11.3% yield). The amide was prepared according to the usual procedure[10] and was recrystallized from benzene, melting at 92.5~93°C (lit.[11] 93°C).

Found: C, 72.34; H, 7.58; N, 9.57. Calcd. for $C_9H_{11}NO$: C, 72.45; H, 7.43; N, 9.39%.

The presence of phenol was identified in the phenolic part by the ferric chloride test.

**Oxidation of Phenyl *n*-Propyl Ketone.**—To a 100 ml. of the selenium dioxide-hydrogen peroxide reagent (0.4 g. of selenium dioxide and 0.2 mol. of hydrogen peroxide) was added 14.8 g. (0.1 mol.) of phenyl *n*-propyl ketone, and the reaction was carried out at 80~82°C for 24 hr. The reaction products were separated in the same manner as described for the oxidation of acetophenone.

The unreacted phenyl *n*-propyl ketone (10.2 g.) was recovered from the neutral part; b. p. 104~108°C (14 mmHg); 2,4-dinitrophenylhydrazone melted at 190~191°C (lit.[9] 191~192°C), mixed melting point with an authentic sample was not depressed.

Propionic acid and butyric acid were identified by the gaschromatography. On distillation, 1.5 g. of a mixture of acids, b. p. 105~110°C (1 mmHg), was obtained. After the mixture was allowed to stand at room temperature for several hours, the crystalline product deposited was filtered and recrystallized from hot water to give 0.6 g. (4.9% yield) of benzoic acid, m. p. 121°C. The filtrate, 0.7 g. (4.3% yield) of $\alpha$-phenyl butyric acid, froze to a crystalline solid, which melted slightly above room temperature (lit.[12] m. p. 43°C). A redistilled sampe showed neutral equivalent 162; calculated for $C_{10}H_{12}O_2$: 164.2. The amide was prepared according to the usual procedure[10] and was recrystallized from benzene-ligroin, melting at 83~84°C (lit.[13] 84°C). The phenol was isolated from the phenolic part, 0.2 g.; the tribromide melted at 94°C (lit.[10] 95°C), mixed melting point with an authentic sample showed no depression.

## Summary

1) Selenium dioxide catalyzed oxidation of phenyl alkyl ketone with hydrogen peroxide in *tert*-butyl alcohol gave $\alpha$-phenyl carboxylic acid which was produced by the rearrangement of the phenyl group to the $\alpha$-carbon atom as shown by Eqs. 2, 4 and 6.

9) G. D. Johnson, *J. Am. Chem. Soc.*, **75**, 2720 (1953).

10) R. L. Shriner, R. C. Fuson and D. Y. Curtin, "The Systematic Identification of Organic Compounds", 4th Ed., John Wiley & Sons, Inc., New York, N. Y. (1956).

11) J. A. King and F. H. H. McMillan, *J. Am. Chem. Soc.*, **68**, 635 (1946).

12) M. M. Rising and T. W. Zee, *J. Am. Chem. Soc.*, **50**, 1211 (1928).

13) *Beilstein*, **9** II, p. 356, Springer-Verlag, Berlin (1946).

Therefore, the reaction mode is quite different from the Willgerodt reaction. The fact described above suggests that similar treatment may be generally applicable to the other aryl alkyl ketones.

2) The reactivity of phenyl alkyl ketone was lower than that of dialkyl ketone, and cleavage reaction was also observed. It is assumed that the cleavage products may be produced partly from the Baeyer-Villiger oxidation product because an active species in this reaction system is considered to be peroxyselenious acid, a kind of peracid.

*Department of Chemical Technology*
*Faculty of Engineering*
*Osaka University*
*Miyakojima-ku, Osaka*

# *Inorganic Extraction Studies on the System of Tri-n-butyl Phosphate—Nitric Acid*

By Tomitaro ISHIMORI and Kenju WATANABE

(Received May 17, 1960)

Tri-*n*-butyl phosphate*, an excellent extracting agent for inorganic salts, has been widely used for the reprocessing of reactor fuel, the separation of some actinide elements from fission products and the analysis of uranium.

Results on the distribution of inorganic salts between TBP and nitric acid solution have been published by a number of investigators. Peppard et al. studied the behavior of scandium[1], yttrium[2], zirconium[1], lanthanide elements[2,3,4,5] and some actinide elements[1,3,5-7] in the extraction from nitric acid solution. McKay et al. also studied in detail the extraction of nitrates of yttrium[8], zirconium[9], lanthanide elements[8,10] and some actinide elements[11-16] with both diluted and undiluted TBP.

Distribution of uranyl[13-31] and thorium nitrate[1,7,11,15,16,20,23-25,32-39] between TBP and nitric acid solution has been studied at various concentrations of TBP, and nitric acid and/or nitrate using aluminum nitrate[18,23,25,26,33],

* Tri-*n*-butyl phosphate is abbreviated as TBP in the present paper.

1) D. F. Peppard, C. W. Mason and J. L. Maier, *J. Inorg. Nucl. Chem.*, 3, 215 (1956).
2) D. F. Peppard, J. P. Faris, P. R. Gray and G. W. Mason, *J. Phys. Chem.*, 57, 294 (1953).
3) D. F. Peppard, W. J. Driscoll, R. J. Sironen and S. McCarty, *J. Inorg. Nucl. Chem.*, 4, 326 (1957).
4) D. F. Peppard, P. R. Gray and M. M. Markus, *J. Am. Chem. Soc.*, 75, 6063 (1953).
5) P. R. Gray, unpublished results quoted in a paper by E. K. Hyde, "Proceedings of International Conference on Peaceful Uses of Atomic Energy", Vol. VII, P/728, Uuited Nations Publication, New York (1956).
6) D. F. Peppard, G. W. Mason, P. R. Gray and J. F. Mech, *J. Am. Chem. Soc.*, 74, 6081 (1952).
7) D. F. Peppard, G. Asanovich, R. W. Atteberry, O. Du Temple, M. V. Gergel, A. W. Gnaedinger, G. W. Mason, V. H. Meschke, E. S. Nuchtman and I. O. Winsch, ibid., 75, 4576 (1953).
8) D. Scargill, K. Alcock, J. M. Fletcher, E. Hesford and H. A. C. McKay, *J. Inorg. Nucl. Chem.*, 4, 304 (1957).
9) K. Alcock, F. C. Bedford, W. H. Hardwich and H. A. C. McKay, ibid., 4, 100 (1957).
10) E. Hesford, E. E. Jackson and H. A. C. McKay, ibid., 9, 279 (1959).
11) E. Hesford, H. A. C. McKay and D. Scargill, ibid., 4, 321 (1957).
12) G. F. Best, H. A. C. McKay and P. R. Woodgate, ibid., 4, 315, (1957).
13) K. Alcock, G. F. Best, E. Hesford and H. A. C. McKay, 6, ibid., 328 (1958).
14) E. Hesford and H. A. C. McKay, *Trans. Faraday Soc.*, 54, 573 (1958).
15) H. A. C. McKay, "Proceedings of International Conference on "Peaceful Uses of Atomic Energy, Vol. VII,P/441, United Nations Publication, New York (1956).
16) J. S. Nairn, D. A. Collins, H. A. C. McKay and A. G. Maddock, "Proceedings of Second International Conference on Peaceful Uses of Atomic Energy," P/1458 (1958).
17) T. C. Runion, AEC Rep., ORNL-874 (1950).
18) T. W. Bartlett, AEC Rep., K-706 (1951).
19) R. L Moore, AEC Rep., AECD-3196 (1951).
20) C. J. Rodden, AEC Rep., TID-10161 (1951).
21) K. Kniel, C. L. Gregory, E. R. Renier and R. H. Reuther, AEC Rep., K-903 (1952).
22) R. L. Andelin, E. L. Anderson and W. H. Mcvey, AEC Rep., IDO-14381 (1956).
23) A. T. Gresky, AEC Rep., CF-56-2-157 (1956).
24) E. K. Hyde, "Proceedings of International Conference on Peaceful Uses of Atomic Energy", Vol. VII P/728, United Nations Publication, New York (1956).
25) T.H. Siddall, III, S. G. Parker and W. E. Pront, AEC Rep., DP-53 (1957).
26) J. W. Codding, Jr., AEC Rep., IDO-14454 (1958).
27) T. J. Collopy, AEC Rep., NLCO-749 (1958).
28) J. W. Codding, W. O. Haas, Jr. and F. K. Heumann, *Ind. Eng. Chem.*, 50, 145 (1958).
29) T. Sato, *J. Inorg. Nucl. Chem.*, 6, 334 (1958).
30) T. Sato, ibid., 9, 188 (1959).
31) K. Naito, This Bulletin 33, 363 (1960).
32) M. R. Anderson, AEC Rep., ISC-116 (1950).
33) R. H. Gercke AEC Rep., UCRL-1493 (1951).
34) C. J. Rodden, AEC Rep., TID-10153 (1952).
35) C. J. Rodden, AEC Rep., TID-10154 (1952).
36) C. J. Rodden. AEC Rep., TID-10157 (1953).
37) M. Smutz, M. E. Whatley and G. L. Bridger, AEC Rep., ISC-415 (1953).
38) R. A. Ewing, S. J. Kiehl, Jr. and A. E. Bearse, AEC Rep., BMI-955 (1954).
39) T. H. Siddall, III., AEC Rep., DP-181 (1956).

sodium nitrate[15,18] or calcium nitrate[7,17] as the salting-out agent. In some cases sulfate[27,37], phosphate[27,37] or fluoride[27,33] was added in order to observe the influence of these anions on the partition of the objectives.

Distribution data for protactinium[40], neptunium[13,16,24,64] and plutonium[12,13,15,16,24,28,41,42] were also presented in the extraction with diluted TBP. According to Yakovlev and Kosyakov[43] extractabilities of americium and curium increase with the concentration of nitrate as salting-out agent in the aqueous solution. Behavior of lanthanide elements[20,23,34,35,44-49] has been often studied in the presence of uranium and/or thorium. The extraction of tetravalent cerium[48,50] from nitric acid solution with TBP was very easy in comparison with other trivalent lanthanide elements. Diluted TBP was used in order to separate zirconium from hafnium[51-53]. The extraction of fission products[23,41,42,48,54] with TBP has been evaluated for the decontamination of fissionable materials. Krieger et al.[48], who presented the extraction data of major long-lived fission products (Cs, Sr, Ru, Zr-Nb and lanthanide elements), observed that cesium was not extracted at all while strontium was extracted very slightly from a solution containing aluminum nitrate. They also mentioned that ruthenium and niobium could be extracted in a yield more than 99% into undiluted TBP. According to Bruce[54], molecular iodine was easily extracted with many diluents for TBP, but iodine extraction may have been minimized by maintaining iodine in the reduced valence state. The extractability of zirconium and niobium, given by Scadden et al.[55], from nitric acid solution containing oxalic acid into undiluted TBP was lower than that from nitric acid alone[1]. Morrison and Beaumont[20] showed that distribution ratio of molybdenum between 30% TBP-kerosene and 1 M nitric acid was 0.060 to 0.088. Diamond's observation[56] shows that molybdenum(VI) is not extracted with TBP from nitric acid. It was reported that the distribution of vanadium was very low between 25% TBP and 5 N nitric acid[57]. The distribution coefficients of ferric, cupric, nickel and chromic nitrate between TBP and nitric acid solution were given by Bartlett[18]. McKay et al[14,58,59] and Tuck[60] studied the system of TBP-diluent-nitric acid.

In this paper are presented the comprehensive and systematic studies on the distribution of ions between undiluted TBP and nitric acid of various concentration.

## Experimental

The general techniques used were described in the previous paper[61]. TBP was purified in the usual way[1-3,8-13], and was used without any dilution. Nitric acid solutions were prepared by diluting concentrated chemically pure nitric acid. The acidity was determined volumetrically whenever necessary. Tracers of sodium and potassium were prepared by irradiation of the nitrates while those of manganese, nickel, germanium and tellurium were prepared from irradiated metals. A nickel tracer was separated from radiochemical impurities by an anion-exchange technique[62]. Germanium and tellurium tracers were used immediately after the separation from their daughters, respectively arsenic and iodine, by solvent extraction[63]. The imported tracers, Rb-86, Sb-124, and Os-191 were used as received. The sources of radioactive tracers other than mentioned above were the same as those shown in the previous paper[61].

The specific counting rate of these radiochemical tracers was higher than $10^4$ count per min. per 100 $\mu$g. Although in some cases the oxidation state and the chemical form of the tracer could not clearly be defined, the most familiar chemical forms were chosen as far as possible. Distribution

40) C. J. Hardy, D. Scargill and J. M. Fletcher, *J. Inorg. Nucl. Chem.*, 7, 257 (1958).
41) B. Goldschmidt, P. Regnaut and I. Prevot, "Proceedings of International Conference on Peaceful Uses of Atomic Energy," Vol. IX, P/349, United Nations Publication, New York (1956).
42) J. R. Flanary, ibid., Vol. IX, P/539.
43) G. N. Yakovlev and V. N. Kosyakov, "Proceedings of Second International Conference on Peaceful Uses of Atomic Energy", Vol. XXVIII P/2127, United Nations Publication, New York (1959).
44) AEC Rep., TID-5154 (1951).
45) R. H. Blackmore, A. E. Bearse and G. D. Calkins, AEC Rep., BMI-261 (1952).
46) L. L. Knapp, M. Smutz and F. H. Spedding, AEC Rep., ISC-766 (1956).
47) J. Bockinski, M. Smutz and F. H. Spedding, *Ind. Eng. Chem.*, 50, 157 (1958).
48) H. L. Krieger, B. Kahn and C. P. Staub, AEC Rep., ORNL-2297 (1957).
49) B. Weaver, F. A. Kappelmann and A. C. Topp, *J. Am. Chem. Soc.*, 75, 3943 (1953).
50) J. C. Warf, ibid., 71, 3257 (1949).
51) G. L. Bridger, B. F. Ruth, G. H. Beyer and W. R. Millard, AEC Rep., ISC-186 (1951).
52) W. R. Millard and R. P. Cox, AEC Rep., ISC-234 (1952).
53) H. A. Wilhelm and R. A. Foos, AEC Rep., ISC-458 (1954).
54) F. R. Bruce, "Proceedings of International Conference on Peaceful Uses of Atomic Energy", Vol. VII, P/719, United Nations Publication, New York (1956).
55) E. M. Scadden and N. E. Ballou, *Anal. Chem.*, 25, 1602 (1953).
56) I. Nelidow and R. M. Diamond, *J. Phys. Chem.*, 59, 710 (1955).
57) C. J. Rodden. AEC Rep., NBL-127 (1956) quoted in NSA Vol. 10, Abstr. No. 3999.
58) K. Alcock, S. S. Grimley, T. V. Hearly, J. Kennedy and H. A. C. Mckay, *Trans. Faraday Soc.*, 52, 39 (1956).
59) T. V. Healy and H. A. C. McKay, ibid., 52, 633 (1956).
60) D. G. Tuck, *J. Chem. Soc.*, 1958, 2783.
61) T. Ishimori, K. Watanabe and E. Nakamura, This Bulletin, 33, 636 (1960).
62) K. A. Kraus and F. Nelson, "Proceedings of International Conference on Peaceful Uses of Atomic Energy", Vol. VII, P/837, United Nations Publication, New York (1956).
63) M. Green and J. A. Kafalas, *J. Chem. Phys.*, 22, 760 (1954).

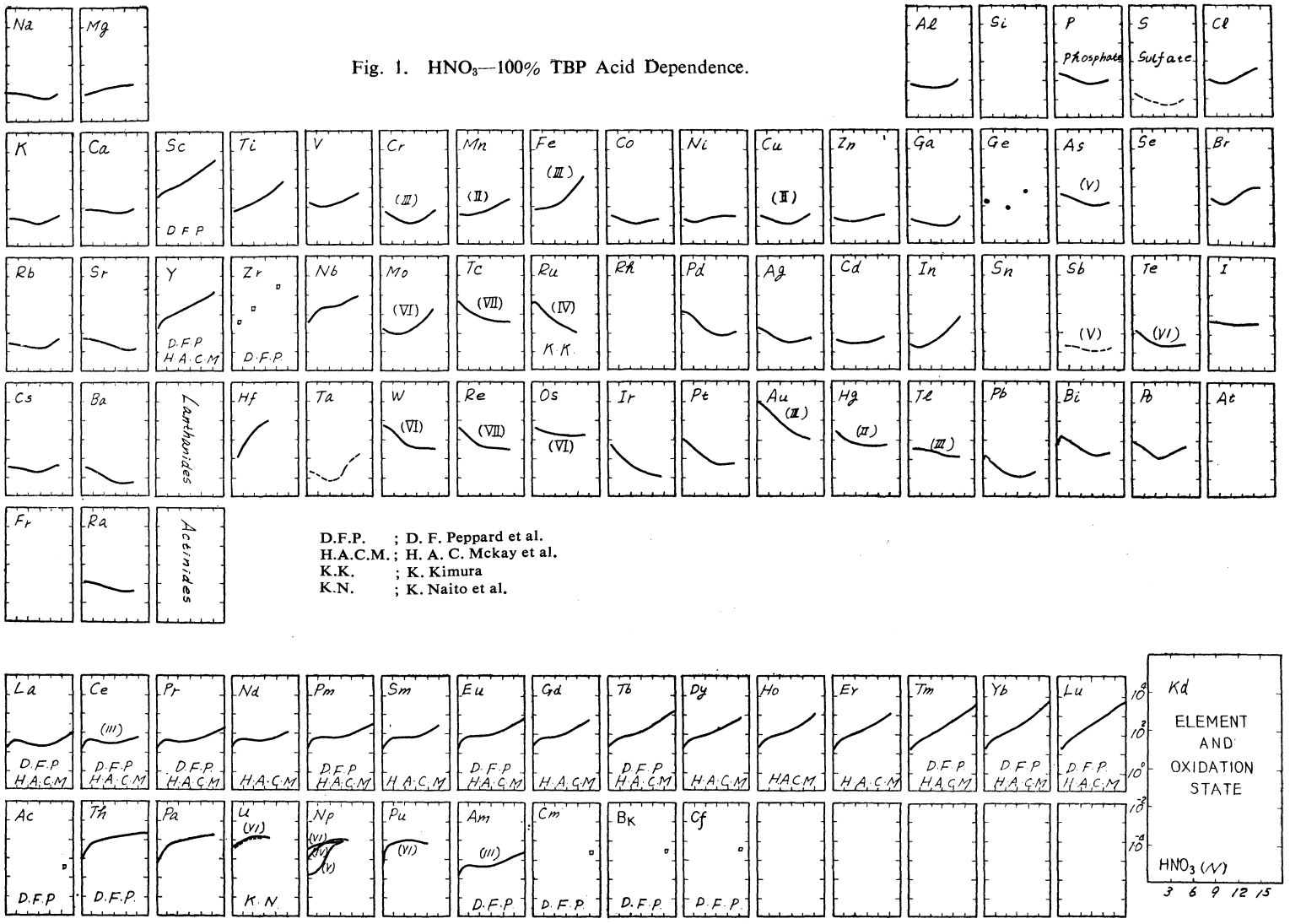



Fig. 1. $HNO_3$—100% TBP Acid Dependence.

ratios were determined radiometrically in the ordinary way[1,3,61,64].

## Results and Discussion

The results are summarized in Fig. 1 as a series of graphs of $\log K_d$ vs. $N$, where $K_d$ is the distribution ratio and $N$ the acidity of nitric acid in normality. Some of the graphs in Fig. 1 were compiled from some published and unpublished results. Data for scandium[1], zirconium[1], thorium[1], americium[3] and some other actinide elements[5] are taken from the work of Peppard and his coworkers. Curves for yttrium[2,8] and lanthanide elements[2,3,8,10] are quoted from the reports of Peppard et al. and McKay et al. Data for ruthenium[65] and uranium(VI)[66] are cited from the observations of Kimura and Naito, respectively. A dotted line for uranium(VI) is based on the result by Bartlett[18]. The curves for hafnium, protactinum and neptunium are taken from the paper[64] of Nakamura et al. The data for plutonium(VI), lead and bismuth were obtained by one of the present authors (T. I.) during his stay in the Argonne National Laboratory, U. S. A.

The $K_d$ values for sulfate and antimony could not be determined exactly, because the activities extracted into the organic phase were very low.

As Fig. 1 shows, four alkali elements behave in a similar way, showing always very low $K_d$ values. There are some similarities in the shape of the acid-dependence curves for chloride and bromide; ruthenium, palladium and platinum. The $K_d$ values of scandium, yttrium and lanthanum increase with the decreasing atomic number, $Z$. Calcium, strontium and barium also show a similar relationship between $K_d$ vs. $Z$ in a high acidity range. As far as these fifteen elements, namely, alkali metals, chloride, bromide, ruthenium, palladium, platinum, calcium, strontium, barium, scandium, yttrium and lanthanum, are concerned, there is a remarkable difference in the shape of $\log K_d$ vs. $N$ curve between TBP-nitric and TBP-hydrochloric acid system. On the other hand, the group of alkali metals, chloride and bromide, ruthenium, palladium and platinum, calcium, strontium and barium, and scandium, yttrium and lanthanum shows a similar $K_d$ vs. $Z$ relationship between TBP-nitric and TBP-hydrochloric system. Among zirconium, hafnium and thorium, thorium gives the highest extractability into TBP from a nitric acid solution while it shows the lowest into TBP from a hydrochloric acid solution.

Concerning the group of zinc, cadmium and mercury, there is a marked similarity both in the shape of acid dependence curve and in values of $K_d$ in the hydrochloric acid system[61]. In the nitric acid system, howerver, the $K_d$ values of these three elements increase with atomic number, showing a noticeable difference between the shape of the acid-dependence curve for mercury and that for two other elements.

The $K_d$ values for 12 N nitric acid were

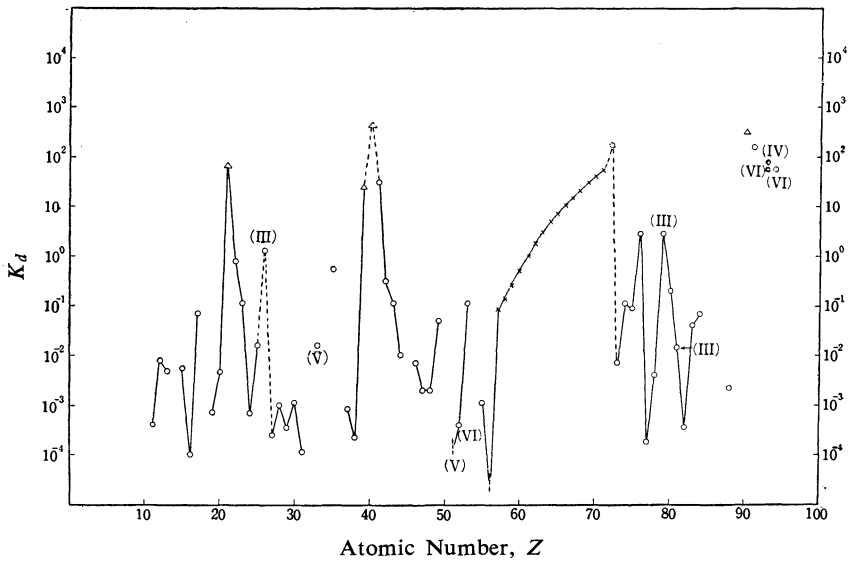



Fig. 2. Relationship between atomic number and $K_d$ values at 12 N $HNO_3$.

64) T. Ishimori and E. Nakamura, This Bulletin, 32, 713 (1959).

65) K. Kimura, unpublished.

66) K. Naito et al., unpublished.

plotted against the atomic number $Z$, in Fig. 2. The values for lanthanides are quoted from the paper of McKay et al.[10] The values for scandium, yttrium, ruthenium and thorium are taken from both published and unpublished works[1-3,65]. There were no data for zirconium, hafnium and neptunium in 12 N nitric acid in the original papers. Accordingly the present authors indicate the values with dotted marks which are estimated from the original data. A regularity in the variation of $K_d$ values seen in Fig. 2 is analogous to that in the TBP-hydrochloric acid system[61]. In $\log K_d$ vs. $Z$ relationship, however, one peak for one long period of the periodic table is seen in the nitric acid system, whereas two peaks are found in the hydrochloric acid system.

Niobium and ferric nitrate give relatively high $K_d$ values in the extraction with TBP from a concentrated nitric acid, while technetium, ruthenium, tungsten, rhenium, osmium and gold are extractable from nitric acid in low concentrations. Protactinum, uranium, neptunium(IV) and -(VI) and plutonium are extracted easily from a nitric acid solution of more than about 3 N.

Fig. 3 gives $K_d$ values for 100% TBP-nitric acid system. This will be convenient for checking the possibility and the efficiency of a mutual separation of a couple of elements chosen arbitrarily. For example, technetium-99 will be separated with TBP from a irradiated molybdenum in 1 N nitric acid solution, because the $K_d$ value for technetium is 18.7 in 1 N nitric acid, while that for molybdenum is 0.02.

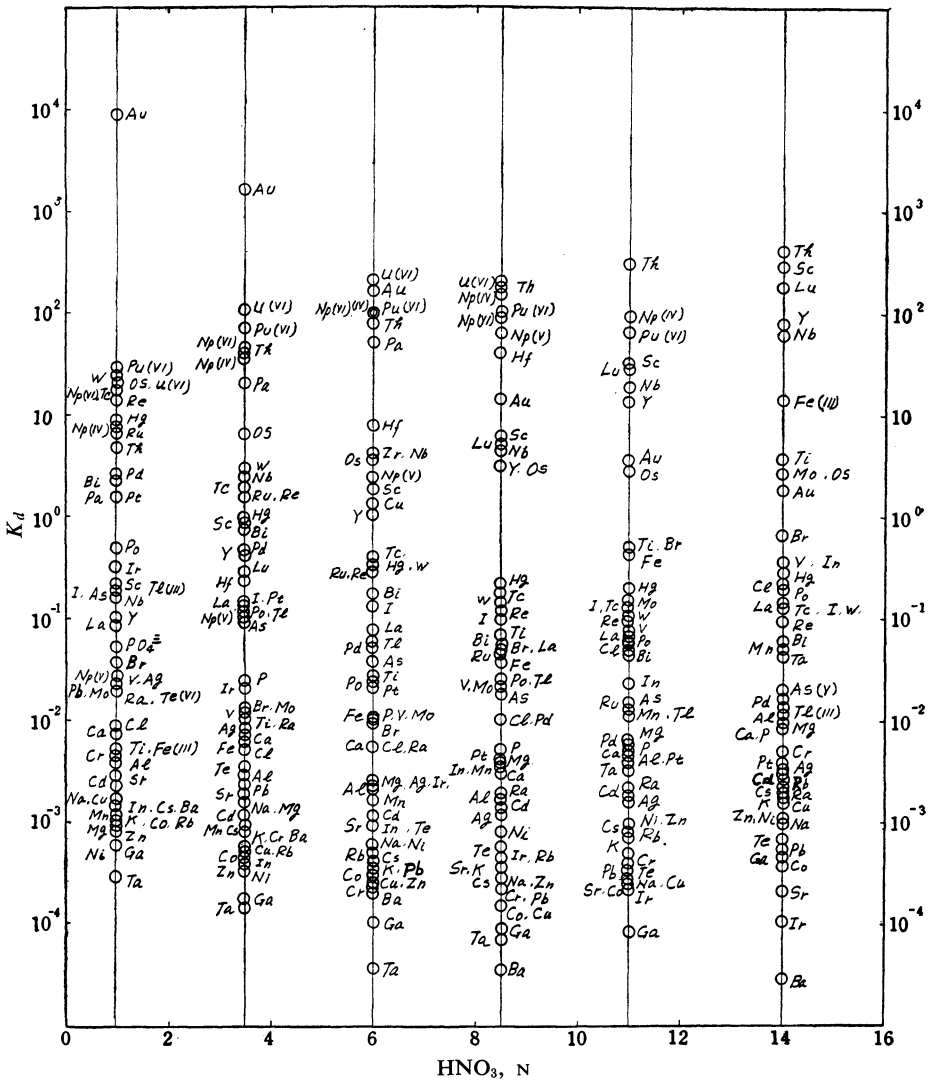



Fig. 3. $K_d$ values in 100% TBP—$HNO_3$ System.

As the $K_d$ values were obtained with a tracer in the present work, the optimum conditions of separation found in Fig. 3 will well fit a chemical separation on a tracer scale. However, some cautions must be paid in macro-scale separations.

Generally most elements give lower $K_d$ values in the TBP-nitric acid system than in the hydrochloric acid system. In other words, it would be easy to find out a favorable condition, where many kinds of element remain in the aqueous phase after TBP extraction from nitric acid solution, while a few kinds of element are extracted into the organic phase. Accordingly, the extraction from nitric media could be applied to a chemical or a radiochemical separation not so widely as that from hydrochloric acid media could be. However, this means that a small number of elements could be isolated selectively. Isolation and group separation of scandium, yttrium, zirconium, hafnium, some actinide and lanthanide elements are promising, according to the TBP extraction data from nitric acid solution of a high acidity. Similarly, extraction from dilute nitric acid well be favorable for the isolation and group separation of technetium and ruthenium.

*Chemistry Division, Tokai Laboratory*
*Japan Atomic Energy Research Institute*
*Tokai, Ibaraki-ken*

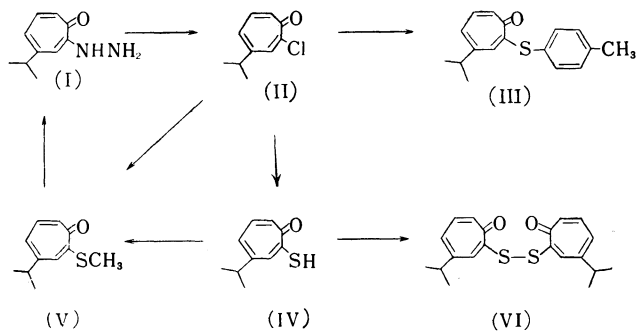
# *4- and 6-Isopropyl-2-mercaptotropones*

By Kazuo MATSUI*

(Received April 22, 1960)

Detailed studies have been made by Nozoe and his co-workers on mercaptotropones[1-4] and mercapto derivatives of 2-phenyltropone has recently been studied by Muroi[5,6]. These studies still leave room for examination of the structure of the parent compound, 2-mercaptotropone, itself with reference to its tautomerism. As a preliminary study to this problem, homologous 4- and 6-isopropyl-2-mercaptotropones were synthesized and some reactions were carried out, which are described herein.

2-Hydrazino-4-isopropyltropone (I) and 2-hydrazino-6-isopropyltropone[7] (VII), obtained from hinokitiol (β-thujaplicin or 4-isopropyltropolone), were converted to 2-chloro-4-isopropyltropone (II) and 2-chloro-6-isopropyltropone[7] (VIII), respectively, and mercapto derivatives were prepared from them.




Scheme 1

* On leave of absence from Tokyo Research Laboratory, Tanabe Seiyaku Co., Ltd.

1) T. Nozoe, M. Sato, and K. Matsui, *Sci. Repts. Tohoku Univ.*, Series I, **37**, 211 (1953).
2) Idem., *Proc. Japan Acad.*, **28**, 408 (1952).
3) Idem., ibid., **28**, 410 (1952).
4) Idem., ibid., **29**, 21 (1953).
5) T. Muroi, *J. Chem., Soc. Japan, Pure Chem. Sec.* (*Nippon Kagaku Zasshi*), **80**, 185 (1959).
6) Idem., ibid., **80**, 303 (1959).
7) S. Seto, *Sci. Repts. Tohoku Univ., Series* I, **37**, 286 (1953).

II easily reacted with potassium salt of *p*-thiocresol when heated in ethanol and formed 4-isopropyl-2-*p*-tolylthiotropone (III) as pale yellow plates, m. p. 110.5~112°C. Heating of II in methanol with four mol. of potassium hydrogensulfide produced 4-isopropyl-2-mercaptotropone (IV) as orange crystals, m. p. 63~65°C, in 80% yield. IV was stable in the air and the benzene layer colored dark red with ferric chloride. Methylation of IV with diazomethane in ether afforded 4-isopropyl-2-methylthiotropone (V) as a yellow oil. The identity of this compound was established by agreement of its ultraviolet spectrum with that of the product obtained by the reaction of II and potassium salt of methanethiol and admixture of their respective 2, 4-dinitrophenylhydrazone, purple needles, m. p. 183°C. Reaction of V with excess of hydrazine by refluxing in methanol for 5 hr. produced I which was identified by admixture of its benzylidene compound, yellow needles, m. p. 203°C, with that of the authentic sample.

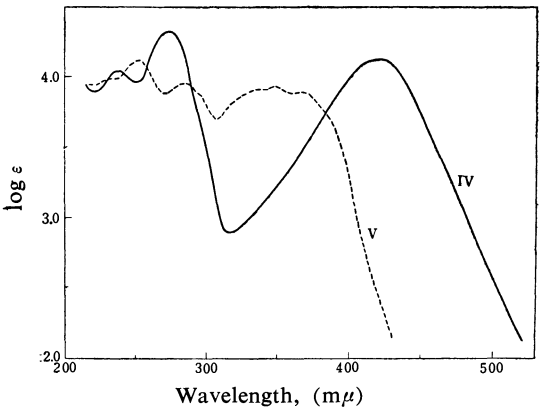
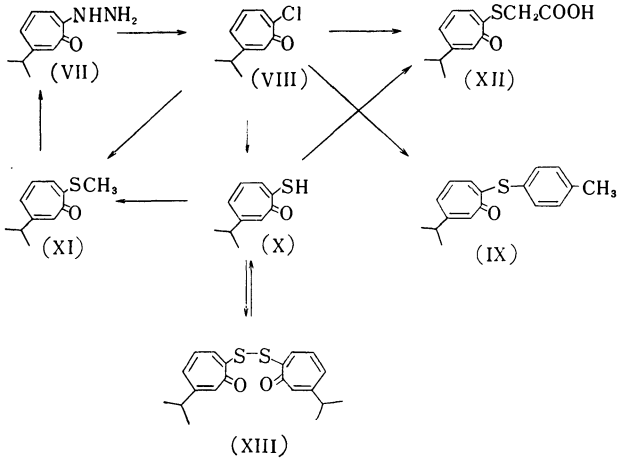



Fig. 1. Ultraviolet absorption spectra[8] of IV and V in methanol.

Application of 0.5 mol. of bromine to ethanolic solution of IV resulted in dehydrogenation from 2 mol. of IV to form 4, 4'-diisopropyl-2, 2'-ditroponyl disulfide (VI) as pale yellow cubic crystals, m. p. 155~156°C.

Heating of VIII with potassium salt of *p*-thiocresol in ethanol afforded 6-isopropyl-2-*p*-tolylthiotropone (IX) as pale yellow plates, m. p. 129~130.5°C. Similarly, application of 4 mol. of potassium hydrogensulfide gave 6-isopropyl-2-mercaptotropone (X) as dark red oil, b. $p._2$ 125~130°C. X was stable in the air like IV and solely formed 6-isopropyl-2-methylthiotropone (XI) as yellow oil by the action of diazomethane. The identity of this compound was established by comparison of its ultraviolet spectrum with that of the product obtained by the reaction of VIII and potassium salt of methanethiol in ethanol and by admixture of respective 2, 4-dinitrophenylhydrazone, purple needles, m. p. 193~195°C.

Heating of XI with excess of hydrazine in methanol for 9 hr. produced VII, which was confirmed by admixture of the benzylidene compound of yellow prisms, m. p. 167°C. The formation of I from V and of VII from XI prove that in substitution reaction of halotropones with thiols, abnormal reaction seen in the case of substitution reaction with amines[9,10] does not take place.




Scheme 2

8) Measured by the Beckman Model DU spectrophotometer.

9) T. Nozoe, S. Seto and T. Sato *Proc. Japan Acad.*, **30**, 473 (1954).

10) T. Sato, *J. Chem. Soc. Japan, Pure Chem. Sec.* (*Nippon Kagaku Zasshi*), **80**, 1056 (1959).

The reaction of the sodium salt of X and sodium monochloroacetate produced 6-isopropyl-2-carboxymethylthiotropone (XII) as pale yellow prisms, m. p. 158~160°C. This compound agreed with the product obtained from the reaction of VIII and potassium thioglycolate through admixture.

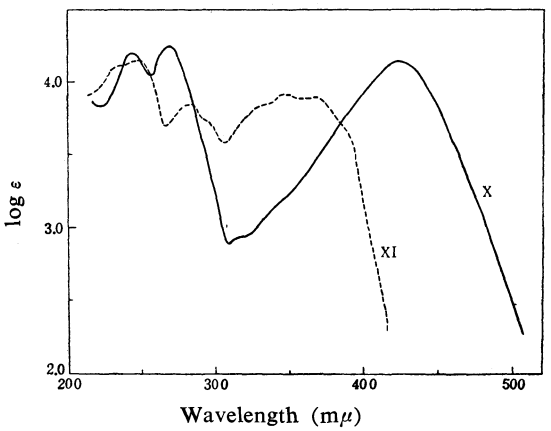
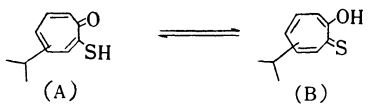



Fig. 2. Ultraviolet absorption spectra of X and XI in methanol.

Bromination of X in ethanol afforded 6, 6'-diisopropyl-2, 2-ditroponyldisulfide (XIII) as pale yellow leaflets, m. p. 210~211°C. XIII is also obtained by tosylation of X in pyridine, while heating of XIII with alkaline aqueous solution of sodium sulfide results in its reduction to form X.




(A) (B)

There are two possible tautomeric structures, A and B, for both IV and X but this problem will be discussed in a separate report, together with that of the parent 2-mercaptotropone.

## Experimental[11]

**4-Isopropyl-2-*p*-tolylthiotropone (III).**—A solution of 80 mg. of *p*-thiocresol, 0.5 ml. of ethanol, and 0.1 ml. of 50% potassium hydroxide was added to a solution of 0.1 g. of 2-chloro-4-isopropyltropone (II) dissolved in 0.3 ml. of ethanol and the mixture was heated on a water bath for a short time. The mixture was diluted with water and the oil that separated out was taken up in benzene. The solid obtained therefrom was recrystallized from cyclohexane to 80 mg. of III as pale yellow plates, m. p. 110.5~112°C.

Found: C, 75.22; H, 6.46. Calcd. for $C_{17}H_{18}OS$: C, 75.51; H, 6.71%[12].

11) All melting points are not corrected.

2, 4-Dinitrophenylhydrazone: Dark red prisms (from ethanol-benzene mixture), m. p. 206~207°C.

Found: C, 60.98; H, 4.73; N, 12.72. Calcd. for $C_{23}H_{22}O_4N_4S$: C, 61.32; H, 4.92; N, 12.44%.

**4-Isopropyl-2-mercaptotropone (IV).**—To a solution of 0.1 g. of II dissolved in 2 ml. of methanol, a solution of potassium hydrogensulfide, prepared by saturation of hydrogen sulfide in a solution of 0.26 ml. of 50% potassium hydroxide in 2 ml. of methanol, was added and the mixture was heated on a water bath for a short time. Methanol was evaporated under a reduced pressure, water was added to the residue, and the solution was treated with activated carbon. The filtrate thereby obtained was acidified with 6N sulfuric acid and the crystals that separated out were collected by filtration. Sublimation of this product under 5 mmHg pressure afforded IV as orange-red crystals m. p. 63~65°C. Yield, 80 mg.

Found: C, 66.39; H, 6.94. Calcd. for $C_{10}H_{12}OS$: C, 66.63; H, 6.71%.

Picryl derivative: Prepared from the potassium salt of IV and picryl chloride, and recrystallized from ethanol to yellow needles, m. p. 174°C.

Found: C, 49.24; H, 3.26; N, 10.88. Calcd. for $C_{16}H_{13}O_7N_3S$: C, 49.10; H, 3.35; N, 10.74%.

**4-Isopropyl-2-methylthiotropone (V).**—i) To a solution of 0.2 g. of II dissolved in 1 ml. of ethanol, 0.2 ml. of 50% potassium hydroxide saturated with methanethiol was added by which exothermic reaction took place. The mixture was diluted with water, extracted with benzene, and the extract was submitted to low pressure distillation, from which 0.2 g. of V was obtained as a yellow oil.

2, 4-Dinitrophenylhydrazone: Purple needles (from ethanol-benzene mixture), m. p. 183°C.

Found: C, 54.21; H, 4.62; N, 14.79. Calcd. for $C_{17}H_{18}O_4N_4S$: C, 54.53; H, 4.85: N, 14.97%.

ii) IV was methylated with diazomethane in ether by the usual process. The product thereby obtained showed good agreement with V obtained above, in ultraviolet absorption spectrum and 2, 4-dinitrophenylhydrazone.

**Reaction of V and Hydrazine.**—A mixture of 30 mg. of V, 0.5 ml. of methanol, and 1 drop of 80% hydrazine hydrate was refluxed for 5 hr., methanol was evaporated under a reduced pressure, and the residue was heated after addition of 2 drops of methanol and 3 drops of benzaldehyde. The crystals that separated out were collected and recrystallized from ethanol to give yellow needles, m. p. 202°C, identical with the bezylidene compound, m. p. 202°C, of 2-hydrazino-4-isopropyltropone (I).

**4, 4'-Diisopropyl-2, 2'-ditroponyl Disulfide (VI).**—A solution of 50 mg. of bromine in 0.5 ml. of ethanol was added to 0.1 g. of IV dissolved in 2 ml. of ethanol, by which crystals began to separate out gradually. After about 30 min. the crystals were collected and recrystallized from ethanol to give 50 mg. of VI as pale yellow, cubic crystals, m. p. 155~156°C.

Found: C, 66.96; H, 5.89. Calcd. for $C_{20}H_{22}O_2S_2$: C, 67.00; H, 6.18%.

12) The microanalyses were carried out by Miss A. Iwanaga and Mr. S. Azumi to whom the author expresses his gratitude.

**6-Isopropyl-2-*p*-tolylthiotropone (IX).**—A solution of 80 mg. of *p*-thiocresol, 0.1 ml. of 50% potassium hydroxide, and 0.5 ml. of ethanol was added to 0.1 g. of 2-chloro-6-isopropyltropone (VIII) in 0.3 ml. of ethanol and the mixture was heated on a water bath for a short time. This was diluted with water, crystals that separated out were collected, and recrystallized from cyclohexane to give 90 mg. of (IX) as pale yellow plates, m. p. 129～130.5°C.

Found: C, 75.19; H, 6.41. Calcd. for $C_{17}H_{18}OS$: C, 75.51; H, 6.71%.

2, 4-dinitrophenylhydrazone: Purple prisms (from ethanol-benzene mixture), m. p. 227～228°C.

Found: C, 61.03; H, 4.76; N, 12.64. Calcd. for $C_{23}H_{22}O_4N_4S$: C, 61.32; H, 4.92; N, 12.44%.

**6-Isopropyl-2-mercaptotropone (X).**—A solution of potassium hydrogensulfide, prepared by saturating hydrogen sulfide in a mixture of 0.46 ml. of 50% potassium hydroxide and 1.5 ml. of methanol was added to the solution of 0.18 g. of VIII dissolved in 0.5 ml. of methanol and the mixture was heated on a water bath for a short time. Methanol was evaporated under a reduced pressure, the residue was dissolved in water, and acidified with 6N sulfuric acid. The oil that separated out was taken up in chloroform and the residue from the chloroform extract was distilled under a reduced pressure, affording 0.13 g. of X as a dark red oil, b. $p._2$ 125～130°C.

Found: C, 66.68; H, 6.48. Calcd. for $C_{10}H_{12}OS$: C, 66.63; H, 6.71%.

2, 4-dinitrophenyl derivative: Prepared from the potassium salt of X and 2, 4-dinitro-chlorobenzene and recrystallized from ethanol to give yellow prisms, m. p. 156～158°C.

Found: C, 55.17; H, 3.85; N, 8.46. Calcd. for $C_{16}H_{14}O_5N_2S$: C, 55.48; H, 4.07; 8.09%.

Picryl derivative: Prepared from the potassium salt of X and picryl chloride, and recrystallized from ethanol to give yellow needles, m. p. 145～147°C.

Found: C, 49.07; H, 3.29; N, 10.96. Calcd. for $C_{16}H_{13}O_7N_3S$: C, 49.10; H, 3.35; N, 10.74%.

**6-Isopropyl-2-methylthiotropone (XI).**—i) To a solution of 0.2 g. of VIII dissolved in 0.5 ml. of ethanol, 0.2 ml. of 50% potassium hydroxide saturated with methanethiol was added, by which an exothermic reaction occurred. The mixture was diluted with water, separated oil was extracted with benzene, and residue from the benzene extract was distilled under a reduced pressure, affording 0.17 g. of XI as a yellow oil.

2, 4-Dinitrophenylhydrazone: Purple needles (from ethanol), m. p. 193～195°C.

Found: C, 54.23; H, 4.48; N, 15.19. Calcd. for $C_{17}H_{18}O_4N_4S$: C, 54.53; H, 4.85; N, 14.97%.

ii) Methylation of X with diazomethane by the usual process afforded a product which was identical with the product obtained in (i) in ultraviolet absorption spectrum and 2, 4-dinitrophenylhydrazone.

**Reaction of XI and Hydrazine.**—A mixture of 0.1 g. of XI, 1 ml. of methanol, and 2 drops of 80% hydrazine hydrate was refluxed for 9 hr. Methanol and excess of hydrazine were removed by low pressure distillation and the residue was heated after addition of 0.5 ml. of ethanol and 5 drops of benzaldehyde. The crystals that separated out were recrystallized from ethanol to give 50 mg. of yellow prisms, m. p. 165～167°C, undepressed on admixture with the benzylidene compound, m. p. 167°C, of 2-hydrazino-6-isopropyltropone (VII).

**2-Carboxymethylthio-6-isopropyltropone (XII).**—(i) A solution of 60 mg. of monochloroacetic acid in 0.5 ml. of 2 N sodium hydroxide and 1 ml. of water was added to the mixture of 0.1 g. of X, 0.3 ml. of 2 N sodium hydroxide, and 1 ml. of water, and the mixture was heated on a water bath for 10 min. by which the solution changed its color from red to yellow. After treatment with activated carbon, the filtrate was acidified with 6N sulfuric acid and the crystals that separated out were collected by filtration. Recrystallization from hydrous ethanol afforded 50 mg. of XII as pale yellow prisms, m. p. 158～160°C.

Found: C, 60.88; H, 5.91. Calcd. for $C_{12}H_{14}O_3S$: C, 60.48; H, 5.92%.

ii) A solution of 50 mg. of thioglycolic acid, 0.3 ml. of 20% potassium hydroxide, and 3 ml. of ethanol was added to the solution of 90 mg. of VIII dissolved in 1 ml. of ethanol, and the mixture was heated on a water bath for 30 min. After evaporation of ethanol under a reduced pressure, water was added to the residue and the solution was treated with activated carbon. The filtrate was acidified with 6 N sulfuric acid and the crystals that precipitated out were recrystallized from hydrous ethanol to give 50 mg. of XII, m. p. 158～159°C, undepressed on admixture with the product obtained in (i).

**6, 6'-Diisopropyl-2, 2'-ditroponyl Disulfide (XIII).**—i) A solution of 50 mg. of bromine in 0.5 ml. of ethanol was added to the solution of 0.1g. of X dissolved in 1 ml. of ethanol, with stirring and ice-cooling. After an hour, the crystals that separated out were collected and recrystallized from benzene-ethanol mixture to give 60 mg. of XIII, as pale yellow leaflets, m. p. 210～211°C.

Found: C, 66.71; H, 6.05. Calcd. for $C_{20}H_{22}O_2S_2$: C, 67.00; 6.18%.

ii) A solution of 50 mg. of X dissolved in 0.3 ml. of pyridine was cooled with ice and 60 mg. of tosyl chloride was added to it, by which the reaction occurred with evolution of heat. The mixture was acidified with 2N hydrochloric acid and the crystals that separated out were recrystallized from a large amount of ethanol affording 30 mg. of XIII, m. p. 210～210.5°C , undepressed on admixture with the product obtained in (i).

Found: C, 67.25; H, 6.03%.

**Reduction of (XIII).**—A mixture of 50 mg. of XIII, 2 ml. of 2N sodium hydroxide, and 50 mg. of sodium sulfide was heated on a water bath for 10 min. by which XIII dissolved completely to form a red solution. After treatment with activated carbon, the filtrate was acidified with 6 N sulfuric acid and the oil that separated was extracted with chloroform. The residue from the chloroform extract was distilled under a reduced pressure to yield 30 mg. of X as a dark red oil, which was identified by ultraviolet absorption spectrum and the picryl derivative.

The present work was carried out while the author was a resident research chemist in the Nozoe Laboratory, Faculty of Science, Tohoku University. The author expresses his deep gratitude to Professor Tetsuo Nozoe for his kind and unfailing guidance throughout this period and to the authorities of Tanabe Seiyaku Co., Ltd. for giving him the chance to study at the above place.

*Department of Chemistry*
*Faculty of Science,*
*Tohoku University*
*Katahira-cho, Sendai*

# *Syntheses of α-, β- and γ-Dolabrins**

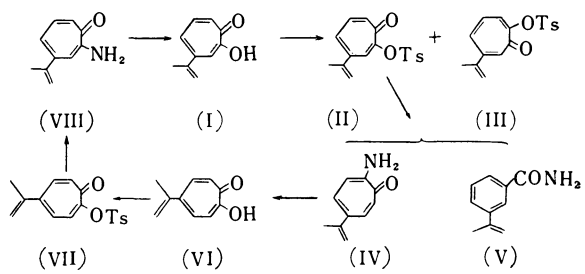
By Tetsuo NOZOE, Toshio MUKAI and Toyonobu ASAO

(Received April 25, 1960)

It is already known that hinokitiol (β-thujaplicin) and α-thujaplicin are present as tropolonic constituents in the essential oil of *Thujoposis dolabrata Sieb. et Zucc*[1]. Recently, the presence of β-dolabrin (4-isopropenyltropolone) in this oil was revealed in this laboratory[2], and more recently, it was also found in other species[3,4]. β-Dolabrin is the first of natural tropolones to possess a double bond in the side chain conjugated to the tropolone ring and it is interesting not only from the point of biogenesis of natural tropolones but also in the study of the chemical nature of such troponoids. For example, oxidation of β-dolabrin easily affords 4-acetyltropolone** in a high yield[2] which is an important starting material for synthesizing colchicine and its allied compounds[5].

Since there are a number of conifers containing α-, β- and γ-thujaplicines, though on different combinations according to species and habitat, there is still a possibility that α- and γ-isomers (3- and 5-isopropenyltropolones) of β-dolabrin might exist in nature[6]. In the present paper will be described the syntheses of isomeric (α-, β- and γ-) dolabrins.

According to Sato[7] in this laboratory, it is possible to convert 4-substituted tropolones to 5-substituted tropolones by utilization of the abnormal substitution of *p*-toluenesufonate of tropolones. Its reverse conversion is also possible. This reaction was applied to β-dolabrin (I). I forms two kinds of tosylates, one of m. p. 128°C and the other of m. p. 82°C, in a good yield. It is certain from the following series of experiments that the tosylate of m. p. 128°C has the structure of II and that of m. p. 82°C, the structure III. Reaction of II with methanol saturated with ammonia gives two kinds of products (IV and V), both corresponding to $C_{10}H_{10}ON$. IV turns green with ferric chloride and forms a picrate. Together with evidence of its ultraviolet spectrum (Fig. 1), IV is known to be an aminotropone derivative, while the ultraviolet spectrum of V (Fig. 1) shows it to be a benzenoid compound formed by rearrangement. Reduction of V affords *m*-cumic acid amide and, therefore, V is 3-isopropenylbenzamide. When II reacts with liquid ammonia, IV is obtained in a good yield but the rearrangement product is not




* Presented at the 11th Annual Meeting of the Chemical Society of Japan, Tokyo, April, 1958.

1) T. Nozoe, A. Yasue and K. Yamane, *Proc. Japan Acad.*, **27**, 15 (1951).

2) T. Nozoe, K. Takase and M. Ogata, *Chem. & Ind.*, **1957**, 1070.

3) J. A. F. Gardner and G. M. Barton, *Can. J. Chem.*, **36**, 1612 (1958).

4) E. Zavarin, R. M. Smith and A. B. Anderson, *J. Org. Chem.*, **24**, 1318 (1959).

** Friedel-Crafts type acylation does not occur in tropolones; Cf. Ref. 6 and P. L. Pauson, *Chem. Revs.*, **55**, 43 (1955).

5) T. Nozoe, K. Takase, J. Shin, Y. Kitahara and K. Doi, Paper presented at the 132nd Convention of the American Chemical Society, New York, September, 1957.

6) T. Nozoe, *Fortsch. Chem. org. Naturstoffe*, **13**, 232 (1956).

7) T. Sato, *J. Chem. Soc. Japan, Pure Chem. Sec.* (*Nippon Kagaku Zasshi*), **80**, 1058 (1959).

obtained. Hydrolysis of IV with alcoholic alkali gives a tropolone derivative (VI), $C_{10}H_{10}O_2$ as colorless scaly crystals, m. p. 101°C, and its reduction affords γ-thujaplicin, indicating that VI is the objective 5-isopropenyltropolone, which may be called γ-dolabrin. $pK_a$ value of VI is 7.17 at 25°C***.

γ-Dolabrin (VI) so obtained can be led back to β-dolabrin by the same process. VI affords only one kind of tosylate (VII) whose reaction with liquid ammonia gives 2-amino-4-isopropenyltropone (VIII) and 4-isopropenylbenzamide (IX). VIII turns green with ferric chloride and is hydrolyzed in alcoholic alkali to β-dolabrin. The structure of IX was also confirmed by its reduction to *p*-cumic acid amide. Reaction of VII with methanolic ammonia gives a small amount of methyl 4-isopropenylbenzoate (X), besides VIII and IX. The ultraviolet spectra of VIII and IX are shown in Fig. 1.

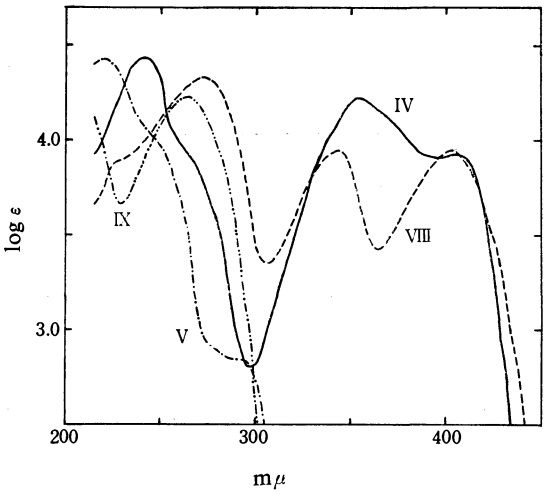



Fig. 1. Ultraviolet absorption spectra of IV, V, VIII and IX in methanol.

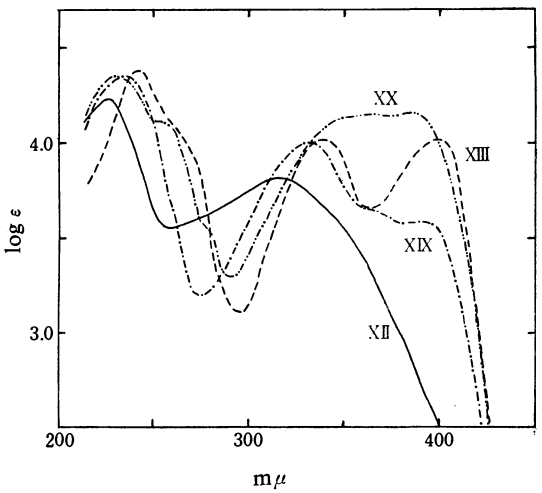



Fig. 2. Ultraviolet absorption spectra of XII, XIII, XIX and XX in methanol.

Reaction of III with liquid ammonia produces an oily substance containing aminotropone and a rearrangement product, 3-isopropenylbenzamide (V). The oily substance was not induced to crystallize or led to form a crystalline derivative such as a picrate but its hydrolysis with alcoholic alkali afforded a small amount of a tropolone derivative (XI) whose copper complex was found by mixed fusion to be identical with the copper complex of α-dolabrin which will be described below. Reaction of III with methanolic ammonia afforded V but the aminotropone derivative was not isolated. The results of the amination of III show that the large steric hindrance of the 7-position to undergo abnormal substitution in III makes it difficult to be attacked by ammonia and rearrangement product V should be formed in a larger amount.

Alkaline hydrolysis of tosylate II gives β-dolabrin and rearrangement product 3-isopropenylbenzoic acid, however acidic hydrolysis of II and III gives β-dolabrin.

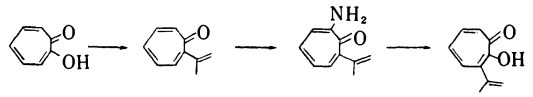
Tropolone is known to form the corresponding 2-alkyltropones by the action of alkyllithium or Grignard reagents[8,9] and this process was attempted for the introduction of isopropenyl group into the tropone ring. Reaction of excess of isopropenyllithium to tropolone afforded an oily substance (XII), $C_{10}H_{10}O$, whose ultraviolet spectrum (Fig. 2) indicated two absorption maxima corresponding to those of tropone[9]. Moreover, the maximum absorption of XII showed a bathochromic shift of 3 and 16 mμ respectively, from those of tropone and it seems appropriate to consider that this shift originates in the conjugation of the side chain double bond with the tropone ring. The infrared spectrum of XII supports the structure as 2-isopropenyltropone. XII is the first tropone derivative with a double bond in the side chain conjugated to the tropone ring and examination of its chemical properties appeared of interest. XII is fairly labile and increased its viscosity when left in the air. Attempted distillation at a reduced pressure resulted in resinification. XII forms an oily hydrochloride but does not produce distinct picrate or 2,4-dinitrophenylhydrazone.

Attempted amination of XII with hydrazine[10]

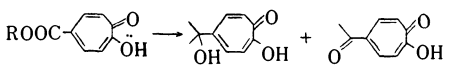
*** $pK_a$ value was measured by Dr. N. Yui of the Institute of Applied Science, Faculty of Technology, Tohoku University, to whom the authors are deeply indebted.

8) W. von E. Doering and C. F. Hiskey, *J. Am. Chem. Soc.*, **74**, 5688 (1952).
9) T. Mukai, This Bulletin, **31**, 1547 (1958).
10) T. Nozoe, T. Mukai, J. Minegishi and T. Fujisawa, *Sci. Repts. Tohoku Univ.*, Series I, **37**, 164 (1954).

turned it black and the 2-aminotropone derivative was not isolated. Reaction of XII with hydroxylamine hydrochloride in pyridine[10] afforded the product as a brown viscous substance in the main with a trace of yellow oily substance (XIII), whose ultraviolet absorption spectrum (Fig. 2) indicated a typical curve for 2-aminotropone derivative. Hydrolysis of XIII with alcoholic alkali gave a very minute amount of a tropolone derivative (XIV), m. p. 36°C, which showed coloration with ferric chloride characteristic of tropolones and easily formed a copper complex, $C_{20}H_{18}O_4Cu$. This copper complex showed no depression of the melting point when fused with the copper complex of XI mentioned above. Paper chromatography of XI and XIV also gave spots with identical $R_f$ value.



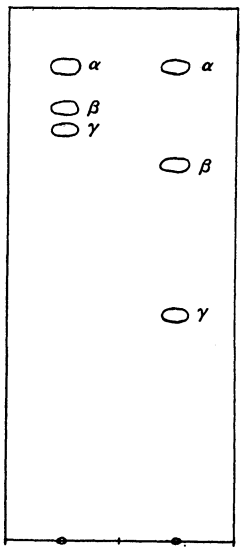
(XII) (XIII) (XIV)



(XVI~XVIII) (XIX) (XX)

Synthesis of γ-dolabrin was attempted by the Grignard reaction of tropolone-5-carboxylic acid alkylester. Methylmagnesium iodide was applied to tropolone-5-carboxylic acid (XV)[11], its methyl ester, and iron complex, but all these compounds were sparingly soluble in ether and the starting compound was recovered in all cases. In order to increase solubility in ether, amyl (XVI), octyl (XVII), and cyclohexyl (XVIII) esters of tropolone-5-carboxylic acid were prepared. Application of about six molar equivalents of methylmagnesium iodide against these esters afforded 5-α-hydroxyisopropyltropolone (XIX) and 5-acetyltropolon (XX). The ultraviolet absorption spectra of XIX and XX are indicated in Fig. 2. The structure of XIX was confirmed from the fact that dehydration of XIX by heating with potassium hydrogensulfate easily afforded γ-dolabrin (VI). XIX turns green in aqueous layer to ferric chloride but the color does not transfer to benzene or chloroform layer. This is the general behavior of hydroxyl or carboxyl derivatives of tropolone. XIX is easily dehydrated and changes partly into VI on heating with acid or by sublimation. 5-Acetyltropolone (XX) is also obtained by oxidation of VI. XX easily forms an oxime, the same as 4-acetyltropolone as already reported[5], and also undergoes condensation with benzaldehyde derivatives to

11) Y. Kitahara, ibid., 40, 74 (1956).




Dolabrin Thujaplicin

Fig. 3. Paper chromatogram of α-, β- and γ-dolabrin and α-, β- and γ-thujaplicin.

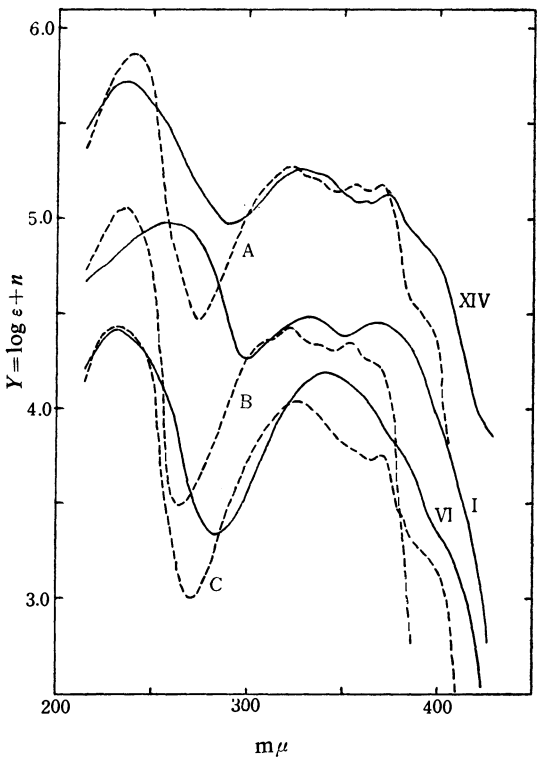



Fig. 4. Ultraviolet absorption spectra of α-, β- and γ-dolabrin (XIV, I and VI), and α-, β- and γ-thujaplicin (A, B and C).

$Y = \log + 1.5$ (for α-series)
$Y = \log + 0.7$ (for β-series)
$Y = \log + 0$ (for γ-series)

form 5-cinnamoyltropolone derivatives.

The work described in this paper has completed the total syntheses of α-, β- and γ-dolabrins, and 4-, and 5-acetyltropolones.

The paper chromatogram**** of α-, β- and γ-dolabrins so obtained is shown in Fig. 3, and their ultraviolet absorption spectra, together with those of corresponding thujaplicins are given in Fig. 4. The spectra of dolabrins show a bathochromic shift from those of corresponding thujaplicins, due to conjugation of the isopropenyl group with the tropolone ring. The absorption of γ-dolabrin in the longer wavelength region differs from that of α- and β-isomers.

## Experimental[12]

**p-Toluenesulfonate (II and III) of β-Dolabrin (I).**—To a solution of 1 g. of β-dolabrin dissolved in 1.5 ml. of pyridine, 1.4 g. of p-toluenesulfonyl chloride was added and the mixture was allowed to stand for about 1 hr. The colorless needles that precipitated out by addition of 4 ml. of ethanol were collected by filtration. Recrystallization of crude crystals, m. p. 124~126°C, from ethanol afforded 820 mg. of II as colorless plates, m. p. 127~128°C. Ethanol was evaporated from the filtrate left after removal of II, water was added to the residue, and the solution was extracted with benzene. The benzene extract was dried, passed through a chromatographic column of alumina, and eluted with benzene. 850 mg. of crystals, m.p. 72~74°C, thereby obtained were recrystallized from ethanol to III as pale yellow scales, m. p. 81~82°C.

Found (for II): C, 64.67; H. 4.66. Found (for III): C, 64.64; H, 4.96. Calcd. for $C_{17}H_{16}O_4S$: C, 64.55; H, 5.10%.

**Reaction of 2-Tosyloxy-4-isopropenyltropone (II) and Ammonia** a) A solution of 300 mg. of II dissolved in 30 ml. of methanol saturated with ammonia was allowed to stand at room temperature for 4 days. Methanol was evaporated under reduced pressure and the residue was treated with benzene, from which 165 mg. of ammonium p-toluenesulfonate was obtained as the insoluble portion. The benzene soluble portion was chromatographed over alumina and eluted with benzene, affording 70 mg. of yellow crystals m. p. 99~102°C. Subsequent elution with ethyl acetate gave 30 mg. of crystals, m. p. 119~123°C. Recrystallization of the former from benzene-cyclohexane mixture afforded IV as yellow needles, m. p. 110~112°C, while that of the latter from benzene-cyclohexane gave V as colorless scales, m. p. 126~126.5°C.

Found (for IV): C, 74.34; H, 6.90; N, 8.09. Found (for V): C, 74.29; H, 6.93; N, 8.75. Calcd. for $C_{10}H_{11}ON$: C, 74.51; H, 6.88; N, 8.69%.

IV forms a picrate of yellow prisms, m. p. 174~175°C (decomp.).

Found: C, 48.80; H, 3.26; N, 14.42. Calcd. for $C_{16}H_{14}O_8N_4$: C, 49.23; H, 3.62; N, 14.36%.

b) A mixture of 200 mg. of II and 13 ml. of liquid ammonia was allowed to stand at room temperature for 2 days and ammonia was evaporated. The residue was extracted with benzene and 60 mg. of IV was obtained. Purification of its filtrate by chromatography afforded 30 mg. of IV but none of V.

**γ-Dolabrin (VI) from 2-Amino-5-isopropenyltropone (IV).**—A mixture of 200 mg. of IV and 500 mg. of sodium hydroxide in 3 ml. of 30% ethanol was refluxed. The yellow crystals that precipitated out were collected, dissolved in water, and the solution was neutralized with 2 N hydrochloric acid, from which 150 mg. of colorless crystals, m. p. 94~96°C, was obtained. Recrystallization from benzene-cyclohexane mixture afforded VI as colorless scales, m. p. 100~101°C.

Found: C, 73.72; H, 5.86. Calcd. for $C_{10}H_{10}O_2$: C, 74.05; H, 6.22%.

I. R. Spectrum: $\tilde{\nu}$ (O-H, C=O, C=C) 3215, 1606, 1595, $\delta$ ($=CH_2$) 907 $cm^{-1}$. (in KBr disk).

Copper complex: Green needles, m. p. over 290°C.

Found: C, 62.02; H, 4.49. Calcd. for $C_{20}H_{18}O_4Cu$: C, 62.24; H, 4.70%.

**Reduction of γ-Dolabrin (VI) and 3-Isopropenylbenzamide (V).**—a) A solution of 20 mg. of VI dissolved in 4 ml. of ethanol, added with 5 mg. of palladium-carbon, was submitted to hydrogenation and 3 ml. of hydrogen was absorbed. Ethanol was evaporated and the crystalline residue was sublimed under reduced pressure. Recrystallization of the sublimate from cyclohexane afforded colorless needles, m. p. 77~78°C, which showed no depression on admixture with γ-thujaplicin, m. p. 80°C.

b) Fifteen mg. of V was hydrogenated by the same way as above to afford 7 mg. of colorless scales, m. p. 94~95°C after recrystallization from benzene-cyclohexane, which showed no depression on admixture with m-cumic acid amide m. p. 95~95.5°C.

**p-Toluenesulfonate (VII) of γ-Dolabrin (VI),**—To a solution of 260 mg. of γ-dolabrin dissolved in 0.5 ml. of pyridine, 360 mg. of p-toluenesulfonyl chloride was added and the mixture was allowed to stand. After about 1.5 hr. 2 ml. of ethanol was added to it and 410 mg. of crystals m. p. 121~124°C was obtained. The filtrate was evaported and the residue was poured into water, separating 70 mg. of crystals m. p. 119~124°C. The combined crystals were recrystallized from ethanol to VII as pale yellow prisms, m. p. 125~126°C.

Found: C, 64.74; H, 5.04. Calcd. for $C_{17}H_{16}O_4S$: C, 64.55; H, 5.10%.

**Reaction of 2-Tosyloxy-5-isopropenyltropone (VII) and Ammonia.**—a) A mixture of 320 mg. of VII dissolved in 15 ml. of liquid ammonia was allowed to stand for 5 days at room temperature,

**** Chromatography is carried out on the paper treated with 17% aqueous solution of phosphoric acid, and benzene used as developing solvent.

12) M. p. are uncorrected. The microanalyses were carried out by Messrs Shin-ichi Ohyama, Kazuyoshi Azumi and Miss Ayako Iwanaga, and infrared spectra were measured with Perkin-Elmer Model 21 double beam spectrophotometer by the member of Prof. Kinumaki's laboratory of the Chemical Research Institute of Non-aqueous solutions, to whom the authors' acknowledgements are hereby extended.

then ammonia was evaporated, and the residue was extracted with benzene. The benzene solution was passed through an alumina layer. The first elution with benzene-ethyl acetate afforded 100 mg. of yellow crystals, m. p. 90~97°C, and subsequent elution with ethyl acetate afforded 30 mg. of colorless crystals, m. p. 181°C. Recrystallization of the former from benzene-petroleum ether afforded VIII as yellow needles, m. p. 100~101°C. The latter was recrystallized from a mixture of ethyl acetate and petroleum ether, affording IX as colorless plates, m. p. 180.5~182°C. Catalytic reduction of IX with polladium-carbon afforded colorless crystals, m. p. 152°C, which showed no depression on admixture with *p*-cumic acid amide, m. p. 153°C.

Found (for VIII): C, 74.17; H, 6.41; N, 8.92. Found (for IX): C, 74.33; H, 6.62; N, 8.62. Calcd. for $C_{10}H_{11}ON$: C, 74.51; H, 6.88; N, 8.69%.

Picrate of VIII: m. p. 130~131°C.

Found: C, 49.72; H, 3.48; N, 14.41. Calcd. for $C_{16}H_{14}O_8N_4$: C, 49.23; H, 3.62; N, 14.36%.

b) A solution of 400 mg. of VII dissolved in 50 ml. of methanol saturated with ammonia was allowed to stand for 4 days at room tepmerature and then the methanol was evaporated. The residue was extracted with benzene, and the benzene-insoluble portion was extracted with water. The insoluble residue was 100 mg. of crystals melting at 180°C. The sparingly soluble portion of benzene extract afforded 30 mg. of the same crystals. Both lots of crystals corresponded to IX. The benzene-soluble portion was chromatographed over alumina and elution with benzene gave 5 mg. of crystals X, m. p. 50~53°C, which showed no depresseon on admixture with methyl *p*-isopropenylbenzoate. The portion eluted with ethyl acetate affored 15 mg. of β-dolabrin, m.p. 51°C, by the same hydrolysis as below.

**Hydrolysis of 2-Amino-4-isopropenyltropone (VIII).**—A solution of 30 mg. of VIII dissolved in a mixture of 150 mg. of potassium hydroxide, and 1 ml. of 50% methanol was refluxed for 3.5 hr. The methanol was then evaporated, 2 ml. of water was added to the residue, and this was extracted with benzene to remove an unreacted substance, the mother liquor was acidified, extracted with benzene, and benzene was evaporated after drying. Recrystallization of its residue from cyclohexane afforded 23 mg. of pale yellow needles, m. p. 54~56°C, which showed no depression on admixture with β-dolabrin

**Reaction of 2-Tosyloxy-6-isopropenyltropone (III) and Ammonia.**—a) A mixture of 2 g. of III and about 20 ml. of liquid ammonia was allowed to stand for 2 days at room temperature. The ammonia was evaporated and the residue was extracted with benzene. The benzene solution was washed with water, dried, and chromatographed over alumina. Elution with benzene afforded 490 mg. of yellow oil (A), and subsequent elution with ethyl acetate afforded 220 mg. of (V), m. p. 124°C. A was refluxed with a mixture of 1 g. of potassium hydroxide, and 5 ml. of 50% ethanol for 8 hr. Ethanol was then evaporated, 5 ml. of water was added to the residue, and this was extracted with benzene. Mother liquor was acidified and extracted with benzene, affording a minute quantity of oil (XI), and this was derived to a copper complex by reaction with copper sulfate solution and 50 mg. of green crystals was obtained. Recrystallization from chloroform-petroleum ether afforded greenish yellow needles, m. p. 250°C (decomp.).

b) A solution of 2 g. of III dissolved in 200 ml. of methanol saturated with ammonia was allowed to stand for 3 days at room temperature and the solvent was evaporated. The residue was dissolved in benzene and 220 mg. of V m. p. 124°C was obtained. The filtrate was evaporated and the residue was refluxed for 2 hr. with a solution of 1 g. of sodium hydroxide in 5 ml. of 50% ethanol. The colorless needles, $C_{10}H_{13}O_2N$, m. p. 179.5~180.5°C (after recrystallization from benzene) were obtained by neutralization of the solution. However, the structure of this acidic substance was not defined.

Found (for m. p. 179.5°C): C, 66.97; H, 7.11; N, 7.73. Calcd. for $C_{10}H_{13}O_2N$: C, 67.02; H, 7.31; N, 7.82%.

**Synthesis of 2-Isopropenyltropone (XII) from Tropolone.** — A solution of 6.4 g. (0.053 mol. eq.) of 2-bromopropene dissolved in 10 ml. of ether was added dropwise into 0.65 g. (0.093 mol. eq.) of lithium in 12 ml. of ether with stirring in nitrogen atmosphere and the mixture was refluxed for 2 hr. After removal of residual lithium pieces, a solution of 1.15 g. (0.0093 mol. eq.) of tropolone dissolved in 50 ml. of ether was added dropwise with stirring and the mixture was stirred for 1 hr. The solution was cooled with ice and 20 ml. of 2 N sulfuric acid was added, the ether layer was separated, and the aqueous layer was extracted with ether. The combined ether solution was washed with sodium chloride solution, passed through an alumina layer to remove unreacted tropolone, and the ether was evaporated from the effluent, leaving 1.5 g. of pale reddish brown oil. Bromination of this oil in glacial acetic acid failed to produce any crystalline derivative. The oil was dissolved in benzene and dry hydrogen chloride gas was passed through this solution. The oily hydrochloride that separated out was collected, decomposed with water, and extracted with ether. The ether extract was washed with water, dried, and passed through a column of alumina. Evaporation of ether from the effluent afforded a reddish brown oil, $n_D^{25}$ 1.6978, which was submitted to elemental analyses and spectral measurement.

Found: C, 81.33; H, 7.01. Calcd. for $C_{10}H_{10}O$: C, 82.16; H, 6.90%.

I. R. spectrum: $\tilde{\nu}$ (C=O, C=C) 1627, 1570~1600, $\delta$ (=$CH_2$) 897 $cm^{-1}$ (in KBr disk).

**Reaction of 2-Isopropenyltropone and Hydroxylamine: (Synthesis of α-Dolabrin (XIV)).** — A solution of 0.2 g. of 2-isopropenyltropone and 0.3 g. of hydroxylamine hydrochloride dissolved in a mixture of 1.5 ml. of dehydrated ethanol and 1.5 ml. of pyridine was refluxed for 2 hr. Ethanol was then evaporated, water was added to the residue, and the solution was extracted with benzene. The benzene extract was washed with water and passed through an alumina layer. First elution with benzene

afforded 20 mg. of red oil (A) and subsequent elution with chloroform and ethanol respectively afforded 10 mg. of yellowish oil (B) and 50 mg. of yellowish brown oil (C). A part of A underwent crystallization but was not purified and it was assumed to be an oxime from its ultraviolet spectrum. $\lambda_{max}^{MeOH}$ mμ (log ε): 223 (4.17), 299 (3.71), 390～400 (3.11).

B also afforded no crystalline picrate but it was assumed from its ultraviolet spectrum to be 2-aminotropone derivative.

It was considered possible that C contains a 2-aminotropone derivative. Therefore, it was refluxed for 2 hr. with 0.2 g. of sodium hydroxide and 2 ml. of 50% ethanol, the ethanol was evaporated, water was added to the residue, and the solution was extracted with chloroform to remove the neutral portion. The aqueous layer was acidified and extracted with chloroform, affording 20 mg. of a brown oil. Distillation of this oil under a reduced pressure gave pale yellow crystals, m. p. 35～36°C, which was dissolved in petroleum ether and derived to a copper complex. The copper comprex came as greenish yellow crystals, m. p. 250°C (decomp.).

Found: C, 61.56; H, 5.15; Cu, 16.29. Calcd. for $C_{20}H_{18}O_4Cu$: C, 62.24; H, 4.70; Cu, 16.46%.

**Synthesis of Esters of Tropolone-5-carboxylic Acid (XV).**—*a) Amyl Ester (XVI).*—To a solution of 600 mg. XV dissolved in 10 ml. of amyl alcohol, 0.15 ml. of conc. sulfuric acid was added and the mixture was refluxed for 2 hr. The solution was filtered to remove carbonized material, the filtrate was concentrated, and the residue was allowed to stand with the addition of ethanol. The residue afforded 450 mg. of crystals melting at 60°C which was recrystallized from petroleum ether to XVI as colorless, scales m. p. 61～62°C. This substance turns red with ferric chloride and the color transfers to the chloroform layer.

Found: C, 66.30; H, 6.74. Calcd. for $C_{13}H_{16}O_4$: C, 66.08; H, 6.83%.

Hydrolysis of this mother liquor with alkali resulted in recovery of 150 mg. of XV, m. p. over 250°C.

*b) Octyl Ester (XVII).* — Obtained by the same method as a) as colorless scales, m. p. 55°C.

Found: C, 69.53; H, 8.12. Calcd. for $C_{16}H_{22}O_4$: C, 69.04; H, 7.97%.

*c) Cyclohexyl Ester (XVIII).*—To a solution of 600 mg. of XV dissolved in 12 ml. of cyclohexanol, 0.6 ml. of conc. hydrochloric acid was added and the mixture was refluxed for 8 hr. The reaction mixture was filtered while hot, the filtrate was concentrated, and allowed to stand. Evaporation was repeated twice and 800 mg. of crystals of m. p. 85°C was obtained as the first crop, and 140 mg. of crystals of m. p. 90°C as the second crop. The combined crystals were recrystallized from ethanol and 60 mg. of tropolone-5-carboxylic acid, m. p. over 250°C, was obtained from the sparingly soluble portion, and 600 mg. of pale brown plates XVIII, m. p. 94～95°C, from the easily soluble portion. Further recrystallization of the latter raised its melting point to 97～98°C.

Found: C, 67.07; H, 6.23. Calcd. for $C_{14}H_{16}O_4$; C, 67.73; H, 6.50%.

**Synthesis of γ-Dolabrin (VI) from the Esters of Tropolone-5-caboxylic Acid.**—a) A solution of 0.5 g. (0.0017 mol. eq.) of XVII dissolved in 10 ml. of ether was added with stirring under ice-cooling to the Grignard reagent from 1.6 g. (0.0113 mol. eq.) of methyl iodide, 0.26 g. (0.0104 mol. eq.) of magnesium, and ether, and the mixture was stirred for 3 hr. Ten ml. of 15% ammonium chloride solution was added to this mixture and the whole mixture was extracted thoroughly with ether. The ether was evaporated, the residue was heated with 10 ml. of 6 N sulfuric acid for 10 min. and the mixture, was extracted with three 5-ml. portions of chloroform, affording 250 mg. of dark brown oil **A**. The mother liquor left after chloroform extraction was extracted with eight 5-ml. portions of ethyl acetate, affording 40 mg. of pale yellow oil (B). A part of B crystallized on being allowed to stand, but its melting point could not be measured. B was submitted to paper chromatography with benzene as a solvent but it did not move with this solvent. A mixture of B and finely divided fused hydrogensulfate was heated for a few minutes at 140°C and the mixture was sublimed under reduced pressure, from which 20 mg. of colorless crystals, m. p. 90～95°C, was obtained. Recrystallization from cyclohexane afforded colorless plates, m. p. 99～100°C, undepressed on admixture with γ-dolabrin. This has indicated that B chiefly contains the objective 5-α-hydroxy-isopropyltropolone (XIX). Some crystals separated out on standing A and 25 mg. of pale yellow crystals, m. p. 178°C, was obtained. It showed no depression of the melting point on admixture with 5-acetyltropolone (XX). The mother liquor left after separation of these crystals was found to contain the octyl ester, XIX, and XX.

b) Reaction of 0.42 g. of the amyl ester (XVI) with 6 molar equivalents of methylmagnesium iodide, as in the case of the above a), was carried out. After completion of the reaction, the product was decomposed with 15 ml. of 6 N sulfuric acid. After separation of the ether layer, the mother liquor was extracted with 20 ml. and 10 ml. of chloloform, and the combined ether and chloroform extracts were washed with eight 10-ml. portions of 8 N sulfuric acid. Evaporation of the solvent from this combined extract left 250 mg. of oil **A**. Sulfuric acid layer and washings were combined, neutralized to pH 4 with dil. potassium hydroxide solution, and the solution continuously extracted with chloroform for 10 hr. Evaporation of chloroform from this extract afforded 80 mg. of oil which underwent crystallization. The crystals were washed out repeatedly with cyclohexane, the cyclohexane was evaporated, and the residue was sublimed under reduced pressure, affording 40 mg. of pale yellow crystals, m. p. 98～99°C, undepressed on admixture with γ-dolabrin (VI). Paper chromatographic examination showed A to be a mixture of the recovered ester, XIX, and XX.

c) A solution of 0.42 g. of the cyclohexyl ester (XVIII) dissolved in 12 ml. of ether was reacted with 6 molar equivalents of methylmagnesium iodide as in the case of (a), stirring for 1 hr. and

refluxed for 30 min. After it was cooled, 15 ml. of 4 N sulfuric acid was added to effect decomposition, extracted with ether, and the ether was evaporated after washing with water and drying over sodium sulfate, affording 250 mg. of yellow oil (A). The sulfuric acid layer was extracted 5 times with 5 ml. of chloroform each time, and the extract was washed with water, dried, and evaporated, to leave 50 mg. of oil. This crystallized immediately and was found to contain chiefly XIX and a small amount of XX. This substance actually gave green coloration in the aqueous layer and pale reddish brown coloration in the chloroform layer with ferric chloride. There was no suitable solvent for recrystallization of the above crystals but on leaving its ethalolic solution, comparatively large plate crystals, m. p. 101~104°C, separated out on the wall of the vessel. A chromatographic test indicated that A contained the recovered ester, XIX, and XX. Crystals separated out on standing A and 15 mg. of XX, m. p. 178~180°C, was obtained. The benzene solution of filtrate was chromatographed over silica gel but it was not successfully separated into its components.

**5-Acetyltropolone (XX) from γ-Dolabrin (VI).**—A solution of 770 mg. of VI dissolved in 27 ml. of formic acid, to which was added 6 ml. of 35% hydrogen peroxide, was stirred at 40°C for 3 hr. and formic acid was distilled off under reduced pressure. Further 7 ml. of 1.2 N sodium hydroxide was added and the mixture was stirred at 40°C for 3 hr. This was acidified with 2 N hydrochloric acid and extracted with chloroform. The aqueous layer was cooled with ice, an aqueous solution of 900 mg. of periodic acid dihydrate was added, mixture was stirred, and 590 mg. of crystals was obtained. The same amount of crystals, 70 mg., was obtained from the chloroform layer. The combined crystals were recrystallized from ethanol to XX as yellow plates, m. p. 182~183°C.

Found: C, 65.69; H, 4.49. Calcd. for $C_9H_8O_3$: C, 65.85; H, 4.91%.

Oxime: Pale yellow plates, m. p. 201~202°C (decomp.).

Found: C, 60.55; H, 4.75; N, 7.81. Calcd. for $C_9H_9O_3N$: C, 60.33; H, 5.00; N, 7.82%.

**Condensation of XX with Benzaldehyde and 3, 4, 5-Trimethoxybenzaldehyde.**—a) A mixture of 650 mg. of XX suspended in 10 ml. of methanol to which was added 700 mg. of benzaldehyde, 1.3 ml. of 5% potassium hydroxide solution, and 15 ml. of water was stirred thoroughly and the orange crystals that separated out were collected by filtration. This substance was dissolved in 100 ml. of water, acidified with 2 N hydrochloric acid, and 900 mg. of yellow needles was recrystallized from ethanol to yellow needles, m. p. 158~159°C.

Found: C, 76.04; H, 4.32. Calcd. for $C_{16}H_{12}O_3$: C, 76.18; H, 4.80%.

b) A mixture of 100 mg. of XX and 150 mg. of trimethoxybenzaldehyde afforded 150 mg. of a condensate of m. p. 207.5~208.5°C after recrystallization from acetic acid.

Found: C, 66.16; H, 5.12. Calcd. for $C_{19}H_{18}O_6$: C, 66.66; H, 5.30%.

The authors gratefully acknowledge financial help for part of the expenses for the present work from the Ministry of Education by a Grant-in-Aid for Scientific Research and from the Sankyo Co., Ltd., and the donation of samples from the Takasago Perfumery Co., Ltd. The writers are indepted to Mr. Yasuo Toyooka for technical assistance.

*Department of Chemistry*
*Faculty of Science*
*Tohoku University*
*Katahira-cho, Sendai*

# *Infrared Spectra of p-Bromophenacyl Esters*

By Hisao NAKATA, Shuzo MATSUO* and Yoshimasa HIRATA

(Received January 6, 1960)

In previous papers[1,2] it has been demonstrated that aureothinic acid and *N*-benzoyl aminotetrahydroaureothinic acid have structures (I) and (II), respectively. The location of an etheric oxygen at an $\alpha$-position of the carboxyl group in these acids was suggested by the comparison of infrared spectra of several model compounds[1] and was established rigorously by oxidative studies[2].

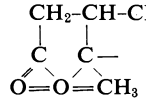
During the course of the structural elucidation of these acids, however, attention was called to the fact that the infrared spectra of their *p*-bromophenacyl esters in chloroform solution show ester carbonyl absorption at

* Institute of Chemical Research, Nippon Shin-yaku Co. Ltd., Nishioji, Hachi-jo, Minami-ku, Kyoto.

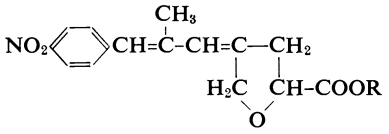
1) H. Nakata, Y. Hirata, K. Okuhara, K. Yamada, T. Naito and K. Iwadare, *J. Chem. Soc. Japan, Pure Chem. Sec.* (*Nippon Kagaku Zasshi*), **79**, 379 (1958).

2) Y. Hirata, H. Nakata and K. Yamada, ibid., **79**, 390 (1958).

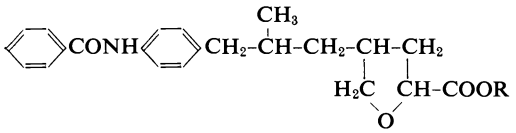
TABLE I. INFRARED SPECTRA OF *p*-BROMOPHENACYL ESTERS ($RCOOCH_2COC_6H_4Br$-*p*) IN CHLOROFORM SOLUTION

| No. | Compound R- | m. p.[a] °C | Ester C=O $cm^{-1}$ | Keto C=O $cm^{-1}$ | $\Sigma(\sigma^*)$[b] |
|---|---|---|---|---|---|
| 1 | *n*-$C_7H_{15}$- | 65～ 66 | 1743 | 1707 | −0.130[c] |
| 2 | *n*-$C_5H_{11}$- | 71～ 72 | 1742 | 1707 | −0.130[c] |
| 3 | *n*-$C_3H_7$- | 62～ 63 | 1743 | 1707 | −0.115 |
| 4 | $C_2H_5$- | 55～ 58 | 1743 | 1705 | −0.100 |
| 5 | $CH_3$- | 75～ 78 | 1744 | 1703 | 0.000 |
| 6 | $C_6H_5CH_2$- | 84～ 86 | 1748 | 1708 | +0.215 |
| 7 | $CH_3OCOCH_2CH_2$-[d] | 105～106 | 1746 | 1708 | +0.254[e] |
| 8 | $CH_3CHClCH_2$- | 75～ 76 | 1749 | 1708 | +0.270[f] |
| 9 | $CH_3CH(OH)$- | 111～112 | 1750 | 1708 | +0.455[f] |
| 10 | H- | 100～101[g] | 1737 | 1706 | +0.490 |
| 11 | $C_2H_5OCH_2$- | 106～107 | 1763 | 1706 | +0.520 |
| 12 | *n*-$C_4H_9OCH_2$- | 90～ 91 | 1764 | 1706 | +0.520 |
| 13 | $HOCH_2$- | 136～138 | 1751 | 1707 | +0.555 |
| 14 | $C_6H_5CONHCH_2$-[h] | 148～149 | 1753 | 1706 | +0.727[i] |
| 15 | $C_6H_5CH(OH)$- | 113～114 | 1750 | 1707 | +0.765 |
| 16 | $C_6H_5OCH_2$- | 149～150 | 1774 | 1707 | +0.850 |
| 17 | $ICH_2$- | 99～100 | 1751 | 1710 | +0.850 |
| 18 | $CH_3CH_2CHBr$- | (oil) | 1753 | 1712 | +0.885[f] |
| 19 | $(C_6H_5)_2C(OH)$- | 154～155 | 1743 | 1710 | +0.960[f] |
| 20 | $ClCH_2$- | 105～106 | 1756 | 1705 | +1.050 |
| 21 | Aureothinic acid (Ia) | 174～175 | 1758 | 1706 | +0.390[f] |
| 22 | *N*-Benzoyl aminotetrahydroaureothinic acid (IIa)[j] | 145～146 | 1758 | 1707 | +0.390[f] |
| 23 | $CH_3COCH(CH_3)CH_2$-[k] | 91 | 1745 | 1698 | +0.099[f] |
| 24 |  [k,l] | 105～106 | 1751 | 1702 | +0.720[m] |

a) All melting points are uncorrected.
b) The value is taken from Taft (Refs. 3 and 4), unless otherwise indicated.
c) Approximated with the value for *n*-$C_4H_9$- substituent.
d) The ester carbonyl group appeared at 1738 $cm^{-1}$.
e) Calculated from the value for $CH_3OCO$- substituent using the inductive parameter of 2.8 (Refs. 3 and 4).
f) Calculated using the additive nature of $\sigma^*$ values (Refs. 3 and 4).
g) T. Kubota and T. Matsuura, *J. Chem. Soc. Japan, Pure Chem. Sec. (Nippon Kagaku Zasshi)*, **72**, 482 (1951).
h) The amide carbonyl group appeared at 1663 $cm^{-1}$.
i) Estimated from the relations $\sigma^*=\sigma_I/0.45$ and $\sigma_I=(\alpha\cdot\sigma_p-\sigma_m)/(\alpha-1)$ (Refs. 3 and 4, and R. W. Taft, Jr. and I. C. Lewis, *J. Am. Chem. Soc.*, **80**, 2436 (1958).), using $\sigma_p$ of +0.078 and $\sigma_m$ of +0.217 (H. H. Jaffe, *Chem. Revs.*, **53**, 191 (1953).) and $\alpha=+0.443$ (J. L. Roberts and H. H. Jaffe, *J. Am. Chem. Soc.*, **81**, 1635 (1959).).
j) The amide carbonyl group appeared at 1660 $cm^{-1}$.
k) R. B. Bradbury and S. Masamune, *J. Am. Chem. Soc.*, **81**, 5201 (1959).
l) The lactone carbonyl group appeared at 1779 $cm^{-1}$.
m) The $\sigma^*$ value for $CH_3COOCH_2$- group was estimated as +1.010 from the same relations cited in foot-note i) of this Table using $\sigma_p$ of +0.31 and $\sigma_m$ of +0.39 (D. H. McDaniel and H. C. Brown, *J. Org. Chem.*, **23**, 420 (1958).), and $\alpha=+0.448$ (J. L. Roberts and H. H. Jaffe, *J. Am. Chem. Soc.*, **81**, 1635 (1959).). The additive nature of $\sigma^*$ values then leads to the value of +0.720 for this $\gamma$-lactone grouping.



(I) R=H, aureothinic acid
(Ia) R=$CH_2COC_6H_4Br$-*p*



(II) R=H, *N*-benzoyl aminotetrahydro-aureothinic acid
(IIa) R=$CH_2COC_6H_4Br$-*p*

1758 $cm^{-1}$, which is considered to be an abnormally high frequency, and it became desirable to examine the infrared spectra of several *p*-bromophenacyl esters. Consequently, twenty *p*-bromophenacyl esters were prepared and their spectra were measured in chloroform solution. The results are summarized in Table I.

The absorption bands of keto carbonyl groups appear in the same frequency range of 1705~1710 $cm^{-1}$. On the other hand, in the spectra of the ester carbonyl groups an etheric function located at an $\alpha$-position of the carboxyl group causes a considerable shift of frequency, as is evident from Table I (compounds No. 11, 12, 16, 21 and 22). While the inductive effect of electronegative $\alpha$-oxygen substituents has usually been cited as the probable cause for the frequency shifts, it has not been possible to differentiate this from direct field effects. A more quantitative understanding of these may be discussed in terms of inductive parameters of the substituents. When the polar substituent constant $\sigma^*$ reported by Taft[3,4] is taken as a measure of inductive effects, the ester carbonyl frequencies presented in Table I define a straight line when plotted against the appropriate $\sigma^*$-values (Fig. 1). The linear correlation obtained is reasonably good and it was found possible to write the following approximate relation:

$$\nu_{C=O}\ cm^{-1} = 1745\ cm^{-1} + 9.1(\Sigma\sigma^*)cm^{-1} \quad (1)$$

It is apparent from Fig. 1 that the absorption bands of both aureothinic (No. 21) and *N*-benzoyl aminotetrahydroaureothinic (No. 22) esters deviate from the correlation line by an amount of 10 $cm^{-1}$. The deviations are more serious with the ethoxy- (No. 11) and *n*-butoxy-acetic (No. 12) esters and even more so with phenoxy-acetic (No. 16). Therefore,

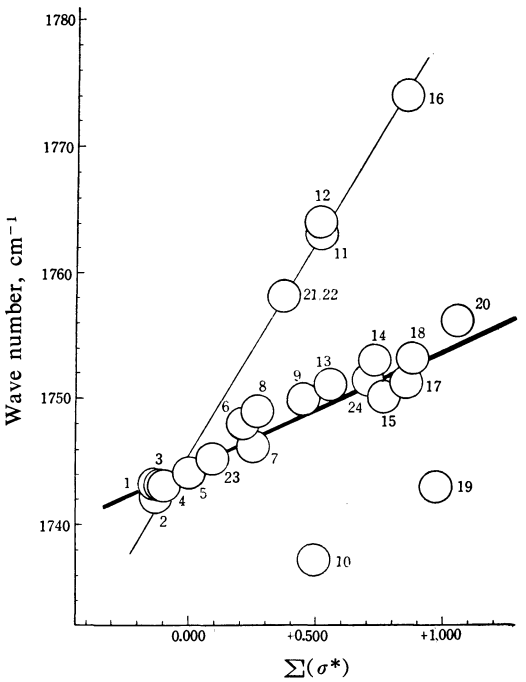



Fig. 1. The linear correlation between polar substituent constants and ester carbonyl frequencies of *p*-bromophenacyl esters. (The numbers refer to the compounds listed in Table II.)

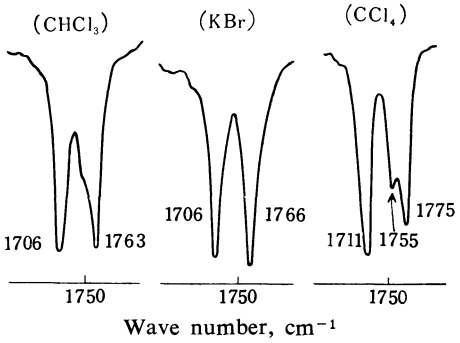


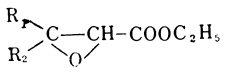

Fig. 2. Infrared spectra of *p*-bromophenacyl ethoxy acetate.

it may be concluded that these deviations are characteristic with esters having an etheric oxygen at their $\alpha$-positions.

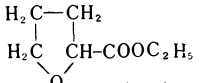
As is shown in Fig. 2, the band of these esters in chloroform solution had a shoulder at a low frequency region, while only a sharp band appeared when the spectrum was measured in the solid state (potassium bromide disks). Recently, House and Blaker[5] have reported that in the carbonyl region glycidic esters such as III and ethyl tetrahydrofuroate (IV) both

3) R. W. Taft, Jr., *J. Am. Chem. Soc.*, **75**, 4231 (1953).
4) R. W. Taft, Jr., in M. S. Newman ed., "Steric Effects in Organic Chemistry", Chapter 13, John Wiley & Sons, Inc., New York (1956).
5) H. O. House and J. W. Blaker, *J. Am. Chem. Soc.*, **80**, 6389 (1958).

exhibited two bands attributable to the presence of two conformations of esters in the solution[6]. The same explanation can be applied to *p*-bromophenacyl esters having an $\alpha$-oxygen substituent.

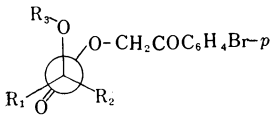


(III)

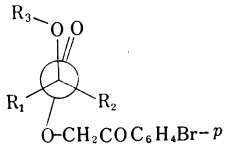


(IV)

These esters would exist in two conformations V and VI in solution. Since the C=O and C-O dipoles are oriented in opposite directions in the conformation V, the spectrum of this structure would be expected to have a normal carbonyl absorption band of *p*-bromophenacyl esters in the range of 1740~1755 $cm^{-1}$, while in the conformation VI, where these dipoles are oriented in the same direction, the direct field effects between these dipoles would be expected, which would result in the carbonyl vibration shifting towards higher frequencies.



(V)



(VI)

These considerations are exactly parallel with those employed in interpret the infrared spectra of $\alpha$-haloketones and $\alpha$-haloesters[7].

The molecular extinctions of the two conformations are not known and the actual concentrations of the two conformations could not be calculated. However, it may be concluded that these esters exist largely as the conformation VI in chloroform solution, since the lower frequency band of the conformation V is a shoulder and since a study of $\alpha$-bromoketo steroids suggests that the molecular extinction of the conformation VI should have a lower value than that of V[8]. Recently, Brown[9] has reported the value 3.36 : 2.77 for the ratio of apparent intensities of the corresponding conformations for ethyl $\alpha$-ethoxy acetate.

To explore the validity of the above presumption, infrared spectra of these esters were examined in carbon tetrachloride solution. As was evident from studies[10] of $\alpha$-bromocyclohexanone in various solvents, the less polar conformation V is stabilized by the less polar solvent so that the spectra of conformations V and VI would be separated from each other. This is actually the case; thus, as is shown in Fig. 2, the spectrum of *p*-bromophenacyl ethoxyacetate in carbon tetrachloride solution exhibits two bands at 1755 and 1775 $cm^{-1}$ in ester carbonyl region corresponding to the conformations V and VI, respectively. The same is true for *n*-butoxyacetic and monochloroacetic esters. The band frequencies of some esters in carbon tetrachloride solution are shown in Table II. Monoiodoacetic ester and $\alpha$-bromobutyric ester did not exhibit two bands even in this non-polar solvent. This observation agrees with the conclusion of Brown[9] that the distribution of two conformations of these esters is controlled largely by the size of the group rather than by the dipole-dipole repulsion.

Table II. Infrared spectra of *p*-bromophenacyl esters ($RCOOCH_2COC_6H_4Br$-*p*) in carbon tetrachloride solution

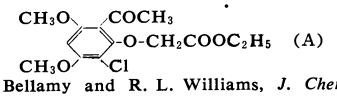
| Compound[a] No.[b] | R- | Ester C=O $cm^{-1}$ | Keto C=O $cm^{-1}$ |
|---|---|---|---|
| 3 | *n*-$C_3H_7$- | 1753 | 1712 |
| 4 | $C_2H_5$- | 1755 | 1712 |
| 5 | $CH_3$- | 1759 | 1712 |
| 6 | $C_6H_5CH_2$- | 1751 | 1711 |
| 8 | $CH_3CHClCH_2$- | 1753 | 1711 |
| 9 | $CH_3CH(OH)$- | 1753 | 1710 |
| 10 | H- | 1745 | 1713 |
| 11 | $C_2H_5OCH_2$- | 1775, 1755 | 1711 |
| 12 | *n*-$C_4H_9OCH_2$- | 1773, 1753 | 1712 |
| 17 | $ICH_2$- | 1754 | 1712 |
| 18 | $CH_3CH_2CHBr$- | 1755 | 1711 |
| 20 | $ClCH_2$- | 1781, 1758 | 1711 |

a) Most of the compounds not listed in this table were sparingly soluble in carbon tetrachloride and their spectra could not be examined.

b) The number refer to the compounds listed in Table I.

Another peculiarity observed in the spectra of most *p*-bromophenacyl esters was the appearance of a set of three strong to medium intensity bands around 1000 $cm^{-1}$, which probably originate from the *p*-bromophenacyl

6) Dawkins and Mulholland noticed that the ester carbonyl band of the ester (A) splitted (1763 and 1753 $cm^{-1}$) even in the solid state (Nujol). See, A. W, Dawkins and T. P. C. Mulholland, *J. Chem. Soc.*, **1959**, 2211.



(A)

7) L. J. Bellamy and R. L. Williams, *J. Chem. Soc.*, **1957**, 4294.

8) R. N. Jones, D. A. Ramsay, F. Herling and K. Dobriner, *J. Am. Chem. Soc.*, **74**, 2828 (1952).

9) T. L. Brown, *J. Am. Chem. Soc.*, **80**, 3513 (1958).

10) J. Allinger and N. L. Allinger, *Tetrahedron*, **2**, 64 (1958).

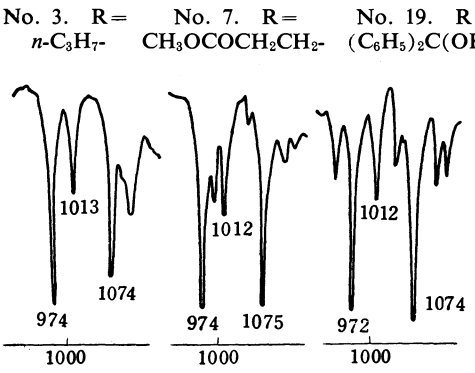



Fig. 3. Characteristic bands of *p*-bromophenacyl ester ($RCOOCH_2COC_6H_4Br$-*p*) around 1000 $cm^{-1}$ ($CHCl_3$).

group. Thus, these bands appear at 1076±2 $cm^{-1}$ (strong), 1014±2 $cm^{-1}$ (medium), and 972±4 $cm^{-1}$ (strong), and are almost independent of the structure of respective acids. These bands are therefore useful for the recognition of *p*-bromophenacyl esters. The characteristic shapes of these bands are shown in Fig. 3.

Provided that direct comparisons of spectra of *p*-bromophenacyl esters with the linear correlation of Eq. 1 are possible, the ester carbonyl absorption band would enable one to evaluate the appropriate $\sum\sigma^*$ value, which, in turn, would predict the nature of substituents around the carboxyl group of the respective acid, since only a few anomalies have been observed in the correlation except for those described above. While the abnormal frequency lowering in formic ester (No. 10) is not unexpected, the cause for the considerable deviation from the correlation in benzilic ester (No. 19) is not known.

Finally it is of interest to note that the frequencies of esters having an etheric function at their $\alpha$-position define another straight line in Fig. 1. Since the abnormally high frequency of these esters is ascribable to the direct field effect of alkoxyl groups, this linear correlation would probably suggest the linearity between the field effect and the inductive effect, at least, for these alkoxyl groups. However, more accurate and sufficient data may be required in order to test such a quantitative correlation.

## Experimental

**General Procedure for Preparation of *p*-Bromophenacyl Esters.** — About 500 mg. of the acid are added to a mixture of 1 ml. of water and 2 ml. of alcohol in a small flask and are neutralized carefully with crystalline sodium bicarbonate. The mixture is warmed very gently on a water bath until evolution of carbon dioxide ceases. The remaining sodium bicarbonate is filtered and the filtrate is added with one or two drops of the acid. Five ml. of alcohol and 500 mg. of *p*-bromophenacyl bromide are added and the mixture is then heated under reflux for 1 hr. Occasionally the addition of a few more milliliters of alcohol may be necessary if a solid separates during the refluxing. The solution is allowed to cool, and the precipitated ester is purified by recrystallization from alcohol or from aqueous alcohol. The melting point of the ester is listed in Table I.

**Infrared Absorption Measurements.**—The spectra were recorded on a Hilger H 800 double beam instrument equipped with sodium chloride optics. Spectra of the solution were measured using 0.16 mm. sodium chloride cells.

The authors wish to express their gratitude to Dr. Isao Satoda, Nippon Shin-yaku Co. for his interest in this research. They are indebted to the Parke Davis Co. for fellowships to H. N. during the course of the research, and are also grateful for a grant from the Ministry of Education.

*Chemical Institute*
*Faculty of Science*
*Nagoya University*
*Chikusa, Nagoya*

# SHORT COMMUNICATIONS

## *Proton Magnetic Resonance Absorption of Aluminum Hydroxides and of their Thermal Dehydration-Products*

By Tokutaro HAGIWARA and Tatsuo SAITO*

(Received February 29, 1960)

The phase transformations occurring in the thermal decomposition of the alumina trihydrate belong, as of old, to the subject of extensive researches. The present authors have now tried to study the thermal dehydration of alumina trihydrate by means of a method of proton magnetic resonance absorption**.

The starting material here employed was a bayerite prepared by a chemical reaction of an aluminum chloride solution with an aqueous ammonia. Each specimen was subjected to the corresponding heating of this starting material during 3 hr. in the air at 100°, 200°, 220°, 250°, 300°, 450° and 600°C, respectively. They were sealed in the evacuated glass tubes which were pumped out to a high vacuum, either at room temperature during 12 hr. or at 110°C during 6 hr., the latter having the purpose of an after-treatment. We call the former group as "a-series" and the latter one as "b-series".

For the NMR measurements, we have used the a.c. modulation technique of the magnetic field at the d.c. magnetic field of about 3100 gauss. The detecting apparatus has the ordinary constitution, which is composed of an autodyne oscillator, an audio-frequency amplifier, a lockin-amplifier and a recording milliammeter.

The measurements of the proton magnetic resonance were also made in the well-known definite hydrargillite, bayerite, böhmite and natural diaspore, respectively. Some reproductions of the experimental line shapes of the proton resonances are shown in Figs. 1 and 2.

As is seen in Fig. 1, the line shapes of the hydrargillite and of the bayerite or the starting material may be presumably understood as being composed of two parts: one is situated at the center with the narrower width and another is of very broad at both sides of it. The line shape of the böhmite shows the signal of the three spin type, while that of the

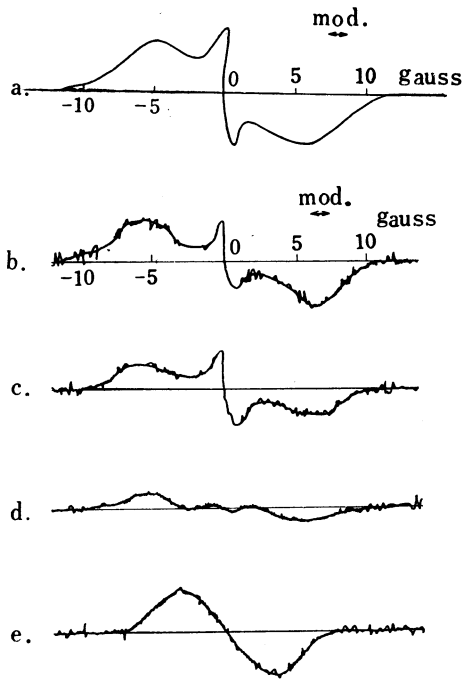



Fig. 1. Recorded derivatives of proton resonance in the starting material and the known, definite hydroxides.
a: Starting material b: Hydrargillite
c: Bayerite d: Böhmite e: Diaspore

TABLE I. THE VALUES OF THE SECOND MOMENTS CALCULATED FROM THE EXPERIMENTAL DERIVATIVES

| Specimen | Second moment (in gauss²) |
|---|---|
| Starting material | 12.9 |
| Bayerite | 13.1 |
| Hydrargillite | 15.2 |
| Böhmite | 14.0 |
| Diaspore | 6.3 |
| Dehydrated at 100°C-(b) | 13.4 |
| 〃 at 200°C-(b) | 13.7 |
| 〃 at 220°C-(b) | 14.0 |
| 〃 at 250°C-(b) | 8.3 |
| 〃 at 300°C-(b) | 6.8 |
| 〃 at 450°C-(b) | 4.3 |
| 〃 at 600°C-(b) | 3.0 |

* Present address; Government Chemical Industrial Research Institute, Tokyo, Honmachi 1-chōme, Shibuya-ku, Tokyo.

** Presented partly at the Symposium on Structural Chemistry, Osaka, Oct. 31, 1954.

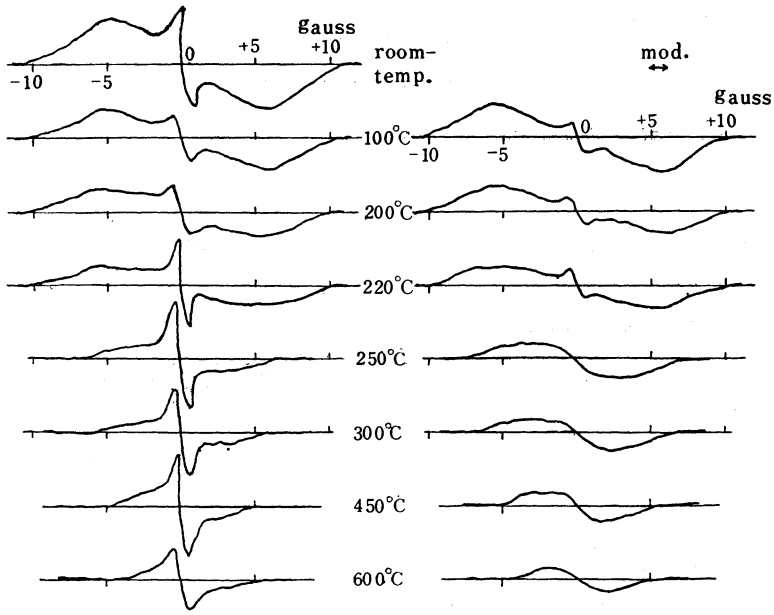



Fig. 2. Recorded derivatives of proton resonance in the a- and b-series—(without and with the after-treatments, in vacuo, 110°C).

diaspore shows the single and narrow line. The values of the second moments calculated from the experimental derivative curves are shown in Table I.

The line shapes of each specimen dehydrated at 100° and 200°C are both similar to that of the starting material. The amplitudes of the central components observed for these line shapes are somewhat reduced by the thermal after-treatment, as in a high vacuum pumping at 110°C, but they yet never disappear by such a treatment. Nevertheless, the line shapes of the specimens dehydrated at about 220°C and higher make quite a difference from above two specimens and the height of the central peaks in these line shapes considerably increases. It is noteworthy that these central peaks, however, disappear by the such after-treatment, as in a high vacuum pumping at 110°C. These interesting behaviors can be seen in Fig. 2. Therefore, we are to suppose that these central peaks in the latter case originate from the water-molecules which are adsorbed by the decomposed products and are in the thermal motion.

Based upon the above experimental fact, the following conclusions can be drawn:

1) The decomposition of this starting material does not occur till the thermal dehydration temperature of about 200°C. This is ascertained in our NMR experiments.

2) The sudden and considerable variation of the central part observed in the line shapes at an about 220°C and higher, seems to show that the first dehydration process of this starting material brings forth an active lower hydroxide, exhibiting very high activity for an adsorption.

3) The gradual decrease of the line width occurring in the range from about 250 to 600°C might be regarded as a result due to the changing of the mixed ratio of the lower hydroxide and alumina phases.

These conclusions will be ascertained by the additional experiment by means of X-ray diffraction method which is in progress in our laboratory.

The authors wish to express their sincere thanks to Professor Tunahiko Shidei and Assistant Professor Syukuro Yano in Kyoto University, under whose continual advice and encouragement the present experiments has been carried out, and also for their so kindness as to allow us the loan of their equipments and the technique throughout this study. This study also has been partly supported under the Scientific Research Expenditure from the Ministry of Education.

*Department of Chemistry*
*Faculty of Science*
*Hiroshima University*
*Hiroshima*

## *Thermal Isomerization of 2-Thenylthiocyanate*

By Kensuke TAKAHASHI, Tyo SONE, Yasuo MATSUKI and Genjiro HAZATO

(Received March 12, 1960)

During the studies of the structural investigation and the identification of thenyl derivatives by means of the NMR technique, we happened upon the occurrence of the thermal isomerization of 2-thenylthiocyanate at about 150°C.

Resonance was observed at 40 mc, the apparatus and the procedure were similar to those previously described[1], and in every sample, cyclohexane was used as an internal reference. The spectrum of the raw product synthesized from thiophene by the procedure of thiocyanomethylation, is shown in Fig. 1a. The lines coming from the aromatic hydrogens in thiophene ring spread over the range of about 20 cps at the low-field side of the spectrum. At the high-field side two lines at 107.5 and 125 cps, referred to cyclohexane signal, are assumed to be the lines coming from the hydrogens of the methylene group. We had expected formerly to be observed only one line coming from this group; whereas, the experimental result showed that the methylene peak was divided into two lines, corresponding to two isomers respectively. After this measurement, the sample was heated at about 150°C for two hours by immersing in a constant temperature bath. In the spectrum of the heated sample, the two lines coming from the methylene hydrogens were found at the same positions but there was a marked difference in their intensities as compared with the non-heated sample, as shown in Fig. 1b. This result indicates the occurrence of a thermal isomerization between two compounds of which our synthesized product consists. The thermal isomerization in allylthiocyanate was firstly shown by Gerlich[2]. Here we have studied the benzyl thiocyanate which shows the thrmal isomerization at about 250°C, reported already by Hennicke[3]. Its spectrum shows two lines coming from methylene and aromatic hydrogens at 96 and 229 cps, referred to cyclohexane signal, respectively. By heating of this compound at about 150°C for two hours, no change of its NMR spectrum was observed in comparison with 2-thenyl derivative, but after heating at about 250°C for two hours, the line coming from the methylene group was found at 111 cps with the other small neighboring peaks, and the lines of the aromatic hydrogens were found at 224 and 228 cps. This phenomenon is assumed as the isomerization from thiocyanate to isothiocyanate which is promoted by heating, the same is the case with that observed in 2-thenyl derivative. The isomerization in question here observed in the NMR spectrum is represented by the shift of the line coming from the methylene group to the lower field, which is attributed to the change of the electronegativity and of the second-order high frequency paramagnetism of the adjacent group. The detailed result on the thiocyanomethylation of thiophene will be published in the Journal of the Chemical Society of Japan, Ind. Chem. Sec.

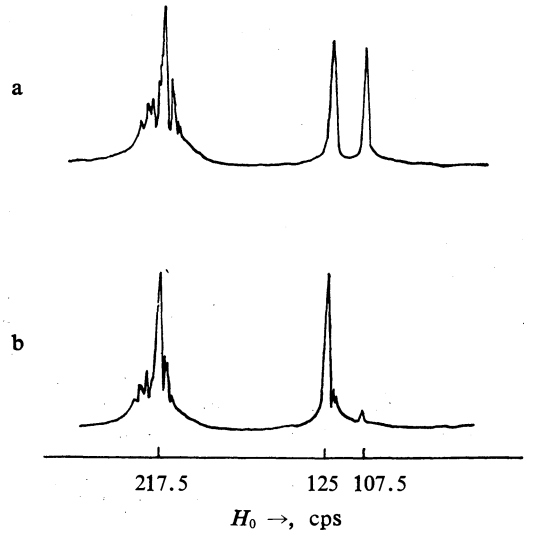



Fig. 1. The proton magnetic resonance spectra of the raw product synthesized from thiophene by thiocyanomethylation, (a) before heating; (b) after heating at about 150°C for two hours. Applied magnetic field increasing from left to right.

*The Chemical Research Institute of Non-aqueous Solutions*
*Tohoku University*
*Katahira-cho, Sendai*

1) K. Takahashi, Y. Matsuki, T. Mashiko and G. Hazato, This Bulletin, 32, 156 (1959).

2) G. Gerlich, *Ann.*, 178, 83 (1875).

3) H. Hennicke, ibid., 344, 24 (1906).

## *On the Electronic Structure of Thiothiophten*

By Kôgorô MAEDA

(Received June 10, 1960)

Recently the structure of a thiothiophten molecule was clarified through the X-ray analysis by Bezzi, Mammi and Garbuglio[1], who proposed a condensed ring system characterized by no-bond resonance structure. On the basis of this peculiar structure, Giacometti and Rigatti[2] have made simple LCAO treatment on the superimposed $\sigma$ and $\pi$ systems of nonlocalized electrons in thiothiophten, by using only $p$ type orbitals for valence states of sulfur atoms. However, since the system involving no-bond resonance structure is somewhat unlikely to occur, an alternative interpretation on the electronic structure of thiothiophten will be given in the present report.

It is possible that a $3p$ electron of the sulfur atom is promoted to a $3d$ orbital and interacts with other $3p$ electrons through $pd$ hybridization[3]. Then it may be reasonable to consider that the central sulfur atom in the straight bond S–S–S of thiothiophten is in a valency state capable of forming the $\sigma$ skeleton of bonds through the $pd$ hybridization. The expected valency state of the central sulfur atom would be in the electron configuration $3s^2 3p^3 3d$; one of $3p$'s, $3p_x$, hybridizes with a $3d$ orbital, going to make up the $\sigma$ bonds of S–S–S in the linear arrangement, and $3p_y$ is adopted to form a C–S $\sigma$ bond with one of $sp^2$ orbitals of the neighboring central carbon atom. These configurations can account for both the so-called abnormal length of the bond between two sulfur atoms[3-5] and the right angle of S–S–C with respect to the central sulfur atom. Thus it might be said that the full $\sigma$ skeleton of the condensed ring system of thiothiophten is composed of the bonds obtained above through the hybridization and other C–S and C–C bonds without introducing the no-bond resonance structure. Over this $\sigma$ ring system covers the $\pi$ electron conjugation system, in which the remaining $3p$ orbital, namely the $3p_z$ orbital participates. The electronic structure of thiothiophten can now be treated according to the usual LCAO approximation without considering the $\sigma$ skeleton.

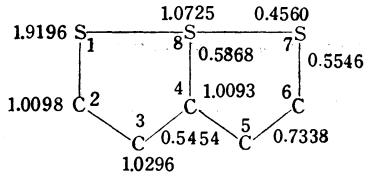



Fig. 1. Molecular diagram of thiothiophten.

In Fig. 1 are given the results obtained by the simple LCAO $\pi$ approximation on thiothiophten. In calculating the molecular diagram, the following assumptions were adopted: All the Coulomb intengrals were taken to be equal to the common value (so-called $\alpha_c$) except for two sulfur atoms $S_1$ and $S_7$ (see Fig. 1), for which a value less by $0.2\beta$ was applied, because the equivalent conjugation systems of thiothiophten in terms of valence bond method are liable to make the atoms positively charged[6]. Furthermore Longuet-Higgins' idea was employed for the two atoms[7]. With respect to the exchange integrals, the standard of the value, $\beta$ was used for all C–C bonds. For S–S and central C–S bonds were given the values $0.3\beta$ and $0.6\beta$, respectively, which are both found in the report of Giacometti and Rigatti[2]. The results given in Fig. 1 are those obtained when the exchange integral of C–S involving $S_1$ or $S_7$ bears the same value as that of C–C. The employment of the value is due to non-symmetrical character between the two bonds on the sulfur atom.

The results obtained in this paper are almost the same as those of Giacometti and Rigatti[2], but they are not necessarily the best. It must be noticed, however, that the results obtained without the help of no-bond resonance idea are appropriate at any rate, although many approximations were necessary in the calculation. The insufficient character of the results may be due to the inadequate values of parameters, which should be determined to predict correctly the values of the dipole moment and resonance energy[6]. Details will be further discussed in subsequent publications.

*Electrotechnical Laboratory*
*Tanashi P. O., Tokyo*

1) S. Bezzi, M. Mammi and C. Garbuglio, *Nature*, **182**, 247 (1958).
2) G. Giacometti and G. Rigatti, *J. Chem. Phys.*, **30**, 1633 (1959).
3) K. Maeda, This Bulletin, **33**, 303 (1960).
4) D. P. Craig, A. Macoll, R. S. Nyholm, L. E. Orgel and L. E. Sutton, *J. Chem. Soc.*, **1954**, 332.
5) D. P. Craig and E. A. Magnusson, ibid., **1956**, 4895.
6) K. Kikuchi, *Sci. Rept. Tohoku Univ. Series* I, **41**, 35 (1957).
7) H. C. Longuet-Higgins, *Trans. Faraday Soc.*, **45**, 173 (1949).

## *Hydration of Thujopsene to Widdrol*

By Shizuo NAGAHAMA

(Received August 18, 1960)

Hydration of thujopsene was first reported by Tanaka and Yamashita[1], who obtained an alcohol $C_{15}H_{26}O$, m. p. 120~122°C, $[\alpha]_D$+115.3° (yield 6%) under mild Bertram-Wahlbaum condition.

In the course of studies on the acid catalyzed isomerization of thujopsene, it was found that thujopsene gave another alcohol which was identified as widdrol by direct comparison with the sample obtained by Erdtman and Thomas[2].

A mixture of oxalic acid (50 g.), water (50 cc.), ethanol (600 cc.) and thujopsene (100 g.) was refluxed for 10 hr. The highest boiling fraction of the reaction products (b. p. 124~129°/5mmHg, 25 g.) solidified on standing and repeated recrystallization of this material from petroleum ether and sublimation under reduced pressure gave widdrol, m. p. 98°C, $[\alpha]_D$+105° (c=0.87), $C_{15}H_{26}O$ (Found: C, 81.02, H, 11.79%). The hydrocarbon fraction (b. p. 105~114°C/5 mmHg, 65 g.) was treated under the same condition as mentioned above and further 4 g. of crude widdrol was obtained. The hydrocarbon fraction (b. p. 104~111°C/5 mmHg, 41 g.) recovered from this reaction mixture underwent the same treatment further to give the product; b. p. 113~114°C/5mmHg, $n_D^{30}$ 1.5022, $d_4^{30}$ 0.9251, $[\alpha]_D$+22.2° (neat), I. R. bands 1638, 888 $cm^{-1}$ (17 g.).

The author wishes to express his gratitude to Professor H. Erdtman and Dr. C. Enzell for kind offer of the precious natural widdrol. He also appreciates the kind guidance of Professor S. Akiyoshi.

*Department of Organic Synthesis*
*Faculty of Engineering*
*Kyushu University*
*Hakozaki, Fukuoka*

1) J. Tanaka and I. Yamashita, *Bull. Osaka Ind. Research Inst.*, **9**, 5 (1958).
2) H. Erdtman and B. R. Thomas, *Acta Chem. Scand.*, **12**, 267 (1958).

# *Non-benzenoid Aromatic Heterocycles. III*[1]. *Conversion of 4-Pyrone Derivatives into 4-Pyridone Derivatives*

By Hiroshi KATO, Takatoshi OGAWA and Masaki OHTA

(Received August 20, 1960)

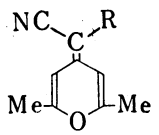
In the first paper of this series[2], the condensation of active methylene compounds with 2, 6-dimethyl-4-pyrone has been reported. In the present communication, the action of amines on these condensation products is described. These compounds are similar to pyrone in their electronic structure, and it is of interest to examine if these compounds are converted into the corresponding pyridone derivatives like pyrones. If the reaction takes place, it will be a valuable route to many pyridone derivatives. As model compounds, 4-(dicyanomethylene)-2, 6-dimethyl-4*H*-pyrane (Ia) and 4-(ethoxycarbonylcyanomethylene)-2, 6-dimethyl-4*H*-pyrane (Ib) were selected. With Ia, the reaction with amines (aniline, benzylamine, hydrazine hydrate) took place and gave the corresponding *N*-substituted 4-(dicyanomethylene)-2, 6-dimethyl-1, 4-dihydropyridines (IIa-c). As to the structure of the reaction product with hydrazine hydrate, two structures, IIc and III, are possible, but the *N*-aminopyridone structure (IIc) was established by condensing it with benzaldehyde to form the benzal derivative (IIg). Although Ia did not react with ammonium chloride, it was converted into pyridone derivative (IId) by heating it in formamide. Of special interest is IId, since it may be isomerized to pyridine derivative IV and would afford a valuable route to many pyridine derivatives*.

Starting from Ib, the corresponding pyridone derivatives (IIe, f) were prepared with benzylamine and hydrazine hydrate, but with aniline or formamide, the starting material was recovered unchanged. It may be worth while to note that the ester group of Ib did not suffer amminolysis.

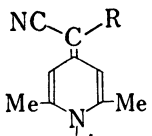
An attempt to prepare 1-thiapyrone derivatives by treatment of Ia and Ib with potassium hydrosulfide was not successful.

---

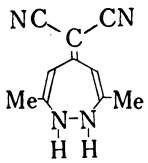
1) Part II. H. Kato, T. Ogawa and M. Ohta, This Bulletin, 33, 1467 (1960).
2) M. Ohta and H. Kato, ibid., 32, 707 (1959).
* After the completion of this work, a review on pyrylium salt by Dimorth[3] appeared, where he briefly reported that he also attempted the reaction of this type and obtained the corresponding pyridine derivatives.
3) K. Dimroth, *Angew. Chem.*, 72, 331 (1960).



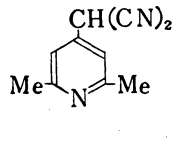
Ia: R=CN
Ib: R=COOEt



IIa: R=CN, R'=Ph
IIb: R=CN, R'=$PhCH_2$
IIc: R=CN, R'=$H_2N$
IId: R=CN, R'=H
IIe: R=COOEt, R'=$PhCH_2$
IIf: R=COOEt, R'=$H_2N$
IIg: R=CN, R'=N=CHPh



III



IV

## Experimental

**Reaction of Ia or Ib with Amines.**—**IIa,** A mixture of Ia (3.5 g.) and an excess of aniline (4 g.) was gently refluxed for an hour. The reaction mixture was washed with dil. hydrochloric acid and the residue (1.0 g., m. p. 310~313°C) was recrystallized from acetic acid giving white needles, m. p. 314~315°C. Yield 20%.

Found: N, 17.11. Calcd. for $C_{16}H_{13}N_3$: N, 16.99%.

Similarly, the following compounds were obtained:

**IIb,** (from Ia and benzylamine; heated at 150°C.) yellow needles (recrystallized from ethanol) m. p. 242~245°C. Yield 34%.

Found: N, 16.28. Calcd. for $C_{17}H_{15}N_3$: N, 16.08%.

**IIc** (from Ia and hydrazine hydrate; heated at 100°C) white needles (recrystallized from acetic acid) m. p. 291~292°C (decomp.) Yield 40%.

Found: N, 30.36. Calcd. for $C_{10}H_{10}N_4$: N, 30.09%.

**IIe,** (from Ib and benzylamine) white needles (recrystallized from ethanol) m. p. 183~184°C. Yield 80%.

Found: N, 9.15. Calcd. for $C_{19}H_{20}O_2N_2$: N, 9.09%.

**IIf,** (from Ib and hydrazine hydrate) pale yellow needles (recrystallized from ethanol) m. p. 217~218°C. Yield 71%.

Found: N, 17.70. Calcd. for $C_{12}H_{15}O_2N_3$: N, 18.02%.

**N-Benzalamino-4-(dicyanomethylene)-2,6-dimethyl-1,4-dihydropyridine (IIg),**—A solution of IIc (0.6 g.) and benzaldehyde (0.4 g.) in acetic acid was refluxed for an hour, and then diluted with water and the precipitate that separated out was collected (0.6 g., m. p, 254~255°C). Recrystallization from acetic acid afforded yellow needles, m. p. 294~295C°.

Found: C, 74.21; H, 5.25; N, 20.00. Calcd. for $C_{17}H_{14}N_4$: C, 74.43; H, 5.14; N, 20.43%.

**4-(Dicyanomethylene)-2,6-dimethyl-1,4-dihydropyridine (IId).**—A solution of Ia (5 g.) in formamide (5 g.) was heated at 150°C for an hour. The crystals which separated out on cooling were collected (1.7 g., m. p. 280~300°C) and recrystallized from formic acid giving yellow needles, m. p. 330~331°C.

Found: C, 70.37; H, 5.36; N, 24.44. Calcd. for $C_{10}H_9N_3$: C, 70.15; H, 5.30; N, 24.55%.

**Reaction of Potassium Hydrosulfide with Ia or Ib,**—When Ia or Ib was refluxed in methanol solution of potassium hydrosulfide, the starting material was recovred unchanged.

The authors are indebted to Mr. Asaji Kondo for performing the microanalyses.

*Laboratory of Organic Chemistry*
*Tokyo Institute of Technology*
*Meguro-ku, Tokyo*

# *Studies on Metal Complex Species Using an Anion Exchange Resin. I. Derivation of Equations and Application to Mercury(II)-Nitrate Complex*

By Hirohiko WAKI

(Received July 16, 1960)

A generalized equation for determining the composition of metal complex species was derived by introducing the complex formation equilibrium in the resin phase, which has not been considered formerly.

When most part of a metallic element exists in the form of $MX_m^{a-bm}$ in the solution phase and $MX_n^{a-bn}$ in the resin phase as a result of complex formation between the metal ion $M^{a+}$ and the anion $X^{b-}$, the following equation may be derived:

$$\log D = (n-a/b)\log[X^{b-}] - (m-a/b)\log(X^{b-}) + K + G \qquad (1)$$

where $D$ represents the distribution coefficient of the metallic element, ( ) and [ ] indicate the concentrations in the solution phase and the resin phase, respectively, and $K$ and $G$ the terms containing the complex formation constant and the activity coefficient in both phases. Under the condition in which $K$ and $G$ are constant,

$$\frac{d\{\log D+(m-a/b)\log(X^{b-})\}}{d\log[X^{b-}]}=n-a/b \quad (2)$$

$$\frac{d\{\log D-(n-a/b)\log[X^{b-}]\}}{d\log(X^{b-})}=-(m-a/b) \quad (3)$$

Accordingly, when $m$ is known and $D$, $(X^{b-})$ and $[X^{b-}]$ are measurable, $n$ can be determined graphically, and $m$ is also obtained when $n$ is known. Even if both are unknown, one of them can be determined when either $(X^{b-})$ or $[X^{b-}]$ is kept constant. Although it is practically impossible to set a condition in which the activity coefficient term is strictly constant, that may be roughly realized when a small quantity of the metallic element is used and the ionic strengths in the two phases are each kept constant by the addition of an indifferent anion, and therefore the complex form may be determined through measurements in the range where the predominant anionic species is $X^{b-}$.

As an application of these equations, adsorption of mercury(II) from a sodium nitrate solution was studied by means of $NaNO_3+NaClO_4$ mixed medium, where $Hg^{2+}$ was employed as $M^{a+}$, $NO_3^-$ as $X^{b-}$ and $ClO_4^-$ as an additional anion. Assuming that mercury is present as $Hg^{2+}$ in a sodium nitrate solution acidified by nitric acid, Eq. 1 is obtained simplified as follows:

$$\log D-2\log(NO_3^-)=(n-2)\log[NO_3^-]+K+G \quad (4)$$

The experiment was carried out by equilibrating 2 g. of an anion exchanger "Dowex 1-X8" (100~200 mesh) of nitrate form with a mixed solution containing 0.1 millimole of mercury(II) nitrate, 0.5 millimole of nitric acid, and a series of mixtures $NaNO_3+NaClO_4$ of various mixing ratios (total concentration is 3 M or 5M), followed by determination of mercury in the solution and nitrate in the resin. Mercury in the resin and nitrate in the solution were determined by subtraction since their total amounts are known. The distribution coefficient of mercury was calculated as

$$D=\frac{\left(\begin{matrix}\text{millimole of Hg adsorbed per}\\ \text{milliequivalent of resin}\end{matrix}\right)}{\left(\begin{matrix}\text{millimole of Hg per}\\ \text{milliliter of solution}\end{matrix}\right)}$$

The ion concentrations in the resin phase were always represented as millimole of the ion per milliequivalent of the resin.

$\log D-2\log(NO_3^-)$ was plotted against logarithm of the nitrate ion concentration in the resin, as shown in Fig. 1. The curves show linearity and their slopes correspond to $n=3.8$ for both cases of 3 M and 5 M of the external total concentration. Accordingly, it may be recognized that most mercury(II) is adsorbed in the form of $Hg(NO_3)_4^{2-}$ from the acidified 3~5 M sodium nitrate solution.

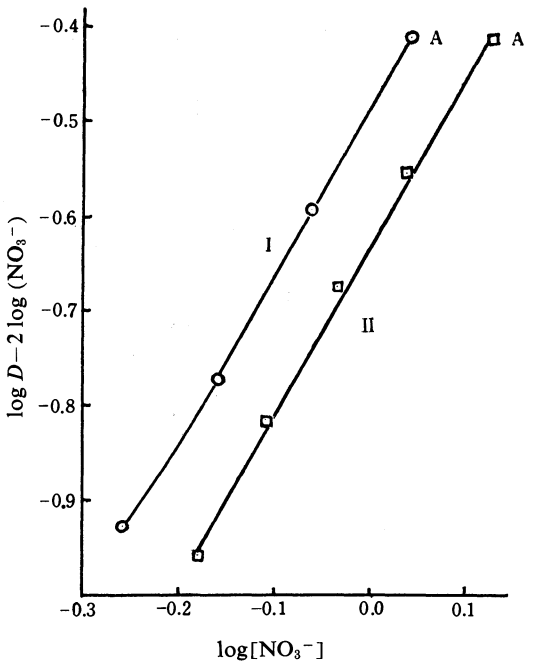



Fig. 1. Distribution coeficient of Hg(II) as a function of the nitrate concentration in the resin phase.
The measurements were carried out at the nitrate-rich range. A is the point in the absence of perchlorate.
I. Total concentration of the external solution is 3 M
II. 〃 5 M

It may also be possible that the lower complex species, such as $Hg(NO_3)^+$ or $Hg(NO_3)_2^0$, exist in the solution. However, since the degree of change in nitrate concentration in the solution phase was much smaller than that in distribution coefficient, the change of the second term on the right side in Eq. 1 may slightly affect the conclusion. Details of this investigation will be reported later.

The author wishes to express his sincere thanks to Professor J. Yoshimura of Kyushu University for his suggestion and encouragement.

*Department of Chemistry*
*Faculty of Science*
*Kyushu University*
*Hakozaki, Fukuoka*

## *Synthesis of Isokinetin, 2-N-furfurylaminopurine and its Leaf-growth Activity (Studies of Isokinetin and its Analogs. Part I)*

By F. Shigeo OKUMURA, Hiroshi KUSAKA and Tetsuji TAKEMATSU

(Received July 11, 1960)

More than fifty kinetin-analogs which belong to 6-(*N*-substituted)-aminopurine, have been prepared and it was found[1] that some of them have a leaf-growth stimulating activity. During the course of this study, our interest was directed to investigate whether the leaf-growth activity is still retained after the furfurylamino group at 6-position of the purine ring migrates to the 2-position.

After making many unsuccessful attempts to synthesize 2-(*N*-furfuryl)-aminopurine, we succeeded in preparing this new compound by the process outlined in Fig. 1.

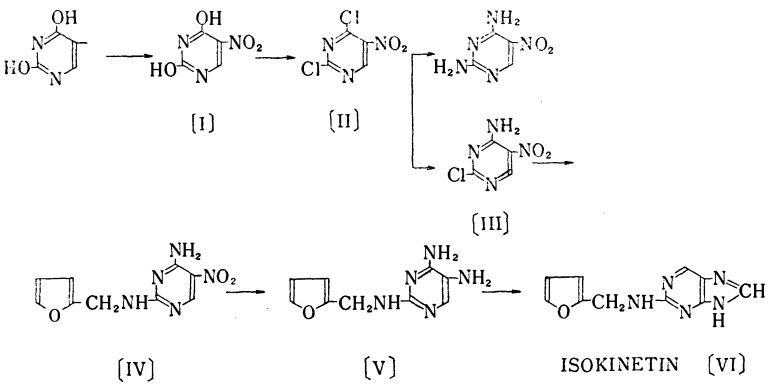
Nitration of uracil with fuming nitric acid gave 2, 6-dihydroxy-5-nitropyrimidine (I) in 90.7% yield, m. p. 294~295°C (Found: N, 26.70. Calcd. for $C_4H_3N_3O_4$: N, 26.75%). This was chlorinated with phosphoroxychloride in the presence of dimethylaniline to give 2, 6-dichloro-5-nitro-pyrimidine (II) in 64% yield.

Amination of II by ammonia in methanol-ether solution gives the mixture of 2, 6-diamino-5-nitro-pyrimidine and 2-chloro-6-amino-5-nitro-pyrimidine (III). However, III can be obtained in 60% yield when amination takes place at low temperature (below 0°C), m. p. of III, 220~221°C, Found: N, 31.95. Calcd. for $C_4H_3N_4O_2Cl$: N, 32.10%. III was then converted into 2-furfurylamino-6-amino-5-nitropyrimidine (IV) in 69.7% yield by refluxing with furfurylamine for 3~4 hr. (m. p, 159~160°C, Found: N, 29.50. Calcd. for $C_9H_9N_5O_3$: N, 29.76%).

IV was finally reduced catalytically with Raney nickel in methanol to give 2-furfuryl-amino-4, 5-diaminopyrimidine (V) which was refluxed with formamide yielding 2-(*N*-furfuryl)-aminopurine (VI) in 24% yield. Tan-colored needle from absolute alcohol, m. p. 195~196°C, (Found: C, 55.88; H, 4.01; N, 32.55. Calcd. for $C_{10}H_9N_5O$: C, 55.55; H, 4.67; N, 32.37%). The ultraviolet spectrum of isokinetin showed almost the same absorption as that of kinetin.

The leaf-growth activity of isokinetin was compared with that of kinetin by using *Rhaphanus cotyledon* by the Takematsu method[2]. The 200 mg./1. solution of kinetin or isokinetin was sprayed by using 0.4 ml. microsprayer on both sides of *Rhaphanus cotyledon*, which was cultured on the sand for 4 days at 15~18°C after coming out the *cotyledon* of *Rhaphanus sativa*. The increase of the leaf-area was measured 5 days after spraying. Isokinetin stimulates leaf-growth, but activity was observed to be about 80% of that of kinetin.

Okumura and Kuraishi[3] observed that kinetin inhibits the growth of the root of *Brassica chinensis L var. amplexicaulis Makino* at the concentration of $10^{-3}$mg./l. In the present communication we have observed the same inhibiting action of both kinetin and isokinetin against the growth of roots of *Rhaphanus sativa* and *Brassica juncea*. Kinetin inhibited the growth of roots remarkably, even in the concentration of 5mg./1. but the inhibiting action of isokinetin was observed only at the concentration of 50 mg./1. or higher. As gibberelline and indol acetic acid has no inhibitory




1) F. S. Okumura et al., This Bulletin, **30**, 194 (1957); **32**, 886, 889, (1959).

2) Method of *Rhaphanus* test and its application, by T. Takematsu (1959).

3) Unpublished work.

effect against the growth of plant roots, this inhibiting action is specific for the kinetin and isokinetin groups.

From the above observation it is clear that there are some interesting relationships between the leaf-growth and root-inhibition among the kinetin and isokinetin groups. Concerning this aspect, further studies are now in progress.

*Department of Chemistry*
*University of Tokushima*
*Tokushima (F. S. O.)*

*Onoda Cement Co.,*
*Yamaguchi (H. K.)*

*Department of Agriculture*
*University of Utsunomiya*
*Utsunomiya (T. T.)*

# *Studies on the Mucilage of the Root of "Tororo-aoi" (Abelmoschus manihot, MEDIC). I. On the Characteristic Colloidal Nature of the Mucilage*

By Saburo INOKAWA

(Received January 22, 1960)

Japanese hand-made paper, as is well known, is very elegant and refined, strong and tenacious, and is considered as a piece of work of Japanese characteristic arts. It is said that its elegance and strength mainly depend upon the properties of "*Neri*" which is indispensable for making Japanese hand-made paper.

"*Neri*" is a plant mucilage, and the mucilage obtained from the root of "*Tororo-aoi*" (*Abelmoschus manihot*, MEDIC) is most widely used. The chemical constituent of this plant mucilage was first investigated by Ozawa[1], and later Oguri[2] studied its distribution in cellular tissue. Oguri et al.[3,4], Machida et al.[5], and Oshibuchi et al.[6] reported that this plant mucilage was mainly made of polyrhamnogalacturonide, which contained rhamnose and galacturonic acid in the ratio of 1 : 1 or 1 : 2, and was accompanied by small quantities of araban, xylan, galactosan, and glucosan. However, concerning the colloidal behavior of this plant mucilage, little work has been done[7,8]. Taking an interest in this mucilage, we have been studying it for several years[9-13]. In this paper, such a purification method in which colloidal characteristics are kept well, was studied and then some colloidal characteristics of the purified mucilage were observed.

## Experimental

**Material.** — Roots of "*Tororo-aoi*" were stored in 0.5% formalin.

**Crude Mucilage.**—The roots were washed with water, ground with a hammer, extracted with distillated water at 0°C for 24 hrs. and the extracted mucilage was filtered through a piece of cotton cloth.

**Viscosity.**—Viscosity determinations were carried out at 20°C by an Ostwald viscometer.

**Intrinsic Viscosity.** — Intrinsic viscosity determinations were carried out at 20°C in 1% sodium chloride solution.

**Spinnability.**—Spinnability was expressed by the maximum length (cm.) of the mucilage threads spun by a rod (7 mm. diameter) raised out of the mucilage. The determinations were carried out at 20°C and the velocity of the ascending of a testing rod was controlled at 4 cm./sec.

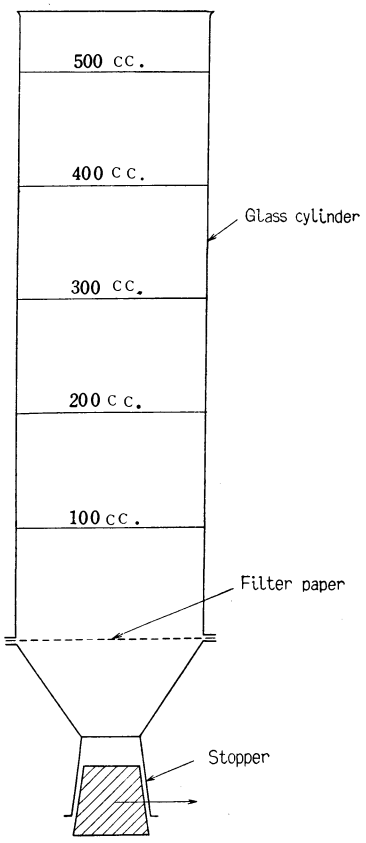



Fig. 1. Apparatus for the measurement of filterability.

1) T. Ozawa, *J. Chem. Soc. Japan, Ind. Chem. Sec.* (*Kogyo Kagaku Zasshi*), **24**, 389 (1922).
2) S. Oguri and H. Kawasaki, ibid., **45**, 307 (1942).
3) S. Oguri and K. Tomamezi, ibid., **46**, 146 (1943).
4) S. Oguri and K. Tomamezi, ibid., **47**, 432 (1944).
5) S. Machida and N. Uchino, *J. Chem. Soc. Japan, Pure Chem. Sec.* (*Nippon Kagaku Zasshi*), **74**, 615 (1954).
6) T. Oshibuchi and H. Kusunose, *J. Agr. Chem. Soc. Japan* (*Nippon Nogei-kagaku Kaishi*), **31**, 481 (1957).
7) S. Machida and N. Uchino, *J. Chem. Soc. Japan, Pure Chem. Sec.* (*Nippon Kagaku Zasshi*), **74**, 183 (1953).
8) I. Shinohara, T. Ono and S. Oguri, *J. Chem. Soc. Japan, Ind. Chem. Sec.* (*Kogyo Kagaku Zasshi*), **61**, 877 (1958).
9) S. Inokawa and R. Goto, *Wood Research* (*Japan*), **No. 14**, 50 (1955).
10) S. Inokawa and R. Goto, ibid., **No. 17**, 50 (1956).
11) S. Inokaxa, R. Goto and A. Takatsuki, ibid., **No. 21**, 26 (1959).
12) S. Inokawa and R. Goto, *J. Chem. Soc. Japan, Pure Chem. Sec.* (*Nippon Kagaku Zasshi*), **79**, 409 (1958).
13) S. Inokawa, R. Goto and I. Morimoto, ibid., **81**, 783 (1960).

**Filterability.** — Filterability means the rate of clogging up a filter paper. The determinations were carried out at 20°C as follows. A filter paper was fitted at the end of a glass cylinder (500 cc.) as in Fig. 1. a) Five hundred cc. of distilled water were poured into the cylinder and the times to filter 100 cc., 200 cc., 300 cc. and 400 cc. of water were measured (respectively, $t_1$, $t_2$, $t_3$ and $t_4$ sec.). b) Five hundred cc. of mucilage were poured into the cylinder, 400 cc. of the mucilage were filtered, and the residual mucilage (100 cc.) was discarded. c) Again, 500 cc. of distillated water were poured into the cylinder, and the times to filter 100 cc., 200 cc., 300 cc. and 400 cc. of water were measured (respectively, $T_1$, $T_2$, $T_3$ and $T_4$ sec.). Mean values of $T_1/t_1$, $T_2/t_2$, $T_3/t_3$ and $T_4/t_4$ are indicated as values for filterability.

**Elasticity.**—Elasticity determinations were carried out at 30°C by Schwedoff's method[14].

## Results and Discussion

**Effect of Heat Treatment on Spinnability, Filterability, Elasticity, and Viscosity, of the Mucilage.**—Although spinnability, filterability, elasticity, and viscosity, of the crude mucilage were considerably large, spinnability, filterability, and elasticity decrease very rapidly by heating at 80°C, as shown in Fig. 2. These are the characteristic properties of the mucilage.

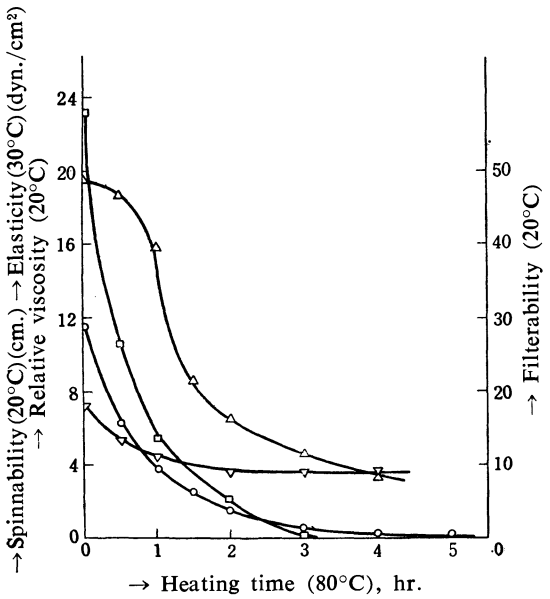



Fig. 2. Effect of heat treatment on the crude mucilage. Concentration of mucilage: 0.20%; $3.2\times10^{-5}$% (filterability).
○, Spinnability △, Filterability
□, Elasticity ▽, Relative viscosity

**Effect of Mixer Treatment on Spinnability, Filterability, Elasticity, and Viscosity, of the Mucilage.**—The crude mucilage in the original state was difficult to filter through a filter paper, but by homogenizing with a mixer, it was made easily filterable. Starch and other impurities contained in the crude mucilage could be removed by the filtration. The change of colloidal properties by mixer treatment is shown in Fig. 3. The spinnability and filterability almost disappeared by mixer treatment but the high elasticity remained. However, the high elasticity decreased considerably by heating or by longer standing in the similar way to that of the crude mucilage. The viscosity decreased rapidly also in the first 1 hr. of heating, the initial rapid fall being followed by a further slow reduction. The white precipitates obtained by the addition of alcohol-ether (8:2) mixture to the mucilage, were composed mainly of rhamnose and galacturonic acid and the mucilage prepared by redissolving the precipitates in water, had nearly equal elasticity to the original mucilage treated by a mixer. The mucilage thus obtained was used in subsequent studies as purified mucilage.

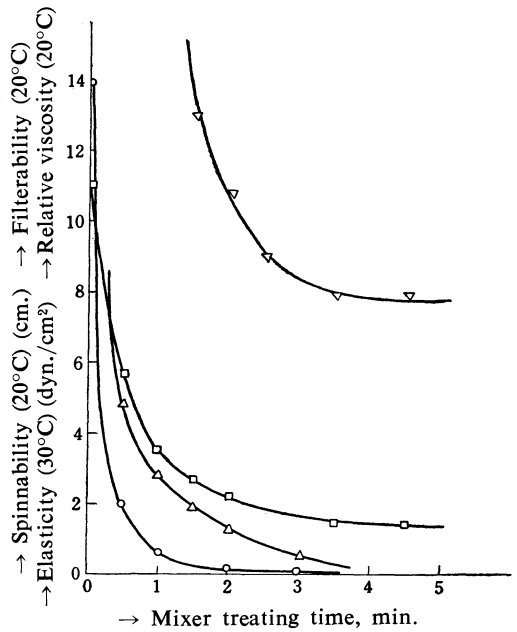



Fig. 3. Effect of mixer treatment on the crude mucilage. Concentration of mucilage: 0.16%; $1.1\times10^{-5}$% (filterability).
○, Spinnability △, Filterability
□, Elasticity ▽, Relative viscosity

**Effect of Heat Treatment on Elasticity and Intrinsic Viscosity of the Purified Mucilage.**—By heating at 80°C for varying periods of time, the elasticity of the purified mucilage fell down very rapidly to nearly zero. The intrinsic viscosity decreased rapidly in the first 30 min. of heating, the initial rapid fall being followed

14) Th. Schwedoff, *J. de Phys.*, [2] 8, 341 (1889).

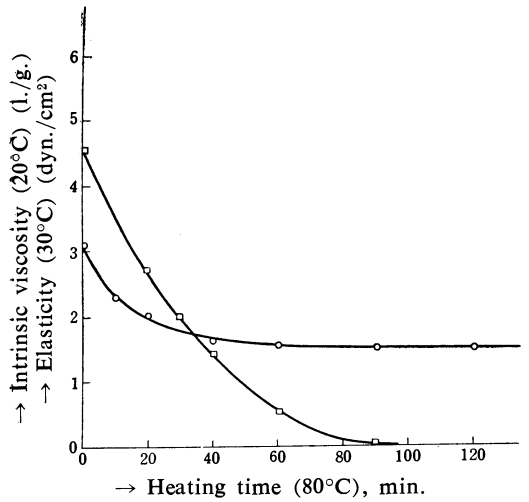



Fig. 4. Effect of heat treatment on the purified mucilage. Concentration of mucilage: 0.37%.
○, Intrinsic viscosity (in 1% NaCl solution)
□, Elasticity

by a slow reduction over a period of some hours as shown in Fig. 4. It seems that the fall of the elasticity does not always depend upon degradation of molecules of the mucin.

**Effect of Electrolytic Groups in the Mucin on Elasticity of the Purified Mucilage.** — 1) Effect of sodium chloride, calcium chloride, disodium ethylenediaminetetraacetate, and sodium oxalate on the elasticity of the purified mucilage was observed (Fig. 5). The elasticity

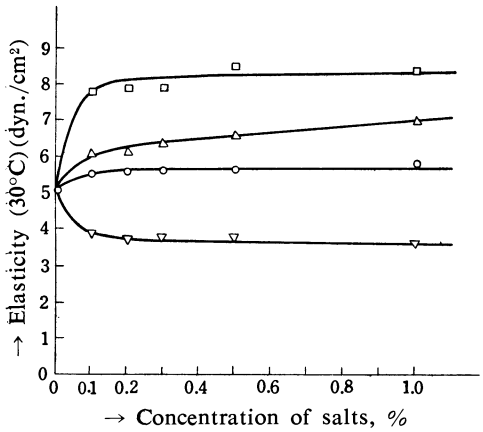



Fig. 5. Effect of addition of salts on the elasticity of the purified mucilage. Concentration of mucilage: 0.37%
○, Sodium chloride
△, Disodium ethylenediaminetetraacetate
□, Sodium oxalate ▽, Calcium chloride

was hardly influenced at all by the addition of sodium chloride, but increased by the addition of disodium ethylenediaminetetraacetate and sodium oxalate which are able to interchange calcium (about 40%) contained in ash of the mucilage, with sodium, and decreased by the addition of calcium chloride. 2) Electrodialysis experiments were carried out. By electrodialysis of the purified mucilage, pH of the mucilage changed from 6.1 to 2.9 and the value for the elasticity of 0.35% mucilage changed from 4.3 (dyn./cm²) to 10 (dyn./cm²). The change of the elasticity of the electrodialyzed mucilage is plotted against the change of pH with the addition of sodium carbonate in Fig. 6. The addition of calcium oxide to

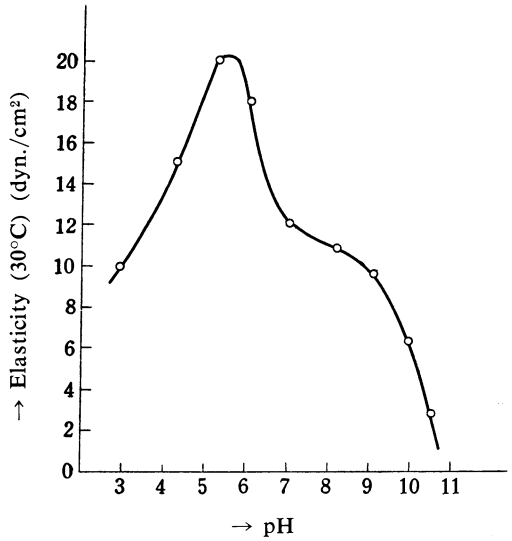



Fig. 6. Effect of pH on the elasticity of the electrodialyzed mucilage. Concentration of mucilage: 0.35%

the electrodialyzed mucilage always decreased the elasticity and at pH 4.2, the value for the elasticity fell to 4.2 (dyn./cm²). From results of above two experiments, it is considered that electrolytic groups in the mucin have effect on the elasticity but are not a major cause for the elasticity.

## Summary

1) The crude mucilage could be filtered after homogenizing by a mixer. By the addition of alcohol-ether mixture to the filtrate, the precipitates were obtained, which gave purified mucilage on redissolving in water.

2) The purified mucilage had noticeable elasticity and could be used for the research work instead of crude mucilage.

3) Some colloidal behavior of the purified mucilage was observed.

The author wishes to express his hearty thanks to Professor R. Goto, Kyoto University,

for his invaluable advice and encouragement throughout this work and to Koshin Kogyo Co. for the generous supply of roots of "*Tororo-aoi*".

*Department of Chemistry*
*Faculty of Science*
*Kyoto University*
*Sakyo-ku, Kyoto*

# *Studies on the Mucilage of the Root of "Tororo-aoi" (Abelmoschus manihot, MEDIC). II. Effect of Heating on the Colloidal Characteristics of the Mucilage*

By Saburo INOKAWA

(Received February 16, 1960)

In the previous paper[1] it has been shown that the elasticity, spinnability, and filterability of the crude mucilage and the elasticity of the purified mucilage decreased remarkably by heating at 80°C for 1~3 hr. Taking an interest in this characteristic of the mucilage, the present investigation was undertaken in order to observe the effect of heating on the mucilage by electron micrography, sedimentation in an ultracentrifuge, and electrophoresis.

## Experimental

**Material.**—Roots of "*Tororo-aoi*" were stored in 0.5% formalin.

**Crude Mucilage and Purified Mucilage.**—These preparations were similar to those described in the previous paper[1].

**Electron Microscope.**—The sample mucilage was mounted on a specimen holder for electron microscopy with a formvar supporting-fiim and dried. After chromium-shadowing the specimen was observed by an electron microscope of the type Shimadzu SM-T4.

**Ultracentrifuge.**—Sedimentation diagrams of an approximately 0.4% solution of mucilage in the presence of a 0.7% sodium chloride were taken by an ultracentrifuge of the type Spinco E under the centrifugal force of 259700 ***g*** at speed of 59780 r. p. m..

**Electrophoresis.**—Electrophoresis patterns of an approximately 0.3% solution of mucilage in a phosphate and sodium chloride buffer of ionic strength 0.02 and 0.18 respectively, were taken by a Tiselius electrophoresis apparatus of the type Hitachi HT-B.

**Elasticity and Intrinsic Viscosity.**—These determinations were the same as those described in the previous paper[1].

## Results and Discussion

**Observations from Electron Micrographs.**—The microscopic observation of network structure, which appears by the addition of methylene blue solution to the crude mucilage, is reported[2]; but the structure has been presumed[3] not to exist originally in the mucilage

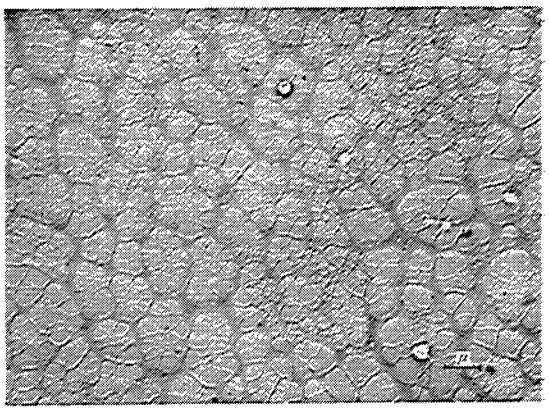


Fig. 1. Electron micrograph of the crude mucilage.
(0.2% aqueous solution) (Cr-shadowing)

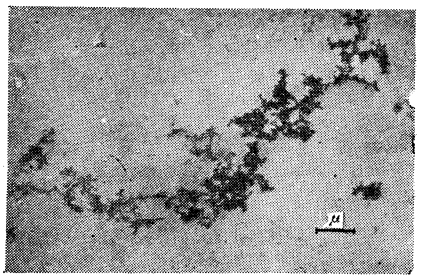


Fig. 2. Electron micrograph of the mucilage heated at 80°C for 3 hr.
(0.2% aqueous solution) (Cr-shadowing)

1) S. Inokawa, This Bulletin, **33**, 1473 (1960).
2) S. Oguri and K. Tomamezi, *J. Soc. Chem. Indust. Japan, (Kogyo Kagaku Zassi)*, **46**, 146 (1943).
3) S. Oguri, I. Shinohara, and T. Ono, *J. Chem. Soc. Japan, Ind. Chem. Sec. (Kogyo Kagaku Zassi)*, **58**, 227 (1955).

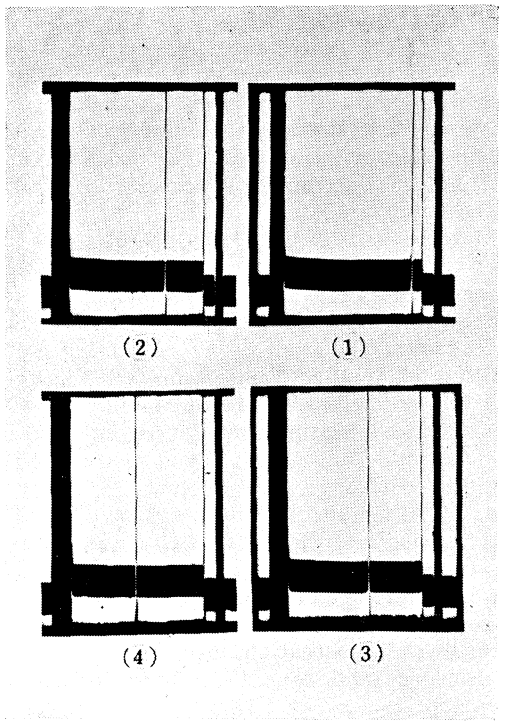



Fig. 3. Sedimentation diagram of the purified fresh mucilage in 0.7% NaCl solution. Speed 59700 r. p. m.; approximate concentration 0.4%; times for each measurement, 16 (1), 90 (2), 112 (3) and 144 (4) min. after reaching full speed.

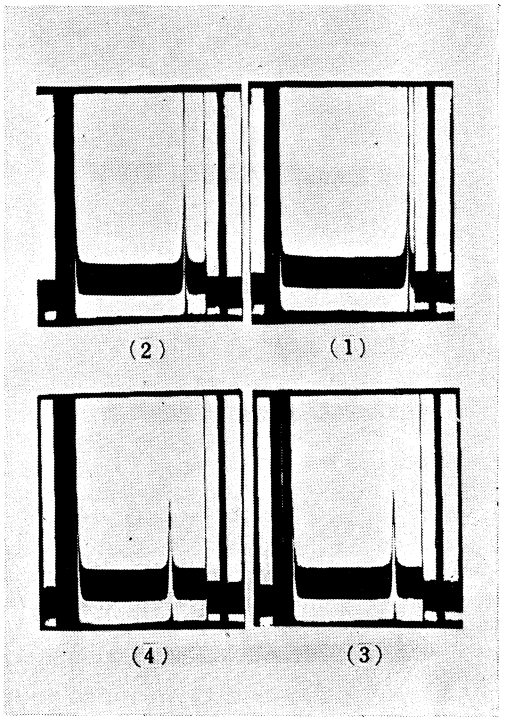



Fig. 4. Sedimentation diagram of the mucilage heated at 80°C for 2 hr. in 0.7% NaCl solution. Speed 59700 r.p.m.; Approximate concentration 0.4%; times for each measurement, 16 (1), 56 (2), 80 (3) and 104 (4) min. after reaching full speed.

but to be formed by an aggregation of composing substances by the addition of the reagent. The present writer has observed that the electron micrograph of the crude mucilage showed a typical network structure as shown in Fig. 1, which by heating at 80°C for 2 hr., was broken to a granular structure as shown in Fig. 2.

**Observation from Sedimentation Diagrams in an Ultracentrifuge.**—Sedimentation diagrams of the purified fresh mucilage and the mucilage heated at 80°C for 2 hr. are shown in Fig. 3 and in Fig. 4 respectively. The shape of the initial strikingly sharp boundary, as a line, of the fresh mucilage, remained perfectly unchanged through sedimentation. The sedimentation boundary of the heated mucilage was also very sharp, but a little spreading of the boundary occurred with the elapse of time. From Figs. 3 and 4 it may be considered that in the fresh mucilage, a network built by a very strong interaction between the mucin molecular chains moves as a whole under the influence of the centrifugal field, and the considerable weakening of the intermolecular force between chains occurs by heat treatment[4].

**Observation from Electrophoresis Patterns.**—Electrophoresis patterns of the purified fresh mucilage and the mucilage heated at 80°C for 2 hr. are shown in Fig. 5 and in Fig. 6, respectively. The initial strikingly sharp ascending pattern[5] of the fresh mucilage remained unchanged through electrophoresis similar to the

TABLE I. RELATIONS BETWEEN pH AND MOBILITY AT 0°C IN PHOSPHATE AND NaCl BUFFER OF IONIC STRENGTH 0.02 AND 0.18

| | pH | 2.1 | 5.3 | 6.9 | 9.6 |
|---|---|---|---|---|---|
| Mobility | Purified fresh mucilage | $1.1\times10^{-5}$ | $1.2\times10^{-4}$ | $1.3\times10^{-4}$ | $2.2\times10^{-5}$ |
| ($cm^2$/sec. V.) | Heated mucilage | $3.0\times10^{-5}$ | $2.6\times10^{-4}$ | $2.4\times10^{-4}$ | $5.0\times10^{-5}$ |

4) In the heated mucilage it was observed that there was something which sedimented rapidly in the initial few minits.

5) The pronounced boundary disturbance in the descending boundary was caused by the adhering of the mucilage on the electrophoresis cell-wall.

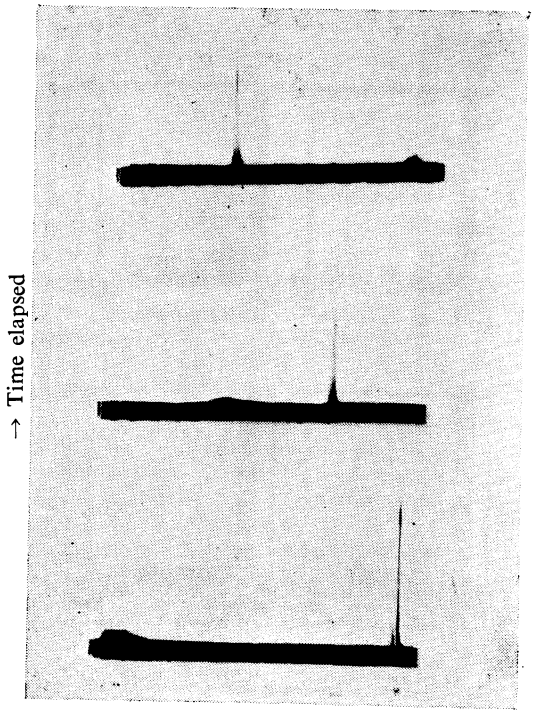



Fig. 5. Electrophoresis pattern of the purified mucilage. Approximate concentration 0.3%; phosphate-NaCl buffer; pH 6.5.

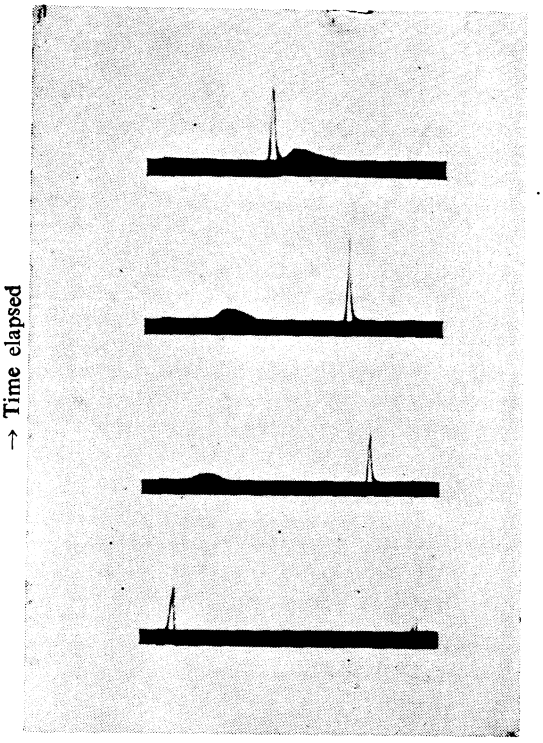



Fig. 6. Electrophoresis pattern of the mucilage heated at 80°C for 2 hr. Approximate concentration 0.3%; phosphate-NaCl buffer; pH 6.5.

centrifugal boundary (Fig. 4). The ascending pattern of the heated mucilage became somewhat broader as time went by. From Figs. 5 and 6 it may also be considered that there exists a very strong interaction between the mucin molecular chains in the fresh mucilage, and that the interaction decreases considerably by heating.

Measurements of the electrophoresis patterns over pH 2.1~9.6 were carried out without observing any change of the shape, and the relations between pH and mobility are tabulated in Table I.

**Effect of Heating Temperature on Elasticity and Intrinsic Viscosity of the Mucilage.**—Relations between heating temperature and decrease of elasticity and intrinsic viscosity of the purified mucilage were observed at heating time of 30, 60 and 90 min. as shown in Fig. 7. The decrease of the elasticity was gradual up to approximately 50°C and then sharp at the higher temperature, but that of intrinsic viscosity was nearly constant. The results seem to indicate that the decrease of elasticity by heating is not caused simply by degradation of mucin molecules. This is also supported by the previous experimental results[6] that

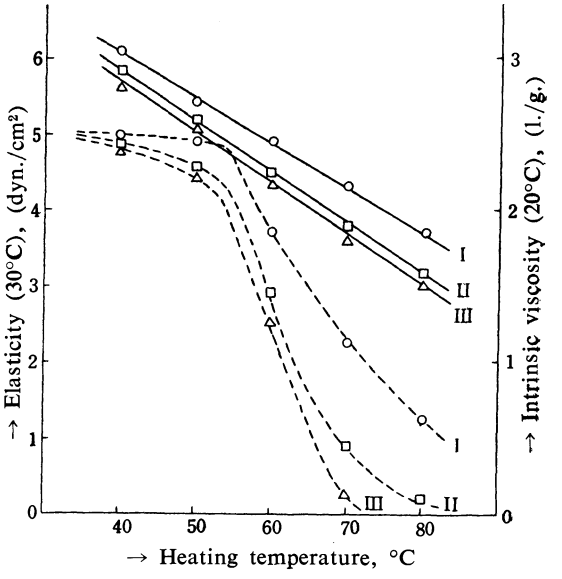



Fig. 7. Relations between heating temperature and decrease of elasticity and intrinsic viscosity.
Mucilage concentration 0.37%
—— Intrinsic viscosity
---- Elasticity
Curve I Heating time 30 min.
Curve II Heating time 60 min.
Curve III Heating time 90 min.

6) S. Inokawa, R. Goto and I. Morimoto, *J. Chem. Soc. Japan, Pure Chem. Sec.* (*Nippon Kagaku Zasshi*), **81**, 783 (1960).

there was no considerable difference in molecular weight between the fresh and the heated mucilage.

**Summary**

1) From electron micrographs it was observed that in the crude mucilage there exists a network structure, but its structure is broken by heating.

2) From sedimentation diagrams and electrophoresis patterns it seems reasonable to assume that in the purified fresh mucilage there exist very strong intermolecular forces like those in gel and these forces decrease markedly by heating.

3) It is conceivable that the degradation of the mucin macromolecule does not play an important role in the marked decrease of the elasticity of the purified fresh mucilage by heating.

Finally the writer wishes to express his hearty thanks to Professor R. Goto, Kyoto University, for his invaluable advice and encouragement throughout this work. He is also indebted to Professor E. Suito and Dr. K. Takiyama of Kyoto University for their help in taking the electron micrographs, to Dr. K. Fukai of Osaka University for taking the sedimentation photographs, to Professor S. Tanaka of Kyoto University for his help in taking electrophoresis photographs. It is also a pleasure to thank Koshin Kogyo Co. for their generous supply of the root of "*Tororo-aoi*".

*Department of Chemistry*
*Faculty of Science*
*Kyoto University*
*Sakyo-ku, Kyoto*

# *Glass Transition of Coal*

By Yuzō SANADA, Naoyuki MOCHIDA and Hidemasa HONDA

(Received September 29, 1959)

The study of mechanical or thermal properties of coal on heating is of great importance in structural investigation and industrial problems. It is well known that coals, especially caking or coking coals, have a polymeric character, and show plastic deformation at room temperature[1] and softening or flow phenomena on heating.[2] It appears, however, that very few detailed investigations on the change of mechanical or thermal properties of coals heated over the range from room temperature to the softening point have yet been made. D. H. Bangham and R. E. Franklin[3] measured the thermal expansion coefficient of three bright coals. They showed that coals have a gradual increase in the thermal expansion coefficient over the range from room temperature to about 300°C. The present authors have measured the change of hardness and volume for several vitrains of every rank over the range from room temperature to about 160°C by using two distinct hardness methods and one dilatometric method, and have found that coals have a few characteristic points over this temperature range.

1) D. W. van Krevelen and J. Schuyer, "Coal Science, Aspects of Coal Constitution", Elsevier, Amsterdam (1957), p. 275.
2) D. W. van Krevelen and J. Schuyer, loc. cit. p. 286.
3) D. H. Bangham and R. E. Franklin, *Trans. Faraday Soc.*, **42B**, 289 (1946).

## Experimental Procedure

**Indentation Hardness Method.**—Coal specimens about 1 cm. wide and 5 cm. long, and about of 2 cm. thick parallel plane were cut perpendicular to the bedding planes, using a motor-driven diamond cutter. One plane of surface perpendicular to the bedding planes of the specimen was highly polished by using glass plates with carborundum and alumina, and woollen cloth with alumina. The specimens were air-dried at room temperature and ordinary humidity.

Fig. 1 shows the experimental apparatus which modified the Akashi micro-hardness tester having a diamond Knoop indenter.[4] The coal specimen, of which the base and two long sides are covered with three electric heating plates settled in a vise, is placed on a steel table with a copper block cooled by water. The position of the vitrain layer can be adjusted by means of screws. The temperature of the vitrain layer is measured by a thermistor surface thermometer located very closely to the indenter and controlled by a suitable variable resistor. The coal specimen is heated at the heating rate of 1°C/min. over the range from room temperature to 160°C. The load of indenter is 100 g. and

4) H. Honda and Y. Sanada, *Fuel*, **36**, 403 (1957).

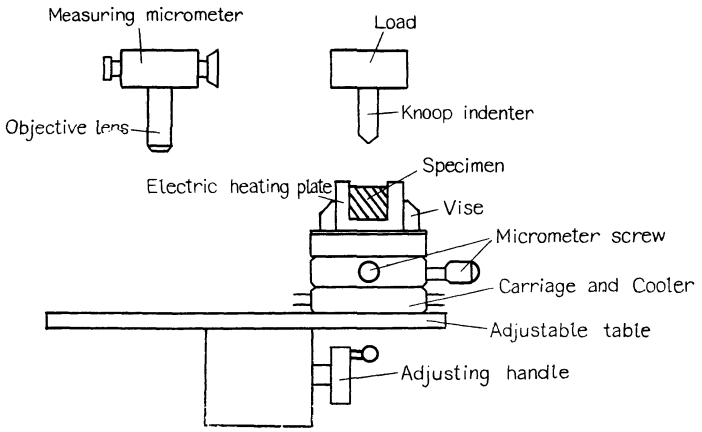



Fig. 1. Apparatus for the determination of the indentation hardness.

the time taken in the duration of the load is 30 sec. The hot impression under the elevated temperature is made every five minutes, i. e. every 5°C. After an impression has been made, the specimen is moved to a new position along the vitrain layer by means of the screw for the distance of 15/100 mm. After all impression have been completed, the furnace is cooled to room temperature and then Knoop hardness numbers are determined from the length of the long diagonal of indentation.

**Pendulum Hardness Method.** — The preparation of coal specimens, the heating method, the heating rate, and the measurements of temperature are the same as those in the case of indentation hardness test.

The apparatus of the pendulum hardness tester of Walker Steele type is given in Fig. 2. It consists of the wedge-type agate fulcrum, two brass arms with weights and a small mirror. The length between the weights at the ends of the arms of the pendulum is 20 cm. The weight of the pendulum is 78 g. The damping of the pendulum hardness tester on the vitrain layer of the specimens is determined by the lamp-and-scale method. The apparatus is held in an air-thermostat. The logarithmic decrement $\lambda$ of the pendulum is given by the following equation, provided that the periodic time is a constant :[5]

$$\lambda = (2.303 \log \theta/\theta')/2n$$

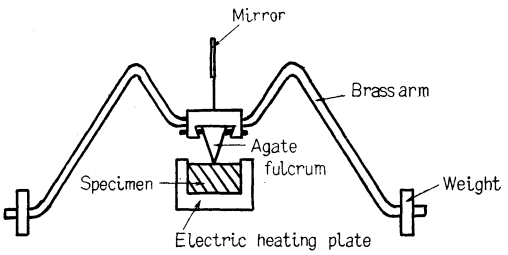



Fig. 2. Apparatus for the determination of the logarithmic decrement.

where $\theta$ and $\theta'$ are the angle from the position of rest, $n$ is the frequency of the pendulum between $\theta$ and $\theta'$. In this experiment, the chosen values of $\theta$ and $\theta'$ were 4° and 3°26′ respectively.

**Dilatometric Method.**—The coal specimen was pulverized to pass through a 30 and stand on a 60 Tyler mesh sieve. The vitrain, of specific gravity less than 1.30, was isolated by the float-or-sink method using mixtures of benzene and carbon tetrachloride. The volume change of vitrain with temperature was measured using a Pyrex glass

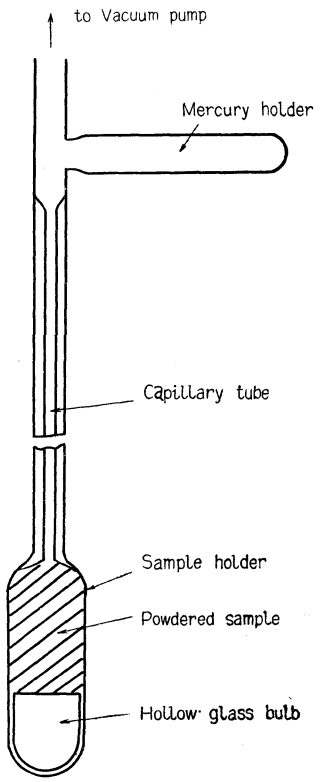



Fig. 3. Modified Bekkedahl's dilatometer.

5) Y. Inoue, K. Kanai and K. Hiroi, *J. Chem. Soc. Japan, Ind. Chem. Sec.* (*Kogyo Kagaku Zasshi*) **59**, 231 (1956).

6) N. Bekkedahl, *J. Research NBS*, **42**, 145 (1949).

TABLE I. ANALYSIS OF VARIOUS VITRAINS

| Source | | Proximate analysis, % | | | | Ultimate analysis (d. a. f.) % | | |
|---|---|---|---|---|---|---|---|---|
| | | Moisture | Ash | V. M. | Fixed Carbon | C | H | O+N+S |
| Brown coal | Tempoku-Menashi | 12.41 | 1.40 | 42.91 | 43.28 | 69.82 | 4.91 | 25.26 |
| | Nakagō | 13.32 | 3.96 | 38.03 | 44.69 | 74.33 | 5.26 | 20.41 |
| Bituminous coal | Takamatsu | 4.67 | 2.29 | 41.10 | 51.94 | 78.95 | 5.01 | 16.04 |
| | Bibai | 2.78 | 3.10 | 41.81 | 52.31 | 80.90 | 5.87 | 13.23 |
| | Ashibetsu | 2.98 | 4.05 | 42.93 | 50.04 | 81.11 | 5.49 | 13.40 |
| | Akabira | 3.01 | 3.21 | 42.50 | 51.28 | 82.29 | 5.92 | 11.79 |
| | Futago | 1.54 | 2.31 | 46.86 | 49.29 | 83.16 | 6.31 | 10.53 |
| | Miike | 1.21 | 3.36 | 43.95 | 51.48 | 84.53 | 6.11 | 9.36 |
| | Ōyūbari | 1.35 | 2.76 | 40.34 | 55.55 | 84.79 | 6.23 | 8.93 |
| | Yūbari | 2.28 | 2.70 | 42.08 | 52.94 | 84.85 | 5.96 | 11.16 |
| | Hashima | 1.24 | 2.09 | 35.91 | 60.76 | 86.59 | 5.56 | 7.85 |
| | Donegan No. 1 (U.S.A) | 1.75 | 1.16 | 31.29 | 65.80 | 87.16 | 5.26 | 7.22 |
| | American (U.S.A.) | 1.55 | 1.17 | 26.26 | 71.02 | 87.68 | 4.80 | 7.52 |
| | Yatake | 1.26 | 3.04 | 20.54 | 75.16 | 88.71 | 4.35 | 6.94 |
| | Shikamachi | 1.16 | 2.52 | 21.16 | 75.16 | 88.76 | 4.70 | 6.54 |
| | Amonate and Bishop (U.S.A.) | 1.06 | 1.40 | 23.53 | 74.01 | 89.16 | 5.19 | 5.20 |
| Anthracite | Uonuki | 1.68 | 1.80 | 10.80 | 85.72 | 91.16 | 3.97 | 4.87 |
| | Hongei (Indo-China) | 2.08 | 0.98 | 6.14 | 90.80 | 93.02 | 3.26 | 3.72 |

dilatometer following the modified Bekkedahl's method[6]. The dilatometer employed in the test is shown in Fig. 3. The dilatometer consists of the capillary tube, the sample holder and the mercury holder. The inner diameter and the length of the capillary tube are 1.5 mm. and about 70 cm. respectively. The inner diameter and the length of the sample holder are 15 mm. and about 13 cm. respectively. One end of the sample holder is left open at first. About 15 g. of the air-dried sample is weighed into the sample holder. A hollow glass bulb, of which the outer diameter is a little smaller than 15 mm. and of which the height is about 3 cm., is settled in the sample holder, and then the end of the sample holder is sealed up. This method makes it possible to avoid any heating of the sample during the sealing operation. Mercury is put in the mercury holder. The coal sample in the dilatometer is evacuated to $10^{-3}$ mmHg for 6 to 8 hr. at room temperature in order to remove gas and then the desired volume of mercury is filled through the capillary. The dilatometer is settled in a stirring liquid paraffin bath, whose temperature is controlled under the heating rate of 1°C/min. The measurements of the height of mercury in the capillary tube were made visually, usually once every minute, from room temperature to 160°C.

The accuracy of determination of the Knoop hardness number itself has already been described in detail.[4] The scatter of the results in this indentation hardness method depends upon the inhomogeneity of the vitrain layer and the temperature control. Though the pendulum hardness is used as a conventional method in the measurements of the glass transition point of high polymers, the scatter of the results in this method may also depend upon the inhomogeneity of vitrain, the temperature control, and the error in the reading of $n$. The dilatometric method is the most conventional and its experimental accuracy is most high in the measurements of the glass transition point of high polymers. The surface temperature of vitrain is easily measured and precisely detected within 1°C by the thermistor having a very small thermo-sensitive element.[7] When the load is applied to the indenter, the surface temperature of vitrain decreases instantaneously. The maximum instantaneous decrease of temperature was about 2°C over the range of 50 to 100°C and about 5°C over the range of 100 to 160°C. In general, the glass transition temperature obtained by the pendulum method is considerably higher than that obtained by the dilatometric method. But this discrepancy becomes smaller by using a wedge instead of two balls as the fulcrum of the pendulum.[8]

The characteristics of various vitrains used are listed in Table I.

## Results and Discussion

The relation between the Knoop hardness number, $H_K$, of air-dried coals and temperature is shown in Fig. 4. For brown coal, $H_K$

7) B. M. Zeffert and S. Hormas, *Anal. Chem.*, 21, 1420 (1949).
8) K. Sato and Y. Inoue, *Chem. High Polymers, Japan (Kobunshi Kagaku)*, 15, 421 (1958).

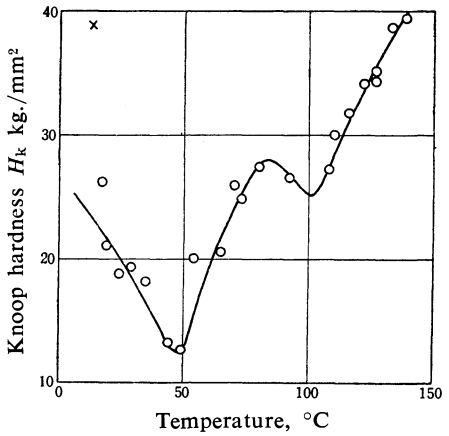



Fig. 4a. Variation of Knoop hardness with temperature for Nakagō brown coal (d. a. f. C=74.33%).

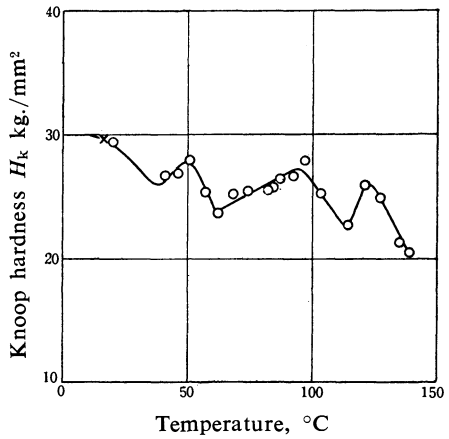



Fig. 4b. Variation of Knoop hardness with temperature for Yūbari coking coal (d. a. f. C=84.85%).

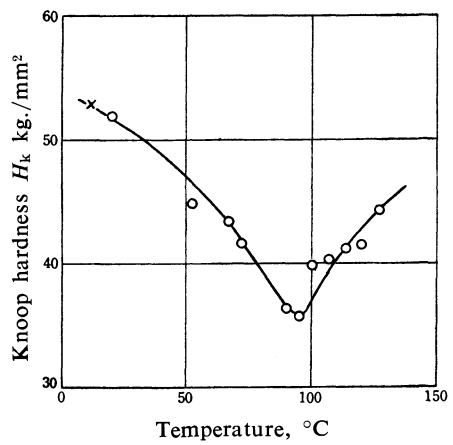



Fig. 4c. Variation of Knoop hardness with temperature for Hongei anthracite (d. a. f. C=93.02%).

decreases with temperature increase to a minimum at about 50°C, increases with temperature to a maximum, decreases again with temperature increase to a second minimum at about 100°C, and then increases with temperature. For bituminous coal $H_k$ shows three minimum values over the range from room temperature to 160°C. For anthracite $H_k$ decreases with temperature increase to a minimum at about 100°C, and then increases with temperature. The temperatures showing the minimum values of $H_k$ of various air-dried vitrains are listed in the first column of Table II. Namely, over this temperature range, air-dried brown coal, bituminous coal and anthracite have two, three and one characteristic points respectively.

After the specimens heated to about 160°C were allowed to cool in an ordinary atmosphere, the Knoop hardness of the specimens was again measured at room temperature. These values of $H_k$ at room temperature are shown by cross marks in Fig. 4. The values of $H_k$ of the cooled bituminous coal and anthracite coincide almost exactly with those of the non-heated original coals respectively. This shows that these coals do not change their chemical constitutions if heated over the range from room temperature to about 160°C. However the value of $H_k$ of the cooled brown coal is much higher than that of the non-heated original brown coal and the cooled brown coal has many tiny cracks on the surface. These phenomena may be attributed to the fact that some chemical reactions such as dehydration occur in the specimen of brown coal by heating over the range from room temperature to about 160°C, as if in the curing of thermosetting plastics, e. g. phenol-formaldehyde resin.

The relations between the logarithmic

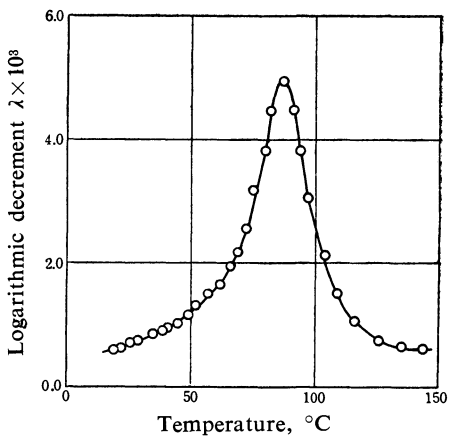



Fig. 5. Variation of logarithmic decrement with temperature for maleic acid-glycol-styrene resin.

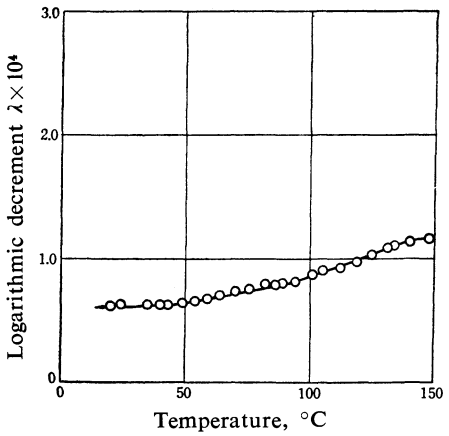



Fig. 6. Variation of logarithmic decrement with temperature for phenol-formaldehyde resin.

decrement, $\lambda$, of the pendulum on maleic acid-glycol-styrene resin, loosely cross-linked linear polymer, and phenol-formaldehyde resin (moulded C state), three-dimensional network polymer, and temperature are shown in Fig. 5 and Fig. 6 respectively. The value of $\lambda$ of maleic acid-glycol-styrene resin increases suddenly with temperature to a maximum at 87°C. Thereafter the value of $\lambda$ decreases suddenly with temperature increase and becomes almost the same at about 150°C as that of room temperature. This change of $\lambda$ with temperature shows a typical glass transition phenomenon of loosely cross-linked linear polymer. Further, the glass transition point of maleic acid-glycol-styrene resin is 87°C. On the other hand, the value of $\lambda$ of phenol-formaldehyde resin increases slowly with the temperature over the range from room temperature to 150°C and does not show a maximum. This change of $\lambda$ with temperature shows a character of three-dimensional network polymer.

The relation between the logarithmic decrement, $\lambda$, of the pendulum on air-dried coals and temperature is shown in Fig. 7. For brown coal $\lambda$ increases with temperature to a maximum at about 50°C, decreases with temperature increase to a minimum, increases again with temperature to a second maximum at about

Table II. Glass transition points of various vitrains

| Source | | Carbon (d. a. f.) % | Glass transition temperature, °C: by indentation hardness method, Air-dried coal $T_{g_1}$ | $T_{g_2}$ | $T_{g_3}$ | by pendulum hardness method, Air-dried coal $T_{g_1}$ | $T_{g_2}$ | $T_{g_3}$ | by dilatometric method, Air-dried coal $T_{g_1}$ | $T_{g_2}$ | $T_{g_3}$ | Strongly dried coal $T_{g_1}$ | $T_{g_2}$ | $T_{g_3}$ |
|---|---|---|---|---|---|---|---|---|---|---|---|---|---|---|
| Brown coal | Tempoku-Menashi | 69.82 | | 50 | 100 | | 50 | 100 | | 50 | 106 | | 52 | — |
| | Nakagō | 74.33 | | 50 | 100 | | 65 | 110 | | 50 | 117 | | | |
| Bituminous coal | Takamatsu | 78.95 | 43 | 70 | 120 | 30 | 57 | 120 | — | 51 | 129 | | | |
| | Bibai | 80.90 | 45 | 80 | 160 | | | | | | | | | |
| | Ashibetsu | 81.11 | 60 | 80 | 120 | 60 | 80 | 145 | | | | | | |
| | Akabira | 82.29 | 30 | 80 | 140 | 35 | 90 | 116 | | | | | | |
| | Futago | 83.16 | 48 | 70 | 105 | | | | | | | | | |
| | Miike | 84.53 | 40 | 65 | 95 | | 92 | 125 | | | | | | |
| | Ōyūbari | 84.79 | 50 | 72 | 96 | 40 | 70 | 140 | | | | | | |
| | Yūbari | 84.85 | 38 | 62 | 113 | 40 | 67 | 135 | 29 | 75 | 145 | 38 | 61 | 133 |
| | Hashima | 86.59 | 25 | 50 | 85 | | | | | | | | | |
| | Donegan No. 1 (U.S.A.) | 87.16 | 35 | 80 | 93 | 30 | | 105 | | | | | | |
| | American (U.S.A.) | 87.68 | 33 | 70 | 120 | | 80 | 110 | | | | | | |
| | Yatake | 88.71 | | | | | | | 34 | 68 | 149 | 20 | 65 | 100 |
| | Shikamachi | 88.76 | 35 | 60 | 105 | 40 | 77 | 120 | | | | | | |
| | Amonate and Bishop (U.S.A.) | 89.16 | 35 | 75 | 105 | | 70 | 120 | | | | | | |
| Anthracite | Uonuki | 91.16 | 25 | | 90 | 25 | | 105 | | | | | | |
| | Hongei (Indo-China) | 93.02 | | | 95 | | | 130 | | | 122 | | | — |

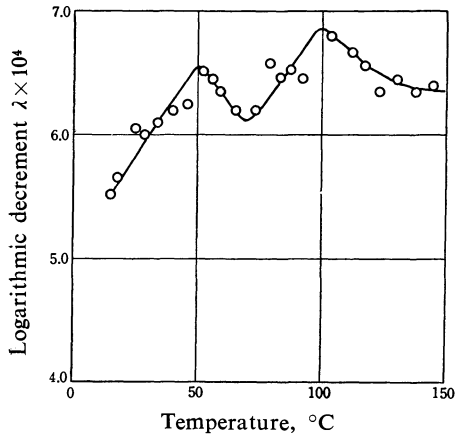



Fig. 7a. Variation of logarithmic decrement with temperature for Tempoku-Menashi brown coal (d. a. f. C=69.82%).

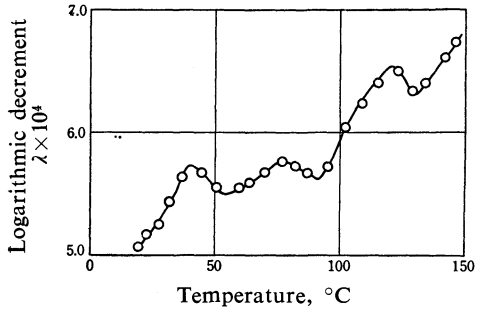



Fig. 7b. Variation of logarithmic decrement with temperature for Shikamachi coking coal (d. a. f. C=88.76%).

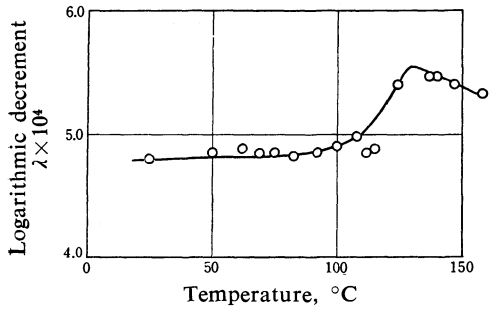



Fig. 7c. Variation of logarithmic decrement with temperature for Hongei anthracite (d. a. f. C=93.02%).

100°C, and then decreases with temperature increase. For bituminous coal $\lambda$ shows three maximum values over the range from room temperature to 160°C. For anthracite $\lambda$ increases with temperature to a maximum at about 130°C and then decreases with temperature increase. The temperature showing the maximum values of $\lambda$ of various air-dried vitrains are listed in the second column of Table II. Over this temperature range, air-dried brown coal, bituminous coal and anthracite have two, three and one characteristic points respectively.

The relation between the reading of mercury height, $V$, in the glass capillary tube of dilatometer containing powdered maleic acid-glycol-styrene resin and temperature is shown in Fig. 8. The value of $V$ increases with temperature and shows a break at 77°C. This change of $V$ with temperature shows a typical glass transition phenomena of loosely cross-linked linear polymer. That is to say, the glass transition point of maleic acid-glycol-styrene resin obtained by the dilatometric method is 77°C and this value is slightly lower than that obtained by the pendulum method.

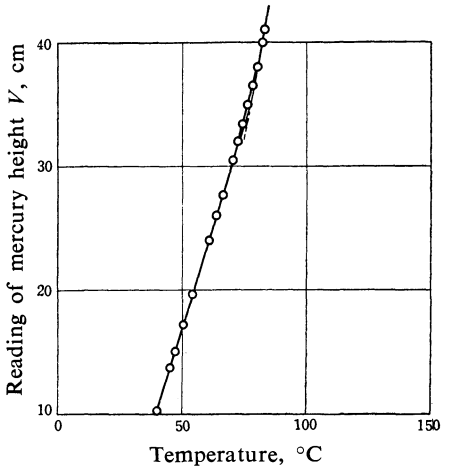



Fig. 8. Variation of reading of mercury height with temperature for maleic acid-glycol-styrene resin.

The relation between the reading of the mercury height, $V$, in the glass capillary tube of dilatometer containing air-dried powdered coals and heating temperature is shown in Fig. 9. As to brown coal $V$ increases suddenly at about 50°C and again at about 100°C. For bituminous coal the sudden increase of $V$ appears three times over the range from room temperature to 160°C, As for anthracite $V$ increases suddenly at about 120°C. The temperatures showing the breaks of $V$-temperature curve of various air-dried vitrains are listed in the third column in Table II. In this case too, the characteristic points of air-dried brown coal, bituminous coal and anthracite are two, three and one respectively.

In order to ensure whether the characteristic points, especially the one at about 100°C, are affected by moisture or combined water of coals or not, the $V$-temperature relations of the samples dried strongly at 130 to 140°C

in vacuo of $10^{-3}$ mmHg for 6 to 8 hr. have been measured using the dilatometer over the range from room temperature to 160°C. The characteristic points in this case are shown in the last column of Table II. For brown coal the break of $V$-temperature curve at about 50°C does not vanish but the one at about 100°C disappears. For bituminous coal the three breaks coincide almost exactly with those of the air-dried sample, though the third break of the strongly dried sample somewhat diminishes. For anthracite the break at about 100°C disappears. Therefore, the $V$-temperature

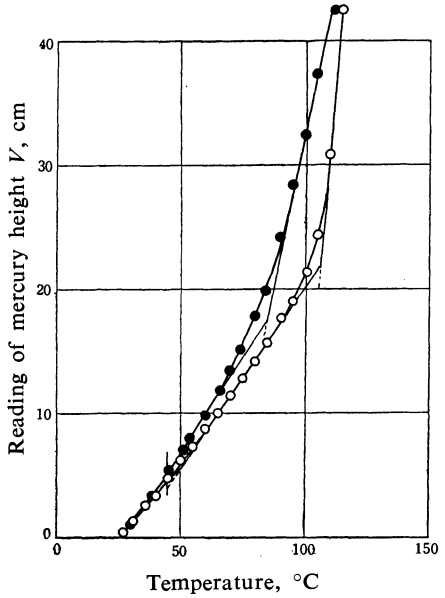



Fig. 9a. Variation of reading of mercury height with temperature for Tempoku-Menashi brown coal (d. a. f. C=69.82%).
○ heating, ● cooling

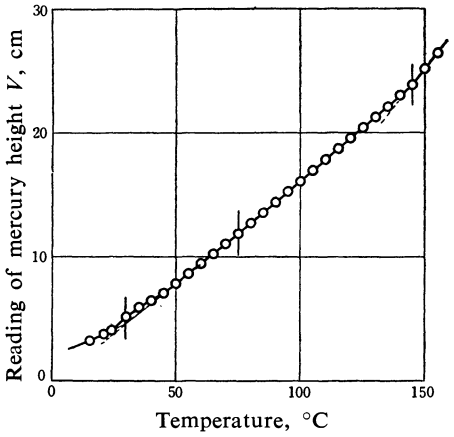



Fig. 9b. Variation of reading of mercury height with temperature for Yūbari coking coal (d. a. f. C=84.85%).

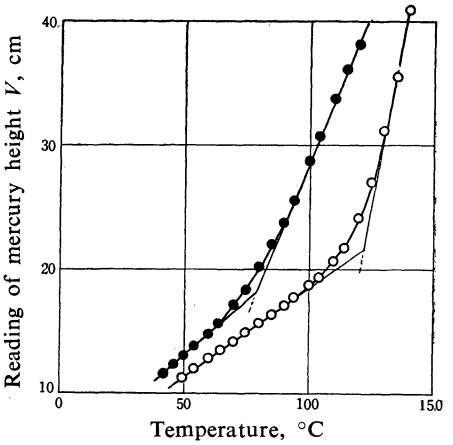



Fig. 9c. Variation of reading of mercury height with temperature for Hongei anthracite (d. a. f. C=93.02%).
○ heating, ● cooling

curve of bituminous coal dried at room temperature in vacuo does not show the thermal hysterisis, though those of brown coal and anthracite dried at room temperature in vacuo have the thermal hysteresis as shown in Fig. 9, if heated coals are cooled under the cooling rate of 1°C/min.

The influence of moisture on the characteristic points is great in brown coal and anthracite, though it is almost negligible in bituminous coal. This may be attributed to the relation between internal surface area and the rank of coal.[9] On the other hand, the glass transition point of completely dried poly(vinylalcohol), one of the hydrophilic polymers, is 73°C. When the moisture content of the sample increases, this glass transition point shifts to a lower temperature and another transition point appears at a higher temperature.[10] Consequently it may be supposed that the effects of moisture on the characteristic points of brown coal are similar to those on the transition points of poly(vinylalcohol). The disappearance of the characteristic point at about 100°C in strongly dried anthracite may be attributed to the cross-linkages among the base units which anthracite has by nature.[11]

When amorphous polymers are heated, in general, they show a minimum of indentation hardness,[12] a maximum of logarithmic decrement of the pendulum[5], and a change of slope of volume-temperature curve[13] at the glass transition point or zone. Table II shows that

9) Y. Kawana, *J. Chem. Soc. Japan, Ind. Chem. Sec. (Kogyo Kagaku Zasshi)*, **61**, 1275 (1958).
10) Y. Sone and I. Sakurada, *Chem. High Polymers, Japan (Kobunshi Kagaku)*, **14**, 574 (1957).
11) H. Honda and Y. Hirose, *Fuel*, **37**, 323 (1958).
12) K. Ito, *J. Japanese Soc. Mech. Eng.*, **58**, 263 (1955).
13) T. Alfrey, Jr., "Mechanical Behavior of High Polymer," Interscience, New York (1948), p. 121.

the temperatures showing minimum values of Knoop hardness, the temperatures showing maximum values of logarithmic decrement and the temperatures showing breaks of $V$-temperature curve of the air-dried vitrain roughly coincide with one another, though the hardness methods and the dilatometric method are independent respectively. Moreover, in the dilatometric method, the temperatures showing breaks of $V$-temperature curve of the strongly dried bituminous coal coincide almost exactly with those of the same air-dried sample and the temperature showing a break of $V$-temperature curve of the strongly dried brown coal also coincides with that of lower temperature of the same air-dried sample. Therefore it seems that these characteristic points, which are not constant but change with experimental time scale etc., are the glass transition points of coals (although D. H. Bangham and R. E. Franklin[3] did not detect them) over the range from room temperature to 160°C, though the influence of adsorbed water films can not be neglected at all.

In an investigation of microplasticity, D. H. Bangham and N. Berkowitz[14] measured the critical deformation force, $F_c$, at which the coal particles flowed to form a translucent film. They found that $F_c$ does not vary uniformly with temperature, but $F_c$ shows its maxima at 120, 200 and 300°C. Also they concluded that the undulating character of the curves representing the variation of $F_c$ with increasing temperature is associated with monolayer films adsorbed on the internal surface of the coal which are evaporated at specific temperatures; the maximum at 120°C, they relate to the loss of water vapor from the coal structure. Results similar to those of D. H. Bangham et al. were reported by C. Ellis[15] following an investigation by a similar method.

On the other hand, J. C. Macrae and A. R. Mitchell[16] studied the shapes of the curves relating failure stress to temperature for two bituminous coals and found that the maxima at 120 and 200°C are closely similar to those reported by both D. H. Bangham et al. and C. Ellis for the $F_c$, at which microplasticity is observable in particles of less than 30 $\mu$ in size. They, however, emphasized that it seems probable that heating to 120°C results in an increase of the failure stress by a mechanism in the nature of a strain relief in which an increased thermal vibration modifies the effect of weakness in the coal structure upon the failure stress and influence of adsorbed water films can not be considered to be wholly acceptable.

The authors' experimental results of bituminous coals may rather give support to the opinion of J. C. Macrae et al. than those of D. H. Bangham et al. and C. Ellis.

*Shigengijutsu-Shikenjo*
*Resources Research Institute*
*Kawaguchi-Saitama, Japan*

14) D. H. Bangham and N. Berkowitz, *Coal Res.*, Dec., 139 (1945).

15) C. Ellis, *Publ. Instn. Gas Engrs.*, **No. 436**, 7 (1953).

16) J. C. Macrae and A. R. Mitchell, *Fuel*, **36**, 423 (1957).

# *Self-consistent Field Molecular Orbital Treatment of Benzenium Ion for a Simplified Model of Hyperconjugation*

By Toshifumi MORITA

(Received December 16, 1959)

Electronic spectra of a number of aromatic carbonium ions were studied theoretically by several investigators[1]. In their explorating work which was greatly suggestive, Muller, Pickett and Mulliken[2] treated the benzenium ion by the simple LCAO MO method including self-consistent technique taking into account the variations of resonance integrals with interatomic distances and of Coulomb integrals with charge distributions. These authors as well as Morita[3,4], who tried to explain spectral shifts of the protonated methyl benzenes by

1) As to a general survey, see, T. Morita, *Progress Reports on Electronic Processes in Chemistry* (Published by the Japanese Research Group on the Electronic States), No. 1, 60 (1959) (in Japanese).

2) N. Muller, L. W. Pickett and R. S. Mulliken, *J. Chem. Phys.*, **21**, 1400 (1953); *J. Am. Chem. Soc.*, **76**, 4770 (1954).

3) T. Morita, *J. Chem. Phys.*, **25**, 1290 (1956).

4) T. Morita, This Bulletin, **31**, 322 (1958).

the methyl substituents, ignored the inter-electronic interaction. In explaining electronic spectra, the self-consistent field molecular orbital (SCF MO) treatment seems to be most satisfactory. Works going along this are those of Mackor et al.[5,6] However, hyperconjugation of the $H_2$–C bond of protonated aromatics was shut out of their computations. When hyperconjugation of the $H_2$ quasi-atom is taken into account, aromatic carbonium ions have odd numbered centers and belong to the so-called "strongly hyperconjugated" system, or system of "isovalent hyperconjugation"[2,7,8]. Morita[9] also indicated that basic properties of isomeric xylenes were interpreted considerably well in terms of hyperconjugation of the $H_2$–C bond in their protonated compounds. Owing to reasons mentioned above, it seems to be of great significance to carry out the SCF MO calculations, taking the hyperconjugative effect into consideration. However, even in the benzenium ion, the simplest of the aromatic carbonium ions, the SCF MO calculation is rather cumbersome and simplification of the model for computation of hyperconjugation may be desired. This paper contains simplification of the model for hyperconjugation in the semiempirical SCF LCAO MO method and discussion of importance of hyperconjugation deduced from the calculated results for the hyperconjugation model compared with those for the bond localization model of the benzenium ion, a prototype of the aromatic carbonium ions.

## A Model for Hyperconjugation in the Semi-empirical SCF MO Method

From the proton magnetic resonance absorption measurement of aromatic carbonium ions, MacLean, van der Waals and Mackor[10] showed that, when a bond was formed between a proton and a carbon atom in an aromatic hydrocarbon ring, valence state of the carbon atom attacked by a proton was altered from $sp^2$- to $sp^3$-hybridization. Accordingly, the configuration of the methylene group constructed at the position of proton attack should be tetrahedral. In a technique for the theory of hyperconjugation, however, it is customary, subject to Mulliken's original idea[11], to assume the $sp^2$-hybridized carbon atom and group orbitals of $H_2$, $\phi_1=2^{-1/2}(1+S)^{-1/2}(h_a+h_b)$ and $\phi_2=2^{-1/2}(1-S)^{-1/2}\times(h_a-h_b)$: ($h_a$, $h_b$: $1s$ orbital of hydrogen atoms a and b; $S$: overlap integral between H atoms). Of the two group orbitals $\phi_1$ and $\phi_2$, $\phi_1$ forms $\sigma$-bond and $\phi_2$ $\pi$-bond, the latter being in conjugation with the benzene ring. Aono[12], in his non-empirical SCF MO treatment of hyperconjugation in methylacetylene, replaced one of the $H_3$ group orbitals by the $2p\pi$ carbon orbital itself and assumed the distance between this orbital and the next carbon to be the same as the length of the C-H bond of the methyl group. We intend, however, in the following way, to treat the orbital $\phi_2$ in question as the quasi-$2p\pi$ orbital and to give a reasonable value of the distance between this quasi-$2p\pi$ and the next lying carbon $2p\pi$ orbitals.

In the SCF MO calculations, the quantities associated with the $\phi_2$ orbital, which embody its characteristics well, are its energy and the effective nuclear charge of $H_2^+$ core. The former determines the valence state ionization potential of the $H_2$ group and the latter contributes to the estimation of interelectronic Coulomb repulsion integrals. In consequence, the matter reduces to the estimation of these quantities. The energy of the $\phi_2$ orbital is calculated from

$$W(\phi_2)=\int \phi_2^* H \phi_2 d\tau \qquad (1)$$

using the Hartree-Fock type Hamiltonian,

$$H=T+U,\ U=-\frac{1}{r_a}-\frac{1}{r_b}+(\phi_1\phi_1 \mid -\frac{1}{2}(\phi_1 \mid \phi_1 \qquad (2)$$

where, $1/r_i$ is the operator showing the potential energy from the $i$'th hydrogen nucleus; $(\phi_1\phi_1 \mid$ and $(\phi_1 \mid \phi_1$ are respectively electronic Coulomb and exchange potential energy operators. $I(H_2)=-W(\phi_2)$ indicates the valence state ionization potential of the $H_2$ group. For the isoelectronic series of C, $N^+$ and $O^{++}$, the empirical relation between valence state ionization potentials ($I_\mu$) and effective nuclear charges ($Z_\mu$) determined using the Slater rule for $2p\pi$ orbitals is formulated by the use of energy values of appropriate valence state[13] and of the atomic spectroscopic data[14]. Knowledge of $I(H_2)$, hence, enables us to obtain the effective nuclear charge $Z(\phi_2)$ associated with the $\phi_2$ orbital. The $Z(\phi_2)$ value is also determined by the alternative method. Subject to Paoloni[15] an empirical relation exists between the nuclear effective charges obtained by the use of Slater rule and one center electronic Coulomb repulsion integrals, for the first row atoms, as follows:

$$(\mu\mu \mid \mu\mu)=3.29_4 Z_\mu \qquad (3)$$

The calculated value of one center Coulomb repulsion integral on the $\phi_2$ orbital, $(\phi_2\phi_2 \mid \phi_2\phi_2)$, allows us to estimate the value of the effective nuclear charge associated with the $\phi_2$ orbital by the use of Eq. 3.

5) A. A. V. Stuart and E. L. Mackor, *J. Chem. Phys.*, **27**, 826 (1957).
6) G. Dallinga, E. L. Mackor and A. A. V. Stuart, *Mol. Phys.*, **1**, 123 (1958).
7) N. Muller and R. S. Mulliken, *J. Am. Chem. Soc.*, **80**, 3489 (1958).
8) R. S. Mulliken, *Tetrahedron*, **5**, 253 (1959).
9) T. Morita, This Bulletin, **32**, 893 (1959).
10) C. MacLean, J. H. van der Waals and E. L. Mackor, *Mol. Phys.*, **1**, 247 (1958).
11) R. S. Mulliken, C. A. Riecke and W. G. Brown, *J. Am. Chem. Soc.*, **63**, 41 (1941); see also, C. A. Coulson, "Valence", Oxford University Press, London (1952), p. 310.
12) S. Aono, *Busseiron Kenkyu*, No. 94, p. 24 (1956).
13) H. A. Skinner and H. O. Pritchard, *Trans. Faraday Soc.*, **49**, 1254 (1953); see also, R. S. Mulliken, *J. Chem. Phys.*, **2**, 782 (1934).
14) Landolt-Börnstein, "Zahlenwerte und Funktionen", I Band, 1 Teil Springer, Berlin (1950); C. E. Moore, "Atomic Energy Levels", Vol. I, N. B. S.. Circular 467 (1949).
15) L. Paoloni, *Nuovo Cimento*, **4**, 410 (1956).

The distance between the quasi-$2p\pi$ and the next lying carbon $2p\pi$ orbitals may be estimated in the following way. The interelectronic Coulomb integral between $\phi_2$ and the next lying carbon $2p\pi$ orbitals is evaluated legitimately by the equation[16] (cf. Fig. 1),

$$(\phi_2\phi_2 \mid 2p\pi C\, 2p\pi C) = [(aa \mid CC) - (ab \mid CC)]/(1-S) \quad (4)$$

The empirical formula indicating the same quantity may be formulated by the Pariser-Parr's method[17] using the value of the effective nuclear charge $Z(\phi_2)$ obtained by either $I_\mu \sim Z_\mu$ relation or Eq. 3, this being a functional relation of the distance $r(H_2\text{-}C)$ between $\phi_2$ and carbon $2p\pi$ orbitals. By putting the value obtained by Eq. 4 into this empirical formula, the distance $r(H_2\text{-}C)$ in question may be evaluated.

Core integral $\beta_{H_2-C}$ between $H_2$ and C can be obtained by the assumption of the proportionality relation,

$$\beta_{H_2-C}/\beta = S_{H_2-C}/S \quad (5)$$

where, $\beta$ is the core integral in benzene molecule; $S$ the overlap integral between two carbon $2p\pi$ orbitals separated by 1.39Å; $S_{H_2-C}$ the overlap integral between carbon $2p\pi$ and next lying $H_2$ quasi-$2p\pi$ orbitals.

As above mentioned, the role of the methylene in the SCF MO method may be understood in the simplified manner.

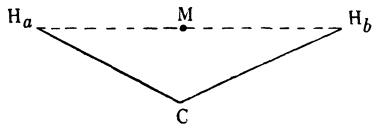



Fig. 1. Assumed geometrical structure of $CH_2$. $C\text{-}H_a = C\text{-}H_b = 1.071$ Å, $\angle H_aCH_b = 120°$.

In the actual calculation, geometrical structure of $C\text{-}H_2$ assumed is the same as that of ethylene by Gallaway and Barker[18] and is indicated in Fig. 1; $C\text{-}H_a = C\text{-}H_b = 1.071$Å, $H_aCH_b = 120°$. (Assumption of $\angle H_aCH_b = 109°28'$ does not seriously affect the calculated results). Semi-empirically calculated values of the quantities determining the model for hyperconjugation are shown in Table I. Although the procedure of this paper goes along the approximation including zero differential overlap by Pariser-Parr[19], or Pople[20], it is desirable to obtain $W(\phi_2)$ with moderate exactness. Indeed, the value calculated with neglect of differential overlap is $-11.834$ eV., and unsuitable for our purpose, if we remember the valence state ionization potential of the $2p\pi$ carbon is 11.54 eV. The value calculated with inclusion of differential overlap is $-11.176$ eV. and this value also may not be said to be appropriate. The moderate value, $-10.256$ eV., is obtained omitting the interelectronic Coulomb integral, $(ab \mid ab)$[21].

Using the value, 2.83, of the effective nuclear charge $Z(\phi_2)$, estimated from Eq. 3, the empirical formula of the interelectronic Coulomb integral $(H_2H_2 \mid CC)$ is obtained as follows,

$$(H_2H_2 \mid CC) = 10.203 - 2.4607r + 0.1933r^2 \quad (r \leqq 2.8A) \quad (6)$$

Substituting the value of $(\phi_2\phi_2 \mid 2p\pi C\, 2p\pi C)$ in the $C\text{-}H_2$ group calculated from Eq. 4 into Eq. 6, the distance $r(C\text{-}H_2)$ between quasi-$2p\pi$ and carbon $2p\pi$ orbitals in the $C\text{-}H_2$ group is estimated as 1.383 and 1.031 Å for the cases with and without differential overlap. (For the case with differential overlap, $r(H_2\text{-}C)$ is estimated to be 1.031 Å from somewhat different equation from Eq. 6 based on somewhat different value of $Z(\phi_2)$). It will be noticed here that when differential overlap is neglected Eq. 4 reduces to

$$(\phi_2\phi_2 \mid 2p\pi C\, 2p\pi C) = (aa \mid CC) \quad (7)$$

It is clear that this approximation 7 is too crude. It is desirable, therefore, to adopt for $r(H_2\text{-}C)$ the middle value between 1.031 and 1.383 Å.

We have performed calculations by the use of some assumed values of $r(H_2\text{-}C)$ between 1.031 and 1.383 Å, and, for $r(H_2\text{-}C) = 1.10$ Å, obtained satisfactory results in agreement with experimental observations. Hence, we describe below on the assumption of $r(H_2\text{-}C) = 1.10$Å. Table I indicates the semi-empirically fixed values of quantities determining the model of hyperconjugation for $C\text{-}H_2$ group (values on the last row of Table I are referred to in the next paragraph).

Somewhat larger value of the C-H distance than that usually accepted in aliphatic hydrocarbons is seen in some papers[22] published after our calculations have finished. Reasonable assumption of $r(H\text{-}C) = 1.11$Å based on these papers leads to $r(H_2\text{-}C) = 1.10$Å by the similar calculations with

16) T. Morita, *J. Chem. Phys.*, **27**, 1442 (1957).
17) R. Pariser and R. G. Parr, ibid., **21**, 767 (1953).
18) W. S. Gallaway and E. F. Barker, ibid., **10**, 88 (1942).
19) R. Pariser and R. G. Parr, ibid., **21**, 466 (1953).
20) J. A. Pople, *Trans. Faraday Soc.*, **49**, 1375 (1953); *J. Phys. Chem.*, **61**, 6 (1957).

21) In the semi-empirical calculation of $W(\phi_2)$, it is assumed that $\int \frac{h_a h_a}{r_b} d\tau = (aa \mid bb)$ and $\int \frac{h_a h_b}{r_b} d\tau = (ab \mid bb) = S(MM \mid bb)$, where M is the midpoint of $H_a$-$H_b$ (Fig. 1). We also obtained $W(\phi_2) = -9.602$ eV. by the non-empirical calculation. Of these four values $W(\phi_2) = -10.256$ eV. is the most appropriate. In our calculations was omitted the correction to be considered in evaluating one center Coulomb repulsion integral $(1s1s \mid 1s1s)$. See, R. D. Brown, *Mol. Phys.*, **1**, 304 (1958).

22) a) K. Kuchitsu, This Bulletin, **32**, 748 (1959); R. A. Bonham, L. S. Bartell and D. A. Kohl, *J. Am. Chem. Soc.*, **81**, 4765 (1959). These authors revealed by the sectormicrophotometer method of electron diffraction that the C-H distances in *n*-butane, *n*-pentane, *n*-hexane and *n*-heptane are 1.100±0.003, 1.118±0.0004, 1.118±0.006 and 1.121±0.007Å, respectively.

b) B. K. Vainshtein, *Kristallografiya*, **3**, 452 (1958); *Chem. Abstr.*, **52**, 19299 (1958). Vainshtein showed that the C-H distance in solid paraffins is 1.123±0.015Å.

c) For ethylene also, recent measurements show somewhat larger value of the C-H distance; see, L. S. Bartell and R. A. Bonham, *J. Chem. Phys.*, **27**, 1414 (1957): H. C. Allen, Jr. and E. K. Plyler, *J. Am. Chem. Soc.*, **80**, 2673 (1958).

d) It ought to be noticed here that the problem of the C-H bond distance has been recently discussed in a wider scope. See, H. J. Bernstein, *J. Phys. Chem.*, **63**, 565 (1959); L. E. Sutton, *Tetrahedron*, **5**, 118 (1959); M. J. S. Dewar and H. N. Schmeising, ibid., **5**, 166 (1959); R. S. Mulliken, ibid., **6**, 68 (1959).

Table I. Semi-empirically fixed values of quantities determining the model of hyperconjugation for C-$H_2$ group

| $W(\phi_2)$ | $(\phi_2\phi_2 \mid \phi_2\phi_2)$ | $Z(\phi_2)$ | $(\phi_2\phi_2 \mid 2p\pi C\,2p\pi C)$ | $r(H_2\text{-}C)$ |
|---|---|---|---|---|
| eV. | eV. | | eV. | Å |
| −10.256 | 9.326 | 2.83 | 7.73 | 1.10 |
| −10.373 | 9.214 | 2.80 | 7.73 | 1.10 |

zero differential overlap to those mentioned above. Values of quantities relating to hyperconjugation of C-$H_2$ group are listed on the last row of Table I, and these are almost identical with those mentioned in the preceding paragraph, hence leading to seriously unaffected results.

At any rate we assume for the orbital of $H_2$ group, which take part in hyperconjugation with the residual part of the molecule, the $2p\pi$ orbital, associated with the effective nuclear charge, 2.83, and standing at a distance, 1.10 Å, from the carbon $2p\pi$ orbital in the methylene group.

The SCF LCAO MO CI calculation for benzenium ion whose co-ordinate system and numbering are as indicated in Fig. 2, is carried out by means of Poples scheme[23] which is based on the theory of Roothaan[24] and combined with Pariser-Parr's approximation[17,19]. The technical procedure for computation is described elsewhere[23,25,26]. What should be stated here is that the core integral $H_{\mu\mu}$ is assumed as follows,

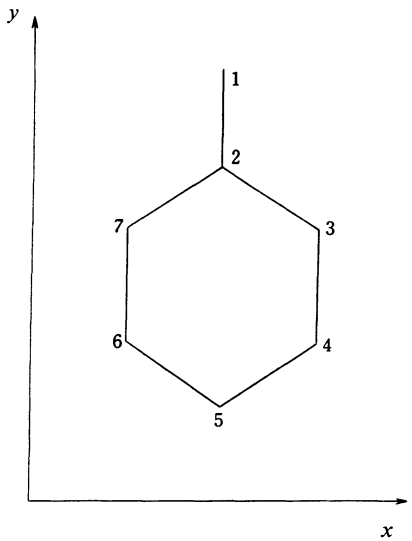



Fig. 2. Co-ordinate system and numbering of benzenium ion for computation.
$\overline{12}=1.10$ Å, $\overline{23}=\overline{34}=\cdots\cdots=\overline{72}=1.39$ Å

$$H_{\mu\mu}=U_{\mu\mu}-\sum_{\alpha(\neq\mu)}{}'(\mu \mid V_\alpha \mid \mu)$$
$$=U_{\mu\mu}-\sum_{\alpha(\neq\mu)}{}' Z_\alpha(\mu\mu \mid \alpha\alpha) \qquad (8)$$

where, $Z_\alpha$ is assumed to be unity.

The approximation of Eq. 8, which Sidman[27] also assumed, leads to that of Pariser and Parr[17,19].

The value of the core integral $\beta$ is taken to be −2.39 eV. except for $\beta_{H_2-C}$ which is estimated to be −4.111 eV. from Eq. 5. Values of valence state ionization potentials are taken from the tables of Skinner and Pritchard[13]. Values of electronic Coulomb repulsion integrals are evaluated using Pariser-Parr's approximations[17].

## Results and Discussion

**(a) Self-consistent Field Molecular Orbitals.** —SCF MO's calculated and expressed by the linear combination of atomic orbitals, $\chi_\mu$, for the models of hyperconjugation and bond localization are shown in Tables II (A) (hyperconjugation) and II (B) (bond localization), which include also the energies, $\varepsilon$, of MO's. The highest occupied molecular orbital is $\phi_3$ in each case and $-\varepsilon_3$ correspond to the ionization potential.

Table II. Calculated self-consistent field molecular orbitals and energies

(A) For the hyperconjugation model

$\varepsilon_1=-21.379$ eV. $\phi_1(1b_2)=0.500\chi_1+0.715\chi_2$
$+0.294(\chi_3+\chi_7)+0.151(\chi_4+\chi_6)+0.143\chi_5$
$\varepsilon_2=-18.381$ eV. $\phi_2(2b_2)=0.248\chi_1+0.239\chi_2$
$-0.103(\chi_3+\chi_7)-0.462(\chi_4+\chi_6)-0.658\chi_5$
$\varepsilon_3=-16.592$ eV. $\phi_3(1a_2)=0.464(\chi_4-\chi_6)$
$+0.534(\chi_3-\chi_7)$
$\varepsilon_4=-8.249$ eV. $\phi_4(3b_2)=0.561\chi_1-0.043\chi_2$
$-0.503(\chi_3+\chi_7)-0.045(\chi_4+\chi_6)+0.416\chi_5$
$\varepsilon_5=-5.607$ eV. $\phi_5(2a_2)=0.534(\chi_4-\chi_6)$
$-0.464(\chi_3-\chi_7)$
$\varepsilon_6=-4.083$ eV. $\phi_6(4b_2)=0.461\chi_1-0.396\chi_2$
$+0.012(\chi_3+\chi_7)+0.408(\chi_4+\chi_6)-0.545\chi_5$
$\varepsilon_7=-2.122$ eV. $\phi_7(5b_2)=0.400\chi_1-0.523\chi_2$
$+0.548(\chi_3+\chi_7)-0.437(\chi_4+\chi_6)-0.274\chi_5$

(B) For the bond localization model

$\varepsilon_1=-19.757$ eV. $\phi_1(1b_2)=0.644\chi_1+0.765\chi_2$
$\varepsilon_2=-19.198$ eV. $\phi_2(2b_2)=0.214(\chi_3+\chi_7)$
$+0.484(\chi_4+\chi_6)+0.664\chi_5$
$\varepsilon_3=-17.056$ eV. $\phi_3(1a_2)=0.457(\chi_4-\chi_6)$
$+0.540(\chi_3-\chi_7)$
$\varepsilon_4=-8.277$ eV. $\phi_4(3b_2)=0.602(\chi_3+\chi_7)$
$+0.085(\chi_4+\chi_6)-0.512\chi_5$
$\varepsilon_5=-6.023$ eV. $\phi_5(2a_2)=0.540(\chi_4-\chi_6)$
$-0.457(\chi_3-\chi_7)$
$\varepsilon_6=-3.684$ eV. $\phi_6(4b_2)=0.765\chi_1-0.644\chi_2$
$\varepsilon_7=-3.678$ eV. $\phi_7(5b_2)=0.304(\chi_3+\chi_7)$
$-0.509(\chi_4+\chi_6)+0.545\chi_5$

23) J. A. Pople, *Proc. Phys. Soc.* (*London*), **A 68**, 81 (1955).
24) C. C. J. Roothaan, *Revs. Mod. Phys.*, **23**, 69 (1951).
25) N. Mataga and K. Nishimoto, *Z. physik. Chem., N. F.*, **13**, 140 (1957).
26) As to the expressions for the interconfigurational matrix elements, see, Ref. 23 and also, R. Pariser, *J. Chem. Phys.*, **24**, 250 (1956). As to the expression for the oscillator strength, see, R. Pariser, loc. cit.
27) J. W. Sidman, ibid., **27**, 429 (1957).

**(b) Electronic Spectra.**—In the calculations with configurational interactions (CI), the singlet configurations considered of excited states for $^1B_1$ symmetry are $V_{3\to4}$, $V_{3\to6}$ and $V_{2\to5}$; those for $^1A_1$ symmetry are $V_{2\to4}$, $V_{3\to5}$ and $V_{1\to4}$. Table III shows, for the hyperconjugation model, the wave functions of excited states with the values of matrix elements.

Electronic spectra theoretically calculated are denoted in Tables IV, V and Fig. 3. The calculated energy of the first transition is, for example, in the case with no configuration interactions, considerably larger for the bond localization model than for the hyperconjugation (Table IV). This suggests that the hyperconjugative effect would possibly be much larger in such a system of isovalent hyperconjugation as benzenium ion than is in the ordinary hyperconjugated molecules.

It is seen in Fig. 3, that the order of excited configurations differs considerably between bond localization and hyperconjugation models.

As the experimental absorption data for protonated compounds of benzene and methylbenzenes are referred those of Reid[28], of Kilpatrick and Hyman[29], as well as of Dallinga, Mackor and Stuart[6]. Among these, the data of Kilpatrick-Hyman and Dallinga-Mackor-Stuart coincide with each other for methylbenzenes. Methyl shifts of the spectra by these investigators are reasonably bathochromic, while are hypsochromic by Reid's measurements. We take up, therefore, the data by Dallinga, Mackor and Stuart, 3700, 2600 and 2000 Å absorptions for benzenium ion, although the experimental extinction curve has not been given explicitly. Theoretical data agree satisfactorily with those experimentally observed (Table V). The oscillator strengths calculated also coincide, in the tendency, with the experimental extinction coefficients by Dallinga, Mackor and Stuart[6] for the protonated compounds of some methylbenzenes. Among these, for example, the mesitylene carbonium ion has the following values of the molar extinction coefficients, 11100, 8800, >13000, respectively, for the first, second and third bands. Further the calculated oscillator strengths by Dallinga, Mackor and Stuart are cited in Table V. These also agree well with our values.

It is striking that the hyperconjugation shift of the first absorption band is, as is seen in Table IV, toward red, while it is, in the Hückel MO calculations, toward blue. Indeed, our Hückel MO calculations using $\alpha_1=\alpha-0.4\beta$ show for the first transition energy the values 1.0709 $(-\beta)$ and 1.0000 $(-\beta)$, of which the former refers to the hyperconjugation and the latter to the bond localization model[30]. By means of the semi-empirical ASMO method also the similar tendency is seen. In performing the semi-empirical ASMO calculations our

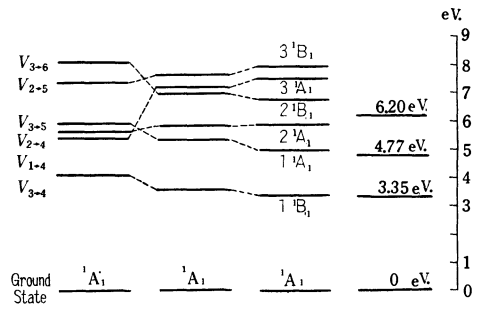



Fig. 3. Observed and calculated $\pi$-electron configurational energy levels.

TABLE III. WAVE FUNCTIONS OF EXCITED STATES WITH THE VALUES OF THE MATRIX ELEMENTS

$^1B_1$-Symmetry

$\Phi(1\,^1B_1)=0.985\,V_{3\to4}-0.017\,V_{3\to6}-0.174\,V_{2\to5}$
$\Phi(2\,^1B_1)=0.082\,V_{3\to4}+0.924\,V_{3\to6}+0.373\,V_{2\to5}$
$\Phi(3\,^1B_1)=0.155\,V_{3\to4}-0.381\,V_{3\to6}+0.911\,V_{2\to5}$
$\{V_{3\to4}\mid V_{3\to6}\}=-0.00988$ eV.
$\{V_{3\to4}\mid V_{2\to5}\}=0.73213$ eV.
$\{V_{3\to6}\mid V_{2\to5}\}=-0.39409$ eV.
$\{V_{3\to4}\mid V_{3\to4}\}=-204.03227$ eV.
$\{V_{3\to6}\mid V_{3\to6}\}=-200.64365$ eV.
$\{V_{2\to5}\mid V_{2\to5}\}=-199.98658$ eV.

$^1A_1$-Symmetry

$\Phi(1\,^1A_1)=0.884\,V_{2\to4}+0.445\,V_{3\to5}+0.143\,V_{1\to4}$
$\Phi(2\,^1A_1)=0.370\,V_{2\to4}-0.854\,V_{3\to5}+0.366\,V_{1\to4}$
$\Phi(3\,^1A_1)=0.285\,V_{2\to4}-0.271\,V_{3\to5}-0.919\,V_{1\to4}$
$\{V_{2\to4}\mid V_{3\to5}\}=-0.45738$ eV.
$\{V_{2\to4}\mid V_{1\to4}\}=-0.52381$ eV.
$\{V_{3\to5}\mid V_{1\to4}\}=0.34067$ eV.
$\{V_{2\to4}\mid V_{2\to4}\}=-202.22097$ eV.
$\{V_{3\to5}\mid V_{3\to5}\}=-201.73760$ eV.
$\{V_{1\to4}\mid V_{1\to4}\}=-200.36226$ eV.

TABLE IV. TRANSITION ENERGIES CALCULATED WITHOUT CONFIGURATION INTERACTIONS

| Bond localization model (eV.) | Hyperconjugation model (eV). |
|---|---|
| 0 (ground state) | 0 (ground state) |
| 4.116 ($V_{3\to4}$) | 3.529 ($V_{3\to4}$) |
| 5.358 ($V_{1\to4}$) | 5.341 ($V_{3\to5}$) |
| 5.621 ($V_{2\to4}$) | 5.824 ($V_{2\to4}$) |
| 5.864 ($V_{3\to5}$) | 6.918 ($V_{3\to6}$) |
| 7.344 ($V_{2\to5}$) | 7.199 ($V_{1\to4}$) |
| 7.959 ($V_{3\to6}$) | 7.575 ($V_{2\to5}$) |

28) C. Reid, *J. Am. Chem. Soc.*, **76**, 3264 (1954).
29) M. Kilpatrick and H. H. Hyman, ibid., **80**, 77 (1958).
30) The Hückel MO method for toluenium and mesitylenium ions also shows the hypsochromic shift for the hyperconjugative effect. See, Refs. 3 and 4.

TABLE V. CALCULATED ELECTRONIC SPECTRA FOR HYPERCONJUGATION MODEL COMPARED WITH EXPERIMENTS

| Symmetry | Polarization | Transition energies for hyperconjugation with CI (eV.) | Transition energies observed (eV.) | Oscillator strengths calculated | |
|---|---|---|---|---|---|
| $1\ ^1B_1$ | x | 3.400 | 3.35 | 0.219[a] | (0.21)[b] |
| $1\ ^1A_1$ | y | 5.025 | 4.77 | 0.012[a] | (0.06)[b] |
| $2\ ^1A_1$ | y | 5.876 | 6.20 | 0.630[a] | (0.99)[b] |
| $2\ ^1B_1$ | x | 6.758 | | 0.117[a] | |
| $3\ ^1A_1$ | y | 7.462 | | 0.017[a] | |
| $3\ ^1B_1$ | x | 7.864 | | 0.354[a] | |

a) These values are calculated by the use of the wave functions in Table III.
b) Values in parentheses are those calculated by Dailinga, Mackor and Stuart; see, Ref. 6.

TABLE VI. ENERGIES OF THE FIRST TRANSITION CALCULATED BY THE HÜCKEL AND PARISER-PARR METHODS

| | Hückel method | Pariser-Parr's method | Modified Hückel method | Modified Pariser-Parr's method |
|---|---|---|---|---|
| Hyperconjugation | 1.0709 $(-\beta)$ | 3.798 eV. | 1.0709 $(-\beta)$ | 3.798 eV. |
| Bond localization | 1.0000 $(-\beta)$ | 3.575 eV. | 1.0833 $(-\beta)$ | 3.864 eV. |

procedure is almost the same as that for toluene by Morita[16]. The value of the core integral $\beta_{H_2-C}$ used is $-4.435$ eV., which is somewhat different from that in the semi-empirical SCF MO method extended in the early part of this paper. Values of the atomic integrals also differ from those used in the SCF MO method. This does not prevent us, however, from judging the calculated results. The calculated energies for the first transition are 3.798 eV. for the hyperconjugation model and 3.575 eV. for the bond localization.

This discrepancy between the results of the SCF MO and ASMO methods might be taken off by introducing the laborious technique of configurational interaction. This seems to be in vain, however, if we take into account the same extent of configurations as in the SCF MO calculations. If any simple modification is tried, however, for the naive and the anti-symmetrized molecular orbital calculations, the identical tendency in all cases will be accomplished.

The modification is done as follows. In the bond localization model, as is seen in Fig. 4, the $\pi$-electron system is cut off into two parts, one being the system 1-2 (A), the other the system 3-4-5-6-7 (B). In the part B, terminal carbons (3 and 7) seem to be electropositive compared to the inner carbons[31]. Consequently, we should give negative value of $\delta$ for the Coulomb integral $\alpha_3$ or $\alpha_7=\alpha+\delta\beta$. We have no thorough materials which suggest the exact way determining the value of $\delta$ in this case. It may not be said, however, that the

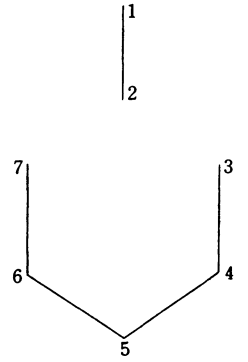



Fig. 4. The effective $\pi$-electron system of the benzenium ion for its bond localization model.

leectropositiveness of the carbon atom 3 or 7 is not satisfactory when it is equated to that of the $H_2$ group. Hence, we assume, for a moment, $\alpha_3=\alpha_7=\alpha-0.4\beta$. The corresponding modification in the ASMO method is to equalize $I_3$ (the valence state ionization potential of the carbon atom 3 or 7) to $I(H_2)$ (the valence state ionization potential of the $H_2$ group, namely $I(H_2)=-W(\phi_2)=-\int\phi_2^*H\phi_2 d\tau$) in the formula expressing the core integral $\alpha_3$ or $\alpha_7$ (Pariser-Parr's notation)

$$\alpha_3=\alpha_7=-I_3-\sum_{\nu\neq 3}{}' (33\mid\nu\nu) \qquad (9)$$

(Although the electronic Coulomb repulsion integrals, $(33\mid\nu\nu)$, have to take different values corresponding to the change in $I_3$, this correction may be omitted for the present purpose.) These modifications in the naive and antisymmetrized molecular orbital methods lead to the

31) R. G. Parr and R. S. Mulliken, *J. Chem. Phys.*, **18**, 1338 (1950).

same tendency as in the SCF MO method with regard to the absorption spectra. Calculated results are indicated in Table VI.

**(c) Charge Densities and Bond Orders.**—Fig. 5 shows $\pi$-electron densities and $\pi$-bond orders calculated for the hyperconjugation and bond localization models.

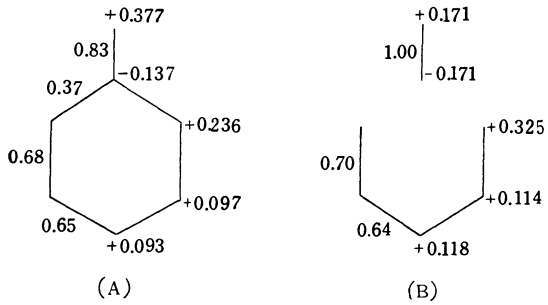



Fig. 5. Calculated formal charges (unit of $+e$) and $\pi$-bond orders of benzenium ion.
A : hyperconjugation, B : bond localization

The proton magnetic resonance spectra of pentamethylbenzene in $CF_3COOH+H_2O\cdot BF_3$ and in $HF+BF_3$ show for the methyl groups the following shifts compared to the benzene proton signal; 196, 199, 204 and 180, 187, 198 (in c/sec.) in each case[10]. The manner in which the assignment of the signals is undertaken is different, according as which model, hyperconjugation or bond localization, is adopted. Namely, the hyperconjugation model predict the signals 196, 199, 204 or 180, 187, 198 (in c/sec.) attributing, in order, to the methyl groups at the positions 3, 4, 5; in contrast, for the bond localization model, these signals should be assigned to the methyl groups at the positions 3, 5, 4 in order. This discrepancy will probably be due to the crudeness of approximations. It will be probably necessary, in the configurational interaction calculations, to take into account further more configurations including the ground state configuration, $V_0$, which is shut out of our computations.

**(d) Hyperconjugation Energy.**—The hyperconjugation energy is obtained by subtracting the energy of hyperconjugation model from that of bond localization one, taking further the compressional energy correction into consideration. The compression energy is evaluated on the assumption of harmonical distortion of a bond. Calculated energy of hyperconjugation is 19.7 kcal./mol., which is much larger than in the case of the ordinary hyperconjugation.

## Summary

Semi-empirical SCF LCAO MO calculations of benzenium ion was undertaken for the model of localization as well as hyperconjugation of the $H_2$–C bond constructed at the position of proton attack. A simplified model of hyperconjugation in the semi-empirical SCF MO method was extended. Calculated results for the hyperconjugation model agreed satisfactorily with the experimental electronic spectra.

Superiority of the SCF MO method to the Hückel MO or ASMO method was indicated in connection with the ordinarily accepted spectral shift through hyperconjugation. Further, some modifications were tried, for the bond localization model, which would have to be taken in the Hückel MO as well as ASMO calculations.

The proton magnetic resonance signals due to methyl substituents in the carbonium ions of methylbenzenes were discussed from charge densities of benzenium ion.

The author wishes to thank Professor T. Titani, Tokyo Metropolitan University, for his interest and to Professors A. Kotera, Tokyo University of Education, and S. Nagakura, the University of Tokyo, and Mr. Y. Mori, Tokyo Institute of Technology, for their kind advices and helpful discussions. This work was financially supported by a grant-in-aid from the Ministry of Education.

*Department of Chemistry*
*Tokyo Metropolitan University*
*Setagaya-ku, Tokyo*

# *Studies on Constituents of Coal Carbonization Light Oil. I. On Saturated Hydrocarbons Contained in High-temperature Coal Carbonization Light Oil*

By Hiroshi YASUI

(Received December 23, 1959)

Constituents and their contents of coal carbonization light oil, are influenced by their carbonization temperature. It has been reported, that components contained in high-temperature coal carbonization light oil differ from those in low-temperature coal carbonization light oil, qualitatively and quantitatively[1,2]. Apparently, such constituents of low-temperature coal carbonization light oil are mainly saturated hydrocarbons and less aromatic and unsaturated hydrocarbons. By contrast, those of high temperature coal carbonization light oil are mainly aromatic and less saturated and unsaturated hydrocarbons. In the studies on the constituents of high-temperature coal carbonization, nearly all the aromatic hydrocarbons contained in the light oil have been determined[3-5]. But the saturated hydrocarbons in the light oil are not present in any large quantity, but separation of these saturated hydrocarbons is difficult, resulting data of such separation being scanty. Saturated hydrocarbons contained in the light oil, previously reported, are *n*-heptane[6-8], octane[9], *n*-decane[10,11] as *n*-paraffin, and 2, 2, 4-trimethylpentane[6,7] and 3-ethyl-3-metylpentane[12] as isoparaffin, and cyclopentane[10], methylcyclopentane[8,10] cyclohexane[7,8,10], methylcyclohexane[10], 1, 2-, 1, 3- and 1, 4-dimethylcyclohexane[10], 1, 3, 5-[13] and 1, 2, 4-trimethylcyclohexane[14] and 1, 2, 4, 5-tetramethylcyclohexane[13] as cycloparaffin. While, the presence of *n*-decane, *n*-undecane and 1, 2, 3, 4-tetramethylcyclohexane in solvent naphtha produced from Yawata Iron & Steel Co., Ltd. in 1949, has been already ascertained by S. Kimura and the author[15]. In this research, the author has ascertained and identified the saturated hydrocarbons contained in benzene[16,17], toluene[17,18] and solvent naphtha fractions[19,20] separated from high-temperature coal carbonization light oil (carbonization temperature, 1250°C) of Yawata Iron & Steel Co., Ltd. in 1952.

## Experimental

**Materials. — Crude Saturated Hydrocarbon Oil Obtained from Benzene Fraction.**—A residual oil after chlorination of benzene fractiton (b. p. 79.5~81°C) at Nihon Kayaku Co., Ltd., which is colorless oil and has $d_4^{20}=0.7755$ and $n_D^{20}=1.444$, was used as material.

**Toluene Fraction.**—Toluene fraction purified by treatment with conc. sulfuric acid, manufactured by Yawata Iron & Steel Co., Ltd. in January, 1952, a colorless oil of b. p. 110.3~111.2°C, $d_4^{20}=0.8633$ and $n_D^{20}=1.493$, was used as material.

**Solvent naphtha.**—Solvent naphtha prepared at Yawata Iron & Steel Co., Ltd. in January, 1952, consisting of 17.8% of 10°-xylene (136~142°C fraction), 40.5% of solvent naphtha I (125~172°C fraction) and 41.7% of solvent naphtha II (149~203°C fraction) in proportion to each rate of production, a pale yellow oil of $d_4^{20}=0.8698$ and $n_D^{20}=1.496$, was used as material.

**Separation of Saturated Hydrocarbon Oil in the Materials.—Saturated Hydrocarbons Contained in Benzene Fraction.**—As benzene was expected to be contained in the material from its physical constants, 500 ml. of it was shaken vigorously with the mixture of 50 ml. of conc. nitric acid ($d_4^{20}=1.42$) and 100 ml. of conc. sulfuric acid ($d_4^{20}=1.84$); and aromatic hydrocarbons were removed. The residual oil was washed by water, neutralized with 10% sodium hydroxide solution, rewashed similarly and dried with calcium chloride to obtain 433 ml. of

1) M. Vahrman, *J. Appl. Chem.*, **2**, 532 (1952).
2) C. H. Lander and R. F. Mackay, "Low Temperature Carbonization", Ernest Benn, Ltd., London, (1924) p. 164.
3) S. Kimura, H. Suzumura and H. Yasui, *J. Japan Tar Ind. Association*, **4**, 35 (1952).
4) H. Steinbrecher and H. Kuhn, *Angew. Chem.*, **50**, 233 (1937).
5) O. Kruber, *Erdöl und Kohle.*, **8**, 637 (1955).
6) J. A. Anderson, C. J. E. Engelder, *Ind. Eng. Chem.*, **37**, 541 (1945).
7) J. Griswold, R. H. Bowden, ibid., **38**, 509 (1946).
8) R. F. Marschner and W. P. Cropper, ibid., **38**, 262 (1946).
9) F. B. Ahrens, *Ber.*, **40**, 848 (1907).
10) H. H. Lowry, "Chemistry of Coal Utilization". Vol. II, John Wiley & Sons, Inc., New York (1947), p. 1357.
11) O. Jacobsen, *Ann.*, **184**, 179 (1877).
12) H. Stinzendorfer, *Oel und Kohle*, **38**, 193 (1942).
13) A. Pictet and M. Bouvier, *Ber.*, **56**, 162 (1923).
14) F. B. Ahrens and L. V. Modzenski, *Z. Angew. Chem.*, **21**, 1411 (1908).
15) S. Kimura and H. Yasui, *J. Chem. Soc. Japan, Pure Chem. Sec.* (*Nippon Kagaku Zasshi*), **74**, 555 (1953).
16) S. Kimura and H. Yasui, ibid., **75**, 163 (1954).
17) H. Yasui, ibid., **78**, 82 (1957).
18) S. Kimura and H. Yasui, ibid., **75**, 300 (1954).
19) H. Yasui, ibid., **78**, 85 (1957).
20) H. Yasui, ibid., **78**, 1213 (1957).

crude saturated hydrocarbon, which has b. p. 85~105°C, $d_4^{20}=0.7711$ and $n_D^{20}=1.430$. Now 300 ml. of this oil was submitted to fractional distillation with metallic sodium and 120 ml. of 78~90°C fraction ($d_4^{20}=0.8059$, $n_D^{20}=1.458$), and 150 ml. of 90~103°C fraction ($d_4^{20}=0.7290$, $n_D^{20}=1.406$) were obtained. But, in the 78~90°C fraction, residual benzene was still expected from its physical constants and ultraviolet spectrum[17]. The residual benzene in this fraction, therefore, was again removed with a mixture of conc. sulfuric acid and conc. nitric acid, and the residual oil and 90~103°C fraction were fractionated by Podbielniak distillation equipment, and 4 per cent by weight of 78~90°C fraction ($d_4^{20}=0.7067$, $n_D^{20}=1.398$) and 96 per cent by weight of 96~100°C fraction ($d_4^{20}=0.7170$, $n_D^{20}=1.405$), were obtained.

**Saturated Hydrocarbons Contained in Toluene Fraction.**—In an iron-pot provided with a stirrer, toluene contained in 169 kg. of toluene fraction, was extracted with 361.7 kg. of conc. sulfuric acid and 2.1 kg. of crude saturated hydrocarbon oil, and about 1.2% by weight of toluene fraction was obtained. Residual toluene in 756 g. of this oil was again removed completely with conc. sulfuric acid. 709 g. of saturated hydrocarbon oil, amounting to about 1.1% of toluene fraction, was obtained. This oil was distilled with metallic sodium and 120~126°C fraction, which has $d_4^{20}=0.7234$ and $n_D^{20}=1.406$, was obtained.

**Saturated Hydrocarbons Contained in Solvent Naphtha.**—In an iron-pot provided with a stirrer, aromatic hydrocarbons contained in 200 kg. of the material, were extracted four times with conc. sulfuric acid (total of 197.34 kg.), and 6.44 kg. of crude saturated hydrocarbon oil, was obtained. Moreover, the residual aromatic hydrocarbon in 760 g. of this oil was removed with conc. sulfuric acid repeatedly and 708 g. of saturated hydrocarbon oil, amounting to about 3% by weight of the material, was obtained. This oil has b. p. 132~198°C, $d_4^{20}=0.7632$ and $n_D^{20}=1.425$. 616 g. of this oil was submitted to the fractional distillation with metallic sodium and six fractions shown in Table I, were obtained.

Total of 118~147°C and 147~161°C fractions were fractionated by Podbielniak distillation equipment, and five fractions shown in Table II were obtained.

Moreover, total of 155~162°C fraction in Table II and 161~172°C, 172~177°C fractions in Table I, were fractionated and three fractions shown in Table III were obtained.

Analyses were carried out on the main fractions of 143.5~155°C in Table II and of 165~174°C in Table III.

TABLE I. FRACTIONS OBTAINED BY FRACTIONAL DISTILLATION OF 616 g. OF 132~198°C FRACTION

| Frac. °C | g. | $d_4^{20}$ | $n_D^{20}$ |
|---|---|---|---|
| 118~147 | 126 | 0.7492 | 1.419 |
| 147~161 | 180 | 0.7551 | 1.421 |
| 161~172 | 97 | 0.7629 | 1.424 |
| 172~177 | 73 | 0.7705 | 1.428 |
| 177~184 | 54 | 0.7749 | 1.431 |
| 184~ | — | 0.7889 | 1.439 |

TABLE II. FRACTIONS OBTAINED BY FRACTIONAL DISTILLATION OF A TOTAL OF 118~147°C AND 147~161°C FRACTIONS

| Frac. °C | g. | $d_4^{20}$ | $n_D^{20}$ |
|---|---|---|---|
| 111.5~132.5 | 19 | 0.7368 | 1.412 |
| 132.5~139 | 20 | 0.7461 | 1.416 |
| 139 ~143.5 | 8 | 0.7486 | 1.416 |
| 143.5~155 | 156 | 0.7502 | 1.418 |
| 155 ~162 | 28 | 0.7605 | 1.422 |

TABLE III. FRACTIONS OBTAINED BY FRACTIONAL DISTILLATION OF A TOTAL OF 155~162°C IN TABLE II AND 161~172°C, 172~177°C FRACTIONS IN TABLE I

| Frac. °C | g. | $d_4^{20}$ | $n_D^{20}$ |
|---|---|---|---|
| 145~147 | 7.5 | 0.7571 | 1.420 |
| 147~165 | 36 | 0.7596 | 1.422 |
| 165~174 | 83 | 0.7643 | 1.425 |

**Identification of *n*-Paraffin.**—*n*-Paraffin was isolated by means of urea adduct[21]. According to an estimation *n*-paraffin contained was about 30% in each fraction. It was added to urea (about 4 mol.) moistened with methanol (about 1 mol.). The suspension was stirred for 30 min. at 25°C and filtered, removing unreacted oil. The mixture of urea adduct and residual urea, were washed with anhydrous ether, which was removed under reduced pressure, and decomposed with water, and oil (*n*-paraffin) was obtained. And, unreacted oil was added to urea moistened with methanol, and treated as mentioned above, repeatedly until oil (*n*-paraffin) was no longer obtained by decomposition with water of urea adduct.

**78~90°C and 96~100°C Fractions.**—These fractions were treated as mentioned above, but oil was not obtained by decomposition with water of the urea adduct[17], suggesting difficulty by means of urea adduct, to separate *n*-paraffin expected to be contained in these fractions as stated by Kuwata and co-workers previously[22].

TABLE IV. ISOLATION OF *n*-PARAFFINS BY MEANS OF UREA ADDUCTS IN 120°~126C, 143.5~155°C AND 165~174°C FRACTIONS

| Frac. | | Oil isolated by means of urea adduct | | | | Residual oil | |
|---|---|---|---|---|---|---|---|
| °C | g. | g. | % for frac. | b. p. °C | $d_4^{20}$ | g. | % for frac. |
| 120 ~126 | 100 | 30 | 30 | 124~125.5 | 0.7035 | 51 | 51 |
| 143.5~155 | 30 | 7.6 | 25 | 149~151 | 0.720 | 18 | 60 |
| 165 ~174 | 30 | 12 | 40 | 165~178 | 0.7306 | 12 | 40 |

21) J. Zimmerschied, R. A. Dinerstein, A. W. Weitkamp and R. F. Marschner, *Ind. Eng. Chem*, **42**, 1300 (1950).

22) T. Kuwata, Y. Mizutani and E. Tamura, *J. Chem. Soc. Japan, Ind. Chem. Sec.* (*Kogyo Kagaku Zasshi*), **55**, 799 (1952).

**120～126°C[18], 143.5～155°C[19] and 165～174°C[20] Fractions.**—*n*-Paraffin contained in the three fractions were isolated by means of urea adduct and the result was shown in Table IV.

**Oil Isolated by Means of Urea Adduct in 120～126°C Fraction.** — Physical constants (Table IV) of this oil are identical with those of *n*-octane[23] (b. p. 125.6°C, $d_4^{20}=0.703$, $n_D^{20}=1.397$). IR spectrum bands[18] (wavelengths; 7.68, 7.87, 8.16, 8.33, 8.8, 9.27, 9.65, 9.95, 10.34, 10.92, 11.4, 11.84, 12.6, 13.08, 13.32, 13.85 $\mu$) of this oil are analogous to those of *n*-octane.

**Oil Isolated by Means of Urea Adduct in 149～151°C Fraction.**—Physical constants (Table IV) of this oil are identical with those of *n*-nonane[23] (b. p. 150.7°C, $d_4^{20}=0.718$, $n_D^{20}=1.406$) and IR spectrum bands[19] (wavelengths; 7.67, 7.94, 8.22, 8.41, 8.81, 9.2, 9.41, 9.58, 10.14, 10.29, 10.79, 11.22, 11.84, 12.05, 12.89, 13.29, 13.86 $\mu$) of this oil are analogous to those of *n*-nonane.

**Oil Isolated by Means of Urea Adduct in 165～174°C Fraction.**—Physical constants (Table IV) of this oil are identical with those of *n*-decane[23] (b. p. 174°C, $d_4^{20}=0.7298$, $n_D^{20}=1.412$). IR spectrum bands[20] (wavelengths; 7.67, 8.01, 8.25, 8.42, 8.81, 9.16, 9.29, 9.92, 10.05, 10.86, 11.15, 11.83, 12.28, 13.0, 13.85 $\mu$) of this oil are analogous to those of *n*-decane.

**Identification of Cycloparaffin.**—Dehydrogenation of the residual oil free from *n*-paraffin, was carried out with Pt-C catalyst at 300～310°C.

**Dehydrogenation[24,25] Catalyst.** — Pt-C catalyst was prepared by Berl's method[24]. About 10 g. of granulated active carbon was mixed with 1 g. of platinum chloride ($PtCl_2 \cdot 2HCl + 6HCl$) dissolved in 25 ml. of water acidified with hydrochloric acid, and the mixture was dried at 110°C with frequent stirring. These were put in a quartz reaction tube (dia., 2 cm., length, 80 cm.) and kept in position by a stopper of glass wool. They were heated to 200°C by electric furnace and the platinum compound was decomposed. Hydrogen was sent to the tube from the entrance until no more hydrochloric acid was formed and a treatment with hydrogen at 300°C was carried out for 30 min.

**Apparatus.**—The sample was dropped into one end of a reaction tube from the sample flask, the dropping velocity regulated by the opening of the cock provided at the lower part of the sample flask, and the oil produced was received from the other end by a receiving flask with an ice-cooled condenser and the gas produced was collected in a gas collector, its pressure being controlled by a pressure

TABLE V. DEHYDROGENATION

Reac. temp. 300～310°C; Dropping velocity 5～6 g./hr.

| Sample | g. | Dehydrogenated oil g. | Gas produced ml. (N. T. P.) | $H_2$* ml. (N. T. P.) |
|---|---|---|---|---|
| (a) | 7 | 4.5 | 828.8 | 812.2 |
| (b) | 10 | 6 | 1906.0 | 1815.2 |
| (c) | 11 | 5.5 | 1261.1 | 1171.0 |
| (d) | 13 | 9.5 | 1330.1 | 1210.6 |
| (e) | 10 | 8.5 | 455.4 | 439.6 |

* The gas produced by dehydrogenation was analyzed by the Hempel method, and the volume of hydrogen produced by dehydrogenation was calculated from the gas produced.

TABLE VI. NITRO-COMPOUNDS OBTAINED BY NITRATION OF DEHYDROGENATED OILS

| | Dehydrogenated oil | Nitro-compound: Obtained: Crude | Obtained: Recrystal. | | Referred[26]: Comp. | |
|---|---|---|---|---|---|---|
| | g. | g. | g. | m. p. °C | | m. p., °C |
| (a) | 0.7 | 0.5 | 0.05 | 88 ～ 90 | *m*-Dinitrobenzene | 90 |
| | | | 0.18 | 69 ～ 70 | 2,4-Dinitrotoluene | 70 |
| (b) | 0.7 | 0.7 | 0.4 | 69.5～ 70 | 〃 | 〃 |
| (c) | 2 | 0.4 | 0.31 | 179 ～181 | 2,4,6-Trinitro-*m*-xylene | 180 |
| | | | 0.02 | 138 ～141 | 2,3,5-Trinitro-*p*-xylene | 140 |
| (d) | 1.5 | 0.8 | 0.45 | 169 ～171 | 3,5-Dinitro-1,2,4-trimethylbenzene | 172 |
| | | | 0.05 | 99 ～100 | Dinitro-1,2,3-trimethylbenzene | 100 |
| (e) | 2 | 0.3 | 0.03 | 230 ～232 | 2,4,6-Trinitro-1,3,5-trimethlybenzene | 232 |
| | | | 0.1 | 179 ～181 | 4,6-Dinitro-1,2,3,5-tetramethylbenzene | 180 |

* All melting points are uncorrected.

23) G. Egloff, "Physical Constants of Pure Hydrocarbons", Vol. I, Reinhold Publ. Corp., New York (1939), p. 49.
24) E. Berl and W. Koerber, *Ind. Eng. Chem., Anal. Ed.*, 12, 175 (1940).
25) S. Komatsu and S. Kimura, *J. Chem. Soc. Japan, Pure Chem. Sec.* (*Nippon Kagaku Zasshi*), 74, 343 (1953).
26) S. P. Mulliken, "A Method for Identification of Pure Organic Compounds", Vol. I., John Wiley & Sons, Inc. (1959), p. 200.

control device. 78~90°C (a) and 96~100°C fractions (b) and each residual oils (c), (d), (e) free from *n*-paraffin in 120~126°C, 143.5~155°C and 165~174°C fractions were dehydrogenated as mentioned above, and the oil condensed in the receiver were subjected to dehydrogenation repeatedly, and the results, shown in Table V, were obtained.

**Identification of Aromatic Hydrocarbons Produced by Dehydrogenation — UV Spectrum of Dehydrogenated Oil**[15-20]. — UV spectra of dehydrogenated oils dissolved in purified cyclohexane, was measured with a Beckman spectrophotometer, model DU and the aromatic hydrocarbons produced by dehydrogenation were estimated from their UV spectra.

**Nitration of Dehydrogenated Oil**[15-20].—Dehydrogenated oil was added to a mixture of 1 vol. of conc. nitric acid and 2 vol. of conc. sulfuric acid and the mixture was heated to boil for five minutes and poured into cold water, and crude nitro-compounds were obtained. These compounds were purified or separated by recrystallization from ethyl alcohol solution, obtaining pure nitro-compounds. The results were shown in Table VI.

The aromatic hydrocarbons contained in each dehydrogenated oil, were determined from UV spectra and Table VI, and the original cycloparaffins contained in (a), (b), (c), (d) and (e) were estimated. The result was shown in Table VII.

TABLE VII. CYCLOPARAFFINS CONTAINED IN (a), (b), (c), (d) AND (e)

| | Cycloparaffin | Ratio* |
|---|---|---|
| (a) | Cyclohexane | 1 |
| | Methylcyclohexane | 4 |
| (b) | Methylcyclohexane | |
| (c) | 1,3-Dimethylcyclohexane | 15 |
| | 1,4-Dimethylcyclohexane | 1 |
| (d) | 1,2,4-Trimethylcyclohexane | 9 |
| | 1,2,3-Trimethylcyclohexane | 1 |
| (e) | 1,3,5-Trimethylcyclohexane | 1 |
| | 1,2,3,5-Tetramethylcyclohexane | 3 |

* The ratio of cycloparaffins contained in each fraction was calculated from weights of nitro-compounds obtained.

TABLE VIII. PHYSICAL CONSTANTS OF OILS, REMOVED AROMATIC HYDROCARBONS CONTAINED IN DEHYDROGENATED OILS

| | Dehydrogenated oil | Oil (saturated hydrocarbon) | | | |
|---|---|---|---|---|---|
| | g. | g. | b. p., °C | $d_4^{20}$ | $n_D^{20}$ |
| (a) | 2.1 | 1.7 | 93 ~ 96 | 0.6865 | 1.389 |
| (b) | 2.2 | 1.5 | 98.5~ 99.5 | 0.6942 | 1.393 |
| (c) | 1.6 | 1.35 | 114 ~116 | 0.7221 | 1.405 |
| (d) | 2.0 | 1.5 | 140 ~145 | 0.7265 | 1.407 |
| (e) | 1.6 | 1.3 | 164 ~166 | 0.7340 | 1.413 |

**Identification of Isoparaffin.**—Aromatic hydrocarbons produced by dehydrogenation were removed from dehydrogenated oils by mixture of 2 vol. of conc. sulfuric acid and 1 vol. of conc. nitric acid or by conc. sulfuric acid[15-20]. The residual oils were washed by water and neutralized with alkaline solution. Similarly rewashed and dried with calcium chloride and distilled with metallic sodium, and the oils, having the physical constants shown in Table VIII were obtained.

IR spectra of these oils were measured with a Baird infrared spectrophotometer and isoparaffins contained in each oil were determined. IR spectrum bands of oil of (a) (wavelengths; 7.45, 7.68, 8.78, 9.30, 9.79, 10.4, 10.74, 11.1, 11.42, 11.57, 12.01, 12.91, 13.54, 13.83 $\mu$) are analogous to those of *n*-heptane. In IR spectrum bands of oil of (b), those of *n*-heptane and 2,2,4-trimethylpentane (wavelengths; 7.7, 8.01, 8.30, 8.56, 9.84, 10.2, 10.82, 11.58, 13.4 $\mu$) were observed. It was observed that IR spectrum bands of oil of (c) contain the bands of the spectrum for 2-methylheptane (wavelengths; 7.45, 7.68, 7.9, 8.55, 9.28, 10.42, 10.56, 10.74, 12.3, 13.06, 13.82 $\mu$) and those of the spectrum for 3-methylheptane (wavelengths; 7.68, 7.9, 9.28, 10.42, 10.95, 11.43, 12.3 $\mu$). In IR spectrum bands of oil of (d), those of 3-methyloctane (wavelengths; 8.7, 9.97, 10.3, 10.48, 10.72, 10.94, 11.22, 11.43, 12.3 $\mu$) and 4-methyloctane (wavelengths; 8.7, 9.26, 10.48, 10.72, 10.94, 11.22, 12.94, 13.5, 13.8 $\mu$) were observed. In IR spectrum of bands of oil of (e), those of 3-methylnonane (wavelengths; 8.6, 9.43, 9.77, 9.96, 10.34, 10.95, 11.2, 13.0, 13.8 $\mu$) and 4-methylnonane (wavelengths; 8.6, 9.24, 10.47, 11.2, 11.86, 12.3, 13.0, 13.6, 13.8 $\mu$) were observed.

## Results and Discussion

The saturated hydrocarbons identified from each fraction and the proportion of *n*-paraffin, isoparaffin and cycloparaffin to each fraction, are shown in Table IX.

It is obvious that saturated hydrocarbons contained in benzene fraction consist of *n*-heptane (about 74.5%), cyclohexane (about 0.1%), methylcyclohexane (about 25.4%) and 2, 2, 4-trimethylpentane (trace). In the saturated hydrocarbons contained in toluene fraction, *n*-octane (30%), mixture of 2-methylheptane and 3-methylheptane (42%) and 1, 3-dimethylcyclohexane (9%) and 1, 4-dimethylcyclohexane (0.5%) were determined. Saturated hydrocarbons contained in solvent naphtha fraction were determined to contain *n*-nonane (about 5.4%), *n*-decane (about 4.7%), mixture of 3-methyloctane and 4-methyloctane (about 10.8%), mixture of 3-methylnonane and 4-methylnonane (about 4.3%), 1,2,4-trimethylcyclohexane (about 0.2%), 1, 2, 4-trimethylcyclohexane (about 2%), 1, 3, 5-trimethylcyclohexane (about 0.1%) and 1, 2, 3, 5-tetramethylcyclohexane (about 0.4%).

The following observations are based on a study of the data presented in this research.

TABLE IX. SATURATED HYDROCARBONS IDENTIFIED AND THE PROPORTION OF *n*-PARAFFIN, ISOPARAFFIN AND CYCLOPARAFFIN TO EACH FRACTION

| Frac. | *n*-Paraffin (%) | Isoparaffin (%) | Cycloparaffin (%) | Aromatic* |
|---|---|---|---|---|
| 78 ~ 90 | *n*-Heptane (87) | None | Cyclohexane (3)<br>Methylcyclohexane (10) | Benzene |
| 96 ~100 | *n*-Heptane (74) | | Methylcyclohexane (26) | |
| 120 ~126 | *n*-Octane (30) | 2-Methylheptane<br>3-Methylheptane (42) | 1,3-Dimethylcyclohexane (9)<br>1,4-Dimethylcyclohexane (0.5) | Toluene |
| 143.5~155 | *n*-Nonane (25) | 3-Methyloctane<br>4-Methyloctane (50) | 1,2,3-Trimethylcyclohexane (1)<br>1,2,4-Trimethylcyclohexane (9) | *o*-Xylene<br>*m*-Xylene<br>*p*-Xylene<br>*o*-Ethyltoluene<br>*m*-Ethyltoluene<br>*p*-Ethyltoluene<br>1,2,4-Trimethylbenzene<br>1,2,3-Trimethylbenzene<br>1,3,5-Trimethylbenzene |
| 165 ~174 | *n*-Decane (40) | 3-Methylnonane<br>4-Methylnonane (37) | 1,3,5-Trimethylcyclohexane (1)<br>1,2,3,5-Tetramethylcyclohexane (3) | |

* Aromatic hydrocarbons in high-temperature coal carbonization light oil prepared at Yawata Iron & Steel Co., Ltd. as identified previously by S. Kimura, H. Suzumura and the author[3].

1) The saturated hydrocarbons contained in benzene, toluene and solvent naphtha fractions are all composed of saturated aliphatic hydrocarbon, about 85%, and cycloparaffinic hydrocarbon, about 15%.

2) The saturated aliphatic hydrocarbons contained in benzene fraction are nearly all *n*-paraffins and the corresponding isoparaffins are expected to be contained in the forerunnings. In the saturated aliphatic hydrocarbons contained in toluene and solvent naphtha fractions, the proportion of contents of *n*-paraffins and isoparaffins are about 1 : 1.5.

3) The isoparaffins, contained in the three fractions mentioned above, are all monomethylparaffins.

4) Comparing cycloparaffins with aromatics, cyclohexane corresponding to benzene, methylcyclohexane to toluene, dimethylcyclohexane to dimethylbenzene and trimethylcyclohexane to trimethylbenzene, are present respectively. In dimethylbenzene isomer, *m*-xylene is the highest in contents, *p*-xylene, half as much as *m*-xylene and *o*-xylene is of trace[3]. Similar tendency is observed in the contents of dimethylcyclohexane isomers, but 1, 2-dimethylcyclohexane can not be identified in this investigation. It is recognized that in trimethylbenzene isomers, much of 1, 2, 4- and 1, 3, 5-isomers are contained, and almost equally[3]. But it has become clear that in trimethylcyclohexane, the content of 1, 2, 4-isomer is more than that of 1, 3, 5-isomer and 1, 2, 3-isomer is of trace. Thereafter a presence of 1, 2, 3, 5- and 1, 2, 3, 4-isomers[15] in tetramethylcyclohexane isomer is observed. They cannot be compared, however, with the corresponding tetramethylbenzene since it is not analyzed yet by the author. It was reported[27] that 1, 2, 4, 5-tetramethylcyclohexane is contained in high-temperature carbonization tar, but the result obtained in this research presents a different result. Moreover, *p*- and *m*-methylethylcyclohexane[3], which correspond to ethyltoluene isomers, are not found.

The author wishes to express his hearty thanks to Professor Sakujirô Kimura of Kyoto University, Professor Tamon Matsu'ura and Professor the late Bunkichi Masumoto of Hiroshima University and Professor Shôzô Tanaka of Kyoto University for their kind guidance and valuable advice throughout this study.

Thanks are also due to Yawata Iron & Steel Co., Ltd. for donation of the materials used

27) K. E. Schulze, *Ber.*, **18**, 3032 (1885).

for this investigation. The author is indebted to Dr. Kenji Kuratani of the University of Tokyo and Sumitomo Chemical Industries Co., Ltd. for the measurement of IR spectra.

*Department of Chemistry*
*Faculty of Science*
*Kyoto University*
*Sakyô-ku, Kyoto*

# *Studies on Constituents of Coal Carbonization Light Oil. II. On Saturated Hydrocarbons Contained in Low-temperature Coal Carbonization Light Oil*

By Hiroshi YASUI

(Received January 6, 1960)

Apparently, constituents of high-temperature coal carbonization light oil are mainly aromatic hydrocarbons and those of low-temperature coal carbonization light oil, are mainly saturated hydrocarbons[1]. But, resulting data of identification of saturated hydrocarbons in low-temperature coal carbonization light oil, are scanty. In 1955, some of them have been reported by A. Jäger and G. Kattwinkel[2] and the following results have been found. 1) The saturated hydrocarbons, contained in low-temperature coal carbonization light oil, consist mainly of straight-chain paraffins. 2) The branched-chain paraffins contained in this oil are all monomethylparaffins. 3) Contents of cycloparaffins are scanty.

Ohyama[3] reported that the neutral oil contained in low-temperature coal carbonization light oil, Ube Kôsan Co., Ltd. production, amounted to about 90 per cent and also the contents of the saturated hydrocarbon in the neutral oil to about 40 per cent. However, the constituents of the individual saturated hydrocarbons in this light oil and their contents have never been ascertained. Therefore, the author has studied on the constituents of the saturated hydrocarbons contained in this oil and found five straight-chain hydrocarbons (*n*-hexane, *n*-heptane, *n*-octane, *n*-nonane and *n*-decane) and five branched-chain hydrocarbons (2-methylhexane, 2-methylheptane, 2-methyloctane, 2-methylnonane and 3-methylnonane) and four cycloparaffins (cyclohexane, methylcyclohexane, 1, 3-dimethylcyclohexane and 1, 3, 5-trimethylcyclohexane) and determined their contents approximately and compared them with the result obtained in a previous paper[4].

1) M. Vahrman, *J. Appl. Chem.*, 2, 532 (1952).
2) A. Jäger und G. Kattwinkel, *Erdöl und Köhle*, 9, 629, 706 (1955).
3) G. Ohyama, "Studies on Ube Coal (Ube-tan no Seijô to Gôsei-yô Gasu oyobi Teion-târu no Seizô to Shori)", Ube Kôsan Co., Ltd., Japan (1951), p. 200.

## Experimental

**Materials.**—Residual oil after extraction of acidic and basic oils in low-temperature coal carbonization light oil (carbonization temperature, 780°C) manufactured by Ube Kôsan Co., Ltd. in August, 1954, with dilute sulfuric acid and alkaline solution, brown colored, was used. This oil kept in a glass reagent bottle for some years and precipitation, amounting to about 1.5 per cent of this oil, was produced. The oil, removing the precipitation by filtration, had a boiling range of 92~265°C, $d_4^{25}=0.8062$ and $n_D^{25}=1.456$. The contents of olefinic, aromatic and saturated hydrocarbons in this oil, were determined to be olefins 9.5 per cent (volume absorbed by 80% $H_2SO_4$), aromatics 49 per cent (volume absorbed by 98% $H_2SO_4$) and saturated hydrocarbons 41.5 per cent (residue) by sulfuric acid absorption method.

**Separation of the Saturated Hydrocarbon Oil.**—Olefinic and aromatic hydrocarbons contained in 320 g. of the material, were removed by extracting with concentrated sulfuric acid. The residual oil was washed by water, neutralized with 10 per cent sodium hydroxide solution, rewashed similarly and dried with calcium chloride to obtain 148 g. of crude saturated hydrocarbon oil (46.2 per cent by weight of the material). This oil was fractionated and 100 g. of 98~220°C fraction, which had $d_4^5=0.7403$ and $n_D^{25}=1.417$, and 45 g. of residual oil, were obtained. Residual aromatic hydrocarbons in 100 g. of 98~220°C fraction, were again removed completely with concentrated sulfuric acid and washed with water and neutralized with alkaline solution and rewashed similarly and dried with calcium chloride and 89 g. (27.8 per cent by weight of the material) of saturated hydrocarbon oil

4) H. Yasui, This Bulletin, 33, 1493 (1960).

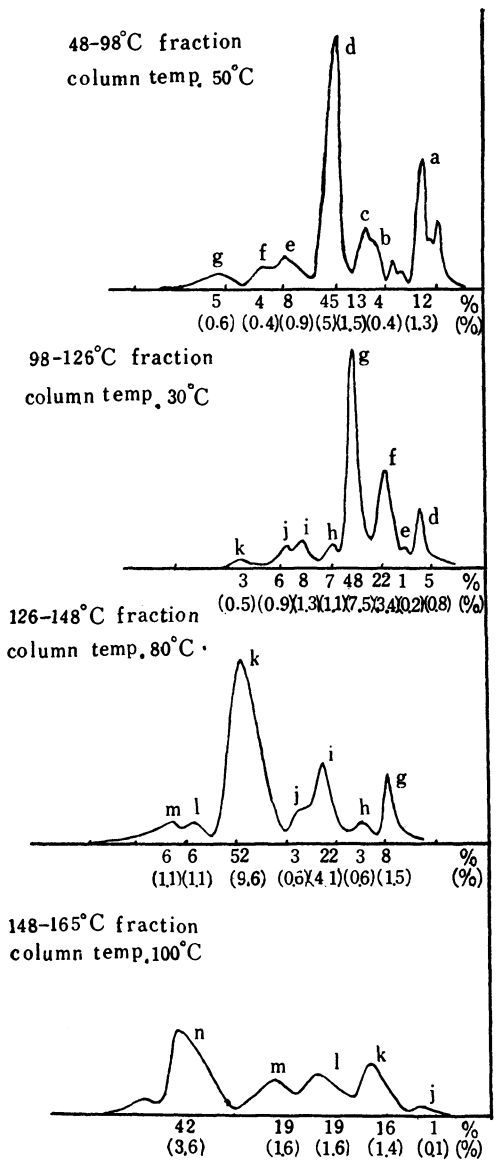



Fig. 1. Gas chromatograms of each fraction. $H_2$ flow rate 100 ml./min.

a ····· *n*-Hexane
b ····· Cyclohexane
c ····· 2-Methylhexane
d ····· *n*-Heptane
e ····· Methylcyclohexane
f ····· 2-Methylheptane
g ····· *n*-Octane
h ····· 1,3-Dimethylcyclohexane
i ····· 2-Methyloctane
j ····· 1,3,5-Trimethylcyclohexane
k ····· *n*-Nonane
l ····· 2-Methylnonane
m ····· 3-Methylnonane
n ····· *n*-Decane
% ····· Per cent of contents to each fraction
(%) ··· Per cent of contents to Sample A

(Sample A), which had $d_4^{25}=0.7397$ and $n_D^{25}=1.414$, was obtained. 87 g. (110 ml.) of this oil was submitted to fractional distillation by Podbielniak equipment with metallic sodium and five fractions shown in Table I, were obtained.

Table I. Fractions obtained by fractional distillation of 87 g. of sample A

| Frac. °C | Main frac. °C | g. | Wt. % | $d_4^{25}$ | $n_D^{25}$ |
|---|---|---|---|---|---|
| 48～ 98 | 87～ 98 | 9.6 | 11.1 | 0.6877 | 1.389 |
| 98～126 | 114～121 | 13.6 | 15.6 | 0.7146 | 1.401 |
| 126～148 | 135～145 | 16.2 | 18.6 | 0.7340 | 1.409 |
| 148～165 | 150～164 | 7.5 | 8.6 | 0.7478 | 1.416 |
| 165～184 | 169～184 | 4.5 | 5.1 | 0.7481 | 1.422 |
| Residue | — | 34.4 | 39.5 | 0.7924 | 1.442 |

Analyses were carried out on 48～98°C, 98～126°C, 126～148°C and 148～165°C fractions in Table I.

**Gas Chromatographic Analysis.**—Gas chromatographic analysis of 48～98°C, 98～126°C, 126～148°C and 148°～165°C fractions was performed with a Perkin-Elmer vapor fractometer. Hydrogen was used as carrier gas and di-*n*-decylphthalate was used as liquid substrate. The identification of the peak in the chromatograms was based on synthetic hydrocarbon data. The retention time of hydrocarbons contained in these fractions was obtained from each synthetic hydrocarbon and comparing the retention times of the peak chromatogram of each synthetic hydrocarbon under identical conditions. Contents of the hydrocarbons in these fractions were calculated from the area of each measurable peak.

**Identification of *n*-Paraffn.**—*n*-Paraffins in these fractions were isolated by means of urea adducts[5]. According to the estimation *n*-paraffin was contained about 50 per cent in each fraction. It was added to urea (about three times in weight of the *n*-paraffin) moistened with methanol (about a fifth of the weight of the urea used). The suspension was stirred for 30 min. at 0°C in 98～126°C, or 20°C in 126～148°C and 148～165°C fractions, and filtered, and unreacted oils were removed. The mixture of urea adduct obtained and the residual urea was washed with anhydrous ether, removed under reduced pressure, decomposed with water, and oil (*n*-paraffin) was obtained. Unreacted oil was once more added to urea moistened with methanol and treated as mentioned above until no more oil (*n*-paraffin) was obtained by decomposition with water of urea adduct. The result was shown in Table II. As stated by the author[4] and Kuwata and co-workers[6] previously, it is difficult to isolate *n*-hexane and *n*-heptane expected to be contained mainly in 48～98°C fraction. Therefore this method was not employed.

**IR Spectra of Oils Obtained by Decomposition with Water of Urea Adducts.**—IR spectra of 48～98°C fraction and oils isolated by decomposition

5) J. Zimmerschied et al., *Ind. Eng. Chem.*, **42**, 1300 (1950).
6) T. Kuwata, Y. Mizutani and E. Tamura, *J. Chem. Soc. Japan, Ind. Chem. Sec.* (*Kogyo Kagaku Zasshi*) **55**, 799 (1952).

TABLE II. ISOLATION OF *n*-PARAFFIN BY UREA ADDUCTS IN 98～126°, 126～148° AND 148～165°C FRACTION

| Fraction | | Oil isolated by urea adduct (*n*-paraffin) | | | | | Residual oil | |
|---|---|---|---|---|---|---|---|---|
| °C | g. | g. | % | b. p., °C | $d_4^{25}$ | $n_D^{25}$ | g. | % |
| 98～126 | 12 | 5.5 | 46 | 120～124 | 0.6983 | 1.396 | 5 | 42 |
| 126～148 | 14 | 6.5 | 54 | 142～151 | 0.7111 | 1.405 | 6.5 | 32 |
| 148～165 | 6.5 | 3.0 | 46 | 152～170 | 0.7248 | 1.410 | 2.2 | 34 |

with water of urea adducts of 98～126°C, 126～148°C and 148～165°C fractions, were measured with an Oh'yô Kôken infrared spectrophotometer.

**48～98°C Fraction.** — In IR spectrum bands of this fraction, those of *n*-hexane (wavelengths; 7.45, 7.73, 8.02, 8.20, 8.6, 8.79, 9.38, 9.46, 9.86, 9.95, 10.29, 11.04, 11.24, 11.31, 11.51, 12.13, 12.6, 12.94, 13.18, 13.78 $\mu$), *n*-heptane (wavelengths; 7.45, 7.68, 7.81, 8.09, 8.27, 8.78, 9.3, 9.79, 10.4, 10.74, 11.1, 11.42, 11.57, 12.01, 12.91, 13.54 13.83 $\mu$), 2-methylhexane (wavelengths; 7.3, 7.41, 7.71, 7.97, 8.18, 8.53, 8.73, 9.3, 9.53, 9.7, 9.85, 10.46, 10.63, 11.0, 11.17, 12.16, 12.81, 13.74 $\mu$), 2-methylheptane (wavelengths; 7.32, 7.46, 7.67, 8.05, 8.28, 8.54, 8.74, 9.22, 9.56, 9.98, 10.41, 10.53, 10.71, 10.88, 11.2, 11.94, 12.31, 13.04, 13.26, 13.81 $\mu$), cyclohexane (wavelengths; 7.4, 7.95, 8.7, 9.1, 9.6, 9.9, 11.1, 11.68 $\mu$) and methylcyclohexane (wavelengths; (7.28, 7.44, 7.69, 8.02, 8.62, 9.06, 9.7, 10.38, 11.02, 11.49, 11.87 $\mu$) were observed.

**Oil Isolated by Decomposition with Water of the Urea Adduct of 98～126°C Fraction.**—Physical constants (Table II) of this oil were analogous to those of *n*-octane[7] (b. p. 125.6°C, $d_4^{20}=0.703$, $n_D^{20}=1.397$). In IR spectrum bands of this oil, those of *n*-heptane, *n*-octane (wavelengths; 7.46, 7.68, 7.87, 8.16, 8.33, 8.8, 9.27, 9.65, 9.95, 10.34, 10.92, 11.1, 11.21, 11.4, 11.84, 12.6, 13.08, 13.52, 13.85 $\mu$) and *n*-nonane (wavelengths; 7.46, 7.67, 7.94, 8.22, 8.81, 9.2, 9.41, 9.58, 10.29, 10.79, 11.22, 11.4, 11.84, 12.05, 12.89, 13.29, 13.86 $\mu$) were observed.

**Oil Isolated by Decomposition with Water of the Urea Adduct of 126～148°C Fraction.**—Physical constants (Table II) of this oil were analogous to those of *n*-nonane[7] (b. p. 150.7°C, $d_4^{20}=0.7111$, $n_D^{20}=1.405$), and in IR spectrum bands of this oil, those of *n*-nonane and *n*-octane were observed.

**Oil Isolated by Decomposition with Water of the Urea Adduct of 148～165°C Fraction.**—Physical constants (Table II) of this oil denoted the values between those of *n*-nonane and *n*-decane[7] (b. p. 174°C, $d_4^{20}=0.7298$, $n_D^{20}=1.412$), and therefore the fraction was expected to be a mixture of *n*-nonane and *n*-decane. In IR spectrum bands of this oil, those of *n*-nonane and *n*-decane (wavelengths; 7.26, 7.45, 7.67, 7.82, 8.01, 8.25, 8.81, 9.16, 9.29, 9.92, 10.05, 10.86, 11.15, 11.83, 12.28, 13.0, 13.85 $\mu$) were observed.

**Gas Chromatographic Analysis.** — The gas chromatographic analysis of oils, obtained by decomposition with water of urea adducts of 98～126°C, 126～148°C and 148～165°C fraction, was performed and chromatograms of these oils were shown in Fig. 2.

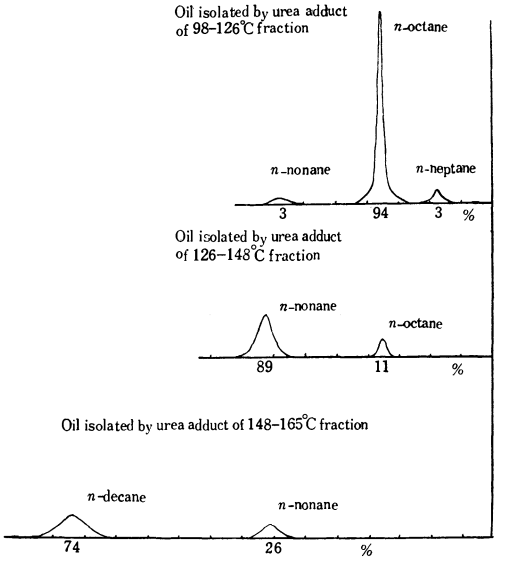



Fig. 2. Gas chromatograms of oils obtained by decomposition with water of urea adducts of each fraction.
Column temp., 100°C; $H_2$ flow rate, 98.6 ml./min.

**Identification of Cycloparaffin and Isoparaffin—IR Spectra.**—IR spectra of residual oils, in 98～126°C, 126～148°C and 148～165°C fractions, are measured with an Oh'yô Kôken spectrophotometer.

**Residual Oil in 98～126°C Fraction Shown in Table II.**—Physical constants of this oil are b. p. 110～125°C, $d_4^{25}=0.7218$, $n_D^{25}=1.404$. In IR spectrum bands of this oil, those of 2-methylheptane, 2-methyloctane (wavelengths; 7.6, 7.67, 7.86, 8.15, 8.33, 8.54, 9.14, 9.3, 9.4, 9.77, 10.18, 10.55, 10.9, 11.25, 11.42, 12.15, 12.7, 13.5, 13.8 $\mu$), 1,3-dimethylcyclohexane (wavelengths; 7.25, 7.66, 7.88, 8.36, 8.6, 8.96, 9.28, 9.45, 10.0, 10.2, 10.53, 10.71, 11.43, 11.72, 12.13 $\mu$) and 1,3,5-trimethylcyclohexane (wavelengths; 7.52, 7.92, 8.53, 8.87, 8.96, 9.35, 9.56, 9.66, 10.0, 10.63, 10.74, 11.84, 11.91, 12.78 $\mu$) were observed.

**Residual Oil in 126～148°C Fraction Shown in Table II.**—Physical constants of this oil are b. p. 139～151°C, $d_4^{25}=0.7406$ and $n_D^{25}=1.414$. In IR spectrum bands of this oil, those of 2-methyloctane, 1,3-dimethylcyclohexane, 2-methylnonane (wavelengths; 7.67, 7.93, 8.21, 8.40, 8.54, 8.76, 9.12, 9.4, 10.07, 10.4, 10.65, 10.9, 11.1, 11.48, 12.0,

7) G. Egloff, "Physical Constants of Pure Hydrocarbons", Vol. I, Reinhold Publ. Corp., New York (1939), p. 49.

12.32, 13.05, 13.6, 13.81 $\mu$), 3-methylnonane (wavelengths; 7.67, 7.83, 8.16, 8.36, 8.66, 9.12, 9.43, 9.94, 11.28, 11.79, 12.2, 12.78, 12.96, 13.6, 13.8 $\mu$) and 1,3,5-trimethylcyclohexane, were observed.

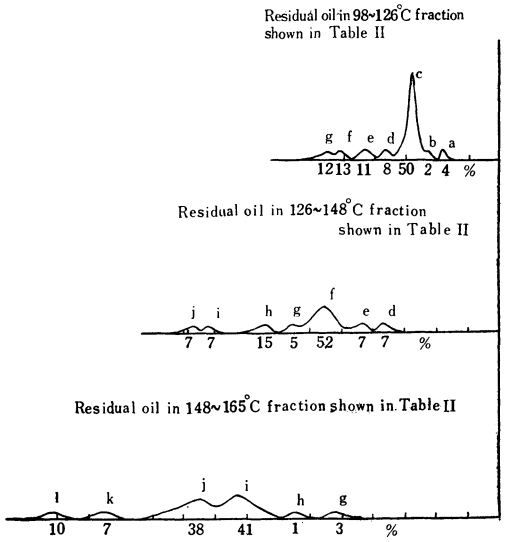



Fig. 3. Gas chromatograms of residual oils in each fraction. Column temp. 100°C; $H_2$ flow rate 98.6 ml./min.

a ····· *n*-Heptane
b ····· Methylcyclohexane
c ····· 2-Methylheptane
d ····· *n*-Octane
e ····· 1,3-Dimethylcyclohexane
f ····· 2-Methyloctane
g ····· 1,3,5-Trimethylcyclohexane
h ····· *n*-Nonane
i ····· 2-Methylnonane
j ····· 3-Methylnonane
k ····· *n*-Decane

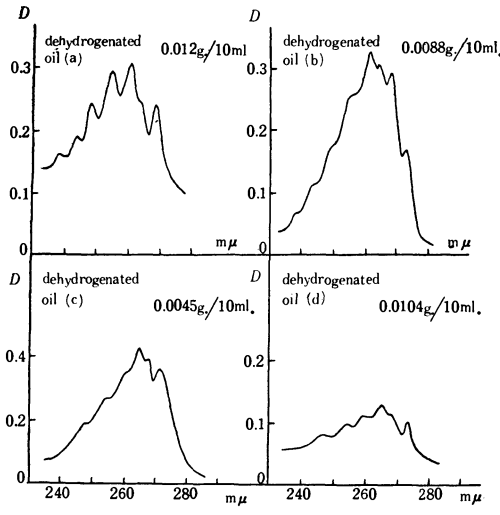



Fig. 4. Ultraviolet spectra of dehydrogenated oils.

**Residual Oil in 148~165°C Fraction Shown in Table II.**—Physical constants of this oil are b. p. 148~164°C, $d_4^{25}=0.7673$ and $n_D^{25}=1.425$. In IR spectrum bands of this oil, those of 2-methylnonane, 3-methylnonane and 1,3,5-trimethylcyclohexane were observed.

**Gas Chromatographic Analysis.**—Gas chromatographic analysis of residual oils, in 98~126°C, 126~148°C and 148~165°C fractions was performed and the chromatograms were shown in Fig. 3.

**Dehydrogenation[4,8].** — Dehydrogenation of 48~98°C fraction (a) and residual oils (b), (c) and (d) in 98~126°C, 126~148°C and 148~165°C fractions shown in Table II, was carried out with Pt-C catalyst prepared by the method described previously[4], at 290~300°C repeatedly, until no hydrogen was producible and by this method, cycloparaffins contained in these fractions were changed to corresponding aromatic hydrocarbons. The result was shown in Table III.

TABLE III. DEHYDROGENATION
REAC. TEMP. 290~300°C; DROPPING VELOCITY 5~6 g./hr.

| Sample | g. | Dehydrogenated oil g. | Gas produced ml. (N. T. P.) | $H_2$* ml. (N. T. P.) |
|---|---|---|---|---|
| (a) | 4 | 2.8 | 284.8 | 263.5 |
| (b) | 4 | 3.0 | 632.9 | 623.8 |
| (c) | 2 | 1.3 | 144.1 | 136.5 |
| (d) | 2 | 1.5 | 48.1 | 40.6 |

* The gas produced by dehydrogenation was analyzed by the Hempel method, and the volume of hydrogen produced was the volume of the gas removed of that of air.

**Identification of Aromatic Hydrocarbons Produced by Dehydrogenation. — Ultraviolet Spectra of the Dehydrogenated Oils.** — Ultraviolet spectra of dehydrogenated oils, dissolved in purified ethanol, were measured with a Beckman spectrophotometer model DU, and were shown in Fig. 4.

**Nitration of Dehydrogenated Oil[9].** — Dehydrogenated oil was added to a mixture of 1 vol. of concentrated nitric acid and 2 vol. of concentrated sulfuric acid and shaken, then boiled for five minutes and poured into cold water, and crude nitro-compounds were obtained. These compounds were separated by fractional recrystallization from ethanol solution, obtaining pure nitro-compounds. The result was shown in Table IV.

From Fig. 3 and Table IV, aromatic hydrocarcons produced by dehydrogenation were confirmed, and their original cycloparaffins and the ratio of their contents were estimated as shown in Table V.

8) E. Berl and W. Koerber, *Ind. Eng. Chem., Anal. Ed.*, 12, 175 (1940).
9) S. P. Mulliken, "A Method for the Identification of Pure Organic Compounds", Vol. I, John Wiley & Sons Inc., New York, p. 200.

TABLE IV. NITRO-COMPOUNDS OBTAINED BY NITRATION OF DEHYDROGENATED OILS

| | Dehydrogenated oil | Nitro-compound: Obtained | | | Nitro-compound: Referred[9] | |
|---|---|---|---|---|---|---|
| | | Crude | Recrystallized | M. p. | Compound | M. p. |
| | g. | g. | g. | °C | | °C |
| (a) | 1.0 | 0.3 | 0.04 | 87~ 90 | *m*-Dinitrobenzene | 90 |
| | | | 0.11 | 67~ 69 | 2,4-Dinitrotoluene | 70 |
| (b) | 1.0 | 0.2 | 0.22 | 66~ 68 | 〃 | 〃 |
| | | | 0.04 | 177~179 | 2,4,6-Trinitro-*m*-xylene | 179 |
| | | | 0.03 | 228~231 | 2,4,6-Trinitro-1,3,5-trimethylbenzene | 232 |
| (c) | 0.75 | 0.2 | 0.03 | 177~180 | 2,4,6-Trinitro-*m*-xylene | 179 |
| | | | 0.04 | 228~232 | 2,4,6-Trinitro-1,3,5-trimethylbenzene | 232 |
| (d) | 1.0 | 0.04 | 0.02 | 230~232 | 〃 | 〃 |

TABLE V. CYCLOPARAFFINS CONTAINED IN (a), (b), (c) AND (d)

| | Cycloparaffin | Ratio* |
|---|---|---|
| (a) | Cyclohexane | 1 |
| | Methylcyclohexane | 3 |
| (b) | Methylcyclohexane | 2 |
| | 1,3-Dimethylcyclohexane | 4 |
| | 1,3,5-Trimethylcyclohexane | 3 |
| (c) | 1,3-Dimethylcyclohexane | 3 |
| | 1,3,5-Trimethylcyclohexane | 4 |
| (d) | 1,3,5-Trimethylcyclohexane | |

* The ratio of cycloparaffins contained in each fraction was calculated from weights of nitro-compounds obtained.

## Results and Discussion

Saturated hydrocarbons identified from the low-temperature coal carbonization light oil produced at Ube Kôsan Co. Ltd. in this research are given below.

It has become clear, that the constituents of the saturated hydrocarbons, contained in this oil, consist of five straight-chain hydrocarbon (*n*-hexane, *n*-heptane, *n*-octane, *n*-nonane and *n*-decane) and five branched-chain hydrocarbon (2-methylhexane, 2-methylheptane, 2-methyloctane, 2-methylnonane and 3-methylnonane) and four cycloparaffins (cyclohexane, methylcyclohexane, 1,3-dimethylcyclohexane and 1,3,5-trimethylcyclohexane). Moreover, percentage of their contents in the saturated hydrocarbon oil (Sample A) separated from the material, is given in the gas chromatograms shown in Fig. 1, and Table VI.

The following observation is based on a study of the data presented in Table VI.

1) Saturated hydrocarbons, contained in the low-temperature coal carbonization light oil, are composed of about 91 per cent of saturated aliphatic hydrocarbon and about 9 per cent of cycloparaffinic hydrocarbon.

2) Saturated aliphatic hydrocarbons contained in this oil, are composed of two parts of *n*-paraffins and one part of isoparaffins.

3) The isoparaffins are all monomethylparaffins and these monomethylparaffins are nearly all 2-methylparaffins.

Comparing the saturated hydrocarbons, contained in high-temperature coal carbonization

TABLE VI. SATURATED HYDROCARBONS IDENTIFIED AND PERCENTAGE OF THEIR CONTENTS IN SAMPLE A

| *n*-Paraffin | | Isoparaffin | | Cycloparaffin | |
|---|---|---|---|---|---|
| Compound | % | Compound | % | Compound | % |
| *n*-Hexane | 1.3 | 2-Methylhexane | 1.5 | Cyclohexane | 0.4 |
| *n*-Heptane | 5.8 | 2-Methylheptane | 3.8 | Methylcyclohexane | 1.1 |
| *n*-Octane | 9.6 | 2-Methyloctane | 5.4 | 1,3-Dimethylcyclohexane | 1.7 |
| *n*-Nonane | 11.5 | 2-Methylnonane | 2.7 | 1,3,5-Trimethylcyclohexane | 1.6 |
| *n*-Decane | 3.6 | 3-Methylnonane | 2.7 | | |
| Total | 31.8 | Total | 16.1 | Total | 4.8 |

light oil produced at Yawata Iron & Steel Co. Ltd., and identified by the author[4], with those identified in this investigation, the following observations are made.

1) Saturated hydrocarbons identified from both low-temperature and high-temperature coal carbonization light oils, consist mainly of saturated aliphatic hydrocarbons of 90 per cent saturated hydrocarbons in low-temperature coal carbonization light oil, and about 85 per cent in high-temperature coal carbonization light oil.

2) In low-temperature coal carbonization light oil, the ratio of contents of *n*-paraffins and isoparaffins is about 2 : 1. In high-temperature coal carbonization light oil, about 1 : 1.5.

3) Isoparaffins, contained in low- and high-temperature coal carbonization light oils, are all monomethylparaffins, and those contained in low-temperature coal carbonization light oil are all 2-methylparaffins, except 3-methylnonane, and the monomethylparaffins contained in high-temperature coal carbonization light oil, consist of 3-methylparaffins and 4-methylparaffins except 2-methylheptane.

F. D. Rossini and B. J. Mair[10] studying the saturated hydrocarbons contained mainly in U. S. A. Mid-Continent, Ponca petroleum concluded that the saturated hydrocarbons consisted mainly of saturated aliphatic hydrocarbons, which contains a large quantity of *n*-paraffin and monomethylparaffin and a trace of branched paraffin which has many branchings. This conclusion is analogous to that of the present studies on saturated hydrocarbons contained in coal carbonization light oil.

The author wishes to express his hearty thanks to Professor Sakujirô Kimura of Kyoto University, Professor Tamon Matsu'ura and the late Professor Bunkichi Masumoto of Hiroshima University and Professor Shôzô Tanaka of Kyoto University for their kind guidance and valuable advice throughout this study.

Thanks are also due to Ube Kôsan Co. Ltd. for donation of the materials used for this investigation. The author is indebted to Yawata Chemical Industries Co. Ltd. for the measurement of gas chromatograms.

*Dapartment of Chemistry*
*Faculty of Science*
*Kyoto University*
*Sakyô-ku, Kyoto*

10) F. D. Rossini and B. J. Mair, *Ind. Eng. Chem. D. S.*, 3, 141 (1958).

# *Thermodynamic Studies on Cobalt Complexes. VI. Solubility of Nitropentamminecobalt(III), cis- and trans-Dinitrotetramminecobalt(III) and Trinitrotriamminecobalt(III) Complexes**

By Motoshichi MORI, Ryokichi TSUCHIYA and Hiroshi FUKUDA

(Received May 11, 1960)

Thermodynamic discussion of the monoacidopentamminecobalt(III) complexes which have $Cl^-$, $NO_3^-$ or $Br^-$ as the anionic ligand was carried out in the preceding paper[1]. In the present study the discussion is extended to the cobalt(III) complexes which have one, two or three nitro groups in the coordination sphere. Solubilities of nitropentamminecobalt(III) chloride, nitrate, bromide and perchlorate, *cis*- and *trans*-dinitrotetramminecobalt(III) chlorides and trinitrotriamminecobalt(III) complex were measured, and the standard free energies of their formation were calculated. The thermodynamic stability of the complexes formed by the substitution of ammonia by one, two or three nitro groups was also discussed.

## Experimental

Nitropentamminecobalt(III) chloride was prepared by the method of Jörgensen[2]. The nitrate, bromide and perchlorate were precipitated by nitric acid ammonium bromide and perchloric acid respectively from the aqueous solution of the

* Read at the 13th Annual Meeting of the Chemical Society of Japan, Tokyo April, 1960.

1) M. Mori and R. Tsuchiya, This Bulletin, 33, 841 (1960).

2) S. M. Jörgensen, *Z. anorg. Chem.*, 17, 463 (1898).

chloride. *cis*- and *trans*-Dinitrotetramminecobalt (III) chlorides and trinitrotriamminecobalt(III) were also prepared by the method of Jörgensen[2-4].

The solubility in the saturated aqueous solution was measured colorimetrically by means of a Hitachi EPU-2 spectrophotometer. Since these nitro-complexes are unstable towards light, equilibrium of the solution was attained in a brown flask immersed in the thermostat to prevent the photo-decomposition.

## Results and Calculation

**Solubility of Nitropentamminecobalt(III) Complexes.** — The results obtained for nitropentamminecobalt(III) chloride, nitrate, bromide and perchlorate are listed in Tables I—IV.

The equilibrium of nitropentamminecobalt-(III) complex in water is expressed by,

$$[Co(NH_3)_5NO_2]X_2(s) = [Co(NH_3)_5NO_2]^{2+}(aq.) + 2X^-(aq.)$$

where X is an anion. If the activities of the cation, the anion and their activity coefficients are expressed by $a_{[Co(NH_3)_5NO_2]^{2+}}$, $a_{X^-}$, $\gamma_{[(Co(NH_3)_5NO_2]^{2+}}$ and $\gamma_{X^-}$ respectively, the equilibrium constant, $K$, is given by

$$K = a_{[Co(NH_3)_5NO_2]^{2+}} \cdot a^2_{X^-} = (m\gamma_{[Co(NH_3)_5NO_2]^{2+}})(2m\gamma_{X^-})^2 = 4m^3\gamma_{[Co(NH_3)_5NO_2]^{2+}} \cdot \gamma^2_{X^-}$$

where $m$ is the solubility in molality. When the mean activity coefficient is expressed by $\gamma_\pm$, the equilibrium constant is given by

$$K = 4m^3\gamma^3_\pm \quad (1)$$

The mean activity coefficient is calculated by the following formula[5] which gives the activity

Table I. Equilibrium of solution for nitropentamminecobalt(III) chloride

| Temp. (°C) | Solubility (Molality $m$) | $1/T\times10^3$ | $\gamma_\pm$ | $K\times10^4$ | log $K$ |
|---|---|---|---|---|---|
| 10.8 | 0.0902 | 3.521 | 0.514 | 3.99 | $\bar{4}$.601 |
| 15 | 0.107 | 3.471 | 0.497 | 6.02 | $\bar{4}$.780 |
| 20 | 0.117 | 3.412 | 0.489 | 7.49 | $\bar{4}$.874 |
| 25 | 0.145 | 3.355 | 0.471 | 12.74 | $\bar{3}$.105 |
| 30 | 0.160 | 3.299 | 0.461 | 16.05 | $\bar{3}$.205 |

Table II. Equilibrium of solution for nitropentamminecobalt(III) nitrate

| Temp. (°C) | Solubility (Molality $m$) | $1/T\times10^3$ | $\gamma_\pm$ | $K\times10^5$ | log $K$ |
|---|---|---|---|---|---|
| 10.8 | 0.0301 | 3.521 | 0.623 | 2.64 | $\bar{5}$.422 |
| 15 | 0.0345 | 3.471 | 0.600 | 3.55 | $\bar{5}$.550 |
| 20 | 0.0419 | 3.412 | 0.590 | 6.04 | $\bar{5}$.781 |
| 25 | 0.0531 | 3.355 | 0.566 | 10.86 | $\bar{4}$.036 |
| 30 | 0.0591 | 3.299 | 0.555 | 14.12 | $\bar{4}$.150 |

Table III. Equilibrium of solution for nitropentamminecobalt(III) bromide

| Temp. (°C) | Solubility (Molality $m$) | $1/T\times10^3$ | $\gamma_\pm$ | $K\times10^4$ | log $K$ |
|---|---|---|---|---|---|
| 10.8 | 0.0360 | 3.521 | 0.605 | 4.13 | $\bar{5}$.616 |
| 15 | 0.0421 | 3.471 | 0.589 | 6.10 | $\bar{5}$.785 |
| 20 | 0.0495 | 3.412 | 0.573 | 9.13 | $\bar{5}$.960 |
| 25 | 0.0587 | 3.355 | 0.556 | 13.91 | $\bar{4}$.143 |
| 30 | 0.0693 | 3.299 | 0.540 | 20.96 | $\bar{4}$.321 |

Table IV. Equilibrium of solution for nitropentamminecobalt(III) perchlorate

| Temp. (°C) | Solubility (Molality $m$) | $1/T\times10^4$ | $\gamma_\pm$ | $K\times10^4$ | log $K$ |
|---|---|---|---|---|---|
| 10.8 | 0.0762 | 3.521 | 0.537 | 2.74 | $\bar{4}$.438 |
| 15 | 0.101 | 3.471 | 0.511 | 5.50 | $\bar{4}$.740 |
| 20 | 0.128 | 3.412 | 0.494 | 10.11 | $\bar{3}$.005 |
| 25 | 0.168 | 3.355 | 0.469 | 19.57 | $\bar{3}$.292 |
| 30 | 0.202 | 3.299 | 0.452 | 30.45 | $\bar{3}$.484 |

3) S. M. Jörgensen, ibid., **17**, 473 (1898).
4) S. M. Jörgensen, ibid., **17**, 469 (1898).
5) J. Kielland, *J. Am. Chem. Soc.*, **59**, 1675 (1937).

coefficient of an ion,

$$\log \gamma_{\text{ion}} = \frac{-0.358z^2\sqrt{2\omega}}{1+0.2325\times10^8 a\sqrt{2\omega}} - \log(1+0.018\,\nu m)$$

where $z$ is the charge of the ion, $\omega$, the ionic strength of the solution, $a$, the closest distance between an ion and another one and $\nu$, the number of ions dissociated from one molecule of the salt.

The logarithm of the equilibrium constant of the solution calculated by Eq. 1 is plotted in Fig. 1 against the reciprocal of the absolute temperature. A straight line is obtained. By the method of least squares the equations of these lines are calculated as follows:

$\log K = 6.243 - 2734/T$ for the chloride

$\log K = 7.636 - 3473/T$ for the nitrate

$\log K = 6.732 - 3156/T$ for the bromide

$\log K = 13.080 - 4715/T$ for the perchlorate

The free energy changes of solution are given as

$$\begin{aligned} \Delta G^\circ &= -RT\ln K = 12510 - 28.56\,T \\ \Delta G^\circ_{298} &= 3991 \text{ cal. for the chloride} \\ \Delta G^\circ &= 15890 - 34.93\,T \\ \Delta G^\circ_{298} &= 5477 \text{ cal. for the nitrate} \\ \Delta G^\circ &= 14440 - 30.79\,T \\ \Delta G^\circ_{298} &= 5262 \text{ cal. for the bromide} \end{aligned} \quad (2)$$

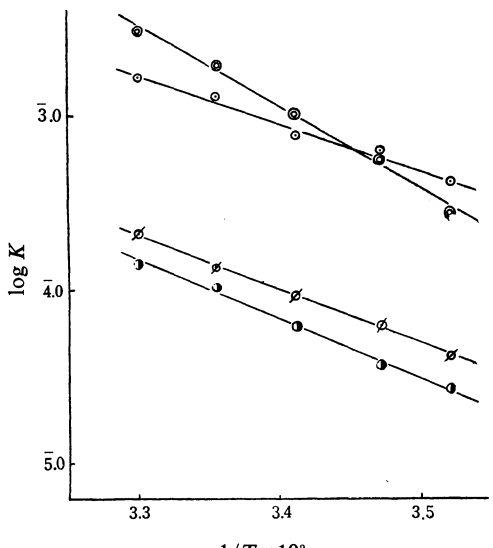



Fig. 1. The relationship between the equilibrium constant of solution and the temperature for nitropentamminecobalt-(III) chloride (⊙), nitrate (◑), bromide (Ø) and perchlorate(◎).

$$\begin{aligned} \Delta G^\circ &= 21570 - 59.84\,T \\ \Delta G^\circ_{298} &= 3728 \text{ cal. for the perchlorate} \end{aligned}$$

From these equations the heats of solution of the chloride, nitrate, bromide and perchlorate are obtained as $\Delta H = 12.51$, 15.89, 14.44 and 21.57 kcal. respectively. The entropy changes for each salt are calculated as $\Delta S^\circ =$ 28.6, 34.9, 30.8 and 59.8 e. u., respectively.

Since the standard free energy of formation of nitropentamminecobalt(III) ion in unit activity is known as $\Delta G^\circ_{f298} = -108.9$ kcal[6]. and the heat of formation as $\Delta H_f = -153.1$ kcal.[7], the relationship between the former and the absolute temperature is calculated as

$$\Delta G^\circ_f = -153100 + 148.3\,T \quad (3)$$

The free energies of formation $Cl^-$, $NO_3^-$, $Br^-$ and $ClO_4^-$ in unit activity were already obtained in the second paper[8] of this series as follows:

$$\begin{aligned} \Delta G^\circ_f &= -40020 + 29.1\,T \text{ for } Cl^- \\ \Delta G^\circ_f &= -49370 + 77.03\,T \text{ for } NO_3^- \\ \Delta G^\circ_f &= -28900 + 14.51\,T \text{ for } Br^- \\ \Delta G^\circ_f &= -31410 + 96.75\,T \text{ for } ClO_4^- \end{aligned} \quad (4)$$

Therefore the standard free energy of formation of nitropentamminecobalt(III) chloride in the solid state is calculated by Eqs. 3, 6 and 4 as

$$\begin{aligned} \Delta G^\circ_f &= -245700 + 235.1\,T \\ \Delta G^\circ_{f\,298} &= -175.6 \text{ kcal.} \end{aligned}$$

The values for the nitrate, bromide and perchlorate of the same complex were calculated by combining respective equations:

$\Delta G^\circ_f = -267700 + 337.3\,T$,

$\Delta G^\circ_{f\,298} = -167.2$ kcal., for the the nitrate

$\Delta G^\circ_f = -225300 + 208.1\,T$,

$\Delta G^\circ_{f\,298} = -163.3$ kcal., for the bromide

$\Delta G^\circ_f = -237500 + 401.6\,T$,

$\Delta G^\circ_{f\,298} = -117.8$ kcal., for the perchlorate

**Solubility of Dinitrotetramminecobalt(III) Complexes.**—The results obtained for *cis*- and *trans*-dinitrotetramminecobalt(III) chlorides are listed in Tables V and VI.

The process of solution of dinitrotetramminecobalt(III) chloride is represented by the following equation,

6) A. B. Lamb and A. T. Larson, *J. Am. Chem. Soc.*, **42**, 2038 (1920).

7) K. B. Yatsimirskii and L. L. Pankowa, *Zhur. Obshchei Khim.*, **18**, 2051 (1948); K. B. Yatsimirskii, "Thermochemie von Komplexverbindungen", Akademie-Verlag, Berlin (1956), p. 179.

8) M. Mori, R. Tsuchiya and Y. Okano, This Bulletin, **32**, 462 (1959).

Table V. Equilibrium of solution for *cis*-dintrotetramminecobalt(III) chloride

| Temp. (°C) | Solubility (Molality $m$) | $1/T\times10^3$ | $\gamma_\pm$ | $K\times10^2$ | log $K$ |
|---|---|---|---|---|---|
| 10 | 0.164 | 3.533 | 0.737 | 1.46 | $\bar{2}$.164 |
| 15 | 0.189 | 3.471 | 0.726 | 1.88 | $\bar{2}$.274 |
| 20 | 0.213 | 3.412 | 0.717 | 2.33 | $\bar{2}$.367 |
| 25 | 0.263 | 3.355 | 0.701 | 3.40 | $\bar{2}$.531 |
| 30 | 0.321 | 3.299 | 0.685 | 4.83 | $\bar{2}$.684 |

Table VI. Equilibrium of solution for *trans*-dinitrotetramminecobalt(III) chloride

| Temp. (°C) | Solubility (Molality $m$) | $1/T\times10^3$ | $\gamma_\pm$ | $K\times10^4$ | log $K$ |
|---|---|---|---|---|---|
| 10 | 0.0319 | 3.533 | 0.847 | 7.30 | $\bar{4}$.863 |
| 15 | 0.0357 | 3.471 | 0.840 | 8.99 | $\bar{4}$.954 |
| 20 | 0.0437 | 3.412 | 0.828 | 13.09 | $\bar{3}$.117 |
| 25 | 0.0521 | 3.355 | 0.817 | 18.12 | $\bar{3}$.258 |
| 30 | 0.0627 | 3.299 | 0.805 | 25.48 | $\bar{3}$.407 |

$$[Co(NH_3)_4(NO_2)_2]Cl(s) = [Co(NH_3)_4(NO_2)_2]^+(aq.) + Cl^-(aq.)$$

When the activities of the cation, the anion and their activity coefficients are expressed by $a_{[Co(NH_3)_4(NO_2)_2]^+}$, $a_{Cl^-}$, $\gamma_{[Co(NH_3)_4(NO_2)_2]^+}$ and $\gamma_{Cl^-}$ respectively, the equilibrium constant of solution, $K$, is given as

$$K = a_{[Co(NH_3)_4(NO_2)_2]^+}\cdot a_{Cl^-} = (m\gamma_{[Co(NH_3)_4(NO_2)_2]^+})(m\gamma_{Cl^-}) = m^2\gamma_{[Co(NH_3)_4(NO_2)_2]^+}\cdot\gamma_{Cl^-} = m^2\gamma^2_\pm,$$

$m$ and $\gamma_\pm$ being the solubility in molality and the mean activity coefficient.

The plots of the logarithm of the above equilibrium constant against the reciprocal of the absolute temperature are given in Fig. 2 as straight lines for both salts. The straight lines are expressed by the following equations:

$$\log K = 5.970 - 2215/T$$

*cis*-$[Co(NH_3)_4(NO_2)_2]Cl$

$$\log K = 5.234 - 2376/T$$

*trans*-$[Co(NH_3)_4(NO_2)_2]Cl$

The free energy changes of solution are given as for the cis salt,

$$\Delta G^\circ = 9111 - 23.87\,T, \quad \Delta G^\circ_{298} = 1995 \text{ cal.} \quad (5)$$

and for the trans salt,

$$\Delta G^\circ = 9556 - 19.42\,T, \quad \Delta G^\circ_{298} = 3767 \text{ cal.} \quad (6)$$

From these equations $\Delta H = 10.13$ kcal. and $\Delta H = 10.87$ kcal. are obtained as the heats of solution of the cis and trans salts respectively and $\Delta S^\circ = 27.3$ e. u. and $\Delta S^\circ = 23.9$ e. u. are obtained as the entropy changes of the cis and trans salts respectively.

Since the energies of formation of *cis*- and *trans*-dinitrotetramminecobalt(III) ions in unit activity are known as $\Delta G^\circ_{f298} = -164.7$ kcal. and $\Delta G^\circ_{f298} = -161.4$ kcal[6]. and their heat of formation as $\Delta H_f = -159.9$ kcal. and $\Delta H_f = -159.1$ kcal[9]. respectively, the relationships between the free energies of formation and the absolute temperature are calculated for the cis salt as,

$$\Delta G^\circ_f = -159900 - 16.10\,T \quad (7)$$

and for the trans salt as,

$$\Delta G^\circ_f = -159100 - 7.72\,T \quad (8)$$

Then the free energy of formation of *cis*-dinitrotetramminecobalt(III) chloride in the solid state is calculated by Eqs. 4, 5 and 7 as

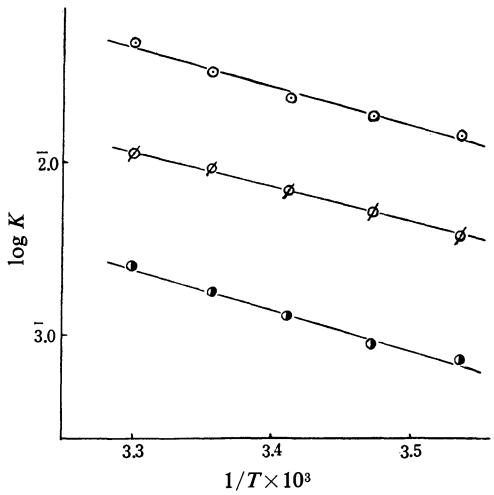



Fig. 2. The relationship between the equilibrium constant of solution and the temperature for *cis*-dinitrotetramminecobalt(III) chloride (⊙), corresponding *trans*-chloride (◑) and trinitrotriamminecobalt(III) complex (∅).

9) K. B. Yatsimirskii and L. L. Pankowa, *Zhur. Obshchei Khim.*, **19**, 623 (1949); K. B. Yatsimirskii, "Thermochemie von Komplexverbindungen", Akademie-Verlag, Berlin (1956), pp. 179, 180.

TABLE VII. EQUILIBRIUM OF SOLUTION FOR TRINITROTRIAMMINECOBALT(III) COMPLEX

| Temp. (°C) | Solubility (Molality $m\times10^3$) | $1/T\times10^3$ | $K\times10^3$ | log $K$ |
|---|---|---|---|---|
| 10 | 3.88 | 3.533 | 3.88 | $\bar{3}.588$ |
| 15 | 5.18 | 3.471 | 5.18 | $\bar{3}.714$ |
| 20 | 6.96 | 3.412 | 6.96 | $\bar{3}.843$ |
| 25 | 9.15 | 3.355 | 9.15 | $\bar{3}.961$ |
| 30 | 11.19 | 3.299 | 11.19 | $\bar{2}.049$ |

$$\Delta G_f^\circ = -210100+40.3\ T,$$
$$\Delta G_{f\,298}^\circ = -198.0 \text{ kcal.}$$

and that of *trans*-dinitrotetramminecobalt(III) chloride by Eqs. 4, 6 and 8 as

$$\Delta G_f^\circ = -210000+45.3\ T,$$
$$\Delta G_{f\,298}^\circ = -196.5 \text{ kcal.}$$

**Solubility of Trinitrotriamminecobalt(III) Complex.** — The results obtained for trinitrotriamminecobalt(III) complex is listed in Table VII.

When the solubility in molality of this complex is expressed by $m$, the equilibrium constant of the solution, $K$, is given by $K=m$. The relationship between the logarithm of $K$ and temperature is shown in Fig. 2 and it is expressed by the equation as below:

$$\log K = 4.696 - 2008/T.$$

The heat of solution is $\Delta H=9.19$ kcal. The free energy change of solution is given as,

$$\Delta G^\circ = 9186 - 21.44\ T,$$
$$\Delta G_{293}^\circ = 2795 \text{ cal.} \qquad (9)$$

The entropy change at 25°C is $\Delta S^\circ_{298}=21.44$ e. u.

The entropy of formation of hexamminecobalt(III) ion, nitropentamminecobalt(III) ion, *trans*- and *cis*-dinitrotetramminecobalt(III) ions were obtained as $-306.9$[8], $-148.3$[10], $7.72$[10] and $16.10$ e. u.[10], respectively. From these values it is found that the entropy of formation increases by 160 e. u., when every one gram equivalent of ammonia is replaced by one gram equivalent of nitro group. Therefore, if it is assumed that the entropy of formation of trinitrotriamminecobalt(III) complex in unit activity in aqueous solution is larger by three times 160 e. u. than that of hexamminecobalt(III) ion in unit activity, the entropy of the former is obtained as $\Delta S^\circ=172$ e. u. As the heat of formation of trinitrotriamminecobalt(III) complex in unit activity in aqueous solution is known as $\Delta H=-160$ kcal.[9], the free energy of formation is obtained as

$$\Delta G_f^\circ = -160000-172\ T,$$
$$\Delta G_{f\,298}^\circ = -211300 \text{ cal.} \qquad (10)$$

By Eqs. 9 and 10 the free energy of formation of trinitrotriamminecobalt(III) complex in the solid state is obtained as

$$\Delta G_f^\circ = -169200-150.6\ T,$$
$$\Delta G_{f\,298}^\circ = -214.1 \text{ kcal.}$$

10) See Eqs. 6, 11 and 10, in this paper.

## Discussion

**Thermodynamic Stability of Nitropentamminecobalt(III) Complexes.** — The solubility, the free energy of solution, the heat of solution and the free energy of formation of nitropentamminecobalt(III) complexes 25°C obtained above are summarized in Table VIII together with the radius of anions[11] forming these complexes. The lattice energy, $U_k$, required for the dissociation of solid complexes into gaseous ions is calculated by using the heat of solution and the heat of hydration of ions[11] which constitute complexes, and the values are shown in Table VIII.

From this table, the order of decrease of the solubility, the free energy of solution, the heat of solution, the lattice energy, the free energy of formation and the thermochemical and thermodynamic stability are found and shown in Table IX.

The same order was found for the solubility, the free energy of solution and the heat of solution of hexamminecobalt(III) complexes[8]. The order of the thermochemical and thermodynamic stability for the above nitropentamminecobalt(III) chloride, nitrate, bromide and perchlorate is in agreement with the order for the corresponding hexamminecobalt(III)[8], aquopentamminecobalt(III)[1] or acidopentamminecobalt(III) complexes[1]. The above order of the thermodynamic quantities may suggest that the ionic bond character between the complex cation and the anions generally diminishes as the ionic radius of the latter decreases, although several cases of reversal between the nitrate and the bromide are found as shown in Table VIII.

**Entropy of Solution of *cis*- and *trans*-Dinitrotetramminecobalt(III) Chlorides.** — The solubility, the free energy of solution, the heat of solution and the entropy of solution

11) K. B. Yatsimirskii, "Thermochemie von Komplexverbindungen", Akademie-Verlag, Berlin (1956), pp. 38—40.

Table VIII. Thermodynamic functions of nitropentamminecobalt(III) complexes at 25°C

| Complex | Solubility in Molality $m$ | Free energy of solution $\Delta G°$ cal. | Heat of solution $\Delta H$ kcal. | Free energy of formation $\Delta G_f°$ kcal. | Radius of anion (Å) | Lattice energy $U_k$ kcal. |
|---|---|---|---|---|---|---|
| $[Co(NH_3)_5NO_2]Cl_2$ | 0.145 | 3991 | 12.51 | −175.6 | 1.81 | 390 |
| $[Co(NH_3)_5NO_2](NO_3)_2$ | 0.0531 | 5477 | 15.89 | −167.2 | 1.89 | 376 |
| $[Co(NH_3)_5NO_2]Br_2$ | 0.0587 | 5262 | 14.44 | −163.3 | 1.96 | 374 |
| $[Co(NH_3)_5NO_2](ClO_4)_2$ | 0.168 | 3728 | 21.57 | −117.8 | 2.36 | 340 |

Table IX. Order of decrease of the thermodynamic quantities

| | |
|---|---|
| Solubility | Chloride>Bromide>Nitrate |
| Free energy of solution | Nitrate>Bromide>Chloride |
| Heat of solution | Nitrate>Bromide>Chloride |
| Lattice energy | Chloride>Nitrate>Bromide>Perchlorate |
| Free energy of formation | Perchlorate>Bromide>Nitrate>Chloride |
| Thermochemical and thermodynamic stability | Chloride>Nitrate>Bromide>Perchlorate |

Table X. Thermodynamic functions of *cis*- and *trans*-dinitrotetramminecobalt(III) chlorides

| Complex | Solubility $m$ | Free energy of solution $\Delta G°$ cal. | Heat of solution $\Delta H$ kcal. | Entropy of solution $\Delta S°$ e. u. |
|---|---|---|---|---|
| *cis*-$[Co(NH_3)_4(NO_2)_2]Cl$ | 0.263 | 1990 | 10.13 | 27.3 |
| *trans*-$[Co(NH_3)_4(NO_2)_2]Cl$ | 0.0521 | 3731 | 10.87 | 23.9 |

of these two isomers at 25°C are summarized in Table X.

As shown in Table X, the cis chloride is more soluble than the trans chloride and the free energy of solution of the former is much lower than that of the latter. The large difference between the free energies of solution is attributed to the fact that the entropy of solution of the cis salt is considerably larger than that of the trans salt, since the heat of solution is approximately the same. In other words, the free energy changes of solution of these two isomers are affected much more by the entropy effect rather than the enthalpy effect.

**Relationship between the Free Energy of Formation and the Number of Coordinated Nitro-groups.** — The free energies of formation of nitropentamminecobalt(III), dinitrotetramminecobalt(III) and hexamminecobalt(III) complexes are plotted against the number of coordinated nitro-groups in Fig. 3. Straight lines were obtained for the chlorides, nitrates, bromides and perchlorates. These four lines all converge at a point which corresponds to the free energy of formation of trinitrotriamminecobalt(III) complexes. It shows that an additivity rule holds between the free energy of formation and the number of nitrogroups.

When the free energy of formation of these complexes and the number of nitrogroups are expressed by $\Delta G_f°$ and $n$ respectively, these straight lines are expressed by

$$\Delta G_f° = an + c, \qquad (11)$$

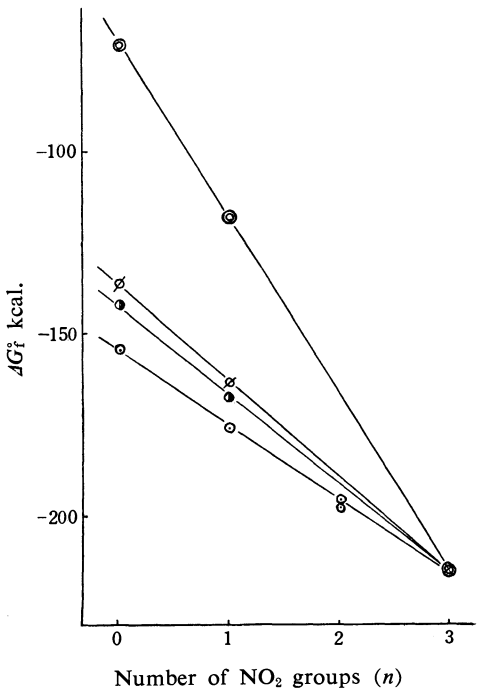



Fig. 3. The relationship between the free energy of formation and the number of nitro-groups coordinated in the series of cobalt(III) nitroammine complexes, that is
$[Co(NH_3)_{6-n}(NO_2)_n]Cl_{3-n}$ (⊙),
$[Co(NH_3)_{6-n}(NO_2)_n](NO_3)_{3-n}$ (◑),
$[Co(NH_3)_{6-n}(NO_2)_n]Br_{3-n}$ (Ø)
and $[Co(NH_3)_{6-n}(NO_2)_n](ClO_4)_{3-n}$ (◎).
(⊗) is trinitrotriamminecobalt(III) complex.

where $c$ is the free energy of formation of a hexamminecobalt(III) complex[8] and $a$ a constant. The constant $a$ gives the difference between the free energy of formation of $[Co(NH_3)_{6-n}(NO_2)_n]X_{3-n}$ and that of $[Co(NH_3)_{6-n-1}(NO_2)_{n+1}]X_{3-n-1}$, which is obtained from Fig. 3 as:

$a=-19.9$ kcal. for chloride

$a=-24.1$ kcal. for nitrate

$a=-26.0$ kcal. for bromide

$a=-47.6$ kcal. for perchlorate

**Free Energy Required for the Dissociation of the Anion from Nitroamminecobalt(III) Complexes.** — The value of $a$ in Eq. 11 for the chlorides is assumed as the sum of the changes of the free energy of formation in two processes such as:

(a) $[Co(NH_3)_6]Cl_3(s) \rightarrow [Co(NH_3)_6]Cl_2(s) \quad \Delta(\Delta G_f^\circ)_a$

(b) $[Co(NH_3)_6]Cl_2(s) \rightarrow [Co(NH_3)_5NO_2]Cl_2(s) \quad \Delta(\Delta G_f^\circ)_b$

that is,

$$a=\Delta(\Delta G_f^\circ)_a+\Delta(\Delta G_f^\circ)_b$$

If it is assumed that the change of the free energy of formation in process (b) is approximately equal to that in the following process,

$[Co(NH_3)_6]^{3+}(aq.) \rightarrow [Co(NH_3)_5NO_2]^{2+}(aq.) \quad \Delta(\Delta G_f^\circ) = -54.4$ kcal.[6]

that is,

$$\Delta(G_f^\circ)_b \fallingdotseq \Delta(G_f^\circ) = -54.4 \text{ kcal.}$$

then the value in the above process (a) is calculated as $\Delta(\Delta G_f^\circ)_a=34.5$ kcal. by using the value $a=-19.9$ kcal. for the chloride. The value $\Delta(\Delta G_f^\circ)_a$ is the free energy required for the elimination of one gram equivalent of chloride ion in the outer coordination sphere frome nitroammin cobalt(III) chloride.

In the same way, the free energies required for eliminating one gram equivalent of $NO_3^-$, $Br^-$ or $ClO_4^-$ in the outer sphere from the respective complexes are calculated as below:

$\Delta(\Delta G_f^\circ)_a=30.3$ kcal. for nitrate

$\Delta(\Delta G_f^\circ)_a=28.4$ kcal. for bromide

$\Delta(\Delta G_f^\circ)_a=6.8$ kcal. for perchlorate

These values show that the dissociation of the anion from cobalt(III) nitroammine complexes becomes more difficult in the order: perchlorate <bromide<nitrate<chloride. This also indicates that the thermodynamic stability of these complexes increases in the same order.

## Summary

1. From the solubility of cobalt(III) nitroammine complexes the thermodynamic stability was found to decrease in the order, chloride> nitrate>bromide>perchlorate.

2. The free energy of solution of *cis*-dinitrotetramminecobalt(III) chloride is lower than that of the trans chloride. This fact is attributed to the abnormally large value of the entropy of solution of the former compared with the latter.

3. Between the free energy of formation of cobalt(III) nitroammine complexes and the number of coordinated nitro-groups there exists a linear relationship.

*Department of Chemistry*
*Faculty of Science*
*Kanazawa University*
*Kanazawa*

# *Thermodynamic Studies on Cobalt Complexes. VII. Solubility of Erdmann's Salt and Related Complexes**

By Motoshichi MORI, Ryokichi TSUCHIYA, Eishin KYUNO and Takashi NISHIDE

(Received May 11, 1960)

Although there have been several investigations[1] on the structure of Erdmann's salt, ammonium tetranitrodiamminecobaltate(III), no thermodynamic study has ever been made on it. In the preceding paper[2] we determined the solubility of nitropentamminecobalt(III), *cis*- and *trans*-dinitrotetramminecobalt(III) and trinitrotriamminecobalt(III) complexes and calculated the standard free energy of formation of solid cobalt(III) ammine complexes containing one, two or three nitrogroups. In the present paper the solubility of the cobalt-(III) ammine complexes containing four nitrogroups, i. e., tetranitrodiamminecobaltate(III) complexes was measured. The solubilities of some of these salts have already been reported[3,4]. In the present study the measurement was extended to several other salts and to different temperatures.

## Experimental

The complexes studied were the following: [I] the so called Erdmann's salt, namely ammonium tetranitrodiamminecobaltate(III) $NH_4[Co(NH_3)_2(NO_2)_4]$, [II] the corresponding potassium salt $K[Co(NH_3)_2(NO_2)_4]$, [III] *cis*-dinitrotetramminecobalt(III) - tetranitrodiamminecobaltate(III) *cis*-$[Co(NH_3)_4(NO_2)_2][Co(NH_3)_2(NO_2)_4]$, and [IV] the corresponding trans isomer among 1-1 valency type salts, [V] nitropentammincobalt(III)-tetranitrodiamminecobaltate(III) $[Co(NH_3)_5NO_2][Co(NH_3)_2(NO_2)_4]_2$ and [VI] chloropentamminecobalt(III)-tetranitrodiamminecobaltate(III) $[Co(NH_3)_5Cl][Co(NH_3)_2(NO_2)_4]_2$ among 1-2 valency type salts and [VII] hexamminecobalt(III) - tetranitrodiamminecobaltate(III) $[Co(NH_3)_6][Co(NH_3)_2(NO_2)_4]_3$ among 1-3 valency type salts.

Erdmann's salt [I] was prepared by the method of Jörgensen[5] and the potassium salt [II] was precipitated from the aqueous solution of I with potassium nitrate. III and IV were prepared by the double decomposition of I and *cis*-dinitrotetramminecobalt(III) nitrate[6] and the trans form chloride[7] respectively. V, VI and VII were prepared by the double decomposition of I and nitropentamminecobalt(III) chloride[8], chloropentamminecobalt(III) chloride[9] and hexamminecobalt(III) chloride[10], respectively.

The measurement of the solubility was made by measuring the cobalt content or the absorbancy of the saturated aqueous solution. The former was carried out by iodometry and the latter with a Hitachi EPU-2 spectrophotometer.

## Results and Calculation

The results of measurement are listed in Tables I—VII. The solubilities are expressed in molality, $m$. The mean activity coefficients $\gamma_\pm$ given for I and II are the values obtained in the first paper of this series[11] and those for the other salts are the values calculated by Debye-Hückel's limiting formula,

$$\log \gamma_\pm = -0.505\, z_+ z_- \sqrt{\mu}$$

where $z_+$ and $z_-$ are the charges of each cation and anion and $\mu$ is the ionic strength of each solution.

**Equilibrium Constant of Solution and Standard Free Energy of Formation of Erdmann's Salt.**— When Erdmann's salt is dissolved in water, the change is expressed by

$$NH_4[Co(NH_3)_2(NO_2)_4]\,(s) = NH_4^+\,(aq.) + [Co(NH_3)_2(NO_2)_4]^-\,(aq.)$$

The equilibrium constant of the solution, $K$, is given as in the preceding paper[2] by $K = m^2\gamma^2_\pm$.

A plot of the logarithm of $K$ against the reciprocal of the absolute temperature is given in Fig. 1 as a straight line, the equation being calculated by the method of least squares as

$$\log K = 0.8981 - 771.8/T$$

The free energy change of solution is given by

$$\Delta G^\circ = 3530 - 4.108\,T, \quad \Delta G^\circ_{298} = 2305 \text{ cal.} \qquad (1)$$

* Read at the 12th Annual Meeting of the Chemical Society of Japan Tokyo April, 1959.

1) Y. Komiyama, This Bulletin, **30**, 13 (1957). Other references in the past were cited in this paper.

2) M. Mori, R. Tsuchiya and H. Fukuda, This Bulletin, **33**, 1503 (1960).

3) J. N. Brönsted and A. Petersen, *J. Am. Chem. Soc.* **43**, 2265 (1921).

4) E. Kyuno, *J. Chem. Soc. Japan, Pure Chem. Sec.* (*Nippon Kagaku Zasshi*), **78**, 1494 (1957).

5) S. M. Jörgensen, *Z. anorg. Chem.*, **17**, 477 (1898).

6) S. M. Jörgensen, ibid., **17**, 473 (1898).

7) S. M. Jörgensen, ibid., **17**, 469 (1898).

8) S. M. Jörgensen, ibid., **17**, 463 (1898).

9) W. A. Hynes, L. K. Yanowsky and M. Schiller, *J. Am. Chem. Soc.*, **60**, 3053 (1938).

10) W. C. Fernelius, "Inorganic Syntheses", Vol. II, McGraw-Hill Book Co., Inc., New York, N. Y. (1946), p. 216.

11) M. Mori and R. Tsuchiya, *J. Chem. Soc. Japan, Pure Chem. Sec.* (*Nippon Kagaku Zasshi*), **79**, 1164 (1958).

TABLE I. SOLUBILITY OF ERDMANN'S SALT

| Temp. (°C) | Solubility (Molality $m$) | $1/T\times10^3$ | $\gamma_\pm$ | $K$ | log $K$ |
|---|---|---|---|---|---|
| 15 | 0.186 | 3.471 | 0.690 | 0.0164 | $\bar{2}.215$ |
| 20 | 0.199 | 3.412 | 0.686 | 0.0186 | $\bar{2}.270$ |
| 25 | 0.209 | 3.355 | 0.681 | 0.0203 | $\bar{2}.308$ |
| 30 | 0.224 | 3.299 | 0.675 | 0.0228 | $\bar{2}.358$ |
| 35 | 0.233 | 3.246 | 0.671 | 0.0244 | $\bar{2}.387$ |

TABLE II. SOLUBILITY OF $K[Co(NH_3)_2(NO_2)_4]$

| Temp. (°C) | Solubility (Molality $m$) | $1/T\times10^3$ | $\gamma_\pm$ | $K\times10^4$ | log $K$ |
|---|---|---|---|---|---|
| 0 | 0.0107 | 3.662 | 0.914 | 1.23 | $\bar{4}.869$ |
| 15 | 0.0364 | 3.471 | 0.847 | 3.08 | $\bar{4}.736$ |
| 20 | 0.0516 | 3.412 | 0.821 | 4.23 | $\bar{4}.627$ |
| 25 | 0.0684 | 3.355 | 0.796 | 5.45 | $\bar{4}.488$ |
| 30 | 0.0969 | 3.299 | 0.763 | 7.39 | $\bar{4}.090$ |

TABLE III. SOLUBILITY OF *cis*-$[Co(NH_3)_4(NO_2)_2][Co(NH_3)_2(NO_2)_4]$

| Temp. (°C) | Solubility (Molality $m\times10^3$) | $1/T\times10^3$ | $\gamma_\pm$ | $K\times10^5$ | log $K$ |
|---|---|---|---|---|---|
| 15 | 4.49 | 3.471 | 0.925 | 1.73 | $\bar{5}.237$ |
| 20 | 6.49 | 3.412 | 0.911 | 3.49 | $\bar{5}.543$ |
| 25 | 8.99 | 3.355 | 0.896 | 6.49 | $\bar{5}.812$ |
| 30 | 11.39 | 3.299 | 0.883 | 10.12 | $\bar{4}.005$ |

TABLE IV. SOLUBILITY OF *trans*-$[Co(NH_3)_4(NO_2)_2][Co(NH_3)_2(NO_2)_4]$

| Temp. (°C) | Solubility (Molality $m\times10^4$) | $1/T\times10^3$ | $\gamma_\pm$ | $K\times10^7$ | log $K$ |
|---|---|---|---|---|---|
| 15 | 4.56 | 3.471 | 0.975 | 1.97 | $\bar{7}.295$ |
| 20 | 6.05 | 3.412 | 0.972 | 3.46 | $\bar{7}.539$ |
| 25 | 8.38 | 3.355 | 0.967 | 6.56 | $\bar{7}.817$ |
| 30 | 11.09 | 3.299 | 0.962 | 11.38 | $\bar{6}.056$ |

TABLE V. SOLUBILITY OF $[Co(NH_3)_5NO_2][Co(NH_3)_2(NO_2)_4]_2$

| Temp. (°C) | Solubility (Molality $m\times10^3$) | $1/T\times10^3$ | $\gamma_\pm$ | $K\times10^9$ | log $K$ |
|---|---|---|---|---|---|
| 10 | 0.670 | 3.532 | 0.906 | 0.892 | $\bar{10}.950$ |
| 15 | 0.928 | 3.471 | 0.887 | 2.24 | $\bar{9}.349$ |
| 20 | 1.12 | 3.412 | 0.879 | 3.81 | $\bar{9}.581$ |
| 25 | 1.46 | 3.355 | 0.865 | 8.07 | $\bar{8}.907$ |
| 30 | 1.62 | 3.299 | 0.857 | 10.71 | $\bar{8}.030$ |

TABLE VI. SOLUBILITY OF $[Co(NH_3)_5Cl][Co(NH_3)_2(NO_2)_4]_2$

| Temp. (°C) | Solubility (Molality $m\times10^3$) | $1/T\times10^3$ | $\gamma_\pm$ | $K\times10^9$ | log $K$ |
|---|---|---|---|---|---|
| 15 | 0.501 | 3.471 | 0.914 | 0.383 | $\bar{10}.584$ |
| 20 | 0.731 | 3.412 | 0.896 | 1.16 | $\bar{9}.066$ |
| 25 | 1.00 | 3.355 | 0.880 | 2.73 | $\bar{9}.436$ |
| 30 | 1.32 | 3.299 | 0.864 | 5.97 | $\bar{9}.776$ |
| 35 | 1.76 | 3.246 | 0.845 | 13.03 | $\bar{8}.115$ |

TABLE VII. SOLUBILITY OF $[Co(NH_3)_6][Co(NH_3)_2(NO_2)_4]_3$

| Temp. (°C) | Solubility (Molality $m\times10^4$) | $1/T\times10^3$ | $\gamma_\pm$ | $K\times10^{14}$ | log $K$ |
|---|---|---|---|---|---|
| 15 | 1.55 | 3.471 | 0.899 | 1.02 | $\bar{14}.010$ |
| 20 | 2.25 | 3.412 | 0.880 | 4.17 | $\bar{14}.620$ |
| 25 | 2.84 | 3.355 | 0.866 | 9.88 | $\bar{14}.995$ |
| 30 | 4.09 | 3.299 | 0.841 | 37.94 | $\bar{13}.579$ |

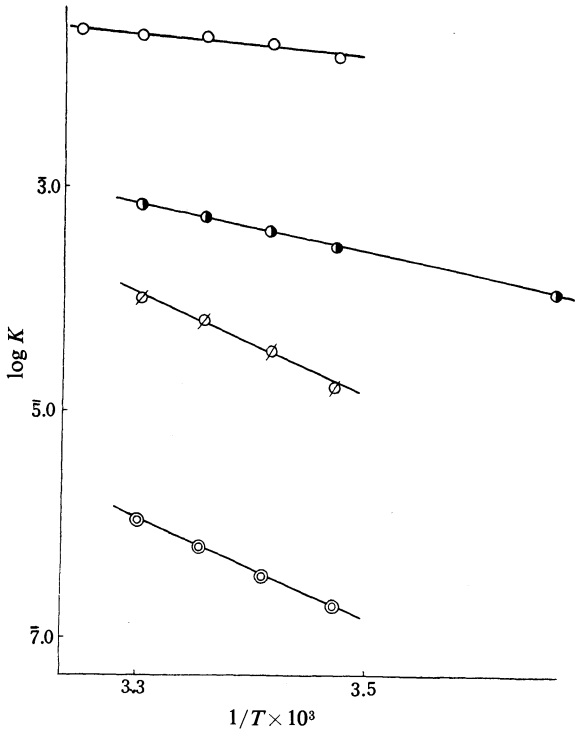



Fig. 1. The relationship between the equilibrium constant of solution and the temperature for Erdmann's salt, $NH_4[(Co\cdot(NH_3)_2(NO_2)_4]$ (○), $K[Co(NH_3)_2(NO_2)_4]$ (◑), *cis*-$[Co(NH_3)_4(NO_2)_2][Co(NH_3)_2\cdot(NO_2)_4]$ (∅), and *trans*-$[Co(NH_3)_4(NO_2)_2]\cdot[Co(NH_3)_2(NO_2)_4]$ (◎).

The heat of solution and the entropy change of solution at 25°C are obtained as $\Delta H=3530$ cal. and $\Delta S^\circ=4.108$ e. u., respectively.

As described in the preceding paper[2], it is found that the entropy of formation of cobalt (III) nitroammine complexes increases by 160 e. u. for each replacement of one gram equivalent of ammonia by one gram equivalent of nitrogroup. Therefore the sum of this value and the entropy of formation of trinitrotriamminecobalt(III) complex in unit activity in aqueous solution, $\Delta S^\circ=172$ e. u., may be regarded as that of tetranitrodiamminecobaltate (III) anion in unit activity in aqueous solution, i. e. $\Delta S^\circ=332$ e. u. Since the heat of formation of the latter is $\Delta H=-164.9$ kcal.[12], the free energy of formation is given by the equation:

$$\Delta G_f^\circ=-164900-332\,T,\quad \Delta G_{f\,298}^\circ=-263.9\text{ kcal.} \tag{2}$$

The free energy of formation of $NH_4^+$ in unit activity is given as[13]

$$\Delta G_f^\circ=-31740-42.74\,T \tag{3}$$

From Eqs. 1, 2 and 3, the free energy of formation of Erdmann's salt in the solid state is calculated as

$$\Delta G_f^\circ=-200200-288.9\,T,$$

$$\Delta G_{f\,298}^\circ=-286.3\text{ kcal.}$$

**Free Energy of Formation of Potassium Tetranitrodiamminecobaltate(III).**—The equilibrium constant of the solution of potassium tetranitrodiamminecobaltate(III) is given by $K=m^2\gamma^2_\pm$ in the same way as that of Erdmann's salt described above. The relationship between $\log K$ and $1/T$ is given by a straight line in Fig. 1, which is expressed by the equation,

$$\log K=3.917-2138/T$$

The free energy change of solution is given as

$$\Delta G^\circ=9777-17.92\,T,\quad \Delta G_{298}^\circ=4436\text{ cal.} \tag{4}$$

and the heat of the solution is $\Delta H=9777$ cal., and the entropy change of the solution at 25°C is $\Delta S^\circ=17.92$ e. u. The free energy of formation of $K^+$ in unit activity in aqueous solution is given as

$$\Delta G_f^\circ=-60040-24.91\,T \tag{5}$$

From Eqs. 2, 4 and 5, the free energy of formation of potassium tetranitrodiamminecobaltate(III) in the solid state is calculated as below:

$$\Delta G_f^\circ=-234700-339\,T,\quad \Delta G_{f\,298}^\circ=-335.8\text{ kcal.}$$

**Free Energy of Formation of *cis*- and *trans*-Dinitrotetramminecobalt(III)-Tetranitrodiamminecobaltates(III).**—The equilibrium constants of solution of these salts are given by $K=m^2\gamma_\pm{}^2$ as above and the relationships between $\log K$ and $1/T$ are given by two straight lines for both salts in Fig. 1, which are expressed for the cis salt by

$$\log K=10.71-4450/T$$

and for the trans salt by

$$\log K=9.014-4532/T$$

The free energy change of solution of the cis salt is obtained as

$$\Delta G^\circ=20350-48.98\,T,\quad \Delta G_{298}^\circ=5751\text{ cal.} \tag{6}$$

and that of the trans salt is obtained as

$$\Delta G^\circ=20730-41.23\,T,\quad \Delta G_{298}^\circ=8438\text{ cal.} \tag{7}$$

The heat of solution and the entropy change of solution of the above cis salt are $\Delta H=20350$ cal. and $\Delta S^\circ=48.98$ e. u. and those of the above trans salt are $\Delta H=20730$ cal. and $\Delta S^\circ=41.23$ e. u., respectively.

12) K. B. Yatsimirskii and L. L. Pankowa, *Zhur. Obshchei Khim.*, **19**, 623 (1949); K. B. Yatsimirskii, "Thermochemie von Komplexverbindungen", Akademie-Verlag, Berlin (1956), p. 180.

13) C. C. Stephenson, *J. Am. Chem. Soc.*, **66**, 1436 (1944).

14) A. E. Hill and J. E. Ricci, *J. Am. Chem. Soc.*, **53**, 4305 (1931).

In the preceding paper[2] the free energy of formation of *cis*- and *trans*-dinitrotetramminecobaltate(III) ions was obtained respectively as

$$\Delta G_f^\circ = -159900 - 16.10\,T \quad (8)$$

$$\Delta G_f^\circ = -159100 - 7.72\,T \quad (9)$$

From Eqs. 2, 6 and 8, the free energy of formation of the cis salt in the solid sate is obtained as

$$\Delta G_f^\circ = -345200 - 299.1\,T,$$

$$\Delta G_{f\,298}^\circ = -434.4 \text{ kcal.}$$

and from Eqs. 2, 7 and 9, that of the trans salt in the solid state is obtained as

$$\Delta G_f^\circ = -344700 - 298.5\,T,$$

$$\Delta G_{f\,298}^\circ = -433.7 \text{ kcal.}$$

**Free Energy of Formation of Nitropentamminecobalt(III)-Tetranitrodiamminecobaltate(III).** —The equilibrium constant of solution of this complex is given by $K = 4\,m^3\gamma^3_\pm$ and a plot of $\log K$ against $1/T$ gives a straight line in Fig. 2, which is expressed by the equation:

$$\log K = 7.530 - 4667/T$$

The free energy change of solution is given by

$$\Delta G^\circ = 21390 - 34.44\,T,$$

$$\Delta G_{298}^\circ = 11130 \text{ cal.} \quad (10)$$

The heat of solution and the entropy change of solution are obtained as $\Delta H = 21.39$ kcal. and $\Delta S^\circ = 34.44$ e. u.. respectively.

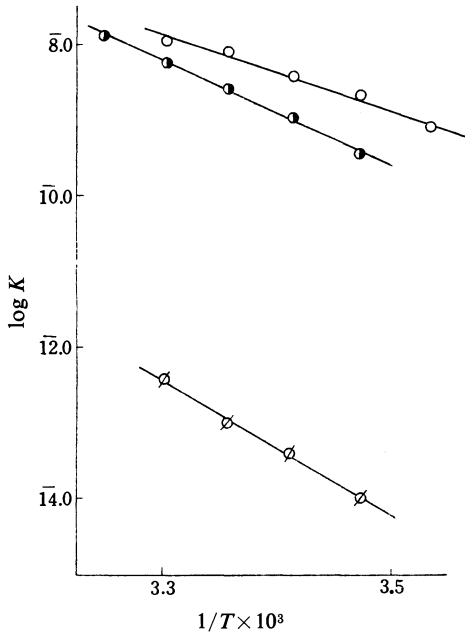



Fig. 2. The relationship between the equilibrium constant of solution and the temperature for $[Co(NH_3)_5NO_2][Co(NH_3)_2(NO_2)_4]_2$ (○), $[Co(NH_3)_5Cl][Co(NH_3)_2(NO_2)_4]_2$ (◑) and $[Co(NH_3)_6][Co(NH_3)_2(NO_2)_4]_3$ (∅).

The free energy of formation of nitropentamminecobalt(III) ion was obtained in the preceding paper[2] as

$$\Delta G_f^\circ = -153100 + 148.3\,T \quad (11)$$

From Eqs. 2, 10 and 11, that of nitropentamminecobalt(III)-tetranitrodiamminecobaltate(III) is obtained as below:

$$\Delta G_f^\circ = -504300 - 481.3\,T,$$

$$\Delta G_{f\,298}^\circ = -647.8 \text{ kcal.}$$

**Free Energy of Formation of Chloropentamminecobalt(III)-Tetranitrodiamminecobaltate(III).** —The equilibrium constant of solution of this complex is also given by $K = 4\,m^3\gamma^3_\pm$ in the same way as the above. A plot of $\log K$ against $1/T$ gives a straight line in Fig. 2 and its equation is calculated as

$$\log K = 13.93 - 6714/T$$

The free energy change of solution is given by

$$\Delta G^\circ = 30710 - 63.72\,T,$$

$$\Delta G_{f\,298}^\circ = 11710 \text{ cal.} \quad (12)$$

The heat of solution is $\Delta H = 30710$ cal. and the entropy change of solution, $\Delta S^\circ = 63.72$ e. u.

The free energy of formation of chloropentamminecobalt(III) ion is obtained from the solubility data[3] and given by the equation,

$$\Delta G_f^\circ = -156100 + 270.9\,T \quad (13)$$

From Eqs. 2, 12 and 13, the free energy of formation of chloropentamminecobalt(III)-tetranitrodiamminecobaltate(III) in the solid state is calculated as

$$\Delta G_f^\circ = -516600 - 329.4\,T,$$

$$\Delta G_{f\,298}^\circ = -614.8 \text{ kcal.}$$

**Free Energy of Formation of Hexamminecobalt(III)-Tetranitrodiamminecobaltate(III).**— The equilibrium constant of solution of this complex is given by $K = 27\,m^4\gamma^4_\pm$ in the same way as that of the hexamminecobalt(III) salts already reported[15]. The logarithm of $K$ is plotted against $1/T$ in Fig. 1 as a straight line, the equation being

$$\log K = 16.83 - 8873/T$$

The free energy change of solution is given by

$$\Delta G^\circ = 40590 - 76.98\,T,$$

$$\Delta G_{298}^\circ = 17640 \text{ cal.} \quad (14)$$

The heat of solution is obtained as $\Delta H = 40590$ cal. and the entropy change of solution as $\Delta S^\circ = 76.98$ e. u.

15) M. Mori, R. Tsuchiya and Y. Okano, This Bulletin, 32, 462 (1959).

TABLE VIII. THERMODYNAMIC FUNCTIONS OF NITROAMMINECOBALT(III) COMPLEXES AT 25°C

| Complex | Solubility | Heat of solution | Equivalent free energy of solution | Entropy change of solution | Lattice energy | Standard free energy of formation |
|---|---|---|---|---|---|---|
| | $m$ | $\Delta H$ cal. | $\Delta G°$ cal. | $\Delta S°$ e.u. | $U$ kcal. | $\Delta G_f^\circ$ kcal. |
| $NH_4[Co(NH_3)_2(NO_2)_4]$ | 0.209 | 3530 | 2305 | | | −286.3 |
| $K[Co(NH_3)_2(NO_2)_4]$ | 0.0684 | 9777 | 4436 | | | −335.8 |
| *cis*-$[Co(NH_3)_4(NO_2)_2]\cdot[Co(NH_3)_2(NO_2)_4]$ | $8.99\times10^{-3}$ | 20350 | 5751 | 48.98 | 101.4 | −434.4 |
| *trans*-$[Co(NH_3)_4(NO_2)_2]\cdot[Co(NH_3)_2(NO_2)_4]$ | $8.38\times10^{-4}$ | 20730 | 8438 | 41.23 | 101.7 | −433.7 |
| $[Co(NH_3)_5NO_2][Co(NH_3)_2(NO_2)_4]_2$ | $1.46\times10^{-3}$ | 21390 | 5565 | | 321.4 | −647.8 |
| $[Co(NH_3)_5Cl]\cdot[Co(NH_3)_2(NO_2)_4]_2$ | $1.00\times10^{-3}$ | 30710 | 5857 | | 323.7 | −614.8 |
| $[Co(NH_3)_6][Co(NH_3)_2\cdot(NO_2)_4]_3$ | $2.84\times10^{-4}$ | 40590 | 5880 | | 664.6 | −863.7 |

In the second paper[15] of this series the free energy of formation of hexamminecobalt-(III) ion was already obtained as

$$\Delta G_f^\circ = -146000 + 307\,T \qquad (15)$$

Therefore, from Eqs. 2, 14 and 15, the free energy of formation of hexamminecobalt(III)-tetranitrodiämminecobaltate(III) in the solid state is given by

$$\Delta G_f^\circ = -681300 - 612\,T,$$
$$\Delta G_{f\,298}^\circ = -863.7 \text{ kcal.}$$

## Discussion

The thermodynamic functions of the nitroamminecobalt(III) complexes at 25°C calculated above are summarized in Table VIII. In this table the free energy of solution is the value for one gram equivalent of each complex, i. e., equivalent free energy of solution.

As shown in this table, the solubilities of these complexes decrease in the order of 1–1, 1–2 and 1–3 valency type salts. In these respects *trans*-$[Co(NH_3)_4(NO_2)_2][Co(NH_3)_2\cdot(NO_2)_4]$ presents a single exception. The equivalent free energies of solution lie within the region between 5500 and 5900 cal. except for *trans*-$[Co(NH_3)_4(NO_2)_2][Co(NH_3)_2(NO_2)_4]$, $K[Co(NH_3)_2(NO_2)_4]$ and Erdmann's salt. This corresponds to the free energy required for breaking a bond between the cation and the anion and hydrating each of the ions when the salt is dissolved.

The free energy of solution of *cis*-dinitrotetramminecobalt(III)-tetranitrodiamminecobaltate(III) is remarkably less than that of the corresponding trans salt. This is due to the fact that the entropy change of solution of the former is much greater than that of the latter. In other words, the entropy effect plays an important role when the cis and trans salts are dissolved in water just as in the case of the *cis*- and *trans*-dinitrotetramminecobalt(III) chloride reported in the preceding paper[2].

The heats of hydration of the complex ions concerned are listed in Table IX[16].

TABLE IX. HEAT OF HYDRATION OF COMPLEX IONS

| Complex ion | Heat of hydration (kcal.) |
|---|---|
| $[Co(NH_3)_4(NO_2)_2]^+$ | −40 |
| $[Co(NH_3)_5NO_2]^{2+}$ | −218 |
| $[Co(NH_3)_5Cl]^{2+}$ | −211 |
| $[Co(NH_3)_6]^{3+}$ | −501 |
| $[Co(NH_3)_2(NO_2)_4]^-$ | −41 |

By using these values and the heats of solution of the cobalt(III) nitroammine complexes described above, their lattice energies are computed. These are also shown in Table VIII.

The standard free energies of formation of four cobalt(III) nitroammine complexes in the solid state are given by:

$$2Co(s) + 6N_2 + 9H_2 + 6O_2 = \textit{cis}\text{-}[Co(NH_3)_4(NO_2)_2][Co(NH_3)_2\cdot(NO_2)_4] \quad \Delta G_f^\circ = -434.4 \text{ kcal.} \qquad (a)$$

$$2Co(s) + 6N_2 + 9H_2 + 6O_2 = \textit{trans}\text{-}[Co(NH_3)_4(NO_2)_2][Co(NH_3)_2\cdot(NO_2)_4] \quad \Delta G_f^\circ = -433.7 \text{ kcal.} \qquad (b)$$

$$3Co(s) + 9N_2 + 27/2H_2 + 9O_2 = [Co(NH_3)_5NO_2][Co(NH_3)_2(NO_2)_4]_2 \quad \Delta G_f^\circ = -647.8 \text{ kcal.} \qquad (c)$$

$$4Co(s) + 12N_2 + 18H_2 + 12O_2 = [Co(NH_3)_6][Co(NH_3)_2(NO_2)_4]_3 \quad \Delta G_f^\circ = -863.7 \text{ kcal.} \qquad (d)$$

16) K. B. Yatsimirskii, "Thermochemie von Komplexverbindungen", Akademie-Verlag, Berlin (1956), p, 38.

By dividing a and b by two, c by three and d by four the following values are obtained:

$$Co(s)+2N_2+9/2H_2+3O_2 = 1/2\ cis\text{-}[Co(NH_3)(NO_2)_2]\cdot[Co(NH_3)_2(NO_2)_4]$$
$$\Delta G_f^\circ = -217.2\ \text{kcal.}$$

$$Co(s)+3N_2+9/2H_2+3O_2 = 1/2\ trans\text{-}[Co(NH_3)_4(NO_2)_2]\cdot[Co(NH_3)_2(NO_2)_4]$$
$$\Delta G_f^\circ = -216.9\ \text{kcal.}$$

$$Co(s)+3N_2+9/2H_2+3O_2 = 1/3\ [Co(NH_3)_5NO_2][Co(NH_3)_2(NO_2)_4]_2 \qquad \Delta G_f^\circ = -215.9\ \text{kcal.}$$

$$Co(s)+3N_2+9/2H_2+3O_2 = 1/4\ [Co(NH_3)_6][Co(NH_3)_2(NO_2)_4]_3$$
$$\Delta G_f^\circ = -215.9\ \text{kcal.}$$

From these values it is found that the free energy of formation of the above-mentioned cobalt(III) nitroammine complexes is proportional to the number of cobalt atoms contained in one molecule of these complexes.

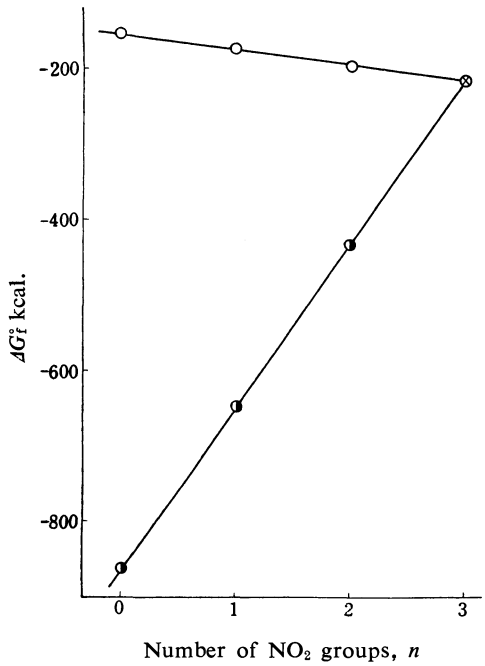



Fig. 3. The relationship between the free energy of formation and the number of nitrogroups co-ordinated in the series of several tetranitrodiamminecobaltates-(III), that is $[Co(NH_3)_{6-n}(NO_2)_n][Co(NH_3)_2(NO_2)_4]_{3-n}$ (◑) and $[Co(NH_3)_{6-n}(NO_2)_n]Cl_{3-n}$ (○).
(⊗) is trinitrotriamminecobalt(III) complex.

When the free energies of formation of the series consisting of $[Co(NH_3)_6][Co(NH_3)_2(NO_2)_4]_3$—$[Co(NH_3)_5NO_2][Co(NH_3)_2(NO_2)_4]_2$—$[Co(NH_3)_4(NO_2)_2][Co(NH_3)_2(NO_2)_4]$ are plotted against the number of $NO_2$ contained in their cations in Fig. 3, a straight line is obtained. This line passes through a point giving the free energy of formation of $[Co(NH_3)_3(NO_2)_3]$. The line for the free energy of formation of the series, $[Co(NH_3)_6]Cl_3$—$[Co(NH_3)_5NO_2]Cl_2$—$[Co(NH_3)_4(NO_2)_2]Cl$, against the number of $NO_2$ also converges to the same point as shown in Fig. 3.

It can be expected that the free energies of formation of $[Co(NH_3)_6][Co(NO_2)_6]$, $[Co(NH_3)_5NO_2][Co(NH_3)(NO_2)_5]$, $[Co(NH_3)_4(NO_2)_2][Co(NH_3)_2(NO_2)_4]$ and $2[Co(NH_3)_3(NO_2)_3]$, are almost equal. The latter three are produced by the successive replacement of $NH_3$ in cation and $NO_2$ in anion of $[Co(NH_3)_6][Co(NO_2)_6]$ with $NO_2$ and $NH_3$ respectively, thus forming a set of coordination isomers. Thus the free energy of formation of $2[Co(NH_3)_3(NO_2)_3]$ is $\Delta G_f^\circ = -428.2$ kcal., that of *cis*-$[Co(NH_3)_4(NO_2)_2][Co(NH_3)_2(NO_2)_4]$ $\Delta G_f^\circ = -434.4$ kcal. and that of the trans salt $\Delta G_f^\circ = -433.7$ kcal., although those of $[Co(NH_3)_6][Co(NO_2)_6]$ and $[Co(NH_3)_5NO_2][Co(NH_3)(NO_2)_5]$ have not been found. These facts mean that the free energy of formation cobalt(III) nitroammine complexes is additive with respect to the $NO_2$ group.

Furthermore, it is also found that the thermodynamic stability of $[Co(NH_3)_5NO_2][Co(NH_3)_2(NO_2)_4]_2$ is greater than that of $[Co(NH_3)_5Cl][Co(NH_3)_2(NO_2)_4]_2$, since the free energy of formation of the former is less than that of the latter.

## Summary

The solubilities of Erdmann's salt, $NH_4[Co(NH_3)_2(NO_2)_4]$, and the following complexes which have the same complex anion, $K[Co(NH_3)_2(NO_2)_4]$, *cis*- and *trans*-$[Co(NH_3)_4(NO_2)_2][Co(NH_3)_2(NO_2)_4]$, $[Co(NH_3)_5NO_2][Co(NH_3)_2(NO_2)_4]_2$, $[Co(NH_3)_5Cl][Co(NH_3)_2(NO_2)_4]_2$ and $[Co(NH_3)_6][Co(NH_3)_2(NO_2)_4]_3$ were measured. Based upon the thermodynamic functions calculated from the above measurement, the free energy of solution, the lattice energy and the free energy of formation of these complexes were calculated and discussed.

*Department of Chemistry*
*Faculty of Science*
*Kanazawa University*
*Kanazawa*

# *Oxidizing Action of Hydroperoxides. IV. On the Oxidation of Aryl Alkyl Ketones*

By Kazuhiro MARUYAMA

(Received March 23, 1960)

This research was started with a view to studying the liquid phase autoxidation of *p*-cymene some years ago. In the liquid phase autoxidation of *p*-cymene in the presence of alkali hydroxide, no resinous product was produced and 8-hydroxy-*p*-cymene, cumic acid and *p*-toluic acid were found, accompanied by a negligibly small amount of *p*-methylacetophenone — an interesting contrast to the autoxidation in the absence of alkali hydroxide. From the studies on the autoxidation of some hydrocarbons, it was observed[1] that alkylhydroperoxides act as a strong oxidizing agent on alkylbenzene and also on some carbonyl compounds*, e. g., the primary carbon atom at $\alpha$-position of the side chain is oxidized to alcohol, to aldehyde and finally to carboxylic acid, the secondary carbon is oxidized to carbonyl group and finally decomposes to yield a mixture of acids and the tertiary carbon atom is oxidized to alcohol and/or decomposes to ketone having a fewer number of carbon atoms. Especially, aryl alkyl ketones are easily split by these oxidizing agents into aromatic carboxylic acid and aliphatic alcohol. Further, in all these oxidation reactions, in contrast to peracid oxidation, no phenolic substances are produced. Also diaryl ketones are not affected by these oxidizing agents — an outstanding difference as compared with the case of the cleavage of ketones by peracids** —, whereas aryl alkyl ketones are affected with great ease. In this paper are reported only the oxidation of aryl alkyl ketones.

## Experimental

**Materials.** — *p*-Methylacetophenone was prepared by the action of acethyl chloride on toluene using anhydrous aluminium chloride as a catalyst. The resulting *p*-methylacetophenone was distilled under reduced pressure using Hempel's column, b. p. 94~95°C/12 mmHg: semicarbazone, m. p. 205°C. Propiophenone was prepared by the action of propionyl chloride on benzene suspending anhydrous aluminum chloride. The resulting propiophenone was completely freed from aluminum ions by shaking with acid and alkali, and was distilled under reduced pressure. B. p. 105°C/20 mmHg, m. p. 21°C. *tert*-Butyl phenyl ketone was synthesized from isopropyl phenyl ketone, following Halle's method[2]. B. p. 220~222°C, 104~106°C/17 mmHg, 2,4-dinitrophenylhydrazone; m. p. 166~168°C. Benzophenone was prepared by the action of benzoyl chloride on benzene suspending anhydrous aluminum chloride. M. p. 47~48°C. Fluorenone was synthesized by the oxidation of commercial grade fluorene, following Fanto's method[3]. M. p. 83~84°C. *p*-Nitrobenzophenone was synthesized by the action of *p*-nitrobenzoyl chloride on benzene suspended with anhydrous aluminum chloride, following Schroeter's method[4]. M. p. 138°C. *tert*-Butylhydroperoxide was synthesized by the action of 30% hydrogen peroxide on *tert*-butanol, following Milas and Surgenor's method[5]. The obtained mixture of *tert*-butylhydroperoxide and di-*tert*-butylperoxide was fractionally distilled under reduced pressure. For the purpose of obtaining highly purified hydroperoxide, this process was repeated four times. B. p. 36°C/19 mmHg. $n_D^{27}$: 1.3967. Cumylhydroperoxide was synthesized by the autoxidation of cumene, following Armstrong, Hall and Quin's method[6]. The obtained cumylhydroperoxide was purified by the fractionation under a high vacuum. B. p. 53~54°C/0.0005 mmHg.

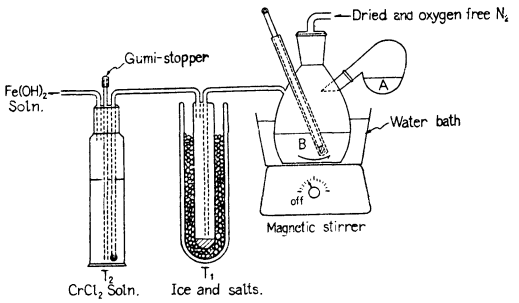



Fig. 1. Reaction apparatus.

**Reaction Apparatus and Procedure.**—The reaction apparatus is shown in Fig. 1. Ketone, monochlorobenzene and finely powdered analytical grade

1) Unpublished work.

* M. S. Kharasch et al. reported that alkylhydroperoxides act as an oxidizing agent on the primary as well as secondary alcohols in alkaline solution (*J. Org. Chem.*, **17**, 207 (1952).

** W. H. Saunders, *J. Am. Chem. Soc.*, **77**, 4679 (1957); W. v. E. Doering and E. Dorfman, ibid., **75**, 5595 (1953); W. G. Dauben and E. Hoerger, ibid., **73**, 1504 (1951), etc.

2) M. A. Haller and Ed. Bauer, *Compt. rend.*, **148**, 72 (1909).

3) R. Fanto, *Monatsh.*, **19**, 584 (1898).

4) G. Schroeter., *Ber.* **42**, 3360 (1909).

5) N. A. Milas and D. Surgenor, *J. Am. Chem. Soc.*, **68**, 1938 (1946).

6) G. P. Armstrong, R. Hall and D. C. Quin, *Nature*, **164**, 834 (1949).

potassium hydroxide were charged in B and hydroperoxide in A. After the air in the reaction vessel (A and B) was substituted completely with dried and purified nitrogen gas and the temperature of the reaction mixture was made to reach 80°C, and then the hydroperoxide was poured into the reaction mixture by rotating the part A by hand. A flow of the nitrogen gas was maintained constantly to 30 cc./min. during the reaction. A vigorous reaction occurred and the temperature of the reaction mixture was raised to about 90°C. Trap $T_1$ was cooled with ice and salt for condensing therein low boiling substances. The oxygen evolved during the reaction was determined at Trap $T_2$ charged with chromous chloride hydrochloric acid solution[7].

**Oxidation.**—*Acetophenone.*—10 g. of acetophenone were dissolved in 150 cc. monochlorobenzene in which 1.3 g. of finely powdered special grade potassium hydroxide were suspended. As an oxidizing agent, 2.0 g. of *tert*-butylhydroperoxide were used. The reaction mixture was agitated by a magnetic stirrer. After the temperature of the reaction mixture reached 80°C, A was gradually rotated to pour the peroxide into B. Then, a vigorous reaction occurred and a white precipitate appeared immediately. Almost all the peroxide was decomposed in the first hour, but about 6 hr. were required to complete the decomposition. After the end of the reaction, the reaction mixture was extracted with a total of 300 g. of water three times. The water extract was acidified with 2 N sulfuric acid and the precipitated benzoic acid was collected, dried and weighed. The filtrate was neutralized with concentrated ammonia water and concentrated to 10 cc., and then subjected to a paperchromatographic analysis. However, no appreciable amount of formic acid was observed. The substances condensed in Trap $T_1$ were gaschromatographically tested and methanol and *tert*-butanol were found to be the main components.

*p-Methylacetophenone.* — 50 g. of *p*-methylacetophenone suspending 1.3 g. of finely powdered potassium hydroxide were charged in B. As an oxidizing agent, 2.0 g. of *tert*-butylhydroperoxide were used. The reaction procedure was in manner similar to that of the acetophenone. The water extract was acidified. Then, *p*-toluic acid was the main reaction product. *p*-Acetylbenzoic acid and formic acid were paperchromatographically detected in the filtrate, but the amounts of acids were too small to be estimated. *p*-Toluic acid (m. p. 176°C) was confirmed by recrystallization and paperchromatography. The condensate of the Trap $T_1$ was analyzed gaschromatographically to find methanol and *tert*-butanol as the main components.

*Propiophenone.*—10 g. of propiophenone were dissolved in 150 cc. monochlorobenzene in which finely powdered 1.7 g. potassium hydroxide suspended. As an oxidizing agent, 2.0 g. of *tert*-butylhydroperoxide were used. After the temperature of the reaction mixture reached 80°C, A was rotated to pour the peroxide into the mixture and a vigorous reaction took place. Then the temperature of the reaction mixture reached as high as 95°C in a few minutes. Almost all the amount of the peroxide was decomposed in the first half hour, but the reaction continued for 6 hr. to complete the decomposition of the peroxide. The water extract was acidified with 2 N sulfuric acid and the acid precipitated was filtrated, dried and weighed. The filtrate was steamdistilled. Acetic acid was found in the distillate. This was estimated by titration. The acetaldehyde and acetone were also detected as 2,4-dinitrophenylhydrazone on a silicagel chromatostrip, but not estimated. From the condensate in Trap $T_1$, ethanol, *tert*-butanol and methanol were respectively detected gaschromatographically (see Fig. 2), but not estimated. A trace of oxygen was detected in Trap $T_2$.

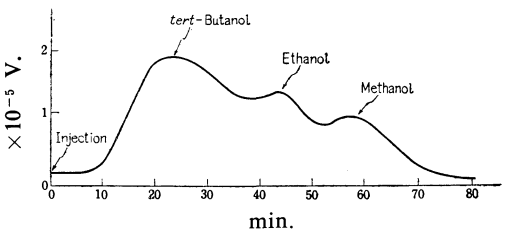



Fig. 2. Gaschromatographic analysis of oxidation products of propiophenone.
Propiophenone $\xrightarrow{tert\text{-}C_4H_9OOH,\ KOH}$ Products
Condition : Sample used : 0.02 ml.
Column temp. : 83°C
Flow rate : $N_2$ 40 ml./min.
Column : Glycerol-Kunirait (20 : 100 w/w)

*tert-Butyl Phenyl Ketone.*—Eight grams of *tert*-butyl phenyl ketone were dissolved in 150 cc. monochlorobenzene suspending 2.8 g. of finely powdered potassium hydroxide. As an oxidizing agent, 10g. of cumylhydroperoxide were used. Cumylhydroperoxide was used to afford facilities for an analysis of low boiling substances, because thermal decomposition products of cumylhydroperoxide will be methanol, aceto-

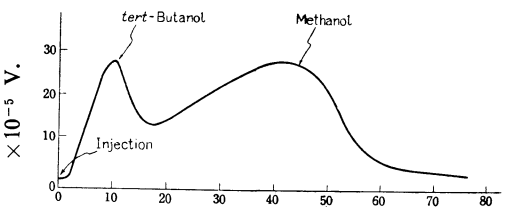



Fig. 3. Gaschromatographic analysis of oxidation products of *tert*-butylphenylketone.
*tert*-Butylphenylketone $\xrightarrow[KOH]{cumylhydroperoxide}$ products
Condition : Sample : 0.03 ml.
Column temp. : 85°C.
Flow rate : $N_2$ 60 ml./min.
Column. : Glycerol-Kunirait (20 : 100 w/w)

7) J. Meis, *Chem. Abstr.*, 8748*d* (1955); H. Karl, *Paliva*, **35**, 8 (1955); *Chem. Abstr.*, 13019*g* (1955); von Pferdton, *Ann.*, **228**, 112 (1885).

TABLE I. OXIDATION OF KETONES BY HYDROPEROXIDES AT 80°C, 6 hr.

| Ketone g. | | Hydroperoxide g. | Recovered ketone g. | Reaction products, g. Acid | Alcohol | Oxygen |
|---|---|---|---|---|---|---|
| Acetophenone | 10 | *tert*-Butyl 2.0 | 9.1 | Benzoic acid 0.50 | (*tert*-Butanol), methanol | None |
| 〃 | 10 | *tert*-Butyl 2.0 | 8.5 | Benzoic acid 0.71 | (*tert*-Butanol), methanol | None |
| *p*-Methyl-acetophenone | 50 | *tert*-Butyl 2.0 | 45 | *p*-Toluic acid 1.0, *p*-acetylbenzoic acid (trace), formic acid (trace) | (*tert*-Butanol), | None |
| 〃 | 50 | *tert*-Butyl 2.0 | 42 | *p*-Toluic acid 1.5, *p*-acetylbenzoic acid (trace), formic acid (trace) | (*tert*-Butanol), methanol | Trace |
| Propiophenone | 10 | *tert*-Butyl 2.0 | 8.3 | Benzoic acid 1.13, acetic acid 0.34, formic acid (trace) | (*tert*-Butanol), ethanol, methanol | None |
| Propiophenone | 17 | *tert*-Butyl 2.0 | — | Benzoic acid 1.13, acetic acid —, formic acid (trace) | (*tert*-Butanol), ethanol, methanol | None |
| *tert*-Butylphenyl ketone | 10 | Cumyl 10 | 9.5 | Benzoic acid 2.5 | (*tert*-Butanol), methanol, ($\alpha$,$\alpha$-dimethyl-benzylalcohol) | None |
| *tert*-Butylphenyl ketone | 0.5 | *tert*-Butyl 1.0 | — | Benzoic acid 0.05 | (*tert*-Butanol), methanol | Trace |
| Benzophenone | 10 | *tert*-Butyl 2.0 | | None reaction | | $O_2$-evolute |
| *p*-Nitrobenzo-phenone | 10 | *tert*-Butyl 2.0 | | None reaction | | $O_2$-evolute |
| Fluorenone | 10 | *tert*-Butyl 2.0 | | None reaction | | $O_2$-evolute |

(*tert*-Butanol and $\alpha$,$\alpha$-dimethylbenzylalcohol are reduction products of *tert*-butylhydroperoxide and cumylhydroperoxide.)

phenone and $\alpha$,$\alpha$-dimethylbenzylalcohol, if the thermal decomposition would occur. On the other hand, the reduction product which could be expected through the reduction of cumylhydroperoxide by ketone, is $\alpha$,$\alpha$-dimethylbenzylalcohol. Treatment of the reaction mixture was almost the same as in the case of propiophenone. From the water extract was obtained benzoic acid which was confirmed by recrystallization and paperchromatography. *tert*-Butanol was detected and estimated as the main component of low boiling substances condensed in the Trap $T_1$. This was confirmed as phenylurethane (m. p. 136°C; Found: C, 67.4; H, 7.4. Calcd. for $C_{11}H_{16}O_2N$: C, 68.3; H, 7.7%) and also gaschromatographic analysis was made. Besides *tert*-butanol, a small amount of methanol was also found.

*Benzophenone, p-Nitrobenzophenone and Fluorenone.* —10 g. of each of all the ketones were dissolved separately in 100 cc. monochlorobenzene in which 2.8 g. of finely powdered potassium hydroxide were suspended. 5 g. of *tert*-butylhydroperoxide were used as an oxidizing agent. Oxidation was carried out in the same apparatus as shown in Fig. 1. After the reaction had finished, the same procedure as before was repeated. None of the oxidation products of the ketones was found and the greater part of unchanged ketones were completely recovered during the reaction. Only oxygen—one of the decomposition products of the hydroperoxide—evolved vigorously in all the cases. *tert*-Butanol, acetone and methanol—the remaining decomposition products of the hydroperoxide itself—were found in the reaction mixture. The experimental results were summarized in Table I.

## Discussion

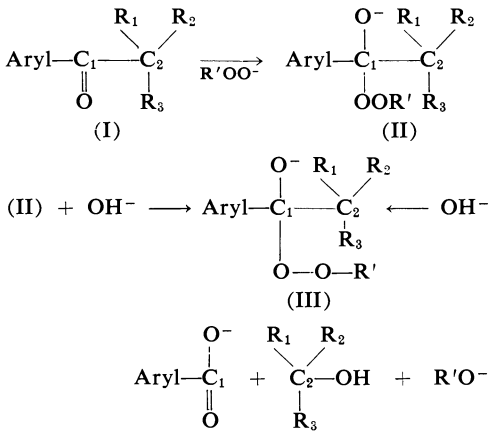
It is likely that for the oxidizing action of hydroperoxides their anions are responsible, because the hydroperoxides themselves can cleave aryl alkyl ketone very slowly or can not do so at all in the absence of alkali hydroxide. Furthermore, in the course of oxidation of alkylbenzenes[8] (*p*-xylene, cumene, ethylbenzene, *p*-cymene and tetralin) by alkali hydroperoxide, the author has observed that potassium hydroxide suspended in alkylbenzene at the beginning of the reaction dissolves nearly completely after the hydroperoxide added and then the oxidation occurs immediately. The alkylbenzenes are oxidized to alcohols, ketones and carboxylic acids. In contrast to this, hydroperoxide alone can not oxidize a side chain of the alkylbenzene in the absence of alkali hydroxide. It may, therefore, be induced

8) K. Maruyama and R. Goto, *Wood Research*, **21**, 12 (1959).

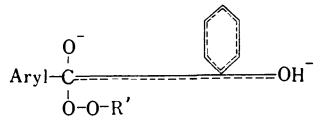
that the anion of hydroperoxide acts as an oxidizing agent. Kharasch et al.[9] asserted that the anion of hydroperoxide is an oxidizing agent in the oxidation of alcohol by hydroperoxide in alkaline solution.

In the oxidation of the above aryl alkyl ketones, the first oxidation products are arylcarboxylc acid and aliphatic alcohol. For example, when propiophenone is oxidized in the above conditions, benzoic acid, ethanol, acetaldehyde and acetic acid are obtained, and it may be seen easily that the latter two products are the second oxidation products. *tert*-Butyl phenyl ketone is also decomposed to benzoic acid and *tert*-butanol (peroxide used, cumylhydroperoxide). Oxidation of both acetophenone and *p*-methylacetophenone yields benzoic acid, *p*-toluic acid and methanol as the main reaction products. However, the methanol provides no direct evidence of alcoholic cleavage originating in the methyl-group of acetophenone or *p*-methylacetophenone, because methanol can be a thermal decomposition product of *tert*-butylhydroperoxide. In spite of the above misgivings, it may be possible to deduce that the methanol would be a cleavage product of acetophenone and also of *p*-methylacetophenone from the estimation of the results of cleavage of propiophenone and *tert*-butyl phenyl ketone; that is, the propiophenone produces ethanol and the *tert*-butyl phenyl ketone produces *tert*-butanol. On the other hand, it seems reasonable to deduce from the experimental results of benzophenone, *p*-nitrobenzophenone and fluorenone that in general diaryl ketones resist the oxidizing agent. This is noticeably different from the cleavage of ketones by peracids, because diaryl ketones are easily cleft by peracids—e. g., peracetic acid—to produce phenols and carboxylic acids[10]. In the cleavage of alkyl aryl ketones by peracids with the exception of cycloalkyl aryl ketones[11], a migration of the aryl group generally occurs, resulting in the formation of phenol.

On the contrary, acetophenone, *p*-methylacetophenone, propiophenone and *tert*-butyl phenyl ketone do not undergo such a cleavage as to yield phenols and carboxylic acids as anticipated from the phenolic cleavage of ketones, that is, the C–C linkage between the carbon atom of benzene and the carbonyl carbon atom resists the attack of hydroperoxide anion and the C–C linkage between the carbonyl carbon atom and the alkyl carbon atom is selectively attacked. For the above reasons, it may be assumed that the oxidation mechanism of ketones by hydroperoxide anion must be kept separated from that of ketones by peracids. Recently, House et al.[12] have reported the cleavage of ketones by alkaline hydrogen peroxide with a poor yield. Based upon the fact that butyrophenone does not cleave to phenol and butyric acid but does cleave to benzoic acid and propionic acid and/or corresponding propanol, they suggest a partly revised oxidation mechanism based on the peracid oxidation mechanism. However, the oxidation mechanism imagined by them hardly explains the results obtained by the present author in the oxidation of diaryl ketones. The author proposes a new oxidation scheme as follows:



In the above assumption, hydroxide anion plays in III a most important role, that is a "pushing action" which is indispensable to the cleavage of ketones. In the case of action of hydroperoxide anion to diaryl ketones resulting in no cleavage, the pushing action of hydroxide anion on $C_2$ which is the benzene ring carbon atom, would not effectively affect it owing to the high potential energy of the transition state represented by IV.



(IV)

Moreover, the fact that with aromatic halides the $S_N2$ type substitution reaction can not easily proceed appears to support a new mechanism, mentioned above. In future, the author has the intention to perform an experiment of oxidation of ketones having an asymmetric carbon atom at $C_2$.

9) M. S. Kharasch et al., *J. Org, Chem.*, **17**, 207 (1952).
10) W. H. Saunders, *J. Am. Chem. Soc.*, **77**, 4679 (1957).
11) S. L. Fries and N. Farnham, ibid., **72**, 5518 (1950).
12) H. O. House and R. L. Wasson, *J. Org. Chem.*, **22**, 1157 (1957).

The author is indebted to Professor R. Goto for his encouragement and discussion throughout this research.

*Department of Chemistry*
*Faculty of Science*
*Kyoto University*

# *Préparation de l'Emulsion à Grand Contraste pour l'Usage Lithographique*

Par Shinichi KIKUCHI et Hirozo UEDA

(Reçu le 13 Février, 1960)

Récemment les pellicules à grand contraste comme Kodalith, Reprolith ont commencé à remplacer les plaques humides dans l'usage lithographique. Les émulsions de cette espèce doivent avoir un grand contraste, une forte densité maximum et une partie inférieure courte de la courbe caractéristique. D-85, dit révélateur contagieux[1] est recommandé pour rendre l'image à grande contraste. Nous avons préparé les émulsions qui s'adaptent à ce révélateur spécial et examiné les conditions de préparation de l'émulsion qui paraissent avoir une influence sur le contraste[2]. Avant d'aborder le développement par D-85 qui est spécial, nous avons essayé de développer les émulsions avec les révélateurs N.S.G. et D-11 dont les formules seront données plus tard.

## Méthode Adoptée

Nous avons pensé qu'un des points les plus importants pour rendre l'image à grand contraste était d'uniformiser les dimensions des grains d'halogénure d'argent. Pour atteindre ce but, nous avons procédé à varier les conditions suivantes:

1. Le mode d'addition du nitrate d'argent dans la solution de bromure de potassium.
2. La concentration en ions argent dans la solution de nitrate d'argent.
3. La vitesse d'addition du nitrate d'argent.
4. L'excès des ions halogènes.
5. Le rapport des concentrations en ions $Cl^-$, $Br^-$ et $I^-$.
6. Le rapport de la concentrations en ions argent à la concentration de gélatine.
7. La concentration de la gélatine.
8. La température.

Nous avons employé dans cette expérience la méthode statistique pour déterminer si quelques-unes de ces conditions ont une influence sur le contraste. La corrélation entre les les conditions et le gamma est jugée par le degré de confiance à 95 et 97%.

## Partie Expérimentale

**Examen des Gélatines Utilisées.**—Dans la première partie de cette étude nous avons examiné les propriétés physico-chimiques et chimiques des gélatines destinées à la préparation de l'émulsion. La teneur en eau de la gélatine a été mesurée par la diminution de poids de la gélatine laissée dans une étuve sèche maintenue à la température constante de 105±5°C. Le point de fusion et le point de congélation ont été mesurés d'après la méthode* recommandée par l'Association des Compagnies Photographiques du Japon. La réaction de Feigl a été examinée de la manière suivante. Environ 1 ml. de la solution de gélatine à 10% qui contient 0.02 g. d'azoture de soude pour 5 ml. de la solution de gélatine, est étendu sur une plaque de verre 2×2 cm. puis laissé à se solidifier. Une heure après, une goutte de solution d'iode (1.268 g. d'iode et 2.5 g. de l'iodure de potassium sont dissous dans 1 litre d'eau distillée) est mise sur la gélatine et cela donne des bulles d'azote suivant la formule: $2NaN_3+I_2=3N_2+2NaI$.

Le nombre de bulle de gaz est compté pendant un quart d'heure et la quantité de bulles est classée entre les valeurs relatives 1 et 10. Cette méthode n'est que qualitative et peut donner une erreur assez élevée quand le nombre de bulles dépasse 40 par 0.5 $cm^2$.

La réaction de Vogel a été examinée de la manière suivante pour montrer le pouvoir réducteur de gélatine. 10 ml. de nitrate d'argent ammoniacal à 6% et 10 ml. de la solution de gélatine à 2% sont mélangés à 32°C et laissés à cette température pendant 24 heures. La couleur de la gélatine est comparée à l'aide d'un colorimètre de Dubosque et le degré de coloration est classé entre les valeurs relatives 1 et 10. Des propriété physico-chimiques des gélatines essayées sont données dans Tableau I.

1) J. A. Yule, *J. Frankl. Inst.*, **239**, 221 (1945).
2) E. J. Wall, "Photographic Emulsions", (1929) pp. 35, 48 et 67; Eder, "Handb. d. Photogrphie", (1927), Bd. 3 Teil I, 3 Aufl; A. Steigmann, "IX e Congré Intern. Photo. Paris", (1936), pp. 372—386.

* Cette méthode est semblable à celle de PAGI qui a paru dans *Bull. Soc. Phot. Sci. Japon*, No. 6, 34 (1956).

TABLEAU I. PROPRIÉTÉS PHYSICO-CHIMIQUES ET CHIMIQUES DES GÉLATINES

| Espèces d'échantillons | Eau % | Point de fusion, °C | Point de congélation, °C | Valeur Feigl | Valeur Vogel |
|---|---|---|---|---|---|
| Nitta No. 3 | 17.7 | 31.9 | 26.0 | 1 | 1 |
| Nippi process | 17.1 | 31.9 | 26.6 | 1 | 2 |
| Nippi ammonia | 16.4 | 30.4 | 25.5 | 10 | 1 |
| Takarazuka 179-5 | 16.5 | 32.5 | 28.5 | 4 | 5 |

**Procédé de Préparation de l'Emulsion.**—*a. Les solutions de réactifs.*—Nous avons préparé les solutions de nitrate d'argent, d'halogénure et de gélatine à température déterminée (45°C). La gélatine est dissoute à 45°C, après d'avoir gonflé dans l'eau. La quantité des solutions est en général de 50 ml.

*b. Addition des solutions et première maturation.*—Les solutions maintenues à 45°C sont mélangées brusquement dans un vase porcelaine et mises à la maturation pendant 20 min. avec agitation. L'appareil d'addition et de maturation est représenté par Fig. 1.

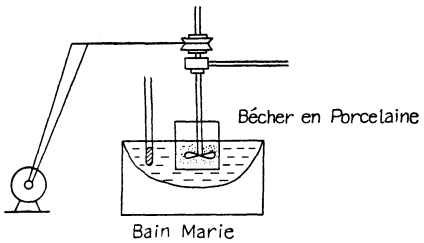



Fig. 1. Bain de maturation.

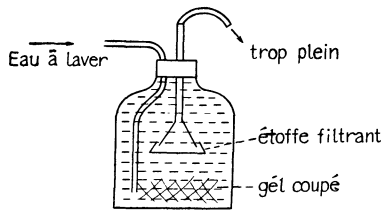



Fig. 2. Appareil de lavage de gél.

*c. Congélation de l'émulsion et son coupage en morceaux.*—Après la première maturation, l'émulsion est mise dans la glace pour la congélation et elle est laissée pendant une nuit dans un frigorifique. Le lendemain matin l'émulsion est coupée par un réseau encadré de bois et formé d'amylan (résine synthétique) dont la maille est de 3 mm. carré. Les émulsions coupées en morceaux sont lavées à l'eau courante dans l'appareil comme dans Fig. 2. La température de l'eau de lavage est maintenue à 14~16°C. La fin de lavage est contrôlée à l'aide du réactif de Nessler qui permet de vérifier s'il reste de l'ammoniaque. Pour 50 ml. d'émulsion une demi-heure de lavage est nécessaire.

*d. 2e Maturation.*—Après le lavage, l'émulsion est mise de nouveau dans un bécher de porcelaine où le gel doit se dissoudre en 1 min. à 45°C. En maintenant l'émulsion à cette température, le plus haut gamma est attteint avec une maturation de 40~70 min. L'agitation mécanique pendant la 2e maturation donne naissance à des bulles quand l'émulsion est étendue sur le verre. On agite donc lentement à la main.

*e. Coulage de l'émulsion sur le verre.*—Le verre de format 119×146 mm. est préalablement lavé, enduit d'une solution d'alun de chrome à 20% et desséché. Avant de coulage, il est porté à 35°C. Le prélèvement de 5 ml. d'émulsion est fait avec une pipette et le coulage est effectué. La couche est nivelée par une tige de verre. La plaque de verre est trans portée sur une planche de verre placée horizontalement et laissée à sécher à l'air à 35°C.

*f. Sensitométrie.*—La sensitométrie se fait par le sensitomètre type I de N.S.G. qui est muni d'un coin ayant une différence de densités successives de 0.15. Les révélateurs employés sont N.S.G. et D-11 à 20°C et ils sont appliqués pendant 4 minutes.

## Résultats

**Propriétés Physico-chimiques et Chimiques des Gélatines Utilisées.** — Les propriétés physico-chimiques et chimiques des gélatines utilisées sont données dans Tableau I. Dans ce tableau les valeurs relatives de Feigl se réfèrent à 1 de Nitta No 3 et 10 de Nippi ammonia et les valeurs de Vogel à 2 de Nippi 61-i et 10 de Nippi FAG 4.

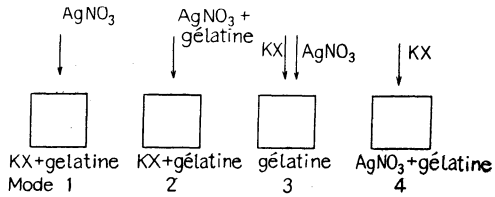



Fig. 3. Différents modes d'addition.

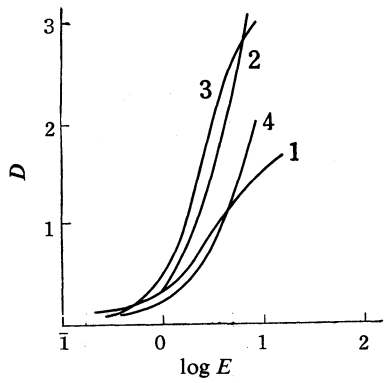



Fig. 4. Courbes caractéristiques.

**Différents Modes d'Addition.** — Nous avons employé quatre différents modes d'addition comme dans Fig. 3. Les résultats sont indiqués dans Tableau II. Prenons un exemple pour illustrer la signification des nombres donnés dans ce tableau. 25 ml. (0.025 g. mole) de la solution de nitrate d'argent 1 M (conc.) sont ajoutés à une solution de gélatine contenant 23.8 ml. de KBr 1.2 M et 1.2 M ml. de KI 1.2 M. Le repport de KBr/KI est de 23.8/1.2=19.8. Cette solution dissout 2.0575 g. de gélatine, ce qui donne le rapport gélatine en gramme/AgX en g. mole 2.0575/0.025=82.3. Dans les conditions où l'iodure est totalement précipité, le rapport AgBr/AgI est 23.56/1.43= 16.3. La quantité totale d'émulsion devient 50 ml. après l'addition.

Dans le mode 2, la quantité de gélatine est divisée en deux parties égales. Les courbes caractéristiques sont données dans Fig. 4 où l'ont voit que c'est le mode 2 qui donne la mailleure courbe avec un gamma élevé.

**Variation de l'Excès d'Halogénure, Rapport des Halogénures et Quantité de Gélatine.**—Dans cette série d'expériences, nous avons fait varier deux facteurs en même temps entre trois qui peuvent influencer les caractéristiques de l'émulsion (Tableaux III et IV). En comparant les résultats, nous avons trouvé qu'une valeur élevée du rapport halogénure d'argent gélatine et un petit excès d'halogénure favorisaient un gamma élevé. La variation du rapport AgCl/AgBr a peu d'effet dans les conditions de ces essais. Si l'on diminue la quantité de gélatine au-delà d'une limite, les grains d'halogénure d'argent sont susceptibles de s'aggroméler avec certaines sortes de gélatine. Nippi Process donne le meilleur résultat. Comme excès

TABLEAU II. RÉSULTATS DE QUATRE MODES D'ADDITION (GÉLATINE, NITTA NO. 3)

| No. d'essais | Mode d'addition | $AgNO_3$ g. mole | Conc. M | KX conc. M | KBr/KI | AgBr/AgI |
|---|---|---|---|---|---|---|
| 1 | 1 | 0.025 | 1 | 1.20 | 19.8 | 16.3 |
| 2 | 2 | 〃 | 〃 | 〃 | 〃 | 〃 |
| 3 | 3 | 〃 | 1.43 | 1.71 | 〃 | 〃 |
| 4 | 4 | 〃 | 1 | 1.20 | 〃 | 〃 |

| No. | Conc. de gélatine gél/AgX | Conc. | 2e Maturation | | $\gamma$(degré de confiance à 95%) | Sensibilité N. S. G. | Voile |
|---|---|---|---|---|---|---|---|
| 1 | 82.3 | 82.3 | 45°C, | 50 min. | 1.58～1.36 | 0.43 | 0.07 |
| 2 | 〃 | 41.2 | 〃 | 〃 | 4.93～3.77 | 0.24 | 0.10 |
| 3 | 〃 | 137 | 〃 | 〃 | 3.72～3.40 | 0.53 | 0.05 |
| 4 | 〃 | 82.3 | 〃 | 〃 | 2.76～2.52 | 0.22 | 0.09 |

TABLEAU III. RÉSULTATS DES EXPÉRIENCES OÙ L'ON FAIT VARIER L'EXCÈS D'HALOGÉNURE, LE RAPPORT DES HALOGÉNURES ET LA QUANTITÉ DE GÉLATINE (NITTA NO. 3, GÉLATINE)

| No. d'essai | $AgNO_3$ g. mole | $AgNO_3$ Conc. M | KX Excès g. mole | KX Conc. M | Rapport KCl/KBr | Rapport AgCl/AgBr |
|---|---|---|---|---|---|---|
| 5 | 0.016 | 0.64 | 0.20 | 0.77 | 1.97 | 1.5 |
| 6 | 〃 | 〃 | 0.90 | 1.24 | 3.74 | 〃 |
| 7 | 〃 | 〃 | 0.20 | 0.77 | 4.74 | 4 |
| 8 | 〃 | 〃 | 0.90 | 1.24 | 8.29 | 〃 |

| No. d'essai | Gélatine Gélatine g. / AgX g. mole | Gélatine Conc. | 2è Maturation | | $\gamma$ | Sensibilité N. S. G. | Voile |
|---|---|---|---|---|---|---|---|
| 5 | 101 | 33<br>33 | 45°C, | 50 min. | 5.42～4.98 | 0.42 | 0.15 |
| 6 | 151 | 49.8<br>49.8 | 〃 | 〃 | 1.51～1.39 | 0.43 | 0.13 |
| 7 | 151 | 49.8<br>49.8 | 〃 | 〃 | 1.98～1.70 | 0.65 | 0.12 |
| 8 | 101 | 33<br>33 | 〃 | 〃 | 3.95～2.05 | 0.43 | 0.14 |

TABLEAU IV. RÉSULTATS DES EXPERIENCES OÙ L'ON FAIT VARIER L'EXCÈS D'HALOGÉNURE, LE RAPPORT DES HALOGÉNURES DANS LES ENVIRONS DE NO. 5 (GÉLATINE NIPPI PROCESS)

| No. d'essai | $AgNO_3$ g. mole | $AgNO_3$ Conc. M | KX Excès g. mole | KX Conc. M | Rapport KCl/KBr | Rapport AgCl/AgBr |
|---|---|---|---|---|---|---|
| 9 | 0.20 | 1 | 0.15 | 0.77 | 1.54 | 1.2 |
| 10 | 〃 | 〃 | 0.25 | 0.84 | 1.76 | 〃 |
| 11 | 〃 | 〃 | 0.15 | 0.77 | 2.23 | 1.8 |
| 12 | 〃 | 〃 | 0.25 | 0.84 | 2.51 | 〃 |
| 13 | 〃 | 〃 | 0.20 | 0.80 | 2.00 | 1.5 |
| 14 | 〃 | 〃 | 0.25 | 0.84 | 2.12 | 〃 |
| 15 | 〃 | 〃 | 0.30 | 0.87 | 2.25 | 〃 |

| No. d'essai | Gélatine: Gélatine g. / AgX g. mole | Gélatine: Conc. | 2è Maturation | $\gamma$ | Sensibilité N. S. G. | Voile |
|---|---|---|---|---|---|---|
| 9 | 100 | 33.5<br>44.5 | 45°C, 80 min. | 2.58～1.94 | 0.55 | 0.29 |
| 10 | 〃 | 〃 | 〃 70 | 3.30～2.48 | 0.50 | 0.14 |
| 11 | 〃 | 〃 | 〃 60 | 2.54～2.14 | 0.35 | 0.21 |
| 12 | 〃 | 〃 | 〃 70 | 3.08～2.68 | 0.35 | 0.18 |
| 13 | 〃 | 〃 | 〃 60 | 3.08～2.72 | 0.45 | 0.20 |
| 14 | 〃 | 〃 | 〃 65 | 2.94～1.90 | 0.90 | 0.08 |
| 15 | 〃 | 〃 | 〃 60 | 3.11～2.15 | 0.91 | 0.16 |

TABKEAU V. BASES DE CALCUL

| No. de coin | Log $E=x_i$ | Densités observées, $D_i$ | | | | | |
|---|---|---|---|---|---|---|---|
| 11 | 0.25 | 2.22 | 2.23 | 2.15 | 2.15 | 2.27 | 2.25 |
| 12 | 0.10 | 1.52 | 1.52 | 1.44 | 1.46 | 1.35 | 1.33 |
| 13 | −0.05 | 0.63 | 0.65 | 0.63 | 0.64 | 0.66 | 0.68 |

| $x_i$ | $(x_i-\bar{x})\times10^{-2}$ | $(x_i-\bar{x})^2\times10^{-4}$ | $D_i$ | $(D_i-\bar{D})\times10^{-2}$ | $(x_i-\bar{x})\times(D_i-\bar{D})\times10^{-4}$ | $\hat{\beta}(x_i-\bar{x})\times10^{-2}$ | $\{(D_i-\bar{D})-\hat{\beta}(x_i-\bar{x})\}^2\times10^{-4}$ |
|---|---|---|---|---|---|---|---|
| 0.25 | 15 | 225 | 2.22 | 79 | 1185 | 78 | 1 |
| | | 〃 | 2.23 | 80 | 1200 | | 4 |
| | | 〃 | 2.15 | 72 | 1080 | | 36 |
| | | 〃 | 2.15 | 72 | 1080 | | 36 |
| | | 〃 | 2.27 | 84 | 1260 | | 36 |
| | | 〃 | 2.25 | 82 | 1230 | | 16 |
| 0.10 | 0 | 0 | 1.52 | 9 | 0 | 0 | 81 |
| | | 〃 | 1.52 | 9 | | | 81 |
| | | 〃 | 1.44 | 1 | | | 1 |
| | | 〃 | 1.46 | 3 | | | 9 |
| | | 〃 | 1.35 | − 8 | | | 64 |
| | | 〃 | 1.33 | −10 | | | 100 |
| −0.05 | −15 | 225 | 0.63 | −80 | 1200 | 78 | 4 |
| | | 〃 | 0.65 | −78 | 1130 | | 0 |
| | | 〃 | 0.63 | −80 | 1200 | | 4 |
| | | 〃 | 0.64 | −79 | 1185 | | 1 |
| | | 〃 | 0.66 | −77 | 1155 | | 1 |
| | | 〃 | 0.68 | −75 | 1125 | | 9 |
| $\bar{x}=0.10$ | | $\Sigma=2700$ | $\Sigma=25.78$ | | $\Sigma=14030$ | | $\Sigma=484$ |

d'halogénure, 25% est le meilleur.

*Manière de traitement des valeurs.*—Pour obtenir les résultats ci-dessus, nous avons employé la manière statistique pour obtenir le gamma probable.

Supposons qu'une relation linéaire existe entre deux valeurs $x$ et $y$ comme suit:

$$y=a_0+b_0x \quad (1)$$

où $a_0$ et $b_0$ sont constants. Les valeurs $y=y_i$ sont obtenues pour $x=x_i$ et $i=1, 2, \cdots\cdots n$. Si $Y_i$ est la valeur obtenue par la méthode de minimum de carrés des valeurs observées,

$$Y_i=a+bx_i$$

L'addition des carrés de déviation entre $y_i$ et $Y_i$ soit minimum:

$$y=\bar{y}+[\sum(x_i-\bar{x})(y_i-\bar{y})/\sum(x_i-\bar{x})^2](x_i-x)$$

$$=\bar{y}+\hat{\beta}(x_i-\bar{x}) \quad (2)$$

où $\bar{y}$ est le moyen de $y_i$, $\bar{x}$ est celui de $x_i$ et $\hat{\beta}$ correspond au gamma. Si l'on prend $S_y$ comme dispersion de $y$ et $n$, comme degré de liberté.

$$S_y=(1/n)\sum[y_i-\{\bar{y}+(\sum(x_i-\bar{x})(y_i-\bar{y})/\sum(x_i-\bar{x})^2)(x_i-\bar{x})\}]^2\equiv\hat{c} \quad (3)$$

Si la fonction $\hat{c}$ (la dispersion du groupe mère) suit la répartition $\chi^2$ du système ayant le degré de liberté $n$, la répartition $t$ est induite de la répartition $\chi^2$ comme suit:

$$t=\sqrt{(n-2)S_x^2}(\hat{\beta}-\gamma)/\sqrt{\hat{c}} \quad (4)$$

d'où

$$\gamma=\hat{\beta}\pm t\sqrt{\hat{c}}/\sqrt{(n-2)S_x^2} \quad (5)$$

où $\gamma$ est le gamma probable et

$$S_x^2=\sum(x_i-\bar{x})^2/n$$

Les auteurs citent un exemple de calcul dans Tableau V.

$$S_x^2=(x_i-\bar{x})/n=2700\times10^{-4}/18=150\times10^{-4}$$

$$\bar{y}=\bar{D}=1.43$$

$$\hat{\beta}=(x_i-\bar{x})(y_i-\bar{y})/(x_i-\bar{x})^2$$

$$=14030\times10^{-4}/2700\times^{-4}=5.20$$

$$\hat{c}=26.9$$

$$n-2=16$$

$t=2.12$ (pour le degré de confiance de 95%)

$$=5.20\pm\frac{2.12\sqrt{26.9}}{\sqrt{16\times150}}=5.20\pm0.22$$

$$=5.42\sim4.98$$

Par cette expérience nous avons voulu examiner l'effet sur gamma en faisant varier la quantité d'excès d'halogénure, du rapport d'ions halogène et la quantité de gélatine. Pour savoir l'effet de trois facteurs il faut faire au moins huit expériences. Mais nous avons fait l'application partielle en employant la méthode du carré latin avec deux niveaux de chaque condition. Le système est schématisé comme Tableau VI.

TABLEAU VI. SYSTÈME DE L'APPLICATION PARTIELLE DU CARRÉ LATIN

| Expérience | Facteurs 1 | 2 | 3 |
|---|---|---|---|
| I | A | C | E |
| II | A | D | F |
| III | B | C | F |
| IV | B | D | E |

Nous avons employé deux niveaux A, B du facteur 1, deux niveaux C, D du facteur 2 et E, F du facteur 3. La valeur obtenue, Val. I de l'équation (6) montre la variation de la différence entre A et B du facteur 1. D'autres facteurs se sont compensés les uns les autres.

TABLEAU VII. RÉSULTATS DES EXPÉRIENCES OÙ L'ON FAIT VARIER LES CONCENTRATIONS DE LA SOLUTION D'ARGENT ET DE LA SOLUTION D'HALOGÉNURE

| No. | $AgNO_3$ | | KX | | 2e Maturation | |
|---|---|---|---|---|---|---|
| | g. mole | Conc. | Excès g. mole | Conc. | Rapport KCl/KBr | Rapport AgCl/AgBr |
| 13 | 0.020 | 1 | 0.20 | 0.80 | 2.00 | 1.5 |
| 16 | 0.022 | 1.09 | 〃 | 0.87 | 〃 | 〃 |
| 17 | 0.024 | 1.20 | 〃 | 0.96 | 〃 | 〃 |
| 18 | 0.027 | 1.34 | 〃 | 1.07 | 〃 | 〃 |
| 19 | 0.030 | 1.50 | 〃 | 1.20 | 〃 | 〃 |

| No. | Gélatine g. / AgX g. mole | Gélatine conc. | 2e Maturation | $\gamma$ | Sensibilité | Voile |
|---|---|---|---|---|---|---|
| 13 | 100 | 33.5 | 45°C, 60 min. | 3.08~2.72 | 0.45 | 0.20 |
| 16 | 92 | 〃 | 〃 75 | 3.22~2.72 | 0.54 | 0.20 |
| 17 | 83.5 | 〃 | 〃 60 | 3.64~3.20 | 0.70 | 0.18 |
| 18 | 75 | 〃 | 〃 60 | 2.73~1.97 | 1.00 | 0.15 |
| 19 | 66.7 | 〃 | 〃 70 | 2.61~2.13 | 0.91 | 0.23 |

TABLEAU VIII. RÉSULTATS DES EXPÉRIENCES OÙ L'ON FAIT VARIER LA QUANTITÉ D'AMMONIAQUE (GÉLATINE WINTERTHUR N4625)

| No. | $AgNO_3$ mole | $AgNO_3$ conc. M | $NH_3$ par 0.025 mole de $AgNO_3$ | KX Excès | KX Conc. M | Rapport KCl/KBr | Rapport AgCl/AgBr |
|---|---|---|---|---|---|---|---|
| 20 | 0.016 | 0.73 | 1 ml. | 0.20 | 0.67 | 2.0 | 1.5 |
| 21 | 〃 | 0.88 | 9.5 | 〃 | 0.59 | 〃 | 〃 |
| 22 | 〃 | 0.88 | 1 | 〃 | 0.59 | 〃 | 〃 |
| 23 | 〃 | 0.73 | 9.5 | 〃 | 0.67 | 〃 | 〃 |

| No. | Gélatine g. / AgX mole | Gélatine conc. | 2e Maturation | $\gamma$ | Sensibilité | Voile |
|---|---|---|---|---|---|---|
| 20 | 101 | 38.5<br>28.9 | 45°C, 55 min. | 3.47～2.37 | 0.90 | 0.43 |
| 21 | 〃 | 46.2<br>25.6 | 〃 65 | 3.78～3.32 | 2.22 | 0.30 |
| 22 | 〃 | 〃 | 〃 45 | 4.30～3.54 | 1.33 | 0.29 |
| 23 | 〃 | 38.5<br>28.9 | 〃 70 | 2.89～2.57 | 1.17 | 0.43 |

TABLEAU IX. RÉSULTATS DES EXPÉRIENCES FAITES AVEC DIVERSES ESPÈCES DE GÉLATINE

| No. | $AgNO_3$ mole | $AgNO_3$ Conc. M | KX Excès | KX Conc. M | Rapport KCl/KBr | Rapport AgCl/AgBr |
|---|---|---|---|---|---|---|
| 24 | 0.20 | 1 | 0.20 | 0.80 | 2.0 | 1.5 |
| 25 | 〃 | 〃 | 〃 | 〃 | 2.38 | 1.8 |
| 26 | 0.16 | 0.88 | 〃 | 0.59 | 2.00 | 1.5 |
| 27 | 0.24 | 1.20 | 〃 | 0.96 | 2.00 | 1.5 |
| 5 | 0.16 | 0.64 | 〃 | 0.77 | 2.00 | 1.5 |

| No. | Gélatines Espèces | Gélatine g. / AgX mole | Conc. | 2e Maturation | $\gamma$ | Sensibilité | Voile |
|---|---|---|---|---|---|---|---|
| 24 | British gélatine | 92.4 | 29.3 | 45°C, 60 min. | 3.37～2.35 | 0.60 | 0.28 |
| 25 | 〃 | 100.5 | 38.5 | 〃 55 | 3.92～2.54 | 0.25 | 0.32 |
| 26 | Winterthur N4625 | 101 | 46.2 | 〃 60 | 4.30～3.54 | 1.33 | 0.29 |
| 27 | Nippi process | 83.5 | 33.5 | 〃 60 | 3.64～3.20 | 0.70 | 0.18 |
| 5 | Nitta No. 3 | 101 | 33 | 〃 50 | 5.42～4.98 | 0.42 | 0.15 |

Val. I = (Résultat I + Résultat II)/2
− (Résultat III + Résultat IV)/2 (6)

Total des carrés moyens :

$$C.F. = (5.20+3.00+1.84+1.45)^2/4 = 11.49^2/4 = 33.005$$

Influence du facteur 1 :

$$S_1 = \{(5.20+3.00)^2+(1.84+1.45)^2\}/2 - C.F. = 6.027$$

d'où s'obtient le rapport de dispersion 602.7.
Influence du facteur 2 :

$$S_2 = \{(5.20+1.84)^2+(3.00+1.45)^2\}/2 - C.F. = 1.627$$

Influence du facteur 3 :

$$S_3 = \{(5.20+1.45)^2+(3.00+1.84)^2\}/2 - C.F. = 0.819$$

D'où les rapports de dispersion des facteurs 2 et 3 sont respectivement 162.7 et 81.9.

D'après le tableau de répartition de $F$, $S_1$ et $S_2$ montrent que les facteurs 1 et 2 sont significatifs et que $S_3$ ne l'est pas pour varier gamma.

**Variation de Concentration de la Solution.**— Nous avons également essayé de faire varier la concentration de la solution d'argent et de la solution d'halogénure. Les résultats sont donnés dans Tableau VII.

Plus la concentration est grande, plus la sensibilité est grande et le gamma est petit. Au-dessus d'une certaine concentration, le voile

TABLEAU X. FORMULES DES RÉVÉLATEURS* D-11 ET N.S.G.

| | D-11 | N. S. G. |
|---|---|---|
| Métol | 1 g. | 3 g. |
| $Na_2SO_3$ | 75 | 50 |
| Hydroquinone | 9 | 6 |
| $Na_2CO_3$ | 25 | 25 |
| KBr | 5 | 1 |
| Eau q.s.p.f. | 1000 ml. | 1000 ml. |

* à diluer pour double volume

TABLEAU XI. GAMMAS OBTENS PAR D-11 ET PAR N. S. G.

| No. des essais | 9 | 10 | 11 | 12 | 13 | 14 | 15 | 16 | 17 | 18 | 19 |
|---|---|---|---|---|---|---|---|---|---|---|---|
| N. S. G. | 2.26 | 2.89 | 2.34 | 2.88 | 2.90 | 2.42 | 2.63 | 3.11 | 3.42 | 2.35 | 2.37 |
| D-11 | 4.65 | 4.02 | 3.09 | 3.47 | 3.36 | 3.71 | 3.71 | 3.22 | 3.84 | 3.56 | 4.12 |

augmente sensiblement trandis que la sensibilité et le gamma diminuent.

**Cas où l'on Ajoute un Excès d'Ammoniaque.** Nous avons essayé d'ajouter un excès d'ammoniaque. Les résultats sont présentés dans Tableau VIII. Dans cette série d'expériences on a également fait varier la quantité de gélatine. Le voile était assez sensible et nous n'avons pas pu obtenir de résultats significatifs et utiles.

**Espèces de Gélatine.**—Nous avons essayé la formule No. 9 avec quatre espèces de gélatine. Nitta No. 3 donne le moindre voile et elle est considérée comme la meilleure parmi ces gélatines (Tableau IX).

**Emploi de Différents Révélateurs.**—Tous les résultats mentionnés jusqu'ici ont été obtenus par le révélateur NSG. D I I donne toujours un gamma plus élevé que le révélateur NSG. Les formules de de deux révélateurs sont données dans Tableau X. La différence entre ces deux gammas dans certains échantillons est donnée dans Tableau XI.

## Conclusion

Dans les conditions que nous avons essayées, le mode 2 d'addition du nitrate d'argent dans KBr avec division de la gélatine en deux parties a donné les résultats les plus conformes au but que nous avous visé proposés. L'observation à microscope électronique semble indiquer que ce mode donne les grains de grandeurs homogènes. Il est préférable de choisir l'excès d'halogénure entre 20 et 30%. Un rapport de la concentration de gélatine à la concentration d'halogénure d'argent voisin de 101 (en unité de gélatine gramme au g. mole de AgX). L'influence de certains autres facteurs n'est pas encore bien déterminée.

*Institut des Sciences Industrielles*
*Université de Tokio*
*Chiba*

# *Graft Polymerization by Pre-heating Method Applied to Polyethylene Containing Benzoyl Peroxide*

By Seizo OKAMURA and Tomonobu MANABE

(Received March 28, 1960)

It has been found by G. Oster that some solid polymers containing photo-sensitizer such as benzophenone could initiate graft polymerization with irradiation by ultra-violet as well as by ionizing rays[1-3]. In those cases, the primary action will be not on the polymer but on the photo-sensitizer, and the decomposed sensitizer fragment may abstract hydrogen atoms from the polymer molecules. The polymer radicals thus formed can initiate graft polymerization or cross-linking reaction.

The ultraviolet pre-irradiation method for graft polymerization or cross-linking reaction cannot be generally applied to thick films or a bundle of fibers because the penetrating power of the rays may be fairly low.

It is found here that some solid polymers containing initiator of radical polymerization of vinyl monomers such as benzoyl peroxide or azobisisobutyronitrile can initiate graft polymerization. This grafting method may be easily applied to thick films or to a bundle of fibres.

## Experimental

A commercial low density polyethylene film of $0.0017\,g.\cdot cm^{-2}$ thickness is soaked for 60 min. in the benzene solution of benzoyl peroxide ($20\,g.\,l^{-1}$) at 50°C, the surface is washed with benzene, and dried. The sample thus obtained contains benzoyl peroxide about 0.2 wt. %. The sample is then heated in air. The sample is sealed with purified methyl methacrylate monomer in a glass tube, and

1) G. Oster and O. Shibata, *J. Polymer Sci.*, **26**, 233 (1957).
2) G. Oster, G. K. Oster and H. Moroson, *J. Polymer Sci.*, **34**, 671 (1959).
3) S. Okamura and T. Manabe, *Isotopes and Radiation*, in press.

then heated in vacuum. After the treatment for graft polymerization, the sample is washed with benzene for about 20 hr. at room temperature in order to extract the homopolymer already formed. The complete extraction, however, will be very hard in such a condition, but some comparison between the graft polymerization conditions may be possible. The sample is then dried and weighed. The amount of graft polymerization will be defined here by

$$\text{graft polymerization \%} = \left( \frac{\text{weight of sample after graft polymerization}}{\text{weight of sample before graft polymerization}} - 1 \right) \times 100$$

The values of grafting thus obtained are rather scattered according to the inhomogeneity of the benzoyl peroxide content and of the sample thickness. Therefore kinetical discussion is omitted here.

## Results

**Time of Pre-heating.**—The effect of time of pre-heating on the graft polymerization is shown in Fig. 1, where the temperature of pre-heating is maintained at 110°C, and the polymerization temperature is 60°C.

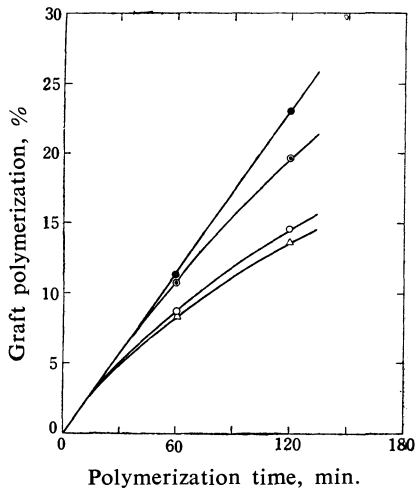



Fig. 1. Effect of time of pre-heating on graft polymerization.
Pre-heating temperature: 110°C
Polymerization temperature: 60°C
Time of pre-heating: -△- 15 min., -○- 30 min., -⊙- 45 min., -●- 60 min.

From the results shown in Fig. 1, it is recognized that the rate of graft polymerization increases with an increase of the time of pre-heating.

**Temperature of Pre-heating.**—The effect of temperature of pre-heating on the graft polymerization is shown in Fig. 2, where the time of pre-heating is maintained at 30 min., and the polymerization temperature is 60°C.

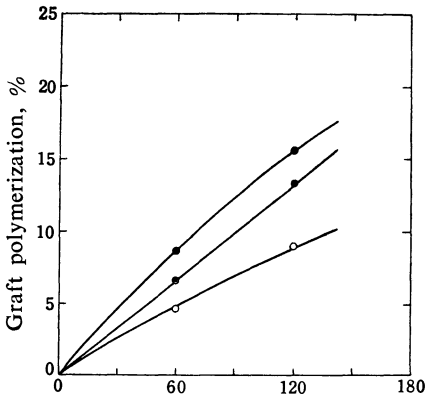



Fig. 2. Effect of temperature of pre-heating on graft polymerization.
Pre-heating time: 30 min.
Polymerization temperature: 60°C
Temperature of pre-heating: -○- 90°C, -⊙- 110°C, -●- 120°C.

From the results shown in Fig. 2, it is found that the rate of graft polymerization increases with the rise of temperature of pre-heating.

**Polymerization Temperature.**—The influence of polymerization temperature on the graft polymerization is represented in Fig. 3, where the pre-heating temperature is maintained at 110°C, and the pre-heating time is 30 min.

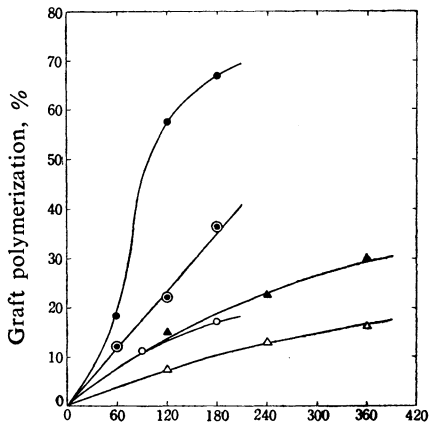



Fig. 3. Effects of polymerization temperature, pre-heating and benzoyl peroxide sensitization on graft polymerization.
Pre-heating: 110°C, 30 min.
-●-
-⊙- No pre-heating
-○- No BPO sensitization
} Polymerization temperature: 70°C
-▲-
-△- No BPO sensitization
} Polymerization temperature: 50°C

**After-effect of Pre-heating.**—The after-effect of pre-heating is shown in Fig. 4, where the pre-heating temperature is maintained at 110°C, the pre-heating time is 30 min. and the polymerization temperature is 60°C.

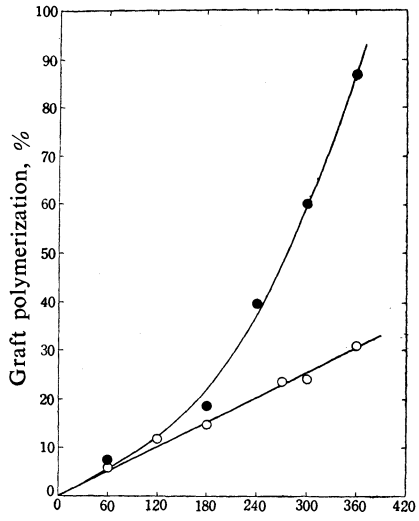



Fig. 4. After effect of pre-heating on graft polymerization.
Pre-heating: 110°C, 30 min.
Polymerization temperature: 60°C
Time interval after pre-heating until polymerization: -○- 4,300 min., -●- 300 min.

From the results represented in Fig. 4, it is shown that the rate of graft polymerization decreases with an increase of time interval after pre-heating until polymerization. And also, the difference of rates between two experiments having different intervals increases with an increase of polymerization time.

## Discussion

The mechanism of graft polymerization reported here may be as follows. I represents the initiator of radical polymerization, P the polymer, M the monomer, and $O_2$ the oxygen respectively.

**Reaction in Pre-heating.**

$I \rightarrow R\cdot$ (1) decomposition of initiator

$R\cdot + P \rightarrow P\cdot + RH$ (2) radical transfer to polymer, production of polymer radical

$P\cdot + O_2 \rightarrow POO\cdot$ (3) production of polymer peroxide radical

$P\cdot + R\cdot \rightarrow$ product (4) disappearence of polymer radical

$P\cdot + P\cdot \rightarrow PP$ (5) cross-linking reaction

$P\cdot + POO\cdot \rightarrow POOP$ (6) production of polymer diperoxide

$POO\cdot + R\cdot \rightarrow POOR$ (7) production of polymer peroxide

**Reaction in Graft Polymerization.**

$I \rightarrow R\cdot$ (8) decomposition of initiator

$POOP \rightarrow PO\cdot + PO\cdot$ (9) decomposition of polymer diperoxide

$POOR \rightarrow PO\cdot + RO\cdot$ (10) decomposition of polymer peroxide

$R\cdot + M \rightarrow RM\cdot$ (11) polymerization by initiator fragment

$PO\cdot + M \rightarrow POM\cdot$ (12) polymerization by polymer diperoxide fragment

$RO\cdot + M \rightarrow ROM\cdot$ (13) polymerization by polymer peroxide fragment

$P\cdot + M \rightarrow PM\cdot$ (14) polymerization by frozen polymer radical at the inside of polymer

$POO\cdot + M \rightarrow POOM\cdot$ (15) polymerization by frozen polymer peroxide radical

The increasing of time and the rise of temperature of pre-heating increase the initiator fragment [R·], and then the increase of graft polymerization may be expected (Figs. 1 and 2). The increase of time interval after pre-heating until polymerization results in the decrease of the concentration of frozen polymer radical (reactions 4 and 5), and then the decrease of graft polymerization may also be expected (Fig. 4). Reaction 14 is expected at the inside of polymer molecule, for the reaction of oxygen with radical (reaction 3) will be very fast.

## Summary

Some solid polymers containing initiator of radical polymerization of vinyl monomers can initiate graft polymerization by heating in air or in vacuo prior to polymerization. In the experiment on polyethylene film containing benzoyl peroxide (monomer: methyl methacrylate), the increase of time (from 0 to 60 min.) and the rise of temperature (from 20 to 120°C) in pre-heating procedure increase the graft polymerization rate. And also, the increase of time interval after pre-heating until polymerization results in the decrease of the graft polymerization rate.

*Department of Textile Chemistry*
*Faculty of Engineering*
*Kyoto University*
*Sakyo-ku, Kyoto*

# *Synthesis of a,α'-Diaminodicarboxylic Acids*

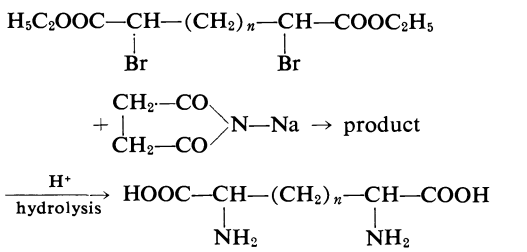
By Koji Toi, Kan Mori and Yoshiharu Izumi

(Received April 11, 1960)

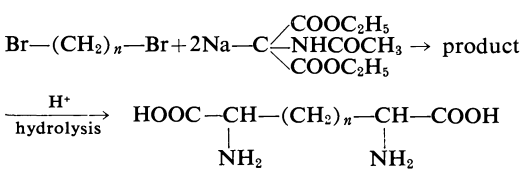
A systematic study of the synthesis of a series of $\alpha,\alpha'$-diaminodicarboxylic acids, containing a number of biologically and biochemically important amino acids, was made, mainly by amination of the corresponding $\alpha,\alpha$-dibromo-compounds using succinimide as an aminating reagent (Method I) and by condensation of diethyl acetamidomalonate with $\alpha,\alpha'$-dibromo-paraffin (Method II).

Among the compounds of this type, of particular interest is $\alpha,\alpha'$-diaminopimelic acid because of its presence in bacterial products[1,2], and because of its role as a precursor in the biosynthesis of lysine[3,4]. $\alpha,\alpha'$-Diaminosuccinic acid, with a chemical structure analogous to aspartic acid, asparagine, $C_4$-dicarboxylic acid and other biologically important substances, has recently been isolated from a natural source[5]. The other amino acids in this series have not yet been found in nature. However, $\alpha,\alpha'$-diaminoglutaric acid is regarded as a precursor in the biosynthesis of $\alpha,\gamma$-diaminobutyric acid.[6] Therefore the availability of these amino acids for biological investigations is desirable.

Method I:



Method II:



Succinimide was first used successfully as an aminating reagent by Akabori, Izumi and Fujiwara for the synthesis of $\alpha,\alpha'$-diaminopimelic acid (D. A. Pim.)[7]. In the present work this method was tried for the preparation of $\alpha,\alpha'$-diaminosuccinic (D. A. Suc.), glutaric (D. A. Glu.) and adipic acid (D. A. Adi.). However it was only successful for D. A. Adi. The diethyl acetamidomalonate method was tested in the preparation of D. A. Adi., D. A. Pim., $\alpha,\alpha'$-diaminosuberic (D. A. Seb.), azelaic (D. A. Aze.), and sebacic acid (D. A. Seb.). It was satisfactory for the synthesis of the three last named. Table I shows the results of the above synthesis.

D. A. Suc. has been prepared by reduction of sodium dihydroxytartarate osazone with sodium amalgam.[8-12] Wenner[13,14] and Mckennis et al.[15] prepared it in high yield by hydrolysis of the corresponding bisbenzylamino compound in the presence of Pd-C and hydrogen at high or atmospheric pressure. In the present work a 44 per cent yield of D. A. Suc. was readily obtained by amination of *meso*-$\alpha,\alpha'$-dibromosuccinate, obtained easily by bromination of diethyl fumarate in sunlight, using succinimide as an aminating reagent.

D. A. Glu. has been prepared by Carter et al.[16] by hydrogenolysis of diethyl pyrazoline-3, 5-dicarboxylate at a high pressure. Hellmann et at.[17] prepared it by reacting diethyl $\alpha$-acetamido - $\alpha$ - dimethylaminomethylmalonateiodomethylate with sodium salt of acetamidomalonate, and by hydrolysis of $\alpha,\alpha'$-diphosphiminoglutaric acid. The final product could not be obtained by amination of diethyl $\alpha,\alpha'$-dibromoglutarate with succinimide. Therefore the method of Carter et al. was reinvestigated. A modification of their procedures

1) E. Work, *Biochem. J.*, **49**, 17 (1951).
2) E. Work and D. L. Dewey, *J. Gen. Microbiol.*, **9**, 394 (1953).
3) D. L. Dewey and E. Work, *Nature*, **169**, 533 (1952).
4) B. D. Davis, ibid., **169**, 534 (1952).
5) F. A. Hochstein, *J. Org. Chem.*, **24**, 679 (1959).
6) H. Hellmann, F. Lingens and E. Frolz, *Chem. Ber.*, **89**, 2433 (1956).
7) S. Akabori, Y. Izumi and T. Fujiwara, *J. Chem. Soc. Japan, Pure Chem. Sec.* (*Nippon Kagaku Zasshi*), **75**, 993 (1954).
8) J. M. Raecgy and J. Tafel, *Chem. Ber.*, **26**, 1980 (1893).
9) J. Tafel, ibid., **20**, 244 (1887).
10) J. Tafel and H. Stern, ibid., **38**. 1589 (1905).
11) J. Tamura, *J. Biochem.*, **27**, 335 (1938).
12) R. Kuhn and F. Zumstein, *Chem. Ber.*, **58**, 1429 (1925).
13) W. Wenner, *J. Org. Chem.*, **13**, 26 (1948).
14) W. Wenner, U. S. Patent, 2,389,099, Nov. 13, 1945.
15) H. Mckennis and A. S. Yard, *J. Org. Chem.*, **23**, 980 (1958).
16) H. E. Carter, F. R. Van Abeel and J. W. Tothrock, *J. Biol. Chem.*, **178**, 325 (1949).
17) H. Hellmann, F. Lingens and E. Frolz, *Chem. Ber.*, **89**, 2433 (1956).

Table I

| Compounds to be synthesized | Method I | | Method II | |
|---|---|---|---|---|
| | Starting material | Yield of product | Starting material | Yield of product |
| D. A. Suc. | *meso*-Diethyl $\alpha, \alpha'$-dibromosuccinic acid | 44% | — | — |
| D. A. Glu. | Diethyl $\alpha, \alpha$-dibromoglutaric acid | Trace | — | — |
| D. A. Adi. | Diethyl $\alpha, \alpha'$-dibromoadipic acid | 73% | Ethylene dibromide | Trace |
| D. A. Pim. | Diethyl $\alpha, \alpha'$-dibromopimelic acid | 81%[7] | Trimethylene dibromide | Trace |
| D. A. Sub. | — | — | Tetramethylene dibromide | 62% |
| D. A. Aze. | — | — | Pentamethylene dibromide | 66% |
| D. A. Seb. | — | — | Hexamethylene dibromide | 79% |

was employed and D. A. Glu. was synthesized in a yield of 33 per cent from glycine ethyl ester hydrochloride without separation of the individual intermediates. The method was as follows: to an aqueous solution of glycine ethyl ester hydrochloride was added an aqueous solution of sodium nitrite. An ethereal solution of methyl acrylate was added without separation of ethyl diazoacetate. Since the product could not be crystallized, the substance was reduced in ethereal solution at a high pressure of hydrogen in the presence of Raney's nickel. It was then hydrolyzed in hydrochloric acid.

Simmonds[18] reported the synthesis of D. A. Adi. and D. A. Pim. by the reaction of phthalimide with the corresponding $\alpha, \alpha'$-dibromo-compounds. Using succinimide instead of phthalimide, these two $\alpha, \alpha'$-dibromo-compounds were converted to D. A. Adi. and D. A. Pim. with comparatively good yields of 73 and 81 per cent, respectively. However, the use of diethyl acetamidomalonate resulted in very poor yields.

D. A. Sub., D. A. Aze., and D. A. Seb. were prepared by Neuberg[19] and Abderhalden et al.[20] from the corresponding $\alpha, \alpha'$-dibromo-compounds and ammonia. Simmonds[19] also reported the preparation of D. A. Seb. by a similar method and of D. A. Seb. and D. A. Aze. in 44 and 39 per cent yields, using acetamidomalonate. In the present work the use of acetamidomalonate resulted in yields of 62, 66, and 79 per cent for D. A. Sub., D. A. Aze. and D. A. Seb., respectively. This method seems the most suitable for these three amino acids, since the starting materials are readily available and the required operations are simple.

It is considered that the low yields of D. A. Suc. and D. A. Glu. in the succinimide method, and of D. A. Adi. and D. A. Pim. in the acetamidomalonate method are probably caused by an inhibition of the reaction by steric hindrance.

Table II. The chromatographic behavior of synthetic diaminodicarboxylic acids

| | $R_f$-value | |
|---|---|---|
| | Fee-form | Hydrochloride |
| D. A. Suc. | 0.0312 | 0.0402 |
| D. A. Glu. | 0.0406 | 0.0522 |
| D. A. Adi. | 0.0455 | 0.0600 |
| D. A. Pim. | 0.0570 | 0.0715 |
| D. A. Sub. | 0.0691 | 0.0878 |
| D. A. Aze. | 0.109 | 0.127 |
| D. A. Seb. | 0.157 | 0.186 |

The above seven amino acids and their hydrochlorides prepared as described above have $R_f$-values shown in Table II on paper chromatography using acetic acid-butanol-water (1 : 4 : 1) as solvent.

## Experimental

**D. A. Suc.** — To a solution of 5.5 g. (0.24 mol.) of sodium in 100 ml. of absolute ethanol was added 30 g. (0.30 mol.) of succinimide. This was heated on a water bath to dissolve the succinimide. To this mixture were added 0.5 g. of potassium iodide and 33 g. (0.10 mol.) of *meso*-$\alpha, \alpha'$-dibromosuccinic acid. The mixture was refluxed on an oil bath for 1 hr. It was cooled and filtered. The filtrate was concentrated in vacuo and the residue was hydrolyzed by refluxing in 100 ml. of concentrated hydrochloric acid and 50 ml. of water for 4 hr. The precipitated succinic acid was removed by filtration and the supernatant was concentrated under reduced pressure. The residual material was dissolved in 70 ml. of methanol and filtered to remove sodium chloride. On neutralization with aniline, D. A. Suc. crystallized immediately as paste or block. This crude solid was washed with 90 per cent methanol. It was dissolved in 100 ml. of warm 20 per cent hydrochloric acid and decolorized. The solution was adjusted to pH 6 with aqueous ammonia and 100 ml. of methanol was added to complete crystallization. White crystalline D. A. Suc. decomposing at 305~310°C was obtained in a yield of 6.0 g. (44 per cent).

Found : C, 32.10 ; H, 5.62 ; N, 18.54. Calcd. for $C_4H_8O_4N_2$ : C, 32.43 ; H, 5.44 ; N, 18.91%.

**D. A. Glu.**—A solution of 12 g. (0.15 mol.) of nitrite and 0.5 g. of sodium acetate in 15 ml. of

18) D. H. Simmonds, *Biochem. J.*, **58**, 520 (1954).
19) C. Neuberg, *Z. phys. Chem.*, **45**, 99 (1905).
20) E. Abderhalden and W. Zeisset; *Fermentforschung*, **9**, 336 (1928).

water was cooled to 0°C and a cold solution containing 14 g. (0.1 mol.) of glycine ethyl ester hydrochloride was added with stirring, external cooling being used to keep the temperature at 0~2°C. After 30 min. 13 g. (0.15 mol.) of methyl acrylate in 25 ml. of ether was added, and rapid stirring was continued for 1 hr. Then 4 ml. of acetic acid was added to the mixture dropwise, and stirring was continued for 1 hr. The ethereal layer was separated. The aqueous layer was extracted with 70 ml. of ether, and the combined ethereal solutions were dried over sodium sulfate. The ether was slowly removed by distillation until the total volume became 40 ml. This solution was then reduced at 80 kg./cm$^2$ by hydrogen in the presence of Raney's nickel for 3 hr. at 60°C and for a further 3 hr. at 120°C. After removal of the catalyst, the filtrate was concentrated under reduced pressure. The residue was hydrolyzed for 3 hr. in 50 ml of boiling concentrated hydrochloric acid. The hydrolysate was decolorized with charcoal and concentrated in vacuo. The residual material was dissolved in 50 ml. of 50 per cent methanol and then 20 ml. of aniline was added with vigorous shaking. D. A. Glu. was crystallized. After storing in a refrigerator, the product was filtered and washed with 10 ml. of water, and then twice with 10 ml. of methanol. The dried product weighed 5.3 g. or 33 per cent of the theoretical yield from glycine ethyl ester hydrochloride. It decomposed at 300~310°C without melting.

Found: C, 36.68 H, 6.40; N, 16.54. Calcd. for $C_5H_{10}O_4N_2$: C, 37.03; H, 6.22; N, 17.28%.

**D. A. Adi.** — This was prepared in a manner similar to that of D. A. Suc. using 5.5 g. (0.24 mol.) of sodium, 30 g. (0.3 g. mol.) of succinimide, and 36 g. (0.1 mol.) of diethyl $\alpha$, $\alpha'$-dibromoadipate. The white crystalline product, reprecipitated from hydrochloric acid and aqueous ammonia, weighed 13.6 g. (73 per cent) and decomposed at 275~277°C without melting.

Found: C, 38.99; H, 7.02; N, 15.49. Calcd. for $C_6H_{12}O_4N_2$: C, 40.90; H, 6.87; N, 15.90%.

**D. A. Pim.**—The preparation of this compound was reported in a previous paper.[1] The yield was 81 per cent, and the decomposition point was 307~310°.

**D. A. Sub.**—To 800 ml. of absolute alcohol containing 19 g. (0.825 mol.) of sodium was added 184 g. (0.85 mol.) of diethyl acetamidomalonate. The mixture was dissolved by heating on a water bath. Then 70 g. (0.324 mol.) of tetramethylenedibromide was added and the mixture was refluxed for 10 hr. The hot reaction mixture was filtered, the residue being washed with hot alcohol. The filtrate and the washings were combined and evaporated in vacuo. The residue was hydrolyzed in 1000 ml. of boiling hydrochloric acid for 5 hr. The mixture was concentrated in vacuo and the dry residue was taken up in 100 ml. of water, and again concentrated to dryness. This operation was repeated once more. Then the dry residue was dissolved in 300 ml. of methanol. A mixture of 80 ml. of pyridine and 300 ml. of methanol was added with shaking and the resulting mixture was let stand overnight to precipitate the crude D. A. Sub. This precipitate was washed with methanol and ether and dried. The yield was 53.5 g. This crude compound was suspended in 1000 ml. of water and dissolved by the addition of 10 per cent sodium hydroxide. An aqueous solution containing 100 g. of copper sulphate was added and the mixture was adjusted to pH 5.4 with 10 per cent sodium hydroxide. The precipitate was washed thoroughly with water and was dissolved in 500 ml. of 3 N hydrochloric acid. It was then treated with hydrogen sulfide to remove the copper. The black precipitate was filtered off, and the filtrate was concentrated in vacuo. The residue was taken up in 400 ml. of methanol. A mixture of 80 ml. of pyridine and 200 ml. of methanol was added with shaking and the resulting mixture allowed to stand. After washing with methanol and ether and drying, 41 g. (62 per cent yield) of white crystalline D. A. Sub. were obtained. This did not decompose below 360°C. Paper chromatography showed a single spot with the $R_f$-value given in Table II.

Found: C, 46.89; H, 7.86; N, 13.79. Calcd. for C, 47.05; H, 7.90; N, 13.72%.

**D. A. Aze.**—This was prepared as above by condensation of 160 g. (0.74 mol.) of diethyl acetamidomalonate with 65 g. (0.283 mol.) of pentamethylenedibromide using 16.8 g. (0.73 mol.) of sodium in 700 ml. of absolute alcohol. The crude product (55.5 g.) was dissolved in 2000 ml. of hot water and 80 g. of basic copper carbonate monohydrate was added. The mixture was heated at boiling point for some time. The precipitate was collected on a suction funnel and thoroughly washed with water. It was dissolved in diluted hydrochloric acid. The solution was saturated with hydrogen sulfide to precipitate the copper sulfide completely. The precipitate was removed by filtration and the filtrate was concentrated in vacuo. The residue was dissolved in 300 ml. of methanol. Neutralization with a mixture of 80 ml. of pyridine and 450 ml. of methanol gave a white crystalline product. This was collected on a suction filter, washed with water, methanol and ether, and dried. 40.5 g. (66 per cent yield) of D. A. Aze. was obtained. This decomposed above 320°C without melting. Paper chromatography of this compound gave a single spot with the $R_f$-value given in Table II.

Found: C, 49.74; H, 8.31; N, 12.81. Calcd. for $C_9H_{18}O_4N_2$: C, 49.53; H, 8.31; N, 12.84%.

**D. A. Seb.**—This compound was prepared in the same way as D. A. Sub. from 23 g. (0.106 mol.) of diethyl acetamidomalonate, 10 g. (0.041 mol.) of hexamethylene dibromide, and 2.3 g. (0.10 mol.) of sodium. The yield was 7.5 g. (79 per cent). It did not decompose below 360°C and gave a single spot on paper chromatography with the $R_f$-value given in Table II.

Found: C, 51.73; H, 8.70; N, 11.96. Calcd. for $C_{10}H_{20}O_4N_2$: C, 51.70; H, 8.68; N, 12.06%.

## Summary

A systematic study was made on the synthesis of $\alpha,\alpha'$-diaminodicarboxylic acids mainly by amination of the corresponding $\alpha,\alpha'$-dibromodicarboxylic acids using succinimide as an

aminating reagent and by condensation of diethyl acetamidomalonate with $\alpha, \omega$-dibromoparaffin.

The authors wish to express their sincere thanks to Professor Shiro Akabori for encouragement and valuable advice throughout this work.

*Division of Organic Chemistry*
*Institute for Protein Research*
*Osaka University Nishi-ku,*
*Osaka (K. T. & Y. I.)*

*Department of General Education*
*Osaka Prefectural University*
*Nakamozu, Sakai (K. M.)*

# *The Ion-Exchange Behavior of Some Neutral Amino Acids*

By Manabu SENŌ and Takeo YAMABE

(Received May 12, 1960)

In many practical works on the separation of amino acids by means of ion-exchangers, some successful procedures using the ion-exchange chromatography have been established. Above all, the displacement development method has been applied with success to the separation by Partridge et al., and Moore and Stein pointed out that the elution method possessed higher resolving power for analytical purposes[1]. However, few fundamental researches have been carried out on the exchange behavior of amino acids on ion-exchange resins[2]. This problem is interesting, since it is expected that weak amphoteric electrolytes such as amino acids exhibit some characteristic behavior concerning the ion-exchange reaction.

In the present paper, the experimental resuls are described on the ion-exchange behavior of some neutral amino acids, particularly the influence of pH on the ion-exchange reaction and some general remarks are presented in this respect. The behavior of the acidic and the basic amino acids toword the ion-exchange resins will be given in the succeeding paper.

## Experimental

Through the present investigation the following reagents were used; amino acids are glycine, DL-alanine and L-leucine, which are commercial special-grade and were used without further purification. The dissociation constants and the isoelectric points of these amino acids are as follows.

| | $pK_1$ | $pK_2$ | pI |
|---|---|---|---|
| Glycine | 2.34 | 9.60 | 5.97 |
| Alanine | 2.34 | 9.69 | 6.00 |
| Leucine | 2.36 | 9.60 | 5.98 |

The ion-exchange resins used were Amberlite resins, IR-120 (4.24) IRC-50 (10.0), IRA-400 (2.15) IR-4B (8.0), the exchange capacities of these resins being given in parentheses in the unit, meq./g. dry resin.

All the experiments were carried out batch-wise. Through a run of measurements, a constant volume, 50 ml., of a solution containing a constant amount, about 2 meq., of amino acid and being adjusted to a desired pH by adding hydrochloric acid or sodium hydroxide, was added onto a constant quantity, about 1 meq., of the ion-exchange resin. The details for each system are given in the following table.

| Amino acids | Total amounts *a* mmol. | H- or OH-form resins, *w* g. dry resin | | | |
|---|---|---|---|---|---|
| | | IR-120 | IRC-50 | IRA-400 | IR-4B |
| Glycine | 1.95 | 0.169 | 0.094 | 0.330 | 0.101 |
| Alanine | 1.98 | 0.166 | 0.111 | 0.331 | 0.180 |
| Leucine | 2.02 | 0.175 | 0.103 | 0.343 | 0.134 |

After being allowed to stand for a few days, which were long enough for the attaining of the ion-exchange equilibrium, the pH and the remaining amount of the amino acid in the solution phase were measured and the adsorbed amount of the amino acid was estimated herefrom.

Amino acids were measured colorimetrically with ninhydrin[3] and pH of the solutions was measured with a glass-electrode pH-meter, model HM-5, Toa Dempa Kogyo Co., Ltd. All the measurements were made at room temperature, 5~15°C.

1) P. B. Hamilton, "Ion Exchangers in Organic and Biochemistry" Ed. by C. Calmon and T. R. E. Kressman, Interscience Publishers, Inc., New York (1957), p. 255.

2) D. T. Englis and H. A. Fiess, *Ind. Eng. Chem.*, **36**, 604 (1944); C. S. Cleaver, R. A. Hardy, Jr. and H. G. Cassidy, *J. Am. Chem. Soc.*, **67**, 1343 (1945); M. E. Carsten and K. Cannan, ibid., **74**, 5950 (1952).

3) K. Satake et al., "Biochemistry I (Seibutu Kagaku I)", Zikken Kagaku Koza, Vol. 23. Maruzen Co., Tokyo (1957), p. 124.

## Results and Discussion

Experimental results were shown in Figs. 1–3, in which the adsorbed amounts of amino acids were plotted against the pH of the equilibrium external solution. As anticipated from the amphoteric nature of amino acids, these are adsorbed by the cation-exchange resins in the pH range lower than its isoelectric point and by the anion-exchange resins in the higher pH range.

As seen in these figures, it was revealed that the maximum adsorption of the neutral amino acids by hydrogen- or hydroxyl-form ion-exchange resins takes place in a rather broad pH range near the isoelectric points, while the acidic and the basic amino acid are extensively adsorbed in a relatively narrow pH range near the isoelectric points, as will be presented in the succeeding paper. Furthermore, it was noticed that, in the case of the sodium or chloride form resins, the amounts of amino acids are remarkably diminished in the pH range near the isoelectric point, compared to the case of the hydrogen- or hydroxyl-form resins. In the lower and the higher pH ranges, the adsorbed amounts of all the amino acids decrease sharply owing to the competitive adsorption of hydrogen or hydroxyl ions.

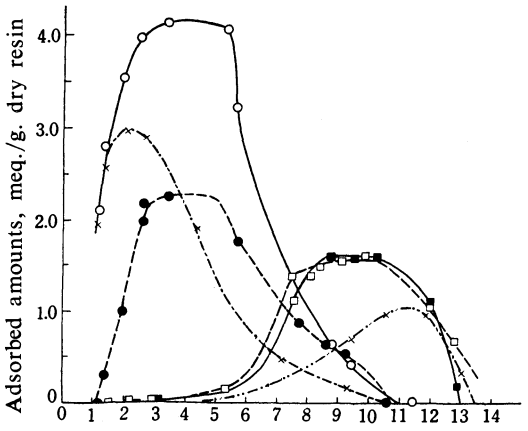



Fig. 1. Adsorption of glycine on ion-exchange resins.
—○— IR-120, H-form
--●-- IRC-50, H-form
--□-- IRA-400, OH-form
—■— IR-4B, OH-form
—·×—· IR-120, Na-form
—·×—·· IRA-400, Cl-form

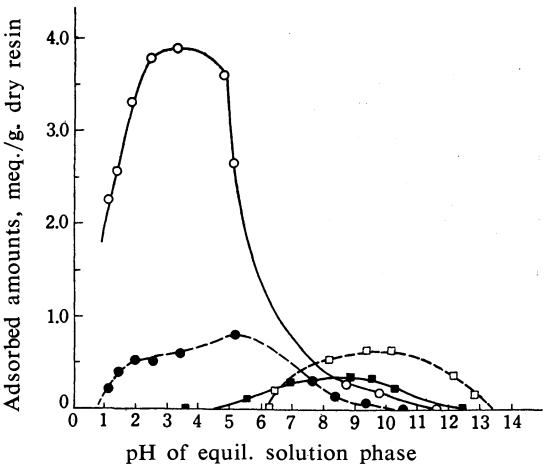



Fig. 2. Adsorption of DL-alanine (symbols are the same as those in Fig. 1).

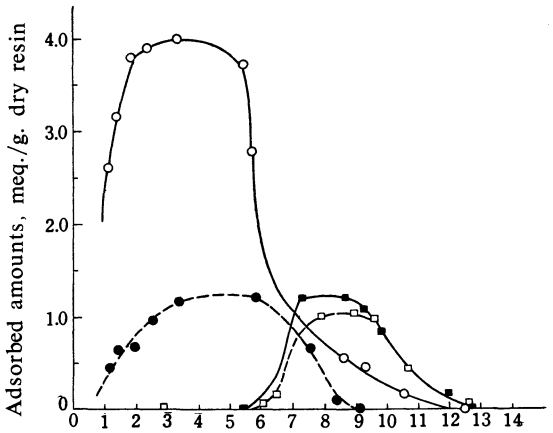



Fig. 3. Adsorption of L-leucine (symbols are the same as those in Fig. 1).

**Adsorption Mechanism of Amino Acids on Ion-Exchange Resins.**—The apparent equilibrium constants defined by

$$\left.\begin{aligned} K_{H}' &= \frac{[A]_r[H^+]_s}{[A]_s[H^+]_r} \\ K_{OH}' &= \frac{[A]_r[OH^-]_s}{[A]_s[OH^-]_r} \end{aligned}\right\} \quad (1)$$

are not constant but depend on pH in the solution phase; $K_H'$ decreases and $K_{OH}'$ increases, with increase of pH, where $[A]_s$, $[H^+]_s$ or $[OH^-]_s$ is concentration in meq./ml. of amino acid, hydrogen or hydroxyl ions in the equilibrium external solution, respectively, and $[A]_r$, $[H^+]_r$ or $[OH^-]_r$ is concentration in meq./(g. dry resin) of amino acid, hydrogen or hydroxyl ions in the resin phase at equilibrium, respectively. It seems that this constancy does not hold, because the dissociation equilibrium of amino acids in the solution is not taken into consideration.

When the neutral amino acid is adsorbed on cation-exchange resin of hydrogen-form,

the amino acid cations that exist in the following equilibrium state,

$$AH^+ \rightleftharpoons A^{\pm} + H^+ \quad \text{(i)}$$

$$A^{\pm} \rightleftharpoons A^- + H^+ \quad \text{(ii)}$$

exchange for hydrogen ions in the ion-exchange resin,

$$RH + AH^+ \rightleftharpoons RAH + H^+ \quad \text{(iii)}$$

and the hydrogen ions are liberated from the cation-exchange resin, resulting in production of more amino acid cations and further exchange of the amino acid cations for the hydrogen ions. The exchange reaction attains the equilibrium through such a repeating process[4].

This adsorption mechanism would be supported by the following empirical facts.

(1) The pH of the external solution remains nearly constant through the adsorption process of amino acids as shown in Table I, in which pH's of the solution phase before and after equilibration of ion-exchange were given in the case of glycine as an example.

TABLE I. pH OF THE SOLUTION PHASE BEFORE AND AFTER EQUILIBRATION OF ION-EXCHANGE OF GLYCINE

| pH of orig. soln. | pH of equil. soln. | pH of orig. soln. | pH of eqil. soln. |
|---|---|---|---|
| Amberlite IR-120, H-form. | | Amberlite IRC-50, H-form. | |
| 1.20 | 1.19 | 1.20 | 1.20 |
| 1.35 | 1.38 | 1.35 | 1.40 |
| 1.90 | 1.90 | 1.98 | 1.98 |
| 2.50 | 2.42 | 2.50 | 2.58 |
| 3.37 | 3.32 | 3.37 | 3.40 |
| 6.60 | 5.30 | 6.60 | 5.60 |
| 8.72 | 5.60 | 8.72 | 7.65 |
| 9.72 | 8.70 | 9.72 | 8.55 |
| 10.80 | 9.39 | 10.80 | 9.20 |
| 12.55 | 12.50 | 12.55 | 12.45 |
| Amberlite IRA-400, OH-form. | | Amberlite IR-4B, OH-form. | |
| 1.35 | 1.48 | 1.35 | 1.52 |
| 2.50 | 2.93 | 2.50 | 3.02 |
| 3.37 | 7.40 | 3.37 | 5.24 |
| 6.60 | 8.00 | 6.60 | 7.45 |
| 8.72 | 8.30 | 8.72 | 8.60 |
| 9.72 | 9.05 | 9.72 | 9.40 |
| 10.80 | 9.80 | 10.80 | 10.10 |
| 12.55 | 11.89 | 12.55 | 11.90 |
| 12.89 | 12.75 | 12.89 | 12.80 |
| Amberlite IR-120, Na-form. | | Amberlite IRA-400, Cl-form. | |
| 1.10 | 1.12 | 1.92 | 1.94 |
| 1.38 | 1.42 | 3.37 | 3.60 |
| 1.92 | 2.09 | 6.60 | 5.25 |
| 2.48 | 2.70 | 9.80 | 9.40 |
| 3.37 | 4.37 | 10.72 | 10.51 |
| 6.60 | 7.16 | 11.98 | 11.81 |
| 9.80 | 9.33 | 13.19 | 13.02 |
| 13.49 | 13.42 | 13.49 | 13.41 |

(2) The amino acids are adsorbed remarkably on the hydrogen- or hydroxyl-form ion-exchanger in the pH range near the isoelectric points, while the amino acid adsorbed on the salt-form ion-exchanger is small in quantity in this pH range.

It should be noticed that the completion of the above-mentioned two processes, i and iii, lead to the same result as the following mechanism[2],

$$RH + A^{\pm} \rightleftharpoons RAH \quad \text{(iv)}$$

However, there is not any evidence that such a process takes place actually.

**Relations between the Adsorbed Amount of Amino Acid and the pH of the External Solution.**—In a case when the neutral amino acid is adsorbed on the hydrogen-form cation-exchanger, the selectivity coefficient is defined as follows:

$$K_H = \frac{[AH^+]_r [H^+]_s}{[AH^+]_s [H^+]_r} \quad (2)$$

where $[A^+]_s$ is the concentration of ion A in the equilibrium external solution in the unit, meq./ml., and $[A^+]_r$ is that in the resin phase in the unit, meq./g. dry resin. Strictly, the activity should be used instead of the concentration in these equations but was not used in the present paper to avoid the troublesome procedure.

The dissociation constants of the neutral amino acids are given as

$$\left.\begin{aligned} K_1 &= \frac{[A^{\pm}]_s [H^+]_s}{[AH^+]_s} \\ K_2 &= \frac{[A^-]_s [H^+]_s}{[A^{\pm}]_s} \end{aligned}\right\} \quad (3)$$

where the term arising from activity coefficient is also neglected.

Under the present experimental condition, that is;

(1) the total amount of amino acid in the system is constant, $a$ meq.,

(2) the amount of the exchangeable ions in the ion-exchange resin is constant, $c$ meq.,

4) Amino acids are taken up from the solution phase into the resin phase by the other processes, such as Donnan adsorption and physical or chemical adsorption, besides the ion-exchange process. Although it is difficult to estimate the contributions of these processes experimentally, it would be safely said on the basis of the preceding reports listed in Ref. 1, that the ion-exchange is the primary process and the other ones have a small contribution to be neglected to a first approximation, excepting for the case of amino acids with benzene rings.

$c=Cw$, where $C$ is the exchange capacity (meq./g. dry resin) of the resin and $w$ is the weight of the resin used,

(3) the volume of the external solution is constant, $v$ ml., the following relationship holds between the exchanged amount of the amino acid, $[AH^+]_r=y$, and the hydrogen ion concentration in the external solution, $[H^+]_s=x$,

$$\frac{(a-wy)(c-wy)}{y}=\frac{vw}{K_H}\frac{x^2+K_1x+K_1K_2}{x} \quad (4)$$

The similar relation is gained in a case when the neutral amino acid is adsorbed on the hydroxyl-form anion-exchanger, where the selectivity coefficient $K_{OH}$ is defined by

$$K_{OH}\frac{[A^-]_r[OH^-]_s}{[A^-]_s[OH^-]_r} \quad (5)$$

The exchanged amount of the amino acid anion, $[A^-]_r=y$, is related to the hydroxyl ion concentration in the equilibrium external solution, $[OH^-]_s=x'$, by the formula

$$\frac{(a-wy)(c-wy)}{y}=\frac{vw}{K_{OH}}\frac{K_1K_2x'^2+K_1K_wx'+K_w^2}{K_1K_2x'} \quad (6)$$

where $K_w$ is the dissociation constant of water.

It must be noted that these relationships are valid for the two-component systems that contain only hydrogen or hydroxyl ions besides amino acid ions.

**$f(x)$ or $f(x')$ Functions.** — It is found that, in the ion-exchange behavior of the weak amphoteric electrolytes such as amino acids, a function of only the concentration of the hydrogen or the hydroxyl ion in the equilibrium solution phase, $f(x)$ or $f(x')$, which appears in the right hands of the Eqs. 4 and 6, gives the characteristic behavior. This function is, for cation exchange,

$$f(x)=\frac{x^2+K_1x+K_1K_2}{x} \quad (7)$$

and for anion exchange

$$f(x')=\frac{K_1K_2x'^2+K_1K_wx'K_w^2}{K_1K_2x'} \quad (8)$$

The numerical values of these functions for amino acids under investigation are given in Table II and shown against pH of the solution phase in Fig. 4[5,6].

The $f(x)$ or $f(x')$ of each amino acid has a minimum at its isoelectric point. At the minimum of $f(x)$ or $f(x')$, the adsorbed amount of the amino acid is the maximum. This can be shown directly by differentiating the Eqs. 4 and 6. It is supported by the present experiment that the adsorbed amount of the amino acid is the maximum at the isoelectric point.

The adsorbed amount of the amino acid is related inversely to the $f(x)$ or $f(x')$. For

TABLE II. $f(x)$ AND $f(x')$ FUNCTIONS

| pH | $\log f(x)$ | | |
|---|---|---|---|
| $(-\log x)$ | Glycine | Alanine | Leucine |
| 0 | 0.002 | 0.002 | 0.002 |
| 1 | $\bar{1}$.021 | $\bar{1}$.021 | $\bar{1}$.017 |
| 2 | $\bar{2}$.164 | $\bar{2}$.164 | $\bar{2}$.155 |
| 3 | $\bar{3}$.746 | $\bar{3}$.746 | $\bar{3}$.729 |
| 4 | $\bar{3}$.669 | $\bar{3}$.669 | $\bar{3}$.649 |
| 5 | $\bar{3}$.661 | $\bar{3}$.661 | $\bar{3}$.641 |
| 6 | $\bar{3}$.660 | $\bar{3}$.660 | $\bar{3}$.640 |
| 7 | $\bar{3}$.661 | $\bar{3}$.661 | $\bar{3}$.641 |
| pH | $\log f(x')$ | | |
| $(-\log K_w/x')$ | Glycine | Alanine | Leucine |
| 6 | $\bar{5}$.600 | $\bar{5}$.691 | $\bar{5}$.600 |
| 7 | $\bar{5}$.601 | $\bar{5}$.692 | $\bar{5}$.601 |
| 8 | $\bar{5}$.611 | $\bar{5}$.700 | $\bar{5}$.611 |
| 9 | $\bar{5}$.697 | $\bar{5}$.772 | $\bar{5}$.697 |
| 10 | $\bar{4}$.146 | $\bar{4}$.173 | $\bar{4}$.146 |
| 11 | $\bar{3}$.017 | $\bar{3}$.020 | $\bar{3}$.017 |
| 12 | $\bar{2}$.002 | $\bar{2}$.002 | $\bar{2}$.002 |
| 13 | $\bar{1}$.000 | $\bar{1}$.000 | $\bar{1}$.000 |
| 14 | 0.000 | 0.000 | 0.000 |

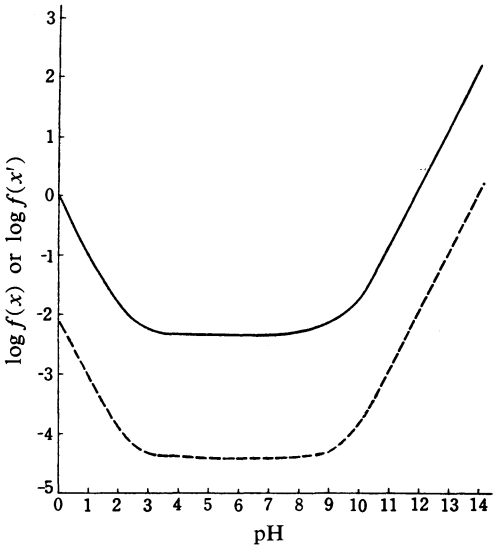



Fig. 4. $f(x)$ and $f(x')$ for glycine, which are shown by a full line and a dotted line, respectively.

5) $f(x)$ is related to $f(x')$ by the formula, $K_wf(x)=K_1K_2f(x')$. Then, for amino acid of which isoelectric point is 7, in this case $K_1K_2=K_w$, $f(x)$ is identical with $f(x')$.

6) $f(x)$ has a practical meaning in the pH range lower than the isoelectric point and $f(x')$ in the higher pH range.

example, the following formula is derived from Eq. 4,

$$y=\frac{ac}{w\left(a+c+\frac{v}{K_H}f(x)\right)}+\frac{a^2c^2}{w\left(a+c+\frac{v}{K_H}f(x)\right)^3}+\cdots\cdots \quad (9)$$

and the similar relation is obtained in another system. From these relations and the dependence of $f(x)$ or $f(x')$ on pH, it is concluded that the maximum adsorption of the neutral amino acids on the hydrogen- or hydroxyl-form exchanger takes place in the broad pH range near the isoelectric point, and this conclusion is also supported experimentally.

**Selectivity Coefficients.**—The selectivity coefficients $K_H$ and $K_{OH}$ were estimated using the above-mentioned experimental data and the formulas and are given in Table III. As for three kinds of neutral amino acids, glycine, alanine and leucine, $K_H$ is very large in comparison with $K_{OH}$. This is partly because the carboxyl group of these amino acids is dissociated more strongly than the amino group and, on this account, the ratio of the concentration of the hydrogen ion to that of the amino acid cation is larger than the ratio of the concentration of the hydroxyl ion to that of the amino acid anion in the equilibrium solution phase[7].

Table III. Selectivity coefficients for ion-exchange of amino acids for hydrogen or hydroxyl ions

| | log $K_H$ | | log $K_{OH}$ | |
|---|---|---|---|---|
| | IR-120 | IRC-50 | IRA-400 | IR-4B |
| Glycine | 0.56 | $\bar{2}.52$ | $\bar{2}.00$ | $\bar{3}.03$ |
| Alanine | 0.41 | $\bar{2}.29$ | $\bar{4}.73$ | $\bar{5}.52$ |
| Leucine | 0.53 | $\bar{2}.43$ | $\bar{3}.24$ | $\bar{4}.38$ |

The order of the selectivity coefficient does not agree with that of the chain length of the amino acid molecule and alanine has smaller $K$ value than that of leucine. This was already reported[8] and it might be considered that a simple adsorption makes a contribution to the uptake of amino acids by ion-exchange resins to some extent in the case of amino acid as glycine which is small in size, and as leucine, which has a long nonpolar chain.

## Summary

The ion-exchange behavior of three kinds of neutral amino acids was examined and the following results were obtained.

1) The ion-exchange behavior of amino acids can be explained when the dissociation equilibrium of amino acids in the solution was taken into account.

2) The maximum adsorption of neutral amino acids on the ion-exchange resins takes place in a rather broad pH range at the isoelectric point.

3) The neutral amino acids are adsorbed more extensively on cation-exchangers than on anion-exchangers. Glycine is adsorbed most extensively and leucine is more adsorbed than alanine.

*Institute of Industrial Science*
*The University of Tokyo*
*Yayoi-cho, Chiba*

7) These ratios are given by
$[H^+]_S/[AH^+]_S=f(x)/[A]_S$
$[OH^-]_S/[A^-]_S=f(x')/[A]_S$
where $[A]_S$ is the concentration of amino acid remaining in the equilibrium solution phase, and, for example, $f(x')=0.087\times10^{-2}\ f(x)$ for glycine.

8) K. Narita, S. Fujiwara and S. Murasawa, This Bulletin, 31, 381 (1958).

# *Syntheses of Peptides Containing Proline. I. Syntheses of Glycyl-L-prolyl-L-leucyl-glycyl-L-proline and its Related Compounds*

By Shumpei SAKAKIBARA and Yutaka NAGAI*

(Received April 1, 1960)

Collagenase is a proteinase with a very high degree of substrate specificity, and its nature has been the object of keen interest of workers both in the fields of biochemistry and medicine. Very recently several preliminary reports[1-4] have been published and we seem to have some clue to look into the whole picture of the action of collagenase.

It had already been shown by several workers[3,5-8] that when collagen was digested with collagenase, most of the *N*-terminal groups belonged to glycine and several amino acids were found at the *C*-terminal ends. Nagai and Noda[2] found that poly-(L-prolyl-L-leucyl-glycyl)[9] was entirely hydrolyzed by collagenase, mostly into tripeptides, glycyl-prolyl-leucine and peptides from both the ends, prolyl-leucyl-glycyl-prolyl-leucine and glycyl-prolyl-leucyl-glycine. Tripeptides similar to the above were also isolated from collagenase digested collagen[7,10]. From these results and also from the accumulated informations[4,6,11-13] of oligopeptides unsusceptible to the action of collagenase, it was contemplated that the substrate specificity of collagenase requires the presence of two proline residues at a proper distance.

The syntheses of peptides containing two proline residues in the sequence of X-Pro-Leu-Gly-Pro-Y which would be a possible good substrate were carried out in our laboratory. The pentapeptide amide, glycyl-L-prolyl-L-leucyl-glycyl-L-proline amide was split by collagenase into two peptides, glycyl-prolyl-leucine and glycyl-proline amide[2]. This pentapeptide amide was the first example of the synthetic oligo-peptide as a good substrate of collagenase, and furnished a good starting inertia for us to elucidate the substrate specificity of the enzyme. Subsequently, many kinds of peptide containing proline, hydroxyproline or sarcosine were synthesized along this line and a preliminary report on an enzymatic test of those peptides has already been published[14].

In the present series of reports, the synthetic studies of those peptides containing proline will be described successively.

## Syntheses of Peptides

In the planning of the synthetic routes of the pentapeptide, a precaution was taken not to use routes passing through dipeptide esters containing proline because free esters of proline dipeptides are considered to have a great tendency for diketopiperazine formation[15]. In the present study, almost all of the possible routes which conformed with the above precaution, as indicated befow, were tried, and the yield, crystallizability and specific rotation of products were compared for each route. The synthetic routes tested were as follows*:

(1) **a.** Z-Gly-$N_3$ + H-Pro-OEt
$\longrightarrow$ {Z-Gly-Pro-OEt}
$\longrightarrow$ Z-Gly-Pro-OH (I)

**b.** Z-Gly-OH + H-Pro-OEt
M.A.
$\longrightarrow$ {Z-Gly-Pro-OEt}
$\longrightarrow$ Z-Gly-Pro-OH (I)

* On leave from Department of Biophysics and Biochemistry, Faculty of Science, the University of Tokyo.

1) W. Harrington and P. H. von Hippel, cited by S. Seifter et al., *J. Biol. Chem.*, **234**, 285 (1959).
2) Y. Nagai and H. Noda, *Biochim. Biophys. Acta*, **34**, 298 (1959).
3) K. Heyns and G. Legler, *Z. physiol. Chem.*, **315**, 288 (1959).
4) W. Grassmann, H. Hörmann, A. Nordwig and E. Wünsch, ibid., **316**, 287 (1959).
5) V. O. Kazakova, V. N. Orekhovich and V. O. Shpikiter, *Doklady Akad. Nauk., S. S. S. R.*, **122**, 657 (1958).
6) S. Michaels, P. M. Gallop, S. Seifter and E. Meilman, *Biochim. Biophys. Acta*, **29**, 450 (1958); *J. Biol. Chem.*, **234**, 285 (1959).
7) S. Akabori, H. Noda, S. Sakakibara and Y. Nagai, *Abstr. IIth Symposium on Enz. Chem. (Japan)*, 109 (1959).
8) I. Mandl, personal communication.
9) H. Kitaoka, S. Sakakibara and H. Tani, This Bulletin, **31**, 802 (1958).
10) R. E. Schrohenloher, J. D. Ogle and M. A. Logan, *J. Biol. Chem.*, **234**, 58 (1959).
11) E. Bidwell and W. E. Van Heyningen, *Biochem. J.*, **42**, 140 (1948).
12) R. Monier, G. Litwack, M. Somlo and B. Labouesse, *Biochim. Biophys. Acta*, **18**, 71 (1955).
13) I. Mandl, H. Zipper and L. T. Ferguson, *Arch. Biochem. Biophys.*, **74**, 465 (1958).
14) Y. Nagai, S. Sakakibara, H. Noda and S. Akabori, *Biochim. Biophys. Acta*, **37**, 567 (1960).
15) J. S. Fruton, *Advances in Protein Chemistry*, **5**, 67 (1949).

* Z= Carbobenzoxy; M. A. = isovaleroyl mixed anhydride method; { } shows a material failed to crystallize, the purity of which is not confirmed by elementary analysis; [ ] shows a material failed to crystallize but obtained as a powder, the purity of which is confirmed by elementary analysis.

(2) Z-Leu-OH + H-Gly-OEt
$\xrightarrow{\text{M.A.}}$ Z-Leu-Gly-OEt (II)
$\longrightarrow$ Z-Leu-Gly-NH-$NH_2$ (III)
II $\longrightarrow$ Z-Leu-Gly-OH (IV)

(3) **a.** Z-Leu-Gly-$N_3$ ($\longleftarrow$ III) + H-Pro-OEt
$\longrightarrow$ Z-Leu-Gly-Pro-OEt (V)

**b.** IV + H-Pro-OEt $\xrightarrow{\text{M.A.}}$ V

(4) Z-Pro-OH + H-Leu-Gly-OEt ($\longleftarrow$ II)
$\xrightarrow{\text{M.A.}}$ Z-Pro-Leu-Gly-OEt (VI)
VI $\longrightarrow$ Z-Pro-Leu-Gly-NH-$NH_2$ (VII)

(5) **a.** Z-Pro-OH + H-Leu-Gly-Pro-OEt ($\longleftarrow$ V)
$\xrightarrow{\text{M.A.}}$ {Z-Pro-Leu-Gly-Pro-OEt} (VIII)

**b.** Z-Pro-Leu-Gly-$N_3$ ($\longleftarrow$ VII) + H-Pro-OEt
$\longrightarrow$ {Z-Pro-Leu-Gly-Pro-OEt} (VIII)
VIII $\longrightarrow$ [Z-Pro-Leu-Gly-Pro-OH]
(IX) $\longrightarrow$ [H-Pro-Leu-Gly-Pro-OH] (X)

(6) **a.** Z-Gly-$N_3$ + H-Pro-Leu-Gly-OEt ($\longleftarrow$ VI)
$\longrightarrow$ Z-Gly-Pro-Leu-Gly-OEt (XI)

**b.** I + H-Leu-Gly-OEt ($\longleftarrow$ II) $\xrightarrow{\text{M.A.}}$
XI $\longrightarrow$ Z-Gly-Pro-Leu-Gly-OH (XII)
XI $\longrightarrow$ Z-Gly-Pro-Leu-Gly-NH-$NH_2$ (XIII)

(7) **a.** Z-Gly-$N_3$ + H-Pro-Leu-Gly-Pro-OEt ($\longleftarrow$ VIII)
$\longrightarrow$ {Z-Gly-Pro-Leu-Gly-Pro-OEt} (XIV)

**b.** I + H-Leu-Gly-Pro-OEt ($\longleftarrow$ V)
$\xrightarrow{\text{M.A.}}$ {Z-Gly-Pro-Leu-Gly-Pro-OEt} (XIV)

**c.** XII + H-Pro-OEt
$\xrightarrow{\text{M.A.}}$ {Z-Gly-Pro-Leu-Gly-Pro-OEt} (XIV)

**d.** Z-Gly-Pro-Leu-Gly-$N_3$ ($\longleftarrow$ XIII) + H-Pro-OEt
$\longrightarrow$ {Z-Gly-Pro-Leu-Gly-Pro-OEt} (XIV)

XIV $\longrightarrow$ Z-Gly-Pro-Leu-Gly-Pro-OH (XV)
$\longrightarrow$ [H-Gly-Pro-Leu-Gly-Pro-OH] (XVI)
XIV $\longrightarrow$ [Z-Gly-Pro-Leu-Gly-Pro-$NH_2$] (XVII)
$\longrightarrow$ [H-Gly-Pro-Leu-Gly-Pro-$NH_2$] (XVIII)

Methods of peptide-bond formation employed in the present study, were the azide method and the isovaleroyl mixed anhydride method[16]. The azide method is well known to be suitable for keeping the optical purity of peptides in the course of the reaction[17]. The mixed anhydride method is a comparatively simple method of the activation of the carboxyl component, and had been used successfully by Ressler and du Vigneaud[18] for the coupling reaction of carbobenzoxy-L-proline and L-leucyl-glycine ethylester. In every case of the azide procedure used in our present study, it was to be noted that carbobenzoxypeptide azide containing proline residue was insoluble in ether, and chloroform was the most suitable solvent for extracting the azide formed. In regard to the acylation of the proline imino group, the azide method was superior to the mixed anhydride method in view of the synthetic yield, crystallizability and melting point of the products. For example, carbobenzoxyglycyl-L-proline (I) which was prepared by the azide method from carbobenzoxyglycine hydrazide and L-proline ethylester was sufficiently pure without recrystallization, and the yield was also satisfactory (m. p. 155°C, yield 75%). On the other hand, the mixed anhydride method gave the substance I with a lower melting point (153°C) in poorer yield (42%). Similar results were obtained in cases of coupling reactions of carbobenzoxy-L-leucyl-glycine with L-proline ethylester, and of carbobenzoxyglycyl-L-prolyl-L-leucyl-glycine with L-proline ethylester. Recently, Bodanszky and du Vigneard[19] have published an interesting communication, in which they proposed the use of carbobenzoxyamino acid *p*-nitrophenylesters for acylation of peptide esters. If their new procedures would be employed in parts of our procedures, better results might be obtained.

Among the synthetic routes for the carbobenzoxypentapeptide ester (XIV), the best result was obtained by route 7-d. Since the

16) J. R. Vaughan, Jr. and R. L. Osato, *J. Am. Chem. Soc.*, **73**, 5553 (1951).
17) M. B. North and G. T. Young, *Chemistry & Industry*, 1567 (1955).
18) C. Ressler and V. du Vigneaud, *J. Am. Chem. Soc.*, **76**, 3107 (1954).
19) M. Bodanszky and V. du Vigneaud, ibid., **81**, 5688 (1959).

substance XIV has not been heretofore crystallized, the synthetic yields for those procedures, 7-b, c and d, were compared with each other on the saponified product XV. The route 7-a was eliminated, since the substance VIII which was used as the intermediate in the route was not crystallized, and purification of which was unsuccessful. Substance XV prepared by route 7-d was readily crystallized under the presence of ethyl acetate, but the same substance XV prepared by route 7-b or 7-c was hard to crystallize. The route 7-b was abandoned for the reason that the crystallizability of the intermediate V was poor and of which yield was rather low. Although both intermediate substances XII and XIII were easily crystallized and were obtained from XI in good yields, mixed anhydride route 7-c was somewhat inferior to azide route 7-d as described above. The intermediate XI was prepared through two routes 6-a and 6-b, and the former was somewhat superior to the latter in synthetic yield. In regard to the optical purity, every preparations (XV) obtained by routes 7-b, c and a showed the same specific rotation after recrystallization.

Carbobenzoxy-L-prolyl-L-leucyl-glycyl-L-proline ethylester (VIII) was prepared not only as an intermediate for the substance XIV, but also as a substrate for collagenase. In the synthesis of the substance VIII, two routes, mixed anhydride procedure (5-a) and azide procedure (5-b), were taken into consideration. Since the substances VIII and its saponified product IX were not crystallized, formation of by-products, separation of which seemed to be difficult, was particularly undesirable. In the similar cases of 7-b and 7-d, which corresponded respectively to 5-a and 5-b, it was observed previously that the former was inferior to the latter in the purity and yield of the product. Then, the route 5-a was not explored in this case. Carbobenzoxy-L-prolyl-L-leucyl-glycine hydrazide (VII), which was used in route 5-b, was water-soluble substance and it was very interesting, that this substance was crystallizable only from toluene and this crystal contained crystallization toluene, which could be removed completely when the compound was heated at 50°C in vacuo.

Peptides or their derivatives containing proline residue in general are hydrophilic and peptides containing two or more proline residues, especially, were hard to be crystallized because of the effect of humidity. It was, however, found that carbobenzoxyglycyl-L-prolyl-L-leucyl-glycyl-L-proline (XV) was an exceptional example of readily crystallizable substance as described above. In this case, both ethyl acetate and water were indispensable for crystallization. When the peptide XV was recrystallized from ethyl acetate which contains equimolar amount of water to the peptide, it formed prisms. The crystal contained one mole each of water, and ethyl acetate per mole of the peptide as crystallization solvent and was fairly stable even when it was kept in the open air. In turn, when the same peptide was recrystallized from water-saturated ethyl acetate, different crystals (plates) were obtained, and they were unstable in the open air and gradually transformed into opaque crystals. A crystallographic study on these phenomena is now in progress by Sasada and Kakudo in our laboratory with X-ray diffraction technique.

As described above, the interesting phenomenon that some kinds of peptide derivatives (VII and XV) have affinity with specific substances (toluene or ethyl acetate) seemed to suggest a possible mode of combination in the enzyme-substrate complex formation. Similarly, the penta-peptide amide (XVIII) which was dried azeotropically by using toluene or ethanol occluded the solvents firmly, and complete removal of the solvents was very hard.

The above mentioned carbobenzoxypentapeptide XV was the best substrate for collagenase as described in the previous communication[14]. The substances IX, XV, XVI and XVIII were all hydrolyzed completely by collagenase within a comparatively short period of time. Studies on the enzymatic digestion of these peptides will be published elsewhere in the near future.

## Experimental*

**Carbobenzoxyglycyl-L-proline (I). — a.** Carbobenzoxyglycine hydrazide (11.2 g., 0.05 mol.) was dissolved in a mixture of acetic acid (40 ml.) and water (80 ml.), and 6 N hydrochloric acid (17 ml., 0.1 mol.) was added into the solution. The mixture was cooled to −5°C, shaken well with a small amount of chloroform and carefully treated with sodium nitrite (3.8 g., 0.055 mol.). The carbobenzoxyglycine azide formed was extracted three times with cold chloroform (total 150 ml.). The combined extract was washed with ice water (50 ml.) and acids for a short time over anhydrous sodium sulfate at −5°C. The dried solution was filtered into a mixture of proline ethylester hydrochloride (10 g., 0.055 mol.) and triethylamine (5.6 g., 0.055 mol.) in chloroform (50 ml.) at −5°C, and allowed to stand overnight at 0~4°C. The reaction mixture was washed successively with 0.5 N hydrochloric acid, water and 5% sodium bicarbonate solution and dried over anhydrous magnesium sulfate. The dried solution was concentrated to syrup under reduced pressure and the residue was redissolved in methanol (100 ml.), and then 2 N sodium hydroxide (25 ml., 0.05 M) was added. After the solution was kept for 2 hr. at room temperature, it was neutralized with 6 N hydrochloric acid, and the methanol

* All melting points were uncorrected.

was removed under reduced pressure. As soon as methanol was removed, colorless prisms appeared. After being stored overnight in a refrigerator, the crystals were filtered off, washed with water and ethyl acetate, and dried in a desiccator. The yield of I with m. p. 154.5~155°C was 75% (11.5 g.). This substance was pure enough without recrystallization for preparing higher peptides. Recrystallization from ethyl acetate of the product (1.4 g.) gave prisms (1.2 g.); m. p. 154.5~155°C, $[\alpha]_D^{15}$ −70.4° (c. 6, ethanol); Bergmann et al.[20] reported m. p. 156°C (corr.).

**b.** Carbobenzoxyglycine (2.1 g., 0.01 M) was dissolved in chloroform (40 ml.) by adding triethylamine (1.0 g., 0.01 M), and then toluene (40 ml.) was added into the solution. The mixture was cooled to −10°C and isovaleroyl chloride (1.2 g., 0.01 M) was added slowly into the solution under stirring. After about 1.5 hr. a solution of proline ethylester hydrochloride (2.16 g., 0.012 M) and triethylamine (1.2 g., 0.012 M) in chloroform (40 ml.) was added into the mixed anhydride solution, and the mixture was allowed to stand overnight at 4°C. The reaction mixture was treated as described above. Yield of I was 42% (1.3 g.); m. p. 152~154°C. Recrystallization from ethyl acetate of the product (1.3 g.) gave fine prisms (1.1 g.); m. p. 153~154°C, $[\alpha]_D^{15}$ −70.2° (c. 5, ethanol).

**Carbobenzoxy-L-leucyl-glycine Ethylester (II).**—This substance was prepared according to the procedures of Vaughan and Osato[16]; yield 70%, m. p. 102~104°C, $[\alpha]_D^{15}$ −26.8° (c. 5.5, ethanol).

**Carbobenzoxy-L-leucyl-glycine Hydrazide (III).**—Into a solution of II (10 g.) in ethanol (40 ml.) was added hydrazine hydrate (8 ml.), and then the mixture was allowed to stand overnight at room temperature. The reaction mixture was concentrated to dryness under reduced pressure and the residual crystalline mass was recrystallized from ethanol and ether to give needles; m. p. 130~132°C, yield 89% (8.5 g.).

Found: C, 56.97; H, 7.29; N, 16.71. Calcd. for $C_{16}H_{24}O_4N_4$: C, 57.13; H, 7.19; N, 16.66%.

**Carbobenzoxy-L-leucyl-glycine (IV).**—This substance was prepared from II according to procedures of Bergmann et al.[21]; m. p. 114~115°C, yield 90%, $[\alpha]_D^{15}$ −26.3° (c. 8, ethanol).

**Carbobenzoxy-L-leucyl-glycyl-L-proline Ethylester (V).—a.** A solution of carbobenzoxy-L-leucyl-glycine azide in chloroform, which was prepared from III (3.4 g.) as in the case of I-a was added into a mixture of proline ethylester hydrochloride (2 g.) and triethylamine (1.1 g.) in chloroform (20 ml.) at −5°C, and the mixture was allowed to stand overnight. The reaction mixture was washed successively with water, 1 N hydrochloric acid, water, 5% sodium bicarbonate and water again, and dried. The dried solution was concentrated to syrup and the residue was crystallized in a refrigerator after treatment with petroleum benzine. The crude crystals formed were triturated with a small amount of ethyl acetate and carefully recrystallized with a small amount of petroleum benzine. The crystals were filtered off, washed with ether and dried in a desiccator in vacuo to give fine needles; m. p. 81~85°C, yield 80% (3.6 g.). Recrystallization of the product from ethyl acetate-petroleum benzine gave needles with m. p. 89~91°C; yield 44% (2.0 g.), $[\alpha]_D^{17}$ −78.0° (c. 6, ethanol). A second crop of the recrystallization was obtained in 11% yield (0.5 g.); m. p. 88~91°C.

Found: C, 61.75; H, 7.25; N, 9.64. Calcd. for $C_{23}H_{33}O_6N_3$: C, 61.72; H, 7.43; N, 9.36%.

**b.** Carbobenzoxy-L-leucyl-glycine (IV) (3.2 g.) was dissolved in chloroform (50 ml.) by adding triethylamine (1 g.) and then toluene (50 ml.) was added to the solution. The mixture was cooled to −10°C and isovaleroyl chloride (1.2 g.) was added slowly to the solution under stirring. After about 1.5 hr. a solution of proline ethylester hydrochloride (2.16 g.) and triethylamine (1.2 g.) in chloroform (40 ml.) was added to the mixed anhydride solution, and then the mixture was allowed to stand overnight at 4°C. The reaction mixture was treated as described above to give a crude product; yield 67% (3 g.). Recrystallization from ethyl acetate-petroleum benzine gave fine needles; m. p. 88~91°C, yield 46% (2.1 g.), $[\alpha]_D^{17}$ −77.8° (c. 4, ethanol).

**Carbobenzoxy-L-prolyl-L-leucyl-glycine Ethylester (VI).**—This substance was prepared according to the procedures of Ressler and du Vigneaud[18]; m.p. 148.5~150.5°C, yield 88~90%. Recrystallization from ethanol-water gave 70% yield, m. p. 150~151.5°C, $[\alpha]_D^{15}$ −81.9° (c. 2, ethanol); second crop from the mother liquor gave 13% yield, m. p. 149~150°C.

**Carbobenzoxy-L-prolyl-L-leucyl-glycine Hydrazide (VII).**—Hydrazine hydrate (2 ml.) was added to a solution of VI (2.24 g.) in ethanol (30 ml.) and then the mixture was allowed to stand overnight at room temperature. The reaction mixture was concentrated to syrup under reduced pressure and the residual syrup was dried by the addition of benzene followed by evaporation under reduced pressure. After the drying procedures were repeated, the residue was crystallized by trituration with toluene (about 10 ml.) and dried over sodium hydroxide at room temperature to give fine needles; yield 91% (2.4 g.), m. p. 76~80°C. This substance contained about one mole of crystallization toluene.

Found: C, 62.82; H, 7.44; N, 14.14. Calcd. for $C_{21}H_{31}O_5N_5 \cdot 3/4C_7H_8$: C, 62.73; H, 7.42; N, 13.94%.

After dryness in vacuo at 50°C, the crystallization toluene was removed.

Found: C, 58.27; H, 7.26; N, 16.40. Calcd. for $C_{21}H_{31}O_5N_5$: C, 58.18; H, 7.21; N, 16.16%.

**Carbobenzoxy-L-prolyl-L-leucyl-glycyl-L-proline (IX).—b.** A carbobenzoxy-L-prolyl-L-leucyl-glycine azide solution, which was prepared from VII (toluene-free 2.15 g.) as in the case of I-a, was added to a mixture of proline ethylester hydrochloride (1 g.) and triethylamine (0.56 g.) in chloroform (20 ml.) at −5°C. After being kept overnight at 4°C, the solution was washed successively with water, 1 N hydrochloric acid, water, 5% sodium bicarbonate solution and again with water, and dried. The dried solution was concentrated to syrup under reduced pressure and the residue was

20) M. Bergmann et al., *Ber.*, **65**, 1192 (1932); *Z. physiol. Chem.*, **212**, 72 (1932).
21) M. Bergmann et al., *J. Biol. Chem.*, **111**, 225 (1935).

redissolved in methanol (30 ml.). 1 N Sodium hydroxide (8 ml.) was added into the methanol solution, and the mixture was allowed to stand for about 3 hr. at room temperature. After neutralizing the reaction mixture with 6 N hydrochloric acid, it was concentrated to syrup under reduced pressure and the remaining oily material was dissolved in 5% sodium bicarbonate solution. The bicarbonate solution was washed well with ethyl acetate and then acidfied with 6 N hydrochloric acid. The separated oil was extracted with chloroform. On evaporation of the solvent a syrup was obtained and was solidified by trituration with petroleum benzine. After dryness in vacuo at 80°C, the amorphous powder amounted to 54% yield (1.4 g.); m.p. 90~120°C (sintered at 90°C), $[\alpha]_D^{17}$ −106.1° (c. 5.5, ethanol).

Found: C, 61.20; H, 7.29; N, 10.38. Calcd. for $C_{26}H_{36}O_7N_4$: C, 60.45; H, 7.02; N, 10.85%.

**L-Prolyl-L-leucyl-glycyl-L-proline (X).**—Palladium-charcoal (5%, 1 g.) was added to a solution of IX (1 g.) in a mixture of methanol (20 ml.) and water (30 ml.), and hydrogen was introduced into the suspension for 3 hr. under stirring. The catalyst was filtered off and washed three times with hot water (total 30 ml.), and then the combined filtrate was concentrated under reduced pressure. The residual syrup was dissolved in small amount of water, and the solution was filtered. The clear solution was concentrated to syrup and the residue was dried by the addition of benzene followed by evaporation under reduced pressure, and then pulverized. After dryness in vacuo at 110°C for about 3 hr., the product amounted to an 80% yield (0.6 g.); deliquescent powder, m. p. 170~180°C (sintered at 147~150°C), $[\alpha]_D^{15}$ −121.5° (c. 5, water).

Found: C, 55.94; H, 7.86; N, 14.32. Calcd. for $C_{18}H_{30}O_5N_4 \cdot 1/6H_2O$: C, 56.09; H, 7.93; N, 14.54%.

Complete dryness of this substance failed because the substance was partially charred when heated at 135°C for 3 hr. in vacuo.

**Carbobenzoxyglycyl-L-prolyl-L-leucyl-glycine Ethylester (XI).—a.** Palladium-charcoal (5%, 5 g.) and 6 N hydrochloric acid (6 ml.) was added to a solution of VI (13.4 g.) in ethanol (200 ml.), and hydrogen was introduced into the suspension for 3 hr. under stirring. The catalyst was filtered off and washed three times with ethanol (total 60 ml.), and then the combined filtrate was concentrated under reduced pressure. The residual syrup was dried by the addition of toluene followed by evaporation under reduced pressure. A carbobenzoxyglycine azide solution, which was prepared from carbobenzoxyglyciues hydrazide (6.7 g.) according to the procednre in the case of I-a was added into a mixture of the prolyl-leucyl-glycine ethylester hydrochloride and triethylamine (3 g.) in chloroform (100 ml.). After storage overnight in a refrigerator at 4°C, the reaction mixture was washed successively with 1 N hydrochloric acid, water, 5% sodium bicarbonate solution and water again, and dried. Evaporation of the solvent gave a syrupy material which was crystallized by the addition of chloroform and petroleum benzine. The yield of the crude product was 80% (12 g.); m. p. 96~101°C (after dryness in vacuo at 80°C). This substance was used for the preparation of XII and XIII without recrystallization. Melting point of this substance rose to 101~104°C after two recrystallization from chloroform and petroleum benzene; $[\alpha]_D^{15}$ −69.9° (c. 5, ethanol).

Found: C, 59.47; H, 7.10; N, 11.15. Calcd. for $C_{25}H_{36}O_7N_4$: C, 59.51; H, 7.19; N, 11.10%.

**b.** The substance II (10 g.) was hydrogenated in ethanol (50 ml.) containing 6 N hydrochloric acid (5 ml.) with 5% palladium-charcoal (4 g.). The catalyst was filtered off and washed three times with ethanol, and then the combined filtrate was concentrated under reduced pressure. The residual syrup was dried by the addition of toluene followed by evaporation under reduced pressure. A mixture of the leucyl-glycine ethylester hydrochloride and triethylamine (3 g.) in chloroform (30 ml.) was added to a mixed anhydride solution at −10°C, which was prepared from I (8 g.), triethylamine (2.65 g.) and isovaleroyl chloride (3.15 g.) in a mixture of chloroform (100 ml.) and toluene (100 ml.) as in the case of I-b. After being kept overnight at 4°C, the reaction mixture was treated in a similar manner to the case of XI-a and a crude product was obtained in a 78% yield (10.3 g.); m. p. 96~101°C (dried in vacuo at 80°C). After several recrystallizations from chloroform-petroleum benzine, this substance melted at 101~105°C; $[\alpha]_D^{15}$ −70.5° (c. 5, ethanol).

**Carbobenzoxyglycyl-L-prolyl-L-leucyl-glycine (XII).**—The crude product of XI-a (5 g.) was dissolved in methanol (50 ml.) and 1 N sodium hydroxide (11 ml.) was added into the solution, and then the mixture was allowed to stand at room temperature for 2 hr. The mixture was neutralized with 6 N hydrochloric acid, and the methanol was distilled under reduced pressure. The crystals formed were filtered off, washed with water and ethyl acetate, and dried; m. p. 184~187°C, yield 87% (4.1 g.). After recrystallization from ethanol-water (1 : 1), this substance melted at 185~188°C; $[\alpha]_D^{15}$ −60.4° (c. 6.5, pyridine).

Found: C, 58.14; H, 6.90; N, 11.76. Calcd. for $C_{23}H_{32}O_7N_4$: C, 57.97; H, 6.77; N, 11.76%.

This substance was prepared from XI-b (3.2 g.) in a yield of 86% (2.6 g.); m. p. 184~188°C, $[\alpha]_D^{15}$ −60.3° (c. 5, pyridine).

**Carbobenzoxyglycyl-L-prolyl-L-leucyl-glycine Hydrazide (XIII).**—The crude XI-a (10.1 g.) was dissolved in ethanol (50 ml.) and hydrazine hydrate (5 ml.) was added to the solution. After being kept overnight at room temperature, the reaction mixture was concentrated to dryness, and the residual syrup was crystallized from ethanol and ether to give long needles; m. p. 155~157°C, yield 97% (9.5 g.). Recrystallization from ethanol and petroleum benzine gave a 94% yield (9.2 g.); m. p. 157~159°C.

Found: C, 56.34; H, 7.04; N, 17.24. Calcd. for $C_{23}H_{34}O_6N_6$: C, 56.31; H, 6.99; N, 17.13%.

This substance was prepared from XI-b (8.8 g.) in a yield of 94% (8.1 g.); m. p. 157~159°C.

**Carbobenzoxyglycyl-L-prolyl-L-leucyl-glycyl-L-proline (XV). — d.** An azide solution which was prepared from XIII (8 g.) as in the case of I-a,

was added to a solution of proline ethylester hydrochloride (3.2 g.) and triethylamine (1.8 g.) in chloroform (20 ml.) at −5°C. The reaction mixture was allowed to stand overnight at 4°C, and was then washed successively with water, 1 N hydrochloric acid, water, 5% sodium bicarbonate solution and water again, and dried. The dried solution was concentrated to syrup under reduced pressure and the residue was redissolved in methanol (100 ml.). 1 N sodium hydroxide (20 ml.) was added into the methanol solution and the mixture was allowed to stand for about 3 hr. at room temperature. After neutralizing the reaction mixture with 6 N hydrochloric acid, it was concentrated to dryness under reduced pressure and the remaining syrup was dissolved in saturated sodium bicarbonate solution. The bicarbonate solution was washed with ethyl acetate and then acidified with 6 N hydrochloric acid. The separated oil was extracted with chloroform and the extract was concentrated to syrup, which was crystallized by trituration with ethyl acetate containing a small amount of water. After storage overnight in a refrigerator, the crystals were filtered off and dried in vacuo at 80°C for about 3 hr. to give 5.0 g. of the first crop. On evaporation of the ethyl acetate washing described above, a slight amount of residue was obtained. The residue was again saponified in the same manner and a second crop (0.6 g.) was obtained. The total yield was 60%. Recrystallization of the product from ethyl acetate containing an equimolar amount of water to the peptide, gave prisms (6 g.) with m. p. 72°C (dec. at 75~77°C), which were dried in the open air. This material contained one mole of ethyl acetate and one mole of water as crystallization solvents.

Found: C, 56.55; H, 7.44; N, 10.39. Calcd. for $C_{28}H_{39}O_8N_5 \cdot C_4H_8O_2 \cdot H_2O$: C, 56.54; H, 7.27; N, 10.30%.

The crystallization solvents could be removed at 80°C in vacuo to give an amorphous powder; m. p. 130~135°C, $[\alpha]_D^{15}$ −128.2° (c. 4, ethanol).

Found: C, 58.49; H, 6.84; N, 12.23. Calcd. for $C_{28}H_{39}O_8N_5$: C, 58.62; H, 6.85; N, 12.21%.

The route XIV-b-XV gave 35% yield of the amorphous powder; $[\alpha]_D^{15}$ −128.2° (c. 4, ethanol). The route XIV-c-XV gave a 45% yield of the same substance; $[\alpha]_D^{15}$ −128.2° (c. 4, ethanol).

**Glycyl-L-prolyl-L-leucyl-glycyl-L-proline (XVI).** —Palladium-charcoal (5%, 1 g.) was added to a solution of XV (1.7 g.) (amorphous powder) in methanol (20 ml.) and water (30 ml.), and hydrogen was introduced into the suspension for 3 hr. under stirring. The catalyst was filtered off and washed three times with hot water (total 30 ml.), and then the combined filtrate was concentrated under reduced pressure. The residual syrup was dissolved in a small amount of water, and the solution was filtered. The clear solution was concentrated to syrup and the residue was dried by the addition of toluene followed by evaporation under reduced pressure, and then pulverized. After dryness in vacuo at 110°C for about 3 hr., the product amounted to a 51% yield (0.8 g.) of deliquescent powder; m. p. 160~167°C, $[\alpha]_D^{15}$ −160.1° (c. 5.5, water.)

Found: C, 53.72; H, 7.65; N, 15.71. Calcd. for $C_{20}H_{33}O_6N_5 \cdot 1/2H_2O$: C, 53.56; H, 7.64; N, 15.62%.

**Carbobenzoxyglycyl-L-prolyl-L-leucyl-glycyl-L-proline Amide (XVII).**—The syrupy material XIV which was prepared from XIII (4.9 g.) according to the procedure XV-d was dissolved in methanol (40 ml.). After being saturated with dry ammonia gas at 0°C, the solution was allowed to stand one week at room temperature in a sealed tube. The reaction mixture was concentrated to syrup under reduced pressure and the residue was dried by the addition of benzene followed by evaporation under reduced pressure. The dried residue was dissolved in hot ethyl acetate and reprecipitated by the addition of petroleum benzine, and dried over phosphrous pentoxide in vacuo at 80°C; yield 63% (3.6 g.), m. p. 118~128°C (sintered at 102~118°C), $[\alpha]_D^{17}$ −117° (c. 4.5, ethanol).

Found: C, 58.73; H, 7.23; N, 14.60. Calcd. for $C_{28}H_{40}O_7N_6$: C, 58.72; H, 7.04; N, 14.68%.

**Glycyl-L-prolyl-L-leucyl-glycyl-L-proline Amide (XVIII).**—Palladium-charcoal (5%, 1 g.) was added to a solution of XVII (1.5 g.) in ethanol (20 ml.) and water (20 ml.), and hydrogen was introduced into the suspension for 3 hr. under stirring. The catalyst was filtered off and washed three times with hot water (total 30 ml.), and then the combined filtrate was concentrated under reduced pressure. The residual syrup was dissolved in a small amount of water, and the solution was filtered. The clear solution was concentrated to syrup and the residue was dried by the addition of ethanol followed by evaporation under reduced pressure, and then pulverized. This material was dried at 110°C in vacuo for 3 hr. before analysis; deliquescent powder, yield of 82% (0.95 g.), m. p. 135~155°C (sintered at 110~115°C), $[\alpha]_D^{17}$ −147.2°C (c. 3.3, ethanol).

Found: C, 54.25; H, 7.76; N, 19.04. Calcd. for $C_{20}H_{34}O_5N_6$: C, 54.78; H, 7.82; N, 19.17%.

## Summary

Glycyl-L-prolyl-L-leucyl-glycyl-L-proline and its related compounds were synthesized for elucidating the substrate specificity of collagenase. In the synthetic study, almost all of the possible routes were tried and the yield, crystallizability and specific rotation of products were compared for each route. Peptides or their derivatives containing two proline residues in general were hydrophilic and hard to be crystallized, but it was found, that carbobenzoxyglycyl-L-prolyl-L-leucyl-glycyl-L-proline was an exceptional example of a readily crystallizable substance and a good substrate for collagenase.

The authors should like to express their thanks to Professor Shiro Akabori of the Institute and Professor Haruhiko Noda of the University of Tokyo for helpful suggestions and guidance in the course of this work.

*Institute for Protein Research*
*Osaka University*
*Joan-cho-36, Kita-ku, Osaka*

# *Crystal Habit Modification of Strontium Sulfate. I. Habit-Modifying Action of Foreign Substances*

By Sadaichi OTANI

(Received March 23, 1960)

Crystals having spherical forms are often found in mineral spherulite which is recognized as a type of radiated crystals. Spherulites have also been prepared artificially by many workers. Popoff[1] studied the two-dimensional spherulites of resorcinol and malonamide, while Lengyel[2] investigated those of several inorganic substances. Three-dimentional spherulites of various inorganic substances were prepared by Morse and others[3] by allowing the reacting solutions to be mixed through diffusion avoiding convection; their best spherulites having spherical forms were obtained in a gelatinous medium. Hence they considered the high viscosity of the medium to be one of the favorable conditions for spherulitic growth. From an ordinary solution, instead of the viscous medium, Patterson[4] obtained spherulitic aggregates of calcium phosphate in the presence of the citrate ion, but the shape of the aggregate was far from being spherical. Recently Miura and his co-workers[5] have succeeded in preparing fine spherical crystals of barium sulfate having nearly uniform size, from an aqueous solution containing citrate ion, and they pointed out the effective utilizations of such crystals in the fundamental study of colloid science and also in the industrial field.

The present author has been interested in the preparation of spherical crystals as well as in the mechanism of their formation, and several attempts have been made regarding these problems. The results obtained will be presented in two parts, of which the first deals with the habit-modifying effect of various substances upon the crystal of strontium sulfate, and the second with the characteristic behavior of the triphosphate ion in the course of deposition and dissolution of strontium sulfate, as well as the mechanism of spherulite formation.

## Experimental

**Reagents.**—Strontium chloride of the reagent grade was purified by repeating three times the alternate crystallization of the dihydrate from a hot solution and then of the hexahydrate from a cold solution. Both potassium sulfate and sodium citrate of the analytical grade were recrystallized from their aqueous solutions. Sodium triphosphate (STP) was prepared by Bell's method[6] and recrystallized from an aqueous solution by adding methanol. Both the EDTA and glycerol used were of the analytical grade. The polyvinyl alcohol (PVA) used had an average molecular weight of $8.5\times10^4$. Both oleylpyridinium chloride and polyethyleneglycol monostearate were furnished by the courtesy of Daiichi Kogyo Seiyaku Co. Ltd. Aerosol OT was of the commercially highest grade.

**Procedure.**—The crystals to be examined were precipitated by mixing a solution of strontium chloride with one of potassium sulfate, in the presence or absence of a third substance in a glass-stoppered flask. To diminish the influence of the container wall upon crystallization, the inside surface of the flask was coated with silicone by the diethyldichlorosilane-treatment. This prevented the precipitate from adhering to the container wall, and thus the crystal growth was not troubled with any steric disturbance of the wall. During mixing and crystallizing, the solutions were violently and continuously shaken with a motor-driven shaker, and the temperature was kept constant within the limits of $\pm0.1$°C.

Foreign substances whose effects were to be examined were added either to the solution of strontium chloride or to one of potassium sulfate, prior to the mixing of these. Sodium citrate, EDTA or condensed phosphates, anyone of which was a complexing agent for metallic cations, was always added to the solution of strontium chloride.

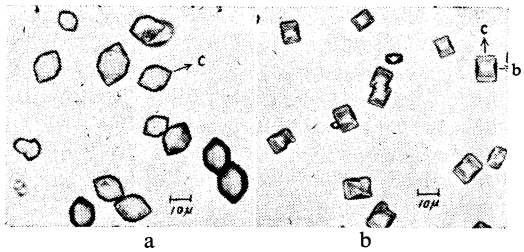
## Results

**Crystals Grown from Mixtures of Strontium Chloride and Potassium Sulfate Solutions.**—First of all, crystals deposited from the solutions prepared by mixing strontium chloride and potassium sulfate solutions without foreign substance were examined. Quite a number of samples were prepared by varying the concentrations and the mixing proportions of the solutions. The concentration range of strontium and sulfate, immediately after mixing, was 0.002~0.1 M.

According to the crystal forms of these samples, they could be classified roughy into

1) B. Popoff, *Latv. Farm. Zurn.*, 1934, 1.
2) E. v. Lengyel, *Z. Krist.*, **97**, 67 (1937).
3) H. W. Morse, C. H. Warren and J. D. H. Donnay, *Am. J. Sci.*, **23**, 421 (1932).
4) D. Patterson, *Nature*, **173**, 75 (1937).
5) M. Miura, T. Nagakane and S. Masaki, *J. Sci. Hiroshima Univ., Ser. A*, **19**, 513 (1956).
6) R. N. Bell, "Inorganic Syntheses", Vol. 3, McGraw-Hill Inc., New York (1950), p. 101.

two large groups. Two microphotographs are shown in Fig. 1 for reference. Fig. 1a represents the crystals of a type obtainable from solutions containing a large excess of sulfate ion and Fig. 1b those of another type from the equivalent mixtures or solutions containing strontium ion in excess. By observing the extinction and retardation of polarized light between the crossed nicols, the orientations of the crystallographic axes were determined, and indicated in the photographs.




a b

Fig. 1. Two samples of crystals grown from mixtures of $SrCl_2$ and $K_2SO_4$ solutions.

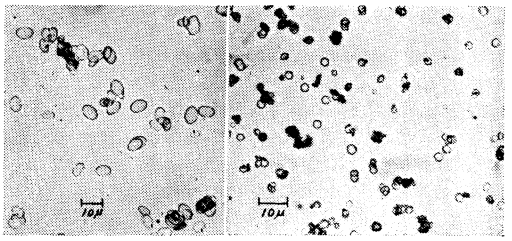
a: 0.017 M $SrCl_2$, 0.10 M $K_2SO_4$
b: 0.10 M $SrCl_2$, 0.017 M $K_2SO_4$

**Effect of Several Additives.** — To inquire whether the viscosity of the medium is an essential factor to the habit modification as reported by Morse and others[3], the effects of glycerol and PVA were tested. In the concentration ranges up to 27% with glycerol and up to 0.4% with PVA, none of these gave any significant influence on the habit of crystals formed.

Then the effects of some surface active agents were examined. Addition of oleylpyridinium chloride or polyethylene glycol monostearate caused a slight increase in the size of the crystals deposited, but the crystal form was hardly influenced by these surface active agents within the concentration limit of 1.0% in each case. Anionic surface active agent Aerosol OT, however, produced a voluminous white precipitate which might be its strontium salt.

**Effect of Sodium Citrate.**—Sodium citrate, even at a very low concentration, has a remarkable effect on the deposition rate and the shape of the crystals. The larger the amount of sodium citrate added, the slower was the deposition rate and the smaller the size of the crystals formed. The shape of the crystals was altered by the addition of sodium citrate in such a way that the edges and corners of the polyhedrons shown in Fig. 1 gradually vanished as the amount of citrate was increased, resulting finally in thin ellipsoids. However, because of the low solubility of strontium citrate, there was a limit to the concentration of the citrate ion in solution, above which the voluminous needle-shaped precipitate appeared.

In Fig. 2 the microphotographs of two samples are shown. These were obtained at 25°C from two separate solutions containing equal amounts of sodium citrate. Both of the solutions from which these crystals were deposited had the same concentration with respect to either of the essential salts as in the previous case (Fig. 1). The electron micrographs of these samples are shown in Fig. 3. Several slenderer figures appearing in Fig. 3a represent the oblique projections of thin ellipsoids (cf. Fig. 7b). Fig. 3b was taken after chromium shadowing at an angle of approximately 22° to the plane of the supporting




a b

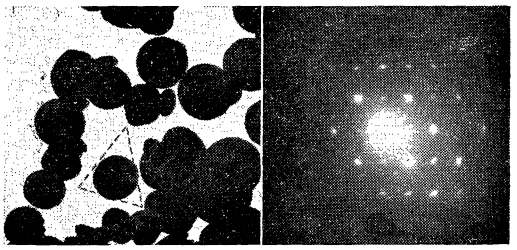
Fig. 2. Two samples of crystals grown from samples solutions containing sodium citrate.

a: 0.071 M $SrCl_2$, 0.10 M $K_2SO_4$, 0.003 M sodium citrate
b: 0.10 M $SrCl_2$, 0.017 M $K_2SO_4$, 0.003 M sodium citrate



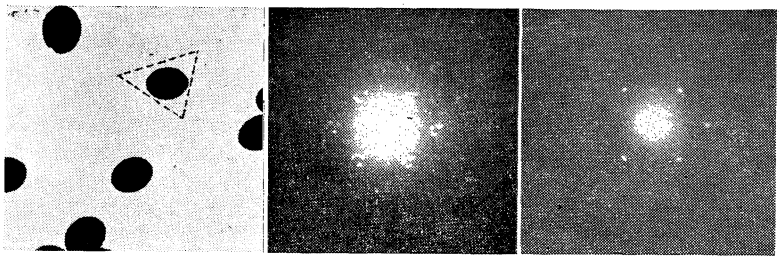
a b

Fig. 3. Electron micrographs of the two a and b shown in Fig. 2.



a b

Fig. 4. Electron micrograph (a) of the sample as one shown in Fig. 2b, and the diffraction pattern (b) of the selected crystal in (a) (surrounded with the triangle).



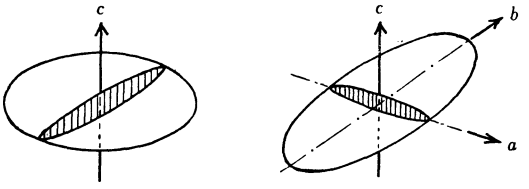
a b c

Fig. 5. Electron micrograph (a) of the same sample as one shown in Fig. 2a, and the diffraction pattern (b and c) of the selected crystal in (a) (surrounded with the triangle).

film. This micrograph shows that the crystals are flat and nearly disk-shaped (cf. Fig. 7a).

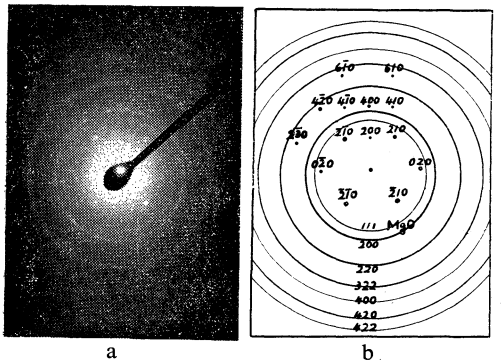
These crystals were then examined by means of an electron microdiffraction technique. The selected-area diffraction of any particle examined gave always an N-pattern as one shown in Fig. 4b or 5c, indicating that these individual crystals are single crystals. For the analysis of the diffraction patterns, the interplanar spacings were determined by comparing these patterns with the Debye-Scherrer rings of magnesium oxide which were taken under a similar condition. For this purpose, the sample crystals and magnesium oxide smoke were mounted together on a supporting film. That is to say, the film on which the sample crystals had already been mounted was exposed to the smoke of burning magnesium. Fig. 6a represents the diffraction pattern of the selected area where both a sample crystal and a large number of fine crystals of magnesium oxide are involved. The Miller indices corresponding to these spots and rings are indicated in Fig. 6b. From this result it is ascertained that the direction of the electron beam in this case was parallel to the *c* axis of the crystal.

Fig. 4b represents the diffraction pattern of the selected crystal shown in Fig. 4a which shows the electron micrograph of the same sample as the one in Fig. 2b. Fig. 5a represents the electron micrograph of the same sample as the one shown in Fig. 2a, and Fig. 5c shows the diffraction pattern of the selected crystal shown in Fig. 5a. Fig. 5b was taken at a current of the intermediate lens which was a little larger than in the case of Fig. 5c. Comparing these three photographs in Fig. 5 with each other, one can easily understand the relation between the orientation of the particle shown in the electron micrograph and that of the same particle in the diffraction pattern. From the fact that the patterns shown in Figs. 4b and 5c coincide with the N-pattern appearing in Fig. 6a, it is revealed that the nearly flat surfaces of these thin ellipsoidal crystals are parallel to the (001) plane. The direction of the largest



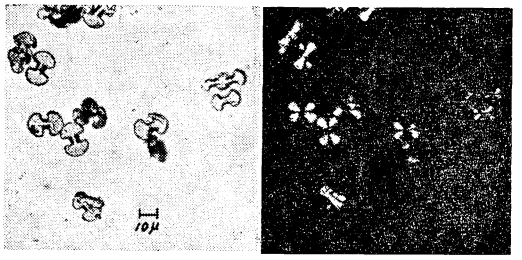

a b

Fig. 7. Shapes and crytsallographic axes of ellipsoidal crystals obtained from solutions containing sodium citrate. Shaded parts indicate the cross sections.




a b

Fig. 6. Diffraction pattern of a selected area where a sample crystal and MgO smoke are mounted together.




a b

Fig. 8. Crystals grown from a solution containing EDTA. (0.013 M $SrCl_2$, 0.05 M $K_2SO_4$, 0.025 M EDTA.)

a: with lower nicol only
b: with crossed nicols

diameter of the crystals shown in Fig. 5a or 2a coincides with that of *b* axis. The axial directions of these crystals are illustrated in Fig. 7.

**Effect of EDTA.**—The crystal habit of strontium sulfate was significantly influenced by EDTA, and it was found that spherulitic aggregates were obtained from a solution containing a relatively large amount of EDTA. One of the remarkable examples is shown in Fig. 8. These photographs were taken with a polarizing microscope with lower nicol only (a) and with the crossed nicols (b). From these photographs, the crystals are seen to be nearly two-dimentional spherulites.

**Effect of Condensed Phosphates.**—The effects of sodium triphosphate (STP) and sodium hexametaphosphate (SHMP) were examined at 25°C. A quite minute amount of these phosphates exerted a great influence on the deposition rate and the crystal habit.

The relation between the composition of the solution and the habit of the crystals obtained in the presence of STP are illustrated in Figs. 9 and 10. Small circles in Fig. 9 indicate the initial concentrations of the three components, strontium chloride, potassium sulfate and STP, the ionic product $[Sr^{2+}][SO_4^{2-}]$ being fixed at 0.001 M$^2$. After examining many solutions having various compositions plotted in the figure, the whole area of the diagram can be divided roughly into six regions A, B,……F. The characteristic behavior of the solution falling in each of these regions is described as follows.

*Region A.*—The effect of STP is insignificant on both the deposition rate and the crystal habit.

*Region B.*—Deposition is retarded noticeably and crystalline aggregates having irregular shapes make their appearance among remarkably modified single crystals (Fig. 10a).

*Region C.*—Retardation of the deposition becomes more significant, and a relatively small number of larger aggregates having irregular shapes (*primary product*) appear in the earlier stage of the process, and later the solution becomes intensely turbid with the deposition of fine single crystals (*secondary product*). Fig. 10b illustrates the primary product.

*Region D.*—Crystal deposition is retarded as well, and crystallization occurs stepwise as in Region C, but the primary product is composed of nearly spherical aggregates as shown in Fig. 10c.

*Region E.*—Spontaneous crystallization is inhibited for a long period of time. However, if the solution was seeded with the crystals obtained from a solution falling in Region D, the seed crystals grow up to larger spheres. The secondary fine crystals also are deposited later.

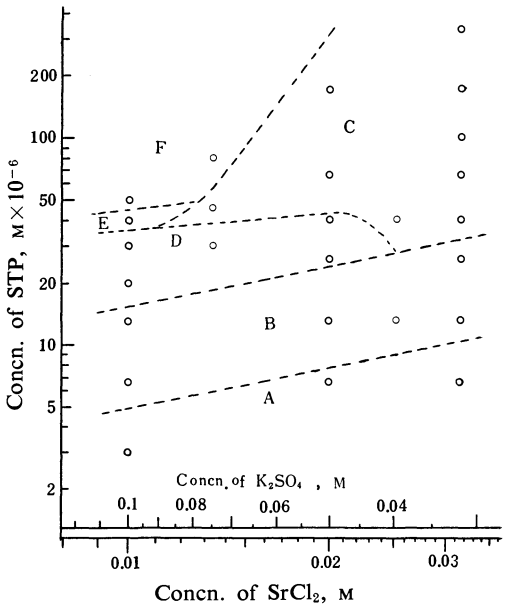



Fig. 9. Composition diagram of $SrCl_2$-$K_2SO_4$-STP-$H_2O$ system.
$[Sr^{2+}][SO_4^{2-}]=0.001$ M$^2$

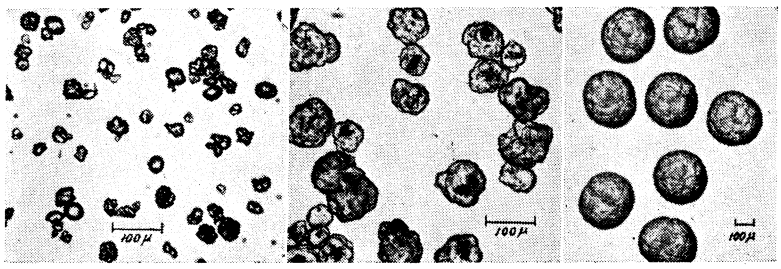



Fig. 10. Crystals grown from solutions containing STP.
a: 0.01 M $SrCl_2$, 0.1 M $K_2SO_4$, $1.3\times10^{-5}$ M STP (Region B)
b: 0.032 M $SrCl_2$, 0.032 M $K_2SO_4$, $6.3\times10^{-5}$ M STP (Region C)
c: 0.01 M $SrCl_2$, 0.1 M $K_2SO_4$, $3.0\times10^{-5}$ M STP (Region D)

*Region F.*—Both spontaneous crystallization and the growth of the seed added are inhibited almost completely.

As the present author was interested in the preparation of spherical crystals, the favorable compositions of the solutions were inquired into for the purpose of examining this process, and it was found that there were the following restrictions on the selection of available compositions. (a) The concentration of STP must be high enough to cause marked habit modification, though there is an upper limit above which no crystallization occurs. (b) The favorable concentration of strontium sulfate is limited to a certain narrow range; below this range crystallization is prevented by so small an amount of STP that the habit-modifying effect does not come into question, while above this range it is impossible to maintain the concentration of STP of sufficiently large value because of the precipitation of sparingly soluble strontium triphosphate. It may be concluded, therefore, that the solution containing a large excess of sulfate ion and a sufficient amount of STP should be recommended for the preparation of well-formed spherical crystals.

Fig. 11, which shows the splinters obtained by crushing the spherical crystal between a pair of microscope slides, makes it clear that the spherical crystal is a kind of spherulite. The arrangement of crystallites can be visualized from microscopic observation of a thin section of the spherulite. Fig. 12a shows a section of a spherulite grown by treating a seed spherulite several times successively with newly prepared solutions of the composition falling in Region E. Fig. 12b illustrates the central portion of the same section in a larger magnification. Fig. 12c shows a micrograph taken with the crossed nicols.

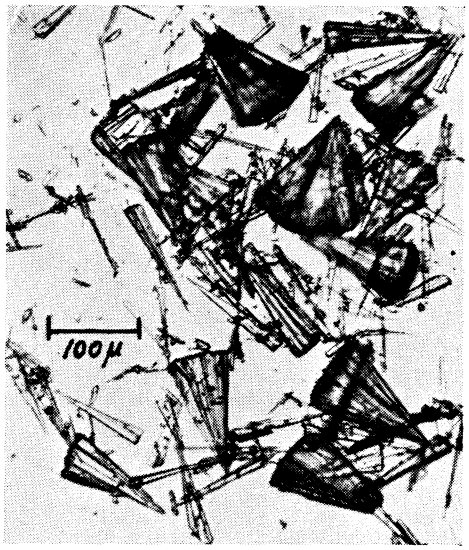



Fig. 11. Splinters of spherulite shown in Fig. 10c.

By certain X-ray examination, it was ascertained that the spherulite was constructed of needle- or wedge-shaped crystallites, each of which was elongated in the direction of *c* axis. The X-ray study was reported in another paper[7].

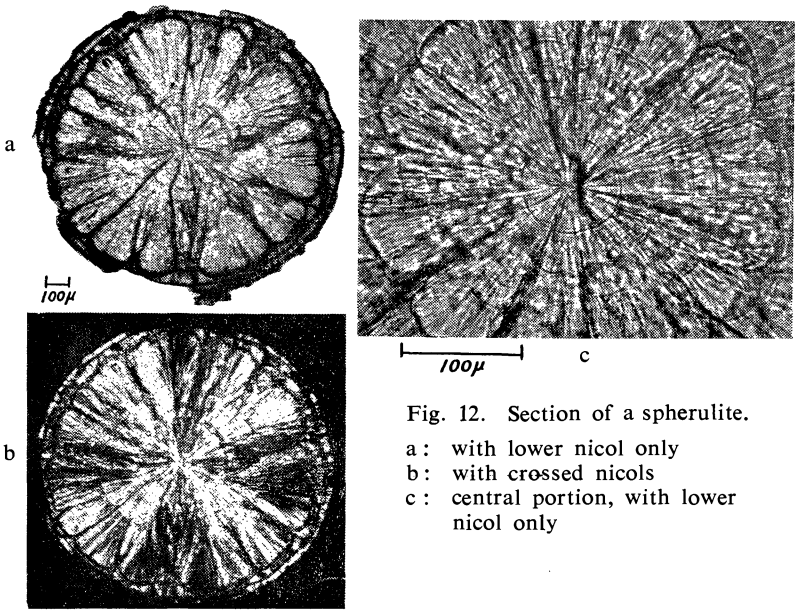



Fig. 12. Section of a spherulite.
a: with lower nicol only
b: with crossed nicols
c: central portion, with lower nicol only

7) Y. Takano and S. Otani, *J. Sci. Hiroshima Univ., Ser. A*, 23, 109 (1959).

The effect of SHMP was also significant and similar to that of STP, and spherulite was obtained from solutions containing a large excess of sulfate and an appropriate amount of SHMP in its concentration range $(3\sim6)\times10^{-5}$ M.

## Discussion

Lambert and Hume-Rothery[8] studied the crystal habit of strontium sulfate precipitated by mixing the strontium chloride solution with sulfuric acid at various concentrations and temperatures. They also investigated the effect of various foreign ions on the precipitation rate, but did not mention the effect on the habit modification. The crystal habits of their products are somewhat different from what was noticed in the present experiments. This discrepancy may be attributed to the difference in the composition of solutions; particularly the difference in acidity may play a dominant role.

From many experimental evidences which have been reported and those of the present work, it is known that the effect of a foreign substance on the crystal habit is very complicated. For example, the citrate ion caused the formation of spherical crystals of barium sulfate[5] on the one hand, and of nearly disk-shaped single crystals of strontium sulfate on the other hand. Another example is the case of spindle-shaped crystals of barium sulfate obtained by Takiyama[9] in the presence of EDTA, which, in the case of strontium sulfate, caused the formation of nearly two-dimensional spherulites.

It is self-evident that the shape of a crystal depends on the relative growth rate in one direction to that in another direction. The growth rate may be affected by the adsorption of foreign substances on crystal faces. According to the peculiarity of each crystal face, the nature and the degree of adsorption may be varied from face to face. Thus a peculiar habit modification might be interpreted by the relation between the crystal structure of the substance to be crystallized and the molecular or ionic structure of the foreign substance added.

The effect of viscosity itself on the crystal habit seems to be insignificant from the experimental results obtained with glycerol or PVA. Referring to the evidence that spherulite can be obtained from ordinary solutions in the presence of a certain impurity, the adsorption, but not the high viscosity, may be the dominant factor for the spherulitic growth. Morse and others' results[3] that the gelatinous medium favored the spherulitic growth may also be attributed to the adsorption of the gelatin itself or of some other impurities possibly involved in it. The mechanism of the spherulitic growth will be discussed in detail in the following paper.

8) B. Lambert and W. Hume-Rothery, *J. Chem. Soc.*, 1926, 2937.
9) K. Takiyama, This Bulletin, **31**, 950 (1958).

## Summary

The effect of various impurities on the crystal habit of strontium sulfate were investigated. Solutions containing citrate ion produced a nearly disk-shaped single crystal whose nearly flat surface was parallel to the (001) plane. Nearly two-dimensional spherulite is obtainable from a solution containing EDTA. A minute amount of sodium triphosphate or sodium hexametaphosphate caused the deposition of a relatively large spherulite having a spherical form, which is composed of numerous needle- or wedge-shaped crystallites elongated in the direction of *c* axis. The habit-modifying action of impurities is discussed in detail.

The author wishes to express his sincere thanks to Professor M. Miura of Hiroshima University for his kind guidance and encouragement throughout this work, and to Professor T. Fujiwara of Hiroshima University for his helpful advice. The author is also indebted to Professor T. Sasaki of Tokyo Metropolitan University, Professor M. Shinagawa of Hiroshima University and Dr. M. Kobayashi of Kobe University for their interest in this work and their kindness in furnishing him with various refined condensed phosphates.

*Department of Chemistry*
*Faculty of Science*
*Hiroshima University*
*Hiroshima*

# *Crystal Habit Modification of Strontium Sulfate. II. Characteristic Effect of Sodium Triphosphate on Crystallization and Mechanism of Spherulite Formation*

By Sadaichi OTANI

(Received March 23, 1960)

In the preceding paper[1] it was reported that the crystal habit of strontium sulfate was remarkably affected by a quite minute amount of sodium triphosphate (STP) added to the solution from which the crystals were deposited, and that the crystallization was retarded and finally came to be practically inhibited, as the amount of STP was increased, provided the concentration of the strontium ion was not over a given value.

Concerning the similar effect of condensed phosphates on the precipitation of various inorganic salts, many works have been published, mostly from the industrial point of view. For example, the effect of metaphosphates on the deposition of calcium carbonate was studied by several workers[2], and the action of triphosphate, metaphosphate, or Quadrafos on the precipitation of gypsum by Burcik[3]. Because of the minuteness of the amount of the phosphates effective in these cases, the prevention of the precipitation could not be ascribed to the sequestration of the component cations by complex formation. Some of the above authors, therefore, attributed the action of these phosphates to the adsorption of them on the crystal nuclei or the growing crystals.

However, the experimental evidences hitherto reported seem to be still insufficient for the reasonable interpretation of the mechanism of these phenomena, and concerning the effect of pure STP on the deposition of strontium sulfate, no work seems to be available in the literature. For the purpose of studying systematically the peculiar effect of STP on the deposition and the crystal habit of strontium sulfate, measurements were made in the present work on the following: (a) deposition rate and (b) dissolution rate of strontium sulfate at various STP contents, (c) surface adsorption of STP on strontium sulfate crystals, and (d) coprecipitation of STP with strontium sulfate. From the results of these experiments, the mechanisms of the habit modification, of the prevention of crystallization and of the spherulite formation will be discussed.

## Experimental and Results

**Inhibition of Crystallization by STP.**—To estimate quantitatively the retardation of the crystal deposition by STP, the rate of crystallization was measured by a conductance method. The reagents used were the same as those in the preceding work[1]. The solution to be examined was prepared

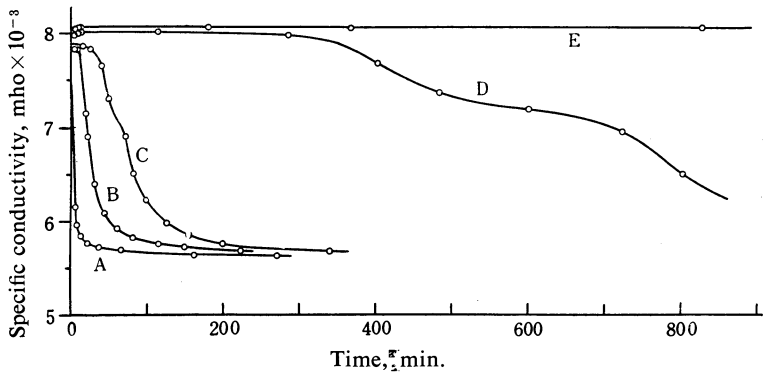



Fig. 1. Conductivity—time curves of 0.02 M $SrSO_4$ solutions containing (A) no STP, (B) $1.0\times10^{-5}$ M STP, (C) $1.5\times10^{-5}$ M STP, (D) $2.0\times10^{-5}$ M STP and (E) $3.0\times10^{-5}$ M STP.

1) S. Otani, This Bulletin, 33, 1543 (1960).
2) L. Rosenstein, U. S. Pat., 2038316 (1936); G. B. Hatch and O. Rice, *Ind. Eng. Chem.*, 31, 51 (1939); R. F. Reitemeier and T. F. Buehrer, *J. Phys. Chem.*, 44, 535, 552 (1940).
3) E. J. Burcik, *Producers Monthly*, 19, No. 1, p. 42 (1954).

in a conductivity cell by mixing equal volumes of potassium sulfate and strontium chloride solutions of equivalent concentration, the latter containing an appropriate amount of STP. Being continuously shaken, the solution was put to the test as to its conductivity at intervals. The results of five runs with different concentrations of STP are illustrated in Fig. 1. The initial concentration of strontium sulfate was fixed at 0.02 M in all cases.

This figure shows how the deposition rate is reduced by a minute amount of STP. Indeed, when the initial concentration of STP amounted to $3.0\times10^{-5}$ M, no change could be detected for a period more than 70 hr. Even if some fine crystals of strontium sulfate were added to this solution, its conductivity remained unchanged for a long period. These facts show that not only the spontaneous crystallization but also the growth of the crystals added was inhibited by STP at this concentration.

The irregularities seen on curves C and D are caused by the stepwise deposition of crystals of two quite different types, one being spherulite and the other fine single crsytals. The comparatively steep decrease in conductivity in the earlier stage corresponds to the growth of the spherulites and that in the later stage to the deposition of fine single crystals.

**Effect of STP on Dissolution.** — The rates of dissolution of strontium sulfate into water and dilute STP solutions of various concentrations were measured by the conductance method at 25°C. The conductivity of the solvent was first measured with a glass-stoppered conductivity cell with 30.0 ml. of the solvent. Then 1.00 ml. of a solution containing 1.00 mg. of strontium sulfate was pipetted into the cell, and the resultant change in conductivity was traced, the solution being shaken continuously. The result is illustrated graphically in Fig. 2.

**Adsorption of STP on Strontium Sulfate.**—The adsorption of STP on strontium sulfate was measured by a radio tracer method with the aid of STP labeled with $^{32}P$.

The labeled STP was prepared, referring to the result of Edward and Herzog[4], by a thermal treatment of the orthophosphate mixture to which radioactive orthophosphate had been added. The product was then recrystallized from an aqueous solution by adding ethanol, and purity was found to be satisfactory for the purpose from a paper chromatographic test. The strontium sulfate used as the adsorbent was precipitated from an equivalent mixture of strontium chloride and potassium sulfate solutions, washed thoroughly with distilled water by decantation, and dried in an oven at 150°C. The particle size of strontium sulfate thus obtained was 3~5 $\mu$ in diameter.

The adsorbed amount of STP was determined by shaking 30.0 ml. of its solution of a known concentration with 0.1000 g. of the adsorbent for an appropriate period and by measuring the radioactivity of the solution before and after treatment. To avoid the dissolution of the adsorbent during the treatment, the STP solution used was prepared by diluting a measured small volume, say 0.1~1 ml., of a rather concentrated stock solution with a given large volume, say 100~500 ml., of a saturated solution of strontium sulfate.

The adsorption rate was estimated by measuring the radioactivity of the solution under investigation at intervals during the shaking. One of the results obtained at $1.0\times10^{-5}$ M of the initial STP concentration at 30°C is shown in Fig. 3, in which the radioactivity is plotted against the time of shaking. The adsorption isotherm obtained at 30.0°C is also illustrated graphically in Fig. 4. It is ascertained

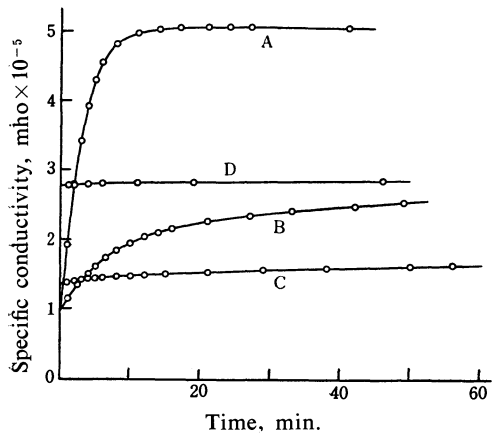



Fig. 2. Conductivity — time curves, showing the dissolution rate of $SrSO_4$ into water and STP solutions.
A: $H_2O$, B: $0.20\times10^{-5}$ M STP, C: $1.0\times10^{-5}$ M STP, D: $4.0\times10^{-5}$ M STP

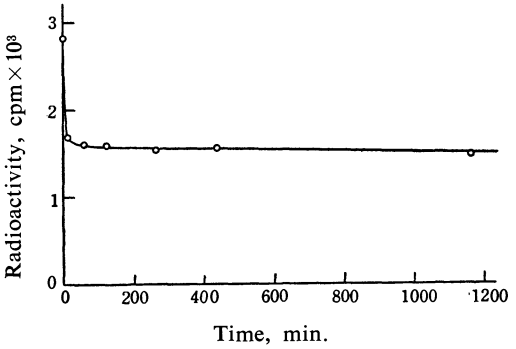



Fig. 3. Radioactivity—time curve, showing adsorption rate of STP on $SrSO_4$ at 30°C.

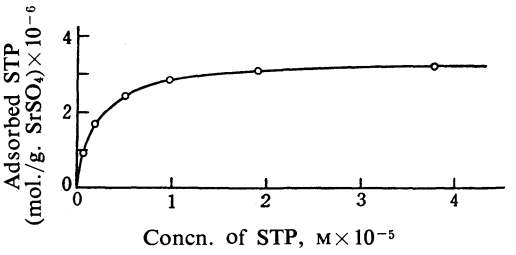



Fig. 4. Adsorption isotherm of STP on $SrSO_4$ at 30.0°C.

4) J. W. Edwards and A. H. Herzog, *J. Am. Chem. Soc.*, 79, 3647 (1957).

that this isotherm is in good agreement with Langmuir's equation.

**Coprecipitation of STP with Strontium Sulfate.** —The coprecipitation was studied with the aid of both the conductance method and the radiotracer technique. The procedures were as follows. Appropriate volumes of strontium chloride, labeled STP, and potassium sulfate solutions, all at 25°C, were pipetted into the conductivity cell in the order just mentioned, and shaken. The decrease in the concentration of strontium sulfate in the solution was traced by conductivity measurement. The radioactivity of the supernatant liquid was measured at intervals during precipitation to trace the decrease in STP concentration. Thus, both amounts of the strontium sulfate and STP precipitated within any desired period were determined simultaneously. One of the results obtained at 25°C is shown with curve A in Fig. 5. This curve illustrates how the amount of coprecipitated STP increases as the crystallization proceeds in a solution where the initial concentrations are 0.02 M with respect to both strontium chloride and potassium sulfate and $1.50\times10^{-5}$ M with respect to STP. In this experiment the solution was constantly shaken during crystallization.

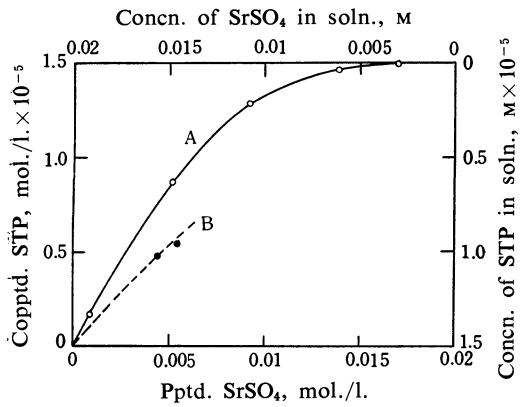



Fig. 5. Coprecipitation of STP with $SrSO_4$.
A: with continuous shaking
B: without shaking

A few measurements were made when solutions were kept unstirred during crystallization. In this case, however, the above-mentioned procedures could not be employed to trace the change in the amount coprecipitated, because the growing crystals were all sedimented at the bottom of the container, thus making the solution inhomogeneous. Therefore, the crystals deposited were filtered off at an appropriate time in the course of crystallization, and weighed after drying. The amount of coprecipitated STP was determined from the radioactivity of the filtrate. The two solid circles in Fig. 5 indicate the values obtained from two runs with solutions having the same composition as that mentioned above.

The mole ratios of STP to strontium sulfate both in the precipitate and the solution were calculated from the data given on curve A in Fig. 5, and are plotted in Fig. 6. The upper curve

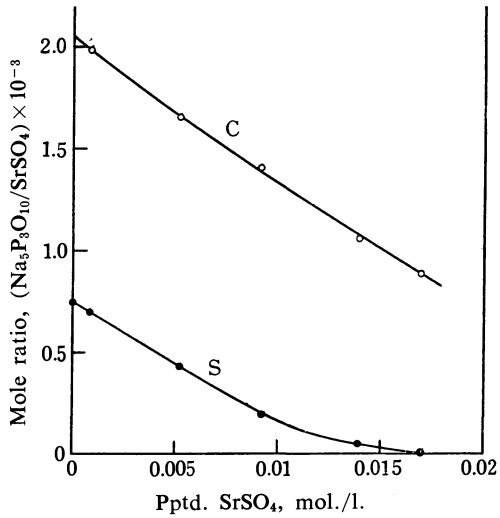



Fig. 6. Mole ratio of STP to $SrSO_4$ during crystallization.
C: in crystal S; in solution

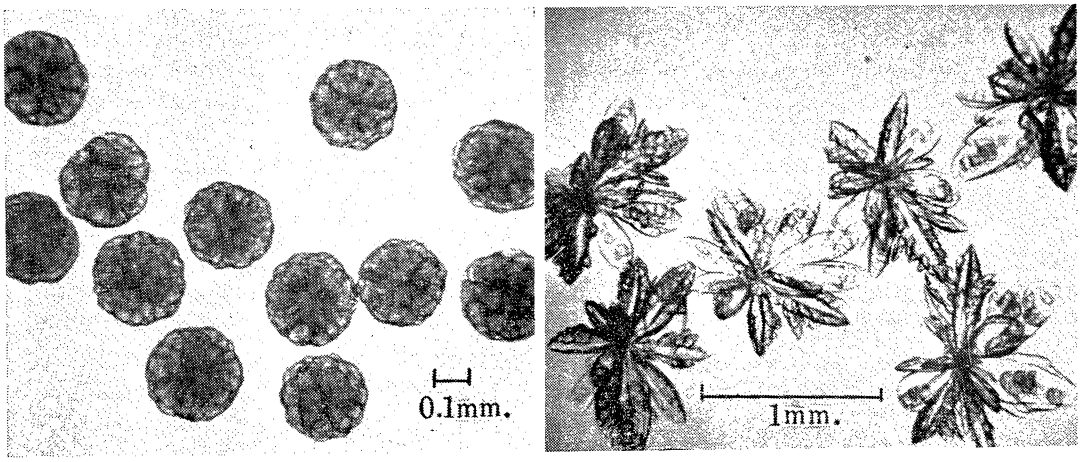
indicates the value in the precipitate and the lower that in the solution.

## Discussion

From the measurements on the crystallization rate, a striking effect of STP was well noticed. As is seen in Fig. 1, an extremely small amount of STP ($3.0\times10^{-5}$ M in its concentration) is quite sufficient to prevent the deposition of crystals from the 0.02 M solution of strontium sulfate. This fact can not be attributed to the complex formation between strontium and triphosphate, in view of the extremely small mole ratio of triphosphate to strontium, namely, 1 : 670.

From the measurements on the dissolution rate, another striking effect of STP was observed. As is seen in Fig. 2, the dissolution of strontium sulfate was retarded by STP even when its concentration was as small as the one in the above-mentioned case. This evidence may possibly be attributed to the adsorption of STP on the crystal surface, because the dissolution can not be hindered directly by the STP existing in the bulk of the solution.

From the measurement of adsorption, the amount of STP adsorbed on strontium sulfate was found to be up to saturation at an extremely low concentration, namely $(2\sim4)\times10^{-5}$ M. Comparison of Fig. 4 with Figs. 1 and 2 reveals the fact that the concentration range within which the amount of adsorbed STP tends to be saturated agrees roughly with the one within which the retardation of crystallization and of dissolution becomes significant. The retardation or prevention of crystallization may accordingly be attributed to the adsorption of STP on the




a b

Fig. 7. Products grown from solutions of $SrSO_4$(0.02 M) containg STP ($1.5\times10^{-5}$ M).
a: with continuous shaking, b: without shaking

crystal nuclei or the growing crystals, and the following mechanism may be considered. The triphosphate ion may be adsorbed preferentially at the active centers of growth on the crystal nuclei or the growing faces of crystals, and the adsorbed triphosphate ion may act as a poison to the layer growth of the crystal faces. The larger the concentration of STP is, the more the active centers will be poisoned and the slower the growth rate will become, and finally, when the concentration of STP exceeds a given value, namely $(3\sim4)\times10^{-5}$ M, at which the adsorption comes to be nearly saturated, all the active centers will be poisoned, and crystallization may be completely inhibited.

Strong interaction between STP and strontium sulfate may be reasonably recognized also from the measurements on coprecipitation. Fig. 6 shows that STP is coprecipitated almost completely with strontium sulfate, the mole ratio of STP to strontium sulfate in the crystal being several times as great as that in the solution.

As is seen from Figs. 5 and 7, agitation of the solution during crystallization has a considerable influence not only on the amount of coprecipitation but also on the crystal habit. Fig. 7a shows the spherulite obtained from a solution with continous shaking (corresponding to curve A in Fig. 5), and Fig. 7b the star-like aggregate from another solution of the same initial composition without shaking (corresponding to curve B in Fig. 5). The difference between the habits of these crystals may be due to the difference in the amount of coprecipitated STP, which can be possibly traced back to the difference in the mode of supply—one by agitation and the other merely by diffusion—of STP from the bulk on the crystal interface.

As already reported[5], the component crystallite of the spherulite or the star-like aggregate is elongated in the direction of *c* axis. This fact means that STP makes the growth rate predominant in the direction of *c* axis. From the above-mentioned poisoning action of the adsorbed STP upon the regular layer growth, it may be concluded that the adsorption of STP is at its minimum on the (001) face as compared with all the other faces, and accordingly the layer growth on this face is least retarded.

Next, the mechanism of spherulite formation will be considered. If radiating fibrillar growth starts from a common center in all directions with an equal growth rate, the growing aggregate will always be spherical. For this to occur, it is necessary to postulate the existence of a cluster of nuclei which has the ability to emit fibrillar crystallites in all directions. In practice, however, the formation of such a cluster of nuclei seems to be improbable, and it may be more acceptable to assume the branching of growing crystallite.

Keller and Waring[6] assumed a periodic branching of fibrils occurring at constant distances with a constant acute angle to explain the "sheaf" formation in the course of spherulitic growth of synthetic high polymers. They proved that the periodicity of branching is a necessary condition for the formation of Popoff's "Zweiblatt"[7] or Morse and Donnay's "sheaf"[8]. Keller and Waring's illustration of

5) Y. Takano and S. Otani, *J. Sci. Hiroshima Univ., Ser. A*, **23**, 109 (1959).
6) A. Keller and J. R. S. Waring, *J. Polymer Sci.*, **17**, 447 (1955).
7) B. Popoff, *Latv. Farm. Zurn.*, **1934**, 1.
8) H. W. Morse and J. D. H. Donnay, *Am. Mineralogist*, **21**, 392 (1936).

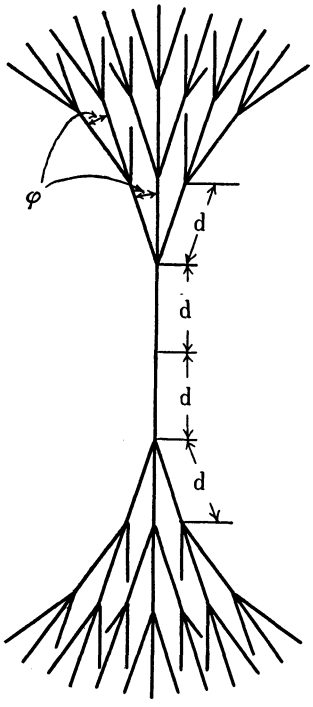



Fig. 8. Schematic diagram showing the sheaf formation through periodic branchings (after Keller and Waring).

the sheaf formation through the periodic branching is reproduced in Fig. 8.

In the present case, the branching of crystallite were recognized from a microscopic observation of the growth process. Fig. 9 shows the development of a seed in a solution containing an appropriate amount of STP. Fig. 9a shows the seed which is one of the splinters obtained by crushing a well-developed spherulite, and Fig. 9b and 9c illustrate the successive stages of its growth. By crushing the product (Fig. 9c), a large number of wedge-shaped smaller crystallites resulted. These are shown in Fig. 9d. By comparing these photographs with each other, it may be seen that radiating crystallization started everywhere on the surface of the seed. This fact may certify that branching of crystallite is induced by STP.

No indication of sheaf formation was observed either in this experiment or in many others mentioned before. However, the formation of spherulite can be interpreted on the basis of the above-mentioned evidence that, under the influence of STP, branchings are accompanied by the growth of strontium sulfate crystal and its growth rate is highly predominant in the direction of *c* axis. Under this condition, the crystal growth must proceed as follows. Starting from a single nucleus, an aggregate crystallites will be formed as a result of successive branchings during the growth, and the number of the crystallites will increase acceleratedly as the growth proceeds. On the other hand, the growth of each crystallite must inevitably be restricted by the steric hindrance of the adjacent ones, and, as a result, only those crystallites of which the direction of the fastest growth happened to coincide nearly with the radial direction may survive. Thus, sooner or later, the aggregate changes to be constructed of a great number of crystallites directed radially, at least near the periphery. Hereafter, the

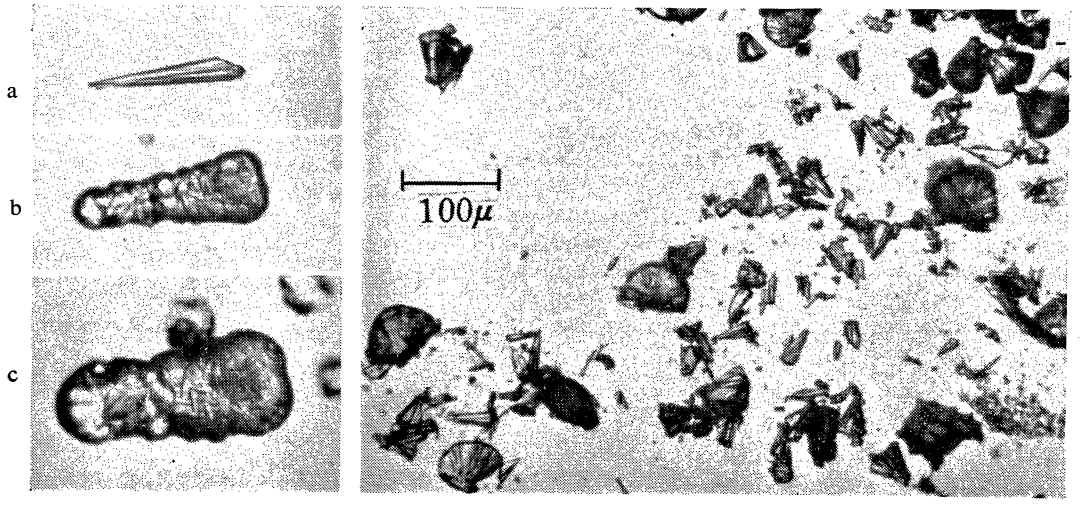



Fig. 9. Spherulitic growth from a seed.
a: seed, b: after 48 min., c: after 190 min., d: splinters obtained by crushing c

shape of the aggregate must gradually approach a sphere, because the growth rate is uniform in all directions in the radial growth.

The above-mentioned concept may explain why such a star-like aggregate as that shown in Fig. 7b is produced, when the solution is kept unstirred. For a moment just after a crystal nucleus begins to grow, it may be supplied with enough STP to cause frequent branchings regardless of the solution being stirred or not. However, as the growth proceeds, the concentration of STP at the immediate vicinity of the growing aggregate may be reduced rapidly because of the consumption of STP due to the selective adsorption (cf. Fig. 6). If the solution is not stirred, STP is supplied merely by diffusion, and hence the branching may ocurr less frequently. Accordingly the resultant aggregate, being composed of a relatively small number of radiated crystallites, gives a star-like appearance.

As to the mechanism of the branching of crystallite, Keller and Waring[6] mentioned twinning and rupture of distorted crystal as possible causes. In the present work, branching is induced by STP, and may be attributed to the adsorption of the latter onto the crystallite. The mechanism of branching may be considered as follows. The adsorbed triphosphate ion could hardly enter into the regular crystal lattice of strontium sulfate because of the unfitness of the size and ionic charge. The crystal lattice may be distorted in the vicinity of the adsorbed triphosphate ion. As the amount of adsorbed triphosphate increases, many ruptures of lattice may appear on the crystal faces owing to the distortions of the lattice. These ruptures may cause branchings of crystallite.

From the above discussion, we may conclude that we shall have a possibility of preparing spherulites of any substance, if we can find an impurity that has the following properties. (1) The impurity is intensely and preferentially adsorbed by the particular crystal faces of the substance in question and (2) the impurity can not make a solid solution or mixed crystal with the substance. A clue to finding such a suitable impurity may possibly be obtained from the knowledge of the relation between the molecular or ionic structure of the impurity and the crystal structure of the substance in question. For the preparation of a spherulite of an inorganic salt, there may be found some suitable impurities among those polyatomic complex ions which have a strong affinity to either of the component ions of the salt.

## Summary

1) The peculiar effect of sodium triphosphate (STP) on the crystallization and the crystal habit of strontium sulfate was studied systematically by measuring (a) the deposition rate and (b) the dissolution rate of strontium sulfate at various STP concentrations, (c) the surface adsorption of STP on strontium sulfate crystal, and (d) the coprecipitation of these salts.

2) The inhibiting action of STP on the deposition and dissolution of strontium sulfate is attributed to the adsorption of STP.

3) The fact that STP makes the growth rate predominant in the direction of *c* axis of strontium sulfate is ascribed to the small adsorption of STP on the (001) faces compared with that on the other faces.

4) The occurrence of the branching of crystallite was ascertained experimentally, and attributed to the ruptures appearing on the crystal faces as a result of the unfitness in the size and ionic charge of the adsorbed triphosphate.

5) The formation process of the spherulite can be interpreted from the fact that the frequent branchings are accompanied by the nearly one-dimentional growth of crystallite.

6) Possibilities of preparing spherulites from other substances are discussed.

The author gratefully acknowledges the guidance and encouragement of Professor M. Miura of Hiroshima University. He also wishes to thank Professor T. Ichikawa of Hiroshima University for his helpful advice and discussions.

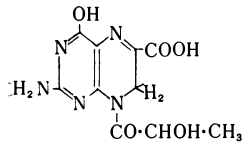
*Department of Chemistry*
*Faculty of Science*
*Hiroshima University*
*Hiroshima*

# *The Structure of the Yellow Pigment from Drosophila*

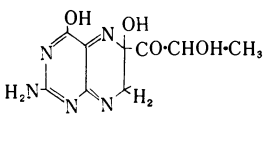
By Saburo NAWA

(Received May 9, 1960)

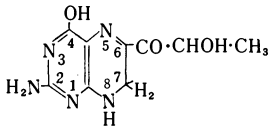
It has been known that the wild type eye-color of *Drosophila melanogaster* is due to the presence of two pigments, the red and the brown. It is of particular interest to study the chemistry of the eye pigments in order to clarify the relationship between genes and biochemical processes, since the various genetic interrelationships are well established in the group of eye-color mutants of *Drosophila*. Hadorn and Mitchell[1] have mentioned for the first time the presence of a yellow pigment, which was later named Sepiapterin by Ziegler-Günder and Hadorn[2], in *Drosophila* by a simple chromatographic technique and that the mutant *sepia* contained much greater amounts of Sepiapterin in comparison with the wild type. In 1954 Nawa and Taira[3] have reported that the yellow pigment, Xanthopterin-B[4], found in the epidermis of the mutant *lemon* of silkworm is a derivative of 2-amino-4-hydroxypteridine and is indistinguishable from Sepiapterin. In the same year Forrest and Mitchell[5] have isolated Sepiapterin as a crystalline form and proposed the structure I for it, although I was later modified to structure II by Forrest et al.[6] In the light of some new experiments on Sepiapterin, however, its structure will be discussed in this paper. And we now wish to propose the structure III for Sepiapterin on the basis of the following findings.



I



II



III

## Experimental

**Isolation of Sepiapterin.** — One handred grams (wet) of flies (*D. melanogaster*, mutant *sepia*) were homogenized in a Waring Blender in 30% ethanol (500 ml.). The suspension was heated at 80°C for 5 min. and allowed to stand overnight in an ice box. The reddish yellow supernatant obtained by centrifugation was concentrated in vacuo to a small volume (about 50 ml.) and then spread on 8 sheets (40×40 cm.) of heavy filter paper (Toyo Roshi Co. Ltd., No. 26). These were then chromatographed with water. The yellow band was cut off and eluted with water. The eluate was then concentrated and chromatographed again on the heavy filter paper (4 sheets) with a mixture of *n*-butanol, acetic acid and water (4 : 1 : 1). After allowing the chromatogram to dry, the appropriate band corresponding to Sepiapterin was eluted with water. The concentrated solution was applied to a column (6×40 cm.) of cellulose powder and developed with water. The fraction of yellow pigment was collected and evaporated to dryness in vacuo. The residue was dissolved in hot water (8 ml.) and allowed to stand overnight in an ice box, when the product (13 mg.) crystallized as orange needles. All the above procedure was carried out in the dark to avoid photolysis. Eight handred gram of flies gave 105 mg. of crystals in repetition of this procedure.

Found: C, 45.9; H, 4.5; N, 29.2. Calcd. for $C_9H_{11}N_5O_3$: C, 45.6; H, 4.7; N, 29.5%.

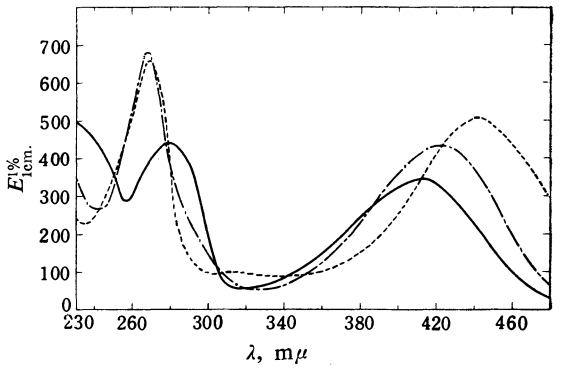



Fig. 1. The ultraviolet absorption of Sepiapterin: ——, at pH 1.0; — — —, at pH 5.0; and - - -, at pH 11.0.

1) E. Hadorn and H. K. Mitchell, *Proc. Nat. Acad. Sci. U. S.*, **37**, 650 (1951).
2) Ziegler-Günder and E. Hadorn, *Z. Vererbungslehre*, **89**, 235 (1958).
3) S. Nawa and T. Taira, *Proc. Japan Acad.*, **30**, 632 (1954).
4) Y. Hirata, K. Nakanishi and H. Kikkawa, This Bulletin, **23**, 76 (1950).
5) H. S. Forrest and H. K. Mitchell, *J. Am. Chem. Soc.*, **76**, 5656, 5658 (1954).
6) H. S. Forrest, D. Hatfield and C. V. Baalen, *Nature*, **183**, 1269 (1959).

The ultraviolet absorption spectra are shown in Fig. 1. (At pH 1, $\lambda_{max}$ 281, 410 m$\mu$, $E^{1\%}_{1cm.}$ 440, 340. At pH 11, $\lambda_{max}$ 268, 440 m$\mu$, $E^{1\%}_{1cm.}$ 665. 510.)

**Air Oxidation in Borax Solution.** — Sepiapterin (25 mg.) was dissolved in 5% borax (50 ml.) and shaken at 35°C for 5 hr. in the dark to avoid photodecomposition, when the yellow color of the solution gradually disappeared and the yellow fluorescence changed to green.

**a) Estimation of 7,8-Dihydroxanthopterin (IV).** —When this reaction mixture was allowed to stand overnight in an ice box, the product (14.6 mg.) precipitated. The compound was recrystallized from 0.25 N sulfuric acid as the sulfate (10.7 mg.).

Found: C, 30.0; H, 3.9; N, 29.2. Calcd. for $C_6H_7N_5O_2 \cdot 1/2H_2SO_4 \cdot H_2O$: C, 29.0; H, 4.0; N, 28.2%.

The ultraviolet absorption curves as shown in Fig. 2a. (At pH 1, $\lambda_{max}$ 276, 305 m$\mu$, $E^{1\%}_{1cm.}$, 535, 310. At pH 11, $\lambda_{max}$ 276 m$\mu$, $E^{1\%}_{1cm.}$ 515.) This compound was readily oxidized to xanthopterin (V) with manganese dioxide in alkaline solution. In neutral solution, moreover, the compound was oxidized to V accompanied by consumption of one mole of iodine. These properties, absorption spectra and $R_f$ values of the compound are perfectly identical with those of the authentic 7,8-dihydroxanthopterin (IV)[7-9]. Some $R_f$ values compared with those for authentic IV (in parentheses) are: *n*-propanol, 1% ammonia (2 : 1), 0.16 (0.16); 2% $K_2HPO_4$, 0.32 (0.32), 3% sodium citrate, 0.35 (0.35). The absorption curves of IV obtained from the catalytic hydrogenation of xanthopterin (Nutritional Biochemicals Co., U. S. A.) are shown in Fig. 2b.

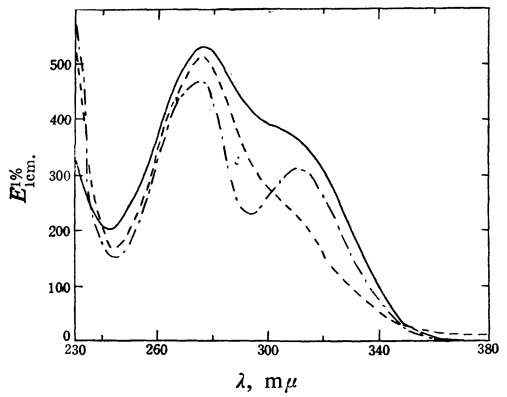



Fig. 2a. The ultraviolet absorption of the product from decomposition of Sepiapterin: ——, at pH 1.0; — — —, at pH 5.0; and - - -, at pH 11.0.

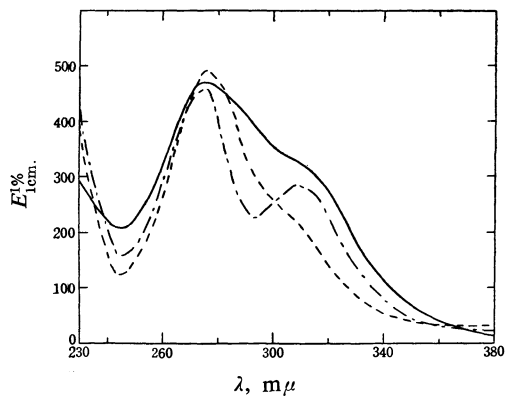



Fig. 2b. The ultraviolet absorption of 7,8-dihydroxanthopterin (IV) obtained from catalytic reduction of xanthopterin: ——, at pH 1.0; — — —, at pH 5.0; and - - -, at pH 11.0.

**b) Characterization of Lactic Acid.** — The supernatant from the reaction mixture mentioned above showed the color reaction[10] characteristic of lactic acid. The supernatant (0.01 ml.) was withdrawn and heated at 100°C for 5 min. with 3 ml. of sulfuric acid and 0.05 ml. of 2% $CuSO_4$. After cooling,, 0.05 ml. of 1.5% *p*-hydroxydiphenyl reagent was added and allowed to stand at 30°C for 30 min. And then the color developed was estimated at 570 m$\mu$ in a Beckman spectrophotometer. From a standard curve obtained from known amounts of lithium lactate, 5 $\mu$g. of Sepiapterin (0.01 ml. of the reaction mixture) was estimated to give 1.5 $\mu$g. of lactic acid (with a molecular weight of 237, the theory for one mole of lactic acid per mole of Sepiapterin is 1.57 $\mu$g.). The remained supernatant was concentrated to a small volume and paper chromatographed in various solvent systems. Some $R_f$ values compared with those for lactic acid (in parentheses) are: *n*-butanol, acetic acid, water (4 : 1 : 1), 0.75 (0.75); ethanol,10% ammonia (4 : 1), 0.77 (0.77); *n*-butanol, pyridine, water (1 : 1 : 1), 0.39 (0.39).

**c) Relationship of Oxygen Uptake, and IV and Lactic Acid Production.** — Sepiapterin (4.7 mg.) was dissolved in 5% borax solution (20 ml.) and each aliquots (2 ml., 0.47 mg.) were shaken in Warburg flasks at 35°C in the dark. At various

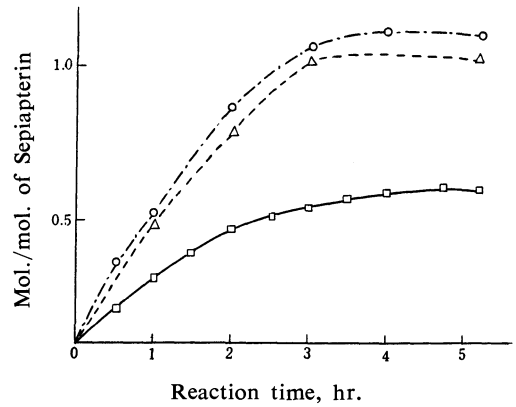



Fig. 3. Air oxidation of Sepiapterin in the presenc of borax: -□-, oxygen consumed; -○-, lactic acid produced; and -△-, 7,8-dihydroxanthopterin produced.

7) B. L. O'Dell, J. M. Vandenbelt, E. S. Bloom and J. J. Pfiffner, *J. Am. Chem. Soc.*, **69**, 250 (1947).
8) W. R. Boon and T. Leigh, *J. Chem. Soc.*, **1951** 1497.
9) G. B. Elion and G. H. Hitchings, *J. Am. Chem. Soc.*, **74**, 3877 (1952).
10) S. B. Barker and W. H. Summerson, *J. Biol. Chem.*, **138**, 535 (1941).

time intervals, oxygen uptake was measured, the amounts of IV produced were calculated using the known extinction constant at 310 mμ at pH 7 and the amounts of lactic acid were determined by the procedure described previously. As shown in Fig. 3, the molar ratio of oxygen consumed, and IV and lactic acid produced was 0.5 : 1 : 1 at all reaction intervals. This reaction did not occur in the absence of oxygen. It should be noted that the rate of reaction is variable. Since the reaction is accerelated by addition of small amounts of heavy metal ions and inhibited by chelating agents, it is concluded that the variable rate is due to the presence of metal-ion impurities.

**Periodate Oxidation.**—A solution of Sepiapterin (2.0 mg.) in 2% sodium bicarbonate (1.2 ml.) was treated with 1% sodium metaperiodate (0.8 ml.) in an ice bath. At various intervals the undestroyed periodate was estimated. Aliquots (0.1 ml.) were withdrawn and quenched in 0.001 N sodium arsenite (1.0 ml.) containing potassium iodide (10 mg.). After 15 min. the samples were titrated with standard potassium iodide-iodine (0.002 N) to a starch end-point. Acetaldehyde was determined by the color development[11] with *p*-hydroxydiphenyl in sulfuric acid. To aliquots (0.01 ml.) was added 0.1% sodium arsenite (0.5 ml.). After 15 min. the solution was treated with sulfuric acid (3 ml.), 2% $CuSO_4$ (0.05 ml.) and 1.5% *p*-hydroxydiphenyl reagent (0.05 ml.) at 30°C for 30 min. The color developed was estimated at 570 mμ. As shown in Fig. 4, the

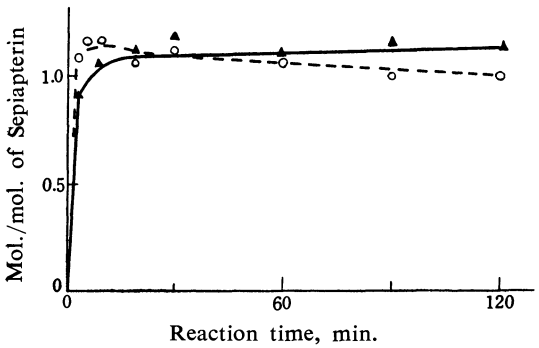



Fig. 4. Periodate oxidation of Sepiapterin: -▲-, periodate consumed; --○--, acetaldehyde produced.

curves of the acetaldehyde production and periodate consumption reached to plateaus as soon as periodate was added to the solution of Sepiapterin. In the reaction the yellow color of the solution rapidly disappeared and the yellow fluorescence changed to green.

**2-Amino-4-hydroxy-7, 8-dihydropteridine-6-carboxylic Acid (VI).**—To a solution of Sepiapterin (20 mg.) in 2% sodium bicarbonate (12 ml.), 1% sodium metaperiodate (8 ml.) was added. After standing 30 min. at 0°C, the reaction mixture was diluted with cold water (20 ml.), applied immediately to a column (5×40 cm.) of cellulose powder and developed with 0.002% ammonia. During the development of the column, the fluorescent products were separated into two bands, major greenish yellow and minor blue fluorescent. The minor blue fluorescent compound (1.6 mg.) was 2-amino-4-hydroxypteridine-6-carboxylic acid (VII) with identity of ultraviolet absorption and its paper chromatographic behavior. The main greenish yellow fluorescent band was collected and a pale greyish residue (7.4 mg.) was obtained by freeze-drying. For convenience, this compound is henceforth referred to as Compound-A.

Found: C, 40.78; H, 3.21; N, 32.75. Calcd. for $C_7H_7N_5O_3$: C, 40.19; H, 3.37; N, 33.48%.

The ultraviolet absorption spectra are shown in Fig. 5. (At pH 1, $\lambda_{max}$ 280, 380 mμ. At pH 11,

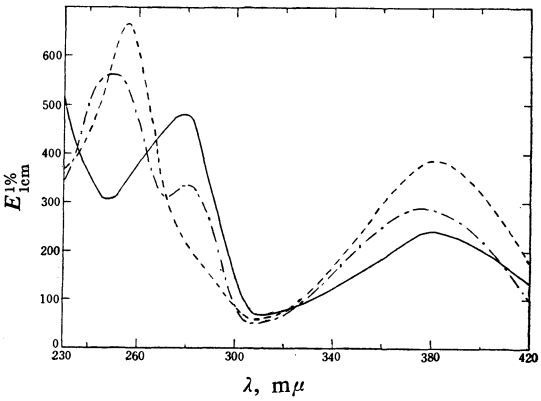



Fig. 5. The ultraviolet absorption of pteridine (VI) obtained from periodate oxidation of Sepiapterin: ——, at pH 1.0; — — —, at pH 5.0; and - - -, at pH 11.0.

$\lambda_{max}$ 255, 380 mμ.) Some $R_f$ values compared with those for VII (in brackets) are: *n*-propanol, 1% ammonia (2 : 1), 0.11 (0.14); *n*-butanol, acetic acid, water (4 : 1 : 1), 0.09 (0.14); 3% sodium citrate. 0.37 (0.53); 5% acetic acid, 0.30 (0.47); 2% $K_2HPO_4$, 0.35 (0.44). Compound-A was comparatively stable to auto-oxidation in neutral solution when stored at 0°C in the dark, but it was readily converted to VII on exposure to light and at that time consumed 0.5 mol. of oxgen. In alkaline solution Compound-A was oxidized into VII with manganese dioxide. In neutral or acidic solution, furthermore, Compound-A consumed 1 mol. of iodine and gave VII. From these results, it is concluded that Compound-A is a dihydro-form of VII, i. e. 2-amino-4-hydroxy-7, 8-dihydropteridine-6-carboxylic acid (VI). This is also confirmed by the following findings.

**a) Reduction of Compound-A with Sodium Borohydride.**—A solution of Compound-A (0.1 mg.) in 0.01 N acetic acid (10 ml.) was treated with sodium borohydride (1 mg.), when the greenish yellow fluorescence of the solution immediately dissappeared. Aliquots of the reaction mixture were adjusted to various pH and the absorption spectra were recorded as shown in Fig. 6. The curves are characteristic of tetrahydropteridies[7,12,13].

11) R. J. Block and D. Bolling, *J. Biol. Chem.*, **130**, 365 (1939).

12) M. Viscontini and H. R. Weilenmann, *Helv. Chim. Acta.*, **41**, 2170 (1958).

13) S. Kaufman, *J. Biol. Chem.*, **234**, 2677 (1959).

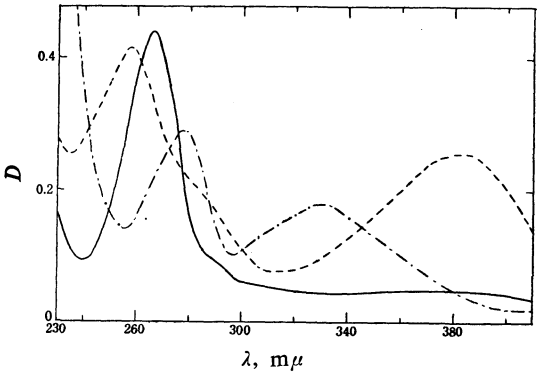



Fig. 6. The absorption of the product resulting from $NaBH_4$ reduction of VI: ——, at pH 1.0; — — —, at pH 5; and - - -, at pH 11.0.

Upon shaking the reaction mixture in air, its fluorescence became blue. Paper chromatography of this solution showed the presence of two blue fluorescent compounds. The major spot was VII and the weaker was 2-amino-4-hydroxypteridine (VIII). Neither VII nor VIII was attacked by $NaBH_4$.

**b) Conversion of Compound-A to 2, 6-Diamino-4-hydroxypteridine (IX).**—A solution of compound-A (0.5 mg.) in 1% ammonia (1 ml.) was heated at 80°C for 30 min. The reaction mixture was applied to a column of cellulose powder and developed with 0.002% ammonia. The main bright green fluorescent band was eluted. The absorption spectra of this eluate in various pH (Fig. 7) correspond to these of 2,6-diamino-4-hydroxypteridine (IX)[14], which were obtained from the catalytic reduction of VIII in dilute ammonia, and the identity of this compound was confirmed by paper chromatographic comparison with the authentic sample. When the compound was incubated with milk xanthine oxidase at pH 8, it was oxidized to a purplish blue

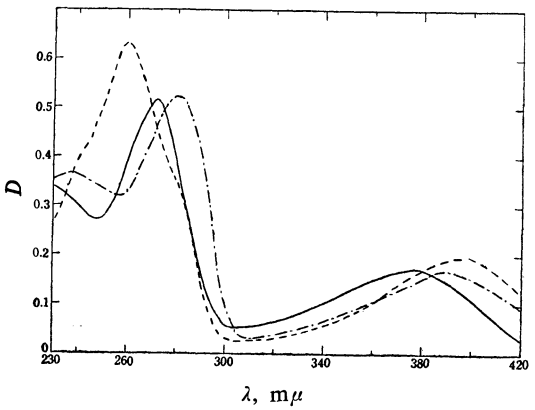



Fig. 7. The absorption of pteridine (IX) obtained from VI by treating with ammonia: ——, at pH 1.0; — — —, at pH 5.0; and - - -, at pH 11.0.

14) C. V. Baalen and H. S. Forrest, *J. Am. Chem. Soc.*, **81**, 1770 (1959).

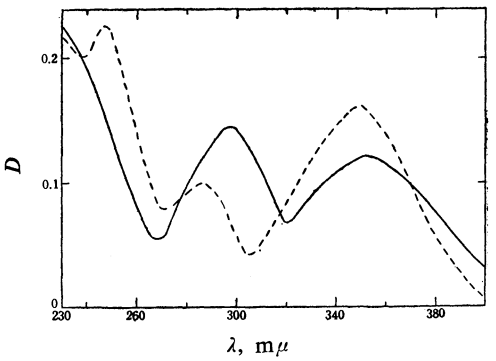



Fig. 8. The absorption of pteridine (X) obtained from IX by treatment with milk xanthine oxidase: ——, at pH 1.0; - - -, at pH 11.0.

fluorescent substance. Its absorption spectra (Fig. 8) resemble those of isoxanthopterin (2-amino-4, 7-dihydroxypteridine)[15]. From the evidence[16,17] that milk xanthine oxidase attacks the 7-position of the pteridine skeleton, it is probable that the substance is 2,6-diamino-4,7-dihydroxypteridine(X).

**Photodecomposition.**—Sepiapterin (0.47 mg., 2.0 μmol.) dissolved in water (2 ml.) was exposed to sunlight in a Warburg flask at 35°C. An oxygen uptake of 50 μl. was observed, when the yellow color of the solution had disappeared. Acetaldehyde (0.086 mg., 1.95 μmol.) was ascertained by the procedure described above. VII (0.39 mg., 1.88 μmol.) was determined using the known optical density for this acid, after separating by paper chromatography.

## Discussion

It has been known that both photodecomposition[3,5] and permanganate oxidation[5] of Sepiapterin gave 2-amino-4-hydroxypteridine-6-carboxylic acid (VII). This shows that Sepiapterin is a 6-substituted pteridine. In connection with the result by Forrest et al.[5], who obtained VII and acetaldehyde from periodate oxidation of Sepiapterin, the present observation that one mole of lactic acid is quantitatively obtained from decomposition of Sepiapterin suggests that the substituent is a lactyl group ($CH_3 \cdot CHOH \cdot CO-$). Since the analytical data indicate that Sepiaterin has three carbon atoms other than its pteridine skeleton, the lactyl group seems to be a sole side chain. The isolation of 7, 8-dihydroxanthopterin (IV) from air oxidation of Sepiapterin suggest whether the 6-hydroxy group of IV is an integral part of the molecule of Sepiapterin or a hydroxylation at the 6-position occurs at

15) A. Albert and H. C. S. Wood, *J. Appl. Chem.* (London), 3, 521 (1953).
16) O. H. Lowry, O. A. Bessey and E. J. Crawford, *J. Biol. Chem.*, **180**, 389 (1949).
17) F. Bergmann and H. Kwietny, *Biochem. et Biophys. Acta*, **26**, 613 (1958).

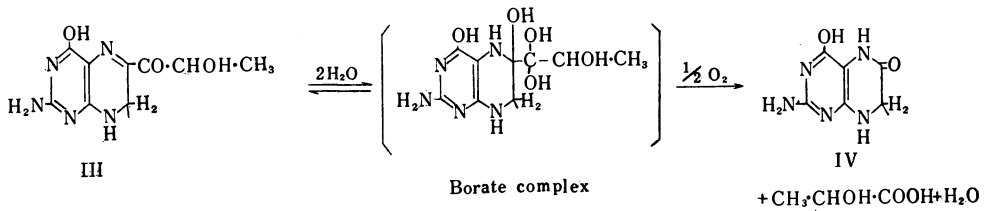



Fig. 9.

the same time as the lactyl side chain is split off. Since this reaction did not occur in the absence of oxygen (0.5 mol. of oxygen were consumed), it is sure that the side chain is split off oxidatively. In this connection, Blakley[18] has reported the production of xanthopterin in aerated solution of dihydro- or tetrahydrofolic acid. It seems reasonable to assume, therefore, that the oxygen atom in the 6-position of IV is oxidatively introduced and then Sepiapterin has no OH group in its 6-position. The finding that the decomposition of Sepiapterin give one mole each of IV and lactic acid accompanied by consumption of 0.5 mol. of oxygen, therefore, suggests that Sepiapterin has the structure 2-amino-4-hydroxy-7, 8-dihydro-6-lactylpteridine (III). From the evidence[19] that polyhydroxy compounds form borate complexes and from the experimental result that 0.5 mol. of oxygen are consumed in the reaction of sepiapterin with borax, the schema shown in Fig. 9 is postulated.

The formation of 2-amino-4-hydroxypteridine-6-carboxylic acid (VII) and acetaldehyde by periodate oxidation of Sepiapterin has been reported by Forrest et al.[5]. However, when in alkaline solution Sepiapterin was treated with periodate, it consumed one mole of periodate to give acetaldehyde and a pteridine different from VII. The pteridine seems to be a dihydro form of VII, i. e. 2-amino-4-hydroxy-7, 8-dihydropteridine-6-carboxylic acid (VI), since it is readily oxidized to VII accompanied by consumption of 0.5 mol. of oxygen or one mole of iodine. Furthermore, the finding that pteridine was converted to 2, 6-diamino-4-hydroxypteridine (IX) by treating with ammonia again supports it to be hydropteridine, in connection with the evidence[14] that the catalytic reduction of 2-amino-4-hydroxypteridine (VIII) in the presence of ammonia gave IX. In progress of our studies, Viscontini and Möhlmann[20] reported that the reduction of Sepiapterin with sodium borohydride give a tetrahydro form of biopterin (2-amino-4-hydroxy-6-(1, 2-dihydroxypropyl)-pteridine )[21-23]. We observed that the sodium borohydride reduction of VI give a compound with a spectrum characteristic of typical tetrahydropteridine[7,12,13], although neither VII nor VIII is affected. Dihydropteridines, therefore, seems to be reduced to the corresponding tetrahydro form by the action of sodium borohydride. It was also found that Sepiapterin is reduced to a tetrahydro form with the enzyme system from chicken liver, which carries out a reaction of dihydrofolic acid to tetrahydrofolic acid. These observations confirm that Sepiapterin is a dihydropteridine. The present result that photodecomposition of Sepiapterin gave one mole each of acetaldehyde and VII accompanied by consumption of one mole of oxygen, is again in accord with the proposed structure III.

Several different pteridines[3,5,6,20,21,23] have already been isolated from *Drosophila*. It has been assumed[3,5,20] that the red pigment found in the wild type has a structure related closely to the yellow pigment (Sepiapterin) and the latter is an intermediate in the synthesis of the former. It is of particular interest that Sepiapterin is a hydropteridine, in connection with the biological significance[24] of hydrofolic acid. Recently, Kaufman[13] reported the role of hydro-form of simple pteridines in the enzymatic oxidation of phenylalanine to tyrosine. It has been, furthermore, known that the mutant *lemon* of silkworm, which accumulates the yellow pigment identical with Sepiapterin in larval epidermis, shows the inhibition of oxidation of phenolic substances in vivo. From these, it may be expected that in the insect the yellow pigment (Sepiapterin) participates in some oxidation-reduction systems, although its biological significance remains to be determined.

## Summary

The yellow pigment (Sepiapterin), occuring in the eyes of *Drosophila melanogaster*,

18) R. L. Blakley, *Biochem. J.*, 65, 331 (1957).
19) J. Böeseken, *Advances in Carbohydrate Chem.*, 4, 189 (1949).
20) M. Viscontini and E. Möhlmann, *Helv. Chim. Acta*, 42, 836. 1679 (1959).
21) H. S. Forrest and H. K. Mitchell, *J. Am. Chem. Soc.*, 77, 4865 (1955).
22) E. L. Patterson, R. Milstrey and E. L. R. Stokstad, ibid., 78, 5868 (1956).
23) M. Viscontini, E. Loeser and P. Karrer, *Helv. Chim. Acta*, 41, 440 (1958).
24) R. L. Blakley, "Current Trends in Heterocyclic Chemistry", A. Albert, editor, Butterworths Scientific Publication, London (1958), p. 140.

decomposed to one mole each of 7, 8-dihydroxanthopterin and lactic acid accompanied by consumption of 0.5 mol. of oxygen. From this and from the results of its photodecomposition and periodate oxidation, it is concluded that the compound has the structure 2-amino-4-hydroxy-7, 8-dihydro-6-lactylpteridine (III).

The author wishes to acknowledge Professor Y. Hirata and Dr. M. Tsujita for their encouragements and criticisms in this work. He is also indebted to Mr. T. Taira for the gift of flies.

*National Institute of Genetics*
*Yata, Mishima, Shizuoka-ken*

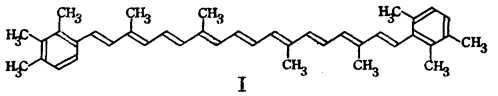
# *Total Syntheses of Renieratene and Renierapurpurin**

By Masaru YAMAGUCHI

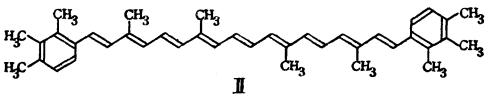
(Received May 11, 1960)

In the present paper are described the total syntheses of renieratene, I, and renierapurpurin, the chemical constitution of the latter having been hitherto unknown. By these works, therefore, the chemical constitution of renieratene has been established beyond doubt and the chemical constitution of renierapurpurin, II, has also been clearly established without any degradation studies.

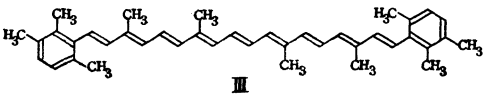
The orange coloration of the sponge *Reniera japonica*, which is considered by zoologists to be identical with *Halichondria panicea*, a species of wide distribution, is mainly due to the presence of a complicated mixture of carotenoids. Fifteen different carotenoids have been isolated from the sponge in crystalline states[1]. The main pigments are, however, carotenoid hydrocarbons which are renieratene, isorenieratene (III), β-carotene and renierapurpurin. Among these pigments, the chemical constitution[2,3] of renieratene and isorenieratene



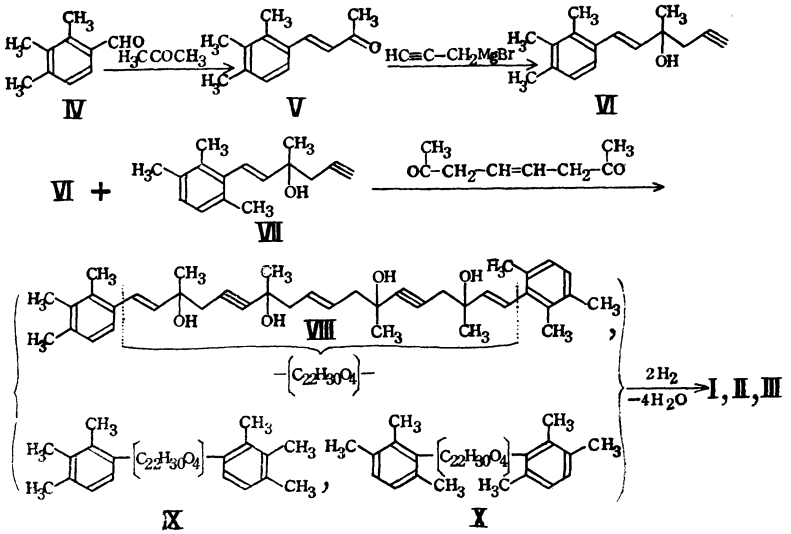
I



II



III

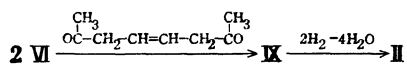


* Pigments of Marine Animals, Part XI. X of this series; T. Mukai, This Bulletin, 33, 1234 (1960).

1) T. Tsumaki, M. Yamaguchi and T. Tsumaki, *J. Chem. Soc. Japan, Pure Chem. Sec.* (*Nippon Kagaku Zasshi*), 75, 297 (1954); M. Yamaguchi, This Bulletin, 30, 111 (1957).

2) M. Yamaguchi, This Bulletin, 31, 739 (1958).

3) M. Yamaguchi, ibid., 31, 51 (1958).



have been elucidated and the total synthesis of the latter has been carried out by the author[4] and later by M. C. Khosla and P. Karrer[5]. On the other hand, however, little progress has been made on the study of the chemical constitution of renierapurpurin because of the limited quantity of the pigment available. It has so far been known that renierapurpurin forms purple plates of m. p. 230°C, exhibits absorption maxima at 544, 504 and 475 mμ in carbon disulfide, and has the formula $C_{40}H_{48}$ (or $C_{40}H_{50}$)[1]. In regard to its constitution, it has been inferred from its absorption maxima and from an analogy to renieratene, etc., that if it contains two triemthylphenyl groups at both ends of the molecule as in renieratene and isorenieratene, the terminal groups should be ones having small steric hindrance between the polyene chain and annular methyl groups. For example 2, 3, 4-trimethylphenyl group satisfies the condition. However, no experiment has been carried out to draw any conclusion on the problem.

The syntheses were carried out according to Karrer's method[6]. 2, 3, 4-Trimethylbenzaldehyde (IV)[2] was condensed with acetone to give 2, 3, 4-trimethylbenzalacetone (V), which was converted into acetylenic alcohol VI by Grignard reaction. A mixture of this acetylenic alcohol and another acetylenic alcohol VII[4] was condensed with octene-2, 7-dione to give a mixture of three isomeric $C_{40}$-diynetetraols (VIII, IX and X). The mixture was partially hydrogenated and then dehydrated, and the chromatographic separations of the product gave renieratene (I), renierapurpurin (II) and isorenieratene (III) in pure states but in low yields. The identity of these pigments with the natural specimens was verified by mixed melting point determinations, mixed chromatographies, and IR- and UV-determinations.

Renierapurpurin was obtained in a better yield in another experiment starting from acetylenic alcohol VI.

Renierapurpurin is the third carotenoid that is proved to contain benzene rings, and the fact that three possible isomers derivable by combinations of 2, 3, 4-trimethylphenyl and 2, 3, 6-trimethylphenyl groups are all present in the sponge, may be considered to provide an important orientation of the biogenesis of this interesting group of carotenoids.

Furthermore these isomers afford a typical example of steric hindrance, the cause of which has been discussed in the previous paper[3]. The absorption maxima (the longest wavelength, in carbon disulfide solution) of renierapurpurin, renieratene and isorenieratene are at 544, 532 and 520 mμ, respectively[2]. The shifts of maxima (12 and 24 mμ) are proportional to the number of 2, 3, 6-trimethylphenyl group in their molecules.

## Experimental

Solutions were evaporated under diminished pressure unless otherwise mentioned. Anhydrous sodium sulfate was employed for drying solutions.

**4-(2, 3, 4-Trimethylphenyl)-3-buten-2-one (V).**—It was prepared from 2, 3, 4-trimethylbenzaldehyde (IV, 22 g., b. p. 133~135°C/20 mmHg), in the way described in 4-(2, 3, 6-trimethylphenyl)-3-buten-2-one in the previous paper[4]. Colorless solid (17.2 g.), b. p. 125~130°C/3 mmHg. On recrystallization from petroleum benzine it formed thick plates of m. p. 70~71°C.

Found: C, 82.87; H, 8.74. Calcd. for $C_{13}H_{16}O$: C, 82.93; H, 8.57%.

From the residue of the distillation, 1, 5-bis-(2, 3, 4-trimethylphenyl)-1, 4-pentadien-3-one (1.6 g.) was obtained in yellow plates when recrystallized from benzene-ethanol, m. p. 150°C.

Found: C, 86.69; H, 8.33. Calcd. for $C_{23}H_{26}O$: C, 86.74; H, 8.23%.

**1-(2, 3, 4-Trimethylphenyl)-3-methyl-1-hexen-5-yn-3-ol (VI).**—Operations of the experiment and the proportions of the reagents are similar to those of the synthesis of 1-(2, 3, 6-trimethylphenyl)-3-methyl-1-hexen-5-yn-3-ol in the previous paper[4]. From $C_{13}$-ketone (V, 13 g.), acetylenic alcohol (VI, 6.1 g.) was obtained as faint colored oil, b. p. 115~120°C (bath temperature)/0.05 mmHg.

Found: C, 84.41; H, 8.92. Calcd. for $C_{16}H_{20}O$: C, 84.16; H, 8.83%.

**$C_{40}$-Diynetetraol Mixture (VIII, IX and X).**—An ethereal solution (ca. 30 cc.) of ethylmagnesium bromide prepared from 3.9 g. of ethyl bromide, was added dropwise to a well-stirred mixture of the above acetylenic alcohol (VI, 2 g.), 1-(2, 3, 6-trimethylphenyl)-3-methyl-1-hexen-5-yn-3-ol (VII, 2 g.)[4], cuprous chloride (50 mg.) and dry ether (20 cc.) during one and a half hours, and the mixture was refluxed for an hour. A solution of 4-octene-2, 7-dione (840 mg.) in dry ether (20 cc.) was added dropwise during thirty minutes under stirring. After refluxing for one hour, the mixture was allowed to stand overnight, and decomposed with 1 N sulfuric acid under ice-cooling. The organic layer was extracted with ether and the ethereal solution was washed with dilute sulfuric acid, aqueous sodium hydrogen carbonate and water, dried and evaporated. The residue (4.8 g.) dissolved in benzene (20 cc.) was adsorbed on alumina (Merck, 80 g.) and the column was washed successively with benzene (100 cc., the eluate gave an oily residue 1.95 g.), with ether (60 cc., residue 0.8 g.) and with ether-methanol 10 : 1 (200 cc., residue 1.8 g.). The last fraction was the mixture

4) M. Yamaguchi, ibid., 32, 1171 (1959).
5) M. C. Khosla and P. Karrer, *Helv. Chim. Acta*, 43, 453 (1960).
6) P. Karrer and C. H. Eugster, ibid., 33, 1172 (1950).

of three isomers of $C_{40}$-diynetetraol and formed a yellowish-colored glass-like mass.

Found: C, 79.91; H, 8.80. Calcd. for $C_{40}H_{52}O_4$: C, 80.50; H, 8.78%.

**Renieratene (I), Renierapurpurin (II) and Isorenieratene (III).**—A solution of the above tetraol mixture (1.5 g.) in ethyl acetate (40 cc.) was filtered through a column of active charcoal (0.3 g.) and shaken with palladium-barium sulfate catalyst (1%, 50 mg.) in an atmosphere of hydrogen. Occasional additions of the small amount of catalyst were necessary until 2 mol. of hydrogen (ca. 116 cc., 9°C/760 mmHg) was absorbed. The catalyst was filtered and the solution was evaporated to glassy residue. A boiling solution of toluene-*p*-sulfonic acid (180 mg., dehydrated by melting in vacuo) in toluene (30 cc.) was added at a time to a boiling solution of the above residue in toluene (40 cc.) and the mixture was boiled for ca. eighty seconds. The greenish brown solution was, as soon as possible, poured into a mixture of a saturated aqueous solution of sodium hydrogen carbonate (300 cc.) and petroleum ether (200 cc.). The petroleum ether solution was then washed once with water and thrice with 90% methanol, dried and evaporated. The reddish-brown residue was dissolved in petroleum ether and chromatographed on alumina (4×20 cm.), giving the following zone: i) dark brown zone (most strongly adsorbed), ii) a broad zone, its color changing from red to orange, iii) an orange brown zone, and iv) faint yellow. The residue of the zone ii) was boiled several times with methanol, and the insoluble residue was rechromatographed on alumina giving the following main zones; a) purplish red (uppermost), b) red and c) orange. The pigment of the zone b) was further purified by rechromatography. The residue of the eluate of each zone was boiled with methanol. The insoluble parts were treated with petroleum ether and ethanol, and each pigment which separated out, was recrystallized several times from suitable solvents. The zone a) gave glistening purple plates (2.4 mg.) of renierapurpurin (from chloroform-ethanol), m. p. 229~230°C, its identity with natural pigment being confirmed by mixed melting point, 229~230°C, by mixed chromatography, and by IR- and UV-spectra (Fig. 1 and Fig. 2). The zone b) gave purplish red fine needles (1.4 mg.) of renieratene (from benzene-ethanol), m. p. 184~185°C, the identity with natural pigment being confirmed by mixed melting point, 184~185°C, by mixed chromatography, and by IR- and UV-spectra. The zone c) gave purplish red find needles (2.0 mg.) of isorenieratene (from benzene-ethanol), m. p. 199~200°C, the identity with natural pigment being confirmed by mixed melting point, 199~200°C, by mixed chromatography, and by UV-spectrum.

Because of the small yields of these pigments, no elementary analysis was carried out.

**$C_{40}$-Diynetetraol (IX).**—It was synthesized from acetylenic alcohol (VI, 3 g.) in the way described above. It formed a faint yellow glass-like mass (1.6 g.).

Found: C, 80.12; H, 8.81. Calcd. for $C_{40}H_{52}O_4$: C, 80.50; H, 8.78%.

**Renierapurpurin (II).**—Tetraol (IX, 1.5 g.) was partially hydrogenated and then dehydrated in the way described above. While petroleum benzine solution of the dehydration product was washed, a part of the pigment was crystallized out, which was filtered off (43 mg.). The mother liquor was chromatographed on alumina from a benzene solution, giving three main zones; i) pink, ii) red and iii) orange. From the zone i), 25 mg. of the pigment was obtained, which was combined with the crystals separated during washing. Several recrystallizations from chloroform-ethanol gave pure renierapurpurin (38 mg.), m. p. 230°C.

Found: C, 90.76; H, 8.99. Calcd. for $C_{40}H_{48}$: C, 90.85; H, 9.15%.

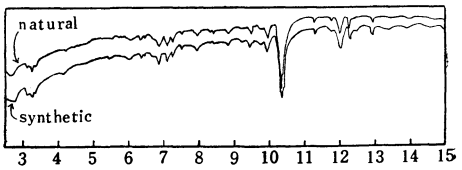



Fig. 1. Infrared spectra of renierapurpurin (KBr disk).

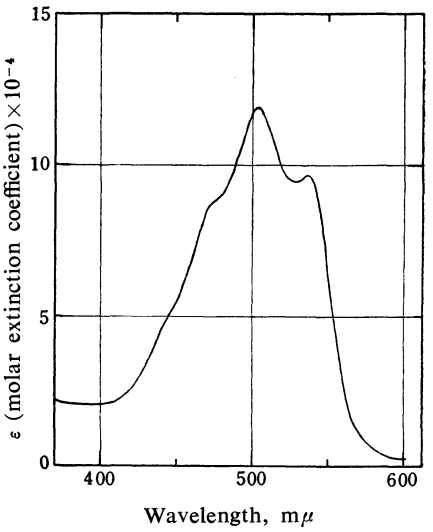



Fig. 2. Absorption curve of renierapurpurin (carbon disulfide).

The author wishes to express his thanks to Professor Tokuichi Tsumaki for his exceedingly kind directions throughout this work. The author also thanks Yoshiya Kanda, Assistant Professor of Structural Chemistry, who kindly provided facilities for measurements of infrared and ultraviolet spectra. The cost of this work has been partially covered by the Scientific Research Grant of the Ministry of Education.

*Department of Chemistry*
*Faculty of Science*
*Kyushu University*
*Hakozaki, Fukuoka*

# *Flow Properties of Aluminum Soaps-Hydrocarbon Systems*

By Sukekuni SHIBA

(Received May 31, 1960)

It has been known that the aluminum soaps dispersed in hydrocarbon oils make stable gels and exhibit a wide variety of flow behaviors. The polymeric natures of the aluminum soaps have been pointed out by many authors[1-3] from the osmotic pressure and viscosity data on aluminum soaps in benzene. These properties indicate that the soap molecules aggregate to form fibrous micelles and are dispersed polymerically with a network structure in hydrocarbon.

Garner, Nissan and Wood[4], studying thermodynamics and rheological behaviors of the aluminum stearate gels in petrol, found that the apparent viscosity at different rates of shear was at first constant, but at higher rates of shear, the apparent viscosity decreased, reaching approximately constant value at very high rates of shear. Weber and Bauer[5], and also Bauer, Weber and Wiberley[6,7], studying the flow properties of aluminum laurate-toluene gels, the effect of peptizers and entrance effects in capillary, by a pressure capillary viscometer over a wide range of mean rates of shear, ranging from $10^{-3}$ to $10^{+6}$ $sec^{-1}$, obtained the shear stress-rate of shear curves, which showed three types of flow: Newtonian flow at low rates of shear, rapid increase in shear rate with shear stress in the region of shear rate above $10^{-2}$ $sec^{-1}$, and constant slope in log-log plot at shear rate above $10^{-2}$ $sec^{-1}$.

Some of the manifold flow properties were clarified by these investigations; however, many aspects of flow behaviors are not fully explained, due to the variability of flow properties with the nature of soaps, solvents, soap concentrations and physical conditions of measurements especially the rate of shear. Measurements with the capillary type viscometers are liable to be affected by the capillary end effects and the changes in properties during the flow. Therefore, it is desirable to take measures under a uniform rate of shear with specimens not subjected to shear. In this investigation, the flow properties of aluminum soaps of various parent fatty acids in hydrocarbon were measured with a concentric cylinder type rotational viscometer of small clearance; the flow properties and especially the time effects under shear were examined.

## Experimental

**Materials.**—The alminum soaps used in this investigation were prepared from purified fatty acids by an aqueous metathetic process. Stearic and palmitic acids were purified from pure acids (Nihon Yushi Co.) by repeated recrystallization from 80 vol.% ethanol. Myristic and lauric acids were purified from commercial reagents by the same method. Capric and caprylic acids were purified from the commercial reagents by distillation under reduced pressure. The purity of the acids was examined by melting points and neutralization equivalents by titration. The physical constants of fatty acids are shown in Table I.

TABLE I. PHYSICAL CONSTANTS OF FATTY ACIDS

| Fatty acid | M. p., °C | | Neut. equiv. | |
|---|---|---|---|---|
| | Found | Lit.[8] | Found | Calcd. |
| Stearic | 69.5 | 69.6 | 281.9 | 284.5 |
| Palmitic | 62.2 | 62.9 | 258.0 | 256.4 |
| Myristic | 54.5 | 54.4 | 229.1 | 228.4 |
| Lauric | 43.3 | 44.0 | 201.3 | 200.3 |
| Capric | 30.1 | 31.3 | 173.1 | 172.3 |
| Caprylic | 14.3 | 16.3 | 143.8 | 144.2 |

Fatty acid was treated with a 40~50% excess sodium hydroxide solution and distilled water to yield an approximately 5% solution of sodium soap. The mixture was heated to dissolve the soap, and the solution was kept completely transparent at 70~80°C for soaps from stearate to laurate and at 50°C for caprate and caprylate. A hot solution of aluminum sulfate was added slowly while being stirred vigorously, until a slight excess was present and precipitation was complete. The precipitated aluminum soap was filtered and washed with distilled water, until free from sulfate. The test for sulfate ion was made by adding barium chloride solution to the filtrate, which was made slightly acidic with hydrochloric acid. The soaps

1) J. W. McBain and E. B. Working, *J. Phys. Colloid Chem.*, **51**, 974 (1947).
2) H. Sheffer, *Canad. J. Research*, **B-26**, 481 (1948).
3) V. R. Gray and A. E. Alexander, *J. Phys. Colloid Chem.*, **53**, 9 (1949).
4) F. H. Garner, A. H. Nissan and G. F. Wood, *Phil. Trans. Roy. Soc.*, **A-243**, 37 (1950).
5) N. Weber and W. H. Bauer, *J. Phys. Chem.*, **60**, 270 (1956).
6) W. H. Bauer, N. Weber and S. E. Wiberley, ibid, **62**, 106 (1958).
7) W. H. Bauer, N. Weber and S. E. Wiberley, ibid, **62**, 1245 (1958).
8) A. W. Ralston, "Fatty Acids and their Derivatives", John Wiley & Sons, Inc., New York (1948), pp. 23-40.

were then dried to constant weight at 110°C, and stored in a desiccator over phosphorus pentoxide. Dried soaps were analysed for aluminum by ignition to oxide. The composition of the soaps is shown in Table II.

TABLE II. COMPOSITION OF ALUMINUM SOAPS

| Aluminum soaps | No. of C atoms in acid | Al wt. % (analysed) | Mole acid per mole Al |
|---|---|---|---|
| Stearate | 18 | 5.04 | 1.72 |
| Palmitate | 16 | 5.80 | 1.62 |
| Myristate | 14 | 5.96 | 1.77 |
| Laurate | 12 | 6.38 | 1.88 |
| Caprate | 10 | 7.36 | 1.87 |
| Caprylate | 8 | 9.17 | 1.72 |

Nujol was used as a vehicle. It is a liquid paraffin of a commercial grade, a paraffin-rich saturated hydrocarbon. The physical properties are as follows; $d_4^{25}=0.8429$, $n_D^{20}=1.467$, $\eta_{25}=0.217$ poise.

**Preparation of Specimen.**—Nujol was added to a weighed quantity of aluminum soap, and the mixture was heated slowly while being stirred until it became a transparent solution at 110~120°C. After maintaining this temperature for 15min. the solution was cooled and stored in a desiccator over phosphorus pentoxide.

**Apparatus.**—A concentric cylinder type rotational viscometer essentially the same as the apparatus developed by Green[9], was used. The outer cylinder was rotated and the torque necessary to keep the inner cylinder stationary was measured by a torsion spring. When the sample is a Bingham body of plastic viscosity $\eta_{pl}$ and yield value $f$, the relation of angular velocity $\omega$, troque $M$, $\eta_{pl}$ and $f$ is given by the Buckingham-Reiner equation[10];

$$\eta_{pl}\omega=(M/4\pi h)(1/r_i^2-1/r_e^2)-f\ln(r_e/r_i) \quad (1)$$

where $r_i$ and $r_e$ are the radii of inner and outer cylinders; $h$ is the height of the immersed part of inner cylinder; $\eta_{pl}$ and $f$ are obtained by the measurement of $M$ corresponding to $\omega$. The shear stress $\tau$ and the rate of shear $D$ at radius $r$ from the center of the cylinder are given by

$$\tau=M/2\pi hr^2 \quad (2)$$

$$D=2\omega/(1/r_i^2-1/r_e^2)r^2 \quad (3)[11]$$

The dimensions of the apparatus are as follows: $2r_i=29$ mm., $2r_e=30$ mm., $h=50$ mm.. rate of revolution 0~400 rpm, torsion constants of the springs $3\times10^3\sim3\times10^5$ dyn. cm./rad. The apparatus was calibrated with viscosity standard oils. The absolute accuracy of the values obtained from dimensions and force constant of the apparatus was within 2%. The end effect was checked, changing the depth of immersion of the inner cylinder. It was found that the end effect was negligible.

**Procedure.**—The speicmen was placed between the cylinders and kept for 15 min. at the measuring temperature. The rate of revolution was raised stepwise, and at each step the equilibrium points where the deflexion of the torsion spring became constant were determined[12]. The down curve was obtained by reducing the rate of revolution down to zero to obtain the rate of shear-shear stress relation corresponding to the state. Measurements were made for systems containing 0.5~4 wt. % soaps in nujol at temperatures 15~75°C.

## Results and Discussion

The aluminum soap-nujol systems give various types of flow. At room temperature, the system containing soaps above 1% makes a gel, and it changes to paste or liquid state by shear. The more diluted system makes a sol with fluidity, which shows linear or non-linear flow properties. At high temperatures above 80°C, the system becomes a homogeneous transparent elastic solution. Thus, the systems show various flow properties and are unstable in regard to shear and time. Therefore, it is necessary to study the change in properties corresponding to the variables.

**Rate of Shear-Shear Stress Curves.**—Examples of the curves exhibiting the rate of shear-shear stress relations are shown in Fig. 1. The lower curves are the equilibrium curves, which are obtained with the elevated rate of shear, and the upper curves are the $D-\tau$ curves (or down curves) for the states of the specimens equilibrated under the highest rates of shear. Two curves coincide for the dilute systems which behave as Newtonian liquids or Bingham plastic bodies. When the concentration is increased, the two curves make a loop. Plastic viscosity

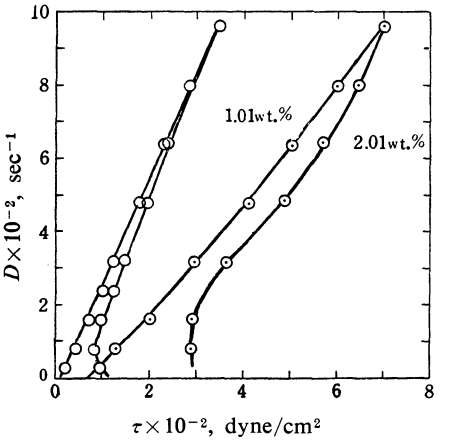



Fig. 1. Rate of shear-shear stress curves for aluminum stearate in nujol at 25°C.

9) H. Green, "Industrial Rheology and Rheological Structures", John Wiley & Sons, Inc., New York (1949), p. 99.

10) M. Reiner, "Deformation and Flow", H. K. Lewis, London (1949), p. 44.

11) For substances which show non-linear flow properties, Eq. 3 can not be used rigorously. In this apparatus, $(r_e-r_i)$ is small enough compared with $r$, so that approximation with Eq. 3 is possible.

12) The specimen was assumed to reach equilibrium when the change in deflexion angle became less than 1/2 deg./min.

and yield value are obtained from the down curve for the state.

Concerning the equilibrium curves, a rapid decrease in viscosity is observed in the range of rate of shear up to 200 $sec^{-1}$. This is in agreement with the results of Weber and Bauer[5], who found a sudden viscosity decrease in the range of rate of shear up to $10^2$ $sec^{-1}$ for aluminum laurate-toluene gels. The curves which they obtained are likely to correspond to the equilibrium curves in this investigation, because the results by these authors will be subject to the effects of shear softening in capillary.

**Ageing.**—The flow properties of the system change with time while standing after preparation. The changes in viscosity and yield value at room temperature (20°C) are shown in Fig. 2. Where the viscosity is obtained from the inclination of the down curve at the rate of shear $5\times10^2$ $sec^{-1}$, for the specimen equilibrated at $10^{-3}$ $sec^{-1}$; the yield values are obtained from the intercepts of the extension of the down curves. Viscosity and yield value increase rapidly with time, exhibiting maximum values at about 4 hr. after preparation, and approach approximately constant values. Therefore, the measurements were carried out between 24~96 hr. after preparation of the specimen. This effect is in agreement with the results of Gray and Alexander[2], and of McBain and Working[1], who obtained the effect of ageing for the benzene solution of aluminum laurate, from flow birefringence and viscosity study. The mechanism of this phenomenon is explained as follows: The system cooled from a hot solution is a metastable jelly containing soap micelles; three dimensional networks of the soap crystallites grow rapidly, and are arranged slowly to the stable state.

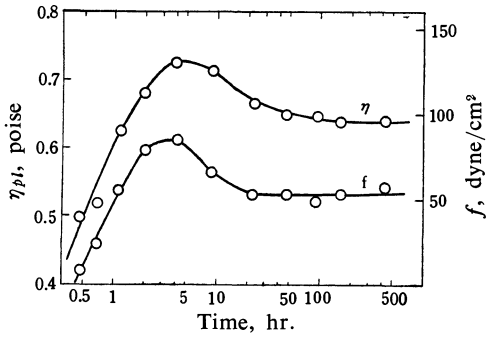



Fig. 2. Ageing of the aluminum stearate in nujol 2.01 wt.%, 25°C.

**Change of Flow Properties under Shear.**—Decrease of shear stress with time under constant rate of shear is shown in Fig. 3. The curve for each rate is obtained for the specimen equilibrated under lower rates of shear. If it is assumed that the contribution of the rheological structures to the shear stress is proportional to the concentration of the structures, $C$, and that the rate of breakdown of the structure is also proportional to $C$, the decrease in shear stress under constant rate of shear is expressed by,

$$\tau-\tau_{eq}=aC \tag{4}$$

$$-\frac{d(\tau-\tau_{eq})}{dt}=-a\frac{dC}{dt}=kC \tag{5}$$

integrating (5)

$$\ln(\tau-\tau_{eq})=\ln(\tau_0-\tau_{eq})-(k/a)t \tag{6}$$

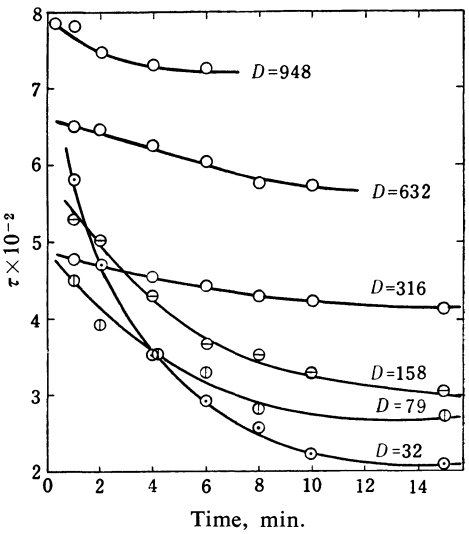



Fig. 3. Decrease of shear stress with time under constant rate of shear.
Aluminum stearate, 2.01 wt.%, 25°C

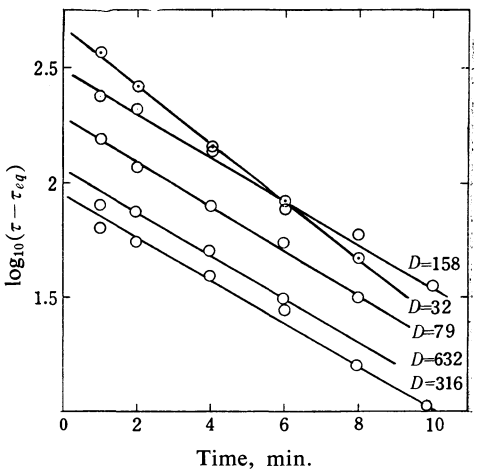



Fig. 4. Rate of degradation of the rheological structure.
Aluminum stearate, 2.01wt.%, 25°C

where $\tau_{eq}$ is the shear stress in quilibrium, $\tau_0$ is the value of $\tau$ at time $t=0$. The decrease in $\log(\tau-\tau_{eq})$ with $t$ is shown in Fig. 4. These results support the assumptions mentioned above. Rates of breakdown under various rates of shear are not constant in general; the rapid breakdown of weak structures under low rate of shear is recognized.

**Examination on Thixotropy**[13].—Flow measurements were repeated to examine the thixotropic recovery, after the specimen was kept standing for some time. The results are shown in Fig. 5. If complete recovery is present, the curves should coincide. However, the curves in subsequent measurements resemble the down curve in the first run, and the breakdown of the structures proceeds by repeated shear. Therefore, in these experimental conditions, thixotropy does not exist even after considerable time.

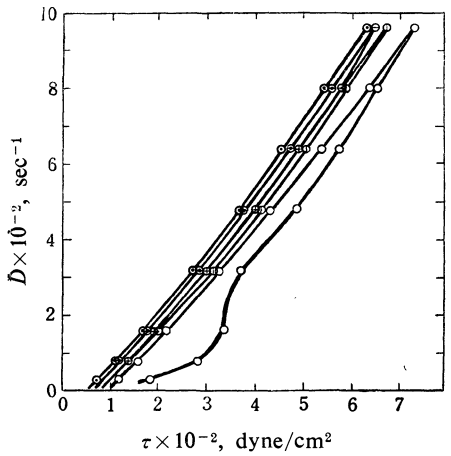



Fig. 5. $D$-$\tau$ curves for repeated shear. Alumium stearate in nujol, 2.01 wt.%, 25°C. ○ 0 hr., ◐ 3 hr., ⊖ 20 hr., ⊙ 72 hr.

Agreements in opinions concerning the time effects of flow behaviors on aluminum soap-hydrocarbon systems have not yet been obtained. Complete recovery was reported by Goldberg and Sandvik[14], and Carver and Van Wazer[15]; whereas, absence of thixotropy was pointed out by Evans and Matthews[16]. Evans states for aluminum greases that the change caused by the applied shearing stress is not thixotropic but

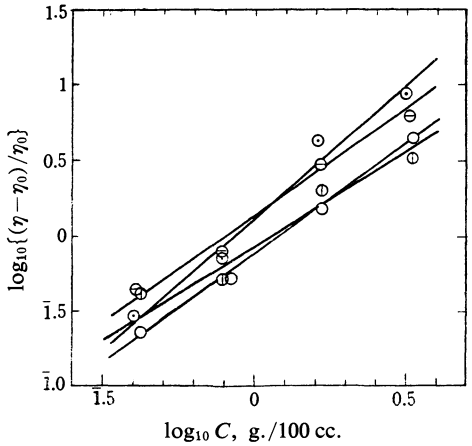



Fig. 6. Concentration dependence of specific viscosity.
○ 15°C, ◐ 25°C ⊖ 50°C, ⊙ 75°C

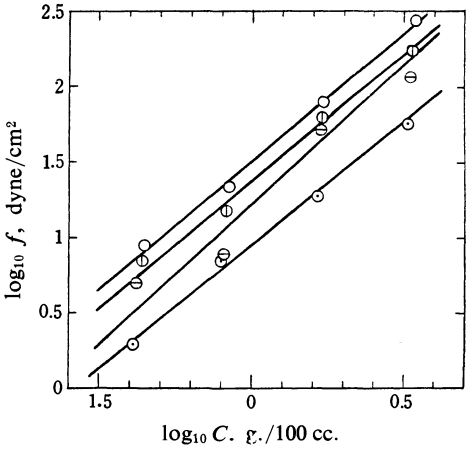



Fig. 7. Concentration dependence of yield values.
○ 15°C, ◐ 25°C, ⊖ 50°C, ⊙ 75°C

appears to be a permanent change in the structure of the grease. Results of this experiment appear to support those of Evans and Matthews. However, the discrepancy of the results obtained by many authors will be ascribed mainly to the experimental conditions; for example, the rate of shear, temperature, concentration and properties of soaps which are not always pure substances. At high temperatures or under a very low rate of shear, it will be possible that the system is thixotropic.

**Effect of Concentration.**—The specific viscosity and yield values for various concentrations and temperatures are shown in Figs. 6 and 7, where the viscosity and yield values are obtained as previously described. These values show an approximately linear relation against $\log C$. That is, the dependence of the viscosity and yield values on concentration is expressed by empirical formulae,

13) It will be adequate to give a general definition of thixotropy in rheological terms as follows: "Thixotropy is the property of a body by virtue of which the ratio of shearing stress to rate of deformation is *temporarily* reduced by previous deformation.", E. K. Fischer, "Colloidal Dispersion", John Wiley and Sons, Inc., New York (1950), p. 183.

14) H. Goldberg and O. Sandvik, *Anal. Chem.*, **19**, 123 (1947).

15) E. K. Carver and J. R. Van Wazer, *J. Phys. Colloid Chem.*, **51**, 751 (1947).

16) D. Evans and J. B. Matthews, *J. Colloid Sci.*, **9**, 60 (1954).

$$\eta=\eta_0(1+aC^m) \quad (7)$$

$$f=bC^n \quad (8)$$

where values of $m$, $a$ and $n$ calculated from the data at 15, 25, 50 and 75°C are, $m$=1.47, 1.30, 1.39, 1.73; $a$=0.73, 0.78, 1.33, 1.33; $n$= 1.72, 1.64, 1.72 and 1.61, respectively.

The systems are considered essentially as colloidal suspensions of soap crystallites in oil. If the soap crystallites are non-attractive rod-like ellipsoidal particles of axial ratio over 20, specific viscosity is given by Simha[17], as a function of axial ratio and volume fraction of the particles. The formula gives very high values of axial ratio corresponding to the measured viscosity values. These facts indicate that it is more appropriate to consider the interaction between soap particles and the network structures in the system.

**Effect of Temperature.**—Viscosity-temperature relation is shown in Fig. 8. In this temperature region, approximately linear relations exist. This shows the absence of serious change in rheological structures in this region. Apparent activation energies of flow and constant $A$, calculated from Andrade equation,

$$\eta=A\exp(\Delta E/RT)$$

are shown in Table III. Decrease in $\Delta E$ with increase in concentration is apparent. This tendency, which is in agreement with the results of Carver et al.[15], will be understandable if it is considered that the flow mechanism, is divided into the usual friction and break down of secondary bonding, and the predominance of the latter mechanism in concentrated systems is considered.

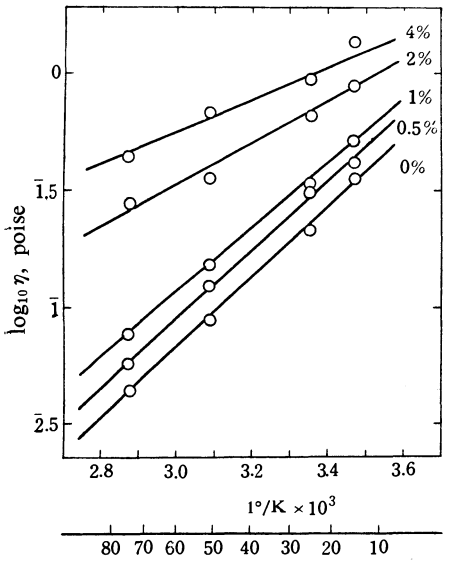



Fig. 8. Viscosity — temperature relations. Aluminum stearate in nujol.

TABLE III. CONSTANTS OF THE ANDRADE FORMULA
(Aluminum stearate in nujol)

| Soap conc. wt. % | $A$ | $\Delta E$, kcal./mol. |
|---|---|---|
| 0.00 | $2.5\times10^{-6}$ | 6.7 |
| 0.50 | $4.3\times10^{-6}$ | 6.6 |
| 0.99 | $9.4\times10^{-6}$ | 6.2 |
| 2.01 | $4.0\times10^{-4}$ | 4.4 |
| 3.99 | $4.7\times10^{-3}$ | 3.2 |

17) R. Simha, *J. Phys. Chem.*, **44**, 25 (1940).

**Effect of the Fatty Acids.**—Results for soaps from various fatty acids are shown in Fig. 9. Soaps from stearate to laurate show similar flow properties, whereas caprate and caprylate show lower values, This fact correlates many other properties of soaps, which change abruptly for soaps below caprate.

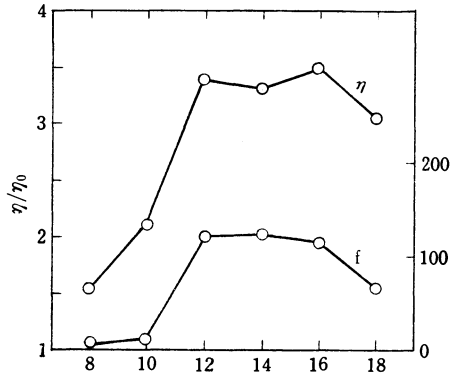



Fig. 9. Viscosity ratio and yield values of various Al soap-nujol gels, 2 wt. %, 25°C.

## Summary

Flow properties of aluminum soap-hydrocarbon systems as viscous liquids or plastic bodies are studied with a concentric rotational viscometer. Results are obtained under the rate of shear up to $10^3$ $sec^{-1}$.

(1) The systems behave as dispersions of soap crystallites with network structures combined by secondary interactions of the particles, and they exhibit marked viscosity increase.

(2) The rheological structures suffer shear breakdown under shear, resulting in decrease in viscosity.

(3) Recovery from the broken structures is impossible, that is, this change is not thixotropic but shear breakdown.

(4) Flow properties change with time while standing at rest.

(5) The effects of concentration, temperature and fatty acids constituting soaps are clarified.

The author wishes to express his thank to Professor H. Akamatu and Dr. T. Nakagawa, both of the University of Tokyo, for their interest and encouragement throughout this investigation.

*Railway Technical Research Institute*
*Kunitachi, Tokyo*

# *Stress Relaxation of Thermo-reversible Gels. Molecular Weight Dependence of Relaxation Spectrum. Polyvinyl Alcohol-Congo Red-Water System**

By Kiyoshi ARAKAWA

(Received May 24, 1960)

In the previous paper[1] the author reported the results of the stress relaxation study of the gels of polyvinyl alcohol-congo red-water system, where the experiment was intended to obtain some knowledge on the concentration dependence of the relaxation spectrum of the gel which was taken as a typical example of thermo-reversible gels of polymeric nature. As a part of the series of rheological studies of thermo-reversible gels[1,2] a stress relaxation experiment has been made for the purpose of studying the molecular weight dependence of the relaxation spectrum of the gel, and the result is reported in the present paper.

## Experimental

**Apparatus.** — A chainomatic balance relaxometer was used to measure the relaxation Young's modulus of the cylindrical gel, which was the same one as that used previously[1], and the schematic diagram of it is shown in Fig. 1. A specimen is compressed to a given strain between a plate attached to a bar and a bottom plate in a double jacket connected to a screw gauge by the rotation of it. The stress in the specimen is automatically balanced with a chain weight by means of a relay and a balancing motor, the ralaxation Young's modulus $E_r$ is calculated form the vertical length of the suspended chain, as follows.

$$E_r = \frac{l}{\Delta l} \cdot \frac{adhg}{bs}$$

$l$ is the height of the cylindrical specimen without strain, $\Delta l$ the amount of the given compression, $s$ the original sectional area of the specimen, $a$ the distance from the fulcrum to the chain, $b$ the distance from the fulcrum to the center of the pressure plate, $d$ the linear density of the chain, $h$ the vertical length of the suspended chain and $g$ is the acceleration of gravity.

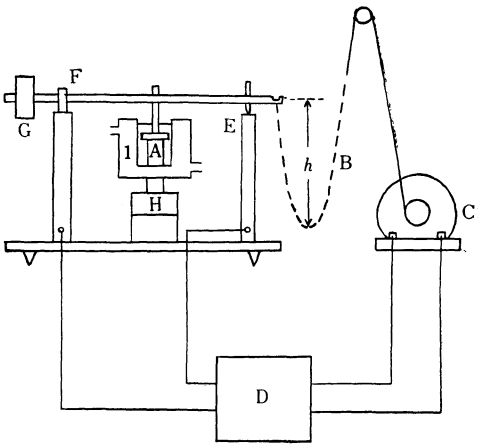



Fig. 1. Chainomatic balance relaxometer.
A: Specimen B: Chain
C: Balancing motor D: Relay
E: Point contact F: Fulcrum
G: Counter weight
H: Micrometer screw
I: Double jacket

**Sample.** — Commercial samples of polyvinyl alcohol were purified by precipitation from aqueous solutions with addition of acetone. The amount of residual acetyl group was smaller than 0.7% by mole for all samples used in this experiment. The values of the intrinsic viscosity $[\eta]_{30°C}$ determined by a capillary viscometer and the molecular weight calculated from those using the formula of Nakajima et al.[3] are given in Table I. Congo red

1) K. Arakawa, This Bulletin, **32**, 1248 (1959).
2) K. Arakawa, This Bulletin, **31**, 842 (1958); K. Arakawa and K. Atsumi, *J. Chem. Soc. Japan, Pure Chem. Sec.* (*Nippon Kagaku Zasshi*), **80**, 133 (1959).
* Partly presented at the Annual Meeting of the Chemical Society of Japan, Tokyo, April, 1960.

3) A. Nakajima and K. Furutati, *Chem. High Polymers* (*Kobunshi Kagaku*) **6**, 460 (1949).

used was Merck's analytical grade chemical. The preparation of testing specimens was made according the same procedure as described in the previous paper[1], except that in the present work an especially designed vessel with a double jacket was used in the dissolution process instead of a conical beaker and a water bath.

The composition of the prepared gel was maintained to be the same for all specimens: polyvinyl alcohol 17.5% and Congo red 1.75% by weight.

TABLE I. MOLECULAR WEIGHT OF POLYVINYL ALCOHOL

| Sample | $[\eta]_{30°C}$(100 cc./g.) | Molecular weight |
|---|---|---|
| I | 0.54 | $3.5\times10^4$ |
| II | 0.66 | $4.9\times10^4$ |
| III | 1.03 | $9.8\times10^4$ |

## Results and Discussion

**Stress Relaxation Data.** — The data of stress relaxation at various temperatures are plotted in the form $(298/T)E_r$ versus $\log t$, where $t$ is time, in Figs. 2a, 2b and 2c. The strain

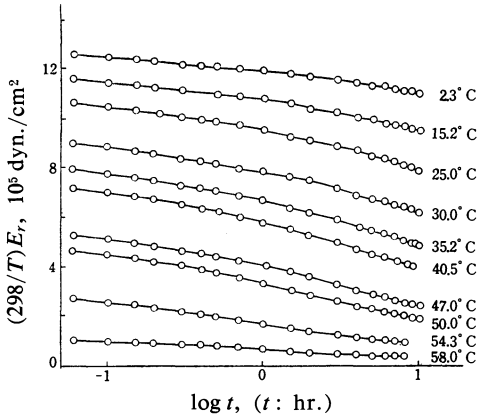



Fig. 2a. Reduced relaxation Young's modulus. Sample I (molecular weight $3.5\times10^4$).

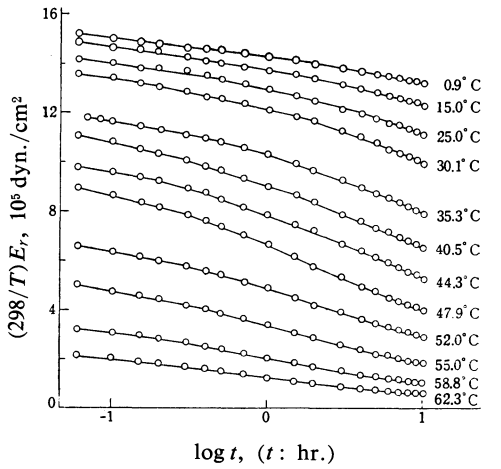



Fig. 2b. Reduced relaxation Young's modulus. Sample II (molecular weight $4.9\times10^4$).

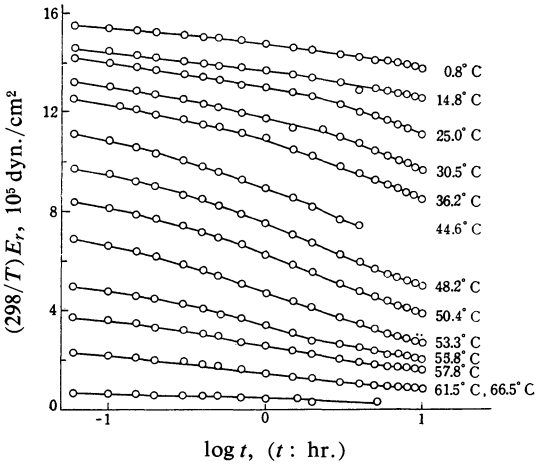



Fig. 2c. Reduced relaxation Young's modulus. Sample III (molecular weight $9.8\times10^4$).

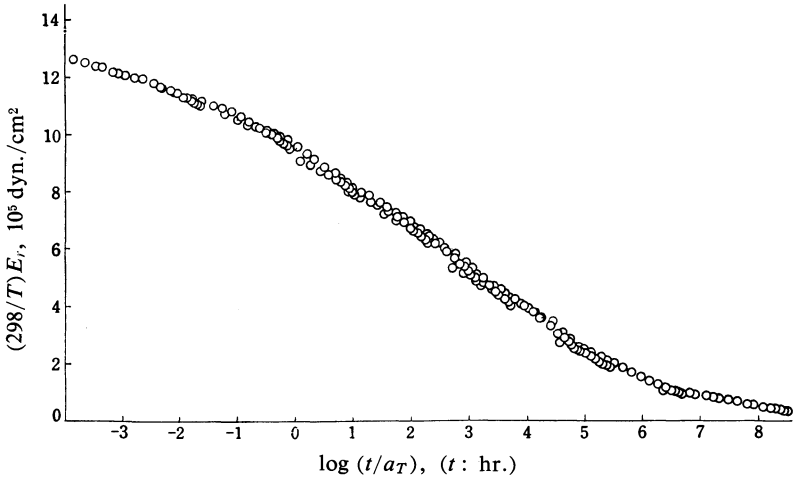



Fig. 3a. Composite relaxation curve at 25°C, Sample I.

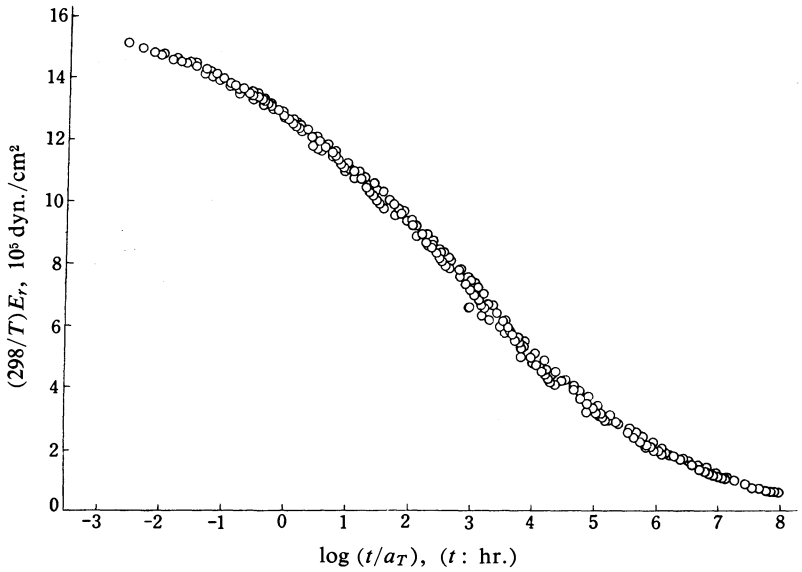



Fig. 3b. Composite relaxation curve at 25°C, Sample II.

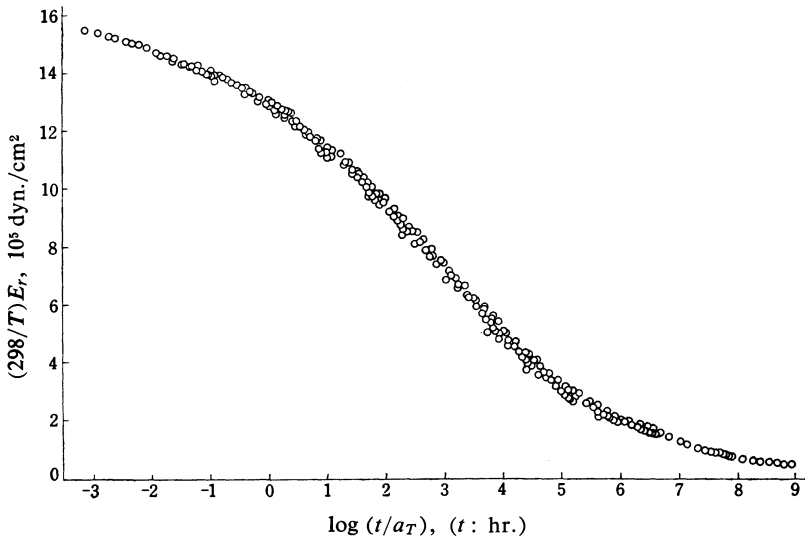



Fig. 3c. Composite relaxation curve at 25°C, Sample III.

applied in this experiment was 15% for all specimens. The data are reduced to 25°C with the multiplication by a factor $298/T$.

According to the time temperature superposition principles[4], each group of relxation curves was superposed to a composite relaxation curve by the horizontal shift of relaxation curves at different temperatures along the $\log t$ axis. The superposition of relaxation curves is good as it is seen in Figs. 3a, 3b and 3c. The density factors was ignored, because its temperature dependence was very small. The shift factors $\log a_T$ are plotted against $T$ in Fig. 4 together with the apparent activation energy $H_a$, which was calculated from the mean $\log a_T$ versus $T$ curve by the following equation.

$$H_a = R\frac{\partial \ln a_T}{\partial(1/T)} \qquad (1)$$

From the Fig. 4 it is seen that $\log a_T$ versus $T$ relation does not obey the W. L. F. equation[5].

**Distribution Functions of Relaxation Times.** —The relaxation spectra $H(\log \tau)$ defined by

4) J. D. Ferry, *J. Am. Chem. Soc.*, **72**, 3746 (1950); F. Schwarzl and A. J. Staverman, *J. Appl. Phys.*, **23**, 838 (1952); C. A. Dahlquist and M. R. Hatfield, *J. Colloid Sci.*, **7**, 253 (1952).

5) M. L. Williams, R. F. Landel and J. D. Ferry, *J. Am. Chem. Soc.*, **77**, 3701 (1955).

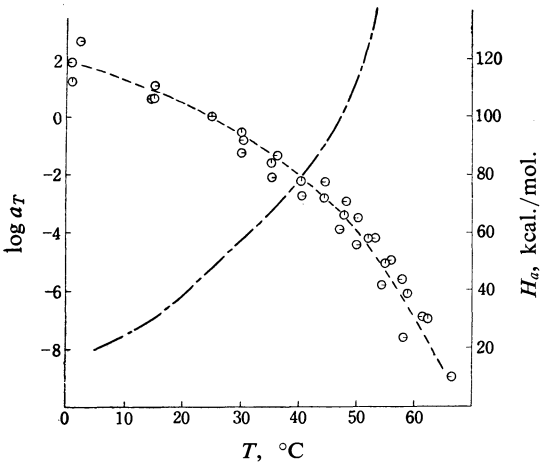



Fig. 4. Temperature dependence of shift factors.
⊖ Sample I, ⊙ Sample II, ⊖ Sample III
----- mean curve of log $a_T$ versus $T$ relation, --- $H_a$

the following Eq. 2 are calculated from the composite relaxation curves shown in Figs. 3a, 3b and 3c by the second order approximation[6].

$$E_r = \int_0^\infty H(\log\tau)\mathrm{e}^{-(t/\tau)}\,\mathrm{d}\log\tau \qquad (2)$$

$$H\left(\log\frac{\tau}{2}\right) = \left[-\frac{\mathrm{d}E_r}{\mathrm{d}\log t} + \frac{1}{2.303}\frac{\mathrm{d}^2E_r}{\mathrm{d}(\log t)^2}\right]_{t=\tau} \qquad (3)$$

The obtained relaxation spectra are plotted against log $\tau$ in Fig. 5. Each spectrum shows the typical box type character, except the structure in details, which is expected to follow a wedge type spectrum at the shorter time region.

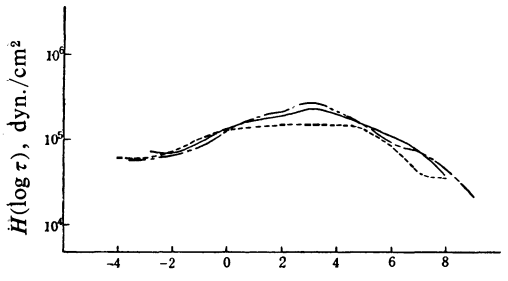



Fig. 5. Relaxation spectra.
----- Sample I
——— Sample II
--- Sample III

They nearly superpose each other at a short time region in Fig. 5. On the longer time side than one hour some difference is seen, and the spectrum goes upwards as the average molecular weight becomes larger, though in the curves of samples II and III the difference is very small and besides, when seen in details, the exchange of the mutual position is found. At the long time end the spectrum of the sample III tends to extend furthest[7].

## Summary and Conclusion

A stress relaxation experiment was made for the gels of polyvinyl alcohol-Congo red-water system using the chainomatic balance relaxometer. Three samples of polyvinyl alcohol whose molecular weight were $3.5\times10^4$, $4.9\times10^4$ and $9.8\times10^4$ were used, and the composition of the gels was maintained to be the same for all specimens: polyvinyl alcohol 17.5% and Congo red 1.75%. The measurement was made to ten hours and the temperature was changed from about 1°C to about 66°C.

The obtained relaxation curves were superposed to a composite relaxation curves for each sample according to the time-temperature superposition principle, and the curves ranging from $10^{-4}$ to $10^9$ hours were obtained, and from those the relaxation spectra were calculated by the second order approximation.

It is seen that the three spectra are nearly all superposed on the shorter time side than one hour and that the maximum value becomes larger as the molecular weight increases, and that the two spectra of the larger molecular weight are very close on the whole, except that at the long time end the spectrum of the largest molecular weight tends to extend further.

It is also seen that the box type spectrum of the gel nearly superposes when the molecular weight is larger than a certain value $M$, where $4.8\times10^4 > M > 3.5\times10^4$, and that the spectrum tends to extend to longer time region as the molecular weight increases.

The author is indebted to Mr. Mineo Watase, Mr. Kokichi Seo and Mr. Hiroshi Osada for their cooperation in carrying out this experiment.

*Department of Chemical Industry*
*Faculty of Engineering*
*Shizuoka University*
*Oiwake, Hamamatsu*

6) F. Schwarzl and A. J. Staverman, *Physica*, **18**, 791 (1952).
7) A. V. Tobolsky, *J. Appl. Phys.*, **27**, 673 (1956).

# *Physical Properties and Crystal Structure of 2-Bromo-2, 3, 3-trimethylbutane**

By Tsutomu KOIDE, Yoshihiro KATO** and Tsutomu ODA

(Received May 23, 1960)

It has been shown that the haloethane derivatives such as 1, 1, 1, 2-tetrachloro-2-methylpropane[1] and other compounds whose molecules are similar to hexamethylethane[2] in shape possess polymorphism and for any temperature range below their melting points they possess molecular orientational or rotational freedom. This freedom in the high temperature modification, which is cubic, seems to be responsible for their relatively high melting points.

Since the van der Waals radius of bromine atom is nearly equal to that of chlorine[3], it is of interest to investigate the behavior of molecules in the solid state for bromo-derivatives of ethane in comparison with the same state of its chloro-derivatives[1,4]. As an example, the authors have studied the crystal structure and the behavior of molecules of 2-bromo-2, 3, 3-trimethylbutane by means of optical, X-ray and differential thermal analysis methods.

## Experimental and Results

**Materials.** — The sample of 2-bromo-2, 3, 3-trimethylbutane was prepared by passing gaseous hydrogen bromide through an ethereal solution of pentamethylethanol, which had been obtained by the Grignard reaction of pinacolone with magnesium bromide in ethereal solution. The final product was twice purified by recrystallization, followed by sublimation in high vacuum ($10^{-5}$ mmHg).

The melting point is found to be 151°C in a sealed capillary tube. The liquid phase vaporizes immediately after melting. The solid is soft and shows plasticity. The density is found to be 1.31 g./cc. at 13°C by the flotation method using an aqueous solution of calcium carbonate.

**Optical Observation.**—Under the polarized microscope, the room temperature phase was found to be isotropic, indicating the crystal to be cubic. Observations were extended to the liquid air temperature. The cryostat for this purpose is shown in Fig. 1. Cooling was made by heat conduction through a copper rod dipped in liquid air. The temperature was measured with a copper-constantan thermo-couple and a millivoltmeter. By cooling, it was observed that the crystal transformed at about −117°C into a different crystalline phase which was optically anisotropic.

**X-ray Measurements.**—*The Crystal Structure of the High Temperature Modification.*—Owing to its extremely high volatility, a single crystal of this substance, sealed in a capillary tube for X-ray measurement, sublimes gradually in few days into a number of smaller crystals in the cooler part of the tube. Therefore, in order to prevent this loss of sample due to sublimation, a glass rod just fitting the glass capillary was inserted to make the remaining free space as small as possible.

Using Cu-$K_\alpha$ radiation ($\lambda = 1.54$ Å) filtered through nickel foil, we prepared a series of 20° oscillation photographs covering a range of about 90° with [011] as the axis of rotation.

Laue photographs were taken with X-ray beams parallel to [100], [110] and [111]. All of the Laue spots were split into two or three parts, but the same crystal showed no splitting in its oscillation photographs when rotated through [110]. Thus the crystal used was not a single crystal, but was composed of several crystallites which were slightly different in orientation. All the efforts to get a single crystal have been unsuccessful, as was the case of 2-chloro-2, 3, 3-trimethylbutane[5]. All the Laue spots were successfully indexed, based upon a cubic lattice having holotesseral symmetry. The point group symmetry of the crystal was found to be $T_d$-$\bar{4}3m$, $O$-43 or $O_h$-$m3m$.

The observed spectra in oscillation photographs can be indexed satisfactorily with a body-centered cubic lattice having a unit cell of the side $a = 7.66$ Å. The observed value of density, 1.31 g./cc., is almost equal to the calculated value, 1.32 g./cc., assuming that two molecules are contained in the unit cell.

**Differential Thermal Analysis (D. T. A.).**—The apparatus used for the D. T. A. was described elsewhere[1]. The temperature range of the measurement was from 90°C to the liquid air temperature. Fig. 2 shows the result of the D. T. A. measurement for warming. The time-temperature curve of Fig. 2 shows the temperature of the used reference substance (sodium chloride) and the differential curve shows the temperature difference between the reference

* Presented at the 11th Annual Meeting of the Chemical Society of Japan, Tokyo, April, 1958.

** Present address,, Daitetsu High School, Matsubara City, Osaka.

1) T. Koide, T. Oda and I. Nitta, This Bulletin, **29**, 738 (1956).

2) D. W. Scott, D. R. Doulsin, M. E. Gross, C. D. Oliver and H. M. Huffman, *J. Am. Chem. Soc.*, **74**. 883 (1954).

3) L. Pauling, "The Nature of the Chemical Bond", Cornell Univ. Press, Ithaca (1948), p. 189.

4) T. Koide, T. Oda and I. Nitta, This Bulletin, **30**, 199 (1957).

5) T. Koide and S. Takeuchi, T. Oda, Y. Yamada and I. Taguchi, ibid., **30**, 680 (1957).

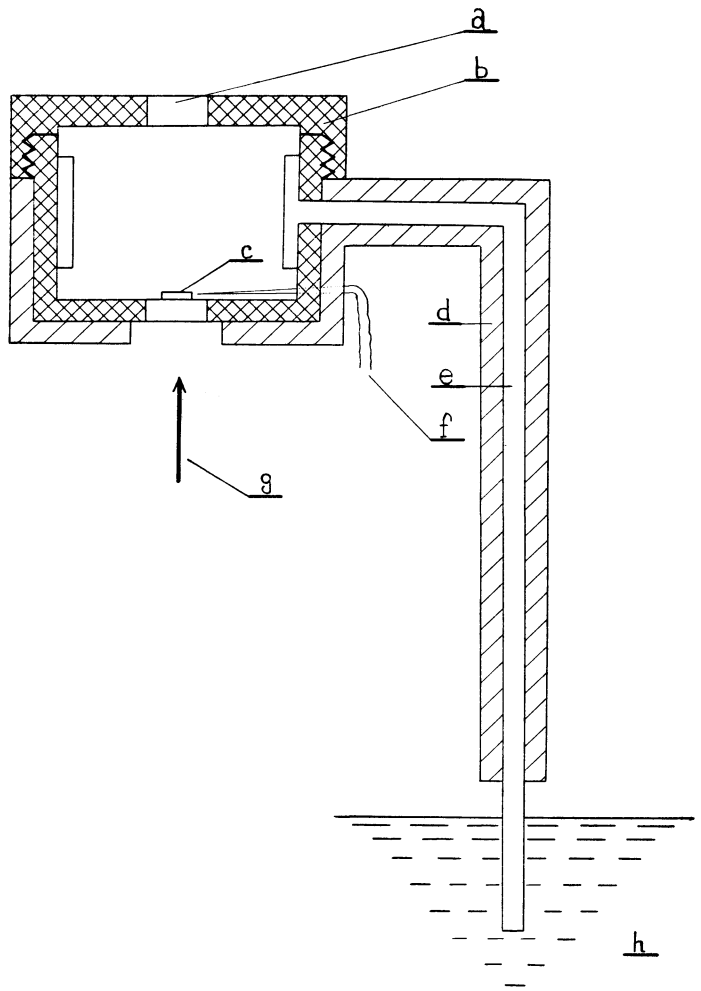



Fig. 1. The cryostat for the optical measurement at low temperature.
a) window (glass), b) bakelite, c) sample, d) thermal insulator, e) copper rod, f) thermocouple, g) polarized light, h) liquid air

substance and the sample. The temperature differences are plotted on an arbitrary scale. There is an anomalous thermal effect at about −114°C (the peak of the differential curve in Fig. 2) for warming and at about −117°C for cooling. This result is in good agreement with the optical observation.

## Discussion

Since there are two molecules in each unit cell with the body-centered cubic lattice, it is reasonable to place the centers of mass of the molecules at the lattice points 0, 0, 0 and 1/2, 1/2, 1/2. The proper symmetry of these points is $T_d$-$\bar{4}3m$, $O$-43 or $O_h$-$m3m$, so that the symmetry of the molecule should have one of these cubic point groups. On the other hand, if we assume that the molecule has the skew configuration (Fig. 3), the highest symmetry that the molecule could have is $C_s$-$m$, the central C-C bond lying on the plane of symmetry. In order that the molecule, which has the symmetry $C_s$-$m$, attains the cubic symmetry, it is necessary to take into consideration some statistical arrangements for explaining the structure of the crystal, as was done in the X-ray studies of other plastic crystals[6].

One of the possibilities that the statistical symmetry of the molecule is as high as $T_d$-$\bar{4}3m$ is that the molecule orientates its central C-C axis parallel to each one of the four body-diagonals statistically equally, so that the C-C axis acquires at least a statistical symmetry

6) C. D. West, *Z. Krist.*, **88**, 195; C. Finbak, *Tids. Kjem, Bergv.*, **17**, 2 (1937); M. Atoji, T. Oda and T. Watanabe, *Acta Cryst.*, 6, 868 (1953); I. Nitta and T. Watanabe, This Bulletin, **13**, 28 (1938); T. Oda and T. Watanabe, *J. Chem. Soc. Japan, Pure Chem. Sec.* (*Nippon Kagaku Zasshi*), **65**, 154 (1944); T. B. Reed and W. N. Lipscomb, *Acta Cryst.*, 6, 108 (1958).

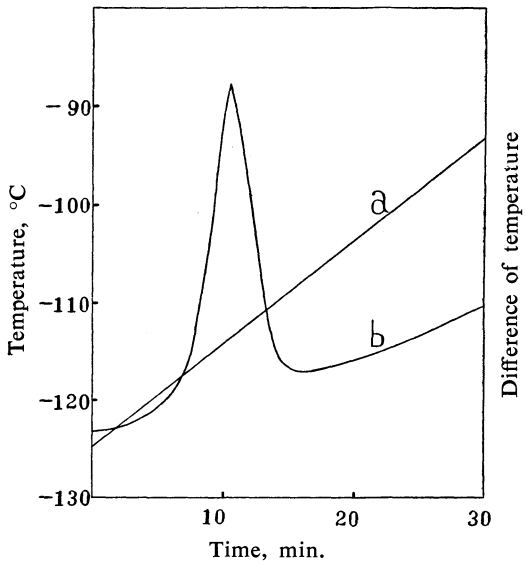



Fig. 2. Differential thermal analysis curve for 2-bromo-2,3,3-trimethylbutane $Br(CH_3)_2C\cdot C(CH_3)_3$.
a) time-temperature curve
b) differential curve

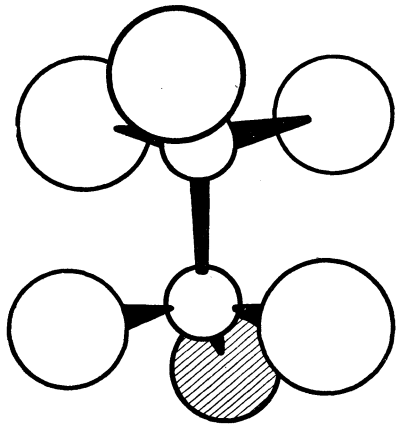


Fig. 3. The assumed model for the free molecule of 2-bromo-2,3,3-trimethylbutane. The small circle represents the carbon atom, the large circle the methyl group and the hatched one the bromine atom.

of 3*m*. Following such a statistical configuration, a calculation of structural factors was carried out, using two models, Ia (Fig. 4) and Ib, which are slightly different from each other. Namely in Ia, the two bromine atoms were assumed to lie statistically on the twenty-four equivalent positions, 24 (*g*)[7] near the three principal axes, and the ten $CH_3$ groups on another set of the same equivalent positions.

7) "International Tables for X-ray Crystallography", Vol. I, Kynoch Press, Birmingham (1952), p. 326.

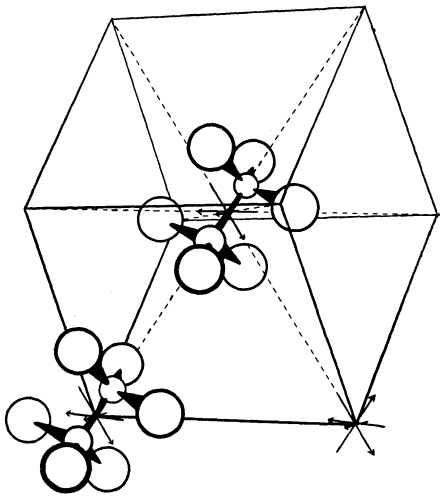


Fig. 4. The model for a statistical configuration, Ia.

In Ib the bromine atoms and the methylic carbon atoms lie separately on two sets of forty-eight equivalent positions, (*h*) with a weight 1/24 for bromine and 5/24 for C. It is to be added here that in these calculations the molecule was assumed to possess the skew form with the C-C and C-Br bond distances, 1.54 and 1.94 Å, and the tetrahedral valency angle.

If half of the molecules, in a statistical sense, rotate their molecular axes around the principal crystal axes through 90°, then the polar molecular axes will be found in eight different directions parallel to the body-diagonals of the crystal. If we add this operation to model Ia, the symmetry of the crystal will become $O^9_h$-*Im*3*m*. We shall call this model IIa. In this model, the polar axes of the molecules will be found in antiparallel orientations, whereas the bromine atoms and methyl groups will remain in almost the same positions as in model Ia. In these two models Ia and IIa, methyl groups and bromine atoms belonging to any two neighbouring molecules are found in trans configuration. By twisting the molecular axis from the positions given by model IIa, we have model IIb (angle of twist ±15°), model IIc (angle of twist ±40°) and model IId (angle of twist ±60°). The symmetry of these three models remains as in IIa.

In addition to these models, which are statistically static, we have also considered model III, in which molecules are rotating spherically around their centers of mass. The crystal will also assume the symmetry of $O^9_h$-*Im*3*m*.

The calculated $|F|$-values based on these models are plotted in Fig. 5, together with the observed data. Curve III is quite different

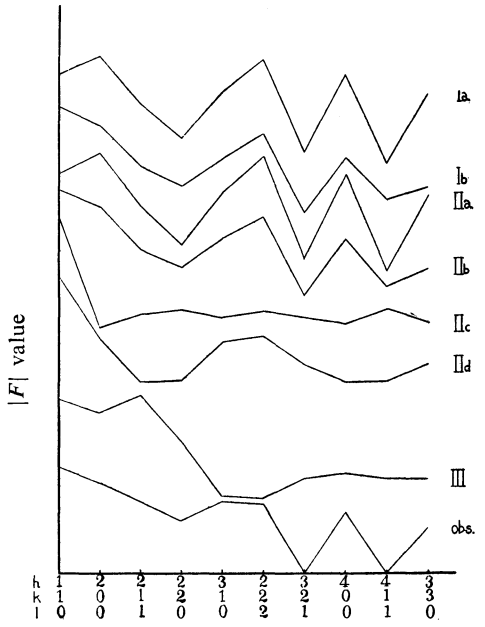



Fig. 5. Observed and calculated values of $|F|$.

from the observed one, suggesting that the free rotation of molecules as a whole in the crystal is ruled out. As a matter of fact, the domain required for the free rotation of the molecules at each lattice point overlaps not only with those of the first neighboring molecules but also with the second neighboring molecules as shown in Fig. 6. The curves for the models IIc and IId also do not agree with the observed one.

The curve Ia agrees fairly well with the observed one. In this model, though there is no appreciable overlap between the first neighboring molecules, there remains the possibility of colliding between the second neighboring molecules (Fig. 6). The agreement between the intensities calculated by model IIb, Ib and the observed ones is the best among all the models so far investigated. In these models, none of the shortest distances between atoms in neighboring molecules exceeds appreciably the sum of the van der Waals radii. It is difficult to decide which one of models, Ib or IIb, is really the case in point. The actual configuration may be expressed by a combination of Ia, Ib, IIa and IIb with appropriate weights.

This statistical structure may throw light on the explanation of the plasticity and rapid decrease of intensity with the increase of diffraction angle.

The orientational disorder of the arrangement of molecules may disappear below the transition temperature. This view is supported by the thermal differential analysis. The change of the optical property from isotropic to an-

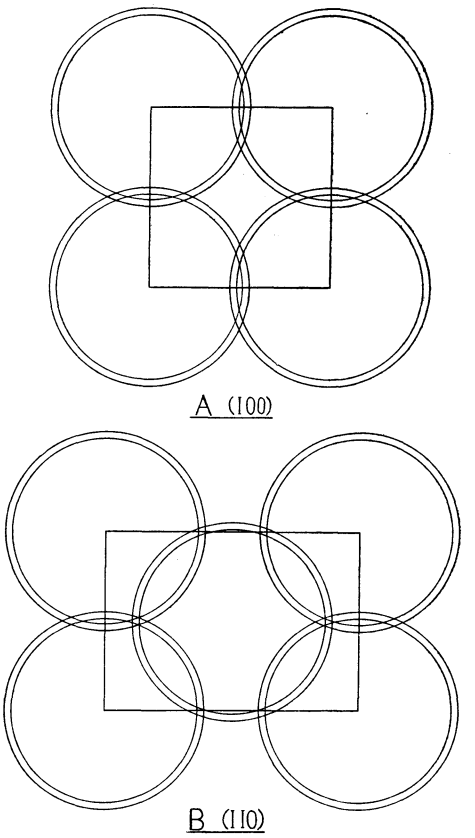



Fig. 6. The required domain for the free rotation of molecule at each lattice point. The radii of these circles are calculated using assumed molecular configuration and van der Waals radii for bromine (outer circles) and methyl groups (inner).
A shows the section parallel to (100).
B shows the section parallel to (110).

isotropic in passing the transition temperature means that the crystal assumes the lower symmetry. This may imply that the arrangement of the molecules becomes more ordered than that of the room temperature phase.

It has been reported that 1, 1, 1, 2-tetrachloro-2-methylpropane[1] and 2-chloro-2, 3, 3-trimethylbutane[4] also give plastic crystals at high temperature. Both of these also belong to the body-centered cubic lattice and the fact that their unit cell dimensions (7.4 and 7.62 Å) are close to the value of the present substance indicates that the free volumes of these molecules are similar.

## Summary

2-Bromo-2, 3, 3-trimethylbutane gives a plastic crystal, which is optically isotropic and has a density of 1.31 g./cc. at 13°C. The X-ray data

can be interpreted on the bases of a body-centered cubic lattice, having $a=7.66$ Å with two molecules in the unit cell. The symmetry interpretation gives a structure of disordered orientation of molecules. It was found, by means of optical and differential thermal analysis methods, that there is a phase transition at about $-114$°C, below which the crystal is of a lower symmetry.

The authors express their hearty thanks to Professor Isamu Nitta, Professor Tokunosuke Watanabé and Dr. Syuzo Seki for their interest during this study. They also express their thanks to Dr. Hiroshi Suga for his help in optical measurements, and to Mr. Yoshiyuki Namba for his discussion. A part of the cost of this research was supported by the Ministry of Education, to which their thanks are due.

*Laboratory of Chemistry*
*Osaka University of*
*Liberal Arts and Education*
*Tennoji, Osaka*

# *Variation of Radiocarbon Concentration in Modern Wood*

By Kunihiko KIGOSHI and Yoshio TOMIKURA

(Received May 27, 1960)

It has recently been pointed out by several authors[1-7] that the atmospheric radiocarbon is increasing because of nuclear tests. The present authors have also detected a remarkable change of the atmospheric radiocarbon concentration after 1953. This recent increase of radiocarbon and the Suess effect[8-10], i.e. the dilution effect of atmospheric radiocarbon by combustion of fossil fuel play an important role in the studies on the carbon dioxide cycle in nature. The present paper presents the results of the measurements on the change of the atmospheric radiocarbon contents in recent years using the carbon in tree rings taken from Honshu Island. We used the tree rings of Japanese cedar (*Crytomeria Japonica*) of which the place of growth and the date of cut were known. The measurements of radiocarbon were made with an acetylene filled proportional counter shielded with iron plates and provided by anticoincidence counters.

1) W. S. Broecker and A. Walton, *Science*, **130**, 309 (1959).
2) G. S. Bien and H. E. Suess, *Z. für Physik*, **154**, 172 (1959).
3) K. O. Munnich and J. C. Vogel, *Naturwiss.*, **45**, 327 (1958).
4) T. A. Rafter and G. J. Fergusson, *Science*, **126**, 557 (1957).
5) T. A. Rafter and G. J. Fergusson, *N. Z. J. Sci. Tech.*, **B38**, 871 (1957).
6) T. A. Rafter and G. J. Fergusson, U. N. Con. on the Peaceful Uses of Atomic Energy, **18**, 526 (1958).
7) Hl. de Vries, *Science*, **128**, 250 (1958).
8) R. Revelle and H. E. Suess, *Tellus*, **9**, 18 (1957).
9) H. R. Brannon, A. C. Daughtry, D. Perry, W. W. Whitaker and M. Williams, *Trans. Am. Geophys. Union*, **38**, 643 (1957).
10) G. J. Fergusson, *Proc. Roy. Soc.*, **A243**, 561 (1958).

## Experimental Procedures

**Apparatus.**—A stainless steel tube proportional counter is placed in the middle of eleven anticoincidence Geiger counters inside of an iron shield of 23 cm. in thickness. The pulses from the proportional counter are delaye 10 micro second and are mixed with the pulses of the anticoincidence counters. The background of the proportional counter is $5.46 \pm 0.3$ counts per minute. The proportional counter used for these experiments has the dimensions of 3.5 cm. in inner diameter and of 52 cm. in length. The center anode is stainless steel wire of 0.05 mm. in diameter. The effective volume of the counter is 420 ml.

**Preparation of Acetylene from a Wood Sample.**—A wood sample is heated in a metal crucible in order to remove the volatile organic substance. This procedure makes the sample charcoal. The charcoal is converted into strontium carbonate by the following procedures; combustion in a current of oxygen, absorption of carbon dioxide in 6 N ammonia water, precipitation of calcium carbonate from an ammonium carbonate solution, evolution of carbon dioxide with hydrochloric acid from the calcium carbonate, absorption of carbon dioxide into ammonia water and precipitation of strontium carbonate. The preparation of acetylene from the strontium carbonate is done in a stainless steel tube which is illustrated in Fig. 1.

The mixture of strontium carbonate (8 g.) and magnesium powder (8 g.) is heated in the stainless steel tube by an electric furnace. The tube is connected to a vacuum line and when the temperature rises to 300~400°C the pumping system is cut by the metal cock. The best way to get a good result is to heat the tube up to 800~900°C for more than 4 hr. Very often a kind of explosion was observed during the heating up to 800°C. The

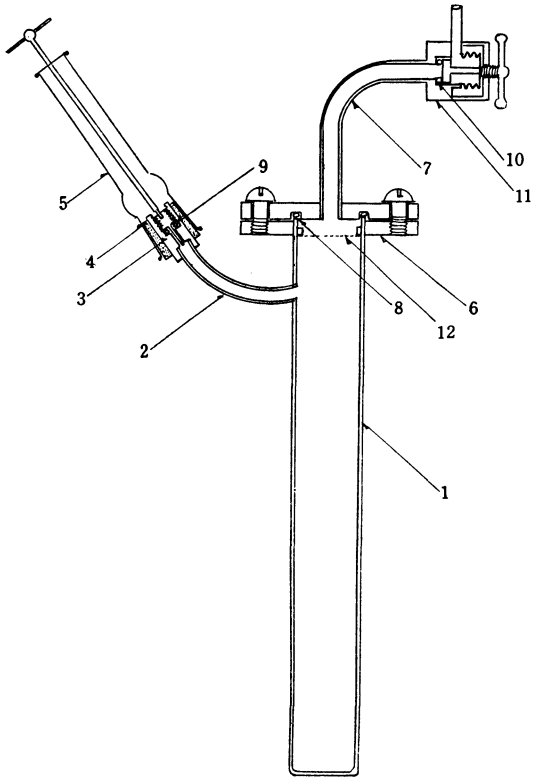



Fig. 1. Tube for preparation of acetylene.
1. Stainless steel tube of 30 mm. in diameter, 780 mm. length
2, 7. Copper tube of 8 mm. in diameter
3. Metal cock for the injection of water
4. Rubber stopper
5. Glass cylinder of 20 mm. in diameter, 150 mm. in length
6. Steel frange
8, 9, 10. O-ring
11. Metal cock
12. Glass filter

explosion can be detected by a sudden temperature rise. The explosion takes place around 450~600°C and if the reaction were stopped just after the explosion, one would get around 60% of acetylene of the calculated value*. Heating up to 800°C after the explosion gives good acetylene yield of 85~95% of the calculated value.

After the preparation of carbide in the stainless steel tube, this is connected to another vacumm line with several cold traps for the purification of acetylene. Acetylene and hydrogen which are evolved by adding water through the side tube to carbide are dried with dry ice in the cold trap. The acetylene is separated from the hydrogen by a trap cooled with liquid nitrogen. The charcoal trap cooled with dry ice removes effectively the contaminated radon from the acetylene. However, since contamination of radon, though it is trace

* When the amount of reaction mixture is large, the temperature rise at the explosion is high enough to produce carbide in fairly good yield.

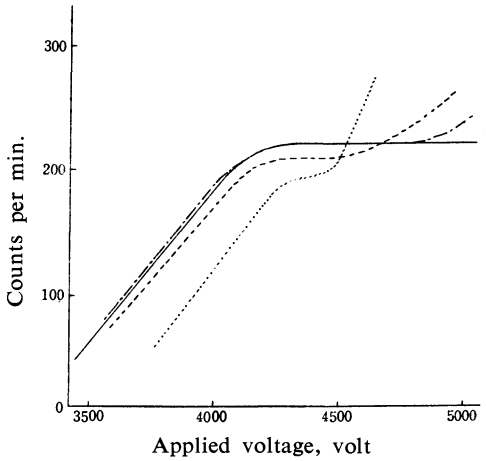



Fig. 2. Characteristic curves of acetylene filled (1 atm.) propertional counter.
——— Pure acetylene
– – – – Acetylene with 0.1% air
– – – 〃 0.2% air
– – – – – – 〃 0.9% air

amount (less than one count per minute), was observed even with these purifications, the acetylene had to be stored in a flask more than three weeks before the activity measurement was made.

**Characteristics of the Acetylene Filled Counter.**—A solid curve in Fig. 2 shows a typical characteristic curve of an acetylene filled proportional counter. The slope of the plateau is constant over the wide range of acetylene pressure within 2% increase per 100 volts. The starting voltage of the plateau is

$$V=(2100+2.98\times P) \text{ volts}, \quad 200<P<800$$

where $P$ is the pressure of acetylene in mmHg. The counter was used with a voltage higher than the starting voltage by 250 volts.

The characteristic curve of the proportional counter changes with the content of impurity of acetylene as is shown in Fig. 2. The allowable maximun amount of impurities such as moisture or air which gives a serious effect on the characteristic curve is abous 0.2% of the total gas. This amount is large enough to operate the counter in a good condition without any special care such as is necessary for the carbon dioxide filled counter that is seriously affected by contaminated air of 0.001% of filling gas[11].

**Effect of the Tritium Activity.**—Fig. 3 shows counts per minute for the different amounts of acetylene gases of modern and dead carbon. There is no change in counts per minute in the case of dead carbon. This indicates that the acetylene produced from dead carbon (from coal or lime) has no activity. The extrapolated values of counts per minute at pressure zero for modern and dead carbon agree with each other within the experimental error of 0.06 count per minute. This shows that the observed activity of the acetyene produced from modern carbon is attributed to the carbon and not to the tritium in acetylene.

11) Hl. de Vries and W. Barendsen, *Physica*, **19**, 987 (1953).

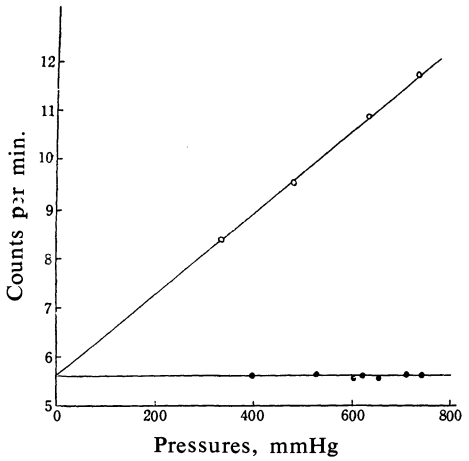



Fig. 3. Relation between counts per minute and pressure of acetylene.
○ Modern carbon, ● Dead carbon

**Counting Procedure.**—Acetylene gas stored more than three weeks is filled in the proportional counter and its characteristic curve is measured. According to the characteristic curve and the pressure in the counter one sets high voltage to be applied. The counting time is usually 48 hr. and the counts are checked every 5 or 10 hr. Background measurements are made for 24 hr. in every two or four days.

## Experimental Results

Table I summarizes the data of the measurements of radiocarbon concentrations in the tree ring samples which were obtained from tree No. 1. Tree No. 1 grew in Akita Prefecture in Honshu Island. This tree has an age of 177 years and was cut in December, 1958. Each tree ring has more than 2 mm. thickness and shows clear boundaries.

The first column of Table I indicates the intervals in which the tree rings grew. The second column shows observed counts per

TABLE I. VARIATION OF C-14 CONCENTRATION IN TREE RINGS GROWN BETWEEN 1789 AND 1950 (Sample tree No. 1)[a]

| Intervals of growth of tree ring | Counts per min. g. carbon | C-14 concentration[b] |
|---|---|---|
| Aug.1782~Sept.1798 | 11.69±0.18 | 0.960±0.015 |
| Aug.1799~Sept.1808 | 12.02±0.18 | 0.986±0.015 |
| Aug.1809~Sept.1818 | 12.19±0.18 | 1.000±0.015 |
| Aug.1819~Sept.1828 | 11.90±0.18 | 0.976±0.015 |
| Aug.1829~Sept.1838 | 12.10±0.18 | 0.988±0.015 |
| Aug.1839~Sept.1848 | 12.19±0.18 | 0.998±0.015 |
| Aug.1849~Sept.1858 | 12.14±0.18 | 0.990±0.015 |
| Aug.1859~Sept.1863 | 12.24±0.18 | 1.000±0.015 |
| Aug.1864~Sept.1868 | 12.24±0.18 | 1.000±0.015 |
| Aug.1869~Sept.1873 | 12.39±0.18 | 1.010±0.015 |
| Aug.1874~Sept.1878 | 12.47±0.14 | 1.015±0.011 |
| Aug.1879~Sept.1883 | 12.49±0.18 | 1.015±0.015 |
| Aug.1884~Sept.1888 | 12.18±0.14 | 0.986±0.011 |
| Aug.1889~Sept.1893 | 12.63±0.18 | 1.028±0.015 |
| Aug.1894~Sept.1998 | 12.40±0.18 | 1.008±0.015 |
| Aug.1899~Sept.1903 | 12.47±0.14 | 1.011±0.011 |
| Aug.1904~Sept.1908 | 12.47±0.18 | 1.011±0.015 |
| Aug.1909~Sept.1913 | 12.52±0.18 | 1.013±0.015 |
| Aug.1914~Sept.1918 | 12.47±0.18 | 1.010±0.015 |
| Aug.1919~Sept.1923 | 12.02±0.18 | 0.974±0.015 |
| Aug.1924~Sept.1928 | 12.20±0.18 | 0.982±0.015 |
| Aug.1929~Sept.1933 | 12.39±0.14 | 1.000±0.011 |
| Aug.1934~Sept.1938 | 12.60±0.18 | 1.017±0.015 |
| Aug.1939~Sept.1943 | 12.02±0.18 | 0.968±0.015 |
| Aug.1944~Sept.1945 | 12.42±0.18 | 1.000±0.015 |
| Aug.1945~Sept.1946 | 12.52±0.14 | 1.011±0.011 |
| Aug.1946~Sept.1947 | 12.10±0.18 | 0.974±0.015 |
| Aug.1947~Sept.1948 | 12.04±0.18 | 0.970±0.015 |
| Aug.1948~Sept.1949 | 12.38±0.18 | 0.997±0.015 |
| Aug.1949~Sept.1950 | 11.78±0.18 | 0.949±0.015 |

a) The data are normalized to the concentration of C-14 of the hypothetical modern wood which would not have been affected by industrial effect and nuclear tests.
b) Grown in Akita Prefecture in Honshu Island.

TABLE II. VARIATION OF C-14 CONCENTRATION IN TREE RINGS GROWN AFTER 1950

| Intervals of growth of tree rings | C-14 concentration in tree rings | | |
|---|---|---|---|
| | Sample No. 1 | Sample No. 2[a] | Sample No. 3[b] |
| Aug. 1950~Sept. 1951 | 1.010±0.015 | | |
| Aug. 1951~Sept. 1952 | 1.000±0.015 | | |
| Aug. 1952~Sept. 1953 | 0.994±0.014 | | |
| Aug. 1953~Sept. 1954 | 1.012±0.014 | | |
| Aug. 1954~Sept. 1955 | 1.034±0.014 | | |
| Aug. 1955~Sept. 1956 | 1.050±0.011 | 1.037±0.011 | |
| Aug. 1956~Sept. 1957 | 1.092±0.015 | 1.081±0.011 | 1.084±0.011 |
| Aug. 1957~Sept. 1958 | 1.122±0.014[c] | 1.083±0.011 | 1.086±0.011 |
| Aug. 1958~Sept. 1959 | | 1.238±0.011 | 1.240±0.011 |

a) Grown on the campus of Gakushuin University in Tokyo.
b) Grown in Mie Prefecture in Honshu Island.
c) This sample includes the tree rings up to December, 1958.

minute for one gram carbon of each sample. The third column gives the concentrations of C-14 in tree rings at the year indicated in the first column. The concentrations are normalized to the mean value of 18 measured concentrations between 1782 and 1913 (Table I). This mean value will be referred to as a concentration of C-14 in hypothetical modern wood which would not have been affected by industrial effect and nuclear tests.

Table II gives a summary of our data on the tree ring samples after 1950. The second column shows the concentrations of C-14 in the samples which were obtained from tree No. 1. The third and the fourth columns give the results on the trees which grew in Tokyo and Mie Prefecture. Tree No. 2 (the third column) was cut in September, 1959, and No. 3 (the fourth column) in August, 1959. These three series of measurements agree well, and indicate a remarkable increase after the autumn of 1958. The errors indicated in Tables I and II include only statistical counting errors (standard deviations).

## Discussion

The tree ring is a sample formed by constant accumulation of carbon from the atmosphere and is dated by clear boundaries. The examination of the data on the concentration of C-14 in the tree rings gives information on the annual average concentration of C-14 in the atmosphere. Moreover, if samples from the same species of tree were used, the differences of the possible isotopic fractionation among the samples might be negligibly small*. These make the tree ring samples adequate for the studies on the annual variation of C-14 concentration in the atmospheric carbon. However there are some questions about the nature of the sample. First, there is a possibility that the carbon which is taken up through the root could be used for assimilation. Second, the carbon dioxide from the pedosphere might be utilized for assimilation by aerial transport to leaf level. Finally there is a question when the organic substance in a certain part of tree ring was synthesized from the carbon dioxide.

The first and the second question had been discussed by W. Whitaker et al.[12] They suggested a possible influence of the uptake of older carbon by the root system as the most likely explanation of differences in radiocarbon contents of trees from different enviroments. If such an influence plays an important role for a tall tree, the increase in radiocarbon contents in tree rings after 1953 would be less than the increases in atmospheric radiocarbon contents. The authors favor the assumption that this influence is negligibly small because the direct experimental evidences on young pea and barley plants show a small amount of uptake of carbon dioxide through the root system[13]. The experimental results of Whitaker et al. on the effect of the aerial transport for carbon dioxide from pedosphere to leaf level show the absence of any significant amount of old carbon cycling from pedosphere to the leaves of trees.

On the circulation of synthesized organic substances in the tree we have some knowledge which will serve to show when the organic substances in a certain part of the tree ring was synthesized from the atmospheric carbon dioxide. The large cells which are adjacent to the boundary of a tree ring are formed in the spring of the year from the carbon dioxide existing in the atmosphere and from the organic substances, which were synthesized after the summer of the preceding year and have been stored in the older tree rings. The cells which are formed after the middle of the summer of the year become smaller. Finally the smallest cells are formed in September forming the boundary of the tree ring. A large part of the organic substances synthesized during the middle of summer and autumn is stored in a newly formed tree ring[14]. The stored organic substances will be used for the formation of new cells in the next spring. It is therefore desirable to cut down the tree in summer for the measurement.

In general it can be said that the tree ring is made by the atmospheric carbon dioxide during August of the preceding year and September of this year. Although formation of boundaries can be influenced easily by the climate of the place where the sample tree grew, the expected error of the indicated intervals of growth of tree rings in Table I and II may be within one month.

Examination of the results listed in Table I shows a constant concentration of C-14 in the atmosphere between 1782 and 1950 within an error of 2%. Fergusson[10] reported 2% depletion of C-14 concentration in the atmospheric carbon dioxide between 1860 and 1954. Although the limits of statistical counting error of the data are rather broad, the present data seem to support the opinion that the depletion is less than 2% between 1782 and 1950.

* The measurements on the isotopic ratio of $^{13}C/^{12}C$ in tree ring carbon by Fergusson[10] and Broecker et al.[1] show a constant value on the samples from a tree or the trees of same species.

12) W. W. Whitaker, S. Valastro, Jr. and M. Williams, *J. Geophys. Res.*, 64 1023 (1959).

13) J. A. J. Stolwijk and K. V. Thimann, *Plant Physiol.*, 32, 513 (1957).

14) J. H. Priestley, *New Phytologist*, 24, 316 (1930).

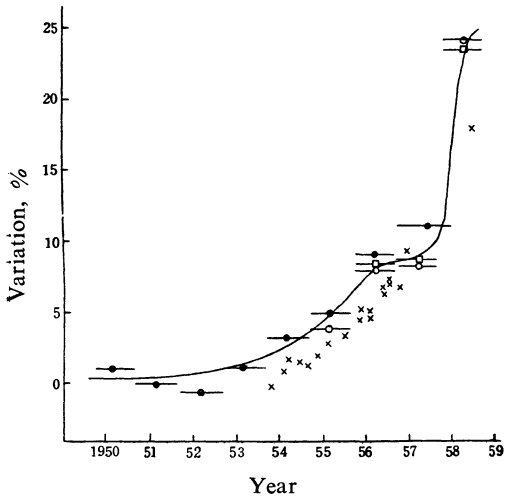



Fig. 4. Variation of C-14 concentration in the atmosphere.

Data of this paper
- ● Akita
- ○ Tokyo
- □ Mie
- —— Interval of growth of tree ring.
- Standard deviation; 1.1~1.5%

Data by Rafter and Fergusson, ×

All the data in Table II as are plotted in Fig. 4 show no essential difference among the three samples except the value of sample No. 1, 1957—1958. Since sample No. 1 was cut in December, 1958 and its last tree ring (1957—1958) was very likely to have incorporated the atmospheric carbon in December, 1958, the higher value corresponds to a sudden increase of atmospheric radiocarbon in the autumn of 1958. It could be concluded that there was no local variation along the south east shore line of Honshu Island from the fact that there is no meaningful difference among the values of the three samples. Bien and Suess[2] reported the variation of C-14 concentration in the tree ring samples up to 1957. These values agree with the present data within the experimental errors. It seems very likely that the local variation of the atmospheric radiocarbon contents is very small, at least in the temperate zone of the northern hemisphere.

In Fig. 4 the plot of the variation of C-14 concentration in the southern atmosphere reported by Rafter and Fergusson[5,6] indicates a systematic delay of the variation to that of the present data. Although the limits of error on the time scale of the present data are rather broad, the delay of the variation of the atmospheric C-14 concentration in the southern hemisphere seems to be several months in length. Broecker and Walton[1] discussed the difference of the atmospheric C-14 concentration between the northern and southern hemispheres. The present result seems to agree with that of Broecker and Walton.

## Summary

1) Using the tree ring samples, the variation of C-14 concentration in the atmosphere since 1782 has been measured by the use of trees growing in Japan. The results show a constant concentration of C-14 in the atmosphere during 1782 and 1950 within the error of 2%.

2) The depletion of C-14 concentration in the atmospheric carbon dioxide between 1782 and 1950 seems to be less than 2%.

3) The observed annual variations on the samples from Tokyo, Akita and Mie Prefectures show almost the same amount of increase after 1953. There is a good agreement between our data and those on the tree ring samples taken in California by Bien and Suess. The concentration of C-14 in the atmosphere averaged over a year seems to have little difference in the temperate zone of the northern hemisphere.

4) The variation of C-14 concentration in the atmosphere of the southern hemisphere seems to follow that of the northern hemisphere with a time lag of several months.

The cooperation of Mr. T. Tokumoto and other officers of the Government Forest Experiment Station and Mr. T. Iwata of the Ise Shrine who supplied the tree samples is gratefully acknowledged. The authors wish to thank Dr. E. Tajima for valuable advice. A part of the expense for this work has been defrayed by the Ministry of Education.

*Department of Physics*
*and Chemistry*
*Gakushuin University*
*Mejiro, Toshima-ku, Tokyo*

# *Spectrophotometric Determination of Bismuth with Xylenol Orange*

By Hiroshi ONISHI and Nasumi ISHIWATARI

(Received May 24, 1960)

Xylenol Orange was first proposed by Körbl and Pribil[1] as a metal indicator for the EDTA titration. Cheng recently described photometric methods for the determination of zirconium[2], hafnium[3], and iron[4] using Xylenol Orange. It does not appear, however, that a photometric method for determining bismuth with this reagent has been reported.

The present paper reports the conditions for the spectrophotometric determination of bismuth with Xylenol Orange including the effect of foreign substances. The composition and formation constant of the bismuth complex are also discussed.

## Experimental

**Apparatus.**—Absorbance measurements were made with a Hitachi Model EPU-2A spectrophotometer, using 1 cm. cells.

**Solutions.** — L-Ascorbic acid, 10 g. in 100 ml. of water, may be used for several days. A 0.1 g. portion of sodium fluoride was dissolved in 100 ml. of water. A 0.10 g. portion of Xylenol Orange, Dotite XO (Dojindo & Co., Ltd., Kumamoto) was dissolved in 100 ml. of water. This solution can be kept for at least one week. Standard bismuth solution was prepared by dissolving 0.500 g. of pure bismuth metal in a few milliliters of nitric acid, evaporating the solution to dryness on a water bath, dissolving the residue in 1 : 9 nitric acid, and making up to 500 ml. From this stock solution (1.00 mg. Bi per ml.) a working standard solution (e.g., 40 p.p.m. Bi) was prepared by dilution.

**Procedure.**—Transfer the sample solution (dilute nitric acid solution) containing 10~80 $\mu$g. of bismuth to 25 ml. volumetric flask and adjust the nitric acid concentration to make the acidity 0.08~0.12 N after diluting to volume. If the acidity of the sample solution is too high, neutralize excess of acid with sodium hydroxide. Dilute the solution to about 15 ml. with water. Add 1 ml. of ascorbic acid solution and allow to stand at room temperature for about 5 min. Next add 1 ml. of sodium fluoride solution, mix, add 1.0 ml. of Xylenol Orange solution. After diluting to the mark with water and mixing, measure the absorbance of the solution in a 1 cm. cell at 530 m$\mu$. Use the reference solution containing the same amounts of Xylenol Orange and other reagents.

## Results and Discussion

The absorption spectra for Xylenol Orange and its bismuth complex are shown in Fig. 1. When a correction is applied for the reagent blank, an absorption peak is found at about 520 m$\mu$. Because the reagent blank against water at 520 m$\mu$ is about twice as much as that at 530 m$\mu$, the wavelength of 530 m$\mu$ has been adopted for the determination of bismuth.

The effect of nitric acid concentration on the absorbance of bismuth complex is shown in Fig. 2. The absorbances were measured against respective reagent blanks. It is seen that the acidity of 0.08~0.12 N is suitable. Perchloric acid or sulfuric acid also gives the same results as does the nitric acid.

As shown in Fig. 3, a practically constant

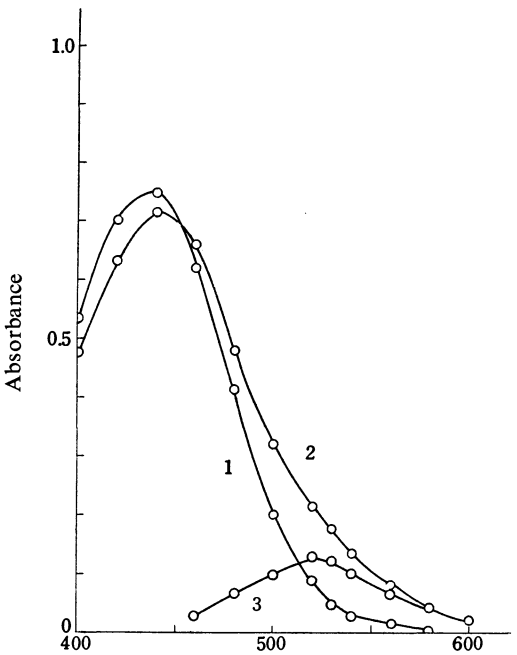



Fig. 1. Absorption spectra;
1. Xylenol Orange (against water),
2. 1.6 p.p.m. Bi (against water),
3. 1.6 p.p.m. Bi (against reagent blank).

1) J. Körbl and R. Pribil, *Chemist-Analyst*, **45**, 102 (1956); J. Körbl, R. Pribil and A. Emr, *Collection Czechoslov. Chem. Communs.*, **22**, 961 (1957).
2) K. L. Cheng, *Talanta*, **2**, 61 (1959).
3) K. L. Cheng, ibid., **3**, 81 (1959).
4) K. L. Cheng, ibid., **3**, 147 (1959).

Table I. Stability of colored solution

| Time after color development, hr. | Absorbance | | | | | |
|---|---|---|---|---|---|---|
| | 40 μg. Bi $HNO_3$ soln.* | 80 μg. Bi $HNO_3$ soln.* | 40 μg. Bi $HNO_3$ soln. | 80 μg. Bi $HNO_3$ soln. | 40 μg. Bi $HClO_4$ soln.* | 40 μg. B. $H_2SO_4$ soln.* |
| About 1/4 | — | 0.244 | 0.104 | 0.207 | — | — |
| 1 | 0.128 | 0.239 | 0.104 | 0.208 | 0.136 | 0.123 |
| 2 | 0.128 | 0.235 | 0.104 | 0.207 | 0.132 | 0.122 |
| 3 | 0.128 | — | 0.103 | 0.207 | 0.134 | 0.120 |
| 16~20(Overnight) | 0.128 | 0.212 | 0.101 | 0.206 | 0.135 | 0.120 |

* Ascorbic acid and NaF were not added.

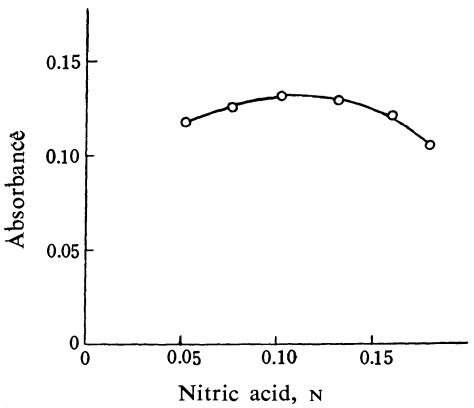



Fig. 2. Effect of nitric acid concentration; 1.6 p.p.m. Bi.

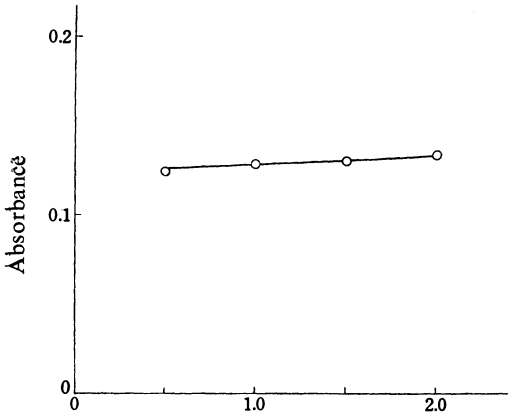



Fig. 3. Effect of Xylenol Orange concentration; 1.6 p.p.m. Bi.

absorbance is obtained by adding more than 0.5 ml. of 0.1% Xylenol Orange solution (final volume=25 ml.). The absorbances were measured against each reagent blank.

Table I shows the stability of the colored solutions. The absorbances remain constant at room temperature for at least 3 hr.

As shown in Fig. 4, absorbance is proportional to bismuth concentration in the range of 0.4 to at least 3 p.p.m. bismuth (10~80 μg. Bi). At 530 mμ the molar extinction coefficient of bismuth is $1.6\times10^4$, or 0.014 μg. Bi/cm² corresponding to $\log I_0/I=0.001$. This sensitivity is comparable to that of the iodide method or the thiourea method[5].

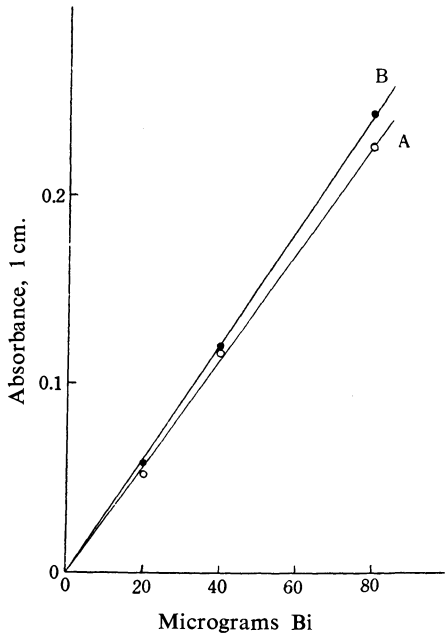



Fig. 4. Absorbance-concentration curve of bismuth;
A. According to the procedure,
B. In the absence of ascorbic acid and NaF.

The effects of many elements on the determination of bismuth were studied under the conditions used in the procedure (Table II). Most of the metals were in the form of nitrate. Microgram amounts of zirconium and thorium can be masked by fluoride ion. The interference of iron(III) can be eliminated by reduction with ascorbic acid. The effect of niobium is

5) E. B. Sandell, "Colorimetric Determination of Traces of Metals", 3rd Ed., Interscience Publishers, Inc., New York (1959), p. 330.

TABLE II. DETERMINATION OF BISMUTH IN THE PRESENCE OF FOREIGN SUBSTANCES
(40.0 μg. of Bi taken in each determination)

| Addition | Bi found, μg. |
|---|---|
| 10 mg. K | 40 |
| 0.2 mg. Cu | 39 |
| 1 mg. Ag[a] | 40 |
| 88 μg. Au[b] | 41 |
| 10 mg. Mg | 39 |
| 10 mg. Ca | 39 |
| 1 mg. Zn | 40 |
| 1 mg. Cd | 40 |
| 2 mg. Hg(II) | 41 |
| 10 mg. Al | 39 |
| 0.1 mg. In | 41 |
| 1 mg. Tl(I) | 41 |
| 0.1 mg. Ti | 39 |
| 50 μg. Zr | 39 |
| 50 μg. Th | 42 |
| 50 μg. Zr, 50 μg. Th, 1 mg. Fe(III) | 37 |
| 5 mg. Sn, 5 mg. Sb[c] | 36 |
| 10 mg. Pb | 40 |
| 5 mg. P (as $KH_2PO_4$) | 39 |
| 0.1 mg. V (as $NH_4VO_3$) | 40 |
| 0.1 mg. Nb[d] | 38 |
| 0.1 mg. Ta | 37 |
| 1 mg. As(III) | 40 |
| 1 mg. As(V) | 40 |
| 0.1 mg. Cr (as $K_2Cr_2O_7$) | 38 |
| 20 μg. Mo (as $NH_4$ molybdate) | 40 |
| 0.1 mg. W (as $Na_2WO_4$) | 39 |
| 10 mg. U(VI) | 40 |
| 0.1 mg. Cl (as NaCl) | 40 |
| 1 mg. Mn(II) | 40 |
| 1 mg. Fe(III) | 39 |
| 2 mg. Co | 41 |
| 2 mg. Ni | 41 |

a) Solution centrifuged after color development.
b) Ascorbic acid not added.
c) Volatilized with $HClO_4$, HBr and HCl.
d) Fumed with $HClO_4$.

removed by fuming with perchloric acid and treating the residue with 2 ml. of hot 1.4 N nitric acid. Apparently niobium is precipitated by this treatment. Absorbance measurements must be made within an hour after color development. (The absorbance increases after that time.) Tin and antimony can be volatilized by treating with perchloric, hydrobromic and hydrochloric acids. Five milligrams each of these elements were evaporated to fumes at about 180°C with 1 ml. of 60% perchloric acid and 2 ml. each of concentrated hydrochloric acid and hydrobromic acid (sp. gr. 1.48). After cooling 2 ml. of hydrobromic acid was again added and the solution was evaporated to dryness. The residue was treated with 2 ml. of 1.4 N nitric acid previous to color development. Silver is precipitated by ascorbic acid, but this can be removed by centrifugation after color development. Molybdenum interferes rather seriously and more than 50 μg. of this element can not be permitted.

The proposed method will probably be applicable to lead-base and tin-base alloys

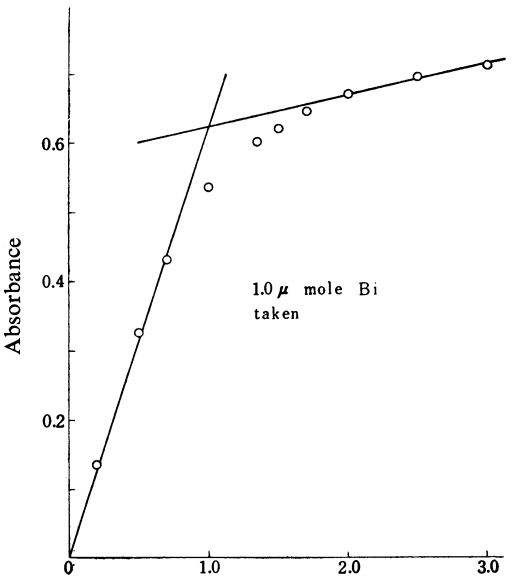



Fig. 5. Mole ratio method.

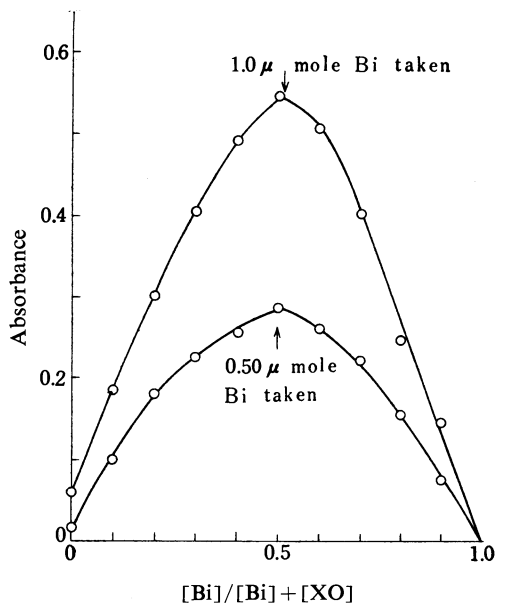



Fig. 6. Method of continuous variation.

after oxychloride precipitation of bismuth[6].

The composition of the bismuth-Xylenol Orange complex was determined by the mole ratio method and by the method of continuous variation (Job's method). The experiments were carried out at room temperatures ranging from 16° to 20°C. From the results obtained (Figs. 5 and 6), a 1 : 1 complex of bismuth with the reagent is indicated. From the fact that Xylenol Orange is an analogue of EDTA, this composition would be expected. On the basis of the data shown in Fig. 6, the formation constant or stability constant of the complex is calculated to be $1\times10^7$ by the method described by Majumdar and Chakrabartty[7] and Cheng[8]. This value is greater than that of the iron(III)-Xylenol Orange complex ($5\times10^5$)[4], and is close to that of the zirconium-Xylenol Orange complex ($4.0\times10^7$)[8].

6) B. Bendigo, R. K. Bell and H. A. Bright, *J. Research Natl. Bur. Standards*, **47**, 252 (1951); R. H. Campbell and M. G. Mellon, *Anal. Chem.*, **32**, 54 (1960).
7) A. K. Majumdar and M. M. Chakrabartty, *Anal. Chim. Acta*, **19**, 372 (1958).
8) K. L. Cheng, *Talanta*, **2**, 266 (1959).

## Summary

A method is described for the spectrophotometric determination of 10~80 μg. of bismuth with Xylenol Orange. The error is not likely to exceed ±10 per cent. The molar extinction coefficient of bismuth in 0.1 N nitric acid solution is $1.6\times10^4$ at 530 mμ. Instead of nitric acid perchloric acid or sulfuric acid may also be used. The interference of small amounts of zirconium, thorium, and iron can be eliminated by masking. Lead and thallium do not interfere with the determination of bismuth. A 1 : 1 complex of bismuth with Xylenol Orange is suggested.

*Japan Atomic Energy Research Institute*
*Tokai, Ibaraki-ken*

# *Studies on Polymerizaton and Depolymerization of ε-Caprolactam Polymer. VIII*. The Solution Viscosity of Poly-ε-capramide of Super-high Degree of Polymerization*

By Naoya OGATA

(Received June 6, 1960)

Several equations have been proposed on the relationship between the intrinsic viscosity $[\eta]$ of poly-ε-capramide in sulfuric acid and the polymerization degree $\overline{P}_n$ or the molecular weight $\overline{M}_n$ as follows:

$$\overline{P}_n = 124[\eta] - 5^{1)}$$

$$\overline{P}_n = 119[\eta]^{2)}$$

$$\overline{P}_n = 170[\eta]_{50\%\ H_2SO_4}{}^{3)}$$

$$\log[\eta] = 0.764(\pm 0.016)\log\overline{M}_n - 3.20^{4)}$$

These equations were proposed on the polymer with polymerization degrees below 300 and with broad molecular weight distribution, which was polymerized in the presence of water.

Poly-ε-capramide of a super-high degree of polymerization and with the sharp molecular weight distribution can be obtained by the so-called rapid polymerization of ε-caprolactam in the presence of alkali catalyst[5]. It is expected that the behaviour of the solution viscosity of poly-ε-capramide of a super-high degree of polymerization would be quite different from that of poly-ε-capramide polymerized in the presence of water.

## Experimental and Results

**Polymerization of ε-Caprolactam**[6]. — Sodium hydroxide was dissolved in ε-caprolactam at 100°C at the amount of 1/100, 1/500, 1/750 and 1/1000 mol./mol. and then carbon dioxide gas was introduced for 30 min. into the molten ε-caprolactam. ε-Caprolactam containing colloidally dispersed sodium carbonate was heated at 290°C under normal

* VII, *Makromol. Chem.*, **30**, 212 (1959).

1) A. Matthes, ibid., **5**, 165 (1950).

2) H. Staudinger and H. Schnell, ibid., **1**, 43 (1947).

3) K. Hoshino and M. Watanabe, *J. Am. Chem. Soc.*, **73**, 4816 (1957).

4) J. R. Schaefgen and P. J. Flory, ibid., **70**, 2709 (1948).

5) W. Griehl, *Faserforsch. u. Textiltech.*, **7**, 207 (1956).

6) H. Yumoto and N. Ogata, This Bulletin, **31**, 907, 913 (1957).

TABLE I. THE RELATION AMONG $C$, $\eta_{rel}$ AND $[\eta]$

| Sample No. | Concentration (g./100 cc.) | | | | | | | $[\eta]$ |
|---|---|---|---|---|---|---|---|---|
| | 0.1 | 0.2 | 0.5 | 1.0 | 1.5 | 2.0 | 3.0 | |
| A | 1.091 | 1.185 | 1.512 | 2.079 | 2.752 | 3.483 | 5.291 | 0.91 |
| B | 1.151 | 1.336 | 1.911 | 3.340 | 5.060 | 6.610 | 11.48 | 1·62 |
| C | 1.246 | 1.553 | 2.634 | 5.421 | 8.708 | 14.34 | 27.66 | 2.51 |
| D | 1.308 | 1.689 | 3.073 | 7.060 | 11.45 | 19.79 | 39.53 | 3.09 |
| E | 1.383 | 1.853 | 3.220 | 7.260 | 12.89 | 23.89 | 51.29 | 3.71 |
| F | 1.476 | 1.942 | 3.789 | 8.753 | 15.52 | 28.18 | 66.82 | 4.47 |
| G | 1.883 | 3.008 | 8.206 | 19.07 | 59.05 | 116.8 | 357.9 | 8.32 |

TABLE II. THE NUMBER OF CARBOXYL AND AMINO GROUPS, AND $\bar{P}_n$ OF THE POLYMER

| Sample No. | $-NH_2$ | | $-COOH$ | |
|---|---|---|---|---|
| | Mol./113 g. | $\bar{P}_n$ | Mol./113 g. | $\bar{P}_n$ |
| A | $1.300\times10^{-2}$ | 77 | $1.010\times10^{-2}$ | 99 |
| B | 0.676 〃 | 148 | 0.501 〃 | 199 |
| C | 0.415 〃 | 241 | 0.189 〃 | 529 |
| D | 0.319 〃 | 314 | 0.145 〃 | 690 |
| E | 0.295 〃 | 339 | 0.120 〃 | 833 |
| F | 0.289 〃 | 347 | 0.098 〃 | 1025 |
| G | 0.155 〃 | 646 | 0.053 〃 | 1910 |

pressure in a nitrogen atmosphere or at 250°C under the reduced pressure of 250 mmHg in a nitrogen atmosphere. After the polymerization, polymers were quickly cooled and washed with water.

**Determination of the Solution Viscosity.**—Polymers were dissolved in 98% sulfuric acid at the concentrations of 0.1, 0.2, 0.5, 1.0, 1.5 and 2.0 g./100 cc. and the relative viscosities of the solutions were determined with the Ostwald's viscometer at 25°±0.01°C. The number of carboxyl groups in the polymers was determined by the alkali titration in benzyl alcohol with phenolphthalein as an indicator, and the number of amino groups was determined by potentiometric titration, in phenol-alcohol solvent (1.7/1.0 in volume)[7].

Table I shows relative viscosities $\eta_{rel}$ of the polymer solutions at various concentrations in 98% sulfuric acid. The number of amino groups in the polymers is about twice as great as that of carboxyl groups, as shown in Table II. Although there have been many discussions on the structure[6,8-12] of the end groups of the alkali-catalyzed poly-ε-capramide, it is assumed that the polymerization degree calculated from the number of amino groups may be correct, since the number of carboxyl groups increases by washing the polymer with water, while that of amino groups does not increase[6,11].

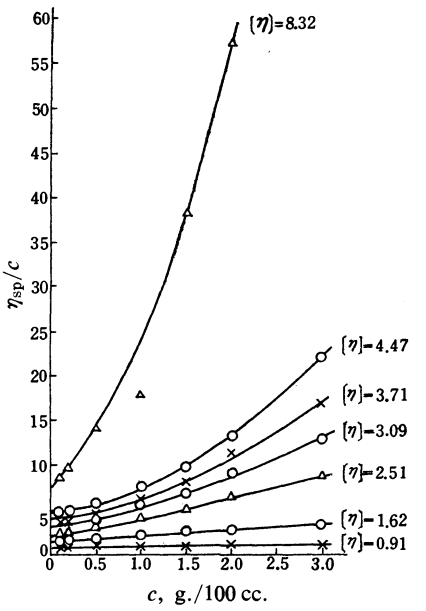



Fig. 1. The relation between $\eta_{sp}/c$ and $c$.

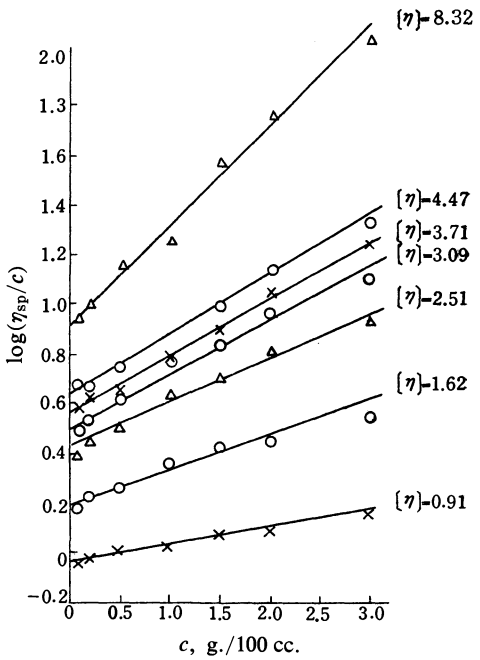



Fig. 2. The relation between $\log(\eta_{sp}/c)$ and $c$.

7) J. E. Waltz and G. B. Taylor, *Anal. Chem.*, **91**, 418 (1947).
8) D. Heikens, *Makromol. Chem.*, **18**, 62 (1956).
9) W. Griehl and S. Schaaf, ibid., **32**, 170 (1959).
10) J. Králíček and J. Šebenda, *J. Polymer Sci.*, **30**, 493 (1958).
11) S. Schaaf, *Faserforsch. u. Textiltech.*, **10**, 224 (1959).
12) A. Hamann, ibid., **9**, 351 (1958).

The relationships between the polymer concentration $c$ (g./100 cc.) in 98% sulfuric acid and $\eta_{sp}/c$ ($\eta_{sp}$ means specific viscosity) shift from a straight line as the polymerization degree increases as shown in Fig. 1. However, as shown in Fig. 2, a linear relation between log ($\eta_{sp}/c$) and $c$ is found and can be expressed as follows:

$$\log(\eta_{sp}/c) = K \cdot c + \log[\eta] \quad (1)$$

where $K$ is a constant and $[\eta]$ the intrinsic viscosity of the polymer, which is obtained by extrapolation of linear log ($\eta_{sp}/c$) vs. $c$ graphs to infinite dilution. The values of $[\eta]$ of the polymers are shown in Table I.

Plotting $K$ against log$[\eta]$, a straight line is obtained as shown in Fig. 3 and the following equation is obtained.

$$K = 0.33 \log[\eta] + 0.05 \quad (2)$$

From Eqs. 1 and 2, Eq. 3 can be derived.

$$\log(\eta_{sp}/c) = 0.05\,c + (0.33\,c + 1)\log[\eta] \quad (3)$$

Plotting $\eta_r$ ($\eta_{rel}$ at $c=1$) against $[\eta]$, a straight line is obtained as shown in Fig. 4, and Eq. 4 is obtained.

$$\eta_r = /2.2[\eta] \quad (4)$$

The relationship between log $\bar{P}_n$ and log $[\eta]$ is in a linear function as shown in Fig. 5, and Eq. 5 is obtained.

$$\bar{P}_{n\,NH_2} = 89[\eta] \quad (5)$$

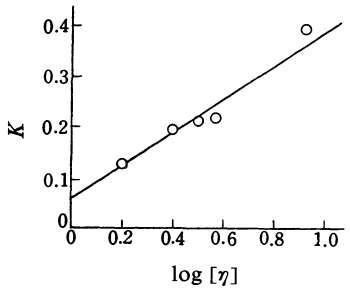



Fig. 3. The relation between $K$ and log $[\eta]$.

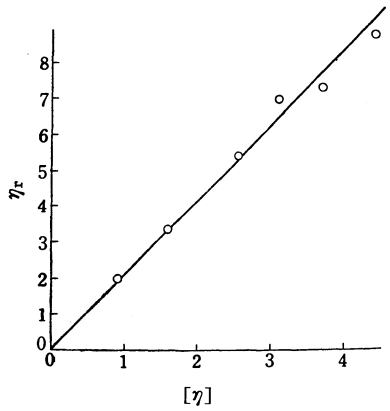



Fig. 4. The relation between $\eta_r$ and $[\eta]$.

From Eqs. 4 and 5, Eq. 6 can be derived.

$$\bar{P}_n = 40.5\,\eta_r \quad (6)$$

Fig. 6 shows the relationship between $\bar{P}_n$ and $\eta_r$ at $c=1$.

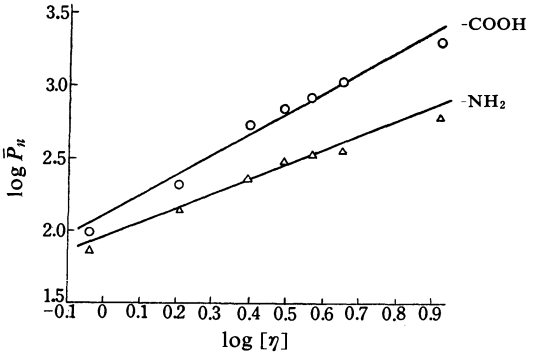



Fig. 5. The relation between log $\bar{P}_n$ and log $[\eta]$.

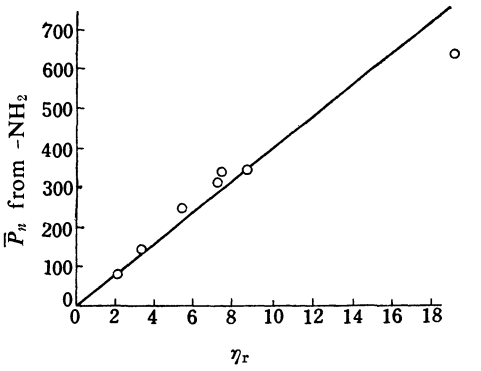



Fig. 6. The relation between $\bar{P}_n$ and $\eta_r$.

**Change in the Polymerization Degree of the Polymer.** — The alkali-catalyzed poly-ε-capramide, which had been washed with water, was preserved in a desiccator with phosphorus pentoxide in a dark place for about 2 years. At that stage, the solution viscosity of the polymers was measured. The polymerization degree of the polymer decreases markedly in comparison with that just after the polymerization and $\bar{P}_n$ becomes about 70, regardless of the initial $\bar{P}_n$.

## Discussion

Generally, it is recognized that the solution viscosity of high polymers can be expressed in the following equation proposed by Huggins,

$$\eta_{sp}/c = [\eta] + k'[\eta]^2 c \quad (8)$$

where $k'$ is approximately constant for a series of polymers in a give solvent. Matthes[1] has recognized that the solution viscosity of poly-ε-capramide in concentrated sulfuric acid is well expressed in Huggins' equation and the same results have been attained by Rybnikář[13].

13) F. Rybnikář, ibid., 9, 500 (1958).

TABLE III. CHANGE IN $\bar{P}_n$ OF THE ALKALI-CATALYZED POLY-ε-CAPRAMIDE

| $\bar{P}_n$ of the polymer just after the polymerization | $\bar{P}_n$ of the polymer after 2 years |
|---|---|
| 454 | 71 |
| 254 | 71 |
| 241 | 64 |
| 208 | 72 |
| 190 | 71 |

Dawydoff[14] has also reported that the relationships between $c$ and $\eta_{sp}/c$ or $\ln \eta_{sq}/c$ are in linear functions in the range of the concentrations of less than 0.1 g./100 cc.

Plotting $\eta_{sq}/c$ against $c$, a straight line is obtained for the alkali-catalyzed poly-ε-capramide of $[\eta] < 2.5$, while the shift from a straight line becomes greater in the polymers of $[\eta] > 2.5$. However, a linear relation between $\log (\eta_{sp}/c)$ and $c$ can be found for the polymers in the wide ranges of the polymerization degrees.

It is expected that the interactions among chain molecules occur strongly, as the polymerization degree of the polymer increases, and a simple equation between $\eta_{sp}/c$ and $c$ is not found. The relationship between $\bar{P}_n$ and $[\eta]$ is a simple equation as that derived by Matthes[1] for the polymer polymerized in the presence of water, but the value of the proportionality constant for the alkali-catalyzed polymer is smaller than that derived by Matthes. This is expected to be due to the difference in the molecular weight distribution.

The polymerization degree of the alkali-catalyzed polymer decreases markedly even at room temperature, as stated before, in spite of the fact that the polymers were preserved in a dry state in a dark place. As it is expected that no chemical or photochemical reactions occur in such moderate state, it is very interesting to ascertain whether the amide-interchange reactions would occur in poly-ε-capramide even at room temperature in solid phase, especially in that of a super-high degree of polymerization.

14) W. Dawdoff, ibid., 8, 267 (1957).

## Summary

The solution viscosity of poly-ε-capramide of a super-high degree of polymerization in 98% sulfuric acid has been investigated. A linear relation between $\log (\eta_{sp}/c)$ and $c$ (g./100 cc.) is found for the alkali-catalyzed polymers of $[\eta] > 2.5$, as expressed by the following equation.

$$\log (\eta_{sp}/c) = 0.05\, c + (0.33\, c + 1) \log [\eta]$$

The relationship between $\bar{P}_n$ and $[\eta]$ is expressed by the following equation.

$$\bar{P}_n = 89\, [\eta]$$

The alkali-catalyzed polymer of a super-high degree of polymerization degrades slowly at room temperature in solid phase.

The author wishes to express his gratitude to Dr. K. Hoshino and Dr. H. Kobayashi for their instruction and permission to publish these results. Thanks are also due to Mr. K. Noishiki, Head of the Nagoya Laboratory, and Mr. T. Takayanagi, Chief Research Chemist, for their helpful and discussion. He also thanks Messrs. M. Nakata and T. Ishikawa who collaborated with him in the experiments.

*Research Department*
*Toyo Rayon Co. Ltd.*
*Minato-ku, Nagoya*

# *Proton Magnetic Resonance of Borazole*[1)]

By Kazuo ITO, Haruyuki WATANABE and Masaji KUBO

(Received June 8, 1960)

The work described in this paper is part of a physicochemical investigation which has as its object the elucidation of the molecular structures and electronic states of borazole and its derivatives. Previous papers of this series have been concerned with the infrared absorptions of some borazole derivatives[2)], the dipole moments of borazole and its derivatives[3)] and the diamagnetic anisotropy of a borazole ring[4)]. The present paper presents the results of investigation on the proton magnetic resonance of borazole. The problem is of particular interest from the standpoint of both chemical shifts and splittings for the following reasons. In the first place, all the NMR spectra which have ever been recorded on compounds having hydrogen atoms attached to boron are outnumbered by the profusion of those on other types of compounds. Secondly, the nuclei of nitrogen $^{14}N$ as well as those of boron isotopes, $^{11}B$ and $^{10}B$, have an electric quadrupole moment capable of affecting through its spin-lattice relaxation the relative broadening of multiplet components. The $^{11}B$ magnetic resonance was also studied in order to facilitate assignments.

## Experimental

**Sample.** — B-Trichloroborazole was prepared by the same method as that described by Brown and Laubengayer[5)]. After being sublimed several times under reduced pressure, it was identified by its melting point 83.5~84.5°C, the value reported in the literature being 83.9~84.5°C [5)]. The infrared spectra[2)] showed absorption bands characteristic of a borazole ring. This compound was reduced to borazole by essentially the same method as that proposed by Schaeffer et al[6)]. differing in that $NaBH_4$ was used as a reducing agent in place of $LiBH_4$ and that triethylene glycol dimethyl ether rather than dibutyl ether was employed as a solvent[7)]. Triethylene glycol dimethyl ether having a boiling point quite different from that of borazole was more suitable than diethylene glycol dimethyl ether suggested by Schaeffer[8)]. Hence, 23.5 g. of sodium borohydride was dissolved in 120 cc. of triethylene glycol dimethyl ether in an atmosphere of dry nitrogen. To this solution, the suspension of 30 g. of B-trichloroborazole in 75 cc. of the same solvent was gradually added at room temperature. Stirring was continued for about 2 hr. After the reaction was over, the product was distilled under reduced pressure and was collected in a trap cooled with dry ice. The yield of crude borazole was about 10 g. Vacuum distillation was repeated several times before use.

**Apparatus and Experimental Procedure.** — The proton magnetic resonance spectrum was recorded at room temperature by means of a JNM-3 high-resolution NMR spectrometer of Japan Electron Optics Laboratory Company operating at 40 Mc./sec. Cyclohexane was used as an internal standard. Accordingly, corrections for the bulk magnetic susceptibility of the sample were not required. It was further confirmed that dilution with carbon tetrachloride did not affect the spectrum in an appreciable manner. The NMR absorption derivative spectrum of $^{11}B$ was also recorded with the same spectrometer operated at 12.6 Mc./sec.

## Results and Discussion

The proton magnetic resonance spectrum obtained is shown in Fig. 1, in which the absorption intensity is plotted against decreasing magnetic field strength. Chemical shifts defined by

$$\delta = 10^6(H_s - H_r)/H_r$$

are also protted along the abscissa. Here, $H_s$ denotes the applied magnetic field for the proton signal of the sample and $H_s$ is that of cyclohexane used as a standard. The signal of cyclohexane was identified by the increase in its intensity on further addition of the standard. Two peaks at $1.4_7$ and $-1.4_9$ were ascribed to spinning side bands, because they shifted depending on the spinning rate.

The spectrum is comprised of a triplet centered at $-4.0_5$ and less intense broad peaks at $2.1_2$, $-1.3_4$ and $-8.2_6$. The triplet was unequivocally assigned to the proton signal of

1) A part of the results presented here has been reported at the 13th Annual Meeting of the Chemical Society of Japan Tokyo, April 5, 1960. A preliminary report has been published in a short communication: K. Ito, H. Watanabe and M. Kubo, *J. Chem. Phys.*, **32**, 947 (1960).

2) H. Watanabe, M. Narisada, T. Nakagawa and M. Kubo, *Spectrochim. Acta*, **16**, 78 (1960). H. Watanabe, T. Totani, T. Nakagawa and M. Kubo, ibid., **16** (1960).

3) H. Watanabe and M. Kubo, *J. Am. Chem. Soc.*, **82**, 2428 (1960).

4) H. Watanabe, K. Ito and M. Kubo, ibid., **82**, 3294 (1960).

5) C. A. Brown and A. W. Laubengayer, ibid., **77**, 3699 (1955).

6) R. Schaeffer, M. Steindler, L. Hohnstedt, H. S. Smith, Jr., L. B. Eddy and H. I. Schlesinger, ibid., **76**, 3303 (1954).

7) L. Hohnstedt and D. T. Haworth, ibid., **82**, 89 (1960).

8) G. W. Schaeffer, private communication.

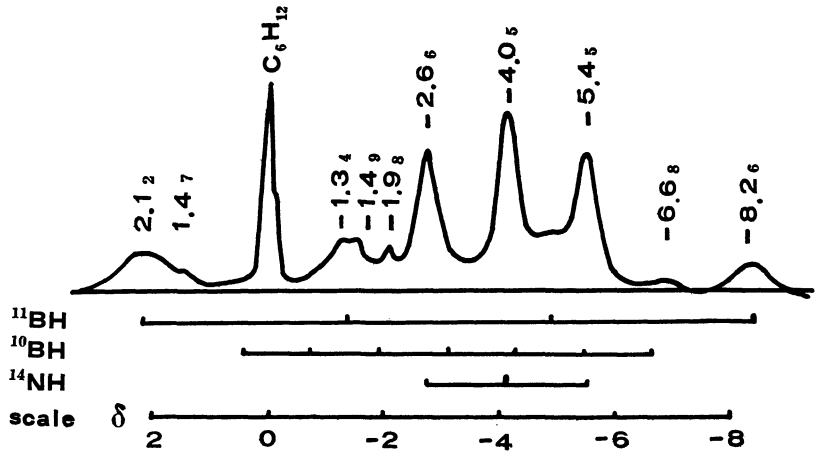



Fig. 1. Proton magnetic resonance spectrum of borazole. The numerical values of shifts are given for major absorption peaks.

$^{14}$NH with a spin coupling constant $J(^{14}NH) = 56$ cps, because the signal is expected to split into three equally spaced peaks owing to the $2I+1$ orientations of a $^{14}$N spin with $I=1$. The spin coupling constant is of the right order of magnitude, since the value for $^{14}NH_3$ is 46 cps[9]. In this triplet pattern, not all of the peaks have the same height, the central line being stronger than the two outer ones, which have the same intensity. Deviation from a simple 1 : 1 : 1 triplet, i. e., the partial collapse of spin multiplets can be ascribed to the presence of $^{14}$N nuclei having an electric quadrupole moment, which gives rise to spin-lattice relaxation in fluctuating electric field gradients. A similar pattern has been shown clearly by Ogg and Ray[9], who compared the proton spectra of anhydrous $^{14}NH_3$ and $^{15}NH_3$. An approximate quantitative theory of this collapse mechanism has been developed by Pople[10], who showed that the broadening of the outer components of the proton triplet spectrum should be three halves as great as that of the central component. Strictly speaking, the outer peaks of the triplet draw together as they broaden. Consequently, the separation between adjacent peaks does not correspond exactly to the spin coupling constant. However, the effect is presumed to be very small in the present case, in which the signals are fairly sharp.

Although the number of hydrogen atoms attached to boron in a borazole molecule is exactly the same as that of hydrogen atoms bonded to nitrogen, the proton signal of BH must be weak, because the abundance ratio of boron isotopes is $^{11}B : {}^{10}B = 81.17\% : 18.83\%$ and also because these isotopes have a greater nuclear spin than that of $^{14}$N, the abundance of which amounts to as much as 99.635%. Therefore, the proton signal of $^{11}$BH must split into four equally spaced peaks in accordance with the spin $I=3/2$ of $^{11}$B. The separation, $3.4_6$, between the two peaks at $2.1_2$ and $-1.3_4$ is equal to half the difference, $6.9_2$, between those at $-1.3_4$ and $-8.2_6$, suggesting the presence of another peak at $-4.8_0$, which, although masked by the $^{14}$NH triplet, appears as a hump between two peaks at $-4.0_5$ and $-5.4_5$ of the triplet. These four peaks complete the proton quartet of $^{11}$BH with $J(^{11}BH) = 138$ cps. This assignment is also consistent with the $^{11}$B NMR spectrum of the same sample. Fig. 2 reproduces the NMR absorption derivative spectrum of $^{11}$B in a borazole molecule. The curve is symmetric across a point, indicating

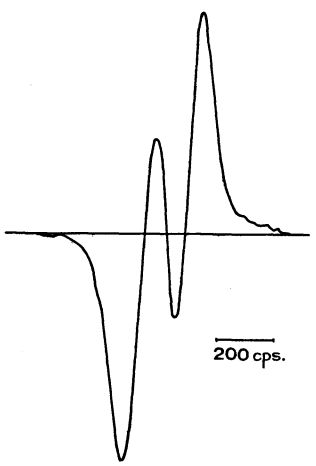



Fig. 2. The NMR absorption derivative spectrum of $^{11}$B of borazole.

9) R. A. Ogg, Jr., and J. D. Ray, *J. Chem. Phys.*, **26**, 1515 (1957).
10) J. A. Pople, *Mol. Phys.*, **1**, 168 (1958).

the presence of two lines of equal intensity separated by 140 cps in good agreement with 138 cps evaluated from the aforementioned proton magnetic resonance spectrum. Philips et al.[11] has carried out the $^{11}B$ magnetic resonance study of boron compounds and reported that $J(^{11}BH)$ was equal to 136 cps for borazole.

The three components of the proton quartet of $^{11}BH$ have practically the same peak height. Although the intensity of the fourth line, which overlaps with the $^{14}NH$ proton triplet, is difficult to estimate exactly, it is very likely that the peak height is the same as those of other members of the quartet. The theory of quadrupole relaxation has already been extended to cover the broadening of multiplet components for protons bonded to nuclei with spin greater than unity[10]. It is predicted that, for spin 3/2, all components of the proton 1 : 1 : 1 : 1 quartet should be broadened equally, instead of showing different peak heights as in the $^{14}NH$ proton triplet. The present results are in agreement with Pople's[10] prediction. A similar quartet pattern having equal spacings and equal peak heights has been shown most clearly for sodium borohydride, $NaBH_4$[12,13]. The partly resolved spectrum of the terminal protons of diborane[13] also appears to be consistent with the prediction.

There are still two weak peaks at $-1.9_8$ and $-6.6_8$ remaining unassigned. A possible interpretation is afforded by the proton signal of $^{10}BH$. If the peak at $-6.6_8$ is assumed to be the outermost low-field member of seven peaks predicted for the signal of protons bonded to $^{10}B$ with its nuclear spin equal to 3, the peak at $-1.9_8$ can be considered to be the third high-field member of the septet, because the center of the $^{11}BH$ quartet must coincide with the central line of the $^{10}BH$ septet. The adequacy of this interpretation is strongly supported by an agreement between the observed spin coupling constant $J(^{10}BH)=48$ cps and the calculated one, 46 cps, based on the observed $J(^{11}BH)=138$ cps and the gyromagnetic ratios $\gamma$ of boron isotopes.

$$\frac{J(^{10}BH)}{J(^{11}BH)}=\frac{\gamma(^{10}B)}{\gamma(^{11}B)}=\frac{4.575}{13.660}$$

where the numerical denominator and numerator are, respectively, the NMR frequencies of $^{11}B$ and $^{10}B$ in Mc. for a 10 kilogauss field. Three peaks between these two observed ones will escape detection owing to overlap with the strong $^{14}NH$ triplet. Two other peaks expected to appear at about $-0.7$ and $+0.5$ have not been observed.

The nuclei of $^{10}B$ have also an electric quadrupole moment. The broadening of multiplet components for protons bonded to nuclei with spin equal to 3 presents an interesting problem from the theoretical point of view. However, it is not feasible to discuss the broadening of the multiplet structure of the septet on the basis of the present investigation.

The proton chemical shifts, $-4.0_5$ and $-3.0_7$, of NH and BH in borazole, as referred to cyclohexane, lead to about $-0.7$ and $+0.3$, respectively, referred to water as a standard[14]. The former differs definitely from the $\delta$ values 4.3~4.5 for secondary alkyl amines[15], and is intermediate between about 2.0 for secondary aryl amines[15] and about $-2.1$ for pyrrole[14]. This is quite reasonable since nitrogen atoms in borazole assume $sp^2$ hybridization and $\pi$-electrons are presumed to migrate to some extent from nitrogen to boron[4,16]. The chemical shift and the spin coupling constant $J(^{11}BH)$ of a BH proton, $+0.3$ and 138 cps, in borazole are closer to those of a terminal proton, $+2.0$ and 125 cps, in diborane, respectively, than to those of a bridge proton, $+6.3$ and 43 cps, in the same molecule[15].

## Summary

The proton and $^{11}B$ magnetic resonances of borazole were recorded at room temperature. The proton magnetic resonance spectrum showed a $^{14}NH$ triplet, a $^{11}BH$ quartet and a part of $^{10}BH$ septet. The broadening of multiplet structure was discussed and the peak heights of the multiplet components were explained in terms of the quadrupole relaxation of nuclei bonded to hydrogen. The chemical shifts and the spin coupling constants were compared with those of related compounds.

The authors wish to thank Dr. T. Seki of Japan Electron Optics Laboratory Company for recording the high-resolution NMR spectra.

*Chemistry Department*
*Faculty of Science*
*Nagoya University*
*Chikusa, Nagoya*

11) W. D. Philips, H. C. Miller and E. L. Muetterties, *J. Am. Chem. Soc.*, **81**, 4496 (1959).
12) R. A. Ogg, Jr., *J. Chem. Phys.*, **22**, 1933 (1954).
13) J. N. Shoolery, *Discussions Faraday Soc.*, **19**, 215 (1955).
14) J. A. Pople, W. G. Schneider and H. J. Bernstein, "High-resolution Nuclear Magnetic Resonance", McGraw-Hill Book Company, Inc., New York (1959).
15) L. H. Meyer, A. Saika and H. S. Gutowsky, *J. Am. Chem. Soc.*, **75**, 4567 (1953).
16) B. L. Crawford, Jr., and J. T. Edsall, *J. Chem. Phys.*, **7**, 223 (1939). C. C. J. Roothaan and R. S. Mulliken, ibid., **16**, 118 (1948). C. W. Rector, G. W. Schaeffer and J. R. Platt, ibid., **17**, 460 (1949).

# *A Quantum-mechanical Approach to the Theory of Aromaticity*

By Kenichi FUKUI, Akira IMAMURA, Teijiro YONEZAWA and Chikayoshi NAGATA

(Received May 28, 1960)

The term "aromatic" originated from a characteristic odor which was possessed by certain substances isolated from various natural products such as benzoic acid (e. g. from gum benzoin), benzaldehyde (bitter-almond oil), cymene (carraway oil), toluene (tolu balsam) and the like. Hence this terminology essentially involved much ambiguousness since originally it was not based upon any scientific concept of classification. Recently the term "aromaticity" has attracted anew the attention of many organic chemists[1] since the discovery and the synthesis of multifarious non-benzenoid "aromatic" compounds such as tropolone, sydnone, ferrocene and numerous derivatives of these compounds[2].

A quantum-mechanical attack on the problem of aromaticity was for the first time delivered by Hueckel in regard to benzene, who presented the so-called $4n+2$ rule[3]. According to his theory, a conjugated compound has $4n+2$ $\pi$ electrons on its ring should exhibit an aromatic character. Although long years have passed since his report, only a very few attempts have been made to approach this problem theoretically. Recent conspicuous developments in the synthetic organic chemistry of non-benzenoid compounds, however, forced pressingly a re-examination of the significance of aromaticity. Craig investigated the compounds containing $d\pi$ electrons by simple LCAO MO treatment and defined two types of aromaticity according to the type of $d\pi$ orbital involved[4]. One of them obeys the $4n+2$ rule while the other is of a novel type in which the rule does not hold.

The researchers mentioned above, however, considered only the energy of $\pi$ electrons and neglected the internuclear repulsion energy. A more dexterous device should accordingly be desired for the elucidation of aromaticity.

The present authors attempted to investigate the aromaticity more minutely from the quantum-chemical point of view. Prior to entering into the main subject it is desirable to define the term "aromaticity". What is meant by aromaticity is of no clear-cut nature and is usually represented by the following characteristics of aromatic compounds.

Aromatic compounds have a plane structure.

Aromatic compounds show a remarkable stability.

Aromatic compounds have a characteristic reactivity.

Aromatic compounds show a peculiarity in such physical properties as ultraviolet absorption spectra[5], molecular refraction[6], magnetic anisotropy[7], and so forth.

Among these properties some have been already solved and explained satisfactorily, while others have yet been left untouched. The distinguished stability of aromatic compounds aroused the present authors' interest above all other things and is mainly discussed in the present paper.

## Energetical Consideration

Classical explanation of the stability of aromatic compounds had been based upon the strain theory, referring to the proposition that a six-membered ring is stable since it undergoes no strain force. However, by means of this theory we can not understand the reason why some five-membered rings such as furan are stable while others such as cyclopentadiene

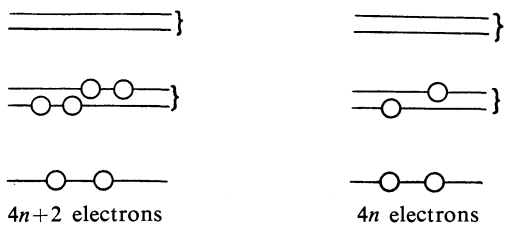



Fig. 1. $\pi$-electron configuration of $(4n+2)$- and $(4n)$-membered rings.

The brace } indicates that two levels are degenerate.

1) R. Robinson, *Tetrahedron*, 3, 323 (1958); H. C. Longuet-Higgins, *Proc. Chem. Soc.*, **1957**, 157.
2) W. Baker and W. D. Ollis, *Quart. Revs. (London)*, **11**, 15 (1957); A. W. Johnson, *J. Chem. Soc.*, **1954**, 1331; T. Nozoe, "Gendai Kagaku", Vol. 10, Iwanami, Tokyo (1957).
3) E. Hueckel, *Z. Physik*, **70**, 204 (1931).
4) D. P. Craig, *J. Chem. Soc.*, **1959**, 997.
5) R. A. Friedel and M. Orchin, "Ultraviolet Spectra of Aromatic Compounds", John Wiley & Sons, Inc., New York (1951); R. Pariser and P. G. Parr, *J. Chem. Phys.*, **21**, 466, 767 (1953).
6) M. Kotake, "Daiyûkikagaku", Vol. 1, Asakura, Tokyo (1958) p. 204..
7) L. Pauling, *J. Chem. Phys.*, **4**, 673 (1936); F. London, *J. de Physique*, **8**, 397 (1937).

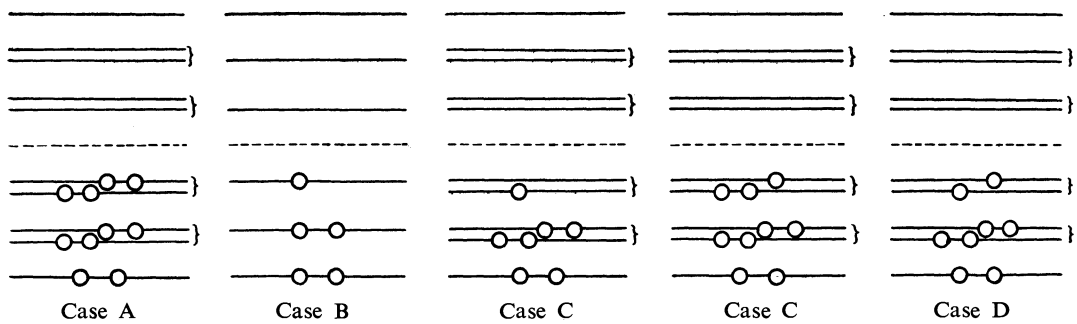



Fig. 2. Electronic configurations which are taken into account in the calculation.
The brace } indicates that two levels are degenerate.

are not. Moreover, recent experiments elucidated that some seven-membered conjugated ring compounds such as tropone and tropolone can exist in a stable form. These facts suggest that, in order to answer the question of aromatic stability, other factors than the strain force, e. g. the magnitude of total $\pi$ electronic energy, should be taken into consideration. For the purpose of attacking this problem, quantum mechanics must obviously be a powerful weapon. Hueckel's $4n+2$ rule was derived by simple LCAO MO treatment[3]. He showed that the electronic configuration of the compound having $4n+2$ electrons on its ring forms a set of closed shells in MO sense analogous to the atomic structure. In the case of $4n$ electrons the complete closed shell structure is impossible as is seen in Fig. 1.

In Hueckel's $4n+2$ rule, however, the effect of electron-electron repulsion and internuclear repulsion had not been taken into account. Accordingly, this rule is not capable of predicting the number of $\pi$ electrons which can exist and be stable on a given membered carbon ring. To overcome this difficulty, the $\pi$ electronic energy is obtained by the formulas utilized by Pople[8]. In the present method the internuclear and electron-electron repulsion energy are considered explicitly and the antisymmetrized product of Hueckel MO were used for the sake of simplicity. Therefore MO is written as

$$\phi_i=\sum_r C_{ir}\phi_r \tag{1}$$

where $\phi_i$ is the $i$th MO and $\phi_r$ represents the AO on the $r$th carbon atom. Electronic configurations which are taken into account are classified into four cases A, B, C and D and these cases are schematically shown in Fig. 2.

For case A Pople gave the total $\pi$ electronic energy including nuclear-nuclear repulsion as follows:

$$\varepsilon_\pi=\sum_r P_{rr}\left(U_{rr}+\frac{1}{4}P_{rr}\gamma_{rr}\right)+2\beta\sum_{r<s}^{*}P_{rs}+\sum_{r<s}\left\{(P_{rr}-1)(P_{ss}-1)-\frac{1}{2}(P_{rs})^2\right\}\gamma_{rs} \tag{2}$$

where $U_{rr}$ is a core matrix element, $\beta_{rs}$ is the resonance integral.

$$\gamma_{rs}=\int\phi_r^*(1)\phi_s^*(2)\frac{e^2}{r_{12}}\phi_r(1)\phi_s(2)\mathrm{d}v_1\mathrm{d}v_2$$

and

$$P_{rs}=2\sum_{i=1}^{n}C_{ir}C_{is} \tag{3}$$

Summation $\sum$ and $\sum^*$ should cover all the atoms and the nearest neighboring atoms, respectively. For the case of regular $n$-membered ring molecules, $U_{rr}$ and $\beta_{rs}$ are constant values represented by $U$ and $\beta$, respectively. In Eq. 2 the internuclear repulsion energy is included in the following form

$$\varepsilon'=\sum_{r<s}Z_rZ_s\gamma_{rs} \tag{4}$$

and $Z_r$ and $Z_s$ are assumed to be unity. For case B the total $\pi$-electronic energy of the non-degenerate system with odd electrons was obtained as follows[8]:

$$\varepsilon_\pi=\sum_r(P^0_{rr}U+P^\alpha_{rr}P^\beta_{rr}\gamma_{rr})+2\beta\sum_{r<s}^{*}P^0_{rs}+\sum_{r<s}\{(P^0_{rr}-1)(P^0_{ss}-1)-[(P^\alpha_{rs})^2+(P^\beta_{rs})^2]\}\gamma_{rs} \tag{5}$$

where

$$P^\alpha_{rs}=\sum_{i=1}^{n}C_{ir}C_{is},\quad P^\beta_{rs}=\sum_{i=1}^{n-1}C_{ir}C_{is}$$

and $$P^\alpha_{rs}=P^\beta_{rs}+P^\beta_{rs} \tag{6}$$

For case C the total $\pi$ electronic energy is obtained by only one electronic configuration for regular $n$-membered ring system, so that the formula for this case is equal to that of case B. For case D the wave functions are chosen as follows.

8) J. A. Pople, *Trans. Faraday Soc.*, **49**, 1375 (1953); A. Brickstock and J. A. Pople, ibid., **50**, 901 (1954).

TABLE I. THE DELOCALIZATION ENERGY OF FIVE-, SIX- AND SEVEN-MEMBERED RING SYSTEMS

| Number of carbon atoms on ring | Number of $\pi$ electrons | Energy of non-conjugated system, e.V. | Energy of conjugated system, e.V. | Difference e.V. |
|---|---|---|---|---|
| 5 | 5 | 5U | 5U− 9.80 | 9.80 |
| | 6 | 6U+10.53 | 6U− 0.48 | 11.01 |
| | 7 | 7U+26.78 | 7U+17.23 | 9.55 |
| 6 | 4 | 4U+ 4.90 | 4U− 6.30 | 11.20 |
| | 5 | 5U | 5U−13.50 | 13.50 |
| | 6 | 6U | 6U−13.88 | 13.88 |
| | 7 | 7U+10.53 | 7U− 2.97 | 13.50 |
| | 8 | 8U+25.96 | 8U+14.76 | 11.20 |
| 7 | 5 | 5U+ 4.38 | 5U−10.17 | 14.55 |
| | 6 | 6U | 6U−17.32 | 17.32 |
| | 7 | 7U | 7U−14.17 | 14.17 |

$$\chi=\frac{1}{\sqrt{2}}\frac{1}{\sqrt{2n!}}\{[\phi_1\bar{\phi}_1\cdots\cdots\phi_n\bar{\phi}_{-n}]-[\phi_1\bar{\phi}_1\cdots\cdots\bar{\phi}_n\phi_{-n}]\} \quad (7)$$

where $\phi_n$ and $\phi_{-n}$ are the molecular orbitals for degenerate levels. In this case we get the total $\pi$ electronic energy by the same method that Pople used as follows:

$$\begin{aligned}\varepsilon_\pi=&\sum_r P_{rr}U+\frac{1}{4}\sum_r\{(P_{rr})^2-(C_{nr})^4-(C_{-nr})^4\\&+6(C_{nr})^2(C_{-nr})^2\}\gamma_{rr}+2\beta\sum_{r<s}{}^{*}P_{rs}\\&+\sum_{r<s}\{(P_{rr}-1)(P_{ss}-1)-\frac{1}{2}(P_{rs})^2\\&-\frac{1}{2}(C_{nr}C_{ns})^2-\frac{1}{2}(C_{-nr}C_{-ns})^2\\&+3(C_{nr}C_{ns})(C_{-nr}C_{-ns})\}\gamma_{rs}\end{aligned} \quad (8)$$

where

$$P_{rs}=2\sum_{j=1}^{n-1}C_{jr}C_{js}+C_{nr}C_{ns}+C_{-nr}C_{-ns} \quad (9)$$

By using these formulas the total $\pi$ electronic energy including internuclear repulsion energy is obtained.

Before performance of calculation it is necessary to consider what kind of quantity can be the measure for aromaticity. In many cases the resonance energy was adopted as the measure for aromaticity[9]. Recently, Craig tried to specify the aromatic character by its symmetry of molecular structures and spin functions[9]. This method, however, is inapplicable to the molecule which lacks sufficient symmetry. In this paper, we intend to compare the stability of the systems of regular $n$-membered ring having $m$ $\pi$ electrons. Since the calculation is restricted to $\pi$ electronic energy and the effect of $\sigma$ bond is neglected, the comparison of stability should be confined to the ring system with the same number of members and variable number of $\pi$ electrons. We, therefore, adopt the energy difference between conjugated regular $n$-membered ring molecule and non-conjugated system that has electrons on each atom as the measure for aromaticity as is shown in Eq. 10.

$$\Delta E=\mathcal{E}\left[\text{⬡}\ \text{or}\ \overset{+}{\text{⬡}}\ \text{or}\ \overset{-}{\text{⬡}}\right]-\mathcal{E}\left[\text{⬡}\right] \quad (10)$$

This measure is nothing but the delocalization energy of the system. The energy of the neutral or ionic non-conjugated system can be given as follows where electron-electron and internuclear repulsions and electron-nuclear attraction are taken into account.

$$\begin{aligned}\varepsilon_{\text{non-conjugated}}=&\sum_{\mu>\nu}(Z_\mu-2)^2\gamma_{\mu\nu}+\sum_{r>s}(Z_r-1)^2\gamma_{rs}\\&+\sum_{r\mu}(Z_\mu-2)(Z_r-1)\gamma_{r\mu}+\sum_{\alpha>\beta}Z_\alpha{}^2\gamma_{\alpha\beta}\\&+\sum_{\alpha,\,r}Z_\alpha(Z_r-1)\gamma_{\alpha r}+\sum_\alpha\gamma_{\alpha\alpha}+nU\end{aligned} \quad (11)$$

where $r$ and $s$ denote the carbon atom which has only one electron on it, $\alpha$ and $\beta$ two electrons, and $\mu$ and $\nu$ none, respectively, and $n$ is the number of $\pi$ electrons. For the sake of simplicity the values of $Z_r$, $Z_\alpha$ and $Z_\mu$ are assumed to be unity. Thus the calculated value is the measure of the stability by delocalization of non-conjugated electrons. Therefore the greater the magnitude of delocalization energy is, the more stable the molecule is. Accordingly this measure is expected to be a good index for aromaticity, since the stability of the molecule is the essential character for aromatic compounds. The atomic integral used in calculation is gained by the semiempirical formulas adopted by Pariser and Parr[5]. For brevity, all the C–C bond distances are assumed to be 1.39 Å referring to that of benzene. Thus

9) D. Ginsburg, "Non-benzenoid Aromatic Compounds", Interscience Publishers Inc., New York (1959).

the obtained results of the delocalization energy are listed in Table I.

As is shown in Table I, infive-, six- and seven-membered ring systems the molecule is most stable when it has six $\pi$ electrons on its ring. In a five-membered ring system this result corresponds to the fact that the five-membered ring molecule with six $\pi$ electrons such as furan, sydnone exists in stable state. Moreover in the seven-membered ring system the stability of tropone and tropolone corresponds to this result. Accordingly, we can explain and extend Hueckel's $4n+2$ rule on the different physical grounds from Hueckel's and combine the rule with the fact that some five- and seven-membered ring molecules with six $\pi$ electrons are stable.

In this connection, it may be worth while to add that another approximate method will contribute to the illustration of $4n+2$ rule. This is the method originally presented by Peter[10] in which the resonance energy is approximately obtained by the perturbation method. The wave function of linear polyenes is utilized as a zero order wave function. The intramolecular bonding between the atoms $r$ and $s$, as is indicated in Fig. 3, is regarded as the perturbation and the stabilization energy due to this bonding is obtained. Result of simple LCAO MO calculation is

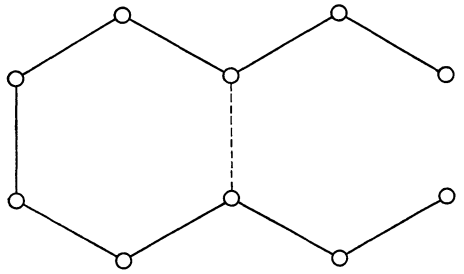


Fig. 3. Scheme for the perturbation method.
Dotted line indicates the new bonding engendered.
Circle and line represent the carbon atom and the C-C bond constructing the linear polyene.

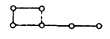
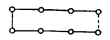
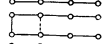
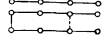
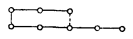
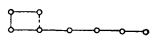
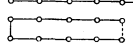
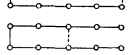
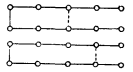
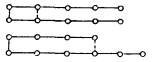
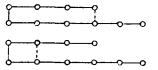
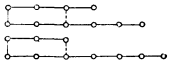
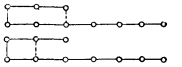
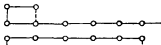
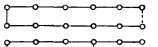
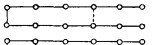
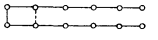
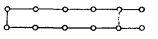
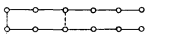
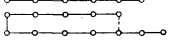
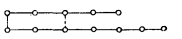
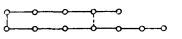
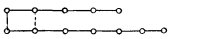
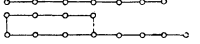
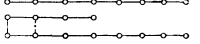
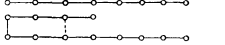
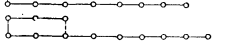
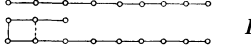
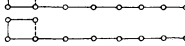
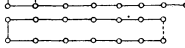
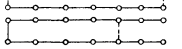
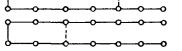
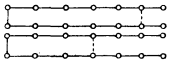
$$\delta\varepsilon = 2P_{rs}\delta\beta_{rs} + \Pi_{rs,rs}(\delta\beta_{rs})^2 + \cdots\cdots \qquad (12)$$

where $\delta\varepsilon$ is the stabilization energy, $P_{rs}$ and $\Pi_{rs,rs}$ are the order of imaginary bond between the atoms $r$ and $s$ and the selfpolarizability of the imaginary bond $r-s$, respectively, each being of the original polyene, and $\delta\beta_{rs}$ denotes the resonance integral of the bond $r-s$.

A glance at Eq. 4 makes it comprehensible that the magnitude of the stabilization energy predominantly depends on the bond order $P_{rs}$. Peter obtained the resonance energy of various

10) D. Peter, *J. Chem. Soc.*, **1958**, 1023.

TABLE II. THE VALUE OF BOND ORDER OF 4-, 6-, 8-, 10-, 12- AND 14-MEMBERED POLYENES

| $n$ | Type of bond formation | Bond order $P_{rs}$ | Number of canonical structure |
|---|---|---|---|
| 4 |  | $P_{1.4} = -0.4473$ | 2 |
| 6 |  | $P_{1.6} = 0.3019$ | 2 |
| |  | $P_{2.5} = -0.0866$ | 1 |
| |  | $P_{1.4} = -0.3874$ | 2 |
| 8 |  | $P_{1.8} = -0.2293$ | 2 |
| |  | $P_{2.7} = -0.3333$ | 2 |
| |  | $P_{3.6} = 0.0340$ | 1 |
| |  | $P_{1.6} = 0.2632$ | 2 |
| |  | $P_{1.4} = -0.3673$ | 2 |
| 10 |  | $P_{1.10} = 0.1855$ | 2 |
| |  | $P_{3.8} = 0.2297$ | 2 |
| |  | $P_{2.9} = -0.0170$ | 1 |
| |  | $P_{4.7} = -0.1278$ | 1 |
| |  | $P_{1.8} = -0.2028$ | 2 |
| |  | $P_{3.6} = -0.2293$ | 2 |
| |  | $P_{2.7} = 0.0440$ | 1 |
| |  | $P_{1.6} = 0.2469$ | 2 |
| |  | $P_{2.5} = -0.1107$ | 1 |
| |  | $P_{1.4} = -0.3576$ | 2 |
| 12 |  | $P_{1.12} = -0.1562$ | 2 |
| |  | $P_{3.10} = -0.1798$ | 2 |
| |  | $P_{5.8} = -0.2938$ | 2 |
| |  | $P_{2.11} = 0.0100$ | 1 |
| |  | $P_{4.9} = 0.0586$ | 1 |
| |  | $P_{1.10} = 0.1660$ | 2 |
| |  | $P_{3.8} = 0.2146$ | 2 |
| |  | $P_{2.9} = -0.0234$ | 1 |
| |  | $P_{4.7} = -0.1377$ | 1 |
| |  | $P_{1.8} = -0.1896$ | 2 |
| |  | $P_{3.6} = -0.3038$ | 2 |
| |  | $P_{2.7} = 0.0485$ | 2 |
| |  | $P_{1.6} = 0.2382$ | 2 |
| |  | $P_{2.5} = -0.1142$ | 1 |
| |  | $P_{1.4} = -0.3523$ | 2 |
| 14 |  | $P_{1.14} = 0.1348$ | 2 |
| |  | $P_{3.12} = 0.1491$ | 2 |
| |  | $P_{5.10} = 0.2000$ | 2 |
| |  | $P_{2.13} = -0.0063$ | 1 |
| |  | $P_{4.11} = -0.0330$ | 1 |
| |  | $P_{6.9} = -0.1491$ | 1 |

Circle written on the line represents the carbon atom which is a member of linear polyene
Dotted line indicates the new bond to be formed.

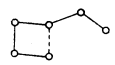
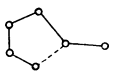
compounds by applying this method and the $4n+2$ rule generally, that is, the molecule in the case that the bond formation makes $4n+2$ ring has the largest resonance energy and therefore more stable than that in the case of $4n$ ring.

If we assume that internuclear repulsion energy stated above does not vary so much according to its geometrical structure, so far as the number of the atoms constituting a molecule does not change, the change of total energy of a molecule may approximately be discussed with an aid of Eq. 4. In many cases that the number of carbon atoms constituting the linear polyene is altered, the value of the bond order was calculated between several carbon-carbon atoms in simple LCAO MO treatment.

The result of calculation is collected in Table II for the cases of four, six, eight, ten, twelve and fourteen carbon atoms. Investigation of this table leads to the conclusion that in a polyene molecule the addition of a bond accompanied with the formation of a $4n+2$ ring stabilizes the molecule, while with the formation of a $4n$ ring it becomes unstable. It may be of interest to examine Table II more carefully to find that in the case of the bond formation with a $4n+2$ ring the corresponding value of bond order increases with the number of describable canonical structures which have alternate single and double bonds, while in $4n$ ring formation the relation is reversed. Hence the number of canonical structures can be a measure for the stability of a $4n+2$ ring molecule but no longer so for $4n$ ring molecules.

The way of estimating the stabilization energy mentioned above can be replaced by the calculation of conjugation energy per electron in perturbed molecule with simple LCAO MO treatment. The relation between these two methods is shown in Table III, in which a good parallelism is seen.

Table III. The parallelism between bond order and conjugation energy

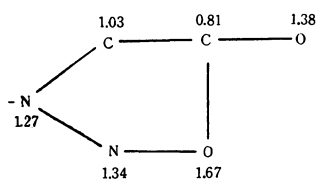
| Molecule | Conjugation energy per electron, $\beta$ | Bond order $P_{rs}$ |
|---|---|---|
|  | 1.100 | −0.3874 |
|  | 1.148 | −0.0866 |
|  | 1.165 | 0.0000 |
|  | 1.244 | 0.0000 |
|  | 1.333 | 0.3019 |

Dotted line indicates the bond formed between atom $r$ and $s$. $\beta$ in parenthesis is the resonance integral of carbon-carbon bond for hydrocarbon.

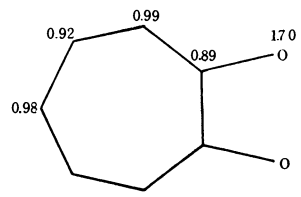
## Electron Distribution

According to the $4n+2$ rule, it is seen that $\pi$ electron distribution should be correlated closely with the stability of aromatic compounds and molecules with the ring containing $4n+2$ $\pi$ electrons may be more stable than those with $4n$ $\pi$ electrons. Therefore the aromatic compound should have the ring which has $4n+2$ $\pi$ electrons on it. With regard to this rule it is non-benzenoid aromatic compounds with substituents such as sydnone, tropone and so on that attract our interest more strongly.

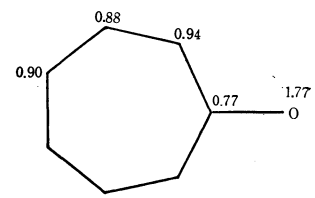
The sum of $\pi$ electron density on the whole ring was obtained in Fig. 4 in the cases of sydnone, tropone and tropolone. These results suggest that in any cases the aromatic compounds tend to form a ring involving $4n+2$ $\pi$ electrons. When the sum of $\pi$ electron density exceeds 6, the 6-membered ring repels electrons to the substituent, and when it is less than 6, the ring attracts electrons to the ring. Further calculation of the electron distribution in some hydrocarbons containing odd-membered ring is done. The result is shown in Table IV, which illustrates that the $(4n+3)$-membered ring repels electrons and $(4n+1)$-membered ring attracts them independently of the ring size. Thus in azulene the seven-membered ring is positively




Sydnone 6.12



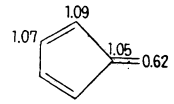
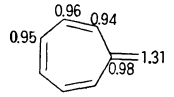
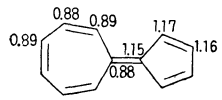
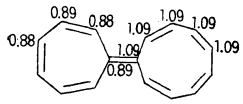
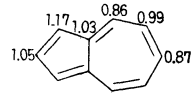

Tropolone 6.58




Tropone 6.21

Fig. 4. Total $\pi$ electron distribution of non-benzenoid aromatic compounds. The value written under the figure is the sum of the $\pi$ electron density of all member atoms constituting the ring.

TALBE IV. $\pi$ ELECTRON DISTRIBUTION OF ODD-MEMBERED RING

| | Sum of the total $\pi$ electron density for $(4n+1)$-membered ring | Formal charge of $(4n+1)$-membered ring | Sum of the total $\pi$ electron density for $(4n+3)$-membered ring | Formal charge of $(4n+3)$-membered ring |
|---|---|---|---|---|
|   | 5.37 | −0.37 | — | — |
|   | — | — | 6.68 | +0.32 |
|   | 5.81 | −0.81 | 6.19 | +0.81 |
|   | 9.81 | −0.81 | 6.19 | +0.81 |
|   | 5.45 | −0.45 | 6.63 | +0.37 |

The value written in figures is the total $\pi$ electron density at each position.

and the five-membered ring negatively charged representing the Fries' rule[11].

The same tendency can also be ascertained by such a perturbation treatmeat as is described above. A $(4n+1)$- or $(4n+3)$-membered ring can be formed as a result of the bond formation between appropriate two atoms in corresponding polyene molecule, as is shown in Fig. 5. This bond formation is considered as

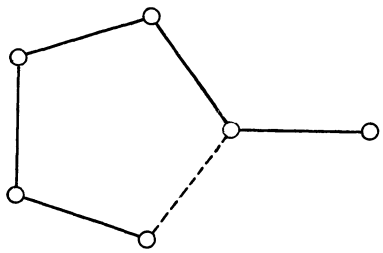


Fig. 5. Adopted model in perturbation method. Circle and line represent the carbon atom and the C-C bond constructing the linear polyene. Dotted line indicates the new bonding engendered.

a perturbation. The wave function for linear polyene is available as a zero order wave function. The total $\pi$ electron density at the $r$th carbon atom, $q_r$, is represented by

$$q_r = 1 + \Pi_{r,st}\delta\beta_{st} + \cdots\cdots \quad (13)$$

where $\delta\beta_{st}$ is the resonance integral of the new bond $s-t$ and $\Pi_{r,st}$ is the atom-bond polarizability of the atom $r$ and the bond $s\cdots\cdots t$ of the original polyene given by

$$\Pi_{r,st} = \frac{\partial q_r}{\partial \beta_{st}} = \sum_{j=1}^{m}\sum_{k=m+1}^{n} \frac{C_{rj}C_{rk}(C_{sj}C_{tk}+C_{tj}C_{sk})}{\varepsilon_j - \varepsilon_k} \quad (14)$$

TABLE V. THE VALUE OF ATOM-BOND POLARIZABILITY AND THE ENERGY DIFFERENCE BETWEEN THE HIGHEST OCCUPIED ORBITAL OF $(4n+1)$- AND $(4n+3)$-MEMBERED RINGS AND $U$

$(4n+1)$-membered ring

| $n$ | $\Pi_{1,2.4n+2}$ $(1/\beta)$ | $\varepsilon_f - U(\beta)$ |
|---|---|---|
| 1 | $\Pi_{1,2.6} = -0.4675$ | 0.6180 |
| 2 | $\Pi_{1,2.10} = -0.3148$ | 0.3474 |
| 3 | $\Pi_{1,2.14} = -0.2383$ | 0.2408 |
| 4 | $\Pi_{1,2.18} = -0.1920$ | 0.1848 |
| 5 | $\Pi_{1,2.22} = -0.1242$ | 0.1474 |

$(4n+3)$-membered ring

| $n$ | $\Pi_{1,2.4n+4}$ $(1/\beta)$ | $\varepsilon_f - U(\beta)$ |
|---|---|---|
| 1 | $\Pi_{1,2.8} = 0.2964$ | −1.2468 |
| 2 | $\Pi_{1,2.12} = 0.2709$ | −0.8310 |
| 3 | $\Pi_{1,2.16} = 0.2127$ | −0.6180 |
| 4 | $\Pi_{1,2.20} = 0.1750$ | −0.4914 |
| 5 | $\Pi_{1,2.24} = 0.1146$ | −0.4068 |

$\Pi_{r,st}$ represents atom-bond polarizability.

$\varepsilon_f$ is energy level of highest occupied orbitals of $(4n+1)$- and $(4n+3)$-membered ring.

$\alpha$ and $\beta$ are Coulomb integral of carbon atom and resonance integral of carbon-carbon bond in polyene, respectively.

11) K. Fries, *Ann. Chem.*, **516**, 248 (1935).

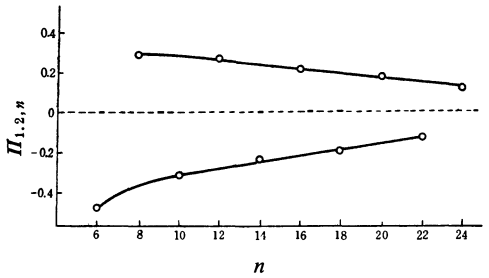



Fig. 6. Atom-bond polarizability and the number of members of linear polyene.

where $C_{rj}$ is the coefficient of the atomic orbital of the $r$th atom in the $j$th molecular orbital in the simple LCAO MO treatment, $\varepsilon_j$ is the energy of the $j$th molecular orbital, and subscript 1, 2, 3,……, $m$ and subscript $m+1$, $m+2$ ……, $n$ denote the occupied and unoccupied molecular orbitals, respectively. The calculated result of $\Pi_{r,st}$ is tabulated in Table V and is also plotted against the number of atoms, $n$, in Fig. 6. In the series of $(4n+3)$-membered rings the value of $\Pi_{r,st}$ is decreased with $n$ and the sum of $\pi$ electron density of the whole ring tends to approach to the limiting value, $4n+2$. A quite reverse tendency is seen in the series of $(4n+1)$-membered rings. That is, $\Pi_{r,st}$ is increased with $n$ and the sum of $\pi$ electron density of the whole ring approaches to the value of $4n+2$. Moreover, it is worth noticing that the absolute value of electronic charge transferred from side chain to ring or in the inverse direction decreases with $n$ in regard to both the $(4n+1)$- and $(4n+3)$-membered rings.

These tendencies may qualitatively be understood from an energetical point of view. The energy levels of $(4n+1)$- and $(4n+3)$-membered rings are given schematically in Fig. 7. In the case of five- and nine-membered rings the charge transfer may occur from side chain to ring and the molecule forms a "closed shell" in a MO sense in order to stabilize itself. On the other hand, in the case of seven-membered ring the direction of the charge transfer is converse.

These circumstances can also be elucidated analytically by using the integral formula for atom-bond polarizability of Coulson[12]. Integral formula for atom-bond polarizability is written as

$$\Pi_{r,st}=(-1)^{s+t}\frac{2}{\pi}\int_{-\infty}^{+\infty}\frac{\Delta_{rt}(iy)\,\Delta_{st}(iy)}{\{\Delta(iy)\}^2}\,dy \tag{15}$$

where $\Delta$ is the secular determinant for the corresponding linear polyene and $\Delta_{rt}$ denotes the secular determinant with row $r$ and column $t$ struck out. Consider a $(4n+1)$-membered ring with a side chain of one carbon atom formed from a $(4n+2)$-membered polyene by a bridging between the 2nd and the $(4n+2)$th atoms of the polyene. The atom-bond polarizability $\Pi_{1,2.4n+2}$ is given by

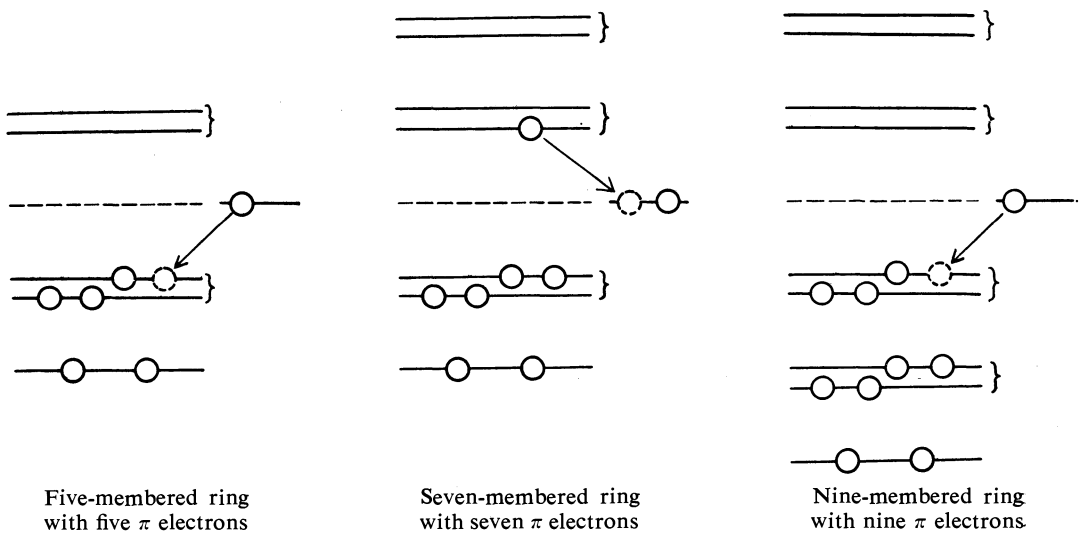
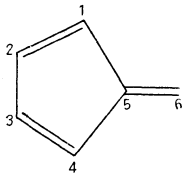
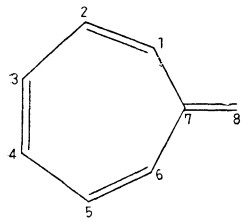



Fig. 7. Energy level of odd-membered ring.
The energy written aside represents that of the side-chain carbon.
The dotted line indicates the $\pi$ electrons transferred and an arrow shows the direction of the electron transfer.

12) C. A. Coulson and H. C. Longuet-Higgins, *Proc. Roy. Soc.*, **A191**, 39 (1947); **A192**, 16 (1947).

TABLE VI. REACTIVITY INDEXES FOR $(4n+1)$- AND $(4n+3)$-MEMBERED RINGS

| Compound | Position | $f_r$(N) | $S_r$(N) | $q_r$ |
|---|---|---|---|---|
|  | 1 | 0.246 | 0.906 | 1.092 |
| | 2 | 0.156 | 0.784 | 1.073 |
| | 5 | 0.073 | 0.598 | 1.047 |
| | 6 | 1.124 | 2.701 | 0.623 |
| **Compound** | **Position** | $f_r$(E) | $S_r$(E) | $q_r$ |
|  | 1 | 0.223 | 2.049 | 0.942 |
| | 2 | 0.100 | 1.071 | 0.962 |
| | 3 | 0.163 | 1.502 | 0.953 |
| | 7 | 0.046 | 0.756 | 0.976 |
| | 8 | 0.982 | 4.744 | 1.311 |

$f_r$, $S_r$ and $q_r$ are frontier electron density, superdelocalizability and total $\pi$-electron density at position $r$, respectively. (N) and (E) denote the reactivity indexes for nucleophilic and electrophilic reaction, respectively.

$$\Pi_{1,2\cdot 4n+2}=(-1)^{2+4n+2}\frac{2}{\pi}\times\int_{-\infty}^{+\infty}\frac{\Delta_{1,2}(iy)\Delta_{1,4n+2}(iy)}{\{\Delta^{(4n+2)}(iy)\}^2}\,dy \tag{16}$$

Following relations are easily proved[12]

$$\Delta_{1,4n+2}(iy)=1,\quad \Delta_{1,2}(iy)=\Delta^{(4n)}(iy)>0$$

and

$$\Delta^{(4n+2)}(iy)<0 \tag{17}$$

where $\Delta^{(4n)}$ and $\Delta^{(4n+2)}$ denote the secular determinants for $(4n)$- and $(4n+2)$-membered polyene, respectively. From Eqs. 13 and 16 with the aid of Eq. 17 it follows that

$$\Pi_{1,2\cdot 4n+2}>0 \quad \text{and} \quad q_1=1+\Pi_{1,2\cdot 4n+2}\delta\beta<1. \tag{18}$$

Hence the total density at the atom of side chain is less than unity, since $\delta\beta$ is negative. In the case of $(4n+3)$-membered ring originated from a $(4n+4)$-membered polyene the following inequalities are obtained in a similar manner.

$$\Pi_{1,2\cdot 4n}<0 \quad \text{and} \quad q_1=1+\Pi_{1,2\cdot 4n}\delta\beta>1 \tag{19}$$

Thus the total density becomes larger than unity.

Moreover, a close relation is observed between the atom-bond polarizability of a polyene and the highest occupied levels of $(4n+1)$- and $(4n+3)$-membered rings formed from the polyene. Table V illustrates this relation with regard to the cases of $(4n+1)$-membered ring formed from $(4n+2)$-membered polyene and $(4n+3)$-membered ring formed from a $(4n+4)$-membered polyene. In the table it is clearly observed that the lower the highest occupied level of $(4n+1)$-membered ring is, ····· and also the higher the highest occupied level of $(4n+3)$-membered ring is, the larger the amount of charge transferred from ring to side chain is. This result also coincides with the fact that the absolute value of the charge transferred decreases with $n$.

Thus a ring in the molecule has a tendency to approach to a $4n+2$ electron ring by the charge transfer to stabilize the molecule. The position to be attacked by a reagent was predicted for azulene in the paper symposium on aromatic character[13]. The attack of reagent was supposed to occur so as to make the ring possess $4n+2$ electrons by the process of reaction. Similarly, from the consideration stated above, it is predicted that the molecule containing a $(4n+1)$-membered ring and a side chain attached to it such as fulvene may be apt to react with a nucleophilic reagent at the side chain carbon. Inversely, in the case of $(4n+3)$-membered ring, an electrophilic reagent is inclined to attack the side chain carbon. Therefore, $4n+2$ rule can be said to govern the orientation of chemical reaction. Further, this rule also suggests a guiding principle in the syntheses of new aromatic compounds. Namely, we should choose an appropriate substituent attached to the ring that makes the ring possess $4n+2$ electrons. If a molecule

13) D. H. Reid, *Tetrahedron*, 3, 339 (1958).

has excessive electrons on its ring, the substituent to be chosen is electron-attracting, and if it has insufficient electrons, an electron-repelling substituent should be introduced to stabilize it.

This has also been supported by several quantum-mechanical theories of chemical reactivity such as the static method[12] and the frontier electron theory[14]. The reactivity indexes used in these theories have been calculated and tabulated in Table VI, showing that the above-mentioned prediction is correct.

*Faculty of Engineering*
*Kyoto University*
*Sakyo-ku, Kyoto*

14) K. Fukui, T. Yonezawa and C. Nagata, *J. Chem. Phys.*, **26**, 831 (1957); **27**, 1247 (1957).

# *Intermediate Compounds in the Catalytic Reduction of Aromatic Nitro Compounds with Raney Nickel Catalyst*[1)]

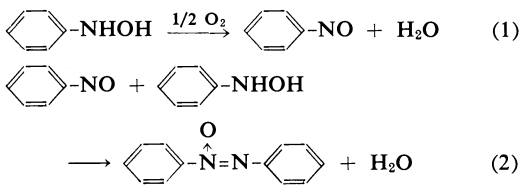
By Akira SUGIMORI*

(Received June 21, 1960)

There have been some studies on the intermediate compounds in the catalytic reduction of nitro compounds with nickel catalysts. Scholnik, Reasenberg and Smith[2)] reported that in the catalytic reduction of sodium *p*-nitrobenzoate with platinized Raney nickel hydrogen uptake stopped when 2 mol. of hydrogen was consumed (3 mol. of hydrogen is required for the complete reduction of a nitro compound to the corresponding primary amine). This would suggest the existence of an intermediate, but they found only the nitro compound and the *p*-aminobenzoate in the reduction product. Shmonina and Sokolski[3)] reported that nitrosobenzene was formed as an intermediate in the catalytic reduction of nitrobenzene with Raney nickel.

The present author studied the partial reduction of aromatic nitro compounds with neutral Raney nickel. Contrary to the above reports, phenylhydroxylamine derivatives were identified as intermediates.

Nitrobenzene (0.01 mol.) was reduced in ethanol solution at 25°C under ordinary pressure with Raney nickel prepared by treating 1.00 g. of nickel-aluminum alloy (Ni, 40%) with 5 ml. of 20% aqueous sodium hydroxide at 50°C and by washing 10 times with cold water and twice with 20 ml. of ethanol. Shaking was stopped when 0.02 mol. of hydrogen was consumed, the catalyst was filtered off, and the filtrate was poured into 300 ml. of ice water. Light white crystals of phenylhydroxylamine were obtained and they were recrystallized from petroleum ether. The melting point was 76~78°C. Found: C, 66.20; H, 6.73. Calcd. for $C_6H_7ON$: C, 66.03; H, 6.47%. This unstable intermediate was easily converted into azoxybenzene on exposure to air according to the following equations:



(1)



(2)

Therefore, the yield of phenylhydroxylamine was calculated from that of azoxybenzene.

In the same way, the partial reduction of *p*-nitroanisole and of ethyl *p*-nitrobenzoate was carried out and the yields of hydroxylamines and amines were determined. The results are shown in Table I. Nitrobenzene and ethyl *p*-nitrobenzoate gave more hydroxylamines than *p*-nitroanisole.

This agrees with the analysis of the curves

TABLE I. THE PRODUCTS OF PARTIAL REDUCTION

| Compound reduced | Yield of hydroxylamine, % | Yield of amine, % |
|---|---|---|
| Nitrobenzene | 77 | 0 |
| Ethyl *p*-nitrobenzoate | 60 | 0 |
| *p*-Nitroanisole | 22 | 40 |

* Present address; Division of Radiation Applications, Japan Atomic Energy Research Institute, Ibaraki-ken.

1) Cf. H. Debus and J. C. Jungers, *Bull. soc. chim. France*, **1959**, 785.

2) S. Scholnik, J. R. Reasenberg, E. Lieber and G. Smith, *J. Am. Chem. Soc.*, **63**, 1192 (1941); J. R. Reasenberg, E. Lieber and G. Smith, ibid., **61**, 384 (1939).

3) V. P. Shmonina and D. V. Sokolski, *Zhur. Obshchei Khim. S. S. S. R.*, **26**, 1759 (1956).

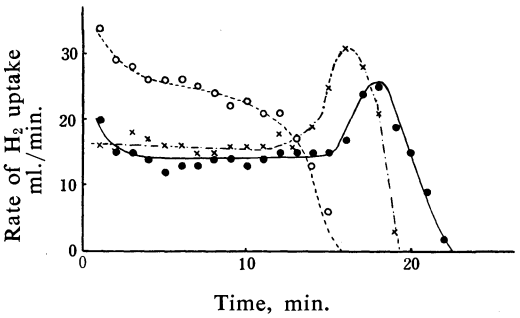



Fig. 1. Rate of Hydrogen uptake.
× Nitrobenzene.
○ *p*-Nitroanisole.
● Ethyl *p*-nitrobenzoate.

of the hydrogen consumption rates in the complete reduction to amines. As is shown in Fig. 1, the reduction rate of *p*-nitroanisole is monotonously decreasing, whereas those of nitrobenzene and ethyl *p*-nitrobenzoate have a remarkable increase towards the end of the reaction. It is likely that this increase in the rate takes place when the hydroxylamines are reduced to the amines. The fact that the hydroxylamines which have greater reduction rates than the parent nitro compounds were isolated as the intermediates in the partial reduction, can be understood from the difference in the affinities of the nitro compounds and hydroxylamines to the nickel catalyst. The nitro compounds with stronger affinities repel the hydroxylamines from the catalyst surface. And it can be said that the affinity difference is greater between nitrobenzene and phenylhydroxylamine and between ethyl *p*-nitrobenzoate (with an electron attracting group) and the corresponding hydroxylamine than between *p*-nitroanisole (with an electron repelling group) and its hydroxylamine. This agrees with the result[4] of the catalytic reduction of nitro compounds with a platinum catalyst.

Therefore, the following sequence of processes is presented:

$$ArNO_2 + Ni \longrightarrow ArNO_2\text{-}Ni \quad (3)$$

$$ArNO_2\text{-}Ni + 2H_2 \longrightarrow ArNHOH\text{-}Ni + H_2O \quad (4)$$

$$ArNHOH\text{-}Ni \begin{cases} \xrightarrow{H_2} ArNH_2 + Ni + H_2O & (5) \\ \xrightarrow{ArNO_2} ArNO_2\text{-}Ni + ArNHOH & (5') \end{cases}$$

$$ArNHOH + Ni \longrightarrow ArNHOH\text{-}Ni \quad (6)$$

$$ArNHOH\text{-}Ni \xrightarrow{H_2} ArNH_2 + Ni + H_2O \quad (7)$$

where Ni means the active center of the nickel catalyst.

The author wishes to express his hearty thanks to Professor Y. Urushibara for his kind guidance and encouragement throughout this work. The author is also very grateful to Dr. M. Kobayashi and Dr. S. Nishimura for their kind discussion.

*Department of Chemistry*
*Faculty of Science*
*The University of Tokyo*
*Hongo, Tokyo*

4) G. Cusmano, *Ann. chim. applicata*, **12**, 123 (1919), *Chem. Abstr.*, **14**, 1314 (1920).

# *Intramolecular Interaction between Hydroxyl Group and π-Electrons. X*[1]*. Tertiary Alcohols Related to Phenethyl Alcohol and 3-Buten-1-ol**

By Michinori Ōki and Hiizu Iwamura

(Received June 16, 1960)

It has been shown in the previous papers[2] that the intramolecular interaction between the hydroxyl group and π-electrons in ω-phenylalkanols and ω-hydroxy-1-alkenes is operative up to phenethyl alcohol and 3-buten-1-ol, respectively. On the other hand, the accumulated data in this laboratory show that there are some alcohols within the above limitation which do not possess the internal interaction, such as 3-cyclohexen-1-ol, and others which have unexpectedly strong O–H stretching absorption ($\nu_{O-H}$) due to the interacting form[3]. The dependence of the occurrence and the

1) Part IX: M. Ōki and H. Iwamura, This Bulletin, 33, 427 (1960).

* The summary of this work was presented at the 13th Annual Meeting of the Chemical Society of Japan, Tokyo, April, 1960.

2) M. Ōki and H. Iwamura, This Bulletin, 32, 567, 1135 (1959).

3) M. Ōki, H. Iwamura and T. Onoda, Unpublished work.

strength of the interaction on the conformation and the configuration of the molecule may inversely be taken advantage of for elucidation of some problems in the stereochemistry of complex organic compounds including natural products. From the point of the above purpose it will be of value at this stage of investigations to supply further fundamental knowledge relating the strength of the interaction to the conformation of the molecule.

While many authors[4] have recently observed the doublet character of $\nu_{O-H}$ of phenethyl alcohol derivatives and 3-buten-1-ol in the infrared absorption, it has been shown by the present authors[2], that their $\nu_{O-H}$ absorptions separate into three (Fig. 1), each being exemplified by the following conformational isomers in Fig. 2, in the case of phenethyl alcohol. The higher two bands are derived from the rotational isomerism about $C_\alpha$–O bond and observed even in saturated alcohols[5]. The highest absorption at about 3636 $cm^{-1}$ (I) has been assigned to the

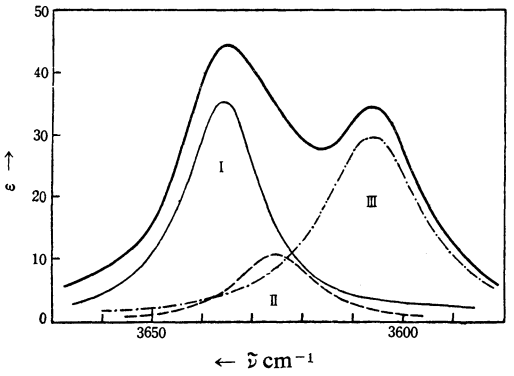



Fig. 1. $\nu_{O-H}$ absorption of phenethyl alcohol.

$\nu_{O-H}$ of the hydroxyl group with its hydrogen atom between two hydrogen atoms attached to the α-carbon atom, while the second at about 3627 $cm^{-1}$ (II) to the $\nu_{O-H}$ with hydroxyl hydrogen between a hydrogen and a carbon atom. The third band at the lowest region of the spectra (III) is of a different kind and has been assigned to $\nu_{O-H}$ of the hydroxyl group having intramolecular interaction with π-electrons of the benzene nucleus. In other words, II and III are the rotational isomers about $C_\alpha$–$C_\beta$ bond.

The triplet nature of the infrared absorption mentioned now, however, does not mean the apparent separation of the absorption curve but that the apparent curve can best be represented by an overlap of three symmetric absorption curves of the type of the Lorentz function[6]. Then nine parameters; $a_i$, $b_i$ and $\nu_i$ ($i=1$, 2 and 3), must be determined in this case and the procedure of the division of the apparent curve is troublesome, whether it is the trial and error method[2] or the least squares method[1]. In the previous paper[1], this difficulty was mentioned and overcome by taking advantage of a tertiary alcohol which shows only doublet $\nu_{O-H}$. The energy of the interaction between an alcoholic hydroxyl group and π-electrons of a benzene nucleus in benzyldimethylcarbinol was thus determined. In the present paper the measurement is extended to the interaction between an alcoholic hydroxyl group and π-electrons of ethylenic double bond in allyldimethylcarbinol. The effect of rotational degrees of freedom on the number of the interacting forms of the molecule and consequently on the apparent $\nu_{O-H}$ curve is also discussed.

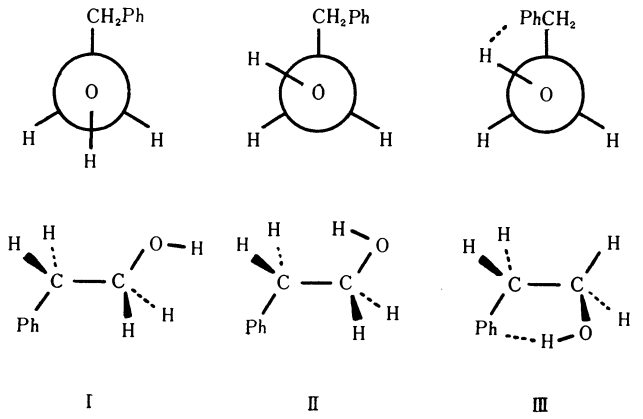



Fig. 2.

4) D. S. Trifan, J. L. Weinmann and L. P. Kuhn, *J. Am. Chem. Soc.*, **79**, 6566 (1957); A. W. Baker and A. T. Shulgin, ibid., **80**, 5358 (1958); I. M. Goldman and R. O. Crisler, *J. Org. Chem.*, **23**, 751 (1958).

5) M. Ōki and H. Iwamura, This Bulletin, **32**, 950 (1959).

6) D. A. Ramsay, *J. Am. Chem. Soc.*, **74**, 72 (1952).

## Experimental

**Measurement and Calculation.**—Measurement of the $\nu_{O-H}$ absorption and the calculation of the band properties and the energy of the interaction were carried out as described previously[1,7], for doublet absorption, Eq. 1 being assumed and six parameters determined by means of the least squares method.

$$D(\nu)=\frac{a_i}{(\nu-\nu_i)^2+b_i^2}+\frac{a_f}{(\nu-\nu_f)^2+b_f^2} \quad (1)$$

**Materials.**—Benzyldimethylcarbinol and allyldimethylcarbinol were prepared by action of acetone on benzyl- and allylmagnesium chlorides, respectively, and their physical constants were as follows: benzyldimethylcarbinol b.p. 70°C/3mmHg, $n_D^{25}$ 1.5158. Found: C, 80.10; H, 9.14. Calcd. for $C_{10}H_{14}O$: C, 79.95; H, 9.39%. (lit.[8], b. p. 59~60°C/1.5 mmHg, $n_D^{25}$ 1.5128): allyldimethylcarbinol b. p. 119°, $n_D^{25}$ 1.4250 (lit.[9], b. p. 118~120°C, $n_D^{17}$ 1.4300).

Dibenzylmethylcarbinol and diallylmethylcarbinol were prepared by action of the corresponding Grignard reagents on ethyl acetate: dibenzylmethylcarbinol b.p. 148°C/3 mmHg, $n_D^{23}$ 1.5686 (lit.[10], b. p. 182°C/15mmHg): diallylmethylcarbinol b. p. 74°C/43 mmHg, $n_D^{23}$ 1.4500 (lit.[11], b. p. 158.4°C). Tribenzylcarbinol and triallylcarbinol were prepared through Grignard reaction between diethyl carbonate and benzyl- and allylmagnesium chlorides, respectively: tribenzylcarbinol m. p. 114~115°C (lit.[12], m. p. 115°C): triallylcarbinol b. p. 82°C/16mmHg, $n_D^{23}$ 1.4682 (lit.[13], b. p. 191~192°C, $n_D^{21}$ 1.468).

## Results and Discussion

The apparent $\nu_{O-H}$ curves of allyldimethylcarbinol at several temperatures are shown in Fig. 3. Each curve can be regarded as an overlap of two Lorentz function curves as is exemplified by the curve at 24°C in Fig. 4, and six parameters determined by applying Eq. 1 to the apparent curves are summarized in Table I. The characteristic tendencies of the dependence of some band properties on temperature such as decrease of the total intensity, increase of the half band-width and shift of the wave numbers to the higher side, are again observed in this case.

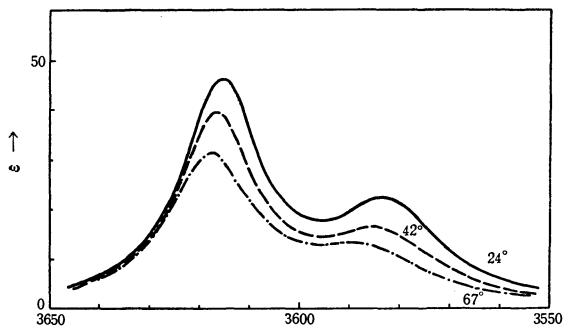



Fig. 3. The apparent $\nu_{O-H}$ absorptions of allyldimethylcarbinol at several temperatures; —— 24°C, - - - 42°C, -·-· 67°C.

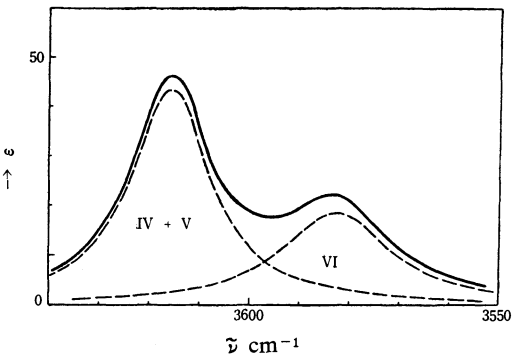



Fig. 4. $\nu_{O-H}$ absorption of allyldimethylcarbinol at 24°C.
—— the observed curve
- - - the divided bands

Table I. The effect of temperature on the $\nu_{O-H}$ absoption of allyldimethylcarbinol

| $1/T\times10^3$ °K$^{-1}$ | $\nu_{O-H}$ | $\nu$ | $a$ | $b$ | $\ln(A_i/A_f)$ |
|---|---|---|---|---|---|
| 3.37 | i | 3582.7 | 21.40 | 13.18 | −0.521 |
| | f | 3615.9 | 26.28 | 9.61 | |
| 3.25 | i | 3583.7 | 21.31 | 13.66 | −0.529 |
| | f | 3616.2 | 25.70 | 9.71 | |
| 3.17 | i | 3583.7 | 19.50 | 14.87 | −0.593 |
| | f | 3616.8 | 23.11 | 9.74 | |
| 3.02 | i | 3585.2 | 16.70 | 15.21 | −0.660 |
| | f | 3617.3 | 21.75 | 10.24 | |
| 2.95 | i | 3587.4 | 15.41 | 15.50 | −0.699 |
| | f | 3618.0 | 21.58 | 10.79 | |

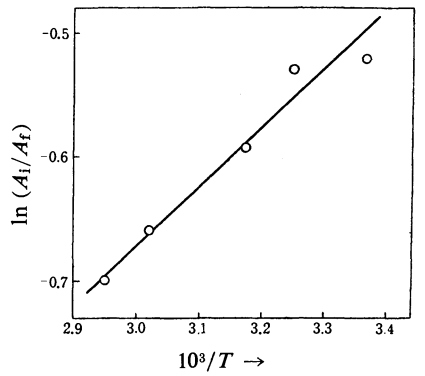



Fig. 5. The temperature dependence of $\ln(A_i/A_f)$.

7) Part VIII: M. Ōki and H. Iwamura, This Bulletin, 33, 717 (1960).
8) R. Heck and S. Winstein, *J. Am. Chem. Soc.*, **79**, 3432 (1957).
9) S. Coffey, *Rec. trav. chim. Pay-Bas*, **41**, 653 (1922).
10) R. Dolique, *Compt. rend.*, **190**, 881 (1930).
11) B. Sorokin, *Ann.*, **185**, 169 (1877).
12) A. A. Morton and J. R. Stevens, *J. Am. Chem. Soc.*, **53**, 4031 (1931).
13) A. Reformatski, *Ber.*, **41**, 4086 (1908).

TABLE II. THE ENERGIES AND THE ENTROPY TERMS OF THE INTERACTION IN ALLYLDIMETHYL- AND BENZYLDIMETHYLCARBINOLS

| Carbinol | $-\Delta H$ (kcal./mol.) | $\Delta S/R-\ln a$ | $\Delta\nu_{max}$ ($cm^{-1}$) |
|---|---|---|---|
| $CH_2$=$CHCH_2CMe_2OH$ | 0.90±0.07 | −2.03±.012 | 33.2 |
| $PhCH_2CMe_2OH$ | 0.54±0.13 | −1.16±0.17 | 21.4 |

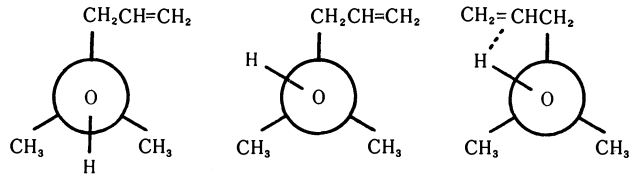



Fig. 6.

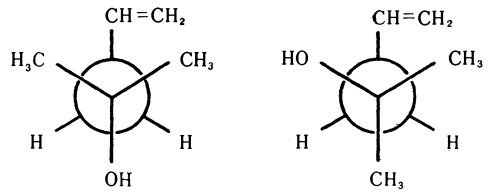
Temperature versus $\ln(A_i/A_f)$ relation is shown in Fig. 5. The values obtained therefrom are tabulated in Table II together with those of benzyldimethylcarbinol reported in the preceding paper[1].

The strengths of the interactions are fairly smaller than those ever estimated. That is, Bamford[14] suggested the energy to be 2~3 kcal./mol. for the interaction between methanol and aromatic nucleus and Schleyer et al.[15] 1.4 kcal./mol. for phenethyl alcohol. However, disappearance of the interacting $\nu_{O-H}$ for 3-cyclohexen-1-ol and β-tetralol seems to suggest, that the energy difference between the free and the interacting molecules is less than 1 kcal./mol. While West[16] has recently shown, that olefins are generally stronger proton-acceptors than simple aromatic hydrocarbons in the intermolecular interaction between the hydroxyl group and π-electrons through measurement of the shift of $\nu_{O-H}$ from free phenol to phenol in hydrocarbons, it is for the first time that the proposition was realized in the intramolecular interaction through the direct energy measurement.

The doublet nature of the $\nu_{O-H}$ of allyldimethylcarbinol as well as benzyldimethylcarbinol shows, that the rotational isomers around $C_\alpha$–O bond can not be distinguished so far as $\nu_{O-H}$ is concerned under the present dispersion of the spectrometer[2]; that is, IV and V in Fig. 6 can not be distinguished and equally give the higher $\nu_{O-H}$ at 3616 $cm^{-1}$. In both forms hydroxyl hydrogen lies between two carbon atoms attached to the α-carbon atom as in *tert*-butyl alcohol[5]. The absorption at 3584 $cm^{-1}$ (VI), on the other hand, can be assigned to the hydroxyl group having internal interaction. In this case, the rotational degree around the $C_\alpha$–$C_\beta$ and $C_\beta$–$C_\gamma$ bonds must be fixed favorably for the interaction, i. e., the hydroxyl group and the group carrying π-electrons must be closely situated.

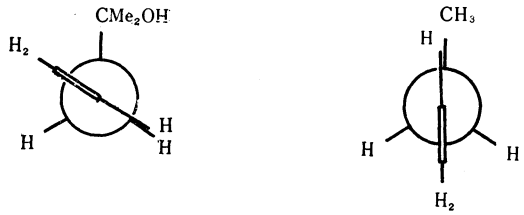
Although it is usual that the energy difference of about one kcal./mol. between two components in an equilibrium mixture makes one at a lower energy level exceedingly predominant, it does not seem to be the case in allyldimethylcarbinol, the ratio $A_i/A_f$ being only 0.59. This could be explained if the absorption intensity per molecule of the interacting $\nu_{O-H}$ is much weaker than that of free $\nu_{O-H}$ and even small $A_i$ represents a large number of the interacting molecules. However, the assumption is rather contradictory to the knowledge of ordinary hydrogen bonding[17] where the absorption intensity increases on hydrogen bond formation because of increased change of the dipole moment accompanying O–H vibrational motion. The possibility may also be excluded from the fact that, as reported previously[2], the sum of the integrated intensities $(A_i+A_f)$ is almost constant throughout the wide range of substituted phenethyl alcohols. It can preferably be explained by considering the statistical factor contributed from the rotational degree of freedom. Rough computation of the number of the possible conformations for allyldimethylcarbinol was made with the assumption that only the staggered conformations are possible for each bond axis. It may reasonably be assumed that both isomers IV and V have not only the same $\nu_{O-H}$ but also almost the same energy in regard to the conformations of the hydroxyl group. As to the $C_\alpha$–$C_\beta$ axis, three conformations VII, VIII and the mirror image of the latter in Fig. 7 are assumed to have the same energy as a first approximation. Strictly speaking, however, VII and VIII are different in that the former has

14) C. H. Bamford, *Discuss. Faraday Soc.*, **16**, 229 (1954).
15) P. von Schleyer et al., *Tetrahedron Letters*, No. 14, p. 1 (1959).
16) R. West, *J. Am. Chem. Soc.*, **81**, 1614 (1959).
17) H. Tsubomura, *J. Chem. Phys.*, **24**, 927 (1956).




VII VIII

Fig. 7.




IX X

Fig. 8.

two gauche type interactions in *n*-butane structure, while the latter a gauche interaction in *n*-butane structure and another gauche interaction in *n*-propyl alcohol. Hence the energy difference between VII and VIII becomes $E_g^{bu.}-E_g^{pr.}$, which may be assumed to be zero[18]. Around the $C_\beta$–$C_\gamma$ bond, only the gauche conformations (IX and its mirror image in Fig. 8) may be permitted as in 1-butene, where two gauche forms are more stable than the trans (X) by 1970 cal./mol.[19] Out of eighteen ($3\times3\times2$) conformations thus possible, only two can take part in the internal interaction and are stabilized by the energy of the interaction. Therefore the ratio, $w_i/w_f=1/8$, must be introduced as a weight in the following Eq. 2;

$$n_i/n_f=w_i/w_f\cdot e^{-(E_i-E_f)/(RT)} \qquad (2)$$

where "$n$" is the number of the molecules. Substitution of the energy of the interaction obtained above gives $n_i/n_f=0.56$ which is in good agreement with $A_i/A_f$ value of 0.59.

The computation was extended to the data of epicholesterol which shows as high $A_i/A_f$ value as 3.14[20]. The molecule has a fairly rigid structure as in Fig. 9 and the freedom of rotation is left only for $C_\alpha$–O axis. Out of three possible conformations, only one can take part

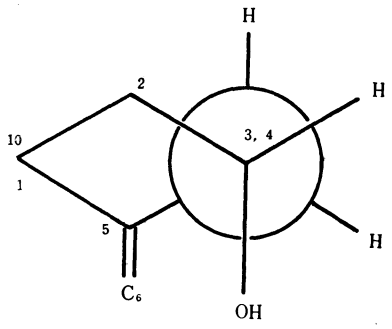



Fig. 9.

in the interaction geometrically, the weight becoming 1/2. As the hydroxyl group is now of the secondary alcohol, it is a stronger proton-donor in hydrogen bonding than those of tertiary alcohols[21], while the ethylenic double bond is regarded to be a stronger proton-acceptor than that of allyldimethylcarbinol, because it possesses three alkyl substituents[14]. The strength of the interaction must therefore be greater than that obtained above and is arbitrarily assumed to be 1.0 kcal./mol[22]. Then $n_i/n_f$ becomes 2.7, which satisfactorily explains why epicholesterol, unlike 3-buten-1-ol, shows larger $A_i/A_f$ value than one.

Benzyldimethylcarbinol may be treated in the same way. The energy difference between two rotational isomers corresponding to VII and VIII would be marked, the latter being more stable, but is neglected for the sake of convenience as no evaluation is possible. As to the $C_\beta$–$C_\gamma$ bond (Fig. 10), every rotational conformation which must be analogous to that of ethylbenzene[23] favors the interaction, and therefore the rotational degree of freedom about this axis is left out of consideration. Thus $w_i/w_f$ becomes 2/7 in all. This value, together with 1/8 in allyldimethylcarbinol, may be regarded to correspond to the entropy terms of the interaction in Table II and well explains the greater absolute value in the latter than in the former, since ln 2/7 is −1.25 and ln 1/8 is −2.08. The energy difference of 0.54 kcal./mol.

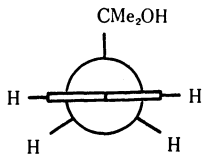



Fig. 10.

18) $E_g^{bu\cdot}$ has been regarded to be 800 cal./mol. (K. S. Pitzer, *J. Chem. Phys.*, **8**, 711 (1940).), while no datum is available for $E_g^{pr\cdot}$, the energy difference between gauche and trans forms in *n*-propyl alcohol.

19) J. G. Aston, S. Isserow and G. J. Szasz, *J. Chem. Phys.*, **12**, 336 (1944); **14**, 67 (1946).

20) M. Ōki and H. Iwamura, This Bulletin, **32**, 307 (1959).

21) L. P. Kuhn, *J. Am. Chem. Soc.*, **76**, 4328 (1954).

22) Assuming that $\Delta\nu_{max}$ is proportional to the energy of the interaction, $-\Delta H=0.9\times34.1/33.2=0.93$ kcal./mol. is obtained, as $\Delta\nu_{max}$ in epicholesterol amounts to 34.1 $cm^{-1}$.

23) F. G. Brickwedde, M. Moskow and R. B. Scott, *J. Chem. Phys.*, **13**, 547 (1945).

TABLE III. $\nu_{O-H}$ OF TERTIARY ALCOHOLS RELATED TO 3-BUTEN-1-OL AND PHENETHYL ALCOHOL

| Alcohol | $\nu_{O-H}$ | $\nu_{max}$ cm$^{-1}$ | $\Delta\nu^{a}_{1/2}$ cm$^{-1}$ | $A\times10^{-3}$ mol$^{-1}$ l. cm$^{-2}$ | $\Delta\nu_{max}$ cm$^{-1}$ | $A_i/A_f$ | $n_i/n_f$ |
|---|---|---|---|---|---|---|---|
| $CH_2$=$CHCH_2CMe_2OH$ | i | 3582.7 | 21.4 | 1.50 | 33.2 | 0.59 | 0.56 |
| | f | 3615.9 | 26.3 | 2.53 | | | |
| $(CH_2$=$CHCH_2)_2CMeOH$ | i | 3580.9 | 25.2 | 2.58 | 33.8 | 1.38 | 1.29 |
| | f | 3614.7 | 20.2 | 1.87 | | | |
| $(CH_2$=$CHCH_2)_3COH$ | i | 3577.8 | 25.4 | 3.87 | 33.9 | 3.37 | 2.25 |
| | f | 3611.7 | 20.4 | 1.15 | | | |
| $PhCH_2CMe_2OH$ | i | 3593.5 | 16.1 | 2.02 | 21.4 | 0.75 | 0.71 |
| | f | 3614.9 | 25.1 | 2.70 | | | |
| $(PhCH_2)_2CMeOH$ | i | 3590.8 | 26.0 | 4.35 | 15.2 | 3.85 | 1.97 |
| | f | 3606.0 | 26.0 | 1.13 | | | |
| $(PhCH_2)_3COH$ | i | 3580.3 | 19.3 | 6.04 | — | — | 4.92 |
| | f | — | — | — | | | |

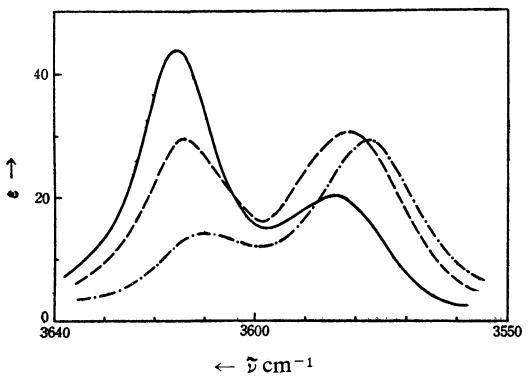



Fig. 11. $\nu_{O-H}$ absorptions of allylcarbinols.
—— $CH_2$=$CHCH_2CMe_2OH$
--- $(CH_2$=$CHCH_2)_2CMeOH$
-·-· $(CH_2$=$CHCH_2)_3COH$

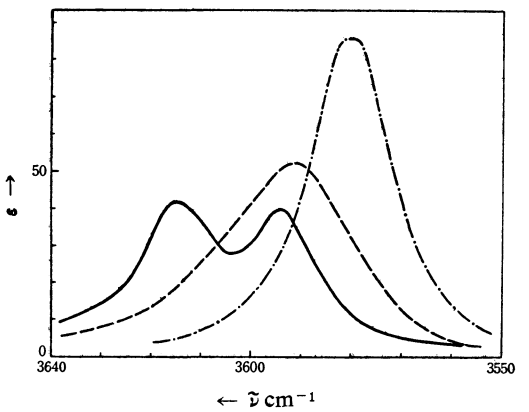



Fig. 12. $\nu_{O-H}$ absorptions of benzylcarbinols.
—— $PhCH_2CMe_2OH$ --- $(PhCH_2)_2CMeOH$
-·-· $(PhCH_2)_3COH$

obtained for benzyldimethylcarbinol was used as the energy of the interaction and $n_i/n_f$ of 0.71 was obtained as shown in Table III.

In order to see these statistical effects on $\nu_{O-H}$ absorption curves, the measurements were extended to some tertiary alcohols related to 3-buten-1-ol and phenethyl alcohol. The apparent $\nu_{O-H}$ absorptions are shown in Figs. 11 and 12, respectively, and the numericals are summarized in Table III, the last column being the $n_i/n_f$ values computed as above. The energies of the interaction tabulated in Table II were applied to the same type of compounds, and this procedure may be justified from the constant $\Delta\nu_{max}$ values in the series of allylcarbinols.

In both series the fair agreement between the observed $A_i/A_f$ and the computed $A_i/A_f$ in the lowest homologs does not always hold true in the higher homologs, especially in benzylcarbinol series. The discrepancy can almost exclusively be attributed to the incorrect assumption made in the computation of the weight, that is, to the effect of steric hindrance which disfavors such conformations with the free hydroxyl group as shown in Fig. 13.

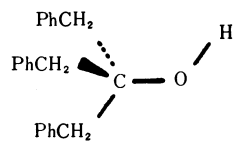



Fig. 13.

It has been shown in this manner, that the ratio of the number of the interacting molecules to the free ones can almost quantitatively be interpreted by considering the statistical or frequency factor of the conformations of the molecules under a given value of the energy of the interaction. In the near future, the computation will be extended to the other organic compounds to explain their $\nu_{O-H}$ absorption curves and the conformations of the molecules.

The authors are indebted to Professor Y. Urushibara and Professor T. Shimanouchi for

their encouragement and discussion throughout this work. The authors' thanks are also due to the Ministry of Education for the Grant in Aid for Fundamental Scientific Research.

*Department of Chemistry*
*Faculty of Science*
*The University of Tokyo*
*Hongo, Tokyo*

# *NMR Spectra of Aliphatic Compounds Containing Oxygen Atoms and the Related Compounds**

By Kenkichi NUKADA

(Received April 13, 1960)

Many works concerning the chemical shifts of functional groups in organic molecules[1-4] have been reported, but the systematic study for the chemical shifts of functional groups containing oxygen atoms has not yet been carried out in detail. In this paper, the author presents the NMR spectra of more than thirty aliphatic compounds containing the oxygen atom and the related compounds such as ethers, formals, acetals, ketal, orthoaliphatic acid esters, polyethylene glycol diethers and cyclic compounds. These compounds contain various types of functional groups such as $CH_3$-O, O-$CH_2$-O, HC$\langle$O, O, etc. Comparing spectra with each other, the author obtained a table of chemical shifts of functional groups. It is also found that there exist some correlations between the chemical shifts of the same type of equivalent protons and the type of alkyl groups bonded to the oxygen atom. The origin of the correlation was considered.

## Experimental

**Measurement of NMR Spectra.**—Spectra were obtained by means of a Varian 4300 B spectrometer (40 Mc). The spectra of both pure liquid benzene solution (volume ratio of solute to benzene equals to 4 : 1) for each sample were obtained and the chemical shifts with respect to proton resonance in benzene were calculated. As a field marker, the spectrum of pure propionic acid was used (Fig. 1). The absolute value of shift was calibrated by the displacement between proton resonances in benzene and cyclohexane (223 cps)[3]. Since it is necessary to maintain all the experimental conditions as stable as possible in the accurate chemical shift measurement, a sweep rate of 1p/$10^7$ per second was used. When necessary to obtain higher resolved spectra, a smaller sweep rate (0.4p/$10^7$) was used. In the latter case, however, the error of chemical shift was considerably increased. The probable error of the measurement in case of rapid passage was within ±2%. Spectra of pure sample were obtained because sometimes it was necessary to check the solvent effect in benzene solution.

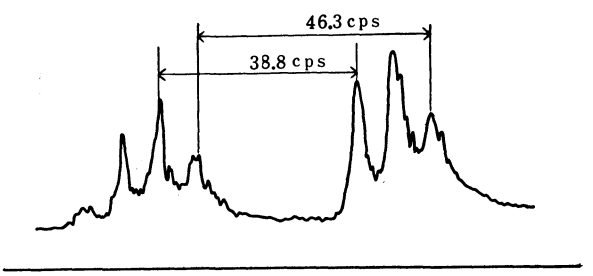



Fig. 1. NMR spectrum of pure propionic acid. This spectrum was used as a field marker, i. e., before and after every chemical shift measurement this spectrum was measured. The absolute values between peaks were calibrated by the displacement between proton resonances in benzene and cyclohexane (223 cps).

**Samples.** — Formals (dimethyl formal, methyl ethyl formal, diethyl formal and diisopropyl formal) and acetals (dimethyl acetal, methyl ethyl acetal and diethyl acetal) were synthesized in the author's laboratory[5]. All the other compounds are commercial products (Tokyo Kasei and Eastman Kodak Co.).

* This is essentially the extension of the work already reported in this Bulletin as a short communication. (K. Nukada and U. Maeda, This Bulletin, 32, 656 (1959)).

1) L. H. Meyer, A. Saika and H. S. Gutowsky, *J. Am. Chem. Soc.* 75, 4567 (1953).

2) V. D. Tiers, "Characteristic Nuclear Magnetic Resonance Shielding Values (Spectral Position) for Hydrogen in Organic Structures", Organic Section, Exploratory NMR Studies, Project 737602, Minnesota Mining and Manufacturing Co. U. S. A. (1958).

3) N. F. Chamberlain, *Anal. Chem.*, 31, 56 (1959).

4) B. L. Bothner-By, C. Naar-Colin and B. L. Shapiro "NMR Spectra and Structure Correlations", (Vol. II), Harvard University, (1958).

5) K. Nukada, *J. Chem. Soc. Japan, Pure Chem. Sec. (Nippon Kagaku Zasshi)*, 80, 976 (1959).

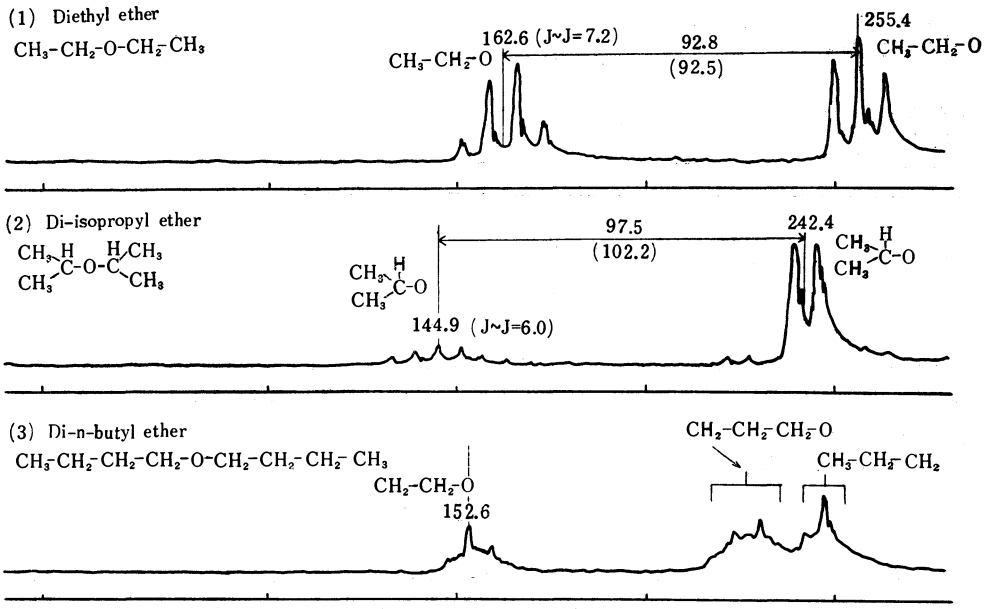

(1) Diethyl ether
CH3-CH2-O-CH2-CH3
162.6 (J~J=7.2)
92.8
(92.5)
255.4
(2) Di-isopropyl ether
97.5
(102.2)
242.4
144.9 (J~J=6.0)
(3) Di-n-butyl ether
CH3-CH2-CH2-CH2-O-CH2-CH2-CH2-CH3
152.6

Fig. 2-1.

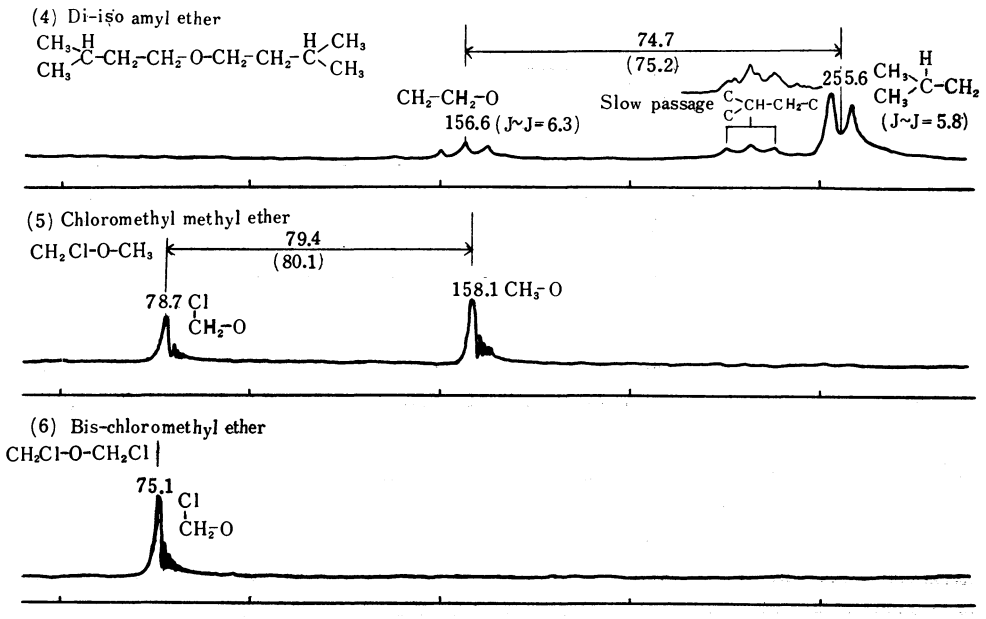

(4) Di-iso amyl ether
74.7
(75.2)
156.6 (J~J=6.3)
Slow passage
255.6
(J~J=5.8)
(5) Chloromethyl methyl ether
CH2Cl-O-CH3
79.4
(80.1)
78.7
158.1
(6) Bis-chloromethyl ether
CH2Cl-O-CH2Cl
75.1

Fig. 2-2.

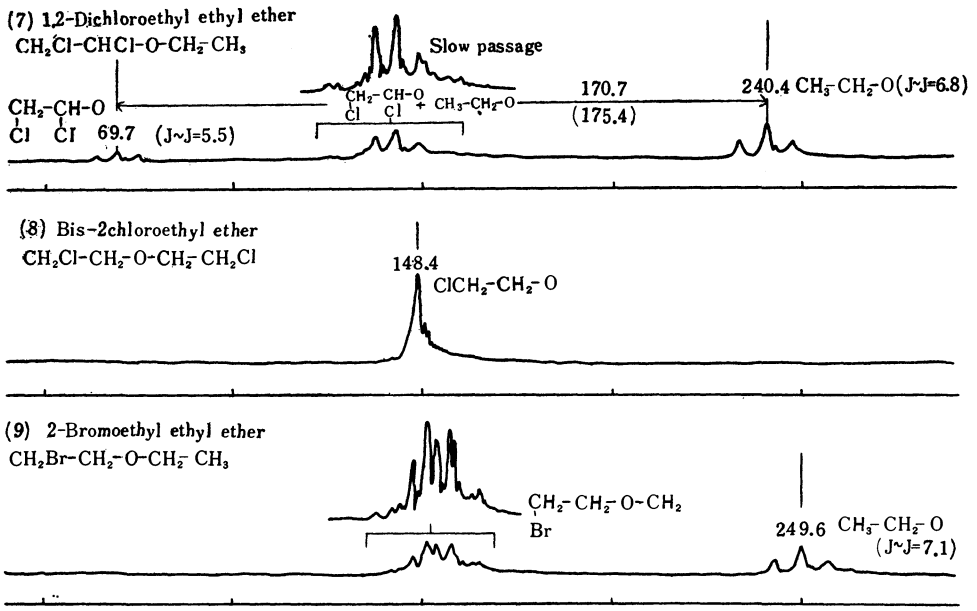

(7) 1,2-Dichloroethyl ethyl ether
CH2Cl-CHCl-O-CH2-CH3
Slow passage
CH2-CH-O
Cl Cl
69.7 (J~J=5.5)
CH2-CH-O + CH3-CH2-O
170.7
(175.4)
240.4 CH3-CH2-O(J~J=6.8)
(8) Bis-2chloroethyl ether
CH2Cl-CH2-O-CH2-CH2Cl
148.4
ClCH2-CH2-O
(9) 2-Bromoethyl ethyl ether
CH2Br-CH2-O-CH2-CH3
CH2-CH2-O-CH2
Br
249.6 CH3-CH2-O
(J~J=7.1)

Fig. 2-3.

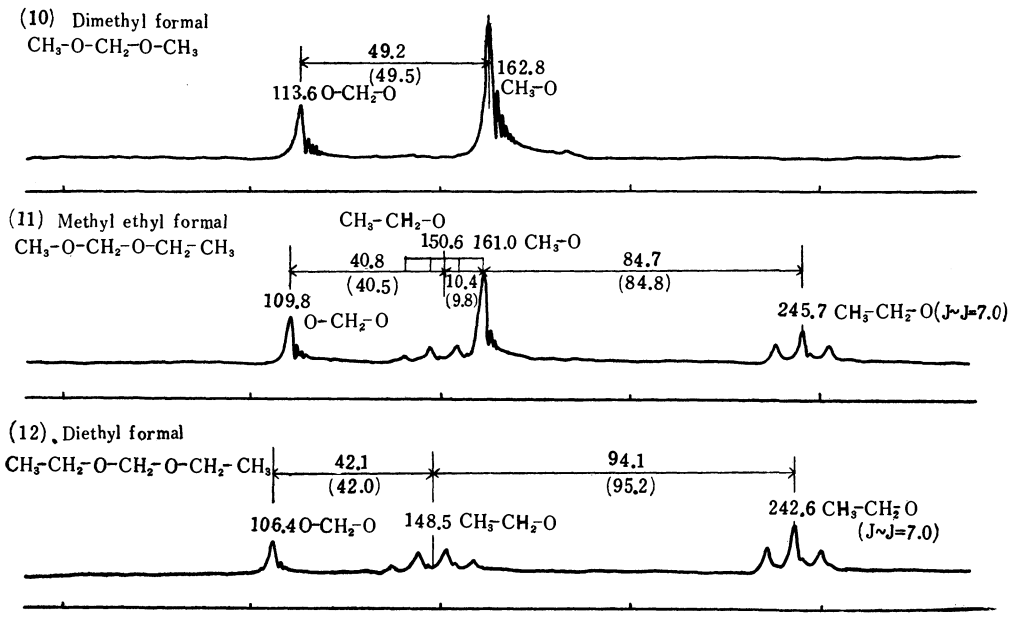

(10) Dimethyl formal
CH3-O-CH2-O-CH3
49.2
(49.5)
113.6 O-CH2-O
162.8
CH3-O
(11) Methyl ethyl formal
CH3-O-CH2-O-CH2-CH3
CH3-CH2-O
150.6 161.0 CH3-O
40.8
(40.5)
10.4
(9.8)
84.7
(84.8)
109.8
O-CH2-O
245.7 CH3-CH2-O(J~J=7.0)
(12) Diethyl formal
CH3-CH2-O-CH2-O-CH2-CH3
42.1
(42.0)
94.1
(95.2)
106.4 O-CH2-O
148.5 CH3-CH2-O
242.6 CH3-CH2-O
(J~J=7.0)

Fig. 2-4.

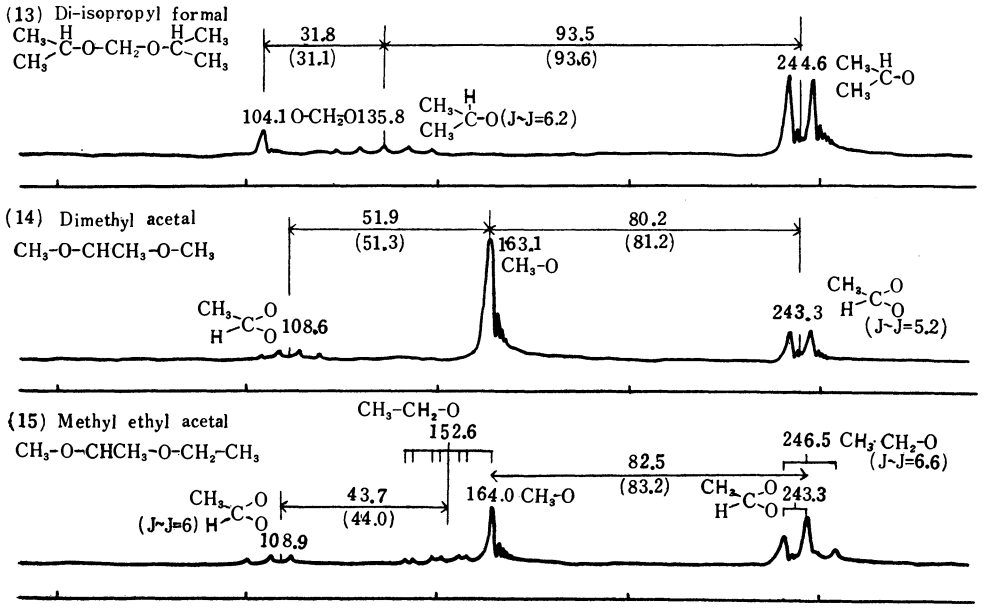

(13) Di-isopropyl formal
31.8
(31.1)
93.5
(93.6)
244.6
104.1
135.8
(J~J=6.2)
(14) Dimethyl acetal
CH3-O-CHCH3-O-CH3
51.9
(51.3)
80.2
(81.2)
163.1
CH3-O
108.6
243.3
(J~J=5.2)
(15) Methyl ethyl acetal
CH3-O-CHCH3-O-CH2-CH3
CH3-CH2-O
152.6
246.5
(J~J=6.6)
82.5
(83.2)
43.7
(44.0)
164.0
243.3
(J~J=6)
108.9

Fig. 2-5.

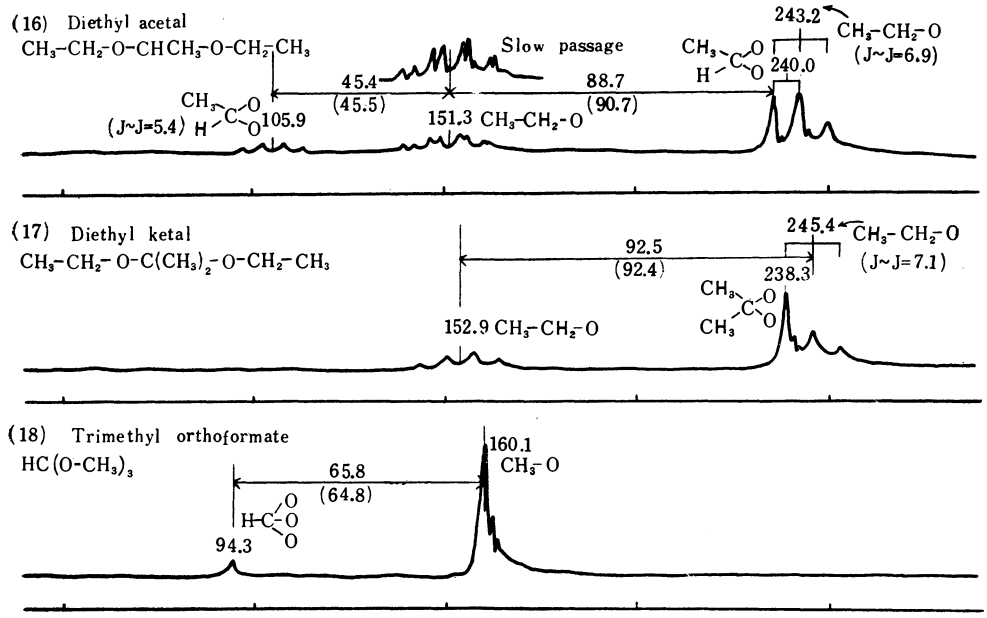

(16) Diethyl acetal
CH3-CH2-O-CHCH3-O-CH2-CH3
Slow passage
243.2
CH3-CH2-O
(J~J=6.9)
45.4
(45.5)
88.7
(90.7)
240.0
(J~J=5.4)
105.9
151.3
(17) Diethyl ketal
CH3-CH2-O-C(CH3)2-O-CH2-CH3
245.4
92.5
(92.4)
238.3
152.9
(18) Trimethyl orthoformate
HC(O-CH3)3
160.1
CH3-O
65.8
(64.8)
94.3

Fig. 2-6.

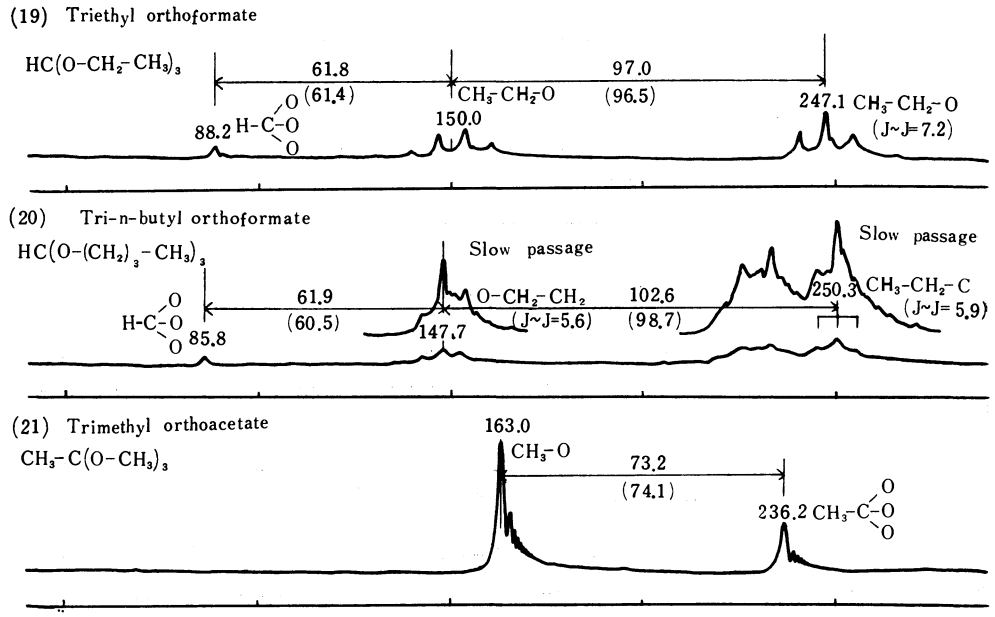

(19) Triethyl orthoformate
HC(O-CH2-CH3)3
61.8
(61.4)
97.0
(96.5)
88.2
150.0
247.1 CH3-CH2-O
(J~J=7.2)
(20) Tri-n-butyl orthoformate
HC(O-(CH2)3-CH3)3
Slow passage
Slow passage
61.9
(60.5)
O-CH2-CH2
(J~J=5.6)
102.6
(98.7)
250.3
CH3-CH2-C
(J~J= 5.9)
85.8
147.7
(21) Trimethyl orthoacetate
CH3-C(O-CH3)3
163.0
CH3-O
73.2
(74.1)
236.2 CH3-C-O

Fig. 2-7.

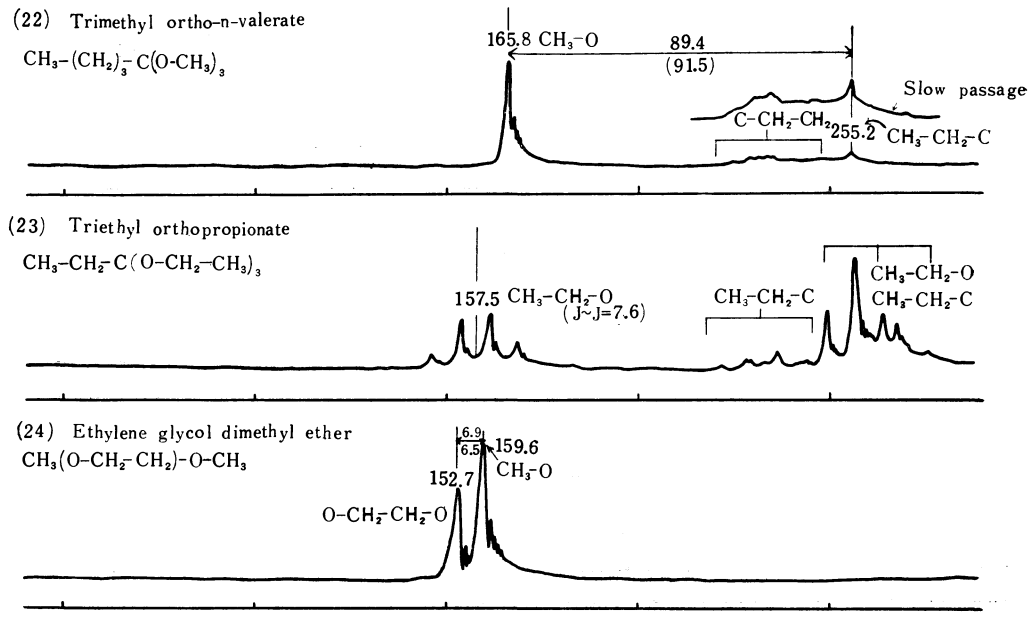

(22) Trimethyl ortho-n-valerate
CH3-(CH2)3-C(O-CH3)3
165.8 CH3-O
89.4
(91.5)
Slow passage
C-CH2-CH2
255.2
CH3-CH2-C
(23) Triethyl orthopropionate
CH3-CH2-C(O-CH2-CH3)3
157.5 CH3-CH2-O
(J~J=7.6)
CH3-CH2-C
CH3-CH2-O
CH3-CH2-C
(24) Ethylene glycol dimethyl ether
CH3(O-CH2-CH2)-O-CH3
6.9
6.5
159.6
CH3-O
152.7
O-CH2-CH2-O

Fig. 2-8.

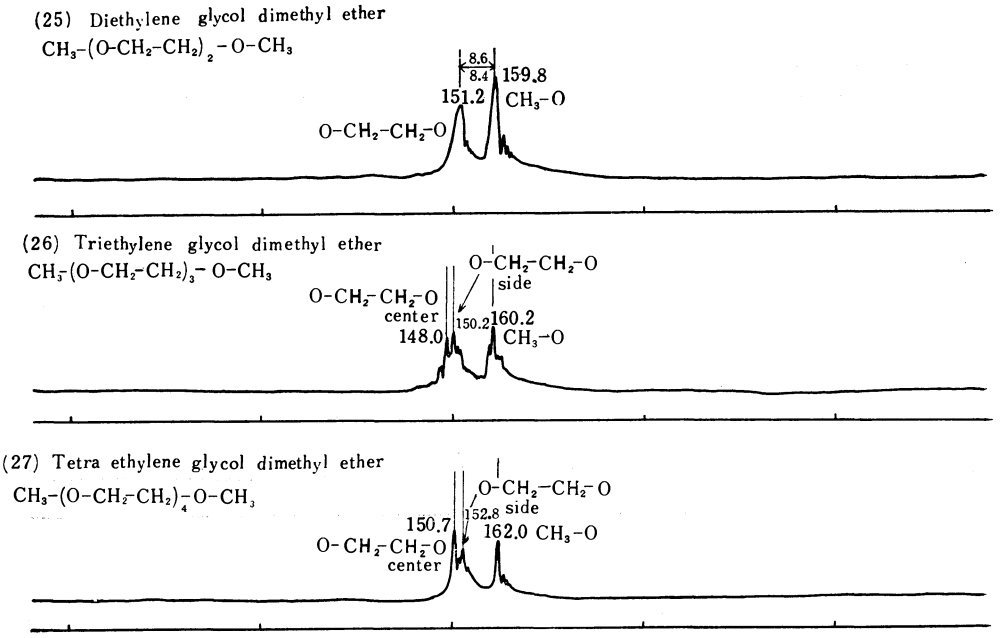



Fig. 2-9.

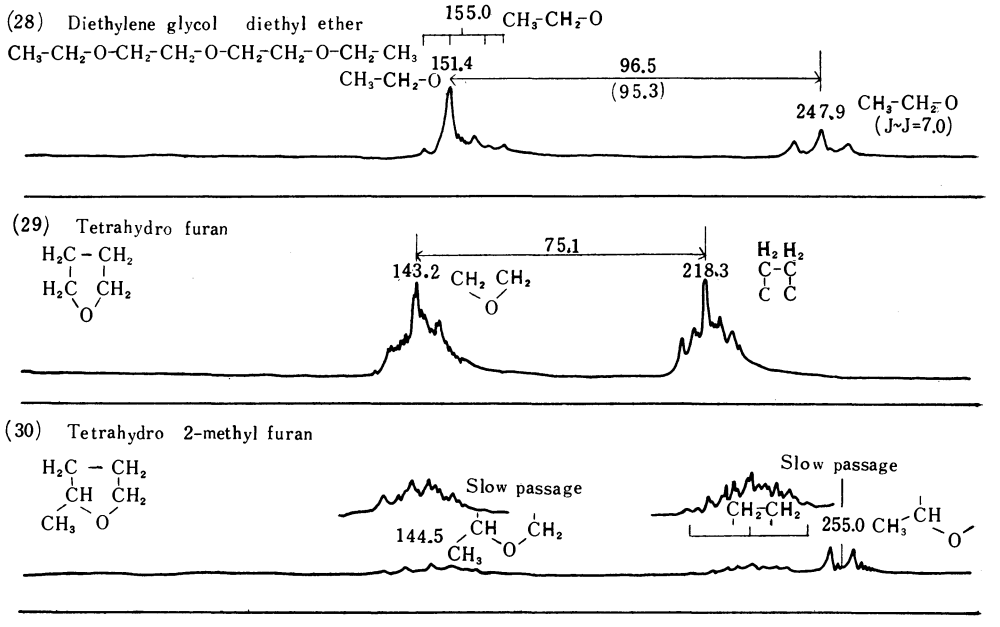



Fig. 2-10.

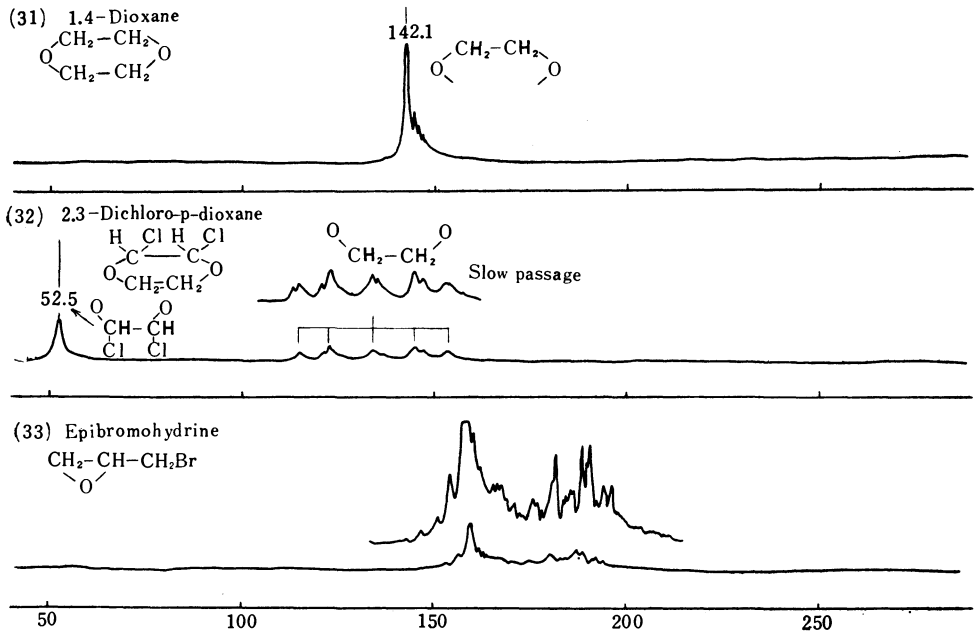



Fig. 2-11.

Fig. 2. NMR spectra of oxygen containing aliphatic compounds. Chemical shift (cps) from benzene protons and assignment are marked on each peak. J-J coupling constant and separation between peaks are also described.

TABLE I. CHEMICAL SHIFT OF FUNCTIONAL GROUP

| Name of group | Type of group | Type of sub-group | Chemical shift cps | Number of samples |
|---|---|---|---|---|
| $CH_3$-C-C-C- | | $\delta_{CH_3}$ | 253.7±3.4 | 3 |
| $CH_3$-$CH_2$-O- | B | $\beta_{CH_3}$ | 246.4±9.0 | 10 |
| $\begin{matrix}CH_3\\CH_3\end{matrix}>$CH-O- | B | $\beta_{CH_3}$ | 243.5±1.1 | 2 |
| $\begin{matrix}CH_3\\CH_3\end{matrix}>C<\begin{matrix}O-\\O-\end{matrix}$ | B | $\beta^2{}_{CH_3}$ | 242.2±2.2 | 3 |
| $CH_3$-C(O-)(O-)(O-) | B | $\beta^3{}_{CH_3}$ | 236.2 | 1 |
| -$CH_2$-C-O- (Five members ring) | B | $\beta_{CH_2}$ (ring) | 218.3 | 1 |
| $CH_3$-O- | A | $\alpha_{CH_3}$ | 161.6±4.2 | 11 |
| -C-$CH_2$-O- | A | $\alpha_{CH_2}$ | 152.9±9.7 | 12 |
| -O-$CH_2$-$CH_2$-O | A | $\alpha\beta_{CH_2}$ | 151.0±3.0 | 5 |
| Cl-$CH_2$-$CH_2$-O- | | $\alpha'\beta_{CH_2}$, $\alpha\beta'_{CH_2}$ | 148.4 | 1 |
| -C-$CH_2$-O- (Five members ring) | A | $\alpha_{CH_2}$ (ring) | 143.9±0.7 | 2 |
| -O-$CH_2$-$CH_2$-O- (Six members ring) | A | $\alpha\beta_{CH_2}$ (ring) | 142.1 | 1 |
| $\begin{matrix}CH_3\\CH_3\end{matrix}>$CH-O- | A | $\alpha_{CH}$ | 140.4±4.6 | 2 |
| -O-$CH_2$-O- | $A^2$ | $\alpha^2{}_{CH_2}$ | 108.5±5.1 | 4 |
| $\begin{matrix}CH_3\\H\end{matrix}>C<\begin{matrix}O-\\O-\end{matrix}$ | $A^2$ | $\alpha^2{}_{CH}$ | 107.8±1.9 | 3 |
| H-C(O-)(O-)(O-) | $A^3$ | $\alpha^3{}_{CH}$ | 89.4±4.9 | 3 |
| Cl-$CH_2$-O- | | $\alpha\alpha'_{CH_2}$ | 76.9±1.8 | 2 |
| $\begin{matrix}Cl\\Cl\end{matrix}>$CH-O- | | $\alpha\alpha'^2{}_{CH}$ | 69.7 | 1 |
| $\begin{matrix}-O\\Cl\end{matrix}>$CH-CH$<\begin{matrix}O-\\Cl\end{matrix}$ (Six members ring) | | $\alpha\alpha'\beta\beta'_{CH}$ | 52.5 | 1 |

TABLE II. CORRELATION BETWEEN CHEMICAL SHIFT AND THE TYPE OF SUBSTITUENT ALKYL GROUP (I)

| Type of molecule | Type of alkyl group | Equivalent proton group | Chemical shift |
|---|---|---|---|
| $HC(OR)_3$ | $CH_3-$ | $HC(O)_3$ | 94.3 |
| | $CH_3-CH_2-$ | | 88.2 |
| | $CH_3-(CH_2)_3-$ | | 85.8 |
| $H_2C(OR_1)(OR_2)$ | $R_1, R_2: CH_3-$ | $H_2C(O)_2$ | 113.6 |
| | $R_1: CH_3-, R_2: CH_3-CH_2-$ | | 109.8 |
| | $R_1, R_2: CH_3-CH_2-$ | | 106.4 |
| | $R_1, R_2: CH_3>CH$ | | 104.1 |
| $CH_3-CH(OR_1)(OR_2)$ | $R_1, R_2: CH_3-$ | $CH_3-CH(O)_2$ | 108.6 |
| | $R_1: CH_3-, R_2: CH_3-CH_2-$ | | 108.9 |
| | $R_1, R_2: CH_3-CH_2-$ | | 105.9 |
| $CH_3-CH(OR_1)(OR_2)$ | $R_1, R_2: CH_3-$ | $CH_3-CH(O)_2$ | 243.3 |
| | $R_1: CH_3-, R_2: CH_3-CH_2-$ | | 343.3 |
| | $R_1, R_2: CH_3-CH_2-$ | | 240.0 |

TABLE III. CORRELATION BETWEEN CHEMICAL SHIFT AND THE TYPE OF SUBSTITUENT ALKYL GROUP (II)

| Type of molecule | Type of alkyl group | Equivalent proton group | Chemical shift |
|---|---|---|---|
| $RC(O-CH_3)_3$ | $H-$ | $-O-CH_3$ | 160.1 |
| | $CH_3-$ | | 163.0 |
| | $CH_3-(CH_2)_3-$ | | 165.8 |
| $RC(O-C_2H_5)_3$ | $H-$ | $-O-CH_2-CH_3$ | 150.0 |
| | $CH_3-CH_2-$ | | 157.5 |
| $R-CH(O-CH_3)_2$ | $H-$ | $-O-CH_3$ | 162.8 |
| | $CH_3-$ | | 163.1 |
| $R-CH(O-CH_3)(O-C_2H_5)$ | $H-$ | $-O-CH_3$ | 161.0 |
| | $CH_3-$ | | 164.0 |
| $R-CH(O-CH_3)(O-C_2H_5)$ | $H$ | $-O-CH_2-CH_3$ | 150.6 |
| | $CH_3-$ | | 152.6 |
| $R_1R_2C(O-C_2H_5)_2$ | $R_1, R_2: H-$ | $-O-CH_2-CH_3$ | 148.5 |
| | $R_1: H-, R_2: CH_3-$ | | 151.3 |
| | $R_1, R_2: CH_3-$ | | 152.9 |
| $R_1R_2C(O-C_2H_5)_2$ | $R_1, R_2: H-$ | $-O-CH_2-CH_3$ | 242.6 |
| | $R_1: H-, R_2: CH_3-$ | | 243.2 |
| | $R_1, R_2: CH_3-$ | | 245.4 |
| $R-CH(O-CH_3)(O-C_2H_5)$ | $H-$ | $-O-CH_2-CH_3$ | 245.7 |
| | $CH_3-$ | | 246.5 |

The purity of some compounds (formals, dimethyl acetal, methyl ethyl acetal, ethers except 1, 2-dichloroethyl ethyl ether, polyethylene glycol diethers and cyclic compounds except tetrahydrofuran and epibromohydrin) was checked by gaschromatograph. The other compounds were found to decompose in the column of gaschromatograph, and in this case the purity was checked by the infrared spectra*. The detailed description of the purification was reported elswhere[5,6].

## Results and Discussion

The spectra obtained may be classified into three types as follows:

a) No peaks overlap with each other, so it is quite easy to assign them from the relative intensity and the appearance of the multiplet structures.

b) Some peaks overlap with each other, but referring to the assignment of class a) it is not so difficult to assign them in most cases.

c) Separation of chemical shift is the same order as J-J splitting. In this paper, the assignment of this class is not given since it is impossible to assign them without exact calculation.

In Fig. 2, the assignment and the value of chemical shifts (in cycle per second) are marked on each peak. The separation between peaks is also shown together with that of pure liquid in parentheses.

* Since the infrared spectra of ketal and orthoaliphatic acid esters have not been reported in the literature, it is impossible to check the purity of these compounds merely by the infrared spectra. Since these compounds were known to decompose gradually to alcohols, esters or to aldehydes in air at room temperature, they were distilled (in vacuo) several times until bands at 3500 $cm^{-1}$ and 1700 $cm^{-1}$ completely disappeared.

6) K. Nukada, *J. Chem. Soc. Japan, Pure Chem. Sec.* (*Nippon Kagaku Zasshi*), **81**, 1028 (1960).

The average values of shifts of all functional groups are listed in Table I and these values are consistent with those listed by Chamberlain[3].

Except for halogenated ethers, all functional groups may be divided into four groups, B, A, $A^2$ and $A^3$ according to the approximate value of shift. These groups include sub-groups $\beta$, $\beta^2$ and $\beta^3$, $\alpha\beta$ and $\alpha$, $\alpha^2$ and $\alpha^3$, respectively. The notation of "the type of sub-group" is defined as follows*: $n$ equivalent protons bonded to $\alpha$ or $\beta$ carbon atoms are designated as $\alpha_{CH_n}$ or $\beta_{CH_n}$. If carbon atoms are at $\alpha$ and/or $\beta$ positions with respect to more than two oxygen atoms, several notations are used, i. e., $\alpha^2{}_{CH_n}$ or $\alpha\beta_{CH_n}$, etc. If the carbon atom is at $\alpha$ position with respect to the chlorine atom the notation $\alpha'$ is used. Practically, the chemical shifts of protons bonded to $\gamma$ or far separated carbon atoms are not influenced by the electronegative atoms interested.

The order of shielding is $B > A > A^2 > A^3$ within the main groups. Further in each group, some correlations are recognized. In groups B and A, the order of shielding is $\beta > \beta^2 > \beta^3$ for $CH_3$ protons and $\alpha > \alpha\beta$ for $CH_2$ protons, respectively. In groups A and $A^2$, the order of shielding is $CH_3 > CH_2 > CH$ for $\alpha$ sub-group and $CH_2 > CH$ for $\alpha^2$ sub-group, respectively.

The correlation between the chemical shift and electronegativity of the functional group being directly related to "the type of group" and "the type of sub-group" is quite reasonable.

Let us next consider the change in chemical shift within each sub-group in more detail. The chemical shift of equivalent protons in some functional groups changes, though very slightly, in homologue. The methyl proton shift of the methoxyl group in $R\text{-}C\langle^{O\text{-}Me}_{O\text{-}Me}_{O\text{-}Me}$, for example, goes to a higher field as the alkyl-group R becomes larger. In another example, the methylene proton shift in $CH_2\langle^{OR_1}_{OR_2}$, goes to a lower field as the alkyl groups $R_1$ and $R_2$ become larger. In Tables II and III, the correlations between the chemical shift and the type of attached alkyl group are shown in the former and the latter cases, respectively. Although the change of chemical shift is very slight and some correction of the solvent effect should be considered, surprisingly regular correlations are obtained.

If it is assumed that after a possible correction due to the solvent effect the order of the magnitude of the chemical shift does not change, the result obtained here will give some information concerning the molecular structure and electron density distribution in the molecule.

The possible explanation for the slight change of chemical shift is as follows:

1) **Steric Effect.**—By the steric repulsion between alkyl groups, the X-C-H bond angle changes slightly, following the slight change in hybridization of the carbon atom in C-H bond.

2) **Inductive Effect.** — As R goes from H through $CH_3$ to higher alkyl groups in R'-O-R, the electron affinity of oxygen atom for R' is lowered causing protons in R' to be more shielded*.

3) **Steric and Inductive Effect.**—As R goes from H to higher alkyl groups in R'-O-R, by the steric hindrance the C-O-C bond angle in R'-O-R increases slightly causing a slight change of hybridization of the oxygen atom and further the increase of electron affinity of the oxygen atom.

4) **Direct Effect.** — As R goes from H to higher alkyl groups, the bond angle in molecules change slightly, causing the slight change of magnetic anisotropy of atoms and then shielding for the protons interested.

At present, it is impossible to decide immediately which cause is predominant, since it is quite difficult to estimate the amounts of the influences of these effects on chemical shift quantitatively. The author could say, however, that at least two causes must be considered since opposite senses are obtained in the correlations shown in Tables II and III.

More detailed discussion concerning this problem will be reported in the near future.

The author wishes to express his sincere thanks to Drs. Y. Mashiko and A. Kuboyama of this Institute and Dr. S. Hattori of Kanazawa University for their valuable discussions, and to Dr. H. Honda and Mr. K. Nagata of the Resources Research Institute and Mr. A Suzuki of this Institute, for their help in the laboratory work.

*Government Chemical Industrial Research Institute of Tokyo*
*Shibuya-ku, Tokyo*

* It is essentially the same as the notation given by Chamberlain. See Ref. 3.

* Dewar described this as I effect of alkyl group in his text book. M. J. S. Dewar, "The Electronic Theory of Organic Chemistry", Oxford Univ. Press, London (1949), p. 52.

# SHORT COMMUNICATIONS

## *Proton Magnetic Resonance in Cocoon*

By Shizuo FUJIWARA* and Makoto NAKAJIMA**

(Received May 16, 1960)

As the application of the nuclear magnetic resonance, we made a preliminary measurement of the proton resonance in cocoon in order to obtain information about the general features of the thermal motions of molecules. The line shape, the width, and the second moments of the absorption curves were investigated in usual way[1].

### Apparatus and Sample

Most part of the apparatus of NMR measurements is same as described by Gutowsky et al.[2], and has been published elsewhere[2]. The magnetic field applied was about 4000 gauss. The intensity of the rf-field, $H_1$, was about 0.1 gauss. The samples were slightly saturated by this strength of $H_1$, but we could not reduce $H_1$ to the lower level. Measurements were made at room temperature as well as at lower temperatures which were obtained by using the Gutowsky's type[2] Dewar vessel. The temperature of the sample was measured by a copper-constantan thermocouple placed 5 mm. apart from the sample.

Several species of cocoon produced by the Tokyo University of Agriculture and Technology were used as the samples which were hereditally different from each other. Measurements of the temperature dependence of the NMR spectrum were made for the species, Shuka×Ginrei. Samples of four species including two yellow, one white, and one red were measured at the room temperature. They have the genes as shown in Table II, and each of them was divided into two parts of the outer and the inner layers.

### Temperature Dependence of the Line Shape

Fig. 1 shows the results of the measurements for Shuka×Ginrei at different temperatures,

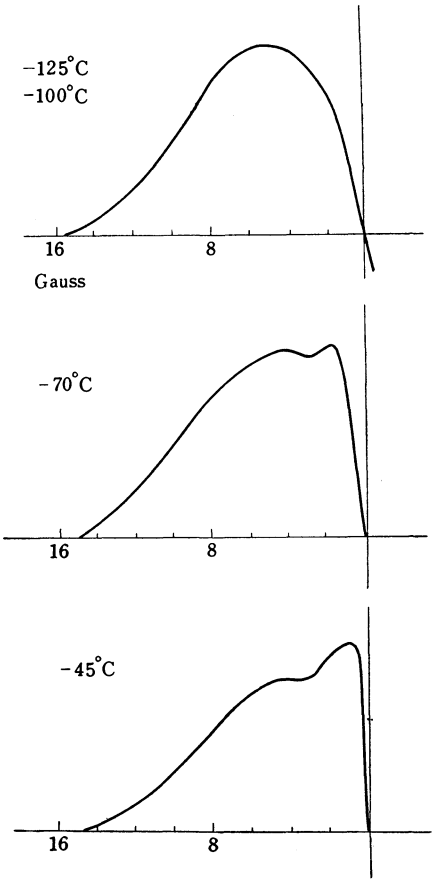



Fig. 1. Proton magnetic resonance in cocoon (species: Shuka×Ginrei). One half of the derivative of the absorption curve is presented as the function of temperature.

where a half of the derivative of each absorption curve is presented. It is noted in the figure that the observed spectrum shows a compound structure, and, moreover, that the relative intensity of the central peak with respect to that of the outer shoulder is much reduced at the lower temperatures, and not detectable at −100°C. The line widths of both the central- and the outer-peaks are not much changed by the temperature.

Besides the principal aminoacids of the silk fibroin, glycine (44%), alanine (26%), and tyrosine (13%), the native cocoon contains sericin. Hence, apart from the amido hydrogens, silk fibroin will contain approximately

* Present address: Department of Chemistry, Faculty of Science, The University of Tokyo, Hongo, Tokyo.
** Tokyo University of Agriculture and Technology, Koganei, Tokyo.

1) General aspect of the proton magnetic resonance in solid will be obtained in Chapter 6 of "Nuclear Magnetic Resonace" by E. R. Andrew, Cambridge University Press, Glasgow (1955), p. 151.

2) H. S. Gutowsky, L. H. Meyer and R. E. McClure, *Rev. Sci. Inst.*, **24**, 644 (1953).

3) S. Fujiwara and S. Hayashi, *Rep. of University of Electro-Communications*, No. 8, 96 (1956).

36% of the protons in methylene groups, but also about 27% in methyl groups, and 36% in CH, OH, or aromatic positions.

Although one may interpret that the existence of a compound structure (as in the cases of polyethylene and polytetrafluoroethylene[4,5] does not necessarily imply that there are two separate regions differing in their degree of motion as proved for natural rubber[6], polymethylmethacrylate[7] and so on, however, we assume that the structure of the observed spectra is due to the net contribution of the protons in different phases, very motional and rigid, since the relative intensity of the central peak is so strongly temperature dependent, and its width is almost independent.

Table I gives the characteristic figures of the spectrum.

As the component I is observable even at −70°C, it can not be attributed to the sorbed water which might be existent in the sample. The line width of II is invariant with temperature over a range of about 130°C, and if our assumption on the structure of the line

TABLE I. NMR LINE WIDTH OF COCOON (SHUKA×GINREI)

| Component | Line width (in gauss) | | | |
|---|---|---|---|---|
| | <−100°C | −70°C | −45°C | 21°C |
| I(narrow) | (−) | (0.8) | 0.8 | 0.8 |
| II(broad) | 8.0 | 8.0 | 8.0 | 8.0 |

The value for I at −70°C was difficult to determine exactly, since its intensity was low.

TABLE II. CHEMICAL COMPOSITION AND THE NMR DATA FOR SEVERAL SPECIES OF COCOON AT 21°C

| Sample | | Layer | Color | Sericine | Amido-N | Carbon | Amido-N | Carbon | $\langle \Delta H^2 \rangle$ | $(\Delta H)_{max.}$ sl. for component II in gauss | Weight % of component I.. |
|---|---|---|---|---|---|---|---|---|---|---|---|
| | | | | Sericine % | % | % | % | % | gauss² | | |
| Osmt × Ci | C | outer | yellow | 36.2 | 0.63 | 47 | 0.36 | 47 | 9.0 | 6.4 | 10.0 |
| | | inner | white | 17.2 | 0.45 | 48 | 0.35 | 48 | 10.8 | 7.0 | 12.5 |
| | Ci | outer | white | 32.8 | 0.65 | 47 | 0.33 | 48 | 9.5 | 7.0 | 11.0 |
| | | inner | yellow | 16.5 | 0.46 | 48 | 0.34 | 47 | 9.8 | 7.5 | 15.7 |
| | +Ci | outer | white | 30.2 | 0.68 | 47 | 0.34 | 48 | 9.7 | 7.0 | 16.0 |
| | | inner | white | 15.4 | 0.48 | 49 | 0.36 | 47 | | | |
| Pk | Pk+c | outer | red | 30.0 | 0.64 | 47 | 0.35 | 48 | 9.7 | 7.9 | 12.0 |
| | | inner | white | 17.7 | 0.51 | 48 | 0.33 | 48 | 11.6 | 8.3 | 14.5 |

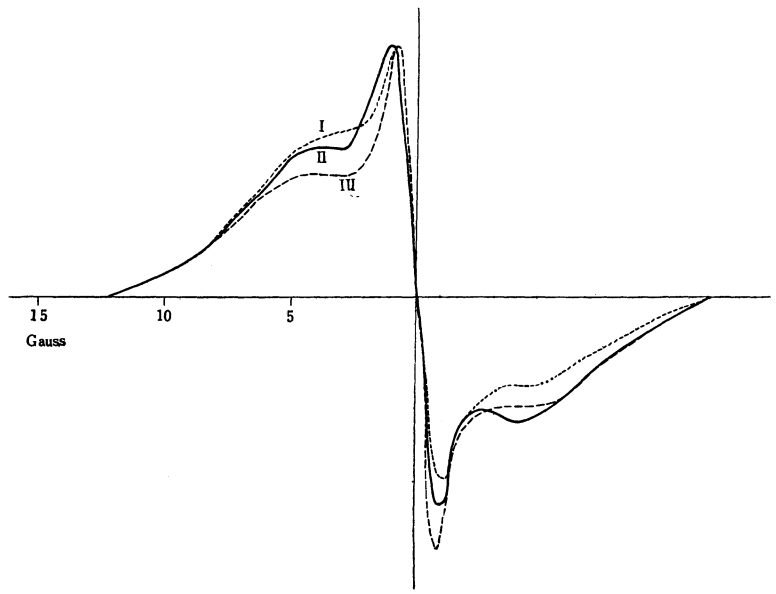



Fig. 2. Derivatives of the NMR absorption spectra for different species of samples at 20°C.
I Shuka×Ginrei, II Osmt, III Pk

4) C. W. Wilson and G. E. Pake, *J. Poly. Sci.*, **10**, 503 (1953).
5) C. W. Wilson and G. E. Pake, *J. Chem. Phys.*, **27**, 115 (1957).
6) H. S. Gutowsky and L. H. Meyer, ibid., **21**, 2122 (1953).
7) J. G. Powles, *Proc. Phys. Soc.*, **69B**, 281 (1956).

shape is correct, this will suggest that the protons in this component are effectively rigid.

The second moments at $-100$ and $-125°C$, where no central peak was observale, were 26.8 and 26.1 gauss$^2$, respectively, and those at $-75°$, $-45°$ and $+21°C$ were 26.1, 24.3 and around 10 gauss$^2$, respectively, which could be explained by the variation of the relative intensities of I and II.

**Line Shapes for Different Species of Cocoon**

Measurements were made for the samples different in species. The results of the measurements were shown in Table II, where the results of the chemical analyses were also shown. Though there is not much difference either in the chemical composition or in the features of the NMR data, among the samples of different species, we notice that the behavior of saturation is different: Fig. 2 shows the normalized derivative curves for the samples, where no saturation effect is observed in the record of Pk, since the each half of the spectrum is completely symmetric with respect to the center of the base line, whereas, in Shuka×Ginrei, the intensity of the right-hand side half is strongly reduced.

Authors thank to Mr. Michio Horinouchi for his assistance in making measurements.

*The University of Electro-Communication*
*Chofu, Tokyo*

## *Separation of Uranium from Fission Products Using Cellulose*

By Noboru Oi

(Received August 16, 1960)

It has been previously known[1] that cellulose has the property of adsorbing metals such as rare earths from impure uranyl nitrate in ether-nitric acid mixture. We could separate uranium from fission products by dissolving uranyl nitrate in organic solvent and percolating the solution through a column of cellulose pulp. Almost all parts of fission products (99% or more) were retained on the cellulose, while uranyl nitrate passed unadsorbed.

Experimental procedure was as follows. A glass tube, 18 mm. in diameter and 10 cm. long, was packed with 1 g. of activated cellulose (100~200 mesh). Uranyl nitrate (1 g.) which includes fission products (about $10^6$~$10^8$ cpm) was dissolved in 5 ml. of the solvent and was transferred to the top of the column. After washing out uranium with further 25 ml. of the solvent, 30 ml. of 0.2 M nitric acid was passed to elute fission products. The activity of the combined organic solvent, nitric acid and the remained cellulose were analyzed by a $\gamma$-scintillation spectrometer.

Organic solvents suitable for this procedure were oxygen-containing compounds which dissolve uranyl nitrate but have small water-insolubility, perhaps less than 2%. Tri-*n*-butylphosphate was found to elute fission products.

The organic solvent was preferably used without nitric acid. Presence of nitric acid enhanced the elution of fission products, especially ruthenium. For example, from 1-month-cooled irradiated uranium, 1% of fission products were eluted by ethyl ether, while 4.5 and 6.6% were eluted by ethyl ether containing 3 and 5% nitric acid, respectively. In this case the ratio of eluted ruthenium was 1 : 18 : 27.

As regards the influence of water in this procedure, it was shown that fission products were eluted more by decreasing the water content of the system. For example, in the case of uranyl dihydrate, fission products were eluted about twice as much as that of uranyl trihydrate. This fact seems to indicate that this separation method resembles to ordinary liquid-liquid extraction. The cellulose seems to act as the water layer.

Behavior of various nuclides in this separation were as follows. Nuclides which were found to contaminate the organic solvent were mainly iodine, ruthenium and cesium. From these, ruthenium is most troublesome. It was eluted 1% by ethyl ether, 4% by *n*-butyl acetateand 20% by methyl isobutyl ketone. Elution of cesium ceases by lowering the initial uranium concentration. Result of the batch method showed that distribution ratio of cesium-137 between *n*-butyl acetate and the cellulose were 2.1 (1.0 M), 9.5 (0.5 M), 450 (0.1 M), and 6300 (0.0 M) in each uranium concentration written in the parentheses. Zirconium and niobium were eluted only to a small extent. Rare earths remained on cellulose.

Example of treatment of 1 g. of 100 days-cooled irradiated uranium are shown in the table. These results may also be improved by lengthening the column or lowering the initial uranium concentration in the solvent.

It seems that this method is also interesting for handling large amounts of irradiated uranium. In this method mass transfer of

1) F. H. Burstall and R. A. Wells, *Analyst*, 76, 396 (1951).

uranium between two different phases is not performed, so that the contamination of fission products is rather small. Moreover uranium can be easily recovered and fission products are condensed on the small amounts of cellulose.

TABLE

| | The amounts of $\gamma$-activity eluted, % |
|---|---|
| Ethyl ether | 0.42 |
| *n*-Butyl acetate | 0.68 |
| Isoamyl acetate | 0.89 |
| Isopropyl acetate | 1.1 |
| Methyl isobutyl ketone | 3.1 |
| Total activity | about $10^7$ $\gamma$ cpm |

The author wishes to express sincere thanks to Mr. Kakuzo Tada of Matsuda Research Laboratory of Tokyo Shibaura Electric Co., Ltd. for kind suggestion and encouragement.

*Matsuda Research Laboratory*
*Tokyo Shibaura Electric Co., Ltd.*
*Kawasaki*

## *The Crystal Structure of Pyridine N-Oxide Hydrochloride and Hydrobromide*

By Yoshiyuki NAMBA, Tsutomu ODA, Hideo ITO and Tokunosuke WATANABE

(Received August 22, 1960)

Pyridine *N*-oxide has recently been a target of investigations by electronic and infrared absorption spectra[1] and by molecular orbital calculations[2], to elucidate its molecular symmetry, bond orders and electronic states, etc. In order to amplify informations about the molecular structure of this compound, the present authors have attempted an X-ray study of its hydrochloride and hydrobromide.

Hydrochloride and hydrobromide of pyridine *N*-oxide were prepared by adding hydrogen chloride or bromide gas to an alcoholic solution of pyridine *N*-oxide. Crystals of these salts were obtained by slow evapolation of alcoholic solutions. They are of a form of a short rod-like prism. The melting points were determined to be 181°C for the hydrochloride and 168°C for the hydrobromide.

No cleavage was observed with both crystals. As these crystals are hygroscopic, we employed a crystal enclosed in a thin-walled capillary made of borosilicate glass for X-ray analyses.

Oscillation and Weissenberg photographs taken with copper $K_\alpha$ radiation ($\lambda=1.54$ Å) indicate that the two crystals are isomorphous and belong to the orthorhombic system. The unit cell dimensions are: $a=11.06\pm0.02$ Å, $b=7.70\pm0.02$ Å, $c=7.25\pm0.02$ Å for the hydrochloride and $a=11.40\pm0.02$ Å, $b=7.87\pm0.02$ Å, $c=7.42\pm0.02$ Å for the hydrobromide. From the density values as determined by the flotation method, each unit cell is found to contain four chemical units. The systematic absences recognized were the $(h\,0\,0)$ reflections with $h$ odd, $(0\,k\,0)$ with $k$ odd and $(0\,0\,l)$ with $l$ odd. Hence the space group was uniquely determined to be $D_2^4$–$P2_12_12_1$. The intensities of $(h\,k\,0)$ and $(h\,0\,l)$ reflections were estimated visually by comparison with calibrated intensity scales, and they were corrected for Lorentz and polarization factors. Approximate temperature and scale factors were obtained by Wilson's method.

From the Patterson projections, $P(uv)$ and $P(uw)$, approximate positions for the halogen atoms were obtained. They are, $x=11/60$, $y=11/60$ and $z=0$. As it was clear that the hydrochloride was more suitable for obtaining atomic positions of light atoms, further analyses were made mainly with the hydrochloride.

A two-dimensional Fourier projection, $\rho(xz)$, was prepared for the hydrochloride using the structure factors whose signs were determined by the chlorine atoms. There appeared in this projection in addition to a predominant peak whose parameter values were those expected for the chlorine atom, a ring-like structure suggesting the location of the skeleton of pyridine *N*-oxide. We calculated the structure factors as a function of the rotation angle of the C···N—O axis of pyridine *N*-oxide within its plane and found that the C···N—O axis is almost parallel with the *c*-axis. In these calculations, we assumed for pyridine *N*-oxide a planar configuration having the symmetry $C_2-2$ with bond lengths, 1.4, 1.4 and 1.3 Å for the C—C, C—N and N—O bonds, respectively. The atomic scattering factors for the carbon, nitrogen and oxygen atoms were those taken from McWeeny's values. In determining the y-coordinates, there remained two possibilites for the orientation of the pyridine *N*-oxide plane referred to the $(0\,1\,0)$ plane. Structure factor calculations for $(h\,k\,0)$ reflections were carried out as a functions of the y-coordinate of the center of the pyridine ring, for the two orientations of its plane ($+30°$, $-30°$), and found a structure which explained fairly well lower order reflections.

1) M. Ito and N. Hata, This Bulletin, **28**, 260 353 (1955).
2) H. H. Jaffe, *J. Am. Chem. Soc.*, **76**, 3527 (1954); **77**, 4441, 4445, 4448, 4451 (1955); T. Kubota, *J. Chem. Soc. Japan, Pure Chem. Sec.* (*Nippon Kagaku Zasshi*), **80**, 578 (1959).

Successive refinements were made. However, as the overlap of light atoms did not permit to give individual atomic coordinate accurately. Therefore an effort was made to improve the y-coordinate of each atom, using the least square method. The $\rho(xz)$ and $\rho(xy)$ are illustrated in Figs. 1 and 2. The atomic arrangement projected along the $c$ and $b$ axes are illustrated in Fig. 3.

The configuration of pyridine *N*-oxide is found to be almost planar. Each chlorine atom is surrounded by six pyridine *N*-oxide groups as neighbors. Namely, if we take a chlorine atom marked (A) in Fig. 3, the neighboring pyridine *N*-oxide groups are those designated by (1), (2), ···, (6). If we assume the pyridine *N*-oxide group behaves as a positive ion and the chlorine atom as an anion, as the results of proton transfer, the structure could be described as an ionic structure. However, the chlorine atom has one oxygen atom at a close distance 2.9 Å ((A)·····O atom of

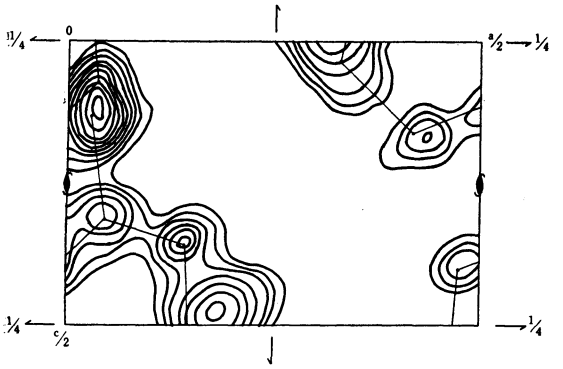



Fig. 1. Electron density map projected on *ac* plane. The intervals of contours for chlorine are twice as much as those for the other atoms.

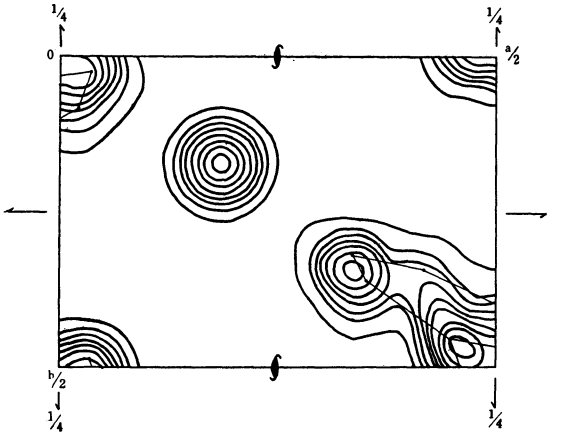



Fig. 2. Electron density map projected on *ab* plane. The intervals of contours for chlorine are twice as much as those for the other atoms.

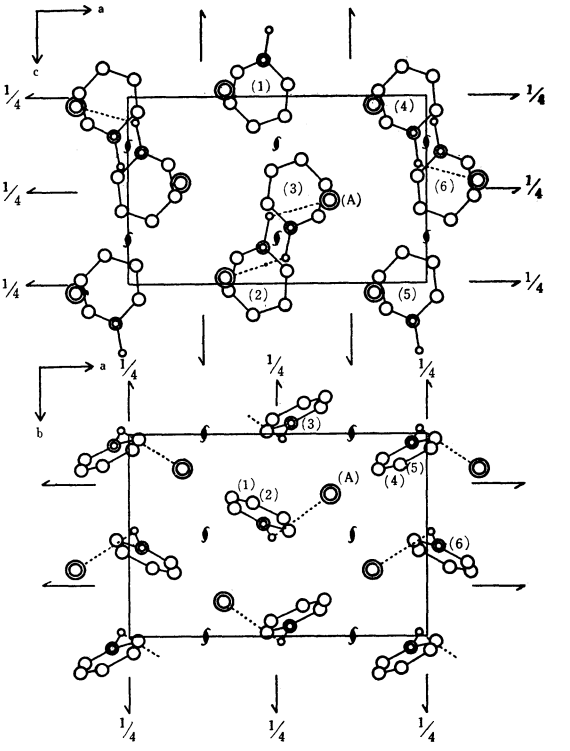



Fig. 3. Projections of the structure, on (010) and (001), showing shorter O···Cl contact with dotted line.
- ○ Oxygen
- ◎ Nitrogen
- ○ Carbon
- ◎ Chlorine anion

pyridine *N*-oxide (2)) which suggests a strong interaction between these two atoms, presumably by a hydrogen bond, O—H···Cl. This point of view is supported by the investigation made by the infrared absorption spectra[3]. If this hydrogen bond is strong enough, pyridine *N*-oxide would form a dipolar molecule with hydrogen chloride, leading to a packing of dipolar molecules. The actual state may be just between two extremes.

We shall postpone discussing the precise configuration of the pyridine *N*-oxide molecule concerning to the electronic state of $\pi$ electrons involved in pyridine ring and those of oxygen atom, in conjugation with each other, untill three-dimensional analyses are made.

*Laboratory of Physical Chemistry*
*Osaka University of Liberal Arts and Education, Minamikawahoricho*
*Tennoji, Osaka (Y. N. and T. O.)*

*Department of Physics, Osaka University, Nakanoshima, Osaka*
*(T. W.)*

3) Y. Matsui and T. Kubota, Presented at the 12th Annual Meeting of the Chemical Society of Japan, Kyoto, April, 1959.

## *The Crystallization of "Allophane" under Hydrothermal Conditions*

By Mitsue KOIZUMI*, Ryôiti KIRIYAMA** and Wataru MURAYAMA**

(Received September 10, 1960)

Allophane, a hydrous silica-alumina mineral, is classified into mineral allophane, soil allophane and "precipitation allophane"[1] from their ways of occurrence. They are almost X-ray amorphous and show the similar thermal behavior characterized by mullite formation at 900~1000°C under atmospheric condition.

In hydrothermal synthesis experiments, crystallization of some amorphous materials, gels or glasses, occurs at fairly low temperatures. In such a condition, phase assemblages more stable than the reactants may easily be formed. An attempt has been made to observe structural differences of allophane and consequently to establish a picture of structural classification of X-ray amorphous minerals by applying the crystallization method under hydrothermal conditions.

The general procedure was to allow samples of allophane to react with water over the range 200~500°C at 1000 atm. $H_2O$ and then to quench into water. The type of pressure vessel used was of the "test-tube" bomb[2]. Running was made for two weeks at maximum. The products were then examined with an X-ray diffractometer.

Soil allophane from Kanuma[3] and Imaichi[4], mineral allophane from Bihoro[5] and precipitation allophane from Asama[6] and Fukazawa[7] were used for the experiment[8]. Synthetic silica-alumina gels prepared by the homogeneous precipitation method over the chemical composition range of $2SiO_2 \cdot Al_2O_3$-$SiO_2 \cdot 5Al_2O_3$ were kindly supplied for this investigation by

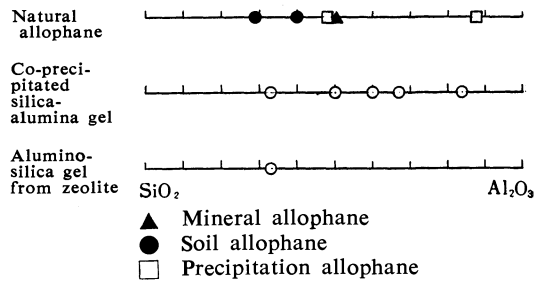



Fig. 1. The chemical composition of the starting materials.

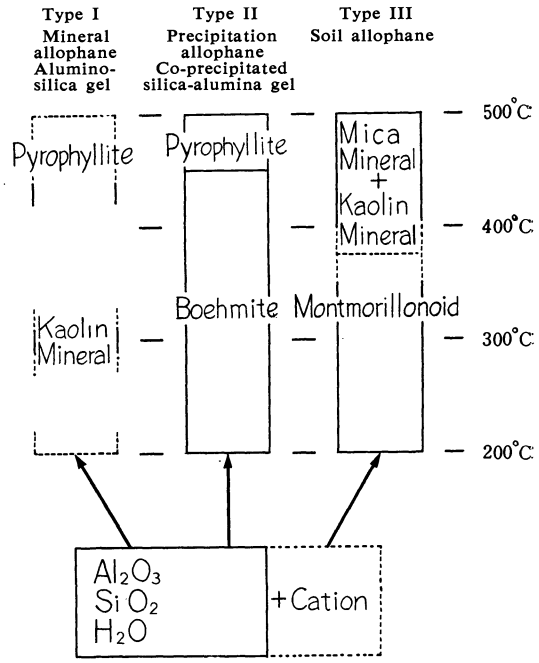



Fig. 2. Diagrammatic representation of phase assemblages obtained from the various starting materials.

Dr. J. Ossaka. The thermal properties of these gels has been studied by Ossaka and found to be identical with those of the natural allophanes[7]. The aluminosilica gel was also prepared from synthetic zeolite, Type A[9], by destructing the framework with hydrochloric acid and then washing sodium ion off with water. The mole ratios of $SiO_2/Al_2O_3$ of these starting materials are illustrated in Fig. 1.

The experimental results are summarized diagrammatically in Fig. 2. Owing to the poor crystallinity of the products, the prcise phase determination was somewhat difficult for several specimens. As indicated in Fig. 2, the crystallization process of the starting materials in this investigation are classified into the following types.

* Present address, Institute of Geological Sciences, College of General Education, Osaka University, Toyonaka, Osaka.

** Present address, The Institute for Scientific and Industrial Research, Osaka University, Sakai, Osaka.

1) This amorphous mineral found from mineral spring was classified by J. Ossaka into a variety of the species of allophane.

2) R. Roy and E. F. Osborn, *Econ. Geol.*, 47, 717 (1952).

3) T. Sudo and J. Ossaka, *Japanese J. Geol. Geogr.*, 22, 215 (1952).

4) R. Morimoto, J. Ossaka and T. Fukuda, *Bull. Earthq. Res. Inst.*, 35, 359 (1957).

5) H. Minato, *Advances in Clay Sci.*, 2, 350 (1960).

6) J. Ossaka, ibid., 2, 339 (1960).

7) J. Ossaka, read before the Annual Meeting of the Mineralogical Society of Japan, Tokyo, June, 1959.

8) The authors are indebted to Dr. J. Ossaka and Dr. H. Minato of the University of Tokyo who kindly supplied the specimens for the experiment.

9) D. W. Breck, W. G. Eversole, R. M. Milton, T. B. Reed and T. L. Thomas, *J. Am. Chem. Soc.*, 78, 5963 (1956).

Type I: From the materials of this type, a kaolin mineral was formed at 300°C, and then pyrophyllite was obtained at 430°C. The mineral allophane and the aluminosilica gel appeared to crystallize in this manner.

Type II: The two samples of precipitation allophane and all the co-precipitated silica-alumina gels with various compositions were classified into this type. It should be noted that, from these samples, only a boehmite phase appeared in the temperature range between 200 and 450°C and above 450°C pyrophyllite was formed.

Type III: The three samples of soil allophane yielded a montmorillonoid phase in the region from 200 to 350°C. The (0 0 1) spacing was 15 Å and expanded to 18 Å when treated with glycol. Above 400°C, a mica and a kaolin mineral were obtained together.

Important factors controlling what phases crystallize from the amorphous minerals may be considered to involve (i) $SiO_2/Al_2O_3$ ratio, (ii) impurity cations and (iii) the gel structure. It is probably possible to remove $SiO_2/Al_2O_3$ ratio out of the major factors on the following basis. Each of the three specimens with the almost same ratio of 2:1, including aluminosilica gel, soil allophane and one of co-precipitated silica-alumina gels, gave a product of its own phase. Such was the case also with mineral allophane, precipitation allophane and co-precipitated gel of the same $SiO_2/Al_2O_3$ ratio of 1:1. The products of type III were obtained only from soil allophane. It is considered that their formation may be effected by the presence of a considerable amount of cation impurities which have been contained in every soil allophane. On the contrary, all the starting materials of the types I and II are chemically free from any cations. It is thus reasonable to assume that gel structure plays a role in deciding the product from the starting materials of the similar chemical composition.

From the preparation method previously mentioned, it is suggested that the co-precipitated gels are homogeneous mixtures of the two species of gel particles, silica and alumina, finely dispersed in each other. This concept is supported by the experimental result that the materials of the type II do not yield an aluminosilicate phase but an alumina mineral, boehmite, in the lower temperature range. Thus the precipitation allophane is possibly considered to be structurally identical with the co-precipitated gel.

Mineral allophane showed the same crystallization behavior with an aluminosilica gel prepared from the zeolite. It is obvious, therefore, the mineral allophane is probably an aluminosilicate with four-coordinated aluminum.

As it is well known, our present knowledge is insufficient to discuss the gel structure precisely. From the above results, however, we may now recommend that study on crystallization under hydrothermal conditions will be applicable to deduce a structure of X-ray amorphous mineral. In this way natural allophane of this investigation can be classified into three groups.

The detailed description of this work will be given elsewhere in near future.

*Faculty of Science*
*Osaka University*
*Nakanoshima, Osaka*

## *Hot-atom Chemistry of Radiocobalt in Nitroammine Cobalt Complex Salts**

By Nobufusa SAITO, Takeshi TOMINAGA and Hirotoshi SANO

(Received September 10, 1960)

The present authors had previously reported[1,2] that radiobromine recoil atoms arising from thermal neutron capture in outer anions of various cobaltammine bromides could substitute in the cobalt coordination sphere to form $^{80m}$Br- or $^{82}$Br-labeled complex cations. In this investigation they found that outer anions of nitroammine cobalt(III) nitrates and nitrites could replace ligand $NH_3$ groups in the radiocobalt coordination sphere when cobalt atom was activated by slow neutron bombardment.

Seven kinds of crystalline complex salts listed in Table I were irradiated in an experimental hole in JRR-1 reactor for one to six hours at pile temperature. Thermal neutron flux was approximately $3\times10^{11}$ n/cm$^2$ sec. After standing for one day at room temperature, the irradiated salts were dissolved in water and $^{60}$Co-labeled species were separated by procedures involving paper electrophoresis[3], paper chromatography[4],

* Presented at the 13th Annual Meeting of the Chemical Society of Japan, Tokyo, April, 1960.

1) N. Saito, H. Sano and T. Tominaga, This Bulletin, 33, 20 (1960).

2) N. Saito, T. Tominaga, and H. Sano, ibid., 33, 120 (1960).

3) M. Maki, *Japan Analyst*, 4, 217 (1955).

4) Y. Yamamoto, A. Nakahara and R. Tsuchida, *J. Chem. Soc. Japan, Pure Chem. Sec.* (*Nippon Kagaku Zasshi*), 75, 114 (1954).

TABLE I. PERCENTAGE DISTRIBUTION OF $^{60}$Co-LABELED SPECIES AFTER THE DISSOLUTION OF IRRADIATED NITROAMMINE COMPLEXES

| Target | $^{60}$Co-labeled species, %* | | | | | | R** |
|---|---|---|---|---|---|---|---|
| | $CoA_6^{3+}$ | $CoA_5NO_{2,3}^{2+}$ | $CoA_4(NO_{2,3})_2^+$ | $CoA_3(NO_{2,3})_3$ | $CoA_2(NO_{2,3})_4^-$ | $Co^{2+}$ | |
| $[Co(NH_3)_6](NO_2)_3$ | 0.9 | 17 | 38 | 13.5 | 9 | 19 | 19 |
| $[Co(NH_3)_6](NO_3)_3$ | 4.5 | 11.5 | 26 | <1.7 | <0.8 | 58 | 3 |
| $[Co(NH_3)_5NO_2](NO_2)_2$ | ≤0.6 | 39 | 18 | 3.9 | 1.4 | 38 | 0.5 |
| $[Co(NH_3)_5NO_2](NO_3)_2$ | ≤0.7 | 34 | 23 | 4.0 | 1.1 | 37 | 0.7 |
| *cis*-$[Co(NH_3)_4(NO_2)_2](NO_3)$ | ~0 | <1.4 | {cis: 47, trans: 4} | 4.2 | 0.9 | 43 | 0.08 |
| *trans*-$[Co(NH_3)_4(NO_2)_2](NO_3)$ | ~0 | 0.5 | {cis: 4.6, trans: 45} | 3.1 | 0.4 | 46 | 0.07 |
| $[Co(NH_3)_3(NO_2)_3]$ | ~0 | ~0 | 0.5 | 55 | ~0 | 44 | 0 |

* "A" denotes an $NH_3$ group in most cases. However, it is possible that small amounts of species with one or two of A's being $H_2O$ may also be present in some cases.

** $R = \frac{\text{Percentage of labeled species containing one more anionic ligand than the target complex}}{\text{Percentage of labeled species containing the same number of anionic ligands as the target complex}}$

ion exchange, or precipitation. The results are summarized in Table I.

As shown in Table I, substitution of ligand $NH_3$ groups by outer anions ($NO_2^-$ or $NO_3^-$) was observed** in most complex salts whenever the substitution product was considerably stable in aqueous solutions. On the contrary, labeled complexes containing less anions in ligands than the target complex were not found in practice after dissolution of almost all the irradiated salts. The factor, *R*, in Table I is the ratio of percentage of labeled species containing one more anionic ligand than the target complex to percentage of labeled species containing the same number of anionic ligands as the target complex. It is interesting that this ratio increases with the increase in electric charge on the target complex ion, or with the increase in number of neighboring outer anions. The results may be generally explained by assuming the electrostatic interaction between the outer anions and the complex ions fragmented more or less during recoil reactions.

It is worth mentioning that cis-trans isomerization of dinitrotetrammine complexes occurs during recoil processes. Cis isomer was found with an enrichment factor of 23±5 in the irradiated *trans*-$[Co(NH_3)_4(NO_2)_2](NO_3)$, while trans isomer with an enrichment factor of 80±10 in the irradiated cis salt.

*Department of Chemistry*
*Faculty of Science*
*The University of Tokyo*
*Hongo, Tokyo*

** This shwos a similarity to the well-known thermal transformation reactions of nitroammine cobalt(III) nitrites.

# *The Electron Spin Resonance Absorption of Molecular Addition Compounds*

By Hiroo INOKUCHI, Kunihiko IKEDA* and Hideo AKAMATU

(Received September 12, 1960)

Recently, a number of molecular complexes formed between electron donors and acceptors have been investigated by the method of electron spin resonance (ESR) and also by the measurement of electrical conductivity[1-3]. On the molecular complexes formed between phenylene diamines and halogenated quinones, Bijl, Kainer and Rose-Innes[3] and also Matsunaga and McDowell[4] reported the existence of unpaired electrons in those complexes. However, it has been found that the observed intensity of ESR absorption fluctuate from specimen to specimen.

In this report, we present the electron spin resonance absorption of the molecular complexes, formed between dimethyl-aniline (I, DMA; liquid) and halogenated benzoquinones (II, *x*-anils) and of those between also tetramethyl-*p*-phenylene diamine (III, TMPD) and *x*-anils as a function of time.

---

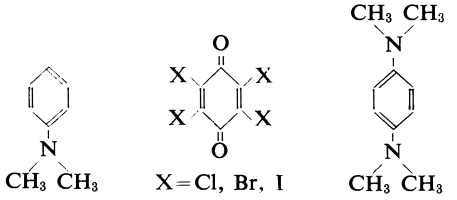
* Present Address: Aeronautical Research Institute, University of Tokyo, Komaba, Meguro-ku, Tokyo.

1) D. D. Eley and H. Inokuchi, Proc. Third Carbon Conf., 91 (1959).
2) D. D. Eley, H. Inokuchi and M. Willis, *Discussions Faraday Soc.*, **28**, 54 (1959).
3) D. Bijl, H. Kainer and A. C. Rose-Innes, *J. Chem. Phys.*, **30**, 765 (1959).
4) Y. Matsunaga and C. A. McDowell, *Nature*, **185**, 916 (1960).

TABLE I. THE PARAMAGNETIC PROPERTIES OF MOLECULAR COMPLEXES FORMED BETWEEN PHENYLENE DIAMINE AND HALOGENATED QUINONES

| Donor | DMA | | | TMPD | | |
|---|---|---|---|---|---|---|
| Acceptor | chloranil | bromanil | iodoanil | chloranil | bromanil | iodoanil |
| Color | blue violet | black violet | black violet | black | brownish black | brownish black |
| $g$-value | $2.0003\pm0.0004$ | $2.0071\pm0.0005$ | $2.0000\pm0.0004$ | $2.0036\pm0.0004$ | $2.0043\pm0.0004$ | $2.0037\pm0.0004$ |
| Line width (gauss) | 20 | 4 (*)<br>32 (†) | 22 | 7 | 13 (*)<br>40 (†) | 22 |
| Spin population (**) | ~0.01% | 5% | 17% | 5% | 7% | 10% |

* Observed with freshly prepared specimen.
† Observed with specimen left for 40 days in air.
** Maximum value.




These complexes were made as follows: 50 mg. of purified $x$-anil were dissolved in 5 cc. of DMA, and one-fifth of its volume of ethanol was added into the solution to precipitate the deep colored molecular complex. After filtration, crystals of the complex were sealed up immediately into glass tubings (diameter 2 mm.) under an atmosphere of argon or oxygen. In the case of TMPD-$x$-anil complexes, the solutions of TMPD and of $x$-anil in benzene were mixed with each other to produce the precipitate of the complex. The precipitate was filtered and washed with a small amount of benzene and of ether successively. These complexes were also kept in glass tubings to prevent a decomposition of TMPD by humidity.

The electron spin resonance absorption spectra of these complexes were observed in association with $x$-band microwave spectrometer, Hitachi MPS-1. The spin concentrations in these complexes were measured in comparison with a standard piece of $\alpha,\alpha'$-diphenyl-$\beta$-picrylhydrazyl or 'violanthrone'*. The $g$-values of these complexes possessed near 2.0 and was estimated from the value of ultramarine which is 2.028.

As illustrated in Table I, it was found that DMA-$x$-anil complexes, for which Bijl et al.[3] observed no ESR signals possess definite ESR absorption around $g=2.0$. This fluctuation of intensity of ESR absorption may depend upon preparation techniques of these complexes. The study of $g$-values of DMA-chloranil and also of DMA-iodoanil, which are fairly smaller than the value of free electron itself ($g=2.0023$), is a noteworthy problem.

In the case of TMPD-$x$-anil molecular complexes (Table I), the spin concentrations changed strongly with great regard to the time after preparation as shown in Fig. 1 for TMPD-bromanil. However, the atmospheric gases surrounding the complexes were not so sensitive to the spin concentration of the complexes excepting TMPD-chloranil.

The ESR absorption curve of TMPD-bromanil complex also changed violently with time in its shape. At first, two ESR absorption peaks, their $g$-values were 2.0030 and 2.0043 respectively, were observed for freshly prepared specimen (curve A of Fig. 2). After a couple of days, a new absorption peak appeared (curve B). However, during a next few days, two of them disappeared and only one ESR absorption peak having $g=2.0043\pm0.0004$ remained (curve C). Through a long period observation, the line width of the

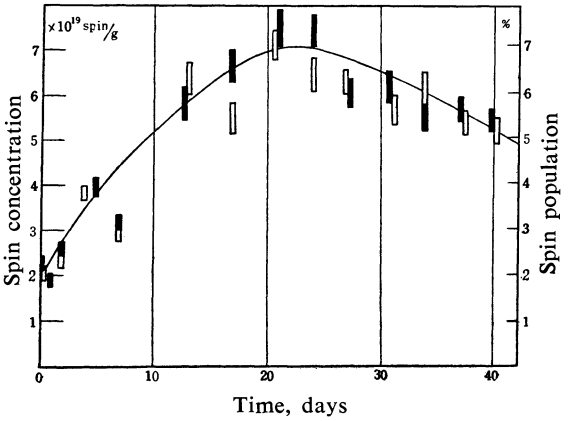



Fig. 1. The time dependence of spin population of tetramethyl-$p$-phenylene diamine-bromanil complex.
■ in air, □ in argon

* Crude violanthrone comprises a small amount of free radicals. This compound can be applied as a substandard piece for the estimation of spin concentration because the free radical is stabilized in the matrix, violanthrone.

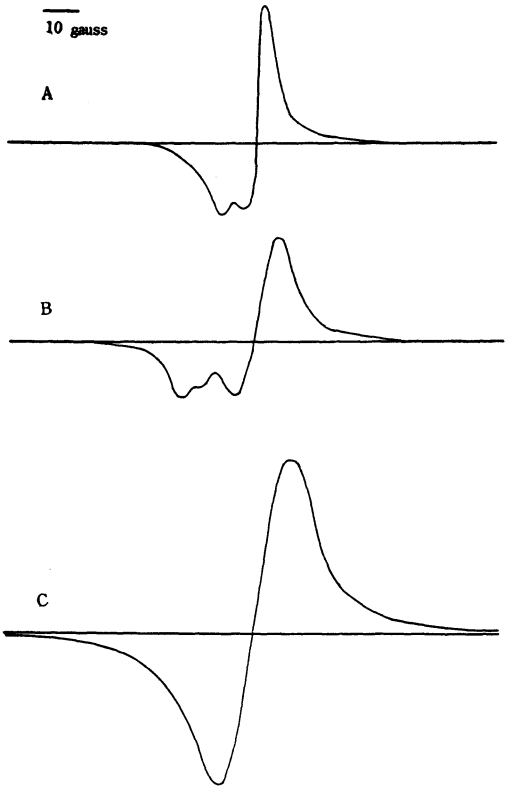



Fig. 2. The derivative curves of electron spin resonance absorption of tetramethyl-*p*-phenylene diamine-bromanil complex in air: (A) for fresh specimen, (B) and (C) for specimen which is exposed in air for 2 days and also for 4 days respectively.

absorption curve was spread from 12~13 gauss to 50 gauss (120 days after preparation).

It seems likely that these changes of spin concentrations and also line widths with time are introduced from the progress of complex formation and/or decomposition of these addition compounds.

*Department of Chemistry*
*Faculty of Science*
*The University of Tokyo*
*Hongo, Tokyo*

# *Detection of End-groups in Polyacrylonitrile by Differential Infrared Spectroscopy*

By Ikuo MATSUBARA

(Received September 19, 1960)

The differential infrared spectroscopy, which is useful for the identification or quantitative estimation of minor constituents in organic substances[1], has been applied to the detection of the end-groups in polyacrylonitrile. As O'Connor et al.[2] have described, the infrared measurements of polymers can be successfully performed with the potassium bromide disk technique, particularly when the samples are obtained in the form of a fine powder or fibers. In the present study the differential analyses of polymers have been carried out with success in combination with the potassium bromide disk technique.

Fig. 1 shows the infrared spectra obtained from the potassium bromide disks of some different polyacrylonitrile samples. The disks were prepared from the mixtures of 400 mg. of potassium bromide and 4 mg. of the sample material, both screened through 250-mesh stainless-steel cloth, by applying a pressure of 8 tons for 10 min. in the evacuated die mount. The infrared spectra were obtained using a Perkin-Elmer model 21 spectrophotometer (with NaCl optics). Samples A and B are polyacrylonitriles of different degrees of polymerization ($\bar{M}_n$=49500 and 11000, respectively)*, both being polymerized by using ammonium persulfate-sodium bisulfite redox system as initiator. Sample C is one polymerized using azo-bis-isobutyronitrile as initiator ($\bar{M}_n$=7000). By inspection of the spectra of samples A and B it has been found that the intensities of the weak shoulder band at 1041 $cm^{-1}$ and the one around 1200 $cm^{-1}$ increase remarkably with the lowering of the degree of polymerization. On the contrary, as is evident from the spectrum of sample C, no such absorption bands of variable intensities are observable at the corresponding frequencies in the case of polyacrylonitrile polymerized using azo-bis-isobutyronitrile as initiator, while the situation is the same for the sample obtained by $\gamma$-ray initiated polymerization. Therefore, it seems that these bands are characteristic of the polymer obtained

1) See for example, D. Z. Robinson, *Anal. Chem.*, **24**, 619 (1952); H. Powell, *J. Appl. Chem.*, **6**, 488 (1956).

2) R. T. O'Connor, E. F. DuPré and E. R. McCall, *Anal. Chem.*, **29**, 998 (1957).

* Measured according to the method of P. F. Onyon, *J. Polymer Sci.*, **22**, 13 (1956).

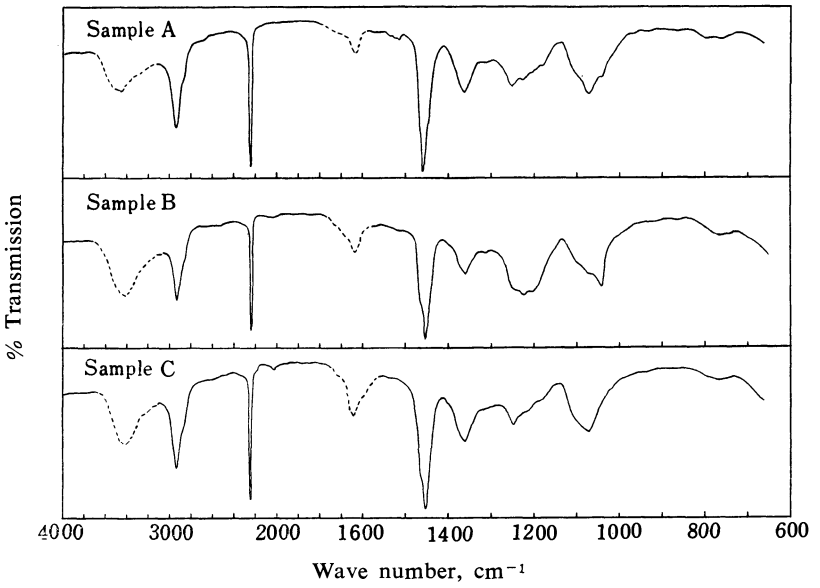



Fig. 1. Infrared spectra of some polyacrylonitriles. Sample A and B were polymerized using ammonium persulfate-sodium bisulfite redox system as initiator ($\overline{M}_n$=49500 and 11000, respectively). Sample C was polymerized using azo-bis-isobutyronitrile as initiator ($\overline{M}_n$=7000). (Dashed lines indicate the absorptions due to water adsorbed by potassium bromide).

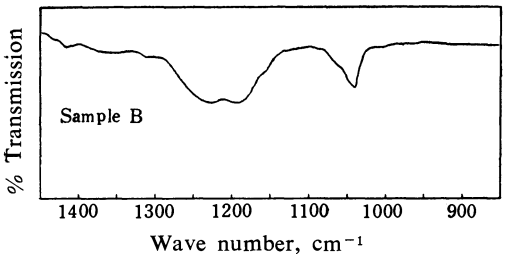



Fig. 2. Differential spectrum of polyacrylonitrile sample B (initiator=ammonium persulfate-sodium bisulfite redox system) against sample C (initiator=azo-bis-isobutyronitrile).

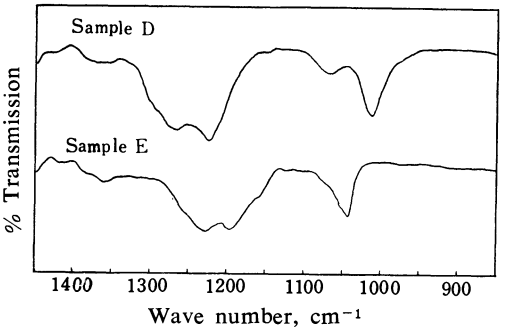



Fig. 3. Differential spectra of polyacrylonitrile sample D (initiator=ammonium persulfate, $\overline{M}_n$=9600) and sample E (initiator=$Fe^{3+}$-sodium bisulfite redox system, $\overline{M}_n$=30300) against sample C (initiator=azo-bis-isobutyronitrile).

using persulfate-bisulfite redox system as initiator. In order to make clear the nature of these bands, the differential method has been applied, in which the disk containing sample B is put in the sample beam of the spectrometer and the absorption bands due to polyacrylonitrile proper are cancelled out by placing the disk containing sample C in the reference beam. The differential spectrum is shown in Fig. 2, in which two independent bands have been separated; one at 1041 $cm^{-1}$ and a doublet with peaks at 1227 and 1190 $cm^{-1}$. It has been predicted from the analyses by tracer methods[3] that, when the persulfate-bisulfite redox system is usedto initiate polymerization, both sulfate and sulfonate end-groups may be introduced into the polymer, and these groups are expected to show characteristic absorptions in the 1200~1000 $cm^{-1}$ region[4]. Therefore, the above two bands are suspected to be due either to the sulfate or sulfonate end-groups. To clarify this point further, two other polyacrylonitrile samples have been examined by the differential method. Sample D was polymerized using ammonium persulfate as initiator ($\overline{M}_n$=9600), and it is expected that the sulfate end-groups

3) Y. Tsuda, *J. Appl. Polymer Sci.*, in press.

4) L. J. Bellamy, "The Infra-red Spectra of Complex Molecules", 2nd Ed., Methuen & Co., Ltd., London (1958), Chapt. 22.

alone may be incorporated in this polymer. Sample E was polymerized using $Fe^{3+}$-sodium bisulfite redox system as initiator ($\overline{M}_n$= 30300), so that the polymer may contain only the sulfonate end-groups. Fig. 3 shows the results of the differential measurements, in which the absorptions due to polyacrylonitrile have been cancelled out by placing sample C in the reference beam. In complete agreement with expectation, the spectrum of sample D corresponds well to those of aliphatic sulfates ($R-O-SO_3^-$), and we may ascribe the doublet with peaks at 1264 and 1224 $cm^{-1}$ to the S-O degenerate stretching vibration, the band at 1065 $cm^{-1}$ to the S-O symmetric stretching vibration of the sulfate ion, while the band at 1011 $cm^{-1}$ may be ascribed to the C-O stretching vibration. In the same way, the spectrum of sample E agrees well with those of aliphatic sulfonates ($R-SO_3^-$)[5], and the doublet with peaks at 1225 and 1195 $cm^{-1}$ may be assigned to the S-O degenerate stretching vibration and the band at 1041 $cm^{-1}$ to the S-O symmetric stretching vibration of the sulfonate ion. Liang and Krimm[6] have reported that there exists a weak shoulder band at 1044 $cm^{-1}$ in the spectrum of polyacrylonitrile and assigned this to a combination or overtone of some skeletal deformation vibrations of this molecule. Although they have not made mention of the initiator by which their polyacrylonitrile sample has been polymerized, it seems quite probable from the above results that this band corresponds to the vibration of the sulfonate end-groups. It is to be wondered why the spectrum of sample B, in which both sulfate and sulfonate end-groups are expected to exist, almost completely agrees with that of sample E and the absorptions due to sulfate end-groups are hardly observable. According to Tsuda's results[3], however, in the polymerization initiated by persulfate-bisulfite redox system the ratio of the concentrations of the sulfate and the sulfonate end-groups produced varies depending on the initial concentrations of the salts and of the acrylonitrile monomer, so that the relative intensities of the absorption bands due to these groups may vary from sample to sample. Therefore, it seems not improbable that the sulfonate end-groups are predominant in the case of sample B.

Quantitative estimations of the end-groups by the differential method were also carried out using the polymers of known end-group contents, and the limit of detectability of both sulfate and sulfonate end-groups by this method is estimated to be about 0.002 millimol./g. polymer.

The author wishes to thank Dr. H. Kobayashi and Dr. K. Kato of Toyo Rayon Co., Ltd. who permitted the publication of this work. He also wishes to thank Mr. H. Kataoka and Mr. K. Shirasaki for their help in experiments.

*Central Research Laboratories*
*Toyo Rayon Co., Ltd.*
*Otsu, Shiga*

5) K. Fujimori, This Bulletin, 32, 850 (1959).
6) C. Y. Liang and S. Krimm, *J. Polymer Sci.*, 31, 513 (1958).

# *Proton Magnetic Resonance Studies on the Thermally Dehydrated Products of Alumina Trihydrate*

By Tatsuo SAITO*

(Received September 21, 1960)

In our previous communication[1], the thermal decomposition of alumina trihydrate was studied from the change of line shapes of proton magnetic resonance absorption in the thermally dehydrated products. In the present communication, the phase transformations accompanied with the thermal dehydration process of alumina trihydrate have been studied from the variation of second moments of the resonance lines in dehydrated products.

The starting material, bayerite, and the detecting apparatus here employed were the same as those used in the previous experiments[1]. The specimens used for the NMR measurements were prepared from this bayerite by the thermal dehydration at 100~800°C which was carried out for 3 hr. in the air. Each specimen was sealed into an evacuated glass tube which was pumped out to a high vacuum at 110°C for 6 hr.

The variation of the second moments calculated from the experimental derivative curves are shown in Fig. 1 as the function of the temperature. Below 220°C, the second moment was 13~14 gauss$^2$ showing no significant change with the temperature. However, in the range from 220 to 400°C the second moment

* Present address, Government Chemical Industrial Research Institute, Tokyo, Honchō 1-Chome, Shibuya-ku, Tokyo.

1) T. Hagiwara and T. Saito, This Bulletin, 33, 1463 (1960).

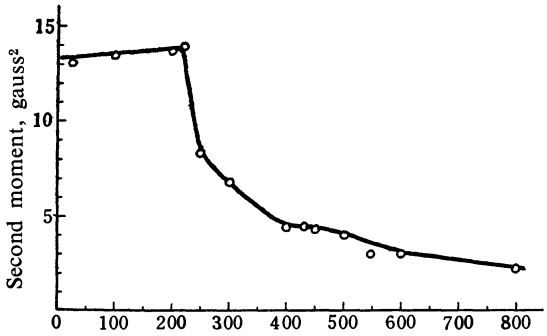



Fig. 1. Variation of the second moments with the temperature in dehydrated products of the starting material.

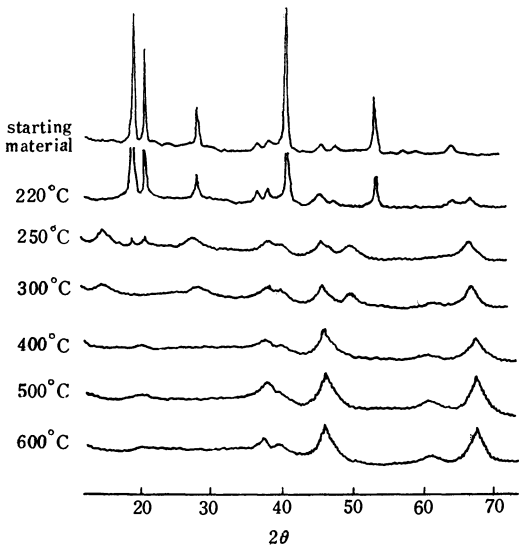



Fig. 2. X-ray diffraction diagrams of the samples dehydrated at various temperatures.

decreases gradually with the rise of temperature, and then at about 400°C the second moment becomes roughly stationary value of 4~5 gauss$^2$. Above 550°C the second moment gradually decreases again.

The above variation of second moments is interpreted as follows:

1) The sudden decrease of second moment at about 220°C seems to show the phase transition from the starting material to the hydrous alumina which has a low value of second moment.

2) The gradual decrease of second moments with the rise of temperature in the range from about 250 to 400°C could be regarded as a result due to the change of mixing ratio of the aluminum hydroxide-hydrous alumina phase.

3) The roughly stationary values of 4~5 gauss$^2$ at about 400~500°C seem to show the phase of hydrous alumina.

The X-ray diffraction study of the compounds was also done. The diffraction diagrams of several specimens which were obtained from this study are shown in Fig. 2. From these diagrams, it is ascertained that the specimens below 220°C having the value of 13~14 gauss$^2$ are crystallographically the same as the starting material, bayerite, and that each specimen at 250° and 300°C shows the diagram of mixed phase of böhmite and $\eta$-alumina, but that the specimens at about 400~500°C having the value of 4~5 gauss$^2$—which are explained to be hydrous alumina—are $\eta$-alumina[2].

It is interesting to note that the transition temperatures of 220 and 400°C are obtained from the variation curve of second moment showing in Fig. 1, while each transition temperature coincides with that of phase transformations obtained from X-ray diffraction studies, respectively.

The author wishes to express his hearty thanks to Professor Tokutaro Hagiwara for his kind direction and also wishes to express his sincere thanks to Professor Tunahiko Shidei and Dr. Syukuro Yano in Kyoto University for their continual guidance and encouragement throughout this study.

*Department of Chemistry*
*Faculty of Science*
*Hiroshima University*
*Hiroshima*

2) A. S. T. M., X-ray powder data file.

## *The Oxygen Effect on Electronic Properties of α, α'-Diphenyl-β-picrylhydrazyl*

By Hiroo INOKUCHI and Minoru KINOSHITA

(Received September 21, 1960)

There is one unpaired electron in each molecule of $\alpha, \alpha'$-diphenyl-$\beta$-picrylhydrazyl. In the study of unpaired spin by means of the method of electron spin resonance (ESR), thereby, this free radical ($g=2.0036\pm0.0003$) is widely used as a standard for estimation of the spin population and also the $g$-value of the applied specimen. However, it has been already known that the ESR absorption spectrum of free radical changes strongly under the influence

TABLE I. THE ELECTRON SPIN RESONANCE ABSORPTION DATA OF D.P.P.H.

| Sample | D.P.P.H.-Single | | | D.P.P.H.-Free | | | D.P.P.H.-Ether | | |
|---|---|---|---|---|---|---|---|---|---|
| | $\Delta H_{msl}$[1] | $\Delta H$[2] | $I$[3] | $\Delta H_{msl}$ | $\Delta H$ | $I$ | $\Delta H_{msl}$ | $\Delta H$ | $I$ |
| Evacuated at 80°C($10^{-6}$ mmHg) for 18 hr. | 1.7 | 3.0 | 1.0 | 1.5 | 2.4 | 1.0 | 1.6 | 2.6 | 1.0 |
| Exposed to air for 2 hr. | 1.7 | 3.0 | 1.0 | 2.25 | 4.2 | 0.9 | 1.75 | 2.9 | 1.0 |
| Exposed to air for 2~3 days. | 1.9 | 3.2 | 1.0 | 2.5 | 4.7 | 0.9 | 1.75 | 2.9 | 1.0 |

1) $\Delta H_{msl}$: Distance between inflection points on absorption curve in gauss.
2) $\Delta H$: Line width at half power of absorption curve in gauss.
2) $I$: Integrated intensity (products of $\Delta H$ and height of the absoption curve) in arbitrary unit.

of gaseous oxygen[1-3]. Further, the existence of stable addition compound between $\alpha, \alpha'$-diphenyl-$\beta$-picrylhydrazyl and a organic solvent*, such as benzene, cyclohexane or ether, has been reported frequently[4]. In this brief report, we are presenting the effects of oxygen on the spin population and also on the electronic conduction of $\alpha, \alpha'$-diphenyl-$\beta$-picrylhydrazyl itself.

The observation of ESR absorption spectra was carried out at room temperature with association of Hitachi MPS-1 type x-band spectrometer. This prime free radical was made from $\alpha, \alpha'$-diphenyl-$\beta$-picrylhydrazine by oxidation with $PbO_2$ in ether. The dependence of the line width and of the intensity of ESR absorption spectra on the three different samples have been observed. One of them, recrystallized from carbon disulfide solution, was a solvent free powdered sample (D.P.P.H.-Free). The second sample was a large single crystal (1.3 mg.) grown from carbon disulfide solution (D.P.P.H.-Single) and the third sample was deposited from ether solution (D.P.P.H.-Ether).

We found that the spin populations in these samples, keeping in vacuo, were coincident with each other as shown in Table I. When these materials were exposed to air, the line width of ESR spectrum of D.P.P.H.-Free was spread remarkably. However, no change of the integrated intensity of ESR absorptions was found practically in spite of broadening of their line widths. These results indicate that the interaction between $\alpha, \alpha'$-diphenyl-$\beta$-picrylhydrazyl and applied solvent or gaseous oxygen is physical instead of chemical one.

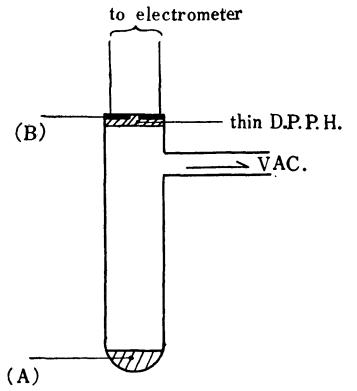



Fig. 1.

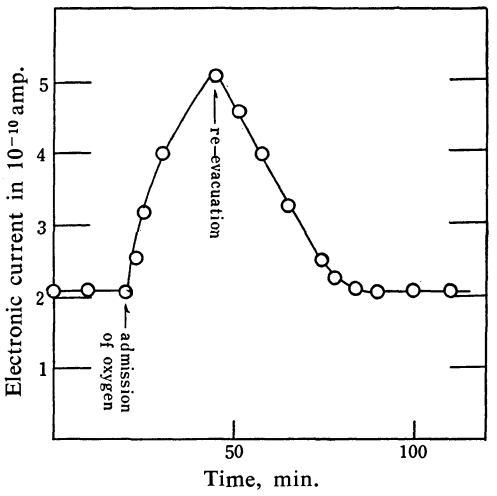



Fig. 2.

We also observed the oxygen effect on the electric conduction of thin D.P.P.H. film. The D.P.P.H. crystal to be evaporated was placed on the bottom (A) of glass vessel as shown in Fig. 1. By heating the vessel, the free radical was evaporated in vacuo to form a continuous thin film inside the top of vessel (B) between the two graphite (colloidal) electrodes. The resistance of this thin film

1) J. J. Lothe and G. Eia, *Acta. Chem. Scand.*, **12**, 1535 (1958).
2) J. E. Bennett and E. J. H. Morgan, *Nature*, **182**, 199 (1958).
3) A. E. Arbuzov, F. G. Volitova, N. S. Grif'yanov and B. M. Kozyrev, *Doklady Akad. Nauk, S. S. S. R.*, **126**, 774 (1959).
* No addition compound between D.P.P.H. and carbon disulfide is found.
4) J. A. Lyons and W. F. Watson, *J. Polymer Sci.*, **16**, 141 (1955).

was observed with association of a vibration-reed electrometer. The admission of oxygen into the vessel caused a marked increase of conduction of the film. However, this effect was reversible as on pumping out the oxygen, then, the resistance of the cell returned to its original value. One of these behaviors is illustrated in Fig. 2. These behaviour also suggests that the interaction between D.P.P.H. and oxygen is almostly phyical. The detail of this work may be submitted in elsewhere.

One of the present authors has already found that the absence of the hydrogen deuterium reaction at the surface of the D.P.P.H. crystals shows that the unpaired electrons in the molecules react with adsorbed hydrogens physically[5].

From these observations, the integrated intensity of ESR absorption of D.P.P.H. is independent on the conditions of preparation and also on the exposing time in the air. Therefore, we can conclude that various sorts of the D.P.P.H. crystals are applied as a standard to estimate the spin population of paramagnetic materials.

The authors express their hearty thanks to Professor H. Akamatu for his direction of this study.

*Department of Chemistry*
*Faculty of Science*
*The University of Tokyo*
*Hongo, Tokyo*

5) D. D. Eley and H. Inokuchi, *Z. Elektrochem.*, 63, 29 (1959).

# *The Distribution of Recoil Tritium in Benzoic Acid*

By Jiro OKAMOTO

(Received September 13, 1960)

Recently, so-called "Recoil labeling" by tritium has been developed in various organic compounds[1,2]. It is a interesting problem to study replacement of hydrogen at various positions of an aromatic ring by recoil tritium. However this has not been reported by far. Therefore, the author investigated the distribution of recoil tritium produced by $^{6}Li(n, \alpha)^{3}H$ reaction in benzoic acid and found the interesting facts as follows. The mixture of benzoic acid and lithium carbonate as tritium source was sealed in a quartz ampoule, in the presence of air. The irradiation was carried out in No. 15 hole of JRR-I for 15 hr. at $2\times10^{11}$ n/cm$^2$ sec. The irradiated material was dissolved in 150 ml. of pure benzene, then 10 g. of pure benzoic acid was added into the solution as carrier. This solution was refluxed for one hour and was immediately filtered to separate insoluble material from the solution, and then benzene solution was evaporated in vacuo and the crystal was dissolved in hot water to remove the labile tritium of the carboxyl group. A liquid scintillation detector (Tracerlab Model CE-1) was used to assay tritium. High voltage of the instrument was chosen at 1700 V. and temperature was kept at $-10°$C.

An outline of the procedures are shown in Fig. 1. The specific activities of the various

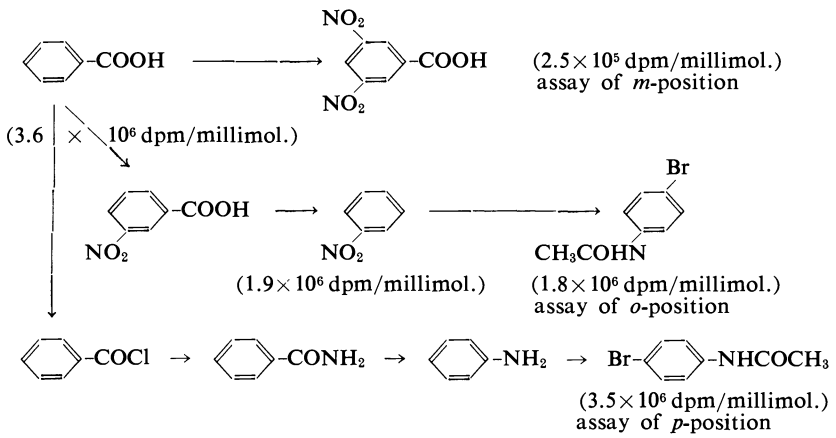



Fig. 1. Derivative and specific activities.

1) F. S. Rowland, A/CONF. 15/P/798.

2) F. S. Rowland and R. Wolfgang, *Nucleonics*, **14**, (8) 58 (1956).

compounds which were derived from the irradiated benzoic acid are also shown in Fig. 1. From these results, the percentage of ortho-, meta- and para-positions were determined. In Fig. 2, the values are shown. As is seen in Fig. 2, the replacement of hydrogen at meta-position by recoil tritium is dominant. Therefore, from the replacement process of recoil tritium in the solid phase in this experiment, it is inferred that tritium reacts after being thermalized. Ivanoff[3] stated that in the

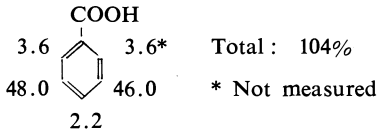



Fig. 2. Distribution of tritium in benzoic acid.

liquid phase, recoil bromine reacts with an aromatic ring after being thermalized. This resulte may support the present author's opinion on the mechanism of replacement reaction of recoil tritium in the solid phase. The furthermore details are to be published later.

*Radioisotope Production Laboratory*
*Japan Atomic Energy Research Institute*
*Tokai, Ibaraki-ken*

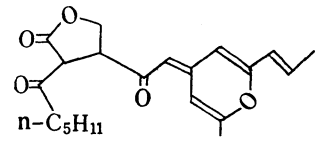
3) M. Ivanoff, *Bull. soc. chim. France*, **1953**, 266 (1953).

## *Monascoflavin**

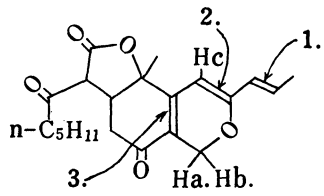
By Mamoru OHASHI, Shosuke YAMAMURA, Akira TERAHARA and Koji NAKANISHI

(Received October 6, 1960)

Structure Ia[1] was forwarded as a working hypothesis for monascoflavin[2-4], $C_{21}H_{26}O_5$, $[\alpha]_{700}^{16}+418$ ($c$: 0.0062 in ethanol), plain positive RD curve, one active hydrogen, three C-$CH_3$, no OH and $OCH_3$. However, the NMR spectra[5], especially the AB type quartet around 140 cps (vs. chloroform, at 56.4 Mc) arising from two protons in monascoflavin and dihydromonascoflavin could not be satisfactorily accounted for by the structure. Further studies on new derivatives, corrections of the molecular formula of hydrogenated products, a re-interpretation of the NMR spectra, and considerations of the biogenetic relations with monascorubrin[6] have led to structure I (or Ib). The mentioned quartet is now comfortably assigned to the methylene protons Ha and Hb. Some pertinent compounds are listed in Table I. The dihydro (II), tetrahydro (III) and hexahydro (IV) derivatives are those in which the double bonds (1), (2) and (3) in I have successively been hydrogenated. The 116 cps peak in I and




Ia




I

II is absent in III and IV, and the peak can be assigned to Hc. Presence of the $n$-$C_5H_{11}CO$ side-chain was shown by the production of capronic acid upon ozonolysis, oxidation with potassium permanganate, or fusion with potassium hydroxide, and production of amylamine upon Beckmann rearrangement of the oxime and hydrolysis. The lactone ring is cleaved and amides are formed, though sluggishly, when monascoflavin and hydrogenated products are treated with various amines, i. e., tetrahydromonascoflavin hexyl amide (V, R=$C_6H_{13}$). The amides, unlike the starting materials, no more showed the appearance or intensification of a ca. 288 m$\mu$ peak upon addition of base, and thus an enolizable $\beta$-keto-$\gamma$-lactone moiety is present in monascoflavin. Compound V (R=H) did not consume lead tetraacetate and this suggested it was not

* Reported at the 1st IUPAC Symposium on Natural Products, Australia, August, 1960.

1) Presented at the 3rd Symposium on the Organic Chemistry of Natural Products, Tokyo, 1959.

2) A. Nishikawa, *J. Arg. Chim. Soc. Japan* (*Nippon Nogeikagaku Kaishi*), **5**, 1007 (1932).

3) H. Salomon and P. Karrer, *Helv. Chim. Acta*, **15**, 18 (1931); P. Karrer and A. Geiger, ibid., **25**, 289 (1941).

4) A. D. G. Powell, A. Robertson and W. B. Whalley, *Chem. Soc. Spec. Publ.* No. 5, 27 (1956).

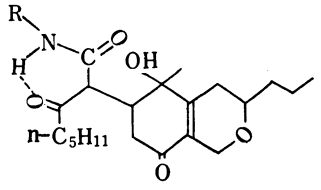
5) M. Ohashi, A. Terahara, K. Nakanishi, I. Yamaguchi and N. Hayakawa, This Bulletin, **33**, 1312 (1960).

6) K. Nakanishi, M. Ohashi, S. Kumasaki and S. Yamamura, *J. Am. Chem. Soc.*, **81**, 6339 (1959).

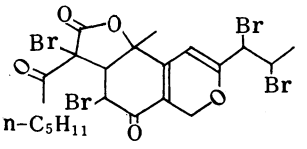
TABLE I. IR AND UV ABSORPTIONS

| Compound | M.p., °C | Solvent | IR -COO- | IR -CO- | IR $\Delta^{\alpha\beta}$CO | UV $\lambda_{max}^{MeOH}$ m$\mu$(log $\varepsilon$) |
|---|---|---|---|---|---|---|
| Mf1.[a] (I) $C_{21}H_{26}O_5$ | 143~145 | $CHCl_3$ | 1786 | 1720 | 1673 | 225(4.21), 288(3.41), 385(4.21) |
| 2H-Mf1. (II) $C_{21}H_{28}O_5$ | 122 | 〃 | 1791 | 1723 | 1672 | 220(3.77), 237(3.61), 364(3.91) |
| 4H-Mf1. (III)[b] $C_{21}H_{30}O_5$ | 136~137 | 〃 | 1790 | 1725 | 1703 | 244(4.03)[c] |
| 6H-Mf1. (IV)[b] $C_{21}H_{32}O_5$ | 211~212 | 〃 | 1778 | 1742[d] 1723 | | |
| 4H-Mf1.-$C_6$-amide[e] (V) $C_{27}H_{41}O_5N$ | 177~178 | 〃 | | 1702 | 1665 | 241[c] |
| nor-4H-Mf1. (VI) $C_{20}H_{30}O_3$ | 41~ 44 | $CCl_4$ | | 1712 | 1668 | 242[c] |
| 4Br-Mf1. (VII) $C_{21}H_{24}O_5Br_4$ | 162~164 | $CHCl_3$ | 1786 | 1711 | 1690 | 225(3.93), 365(3.95) |

a) Abbreviation for monascoflavin.
b) Tetra- and hexahydromonascoflavin were formulated as the hexa- and octahydro derivatives, respectively, in reference 5.
c) The difference with the calculated $\lambda_{max}$ of 249 m$\mu$ is presumably caused by a transannular effect of the oxygenic *p* electrons on the $\alpha\beta$-unsaturated system. A similar effect has been reported for nitrogen: A. Marchant and A. R. Pinder, *J. Chem. Soc.*, **1956**, 327.
d) This unusually high $\nu_{C=O}$ value for a six-membered ring ketone is due to ring strain imposed by the $\gamma$-lactone. A similar effect is observed when the 1703 $cm^{-1}$ band in III is compared with the 1668 $cm^{-1}$ band in VI.
e) Amide I and II bands at 1665 and 1520 $cm^{-1}$, respectively.

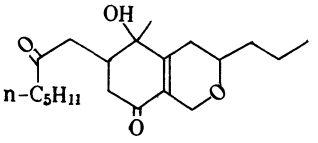


V

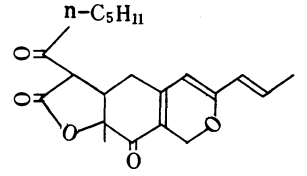


VII

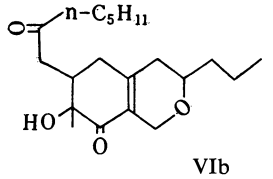
an $\alpha$-ketol. Ozonolysis of I and II gave acetaldehyde and butyric acid, respectively, while base hydrolysis of I and II gave crotonic acid and butyric acid, respectively. These results show that a propenyl side-chain is attached to the $\alpha$-position of the pyran ring and that it should be conjugated with the $\alpha$, $\beta$-unsaturated carbonyl group (to permit the occurrence of a vinylogous $\beta$-diketone cleavage). The conspicuous methyl peak at 330 cps in I remains constant and uncoupled in II-IV[5], and the position is lower than ordinary methyl peaks by ca. 30 cps. This, coupled with the production of methylglyoxal from the ozonolysis of I places a methyl group on a tertiary carbon atom bearing a oxygenic function (the lactone ring). Tetrabromomonascoflavin (VII) has no active hydrogen. Furthermore, the +17 $cm^{-1}$ shift of the 1673 $cm^{-1}$ band of I suggests that the $\alpha$-position of the $\alpha$, $\beta$-unsaturated carbonyl group must be substituted by an equatorial bromine. Boiling III in 20% alkali under nitrogen yielded VI. The facts mentioned are best explained by structure I.



VI



Ib



VIb

The alternative structure Ib is also conceivable

but it is difficult to account for the 1690 $cm^{-1}$ band in tetrabromo-monascoflavin and the non-consumption of lead tetraacetate by V(R=H). However, Ib is the conclusion reached by English chemists[7] who base their conclusion on analogies with other azaphilones, e.g., monascorubrin[8], the structure of which also differs from that of the present authors[6,9], and the fact that nortetrahydromonascoflavin (VIb instead of VI) consumed periodic acid with the production of a methyl ketone. These inconsistencies will be settled in the near future.

We are grateful to Professor E. Nishikawa, formerly of Nagoya University, for an abundant supply of starting material and suggestions.

*Department of Chemistry*
*Faculty of Science*
*Tokyo University of Education*
*Bunkyo-ku, Tokyo*
*(M. O., A. T. and K. N.)*

*Chemical Institute*
*Nagoya University*
*Chikusa-ku, Nagoyo*
*(S. Y.)*

7) The authors are most grateful to Dr. W. B. Whalley, University of Liverpool, for informing us of their results prior to publication and for discussion at the IUPAC Symposium.

8) B. C. Fielding, F. J. Haws, J. S. E. Holker, A. D. G. Powell, A. Robertson, D. N. Stanway and W. B. Whalley, *Tetrahedron Letters*, No. 5, 24 (1960).

9) M. Ohashi, A. Terahara and K. Nakanishi, This Bulletin, 33, 1311 (1960).

# *Intramolecular Interaction between Hydroxyl Group and π-Electrons. XI*[1]. *High Resolution Proton Magnetic Resonance Spectra of Tertiary Alcohols Having π-Electrons*

By Michinori Ōki and Hiizu Iwamura

(Received October 8, 1960)

It has been shown through infrared studies[1] that the intramolecular interaction between hydroxyl groups and π-electrons shifts the O–H stretching vibration ($\nu_{O-H}$) to lower frequencies in comparison with an ordinary hydrogn bonding. In connection with recent high resolution nuclear magnetic resonance spectroscopy which has successfully been applied to the study of hydrogen bonding[2], variation of the proton resonance of some alcohols with concentration changes in carbon tetrachloride was studied in order to detect any effect of the aforementioned interaction to the NMR spectra, which must give rise to a different magnetic shielding of hydroxylic proton of the interacting form from that of the free one.

A Varian model V-4300 high resolution NMR spectrometer was operated at 56.4 Mc/sec. Samples include *tert*-amyl alcohol, allyldimethylcarbinol, benzyldimethylcarbinol and tribenzylcarbinol. Preparations and purities of the samples are specified in the preceding paper[1]. Measurements were carried out at 20°C, the samples being dissolved in a given amount of carbon tetrachloride and sealed in glass tubes with the outer diameter of 5 mm. The magnetic field was swept twice in both decreasing and increasing directions and the average of the records of both directions of the sweep taken. The calibration of the sweep rate was made by recording the spectrum of toluene and by reading the separation of the two peaks as 4.90 ppm[3]. The chemical shift ($\delta$) was referred to water as an external standard and corrected for bulk diamagnetic susceptibilities of *tert*-amyl alcohol, allyldimethylcarbinol and benzyldimethylcarbinol, $-\chi_v \times 10^6$ being 0.644, 0.585 and 0.696[4], respectively.

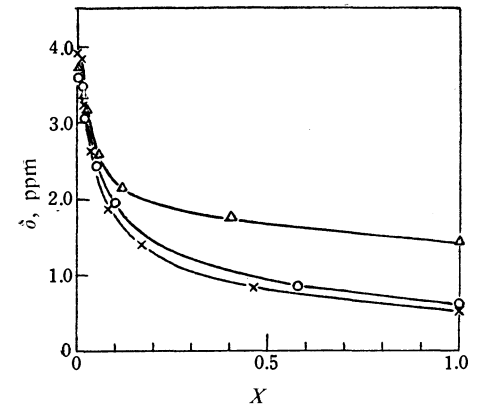
While the absorption lines assigned to hydrogen attached to carbon atom shifted less than 0.5 ppm from thet pure liquid to the sample at infinite dilution, that of hydroxyl proton showed a marked concentration dependence as shown in Figs. 1 and 2. On dilution, the chemical shifts gradually moved to higher magnetic field and at about 0.02 mol. fraction a reversal of the curvature was observed with three carbinols. This phenomenon is understood to be characteristic of a system consisting of monomer, dimer and high polymer[2a]. Tribenzylcarbinol showed, unlike these, no association pattern within the measured concentration range. The curves were extrapolated to infinite dilution and the chemical shifts of pure monomers obtained. Under these conditions, *tert*-amyl alcohol is quite free from association and tribenzylcarbinol possesses only

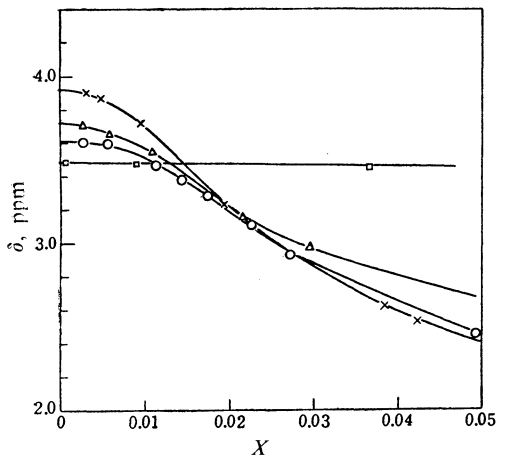
1) Part X: M. Ōki and H. Iwamura, This Bulletin, 33, 1600 (1600); see also the foregoing papers.

2) a) E. D. Becker and U. Liddel, *J. Mol. Spectroscopy*, 2, 1 (1958), and others cited in the literature. b) The NMR study of the interaction pertaining to the π-electron system was presented by N. Nakagawa at the Symposium on Structural Chemistry, the Chemical Society of Japan, Tokyo, September, 1959, phenylacetylene being the example.

3) N. F. Chamberlain, *Anal. Chem.*, 31, 56 (1959).

4) Measurements were kindly made by Mr. Minoru Kinoshita, to whom the authors, thanks are due.




Figs. 1 and 2. Chemical shifts of the OH proton resonance, $\delta$ in ppm, vs. mole fraction of alcohols, $X$.

I. *tert*-Amyl alcohol -×-×-
II. Allyldimethylcarbinol -○-○-
III. Benzyldimethylcarbinol -△-△-
IV. Tribenzylcarbinol -□-□-

the hydroxyl group which is intramolecularly interacting with $\pi$-electrons of the benzene nucleus, while allyldimethylcarbinol and benzyldimethylcarbinol are in equilibrium mixtures of free and interacting hydroxyl groups. The composition of the equilibrium estimated from the integrated intensities of infrared absorption is added to the last column in Table I.

TABLE I. CHEMICAL SHIFTS AND THE COMPOSITION AT INFINITE DILUTION IN CARBON TETRACHLORIDE

| | $\delta_{X=0}$ ppm | $\Delta\delta$ ppm | Mole fraction of the interacting form |
|---|---|---|---|
| *tert*-Amyl alcohol | 3.92 | 0 | 0 |
| Allyldimethylcarbinol | 3.61 | 0.31 | 0.37 |
| Benzyldimethylcarbinol | 3.72 | 0.20 | 0.43 |
| Tribenzylcarbinol | 3.49 | 0.43 | 1 |

In contrast with the infrared spectra which show separate $\nu_{O-H}$ bands, the NMR spectra of hydroxyl proton are absolutely single. This must be attributed to the short lifetime and rapid exchange of free and interacting forms of these carbinols. The single proton resonance is therefore observed at the field corresponding to the average shielding of the two forms. When $\delta$ value of *tert*-amyl alcohol is taken as the chemical shift of purely free tertiary alcohols and that of tribenzylcarbinol as that interacting form, the composition of the equilibrium of benzyldimethylcarbinol may be computed from its $\delta$ value. The $\Delta\delta$ (0.20) of benzyldimethylcarbinol is divided by 0.43 and the quotient (0.47 mole fraction) is found to be in good agreement with the infrared datum (0.43). Unfortunately, the true chemical shift of hydroxyl proton taking part in the interaction with $\pi$-electrons of ethylenic linkage can not be determined because of lack of the sample which possesses only the interacting form. Assuming that the observed $\delta_{X=0}$ value of allyldimethylcarbinol is a weighted mean between free and interacting forms, the $\delta$ value of the interacting form can be estimated with use of composition datum (0.37 mole fraction) obtained from the infrared spectra. Thus $\Delta\delta$ is 0.31/0.37 or 0.838 ppm, $\delta$ being 3.08 ppm. Therefore, it may be said that, with the intramolecular interaction of the hydroxyl group with $\pi$-electrons of ethylenic linkage, the magnetic shielding of tertiary hydroxyl proton becomes less and $\delta$ value shifts to the lower magnetic field by less than one ppm. The chemical shift of the hydroxyl proton having interaction with $\pi$-electrons of the benzene nucleus is 0.41 ppm higher than this value. The ring current diamagnetic effect must be operative in the latter case. More precise evaluation is in progress in the hope of obtaining the knowledge about the geometry of the interacting form.

*Department of Chemistry*
*Faculty of Science*
*The University of Tokyo*
*Hongo, Tokyo*

## *Association Shifts of NMR Spectra of Phenylacetylene**

By Naoya NAKAGAWA** and
Shizuo FUJIWARA***

(Received October 15, 1960)

Solvent effects have recently attracted the attention of several workers in the investigations of the chemical shift phenomena of proton magnetic resonance in the -OH, -COOH, -NH, and $-SO_3H$ groups of organic compounds. The results of NMR measurements were interpreted in terms of proton exchange and of hydrogen-bond formation[1]. Some of the most interesting results of these investigations are that obtained by Huggins, Pimentel and Shoolery[2], and by Korinek, Reeves and Schneider[3,4] for chloroform, which revealed us the fact that the association of the chloroform molecules can be studied by the proton resonance shifts of chloroform.

Since this technique is quite useful for the investigations of intermolecular interactions in liquid state, we made measurements of the solvent effects on the proton resonance shifts of phenylacetylene. The apparatus used for NMR measurements was constructed at the University of Electro-Communications and was operated at 27 Mc. In each of these samples, molecules are assumed to be associated with each other (self-association) or with solvent molecules; hence, the results of these measurements can be compared to those of chloroform.

Fig. 1 shows the results of NMR measurements of the solvent effects for the ethinyl proton of phenylacetylene. The resonance position of the ethinyl proton is shifted to lower field by the addition of solvents such as $Et_3N$, $Et_2NH$, $Et_2O$, EtOH, and $Me_2CO$. This can be explained as being due to hydrogen bonding with nitrogen or with oxygen atoms of the solvent molecules. The high-field shift observed in the system with benzene

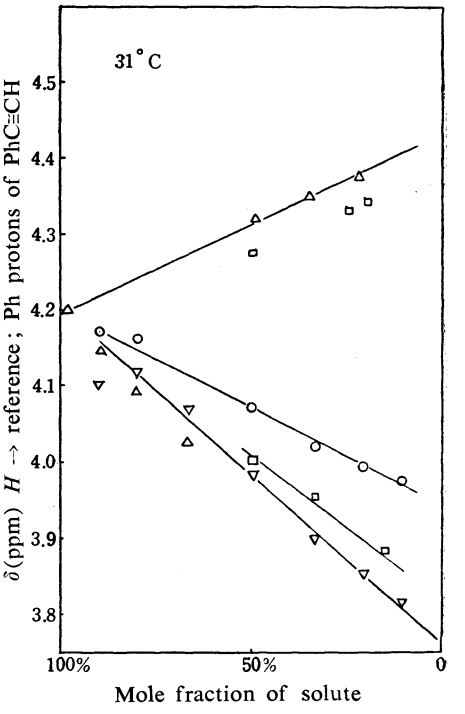



Fig. 1. Chemical shifts of C≡CH of PhC≡CH.
Solvent, △ $C_6H_{12}$, □ $CCl_4$
○ $Et_3N$, □ $Me_2CO$, ▽ $Et_2NH$,
△ EtOH

is explained, as in the case of chloroform, by hydrogen bonding with the $\pi$-electrons of benzene. On the other hand, the high-field shifts observed in the system with carbon tetrachloride and with cyclohexane may be explained by assuming that the self-association of phenyl acetylene molecules is broken by the solvent molecules. This may be regarded as evidence for the proposition that the phenylacetylene molecules are associated with each other through interaction of the triple-bond $\pi$-electrons. This conclusion seems to be consistent with the finding of West in the infrared spectra of triple-bond compounds[5].

The authors thank to Mr. Hiroshi Shimizu of the University of Tokyo for valuable discussions.

*Department of General Education*
*Nagoya University*
*Nagoya (N. N.)*

*Department of Chemistry*
*Faculty of Science*
*University of Electro-Communications*
*Chofu, Tokyo (S. F.)*

* Presented at the Symposium of Structural Chemistry, the Chemical Society of Japan, Tokyo, September, 1959.

** Present address: University of Electro-Communications, Chofu, Tokyo.

*** Present address: Department of Chemistry, Faculty of Science, The University of Tokyo, Tokyo.

1) J. A. Pople, W. G. Schneide and H. J. Bernstein, "High-resolution Nuclear Magnetic Resonance", McGraw-Hill, New York (1959), p. 401.

2) C. M. Huggins, G. C. Pimentel, and J. N. Shoolery, *J. Chem. Phys.*, 23, 1244 (1955).

3) G. J. Korinek and W. G. Schneider, *Can. J. Chem.*, 35, 1157 (1957).

4) L. W. Reeves and W. G. Schneider, ibid., 36, 251 (1957).

5) R. West lectured at the Symposium of Electronic States of Molecules, the Chemical Society of Japan, September, 1959, Tokyo.

# *The Anodic Behavior of Cathodically Prepolarized Bright Platinum Electrode in Sulfuric Acid Solution*

By Shigeo SHIBATA

(Received December 23, 1959)

Numerous accounts[1-19] have been published on the charging curve which is a variation of potential with quantity of electricity passed when a platinum electrode is forced from the equilibrium potential of hydrogen to the oxygen evolution potential with a steady direct current. The curve was distinguished principally into three stages: an initial slow rise of potential which is generally considered to correspond to ionization of hydrogen atoms which have been adsorbed on the electrode surface, rapid linear rise for charging a double layer, and finally a slow linear change to deposition of oxygen which forms an adsorbed or an oxide layer prior to the evolution of gas. In addition, Pearson and Butler[5] and also Hickling[10] found that, when the electrode was first cathodically polarized and anodic current was passed, a new stage, which consists of a horizontal portion of steady potential, which we call stage $\alpha'$, appeared prior to the above-mentioned three stages. Pearson and Butler considered this stage to be attributable to the ionization of free hydrogen in the solution, but Hickling explained that it may be more complex than this simple view. As to the behavior of the stage $\alpha'$, Breiter, Knorr and Völkl[16] found that it is considerably lengthened when the electrode was cathodically prepolarized with high current density (c. d.). They have considered that this phenomenon was ascribed to bubbles which evolved on the surface of the electrode by cathodic prepolarization. Experimental or theoretical studies on the stage $\alpha'$ have been done by these authors, nevertheless the results of those studies are not satisfactory, because they are only qualitative and imperfect. The present investigation was undertaken to throw some light on this problem.

## Experimental

In order to establish a suitable condition for the observation, a network as shown diagrammatically in Fig. 1, similar in principle to that used by Breiter et al.[16], was used. An electrolysis cell can be fed with a steady current from Circuit I as well as from Circuit II, these currents being opposite to each other in direction, with regulated power supplies P and P'. R and R' are variable high

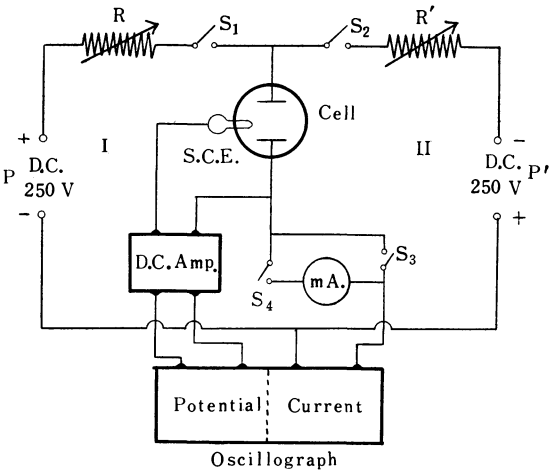



Fig. 1. Circuit diagram.

resistances. When, at first, the switch $S_1$ is closed, a steady current $i_k$ supplied from Circuit I begins to pass through the cell. At a suitable instant the switch $S_2$ is closed, the other switch being left as it is, so that a steady current $i_a'$ supplied from Circuit II, which is opposite in direction and larger in magnitude, superposes with the former, resulting in a current with the same direction as that of the latter and the amount of $i_a = i_a' - i_k$.

1) F. P. Bowden, *Proc. Roy. Soc.*, **125A**, 446 (1929).
2) J. A. V. Butler and G. Armstrong, ibid., **137A**, 604 (1932).
3) G. Armstrong, F. R. Himthworth and J. A. V. Butler, ibid., **143A**, 89 (1933).
4) J. A. V. Butler and G. Drever, *Trans. Faraday Soc.*, **32**, 427 (1936).
5) J. D. Pearson and J. A. V. Butler, ibid., **34**, 1163 (1938).
6) B. Ershler and A. Frumkin, ibid., **35**, 464 (1939).
7) J. A. V. Butler, "Electrocapillarity", Methuen & Co. Ltd., London (1940), p. 174.
8) J. A. V. Butler and G. Armstrong, *J. Chem. Soc.*, **1943**, 743.
9) A. L. Ferguson and M. B. Towns, *Trans. Electrochem. Soc.*, **83**, 271, 285 (1943).
10) A. Hickling, *Trans. Faraday Soc.*, **41**, 333 (1945).
11) A. Hickling, ibid., **42**, 518 (1946).
12) G. Armstrong and J. A. V. Butler, *Discussion Faraday Soc.*, **1**, 122 (1947).
13) B. Ershler, ibid., **1**, 269 (1947).
14) A. Hickling and D. Taylor, *Trans. Faraday Soc.*, **44**, 262 (1948).
15) El Wakkad and S. H. Emara, *J. Chem. Soc.*, **1952**, 461.
16) M. Breiter, C. A. Knorr and W. Völkl, *Z. Electrochem.*, **59**, 681 (1955).
17) M. Becker and M. Breiter, ibid., **60**, 1080 (1956).
18) K. J. Vetter and D. Berndt, ibid., **62**, 378 (1958).
19) J. Giner, ibid., **63**, 386 (1959).

The potential changes of the working electrode, measured against a saturated calomel electrode, were recorded by means of a mechanical oscillograph. All potentials referred to are on the hydrogen scale. Switch $S_2$ was geared with a shutter of the oscillograph. The electrolysis cell used was of H type as previously described[20]. The working electrode of bright platinum plate having an area of one square centimeter per side, the back side of which was covered with a thin layer of molten glass, was placed in one compartment, and an antipodal electrode of platinized platinum plate, having an apparent area of 2 cm², was placed in the other compartment. 1 N sulfuric acid solution made with G. R. sulfuric acid and conductivity water redistilled several times with a silica still was used as the electrolyte. Prior to use, the working electrode was carefully cleaned with hot chromic acid, hot concentrated nitric acid and finally with distilled water, and then activated by anodic polarization with a current of 100 mA./cm² for one hour in 1N sulfuric acid solution, reduced cathodically, and introduced into the cell containing the electrolyte saturated with hydrogen. After passing purified hydrogen through the electrolyte for 10 min., the cell was let stand for 5 min. with or without the passing of a given cathodic current, till it was polarized for the oscillographic observation. All experiments were carried out in a thermostat of 15°C.

## Results

It was observed that the horizontal stage $\alpha'$ which is characteristic of the prepolarized electrode could be clearly found also for the nonpolarized electrode in the solution saturated with hydrogen at low anodic polarization c. d. as shown in Fig. 2(A). Fig. 3(A) shows a plot

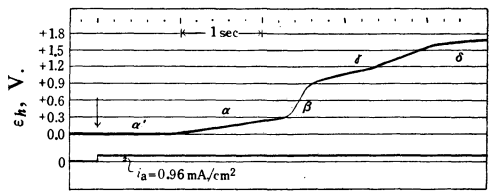



Fig. 2(A). Anodic oscillogram of the nonpolarized electrode in 1 N sulfuric acid solution saturated with hydrogen.

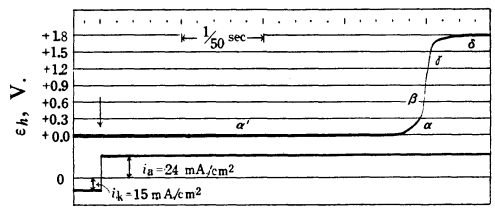



Fig. 2(B). Anodic oscillogram of the prepolarized electrode in 1 N sulfuric acid solution saturated with hydrogen.

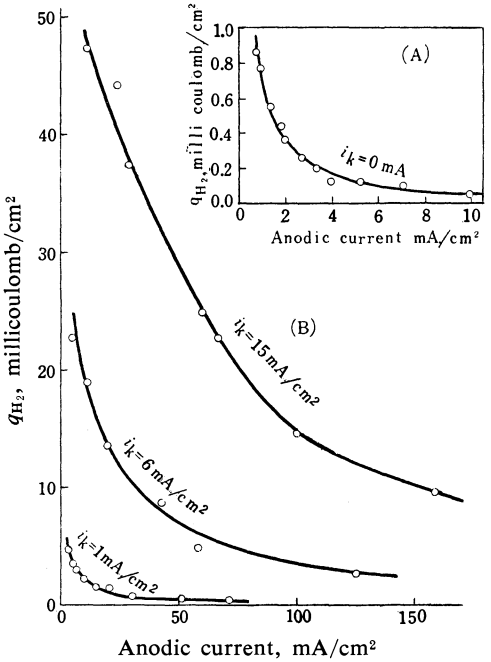



Fig. 3. Variation of $q_{H_2}$ with anodic polarizing c. d.
(A) The nonpolarized electrode
(B) The cathodically prepolarized electrode

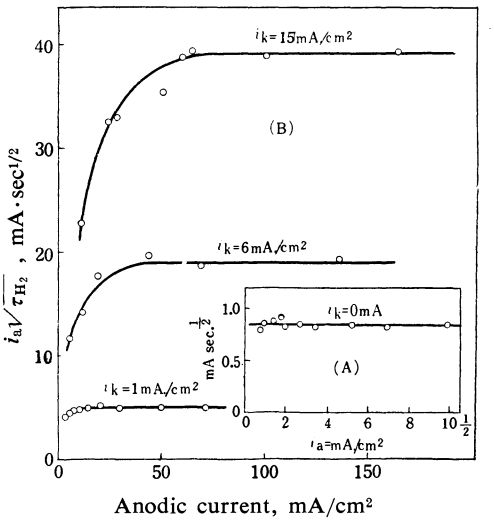



Fig. 4. Dependence of $i_a\sqrt{\tau_{H_2}}$ on anodic polarizing c. d.
(A) The nonpolarized electrode
(B) The prepolarized electrode

of $q_{H_2}$, the quantities of electricity required in stage $\alpha'$, against the anodic c. d. As to the relation between the anodic polarization c. d. $i_a$ and the transition time $\tau_{H_2}$ of the stage $\alpha'$, Sand's equation is applicable[21]. As seen in

20) S. Shibata, *J. Chem. Soc. Japan, Pure Chem. Soc. (Nippon Kagaku Zasshi)*, **79**, 239 (1958).

21) H. J. S. Sand, *Phil. Mag.*, **1**, 45 (1901).

Fig. 4(A), $i_a\sqrt{\tau_{H_2}}$ is independent of $i_a$. Taking the diffusion coefficient $D$ as $4.7\times10^{-5}$ cm./sec.[22], we can compute the value of $C^0$, the result being obtained as $7.67\times10^{-4}$ mol./l., which is in good agreement with the solubility of hydrogen $7.3\times10^{-4}$ mol./l.[23] Consequently, the electrode reaction at the stage $\alpha'$ in this case is ionization of hydrogen molecule in the solution and its reaction rate is controlled by diffusion of the hydrogen.

When the electrode was led from a cathodically polarized state with a given c. d. immediately to an anodically polarized state, the stage $\alpha'$ was lengthened considerably, as shown in Fig. 2(B). In Fig. 3(B), $q_{H_2}$ is traced in relation with the polarization c. d. The value of $q_{H_2}$ decreased with the increase of $i_a$ when $i_k$ is kept unchanged, and increased with the increase of $i_k$ when $i_a$ is kept unchanged. It was found that for a given $i_k$ the function $i_a\sqrt{\tau_{H_2}}$ in Sand's equation increased with the increase of $i_a$ in the range of low $i_a$, but tended to a definite value when $i_a$ grew sufficiently. This can be seen in Fig. 4(B). The concentration of hydrogen in the vicinity of the electrode polarized cathodically was computed with Sand's equation, taking the constant value of $i_a\sqrt{\tau_{H_2}}$ at large $i_a$. The results obtained were 4.08, 16.2 and $32.8\times10^{-3}$ mol./l. for the cathodic c. d.'s of 1, 6 and 15 mA/cm$^2$, respectively.

The behavior of $q_{H_2}$ under the turbulence of the electrolyte were studied with the rotated electrode at various rates varying up to 1500 r. p. m., $i_k$ and $i_a$ being kept unchanged. The result thus obtained is shown in Fig. 5. It is seen in this figure that $q_{H_2}$ decreases quickly with the increase of the rate of rotation in the range of low rotations. This can be attributed to the removal of the hydrogen accumulated owing to the prepolarization in the solution in the vicinity of the electrode, but as the rotation becomes vigorous, the rate of this decrease diminishes. As the rate exceeds 1000 r. p. m., the value of $q_{H_2}$ tends to a constant value independent of $i_a$ and $i_k$. This value is coincident to that of the nonpolarized electrode, and suggests the vanishing of the accumulated hydrogen.

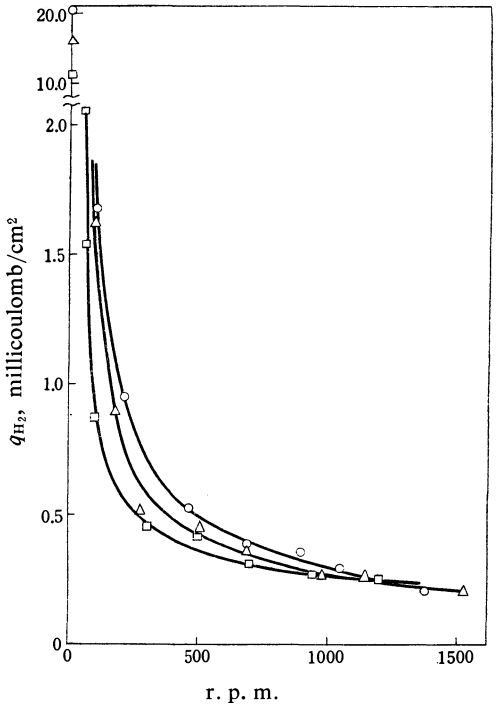



Fig. 5. Variation of $q_{H_2}$ of the prepolarized electrode with number of rotation per min.

| | $i_k$, mA/cm$^2$ | $i_a$, mA/cm$^2$ |
|---|---|---|
| —○— | 8.85 | 5.0 |
| —△— | 3.0 | 5.0 |
| —□— | 8.85 | 15.3 |

## Discussion

The fact that we have found several phenomena which need to be attributed to accumulation of hydrogen in the vicinity of the electrode leads us to assume the existence of temporary supersaturation of hydrogen. It was reported in the experiment performed by Clamroth and Knorr[24] with an active palladium electrode that the maximum value of the diffusion overpotential of the hydrogen on the cathode was $-30\sim-60$ mV. This corresponds to the fact that the concentration of hydrogen in the solution near the electrode is as 10~100 times large as the saturation value at 1 atm. As such a state of high concentration must be very unstable. At the instant of the shut-off of the cathodic current the concentration should begin to fall irreversibly due to the exclusion from the solution. This process is also confirmed in the present results in the behavior of $i_a\sqrt{\tau_{H_2}}$ in reference to $i_a$. As seen in Fig. 4(B) the value of $i_a\sqrt{\tau_{H_2}}$ diminished considerably as $i_a$ decreased. This discrepancy can not be understood unless it is attributed to the spontaneous exclusion of hydrogen from the solution due to the supersaturation. In order to study this point in detail, the following observation was performed. After the steady current which had kept the electrode cathodically polarized, was shut off, the electrode was left as it was for a suitable time elapse—say $t$—till a steady anodic current was switched on,

22) "International Critical Tables", Vol. V, McGraw-Hill Book Co. Inc., New York (1929), p. 63.
23) A. Seidell, "Solubilities of Organic and Inorganic Compounds", Van Nostrand Co., New York (1940), p. 557.
24) R. Clamroth and C. A. Knorr, *Z. Electrochem.*, **57**, 399 (1953).

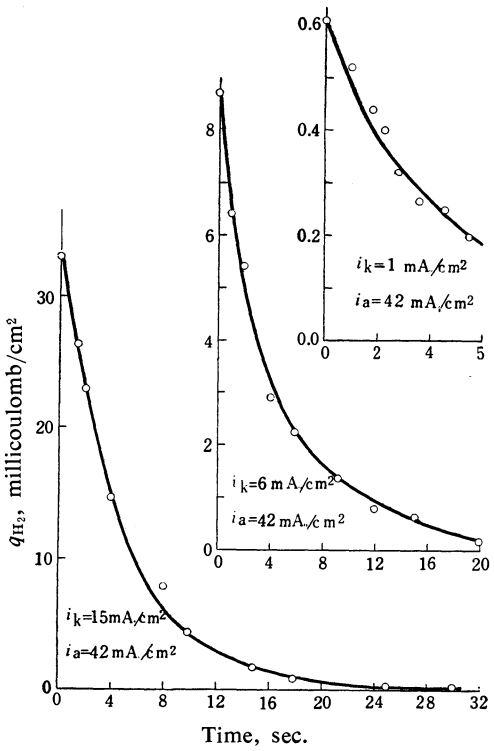



Fig. 6. Decay of $q_{H_2}$ with standing time.

the oscillographic observation taking place simultaneously. Fig. 6 shows the relation between $q_{H_2}$ and $t$. In this figure, we can see the $q_{H_2}$ decreases with the time $t$, in a manner closely resembling that of the decrease of reactant in the usual chemical reaction of first order. That is to say, the spontaneous reduction of the concentration of the hydrogen should obey the following equation

$$-dc/dt = k({}_tC - C^0) \qquad (1)$$

where ${}_tC$ is the concentration of hydrogen in the vicinity of the electrode at the time elapse $t$ from the instant of the shut-off of the polarizing current and $k$ a proportional constant. Solving this equation, we obtain

$$t = -\frac{1}{k} \ln \frac{{}_tC - C^0}{{}_0C - C^0} \qquad (2)$$

where ${}_0C$ is the concentration in the vicinity of the electrode at $t=0$. As the anodic current is sufficiently large (42 mA/cm² in this experiment) for the spontaneous decrease of the concentration of the hydrogen by exclusion during $\tau_{H_2}$ to be disregarded, $\sqrt{\tau_{H_2}}$ is proportional to $C$ as Sand's equation requires. Consequently, the total decrease of $q_{H_2}$ during $t$ can be regarded as corresponding to the decrease of $C$.

$$t = -\frac{1}{k} \ln \frac{\sqrt{{}_t\tau_{H_2}} - \sqrt{\tau^0_{H_2}}}{\sqrt{{}_0\tau_{H_2}} - \sqrt{\tau^0_{H_2}}} \qquad (2')$$

where ${}_t\tau_{H_2}$ is the transition time of stage $\alpha'$ consecutive to the unpolarizing time interval $t$, and ${}_0\tau_{H_2}$ that for $t=0$. When ${}_0C \gg C^0$, also ${}_tC \gg C^0$, Eqs. 2 and 2′ can be simplified as

$$t = -1/k \ln ({}_tC/{}_0C) \qquad (3)$$

$$= -1/2k \ln ({}_t\tau_{H_2}/{}_0\tau_{H_2}) \qquad (3')$$

It is seen from Fig. 7 that a plot of $\log({}_t\tau_{H_2}/{}_0\tau_{H_2})$ against standing time $t$ is linear. From the slope of this line, the value of the rate constant was evaluated as 0.101 sec.

Now, since we can reasonably say that the rate of decay of hydrogen concentration in the vicinity of the electrode, which led from the cathodically polarized state, consists of the superposition of the decay due to the diffusion and the spontaneous decrease due to the supersaturation, it can be expressed mathematically as follows,

$$\frac{\partial C(x,t)}{\partial t} = D\frac{\partial^2 C(x,t)}{\partial x^2} - k\{C(x,t) - C^0\} \qquad (4)$$

where $C(x,t)$ is the concentration of hydrogen at a point $x$ apart from the electrode surface at time $t$. While the concentration near the electrode polarizing cathodically should fall from the surface toward the bulk solution in macroscopical range, it would be natural to assume that through the thin layer in the vicinity of the surface, in which the diffusion zone would be formed during $\tau_{H_2}$ in the subsequent anodic polarization, the concentration

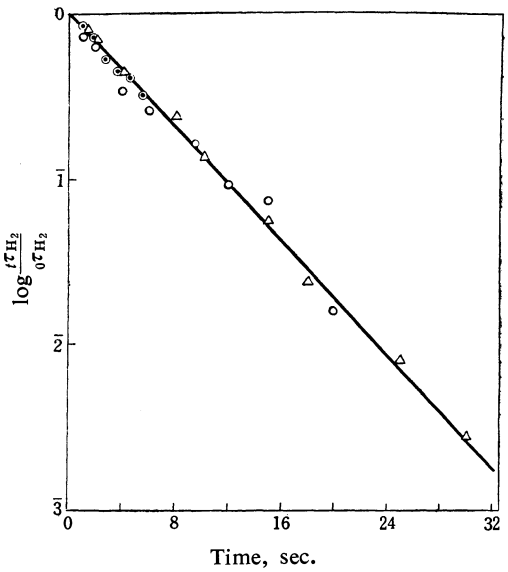



Fig. 7. A plot of $\log \frac{t\tau_{H_2}}{0\tau_{H_2}}$ against standing time.

$i_k$
—⊙— 1 mA/cm²
—○— 6 mA/cm² } $i_a$=42 mA/cm²
—△— 15 mA/cm²

is constant. So the initial condition can be taken as

$$C(x, 0) = {}_0C \tag{5}$$

The boundary condition is

$$D\left(\frac{\partial C(x, t)}{\partial x}\right)_{x=0} = \frac{i_a}{2F} \tag{6}$$

The solution of Eq. 4 which satisfies the conditions 5 and 6 is given by

$$\begin{aligned} C(x, t) = {}&{}_0C \exp(-kt) + C^0\{1-\exp(-kt)\} \\ &- \frac{i_a}{2F\sqrt{Dk}} \exp\left(-\sqrt{\frac{k}{D}}x\right) \\ &+ \frac{i_a}{4F\sqrt{Dk}}\left\{\exp\left(-\sqrt{\frac{k}{D}}x\right)\operatorname{erfc}\left(\sqrt{kt} - \frac{x}{2\sqrt{Dt}}\right)\right. \\ &\left. + \exp\left(\sqrt{\frac{k}{D}}x\right)\operatorname{erfc}\left(\sqrt{kt} + \frac{x}{2\sqrt{Dt}}\right)\right\} \end{aligned} \tag{7}$$

The variation of the concentration at $x=0$ is

$$\begin{aligned} C(0, t) = {}&{}_0C \exp(-kt) + C^0\{1-\exp(-kt)\} \\ &+ \frac{i_a}{2F\sqrt{Dk}} \operatorname{erfc}(\sqrt{kt}) \end{aligned} \tag{8}$$

If we assume that $C(0, \tau_{H_2}) \approx 0$, then

$$\begin{aligned} &{}_0C \exp(-k\tau_{H_2}) + C^0\{1-\exp(k\tau_{H_2})\} \\ &= \frac{i_a}{2F\sqrt{Dk}} \operatorname{erf}(\sqrt{k\tau_{H_2}}) \end{aligned} \tag{9}$$

If $k \to 0$, we obtain Sand's equation. When ${}_0C \gg C^0$ or $\tau_{H_2}$ is sufficiently small, the second term on the left side of Eq. 9 can be neglected against other terms; then we have

$${}_0C \exp(-k\tau_{H_2}) = \frac{i_a}{2F\sqrt{Dk}} \operatorname{erf}(\sqrt{k\tau_{H_2}}) \tag{10}$$

Taking logarithumus of both sides of the equation, this becomes

$$\begin{aligned} \log i_a = {}&\log 2F\sqrt{Dk}\ {}_0C - \{k\tau_{H_2}/2.303 \\ &+ \log \operatorname{erf}(\sqrt{k\tau_{H_2}})\} \end{aligned} \tag{11}$$

$$= \log 2F\sqrt{Dk}\ {}_0C - f(\tau_{H_2}) \tag{11'}$$

where $f(\tau_{H_2})$ in Eq. 11′ expresses the second term on the right hand side of Eq. 11. Eq. 11 is in favour of the experimental results as shown in Fig. 8. If we write ${}_0i_a$ anodic c. d. at $f(\tau_{H_2})=0$, it is obtained, by using Eq. 11′, that

$${}_0i_a = 2F\sqrt{Dk}\ {}_0C \tag{12}$$

By means of Eq. 12 it is possible to calculate the initial concentration ${}_0C$ if ${}_0i_a$ is known. Using the value of ${}_0i_a$ obtained by extrapolating the curve to $f(\tau_{H_2})=0$ in Fig. 8, ${}_0C$ at cathodic c. d.'s of 1, 6 and 15 mA/cm$^2$ was evaluated as 4.0, 14.3 and $30.0\times10^{-3}$ mol./l., respectively. These were in good agreement with the values obtained by calculation with Sand's equation at large $i_a$.

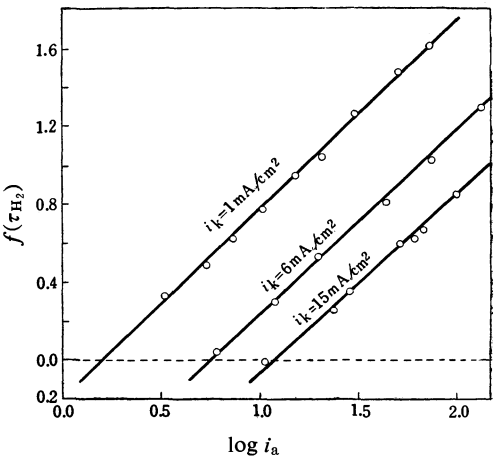



Fig. 8. Relation between $f(\tau_{H_2})$ and log $i_a$.

## Summary

The anodic charging curves of a cathodically prepolarized bright platinum electrode in 1 N sulfuric acid solution saturated with hydrogen have been studied by means of a mechanical oscillograph.

The behavior of stage $\alpha'$ for anodic polarizing c. d. can be explained on the assumption that its stage is due to the molecular hydrogen accumulated in the vicinity of the electrode during the cathodic prepolarization, and that the concentration of the accumulated hydrogen decreases in the same manner as the chemical reaction of first order.

The author's warmest thanks are due to Professor H. Yoshisaki for encouragement and advice, and to Professor T. Terasaki for helpful suggestions.

*Department of Chemistry*
*Faculty of Liberal Arts and Science*
*Yamagata University*
*Koshirakawa, Yamagata*

## Appendix

On writing

$$C_1(x, t) = C(x,t) - C^0 \tag{13}$$

Eq. 4 becomes

$$\frac{\partial C_1(x, t)}{\partial t} = D\frac{\partial^2 C_1(x,t)}{\partial x^2} - kC_1(x,t) \tag{14}$$

and the initial condition is given by

$$\begin{aligned} C_1(x,0) &= {}_0C - C^0 \\ &= B \end{aligned} \tag{15}$$

the boundary condition 6 do not change.

We may attempt to find a solution of Eq. 14 by putting

$$C_1(x,t) = \phi(x) + \varphi(x,t) \tag{16}$$

where $\psi(x)$ is a function of $x$, $\varphi(x,t)$ is of $x$ and $t$. We have to satisfy

$$\frac{\partial\psi(x)}{\partial t}=D\frac{\partial^2\psi(x)}{\partial x^2}-k\psi(x) \tag{17}$$

and

$$\frac{\partial\varphi(x,t)}{\partial t}=D\frac{\partial^2\varphi(x,t)}{\partial x^2}-k\varphi(x,t) \tag{18}$$

The general solution of Eq. 17 is

$$\psi(x)=Ae^{-\sqrt{(k/D)}x} \tag{19}$$

where $A$ is an integration constant. Substitution by the boundary condition 6, yields

$$D\left(\frac{\partial\psi(x)}{\partial x}\right)_{x=0}=-DA\sqrt{\frac{k}{D}}$$
$$=i_a/2\boldsymbol{F}$$

Thus, we obtain

$$\psi(x)=\frac{i_a}{2\boldsymbol{F}\sqrt{Dk}}e^{-\sqrt{(k/D)}x} \tag{20}$$

If we put

$$\varphi(x,0)=\boldsymbol{B}-\psi(x) \tag{21}$$
$$=\phi(x) \tag{21'}$$

the function $C_1(x,t)$ of Eq. 16 satisfy the initial condition (15), i. e.

$$C_1(x,0)=\psi(x)+\varphi(x,0)$$
$$=\boldsymbol{B}$$

The function $\varphi(x,t)$ must satisfy also the boundary condition

$$D\left(\frac{\partial\varphi(x,t)}{\partial x}\right)_{x=0}=0 \tag{22}$$

The general solution of Eq. 18 is

$$\varphi(x,t)=e^{-(D\alpha^2+k)t}\cos\alpha x \tag{23}$$

According to Fourie's integral theorem we obtain

$$\varphi(x,t)=\frac{2}{\pi}\int_0^\infty d\alpha\int_0^\infty\phi(\lambda)e^{-(D\alpha^2+k)t}\cos\alpha x\cos\alpha\lambda d\lambda \tag{24}$$

Summing Eq. 19 and the integrated result of Eq. 24, and using Eq. 13 we obtain the solution 7.

# *Absorption Spectra of Nitrobenzene Derivatives. I. Spectral Features of o-, m- and p-Isomers*

By Kimio SEMBA*

(Received May 26, 1960)

It is well known that molecules having electron attracting groups such as nitro, carbonyl and corboxyl groups exhibit intense absorption spectra in the near ultraviolet or visible region[1]. Recently, Nagakura and Tanaka[2] presented a new theory (molecular energy level diagram method) based on the molecular orbital theory treating the electron migration between two $\pi$-electron systems. According to their theory, it is possible to interpret strong absorption bands of some aromatic nitro compounds in terms of the intramolecular charge transfer spectra.

The intramolecular charge transfer in nitrobenzene means the interaction of the highest occupied orbital of benzene ($H_B$) with the lowest vacant orbital of nitro group ($V_S$). In nitrobenzene derivatives there are appreciable interactions between the molecular orbitals of monosubstituted benzenes and those of the nitro groups[3]. Considering the energy values and symmetry properties of these orbitals, one sees that the interaction between the highest occupied orbital of the monosubstituted benzene and the lowest vacant orbital (anti-bonding $\pi$-orbital) of the nitro group is especially important.

The molecular energy-level diagrams of benzene, aniline and nitromethane[2] are shown in Fig. 1. The intramolecular charge transfer transition may occur as a result of interactions between two split orbitals ($H_{x1}$ and $H_{x2}$) in aniline and the lowest vacant orbital $V_S$ of the nitro group. These transitions are generally accompanied by a large electronic transfer and have been designated as intramolecular charge transfer transition[2].

According to Nagakura and Tanaka's theory, there is no interaction between $H_{x2}$ and $V_S$, and only one transition due to the $H_{x1}$ and $V_S$ interaction can be observed for a *p*-isomer. On the other hand, in *o*- and *m*-isomers the

* Present address: Research Laboratory, Kurosaki Firebrick Mfg. Co., 535, Fujita, Yawata.

1) L. Dede and A. Rosenberg, *Ber.*, **67**, 147 (1934); W. D. Kumler, *J. Am. Chem. Soc.*, **68**, 1184 (1946).

2) S. Nagakura and J. Tanaka, *J. Chem. Phys.*, **22**, 236 (1954); S. Nagakura, ibid., **23**, 1441 (1955).

3) J. Tanaka and S. Nagakura, ibid., **24**, 1274 (1956); *J. Chem. Soc. Japan, Pure Chem. Sec.* (*Nippon Kagaku Zasshi*), **78**, 1200 (1957).

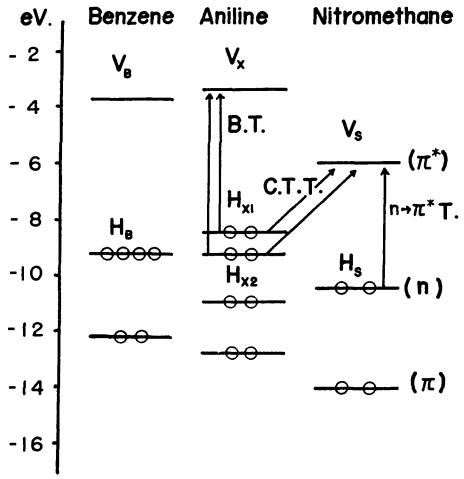



Fig. 1. Molecular energy level diagrams of benzene, aniline and nitromethane.

two orbital $H_{x1}$ and $H_{x2}$ can interact with $V_S$, and two transfer transitions of the charge transfer type may be expected for these isomers.

In this paper the intramolecular charge transfer spectra (250~400 m$\mu$) of *o*-, *m*- and *p*-nitrophenol, -nitroanisole, -nitroaniline and -nitro-*N*-dimethylaniline are measured in *n*-hexane, and their spectral features together with the effect of substituents on them are discussed according to Nagakura and Tanaka's theory.

The migration effects of electron donating groups on absorption spectra of *o*-, *m*- and *p*-nitroaniline are considered in aqueous and hydrochloric acidic solutions and the existence of simple equilibria between these isomers and protons is indicated.

## Experimental

Absorption spectra were recorded by a Hitachi automatic recording spectrophotometer type EPS-2, using quartz cells of 1 cm. in path length. Infrared spectra were obtained by another Hitachi double beam infrared spectrophotometer type EPI-2 with 0.1 mm. rock salt cells.

Solvents, *n*-hexane, methanol, ethanol, chloroform and ethyl ether, were purified by the method recommended by Weissberger and Proskauer[4].

*o*-, *m*- and *p*-Nitrophenol, -nitroanisole and -nitroaniline of Tokyo Chemical Industry Co. special grade were used. *m*- and *p*-Nitro-*N*-dimethylaniline were synthesized according to Fich's method[5] by nitration of *N*-dimethylaniline, and were recrystallized several times from ethanol and benzene, respectively. These samples were thought to be pure enough and no further purification was carried out.

4) A. Weissberger and E. S. Proskauer, "Organic Solvent", Interscience Publishers, Inc., New York (1955).
5) H. M. Fich, "Organic Syntheses", Vol. 27, p. 62.

## Results and Discussion

**Spectral Features of *o*-, *m*- and *p*-Isomers.**— Absorption maxima of the nitrobenzene derivatives in *n*-hexane are collected in Table I.

Table I. Absorption maxima of nitrobenzene derivatives in *n*-hexane

| Molecule | Absorption maxima, m$\mu$ | | | |
|---|---|---|---|---|
| *o*-Derivatives | | | | |
| Nitrophenol | 212.6 | — | 271.0* | 347.0* |
| Nitroanisole | 214.5 | — | 251.2* | 307.5* |
| Nitroaniline | 229.0 | 244.0 | 269.0* | 376.0* |
| *m*-Derivatives | | | | |
| Nitrophenol | 222.4 | — | 258.0* | 312.0* |
| Nitroanisole | 225.2 | — | 261.7* | 320.4* |
| Nitroaniline | 229.0 | 249.0 | 266.0* | 344.0* |
| Nitro-*N*-dimethylaniline | — | 248.0 | — | 382.5* |
| *p*-Derivatives | | | | |
| Nitrophenol | 224.3 | — | 285.0* | 334.0** |
| Nitroanisole | 225.8 | — | 293.0* | — |
| Nitroaniline | 226.0 | — | 320.0* | — |
| Nitro-*N*-dimethylaniline | — | — | 348.0* | — |

* Intramolecular charge transfer bands.
** Band due to $n\rightarrow\pi^*$ transition.

It is noted from Table I and Fig. 2 (the absorption spectra of *o*-, *m*- and *p*-nitroaniline) that the spectra of *o*- and *m*-nitrobenzene derivatives resemble each other in the point that they show two kinds of absorption bands in the ultraviolet and visible regions, one at 260 m$\mu$ and the other at 350~380 m$\mu$. On the other hand, the *p*-isomer spectrum is quite different from those of the other isomers, except for the band at 220 m$\mu$.

These spectral characteristics have already been pointed out by Kumler[1], and were interpreted on the basis of the "electron oscillation" theory proposed by Lewis and Calvin[6]. However, Kumler's interpretation must be reconsidered from the standpoint of recent theories.

From the positions and intensities of these absorption bands we may assign the bands at 260 and 350~380 m$\mu$ for the *o*- and *m*-isomers and the band at 300 m$\mu$ for the *p*-isomer to the intramolecular charge transfer transitions in these molecules. Thus we have two intramolecular charge transfer bands for *o*- and *m*-isomers and only one for the *p*-isomer (Table I). These characteristic features of the intramolecular charge transfer spectra for the three isomers of nitrobenzene derivatives have been well explained by the molecular orbital theories cited above[3].

6) G. N. Lewis and M. Calvin, *Chem. Revs.*, **25**, 273 (1939).

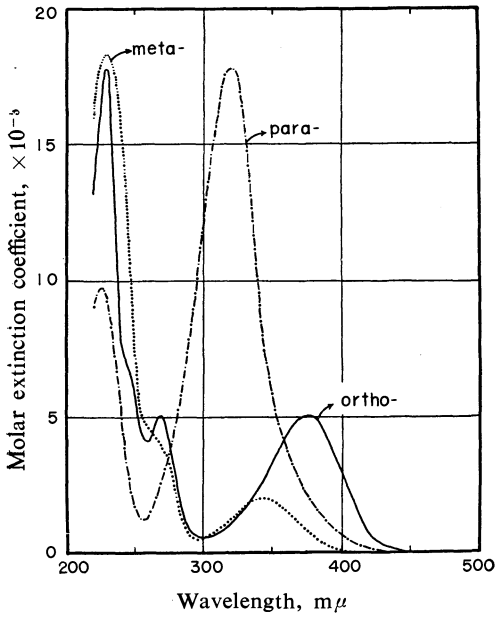



Fig. 2. Absorption spectra of *o*-, *m*- and *p*-nitroaniline, all in *n*-hexane.

The intramolecular charge transfer spectrum of *p*-nitroaniline is much stronger ($\varepsilon \sim 10000$) than those of the *o*- and *m*-nitroaniline (Fig. 2). The coefficient* of the AO at the para-position in the $H_{x1}$-MO of a monosubstituted benzene (aniline) is greater than those of ortho- and meta-AO's, giving rise to stronger absorption for the *p*-isomer than for other isomers[3]. The intensities of the bands at 260 mμ for the *o*- and *m*-isomers are nearly equal ($\varepsilon \sim 5000$) and the longer wavelength band at 350~380 mμ for the *o*-isomer is stronger than the band of the *m*-isomer. The same relations among intensities of the intramolecular charge transfer bands can also be observed for the spectra of other nitrobenzene derivatives studied in this paper.

Absorption bands of *o*-nitrophenol and *o*-nitroaniline, due to transitions of the same type appear at longer wavelengths than those of the *m*-isomers. On the other hand, the bands of *m*-nitroanisole appear at longer wavelengths than those of the *o*-isomer. These facts may be explained in terms of intramolecular hydrogen bondings[3] which can be formed in these ortho compounds as shown in Fig. 3. The formations of these intramolecular hydrogen bondings are evident from infrared absorptions as shown in Figs. 4 and 5. The OH group in *o*-nitrophenol shows a very broad infrared absorption band at 3200 $cm^{-1}$, and the $NH_2$ group in *o*-nitroaniline shows less broad absorptions at 3510 and 3380 $cm^{-1}$. On

* See ref. 3.

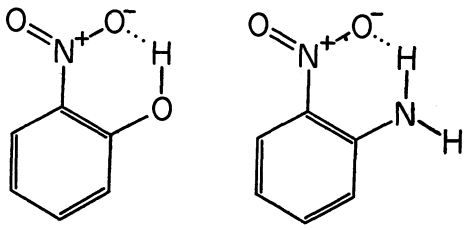


Fig. 3. Intramolecular hydrogen bondings in *o*-nitrophenol and *o*-nitroaniline.

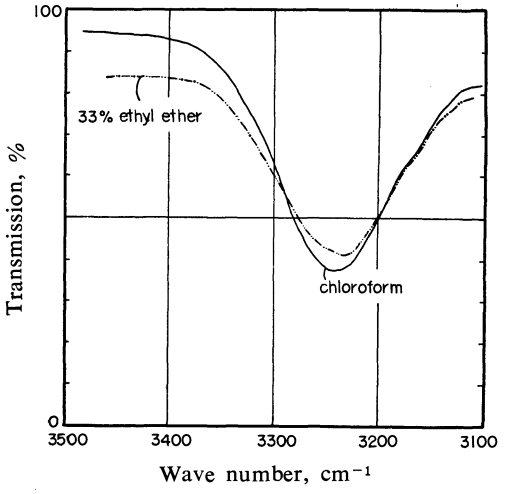



Fig. 4. Infrared absorption of *o*-nitrophenol in chloroform.

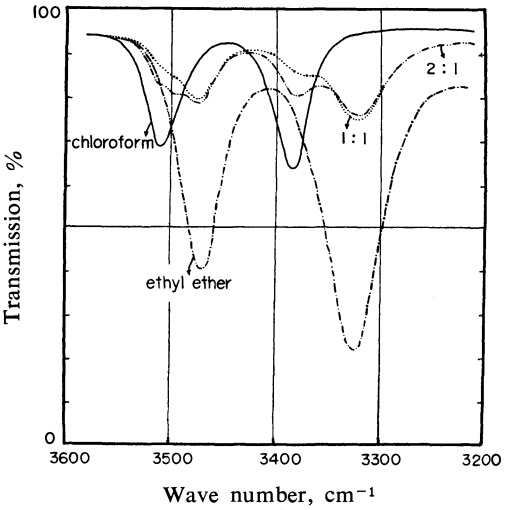



Fig. 5. Infrared absorption of *o*-nitroaniline in chloroform (-·-·- 33% ethyl ether, ····· 50% ethyl ether).

the addition of ethyl ether the former does not shift but the latter groups shift to longer wavelengths. These facts indicate that in *o*-nitrophenol intramolecular hydrogen bonding

is too strong to allow an intermolecular hydrogen bonding between the solute and ethyl ether molecules but in *o*-nitroaniline the intermolecular hydrogen bonding is formed to a large extent, as shown in Fig. 6.

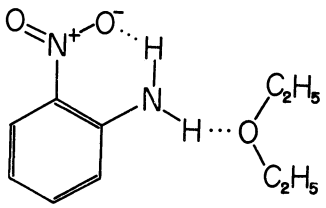


Fig. 6. Intermolecular hydrogen bonding between *o*-nitroaniline and ethyl ether.

The band at 220 m$\mu$ in the spectra of *o*-, *m*- and *p*-isomers may be associated with the transition of another charge transfer type[7]. Absorption shoulders are observed at 240~250 m$\mu$ for *o*- and *m*-nitroaniline (Table I).

**Effect of Substituents on Absorption Spectra.** —Next we shall study the effect of electron donating groups on the absorption spectra in nitrobenzene derivatives. Usually this effect is divided into resonance and inductive effects. In the present case only the resonance effect is of interest, and so we neglect the inductive effect.

According to the perturbation theory the resonance effect is associated with the transfer of an electron from a $\pi$-orbital of the substituent into a vacant orbital of the conjugated system. The effect of the substituents on absorption spectra of benzene derivatives has been explained in terms of the relative stabilization of the ground and excited states[8]. The stabilization energies of these states are closely connected with electron migration from the substituents into the ring, and as generally the stabilization is much greater in the excited state, red shifts of absorption bands are expected with the increasing electron migration.

As seen from Table I, the absorption bands of the *m*- and *p*-isomers shift to the longer wavelengths in the order of OH, $OCH_3$, $NH_2$ and $N(CH_3)_2$ groups. These spectral shifts are very similar to those of monosubstituted benzene derivatives. However, the shifts for *o*-isomers are of somewhat different nature on account of ortho-effects involving effects of intramolecular hydrogen bonding and of steric hindrance.

On comparing nitrophenol with nitroaniline the ionization energy of the $NH_2$ group is much smaller than that of the OH group[9], leading to a much larger electron migration from the $NH_2$ group than from the OH group. Consequently nitroaniline shows a red shift of absorption maximum as compared with nitrophenol. The same type of shifts has been observed for monosubstituted benzenes, phenol and aniline, the latter showing the absorption at the longer wavelength.

On the other hand, we find the absorption maximum of nitrophenol on the blue side of the nitroanisole maximum. Matsen et al.[10] found that the O–O band of phenol is at a longer wavelength than that of anisole and from this they concluded that the resonance of the OH group with the benzene ring is much stronger than that of an alkoxy group ($OCH_3$ or $OC_2H_5$). However, from our result we can assume that the electron migration from the $OCH_3$ group is greater than that from the OH group because of the hyperconjugation effect of the $CH_3$ group. The same consideration may be taken for the $NH_2$ and $N(CH_3)_2$ groups, as the absorption maximum of nitro-*N*-dimethylaniline appears at the longer wevelength than that of nitroaniline.

**Effect of Electron Migration on Absorption Spectra.** — As mentioned above, the shifts of intramolecular charge transfer spectra are very much influenced by the amount of electron migration from electron donating substituents into the benzene ring. For the sake of simplicity we limited our consideration to the case of nitroaniline in aqueous or hydrochloric acidic solution.

The amount of electron migration from the $NH_2$ group of nitroaniline will decrease by addition of hydrochloric acid to the aqueous solution, since the lone pair electrons of the N-atom in the $NH_2$ group will be fixed by a proton according to the following scheme

$$-NH_2 + H^+ \rightleftharpoons -NH_3^+$$

and the electron migration into the ring will be arrested. Then the absorption spectrum of nitroaniline will resemble that of nitrobenzene.

This expectation is satisfactorily supported by the experimental results as shown in Figs. 7, 8 and 9. The absorption spectra of *o*-, *m*- and *p*-nitroaniline in aqueous solutions approach to that of nitrobenzene with the increasing concentration of hydrochloric acid, and finally they all become the same as the spectrum of nitrobenzene with respect to absorption intensities and wavelengths.

7) J. Tanaka, *J. Chem. Soc. Japan, Pure Chem. Sec.* (*Nippon Kagaku Zasshi*), **79**, 1114 (1958).

8) K. F. Herzfeld, *Chem. Revs.*, **41**, 233 (1947); W. W. Robertson and F. A. Matsen, *J. Am. Chem. Soc.*, **72**, 5252 (1950); H. Baba and S. Nagakura, *J. Chem. Soc. Japan, Pure Chem. Sec.* (*Nippon Kagaku Zasshi*), **72**, 72 (1951); M. Tuboi, This Bulletin, **25**, 369 (1952); K. Semba, *J. Chem. Soc. Japan, Pure Chem. Sec.* (*Nippon Kagaku Zasshi*), **77**, 333, 338 (1956).

9) W. C. Price, *Chem. Revs.*, **41**, 257 (1947).

10) W. W. Robertson, A. J. Seriff and F. A. Matsen, *J. Am. Chem. Soc.*, **72**, 1539 (1950).

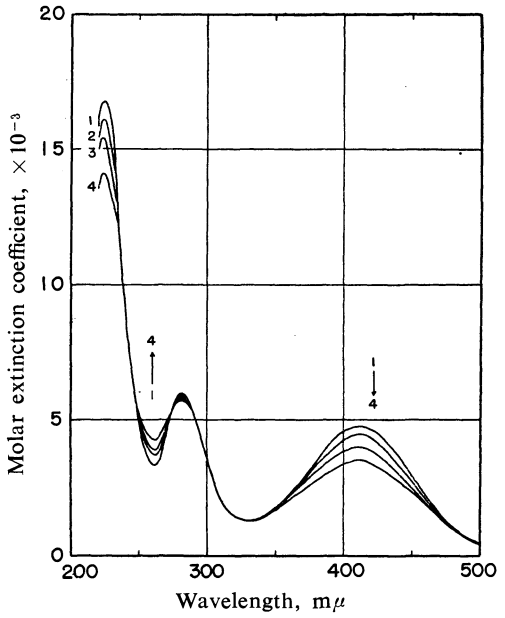



Fig. 7. Absorption spectra of *o*-nitroaniline ($4.18\times10^{-5}$ mol./l.) in water in the presence of hydrochloric acid, at 29°C.
Curve 1: aqueous solution.
Curve 2: concentration of hydrochloric acid $9.16\times10^{-2}$ mol./l.
Curve 3: $2.75\times10^{-1}$ mol./l.
Curve 4: $4.58\times10^{-1}$ mol./l.

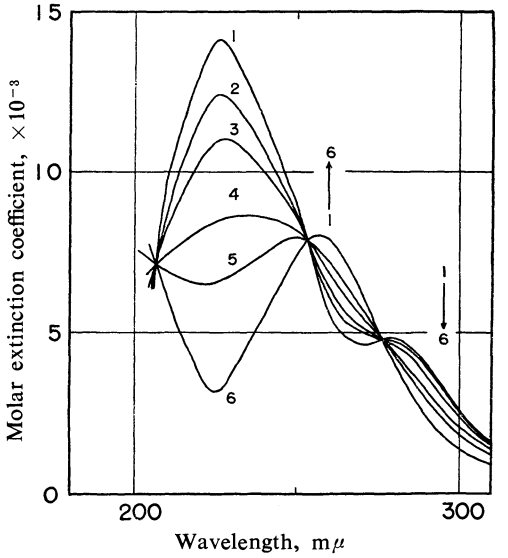



Fig. 8. Absorption spectra of *m*-nitroaniline ($5.78\times10^{-5}$ mol./l.) in water in the presence of hydrochloric acid, at 29.5°C.
Curve 1: aqueous solution.
Curve 2: concentration of hydrochloric acid $9.16\times10^{-4}$ mol./l.
Curve 3: $1.83\times10^{-3}$ mol./l.
Curve 4: $4.58\times10^{-2}$ mol./l.
Curve 5: $9.16\times10^{-2}$ mol./l.
Curve 6: $4.58\times10^{-1}$ mol./l.

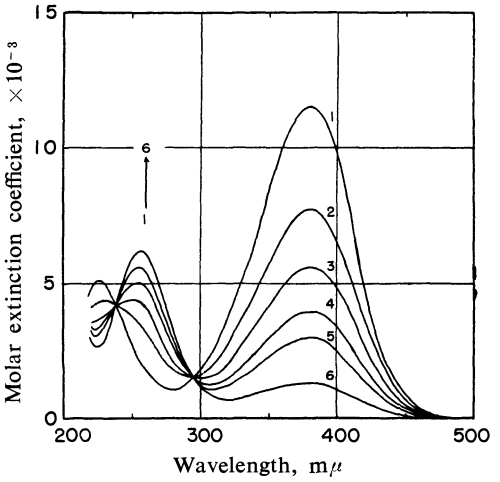
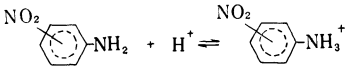



Fig. 9. Absorption spectra of *p*-nitroaniline ($1.02\times10^{-4}$ mol./l.) in water in the presence of hydrochloric acid, at 26°C.
Curve 1: aqueous solution.
Curve 2: concentration of hydrochloric acid $4.58\times10^{-2}$ mol./l.
Curve 3: $9.16\times10^{-2}$ mol./l.
Curve 4: $1.83\times10^{-1}$ mol./l.
Curve 5: $2.75\times10^{-1}$ mol./l.
Curve 6: $6.41\times10^{-1}$ mol./l.

Isosbestic points observed for the spectra of all the isomers can be explained by assuming the following equilibrium

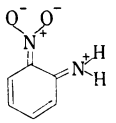


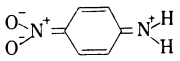

From the experimental results the equilibrium constants and differences of free energy are evaluated, as listed in Table II.

TABLE II. EQUILIBRIUM CONSTANTS AND FREE ENRGY DIFFERENCES FOR *o*-, *m*- AND *p*-NITROANILINE

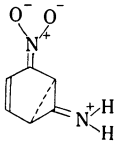
| Molecule | Equilibrium constant | Free enrgy difference kcal./mol. |
|---|---|---|
| *o*-Nitroaniline | 3.5 | −0.75 (at 29°C) |
| *m*-Nitroaniline | 200 | −3.3 (at 29.5°C) |
| *p*-Nitroaniline | 10.8 | −1.4 (at 26°C) |

The equilibrium constant for the *m*-isomer is much larger than those for other isomers, and the *m*-isomer requires a very small amount of hydrochloric acid to reach equilibrium. This may be due to the meta-directing property of the $NO_2$ group. The meta-position is more negative compared with other positions as the $NO_2$ group has the meta-directing power, and the proton affinity of the N-atom in the *m*-isomer is large (formation of *m*-nitroanilinium ion). The same conclusion may be reached from the viewpoint of the resonance theory. In the *o*- and *p*-isomers the *o*- and *p*-quinoid structures





contribute largely, while in the *m*-isomer the contribution of the *m*-quinoid structure



is expected to be small. From this fact we may conclude that the electron migrations from the $NH_2$ group in the *o*- or the *p*-isomer are large, and that in the *m*-isomer a proton may easily be bonded to the N-atom.

The small value of the equilibrium constant for the *o*-isomer is probably due to steric hindrance.

***n*→*π** Transition**— The absorption band of nitrobenzene due to the $n\rightarrow\pi^*$ electronic transition was observed by Wolf and Herold[11] and by Wenzel[12]. The absorption due to the $n\rightarrow\pi^*$ transition is characterized by its weak intensity and so can not be observed if a strong absorption band lies in the same wavelength region.

In the present work the absorption shoulder with the molar extinction coefficient of about 1000 is observed for *p*-nitrophenol at about 334 m$\mu$. Although this absorption shoulder shifts to the longer wavelengths, in methanol, ethanol and water, it may be assigned to the $n\rightarrow\pi^*$ transition owing to its weakness of intensity. However, we could not observed this weak band in detail owing to the disturbance of the strong intramolecular charge transfer band which overlaps the weak band.

11) K. L. Wolf and W. Herold, *Z. physik. Chem.*, **B13**, 201 (1931).
12) A. Wenzel, *J. Chem. Phys.*, **22**, 1623 (1954).

## Summary

The intramolecular charge transfer spectra of some nitrobenzene derivatives were measured in *n*-hexane. The general features of the absorption spectra and the effect of substituents on the absorption spectra were considered from the concept of the intramolecular charge transfer. The migration effect of electron donating groups was discussed for the nitroaniline in aqueous and hydrochloric acidic solutions. Also other absorption due to the $n\rightarrow\pi^*$ transition of nitro group was considered.

The author wishes to thank Professor S. Imanishi and Dr. Y. Kanda of Kyushu University for their kind advice and encouragement thoughout this investigation, and Dr. M. Ito for his helpful and valuable discussions. The author also wishes to thank Drs. Y. Kora and T. Ikenoue of Kurosaki Firebrick Mfg. CO. for their kind encouragement.

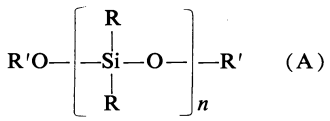
*Department of Chemistry*
*Faculty of Science*
*Kyushu University*
*Hakozaki, Fukuoka*

# *Alkylalkoxypolysiloxanes. IX*[1]. *Methylethoxypolysiloxanes Containing the Trimethylsiloxy Group*

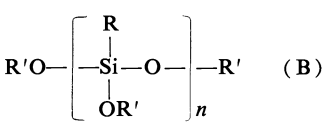
By Minoru SAKIYAMA and Rokuro OKAWARA

(Received June 21, 1960)

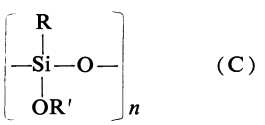
Many alkylalkoxypolysiloxanes have hitherto been synthesized. They have following general formulas, and each was prepared from only one kind of alkylchlorosilane.



(A)



(B)



(C)

1) Part VIII of this series, R. Okawara and M. Katayama, This Bulletin, 33, 659 (1960).

$$R-\left[\begin{array}{c} OR' \\ | \\ -Si-O- \\ | \\ OR' \end{array}\right]_n-R' \quad (D)$$

R, R'=alkyl group

In this paper, the syntheses and properties of the lower members of linear and branched methylethoxypolysiloxanes involving the trimethylsiloxy group $(CH_3)_3SiO$ are described.

Compounds which belong to series A to D have been synthesized by one of the following methods:

(1) partial hydrolysis of dialkyldialkoxysilane or alkyltrialkoxysilane[2]

(2) sodium hydrogen carbonate treatment of partially alcoholyzed alkylchlorosilanes[3]

(3) thermal condensation between Si–OR and Si–Cl[4]

(4) hydrolysis of partially alcoholyzed alkylchlorosilanes in wet pyridine[5].

Method 4 is different from 1 in that the former takes into account the difference in reactivity toward water between the Si–Cl and the $Si-OC_2H_5$ bonds. It appears that the ethoxy groups reacted quite randomly with $H_2O$ to decrease the yield in method 1, especially when two kinds of methylethoxysilane were used. Therefore, method 1 was not examined. Also the results of some experiments showed that methods 2 and 3 were not conveniently applicable to the preparation. In consequence, method 4 was adopted. Partially ethanolyzed silicon tetrachloride, methyltrichlorosilane and dimethyldichlorosilane were mixed separately with trimethylchlorosilane and cohydrolyzed in wet pyridine in benzene containing the calculated amount of water. The products of hydrolysis were fractionally distilled. The details of the reactions are summarized in Table I. The desired products were obtained in moderate yield. This method is based on the difference of reactivity towards water between the Si–Cl and $Si-OC_2H_5$ bonds. As the $Si-OC_2H_5$ bond is also known to hydrolyze rapidly, particularly in an acidic medium, a slightly basic medium of wet pyridine in benzene was used. The properties of the compounds obtained by the fractionation through a highly efficient Stedman column are given in Table II.

The infrared spectra of these compounds give additional information about the characteristic vibrations of the ethoxy group and the methyl group attached to the silicon atom. Infrared spectra of some types of methylethoxypolysiloxanes have been reported[6]. The spectra obtained for the compounds studied here are similar to those of the methylethoxypolysiloxanes cited above in the region 1300 to 3500 $cm^{-1}$. The spectra in the region 700 to 1300 $cm^{-1}$ are presented on Fig. 1. Frequencies and assignments are shown in Table III.

A sharp band near 1250 $cm^{-1}$ is known to be characteristic of the symmetric deformation of the methyl groups attached directly to a silicon atom. The spectra in Fig. 1 show that, except in $(CH_3)_3SiOSi(CH_3)_2OC_2H_5$, this band is a doublet. The compounds $[(CH_3)_3SiO]_3SiCH_3$ and $[(CH_3)_3SiO]_4Si$ have been reported[7] to show a doublet in the same region.

Wright et al.[7] reported that the characteristic bands of the unit $(CH_3)_3SiO$ lie at 754~756 $cm^{-1}$ and 841 $cm^{-1}$, that of $(CH_3)_2SiO$ at 800~814 $cm^{-1}$ and that of $CH_3SiO$ at 800 $cm^{-1}$. Table III shows that the same bands are observed in the spectra of our compounds containing these particular groups, except that the 800 $cm^{-1}$ band of the $(CH_3)_2SiO$ unit is split into a doublet.

A band near 960 $cm^{-1}$ is connected with the C–C stretching vibration of the $C_2H_5O$ group, and those in the region 1000 to 1150 $cm^{-1}$ are related to Si–O–Si and Si–O–C skeletal vibrations. Of the latter, the band near 1100 $cm^{-1}$ decreases in intensity with the substitution of ethoxy groups by trimethylsiloxy groups. The C–O bond is believed to contribute greatly to this absorption band. A similar tendency in intensity is seen for the bands near 780 $cm^{-1}$ and 1160 $cm^{-1}$.

## Experimental

**Starting Materials.** — Trimethylchlorosilane (I), dimethyldichlorosilane and methyltrichlorosilane were supplied by the Shin-etsu Chem. Ind. Co. Silicon tetrachloride was obtained by the reaction of silicon with chlorine. Those chlorosilanes were partially alcoholyzed with ethanol below 5°C in a three-necked flask with an efficient stirrer, a reflux condenser and a dropping funnel. Then the mixture was warmed to 50°C to complete the reaction and it was fractionally distilled through a Stedman column of about 30 theoretical plates. Boiling points and chlorine content are shown in Table I. The experimental value for the chlorine content of triethoxychlorosilane was considerably less than the calculated value. This is thought to be due to contamination by tetraethoxysilane which has a boiling point close to that of triethoxychlorosilane. This mixture (VII) was used for the source of triethoxychlorosilane without further purification.

**Sodium Hydrogen Carbonate Treatment of the Mixture of I and II.**—To the refluxing mixture of

2) H. J. Fletcher and M. J. Hunter, *J. Am. Chem. Soc.*, 71, 2919, 2922 (1949).
3) R. Okawara et al., This Bulletin, **28**, 360, 364, 367 (1955).
4) R. Okawara et al., ibid., **27**, 428, 582 (1954).
5) R. Okawara et al., ibid., **31**, 22 (1958); **33**, 659 (1960).
6) R. Okawara, ibid., **31**, 154 (1958).
7) N. Wright and M. J. Hunter, *J. Am. Chem. Soc.*, **69**, 803 (1947).

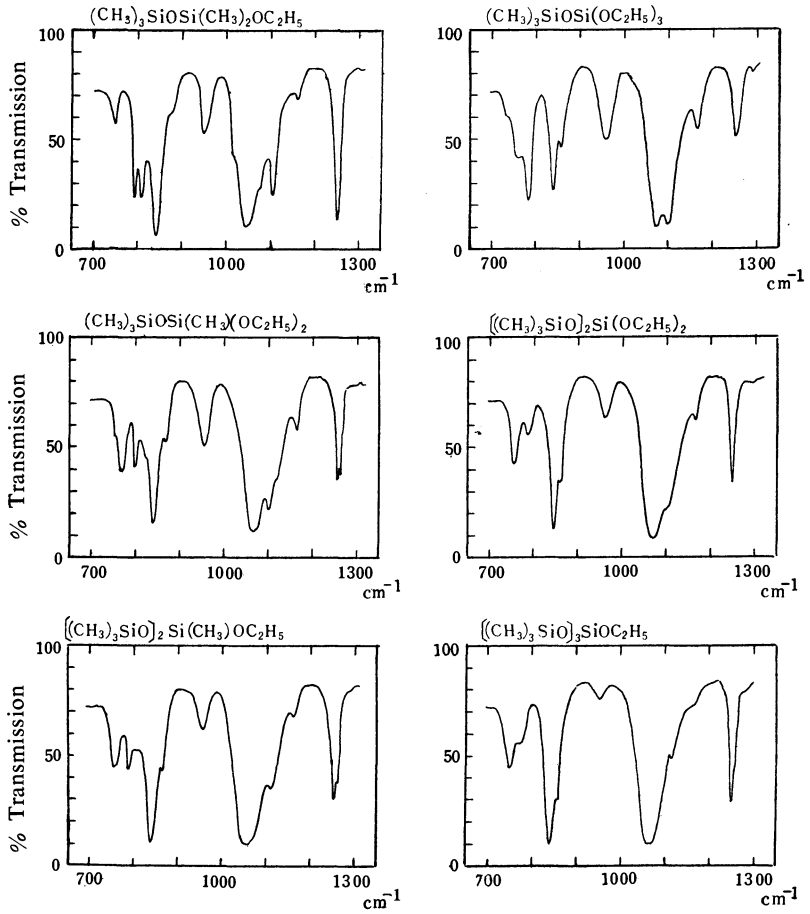



Fig. 1. Infrared spectra of methylethoxypolysiloxanes containing the trimethylsiloxy group.

I (21.8 g., 0.2 mol.) and II (27.8 g., 0.2 mol.), sodium hydrogen carbonate (16.8 g., 0.2 mol.) was added in portions. A reaction occurred violently with the evolution of hydrogen chloride and carbon dioxide. After completion of the reaction, the mixture (20 g.) was fractionally distilled. No plateau was found corresponding to $(CH_3)_3SiOSi(CH_3)_2$-$OC_2H_5$. It was thought from the distillation curve that the product was a complex mixture of methylethoxysilanes and -polysiloxanes.

**Attempts to Condense I and Tetraethoxysilane Thermally.**—A mixture of I (11 g., 0.1 mol.) and tetraethoxysilane (52 g., 0.25 mol.) was refluxed at 124°C for 20 hr., but no reaction occurred. The starting materials were recovered by the fractional distillation of the reaction mixture.

A mixture of I (22 g., 0.2 mol.) and tetraethoxysilane (21 g., 0.1 mol.) was passed through an electrically-heated quartz tube of 40 cm. length and 5 cm. diameter at 300°C for 4.5 hr. The condensate (40 g.) was fractionally distilled. Unreacted tetraethoxysilane was obtained, along with hexaethoxydisiloxane, which could be produced from the partial hydrolysis of tetraethoxysilane by a small amount of water remaining in the reaction tube or formed by oxidation of the ethoxy groups. Between the plateaus of these two compounds, a small plateau having a high refractive index ($n_D^{20}$ 1.3862. reported[8] for $(C_2H_5O)_4Si$: $n_D^{20}$ 1.3837) was found. The thermal condensation: $Si\text{-}Cl + C_2H_5O\text{-}Si \rightarrow Si\text{-}O\text{-}Si + C_2H_5Cl$ might have occurred in this experiment, but the yield was too low to apply this method to the synthesis.

**Hydrolysis of Chlorosilane Mixture in Wet Pyridine.**—The details of each experiment are given in Table I.

The typical operation was as follows. The hydrolyzing mixture consisting of benzene and the calculated amount of pyridine and water was placed in a three-necked flask with an efficient stirrer, a reflux condenser and a dropping funnel. The mixture of I and II to VII was added to the hydrolyzing mixture which was cooled with an ice-bath. The rate of addition was controlled, so that the white smoke of the chlorosilane-pyridine adduct would not be evolved from the top of the reflux condenser. After addition, the mixture was stirred for 1 hr. at room temperature. Whenever

8) D. F. Peppard et al., ibid., **68**, 77 (1946).

TABLE I. HYDROLYSIS OF CHLOROSILANE MIXTURE IN WET PYRIDINE

| Exp. No | Chlorosilane mixture: $(CH_3)_3SiCl$ g. (mol.) | Chlorosilane mixture: Ethoxychlorosilane g. (mol.) | Benzene as diluent ml. | Yield of condensate (% theory) | Main product $R=(CH_3)_3SiO$ | Yield g. |
|---|---|---|---|---|---|---|
| 1 | 43.6 (0.4) | II* 55.5 (0.4) | 100 | 46 (60) | $RSi(CH_3)_2(OC_2H_5)$ | 14 |
| 2 | 65.4 (0.6) | III 47.7 (0.3) | 100 | 63 (79) | $R_2Si(CH_3)(OC_2H_5)$ | 26 |
| 3 | 43.6 (0.4) | III 63.6 (0.4) | 80 | 47 (64) | $R_2Si(CH_3)(OC_2H_5)$ | 15 |
| 4 | 27.3 (0.25) | IV 53.4 (0.25) | 100 | 35 (66) | $RSi(CH_3)(OC_2H_5)_2$ | 18 |
| 5 | 59.9 (0.55) | V 29.9 (0.17) | 50 | 30 (52) | $R_3Si(OC_2H_5)$ | 9 |
| 6 | 54.4 (0.5) | VI 47.3 (0.25) | 100 | 57 (69) | $R_2Si(OC_2H_5)_2$ | 31 |
| 7 | 19.0 (0.17) | VII 50.0 ( — ) | 25 | 38 (—) | $RSi(OC_2H_5)_3$ | 20 |

* II $(CH_3)_2Si(OC_2H_5)Cl$ b. p. 95°C, Calcd. for II : Cl, 25.6. Found : Cl, 25.9%.
III $CH_3Si(OC_2H_5)Cl_2$ b. p. 100°C, Calcd. for III : Cl, 44.6. Found : Cl, 44.1%.
IV $CH_3Si(OC_2H_5)_2Cl$ b. p. 126°C, Calcd. for IV : Cl, 19.9. Found : Cl, 20.2%.
V $Si(OC_2H_5)Cl_3$ b. p. 102°C, Calcd. for V : Cl, 59.2. Found : Cl, 58.2%.
VI $Si(OC_2H_5)_2Cl_2$ b. p. 136°C, Calcd. for VI : Cl, 37.6. Found : Cl, 38.0%.
VII A mixture of $Si(OC_2H_5)_3Cl$ with $Si(OC_2H_5)_4$ b. p. 156°C, Calcd. for $Si(OC_2H_5)_3Cl$ : Cl, 17.5. Found : Cl, 10.3%.

TABLE II. METHYLETHOXYPOLYSILOXANES
$R=(CH_3)_3SiO$

| Methylethoxypolysiloxanes | B. p. °C/mmHg | Refractive index $n_D^{20}$ | Density $d_D^{20}$ | Molar refr. Found (Calcd.)* | % Si Found (Calcd.) |
|---|---|---|---|---|---|
| $RSi(CH_3)_2(OC_2H_5)$ | 129.6/760 | 1.3844 | 0.8324 | 54.08 (54.31) | 29.5 (29.20) |
| $RSi(CH_3)(OC_2H_5)_2$ | 154.9/760 | 1.3870 | 0.8766 | 59.72 (59.70) | 25.5 (25.26) |
| $RSi(OC_2H_5)_3$ | 177.3/760 | 1.3868 | 0.9110 | 65.13 (65.09) | 22.1 (22.25) |
| $R_2Si(CH_3)(OC_2H_5)$ | 170.0/760 | 1.3880 | 0.8623 | 72.95 (72.95) | 31.9 (31.62) |
| $R_2Si(OC_2H_5)_2$ | 182.8/760 | 1.3880 | 0.8915 | 78.50 (78.34) | 29.2 (28.41) |
| $R_3Si(OC_2H_5)$ | 194.5/760 | 1.3888 | 0.8803 | 91.48 (91.59) | 33.2 (32.98) |

* Calculated from bond refractivities by E. L. Warrick, *J. Am. Chem. Soc.*, **68**, 2455 (1946).

TABLE III. INFRARED SPECTRA OF TRIMETHYLSILOXYETHOXYSILOXANES : POSITIONS OF BANDS (IN $cm^{-1}$)
$R=(CH_3)_3SiO$

| $RSi(CH_3)_2OC_2H_5$ | $RSi(CH_3)(OC_2H_5)_2$ | $R_2Si(CH_3)OC_2H_5$ | $RSi(OC_2H_5)_3$ | $R_2Si(OC_2H_5)_2$ | $R_3Si(OC_2H_5)$ | Assignment |
|---|---|---|---|---|---|---|
| 749 | 751 | 757 | 757 | 753 | 751 | $(CH_3)_3SiO_{1/2}$ |
| | 768 | | 783 | 786 | 771 | |
| 791, 809 | 798 | 788 | | | | $(CH_3)_2SiO$, $CH_3SiO_{3/2}$ |
| 842 | 841 | 841 | 840 | 842 | 842 | $(CH_3)_3SiO_{1/2}$ |
| 875 | 867 | 867 | 856 | 859 | 860 | |
| 950 | 956 | 956 | 961 | 959 | 955 | C-C str. |
| 1022 | | | | | | |
| 1054 | 1067 | 1061 | 1073 | 1067 | 1065 | SiOSi |
| 1082 | 1100 | 1112 | 1098 | 1098 | 1114 | |
| 1106 | 1117 | | | | | |
| 1162 | 1164 | 1162 | 1164 | 1164 | 1163 | |
| 1255 | 1254 | 1254 | 1252 | 1252 | 1251 | $CH_3$(-Si) |
| | 1263 | 1261 | 1260 | 1260 | 1259 | |

the chlorosilane odor still remained, several drops of wet pyridine were added. The mixture was washed with cold water, and then dried with sodium sulfate. Benzene was removed by distillation, followed by a fractionation through a Stedman type column of about 50 theoretical plates.

**Determination of Silicon Content.**—It is known that when methylpolysiloxanes containing the trimethylsiloxy group are decomposed by the action of concentrated sulfuric acid, volatile decomposition products are evolved. Therefore this method cannot be applied to the determination of silicon content in these compounds. In this study, about 0.5 g. of the sample was decomposed by sodium peroxide in a Paar bomb.

**Infrared Spectra.**—A Hilger H800 spectrometer with a sodium chloride prism was used. Spectra were taken in carbon disulfide solution in the region 700 to 1400 $cm^{-1}$ and in carbon tetrachloride solution in the region 1300 to 3500 $cm^{-1}$. The concentrations were 3% in both cases.

## Summary

(1) Methylethoxypolysiloxanes containing the trimethylsiloxy group have been prepared.

(2) The infrared spectra of these compounds are discussed.

*Department of Applied Chemistry*
*Faculty of Engineering*
*Osaka University*
*Miyakojima, Osaka*

# *Diffusion in Glycerol-Water Mixture*

By Yasunori NISHIJIMA* and Gerald OSTER

(Received June 24, 1960)

When the diffusion coefficient is concentration dependent, the diffusion curve, in which the concentration gradient is plotted against distance, will no longer be symmetric with respect to the position of the original boundary. In such a skewed curve, the maximum position of the concentration gradient is displaced to the solvent side or to the solution side depending on whether the concentration dependence is positive or negative, respectively. The degree of skewness of the curve is a measure of the extent of the concentration dependence of the diffusion coefficient.

The concentration dependence of diffusion coefficient, especially in the case of polymer solutions, has been studied[1-4].

This dependence is attributed to a thermodynamic factor and to a hydrodynamic factor. In most cases, these factors act in opposite directions and partly counterbalance the resultant concentration dependence of the diffusion coefficient. The thermodynamic factor is due to the non-ideality of the solution and usually contributes to the positive dependence, that is, to increase the rate of diffusion with increasing concentration. On the other hand, the hydrodynamic factor tends to slow down the diffusion rate with increasing concentration. This factor is attributed to the concentration dependence of the frictional coefficient of the diffusing particles. When the size and shape of the diffusing particles are independent of the concentration, the hydrodynamic factor can be estimated from the local viscosity of the medium in which the particles are diffusing[5]. It has not been entirely clear, however, how one can determine the local viscosity of the medium. In the case of very dilute solutions, the local viscosity is approximated by the solvent viscosity, whereas, at higher solute concentrations, the local viscosity is apparently somewhere between the solvent viscosity and the solution, or macroscopic, viscosity. In the case of solutions of small molecules such as glycerol-water mixtures, we have found that the local viscosity, obtained from fluorescence measurements of Auramine O, equals the macroscopic viscosity of solution[6].

It is the purpose of the present paper to investigate the concepts mentioned above using the glycerol-water system as an example, and

* Present address, Department of Textile Chemistry, Kyoto University, Kyoto.

1) C. O. Beckmann and J. L. Rosenberg, *Ann. N. Y. Acad. Sci.*, **46**, 329 (1945).

2) S. J. Singer, *J. Chem. Phys.*, **15**, 341 (1947).

3) N. Gralen, *Inaugural Dissertation, Uppsala* (1944).

4) Y. Nishijima and H. Inagaki, *J. Chem. Soc. Japan, Pure Chem. Sec.* (*Nippon Kagaku Zasshi*), **73**, 191 (1952).

5) Y. Nishijima and G. Oster, *J. Polymer Sci.*, **19**, 337 (1956).

6) G. Oster and Y. Nishijima, *J. Am. Chem. Soc.*, **78**, 1581 (1956).

covering a wide range of concentrations. The diffusion measurements were carried out in an interferometric micro-diffusion apparatus[5].

## Experimental

**Apparatus.**—We have developed a simple interferometric microdiffusion method which employs an ordinary light microscope. The diffusion cell is an optical wedge consisting of two partially-reflecting microscope slides and placed on the microscope stage. Small drops of the liquids are introduced into the cell to form a sharp boundary readily. Since the cell is very thin, convection currents are eliminated and hence rigid temperature control is unnecessary and the temperature was maintained in the vicinity of 25°C. The time required for diffusion measurements in the micro method is reduced by several thousand-fold that required in a conventional diffusion apparatus. The interference fringes produced in the cell are photographed every minute. Since each fringe represents a contour line of constant optical path in the wedge, the refractive index gradient is easily determined. The details of this method have been treated elsewhere[5].

## Results

To insure high accuracy, the diffusion measurements were carried out between several pairs of glycerol-water mixtures varying in concentrations ranging from pure water to 93% glycerol by weight. An example of a normalized diffusion curve obtained by our method is given in Fig. 1. For higher glycerol concentrations the curve is even more skewed in the direction of the higher concentration side.

The diffusion coefficient $D(c)$ as a function of concentration may be calculated from Boltzmann's equation[7]

$$D(c) = -\frac{1}{2t} \cdot \frac{dx}{dc} \int_0^c x dc \qquad (1)$$

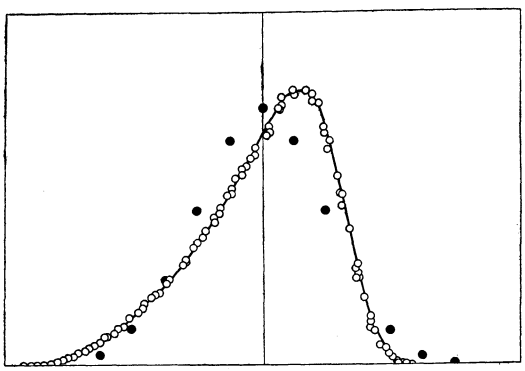


Fig. 1. Normalized diffusion curve: 62% glycerol against pure water (water on left); Open circles: experimental points. Black dots: Gaussian curve.

7) L. Boltzmann, *Ann. Physik*, 53, 959 (1894).

where $c$ is the concentration, $x$ is the distance along the direction of diffusion, and $t$ is the time. In the present study, the diffusion coefficients were calculated from Boltzmann's equation utilizing normalized coordinates. The diffusion coefficient as a function of glycerol concentration is given in Fig. 2. The fact that the slope is negative, shows that the hydrodynamic factor is predominant. Since this curve is not linear, simple graphical methods for evaluating the concentration dependence[3,8] are not valid because such methods assume linearity. A general statistical method for analyzing slightly skewed curves has been developed[9], but is not valid for high glycerol concentration since the diffusion curves are highly skewed (see, for example, Fig. 1).

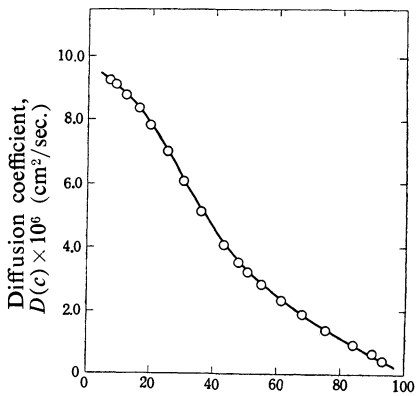



Fig. 2. Diffusion coefficient of glycerol as a function of concentration.

## Discussion

The diffusion coefficient in non-ideal solution is given by the equation[10]

$$D(c) = \frac{RT}{f} \cdot \frac{d \ln a_2}{d \ln c} \qquad (2)$$

where $f$ is the frictional coefficient of the diffusing particles, $a_2$ is the activity of the solute at concentration $c$, $R$ is the gas constant, and $T$ is the absolute temperature. We have calculated the thermodynamic factor, $d \ln a_2 / d \ln c$, in Eq. 2 from literature values of the vapor pressures of glycerol-water mixtures[11]. The frictional coefficient $f$ is proportional to the local viscosity of the medium. Hence, if the local viscosity is identical with the macroscopic, or solution, viscosity this hydrodynamic

8) H. Inagaki and Y. Nishijima, *J. Chem. Soc. Japan Pure Chem. Sec.* (*Nippon Kagaku Zasshi*), 72, 888 (1951).
9) Y. Nishijima and G. Oster, *J. Chem. Phys.*, 24, 269 (1957).
10) L. Onsager and R. M. Fuoss, *J. Phys. Chem.*, 36, 2689 (1932).
11) C. S. Miner and N. N. Dalton, "Glycerol", Reinhold Publishing Co., N. Y. (1953), p. 269.

TABLE I. CORRECTION FACTORS FOR THE DIFFUSION COEFFICIENT

| Glycerol conc. (wt. %) | 10 | 20 | 30 | 40 | 50 | 60 | 70 | 80 | 90 |
|---|---|---|---|---|---|---|---|---|---|
| $(d \ln a_2/d \ln c)$ | 1.0 | 1.2 | 1.4 | 1.7 | 2.0 | 2.3 | 2.8 | 3.2 | 3.5 |
| Viscosity | 1.15 | 1.54 | 2.16 | 3.18 | 5.04 | 8.82 | 17.96 | 45.86 | 163.6 |

factor should be proportional to observed viscosities of the glycerol-water mixtures. These correction factors are given in Table I. Applying these correction factors to the data of Fig. 2, we obtain the curve shown in Fig. 3.

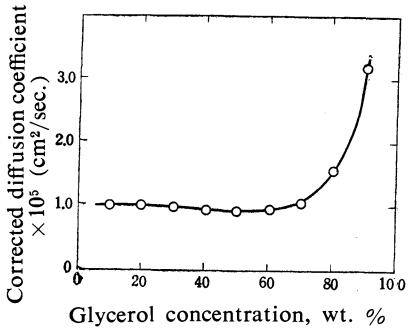



Fig. 3. Corrected diffusion coefficient of glycerol.

The corrected diffusion coefficient illustrated in Fig. 3 is sensibly independent of concentration up to 70% glycerol above which it rises rapidly. The increased mobility at very high glycerol concentrations could be due to a decreased hydration of the glycerol molecules. Vapor pressure measurements of glycerol-water mixtures have been interpreted in terms of a decrease of hydration with increasing concentration of glycerol[12]. More direct measurements, however, such as obtained from nuclear magnetic resonance, could better indicate changes in hydration.

## Summary

Diffusion studies of glycerol in glycerol-water mixtures ranging from zero to 93% glycerol were carried out using the micro-interferometric method. For higher concentration of glycerol the diffusion coefficient decreases strongly with increasing concentration and the diffusion curves are highly skewed. Applying thermodynamic and hydrodynamic correction obtained from vapor pressure measurements and solution viscosities, respectively, the diffusion coefficient was found to be sensibly independent of glycerol concentration up to about 70% after which it rises. The increased mobility at very high glycerol concentrations is attributed to a decreased hydration of the glycerol molecules under these conditions.

*Department of Chemistry*
*Polytechnic Institute of Brooklyn*
*Brooklyn 1, New York U.S.A.*

12) P. E. Perman and T. W. Price, *Trans. Faraday Soc.*, 8, 68 (1912).

# *Formaldehyde Resins. LIII. The Acid-catalyzed Reaction of Acid Amide with Formaldehyde*

By Minoru IMOTO and Mitsue KOBAYASHI

(Received June 23, 1960)

As is well known, acid amides react with formaldehyde to give methylol amides, in the presence of acid- or base-catalysts. Since urea resin is produced by this kind of reaction, many studies have been made[1-3]. Recently, Ugelstadt[4] made a kinetic study of the reactions of propylamide, monochloroacetamide and benzamide with formaldehyde, and concluded that, in acid solution, the reaction rate was represented by

$$v=\frac{-\mathrm{d}[CH_2O]}{\mathrm{d}t}=\text{const.}\,[R\text{-}CONH_2]\,[CH_2O] \quad (1)$$

Furthermore, the following mechanism was

1) A. Einhorn, *Ann.*, **343**, 207 (1905).
2) G. A. Crowe, Jr. and C. C. Lynch, *J. Am. Chem. Soc.*, **71**, 3731 (1949); **72**, 3622 (1950).
3) A. Iliceto, *Ann. chim. applicata*, **43**, 516 (1953).
4) J. Ugelstadt, The reaction of formaldehyde with amides, and the alkaline hydrolysis of alkoxymethyl ureas. *Dissert. at Norges Tekniske Hogskole* (1955).

proposed for this reaction:

$$\text{i)}\quad CH_2O+HA \underset{k_{-1}}{\overset{k_1}{\rightleftharpoons}} \overset{+}{C}H_2OH+A^-$$

$$\text{ii)}\quad R\text{-}CONH_2+\overset{+}{C}H_2OH \xrightarrow{k_2} [R\text{-}CONH_2CH_2OH]^+$$

$$\text{iii)}\quad [R\text{-}CONH_2CH_2OH]^+ + A^- \rightleftharpoons R\text{-}CONHCH_2OH+HA$$

in which step ii is rate determining. In order to justify this mechanism, it may be useful to examine how the reaction rate is influenced by the polar character of R in $R\text{-}CONH_2$. In the present paper, the acid-catalyzed reactions of ten acid amides with formaldehyde were studied kinetically. The results obtained were as follows: (i) An equation identical with that of Ugelstadt was obtained. (ii) The reaction rate constant ($k$) was estimated for each acid amide, (iii) It was confirmed that the values of $k$ fitted Hammett's equation. (iv) The reaction mechanism was discussed.

## Experimental

**Materials.** — The acid amides were synthesized from the corresponding carboxylic acids according to the following scheme;

$$R\text{-}COOH \xrightarrow[PCl_3]{SOCl_2 \text{ or}} R\text{-}COCl \xrightarrow{NH_4OH} R\text{-}CONH_2$$

The acid amides obtained were purified by repeating recrystalizations. Thus six kinds of substituted benzamides and four kinds of aliphatic amides were prepared; *p*-methoxybenzamide (m. p., 105°C, recrystalized from water-methanol), benzamide (m. p., 128°C, from water-methanol), *p*-chlorobenzamide (m. p., 177.7°C, from water-methanol), *p*-bromobenzamide (m. p., 190°C, from water-methanol), *m*-nitrobenzamide (m. p., 142.5°C, from water-methanol), *p*-nitrobenzamide (m. p., 199°C, from water-ethanol), acetamide (m. p., 80°C from chloroform-ligroin), propylamide (m. p., 79°C, from chloroform-ligroin), *n*-butylamide (m. p., 115°C, from ethylacetate-ligroin) and isobutylamide (m. p., 128°C, from chloroform-ligroin).

The aqueous solution of formaldehyde was prepared by the following procedure; a mixture of para-formaldehyde and water was distilled after refluxing for several hours. The distillate was diluted to a concentration of 1 mol./l.

As catalyst 0.6580 N (in the case of substituted benzamide) or 1.014 N (in the case of aliphatic amide) hydrochloric acid was used.

Commercial dioxane was refluxed for 17 hr. with 10% of its volume of 1 N hydrochloric acid to remove acetaldehyde, under a current of nitrogen. To remove water, the dioxane was treated with a concentrated solution of potassium hydroxide, then allowed to stand over pellets of potassium hydroxides for 1 day and dried over sodium for several hours. It was rectified three times and the fraction above 100.5°C was used.

**Kinetic Procedures.** — All reactions were carried out at 60±0.05°C. The reaction rates were measured according to the following procedures; A required amount of acid amide was weighed into a 50 ml. measuring flask. The acid amide was dissolved in 20 ml. dioxane and then 4 ml. (in the case of substituted benzamide) or 2 ml. (in the case of aliphatic amide) of the catalyst (hydrochloric acid) was added. The flask was placed in a thermostat at 60±0.05°C for at least 30 min. The formaldehyde solution and distilled water were also kept at the same temperature. A required amount of the formaldehyde solution was added to the flask from a hole pipette. Then immediately the solution was diluted to 50 ml. with distilled water. After thorough mixing, the solution was brought into the reaction vessel which was placed in the thermostat. The time when all the reactants were mixed was taken as zero. And 8—10 aliquotes of 5 ml. were taken by a pipette at suitable time intervals. The aliquote was run into a phosphate buffer solution (pH=7.1). The time when the pipette had run empty was taken as zero. Five millilitre of 0.1 N or 0.15 N potassium cyanide was added immediately and the solution was allowed to stand for 10 min. at room temperature. Then were added 10 drops of a diphenyl carbazone solution (1% in methanol), followed by 1 N nitric acid until a light orange-yellow color appeared. The solution was then immediately titrated with 0.03 N or 0.05 N mercuric nitrate until a violet color developed. The consumed amount of $CH_2O$ was calculated for each reaction time.

## Results and Discussion

**Reaction-orders of the Reactants.**—To derive a rate equation of the reaction, the effects of the concentrations of each reactant on the rates were investigated. The study was carried out first on benzamide.

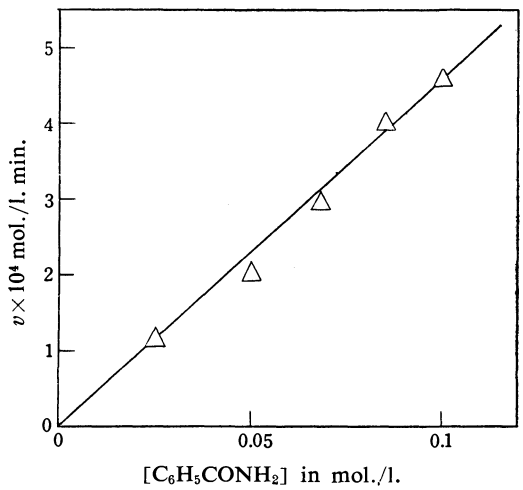



Fig. 1. The relation between the reaction rates and the concentrations of benzamide. Reaction conditions; $[CH_2O]$···0.05 mol./l.; [HCl]···0.05264 N; temp. 60°C.

a) *The Concentrations of Benzamide.*—Keeping the concentrations of formaldehyde and hydrochloric acid constant, the concentration of benzamide was changed from 0.025 to 0.1 mol./l. As shown in Fig. 1, the linear relationship was obtained between the reaction rates and the concentrations of benzamide. The reaction, therefore, was decided to be of first order with regard to the concentrations of benzamide.

b) *The Concentration of Formaldehyde.*—Keeping the concentrations of benzamide and hydrochloric acid constant, the concentration of formaldehyde was changed from 0.015 to 0.05 mol./l. As shown in Fig. 2, the linear relationship was obtained between the reaction rates and the concentrations of formaldehyde. So the reaction was also of first order with formaldehyde.

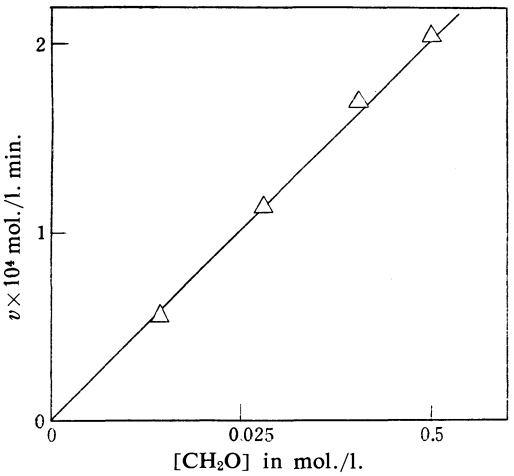



Fig. 2. The relation between the reaction rates and the concentrations of formaldehyde.
Reaction conditions; [$C_6H_5CONH_2$]···0.05 mol./l.; [HCl]···0.05264 N; temp. 60°C.

c) *The Concentrations of Hydrochloric Acid.*—Keeping the concentrations of R-$CONH_2$ and formaldehyde constant, the amount of the catalyst included in 50 ml. of the solution was changed from 2 ml. to 6 ml. The pH of the reaction system and the consumption rate of formaldehyde were measured. As shown in Fig. 3, a linear relationship was observed between the consumption rate of formaldehyde ($v$) and the concentration of hydrochloric acid. But as Fig. 4 shows, the relationship between $v$ and pH is not linear. From the results, it was assumed that this reaction proceeded by a mechanism of general acid-catalysis and the reaction order of hydrochloric acid was unity.

d) *Rate Equation.*—From the results obtained above, the experimental rate equation is represented as follows;

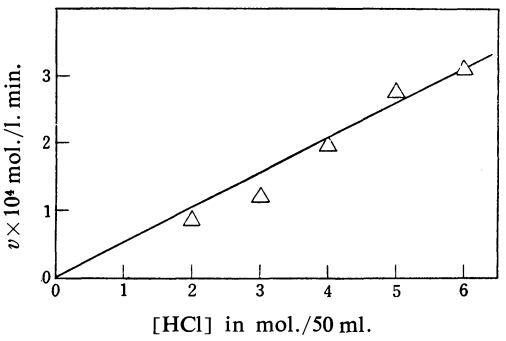



Fig. 3. Plot of the reaction rates against the concentrations of the hydrochloric acid.
Reaction conditions; [$C_6H_5CONH_2$]...0.05 mol./l.; [$CH_2O$]···0.05 mol./l.; temp. 60°C.

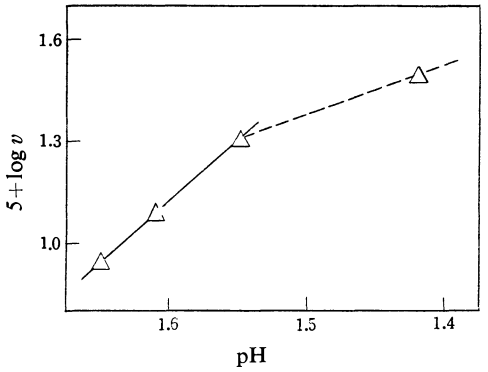



Fig. 4. Plot of the reaction rates against pH.

$$v=\frac{-\mathrm{d}[CH_2O]}{\mathrm{d}t}=k'[HCl]\,[R\text{-}CONH_2]\,[CH_2O] \quad (2)$$

Since [HCl] was assumed to be constant during the reaction, Eq. 2 was simplified to

$$v=k\,[R\text{-}CONH_2]\,[CH_2O] \quad (3)$$

To examine whether the Eq. 3 obtained for benzamide is also applicable to the other amides or not, this equation was tested for acetamide. When the initial concentrations of formaldehyde and acetamide were both a mol./l. and the consumption of formaldehyde was $x$ mol./l., Eq. 4 may be adopted in order to confirm the correctness of Eq. 3.

$$\frac{x}{a(a-x)}=kt \quad (4)$$

A linear relationship was obtained between $\frac{x}{a(a-x)}$ and $t$, at the initial stage of the reaction. (see Fig. 5) Accordingly, Eq. 3 was well supported. The deviation from the linearity at longer reaction time was attributed to the reversed reaction. For the other nine amides, the values of $k$ were estimated by the

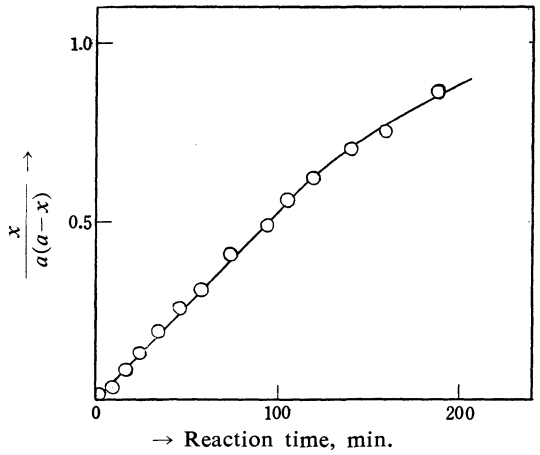



Fig. 5. Plot of $\frac{x}{a(a-x)}$ vs. reaction time.
Reaction conditions; $[CH_3CONH_2]$···0.1 mol./l.; [HCl]···0.02028 N; $[CH_2O]$···0.1 mol./l.; solvent···water; temp. 60°C.

TABLE I. RATE CONSTANTS FOR SUBSTITUTED BENZAMIDES

| Acid amide | $k\dagger \times 10^3$ |
|---|---|
| *p*-Methoxybenzamide | 19.4 |
| Benzamide | 8.16 |
| *p*-Chlorobenzamide | 4.95 |
| *p*-Bromobenzamide | 4.56 |
| *m*-Nitrobenzamide | 1.36 |
| *p*-Nitrobenzamide | 1.25 |

† $[R\text{-}CONH_2]$ 0.05 mol./l., $[CH_2O]$ 0.05 mol./l., [HCl] 0.05364 mol./l., temp. 60°C.

TABLE II. RATE CONSTANTS FOR ALIPHATIC AMIDES

| Acid amide | $k\dagger \times 10^3$ | $\sigma^-$ | $E_s$ |
|---|---|---|---|
| Acetamide | 3.37 | 0.00 | 0.00 |
| Propylamide | 5.19 | −0.10 | −0.07 |
| *n*-Butylamide | 3.29 | −0.115 | −0.36 |
| Isobutylamide | 2.55 | −0.190 | −0.47 |
| Benzamide | 3.12 | +0.610 | +1.24 |

† Reaction conditions are; $[R\text{-}CONH_2]$ 0.1 mol./l., $[CH_2O]$ 0.1 mol./l., [HCl] 0.02028 N, temp. 60°C.

Eq. 3. The results are given in Tables I and II.

**The Effects of the Polar Character on Reaction Rates.**—These values of $k$ were correlated with Hammett's[5] and Taft-Ingold's[6] equations. The linear relationships were obtained as Figs. 6 and 7.

The two equations were as follows;

$$\log \frac{k}{k_0} = -1.10\,\sigma$$

for the substituted benzamides.

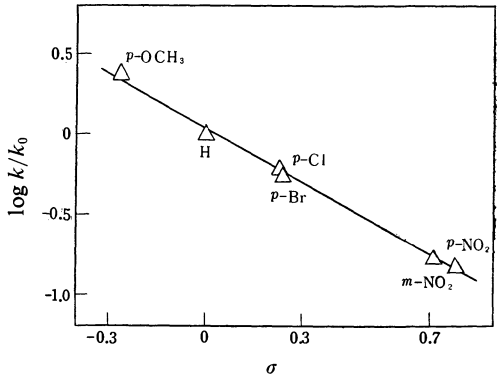



Fig. 6. Hammett equation plot
$\log k/k_0$ vs. $\sigma$ for substituted benzamides.
$\log k/k_0 = -1.10\,\sigma$

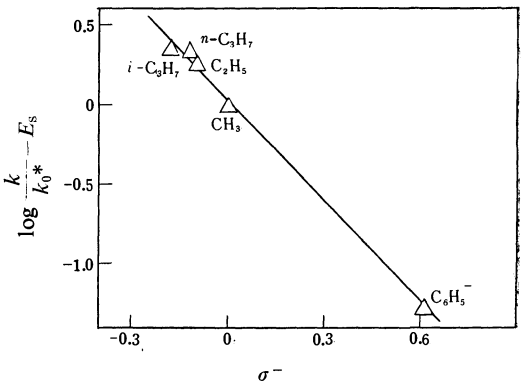



Fig. 7. Taft-Ingold equation plot
$\log \frac{k}{k_0^*} - E_s$ vs. $\sigma^-$ for aliphatic amides.

$$\log \frac{k}{k_0^*} - E_s = -2.16\,\sigma^-$$

$$\log \frac{k}{k_0^*} - E_s = -2.16\,\sigma^-$$

for the aliphatic acid amides. The rate constants for benzamide and acetamide were denoted by $k_0$ and $k_0^*$ respectively.

The negative values of $\rho$ indicate that introducing of the electron releasing groups increases the reaction rate.

**The Effect of the Polar Character on the Activation Energy and the Activation Entropy.**—For *p*-methoxybenzamide, benzamide and *p*-nitrobenzamide, the activation energies were calculated according to Arrhenius equation. (see Table III and Fig. 8). Using the values of the activation energy $\Delta E^+$ thus obtained, the activation entropies $\Delta S^+$ were calculated according to the following equation,

$$k = \kappa \cdot \frac{kT}{h} \cdot e^{-\Delta E^+/RT} \cdot e^{\Delta S^+/R}$$

5) L. P. Hammett, "Physical Organic Chemistry", McGraw-Hill Book Co., New York (1940), p. 184.

6) M. S. Newman, "Steric Effects in Organic Chemistry", John Willy & Sons Inc., New York (1956), p. 586.

where transmission coefficient denoted by $\kappa$ was assumed to be unity. The results are given in the third column of Table III.

It seems reasonable to consider that the higher value of $k$ for the amide having a more electron-releasing group is due mainly to the lower activation energy. The compensation rule is likely to exist for each amide.

Table III. Activation energies and activation entropies for substituted benzamide

| Acid amide | $\Delta E^{\ddagger}$ kcal./mol. | $\Delta S^{\ddagger}$ cal./deg. |
|---|---|---|
| *p*-Methoxybenzamide | 17.1 | −23.86 |
| Benzamide | 20.2 | −16.30 |
| *p*-Nitrobenzamide | 23.5 | −10.16 |

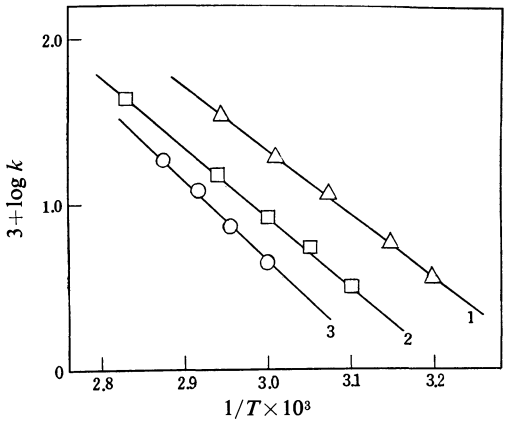



Fig. 8. Temperature dependence of the rate constants.
Upper curve; *p*-methoxybenzamide
Middle curve; benzamide
Lower curve; *p*-nitrobenzamide

**Reaction Mechanism of Benzamide with Formaldehyde.**—From the reaction mechanism having been introduced by Ugelstadt, it follows that

$$v=\frac{-d[CH_2O]}{dt}$$

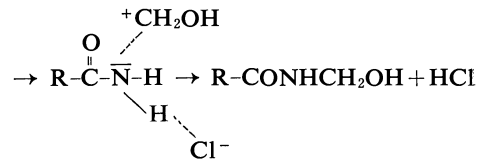
$$=\frac{k_1}{k_{-1}}k_2[HCl][R\text{-}CONH_2][CH_2O]$$

$$=k[CONH_2][CH_2O]$$

Taking into account of his hypothesis that the step of attacking of $^{+}CH_2OH$ on the lone-pair of the nitrogen atom in $-CONH_2$ is rate determining, we could expect that the larger rate constant was observed for the amide having higher electron density at the nitrogen atom. Therefore our results can be well explained with this mechanism. But on the other hand, another mechanism, a $S_E2$ mechanism, may be also possible, as follows:

i) $CH_2O+HCl \rightleftharpoons {}^{+}CH_2OH+Cl^{-}$

ii) $R\text{-}CONH_2+{}^{+}CH_2OH+Cl^{-}$




In this mechanism, the step ii is rate determining.

Which mechanism is more correct remains undetermined.

**On the Existence of $RCONH_3^{+}$.** — Notwithstanding a weak basicity of nitrogen atom of acid amides, it was proved from a spectroscopic study that the addition of a cation to the nitrogen atom was probable.

The infrared spectrum of hydrochloric acid salt of *p*-methoxybenzamide (1 : 1) at solid state (nujol) was compared with that of *p*-methoxybenzamide (see Fig. 9).

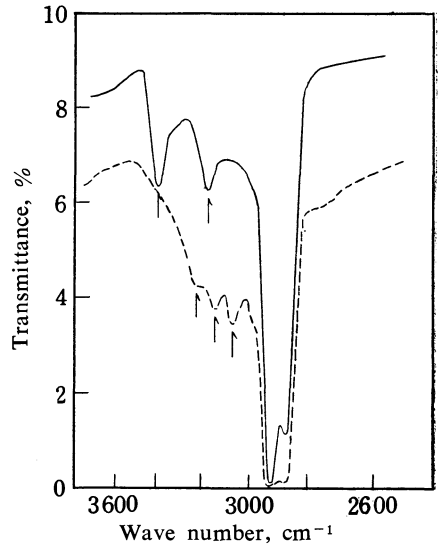



Fig. 9. The infrared spectra of *p*-methoxybenzamide and its hydrochloric acid salt.
Solid line ··· *p*-methoxybenzamide
Dotted line ··· hydrochloric acid salt

The absorption bands at 3382 and 3170 $cm^{-1}$ of the amide may be assigned to the stretching vibrations of the $NH_2$ group under the influence of hydrogen bonding. Comparing with Hopkin's result about urea nitrate[7], the 3237, 3150 and 3068 $cm^{-1}$ bands may be decided as due to the stretching vibrations of $NH_3^{+}$. The disappearance of the 3382 $cm^{-1}$ band in the salt shows an absence of free $NH_2$ group in the molecule.

7) M. Davies and L. Hopkins, *Trans. Faraday Soc.*, 53, 1563 (1957).

From the facts cited above, we may reasonably assume the structure of the salt as $R-\overset{\overset{O}{\|}}{C}-\overset{+}{N}H_3Cl^-$.

*Institute of Polytechnics*
*Osaka City University*
*Minami-Ogimachi*
*Osaka*

# *Formation of Benzenecarboxylic Acids from Bituminous Coal by Means of Oxygen-oxidation in Alkaline Medium*

By Yoshio KAMIYA

(Received June 29, 1960)

The oxidation of coal has been an important method of studying the structure of coal and of obtaining products such as benzenecarboxylic acids. The first systematic work was that of Fischer[1] and Schrader who used air to oxidize suspensions of coal in aqueous sodium carbonate. Oxidation of coal in alkaline permanganate solution was carried out by Bone[2] and coworkers, and most of the benzenecarboxylic acids were isolated. Oxygen-oxidation in aqueous caustic alkali was carried out by Howard[3] and coworkers, who obtained aromatic polycarboxylic acids in good yield from bituminous coal. It is hoped that better reaction methods and conditions will be found by further detailed experiments.

In this paper oxygen-oxidation of coal carried out in aqueous solution of sodium or potassium carbonate, in order to investigate the influence of reaction conditions, is discussed. Various benzenecarboxylic acids were separated from the oxidized product and were identified.

## Experimental

The sample used in the experiment was a Japanese bituminous coal, Shikamachi, the analytical result of which is given below :—

Moisture 1.2% ; Ash 19.8% ; C (d. a. f.) 87.3% ; H(d. a. f.) 5.4%.

*Oxidation Procedure A.*—A suspension of 6 g. of coal (through 100 mesh) in 200 ml. of sodium carbonate aqueous solution of various concentrations was treated with oxygen (initial pressure 30 kg./cm$^2$/0°C) at 250°C for 90 min. in a 600 ml. shaking type autoclave (agitation frequency 100/min.).

*Oxidation Procedure B.* — A suspension of 85 g. of coal in 1.5 l. of aqueous solution of sodium or potassium carbonate was treated with oxygen at 250~280°C in a 3 l. autoclave electro-magnatically agitated ; the reaction gases discharged continuously from the vessel at the rate of 2 l./min. were found to contain about 30% (average) of carbon dioxide.

*Analysis of Oxidation Products.* — The reaction product was filtered to remove residue and the filtrate was acidified with sulfuric acid to pH 1.5. Water-insoluble acids were filtered off and weighed after vacuum drying. The filtrate was saturated with sodium sulfate at 25°C and extracted twice with methyl ethyl ketone equal to 80% of the volume of the total filtrate. The total acids extracted were considered to represent "Aromatic acids" after vacuum drying at 100°C and removal of oxalic acid. Oxalic acid was precipitated with acetic acid and calcium chloride, and the precipitate was decomposed with sulfuric acid and titrated with permanganate solution. The oxalic acid was confirmed as dihydrate by the determination of equivalent weight 64 and melting point 100~101°C.

*Esterification of Aromatic Acid.*—150 g. of aromatic acids were dissolved in a mixture of 450 g. of methanol and 36 g. of sulfuric acid and kept at 110°C for 5 hr. The reaction products were extracted with ethylene dichloride and aqueous solution of sodium carbonate. The acidic esters were re-esterified under similar conditions repeatedly.

## Results and Discussion

**Reaction Conditions.** — The results of procedure A are shown in Fig. 1. An increase in the ratio of sodium carbonate to coal caused an increment in the reaction rate as well as in the yield of aromatic acids. The ratio of 8.7 : 1 corresponds approximately to the weight of sodium carbonate required to convert all the carbon dioxide into sodium bicarbonate. The yield of oxalic acid was 1.4% when the ratio was 10 : 1, but less than 0.5% when it was lower 7 : 1. When sodium hydroxide was used, the yields of products were as shown in Table I.

1) F. Fischer and H. Schrader, *Gesammelte Abhandlungen zur Kenntnis der Kohle*, **4**, (1920); **5**, (1922).
2) W. A. Bone, L. Horton and S. G. Ward, *Proc. Roy. Soc.*, **A127**, 480 (1930).
3) H. C. Howard et al., *J. Am. Chem. Soc.*, **61**, 2398 (1939); *Ind. Eng. Chem.*, **44**, 2784 (1952).

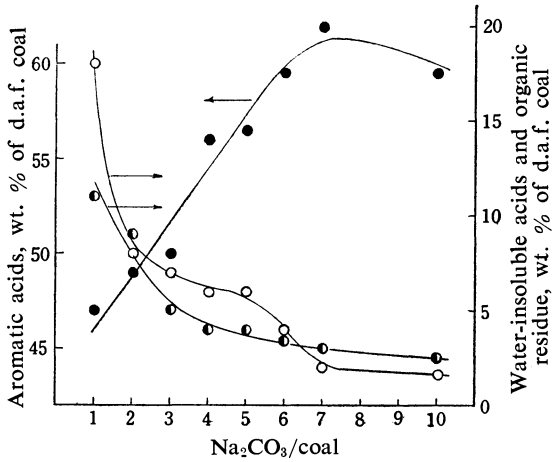



Fig. 1. Influence of the ratio of sodium carbonate to coal.
Procedure A
● Aromatic acids
○ Water-insoluble acids
◐ Organic residue

TABLE I. THE YIELDS OF OXIDATION PRODUCTS USING SODIUM HYDROXIDE AQUEOUS SOLUTION
Procedure A, NaOH/coal=3.4

Yields, wt. % of d.a.f. coal
Aromatic acids 61.3%, Water-insoluble acids 6.8%, Oxalic acid 13.2%, Organic residue 1.2%, Carbon dioxide carbon/coal carbon 0.498

Accordingly, it is seen that if enough sodium carbonate is present, the yield of aromatic acids is the same as in the case of sodium hydroxide.

A portion (200 ml.) of the reaction product from procedure B* was resubmitted to oxidation under two different conditions (Table II)

TABLE II. OXIDATION OF REACTION PRODUCT

| Oxidation condition | Yield of acids, wt. % of d.a.f. coal | |
|---|---|---|
| | Water-insoluble acids | Aromatic acids |
| Before reoxidation | 61.2 | 34.2 |
| Procedure A | 0.8 | 17.0 |
| Procedure A 34 g. of NaOH added | 3.4 | 55.2 |

to investigate the influence of alkali on the decomposition of the acids produced. It was observed that when the ratio of alkali to coal was small the decomposition rate of aromatic acids and water-insoluble acids was high.

During oxidation reaction equilibrium was reached:

$$Na_2CO_3+CO_2+H_2O \rightleftarrows 2NaHCO_3$$

* 250°C, 120 min., $Na_2CO_3$/coal=1, oxygen partial pressure 10 kg./cm², agitation frequency 85/min.

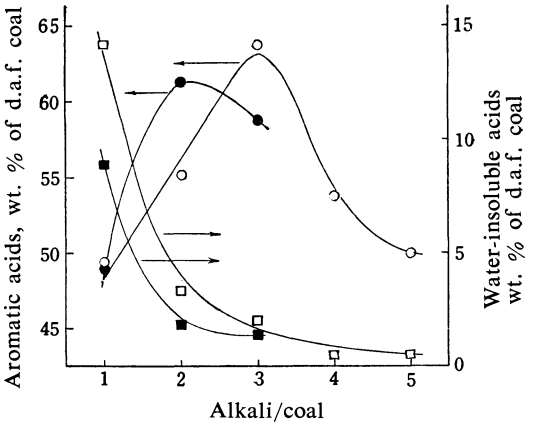



Fig. 2. Influence of the ratio of alkali to coal.
Procedure B, 270°C, 120 min.,
Oxygen partial pressure (average) 14 kg./cm² ($K_2CO_3$), 17 kg./cm² ($Na_2CO_3$),
Agitation frequency 85/min.
● Aromatic acids ($Na_2CO_3$)
○ Aromatic acids ($K_2CO_3$)
■ Water-insoluble acids ($Na_2CO_3$)
□ Water-insoluble acids ($K_2CO_3$)

So it was inferred that bleeding the reactor to remove carbon dioxide would result in good yield of aromatic acids, even when the ratio of alkali to coal was not large. Results of procedure B are shown in Fig. 2. The relations were found to be independent of the kind of alkali at the same molar ratio, when the normality of solution was chosen instead of alkali coal weight ratio. Good acids yields were obtained when the ratio of alkali to coal was higher than 2:1.

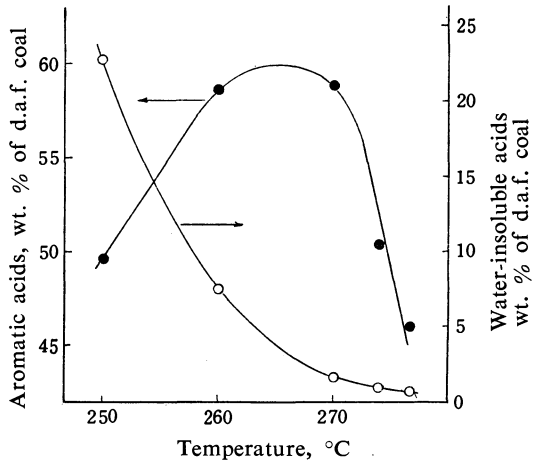



Fig. 3. Influence of temperature.
Procedure B, 120 min. $Na_2CO_3$ 255 g.
Oxygen partial pressure (average) 17 kg./cm², Agitation frequency 85/min.
● Aromatic acids
○ Water-insoluble acids

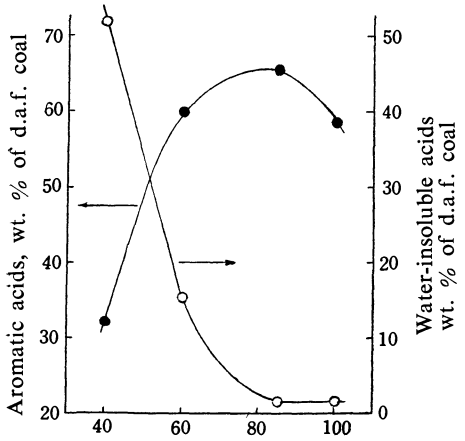



Fig. 4. Influence of agitation.
Procedure B, $K_2CO_3$ 255 g., 270°C, 120 min.,
Oxygen partial pressure (average) 14 kg./cm²
● Aromatic acids
○ Water-insoluble acids

Generally, the reaction rate was doubled for every 10°C rise in temperature. There is also an optimum temperature as shown in Fig. 3. The effect of agitation is also important as shown in Fig. 4.

TABLE III. REACTION CONDITIONS FOR OPTIMUM YIELDS OF AROMATIC ACIDS

| | | |
|---|---|---|
| Reaction conditions | | |
| Alkali used | $Na_2CO_3$ | $K_2CO_3$ |
| Alkali/Coal (wt. basis) | 3 | 3 |
| Temperature (°C) | 270 | 270 |
| Time (min.) | 120 | 120 |
| Total pressure (kg./cm²) | 70 | 72 |
| Oxygen pressure (average, kg./cm²) | 14 | 14 |
| Agitation frequency (per min.) | 85 | 85 |
| Yield (wt. % of d.a.f. coal) | | |
| Aromatic acids | 60.8 | 63.9 |
| Water-insoluble acids | 3.8 | 2.1 |
| Oxalic acid | 0.2 | 2.8 |
| Organic residue | 3.1 | 1.5 |

TABLE IV. PROPERTIES OF ACIDS PRODUCED UNDER OPTIMUM CONDITIONS

| Color | | Aromatic acids yellow | Water-insoluble acids dark brown |
|---|---|---|---|
| Elementary analysis | C(%) | 54.5 | 66.0 |
| | H(%) | 3.7 | 3.0 |
| Molecular weight | | 250 | — |
| Equivalent weight | | 80 | 130 |

Remarks: Ash contents of these acids were less than 0.1%.

Details of the optimum reaction conditions and the yield of products are given in Table III. The properties of the acids are given in Table IV.

The coal oxidation process may be expressed as follows: Coal $\xrightarrow{I}$ Water-insoluble acids $\xrightarrow{II}$ Aromatic acids $\xrightarrow{III}$ $CO_2$, $H_2O$. If the ratios of the reaction speeds of these steps are independent of any reaction factors, good correlation between the yields of products should be observed. The relations between water-insoluble acids and aromatic acids are plotted in Fig. 5, and found the mechanism of the reaction is not changed by altering temperature, pressure and agitation. When the alkali coal ratio is 1 : 1, the first step becomes slow and the third fast. The oxidation mechanism depends upon the ratio of alkali to coal.

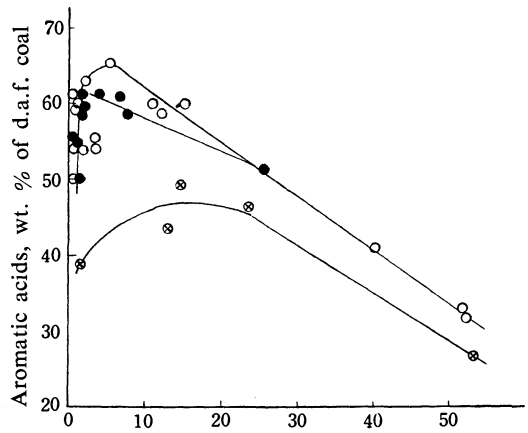



Fig. 5. Relations between water-insoluble acids and aromatic acids.
Procedure B, 250~280°C, 120 min.,
Oxygen partial pressure (average) 7~21 kg./cm², Agitation frequency 55~100/min.
○ $K_2CO_3$/coal=2~5
⊗ $K_2CO_3$/coal=1
● $Na_2CO_3$/coal=2 or 3

**Separation of Benzenecarboxylic Acids.**—From the industrial point of view, the most favorable oxidation medium may be sodium carbonate, because of its smaller corrosive effect, low cost and the possibility of its easy recovery. Benzenecarboxylic acids were separated from the aromatic acids which were obtained by the sodium carbonate process under the optimum conditions.

By the first and second esterification 128 g. of neutral esters (Fraction A) were obtained, and by the third and fourth 15 g. (Fraction B) were obtained. Residual acidic materials were completely hydrolysed with alkali and 6 g. of acids (Fraction C) were recovered.

TABLE V. ANALYTICAL CHARACTERISTICS OF ISOLATED ACIDS AND ESTERS

| Component | Elementary analysis (%) C | H | Equivalent weight | Melting point | Remarks |
|---|---|---|---|---|---|
| Phthalic acid | 57.45 (57.45) | 3.66 (3.64) | 83 (83) | Anhydride 131°C *p*-Nitrobenzyl ester 155°C | |
| Isophthalic acid | 57.69 (57.45) | 3.45 (3.64) | 83 (83) | Dimethyl ester 65°C *p*-Nitrobenzyl ester 201~202°C | Barium salt water-soluble |
| Terephthalic acid | 57.53 (57.45) | 3.45 (3.64) | 83 (83) | Dimethyl ester 139~140°C | |
| Trimellitic acid | 51.52 (51.41) | 3.01 (2.85) | 70.5 (70) | Acid 224~225°C | Barium salt water-soluble |
| Hemimellitic acid trimethyl ester | 56.80 (57.14) | 4.57 (4.78) | 84 (84) | Trimethyl ester 100°C | |
| Trimesic acid trimethyl ester | 51.21 (51.41) | 2.84 (2.85) | 83.5 (84) | Trimethyl ester 143~144°C | |
| 1,2,3,4-Benzene-tetracarboxylic acid tetramethyl ester | 54.35 (54.19) | 4.83 (4.52) | 77.5 (77.5) | Acid 237~240°C Tetramethyl ester 130°C | |
| 1,2,3,5-Benzene-tetracarboxylic acid tetramethyl ester | 54.42 (54.19) | 4.76 (4.52) | 78.2 (77.5) | Tetramethyl ester 112~113°C | |
| 1,2,4,5-Benzene-tetracarboxylic acid tetramethyl ester | 54.28 (54.19) | 4.67 (4.52) | 77.9 (77.5) | Tetramethyl ester 141.5°C | |
| Benzenepenta-carboxylic acid pentamethyl ester | 52.31 (52.18) | 4.01 (4.38) | 74.6 (73.5) | Pentamethyl ester 147~148°C | |
| Mellitic acid | | | 56.8 (57.0) | Acid 282~285°C | Insoluble in ammonia |
| Naphthalenetri-carboxylic acid | 60.54 (60.00) | 3.59 (3.08) | 87.0 (86.7) | | Naphthalene was obtained after decarboxylation*. |

Figures in brackets have been calculated.
* Dissolved in aqueous solution of sodium carbonate and treated at 450°C.

Fraction A was separated into nine fractions by means of vacuum distillation at 120~300°C (packed column, I. d. 10 mm., height 26 cm.). From the distillate nine benzenecarboxylic acids (di-, tri- and tetra-) were isolated by means of solubility difference, using acids, barium salts or methyl esters in solution, and identified (Table V). Infrared spectra of the benzenecarboxylic acids were compared with those of the pure substances and confirmed the identifications. Traces of benzoic acid were isolated by means of counter-current distribution (solvent: ethyl ether and water) from phthalic acid fraction. Naphthalene-carboxylic acid was separated as follows; the ethyl ether soluble part of a distillate (4 mmHg, 225~300°C) was hydrolysed, the filtrate of barium salts in solution was extracted with ethyl ether after acidification, and the extracted acid in ethyl ether solution was purified by washing with water.

Fraction B was submitted to chromatography (column alumina, developer carbon tetrachloride) and recrystallization, and as a result benzene tetra- and penta-carboxylic acids were isolated. From Fraction C mellitic acid was isolated.

The yields of benzenecarboxylic acids from the aromatic acids were as follows:

| | | |
|---|---|---|
| Benzenedicarboxylic acids | | 7.1% |
| Phthalic acid | 5.9% | |
| Isophthalic acid | 1.1% | |
| Terephthalic acid | 0.1% | |
| Benzenetricarboxylic acids | | 16.2% |
| Hemimellitic acid | 4.9% | |
| Trimellitic acid | 10.9% | |
| Trimesic acid | 0.4% | |
| Benzenetetracarboxylic acids mainly 1, 2, 4, 5- and 1, 2, 3, 4- | | 17.3% |
| Benzenepentacarboxylic acid | | 1.9% |
| Mellitic acid | | 0.3% |

The total yield of benzenecarboxylic acids was 43% of aromatic acids and 25% of coal (d.a.f.). The ratio of di- tri- and tetra-benzenecarboxylic acids was approximately 1 : 2 : 2.

Acknowledgment is made to professor S. Ando for his support and advice in the experiments.

*Department of Applied Chemistry*
*Faculty of Engineering*
*The University of Tokyo*
*Hongo, Tokyo*

# *Charge-transfer Complexes between Iodine and Various Aliphatic Amines*

By Hiroshi YADA, Jiro TANAKA and Saburo NAGAKURA

(Received June 21, 1960)

In 1949 Benesi and Hildebrand[1] found an absorption band characteristic of the iodine complex with benzene. They demonstrated that this absorption band belongs to neither of the component molecules but is due to the interaction between them. Mulliken[2] succeeded in interpreting it as the intermolecular charge-transfer absorption, namely, the absorption inherent to the charge-transfer complex caused by the interaction between an electron donor and an electron acceptor. Since that time complexes of this kind consisting of various combinations of electron donors and acceptors have been studied from both experimental and theoretical points of view[3,4]. Especially, the complexes containing iodine as electron acceptor have been investigated extensively by many authors[3-7].

Nagakura[8] studied spectroscopically the complex between triethylamine and iodine in *n*-heptane. He concluded that the system does not exist as the ammonium salt like $(R_3IN)^+I^-$ but does as the charge-transfer complex represented by the resonance hybrid between the no-bond structure, $R_3N\cdots\cdots I_2$ and the dative (charge-transfer) structure, $R_3N^+-I_2^-$, and also showed that this complex is the most stable among the iodine complexes studied so far, as is seen from its great heat of formation of 12.0 kcal./mol. Further, Nagakura and Tsubomura[9] determined the dipole moment of this complex to be 11.3D in dioxane solution. This fact is conceivably interesting in showing that the contribution of the dative structure amounts to or probably exceeds 50% for this complex and that the complex may be regarded as an intermediate stage for the ammonium salt formation process shown as follows: $R_3N+I_2\rightarrow R_3IN^++I^-$. In fact it has been observed that the complex is easily converted into the corresponding ammonium salt when a slight amount of moisture is present.

In the present paper, the above-mentioned study is extended to iodine complexes with aliphatic amines other than triethylamine. The electron donors used in the present study are ammonia, methylamine, ethylamine, *n*-butylamine, dimetylamine, trimethylamine, tri-*n*-propylamine, tri-*n*-butylamine and piperidine. One of our principal purposes is to discuss the relation between the stability of the complexes and the structures of amine molecules as electron donors, special attention being concentrated on the effect of the alkyl group upon the electron donating power and steric repulsion of various amines. Another principal purpose is to obtain accurate and profound knowledge concerning the spectroscopic properties of the amine-iodine complexes. This is useful for discussing the mechanism of the complex formation.

## Experimental

**Purification of Materials.**—Commercial iodine of G. P. grade was sublimed first with calcium oxide and potassium iodide, and sublimed again under nitrogen atmosphere. It was kept in a desiccator with phosphorus pentoxide as a drying agent. *n*-Heptane of Enjay Co. was shaken with sulfuric acid, dried with calcium chloride and sodium metal successively, and distilled with a distilling column of 60 plates made by Tokyo Kagaku Seiki Co.

1) H. A. Benesi and J. H. Hildebrand, *J. Am. Chem. Soc.*, **71**, 2703 (1949).
2) R. S. Mulliken, ibid, **74**, 811 (1952); *J. Phys. Chem.*, **56**, 801 (1952).
3) L. J. Andrews, *Chem. Revs.*, **54**, 713 (1954).
4) S. P. McGlynn, ibid., **58**, 1113 (1958).
5) T. Kubota, *J. Chem. Soc. Japan, Pure Chem. Sec. (Nippon Kagaku Zasshi)*, **80**, 578 (1959).
6) C. Reid and R. S. Mulliken, *J. Am. Chem. Soc.*, **76**, 3869 (1954).
7) S. Aono, *Prog. Theor. Phys.*, **20**, 133 (1958).
8) S. Nagakura, *J. Am. Chem. Soc.*, **80**, 520 (1958).
9) S. Nagakura and H. Tsubomura, *J. Chem. Phys.*, **27**, 819 (1957).

Ammonia generated from its aqueous solution by adding concentrated aqueous alkali was liquefied by coolng with dry ice and acetone mixture and dried with a piece of sodium metal. The dry ammonia thus obtained was led into *n*-heptane to prepare the stock solution. This stock solution was diluted to a desired concentration immediately before use. Methylamine, ethylamine, dimethylamine and trimethylamine were purified by distilling at low temperatures with activated alumina immediately before use for spectrophotometric measurements. The concentrations of ammonia, methylamine, dimethylamine and trimethylamine were determined by titration. *n*-Butylamine, diethylamine and piperidine were distilled twice with activated alumina to remove a trace of water. Tri-*n*-propylamine and tri-*n*-butylamine were shaken with acetic anhydride to remove primary and secondary amines contained as impurities, dried with activated alumina and then distilled twice under reduced pressure.

**Method.** — A Cary recording spectrophotometer Model 14 was used for measuring absorption spectra. The temperature of the absorption cell was kept constant during the measurements by using the thermospacer through which water of constant temperature was circulating. A quartz cell with a glass stopper ($10\pm0.01$ mm. light path) was used for the measurements in the ultraviolet region and a quartz cell with $100\pm0.2$ mm. light path was also used for the measurements in the visible region. In the present experiments, the concentrations of iodine and aliphatic amines were taken as low as possible. The actual values of the concentration were in the order of $10^{-5}$ and $10^{-3}\sim10^{-4}$ mol./l. for iodine and aliphatic amines, respectively. Under these conditions, the mixed solutions of iodine and amines were proved spectroscopically to exist in stable equilibrium for several hours. For the system of iodine and ammonia, however, the donor concentration amounted to the order of $10^{-2}$ mol./l., since the equilibrium constant for this system was rather small compared with those the other systems[10]. In this case the shape of the shifted visible band of iodine, which was used for the calculation of equilibrium constants in this case, was observed to be slightly dependent on the donor concentration. It was evident, however, that the effect was not so great as to affect the calculated equilibrium constants. Special care was taken to get rid of moisture in the procedure of preparing the mixed solutions, since even the existence of a slight amount of water is supposed to produce the $I_3^-$ ion whose strong absorption peaks appear in the vicinity of the two kinds of absorption bands, namely the charge-transfer band and the shifted visible band of iodine.

## Results and Discussion

Generally speaking, all the amine-iodine complexes under present consideration show the same spectroscopic features as the triethylamine-iodine complex described in the previous paper does[8]. Some typical examples of the absorption spectra measured in the present study are shown in Figs. 1—4. As is revealed from these figures, the absorption spectra of the iodine-amine systems commonly show two characteristic bands at 410~430 m$\mu$ and 230~280 m$\mu$ wavelength regions. By comparison with the iodine-triethylamine system reported in the previous paper[8], it is evident that the shorter and longer wavelength bands are respectively the charge-transfer band and the blue-shifted one of the visible band of iodine which ordinarily appears at 520 m$\mu$ in *n*-heptane. The maximum wavelengths ($\lambda_{CT}$, $\lambda_{vis}$) of these two kinds of absorption bands are given in Table I, together with the peak intensity ($\varepsilon_{CT}$) for the charge-transfer band. Further, from the analysis of these spectroscopic data, it was concluded that all the electron donors under consideration form stable 1 : 1 complexes with iodine in *n*-heptane. Since the details of the analytical method was described in the previous paper[8], it seems tedious to repeat

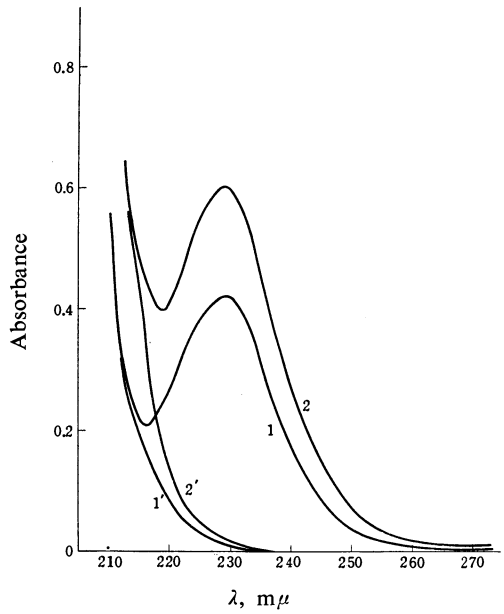



Fig. 1. The near ultraviolet absorption measured at 20°C with mixed solution of ammonia and iodine in *n*-heptane. The concentration of iodine is $7.35\times10^{-5}$ mol./l. The concentrations of ammonia are $5.70\times10^{-3}$ and $1.14\times10^{-2}$ mol./. for curves 1 and 2, respectively. Curves 1′ and 2′ are the absorption curves for the pure ammonia solutions with the concentrations corresponding to curves 1 and 2, respectively. The iodine solution of $7.35\times10^{-5}$ was used as reference with the measurement of curves 1 and 2. The light path was 10 mm. in all cases.

10) With the amine concentration over this limit value the shape of the two bands apparently changed and their peaks seemed to shift towards longer and shorter wavelengths for the charge-transfer band and the shifted visible band of iodine respectively. This phenomenon is the same as that observed by Reid and Mulliken in the case of pyridine-iodine system. In this case it is likely that complicated phenomena other than 1 : 1 equilibrium occur.

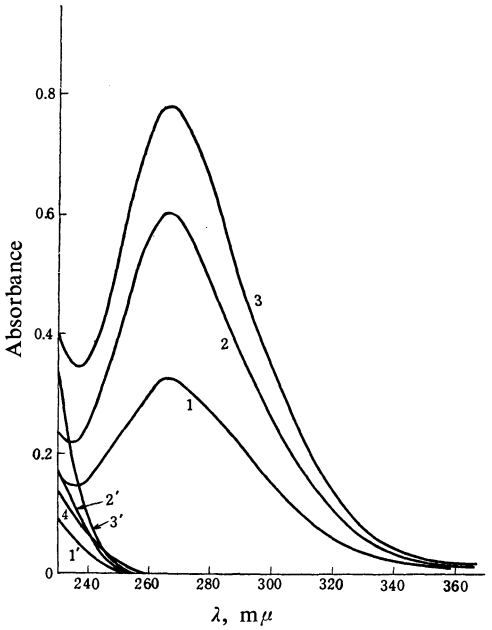



Fig. 2. The near ultraviolet absorption measured at 20°C with the mixed solution of trimethylamine and iodine. The concentration of iodine is $3.00\times10^{-5}$ mol./l. The concentrations of trimethylamine are $2.04\times10^{-4}$, $4.08\times10^{-4}$ and $7.45\times10^{-4}$ mol./l. for curves 1, 2 and 3, respectively. Curves 1', 2' and 3' are the absorptions for the pure trimethylamine solutions with the concentrations corresponding to curves 1, 2 and 3, respectively. Curve 4 is for the pure iodine solution. The light path was 10 mm. in all cases.

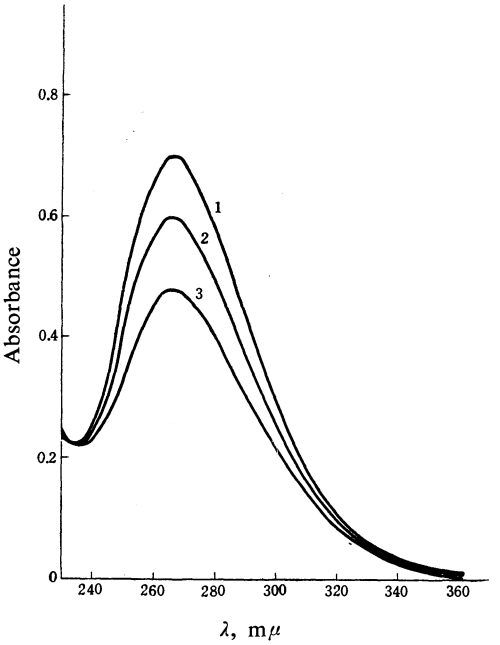



Fig. 3. The temperature dependency of the near ultraviolet absorption of the mixed solution of trimethylamine and iodine. The concentrations of iodine and trimethylamine are $3.00\times10^{-5}$ and $4.08\times10^{-4}$ mol./l., respectively. 10 mm. light path.

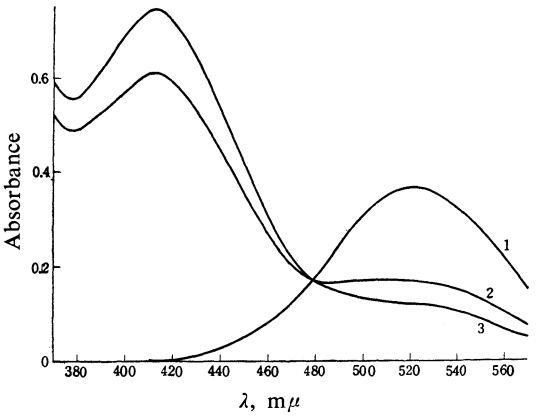
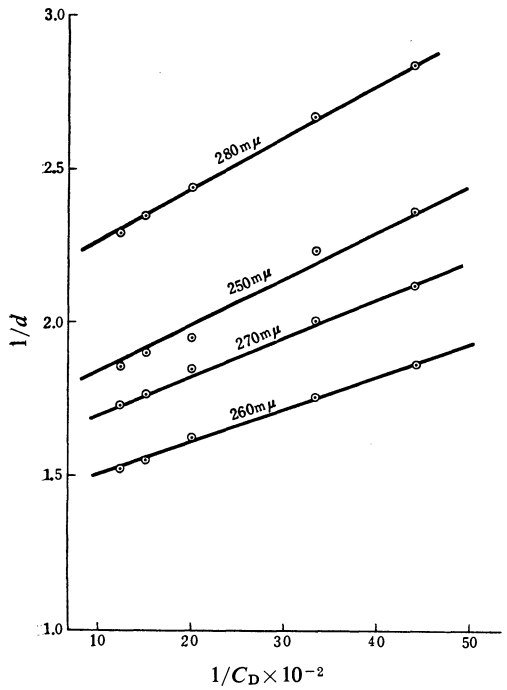



Fig. 4. The visible band of the mixed solution of tri-*n*-butylamine and iodine. The concentration of iodine is $3.97\times10^{-5}$ mol./l. The concentrations of tri-*n*-butylamine are 0, $8.34\times10^{-4}$ and $1.294\times10^{-3}$ mol./l. for the curves 1, 2 and 3, respectively. 100 mm. light path.

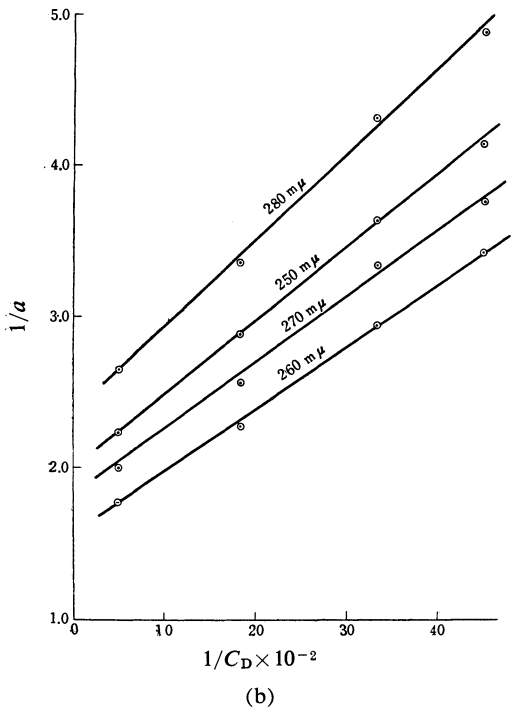
here an account of it. Hence, our description on the evaluation of the equilibrium constants ($K$) will be made only in brief.

The actual evaluation of $K$ was made by the two following methods; one is Benesi and Hildebrand's method and the other is the method which was applied successfully to some hydrogen-bonded systems and also to the triethylamine-iodine system[8,11]. Fig. 5 shows that Benesi and Hildebrand relation is satisfied for the systems under consideration. The $K$ values obtained by these two methods were in complete agreement with each other within the range of experimental errors. For most of the systems under consideration, both the charge-transfer band and the shifted iodine visibie band were used for the evaluation of $K$. However, for the system containing ammonia or methylamine as the electron donor, $K$ was evaluated from the blue-shifted iodine band alone. This is because the charge-transfer bands of these two systems, which appeared at shorter wavelengths compared with those of the other systems, overlap to some extent with the band at some 190 mμ pertinent to the electron donors and therefore are not suitable for the accurate evaluation of $K$. The $K$ values at various temperatures obtained in the present study are given in Table I. Then the values of $R\ln K$ were plotted against the reciprocals of the absolute temperatures ($T$) at which

11) S. Nagakura, *J. Am. Chem. Soc.*, 76, 3070 (1954).




(a)




(b)

Fig. 5. Benesi-Hildebrand's plots for the diethylamine-iodine complex: a, at 10°C; b, at 30°C. $C_D$ and $d$ are the concentration of electron donor and the absorbance of the solution.

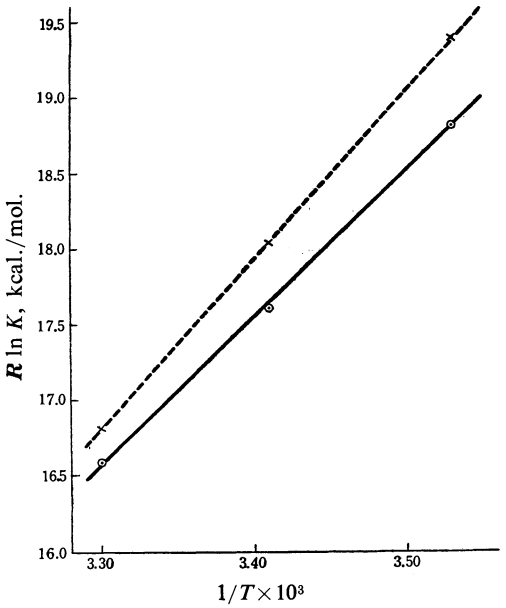



Fig. 6. The relations between $R \ln K$ and $1/T$ for the diethylamine (—○—) and piperidine (---×---) complexes.

equilibrium constants were obtained. The linear relationship between these two quantities is shown in Fig. 6 for some typical systems. The heat of formation ($\Delta H$) and the entropy change ($\Delta S$) for the complex formation were obtained from the slope of the straight line and its intersection with ordinate, respectively (actually by the use of the least squares method). The results are shown in Table I, together with the ionization potentials ($I_p$) cited from literatures[12,13] for convenience of discussion. Some notable facts deduced from the results in Table I will be discussed below.

**Heat of Formation and Entropy Change.**— The $|\Delta H|$ values change widely from 4.8 kcal./mol. for the ammonia complex to 12.3 kcal./mol. for the tri-*n*-propylamine complex. A similar tendency can also be seen with $|\Delta S|$. Moreover, it is evident from Table I that both of these quantities generally increase with the decreasing ionization potential of the electron donor. This relationship between $|\Delta H|$ and $I_p$ is completely consistent with the expectation from Mulliken's charge-transfer theory. Therefore this fact certainly supports the interpretation that the iodine-amine complexes under consideration are of Mulliken's charge-transfer type.

It is worthy of notice that the values of $|\Delta H|$ and $|\Delta S|$ increase regularly by replacing

12) K. Watanabe and J. R. Mottle, *J. Chem. Phys.*, **26**, 1773 (1957).
13) K. Higasi, I. Omura and T. Tsuchiya, *Monograph Series of the Research Institute of Applied Electricity, Hokkaido University*, No. 4 (1954—7), Appendix.

TABLE I. SPECTROSCOPIC AND THERMAL DATA OF VARIOUS IODINE-AMINE COMPLEXES OBTAINED IN THE PRESENT EXPERIMENT, TOGETHER WITH THE IONIZATION POTENTIAL DATA ($I_p$)

| Electron donor | $\lambda_{CT}^{obs}$ mμ | $\varepsilon_{CT}$ $\times 10^{-4}$ | $\lambda_{vis}^{obs}$ mμ | $K$ 10°C | 20°C | 25°C | 30°C | 40°C | $-\Delta H$ kcal./mol. | $-\Delta S$ e. u. | $I_p$[12,13] eV. |
|---|---|---|---|---|---|---|---|---|---|---|---|
| Ammonia | 229 | 2.34 | 430 | 89 | 67 | | | | 4.8 | 8.0 | 10.154 |
| $MeNH_2$ | 245 | 2.12 | 418 | | 530 | | 330 | | 7.1 | 12.3 | 8.97 |
| $EtNH_2$ | 246 | 2.26 | 417 | | 720 | 560 | 480 | 320 | 7.4 | 12.3 | 8.86 |
| *n*-$BuNH_2$ | 247 | 2.48 | 417 | | 1230 | | 770 | 480 | 8.4 | 14.8 | 8.71 |
| $Me_2NH$ | 256 | 2.68 | 412 | | 6800 | | 4200 | 2560 | 9.8 | 15.9 | 8.24 |
| $Et_2NH$ | 260 | 2.50 | 410 | 13000 | 7120 | | 4260 | | 9.7 | 18.4 | 8.01 |
| piperidine | 260 | 2.97 | 410 | 16200 | 9400 | | 4900 | | 10.3 | 16.1 | |
| $Me_3N$ | 266 | 3.13 | 414 | | 12100 | 7540 | 6240 | 4370* | 12.1 | 22.6 | 7.82 |
| $Et_3N$[8] | 278 | 2.56 | 414 | | 6320 | 4690 | 3310 | 1740 | 12.0 | 23.5 | 7.50 |
| *n*-$Pr_3N$ | 281 | 2.38 | 414 | 2930 | 1390 | | 740 | | 12.1 | 26.6 | 7.23 |
| *n*-$Bu_3N$ | 281 | 2.50 | 414 | 3900 | 1600 | | | | 12.3 | 27.8 | |

* This value was obtained at 35°C.

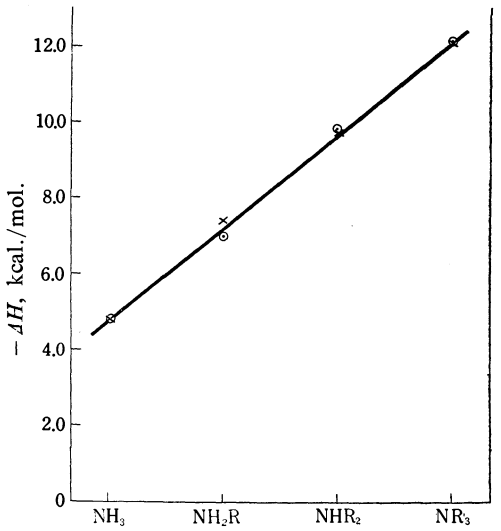



Fig. 7. The effect of successive substitution of alkyl groups for hydrogen atoms of ammonia on the heat of formation.

○: R=Me ×: R=Et

successively hydrogen atoms of ammonia by fixed kinds of alkyl groups. A typical example exhibiting such a tendency is given in Fig. 7. This figure shows that $|\Delta H|$ changes linearly with the number of the methyl or ethyl group introduced into the ammonia molecule. This seems to be interesting in meaning that the effect of the alkyl substitution upon the magnitudes of this quantity may be additive. According to the present experimental results, the $|\Delta H|$ value increases by 2.4 kcal./mol. by replacement of a hydrogen atom of ammonia by a methyl or ethyl group.

Next let us add some notes on the direct relation between $|\Delta H|$ and $|\Delta S|$. As was already pointed out by several authors[14], $\Delta H$'s are often known to change in a linear fashion with $\Delta S$'s for a series of related reactions or equilibria involving moderate changes in structure. For example, Keefer and Andrews[15]

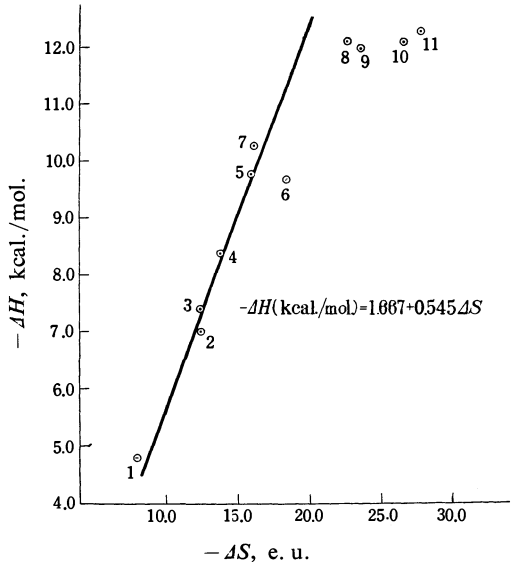



Fig. 8. The relation between the heats of formation and entropies. The numbers in Figs. 8-10 represent the kind of electron donors: 1, ammonia; 2, methylamine; 3, ethylamine; 4, *n*-butylamine; 5, dimethylamine; 6, diethylamine; 7, piperidine; 8, trimethylamine; 9, triethylamine 10, tri-*n*-propylamine; 11, tri-*n*-butylamine. The value for triethylamine is taken from Ref. 11.

14) For example, see J. E. Leffler, *J. Org. Chem.*, **20**. 1202 (1955).

15) R. M. Keefer and L. J. Andrews, *J. Am. Chem. Soc.*, **77**, 2164 (1955).

reported that such a linear relationship holds good for a series of substituted benzene-iodine complexes.

As is clear from Fig. 8, the linear relationship between $|\Delta H|$ and $|\Delta S|$ seems to hold for most amine complexes studied in the present paper, too. However, the points for the complexes including diethylamine and four tertiary amines as electron donors apparently deviate rightwards from the straight line. In the complex formation of iodine with these amines involving bulky substituent groups, the steric strain may actually bring about a great decrease of freedom in the motion of the substituent groups. This is probably the reason why the complexes including these amines as electron donors show greater entropy change than that expected from the linear relationship in Fig. 8. Such deviation from the linear relationship was also observed by Keefer and Andrews with the hexaethylbenzene-iodine complex[15]. Excluding the members deviating from the straight line, one can evaluate the isokinetic temperature[14] to be 545°K for amine-iodine systems.

**The Relation between $|\Delta H|$ and Hammett's Constant.** — When the linear relationship is satisfied between $\Delta H$ and $\Delta S$ in a series of related reactions or equilibria, the same relationship is known to be always satisfied between Hammett's substituent constant $\sigma$ and $\Delta H$, too. In fact, on the basis of the experimental results by Brown et al.[16], Taft[17] pointed out that $\Delta H$ values of $Me_3BNR_3$ complexes change linearly with the $\sigma^*$ values of substituent groups of amines, so far as the steric strain due to the substituent groups may be regarded as small. A similar relation may be expected to hold for the present case. In Fig. 9 are plotted the heats of formation of the iodine-amine complexes against $\sigma^*$ values for alkyl groups of various amine components. The $\sigma^*$ values taken here are the same as those employed by Taft[18] for the trimethylboron-amine complexes. Inspection of the figure reveals to us that, as expected from Hammett's rule, the linear relationship is well satisfied for almost all the points except for those of triethyl-, tri-*n*-propyl-, tri-*n*-butyl-amines. The discrepancy observed with these three tertiary amine complexes may reasonably be thought to be caused by the steric strain. This fact is consistent with the conclusion derived from the $|\Delta H|-|\Delta S|$ relationship mentioned in the preceding paragraph. Taft also pointed out the existence of a similar discrepancy for the $Me_3B\cdot NR_3$ complexes. By excluding the cases of the donors deviating from the straight line in Fig. 9, the value of reaction constant $\rho$ can be calculated to be $-4.84$ for the amine-iodine complexes.

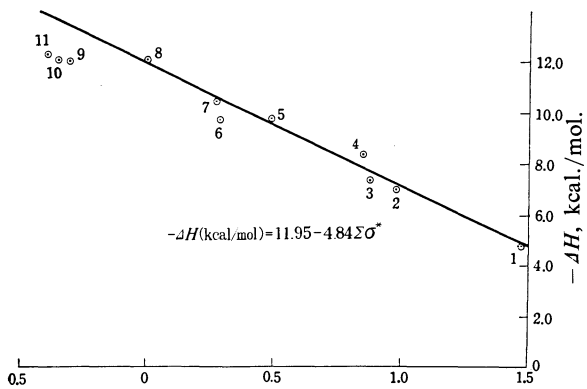



Fig. 9. Hammett's plot between the heat of formation and $\sigma^*$. The straight line is drawn by applying the least squares method to the points 1—5 and 7.

**The Relation between Wavelengths of Charge-transfer Bands and Ionization Potentials of Electron Donors.**—In Fig. 10 the transition energies ($h\nu_{CT}^{obs}$) of the charge-transfer spectra are plotted versus the ionization potentials of electron donors. As is clearly seen from this figure and Table I, the lower the ionization potentials of electron donors are, the smaller the transition energies of the charge-tranfer bands. This tendency can naturally be expected from Mulliken's theory and has already been observed by several investigators for iodine complexes with aromatic hydrocarbons and other electron donors[14,15]. However, the present results are thought to be more reliable and systematic compared with results obtained with some other iodine complexes, because for the present systems the charge-transfer bands appear at the suitable wavelength region where the bands do not overlap with those inherent to the component molecules and therefore the accurate determination of the maximum wavelength is possible.

Concerning the relation between the ionization potential of the electron donor and the transition energy of the charge-trasfer absorption band, Mulliken's charge-transfer theory gives the following formula:

$$h\nu_{CT}=I_p-A+2\beta^2/(I_p-A) \qquad (1)$$

16) H. C. Brown and R. B. Johannesen, ibid., 75, 16 (1653) and other papers.
17) R. W. Taft, Jr., "Steric Effects in Organic Chemistry", Edited by M. S. Newman, John Wiley & Sons, Inc., New York (1956), p. 632.
18) Ref. 17, p. 619. $\Sigma\sigma^*$ for piperidine is assumed to be the sum of $\sigma^*$ values of ethyl and *n*-propyl groups.
19) R. S. Mulliken, *Rec. trav. chim. Pays-Bas*, 75, 845 (1956).

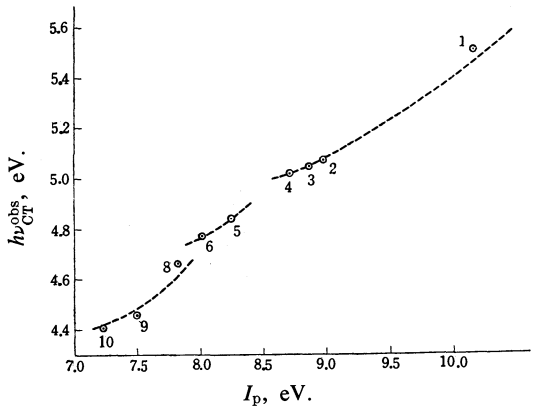



Fig. 10. The relation between the transition energies ($h\nu_{CT}^{obs}$) of the charge-transfer absorption bands and the ionization potentials of the electron donors ($I_p$).

where $\beta$ means the exchange integral between electron donating and electron accepting orbitals, and $A$ represents the electron affinity of the acceptor plus the attraction energy between the component molecules in the charge-transfer structure. Hastings et al.[15] found empirically that Eq. 1 with constant $A$ and $\beta$ fits well the observed $h\nu_{CT}$ values of the complexes of a large number of donor molecules with iodine. However, in the present iodine complexes where the value of $|I_p-A|$ can not be thought to be considerably large as compared with $|\beta|$ and the interaction between the component molecules is apparently great as revealed from the $\Delta H$ values, it looks better to adopt the following equation which can be derived by treating the resonance interaction of the no-bond structure with the dative (charge-transfer) structure with the aid of a variation method:

$$h\nu_{CT}=\sqrt{(I_p-A)^2-4s\beta(I_p-A)+4\beta^2}/(1-s^2) \quad (2)$$

where $s$ means the overlap integral between the electron donating and accepting orbitals, and the other notations in Eq. 2 are the same as those in Eq. 1. From either of these formulas, the linear relationship between $I_p$ and $h\nu_{CT}$ may be expected when the magnitude of $I_p-A$ is overwhelmingly greater than $|\beta|$. In fact, Ham, Platt and McConnell[20] pointed out that the expected relationship is fulfilled for the $h\nu_{CT}^{obs}$ and $I_p$ values observed with a number of iodine complexes.

By the first glance at Fig. 10, it may be revealed that all the points in the figure fit fairly well a straight line. However, in view of the fact that the observed $h\nu_{CT}^{obs}$ values of iodine complexes with various primary or tertiary amines show a tendency to converge to a constant value (5.0 and 4.4 eV. for primary and tertiary amines respectively), it looks better to interpret the results as follows: All the points in Fig. 10 are divided into three parts, according to whether the electron donor is ammonia and primary amines, secondary amines, or tertiary amines. Further, each part of them can conceivably be represented by a hyperbola as expected from Eq. 2.

In other words, it may be said that no parameter in Eq. 2 is a constant commonly used for all the iodine complexes under consideration but rather a constant characteristic of each part. In this connection, it seems interesting to evaluate the actual values of these parameters in such a manner as to fit the observed relationship between $I_p$ and $h\nu_{CT}^{obs}$ as well as possible.

Under the reasonable approximation that the exchange integral $\beta$ is proportional to the overlap integral $s$, namely $\beta=\alpha s$, Eq. 2 can be changed as follows:

$$(1-s^2)h\nu_{CT}=\{(I_p-A)^2-4(I_p-A)\alpha s^2+4\alpha^2 s^2\}^{1/2} \quad (3)$$

Here $\alpha$ is a constant which may be commonly determined independently of the kind of amine. The structure of the trimethylamine–iodine complex was studied by Strømme[22] with the aid of X-ray crystal analysis method and was determined as shown in Fig. 11. On the basis

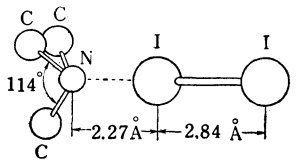



Fig. 11. The spatial configuration for the trimethylamine–iodine complex based on Strømme's X-ray crystal analysis[22].

of this structure, the overlap integral $s_t$ for the tertiary amine–iodine complex system can be evaluated at 0.293. In this case, the 5p $\sigma^*$ antibonding orbital of iodine and the s-p hybridized nonbonding electron orbital of nitrogen are assumed to be electron accepting and donating orbitals, respectively. In that case the proportion of s-p hybridization was determined from the ∠C–N–C bond angle. By the use of the value of $s_t$ and the observed $h\nu_{CT}^{obs}$ and $I_p$ values, the parameter $A_t$ for the tertiary amine complexes and the common

20) H. McConnell, J. S. Ham and J. R. Platt, *J. Chem. Phys.*, **21**, 66 (1953).
21) S. H. Hastings, J. L. Schiller and F. A. Matsen, *J. Am. Chem. Soc.*, **75**, 2900 (1953).
22) O. Strømme, *Acta Chem. Scand.*, **13**, 268 (1959).

parameter $\alpha$ can be evaluated at 7.60 and $-7.14$ eV., respectively. Further, by applying commonly this $\alpha$ value to the secondary and primary amine systems, the parameters for these systems ($s_s$, $s_p$, $A_s$ and $A_p$) can be determined. These results are tabulated in Table II, together with the values of $\beta_p$, $\beta_s$ and $\beta_t$.

Table II. The calculated values of parameter in Eq. 3

| | $A$ (eV.) | $s$ | $\beta$ (eV.) |
|---|---|---|---|
| Primary amines and ammonia | 9.85 | 0.327 | $-2.32$ |
| Secondary amines | 8.21 | 0.308 | $-2.20$ |
| Tertiary amines | 7.60 | 0.293 | $-2.09$ |

From Table II it is clear that $A$, $s$ and $|\beta|$ values decrease in the order of primary amine > secondary amine > tertiary amine. The explanation for this tendency will be given below. The bulky alkyl groups attached to the nitrogen atom of the amine molecule probably cause the increase in the steric repulsion with the opponent iodine molecule. Actually the existence of the steric hindrance for the cases of the triethylamine, tri-*n*-propylamine and tri-*n*-butylamine complexes was shown in the preceding paragraph. This steric repulsion may conceivably bring about the increase in the N–I distance of the complex, in the order of the primary amine<secondary amine < tertiary amine. This means that $s$, $|\beta|$ and the magnitude of the electrostatic attraction in the dative (charge-transfer) structure decrease in the following order: primary amine > secondary amine > tertiary amine. Moreover, $A$ is considered to be the sum of the electron affinity of electron acceptor and the electrostatic attraction between component molecules in the complexed state. Therefore the values of $A$ turn out to decrease in the above order, even if the electron affinity of iodine may be regarded as a constant. Since the latter value is usually assumed to be 1.8 eV.[23], it is easily seen from the $A$ values given in Table II that the absolute values of the electrostatic attraction terms then amount to some 8.0, 6.4 and 5.8 eV. for the complexes including ammonia and primary amines, secondary amines, and tertiary amines, respectively.

## Summary

Mulliken's charge-transfer type molecular complexes between iodine and various aliphatic amines were studied spectrophotometrically in *n*-heptane solutions. The electron donor components used in the present study include ammonia, primary amines (methyl-, ethyl- and *n*-butyl-), secondary amines (dimethyl-, diethyl- and piperidine), and also tertiary amines (trimethyl-, tri-*n*-propyl- and tri-*n*-butyl-). The charge-transfer absorption bands characteristic of molecular complexes of this kind appeared between 229 and 281 m$\mu$ depending on the kind of amines used as electron donors. The stable equilibria of 1 : 1 complex formation were verified for all the systems. The equilibrium constants ($K$) were determined at various temperatures and the heats of formation ($\Delta H$) and entropy changes ($\Delta S$) were evaluated. The values of $\Delta H$ range from $-4.8$ kcal./mol. for ammonia complex to $-12.3$ kcal./mol. for tri-*n*-butylamine complex, and $\Delta S$ also changes from $-8.0$ e. u. for the former and $-27.8$ e. u. for the latter. The effect of successive replacement of hydrogen atoms of ammonia by methyl or ethyl groups on the value of $\Delta H$ was shown to be additive. From the data of $\Delta H$ and $\Delta S$ it was concluded that there exists a linear relation between these two quantities for the iodine complexes with all the primary amines and secondary amines having rather small substituent groups like methyl. The deviation from the linear relation was observed with the complexes including diethylamine and tertiary amines as electron donors. These amines with bulky substituent groups may be expected to exert a great steric hindrance in the case of the molecular complex formation. Further it was shown that the plots of $\Delta H$'s against $\sigma^*$'s (Hammett's substituent constant) fit the straight line, except for those of the iodine complexes with triethylamine, tri-*n*-propylamine and tri-*n*-butylamine. With the aid of the spatial configuration derived from X-ray crystal analysis data for the trimethylamine–iodine complex, one could evaluate the three parameters (overlap integral ($s$), exchange integral ($\beta$) and effective electron affinity ($A$)) which are necessary for explaining reasonably the relation between the transition energies of the charge-transfer bands and the ionization potentials of electron donors. For example, the $\beta$ values thus estimated were $-2.09$, $-2.20$ and $-2.32$ eV. for the complexes with primary, secondary and tertiary amines, respectively.

*The Institute for Solid State Physics*
*The University of Tokyo*
*Shinryudo-cho, Minato-ku, Tokyo*

23) R. S. Mulliken, *J. Am. Chem. Soc.*, 72, 600 (1950).

# *Studies on Pelletierine. I. Isolation of Pelletierine from Pomegranate Root Bark**

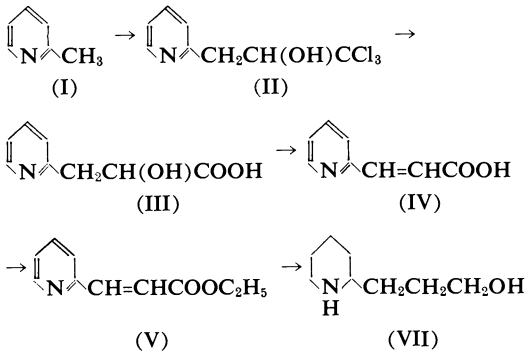
By Shigeru KUWATA

(Received November 28, 1959)

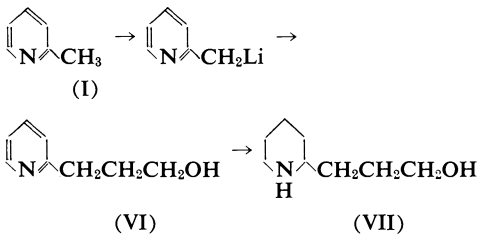
Pelletierine, an alkaloid which was found in pomegranate bark together with isopelletierine, methylisopelletierine and pseudopelletierine, and long regarded as the most anthelmintic component of the bark-extracts, was assigned the structure 3-(2-piperidyl)-propionaldehyde by Hess and Eichel already in 1917[1]. But no one has been able to succeed in the synthesis of this compound in spite of its very simple structure. This fact has been shedding some doubt upon the reliability of this structure.

According to Hess and Eichel, pelletierine is stable to oxidation and the corresponding propionic acid has never been obtained by the action of chromic acid in sulfuric acid, while part of the base is recovered unchanged and the rest is decomposed under the liberation of ammonia. From general properties of primary alcohol it will be expected that, when 3-(2-piperidyl)-1-propanol is oxidized with chromic acid, the corresponding aldehyde would be formed at least at the first oxidation step, and if this aldehyde is pelletierine as has been assumed, this may not be oxidizable further and must be isolated from the oxidation products. In order to scrutinize this idea, 3-(2-piperidyl)-1-propanol, which was prepared in the scheme of Eq. 1 or 2, was treated with chromic acid. This material, on being oxidized with chromic acid just sufficient to convert it into the aldehyde, gave no product corresponding to the aldehyde either at room temperature or at a higher one. By more drastic conditions using excess chromic acid, a colorless crystalline product was isolated as hydrochloride, which proved to be 3-(2-piperidyl)-propionic acid hydrochloride. These results show apparently that it is very difficult to assign the aldehyde structure to pelletierine.

Equation 1




Equation 2




The alternatively suggested structure for this alkaloid is 1-(2-piperidyl)-2-propanone, i. e., isopelletierine[2-7]. For instance, Galinovsky and Vogl[2], or Wibaut and Hirschel[7] asserted the identity of pelletierine with isopelletierine by comparing the derivatives of both compounds.

But it should be mentioned that the isolation of pelletierine, the most important material for these discussions, has never been attempted by tracing the reports of Hess and Eichel as closely as possible, and its physical properties or chemical behaviors have never been re-examined. Therefore one has been compelled to rely on their reports regarding the properties of this alkaloid. On re-examining their reports, however, a few descriptions are found unacceptable in some respects. For instance, constants of isopelletierine and its derivatives used for the comparison with those of pelletierine and its derivatives[8] are considerably different from those given later by

* This work was partly presented at the 10th and 11th Annual Meetings of the Chemical Society of Japan, April 6, 1957 and April 5, 1958.

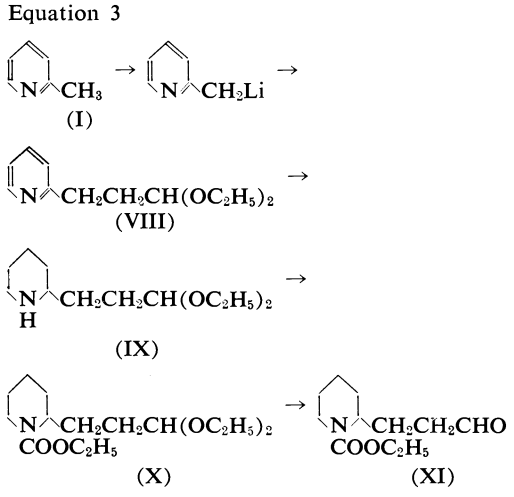
1) K. Hess and A. Eichel, *Ber.*, **50**, 1192 (1917).
2) F. Galinovsky and O. Vogl, *Monatsh.*, **83**, 1055 (1952).
3) F. Galinovsky and R. Höllinger, ibid., **85**, 1012 (1954).
4) O. Vogl and G. Bianchetti, ibid., **86**, 1024 (1955).
5) J. P. Wibaut et al., *Rec. trav. chim.*, **73**, 102 (1954).
6) J. P. Wibaut and U. Hollstein, *Konincl. Ned. Akad. Wetenshap., Proc. Ser.*, **B59**, 426 (1956): *Chem. Abstr.*, **51**, 11364i (1957).
7) J. P. Wibaut and M. I. Hirschel, *Rec. trav. chim.*, **75**, 225 (1956).
8) K. Hess and A. Eichel, *Ber.*, **50**, 1386 (1917).

Hess himself[9] or by other researchers[10,11].

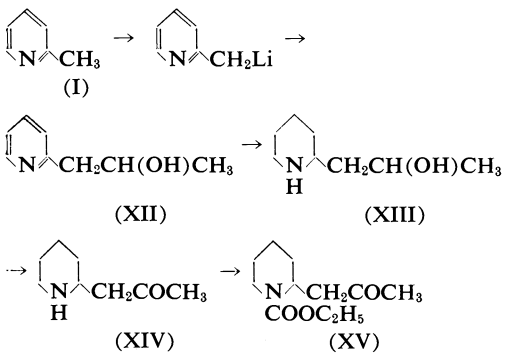
In order to compare pelletierine with isopelletierine decidedly, it will be most necessary to isolate the same sample of pelletierine as that which was obtained by Hess, and to re-examine its properties in the first step. Therefore the tracing of the Hess' experiment by using 60 kg. of powder of pomegranate root bark was attempted. The method of isolation was essentially the same as that which had been adopted by Hess and Eichel[8,12], and "pelletierine" was isolated in the form of urethane, having the same boiling point (b. p. 164~166°C at 20 mmHg; lit.[8] b. p. 169~170°C at 21 mmHg). In this method, some procedures were modified with the same results, and these could be confirmed by the preliminaly paper chromatographic test.

3-(2-Piperidyl)-propionaldehyde urethane and isopelletierine urethane, the partners for the comparison, were prepared according to Eqs. 3 and 4, respectively.

Equation 3



Equation 4



9) K. Hess and O. Littmann, *Ann.*, **494**, 7 (1932).
10) J. Meisenheimer and E. Mahler, ibid., **462**, 301 (1928).
11) P. I. Mortimer and W. Wilkinson, *J. Chem. Soc.*, **1957**, 3967.
12) Another method of isolating pelletierine was also reported by Hess, *Ber.*, **52**, 1005 (1919).

Now, "pelletierine urethane", thus obtained from natural sources, was compared with the synthetic samples of 3-(2-piperidyl)-propionaldehyde urethane and isopelletierine urethane.

Table I. Physical constants of the three urethanes

| Urethane | B. p., °C mmHg | $n_D^{20}$ |
|---|---|---|
| 3-(2-Piperidyl)-propionaldehyde urethane | 122~124 (2.5) | 1.4792 |
| 1-(2-Piperidyl)-2-propanone urethane | 131~132 (3.5) | 1.4715 |
| Pelletierine urethane from natural sources | 131~131.5 (3.5) | 1.4711 |

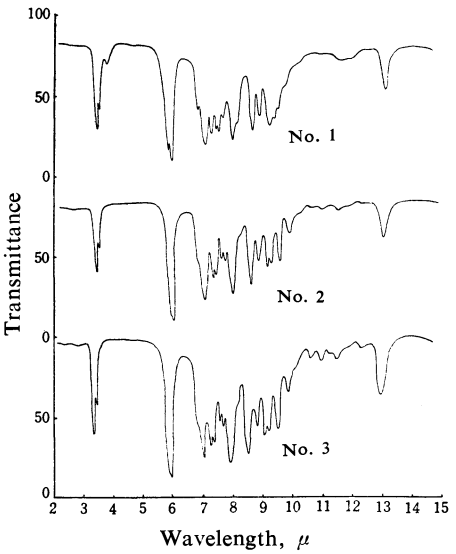



Fig. 1. I. R. of three urethanes.
No. 1: 3-(2-Piperidyl)-propionaldehyde urethane
No. 2: Pelletierine urethane from natural sources
No. 3: 1-(2-Piperidyl)-2-propanone urethane

The physical constants of these urethanes are listed in Table I.

From Table I, it may be recognized that the constants of urethane of pelletierine isolated from natural sources agree well with those of isopelletierine urethane but not with those of 3-(2-piperidyl)-propionaldehyde urethane.

In Fig. 1, in which the infrared spectra of these three urethanes are shown, the spectrum of pelletierine urethane agrees well with that of isopelletierine urethane[13], and not with that of 3-(2-piperidyl)-propionaldehyde urethane. It is remarkable that it never shows

13) This result agrees with the one obtained using hydrobromide by J. P. Wibaut and M. I. Hirschel: Ref. 7.

peaks at 2700 $cm^{-1}$ and 1710 $cm^{-1}$ corresponding to the aldehyde group. Further, these peaks are recognizable in the spectrum of neither the fore-running nor the after-running of "pelletierine urethane".

This fact shows that, in this sample, the compounds having the aldehyde group are never contained even in a small amount. This may be a decided bit of evidence for the absence of 3-(2-piperidyl)-propionaldehyde in the pomegranate bark.

Thus, from the above mentioned points, the author concludes that what has been named pelletierine is nothing but isopelletierine.

## Experimental

**1, 1, 1-Trichloro-2-hydroxy-3-(2-pyridyl)-propane (II).** — 1) 2-Picoline (I) (93 g.) and anhydrous chloral (14 g.) were heated in amyl- or butylacetate (310 g.) for 11~12 hr. at 120~130°C according to Einhorn[14]. The product formed into colorless needle crystals (from ethanol); m. p. 201~202°C (decomp.) (lit.[14] 201~202°C (decomp.)). The yield was 40%.

2) Excess I (1000 cc.) and anhydrous chloral (500 g.) were heated to 110~113°C for 40 hr. according to Tullock and McElvain[15]. The same compound as the above was obtained in 65% yield.

**3-(2-Pyridyl)-lactic Acid (III).**—The compound II was hydrolysed with sodium carbonate as described by Einhorn[14]. III formed into colorless prismatic crystals, m. p. 124~125°C (from ethanol) (lit.[14] m. p. 124~125°C). The yield was 80%.

**3-(2-Pyridyl)-acrylic Acid (IV).**—1) III was dehydrated as described by Einhorn[14]. IV formed into colorless needles, m. p. 204~205°C (decomp.) (lit.[14] m. p. 204~205°C (decomp.)). The yield was 81%.

2) The same compound was obtained from II according to the method of King[16] with some modifications.

A solution of II (341 g.) in ethanol (1100 cc.) was added dropwise with stirring during 5 hr. to a boiling solution of potassium hydroxide (408 g.) in ethanol (2600 cc.). After potassium chloride was filtered off, the filtrate was dried up and kept at 75~79°C at 11~12 mmHg for 24 hr. The cake obtained was dissolved in water and acidified to pH 4 with hydrochloric acid. The precipitate, after being collected and washed with water, gave the acid IV. The yield was 163 g.

**Ethyl 3-(2-pyridyl)-acrylate (V).** — The acid IV was esterified in 67% yield as described in the literature[14]; b. p.$_{14}$ 152.5~153°C; b. p.$_{11}$ 143~147°C (lit.[14] b. p.$_{11}$ 142~145°C).

**3-(2-Pyridyl)-1-propanol (VI).**—2-Picolyl lithium prepared from I (23 g.) and phenyl lithium, which was, in turn, prepared from phenyl bromide (40 g.) and lithium (3.5 g.) in dry ether (200 cc.), was condensed with ethylene oxide (10 g.) as described in Org. Synth.[17]; b. p.$_{7}$ 128~131°C (lit.[17] b. p.$_{4}$ 116~118°C). The yield was 32%.

**3-(2-Piperidyl)-1-propanol (VII).**—1) The ester V was reduced in 28% yield with metallic sodium and ethanol according to Tullock and McElvain[15]. Replacing ethanol with cyclohexanol gave the same result without varying the yield of the reduction product; b. p.$_{3}$ 102~105°C (lit.[15] b. p.$_{3}$ 102~105°C).

2) The alcohol VI (21.5 g.) in dioxane (10 cc.) was hydrogenated over Raney nickel (ca. 0.2 g.) at 130~140°C with hydrogen at an initial pressure of 90 kg./$cm^2$ for about 4 hr.; b. p.$_{5}$ 121~125°C, $n_D^{25}$ 1.4866 (lit.[18] $n_D^{25}$ 1.4863). The yield was 14 g.

**Oxidation of VII with Chromic Acid.**—*1) Mild Oxidation.*—To the propanol VII (8.6 g., 0.06 mol.) in glacial acetic acid (80 cc.) was added chromic acid (4 g., 0.04 mol. = 0.06 equivalent of O) in water (4 cc.) dropwise with stirring at room temperature (30°C), then stirred for 2 hr. more at this temperature. No change of color was observed during this period. The bath temperature was gradually raised, and at about 80°C the color promptly turned green. After being stirred for 10 min. at 80°C and 2 hr. at 50°C, the acetic acid was evaporated. Then the residue was dissolved in water, made alkaline with sodium hydroxide when a considerable amount of tarry material, which dissolved neither in ether nor in water, was separated and the aqueous solution was extracted with ether. After drying, the ether extract was distilled in the stream of hydrogen under reduced pressure. There was obtained 1.7 g. of the fraction of b. p.$_{21}$ 143~145°C, and its refractive index ($n_D^{25}$ 1.4848) was found to be the same as that of the starting material. The residue (2.7 g.) could not be distilled in an oil-bath at 250°C under a pressure of 5 mmHg. No fore-running fraction, the boiling point of which corresponds to that of pelletierine could be recognized.

*2) Violent Oxidation.* — The propanol VII (4 g.) was added dropwise to a mixture of chromic acid (4 g.), concentrated sulfuric acid (16 g.) and water (50 cc.) with shaking. A considerable amount of heat was evolved and the color immediately turned green. Then it was heated with occasional shaking for 1 hr. at 90~100°C. After the inorganic ions were removed by the method of Koenig and Hoppe[19], the aqueous solution was acidified with hydrochloric acid, decolorized and concentrated to dryness. An alcoholic extract of the residue was evaporated in vacuo. From the syrupy residue were separated needle crystals after being allowed to stand in a refrigerator overnight. The crystals were filtered from extremely viscous liquid, washed thoroughly with ethanol and recrystallized from ethanol. The needle crystals thus obtained melted at 186~187°C and were not depressed by admixture with an authentic sample of 3-(2-piperidyl)-propionic acid hydrochloride.

**1, 1-Diethoxy-3-(2-pyridyl)-propane (VIII).**—According to Spielman et al.[20] VIII was synthesized

14) A. Einhorn, *Ann.*, **265**, 208 (1891).
15) C. W. Tullock and S. M. McElvain, *J. Am. Chem. Soc.*, **61**, 961 (1939).
16) J. A. King et al., *J. Org. Chem.*, **16**, 1100 (1951).
17) L. A. Walter, "Organic Syntheses" **23**, 83 (1943).
18) R. R. Burtner and J. M. Brown, *J. Am. Chem. Soc.*, **69**, 631 (1947).
19) W. Koenig and G. Hoppe, *Ber.*, **35**, 1348 (1902); **36**, 2906 (1903).
20) M. A. Spielman et al., *J. Org. Chem.*, **6**, 780 (1941).

with the reaction of 2-picolyl lithium and bromoacetal, which was prepared by the method of Org. Synth.[21]; b. p.$_{7}$ 128~129°C (lit.[20] b. p.$_{8}$ 128°C). The yield was 15% (based on lithium).

**1, 1-Diethoxy-3-(2-piperidyl)-propane (IX).**—The acetal VIII (30 g.) in ethanol (200 cc.) was hydrogenated over Raney nickel (ca. 5 g.) at 130~140°C with hydrogen at an initial pressure of 105 kg./cm$^2$ for about 2 hr.; b. p.$_{6}$ 117~120°C, $n_D^{20}$ 1.4540 (lit.[20] b. p.$_{3}$ 101~106°C, b. p.$_{1}$ 91~92°C, $n_D^{25}$ 1.4568). The yield was 20 g.

***N*-Ethoxycarbonyl-1, 1-diethoxy-3-(2-piperidyl)-propane (X).**—The acetal IX was converted into its urethane with ethyl chloroformate and sodium hydroxide by Spielman's method[20]; b. p.$_{3.5}$ 152~156°C, $n_D^{20}$ 1.4612 (lit.[20] b. p.$_{2}$ 146~147°C, $n_D^{25}$ 1.4580). The yield was 74%.

***N*-Ethoxycarbonyl-3-(2-piperidyl)-propionaldehyde (XI).**—The acetal X was hydrolyzed in 95% acetic acid by Spielman's method[20]; b. p.$_{2.5}$ 122~124°C, $n_D^{20}$ 1.4792 (lit.[20] b. p.$_{1}$ 119~121°C, $n_D^{25}$ 1.4771). The yield was 69%.

**1-(2-Pyridyl)-2-propanol (XII).** — According to Org. Synth.[17] the propanol XII was prepared by the condensation of acetaldehyde with 2-picolyl lithium; b. p.$_{17}$ 114~119°C (lit.[17] b. p.$_{17}$ 116~117°C). The yield was 56% based on I.

**1-(2-Piperidyl)-2-propanol (XIII).**—The propanol XII (184.5 g.) in dioxane (100 cc.) was hydrogenated over Raney nickel (ca. 12 g.) at 130°C with hydrogen at an initial pressure of 120 kg./cm$^2$ for 3 hr.; b. p.$_{13}$ 108~113°C (lit.[10] b. p.$_{16}$ 115~120°C). The yield was 158.5 g.

**1-(2-Piperidyl)-2-propanone (Isopelletierine) (XIV).**—The propanol XIII (11.4 g.) was oxidized to isopelletierine with chromic anhydride (6 g.) in glacial acetic acid (80 cc.) by the method of Meisenheimer and Mahler[10]. The fraction distilling below 105°C at 15 mmHg was collected (8 g.). Rectification yielded the fraction of b. p.$_{7}$ 79~80°C, b. p.$_{21}$ 101.2°C, $n_D^{20}$ 1.4661, $d_4^{20}$ 0.9587 (lit. b. p.$_{10}$ 86°C[10], b. p.$_{14}$ 91~92°C[9], $n_D^{20}$ 1.46687[9], $d_4^{20}$ 0.9624[9]).

Found: N, 10.05. Calcd. for $C_8H_{15}ON$: N, 9.92%.

Hydrobromide; colorless needles (from acetone), m. p. 139~140°C (lit. m. p. 137°C[5,10], 138°C[11]).

Picrate; yellow needles (from ethanol), m. p. 151.5~152°C (lit. m. p. 148~149°C[2], 149~150°C[11]).

***N*-Ethoxycarbonyl-1-(2-piperidyl)-2-propanone (XV).**—The pure isopelletierine, obtained by treating the pure hydrobromide with sodium hydroxide and rectifying the free base, was treated with ethyl chloroformate in the presence of sodium hydroxide by the usual method; colorless viscous liquid, b. p.$_{3.5}$ 131~132°C, b. p.$_{20}$ 165~166°C, $n_D^{20}$ 1.4715.

Found: N, 6.60. Calcd. for $C_{11}H_{19}O_3N$: N, 6.57%.

**"Pelletierine"**

The samples of the pomegranae bark used in this experiment were as follows:

*Powder of Pomegranate Root Bark (Sample I):*—Gathered at the north-bank of the River Yoshino, in Tokushima Prefecture, Japan; dried for several days and ground to fine powder.

*Powder of Pomegranate Root (Sample II).*—From the pomegranate cultured in this laboratory; used immediately after gathering.

*Powder of Pomegranate Bark (Sample III).*—Purchased from drug store; when it was gathered was unknown.

**Preparation of the Sample for Paper-chromatography.** — *1) Method of Wibaut et al.*[5]: — Sample (common to I, II and III) was boiled with methanol, filtered and methanol was distilled off under diminished pressure. The residue was warmed with 10% hydrochloric acid at about 60°C and filtered. The filtrate was washed with chloroform and, after alkalifying with sodium hydroxide extracted with chloroform. The extract was shaken with 10% hydrochloric acid again, then the aqueous layer was condensed under reduced pressure.

*2) Hydrochloric Acid-Methanol Extraction.*—Sample was boiled with methanol containing hydrochloric acid, filtered and condensed under reduced pressure. The syrup thus obtained was extracted with 10% hydrochloric acid and treated as above.

*3) Method of Hess and Eichel*[8],**.—The mixture of sample and sodium hydroxide solution was placed in Soxhlet's apparatus and extracted with ether. The ether extract was treated with 10% hydrochloric acid and the hydrochloric acid extract was condensed.

**Chromatography.** — *Paper:* — Toyo filter paper No. 50 for chromatography (paper was allowed to stand over 24 hr. with saturated vapor of developer before use).

*Developer.* — *n*-Butyl alcohol: con. hydrochloric acid: water=100 : 8 : ca. 20 (in volume) (the upper layer of the mixture was used as developer).

*Method of Development.*—Descending method.

*Colorizing Agent:*—Dragendorf's resgent.

The experimental results are shown in Table II.

Table II. Results of paper chromatographic analyses

| Sample | Method of preparation | $R_f$ | | |
|---|---|---|---|---|
| I | 1 | 0.37 | 0.45 | 0.57 |
| I | 2 | 0.37 | 0.46 | |
| I | 3 | 0.39 | 0.46 | |
| II | 1 | 0.39 | 0.49 | |
| III | 1 | 0.35 | 0.42 | |
| Root bark[5] | | 0.16 | 0.34 | 0.43 |
| Pseudopelletierine[5] | | 0.32~0.34 | | |
| *dl*-Methylisopelletierine[5] | | 0.41~0.45 | | |
| *dl*-Isopelletierine[5] | | 0.48~0.53 | | |

**Isolation of Pelletierine.** — Sixty kg. of sample I was extracted by boiling methanol three times, each for 10 hr. The extracts were condensed to syrup and warmed for some time with 10% hydrochloric acid on 60°C and filtered from resinous material. The filtrate was washed with chloroform, the residual aqueous layer was made alkaline with

21) S. M. McElvain and D. Kundiger, *Organic Syntheses*, 23, 8 (1943).

** Instead of calcium hydroxide and chloroform, sodium hydroxide and ether were used, respectively.

sodium hydroxide and extracted with chloroform. The chloroform extract was treated with 10% hydrochloric acid, the aqueous solution was, after condensing, dried up in a desiccator, and thus the mixture of alkaloidhydrochlorides was obtained. The yield was 160 g. This hydrochloride was dissolved in water, and after weakly alkalifying with aqueous sodium bicarbonate solution, extracted with ether. From this ether extract pseudopelletierine was obtainable. The aqueous solution was strongly alkalified with sodium hydroxide and extracted with ether repeatedly until the ether layer became colorless. After drying with sodium hydroxide and distilling off the solvent, the ether extract was distilled under reduced pressure in the atmosphere of hydrogen, then the fraction of 102~113°C at 20 mmHg was collected. The yield was 64.1 g. (The greater part of this fraction was distilled at 104~105°C at 20 mmHg, and, when rectified, the liquid of b. p.$_9$ 86~86.2°C and $n_D^{20}$ 1.4665 was obtained. During distillation in the atmosphere of hydrogen, this liquid kept completely colorless, but it became pink at once when it was allowed to make a contact with air, and then turned dark red in time).

The mixture of the fraction of b. p.$_{20}$ 102~113°C (31.9 g.), sodium hydroxide (45 g.) and water (160 cc.) was stirred and cooled below 10°C. To this suspension, ethyl chloroformate (36 g.) was added gradually. The reaction product was extracted with ether and the extract dried with sodium hydroxide freed from the solvent, and distilled under reduced pressure; thus the fraction which boils at 164~166°C at 19 mmHg was obtained (lit.[8] b. p.$_{21}$ 169~170°C). The yield was 13.3 g. After rectification, viscous colorless liquid of b. p.$_{3.5}$ 131~131.5°C and $n_D^{20}$ 1.4711 was obtained.

**Infrared Absorption Spectra.** — These measurements were taken with a Perkin-Elmer spectrophotometer, Model 21 with sodium chloride prism).

Phase: liquid

Thickness: ca. 0.01 mm.

The author desires to state with sincere thanks that this work was commenced under the direction of the late Professor Ryuzaburo Nodzu and he wishes to express his profound gratitude to Professor Ryozo Goto of Kyoto University and to Professor Hiroshi Watanabe of Kōnan-University for thier invaluable advice and cordial encouragement throughout the work. He also thanks the Research Laboratory of Takeda Pharmaceutical Industries for infrared measurements and Miss. T. Nagahama and Mr. Y. Kaneko for their collaboration with him in the experiments.

*Laboratory of Chemistry*
*Faculty of Science*
*Konan-University*
*Okamoto, Higashinada, Kobe*

# *Studies on Pelletierine. II. On the Structure of the So-called Pelletierine Proposed by Hess**,***

By Sigeru KUWATA

(Received January 6, 1960)

As reported in the previous paper[1], the author has isolated pelletierine by tracing the same method as that of Hess and Eichel and has compared it with synthetic samples of 3-(2-piperidyl)-propionaldehyde and 1-(2-piperidyl)-2-propanone in the form of urethane, as the result of which he has reached the conclusion that pelletierine is the same as isopelletierine, 1-(2-piperidyl)-2-propanone.

But the problem remains that the chemical reactions of pelletetierine, on the basis of which Hess and Eichel have assigned to it the structure of 3-(2-piperidyl)-propionaldehyde, should be explained with isopelletierine.

The most important reactions used by them for the determination of the structure of pelletierine were the following two[2]:

1) $C_8H_{15}ON$ (pelletierine) $\xrightarrow{H_2NNH_2}$ $C_8H_{17}N_3$ $\xrightarrow{EtONa}$ $C_8H_{17}N$ (coniine)

2) $C_8H_{15}ON$ (pelletierine) $\xrightarrow{H_2NOH}$ $C_8H_{16}ON_2$ $\xrightarrow{PCl_5}$ $C_8H_{14}N_2$ (I) $\xrightarrow{KOH\text{-}EtOH,\ HCl\text{-}EtOH}$ the compound II, assumed to be ethyl 3-(2-piperidyl)-propionate hydrochloride

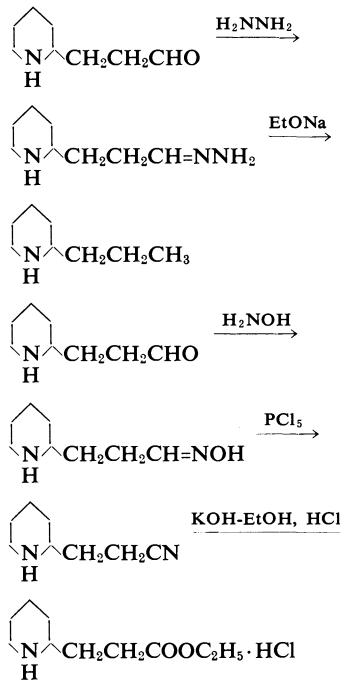
* This work was partly presented at the 12th Annual Meeting of the Chemical Society of Japan, April 4, 1959.

** Immediately before the publication of this paper, the author received a publication of the *J. Am. Chem. Soc.*, in which R. L. Augustine reported the rearrangement of isopelletierine-oxime obtaining the same results; ibid., **81**, 4664 (1959).

1) S. Kuwata, This Bulletin, **33**, 1668 (1960).

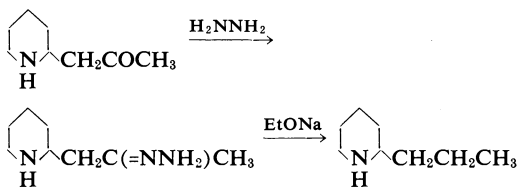
2) K. Hess and A. Eichel, *Ber.*, **50**, 1192 (1917).

Assigning the aldehyde structure to pelletierine, they have explained these reactions as follows:

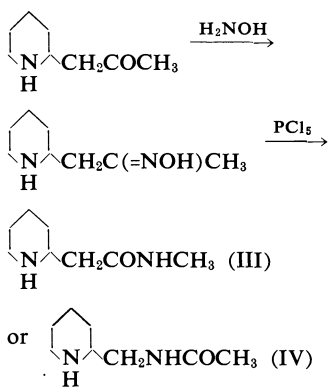
3) 

4) 

In reaction 1, the aldehyde may be replaceable by the ketone (isopelletierine) with the same final reaction product:



But in reaction 2, the product will be entirely different according to the structure of the starting material. Although the production of nitrile is expected from the aldehyde, from the ketone the amide III or IV will be obtainable by the Beckmann rearrangement:



Then, if the compound I is nitrile, as Hess has evaluated, the reaction must involve a skeletal rearrangement which has never been observed hitherto. Or if Hess' evaluation is incorrect, the question as to what structure should be assigned to it remains.

In order to clarify these situations the author has traced reaction 2 using isopelletierine-oxime under the same conditions described by Hess. Thus isopelletierine-oxime was treated with freshly sublimed phosphorus pentachloride in phenetole. The reaction proceeded, as described in the literature[2], with remarkable evolution of heat, and a brown syrupy material was produced, from which, after rectification, the compound which boiled at 104~106°C at 15 mmHg was obtained. When it was purified through picrate, a colorless liquid, boiling at 102~103°C at 10 mmHg, was obtained. This material showed complete agreement with the compound I that Hess and Eichel had obtained from pelletierine-oxime; the comparison between the two is shown in Table I.

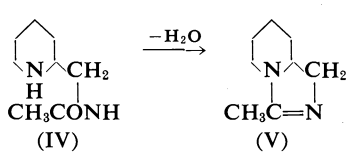
Table I. The properties of the compounds obtained from the reaction of oxime and rhosphorus pentoxide

| Oxime | Molecular formula | B. p., °C (mmHg) | M. p. of picrate, °C |
|---|---|---|---|
| Isopelletierine-oxime | $C_8H_{14}N_2$ | 104~106(15)<br>102~103(10)* | 174~175 |
| Pelletierine-oxime[2] | $C_8H_{14}N_2$ | 105~108(15)<br>104~106(15)* | 175~176 |

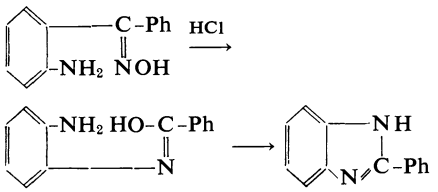
* Purified through picrate.

Thus it was ascertained that the reaction is reproducible with isopelletierine.

This compound I cannot be nitrile, for its infrared spectrum shows no absorption between 4.0 $\mu$ and 5.0 $\mu$. It is also certain from analytical data that this compound I is neither the amide III nor IV, though the most probable reaction in this case may be the Beckmann rearrangement. On comparing the two formulae, $C_8H_{14}N_2$ of the compound I, and $C_8H_{16}ON_2$ of the amide, it will be easily seen that the difference is just one molecule of water. This fact may allow one to suppose that the compound I may be producible by intramolecular dehydration of the amide, produced by the Beckmann rearrangement of the keto-oxime. Such a dehydration is difficult sterically with formula III, but with formula IV, the following ring closure may be brought on:

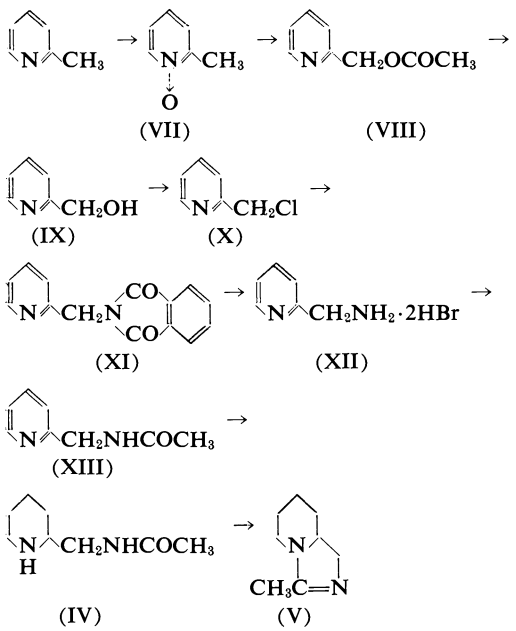


An analogous dehydration has been illustrated, in fact, with *o*-aminobenzophenoneoxime, which provides benzenylphenyleneamidine by the Beckmann rearrangement according to the following scheme[3]:



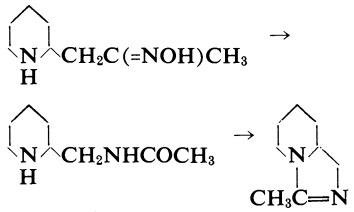
For the purpose of confirming the correctness of this assumption, 2-acetamidomethylpiperidine (IV) was synthesized by another route, and its dehydrative cyclization was attempted by treating it with phosphorus oxychloride, according to the method of Bower[4] (Eq. 1).

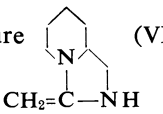
Eq. 1

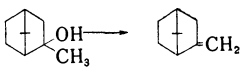


The compound V thus obtained boiled at 103~106°C at 11 mmHg and its picrate melted at 174~175°C. This was never depressed when it was mixed with the picrate of I. The identity of both picrates was also confirmed by the Debye-Scherrer diagram.

From these results, the author thinks that the real structure of the compound I, to which Hess and Eichel assigned 3-(2-piperidyl)-propionitrile, should be represented by V, and the reaction should be explained as shown in the following scheme:



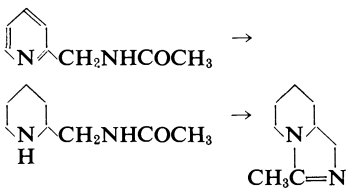
An alternative structure  (VI), however, may also be assumable for the compound I, because such a structure, having the terminal vinyl group, can be seen in some cases as $\alpha$-fenchene from methyl-$\alpha$-fenchocamphorol by intramolecular dehydration[5]:



However, on treating the compound I with ozone, no formaldehyde can be detected, so structure V, and not VI, should be assigned to this compound. The fact that its near infrared spectrum shows no absorption at ca. 1640 m$\mu$ and ca. 2130 m$\mu$ corresponding to $CH_2=C\langle$[6], may also support this conclusion.

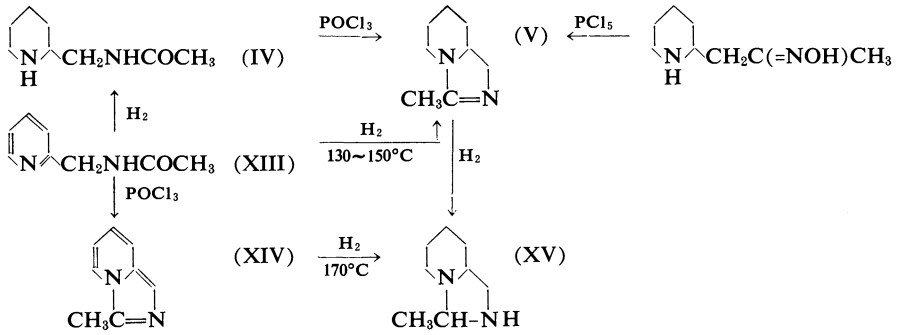
Another proof of structure V for this substance was also found in another way. When this compound was reduced catalytically, a colorless liquid, b. $p._{14}$ 85~100°C, which gave crystalline styphnate of m. p. 183~185°C, was obtained. This compound proved identical, by the mixed melting point of both the styphnates, with 2-methyl-1, 3-diazabicyclo[4 : 3 : 0]-nonane obtained by reducing 3-methyl-2; 3a-diazaindene catalytically.

The compound V was also found to be producible when 2-acetamidomethylpyridine was hydrogenated in ethanol at 130~150°C over Raney nickel, the reaction of which would probably be represented by the scheme:



This fact may be a proof that *N*-acetamidomethylpiperidine can be easily cyclized into the bicyclic compound V. The relationship among these bicyclic compounds will be shown diagramatically as follows.

3) J. Meisenheimer and H. Meis, *Ber.*, **57**, 289 (1924).
4) J. D. Bower and R. G. Ramage, *J. Chem. Soc.*, **1955**, 2834.
5) J. L. Simonsen, "The Terpenes", Vol. II, Cambridge University Press (1949), p. 540.
6) Private communication from Mr. M. Nishikawa of the Research Laboratory, Takeda Pharmaceutical Industries, Ltd.; cf. R. H. Holman, *Anal. Chem.*, **28**, 1533 (1956); W. Kaye, *Spectrochimica Acta*, **6**, 257 (1954).




Hess and Eichel treated their "nitrile", the compound I, with alcoholic potash, then with alcoholic hydrochloric acid, and obtained the compound II, which they believed to be ethyl 3-(2-piperidyl)-propionate hydrochloride on the basis of its analytical data and the comparison of the melting points of both the compounds as well as their gold salts. On re-examining their description, one will see that these evidences have some weak points. It is true that analytical data given by them, C, 54.39; H, 9.10, agree well with those for the ester hydrochloride (C, 54.10; H, 9.08), but, those of N and Cl are not given by them. The comparison between the melting points is also not decisive, because it is not dependent on the mixed melting point method. From these situations it seems necessary to re-examine the nature of the hydrolysis product obtained by Hess and Eichel from their "nitrile".

Thus the author wanted to trace their experiments as accurately as possible, but their description of the reaction conditions is not so definite. They state, "Das Nitril wurde mit einer 5-prozentigen alkoholischen Kaliumhydroxydlösung kurze Zeit auf dem Wasserbade erwärmt" and "1 Stunde mit alkoholischer Salzsäure gekocht." In alkali treatment, the volume of alkali solution, the temperature and the reaction time, and in acid treatment the concentration of hydrochloric acid and its volume, are not definite. Thus the reaction was carried out by varying the conditions, and various results were obtained, which are summarized in Table II. Unfortunately in all these cases no crystalline product corresponding to Hess' "ethyl 3 (2-piperidyl)-propionate hydrochloride" could be isolated, but in one case yellow crystalline gold salt (m. p. about 90~95°C, C, 18.51; H, 3.00; Au, 48.40) was obtained from the semisolid hydrolyzate. On recrystallization it gave red needles (m. p. about 120°C, C, 22.30; H, 3.34; Au, 47.05), which seemed to resemble the gold salt of ethyl 3-(2-piperidyl)-propionate hydrochloride (m. p. 128°C, C, 22.87; H, 3.84), as far as the melting point and contents of C and H were concerned, but it was quite apparent from the difference in color (the authentic sample of the gold salt of ethyl 3-(2-piperidyl)-propionate hydrochloride is yellow) as well as from the Au-contents that the two compounds were not identical. Though it is impossible to decide, however, whether the gold salt obtained here was the same compound as Hess and Eichel have isolated, because they have never reported the nature of their compound except its melting point, it may be said at least that by treating the compound I according to their method, a gold salt resembling the one reported by them is obtainable.

On the grounds which have been described hitherto, the author believes that he can deduce the conclusion that pelletierine, to which Hess and Eichel have assigned the structure 3-(2-piperidyl)-propionaldehyde, is nothing but isopelletierine, 1-(2-piperidyl)-2-propanone. By this conclusion can easily be solved many conflicts, arising from the assumption that pelletierine is 3-(2-piperidyl)-propionaldehyde, e. g. a confilict that pelletierine is stable against oxidation, and can not be oxidized into 3-(2-piperidyl)-propionic acid with chromic acid, or a conflct that it can be isolable without any special care, though 3-(2-piperidyl)-propionaldehyde can not be synthesized by any method on account of its extreme instability. The reaction of pelletierine that Hess and Eichel used for the determination of the structure is also easily explainable with isopelletierine, when 3-(2-piperidyl)-propionitrile is replaced by 2-methyl-1, 3-diazabicyclo [4 : 3 : 0]-2-nonene (V) with the same molecular formula. This conclusion also agrees with the finding by Wibaut and Hollstein[7] that 3-(2-piperidyl)-propionaldehyde has no anthelmintic activity, while 1-(2-piperidyl)-2-propanone (isopelletierine) is strongly anthelmintic.

7) J. P. Wibaut and U. Hollstein, *Konincl. Ned. Akad. Wetenschap., Proc. Ser.*, **B59**, 426 (1956); *Chem. Abstr.*, **51**, 11364*i* (1957).

## Experimental

**Isopelletierine-oxime.**—To the solution of $NH_2OH \cdot HCl$ (20 g.) and NaOAc (20 g.) in water (40 cc.) was added isopelletierine (16 g.) in methanol (18 cc.). After standing at room temperature overnight, the solution was made alkaline with sodium hydroxide and was extracted with ether. After drying and distilling off the solvent, the residue (colorless needle crystals, m. p. 97~99°C) was distilled under reduced pressure; b. $p._{10}$ 148~152°C (lit.[8] b. $p._{2.5}$ 134°C, b. $p._{5.6}$ 146°C). The yield was 12.5 g. After boiling the viscous distillate with petroleum ether and cooling, needle crystals were separated; m. p. 105~106°C (from ether). (As to the melting points for the two isomers, Mortimer et al.[8] have reported 105.5°C and 90°C, while Hess and Eichel[2] have reported 96~97°C and 80°C for pelletierine-oxime. The author used the higher melting isomer for the next reaction because it was also the higher one that Hess and Eichel had used for the reaction with phosphorus pentachloride).

**The Reaction of Isopelletierine-oxime with Phosphorus Pentachloride.**—According to a method just the same as Hess and Eichel's[2], isopelletierine-oxime (m. p. 105~106°C) (4.4 g.) was dissolved into freshly rectified anhydrous hot phenetole (10 cc.) and cooled to about 35~40°C, and this solution was added dropwise into a phenetole (30 cc.) solution of freshly sublimed phosphorus pentachloride (9 g.). At the beginning, the oxime precipitated gelatinously, but after some time it turned into a dark brown mass with violent evolution of heat and hydrochloric acid gas, and precipitated to the bottom. After several hours, phenetole was distilled off under reduced pressure at the temperature of 70~85°C, and the residue was dissolved in water while cooling. After the removal of residual phenetole by extraction with ether, the solution was made alkaline with sodium hydroxide and extracted with ether. The ether extract was dried with potassium hydroxide, freed from ether and distilled under diminished pressure. Thus the fraction boiling at 104~106°C at 15 mmHg was gathered. The yield was 1.2 g. After being converted into picrate, recrystallized and regenerated by sodium hydroxide the purified sample was obtained, boiling at 102~103°C at 10 mmHg; $n_D^{25}$ 1.4973.

Found: C, 68.83; H, 10.14; N, 19.17. Calcd. for $C_8H_{14}N_2$: C, 69.52; H, 10.21; N, 20.27%.

The error of the analysis would probably be attributable to the hygroscopicity of this material.

Picrate: yellow needles, m. p. 174~175°C (from ethanol).

Found: C, 45.82; H, 4.72; N, 18.88. Calcd. for $C_{14}H_{17}O_7N_5$: C, 45.77; H, 4.67; N, 19.07%.

**2-Picoline *N*-Oxide (VII).**—The compound VII was obtained in 90% yield from the reaction of 2-picoline and hydrogen peroxide in acetic acid by the method of Boekelheide[9]; b. $p._{25}$ 146~148°C (lit.[9] b. $p._{15}$ 123~124°C).

**2-Pyridylmethanol Acetate (VIII).**—The compound VII was converted into VIII in 79% yield by the action of acetic anhydride according to Boekelheide[9]; b. $p._{18}$ 117~119°C (lit.[9] b. $p._{22}$ 115~118°C).

**2-Pyridylmethanol (IX).**—The acetate VIII was hydrolyzed with 10% hydrochloric acid in 70% yield according to Kobayashi[9]; b. $p._{17}$ 118~121°C (lit[10] b. $p._{16}$ 111~115°C); picrate, m. p. 160~161°C (lit.[9] m. p. 160.5~161°C).

**2-Pyridylmethylchloride (X).**—According to Itai[11], X was obtained by the reaction of the alcohol IX and phosphorus trichloride in 60% yield; b. $p._{21}$ 87°C (lit.[11] b. $p._5$ 70~80°C).

**2-Pyridylmethylamine Hydrobromide (XII).**—The chloride X (35 g.), potassium phthalimide (50 g.) and dimethylformamide (300 cc.) were heated at 90~100°C for about 5 hr. in water bath. When water was added to the reaction product after removal of the solvent under reduced pressure, all the contents of the vessel solidified (solid XI weighed 72 g.) After washing thoroughly with water and dilute sodium carbonate solution, the solid was boiled for 2 hr. with 48% HBr (300 cc.) in oil-bath, and phthalic acid, which separated on cooling, was filtered off. Being decolorized and condensing the filtrate, 60 g. of the crude XII was obtained. From 10 g. of this salt, after treating with sodium hydroxide, extracting with chloroform and distilling the extract, 2.5 g. of the free amine, boiling at 81°C at 5 mmHg, was obtained (lit.[4] b. $p._{20}$ 95~98°C).

**2-Acetamidomethylpyridine (XIII).**—To the mixture of XII (30 g.) and 30% sodium hydroxide solution (240 cc.), acetyl chloride (30 cc.) was added gradually with stirring, keeping the temperature below 20°C. The reaction product was extracted with chloroform, dried with sodium sulfate and distilled under diminished pressure; b. $p._3$ 145~149°C (lit.[4] b. $p._5$ 160~163°C), $n_D^{25}$ 1.5430; picrate, m. p. 169~170°C (Found: N, 18.14%).

**2-Acetamidomethylpiperidine (IV).**—The amide XIII (5 g.) in dioxane (30 cc.) was hydrogenated over Raney nickel with hydrogen of initial pressure of 70 kg./cm² for 2 hr.; b. $p._{14}$ 158~165°C, $n_D^{25}$ 1.5205. This was proved to be a mixture of XIII and IV, because from this distillate two picrates were obtained. One was hardly soluble in ethanol and melted at 169~170°C and was confirmed as the picrate of unreacted XIII by mixed melting point determination. Another, the picrate of IV, was easily soluble in ethanol and melted at 153~155°C.

*Anal. of picrate of IV.* Found: N, 17.85. Calcd. for $C_{14}H_{19}O_8N_5$: N, 18.18%.

The distillate was used for the next reaction without further separation.

**Cyclization of IV by Phosphoryl Chloride.**—A mixture of IV (5.6 g.) and phosphoryl chloride (20 cc.) in benzene (50 cc.) was refluxed for 3 hr. in water bath. Benzene was distilled off, and the residue was dissolved in water, made alkaline with sodium hydroxide and extracted with chloroform.

8) P. I. Mortimer and S. Wilkinson, *J. Chem. Soc.*, **1957**, 3967.

9) V. Boekelheide and W. J. Linn, *J. Am. Chem. Soc.*, **76**, 1286 (1954); cf. G. Kobayashi and S. Furukawa, *Pharm. Bull. (Japan)*, **1**, 347 (1953).

10) W. M. Edwards and P. C. Teague, *J. Am. Chem. Soc.*, **71**, 3548 (1949).

11) T. Itai and H. Ogura, *J. Pharm. Soc. Japan (Yakugaku Zasshi)*, **75**, 296 (1955).

The extract, dried with sodium sulfate and after removal of the solvent, was distilled under diminished pressure, and was obtained the fraction of b. $p._{11}$ 103~106°C, $n_D^{25}$ 1.5011. The yield was 0.5 g. Its picrate melted at 174~175°C, and showed no depression of the melting point when mixed with the picrate of the reaction product of isopelletierine-oxime and phosphorus pentachloride. Both picrates showed identical Debye-Scherrer diagram.

*Anal. of picrate.* Found: C, 45.66; H, 4.64. Calcd. for $C_{14}H_{17}O_7N_5$: C, 45.77; H, 4.67%.

**Cyclization of XIII to 3-Methyl-2; 3a-diazaindene (XIV) with Phosphoryl Chloride.** — According to Bower and Ramage[4], the compound XIII (4 g.) and phosphoryl chloride (8 cc.) in benzene (24 cc.) were heated under gentle reflux for 4 hr. After distilling off benzene and the remaining phosphoryl chloride under reduced pressure, water was added to the residue, which was made alkaline and extracted with chloroform. After removal of solvent, the residue was distilled under reduced pressure; b. $p._7$ 120~134°C (mainly distilled at b. $p._7$ 134°C) (lit.[4] b. $p._4$ 112~117°C); $n_D^{25}$ 1.5951. The yield was 2.5 g.

Picrate: yellow amorphous crystals, m. p. 210°C (darkened over 200°C) (lit.[4] m. p. 221°C (decomp.)).

Found: C, 46.31; H, 3.46. Calcd. for $C_{14}H_{11}O_7N_5$: C, 46.54; H, 3.07%.

**Reduction of 2-Methyl-1,3-diazabicyclo[4:3:0]-2-nonene (V) to 2-Methyl-1,3-diazabicyclo[4:3:0]-nonane (XV).**—V was hydrogenated over Raney nickel in ethanol with hydrogen having an initial pressure of 95 kg./cm² at 150°C for 3.15 hr. After removal of the catalyst and solvent, the reduction product was distilled under diminished pressure; b. $p._{14}$ 85~100°C. Styphnate: amorphous yellow crystals, m.p. 183~185°C.

*Anal. of styphnate.* Found: C, 43.52; H, 5.06. Calcd. for $C_{14}H_{19}O_8N_5$: C, 43.64; H, 4.97%.

**Reduction of XIV to XV.**—The compound XIV was hydrogenated over Raney nickel in ethanol with hydrogen having an initial pressure of 95 kg./cm² at 170°C for 4 hr. After removal of the catalyst and solvent, the reduction product was distilled under reduced pressure; b. $p._{12}$ 96~98°C, $n_D^{25}$ 1.4600. Styphnate: amorphous yellow crystals, m. p. 183~185°C. This styphnate was identical with the one of XV derived from V, which was confirmed by mixed melting point determination and the comparison of their IR spectra.

**Reduction of XIII in Ethanol.**—The amide XIII (16 g.) in ethanol (20 cc.) was hydrogenated over Raney nickel (ca. 1 g.) with hydrogen having an initial pressure of 130 kg./cm² for 4 hr. at 130~150°C. Distilling the reaction product, after removal of solvent, the following distillates were obtained.

(A) b. $p._{11}$ ~91°C, 4.1 g.

(B) b. $p._{11}$ 91°C~b. $p._{12}$ 158°C, very little.

(C) b. $p._{12}$ 158~163°C (mainly distilled at 162~163°C), 5.6 g.; $n_D^{25}$ 1.5196.

A portion boiling at 102~108°C at 11 mmHg ($n_D^{25}$ 1.4975) in the fraction B formed the picrate, m. p. 174~175°C (needle crystals from ethanol), and this picrate showed no depression of melting point when mixed with the picrate of V, prepared by the action of phosphorus pentachloride upon isopelletierine-oxime. The identitly of both the picrates was also confirmed by the Debye-Scherrer diagram.

*Anal. of the picrate.* Found: C, 46.02; H, 4.79. Calcd. for $C_{14}H_{17}O_7N_5$: C, 45.77; H, 4.67%.

Treating the fraction C with phosphoryl chloride in benzene as mentioned previously, liquid of b. $p._{11}$ 103~106°C and $n_D^{25}$ 1.4985 was obtained, the picrate of which melted at 174~175°C and showed no depression of melting point when mixed with the picrate of V. From the residue, after removal of the liquid (b. $p._{11}$ 103~106°C), the picrate of m. p. 200°C (decomp.) was obtained and showed no depression of melting point when mixed with the picrate of XIV.

Fraction A mainly distilled at 80~83°C at 13 mmHg on redistillation; $n_D^{25}$ 1.4628, $d_4^{25}$ 0.9142. Styphnate melted at 123~125°C (Found: C, 43.69; H, 5.65%).

**Treatment of the Compound V, Obtained from the Reaction of Isopelletierine-oxime with Phosphorus Pentachloride, with Alcoholic Potassium Hydroxide and Alcoholic Hydrochloric Acid.**—V was heated in waterbath with 5% alcoholic potassium hydroxide and the solution was evaporated to

Table II. Conditions and results of alcoholic potassium hydroxide and alcoholic hydrochloric acid treatment of V

| Exp. No. | V g. | KOH g. | EtOH cc. | Time | HCl | EtOH cc. | Time | Product |
|---|---|---|---|---|---|---|---|---|
| 1 | 0.8 | 1.5 | 30 | reflux 2 hr. | saturate | 30 | reflux 1 hr. | Syrupy, hygroscopic, insoluble in hot acetone; crystalline gold salt could not obtained. |
| 2 | 0.5* | 0.5 | 10 | reflux 0.5 hr. | bubbling | 10 | reflux 1 hr. | Needle crystals separated on standing, insoluble in hot acetone, m. p. 190~192°C. |
| 3 | 1.2 | 1 | 20 | warm ca. 60°C 30 min. | conc. HCl 5 cc. | 15 | reflux 1 hr. | Syrupy, soluble in hot acetone; gold salt formed into red needles** (from $H_2O$), m. p. ca. 120°C. |

* Purified material through picrate.

** By adding $AuCl_3$ solution to the syrupy material dissolved in water, yellow amorphous gold salt was obtained, m. p. 90~95°C (Found: C, 18.51; H, 3.00; Au, 48.40%). By recrystallization of this salt from $AuCl_3$ solution, yellow needles were obtained, but from water, there obtained red needles melting at about 120°C (Found: C, 22.30; H, 3.34; Au, 47.05%).

dryness after acidifying with concentrated hydrochloric acid. The dried crystallinematter was extracted with ethanol. After removal of the solvent the extract was refluxed with an alcoholic hydrochloric acid. After 1 hr.'s refluxing, the solution was evaporated under reduced pressure. A part of the residue was dissolved in water and the aqueous gold chloride was added. The conditions of the experiments and the properties of the residues or gold salts were listed in Table II.

The author wishes to express his sincere gratitude to Professor Ryozo Goto of Kyoto University and Hiroshi Watanabe of Kōnan-University for their invaluable advice and cordial encouragement throughout the work. He also thanks Miss C. Higashi of the Institute for Chemical Research of Kyoto University, for elementary analyses, the Research Laboratory of Takeda Pharmaceutical Industries, Ltd. for infrared spectra, Debye-Scherrer measurements and elementary analyses. Further he extends his thanks to Mr. H. Kawai and Mr. Y. Nakatake who collaborated with him in this experiment.

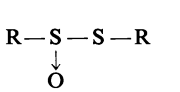
*Laboratory of Chemistry*
*Faculty of Science*
*Konan-University*
*Okamoto, Higashinada, Kobe*

# *Studies on Anti-cancer Agents. V. Desulfurization by Hydrazine Hydrate. II. The Reaction of Benzyl and Piperonyl Disulfide with Hydrazine**

By Tetsuji KAMETANI, Keiichiro FUKUMOTO, Yumiko SATOH**
Takashi TESHIGAWARA and Osamu UMEZAWA***

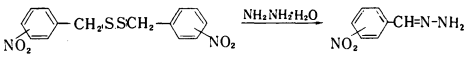
(Received April 20, 1960)

In the preceeding paper[1-3] Kametani and co-workers described the fact that three kinds of alkyl thiolsulfinates, namely, isobutyl, *tert*-butyl and *n*-amyl thiolsulfinates (I) were recognized to be effective against Ehrlich ascites tumor by their screening test among various thiolsulfinates synthesized by us, but almost all of these compounds are unstable for heat and irritative for the skin and eyes, so it is difficult to use them as anti-cancer agents. Among them, only dibenzyl thiolsulfinate (II) was found to form stable crystals, so we tried to synthesize various kinds of dibenzyl thiolsulfinate derivatives, bearing various functional groups in the phenyl nuclei, for instance, nitro, amino and so on.

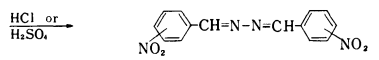


I: R=isobutyl, *tert*-butyl-, *n*-amyl-
II: R=$C_6H_5$-
III: R=*p*-$NH_2C_5H_4$-

As we reported previously[4], the first attempt to reduce nitrobenzyl disulfide to the corresponding amino derivative (III) by means of hydrazine hydrate resulted in the formation of nitrobenzal hydrazine (V) or nitrobenzaldazine (VI) as the results of an unexpected desulfurization reaction indicated below.



(IV) (V)



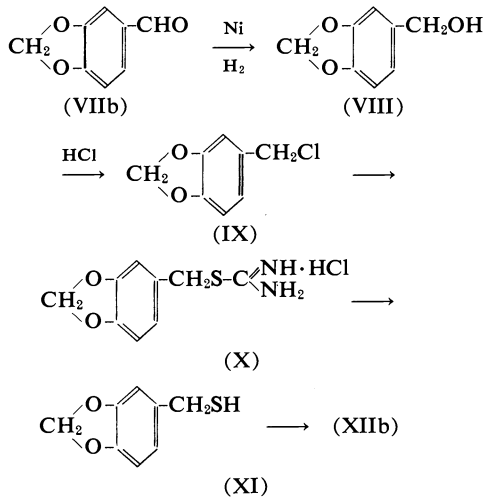
(VI)

In this paper desulfurization reaction was examined in the case of benzyl (XIIa) or piperonyl disulfide (XIIb), which has no electron-attractive radical, namely, the nitro group. The piperonyl disulfide (XIIb) was prepared according to the following reaction scheme. In this case, crossed-Cannizzaro reaction was applied the first time to obtain piperonyl alcohol, but the catalytic hydrogenation was found to be more excellent.

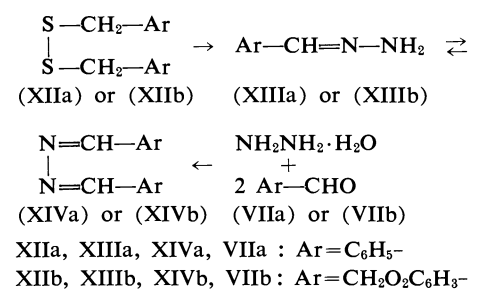
* Presented at the 13th Annual Meeting of the Pharmaceutical Society of Japan, Tokyo, April, 1960.

** Present Address: Pharmaceutical Institute, School of Medicine, Tohoku University, Kitayobancho, Sendai.
*** Present Address: Kowa Chemical Institute, Honcho, Chuo-ku, Tokyo.

1) T. Kametani, K. Fukumo to and O. Umezawa, *Yakugaku Kenkyu*, **31**, 60 (1959).
2) ibid., **31**, 125 (1959).
3) ibid., **31**, 132 (1959).
4) T. Kametani, K. Fukumoto, Y. Takayanagi, T. Teshigawara and O. Umezawa, *Chem. Pharm. Bull.*, in press.



When benzyl disulfide was heated with an excess of hydrazine hydrate, desulfurization occurred giving a small amount of yellowish crystals, which agreed with an authentic sample of m. p. 93°C[5] of benzaldazine (XIVa) by a mixed melting point test. As it was known that this compound XIVa turned to benzal hydrazine (XIII) by heating with hydrazine hydrate[6], the former substance was heated with an excess of hydrazine hydrate and it was observed that the color of the reaction mixture changed to colorless from yellow, indicating the formation of benzal hydrazine (XIIIa). This substance is known to be comparatively unstable against moisture in the air and easily decomposes to benzaldazine and hydrazine hydrate[7], therefore it seems possible that the benzal hydrazines initially formed from the disulfides give the corresponding benzaldazines by a prolonged period of reaction. Similarly, dipiperonyliden hydrazine (XIVb) was obtained from piperonyl disulfide and was proved to be identical with an authentic sample which was synthesized from piperonal and hydrazine hydrate[8].



XIIa, XIIIa, XIVa, VIIa : Ar=$C_6H_5$-
XIIb, XIIIb, XIVb, VIIb : Ar=$CH_2O_2C_6H_3$-

5) Th. Curtius and R. Jay, *J. prakt. Chem.*, [2] **39**, 44 (1889).
6) Th. Curtius and H. Franzen, *Ber.*, **35**, 3236 (1902).
7) Th. Curtius and L. Pflug, *J. prakt. Chem.*, [2] **44**, 537 (1891).
8) D. Vorländer, *Ber.*, **39**, 807 (1906).

## Experimental

**The Reaction of Dibenzyl Disulfide with Hydrazine Hydrate.** — The mixture of dibenzyl disulfide (1 g.) and 80% $NH_2NH_2 \cdot H_2O$ (2 ml.) was refluxed. After 30 min., an evolution of a gas containing sulfur and the deposition of a small amount of grayish-white substance on the inner tube of the condenser was observed. After 13 hr. of reflux, the reaction mixture was treated with hydrochloric acid and then extracted with ether. Then an ethereal extract was washed with water, dried on sodium sulfate and evaporated, resulting in a yellow viscous substance. This was recrystallized from dilute acetone giving yellow needles of m. p. 91~92°C in poor yield. This was found to be identical with the authentic sample described below.

**Benzaldazine (XIVa).**—To benzaldehyde (2 g.), 1.1 g. of 80% $NH_2NH_2 \cdot H_2O$ was gradually added at room temperature and considerable heat generation which accompanied the separation of yellow needles was observed. After recrystallization from ethanol, 1.3 g. (68.4%) of yellow, long needles (m. p. 93°C)[5] were obtained***.

**Piperonyl Thiuronium Chloride (X).**—Piperonyl chloride (5 g.) was added to thiourea (2.2 g.) in 99% ethanol (33 ml.) and the mixture was heated for 1.5 hr. The solvent was removed by distillation and a small quantity of ether was added to induce crystallization. The solid was collected by filtration. Colorless prisms (m. p. 201°C) were obtained by recrystallization from ethanol. Yield, 5.3 g., 73.6% of theoretical.

Found : C, 43.17 ; H, 4.00. Calcd. for $C_9H_{11}O_2 \cdot NSCl$ : C, 43.81 ; H, 4.49%.

**Piperonyl Mercaptan (XI).** — Thiuronium salt (5 g.) was admixed with 10% sodium hydroxide (34 ml.) and refluxed for 1.5 hr. on an oil bath. In this case an evolution of ammonia gas was observed. After cooling, the mixture was acidified with hydrochloric acid and extracted with ether. After being treated as usual, a fraction of 116~118°C/5 mmHg. (1.5 g., 44.1% of theoretical) was obtained by distillation in vacuo.

**Piperonyl Disulfide (XIIb).**—Iodine (1.2 g.) was gradually added to the stirred mixture of pyridine (1 g.) and piperonyl mercaptan (1.5 g.) at 15°C. After 1.5 hr., the reaction mixture was poured into water (50 ml.) and extracted with benzene, the extract was washed with saturated sodium thiosulfate, hydrochloric acid and water, successively and then evaporated. The residue was recrystallized from ethanol forming yellowish-white crystals (0.5 g., 35.8% of theoretical) of m. p. 68°C[9].

**The Reaction of Piperonyl Disulfide with Hydrazine Hydrate.**—The mixture of piperonyl disulfide (1 g.) and 80% $NH_2NH_2 \cdot H_2O$ (1.5 g.) was heated for 26 hr. and extracted with ether. The ethereal extract was evaporated after drying on sodium sulfate and the residue was recrystallized from acetone giving yellow needles (0.2 g., 22% of theoretical), m. p. 201°C. This was proved to be identical with an authentic sample prepared by the following method.

**** According to Ref. 5, this reaction was carried out in the presence of alkali.
9) W. Manchot and Chr. Zahn, *Ann.*, **345**, 326 (1905).

**Dipiperonyliden Hydrazine (Piperonal Azine) (XVb).**—Hydrazine hydrate (0.1 g.) was added to the mixture of piperonal (0.4 g.) and ethanol (1 ml.). After a few minutes a small amount of water was added, a white crystal separating from it. This was recrystallized from dilute acetic acid giving yellow crystals (0.2 g., 50.1% of theoretical), m. p. 202~203°C.

## Summary

The desulfurization reaction which was reported in the previous paper in case of the reaction of *p*-nitrobenzyl disulfide and hydrazine hydrate was also observed in the similar reaction of benzyl and piperonyl disulfide. The reaction product was found to be benzaldazine derivative instead of the derivative of benzal hydrazine.

*Pharmaceutical Institute*
*School of Medicine*
*Tohoku University*
*Kitayobancho, Sendai*

# *Behavior of Some Impurities in the Electro-refining of Iron*

By Shumpei OKA*, Takashi MUKAIBO and Hirokazu AIKAWA

(Received April 21, 1960)

Knowledge concerning the behavior of trace impurities during electrolysis is important in preparing high purity electrolytic iron. The production of electrolytic iron has a long history[1,2], but very few investigations have been reported on the behavior of trace impurities[3].

Selecting the sulfate bath as an example, the authors studied the behavior of orthophosphate, sulfate and zinc ions in the electrolyte as well as the behavior of silver plated on anodes. The difficulty of trace analysis was avoided by using phosphorus-32, sulfur-35, zinc-65 and silver-110 as radioactive tracers.

## Experimental

Experiments were carried out separately with phosphate, sulfate and zinc ions in a bath and also with silver plated on anodes. Phosphate, sulfate and zinc ions were added to the electrolyte with corresponding radioisotopes. Silver was plated anodes without applying electricity in the cyanide bath containing silver-110.

After 48 hours' electrolysis, the distribution of the added radioisotope was determined by a suitable radiation counter. The contents of each element in the deposited iron were calculated from the concentration of the carrier.

**Electrolysis.**—An assembly having a high enough scale and the stability to discuss the behavior of impurities during the electrolysis has been constructed. The main features of the equipment are the special cathode frame designed to improve the current distribution on the cathode, liquid suppliers which feed the solution to electrolytic cell, and water bath to make up for the loss due to the evaporation of water. The supply solution for the electrolytic cell contains a sufficient amount of sulfuric acid to keep proper pH-values during long operations. The details of the assembly were reported elsewhere[4] with the results of re-electrolysis of electrolytic iron. In the following experiments the electrolytic iron was also used as an anode material.

The conditions of electrolysis are: temperature 60°C, current density 2 amp./dm$^2$, pH 5~6, 1 M/l. Mohr's salt solution and the period of deposition, 48 hrs. According to Mukai's work[5], sodium *n*-butylsulfonate was added to the bath at the concentration of 1 g./l. in order to protect the deposited metal from dendrite formation and to attain a high current efficiency.

**Measurements of Radioactivity.**—Phosphorus-32 emits a $\beta$-ray of maximum energy 1.71 MeV., which is strong enough to be measured by a liquid immersion type counter. Measurements were carried out by using 20 ml. of the sample solution containing 2 N hydrochloric acid and the correction was made for the absorption due to iron in the solution.

Autoradiography was applied to obtain some information on the distribution of phosphorus in the deposited iron. As the activity of the sample was very weak, X-ray emulsion was selected as a sensitive material. The specimen was moulded in

* Present address, Graduate School, Science and Engineering, Nihon University, Surugadai, Chiyoda-ku, Tokyo.

1) V. Engelhardt, "Taschenbuch der Electrochemie", Akademische Verlagsgesellschaft m. b. H., Leipzig (1931), p. 219.

2) W. M. Shafer and C. R. Harr, *J. Electrochem. Soc.*, **105**, 413 (1958).

3) G. A. Moore, *J. of Metals*, **5**, 1443 (1953).

4) S. Oka and T. Mukaibo, *Annual Report of the Engineerig Research Inst., Univ. of Tokyo*, **18**, No. 2, 14, (1960).

5) M. Mukai, *J. Electrochem. Soc. Japan*, (*Denki-Kagaku*) **20**, 215 (1952).

synthetic resin and an X-ray film was contacted on the polished plane which was coated with thin collodion film. Exposure was continued for three months.

Sulfur-35 emits a $\beta$-ray of maximum energy 0.167 MeV. and a gas flow counter was used for the measurements of its radioactivity. The samples were prepared in the form of barium sulfate precipitates and the self-absorption was corrected. The activity of sulfur-35 in the surface layer of the deposited iron was measured directly by the gas flow counter without separating the iron, because the $\beta$-ray of sulfur-35 has the maximum range of about 0.05 mm. in iron.

Silver-110 and zinc-65 emit $\gamma$-rays and were measured by a well type scintillation counter using liquid samples without the elimination of co-existing iron.

## Results

**Phosphate Ion.** — Electrolysis was repeated several times at different concentrations of the carrier in the electrolyte. Results are illustrated in Table I.

Table I. Distribution of phosphorus after electrolysis

| Concentration of phosphate ion* | 0.00 | 0.66 | 3.30 | 4.96 | 6.60 |
|---|---|---|---|---|---|
| Distribution (%) | | | | | |
| Electrolyte | 1.0 | 1.0 | 1.0 | 0.7 | 0.1 |
| Precipitate | 61.9 | 62.0 | 36.8 | 32.4 | 25.8 |
| Deposited iron | 8.0 | 24.3 | 55.3 | 62.2 | 73.1 |
| Recovery | 70.9 | 87.3 | 93.1 | 95.3 | 98.9 |
| Phosphorus in deposited iron** | + | 0.038 | 0.86 | 1.9 | 2.3 |

* Concentration of the carrier added is expressed in P g./l.
** Weight percentage.
\+ Far less than 0.0004. The value was estimated by using the specific activity of carrier concentration, 0.66 g./l.

When the concentration of phosphate ion was higher than 3 g./l. in the electrolyte as phosphorus, more than half of the added phosphate ions were deposited on the cathode. On the contrary, at the concentration lower than 3 g./l. co-precipitation of phosphate ions with iron hydroxide was dominant over the deposition on the cathode. The recovery of phosphorus-32 became difficult with the decrease of the concentration of the carrier.

The concentration of phosphate ion in the electrolyte decreased rapidly at the beginning of electrolysis and almost all of the added phosphate ions were eliminated by the end of electrolysis.

Autoradiography was applied to the vertical section of the deposited metal. Fig. 1a shows a typical pattern of the autoradiograph obtained from the section illustrated in Fig. 1b. The high concentration of phosphorus near the mother plate was observed, even when pits or dendrites were formed. The distribution coincides with the observed decrease of the concentration of phosphate ion in the bath at the beginning of electrolysis.

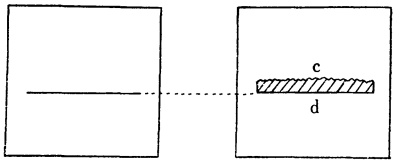



Fig. 1a Fig. 1b

Fig. 1a: Autoradiograph.
Fig. 1b: Section of the specimen.
c: Solution side
d: Mother plate side

By applying the same method of autoradiography on the horizontal plane of the deposited metal, the flat distribution of phosphorus was observed.

**Sulfate Ion.**—The concentration of sulfate ion was about 2 g.-ion/l. in the sulfate bath and sulfur-35 was added to the electrolyte in the form of sulfate ion. The deposited metal from this bath was proved to contain 0.017~0.018 wt. per cent of sulfur by measuring the radioactivity.

Five washing steps were applied to the deposited metal. The effect of washing on the sulfur contents of the surface layer of the metal is illustrated in Fig. 2.

The solution side of the deposited metal had a higher activity than the mother plate side at the beginning of washing. By washing,

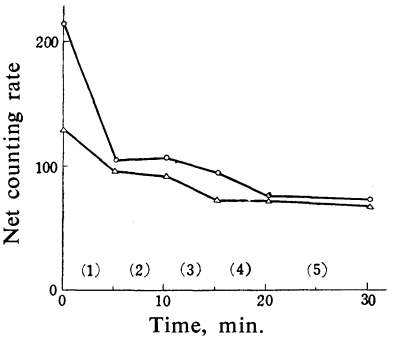



Fig. 2. Effect of washing on sulfur contents.
○ Solution side, △ Mother plate side
Conditions of washing:
(1) Boil in hot water for 5 minutes.
(2) Boil in hot water for 5 minutes.
(3) Immerse in 60°C 0.01 N HCl for 5 minutes.
(4) Immerse in 60°C 0.1 N HCl for 5 minutes.
(5) Boil in hot water for 10 minutes.

the activity of both sides decreased to the same level and the contents of sulfur was reduced from 0.018 to 0.008 wt. per cent.

Autoradiography was tried in vain on the deposited metal. The sulfur seems to have been removed from the surface of the specimen during the wet polishing process.

**Zinc Ion.**—Experiments were carried out at the concentration of added zinc carrier 0.65 and 1.30 mg./l. in the electrolyte. In both cases, nearly 90% of the added zinc-65 ions were deposited on the cathode. A part of the remaining 10% was co-precipitated with iron hydroxide and the rest remained in the electrolyte.

**Silver Plated on Anodes.** — After 48 hours' electrolysis, over 90% of the silver ions that were separated from anodes were precipitated with iron hydroxide and only about 2% were deposited on the cathode. The amount of silver plated on anodes was calculated as 0.47 ppm in iron from the amout of silver separated from anodes by electrolysis. About 0.008 ppm of silver against iron were included in the deposited iron.

**Summary**

Phosphate ions were found to deposit themselves on the cathode like a cation. This phenomenon suggests the formation of a complex ion which has positive charges. The results on sulfur confirms the importance of washing which was pointed out by Schafer and Harr[2] in achieving low values of total sulfur in the deposited metal. Silver was eliminated effectively by electrolysis, but it will be still difficult to remove zinc from iron by electrolysis.

The experiments on radioisotopes were performed in the Radioisotope Laboratory of the University of Tokyo. The authors are indebted to Toho Zinc Co. for financial aid in performing these experiments.

*Department of Applied Chemistry*
*Faculty of Engineering*
*The University of Tokyo*
*Hongo, Tokyo*

# *Synthesis of Several Ketones from Acetaldehyde and Propylene by Gamma-ray Irradiation**)

By Kozo HIROTA and Motoyoshi HATADA

(Received May 2, 1960)

It has been reported[1] mostly in the patent literature that some ketones are synthetized by a chain mechanism from aldehydes and terminal olefins at 60~100°C, using benzoyl peroxide, acetyl peroxide etc. as initiator. The reaction is believed to involve the sequence,

$$RCHO \rightarrow R\dot{C}O + H$$

$$R\dot{C}O + CH_2{=}CHR' \rightarrow RCOCH_2\dot{C}HR'$$

$$RCOCH_2\dot{C}HR' + RCHO \rightarrow RCOCH_2CH_2R' + R\dot{C}O$$

A similar reaction has been initiated photochemically at room temperature. However, the reaction ought to proceed more easily by use of gamma-ray irradiation without any chemical initiator, because of its powerful action of producing free radicals. Such being the situation, it is interesting to investigate the above expectation in the system of acetaldehyde and propylene, because the yield of ketones was low when a chemical initiator was used[2]. It is the purpose of the present paper to report the result actually carried out.

## Experimental

**Materials.**—*Acetaldehyde* was prepared by heating commercial paraaldehyde at 70°C, which had been purified by distillation, with a small amount of concentrated sulfuric acid. The final product was purified by repeating vacuum distillation twice. *Propylene* was prepared by dehydrating the middle fraction of the distillate of commercial isopropyl alcohol on alumina kept at 400°C. Impurities of the samples were found to be within 0.5% with mass-spectrometry and gas-chromatography.

**Procedure.** — All the samples were carefully deaerated by evacuation, then keeping them at

* Preliminary report: the 3rd Isotope Symposium of Japan, R. 31, Tokyo, Sept. 15, 1959.

1) Cf. C. Walling, "Free Radicals in Solution", John Wiley & Sons, New York (1957), p. 273,

2) F. C. Ladd, U. S. Pat., 2,517, 684 (Aug. 8, 1950).

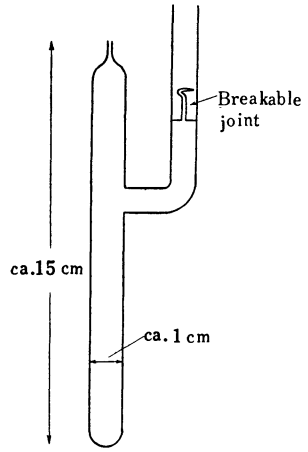



Fig. 1. Irradiation tube.

−190°C, enclosed and irradiated in the glass tube shown in Fig. 1. *Irradiation* was carried out on the samples enclosed in the tube with the Co-60 source (1000 curie) installed at Osaka Laboratory of JARRP. The dose rate was measured with the Fricke dosimeter. After irradiation, products were taken out from the tube by use of a breakable joint and were put to analysis.

**Analysis.**—After the amount of gaseous products was determined with the Saunder-Taylor apparatus, they were analyzed quantitatively by the mass-spectrometric method (apparatus: Hitachi RMU-5). Liquid products were analyzed by the gas-chromatographic method (apparatus: Shimadzu GClA; carrier gas: helium). Final identification of each product was made, however, by resorting to mass-spectrometry and infrared spectrometry on the samples fractionated by the gas-chromatograph except in the case of the higher boiling products, the chemical structure of which was estimated from their retention time.

## Results and Discussion

The gaseous products were hydrogen, methane and carbon monoxide, their $G$ values being small as shown in Table I. From the liquid products, methylpropylketone (MPK), methylhexylketone (MHK), and methylnonylketone (MNK) could be identified by the gas-chromatographic method, using a high vacuum-oil-column (length 2.45 m.) at 180°C. The peak of MPK separated into two parts when the column charged with dioctyl phthalate was used. The peak which was larger in area by several times was found to be normal MPK (M*n*PK), while the other was its isomer, i.e., methylisopropylketone (M*i*PK). It is noteworthy that MPK's, MHK and MNK correspond to the ketones produced by the addition of one, two and three molecules of propylene to an acetaldehyde molecule, respectively.

Table I. Examples of the experiment

Amounts of products are expressed in mol.$\times 10^{-4}$; numbers in parentheses are $G$ values.

| Experiment | 1 | 2 | 3 |
|---|---|---|---|
| Acetaldehyde (mol.) | 0.053 | 0.053 | 0.116 |
| Propylene (mol.) | 0.05 | 0.031 | 0.032 |
| $R$=acetaldehyde/propylene | $1.0_4$ | $1.7_1$ | $3.6_2$ |
| Total dose (r) | $7\times10^7$ | $1\times10^7$ | $2\times10^7$ |
| Dose rate (r/hr.) | $12.2\times10^4$ | $1.9\times10^4$ | $1.4\times10^4$ |
| Products: Hydrogen | 2.24(0.64) | 0.5 (1.4) | — |
| Products: Carbon monoxide | 1.16(0.35) | 0.38(1.0) | — |
| Products: Methane | 0.17(0.05) | 0.11(0.2) | — |
| Products: MPK (M*i*PK) | 6.0 (1.8) | 2.8 (7.0) | 8.7(5.7) |
| Products: MPK (M*n*PK) | 29.0 (9.0) | 2.4 (68) | 128 (83) |
| Products: MHK | 20 (6.0) | 19.5 (60) | 39 (28) |
| Products: MNK | 6.0 (1.8) | 4.3 (1.4) | 5.0(3.3) |

Considering that aldehyde is more sensitive to radiation than propylene and also that irradiation is carried out at room temperature, these ketones may be produced via acetyl radical by the following scheme:

$$CH_3CHO \rightsquigarrow CH_3\dot{C}O$$

$$CH_3\dot{C}O + CH_2{=}CHCH_3 \xrightarrow{k_{p0}} CH_3COCH_2\dot{C}HCH_3$$

$$CH_3COCH_2\dot{C}HCH_3 + CH_3CHO \xrightarrow{k_{p1}} CH_3COCH_2CH_2CH_3 + CH_3\dot{C}O$$

$$CH_3COCH_2\dot{C}HCH_3 + CH_2{=}CHCH_3 \xrightarrow{k_{p1}} CH_3COCH_2\underset{\displaystyle CH_2\dot{C}HCH_3}{\underset{|}{C}}HCH_3$$

$$CH_3COCH_2\underset{\displaystyle CH_2\dot{C}HCH_3}{\underset{|}{C}}HCH_3 + CH_3CHO \xrightarrow{k_{d2}} CH_3COCH_2\underset{\displaystyle CH_2CH_2CH_3}{\underset{|}{C}}HCH_3 + CH_3\dot{C}O$$

$$CH_3COCH_2\underset{\displaystyle CH_2CH_2CH_3}{\underset{|}{C}}HCH_2\dot{C}HCH_3 + CH_2{=}CHCH_3 \xrightarrow{k_{p2}} CH_3COCH_2\underset{\displaystyle CH_3}{\underset{|}{C}}HCH_2\underset{\displaystyle CH_3}{\underset{|}{C}}HCH_2\dot{C}HCH_3$$

The above scheme coincides with the result that the $G$ values of the produced ketones are higher than that of usual radiation-induced reaction. The produced ketones may therefore be expressed generally by $RCO(C_{3n}H_{6n+1})$, thus M*n*PK, MHK and MNK being the ketones, $n$ of which corresponds to 1, 2 and 3, respectively. However, the presence of a

small amount of M*i*PK indicates a process slightly different from the above; i. e. the addition of acetyl radical to $\beta$-carbon of propylene as follows:

$$CH_3\dot{C}O+CH_2=CHCH_3 \longrightarrow$$

$$CH_3CO-\underset{\cdot CH_2}{\overset{H}{C}}-CH_3 \xrightarrow{RCHO} CH_3CO-\underset{CH_3}{\overset{H}{C}}-CH_3$$

According to the mechanism, higher homologues of the ketone ($n=4, 5, 6\cdots\cdots$) must be produced besides, even though in smaller amount. Actually they could not be identified in the residues of vacuum-distillation of the product, but their existence can be estimated by the following reasoning. In Fig. 2, molar fractions $F_n$ of each ketone produced by the ratio $1:n$ are plotted against aldehyde/propylene ($R$) as the abscissa, making the total dose and dose rate constant, i. e., at $2.3\times10^7$ r and $4.7\times10^4$ r/hr. respectively. The full line denotes the theoretical one[3], calculated by the formula,

$$F_n=\frac{C_nR}{\prod_{i=1}^{n}(C_iR+1)} \qquad (3)$$

where $C_n$'s are transfer constants, $k_{dn}/k_{pn}$. When the following values were adopted, in actual calculation, $C_1=0.84$, $C_2=1.64$ and $C_3=6.1$, good coincidence between theoretical and observed data is obtained. Considering this result, even $C_4$ must be so large that homologues of ketone higher than MNK can be neglected practically, even though they are produced. Actually, if $C_4$ is assumed to be 20 and $F_4$ is calculated, it is very small as shown by the dotted line in Fig. 2.

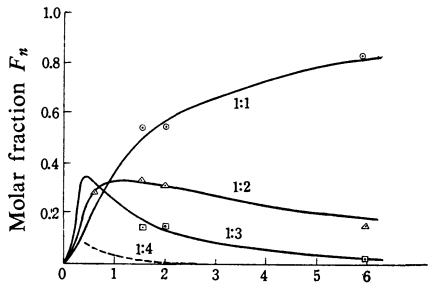



Fig. 2. Molar fraction of produced ketones vs. $R$*.
Dose rate, $4.7\times10^4$ r/hr.
Total dose, $2.3\times10^7$ r.
— Theoretical curves calculated by Eq. 3.

* In Fig. 2~5, $1:n$ means the ketone produced by one mole of aldehyde and $n$ moles of propylene.

3) Cf. p. 245 of Ref. 1.

The terminating processes which follow the above propagating processes in the chain reaction must be ascribed to some recombination processes between radicals, e. g.

$$2CH_3\dot{C}O \longrightarrow (CH_3CO)_2$$

or $$CH_3\dot{C}O+CH_3CO(C_3H_6)_n\dot{C}H_2CHCH_3$$
$$\longrightarrow CH_3CO(C_3H_6)_{n+1}COCH_3$$

Such processes may be reasonable if the fact that the yields of the ketones decrease with increasing dose rate as shown later is taken into account. However the products resulting from the recombination process could not be detected, probably because of their lower yields and of their larger retention time in the gas-chromatogram.

As shown in Fig. 3, where dose rate and total dose were kept constant at $4.7\times10^4$ r/hr. and $2.3\times10^7$ r., respectively, the amount of hydrogen was practically constant, while those of methane and carbon monoxide increased; this tendency is concordant with the expectation that the decomposition products of acetaldehyde increase with $R$.

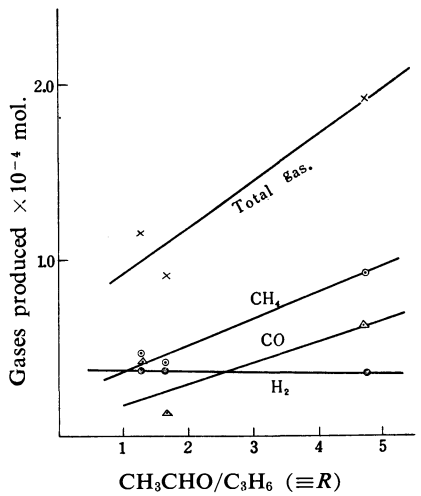



Fig. 3. Gases produced vs. $R$ (molar ratio of acetaldehyde and propylene in the feed).
Total dose, $2.3\times10^7$ r.
Dose rate, $4.7\times10^4$ r/hr.

The effect of total dose on the ketones produced is shown in Fig. 4 where the dose rate and $R$ were kept constant at $15.6\times10^4$ r/hr. and 1.6, respectively. It was found that the amounts of MPK, MHK and MNK increased with the total dose, but not linearly in the cases of MHK and MNK. This result may be explained by the fact the reaction order of propylene was greater than that of aldehyde in the cases of MHK and MNK, considering that the amount of the unreacted

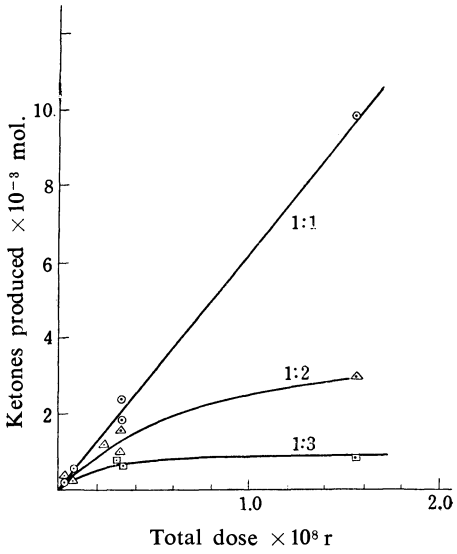



Fig. 4. Ketones produced vs. total dose. $R=1.6$, dose rate, $15.6\times 10^4$ r/hr.

propylene was very small in the case of the highest total dose. The gases produced increased practically linearly against the total dose, but the amounts of hydrogen and methane were the same in the order of magnitude, while the amount of carbon monoxide was much smaller. Of course the order of their magnitude varied according to $R$ as shown in Fig. 3.

In Fig. 5, the logarithm of the amounts of liquid products is plotted against the logarithm of the dose rate where the total dose and $R$ were kept $2.3\times 10^7$ r and 1.6, respectively. As compared with the liquid products, the amounts of the gaseous products were practically not affected by the dose rate, though the amounts of hydrogen and carbon monoxide decreased slightly while that of methane increase. The amounts of ketones decreased markedly against the dose rate, but a linear relation does not exist in Fig. 5. Such a result ought not to be obtained if the bimolecular termination of $CH_3\dot{C}O$ be realized as was done in the above reaction sceeme. However, since the data are still insufficient to derive any conclusion in regard to the mechanism, i. e., the number of measurements was small, and concentration of propylene was not constant during the reaction in some of the measurements, a definite conclusion on the effect of dose rate will be postponed to later research.

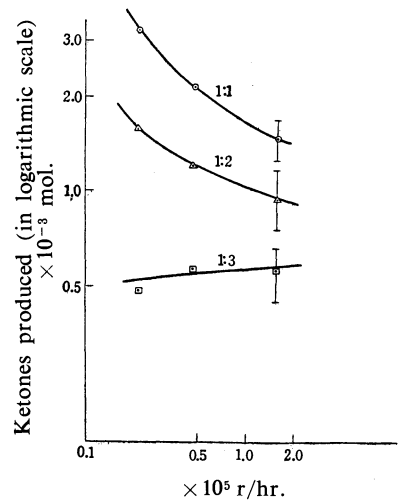



Fig. 5. The amounts of ketones produced vs. irradiation dose rate. $R=1.6$, total dose $2.3\times 10^7$ r.

Finally we will see what can be said about this reaction if it is considered as a synthetic method. First, it is favorable for this method that the total yield of the produced ketones was larger than that of the method by which some chemical initiator is used. For instance in No. 3 in Table I, conversion of propylene into MPK, MHK and MNK amounted to 72%, the sum of their $G$ values being 120. Second, $G$ values will be increased markedly, if the temperature of the system is raised as much as possible. This expectation has been confirmed to some degree in the system of acetaldehyde and isobutylene[4]. However, it is interesting hereafter to determine the upper limit of the reaction temperature, considering that acetyl radical inclines to decompose into $CH_3$ and CO according to the degree of the temperature.

## Summary

It has been found that methylpropylketone and other higher ketones are synthetized with relatively high $G$ values by gamma-ray irradiation on mixtures of acetadehyde and propylene at room temperature, and that the reaction proceeds by a chain mechanism, with acetyl radical produced thereby as the initiator.

We express sincere thanks to Mr. S. Iizuka for his kind advice and also to Mr. J. Takezaki for his assistance in mass-spectrometry.

*Osaka Laboratory*
*Japanese Association for Radiation Research on Polymers*
*Mii, Neyagawa City*
*Osaka (K. H. and M. H.)*

*Department of Chemistry*
*Faculty of Science*
*Osaka University*
*Nakanoshima, Kita-ku*
*Osaka (K. H.)*

4) K. Hirota, S. Iizuka and M. Hatada, *Abstracts of the 13th Annual Meeting of Chemical Society of Japan*, 49 (1960).

# *Spectrophotometric Determination of Traces of Boron in Thorium**

By Hiroshi ONISHI, Nasumi ISHIWATARI and Hitoshi NAGAI

(Received May 24, 1960)

Although a few reports[1,2] have been published of the chemical determination of boron in thorium metal, no paper seems to be available pertaining to its determination in thorium oxide. This is probably due to the fact that it is very difficult to dissolve the oxide. Nitric acid or hydrochloric acid in the presence of a small amount of fluoride dissolves the oxide. However, this method of solution will not be directly applicable to the photometric determination of boron because of the interference of fluoride.

The authors have found that strong phosphoric acid[3] dissolves both thorium oxide and metal relatively easily. On the basis of this finding, a method has been developed for the determination of as little as a few tenths of a part per million of boron in thorium oxide or metal. After the dissolution of the sample, boron is separated as methyl borate, and finally determined by the curcumin method[4].

## Experimental

**Apparatus.** — The quartz distilling apparatus and the spectrophotometer were the same as those described before[4].

**Reagents.**—*Strong Phosphoric Acid.*—Prepare from 85% orthophosphoric acid according to the direction of Kiba[3]. The orthophosphoric acid should preferably contain less than 0.05 ppm of B. When such an acid is not obtainable, purify it as follows. Transfer 150 ml. of 85% phosphoric acid, 30 ml. of water (redistilled), and 500 ml. of redistilled methanol to a one-liter quartz distilling flask. Connect the condenser, and heat the flask in a water bath, and continue distillation until no more liquid comes out. Add 150 ml. of water and distil again. Transfer the residue to a 500 ml. quartz beaker, and heat at 150~200°C for several hours. Cool, add 150 ml. of water, and repeat heating as above. Add 100 ml. of water and heat at 200~250°C until boiling ceases. Finally add 100 ml. of water and heat at 200~280°C until boiling ceases. Cool, and prepare the strong phosphoric acid in a suitable apparatus by heating the purified acid to 300°C.

Other solutions used were the same as those described previously[4].

**Procedure.**—Transfer 1.00 g. of thorium oxide or thorium metal sample to the distilling flask and add 5.0 ml. of the strong phosphoric acid using a syringe. Heat the flask on a sand bath at 200~250°C and shake the contents occasionally to hasten the solution of the sample. Stop heating when a clear sample solution has been obtained.

To the cold solution add 3 ml. of water (redistilled) and mix. Connect the flask with the condenser through the adapter, and immerse the flask in a one-liter beaker containing water (this serves as a water bath). Place a 100 ml. platinum dish containing 7.0 ml. of 0.1 N calcium hydroxide suspension and 10 ml. of water under the condenser. Add 20 ml. of methanol (redistilled) and mix the solution with a polyethylene rod and wash the rod with 10 ml. of methanol. Connect the tap funnel, and raise the temperature of the bath slowly to boiling point. Continue heating until no more liquid comes out. (This distillation will take 15~20 min.)

Remove the burner and replace the hot water by cold water. Add 20 ml. of methanol through the tap funnel and distil again. (This second distillation will take 10~15 min.) Lower the dish and wash down the stem of the condenser with water. Mix the distillate and washings and confirm the fact that the solution is alkaline. Evaporate the solution gently to dryness on a water bath.

To the residue add 2 ml. of water and 4.0 ml. of curcumin-oxalic acid solution (0.40 g. of curcumin and 50 g. of oxalic acid in one liter of ethanol). Then continue according to the directions previously described[4]. When the amount of boron is found by referring to the standard curve that has been prepared by omitting the separation step, a correction of +15 per cent is advisable.

*Note.* — Instead of the distilling flask, a quartz dish may be used for the dissolution of the sample. In this case, the process of solution is accelerated by stirring with a quartz rod. The clear sample solution should be transferred to the distilling flask while the solution is hot.

## Results and Discussion

As pointed out by Rodden[5], thorium oxides that have been highly ignited are very difficult to dissolve. In the present work, thorium oxides that had been prepared by heating

* Presented at the 13th Annual Meeting of the Chemical Society of Japan, Tokyo, April 1960.

1) J. P. Burelbach and R. J. March, ANL-5240 (1953).

2) A. R. Eberle and M. W. Lerner, *Anal. Chem.*, 32, 146 (1960).

3) T. Kiba, *Chemistry and Chem. Ind.* (*Kagaku to Kogyo*), 11, 730 (1958).

4) H. Onishi, N. Ishiwatari and H. Nagai, This Bulletin, 33, 830 (1960).

5) C. J. Rodden, *Proceedings Internatl. Conf. Peaceful Uses Atomic Energy*, 8, 197 (1956).

thorium nitrate to 500 and 700°C were dissolved in strong phosphoric acid within 1 and 2 hr., respectively (quartz dish). When the distilling flask is used, a longer time is required.

The effects of phosphoric acid and thorium on the determination of boron are shown in Table I. Seven milliliters of 0.1 N calcium hydroxide suspension and the foreign substance, with or without 1 μg. of boron, were evaporated to dryness and then subjected to color development. The addition of 0.18 meq. of phosphoric acid resulted in about a 40 per cent decrease in absorbance. However, as shown below, no significant quantity of phosphoric acid comes out during methanol distillation.

Table I. Effect of phosphoric acid and thorium on the determination of boron*

| Addition | Absorbance | | |
|---|---|---|---|
| | Blank | 1.0 μg. B | Difference |
| — | 0.060 | 0.370 | 0.310 |
| 0.30 ml. 0.18 N $H_3PO_4$ | 0.060 | 0.340 | 0.280 |
| 0.50 ml. 0.18 N $H_3PO_4$ | 0.061 | 0.314 | 0.253 |
| 1.0 ml. 0.18 N $H_3PO_4$ | 0.050 | 0.246 | 0.196 |
| 0.56 mg. Th (as $ThCl_4$) | 0.056 | 0.357 | 0.301 |
| 1.1 mg. Th (as $ThCl_4$) | 0.055 | 0.325 | 0.270 |

* In the presence of 0.7 meq. of $Ca(OH)_2$.

Table II. Effect of water on the distillation of boron

In each case 5.0 ml. of strong phosphoric acid was used.

| Water added, ml. | Recovery of 1 μg. B, %* |
|---|---|
| 1.0 | 79 |
| 2.0 | 78 |
| 3.0 | 89 |
| 4.0 | 81 |
| 5.0 | 92 |
| 6.0 | 72 |

* Average of duplicate experiments.

Table II shows the effect of water on the distillation of boron. When water was not added to 5.0 ml. of strong phosphoric acid, methanol distillation was not successful. This was probably due to the formation of methyl phosphate. In the table recoveries were calculated by referring to the standard curve obtained without distillation of boron. In the subsequent work, 3.0 ml. of water was adopted.

Table III summarizes the results of methanol distillation of boron in the absence of thorium. The distillation was made according to the proposed procedure. The reagent blank against the blank of direct color development was about 0.2 μg. of boron. The average recovery

Table III. Distillation of boron from phosphoric acid solution

5.0 ml. of strong phosphoric acid solution was heated at 200~250°C for 2 hr. After cooling 3 ml. of water was added and MeOH distillation followed.

| B taken, μg. | B found, μg. | Average recovery, % |
|---|---|---|
| 0.20 | 0.17, 0.17 | 85 |
| 0.50 | 0.46, 0.45, 0.47, 0.39 | 88 |
| 1.00 | 0.88, 0.81, 0.90 0.79, 0.90, 0.88 | 86 |

Table IV. Determination of boron in thorium oxide

| B added, ppm | B found, ppm* |
|---|---|
| 0.20 | 0.22, 0.18 |
| 0.50 | 0.46, 0.45 |
| 1.00 | 0.86, 0.92 |

* Includes the original B content of thorium oxide (<0.05 ppm B).

Table V. Determination of boron in standard thorium oxides and thorium metal

| Sample | Boron, ppm | |
|---|---|---|
| | NBL | Proposed method |
| NBL-26-6, $ThO_2$ | 2 | 1.8, 1.9 |
| NBL-26-5, $ThO_2$ | 3 | 2.9, 2.7 |
| NBL-26-3, $ThO_2$* | 4.4 | 4.7, 4.4 |
| NBL analyzed sample No. 19 Th** | about 1 | 0.58, 0.46, 0.46, 0.43 |

* Other certified values, based on metal (in ppm): 100 each Al, Fe, Mo, P, Si, V, Zn, 35 Be, 10 each Bi, Co, Cu, Mg, Mn, Ni, Pb, Sn, 1 each Ag and Cd.

** Other certified values (in ppm): about 20 Al, about 150 Be, <10 Ca, <5 Cu, 140 Fe, <10 Mg, about 2 Mn, about 10 Ni, about 4 Pb, about 20 Si, about 2 U, 60 N, 230 C.

of 0.2 to 1 μg. of boron is calculated to be 86%. The standard deviation for 1 μg. of boron is 5.6%. The recovery of 86% is comparable to that of the methanol distillation from a sulfuric acid medium[4].

Known amounts of boron were added to thorium oxide (1 g., Société de Produits Chimique des Terres Rares, France) and the boron was determined by the proposed procedure except that +15% were not applied (Table IV). A recovery of about 86% is indicated after correcting for the original boron content of the sample.

The standard samples of thorium oxide and thorium metal, issued by the New Brunswick Laboratory (NBL), were analyzed by the proposed method, and the results are shown in Table V. It is seen that the NBL values for

thorium oxide samples agree quite well with the values obtained by applying the proposed method. Because the NBL value for the thorium metal is very approximate, it is not possible to check the accuracy of the proposed method directly. Duplicate analyses of the thorium metal that was converted into oxide by heating to 600°C for several hours gave 0.67 and 0.59 ppm B (average 0.63 ppm). Since this average agrees within an experimental error with the average of 0.48 ppm (Table V), it is not likely that insoluble boron remains after dissolution of thorium metal in strong phosphoric acid. Furthermore, the average value of 0.48 ppm B agrees reasonably well with the value of 0.35 ppm which was obtained by the spectrochemical determination employing the carrier distillation technique[6]. Consequently, it is considered that the proposed method is successfully applicable to thorium metal. As curcumin can not be used in the method described by Eberle and Lerner[2], the proposed method seems to be more practicable.

6) T. Nakazima and H. Fukushima, *Japan Analyst (Bunseki Kagaku)*, **9**, 830 (1960).

**Summary**

Procedure is described for the spectrophotometric determination of a few tenths of a part per million of boron in thorium oxide or metal. The sample was brought into solution with strong phosphoric acid. After diluting the solution with water, boron was separated by distillation as methyl borate, and finally determined by the curcumin method. The error is not likely to exceed ±0.1 ppm for 0.2~1 ppm of boron.

The authors are indebted to Mr. T. Nakazima and Mr. H. Fukushima of this institute for spectrographic analysis of thorium metal.

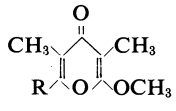
*Japan Atomic Energy Research Institute*
*Tokai, Ibaraki-ken*

# *Correlation of Reaction Rates and Product Stabilities. I. The Methylation of Pyrononeswith Diazomethane*[1-3]

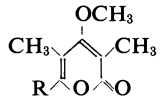
By Hisao NAKATA

(Received February 22, 1960)

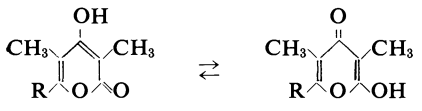
The skeletal structures of aureothin and isoaureothin have recently been established as I and II, respectively[1]. The relative stabilities of these two compounds are so different that aureothin isomerizes readily to the more stable isoaureothin derivatives especially under acidic conditions[4]. The isomerization reaction has so far been considered to be an irreversible process involving a certain drastic structural change since the reverse isomerization reaction has not been observed during the course of the structural elucidation studies.



(I) Aureothin

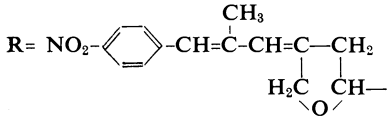


(II) Isoaureothin



(IIIα) (IIIγ)

Desmethylisoaureothin



However, as was shown in the previous paper[1], the constitutional difference between I and II is only in their pyrone rings, and therefore, two tautomeric structures of IIIα and IIIγ are possible for the demethylated product, desmethylisoaureothin. In order to confirm rigorously the structural correlation between

1) Structure of Aureothin. VIII. Part VII of this series K. Yamada, H. Nakata and Y. Hirata, *J. Chem. Soc. Japan, Pure Chem. Sec.* (*Nippon Kagaku Zasshi*), **81**, 340 (1960).

2) Presented at the 12th Annual Meeting of the Chemical Society of Japan, Kyoto, April, 1959.

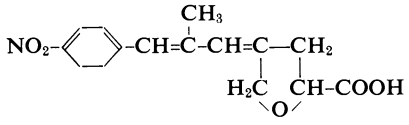
3) A preliminary communication of this work has appeared. See, H. Nakata, S. Takahashi, K. Yamada and Y. Hirata, *Tetrahedron Letters*, No. 16, 9 (1959).

4) Y. Hirata, K. Okuhara, H. Nakata, T. Naito and K. Iwadare, *J. Chem. Soc. Japan, Pure Chem. Sec.* (*Nippon Kagaku Zasshi*), **78**, 1700 (1957).

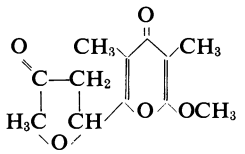
aureothin and isoaureothin, it was felt to be desirable to perform the reverse isomerization reaction.

In the present investigation, desmethylisoaureothin (III$\alpha$) is methylated with diazomethane under the special condition derived from the theory of Arndt's kinetically interplayed methylation reaction. Satisfactory results are obtained.

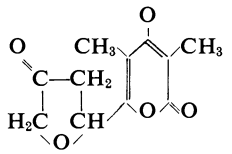
**Tautomerism of Pyronone Derivatives.** — Although previous studies[5] suggest the structure of desmethylisoaureothin as III$\alpha$ having an $\alpha$-pyrone ring, a more definite evidence[1] is now available. Subtraction of the ultraviolet absorption curve of aureothinic acid (IV)[6] from the curve of desmethyl isoaureothin affords the spectrum of the residual pyrone



(IV) Aureothinic acid



(V) Aureonone



(VI) Isoaureonone

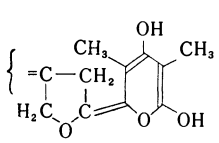
fragment. The resultant spectrum does not agree with the spectrum of aureonone (V)[1] but is well superimposable on the spectrum of isoaureonone (VI)[1]. This indicates, that the tautomeric form of the $\alpha$-pyrone structure III$\alpha$ predominates desmethylisoaureothin even in solution. Data of infrared spectra of those compounds[1] also support the conclusion. Therefore, the theoretically conceivable equilibrium III$\alpha$ $\rightleftarrows$ III$\gamma$ lies almost at the III$\alpha$ side[7] and III$\gamma$ is thermodynamically less stable than III$\alpha$. The same is true for their methylated products, aureothin and isoaureothin; the former is less stable than the latter[4]. It was reported also in other pyronone derivatives that the $\gamma$-pyrone isomer is usually less stable and in solution the $\alpha$-pyrone alternative predominates[9-13].

**Theory of Kinetically Interplayed Methylation.** — When a proton transfers from tautomeric acids to bases, it has been observed[14,15] that the proton is lost most quickly from a least stable tautomer. This proton mobility is characterized as the *dynamic acidity*[16,17] and should be differentiated from the so-called acidity in the equilibrium state (*static acidity* in the strict sense)[18,19]. The dynamic acidity correlates with the activation energy of the proton transfer process and the static acidity correlates with the free energy difference between the acid and its conjugated base[20]. The reactivity of a given acid depends on the dynamic acidity of the acid particularly in the reaction, where the proton plays a dominant role; thus, it may be concluded that the reactivity of the acid towards diazomethane is proportional to its dynamic acidity[17,18,23-28]. The less stable isomeric acid has a larger dynamic acidity and is methylated with diazomethane more quickly than the stable isomer,

5) T. Naito, Y. Hirata, K. Okuhara and K. Iwadare, ibid., 374 (1958).

6) Y. Hirata, H. Nakata and K. Yamada, ibid., **79**, 390 (1958).

7) Recently, Yamazaki[8] has ascertained the percentage of enol of desmethylisoaureothin in various solvents. Although she reported the values 46.0 and 41.5% in ethanol and 25.0 and 22.2% in chloroform, no indications of such a result are observed from the infrared spectra[1] of desmethylisoaureothin, and our present conclusion that desmethylisoaureothin exists largely as III$\alpha$ (one of the enol forms) also does not agree with her. Moreover, the reported values in formic acid and in methanol are over 100%, the reason of which attributed to the presence of the dienol form of desmethylisoaureothin. However, it is unlikely to consider any dienol form of this compound. If we were forced to assume the following dienol structure, this would contradict with our previous observation[4] that desmethylisoaureothin is optically active and has a definite sign of rotation in solution.



8) F. Yamazaki, ibid., **79**, 1204 (1958).

9) I. Chmielewska and J. Cieslak, *Przemysl. Chem.*, **8**, 196 (1952).

10) R. H. Wiley and C. H. Jarboe, *J. Am. Chem. Soc.*, **78**, 624 (1956).

11) J. Cieslak, *Roczniki Chem.*, **32**, 837 (1958).

12) I. Chmielewaka, J. Cieslak, K. Gorczynska, B. Kontnik and K. Pitakowska, *Tetrahedron*, **4**, 36 (1958).

13) D. Herbst, W. B. Mors, O. R. Gottlieb and C. Djerassi, *J. Am. Chem. Soc.*, **81**, 2427 (1959).

14) A. G. Catchpole, E. D. Hughes and C. K. Ingold, *J. Chem. Soc.*, **1948**, 11.

15) C. K. Ingold, "Structure and Mechanism in Organic Chemistry", Cornell University Press, New York (1953), p. 565.

16) F. Arndt, in J. Mitchell, Jr., I. M. Kolthoff, E. S. Proskauer and A. Weissberger ed., "Organic Analysis", Vol. I, Interscience Publishers Inc., New York (1953), p. 197.

17) W. Hückel, "Theoretische Grundlagen der Organischen Chemie", Vol. I. 8th Ed., Akademische Verlagsgesellschaft, Leipzig (1956), p. 306.

18) C. Gustafsson, *Suomen Kemistilehti*, **18B**, 11 (1945).

19) F. Arndt, "Statische und Dynamische Acidität", Vol. VIII, Abhandlungen der Braunschweigischen Wissenschaftlichen Gesellschaft (1956), p. 1.

20) Parallelisms between dynamic acidity and static acidity have frequently been observed. See Refs. 15, 21, 22 and 33.

21) J. E. Leffler, "The Reactive Intermediates of Organic Chemistry", Interscience Publishers Inc., New York (1956), p. 187.

22) R. W. Taft, Jr., *J. Am. Chem. Soc.*, **79**, 5075 (1957).

23) B. Eistert, "Tautomerie und Mesomerie", Ferdinand Enke, Stuttgart (1938), p. 43.

24) J. D. Roberts, W. Watanabe and R. E. McMahon, *J. Am. Chem. Soc.*, **73**, 760 (1951).

25) J. D. Roberts and J. A. Yancey, ibid., **73**, 1011 (1951).

26) C. K. Hancock and J. S. Westmoreland, ibid., **80**, 545 (1958).

27) J. Hine and W. C. Bailey, Jr., ibid., **81**, 2075 (1959).

28) Ref. 16, p. 202.

though the equilibrium concentration of the former is less than that of the latter in the solution.

Since the methylation reaction with diazomethane produces an exceedingly stable nitrogen molecule, the process undoubtedly does not have high energy requirements and, indeed, may even be somewhat exothermic[29-31]. The activation energy is correspondingly rather small and the transition state of the methylation reaction would resemble the starting material closely[32,33] in topology[34] and in geometry[34].

When two tautometric acids, A-OH and G-OH, are methylated with diazomethane, the reaction may proceed according to the following mechanistic scheme[16,37] where $A\text{-}OCH_3$ is produced only from A-OH and $G\text{-}OCH_3$ only from G-OH. Because of the resemblance of the transition state to the starting materials it

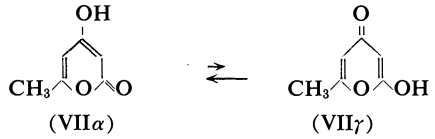
$$\begin{array}{ccc} CH_2N_2 + A\text{-}OH & \underset{k_-}{\overset{k_+}{\rightleftarrows}} & G\text{-}OH + CH_2N_2 \\ \downarrow k_a & & \downarrow k_g \\ A\text{-}OCH_3 & & G\text{-}OCH_3 \end{array}$$

seems unlikely to consider any other reaction processes of indirect methylation involving the rearrangement of the reaction centre.

Arndt[16,19,38] has discussed in detail the kinetic interplay between methylation reactions (velocities $k_a$ and $k_g$) and prototropic rearrangement reactions (velocities $k_+$ and $k_-$), and drawn the following conclusions. If the concentrated diazomethane solution is added to the tautomeric mixture of A-OH and G-OH, the product proportions $G\text{-}OCH_3/A\text{-}OCH_3$ are not very different from the ratio of G-OH/A-OH, which is the ratio of the initial equilibrium concentrations of the respective acids. On the other hand, if the concentration of diazomethane is maintained at a low level, the ratio of $G\text{-}OCH_3/A\text{-}OCH_3$ will be larger than G-OH/A-OH, provided that G-OH has a larger dynamic acidity than A-OH.

Consequently, it may be expected that the product proportions of the two isomeric methyl ethers depend on the time required for the addition of the diazomethane solution, the more gradually the addition of the diazomethane solution, the more will increase the proportions of the methylated product of the less stable isomeric acid having the larger dynamic acidity.

**Diazomethane Methylation of Pyronone Derivatives.** — Although literatures contain several references to the diazomethane methylation of 2,4-pyronone derivatives such as 6-methyl-2,4-pyronone (triacetic lactone) (VII), the results obtained have been the subject of considerable controversy[9,10,39-41].



(VII$\alpha$) (VII$\gamma$)

6-Methyl-2,4-pyronone (triacetic lactone)



(VIII$\alpha$) 6-Methyl-4-methoxy-$\alpha$-pyrone

(VIII$\gamma$) 6M-ethyl-2-methoxy-$\gamma$-pyrone

Recently, there appeared an extensive study[13] of this methylation reaction and it was concluded that the products were usually mixtures of two possible isomers, the actual proportions depending on the nature of other substituents[42]. Several results in other 2,4-pyronone derivatives were also reported[11,12,43-47]. However,

29) D. J. Cram and J. Allinger, *J. Am. Chem. Soc.*, **79**, 2866 (1957).
30) A. Streitwieser, Jr., and W. D. Schaeffer, ibid., **79**, 2888 (1957).
31) A. Streitwieser, Jr. *J. Org. Chem.*, **22**, 861 (1957).
32) J. E. Leffler, *Science*, **117**, 340 (1953).
33) G. S. Hammond, *J. Am. Chem. Soc.*, **77**, 334 (1955).
34) It seems reasonable to distinguish the terms *topology* and *geometry* of the transition state from the term *structure* of reactants or of products, as seen in Refs. 32, 35 and 36. Although the transition state lies somewhere between the reactants and the products, it may not have any definite structure in the ordinary sense, since the arrangement of atoms of the reacting molecules varies with the time in passing over the transition state. The *topology* represents the linkage of atoms of the reacting molecules in the transition state, and may correspond to the *constitution* of the molecule in the static state. The *geometry* represents the spacial orientations of atoms of the reacting molecules in the transition state, and may correspond to the *configuration* and the *conformation* of the molecule in the static state.
35) J. E. Leffler and E. Grunwald, in S. L. Friess and A. Weissberger ed., "Technique of Organic Chemistry", Vol. VIII (Investigation of Rates and Mechanisms of Reactions), Interscience Publishers Inc., New York (1953), pp. 326, 329.
36) Ref. 21, p. 116.
37) R. Huisgen, *Angew. Chem.*, **67**, 445 (1955).
38) F. Arndt, ibid., **61**, 397 (1949).
39) F. Arndt and B. Eistert, *Ber.*, **68**, 1572 (1935).
40) F. Arndt and S. Avan, ibid., **84**, 343 (1951).
41) S. Janiszewska-Drabarek, *Roczniki Chem.*, **27**, 456 (1953).
42) Chmielewska and co-workers observed, that two series of isomeric methyl ethers were obtained on the methylation of 3-substituted 4-hydroxycoumarins with diazomethane and that product proportions were distinctly affected by the type of substituent in position 3. The author is indebted to Professor I. Chmielewska of Warsaw University for her kind information of this result (private communication to K. Yamada of this Institute). See, J. Cieslak, S. Lewak and I. Chmielewska, *Roczniki Chem.*, **33**, 349 (1959).
43) W. Borsche and C. K. Bodenstein, *Ber.*, **62**, 2515 (1929).
44) I. Chmielewska and J. Cieslak, *Roczniki Chem.*, **28**, 38 (1954).
45) R. B. Woodward and G. Small, Jr., *J. Am. Chem. Soc.*, **72**, 1297 (1950).
46) H. Stetter and C. W. Schellhammer, *Ann.*, **605**, 58 (1957).
47) E. Ziegler and E. Nolken, *Monatsh.*, **89**, 391 (1958).

as far as the author is aware, little attention has been paid to investigate the relation between the product proportions and the reaction condition employed[48]. Thus, the diazomethane methylation of 6-methyl-2, 4-pyronone (VII) was first examined.

## Results and Discussion

The methylation was carried out by addition of ethereal solution of diazomethane[49] to a suspension of VII in dry ether, and the two isomeric methyl ethers, VIII$\alpha$ and VIII$\gamma$, were separated by the technique of Polish workers[9,50]. Product proportions are calculated as the percentage of the total weight of the methylated products isolated. The results are summarized in Table I.

Table I. Product proportions of diazomethane methylation

| The time required for the addition of the diazomethane solution | Average product proportions | |
|---|---|---|
| i) 6-Methyl-2,4-pyronone (VII) : | VIII$\gamma$ % | VIII$\alpha$ % |
| Very rapidly | 0 | 100 |
| 4 hr. | 26 | 74 |
| 8 hr. | 31 | 69 |
| 18 hr. | 33 | 67 |
| ii) Desmethylisoaureothin (III) : | I, % | II, % |
| Very rapidly | 0 | 100 |
| 2~4 hr. | 0 | 100 |
| 18 hr. | 2 | 98 |

On the basis of these data, it should be emphasized that the more gradually the addition of the diazomethane solution, the more will increase the proportions of the $\gamma$-pyrone methyl ether, VIII$\gamma$.

6-Methyl-2, 4-pyronone (VII) would exist in solution as a tautomeric mixture of VII$\alpha$ and VII$\gamma$. Spectral data[9,10] suggest, that in either solution the tautomeric form of an $\alpha$-pyrone structure (VII$\alpha$) predominates. This means VII$\gamma$ is thermodynamically less stable, and has a larger dynamic acidity, than VII$\alpha$. The observed results presented in Table I are therefore in good agreement with the theoretical prediction that the gradual addition of diazomethane will give rise to the increase of percentages of the less stable isomeric methyl ether in the over-all product.

The same is true in the case of methylation of desmethylisoaureothin (III). As is shown in Table I, aureothin (I) was obtained only when the diazomethane solution was added very gradually. Accordingly, the reverse isomerization reaction was also solved satisfactorily.

From these data the structural correlation of aureothin (I) and isoaureothin (II) was confirmed. It is also indicated that the desmethyl derivative of aureothin does exist in solution as a tautomeric mixture of III$\alpha$ and III$\gamma$[51]. Desmethylaureothin (III$\gamma$) has not been known so far, since its concentration in solution is presumably very small as compared with that of the stable isomer, desmethylisoaureothin (III$\alpha$).

Moreover, the present results support the conclusion[1] that desmethylisoaureothin has the structure III$\alpha$ also in the solid state, since the methylation reaction was carried out for the ether suspension of desmethylisoaureothin[52].

The skeletal structure of aureothin (I) thus being established rigorously, emphasis must be given for the structural peculiarity of this compound. Aureothin has a nitro group which is as yet a rather rare function in natural products. Only few other examples were known, including chloramphenicol[60], hiptagenic acid[61], azomycin[62], and aristolochic acid[63]. Among

48) Herbst et al.[13] reported the product ratio, VIII$\alpha$: VIII$\gamma$ as 64 : 19, which did not agree with the ratio 72 : 20 of Janiszewaka-Drabarek[41]. They also noticed that different proportions were observed under the condition described by Wiley and Jarboe[10] but no explanation of this result was given.

49) F. Arndt, "Organic Syntheses", Coll. Vol. II, John Wiley and Sons Inc., New York (1943), p. 165.

50) I. Chmielewska, J. Cieslak and T. Kraczkiewicz, *Roczniki Chem.*, **30**, 1009 (1956).

51) If III$\gamma$ does not exist in solution, aureothin (I) will not be obtained and the sole product, independently of the reaction condition, will be II, since I is considered to be produced only through III$\gamma$ in the above mechanistic scheme.

52) It seems reasonable to assume that the equilibrium A—OH$\rightleftarrows$G—OH is not held in the solid state. If the crystal consists from the less stable G—OH, the tautomer is first formed when the crystal is dissolved into solution must be G—OH. The next step of the reaction will be either the methylation of this newly formed G—OH to G—$OCH_3$ or its rearrangement to the more stable A—OH. Since G—OH is methylated more rapidly than A—OH, when the methylation takes place immediately by the addition of the concentrated diazomethane solution, the methylation reaction should occur preferentially and the rearrangement reaction will lag behind, so that diazomethane will have little chance to react with A—OH. In this case, therefore, the percentage of the less stable methyl ether, G—$OCH_3$, will increase in the over-all product, when the concentrated diazomethane solution is added rapidly. This is quite contrary to the observed tendency. The method used in Ref. 53 may generally be utilized to show which possible tautomeric structure is represented by the crystals. Several applications have recently been reported. See Refs. 54—59.

53) Ref. 16, p. 217 and 239.

54) F. Arndt, L. Ergener and O. Kutlu, *Chem. & Ind.*, 1950, 565.

55) L. Ergener, *Rev. faculte sci. univ. Istanbul*, **A15**, 96, 103 (1950).

56) F. Arndt, L. Loewe, R. Ün and E. Ayca, *Ber.*, **84**, 319 (1951).

57) F. Arndt, L. Loewe and E. Ayca, ibid., **84**, 329 (1951).

58) F. Arndt, L. Ergener and L. Kutlu, *Chem. Ber.*, **86**, 951, 957 (1953).

59) Ref. 17, pp. 290, 291 and 294.

60) M. C. Rebstock, H. M. Crooks, Jr., J. Contoulis and Q. R. Bartz, *J. Am. Chem. Soc.*, **71**, 2458 (1949).

61) C. L. Carter and W. J. McChesney, *Nature*, **164**, 575 (1949).

62) S. Nakamura, *Pharm. Bull.*, **3**, 379 (1955).

them, aureothin is the third nitro compound obtained from nature[64]. Moreover, aureothin has the substituted 2-methoxy-$\gamma$-pyrone structure. All other methylated 2,4-pyrononones which have so far been encountered in nature are 4-methoxy-$\alpha$-pyrones, such as yangonin[11,12,43,44], anibine[65], 4-methoxyparacotoin[65,66] and 5,6-dehydrokavain[66].

## Experimental

**6-Methyl-2,4-pyronone (VII).** — 6-Methyl-2,4-pyronone was prepared from dehydroacetic acid[67].

**Methylation of 6-Methyl-2,4-pyronone.** — About 100 ml. of a dilute ethereal solution of diazomethane prepared[49] from 10 g. of nitrosomethylurea was added, with vigorous stirring, to a suspension of 1 g. of 6-methyl-2,4-pyronone (VII) in dry ether over various periods. All traces of atmospheric moisture were excluded and the temperature of the reaction mixture was maintained at 10~15°C during the addition of the diazomethane solution. After all the diazomethane had been added, stirring was continued for about one hour. All solids gradually dissolved, and finally a light yellow solution was obtained. The resulting mixture was evaporated to dryness in vacuo. The solid was then extracted with seven 50 ml. portions of petroleum ether (b. p. 30~60°C). A small amount of a dark sticky solid remained. The combined extracts were filtered to remove any insoluble impurities and were again evaporated to dryness in vacuo. The crystals thus obtained were dried in a vacuum desiccator over calcium chloride. The procedure for the separation of the two isomeric methyl ethers was the same as that described by Chmielewska et al.[9,50]. The above crystals were dissolved in 50 ml. of anhydrous ether and the solution was cooled below 0°C and was treated with dry hydrogen chloride. The insoluble hydrochloride of VIII$\gamma$ separated immediately and was filtered and dried. The isomeric VIII$\alpha$ remained in solution and was obtained after evaporation of the solvent. The crude 6-methyl-4-methoxy-$\alpha$-pyrone (VIII$\alpha$) exhibited m. p. 84~88°C. Recrystallization from petroleum ether gave pure material, m. p. 87~88°C. The hydrochloride of VIII$\gamma$ was suspended in anhydrous ether, and about 0.5 ml. of diethylamine was added and the mixture was set aside overnight. Insoluble diethylamine hydrochloride was then filtered and the evaporation of the solvent gave free 6-methyl-2-methoxy-$\gamma$-pyrone (VIII$\gamma$), m. p. 88~93°C. After recrystallization from petroleum ether it melted at 94~95°C.

The product proportions shown in Table I are calculated as the percentage of the total weight of the methylated products isolated, data of which are listed in Table II.

TABLE II. PRODUCT YIELDS OF DIAZOMETHANE METHYLATION OF 6-METHYL-2,4-PYRONONE (VII)

| The time required for the addition of the diazomethane solution | Solvent | Product yields mg. | |
|---|---|---|---|
| | | VIII$\gamma$ | VIII$\alpha$ |
| Very rapidly | Ether | 0 | 600 |
| 4 hr. | Ether | 180 | 550 |
| 8 hr. | Ether | 190 | 430 |
| 18 hr. | Ether | 250 | 500 |
| Very rapidly | Acetone | 0 | 400 |
| 4 hr. | Acetone | 120 | 330 |

Table II includes some additional data of the methylation in acetone solvent. The results are essentially the same with those in ether except for the recovery of about 300 mg. of the unchanged starting material (VII).

**Methylation of Desmethylisoaureothin (III).** — To a suspension of 870 mg. of desmethylisoaureothin (III) in 30 ml. of dry ether was added, dropwise, 50 ml. of ethereal diazomethane solution prepared[49] from 1 g. of nitrosomethylurea over a period of 18 hr. with vigorous stirring. During this period, the temperature of the reaction mixture was maintained at 10~15°C and all traces of atmospheric moisture were excluded. After all the diazomethane solution had been added, stirring was continued for 2 hr. The light yellow crystalline solid was then filtered and washed with three 10 ml. portions of ether. The ether washings were combined with the filtrate. The solid separated was recrystallized from ethanol and there was obtained 620 mg. of isoaureothin (II), light yellow needles, m. p. 146~147°C, undepressed upon admixture with an authentic sample.

It is interesting to note that aureothin does not form a hydrochloride, though it has a $\gamma$-pyrone structure. Therefore, two isomeric methyl ethers, I and II, were separated by fractional crystallization from ethanol. Thus, the above ether filtrate and washings were combined and were evaporated to dryness in vacuo. Recrystallization of the resulting solid from ethanol gave a mixture of crystals of yellow prisms and of a small amount of light yellow needles. Two additional recrystallizations from ethanol gave 10 mg. of aureothin (I), yellow prisms, m. p. 152~153°C, undepressed upon admixture with an authentic sample.

The author is indebted to Professor Yoshimasa Hirata of this University for his valuable discussions and encouragement during this investigation. The author wishes to express his gratitude to Mr. Sho Takahashi for technical assistance in some of the experiments reported here. He is also grateful to Mr. Kiyoyuki Yamada for kindly calling the Professor Chmielewska's paper to his attention.

*Chemical Institute*
*Faculty of Science*
*Nagoya University*
*Chikusa, Nagoya*

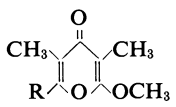
63) M. Pailer, L. Belohlave and E. Simonitsh, *Monatsh.*, **87**, 249 (1956).
64) Y. Hirata, K. Okuhara and T. Naito, *Nature*, **173**, 1101 (1954).
65) W. B. Mors, O. R. Gottlieb and C. Djerassi, *J. Am. Chem. Soc.*, **79**, 4507 (1957).
66) O. R. Gottlieb and W. B. Mors, *J. Org. Chem.*, **24**, 17 (1959).
67) J. Collie, *J. Chem. Soc.*, **59**, 607 (1891).

# *Correlation of Reaction Rates and Product Stabilities. II*[1]. *The Methylation of Pyronones with Dimethyl Sulfate*[2,3]

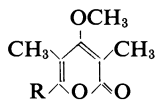
By Hisao NAKATA

(Received March 22, 1960)

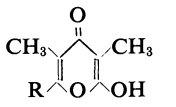
In the previous paper[1] of this series it was reported that the methylation of desmethylisoaureothin (III$\alpha$) with diazomethane under a certain specific experimental condition afforded both aureothin (I) and isoaureothin (II). The product proportion of the two isomeric methyl ethers, viz., I : II, was 1 : 60. A more effective methylation reaction leading to a high yield of aureothin is necessary for preparative purposes since the transformation would be involved in the final stage of the total synthesis of aureothin.



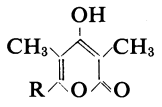
(I) Aureothin



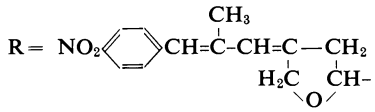
(II) Isoaureothin



(III$\gamma$) Desmethylaureothin



(III$\alpha$) Desmethylisoaureothin



The present investigation is concerned with an experiment on the methylation reaction of enolate anions of 2, 4-pyronone derivatives, the reaction that was chosen for scrutiny for reasons given in the following section. It was shown that the methylation with dimethyl sulfate was successful, and that aureothin was obtained from desmethylisoaureothin in fairly good yield. However, the product proportions of both isomers obtained were incompatible with those predicted by the general rule of this type of reaction. The scope of the reaction and some theoretical implications of the results are briefly discussed.

1) Part I of this series, H. Nakata, This Bulletin, **33**, 1688 (1960).

2) Structure of Aureothin. IX. Part VIII of this series Ref. 1.

3) Presented at the 12th Annual Meeting of the Chemical Society of Japan, Kyoto, April, 1959. A preliminary communication of a part of this work has also appeared. See, H. Nakata, S. Takahashi, K. Yamada and Y. Hirata, *Tetrahedron Letters*, No. 16, 9 (1959).

## Theory of Kinetically Controlled Methylation

The previous investigation[4] on the tautomerism of several 2, 4-pyronones indicates that the $\alpha$-pyrone derivatives are generally more stable than the isomeric $\gamma$-pyrone alternatives. This is well exemplified by the fact[1,5] that isoaureothin (II) and desmethylisoaureothin (III$\alpha$) are, respectively, more stable than aureothin (I) and desmethylaureothin (III$\gamma$.)

Because of this stability sequence of I and II, no equilibrium-controlled[6] methylation reaction of either III$\gamma$ or III$\alpha$ is expected to afford less stable aureothin (I) predominantly, since in the equilibrium-controlled reaction the proportion of the products is a function of only their relative stabilities, and is completely independent of reaction mechanism and rate. On the contrary, in a kinetically controlled reaction relative yields of the products depend only on the relative rates at which they are produced, and are independent of their relative stabilities. Accordingly, an appropriate kinetically controlled reaction must be employed for the purpose of obtaining aureothin (I) in comparatively high yield.

Even in the kinetically controlled reactions, however, there are many instances in which the most stable products are formed at the most rapid rates, and the kinetic control and the equilibrium-control of the reaction frequently give similar product proportions. The reactions of this type are in most cases endothermic processes where the products will provide the best models for the transition

4) For summaries of existing data on the tautomerism of several 2,4-pyronone derivatives, see Ref. 1 and references cited therein.

5) Y. Hirata, K. Okuhara, H. Nakata, T. Naito and K. Iwadare, *J. Chem. Soc. Japan, Pure Chem. Sec.* (*Nippon Kagaku Zasshi*), **78**, 1700 (1957).

6) Ingold and his co-workers[7,8] have used the term "thermodynamically controlled reaction" instead of "equilibrium-controlled reaction"[9].

7) A. G. Catchpole, E. D. Hughes and C. K. Ingold, *J. Chem. Soc.*, **1948**, 11.

8) C. K. Ingold, "Structure and Mechanism in Organic Chemistry", Cornell University Press, New York (1953), pp. 565,

9) D. J. Cram and G. S. Hammond, "Organic Chemistry", McGraw-Hill Book Co., Inc., New York (1959), p. 192.

state of the reaction[10,11]. These reactions are usually associated with the production of unstable intermediates from stable starting substances.

On the other hand, if starting substances are of highly reactive unstable species, a different situation occurs. The unstable reactant may probably be destroyed in a very fast, exothermic reaction. The activation energy is correspondingly rather small and the transition state of the reaction may resemble the reactant closely[10,11] in topology and in geometry[12].

When the reactant possesses two different reactive positions, its reaction at one or the other of its reaction centers will give two isomeric products. As is seen in ambident ions[15], such a dual reactivity is best attained when the reactant is an ion, the ionic charge of which spreads over a conjugated system covering these two reaction centers[16,17]. Moreover, the destruction of unstable organic ions, e. g., carbonium ions or carbanions, may be an exothermic process[10]. Thus, of particular importance for the reaction in question will be the fact that the reactant has ionic, conjugatively delocalized electrons distributed between its two reaction centers. Such structural requirements provide the reactant, not only with a dual reactivity, but with an enhanced reactivity as well.

Since the transition states leading to the two products in these reactions have considerable resemblance to the common starting ion, it might be expected that they would resemble each other more than do the two isomeric products[18]. Therefore, the less stable isomer will be obtained in a higher percentage in the kinetically controlled reaction than in the equilibrium-controlled one.

Consequently, the foregoing discussion leads to the conclusion that the following set of conditions is required for a given reaction in which the less stable isomeric product is obtained preferentially.

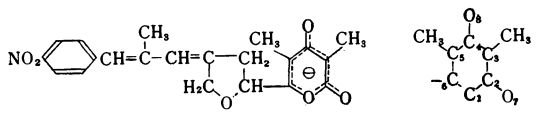
*1) The reactant must have two different reactive positions mutually conjugated. The reaction upon these affords the two isomeric products.*

*2) The reactant must be a highly reactive unstable species so as to make its reaction exothermic.*

*3) The reaction employed must be kinetically controlled.*

In the present case, methylation of the sodium salt of desmethylisoaureothin seems to be advantageous for the following three reasons.

1) As is the case in other enolate ions of $\beta$-dicarbonyl derivatives, the anion of the salt will probably have the structure IV in which the ionic, conjugatively delocalized electrons are distributed over the pyronone skeleton including the two exocyclic oxygen atoms, $O_7$ and $O_8$. The methylation reaction at one or the other of these oxygens will give either of the two isomeric methyl ethers, viz., I or II.



(IV) Enolate ion of desmethylisoaureothin

2) Although the sodium salt of desmethylisoaureothin is prepared easily and is considerably stable in alkaline solution[5,19], the enolate ion is at any rate a kind of organic ion, and it will have an enhanced reactivity towards any electrophilic reagents[20]. As in ionic inorganic reactions the destruction process of such a reactive ionic species is expected to be a very fast and, presumably, exothermic reaction.

3) Since the methyl ether groupings of aureothin (I) and isoaureothin (II) are relatively stable in neutral or in weakly alkaline mediums[5], no demethylation reaction of either compound will take place under such mild conditions. Therefore, if the methylation reaction is carried out under these conditions, it will be an irreversible, and thus will be a kinetically controlled process.

The next problem was to decide the actual experimental conditions, i. e., the reagent, the

10) G. S. Hammond, *J. Am. Chem. Soc.*, **77**, 334 (1955).

11) J. E. Leffler, *Science*, **117**, 340 (1953).

12) The terms *topology* and *geometry* of the transition state[11,13,14] have been defined previously[1], differentiating from the term *structure* of reactants or of products. The *topology* represents the linkage of atoms of the reacting molecules in the transition state, and may correspond to the *constitution* of the molecule in the static state. The *geometry* represents the spacial orientations of atoms of the reacting molecules in the transition state, and may correspond to the *configuration* and the *conformation* of the molecule in the static state. The topology and the geometry reflect the *dynamic* aspect of molecules.

13) J. E. Leffler and E. Grunwald, in S. L. Friess and A. Weissberger ed., "Technique of Organic Chemistry", Vol. VIII (Investigation of Rates and Mechanism of Reactions), Interscience Publishers Inc., New York (1953), p. 326 and 329.

14) J. E. Leffler, "The Reactive Intermediates of Organic Chemistry", Interscience Publishers., Inc., New York (1956), p. 116.

15) N. Kornblum, R. A. Smiley, R. K. Blackwood and D. C. Iffland, *J. Am. Chem. Soc.*, **77**, 6269 (1955).

16) A. N. Nesmeyanov and M. I. Kabachnik, *Zhur. Obshchei Khim.*, **25**, 41 (1955).

17) A. N. Nesmeyanov and M. I. Kabachnik, *Experientia, Suppl.*, No. 2, 49 (1955).

18) J. Hine, "Physical Organic Chemistry", McGraw-Hill Book Co., Inc., New York (1956), p. 232.

19) K. Yamada, H. Nakata and Y. Hirata, *J. Chem. Soc. Japan, Pure Chem. Sec.* (*Nippon Kagaku Zasshi*), **81**, 340 (1960).

20) It should be noted that generally there is no necessary relation among the synthetic ease of the compound, its reactivity, and its stability[21].

21) G. W. Wheland, "Advanced Organic Chemistry", 2nd Ed., John Wiley & Sons Inc., New York (1949), p. 366.

solvent, and the reaction temperature, of the methylation.

In general the alkylation of β-diketones and β-keto-esters is complicated by the possibility that the alkyl group may be introduced either on an oxygen atom (O-alkylation) or on a carbon atom (C-alkylation). As is expected from the structural formula IV, the pyronone enolate ion has at least three reactive positions of $C_3$, $O_7$ and $O_8$. For the present purpose the predominant O-alkylation is desirable and the methylation at the carbon atom $C_3$ must be avoided.

The most important factor affecting the nature of oxygen versus carbon alkylation is the electrophilicity of the alkylating agent. It has been reported[16,17] that when a bond between oxygen and a metal is strongly ionized, e.g., in a typical sodium enolate, a cationic reagent having a strongly electrophilic character will react preferentially at the oxygen atom. This can be generalized[15] in the following way. In the reaction of an ambident ion, the greater is the electrophilicity of the reagent, the greater is the preference for covalency formation with the atom of higher electronegativity[22].

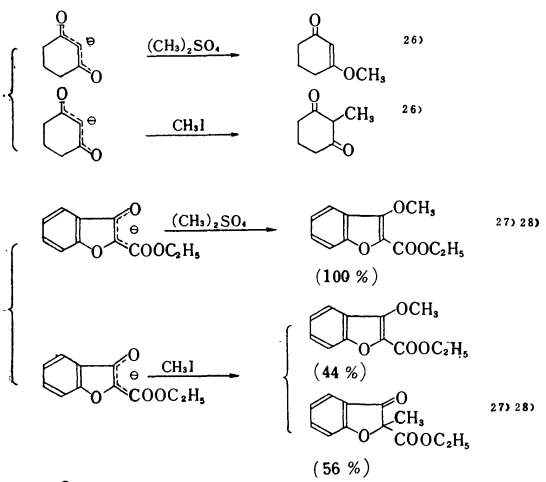
Of available methylating agents, dimethyl sulfate was preferred to methyl iodide on this basis. The fact[25] that dimethyl sulfate usually attacks the more electronegative atom of ambident anions reveals the strongly electrophilic character of the reagent[32].

In the reaction of IV with dimethyl sulfate, the magnitude of the anionic charge will be more or less reduced as the reaction proceeds. Therefore, the less polar solvent, and thus the solvent having a smaller $Y$-value[33,34], may promote the reaction[35,36]. Anhydrous acetone is considered to be a good solvent in this connection[37]. Furthermore, acetone is an aprotic solvent[39] and may prevent solvolytic decomposition of dimethyl sulfate.

The reaction temperature should be low enough to keep the reaction condition mild and less drastic. This is a direct consequence of the requirement that the methylation reaction must be kinetically controlled[40].

## Results

The sodium salt of desmethylisoaureothin was prepared by dissolving the enol III$\alpha$ into 2 N sodium hydroxide solution, and was separated as light yellow needles. The salt had no distinct melting point and decomposed at about 207~210°C without melting. It was insoluble in non-hydroxylic solvents such as benzene. These properties indicated the ionic character of the salt[23,42] as was formulated in IV.




$CN^{\ominus}+(CH_3)_2SO_4 \rightarrow CH_3-CN(75\%)+CH_3-NC(25\%)$[29,30]
$CN^{\ominus}+CH_3I \rightarrow CH_3-CN(100\%)$[29,30]
$NO_2^{\ominus}+(CH_3)_2SO_4 \rightarrow CH_3-NO_2(25\%)+CH_3-ONO(75\%)$[30]
$NO_2^{\ominus}+CH_3I \rightarrow CH_3-NO_2(100\%)$[31]

22) The alkylation of ambident anions has been discussed comprehensively but in a completely different way by Brändström[23,24].
23) A. Brändström, *Arkiv Kemi*, 6, 155 (1953).
24) A. Brändström, *Arkiv Kemi*, 7, 81 (1954).
25) Some typical examples are found in the literature[26-31].
26) H. Stetter and W. Dierichs, *Chem. Ber.*, 85, 61 (1952).
27) K. Auwers, *Ber.*, 45, 994 (1912).
28) K. Auwers, *Ann.*, 393, 338 (1912).
29) A. Williamson, *J. prakt. Chem.*, [1], 61, 60 (1854).
30) F. Kaufler and C. Pomeranz, *Monatsh.* 22, 495 (1901).
31) V. Meyer, *Ann.*, 171, 33, 35 (1874).
32) Nesmeyanov and Kabachnik[16,17] also reported that dimethyl sulfate has greater electrophilicity than methyl iodide.
33) E. Grunwald and S. Winstein, *J. Am. Chem. Soc.*, 70, 846 (1948).
34) A. H. Fainberg and S. Winstein, ibid., 78, 2770 (1956).
35) Ref. 8, pp. 345~355.
36) A. E. Remick, "Electronic Interpretations of Organic Chemistry", 2nd Ed., John Wiley & Sons Inc., New York (1949), pp. 272~284.
37) The selection of acetone as a solvent might give rise to a slight disadvantage to the preferential O-alkylation[15-17,23,24]. As was reported in Ref. 38 recently, however, this is not necessarily the case.
38) D. Y. Curtin and R. R. Fraser, *J. Am. Chem. Soc.*, 80, 6016 (1958).
39) L. P. Hammett, "Physical Organic Chemistry", McGraw-Hill Book Co., Inc., New York (1940), p. 288.
40) Selectivity of oxygen versus carbon alkylation may probably be affected by temperature. The corresponding rate equation becomes $\ln(k_o/k_c) = -(\Delta\Delta H^{\neq}/RT)+(\Delta\Delta S^{\neq}/R)$. where $\Delta\Delta H^{\neq} = \Delta H_o^{\neq} - \Delta H_c^{\neq}$ and $\Delta\Delta S^{\neq} = \Delta S_o^{\neq} - \Delta S_c^{\neq}$, the subscripts o and c referring to O- and C-alkylation, respectively. In the present case, $k_o/k_c$ will presumably decrease with the increase of the reaction temperature since the choice of the reagent would enable one to assume $\Delta H_o^{\neq} < \Delta H_c^{\neq}$. Accordingly, the low temperature is favored. Dewar[41] has suggested that for very reactive cationic reagents the quantity $\Delta\Delta H^{\neq}$ will be small. If this is actually the case, then the selectivity will have a relatively small temperature dependence. For further detailed discussion and criticism of Dewar's argument, see Ref. 23.
41) M. J. S. Dewar, "The Electronic Theory of Organic Chemistry", Oxford University Press, London (1949), p. 104.
42) Sidgwick and Brewer[43] have classified many alkali metal derivatives of β-dicarbonyl compounds into salts and covalent compounds from observations of melting point and of solubility in benzene.
43) N. V. Sidgwick and F. M. Brewer, *J. Chem. Soc.*, 1925, 2379.

TABLE I. METHYLATION OF DESMETHYLISOAUREOTHIN (III$\alpha$) WITH DIMETHYL SULFATE

| | Solvent | Time of refluxing hr. | Total yield % | Product proportions % | |
|---|---|---|---|---|---|
| | | | | I | II |
| III$\alpha$-sodium salt | Acetone | 6 | 62 | 41 | 59 |
| III$\alpha$-sodium salt | Acetone | 5 | 63 | 27 | 73 |
| III$\alpha$-sodium salt+$K_2CO_3$ | Acetone | 6 | 41 | 38 | 62 |
| III$\alpha$-sodium salt+$K_2CO_3$ | Acetone | 6 | 68 | 29[a] | 71[a] |
| III$\alpha$+$K_2CO_3$ | Acetone | 6 | 46 | 18[a] | 82[a] |
| III$\alpha$+I[b]+$K_2CO_3$ | Acetone | 6 | 72 | 16[a] | 84[a] |

a) Data from the infrared analysis.
b) Recovery of added I was estimated as 83% from a separate experiment. See experimental section.

TABLE II. METHYLATION OF 6-METHYL-2,4-PYRONONE (V) AND OF 4-HYDROXYCOUMARIN (VI) WITH DIMETHYL SULFATE

| | Solvent | Time of refluxing hr. | Total yield % | Product proportions % | |
|---|---|---|---|---|---|
| i) 6-Methyl-2,4-pyronone (V): | | | | VII$\gamma$ | VII$\alpha$ |
| V-sodium salt+$K_2CO_3$ | Acetone | 1 | 58 | 0 | 100 |
| V-sodium salt+$K_2CO_3$ | Acetone | 6 | 35 | 0 | 100 |
| V-sodium salt+$K_2CO_3$ | Ether | 6 | >26[a] | 0 | 100 |
| V-triethylammonium salt +$K_2CO_3$ | Acetone | 6 | 34 | 0 | 100 |
| V-silver salt+$K_2CO_3$ | Acetone | 6 | 16 | 0 | 100 |
| V+$K_2CO_3$ | Acetone | 6 | 69 | 0 | 100 |
| V-sodium salt+VII$\gamma$+$K_2CO_3$ | Acetone | 4 | 69 | 0[b] | 100 |
| V-sodium salt+VII$\gamma$+$K_2CO_3$ | Ether | 6 | 36[c] | 0[d] | 100 |
| ii) 4-Hydroxycoumarin (VI): | | | | VIII$\gamma$ | VIII$\alpha$ |
| VI-sodium salt+$K_2CO_3$ | Acetone | 6 | 85 | 0 | 100 |

a) A small amount of V was recovered.
b) Recovery of added VII$\gamma$ was 90%.
c) About 40% of V was recovered unchanged.
d) Recovery of added VII$\gamma$ was 71%.

Since the sodium salt was practically insoluble in anhydrous acetone the methylation reaction was first attempted in water-acetone mixture (4 : 1) at 0°C for 1.5 hr. Under these conditions, however, only the starting material III$\alpha$ was recovered unchanged. Consequently, it seemed desirable to employ the more forced condition. Thus, the salt was suspended in anhydrous acetone and the mixture was refluxed with dimethyl sulfate for 6 hr.[44]. Upon employing the fractional crystallization of the resulting mixture, there were actually isolated both aureothin (I) (25% yield) and isoaureothin (II) (37% yield).

This result provided an additional and unambiguous evidence for the reverse isomerization reaction[1] of desmethylisoaureothin derivatives into aureothin, and accordingly, the structural correlation between them was rigorously established.

As might be anticipated from the scrutiny for the reaction conditions discussed in the preceding section, the yield of the less stable isomeric methyl ether I was satisfactory in this methylation reaction. However, attention was called to the relative product proportions of both methyl ethers.

The separation of two isomeric methyl ether derivatives of 2,4-pyrononeses is usually accomplished by taking advantage of the fact that $\gamma$-pyrones form ether-insoluble hydrochlorides[47,48]. In the present case, however, the hydrochloride of aureothin (I) could not be formed, and both isomers were separated by the fractional crystallization from alcohol.

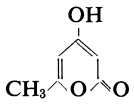
In order to determine more accurately, the relative amounts of isomeric I and II in a

44) Since the reaction was carried out in acetone suspension, the selectivity of oxygen versus carbon alkylation might be affected by the so-called heterogeneity factor[45,46].
45) G. A. Russell, *J. Am. Chem. Soc.*, **81**, 2017 (1959).
46) N. Kornblum and A. P. Lurie, ibid., **81**, 2705 (1959).
47) I. Chmielewska and J. Cieslak, *Przemystl. Chem.*, **8**, 196 (1952).
48) I. Chmielewska and J. Cieslak and T·Kraczkiewicz, *Roczniki Chem.*, **30**, 1009 (1956).

reaction mixture, it seems desirable to use an analytical technique by infrared spectra rather than the troublesome fractional crystallization. Essentially the same method as that described by Zimmerman and his co-workers[49-51] was employed here. The method proved to be accurate to ±2% of aureothin (note Table III in the Experimental Section for analysis of known mixtures of I and II).

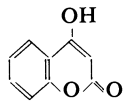
Repetition of the methylation experiments showed that the relative amounts of aureothin (I) were always less than those of isoaureothin (II) (Table I). This is incompatible with the general rule of the kinetically controlled reaction[7,8]. The rule states that the less stable isomeric product is formed more rapidly from a given ambident ion, i. e., the less stable isomer should be obtained in a higher percentage over-all product.

Since it appeared of interest to investigate further the general feature of this reaction, the methylations of 6-methyl-2, 4-pyronone (triacetic lactone, V)[4] and of 4-hydroxycoumarin (VI)[52] with dimethyl sulfate were examined. These compounds may probably serve as good models of desmethylisoaureothin (III$\alpha$). 6-Methyl-2, 4-pyrone (V) is expected to afford two possible isomeric methyl ethers, VII$\gamma$ and VII$\alpha$, of which the latter is more stable[4]. Similarly, 4-hydroxycoumarin (VI) will give both VIII$\gamma$ and VIII$\alpha$. The method for quantitative separation of each isomeric methyl ether has been established[47,48], utilizing the hydrochloride formation of VII$\gamma$ and of VIII$\gamma$. The results are shown in Table II.



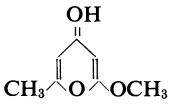
(V)

6-Methyl-2, 4-pyronone (triacetic lactone)



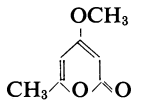
(VI)

4-Hydroxycoumarin



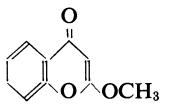
(VII$\gamma$)

6-Methyl-2-methoxy-$\gamma$-pyrone



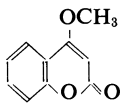
(VII$\alpha$)

6-Methyl-4-methoxy-$\alpha$-pyrone



(VIII$\gamma$)

2-Methoxy-$\gamma$-chromone



(VIII$\alpha$)

4-Methoxy-$\alpha$-chromone

The most striking aspect of the results of the methylation experiments summarized in Table II is the exclusive formation of the more stable methyl ethers under all conditions. This is again quite contrary to the general rule of Ingold[7,8].

Prior to discussion of these contrasted results of methylation reactions, an important point must be established. It is to demonstrate that the methylation reaction is undoubtedly a kinetically controlled process. If the reaction are, not kinetically, but equilibrium-controlled, the preferential formation of the more stable product is understandable, and the results are, of course, far from our problem.

In order to test this possibility, the methylation reaction of the sodium salt of V in acetone and in ether solvent was repeated in the presence of 6-methyl-2-methoxy-$\gamma$-pyrone (VII$\gamma$). From each run there was obtained nearly the same amount of VII$\alpha$ as in the previous experiments and the added VII$\gamma$ was almost quantitatively recovered unchanged (Table II, footnotes b and d). If the methylation reaction had been reversible, the less stable, added VII$\gamma$ would be converted into the more stable VII$\alpha$ by demethylation, isomerization, followed by re-methylation. However, the recovery of VII$\gamma$ and the material balance indicated that this was not the case. Therefore, the two possible products are not interconvertible under the reaction condition, and the possibility that the reaction might be an equilibrium-controlled process is rigorously excluded. Furthermore, it was also shown by these experiments that the absence of VII$\gamma$ in a reaction mixture was not due to any decomposition of it during working-up processes.

Some additional data on the exclusive formation of the more stable methyl ether in 2, 4-pyronone derivatives are available from the literature, though each reaction was not specified as a kinetically controlled process[55-57].

## Discussion

Ingold's rule[7,8] of the kinetically controlled reaction is acceptable for a wide variety of reactions including the recombination of allylic

49) H. E. Zimmerman, *J. Am. Chem. Soc.*, **78**, 1168 (1956).
50) H. E. Zimmerman and H. J. Giallombardo, ibid., **78**, 6259 (1956).
51) H. E. Zimmerman and T. W. Cutshall, ibid., **81**, 4305 (1959).

52) Two tautomeric structures are possible for 4-hydroxycoumarin. As in other 2,4-pyronone derivatives[4], the $\alpha$-chromone structure VI is more stable than the alternative $\gamma$-chromone structure[53,54].
53) F. Arndt, L. Loewe, R. Ün and E. Ayca, *Ber.*, **84**, 319 (1951).
54) R. A. Abramovitch and J. R. Gear, *Can. J. Chem.*, **36**, 1501 (1958).
55) S. Janiszewska-Drabarek, *Roczniki Chem.*, **27**, 456 (1953).
56) W. Borsche and C. K. Bodenstein, *Ber.*, **62**, 2515 (1929).
57) I. Chmielewska, J. Cieslak, K. Gorczynska, B. Kontnik and K. Pitakowska, *Tetrahedron*, **4**, 36 (1958).

carbonium ions with anions, the protonation of anions of aliphatic nitro compounds, and those of β-dicarbonyl compounds. From the present results, however, one might conclude that the rule has not entirely general applicability. It will be of interest to re-examine the scope and limitations of the rule in connection with the correlation between reaction rates and product stabilities. This point will be discussed in detail in a subsequent publication of this series, but a brief discussion is given here.

Ingold's rule is based on the consideration[8] that the least stable starting ambident ion is converted into the energetically less different unstable isomeric product with a less drastic electronic reorganization involving less activation energy, than into the electronically and energetically very different stable isomeric product. This seems to be in accordance with Hammond's postulate[10], which states that an interconversion of two states will involve only a small reorganization of the molecular structures if these two states occur consecutively during a reaction process and have nearly the same energy content.

In fact, in most reactions which have so far been associated with the rule, the structure of a given ambident ion has close resemblance to the less stable product. For example, the enolate ion of ethyl acetoacetate has a structure similar to that of the enol[58-60], and thus, treatment of it with dry hydrogen chloride actually gives almost exclusively the less stable enol[61].

If, however, the least stable ambident ion structurally resembles more the stable product than the unstable one, the reverse situation can occur; the most stable isomer will be formed more rapidly than the less stable isomer. The present results of the preferential formation of the more stable methyl ethers in all reactions may be explicable if one considers that the structure of the pyronone enolate ion resembles more the structure of the more stable α-pyrone isomer than that of γ-pyrone isomer. The simple molecular orbital calculation of the charge distributions in the pyronone enolate ion supported this consideration. The details will be reported in a forthcoming paper.

Although the above formulation is in agreement with the orignial idea of Ingold and of Hammond, i. e., the less drastic the structural change the less will be the activation energy of the reaction, it is worthy to note that the structure of the least stable ambident ion does not always resemble the structure of the less stable isomer.

Finally, it may require comment as to why the structure of the ambident ion has resemblance to the more stable isomer in the present special type of compound. Generally, the stabilities of two tautomeric substances depend on two competitive factors[62-65], i. e., *prototropic expenditure of work* and *electronic delocalization*[66], the former being a dominant factor in most keto-enol systems[67]. On the contrary, in the α-pyrone-γ-pyrone system, it seems reasonable to assume that this factor will be more or less of minor importance, since both isomers of a given 2, 4-pyronone have similar O-H functions. Therefore, the relative stabilities of the two isomers will probably be due to the electronic delocalization. This means that the more stable α-pyrone structure is more favorable for the electronic delocalization than the less stable γ-pyrone structure. On the other hand, the electrons should be most favorably distributed in the pyronone enolate ion. Accordingly, the structural resemblance between the ion and the more stable α-pyrone isomer is expected to exist.

## Experimental

**Sodium Salt of Desmethylisoaureothin (IIIα).**— Desmethylisoaureothin (IIIα,) m. p. 196~198°C[5] (1 g.) was dissolved in 30 ml. of hot 2 N sodium hydroxide solution. A clear brown solution was obtained. The crystals which separate on cooling were collected, washed with a small amount of cold alcohol, and dried. Light yellow needles. Yield 1.1 g. The salt had no distinct melting point and decomposed at about 207~210°C without melting.

**Methylation of Sodium Salt of IIIα.** — The sodium salt (1.1 g.) prepared from 1 g. of desmethylisoaureothin (IIIα) was suspended in 40 ml. of anhydrous acetone. Dimethyl sulfate (0.7 g.) was added to the suspension and the mixture was refluxed for 6 hr., and was then set aside overnight. The mixture was again warmed on water bath for 5 min. and was filtered. By concentration of the filtrate to 5 ml. in vacuo a yellow crystalline solid separated, which was filtered. Twice recrystallizations from alcohol gave yellow needles, m. p. 146°C, undepressed upon admixture with an authentic

58) B. Eistert, "Tautomerie und Mesomerie", Ferdinand Enke, Stuttgart (1938), p. 125.
59) H. Henecka, "Chemie der Beta-Dicarbonyl-Verbindungen", Springer Verlag, Berlin (1950), p. 29.
60) W. Hückel, "Theoretische Grundlagen der Organischen Chemie", Vol. I, 8th Ed., Akademische Verlagsgesellschaft, Leipzig (1956), pp. 280 and 322.
61) L. Knorr, O. Rothe and H. Averbeck, *Ber.*, **44**, 1143 (1911).
62) F. Arndt and C. Martius, *Ann.*, **499**, 228 (1932).
63) Ref. 59, pp. 15~20.
64) Ref. 60, pp. 301~313.
65) G. Briegleb and W. Strohmeier, *Angew. Chem.*, **64**, 409 (1952).
66) In Arndt's terminology[62], these are "Prototropie" (prototroper Arbeitsaufwand) and "Enotropie" (elektromerer Effekt), respectively. See also, *Chem. Abstr.*, **27**, 2132 (1933).
67) Ref. 21, p. 613.

sample of isoaureothin II. Yield 200 mg. Spontaneous evaporation of each mother liquor of this recrystallization gave 60 mg. of brownish yellow prisms, m. p. 151~152°C, undepressed on admixture with an authentic sample of aureothin I. The infrared spectrum of this material was identical with that of I. The above acetone filtrate was diluted with 30 ml. of water. The separated brown oil crystallized after 2 days. Recrystallization from alcohol gave additional 180 mg. of isoaureothin (II). The mother liquor was evaporated as above, and 205 mg. of aureothin I, m. p. 150~151°C was obtained as brownish yellow prisms. Total yield 62% (aureothin, 265 mg.; isoaureothin, 380 mg.). When the reaction mixture was refluxed for 5 hr., there was obtained 40 mg. of I and 110 mg. of II from 230 mg. of III$\alpha$ (total yield 63%). In another run, the reaction mixture was refluxed with 2 g. of anhydrous potassium carbonate. From 1 g. of the sodium salt, 150 mg. of I and 250 mg. of II were obtained (total yield 41%). In each case, none of the starting material of III$\alpha$ was recovered.

**Attempt on Methylation of Sodium Salt of III$\alpha$ at Low Temperature.** — The sodium salt of III$\alpha$ (500 mg.) was dissolved in 25 ml. of water-acetone mixture (4 : 1). This yellow solution was cooled below 0°C and 4 drops of dimethyl sulfate was added. The mixture was stirred for 30 min. at 0°C and then for another 1 hr. at room temperature. The solution was concentrated to 10 ml. in vacuo and neutralized with dilute acetic acid. A precipitated yellow solid was collected and washed with cold water. Recrystallization from alcohol gave yellow needles, m. p. 195~198°C, undepressed upon admixture with an authentic desmethylisoaureothin III$\alpha$. Recovery 230 mg.

**Quantitative Infrared Analyses.**—Essentially the same analytical technique as that described by Zimmerman and his co-workers[49-51] was employed. All spectra were measured as potassium bromide pellets. It was found that aureothin I exhibited a sharp maximum at 1260 $cm^{-1}$ (optical density= 0.5528; 1.05 mg.-sample) while isoaureothin II had a minimum at this frequency (optical density= 0.0603; 1.06 mg. -sample). The spectrum of isoaureothin II possessed a sharp maximum at 1230 $cm^{-1}$ (optical density=0.3098; 1.06 mg.-sample) while aureothin I had a minimum at this frequency (optical density=0.0969; 1.05 mg.-sample). These two bands were well separated and were selected as the key bands for analysis. Desmethylisoaureothin III$\alpha$ had no intense band in the range 1300~1220 $cm^{-1}$.

The following equation was used: $R = Q \times F$. Here $R$ is the ratio of aureothin I to isoaureothin II, viz., $R$=I/II.

$$Q = \frac{D_m' D_i'' - D_m'' D_i'}{D_m'' D_a' - D_m' D_a''}$$

The $D_m$'s, $D_a$'s and $D_i$'s are optical densities of a given mixture, pure aureothin, and pure isoaureothin, respectively. The superscripts refer to the analytical frequencies of 1260 (') and 1230 ('') $cm^{-1}$. $F$ was determined empirically from the values of $Q$ and $R$ for known mixtures as shown in Table III. The average value of $F$=0.848 was used in calculating the results in the last two columns of Table III. The optical densities used were calculated from the transmittances directly without any consideration of background absorption.

In each case the unknown was prepared by grinding evenly the isomeric mixture with double portions of potassium bromide. An appreciable amount of this well ground mixture was taken as an analytical sample. The sample was ground evenly with 150 mg. of potassium bromide for 5 min. and the mixture was placed under 8 ton/$cm^2$ in a 1.30 cm. diameter casing. The spectra were recorded on a Koken IR-S double beam instrument equipped with sodium chloride optics. The optical density of all mixtures, known and unknown, was taken as zero at 1850 $cm^{-1}$. The best results were obtained when the percentage transmission of both key bands of mixtures was in the range 25~80%. Analyses were made in duplicate in nearly all experiments.

**Repetition of the Methylation Experiment.** — Desmethylisoaureothin III$\alpha$ was converted into its sodium salt (from 400 mg. of III$\alpha$). The salt was suspended in 25 ml. of dry acetone. Nine drops of dimethyl sulfate and 2 g. of anhydrous potassium carbonate were added and the mixture was refluxed for 6 hr. The reaction mixture was worked up as in the foregoing experiment. There was obtained 280 mg. (total yield 68%) of isomeric mixture, which was used for infrared analysis.

No. 1 $D_m'$=0.2148, $D_m''$=0.2365, $Q$=0.474,
Calcd. $R$=0.402, Calcd. I %=28.6%

Nd. 2 $D_m'$=0.5688, $D_m''$=0.6196, $Q$=0.483,
Calcd. $R$=0.409, Calcd. I %=29.1%
Average I %=28.9%

TABLE III. ANALYSIS OF KNOWN MIXTURES OF AUREOTHIN AND ISOAUREOTHIN

| Actual I, % | $D_m'$ | $D_m''$ | $Q$ | Actual $R$ | Calcd. $F$ | Calcd. $R$ | Calcd. I, % |
|---|---|---|---|---|---|---|---|
| 0.0 | 0.0603 | 0.3098 | — | — | — | — | — |
| 14.0 | 0.2148 | 0.4200 | 0.194 | 0.163 | 0.836 | 0.165 | 14.2 |
| 22.4 | 0.1939 | 0.2756 | 0.325 | 0.289 | 0.889 | 0.275 | 21.6 |
| 30.6 | 0.2758 | 0.3189 | 0.508 | 0.439 | 0.864 | 0.432 | 30.2 |
| 32.6 | 0.4560 | 0.4319 | 0.592 | 0.485 | 0.820 | 0.502 | 33.4 |
| 41.9 | 0.3768 | 0.2677 | 0.902 | 0.721 | 0.800 | 0.765 | 43.3 |
| 47.1 | 0.4322 | 0.2842 | 1.009 | 0.889 | 0.889 | 0.856 | 46.2 |
| 61.4 | 0.6375 | 0.3100 | 1.786 | 1.595 | 0.894 | 1.515 | 60.3 |
| 84.2 | 0.4684 | 0.1192 | 6.690 | 5.300 | 0.793 | 5.671 | 85.2 |
| 100.0 | 0.5528 | 0.0969 | — | — | — | — | — |

The infrared spectrum of this mixture did not exhibit a band at 1195 $cm^{-1}$, indicating the absence of III$\alpha$.

**Methylation of III$\alpha$ with Dimethyl Sulfate and Potassium Carbonate.** — A solution of desmethylisoaureothin III$\alpha$ in anhydrous acetone (500 mg. in 30 ml.) was refluxed with 20 drops of dimethyl sulfate and 2 g. of potassium carbonate for 6 hr. The resulting yellow solution was evaporated to dryness in vacuo. A yellow crystalline solid was obtained. Three recrystallizations from alcohol gave 150 mg. of pure isoaureothin II. From mother liquors of the recrystallization, there was isolated 90 mg. of isomeric mixture, which was subjected to infrared analysis.

No. 1 $D_m'=0.2923$, $D_m''=0.1937$, $Q=1.071$,
Calcd. $R=0.909$, Calcd. I %=47.7%

No. 2 $D_m'=0.4202$, $D_m''=0.2679$, $Q=1.062$,
Calcd. $R=0.900$, Calcd. I %=47.3%
Average I %=47.5%

The infrared spectrum of this mixture did not exhibit a band at 1195 $cm^{-1}$, indicating the absence of III$\alpha$. Therefore, the total yield was 46%, 43 mg. of I and 197 mg. of II.

**Methylation of III$\alpha$ in the Presence of I.** — Desmethylisoaureothin (III$\alpha$) (300 mg.) was methylated as above in the presence of 200 mg. of aureothin (I). There was isolated 390 mg. of isomeric mixture, which was subjected to infrared analysis.

No. 1 $D_m'=0.4953$, $D_m''=0.2840$, $Q=1.252$,
Calcd. $R=1.062$, Calcd. I %=51.4%

No. 2 $D_m'=0.2365$, $D_m''=0.1367$, $Q=1.236$,
Calcd. $R=1.049$, Calcd. I %=51.2%
Average I %=51.3%

The infrared spectrum of the mixture did not exhibit a band at 1195 $cm^{-1}$, indicating the absence of III$\alpha$. The analysis showed that the mixture contained 202 mg. of I and 188 mg. of II. In a separate experiment, 200 mg. of I alone was treated under the same reaction condition as above. It resulted in 83% recovery (165 mg.) of I. Thus, the actual methylation products were 37 mg. of I and 188 mg. of II. Total Yield 72%.

**6-Methyl-2,4-pyronone (V).** — 6-Methyl-2,4-pyronone was prepared from dehydroacetic acid[68].

**Sodium Salt of 6-Methyl-2, 4-pyronone.** — The general procedure for preparation of sodium salts of $\beta$-dicarbonyl compounds was used[69]. Alcoholic sodium ethoxide solution prepared from 0.5 g. of metallic sodium and 15 ml. of ethanol was added to a solution of 3 g. of V in 30 ml. of ethanol. The mixture was concentrated to 20 ml. in vacuo and then 100 ml. of ether was added. The precipitated white solid was collected, washed with acetone, and dried. Yield 2.5 g.

**Methylation of Sodium Salt of V in Acetone.**— One gram of the sodium salt and 2 g. of anhydrous potassium carbonate was suspended in anhydrous acetone, and 1.8 ml. of dimethyl sulfate was added to the suspension. The mixture was refluxed for 1 hr. with occasional shaking. The reaction mixture was filtered while still hot, and the filtrate was evaporated to dryness in vacuo. The resulting solid was extracted with seven 50 ml. portions of petroleum ether (b. p. 30~60°C). A relatively large amount of dark solid remained. The combined extracts were filtered to remove any insoluble impurities and were evaporated to dryness in vacuo, and finally dried in a vacuum desiccator over calcium chloride. The crystalline solid thus obtained was dissolved in 50 ml. of anhydrous ether. The solution was cooled below 0°C and was treated with dry hydrogen chloride. None of the hydrochloride of 6-methyl-2-methoxy-$\gamma$-pyrone (VII$\gamma$) was precipitated. After evaporation of the solvent crude 6-methyl-4-methoxy-$\alpha$-pyrone (VII$\alpha$) was obtained. Recrystallization from petroleum ether gave pure material, m. p. 87~88°C, undepressed upon admixture with an authentic sample[1]. Yield 550 mg. (58%). The above dark solid, which remained from the petroleum ether extraction, was again extracted with anhydrous ether. Treatment of the extracts with dry hydrogen chloride gave no precipitate.

In another run, after the filtration of the initial reaction mixture, the filtrate was concentrated in vacuo over 1 g. of freshly added anhydrous potassium carbonate to prevent any possible acid-catalyzed decomposition of VII$\gamma$ during the working-up process. The final results were essentially the same as those described above, and no VII$\gamma$ was obtained.

When the reaction mixture was refluxed for 6 hr., only VII$\alpha$ was obtained. Yield 330 mg. (35%).

**Methylation of Sodium Salt of V in Ether.**—In 20 ml. of anhydrous ether 1 g. of the sodium salt and 2 g. of potassium carbonate was suspended, to which 2 g. of dimethyl sulfate was added. The mixture was refluxed for 6 hr. After removing the potassium carbonate, the ether filtrate was treated with dry hydrogen chloride. No precipitate was formed. The solution was then concentrated in vacuo. Recrystallization of the resulting solid from petroleum ether gave 250 mg. of VII$\alpha$. Since V was sparingly soluble in ether, unchanged V remained in potassium carbonate residue. The above filtrated solid was dissolved in water and the solution was acidified with dilute sulfuric acid. A small amount of V separated as fine needles, m. p. 186~188°C.

**Triethylammonium Salt of V.** — About 2 ml. of triethylamine was added to a solution of 1 g. of V in 5 ml. of ethanol. Evaporation of the solvent in vacuo gave a colorless oil. Attempts to crystallize the salt from the oil were unsuccessful, and the oil was used without further purification. When the oil was dissolved in water, the initial V was precipitated as a white crystal.

**Methylation of Triethylammonium Salt of V.**— The above oily material (1 g.) was methylated. The procedures used for separation and purification of products were essentially the same as those described above. Only VII$\alpha$ was obtained. Yield 210 mg. (34%).

**Methylation of Silver Salt of V.**—The silver

68) J. Collie, *J. Chem. Soc.*, 59, 607 (1891).
69) S. M. McElvain and K. H. Weber, *J. Am. Chem. Soc.*, 63, 2192 (1941).

salt of V was prepared according to the directions of Janiszewska-Drabarek[55]. Methylation was carried out as above. The yield was low, VII$\alpha$ 150 mg. (16%).

**Methylation of V with Dimethyl Sulfate and Potassium Carbonate.** — In 15 ml. of anhydrous acetone 850 mg. of V was dissolved. The solution was refluxed with 5 g. of potassium carbonate and 2 ml. of dimethyl sulfate for 6 hr. Concentration of the filtrate of the reaction mixture gave an oily material containing crystals. The procedures for separation of the isomeric methyl ethers were essentially the same as those described above. Only VII$\alpha$ was obtained. Yield 650 mg. (69%).

**Methylation of Sodium Salt of V in the Presence of VII$\gamma$.**—The mixture of 1 g. of the sodium salt, 100 mg. of 6-methyl-2-methoxy-$\gamma$-pyronoe (VII$\gamma$)[1], 2 g. of potassium carbonate, and 2 ml. of dimethyl sulfate was refluxed in anhydrous acetone for 4 hr. The filtrate of the reaction mixture was concentrated in vacuo and the resulting solid was dissolved in 60 ml. of dry ether. A small amount of insoluble material remained and was discarded. The ether solution was cooled and was treated with dry hydrogen chloride. The hydrochloride of VII$\gamma$ was precipitated immediately, and was collected and dried (120 mg.). The isomeric VII$\alpha$ remained in solution and was obtained after evaporation of the solvent. Yield 650 mg. (69%). The free VII$\gamma$ was recovered from the above hydrochloride on treatment with diethylamine[47,48]. Yield 90 mg. (recovery 90%).

In another run, the mixture of 1 g. of the sodium salt, 140 mg. of VII$\gamma$, 2 g. of potassium carbonate, and 2 ml. of dimethyl sulfate was refluxed in anhydrous ether for 6 hr. The ether layer of the reaction mixture was cooled and treated with dry hydrogen chloride. About 130 mg. of hydrochloride of VII$\gamma$ was obtained. This was transformed to free VII$\gamma$ as above. Yield 100 mg. (recovery 71%). The ehter solution was concentrated and the solid thus obtained was recrystallized from petroleum ether. Yield 200 mg. VII$\alpha$ (36%). The filtrated potassium carbonate residue was dissolved in 20 ml. of water. Acidifying with dilute sulfuric acid gave white needles, m. p. 187~189°C, undepressed upon admixture with an authentic sample of V. Recovery 350 mg. (40%).

**4-Hydroxycoumarin (VI).** — Acetylation of 75 g. of methyl salicylate with 75 g. of acetic anhydride in 20 ml. of pyridine gave 80 g. of methyl acetyl salicylate. Treatment of this methyl acetyl salicylate with 9.6 g. of metallic sodium yielded 26 g. of 4-hydroxycoumarin (VI[70].) After recrystallization from water it exhibited m. p. 204~205°C.

**Sodium Salt of 4-Hydroxycoumarin (VI).** — 4-Hydroxycoumarin (VI) (4 g.) was dissolved in 20 ml. of ethanol and alcoholic sodium ethoxide solution prepared from 0.5 g. of metallic sodium and 10 ml. of ethanol was added. The mixture was concentrated in vacuo to 15 ml. and then 100 ml. of ether was added. The precipitated white solid was filtered and dried. Yield 3.4 g.

**Methylation of Sodium Salt of VI.** — One gram of the sodium salt of VI and 2 g. of potassium carbonate were suspended in anhydrous acetone, and the mixture was refluxed with 1.5 ml. of dimethyl sulfate for 6 hr. The acetone layer was treated as described in the literature[55] to separate each isomeric methyl ether. Only 4-methoxy-$\alpha$-chromone (VIII$\alpha$) was obtained. m. p. 125~126°C. Yield 810 mg. (85%).

The author is indebted to Professor Yoshimasa Hirata of this University for his valuable discussions and encouragement during this investigation. The author also wishes to express his gratitude to Mr. Sho Takahashi for technical assistance in some of the experiments reported here.

*Chemical Institute*
*Faculty of Science*
*Nagoya University*
*Chikusa, Nagoya*

70) H. Pauly and K. Lockemann, *Ber.*, **48**, 28 (1915).

# *The Transition Phenomenon of Unsaturated Polyester Resin*

By Kōji TANAKA

(Received March 22, 1960)

So far, the author has studied the relationship between the structure and the transition phenomenon of high polymers such as polyethylene and polyvinylalcohol by volume dilatometry and the nuclear magnetic resonance absorption method. As to polyethylene[1], a crystalline polymer, investigation was made of the effect of the degree of crystallinity and of the degree of chain branching on its transition temperature, and on polyvinylalcohol[2] a study was made of the relationship between the hydroxyl group and the transition phenomenon. There is a report[3] that the glass transition temperature of non-crystalline polymer such as atactic polystyrene largely depends upon the degree of polymerization and that the mechanism of the transition phenomenon can be made clear from the standpoint of rate process. Unsaturated polyester resin (unsaturated alkyd resin) crosslinked by a vinyl compound is a non-crystalline polymer having a three dimensional network. Therefore it is expected that the mechanism of the transition phenomenon of the resin differs from that of non-crystalline polymer such as atactic polystyrene, even if the polyester resin itself shows some transition phenomenon.

Polyester resin in a broad sense includes all the high molecular compounds in which the ester linkage between the carboxyl group and the hydroxyl group is the principal element for the formation of high polymer. In the present paper, however, it stands for the polyester resin in a narrow sense; that is, the unsaturated polyester resin crosslinked by a vinyl compound such as styrene and vinylacetate. As is well known, the polyester resin has many good points in comparison with other synthetic resins. For example it excels in such chemical properties as resistance against acid, alkali, water, oil and organic solvent, as well as in electrical property. Above all arc resistance is its distinguishing character. The completely crosslinked polyester resin is hard and brittle at room temperature and below at about $-5°C$ it becomes more brittle, but above 60°C it becomes abruptly flexible. It seems that there is scarcely found any paper describing at what temperature and by what transition mechanism such a change of property occurs. The dilatometric study by the authors showed that this resin had two transition points of second order and the upper transition temperature was charged by the amount of vinyl compound, and in addition it was investigated by nuclear magnetic resonance absorption method from what struct ture and molecular motion these transition phenomena arose.

1) K. Tanaka, This Bulletin, **33**, 1060, 1133 (1960).
2) K. Tanaka et al., This Bulletin, **29**, 843 (1956); **30**, 197, 428 (1957).
3) T. G. Fox and P. J. Flory, *J. Appl. Phys.*, **21**, 581 (1950).

## Experimental

**Samples.**—MD-S-O: This sample was prepared by mixing maleic anhydride and diethyleneglycol in the mole ratio of 1 to 1 and by heating the mixture at 180°C for six hours with stirring under nitrogen atmosphere.

MAD-S-O: This sample was prepared by mixing maleic anhydride, adipic acid, and diethyleneglycol in the mole ratio of 9 to 1 to 10 and by heating the mixture at 180°C for four hours with stirring under nitrogen gas atmosphere.

These two samples were viscous liquids having no crosslinking structure and were used as starting substances for the preparation of other samples, that is, all other samples were prepared by adding styrene to MD-S-O or MAD-S-O in the ratio shown in Table I and by heating at 80°C for three hours between glass plates, and in addition after-cure treatment was performed at about 100°C for three hours.

TABLE I. THE AMOUNT OF STYRENE IN THE SAMPLES OF POLYESTER RESIN

| Sample | Styrene monomer wt. % | The ratio of C=C group to styrene monomer |
|---|---|---|
| MD-S-0 | 0.0 | 1 : 0 |
| MD-S-1 | 10.0 | 1 : 0.20 |
| MD-S-2 | 20.0 | 1 : 0.45 |
| MD-S-3 | 30.0 | 1 : 0.77 |
| MD-S-4 | 35.9 | 1 : 1 |
| MAD-S-0 | 0.0 | 1 : 0 |
| MAD-S-1 | 10.0 | 1 : 0.22 |
| MAD-S-2 | 20.0 | 1 : 0.50 |
| MAD-S-3 | 30.2 | 1 : 1 |
| MAD-S-4 | 40.0 | 1 : 1.35 |

**Volume Dilatometry.**—The details about this procedure were omitted as they had been described already[1]. Mercury was used as a confining liquid and the temperature range covered was from the

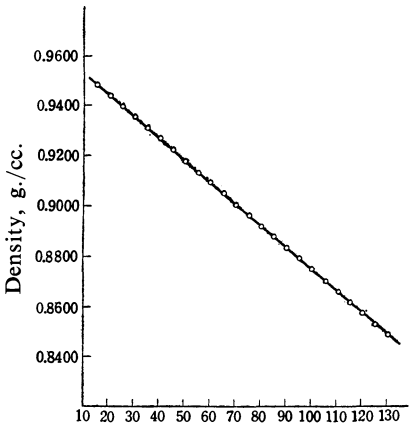



Fig. 1. The density-temperature relationship of silicone oil.

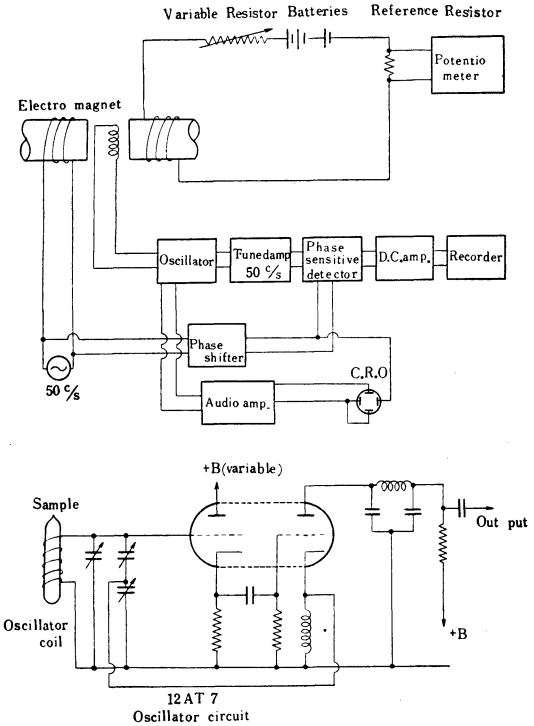



Fig. 2. The constitution of the apparatus for nuclear magnetic resonance absorption.

freezing point of mercury to about 120°C. The bath temperature was varied about five degrees at a time and 20 min. were taken before every measurement in order to let the sample attain equilibrium temperature.

**Hydrostatic Method of Measuring Density.— Apparatus.** — *Balance.* — An ordinary chemical-balance remodeled a little was used. (sensitivity 1/5 mg.)

*Thermostat.*—The chrome-plated vessel with stirrer and two heaters of 500 W. was used. It could accomodate two litters of liquid. Temperature control was performed by connecting the Ostwald-type mercury regulator to micro relay in the range of ±0.05 degree.

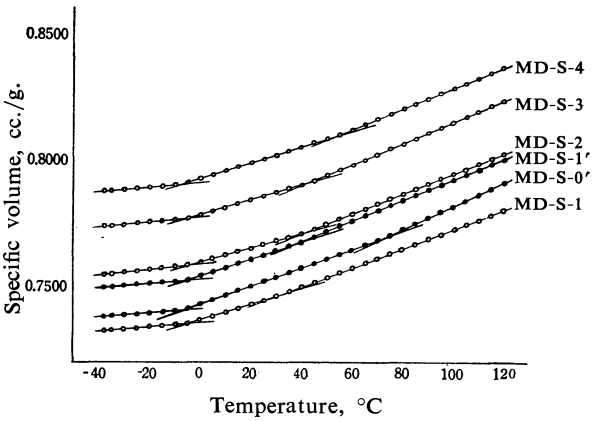



Fig. 3. The volume-temperature curves for the samples of MD series.

*Dipping Liquid.*—As a dipping liquid silicone oil was used. Its qualities were as follows; viscosity 10 c. s. at 25°C, freezing point −65°C, boiling point 200°C, flash point 163°C, and thermal conductivity 0.00032.

*Procedure.*—The sample was connected to the balance with terylene fiber and dipped into silicone oil, and the density was measured in the temperature range from room temperature to 120°C. The temperature was raised five degrees at a time and 15 min. were taken before every measurement.

*Calculation.*—The calculation of density at every temperature, $d_t$ was performed according to the following expression,

$$d_t = \frac{W}{W - W_t} \times \rho_t$$

where $W$ was the weight of the sample in air, $W_t$ that in silicone oil and $\rho_t$ the density of silicone oil at the measured temperature. The density-temperature relationship of silicone oil was determined by volume dilatometry in the temperature range from room temperature to 130°C and shown in Fig. 2.

**Nuclear Magnetic Resonance Absorption Method.** — The usual apparatus consisting of an autodyne oscillator, a lock-in-amplifier, and a recorder was used (Fig. 3). The field intensity was about 3000 gauss. The sample was sealed in the evacuated glass tube.

## Results

Dilatometric study was perfomed for the samples of MD series. Specific volume-temperature curves obtained are shown in Fig. 4. In the figure MD-S-O′ is the sample MD-S-O gelatinized by heating at 110°C for three days and MD-S-1′ the sample MD-S-1 after-cured at 100°C for a day.

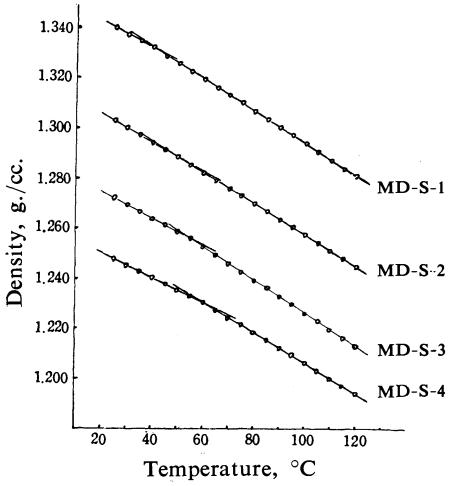



Fig. 4. The density-temperature curves for the samples of MD series.

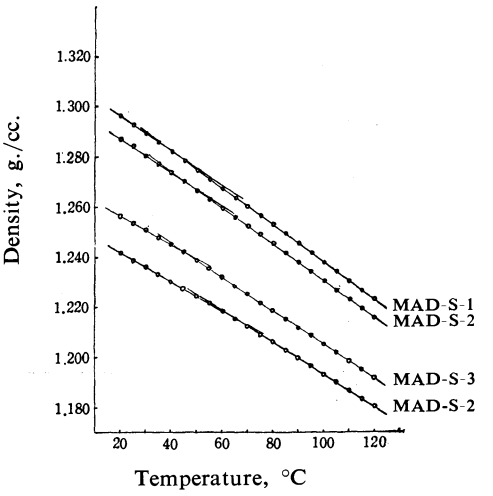



Fig. 5. The density-temperature curves for the samples of MAD series.

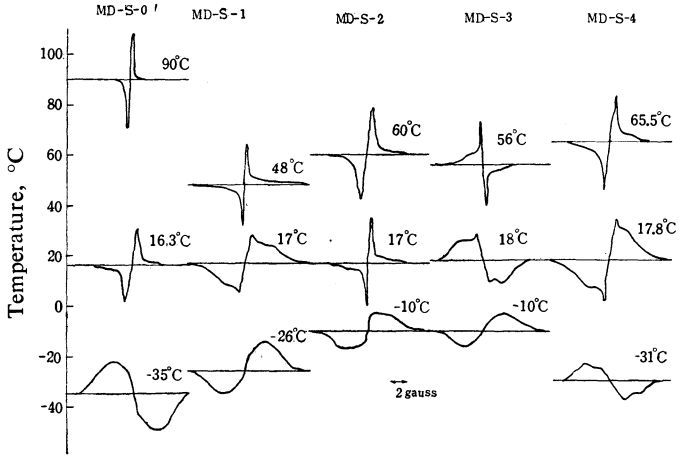



Fig. 6. The derivative absorption curves for the samples of polyester resin.

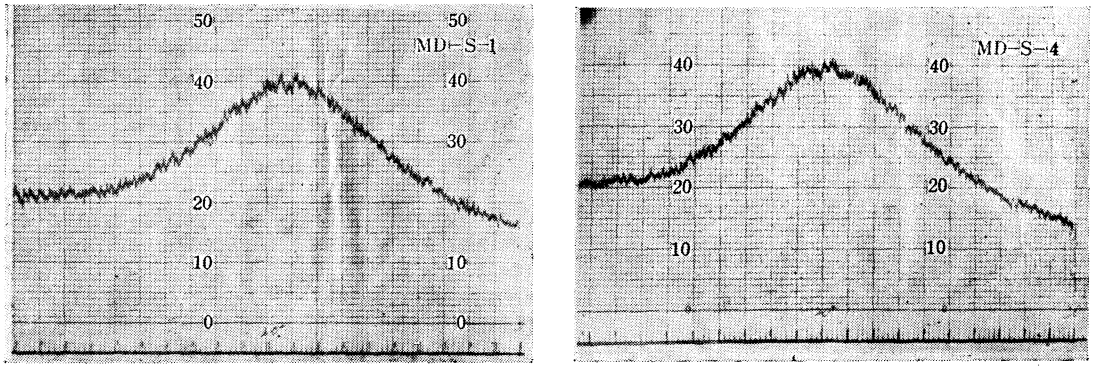



Fig. 7. The X-ray diffraction diagrams for MD-S-1 and MD-S-4.

Hydrostatic study was carried out for all the samples except MD-S-0 and MAD-S-0. Density-temperature curves obtained are illustrated in Figs. 5 and 6.

As is shown in Fig. 2, two second order transition points were observed for each sample of MD series. These temperatures are listed in Table II with the results for MD and MAD series by hydrostatic method.

In Fig. 7 are shown derivative line shapes by nuclear magnetic resonance absorption method for the samples of MD series and the values of second moment, $<\Delta H^2>$, obtained from the derivative curves above and below two second-order transition temperatures for each sample of MD series are listed in Table III.

Table II. The second order transition temperatures of the samples of polyester resin (in °C)

| Sample | Dilatometric result | | Hydrostatic results |
|---|---|---|---|
| | Lower point | Upper point | |
| MD-S-0′ | −6.5 | 77.9 | — |
| MD-S-1 | −3.5 | 36.0 | 40.0 |
| MD-S-1′ | −6.0 | 39.7 | — |
| MD-S-2 | −3.0 | 40.3 | 50.0 |
| MD-S-3 | −4.9 | 46.0 | 55.0 |
| MD-S-4 | −5.8 | 57.4 | 60.0 |
| MAD-S-1 | — | — | 39.0 |
| MAD-S-2 | — | — | 42.0 |
| MAD-S-3 | — | — | 45.0 |
| MAD-S-4 | — | — | 60.0 |

Table III. The second moment, (in gauss$^2$) $<\Delta H^2>$, at temperatures above and below the two second-order transition temperatures for the samples of polyester resin

| Sample | $<\Delta H^2>$ (°C) | $<\Delta H^2>$ (°C) | $<\Delta H^2>$ (°C) | $<\Delta H^2>$ (°C) |
|---|---|---|---|---|
| MD-S-0′ | 0.25 (81.3) | 5.2 (15.0) | 13.7 (−10.0) | 19.8 (−78.0) |
| MD-S-1 | 3.0 (84.2) | 12.9 (16.8) | 14.7 (−26.0) | 17.3 (−48.0) |
| MD-S-2 | 3.1 (70.2) | 12.2 (0.0) | 14.3 (−17.0) | 15.6 (−50.0) |
| MD-S-3 | 5.7 (108.0) | 11.6 (18.0) | 14.3 (−10.0) | 16.0 (−45.0) |
| MD-S-4 | 5.7 (65.0) | 13.5 (18.0) | 13.7 (−31.0) | — |

## Discussion

As was mentioned already, the dilatometric study on the samples of MD series showed that they have two transition points of second-order, and the one was observed below 0°C and the other above room temperature. The transitions below 0°C were observed at nearly equal temperatures for all the samples, while apart from MD-S-0′ and MD-S-1′, those above room temperature were observed at the higher temperature for the sample crosslinked by the larger amount of styrene. Hydrostatic study above room temperature also showed a similar tendency for the samples of MD series and MAD series. Therefore the transition above room temperature is considered to be associated with the crosslinkng structure of the sample. The three dimensional net structure of polyester resin caused by the crosslinking with styrene will become more compact with the increasing amount of styrene until the sample is completely crosslinked. Hence, it is considered that the segmental motion of the polymer is restricted more severely and that the transiton occurs at a higher temperature with the increase of the amount of styrene. This result is well consistent with the result obtained from dielectric measurement by Nakajima and Ishikawa[4] who found two dielectric absorptions at the temperatures above room temperature and below 0°C for the samples of polyester resin. The specific volume of the samples of MD series increases with the increasing amount of styrene. Probably the reason is that the molecular interval is extended by the crosslinking by styrene. Fig. 5 also shows a similar result and the values of density are well consistent with those obtained from Fig. 4.

For MD-S-0′, the lower transition occurs at a temperature almost equal to that of other samples, but the upper transition occurs at 77.9°C, which is higher than that of any other samples. Probably the sample was crosslinked without styrene by the long-time heating and in the sample of this sort the segmental motion was restricted more severely than in the sample completely crosslinked by styrene.

For MD-S-1′, in which the crosslinkings without styrene are considered to exist in addition to those with styrene, only a slight rise of the upper transition temperature was observed. It is likely that the crosslinking without styrene was limited by the styrene contained already in the polymer.

For the samples of MAD series, it was also found that the density decreasing with the increase of the amount of styrene, though it was less affected by the amount of styrene than those of the MD series. In comparing Fig. 6 with Fig. 5, densities and the transition temperature of the sample of MAD series are always lower than those of the sample of MD series containing an equal amount of styrene. Adipic acid does not have C=C bond and is not

4) T. Nakajima and E. Ishikawa, *Bull. Electrotech. Lab. (Japan)*, **20**, 20 (1956).

crosslinked by styrene, so it is considered that an almost constant spaces are always kept at the vicinity of this atomic group and the segmental motion is not so restricted there. For MAD-S-4, the densities are always smaller than those of others of MAD series and the transition temperature is higher. This sample contains an excess amount of styrene and it is considered that it consists of the mixture of MAD-S-3 and styrene polymer or that it is crosslinked by a dimer or trimer of styrene in addition to the crosslinking by the monomer. If the structure of this sample is of the latter type, the molecular interval will be partly wider than that of MAD-S-3, so the decrease of density is reasonable. However, if so, the lowering of the transition point must be observed because the restriction of mobility became smaller than MAD-S-3. The density of polystyrene is about 1.05 at room temperature and the second order transition temperature is around 80°C. Therefore it is considered that the decrease of density and the rise of transition temperature is due to the existence of styrene polymer.

It is considered generally that the second order transition temperature of the crystalline polymer and the non-crystalline one is the point at which the amorphous region of the polymer starts the large-scale segmental motion or at which side chains and molecular terminal groups start the motion. What is, then, the origin of these two second-order transition points of the crosslinked polymer observed? The X-ray diffraction diagrams for the two samples of MD series are shown in Fig. 8. These diagrams did not give any peaks showing the existence of the crystalline part. Therefore the samples investigated are considered to have random network of three-dimensions.

According to Nakajima and Ishikawa[4], polar groups attributed to dielectric absorption at a lower temperature are hydroxyl groups at the molecular terminal and free water contained in the polymer, and those at a higher temperature are ester and ether groups whose mobility is affected by crosslinking by styrene. However, it is not considered that the transition at a lower temperature is attributable only to the molecular-end groups and free water, since, as is shown in Table III, the second moment obtained from the derivative curve in Fig. 7 shows the remarkable change at the vicinity of the lower second-order transition point of each sample. In addition, the amount of protons in the motional state estimated from the derivative curves at the vicinity of room temperature, each of which consists of the absorption curve of protons in the rigid state and that of protons in the motional state, is more than 30% in all the samples investigated and the value of 30% is too large to be considered as protons in the molecular terminal groups and in free water. Therefore it is considered that the second-order transition point at a lower temperature range is the one at which protons in diethyleneglycol located at a place distant from the crosslinking point in the sample of polyester resin start the motion. At the temperature above the upper second-order transition point the narrowing of the movement of protons occurs and a sharp derivative curve was obtained. Therefore the transition point is the temperature at which the Brownian motion of the whole molecule becomes violent. But unlike an amorphous polymer such as atactic polystyrene, it is interesting that the shoulders of the derivative curve are observed at the temperature range above the transition temperature till near the temperature at which thermal degradation of the sample takes place and also that the existence of protons in rigid state (which are considered to be protons at the vicinity of crosslinking points) is recognized.

The author wishes to express his thanks to Professor Masatami Takeda for his able leadership. He is also indebted to Mr. Hiromi Tanno and Miss Masako Yoshida for their assistance in experimental work.

*Tokyo College of Science*
*Kagurazaka, Shinjuku-ku, Tokyo*

# *On the Thermal Dissociation of Organic Compounds*[1]. *XV. Thermal Dissociation of Urethans in the Presence of Aromatic Amines*

By Teruaki MUKAIYAMA and Toyohiko AKIBA

(Received March 15, 1960)

In the previous papers of this series[2,3] it was shown that, in the presence of amines, urethans dissociate into their component compounds via Eqs. 1 and 2.

$$R\text{-}NHCOOR' \rightleftharpoons R\text{-}N{=}C{=}O + HO\text{-}R' \quad (1)$$

$$R\text{-}N{=}C{=}O + H_2N\text{-}R'' \rightleftharpoons R\text{-}NHCONH\text{-}R'' \quad (2)$$

During the process of dissociation, the nitrogen atom of urethan donates a proton to form an isocyanate, and the oxygen atom accepts a proton to form an alcohol. Therefore, the dissociation reaction involves a double transfer of its protons, namely protonation and deprotonation of urethans by the action of a basic medium.

If Eq. 1 is the rate-determining step of the reactions, the dissociation rate can be followed by measuring the amount of amine remaining at various time intervals. In the case of the dissociation of *N*-phenyl-phenylurethan in the presence of aliphatic amines, such as di-*n*-butyl amine and benzyl amine, the plot for the second order reaction shows a straight line throughout a large portion of the reaction. However, the rate of the dissociation of urethan in weak basic medium, such as anilines, is much slower than in aliphatic amines and shows a tendency of increasing rate as the dissociation proceeds. In this case the rate deviates considerably from the true second-order kinetics.

It seems that the anomalous acceleration of the dissociation is due to the reaction products, urea and phenol. The acceleration of dissociation was therefore examined on the basis of the results obtained from experiments repeated with adding various amounts of urea and phenol in the initial process.

The acceleration of a reaction brought about by the products formed is called "products catalyzed reaction" and in the case of this dissociation, it was found that urea accelerates the dissociation much more than phenol. The products catalyzed reaction found in the thermal dissociation of urethan in aromatic amines makes the mechanism of dissociation of urethan in a weak base more complicated than that in a strong base, such as aliphatic amines.

On the other hand, under the present experimental condition, the dissociation of urethan could not be observed in the absence of anilines, even when urea or phenol is present. And it can be concluded that the coexistence of anilines is a necessary condition for urea or phenol to accelerate the dissociation.

In order to clarify the behavior of urea which accelerate the dissociation, the rates of dissociation of urethans in amine solution in the presence of ureas and analogous compounds, such as amide, were determined. The results can thus be explained by considering the acceptance of a proton by the accelerators from the urethan-amine complex in the transition state and to promote it to dissociate.

## Experimental

**Procedure.** — The experimental procedure was essentially that used in the earlier investigation[2,3]. The amount of amine remaining was determined by titrating with 0.05 N perchloric acid in glacial acetic acid, using Crystal Violet as indicator. The perchloric acid glacial acetic acid solution was prepared according to the method of Markunas[4].

**Materials.**—*N*-Phenyl-phenylurethan, m. p. 122~123°C, and *N*-phenyl-*p*-chlorophenyl urethan, m. p. 120~121°C, were prepared from phenyl isocyanate and the corresponding phenols, and recrystallized from aqueous ethanol.

The physical properties for amines and accelerators are listed in Table I.

Determination of dissociation rate: As described in the introduction, the rates of the dissociation of urethan in the presence of aliphatic amines followed true second-order kinetics. However, the rates of the dissociation in aromatic amines showed anomalous acceleration of the dissociation, as shown in Fig. 1, which might have been caused by the reaction products, urea and phenol. Therfore, the rates of the dissociation, which are the initial

1) This investigation was performed at the Gakushuin University.
2) T. Mukaiyama and M. Iwanami, *J. Am. Chem. Soc.*, **79**, 73 (1957).
3) T. Mukaiyama, T. Akiba and T. Asahi, This Bulletin, **33**, 1137 (1960).
4) P. C. Markunas and J. A. Riddick, *J. Ann. Chem.*, **23**, 337 (1951).

TABLE I. BOILING POINTS AND $pK_b$ VALUES FOR AMINES

| Amines | B. p., °C/mmHg | $pK_b$ | Amines | B. p., °C/mmHg | $pK_b$ |
|---|---|---|---|---|---|
| Aniline | 184.4 | 9.30 | *m*-Chloroaniline | 230.5 | 10.40 |
| *o*-Toluidine | 200 | 9.47 | *p*-Chloroaniline | 232 | 12.00 |
| *m*-Toluidine | 203 | 9.30 | *N*-Methylaniline | 195.5 | 9.60 |
| *p*-Toluidine | 200.5 | 9.70 | *N*-Ethylaniline | 204 | 9.38 |
| *o*-Anisidine | 225 | 9.70 | *N*-*n*-Butylaniline | 240 | |
| *m*-Anisidine | 250~1 | | *N*-Benzylaniline | 201~3/37 | |
| *p*-Anisidine | 244 | 8.82 | | | |

Melting points and boiling points for accelerators.

| $RC_6H_4NHCOOCH_2C_6H_5$ R | M. p. °C | | M. p. (b. p.) °C |
|---|---|---|---|
| H | 78 | Diethylbenzamide | (280~2) |
| *m*-Nitro | 115.5~116 | Benzanilide | 163 |
| *p*-Nitro | 155 | Benz-*p*-toluidide | 157~8 |
| *p*-Methoxy | 98.5~ 99 | *sym*-Diphenylurea | 234 |
| *o*-Chloro | 110 | Triphenylurea | 136 |
| *p*-Methyl | 82.5~ 83 | Tetraphenylurea | 183 |
| Acetanilide | 113~4 | *N*,*N*-Diphenyl-*N'*,*N'*-diethylurea | 41~41.5 |
| Benzsulfoamide | 156 | | |
| Benzamide | 130 | | |
| Phthalimide | 238 | | |
| Diphenylbenzamide | 177 | | |

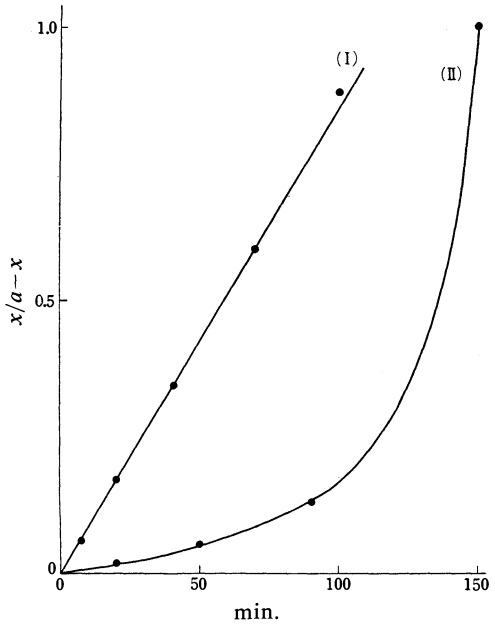



Fig. 1. Second-order plots of the thermal dissociation of *N*-phenyl phenylurethan in di-*n*-butyl amine—nitrobenzene solution at 45°C (I) and that in *p*-chloroaniline—nitrobenzene solution at 165°C (II).

gradiencies, obtained from the titration curve of the residual amine, were measured before appreciable quantities of products, urea and phenol, are formed. The initial rates show substantial variations in their dependence upon the concentration of the amines, or the accelerators, as shown in Tables IV—VI.

## Results and Discussion

As reported in earlier papers[5], the rates of the dissociation of urethan in the presence of amines increased with the basicity of the medium. As shown in Table II, the rates of

TABLE II. THE INITIAL RATES OF THE THERMAL DISSOCIATION OF *N*-PHENYL PHENYLURETHAN IN ALIPHATIC AND AROMATIC AMINES—NITROBENZENE SOLUTION

| Amines | °C | Initial rate $V_0 \times 10^5$ mol./min. |
|---|---|---|
| Aniline | 165 | 0.0303 |
| *p*-Toluidine | 165 | 0.0161 |
| *N*-Methylaniline | 165 | 0.261 |
| *N*-Ethylaniline | 165 | 0.381 |
| Diisobutylamine | 89 | 1.25 |
| Cyclohexylamine | 89 | 3.03 |
| *n*-Hexylamine | 89 | 4.26 |
| 2-Ethylhexylamine | 89 | 1.87 |

the dissociation using aliphatic amines are much faster than those with aromatic ones.

The dissociation rates of urethan in the presence of aromatic amines with electron-donating substituents, such as anisidine and *N*-alkyl aniline, are much greater than those

5) T. Mukaiyama and Y. Hoshino, *J. Am. Chem. Soc.*, **78**, 1756 (1956).

in aromatic amines with electron-withdrawing substituents, such as *m*- and *p*-chloroanilines, as tabulated in Table III.

TABLE III. THE INITIAL RATES OF THE THERMAL DISSOCIATION OF *N*-PHENYL-*m*-CHLOROPHENYL-URETHAN IN AN AMINE—NITROBENZENE SOLUTIONS

| Amines | °C | $V_0 \times 10^6$ mol./min. |
|---|---|---|
| Aniline | 145 | 0.52 |
| *o*-Anisidine | 145 | 0.91 |
| *p*-Anisidine | 145 | 1.79 |
| *m*-Chloroaniline | 145 | 0.05 |
| *p*-Chloroaniline | 165 | 0.25 |
| *o*-Toluidine | 145 | 0.208 |
| *m*-Toluidine | 145 | 0.406 |
| *p*-Toluidine | 145 | 0.659 |
| *N*-Methylaniline | 145 | 1.87 |
| *N*-Ethylaniline | 145 | 2.22 |
| *p*-Aminophenol | 115 | 6.25 |
| *m*-Aminophenol | 165 | 2.54 |

As shown in Fig. 1, an anomalous acceleration of dissociation occurs after about 20% of the urethan dissociated in the presence of aromatic amines. This phenomenon was not observed, when urethan is dissociated in the presence of aliphatic amines, which are stronger bases than aromatic ones. Assuming that the acceleration might be caused by urea and phenol, which are produced during the dissociation, 2.5 equimolecular proportions of *sym*-diphenylurea and phenol were added to the reaction system in advance. Consequently the amount of amines remaining decreased remarkably by the addition of both urea and phenol, as shown in Fig. 2. The acceleration of the reaction aided by the products is generally called " products catalyzed reaction ".

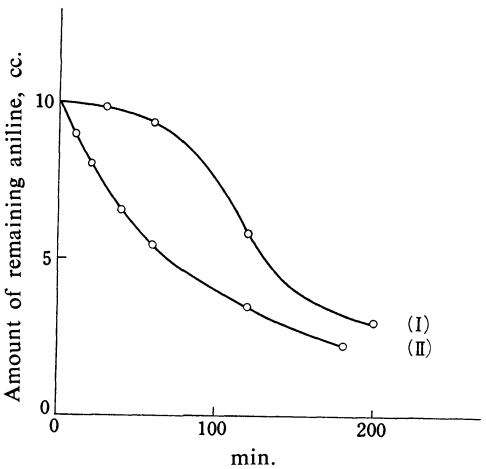



Fig. 2. Catalyzed thermal dissociation of *N*-phenyl *m*-chlorophenyl urethan with additional accelerators in aniline—nitrobenzene solution at 165°C.

| *N*-Phenyl *m*-chlorophenyl urethan | Aniline | *m*-Chloro-phenol | *sym*-Di-phenylurea |
|---|---|---|---|
| (I) 1 mol. | 1 mol. | 0 | 0 |
| (II) 1 mol. | 1 mol. | 2.5 mol. | 2.5 mol. |

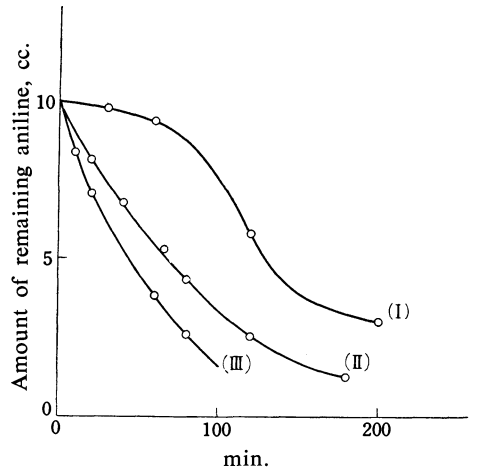



Fig. 3a. Catalyzed thermal dissociation of *N*-phenyl *m*-chlorophenyl urethan with additional accelerator in aniline—nitrobenzene solution at 165°C.

| *N*-Phenyl *m*-chlorophenyl urethan | Aniline | *sym*-Di-phenylurea |
|---|---|---|
| (I) 1 mol. | 1 mol. | 0 |
| (II) 1 mol. | 1 mol. | 1 mol. |
| (III) 1 mol. | 1 mol. | 2 mol. |

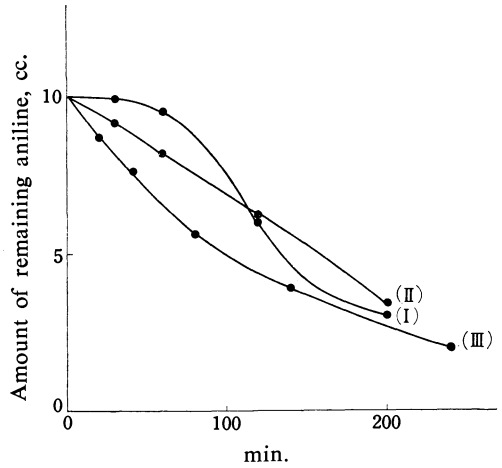



Fig. 3b. Catalyzed thermal dissociation of *N*-phenyl *m*-chlorophenyl urethan with additional accelerator in aniline—nitrobenzene solution at 165°C.

| *N*-Phenyl *m*-chlorophenyl urethan | Aniline | *m*-Chloro-phenol |
|---|---|---|
| (I) 1 mol. | 1 mol. | 0 |
| (II) 1 mol. | 1 mol. | 0.5 mol. |
| (III) 1 mol. | 1 mol. | 1.0 mol. |

Similar results are shown by Baker[6] in the addition reaction of isocyanate with alcohol, a reversal of the present type of dissociation.

On the other hand, under the present experimental conditions, the dissociation of urethan could not be observed in the absence of anilines even when urea or phenol is present. It can be concluded that the coexistence of anilines is a necessary condition for urea or phenol to accelerate the dissociation.

In the present experiment, the catalytic activities of products or urea and phenol, adding them individually, were demonstrated by varying molar ratios of urethan, 0.5 to 2.5, as shown in Fig. 3 and Table IV.

TABLE IV. THE INITIAL RATES OF THE CATALYZED DISSOCIATION OF *N*-PHENYL *m*-CHLOROPHENYL URETHAN (1 MOL.) WITH ADDED ACCELERATORS IN AN AMINE (1 MOL.)—NITROBENZENE SOLUTION

$V_0 \times 10^6$ mol./min.

| Added accelerators | Mol. | Aniline 165°C | *p*-Chloro aniline 165°C | *p*-Toluidine 145°C |
|---|---|---|---|---|
| None | | 0.902 | 0.24 | 0.66 |
| *m*-Chlorophenol | 0.5 | 2.61 | 1.5 | 6.3 |
| | 1.0 | 5.42 | 1.25 | 3.13 |
| | 1.5 | 1.63 | 1.5 | 4.10 |
| | 2.0 | 2.19 | 1.67 | 3.58 |
| | 2.5 | | 2.40 | 13.0 |
| *sym*-diphenylurea | 0.5 | 1.97 | 0.28 | 3.57 |
| | 1.0 | 10.38 | 5.06 | 4.60 |
| | 1.5 | 14.5 | 3.16 | 7.92 |
| | 2.0 | 13.32 | 13.7 | 21.4 |
| | 2.5 | 17.65 | 21.5 | 22.4 |
| *sym*-Diphenylurea and *m*-chlorophenol | 0.5 | 6.88 | 3.2 | 11.7 |
| | 1.0 | 12.5 | 3.7 | 4.73 |
| | 1.5 | 9.07 | 9.9 | 24.17 |
| | 2.0 | 9.38 | 21.0 | 14.5 |
| | 2.5 | | 33.3 | 35.0 |

As shown in Table IV, the rate of the catalyzed dissociation is much greater in the presence of urea than of phenol, and it increases concomitantly with increasing concentrations of urea. However, the increase of rate by varying the initial concentration of phenol could be scarcely observed. Therefore, the acceleration of reaction due to the products is caused chiefly by urea. In aromatic amine series, the accelerating action of urea becomes more effective, when a weak base is used. For example, the ratio of the rates in the presence and in the absence of urea in *p*-chloroaniline is 110 : 1, while that in *p*-toluidine, the stronger base, is 40 : 1.

In order to investigate the catalytic activity of ureas, urethans and acid amides, having both an active hydrogen atom and a basic nitrogen atom and exhibiting the same amphoteric character as urea, were used as accelerators.

TABLE V. THE INITIAL RATES OF THE CATALYZED DISSOCIATION OF *N*-PHENYL PHENYLURETHAN WITH ADDED ACCELERATOR IN A *p*-TOLUIDINE —NITROBENZENE SOLUTION

| | Urethan | *p*-Toluidine | *m*-Chlorophenol | Accelerator |
|---|---|---|---|---|
| mol. | 1 | 1 | 2.5 | 2.5 |

| Accelerator | °C | $V_0 \times 10^6$ mol./min. |
|---|---|---|
| $R\text{-}C_6H_4NHCOOCH_2C_6H_5$ | | |
| R: H | 145 | 1.43 |
| *m*-Nitro | 145 | 0.25 |
| *p*-Nitro | 145 | 1.63 |
| *p*-Methoxy | 145 | 2.12 |
| *p*-Chloro | 145 | 2.08 |
| *p*-Methyl | 145 | 5.16 |
| Acetanilide | 165 | 9.00 |
| Benzenesulfonamide | 165 | 5.9 |
| Benzamide | 115 | 2.72 |
| Phthalimide | 145 | 4.98 |

The initial rates of dissociation in the presence of these accelerators (Tables IV—VI) represent the relative catalytic activities and the order of the acceleration ability is as follows;

benzamide$\gg$ *sym*-diphenylurea$\gg$ phthalimide $>$ *N*-phenyl benzyl urethans$>$ acetanilide $>$ benzenesulfonamide.

From this observation, benzamide and *sym*-diphenylurea appear to have greater activity of acceleration as compared to phthalimide and sulfonamide. It can be shown that sulfonamide and phthalimide, having more acidic hydrogen atoms, are less effective than benzamide and urea.

The thermal dissociation of urethan was carried out in various anilines by adding ureas or benzamides substituted with alkyl or aryl groups for hydrogen atom, in equimolecular proportion, as shown in Table VI. Table VI shows that benzamide and *N*, *N*-diphenyl-*N'*, *N'*-diethylurea possess remarkable catalytic activities, while diphenylbenzamide is hardly effective. Accordingly, the relative order of activity of the accelerators is as follows;

benzamide$\gg$ *N*, *N*-diphenyl-*N'*, *N'*-diethylurea $>$ *sym*-diphenylurea$>$ triphenylurea $\geqq$tetraphenylurea$\geqq$diethylbenzamide $>$ benz-*p*-toluidide$>$ benzanilide $>$ diphenylbenzamide$\geqq$none

As presented in the above order, benzamide accelerates the reaction very remarkably. The

6) J. W. Baker and J. B. Holdsworth, *J. Chem. Soc.*, 1943, 713.

TABLE VIa. THE INITIAL RATES OF THE CATALYZED DISSOCIATION OF *N*-PHENYL *o*-CHLOROPHENYL URETHAN WITH ADDED ACCELERATORS IN AN ANILINE—NITROBENZENE SOLUTION

$V_0 \times 10^5$ mol./min. at 145°C

| Accelerators | Anilines | | | | | | | |
|---|---|---|---|---|---|---|---|---|
| | Aniline | *p*-Methyl | *p*-Methoxy | *p*-Chloro | *N*-Methyl | *N*-Ethyl | *N*-*n*-Butyl | *N*-Benzyl |
| None | 0.02 | 0.035 | 0.12 | 0.019 | 0.019 | 0.110 | 0.107 | 0.005 |
| *sym*-Diphenylurea | 0.21 | 0.681 | 0.707 | 0.022 | 0.711 | 1.06 | 0.57 | 0.078 |
| Triphenylurea | 0.213 | 0.142 | 0.024 | 0.025 | | | | |
| Tetraphenylurea | 3.43 | 0.073 | 0.243 | 0.018 | 0.184 | 7.37 | 0.326 | 0.109 |
| *N*, *N*-Diphenyl-*N'*, *N'*-diethylurea | 6.14 | 0.078 | 0.922 | 0.066 | 1.32 | | | 0.306 |
| Benzamide | 1.51 | 2.00 | 2.07 | 0.598 | 1.10 | 2.11 | 1.08 | 0.415 |
| Benzanilide | 0.026 | 0.065 | 0.128 | 0.007 | 1.58 | 2.00 | 0.025 | 0.015 |
| Benz-*p*-toluidide | 0.060 | 0.067 | 0.245 | 0.012 | 0.052 | 6.84 | 0.078 | 0.050 |
| Diphenylbenzamide | 0.021 | 0.063 | 0.148 | 0.008 | 0.039 | 0.113 | 0.097 | 0.012 |
| Diethylbenzamide | 0.033 | 0.130 | 0.259 | 0.038 | 0.148 | 0.116 | 0.096 | 0.020 |

TABLE VIb. THE INITIAL RATES OF THE CATALYZED DISSOCIATION OF *N*-PHENYL PHENYL-URETHAN WITH ADDED ACCELERATORS IN AN ANILINE—NITROBENZENE SOLUTION

$V_0 \times 10^6$ mol./min. at 165°C

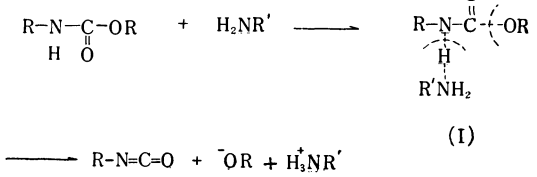
| Accelerators | Anilines | | | |
|---|---|---|---|---|
| | Aniline | *p*-Methyl | *N*-Methyl | *N*-Ethyl |
| None | 0.303 | 0.161 | 2.60 | 3.81 |
| *sym*-Diphenylurea | 1.59 | 1.51 | 3.02 | 9.17 |
| Benzaniline | 0.098 | 0.232 | 0.553 | 0.917 |
| Benz-*p*-toluidide | 0.419 | 0.446 | 0.473 | |
| Benzamide | 7.14 | 0.758 | 5.41 | 9.63 |
| Diphenylbenzamide | 0.071 | 0.589 | 0.330 | 10.6 |
| Diethylbenzamide | 0.58 | 0.107 | 0.91 | 0.089 |

order [*N*, *N*-diphenyl-*N'*-*N'*-diethylurea> tetraphenylurea and diethylbenzamide> diphenylbenzamide] indicates that in similar compounds such as urea and benzamide, diethyl derivatives catalyze more strongly than diphenyl derivatives. Furthermore, the order of urea compounds, *N*, *N*-diphenyl-*N'*-*N'*-diethylurea> *sym*-diphenylurea> tetraphenylurea, indicates that the hydrogen atom attached to the nitrogen atom is not effective in accelerating the dissociation, but the character of the nitrogen atom is the responsible factor. It is considered that the ability of a compound to accelerate the dissociation is attributed to the electrical and structural character of nitrogen atom which is capable of receiving a proton.

In view of the above discussion, it has been observed that the rate of dissociation of urethan, including a double transfer of its proton, in a strong basic or acidic medium is faster than that in a weak basic or acidic medium. This indicates that the rate of dissociation is dependent on the acidic or basic strength of the medium. However, the rate of dissociation is enhanced in a medium containing a mixture of weak base and acid, such as aniline and phenol, rather than in a medium containing the individual compounds.

## Reaction Mechanism

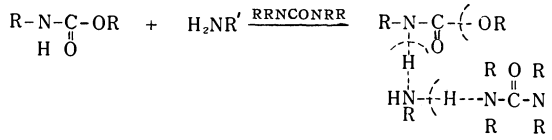
The scheme of the uncatalyzed dissociation of urethan in the presence of an organic base is illustrated as follows;



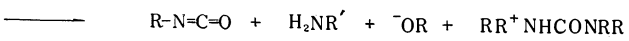
(I)

In state I, amine behaves as such as to accept a proton which results in the formation of a complex with urethan. State I then dissociates through a shift of a pair of electrons. The catalytic activity of an amine, which assists in the proton transfer of urethan at state I is affected by the basicity of amine as shown in Table II.

The scheme of the dissociation of urethan in an aromatic amine medium in the presence of an accelerator is illustrated as follows;



(II)



In state II, the amine behaves in such a manner as to accept a proton, and the accelerator encourages the deprotonation of the amine to proceed. That is, an accelerator accepts a hydrogen atom from the amine–urethan complex (state II) and induces the amine to take up the hydrogen atom from urethan, hence the dissociation proceeds more readily. Therefore, the accelerator plays an important role in promoting the dissociation of the amine-urethan complex by participating in the proton transfer.

## Summary

*N*-Phenyl phenylurethans dissociate readily into their component compounds in the presence of aliphatic amines and the plot for the second order reaction shows a straight line throughout a large portion of the dissociation. However, the rate of the dissociation of urethans in aromatic amines is much slower than in aliphatic ones and shows a tendency of increasing rate as the dissociation proceeds. The anomalous acceleration of the dissociation is due to the reaction products, urea and phenol.

In order to clarify the behavior of urea which accelerates the dissociation effectively, the rates of the dissociation of urethans in the presence of ureas and analogous compounds, such as urethans and amides, were determined.

The mechanism of the dissociation of urethans in aromatic amines which involve the product catalyzed reaction was discussed.

The authors wish to express their hearty thanks to Professor Toshio Hoshino for his encouragement throughout the course of this experiment and to Mr. Keishi Katsuno and Mr. Yohichi Nakamura for their assistance.

*Department of Chemistry*
*Tokyo Institute of Technology*
*Meguro-ku, Tokyo*

# *The Dehydration Reactions of Aldoximes*

By Teruaki MUKAIYAMA and Tsujiaki HATA

(Received May 4, 1960)

The dehydration reactions of nitroparaffin and aldoxime with isocyanate, carbodiimide, acetylenic ether and ketene acetal have been described in the previous papers[1,2]. In one of the preceding papers, it was proposed that compounds containing a triple bond or a twinned double bond may be used as a useful dehydrating reagent. In addition, the dehydration reaction of aldoxime with ketene acetal containing a double bond and two alkoxyl groups turns out to be also successful. It is also known that iminochloride[3] containing a double bond and a chlorine atom reacts with water much more easily, yielding acid amide rather than nitrile containing a triple bond. These results lead to conclusion that not only the compounds containing a triple bond or a twinned double bond but also the compounds containing a double bond and an atom or atomic group, such as halogen alkoxyl or acyloxyl groups, would become effective dehydrating reagents.

Referring to the above results it appears

1) T. Mukaiyama and T. Hoshino, *J. Am. Chem. Soc.*, **82**, 5339 (1960).

2) T. Mukaiyama and T. Hata, This is now presented to this Bulletin.

3) J. v. Braun, F. Jostes and W. Münch, *Ann.*, **453**, 113 (1927).

feasible to extend the dehydration reactions of nitroparaffin and aldoxime by using vinyl ether or vinyl acetate in place of acetylenic ether described in the preceding paper. Firstly, the reaction of vinyl *n*-butyl ether and aldoxime is tested in the presence of tertiary alkyl amine, but no reaction occurs and the starting materials are recovered quantitatively. The dehydration reaction is also not observed, when vinyl acetate is treated with benzaldoxime under the same condition.

It is known that the addition reaction[4] of vinyl acetate with an alcohol to form an acetal is well conducted in the presence of boron trifluoride and mercuric oxide. Accordingly, vinyl acetate and benzaldoxime are reacted in the presence of a catalytic amount of boron trifluoride and yellow mercuric oxide in place of a basic catalyst. A violent reaction takes place and benzonitrile, acetaldehyde and acetic acid are obtained in good yields.

$$CH_2{=}CH{-}OAc + C_6H_5CH{=}NOH \rightarrow \left[\begin{array}{l} CH_3CH(OAc)(ON{=}CHC_6H_5) \end{array}\right] \rightarrow C_6H_5C{\equiv}N + CH_3CHO + AcOH$$

(I)

Analogous to the explanation used for the dehydration with acetylenic ether, it is reasonable to consider that the reaction proceeds through an intermediate I which gives nitrile and hemiacylal. The latter decomposes to give acetaldehyde and acetic acid.

By the same method, the reaction of vinyl ether and aldoxime gives nitrile in equally good yield along with acetaldehyde and acetal.

$$2CH_2{=}CH{-}OR + R'CH{=}NOH \rightarrow CH_3CH(OR)(ON{=}CHR') \rightarrow R'C{\equiv}N + CH_3CHO + CH_3CH(OR)_2$$

(II)

In order to evaluate experimentally the intermediate of the reaction, namely the addition compound of vinyl ether and aldoxime, the isolation of the compound II is tried. Since the catalysts, boron trifluoride and mercuric oxide, may accelerate both the initial addition reaction and the subsequent decomposition reaction, an equimolar amount of triethyl amine to neutralize boron trifluoride is added to the reaction system of vinyl ether and aldoxime immediately after the liberation of heat ceases. By this method the addition compound is isolated in high yield. And the addition compound is observed to decompose on heating in the presence of a catalytic amount of boron trifluonide and mercuric oxide to give 82% yield of nitrile. Consequently, it can be concluded that the coexistence of boron trifluoride and mercuric oxide is effective in accelerating the decomposition of the associated addition compounds with vinylogs, and conducts the dehydration of aldoximes. The decomposition of the adduct II cannot be observed in the absence of the said catalysts and it is recovered quantitatively after refluxing for 7 hr. in benzene.

Further, it is confirmed that benzaldoxime is recovered unchanged, when it is refluxed for 6 hr. in the presence of a catalytic amount of boron trifluoride in benzene. It can be concluded that the dehydration reaction of benzaldoxime is conducted with vinyl ether or vinyl acetate.

In order to examine the possibility of dehydration of aldoximes with vinylogs having an electron-withdrawing substituent which usually show different reactions from vinyl ether or vinyl acetate, acrylonitrile is reacted with benzaldoxime in the presence of a catalytic amount of boron trifluoride and mercuric oxide. No reaction is then observed and the starting materials are recovered. On the other hand, the addition reaction of acrylonitrile with aldoxime is known as an example of cyanoethylation[5] when strong bases are used. The addition compound of acrylonitrile and benzaldoxime is synthesized initially according to the method of Bruson and Riener and it is successfully decomposed to give nitrile and ethylene cyanohydrin on heating in the presence of a catalytic amount of boron trifluoride and mercuric oxide.

$$CH_2{=}CH{-}C{\equiv}N + C_6H_5CH{=}NOH \xrightarrow[\text{or Triton B}]{KOH} C_6H_5CH{=}NOCH_2CH_2C{\equiv}N \xrightarrow{HgO\text{-}BF_3} HOCH_2CH_2C{\equiv}N + C_6H_5C{\equiv}N$$

In the next place, the dehydration reaction of aldoxime with a compound containing carbon-oxygen double bond is studied. It is generally shown that carbonyl compounds react with water to form unstable *gem*-dihydroxy compounds which exist in equilibrium with the starting materials and can scarcely be isolated. On this basis, it is said that these compounds cannot be used as a dehydrating reagent in the present type of reaction. It is, however, known that benzil containing two carbonyl groups reacts with water to form a stable benzilic acid and this is considered to be an example of carbonyl compounds as a dehydrating reagent. The reaction of benzil with aldoxime in the presence of a small

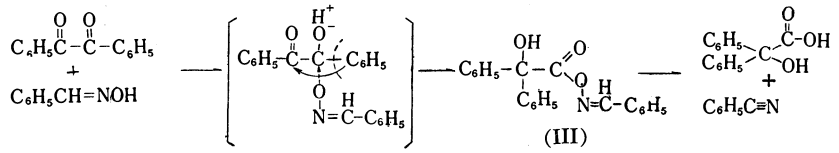
4) W. J. Croxall, F. J. Glavis and H. T. Neher, *J. Am. Chem. Soc.*, **70**, 2805 (1948).

5) H. A. Bruson and T. W. Riener, U. S. Pat., 2352514 *Chem. Abstr.* **38**, 5506 (1944).

amount of potassium hydroxide is tried and nitrile and benzilic acid are obtained as expected.

$$C_6H_5CO—COC_6H_5 + C_6H_5CH=NOH \xrightarrow{KOH} C_6H_5C\equiv N + (C_6H_5)_2(OH)C—COOH$$

The reaction can be shown by the following scheme which involves the initial formation of the addition compound of benzil and aldoxime, and the subsequent rearrangement of the phenyl group to form III. This decomposes to nitrile and benzilic acid by transferring its hydrogen atom.



(III)

Further, in the course of preparing acetylenic ether according to the method of Arens[6], it is found that the intermediate, $\alpha,\beta$-dibromoethyl methyl ether, reacts violently with water to form bromoacetaldehyde and hydrogen bromide. On the consideration that such compounds which readily react with water can be used as a dehydrating reagent of the present type of dehydration, the reaction of $\alpha,\beta$-dibromoethyl methyl ether with aldoxime is tried and nitrile results quantitatively along with hydrogen bromide.

$$CH_2BrCHBr—O—CH_3 + C_6H_5CH=NOH \rightarrow \left[CH_2BrCH(—OCH_3)—ON=CHC_6H_5\right] \rightarrow C_6H_5C\equiv N + (CH_2BrCHO)_3 + HBr$$

(IV)

This reaction can be explained by introducing the intermediate IV which is yielded by the reaction of aldoxime and the ether. The IV, which is similar to the addition compound of vinyl ether and aldoxime, decomposes to give nitrile and hemiacetal. The latter decomposes to aldehyde and alcohol.

Similarly, nitrile is obtained quantitatively when aldoxime is reacted with $\alpha,\beta$-dibromoethyl acetate and $\alpha,\beta$-dibromopropionitrile respectively as shown in the following equations.

$$CH_2BrCHBr—OAc + C_6H_5CH=NOH \rightarrow C_6H_5C\equiv N + AcOH + (CH_2BrCHO)_3 + HBr$$

$$CH_2BrCHBr—C\equiv N + C_6H_5CH=NOH \rightarrow C_6H_5C\equiv N + HBr$$

These reactions are carried out in the absence of a catalyst, and the initially formed hydrogen bromide may be considered to accelerate the reactions.

On the other hand, the treatment of benzaldoxime with $\alpha,\beta$-dibromoethylbenzene yields the dehydrated product of bonzonitril and water in high yields, and the starting material of dibromo compound is unexpectedly recovered. The recovery of the dibromo compound can be satisfactorily explained by considering the replacement reaction of initially formed $\beta$-hydroxy-$\beta$-phenylethylbromide with hydrogen bromide, as shown in the following equations. The unexpected isolation of water is considered to be due to the low reactivity of $\alpha,\beta$-dibromoethylbenzene with water as compared with $\alpha,\beta$-dibromoethylmethyl ether and $\alpha,\beta$-dibromoethyl acetate.

$$CH_2BrCHBr—C_6H_5 + C_6H_5CH=NOH \rightarrow \left[CH_2BrCH(—C_6H_5)—ON=CHC_6H_5\right] + HBr$$

(V)

$$V \rightarrow C_6H_5C\equiv N + CH_2BrCH(—C_6H_5)—OH$$

(VI)

$$VI + HBr \rightarrow CH_2BrCHBr—C_6H_5 + H_2O$$

## Experimental

**Reaction of $\alpha$-Benzaldoxime with Vinyl Acetate.**—A solution of 10 drops of boron trifluoride (40% ether solution) and 0.6 g. of yellow mercuric oxide in 10 ml. dry benzene was added dropwise over a 30-min. period to a solution of vinyl acetate (16 g., 0.186 mol.) and $\alpha$-benzaldoxime (11.3 g., 0.093 mol.) in 20 ml. dry benzene with continuous stirring. Then acetaldehyde and benzene were distilled into a 2, 4-dinitrophenylhydrazine solution. The yield of acetaldehyde 3.6 g., (44% of theoretical) was calculated from the yield of acetaldehyde 2,4-dinitrophenylhydrazone thus obtained. The liquid residue was distilled to give acetic acid 8.1 g., (72% of theoretical), b. p. 55C° (61 mmHg) and benzonitrile 8.7 g., (91% of theoretical), b. p. 85~87°C (23 mmHg) was obtained.

**Reaction of *n*-Heptanaldoxime with Vinyl Methyl Ether.**—To a solution of *n*-heptanaldoxime (5 g., 0.039 mol.) and methyl vinyl ether (5 g., 0.089 mol.) were added 2 drops of boron trifluoride (40% ether solution) and 0.1 g. of yellow mercuric

6) J. F. Arens, *Rec. trav. chim.* Pays-Bas, **74**, 271 (1955).

oxide. After shaking the mixture for 30 min., it became clear, and then it was heated under reflux for 5 hr. After removing acetaldehyde and benzene, acetaldehyde dimethyl acetal 3.5 g., (89% of theoretical), b. p. 64~66C° and heptanitrile 1.7 g., (40% of theoretical), b. p. 54°C (8 mmHg) were obtained.

**Reaction of α-Benzaldoxime with Vinyl Methyl Ether.**—To a solution of α-benzaldoxime (15 g., 0.123 mol.) and methyl vinyl ether (15 g., 0.268 mol.) in 20 ml. dry denzene were added 5 drops of boron trifluoride (40% ether solution) and 0.3 g. of yellow mercuric oxide. After shaking the mixture for 30 min., it was heated under reflux for 6 hr. After removal of acetaldehyde and benzene, acetaldehyde dimethyl acetal 4.0 g., (34% of theoretical), b. p. 62~64°C and benzonitrile 10.2 g., (80% of theoretical), b. p. 48~50°C (3 mmHg) were obtained.

**Addition Compound of α-Benzaldoxime and Ethyl Vinyl Ether.**—To a solution of ethyl vinyl ether (3.6 g., 0.05 mol.) and 0.05 g. of yellow mercuric oxide in 10 ml. dry benzene was added dropwise a solution of α-benzaldoxime (6.1 g., 0.05 mol.) and 2 drops of boron trifluoride (40% ether solution) in 5 ml. dry benzene with continuous stirring over a 10-min. period at room temperature. The reaction mixture became warm and clear soon. After rapid cooling, 4 drops of triethyl amine was added to the solution. After removal of benzene, an attempt was made to distil the liquid residue. Addition compound of benzaldoxime and ethyl vinyl ether 7.8 g., (80% of theoretical), b. p. 92~93°C (4.5 mmHg) was obtained.

Found: C, 68.62; H, 7.86; N, 7.41. Calcd. for $C_{11}H_{15}O_2N$: C, 68.37; H, 7.82; N, 7.25%.

**Decomposition of the Addition Compound of α-Benzaldoxime and Ethyl Vinyl Ether.**—To a solution of the addition compound of α-benzaldoxime and ethyl vinyl ether (1.9 g., 0.01 mol.) in 10 ml. dry ether were added 5 drops of boron trifluoride (40% ether solution) and yellow mercuric oxide (0.05 g.). Then the mixture was heated under reflux for 7 hr. After removal of acetaldehyde and ether, ethanol 0.4 g., (87% of theoretical), b. p. 77~78°C and benzonitrile 0.85 g., (83% of theoretical), b. p. 69°C (10 mmHg) were obtained.

**Reaction of α-Benzaldoxime with Acrylonitrile.**—To a solution of α-benzaldoxime (8 g., 0.066 mol.) and acrylonitrile (3.5 g., 0.066 mol.) in 15 ml. dry benzene was added 0.2 g. of potassium hydroxide. The mixture was heated under reflux for 5 hr. After removal of benzene, the addition compound of α-benzaldoxime and acrylonitrile 5.2 g., (45% of theoretical), b. p. 150°C (6 mmHg) was obtained.

Found: N, 16.12. Calcd. for $C_{10}H_{10}N_2O$: N, 16.09%.

The same result was obtained when Triton B was used in place of potassium hydroxide.

**Decomposition of the Addition Compound of α-Benzaldoxime and Acrylonitrile.**—To a solution of the above mentioned addition compound (5.2 g., 0.03 mol.) in 10 ml. dry benzene were added 10 drops of boron trifluoride (40% ether solution) and 0.1 g. of yellow mercuric oxide. The mixture was heated under reflux for 12 hr. After removal of benzene, benzonitrile 1.6 g., (44% of theoretical), b. p. 188~189°C and ethylene cyanohydrin 0.7 g., (33% of theoretical), b. p. 221~223°C were obtained.

**Reaction of α-Benzaldoxime with Benzil.**—To a mixture of α-benzaldoxime (1.2 g., 0.01 mol.) and benzil (2.1 g., 0.01 mol.) was added 0.1 g. of well-ground potassium hydroxide. After the mixture was heated on the water-bath for 30 min., it was left on stand for 5 days at room temperature and a large amount of benzilic acid was separated. It was filtered and washed with light petroleum ether and recrystallized from 95% ethanol, 0.5 g., (22% of theroetical), m. p. 150°C. After removal of the low boiling point fractions from the filtrate, benzonitrile 0.2 g., (20% of theoretical), b. p. 78~80°C (18 mmHg) was obtained.

**Reaction of α-Benzaldoxime with α, β-Dibromoethyl Methyl Ether.**—α-Benzaldoxime (6.7 g., 0.055 mol.) was added dropwise to a solution of α, β-dibromoethyl methyl ether in 10 ml. dry benzene with continuous stirring at room temperature. A large amount of white precipitate separated, and then it dissolved with evolving hydrogen bromide, when the mixture was heated under reflux. After heating the mixture for 6 hr., the resulting solution was distilled under reduced pressure and benzonitrile 5.3 g., (93% of theoretical), b. p. 75° (17 mmHg) was obtained. From the residue a small amount of bromoacetaldehyde trimer, m.p. 102~104°C, was obtained.

**Reaction of α-Benzaldoxime with α, β-Dibromoethyl Acetate.**—α-Benzaldoxime (9.9 g., 0.081 mol.) was added dropwise to a solution of α, β-dibromoethyl acetate (20 g., 0.081 mol.) in 20 ml. dry benzene with continuous stirring. After the mixture was heated under reflux for 2 hr., the resulting solution was worked up in the usual manner and acetic acid 2.2 g., (46% of theoretical), b. p. 118°C and benzonitrile 4.8 g., (57% of theoretical), b. p. 61~63°C (7 mmHg) were obtained. From the residue a small amount of bromoacetaldehyde trimer, m. p. 103~104°, was obtained.

**Reaction of α-Benzaldoxime with α, β-Dibromopropionitrile.**—α-Benzaldoxime (11.4 g., 0.094 mol.) was added dropwise to a solution of α, β-dibromopropionitrile (20 g., 0.094 mol.) in 20 ml. dry benzene with continuous stirring. After heating the mixture under reflux for 3 hr., the resulting solution was worked up in the usual manner, benzonitrile 9.7 g., (98% of theoretical), b. p. 77~78°C (15 mmHg) was obtained.

**Reaction of α-Benzaldoxime with α, β-Dibromoethylbenzene.**—α-Benzaldoxime (2.4 g., 0.05 mol.) was added to a solution of α, β-dibromoethylbenzene (5.3 g., 0.05 mol.) in 15 ml. dry benzene. The mixture was heated under reflux for 5 hr. After removal of benzene, water and benzonitrile were distilled and water 2.0 g., (56% of theoretical) and benzonitrile 1.3 g., (65% of theoretical), b. p. 76~78°C (15 mmHg) were obtained. α, β-Dibromoethylbenzene 3.7 g., (70% of theoretical), b. p. 137~139°C (15 mmHg) was recovered.

The authors wish to express their hearty thanks to Professor Toshio Hoshino for his encouragement and to Mr. Senichiro Takeda and Mr. Tomohiko Tsuchiya for their help

throughout the course of this experiment. Thanks are also due to Mr. Asaji Kondo for the microanalyses.

*Department of Chemistry*
*Tokyo Institute of Technology*
*Meguro-ku, Tokyo*

# *A Kinetic Study of Addition Reaction of Vinyl Ether with Carboxylic Acids*

By Teruaki MUKAIYAMA and Hiroyuki NOHIRA

(Received June 1, 1960)

The addition reactions of vinyl ethers with carboxylic acids have been known to give hemiacetal esters (I) in high yields in the presence of a catalytic amount of strong acids, such as hydrochloric acid, sulfuric acid and phosphoric acid.

$$CH_2{=}CH{-}OR + R'COOH \rightarrow CH_3{-}\underset{\displaystyle OCOR'}{\overset{\displaystyle H}{\overset{|}{\underset{|}{C}}}}{-}OR \quad [I] \qquad (1)$$

There are numerous publications in the literature on the addition reactions of vinyl ethers with compounds containing active hydrogen, such as alcohols, phenols and carboxylic acids[1-4]; however, there have been no papers published on the kinetic study of the reactions of vinyl ethers except on their hydrolysis[5,6].

In the present investigation, the rates of the addition reaction of *n*-butyl vinyl ether with carboxylic acids in dioxane and toluene have been measured in order to study the mechanism of the addition reactions.

## Experimental

**Materials.**—*n*-Butyl vinyl ether was obtained from commercial source and purified as follows; the vinyl ether was washed several times with equal volumes of water containing a small amount of sodium carbonate, dried over potassium hydroxide and distilled from metallic sodium through a 30 cm. long column, b. p. 93.0~94.0°C.

Carboxylic acids were also obtained from a commercial source and purified by distillation or recrystallization. Melting points or boiling points and p*K*a of the carboxylic acids used are listed in Table. I.

**Solvent.**—Dioxane (b. p. 101.3°C), toluene (b. p. 111°C) and anisole (b. p. 154°C) were purified by being stored over metallic sodium wire and being distilled from metallic sodium.

**General Kinetic Method.**—In a 50 ml. volumetric flask a solution of *n*-butyl vinyl ether in dioxane was prepared which was exactly 3.00 mol./l. with respect to the vinyl ether. The exact molarity of the solution was determined by iodometry[7]. Similarly, a solution of the corresponding carboxylic acids of appropriate concentration was prepared.

As a typical run, 20 ml. of the carboxylic acid

TABLE I. LIST OF CARBOXYLIC ACIDS USED

| Acid | B. p. | $pK_a^{25°C}$ | Acid | M. p. | $pK_a^{25°C}$ |
|---|---|---|---|---|---|
| Acetic | 118.5 | 4.76 | Benzoic acid | 121.7 | 4.17 |
| Propionic | 141.0 | 4.88 | *o*-$NO_2$- | 148 | 2.21 |
| *n*-Butyric | 162.5 | 4.82 | *o*-Br- | 149 | 2.82 |
| *n*-Valeric | 187.0 | 4.81 | *o*-Cl- | 141 | 2.89 |
| *n*-Caproic | 205.0 | 4.85 | *m*-$NO_2$- | 142 | 3.46 |
| Monochloroacetic | 189.5 | 2.81 | *m*-$CH_3$- | 111 | 4.28 |
| | | | *p*-$NO_2$- | 240 | 3.40 |
| | | | *p*-$CH_3O$- | 184 | 4.49 |
| | | | 3.5, Di-$NO_2$- | 205 | 2.80 |

1) N. A. Gershtein and M. F. Shostakovskii, *Zhur. Obshchei Khim.* (*J. Gen. Chem.*), **21**, 1452 (1951); *Chem. Abstr.*, **46**, 3001 (1952).
2) M. Levas, *Ann. chim.* (*Paris*), **7**, 697 (1952).
3) C. E. Schildknecht, A. O. Zoss and C. Mckinly, *Ind. Eng. Chem.*, **39**, 180 (1947).
4) W. Reppe, *Ann.*, **601**, 81 (1956).
5) A. Zahorka und K. Weimann, *Monatsh.* **71**, 229 (1938).
6) E. N. Prolezhava, E. S. Shapiro and M. F. Shostakovskii, *Zhur. Obshchei Khim.* (*J. Gen. Chem.*), **18**, 1663 (1948); *Chem. Abstr.*, **43**, 3272 (1949).
7) S. Siggia and R. L. Edsberg, *Anal. Chem.*, **20**, 762 (1948).

solution was placed in a 30 ml. reaction tube, and immersed in a thermostat for 20 min. to obtain a constant temperature. To start the reaction, 5 ml. of the vinyl ether solution was pipetted into the carboxylic acid solution. Two milliliter aliquots of this solution were withdrawn from time to time by means of a pipet and put into the mixture of 15 ml. of standard 0.1 N iodine solution and 15 ml. of methanol in a 100 ml. erlenmyer flask. After the mixture was stirred for 5 min., the excess iodine was titrated with standard 0.1 N sodium thiosulfate solution.

When toluene or anisole was used as the solvent, 0.5 N iodine solution and a large excess of methanol were used to make the titrating mixture homogeneous.

## Results and Discussion

Fig. 1 shows plots of percentage reaction against time (min.) for the reaction of *n*-butyl vinyl ether and monochloroacetic acid in dioxane at 60.0°C with various initial concentrations of reactants. The order of the reaction was determined by van't Hoff's initial rate method, and 0.95±0.1 order with respect to vinyl ether and 2.05±0.1 order with respect to carboxylic acid are obtained. Hence, the kinetic equation of the reaction is expressed by

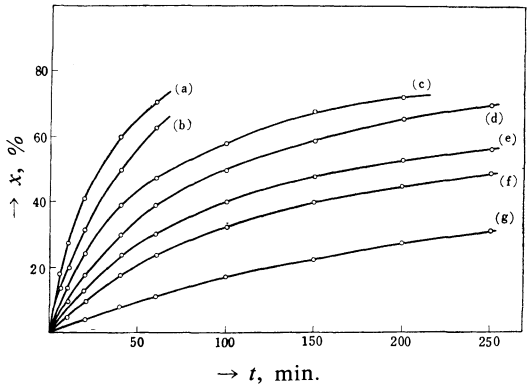



Fig. 1. The addition reactions of *n*-butyl vinyl ether with monochloroacetic acid in dioxane at 60°C.
The plots of percentage reaction *x* against time by various concentration:

| Run | a) | b) | c) | d) | e) | f) | g) |
|---|---|---|---|---|---|---|---|
| *n*-Butyl vinyl ether, mol./l. | 0.6 | 0.5 | 1.2 | 1.0 | 0.6 | 0.5 | 0.3 |
| Monochloro-acetic acid mol./l. | 1.2 | 1.0 | 0.6 | 0.5 | 0.6 | 0.5 | 0.3 |

$$-\frac{dC}{dt}=kAB^2 \qquad (2)$$

where the symbols $A$, $B$ and $C$ represent the concentrations of vinyl ether, carboxylic acid and product, respectively.

Eq. 2 may be integrated to give Eq. 3 or 4.

For $A_0 \neq B_0$,

$$2.303 \log \frac{A_0(B_0-C)}{B_0(A_0-C)}+\frac{B_0-A_0}{B_0}-\frac{B_0-A_0}{B_0-C}=(B_0-A_0)^2kt \qquad (3)$$

For $A_0=B_0$,

$$\frac{2A_0C-C^2}{(A_0-C)^2}=2A_0^2kt \qquad (4)$$

where $A_0$ and $B_0$ represent the initial concentrations of vinyl ether and carboxylic acid, respectively.

For individual runs with varvious initial concentrations shown in Fig. 1, the third order rate constants were calculated by the Eq. 3 or 4 at appropriate percentage reaction. The rate constants are determined along the abovementioned way in such a large range of reaction, i.e. from 10% to 60% completion. Table II shows these rate constants and leads to the fact that these constants are very close together in magnitude (the average value of the rate constant is $4.06\times10^{-4}$ mol$^{-2}$ sec$^{-1}$).

Similarly, the third order rate constants of the reaction of *n*-butyl vinyl ether with aliphatic and aromatic carboxylic acids are obtained (Tables III and IV). The plots of the logarithm of the rate constants vs. threciprocal absolute temperature gave satisfactory straight lines from which activation energies and entropies of activation were obtained (Table IV).

The effects of the substituents of carboxylic acids on this addition reaction are noted as follows:

(1) The rate increases as the acidity of carboxylic acid increases.

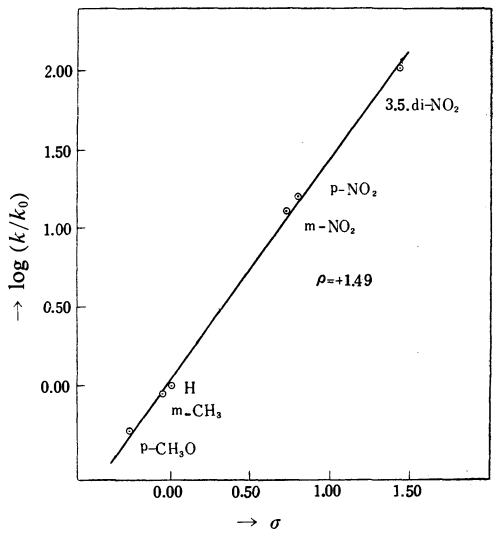



Fig. 2. Plots of log ($k/k_0$) against the Hammett $\sigma$-values.

TABLE II. THE RATE CONSTANTS FOR THE ADDITION REACTION OF *n*-BUTYL VINYL ETHER WITH MONOCLOROACETIC ACID IN DIOXANE AT 60°C

| Run | Initial concentration (mol./l.) V. E. | ClAcOH | $k\times10^{-4}$ mol$^{-2}$ sec$^{-1}$ | | | | | | |
|---|---|---|---|---|---|---|---|---|---|
| | | $x$ (%)=10 | 20 | 30 | 40 | 50 | 60 | 70 | Average |
| a | 0.6 | 1.2 | — | 4.11 | 4.05 | 3.97 | 4.15 | 4.12 | 3.95 | 4.06 |
| b | 0.5 | 1.0 | — | 4.08 | 3.99 | 3.93 | 4.02 | 4.10 | — | 4.02 |
| c | 1.2 | 0.6 | — | 4.02 | 4.05 | 4.08 | 4.00 | 3.99 | 4.12 | 4.04 |
| d | 1.0 | 0.5 | — | 3.98 | 3.85 | 4.05 | 4.03 | 3.90 | — | 3.96 |
| e | 0.6 | 0.6 | 4.20 | 4.09 | 4.22 | 4.03 | 3.97 | — | — | 4.10 |
| f | 0.5 | 0.5 | 4.11 | 4.08 | 4.15 | 4.23 | 4.17 | — | — | 4.15 |
| g | 0.3 | 0.3 | 3.98 | 4.08 | 4.07 | — | — | — | — | 4.05 |
| | | | | | | | | | Average | 4.06 |

TABLE III. THE RATE CONSTANTS, THE ACTIVATION ENERGIES AND THE ENTROPIES OF ACTIVATION OF THE ADDITION REACTIONS OF *n*-BUTYL VINYL ETHER WITH CARBOXYLIC ACIDS IN DIOXANE

| Carboxylic acid | $k\times10^{-5}$ mol$^{-2}$ sec$^{-1}$ 70°C | 60°C | 50°C | 40°C | 30°C | $E$ (kcal.) | $-\Delta S^{\neq}$ (e. u.) |
|---|---|---|---|---|---|---|---|
| Acetic | 0.99 | 0.46 | 0.20 | — | — | 16.5 | 33.0 |
| Monochloroacetic | — | 40.6 | 18.5 | 8.69 | 3.95 | 15.6 | 27.4 |
| Benzoic | 3.14 | 1.48 | 0.73 | 0.32 | — | 16.2 | 32.2 |
| 3.5, Di-$NO_2$- | — | 190.0 | 97.5 | 51.1 | — | 13.9 | 29.9 |
| *o*-$NO_2$- | — | 150.0 | 67.5 | 32.5 | 15.3 | 14.7 | 27.5 |
| *m*-$NO_2$- | — | 20.0 | 10.1 | 4.80 | 2.20 | 14.8 | 31.4 |
| *p*-$NO_2$- | 43.8 | 23.3 | 10.9 | — | — | 14.7 | 31.2 |
| *m*-$CH_3$- | 2.84 | 1.37 | 0.62 | 0.29 | — | 16.2 | 32.3 |
| *p*-$CH_3O$- | 1.83 | 0.79 | 0.34 | — | — | 17.5 | 29.5 |
| *o*-Br- | 31.2 | 15.0 | 7.40 | 3.75 | — | 15.1 | 31.0 |
| *o*-Cl- | 26.0 | 13.0 | 6.65 | 3.15 | — | 15.4 | 32.5 |

TABLE IV. THE RATE CONSTANTS OF THE ADDITION REACTION OF *n*-BUTYL VINYL ETHER WITH ALIPHATIC CARBOXYLIC ACIDS IN TOLUENE AT 60°C

| Carboxylic acid | Acetic | Propionic | *n*-Butyric | *n*-Valeric | *n*-Caproic |
|---|---|---|---|---|---|
| $k\times10^{-5}$ mol$^{-2}$ sec$^{-1}$ | 8.70 | 3.66 | 3.05 | 1.67 | 1.01 |

(2) The effect of substituents in meta and para substituted benzoic acids nearly follows the Hammett equation. As shown in Fig. 2, $\log k$ is approximately a linear function of the substituent constants $\sigma$ given by Hammett[8], and the gradient of the plots gave a value for the reaction constant $\rho$ of +1.49.

(3) In ortho substituted benzoic acids, the reaction is not so fast as expected from their acidities, which may be attributed to the steric hindrance of the ortho substituents.

(4) In fatty acids, the rate decreases as the length of carbon chain increases.

These results lead to the conclusion that the reaction takes place in two stages, namely the initial formation of an intermediate complex in equilibrium with vinyl ether and carboxylic acid and followed by the reaction of the complex with another carboxylic acid via rate determining step.

8) L. P. Hammett, "Physical Organic Chmistry", McGraw-Hill Book Co., Inc., New York, N. Y. (1941), p. 188.

$$CH_2{=}CH{-}OC_4H_9 + RCOOH \underset{K}{\rightleftarrows} [RCOOH\cdots CH_2{=}CH{-}OC_4H_9] \quad (5)$$

$$\text{Complex} + RCOOH \xrightarrow[k']{} CH_3{-}\overset{H}{\underset{O}{\underset{|}{\overset{|}{C}}}}{-}OC_4H_9 + RCOOH \quad (6)$$
$$\qquad\qquad\qquad\qquad\qquad\qquad\qquad\qquad\qquad\qquad\quad COR$$

For the first stage, the concentration of the complex is found to be

$$[\text{Complex}] = K[CH_2{=}CH{-}OC_4H_9][RCOOH] \quad (7)$$

where $K$ is the equilibrium constant of this stage.

For the second stage, the rate of formation of the product is given by

$$\frac{d[\text{product}]}{dt} = k'[\text{complex}][RCOOH] \quad (8)$$

where $k'$ is the rate constant of this stage.

The over-all kinetic equation, therefore, expressed as

$$\frac{d[\text{product}]}{dt} = k'K[CH_2{=}CH{-}OC_4H_9][RCOOH]^2 \quad (9)$$

It is natural to consider that $K$ is directly proportional to $K_a$, the dissociation constant of the carboxylic acid used. Since a linear Hammett relation is observed, the experimental rate constant $k$ becomes directly proportional to $K_a$,

$$K \propto K_a \quad \text{and} \quad k = k'K \quad (10)$$

The results show that $k'$, the rate constant of the second stage, is not largely influenced by nucleophilic nature of carboxylic acid.

This two-stage mechanism was further ascertained by the following experiments.

Eq. 11 is given, when two kinds of carboxylic acids are reacted competitively with vinyl ether in a kinetic run,

$$-\frac{dA}{dt} = k_1AB_1^2 + k_2AB_1B_2 + k_3AB_2^2 \quad (11)$$

where $A$ is the concentration of *n*-butyl vinyl ether, $B_1$ and $B_2$ are those of two carboxylic acids, respectively.

Fig. 3 shows plots of percentage reaction against time (min.) for the competitive reaction of vinyl ether (0.6 mol./l.) with monochloroacetic acid $B_1$ (0.6 mol./l.) and acetic acid $B_2$ (0.6 mol./l.) in dioxane at 60°C.

From Eq. 11 by use of rate constants, $k_1 = 4.06\times10^{-4}$ mol$^{-2}$sec$^{-1}$ and $k_3 = 4.6\times10^{-6}$mol$^{-2}$ sec$^{-1}$, which have been obtained in the separate experiment listed in Table III, the value of $k_2$ can be estimated graphically by initial rate given in Fig. 3. It is $4.0\times10^{-4}$ mol$^{-2}$ sec$^{-1}$ and the kinetic equation can be expressed as follows.

$$-\frac{dA}{dt} = 4.07\times10^{-4}AB_1^2 + 4.0\times10^{-4}AB_1B_2 + 4.6\times10^{-6}AB_2^2 \quad (12)$$

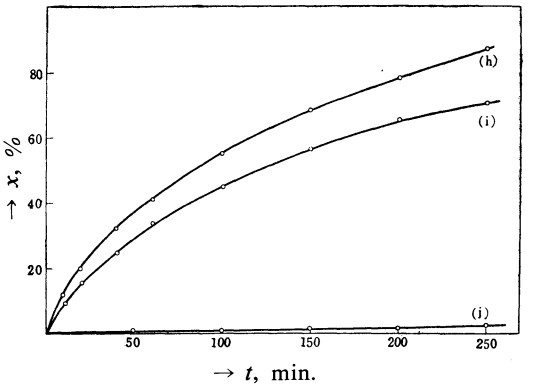
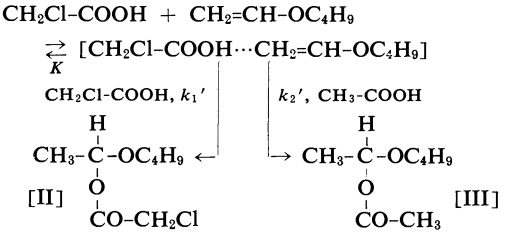



Fig. 3. The competitive addition reactions of *n*-butyl ether with two carboxylic acids in dioxane at 60°C.
The plots of percentage reaction $x$ against time;

| Run | h) | i) | j) |
|---|---|---|---|
| *n*-Butyl vinyl ether, mol./l. | 0.6 | 0.5 | 0.5 |
| Monochloroacetic acid mol./l. | 0.6 | 0.5 | — |
| Acetic acid, mol./l. | 0.6 | 0.5 | 0.5 |




By the separate experiment, it was ascertained that the ratio of the formation of II and III was 4 : 3. Since $k_1$ and $k_2$ are nearly the same values, this gives further experimental support for the above mentioned consideration that the first step, the formation of the complex from vinyl ether and carboxylic acid, is a dominant factor in this reaction and the rates of second step, $k_1'$ and $k_2'$, are nearly equal.

The reaction of *n*-butyl vinyl ether with acetic acid is accelerated by a catalytic amount of phosphoric acid. In a similar fashion as described in the case of the above mentioned competitive reaction of two carboxylic acids, Eq. 11 is also available to this reaction when $A$, $B_1$ and $B_2$ represent the concentrations of the vinyl ether, phosphoric acid and the acetic acid, respectively. Since $B_1$ and $k_3$, the rate constant of self catalyzed reaction of acetic acid, are very small values, both the first term, $k_1AB_1^2$, and the third term, $k_3AB_2^2$, are small compared with the second term, $k_2AB_1B_2$. Then, the kinetic equation is given as follows;

$$-\frac{dA}{dt} = k_2AB_1B_2 \quad (13)$$

Fig. 4 shows plots of $\log\{(200-x)/(100-x)\}$ (where $x$ represents percentage reaction of the vinyl ether) against time for the reaction of *n*-butyl vinyl ether (initial concentration 0.6 mol./l.) and acetic acid (initial concentration 1.2 mol./l.) in dioxane at 50°C with various concentrations of phosphoric acid, a—e.

The rates of reaction increase linearly as the concentration of phosphoric acid increases, and second order plots have a sufficiently straight lines from which the rate constants $k_2$ have been obtained (Table IV). It was confirmed that the reaction is a general acid catalyzed reaction similar to the results obtaind in the case of hydrolysis of vinyl ether[5,6].

TABLE V. THE RATE CONSTANTS OF THE ADDITION REACTION OF *n*-BUTYL VINYL ETHER WITH MONOCHLOROACETIC ACID IN VARIOUS SOLVENTS AT 30°C

| Solvent | $k$, $mol^{-2}\,sec^{-1}$ | Solvent | $k$, $mol^{-2}\,sec^{-1}$ |
|---|---|---|---|
| Dioxane | $3.95\times10^{-5}$ | Toluene 5+dioxane 1 | $9.1\times10^{-3}$ |
| Anisole | $1.34\times10^{-3}$ | Toluene 2+dioxane 1 | $2.1\times10^{-3}$ |
| Toluene | $2.08\times10^{-2}$ | Toluene 1+dioxane 2 | $0.7\times10^{-3}$ |
| | | Toluene 11+ether 1 | $3.3\times10^{-3}$ |

TABLE VI. THE RATE CONSTANTS OF THE ADDITION REACTION OF *n*-BUTYL VINYL ETHER WITH ACETIC ACID IN THE PRESENCE OF A CATALYTIC AMOUNT OF PHOSPHORIC ACID IN DIOXANE AT 50°C

| Run | $[H_3PO_4]$, mol./l. | $k'[H_3PO_4]$, $mol^{-1}\,sec^{-1}$ | $k'$, $mol^{-2}\,sec^{-1}$ |
|---|---|---|---|
| a | $4.8\times10^{-4}$ | $1.50\times10^{-5}$ | $3.1\times10^{-1}$ |
| b | 9.6 〃 | 2.60 〃 | 2.7 〃 |
| c | 13.8 〃 | 4.40 〃 | 3.0 〃 |
| d | 24.0 〃 | 8.15 〃 | 3.4 〃 |
| e | 48.0 〃 | 15.8 〃 | 3.3 〃 |

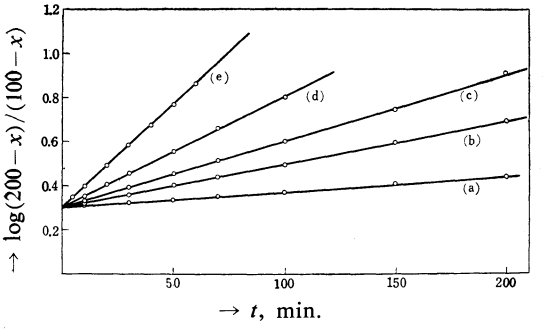
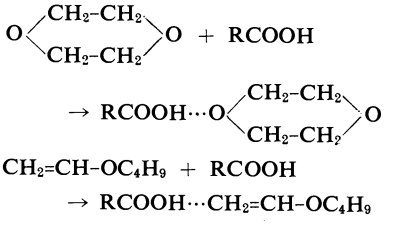



Fig. 4. The addition reaction of *n*-butyl vinyl ether with acetic acid in the presence of a catalytic amount of phosphoric acid in dioxane at 50°C.

In addition, the rates of this reaction are remarkably influenced by the nature of the solvent used. Table V shows the rate constants of the reaction of chloroacetic acid with *n*-butyl vinyl ether in dioxane, anisole and toluene at 30°C. In toluene the reaction is faster by 520 times than in dioxane. In anisole the reaction is not so fast as in toluene but still it is faster by 34 times than in dioxane. It was also observed that the addition of a small amount of dioxane or diethyl ether to toluene solution retards the reaction considerably.

Possible formation of complex from carboxylic acid and solvent containing ether linkage such as dioxane, competes with the formation of the above-mentioned complex from vinyl ether and carboxylic acid, and decreases the concentration of the latter which is the necessary intermediate to form the product, hemiacetal ester. This is a reason why the reaction is very slow in dioxane.




**Summary**

The rate constants, the activation energies and the entropies of activation of the addition reactions of *n*-butyl vinyl ether with carboxylic acids in dioxane, anisole and toluene were determined. It was found that the reaction is first order with respect to vinyl ether and second order with respect to carboxylic acid, and the rate of the reaction increases as the acidity of carboxylic acid increases and a linear Hammett relation is observed in the reaction of meta and para substituted benzoic acids. In the presence of a catalytic amount of phosphoric acid, the rate increases linearly with its concentration. The addition involves two stages, namely the initial formation of intermediate complex from vinyl ether and carboxylic acid, followed by the reaction of the complex with another carboxylic acid. In addition, the solvent effect has been clarified and a general acid catalyzed reaction has been discussed in view of these results.

The authers wish to express their hearty thanks to Professor Toshio Hoshino for his encouragement throughout the course of this experiment.

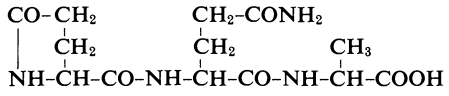
*Department of Chemistry*
*Tokyo Institute of Technology*
*Meguro-ku, Tokyo*

# *Studies on Peptides. VIII. The Synthesis of α,γ-Glutamyl Peptides and the Cleavage Reactions of their γ-Glutamyl Peptide Linkages*[1]

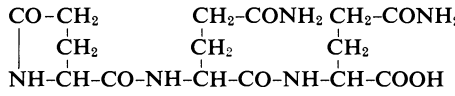
By Tetsuo SHIBA and Takeo KANEKO

(Received May 13, 1960)

In previous papers[2,3], the structure of eisenine, tripeptide isolated from the brown marine alga *Eisenia bicyclis* Setchell[4,5], had been confirmed by synthesis. Eisenine was thus shown to be L-pyroglutamyl-L-glutaminyl-L-alanine (I). A similar tripeptide, fastigiatine, had been obtained by Fruton and his coworkers from the American marine alga *Pelvetia fastigiata*[6].



(I)



(II)

They suggested that fastigiatine is L-pyroglutamyl-L-glutaminyl-L-glutamine (II)[6]. However, our synthetic results have shown that this structure can not explain the physical constants of natural fastigiatine[1,7]. Nevertheless, even if this structure is not correct, a pyrrolidone ring is certainly present in the molecule of fastigiatine. During the course of our investigations on these two naturally occurring peptides, eisenine and fastigiatine, the fact, that both contain a pyrrolidone ring, seemed to us to be of particular interest.

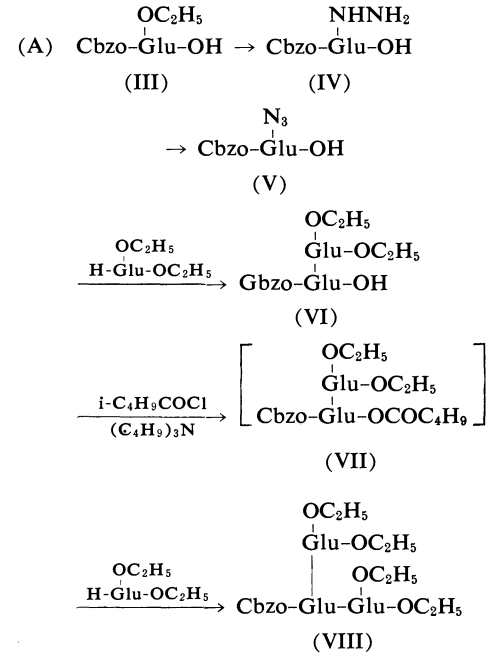
With regard to the mechanism of formation of such a pyrrolidone ring, two possibilities were considered. One of them is a biosynthetic process in which only the γ-glutamyl peptide linkage of an α,γ-glutamyl peptide existing in the living cell is cleft enzymatically thus forming the pyroglutamyl peptide. With regard to this mechanism, Woodward and Reihart[8] reported that γ-glutamyl transpeptidase obtained from kidney, cleft selectively the γ-glutamyl peptide linkage in glutathione and that pyrrolidone carboxylic acid was produced. Connell and Hanes[9], in discussing this cleavage reaction, suggested that the γ-glutamyl peptide linkage had not been split by pure transpeptidase but by γ-glutamyl lactamase.

The second possibility is a non-enzymatic formation of the pyrrolidone ring. When a powder of the alga is heated in aqueous ethyl alcohol on a boiling water bath in order to extract the peptide, the original α,γ-glutamyl peptide or glutaminyl peptide may be converted to a pyroglutamyl peptide such as eisenine or fastigiatine. In general, the γ-glutamyl peptide bond is much more labile than the α-peptide bond. Ellfolk and Synge[10], as well as Hird and Springell[11], have pointed out that pyrrolidone carboxylic acid was produced from glutathione in a non-enzymatic reaction rather than an enzymatic one. Young and his coworkers[12,13] have observed a similar non-enzymatic reaction in the cases of several γ-glutamyl peptides. Glutamine or glutaminyl peptides are also easily cyclized to pyrrolidone carboxylic acid or to a pyroglutamyl peptide respectively by merely heating their aqueous solutions[7,14,15]. Although the non-enymatic formation of pyrrolidone carboxylic acid from a γ-glutamyl peptide or of a pyroglutamyl peptide from a glutaminyl peptide has been studied, it is not certain whether a pyroglutamyl peptide can be produced by cleavage of α,γ-glutamyl peptide. In the present investigation several α,γ-glutamyl peptides were synthesized and their selective cleavage reactions were studied.

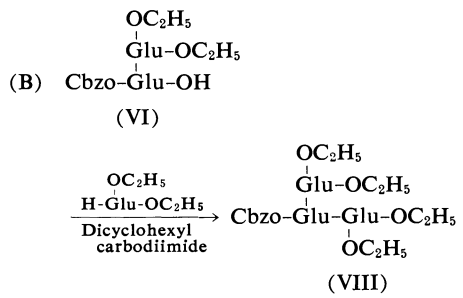
A few methods for the synthesis of α,γ-glutamyl peptides were investigated in a case of the tetraethyl ester of carbobenzyloxy-α,γ-L-glutamyl di-L-glutamic acid. The first method (A) was based on the following reactions.

1) For the previous publication see T. Shiba and S. Imai, *J. Chem. Soc. Japan, Pure Chem. Sec.* (*Nippon Kagaku Zasshi*), **80**, 497 (1959).
2) T. Kaneko, T. Shiba, W. Watarai, S. Imai, T. Shimada and K. Ueno, *Chem. & Ind.*, **1957**, 986.
3) T. Shiba, *J. Chem. Soc. Japan Pure Chem. Sec.* (*Nippon Kagaku Zasshi*), **80**, 492 (1959).
4) T. Ohira, *J. Agr. Chem. Soc. Japan* (*Nippon Nogei-Kagaku Kaishi*), **15**, 370 (1939).
5) T. Ohira, ibid., **16**, 293 (1940).
6) C. A. Dekker, D. Stone and J. S. Fruton, *J. Biol. Chem.*, **181**, 719 (1949).
7) T. Shiba, S. Imai and T. Kaneko, This Bulletin, **31**, 244 (1958).
8) G. E. Woodward and F. C. Reinhart, *J. Biol. Chem.*, **145**, 471 (1942).
9) G. E. Connell and C. S. Hanes, *Nature*, **177**, 377 (1956).
10) N. Ellfolk and R. L. Synge, *Biochem. J.*, **59**, 523 (1955).
11) F. J. R. Hird and P. H. Springell, ibid., **56**, 417 (1954).
12) W. J. LeQuesne and G. T. Young, *J. Chem. Soc.*, **1952**, 594.
13) D. A. Rowlands and G. T. Young, ibid., **1952**, 3937.
14) J. Melville, *Biochem. J.*, **29**, 179 (1935).
15) K. Narita, *Biochim. et Biophys. Acta*, **30**, 352 (1958).

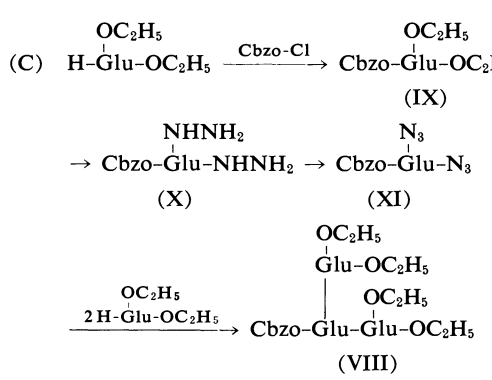
Carbobenzyloxy-$\gamma$-L-glutamyl azide (V) obtained from $\gamma$-ethyl carbobenzyloxy-L-glutamate (III) via the hydrazide (IV), was condensed with diethyl-L-glutamate to give the carbobenzyloxy-$\gamma$-dipeptide diethyl ester (VI). This diester VI was then combined with diethyl-L-glutamate via its mixed anhydride VII with isovaleric acid to obtain tetraethyl carbobenzyloxy-$\alpha$, $\gamma$-L-glutamyl di-L-glutamate (VIII).



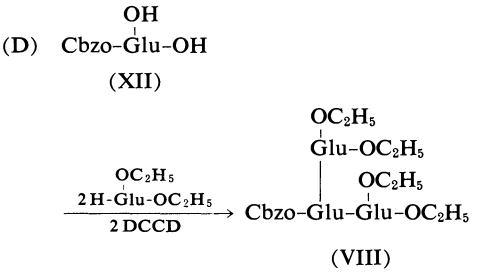
In the second method B, diethyl carbobenzyloxy-$\gamma$-L-glutamyl-L-glutamate (VI), synthesized as in method A, was coupled with diethyl-L-glutamate by means of dicyclohexyl carbodiimide. Method B gives a better yield of VIII than method A. However, both methods have the disadvantage of giving poor yields of the intermediate VI from the azide V and of requiring many synthetic steps.



Booth and his collaborators had synthesized the same carbobenzyloxy tetraester (VIII)[16]. Their method was based on the preparation of diethyl carbobenzyloxy-$\alpha$-glutamyl glutamate, followed by its conversion into VIII via the acid chloride method. Their synthesis suffers from similar defects as methods A and B. Later, they succeeded in condensing one mole of *p*-nitrobenzoyl-$\alpha$, $\gamma$-glutamyl diazide with two moles of diethyl glutamate, thus forming in a single reaction tetraethyl *p*-nitrobenzoyl-$\alpha$, $\gamma$-glutamyl diglutamate[17]. In our third method C this diazide method was applied to the carbobenzyloxy derivative. Diethyl carbobenzyloxy-L-glutamate (IX) was obtained in good yield by the direct carbobenzyloxylation of diethyl L-glutamate. This diethyl ester (IX) was then converted into the dihydrazide (X,) and then to the diazide (XI), which was combined with two moles of diethyl L-glutamate to form tetraethyl carbobenzyloxy-$\alpha$, $\gamma$-L-glutamyl di-L-glutamate (VIII). Method C was superior to methods A and B, because the synthetic path became shorter and an overall yield of 48% in reactions X to VIII was obtained.



In our last method D, carbobenzyloxy-L-glutamic acid was directly coupled with two moles of diethyl L-glutamate using two moles of dicyclohexyl carbodiimide. The starting material for this reaction is easily available, only one step is required in order to obtain the desired product and an excellent yield (88%) is obtained. Therefore, this method is superior to the other methods.



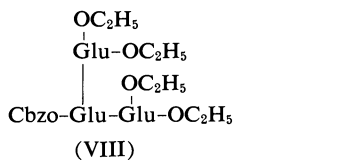
The carbobenzyloxy tetraester obtained through such methods, was difficult to crystal-

16) J. H. Mowat et al., *J. Am. Chem. Soc.*, **70**, 1096 (1948).

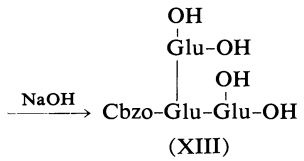
17) J. H. Mowat et al., ibid., **71**, 2308 (1949).

lize, but was obtained as a gelatinous precipitate upon addition of petroleum ether to its solution in ethyl acetate. Several samples of VIII showed varying melting points due to the occlusion of solvent, but their infrared spectra were all identical.

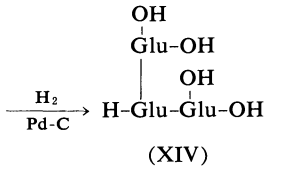
Carbobenzyloxy tetraester (VIII) prepared according to method D, was then hydrolyzed to carbobenzyloxy-$\alpha,\gamma$-L-glutamyl di-L-glutamic acid (XIII), which was obtained as a syrup that did not crystallize. Compound XIII was hydrogenated to $\alpha,\gamma$-L-glutamyl di-L-glutamic



(VIII)



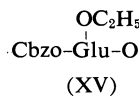
(XIII)



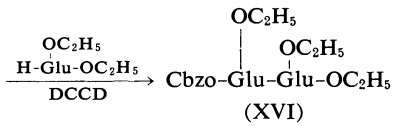
(XIV)

acid (XIV), which had a tendency to decompose during evaporation in vacuo and therefore was lyophilized.

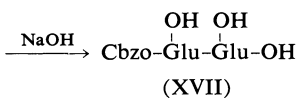
As preliminary experiment for our method D, $\gamma$-ethyl carbobenzyloxy-L-glutamate (XV) was coupled with diethyl L-glutamate using dicyclohexyl carbodiimide. Triethyl carbobenzyloxy-$\alpha$-L-glutamyl-L-glutamate (XVI) was thus obtained in a good yield. Compound XVI was then hydrolyzed to carbobenzyloxy-$\alpha$-L-glutamyl-L-glutamic acid (XVII), which was hydrogenated to $\alpha$-L-glutamyl-L-glutamic acid (XVIII).



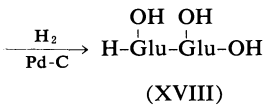
(XV)



(XVI)



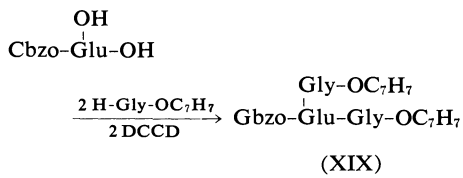
(XVII)



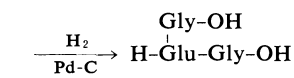
(XVIII)

For the purpose of preparing $\alpha$-glutamyl dipeptides, the method of Bergmann and Zervas[18], in which carbobenzyloxy glutamic anhydride is coupled with an amino acid ester, has hitherto mostly employed. The reaction products, however, always contained a small amount of $\gamma$-peptide as a by-product, which must be separated from the $\alpha$-isomer by means of successive extractions or a countercurrent distribution. Therefore, the anhydride method is not only very tedious, but also disadvantageous as far as its yield is concerned. In contrast, method D is believed to be a better synthetic approach to $\alpha$-glutamyl peptides, since these defects are eliminated.

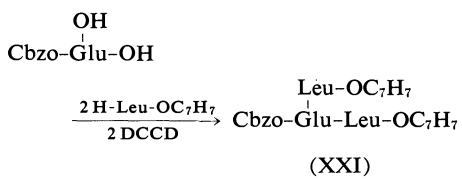
Subsequently, $\alpha,\gamma$-L-glutamyl diglycine (XX), $\alpha,\gamma$-L-glutamyl di-L-leucine (XXII) and $\alpha,\gamma$-L-glutamyl di-Laspartic acid (XXIV) were also synthesized according to method D except that the amino acid benzyl esters were used in place of the ethyl esters. The benzyl esters of carbobenzyloxy-$\alpha,\gamma$-glutamyl petides (XIX, XXI, XXIII) were hydrogenated to the $\alpha,\gamma$-glutamyl peptides (XX, XXII, XXIV) in one step. The hydrolysis step required for ethyl esters was thus eliminated.



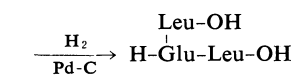
(XIX)



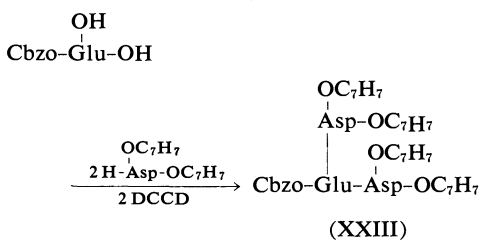
(XX)



(XXI)

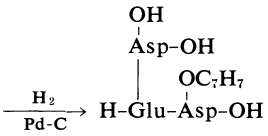


(XXII)



(XXIII)

18) M. Bergmann and L. Zervas, *Ber.*, 65, 1192 (1932).



(XXIV)

The hydrogenolysis of the benzylesters (XIX, XXI, XXIII) was carried out in open vessels after the addition of palladium-charcoal (10%). In the case of peptides of glycine XIX and of leucine XXI, this hydrogenolysis took place readily, while tetrabenzyl carbobenzyloxy-$\alpha,\gamma$-glutamyl diaspartate (XXIII) was difficult to hydrogenate, probably owing to its steric structure; the hydrogenated product XXIV could not be obtained in a pure state.

For the purpose of the preparation of $\alpha,\gamma$-L-glutamyl di-L-lysine by a similar synthetic method, $\varepsilon$-carbobenzyloxy-L-lysine methyl ester hydrochloride (XXV) and $\varepsilon$-carbobenzyloxy-L-lysine benzyl ester hydrochloride (XXVI) were synthesized. The former (XXV) had been prepared from $\varepsilon$-carbobenzyloxy-$\alpha$-carboxyl-L-lysine anhydride and methyl alcoholic hydrochloric acid by Bergmann and his coworkers[19]. Our advantageous method or preparation of $\varepsilon$-carbobenzyloxy lysine ester hydrochloride was based on the esterification of $\varepsilon$-carbobenzyloxy-L-lysine obtained from copper lysinate and carbobenzyloxy chloride[20]. $\varepsilon$-Carbobenzyloxy-L-lysine was esterified with thionyl chloride in methyl alcohol for benzyl alcohol to yield the methyl ester hydrochloride (XXV) and the benzyl ester hydrochloride (XXVI) respectively without decomposition of the carbobenzyloxy group. The condensation reactions of these lysine esters with carbobenzyloxy glutamic acid in the presence of dicyclohexyl carbodiimide were not successful. Complex mixtures were obtained in all cases. This failure may be due to the molecular structures of XXV and XXVI. However, these cabobenzyloxylysine ester hydrochlorides (XXV and XXVI) may be useful intermediates in the syntheses of other lysine peptides.

$$\text{Cbzo-NH(CH}_2)_4\text{CH(NH}_2\cdot\text{HCl)COOCH}_3$$

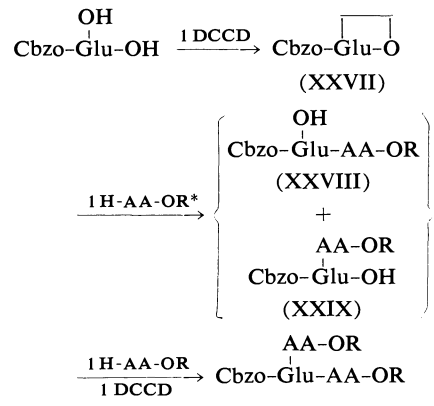
(XXV)

$$\text{Cbzo-NH(CH}_2)_4\text{(NH}_2\cdot\text{HCl)COOCH}_2\text{C}_6\text{H}_5$$

(XXVI)

In the course of all condensation reactions in the presence of cyclohexyl carbodiimide, pure dicyclohexyl urea always separated in crystalline form from the reaction mixture. In order to use it repeatedly for other reactions, dicyclohexyl carbodiimide was recovered from dicyclohexyl urea in fair yield according to the method of Amiard and Heymes[21].

Concerning the mechanism of the condensation reaction in the presence of dicyclohexyl carbodiimide, we supposed at first that two moles of amino acid ester would combine simultaneously with one mole of carbobenzyloxy glutamic acid in the presence of two moles of dicyclohexyl carbodiimide. However, when solutions of one mole of carbobenzyloxy-glutamic acid and of two moles of dicyclohexyl carbodiimide were mixed before the addition of any amino acid ester, it was observed that nearly one mole of dicyclohexyl urea separated out immediately. When two moles of amino acid ester were then added to the filtrate from this urea derivative, the expected $\alpha,\gamma$-glutamyl peptide was obtained in good yield and another mole of dicyclohexyl urea was formed at the same time. Therefore, the reactioncan be better explained by a three step mechanism as follows. In the first step, one mole of carbobenzyloxy glutamic acid reacts with one mole of dicyclohexyl carbodiimide to form carbobenzyloxy-glutamic anhydride (XXVII). In the second step, the anhydride ring is opened by one mole of amino acid ester according to the same mechanism as in the method of Bergmann and Zervas[18] with the formation of a mixture of $\alpha$- and $\gamma$-dipeptide derivatives XXVIII and XXIX. In the third step, these condense with another mole of amino acid ester by the action of one mole of dicyclohexyl carbodiimide to give a single product XXX.



(XXVII)

(XXVIII)

(XXIX)

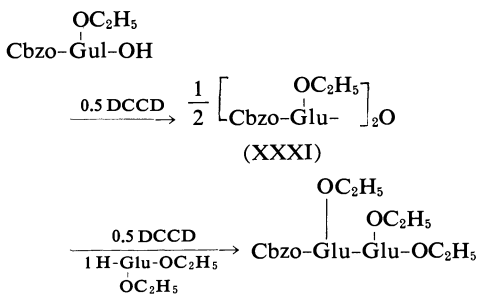
(XXX)

In fact, when one mole of carbobenzyloxy-L-glutamic acid and one mole of dicyclohexyl carbodiimide were mixed, about 0.9 mol. of

19) M. Bergmann, L. Zervas and W. F. Ross, *J. Biol. Chem.*, **111**, 245 (1935).
20) A. Neuberger and F. Sanger., *Biochem. J.*, **37**, 515 (1943).
21) G. Amiard and R. Heymes, *Bull. soc. chim. France*, 1956, 1360.
* -AA-=amino acid residue, -NH-CH(R)-CO-.

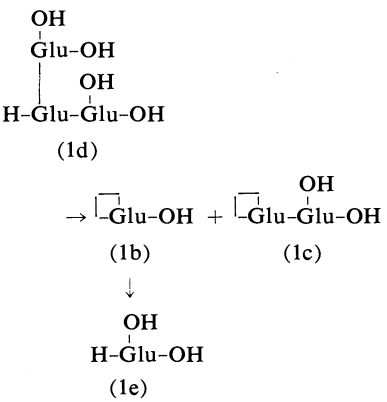
dicyclohexyl urea was always obtained as a precipitate; hence it appears that carbobenzyloxy glutamic anhydride (XXVII) must be formed, but all efforts to crystallize it from the reaction mixture were unsuccessful. Although the formation of the anhydride (XXVII) could not be directly proven, the above mentioned mechanism could be demonstrated indirectly by the following experiment. When one mole of pure carbobenzyloxy-L-glutamic anhydride (XXVII), prepared from carbobenzyloy glutamic acid and acetic anhydride by the usual method, was reacted with two moles of glycine benzyl ester by means of one mole of dicyclohexyl carbodiimide, dibenzyl-carbobenzyloxy-$\alpha$, $\gamma$-L-glutamyl diglycinate (XIX) was obtained in very good yield (92%). This supports the above described three-step mechanism.

When the synthesis of $\alpha$-glutamyl glutamic acid (XVIII) was carried out in a stepwise fashion, i.e. when $\gamma$-ethyl carbobenzyloxy-L-glutamate was mixed with a solution of dicyclohexyl carbodiimide, before diethyl L-glutamate was added, a precipitate of dicyclohexyl urea was also observed. It is assumed, that in this case one mole of the carbobenzyloxy-$\gamma$-ester and a half mole of dicyclohexyl carbodiimide form an intermolecular anhydride XXXI, which then reacts with one mole of diethyl glutamate by means of a half mole of dicyclohexyl carbodiimide in a similar manner as the $\alpha,\gamma$-glutamyl peptide diester (XXX) is assumed to be formed from carbobenzyloxy-glutamic anhydride (XXVII).

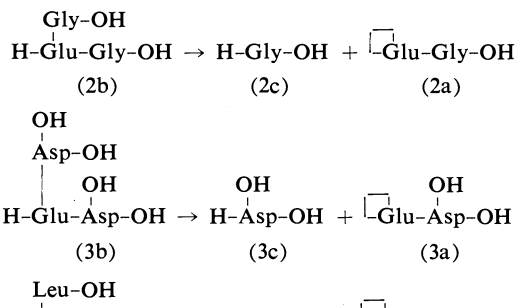


Muramatsu and Hagitani[22] have shown that formyl-$\beta$-alanine can also be converted to its bimolecular anhydride by means of dicyclohexyl carbodiimide. Only a small amount of other information on the formation of anhydrides by the reaction of dicyclohexyl carbodiimide with *N*-substituted-$\alpha$-amino acids is available.

Finally, the cleavage of four $\alpha,\gamma$-glutamyl peptides, as well as of $\alpha$-glutamyl glutamic acid and of $\gamma$-glutamyl glutamic acid, caused by heating the aqueous solutions of these peptides, was investigated. The results are presented in Figs. 1—6. In the case of $\alpha,\gamma$-L-glutamyl di-L-glutamic acid (1d), a small amount of pyrrolidone carboxylic acid (1b) was split off after only one week at 40°C. However, at 100°C both pyrrolidone carboxylic acid (1b) and glutamic acid (1e) began to appear already after one hour. The $\alpha,\gamma$-peptide (1d) disappeared completely after nine hours, while a new spot 1c appeared after three hours and became gradually stronger on longer heating. It was not colored by ninhydrin, but colored by Bromothymol Blue, and is supposed to be pyroglutamyl glutamic acid. From the result of this experiment, it was concluded that $\alpha,\gamma$-glutamyl diglutamic acid in aqueous solution was decomposed at 100°C to pyrrolidone carboxylic acid and or glutamic acid and pyroglutamyl glutamic acid by a selective cleavage of its $\gamma$-peptide linkage as shown below.

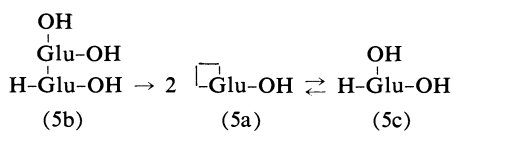


The cleavage of $\alpha,\gamma$-L-glutamyl diglycine (Fig. 2), $\alpha,\gamma$-L-glutamyl di-L-aspartic acid (Fig. 3), and $\alpha,\gamma$-L-glutamyl di-L-leucine (Fig. 4) proceeded in a similar manner. The decompositions began after one hour at 100°C and were completed after ten to twenty hours. These cleavage reactions may be represented as follows.



22) I. Muramatsu and S. Hagitani, *J. Chem. Soc. Japan, Pure Chem. Sec.* (*Nippon Kagaku Zasshi*), **80**, 1497 (1959).

In the course of the decomposition of γ-glytamyl glutamic acid (Fig. 5), the Bromothymol Blue positive spot (5a) of pyrrolidone carboxylic acid appeared before the ninhydrin spot of glutamic acid (5c). Since Bromothymol Blue is a less sensitive reagent than ninhydrin, this indicates that both glutamic acid residues of the dipeptide were first decomposed to pyrrolidone carboxylic acid, which was then converted to glutamic acid.




On the other hand, α-L-glutamyl glutamic acid was rather stable and began to decompose after only twenty hours (Fig. 6).

From the results of this invesigation it may be concluded that α, γ-glutamyl peptides are subject to the selective cleavage of the γ-peptide bond on heating of the aqueous solutions, with the formation of a pyroglutamyl peptide and an amino acid. The rate of the decomposition was independent of the nature of the amino acid linked to the γ-glutamyl caboxyl group. On the basis of the cleavage reactions described above it is reasonable to assume that the pyroglutamyl peptides of marine algae were formed from glutaminyl peptides or from α, γ-glutamyl peptides in the course of the heating during their isolation.

## Experimental

**Diethyl Carbobenzyloxy-L-glutamate (IX).**—A solution of 83 g. (0.35 mol.) of diethyl L-glutamate hydrochloride in 500 ml. of water was mixed with 44 ml. of an aqueous solution of 4 N sodium carbonate. To this solution of pH 7~8, 70 g. (0.41 mol.) of carbobenzyloxy chloride and 50 ml. of an aqueous solution of 4 N sodium carbonate were added. The reaction mixture was vigorously stirred at room temperature (25°C) for three hours. It was extracted twice with 100 ml. of ether. The combined extract was washed with aqueous sodium carbonate, dried with sodium sulfate, and then evaporated in vacuo to a syrupy residue, which crystallized after two weeks' standing at room temperature; yield 103 g. (89%). It was recrystallized from ethyl alcohol and water, needles, m. p. 39~42°C.

Found: C, 60.91; H, 6.73; N, 4.04. Calcd. for $C_{17}H_{23}O_6N$: C, 60.52; H, 6.87; N, 4.15%.

In order to confirm the optical purity of the product, 4.1 g. was dissolved in 80 ml. of 1 N sodium hydroxide solution at room temperature during two hours. Then, the solution was acidified with 5 N hydrochloric acid and extracted with ethyl acetate. The extract was shaken with an aqueous solution of 1 N sodium carbonate. The aqueous layer was separated, acidified and extracted with ethyl acetate. This extract was evaporated in vacuo to a residue, which was hydrogenated in 20 ml. of methyl alcohol and 20 ml. of water in an open vessel in the presence of 100 mg. of 5% palladium-charcoal. After filtration of the catalyst and evaporation of the filtrate a residue was obtained, which was crystallized from water; yield, 0.4 g. On recrystallization, 255 mg. of pure L-glutamic acid was obtained. The overall yield from carbobenzyloxy diester (IX) was 14 percent. $[\alpha]_D^{25}$ −31.8° (*c*, 2.74, 2 N HCl).

Found: C, 40.34; H, 6.17; H, 9.44. Calcd. for $C_5H_9O_4N$; C, 40.81; H, 6.17; N, 9.52%.

**Carbobenzyloxy-L-glutamic Dihydrazide (X).**—To a solution of 72 g. of diethyl carbobenzyloxy-L-glutamate (IX) in 150 ml. of 99% ethyl alcohol, 100 ml. of 90% hydrazine hydrate was added with stirring during forty-five minutes. The temperature of the reaction mixture was kept below 30°C. When a large amount of a solid product formed during the reaction, another 100 ml. of ethyl alcohol was added. Vigorous stirring was continued for one hour and a half. The white precipitate formed was filtered and then was dissolved in 5 N hydrochloric acid. A solution of sodium acetate was carefully added until a pH of 4 was reached. After standing overnight, 40 g. of fine needles were obtained; yield 60%, m. p. 183~184°C (decomp.). $[\alpha]_D^{21}$ −14.2° (*c*, 3.05, 2 N HCl). Recrystallization from hydrochloric acid and aqueous sodium acetate gave crystals of m. p. 203~204°C (dec.).

Found: C, 50.57; H, 5.91; N, 22.60. Calcd. for $C_{13}H_{19}O_4N_5$: C, 50.49; H, 6.15; N, 22.64%.

**Tetraethyl Carbobenzyloxy-α, γ-L-glutamyl Di-L-glutamate (VIII). Method A.**—Diethyl carbobenzyloxy-γ-L-glutamyl glutamate (VI) prepared from 6.0 g. (0.02 mol.) of carbobenzyloxy-γ-L-glutamyl hydrazide by the azide method[23], was dissolved in 25 ml. of toluene and 25 ml. of chloroform, and 3.7 g. (0.02 mol.) of tri-*n*-butylamine and 2.4 g. (0.02 mol.) of isovaleryl chloride were added with stirring to the solution kept below 5°C. Stirring was continued for two hours while the temperature of the reaction mixture was kept at 0°C. A solution of free diethyl glutamate prepared from 4.8 g. (0.02 mol.) of diethyl L-glytamate hydrochloride and 3.7 g. (0.02 mol.) of tri-*n*-butylamine, in 50 ml. of chloroform, was added dropwise below 0°C within ten minutes. The reaction mixture was stirred for three hours between 0° and −10°C, then permitted to stand at room temperature for a few hours. The reaction mixture was washed with water, 3% aqueous sodium bicarbonate, 0.5% hydrochloric acid and water, and dried with sodium sulfate. Upon addition of petroleum ether crystals formed, which were filtered and dried over phosphorus pentoxide in vacuo; yield, 5.9 g. (45% based on carbobenzyloxy-L-glutamyl-γ-hydrazide), m. p. 133~134°C (sintered at 103~104°C). The melting point could be raised up to 134~136°C* (sintered at 106~108°C) by

23) T. Shiba and S. Imai, *J. Chem. Soc. Japan, Pure Chem. Sec.* (*Nippon Kagaku Zasshi*), **80**, 176 (1959).

* J. H. Mowat, Y. Subborow et al. (*J. Am. Chem. Soc.*, 71, 2308 (1949)) have synthesized tetraethyl carbobenzyloxy-α, γ-L-glutamyl-L-glutamate from tetraethyl *p*-nitrobenzoyl-α, γ-L-glutamyl-L-glutamate by replacing the *p*-nitrobenzoyl group with a carbobenzyloxy group. Their sample had a melting point of 140.5~142.0°C (sintered at 105~107°C).

recrystallization from ethyl alcohol and water. $[\alpha]_D^{23}-15.9°$ ($c$, 3.01, 99% EtOH).

Found: C, 56.62; H, 7.16; N, 6.67. Calcd. for $C_{31}H_{45}O_{12}N_3$: C, 57.13; H, 6.96; N, 6.45%.

**Method B.**—To a solution of 5.7 g. (0.035 mol.) of diethyl glutamate hydrochloride in 50 ml. of tetrahydrofuran, 1.7 g. of triethylamine was added and the triethylamine hydrochloride formed was filtered off. To the solution of the free ester, 7.6 g. (0.0163 mol.) of diethyl carbobenzyloxy-$\gamma$-L-glutamyl-L-glutamate (VI) and 3.4 g. (0.0163 mol.) of dicyclohexyl carbodiimide in 50 ml. of tetrahydrofuran were added. After stirring for five hours, 0.4 ml. of glacial acetic acid was added and stirring was continued for another hour in order to decompose unreacted carbodiimide. After filtrations of the dicyclohexyl urea, which weighed 3.3 g. (89%) and melted at 228~229°C, the filtrate was evaporated in vacuo. The syrupy residue was dissolved in ethyl acetate, the solution was washed with dilute hydrochloric acid, aqueous potassium bicarbonate and water, dried with sodium sulfate and concentrated in vacuo. The gelatinous residue was recrystallized from ethyl acetate and petroleum ether to give 8.8 g. (83%) of a colorless powder, m. p. 124~127°C (sintered at 92~98°C).

Found: C, 56.85; H, 6.92; N, 6.69. Calcd. for $C_{31}H_{45}O_{12}N_3$: C, 57.13; H, 6.95; N, 6.45%.

**Method C.**—In a mixture of 50 ml. of water, 15 ml. of concentrated hydrochloric acid and 50 ml. of chloroform, 6.2 g. (0.02 mol.) of carbobenzyloxy-L-glutamic dihyrazide (X) was dissolved. After cooling to 0°C, 30 ml. of an aqueous solution of 5.5 g. (0.08 mol.) of sodium nitrite was added dropwise within ten minutes. The reaction temperature must not exceed 5°C. After stirring for one hour at 0°C, the aqueous layer was separated and extracted twice with 30 ml. of chloroform. The combined chloroform solution was washed twice with cold water and dried with sodium sulfate. A solution of diethyl L-glutamate was prepared by dissolving 24.0 g. (0.10 mol.) of diethyl L-glutamate hydrochloride and 20.5 g. (0.20 mol.) of potassium bicarbonate in 50 ml. of water and extracting this solution three times with 50 ml. of chloroform. The combined extract was washed with water and dried with sodium sulfate. The solution of diazide obtained above was added dropwise during five minutes to this solution, while the temperature was kept at −5°C. The reaction mixture was stirred for two hours between −10°C to 0°C, and then permitted to stand overnight at room temperature. The reaction mixture was washed with dilute hydrochloric acid and then with a small amount of water, dried with sodium sulfate and evaporated in vacuo. The syrupy residue was reprecipitated from ethyl acetate and petroleum ether. The gelatinous precipitate was filtered and crystallized from ethyl alcohol and water to yield crystals, which after drying for a day in vacuo at 65°C weighed 6.3 g. (48%), m. p. 129~131°C (sintered at 99~102°C).

Found: C, 56.88; H, 6.82; N, 6.76; Calcd. for $C_{31}H_{45}O_{12}N_3$: C, 57.13; H, 6.96; N, 6.45%.

**Method D.**—A solution of 5.6 g. (0.02 mol.) of carbobenzyloxy-L-glutamic acid (XII) in 25 ml. of tetrahydrofuran and a solution of 10.0 g. (0.048 mol.) of dicyclohexyl carbodiimide 25 ml. of tetrahydrofuran were mixed. White crystalline dicyclohexyl urea began to form after a few minutes. Without removing the precipitate, a solution of diethyl L-glutamate was added. This solution had been prepared by adding 6.0 g. (0.06 mol.) of triethylamines to a solution of 14.3 g. (0.06 mol.) of diethyl L-glutamate hydrochloride in 30 ml. of tetrahydrofuran and removing the triethylamine hydrochloride formed by filtration. After the addition of the diethyl L-glutamate, the reaction mixture was stirred for five hours and then allowed to stand overnight. In order to decompose unreacted carbodiimide, 0.5 ml. of glacial acetic acid was added to the reaction mixture and the precipitate of dicyclohexyl urea (8.3 g.) was filtered off. The filtrate was evaporated in vacuo and the residue was dissolved in 100 ml. of ethyl acetate. The solution was washed with dilute hydrochloric acid, aqueous potassium bicarbonate and water and then dried with sodium sulfate. Upon addition of petroleum ether a gelatinous precipitate was obtained, which was filtered and dried in vacuo over phosphorus pentoxide; yield 11.4 g. (88%), m. p. 85~91°C. A recrystaillzed sample melted at 118~120°C (sintered at 102~104°C).

Found: C, 56.89; H, 6.73; N, 6.93. Calcd. for $C_{31}H_{45}O_{12}N_3$: C, 57.13; H, 6.96; N, 6.45%.

**$\alpha,\gamma$-L-Glutamyl Di-L-glutamic Acid (XIV).**—To a solution of 29.5 g. (0.045 mol.) of tetraethyl carbobenzyloxy-$\alpha,\gamma$-L-glutamyl di-L-glutamate in 100 ml. of 1 N sodium hydroxide was added. After standing for one hour at room temperature the reaction mixture was neutralized with 2 N hydrochloric acid, then concentrated to about 100 ml. in vacuo, acidified to Thymol Blue and extracted five times with 100 ml. of ethyl acetate. The extract was shaken five times with aqueous sodium carbonate. The combined aqueous layers were neutralized, concentrated to 200 ml., acidified and extracted again six times with 100 ml. of ethyl acetate. The extracted was dried with sodium sulfate and evaporated in vacuo to 20 g. of a syrup, which did not crystallize; yield 82%.

A solution of 7.0 g. of syrupy carbobenzyloxy-$\alpha,\gamma$-L-glutamyl di-L-glutamic acid in 100 ml. of methyl alcohol and 100 ml. of water, was hydrogenated by the usual method using 1.0 g. of 5% palladium-charcoal. After the catalyst was filtered off, the filtrate was concentrated in vacuo below 35°C to a volume of about 100 ml., and then lyophilized; yield 3.6 g. (96%), m. p. 121~123°C (dec.). $[\alpha]_D^{30}+1.4°$ ($c$, 2.55, 2 N HCl).

Found: C, 42.55; H, 6.27; N, 10.07. Calcd. for $C_{15}H_{23}O_{10}N_3\cdot H_2O$: C, 42.55; H, 5.95; N, 9.93%.

**Triethyl Carbobenzyloxy-$\alpha$-L-glutamyl-L-glutamate (XVI).**—To a solution of 5.8 g. (0.024 mol.) of diethyl-L-glutamate hydrochloride in 50 ml. of tetrahydrofuran, 1.6 g. of triethylamine was added. After removal of the triethylamine hydrochloride formed, the filtrate was poured to a mixture of 5.0 g. (0.016 mol.) of $\gamma$-ethyl carbobenzyloxy-L-glutamate (XV) and 3.6 g. (0.017 mol.) of dicyclohexyl carbodiimide in 50 ml. of tetrahydrofuran. The reaction mixture was stirred for three hours, and

then treated with 0.5 ml. of glacial acetic acid to decompose the excess of carbodiimide. The insoluble dicyclohexyl urea was removed by filtration and washed; Yield 3.2 g. (84%). The solvent was replaced by ethyl acetate and the solution was washed with dilute hydrochloric acid, aqueous potassium bicarbonate and water. After drying with sodium sulfate the solvent was evaporated in vacuo to a residue, which was crystallized from ethyl acetate and petroleum ether; yield 6.5 g. (81%), m. p. 60~64°C (sintered at 45~52°C).

Found: C, 58.72; H, 7.03; N, 5.83. Calcd. for $C_{24}H_{34}O_9N_2$: C, 58.29; H, 6.93; N, 5.67%.

**Carbobenzyloxy-α-L-glutamyl-L-glutamic Acid (XVII).**—To a solution of 6.2 g. (0.0125 mol.) of carbobenzyloxy triester (XVI) in 50 ml. of methyl alcohol, 50 ml. of 1 N sodium hydroxide was added. After standing at room temperature for two and a half hours a small amount of undissolved substance was removed by filtration and the filtrate was acidified with 2 N hydrochloric acid and extracted fou times with ethyl acetate. The dried extract was evaporated in vacuo to a syrup, which was dissolved in 100 ml. of hot water. On cooling, crystals formed which were recrystallized from aqueous ethyl alcohol; yield 2.8 g. (54%), m. p. 161~164°C (decomp.) (sinters at 139°C).

Found: C, 53.13; H, 5.92; N, 7.03. Calcd. for $C_{18}H_{22}O_9N_2$: C, 53.68; H, 5.40; N, 6.83%.

**α-L-Glutamyl-L-glutamic Acid (XVIII).**—A solution of 1.9 g. of carbobenzyloxy dipeptide XVII in 40 ml. of methyl alcohol and 20 ml. of water was hydrogenated using 5% palladium-charcoal. The catalyst was filtered off and washed with hot water. The filtrate and the washings were combined and evaporated in vacuo. The residue was crystallized from water and ethyl alcohol; yield 0.9 g. (61%), m.p. 178~179°C (decomp.). Its infrared spectrum was completely identical with that of α-L-glutamyl-L-glutamic acid prepared from carbobenzyloxy glutamic anhydride according to Bergmann's method.

Found: C, 43.30; H, 5.63; N, 9.99. Calcd. for $C_{10}H_{16}O_7N_2$: C, 43.48; H, 5.84; N, 10.14%.

**Di-benzyl Carbobenzyloxy-α, γ-L-glutamyl Diglycinate (XIX).** — Benzyl glycinate-*p*-toluenesulfonate was prepared according to the method of Izumiya and Makisumi[24]. To a solution of 15.0 g. (0.045 mol.) of this ester salt (m. p. 130~131°C) in 100 ml. of chloroform, 4.5 g. (0.045 mol.) of triethylamine was added. The mixture was poured into a solution of 5.6 g. (0.020 mol.) of carbobenzyloxy-L-glutamic acid in 100 ml. of tetrahydrofuran. Then a solution of 11.0 g. (0.053 mol.) of dicyclohexyl carbodiimide in 100 ml. of tetahydrofuran was added. After the reaction mixture was stirred at room temperature for seven hours, the cyclohexyl urea formed was filtered off; weight 4.4 g. (50%). A small amount of glacial acetic acid was added to the filtrate. After two hours' stirring the reaction mixture was evaporated in vacuo and the residue was dissolved in ethyl acetate. Undissolved dicyclohexyl urea was filtered off. Upon addition of petroleum ether to the filtrate a precipitate was obtained which was recrystallized from ethyl alcohol, and dried in vacuo over phosphorus pentoxide; yield 5.5 g. (48%), m. p. 146~149°C.

Found: C, 64.25; H, 5.76; N, 7.48. Calcd. for $C_{31}H_{33}O_8N_3$: C, 64.68; H, 5.78; N, 7.30%.

**α, γ-L-Glutamyl Diglycine (XX).** — A solution of 5.1 g. of dibenzyl ester XIX in 50 ml. of dioxane, 50 ml. of methyl alcohol and 50 ml. of water, was hydrogenated by the usual method using 1.0 g. of 5% palladum-charcoal. After the catalyst was filtered off, the filtrate was evaporated in vacuo and the residue was lyophilized; yield 1.6 g. (70%), m. p. 73~77°C (sintered at about 68°C). It was dried in vacuo over phosphorus pentoxide for an elementary analysis. $pK'_{a_1}$ 2.70; $pK'_{a_2}$ 3.69; $pK'_{a_3}$ 8.02.

Found: C, 38.75; H, 6.03; N, 14.56; MW, 290. Calcd. for $C_9H_{15}O_6N_3 \cdot H_2O$: C, 38.71; H, 6.14; N, 15.05%, MW, 279.

The molecular weight was calculated from the neutralization equivalent as dibasic acid.

**Diethyl Carbobenzyloxy-α, γ-L-glutamyl Di-L-leucinate (XXI).**—A solution of 7.0 g. (0.025 mol.) of carbobenzyloxy-L-glutamic acid in 75 ml. of tetrahydrofuran and a solution of 3.4 g. (0.065 mol.) of dicyclohexyl carbodiimide in 75 ml. of tetrahydrofuran were mixed. Without removing the precipitate of dicyclohexyl urea which formed, a solution of benzyl L-leucinate was added. This solution had been prepared by adding 6.5 g. (0.065 mol.) of triethylamine to a suspension of 23.6 g. (0.06 mol.) of benzyl L-leucinate-*p*-toluenesulfonate[24] (m. p. 154~155°C) in 150 ml. of chloroform. After the addition of the benzyl L-leucinate, the reaction mixture was stirred for five hours. The precipitate of dicyclohexyl urea was removed by filtration and washed with tetrahydrofuran; weighte 8.3 g. (57%). After addition of a small amount of glacial acetic acid and filtration of a further precipitate (2.2 g.), the filtrate was evaporated to dryness in vacuo. The residue was dissolved in ethyl acetate and washed with water, dilute sodium bicarbonate, dilute hydrochloric acid and water. The solvent was removed and petroleum ether was added to the residue. After cooling, a gelatinous precipitate formed. It was recrystallized from ethyl alcohol and water, and dried in vacuo over phosphorus pentoxide; yield 10.9 g., m. p. 107~116°C (softened at 98°C). From the mother liquor, 3.1 g. of crystals were obtained; total yield 82%.

Found: C, 67.86; H, 7.11; N, 6.53. Calcd. for $C_{39}H_{49}O_8N_3$: C, 68.10; H, 7.18; N, 6.11%.

**α, γ-L-Glutamyl Di-L-leucine (XXII).**—A solution of 5.0 g. of dibenzyl ester XXI in 30 ml. of methyl alcohol, 80 ml. of dioxane and 30 ml. of water was hydrogenated using 1.0 g. of 5% palladium-charcoal. After filtration of the catalyst, the filtrate was concentrated in vacuo to a volume of about 65 ml. The remaining solvent was removed by lyophilization; yield 1.8 g. (67%), m. p. 137~141°C (softened at 134°C, $pK'_{a_1}$ 2.81; $pK'_{a_2}$ 3.75; $pK'_{a_3}$ 8.07). The molecular weight was calculated from the neutralization equivalent as a dibasic acid.

Found: C, 52.65; H, 8.37; N, 10.13; MW, 464. Calcd. for $C_{17}H_{31}O_6N_3 \cdot H_2O$: C, 52.22; H, 8.51; N, 10.75%; MW, 391.

24) N. Izumiya and S. Makisumi, *J. Chem. Soc. Japan, Pure Chem. Sec.* (*Nippon Kagaku Zasshi*), **78**, 1768 (1957).

**Tetrabenzyl Carbobenzyloxy-α, γ-L-glutamyl Di-L-aspartate (XXIII).**—To a suspension of 31.0 g. (0.070 mol.) of dibenzyl-L-aspartate-*p*-toluenesulfonate (m. p. 152°C)[24] in 200 ml. of chloroform, 7.0 g. (0.070 mol.) of triethylamine was added to give a clear solution of the free ester. Solution of 7.0 g. (0.025 mol.) of carbobenzyloxy-L-glutamic acid in 100 ml. of tetrahydrofuran and of 14.5 g. (0.070 mol.) of dicyclohexyl carbodiimide in 100 ml. of tetrahydrofuran were added to the solution of the free ester with ice-cooling. The mixture was then stirred at room temperature for nine hours. A gelatinous precipitate was filtered off. This precipitate seemed to be a mixture of the expected tetrabenzyl ester and dicyclohexyl urea. Therefore, it was extracted with tetrahydrofuran and the extract was evaporated. The residue was dissolved in ethyl alcohol and tetrahydrofuran, and crystallized by adding water to the solution. Recrystallization from the same solvents gave 7.6 g. of crystals, m. p. 139~145°C. Some dicyclohexyl urea which had separated out from the mother liquor of the gelatinous precipitate was removed by filtration, and the filtrate was washed with acid, aqueous sodium bicarbonate and water. Upon addition of petroleum ether a precipitate formed which was recrystallized from a mixture of ethyl acetate, tetrahydrofuran and petroleum ether; weighted 4.5 g., m. p. 152~158°C (softened at 145°C). The total yield was 12.1 g. (56%).

Found: C, 67.11; H, 5.75; N, 4.91. Calcd. for $C_{49}H_{49}O_{12}N_3$: C, 67.51; H, 5.63; N, 4.88%.

**α, γ-L-Glutamyl Di-L-aspartic Acid (XXIV).**—A solution of 3.0 g. of compound XXIII in 30 ml. of methyl alcohol, 90 ml. of dioxane and 30 ml. of water, was hydrogenated using 0.7 g. of 5% palladium-charcoal. After filtration of the catalyst, the filtrate and the washings were combined, concentrated in vacuo to about 30 ml. and then lyophilized to a solid, which weighed 1.2 g., m. p. 58~63°C. Elementary analysis, however, indicated that this substance was a mixture of the expected compound XXIV and starting material XXIII. Therefore, 0.7 g. of this substance was again hydrogenated. A paper chromatogram of the reduction product showed only one ninhydrin-positive spot but elementary analysis showed that the substance was still not pure.

**Methyl ε-Carbobenzyloxy-L-lysinate Hydrochloride (XXV).**—To a suspension of 2.0 g. (0.072 mol.) of ε-carbobenzyloxy-L-lysine[20], m. p. 248~250°C (decomp.) in 15 ml. of methyl alcohol, 1.0 g. (0.084 mol.) of thionyl chloride was added dropwise at 0°C. The reaction mixture was permitted to stand one hour and a half in a water bath of 40°C and then twenty hours at 25°C. After evaporated to dryness in vacuo, water was added to a residue and evaporated again in vacuo. Addition of water followed by evaporation was repeated several times to remove the excess of thionyl chloride and hydrochloric acid. The residue was crystallized from 99% ethyl alcohol-ethyl acetate. Pure ester hydrochloride was obtained after recrystallization from the same solvent; weighted 2.0 g. (84%), m. p. 113~114°C (sintered at 111°C).

Found: C, 54.21; H, 6.80; N, 8.41; Cl, 10.99. Calcd. for $C_{15}H_{23}O_4N_2Cl$: C, 54.30; H, 7.24; N, 8.45; Cl, 10.71%.

**Benzyl ε-Carbobenzyloxy-L-lysinate Hydrochloride (XXVI).**—To a suspension of 1.7 g. (0.006 mol.) of ε-carbobenzyloxy-L-lysine[20] in 10 ml. of benzyl alcohol there was added dropwise at −10°C, 0.9 g. (0.0076 mol.) of thionyl chloride. The reaction mixture was permitted to stand at 40°C for four hours, and then at 29°C for twenty three hours. It was then concentrated in vacuo. Upon addition of ether, gelatinous precipitate formed, which was filtered off, washed with ether, and recrystallized from 99% ethyl alcohol-ether; weight 0.5 g., m. p. 131°C. A second crop of ester hydrochloride was obtained from the mother liquor by addition of more ether; weight 0.2 g. The total yield was 24%. A sample recrystallized from the same solvent for elementary analysis melted at 133~134°C.

Found: C, 61.34; H, 6.84; N, 6.98; Cl, 8.55. Calcd. for $C_{21}H_{27}O_4N_2Cl$: C, 61.98; H, 6.69, N, 6.89; Cl, 8.71%.

**Recovery of Dicyclohexyl Carbodiimide from Dicyclohexylurea.**—To 49.5 g. (0.22 mol.) of dicyclohexyl urea, 90 g. of pyridine and 43.9 g. (0.22 mol.) of *p*-toluenesulfonyl chloride were added. The reaction mixture was stirred for one and a half hours at 70~75°C, whereby a faintly yellow precipitate formed. After cooling, petroleum ether was added. The reaction mixture was filtered, and a small amount of triethylamine was added to the filtrate which was then boiled for one hour. A brown precipitate separated out and was filtered off. The filtrate was evaporated in vacuo to a syrup, which was distilled under reduced pressure. It solidified at room temperature; yield 31.8 g. (70%), b. p. 120~130°C/3 mmHg.

**Cleavage Reactions of α, γ-Glutamyl Peptides in Hot Water.**—Solutions of 200~300 mg. samples of α,γ-glutamyl diglutamic acid, α,γ-glutamyl diglycine, α,γ-glutamyl diaspartic acid, α,γ-glutamyl dileucine, γ-glutamyl glutamic acid and α-glutamyl glutamic acid in 20~30 ml. of distilled water were heated in a boiling water bath. An aliquot of each solution was chromatographed using *n*-butyl alcohol-acetic acid-water (4 : 1 : 2) as a developing solvent. The chromatograms were then sprayed first with bromothymol blue in 95% ethyl alcohol and then with ninhydrin in *n*-butyl alcohol. The original peptides were revealed by bromothymol blue as well as by ninhydrin except in the case of α,γ-glutamyl dileucine which showed coloration only with ninhydrin (Figs. 1—6).

In Fig. 1, the spot 1d is the original peptide XIV. After heating the solution for one hour at 100°C, pyrrolidone carboxylic acid (1b) and glutamic acid (1e) were formed. A spot (1c) is supposed to be pyroglutamyl glutamic acid because it was not colored by ninhydrin but only by bromothymol blue. The original peptide (1d) disappeared completely after seven hours. An unknown spot (1a) appeared after twenty-one hours' heating. In another experiment in which the solution was heated at 40°C, the original peptide (1d) was hardly decomposed at all even after one week (Fig. 1).

Fig. 2 shows that the peptide XX (2b) was

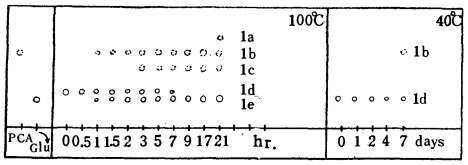



Fig. 1. The cleavage reaction of $\alpha,\gamma$-L-glutamyl di-L-glutamic acid.

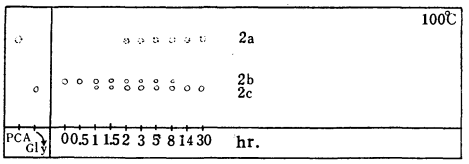



Fig. 2. The cleavage reaction of $\alpha,\gamma$-L-glutamyl diglycine.

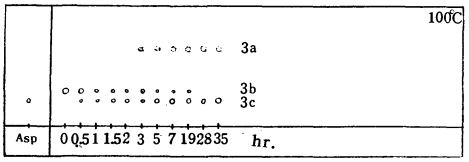



Fig. 3. The cleavage reaction of $\alpha,\gamma$-L-glutamyl di-L-aspartic acid.

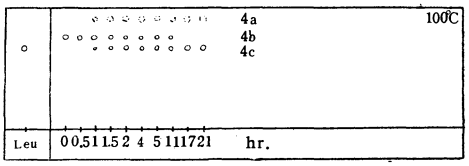



Fig. 4. The cleavage reaction of $\alpha,\gamma$-L-glutamyl di-L-leucine.

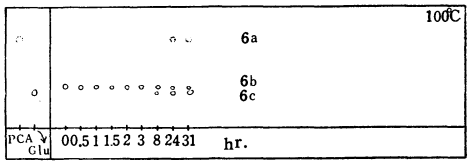



Fig. 5. The cleavage reaction of $\gamma$-L-glutamyl-L-glutamic acid.

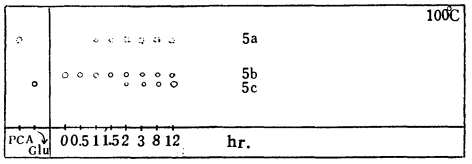



Fig. 6. The cleavage reaction of $\alpha$-L-glutamyl-L-glutamic acid.

○: Ninhydrin coloration, ◌: Bromothymol blue coloration, PCA: Pyrrolidone carboxylic acid.

completely decomposed after eight hours, while glycine (2c) and pyroglutamyl glycine (2a) were formed. Spot 2a was an acidic substance like spot 1c without a free amino group and its structure was shown by the following experiment to be pyroglutamyl glycine. The peptide XX was refluxed with water for eight hours, and then Dowex 50 (H form) was added to the solution until a pH of 1.94 was reached. After filtration the filtrate was evaporated in vacuo to a syrup, which was shown by paper chromatography to be identical with 2a. This syrupy substance was hydrolyzed by 6 N hydrochloric acid at 100°C for eight hours. A two-dimensional paper chromatogram of the hydrolyzate showed two ninhydrin-positive spots of glutamic acid and glycine. Therefore, spot 2a must be due to pyroglutamyl glycine.

Fig. 3 shows the decomposition of the peptide XXIV. It was completely decomposed after twenty eight hours, while aspartic acid (3c) and pyroglutamyl aspartic acid (3a) began to appear after half an hour and three hours respectively.

The cleavage of the peptide XXII is shown in Fig. 4. A spot of the original peptide (4b) disappeared after seventeen hours, while pyroglutamyl leucine (4a) and leucine (4c) appeared.

In Fig. 5, spots 5a, 5b and 5c correspond to pyrrolidone carboxylic acid, original $\gamma$-glutamyl glutamic acid and glutamic acid, respectively. Pyrrolidone carboxylic acid (5a) appeared before glutamic acid (5c).

Fig. 6 shows that in contrast to the peptides in Figs. 1—5 $\alpha$-glutamyl glutamic acid (6b) could not be completely decomposed even after thirty-one hours, and that glutamic acid (6c) and pyroglutamic acid (6a) appeared only after weight and twenty-eight hours respectively.

**Reaction between Carbobenzyloxy Glutamic Acid and Dicyclohexyl Carbodiimide.**—A solution of 3.7 g. (0.018 mol.) of dicyclohexyl carbodiimide in 30 ml. of tetrahydrofuran was added to a solution of 5.0 g. (0.018 mol.) of carbobenzyloxy-L-glutamic acid in 30 ml. of tetrahydrofuran. A precipitate of dicyclohexyl urea separated out immediately. After stirring at room temperature (20°C) for four hours the dicyclohexyl urea was filtered off; weight 3.8 g., m. p. 228~229.5°C. The filtrate was evaporated to dryness in vacuo and the residue was dissolved in ethyl acetate. A small amount (0.2 g.) of undissolved dicyclohexyl urea was filtered off again. The total weight of dicyclohexyl urea obtained in the two crops was 4.0 g. It corresponds almost to the theoretical amount expected from the dehydration reaction. The filtrate was again evaporated to a syrup which could not be crystallized.

**Synthesis of Dibenzyl Carbobenzyloxy-$\alpha,\gamma$-L-glutamyl Diglycinate from Carbobenzyloxy-L-glutamic Anhydride.**—A solution of 2.6 g. (0.010 mol.) of carbobenzyloxy-L-glutamic anhydride[23], synthesized from carbobenzyloxy-L-glutamic acid and acetic anhydride, in 50 ml. of tetrahydrofuran was prepared. Solutions of 7.8 g. (0.023 mol.) of benzyl glycinate-*p*-toluenesulfonate[24] and 4.3 g. (0.023 mol.) of tri-*n*-butylamine in 100 ml. of tetrahydrofuran and of 2.3 g. (0.011 mol.) of dicyclohexyl carbodiimide in 10 ml. of tetrahydrofuran were then

added at room temperature. The reaction mixture was stirred for six hours and the crystal of dicyclohexyl urea was filtered off; weight 1.4 g. (56%), m. p. 228~230°C. While the filtrate was concentrated, a large amount of a crystalline material separated out, which was collected by filtration, suspended in 0.25 N aqueous sodium carbonate, filtered and washed carefully with water; yield 5.3 g. (92%), m. p. 145~149°C. This crystalline material was suspended in 50 ml. of 2 N hydrochloric acid, filtered, washed with water and then recrystallized from ethyl alcohol to give 4.2 g. of pure crystals, m. p. 152~154°C (sintered at 148°C). The infrared spectrum was identical with the one of the ester (XIX) prepared directly from carbobenzyloxy glutamic acid.

Found: C, 64.70; H, 5.84; N, 7.31. Calcd. for $C_{31}H_{33}O_8N_3$: C, 64.68; H, 5.78; H, 7.30%.

The authors wish to thank Mr. Kazunobu Ono for his assistance in the experiments, Dr. Hans J. Cahnmann, National Institutes of Health, U. S. A., for his generous advice on preparing this manuscript and Ajinomoto Co. Inc. for their kind gift of various amino acids.

*Department of Chemistry*
*Faculty of Science*
*Osaka University*
*Nakanoshima, Osaka*

# *Leaching of Andesite in Acid Media*

By Hiroshi KAMIYA

(Received June 2, 1960)

"Leaching" is a term often used in geology. There is little geochemical study on the leaching process of rocks.

In many epithermal deposits such as sulfur, iron sulfide, opal and alunite ores, the original host rocks have been altered with acid leaching and other processes, and transformed into various altered zones.

Leaching action of surface and ground waters takes part in weathering processes at ordinary temperature and pressure.

As a result, it is important to investigate under natural conditions the behavior of chemical elements, which are abundant in the host rocks as constituents of rock-forming minerals, in order to consider the mechanism of weathering and the alteration of host rocks in the zone of oxidation.

In the study on the behavior of chemical elements, the concept "mobility" has been introduced by many investigators. The relative mobility of some elements in hydrothermal condition has been established by Bakhmutov[1]. Moreover, in weathering processes including leaching, migration and fixation of constituents of the host rocks by actions of ground and surface waters, their mobilities have been discussed[2].

Mobility defined in this way is affected by pH and oxidation-reduction potentional of the environments and many other factors.

Elements may move not only as ions, but as colloids or detrial fragments of original minerals. The movement of the elements as emanation, moreover, may take place, where volcanic gasses take part in the formation of altered rocks.

The above-mentioned discussions are based on no theory or experiments but on field data and observations, as well as on the analysis of natural substances.

The initial processes of both alteration and weathering are chemical and physical decompositions of rocks. Concerning this, solubility of rocks and minerals in water has been measured[3-5].

The present experiment was carried out to investigate what mobility the constituents of rock-forming minerals have, as mainly ions in various acid media in the presence of a sufficient quantity of air.

It is the aim of this study to obtain quantitative data on a leaching action which may play a serious role in weathering and alteration of rocks in the zone of oxidation.

1) L. A. Bakhmutov, *A Translation of Geokhimiya*, No. 1, 83 (1958).
2) D. H. Anderson and H. E. Hawkes, *Geochim. et Cosmochim. Acta*, **14**, 204 (1958).
3) M. D. Dorfman, *A Translation of Geokhimiya*, No. 5, 537 (1958).
4) D. Carroll and H. C. Starkéy, *Geochim. et Cosmochim. Acta*, **16**, 83 (1959).
5) L. K. Yakhontova, *A Translation of Geokhimiya*, No. 1, 95 (1958).

## Experimental

**Sample.**—Like other sulfur deposits, various kinds of altered rocks consisting of secondary minerals, such as opal, alunite and kaoline, were found around sulfur ore bodies of Ogushi Mine in Gumma Prefecture.

It has been recognized there that one of the original host rocks thus hydrothermally altered is augite hypersthene-andesite. The least altered andesite was powdered to 150~200 meshes and used for the present leaching experiment. The chemical composition and mode of the andesite are shown in Tables I and II.

TABLE I. CHEMICAL COMPOSITION OF ANDESITE

| Constituent | Content (%) |
|---|---|
| $SiO_2$ | 55.8 |
| $Al_2O_3$ | 18.8 |
| FeO | 4.1 |
| $Fe_2O_3$ | 3.4 |
| MgO | 3.8 |
| CaO | 7.5 |
| $Na_2O$ | 2.1 |
| $K_2O$ | 1.0 |
| $H_2O$ (−) | 3.0 |
| $H_2O$ (+) | 1.4 |
| Total | 100.9 |

TABLE II. VOLUME PERCENTAGE OF THE CONSTITUTENTS OF THE ANDESITE

| | | |
|---|---|---|
| Phenocryst | Plagioclase | 38 |
| | Hypersthene | 9 |
| | Augite | 8 |
| | Magnetite | 5 |
| Groundmass | | 33 |
| Alteration product | | 7 |
| Total | | 100 |

**Equipment.**—A polyethylene 500 ml. bottle, which contained 200 ml. of leaching acid or water to suspend the powdered sample, was placed on a water bath. This leaching bottle was fitted with a two-hole rubber stopper carrying a polyethylene tube of 5 mm. diameter attached to a flow-meter of air through a washing bottle and reached nearly to the bottom of the leaching bottle so that the leaching acid or water in it would be well stirred by the introduction of air, and also carrying a condenser connected to an aspirator.

For all equipment polyethylene was used because glass could introduce silica and sodium.

**Procedure.**—The flow of air was regulated with the aspirator so that the air would be bubbled through the solution at the rate of 2 l. per minute.

As its temperature was raised up to approximately 90°C, 2 g. of the powdered sample was suspended in it. The leaching experiments were carried out at 90±3°C.

After 5 min., 30 min., 1, 2 and 3 hr. from addition of the sample, the treatment was stopped immediately, and the leachates were centrifuged and analyzed.

For this experiment were used 0.1, and 0.01, 0.001 N sulfuric acids and distilled water.

**Analytical Method.**—The leachates were analyzed for silica, aluminum, iron, calcium, magnesium, sodium and potassium which are abundant in the rock.

1) *$SiO_2$.*—Silica was determined colorimetrically by a molybdenum blue method which would determine only dissolved silica, but no colloidal silica.

2) *Fe.*—Colorimetric estimation of total iron was carried out by reduction of all the iron to ferrous state, using hydroxylamine, and then by measurement of transmittance of a red color developed with $\alpha, \alpha'$-dipyridyl. Ferrous iron was determined by adding $\alpha, \alpha'$-dipyridyl with no reducing agents, reading the transmittance and comparing with a calibration curve. Ferric iron was determined by difference from the sum of the two.

3) *Al.*—Total iron and aluminum was detemined by back titration of a small excess of EDTA with a standard zinc sulfate solution using dithizone as an indicator after addition of sodium acetate buffer. Then, aluminum was determined from the amount of total iron and aluminum after deducting the amount of iron obtained by colorimetric method.

4) *Ca and Mg.*—Total calcium and magnesium were determined by titrating with EDTA in the presence of Eriochrome Black T at pH 10 after removal of iron and aluminum. Next calcium was determined by titration with EDTA using NANA* indicator in strong alkaline solution, and finally the amount of magnesium was calculated by subtracting the amount of calcium from the combined amount.

5) *Na and K.*—Sodium and potassium were determined by means of flame photometry.

## Results and Discussion

**Leaching of Seven Constituents.**—The amounts of seven constituents, $SiO_2$, Al, Fe, Ca, Mg, Na and K leached out of 2 g. sample with sulfuric acid or water at 5 min., 30 min., 1, 2 and 3 hr., respectively, after starting the leaching are arranged in Table III. They are plotted against time in Fig. 1.

As change in pH of the leaching media might have an influence on the leaching, it was desirable to keep the pH of them constant and to maintain the original leaching conditions. However, the experiment under pH-constant condition was not carried out, because the use of buffer solutions, for instance, would make it difficult to detect small amount of constituents leached out of the rock and have an effect on the leaching. Ranges from initial to final pH of the leaching acid or water are given in Fig. 1.

Among the constituents leached, only silicon

* NANA is a commercial name which has chemical formula of 2-hydroxy-1-(2'-hydroxy-4'-sulfo-1-naphthylazo)-3-naphthoic acid.

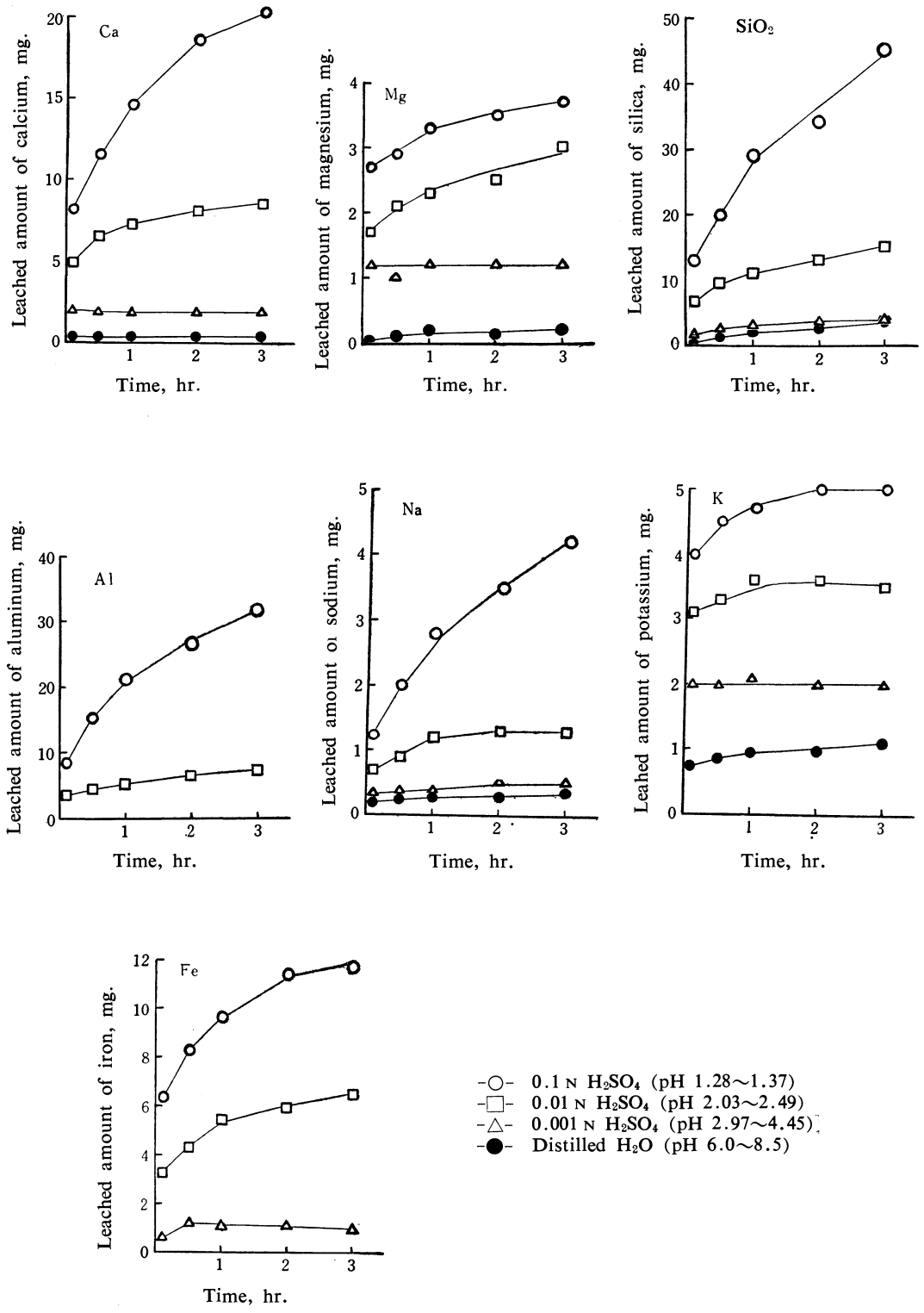



Fig. 1. Leaching-curve of seven constituents plotted against time.

TABLE III. SEVEN CONSTITUENTS LEACHED OUT OF 2 g. POWDERED SAMPLE WITH 200 ml. SULFURIC ACID AND WATER

| | Time | Na (mg.) | K (mg.) | Ca (mg.) | Mg (mg.) | $Fe^{2+}$ (mg.) | $Fe^{3+}$ (mg.) | Al (mg.) | $SiO_2$ (mg.) | pH |
|---|---|---|---|---|---|---|---|---|---|---|
| | 5 min. | 1.2 | 4.0 | 8.2 | 2.7 | 5.6 | 0.7 | 8.5 | 13 | 1.31 |
| 0.1 N-$H_2SO_4$ | 30 min. | 2.0 | 4.5 | 11.6 | 2.9 | 6.3 | 2.0 | 15.2 | 20 | 1.33 |
| (pH 1.28) | 1 hr. | 2.8 | 4.7 | 14.6 | 3.3 | 6.4 | 3.3 | 21.2 | 29 | 1.34 |
| | 2 hr. | 3.5 | 5.0 | 18.5 | 3.5 | 7.8 | 3.6 | 26.5 | 34 | 1.35 |
| | 3 hr. | 4.2 | 5.0 | 20.2 | 3.7 | 8.5 | 3.2 | 31.6 | 45 | 1.37 |
| | 5 min. | 0.7 | 3.1 | 4.9 | 1.7 | 3.2 | <0.1 | 3.4 | 6.5 | 2.20 |
| 0.01 N-$H_2SO_4$ | 30 min. | 0.9 | 3.3 | 6.5 | 2.1 | 4.1 | 0.2 | 4.4 | 9.5 | 2.28 |
| (pH 2.03) | 1 hr. | 1.2 | 3.6 | 7.2 | 2.3 | 5.3 | <0.1 | 5.2 | 11 | 2.35 |
| | 2 hr. | 1.3 | 3.6 | 8.0 | 2.5 | 5.7 | 0.2 | 6.6 | 13 | 2.42 |
| | 3 hr. | 1.3 | 3.5 | 8.5 | 3.0 | 6.2 | 0.2 | 7.3 | 15 | 2.49 |
| | 5 min. | 0.35 | 2.0 | 2.0 | 1.2 | 0.67 | <0.05 | 0.2 | 1.6 | 3.89 |
| 0.001 N-$H_2SO_4$ | 30 min. | 0.37 | 2.0 | 1.9 | 1.0 | 1.1 | 0.1 | 0.2 | 2.6 | 4.33 |
| (pH 2.97) | 1 hr. | 0.40 | 2.1 | 1.8 | 1.2 | 1.0 | 0.1 | 0.3 | 3.0 | 4.37 |
| | 2 hr. | 0.43 | 2.0 | 1.8 | 1.2 | 1.1 | <0.05 | 0.2 | 3.9 | 4.42 |
| | 3 hr. | 0.42 | 2.0 | 1.8 | 1.2 | 0.9 | 0.1 | 0.3 | 4.0 | 4.45 |
| | 5 min. | 0.21 | 0.75 | 0.3 | <0.1 | <0.05 | — | 0.1 | 0.6 | 7.4 |
| Distilled $H_2O$ | 30 min. | 0.24 | 0.87 | 0.2 | 0.1 | <0.05 | — | 0.1 | 1.4 | 7.7 |
| (pH 6.0) | 1 hr. | 0.28 | 0.95 | 0.2 | 0.2 | <0.05 | — | 0.2 | 2.2 | 8.2 |
| | 2 hr. | 0.28 | 0.97 | 0.3 | 0.1 | <0.05 | — | 0.2 | 2.8 | 8.5 |
| | 3 hr. | 0.34 | 1.1 | 0.3 | 0.2 | <0.05 | — | 0.2 | 3.6 | 8.5 |

is represented as $SiO_2$, because it would be leached in the form of oxide[6].

As shown in Fig. 1, time of leaching, generally, tends to increase the amount of constituents leached. The leaching is very rapid for an initial stage of the experiment, but becomes retarded gradually later, as the concentration of constituents in the leachate appears to approach the limit of their solubility in the leaching acid or water.

The lower pH of the leaching media is, the larger initial leached amount and its increment are. At a high pH of the leaching media such as 0.001 N sulfuric acid and distilled water, time of leaching hardly increases the initial leached amount of several constituents.

The rock contains both ferrous and ferric irons. There existed more ferrous than ferric iron in the leachate of 0.1 N sulfuric acid, and in the leachate of 0.01 N and 0.001 N sulfuric acids and distilled water ferric iron was hardly detected. As the leached ferrous iron might be oxidized to ferric state by bubbled air, it should not be concluded that all the ferric iron in the leachate came only of one kind in the rock. Therefore, the leaching curve of total iron is drawn without a distinction between ferric and ferrous irons in Fig. 1.

With 0.001 N sufuric acid the leaching of iron proceeds during the first 30 min. of the experiment, but prolongation of it decreases its amount in the leachate. This decrease may be caused by reprecipitation of iron once leached owing to an increase of pH.

**Initial Leaching.**—As already described, the initial leaching is very rapid. A considerable amount of constituents was leached out of the rock even during the first 5 min. of experiment.

Each straight line, which is drawn through the first two points representing the leached amount at 5 and 30 min. on the curves given in Fig. 1, does not pass through the origin, but intercepts the axis of the leached amounts. The value of this interception may be thought to correspond to the initial leached amount. In 0.1 N sulfuric acid, for example, this amount of potassium reached 80 per cent of its amount leached up to the end of the experiment.

The initial leaching ratio, that is, the ratio of the initial leached amount of each constituent, obtained in this way, to its content in the original rock was calculated. In Fig. 2 these ratios are plotted against initial pH of the leaching acid or water used for the experiment.

Fig. 2 shows that the initial leaching ratio of every constituent decreases with an increase of pH. The ratio of potassium is the largest among the constituents under the experimental conditions, that is, at pH range 1 to 6. On the contrary, that of silica is the smallest. The ratio of sodium belongs to a rather small

6) H. Mukaiyama, *Min. Geol.*, 4, 195 (1954).

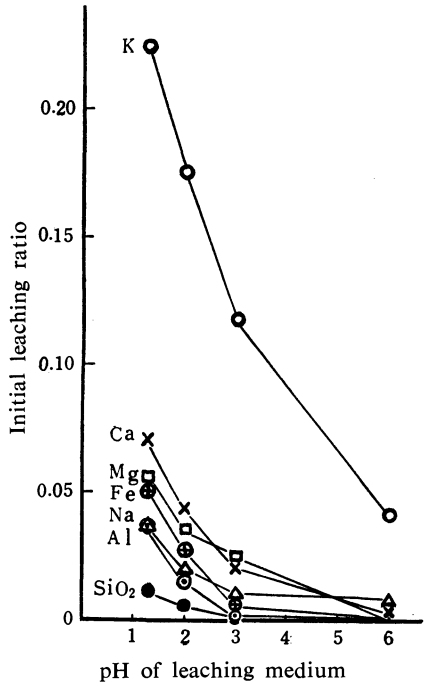



Fig. 2. Relation between initial leaching ratio and pH of leaching medium.

group at low pH, but is large next to that of potassium at pH 6.

Above pH 3 the ratios of aluminum and iron are much the same to that of silica.

**Increasing Rate of Leached Amount.** — The leaching of the constituents out of the rock proceeds at a certain increasing rate, whereupon it becomes gradually retarded.

During three hours of the leaching experiment an average increment per hour of the amount of each constituent excepting the initial leached amount was obtained from the curve in Fig. 1. This increasing rate expresses an average slope of the curve which passes through the five points corresponding to the amount leached at each time.

The ratio of this rate to the content of each constituent in the rock was calculated and plotted against the intermediate value of initial and final pH of the leaching acid or water in Fig. 3.

With an increase of pH, the increasing ratio defined in this way has the same tendency to decrease as the initial leaching ratio has. However, the increasing rate of several constituents is too small to be recognized in 0.001 N

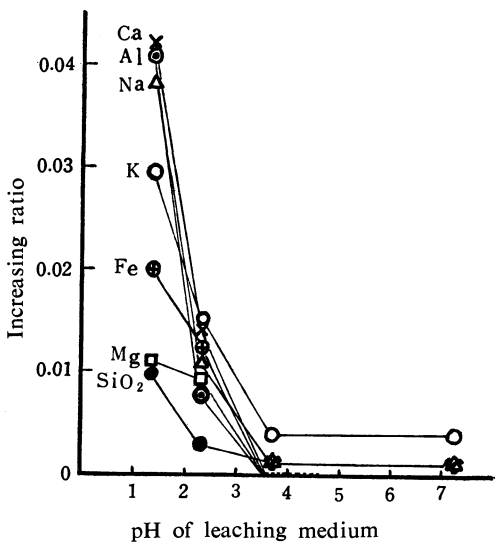



Fig. 3. Relation between increasing ratio and pH of leaching medium.

sulfuric acid and distilled water. In general, the leaching of all the constituents out of the rock is retarded at high pH. For this reason a small increasing rate need not be discussed in detail.

The curves of the increasing ratio in Fig. 3 differ somewhat from the curves of the initial leaching ratio in Fig. 2.

At pH 1 calcium, aluminum and sodium refer to a group of large ratio, next to which are potassium and iron. The ratio of magnesium and silica are small at this pH. Raising of pH changes the order of the ratios at pH 1. At pH 2 aluminum, which has a large ratio at pH 1, belongs to a group of smaller ratio, and on the other hand potassium is the top of them. Magnesium has less difference of the ratio than other constituents at pH range 1 to 2.

**A Comparison between Initial Leaching Ratio and Increasing Ratio.**—In Table IV are given the following ratios of each constituent at pH's 1 and 2.

$$\frac{\text{Increasing ratio (shown in Fig. 3)}}{\text{Initial leaching ratio (shown in Fig. 2)}}$$

Table IV shows that the leaching of potassium is very rapid at an initial stage but becomes retarded soon, that is, the average slope of its leaching curve is less steep than the other constituents in Fig. 1, and that on the contrary

Table IV. Increasing ratio/initial leaching ratio

| | Na | K | Ca | Mg | Fe | Al | $SiO_2$ |
|---|---|---|---|---|---|---|---|
| 0.1 N-$H_2SO_4$ | 1.1 | 0.1 | 0.6 | 0.2 | 0.4 | 1.1 | 0.9 |
| 0.01 N-$H_2SO_4$ | 0.6 | 0.1 | 0.3 | 0.3 | 0.4 | 0.5 | 0.6 |

the increasing rate of sodium, aluminum and silica is superior to the initial leaching.

As a result, every constituent has a characteristic initial leaching ratio and increasing ratio which may depend on mineral composition of the rock or other factors.

The least mobility of silica in the present experiment agrees in Shimada's conclusion that action of sulfuric acid could cause aluminum, iron etc. originally present in rocks to be removed leaving silica to form siliceous rocks[7].

Though a leaching process of rocks would be very complicated under natural conditions, the effect of pH on it is the most important one of many environmental factors.

The writer wishes to express his indebtedness to Professor K. Noguchi for having been good enough to read this manuscript, to Dr. T. Sudo for helpful advice and encouragement and to Dr. J. Ossaka and Mr. M. Ichikuni for help and advice with regard to the analytical techniques. His acknowledgement is also due to the staff of the Ogushi Mine for help in the collection of specimens.

*Department of Chemistry*
*Faculty of Science*
*Tokyo Metropolitan University*
*Setagaya, Tokyo*

7) K. Shimada, *J. Chem. Soc. Japan. Pure Chem. Sec.* (*Nippon Kagaku Zasshi*), **80**, 263 (1959).

# SHORT COMMUNICATIONS

## *Chlorination of Guaiacol Relating to Bleaching Mechanism of Pulp*

By Koichiro SATO and Hiroshi MIKAWA

(Received September 6, 1960)

To make clear the mechanism of chlorination of lignin by an aqueous chlorine solution, chlorination of lignin and model compounds[1] have been investigated since some years ago.

In advance of the investigation of the behavior of complex lignin-like models against aqueous chlorine solution, guaiacol was investigated first. Because, it is expected that this simple case will show the fundamental principle of the chlorination reaction of the benzene nucleus.

As quite recently C. Dence and K. Sarkanen[2] have reported similar investigations, the results obtained in our laboratory till now are summarized and reported briefly as follows.

A homogenous aqueous solution of guaiacol (128 g. guaiacol in 7 l. of water) was treated 7.5 l. of aqueous chlorine solution (molar ratio 1 : 1) for about 1/2 hr. at 0°C. A small amount of sodium sulphite solution was added to destroy the excess of remaining chlorine or hypochlorous acid if any, and the pH of the solution was adjusted to nine with sodium hydroxide. Sodium borohydride was added in order to reduce the quinoidal structure to pyrocatechol structure to prevent the polymerization of quinoidal structure if any. Then, the solution was acidified, resinous products separated (I), and the whole was extracted continuously with chloroform (II) followed, by ether (III).

I and II were distilled in vacuo into four fractions respectively, each fraction was examined gas chromatographically, and the fractions containing similar components were combined.

From the five fractions thus obtained the following compounds were separated and identified.

1) Guaiacol: The compound was separated as 3, 5-dinitrobenzoate, m. p. 137~139°C, which was not depressed on admixture with the authentic sample. (Found: $OCH_3$, 10.25. Calcd. for $C_{14}H_{10}O_7N_2$: $OCH_3$, 9.75%.)

2) 5-Chloroguaiacol*: The compound was separated as 3, 5-dinitrobenzoate, m. p. 170~171.5°C, which was not depressed on admixture with the authentic sample. (Found: C, 47.71; H, 3.20; Cl, 10.08; $OCH_3$, 8.77. Calcd. for $C_{14}H_9O_7N_2Cl$: C, 47.68; H, 2.55; Cl, 10.07; $OCH_3$, 8.79%.)

3) 4, 5-Dichloroguaiacol: White needles, m. p. 71~73°C, which was not depressed on

1) K. Sato, K. Ebisawa and H. Mikawa, *J. Chem. Soc. Japan, Ind. Chem. Sec* (*Kogyo Kagaku Zasshi*), **61**, 1090 (1958).
2) C. Cence and K. Sarkanen, *Tappi*, **43**, No. 1, 83 (1960).

* Named according to Beilstein's Handbook.

admixture with the authentic sample. (Found: C, 43.68; H, 3.29; Cl, 36.65. Calcd. for $C_7H_6O_2Cl_2$: C, 43.55; H, 3.13; Cl, 36.74%.)

4) Trichloroguaiacol: Pale yellow needles, melting at 103~106°C. (Found: C, 37.58; H, 2.41; $OCH_3$, 13.91. Calcd. for $C_7H_5O_2Cl_3$: C, 36.94; H, 2.21; $OCH_3$, 13.62%.) The positions of chlorine atoms are not settled as yet.

5) 3, 3'-Dimethoxy-4,4'-dihydroxydiphenyl: White prisms, melting at 166~167°C. (Found: C, 67.71; H, 5.73; $OCH_3$, 25.75; Cl, 0.00. Calcd. for $C_{12}H_8O_2(OCH_3)_2$: C, 68.28; H, 5.73; $OCH_3$, 25.21%). Diacetyl derivative, melting at 200.5~202°C. (Found: C, 65.35; H, 5.95; mol. wt. (Rast), 336. Calcd. for $C_{18}H_{18}O_6$: C, 65.44; H, 5.49%; mol. wt., 330.32). Dimethyl derivative (biveratrol), melting at 132~133°C. (Found: C, 69.85; H, 6.72; mol. wt. (Rast), 273. Calcd. for $C_{16}H_{18}O_4$: C, 70.05; H, 6.61%; mol. wt., 274.30).

Melting points of the diphenyl and its two derivatives agree well with the values reported in literatures[3,4]. The diphenyl has one phenolic hydroxyl group per methoxyl group, according to the so-called $\Delta\varepsilon$-method of Aulin-Erdtman[5].

From the fraction III the following compounds were separated and identified.

1) Pyrocatechol: White prisms, melting at 103.5~104.5°C, undepressed on admixture with the authentic sample. (Found: C, 65.33; H, 5.54. Calcd. for $C_6H_6O_2$: C, 65.44; H, 5.49%.)

2) 3-Chloropyrocatechol: The compound was isolated as mono carboxymethyl ether, melting at 122~123.5°C, undepressed on admixture with the authentic sample of 3-chlorocatechol monocarboxymethyl ether. (Found: C, 47.70; H, 3.71; Cl, 17.71. Calcd. for $C_8H_7O_4Cl$: C, 47.43; H, 3.46; Cl, 17.52%). The position of the carboxymethyl group of the mono-ether is not determined. Diether was not prepared, as it was found to be difficult to etherify both hydroxyl groups of 3-chloropyrocatechol by an usual method.

Results so far obtained on the effects of aqueous chlorine water on the guaiacol nucleus are summarized as follows:

1) Methoxyl group is demethylated to give methanol in high yield[1].

2) Isolation of pyrocatechol suggests that demethylation can occur without introduction of any chlorine atoms into the nucleus.

3) One to three chlorine atoms are introduced without cleavage of methoxyl groups.

4) It seems therefore to be probable that chlorination of the nucleus and the demethylation of methoxyl group are independent reactions.

5) Guaiacol dimerizes by dehydrogenation.

Details of this work will be published later.

*Research Laboratory*
*of the Kokusaku Pulp Ind. Co. Ltd.,*
*Kamiochiai, Shinjuku, Tokyo*

3) F. Fichter and W. Dietrich, *Helv. Chim. Acta*, **7**, 131 (1924).

4) S. Tamura, K. Okuma, Y. Miyao and N. Haramaki, *J. Agr. Chem. Soc. Japan (Nippon Nogei-Kagaku Kaishi)*, **27**, 877 (1953).

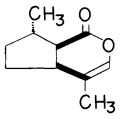
5) Aulin-Erdtman, *Svensk Papperstidn*, **55**, 745 (1952).

## *The Synthesis of dl-Nepetalactone*

By Takeo SAKAN, Akira FUJINO,
Fujio MURAI, Akio SUZUI
and Yasuo BUTSUGAN

(Received September 10, 1960)

The authors wish to report the synthesis of *dl*-nepetalactone, the levorotatory form of which was first isolated in 1941 from the oil of catnip plant, *Nepeta cataria* L., by S. M. McElvain et al.[1], and was later shown clearly to be I[2,3].

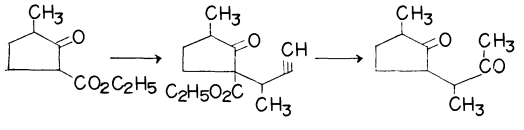


I

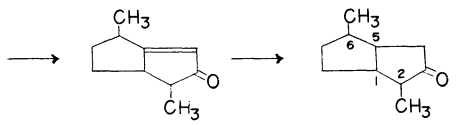
Ethyl 3-methyl-2-oxocyclopentanecarboxylate[4] (II) was condensed with 3-bromobutyne[5] to give III, b. p. 99°C/1 mmHg ($\nu_{C\equiv C}$ 4.72 $\mu$, $\nu_{C=O}$ 5.72 $\mu$, 5.86 $\mu$), which was, after hydration, hydrolyzed to diketone IV, b. p. 86°C/1 mmHg (Found: C, 70.97; H, 9.44. Calcd. for $C_{10}H_{16}O_2$: C, 71.39; H, 9.59%) ($\nu_{C=O}$ 5.78 $\mu$, 5.86 $\mu$). IV was converted through intramolecular condensation into bicyclic $\alpha,\beta$-unsaturated ketone V, b. p. 66~70°C/1 mmHg ($\lambda_{max}^{EtOH}$ 240 m$\mu$, $\varepsilon=21{,}000$; $\nu_{C=O}$ 5.88 $\mu$, $\nu_{C=C}$ 6.01 $\mu$). Semicarbazone: m. p. 188~189°C; 2, 4-dinitrophenylhydrazone: m. p. 213°C. Catalytic hydrogenation of V afforded saturated ketone VI, b. p. 72~75°/2 mmHg (Found: C, 78.57; H, 10.57. Calcd. for $C_{10}H_{16}O$: C, 78.89; H, 10.59%) ($\nu_{C=O}$

1) S. M. McElvain, R. D. Bright and P. R. Johnson, *J. Am. Chem. Soc.*, **63**, 1558 (1950).
2) J. Meinwald, ibid., **76**, 4571 (1954).
3) R. B. Bates, E. J. Eisenbraun and S. M. McElvain, ibid., **80**, 3420 (1958).
4) W. Dieckmann, *Ann.*, **317**, 37 (1903).
5) M. T. Rogers and M. B. Panish, *J. Am. Chem. Soc.*, **77**, 3684 (1955).

5.78 $\mu$), likely fulfilling the stereochemical requirements ($H_{(C-1)}-H_{(C-5)}-H_{(C-6)}$: cis-trans). 2, 4-Dinitrophenylhydrazone of VI: m. p. 87~88°C.



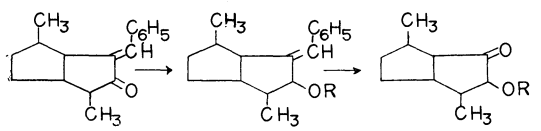
II III IV



V VI

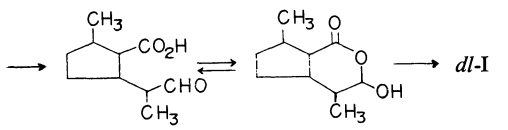
To make sure the above stereospecificity, the benzylidene derivative (VII), b. p. 110~120°C/0.005 mmHg ($\lambda_{max}^{EtOH}$ 303 m$\mu$, $\varepsilon$=13,000; $\nu_{C=O}$ 5.86 $\mu$, $\nu_{C=C}$ 6.18 $\mu$) (2, 4-dinitrophenylhydrazone: m. p. 181~182°C), of VI was ozonolyzed. A dicarboxylic acid, $C_{10}H_{16}O_4$ (Found: C, 60.29; H, 8.29. Calcd.: C, 59.98; H, 8.05%), m. p. 124.5~126°C, was obtained as an oxidation product. As the IR spectrum of this compound in carbon disulfide was in good accord with that of one (m. p. 85°C[3]) of nepetalinic acids, the acid in hand was distinctly racemic *cis-trans*-nepetalinic acid (m. p. in lit.[6]: 127°C).

Then VII was reduced with sodium borohydride to unsaturated alcohol VIIIa, b. p. 110~128°C/0.015 mmHg ($\nu_{OH}$ 2.98 $\mu$). Acetylation of VIIIa yielded a crystalline acetate (VIIIb), m. p. 120~121°C (Found: C, 79.90; H, 8.55. Calcd. for $C_{19}H_{24}O_2$: C, 80.24; H, 8.51%) and an oily one (VIIIb'), b. p. 105~108°C/0.025 mmHg (Found: C, 80.09; H, 9.00%) ($\nu_{C=O}$ 5.77 $\mu$), the latter predominating much over the former.



VII VIII IX

a: R=H, b, b': R=COCH$_3$



$X_A$ $X_B$

When VIIIb was, after ozonolysis and hydrolysis, oxidized with permanganate, a dicarboxylic acid, $C_{10}H_{16}O_4$ (Found: C, 60.11; H, 8.26%), m. p. 158~159°C, was the only product, which showed an IR absorption undoubtedly different from that given by either of the nepetalinic acids (m. p. 85°C and m. p. 117~118°C). Therefore, the crystalline acetate might result from the ketone of cis-cis-series corresponding to VI, formed in a small quantity in the process IV → V → VI.

VIIIb' was ozonolyzed to $\alpha$-acetoxyketone IXb, b. p. 70~73°C/0.05 mmHg (Found: C, 68.17; H, 8.84. Calcd. for $C_{12}H_{18}O_3$: C, 68.54; H, 8.63%). On treatment with diluted alkali, IXb afforded $\alpha$-ketol IXa ($\nu_{OH}$ 2.89 $\mu$, $\nu_{C=O}$ 5.80 $\mu$), which was too unstable to be distilled, and was immediately oxidized with periodate to aldehyde carboxylic acid $X_A$. The product, with some charactor of lactol $X_B$, was dehydrated to *dl*-nepetalactone (*dl*-I), b. p. 135°C (bath temp.)/7 mmHg ($\nu_{C=O}$ 5.68 $\mu$, $\nu_{C=C}$ 5.93 $\mu$) by heating at about 200°C. The synthesized lactone accorded in all respects with the natural lactone in their IR charts except only a slight difference of the absorption intensities near 11.4 and 12.2 $\mu$.

The authors are grateful to Professor S. M. McElvain for his kind offer of the spectrum chart of nepetalactone for the identification.

*Institute of Polytechnics*
*Osaka City University*
*Kita-ku, Osaka*

6) K. J. Clark, G. I. Fray, R. H. Jaeger and Sir R. Robinson, *Tetrahedron*, 6, 217 (1959).

## *Retention of Mn-56 in Neutron-irradiated Potassium Permanganate*

By Hirotoshi SANO

(Received October 27, 1960)

Although the behavior of radioactive manganese atoms produced by $(n, \gamma)$ reaction on permanganate has been studied by several investigators[1,8,9], no information is available on the effect of irradiation temperature on the retention of radio manganese as permanganate. It has been reported that the retention tends to decrease as the irradiation temperature lowers down to dry-ice or liquid-nitrogen temperature in various inorganic salts such as

1) W. F. Libby, *J. Am. Chem. Soc.*, 61, 1930 (1940); W. Rieder, E. Broda and J. Erber, *Monatsh.*, **81**, 657 (1950); K. J. McCallum and A. G. Maddock, *Trans. Faraday Soc.*, **49**, 1150 (1953).

TABLE I. EFFECT OF TEMPERATURE AT BOMBARDMENT SITE

| Sample | Length of irradiation, min. | Storage time, min. | Retention, % (Irradiation temperature) −196°C | −72°C | 25°C | 90~190°C |
|---|---|---|---|---|---|---|
| Crude $KMnO_4$ | 150 | 30 | — | 16.7±0.6 | 15.2±0.4 | — |
| Recrystallized $KMnO_4$ | 140 | 〃 | 23.8±0.6 | 23.1±0.4 | 21.2±0.3 (21.6±0.2)[a] | — |
| 〃 | 150 | 〃 | 23.3±0.5 | — | 21.8±0.3 | 38.8±0.4 |
| 〃 | 〃 | 〃 | 23.0±0.5 | 21.0±0.4 | 20.0±0.3 | — |
| 〃 | 〃 | 〃 | 23.5±0.5 | 23.3±0.4 | 20.8±0.3 (21.6±0.2)[a] | — |

a) Sample was irradiated in a paraffin block (5 cm. thickness). It has been known that the neutron energy has no effect on the retention as $KMnO_4$[8].

TABLE II. EFFECT OF STORAGE TEMPERATURE AFTER BOMBARDMENT

| Sample | Length of irradiation, min. | Storage time, min. | Retention, % (Storage temperature) −196°C | −72°C | 25°C | 85~180°C |
|---|---|---|---|---|---|---|
| Recrystallized $KMnO_4$ | 60 | 100 | 19.3±0.3 | — | 20.5±0.3 | — |
| 〃 | 90 | 〃 | — | 19.2±0.3 | 19.0±0.3 | — |
| From Aten's data[9] | — | 120 | — | — | 21~26 | 35~74 |

$K_3Co(CN)_6$[2], $K_2ReCl_6$[3], $KIO_3$[4], $K_3AsO_4$[5], $K_2CrO_4$[6] and $[Co(NH_3)_5Br](NO_3)_2$[7].

A seriess of experiments have been carried out by the present author to study the effect of temperature on retention of recoil radio manganese as permanganate. About one-half gram of potassium permanganate in small crystals was placed in separate glass tubes. For low temperature bombardments, the glass tubes were dipped in either liquid nitrogen or dry-ice–etheanol, while they were warmed by preheated oil for high-temperature bombardments. The samples were exposed for two to three hours to neutrons at a flux of ca. $10^7$ $n/cm^2$ sec. The maximum energy of neutrons produced by Be–D reaction was ca. 7 MeV. All bombardments were made in the presence of air. Following the bombardments, the samples were dissolved in distilled water and mixed with a small amount of manganese sulfate solution. The resulting manganese dioxide was filtered through a paper filter without suction. Both the precipitate and the filtrate were reduced with sodium sulfite. The activity of the resulting solution was measured with a dipping type G-M counter, and decay curve was determined. In another series of experiments, the samples were bombarded for 1 to 1.5 hr. at room temperature and then stored for nearly two hours at various temperatures. They were treated in the same way as described above. The results are summarized in Tables I and II.

It is worth mentioning that the bombardment at dry-ice–ethanol or liquid-nitrogen temperature always resulted in slightly higher retentions than the room temperature bombardment did. The results seem to be peculiar as compared with these obtained for other inorganic salts[2-7], in which the retension tends to decrease as the temperature lowers. The bombardment at 90~190°C resulted in highest retentions. This is probably due to an effect similar to thermal annealing. It is seen from Table II that the storage at dry-ice–ethanol or liquid-nitrogen temperature has little effect on the retention.

The author acknowledges the helpful advice given by Professor Nobufusa Saito, and the Institute of Physical and Chemical Research for irradiating samples.

*Department of Chemistry*
*Faculty of Science*
*The University of Tokyo*
*Hongo, Tokyo*

2) H. Rauscher and G. Harbottle, *J. Inorg. Nucl. Chem.*, **4**, 155 (1957).
3) W. Herr, *Z. Elektrochem.*, **56**, 911 (1952).
4) N. Saito, H. Sano and R. Shiomi, Presented at the Symposium on Radiochemistry, Kyoto, 1958.
5) N. Saito and I. Tomita, ibid.
6) G. Harbottle, *J. Chem. Phys.*, **22**, 1083 (1954).
7) N. Saito, H. Sano and T. Tominaga, This Bulletin, **33**, 20 (1959).
8) E. Broda and W. Rieder, *J. Chem. Soc.*, 1949, (s) 356 W. Rieder, *Acta Phys. Austriaca*, **4**, 290 (1950).
9) A. H. W. Aten, Jr. and J. B. M. van Berkum, *J. Am. Chem. Soc.*, **72**, 3273 (1952).

# *Transport Behavior of Some Inorganic Cations across Ion-exchange Membranes. Preferential Impermeability of Barium Ions across Sulfonic Acid Membrane*

By Takeo YAMABE, Manabu SENŌ, Tatuo TANAKA and Ichiro KAMII

(Received September 20, 1960)

It appears to be generally accepted that the permselectivity of a given ion across ion-exchange membranes is closely related to the selectivity of the ion in the ion-exchange equilibria, while the mobilities of ions in solution and membranes are one of the most important factors that have effects on the permeability. In fact, as shown already by one of the authors[1], the order of the permselectivity of cations across a heterogeneous sulfonated styrene cation-exchange membrane[2] is as follows: $H^+ > K^+ > NH_4^+ > Ca^{2+} > Mg^{2+} > Na^+$, and it was recognized that the ion with the larger mobility and the larger selectivity in the ion-exchange reaction possesses the larger permselectivity. In the present communication, it is reported that barium ions show a peculiar transport behavior in the electrodialyses using ion-exchange membranes. As shown in Table I, barium ions show an extraordinarily small permeability, in spite of their very large selectivity in the ion-exchange equilibria.

TABLE I. PERMSELECTIVITIES OF ALKALI-EARTH METAL IONS

| Ions | Permselectivity* | Selectivity of ion-exchange** | Mobility in inf. dil. soln. |
|---|---|---|---|
| M | $T^M_{Na}$ | $K^M_{Na}$ | cm²/V. sec. |
| $Ca^{2+}$ | 1.24[7] | 2.60 | $5.29\times10^{-4}$ |
| $Mg^{2+}$ | 1.13[1] | 1.66 | 4.66 〃 |
| $Ba^{2+}$ | 0.70 | 5.81 | 5.70 〃 |

* Experimental conditions used: Current density 0.02 amp./cm², concentration of stock solution (2-component, ratio 1 : 1) 0.1 N, time 2∼4 hr.

** Data of O. D. Bonner et al. on Dowex 50 X8[8].

This result may be interpreted as follows: The large selectivity of barium ions is owing to the formation of a complex salt with the sulfonated group which dissociates scarecely, resulting in the relatively small concentration of barium ions in unrestricted state[3]. The small concentration of free ions in membranes leads to their small permselectivity. In general, the most predominant factors in determining the permeability of ions across membranes are the mobility and the concentration of unbound ions in membranes, but not the selectivity in the ion-exchange equilibria. The transport behavior of barium ions is one of the confirmative evidences for the deduction and it is also supported by the permeability of some heavy metal ions[6].

The experimental procedure was the same as those given in the preceding papers[1,7], i. e., from the electrodialysis data using a multi-compartment cell with cation- and anion-exchange membranes alternatively, the permselectivity coefficients were calculated according to the equation

$$T^B_A = \left(\frac{t^+_B - t^-_B}{t^+_A - t^-_A}\right) \Big/ \left(\frac{c_B}{c_A}\right) = \frac{r_B - 1}{r_A - 1}$$

where $t^+_A$ and $t^+_B$ are the transport numbers of ion A and B across a cation-exchange membrane, $t^-_A$ and $t^-_B$ are those across an anion-exchange membrane, $c_A$ and $c_B$ are concentrations of ion A and B in the stock solution and $r_A$ and $r_B$ are concentration ratios of ion A and B obtained directly from experimental data. If transport numbers of cations across an anion-exchange membrane are small and remain nearly constant, independently of the kind of cations, this coefficient should be a mesure of the permselectivity of given cations across a cation-exchange membrane. It will be permissible to think that this conditions is fulfilled in this experiment.

*The Institute of Industrial Science*
*The University of Tokyo*
*Yayoi-cho, Chiba (T. Y. & M. S.)*

*Showa College of Pharmacy*
*Tsurumaki-cho, Setagaya*
*Tokyo (T. T. & I. K.)*

1) T. Yamabe and Y. Tanaka, *J. Chem. Soc. Japan, Ind. Chem. Sec.* (*Kogyo Kagaku Zasshi*), **63**, 1342 (1960).

2) This membrane was prepared with pulverized Amberlite IR-120 and the other membranes used in the present experiments were prepared with Amberlite ion-exchange resin powder.

3) It is suggested by the formation of a water-insoluble barium salt with toluenesulfonic acid and is also supported by the swelling behavior[4] and the electric conductivity data[5] of barium-form resin.

4) M. Senō and T. Yamabe, presented at the 9th Annual Meeting of the Society of Polymer Science, Osaka, May 29, 1960.

5) E. Heymann and I. J. O'Donnell, *J. Colloid Sci.*, **4**, 405 (1949); A. O. Jakubovic, G. J. Hills and J. A. Kitchener, *Trans. Faraday Soc.*, **55**, 1570 (1959).

6) M. Senō, T. Saito and T. Yamabe, This Bulletin, **33**, 563 (1960).

7) T. Yamabe, M. Senō and T. Tanaka, *Bull. of Soc. of Salt Sci. Japan* (*Nihon Shio Gakkai-shi*), to be published.

8) It is structurally identical with Amberlite IR-120. Moreover, it was revealed that nearly the same ion-exchange reactions take place for both the heterogeneous ion-exchange membrane and the ion-exchange resin, from which the membrane is prepared.
T. Yamabe and T. Saito, *J. Chem. Soc. Japan, Ind. Chem. Sec.* (*Kogyo Kagaku Zasshi*), **63**, 1848 (1960).

## *Molecular Rotations of Polyhydroxycyclohexanes in Relation to their Structures*[1]

By Shukichi YAMANA

(Received November 5, 1960)

Availability of PM-method[2] for the case of $[M]_D^{20}(W)$[3] of polyhydroxycyclohexanes of C1 conformation was tested here. Names of several substances under discussion, together with the orientation of the unit groups, (OH), in their molecules and their $[M]_D^{20}(W)$ are shown in Table I[4]. At first, by using the theoretical

1) Presented at the Symposium on the Structural Chemistry of the Chemical Society of Japan, Sapporo, August 5, 1960.

2) S. Yamana, This Bulletin, **31**, 558 (1958).

3) $[M]_D^{20}$ (W) is a notation which represents the optical molecular rotation of the plane polarized light of wavelength of D-line at 20°C by an aqueous solution of an optically active substance. $[\mu]_{D\,obs}^{20}$ means a corresponding partial molecular rotation which is caused by the dynamical coupling effect between any two members of unit groups in the molecule.

$$\therefore \quad [M]_D^{20}(W) = \sum [\mu]_{D\,obs}^{20} = \sum_{i \neq k} \zeta_i \zeta_k [\mu]_{D\,calcd}^{20}$$

(Ref. Eq. 3 in the previous paper[2]). Here, $[\mu]_{D\,calcd}^{20}$ is the calculated value by using Kirkwood's theoretical formulae and $\zeta_i$ and $\zeta_k$ are adjustable parameters.

4) The central group, cyclohexane-ring, does not appear in the calculation.

TABLE I

| Name Cyclohexane | Orientation of unit group, (OH) | Obs. $[M]_D^{20}$(W)[5] | Calcd. $\sum[\mu]_{Dobs}^{20}$[12] | Calcd. Whiffen[9] |
|---|---|---|---|---|
| (−) 1/2 diol | [(1β), (2α)] | −48.2[6] | −42.7(−42.7) | −45 |
| (+) 3/1,2 triol | [(1α), (2α), (3β)] | 92.0[7] | 92.2(96.3) | 90 |
| (−) 1,2,3/4 tetrol | [(1β), (2β), (3β), (4α)] | −49.2[7] | −49.5(−53.6) | −45 |
| (+) 3/1,2,4 tetrol | [(1α), (2α), (3β), (4α)] | 53.9[6] | 49.5(53.6) | 45 |
| (−) 1,3/2,4 tetrol | [(1β), (2α), (3β), (4α)] | −42.7[7] | −42.7(−42.7) | −45 |
| (+) 3,5/1,2,4 pentitol | [(1α), (2α), (3β), (4α), (5β)] | 86.2[8] | 85.4(85.4) | 90 |
| (+) 1,3,4/2,5 pentitol | [(1β), (2α), (3β), (4β), (5α)] | 42[9] | 49.5(53.6) | 45 |
| (+) 3,5,6/1,2,4 hexitol | [(1α), (2α), (3β), (4α), (5β), (6β)] | 117[9] | 128.1(128.1) | 135 |

TABLE II. $[\mu]_{Dcalcd}^{20}\{3/(n^2+2)\}$ AND $[\mu]_{Dobs}^{20}$[3], CAUSED BY THE DYNAMICAL COUPLING EFFECT BETWEEN ANY TWO MEMBERS OF UNIT GROUPS IN POLYHYDROXYCYCLOHEXANE OF C1 CONFORMATION

| | 6β | 6α | 5β | 5α | 4β | 4α | 3β | 3α | 2β | 2α |
|---|---|---|---|---|---|---|---|---|---|---|
| 1α | 0 | $-A$ | $-B$ | 0 | 0 | 0 | $B$ | 0 | 0 | $A$ |
| 1β | $-A$ | $A$ | 0 | $B$ | 0 | 0 | 0 | $-B$ | $A$ | $-A$ |
| 2α | $-B$ | 0 | 0 | 0 | $B$ | 0 | $A$ | $-A$ | | |
| 2β | 0 | $B$ | 0 | 0 | 0 | $-B$ | $-A$ | 0 | | |
| 3α | 0 | 0 | $B$ | 0 | 0 | $A$ | | | | |
| 3β | 0 | 0 | 0 | $-B$ | $A$ | $-A$ | | | | |
| 4α | $B$ | 0 | $A$ | $-A$ | | | | | | |
| 4β | 0 | $-B$ | $-A$ | 0 | | | | | | |
| 5α | 0 | $A$ | | | | | | | | |
| 5β | $A$ | $-A$ | | | | | | | | |

Note :

| | $[\mu]_{Dcalcd}^{20}\{3/(n^2+2)\}$ | $[\mu]_{Dobs.}^{20}$ |
|---|---|---|
| $A$ | 11.73 (6.50)[12] | 42.7 (42.7) |
| $B$ | 1.88 (1.66) | 6.8 (10.9) |

formulae of Kirkwood[10], all $[\mu]_{Dcalcd}^{20}\{3/(n^2+2)\}$'s possible in the molecule were calculated[11] and given in Table II. Next, by using these values of $[\mu]_{Dcalcd}^{20}\{3/(n^2+2)\}$ and an adjustable parameter, $\zeta_{OH}$, the following equation was obtained.

$[M]_D^{20}$(W) of (−)1, 3/2, 4 tetrol, −42.7 $\equiv\sum[\mu]_{Dobs}^{20}$ of (−)1, 3/2, 4 tetrol $=(1\beta)\,\bar{\times}\,(2\alpha)+(1\beta)\,\bar{\times}\,(3\beta)+(1\beta)\,\bar{\times}\,(4\alpha)+(2\alpha)\,\bar{\times}\,(3\beta)+(2\alpha)\,\bar{\times}\,(4\alpha)+(3\beta)\,\bar{\times}\,(4\alpha)$[13] $=\{(n^2+2)/3\}\zeta^2_{OH}\{(1\beta)\times(2\alpha)+(1\beta)\times(3\beta)+(1\beta)\times(4\alpha)+(2\alpha)\times(3\beta)+(2\alpha)\times(4\alpha)+(3\beta)\times(4\alpha)\}$[14] $=\{(n^2+2)/3\}\zeta^2_{OH}(-11.73+0+0+11.73+0-11.73)$

$$\therefore\quad \zeta^2_{OH}=3.6402\{3/(n^2+2)\}$$

or

$$\zeta_{OH}=1.9079\{3/(n^2+2)\}^{1/2}$$

The values of $A$ and $B$ for $[\mu]_{Dobs}^{20}$ in Note of table II, can be obtained by multiplying those for $[\mu]_{Dcalcd}^{20}\{3/(n^2+2)\}$ by $\zeta^2_{OH}\{(n^2+2)/3\}$. By using the values of $[\mu]_{Dobs}^{20}$ in Table II, $\sum[\mu]_{obs}$ of all polyhydroxycyclohexanes were calculated and given in the fourth column of Table I. Referring to Table I, it becomes apparent that PM-method is more suitable one to estimate $[M]_D^{20}$(W) of polyhydroxycyclohexanes than Whiffen's method[9], especially when the optical center is located at the center of mass of a bond.

The author wishes to express his sincere thanks to Professor T. Yamamoto, Kyoto University, for his advice and encouragement.

*Department of Chemistry*
*Kyoto Gakugei University*
*Fushimi-ku, Kyoto*

5) From the standpoint that $\partial[M]_D(W)/\partial T$ is small, some values were presumed from $[M]_D(W)$ which had been observed in the neighborhood of 20°C but not exactly at 20°C.

6) Th. Posternak, D. Reymond and H. Friedli, *Helv. Chim. Acta*, **38**, 205 (1955).

7) Th. Posternak and D. Reymond, ibid., **38**, 195 (1955).

8) Th. Posternak, ibid., **33**, 343 (1950).

9) D. H. Whiffen, *Chemistry and Industry*, **1956**, 964.

10) S. Yamana, This Bulletin, **30**, 203 (1957).

11) The molecular model of a cyclohexane derivative and optical data of (OH) are assumed as follows. The length of C-C bond is 1.54Å, and that of C-O bond is 1.42Å. The valency angle of C atom is 109° 28′. Mean polarizability, $\alpha$, of (OH) is $1.40\times10^{-24}$ (cc.). Anisotropy ratio, $\beta$ of (OH) is 0.35[10].

12) The values, calculated by supposing that the optical center of (OH) is located at its O atom, are given in parentheses.

13) S. Yamana, This Bulletin, **30**, 916 (1957).

14) Ref. Eq. 32 in the foot-note 32 of the previous paper[2].

## *Reaction of Enamines. I. The Preparation of Thiocarbonyl Compounds*

By Yujiro NOMURA and Yoshito TAKEUCHI

(Received November 9, 1960)

The reactions of enamines[1-3] have been well investigated[4-6]. We have paid attention to the reactivities of enamines and found that thiocarbonyl compounds were obtained by the reaction between enamines and hydrogen sulfide. Thiocarbonyl compounds are usually prepared by the treatment of an acid solution of the corresponding carbonyl compounds with hydrogen sulfide. This method is, however, often likely to lead to the formation of trimers, but our new method is successful in preparing monomeric compounds in good yield.

Twenty grams of 1-morpholino-1-cyclohexene[7] was dissolved in 90 cc. of dimethylformamide and hydrogen sulfide was introduced for six hours with ice cooling. The exothermic reaction occurred and the reaction mixture became faint yellow. Yellow oil separated at once when 100 cc. of 6 N hydrochloric acid was added with stirring and ice cooling.

After adding 100 cc. of water, the oil was extracted with petroleum ether, washed several times with water, dried and distilled in vacuo under nitrogen. The pink liquid, b. p.* 77~78°C/15 mmHg, with disagreeable odour was obtained, whose color was gradually faded away on standing[8].

Yield 10.0 g. (73% theoretical).

The product gave 2, 4-dinitrophenylhydrazone, m. p. 159~160°C, which showed no m. p. depression on admixture with cyclohexanone 2, 4-dinitrophenylhydrazone.

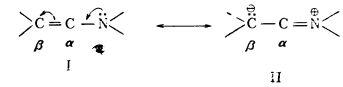
IR spectrum of the product in carbon tetrachloride solution indicated the existence of C=S bond (medium intensity band at 1130 $cm^{-1}$) and the lack of C=O bond of cyclohexanone (strong intensity band at 1705 $cm^{-1}$).

All these facts lead us to identify this product as cyclohexanethione.

By practically the same method, cyclopentanethione was prepared in considerably good yield. From 47.4 g. of 1-morpholino-1-cyclopentene[9] in 200 cc. of dimethylformamide was obtained 23.2 g. (68% theoretical) of cyclopentanethione, b. p.** 63~65°C/8 mmHg. This gave 2, 4-dinitrophenylhydrazone, m. p. 145~146°C, which was found, by means of the mixed melting point test, to be identical with cyclopentanone 2, 4-dinitrophenylhydrazone.

IR spectrum had no absorption at 1740 $cm^{-1}$ ($\nu_{C=O}$ of cyclopentanone).

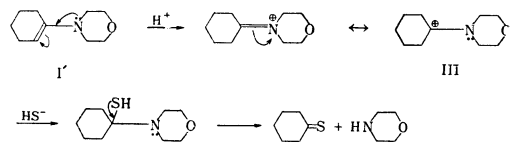
Enamines have two mesomeric forms, enamine-form I and iminoform II.



I II

The reaction of enamines proceeds in most cases through the attack of electrophilic reagent at $\beta$-carbon atom of imino-form II, but nucleophilic attack at $\alpha$-carbon atom has also been reported[6].

It is postulated that the reaction of enamines and hydrogen sulfide occurs by the nucleophilic attack of $HS^-$ ion on the protonated enamine intermediate (III) as follows.



I' III

We continue to explore the full scope of the reaction of enamines with hydrogen sulfide. The results of the further investigation will be reported in more detail later.

*Department of Chemistry*
*College of General Education*
*The University of Tokyo*
*Meguro-ku, Tokyo*

1) C. Mannich and H. Davidsen, *Ber.*, **69**, 2106 (1936).
2) F. W. Heyl and M. E. Herr, *J. Am. Chem. Soc.*, **75**, 1918 (1953).
3) G. Opitz, H. Hellmann and H. W. Schubert, *Ann.*, **623**, 112 (1959).
4) P. L. deBenneville and J. H. Macartney, *J. Am. Chem. Soc.*, **72**, 3073 (1950).
5) G. Stork, R. Terrell and J. Szmuszkovicz, ibid., **76**, 2029 (1954).
6) R. F. Parcell, ibid., **81**, 2596 (1959).
7) S. Hünig, E. Benzing and E. Lücke, *Chem. Ber.*, **90**, 2833 (1957).
8) D. C. Sen, *J. Indian Chem. Soc.*, **13**, 268 (1935). Cf. *Chem. Abstr.* **31**, 6340⁴ (1936).
9) S. Hünig and W. Lendle, *Chem. Ber.*, **93**, 909 (1960).

* The reported b. p.[8] 76°C/15mmHg.
** The reported b. p.[8] 86~88°C/10mmHg.